Design, synthesis and fluorescent characterisation of 2,5-dihydro-1,2,3-triazines.

NUI MAYNOOTH

Ollscoil na hÉireann Má Nuad

PhD. Thesis

Presented to the Department of Chemistry,
Faculty of Science and Engineering,
National University of Ireland Maynooth,
Maynooth,
Co. Kildare,
Ireland.
in requirements for the Degree of:

MHE02 Philosophiae Doctor Research Degree in Chemistry

By

Dean Edward St. Mart BSc.

October 2013

Supervisor / Head of Department: Dr. John C. Stephens

Declaration of Authorship

I hereby certify that this thesis has not been submitted before, in whole or in part, to this or any other university for any degree and is, except where stated, the original work of the author.

Signed: _____ Date: _____

Dean Edward St. Mart B.Sc.

Dedication

To my parents, Christian and Modey, for your constant support throughout my life.

To my grandparents, Roger and Suzanne, Thomas and Alice, who always believed in my potential and the encouragement to do something important with my life.

In loving memory of
(Gran) Roger St. Mart and Cathy Wolfe.

"When you feel like giving up,
remember why you started in the first place….."

Acknowledgements

I would first like to express my gratitude to my supervisor, Dr. John Stephens, for his constant encouragement and time throughout my PhD. Thank you for the opportunity to be part of a talented research group. I am very grateful for to have had the opportunity to apply and succeed in being selected to attend the 60th Lindau Meeting of the Nobel Laureates; that is an experience I will never forget. I will always value the friendship you've shown to me and all the lessons I have learned from being your student.

To Dr. Alan Ryder and Dr. Denisio Togashi at NUI Galway; thank you for introducing me to the fascinating world of fluorescence. Every visit to your lab was an enjoyable experience; especially the summer of 2011 I spent living in Galway researching at your laboratory. The discussions which we had and knowledge you have both imparted on me will not be forgotten. To Prof. Luke Burke; it was a pleasure to meet you and hear your intriguing stories of touring European universities in past times. I am very grateful for the computational work which you performed and enjoyed the discussions I partook with you. To Dr. Elisa Fadda, your help with computational calculations came at an invaluable time. To Prof. Vickie McKee and Prof. Patrick Mc Ardle for their help of x-ray crystal structure determination of several compounds. IRC for EMBARK postgraduate research scholarship and NUI Maynooth for Pat and John Hume Scholarship.

To all the lecturing staff at NUI Maynooth; thank you for all your support, both as an undergraduate and postgraduate. To all the technical staff at NUI Maynooth; Ollie, Barbaara, Ria, Anne, Walter, Orla and Noel for all your help. To Dr. Ken Maddock, for our interesting talks about art, science and exercise, and co-developer of the "super" steam distillation apparatus.

To all the members of the Dr. John Stephens research group; thank you for making the time as a member of the group a memorable experience. To all postgraduates of the NUIM Chemistry Department, both past and present, I wish everyone the best in their future endevaours.

To Wayne; for sharing a bench in the beginning and the company when working late nights in the lab. To Pauraic; for your deep passion of chemistry and our discussions of everything from sport and nutrition to chemistry. To Laura, for all your constant

encouragement and support. Wayne, Pauraic and Louise; thank you for a place to stay on all our nights out in Maynooth, I hope all our friendship remains into the future.

To all my friends from home and those I have made along the way, either through university, work, kickboxing or bodybuilding; you've all made this a much easier experience. To my Aunty Sharon, for all her support and kindness over the years. To my Uncle Lukey, for all his inspiration when I was younger.

To my grandparents, for all your support when I was growing up; you have helped shape me into who I am today. To Gran, you always said to me to be a proud person in life, that education was very important and to do something significant with my life. I hope I have made you proud.

To my dogs; Toby, who sadly passed away at beginning of this journey after being my best friend for 17 years, and to Toki and Ace for their unconditional love no matter the time of day. To my brother, Ashley; although we argue, I will always love and support you in life. You're future is bright if you focus and apply your potential.

Finally, to my parents; words can't describe the support you have given me both in my academic and leisurely pursuits. You have not denied me anything throughout my life and have always encouraged me to pursue greater things. Your love has helped me through difficult times and I shall always be eternally grateful to you both.

Abstract

Design, synthesis and fluorescent characterisation of 2,5-dihydro-1,2,3-triazines.

Dean Edward St. Mart (PhD)

National University of Ireland Maynooth, 2013

The extrinsic labelling of biomolecules for identification and/or quantification is a common methodology used in the lifesciences. This labelling, for example, can be carried out with (i) radioactive markers or (ii) compounds with absorption and/or fluorescence properties. With the advent of confocal microscopy and live cell imaging, fluorescence offers the tools to visualise and quantify the chemical and biochemical processes in living cells. The subject of this thesis concerns the synthesis and investigation of the fluorescence of a new class of organic fluorophores; the 2,5-dihydro-1,2,3-triazines.

A series of fluorescent 2,5-dihydro-1,2,3-triazines were synthesized *via* an interesting Huisgen 1,3-dipolar cycloaddition between 2,4,5-triphenyl-1,2,3-triazolium-1-arylaminide 1,3-dipoles and terminal alkyne propiolates. The initial cycloadduct undergoes a sigmatropic rearrangement followed by a ring expansion to generate the 2,5-dihydro-1,2,3-triazine fluorophore. The synthesis of 2,5-dihydro-1,2,3-triazine fluorophores with different structural changes, and the affect these changes had on the photophysics of the fluorophores was investigated. This was undertaken with a view to better understanding the fluorescence of this new class of fluorophore and to developing a fluorophore capable of conjugating to biomolecules. Several modifications were explored including (i) substituting the imine phenyl and N2 phenyl rings with heavy atoms, (ii) changing the methyl ester to a methyl ketone or 4-substituted phenyl ester, (iii) varying the substituent on the imine carbon and (iv) removing the phenylimine group.

In collaboration with Dr. Alan G. Ryder at NUI Galway and Prof. Luke A. Burke at Rutgers University, New Jersey; a full fluorescence charaterisation was performed building on preliminary photophysical studies. Steady state ultraviolet absorption, fluorescence spectroscopy and time domain lifetime measurements were conducted in order to elucidated a model of fluorescence for the 2,5-dihydro-1,2,3-triazines. These measurements in combination with TD-DFT calculations (relative energies, dipole moments, oscillator strength and calculated transition wavelength), courtesy of Prof. Luke A. Burke, allowed us

to generate a photophysical model that explains the fluorescence of the 2,5-dihydro-1,2,3-triazines. It was found that three structures may exist for the 2,5-dihydro-1,2,3-triazines: **g0** (optimized for S_0), **g1** (optimized for S_1) and, **g2** (optimized for S_2) and that the positioning of the imine and carbonyl ester on the triazine is very important in dictating the fluorescent and electronic properties. It was found that the phenylimine group is essential for the long lived fluorescence of the 2,5-dihydro-1,2,3-triazines. Furthermore, we propose that in order to maintain fluorescence the phenylimine group must have substituents small enough to allow the imine group to remain in plane with the carbonyl group. The energies of the excited states appeared to be affected by the interaction of the carbonyl with the imine hydrogen and by changes in electron density at the carbonyl group. A significant red shift was observed in the fluorescence emission in both cases where the methoxy group on the ester carbonyl was replaced with a less potent electron donating group or an electron withdrawing group *e.g.* methyl or benzotriazole group.

An extensive solvent fluorescent study was performed; ultraviolet absorption, fluorescence spectroscopy and time domain lifetime measurements. It was found that the 2,5-dihydro-1,2,3-triazine fluorophores were not affected by the solvent or microenvironment as no solvatochromism was observed in both the ground and excited state. The photostability of triazine **3a** in toluene was proven to be exceptional when placed under constant irradiation at 310 nm excitation in a spectrometer. When **3a** in toluene was exposed to intense UV illumination in the dark over a 6 hour period, the photostability was slightly greater than when compared to a standard, quinine sulphate in 0.1M sulphuric acid. The fluorophores are also not susceptible to collisional quenching by molecular oxygen. Degassing of a solution of triazine **3a** in toluene and measurement of its time correlated photon counting lifetime over a 35 minute only resulted in a 3 % increase in the intensity weighted average lifetime, as was also the case for triazine **10a**.

Substituting the 4-position of the imine phenyl and N2 phenyl rings with heavy atoms had very little effect on the molecule's energy levels, and the heavy atom effect was observed to be small in these cases. Changing from a methyl ester to a family of 4-substituted phenyl esters appeared to have only minor influence on the photophysics, supported by computational calculations by Dr. Elisa Fadda (NUI Maynooth). Although, the 4-NO_2 phenyl ester did display some solvent sensitivity, we believe that this is due to the NO_2 group itself interacting with the solvent system as opposed to its affect on the ester group.

The synthesis of propiolates containing stable activating groups (for coupling reactions) was performed. Their subsequent use in the 1,3-dipolar cycloaddition provided access to 2,5-dihydro-1,2,3-triazines containing the activating groups. These activated triazines are capable of conjugation to biomolecules. This approach generated an acylbenzotriazole and an isothiocyanate activated 2,5-dihydro-1,2,3-triazine. The acylbenzotriazole 2,5-dihydro-1,2,3-triazine was successfully coupled with L-alanine.

Table of Contents

Chapter 1: Introduction

1.1 ABSORPTION OF LIGHT AND EXCITED ELECTRONIC STATES.

The absorption of light by a molecule results in an electronic transition within the molecule. Such a transition involves the promotion of an electron from the highest occupied molecular orbital (HOMO) to the lowest unoccupied molecular orbital (LUMO). The energy difference between the excited state and the ground state should be consistent with the energy of the absorbed photon for the creation of an excited state.[1] The energy of the photon can be then described as:

$$E = h\nu = E_e - E_g \qquad 1.1.1$$

where E_e and E_g are the energies of the excited and ground states respectively, h is Planck's constant, and ν is the frequency of light.

The efficiency of light absorption at wavelength λ by a molecule is expressed by the Beer-Lambert law:

$$A(\lambda) = log\ (I_\lambda^O / I_\lambda) = \varepsilon(\lambda) * l * c \qquad 1.1.2$$

where $A(\lambda)$ is the measured absorbance, I_λ^O and I_λ are the light intensities of the incident and transmitted light respectively, $\varepsilon(\lambda)$ is the molar extinction coefficient, l is the absorption path length and c is the molar concentration of the absorbing species.[2]

Within each electronic state exist a set of vibrational states that correspond to different vibrational energies of the molecule governed by infrared frequencies. These vibrational states are in turn are associated with a set of rotational states that correspond to microwave frequencies.[1]

The total energy, E, of a particular state of a molecule can be represented as the sum of the electronic energy, E_{el}, the vibrational energy, E_{vib}, and the rotational energy, E_{rot}:

$$E = E_{el} + E_{vib} + E_{rot} \qquad 1.1.3$$

The overall change of energy as a result of the absorption of a photon of light is:

$$\Delta E = \Delta E_{el} + \Delta E_{vib} + \Delta E_{rot} \qquad 1.1.4$$

The absorption of a photon by a molecule is usually to a vibrational level above the 'zeroth' vibrational level of the excited singlet state.

An absorption spectrum maps out the energy difference between the ground state and the several vibrational levels of the excited singlet states. According to Boltzman distribution, at room temperature the majority of molecules exist in the lowest vibrational energy level of the ground state S_0.

For the first singlet excited state (S_1), the light absorption process occurs very rapidly (10^{-15} seconds) to form S_1. There is no change in the nuclear coordinates of the molecule during the absorption process and is known as a Frank Condon transition.

If absorption occurs to S_2, an internal conversion from the lowest vibrational level of S_2 to an upper vibrational level of S_1 results, with the molecule losing the excess vibrational energy through collision with solvent molecules and ends up in the lowest vibrational level of S_1. Thus, within 10^{-13} to 10^{-14} seconds of excitation the molecule is in the lowest (0^{th}) vibrational level of S_1, termed $S_1(0)$. Such a metastable state can now undergo a number of competing processes unavailable to the ground state.[1]

Typically, the excited state exists for a period of nanoseconds after which the molecule can return to the ground state either by radiative energy loss produced by the emission of a photon or by other possible de-excitation pathways (Figure 1.2.1).[3]

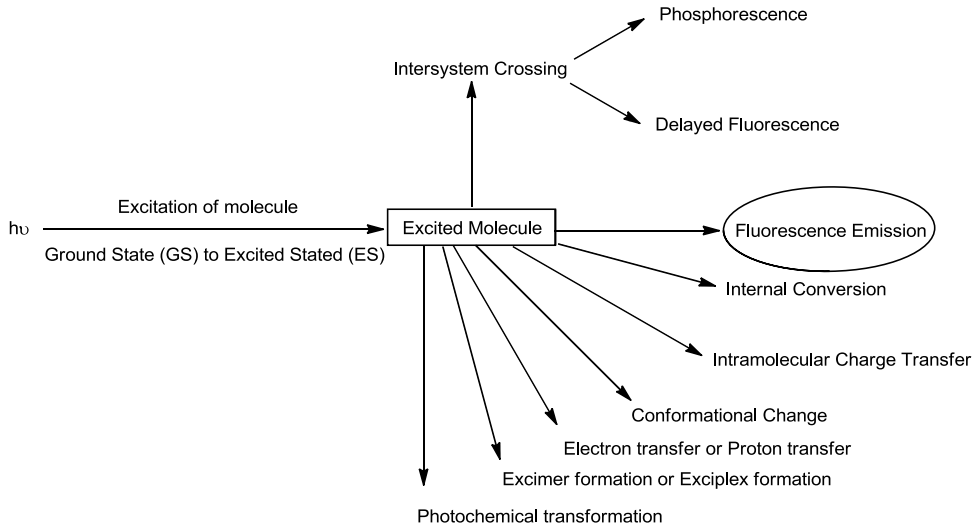

Figure 1.1.1. Possible de-excitation pathways following excitation.[3]

1.2 FLUORESCENCE.

Fluorescence is the process in which a molecule absorbs light of a given wavelength, and subsequently emits a photon of light of a different, usually longer, wavelength. Named after the Polish physicist Alexander Jablonski, a Jablonski diagram is a convenient way to illustrate the photon absorption processes and deactivation processes of the excited states (Figure 1.2.1).[1]

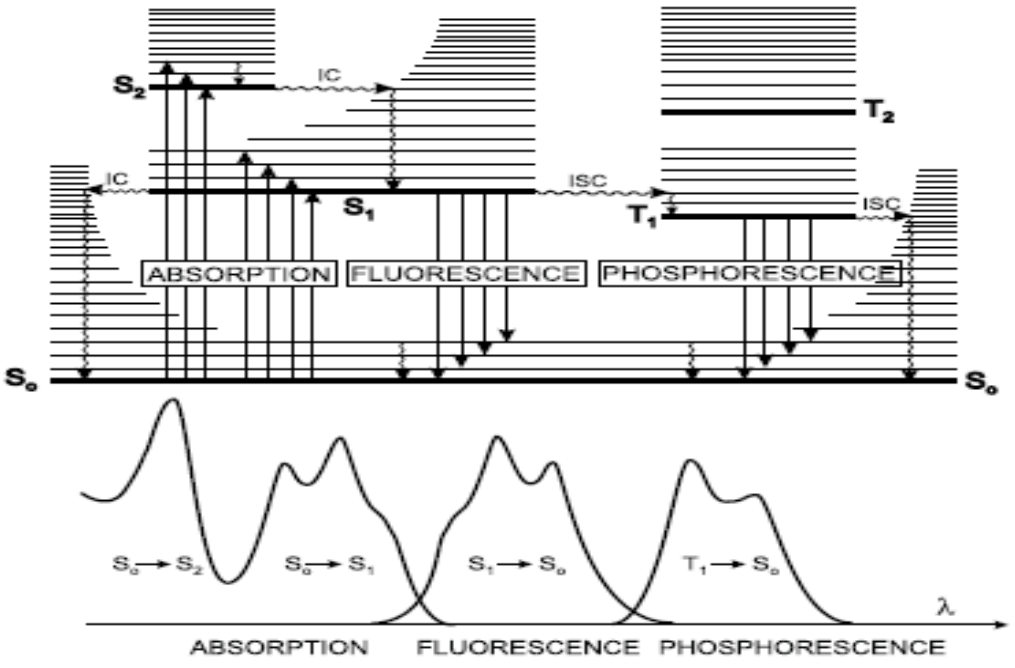

Time scale of fluorescence events:	
Absorption:	10^{-15} s
Vibrational relaxation:	10^{-12} to 10^{-15} s
Lifetime of singlet excited state, S_1:	10^{-12} to 10^{-7} s → Fluorescence
Intersystem crossing:	10^{-10} to 10^{-8} s
Internal conversion:	10^{-11} to 10^{-5} s
Lifetime of triplet excited state, T_1:	10^{-6} to 1 s → Phosphorescence

Figure 1.2.1. A Jablonski diagram showing the relative positions of the absorption, fluorescence and phosphorescence spectra as well as the electronic singlet excited states S_0, S_1 and S_2. Reproduced.[2]

Absorption of a photon results in promotion to one of the vibrational energy levels of S_1 or S_2; depending on the level of the absorbed energy. The energy loss in the excited state is due to vibrational relaxation, and therefore the energy of the emitted photon is lower in energy and of longer wavelength than the absorbed photon. The difference in energy or wavelength ($h_{\nu\ absorbance} - h_{\nu\ fluorescence}$) is known as the Stokes shift; an important parameter which can provide important information on the environment of the excited states based on solvatochromic shifts.

A molecule may also undergo intersystem crossing from S_1 to the first triplet state T_1, resulting in emission of a photon termed phosphorescence. This transition is forbidden but can occur due to spin-orbit coupling.[2] The process is longer lived (milliseconds to seconds) and of lower energy and higher wavelength than fluorescence.

Other interactions may compete with fluorescence in the excited state (i.e. energy transfer, proton transfer, electron transfer) provided they occur within the average time which the molecules exists in the excited state.[1]

1.2.1 Fluorescence Emission and Excitation Spectra.

Molecules which exhibit fluorescence are called fluorophores, and each can generate three characteristic spectra; absorption, emission, and excitation (Figure 1.2.1).

The emission spectrum is the wavelength distribution of the fluorescence intensity, measured at a single constant excitation wavelength and can be represented on a wavenumber (cm^{-1}) or wavelength (nm) scale.[4] The shape of the emission band is generally a mirror image of the longest wavelength absorption, provided the ground state vibrational levels are similar to those in the excited state.

The fluorescence intensity, I_F, is quantitatively dependent on the absorbance of the sample, as well as the fluorescence quantum yield of the fluorophore, Φ_F, and the intensity of the incident light, I_0, where:

$$I_F = \Phi_F * I_0 * (1 - e^{-\varepsilon lc}) \qquad 1.2.1$$

and ε is the molar extinction coefficient, l is the optical path length and, c is the molar concentration of the fluorophore. If the intensity of the incident light is constant, then the concentration of the fluorophore will have a linear relationship to the fluorescence intensity.

The fluorescence quantum yield, Φ_F, is defined as the fraction of excited molecules that return to the ground state S_0 with the emission of fluorescent photons and is usually determined by comparison with a fluorescence standard (e.g. Rhodamine 110). The fluorescence standard is so as to be preferably excited close to the same wavelength as the compound under investigation, and so as to have a fluorescence spectrum covering a similar wavelength range. The fluorescence quantum yield, Φ_F, is calculated using Equation 1.2.2:

$$\Phi_F = \Phi_{F(R)} * (n^2 / n^2_{(R)}) * (I / I_{(R)}) * (OD_{(R)} / OD) \qquad 1.2.2$$

where R is the reference solution, n is the refractive index of the solvent, OD is the optical density (absorbance), and I is the integrated area under the fluorescence spectra. However due to the small additive errors in measuring the absorbances at the excitation wavelength, the correction factors of the detection system and the quantum yield of the standard, the accuracy of the determination of fluorescence quantum yields cannot be better than 5–10%.[2,4]

Kasha's rule states that photon emission (fluorescence or phosphorescence) occurs only from the lowest excited state of a given multiplicity.[3] The rule is relevant in understanding the emission spectrum of an excited molecule. Upon absorbing a photon, a molecule in its electronic singlet ground state (S_0) may be excited to any of a set of higher electronic states (denoted S_n where $n>0$).

However, according to Kasha's rule, photon emission (fluorescence) is expected to generally occur only from the lowest excited state, S_1.

Since only one state is expected to yield emission, one may also surmise that the emission wavelength is independent of the excitation wavelength.

The rule can be explained by the Franck–Condon factors for vibronic transitions. The Franck–Condon factor (vibrational overlap integral) expresses the degree of overlap between the vibrational wavefunctions for a given pair of energy levels that differ in both vibrational and electronic quantum number.

The greater the overlap, the quicker the molecule can undergo a transition from a higher to lower level, with overlap being greatest when the two vibrational levels are close in energy.

In most molecules, the vibrationless levels of the excited states all lie close together, so molecules in upper states quickly reach the lowest excited state, $S_1(0)$, before they have time to fluoresce. This process is known as internal conversion (IC).

However, if the energy gap between higher electronic excited states and $S_1(0)$ is greater (*e.g.* the gap between S_2 and S_1), fluorescence (*e.g.* from S_2) will occur in competition with IC.[5]

This is an exception to Kasha's rule and such exceptions can arise when there are large energy gaps between excited states. An example is an isomer of naphthalene; azulene (Figure 1.2.2). Due to the $S_0 \rightarrow S_1$ transition having a weak absorption in relation to the absorption of the $S_0 \rightarrow S_2$, fluorescence emission occurs from S_2 to S_0 but no emission is observed for S_1 to S_0.[5]

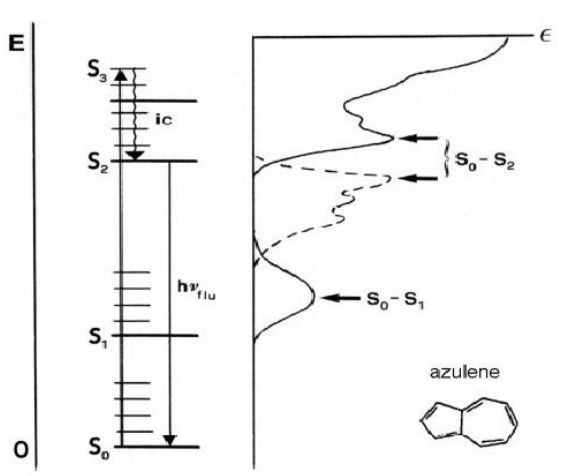

Figure 1.2.2. Jablonski diagram showing $S_0 \rightarrow S_2$ transition, absorption (-) and fluorescence spectra (--) of azulene. Reproduced.[5]

The fluorescence excitation spectrum shows the variation in fluorescence intensity as a function of the excitation wavelength for a fixed emission wavelength. As fluorescence intensity is proportional to the concentration at low absorbances, and provided there is only one species in the ground state, the excitation spectrum is generally identical in shape to the absorption spectrum. If there are several species present in the ground state (e.g. tautomeric forms, aggregates), the excitation and absorption spectra are no longer superimposable.[2]

1.2.2 Fluorescence Lifetime.

The fluorescence lifetime (τ) is defined as the average time a fluorophore stays in the excited state before returning to the ground state, expressed as the inverse of the total depopulation rate:

$$\tau = 1 / k_r + k_{nr} \qquad 1.2.3$$

where k_r is the rate of radiative deactivation through emission of fluorescence and k_{nr} is the rate of radiationless decay (sum of rate constants for internal conversion and intersystem crossing).

The fluorescent lifetime is an important parameter as it provides information on the time available for the excited fluorophore to interact with its microenvironment. However, it is important to note that it is a statistical average and that not all fluorophores will emit at a time delay equal to the lifetime; some emitting quicker than others. At present there are two dominant methods for time resolved measurements; time-domain and frequency domain techniques, both of which yield equivalent data.[6]

1.2.3 Fluorophores.

Fluorophores can be generally categorized into two groups; intrinsic fluorophores which occur naturally, and extrinsic fluorophores which can be added to a sample to provide fluorescence when none exists or to change the spectral properties of the sample.[7] Intrinsic fluorophores include the aromatic amino acids tryptophan, tyrosine and phenylalanine, with UV absorbance and emission from proteins owing generally to the indole groups of tryptophan residues (Figure 1.2.3).

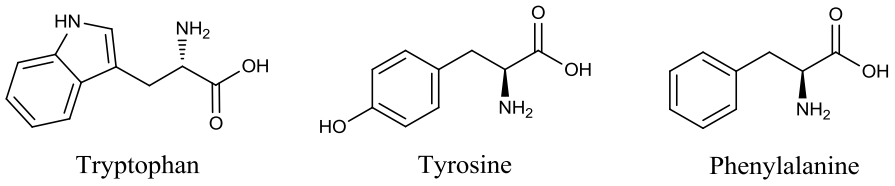

Tryptophan Tyrosine Phenylalanine

Figure 1.2.3. Structures of intrinsic biochemical fluorophores.[7]

More often than not, one finds that molecules of interest are nonfluorescent. For proteins, it is generally desirable to label them with chromophores with longer excitation and emission wavelengths than the aromatic amino acids. There are several useful references that provide detailed information on the correct selection of a chromophore for a given purpose.[8,9] Numerous fluorophores are available for covalent or non-covalent labeling of proteins, with increasing interest focusing on red and near-infrared (NIR) dyes such as cyanine (Figure 1.2.4). This is due to their longer excitation wavelengths, decreased autofluorescence and detectability over background.[7]

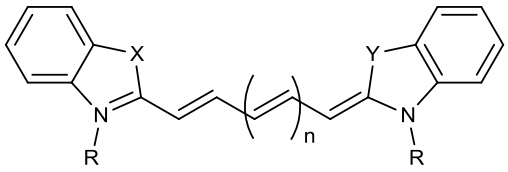

X, Y = O, S $(CH_2(CH_3)_2$
n = 0 to 4
R = $(CH_2)_xSO_3^-$

Figure 1.2.4. Basic structure of cyanine dyes.[9]

Numerous fluorophores are available for covalent and non covalent labeling of proteins. The covalent probes generally contain a variety of activating groups for coupling with amines and sulfhydryl side chains of proteins.

Fluorescein is an example of a popular extrinsic probe with a long absorption maximum near 480 nm, emission wavelength at 510 nm, high quantum yield and insensitivity to its local environment (Figure 1.2.5). Fluorescein isothiocyanate (FITC) is often used as a label for either sulfhydryl groups or amines within a target protein. However, due to its small Stokes shift, fluorescein tends to self-quench leading to a decrease in fluorescence intensity.[7]

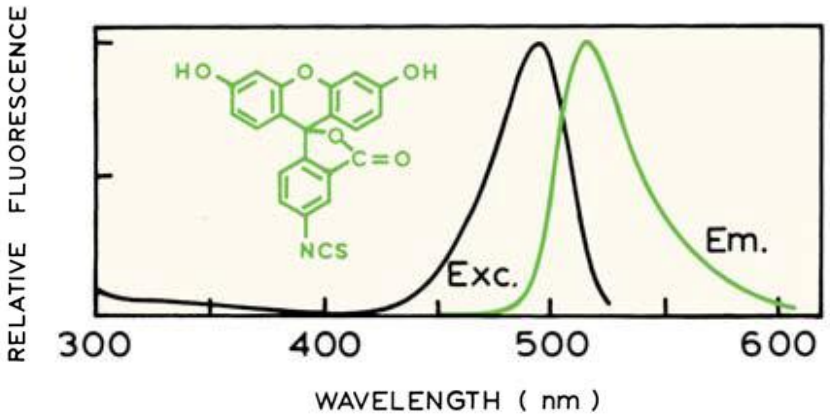

Figure 1.2.5. Excitation and emission spectra of FITC. Reproduced.[7]

1.3 SOLVATOCHROMISM, ENVIRONMENTAL AND MOLECULAR STRUCTURE EFFECTS ON FLUORESCENCE.

Solvent polarity and the local environment can have a significant effect on the emission of a fluorophore. Factors which effect fluorescence emission spectra and quantum yield include solvent polarity and viscosity, temperature and the rate of solvent relaxation, the rigidity of the local environment, hydrogen bonding, pH, proton transfer and excited state reactions.[10] This may result in an increase or decrease in absorption or fluorescence intensity and/or spectral shift, or an increase or decrease in fluorescence lifetime. One common use of solvent effects is in the determination of polarity of the binding site of a targeted macromolecule.[10]

A solvatochromic compound is one which will exhibit a change in shape, location or intensity of the absorption or emission spectra with changing solvent polarity. Negative solvatochromism refers to a hypsochromic shift (toward blue region); and positive solvatochromism is observed with a bathochromic shift (toward red region) with respect to an increase in solvent polarity. Reverse solvatochromism is observed with an alteration from hypsochromic to bathochromic (or the opposite) with an increase in solvent polarity.[10]

1.3.1 Effects of solvent polarity and estimation of polarity using fluorescence.

Typically, a fluorophore is usually excited to an excited vibrational level within S_1, with excess vibrational energy being rapidly lost to the solvent. If excitation occurs to S_2, rapid decay occurs to S_1 in 10^{-12} seconds due to internal conversion. Typically, the fluorophore has a greater dipole moment in the excited state (μ_E) than in the ground state (μ_G). Due to stabilization of the excited state by polar solvent molecules, the energy of the excited state is lowered due to reorientation or relaxation of the solvent dipoles around μ_E. As the solvent polarity is increased, a more pronounced effect is observed, resulting in emission at longer wavelengths or lower energies, resulting in a red shift of the spectrum being observed. This change in spectral shift and fluorescence emission can then be correlated to solvent polarity. In general, only fluorophores that are themselves polar

display a considerable sensitivity to solvent polarity. Figure 1.3.1 shows a Jablonski diagram indicating the differences in relaxation energy between a less polar solvent ($h\nu_F$), more polar solvent ($h\nu'_F$) and the original fluorescence spectra without solvatochromic influence (F). The relaxation time for more polar solvents is slightly longer resulting in a lower energy emission ($h\nu'_F$) causing the spectra to be red-shifted as seen in the spectra at the bottom of Figure 1.3.1. A visual example is given in Figure 1.3.2, detailing the red-shift observed in the emission spectra of 1-dimethylamino-5-naphthylsulfonyl (DNS) in solvents of increasing polarity.

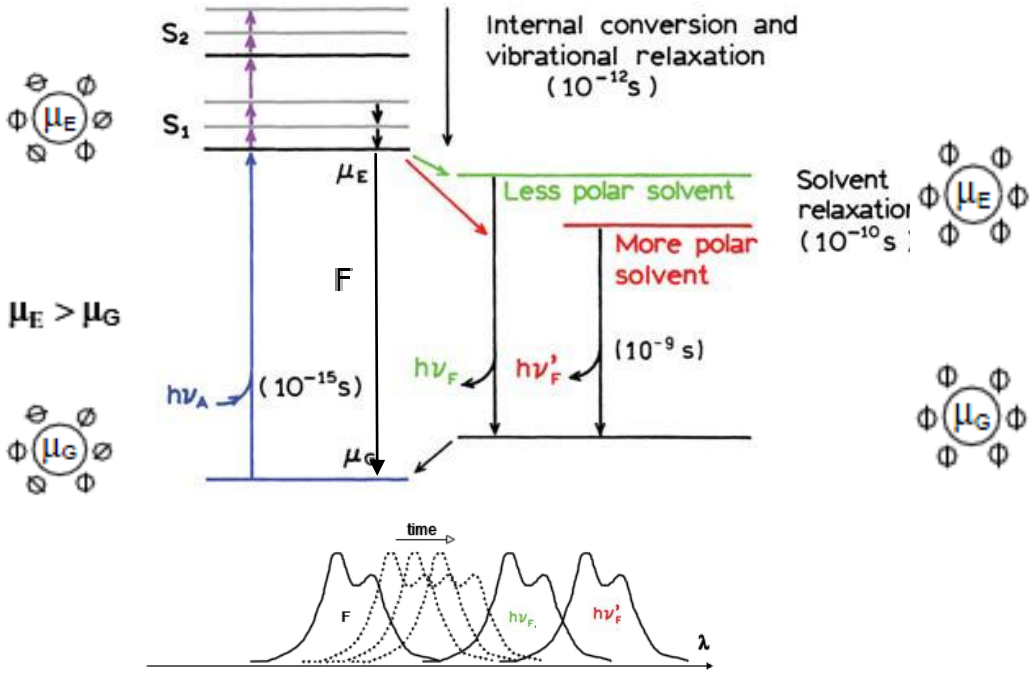

Figure 1.3.1. Jablonski diagram for fluorescence with solvent relaxation. The small circles with lines through them represent the solvent and their dipole moments. Edited.[10]

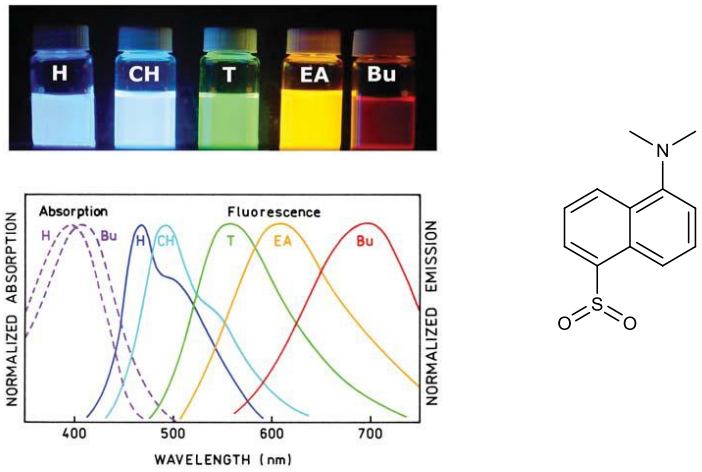

Figure 1.3.2. Emission spectra of 1-dimethylamino-5-naphthylsulfonyl (DNS) in solvents of increasing polarity from hexane (H) to n-butanol (Bu). Reproduced.[10]

With regard to solvents, polarity is defined as *"all possible, non-specific and specific, intermolecular interactions between solute ions or molecules and solvent molecules, excluding such interactions leading to definite chemical alterations of the ions or molecules of the solute"*.[11] This generalization is often explained through the use of dielectric constants (now referred to as relative permittivity), dipole moments, and refractive indexes as physical polarity parameters.

Due to an insufficient definition of solvent polarity through a single physical parameter, there now exists several empirical scales of solvent polarity. Such scales are generated using spectroscopic methods which describe individual solvent-solute molecular interactions. The most widely used solvent polarity scales based on solvatochromic measurements include:

1. The *ET(30)* scale of solvent polarity by Dimroth and Reichardt.[12]
2. The α and β scales of Kamlet and Taft which describe the solvent's hydrogen bond donating (α) and hydrogen bond accepting (β) ability.[13-15]
3. The π^* scale of solvent polarity/dipolarizability by Kamlet, Taft and Abboud.[15, 16]
4. The solvent scales of *solvent dipolarity/polarizability (SPP)*, *solvent basicity (SB)* and *solvent acidity (SA)* by Catalan *et al*.[17-19]

Despite the variety of solvent scales available, most have been found to more or less correlate with each other.[20]

1.3.2 Effects of temperature and viscosity on fluorescence.

For fluid solvents, one can assume that solvent relaxation occurs completely before emission. Generally an increase in temperature results in a decrease in the fluorescence quantum yield and lifetime due to an increased efficiency of the non radiative processes associated with a temperature increase (solvent molecule collisions, intermolecular vibrations and rotations etc.).[2] However, at lower temperatures the solvent can become more viscous, allowing a greater time for solvent reorientation to occur. Because of the decreased rate in solvent motion, the effects of low temperature are similar to the effects of solvents of low polarity, with emission occurring from the unrelaxed state at low temperature.[10]

Fluorescent quantum yields can often be dependent on solvent viscosity, due to molecular mechanics in the excited state. In highly viscous solvents, distortion or rotation of the molecule is more difficult and the decay is radiative; while in a less viscous environment the molecule may display an internal rotation or charge transfer resulting in radiationless decay.[7]

The emission intensity of a fluorophore may also be effected by solvent temperature, with the best known example being trans-stilbene with the intensity decay being dependent on temperature due to rotation around the central ethylene double bond in the excited state.[10] In the ground state for *trans*-stilbene, a large energy barrier exists for rotation to occur about the bond, whilst in the excited state, the energy barrier is much smaller. Rotation about this bond occurs in about 70 ps for trans-stilbene with a return to the ground state, but for *cis*-stilbene this rotation is even more rapid (~ 1 ps) which results in a much shorter fluorescence lifetime (Figure 1.3.3).[10]

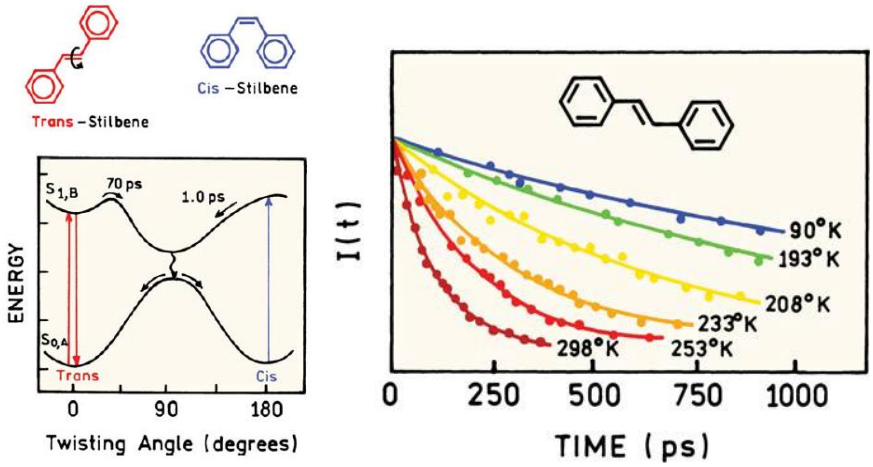

Figure 1.3.3. Excited state isomerization of stilbene between the *trans* and *cis*, and the fluorescence intensity decay of *trans*-stilbene in methylcyclohexane:isohexane, showing a decrease in fluorescence intensity due to bond rotation as temperature is increased. Reproduced.[10]

1.3.3 Effects of molecular structure on fluorescence.

Most fluorescent compounds are aromatic. Generally, a shift in the absorption and fluorescence spectra to longer wavelengths is observed upon increasing the degree of conjugation (π system). $\pi \rightarrow \pi^*$ transitions are the lowest lying transitions in aromatic hydrocarbons but when a heteroatom is involved in the π system, an $n \rightarrow \pi^*$ transition may be the lowest lying. Such an $n \rightarrow \pi^*$ transition is generally seen with most *azo* compounds and nitrogen heterocycles.[2]

In general, the presence of heavy atoms as substituents on aromatic molecules (e.g. Br, I) results in fluorescence quenching known as the internal heavy atom effect. This is due to increased probability of intersystem crossing, which is favored by spin–orbit coupling, leading to conversion to the triplet state which in turn leads to non-fluorescent phosphorescent emission. However, this effect can be small for some aromatic hydrocarbons if:

(i) the fluorescence quantum yield is large so that de-excitation by fluorescence emission dominates all other de-excitation processes;

(ii) the fluorescence quantum yield is very low so that the increase in efficiency of intersystem crossing is relatively small;
(iii) there is no triplet state energetically close to the fluorescing state.[2]

The lowest-lying transitions of aromatic hydrocarbons are of the $\pi \rightarrow \pi^*$ type, which are characterized by high molar absorption coefficients and relatively high fluorescence quantum yields. When a heteroatom is involved in the π-system, an $n \rightarrow \pi^*$ transition may be the lowest-lying transition which has a much slower radiative lifetime and cannot compete with dominative non-radiative processes, resulting in lower fluorescence quantum yields. The energy of the $n \rightarrow \pi^*$ state can also become lower than that of the $\pi \rightarrow \pi^*$ state in some solvents.

In general, aromatic substitution with electron-donating groups (OH, OCH_3, NH_2 *etc*.) induces an increase in the molar absorption coefficient and a shift in both absorption and fluorescence spectra.

Some aromatic carbonyl compounds have low-lying $\pi \rightarrow \pi^*$ excited states. If an $n \rightarrow \pi^*$ state lies only slightly higher in energy, the fluorescence quantum yield strongly depends on the polarity of the solvent; this is known as the proximity effect.

When the polarity and the hydrogen bonding power of the solvent increases, the $n \rightarrow \pi^*$ state can shift to higher energy. The $\pi \rightarrow \pi^*$ state is now shifted to a lower energy state (*i.e.* lowest-lying transition) resulting in relatively high fluorescence quantum yields. Therefore, a fluorophore may display intense fluorescence in polar solvents but weak fluorescence in nonpolar solvents.[2]

In general, the fluorescence of aromatic hydrocarbons possessing an NO_2 substituent is difficult to detect due to the existence of a low-lying $n \rightarrow \pi^*$ transition, as a result of the strong electron-withdrawing power of the NO_2 group which explains the efficient intersystem crossing process. Many nitro-aromatic containing fluorophores are phosphorescent and the absence of detectable fluorescence is likely to be due to a high rate of $S_1 \rightarrow S_0$ internal conversion (nonradiative de-excitation), which may be related to the considerable charge-transfer character of the excited state.[2]

Water solubility of many fluorophores is achieved by substituting sulfonate groups (SO_3H). Fortunately, these groups only slightly effect the fluorescence characteristics of the parent molecule and typically result in a small red-shift of the fluorescence spectrum with the fluorescence quantum yield only slightly decreased.[2]

1.4 1,3-DIPOLAR CYCLOADDITIONS.

Cycloadditions are ring closure reactions which involve cyclic electron shifts, whereby the number of σ bonds increase at the expense of π bonds.[21] In 1960, a general principle for the synthesis of five membered rings known as the 1,3-dipolar cycloaddition was introduced; whereby a 1,3-dipole reacts with a multiple bond system known as the dipolarophile.

A 1,3-dipole is defined as an *a*-*b*-*c* structure, divided into two different types: the allyl anion type and the propargyl-allenyl anion type (Figure 1.4.1). The allyl anion type is characterized by a bent structure with four electrons in three parallel p_z orbitals perpendicular to the plane of the dipole. Two resonance structures exist in which the three centers have an electron octet, and two resonance structures in which *a* or *c* has an electron sextet. The central atom *b* can be nitrogen, oxygen or sulfur.

The propargyl-allenyl anion type has an extra π orbital in the plane orthogonal to the allenyl anion type molecular orbital (MO), and therefore is not directly involved in the resonance structures and reactions of the dipole. The propargyl-allenyl anion type is linear and the central atom *b* is limited to nitrogen.[22] The identity of allenyl type 1,3-dipoles containing nitrogen and oxygen, as well as propargyl-allenyl type 1,3-dipoles which contain nitrogen only are given in Figure 1.4.2.

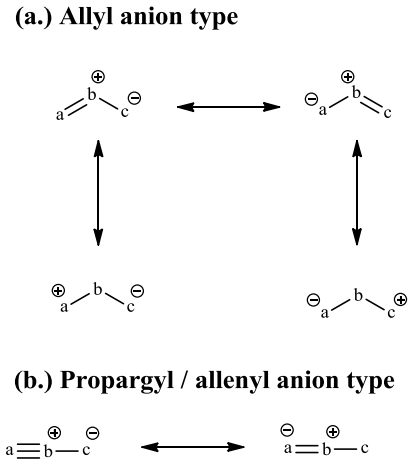

Figure 1.4.1. The basic resonance structures of 1,3-dipoles.[22]

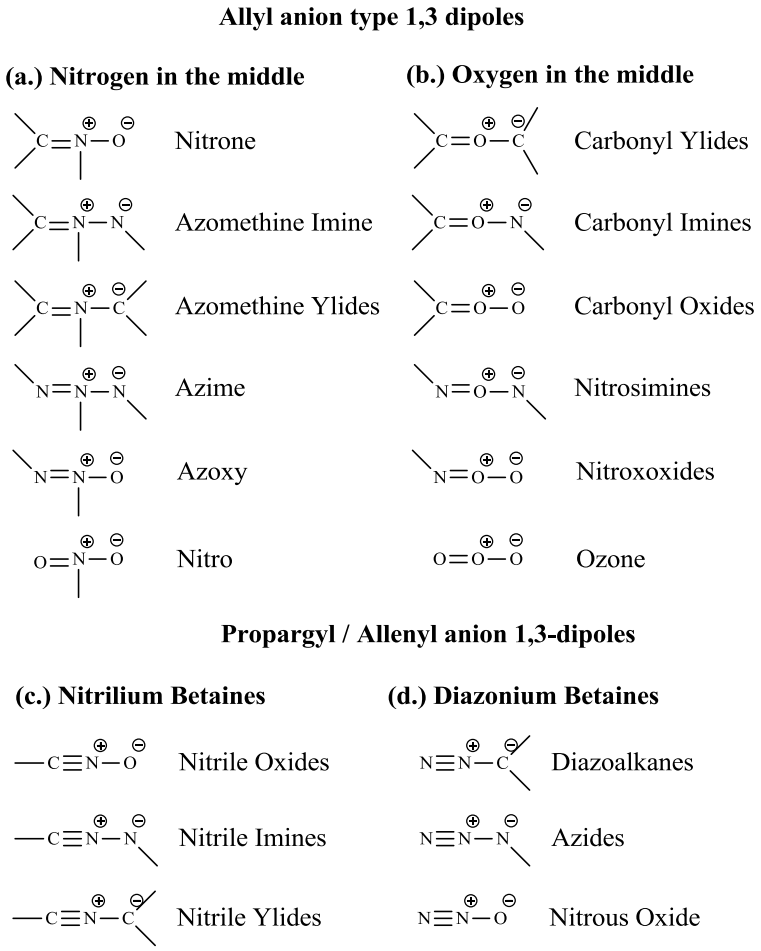

Figure 1.4.2. Classification of 1,3-dipoles.[22]

1.4.2 Stereoselectivity and Sustman classification of 1,3-dipolar cycloadditions.

On the basis of the stereospecificity of the 1,3-dipolar cycloaddition, it is now accepted to occur *via* a concerted mechanism.[23,24] The transition state of the concerted mechanism has been shown to be controlled by the frontier molecular orbitals (FMO) of the substrates, in which the $LUMO_{dipole}$ can interact with the $HOMO_{dipolarophile}$ and the $HOMO_{dipole}$ with the $LUMO_{dipolarophile}$. Sustman has classified 1,3-dipolar cycloadditions into three types on the basis of the relative FMO energies (Figure 1.4.3).

In **Type I** (normal electron demand), the dominant FMO interaction is between the $HOMO_{dipole}$ with the $LUMO_{dipolarophile.}$

In **Type II** (neutral electron demand), the FMO energies of both HOMO and LUMO are similar, implying both HOMO-LUMO interactions are important.

In **Type III** (inverse electron demand), the dominant interaction is between the $LUMO_{dipole}$ and the $HOMO_{dipolarophile}$.

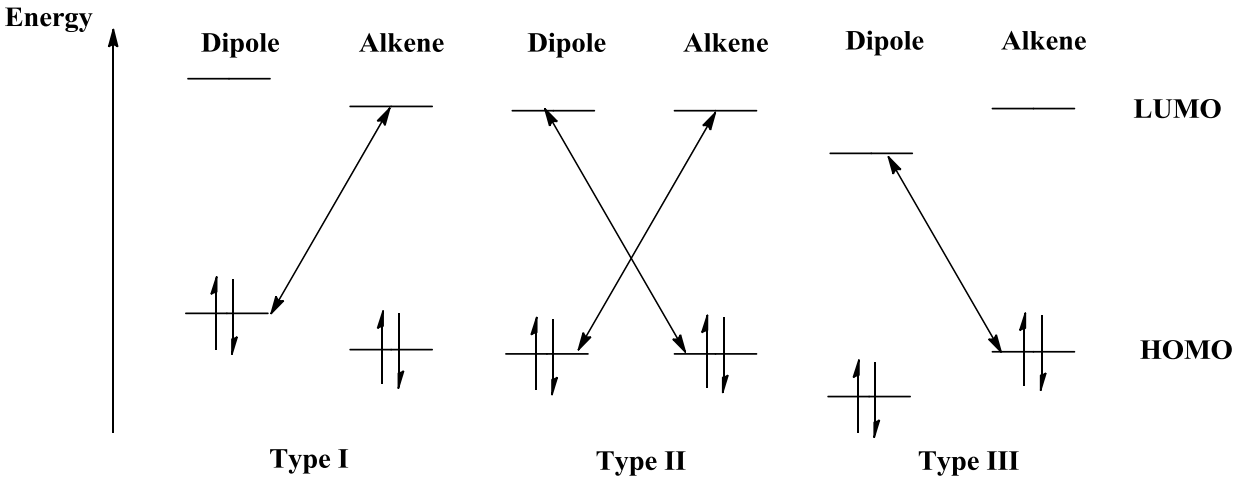

Figure 1.4.3. Sustman classification of 1,3-dipolar cycloadditions based on relative energies of FMOs.[22]

The stereochemistry of a 1,3-dipolar cycloaddition can be controlled to produce products which retain the stereochemistry of the original substrates. This can be done by choosing appropriate substrates, or by coordination of a metal complex acting as a catalyst. The 1,3-dipolar cycloaddition of benzonitrile oxide with *trans*-dideuterated ethylene gives exclusively the *trans* isoxaline.[22] If the mechanism occurred *via* a diradical intermediate as proposed by Firestone, 180^{o} rotation of the terminal bond could occur giving rise to a mixture of both *cis* and *trans* isomers (Figure 1.4.4.).[25]

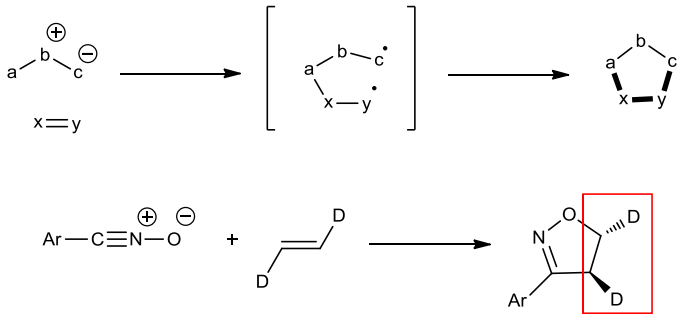

Figure 1.4.4. 1,3-Dipolar cycloaddition of benzonitrile oxide with *trans*-dideuterated ethylene gives exclusively the *trans* isoxaline.[22]

1.5 1,2,3-TRIAZOLIUM-1-AMINIDE 1,3-DIPOLES.

The isomerism of phenylhydrazones of α-dicarbonyl compounds has been a topic of interest historically. Scheme 1.5.1 shows the possible isomers of the 1,2-bis(phenyl)hydrazone system, which are the *E,E*, the *E,Z*, and the *Z,Z*; all of which have been identified. The reaction of benzil with phenylhydrazine results in the isolation of only the *E,E* isomer.[26]

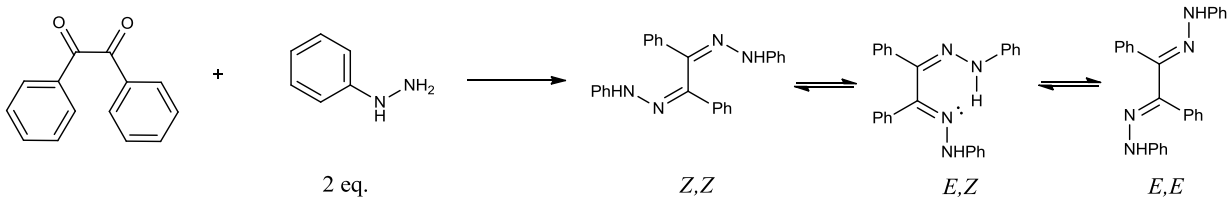

Scheme 1.5.1. Isomers of 1,2-bis(phenyl)hydrazone of benzil.

The oxidation of each of the isomers gives the same *trans-azo* compound; 1,2-diphenyl-(*E*)-1,2-bis(phenyldiazenyl)ethane, which in solution can undergo a facile *E-Z* isomerisation. 1,2-Diphenyl-(*Z*)-1,2-bis(phenyldiazenyl)ethane exists in equilibrium with a cyclic 1,2,3-triazolium-1-imide form (Scheme 1.5.2). This has been reported to be observed by variable temperature ^{1}H NMR, with the symmetrical diazo *Z* form being observed at -40 ^{o}C; whilst at 23 ^{o}C the compound has cyclised and no longer shows symmetry or characteristic arylazo proton shifts.[27] This latter form is a reactive 1,3-dipole which dominates the reactivity of this system. [28-32]

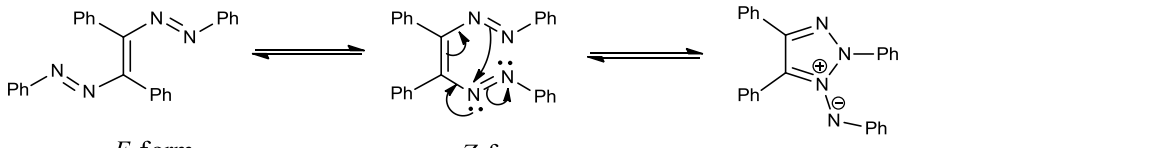

Scheme 1.5.2. Electrocyclisation of 1,2-diphenyl-(Z)-1,2-bis(phenyldiazenyl)ethane.

1.5.1 Synthetic derivatives of 1,2,3-triazolium-aminide 1,3-dipoles.

When 1,2-bis(areneazo)cycloalkenes are used, interesting new tricyclic azapropellanes are obtained (Scheme 1.5.3).[32] The reactions are stereospecific (> 99%), with the *cis*- and *trans*- isomers identifiable by the dihedral coupling constant $J(H_A - H_B)$ of ~ 9 Hz and dihedral angle ~ 0°. This provided a model for the *endo*-H_A and $-H_B$, which allowed identification of other possible *trans*- isomeric structures.

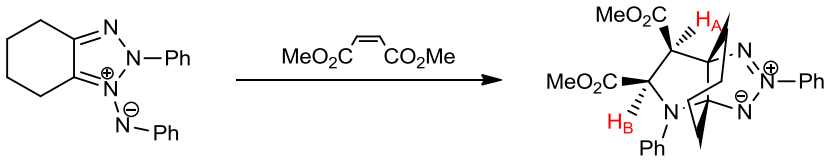

Scheme 1.5.3. Tricyclic azapropellanes obtained when 1,2-bis(areneazo)cycloalkenes are used.[32]

Such reactions are seen as concerted 1,3-dipolar cycloadditions involving a 1,4-N→C sigmatropic rearrangement. However, it has been noted that it could be also viewed as a multistep Michael reaction involving initial nucleophilic addition of the exocyclic -N^- terminal of the dipole to the dipolarophile creating a new N-C bond followed by subsequent ring closure and cleavage of the N-N bond. This mechanism would result in a loss in stereochemistry due to rotations around single bonds in a number of intermediates. The stereospecificity of the reaction supports what is now the favoured mechanism; a concerted 1,3-dipolar cycloaddition-sigmatropic rearrangement.

The *exo*-arrangment of substituents in the products, as mentioned previously, requires an initial *endo*-cycloaddition. The azomethine imide dipole is an electron rich structure and would be expected to give dipole-HOMO-controlled reactions.[21] The required *endo*-orientation of substituents containing π-bonds is accessible due to favourable secondary orbital interactions or opposed alignment of dipoles.[32] Figure 1.5.1 shows the favourable orbital interactions between the azomethine imide dipole and dimethyl maleate to give a constructive *endo*-cycloaddtion.

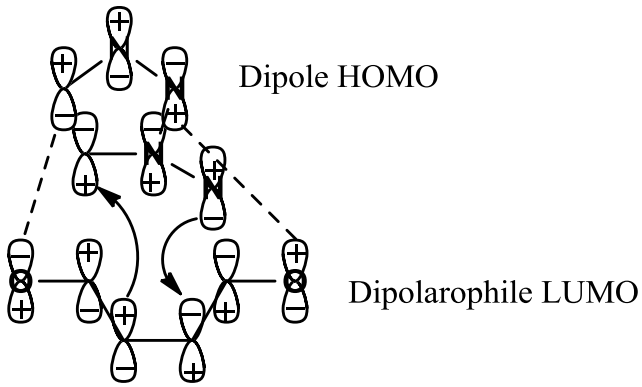

Figure 1.5.1. Favoured *endo*-transition state. Primary orbital interactions shown as curly arrows and secondary orbital interactions as dashed lines.

Rapid rearrangement after the initial cycloaddition results in the N-N-N chain being carried intact through a range of steps, providing an important synthetic route to monocyclic hetero-1,2,3-triazines such as thiatriazines and oxatriazines.[33,34] The broad synthetic scope of 1,2,3-triazolium-1-aminides as 1,3-dipoles has been comprehensively reviewed by Butler *et al*. and Rodina *et al*.[35,36]

1.6 TRIAZINES.

Triazines are a six membered ring containing three nitrogen atoms, of which there are three possible structures; 1,2,3-triazine, 1,2,4-triazine (1,3,4-triazine) and 1,3,5-triazine (Figure 1.6.1).

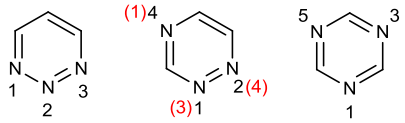

Figure 1.6.1. Possible triazine structures.

1.6.1 1,3,5-Triazines.

1,3,5-Triazine, known as the symmetrical triazine (*s*-triazine or *sym*-triazine), has alternating nitrogen and carbon atoms around one ring and is found in some important compounds, including cyanuric acid (1,3,5-triazine-2,4,6-triol), melamine (1,3,5-triazine-2,4,6-triamine), ammeline (4,6-diamino-2-hydroxy-1,3,5-triazine), and acetoguanamine (6-methyl-1,3,5-triazine-2,4-diamine). Melamine and ammeline have found importance as fire retardant agents as they have been shown to exhibit a high degree of thermal stability.[37, 38]

2,4,6-Trichloro-1,3,5-triazine (TCT or cyanuric chloride, Figure 1.6.2) is a valuable synthetic reagent as one can take advantage of the temperature dependent stepwise substitution of its three chlorine atoms by different nucleophiles. TCT is also a useful coupling reagent in the formation of macrocyclic lactones.[39,40] Recently, it has been reported that when TCT is incorporated into reactive fluorescent dyes, it is able to react with hydroxy groups from cellulose and amino or thiol groups from proteins, making it a useful molecular link between a fluorescent dye and an organic matrix.[41]

2-Hydroxyphenyl-1,3,5-triazines (Figure 1.6.2) have been widely used as UV absorbers for polymers. They can absorb ultraviolet radiation which would otherwise damage the polymer and transform it into vibrational energy by an efficient radiationless deactivation pathway. This has been shown to be due to an excited state intramolecular proton transfer (ESIPT) in the excited singlet state S_1 which is followed by fluorescence

emission with a very large Stokes shift and high quantum yields from the proton transferred S_1' state.[42]

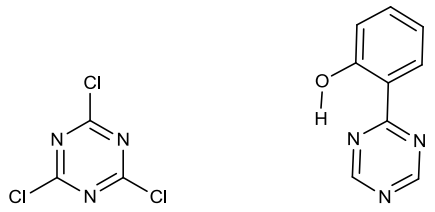

Figure 1.6.2. Structures of 2,4,6-trichloro-1,3,5-triazine (TCT) and 2-hydroxyphenyl-1,3,5-triazines.

A new 1,3,5-triazine tripod system for a 4,4-difluoro-4-bora-3a,4a-diaza-*s*-indacene (BODIPY) fluorophore has recently been described with quantum efficiencies as high as 0.84 (Figure 1.6.3).[40] In addition to the fluorophore, two other different functional groups may be incorporated onto the 1,3,5-triazine tripod; where one position is a binding subunit, such as di-(2-picolyl)amine (DPA), for metal ions; and the other an auxiliary group. This auxiliary group may confer additional chemical or physical properties on the product such as solubility or fine tuning of fluorescent behavior by a selective photo induced electron transfer process.

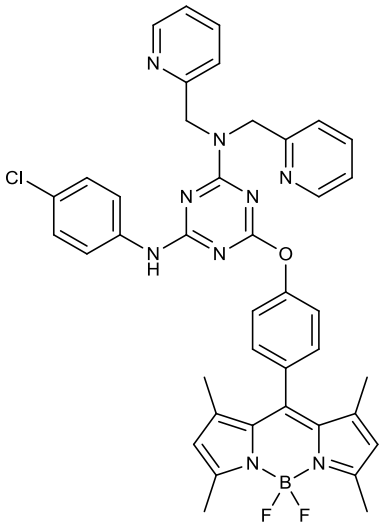

Figure 1.6.3. 1,3,5-Triazine tripod BODIPY fluorophore system with Hg^{2+} binding subunit, and a quantum yield of 0.84.[40]

1.6.2 1,2,4-Triazines.

1,2,4-Triazine, known as the asymmetrical triazine (*as*-triazine or *asymm*-triazine), and its derivatives have been widely studied since many have been reported to have promising biological activities.[43] The 1,2,4-triazine structure is a prominent structural motif in numerous natural and synthetic biologically active compounds such as the well known antiviral drug azaribine (Figure 1.6.4).[44]

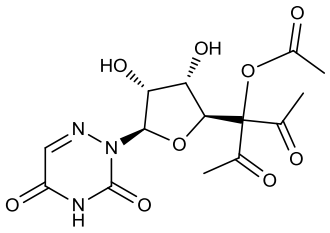

Figure 1.6.4. Structure of the antiviral drug azaribine (3-((2S,3S,4R,5R)-5-(3,5-dioxo-4,5-dihydro-1,2,4-triazin-2(3H)-yl)-3,4-dihydroxytetrahydrofuran-2-yl)-2,4-dioxopentan-3-yl acetate).

The literature describing 1,2,4-triazine and its derivatives detail various methods of preparation with 1,2-dicarbonyl compounds being the most common starting materials used for the synthesis.[52-54]

Laakso *et al*. reported the condensation of acylhydrazides with benzil, in acetic acid containing ammonium acetate, to give 5,6-diphenyl-1,2,4-triazines with various aromatic and heterocyclic groups attached at position 3. Thirumurugan *et al*. describe an efficient and high yielding synthesis for biaryl-3-pyridinyl-1,2,4-triazine which displays good fluorescent properties and a selective nature for Fe(III) ions. The Thirumurugan synthesis employs a condensation of cinnamils with pyridine carboxytrisamidrazone either by conventional heating or microwave irradiation.[45,44]

Some 1,2,4-triazines have been found to be efficient fluorescent chemosensors for transition metals, whilst newly developed two-photon absorption (TPA) systems based on the 1,2,4-triazine chromophore have recently been discovered.[46,47] Bidentate Schiff bases derived from the condensation reaction of 5-bromothiophene-2-carboxaldehyde with 4-amino-3-mercapto-6-methyl-5-oxo-[1,2,4]triazine complexed to cobalt, nickel, copper and zinc have been reported to exhibit strong fluorescence emission, whilst also demonstrating biological activity as antimicrobial agents. Antibacterial and antifungal activity of the Schiff bases was greatly enhanced when coordinated to a metal ion with minimum inhibitory concentrations (MIC) ranging from 32 to 128 μg/mL against Gram-positive bacteria.[48]

1.6.3 1,2,3-Triazines.

Of the three possible triazine systems, the 1,2,3-triazine, known as vicinal triazine (*v*-triazine or *vic*-triazine) is certainly the least studied class. Apart from the initial charaterisation of the unsubstituted 1,2,3-triazine, very few studies have been carried out to date on the physical and chemical properties since they were first synthesized by Ohsawa in 1981.[49]

1.6.3.1 Fluorescent thieno-1,2,3-triazine-4-ones.

Thieno-1,2,3-triazine-4-ones first synthesized by Henriksen have shown particular promise as antidepressants (Figure 1.6.6).[50,51] It was noted by Henriksen that the 5-(methylthio)-4-oxo-3,4-dihydrothieno[3,4-d][1,2,3]triazine derivatives were intense yellow solids, and even more characteristic was there strong yellow fluorescence in solution and long wavelength absorption maximum around 390 nm.

Reopening an investigation on the above compounds in 2009 resulted in a systematic photophysical charaterisation of the solvatochromic nature of this class of small molecules. Interestingly, the compounds are thermally stable as the original compounds were studied after being stored in Pyrex vessels for 35 years. They also have impressive chemical resistance as exemplified by the use of concentrated hydrochloric acid and 2M sodium hydroxide in their preparation and purification.[52]

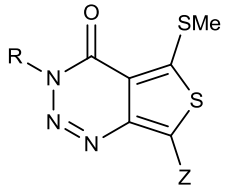

R = H or Me

Z = CO_2Et, COMe, COPh, $CONH_2$, CONHMe, or CO_2Me

Figure 1.6.6. 2-Methylthio-5-(Z-carbonyl)thieno-[3,4-e]-3,4-dihydro-1,2,3-triazine-4-one derivatives synthesized by Henriksen *et al*.[50]

It was found that the colour of fluorescence as well as the quantum yields and lifetimes could be altered by changing the substitution pattern and solvent. A decrease in fluorescence quantum yield was observed when solvent polarity was increased, and in protic solvents. A red-shifted emission was also observed indicating a high dipole moment in the excited state and specific solvent interaction in the excited state. This is in accord with the polar character of the singlet excited charge transfer state. Spectral calculations revealed the first excited state to be dominated by a HOMO-LUMO transition accompanied by a charge transfer. [50]

Most recently, 3H-benzo[4, 5]thieno[2, 3-d][1, 2, 3] triazin-4-ones have been shown to exhibit inhibition of vascular endothelial growth factor receptor-2 (VEGFR-2), as well as anti-hyperlipidemic (elevation of lipid concentration in blood) activity.[53]

1.6.3.2 Fluorescent 2,5-dihydro-1,2,3-triazines.

The main topic of this thesis centres on the synthesis and fluorescent characterization of another interesting class of fluorescent 1,2,3-triazines; the 2,5-dihydro-1,2,3-triazines (Figure 1.6.7) first reported by Butler *et al*.[54] Interestingly, these 1,2,3-triazine derivatives show a dual UV absorption at ~310 and 400 nm with fluorescent emission at *ca.* 480 and 528 nm (for excitation at both ~310 and ~400 nm); as well as a significant Stokes shift of ~ 200 nm at 310 nm excitiation.

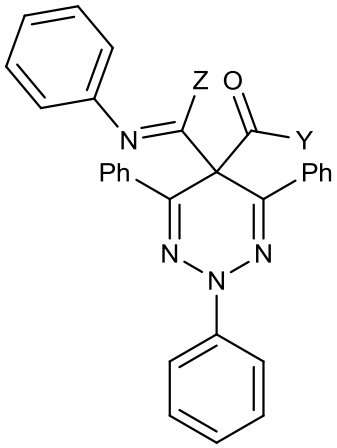

Figure 1.6.7. General structure of the 2,5-dihydro-1,2,3-triazine reported by Butler *et al*. [54]

Chapter 2: Materials and Methods

2.1 ORGANIC SYNTHESIS.

Melting points were measured on a Stuart melting point apparatus. Infra-red (IR) spectra were measured on a Perkin-Elmer Spectrum 2000 FT-IR spectrophotometer. Nuclear Magnetic Resonance (NMR) spectra were measured on a Bruker Avance 300 spectrometer using tetramethylsilane as an internal reference for ^{1}H shifts. Coupling constants *J* are given in Hz. Multiplicity as follows: s (singlet), d (doublet), appd (apparent doublet), t (triplet), appt (apparent triplet), m (multiplet). Electrospray (ESI) mass spectra were collected on an Agilent Technologies 6410 Time of Flight LC/MS. The interpretation of mass spectra was aided by the program "Agilent Masshunter Workstation" software. Yields refer to isolated amount of compound unless stated otherwise. Solvents were purified according to literature procedures.[55]

The following chemicals were purchased and used as received:

Sigma Aldrich:

Benzil, phenylhydrazine, *p*-chlorophenylhydrazine, *p*-bromophenylhydrazine, manganese dioxide, methyl propiolate, methyl phenylpropiolate, dimethyl acetylenedicarboxylate, sodium deuteroxide, D_2O, chloroform-d_1, 4-dimethylaminopyridine, 1,3-dicyclohexylcarbodiimide, L-alanine, 4-aminophenol, thiophosgene.

Acros Organics (Fischer):

3-Butyn-2-one, methyl-2-butyn-oate, phenol, *p*-cresol, 4-methoxyphenol, 4-nitrophenol, 1H-benzotriazole.

Fissons Scientific:

Lead dioxide.

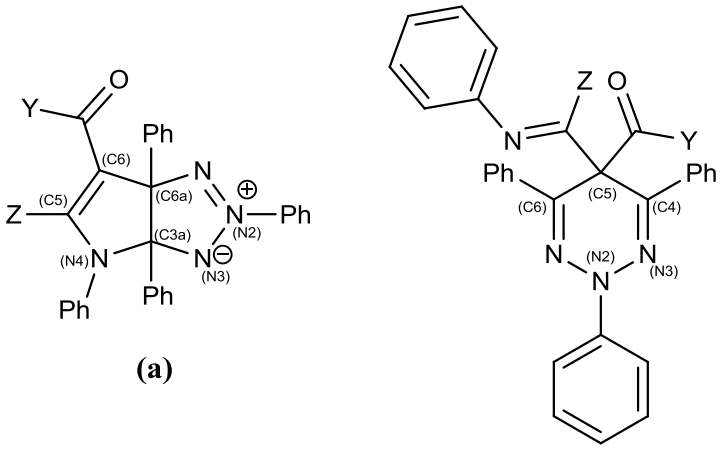

Figure 2.1.1. Numbering schemes for (a) fused 2,3a,4,6a-tetraphenyl-3,3a,4,6a-tetrahydropyrrolo[2,3-d]-[1,2,3]-triazol-2-ium-3-ides and (b) 2,5-dihydro-1,2,3-triazines.

2.1.1 Synthesis for Chapter 4.

Synthesis of 1,2-bis(phenyl)hydrazone of benzil (1).[35]

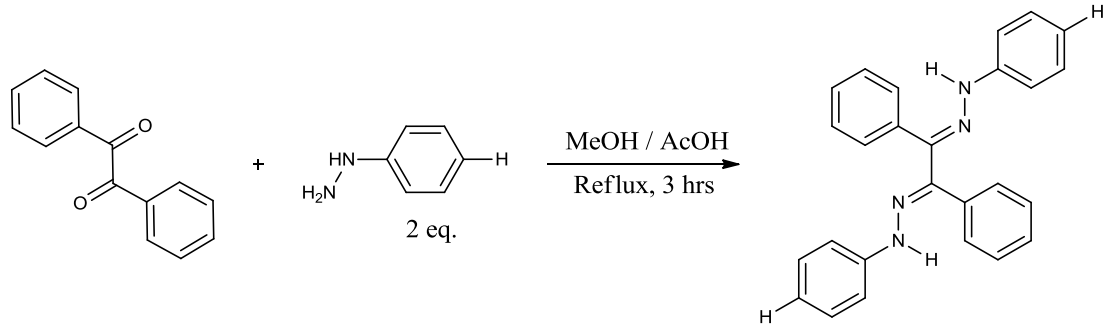

A solution of benzil (3.239 g, 15.365 mmol), phenylhydrazine (3.02 cm^3, 30.729 mmol) and glacial acetic acid (4.39 mL) in methanol (32 mL) was stirred under reflux for 3 hrs. After the reflux period, the solution was allowed to cool on ice and the pure 1,2-bis(phenyl)hydrazone of benzil precipitated. The precipitate was collected under suction, washing with ice cold methanol, as a bright yellow solid (4.69 g, 78.3 %).

m.p: 222 – 224 ^oC (from methanol).

Literature m.p: 234 ^oC (from ethanol).[35]

IR (NaCl) ν_{max} 1641 cm^{-1} (C=N).

^1H NMR (300 MHz $CDCl_3$): δ 6.93-6.98 (m, 2H, Ar), 7.13-7.47 (m, 14H, Ar), 7.76-7.79 (m, 4H, Ar).

HRMS *m/z* 391.1904 ($[M + H]^+$, $C_{26}H_{23}N_4$ requires 391.1917).

Matches literature.[35]

Synthesis of 2,4,5-triphenyl-1,2,3-triazolium-1-phenylaminide (2a).[54]

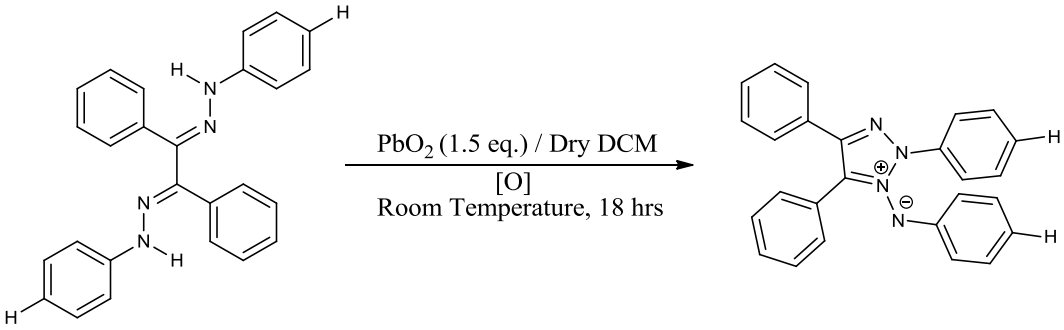

A suspension of 1,2-bis(phenyl)hydrazone of benzil (4.416 g, 11.367 mmol) in dry dichloromethane (133 mL) was treated with an excess of lead dioxide (4.078 g, 17.051 mmol) and stirred for 18 hours at ambient temperature. The lead salts were removed by filtration through a bed of celite washing with dichloromethane, and the filtrate evaporated to dryness under reduced pressure. The crude product was dissolved in the minimum amount of hot toluene (heated to approximately 110^{o}C), to which ice chilled petroleum ether (b.p 60-80 ^{o}C) was added dropwise. Pure 2,4,5-triphenyl-1,2,3-triazolium-1-phenylaminide precipitated as a dark red/brown solid and collected by suction filtration (3.450 g, 78.1 %).

m.p: 178 - 179 ^{o}C from (toluene:petroleum ether b.p. 60 – 80 ^{o}C).

Literature m.p: 178 – 179 ^{o}C (from toluene:petroleum ether b.p. 60 – 80 ^{o}C).[54]

IR (NaCl) ν_{max} 1592 cm^{-1} (C=N).

^{1}H NMR (300 MHz $CDCl_3$): δ 6.89-7.03 (appt, 2H, Ar), 7.34-7.49 (m, 14H, Ar), 7.56-7.63 (m, 4H, Ar).

HRMS *m/z* 389.1764 ($[M + H]^+$, $C_{26}H_{21}N_4$ requires 389.1761).

Matches literature.[54]

Synthesis of 2,4,5-diphenyl-1,2,3-triazolium-1-phenylaminide (2b).

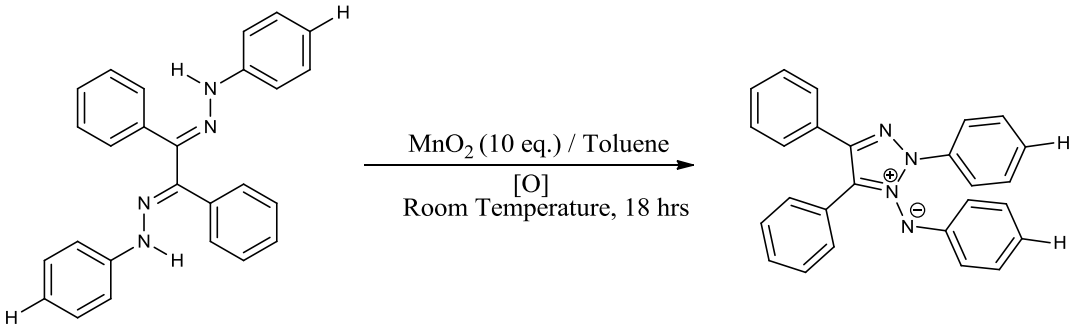

A suspension of 1,2-bis(phenyl)hydrazone of benzil (0.402 g, 1.029 mmol) in toluene (30 mL) was treated with an excess of manganese dioxide (0.895 g, 10.297 mmol) and stirred for 18 hrs at ambient temperature. The manganese salts were removed by filtration through a Nylon 66 membrane (0.45μm x 47μm) and the filtrate evaporated to dryness under reduced pressure to yield 2,4,5-diphenyl-1,2,3-triazolium-1-phenylaminide as a dark red/brown solid (0.376 g, 94 %).

m.p: 178 – 179 ^{o}C (from toluene).

Literature m.p: 178 – 179 ^{o}C (from toluene:petroleum ether b.p. 60 – 80 ^{o}C).[54]

IR (NaCl) ν_{max} 1592 cm^{-1} (C=N).

^{1}H NMR (300 MHz $CDCl_3$): δ = 6.89-7.03 (t, 2H, Ar), 7.34-7.49 (m, 14H, Ar), 7.56-7.63 (m, 4H, Ar).

HRMS *m/z* 389.1764 ($[M + H]^+$, $C_{26}H_{21}N_4$ requires 389.1761).

Matches literature.[54]

Synthesis of 5-methoxycarbonyl-5-(N-phenylformimidoyl)-2,4,6-triphenyl-2,5-dihydro-1,2,3-triazine (3a) and 6-methoxycarbonyl-2,3a,4,6a-tetraphenyl-3,3a,4,6a-tetrahydropyrrolo[2,3-d]-[1,2,3]-triazol-2-ium-3-ide (3b).[54]

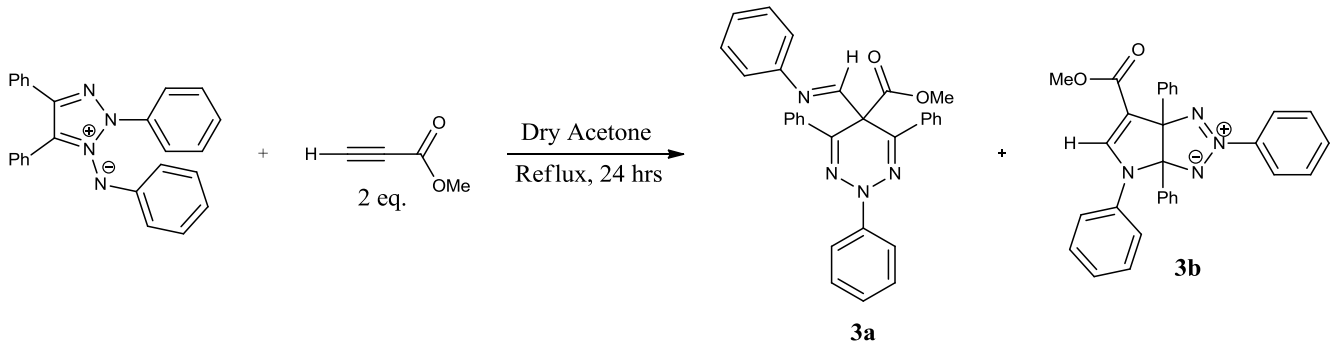

A suspension of 2,4,5-triphenyl-1,2,3-triazolium-1-phenylaminide (1.988 g, 5.117 mmol) in dry acetone (40 mL) was treated with an excess of methyl propiolate (0.91 mL, 10.23 mmol) and stirred under reflux for 24 hrs. The solvent was removed under reduced pressure and the residue was placed, dry loaded (silica 230 – 400 mesh ASTM), on a silica gel column (230 – 400 mesh ASTM). Elution with 1:6 v/v ethyl acetate:n-hexane gave 5-methoxycarbonyl-5-(N-phenylformimidoyl)-2,4,6-triphenyl-2,5-dihydro-1,2,3-triazine (**3a**) (R_f: 0.36 - 1:6 v/v ethyl acetate:n-hexane) as a bright yellow/green solid which displays intense bright green fluorescence when exposed to 365 nm UV light (1.455g, 58.2 %).

Changing of solvent gradient to 1:3 v/v ethyl acetate:n-hexane afforded 6-methoxycarbonyl-2,3a,4,6a-tetraphenyl-3,3a,4,6a-tetrahydropyrrolo[2,3-d][1,2,3]-triazol-2-ium-3-ide (**3b**) (R_f: 0.05 - 1:6 v/v ethyl acetate:n-hexane) as a bright yellow solid (0.24 g, 9.6 %).

5-Methoxycarbonyl-5-(N-phenylformimidoyl)-2,4,6-triphenyl-2,5-dihydro-1,2,3-triazine (3a).

m.p: 146 – 147 ^{o}C (from ethyl acetate:n-hexane 1:6 v/v).

Literature m.p: 146 – 147 ^{o}C (from ethanol).[54]

IR (NaCl) ν_{max} 1740 cm^{-1} (C=O).

^{1}H NMR (300 MHz $CDCl_3$): δ 3.53 (s, 3H, O-CH_3), 6.77-6.80 (d, 2H, *J* = 8.3 Hz, H_{ortho} iminyl N-C_6H_5), 7.10-7.42 (m, 12H, Ar), 7.76-7.93 (m, 6H, Ar), 8.49 (s, 1H, N=CH).

HRMS *m/z* 473.1951 ($[M + H]^+$, $C_{30}H_{25}N_4O_2$ requires 473.1972).

Matches literature.[54]

6-Methoxycarbonyl-2,3a,4,6a-tetraphenyl-3,3a,4,6a-tetrahydropyrrolo[2,3-d]-[1,2,3]-triazol-2-ium-3-ide (3b).

m.p: 164 – 166 ^{o}C (from ethyl acetate:n-hexane 1:6 v/v).

Literature m.p: 164 – 166 ^{o}C (from ethanol).[54]

IR (NaCl) ν_{max} 1697 cm^{-1} (C=O).

^{1}H NMR (300 MHz $CDCl_3$): δ 3.66 (s, 3H, O-CH_3), 6.92-7.02 (m, 10H, Ar), 7.15-7.26 (m, 4H, Ar), 7.50-7.62 (m, 4H, Ar), 8.42 (s, 1H, 5-CH), 8.43-8.46 (m, 2H, Ar).

HRMS *m/z* 473.1961 ($[M + H]^+$, $C_{30}H_{25}N_4O_2$ requires 473.1972).

Matches literature.[54]

Synthesis of 5-methoxycarbonyl-5-(N-phenylformimidoyl)-2,4,6-triphenyl-2,5 dihydro-1,2,3-triazine (3a-2).

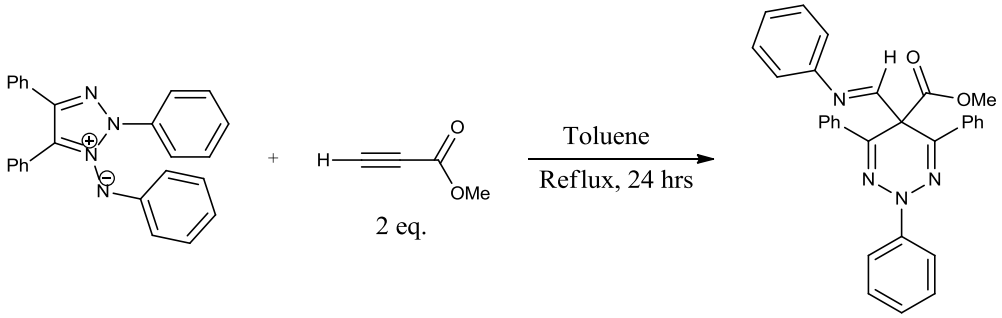

A suspension of 2,4,5-triphenyl-1,2,3-triazolium-1-phenylaminide (1.988 g, 5.117 mmol) in toluene (30 mL) was treated with an excess of methyl propiolate (0.91 mL, 10.23 mmol) and stirred under reflux for 24 hrs. The solvent was removed under reduced pressure and the residue was placed, dry loaded (silica 230 – 400 mesh ASTM), on a silica gel column (230 – 400 mesh ASTM). Elution with 1:6 v/v ethyl acetate:n-hexane gave 5-methoxycarbonyl-5-(N-phenylformimidoyl)-2,4,6-triphenyl-2,5-dihydro-1,2,3-triazine (R_f: 0.36 - 1:6 v/v ethyl acetate:n-hexane) as a bright yellow/green solid which displays intense bright green fluorescence when exposed to 365nm UV light (2.1 g, 84 %).

m.p: 146 – 147 ^{o}C (from ethyl acetate:n-hexane 1:6 v/v).

Literature m.p: 146 – 147 ^{o}C (from ethanol).[54]

IR (NaCl) ν_{max} 1740 cm^{-1} (C=O).

^{1}H NMR (300 MHz $CDCl_3$): δ 3.53 (s, 3H, O-CH_3), 6.77-6.80 (d, 2H, J = 8.3 Hz, H_{ortho} iminyl N-C_6H_5), 7.10-7.42 (m, 12H, Ar), 7.76-7.93 (m, 6H, Ar), 8.49 (s, 1H, N=CH).

HRMS *m/z* 473.1951 ($[M + H]^+$, $C_{30}H_{25}N_4O_2$ requires 473.1972).

Matches literature.[54]

Synthesis of 1,2-bis(4-chlorophenyl)hydrazone of benzil (4).[56]

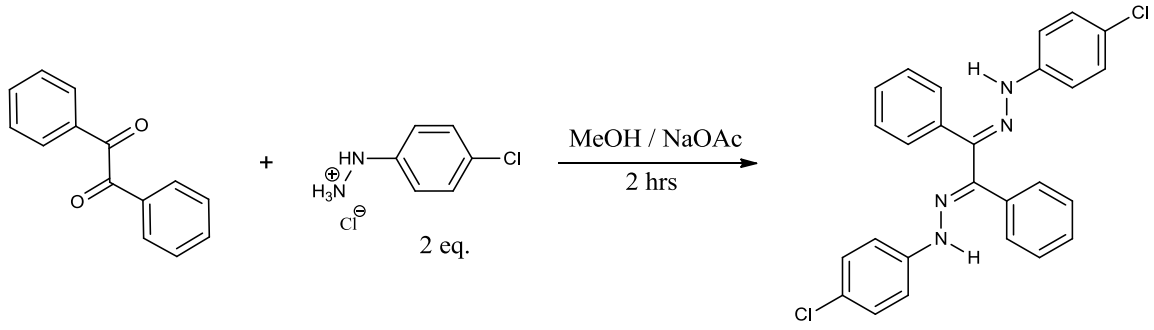

A solution of benzil (0.687 g, 3.265 mmol), 4-chlorophenylhydrazine hydrochloride (1.167 g, 6.530 mmol), sodium acetate trihydrate (4.485 g, 32.652 mmol) in ethanol (13 mL) was stirred under reflux for 2 hrs. The solution was allowed to cool to room temperature and sodium chloride was filtered off by suction filtration. The filter was washed using a minimum amount of dichloromethane. The filtrate was collected and solvent removed under reduced pressure. The residue was subjected to a hot recrystallisation from ethanol. Pure 1,2-bis(4-chlorophenyl)hydrazone of benzil precipitated as a yellow solid and was collected, washing with ice cold methanol (0.834 g, 55.6 %).

m.p: 216 – 217 ^{o}C (from ethanol).

Literature m.p: 190 ^{o}C (from aqueous ethanol).[56]

IR (NaCl) ν_{max} 1598 cm^{-1} (C=N).

^{1}H NMR (300 MHz $CDCl_3$): δ 6.96-6.99 (appd, 2H, Ar), 7.11-7.17 (m, 5H), 7.23-7.39 (m, 13H).

HRMS *m/z* 459.1158 ($[M + H]^+$, $C_{26}H_{21}Cl_2N_4$ requires 459.1138).

Matches literature.[56]

Synthesis of 2-(4-chlorophenyl)-4,5-diphenyl-1,2,3-triazolium-1-(4-chlorophenyl)-aminide (5).[54]

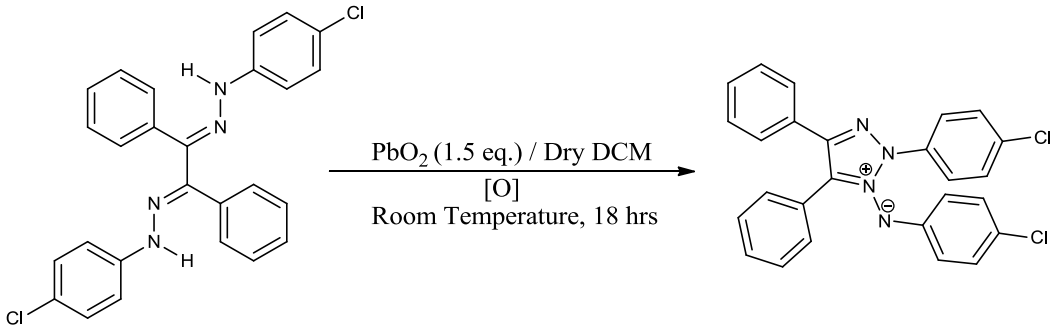

A suspension of 1,2-bis(4-chlorophenyl)hydrazone of benzil (2.66 g, 5.79 mmol) in dry dichloromethane (68 mL) was treated with an excess of lead dioxide (3.374 g, 8.659 mmol) and stirred for 18 hrs at ambient temperature. The lead salts were removed by filtration through a bed of celite washing with dichloromethane, and the filtrate evaporated to dryness under reduced pressure. The crude product was dissolved in the minimum amount of hot toluene (heated to approximately 110^{o}C), to which ice chilled petroleum ether (b.p 60-80 ^{o}C) was added dropwise. Pure 2-(4-chlorophenyl)-4,5-diphenyl-1,2,3-triazolium-1-(4-chlorophenyl)-aminide precipitated as a dark red/brown solid and was collected by suction filtration (1.948 g, 73.6 %).

m.p: 194 – 195 ^{o}C (from toluene:petroleum ether b.p. 60 – 80 ^{o}C).

Literature m.p: 187 – 188 ^{o}C (from toluene:petroleum ether b.p. 60 – 80 ^{o}C).[54]

IR (NaCl) ν_{max} 1588 cm^{-1} (C=N).

^{1}H NMR (300 MHz $CDCl_3$): δ 6.69–6.99 (m, 3H, Ar), 7.10-7.29 (m, 3H, Ar), 7.47-7.60 (m, 8H, Ar), 7.62-7.68 (m, 4H, Ar).

HRMS *m/z* 457.0989 ($[M + H]^+$, $C_{26}H_{19}Cl_2N_4$ requires 457.0981).

Matches literature.[54]

Synthesis of 5-methoxycarbonyl-5-N-((4-chlorophenyl)lformimidoyl)-2-(4-chlorophenyl)-4,6-diphenyl-2,5-dihydro-1,2,3-triazine (6a) and 6-methoxycarbonyl-3a,6a-diphenyl-2,4-bis(p-chlorophenyl)-3,3a,4,6a-tetrahydropyrrolo[2,3-d][1,2,3]-triazol-2-ium-3-ide (6b).[54]

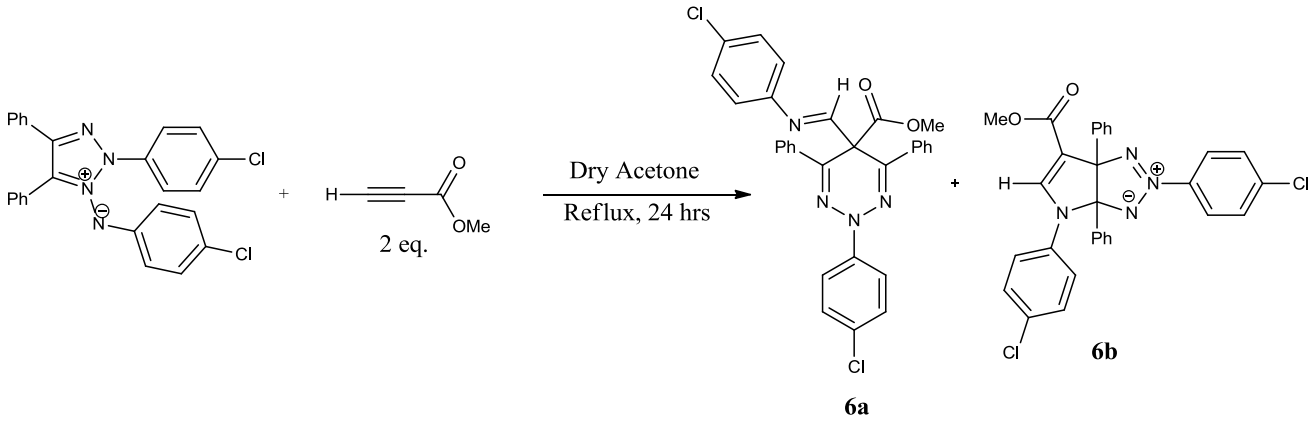

A suspension of 2-(4-chlorophenyl)-4,5-diphenyl-1,2,3-triazolium-1-(4-chlorophenyl)-aminide (1.230 g, 2.69 mmol) in dry acetone (20 cm^3) was treated with an excess of methyl propiolate (0.48 cm^3, 5.38 mmol) and stirred under reflux for 24 hrs. The solvent was removed under reduced pressure and the residue was placed, dry loaded (silica 230 – 400 mesh ASTM), on a silica gel column (230 – 400 mesh ASTM). Elution with 1:6 v/v ethyl acetate:n-hexane gave 5-methoxycarbonyl-5-N-((4-chlorophenyl)lformimidoyl)-2-(4-chlorophenyl)-4,6-diphenyl-2,5-dihydro-1,2,3-triazine (**6a**) (R_f: 0.35 - 1:6 v/v ethyl acetate:n-hexane) as a bright yellow/green solid which displays intense bright green fluorescence when exposed to 365 nm UV light (1.069 g, 71.3 %).

Changing of solvent gradient to 1:3 v/v ethyl acetate:n-hexane afforded 6-methoxycarbonyl-3a,6a-diphenyl-2,4-bis(p-chlorophenyl)-3,3a,4,6a-tetrahydropyrrolo[2,3-d][1,2,3]-triazol-2-ium-3-ide (**6b**) (R_f: 0.05 - 1:6 v/v ethyl acetate:n-hexane) as a bright yellow solid (0.43 g, 28.7 %).

5-Methoxycarbonyl-5-N-((4-chlorophenyl)lformimidoyl)-2-(4-chlorophenyl)-4,6-diphenyl-2,5-dihydro-1,2,3-triazine (6a).

m.p: 158 – 159 ^{o}C (from ethyl acetate:n-hexane 1:6 v/v).

Literature m.p: m.p: 158 – 159 ^{o}C (from ethanol).[54]

IR (NaCl) ν_{max} 1743 cm^{-1} (C=O).

^{1}H NMR (300 MHz $CDCl_3$): δ 3.54 (s, 3H, O-CH_3), 6.69-6.71 (d, 2H) 7.18-7.21 (d, 2H J_{AB} = 8.5 Hz, iminyl N-C_6H_4-Cl-*p*, AA′BB′), 7.25-7.45 (m, 8H, Ar), 7.72-7.75 (m, 4H, Ar), 7.81-7.84 (d, 2H, J_{AB} = 8.9 Hz, 2-N-C_6H_4-Cl-*p*, AA′BB′), 8.48 (s, 1H, N=CH).

HRMS *m/z* 541.1178 ($[M + H]^+$, $C_{30}H_{23}Cl_2N_4O_2$ requires 541.1193).

Matches literature.[54]

6-Methoxycarbonyl-3a,6a-diphenyl-2,4-bis(p-chlorophenyl)-3,3a,4,6a-tetrahydropyrrolo[2,3-d][1,2,3]-triazol-2-ium-3-ide (6b).

m.p: 163 – 164 ^{o}C (from ethyl acetate:n-hexane 1:6 v/v).

Literature m.p: 163 – 164 ^{o}C (from ethanol).[54]

IR (NaCl) ν_{max} 1703 cm^{-1} (C=O).

^{1}H NMR (300 MHz $CDCl_3$) δ = 3.66 (s, 3H, O-CH_3), 6.89-6.99 (m, 10H, Ar), 7.01-7.17 (m, 4H, Ar), 7.50-7.53 (d, 2H, J_{AB} = 8.9 Hz, 2-N-C_6H_4-Cl-*p*, AA′BB′), 8.34 (s, 1H, 5-CH), 8.38-8.41 (m, 2H, Ar).

HRMS *m/z* 541.1209 ($[M + H]^+$, $C_{30}H_{23}Cl_2N_4O_2$ requires 541.1193).

Matches literature.[54]

Synthesis of 1,2-bis(4-bromophenyl)hydrazone of benzil (7).[56]

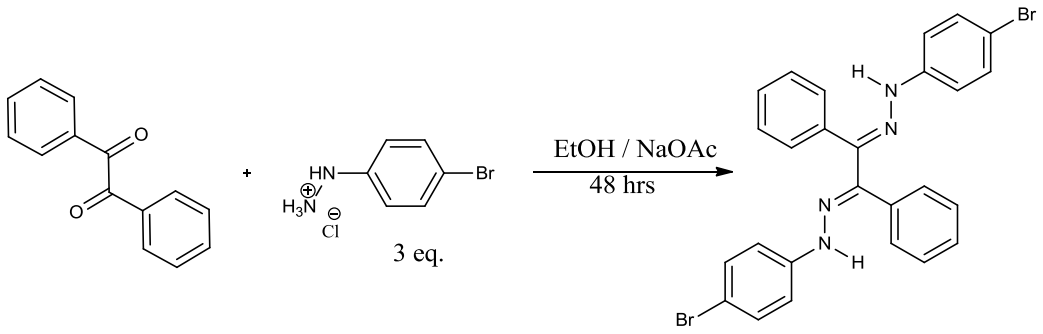

A solution of benzil (0.383 g, 1.833 mmol), 4-bromophenylhydrazine hydrochloride (0.819 g, 3.666 mmol), sodium acetate trihydrate (0.499 g, 3.666 mmol) in ethanol (25 mL) was stirred under reflux for 48 hrs. The solution was allowed to cool to room temperature and sodium chloride was filtered off by suction filtration. The filter was washed using a minimum amount of dichloromethane. The filtrate was collected and solvent removed under reduced pressure. The residue was subjected to a hot recrystallisation from ethanol. Pure 1,2-bis(4-bromophenyl)hydrazone of benzil precipitated as a yellow solid and was collected, washing with ice cold methanol (0.628 g, 62.8 %).

m.p: 233^{o}C (from ethanol).

Literature m.p: 233^{o}C (from benzene/ethanol).[56]

IR (NaCl) ν_{max} 1266 cm^{-1} (C=N).

^{1}H NMR (300 MHz $CDCl_3$): δ 6.96-6.99 (appd, 2H, Ar), 7.11-7.17 (m, 5H, Ar), 7.23-7.39 (m, 13H, Ar).

HRMS *m/z* 547.0154 ($[M + H]^+$, $C_{26}H_{21}Br_2N_4$ requires 547.0128).

Matches literature.[56]

Synthesis of 2-(4-bromophenyl)-4,5-diphenyl-1,2,3-triazolium-1-(4-bromophenyl)-aminide (8).[31]

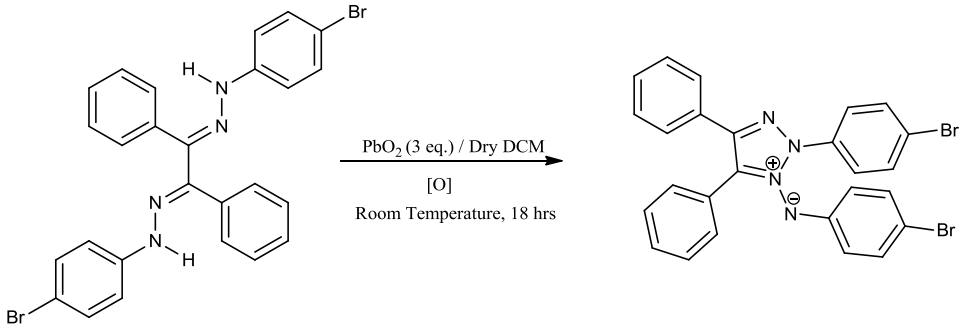

A suspension of 1,2-bis(4-bromophenyl)hydrazone of benzil (0.425 g, 0.775 mmol) in dry dichloromethane (15 mL) was treated with an excess of lead dioxide (0.556 g, 2.325 mmol) and stirred for 60 hrs at ambient temperature. The lead salts were removed by filtration through a bed of celite, and the filtrate evaporated to dryness under reduced pressure. The crude product was dissolved in the minimum amount of toluene and then heated to approximately 110^{o}C, to which ice chilled petroleum ether (b.p 60-80 ^{o}C) was added dropwise. Pure 2-(4-bromophenyl)-4,5-diphenyl-1,2,3-triazolium-1-(4-methoxyphenyl)-aminide precipitated as a black solid and was collected by suction filtration (0.250 g, 59.1 %).

m.p: 185 – 186 ^{o}C (from toluene:petroleum ether b.p. 60-80 ^{o}C).

Literature m.p: 197 – 199 ^{o}C (from toluene:petroleum ether b.p. 60-80 ^{o}C).[54]

IR (NaCl) ν_{max} 1266 cm^{-1} (C=N).

^{1}H NMR (300 MHz $CDCl_3$): δ 6.94-6.97 (m, 3H, Ar), 7.28-7.54 (m, 15H, Ar).

HRMS *m/z* 544.9947 ($[M + H]^+$, $C_{26}H_{19}Br_2N_4$ requires 544.9971).

Matches literature.[31]

Synthesis of 5-methoxycarbonyl-5-N-((4-bromophenyl)lformimidoyl)-2-(4-bromophenyl)-4,6-diphenyl-2,5-dihydro-1,2,3-triazine (9a) and 6-methoxycarbonyl-3a,6a-diphenyl-2,4-bis(p-bromophenyl)-3,3a,4,6a-tetrahydropyrrolo[2,3-d][1,2,3]-triazol-2-ium-3-ide (9b).[54]

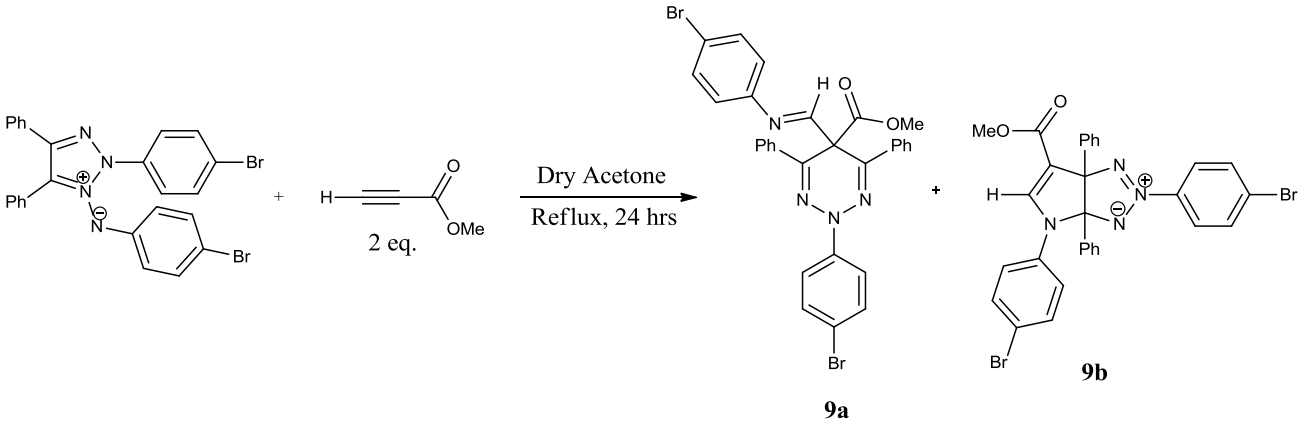

A suspension of 2-(4-bromophenyl)-4,5-diphenyl-1,2,3-triazolium-1-(4-bromophenyl)-aminide (0.1 g, 0.184 mmol) in dry acetone (5 mL) was treated with an excess of methyl propiolate (0.033 mL, 0.367 mmol) and stirred under reflux for 24 hrs. The solvent was removed under reduced pressure and the residue was placed, dry loaded (silica 230 – 400 mesh ASTM), on a silica gel column (230 – 400 mesh ASTM). Elution with 1:6 v/v ethyl acetate:n-hexane gave 5-methoxycarbonyl-5-N-((4-bromophenyl)lformimidoyl)-2-(4-bromophenyl)-4,6-diphenyl-2,5-dihydro-1,2,3-triazine (**9a**) (R_f: 0.36 - 1:6 v/v ethyl acetate:n-hexane) as a bright yellow/green solid which displays green fluorescence when exposed to 365 nm UV light (0.098 g, 85.2 %).

Changing of solvent gradient to 1:3 v/v ethyl acetate:n-hexane afforded 6-methoxycarbonyl-3a,6a-diphenyl-2,4-bis(p-bromophenyl)-3,3a,4,6a-tetrahydropyrrolo[2,3-d][1,2,3]-triazol-2-ium-3-ide (**9b**) (R_f: 0.05 - 1:6 v/v ethyl acetate:n-hexane) as a dark yellow solid (0.005 g, 4.34 %).

5-Methoxycarbonyl-5-N-((4-bromophenyl)lformimidoyl)-2-(4-bromophenyl)-4,6-diphenyl-2,5-dihydro-1,2,3-triazine (9a).

m.p: 163 – 164 ^{o}C (from ethyl acetate:n-hexane 1:6 v/v).

Literature m.p: 163 – 164 ^{o}C (from ethanol).[54]

IR (NaCl) ν_{max} 1737 cm^{-1} (C=O).

^{1}H NMR (300 MHz $CDCl_3$): δ 3.54 (s, 3H, O-CH_3), 6.62-6.65 (d, 2H, *J* = 8.5 Hz, H_{ortho} iminyl N-C_6H_4-Br-*p*), 7.32-7.4 (m, 8H, Ar), 7.47-7.5 (d, 2H, *J* = 9 Hz, H_{ortho} 2-N-C_6H_4-Br-*p*), 7.71-7.78 (m, 6H, Ar), 8.48 (s, 1H, N=CH).

HRMS *m/z* 629.0175 ($[M + H]^+$, $C_{30}H_{23}Br_2N_4O_2$ requires 629.0182).

Matches literature.[54]

6-Methoxycarbonyl-3a,6a-diphenyl-2,4-bis(p-bromophenyl)-3,3a,4,6a-tetrahydropyrrolo[2,3-d][1,2,3]-triazol-2-ium-3-ide (9b).

m.p: 169 – 170 ^{o}C (from ethyl acetate:n-hexane 1:6 v/v).

Literature m.p: 169 – 170 ^{o}C (from ethanol).[54]

IR (NaCl) ν_{max} 1696 cm^{-1} (C=O).

^{1}H NMR (300 MHz $CDCl_3$): δ 3.66 (s, 3H, O-CH_3), 6.88-6.94 (m, 10H, Ar), 7.07-7.10 (d, 2H, *J* = 8.8 Hz, 4-N-C_6H_4-Br-*p*, AA′BB′), 7.25-7.28 (d, 2H, *J* = 8.8 Hz, 4-N-C_6H_4-Br-*p*, AA′BB′), 7.66-7.69 (d, 2H, *J* = 8.9 Hz H_{ortho} 2-N-C_6H_4-Br-*p*), 8.3 (s, 1H, 5-CH), 8.34-8.36 (m, 2H, Ar).

HRMS *m/z* 629.0142 ($[M + H]^+$, $C_{30}H_{23}Br_2N_4O_2$ requires 629.0182).

Matches literature.[54]

Synthesis of 5-propan-one-5-(N-phenylformimidoyl)-2,4,6-triphenyl-2,5-dihydro-1,2,3-triazine (10a) and 6-acetyl-2,3a,4,6a-tetraphenyl-4,6a-dihydro-3aH-pyrrolo[2,3-d][1,2,3]triazol-2-ium-3-ide (10b).

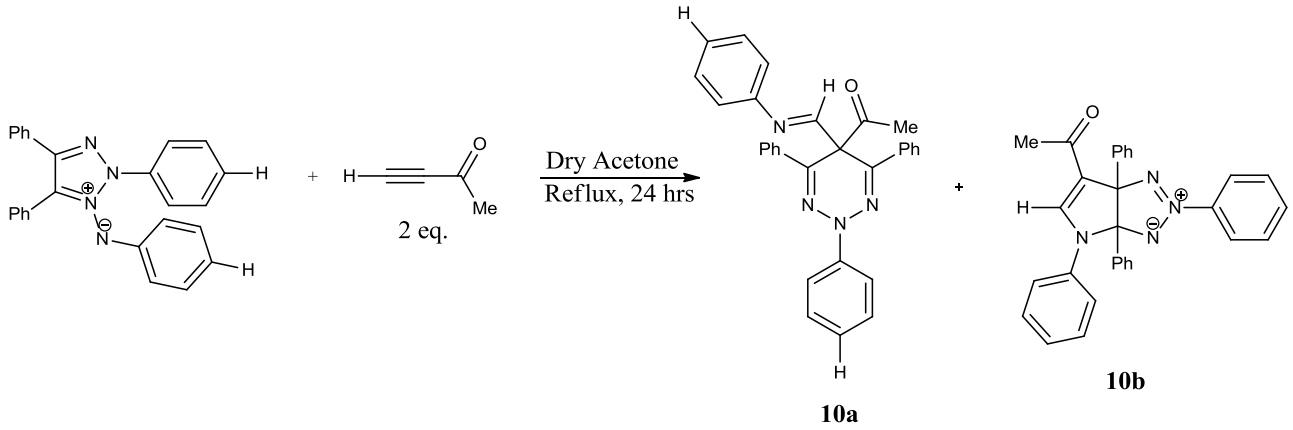

A suspension of 2,4,5-triphenyl-1,2,3-triazolium-1-phenylaminide (0.255 g, 0.657 mmol) in dry acetone (10 mL) was treated with an excess of 3-butyn-2-one (0.102 mL, 1.314 mmol) and stirred under reflux for 24 hrs. The solvent was removed under reduced pressure and the residue was placed, dry loaded (silica 230 – 400 mesh ASTM), on a silica gel column (230 – 400 mesh ASTM). Elution with 1:6 v/v ethyl acetate:n-hexane gave 5-propan-one-5-(N-phenylformimidoyl)-2,4,6-triphenyl-2,5-dihydro-1,2,3-triazine (R_f : 0.36 - 1:6 v/v ethyl acetate:n-hexane) as a dark orange solid which displays intense bright yellow/green fluorescence when exposed to 365 nm UV light (0.118 g, 39.3 %).

Changing of solvent gradient to 1:3 v/v ethyl acetate:n-hexane afforded 6-acetyl-2,3a,4,6a-tetraphenyl-4,6a-dihydro-3aH-pyrrolo[2,3-d][1,2,3]triazol-2-ium-3-ide (**10b**) (R_f: 0.05 - 1:6 v/v ethyl acetate:n-hexane) as a dark yellow solid (0.178 g, 59.3 %).

5-Propan-one-5-(N-phenylformimidoyl)-2,4,6-triphenyl-2,5-dihydro-1,2,3-triazine (10).

m.p: 174 – 175 ^{o}C (from ethyl acetate:n-hexane 1:6 v/v).

IR (NaCl) ν_{max} 1717 cm^{-1} (C=O).

^{1}H NMR (300 MHz $CDCl_3$): δ 3.18 (s, 3H, O=C-CH_3), 6.72-6.75 (d, 2H, *J* = 8.3 Hz, H_{ortho} iminyl N-C_6H_5), 7.13-7.80 (m, 16H, Ar), 7.98-8.0 (m, 2H, Ar), 8.85 (s, 1H, N=CH).

^{13}C NMR (75 MHz $CDCl_3$) δ = 27.9 (CH_3), 58.3 (C5), 114.8, 119.0, 122.5, 125, 127.9, 128.6, 143.9, 150.2 (aromatics, overlapping signals), 133.8, 135.5 (C4 and C6), 161.5 (N=CH), 203.7 (C=O).

HRMS *m/z* 457.2004 ([M + Na]$^{+}$, $C_{30}H_{25}N_4O$ requires 457.2023).

6-Acetyl-2,3a,4,6a-tetraphenyl-4,6a-dihydro-3aH-pyrrolo[2,3-d][1,2,3]triazol-2-ium-3-ide (10a).

m.p: 170 – 172 ^{o}C from (from ethyl acetate:n-hexane 1:6 v/v).

IR (NaCl) ν_{max} 1638 cm^{-1} (C=O).

^{1}H NMR (300 MHz $CDCl_3$): δ 3.13 (s, 3H, O=C-CH_3), 6.9-7.01 (m, 11H, Ar), 7.15-7.21 (m, 2H, Ar), 7.24-7.29 (m, 2H, Ar), 7.51-7.63 (m, 3H, Ar) 8.43 (s, 1H, 5-CH), 8.44-8.46 (m, 2H, Ar).

^{13}C NMR (75 MHz $CDCl_3$) δ = 26.7 (CH_3), 91.7, 105.1 (C6a and C3a), 114.8, 117.8, 121.9, 122.2, 126.1, 126.6, 127.39, 127.6, 127.9, 128.1, 130.8, 134.5, 136.6, 139.3 (aromatics, overlapping signals), 147.6 (C5), 192 (C=O).

HRMS *m/z* 479.1851 ([M + Na]$^{+}$, $C_{30}H_{24}N_4NaO$ requires 479.1842).

2.1.2 Synthesis for Chapter 5.

Synthesis of 5-methoxycarbonyl-5-(N-phenylimino(ethyl))-2,4,6-triphenyl-2,5-dihydro-1,2,3-triazine (11b).

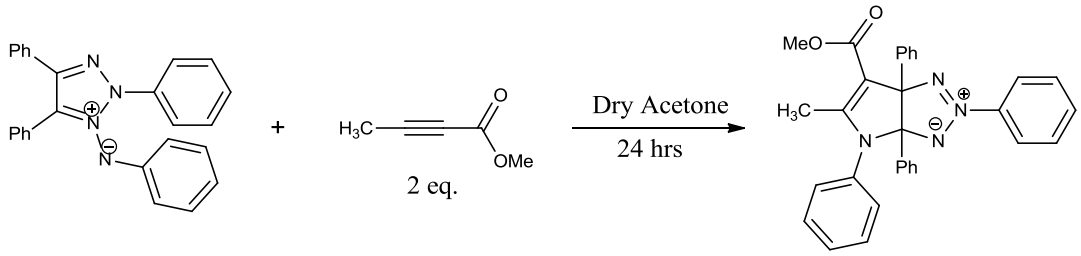

A suspension of 2,4,5-triphenyl-1,2,3-triazolium-1-phenylaminide (0.239 g, 0.617 mmol) in dry acetone (8 mL) was treated with an excess of methyl-2-butyn-oate (0.123 cm^3, 1.234 mmol) and stirred under reflux for 24 hours. The solvent was removed under reduced pressure and the residue was placed, dry loaded (silica 230 – 400 mesh ASTM), on a silica gel column (230 – 400 mesh ASTM). Elution with 1:6 v/v ethyl acetate:n-hexane gave 6-(methoxycarbonyl)-5-methyl-2,3a,4,6a-tetraphenyl-4,6a-dihydro-3aH-pyrrolo[2,3-d][1,2,3]triazol-2-ium-3-ide (R_f: 0.05 - 1:6 v/v ethyl acetate:n-hexane) as a dark yellow solid (0.242 g, 80.7 %).

m.p: 163 – 164 ^oC (from dichloromethane:toluene 1:1 v/v).

IR (NaCl) ν_{max} 1680 cm^{-1} (C=O).

^1H NMR (300 MHz $CDCl_3$): δ 2.46 (s, 3H, C=C-CH_3), 3.56 (s, 3H, O=C-CH_3), 6.80-6.97 (m, 10H, Ar), 7.11-7.28 (m, 5H, Ar), 7.55-7.60 (m, 3H, Ar), 8.38-8.42 (m, 2H, Ar).

^{13}C NMR (75 MHz $CDCl_3$): δ 13.7 (CH_3), 49.4 (O-CH_3), 90.8, 100.7 (C6a and C3a), 103.7 (C-6), 121.9, 125.5, 126.1, 126.3, 126.4, 126.5, 126.8, 126.9, 130.5, 135.6, 137.6, 137.8, 139.6 (aromatics, overlapping signals), 163.3 (C5), 165.8 (C=O).

HRMS *m/z* 487.2104 ($[M + H]^+$, $C_{31}H_{27}N_4O_2$ requires 487.2129).

Synthesis of 5-methoxycarbonyl-5-(N-phenylimino(ethyl))-2,4,6-triphenyl-2,5-dihydro-1,2,3-triazine (11a).

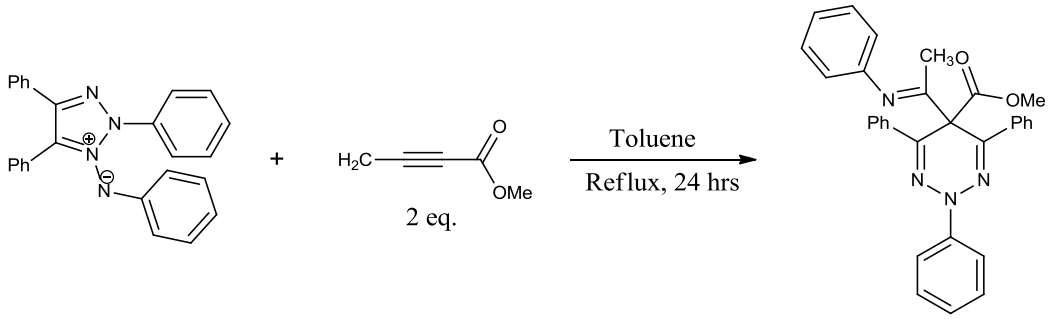

A suspension of 2,4,5-triphenyl-1,2,3-triazolium-1-phenylaminide (0.239 g, 0.617 mmol) in dry toluene (10 mL) was treated with an excess of methyl-2-butyn-oate (0.123 mL, 1.233 mmol) and stirred under reflux for 24 hrs. The solvent was removed under reduced pressure and the residue was placed, dry loaded (silica 230 – 400 mesh ASTM), on a silica gel column (230 – 400 mesh ASTM). Elution with 1:6 v/v ethyl acetate:n-hexane and hot recrystallisation from ethanol gave 5-methoxycarbonyl-5-(N-phenylimino(ethyl))-2,4,6-triphenyl-2,5-dihydro-1,2,3-triazine (R_f: 0.36 - 1:6 v/v ethyl acetate:n-hexane) as a dark yellow solid which does not fluoresce when exposed to 365 nm UV light, however the molecule exhibits weak green fluorescence when in solution (0.241 g, 80%).

m.p: 189 ^{o}C (from ethanol).

IR (NaCl) ν_{max} 1740 cm^{-1} (C=O).

^{1}H NMR (300 MHz $CDCl_3$): δ 1.05 (s, 3H, N=C-CH_3), 3.80 (s, 3H, O=C-CH_3), 6.64-6.67 (d, 2H, *J* = 8.3 Hz, H_{ortho} iminyl N-C_6H_5), 6.99 (m, 1H, Ar), 7.04 (m, 1H, Ar), 7.12-7.28 (m, 2H, Ar), 8.37-7.45 (m, 8H, Ar), 7.89-7.95 (m, 6H, Ar).

^{13}C NMR (75 MHz $CDCl_3$): δ 20.0 (CH_3), 53.1 (C-5), 61.1 (O-CH_3), 123.8, 123.9, 128.8, 129.0, 129.6, 135.2, 136.4, 145.7, 150.1, (aromatics, overlapping signals), 128.1, 130.2 (C4 and C6), 168.1 (N=C), 169.9 (C=O).

HRMS *m/z* 487.2148 ($[M + H]^+$, $C_{31}H_{27}N_4O_2$ requires 487.2129).

Synthesis of 5-methoxycarbonyl-5-(phenyl(imino(methyl)))-2,4,6-triphenyl-2,5-dihydro-1,2,3-triazine (12).

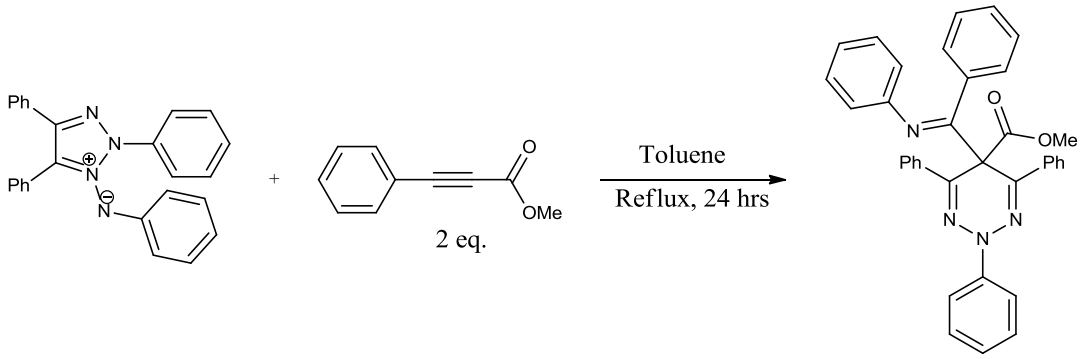

A suspension of 2,4,5-triphenyl-1,2,3-triazolium-1-phenylaminide (0.106 g, 0.273 mmol) in dry toluene (6 mL) was treated with an excess of methyl phenylpropiolate (0.1 mL, 0.7 mmol) and stirred under reflux for 24 hrs. The solvent was removed under reduced pressure and the residue was placed, dry loaded (silica 230 – 400 mesh ASTM), on a silica gel column (230 – 400 mesh ASTM). Elution with 1:6 v/v ethyl acetate:n-hexane gave 5-methoxycarbonyl-5-(N-phenylimino(ethyl))-2,4,6-triphenyl-2,5-dihydro-1,2,3-triazine (R_f: 0.36 - 1:6 v/v ethyl acetate:n-hexane) as a pale white solid which does not fluoresce when exposed to 365 nm UV light (0.1 g, 75.33 %).

m.p: 168 - 170 ^{o}C (from ethanol).

IR (NaCl) ν_{max} 1641 cm^{-1} (C=O).

^{1}H NMR (300 MHz $CDCl_3$): δ 3.18 (s, 3H, O-CH_3), 6.5-6.53 (appd, 2H, *J* =7.3 Hz, Ar), 6.79-6.84 (appt, 1H, *J* = 7.4 Hz, Ar), 6.99-7.04 (m, 6H, Ar), 7.25-7.3 (m, 8H, Ar), 7.42-7.47 (appt, 2H, *J* = 8.5 Hz, Ar), 7.53-7.58 (m, 4H, Ar), 7.98-8.01 (appd, 2H, *J* = 7.8 Hz, Ar).

^{13}C NMR (75 MHz $CDCl_3$): δ 52.4 (C5), 61.9 (O-CH_3), 116.6, 119.9, 123.4, 124.0, 127.5, 127.8, 128.3, 134.5, 135.7, 136.8, 146.1, 149.4 (aromatics, overlapping signals), 134.5, 135.7 (C4 and C6), 168.9 (N=C), 170.8 (C=O).

HRMS *m/z* 549.2339 ($[M + H]^+$, $C_{36}H_{29}N_4O_2$ requires 549.2285).

Synthesis of 5-methoxycarbonyl-5-(2-methoxy-2-oxo-1-(phenylimino(ethyl)))-2,4,6-triphenyl-2,5-dihydro-1,2,3-triazine (13).[57]

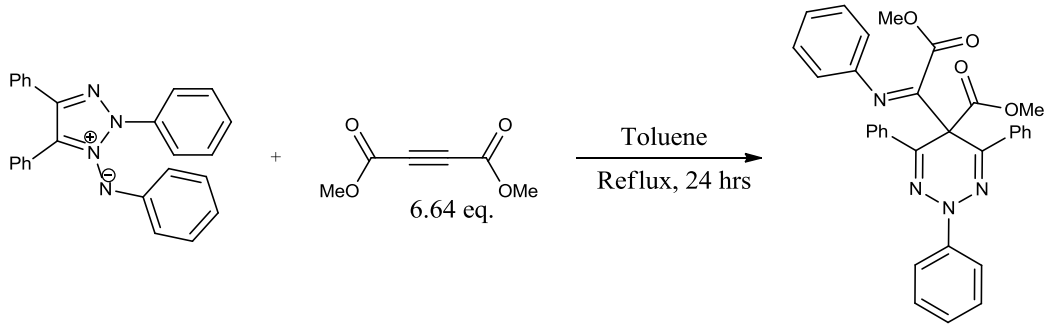

A suspension of 2,4,5-triphenyl-1,2,3-triazolium-1-phenylaminide (0.438 g, 1.129 mmol) in dry toluene (15 mL) was treated with an excess of dimethyl acetylenedicarboxylate (DMAD) (0.92 mL, 7.51 mmol) and stirred under reflux for 24 hrs. The solvent was removed under reduced pressure and the residue was placed, dry loaded (silica 230 – 400 mesh ASTM), on a silica gel column (230 – 400 mesh ASTM). Elution with 1:6 v/v ethyl acetate:n-hexane gave 5-methoxycarbonyl-5-(2-methoxy-2-oxo-1-(phenylimino(ethyl)))-2,4,6-triphenyl-2,5-dihydro-1,2,3-triazine (R_f: 0.36 - 1:6 v/v ethyl acetate:n-hexane) as a yellow solid which does not fluoresce when exposed to 365 nm UV light (0.453 g, 75.6 %).

IR (NaCl) ν_{max} 1746 cm^{-1} (C=O), 1730 cm^{-1} (C=O).

m.p: 144 – 146 ^{o}C (from ethyl acetate:n-hexane 1:6 v/v).

Literature m.p: 151 – 152 ^{o}C (from methanol).[57]

^{1}H NMR (300 MHz $CDCl_3$): δ 2.91 (s, 3H, O-CH_3), 3.74 (s, 3H, O-CH_3), 6.48-6.49 (d, 2H, *J* = 8.3 Hz, H_{ortho} iminyl N-C_6H_5), 7.01-7.08 (appt, 1H, Ar), 7.11-7.23 (m, 4H, Ar), 7.36-7.41 (m, 7H, Ar) 7.82-7.90 (m, 6H, Ar).

HRMS *m/z* 531.2031 ($[M + H]^+$, $C_{32}H_{27}N_4O_4$ requires 531.2027).

Matches literature.[57]

Synthesis of methyl [3- ^{2}H] propiolate (14).[58]

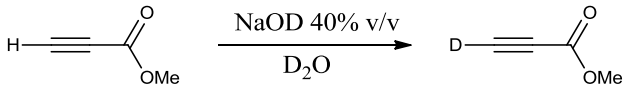

To a stirred solution of methyl propiolate (0.070 mL, 0.8107 mmol) in D_2O (1 mL), was added 40% v/v sodium deuteroxide in D_2O (0.1 mL) and stirred overnight at room temperature. The organic layer was extracted with $CDCl_3$ (2 x 5 mL), washed with D_2O, dried over calcium chloride and filtered. The resulting colourless solution was sufficiently pure for the next step (0.069 g, 100 %).

^{1}H NMR (300 MHz $CDCl_3$): δ 3.48 (s, 3H, OCH_3).

Matches literature.[58]

Synthesis of 5-methoxycarbonyl-5-(N-phenylform-D-imidoyl)-2,4,6-triphenyl-2,5-dihydro-1,2,3-triazine (15).

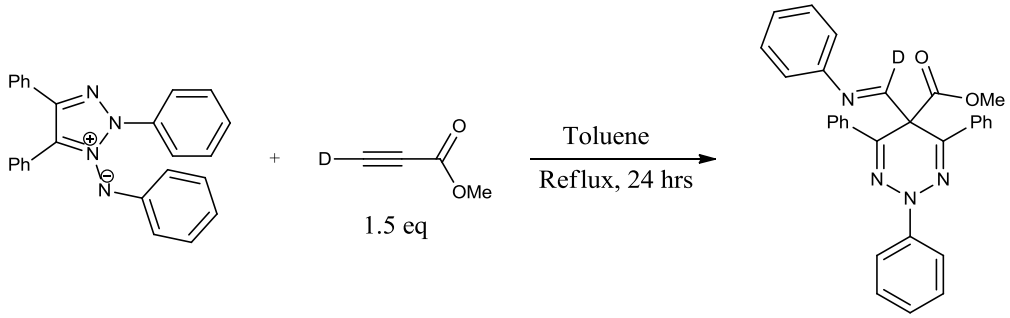

To the solution of methyl [3-^{2}H] propiolate (0.069 g, 0.810 mmol) previously prepared in $CDCl_3$ was added 2,4,5-triphenyl-1,2,3-triazolium-1-phenylaminide (0.472 g, 1.216 mmol) and toluene (15 mL) before being stirred under reflux for 24 hrs. The solvent was removed under reduced pressure and the residue was placed, dry loaded (silica 230 – 400 mesh ASTM), on a silica gel column (230 – 400 mesh ASTM). Elution with 1:6 v/v ethyl acetate:n-hexane gave 5-methoxycarbonyl-5-(N-phenylform-D-imidoyl)-2,4,6-triphenyl-2,5-dihydro-1,2,3-triazine (R_f: 0.36 - 1:6 v/v ethyl acetate:n-hexane) as a bright yellow/green solid which displays intense bright green fluorescence when exposed to 365 nm UV light (0.292 g, 76.3 %).

m.p: 145 ^{o}C (from ethyl acetate:n-hexane 1:6 v/v).

IR (NaCl) ν_{max} 1737 cm^{-1} (C=O).

^{1}H NMR (300 MHz $CDCl_3$): δ 3.54 (s, 3H, O-CH_3), 6.78-6.79 (d, 2H, *J* = 8.3 Hz, H_{ortho} iminyl N-C_6H_5), 7.1-7.12 (appt, 2H, Ar), 7.15-7.7.25 (m, 2H, Ar), 7.36-7.42 (m, 8H, Ar), 7.75-7.79 (m, 4H, Ar), 7.89-7.92 (d, 2H, *J* = 8.9 Hz H_{ortho} 2-N-C_6H_5).

^{13}C NMR (75 MHz $CDCl_3$): δ 53.3 (C5), 53.4 (O-CH_3), 116, 120.3, 123.5, 126.2, 128.4, 128.6, 128.8, 128.9, 129.5, 145.2, 150.9 (aromatics, overlapping signals), 134.8, 135.2 (C4 and C6), 170.2 (C=O).

HRMS *m/z* 474.1916 ([M + H]$^{+}$, $C_{30}H_{24}DN_4O_2$ requires 474.1962).

2.1.3. Synthesis for Chapter 6.

Synthesis of 5-methoxycarbonyl-5-H-2,4,6-triphenyl-2,5-dihydro-1,2,3-triazine (16).[54]

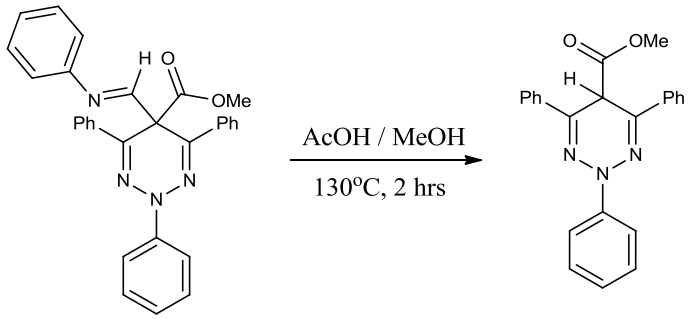

Acetic acid (0.07 mL, 11.76 mmol) was added to 5-methoxycarbonyl-5-(N-phenylformimidoyl)-2,4,6-triphenyl-2,5-dihydro-1,2,3-triazine (0.556 g, 1.176 mmol) in methanol (1 mL) and heated for 2 hrs at 130^{o}C. The solution was allowed to cool to room temperature before washing with saturated aqueous sodium bicarbonate (10 mL), and extracting with diethyl ether (30 mL). The organic layer was dried over magnesium sulphate and filtered. The solvent was removed under reduced pressure and the residue was placed, dry loaded (silica 230 – 400 mesh ASTM), on a silica gel column (230 – 400 mesh ASTM). Elution with 1:6 v/v ethyl acetate:n-hexane gave 5-methoxycarbonyl-5-H-2,4,6-triphenyl-2,5-dihydro-1,2,3-triazine (R_f: 0.36 (1:6 v/v ethyl acetate:n-hexane) as a bright yellow/green solid, which displays bright green fluorescence when exposed to 365nm UV light, upon removal of solvent under reduced pressure (0.432 g, 99.3 %).

m.p: 193-195 ^{o}C (from ethyl acetate:n-hexane 1:6 v/v).

Literature m.p: 193-196 ^{o}C (from dichloromethane:n-hexane.[54]

IR (NaCl) ν_{max} 1740 cm^{-1} (C=O).

^{1}H NMR (300 MHz $CDCl_3$): δ 3.64 (s, 3H, O-CH_3), 5.32 (s, 1H, 5-CH), 7.12-7.17 (m, 1H, Ar), 7.50-7.40 (m, 8H, Ar), 7.95-8.04 (m, 6H, Ar).

HRMS *m/z* 370.1539 ($[M + H]^+$, $C_{23}H_{20}N_3O_2$ requires 370.1556).

Matches literature.[54]

Synthesis of 5-methoxycarbonyl-5-H-2-(4-chlorophenyl-4,6-diphenyl-2,5-dihydro-1,2,3-triazine (17).

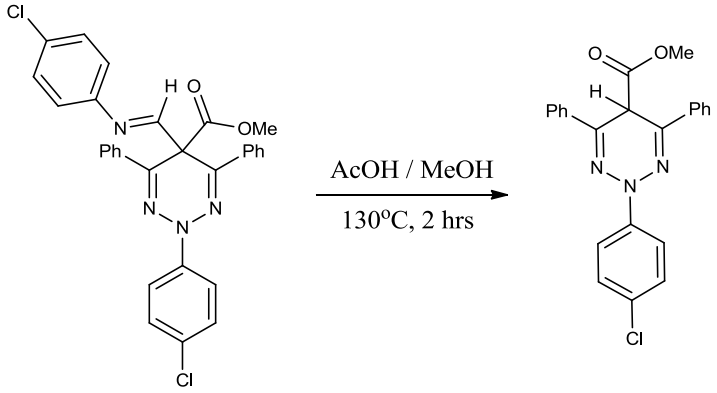

Acetic acid (0.06 mL, 1.11 mmol) was added to 5-methoxycarbonyl-5-N-((4-chlorophenyl)formimidoyl))-2-(4-chlorophenyl)-4,6-diphenyl-2,5-dihydro-1,2,3-triazine (0.06 g, 0.11 mmol) in methanol (1 mL) and heated for 2 hrs at 130°C. The solution was allowed to cool to room temperature before washing with saturated aqueous sodium bicarbonate (10mL), and extracting with diethyl ether (30 mL). The organic layer was dried over magnesium sulphate and filtered. The solvent was removed under reduced pressure and the residue was placed, dry loaded (silica 230 – 400 mesh ASTM), on a silica gel column (230 – 400 mesh ASTM). Elution with 1:6 v/v ethyl acetate:n-hexane gave 5-methoxycarbonyl-5-H-2-(4-chlorophenyl)-4,6-diphenyl-2,5-dihydro-1,2,3-triazine (R_f: 0.36 - 1:6 v/v ethyl acetate:n-hexane) as a bright yellow/green solid which displays bright green fluorescence when exposed to 365 nm UV light (0.04 g, 84 %).

m.p: 171 - 173 °C (from ethyl acetate:n-hexane 1:6 v/v).

IR (NaCl) ν_{max} 1641 cm^{-1} (C=O).

^{1}H NMR (300 MHz $CDCl_3$): δ 3.65 (s, 3H, O-CH_3), 5.32 (s, 1H, 5-CH), 7.36-7.49 (m, 8H, Ar), 7.86-7.89 (d, 2H, *J* = 8.8 Hz H_{ortho} 2-N-C_6H_4-Cl-*p*), 7.99-8.02 (m, 4H, Ar).

^{13}C NMR (75 MHz $CDCl_3$): δ 37.3 (C5), 52.2 (O-CH_3), 116.3, 125.6, 127.6, 127.7, 127.8, 128.9, 143.2 (aromatics, overlapping signals), 132.9, 133.4 (C4 and C6), 166.5 (C=O).

HRMS *m/z* 404.1155 ($[M + H]^+$, $C_{23}H_{19}ClN_3O_2$ requires 404.1160).

Synthesis of 5-methoxycarbonyl-5-H-2-(4-bromophenyl-4,6-diphenyl-2,5-dihydro-1,2,3-triazine (18).

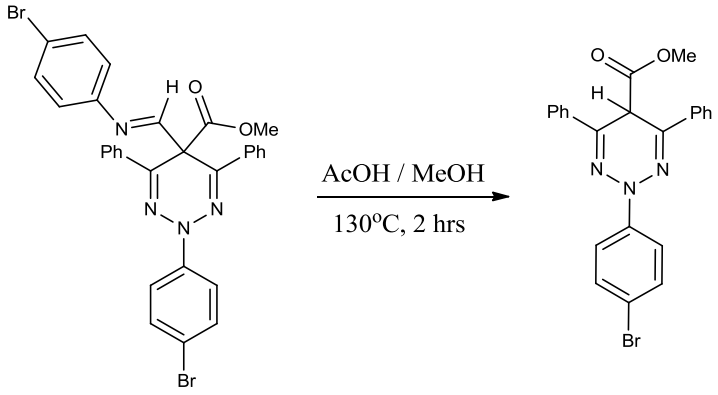

Acetic acid (0.03 mL, 0.51 mmol) was added to 5-methoxycarbonyl-5-N-((4-bromophenyl)formimidoyl))-2-(4-bromophenyl)-4,6-diphenyl-2,5-dihydro-1,2,3-triazine (0.032 g, 0.051 mmol) in methanol (1 mL) and refluxed for 2 hrs at 130^{o}C. The solution was allowed to cool to room temperature before washing with saturated aqueous sodium bicarbonate (10 mL), and extracting with diethyl ether (30 mL). The organic layer was dried over magnesium sulphate and filtered. The solvent was removed under reduced pressure and the residue was placed, dry loaded (silica 230 – 400 mesh ASTM), on a silica gel column (230 – 400 mesh ASTM). Elution with 1:6 v/v ethyl acetate:n-hexane gave 5-methoxycarbonyl-5-H-2-(4-bromophenyl)-4,6-diphenyl-2,5-dihydro-1,2,3-triazine (R_f: 0.36 - 1:6 v/v ethyl acetate:n-hexane) as a bright yellow/green solid which displays bright green fluorescence when exposed to 365nm UV light (0.022 g, 95.7 %).

m.p: 179 - 180 ^{o}C (from ethyl acetate:n-hexane 1:6 v/v).

IR (NaCl) ν_{max} 1638 cm^{-1} (C=O).

^{1}H NMR (300 MHz $CDCl_3$) δ = 3.66 (s, 3H, O-CH_3), 5.32 (s, 1H, 5-CH), 7.37-7.60 (m, 8H, Ar), 7.80-7.97 (m, 2H, Ar), 8.04-8.05 (m, 4H, Ar).

^{13}C NMR (75 MHz $CDCl_3$): δ 37.4 (C5), 52.2 (O-CH_3), 115.3, 116.7, 125.6, 127.7, 128.9, 130.7, 143.7 (aromatics, overlapping signals), 133, 133.4 (C4 and C6), 166.5 (C=O).

HRMS *m/z* 448.0646 ($[M + H]^+$, $C_{23}H_{19}BrN_3O_2$ requires 448.0655).

Synthesis of 5-propanone-5-H-2,4,6-triphenyl-2,5-dihydro-1,2,3-triazine (19).

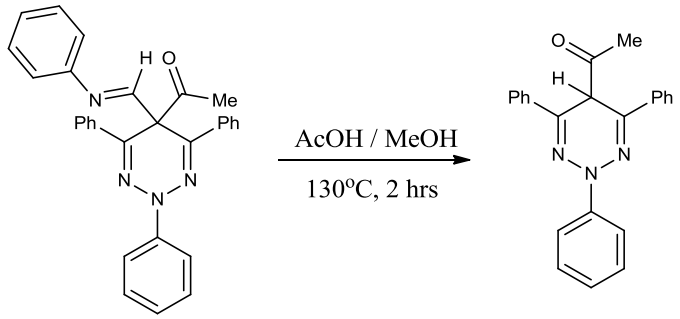

Acetic acid (0.024 mL, 0.438 mmol) was added to 5-propanone-5-(N-phenylformimidoyl)-2,4,6-triphenyl-2,5-dihydro-1,2,3-triazine (0.02 g, 0.044 mmol) in methanol (1 mL) and refluxed for 2 hrs at 130^{o}C. The solution was allowed to cool to room temperature before washing with saturated aqueous sodium bicarbonate (10mL), and extracting with diethyl ether (30 mL). The organic layer was dried over magnesium sulphate and filtered. The solvent was removed under reduced pressure and the residue was placed, dry loaded (silica 230 – 400 mesh ASTM), on a silica gel column (230 – 400 mesh ASTM). Elution with 1:6 v/v ethyl acetate:n-hexane gave 5-propanone-5-H-2,4,6-triphenyl-2,5-dihydro-1,2,3-triazine (R_f: 0.36 - 1:6 v/v ethyl acetate:n-hexane) as a bright yellow/green solid which displays bright green fluorescence when exposed to 365nm UV light (0.014 g, 93.3 %).

m.p: 109 – 110 ^{o}C (from ethyl acetate:n-hexane 1:6 v/v).

IR (NaCl) ν_{max} 1638 cm^{-1} (C=O).

^{1}H NMR (300 MHz $CDCl_3$): δ 2.07 (s, 3H, O=C-CH_3), 5.32 (s, 1H, 5-CH), 7.13-7.19 (m, 1H, Ar), 7.40-7.50 (m, 8H, Ar), 7.94-8.02 (m, 6H, Ar).

^{13}C NMR (75 MHz $CDCl_3$) δ 28.6 (C5), 47.7 (CH_3), 115.1, 122.6, 125.6, 127.7, 127.9, 128.9, 144.6 (aromatics, overlapping signals), 133.6, 134.1 (C4 and C6), 200.6 (C=O).

HRMS *m/z* 354.1605 ($[M + H]^+$, $C_{23}H_{20}N_3O$ requires 354.1601).

2.1.4. Synthesis for Chapter 7.

Synthesis of phenyl propiolate (20). [59]

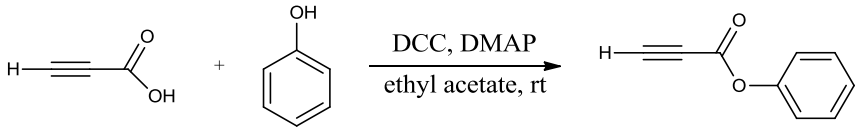

To a stirred solution of phenol (0.941 g, 10 mmol) and 4-dimethylaminopyridine (0.015 g, 0.125 mmol) in freshly distilled ethyl acetate (10 mL), suspended in an ice bath under nitrogen atmosphere was added propiolic acid (0.61 mL, 10 mmol). Following 10 min period of stirring, 1,3-dicyclohexylcarbodiimide (2.06 g, 10 mmol) in freshly distilled ethyl acetate (10 mL) under nitrogen was added *via* syringe and a white precipitate formed. The ice bath was removed after 10 min and the reaction mixture was stirred at ambient temperature for a further 22 hrs, before it was filtered and the filter cake washed with ethyl acetate (6 x 5 mL) until white. The dark red filtrate was concentrated under reduced pressure. The residue was loaded in chloroform on a silica gel column (230-400 mesh ASTM). Elution with chloroform gave phenyl propiolate (R_f: 0.71 - chloroform) as a pale light yellow oil upon removal of the solvent under reduced pressure (0.77 g, 53 %).

IR (NaCl) ν_{max} 1641 cm^{-1} (C=O).

^1H NMR (300 MHz $CDCl_3$): δ 3.06 (s, lH, C≡C-H), 7.12-7.16 (m, 2H, Ar), 7.24-7.38 (m, 1H, Ar), 7.40-7.43 (m, 2H, Ar).

HRMS *m/z* 147.0433 ($[M + H]^+$, $C_9H_7O_2$ requires 147.0441).

Matches literature.[59]

Synthesis of 5-phenylcarboxylate-5-(N-phenylformimidoyl)-2,4,6-triphenyl-2,5-dihydro-1,2,3-triazine (21).

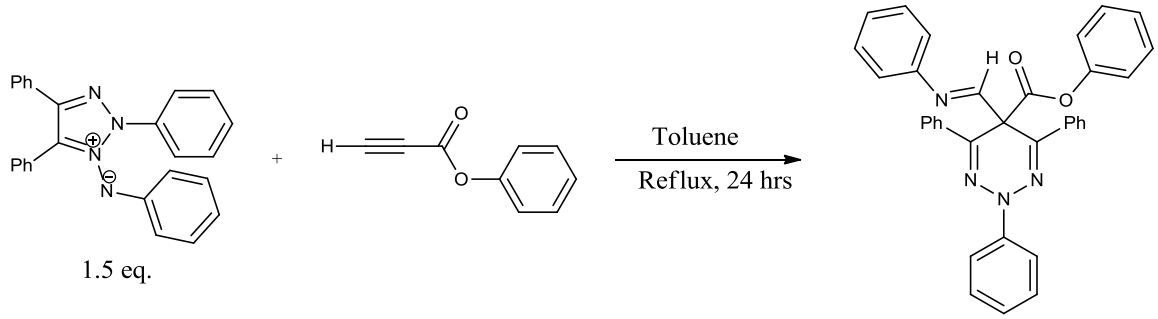

2,4,5-Triphenyl-1,2,3-triazolium-1-phenylaminide (0.374 g, 0.964 mmol) and phenyl propiolate (0.094 g, 0.643 mmol) in toluene (4 mL) was stirred under reflux for 24 hrs. The solvent was removed under reduced pressure and the residue was placed, dry loaded (silica 230 – 400 mesh ASTM), on a silica gel column (230 – 400 mesh ASTM). Elution with 1:8 v/v ethyl acetate:n-hexane gave 5-phenylcarboxylate-5-(N-phenylformimidoyl)-2,4,6-triphenyl-2,5-dihydro-1,2,3-triazine (R_f: 0.36 - 1:8 v/v ethyl acetate:n-hexane) as a bright yellow solid which displays green fluorescence when exposed to 365 nm UV light (0.288 g, 84 %).

m.p: 88 ^{o}C (from ethyl acetate:n-hexane 1:8 v/v).

IR (NaCl) ν_{max} 1641 cm^{-1} (C=O).

^{1}H NMR (300 MHz $CDCl_3$): δ 6.01-6.04 (d, 2H, *J* = 7.7 Hz H_{ortho} O-C_6H_5), 6.87- 7.47 (m, 17H, Ar), 7.83-7.88 (m, 4H, Ar) 7.92-7.93 (d, 2H, *J* = 8.5 Hz H_{ortho} 2-N-C_6H_5), 8.59 (s, 1H, N=CH).

^{13}C NMR (75 MHz $CDCl_3$): δ 54 (C5), 116.1, 120.6, 123.6, 126.2, 126.5, 128.7, 128.5, 128.8, 129.0, 129.3, 129.7, 145.2, 149.9 (aromatics, overlapping signals), 134.5, 134.9 (C4 and C6), 157.7 (N=CH), 176.5 (C=O).

HRMS *m/z* 535.2117 ($[M + H]^+$, $C_{35}H_{27}N_4O_2$ requires 535.2129).

Synthesis of p-tolyl propiolate (22).[59]

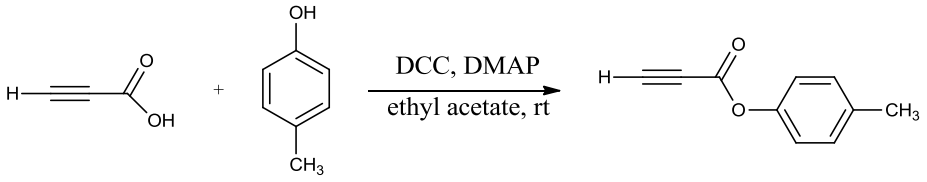

To a stirred solution of p-cresol (1.081g, 10 mmol) and 4-dimethylaminopyridine (0.015 g, 0.125 mmol) in freshly distilled ethyl acetate (10 mL), suspended in an ice bath under nitrogen atmosphere, was added propiolic acid (0.61 cm^3, 10 mmol). Following a 10 min period of stirring, 1,3-dicyclohexylcarbodiimide (2.06 g, 10 mmol) in freshly distilled ethyl acetate (10 mL) under nitrogen was added *via* syringe and a white precipitate formed. The ice bath was removed after 10 min and the reaction mixture was stirred at ambient temperature for a further 22 hrs, before it was filtered and the filter cake washed with ethyl acetate (6 x 5 mL) until white. The dark red filtrate was concentrated under reduced pressure. The residue was loaded in chloroform on a silica gel column (230-400 mesh ASTM). Elution with chloroform gave p-tolyl propiolate (R_f: 0.76 - chloroform) as a pale yellow oil upon removal of the solvent under reduced pressure (1.15 g, 71.6 %).

IR (NaCl) ν_{max} 1730 cm^{-1} (C=O).

^{1}H NMR (300 Hz $CDCl_3$) δ = 2.26 (s, 3H, CH_3), 3.01 (s, 1H, C≡C-H), 7.01-7.10 (d, 2H, *J* = 8.5 Hz O-C_6H_4-CH_3-*p*, AA′BB′), 7.15-7.2 (d, 2H, *J* = 8.5 Hz O-C_6H_4-CH_3-*p*, AA′BB′).

HRMS *m/z* 161.0595 ($[M + H]^+$, $C_{10}H_9O_2$ requires 161.0597).

Matches literature.[59]

Synthesis of 5-tolylcarboxylate-5-(N-phenylformimidoyl)-2,4,6-triphenyl-2,5-dihydro-1,2,3-triazine (23).

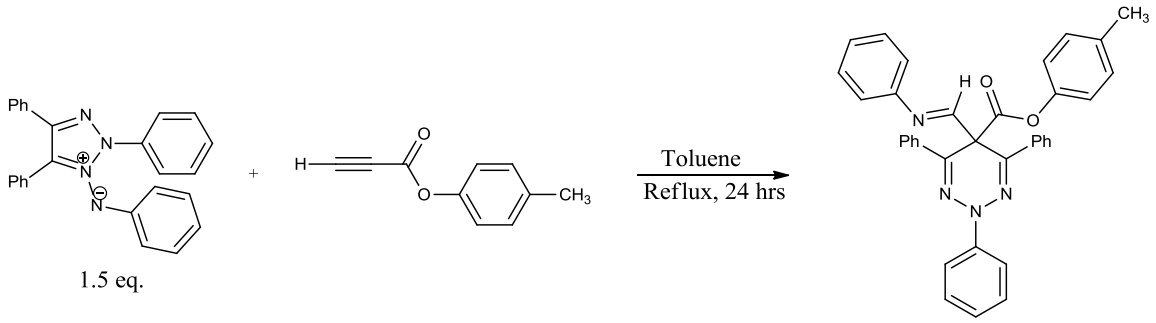

2,4,5-Triphenyl-1,2,3-triazolium-1-phenylaminide (0.349 g, 0.899 mmol) and 4-tolyl propiolate (0.096 g, 0.599 mmol) in toluene (4 mL) was stirred under reflux for 24 hours. The solvent was removed under reduced pressure and the residue was placed, dry loaded (silica 230 – 400 mesh ASTM), on a silica gel column (230 – 400 mesh ASTM). Elution with 1:8 v/v ethyl acetate:n-hexane gave 5-tolylcarboxylate-5-(N-phenylformimidoyl)-2,4,6-triphenyl-2,5-dihydro-1,2,3-triazine **(**R_f: 0.36 - 1:8 v/v ethyl acetate:n-hexane) as a bright yellow solid which displays green fluorescence when exposed to 365 nm UV light (0.304 g, 92.7 %).

m.p: 90 ^{o}C (from ethyl acetate:n-hexane 1:8 v/v).

IR (NaCl) ν_{max} 1641 cm^{-1} (C=O).

^{1}H NMR (300 MHz $CDCl_3$): δ 2.25 (s, 3H, CH_3-*p*), 5.98-5.99 (appd, 2H, *J* = 8.44 Hz H_{ortho} 2-N-phenyl ring) 6.94-6.98 (d, 2H, *J* = 8.47 Hz H_{ortho} iminyl N-C_6H_5) 7.02-7.05 (appd, 2H, *J* = 8.51 Hz O-C_6H_4-CH_3-*p*, AA′BB′) 7.17-7.52 (m, 12H, Ar), 7.89-7.93 (m, 4H, Ar), 8.00-8.02 (d, 2H, *J* = 8.85 Hz O-C_6H_4-CH_3-*p*, AA′BB′), 8.49 (s, 1H, N=CH).

^{13}C NMR (75 MHz $CDCl_3$): δ 20.8 (CH_3-*p*), 54 (C5), 116.1, 120.2, 120.6, 123.6, 126.5, 128.5, 128.6, 129.0, 129.7, 129.8, 129.9, 134.9, 145.2, 147.6 (aromatics, overlapping signals), 134.5, 135.9 (C4 and C6), 157.7 (N=CH), 168.7 (C=O).

HRMS *m/z* 549.2311 ($[M + H]^+$, $C_{36}H_{29}N_4O_2$ requires 549.2285).

Synthesis of 4-methoxyphenyl propiolate (24).[59]

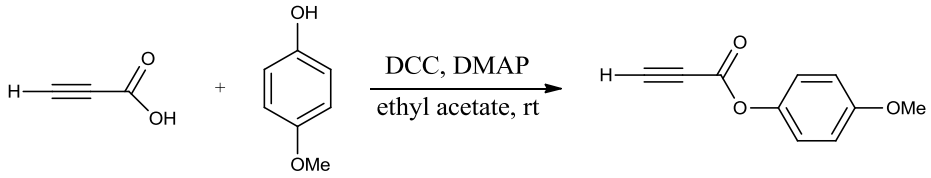

To a stirred solution of 4-methoxyphenol (1.24 g, 10 mmol) and 4-dimethylaminopyridine (0.015 g, 0.125 mmol) in freshly distilled ethyl acetate (10 mL), suspended in an ice bath under nitrogen atmosphere was added propiolic acid (0.61 mL, 10 mmol). Following a 10 min period of stirring, 1,3-dicyclohexylcarbodiimide (2.06 g, 10 mmol) in freshly distilled ethyl acetate (10 mL) under nitrogen was added *via* syringe and a white precipitate formed. The ice bath was removed after 10 min and the reaction mixture was stirred at ambient temperature for a further 22 hrs, before it was filtered and the filter cake washed with ethyl acetate (6 x 5 mL) until white. The dark red filtrate was concentrated under reduced pressure. The residue was loaded in chloroform on a silica gel column (230-400 mesh ASTM). Elution with chloroform gave 4-methoxyphenyl propiolate (R_f: 0.65 - chloroform) as a pale yellow oil upon removal of the solvent under reduced pressure (1.35 g, 76.7 %).

IR (NaCl) ν_{max} 1733 cm^{-1} (C=O).

^{1}H NMR (300 MHz $CDCl_3$): δ 3.07 **(**s, lH, C≡C-H), 3.80 (s, 3H, OCH_3-*p*), 6.85-6.9 (d, 2H, *J* = 8.5 Hz O-C_6H_4-OCH_3-*p*, AA′BB′), 7.05-7.10 (d, 2H, *J* = 8.5 Hz O-C_6H_4-OCH_3-*p*, AA′BB′).

HRMS *m/z* 177.0552 ($[M + H]^+$, $C_{10}H_9O_3$ requires 177.0546).

Matches literature.[59]

Synthesis of 5-(4-methoxyphenyl)carboxylate-5-(N-phenylformimidoyl)-2,4,6-triphenyl-2,5-dihydro-1,2,3-triazine (25).

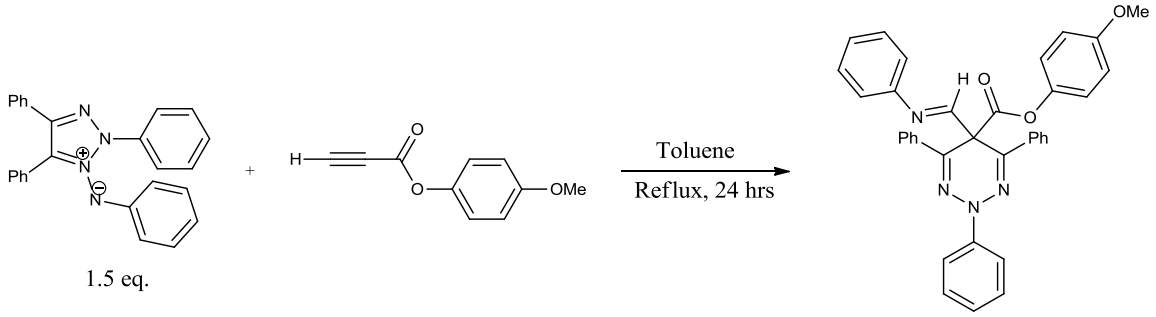

2,4,5-Triphenyl-1,2,3-triazolium-1-phenylaminide (0.261 g, 0.672 mmol) and 4-methoxyphenyl propiolate (0.078 g, 0.448 mmol) in toluene (4 mL) was stirred under reflux for 24 hrs. The solvent was removed under reduced pressure and the residue was placed, dry loaded (silica 230 – 400 mesh ASTM), on a silica gel column (230 – 400 mesh ASTM). Elution with 1:6 v/v ethyl acetate:n-hexane gave 5-(4-methoxyphenyl)carboxylate-5-(N-phenylformimidoyl)-2,4,6-triphenyl-2,5-dihydro-1,2,3-triazine **(**R_f: 0. 36 - 1:6 v/v ethyl acetate:n-hexane) as a bright yellow/green solid which displays green fluorescence when exposed to 365 nm UV light (0.238 g, 94.4 %).

m.p: 78 ^{o}C (from ethyl acetate:n-hexane 1:6 v/v).

IR (NaCl) ν_{max} 1641 cm^{-1} (C=O).

^{1}H NMR (300 Hz $CDCl_3$) δ = 3.70 (s, 3H, OCH_3-*p*), 5.96-5.99 (d, 2H, *J* = 8.9 Hz O-C_6H_4-OCH_3-*p*, AA′BB′), 6.64-6.67 (d, 2H, *J* = 8.9 Hz O-C_6H_4-OCH_3-*p*, AA′BB′), 7.02-7.05 (d, 2H, *J* = 8.3 Hz H_{ortho} iminyl N-C_6H_5), 7.17-7.19 (m, 2H, Ar), 7.22-7.36 (m, 2H, Ar) 7.50-7.59 (m, 8H, Ar), 7.89-7.92 (m, 4H, Ar), 7.99-8.01 (d, 2H, *J* = 8.8 Hz H_{ortho} 2-N-C_6H_5), 8.66 (s, 1H, N=CH).

^{13}C NMR (75 MHz $CDCl_3$): δ 54 (OCH_3-*p*), 55.4 (C5), 114.3, 116.2, 120.6, 121.3, 123.7, 126.5, 128.5, 128.6, 128.9, 129.05, 129.7, 143.4, 145.2, 157.5 (aromatics, overlapping signals), 134.6, 135 (C4 and C6), 157.7 (N=CH), 168.9 (C=O).

HRMS *m/z* 565.225 ([M + H]$^{+}$, $C_{36}H_{29}N_4O_3$ requires 565.2234).

Synthesis of 4-nitrophenyl propiolate (26).[59]

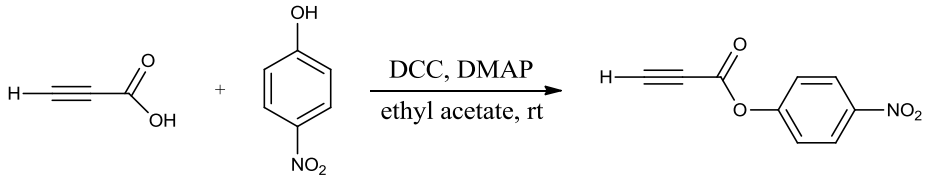

To a stirred solution of 4-nitrophenol (1.39 g, 10 mmol) and 4-dimethylaminopyridine (0.015 g, 0.125 mmol) in freshly distilled ethyl acetate (10 mL) suspended in an ice bath under nitrogen atmosphere, was added propiolic acid (0.61 mL, 10 mmol). Following a 10 min period of stirring, 1,3-dicyclohexylcarbodiimide (2.06 g, 10 mmol) in freshly distilled ethyl acetate (10 mL) under nitrogen was added dropwise to the stirring solution *via* syringe and a white precipitate formed. The ice bath was removed after 10 min and the reaction mixture was stirred at ambient temperature for a further 22 hrs, before it was filtered and the filter cakewashed with ethyl acetate (6 x 5 mL) until white. The yellow filtrate was concentrated under reduced pressure. The residue was loaded in chloroform on a silica gel column (230-400 mesh ASTM). Elution with 3:1 v/v dichloromethane:n-hexane gave 4-nitrophenyl propiolate (R_f: 0.33 - 3:1 v/v dichloromethane:n-hexane) as a white colourless solid upon removal of the solvent under reduced pressure (1.705 g, 89.2 %).

m.p: 136 – 137 ^{o}C (from dichloromethane:n-hexane 1:1 v/v).

Literature m.p: 136 – 137 ^{o}C (from dichloromethane:n-hexane 1:1 v/v).[59]

IR (NaCl) ν_{max} 1743 cm^{-1} (C=O).

^{1}H NMR (300 MHz $CDCl_3$): δ 3.17 (s, 1H, C≡C-H), 7.33-7.38 (d, 2H, *J* = 8.5 Hz O-C_6H_4-NO_2 -*p*, AA′BB′) 8.27-8.32 (d, 2H, *J* = 8.5 Hz O-C_6H_4- NO_2-*p*, AA′BB′).

HRMS *m/z* 192.0282 ($[M + H]^+$, $C_9H_6NO_4$ requires 192.0291).

Matches literature.[59]

Synthesis of 5-(4-nitrophenyl)carboxylate-5-(N-phenylformimidoyl)-2,4,6-triphenyl-2,5-dihydro-1,2,3-triazine (27).

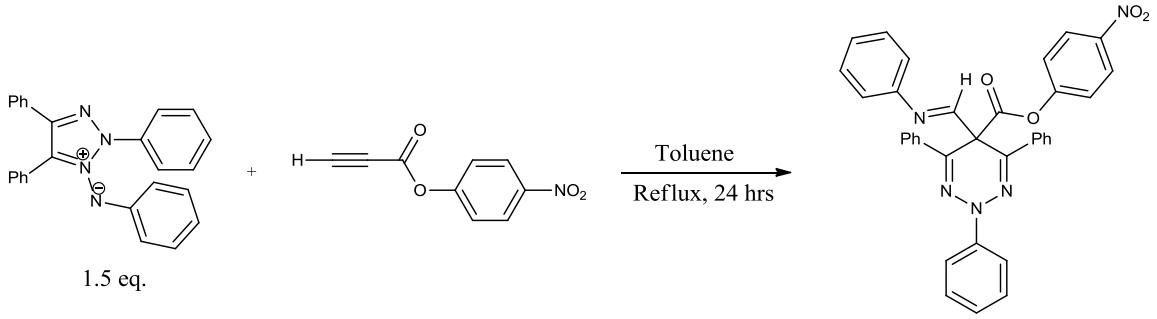

2,4,5-Triphenyl-1,2,3-triazolium-1-phenylaminide (0.1 g, 0.258 mmol) and 4-nitrophenyl propiolate (0.032 g, 0.172 mmol) in toluene (3 mL) was stirred under reflux for 24 hrs. The solvent was removed under reduced pressure and the residue was placed, dry loaded (silica 230 – 400 mesh ASTM), on a silica gel column (230 – 400 mesh ASTM). Elution with 1:6 v/v ethyl acetate:n-hexane gave 5-(4-nitrophenyl)carboxylate-5-(N-phenylformimidoyl)-2,4,6-triphenyl-2,5-dihydro-1,2,3-triazine (R_f: 0.36 - 1:6 v/v ethyl acetate:n-hexane) as a bright yellow/green solid which displays weak green fluorescence when exposed to 365 nm UV light **(**0.83 g, 83 %).

m.p: 80 - 82 ^{o}C (from ethyl acetate:n-hexane 1:6 v/v).

IR (NaCl) ν_{max} 1761 cm^{-1} (C=O).

^{1}H NMR (300 MHz $CDCl_3$): δ = 6.13-6.18 (d, 2H, *J* = 9.0 Hz H_{ortho} O-C_6H_4-NO_2-*p*), 6.99-7.02 (d, 2H, *J* = 8.6 Hz H_{ortho} iminyl N-C_6H_5), 7.14-7.22 (m, 2H, Ar), 7.28-7.39 (m, 2H, Ar), 7.42-7.49 (m, 8H, Ar), 7.81-7.84 (m, 4H, Ar), 7.93-8.02 (m, 4H, Ar), 8.53 (s, 1H, N=CH).

^{13}C NMR (75 MHz $CDCl_3$): δ 54.4 (C5), 116.2, 120.6, 125.1, 126.8, 128.7, 128.9, 129.1, 129.9, 145.1, 145.7, 150.4, 154.4 (aromatics, overlapping signals), 133.7, 134.7 (C4 and C6), 156.8 (N=CH), 167.8 (C=O).

HRMS *m/z* 580.1988 ($[M + H]^+$, $C_{35}H_{26}N_5O_4$ requires 580.1979).

2.1.5 Synthesis for Chapter 8.

Synthesis of 1-(1H-benzo[d][1,2,3]triazol-1-yl)prop-2-yn-1-one (28).[60]

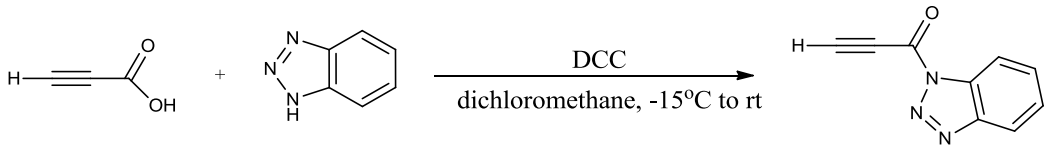

To a stirred solution of propiolic acid (0.613 mL, 10 mmol) in dichloromethane (25 mL) was added 1H-benzotriazole (1.191 g, 10 mmol) and 1,3-dicyclohexylcarbodiimide (2.291 g, 11 mmol) at -15°C and allowed to warm to room temperature. The solution was then allowed to stir for 22 hrs. The dicyclohexylurea was removed by filtration and washed with ethyl acetate (5 x 10 mL) and the filtrate evaporated under reduced pressure. The residue was dissolved in minimum amount of dichloromethane, and the product crystallised by the dropwise addition of petroleum ether (b.p 60-80 °C) as a pale brown "fluffy" solid (1.175 g, 68.7 %).

m.p: 99 °C (from dichloromethane:petroleum ether (b.p 60-80 °C)).

Literature m.p: 99 °C (from ethyl acetate:hexanes 1:4).[60]

IR (NaCl) ν_{max} 1694 cm^{-1} (C=O).

^1H NMR (300 MHz $CDCl_3$): δ 3.87 (s, 1H, H≡C), 7.53-7.59 (appt, 1H, Ar), 7.68-7.73 (appt, 1H, Ar), 8.15-8.18 (d, 1H, J = 8.2 Hz benzotriazole C_6H_4 AA′BB′) 8.24-8.27 (d, 1H, J = 8.2 Hz benzotriazole C_6H_4 AA′BB′).

HRMS *m/z* 172.0505 ($[M + H]^+$, $C_9H_6N_3O$ requires 172.0505).

Matches literature.[60]

Synthesis of 5-(1H-benzotriazol-1yl)-5-(N-phenylformimidoyl)-2,4,6-triphenyl-2,5-dihydro-1,2,3-triazine (29).

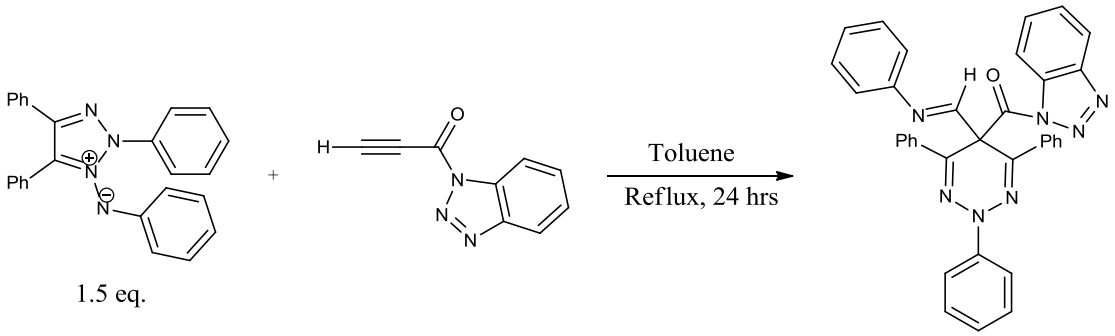

2,4,5-Triphenyl-1,2,3-triazolium-1-phenylaminide (0.680 g, 1.752 mmol) and 1-(1H-benzo[d][1,2,3]triazol-1-yl)prop-2-yn-1-one (0.20 g, 1.17 mmol) in toluene (20 mL) was stirred under reflux for 24 hrs. The solvent was removed under reduced pressure and the residue was placed, dry loaded (silica 230 – 400 mesh ASTM), on a silica gel column (230 – 400 mesh ASTM). Elution with 1:6 v/v ethyl acetate:n-hexane gave 5-(1H-benzotriazol-1yl)-5-(N-phenylformimidoyl)-2,4,6-triphenyl-2,5-dihydro-1,2,3-triazine (R_f: 0.36 - 1:6 v/v ethyl acetate:n-hexane) as a bright yellow/green solid which displays yellow fluorescence when exposed to 365nm UV light (0.54 g, 83 %).

m.p: 130 ^{o}C (from ethyl acetate:n-hexane 1:6 v/v).

IR (NaCl) ν_{max} 1721 cm^{-1} (C=O).

^{1}H NMR (300 MHz $CDCl_3$): δ 7.10-7.25 (m, 10H, Ar), 7.28-7.49 (m, 6H, Ar), 7.68-7.72 (appd, 4H, Ar), 7.79-7.82 (d, 1H, *J* = 8.2 Hz benzotriazole C_6H_4 AA′BB′), 7.94-8 (appt, 3H, Ar), 8.93 (s, 1H, N=CH).

^{13}C NMR (75 MHz $CDCl_3$): δ 53.7 (C5), 113.8, 116.0, 120.0, 120.7, 123.4, 126.4, 126.6, 128.1, 128.3, 128.8, 129.0, 129.4, 144.3, 145.2, 150.8 (aromatics, overlapping signals), 134.8, 134.7 (C4 and C6), 156.2 (N=CH), 168.9 (C=O).

HRMS *m/z* 560.2208 ([M + H]$^{+}$, $C_{35}H_{26}N_7O$ requires 560.2193).

Synthesis of 5-((carboxyamido) propanoic acid)-5-(N-phenylformimidoyl)-2,4,6-triphenyl-2,5-dihydro-1,2,3-triazine (30).

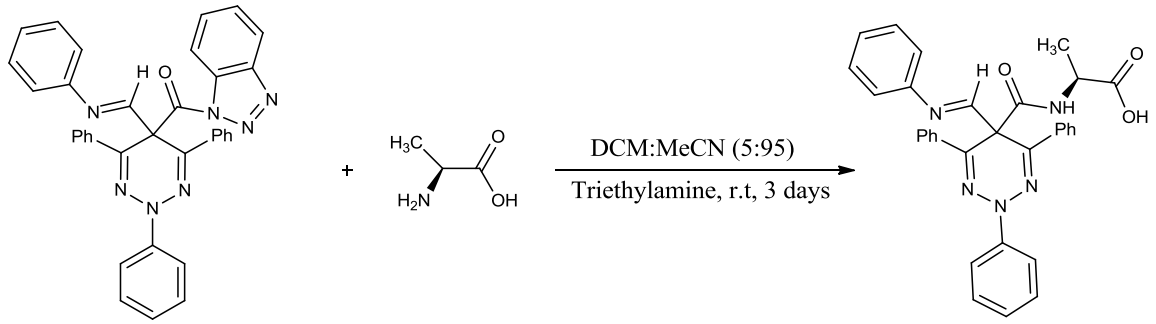

To a solution of 5-(1H-benzotriazol-1yl)-5-(N-phenylformimidoyl)-2,4,6-triphenyl-2,5-dihydro-1,2,3-triazine (0.050 g, 0.0893 mmol) in dichloromethane:acetonitrile (5:95, 0.25:4.75 mL) was added L-alanine (0.008 g, 0.0893 mmol) and triethylamine (0.013 mL, 0.0982 mmol) and allowed to stir for 72 hours. The solvent was removed under reduced pressure and the residue was placed, dry loaded (silica 230 – 400 mesh ASTM), on a silica gel column (230 – 400 mesh ASTM). Elution with gradient from 1:6 v/v ethyl acetate:n-hexane to 1:1 v/v ethyl acetate:methanol gave 5-((carboxyamido) propanoic acid)-5-(N-phenylformimidoyl)-2,4,6-triphenyl-2,5-dihydro-1,2,3-triazine (R_f: 0.05 - ethyl acetate:petroleum ether 1:6 v/v) as a bright yellow/green solid which displays green fluorescence when exposed to 365 nm UV light (0.040 g, 85 %).

m.p: 136 ^oC (from chloroform:petroleum ether (b.p 60-80 ^oC)).

IR (NaCl) ν_{max} 1631 cm^{-1} (C=O).

^1H NMR (300 MHz DMSO-d6): δ 0.89-0.91 (d, 3H, *J*= 6.8 Hz, CH_3), 3.59-3.68 (m, 1H, C-H), 6.89-6.72 (d, 2H, *J* = 7.5 Hz H_{ortho} iminyl C_6H_5), 7.12-7.28 (m, 3H, Ar), 7.39-7.50 (m, 8H, Ar), 7.81-7.89 (m, 7H, Ar), 8.98 (s, 1H, N=CH) - (COOH signal not observed).

^{13}C NMR (75 MHz DMSO-d6): δ 17.4 (CH_3), 50.3 (α carbon; $\underline{C}$-CH_3) 50.9 (C5), 115.2, 119.8, 126.2, 127.4, 128.3, 129.3, 138.1 144.3 (aromatics, overlapping signals), 134.5, 134.6 (C4 and C6), 150.3 (N=CH), 164.3 (C=O) 167.8 (C=OOH).

HRMS *m/z* 530.2096 ($[M + H]^+$, $C_{32}H_{27}N_5O_3$ requires 530.2114).

Synthesis of 4-isothiocyanatophenol (31).[61]

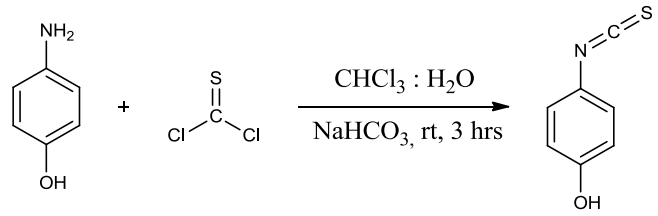

To 4-aminophenol (1.091 g, 10 mmol) in a mixture of chloroform (60 mL) and aqueous sodium hydrogen carbonate (1.68 g in 80 mL of water) was added thiophosgene (1.53 mL, 10 mmol) and allowed to stir at room temperature for 3 hrs. The organic layer was washed with water (3 x 50 mL). The solvent was removed under reduced pressure and the residue placed on a silica gel column (230-400 mesh ASTM). Elution with 3:1 v/v dichloromethane:petroleum ether (b.p 60-80 ^{o}C) gave 4-isothiocyantophenol (R_f: 0.2 - chloroform) as a dark red oil upon removal of solvent (1.23 g, 81.5 %).

^{1}H NMR (300 MHz $CDCl_3$): δ 5.03 (s, 1H, -OH), 6.77-6.8 (d, 2H, *J* = 8.9 Hz, C_6H_4-NCS-*p*, AA′BB′) 7.10-7.13 (d, 2H, *J* = 8.9 Hz, C_6H_4-NCS-*p*, AA′BB′).

Matches literature.[61]

Synthesis of 4-isothiocyanatophenyl propiolate (32).

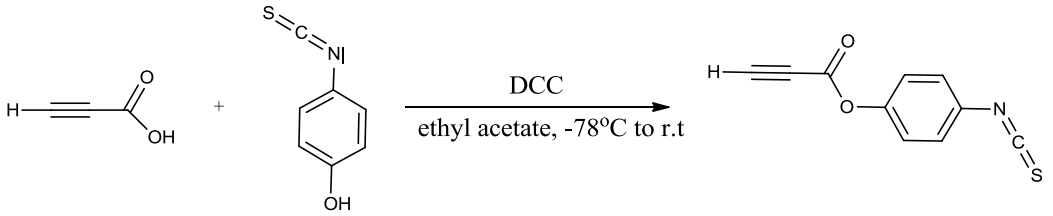

To a stirred solution of 4-isothiocyanatophenol (1.231 g, 8.142 mmol) in ethyl acetate (4 mL) was added propiolic acid (0.501 mL, 8.142 mmol) at -78^{o}C. Following a 10 min period of stirring, 1,3-dicyclohexylcarbodiimide (1.679 g, 8.142 mmol) dissolved in ethyl acetate (4 mL) was added dropwise to the stirring solution *via* syringe and the reation was allowed to warm to room temperature. A white precipitate formed and the reaction mixture was stirred for a further 22 hrs, before it was filtered and the filter cake washed with ethyl acetate (6 x 5 mL) until white. The yellow filtrate was concentrated under reduced pressure. The residue was loaded on a silica gel column (230-400 mesh ASTM) and eluted with chloroform. Upon removal of the solvent under reduced pressure, the residue was dissolved in minimum amount of dichloromethane, and the product crystallised by the dropwise addition of petroleum ether (b.p 60-80 ^{o}C) to yield 4-isothiocyanatophenyl propiolate (R_f: 0.8 - chloroform) as pale white needles (0.727 g. 44 %).

m.p: 76 ^{o}C (from dichloromethane:petroleum ether (b.p 60-80 ^{o}C)).

IR (NaCl) ν_{max} 2123 cm^{-1} (NCS).

^{1}H NMR (300 MHz $CDCl_3$) δ = 3.11 (s, 1H, C≡C-H), 7.14- 7.17 (d, 2H, *J* = 9.0 Hz, H_{ortho} -O-C_6H_4- NCS-*p*), 7.24-7.26 (d, 2H, *J* = 4.67 Hz, H_{meta} –O-C_6H_4-NCS-*p)*

^{13}C NMR (75 MHz $CDCl_3$) δ = 73.8 (C≡C-H), 77.4 (C≡C-H), 122.6, 126.9, 129.6, 148.1 (aromatics, overlapping signals), 135.5 (N=C=S), 150.4 (C=O).

HRMS *m/z* 204.0113 ([M + H]$^{+}$, $C_{10}H_6NO_2S$ requires 204.0114).

Synthesis of 5-(4-isothiocyanatophenyl)carboxylate-5-(N-phenylformimidoyl)-2,4,6-triphenyl-2,5-dihydro-1,2,3-triazine (33).

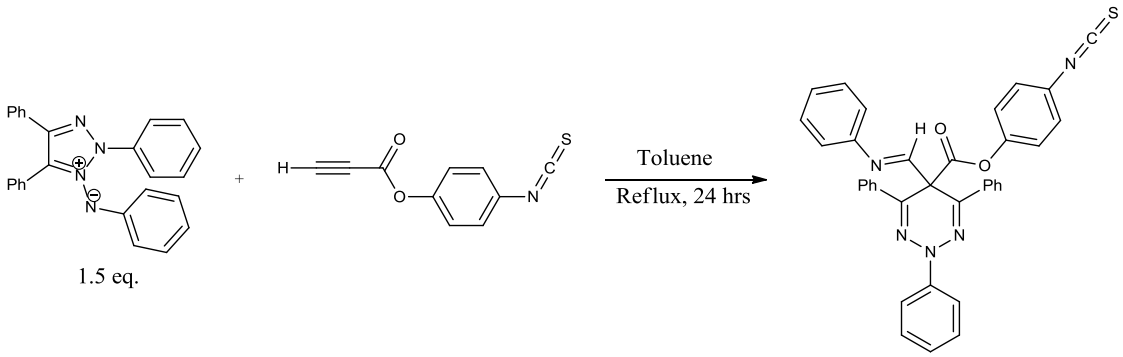

2,4,5-Triphenyl-1,2,3-triazolium-1-phenylaminide (0.118 g, 0.304 mmol) and 4-isothiocyanatophenyl propiolate (0.051 g, 0.253 mmol) in toluene (4 mL) was stirred under reflux for 24 hrs. The solvent was removed under reduced pressure and the residue was placed, dry loaded (silica 230 – 400 mesh ASTM), on a silica gel column (230 – 400 mesh ASTM). Elution with gradient from 100: 0 petroleum ether :dichloromethane v/v to 94:6 petroleum ether :dichloromethane v/v gave 5-(4-isothiocyanatophenyl)carboxylate-5-(N-phenylformimidoyl)-2,4,6-triphenyl-2,5-dihydro-1,2,3-triazine (R_f: 0.1 - petroleum ether (b.p 60-80 ^oC)) as a bright yellow/green solid which displays weak green fluorescence when exposed to 365 nm UV (0.070 g, 46.7 %).

m.p: 96 ^oC (from dichloromethane:petroleum ether (b.p 60-80 ^oC)).

IR (NaCl) ν_{max} 2099 cm^{-1} (NCS).

^1H NMR (300 MHz $CDCl_3$): δ 5.95-5.97 (d, 2H, *J* = 8.77 Hz, H_{ortho} -O-C_6H_4-NCS-*p*), 6.94-7.00 (m, 4H, Ar), 7.13-7.32 (m, 4H, Ar), 7.39-7.47 (m, 8H, Ar), 7.80-7.84 (m, 4H, Ar), 7.93-7.95 (d, 2H, *J* = 7.85 Hz, H_{ortho} iminyl C_6H_5), 8.55 (s, 1H, N=CH).

^{13}C NMR (75 MHz $CDCl_3$): δ 53.1 (C5), 115.1, 121, 122.8, 125.6, 127.6, 127.8, 128.0, 128.8, 144.0, 147.2, 149.4 (aromatics, overlapping signals), 133.0, 133.7 (C4 and C6), 135.3 (N=C=S), 156.1 (N=CH), 167.3 (C=O).

HRMS *m/z* 592.1780 ($[M + H]^+$, $C_{36}H_{26}N_5O_2S$ requires 592.1802).

2.2 FLUORESCENCE SPECTROSCOPY †.

The following spectroscopic grade solvents were purchased from Sigma Aldrich. Prior to use, all solvents were dried over activated 3Å molecular sieves.[55]

Toluene, 1,4-dioxane, ethyl acetate, chloroform, 2-methyl-2-butanol, N,N-dimethylformamide, acetonitrile, propylene carbonate, 1-octanol, 1-hexanol, 1-butanol, 1-pentanol, 1-propanol, acetic acid, ethanol, 1,5-pentanediol, 1,3-butanediol, 1,4-butanediol, 1,3-propanediol, methanol, 1,2-ethanediol, 2,2,2-trifluoroethanol, ethanol-d^1 (EtOD), methanol-d^1 (MeOD), trifluoroacetic acid.

2.2.1 Sample preparation for fluorescent measurements.

All samples were prepared using the exact procedure as below. An example for the preparation of a 1 x 10^{-5} M solution of **3a** in toluene is given.

0.2362 g (5 mmol) of **3a** was weighed out on a 4 digit decimal place balance into a 1 mL eppendorf and was dissolved in 1 mL of dichloromethane using a 1000 μL Gilson pipette to give a stock solution with a concentration of 5 x 10^{-3} M. 10 μL (5 mmol) of the stock solution was transferred to a 5 mL volumetric flask using a 20 μL Gilson pipette and the solvent was gently evaporated from the volumetric flask using an air pump. Toluene was added up to the mark of the 5 mL volumetric flask and the flask was inverted 10 times and sonicated until all visible traces of the green residue on the bottom of the glassware appeared to be dissolved in solution. The resulting solution was assumed to have a maximum concentration of 1 x 10^{-5} M.

† All fluorescence experimental work was performed at Dr. Alan G. Ryder's Nanoscale Biophotonics Laboratory at the National University of Ireland, Galway (NUIG).

2.2.2 UV/Vis absorption measurements.

Absorption spectra of all molecules were recorded on a Perkin-Elmer Lambda 950 with the sample held in a 10 x 2 cm path length, Teflon stoppered, quartz cuvette at room temperature. All samples recorded had a concentration of 1 x 10^{-5} M. Data analysis was carried out using the Origin (Version 7.0) software package. All measurements were made at room temperature (~20 ^{o}C) under normal ambient conditions.

2.2.3 Steady state fluorescence measurements.

Steady state fluorescence spectra were obtained using a Cary Eclipse (Varian) spectrophotometer, with slits set to 5 mm for emission and excitation spectra measurements. Samples were excited at 310 and 400 nm, held in a 10 x 2 cm path length, Teflon stoppered, quartz cuvette at room temperature. Excitation spectra were recorded with emission set at 480, 520 and 600 nm. All samples recorded had a concentration of 1 x 10^{-5} M. The fluorescence spectra of the solvent were recorded at both excitation wavelengths (310 and 400 nm) to check for any solvent scatter. Data analysis and band fitting was carried out using the Origin (Version 7.0) software package. All measurements were made at room temperature (~20 ^{o}C) under normal ambient conditions.

2.2.3 Fluorescent quantum yields.

The fluorescence quantum yield, Φ_F, was calculated using Equation 1.2.2:

$$\Phi_F = \Phi_{F(R)} * (n^2 / n^2_{(R)}) * (I / I_{(R)}) * (OD_{(R)} / OD) \qquad 1.2.2$$

where $_{(R)}$ is the reference solution, n is the refractive index of the solvent, OD is the optical density (absorbance), and I is the integrated area under the fluorescence spectra.

The reference chosen was Rhodamine 110 and its emission spectra was recorded in deionised water at a concentration of 1 x 10^{-5} M at 310 and 400 nm excitation. The $\Phi_{F(R)}$ was taken to be 0.93 at both 310 and 400 nm excitation taken from the work investigated by Magde *et al*.[62,63]

2.2.4 Steady state fluorescence photodegradation study.

3a was subjected to constant excitation at 310 nm for 900 minutes using a Perkin Elmer LS50 B spectrophotometer, with slits set to 5 mm, at a concentration of 1 x 10^{-5} M. Spectra were recorded using two solvents, toluene and methanol.

Following this, the sample of **3a** in toluene was then exposed to strong UV irradiation in the dark and emission spectra recorded with excitation at 310 and 400 nm over a period of 6 hours. Quinine sulfate at a concentration of 1 x 10^{-5} M in 1M sulfuric acid was used as a standard for comparison, excitation at 350 nm. All measurements were made at room temperature (~20 ^{o}C) under normal ambient conditions.

2.2.5 Fluorescence lifetime measurements.

Magic-angle fluorescence decays were measured recorded using a Time Correlated Single Photon Counting (TCSPC) Fluotime 200 system using a pulsed laser diode (405 nm) excitation source (Picoquant GmbH). The pulsed excitation light was filtered to remove any spurious long wavelength emissions. Measurements were made at a count rate of less than 1% of the pulse rate to maintain Poisson statistics. Typical full widths at half maximum (fwhm), obtained for instrument response function were in the order of a hundred picoseconds. The instrument response function (IRF) was collected under the same conditions as the sample using a clean quartz slide. Fluorescence lifetimes were extracted from the measured decay curves using the FluoFit program (PicoQuant, Germany), which implements nonlinear least squares error minimization analysis. The final quoted result was determined by the fit, with a χ^2 value less than 1.2 being favourable and a residual trace

that was symmetric about the zero axis. All measurements were made at room temperature (~20 ^{o}C) under normal ambient conditions.

2.2.6 Fluorescence lifetime deoxygenation study.

Fluorescence lifetimes were measured for **3a** and **10a** in toluene at a concentration of 1 x 10^{-5} M. Argon gas was bubbled through the solution inside the cuvette, and the fluorescence lifetime was recorded after 10 and 35 minutes as per the method described in 2.2.2.

Chapter 3: Model of fluorescence for N=C-H and N=C-CH_3 triazine.

3.1 INTRODUCTION.

The focus of this project was to initially elucidate the model of fluorescence for the 2,5-dihydro-1,2,3-triazines, originally reported by Butler *et al*, through steady state ultraviolet absorption and fluorescence spectroscopy and time domain lifetime measurements. However, upon initial analysis of the results obtained, the emission properties of these 2,5-dihydro-1,2,3-triazine fluorophores (Figure 3.2.1) were found to be very complex (Chapter 4, Section 4.3 and Chapter 5, Section 5.3). As a result a theoretical study was undertaken to help understand the photophysics of the 2,5,-dihydro-1,2,3-triazine.

All the theoretical calculations and computational modelling was carried out by Professor Luke A. Burke and not by me. They are included in the thesis as they are essential for explaining the complex photophysics of the 2,5-dihydro-1,2,3-triazine fluorophores. I contributed to the interpretation of these calculations to help generate the photophysical model.

As 400 nm is a much more accessible excitation wavelength for microscopy and spectroscopy, most of the subsequent photochemical charaterisation was undertaken using the excitation wavelength of 400 nm.

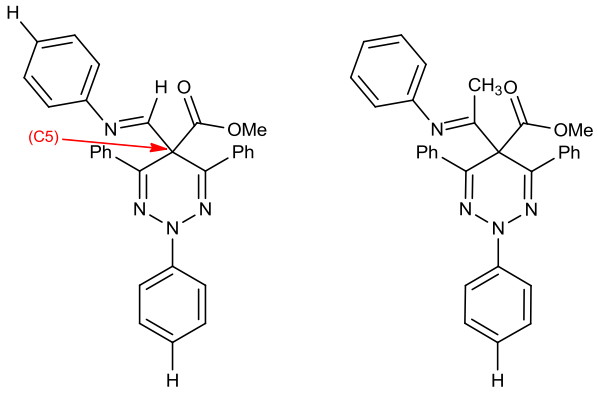

Figure 3.2.1. Structures of N=C-H (**3a**) and N=C-CH_3 triazine (**11a**).

Time-dependent density functional theory (TD-DFT) is now the most widely used theoretical approach to compute the energy of excited states (ES) and their properties such as geometries, dipole moment (DM), transition moments, and densities.

3.2 RESULTS AND DISCUSSION.

3.2.1 Theoretical calculations to elucidate model.

All calculations were performed by Professor Luke Burke with the A02 version of Gaussian09 using the PBE0 functional and default parameters and thresholds. The polarity effect of a solvent matrix was simulated with the use of the polarizable continuum model (PCM) using the polar aprotic acetonitrile (MeCN) parameter throughout the study.

All ground state (GS, S_0) structures were optimized and vibrationally characterized with analytical second derivatives using the 6-31G(d) basis set, followed by re-optimization with the 6-31+G(d) basis set.

The geometries of the S_1 and S_2 ES were obtained using the TD-DFT gradients available and it was found that the geometry of the S_2 state has overall C_s symmetry, *vide infra*.

During the optimization of S_2 the procedure had to be stopped whenever there was an inversion of the energies of the first two states. Otherwise, the program can continue to optimize to a structure on the S_1 surface, which is most likely a rotational transition state structure with C_s symmetry. Whenever the cross over occurred, the geometry of the last structure with the correct energy ordering was slightly modified and a new optimization path was followed until the optimization thresholds were obtained for the S_2 state.

This frequent inversion of energy levels in S_2 precludes the calculation of vibrational frequencies by the numerical techniques available to TD-DFT and the application of the State Specific approximation in the PCM model to account for solvent reorganization around the equilibrium structure of the ES.

It was found that the S_1 and S_2 states are structurally similar and can be clearly identified due to large differences in oscillator strength f and dipole moment μ (*density* keyword in Gaussian).

The reordering of energy levels made the search for the absolute minima **g3** and **g4** for S_3 and S_4 impossible, but in any case useless since S_2, S_3, and S_4 are shown to be all vibrational accessible to each other.

3.2.1.2 Theoretical structures. (Courtesy of Professor Luke A. Burke).

An optimized structure was obtained for each of the S_0, S_1, and S_2 states of N=C-H (**3a**), and N=C-CH_3 (**11a**) triazine molecules, for each theoretical method chosen.

The optimized structures are designated **g0**, **g1**, and **g2**, and each corresponds to the energy minimum for S_0, S_1, and S_2, respectively (Figure 3.2.2).

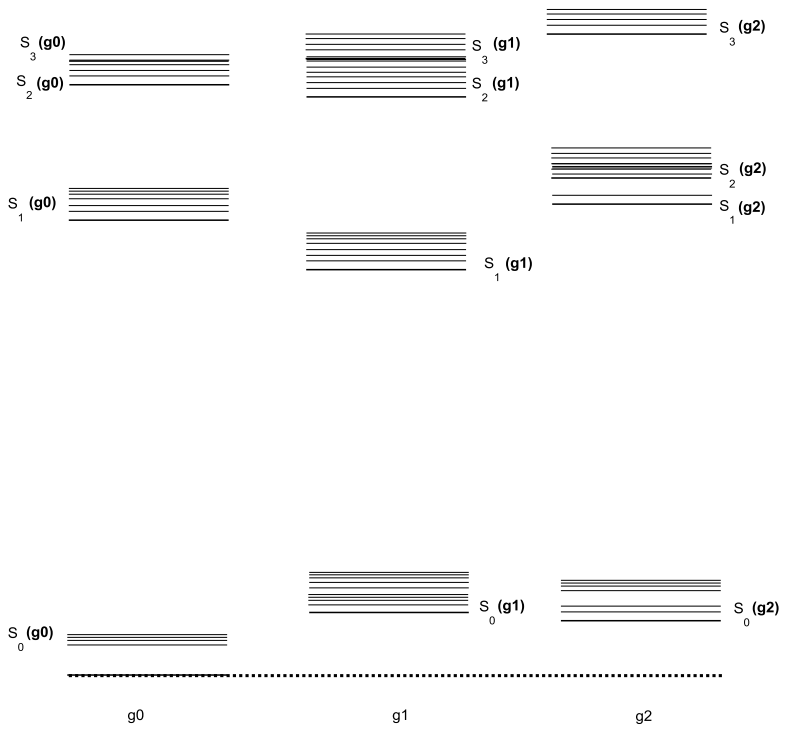

Figure 3.2.2. Schematic representation of transition energy levels relative to the calculated "**g**" optimised structures.

It must be noted that there are only three structures:

1. **g0** (optimized for S_0).
2. **g1** (optimized for S_1).
3. **g2** (optimized for S_2).

This means that for a given structure, say **g0**, the ordering for the energy levels above S_0; S_2 and S_3 are variable until the computation finds a local minimum for S_1, S_2 and S_3. The same is applied for **g1** (fixing S_1) and **g2** (fixing S_2).

Figure 3.2.3 and 3.2.4 shows the **g0**, **g1**, and **g2** structures for N=C-H triazine, and N=C-CH_3 triazine using 6-31+G(d)/MeCN calculation.

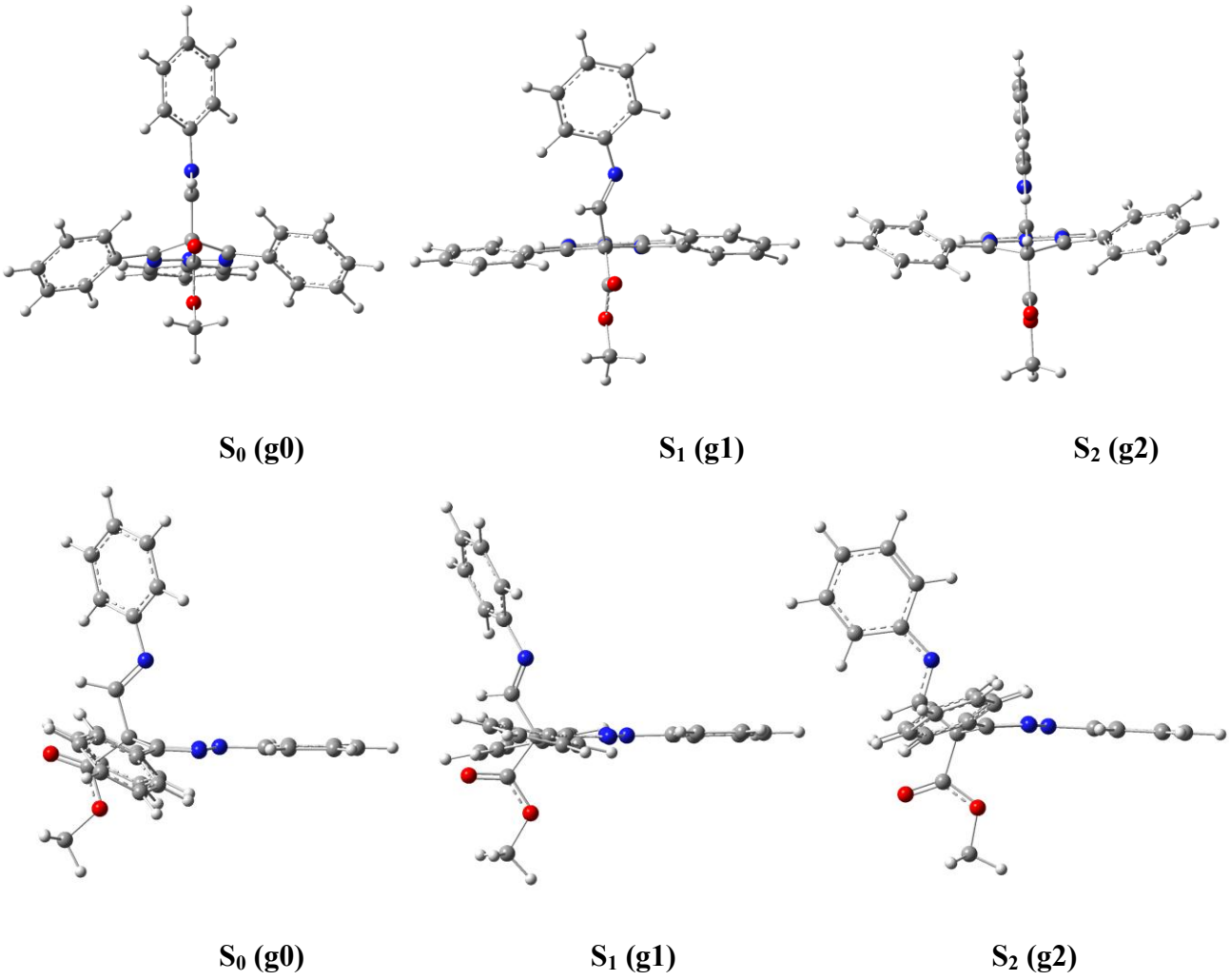

Figure 3.2.3. The S_0 (**g0**), S_1 (**g1**), and S_2 (**g2**) structures for N=C-H triazine (**3a**) rear view through the triazine axis (top) and side view (bottom) using 6-31+G(d)/MeCN calculation.

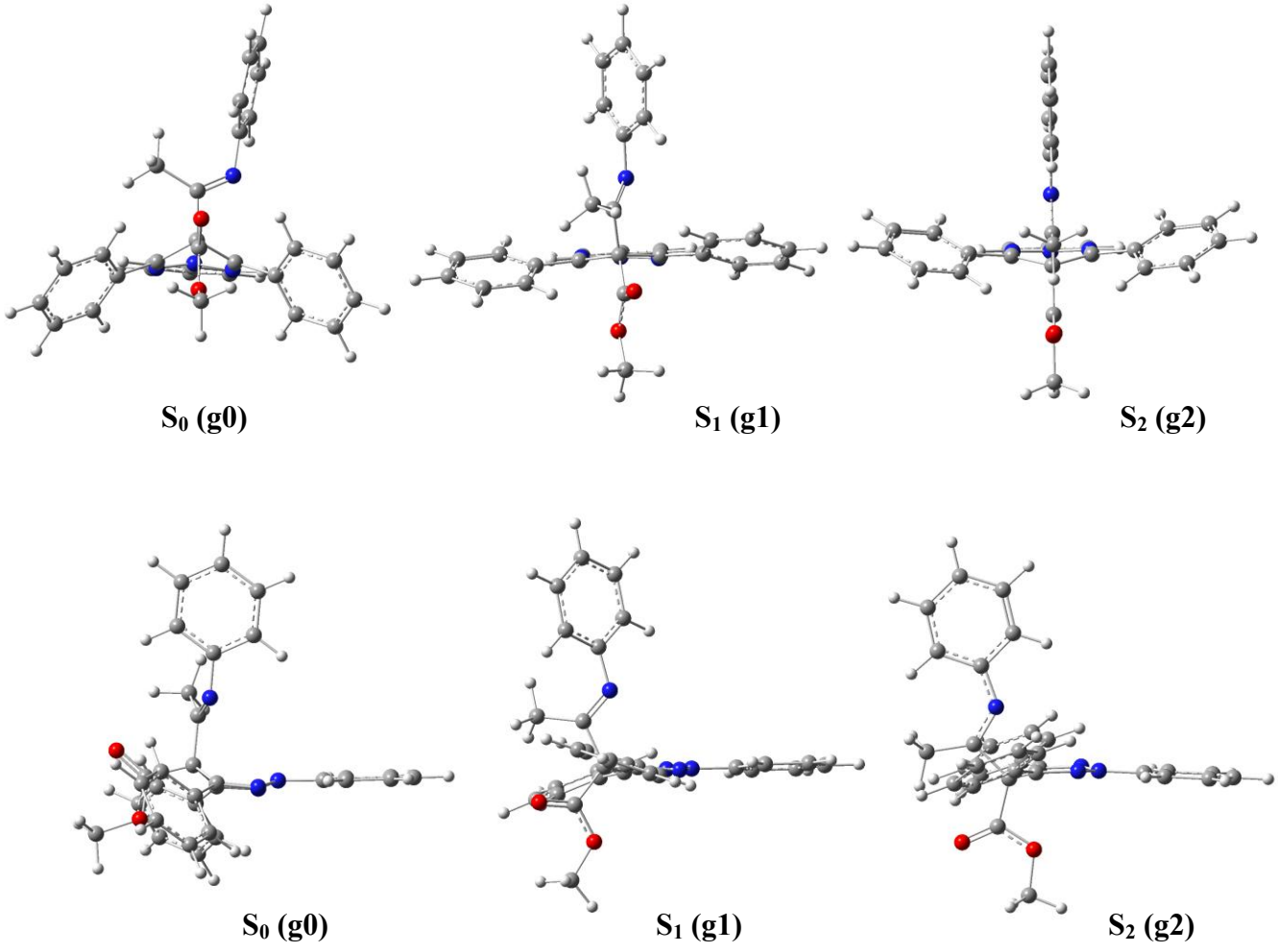

Figure 3.2.3. The S_0 (**g0**), S_1 (**g1**), and S_2 (**g2**) for N=C-CH_3 triazine (**11a**) with rear view through the triazine axis (top), side view (bottom) using 6-31+G(d)/MeCN calculation.

Using planarity of the dihydro-triazine ring as a motif, the three states for both N=C-H triazine and N=C-CH_3 triazine takes the following forms:

1. **g0**, triazine ring in an envelope conformation with the ester equatorial and the imine axial; giving a pseudo-plane of symmetry through the triazine.
2. **g1**, triazine ring in a flat conformation with a coplanar N-2 phenyl and twisted C-4 and C-6 phenyls; giving a pseudo-C_2 axis of symmetry.
3. **g2**, triazine ring in an envelope conformation with the ester axial and the imine equatorial; giving total Cs symmetry.

There is only one stable envelope conformation for **g0** and **g2**, as reoptimization with the imine and ester in reversed axial and equatorial positions leads to the original conformation.

Both N=C-H triazine and N=C-CH_3 triazine can be considered nearly structurally equivalent to each other when in the **g1** and **g2** geometries.

In both N=C-H triazine and N=C-CH_3 triazine, the minimum energy S_2 (**g2**) state has C_s symmetry with the imine and its phenyl group in the C_s plane; and the S_1 state has the C=N of the imine rotated 40^o out of plane; while its phenyl group lies 35^o out of plane with the imine π bond.

In N=C-H triazine, the GS **g0** structure can be considered quite close to the symmetric **g2** structure, with the C=N being only 2^o rotated out of plane and the phenyl 35^o out of plane.

The major difference in the GS **g0** geometries is that, in N=C-H triazine, the imine *C-H* bond is held nearly (ca. 2^o) in the triazine pseudo-plane, while in N=C-CH_3 triazine, the imine *C-CH3* is rotated (ca. 70^o) out of the triazine pseudo-plane.

Thus, the variation of structure between N=C-H triazine (**3a**) and N=C-CH_3 triazine (**11a**) involves the rotation of the imine group (H or CH_3) over the triazine ring (plus the usual π bond length alternation between the GS and ES).

In N=C-H triazine, the imine hydrogen N=C-*H* interacts with the ester carbonyl lone pair, thus holding the imine and ester in-plane or nearly in-plane for S_0, S_1, and S_2. All three geometries **g0**, **g1**, and **g2** are close to one another and thus are vibrationally accessible in the GS S_0.

While in N=C-CH_3 triazine, **g0** differs significantly from **g1** and **g2**, rendering the ES geometries vibrationally inaccessible from **g0**. The imine methyl group (N=C-CH_3) interaction held out of plane with the ester accounts for the different electronic properties of N=C-CH_3 triazine in the GS compared to N=C-H triazine.

Refer to Appendix A.6 for further comment.

3.2.1.3 Theoretical energetic and properties.

The TD-DFT calculation returns properties for each of states based on a particular structural geometry. For example, Figure 3.2.2 shows the first "vertical transition" out of the ground state structure to the ES, S_1, and its properties is reported as "S_1 (**g0**)".

After the optimized geometry (**g1**) of the first ES, S_1, is found, then the properties of the second ES, S_2, "vertical transition" out of the **g1** structure is reported as "S_2 (**g1**)". All geometric parameters are reported for the 6-31+G(d) optimized structures in MeCN.

The energies relative to that for S_0 at **g0** (S_0 (**g0**)) (in cm^{-1}) are given in Table 3.1 for S_0 through S_3 at the geometries of the three optimized structures, **g0**, **g1**, and **g2**, as well as the dipole moments μ (in D) (*e.g.* transition dipole moment between S_0 (**g0**) and S_1 (**g0**) is 6.25 D).

The transition energies (in nm) are provided in Table 3.2 relative to S_0 at the structures **g0**, **g1**, and **g2** as well as the oscillator strengths *f* (in a.u.).

Fortunately for identification of the states in N=C-H and N=C-CH_3 triazine, the values of a physical property such as μ and *f* are quite different in nearby states.

	N=C-H (6-31+d, MeCN)			N=C-CH_3 (6-31+d, MeCN)		
	Relative Energy levels (cm^{-1})					
E. level	***g0***	***g1***	***g2***	***g0***	***g1***	***g2***
S_0	0	3085	2907	0	3660	5422
S_1	22901	20523	23759	27082	21667	26212
S_2	29727	29166	24970	30733	30659	27705
S_3	30889	31037	32283	33353	30482	34456

	N=C-H (6-31+d, MeCN)			N=C-CH_3 (6-31+d, MeCN)		
	Calculated Dipole Moment, μ(D)					
E. level	***g0***	***g1***	***g2***	***g0***	***g1***	***g2***
S_0	3.61	3.39	2.68	3.95	3.81	3.25
S_1	6.25	4.69	4.51	3.88	3.66	3.24
S_2	11.69	8.69	15.91	6.22	10.79	12.67
S_3	5.16	13.79	2.91	14.19	3.42	3.31

Table 3.1. Calculated energies (cm^{-1}) and transition dipole moments ($\mu(D)$) for N=C-H and N=C-CH_3 triazine molecules in MeCN.

	N=C-H (6-31+d, MeCN)			N=C-CH_3 (6-31+d, MeCN)		
	Calculated transition wavelength, nm.					
E. level	***g0***	***g1***	***g2***	***g0***	***g1***	***g2***
$S_{1\rightarrow0}$	437	573	480	369	555	481
$S_{2\rightarrow0}$	336	383	453	325	370	449
$S_{3\rightarrow0}$	324	358	340	300	373	344
$S_{4\rightarrow0}$	321	344	336	297	330	337

	N=C-H (6-31+d, MeCN)			N=C-CH_3 (6-31+d, MeCN)		
	Calculated oscillator strength, a.u.					
E. level	***g0***	***g1***	***g2***	***g0***	***g1***	***g2***
$S_{1\rightarrow0}$	0.2738	0.3409	0.3706	0.4140	0.3401	0.3322
$S_{2\rightarrow0}$	0.1156	0.4119	0.0131	0.6449	0.2847	0.0150
$S_{3\rightarrow0}$	0.5736	0.0989	0.9522	0.0862	0.3953	0.7930
$S_{4\rightarrow0}$	0.4925	0.3797	0.1033	0.0847	0.2121	0.1980

Table 3.2. Calculated transition wavelengths (nm), and oscillator strengths (a.u.) for N=C-H and N=C-CH_3 triazine molecules in MeCN.

3.2.2 Steady-state emission spectroscopy of N=C-H triazine.

The fluorescence of the aforementioned 2,5-dihyrdo-1,2,3-triazine fluorophores is complex with three or more emission bands being observed depending on the excitation wavelength. Figure 3.2.8 shows the difference in the absorption spectrum between N=C-H triazine and N=C-CH_3 triazine. The computational model indicates that emission for N=C-H triazine occurs from three different S_1 excited states, whereas for the N=C-CH_3 triazine, emission is observed from both S_2 and S_1 ES (*vide infra*).

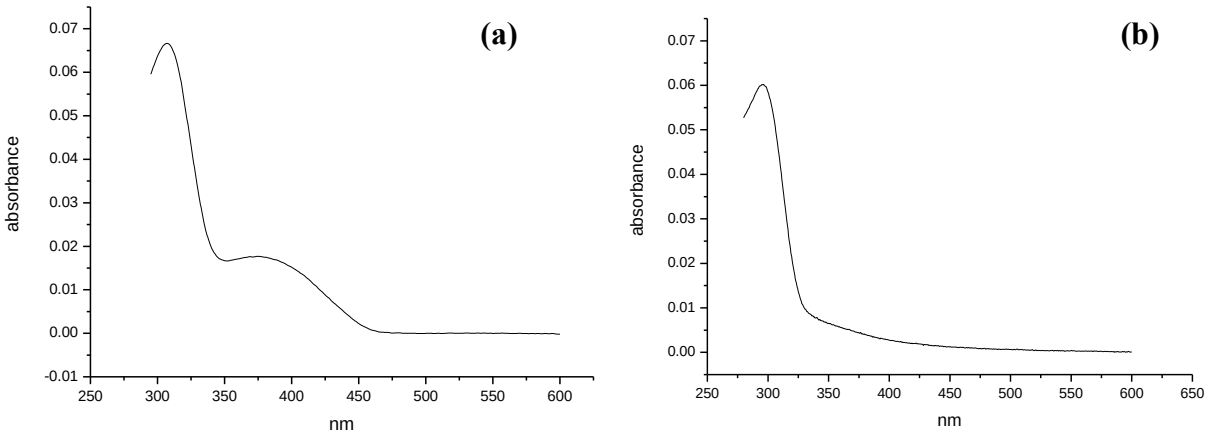

Figure 3.2.8. Ultraviolet-visible absorption spectra collected in acetonitrile for: (a) N=C-H triazine and (b) N=C-CH_3 triazine.

For N=C-H triazine in acetonitrile, excitation into either the 310 or 400 nm absorption bands generates a complicated, green fluorescence emission band centered at 517 nm for 310 nm excitation and 511 nm for 400 nm excitation. For excitation at 400 nm, the emission centered at 517 nm is comprised of three separate emission bands: ~470 nm, ~510 nm, and ~548 nm (Figure 3.2.9 and Table 3.3). Excitation in the UV at 310 nm shows an additional weakly emitting band at ~350 nm which is seen in only a select number of solvents (and not in aceotnitrile). Overall, the broad green emission band only shows a small blue-shift (band maximum, 517 to 511 nm) as the excitation wavelength increases from 310 to 400 nm.

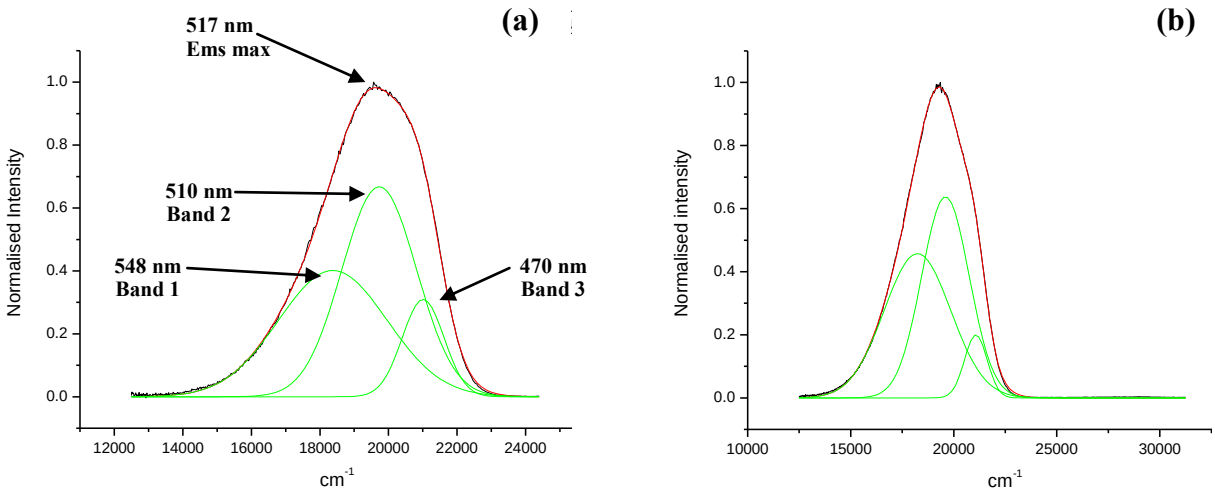

Figure 3.2.9. Steady-state fluorescence emission spectra collected in acetonitrile for: (a) N=C-H triazine with 400 nm excitation; (b) N=C-H triazine with 310 nm excitation. A concentration of 1.5 x 10^{-5} M was used for all measurements.

Molecule	λ_{ex}	Φ	λ max_{em} Band 1 cm^{-1} (nm)	Fwhm* (Rel. area)	λ max_{em} Band 2 cm^{-1} (nm)	Fwhm (Rel. area)	λ max_{em} Band 3 cm^{-1} (nm)	Fwhm (Rel. area)	λ max_{em} Band 4 cm^{-1} (nm)	Fwhm (Rel. area)
N=C-H	310	0.54	18238 (548)	3232 (47%)	19598 (510)	2308 (46%)	21073 (475)	1097 (7%)	~350 nm (v. weak)	Too weak to fit.
N=C-H	400	0.54	18377 (544)	3166 (41%)	19730 (507)	2176 (47%)	21011 (476)	1223 (12%)	--	--

Table 3.3. Fluorescent Quantum Yield (Φ), and band maxima for Gaussian deconvoluted emission spectra of N=C-H triazine.

* Full width at half maximum (fwhm).

3.2.2.2 Proposed model of fluorescence emission of N=C-H triazine at 310 nm.

The 310 nm excitation of N=C-H triazine is thought to be primarily the S_0 to either S_2 or S_3 transition with the molecule having structure **g0** in the GS (Figure 3.2.10). In S_2 and S_3, the **g0** structure has very similar predicted energies (ΔE = 1162 cm^{-1}) and therefore can conclude that internal conversion down to S_2 will be facilitated.

The S2 (**g0**) state, vibrationally relaxes to the lowest vibronic e-level and returns to the ground S_0 state/structure with emission of a photon at ~350 nm. However, this emission band is very weak and is barely visible in most solvents. What is generally observed is a very strong, complex emission band at ~520 nm.

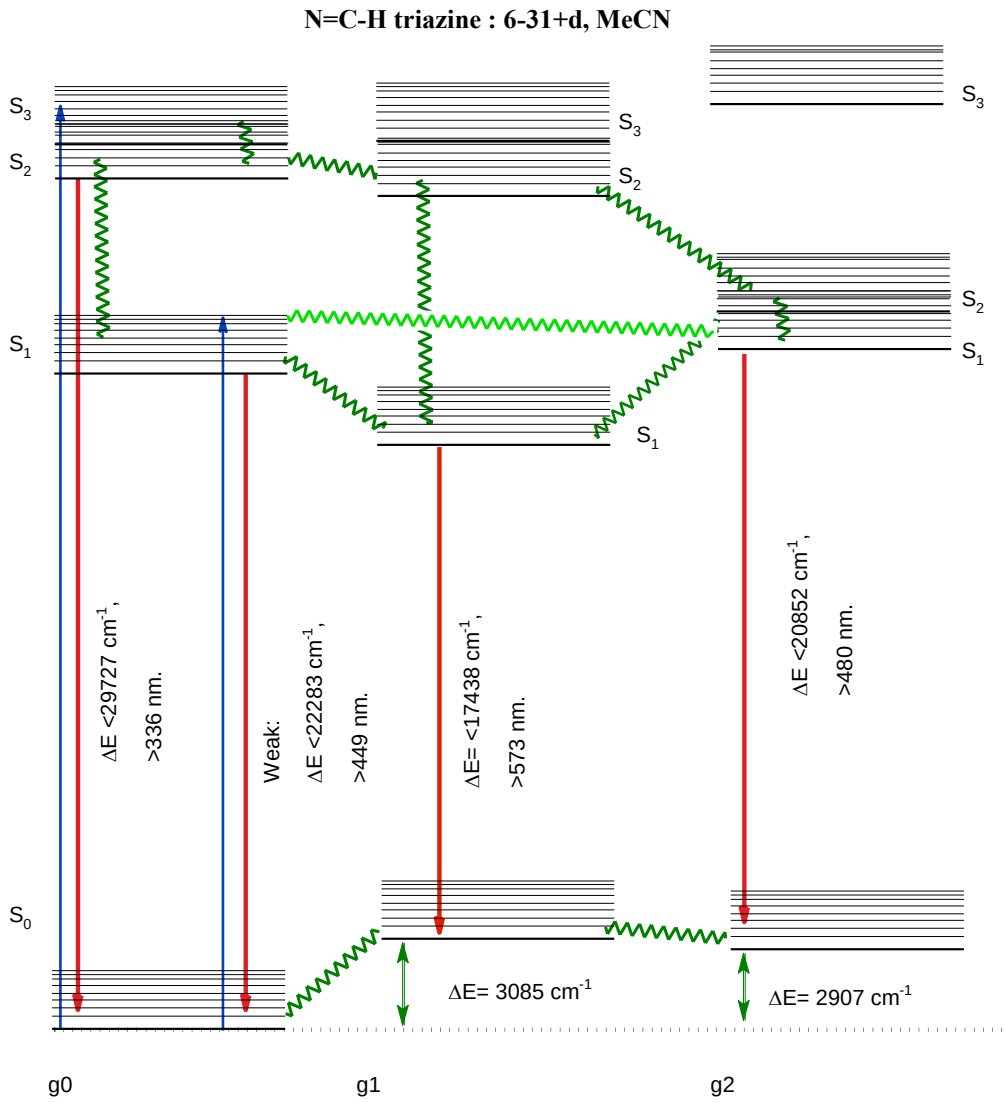

Figure 3.2.10. Proposed photophysical scheme for the N=C-H triazine molecule, showing the transitions and correlation with energy levels. Separations based on the U-31+d data in MeCN.

What can be suggested is that extensive internal conversion (IC) and cross over into the different vibronic states of the closely related structures is occurring. This leads to emission from the S_1 (**g0**), S_1 (**g1**) and S_1 (**g2**) states at wavelengths of <555 nm, >480 nm, and ~> 450 mm respectively.

The justification can be based on the molecular modeling and the following observations. The S_2 (**g0**) excited state is very close to that of the S_2 (**g1**) and S_2 (**g2**) excited states with ΔE = -561 cm^{-1} and -4757 cm^{-1} respectively. Therefore the excited molecule in S_2 (**g0**) has five options for emission:

1. S_2 (**g0**) IC down to S_1 (**g0**) with emission of a photon back to GS, proposed to be the short wavelength band (predicted at ~450 nm, observed at ~470 nm in MeCN, 7 % of fitted area).

2. S_2 (**g0**) to IC to S_2 (**g1**), and then IC down to the S_1 (**g2**) lowest energy level, followed by $S_{1\rightarrow0}$ (**g2**) emission. This is proposed to be the middle band (predicted at 480 nm, observed at ~503 nm, 46 % of fitted area).

3. IC from S_2 (**g0**) down into the S_1 (**g0**) states, then IC across into S_1 (**g1**) followed by $S_{1\rightarrow0}$ (**g1**) with emission of a photon, assumed to be the long wavelength emission band (predicted ~573 nm, observed at~540 nm, 47% of fitted area).

3(b). S_2 (**g0**) can IC to S_2 (**g1**) and then IC down to the S_1 (**g1**) lowest energy level,followed by $S_{1\rightarrow0}$ (**g1**) emission. This is a second pathway for the long wavelength emission.

3(c). S_2 (**g0**) to IC to S_2 (**g2**), and then IC down to the S_1 (**g2**) lowest energy level, then cross over into the lower energy S_1 (**g1**) state, which then emits as a third pathway at the long wavelength ($S_{1\rightarrow0}$ (**g1**) emission).

This agrees with the experimental evidence, both in terms of band energies and band intensities.

The band area for the long wavelength emission band is much greater than for all the other emission bands (47 %). This is as expected since the S_1 (**g1**) state can be populated by three separate routes, and has a relatively large calculated oscillator strength, f = 0.3409.

The S_1 (**g2**) state is accessible *via* two routes; either by IC from S1 (**g0**) to S1 (**g2**), or S_2 (**g0**) to IC to S_2 (**g1**), and then IC down to the S_1 (**g2**) lowest energy level, and the band area is again relatively large (46 %) and the calculated oscillator strength is again large, f =0.3706.

Finally, the proportion of the emission from S_1 (**g0**) is the smallest by area (7 %) as there is only one route to populate this state, and it has the smallest relative oscillator strength, f = 0.2738.

3.2.2.2 Proposed model of fluorescence emission of N=C-H triazine at 400 nm.

400 nm excitation of N=C-H triazine is believed to be the S_0 (**g0**) to S_1 (**g0**) transition. The S_1 (**g0**) excited state is also very close to that of the S_1 (**g1**) and S_1 (**g2**) excited states structures with ΔE = -2378 cm^{-1} and +858 cm^{-1} which indicates that there should be significant overlap of the vibronic states, and high rates of IC.

Thus we get emission from the S_1 (**g0**), S_1 (**g1**) and S_1 (**g2**) states at wavelengths of <555 nm, >480 nm, and ~> 450 mm respectively in a similar fashion to the 310 nm excitation, however, there are differences.

The 400 nm excited N=C-H triazine molecule in MeCN at S_1 (**g0**) has four options for emission (Figure 3.2.10):

1. S_1 (**g0**) vibrationally relaxes down to lowest vibrational energy level in S_1 (**g0**), with emission of a photon back to GS (predicted at ~450 nm, observed at ~470 nm, 12 % of fitted area).

2. The photon energy at 400 nm is high enough to excite the upper vibrational energy levels in S_1 (**g0**). This is expected to be higher than the lower vibronic levels in S_1 (**g2**) and so it is proposed that this transition is very favorable and thus $S_{1\rightarrow0}$ (**g2**) emission can occur, assumed as the middle band at ~500 nm (47 % of fitted area).

3. S_1 (**g0**) IC across into the S_1 (**g1**) lowest energy level with emission of a photon from this band down to the S_0 (**g1**) GS, postulated as the long wavelength emission band (predicted ~573 nm, observed at~540 nm, 41 % of fitted area).

3(b). The molecule in the S_1 (**g2**) can of course IC to S_1 (**g1**), the second pathway for the long wavelength emission.

The major difference in the emission spectra between the 310 and 400 nm spectra involves the proportion of the short wavelength $S_{1\rightarrow0}$ (**g0**) emission which increases from 7 to 12% (by integrated area) as the excitation wavelength increases.

3.2.2.3 Proposed model of fluorescence emission of N=C-CH_3 triazine.

For the N=C-CH_3 triazine molecule, the absorption spectrum changes dramatically and we do not observe a strong band at ~400 nm. For N=C-CH_3 triazine, excitation at 400 nm results in virtually no fluorescence emission. All that is observed is a very weak and noisy single emission and at ~520 nm (Figure 3.2.11 (a)).

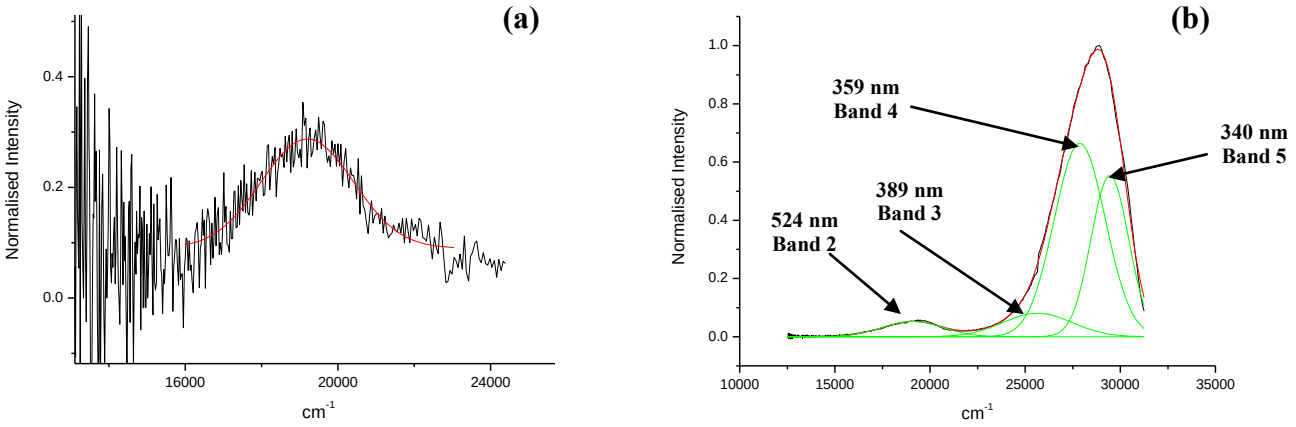

Figure 3.2.11. Steady-state fluorescence emission spectra collected in acetonitrile for: (a) N=C-CH_3 triazine with 400 nm excitation; and (b) N=C-CH_3 triazine with 310 nm excitation. A concentration of 1.5 x 10^{-5} M was used for all measurements.

Molecule	**λ_{ex}**	**Φ**	**λ max_{em} Band 2 cm^{-1} (nm)**	**Fwhm* (Rel. area)**	**λ max_{em} Band 3 cm^{-1} (nm)**	**Fwhm (Rel. area)**	**λ max_{em} Band 4 cm^{-1} (nm)**	**Fwhm (Rel. area)**	**λ max_{em} Band 5 cm^{-1} (nm)**	**Fwhm (Rel. area)**
N=C-CH_3	310	0.18	19082 (524)	3167 (5%)	25648 (389)	3607 (9%)	27871 (359)	2686 (53%)	29450 (340)	1977 (33%)
N=C-CH_3	400	0.02	19198 (521)	2423 (100%)	--	--	--	--	--	--

Table 3.4. Fluorescent Quantum Yield (Φ), and band maxima for Gaussian deconvoluted emission spectra of N=C-CH_3 triazine molecules in acetonitrile.

* Full width at half maximum (fwhm).

Excitation at 400 nm populates the S_1 (**g0**) state which then IC to the S_1 (**g1**) state where it vibrationally relaxes before emitting a photon. This $S_{1\rightarrow0}$(**g0**) emission is very weak because the change in dipole moment (0.07 μ(D)) is very small although the calculated oscillator strength is relatively large (*f* = 0.4140) (Table 3..2).

However, once excited at ~310 nm, a strong tri-band emission centred at ~350 nm is observed. This UV excitation populates the S_3 (**g0**) and S_2 (**g0**) ES (Figure 3.2.12), and the molecule can revert to the ground state by fluorescence *via* a number of internal conversion/vibrational relaxation pathways:

1. $S_{2\rightarrow0}$ (**g0**) emission (33% of the fitted area) observed at ~340 nm (predicted >325 nm).

2. $S_{1\rightarrow0}$ (**g0**) emission (53% of the fitted area) observed at ~360 nm (predicted 369 nm),

3. S_3 (**g0**) or S_2 (**g0**) IC to S_2/S_3 (**g1**) states followed by $S_{2\rightarrow0}$(**g1**) emission (9% of the fitted area) observed at ~390 nm (predicted >370 nm),

4. S_2/S_3 (**g1**) or S_1 (**g0**) states IC down into S_1 (**g1**) followed by $S_{1\rightarrow0}$ (**g1**) emission (5% of the fitted area) which is observed at ~520 nm (predicted >550 nm).

The predicted oscillator strengths *f* also support these assignments for the emission bands, with $S_{2\rightarrow0}$ (**g0**) *f* = 0.6449, $S_{1\rightarrow0}$ (**g0**) *f* = 0.4140, $S_{2\rightarrow0}$ (**g1**) *f* = 0.2847, and $S_{1\rightarrow0}$ (**g1**) *f* = 0.3401.

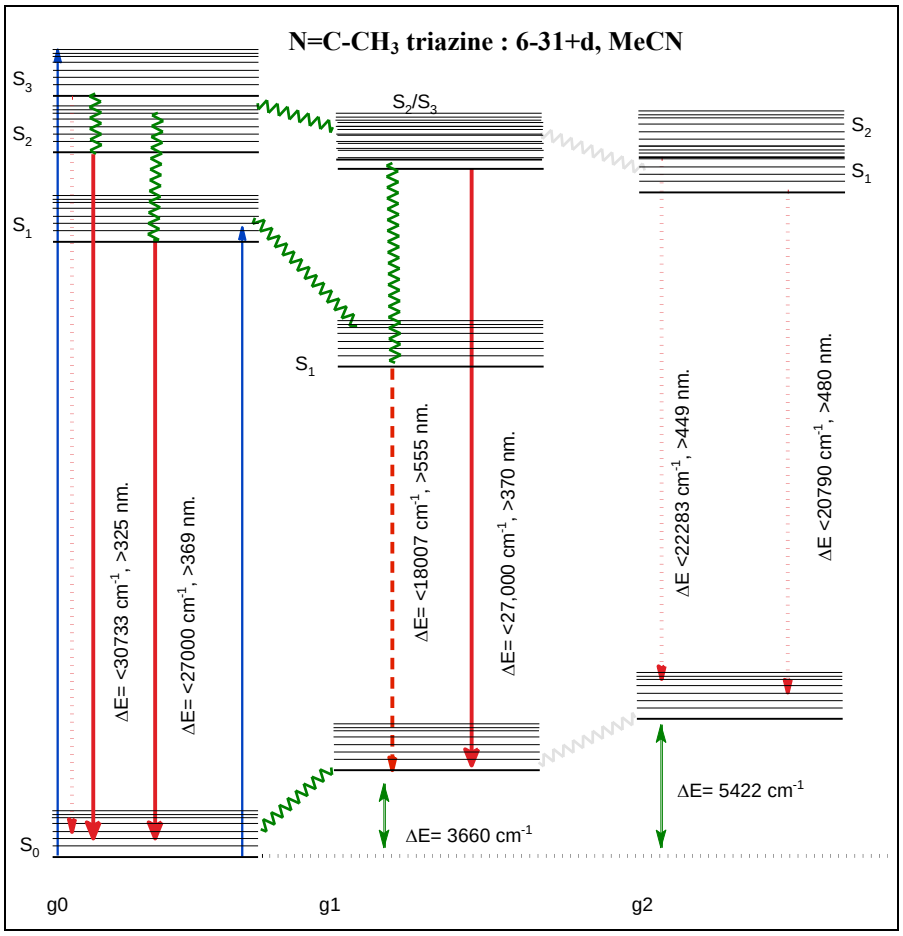

Figure 3.2.12. Proposed photophysical scheme for N=C-CH_3 triazine, showing the transitions and correlation with energy levels. Separations based on the 6-31+G(d)/MeCN calculations.

3.3 CONCLUSION.

To date, apart from the fluorescent 2,5-dihydro 1,2,3-triazine derivatives reported by Butler *et al*., there has only been one other class of fluorescent 1,2,3-triazines reported in the literature.[52, 54]

The complex fluorescence emission of N=C-H triazine was elucidated in comparison to N=C-CH_3 triazine, which when excited at 400 nm results in virtually no fluorescence emission. With the aid of TD-DFT calculations, courtesy of Professor Luke A. Burke; three structures were calculated with analytical second derivatives using the 6-31G(d) basis set: **g0** (optimized for S_0), **g1** (optimized for S_1) and, **g2** (optimized for S_2).

For 310 nm excitation of N=C-H triazine, an S_0 to either S_2 or S_3 transition with the molecule having structure **g0** in the GS is thought to be the model of fluorescence with extensive IC into the different vibronic states of closely related structures occurring, leading to emission from the S_1 (**g0**), S_1 (**g1**) and S_1 (**g2**) states.

Based on calculated oscillator strengths *f*, it was proposed that following excitation to either S_3 (**g0**) or S_2 (**g0**), the tri-band emission can be resolved as emission from the S_1 (**g1**) state *via* three distinct paths being attributed to the long wavelength emission band (observed at ~540 nm), emission from S_1 (**g2**) composing the middle wavelength band (observed at ~503 nm) and finally S_2 (**g0**) IC down to S_1 (**g0**) with emission of photon when returning to GS is attributed to the short wavelength band (observed at ~470 nm).

For 400 nm excitation of N=C-H triazine, the model of fluorecence is reasoned to be an S_0 (**g0**) to S_1 (**g0**) transition with emission from the S_1 (**g0**), S_1 (**g1**) and S_1 (**g2**) states in a similar fashion to the 310 nm excitation. Ultimately, the major difference in the emission spectra between the 310 and 400 nm spectra involves the proportion of the short wavelength $S_{1\rightarrow0}$ (**g0**) emission which increases as the excitation wavelength increases.

For N=C-CH_3 triazine, excitation at 400 nm results in virtually no fluorescence emission due to population of the S_1 (**g0**) state (observed as a weak band at ~520 nm). As the calculated change in dipole moment is small, the $S_{1\rightarrow0}$ (**g0**) emission is expected to be very weak.

However, excitation at ~310 nm results in a strong tri-band emission centred at ~350 nm. 310 nm excitation populates the S_3 (**g0**) and S_2 (**g0**) ES, and the molecule can

revert to the ground state by fluorescence *via* a number of IC or vibrational relaxation pathways: $S_{2\rightarrow0}$ (**g0**), $S_{1\rightarrow0}$ (**g0**), $S_{2\rightarrow0}$ (**g1**), and $S_{1\rightarrow0}$ (**g1**).

In conclusion, the significant difference, which accounts for the distinction between the fluorescent and electronic properties of N=C-H and N=C-CH_3 triazine was found computationally to be ultimately due to the positioning of the imine and ester of N=C-H triazine. The imine and ester of N=C-H triazine are held in-plane or nearly in-plane due to an interaction between the imine hydrogen and the ester carbonyl lone pair for S_0, S_1, and S_2; whilst in N=C-CH_3 triazine the imine methyl group N=C-CH_3 interaction holds it out of plane with the ester. Thus, the major differences of structure between N=C-H triazine and N=C-CH_3 triazine involves the rotation of the imine group (H or CH_3) over the triazine ring.

In light of this, it can be postulated that for the development of new fluoresecent derivatives of the 2,5-dihydro-1,2,3-triazine, the imine hydrogen and carbonyl must be preserved in the structure for the retention its fluorescent properties. Once this is retained, such areas as the N-2 phenyl ring and imine phenyl ring could be modified to effect the HOMO-LUMO transition dipole (See Appendix A.6, Figure A.6.1 and A.6.2), and thus either lower (red-shifting) or increase (blue-shifting) the emission energy to produce a spectral shift.

Figure 3.2.13 shows two structures which have been shown theoretically to emit in the near-infrared (NIR) region by effecting the electron density of the N-2, imine and middle phenyl rings by substitution. Such structures may be synthesised and investigated in future, whilst Figure 3.2.14 proposes two other structures which may lower the HOMO-LUMO gap by increasing the conjugation within the triazine π aromatic system.

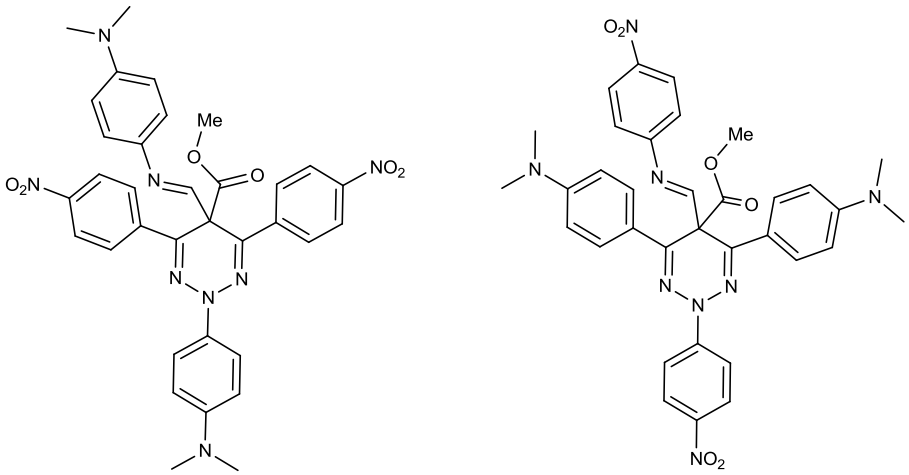

Figure 3.2.13. Proposed structures of modified 2,5-dihyrdo-1,2,3-triazines which show from preliminary theoretical calculations to exhibit strong absorptions in the near-infrared (~ 800 nm).

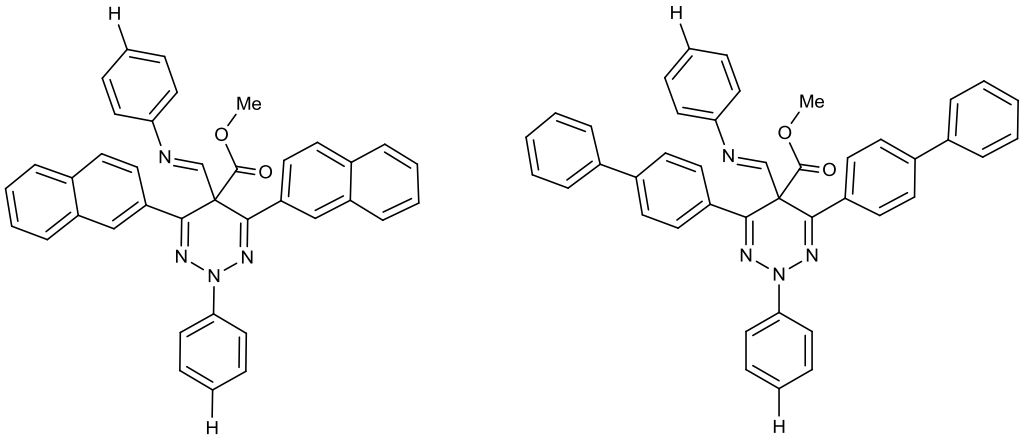

Figure 3.2.14. Increasing the conjugation within the triazine π aromatic system may reduce HOMO-LUMO energy gap, resulting in a lower energy red-emitting flurophore.

Chapter 4: 2,5-Dihydro-1,2,3-triazines with substituted aryl groups.

4.1 INTRODUCTION.

In comparison with 1,2,4- and 1,3,5- triazine structures, the 1,2,3-triazine system is less studied. This is due to its low stability and limited synthetic routes. Before 1979, monocyclic 1,2,3-triazines were limited to 4,5,6-trisubstitued products as the general method for their preparation was by rearrangement of trisubstituted cyclopropenyl azides.[64]

1,2,3-triazines are of interest as they are a potential route to azete precursors by photolysis of the corresponding 4,5,6-trisubstituted 1,2,3-triazines.[64] Monocyclic 1,2,3-triazines are π deficient and react with nucleophilic reagents such as Grignard reagents. The 4,6-disubstitued 1,2,3-triazines undergoing nucleophilic attack at the N2 and C5 atoms, to yield 2,5-dihydro 1,2,3-triazines (Figure 4.1.1).[65]

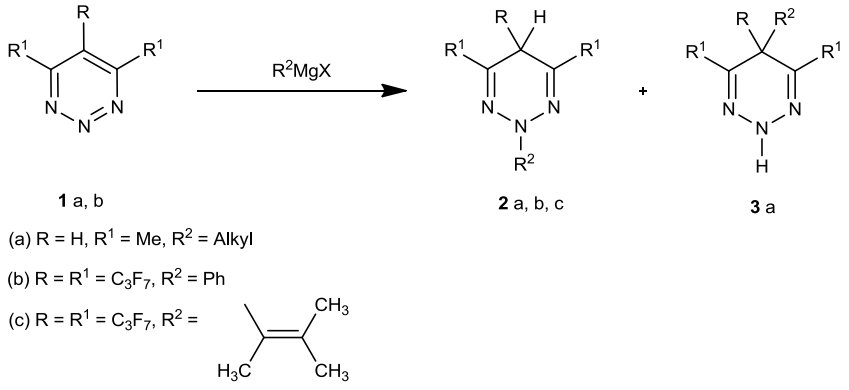

Figure 4.1.1. Synthetic route to 2,5-dihydro 1,2,3-triazines from monocyclic 1,2,3-triazines.[65]

This chapter is focused on the discussion of a simple one-pot reaction to produce known fluorescent 2,5-dihydro-1,2,3-triazine derivatives, and investigation of their interesting dual emission fluorescent properties.[54]

4.1.2 Synthesis of fluorescent 2,5-dihydro 1,2,3-triazines.

The reaction of 1,2,3-triazolium-1-phenylaminide 1,3-dipoles with unsymmetrical propiolate esters leads to the formation of the substituted 1,2,3-triazine derivatives *via* the isolatable fused pyrrolo[2,3-d]-triazoline first generation intermediate.

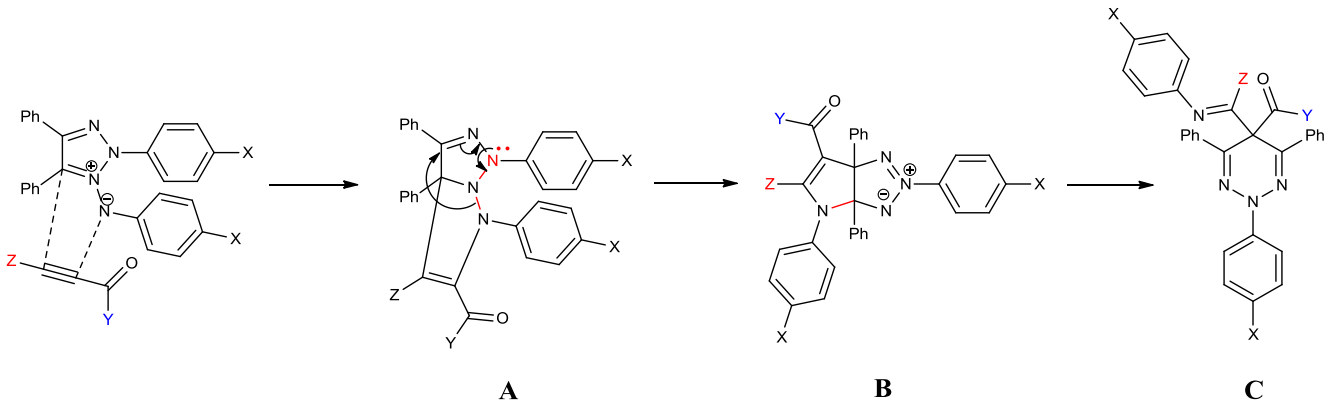

Scheme 4.1.1. General synthetic scheme to 2,5-dihydro 1,2,3-triazines from 1,2,3-triazolium 1-aminide 1,3-dipoles.

It has been established that the 1,2,3-triazolium-1-aminide is a **Type I** 1,3-dipole as it undergoes $HOMO_{dipole}$ controlled Huisgen cycloadditions.[66] The initial cycloadduct **A** undergoes a symmetry allowed suprafacial 1,4-electrocyclic rearrangement to give the fused pyrrolo[2,3-d]-triazoline **B**, due to the labile exocyclic N-N bond (Scheme 4.1.1), where the four π electrons are delocalized over three atoms. This 1,4-sigmatropic rearrangement is a heteroanalogue of the 1,5-sigmatropic rearrangement of 1,3-dienes in carbon chemistry. With 1,5-sigmatropic rearrangements the four π electrons are delocalized over four carbon atoms, resulting in a 1,5-migration across two π bonds. Originally, the product from the reaction between 2,4,5-triphenyl-1,2,3-triazolium-1-phenylaminide 1,3-dipole and terminal propiolate was thought to be structure **A**, the direct cycloadduct.[29, 67]

Subsequently, the product was shown to be structure **B** and this was supported by ^{13}C NMR data, which include key quaternary bridgehead carbon signals that appear *circa* 92 and 105 ppm. Attempts to isolate compound **A** by carrying out the reaction at 0°C resulted in no reaction or **B** being isolated in lower yields.[28, 29]

If a H-atom is the Z substituent at C5 (compound **B**, Scheme 4.1.1, Figure 4.1.2) and there is a double bond between C5 and C6, an additional rearrangement can occur in situ. A cleavage of the C3a-N4 bond, resulting in ring expansion and generation of the 2,5-dihydro 1,2,3-triazine product, compound **C**.

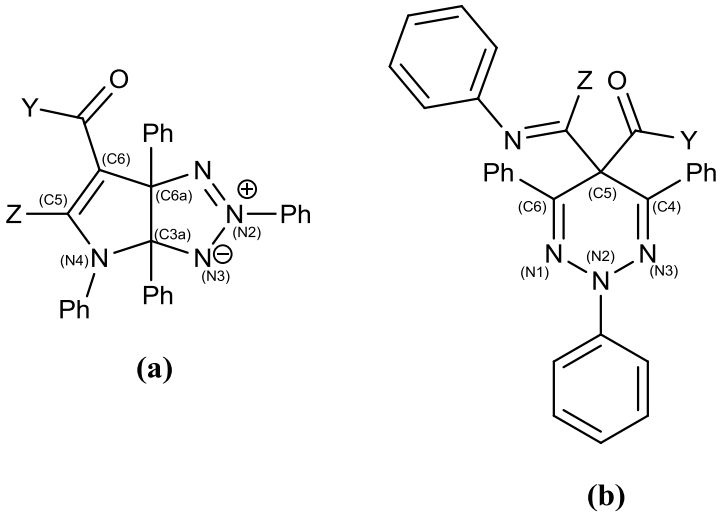

Figure 4.1.2. Numbering schemes for (a) fused 2,3a,4,6a-tetraphenyl-3,3a,4,6a-tetrahydropyrrolo[2,3-d]-[1,2,3]-triazol-2-ium-3-ides and (b) 2,5-dihydro-1,2,3-triazines.

Of interest, is the planar symmetrical nature of the atoms comprising the C-N-N-N-C system in compound **C** in which the N1-N2-N3 and C-N-N bond angles are 121 ^{o} and 116^{o} respectively. This is in contrast to the buckled nature of the C-C-C region which based on X-ray crystallography studies have almost normal C-C bond lengths and tetrahedral bond angles.[54,68]

4.1.3 Oxidation of bis-phenylhydrazones to 1,2,3-triazolium-1-phenylaminide 1,3-dipoles.

Bis-arylhydrazones of benzil can be prepared by refluxing benzil with an excess of the appropriate arylhydrazine and acetic acid.[56] There are some cases which fail to give bis-arylhydrazones and instead result in the isolation of mono-hydrazones (Figure 4.1.3).[56]

Whilst the benzil bis-arylhydrazones exist in several forms (Section 1.5, Scheme 1), mono-arylhydrazones are believed to exist in one form only; the *syn* form which is stabilized by a hydrogen-bonded chelated ring.[56]

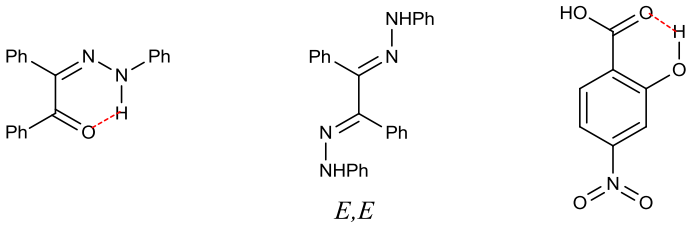

Figure 4.1.3. Mono-phenylhydrazone of benzil showing hydrogen-bonded chelated ring and the *E,E* form of 1,2-bis(pheny)lhydrazone of benzil; 4-nitro-salicylaldehyde.

We observed this firsthand in a failed attempt to synthesise 1,2-bis(4-nitrophenyl)hydrazones of benzil, which resulted in the generation of the monohydrazone exclusively. This is perhaps due to a substituent effect from the *p*-nitro stabilizing the intramoleular hydrogen bond (Figure 4.1.3). Such has been shown by computation methods using salicylaldehyde whereby substituents in the para position (*e.g.* NO_2) with respect to the OH stabilize the intramolecular hydrogen bond. [69]

Oxidations of bis(hydrazone) systems has received considerable interest in the past due to the unexpected structures which are encountered among the products.

Active manganese dioxide (MnO_2) in solvents of neutral pH has been reported to oxidize phenylhydrazones *via* a free radical mechanism involving hydrogen abstraction, similar to the lead tetra-acetate ($Pb(C_2H_3O_2)_4$) oxidation of phenylhydrazones.[70]

Under acidic conditions, oxidation of bis-arylhydrazones of benzil at refluxing temperature in toluene results in the formation of 2,4,5-triphenyl-1,2,3-triazole. Treating 1,2-bis(phenyl)hydrazone with sulphuric acid or palladium-carbon in aqueous ethanol results in cyclisation to generate 2,4,5-triphenyl-1,2,3-triazole.[26, 28]

Other cyclising agents include potassium dichromate ($K_2Cr_2O_7$) in 50 % acetic acid, copper (II) chloride ($CuCl_2$) in methanol, acetic anhydride, nitric acid in 1:3 v/v methanol:chloroform, 10% iodine in ether with 6% sodium ethoxide and thallium acetate ($Tl(OAc)_3$) in acetic acid.[26, 27, 56]

Nickel peroxide (NiO_2) oxidation of 1,2-bis(phenyl)hydrazone of benzil is reported to behave similarly to manganese dioxide; again giving 2,4,5-triphenyl-1,2,3-triazoles chiefly.[71]

The rearrangement from bis(areneazo)alkenes to 1,2,3-triazoles is reported by George *et al*. to be due to the loss of phenylnitrene when the mesoionic form is heated whilst Butler *et al*. put forward that it may be seen as a 3,3-sigmatropic migration (Figure 4.1.4).[27, 28]

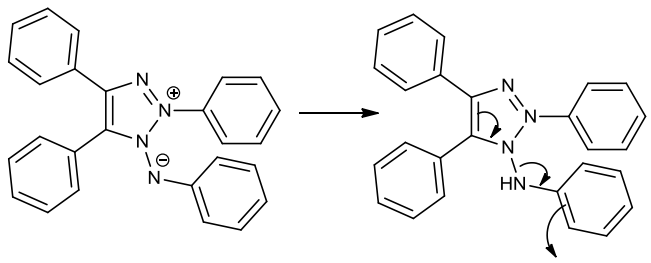

Figure 4.1.4. Proposed method of rearrangement of cyclised bis(areneazo)alkenes to 1,2,3-triazoles by loss of phenylnitrene.[27]

However, the oxidation of glyoxal osazone using activated manganese dioxide at room temperature results in the formation of (*Z*)-1,2-bis((*E*)-phenyldiazenyl)ethene in 94 % yield and no observable triazole (Scheme 4.1.1).[70]

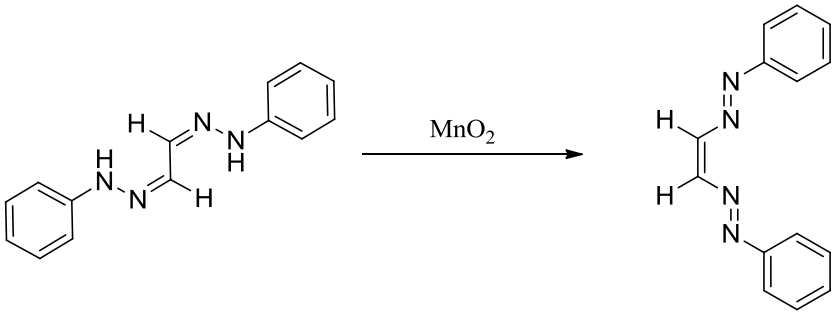

Scheme 4.1.1. Oxidation of glyoxal osazone using activated manganese dioxide at room temperature to form (*Z*)-1,2-bis((*E*)-phenyldiazenyl)ethene.[70]

4.1.4 Dual excitation fluorescent probes.

Fluorophores which exhibit dual excitation are of particular interest in biological imaging.[72] Generally, the two excitation wavelengths can be monitored at a single emission wavelength, which is measured independently for each excitation band. This can then be used to calculate the ratio of bound to free intracellular targets of interest by monitoring the changes in fluorescence emission intensity and is known as the ratio method.[73]

The popular dual excitation fluorescent probe Fura-2 (Figure 4.1.5) is best known for intracellular calcium imaging. Fura-2 can be dual excited at 340 and 380 nm and monitored at a single emission wavelength to obtain a ratio of bound to free intracellular calcium as revealed by the changes in fluorescence emission intensity. [73]

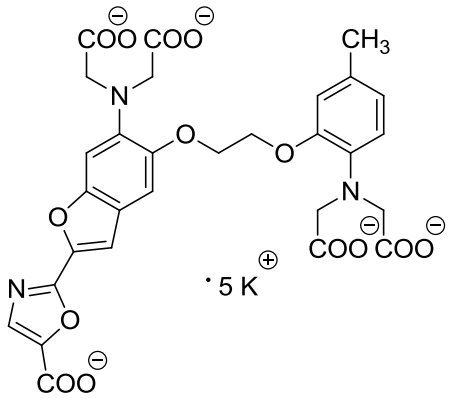

Figure 4.1.5. Structure of the dual excitation probe Fura-2.

4.2 RESULTS AND DISCUSSION (SYNTHESIS).

Refer to Chapter 2, Section 2.1 for experimental procedure and results.

4.2.1 Synthesis of 1,2,3-triazolium-1-aminide 1,3-dipoles.

The 1,2 bis-arylhydrazones of benzil were synthesized by reacting an excess of the desired arylhydrazine with benzil, in the presence of acetic acid, to yield the 1,2,-bisphenylhydrazone of benzil for phenylhydrazine (Scheme 4.2.1, **1**, 78 % yield). A similar methodology was applied to the synthesis of 1,2-bis(4-chlorophenyl)hydrazone of benzil (**4**, 55 % yield), and 1,2,-bis(4-bromophenyl)hydrazone of benzil (**7**, 63 % yield) using 4-chlorophenylhydrazine and 4-bromophenylhydrazine respectively.

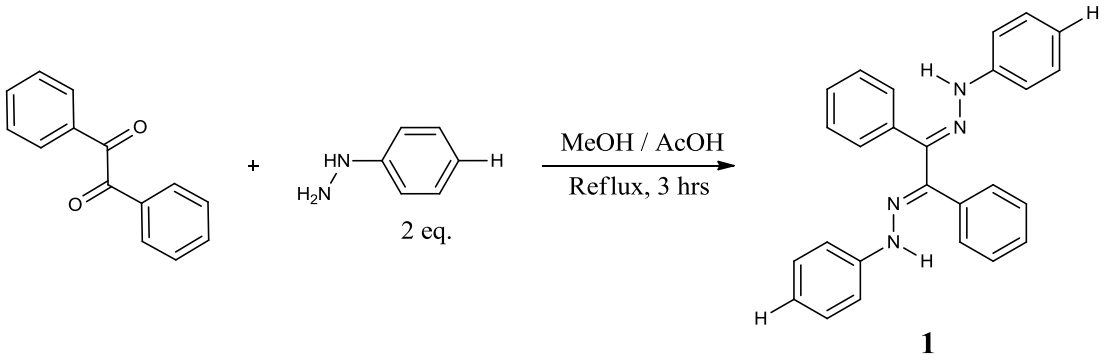

1

Scheme 4.2.1. Synthesis of 1,2-bisphenylhydrazone of benzil.

However, 4-chlorophenylhydrazine (Scheme 4.2.2) and 4-bromophenylhydrazine are commercially available as the respective hydrochloride salt. In order for the reaction to proceed, the amine must be deprotonated to allow nucleophilic addition to the carbonyl of benzil to occur. Sodium acetate trihydrate was used as base, thus producing the required acid catalyst, acetic acid *in situ* and also sodium chloride as a by-product.

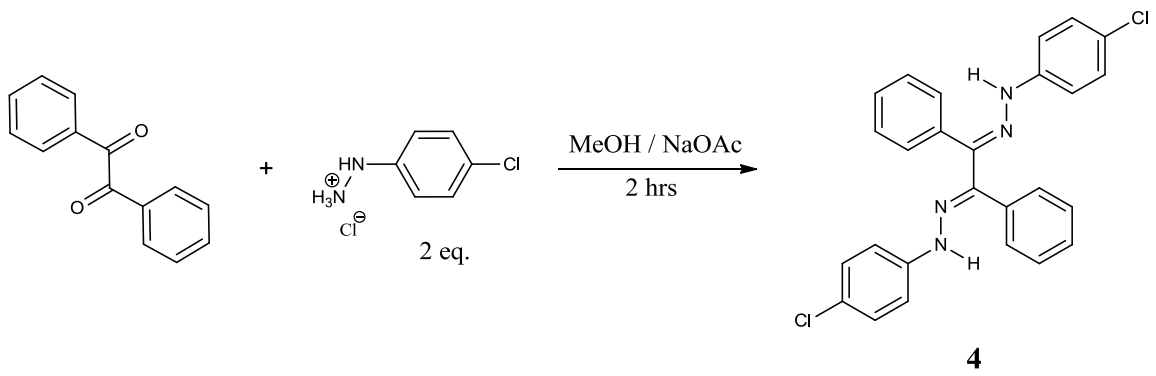

4

Scheme 4.2.2. Synthesis of 1,2-bis(4-chlorophenyl)hydrazone of benzil.

Oxidation of the bisarylhydrazones of benzil was carried out using lead(IV) dioxide and stirring in dry dichloromethane at room temperature to give the corresponding 2,4,5-triphenyl-1,2,3-triazolium-1-arylaminide 1,3-dipole in yields of 78 % (**2**, X = H), 73 % (**5**, X = Cl) and 63 % (**8**, X = Br).

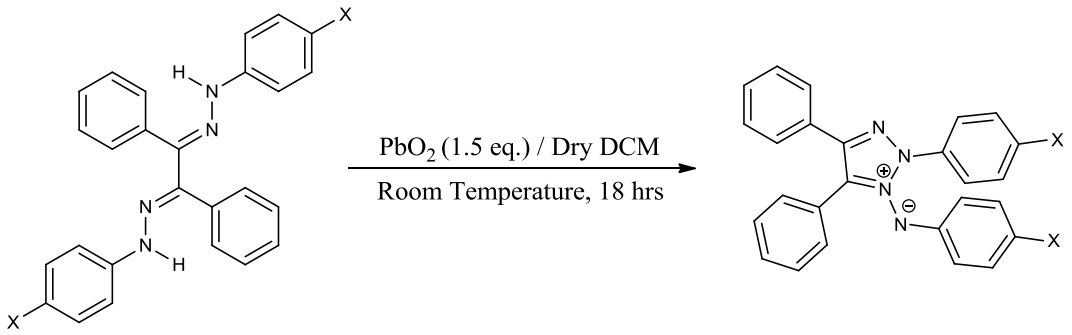

1 X = H
4 X = Cl
7 X = Br

2 X = H
5 X = Cl
8 X = Br

Scheme 4.2.3. Oxidation of 1,2-bis-arylhydrazones of benzil to the corresponding 2,4,5-triphenyl-1,2,3-triazolium-1-arylaminide 1,3-dipole using lead(IV) dioxide.

In spite of this an investigation was undertaken to identify "greener" methods for the synthesis of the 1,2,3-triazolium-1-aminide 1,3-dipoles. Principle 3 of the 12 Principles of Green Chemistry states the use of *"Less Hazardous Chemical Syntheses – To design synthetic methods to use and generate substances that minimize toxicity to human health*

and the environment".[74] Thus, the potential to eliminate the requirement for lead dioxide was examined.

It was found that not all commercially available lead dioxide reagents can successfully oxidize bisphenylhydrazones of benzil to produce 1,2,3-triazolium-1-phenylaminide 1,3-dipoles. Reactions were always performed successfully using "brown" lead(IV) dioxide, but when "black" lead(IV) dioxide was tested no reaction was observed. The same result occurred using lead(II) dioxide and "red" lead(II,IV) dioxide.

In the past it has been reported that commercial manganese(IV) dioxide was found to commonly have a lower activity and often be inactive.[75] When preparing "active" manganese dioxide it is reported to be essential to precipitate it in the presence of base or to treat it with base after precipitation and before drying.[75] Both under- and over-drying has also been found to reduce the activity of the oxide.[75] The "active" manganese dioxide is a hydrated oxide.[75] Based on this it could be argued that the "black" and "red" lead dioxide had not undergone the same "activating" procedures as the "brown" lead dioxide and hence were unable to oxidize our hydrazones.

As described in Section 4.2.2, manganese dioxide may be a useful reagent for the preparation of 1,2,3-triazolium-1-phenylaminide-1,3-dipoles, providing the correct conditions are used. Performing the oxidation at room temperature with a 10 equivalent excess and stirring in toluene allowed the 1,2-bisphenylhydrazone of benzil to be successfully oxidized to the 2,4,5-triphenyl-1,2,3-triazolium-1-phenylaminide 1,3-dipole in a 94 % yield.

When column chromatography was performed on the product of the 1,3-dipolar cycloaddition between 2,4,5-triphenyl-1,2,3-triazolium-1-phenylaminde 1,3-dipole and methyl propiolate, an unknown product was isolated. An x-ray crystal structure was successfully grown and the structure determined was found to be 2,4,5-triphenyl-1,2,3-triazole (Figure 4.2.1).

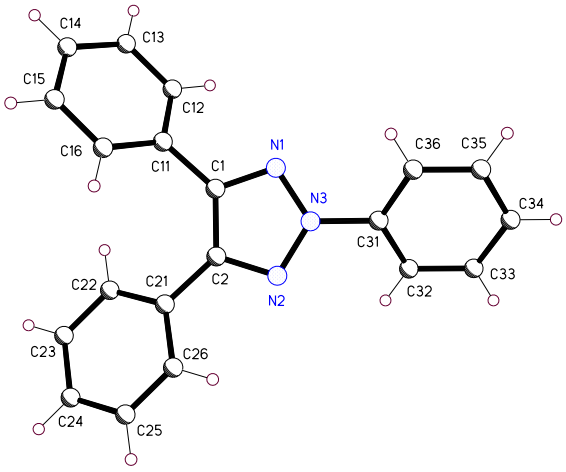

Figure 4.2.1. X-ray crystal structure for 2,4,5-triphenyl-1,2,3-triazole.

From the literature discussed in Section 4.2.2, a small percentage of 2,4,5-triphenyl-1,2,3-triazole can be produced during the oxidation of the arylhydrazone. In addition to the x-ray crystal structure, the ^{1}H NMR spectrum, (m, 6H, 7.38-7.40), (m, 3H, 7.47-7.52), (m, 4H, 7.63-7.86), (d, 2H, 8.17-8.19), allowed clear identification of the 2,4,5-triphenyl-1,2,3-triazole. The presence of the 1,2,3-triazole can be identified in the ^{1}H NMR spectrum of 2,4,5-triphenyl-1,2,3-triazolium-1-phenylaminide as a doublet at 8.17-8.19 ppm (4.5 % impurity, Figure 4.2.2).

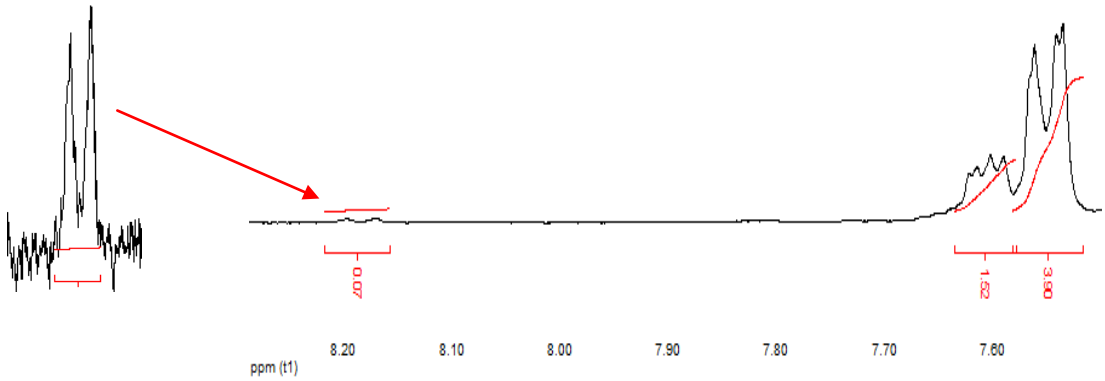

Figure 4.2.2. 2,4,5-triphenyl-1,2,3-triazole can be identified in the ^{1}H NMR spectrum of 2,4,5-triphenyl-1,2,3-triazolium-1-phenylaminide as a doublet at 8.17-8.19 ppm (zoomed on left).

4.2.2 1,3-Dipolar cycloadditions of 1,2,3-triazolium-1-arylaminide 1,3-dipoles with methyl propiolate and 3-butyn-2-one.

As previously discussed, the use of a terminally monosubstituted alkyne (*e.g.* methyl propiolate, Z = H) allows a 1,4 N→C sigmatropic rearrangement to occur within the initial cycloadduct, which then undergoes a further *in situ* rearrangement to generate the fused pyrrolo[2,3-d]-triazoline "first generation" products, **3b**, **6b** and **9b** (10 %, 29 % and 4 % yields respectively) (Scheme 4.2.4).

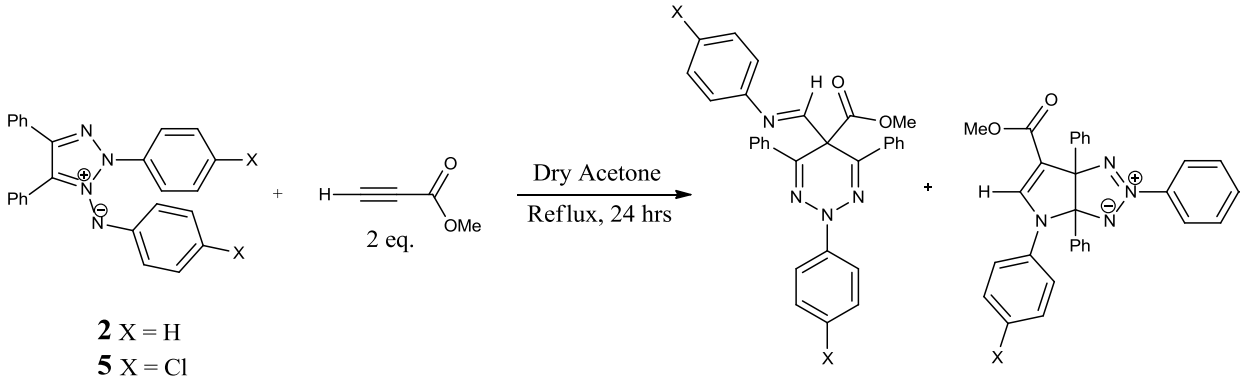

2 X = H
5 X = Cl
8 X = Br

3a X = H
6a X = Cl
9a X = Br

3b X = H
6b X = Cl
9b X = Br

Scheme 4.2.4. 1,3-dipolar cycloaddition of 1,2,3-triazolium-1-arylaminide 1,3-dipoles with methyl propiolate to generate 2,5-dihydro-1,2,3-triazines with substituted aryl groups.

The structure of the fused pyrrolo[2,3-d]-triazoline "first generation" products (**3b**, **6b** and **9b**) are supported by ^{1}H and ^{13}C NMR spectra, and also HRMS and IR spectroscopy. The ^{1}H NMR spectra of **3b**, **6b** and **9b** all exhibit two characteristic singlets; the methoxy group as a singlet at ~3.66 ppm, as well as the hydrogen at C5 observed at ~8.4 ppm (Figure 4.1.2). Such deshielding is to be expected due to the delocalization between the C5 and C6 double bond and the carbonyl, thus making C5 more electropositive resulting in a more deshielded hydrogen. This is also observed in the ^{13}C NMR spectra whereby the deshieled C5 carbon is observed at ~149 ppm. The ^{13}C NMR spectrum of **3b**, **6b** and **9b** also exhibit key quaternary bridgehead carbons; C3a and C6a (Figure 4.1.2) that appear at ~92 and ~105 ppm. A quaternary ^{13}C NMR signal at ~165 ppm confirms the presence of a carbonyl and this is supported by the IR spectrum with the C=O stretch being

observed at ~1698 cm^{-1}. The structure elucidation is also supported by an x-ray crystal structure which had not been previously published. An interesting "stick-man" structure can be observed when the molecule is viewed from the front, with the two bridgehead phenyl groups pointing underneath the ring to form the "legs" and C6 carbonyl and N4-phenyl group making the "arms".

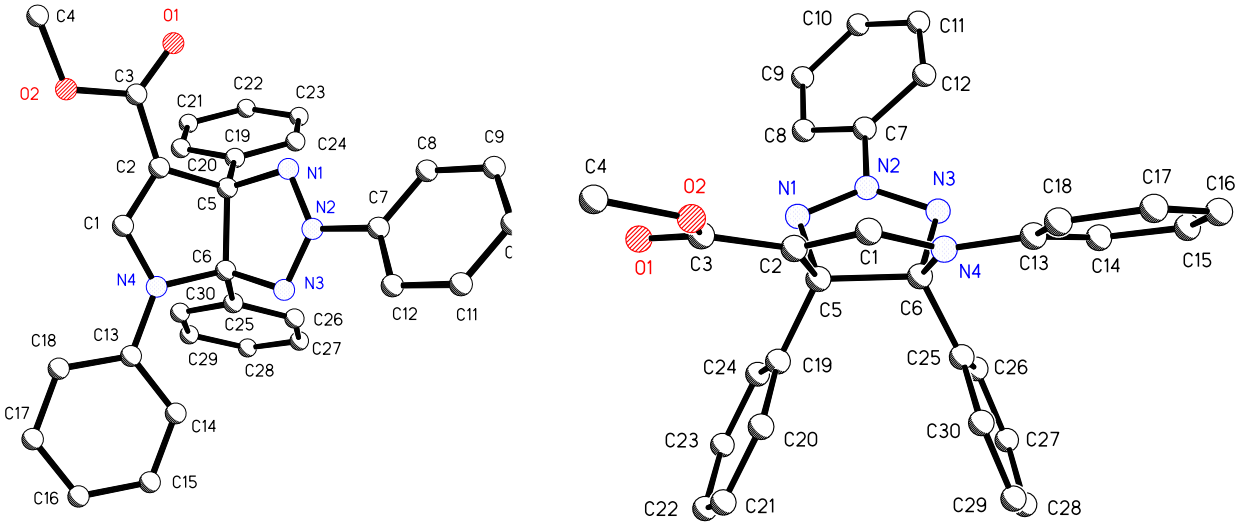

Figure 4.2.1. X-ray crystal structure for 6-methoxycarbonyl-2,3a,4,6a-tetraphenyl-3,3a,4,6a-tetrahydropyrrolo[2,3-d]-[1,2,3]-triazol-2-ium-3-ide.

Ring expansion of **3b**, **6b** and **9b** produces the "second generation" product; a fluorescent 2,5-dihydro-1,2,3-triazine in yields of 58 % (**3a**), 71 % (**6a**) and 85 % (**9a**). The structure of the isolated products were identified using ^{1}H and ^{13}C NMR spectra, supported by HRMS and IR spectroscopy. As discussed in Section 4.1.2, the reaction is highly regioselective and only one isomer is isolated for each of **3b**, **6b** and **9b**. This is supported as only one singlet is observed for the imine hydrogen at ~8.5 ppm in the ^{1}H NMR spectra. The same is also observed for the methoxy group with one singlet present at ~3.53 ppm in the ^{1}H NMR spectrum. The ^{13}C NMR spectrum of **3a**, **6a** and **9a** show the presence of an imine carbon at ~160 ppm. They also exhibit a key quaternary carbon signal for C5 at ~53 ppm, as well as a quaternary carbon signal at ~170 ppm which again confirms the presence of a carbonyl and is supported by the IR spectrum with the C=O stretch being observed at ~1698 cm^{-1}.

When the cycloaddition is performed using 3-butyn-2-one (Scheme 4.2.3), the methyl ester can be successfully replaced with a methyl ketone generating a new triazine analogue (**10a**) in a 39 % yield. This new triazine displays intense yellow fluorescence in solution.

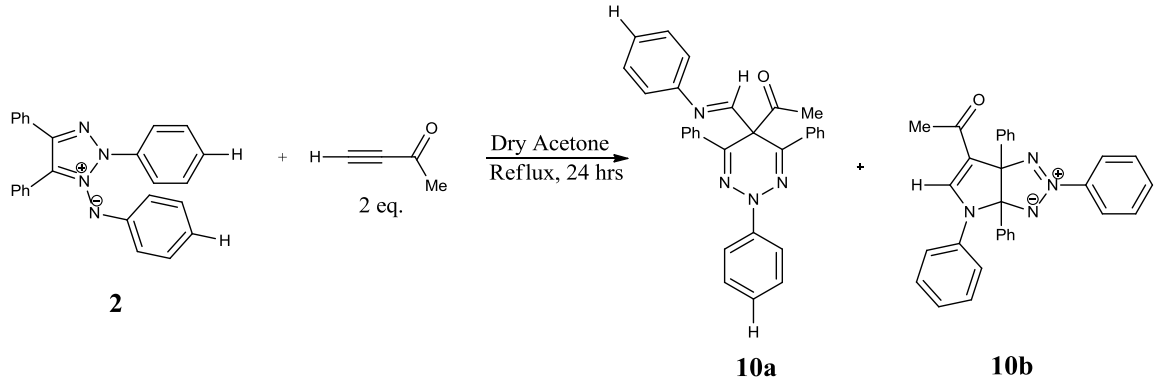

Scheme 4.2.3. 1,3-Dipolar cycloaddition of 2,4,5-triphenyl-1,2,3-triazolium-1-phenylaminide 1,3-dipole (**2**) with 3-butyn-2-one to generate a methyl ketone triazine analogue.

The structures of the new products were again identified using ^{1}H and ^{13}C NMR spectra, supported by HRMS and IR spectroscopy. The fused pyrrolo[2,3-d]-triazoline "first generation" product **10b** was also isolated in a 59 % yield. Again, the ^{1}H NMR spectrum of **10b** exhibits the two expected singlets. As the carbonyl is substituted now with a methyl ketone, the ^{1}H signal for the methoxy group (O-CH_3, 3.66 ppm) is expected to be replaced with a signal for the CH_3 group of the ketone, and was observed as a singlet at 3.13 ppm. Once more, the deshielded hydrogen of C5 is also observed at 8.43 ppm and 147.6 ppm in the ^{1}H and ^{13}C NMR spectra respectively. The ^{13}C NMR spectrum of **10b** also exhibits the key quaternary bridgehead carbons; C3a and C6a (Figure 4.1.2) at 91.6 and 105.1 ppm. A quaternary ^{13}C NMR signal at 192 ppm also confirms the presence of a carbonyl and this is supported by the IR spectrum with the C=O stretch being observed at 1638 cm^{-1}.

The "second generation" fluorescent 2,5-dihydro-1,2,3-triazine product **10a** was iolsated in a 39 % yield. The reaction is also highly regioselective and only one isomer is isolated for **10b**. Again for **10a**, only the singlet is observed for the imine hydrogen at 8.85

ppm and 161.5 ppm in the ^{1}H and ^{13}C NMR spectra respectively. A singlet for the CH_3 group of the ketone appears as a singlet at 3.18 ppm and 27.9 ppm for the ^{1}H and ^{13}C NMR spectra in that order. The quaternary carbon signal for C5 is observed at 58.3 ppm, as well as a quaternary carbon signal at 203.7 ppm, which again confirms the presence of a carbonyl and is again supported by the IR spectrum with the C=O stretch being observed at 1717 cm^{-1}.

4.3 RESULTS AND DISCUSSION (FLUORESCENCE SPECTROSCOPY).

Refer to Chapter 2, Section 2.2 for experimental procedures.

Refer to Appendix of Results 1.1, 1.2, 1.3 and 1.4 for complete set of solvatochromic results, tables and graphs.

4.3.1 Steady state fluorescence study.

The initial published fluorescence study of the 1,2,3-triazine fluorophores was very cursory and restricted to the emission properties in two solvents, toluene and methanol and the precise photophysical mechanism of emission was not elucidated.[54]

Therefore, a detailed steady state solvatochromism study was undertaken for the 2,5-dihydro-1,2,3-triazines with substituted aryl groups (**3a**, **6a**, **9a** and **10a**). For this, a selection of 24 solvents were chosen; varying from protic to aprotic and across a significant range of $E_T(30)$ values of solvent polarity (Refer to Appendix A.2 for list of solvents and solvatochromic values).

Following collection of the data, analysis against normalized solvent polarity (E_T^N), solvent hydrogen bonding donating/accepting ability (α and β), solvent polarizability (π^*), viscosity (η(Cp)) and dipole moment (μ) was performed for each fluorophore using the software package Origin 7.0.

The aim of the study was to identify any possible ground state solvent interactions which may influence their fluorescent behavior, and to investigate if these fluorophores displayed any sensitivity toward the nature of the solvent and their environment.

4.3.1.1 Ultraviolet Visible Absorption Spectra.

The UV-visible spectra of the compounds (**3a**, **6a**, **9a** and **10a**) show two major absoprtion bands (~310 and ~400 nm) which are not strongly effected by changing the nature of the solvent, meaning there is very little solvent-ground state interaction (Figures 4.3.3). This is also evident when examining the λ_{abs} maximum values for both bands of **3a** (Table 4.1) and is supported by the normalized UV-visible spectra where only small changes are observed in the band positions (Figures 4.3.4).

Solvent	Code	X	Y	Band 1 λ_{abs}max (nm)	Band 2 λ_{abs}max (nm)
Toluene	**3a**	H	OMe	312	385
1,4-Dioxane	**3a**	H	OMe	309.5	379
Ethyl acetate	**3a**	H	OMe	308	380.5
Chloroform	**3a**	H	OMe	311.5	388.5
2-Methyl-2-butanol	**3a**	H	OMe	308.5	377
N,N-dimethylformamide	**3a**	H	OMe	309	384.5
Acetonitrile	**3a**	H	OMe	307	374.5
Propylene carbonate	**3a**	H	OMe	308	381
1-Octanol	**3a**	H	OMe	309.5	387
1-Hexanol	**3a**	H	OMe	309.5	388
1-Butanol	**3a**	H	OMe	310	380.5
1-Pentanol	**3a**	H	OMe	311	391
1-Propanol	**3a**	H	OMe	308.5	386.5
Acetic acid	**3a**	H	OMe	307	388
Ethanol	**3a**	H	OMe	306.5	376.5
1,5-Pentanediol	**3a**	H	OMe	312.5	391.5
1,3-Butanediol	**3a**	H	OMe	307	391.5
1,4-Butanediol	**3a**	H	OMe	308.5	379.5
1,3-Propanediol	**3a**	H	OMe	309.5	391
Methanol	**3a**	H	OMe	306.5	386.5
1,2-Ethanediol	**3a**	H	OMe	308	387
2,2,2-Trifluoroethanol	**3a**	H	OMe	300.5	375
d-Ethanol	**3a**	H	OMe	307	385.5
d-Methanol	**3a**	H	OMe	306.5	385.5

Table 4.1. λ_{abs} maximum values for the UV absorption bands of **3a**.

This is in contrast to reported unsubstituted 1,2,3-triazines where extensive hydrogen bonding to the nitrogen atoms is observed (Figure 4.3.1). For unsubstituted 1,2,3-triazines, the N atoms can interact strongly with solvent molecules *via* hydrogen bonding leading to significant changes in absorption spectra.[50, 76]

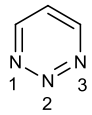

Figure 4.3.1. Unsubstituted 1,2,3-triazine.

The lack of hydrogen bonding in the ground state is confirmed by the fact that the absorption spectrum of **3a** is the same in methanol-d as it is for methanol (Figure 4.3.2).

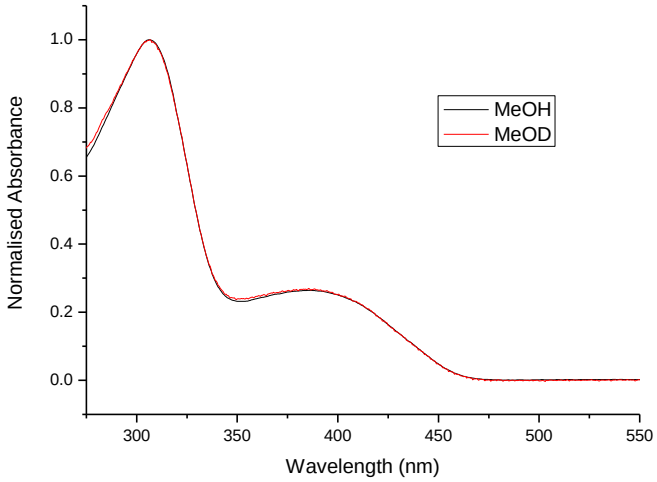

Figure 4.3.2. Normalised ultraviolet visible absorption spectra of **3a** in methanol and methanol-d.

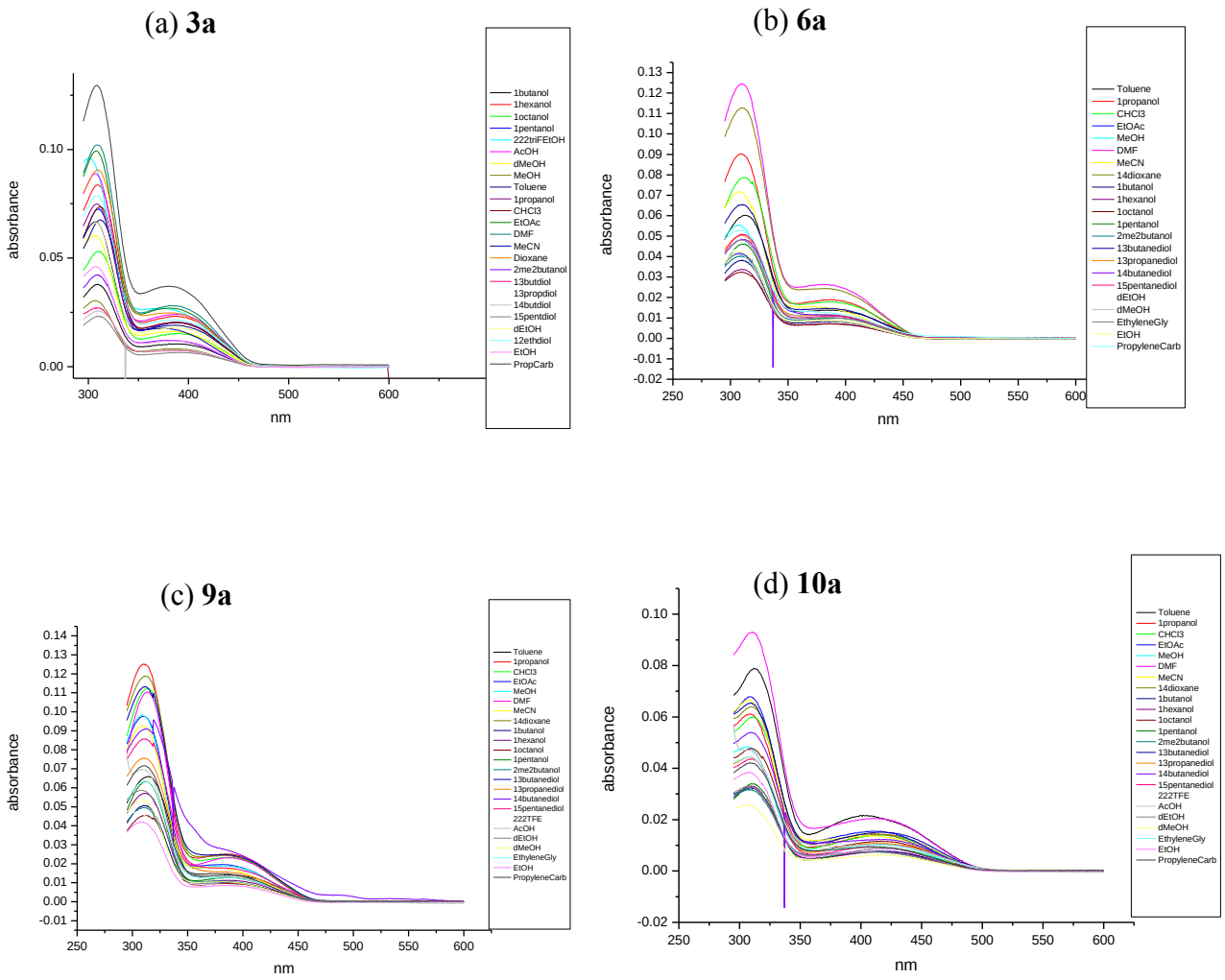

Figure 4.3.3. Ultraviolet visible absorption spectra for the 2,5-dihydro-1,2,3-triazines with substituted aryl groups (**3a**, **6a**, **9a** and **10a**) recorded at an assumed maximum concentration of 1 x 10^{-5} M.

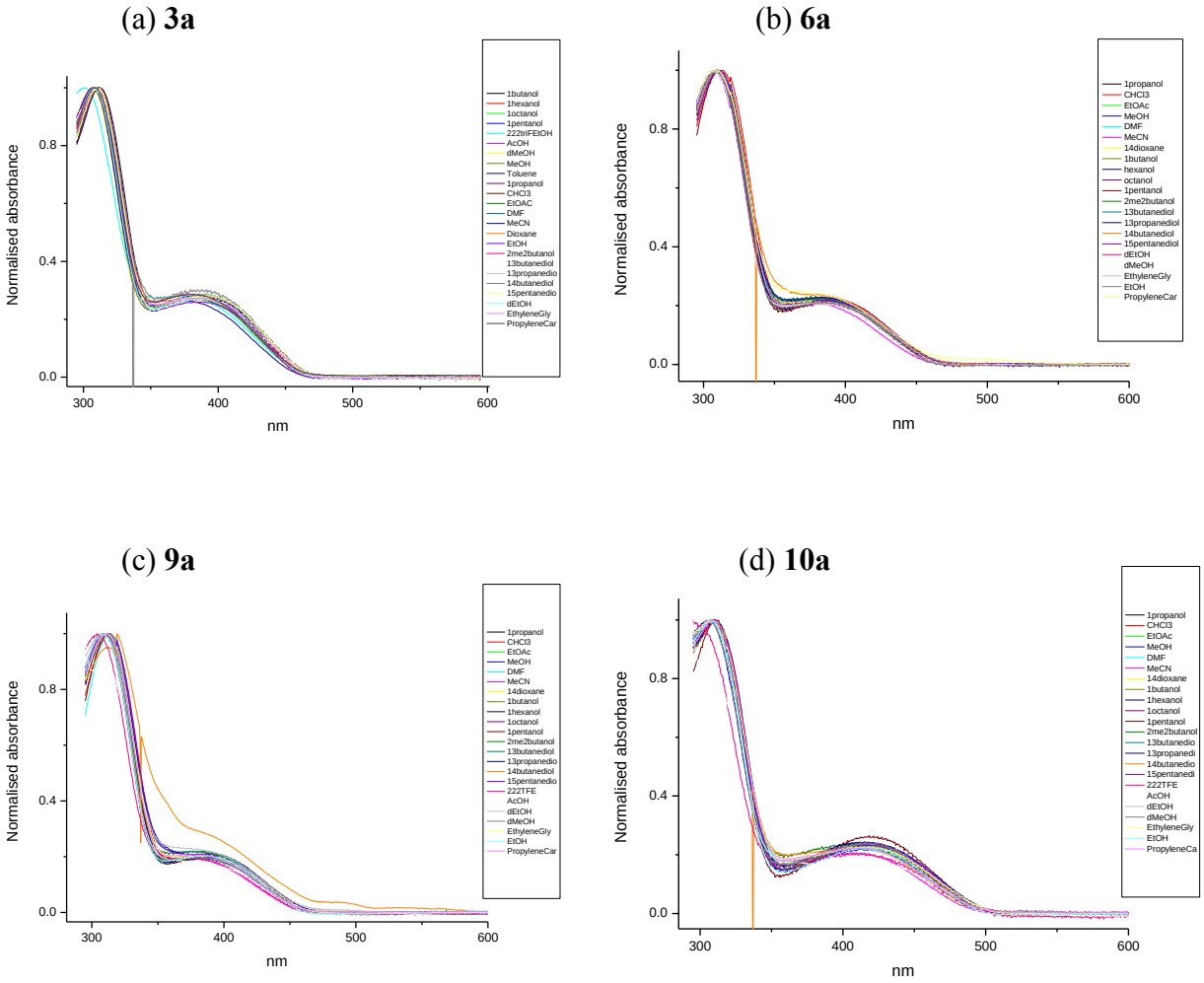

Figure 4.3.4. Normalised ultraviolet visible absorption spectra for the 2,5-dihydro-1,2,3-triazines with substituted aryl groups (**3a**, **6a**, **9a** and **10a**).

4.3.1.2 Fluorescence Emission Spectra.

For the 2,5-dihydro-1,2,3-triazines with substituted aryl groups (**3a**, **6a**, **9a** and **10a**) excitation into either of the absorption bands (310 or 400 nm) generates a complicated, green fluorescence emission band centered at ~520 nm. This emission band appears to be only effected slightly by changing the nature of the solvent (Figures 4.3.6 and 4.3.7). This is supported by the fact that very small solvatochromism is observed in the position of the emission band maximum when observing the normalised fluorescence spectra (Figure 4.3.8 and 4.3.9). The deconvoluted emission spectra for 400 nm excitation consists of three separate emission bands: ~470 nm (Band 3), ~510 nm (Band 2), and ~540 nm (Band 1). The nature of these three emission bands has been discussed in Chapter 3 (Figure 4.3.5). Excitation at 310 nm generates the same three bands (Band 1, 2 and 3) and a weak emission centered at ~350 nm (Figure 4.3.9). The weak emission at 350nm consists of two separate emission bands: ~380nm (Band 4) and ~350 nm (Band 5) due to the population of the S_3 (**g0**) and S_2 (**g0**) ES and seems to only be evident in the long chain diol solvents (*e.g.* 1,4-butanediol, Figure 4.3.5 and 4.3.6).

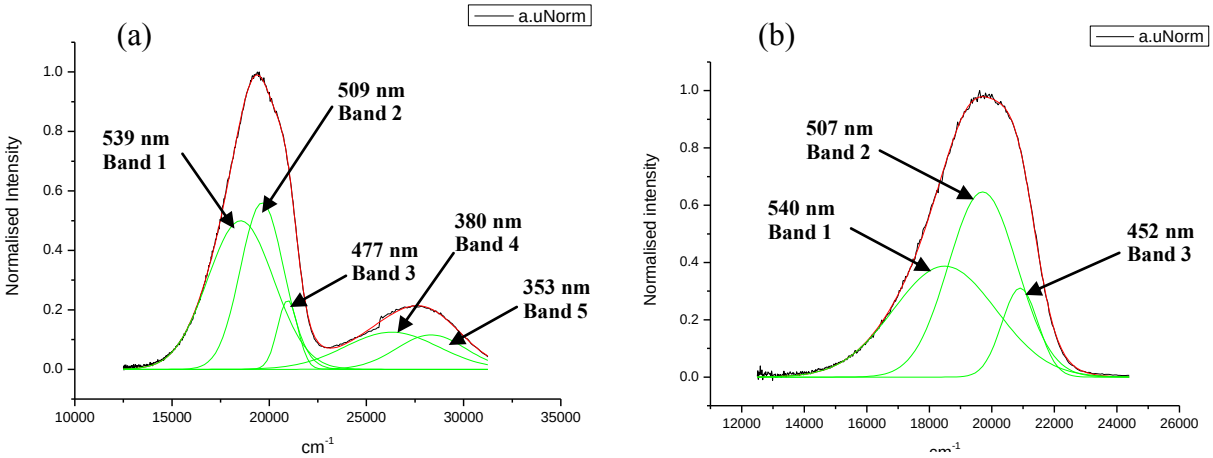

Figure 4.3.5. Gaussian model fits of the normalised fluorescence emission spectrum of **3a** recorded in 1,4-butanediol for (a) 310 nm and (b) 400 nm excitation.

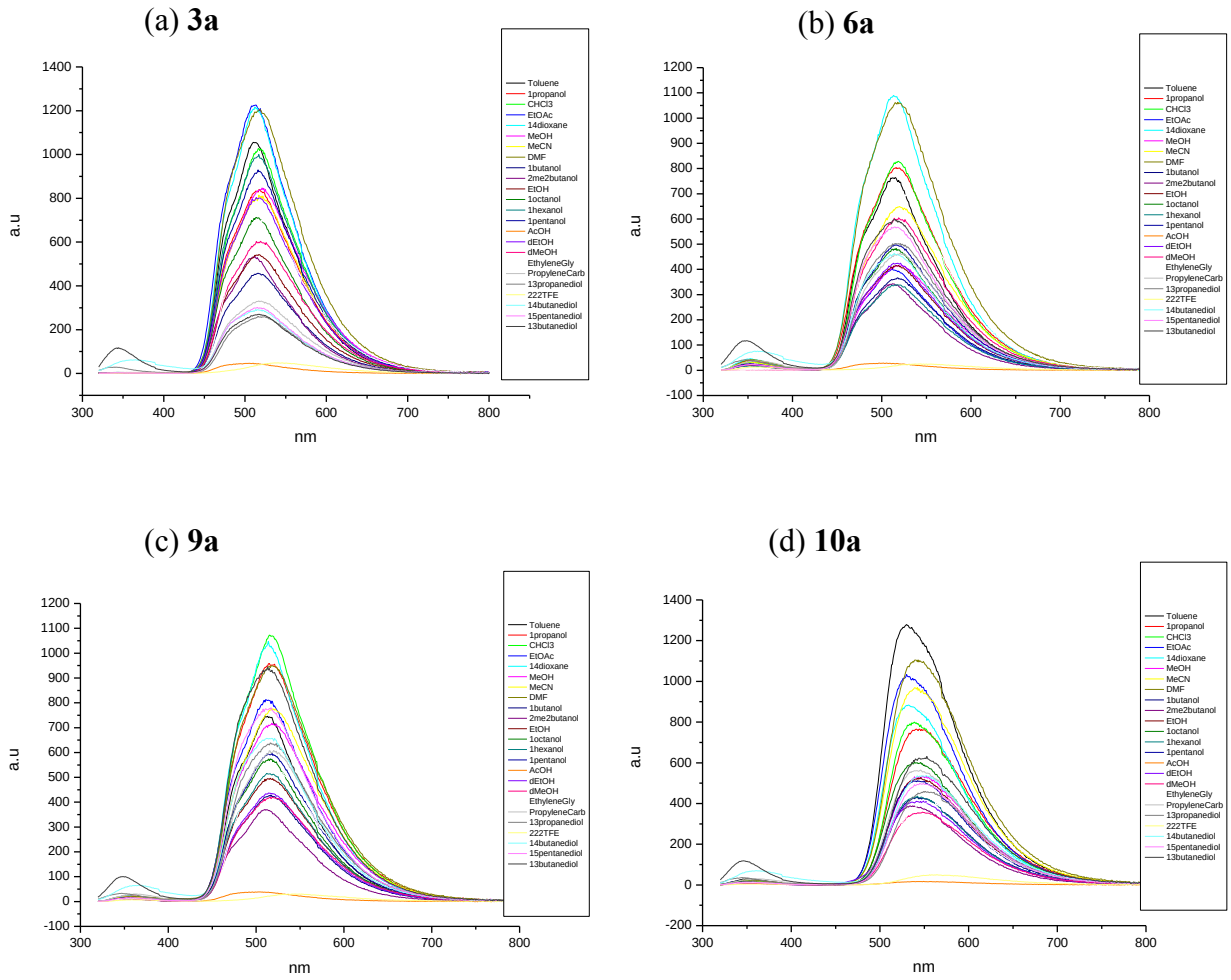

Figure 4.3.6. Summary of fluorescent emission spectra at 310 nm excitation for the 2,5-dihydro-1,2,3-triazines with substituted aryl groups (**3a**, **6a**, **9a** and **10a**) recorded at an assumed maximum concentration of 1 x 10^{-5} M.

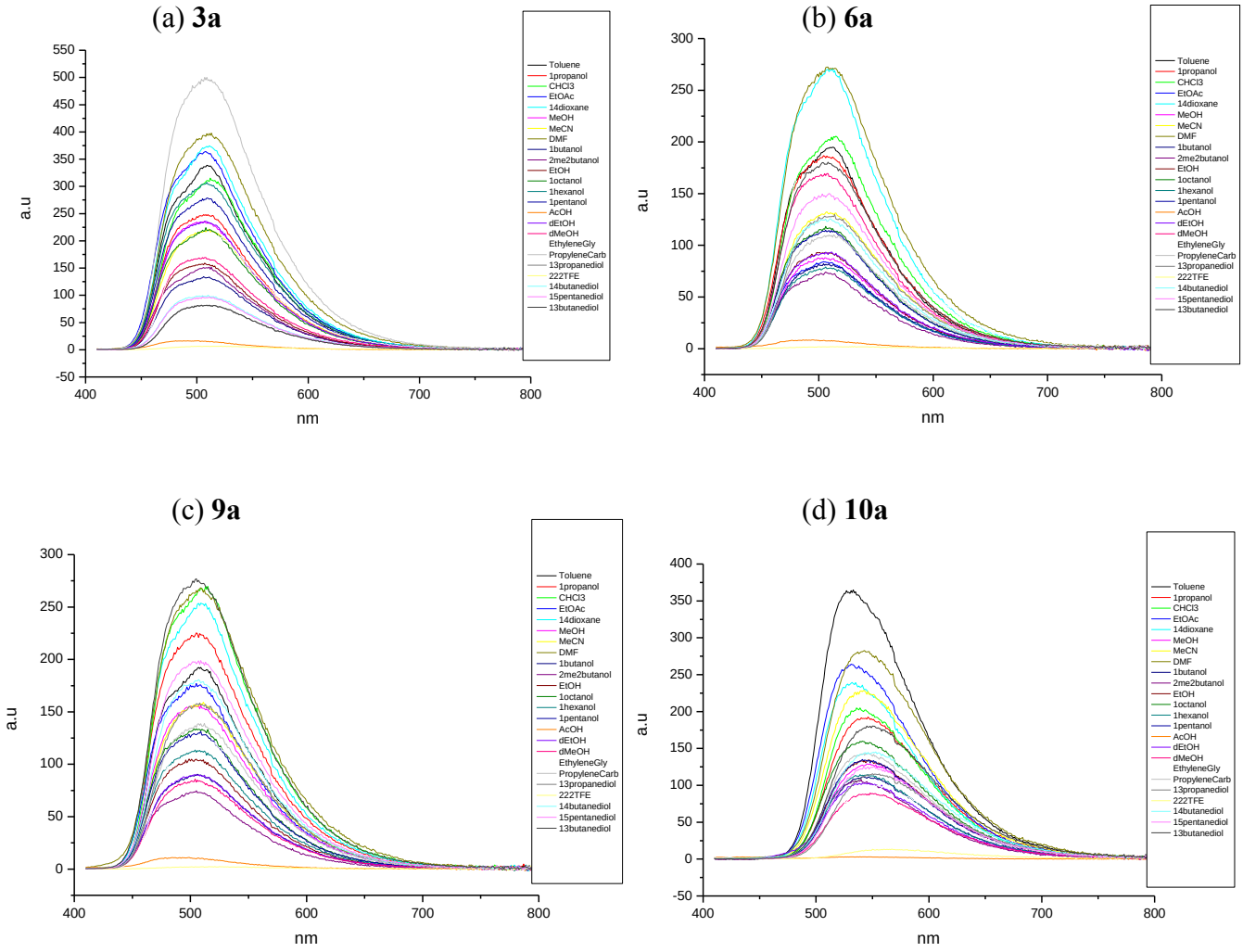

Figure 4.3.7. Summary of fluorescent emission spectra at 400 nm excitation for the 2,5-dihydro-1,2,3-triazines with substituted aryl groups (**3a**, **6a**, **9a** and **10a**) recorded at an assumed maximum concentration of 1 x 10^{-5} M.

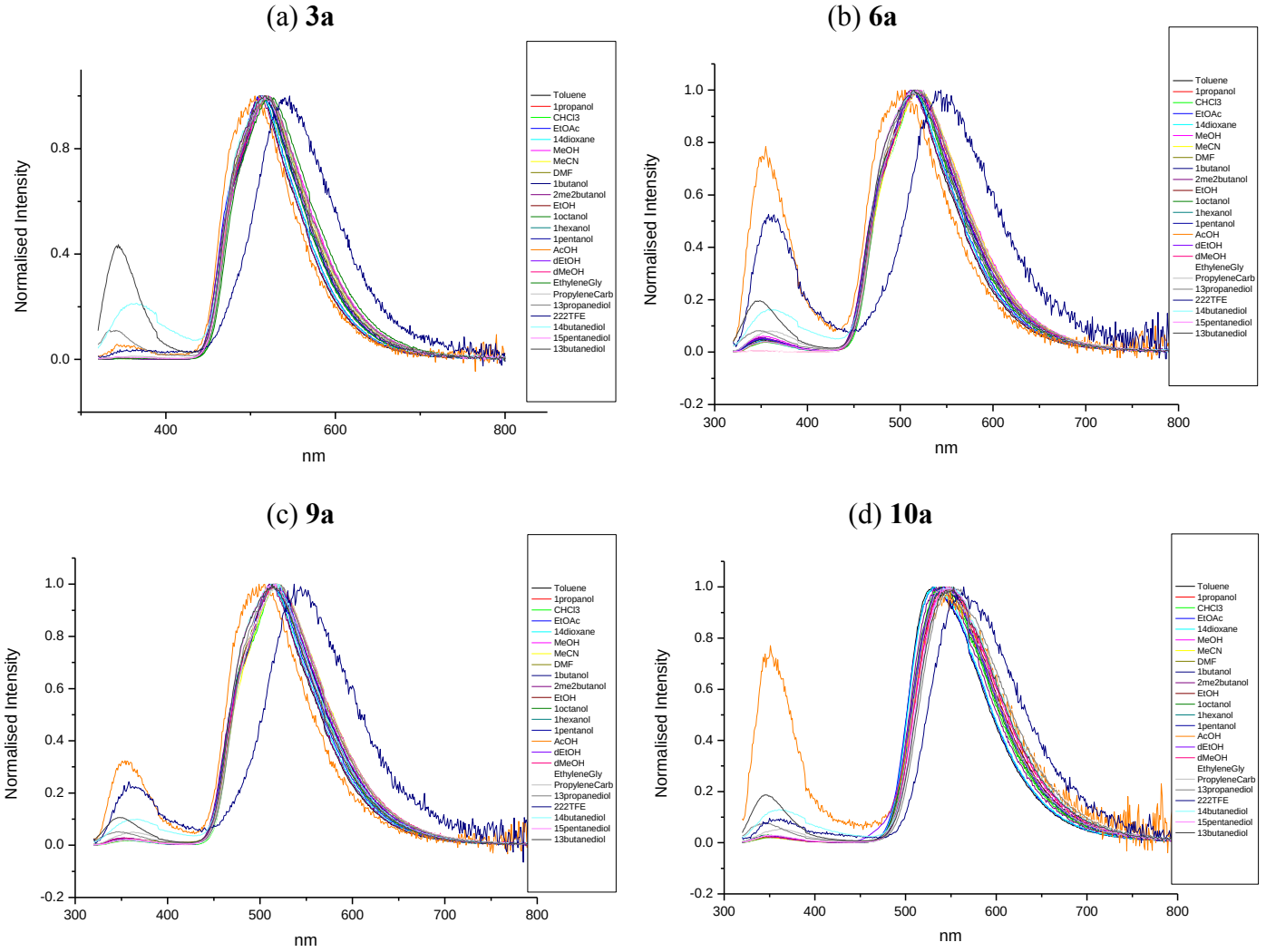

Figure 4.3.8. Summary of normalized fluorescent emission spectra at 310 nm excitation for the 2,5-dihydro-1,2,3-triazines with substituted aryl groups (**3a**, **6a**, **9a** and **10a**)

.

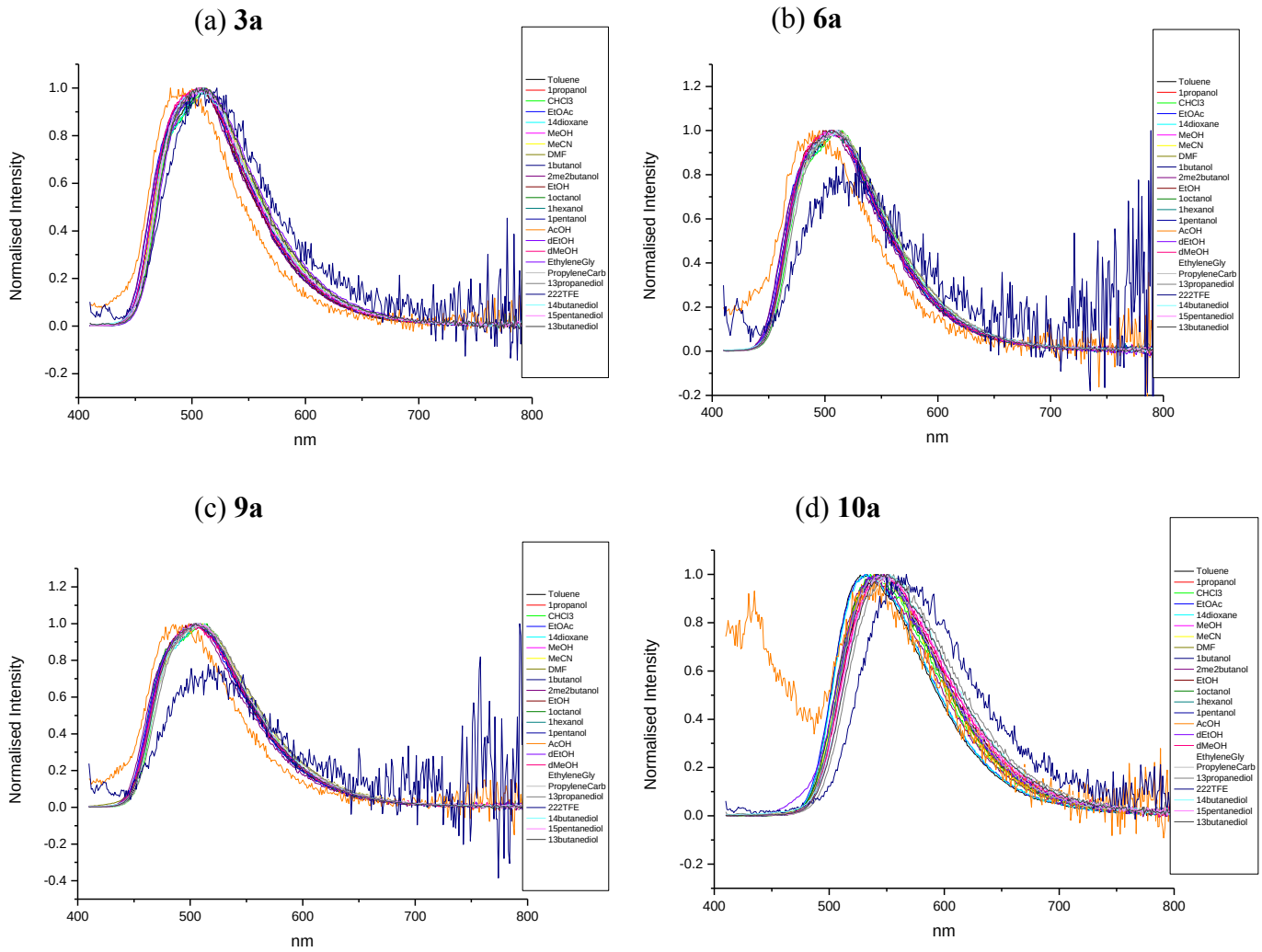

Figure 4.3.9. Summary of normalized fluorescent emission spectra at 400 nm excitation for the 2,5-dihydro-1,2,3-triazines with substituted aryl groups (**3a**, **6a**, **9a** and **10a**).

An extensive range of solvents were investigated but only small solvatochromic trends were observed. As a result, it is more informative to compare the minimum and maximum values for each compound, regardless of solvent. Hence, the solvent will vary in the following tables. For a full summary of all results and solvatochromic values refer to Appendix of Results, 1.1, 1.2, 1.3 and 1.4.

The observed emission peak maximum at 310 nm excitation (Table 4.2 (a)) ranges from 520 nm (**9a** in propylene carbonate), 521 nm (**6a** in ethylene glycol), 525 nm (**3a** in ethylene glycol) to 555 nm (**10a** in ethylene glycol). The observed emission peak maximum at 400 nm excitation (Table 4.2 (b)) ranges from 513 nm (**3a** in N,N-dimethylformamide), 515 nm (**9a** in chloroform), 521 nm (**6a** in propylene carbonate) to 555 nm (**10a** in ethylene glycol).

(a)

Code	X	Y	Solvent	$\lambda_{310\ nm\ ems}$ (min)
3a	H	OCH_3	Toluene	510
6a	Cl	OCH_3	Ethyl Acetate	511
9a	Br	OCH_3	Toluene	510
10a	H	CH_3	2-Methyl-2-butanol	537

Solvent	$\lambda_{310\ nm\ ems}$ (max)
Ethylene Glycol	525
Ethylene Glycol	521
Propylene Carbonate	520
Ethylene Glycol	555

(b)

Code	X	Y	Solvent	$\lambda_{400\ nm\ ems}$ (min)
3a	H	OCH_3	Methanol	504
6a	Cl	OCH_3	Ethanol	498
9a	Br	OCH_3	1-Octanol	503
10a	H	CH_3	Ethyl Acetate	531

Solvent	$\lambda_{400\ nm\ ems}$ (max)
N,N-dimethylformamide	513
Propylene Carbonate	521
Chloroform	515
Ethylene Glycol	555

Table 4.2. Summary of (a) observed emission peak maximum for 310 nm excitation (minimum and maximum value) of **3a**, **6a**, **9a** and **10a** and (b) emission band maximum for 400 nm excitation (minimum and maximum value) of **3a**, **6a**, **9a** and **10a**.

In general, the calculated quantum yields for **3a**, **6a**, **9a** and **10a** range from moderate to high (Figure 4.3.10). For 310 nm excitation, the maximum quantum yield for **3a, 6a**, **9a** and **10a** were calculated to be 0.76 in toluene, 0.75 in ethylene glycol, 0.61 in 1-octanol and 0.83 in toluene respectively (Table 4.3 (a)). Similarly the maximum quantum

yield for **3a, 6a**, **9a** and **10a** for 400 nm excitation, was calculated to be 0.79 in toluene, 0.93 in ethylene glycol, 0.63 in toluene and 0.75 in toluene (Table 4.3 (b)).

(a)

Code	X	Y	Solvent	$\Phi_{310\ nm\ ems}$ (min)
3a	H	OCH_3	Propylene Carbonate	0.13
6a	Cl	OCH_3	Methanol	0.35
9a	Br	OCH_3	Methanol	0.33
10a	H	CH_3	Ethylene Glycol	0.48

Solvent	$\Phi_{310\ nm\ ems}$ (max)
Toluene	0.76
Ethylene Glycol	0.75
1-Octanol	0.61
Toluene	0.83

(b)

Code	X	Y	Solvent	$\Phi_{400\ nm\ ems}$ (min)
3a	H	OCH_3	Methanol	0.32
6a	Cl	OCH_3	Methanol	0.3
9a	Br	OCH_3	Ethanol-d	0.28
10a	H	CH_3	Ethylene Glycol	0.47

Solvent	$\Phi_{400\ nm\ ems}$ (max)
Toluene	0.79
Ethylene Glycol	0.93
Toluene	0.63
Toluene	0.75

Table 4.3. Summary of (a) minimum and maximum quantum yield (**Φ**) values for **3a**, **6a**, **9a** and **10a** at 310 nm excitation and (b) minimum and maximum quantum yield (**Φ**) values for **3a**, **6a**, **9a** and **10a** at 400 nm excitation.

However there are two exceptions; acetic acid and 2,2,2-trifluoroethanol, both of which dramatically quench the fluorescence intensity as well as attribute to very low quantum yields for all compounds (Figure 4.3.10). It is thought a possible reason for this is hydrogen bonding of 2,2,2-trifluoroethanol (α value of 1.51) and acetic acid (α value of 1.12) to the triazine nitrogens, the imine nitrogen or the carbonyl oxygen, which could effect the imine and carbonyl interaction. Acetic acid, with a pKa of 4.75, may be involved in the protonation or partial protonation of the carbonyl or imine and again may effect the imine-carbonyl interaction. In light of this, a fully study is yet to be performed to support this hypothesis.

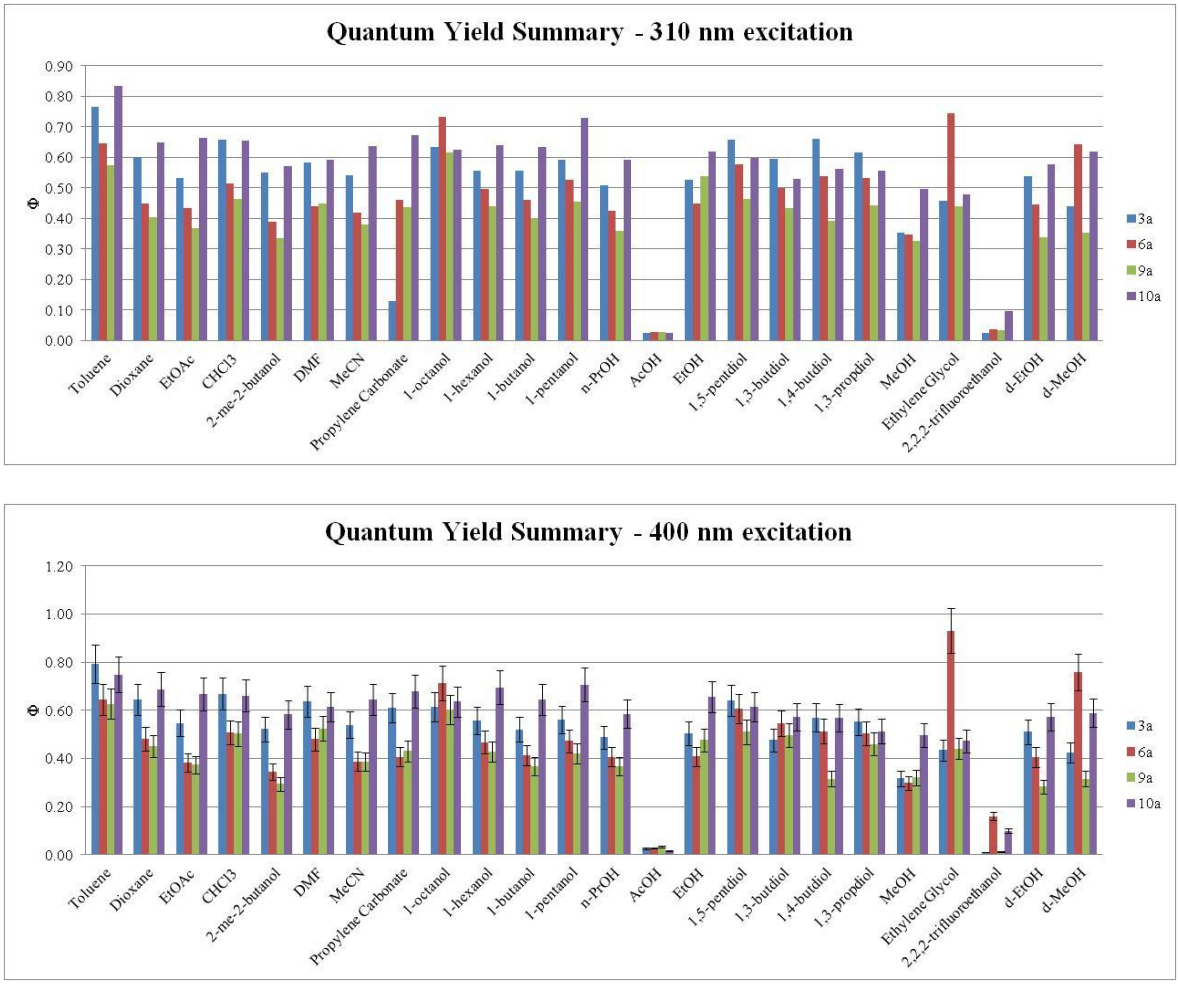

Figure 4.3.10. Graphical summary of quantum yield (**Φ**) values for **3a**, **6a**, **9a** and **10a**.

From Table 4.1 and 4.2, it is evident that a marked difference in emission can be observed by changing the carbonyl to a ketone (**10a**) rather than a methyl ester (**3a**, **6a** and **9a**). The quantum yield is generally larger for both 310 and 400 nm excitation (Table 4.3) and a significant red-shift in the emission peak maximum is observed (Table 4.2). These effects may be a resultant of the change in electron density at the carbonyl group. Computational calculations comparing the dipole moment of ketones to esters suggest there is a considerable difference in electron density and dipole moment (for further discussion see Chapter 7, Section 7.3.1.2).

For **3a**, the emission peak maximum for excitation at 310 nm has a maximum value in ethylene glycol at 525 nm whilst for **10a**, a 30 nm red shift in the emission peak maximum value is observed at 555 nm in ethylene glycol.

An even larger red-shift of 42 nm is observed for 400 nm excitation, where the emission peak maximum has a maximum value for **3a** is 513 nm in N,N-dimethylformamide, whilst for **10a** the value is 555 nm in ethylene glycol (Table 4.2).

For the 4-Cl and 4-Br triazine derivatives (**6a** and **9a**), the emission properties are virtually identical to the parent triazine **3a** and the relative intensities and areas of the three fitted emission bands do not change significantly between the three different molecules (Tables 4.4, 4.5, 4.6 and 4.7). There is a slight decrease in quantum yield (Table 4.3). However, this decrease in quantum yield is not so large as to preclude the use of these substituted triazine derivatives. This suggests that substitution at the 4-position of the imine phenyl and N2 phenyl rings with heavy atoms which originate from the 4-substitued arylhydrazines (*e.g.* 4-chlorophenylhydrazine) at the start of the synthesis, has very little effect on the molecule's energy levels. It also suggests that the heavy atom effect (*e.g.* spin-orbit coupling and, or intersystem crossing to the triplet state) is small as either (i) the de-excitation by fluorescence emission of these fluorophores dominates all other de-excitation processes or (ii) there is no triplet state energetically close to any of the fluorescing states.[2]

Analysis against normalized solvent polarity (E_T^N), solvent hydrogen bonding donating/accepting ability (α and β), solvent polarizability (π^*), viscosity (η(Cp)) and dipole moment (μ) was performed for each fluorophore. However, the solvatochromic analysis of all components (band position, area percentage of band to overall fit, band width, area ratios and band fwhm) of the deconvoluted spectra of the compounds revealed that the distribution of the data was fairly random (Appendix of Results, 1.1, 1.2, 1.3 and 1.4).

Table 4.4 shows the minimum and maximum values of the Gaussian band positions of the deconvoluted 310 nm excitation spectra (Figure 4.3.5) and Table 4.5 lists the minimum and maximum percentage area values. Tables 4.6 shows the minimum and maximum values of the Gaussian band positions of the deconvoluted 400 nm excitation spectra and Table 4.7 lists the minimum and maximum percentage areas.

Code	X	Y	Solvent	$\lambda_{310\ nm\ ems}$ Band 1 (nm) (min)
3a	H	OCH_3	2-Methyl-2-butnaol	533
6a	Cl	OCH_3	2-Methyl-2-butanol	534
9a	Br	OCH_3	2-Methyl-2-butanol	533
10a	H	CH_3	Toluene	582

X	Y	Solvent	$\lambda_{310\ nm\ ems}$ Band 1 (nm) (max)
H	OCH_3	Ethylene Glycol	554
Cl	OCH_3	Acetonitrile	550
Br	OCH_3	Ethylene Glycol	552
H	CH_3	Ethylene Glycol	609

Code	X	Y	Solvent	$\lambda_{310\ nm\ ems}$ Band 2 (nm) (min)
3a	H	OCH_3	2-Methyl-2-butanol	503
6a	Cl	OCH_3	2-Methyl-2-butanol	505
9a	Br	OCH_3	2-Methyl-2-butanol	504
10a	H	CH_3	Toluene	545

X	Y	Solvent	$\lambda_{310\ nm\ ems}$ Band 2 (nm) (max)
H	OCH_3	Ethylene Glycol	515
Cl	OCH_3	Ethylene Glycol	515
Br	OCH_3	Ethylene Glycol	513
H	CH_3	Ethylene Glycol	567

Code	X	Y	Solvent	$\lambda_{310\ nm\ ems}$ Band 3 (nm) (min)
3a	H	OCH_3	2-Methyl-2-butanol	468
6a	Cl	OCH_3	2-Methyl-2-butanol	468
9a	Br	OCH_3	2-Methyl-2-butanol	467
10a	H	CH_3	Toluene	515

X	Y	Solvent	$\lambda_{310\ nm\ ems}$ Band 3 (nm) (max)
H	OCH_3	Ethylene Glycol	479
Cl	OCH_3	Ethylene Glycol	479
Br	OCH_3	Ethylene Glycol	478
H	CH_3	Ethylene Glycol	531

Code	X	Y	Solvent	$\lambda_{310\ nm\ ems}$ Band 4 (nm) (min)
3a	H	OCH_3	1,3-Propanediol	344
6a	Cl	OCH_3	1,3-Propanediol	350
9a	Br	OCH_3	1,3-Propanediol	350
10a	H	CH_3	1,3-Propanediol	346

X	Y	Solvent	$\lambda_{310\ nm\ ems}$ Band 4 (nm) (max)
H	OCH_3	1,4-Butanediol	380
Cl	OCH_3	1,4-Butanediol	391
Br	OCH_3	1,3-Butanediol	374
H	CH_3	1,4-Butanediol	421

Code	X	Y	Solvent	$\lambda_{310\ nm\ ems}$ Band 5 (nm) (min)
3a	H	OCH_3	1,3-Propanediol	338
6a	Cl	OCH_3	1,3-Butanediol	343
9a	Br	OCH_3	-	-
10a	H	CH_3	1,3-Butanediol	346

X	Y	Solvent	$\lambda_{310\ nm\ ems}$ Band 5 (nm) (max)
H	OCH_3	1,4-Butanediol	353
Cl	OCH_3	1,4-Butanediol	354
Br	OCH_3	1,3-Butanediol	346
H	CH_3	1,4-Butanediol	360

Table 4.4. Summary of Guassian band maximum positions from deconvoluted spectra (minimum and maximum values) for **3a**, **6a**, **9a** and **10a** at 310 nm excitation.

Code	X	Y	Solvent	$\lambda_{310\ nm\ ems}$ Band 1 Area % (min)
3a	H	OCH_3	1,3-Butanediol	36.3
6a	Cl	OCH_3	1,3-Butanediol	39.37
9a	Br	OCH_3	1,3-Butanediol	41
10a	H	CH_3	1,3-Butanediol	23.58

X	Y	Solvent	$\lambda_{310\ nm\ ems}$ Band 1 Area % (max)
H	OCH_3	2-Methyl-2-butanol	59.26
Cl	OCH_3	2-Methyl-2-butanol	55.23
Br	OCH_3	2-Methyl-2-butanol	58
H	CH_3	1,4-Dioxane	35.15

Code	X	Y	Solvent	$\lambda_{310\ nm\ ems}$ Band 2 Area % (min)
3a	H	OCH_3	1,3-Butanediol	27.33
6a	Cl	OCH_3	2-Methyl-2-butanol	32.75
9a	Br	OCH_3	2-Methyl-2-butanol	31.49
10a	H	CH_3	Acetonitrile	46.11

X	Y	Solvent	$\lambda_{310\ nm\ ems}$ Band 2 Area % (max)
H	OCH_3	Acetonitrile	46.43
Cl	OCH_3	Ethylene Glycol	45.27
Br	OCH_3	Acetonitrile	45.74
H	CH_3	1,3-Butanediol	58.86

Code	X	Y	Solvent	$\lambda_{310\ nm\ ems}$ Band 3 Area % (min)
3a	H	OCH_3	1,3-Butanediol	5.49
6a	Cl	OCH_3	Methanol	6.15
9a	Br	OCH_3	Acetonitrile	6.26
10a	H	CH_3	1,4-Dioxane	17.79

X	Y	Solvent	$\lambda_{310\ nm\ ems}$ Band 3 Area % (max)
H	OCH_3	1,5-Pentanediol	8.36
Cl	OCH_3	1,5-Pentanediol	8.7
Br	OCH_3	Chloroform	9.22
H	CH_3	Ethylene Glycol	22.04

Code	X	Y	Solvent	$\lambda_{310\ nm}$ Band 4 Area % (min)
3a	H	OCH_3	1,3-Propanediol	8.31
6a	Cl	OCH_3	N,N-dimethylformamide	3.66
9a	Br	OCH_3	Chloroform	1.17
10a	H	CH_3	Acetonitrile	2.38

X	Y	Solvent	$\lambda_{310\ nm}$ Band 4 Area % (max)
H	OCH_3	1,3-Butanediol	15.14
Cl	OCH_3	1,3-Propanediol	8.6
Br	OCH_3	1,4-Butanediol	11.38
H	CH_3	1,3-Propanediol	9.44

Code	X	Y	Solvent	$\lambda_{310\ nm\ ems}$ Band 5 Area % (min)
3a	H	OCH_3	1,3-Propanediol	3.52
6a	Cl	OCH_3	1,3-Butanediol	9.05
9a	Br	OCH_3	-	-
10a	H	CH_3	1,3-Butanediol	13.63

X	Y	Solvent	$\lambda_{310\ nm\ ems}$ Band 5 Area % (max)
H	OCH_3	1,3-Butanediol	15.72
Cl	OCH_3	1,4-Butanediol	10.99
Br	OCH_3	1,3-Butanediol	6.96
H	CH_3	1,4-Butanediol	13.86

Table 4.5. Summary of area percentages for Gaussian band fits (minimum and maximum values) for **3a**, **6a**, **9a** and **10a** at 310 nm excitation.

Code	X	Y	Solvent	$\lambda_{400\ nm\ ems}$ Band 1 (nm) (min)
3a	H	OCH_3	Toluene	524
6a	Cl	OCH_3	2-Methyl-2-butanol	535
9a	Br	OCH_3	2-Methyl-2-butanol	533
10a	H	CH_3	1,4-Dioxane	582

X	Y	Solvent	$\lambda_{400\ nm\ ems}$ Band 1 (nm) (max)
H	OCH_3	Ethylene Glycol	548
Cl	OCH_3	Ethylene Glycol	548
Br	OCH_3	Ethylene Glycol	548
H	CH_3	1,3-Propanediol	610

Code	X	Y	Solvent	$\lambda_{400\ nm\ ems}$ Band 2 (nm) (min)
3a	H	OCH_3	2-Methyl-2-butanol	500
6a	Cl	OCH_3	2-Methyl-2-butanol	500
9a	Br	OCH_3	2-Methyl-2-butanol	499
10a	H	CH_3	Toluene	545

X	Y	Solvent	$\lambda_{400\ nm\ ems}$ Band 2 (nm) (max)
H	OCH_3	Ethylene Glycol	510
Cl	OCH_3	Ethylene Glycol	510
Br	OCH_3	Ethylene Glycol	510
H	CH_3	Ethylene Glycol	567

Code	X	Y	Solvent	$\lambda_{400\ nm\ ems}$ Band 3 (nm) (min)
3a	H	OCH_3	2-Methyl-2-butanol	469
6a	Cl	OCH_3	2-Methyl-2-butanol	468
9a	Br	OCH_3	Ethyl Acetate	470
10a	H	CH_3	Ethyl Acetate	515

X	Y	Solvent	$\lambda_{400\ nm\ ems}$ Band 3 (nm) (max)
H	OCH_3	Ethylene Glycol	480
Cl	OCH_3	Ethylene Glycol	480
Br	OCH_3	Ethylene Glycol	479
H	CH_3	Ethylene Glycol	532

Table 4.6. Summary of Guassian band maximum positions from deconvoluted spectra (minimum and maximum values) for **3a**, **6a**, **9a** and **10a** at 400 nm excitation.

Code	X	Y	Solvent	$\lambda_{400\ nm\ ems}$ Band 1 Area % (min)
3a	H	OCH_3	Methanol	40.67
6a	Cl	OCH_3	1,5-Pentanediol	36.26
9a	Br	OCH_3	Methanol	37.8
10a	H	CH_3	1-Propanol	22.06

X	Y	Solvent	$\lambda_{400\ nm\ ems}$ Band 1 Area % (max)
H	OCH_3	Toluene	50.7
Cl	OCH_3	Toluene	48
Br	OCH_3	N,N-dimethylformamide	45.93
H	CH_3	1,4-Butanediol	43.07

Code	X	Y	Solvent	$\lambda_{400\ nm\ ems}$ Band 2 Area % (min)
3a	H	OCH_3	Toluene	38.89
6a	Cl	OCH_3	Toluene	40.27
9a	Br	OCH_3	2-Methyl-2-butanol	44.33
10a	H	CH_3	1,4-Butanediol	38.92

X	Y	Solvent	$\lambda_{400\ nm\ ems}$ Band 2 Area % (max)
H	OCH_3	Acetonitrile	46.85
Cl	OCH_3	1,5-Pentanediol	51.42
Br	OCH_3	Methanol	48.39
H	CH_3	Methanol	51.61

Code	X	Y	Solvent	$\lambda_{400\ nm\ ems}$ Band 3 Area % (min)
3a	H	OCH_3	1,4-Dioxane	9.42
6a	Cl	OCH_3	2-Methyl-2-butanol	9.55
9a	Br	OCH_3	N,N-dimethylformamide	9.27
10a	H	CH_3	1,4-Butanediol	17.99

X	Y	Solvent	$\lambda_{400\ nm\ ems}$ Band 3 Area % (max)
H	OCH_3	Ethylene Glycol	12.67
Cl	OCH_3	Methanol	13.65
Br	OCH_3	Methanol	13.8
H	CH_3	1-Propanol	26.31

Table 4.7. Summary of area percentages for Gaussian band fits (minimum and maximum values) for **3a**, **6a**, **9a** and **10a** at 400 nm excitation.

The only significant difference is observed in the position of the bands and area percentage contribution when the methyl ester triazines **3a**, **6a**, **9a**, are compared to the ketone substituted triazine **10a**.

For example at 310 nm excitation, **3a** has a maximum value of 554 nm in ethylene glycol for Band 1 whilst for **10a** the value is significantly redshifted at a maximum of 609 nm in ethylene glycol. The maximum percentage contribution Band 1 has to the fit is 59.26 % in 2-methyl-2-butanol for **3a**, whilst it is much lower in **10a** at 35.15 % in 1,4-dioxane. For Band 3, **3a** has a maximum value of 479 nm in ethylene glycol whilst for **10a** the value is again redshifted at a maximum at 531 nm in ethylene glycol. The maximum percentage contribution Band 3 has to the fit is now much lower at 8.36 % in 1,5-pentanediol for **3a**, whilst being much higher in **10a** at 22.04 % in ethylene glycol. This is also observed for 400 nm excitation (Table 4.7) where the maximum percentage contribution Band 3 has to

the fit is 12.67 % in ethylene glycol for **3a**, whilst being much higher in **10a** at 26.31 % in 1-propanol.

Therefore, according to the model (Chapter 3, Section 3.2.2.2), this increase in the area contribution of Band 3 from the presence of a ketone in **10a** compared to the methyl ester **3a**, causes an increased rate of IC from S_2 (**g0**) to S_1 (**g0**) for 310 nm excitation and an increased rate of S_1 (**g0**) emission for 400 nm excitation.

However, the analysis of the Gaussian model fit data show that the compounds only exhibit slight solvatochromic behaviour. A multiple linear regression analysis on **3a** (Table 4.8 and 4.9) against the solvatochromic values α, β and π* was performed. The emission peak maximum, Gaussian band positions, quantum yield and UV-visible absorbance were correlated against for both 310 and 400 nm excitation which showed no significant correlations (a linear correlation is supported when r^2 approaches unity *i.e.* 1).

Observing Table 4.7, a significant trend is observed between the calculated and the observed position of Band 4 (r^2 = 0.99). However, this band is only observed in 5 solvents that are very similar (acetic acid, 1,3-butanediol, 1,4-butanediol, 1,3-propanediol and 2,2,2-trifluoroethanol) and makes the correlation sample size very small, other parameters have a sample size of 24 solvents (Figure 4.3.11).

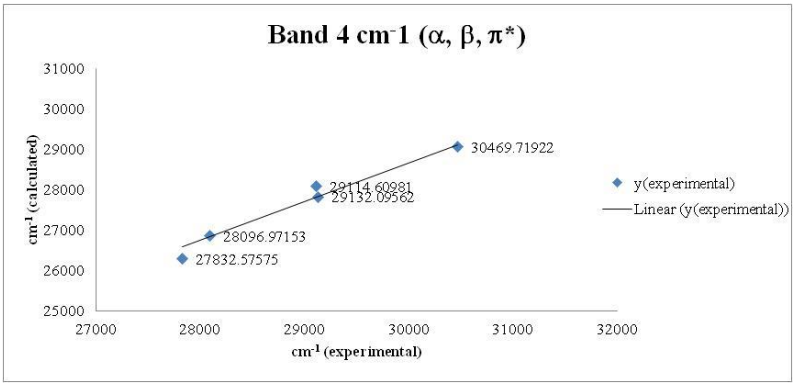

Figure 4.3.11. Linear regression analysis of the experimental position of Band 4 (cm^{-1}) versus the calculated position when correlated against α,β, and π*.

Y	y_o	a_α	b_β	c_{π^*}	r^2
$\lambda_{ems\ max\ (32258\ cm^{-1})}$	19504.26 ± 233.48	-315.64 ± 120.48	306.34 ± 185.68	-214.23 ± 289.54	**0.35**
Band 1 cm^{-1} (Gaussian Fit)	18858.78 ± 186.00	-176.56 ± 95.98	-54.95 ± 147.92	-523.73 ± 230.67	**0.34**
Band 2 cm^{-1} (Gaussian Fit)	19857.65 ± 202.35	-347.59 ± 104.42	348.84 ± 160.93	-380.65 ± 250.94	**0.50**
Band 3 cm^{-1} (Gaussian Fit)	21544.98 ± 62.16	-96.75 ± 40.77	-35.21 ± 61.27	-594.67 ± 75.86	**0.80**
Band 4 cm^{-1} (Gaussian Fit)	16666.25 ± 650.14	7166.03 ± 297.26	8639.10 ± 283.05	-835.61 ± 402.68	**0.99**
Band 5 cm^{-1} (Gaussian Fit)	-	-	-	-	-
Φ (32258 cm-1)	0.55 ± 0.17	-0.22 ± 0.09	0.24 ± 0.14	-0.10 ± 0.22	**0.32**
Abs (32258 cm-1)	0.10 ± 0.02	-0.01 ± 0.01	-0.03 ± 0.02	-0.01 ± 0.03	**0.19**

Table 4.8. Estimated from the equation ($y = y_0 + a_\alpha*\alpha + b_\beta*\beta + c_{\pi^*}*\pi^*$), coefficients ($y_o$, a_α, b_β, c_{π^*}), their standard errors and correlation coefficients (r) for the multiple linear regression analysis for **3a** at 310 nm excitation against the solvatochromic values α, β and π*.

y	y_o	a_α	b_β	c_{π^*}	r^2
$\lambda_{ems\ max\ (25000\ cm^{-1})}$	19625.23 ± 296.69	101.05 ± 153.10	147.21 ± 235.95	-141.19 ± 367.93	**0.06**
Band 1 cm^{-1} (Gaussian Fit)	18796.29 ± 394.65	-201.81 ± 203.65	217.04 ± 313.86	-495.87 ± 489.41	**0.13**
Band 2 cm^{-1} (Gaussian Fit)	20059.32 ± 100.11	-213.96 ± 51.66	196.56 ± 79.61	-452.84 ± 124.15	**0.68**
Band 3 cm^{-1} (Gaussian Fit)	21484.91 ± 74.11	-203.04 ± 38.24	71.53 ± 58.93	-604.37 ± 91.90	**0.81**
Φ (25000 cm-1)	0.60 ± 0.12	-0.33 ± 0.06	0.17 ± 0.09	-0.00 ± 0.15	**0.61**
Abs (25000 cm-1)	0.02 ± 0.00	-0.00 ± 0.00	-0.00 ± 0.00	-0.00 ± 0.00	**0.18**

Table 4.9. Estimated from the equation ($y = y0 + a\alpha*\alpha + b\beta*\beta + c\pi^{**}\pi^*$), coefficients (yo, aα, bβ, cπ*), their standard errors and correlation coefficients (r) for the multiple linear regression analysis for 3a at 400 nm excitation against the solvatochromic values α, β and π*.

4.3.1.3 Photodegradation and photobleaching of 3a.

When **3a**, in toluene, is irradiated at 310 nm excitation in a conventional spectrometer, no significant decrease in emission intensity is observed over a period of constant illumination of ~900 minutes (Figure 4.3.12). This indicates that these molecules are potentially very useful as photostable fluorophores.

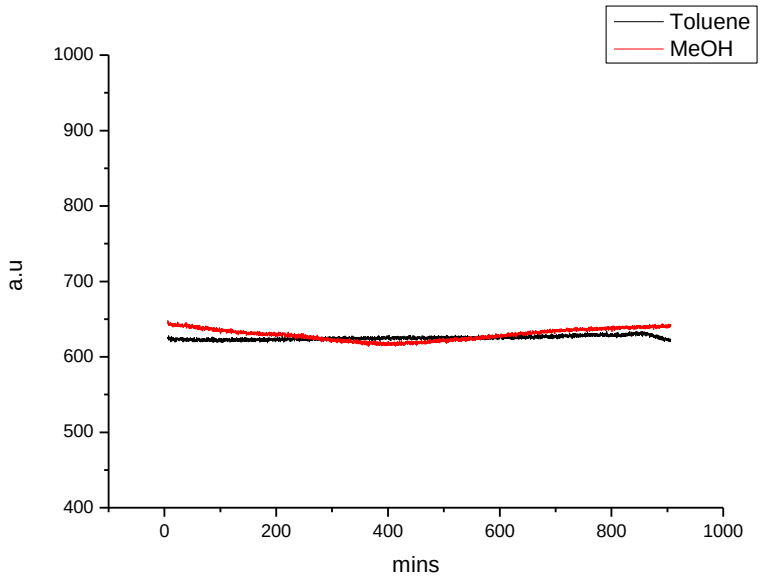

Figure 4.3.12. Attempted photobleaching of **3a** under 310 nm irradiation for 900 minutes in toluene and methanol.

A more intense UV illumination was then performed using a UV lamp whereby two cuvettes; one containing quinine sulphate in 0.1M H_2SO_4, and the other containing **3a** in toluene were irradiated for 6 hours. The emission spectra was recorded at 310 and 400 nm excitation for **3a**, and 350 nm excitation for quinine sulphate after 30 minutes illumination, 60 minutes and 90 minutes illumination, and then every 90 minutes thereafter. Figure 4.3.13 shows the emission spectra of **3a** at 310 nm (a) and 400 nm (b) excitation and quinine sulphate (c) at 350 nm excitation over the period of six hours of constant UV illumination. Observing the emission spectra for each shows a drop in fluorescence intensity which is fairly modest at <20 %.

(a) **3a** 310 nm excitation

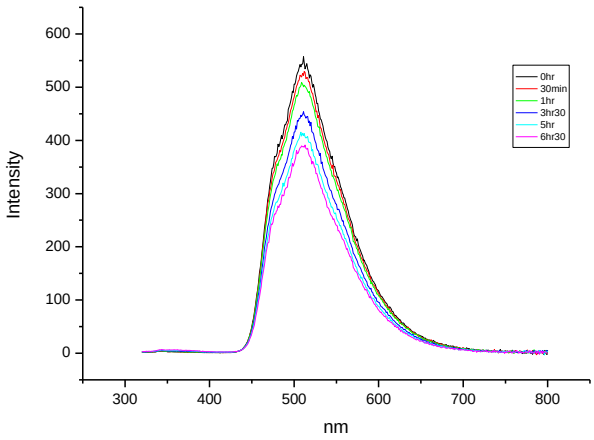

(b) **3a** 400 nm excitation

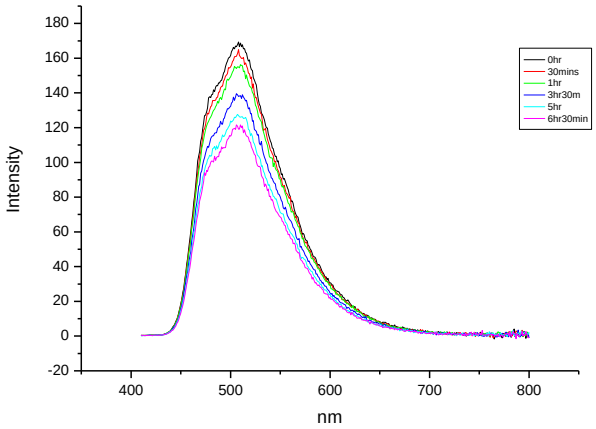

(c) Quinine sulphate 350 nm excitation

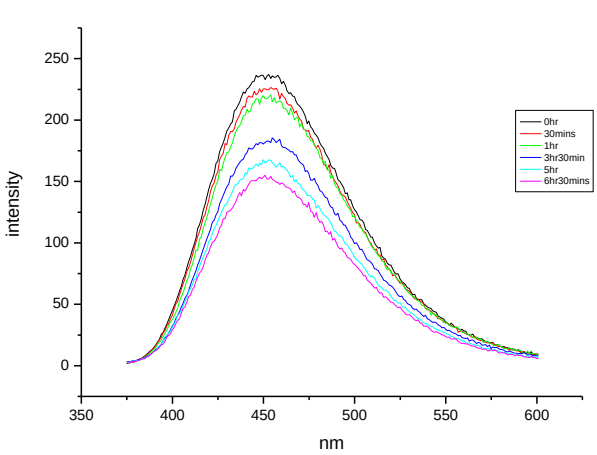

(d) Summary

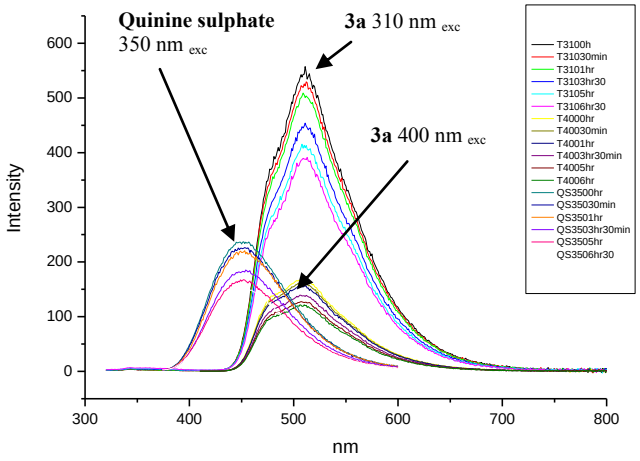

Figure 4.3.13. Emission spectra of **3a** at (a) 310 nm (T310) and (b) 400 nm (T400) excitation and (c) quinine sulphate at 350 nm excitation (QS350) over a period of six hours of constant UV illumination and, (d) a summary of the three spectra overlayed.

In addition, the normalized emission spectra for **3a** and quinine sulphate (Figure 4.3.14) show that the emission profiles remain unchanged after six hours of constant illumination, ultimately indicating no effect is being observed on the energies of the excited states.

(a) **3a** 310 nm excitation

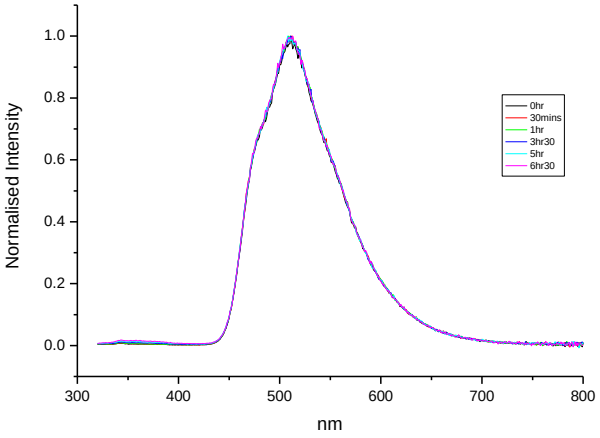

(b) **3a** 400 nm excitation

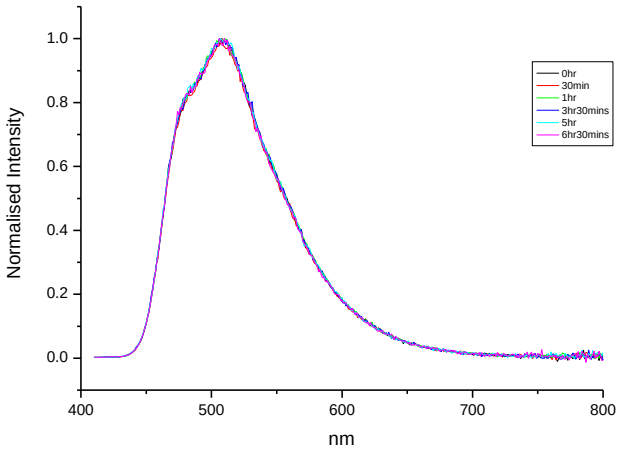

(c) Quinine sulphate 350 nm excitation

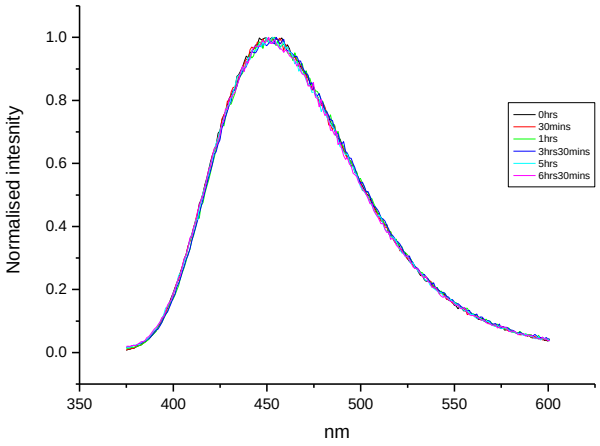

Figure 4.3.14. Normalised emission spectra of **3a** at 310 nm (a) and 400 nm (b) excitation, and quinine sulphate (c) at 350 nm excitation, over a period of six hours of constant UV illumination.

The photostability of **3a** relative to quinine sulphate is very good. By plotting the integrated areas of the emission spectra, the ~20 % decrease in emission intensity is clearly observed. However, when the normalised spectra are compared, both **3a** and quinine sulphate appear to experience the same decrease in intensity until the 210 minute mark, after which the intensity of **3a** decreases much more slowly than quinine sulphate. (Figure 4.3.12 (b)). Quinine sulphate is known to be very stable, hence its adoption as a

fluorescence photobleaching standard. Quinine sulphate in 0.05 M H_2SO_4 has been shown to be stable to +/– 1 percent when stored in the dark and measured for six months.[77]

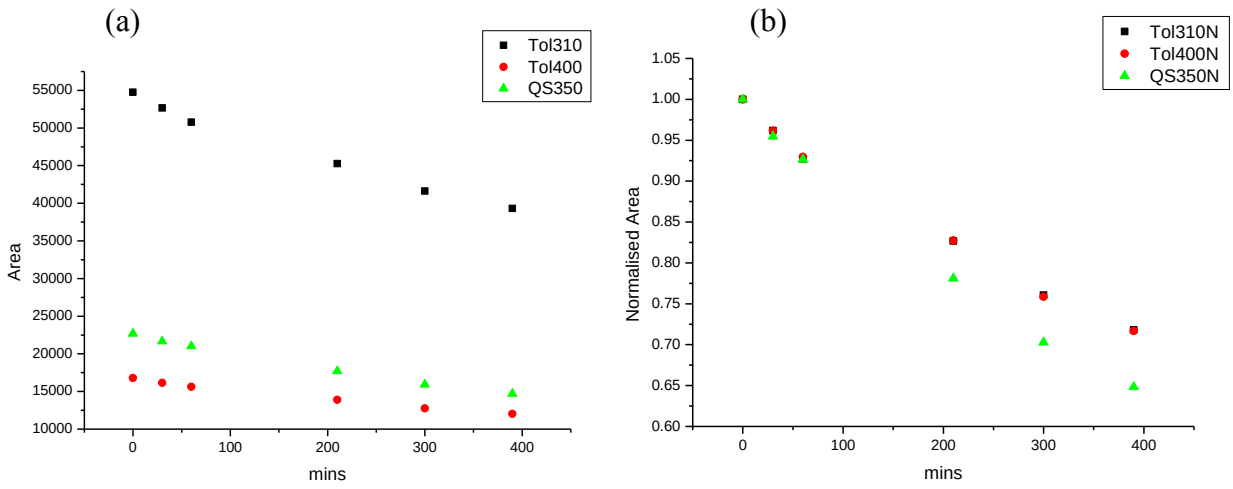

Figure 4.3.15. Comparison of integrated areas from (a) raw emission spectra of **3a** in toluene for 310 and 400 nm excitation (Tol310 and Tol400), and quinine sulphate at 350 nm excitation (QS350) and (b) normalized emission spectra of **3a** in toluene for 310 and 400 nm excitation (Tol310N and Tol400N), and quinine sulphate at 350 nm excitation (QS350N) over the six hour period of constant UV illumination.

A reduction in the fluorescence intensity can also be observed when **3a** is subjected to temperatures higher than 20 ^{o}C. At 60 ^{o}C, a ~40 % decrease in fluorescence intensity for **3a** in toluene can be observed for both 310 and 400 nm excitation (Figure 4.3.16). This is presumed to be due to dynamic quenching as a result of increased mobility at higher temperature. Such an increase in mobility results in an increase in non-radiative deactivation processes (*e.g.* solvent collisions) in the excited state. Nevertheless, this effect is non-destructive as upon cooling the solution back to 20 ^{o}C and allowing time to equilibrate, the original intensity is observed (Figure 4.3.16).

(a) **3a** 310 nm excitation (b) **3a** 400 nm excitation

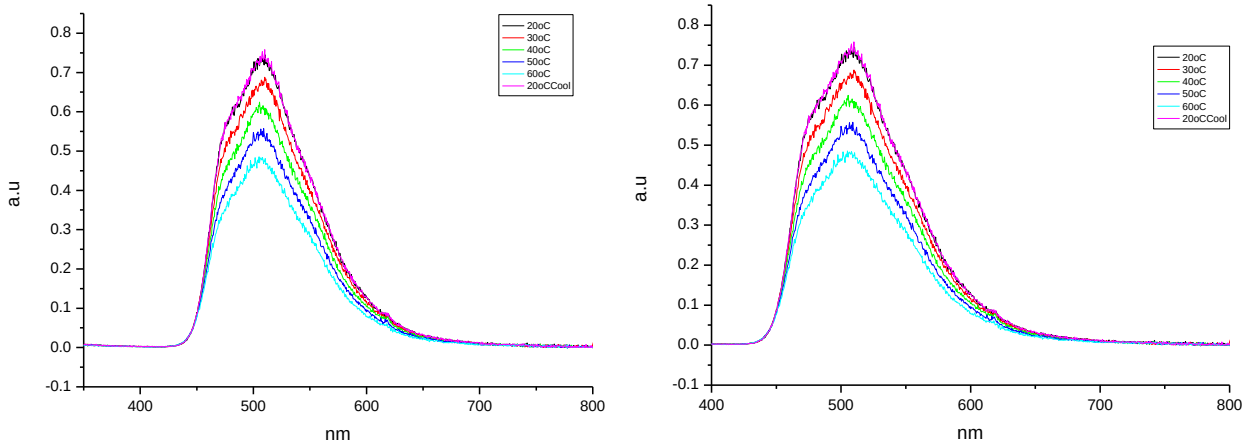

Figure 4.3.16. Fluorescence emission spectra of **3a** recorded at 310 and 400 nm excitation at varying temperature (20 ^{o}C to 60 ^{o}C) in toluene.

4.3.2 Time resolved fluorescence measurements.

The fluorescence lifetime behaviour of these triazine fluorophores is complex, and dependent on the emission and excitation wavelengths. Using a 405 nm laser diode excitation source, the fluorescent lifetime behaviour of the 400 nm emission of **3a**, **6a**, **9a** and **10a** could be investigated by time correlated single photon counting (TCSPC).

The sample is excited with a pulse of light and the time is measured between the excitation pulse and the observed photon and stored in a histogram to generate a decay curve at a particular emission wavelength ((470, 490, 520, 540, or 570 for **3a**, **6a**, **9a** or 490, 520, 540, 570 and 600 nm for **10a**). For TCSPC, the conditions are adjusted so that less than one photon is detected per laser pulse. The x-axis is the time difference and the y-axis the number of photons detected for this time difference. The data is then analysed by the nonlinear least squares (NLLS) method. The value of χ^2(reduced) and visual examination of the residuals and fitted function (traced along decay curve) can be used to judge the goodness of fit. The residuals are the differences between the measured data and the fitted function (Figure 4.3.17).[6]

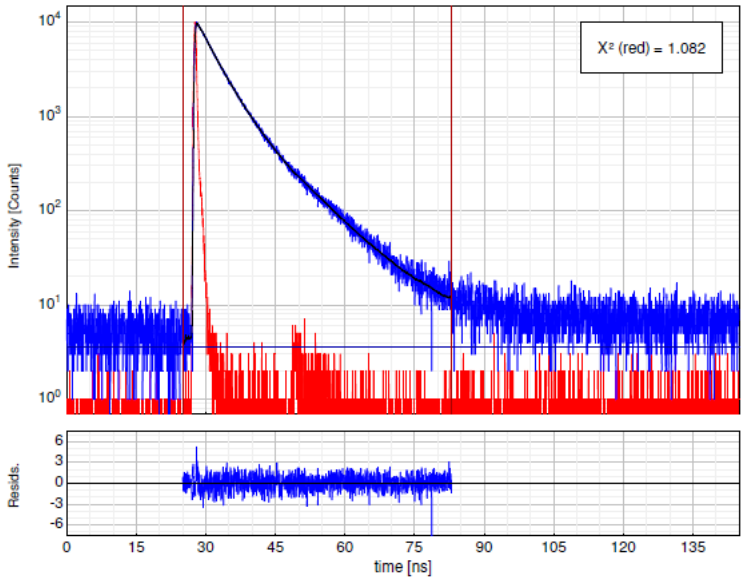

Figure 4.3.17. Example of a TCSPC decay for **3a** in toluene at 470 nm.

For all of the species (**3a**, **6a**, **9a** and **10a**), the fluorescence decay could be fitted to a 2 or 3 exponential term. The two or three fit decay is composed of:

1. A short lived component (τ_1) with values ranging from 0.2 to 3 ns.
2. A medium component (τ_2) ranging from 2 to 7 ns.
3. A long lived component (τ_3) which ranges from 6 to 14.5 ns.

Fitting of the decay data was performed using the Fluofit software using a free fit method rather than a global fit across all wavelengths. If the data is free fitted, the function is allowed to freely assign values for both the decay times (τ_i) and amplitudes of the components (α_i) to obtain a goodness of fit for each individual lifetime decay (*e.g.* 470 nm for **3a**). Whilst a global fit assigns fixed parameter values for each decay time across a selected range of data (*e.g.* 470, 490, 520, 540, 570 and 600 nm) and searches for the local minimum for the amplitudes of the components (α_i).

However the method of fit, whether free or fixed globally, only had minor influence on the intensity weighted average lifetime (τ_f) with a 3 % difference (6.3 ns versus 6.45 ns) being observed between the free fit and global fit at 470 nm for **3a** (Table 4.9).

Code	λ (nm)	Solvent	τ_1 (ns)	A_1 (%)	τ_2 (ns)	A_2 (%)	τ_3 (ns)	A_3 (%)	τ_f (ns) (Intensity Weighted)	χ^2
Free Fit										
3a	470	Acetonitrile	-	-	4.78	68.4	9.6	31.6	6.3	1.19
3a	490	Acetonitrile	-	-	4.95	64.7	10.6	35.3	6.9	1.04
3a	520	Acetonitrile	-	-	5.13	49.7	12.3	50.3	8.7	1.06
3a	540	Acetonitrile	-	-	5.21	40.4	12.6	59.7	9.6	1.09
3a	570	Acetonitrile	-	-	5.33	28.7	12.9	71.3	10.7	1.10
Global Fit										
3a	470	Acetonitrile	-	-	5.16	81.97	12.29	18.03	6.45	1.197
3a	490	Acetonitrile	-	-	5.16	73.49	12.29	26.51	7.05	1.12
3a	520	Acetonitrile	-	-	5.16	50.39	12.29	49.61	8.7	1.074
3a	540	Acetonitrile	-	-	5.16	38.73	12.29	61.27	9.53	1.123
3a	570	Acetonitrile	-	-	5.16	25.18	12.29	74.82	10.58	1.177

Table 4.10. Comparison of the free fit and global fit fluorescence lifetime data **3a** in acetonitrile measured at a variety of emission wavelengths nm using a 405 nm (laser diode) excitation sources. A_i represents the fractional intensities, while τ_i are the individual lifetime components and $\langle \tau \rangle_f$ is the intensity weighted average lifetime.

For **3a** in acetonitrile (Table 4.10), the average lifetime increases with emission wavelength. The fluorescence decay fits to a bi-exponential model and when the data is globally fitted, the medium lifetime (5.16 ns) fraction decreases from 82 % to 25 % as one goes from 470 nm to 570 nm emission with a corresponding increase of 18 % to 75 % in the long lifetime component.

(a)

Code	λ (nm)	Solvent	τ_1 (ns)	A_1 (%)	τ_2 (ns)	A_2 (%)	τ_3 (ns)	A_3 (%)	τ_f (ns) (Intensity Weighted)	χ^2
Free Fit										
6a	470	Acetonitrile	0.36	1.3	4.2	69.4	7.6	29.3	5.2	1.05
6a	490	Acetonitrile	0.39	1.3	4.4	71.7	9.1	27	5.6	1.09
6a	520	Acetonitrile	0.56	1.0	4.6	63.3	12.3	35.7	7.3	1.07
6a	540	Acetonitrile	0.37	0.7	4.5	51.6	12.2	47.7	8.2	1.12
6a	570	Acetonitrile	2.4	5.6	5.4	43.4	13.7	51.1	9.5	1.10
Global Fit										
6a	470	Acetonitrile	2.12	7.61	5.05	86.07	13.16	6.32	5.34	1.09
6a	490	Acetonitrile	2.12	6.21	5.05	81.61	13.16	12.18	5.86	1.09
6a	520	Acetonitrile	2.12	4.7	5.05	63.99	13.16	31.31	7.45	1.09
6a	540	Acetonitrile	2.12	3.86	5.05	54.04	13.16	42.1	8.35	1.12
6a	570	Acetonitrile	2.12	3.44	5.05	41.97	13.16	54.59	9.38	1.15

(b)

Code	λ (nm)	Solvent	τ_1 (ns)	A_1 (%)	τ_2 (ns)	A_2 (%)	τ_3 (ns)	A_3 (%)	τ_f (ns) (Intensity Weighted)	χ^2
Free Fits										
9a	470	Acetonitrile	0.32	1.3	3.7	65	6.5	34	4.6	1.13
9a	490	Acetonitrile	0.27	1.3	3.9	68.3	7.9	30.4	5.0	1.12
9a	520	Acetonitrile	1.9	6.5	4.6	65.1	12.7	28.4	6.7	1.11
9a	540	Acetonitrile	0.37	1	4.2	58	12.4	41	7.5	1.08
9a	570	Acetonitrile	0.8	1	4.3	48	12.8	51	8.6	1.06
Global Fits										
9a	470	Acetonitrile	2.39	15.86	4.78	79.83	12.78	4.31	4.74	1.17
9a	490	Acetonitrile	2.39	12.53	4.78	77.28	12.78	10.19	5.29	1.14
9a	520	Acetonitrile	2.39	10.02	4.78	61.6	12.78	28.38	6.81	1.13
9a	540	Acetonitrile	2.39	8.29	4.78	53.84	12.78	37.87	7.61	1.10
9a	570	Acetonitrile	2.39	7.98	4.78	42.42	12.78	49.59	8.55	1.16

Table 4.11. Comparison of the free fit and global fit fluorescence lifetime data for (a) **6a** and (b) **9a** in acetonitrile measured at a variety of emission wavelengths nm using a 405 nm (laser diode) excitation sources.

The 4-Cl and 4-Br derivatives (**6a** and **9a**) have very different lifetime behavior to **3a**, with a tri-exponential model being required to fit the decay curves. For the globally fittred 4-Cl species in acetonitrile (Table 4.11 (a)), a new short lifetime (2.1 ns) component is observed and a notable increase in the longer lived lifetime, up to ~13.17 ns, with a significant decrease in the lifetime of the medium lifetime component, down to ~5.0 ns. Overall this shows up as a decrease in the intensity averaged lifetime of **6a** of ~17 % at 490 nm and ~14 % at 570 nm versus **3a** (Table 4.10). For **6a**, the maximum value for the intensity weighted lifetime at 470 nm is 6.7 ns in 1,5-pentanediol, whilst at 570 nm, the maximum value for the intensity weighted lifetime is again much longer at 10.69 ns in 1,5-pentanediol (Table 4.11 (a)).

For **9a** (Table 4.11 (b)), the effect is more marked with decreases in the intensity averaged lifetime of **9a** of 26 % at 490 nm and 20 % at 570 nm relative to **3a**. Similarly to **6a**, the maximum value for the intensity weighted lifetime for **9a** at 470 nm excitation is 6.72 ns in 1,5-pentanediol, whilst at 570 nm excitation, the maximum value of the intensity weighted lifetime is 10.2 ns in 1,5-pentanediol (Table 4.11 (b)).

An extensive range of solvents were investigated but small trends were only observed. As a result, it is more informative to compare the minimum and maximum values for each compound, regardless of solvent. Hence, the solvent will vary in the following tables. For a full summary of the data refer to Appendix of Results, 1.1, 1.2, 1.3 and 1.4.

Table 4.12 lists the minimum and maximum intensity weighted average lifetimes for **3a**, **6a**, **9a** and **10a** at the lowest (470 and 490 nm) and highest emission wavelengths (570 and 600 nm). For example, **3a** has a maximum value for the intensity weighted lifetime at 470 nm of 6.87 ns in propylene carbonate, whilst at 570 nm, the maximum value of the intensity weighted lifetime is much longer at 11.09 ns in propylene carbonate, with similar increases for **6a** and **9a** (Table 4.12).

Like with the emission spectra, a difference is observed in the lifetime between **10a** and **3a**. The long lived component τ_3 has a maximum value of 10.59 ns in chloroform for **3a** and contributes to 29.16 %, whereas for **10a**, the longer lived component τ_3 has a maximum value of 14.68 ns in acetonitrile but now contributes to 95.21 % of the fitted

lifetime (Table 4.13). This results in a two fold increase in the maximum value for the intensity average lifetime at 490 nm for **10a** of 13.95 ns in ethyl acetate, versus 6.87 ns in propylene carbonate at 470 nm for **3a** (Table 4.12).

Code	X	Y	Wavelength (nm)	Solvent	τ_f (ns) Intensity Weighted (min)
3a	H	OCH_3	470	Methanol	4.16
6a	Cl	OCH_3	470	2-Methyl-2-butanol	4.16
9a	Br	OCH_3	470	Ethyl Acetate	4.05
10a	H	CH_3	490	1,4-Butanediol	10.08

Wavelength (nm)	Solvent	τ_f (ns) Intensity Weighted (max)
470	Propylene Carbonate	6.87
470	1,5-Pentanediol	6.7
470	1,5-Pentanediol	6.72
490	Ethyl Acetate	13.95

Code	X	Y	Wavelength (nm)	Solvent	τf (ns) Intensity Weighted (min)
3a	H	OCH_3	570	Methanol	7.15
6a	Cl	OCH_3	570	Methanol	7.3
9a	Br	OCH_3	570	Methanol	6.9
10a	H	CH_3	600	Ethylene Glycol	11.79

Wavelength (nm)	Solvent	τf (ns) Intensity Weighted (max)
570	Propylene Carbonate	11.09
570	1,5-Pentanediol	10.69
570	1,5-Pentanediol	10.2
600	Acetonitrile	14.69

Table 4.12. Summary of the minimum and maximum intensity weighted average lifetimes (τ_f) of the 2,5-dihydro-1,2,3-triazines with substituted aryl groups at 470 / 490 and 570 / 600 nm excitation.

Tables 4.13 and 4.14 list the minimum and maximum values for the decay times (τ_i) and their corresponding fractional intensities (A_i) for **3a**, **6a**, **9a** at 470 and 570 nm emission, and at 490 and 600 nm emission for **10a**.

Observing **3a**, **6a** and **9a** (Table 4.13 and 4.14), τ_2 contributes the most to the decay at 470 nm (70.78 to 85.71 %), whilst at 570 nm there is an increase in the contribution from the longer lived τ_3 state (29.16 % at 470 nm to 51.7 % at 570 nm for **3a**) and subsequent decrease in the maximum contribution from τ_2 (70.78 to 40.48 %). Again, it is clearly evident that for **10a**, the longer lived τ_3 contributes the most to the decay at both 490 and 600 nm (95.21 % at 490 nm to 100 % at 600 nm).

Code	X	Y	nm	Solvent	τ_1 (ns) (min)	A_1 (%)
3a	H	OCH_3	470	1-Propanol	0.19	1.96
6a	Cl	OCH_3	470	1-Propanol	0.22	2.8
9a	Br	OCH_3	470	1-Propanol	0.22	3.32
10a	H	CH_3	490	1,4-Dioxane	0.22	0.54

X	Y	nm	Solvent	τ_1 (ns) (max)	A_1 (%)
H	OCH_3	470	1-Octanol	0.60	4.69
Cl	OCH_3	470	1-Octanol	0.59	6.58
Br	OCH_3	470	1,5-Pentanediol	0.48	4.55
H	CH_3	490	1,3-Butanediol	0.41	10.82

Code	X	Y	nm	Solvent	τ_2 (ns) (min)	A_2 (%)
3a	H	OCH_3	470	Ethylene Glycol	2.05	12.27
6a	Cl	OCH_3	470	1,4-Butanediol	2.86	17.09
9a	Br	OCH_3	470	1,4-Butanediol	3.11	21.79
10a	H	CH_3	490	Ethyl Acetate	0.41	10.82

X	Y	nm	Solvent	τ_2 (ns) (max)	A_2 (%)
H	OCH_3	470	Propylene Carbonate	5.53	70.78
Cl	OCH_3	470	1-Hexanol	4.95	85.71
Br	OCH_3	470	1-Hexanol	4.47	83.34
H	CH_3	490	Methanol	4.95	5.1

Code	X	Y	nm	Solvent	τ_3 (ns) (min)	A_3 (%)
3a	H	OCH_3	470	1,4-Butanediol	6.61	61.28
6a	Cl	OCH_3	470	Ethanol	6.05	44.86
9a	Br	OCH_3	470	1-Butanol	5.79	35.42
10a	H	CH_3	490	Ethylene Glycol	12.01	88.49

X	Y	nm	Solvent	τ_3 (ns) (max)	A_3 (%)
H	OCH_3	470	Chloroform	10.59	29.16
Cl	OCH_3	470	1-Hexanol	10.84	8.68
Br	OCH_3	470	2-Methyl-2-butanol	10.49	9.62
H	CH_3	490	Acetonitrile	14.68	95.21

Table 4.13. Summary of the minimum and maximum values for the lifetime decay components of the three exponential fit for the decay at 470 nm (490 nm for **10a**) emission for the 2,5-dihydro-1,2,3-triazines with substituted aryl groups; where τ_i is the decay time and A_i is the fractional intensity.

Code	X	Y	nm	Solvent	τ_1 (ns) (min)	A_1 (%)
3a	H	OCH_3	570	N,N-Dimethylformamide	0.13	0.82
6a	Cl	OCH_3	570	1-Butanol	0.32	1.58
9a	Br	OCH_3	570	1,4-Dioxane	0.22	1.16
10a	H	CH_3	600	1-Pentanol	0.34	0.56

X	Y	nm	Solvent	τ_1 (ns) (max)	A_1 (%)
H	OCH_3	570	1,4-Butanediol	2.84	13.58
Cl	OCH_3	570	1,4-Butanediol	2.99	8.18
Br	OCH_3	570	1,3-Propanediol	3.95	8.27
H	CH_3	600	1-Octanol	0.64	0.96

Code	X	Y	nm	Solvent	τ_2 (ns) (min)	A_2 (%)
3a	H	OCH_3	570	2-Methyl-2-butanol	3.67	11.62
6a	Cl	OCH_3	570	Toluene	4.11	23.28
9a	Br	OCH_3	570	Toluene	3.93	27.94
10a	H	CH_3	600	Ethylene Glycol	2.35	3.67

X	Y	nm	Solvent	τ_2 (ns) (max)	A_2 (%)
H	OCH_3	570	1,5-Pentanediol	6.56	48.04
Cl	OCH_3	570	1,4-Butanediol	7.16	51.57
Br	OCH_3	570	1,4-Butanediol	7.04	52.66
H	CH_3	600	1,5-Pentanediol	7.56	11.7

Code	X	Y	nm	Solvent	τ_3 (ns) (min)	A_3 (%)
3a	H	OCH_3	570	Toluene	9.67	93.8
6a	Cl	OCH_3	570	Toluene	9.97	76.62
9a	Br	OCH_3	570	Toluene	9.71	72.06
10a	H	CH_3	600	Ethylene Glycol	12.15	96.33

X	Y	nm	Solvent	τ_3 (ns) (max)	A_3 (%)
H	OCH_3	570	1,3-Butanediol	13.5	51.7
Cl	OCH_3	570	1,3-Butanediol	14.59	47.71
Br	OCH_3	570	1,3-Butanediol	13.86	47.06
H	CH_3	600	Acetonitrile	14.69	100

Table 4.14. Summary of the minimum and maximum values for the lifetime decay components of the three exponential fit for the decay at 570 nm (600 nm for **10a**) emission for the 2,5-dihydro-1,2,3-triazines with substituted aryl groups; where τ_i is the decay time and A_i is the fractional intensity.

Analysis of the intensity weighted average lifetimes, 470 nm intensity weighted lifetime and 570 nm intensity weighted lifetime (and their respective decay times) against the normalized solvent polarity (E_T^N), solvent hydrogen bonding donating/accepting ability (α and β), solvent polarizability (π^*), viscosity (η(Cp)), dielectric constant (ε) and dipole moment (μ) was performed for each fluorophore. However, the solvatochromic analysis of all components again revealed no significant trends and the distribution of the data was fairly random (Appendix of Results, 1.1, 1.2, 1.3 and 1.4). Similar to the emission, a multiple linear regression analysis on the lifetime of **3a** (Table 4.15) against the solvatochromic values α, β and π^* was performed. The intensity weighted average lifetimes at 470 and 570 nm and their respective individual decay times (τ_1, τ_2, and τ_3) were correlated against but again showed no significant correlations (a linear correlation is supported when r^2 approaches unity *i.e.* 1).

y	y_o	a_α	b_β	c_{π^*}	r^2
τ_f (Intensity weighted, 470nm)	6.65 ± 1.37	-0.71 ± 0.70	-0.56 ± 1.09	-0.61 ± 1.70	**0.08**
τ_1 (Intensity weighted, 470nm)	2.83 ± 1.86	-1.54 ± 0.96	-2.42 ± 1.48	2.03 ± 2.31	**0.29**
τ_2 (Intensity weighted, 470nm)	9.19 ± 2.08	-2.74 ± 1.07	-2.98 ± 1.65	-0.13 ± 2.58	**0.39**
τ_3 (Intensity weighted, 470nm)	12.79 ± 2.34	-0.63 ± 1.28	-0.44 ± 2.28	-5.17 ± 2.63	**0.43**
τ_f (Intensity weighted, 570nm)	12.57 ± 2.22	-1.59 ± 1.14	-1.03 ± 1.76	-2.70 ± 2.75	**0.16**
τ_1 (Intensity weighted, 570nm)	2.21 ± 2.23	-1.45 ± 1.07	-2.82 ± 1.61	4.98 ± 2.84	**0.45**
τ_2 (Intensity weighted, 570nm)	8.70 ± 3.69	-1.24 ± 1.90	-4.92 ± 2.94	3.74 ± 4.58	**0.21**
τ_3 (Intensity weighted, 570nm)	9.88 ± 1.29	0.18 ± 0.70	1.27 ± 1.26	2.77 ± 1.45	**0.39**

Table 4.15. Estimated from equation ($y= y_0 + a_\alpha*\alpha + b_\beta*\beta + c_{\pi^*}*\pi^*$), coefficients ($y_o$, a_α, b_β, c_{π^*}), their standard errors and correlation coefficients (r) for the multiple linear regression analysis of the time domain fluorescent lifetimes and components of **3a** at 405 nm excitation.

4.3.2.1 Influence of molecular oxygen on the fluorescence lifetime of 3a and 10a – deoxygenation lifetime study.

Precautions were taken to ensure dry solvents were used for all studies but the presence of molecular oxygen needed to be considered as it is known that molecular oxygen is a powerful collisional quencher in the excited state.[3] It was thought that deoxygenating the solvent may cause a marked increase in lifetime of the 2,5-dihydro-1,2,3-triazines with substituted aryl groups if the fluorophore is susceptible to quenching by molecular oxygen. The lifetime was recorded in toluene prior to deoxygenation, and then was subject to argon being passed through the solution over a period of 35 minutes, with a measurement performed after 10 minutes and finally at 35 minutes.

Table 4.16 shows the intensity weighted average lifetimes of **3a** measured at 470 nm and 570 nm at different times following degassing of the solution with Argon gas. The results showed that the decay times and fractional intensities do not vary over the 35 minute period, with only a 3 % increase (8.74 to 9.00 ns) in the intensity weighted average lifetime at 570 nm excitation for **3a** after 35 minutes.

Table 4.17 shows the intensity weighted average lifetimes of **10a** measured at 490 nm and 600 nm at different times following degassing of the solution with Argon gas. Again, the decay times and fractional intensities do not vary over the 35 minute period, with only a 2 % increase (12.45 to 12.88 ns) in the intensity weighted average lifetime at 600 nm excitation for **10a** after 35 minutes.

From the results (Tables 4.16 and 4.17), it is evident that the 2,5-dihydro-1,2,3-triazine fluorophore is uneffected by collisional quenching due to molecular oxygen. These results are encouraging as they, along with the results presented in Section 4.1.3.1, suggest that the 2,5-dihydro-1,2,3-triazines are very photostable organic fluorophores.

Code	X	Y	Wavelength (nm)	Time (mins)	Solvent	τ_1 (ns)	A_1 (%)	τ_2 (ns)	A_2 (%)	τ_f (ns) (Intensity Weighted)	χ^2
3a	H	OCH_3	470	0	Toluene	3.87	63.8	9.36	36.2	5.85	1.118
3a	H	OCH_3	470	10	Toluene	3.73	60.07	9.79	39.93	6.15	1.126
3a	H	OCH_3	470	35	Toluene	3.41	57.83	9.19	42.17	5.85	1.118
3a	H	OCH_3	570	0	Toluene	4.07	17.44	9.72	82.56	8.74	1.117
3a	H	OCH_3	570	10	Toluene	4.3	17.19	10.19	82.81	9.18	1.104
3a	H	OCH_3	570	35	Toluene	4.07	16.05	9.95	83.95	9.00	1.13

Table 4.16. Summary of Time Correlated Single Photon Counting (TCSPC) fluorescent lifetimes (intensity weighted) of **3a** measured at 470 nm and 570 nm at different times following degassing of the solution with Argon gas.

Code	X	Y	Wavelength (nm)	Time (mins)	Solvent	τ_1 (ns)	A_1 (%)	τ_2 (ns)	A_2 (%)	τ_f (ns) (Intensity Weighted)	χ^2
10a	H	OCH_3	490	0	Toluene	0.96	1.3	12.60	98.7	12.45	1.128
10a	H	OCH_3	490	10	Toluene	1.95	2.71	12.92	97.29	12.62	1.21
10a	H	OCH_3	490	35	Toluene	1.99	3.46	12.83	96.54	12.45	1.221
10a	H	OCH_3	600	0	Toluene	-	-	12.63	100	12.63	1.162
10a	H	OCH_3	600	10	Toluene	-	-	13.02	100	13.02	1.134
10a	H	OCH_3	600	35	Toluene	-	-	12.88	100	12.88	1.149

Table 4.17. Summary of Time Correlated Single Photon Counting (TCSPC) fluorescent lifetimes (intensity weighted) of **10a** measured at 470 nm and 600 nm at different times following degassing of the solution with Argon gas.

4.4 CONCLUSION.

The synthesis of the discussed 2,5-dihydro-1,2,3-triazine fluorophores is a facile one pot high yielding synthesis, which employs a 1,3-dipolar cycloaddition of 2,4,5-triphenyl-1,2,3-triazolium-1-phenylaminide 1,3-dipoles with an appropriate terminal propiolate. The use of methyl propiolate (Z = H) allowed a 1,4 N→C sigmatropic rearrangement to occur within the initial cycloadduct to generate the fused pyrrolo[2,3-d]-triazoline "first generation" products, **3b**, **6b** and **9b** (10 %, 29 % and 4 % yields respectively). The key quaternary bridgehead carbons; C3a and C6a (Figure 4.1.2) appear at ~92 and ~105 ppm in the ^{13}C spectrum. Ring expansion of **3b**, **6b** and **9b** produced the "second generation" product; a fluorescent 2,5-dihydro-1,2,3-triazine in yields of 58 % (**3a**), 71 % (**6a**) and 85 % (**9a**).

For the 2,5-dihydro-1,2,3-triazines with substituted aryl groups (**3a**, **6a**, **9a** and **10a**) excitation into either of the UV-visible absorption bands (310 or 400 nm) generated a complicated, green fluorescence emission band centered at ~520 nm that is uneffected by changing the nature of the solvent (Figures 4.3.6 and 4.3.7). This is supported by the fact that no solvatochromism was observed in position of the emission band maximum when observing the normalised fluorescence spectra. For the 4-Cl and 4-Br triazines (**3a** and **6a**), the emission properties were found to be virtually identical to **3a**.

10a was synthesized as the product from the cycloaddition between 2,4,5-triphenyl-1,2,3-triazolium-1-phenylaminide 1,3-dipole and 3-butyn-2-one, which resulted in a 2,5-dihydro-1,2,3-triazine with a methyl substituted carbonyl. This minor structural difference brought about a significant change to the energy of the emission spectrum, resulting in a red-shifted spectra versus the methyl ester triazine **3a**. By substituting a ketone, it is believed an increased rate of IC from S_2 (**g0**) to S_1 (**g0**) with emission of a photon back to GS is observed. Likewise, an increase in the quantum yield at 310 nm excitation (0.83 in toluene for **10a** versus 0.76 in toluene for **3a**) and a longer lived intensity average fluorescent lifetime resulted (13.95 ns in ethyl acetate for **10a** at 490 nm excitation versus 6.87 ns in propylene carbonate for **3a** at 470 nm excitation).

The photostability of **3a** was proven to be exceptional when compared to quinine sulphate. A solution of **3a** in toluene was placed under constant irradiation at 310 nm

excitation in a spectrometer as well as being subjected to an intense UV illumination in the dark over a 6 hour period. Quinine sulphate in 0.1M sulphuric acid was used as a standard. This resulted in a slight drop in the fluorescence intensity which was fairly modest at <20 %. Observing the normalised emission profiles, they remained unchanged after the six hours of constant illumination, ultimately indicating no effect was being observed on the energies of the excited states. When a solution of **3a** was heated, a non-destructive quenching process was observed with a decrease in fluorescence intensity of ~40 % for 310 and 400 nm excitation at 60 ^{o}C. Upon cooling back to 20 ^{o}C, the original fluorescence intensity was observed.

Degassing of a solution of **3a** in toluene and measurement of its TCSPC lifetime over a 35 minute only resulted in a 3 % increase (8.74 to 9.00 ns) in the intensity weighted average lifetime at 570 nm emission, with the decay times and fractional intensities found to not vary. This was also the case for **10a**, with only a 2 % increase (12.45 to 12.88 ns) in the intensity weighted average lifetime at 600 nm emission being observed after 35 minutes. Therefore, the use of dry solvent is proven sufficient for future measurements as the fluorophores are not susceptible to collisional quenching by molecular oxygen.

In light of the results presented, it is evident that the 2,5-dihydro-1,2,3-triazines show promise as dual excitation (310 or 400 nm) fluorophores, both of which generate similar green fluorescence emission bands centered at ~520 nm, that is uneffected by changing the nature of the solvent. This is of benefit as the lack of solvatochromism means that the fluorophore's photophysics can be well predicted within a biological environment as the polarity of the microenvironment will not effect the fluorescent properties. Furthermore, this lack of solvatochromism along with their outstanding photostability and long lived lifetime properties make them very suitable and promising as future biological probes pending further structural modification to allow conjugation to biological molecules.

Chapter 5: Imine substituted (N=C-Z) 2,5-dihydro-1,2,3-triazines.

5.1 INTRODUCTION.

The work reported by Butler *et al*. focused on the use of terminal propiolate esters as the dipolarophile, resulting in a N=C-H imine functionality in the final 2,5-dihydro-1,2,3-triazine.[54] We postulated that the presence of the N=C-H imine hydrogen was important for fluorescence. In order to investigate this theory, a synthetic route to a family of 2,5-dihydro-1,2,3-triazines with different substituents on the imine carbon was developed *i.e.* N=C-Z (where Z = CH_3, Ph, COOMe or D) instead of N=C-H for the parent triazine **3a**. This synthetic route employs a commercially available terminally substituted alkyne dipolarophile with the terminal hydrogen now replaced (Scheme 5.1.1).

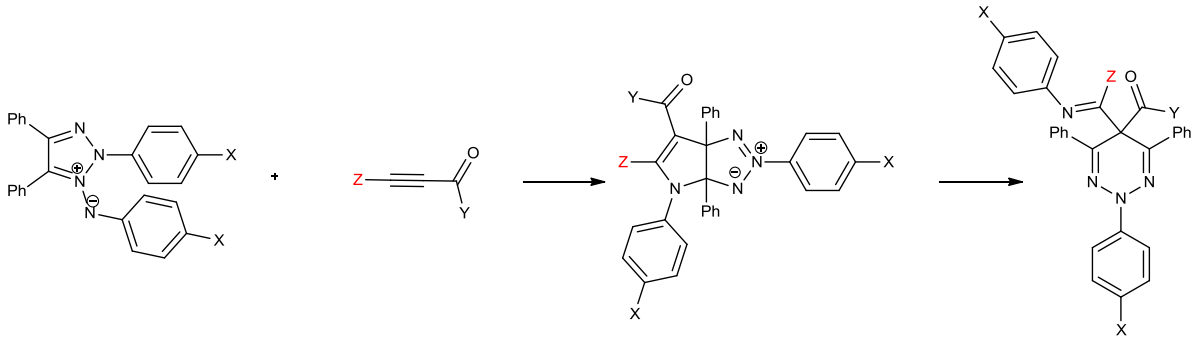

Scheme 5.1.1. General synthetic scheme to produce imine substituted (N=C-Z) 2,5-dihydro 1,2,3-triazines from terminally substituted propiolates.

5.2 RESULTS AND DISCUSSION (SYNTHESIS).

Refer to Chapter 2, Section 2.1.2 for experimental procedure and results.

5.2.1 1,3-Dipolar cycloadditions of 2,4,5-triphenyl-1,2,3-triazolium-1-aminide 1,3-dipoles with terminally substituted propiolates.

The 2,5-dihydro-1,2,3-triazines are typically synthesised by refluxing the corresponding 1,2,3-triazolium-1-aminide dipole and an appropriate alkyne in dry acetone.[54] However, under these conditions the reaction using the terminal alkyne methyl-2-butynoate (Z = CH_3) produced the pyrrolo[2,3-d][1,2,3]triazol-2-ium-3-ide intermediate (**11b**) in a 81 % yield, with no 2,5-dihydro-1,2,3-triazine isolated (Scheme 5.2.1).

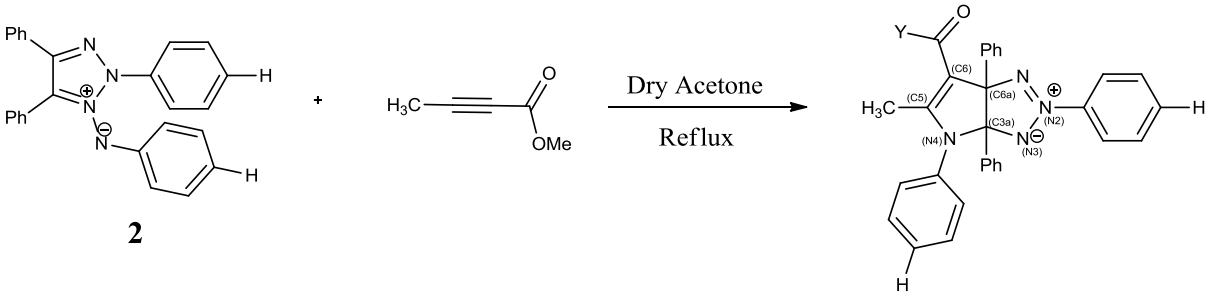

Scheme 5.2.1. 1,3-Dipolar cycloaddition of 1,2,3-triazolium-1-phenylaminide 1,3-dipole (**2)** with methyl-2-butynoate yields only pyrrolo[2,3-d][1,2,3]triazol-2-ium-3-ide intermediate (**11b**) by acetone reflux.

It was suspected that the activation energy barrier for the ring expansion from the pyrrolo[2,3-d][1,2,3]triazol-2-ium-3-ide intermediate (**11b**, Scheme 5.2.1) to the 2,5-dihydro-1,2,3-triazine (**11a**) was higher for the reaction using methyl-2-butynoate (Z = CH_3) compared to using methyl propiolate (Z = H). Refluxing in dry toluene, instead of dry acetone, successfully allowed the ring expansion to occur, producing the desired methyl substituted iminie 2,5-dihydro-1,2,3-triazine (**11a**) in an isolated yield of 80 % with no pyrrolo[2,3-d][1,2,3]triazol-2-ium-3-ide intermediate (**11b**) being isolated.

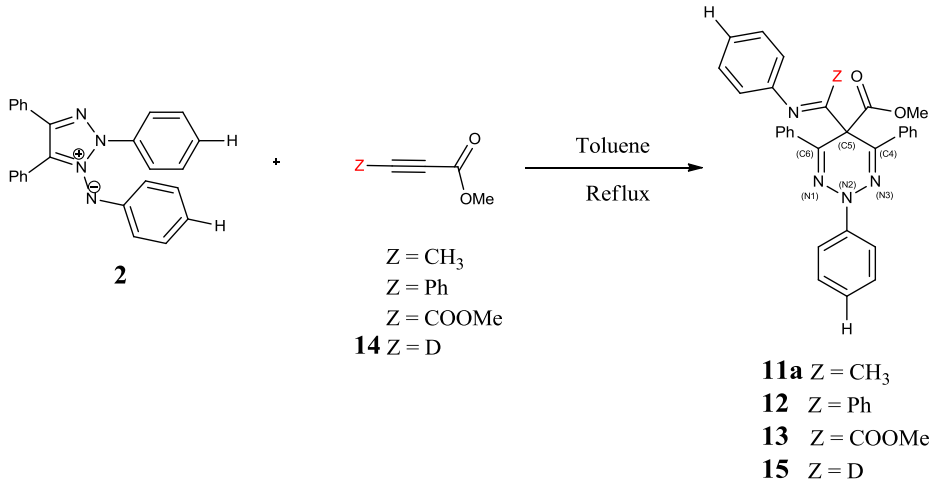

Scheme 5.2.2. 1,3-Dipolar cycloaddition of 1,2,3-triazolium-1-phenylaminide 1,3-dipole (**2**) with terminally substituted propiolates to produce imine substituted (N=C-Z) 2,5-dihydro 1,2,3-triazines by toluene reflux.

The structures of **11b** and **11a** were identified using ^{1}H and ^{13}C NMR spectra and supported by HRMS and IR spectroscopy. As discussed in Chapter 4, the reaction is again highly regioselective and only one isomer is isolated for each of **11b** and **11a**.

The ^{1}H NMR spectra of **11b** again exhibits two characteristic singlets; the methoxy group at 3.56 ppm, as well as the methyl group at C5 at 2.46 ppm with the corresponding signals in the ^{13}C spectrum occurring at 13.7 and 49.4 ppm respectively. The C5 carbon of **11b** is observed at a deshieled 163.3 ppm with the expected key quaternary bridgehead carbons, C3a and C6a, appearing at 90.8 and 100.7 ppm. A quaternary ^{13}C NMR signal at 165.8 ppm confirmed the presence of a carbonyl and this is supported by the IR spectrum with the C=O stretch being observed at 1680 cm^{-1}.

The characteristic imine hydrogen signal observed at 8.49 ppm for **3a** (Z = H), is no longer observed in the ^{1}H spectrum of **11a**. Instead, a singlet is observed for the methyl group of the substituted imine at 1.05 ppm and 20 ppm in the ^{1}H and ^{13}C NMR spectra respectively. Again, similar to **3a**, the methoxy group is observed as only a singlet at 3.8 ppm. The ^{13}C NMR spectrum of **11a** shows the presence of an imine carbon at 168.1 ppm, the key quaternary carbon signal for C5 at 53.1 ppm, as well as a quaternary carbon signal at 169.9 ppm which again confirms the presence of a carbonyl and is supported by the IR spectrum with the C=O stretch being observed at 1641 cm^{-1}.

When the cycloaddition between 2,4,5-triphenyl-1,2,3-triazolium-1-phenylaminide (**2**) was performed using methyl phenylpropiolate (Z = Ph), under reflux in toluene, a phenyl imine substituted 2,5-dihydro-1,2,3-triazine (**12**) was successfully isolated in 75 % yield with no pyrrolo[2,3-d][1,2,3]triazol-2-ium-3-ide intermediate being isolated.

When the disubstituted alkyne, dimethyl acetylenedicarboxylate (Z = COOMe) is used, the synthesis generates an carbonyl ester imine substituted 2,5-dihydro-1,2,3-triazine (**13**). Unlike the previously reported 2,5-dihydro-1,2,3-triazines (**3a**, **6a** and **9a**), this was the first not to display fluorescence when in solution. This compound had been previously reported in the literature by Butler *et al.* who employed a thermolytic ring expansion of pyrrolo[2,3-d]-1,2,3-triazoles to give the 2,5-dihydro-1,2,3-triazine (**13**) in an 81 % yield.[57] Performing the cycloaddition in refluxing toluene afforded the triazine **13** in an isolated yield of 75 % following column chromatography with no pyrrolo[2,3-d][1,2,3]triazol-2-ium-3-ide intermediate being isolated. The structures of **12** and **13** were identified using ^{1}H and ^{13}C NMR spectra and supported by HRMS and IR spectroscopy. The ^{1}H NMR spectrum of **12** again exhibits a characteristic singlet for the methoxy group at 3.18, whilst **13** shows two singlets for both its methoxy groups at 2.91 and 3.74 ppm. The ^{13}C NMR spectrum of **12** and **13** show the presence of an imine carbon at 168.9 and 156 ppm respectively and a quaternary carbon signal for C5 at 52.4 and 50.6 ppm for **12** and **13** respectively. A quaternary carbon signal at 170.8 ppm confirms the presence of a carbonyl in **12**, whilst two quaternary carbon signals are observed for **13** at 159.3 and 168 ppm for both its carbonyl. This is supported by the IR spectrum with the C=O stretch being observed at 1641 cm^{-1} for **12**, and two C=O stretches observed for **13** at 1730 and 1746 cm^{-1}.

We wanted to investigate the effect of replacing the imine hydrogen with a deuterium would have on the fluorescent properites of **3a**. To do this it was necessary to perform the cycloaddition using the deuterated propiolate ester; methyl [3-^{2H}] propiolate (**14)** (Z = D) rather than methyl propiolate (Z = H). To this point, all the alkynes utilized were commercially available, however methyl [3-^{2H}] propiolate had to be synthesized *via* a base catelysed hydrogen deuterium exchange. Methyl propiolate in D_2O was treated with 40% v/v sodium deuteroxide in D_2O and stirred overnight at room temperature. The reaction mixture was extracted using $CDCl_3$ and washed with D_2O before being dried over calcium chloride. The ^{1}H NMR spectrum indicated hydrogen deuterium exchange had

occurred as the only singlet observed was for the methoxy group at 3.48 ppm with no singlet appearing for the alkyne hydrogen. Further purification was not performed due to the volatile nature of methyl propiolate and the filtered colourless solution of methyl [3-^{2H}] propiolate (**14)** in chloroform was considered sufficiently pure for the subsequent cycloaddition. When the cycloaddition between 2,4,5-triphenyl-1,2,3-triazolium-1-phenylaminide (**2**) was performed using methyl [3-^{2H}] propiolate (**14)** (Z = D), under reflux in toluene, a deuterium imine substituted 2,5-dihydro-1,2,3-triazine (**15**) was successfully isolated in 76 % yield with no pyrrolo[2,3-d][1,2,3]triazol-2-ium-3-ide intermediate being isolated. The structure of **14** was identified using ^{1}H and ^{13}C NMR spectra and supported by HRMS and IR spectroscopy. The characteristic imine hydrogen signal observed at 8.49 ppm for **3a** (Z = H), is no longer observed in the ^{1}H NMR spectrum of **15** (Z = D) due being substituted with a deuterium. The ^{1}H NMR spectrum of **15** again exhibits the characteristic singlet for the methoxy group at 3.54 ppm. The key quaternary carbon signal for C5 is observed at 53.3 ppm, and C4 and C6 are 134.8 and 135.2 ppm. A quaternary carbon signal at 170.2 ppm confirmed the presence of a carbonyl and was supported by the IR spectrum with the C=O stretch being observed at 1737 cm^{-1} for **15**.

The structures of **11a** and **13** are further supported by x-ray crystal structures which had not been previously published.

Interestingly, the crystal structure for **11a** (Figure 5.2.1) shows the methyl group at C(25) to be placed over the plane of the triazine ring, with the methoxy carbonyl group at C(14) pointing to the back. The planarity of the triazine ring is also distorted as the phenyl rings of C(15) and C(13) are being held out of plane to the triazine core. The placement of the imine methyl group over the triazine ring in the x-ray crystal structure supports the photophysical model of hindered rotation which holds the imine methyl group out of plane to the methoxy carbonyl, which ultimately affects the excited state electronics (Chapter 3).

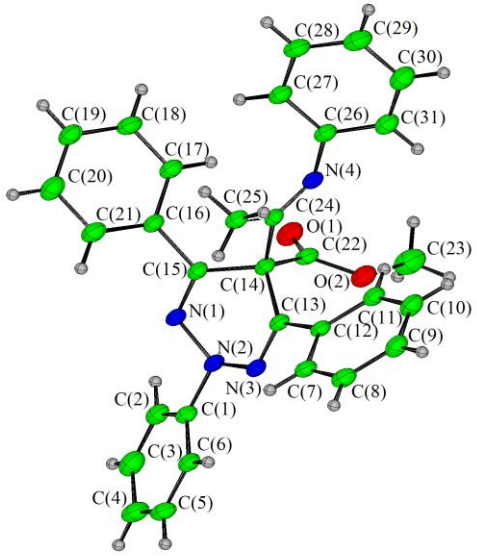

Figure 5.2.1. X-ray crystal structure of **11a**.

Similarly, the crystal structure for **13** (Figure 5.2.2) shows the methoxy carbonyl group at C(24) to be again placed over the plane of the triazine ring, with the methoxy carbonyl group at C(14) pointing to the back. The distortion of the planarity of the triazine ring is again clearly evident from the positioning of the phenyl rings of C(13) and C(15) being held out of plane to the triazine core. Again, the placement of the imine methoxy carbonyl group over the triazine ring in the x-ray crystal structure supports the photophysical model of the hindered rotation which holds the imine methoxy carbonyl group out of plane to the methoxy carbonyl group of C(14) , which ultimately affects the excited state electronics (Chapter 3).

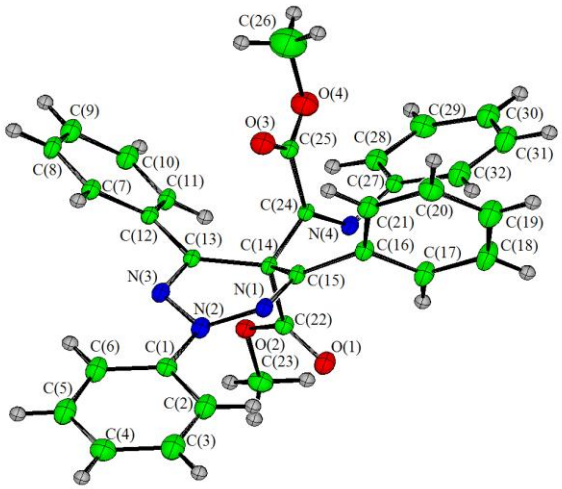

Figure 5.2.2. X-ray crystal structure of **13**.

5.3 RESULTS AND DISCUSSION (FLUORESCENCE SPECTROSCOPY).

Refer to Chapter 2, Section 2.2.1 for experimental procedures.

Refer to Appendix of Results 2.1, 2.2, 2.3 and 2.4 for complete set of solvatochromic results, tables and graphs.

5.3.1 Steady state fluorescence study.

A detailed steady state solvatochromism study was undertaken for the imine substituted (N=C-Z) 2,5-dihydro-1,2,3-triazine fluorophores (**11a**, **12**, **13** and **15**) with 12 solvents selected: toluene, 1,4-dioxane, chloroform, acetonitrile, 1-octanol, 1-hexanol, 1-butanol, 1-pentanol, 1-propanol, acetic acid, methanol and 2,2,2-trifluoroethanol (Refer to Appendix A.2 for complete list of solvents and solvatochromic values).

Analysis was again performed against normalized solvent polarity (E_T^N), solvent hydrogen bonding donating/accepting ability (α and β), solvent polarizability (π^*), viscosity (η(Cp)) and dipole moment (μ) for each fluorophore, using the software package Origin 7.0, in order to identify any possible ground state solvent interactions which may influence their fluorescence emission.

5.3.1.1 Ultraviolet Visible absorption spectra.

Interestingly, the nature of the imine carbon substitution now causes a significant change to the ground state absorption and photophysics. In particular, a higher energy absorption at ~300 nm, that is blue shifted compared to **3a** (N=C-H) is observed and the strong absorption band at ~400 nm for **3a** (inset, Figure 5.3.1) is no longer observed except in the case of **15** (**Z** = **D**) (Figure 5.3.1). Like the 2,5-dihydro-1,2,3-triazines with substituted aryl groups, the imine substituted fluorophore is not effected by changing the nature of the solvent, (Figures 5.3.1). This is clearly evident as there is no change in the band positions for the normalized UV-visible spectra (Figures 5.3.2).

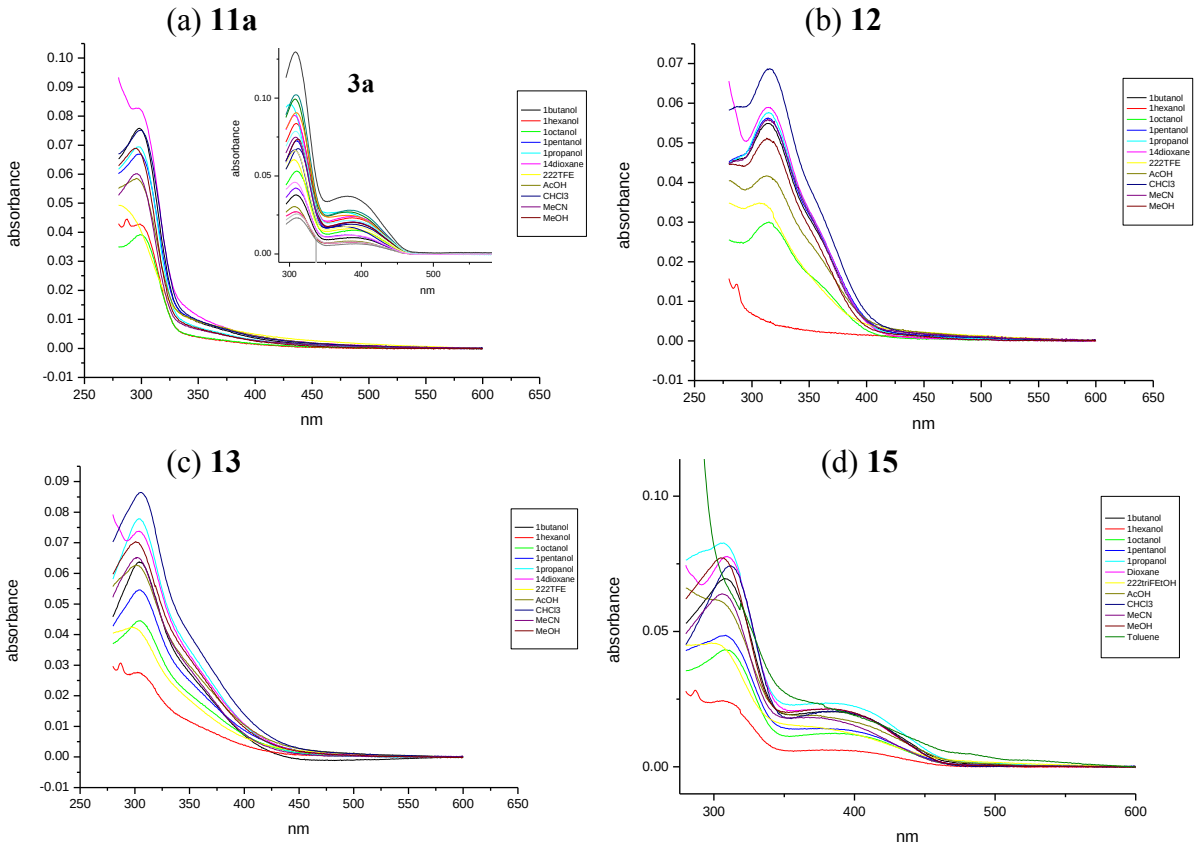

Figure 5.3.1. Ultraviolet visible absorption spectra for the imine substituted 2,5-dihydro-1,2,3-triazines (**11a**, **12**, **13** and **15**) recorded at an assumed maximum concentration of 1 x 10^{-5} M, , with **3a** (inset) for comparison.

.

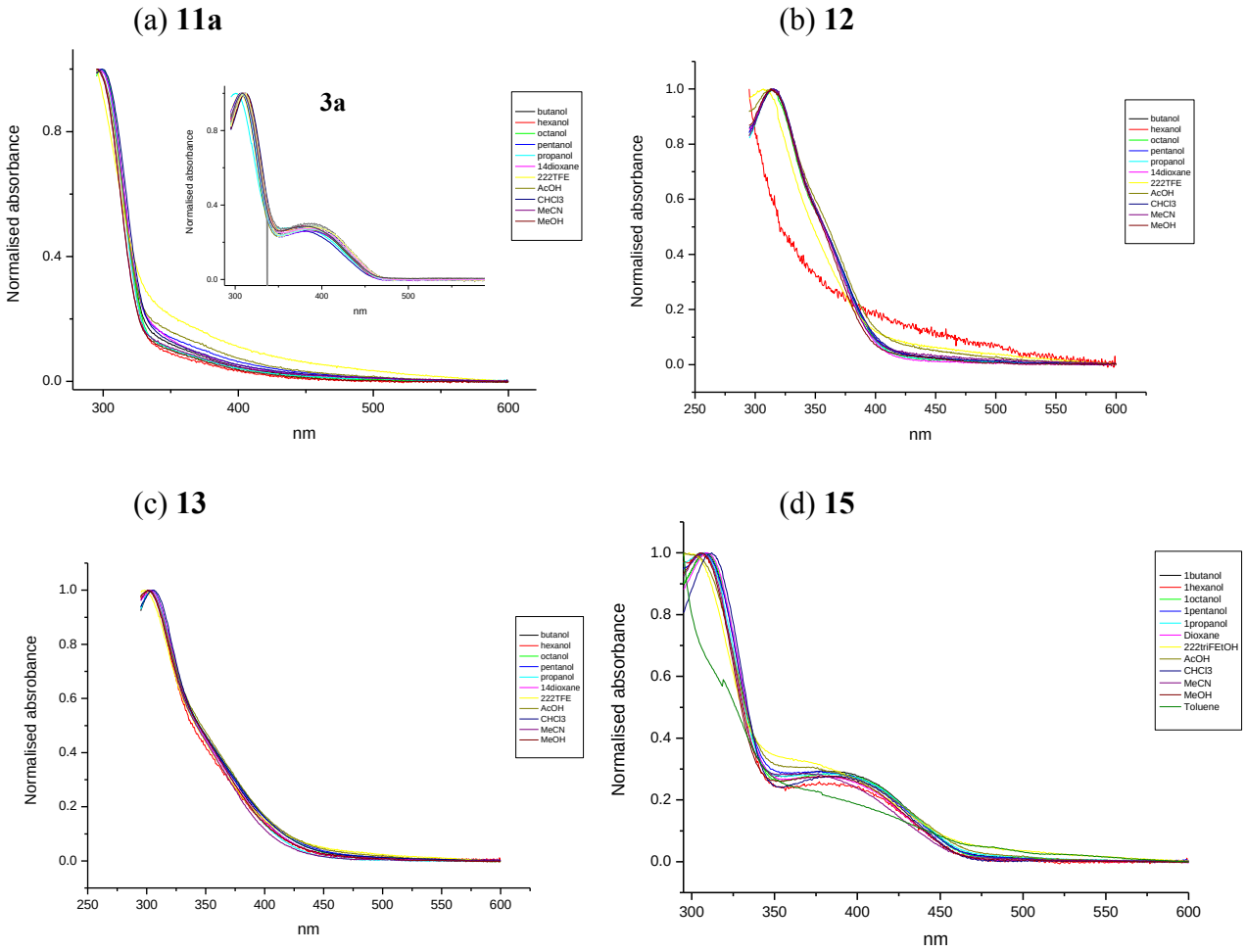

Figure 5.3.2. Normalised ultraviolet visible absorption spectra for the imine substituted 2,5-dihydro-1,2,3-triazines (**11a**, **12**, **13** and **15**), with **3a** (inset) for comparison.

5.3.1.2 Fluorescence emission spectra.

The fluorescence emission spectra of **11a** (N=C-CH_3) at 310 nm excitation now shows a weak intensity band at *ca.* 500 nm and a new intense tri-band emission at *ca.* 350 nm (Figure 5.3.3, Band 3, 4 and 5) which has been shown in Chpater 3 to be due to population of the S_3 (**g0**) and S_2 (**g0**) ES. This is similar to the weakly emitting band at ~350 nm which is seen in the long chain diol solvents for **3a**, **6a** and **9a** after excitation at 310 nm (Chapter 4, Figure 4.3.6).

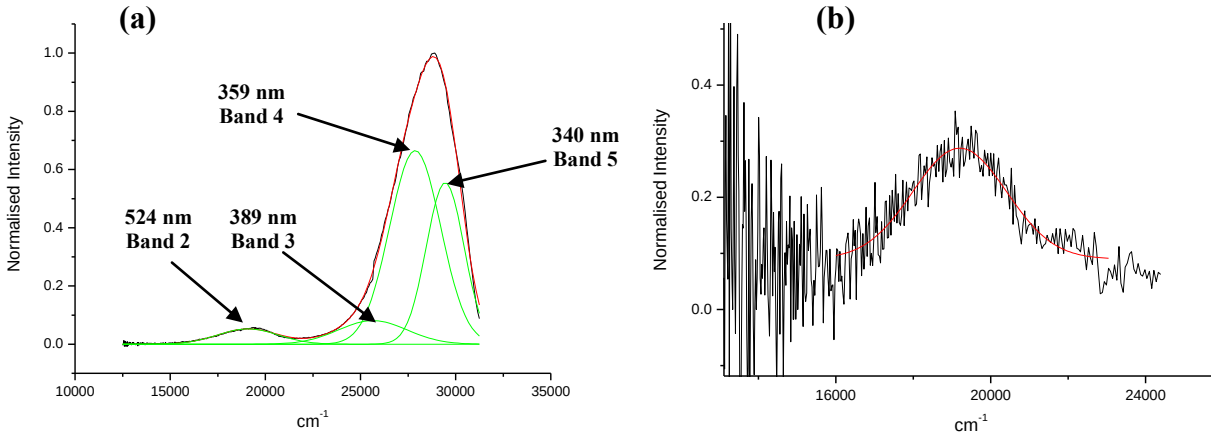

Figure 5.3.3. Gaussian model fits of the normalised fluorescence emission spectrum of **11a** recorded in acetonitrile for (a) 310 nm and (b) 400 nm excitation.

The emission spectra at *ca.* 350 nm following 310 nm excitation for **11a** again appears to be uneffected by changing the nature of the solvent, which is similar to the 2,5-dihydro-1,2,3-triazines with substituted aryl groups (Figure 5.3.4). This is supported by the fact that no solvatochromism is observed in position of the emission band maximum when observing the normalised fluorescence spectra of **11a** (Figure 5.3.5).

Excitation at 400 nm results in virtually no fluorescence emission for **11a** and all that is observed is a very weak and noisy single emission at ~510 nm (Figure 5.3.6). This has been shown in Chapter 3 to be due to the population of S_1 (**g0**) which intersystem crosses to S_1 (**g1**) with a small change in dipole moment.

Chapter 3 also explained that the major conformational difference between N=C-H (**3a**) and N=C-CH_3 (**11a**) triazine involved the extent of rotation of the imine group (Z = H or CH_3) over the triazine ring and that this has a pronounced effect on the fluorescence emission. Therefore, we postulated that synthesising structures with a bulky substituent such as a phenyl or carboxy ester substituted on the imine carbon (**12** Z = Ph and **13** Z = COOMe) could generate a significant change in fluorescence properties. This change could be explained by the proposal that the imine and ester can no longer be held in-plane which ultimately effects the dipole transition moment. This distortion has been shown in the x-ray crystal structure (Figure 5.2.2) obtained for **13** (Z = COOMe), whereby the planarity of the triazine ring has been distorted due to the carboxy ester extending out over the ring. As a result, under both 310 and 400 nm excitation, only very weakly emitting species are observed for both **12** and **13** (Figure 5.3.4 and 5.3.5, inset is zoomed spectra).

For the deuterium imine substituted 2,5-dihydro-1,2,3-triazine (**15** Z = D), virtually the same steady state fluorescence emission behaviour was observed as found for **3a** (N=C-H) was observed (Figure 5.3.4, 5.3.5). Again as for **3a**, the emission spectra for **15** appear to be uneffected by changes in the nature of the solvent. This is supported by the fact that no solvatochromism is observed in position of the emission band maximum when observing the normalised fluorescence spectra of **15** (Figure 5.3.6 and 5.3.7).

The observed emission peak maximum (minimum and maximum value) at 310 nm excitation for **11a**, **12**, **13** and **15** are given in Table 5.1 (a) and range from 352 nm (**11a** in chloroform), 515 nm (**12** in chloroform) to 519 nm (**15** in chloroform) versus 525 nm for **3a** in ethylene glycol.

The observed emission peak maximum (minimum and maximum value) at 400 nm excitation for **11a**, **12**, **13** and **15** are given in Table 5.1 (b) and range from 512 nm (**15** in 1-octanol), 523 nm (**11a** in acetonitrile and **12** in methanol) and can be compared with 513 nm for **3a** in acetonitrile. Peak maxima values could not be obtained from the weak emission spectra for **15** (Z = COOMe).

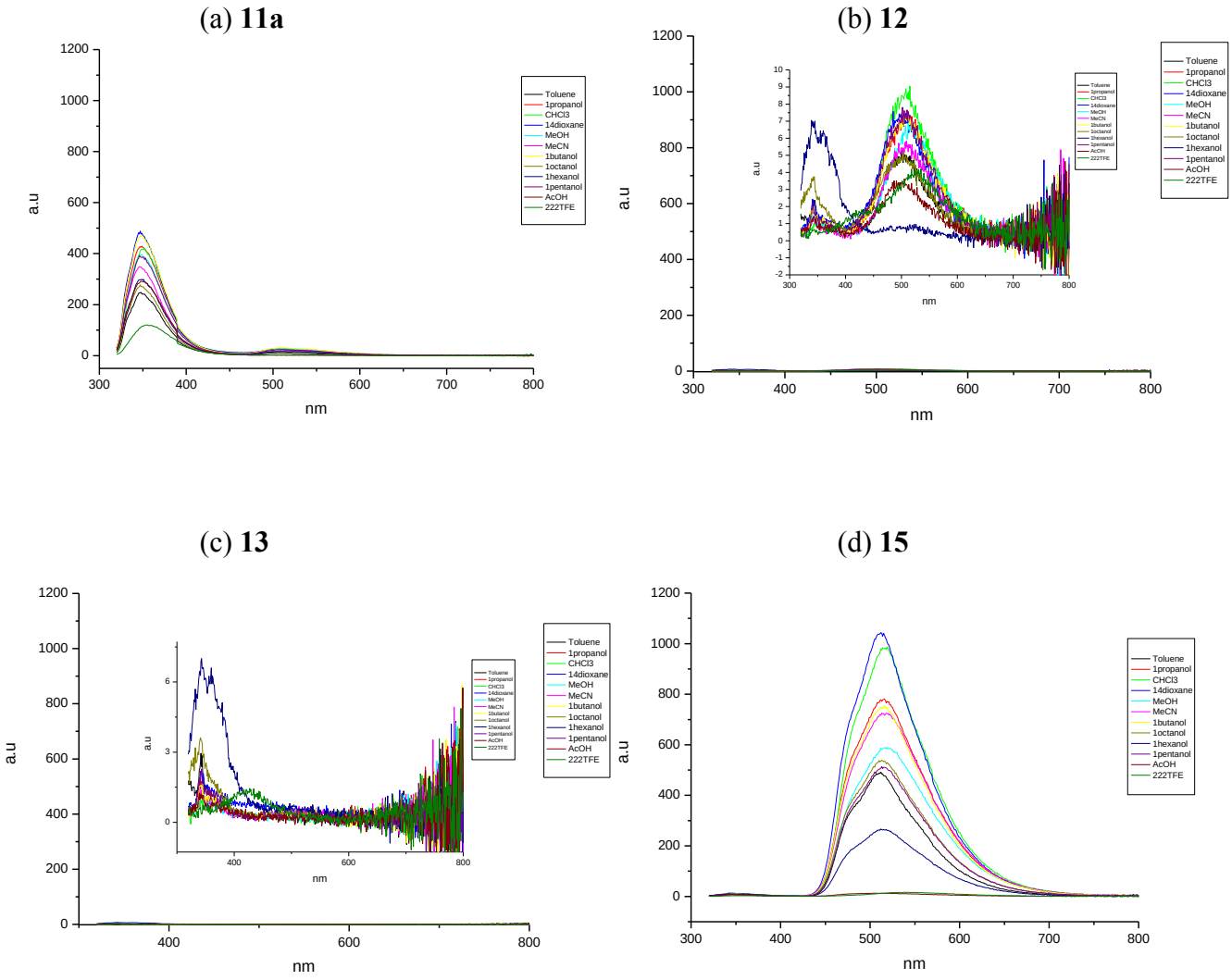

Figure 5.3.4. Summary of fluorescent emission spectra at 310 nm excitation for the imine substituted 2,5-dihydro-1,2,3-triazines (**11a**, **12**, **13** and **15**) recorded at an assumed maximum concentration of 1 x 10^{-5} M.

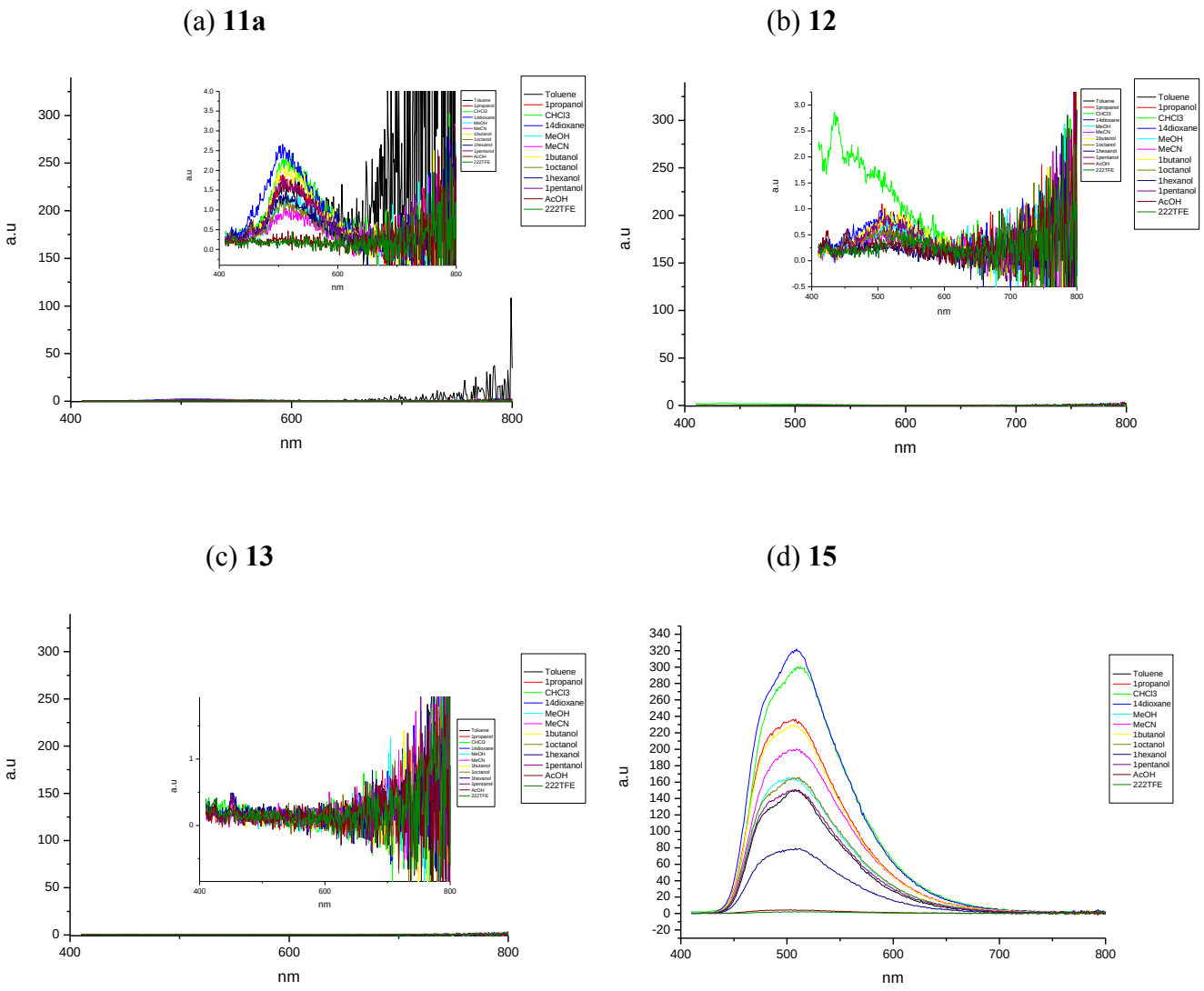

Figure 5.3.5. Summary of fluorescent emission spectra at 400 nm excitation for the imine substituted 2,5-dihydro-1,2,3-triazines (**11a**, **12**, **13** and **15**) recorded at an assumed maximum concentration of 1 x 10^{-5} M.

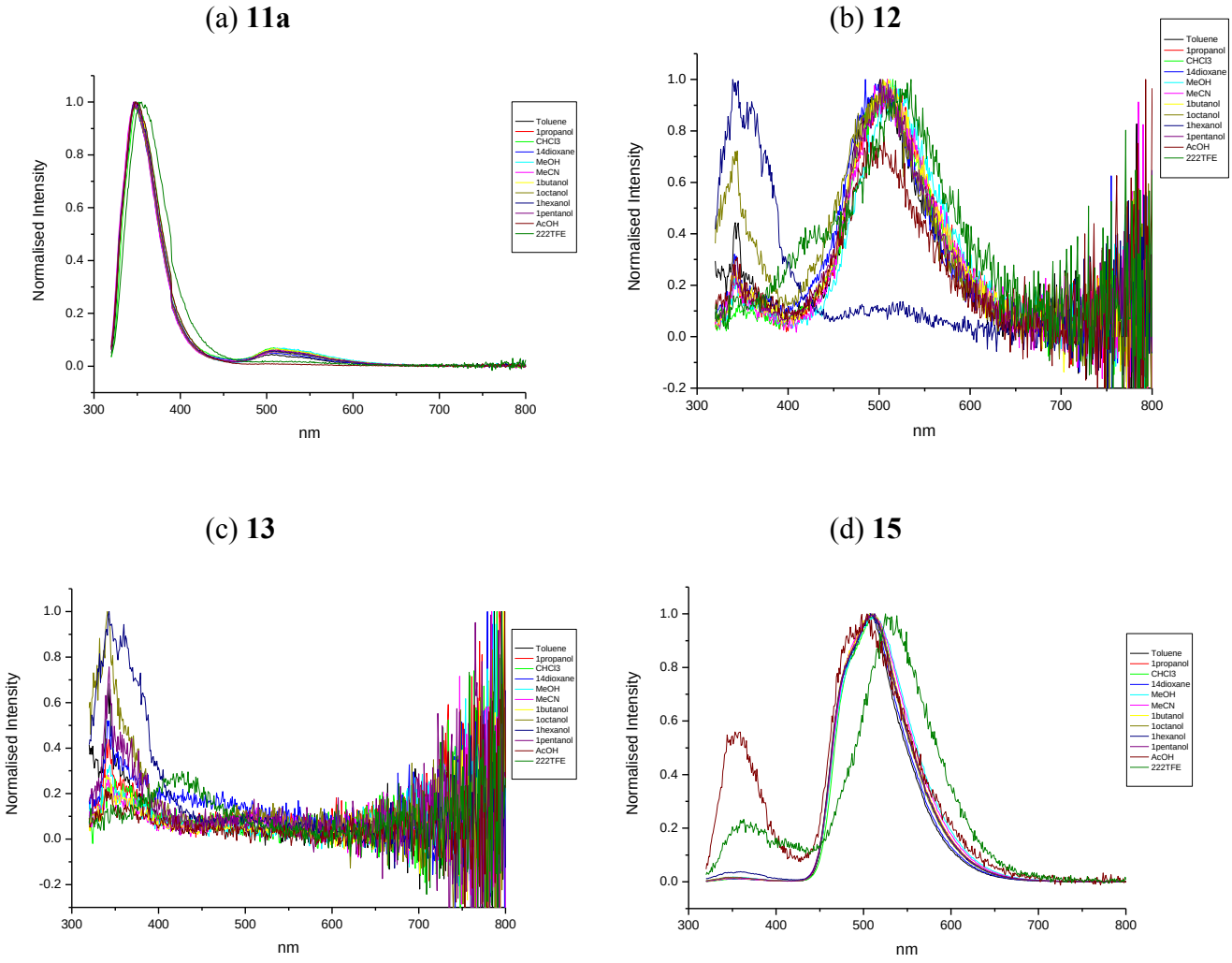

Figure 5.3.6. Summary of normalized fluorescent emission spectra at 310 nm excitation for the imine substituted 2,5-dihydro-1,2,3-triazines (**11a**, **12**, **13** and **15**).

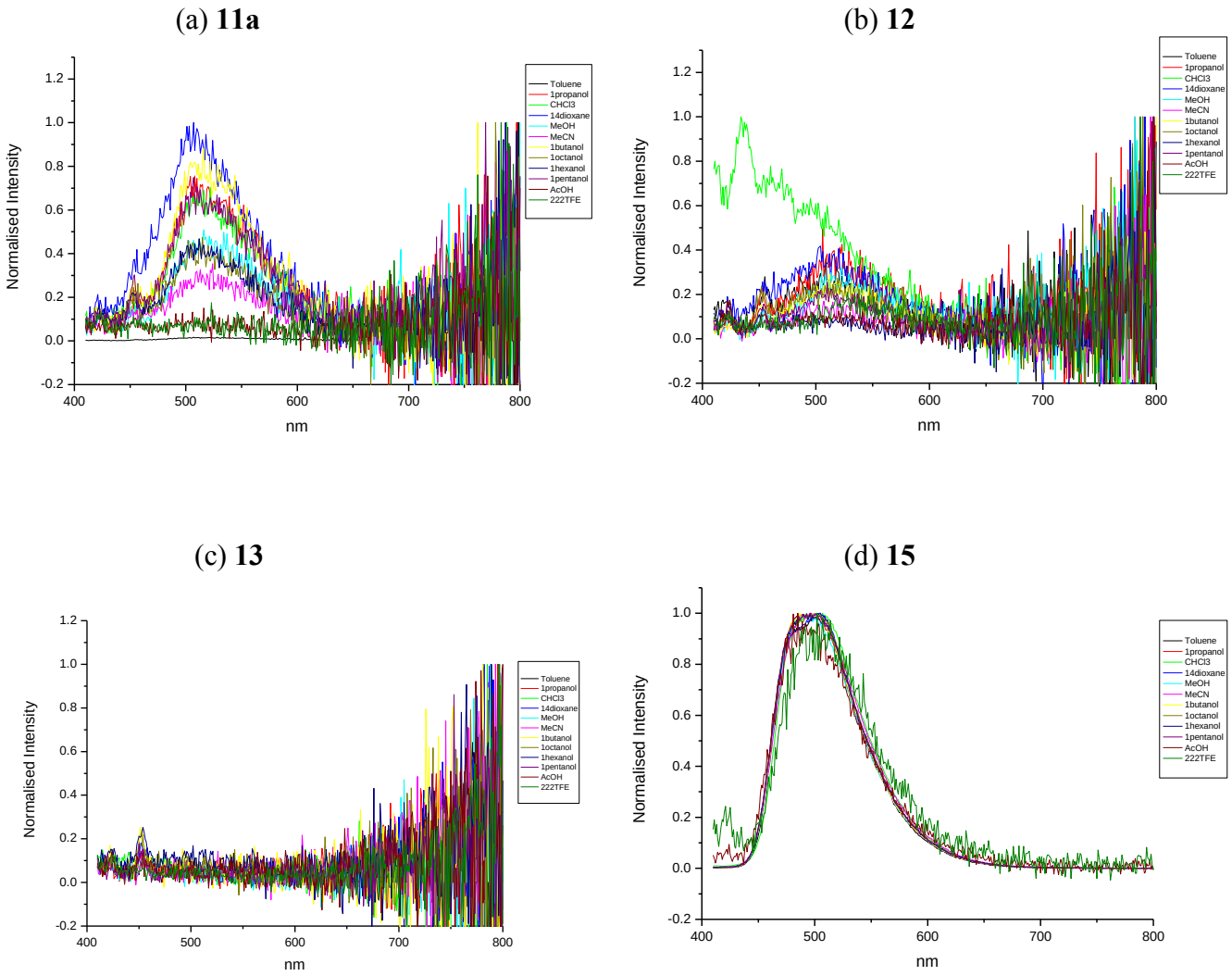

Figure 5.3.7. Summary of normalized fluorescent emission spectra at 400 nm excitation for the imine substituted 2,5-dihydro-1,2,3-triazines (**11a**, **12**, **13** and **15**).

(a)

Code	Z	Solvent	$\lambda_{310\ nm\ ems}$ (min)	Solvent	$\lambda_{310\ nm\ ems}$ (max)
3a	H †	Toluene	510	Ethylene Glycol	525
11a	CH_3	Acetonitrile	346	Chloroform	352
12	Ph	1-Hexanol	339	Chloroform	515
13	COOMe *	-	-	-	-
15	D	Toluene	512	Chloroform	519

(b)

Code	Z	Solvent	$\lambda_{400\ nm\ ems}$ (min)	Solvent	$\lambda_{400\ nm\ ems}$ (max)
3a	H †	Methanol	504	N,N-dimethylformamide	513
11a	CH_3	1-Pentanol	506	Acetonitrile	523
12	Ph	1,4-Dioxane	504	Methanol	523
13	COOMe *	-	-	-	-
15	D	Methanol	502	1-Octanol	512

Table 5.1. Summary of (a) observed emission peak maximum for 310 nm excitation (minimum and maximum value) of **11a**, **12**, **13** and **15** and (b) emission band maximum for 400 nm excitation (minimum and maximum value) of **11a**, **12**, **13** and **15**.

† Included for comparison.
* Peak maxima values too difficult to obtain from emission spectra for **13** (Z = COOMe)

An extensive range of solvents were investigated but only small solvatochromic trends were observed. As a result, it is more informative to compare the minimum and maximum values for each compound, regardless of solvent. Hence, the solvent will vary in the following tables. For a full summary of all results and solvatochromic values refer to Appendix of Results, 2.1, 2.2, 2.3 and 2.4.

In general, the calculated quantum yields for **11a**, **12** and **13** are much lower than the 2,5-dihydro-1,2,3-triazines with substituted aryl groups. For 310 nm excitation, the maximum quantum yield for **11a, 12** and **15** were calculated to be 0.22 in 1-hexanol, 0.05 in 1-hexanol and 0.63 in chloroform respectively (Table 5.2 (a)). Similarly the maximum quantum yield for **11a, 12**, and **15** for 400 nm excitation, were calculated to be to be 0.07 in toluene, 0.02 in chloroform, and 0.64 in 1,4-dioxane (Table 5.2 (b)). The quantum yields for **13** are 0 in all solvents, both at 310 and 400 nm excitation.

In comparison to **3a** (Z = H), the quantum yields are much lower for **11a**, **12** and **13** (Figure 5.3.8). However, for **15** (Z = D) only a slight difference is observed in the maximum value of the quantum yields; 0.63 in chloroform for **15** versus 0.76 in toluene for **3a** at 310 nm excitation, and 0.64 in 1,4-dioxane for **15** versus 0.79 in toluene for **3a** at 400 nm excitation. This indicates that substitution of the imine hydrogen for deuterium only has a minor effect on the fluorescence efficiency of **3a**.

Again there are two exceptions; acetic acid and 2,2,2-trifluoroethanol, both of which dramatically quench the fluorescence intensity as well as attribute to very low quantum yields for all compounds (Figure 5.3.8). Again it is possible that 2,2,2-trifluoroethanol and acetic acid are both capable of hydrogen bonding to the triazine nitrogens, the imine nitrogen or the carbonyl oxygen which would further effect the imine and carbonyl interaction but again this needs more investigation to support this hypothesis.

(a)

Code	Z	Solvent	$\Phi_{310\ nm}$ (min)	Solvent	$\Phi_{310\ nm}$ (max)
3a	H †	Propylene Carbonate	0.13	Toluene	0.76
11a	CH_3	Toluene	0.14	1-Hexanol	0.22
12	Ph	Toluene	0.01	1-Hexanol	0.05
13	COOMe	-	-	-	-
15	D	Methanol	0.34	Chloroform	0.63

(b)

Code	Z	Solvent	$\Phi_{400\ nm}$ (min)	Solvent	$\Phi_{400\ nm}$ (max)
3a	H †	Methanol	0.32	Toluene	0.79
11a	CH_3	Acetontirile	0.02	Toluene	0.07
12	Ph	Toluene	0	Chloroform	0.02
13	COOMe	-	-	-	-
15	D	Methanol	0.29	1,4-Dioxane	0.64

Table 5.2. Summary of (a) minimum and maximum quantum yield (**Φ**) values for **11a**, **12**, **13** and **15** at 310 nm excitation and (b) minimum and maximum quantum yield (**Φ**) values for **11a**, **12**, **13** and **15** at 400 nm excitation.

† Included for comparison.

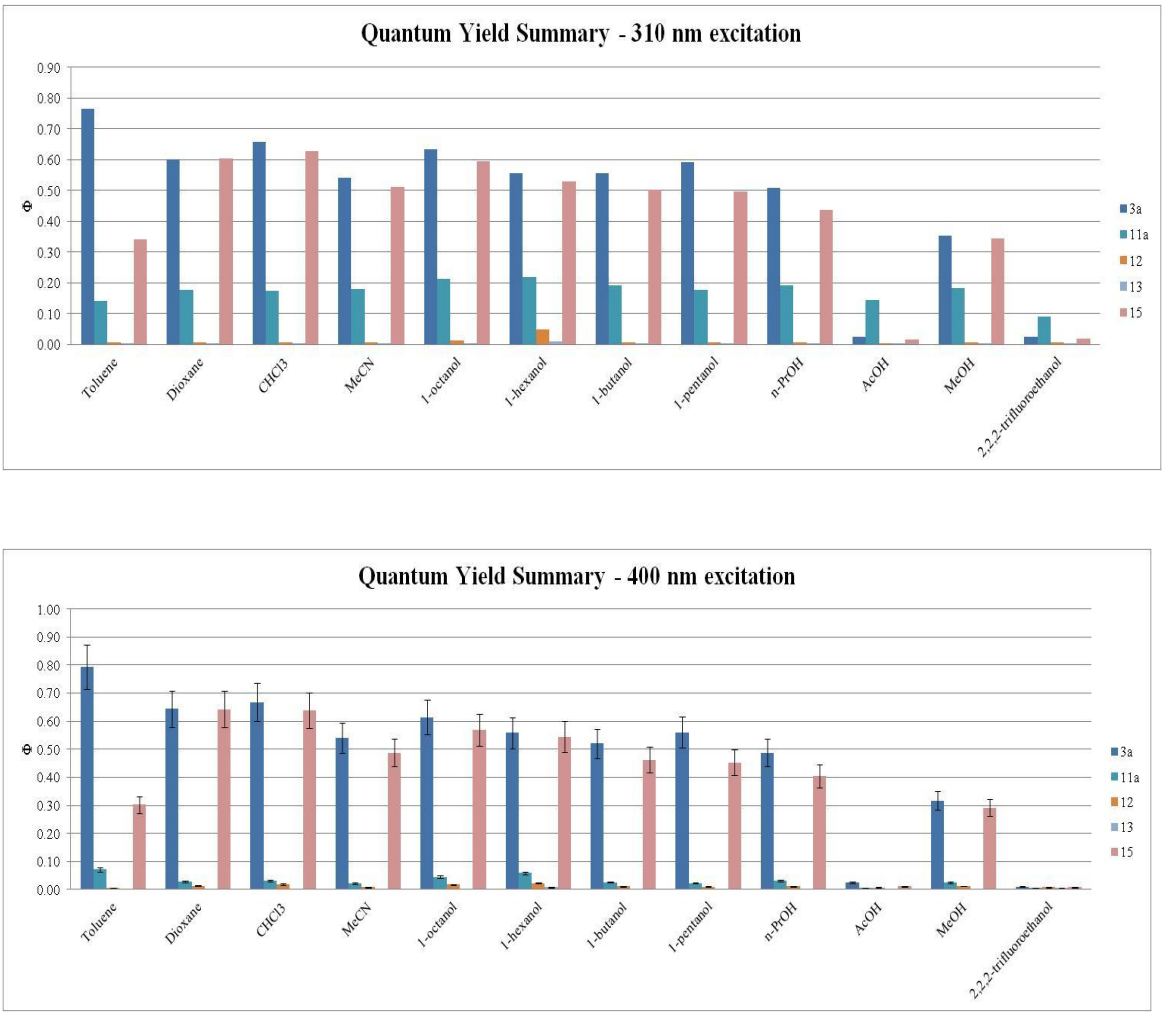

Figure 5.3.8. Graphical summary of quantum yield (**Φ**) values for the imine substituted (N=C-Z) 2,5-dihydro-1,2,3-triazines (**11a**, **12**, **13**, and **15**) versus **3a** (N=C-H).

Analysis against normalized solvent polarity (E_T^N), solvent hydrogen bonding donating/accepting ability (α and β), solvent polarizability (π^*), viscosity (η(Cp)) and dipole moment (μ) was again performed for each fluorophore. However, the solvatochromic analysis of all components (band position, area percentage of band to overall fit, band width, area ratios and band fwhm) of the deconvoluted spectra of the compounds revealed that the distribution of the data was fairly random (Appendix of Results, 2.1, 2.2, 2.3 and 2.4.).

Table 5.3 shows the minimum and maximum values of the Gaussian band positions of the deconvoluted 310 nm excitation spectra and Table 5.4 lists the minimum and maximum percentage area values.

Tables 5.5 shows the minimum and maximum values of the Gaussian band positions of the deconvoluted 400 nm excitation spectra and Table 5.5 lists the minimum and maximum percentage areas.

Code	Z	Solvent	$\lambda_{310\ nm\ ems}$ Band 1 (nm) (min)	Solvent	$\lambda_{310\ nm\ ems}$ Band 1 (nm) (max)
3a	H	2-Methyl-2-butnaol	533	Ethylene Glycol	554
11a	CH_3	-	-	-	-
12	Ph	1-Octanol	500	Acetonitrile	518
13	COOMe	-	-	-	-
15	D	Toluene	532	Methanol	548

Code	Z	Solvent	$\lambda_{310\ nm\ ems}$ Band 2 (nm) (min)	Solvent	$\lambda_{310\ nm\ ems}$ Band 2 (nm) (max)
3a	H	2-Methyl-2-butanol	503	Ethylene Glycol	515
11a	CH_3	1,4-Dioxane	516	Methanol	526
12	Ph	1-Octanol	454	1-Propanol	508
13	COOMe	1-Octanol	463	1-Hexanol	497
15	D	Toluene	504	Methanol	510

Code	Z	Solvent	$\lambda_{310\ nm\ ems}$ Band 3 (nm) (min)	Solvent	$\lambda_{310\ nm\ ems}$ Band 3 (nm) (max)
3a	H	2-Methyl-2-butanol	468	Ethylene Glycol	479
11a	CH_3	Toluene	385	Methanol	410
12	Ph	1-Octanol	337	1-Hexanol	359
13	COOMe	1-Octanol	338	1,4-Dioxane	369
15	D	1,4-Dioxane	470	Chloroform	474

Code	Z	Solvent	$\lambda_{310\ nm\ ems}$ Band 4 (nm) (min)	Solvent	$\lambda_{310\ nm\ ems}$ Band 4 (nm) (max)
3a	H	1,3-Propanediol	344	1,4-Butanediol	380
11a	CH_3	Toluene	358	Methanol	361
12	Ph	-	-	1-Hexanol	331
13	COOMe	1-Pentanol	342	1,4-Dioxane	343
15	D	1-Octanol	348	Chloroform	354

Code	Z	Solvent	$\lambda_{310\ nm\ ems}$ Band 5 (nm) (min)	Solvent	$\lambda_{310\ nm\ ems}$ Band 5 (nm) (max)
3a	H	1,3-Propanediol	338	1,4-Butanediol	353
11a	CH_3	Acetonitrile	339	Chloroform	341
12	Ph	-	-	-	-
13	COOMe	-	-	-	-
15	D	-	-	-	-

Table 5.3. Summary of Guassian band maximum positions from deconvoluted spectra (minimum and maximum values) for **11a**, **12**, **13** and **15** at 310 nm excitation.

Code	Z	Solvent	$\lambda_{310\ nm}$ Band 1 Area % (min)
3a	H	1,3-Butanediol	36.3
11a	CH_3	-	-
12	Ph	1-Propanol	28.32
13	COOMe	-	-
15	D	Methanol	46.8

Z	Solvent	$\lambda_{310\ nm}$ Band 1 Area % (max)
H	2-Methyl-2-butanol	59.26
CH_3	-	-
Ph	Methanol	82.86
COOMe	-	-
D	Toluene	59

Code	Z	Solvent	$\lambda_{310\ nm}$ Band 2 Area % (min)
3a	H	1,3-Butanediol	27.33
11a	CH_3	Toluene	3.94
12	Ph	1-Hexanol	10.82
13	COOMe	1-Hexanol	8.88
15	D	Toluene	30

Z	Solvent	$\lambda_{310\ nm}$ Band 2 Area % (max)
H	Acetonitrile	46.43
CH_3	Chloroform	5.81
Ph	1-Propanol	58.35
COOMe	1-Octanol	25.86
D	Methanol	44

Code	Z	Solvent	$\lambda_{310\ nm}$ Band 3 Area % (min)
3a	H	1,3-Butanediol	5.49
11a	CH_3	Methanol	3.54
12	Ph	1-Butanol	11.6
13	COOMe	1,4-Dioxane	68.5
15	D	Methanol	6.94

Z	Solvent	$\lambda_{310\ nm}$ Band 3 Area % (max)
H	1,5-Pentanediol	8.36
CH_3	Toluene	12.4
Ph	1-Hexanol	68.64
COOMe	Methanol	100
D	Toluene	9.36

Code	Z	Solvent	$\lambda_{310\ nm}$ Band 4 Area % (min)
3a	H	1,3-Propanediol	8.31
11a	CH_3	Acetonitrile	53.45
12	Ph	-	-
13	COOMe	1-Pentanol	10.64
15	D	Chloroform	1.16

Z	Solvent	$\lambda_{310\ nm}$ Band 4 Area % (max)
H	1,3-Butanediol	15.14
CH_3	Methanol	56.74
Ph	1-Hexanol	20.53
COOMe	Acetonitrile	81.73
D	1-Hexanol	4.69

Code	Z	Solvent	$\lambda_{310\ nm}$ Band 5 Area % (min)
3a	H	1,3-Propanediol	3.52
11a	CH_3	Chloroform	28.69
12	Ph	-	-
13	COOMe	-	-
15	D	-	-

Z	Solvent	$\lambda_{310\ nm}$ Band 5 Area % (max)
H	1,3-Butanediol	15.72
CH_3	Methanol	34.02
Ph	-	-
COOMe	-	-
D	-	-

Table 5.4. Summary of area percentages for Gaussian band fits (minimum and maximum values) for **11a**, **12**, **13** and **15** at 310 nm excitation.

Code	Z	Solvent	$\lambda_{400\ nm\ ems}$ Band 1 (nm) (min)
3a	H	Toluene	524
11a	CH_3	-	-
12	Ph	-	-
13	COOMe	-	-
15	D	Toluene	531

Z	Solvent	$\lambda_{400\ nm\ ems}$ Band 1 (nm) (max)
H	Ethylene Glycol	548
CH_3	-	-
Ph	-	-
COOMe	-	-
D	Acetonitrile	541

Code	Z	Solvent	$\lambda_{400\ nm\ ems}$ Band 2 (nm) (min)
3a	H	2-Methyl-2-butanol	500
11a	CH_3	1,4-Dioxane	512
12	Ph	Chloroform	437
13	COOMe	-	-
15	D	1,4-Dioxane	502

Z	Solvent	$\lambda_{400\ nm\ ems}$ Band 2 (nm) (max)
H	Ethylene Glycol	510
CH_3	Toluene	526
Ph	Methanol	524
COOMe	-	-
D	Chloroform	505

Code	Z	Solvent	$\lambda_{400\ nm\ ems}$ Band 3 (nm) (min)
3a	H	2-Methyl-2-butanol	469
11a	CH_3	-	-
12	Ph	-	-
13	COOMe	-	-
15	D	1,4-Dioxane	471

Z	Solvent	$\lambda_{400\ nm\ ems}$ Band 3 (nm) (max)
H	Ethylene Glycol	480
CH_3	-	-
Ph	-	-
COOMe	-	-
D	Chloroform	475

Table 5.5. Summary of Guassian band maximum positions from deconvoluted spectra (minimum and maximum values) for **11a**, **12**, **13** and **15** at 400 nm excitation.

Code	Z	Solvent	$\lambda_{400\ nm}$ Band 1 Area % (min)
3a	H	Methanol	40.67
11a	CH_3	-	-
12	Ph	-	-
13	COOMe	-	-
15	D	Methanol	40.52

Z	Solvent	$\lambda_{400\ nm}$ Band 1 Area % (max)
H	Toluene	50.7
CH_3	-	-
Ph	-	-
COOMe	-	-
D	Toluene	51.54

Code	Z	Solvent	$\lambda_{400\ nm}$ Band 2 Area % (min)
3a	H	Toluene	38.89
11a	CH_3	-	-
12	Ph	-	-
13	COOMe	-	-
15	D	Toluene	37.66

Z	Solvent	$\lambda_{400\ nm}$ Band 2 Area % (max)
H	Acetonitrile	46.85
CH_3	Toluene	100
Ph	Toluene	100
COOMe	-	-
D	Acetonitrile	46.12

Code	Z	Solvent	$\lambda_{400\ nm}$ Band 3 Area % (min)
3a	H	1,4-Dioxane	9.42
11a	CH_3	-	-
12	Ph	-	-
13	COOMe	-	-
15	D	1,4-Dioxane	9.72

Z	Solvent	$\lambda_{400\ nm}$ Band 3 Area % (max)
H	Ethylene Glycol	12.67
CH_3	-	-
Ph	-	-
COOMe	-	-
D	Methanol	13.67

Table 5.6. Summary of area percentages for Gaussian band fits (minimum and maximum values) for **11a**, **12**, **13** and **15** at 400 nm excitation.

From Tables 5.4 and 5.5, a difference can be observed between the area percentage contribution of the fitted bands for **11a** and **3a** at 310 nm excitation. For **3a**, Band 2 has a maximum percentage contribution of 46.43 % in acetonitrile, whilst for **11a** it is 5 % in acetonitrile. Band 3 has a maximum percentage contribution of 8.36 % in 1,5-pentanediol for **3a** whereas the value is 12.4 % in toluene for **11a**. Band 4 and 5 have a maximum percentage contribution of 15.14 % and 15.72 % respectively in 1,3-butanediol for **3a**. From this, the increase in S_2(**g0**) and S_1(**g0**) emission for **11a**, can be seen from the percentage contributions from Band 4 and Band 5, with a maximum percentage contribution of 56.74 % and 34.02 % respectively in methanol.

From Tables 5.4, 5.5, 5.6 and 5.7, it is evident that a deuterium substituition has very little effect on the nature of the excited states, with the band positions and area percentage contributions in close agreement with **3a** (Z = H). For example at 310 nm excitation, **15** has a maximum value of 548 nm in methanol for Band 1 whilst for **3a** the value is 554 nm in ethylene glycol. Similarly the maximum area percentage contribution of Band 1 for **15** is 59 % in toluene and 59 % in 2-methyl-2-butanol for **3a**.

Further analysis of the Gaussian model fit data showed no trend or evidence of solvatochromic behaviour. A multiple linear regression analysis on **11a** (Table 5.7 and 5.8) against the solvatochromic values α, β and π^* was performed. The emission peak maximum, Gaussian band positions, quantum yield and UV-visible absorbance were correlated against for both 310 and 400 nm excitation which showed no significant correlations (a linear correlation is supported when r^2 approaches unity *i.e.* 1).

y	y_o	a_α	b_β	c_{π^*}	r^2
$\lambda_{ems\ max\ (32258\ cm^{-1})}$	28135.00 ± 269.90	-355.02 ± 72.56	594.67 ± 138.40	861.34 ± 410.21	**0.82**
Band 1 cm^{-1} (Gaussian Fit)	-	-	-	-	**-**
Band 2 cm^{-1} (Gaussian Fit)	19790.73 ± 164.98	-191.36 ± 73.35	-191.67 ± 97.17	-793.95 ± 251.35	**0.80**
Band 3 cm^{-1} (Gaussian Fit)	26678.20 ± 1231.15	23.63 ± 330.99	-989.77 ± 631.34	-1411.55 ± 1871.20	**0.27**
Band 4 cm^{-1} (Gaussian Fit)	27833.19 ± 252.89	-174.86 ± 67.99	77.29 ± 129.68	-6.63 ± 384.37	**0.50**
Band 5 cm^{-1} (Gaussian Fit)	29235.45 ± 177.74	-159.94 ± 47.78	212.82 ± 91.14	210.20 ± 270.15	**0.68**
Φ (32258 cm-1)	0.17 ± 0.06	-0.02 ± 0.01	0.06 ± 0.03	-0.04 ± 0.09	**0.68**
Abs (32258 cm-1)	0.08 ± 0.03	-0.019 ± 0.00	-0.01 ± 0.01	-0.027 ± 0.04	**0.52**

Table 5.7. Estimated from the equation ($y = y_0 + a_\alpha*\alpha + b_\beta*\beta + c_{\pi^*}*\pi^*$), coefficients ($y_o$, a_α, b_β, c_{π^*}), their standard errors and correlation coefficients (r) for the multiple linear regression analysis for **11a** at 310 nm excitation against the solvatochromic values α, β and π*.

y	y_o	a_α	b_β	c_{π^*}	r^2
$\lambda_{ems\ max\ (25000\ cm^{-1})}$	20195.04 ± 454.26	-394.39 ± 201.98	253.03 ± 267.56	-1273.89 ± 692.08	**0.64**
Band 1 cm^{-1} (Gaussian Fit)	-	-	-	-	**-**
Band 2 cm^{-1} (Gaussian Fit)	19184.26 ± 446.58	-41.29 ± 165.88	79.40 ± 261.36	31.10 ± 677.55	**0.02**
Band 3 cm^{-1} (Gaussian Fit)	-	-	-	-	**-**
Φ (25000 cm-1)	0.13 ± 0.03	-0.00 ± 0.01	-0.03 ± 0.01	-0.15 ± 0.05	**0.55**
Abs (25000 cm-1)	0.03 ± 0.02	-0.00 ± 0.00	-0.01 ± 0.01	-0.03 ± 0.03	**0.40**

Table 5.8 Estimated from the equation ($y = y_0 + a_\alpha*\alpha + b_\beta*\beta + c_{\pi^*}*\pi^*$), coefficients ($y_o$, a_α, b_β, c_{π^*}), their standard errors and correlation coefficients (r) for the multiple linear regression analysis for **11a** at 400 nm excitation against the solvatochromic values α, β and π*.

5.3.2 Time resolved fluorescence measurements.

The fluorescence lifetime behaviour of the imine substituted (N=C-Z) 2,5-dihydro-1,2,3-triazine fluorophores is completely different to the hydrogen substituted parent structure **3a** (N=C-H). Similarly to the 2,5-dihydro-1,2,3-triazines with substituted aryl groups, the fluorescence decay of all the species (**11a**, **12**, **13** and **15**) could be fitted to a 2 or 3 exponential term.

As only a 405 nm excitation source was used to investigate the fluorescent lifetime behavior of the 2,5-dihydro-1,2,3-triazines with substituted aryl groups, only the 400 nm emission band lifetime was investigated for those compounds reported in Chapter 4, Section 4.3.2. By using a 295 nm LED excitation source, the lifetime of the 310 nm excitation fluorescence band centered at ~350 nm could be investigated for **11a**, **12**, and **13** at 330 and 350 nm. For the 310 nm emission band centered at ~500 nm for **15**, the lifetime of the outer edges of the emission could be investigated at 470 nm and 570 nm using the 295 nm LED excitation source.

Fitting of the decay data was performed using the Fluofit software using a free fit method. The χ^2 (goodness of fit) values are a little high for the LED excited measurements. This is mostly due to misfits at the beginning of the decay traces and is largely attributed to light scatter and small mismatches between the instrument response and fluorescence decay data. Due to extremely low photon counts and poor decay curves, an accurate fit could not be obtained for the lifetimes of **12** and **13**.

The 330 and 350 nm (295 nm LED excitation) two fit decay for N=C-CH_3 (**11a**) is composed of:

1. A very fast component (τ_1) with values ranging from 0.99 to 1.5 ns.
2. A medium/long component (τ_2) with values ranging from ~3.7 to 8.3 ns.

Whilst for **15**, the 470 and 570 nm (295 nm LED excitation) three fit decay is composed of:

1. A short lived component (τ_1) with values ranging from ~0.26 to 11.5 ns.
2. A medium component (τ_2) ranging from values of 2.73 to 6.64 ns.
3. A long lived component (τ_3) which ranges from 9.23 to 13.91 ns.

An extensive range of solvents were investigated but only small trends were observed. As a result, it is more informative to compare the minimum and maximum values for each compound, regardless of solvent. Hence, the solvent will vary in the following tables. For a full summary of the data refer to Appendix of Results, 2.1, 2.2, 2.3 and 2.4.

Table 5.9 lists the minimum and maximum intensity weighted average lifetimes for **11a** and **15** at the lowest (330 / 470 nm) and highest emission wavelength (350 / 570 nm) using a 295 nm LED excitation source.

11a has a maximum value for the intensity weighted lifetime at 330 nm of 1.8 ns in 1-hexanol, whilst at 350 nm, the maximum value of the intensity weighted lifetime is slightly shorter at 1.52 ns in 1-octanol (Table 5.9). For **15**, the maximum value for the intensity weighted lifetime at 470 nm is 7.54 ns in chloroform, whilst at 570 nm, the maximum value of the intensity weighted lifetime is much longer at 11.81 ns in 1-octanol. This indicates that the lifetime of the 310 nm emission is relatively long lived for **15**, and suggests that it is similar in nature to the 310 nm excitation emission centered at ~500 nm for **3a**.

Code	Z	Wavelength (nm) – LED	Solvent	τ_f (ns) (Intensity Weighted) (min)	Wavelength (nm) - LED	Solvent	τ_f (ns) (Intensity Weighted) (max)
3a	CH_3	350	Chloroform	1.07	350	1-Hexanol	1.52
11a	Ph *	-	-	-	-	-	-
12	COOMe *	-	-	-	-	-	-
13	D	570	Methanol	2.51	570	1-Octanol	11.81
15							

Code	Z	Wavelength (nm) – LED	Solvent	τ_f (ns) (Intensity Weighted) (min)	Wavelength (nm) - LED	Solvent	τ_f (ns) (Intensity Weighted) (max)
3a	CH_3	330	Chloroform	1.06	330	1-Hexanol	1.8
11a	Ph *	-	-	-	-	-	-
12	COOMe *	-	-	-	-	-	-
13	D	470	Methanol	2.36	470	Chloroform	7.54
15							

Table 5.9. Summary of the minimum and maximum intensity weighted average lifetimes (τ_f) of the imine substituted (N=C-Z) 2,5-dihydro-1,2,3-triazines recorded using a 295 nm LED excitation source.

Tables 5.10 lists the minimum and maximum values for the decay times (τ_i) and their corresponding fractional intensities (A_i) for **11a** (330 and 350 nm emission) and **15** (470 and 570 nm emission) using a 295 nm LED excitation source.

For **11a** (Table 5.10 (a)), it is clear that the majority of the intensity weighted average lifetime is composed of the fast component τ_1 (0.99 to 1.16 ns, with up to 98.74 % fractional intensity), with the medium/long component τ_2 (3.67 to 8.14 ns) being the remainder of the decay at 330 and 350 nm (295 nm LED excitation source). For **15**, the intensity weighted average lifetime is composed in majority of the medium component τ_2 (up to 72.88 %) at 470 nm, whilst at 570 nm, similarly to 405 nm excitation, there is an increase in the contribution from the longer lived τ_3 state (up to 93.24 %) and subsequent decrease in the maximum contribution from τ_2 (72.88 to 41.02 %) for 295 nm LED excitation.

(a)

Z	Waevlength (nm) - LED	Solvent	τ_1 (ns) (min)	A_1 (%)
CH_3	330	Chloroform	1.01	98.74
CH_3	350	Toluene	0.99	98.21

Z	Waevlength (nm) - LED	Solvent	τ_1 (ns) (max)	A_1 (%)
CH_3	330	1-Octanol	1.16	92.38
CH_3	350	1-Octanol	1.12	89.96

Z	Waevlength (nm) - LED	Solvent	τ_3 (ns) (min)	A_3 (%)
CH_3	330	-	-	-
CH_3	350	-	-	-

Z	Waevlength (nm) - LED	Solvent	τ_3 (ns) (max)	A_3 (%)
CH_3	330	-	-	-
CH_3	350	-	-	-

Z	Waevlength (nm) - LED	Solvent	τ_2 (ns) (min)	A_2 (%)
CH_3	330	Methanol	5.05	0.88
CH_3	350	Methanol	3.67	0.93

Z	Waevlength (nm) - LED	Solvent	τ_2 (ns) (max)	A_2 (%)
CH_3	330	1-Butanol	8.14	2.92
CH_3	350	1-Hexanol	7.97	6.11

(b)

Z	Waevlength (nm) - LED	Solvent	τ_1 (ns) (min)	A_1 (%)
D	470	Methanol	2.79	72.88
D	570	1,4-Dioxane	0.26*	41.02
D	570	Methanol	1.92	58.98

Z	Waevlength (nm) - LED	Solvent	τ_1 (ns) (max)	A_1 (%)
D	470	Chloroform	5.73	70.24
D	570	1,4-Dioxane	1.55*	2.29
D	570	1-Octanol	11.5	35.55

Z	Waevlength (nm) - LED	Solvent	τ_3 (ns) (min)	A_3 (%)
D	470	1-Butanol	9.23	22.79
D	570	Toluene	10.11	93.24

Z	Waevlength (nm) - LED	Solvent	τ_3 (ns) (max)	A_3 (%)
D	470	1-Hexanol	12.71	16.01
D	570	1-octanol	13.91	50.37

Table 5.10. Summary of the minimum and maximum values for the lifetime decay components of (a) **11a** (330 and 350 nm emission) and (b) **15** (470 and 570 nm emission) using a 295 nm LED excitation source.

Similar to the emission, no solvatochromic behavior was observed for the 295 nm LED excitation fluorescent lifetime. The only trend observed was for the intensity weighted average lifetime for **11a** (330 and 350 nm) versus dipole moment (μ(D)) of the solvent

* Due to extremely low photon counts and poor decay curves, an accurate fit could not be obtained.

(Figure 5.3.9). An "on switch" trend is observed in intensity weighted lifetime as the solvent dipole moment increases from 1,4-dioxane (μ(D) of 0) to 2,2,2-trifluoroethanol (μ(D) of 2.46); acetonitrile (μ(D) of 3.92) being the outliers. This would indicate that the lifetime of the 310 nm emission for **11a** is sensitive to the dipole moment of the solvent, but shall require further investigation.

Figure 5.3.9. Intensity weighted average lifetimes (τ_f) at 330 and 350 nm (295 nm LED) of **11a** versus μ(D).

The instrument was then configured with a 405 nm laser diode excitation source and the lifetime of the 400 nm emission band centred at 500 nm was examined for both **11a** (Z = CH_3) and **15** (Z = D).

Due to extremely low counts and poor quality decay curves, fitting of the fluorescence lifetime of the 400 nm excitation band centred at 500 nm could only be done for **11a** in 1,4-dioxane and chloroform.

Table 5.11 lists the minimum and maximum intensity weighted average lifetimes for **11a** and **15** at 500 nm emission using a 405 nm laser diode excitation source and is compared to **3a** at 490 nm emission.

In comparison to **3a** (Z = H) at 490 nm emission, where the intensity weighted average lifetime has a maximum value of 7.44 ns in propylene carbonate, the intensity weighted average lifetime of **11a** is considerably faster at 500 nm emission with a maximum value of 3.88 ns in 1,4-dioxane. Whereas for **15** (Z = D) the intensity weighted

average lifetime is slightly longer with a maximum value of 8.24 ns in 1,4-dioxane (Table 5.11).

Code	Z	Wavelength (nm) – Laser	Solvent	τ_f (ns) (Intensity Weighted) (min)	Wavelength (nm) - Laser	Solvent	τ_f (ns) (Intensity Weighted) (max)
3a	H	490	Methanol	4.49	490	Propylene Carbonate	7.44
11a	CH_3	500	Chloroform	2.81	500	1,4-dioxane	3.88
12	Ph *	-	-	-	-	-	-
13	COOMe *	-	-	-	-	-	-
15	D	500	1-hexanol	1.18	500	1,4-dioxane	8.24

Table 5.11. Summary of the minimum and maximum intensity weighted average lifetimes (τ_f) of the imine substituted (N=C-Z) 2,5-dihydro-1,2,3-triazines using a 405 nm laser diode excitation source.

The minimum and maximum values for the decay times (τ_i) and their corresponding fractional intensities (A_i) for **11a** and **15** at 500 nm excitation using a 405 nm laser diode excitation source are given in Tables 5.12.

Code	Z	Wavelength (nm)	Solvent	τ_1 (ns) (min)	A_1 (%)	Z	Waevlength (nm)	Solvent	τ_1 (ns) (max)	A_1 (%)
3a	H	490	N,N-dimethylforamide	0.22	0.97	H	490	Ethylene Glycol	1.19	3.95
11a	CH_3	500	1,4-Dioxane	0.29	22.53	CH_3	500	Chloroform	0.62	7.82
15	D	500	1-Pentanol	0.34	2.02	D	500	Methanol	1.28	17.86

* Due to extremely low photon counts and poor decay curves, an accurate fit could not be obtained.

Code	Z	Wavelength (nm)	Solvent	τ_2 (ns) (min)	A_2 (%)
3a	H	490	1,4-Dioxane	3.29	66.47
11a	CH_3	500	Chloroform	1.5	65.28
15	D	500	Methanol	2.62	82.14

Z	Waevlength (nm)	Solvent	τ_2 (ns) (max)	A_2 (%)
H	490	N,N-dimethylformamide	5.65	69.75
CH_3	500	1,4-dioxane	3.57	56.51
D	500	Chloroform	5.5	57.28

Code	Z	Wavelength (nm)	Solvent	τ_3 (ns) (min)	A_3 (%)
3a	H	490	Ethylene Glycol	7.38	33.41
11a	CH_3	500	Chloroform	6.52	27.4
15	D	500	Toluene	9.78	55.37

Z	Wavelength (nm)	Solvent	τ_3 (ns) (max)	A_3 (%)
H	490	1-Hexanol	11.73	24.14
CH_3	500	1,4-Dioxane	8.56	20.96
D	500	1-Pentanol	11.84	27.55

Table 5.12. Summary of the minimum and maximum lifetime decay components of the imine substituted (N=C-Z) 2,5-dihydro-1,2,3-triazines using a 405 nm laser diode excitation source; where A_i is the fractional intensity.

The majority of the lifetime at 500 nm for **11a** is composed of the short lived species τ_2 (1.5 to 3.57 ns), with the remainder being equally composed of a very fast component τ_1 (0.29 to 0.62 ns) and a long lived component τ_3 (6.52 to 8.56 ns).

The intensity weighted average lifetime of **15** is similar to **3a**, only being ~0.8 ns faster (Table 5.11). From Table 5.12, the slightly longer values for τ_3 (9.78 to 11.84 ns) accounts for the slightly longer lived lifetime of **15**.

Analysis of the intensity weighted average lifetimes (295 nm LED and 405 nm laser diode exctitation source), 330 and 350 nm intensity weighted lifetimes (295 nm LED) and 500 nm intensity weighted lifetime (405 nm laser diode), and their respective decay times against the normalized solvent polarity (E_T^N), solvent hydrogen bonding donating/accepting ability (α and β), solvent polarizability (π^*), viscosity (η(Cp)), dielectric constant (ε) and dipole moment (μ) was performed for each fluorophore.

However, the solvatochromic analysis of all the components revealed the distribution of data to be fairly random (Appendix of Results, 2.1, 2.2, 2.3 and 2.4).

5.4 CONCLUSION.

One of the interesting things about these molecules is the fact that small structural changes, in the appropriate position, can have a very large effect on the photophysical behaviour.

From Chapter 4, it is known that if the structural changes are outside of the molecular core, then the spectroscopic differences appear to be relatively small as seen

when the 4-position of the upper and lower phenyl rings are substituted with heavy atoms (**6a** and **9a**).

For this particular family, the imine substituted (N=C-Z) variants, the structural change applied was substitution at the imine carbon (Z = CH_3, Ph, COOMe, or D) and in doing so, a significant change in fluorescence was observed. We postulate that due to these structural modifications, the imine and ester are no longer held in-plane, which effects the fluorescence behavior by altering the dipole transition moment.

The substitution is easily accomplished synthetically by utilizing a terminally substituted alkyne dipolarophile, most of which are commercially available, in the 1,3-dipolar cycloaddition. However, thermolytic ring expansion of the pyrrolo[2,3-d]-1,2,3-triazolium intermediate did not occur under "normal" conditions (*i.e.* dry acetone reflux) when methyl-2-butynoate (Z = CH_3) was used. Investigation of the literature suggested that this is due to a higher energy barrier for the ring expansion which was overcome by simply refluxing in toluene to produce the 2,5-dihydro-1,2,3-triazines: **11a**, **12**, **13** and **15** in yields of 80 %, 75 %, 75 % and 76 % respectively).

Interestingly, the nature of the imine carbon substitution caused a significant change to the ground state absorption and photophysics. A higher energy absorption at ~300 nm, that is blue shifted compared to **3a** was observed for **11a**. The strong absorption band at ~400 nm was no longer observed except in the case of **15** (Z = D) which shares similarities to **3a** (Z = H).

The 310 nm excitation of **11a** now shows a weak intensity at *ca.* 500 nm and a new intense tri-band emission at *ca.* 350 nm that is uneffected by changing the nature of the solvent. This is supported by the fact that in the normalised fluorescence sprectra no solvatochromism was observed in position of the emission band maximum. In general, the calculated quantum yields for **11a**, **12** and **13** were much lower than **3a**. Excitation at 400 nm resulted in virtually no fluorescence emission for **11a** with either a very weak or noisy single emission at ~510 nm.

Bulky substituents, such as a phenyl or carboxy ester substituted on the imine carbon (**12**, Z = Ph and **13**, Z = COOMe) generate a significant change in fluorescence properties. We believe that the imine and ester can no longer be held in-plane and that this

ultimately effects the dipole transition moment. As a result, under both 310 and 400 nm excitation, only very weakly emitting species are observed for both **12** and **13**. However, in the case of a deuterium substituent (**15**) the fluorescent properties were almost the same for the hydrogen substituted parent structure (**3a**).

By using a 295 nm LED excitation source, the lifetime of the 310 nm excitation fluorescence band centered at ~350 nm could be investigated for **11a** and was found to be quite short lived (1.8 ns in 1-octanol). As the lifetime of the 310 nm emissions was not investigated in the study of **3a**, and as **15** is similar in fluorescent behavior, the lifetime of the emission of **15** for 310 nm excitation was investigated whilst the 295 nm LED excitation source was set up. At 570 nm emission, the intensity weighted lifetime of **15** is 11.81 ns in 1-octanol, which indicated that the lifetime of the 310 nm emission is relatively long lived for **15**. We therefore believe that the same result would be obtained for the lifetime of the 310 nm excitation for **3a**.

This work identified an important structural element to this class of fluorphore was identified. The synthesis of novel fluorophores of this class in future will require that the imine is substituted with smaller substituents so as to maintain the rotation of the imine group and hence allow it to remain in plane with the carbonyl. We believe that it is this that ultimately controls the fluorescence emission and fluorescence efficiency.

.

Chapter 6: Imine hydrolysis of the 2,5-dihydro-1,2,3-triazines with substituted aryl groups.

6.1 INTRODUCTION.

The 2,5-dihydro-1,2,3-triazine compounds discussed thus far are reasonably stable compounds and can be stored as a solid, under dry conditions, for several months. However, the imine functionality of **3a** (N=C-H) is susceptible to hydrolysis and as a result dry solvents must be used in the preparation of these 2,5-dihydro-1,2,3-triazines.[54]

When the reaction is carried out using wet acetone a small quantity of a new product, 5-H 2,5-dihydro 1,2,3-triazine (**16**), is encountered resulting from the hydrolytic degradation of **3a**.

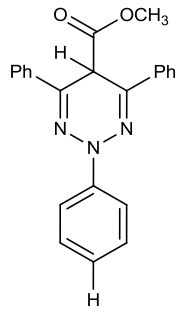

16

Figure 6.1.1. General structure of 5-H 2,5-dihydro-1,2,3-triazine (**16**).

It is known that solid tumors tend to have a more acidic microenvironment than normal tissues, as demonstrated in murine tumor models whereby the extracellular environment is acidic relative to the intracellular environment.[78] We postulated that this may limit the use of **3a** as a fluorescent pH or environment probe as the imine may be susceptible to hydrolysis at extracellular pH resulting in a mixture of fluorescent species being present.

Therefore, we considered that **16** itself may be more suitable as a future conventional fluorophore. Hence, a deliberate approach to hydrolyzing **3a** in an efficient manner was investigated. Previously Butler *et al.* had reported the generation of **16** *via* a long seven day reflux.[54] We undertook an investigation to find an efficient synthesis of **16** and a study of its fluorescent properties.

6.2 RESULTS AND DISCUSSION (SYNTHESIS).

Refer to Chapter 2, Section 2.1.3 for experimental procedure and results.

6.2.1 Imine hydrolysis of the 2,5-dihydro-1,2,3-triazines with substituted aryl groups.

The hydrolysis of imines is generally a facile reaction assisted by acid catalysis, whereby protonation of the imine nitrogen results in the formation of an iminium ion. This iminium ion undergoes nucleophilic attack by water and subsequent elimination of an amine moiety to yield an oxonium ion, which in turn can then be deprotonated to give a ketone.[79]

Hydrolysis of the 2,5-dihydro-1,2,3-triazine involves the acid catalyzed addition of water to the imine resulting in (a) competitive fragmentation to give formanilide and the hydrolysed product, or (b) a formylated triazine at C-5 which undergoes air oxidation of the formyl group and subsequent decarboxylation to give the hydrolysed 5-H 2,5-dihydro 1,2,3-triazine (Scheme 6.2.1).[54,80]

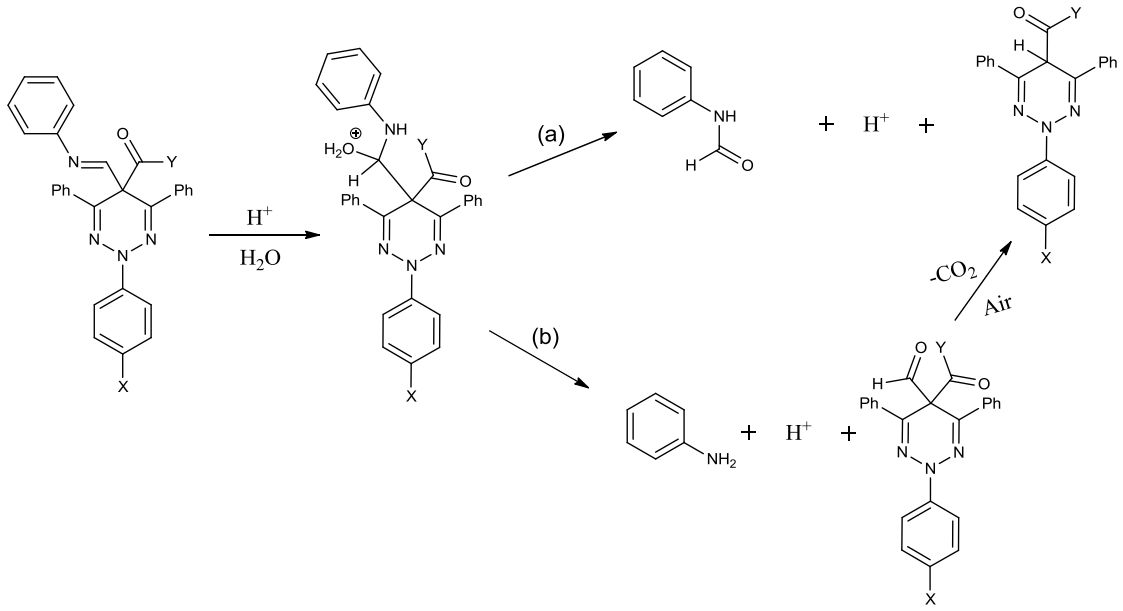

Scheme 6.2.1. Proposed mechanism of hydrolysis of 2,5-dihydro-1,2,3-triazine.

When the degradation was carried out in a 1:1 (v/v) EtOD-D_2O mixture, the C-5 position became deuterated confirming the presence of a carbanion. [54,80] This susceptibility of the 2,5-dihydro-1,2,3-triazines to hydrolysis also manifests itself during the purification of 2,5-dihydro-1,2,3-triazines with substituted aryl groups, namely during column chromatography. The acidic nature of the silica gel used during flash chromatography purification appears to promote the imine hydrolysis, albeit to a small extent.

The previously reported method for hydrolysis (Table 6.1, entry 1) was inefficient, taking a week to afford desirable yields, and was also problematic in terms of the final column chromatography purification process. The retention factor (R_f) value of the hydrolysed product is the same as parent molecule, both can be identified as a mixture of a green/light blue fluorescence spot when viewed under UV illumination. As a result, we aimed to develop a highly efficient method with full conversion and avoiding difficult column chromatography.

The initial reaction conditions chosen were similar to the original aqueous ethanol reflux but with hydrochloric acid added as an acid catalyst (Table 6.1, entry 2). This reaction yielded a complex mixture of unidentifiable products.

Entry	Reaction Conditions	Time	Yield (%)
1	EtOH, H_2O, 100 ^oC [54]	1 week	50 % *
2	EtOH, HCl, 100 ^oC	24 hrs	Complex mixture

Table 6.1 Attempted reaction conditions for imine hydrolysis of Ph triazine.

It was assumed that the reaction conditions using hydrochloric acid were too harsh and the use of a weaker acid, acetic acid, was investigated (Table 6.2). A 5 hr reflux in neat acetic acid (Table 6.2, entry 1) also produced a complex mixture of products, although some of the desired product was generated as can be seen by the presence of the C5 hydrogen signal at 5.32 ppm in the ^1H NMR spectrum (Figure 6.2.1.).

* Impure isolated yield.

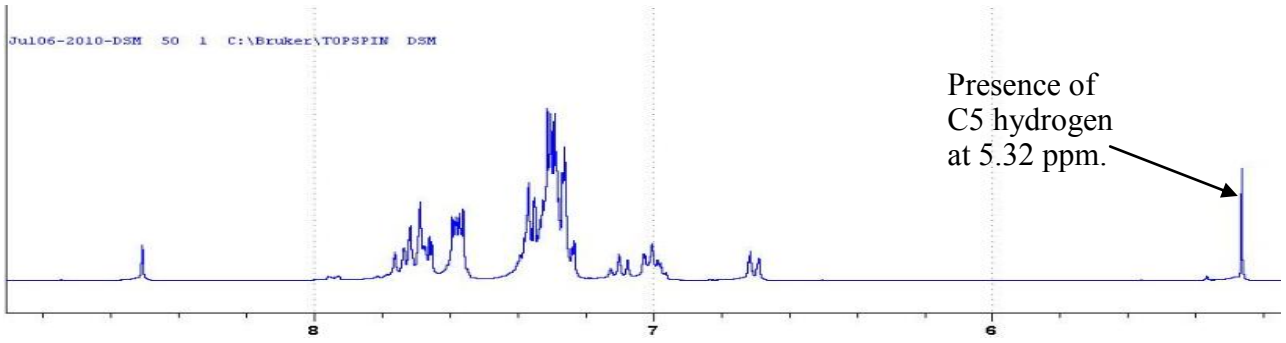

Figure 6.2.1. ^{1}H NMR spectrum of **3a** following a 5 hr reflux in acetic acid.

Entry	Reaction Conditions	Time	Result
1	Acetic acid, 120 ^{o}C	5 hrs	Desired product with complex mixture
2	Acetic acid, 120 ^{o}C	15 mins to 2 hrs*	Complex mixture with increasing product to starting material ratio
3	Acetic acid, 20 ^{o}C	1 week	Desired product with complex mixture
4	Acetic acid (10 mol excess), MeOH, 120 ^{o}C	2 hrs	99 % yield of desired product

Table 6.2. Attempted reaction conditions for the imine hydrolysis of **3a** using acetic acid.

An NMR time course investigation was undertaken (Table 6.2, entry 2) whereby a small quantity was removed from the reaction every 15 minutes over the course of a 2 hour period. The sample was washed with saturared aqueous sodium bicarbonate, extracted with diethyl ether, dried using magnesium sulphate and filtered. The solvent was then removed under reduced pressure and the ^{1}H NMR spectrum was recorded of the residue in $CDCl_3$. Although an increase in product to starting material ratio was observed over the 2 hour period, it was accompanied by the generation of a complex reaction mixture of products (Figure 6.2.2). Stirring the starting material in neat acetic acid at 20 ^{o}C for 1 week (Table 6.2, entry 3) resulted in the generation of the desired product but again this was accompanied by the production of several unidentifiable by-products.

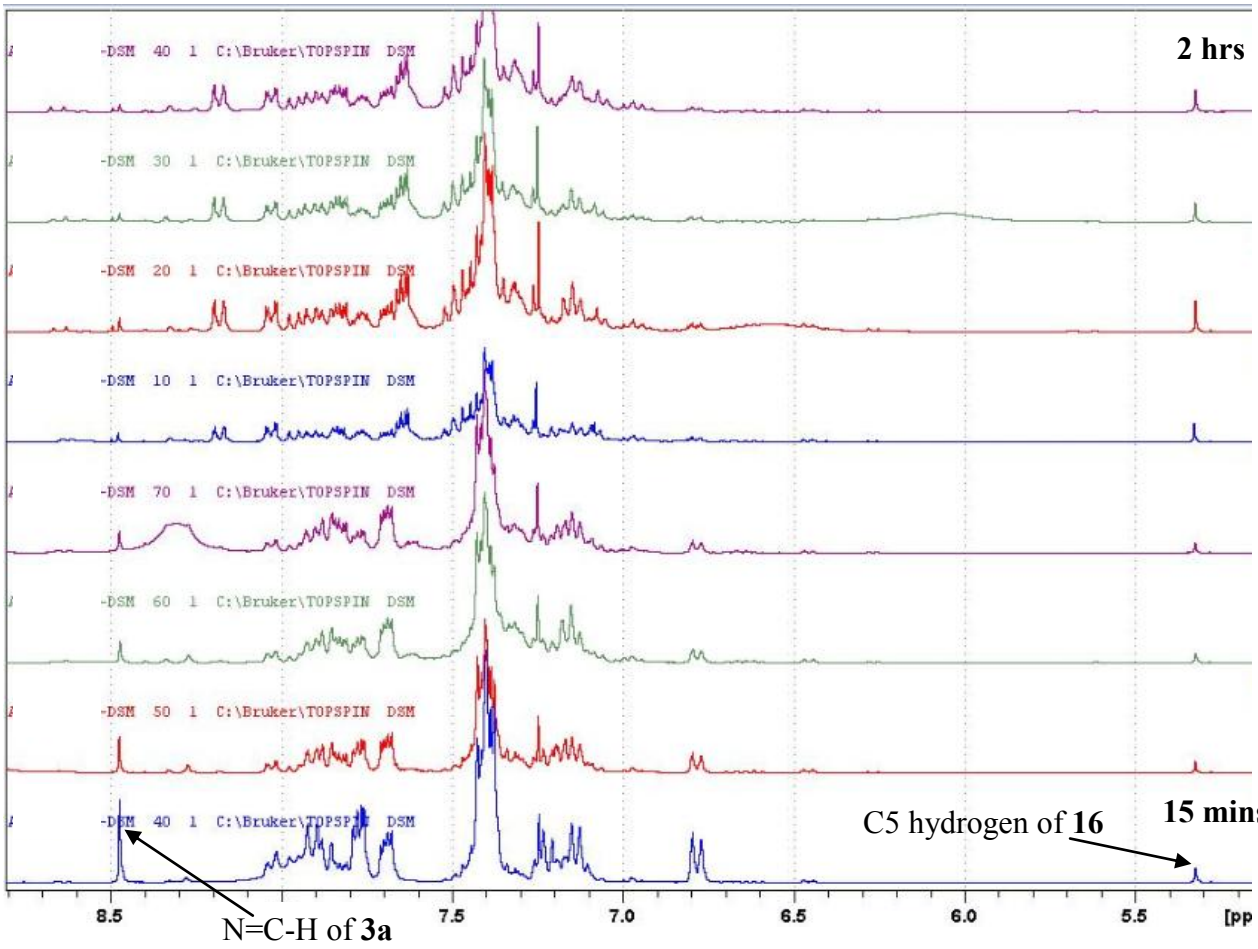

Figure 6.2.2. NMR spectra of **3a** in acetic acid recorded every 15 minutes as reaction was performed under reflux.

We concluded that the reaction conditions were still too harsh and decided to lower the concentration of acid and use a wet co-solvent, methanol. Heating the reaction mixture to 120 ^{o}C for 2 hours (Table 6.2, entry 4) allowed the reaction to go to completion and the desired product **16** was isolated in a 99 %yield. This same methodology was successfully applied to the hydrolysis of the other 2,5-dihydro-1,2,3-triazines with substituted aryl groups **6a**, **9a** and **10a** with isolated yields of 84 %, 96 % and 93 % respectively.

In all cases, the structure was identified using ^{1}H and ^{13}C NMR spectra and supported by HRMS and IR spectroscopy. A confident assignment can be made based on the characteristic C5 hydrogen ^{1}H NMR signal observed at 5.31 ppm for **16** as well as the

* Samples were taken every 15 minutes and analysed *via* ^{1}H NMR.

disappearance of the imine N=C-H proton signal at 8.47 in the ^{1}H NMR spectrum and carbon signal at 159 ppm in the ^{13}C spectrum (Figure 6.2.3).

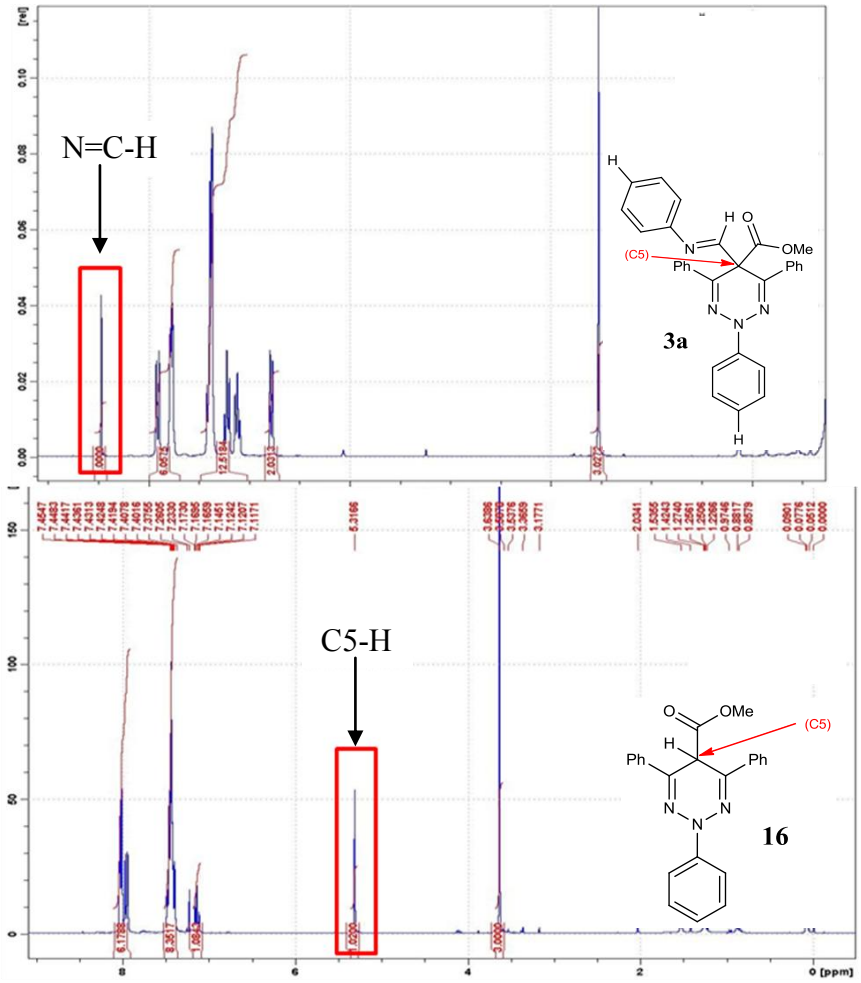

Figure 6.2.3. NMR spectra of **3a** and **16** recorded in chloroform.The disappearance of the imine hydrogen at 8.49 ppm and appearance of a new signal for the C5 hydrogen at 5.32 ppm for **16** are highlighted.

They also exhibit a key quaternary carbon signal for C5 at ~37 ppm, as well as a quaternary carbon signal at ~166 ppm which confirms the presence of a carbonyl and is supported by the IR spectrum with the C=O stretch being observed at ~1641 cm^{-1}.

Interestingly, the new hydrolysed fluorophore **16** now exhibits blue/green fluorescence in solution upon UV irradiation, evident in the photograph shown in Figure 6.2.4.

Figure 6.2.4. Solutions of **3a** and **16** in chloroform under UV irradiation.

6.3 RESULTS AND DISCUSSION (FLUORESCENCE SPECTROSCOPY).

Refer to Chapter 2, Section 2.2.1 for experimental procedure and results.

Refer to Appendix of Results 3.1, 3.2, 3.3 and 3.4 for complete set of solvatochromic results, tables and graphs.

6.3.1 Steady state fluorescence study.

A detailed steady state solvatochromism study was undertaken for the imine hydrolysed 2,5-dihydro-1,2,3-triazine fluorophores (**16**, **17**, **18** and **19**) with 12 solvents selected: toluene, 1,4-dioxane, chloroform, acetonitrile, 1-octanol, 1-hexanol, 1-butanol, 1-pentanol, 1-propanol, acetic acid, methanol and 2,2,2-trifluoroethanol (Refer to Appendix A.2 for complete list of solvents and solvatochromic values).

Analysis was again performed against normalized solvent polarity (E_T^N), solvent hydrogen bonding donating/accepting ability (α and β), solvent polarizability (π^*), viscosity (η(Cp)) and dipole moment (μ) for each fluorophore, using the software package Origin 7.0, in an attempt to identify any possible ground state solvent interactions which may influence their fluorescence emission.

6.3.1.1 Ultraviolet Visible absorption spectra.

Removal of the phenylimine group and its replacement with a hydrogen at C-5 causes a minor change to the ground state absorption and photophysics. A lower energy absorption that is red-shifted at ~325 nm compared to **3a** (~310 nm) and a broad absorption band at ~390 nm is observed. Similar to **3a**, both absorption bands are not strongly effected by changing the nature of the solvent (Figures 6.3.1), which is clearly evident in the normalized UV-visible spectra where there is no change in the band positions (Figures 4.3.4).

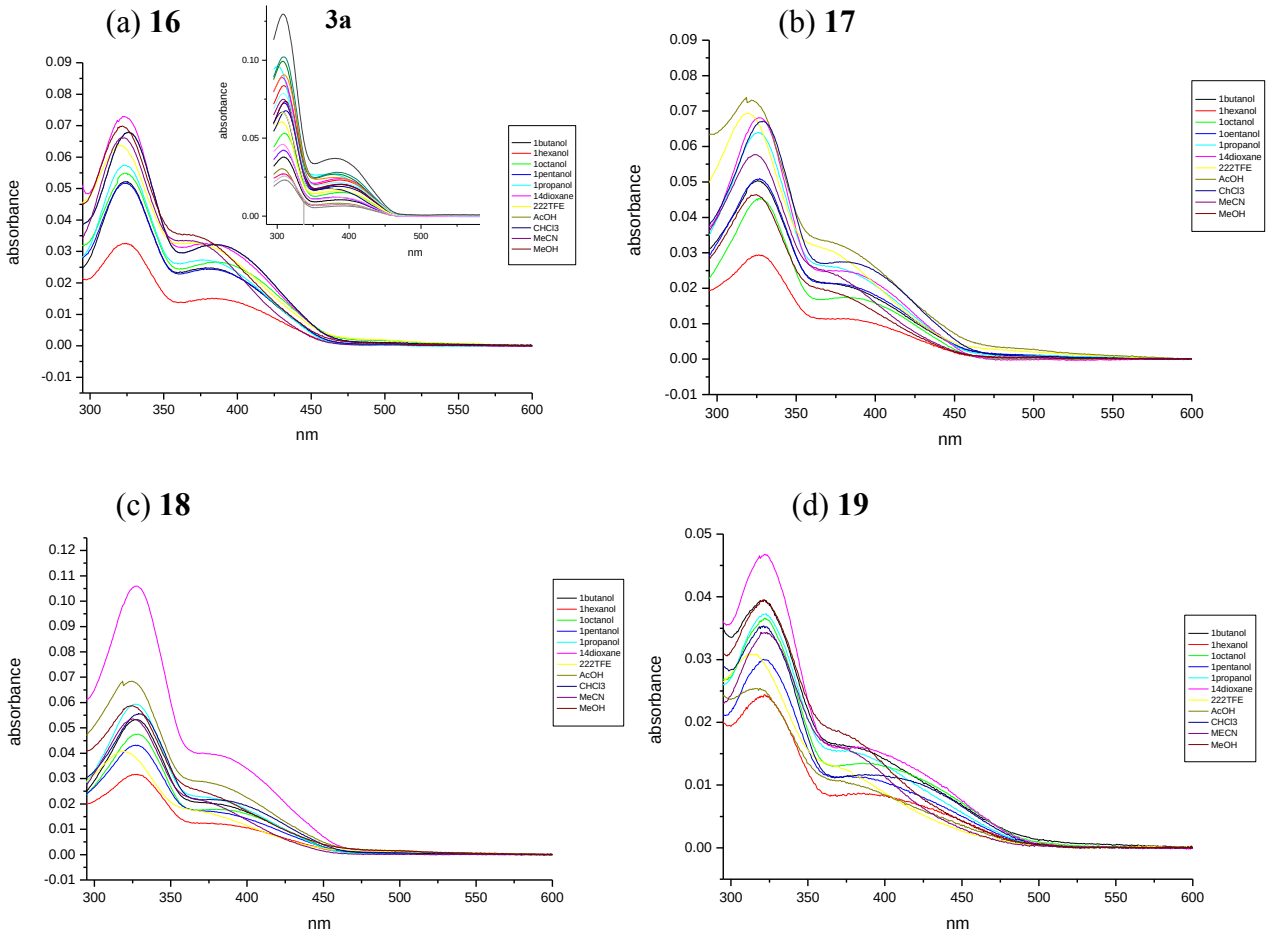

Figure 6.3.1. Ultraviolet visible absorption spectra for the imine hydrolysed 2,5-dihydro-1,2,3-triazines (**16**, **17**, **18** and **19**) recorded at an assumed maximum concentration of 1 x 10^{-5} M, with **3a** (inset) for comparison.

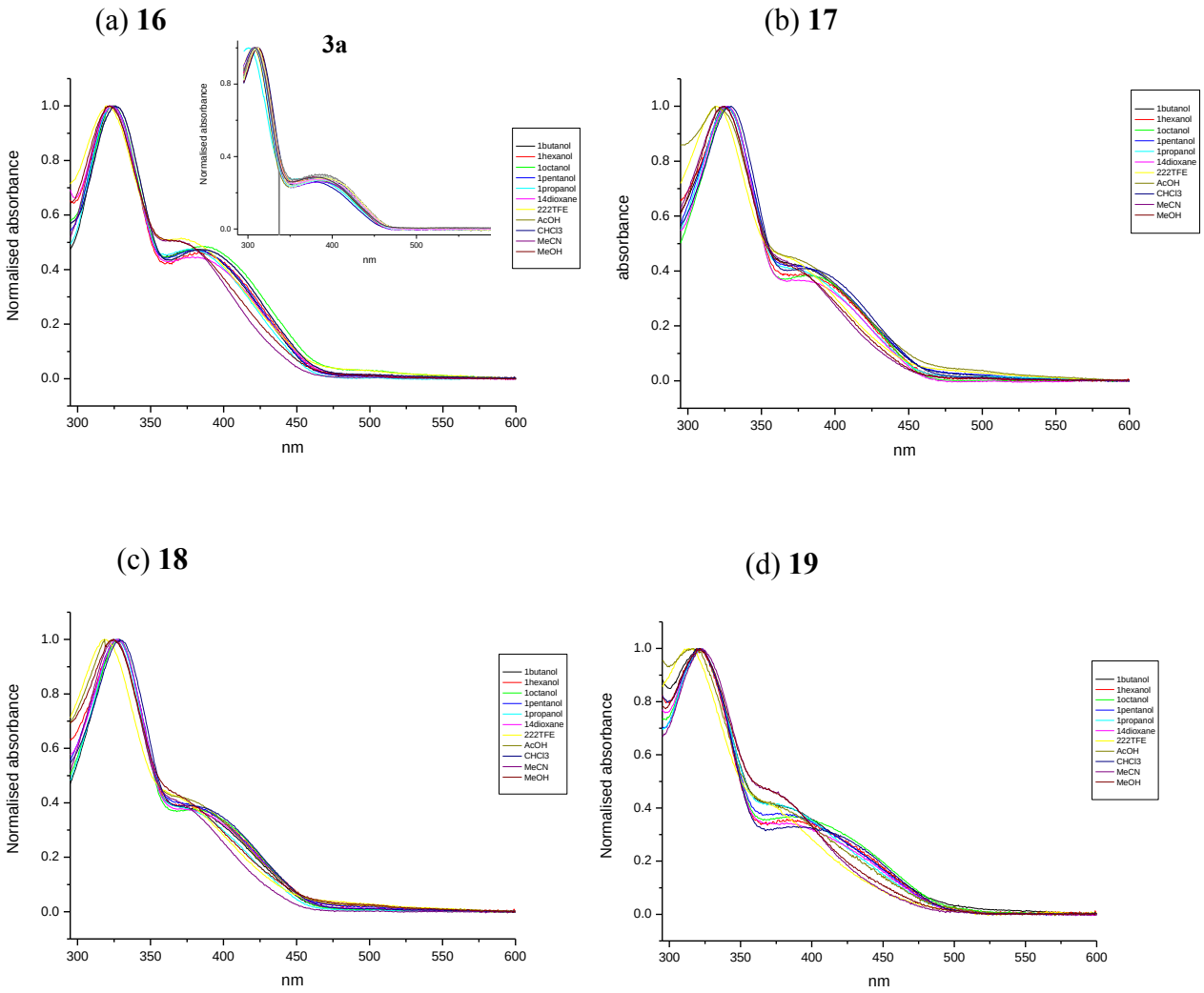

Figure 6.3.2. Normalised ultraviolet visible absorption spectra for the imine hydrolysed 2,5-dihydro-1,2,3-triazines (**16**, **17**, **18** and **19**), with **3a** (inset) for comparison.

6.3.1.2 Fluorescence emission spectra.

For all of the imine hydrolysed 2,5-dihydro-1,2,3-triazine fluorophores, excitation into either of the absorption bands (310 and 400 nm) results in a green/blue fluorescence emission band centred at ~480 nm that is blue-shifted compared to **3a** (~520 nm) and is also uneffected by the nature of the solvent (Figures 6.3.4, and 6.3.5). This is supported in the normalised fluorescence spectra where no change is observed in the position of the emission band maximum (Figure 6.3.6 and 6.3.7). The deconvoluted spectra at 400 nm excitation (Figure 6.3.3) consist of three emission bands: ~470 nm (Band 3), ~500 nm (Band 2), and ~530 nm (Band 1) that are of higher energy compared to **3a;** ~510 nm (Band 2), and ~540 nm (Band 1). Excitation at 310 nm emission also consists of three separate emission bands: ~495 nm (Band 3), ~510 nm (Band 2), and ~530 nm (Band 1). Also a single weakly emitting band at ~350 nm (Band 4) is obsevred which is assumed to be due to the population of the S_3 (**g0**) and S_2 (**g0**) ES (similar to **3a** although a fifth band (Band 5) was not found). This emission (Band 4) is only observed in 1-hexanol for **16** but is more noticeable for **17** and **18** where the N-2 phenyl ring is substituted with a heavy atom (Figure 6.3.4).

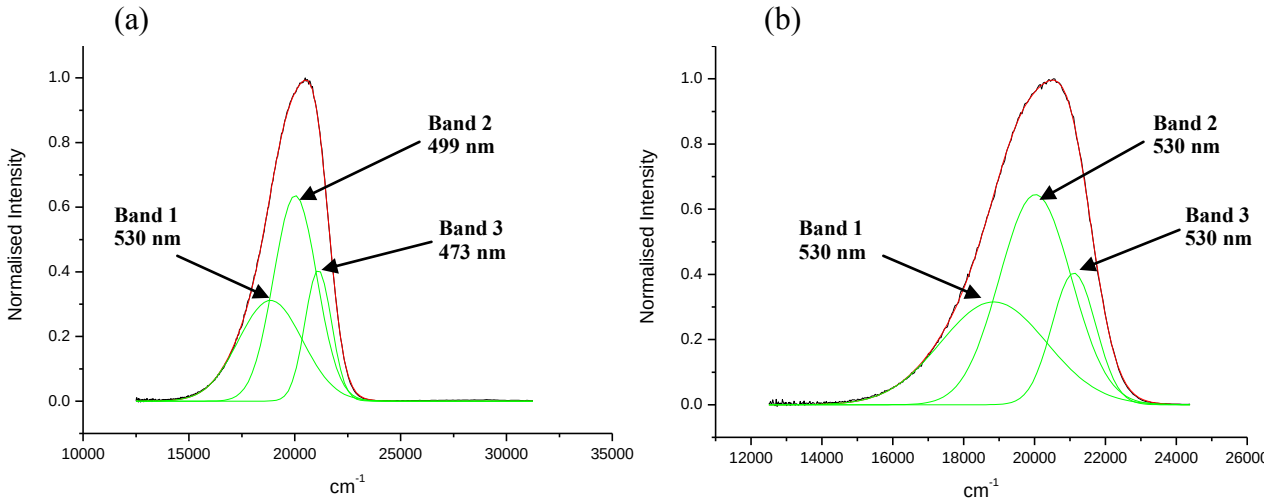

Figure 6.3.3. Gaussian model fits of the normalised fluorescence emission spectrum of **16** recorded in acetonitrile for (a) 310 nm and (b) 400 nm excitation.

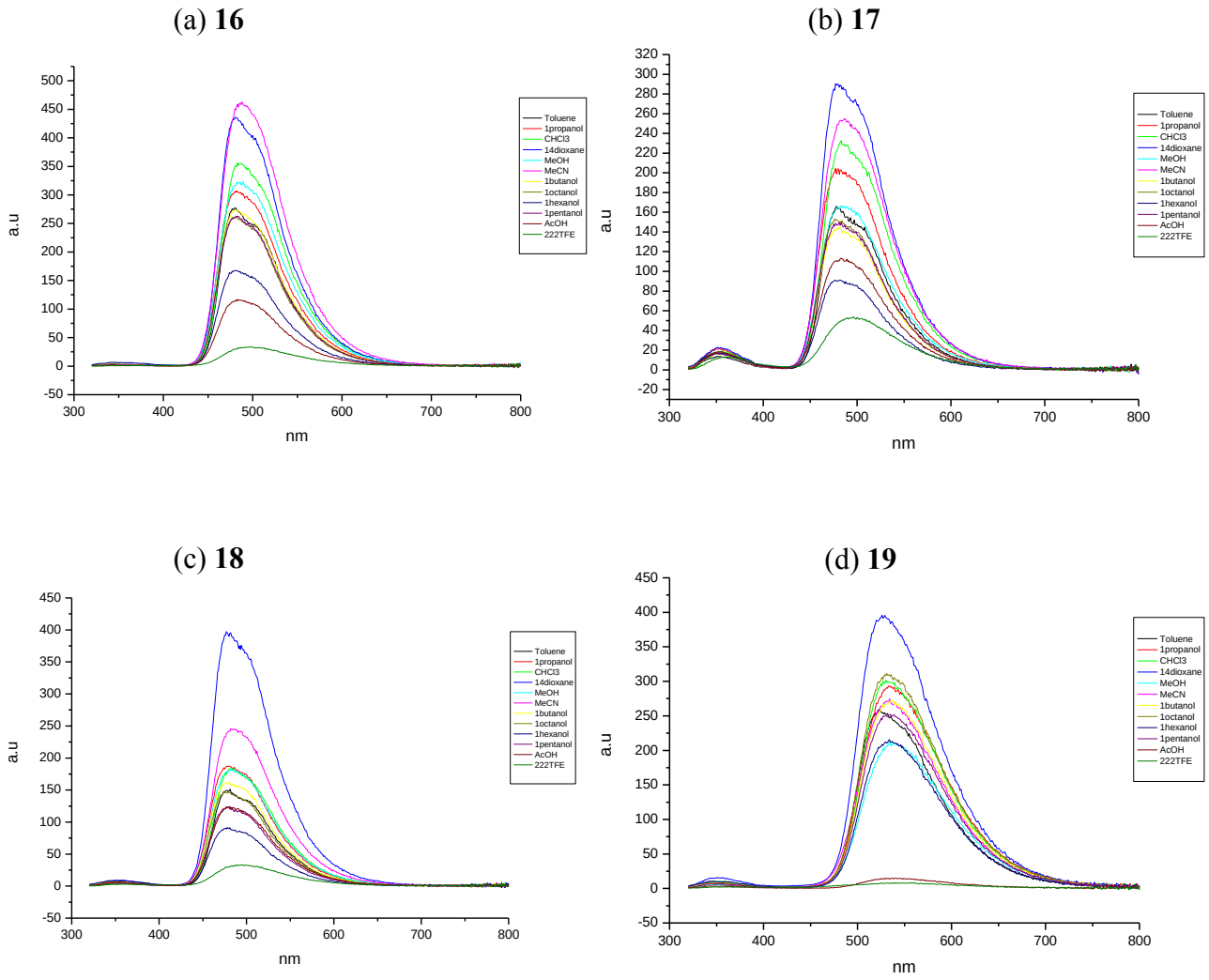

Figure 6.3.4. Summary of fluorescent emission spectra at 310 nm excitation for the imine hydrolysed 2,5-dihydro-1,2,3-triazines (**16**, **17**, **18** and **19**) recorded at an assumed maximum concentration of 1 x 10^{-5} M.

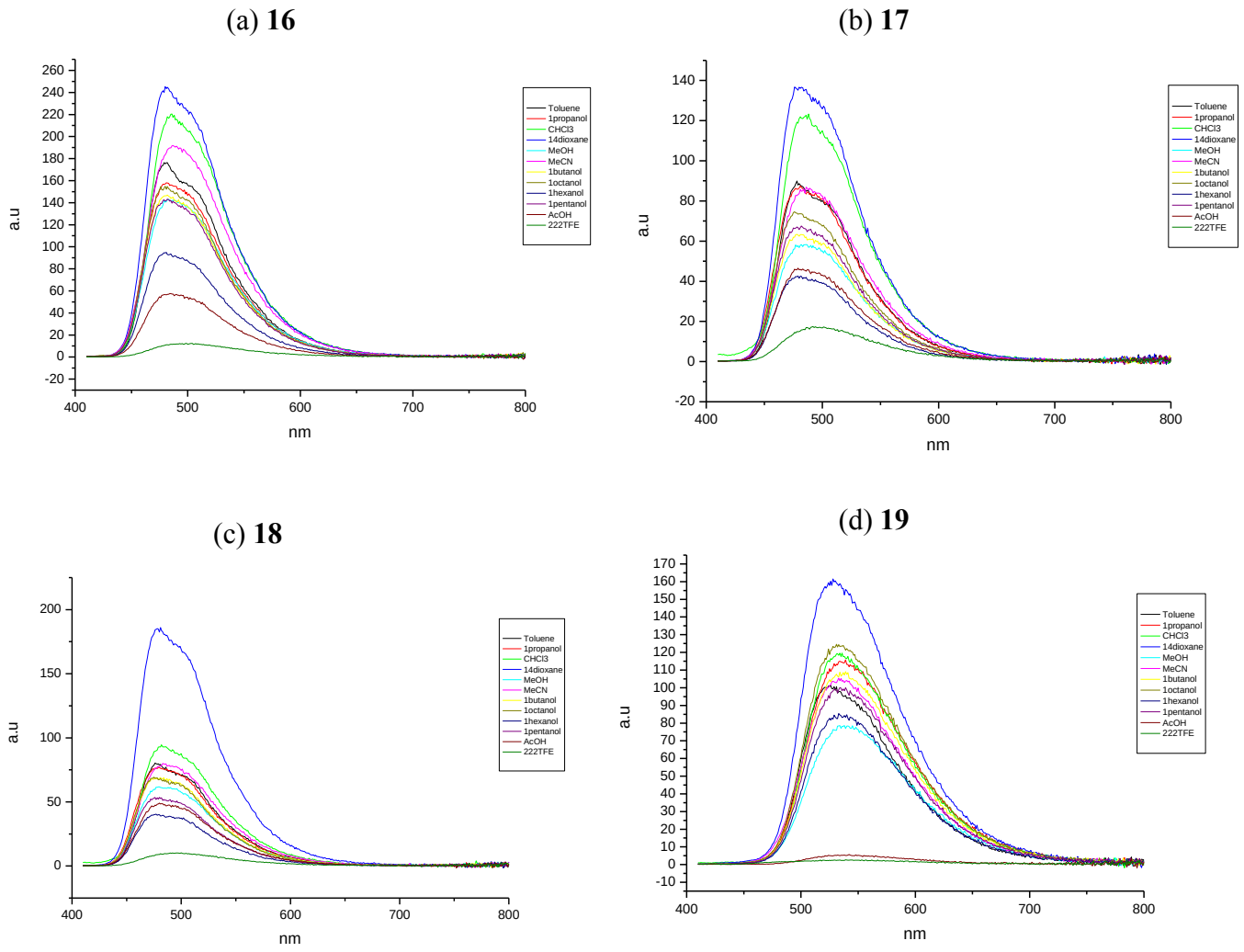

Figure 6.3.5. Summary of fluorescent emission spectra at 400 nm excitation for the imine hydrolysed 2,5-dihydro-1,2,3-triazines (**16**, **17**, **18** and **19**) recorded at an assumed maximum concentration of 1 x 10^{-5} M.

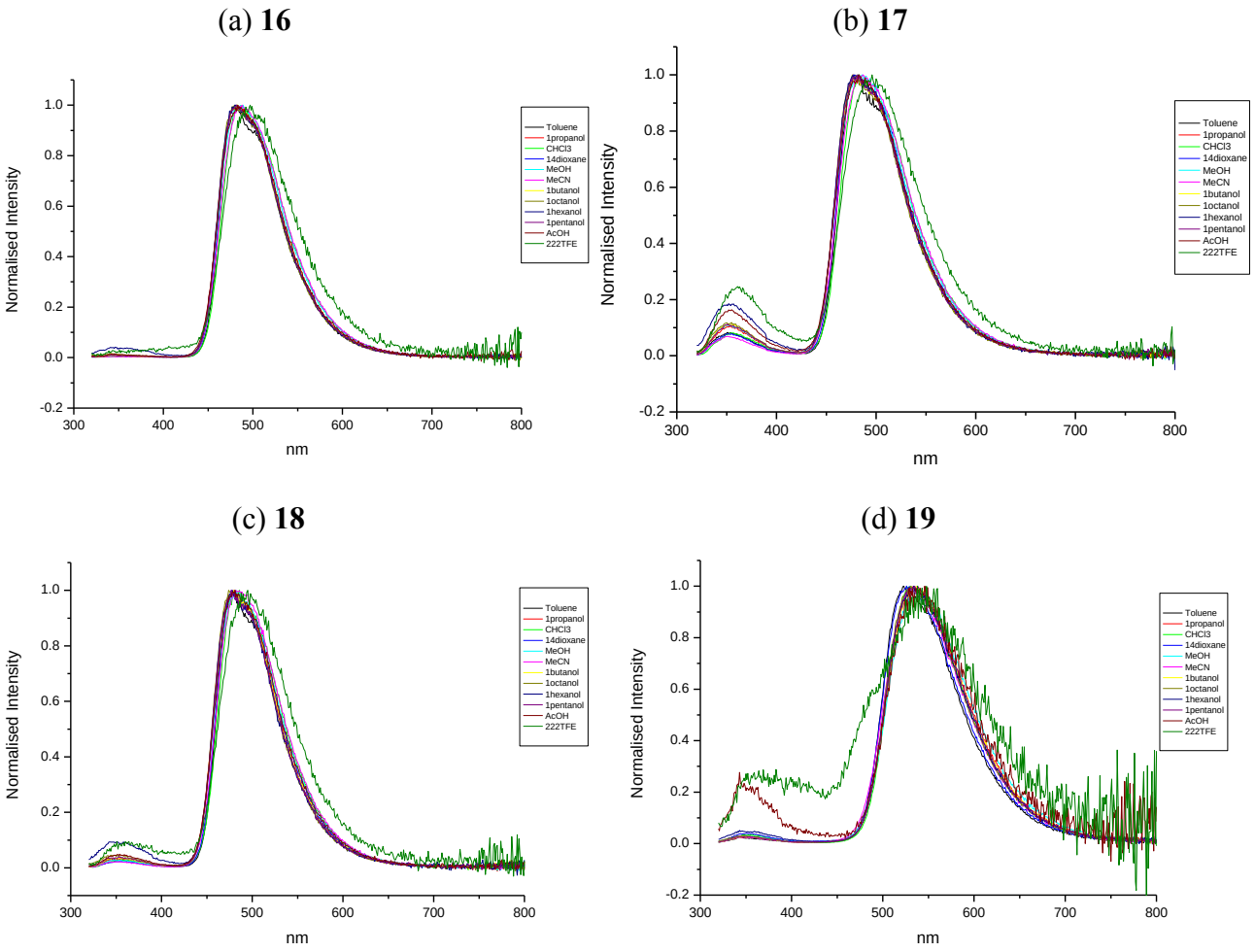

Figure 6.3.6. Summary of the normalized fluorescent emission spectra at 310 nm excitation for the imine hydrolysed 2,5-dihydro-1,2,3-triazines (**16**, **17**, **18** and **19**).

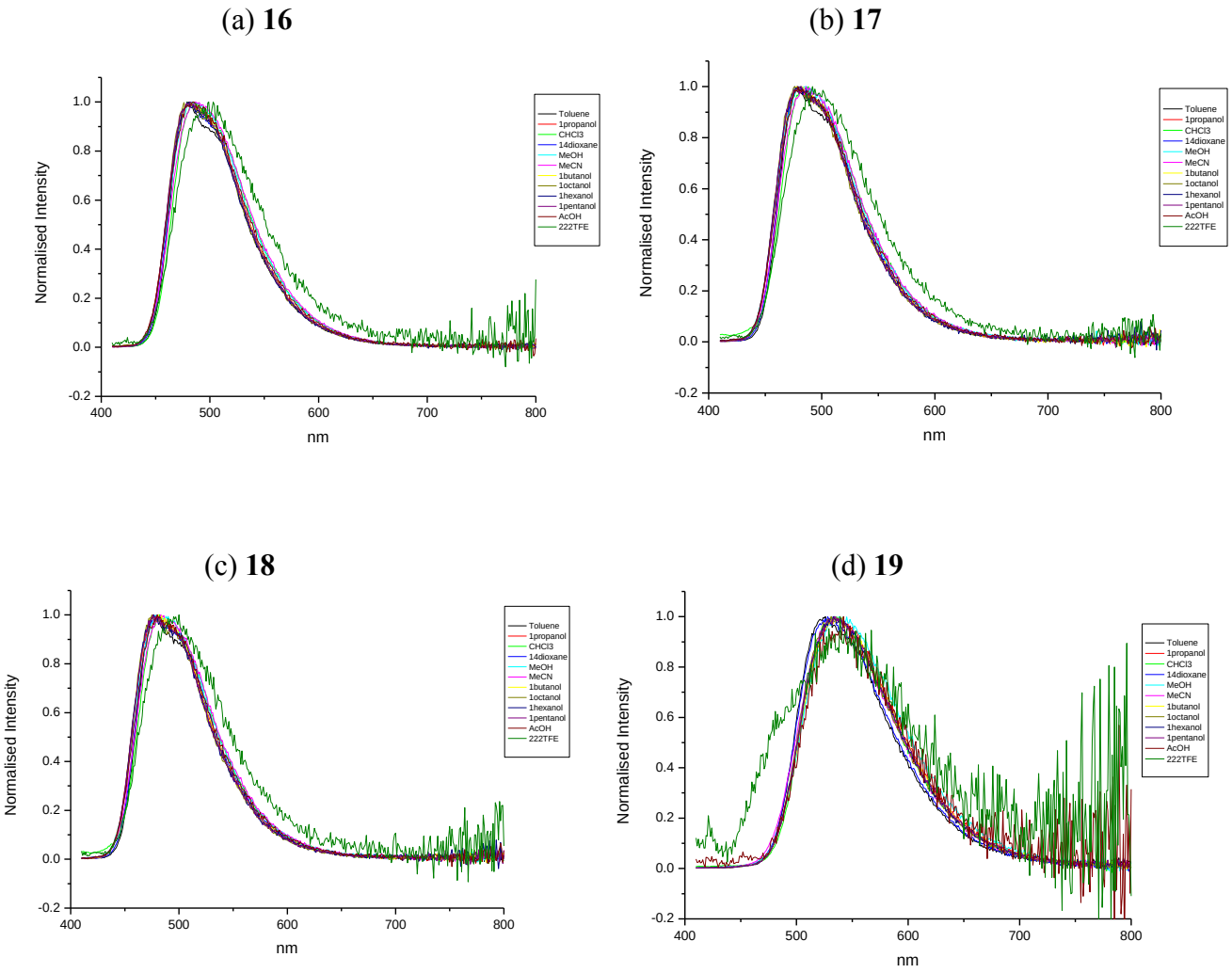

Figure 6.3.7. Summary of the normalised fluorescent emission spectra at 400 nm excitation for the imine hydrolysed 2,5-dihydro-1,2,3-triazines (**16**, **17**, **18** and **19**).

An extensive range of solvents were investigated but only small solvatochromic trends were observed. As a result, it is more informative to compare the minimum and maximum values for each compound, regardless of solvent. Hence, the solvent will vary in the following tables. For a full summary of all results and solvatochromic values refer to Appendix of Results, 3.1, 3.2, 3.3 and 3.4.

The observed peak maximum at 310 nm excitation (Table 6.3, (a)) ranges from 486 nm (**18** in chloroform), 487 nm (**17** in acetonitrile), 489 nm (**16** in methanol) to 537 nm (**19** in 1-butanol). They are all considerably blue shifted compared to 525 nm for **3a** (in ethylene glycol). For 400 nm excitation (Table 6.3, (b)), the observed peak maximum ranges from 483 nm (**18** in acetonitrile), 487 nm (**16** in acetonitrile), 488 nm (**17** in chloroform) to 539 nm (**19** in 1-butanol). Again, they are also considerably blue shifted compared to 513 nm for **3a** (in N,N-dimethylformamide).

(a)

Code	X	Y	Solvent	$\lambda_{310\ nm\ ems}$ (min)	Solvent	$\lambda_{310\ nm\ ems}$ (max)
3a (N=C-H)	H	OCH_3	Toluene	510	Ethylene Glycol	525
16	H	OCH_3	Toluene	480	Methanol	489
17	Cl	OCH_3	1-Octanol	476	Acetonitrile	487
18	Br	OCH_3	1-Octanol	474	Chloroform	486
19	H	CH_3	Toluene	523	1-Butanol	537

(b)

Code	X	Y	Solvent	$\lambda_{400\ nm\ ems}$ (min)	Solvent	$\lambda_{400\ nm\ ems}$ (max)
3a (N=C-H)	H	OCH_3	Methanol	504	N,N-dimethylformamide	513
16	H	OCH_3	Toluene	479	Acetonitrile	487
17	Cl	OCH_3	1,4-Dioxane	476	Chloroform	488
18	Br	OCH_3	1-Octanol	475	Acetonitrile	483
19	H	CH_3	Toluene	526	1-Butanol	539

Table 6.3. Summary of (a) observed emission peak maximum for 310 nm excitation (minimumand maximum value) of **16**, **17**, **18** and **19** and (b) emission band maximum for 400 nm excitation (minimum and maximum value) of **16**, **17**, **18** and **19**.

The calculated quantum yields for **16**, **17**, **18** and **19** are significantly smaller than the parent phenylimine (N=C-H) substituted 2,5-dihydro-1,2,3-triazine **3a** (Figure 6.3.8). For 310 nm excitation, the maximum quantum yield for **16**, **17**, **18** and **19** were calculated to be 0.29 in acetonitrile, 0.22 in 1,4-dioxane, 0.2 in acetonitrile and 0.46 in chloroform respectively (Table 6.4 (a)) and can be compared to 0.76 in toluene for **3a**. At 400 nm excitation, the maximum quantum yields for **16**, **17**, **18** and **19** were similar and calculated to be 0.28 in 1,4-dioxane, 0.21 in 1,4-dioxane, 0.2 in toluene and 0.45 in chloroform respectively (Table 6.4 (b)), and can again be compared to 0.79 in toluene for **3a**.

(a)

Code	X	Y	Solvent	$\Phi_{310\ nm}$ (min)
3a (N=C-H)	H	OCH_3	Propylene Carbonate	0.13
16	H	OCH_3	Methanol	0.18
17	Cl	OCH_3	1-Butanol	0.14
18	Br	OCH_3	Methanol	0.13
19	H	CH_3	Methanol	0.25

Solvent	$\Phi_{310\ nm}$ (max)
Toluene	0.76
Acetonitrile	0.29
1,4-Dioxane	0.22
Acetonitrile	0.2
Chloroform	0.46

(b)

Code	X	Y	Solvent	$\Phi_{400\ nm}$ (min)
3a (N=C-H)	H	OCH_3	Methanol	0.32
16	H	OCH_3	Methanol	0.17
17	Cl	OCH_3	1-Butanol	0.12
18	Br	OCH_3	Methanol	0.11
19	H	CH_3	Methanol	0.23

Solvent	$\Phi_{400\ nm}$ (max)
Toluene	0.79
1,4-Dioxane	0.28
1,4-Dioxane	0.21
Toluene	0.2
Chloroform	0.45

Table 6.4. Summary of (a) minimum and maximum quantum yield (**Φ**) values for **16**, **17**, **18** and **19** at 310 nm excitation and (b) minimum and maximum quantum yield (**Φ**) values for **11a**, **12**, **13** and **15** at 400 nm excitation.

Similar to **3a**, acetic acid and trifluoroethanol cause significant quenching of the fluorescence intensity and quantum yield of the imine hydrolysed 2,5-dihydro-1,2,3-triazines (Figure 6.3.8). Again this is potentially due to hydrogen bonding by 2,2,2-trifluoroethanol, or protonation of the carbonyl oxygen by acetic acid. However, this is yet to be fully investigated in support of this hypothesis.

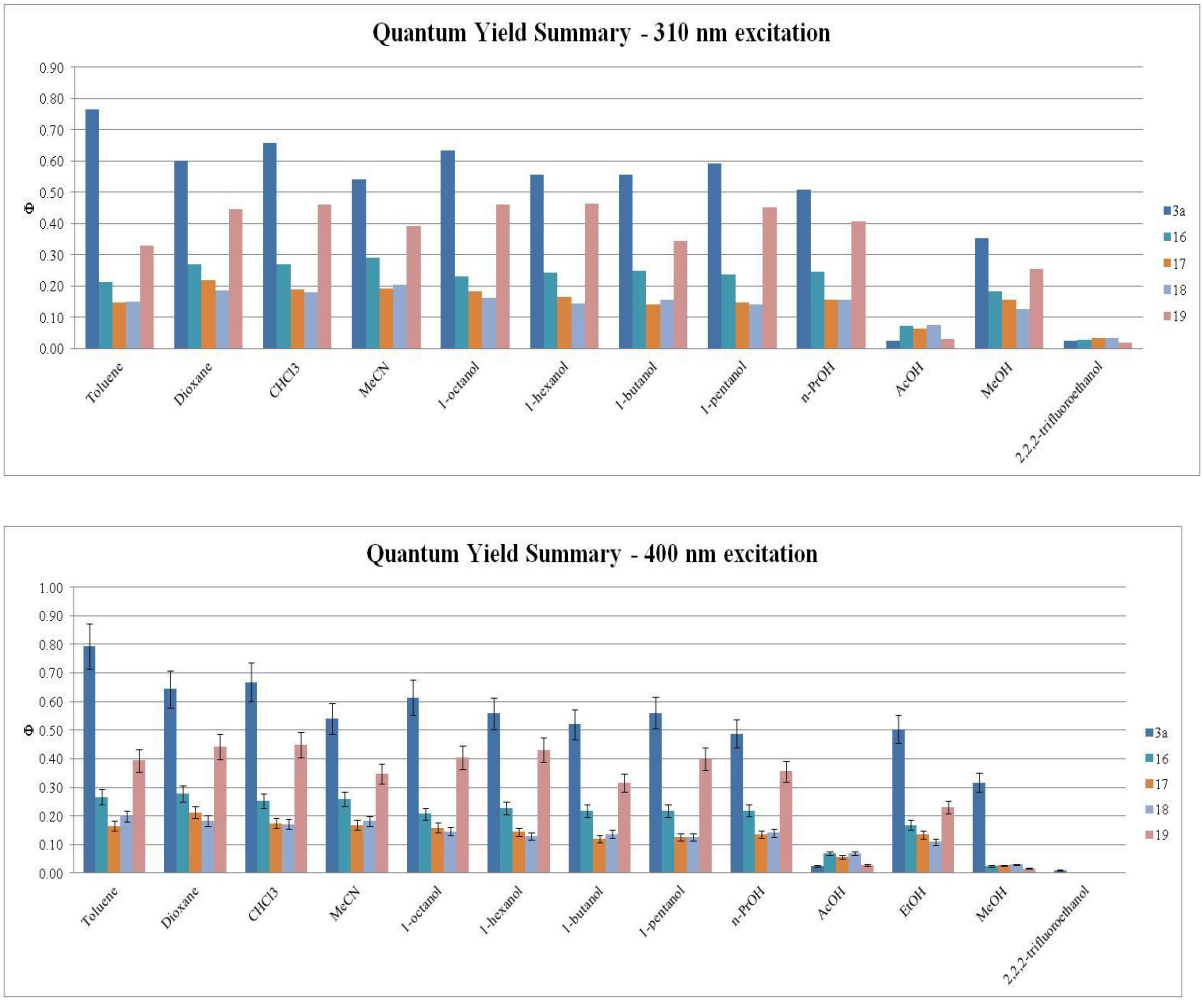

Figure 6.3.8. Graphical summary of quantum yield (**Φ**) values for the imine hydrolysed 2,5-dihydro-1,2,3-triazines (**16**, **17**, **18**, and **19**) versus **3a** (N=C-H).

When compared to its unhydrolysed form **10a**, **19** is blue shifted with a maximum emission value at 310 nm excitation of 537 nm in 1-butanol compared to 555 nm in ethylene glycol for **10a**. At 400 nm excitation, a maximum emission value of 539 nm in 1-butanol is observed for **19** compared to 555 nm in ethylene glycol for **10a** (Chapter 4, Table 4.1).

Comparing **16** to **19**, one can note a significant difference of 48 nm between the maximum emission values at 310 nm excitation; 489 nm in methanol for **16**, and 537 nm in 1-butanol for **19**. Likewise for 400 nm excitation, the emission maximum values differ by 52 nm; 487 nm in acetonitrile for **16** and 539 nm in 1-butanol for **19** (Table 6.3). The maximum calculated quantum yield is again larger for **19** at both 310 and 400 nm excitation (Table 6.4 and Figure 6.3.8), and is ~1.5 times more efficient than **16** (*e.g.* 0.46 in chloroform for **19** versus 0.29 in acetonitrile for **16** at 310 nm excitation).

For the 4-Cl and 4-Br derivatives (**17** and **18**), the emission properties are very similar to **16** in that the relative intensities and areas of the emission bands show little change between the three different molecules. The quantum yields for the 4-Cl and 4-Br derivatives (**17** and **18**) are slightly lower when compared with **16** (Table 6.4).

This indicates again that the substitution at the 4-position of the N2 phenyl ring with heavy atoms has very little effect on the molecule's energy levels. The decrease in quantum yield is again not so large as to preclude the use of triazine derivatives with a substitution in the 4-position of the N2 phenyl ring as fluorophores (Figure 6.3.8).

Analysis against normalized solvent polarity (E_T^N), solvent hydrogen bonding donating/accepting ability (α and β), solvent polarizability (π^*), viscosity (η(Cp)) and dipole moment (μ) was performed for each fluorophore. However, the solvatochromic analysis of all components (band position, area percentage of band to overall fit, band width, area ratios and band fwhm) of the deconvoluted spectra of the compounds revealed the distribution of the data to be fairly random (Appendix of Results, 3.1, 3.2, 3.3 and 3.4).

Table 6.5 shows the minimum and maximum values of the Gaussian band positions of the deconvoluted 310 nm excitation spectra (Figure 6.3.3) and Table 6.6 lists the minimum and maximum percentage area values. Tables 6.7 shows the minimum and maximum values of the Gaussian band positions of the deconvoluted 400 nm excitation spectra and Table 6.8 lists the minimum and maximum percentage areas.

At 310 nm excitation (Table 6.5 and 6.6), Band 1 has a maximum value at 530 nm in acetonitrile for **16** whilst for **19** the value is significantly red shifted with a maximum value at 577 nm in methanol (Band 1 has a maximum value at 554 nm in ethylene glycol for **3a**). The red shift is also observed for Band 2 and Band 3; 510 nm in toluene for **16** compared with 533 nm in methanol for **19**; and 501 nm in toluene for **16** and 521 nm in methanol for **19** respectively.

In comparison to **3a** (N=C-H), the S_1 (**g1**) emission state (Band 1) and S_1 (**g2**) (Band 2) are higher in energy for **16**, **17**, **18** and **19**, with the S_1 (**g0**) emission state (Band 3) being lower in energy than the phenylimine parent **3a** at 310 nm excitation. This indicates that the removal of the phenylimine is effecting the energy of the fluorescent states of **16**, **17**, **18** and **19** compared to the unhydrolysed phenylimine parent **3a**.

The maximum area percentage contributions also differ significantly to **3a** (N=C-H) at 310 nm excitation but are similar between **16** and **19**. Band 1 having a maximum contribution of 43.15 % in toluene for **16** and 42.53 % in 1,4-dioxane for **19** compared with 59.26 % in 2-methyl-2-butanol for **3a**. Band 3 has a maximum contribution of 26.34 % in toluene for **16** and 20.27 % in acetonitrile for **19** compared with 8.36 % in 1,5-pentanediol for **3a**. This indicates that the removal of the phenylimine is ultimately leading to an increase in the lower energy S_1 (**g0**) emission state at 310 nm excitation.

Although the energy of the emission states are lower (red shifted) for **19**, the population of the excited states compared to **16** are similar (Table 6.6 and 6.8) which would indicate that substitution of the carbonyl has little effect on how the excited states are populated for the hydrolysed 2,5-dihydro-1,2,3-triazines but does effect the energies of the transitions.

Code	X	Y	Solvent	$\lambda_{310\ nm\ ems}$ Band 1 (nm) (min)
3a (N=C-H)	H	OCH_3	2-Methyl-2-butnaol	533
16	H	OCH_3	Toluene	521
17	Cl	OCH_3	1-Hexanol	517
18	Br	OCH_3	1-Octanol	518
19	H	CH_3	1,4-Dioxane	567

Code	X	Y	Solvent	$\lambda_{310\ nm\ ems}$ Band 1 (nm) (max)
3a (N=C-H)	H	OCH_3	Ethylene Glycol	554
16	H	OCH_3	Acetonitrile	530
17	Cl	OCH_3	Acetonitrile	527
18	Br	OCH_3	Acetonitrile	526
19	H	CH_3	Methanol	577

Code	X	Y	Solvent	$\lambda_{310\ nm\ ems}$ Band 2 (nm) (min)
3a (N=C-H)	H	OCH_3	2-Methyl-2-butanol	503
16	H	OCH_3	1-Octanol	495
17	Cl	OCH_3	1-Propanol	493
18	Br	OCH_3	1-Butanol	492
19	H	CH_3	Toluene	540

Code	X	Y	Solvent	$\lambda_{310\ nm\ ems}$ Band 2 (nm) (max)
3a (N=C-H)	H	OCH_3	Ethylene Glycol	515
16	H	OCH_3	Toluene	510
17	Cl	OCH_3	Toluene	500
18	Br	OCH_3	Toluene	499
19	H	CH_3	Methanol	553

Code	X	Y	Solvent	$\lambda_{310\ nm\ ems}$ Band 3 (nm) (min)
3a (N=C-H)	H	OCH_3	2-Methyl-2-butanol	468
16	H	OCH_3	1-Octanol	495
17	Cl	OCH_3	1-Octanol	468
18	Br	OCH_3	1-Butanol	467
19	H	CH_3	Toluene	512

Code	X	Y	Solvent	$\lambda_{310\ nm\ ems}$ Band 3 (nm) (max)
3a (N=C-H)	H	OCH_3	Ethylene Glycol	479
16	H	OCH_3	Toluene	501
17	Cl	OCH_3	Chloroform	474
18	Br	OCH_3	Chloroform	472
19	H	CH_3	Methanol	521

Code	X	Y	Solvent	$\lambda_{310\ nm\ ems}$ Band 4 (nm) (min)
3a (N=C-H)	H	OCH_3	1,3-Propanediol	344
16	H	OCH_3	-	-
17	Cl	OCH_3	1-Octanol	355
18	Br	OCH_3	1-Octanol	352
19	H	CH_3	1-Octanol	350

Code	X	Y	Solvent	$\lambda_{310\ nm\ ems}$ Band 4 (nm) (max)
3a (N=C-H)	H	OCH_3	1,4-Butanediol	380
16	H	OCH_3	1-Hexanol	351
17	Cl	OCH_3	Chloroform	359
18	Br	OCH_3	Chloroform	360
19	H	CH_3	Methanol	356

Table 6.5. Summary of Guassian band maximum positions from deconvoluted spectra (minimum and maximum values) for **11a**, **12**, **13** and **15** at 310 nm excitation.

Code	X	Y	Solvent	$\lambda_{310\ nm}$ Band 1 Area % (min)
3a (N=C-H)	H	OCH_3	1,3-Butanediol	36.3
16	H	OCH_3	Acetonitrile	34.22
17	Cl	OCH_3	Acetonitrile	32.45
18	Br	OCH_3	1-Hexanol	33.19
19	H	CH_3	1-Hexanol	34.48

Code	X	Y	Solvent	$\lambda_{310\ nm}$ Band 1 Area % (max)
3a (N=C-H)	H	OCH_3	2-Methyl-2-butanol	59.26
16	H	OCH_3	Toluene	43.15
17	Cl	OCH_3	Toluene	39.48
18	Br	OCH_3	Toluene	40.91
19	H	CH_3	1,4-Dioxane	42.53

Code	X	Y	Solvent	$\lambda_{310\ nm}$ Band 2 Area % (min)
3a (N=C-H)	H	OCH_3	1,3-Butanediol	27.33
16	H	OCH_3	Toluene	30.5
17	Cl	OCH_3	Toluene	28.56
18	Br	OCH_3	Toluene	32.06
19	H	CH_3	1,4-Dioxane	36.38

Code	X	Y	Solvent	$\lambda_{310\ nm}$ Band 2 Area % (max)
3a (N=C-H)	H	OCH_3	Acetonitrile	46.43
16	H	OCH_3	Acetonitrile	47.3
17	Cl	OCH_3	Acetonitrile	43.85
18	Br	OCH_3	Acetonitrile	46.29
19	H	CH_3	1-Pentanol	43.05

Code	X	Y	Solvent	$\lambda_{310\ nm}$ Band 3 Area % (min)
3a (N=C-H)	H	OCH_3	1,3-Butanediol	5.49
16	H	OCH_3	Methanol	17.68
17	Cl	OCH_3	1-Hexanol	13.9
18	Br	OCH_3	1-Hexanol	15.95
19	H	CH_3	Toluene	15.59

Code	X	Y	Solvent	$\lambda_{310\ nm}$ Band 3 Area % (max)
3a (N=C-H)	H	OCH_3	1,5-Pentanediol	8.36
16	H	OCH_3	Toluene	26.34
17	Cl	OCH_3	Toluene	22.88
18	Br	OCH_3	Toluene	23.24
19	H	CH_3	Acetonitrile	20.27

Code	X	Y	Solvent	$\lambda_{310\ nm}$ Band 4 Area % (min)
3a (N=C-H)	H	OCH_3	1,3-Propanediol	8.31
16	H	OCH_3	-	-
17	Cl	OCH_3	Acetonitrile	7.09
18	Br	OCH_3	Acetonitrile	2.52
19	H	CH_3	Toluene	3.34

Code	X	Y	Solvent	$\lambda_{310\ nm}$ Band 4 Area % (max)
3a (N=C-H)	H	OCH_3	1,3-Butanediol	15.14
16	H	OCH_3	1-Hexanol	6.09
17	Cl	OCH_3	1-Hexanol	19.36
18	Br	OCH_3	1-Hexanol	12.49
19	H	CH_3	1,4-Dioxane	5.36

Table 6.6. Summary of area percentages for Gaussian band fits (minimum and maximum values) for **16**, **17**, **18** and **19** at 310 nm excitation

Code	X	Y	Solvent	$\lambda_{400\ nm\ ems}$ Band 1 (nm) (min)
3a (N=C-H)	H	OCH_3	Toluene	524
16	H	OCH_3	Toluene	523
17	Cl	OCH_3	Chloroform	514
18	Br	OCH_3	Chloroform	512
19	H	CH_3	1,4-Dioxane	569

Code	X	Y	Solvent	$\lambda_{400\ nm\ ems}$ Band 1 (nm) (max)
3a (N=C-H)	H	OCH_3	Ethylene Glycol	548
16	H	OCH_3	Chloroform	531
17	Cl	OCH_3	Acetonitrile	528
18	Br	OCH_3	Acetonitrile	527
19	H	CH_3	Methanol	583

Code	X	Y	Solvent	$\lambda_{400\ nm\ ems}$ Band 2 (nm) (min)
3a (N=C-H)	H	OCH_3	2-Methyl-2-butanol	500
16	H	OCH_3	1-Octanol	496
17	Cl	OCH_3	1-Octanol	494
18	Br	OCH_3	1-Pentanol	492
19	H	CH_3	Toluene	541

Code	X	Y	Solvent	$\lambda_{400\ nm\ ems}$ Band 2 (nm) (max)
3a (N=C-H)	H	OCH_3	Ethylene Glycol	510
16	H	OCH_3	Toluene	502
17	Cl	OCH_3	Chloroform	501
18	Br	OCH_3	Toluene	499
19	H	CH_3	Methanol	553

Code	X	Y	Solvent	$\lambda_{400\ nm\ ems}$ Band 3 (nm) (min)
3a (N=C-H)	H	OCH_3	2-Methyl-2-butanol	469
16	H	OCH_3	1-Octanol	470
17	Cl	OCH_3	1-Octanol	468
18	Br	OCH_3	1-Octanol	467
19	H	CH_3	Toluene	512

Code	X	Y	Solvent	$\lambda_{400\ nm\ ems}$ Band 3 (nm) (max)
3a (N=C-H)	H	OCH_3	Ethylene Glycol	480
16	H	OCH_3	Chloroform	476
17	Cl	OCH_3	Chloroform	475
18	Br	OCH_3	Chloroform	473
19	H	CH_3	Methanol	520

Table 6.7. Summary of Guassian band maximum positions from deconvoluted spectra (minimum and maximum values) for **11a**, **12**, **13** and **15** at 400 nm excitation.

Code	X	Y	Solvent	$\lambda_{400\ nm}$ Band 1 Area % (min)
3a (N=C-H)	H	OCH_3	Methanol	40.67
16	H	OCH_3	Acetonitrile	30.81
17	Cl	OCH_3	1-Pentanol	33.65
18	Br	OCH_3	Methanol	33.04
19	H	CH_3	Acetonitrile	26.07

Code	X	Y	Solvent	$\lambda_{400\ nm}$ Band 1 Area % (max)
3a (N=C-H)	H	OCH_3	Toluene	50.7
16	H	OCH_3	Toluene	41.64
17	Cl	OCH_3	Chloroform	51.81
18	Br	OCH_3	Chloroform	50.46
19	H	CH_3	1,4-Dioxane	43.85

Code	X	Y	Solvent	$\lambda_{400\ nm}$ Band 2 Area % (min)
3a (N=C-H)	H	OCH_3	Toluene	38.89
16	H	OCH_3	Toluene	32.34
17	Cl	OCH_3	Chloroform	31.11
18	Br	OCH_3	Toluene	30.74
19	H	CH_3	1,4-Dioxane	39.32

Code	X	Y	Solvent	$\lambda_{400\ nm}$ Band 2 Area % (max)
3a (N=C-H)	H	OCH_3	Acetonitrile	46.85
16	H	OCH_3	Acetonitrile	52.85
17	Cl	OCH_3	1-Pentanol	47.27
18	Br	OCH_3	Methanol	48.86
19	H	CH_3	Acetonitrile	50.11

Code	X	Y	Solvent	$\lambda_{400\ nm}$ Band 3 Area % (min)
3a (N=C-H)	H	OCH_3	1,4-Dioxane	9.42
16	H	OCH_3	Acetonitrile	16.33
17	Cl	OCH_3	Methanol	16.90
18	Br	OCH_3	Chloroform	16.67
19	H	CH_3	Toluene	16.78

Code	X	Y	Solvent	$\lambda_{400\ nm}$ Band 3 Area % (max)
3a (N=C-H)	H	OCH_3	Ethylene Glycol	12.67
16	H	OCH_3	Toluene	26
17	Cl	OCH_3	Toluene	24.27
18	Br	OCH_3	Toluene	25.91
19	H	CH_3	Acetonitrile	23.81

Table 6.8. Summary of area percentages for Gaussian band fits (minimum and maximum values) for **16**, **17**, **18** and **19** at 400 nm excitation

Analysis of the Gaussian model fit data showed no trend nor exhibited solvatochromic behaviour. A multiple linear regression analysis on **16** (Table 6.9 and 6.10) against the solvatochromic values α, β and π^* was performed. The emission peak maximum, Gaussian band positions, quantum yield and UV-visible absorbance were correlated against for both 310 and 400 nm excitation which showed no significant correlations (a linear correlation is supported when r^2 approaches unity i.e. 1).

y	y_o	a_α	b_β	c_{π^*}	r^2
$\lambda_{ems\ max\ (32258\ cm^{-1})}$	21429.46 ± 322.59	-201.46 ± 86.72	-30.20 ± 165.42	-1153.71 ± 490.30	**0.73**
Band 1 cm^{-1} (Gaussian Fit)	19434.41 ± 228.58	12.28 ± 61.45	-126.10 ± 117.21	-676.36 ± 347.41	**0.36**
Band 2 cm^{-1} (Gaussian Fit)	19950.44 ± 240.66	214.26 ± 64.70	47.27 ± 123.41	25.07 ± 365.78	**0.62**
Band 3 cm^{-1} (Gaussian Fit)	21135.00 ± 102.97	17.94 ± 38.25	180.26 ± 60.26	-83.75 ± 156.23	**0.81**
Band 4 cm^{-1} (Gaussian Fit)	-	-	-	-	-
Φ (32258 cm-1)	0.26 ± 0.13	-0.13 ± 0.03	0.07 ± 0.06	-0.01 ± 0.19	**0.71**
Abs (32258 cm-1)	0.02 ± 0.02	-0.00 ± 0.00	-1.68E-4 ± 0.01	0.05 ± 0.03	**0.52**

Table 6.9. Estimated from the equation ($y = y_0 + a_\alpha*\alpha + b_\beta*\beta + c_{\pi^*}*\pi^*$), coefficients ($y_o$, a_α, b_β, c_{π^*}), their standard errors and correlation coefficients (r) for the multiple linear regression analysis for **16** at 310 nm excitation against the solvatochromic values α, β and π*.

y	y_o	a_α	b_β	c_{π^*}	r^2
$\lambda_{ems\ max\ (25000\ cm^{-1})}$	21164.15 ± 321.16	-267.21 ± 86.34	181.39 ± 164.69	-764.71 ± 488.12	**0.78**
Band 1 cm^{-1} (Gaussian Fit)	19353.84 ± 324.15	-217.46 ± 87.14	126.00 ± 166.22	-641.56 ± 492.67	**0.69**
Band 2 cm^{-1} (Gaussian Fit)	19914.20 ± 126.76	-51.38 ± 34.08	298.55 ± 65.00	41.81 ± 192.67	**0.86**
Band 3 cm^{-1} (Gaussian Fit)	21119.09 ± 111.18	-55.63 ± 29.89	243.28 ± 57.01	-72.72 ± 168.98	**0.87**
Φ (25000 cm-1)	0.34 ± 0.09	-0.14 ± 0.02	0.02 ± 0.04	-0.11 ± 0.14	**0.84**
Abs (25000 cm-1)	0.03 ± 0.01	-0.00 ± 0.00	-0.002 ± 0.00	-0.00 ± 0.01	**0.38**

Table 6.10. Estimated from the equation ($y = y_0 + a_\alpha*\alpha + b_\beta*\beta + c_{\pi^*}*\pi^*$), coefficients ($y_o$, a_α, b_β, c_{π^*}), their standard errors and correlation coefficients (r) for the multiple linear regression analysis for **16** at 400 nm excitation against the solvatochromic values α, β and π*.

6.3.2 Time resolved fluorescence measurements.

Using a 405 nm laser diode excitation source, the fluorescent lifetime behaviour of the 400 nm emission of **16**, **17**, **18** and **19** was investigated by time correlated single photon counting (TCSPC) at wavelengths of 470, 490, 520, 540, or 570 for **16**, **17** and **18**; and 470, 490, 520, 540, 570 and 600 nm for **19** due to its red shifted emission.

For all of the species (**16**, **17**, **18** and **19**), the fluorescence decay could be fitted to a 2 or 3 exponential term, composed of:

1. A short lived component (τ_1) which ranges in value from 0.19 to 1.4 ns
2. A medium component (τ_2) that ranges from 1.17 to 3.59 ns.
3. A long lived component (τ_3) which ranges from 2 to 9.53 ns.

Table 6.11 lists the minimum and maximum intensity weighted average lifetimes for **16**, **17**, **18** and **19** at the lowest (470 nm) and highest emission wavelength (570 / 600 nm). Interestingly removal of the phenylimine group had a significant effect on the fluorescence lifetimes of the triazines. For example, the fluorescent lifetime of **16** was notably much shorter than the unhydrolysed triazine **3a**; having a maximum intensity weighted average lifetime of 3.49 ns in acetonitrile for **16** compared with 6.87 ns at 470 nm in propylene carbonate for **3a** (Table 6.11). The 4-Cl and 4-Br derivatives (**17** and **18**) differ again to the unsubstituted parent **16**, where the average intensity weighted lifetimes are ~27 % and 29 % shorter respectively at 470 nm, and ~27 % and 30 % shorter at 570 nm respectively when compared to **16** (Table 6.11)

An extensive range of solvents were investigated but small trends were only observed. As a result, it is more informative to compare the minimum and maximum values for each compound, regardless of solvent. Hence, the solvent will vary in the following tables. For a full summary of the data refer to Appendix of Results, 3.1, 3.2, 3.3 and 3.4.

Code	X	Y	nm	Solvent	τ_f (ns) (Intensity Weighted) (min)
3a (N=C-H)	H	OCH_3	470	Methanol	4.16
16	H	OCH_3	470	1-Octanol	2.52
17	Cl	OCH_3	470	1-Octanol	1.6
18	Br	OCH_3	470	1-Butanol	1.72
19	H	CH_3	470	1-Propanol	2.36

Code	X	Y	nm	Solvent	τ_f (ns) (Intensity Weighted) (max)
3a (N=C-H)	H	OCH_3	470	Propylene Carbonate	6.87
16	H	OCH_3	470	Acetonitrile	3.49
17	Cl	OCH_3	470	Acetonitrile	2.56
18	Br	OCH_3	470	Acetonitrile	2.48
19	H	CH_3	470	1,4-Dioxane	5.63

Code	X	Y	nm	Solvent	τf (ns) (Intensity Weighted) (min)
3a (N=C-H)	H	OCH_3	570	Methanol	7.15
16	H	OCH_3	570	Methanol	2.67
17	Cl	OCH_3	570	1-Octanol	1.75
18	Br	OCH_3	570	1-Hexanol	1.65
19	H	CH_3	600	Methanol	7.96

Code	X	Y	nm	Solvent	τf (ns) (Intensity Weighted) (max)
3a (N=C-H)	H	OCH_3	570	Propylene Carbonate	11.09
16	H	OCH_3	570	Acetonitrile	3.63
17	Cl	OCH_3	570	Acetonitrile	2.67
18	Br	OCH_3	570	Acetonitrile	2.57
19	H	CH_3	600	Chloroform	10.44

Table 6.11. Summary of the minimum and maximum intensity weighted average lifetimes (τ_f) of the imine hydrolysed 2,5-dihydro-1,2,3-triazines at 470 and 570 nm emission.

Table 6.12 and 6.13 list the minimum and maximum values for the decay times (τ_i) and their corresponding fractional intensities (A_i) for **16**, **17**, **18** at 470 and 570 nm emission, and at 470 and 600 nm emission for **19**. The shortening of the fluorescence lifetime of the hydrolysed triazines appears to be due to a significant shortening of the long lived component (τ_3); having a maximum value of 4.14 ns at 470 nm in acetonitrile for **16** against 10.59 ns at 470 nm in chloroform for **3a** (Table 6.12).

Once again a change in the electron density at the carbonyl group, *i.e.* comparing **19** and **16**, causes a change in the fluorescence lifetime. As previously mentioned, computational calculations comparing the dipole moment of ketones to esters suggest there is a considerable difference in electron density and dipole moment (for further discussion see Chapter 7, Section 7.3.1.2). The presence of the keto group (**19**) resulted in a much longer lived state (τ_3); 9.1 ns in 1-butanol compared to 4.14 nm in acetonitrile for **3a** at 470 nm emission and 12.82 ns in chloroform compared to 5.44 ns in 1-octanol for **3a** at 570 nm excitation. This results in an almost three fold increase in the maximum intensity average

lifetime at 570 nm from 3.63 ns in acetonitrile for **16** to 10.44 ns in ethyl acetate for **19** (Table 6.11).

Code	X	Y	nm	Solvent	τ_1 (ns) (min)	A_1 (%)
3a (N=C-H)	H	OCH_3	470	1-Propanol	0.19	1.96
16	H	OCH_3	470	1-Octanol	0.19	11.73
17	Cl	OCH_3	470	1,4-Dioxane	0.29	1.45
18	Br	OCH_3	470	Methanol	0.26	4.12
19	H	CH_3	470	1-Propanol	0.27	68.72

Code	Solvent	τ_1 (ns) (max)	A_1 (%)
3a (N=C-H)	1-Octanol	0.60	4.69
16	1-Propanol	1.4	7.04
17	1-Pentanol	0.59	10.32
18	1-Octanol	0.79	20.72
19	Acetonitrile	0.63	26.77

Code	X	Y	nm	Solvent	τ_2 (ns) (min)	A_2 (%)
3a (N=C-H)	H	OCH_3	470	Ethylene Glycol	2.05	12.27
16	H	OCH_3	470	Methanol	1.52	23.36
17	Cl	OCH_3	470	Toluene	1.17	16.81
18	Br	OCH_3	470	1-Pentanol	1.18	35.5
19	H	CH_3	470	Chloroform	1.64	26.64

Code	Solvent	τ_2 (ns) (max)	A_2 (%)
3a (N=C-H)	Propylene Carbonate	5.53	70.78
16	1-Hexanol	2.53	76.21
17	1-Pentanol	1.8	81.25
18	Acetonitrile	1.95	57.88
19	Methanol	2.56	24.7

Code	X	Y	nm	Solvent	τ_3 (ns) (min)	A_3 (%)
3a (N=C-H)	H	OCH_3	470	1,4-Butanediol	6.61	61.28
16	H	OCH_3	470	Methanol	2.95	76.64
17	Cl	OCH_3	470	1-Propanol	2.16	60.08
18	Br	OCH_3	470	1-Octanol	2.00	79.28
19	H	CH_3	470	Acetonitrile	6.95	44.12

Code	Solvent	τ_3 (ns) (max)	A_3 (%)
3a (N=C-H)	Chloroform	10.59	29.16
16	Acetonitrile	4.14	65.62
17	Acetonitrile	3.11	62.5
18	1-hexanol	3.55	4.92
19	1-butanol	9.1	34.82

Table 6.12. Summary of the minimum and maximum values for the lifetime decay components of the three exponential fit for the decay at 470 nm excitation for the imine hydrolysed 2,5-dihydro-1,2,3-triazines; where τ_i is the decay time and A_i is the fractional intensity.

Code	X	Y	nm	Solvent	τ_1 (ns) (min)	A_1 (%)
3a (N=C-H)	H	OCH_3	570	N,N-Dimethylformamide	0.13	0.82
16	H	OCH_3	570	1-Octanol	0.23	7.7
17	Cl	OCH_3	570	1-Octanol	0.2	15.28
18	Br	OCH_3	570	Chloroform	0.29	3.52
19	H	CH_3	570	1-Butanol	0.33	1.22

Code	Solvent	τ_1 (ns) (max)	A_1 (%)
3a (N=C-H)	1,4-Butanediol	2.84	13.58
16	1-Hexanol	0.77	4.12
17	1-Propanol	0.85	10.54
18	1-Propanol	1.09	9.61
19	1-Hexanol	0.44	0.79

Code	X	Y	nm	Solvent	τ_2 (ns) (min)	A_2 (%)
3a (N=C-H)	H	OCH_3	570	2-Methyl-2-butanol	3.67	11.62
16	H	OCH_3	570	Methanol	1.57	21.91
17	Cl	OCH_3	570	Toluene	1.44	24.59
18	Br	OCH_3	570	Methanol	1.49	34.19
19	H	CH_3	570	Toluene	3.59	36.1

Code	Solvent	τ_2 (ns) (max)	A_2 (%)
3a (N=C-H)	1,5-Pentanediol	6.56	48.04
16	Toluene	3.09	82.23
17	1,4-Dioxane	2.05	55.88
18	Toluene	2.00	35.77
19	Chloroform	9.14	64.62

Code	X	Y	nm	Solvent	τ_3 (ns) (min)	A_3 (%)
3a (N=C-H)	H	OCH_3	570	Toluene	9.67	93.8
16	H	OCH_3	570	Methanol	2.98	78.09
17	Cl	OCH_3	570	Methanol	2.64	37.07
18	Br	OCH_3	570	Methanol	2.38	61.44
19	H	CH_3	570	Methanol	9.53	71.93

Code	Solvent	τ_3 (ns) (max)	A_3 (%)
3a (N=C-H)	1,3-Butanediol	13.5	51.7
16	1-Octanol	5.44	8.67
17	1-Pentanol	5.58	3.43
18	1-Pentanol	4.05	3.97
19	Chloroform	12.82	35.38

Table 6.13. Summary of the minimum and maximum values for the lifetime decay components of the three exponential fit for the decay at 570 nm excitation for the imine hydrolysed 2,5-dihydro-1,2,3-triazines; where τ_i is the decay time and A_i is the fractional intensity.

Analysis of the intensity weighted average lifetimes, 470 nm intensity weighted lifetime and 570 nm intensity weighted lifetime (and their respective decay times) against the normalized solvent polarity (E_T^N), solvent hydrogen bonding donating/accepting ability (α and β), solvent polarizability (π^*), viscosity (η(Cp)), dielectric constant (ε) and dipole moment (μ) was performed for each fluorophore. However, the solvatochromic analysis of all components revealed no significant trends and the distribution of the data was fairly random (Appendix of Results, 3.1, 3.2, 3.3 and 3.4). Similar to the emission, a multiple linear regression analysis on the lifetime of **16** (Table 6.14) against the solvatochromic values α, β and π^* was performed. The intensity weighted average lifetimes at 470 and 570 nm and their respective individual decay times (τ_1, τ_2, and τ_3) were correlated against but again showed no significant correlations were observed (a linear correlation is supported when r^2 approaches unity *i.e.* 1).

y	y_o	a_α	b_β	c_{π^*}	r^2
τ_f (Intensity weighted, 470nm)	3.40 ± 1.35	-1.71 ± 0.36	0.44 ± 0.69	0.04 ± 2.05	**0.76**
τ_f (Amplitude weighted, 470nm)	2.27 ± 1.58	-1.74 ± 0.42	0.40 ± 0.81	1.59 ± 2.40	**0.68**
τ_1 (Intensity weighted, 470nm)	-2.31 ± 3.94	0.39 ± 1.37	1.51 ± 2.16	3.07 ± 4.86	**0.15**
τ_2 (Intensity weighted, 470nm)	3.01 ± 1.55	0.27 ± 0.41	-0.38 ± 0.79	-1.54 ± 2.36	**0.07**
τ_3 (Intensity weighted, 470nm)	3.24 ± 1.21	0.16 ± 0.44	-0.27 ± 0.70	0.97 ± 1.83	**0.16**
τ_f (Intensity weighted, 570nm)	3.54 ± 1.37	-1.75 ± 0.36	0.475 ± 0.70	-0.02 ± 2.08	**0.77**
τ_f (Amplitude weighted, 570nm)	2.66 ± 1.65	-1.82 ± 0.44	0.18 ± 0.84	1.15 ± 2.51	**0.69**
τ_1 (Intensity weighted, 570nm)	1.29 ± 1.27	0.16 ± 0.33	-0.49 ± 0.62	-1.30 ± 2.20	**0.20**
τ_2 (Intensity weighted, 570nm)	4.52 ± 0.94	-0.91 ± 0.25	-0.22 ± 0.48	-3.05 ± 1.42	**0.78**
τ_3 (Intensity weighted, 570nm)	6.59 ± 2.00	0.42 ± 0.53	-1.59 ± 1.02	-3.19 ± 3.04	**0.24**

Table 6.14. Estimated from equation ($y = y_0 + a_\alpha*\alpha + b_\beta*\beta + c_{\pi^*}*\pi^*$), coefficients ($y_o$, a_α, b_β, c_{π^*}), their standard errors and correlation coefficients (r) for the multiple linear regression analysis of the time domain fluorescent lifetimes and components of **16** at 405 nm excitation.

6.4 CONCLUSION.

The 2,5-dihydro-1,2,3-triazines described so far in this thesis have been reasonably stable compounds that can be stored as a solid, under dry conditions, for several months. However, the imine functionality of **3a** (N=C-H) is susceptible to hydrolysis. This may limit the use of **3a** as a fluorescent biological probe as the imine may be susceptible to hydrolysis at extracellular pH resulting in the presence of two different fluorescent species. The hydrolysis of the 2,5-dihydro-1,2,3-triazines with substituted aryl groups affords a smaller fluorophore with enhanced chemical stability to the phenylimine triazines.

The generation of **16** was initially reported *via* a long seven day reflux.[54] An investigation to find a more efficient synthesis of **16** was undertaken, which led to the development of a mild two hour acid catalysed imine hydrolysis of the phenylimine using 10 mol % acetic acid, methanol and heating to 120 ^{o}C. This methodology generated the hydrolysed 2,5-dihydro-1,2,3-triazines (**16**, **17**, **18** and **19**), from their corresponding phenylimine substituted triazine (**3a**, **6a**, **9a** and **10a**), in yields of 99 %, 84 %, 96 % and 93 % respectively.

Removal of the phenylimine group and its replacement with a hydrogen at C5, caused only minor change to the ground state absorptions. A lower energy absorption that is red-shifted at ~325 nm compared to **3a** (~310 nm) and a broad absorption band at ~390 nm was observed. Excitation into either of the absorption bands (310 and 400 nm) resulted in a green/blue fluorescence emission band centred at ~480 nm that was blue-shifted compared to **3a** (~520 nm) and is also uneffected by the nature of the solvent (Figures 6.3.4, and 6.3.5). This is supported by the normalised fluorescence spectra where no change was observed in the position of the emission band maximum. For the 4-Cl and 4-Br derivatives (**17** and **18**), the emission properties were almost the same as those for **16**.

Comparing methyl ester **16** and keto hydrolysed 2,5-dihydro-1,2,3-triazine **19**, a red shift was observed for the ketone substituted **19**. The maximum calculated quantum yield was again larger for **19** at both 310 and 400 nm excitation and was ~1.5 times more efficient than **16**. Although the energy of the emission states have changed for **19**, the

population of the excited states were similar to **16**. Therefore, it is believed that substitution of the carbonyl has little effect on how the excited states are populated for the hydrolysed 2,5-dihydro-1,2,3-triazines but does effect the energies of the transitions *i.e.* a ketone significantly decreases the energy difference between the excited states and ground state versus a methyl ester, resulting in a red shifted spectra.

The intensity weighted average fluorescent lifetime of the hydrolysed triazine was found to be much shorter (~3 ns) than the phenylimine parent due to a significant shortening of the long lived component (τ_3) of the fluorescent decay *e.g.* 4.14 ns at 470 nm in acetonitrile for **16** compared to 10.59 ns at 470 nm in chloroform for **3a**.

Currently, the photostability of the hydrolysed 2,5-dihydro-1,2,3-triazines are being investigated by our collaborator Dr. Alan G. Ryder at NUIG. Although the fluorescence efficiency of **16** is much less than the phenylimine substituted **3a** (N=C-H), *e.g.* 0.29 in acetonitrile for **16** compared to 0.76 in toluene for **3a** at 310 nm excitation, it is possible that the structurally simpler **16** will be a more suitable candidate for future conjugation to biological molecules due to its superior chemical stability when compared to **3a**.

Chapter 7: Substituted phenyl ester 2,5-dihydro-1,2,3-triazines.

7.1 INTRODUCTION.

So far in this thesis, the effect of structural changes within the fluorophore has been investigated and discussed. Such changes included substituting the imine phenyl and N2 phenyl rings with heavy atoms, changing the methyl ester to a methyl ketone, and varying the substituent on the imine carbon.

Changing the methyl ester to a methyl ketone, and hence changing the electron density in the carbonyl group had a marked effect on the photophysics. We were interested in further exploring this effect. As such, we designed and synthesized the phenyl ester triazine family (Scheme 7.1.1).

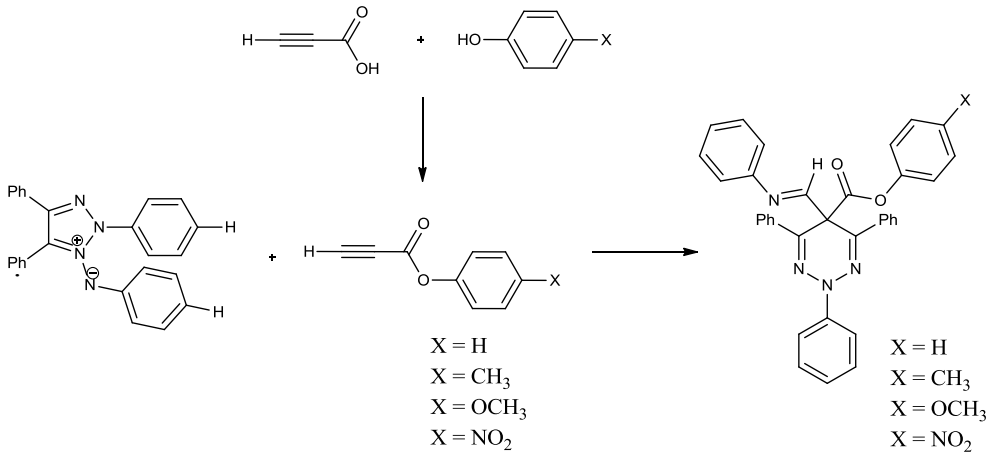

Scheme 7.1.1. Synthesis of 4-substituted phenyl ester derivatives of **3a** from 4-substituted phenyl propiolates.

The proposed synthetic route to the phenyl ester triazines utilised a Steglich esterification between propiolic acid and various phenols to produce the required 4-substituted phenyl propiolates. These propiolates could then partake in 1,3-dipolar cycloadditions with 2,4,5-triphenyl-1,2,3-triazolium-1-phenylaminide 1,3-dipole to give the final triazines.[59]

7.2 RESULTS AND DISCUSSION (SYNTHESIS).

Refer to Chapter 2, Section 2.1.4 for experimental procedure and results.

7.2.1 Steglich esterification of propiolic acid and 4-substituted phenols to generate 4-substituted phenyl propiolates.

The Steglich esterification is a useful mild reaction employing N,N-dicyclohexylcarbodiimide (DCC) in the conversion of carboxylic acids to esters. The Steglich esterification is often used with sterically demanding substrates. The carboxylic acid forms an O-acylisourea intermediate, which "activates" the carbonyl making it more reactive toward nucleophilic attack. An alcohol can then add to the activated carboxylic acid followed by hydrolysis to form dicyclohexylurea (DHU) as an insoluble byproduct and the desired ester (Figure 7.2.1 (a)).

The addition of 5 mol % dimethylaminopyridine (DMAP) is important for the efficient formation of esters (this is not so for amide formation as amines are typically more nucleophilic than alcohols). It is believed to be due to the fact that DMAP is a stronger nucleophile than the alcohol and reacts with the O-acylisourea to form an active amide which in turn reacts rapidly with alcohols to form the desired esters (Figure 7.2.1 (b)).

The above Steglich esterification was utilized to produce 4-substituted phenyl propiolates from propiolic acid and various phenols.

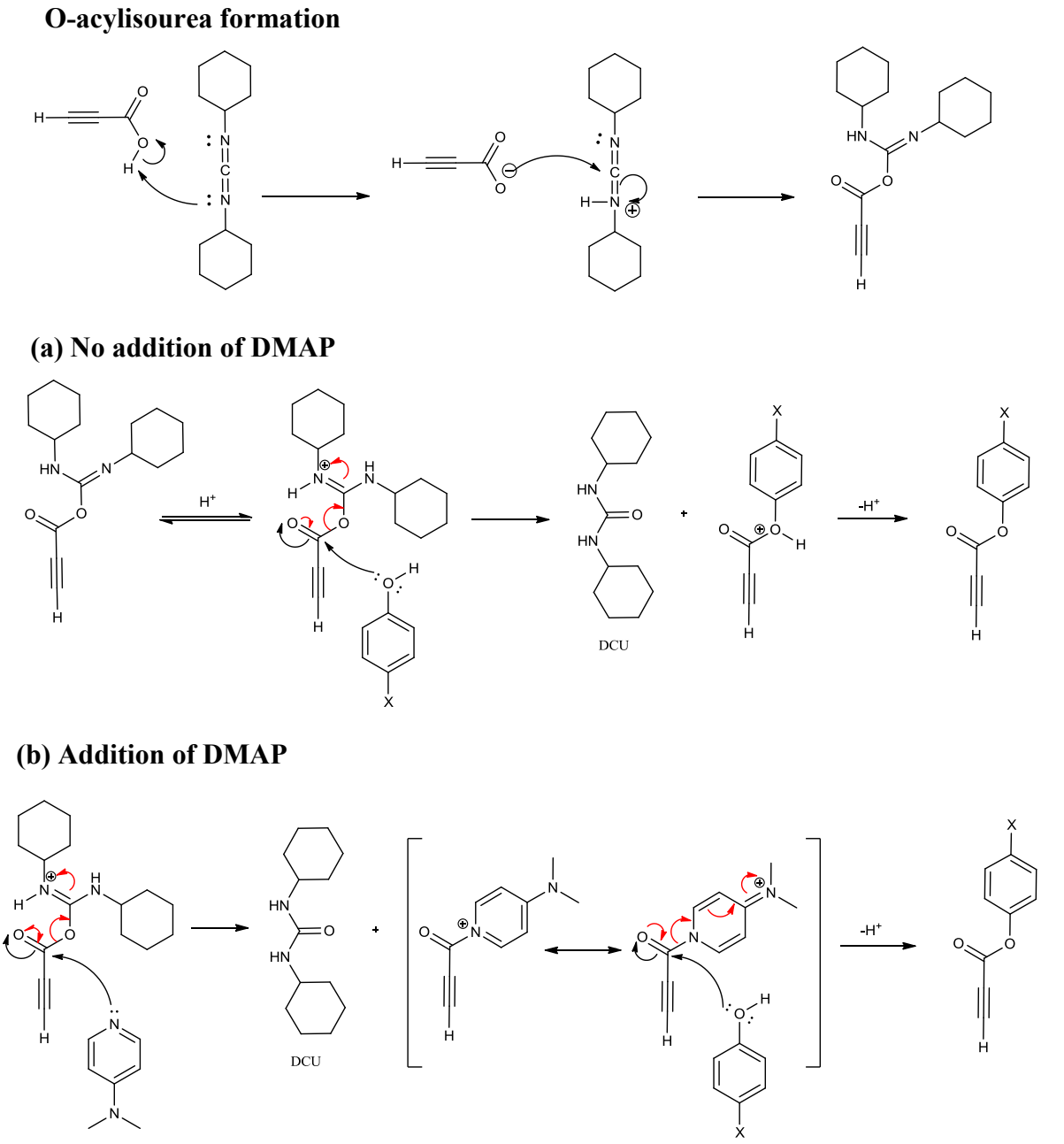

Figure 7.2.1. Proposed mechanism for the Steglich esterification of propiolic acid and 4-substituted phenols to produce 4-substituted phenyl propiolates (a) without the addition of DMAP and (b) with the addition of DMAP.

It has been published that phenols may also partake in a Michael-type addition to a reactive triple bond (*e.g.* propiolates) and can occur very effectively under typical conditions of esterification (*i.e.* in the presence of DCC and DMAP at ambient temperature). This results in the creation of phenoxyacrylic acid phenyl esters *via* one pot esterification and Michael-type addition.[59] This occurs when a two-fold excess of the phenol is used and can be avoided by using an excess of propiolic acid. In order to avoid this unwanted Michael-type addition, we carefully considered the reaction conditions, using only one equivalent of the phenol as described by Bialecka-Florjańczyk.[59]

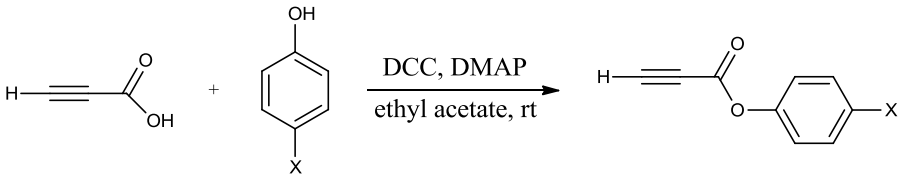

X = H
X = CH_3
X = OCH_3
X = NO_2

20 X = H
22 X = CH_3
24 X = OCH_3
26 X = NO_2

Scheme 7.2.1. Synthesis of 4-substituted phenyl propiolates from propiolic acid and 4-substituted phenols.

By using an equimolar amount of propiolic acid and one of the following phenols (phenol, *p*-cresol, 4-methoxyphenol, and 4-nitrophenol) under the above conditions, the 4-substituted phenyl propiolates; **20**, **22**, **24** and **26** were isolated in yields of 53 %, 72 %, 76 %, and 89 % respectively following purification by column chromatography.

The structure of the isolated products were identified using ^{1}H and ^{13}C NMR spectra and supported by HRMS and IR spectroscopy. The alkynes were identified by their characteristic terminal hydrogen signal in the ^{1}H NMR spectra at ~3.06 ppm.[59]

Compound **22** produced another singlet at 2.26 ppm for the *p*-CH_3 with **24** displaying a singlet at 3.8 ppm for the *p*-OCH_3 in the ^{1}H NMR spectra. Compounds **22**, **24** and **26** also exhibits AA'BB' coupling (*J* values of 8.5 Hz.) for the aromatic ring doublets in the region of 7.0 to 8.32 ppm. The presence of a carbonyl was confirmed by IR spectroscopically with a C=O stretch in the region of ~1641 cm^{-1}.

7.2.2 1,3-Dipolar cycloadditions of 2,4,5-triphenyl-1,2,3-triazolium-1-phenylaminide 1,3-dipole with 4-substituted phenyl propiolates.

The reaction of 2,4,5-triphenyl-1,2,3-triazolium-1-phenylaminide 1,3-dipoles and the appropriate 4-substituted phenyl propiolate (Scheme 7.2.2) results in a fluorescent 2,5-dihydro-1,2,3-triazine containing a phenyl ester functionality. The electron density of the carbonyl group is varied depending on the substituent at the 4-position of the phenyl esters.

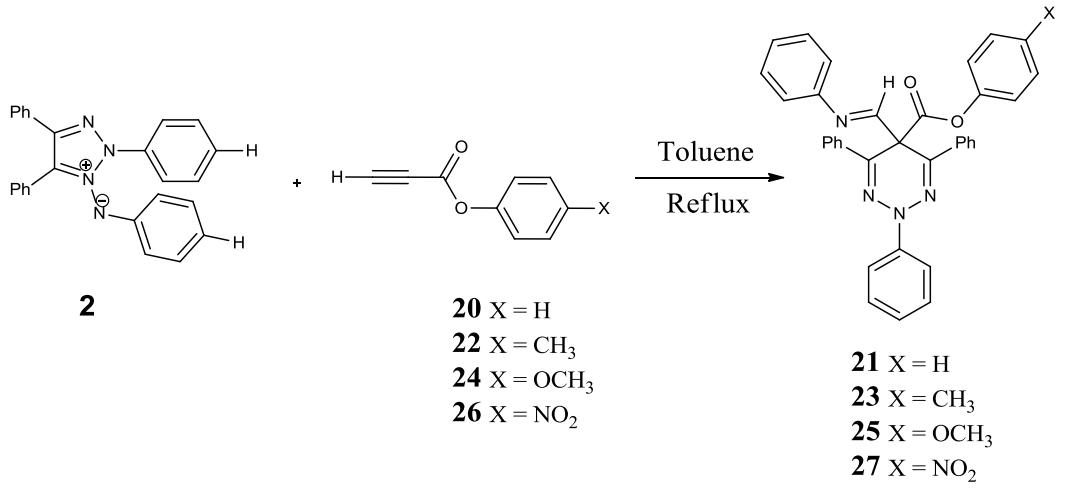

2

20 X = H
22 X = CH_3
24 X = OCH_3
26 X = NO_2

21 X = H
23 X = CH_3
25 X = OCH_3
27 X = NO_2

Scheme 7.2.2. Synthesis of 4-substituted phenyl ester triazines from 4-substituted phenyl propiolates.

As previously discussed (Chapter 5, Section 5.2.1), the use of a high reaction temperature in the cycloaddition between 2,4,5-triphenyl-1,2,3-triazolium-1-phenylaminide 1,3-dipoles and methyl propiolate improves conversion to the 2,5-dihydro-1,2,3-triazine. As such, the cycloaddition using the appropriate 4-substituted phenyl propiolate was performed using a toluene reflux.

Typically, propiolates and substituted terminal alkynes are volatile substrates (*e.g.* methyl propiolate) resulting in the easy removal of an excess of the reactant upon reaction completion. However, all the 4-substituted phenyl propiolates are non volatile and any excess would have to be removed using column chromatography. Therefore, to aid in the purification, an excess of the 2,4,5-triphenyl-1,2,3-triazolium-1-phenylaminide 1,3-dipole was used to ensure full conversion of the phenyl propiolate to the desired phenyl ester substituted 2,5-dihydro-1.2.3-triazine. Triazines **21**, **23**, **25** and **27** were generated in yields

of 84 %, 93 %, 94 % and 83 % respectively. A small amount of 2,4,5-triphenyl-1,2,3-triazole was isolated during purification and had been carried through with the 1,3-dipole starting material. It is a by product from the oxidation of the 1,2-bisphenylhydrazone of benzil to 2,4,5-triphenyl-1,2,3-triazolium-1-phenylaminide 1,3-dipole.

In all cases, the structure was identified using ^{1}H and ^{13}C NMR spectra and supported by HRMS and IR spectroscopy. As discussed in Section 4.1.2, the reaction is again highly regioselective and only one isomer is isolated for each of **21**, **23**, **25** and **27**. This is supported as only one singlet is observed for the imine hydrogen at ~8.5 ppm and in the ^{1}H NMR spectra. The ^{13}C NMR spectrum of **21**, **23**, **25** and **27** show the presence of an imine carbon at ~160 ppm. They also exhibit the key quaternary carbon signal for C5 at ~53 ppm, as well as a quaternary carbon signal at ~170 ppm which again confirms the presence of a carbonyl and is supported by the IR spectrum with a C=O stretch observed at ~1698 cm^{-1}.

Compound 23 (X = CH_3) also exhibits a characteristic singlet at 2.25 ppm and 20.8 ppm for the *p*-CH_3 whilst **25** (X = OCH_3) displayed a singlet at 3.7 ppm and 54 ppm for the *p*-OCH_3 in the ^{1}H and ^{13}C NMR spectra respectively.

7.3 RESULTS AND DISCUSSION (FLUORESCENCE SPECTROSCOPY).

Refer to Chapter 2, Section 2.2.1 for experimental procedure and results.

Refer to Results Appendix 4.1, 4.2, 4.3 and 4.4 for complete set of solvatochromic results, tables and graphs.

7.3.1 Steady state fluorescence study.

A detailed steady state solvatochromism study was undertaken for the phenyl ester substituted 2,5-dihydro-1,2,3-triazine fluorophores (**21**, **23**, **25** and **27**) with 12 solvents selected: toluene, 1,4-dioxane, chloroform, acetonitrile, 1-octanol, 1-hexanol, 1-butanol, 1-pentanol, 1-propanol, acetic acid, methanol and 2,2,2-trifluoroethanol (Refer to Appendix A.2 for complete list of solvents and solvatochromic values).

Analysis was again performed against normalized solvent polarity (E_T^N), solvent hydrogen bonding donating/accepting ability (α and β), solvent polarizability (π^*), viscosity (η(Cp)) and dipole moment (μ) for each fluorophore, using the software package Origin 7.0, in order to identify any possible ground state solvent interactions which may influence their fluorescence emission.

7.3.1.1 Ultraviolet Visible absorption spectra.

The ground state absorptions for the phenyl ester triazines do not change in comparison with the methyl ester triazine (**3a**, Chapter 4, Section 4.3.1.1). An absorption at ~310 nm and a broad absorption band at ~390 nm are observed and are not strongly effected by changing the nature of the solvent (Figure 7.3.1). This is clearly evident in the normalized UV-visible spectra which show no change in the band positions (Figures 7.3.2).

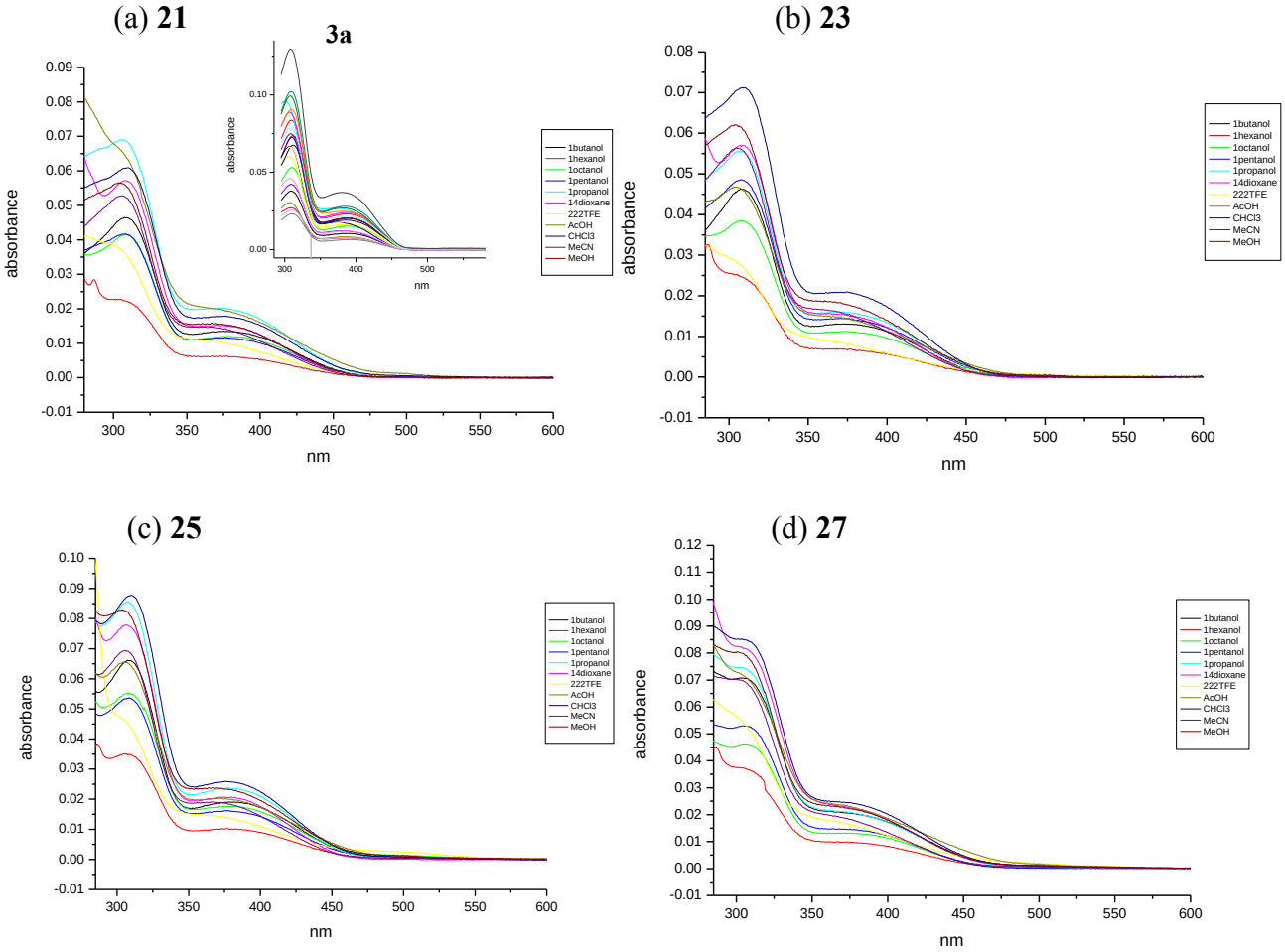

Figure 7.3.1. Ultraviolet visible absorption spectra for the imine hydrolysed 2,5-dihydro-1,2,3-triazines (**21**, **23**, **25** and **27**), with **3a** (inset) for comparison recorded at an assumed maximum concentration of 1 x 10^{-5} M.

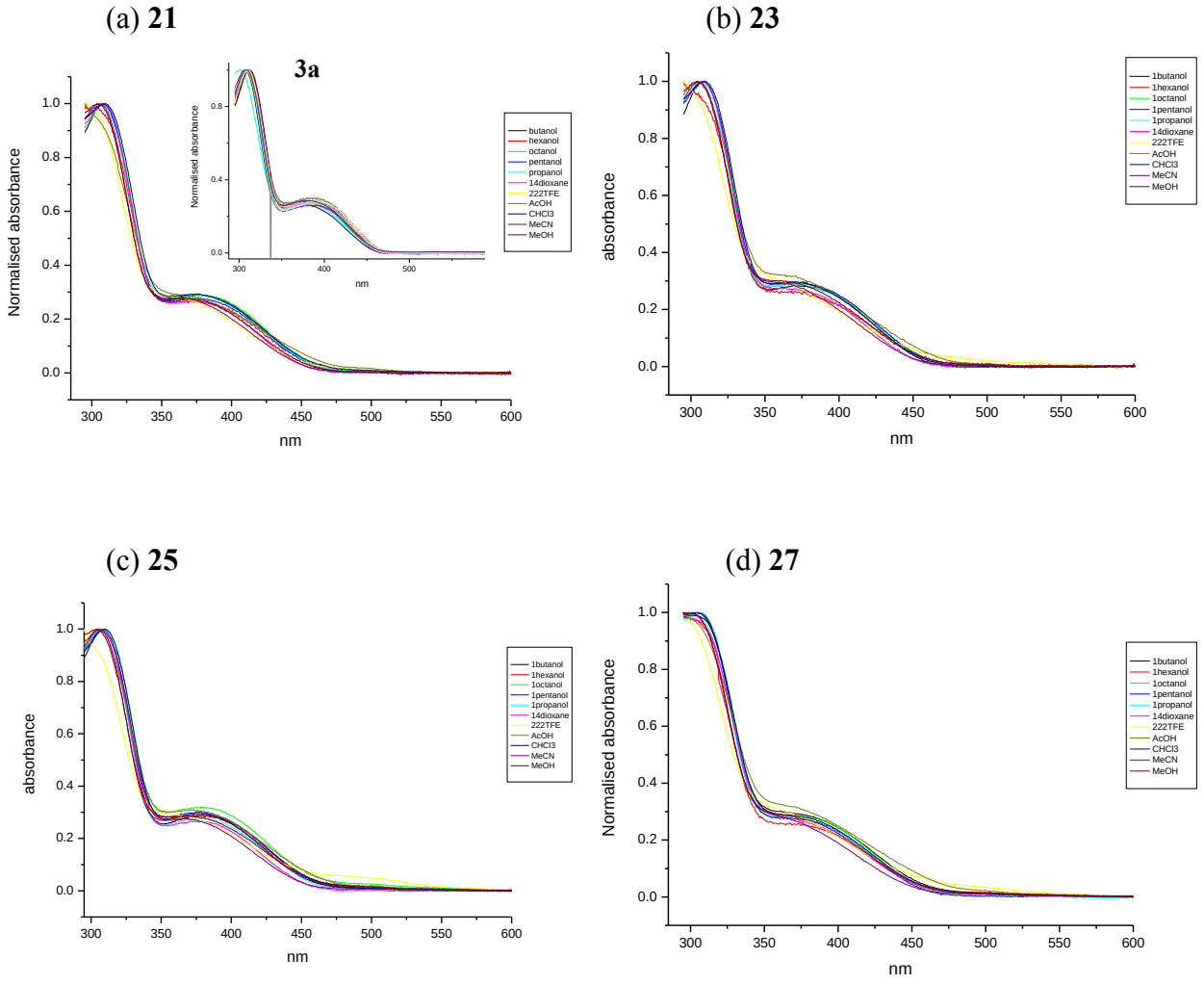

Figure 7.3.2. Normalised ultraviolet visible absorption spectra for the imine hydrolysed 2,5-dihydro-1,2,3-triazines (**21**, **23**, **25** and **27**), with **3a** (inset) for comparison

7.3.1.2 Fluorescence emission spectra.

Like the methyl ester triazine (Chapter 4), excitation into either of the absorption bands (310 or 400 nm) for the phenyl ester triazines (**21**, **23**, **25** and **27**) results in a similar complicated, green fluorescence emission band centered at ~520 nm. For **21**, **23** and **25** the emission band appears to be uneffected by changing the nature of the solvent (Figure 7.3.4 and 7.3.5). The deconvoluted spectra at 400 nm excitation (Figure 7.3.3) consists of three emission bands similar to **3a**: ~480 nm (Band 3), ~510 nm (Band 2), and ~540 nm (Band 1). Excitation at 310 nm emission also consists of three separate emission bands: ~480 nm (Band 3), ~510 nm (Band 2), and ~540 nm (Band 1). In addition, a single weakly emitting band at ~350 nm (Band 4) is obsevred which is assumed once more to be due to the population of the S_3 (**g0**) and S_2 (**g0**) ES as suspected for **3a**.

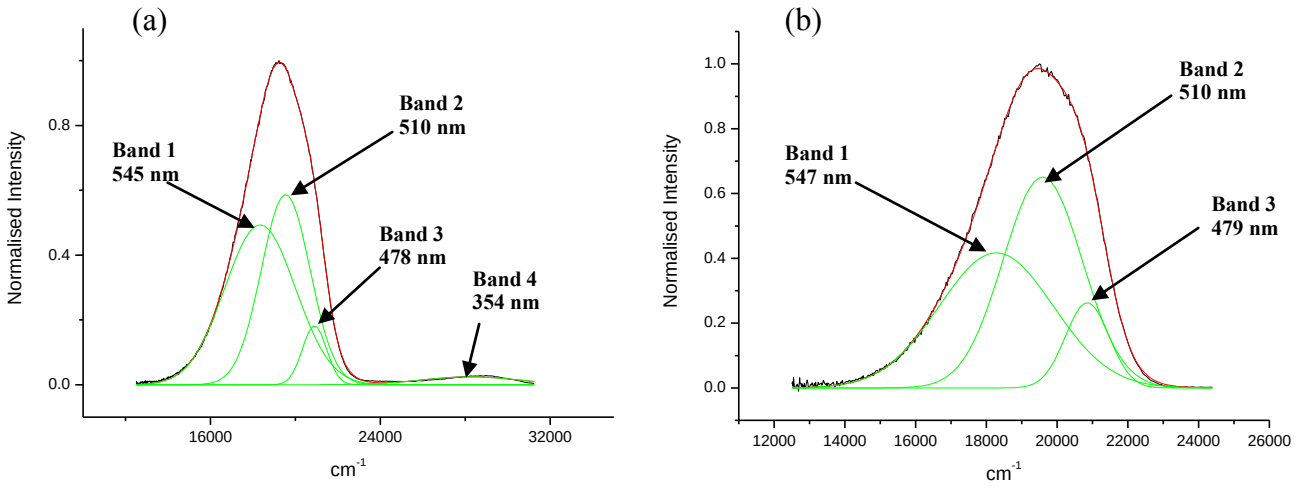

Figure 7.3.3. Gaussian model fits of the normalised fluorescence emission spectrum of **21** recorded in acetonitrile for (a) 310 nm and (b) 400 nm excitation.

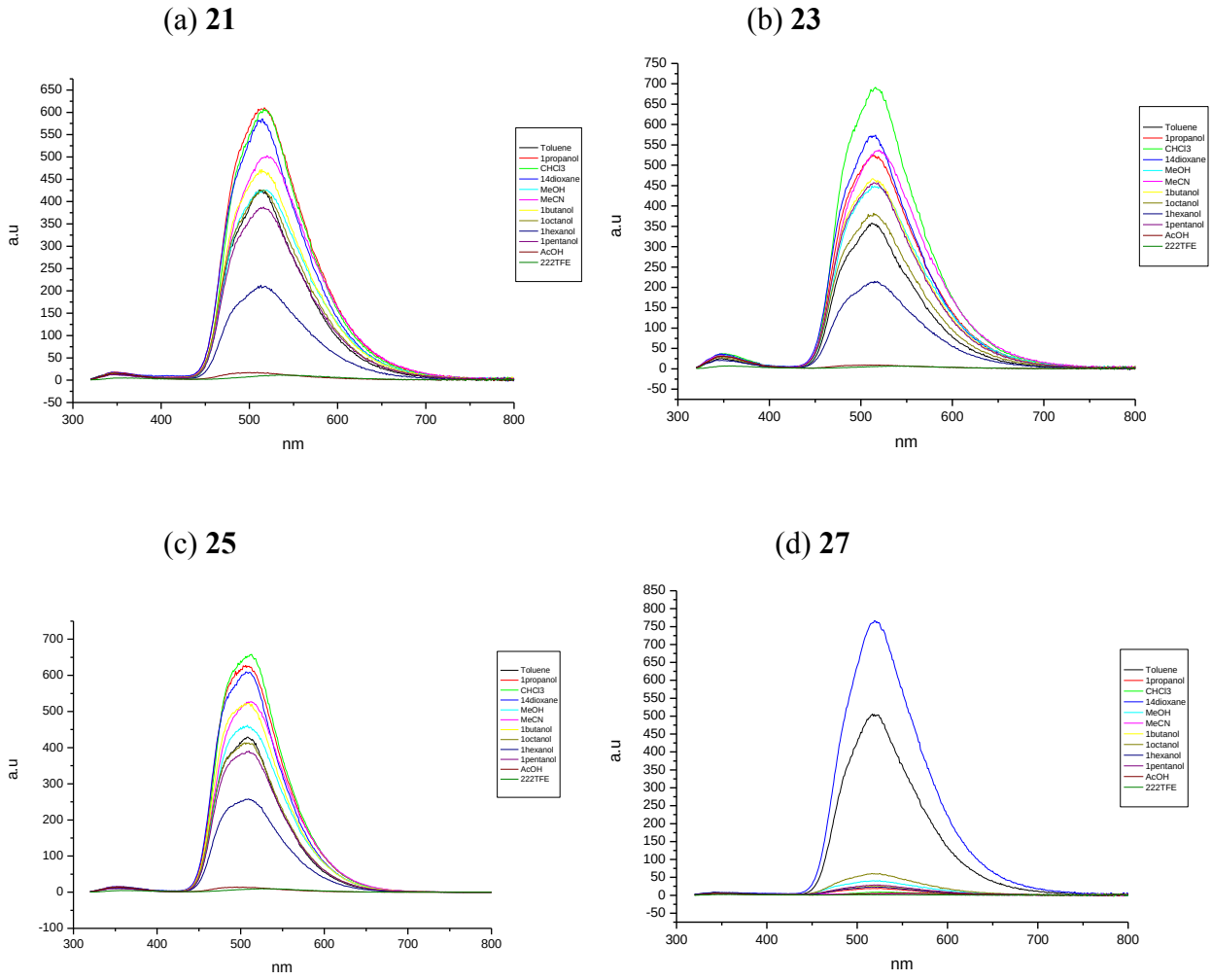

Figure 7.3.6. Summary of fluorescent emission spectra at 310 nm excitation for the phenyl ester substituted 2,5-dihydro-1,2,3-triazines (**21**, **23**, **25** and **27**) recorded at an assumed maximum concentration of 1 x 10^{-5} M.

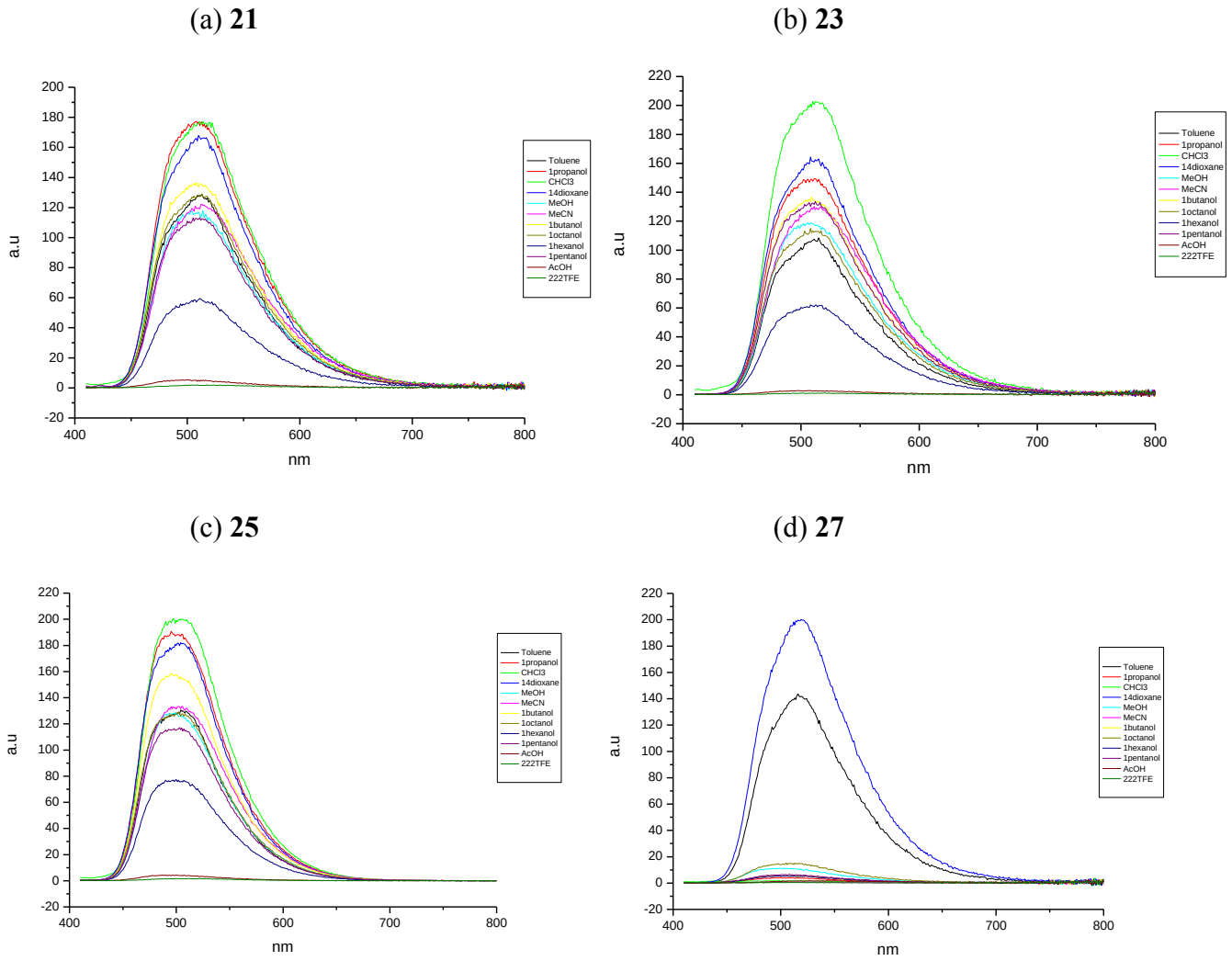

Figure 7.3.7. Summary of fluorescent emission spectra at 400 nm excitation for the phenyl ester substituted 2,5-dihydro-1,2,3-triazines (**21**, **23**, **25** and **27**) recorded at an assumed maximum concentration of 1 x 10^{-5} M.

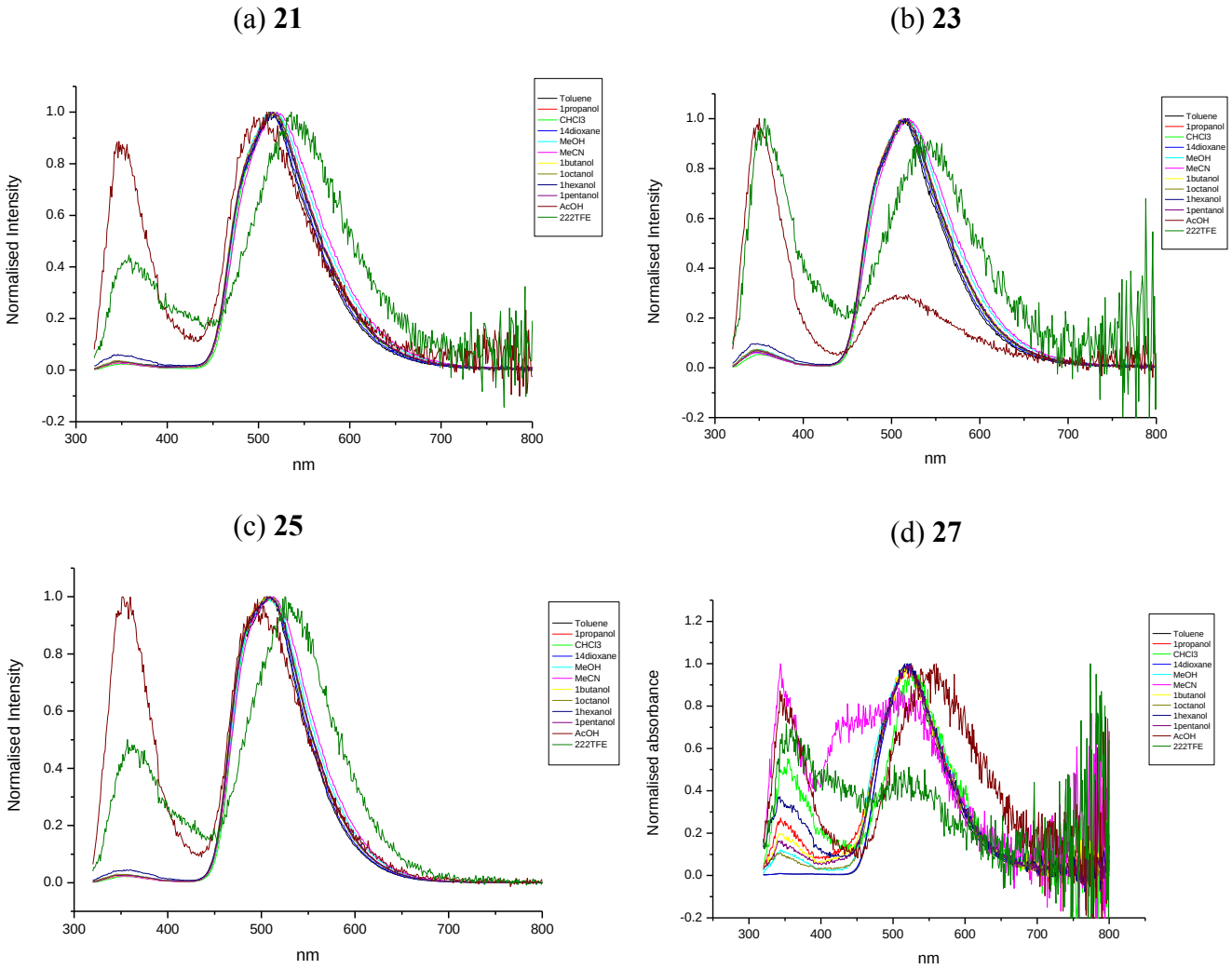

Figure 7.3.8. Summary of the normalized fluorescent emission spectra at 310 nm excitation for the phenyl ester substituted 2,5-dihydro-1,2,3-triazines (**21**, **23**, **25** and **27**).

.

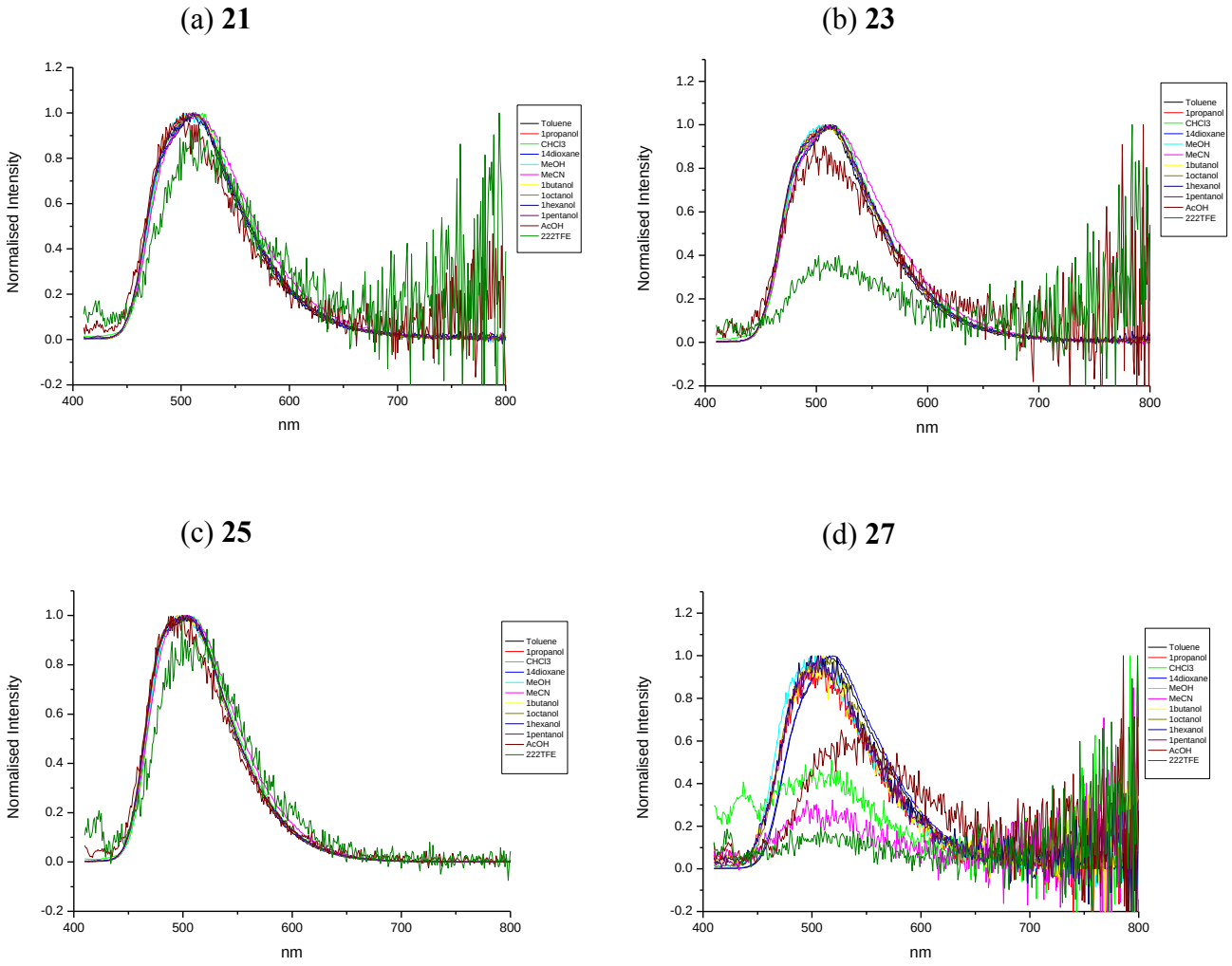

Figure 7.3.9. Summary of the normalized fluorescent emission spectra at 400 nm excitation for the phenyl ester substituted 2,5-dihydro-1,2,3-triazines (**21**, **23**, **25** and **27**).

An extensive range of solvents were investigated but only small solvatochromic trends were observed. As a result, it is more informative to compare the minimum and maximum values for each compound, regardless of solvent. Hence, the solvent will vary in the following tables. For a full summary of all results and solvatochromic values refer to Appendix of Results, 4.1, 4.2, 4.3 and 4.4.

The observed emission peak maximum at 310 nm excitation (Table 7.1 (a)) ranges from 519 nm (**25** in propylene carbonate), 520 nm (**21** and **23** in acetonitrile) to 525 nm (**27** in 1-octanol) and compares to 525 nm for **3a** in ethylene glycol. The observed emission peak maximum at 400 nm excitation (Table 7.1 (b)) ranges from 514 nm (**21** in chloroform), 515 nm (**23** in toluene), 516 nm (**25** in acetonitrile) to 519 nm (**27** in 1,4-dioxane) and compares to 513 nm for **3a** in N,N-dimethylformamide.

(a)

Code	X	Solvent	$\lambda_{310\ nm\ ems}$ (min)	Solvent	$\lambda_{310\ nm\ ems}$ (max)
3a	-	Toluene	510	Ethylene Glycol	525
21	H	Toluene	512	Acetonitrile	520
23	CH_3	Toluene	512	Acetonitrile	520
25	OCH_3	1,4-Dioxane	512	Methanol	519
27	NO_2	Acetonitrile	509	1-Octanol	525

(b)

Code	X	Solvent	$\lambda_{400\ nm\ ems}$ (max)	Solvent	$\lambda_{400\ nm\ ems}$ (max)
3a	-	Methanol	504	N,N-dimethylformamide	513
21	H	1-Butanol	508	Chloroform	514
23	CH_3	Methanol	506	Toluene	515
25	OCH_3	1-Propanol	506	Acetonitrile	516
27	NO_2	1-Propanol	500	1,4-Dioxane	519

Table 7.1. Summary of (a) observed emission peak maximum for 310 nm excitation (minimum and maximum value) of **21**, **23**, **25** and **27** and (b) emission band maximum for 400 nm excitation (minimum and maximum value) of **21**, **23**, **25** and **27**.

In general, the calculated quantum yields for **21**, **23**, **25** and **27** are moderate in comparison to the methyl ester triazine **3a**. For 310 nm excitation, the maximum quantum yield for **21**, **23**, **25** and **27** were calculated to be 0.5 in 1-octanol, 0.49 in 1-octanol, 0.47 in 1,4-dioxane and 0.44 in 1,4-dioxane respectively compared to 0.76 in toluene for **3a** (Table 7.2 (a)). Similarly for 400 nm excitation, the maximum quantum yield for **21**, **23**, **25** and **27** were calculated to be 0.54 in 1,4-dioxane, 0.53 in 1,4-dioxane, 0.52 in 1,4-dioxane and 0.45 in 1,4-dioxane in that order, compared to 0.79 in toluene for **3a** (Table 7.2 (b)).

(a)

Code	X	Solvent	$\Phi_{310\ nm}$ (min)	Solvent	$\Phi_{310\ nm}$ (max)
3a	-	Propylene Carbonate	0.13	Toluene	0.76
21	H	Toluene	0.27	1-Octanol	0.5
23	CH_3	Toluene	0.31	1-Octanol	0.49
25	OCH_3	1-Butanol	0.32	1,4-Dioxane	0.47
27	NO_2	Chloroform	0.01	1,4-Dioxane	0.44

(b)

Code	X	Solvent	$\Phi_{400\ nm}$ (min)	Solvent	$\Phi_{400\ nm}$ (max)
3a	-	Methanol	0.32	Toluene	0.79
21	H	Toluene	0.20	1,4-Dioxane	0.54
23	CH_3	Toluene	0.31	1,4-Dioxane	0.53
25	OCH_3	Methanol	0.29	1,4-Dioxane	0.52
27	NO_2	Chloroform	0.01	1,4-Dioxane	0.45

Table 7.2. Summary of (a) minimum and maximum quantum yield (**Φ**) values for **21**, **23**, **25** and **27** at 310 nm excitation and (b) minimum and maximum quantum yield (**Φ**) values for **21**, **23**, **25** and **27** at 400 nm excitation.

Similar to **3a**, acetic acid and trifluoroethanol again cause significant quenching to the fluorescence intensity and quantum yield of the phenyl ester 2,5-dihydro-1,2,3-triazines, which again is potentially due to hydrogen bonding of 2,2,2-trifluoroethanol to the triazine nitrogens, the imine nitrogen or the carbonyl oxygen, which could effect the imine and carbonyl interaction or partial protonation of the carbonyl oxygen by acetic acid (Figure 7.3.10). A fully study is yet to be performed in support of this hypothesis.

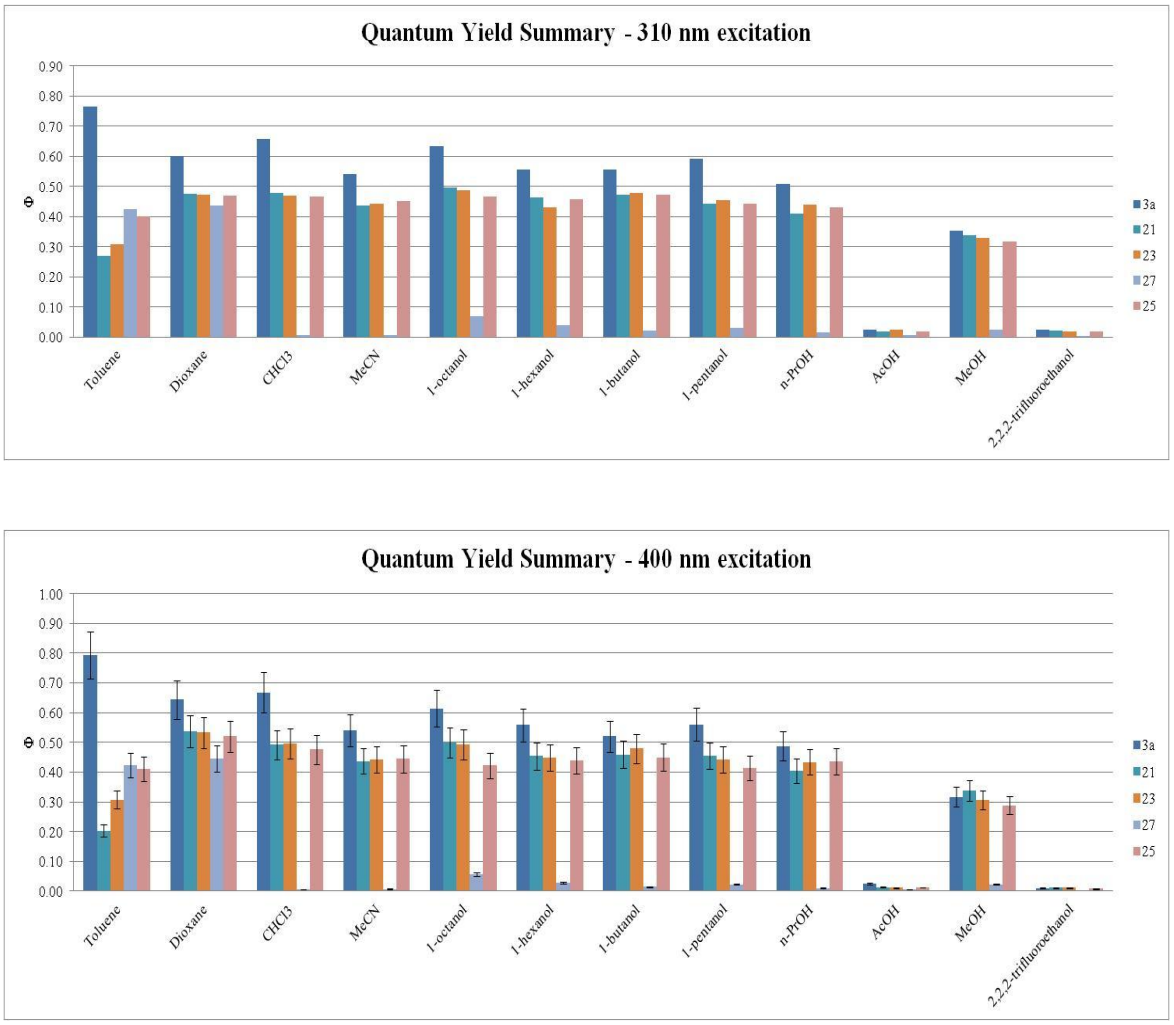

Figure 7.3.10. Graphical summary of quantum yield (**Φ**) values for the phenyl ester substituted 2,5-dihydro-1,2,3-triazines (**21**, **23**, **25**, and **27**) versus **3a** (N=C-H).

The difference in quantum yield varies only slightly between **21**, **23** and **25** (Figure 7.3.10), but when substituted with a *p*-NO_2 (**27**) it becomes evident that the fluorescence of the molecule is exhibiting solvent selectivity as the *p*-NO_2 substituent produces a surprising quenching effect in most solvents, bar toluene and 1,4-dioxane (Figure 7.3.4, 7.3.5 and 7.3.10).

It is known that in general the fluorescence of aromatic hydrocarbons possessing an NO_2 substituent is not detectable due to low-lying $n \rightarrow \pi^*$ transitions which contributes to an efficient intersystem crossing process that out competes radiative processes (*i.e.* phosphorescence). A result of the strong electron-withdrawing power of a NO_2 group there is a high rate of $S_1 \rightarrow S_0$ internal conversion (radiationless de-excitation) that is likely to be the cause of the absence of detectable fluorescence.

The fluorescence of the *p*-NO_2 phenyl ester triazine (**27**) is observed in the nonpolar aprotic solvents toluene and 1,4-dioxane which have normalized polarity (E_T^N) values of 0.099 and 0.164, hydrogen bonding donating (α) values of 0 for both and dipole moment (μ) values of 0.37 and 0 respectively. This is in comparison to the other aprotic solvents chloroform and acetonitrile studied which exhibit weak fluorescence and have higher normalized polarity (E_T^N) values of 0.259 and 0.46, higher hydrogen bonding donating (α) values of 0.44 and 0.19 and larger dipole moment (μ) values of 1.04 and 3.92 respectively.

Quenching was also observed in the protic polar alcohol series studied (1-octanol, 1-hexanol, 1-butanol, 1-pentanol and 1-propanol) with (E_T^N) values ranging from 0.537 to 0.762, hydrogen bonding donating (α) values ranging from 0.28 to 0.98 and dipole moment (μ) values ranging from 1.55 and 1.8.

The quenching of **27** therefore appears to be influenced by the polarity of the solvent (and solvent dipole moment) and hydrogen bonding ability of the solvent with fluorescence observed in aprotic solvents of low polarity (and solvent dipole moment) with no hydrogen bonding ability.

Observing the deconvoluted spectra of **27** in chloroform, acetonitrile and methanol (Figure 7.3.11) and the normalized Gaussian band fit positions and area contributions (Tables 7.3), it is clear that a change in the emission properties is occurring. Only toluene and 1,4-dioxane exhibit the typical emission bands as the other phenyl ester triazines at 310 nm excitation: ~480 nm (Band 3), ~510 nm (Band 2), and ~540 nm (Band 1) and have only slight changes in the contributions compared to the methyl ester triazine **3a:** 5 % versus 7 % for **3a** (Band 3), 40 % versus 46 % for **3a** (Band 2) and 54 % versus 47 % for **3a** (Band 1) and this suggests increased IC from S_2 (**g0**) to yield S_1 (**g1**) emission (Band 1) and

decreased IC from S_2 (**g0**) to yield S_1 (**g2**) emission in comparison to when a methyl ester is substituted.

Taking chloroform and methanol as examples, we see that the 480 nm emission band (Band 3) which is associated with emission from the S_1 (**g0**) state is not found at 310 nm excitation. What is observed however are emission bands at ~380 and ~350 nm (Band 4 and 5) for the quenching solvents†, which are associated with S_2 (**g0**) and S_3 (**g0**). Therefore, it is thought that the solvent is hydrogen bonding to the nitro group oxygens promoting radiationless de-excitation from the S_3 (**g0**) or S_2 (**g0**) excited state, or in the case of the aprotic solvents acetonitrile and chloroform the dipole moment of the solvent appears to be promoting radiationless de-excitation and thus preventing the other fluorescent emission processes from occurring.

For 400 nm excitation (Table 7.4), S_1 (**g0**) emission (Band 3) and S_1 (**g1**) emission (Band 1) is observed for all solvents except chloroform and acetonitrile. Chloroform and acetonitrile appear to only exhibit weak fluorescence from the S_1 (**g2**) state that is of higher energy (500 nm) in both chloroform and acetonitrile versus 510 nm in toluene. However, S_1 (**g2**) emission (Band 2) is not observed for the polar protic solvents except for 1-octanol, possibly due to the higher viscosity of 1-octanol. This may make the S_1 (**g2**) transition more favourable from S_1 (**g0**) as we see a significant contribution from this state for 1-octanol (55 %) as compared to a non viscous solvent like toluene (44 %) (Table 7.4). Therefore, it is believed that upon being excited at 400 nm excitation, radiationless de-excitation from the S_1 (**g0**) or S_1 (**g1**) (which can be reached by internal conversion from S_1 (**g0**)) is promoted for the polar protic solvents in a similar fashion to 310 nm excitation. However, for chloroform and acetonitrile, the S_1 (**g0**) to S_1 (**g2**) transition appears to be promoted followed by radiationless de-excitation, with the energy of the S_1 (**g2**) state being higher in energy than in aprotic, non-hydrogen bonding solvents.

† Chloroform, acetonitrile, 1-octanol, 1-hexanol, 1-butanol, 1-pentanol and 1-propanol.

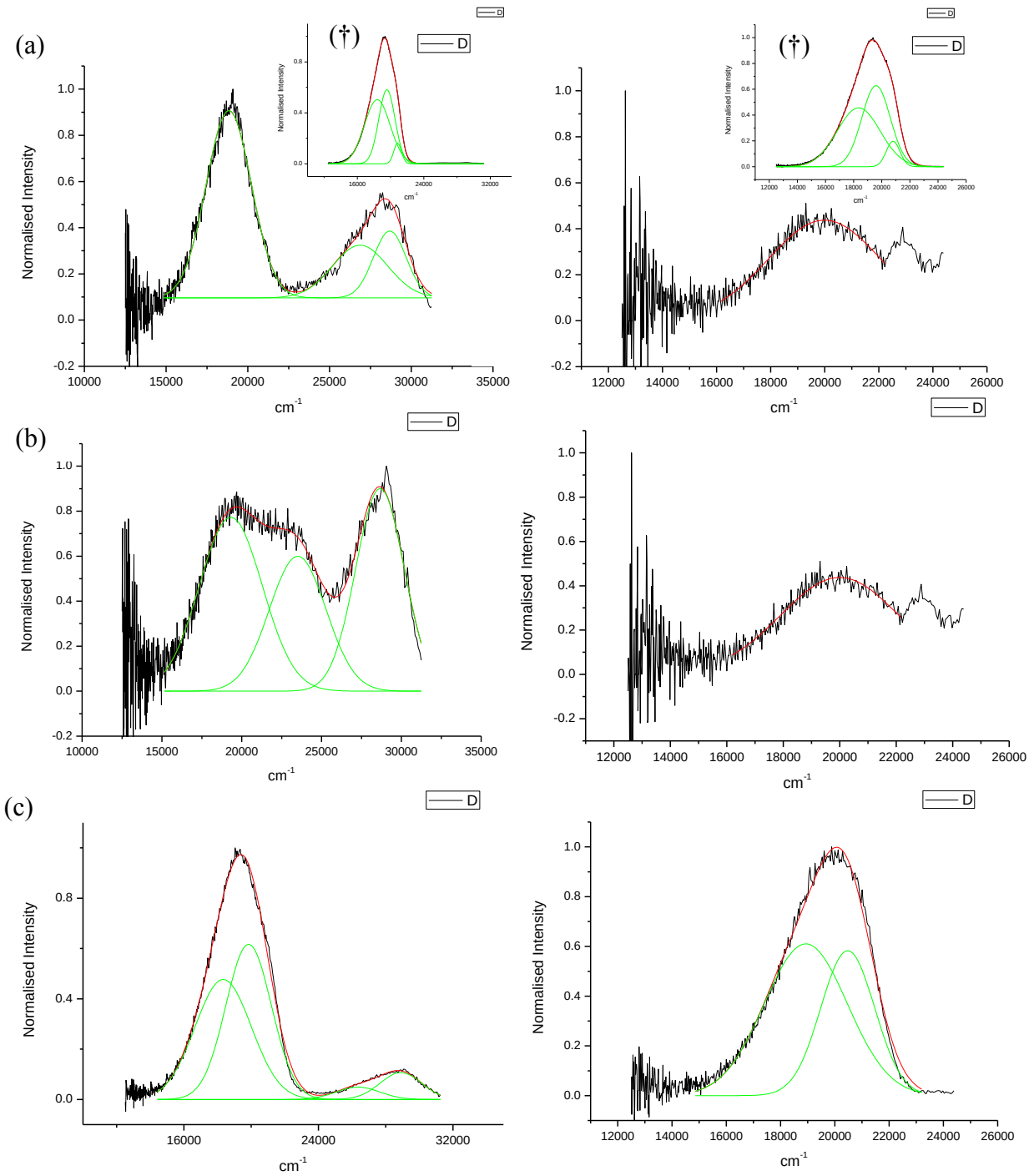

Figure 7.3.11. Gaussian model fit of the normalised fluorescence emission spectrum of **27** recorded in (a) chloroform ((†) toluene), (b) acetonitrile and (c) methanol at 310 nm (left) and 400 nm (right) excitation.

(a)

Solvent	λ max$_{em}$ Band 1 (nm)	λ max$_{em}$ Band 2 (nm)	λ max$_{em}$ Band 3 (nm)	λ max$_{em}$ Band 4 (nm)	λ max$_{em}$ Band 5 (nm)
Toluene	543.45	511.27	479.75	-	-
1,4-Dioxane	543.64	512.02	478.79	-	-
Chloroform	530.81	-	-	372.13	348.59
Acetonitrile	-	517.72	-	425.41	348.85
1-Octanol	551.08	509.92	-	408.05	346.58
1-Hexanol	539.78	503.67	-	352.93	341.84
1-Butanol	-	520.23	-	412.30	352.52
1-Pentanol	-	521.33	-	411.50	352.27
1-Propanol	-	520.15	-	412.99	351.27
Acetic acid	568.21	515.47	-	357.91	342.57
Methanol	545.32	503.80	-	379.44	346.02
2,2,2-Trifluoroethanol	-	525.83	-	404.44	352.19

(b)

Solvent	Band 1 Area (%)	Band 2 Area (%)	Band 3 Area (%)	Band 4 Area (%)	Band 5 Area (%)
Toluene	54.63	40.07	5.29	-	-
1,4-Dioxane	56.32	39.06	4.61	-	-
Chloroform	62.41	-	-	21.42	16.15
Acetonitrile	-	38.56	-	26.86	34.57
1-Octanol	32.70	55.62	-	1.34	10.32
1-Hexanol	32.21	41.88	-	25.12	0.78
1-Butanol	-	81.69	-	2.39	15.90
1-Pentanol	-	84.10	-	1.89	14.00
1-Propanol	-	76.99	-	3.83	19.17
Acetic acid	42.30	11.96	-	40.71	5.01
Methanol	43.63	45.65	-	3.46	7.23
2,2,2-Trifluoroethanol	-	26.92	-	43.33	29.74

Table 7.3. Summary of (a) Guassian band positions and (b) area percentages for the Gaussian band fits from the deconvoluted spectra of **27** at 310 nm excitation.

Solvent	λ max$_{em}$ Band 1 (nm)	λ max$_{em}$ Band 2 (nm)	λmax$_{em}$ Band 3 (nm)	Band 1 Area (%)	Band 2 Area (%)	Band 3 Area (%)
Toluene	544.67	510.32	480.65	48.92	44.36	6.71
1,4-Dioxane	545.98	510.91	479.98	48.04	45.49	6.45
Chloroform	-	500.19	-	-	100	-
Acetonitrile	-	500.11	-	-	100	-
1-Octanol	544.03	506.43	478.26	39.27	53.26	7.45
1-Hexanol	536.44	-	495.07	52.37	-	47.62
1-Butanol	533.57	-	494.03	54.80	-	45.19
1-Pentanol	536.04	-	494.77	52.96	-	47.03
1-Propanol	533.88	-	493.06	54.57	-	45.42
Acetic acid	539.95	-	-	100	-	-
Methanol	528.25	-	488.40	61.76	-	38.23
2,2,2-Trifluoroethanol	-	510.38	-	-	100	-

Table 7.4. Summary of the Guassian band positions and area percentages for the Gaussian band fits from the deconvoluted spectra of **27** at 400 nm excitation.

Table 7.6 shows the minimum and maximum values of the Gaussian band positions of the deconvoluted 310 nm excitation spectra for **21**, **23** and **25** (Figure 7.3.3) and Table 7.7 lists the minimum and maximum percentage area values. Tables 7.8 shows the minimum and maximum values of the Gaussian band positions of the deconvoluted 400 nm excitation spectra for **21**, **23** and **25** and Table 7.9 lists the minimum and maximum percentage areas contributions.

The emission properties are almost identical across the phenyl ester triazine family and the relative intensities and areas of the emission bands do not change significantly between **21**, **23** and **25** (Tables 7.6, 7.7, 7.8 and 7.9). They all exhibit the same emission bands as the methyl ester triazine (**3a**) at both 310 and 400 nm excitation: ~480 nm (Band 3), ~510 nm (Band 2), and ~540 nm (Band 1) as well as having similar contributions compared to the methyl ester triazine **3a** (*e.g.* the contributions at 400 nm excitation are ~50 % (Band 1) ~46 % (Band 2) and ~13 % (Band 1) for **21**, **23**, **25** and **3a** (Table 7.9)).

This would indicate that changing the from a methyl ester carbonyl to a 4-substituted phenyl ester with the exception of *p*-NO_2 has only a minor influence on the photophysics of the 2,5-dihydro-1,2,3-triazines. In general, we see little change in fluorescence when compared to **3a** at either 310 or 400 nm excitation.

In order to help explain the unexpected lack of change in fluorescence with the family of phenyl ester triazines, we undertook a computational study exploring the electron density of the carbonyl group. The computational calculations were carried out by a collaborator, Dr Elisa Fadda, NUI Maynooth. The C=O dipole, and charge on the carbon and oxygen atoms were calculated for the esters; methyl acetate (as a model for **3a**), phenyl acetate (as a model for **21**) and 4-methoxyphenyl acetate (as a model for **25**), **Figure 7.3.12.** A ketone, propan-2-one, and an acylbenzotriazole, 1-(1H-benzo[d][1,2,3]triazol-1-yl)ethanone (Figure 7.3.12) was also investigated as models for **10a** and **29** respectively. We modeled **10a** and **29** as a distinct change in the energy of the fluorescence was observed for both **10a** and **29** (Chapter 4 and Chapter 8). Table 7.5 reports the calculated results for each of the compounds. All molecules were built by Dr. Fadda with version 9.4 of Maestro (Academic License); their geometry was optimized with version 6.5 of TURBOMOLE at the b97d//def2-TZV(P) level of theory; within the resolution of the identity approximation and in redundant internal coordinates. b97d represents the b97 GGA functional augmented

with Grimme dispersion contribution. Atom charges were obtained through fitting of the electrostatic potential (ESP) with Bragg-Slater radii. .

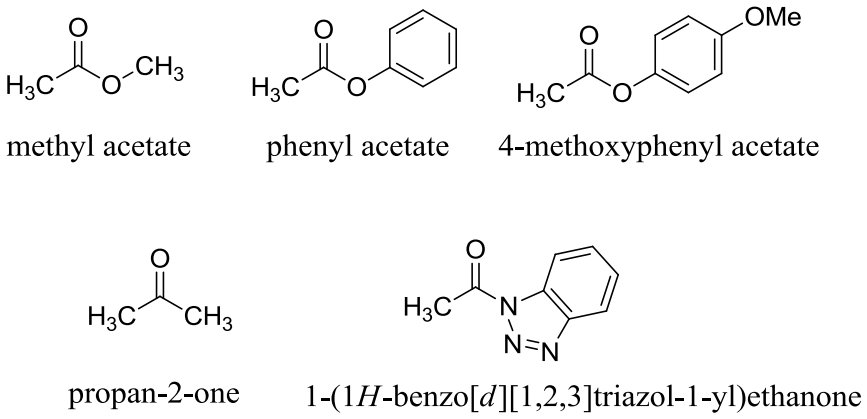

Figure 7.3.12. Compounds used to investigate the carbonyl electronics.

Compound	Charge Carbon	Charge Oxygen	C=O dipole (D)
Methyl acetate	0.7376	-0.5401	1.1481
Phenyl acetate	0.7496	-0.5637	1.0749
4-Methoxyphenyl acetate	0.7517	-0.5685	1.0604
Propan-2-one	0.4875	-0.4929	-0.0316
1-(1H-benzo[d][1,2,3]triazol-1-yl)ethanone	0.3792	-0.4630	-0.4878

Table 7.5. Summary of the calculated C=O dipoles and charges on the carbon and oxygen atoms.

The results of the computational study indicated that the carbonyl group of the esters are characterized by a C=O dipole of ~ 1.1 D and that there was little change in electron density at the carbonyl as you move from a methyl ester to a phenyl ester to a *p*-methoxy phenyl ester (Table 7.5). The resonance effect of a *p*-substituted methoxy group appears to have little influence on the carbonyl's electronics. This lack of change in electron density, at these ester carbonyls, may explain the lack of change in fluorescence between the phenyl ester triazines **21**, **23** and **25** when compared to the methyl ester triazine

3a. For the phenylimine substituted triazines, **10a** and **29**, we proposed that a key component in our model of fluorescence was the interaction between the carbonyl group and the imine C-H (Chapter 3). The calculated charge on the oxygen atom for the esters were all similar (-0.5401, -0.5637, -0.5685 for methyl acetate, phenyl acetate, and 4-methoxyphenyl acetate respectively, Table 7.5) and as such the methyl and phenyl ester triazines may be expected to have a carbonyl:imine C-H interaction of similar strength and hence may in part help explain their similar fluorescence.

However, when the carbonyl on the triazine is substituted with a methyl ketone (**10a** and **19**, Chapter 4 and 6) or a N-acylbenzotriazole (**29**, Chapter 8, Section 8.2.1), a lower energy emission is observed for the fluorescence in both cases, when compared to the methyl ester triazine **3a**.

This change in fluorescence may be associated with the marked difference between the calculated electron densities of the carbonyl when an ester (*e.g.* methyl acetate, calculated C=O dipole moment of 1.1481 D) is compared to a ketone (*e.g.* propan-2-one, calculated C=O dipole moment of -0.0316 D) or N-acylbenzotriazole (*e.g.* 1-(1H-benzo[d][1,2,3]triazol-1-yl)ethanone, calculated C=O dipole moment of -0.4878 D).

Furthermore, as previously discussed, our model of fluorescence (**10a** and **29**, Chapter 3) suggests that a key interaction exists between the imine C-H and the carbonyl group. Based on these calculations, this interaction could be stronger for the ester substituted triazines (*e.g.* **3a** and **21**) as the carbonyl oxygen's have a higher calculated negative charge (-0.5401, -0.5637, -0.5685 for methyl acetate, phenyl acetate, and 4-methoxyphenyl acetate respectively) compared to the ketone substituted triazine (**10a**) and N-acylbenzotriazole substituted triazine (**29**), as the calculated charge on the oxygen were found to be lower (-0.4929 for propan-2-one and -0.4630 and 1-(1H-benzo[d][1,2,3]triazol-1-yl)ethanone). This change in the strength of the carbonyl:imine C-H interaction may directly affect the fluorescent properties.

Code	X	Solvent	$\lambda_{310\ nm\ ems}$ Band 1 (nm) (min)
3a	-	2-Methyl-2-butnaol	533
21	H	1-Pentanol	525
23	CH_3	Toluene	533
25	OCH_3	Toluene	537

Code	X	Solvent	$\lambda_{310\ nm\ ems}$ Band 1 (nm) (max)
3a	-	Ethylene Glycol	554
21	H	Acetonitrile	545
23	CH_3	Acetonitrile	546
25	OCH_3	Methanol	548

Code	X	Solvent	$\lambda_{310\ nm\ ems}$ Band 2 (nm) (min)
3a	-	2-Methyl-2-butanol	503
21	H	1,4-Dioxane	507
23	CH_3	Toluene	507
25	OCH_3	1,4-Dioxane	506

Code	X	Solvent	$\lambda_{310\ nm\ ems}$ Band 2 (nm) (max)
3a	-	Ethylene Glycol	515
21	H	Acetonitrile	512
23	CH_3	Acetonitrile	511
25	OCH_3	Acetonitrile	511

Code	X	Solvent	$\lambda_{310\ nm\ ems}$ Band 3 (nm) (min)
3a	-	2-Methyl-2-butanol	468
21	H	1,4-Dioxane	475
23	CH_3	1,4-Dioxane	474
25	OCH_3	1,4-Dioxane	474

Code	X	Solvent	$\lambda_{310\ nm\ ems}$ Band 3 (nm) (max)
3a	-	Ethylene Glycol	479
21	H	Methanol	479
23	CH_3	Methanol	479
25	OCH_3	Methanol	479

Code	X	Solvent	$\lambda_{310\ nm\ ems}$ Band 4 (nm) (min)
3a	-	1,3-Propanediol	344
21	H	1-Octanol	353
23	CH_3	1-Octanol	352
25	OCH_3	1-Octanol	351

Code	X	Solvent	$\lambda_{310\ nm\ ems}$ Band 4 (nm) (max)
3a	-	1,4-Butanediol	380
21	H	1-Pentanol	361
23	CH_3	Chloroform	355
25	OCH_3	Chloroform	355

Table 7.6. Summary of Guassian band maximum positions from deconvoluted spectra (minimum and maximum values) for **21**, **23**, **25** and **27** at 310 nm excitation.

Code	X	Solvent	$\lambda_{310\ nm}$ Band 1 Area % (min)
3a	-	1,3-Butanediol	36.3
21	H	Methanol	47.69
23	CH_3	Methanol	44.35
25	OCH_3	Methanol	44.94

Code	X	Solvent	$\lambda_{310\ nm}$ Band 1 Area % (max)
3a	-	2-Methyl-2-butanol	59.26
21	H	Toluene	56.05
23	CH_3	Toluene	54.46
25	OCH_3	Toluene	51.89

Code	X	Solvent	$\lambda_{310\ nm}$ Band 2 Area % (min)
3a	-	1,3-Butanediol	27.33
21	H	1-Pentanol	28.28
23	CH_3	Toluene	29.82
25	OCH_3	Toluene	36.84

Code	X	Solvent	$\lambda_{310\ nm}$ Band 2 Area % (max)
3a	-	Acetonitrile	46.43
21	H	Acetonitrile	40.79
23	CH_3	Methanol	40.44
25	OCH_3	Methanol	43.24

Code	X	Solvent	$\lambda_{310\ nm}$ Band 3 Area % (min)
3a	-	1,3-Butanediol	5.49
21	H	Acetonitrile	6.27
23	CH_3	Acetonitrile	6.65
25	OCH_3	Acetonitrile	7.38

Code	X	Solvent	$\lambda_{310\ nm}$ Band 3 Area % (max)
3a	-	1,5-Pentanediol	8.36
21	H	1-Pentanol	13.65
23	CH_3	Toluene	8.5
25	OCH_3	Methanol	8.84

Code	X	Solvent	$\lambda_{310\ nm}$ Band 4 Area % (min)
3a	-	1,3-Propanediol	8.31
21	H	Chloroform	2.78
23	CH_3	Chloroform	5.42
25	OCH_3	Chloroform	2.31

Code	X	Solvent	$\lambda_{310\ nm}$ Band 4 Area % (max)
3a	-	1,3-Butanediol	15.14
21	H	1-Hexanol	7.61
23	CH_3	1-Hexanol	10.41
25	OCH_3	1-Hexanol	5.22

Table 7.7. Summary of area percentages for Gaussian band fits (minimum and maximum values) for **21**, **23**, **25** and **27** at 310 nm excitation.

Code	X	Solvent	$\lambda_{400\ nm\ ems}$ Band 1 (nm) (min)
3a	-	Toluene	524
21	H	Chloroform	535
23	CH_3	Chloroform	532
25	OCH_3	Chloroform	536

Code	X	Solvent	$\lambda_{400\ nm\ ems}$ Band 1 (nm) (max)
3a	-	Ethylene Glycol	548
21	H	Acetonitrile	547
23	CH_3	Acetonitrile	546
25	OCH_3	Acetonitrile	546

Code	X	Solvent	$\lambda_{400\ nm\ ems}$ Band 2 (nm) (min)
3a	-	2-Methyl-2-butanol	500
21	H	Toluene	505
23	CH_3	Toluene	505
25	OCH_3	1,4-Dioxane	505

Code	X	Solvent	$\lambda_{400\ nm\ ems}$ Band 2 (nm) (max)
3a	-	Ethylene Glycol	510
21	H	Acetonitrile	510
23	CH_3	Acetonitrile	510
25	OCH_3	Acetonitrile	510

Code	X	Solvent	$\lambda_{400\ nm\ ems}$ Band 3 (nm) (min)
3a	-	2-Methyl-2-butanol	469
21	H	1,4-Dioxane	475
23	CH_3	1,4-Dioxane	475
25	OCH_3	1,4-Dioxane	474

Code	X	Solvent	$\lambda_{400\ nm\ ems}$ Band 3 (nm) (max)
3a	-	Ethylene Glycol	480
21	H	Methanol	480
23	CH_3	Methanol	480
25	OCH_3	Methanol	479

Table 7.8. Summary of Guassian band maximum positions from deconvoluted spectra (minimum and maximum values) for **21**, **23**, **25** and **27** at 400 nm excitation.

Code	X	Solvent	$\lambda_{400\ nm}$ Band 1 Area % (min)
3a	-	Methanol	40.67
21	H	Methanol	40.87
23	CH_3	Methanol	41.12
25	OCH_3	Methanol	41.42

Code	X	Solvent	$\lambda_{400\ nm}$ Band 1 Area % (max)
3a	-	Toluene	50.7
21	H	Chloroform	53.39
23	CH_3	Chloroform	55.94
25	OCH_3	Chloroform	51.4

Code	X	Solvent	$\lambda_{400\ nm}$ Band 2 Area % (min)
3a	-	Toluene	38.89
21	H	Chloroform	36.76
23	CH_3	Chloroform	33.73
25	OCH_3	Chloroform	38.67

Code	X	Solvent	$\lambda_{400\ nm}$ Band 2 Area % (max)
3a	-	Acetonitrile	46.85
21	H	Acetonitrile	46.61
23	CH_3	Acetonitrile	46.67
25	OCH_3	1-Hexanol	46.8

Code	X	Solvent	$\lambda_{400\ nm}$ Band 3 Area % (min)
3a	-	1,4-Dioxane	9.42
21	H	1,4-Dioxane	9.31
23	CH_3	1,4-Dioxane	9.03
25	OCH_3	1,4-Dioxane	8.84

Code	X	Solvent	$\lambda_{400\ nm}$ Band 3 Area % (max)
3a	-	Ethylene Glycol	12.67
21	H	Methanol	13.6
23	CH_3	Methanol	13.01
25	OCH_3	Methanol	13.17

Table 7.9. Summary of area percentages for Gaussian band fits (minimum and maximum values) for **21**, **23**, **25** and **27** at 400 nm excitation.

Analysis against normalized solvent polarity (E_T^N), solvent hydrogen bonding donating/accepting ability (α and β), solvent polarizability (π^*), viscosity (η(Cp)) and dipole moment (μ) was performed for each fluorophore. However, the solvatochromic analysis of all components (band position, area percentage of band to overall fit, band width, area ratios and band fwhm) of the deconvoluted spectra of the compounds revealed the distribution of the data to be fairly random (Appendix of Results, 4.1, 4.2, 4.3 and 4.4).

The analysis of the Gaussian model fit data show no trend nor exhibit solvatochromic behaviour. A multiple linear regression analysis on **21** (Table 7.10 and 7.11) against the solvatochromic values α, β and π^* was performed. The emission peak maximum, Gaussian band positions, quantum yield and UV-visible absorbance were

correlated against for both 310 and 400 nm excitation which showed no significant correlations (a linear correlation is supported when r^2 approaches unity i.e. 1).

y	y_o	a_α	b_β	c_{π^*}	r^2
$\lambda_{ems\ max\ (32258\ cm^{-1})}$	19639.54 ± 588.39	-212.83 ± 158.18	179.78 ± 301.73	-437.86 ± 894.28	**0.38**
Band 1 cm^{-1} (Gaussian Fit)	19203.00 ± 447.94	-183.37 ± 120.42	6.24 ± 229.70	-962.72 ± 680.81	**0.53**
Band 2 cm^{-1} (Gaussian Fit)	19601.26 ± 881.49	-285.86 ± 236.98	407.98 ± 452.03	13.81 ± 1339.75	**0.29**
Band 3 cm^{-1} (Gaussian Fit)	21322.79 ± 130.02	-118.84 ± 57.81	-18.11 ± 76.58	-531.35 ± 198.09	**0.68**
Band 4 cm^{-1} (Gaussian Fit)	28028.45 ± 1648.74	-1163.72 ± 443.25	1247.06 ± 845.48	-319.05 ± 2505.88	**0.62**
Φ (32258 cm-1)	0.59 ± 0.32	-0.20 ± 0.08	0.15 ± 0.16	-0.32 ± 0.49	**0.60**
Abs (32258 cm-1)	0.05 ± 0.04	-0.01 ± 0.01	-0.00 ± 0.02	0.02 ± 0.06	**0.28**

Table 7.10. Estimated from the equation ($y = y_0 + a_\alpha*\alpha + b_\beta*\beta + c_{\pi^*}*\pi^*$), coefficients ($y_o$, a_α, b_β, c_{π^*}), their standard errors and correlation coefficients (r) for the multiple linear regression analysis for **21** at 310 nm excitation against the solvatochromic values α, β and π*.

y	y_o	a_α	b_β	c_{π^*}	r^2
$\lambda_{ems\ max\ (25000\ cm^{-1})}$	19274.29 ± 416.71	-19.77 ± 112.03	251.89 ± 213.69	314.42 ± 633.35	**0.18**
Band 1 cm^{-1} (Gaussian Fit)	19178.48 ± 298.44	56.77 ± 80.23	-388.40 ± 153.04	-948.91 ± 453.59	**0.44**
Band 2 cm^{-1} (Gaussian Fit)	19717.75 ± 571.36	86.19 ± 153.60	-3.56 ± 292.99	-32.59 ± 868.39	**0.04**
Band 3 cm^{-1} (Gaussian Fit)	21333.08 ± 140.59	-139.45 ± 62.51	-26.43 ± 82.81	-591.10 ± 214.19	**0.70**
Φ (25000 cm-1)	0.54 ± 0.36	-0.22 ± 0.09	0.18 ± 0.18	-0.25 ± 0.56	**0.57**
Abs (25000 cm-1)	0.02 ± 0.01	-0.00 ± 0.00	-0.00 ± 0.00	-0.01 ± 0.02	**0.28**

Table 7.11. Estimated from the equation ($y = y_0 + a_\alpha*\alpha + b_\beta*\beta + c_{\pi^*}*\pi^*$), coefficients ($y_o$, a_α, b_β, c_{π^*}), their standard errors and correlation coefficients (r) for the multiple linear regression analysis for **21** at 400 nm excitation against the solvatochromic values α, β and π*.

7.3.2 Time resolved fluorescence measurements.

Similar to the fluorescence emission, the phenyl ester triazines (**21**, **23**, **25** and **27**) deviate only slightly in their fluorescence lifetime behaviour compared to the methyl ester triazine (**3a**). Again all of the fluorescence decay species could be fitted to a 2 or 3 exponential term:

1. A short lived component (τ_1) with values ranging from 0.17 to 1.56 ns.
2. A medium component (τ_2) ranging from values of 3.45 to 6.03 ns.
3. A long lived component (τ_3) which ranges from 5.76 to 13.54 ns.

An extensive range of solvents were investigated but small trends were only observed. As a result, it is more informative to compare the minimum and maximum values for each compound, regardless of solvent. Hence, the solvent will vary in the following tables. For a full summary refer to Appendix of Results, 4.1, 4.2, 4.3 and 4.4.

Table 7.12 lists the minimum and maximum intensity weighted average lifetimes for **21**, **23**, **25** and **27** at the lowest (470 nm) and highest emission wavelengths (570 nm). Compound **21** has a maximum value for the intensity weighted lifetime at 470 nm emission of 6.28 ns in chloroform, whilst at 570 nm emission, the maximum value of the intensity weighted lifetime is much longer at 11.19 ns in propylene carbonate. Similar values were observed for **23** and **25** (Table 7.12). This is almost in agreement with the values observed for the methyl ester triazine **3a**; 6.87 ns in propylene carbonate at 470 nm emission and 11.09 ns in propylene carbonate at 570 nm emission.

However, a difference is observed in the lifetime for **27** (X = NO_2), which exhibits a much shorter lifetime at 470 nm and 570 nm emission in the solvents that effect and quench the fluorescence (*e.g.* 0.45 ns in 1-octanol at 470 nm and 2.18 ns in acetonitrile at 570 nm). This is in stark contrast to the longer lifetimes of **21**, **23** and **25** (Table 7.12). Again like the fluorescence emission, the lifetime for **27** is uneffected in toluene and 1,4-dioxane, and has

similar maximum intensity weigthed average lifetimes as **21**, **23** and **25**: 6.92 ns in toluene at 470 nm and 10.86 ns in 1,4-dioxane at 570 nm emission.

Code	X	Wavelength (nm)	Solvent	τ_f (ns) (Intensity Weighted) (min)
3a	-	470	Methanol	4.16
21	H	470	Methanol	5.01
23	CH_3	470	Methanol	4.69
25	OCH_3	470	Methanol	4.73
27	NO_2	470	1-octanol	0.45

Code	X	Wavelength (nm)	Solvent	τ_f (ns) (Intensity Weighted) (max)
3a	-	470	Propylene Carbonate	6.87
21	H	470	Chloroform	6.28
23	CH_3	470	1-Octanol	6.22
25	OCH_3	470	1-Octanol	6.71
27	NO_2	470	Toluene	6.92

Code	X	Wavelength (nm)	Solvent	τf (ns) (Intensity Weighted) (min)
3a	-	570	Methanol	7.15
21	H	570	Methanol	8.27
23	CH_3	570	Methanol	7.79
25	OCH_3	570	Methanol	7.75
27	NO_2	570	Acetonitrile	2.18

Code	X	Wavelength (nm)	Solvent	τf (ns) (Intensity Weighted) (max)
3a	-	570	Propylene Carbonate	11.09
21	H	570	Acetonitrile	11.19
23	CH_3	570	1-octanol	11.12
25	OCH_3	570	Acetonitrile	10.99
27	NO_2	570	1,4-dioxane	10.86

Table 7.12. Summary of the minimum and maximum intensity weighted average lifetimes (τ_f) of the phenyl ester substituted 2,5-dihydro-1,2,3-triazines at 470 and 570 nm emission.

Tables 7.13 and 7.14 list the minimum and maximum values for the decay times (τ_i) and their corresponding fractional intensities (A_i) for **21**, **23** and **25** at 470 and 570 nm emission.

For **21**, **23** and **25** (Table 7.13 and 7.14), τ_2 contributes the most to the decay at 470 nm (68 to 83 %). At 570 nm there is an increase in the contribution from the longer lived τ_3 state (*e.g.* 15 % at 470 nm to 70 % at 570 nm for **21**) and subsequent decrease in the maximum contribution from τ_2 (*e.g.* 80 to 35 % for **21**).

Code	X	nm	Solvent	τ_1 (ns) (min)	A_1 (%)
3a	-	470	1-Propanol	0.19	1.96
21	H	470	Methanol	0.17	5.05
23	CH_3	470	1-Octanol	0.24	7.15
25	OCH_3	470	1-Propanol	0.18	1.42

Code	X	nm	Solvent	τ_1 (ns) (max)	A_1 (%)
3a	-	470	1-Octanol	0.60	4.69
21	H	470	Chloroform	1.49	10.01
23	CH_3	470	Chloroform	1.19	6.42
25	OCH_3	470	Chloroform	1.56	6.22

Code	X	nm	Solvent	τ_2 (ns) (min)	A_2 (%)
3a	-	470	Ethylene Glycol	2.05	12.27
21	H	470	Toluene	3.87	71.01
23	CH_3	470	Toluene	3.45	67.87
25	OCH_3	470	Toluene	3.59	68.07

Code	X	nm	Solvent	τ_2 (ns) (min)	A_2 (%)
3a	-	470	Propylene Carbonate	5.53	70.78
21	H	470	1-butanol	5.57	79.59
23	CH_3	470	1-pentanol	5.54	82.32
25	OCH_3	470	1-hexanol	5.61	83.43

Code	X	nm	Solvent	τ_3 (ns) (min)	A_3 (%)
3a	-	470	1,4-Butanediol	6.61	61.28
21	H	470	Methanol	7.12	23.04
23	CH_3	470	Methanol	6.31	34.56
25	OCH_3	470	Methanol	5.76	53.27

Code	X	nm	Solvent	τ_3 (ns) (max)	A_3 (%)
3a	-	470	Chloroform	10.59	29.16
21	H	470	Chloroform	13.54	15.4
23	CH_3	470	1-Pentanol	11.00	14.34
25	OCH_3	470	1-Octanol	12.39	23.19

Table 7.13. Summary of the minimum and maximum values for the lifetime decay components of the three exponential fit for the decay at 470 nm emission for the phenyl ester substituted 2,5-dihydro-1,2,3-triazines (**21**, **23** and **25**); where τ_i is the decay time and A_i is the fractional intensity.

Code	X	nm	Solvent	τ_1 (ns) (min)	A_1 (%)
3a	-	570	N,N-Dimethylformamide	0.13	0.82
21	H	570	Methanol	0.17	2.77
23	CH_3	570	1-Octanol	0.22	1.36
25	OCH_3	570	1-Octanol	0.14	2.62

Code	X	nm	Solvent	τ_1 (ns) (max)	A_1 (%)
3a	-	570	1,4-Butanediol	2.84	13.58
21	H	570	Chloroform	0.34	0.23
23	CH_3	570	Methanol	0.40	1.4
25	OCH_3	570	Methanol	0.44	1.74

Code	X	nm	Solvent	τ_2 (ns) (min)	A_2 (%)
3a	-	570	2-Methyl-2-butanol	3.67	11.62
21	H	570	Toluene	3.74	10.86
23	CH_3	570	Toluene	3.64	13.97
25	OCH_3	570	Toluene	3.83	11.83

Code	X	nm	Solvent	τ_2 (ns) (max)	A_2 (%)
3a	-	570	1,5-Pentanediol	6.56	48.04
21	H	570	1-Pentanol	5.90	35.05
23	CH_3	570	1-Octanol	6.03	27.29
25	OCH_3	570	1-Pentanol	5.86	37.33

Code	X	nm	Solvent	τ_3 (ns) (min)	A_3 (%)
3a	-	570	Toluene	9.67	93.8
21	H	570	Toluene	9.81	89.14
23	CH_3	570	Toluene	9.63	86.03
25	OCH_3	570	Toluene	9.73	88.17

Code	X	nm	Solvent	τ_3 (ns) (max)	A_3 (%)
3a	-	570	1,3-Butanediol	13.5	51.7
21	H	570	Acetonitrile	13.69	70
23	CH_3	570	1-Butanol	13.47	58.34
25	OCH_3	570	1-Pentanol	13.49	62.67

Table 7.14. Summary of the minimum and maximum values for the lifetime decay components of the three exponential fit for the decay at 570 nm emission for the phenyl ester substituted 2,5-dihydro-1,2,3-triazines (**21**, **23** and **25**); where τ_i is the decay time and A_i is the fractional intensity.

As was observed in the fluorescence emission data, a noticeable change is observed in the fluorescence lifetime data when the phenyl ester is substituted with a *p*-NO_2 group (**27**). When we compare the data for **27** in an aprotic solvent (toluene) to a protic solvent (methanol), we see that the long lived component (τ_3) is significantly shorter in protic solvents at 470 nm; 10.62 ns in toluene vs 5.30 ns in methanol (Table 7.15). This results in an almost two fold decrease in the intensity weight average lifetime; 6.93 ns in toluene and 3.95 ns in methanol.

Code	Wavelength (nm)	Solvent	τ_1 (ns)	A_1 (%)	τ_2 (ns)	A_2 (%)	τ_3 (ns)	A_3 (%)	τ_f (ns) (Intensity Weighted)
27	470	Toluene	-	-	3.94	55.31	10.62	44.69	6.93
27	470	Methanol	0.41	2.06	3.33	63.59	5.30	34.35	3.95
27	570	Toluene	-	-	4.02	2.26	10.81	97.74	10.66
27	570	Methanol	2.35	4.4	4.00	60.11	12.22	35.49	6.85

Table 7.15. Summary of the lifetime decay components of **27** at 470 and 570 nm in an aprotic nonpolar solvent (toluene) and protic polar solvent (methanol); where τ_i is the decay time and A_i is the fractional intensity.

Analysis of the intensity weighted lifetime, 470 and 570 nm intensity weighted lifetime (and their respective decay times) against the normalized solvent polarity (E_T^N), solvent hydrogen bonding donating/accepting ability (α and β), solvent polarizability (π^*), viscosity (η(Cp)), dielectric constant (ε) and dipole moment (μ) was performed for each fluorophore. However, the solvatochromic analysis of all components revealed no significant trends and the distribution of the data was fairly random (Appendix of Results, 4.1, 4.2, 4.3 and 4.4). Similar to the emission data, a multiple linear regression analysis on the lifetime of **21** (Table 7.16) against the solvatochromic values α, β and π^* was performed. The intensity weighted average lifetimes at 470 and 570 nm and their respective individual decay times (τ_1, τ_2, and τ_3) were correlated against but again showed no significant correlations (a linear correlation is supported when r^2 approaches unity *i.e.* 1).

y	y_o	a_α	b_β	c_{π^*}	r^2
τ_f (Intensity weighted, 470nm)	8.15 ± 3.02	-2.89 ± 0.81	1.66 ± 1.55	-3.72 ± 4.60	**0.74**
τ_f (Amplitude weighted, 470nm)	3.74 ± 2.41	-3.45 ± 0.64	1.15 ± 1.23	2.40 ± 3.66	**0.79**
τ_1 (Intensity weighted, 470nm)	2.83 ± 1.03	-0.18 ± 0.26	-1.35 ± 0.47	-2.80 ± 1.70	**0.69**
τ_2 (Intensity weighted, 470nm)	6.05 ± 2.97	-1.53 ± 0.79	1.61 ± 1.52	-2.87 ± 4.51	**0.57**
τ_3 (Intensity weighted, 470nm)	21.09 ± 5.34	-0.78 ± 1.43	-4.91 ± 2.74	-16.59 ± 8.12	**0.44**
τ_f (Intensity weighted, 570nm)	13.43 ± 6.23	-5.27 ± 1.67	3.43 ± 3.19	-5.95 ± 9.47	**0.69**
τ_f (Amplitude weighted, 570nm)	10.54 ± 4.97	-6.27 ± 1.33	1.82 ± 2.55	-1.86 ± 7.55	**0.77**
τ_1 (Intensity weighted, 570nm)	0.70 ± 0.22	-0.01 ± 0.09	-0.22 ± 0.11	-0.61 ± 0.42	**0.77**
τ_2 (Intensity weighted, 570nm)	5.00 ± 2.79	-1.95 ± 0.75	2.74 ± 1.43	-1.18 ± 4.24	**0.69**
τ_3 (Intensity weighted, 570nm)	10.13 ± 6.65	-4.34 ± 1.79	6.02 ± 3.41	1.26 ± 10.12	**0.60**

Table 7.16. Estimated from equation ($y = y_0 + a_\alpha*\alpha + b_\beta*\beta + c_{\pi^*}*\pi^*$), coefficients ($y_o$, a_α, b_β, c_{π^*}), their standard errors and correlation coefficients (r) for the multiple linear regression analysis of the time domain fluorescent lifetimes and components of **21** at 405 nm excitation against the solvatochromic values α, β and π*.

7.4 CONCLUSION.

Chapter 4 discussed the marked effect that changing the methyl ester to a methyl ketone, and hence changing the electron density in the carbonyl group, had on the photophysics. It was hoped that by substituting a phenyl ester in place of the methyl ester, that the electronic nature of the carbonyl may be affected by substituting *para* electron donating and electron withdrawing groups on the phenyl ester.

The proposed synthetic route to the phenyl ester triazines utilised a Steglich esterification, between propiolic acid and various phenols to produce the required 4-substituted phenyl propiolates (**20**, **22**, **24** and **26**) in yields of 53 %, 72 %, 76 % and 89 % in that order. These propiolates were then used in a 1,3-dipolar cycloaddition with 2,4,5-triphenyl-1,2,3-triazolium-1-phenylaminide 1,3-dipole to produce the substituted phenyl ester triazines (**21**, **23**, **25** and **27**) in yields of 84 %, 98 %, 94 % and 83 % respectively.

The emission properties are almost identical across the phenyl ester triazine family (**21**, **23** and **25)** except for **27** (X = NO_2), exhibiting a complicated, green fluorescence emission band centered at ~520 nn. The same deconvoluted emission bands and similar contributions at both 310 and 400 nm excitation compared to the methyl ester triazine **3a** were found. Similarly, the emission of the phenyl ester triazines is uneffected by the nature of the solvent and this is confirmed in the normalised fluorescence spectra where no change is observed in the emission band maximum (Figure 7.3.8 and 7.3.9). Similar to the fluorescence emission, the phenyl ester triazines (**21**, **23**, **25** and **27**) deviated only slightly in their fluorescence lifetime behaviour compared to the methyl ester triazine (**3a**) (*e.g.* the maximum value for the intensity weighted lifetime at 470 nm for **21** was 6.28 ns in chloroform versus 6.87 ns in propylene carbonate for the methyl ester triazine **3a)**.

However, the *p*-NO_2 phenyl ester triazine (**27**) was an exemption to this. The fluorescence of **27** was only observed in the nonpolar aprotic solvents toluene and 1,4-dioxane, both being aprotic solvents of low polarity (and solvent dipole moment) with no hydrogen bonding ability. This was in comparison to the other aprotic solvents chloroform and acetonitrile and the protic polar alcohol series (1-octanol, 1-hexanol, 1-butanol, 1-pentanol and 1-propanol) which all exhibited fluorescence quenching.

Compound **27**, in toluene and 1,4-dioxane, exhibited the typical emission bands as observed for the other phenyl ester triazines at 310 nm excitation: ~480 nm (Band 3), ~510 nm (Band 2), and ~540 nm (Band 1) which was also similar to those of the methyl ester triazine **3a**. However, in chloroform for example, the 480 nm emission band (Band 3) was not found at 310 nm excitation which is associated with emission from the S_1 (**g0**) state. What was observed however was emission bands at ~380 and ~350 nm (Band 4 and 5) which are associated with S_2 (**g0**) and S_3 (**g0**). It is believed that the solvent is hydrogen bonding to the nitro group oxygens promoting radiationless de-excitation from the S_3 (**g0**) or S_2 (**g0**) excited state. In the case of the aprotic solvents acetonitrile and chloroform the dipole moment of the solvent is possibly promoting an efficient intersystem crossing process by solvation and thus preventing the other fluorescent emission processes from occurring.

For 400 nm excitation of **27** (Table 7.4), S_1 (**g0**) emission (Band 3) and S_1 (**g1**) emission (Band 1) were observed for all solvents except chloroform and acetonitrile. For the polar protic solvents, radiationless de-excitation from the S_1 (**g0**) or S_1 (**g1**) excited state appears to be the mechanism of quenching. However, for chloroform and acetonitrile, the S_1 (**g0**) to S_1 (**g2**) transition appears to be more favourable followed by radiationless de-excitation.

Therefore in light of the work presented, the substitution of the carbonyl with a phenyl ester rather than a methyl ester and substitution of the 4-position of the phenyl ester (except *p*-NO_2) has only minor influence on the photophysics of the 2,5-dihydro-1,2,3-triazines. No significant change in fluorescence is observed when compared to **3a** at either 310 or 400 nm excitation.

In order to explain the unexpected lack of change in fluorescence with the family of phenyl ester triazines, a computational study was undertaken to investigate the electron density at the carbonyl group. Calculated values for the C=O dipole, and charge on the carbon and oxygen atoms for the esters; methyl acetate, phenyl acetate, and 4-methoxyphenyl acetate were obtained. The results of the computational study indicated that there was little change in electron density at the carbonyl as you move from a methyl ester to a phenyl ester to a *p*-substituent methoxy ester. This lack of change in electron density

may explain the lack of change in fluorescence between the phenyl ester triazines **21**, **23** and **25** when compared to the methyl ester triazine **3a**.

As a distinct change in the energy of the fluorescence is observed when the triazine carbonyl is a ketone **10a** or N-acylbenzotriazole **29**, propan-2-one and 1-(1H-benzo[d][1,2,3]triazol-1-yl)ethanone were also investigated computationally. It may be concluded that the change in fluorescence is associated with the marked change in calculated electron densities of the carbonyl; 1.1481 D for a methyl ester compared to -0.0316 D and -0.4878 D for a ketone and N-acylbenzotriazole respectively.

Furthermore our model of fluorescence for **10a** and **29** suggests that a key interaction exists between the imine C-H and the carbonyl group. Our calculations, charge on oxygen, suggest that this interaction will be stronger for ester substituted triazines (*e.g.* **3a** and **21**) compared to the ketone substituted triazine (**10a**) and N-acylbenzotriazole substituted triazine (**29**) due to their larger calculated charge on oxygen. This change in the strength of the carbonyl:imine C-H interaction may directly affect the fluorescent properties.

We do not see an effect on the populations or emission band energies when a phenyl ester is substituted over a methyl ester. As such a phenyl ester triazine, with a suitably reactive group in the *para* position of the phenyl ester, may offer a promising method for the labeling of biomolecules without negatively affecting the fluorescence. Such a methodology could capitalize on the usefulness of the Steglich esterification of propiolic acid to generate an activated *para*-substituted phenyl propiolate and ultimately a phenyl ester 2,5-dihydro-1,2,3-triazine analogue with a suitable substitute for bioconjugation (e.g. a *para* isothiocyanate). Its fluorescent properties may be predicted to closely resemble that of **21** (and **3a**) in light of the work in this chapter. This concept is discussed further in Chapter 8.

.

Chapter 8: Towards the fluorescent labeling of biomolecules.

8.1 INTRODUCTION.

In recent years, fluorescent labeling of biological targets of interest has received particular attention due to advances in both fluorescence instrumentation and the synthesis of new fluorophores. Through covalent and non-covalent labeling with organic fluorophores, fluorescent conjugates or complexes of a sample analyte can be produced. Such conjugates or complexes can show fluorescence from short (*ca.* 400 nm ultraviolet region, *e.g.* dansyl chloride), to medium (*ca.* 550 nm visible region. *e.g.* fluorescein), or very long (*ca.* 900 nm near-infrared region. *e.g.* cyanines) depending on the chosen fluorescent marker.[9]

Fluorophores, such as dansyl enjoy widespread use but their excitation and emission spectra overlap significantly with cellular autofluorescence. This overlap poses a problem as it limits their usefulness in live cells.[81] Fluorophores with emission shifted to the red are desirable as a possible decrease in the overlap with the autofluorescence from biological materials is to be expected. Therefore, the synthesis and photophysical investigation of organic fluorophores with absorption and emission at long wavelengths is of importance.

Luckily, it is now possible in most cases to choose a fluorophore with the necessary fluorescent properties for a given role. However, there is still a strong need for new fluorophores or known fluorophores with improved water solubility, high quantum yield, and excitation and emission maxima beyond 600 nm.[9]

An additional requirement, which must also be considered, is that the fluorophore must also possess a functional group capable of efficiently coupling to a biomolecule, for example be readily incorporated regiospecifically at the C- or N- terminus of a protein.[7,82] Fluorophores such as the xanthenes, rhodamines and fluorescein; or the Alexa-fluor dyes generally require relatively long, flexible linkers between the protein and the fluorescent probe which may interfere with “flexibility” and conformation of the protein.[81,82]

Amine-reactive probes are widely used to modify proteins, peptides, ligands, synthetic oligonucleotides and other biomolecules. The most significant factors relating to an amine's reactivity are its class (aliphatic or aromatic) and its basicity.[83]

Virtually all proteins have lysine residues and most proteins have a free amine at the N-terminus. Lysine residues are generally the primary targets for the amine modification of proteins but there is usually a trade-off between the degree of labeling and functional properties. This is because conjugates with a high degree of labeling tend to precipitate out of solution or bind nonspecifically.[83]

A pH of 8.5 to 9.5 is usually optimal for modifying lysine residues. In general, the α-amino group at the N-terminus of a protein has a pKa of ~9, so a reaction at near neutral pH can sometimes be performed.[83]

A limitation to the use of amine reactive probes is that although amine acylation should be carried out above pH 8.5, the reactants tend to degrade in the presence of water, with the rate increasing as the pH increases. Alternativly protein modification by isothiocyanates usually requires a pH > 9 for optimal conjugations which may be problematic when working with base-sensitive proteins.

Aromatic amines are very weak bases, unprotonated at pH 7 and weaker nucleophiles compared to aliphatic amines. Modification of these relatively uncommon groups in biomolecules requires a highly reactive reagent such as an isothiocyanates or acid halide.[83]

Taking this into account, it was decided to design a fluorophore based on the aromatic 2,5-dihydro-1,2,3-triazine (**3a**) that could be used to label biomolecules *e.g* proteins. With this in mind two routes were chosen, involving (a) "activation" of the carbonyl with a benzotriazole (Bt) group, making it more reactive toward nucleophilic substitution *e.g.* an amino group of an amino acid or peptide, and (b) the incorporation of an isothiocyanate (N=C=S) reactive functional group that could react with amines *e.g.* N-terminus of an amino acid or peptide.

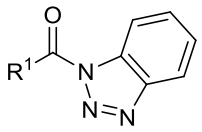

(a) N-acylbenzotriazole

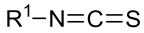

(b) Isothiocyanate

Figure 8.1.1. Two potential routes for bioconjugation (a) a benzotriazole (Bt) group and (b) the incorporation of an isothiocyanate (N=C=S) reactive functional group.

8.1.2 Peptide bond formation.

The procedure used to combine an amino acid with a carbonyl containing compound is known as a coupling reaction. Generally, coupling involves attack of the amino group of the amino acid at the carbonyl carbon atom of the carbonyl-containing component, whereby the carbonyl has previously been "activated" by the introduction of an electron withdrawing group / leaving group (Scheme 8.1.1).[84]

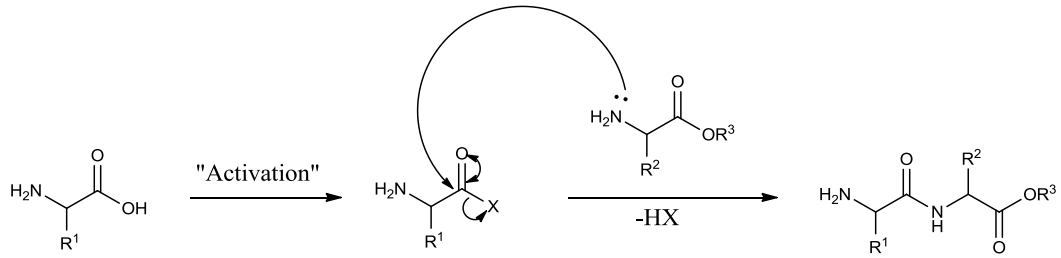

Scheme 8.1.1. Peptide bond formation.

The activated compound may be a shelf-stable reagent such as an active ester or a compound of intermediate stability such as an acyl halide. Most coupling reagents can be applied to the coupling of N-protected amino acids but not all can be applied to the coupling of peptides *e.g.* acyl halides are not favourable to couple peptides due to potential hydrolysis and cleavage of the activating group.[84]

However, this activation step poses a problem in that loss of chirality of the amino acid undergoing activation can occur. This has been reported to occur *via* two base catalysed paths: (a) direct enolization of the carbonyl, and (b) formation of a 5(4H)-oxazolone).[84]

8.1.2.2. Carbodiimides.

A traditional way to form peptide bonds is using dicyclohexylcarbodiimide (DCC); a carbodiimide which contains two nitrogen atoms that are weakly basic but can react with an acid to generate an O-acylisourea. This reactive species can undergo aminolysis in the presence of an amine to generate a peptide. Also, they may form symmetrical anyhydrides if excess carboxylic acid is present, or cyclise to an oxazolone; both of which can yield a peptide by aminolysis.

In some cases, the O-acylisourea may rearrange to a stable inert N-acylurea (Scheme 8.2.1). This process consumes starting material acid without generating any product peptide and is generally very fast in N,N-dimethylformamide (DMF) and slower in dicholormethane (DCM). This makes DCC unsuitable for couplings involved fluorenylmethoxycarbonyl (Fmoc) protected amines which are generally performed in DMF. The use of N-hydroxy derivatives (*e.g.* benzotriazole (Bt)) to first generate active esters can suppress the formation of N-acylurea.[84]

Therefore, carbodiiminde coupling reactions are generally performed with at either 4 ^{o}C or 25 ^{o}C using DCM as solvent. For large-scale synthesis, 4 ^{o}C is recommended because of the exothermic nature of the reaction.[84] A successful coupling is often indicated by the generation of a white precipitate of dicyclohexylurea (DCU), depending on the solvent, but generally the addition of diethyl ether will precipitate the DCU allowing it to removed by filtration. However, sometimes traces of DCU can remain in solution and can be difficult to remove chromatographically.[84]

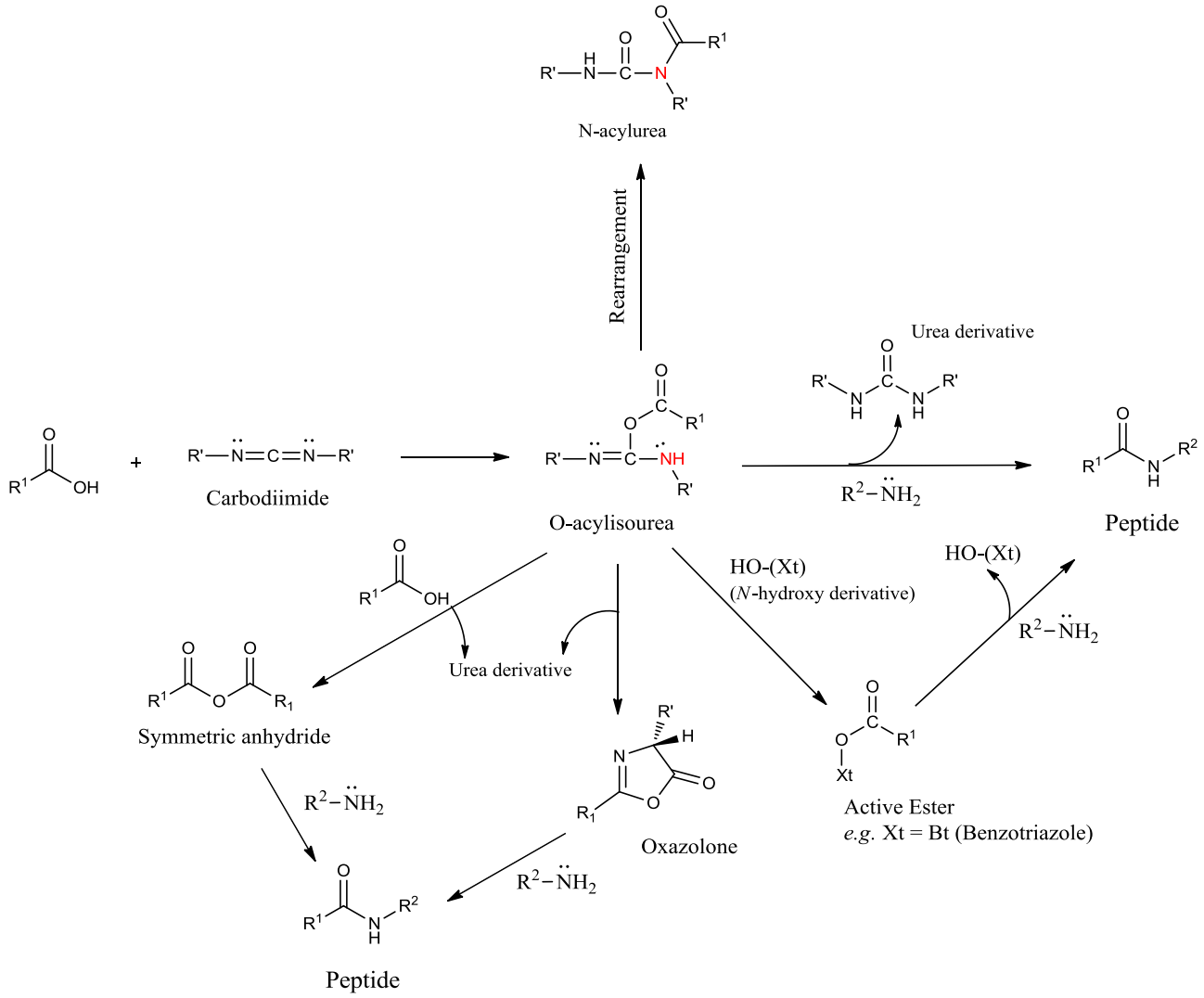

Scheme 8.2.1. Carbodiimide mediated peptide bond formation.

8.1.2.3. Acylbenzotriazoles.

N-protected-acylbenzotriazoles are effective intermediates for the preparation of peptides *via* N-acylation. They can be prepared using two methods starting directly from the carboxylic acid.[84]

The first method involves substitution of the carboxylic acid with a sulfonyl group from sulfonylbenzotriazole, which in the presence of triethylamine (Et_3N) and benzotriazole (Bt) transforms into the desired acylbenzotriazole (Scheme 8.2.2 (a)).

The second method involves treatment of the carboxylic acid with 1,1'-sulfinylbis(1H-benzotriazole) (BtSOBt), which is prepared in situ from thionyl chloride and an excess of benzotriazole (Scheme 8.2.2 (b)).[60]

N-acylbenzotriazoles are advantageous over acyl chlorides as they are generally resistant to short periods of contact with water. As a result, N-acylbenzotriazoles are suitable for reactions which involve mixed aqueous solvent systems, as often is the case for reactions using free amino acids. N-protected-aminoacyl-benzotriazoles can be isolated relatively easily, are stable at room temperature for months, and can be generally handled without special procedures to exclude air or moisture.[60, 84] Lastly, the reagents involved in the preparation are inexpensive making it a cost effective coupling methodology.

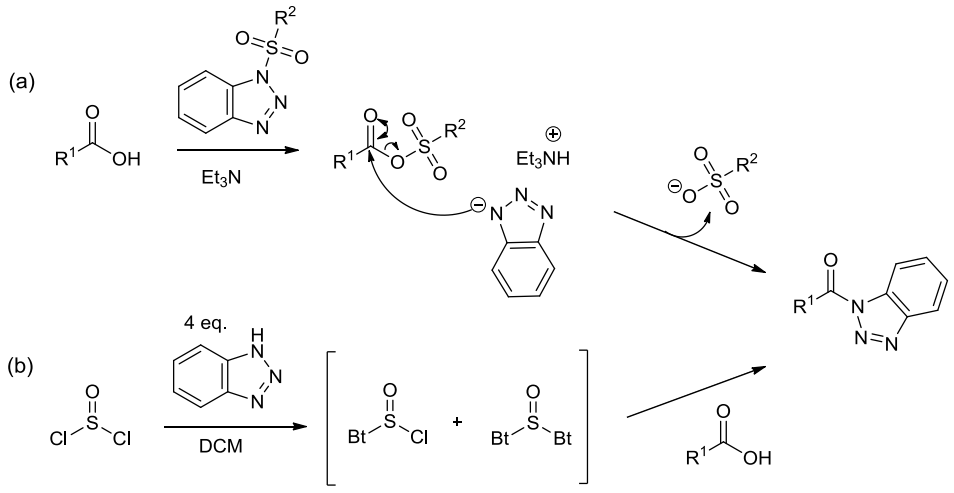

Scheme 8.2.2. Preparative routes to N-acylbenzotriazoles.

8.1.2.4. Isothiocyanates.

Amine-reactive dyes are often used to prepare bioconjugates for immunochemistry *e.*g labeling of antibodies.[83] In these applications, the stability of the chemical bond between the dye and biomolecule is of critical importance.

The bioconjugate will typically be studied within a biochemically complex sample, and more often than not, it will often be subjected to a series of post-processing steps. The integrity of the labeled sample must be maintained throughout the purification process if any useful relationship to the abundance or localization of the bioconjugate's molecular target is to be obtained from the fluorescence emission generated by the dye.[83]

Isothiocyanates (R–N=C=S) are moderately reactive but quite stable in water and most solvents. They form thioureas upon reaction with amines, which generally are stable and can be isolated (Scheme 8.3.3). It has been reported that antibody conjugates prepared from fluorescent isothiocyanates can deteriorate over time, which in recent times has prompted the use of fluorescent succinimidyl esters for synthesising bioconjugates.[83] For example, the thiourea formed by the reaction of fluorescein isothiocyanate with amines is believed to be susceptible to the conversion of a guanidinium cation by concentrated ammonia.[85] Despite the growing number available of amine-reactive fluorophores for selection, fluorescein isothiocyanate (FITC) is still widely used as a reactive fluorescent dyes for preparing fluorescent bioconjugates.[7, 83]

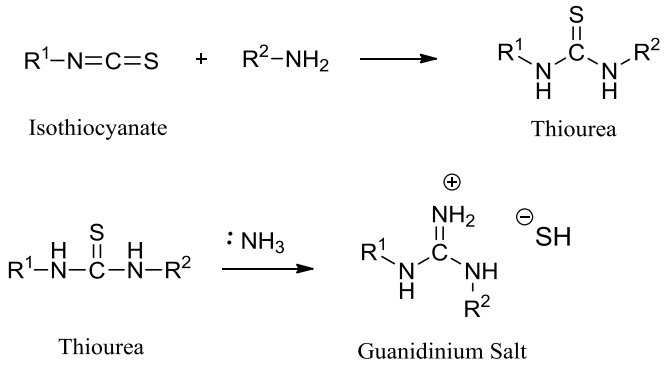

Scheme 8.3.3. Reaction of a primary amine with isothiocyanates to generate a thiourea. Conversion of the thiourea to a guanidinium salt may occur in ammonia solution.

8.2 RESULTS AND DISCUSSION.

Refer to Chapter 2, Section 2.1.5 for experimental procedure and results.

8.2.1 Synthesis of an acylbenzotriazole activated aromatic 2,5-dihydro-1,2,3-triazine.

Looking at the structure of **3a**, it is unlikely that the ester will be susceptible to nucleophilic attack by amines and this makes it a doubtful candidate for biological applications. Therefore, a post synthesis structural modification to **3a** is unlikely to be a useful strategy to produce a fluorophore capable of conjugation.

As mentioned in Section 8.2.2.3, acylbenzotriazoles are useful "activating" groups. It was thought that if benzotriazole could be substituted on the 2,5-dihydro-1,2,3-triazine structure then peptide conjugation would be feasible by reaction with the free amine of an amino acid (under appropriate conditions). The most accessible position for substitution is the carbonyl, dictated by the alkyne propiolate used in the 1,3-dipolar cycloaddition.

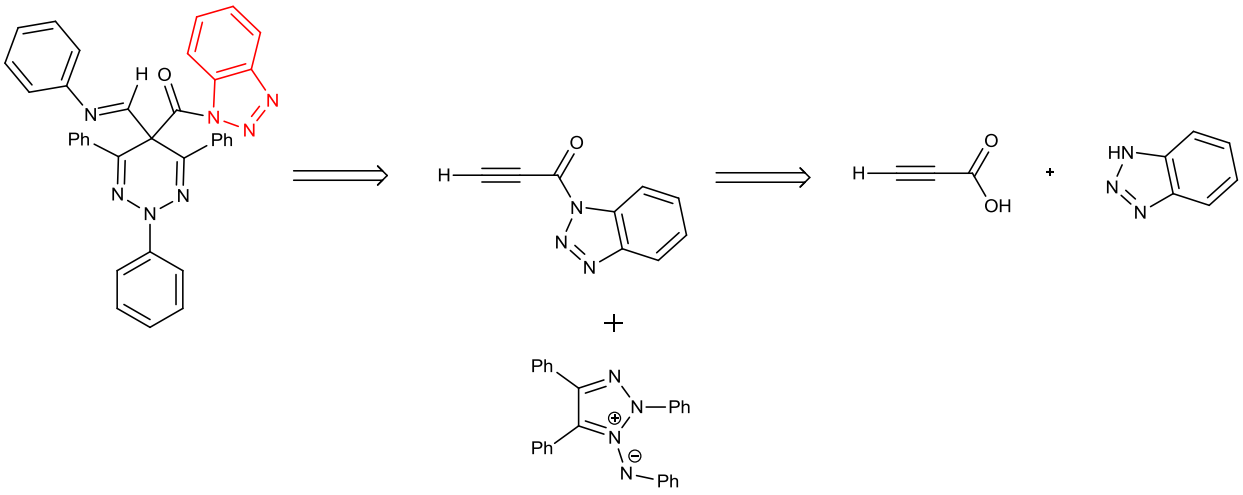

Scheme 8.2.1. Retrosynthetic analysis to produce an acylbenzotriazole substituted 2,5-dihydro-1,2,3-triazine starting from propiolic acid and 1H-benzotriazole.

Retrosynthetically (Scheme 8.2.1), if a propiolate that is substituted with an acylbenzotriazole was synthesized and participated in a 1,3-dipolar cycloaddition with

2,4,5-triphenyl-1,2,3-triazolium-1-phenylaminide 1,3-dipole, an acylbenzotriazole substituted 2,5-dihydro-1,2,3-triazine would be the product.

The synthesis of 1-(1H-benzo[d][1,2,3]triazol-1-yl)prop-2-yn-1-one (**28**) was reported by Katrizky where propiolic acid was treated with an excess of benzotriazole and thionyl chloride.[60] However, in our hands a non reaction was observed following several attempts using this method.

From Chapter 7, it is known that the reaction between carboxylic acids and amines under DCC coupling conditions occurs with relative ease. Therefore, it was thought that 1-(1H-benzo[d][1,2,3]triazol-1-yl)prop-2-yn-1-one could be alternatively synthesized by coupling 1H-benzotriazole and propiolic acid under the same condtions as used for the Steglich esterification. The approach proved successful and following filtration of the insoluble DCU, the desired product was obtained in a 69 % yield following recrystallisation. The structure of the isolated product was identified using ^{1}H and ^{13}C NMR spectra and supported by HRMS and IR spectroscopy. The characteristic terminal hydrogen signal can be identified in the ^{1}H NMR spectra as a singlet at 3.87 ppm. The presence of a carbonyl is confirmed by C=O stretch being observed in the IR spectrum at 1694 cm^{-1}.[60]

The 1,3-dipolar cycloaddition between 2,4,5-triphenyl-1,2,3-triazolium-1-phenylaminide 1,3-dipole (**2**) and 1-(1H-benzo[d][1,2,3]triazol-1-yl)prop-2-yn-1-one (**28**), under reflux in toluene, resulted in a fluorescent 2,5-dihydro-1,2,3-triazine (**29**) that was "activated" at the carbonyl with a benzotriazole group. Analogous to **10a**, the new fluorophore, **29** displays intense yellow fluorescence in solution. The structure of the isolated product was again identified using ^{1}H and ^{13}C NMR spectra and supported by HRMS and IR spectroscopy.

The reaction is again highly regioselective and only one isomer is isolated for **29**. This is supported by the fact that only one singlet is observed for the imine hydrogen at 8.93 ppm in the ^{1}H NMR spectra. The ^{13}C NMR spectrum of **29** also shows the presence of an imine carbon at 156.2 ppm and a quaternary carbon signal for C5 at 53.7 ppm. A carbonyl carbon signal at 168.9 ppm is also present, which is supported by the IR C=O stretch at 1721 cm^{-1}.

With the goal of activating the carbonyl now achieved, a peptide conjugation reaction was performed on **29** using a procedure similar to that reported by Katritzy for the conjugation of an activated N-acylbenzotriazole coumarin fluorophore and various chiral amino acids (Scheme 8.2.2).[82]

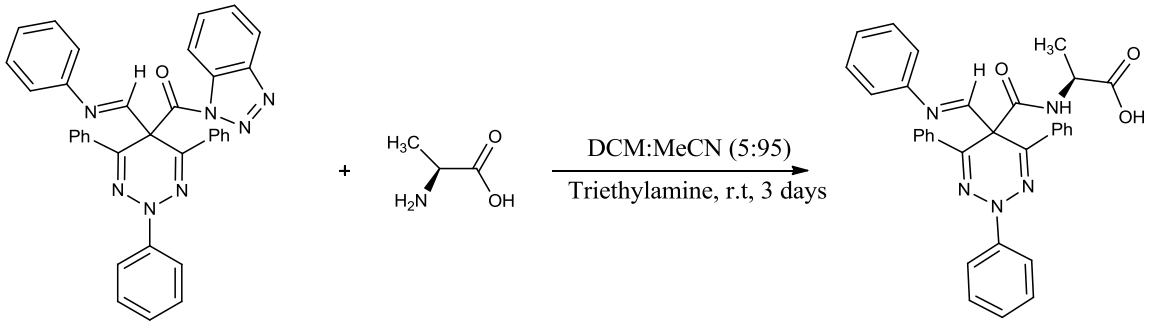

29 **30**

Scheme 8.2.2. Conjugation of L-alanine to the acylbenzotriazole activated aromatic 2,5-dihydro-1,2,3-triazine **29**.

L-alanine was chosen for conjugation due to its R side group being a simple methyl group. Using a solvent system of 5:95 v/v dichloromethane:acetonitrile along with triethylamine as base, the desired conjugated product 5-((carboxyamido) propanoic acid)-5-(N-phenylformimidoyl)-2,4,6-triphenyl-2,5-dihydro-1,2,3-triazine (**30**) was isolated in 85 % yield following column chromatography.

The structure of the isolated product **30** was identified using ^{1}H and ^{13}C NMR spectra and supported by HRMS and IR spectroscopy. A singlet was observed for the imine hydrogen at 8.99 ppm in the ^{1}H NMR spectra. The ^{13}C NMR spectrum of **30** shows the presence of the imine carbon at 150.3 ppm and a quaternary carbon signal for C5 at 50.9.

The conjugation of L-alanine is supported by the presence of a doublet at 0.89-0.93 ppm and a multiplet at 3.59-3.68 ppm that integrated for 3 hydrogens and a single hydrogen respectively. These signals are assigned as the CH_3 group and the hydrogen of the alpha carbon of L-alanine. The CH_3 group and alpha carbon were observed at 17.4 and 50.9 ppm in the ^{13}C NMR spectrum. Two signals at 164.3 and 167.8 ppm were also observed and are assigned as the two carbonyls which is supported by the IR C=O stretches at 1641 and 1741 cm^{-1}.

Another interesting observation is that the conjugation reaction can be monitored *via* its fluorescence. When substituted with an acylbenzotriazole, triazine **29** exhibits bright yellow fluorescence, similar to the ketone substituted triazine **10a**. Once the conjugation has occurred, and the carbonyl of **30** is now an amide, the energy of the fluorescence is blue-shifted resulting in green fluorescence as previously observed for the methyl ester triazine **3a** (Figure 8.2.1). As previously discussed, computational calculations comparing the dipole moment of a N-acylbenzotriazole to esters suggested there is a considerable difference in electron density and dipole moment between the two compound classes (Chapter 7, Section 7.3.1.2).

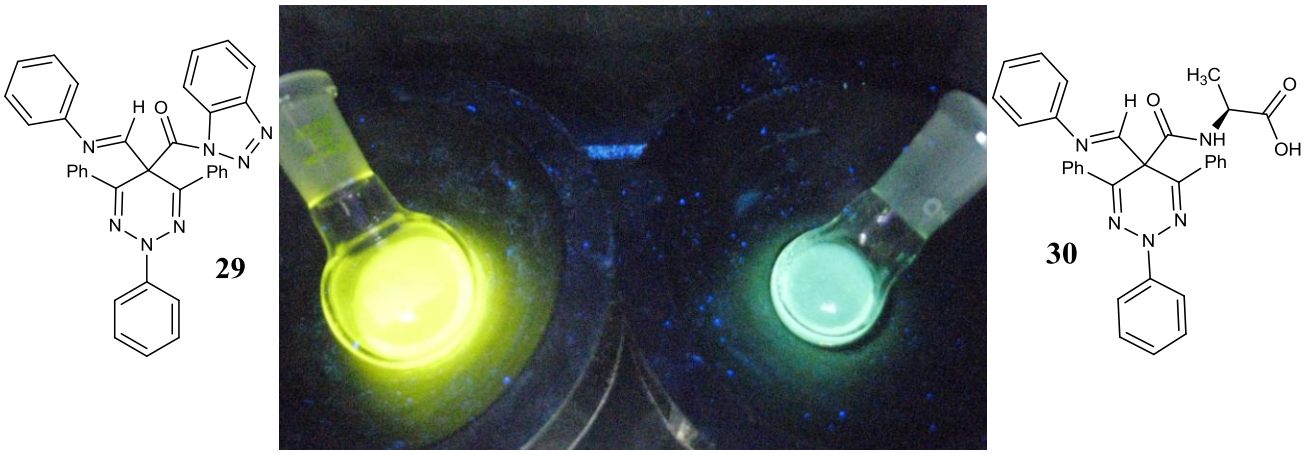

Figure 8.2.1. Fluorescence observed under UV irradiation when the carbonyl is activated with a benzotriazole (**29**, yellow, left) and the amino acid conjugated product (**30**, green, right).

However, this is only based on a laboratory observation. A detailed steady state absorption and fluorescence study is yet to be performed on both **29** and **30**.

8.2.2 Synthesis of a substituted phenyl ester isothiocyanate triazine.

As isothiocyanates are well known for their reaction with amines, it was decided to explore the use of an isothiocyanate as a second method for conjugation. It was proposed that an isothiocyanate could be incorporated *via* a 1,3-dipolar cycloaddition between 4-isothiocyanatophenyl propiolate and 2,4,5-triphenyl-1,2,3-triazolium-1-phenylaminide 1,3-dipole. To do that we could exploit the chemistry already used in the synthesis of the 4-substituted phenyl propiolates (Chapter 7). Retrosynthetically, this would provide a phenyl ester 2,5-dihydro-1,2,3-triazine substituted with an isothiocyanate at the 4-position (Scheme 8.2.3).

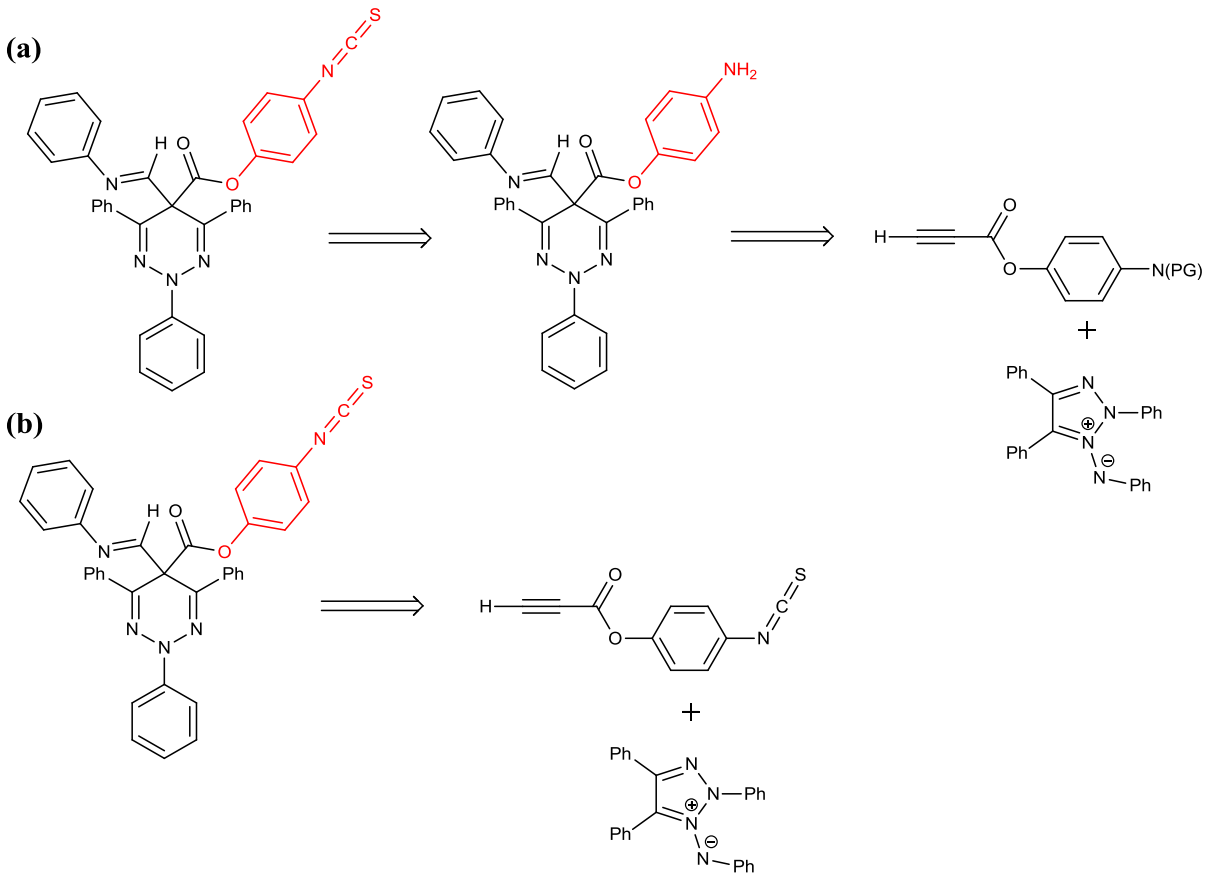

Scheme 8.2.3. Retrosynthetic routes to produce an substituted phenyl ester isothiocyanate 2,5-dihydro-1,2,3-triazine.

Firstly, it was neccesary to synthesise a propiolate containing either (a) a propiolate with a protected amine that could be transformed to an isothiocyanate following the 1,3-dipolar cycloaddition or (b) a propiolate substituted with a isothiocyanate directly (Scheme 8.2.3).

Exploiting the chemistry used in the synthesis of the 4-substituted phenyl propiolates, 4-aminophenol could be coupled to propiolic acid to generate the required alkyne. However, the amino group of 4-aminophenol would have to be protected prior to performing the Steglich esterification. Otherwise the nucleophilic amine group could attack instead of the alcohol. Two groups commonly used in the protection of amines are di-tert-butyl dicarbonate (t-Boc) and fluorenylmethyloxycarbonyl (Fmoc), both of which can be removed under mild conditions.

Considering the first strategy (Scheme 8.2.4), 4-aminophenol would be protected with a t-Boc and then subsequently coupled to propiolic acid. However, upon protecting 4-aminophenol successfully with t-Boc, it was realized that the acid conditions employed to remove t-Boc groups would not be suitable as the 2,5-dihydro-1,2,3-triazine would be susceptible to hydrolysis under those conditions. Hence the coupling of propiolic acid and the t-Boc protected aminophenol was abandoned.

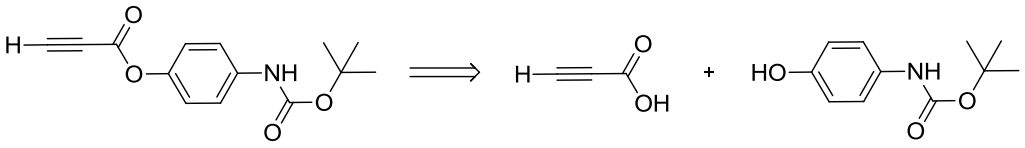

Scheme 8.2.4. Retrosynthetic analysis to produce a propiolate from t-Boc protected 4-aminophenol.

The second strategy (Scheme 8.2.5) involved protecting 4-aminophenol with an Fmoc group before coupling to propiolic acid. Fmoc is deprotected by stirring at room temperature in the base piperidine. However, upon protecting 4-aminophenol successfully with Fmoc, a problem lay with the solubility of the Fmoc protected 4-aminophenol. It was found to be insoluble in most solvents, except DMF, and could not be coupled successfully with propiolic acid.

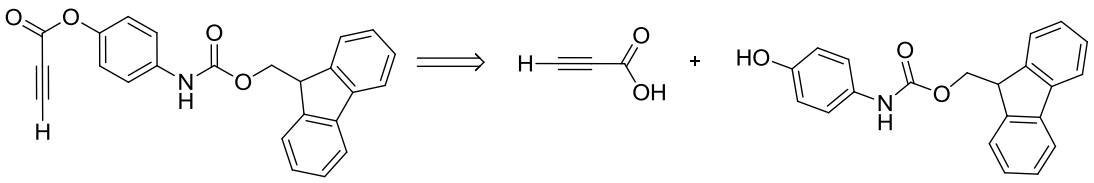

Scheme 8.2.5. Retrosynthetic analysis to produce a propiolate containing a protected Fmoc amine.

It was then decided to try the direct reaction of 4-aminophenol with thiophosgene to produce 4-isothiocyanatophenol. This would be ready for coupling with propiolic acid, using DCC, to give the desired isothiocyanate substituted propiolate (Scheme 8.2.6).

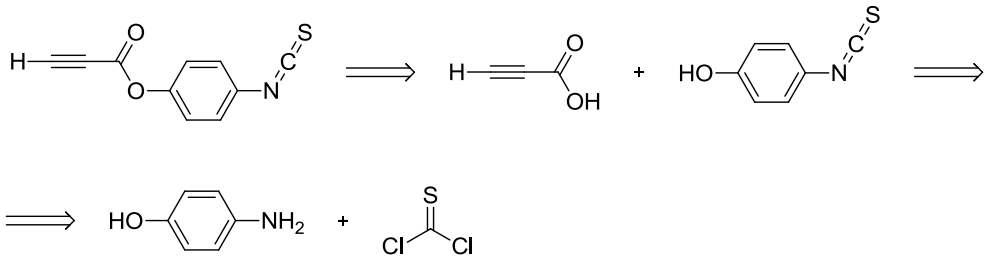

Scheme 8.2.6. Retrosynthetic analysis to produce 4-isothiocyanatophenyl propiolate from 4-isothiocyanatophenol.

First, 4-aminophenol was treated with thiophosgene to generate 4-isothiocyanatophenol (**31**) in an 82 % yield following column chromatography. The structure of the isolated product was identified using ^{1}H and ^{13}C NMR spectra and supported by HRMS and IR spectroscopy. A singlet at 5.03 ppm was observed for the OH as well as two doublets at 6.77-7.13 ppm, which exhibit AA'BB' coupling (J = 8.9 Hz) and was assigned as the aromatic hydrogens.[61]

Exploiting the chemistry already used in the synthesis of the 4-substituted phenyl propiolates; an equimolar amount of propiolic acid and 4-isothiocyantophenol were coupled under the same conditions as the 4-substituted phenyl propiolates. The method proved successful, with the isolation of 4-isothiocyanatophenyl propiolate (**32**) in a 44 % yield following recrystallisation. The structure of the isolated product was identified using ^{1}H and ^{13}C NMR spectra and supported by HRMS and IR spectroscopy. The alkyne was

identified by its characteristic terminal hydrogen signal in the ^{1}H NMR spectra as a singlet at 3.11 ppm. The ^{13}C NMR spectra showed two signals at 73.8 and 77.4 ppm for the alkyne carbons, a signal at 135.5 ppm for the isothiocyanate carbon and another at 150.4 ppm for the carbonyl carbon. The presence of an isothiocyanate is confirmed by the N=C=S stretch in the IR spectrum observed as a broad band at 2123 cm^{-1}.

As isothiocyanates are potential dipolarophiles, it was anticipated that the cycloaddition between 4-isothiocyanatophenyl propiolate and 2,4,5-triphenyl-1,2,3-triazolium-1-phenylaminide 1,3-dipole could potentially result in a cycloaddition between the 1,3-dipole and the double bond of the isothiocyanate.[86] However, in practice this did not occur, and the 1,3-dipolar cycloaddition between 4-isothiocyanatophenyl propiolate and an excess of 2,4,5-triphenyl-1,2,3-triazolium-1-phenylaminide 1,3-dipole (Scheme 8.2.7) resulted in the formation of a substituted phenyl ester isothiocyanate 2,5-dihydro-1,2,3-triazine (**33**). Triazine **33** was isolated in a 47 % yield following column chromatography.

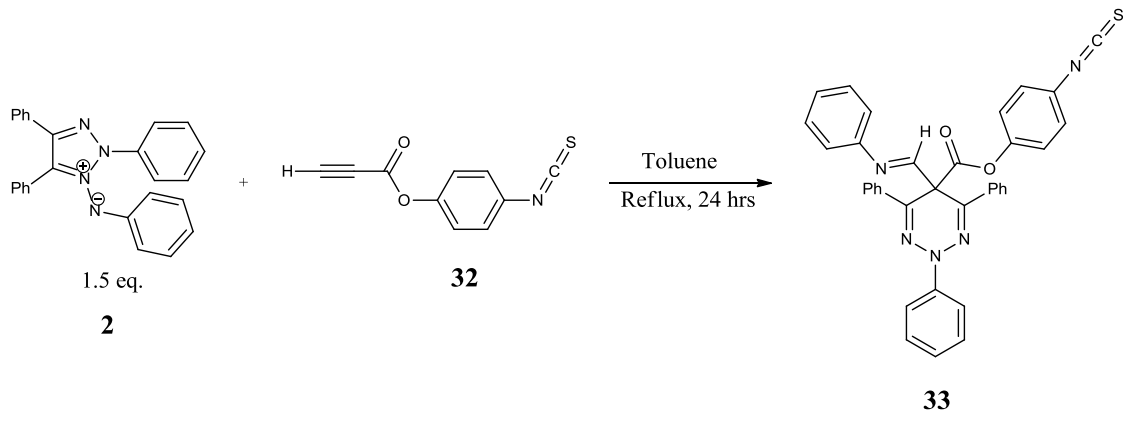

Scheme 8.2.7. Synthesis of the substituted phenyl ester isothiocyanate triazine (**33**) from 4-isothiocyanatophenyl propiolate (**32**).

The structure of **33** was identified using ^{1}H and ^{13}C NMR spectra and supported by HRMS and IR spectroscopy. A singlet was observed for the imine hydrogen at 8.55 ppm in the ^{1}H NMR spectra. The ^{13}C NMR spectrum of **33** shows the presence of the imine carbon at 156.1 ppm and a quaternary carbon signal for C5 at 53.1. A confident assignment can be made for the presence of an isotiocynate based on the ^{13}C characteristic signal for the N=C=S observed at 135.3 ppm as well as the broad IR signal for the N=C=S observed at 2099 cm^{-1}.

A conjugation reaction was attempted between **33** and L-alanine but gave a complex mixture, and therefore requires further study. A detailed steady state absorption and fluorescence study is also yet to be performed on **33**. However, it is anticipated that the photophysics of **33** would behave similarly to the substituted phenyl ester triazines (**21**, **23** and **25**) as presented in Chapter 7. Therefore, it is assumed that the transformation of the isothiocyanate to a thiourea, by conjugation, will again only have minor influence on the photophysics when compared to the phenyl ester triazines.

8.4 CONCLUSION.

Fluorescence in the life sciences has received interest of late as a non-destructive way of tracking or analysing biological molecules. As relatively few cellular components are naturally fluorescent, a protein or other component can be "labelled" with an extrinsic fluorophore. In many cases a fluorophore can be chosen that is suitable for the sample molecule in question.[8, 9] However, there is still a need for new fluorophores with improved water solubility, high quantum yields and excitation / emission maximum beyond 600 nm.

It was initially reported that the 2,5-dihydro-1,2,3-triazine (**3a**) showed promise as a biological probe due to its unique dual band emission (310 and 400 nm excitation) and considerable large Stoke's shift (120-180 nm).[54] Intrinsic fluorescence is normally observed at wavelengths of 280 to 295 nm (*e.g.* tryptophan residues are excited at 280 nm).[7] Therefore, the 400 nm excitation of the 2,5-dihydro-1,2,3-triazine has value in that it still has a considerably large Stoke's Shift (~120 nm) that avoids the possibly of self quenching and also avoids the possibility of autofluorescence from an excited biological sample.

However, the problem lay in the structure of **3a** which is unsuitable for conjugation. The most accessible position for substitution is the carbonyl, which by retrosynthetic analysis is dictated by the alkyne propiolate used in the 1,3-dipolar cycloaddition. For that reason, novel analogues were synthesized, **29** and **33**, providing two unique strategies for the conjugation of the 2,5-dihydro-1,2,3-triazine fluorophore with biomolecules.

As the stability of benzotriazoles as "activating" groups is well known, the first strategy involved the generation of an acylbenzotriazole "activated" propiolate alkyne.[60] The synthesis of 1-(1H-benzo[d][1,2,3]triazol-1-yl)prop-2-yn-1-one (**28**) by coupling 1H-benzotriazole and propiolic acid proved successful and was obtained in a 69 % yield following recrystallisation. This provided the necessary propiolate that was used to generate an acylbenzotriazole activated 2,5-dihydro-1,2,3-triazine (**29**) in 83 % yield following the 1,3-dipolar cycloaddition of **28** with **2**.

The novel benzotriazole activated 2,5-dihydro-1,2,3-triazine (**29**) shows good potential as a candidate for peptide conjugation as the fluorophore was successfully coupled with L-alanine to generate **30** in an 85 % yield. Similar to the ketone substituted **10a**,

compound **29** exhibited a strong yellow fluorescence in solution. Interestingly, the conjugation of **29** with an amino acid can be monitored visually as the generation of an amide at the carbonyl causes a visual blue-shift to the fluorescence in solution.

It is worth noting that by coupling **29** to an octa-arginine cell penetrating polypeptide the water solubility of the 2,5-dihydro-1,2,3-triazine fluorophore may be improved. This concept is currently under investigation in collaboration with Dr. Marc Dovecelle at RCSI (Figure 8.4.1).[87]

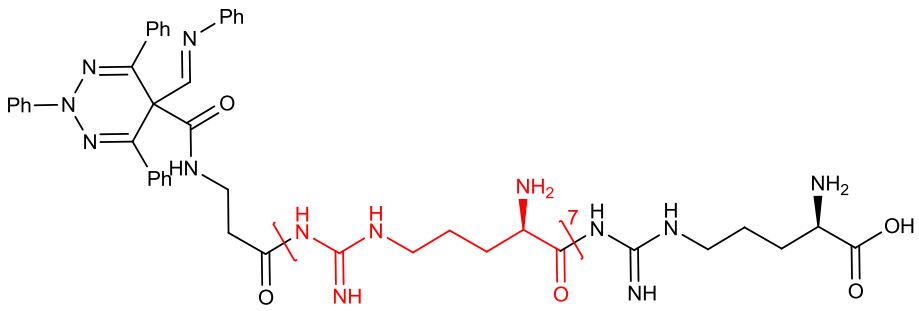

Figure 8.4.1. Structure of the octa-arginine cell penetrating 2,5-dihydro-1,2,3-triazine.

The second strategy involved the incorporation of an isothiocyanate group by integrating a phenyl ester into the 2,5-dihydro-1,2,3-triazine structure as before (Chapter 7). By reacting 4-aminophenol with thiophosgene, 4-isothiocyanatophenol (**31**) was synthesized (82 % yield). This was then coupled with propiolic acid, using DCC conditions, to generate an isothiocyanate containing alkyne, 4-isothiocyanatophenyl propiolate (**32**). Alkyne **32** was isolated in a 44 % yield following recrystallisation. Although isothiocyanates are potential dipolarophiles, the 1,3-dipolar cycloaddition between 4-isothiocyanatophenyl propiolate and an excess of 2,4,5-triphenyl-1,2,3-triazolium-1-phenylaminide 1,3-dipole generated the substituted phenyl ester isothiocyanate 2,5-dihydro-1,2,3-triazine (**33**) only and was isolated in a 47 % yield.

It is anticipated that the photophysics of **33** will be similar to the substituted phenyl ester triazines (**21**, **23** and **25**) that have been studied and that the subsequent coupling of an amino acid to generate a thiourea on the phenyl ester will only have minor influence on the photophysics.

A full detailed fluorescence study is yet to be performed on the new analogues, **29** and **33**, but both show great potential as extrinsic fluorophores for peptide conjugation. It is anticipated that the conjugated 2,5-dihydro-1,2,3-triazine fluorophore will exhibit the same dual excitation, fluorescence efficiency and relative photostability as reported for **3a** (Chapter 4, Section 4.3.1.3).

It is hoped future work shall focus on improving the water solubility and to identify analogues capable of further decreasing the excited state energy to generate NIR emitting fluorophores. As a novel class of dual excitation fluorophores, the future of 2,5-dihydro-1,2,3-triazine fluorophores capable of intracellular imaging appears to be bright.

Chapter 9: Summary and Conclusion.

This PhD focused on investigating the effect structural changes within the 2,5-dihydro-1,2,3-triazine fluorophore had on its photophysics with a view to developing a fluorophore capable of conjugating to biomolecules. Several modifications were explored including substituting the imine phenyl and N2 phenyl rings with heavy atoms, changing the methyl ester to a methyl ketone or 4-substituted phenyl ester, varying the substituent on the imine carbon, and removing the phenylimine group.

Through the aid of TD-DFT calculations, courtesy of Professor Luke A. Burke; we concluded that three structures may exist for the 2,5-dihydro-1,2,3-triazines: **g0** (optimized for S_0), **g1** (optimized for S_1) and, **g2** (optimized for S_2). From these calculations, a photophysical model was generated explaining the fluorescence of **3a** (N=C-H) and the methyl substituted imine derivative **11a** (N=C-CH_3).

For 310 nm excitation of N=C-H triazine (**3a**) the molecule is believed to have the **g0** structure in the GS, and an S_0 (**g0**) to S_2 (**g0**) transition then occurs due to the large change in dipole moment. Extensive IC into the different vibronic states of closely related structures occurs which leads to emission from the S_1 (**g0**), S_1 (**g2**) and S_1 (**g1**) states. The complicated tri-band emission centred at ~520 nm for 310 nm exciation of **3a** was resolved as:

1. Emission from the S_1 (**g1**) state *via* three distinct paths being attributed to the long wavelength emission band observed at ~540 nm,
2. S_2 (**g0**) IC to S_1 (**g2**) with emission of a photon composing the middle wavelength band observed at ~503 nm,
3. S_2 (**g0**) IC down to S_1 (**g0**) with emission of photon when returning to GS and is attributed to the short wavelength band observed at ~470 nm.

For 400 nm excitation of **3a**, the model of fluorecence was reasoned to be an S_0 (**g0**) to S_1 (**g0**) transition with emission from the S_1 (**g0**), S_1 (**g1**) and S_1 (**g2**) states in a similar fashion to the 310 nm excitation.

For the 4-Cl and 4-Br aromatic substituted triazine derivatives (**6a** and **9a**), the emission properties are virtually identical to the parent triazine **3a**. This indicated that substitution at the 4-position of the imine phenyl and N2 phenyl rings with heavy atoms has very little effect on the molecule's energy levels and that the heavy atom effect is small in these cases. Ultimately, the major difference between 310 and 400 nm excitation for the 2,5-dihydro-1,2,3-triazines with substituted aryl groups (**3a**, **6a**, **9a**) involves the proportion of the short wavelength $S_{1\rightarrow0}$ (**g0**) emission (~470 nm) which increases as the excitation wavelength increases.

When the carbonyl is substituted with a methyl ketone (**10a**) instead of a methyl ester (**3a**), a significant change to the energy of the emission spectrum is observed. The populations of the excited states are also different in comparison to **3a**. We believe an increased rate of IC from S_2 (**g0**) to S_1 (**g0**) with emission of a photon back to GS (Band 3) is observed as the energy of the transition is lower (Band 3, 531 nm for **10a** vs 479 nm for **3a**, both in ethylene glycol at 310 nm excitation, Chapter 4, Table 4.3).

Based on calculations performed by Dr. Elisa Fadda, we suggest that change in fluorescence is associated with the marked difference between the calculated electron densities of the carbonyl of an ester and ketone. The calculated observations can also be associated to the model of fluorescence based on the in-plane imine hydrogen interaction with the carbonyl group. Based on the calculations, it is now known that this interaction could be expected to be stronger for the ester substituted triazines (*e.g.* **3a** and **21**) as the carbonyl oxygen's have a higher calculated negative charge (*e,g.* -0.5401 for methyl acetate) compared to the ketone substituted triazine (**10a**) as the calculated charge on the oxygen was found to be less electronegative (-0.4929 for propan-2-one). The weaker interaction as well as the lower dipole moment appears to account for why a lower energy emission is observed when the carbonyl is changed from an ester to a ketone.

For the imine substituted N=C-CH_3 triazine (**11a**), excitation at 400 nm results in virtually no fluorescence emission resulting from population of the S_1 (**g0**) state which is observed as a weak band at ~520 nm. This is believed to be due to the calculated change in dipole moment being small for the $S_{1\rightarrow0}$ (**g0**) emission (based on dipole moment calculations).

However, excitation at ~310 nm results in a strong tri-banded emission centred at ~350 nm. This is believed to be S_0 (**g0**) populating the S_3 (**g0**) and S_2 (**g0**) ES upon excitation. The molecule can then revert to the ground state by fluorescence *via* a number of IC or vibrational relaxation pathways: $S_{2\rightarrow0}$ (**g0**), $S_{1\rightarrow0}$ (**g0**), $S_{2\rightarrow0}$ (**g1**), and $S_{1\rightarrow0}$ (**g1**).

We believe that what ultimately accounts for the significant difference in the fluorescent and electronic properties of **3a** and **11a** is the positioning of the imine and ester. The imine and ester of N=C-H triazine are held in-plane or nearly in-plane due to an interaction between the imine hydrogen and the ester carbonyl lone pair for S_0, S_1, and S_2 for **3a**. However in **11a**, the imine methyl group N=C-CH_3 is held out of plane with the ester, which ultimately effects the transition dipole moments and fluorescence.

Bulky substituents such as a phenyl or carboxy ester substituted on the imine carbon (**12**, Z = Ph and **13**, Z = COOMe) generates a significant change in fluorescence properties compared to **3a**. Here the imine and ester can no longer be held in-plane and again this ultimately effects the dipole transition moment. As a result, under both 310 and 400 nm excitation only very weakly emitting species are observed. Therefore, the imine must be substituted with smaller substituents so as to maintain the rotation of the imine group, which allows it to remain in plane with the carbonyl.

In the case of a deuterium being substituted on the imine carbon (**15**), the fluorescent properties were almost the same as the hydrogen substituted parent structure (**3a**).

Removal of the phenylimine group results in a blue-shifted fluorescence emission band centred at ~480 nm compared to the phenylimine substituted **3a** (~520 nm). The fluorescence efficiency is also effected *e.g.* for 310 nm excitation, the maximum quantum yield for **16** was calculated to be 0.29 in acetonitrile compared to 0.76 in toluene for **3a**. The intensity weighted average fluorescent lifetime of the hydrolysed triazine is also effected compared to the phenylimine substituted **3a**. It is much shorter (~3 ns) than the phenylimine parent (~10 ns) due to a significant shortening of the long lived component (τ_3) of the fluorescent decay. For the 4-Cl and 4-Br derivatives (**17** and **18**), the emission properties were almost the same as **16**, again indicating that substitution at the 4-position of the N2 phenyl ring has very little effect on the molecule's energy levels and that the heavy atom effect is small in these cases.

Similar to the comparison between **10a** and **3a**, a red shift is observed in the emission for the ketone hydrolysed 2,5-dihydro-1,2,3-triazine **19** when compared with the methyl ester hydrolysed 2,5-dihydro-1,2,3-triazine **16**. Although the energy of the emission states changes for **19**, the population of the excited states compared to **16** are similar. This would suggest that substitution of the carbonyl has little effect on how the excited states are populated for the hydrolysed 2,5-dihydro-1,2,3-triazines but does effect the energies of the transitions. We suggest that this lower energy emission is associated with a change in dipole moment between the hydrolysed methyl ester triazine **16** and hydrolysed methyl ketone triazine **19**, based on the calculations performed by Dr. Fadda

In comparison to **3a** (N=C-H), the S_1 (**g1**) emission state (Band 1) and S_1 (**g2**) (Band 2) are higher in energy for **16**, **17**, **18** and **19**, with the S_1 (**g0**) emission state (Band 3) being lower in energy than the phenylimine parent **3a**. This suggests that the removal of the phenylimine is effecting the energy of the fluorescent states of **16**, **17**, **18** and **19** compared to the unhydrolysed phenylimine parent **3a**. This is ultimately leading to an increase of the lower energy S_1 (**g0**) emission state at 310 nm excitation (26.34 % in toluene for **16** and 20.27 % in acetonitrile for **19** versus 8.36 % in 1,5-pentanediol for **3a**).

The substitution of a phenyl ester on the aromatic 2,5-dihydro-1,2,3-triazine (**21**, **23** and **25**) results in a similar complicated, tri-banded green fluorescence emission centered at ~520 nm that are of similar energy to the methyl ester triazines (**3a**, **6a** and **9a**). This indicated that the substitution of the carbonyl with a phenyl ester rather than a methyl ester and substitution of the 4-position of the phenyl ester (except *p*-NO_2) has only minor influence on the photophysics of the 2,5-dihydro-1,2,3-triazines. In these cases we don't observe a distinct change in fluorescence (populations or emission band energies) when compared to **3a** at either 310 or 400 nm excitation. We believe that the lack of change in fluorescence with the family of phenyl ester triazines compared to the methyl ester triazine **3a** is due to the similar nature of the electron density at the carbonyl of a methyl ester and the carbonyl of a phenyl ester, based on computational calculations.

The exception is with a *p*-NO_2 substituted phenyl ester (**27**), whereby the nitro groups appear to promote radiationless de-excitation from the **g0** excited state.

In conclusion, this thesis may be summarized as follows:

- The 2,5-dihydro-1,2,3-triazine fluorophores do not appear to be effected by the solvent or microenvironment as no solvatochromism was observed in both the ground state and excited state.
- The fluorescence of the 2,5-dihydro-1,2,3-triazines is quenched completely in acetic acid and 2,2,2-trifluoroethanol but the process is yet to be fully investigated.
- Substitution at the 4-position of the imine phenyl and N2 phenyl rings has very little effect on the molecule's energy levels and that the heavy atom effect is small in these cases.
- The phenylimine group is essential for the long lived fluorescence of the 2,5-dihydro-1,2,3-triazines with substituted aryl groups.
- In order to maintain fluorescence, the phenylimine group must be substituted with substituents small enough to maintain the rotation of the imine group and allow it to remain in plane with the carbonyl.
- Removal of the phenylimine increases the energy of the emission states, but results in a less efficient and shorter lived fluorescence.
- If the dipole moment of the carbonyl is decreased or a more efficient in plane interaction of the carbonyl lone pair with the imine hydrogen is achieved, the energy of the emission may possibly be lowered resulting in a red-shifted emission.
- Substituting the methyl ester to a 4-substituted phenyl ester has only minor influence on the photophysics due to the similar electron densities at the carbonyl of a methyl ester and a carbonyl of a phenyl ester.
- The synthesis of propiolates containing stable activating groups provides an accessible route to generating 2,5-dihydro-1,2,3-triazines capable of conjugation to biomolecules.

Appendices

A.1 FLUORESCENCE SPECTROSCOPY SOLVATOCHROMIC ANALYSIS.

Refer to Appendix of Results (pdf file on disc attached at back of thesis) for raw fluorescence spectroscopic data and full data analysis for all compounds.

A.2 SOLVATOCHROMIC VALUES OF SOLVENTS INVESTIGATED.

Solvent	Protic Nature	Viscosity η(Cp) (at 25°C)	Polarity $E_T(30)$	Polarity Normalized E_T^N	HBD ability α	HBA ability π	Polarity/Polarizability π*	Dielectric Constant ε	Dipole Moment μ (D)
Toluene	**Aprotic**	0.56	33.9	0.099	0	0.11	0.54	2.379	0.37
1,4-Dioxane	**Aprotic**	1.177	36	0.164	0	0.37	0.55	2.2189	0
Ethyl acetate	**Aprotic**	0.423	38.1	0.228	0	0.45	0.55	6.0814	1.78
Chloroform	**Aprotic**	0.537	39.1	0.259	0.44	0	0.58	4.8069	1.04
2-Methyl-2-butanol	**Protic**	3.55	41	0.318	0.29	0.52	0.4	5.7	1.82
N,N-dimethylformamide	**Aprotic**	0.794	43.2	0.386	0	0.69	0.88	38.25	3.82
Acetonitrile	**Aprotic**	0.369	45.6	0.46	0.19	0.31	0.75	36.64	3.92
Propylene Carbonate	**Aprotic**	2.48	46	0.472	0	0.4	0.83	66.14	4.9
1-Octanol	**Protic**	7.29	48.1	0.537	0.77	0.81	0.4	10.3	1.8
1-Hexanol	**Protic**	4.58	48.8	0.559	0.8	0.84	0.4	13.03	1.8
1-Butanol	**Protic**	2.54	49.7	0.586	0.79	0.88	0.47	17.84	1.66
1-Pentanol	**Protic**	3.62	49.1	0.586	0.28	0.93	0.4	15.13	1.7
1-Propanol	**Protic**	1.945	50.7	0.617	0.76	0.84	0.48	20.8	1.55
Acetic Acid	**Protic**	1.056	51.7	0.648	1.12	0.45	0.64	6.2	1.7
1,5-Pentanediol	**Protic**	1.074	51.9	0.654	0.86	0.75	0.54	25.3	1.69
Ethanol	**Protic**	96.05	51.9	0.654	0.7	0.82	0.76	26.2	2.5
1,3-Butanediol	**Protic**	97.25	52.8	0.682	0.76	0.74	0.75	28.8	2.5
1,4-Butanediol	**Protic**	72.618	53.5	0.704	0.63	0.68	0.93	31.9	2.58
1,3-Propanediol	**Protic**	40.067	54.9	0.747	0.9	0.77	0.84	35.1	2.5
Methanol	**Protic**	0.544	55.4	0.762	0.98	0.66	0.6	33	1.7
Ethylene Glycol	**Protic**	16.06	56.3	0.79	0.9	0.52	0.92	41.4	2.28
2,2,2-Trifluoroethanol	**Protic**	1.78	59.8	0.898	1.51	0	0.73	27.68	2.46
Ethanol-d	**Aprotic**	1.106	-	-	-	-	-	-	-
Methanol-d	**Aprotic**	0.558	-	-	-	-	-	-	-

Table A.1. Solvatochromic values used for fluorescence analysis. [15, 88, 89, 90, 91, 92]

Note: Values at ambient temperature unless otherwise specified.

A.3 SELECTED INFRARED SPECTRA.

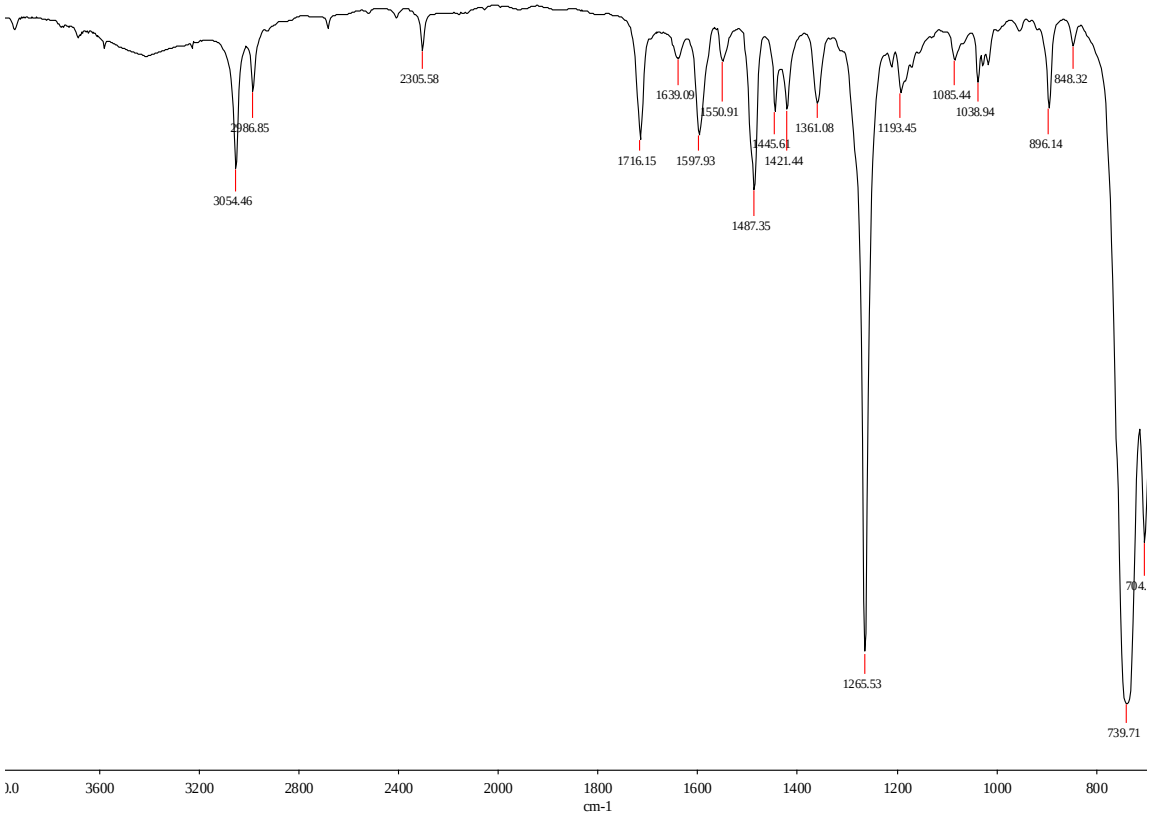

A.3.1. Infrared spectra of **10a**.

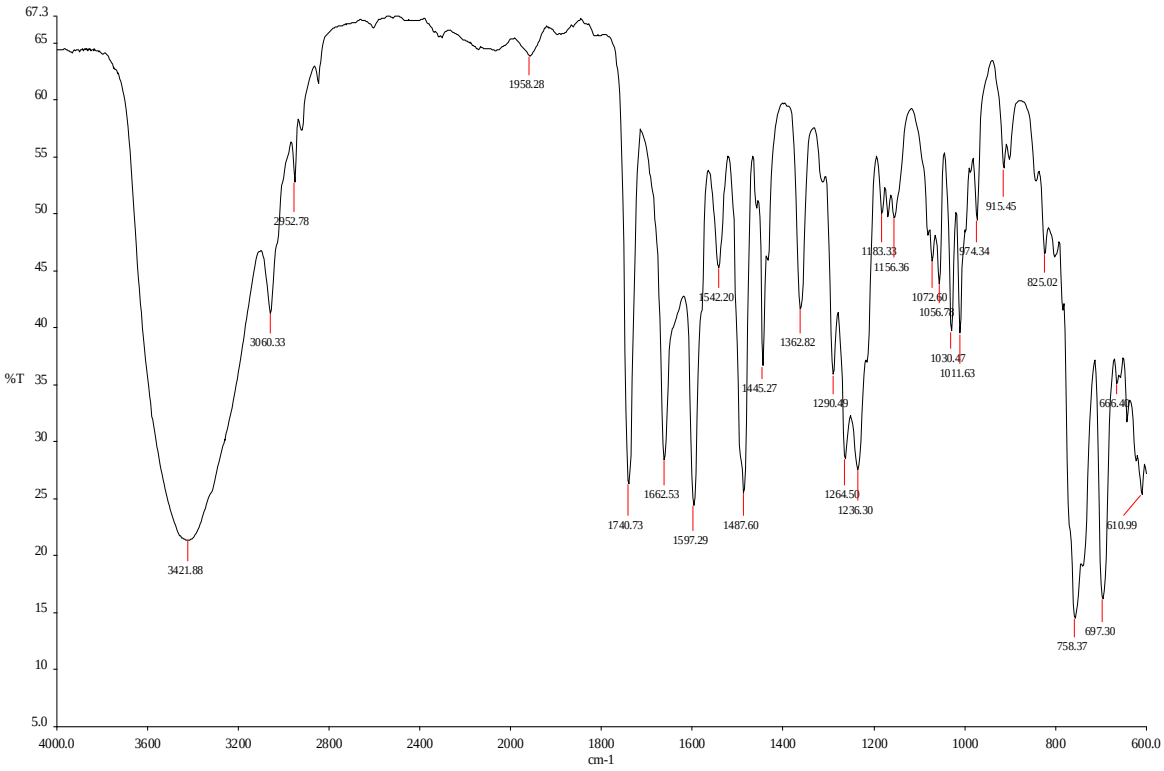

A.3.2 Infrared spectra of **11a**.

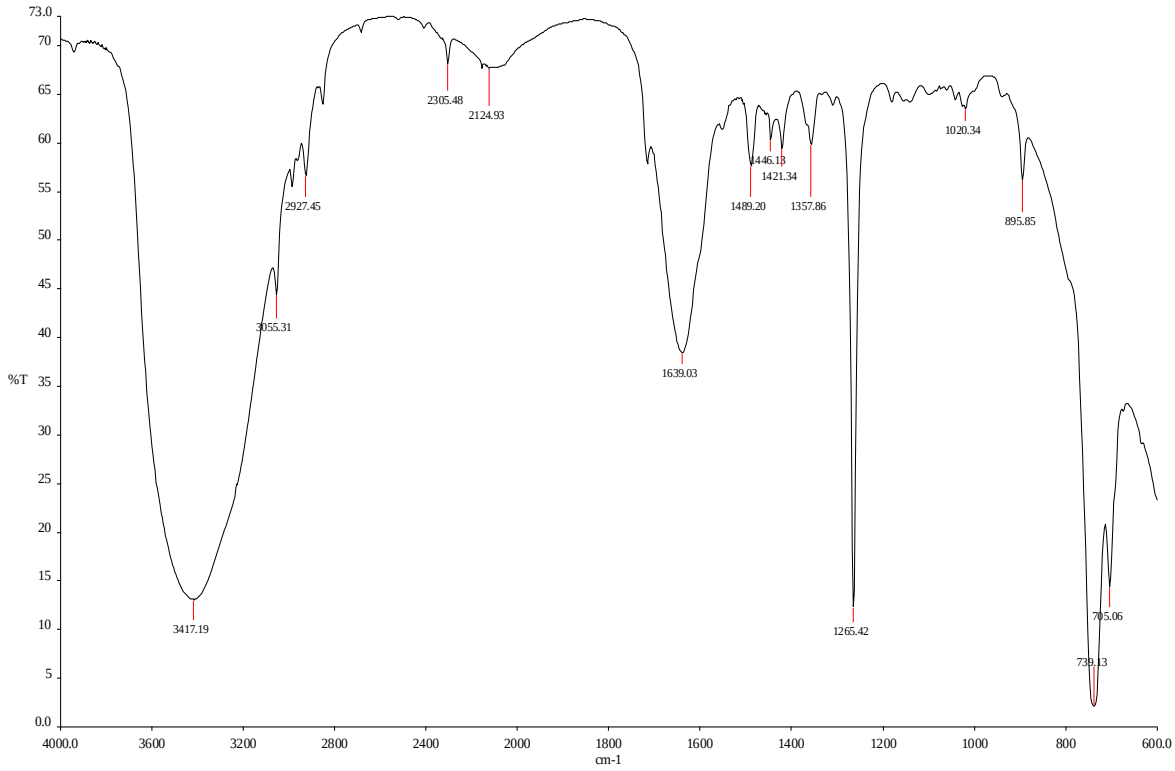

A.3.3. Infrared spectra of **19**.

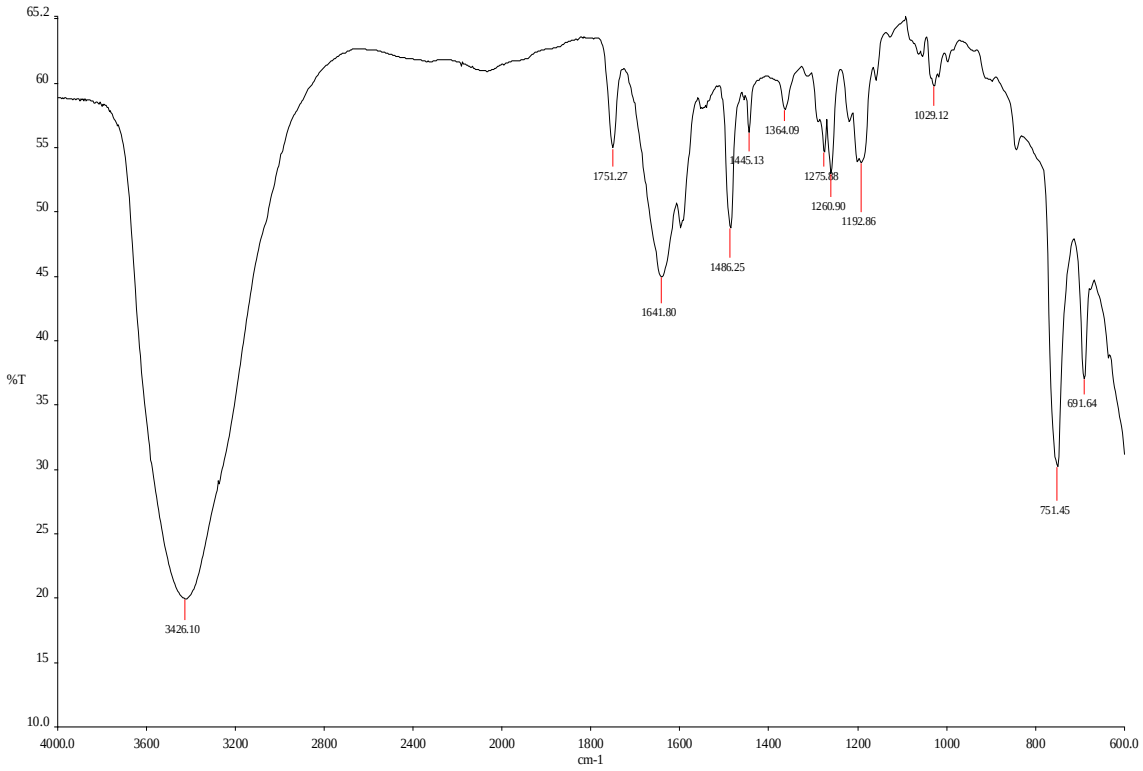

A.3.4. Infrared spectra of **21**.

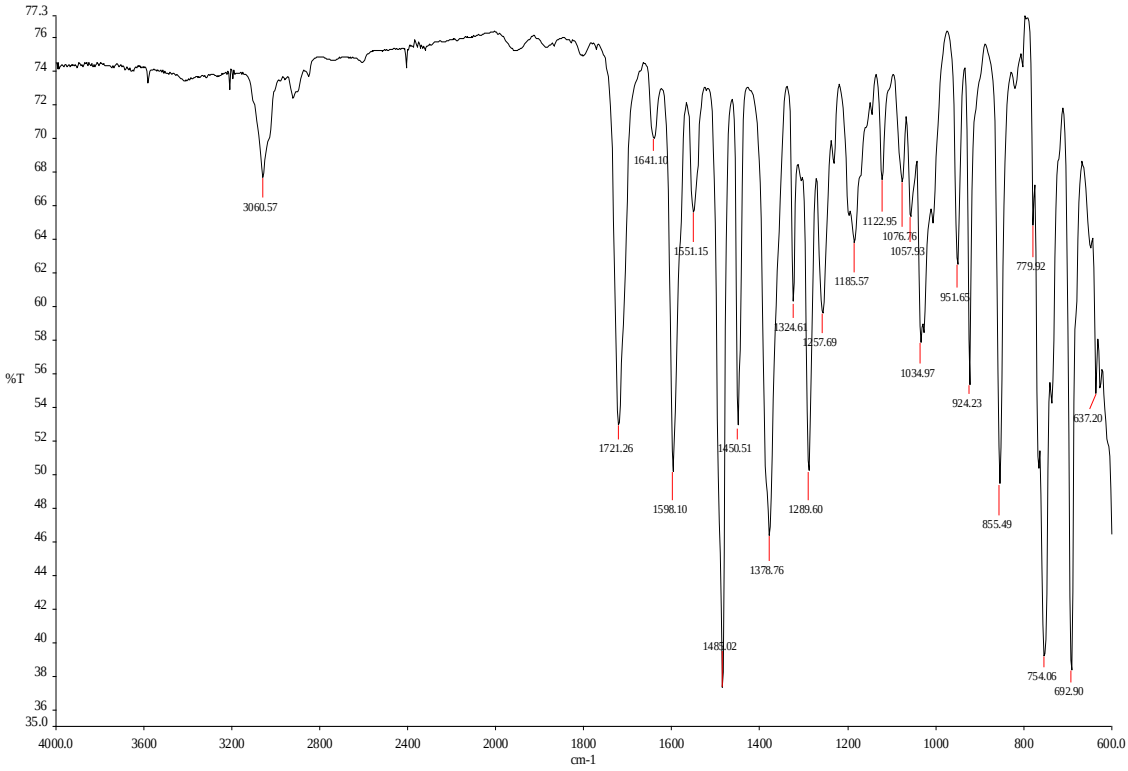

A.3.5. Infrared spectra of **30**.

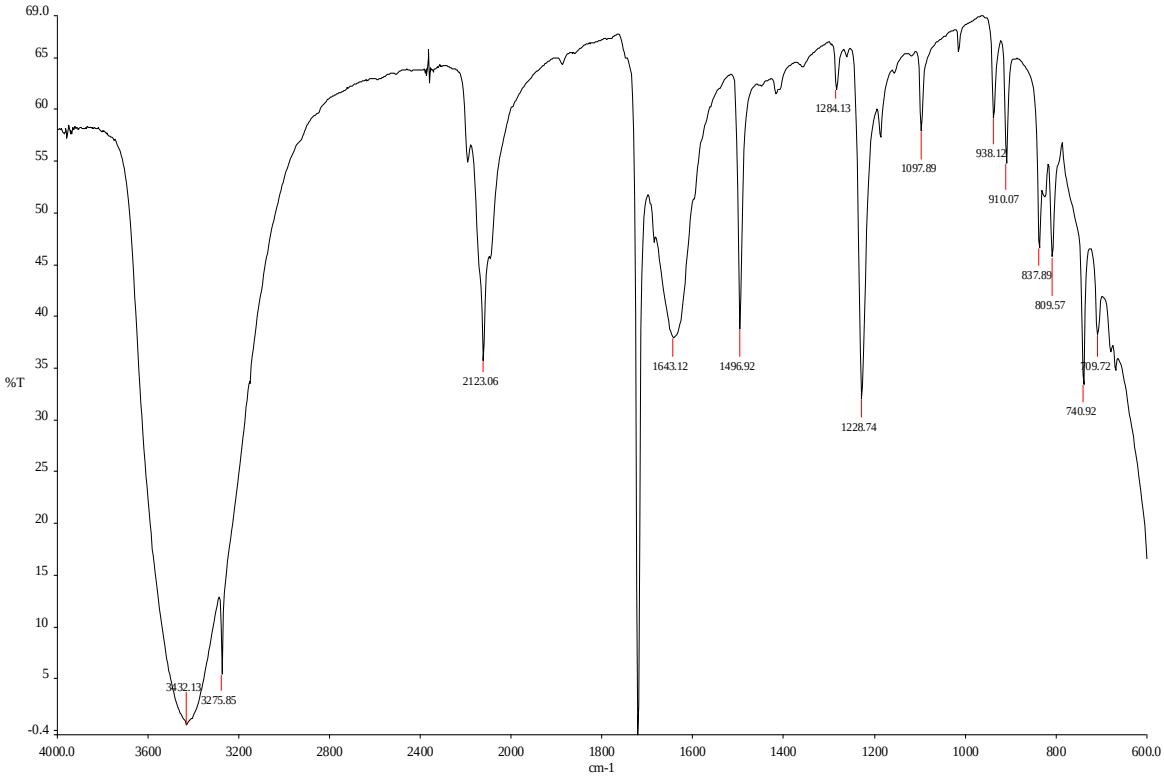

A.3.6. Infrared spectra of **32**.

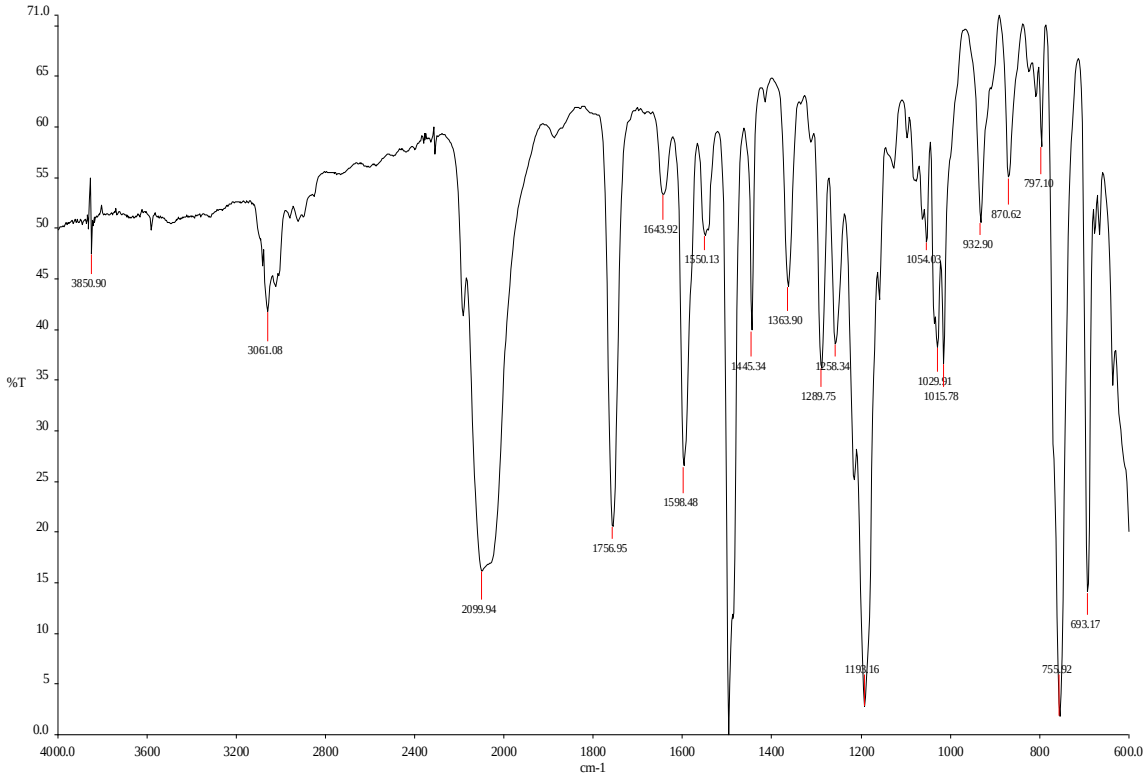

A.3.7. Infrared spectra of **33**.

A.4 SELECTED NMR SPECTRA.

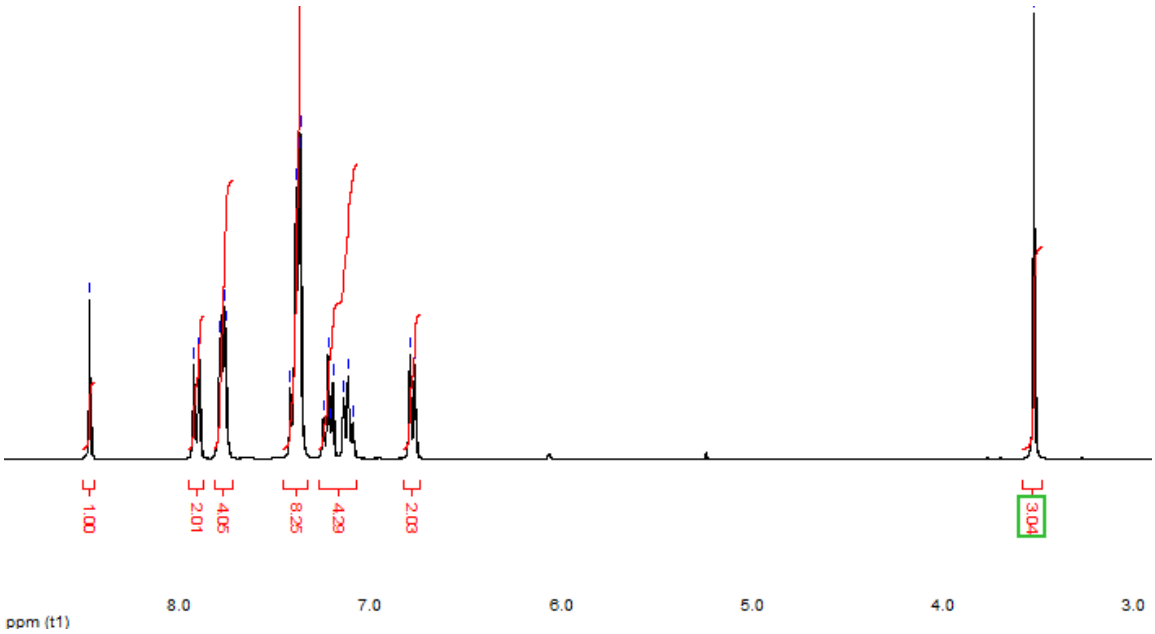

A.4.1. ^{1}H NMR spectra of **3a**

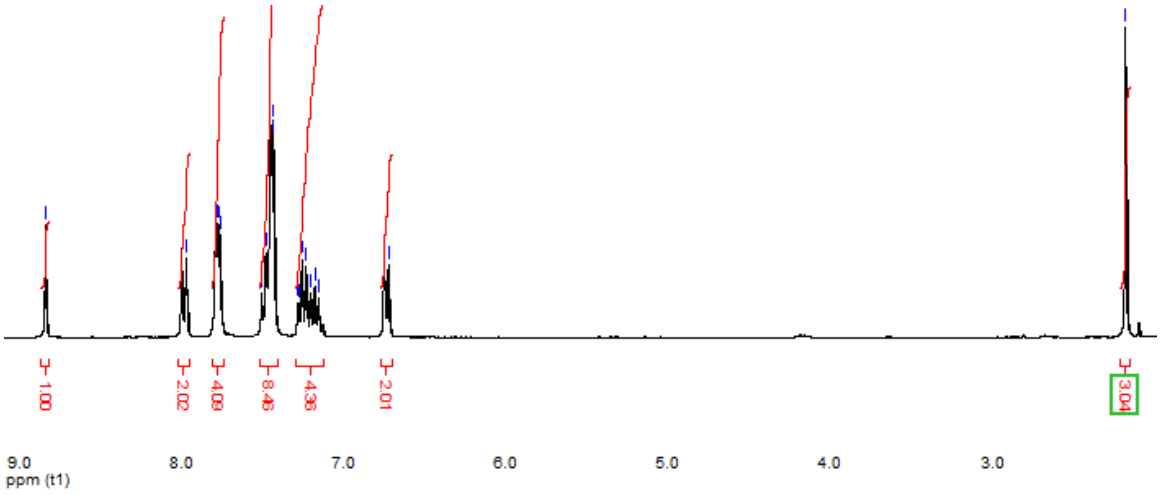

A.4.2. ^{1}H NMR spectra of **10a**.

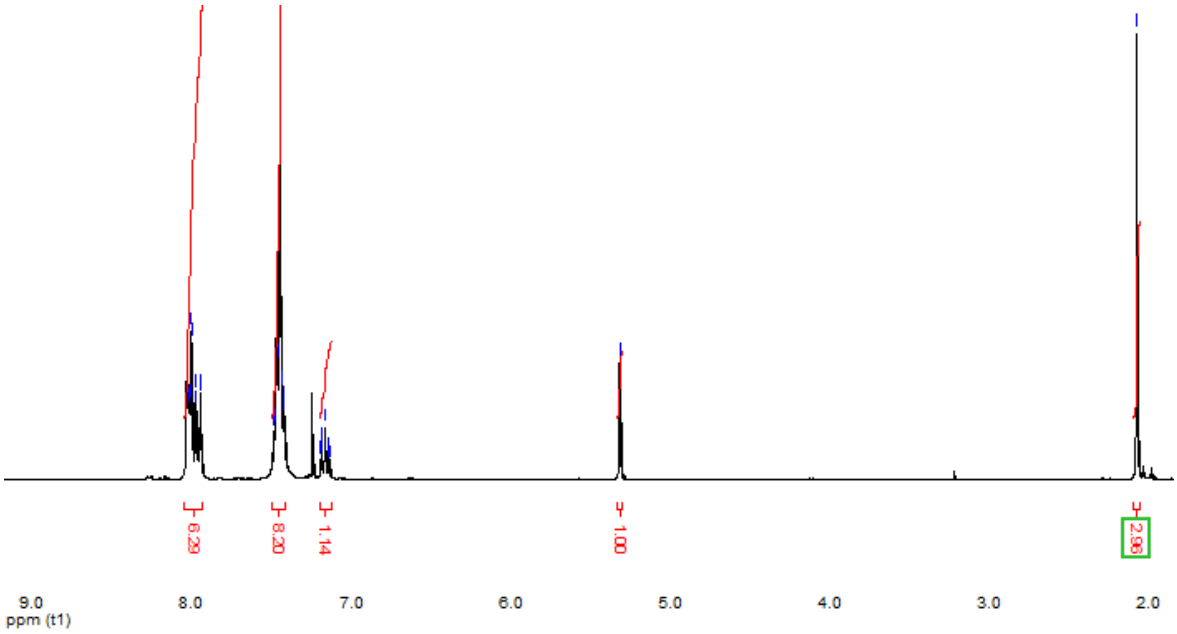

A.4.3. ^{1}H NMR spectra spectra of **19**.

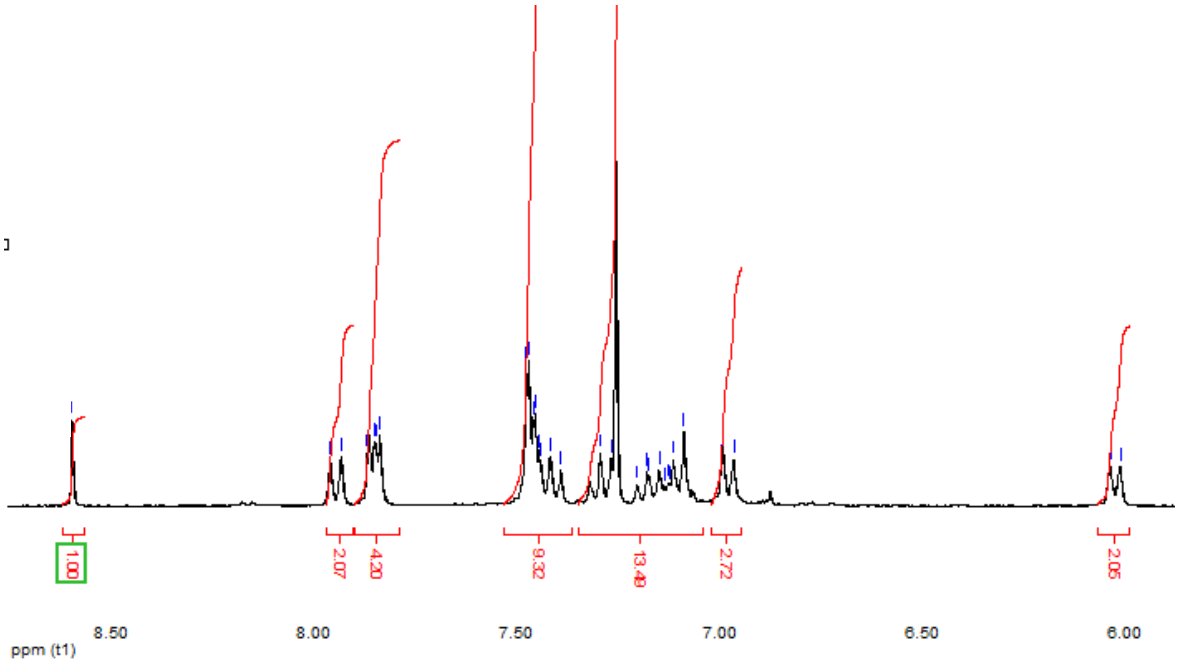

A.4.4. ^{1}H NMR spectra spectra of **21**.

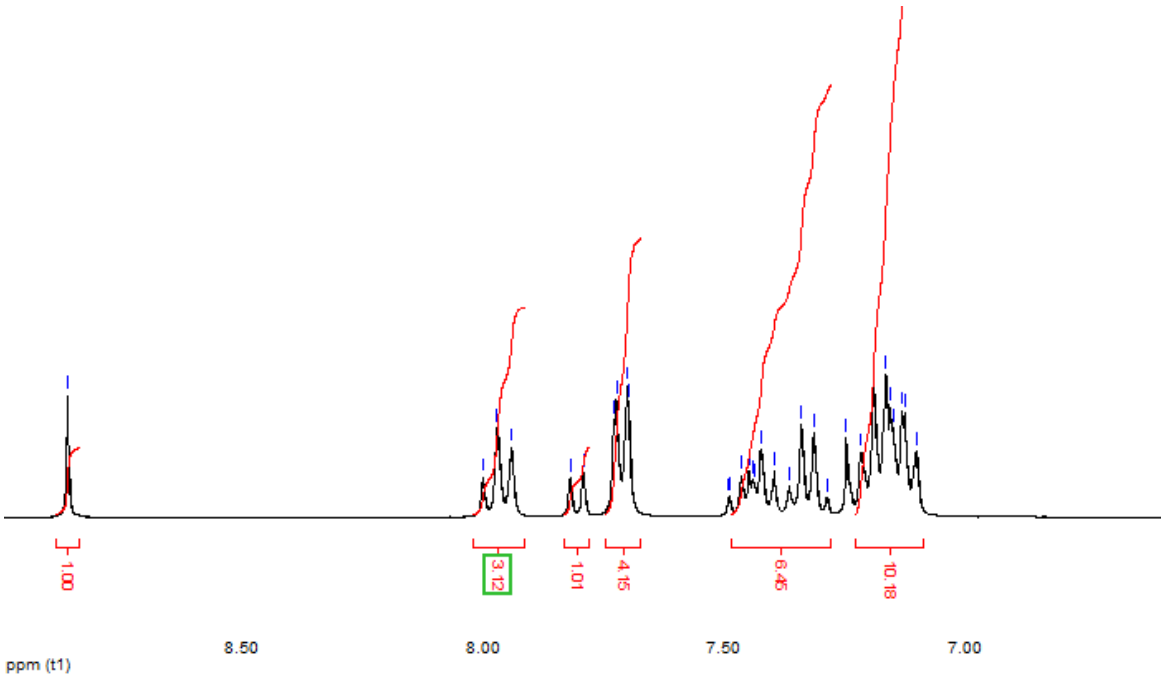

A.4.5. ^{1}H NMR spectra spectra of **29**.

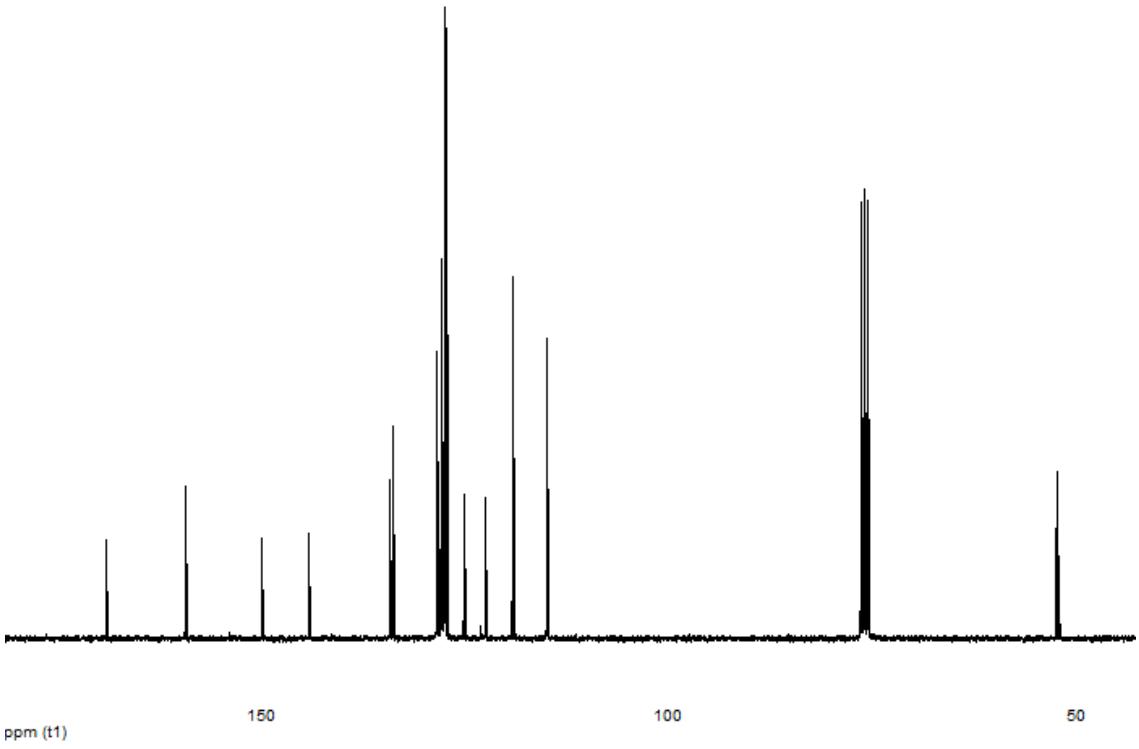

A.4.6. ^{13}C NMR spectra spectra of **3a**.

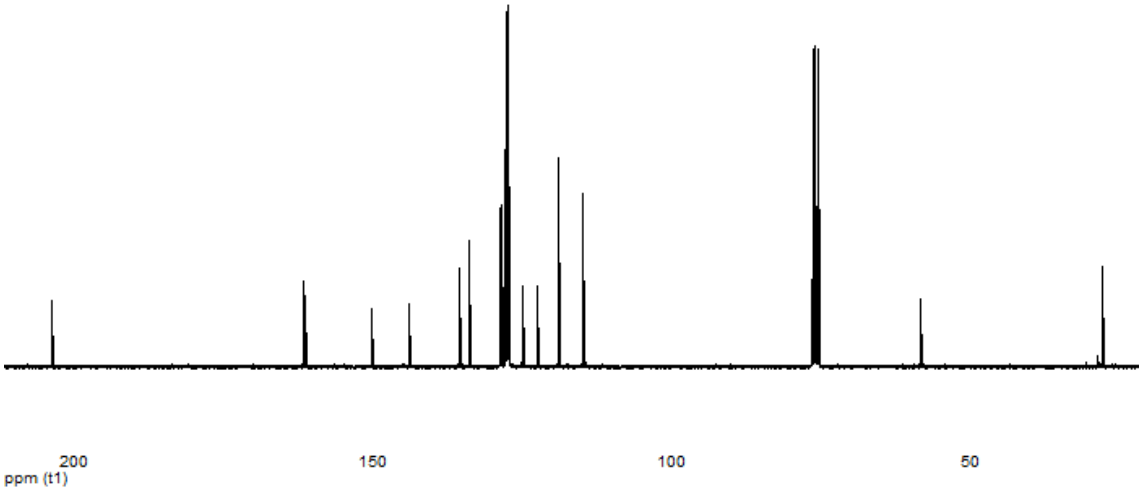

A.4.7. ^{13}C NMR spectra spectra of **10a**.

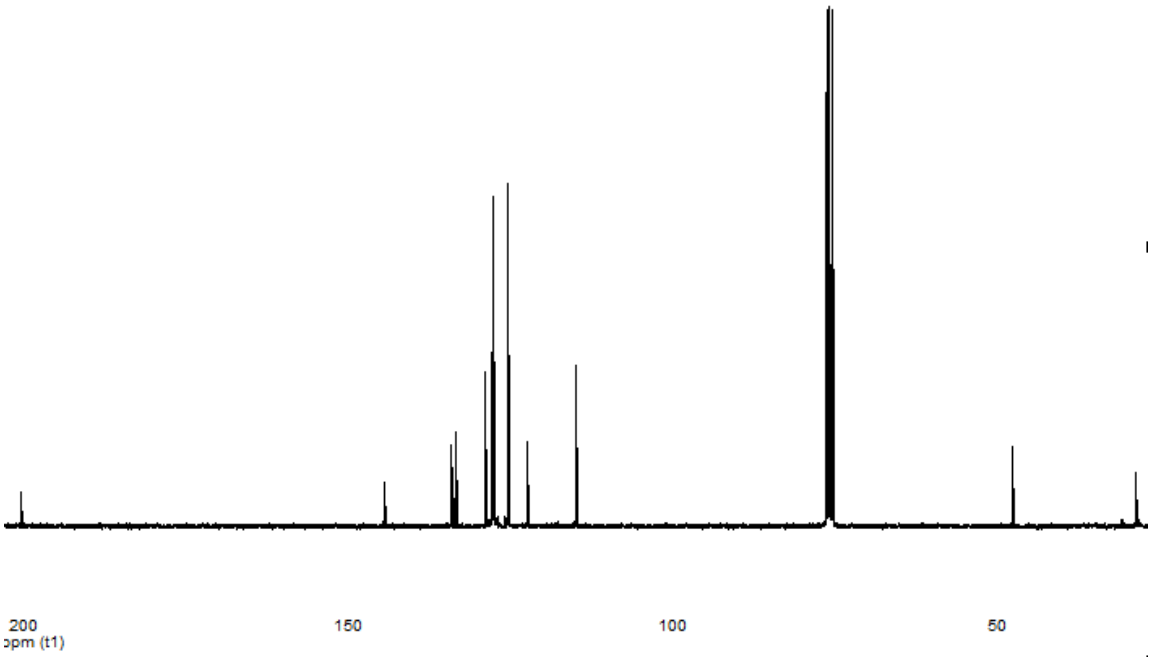

A.4.8. ^{13}C NMR spectra spectra of **19**.

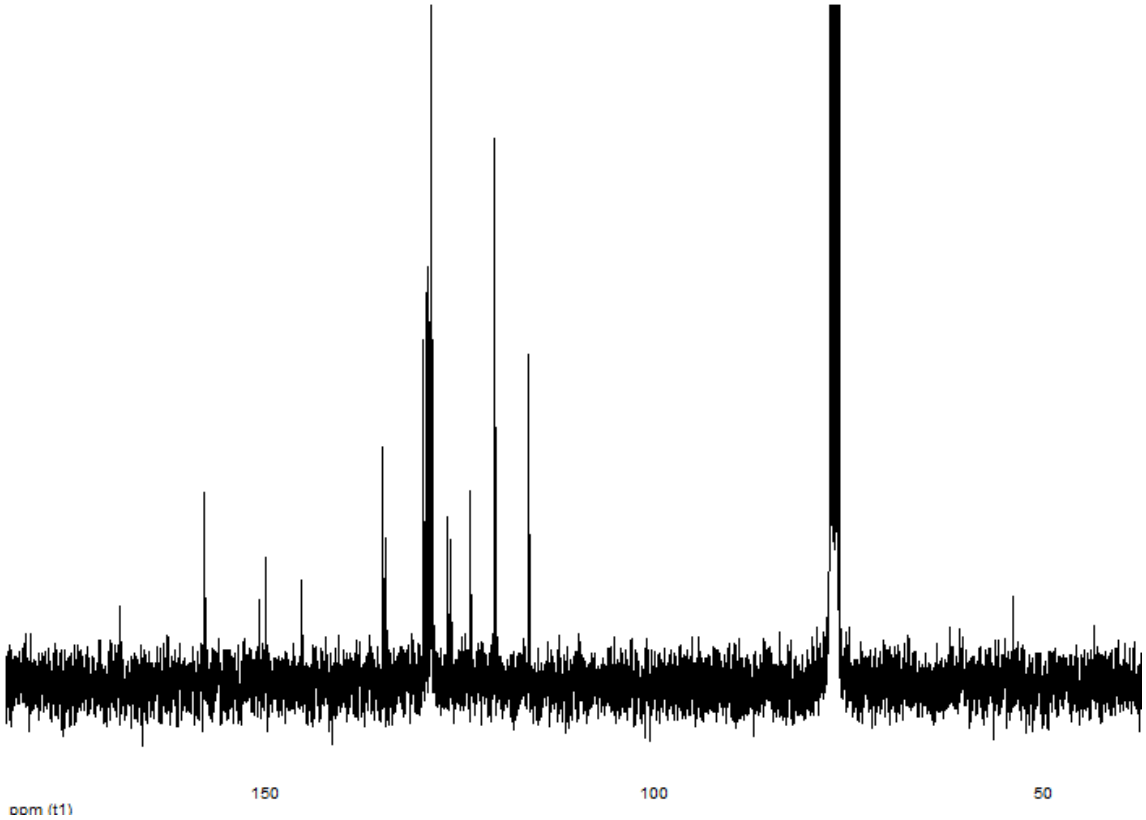

A.4.9. ^{13}C NMR spectra spectra of **21**.

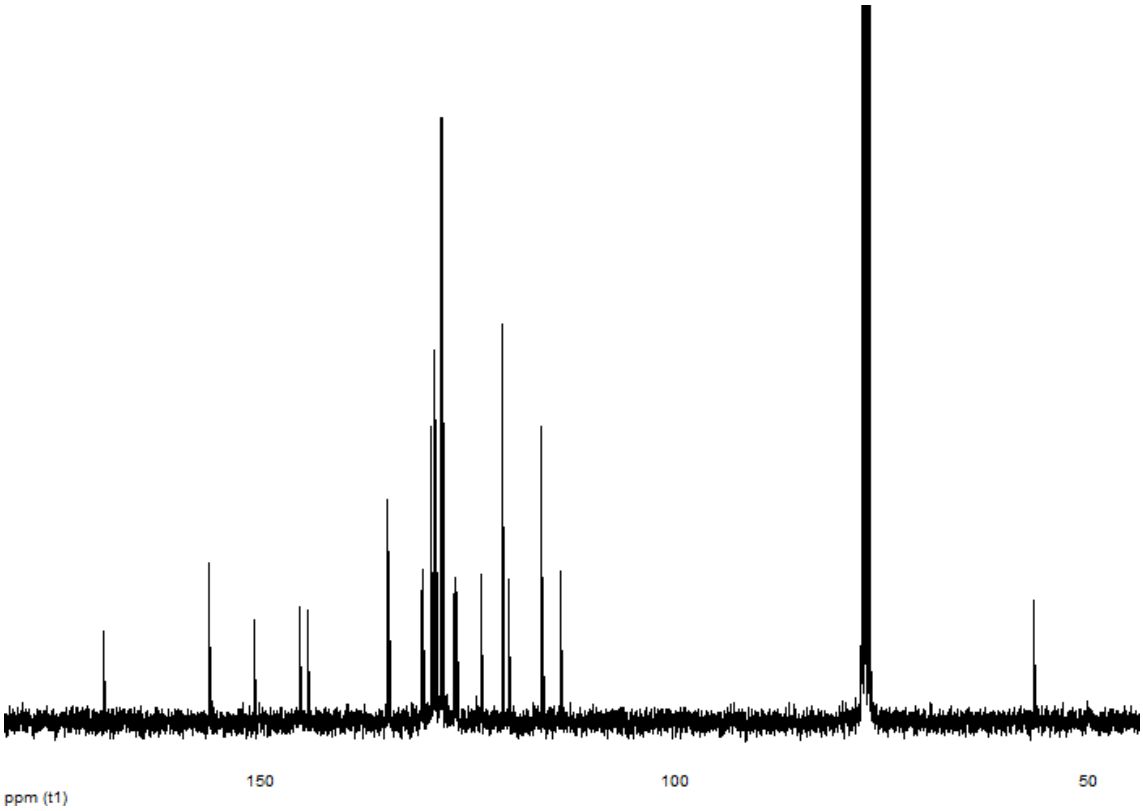

A.4.10. ^{13}C NMR spectra spectra of **29**.

A.5 X-RAY CRYSTALLOGRAPHY DATA.

A.5.1 2,4,5-Triphenyl-1,2,3-triazole.

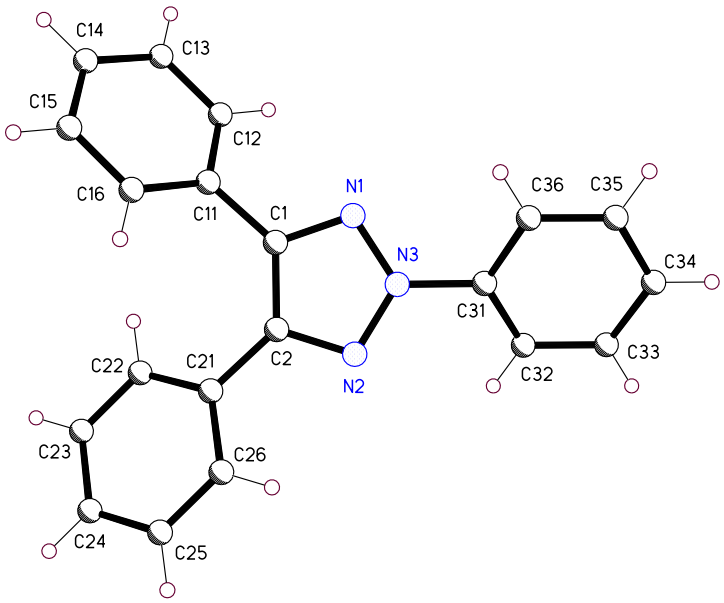

The data were collected at 150(2)K on a Bruker Apex II CCD diffractometer using MoK_α radiation (λ = 0.71073Å). The structure was solved by direct methods and refined on F^2 using all the reflections*. All the non-hydrogen atoms were refined using anisotropic atomic displacement parameters and hydrogen atoms were inserted at calculated positions using a riding model. Parameters for data collection and refinement are summarised in Table 1.

* G.M. Sheldrick, Acta Cryst. 2008, A64, 112-122.

Table 1. Crystal data and structure refinement for 2,4,5-Triphenyl-1,2,3-triazole.

Identification code	jsdmso	
Empirical formula	C20 H15 N3	
Formula weight	297.35	
Temperature	150(2) K	
Wavelength	0.71073 Å	
Crystal system	Orthorhombic	
Space group	Pbca	
Unit cell dimensions	a = 19.614(5) Å	α= 90°.
	b = 7.632(2) Å	β= 90°.
	c = 20.305(5) Å	γ = 90°.
Volume	3039.2(14) $Å^3$	
Z	8	
Density (calculated)	1.300 Mg/m^3	
Absorption coefficient	0.078 mm^{-1}	
F(000)	1248	
Crystal size	0.41 x 0.34 x 0.34 mm^3	
Crystal description	yellow block	
Theta range for data collection	2.01 to 28.34°.	
Index ranges	-26<=h<=26, -10<=k<=10, -27<=l<=26	
Reflections collected	29108	
Independent reflections	3790 [R(int) = 0.0314]	
Completeness to theta = 28.34°	100.0 %	
Absorption correction	Semi-empirical from equivalents	
Max. and min. transmission	0.9738 and 0.9685	
Refinement method	Full-matrix least-squares on F^2	
Data / restraints / parameters	3790 / 0 / 208	
Goodness-of-fit on F^2	1.031	
Final R indices [I>2sigma(I)]	R1 = 0.0380, wR2 = 0.0945	
R indices (all data)	R1 = 0.0479, wR2 = 0.1018	
Largest diff. peak and hole	0.280 and -0.219 e.$Å^{-3}$	

Table 2. Atomic coordinates (x 10^4) and equivalent isotropic displacement parameters ($Å^2$x 10^3) for jsdmso. U(eq) is defined as one third of the trace of the orthogonalized U^{ij} tensor.

	x	y	z	U(eq)
N(1)	2608(1)	2684(1)	2738(1)	27(1)
C(1)	1958(1)	2696(1)	2535(1)	25(1)
C(2)	1534(1)	2960(1)	3091(1)	25(1)
N(2)	1930(1)	3100(1)	3625(1)	27(1)
N(3)	2562(1)	2929(1)	3388(1)	27(1)
C(11)	1810(1)	2453(1)	1829(1)	24(1)
C(12)	2205(1)	1287(2)	1464(1)	30(1)
C(13)	2099(1)	1083(2)	794(1)	37(1)
C(14)	1601(1)	2050(2)	476(1)	37(1)
C(15)	1210(1)	3222(2)	832(1)	33(1)
C(16)	1311(1)	3426(2)	1505(1)	28(1)
C(21)	786(1)	3056(1)	3165(1)	24(1)
C(22)	349(1)	2155(1)	2740(1)	27(1)
C(23)	-352(1)	2230(2)	2831(1)	30(1)
C(24)	-626(1)	3191(2)	3347(1)	34(1)
C(25)	-195(1)	4089(2)	3771(1)	34(1)
C(26)	505(1)	4025(2)	3682(1)	29(1)
C(31)	3148(1)	3028(1)	3801(1)	26(1)
C(32)	3101(1)	2469(2)	4449(1)	33(1)
C(33)	3670(1)	2594(2)	4850(1)	35(1)
C(34)	4278(1)	3241(2)	4605(1)	33(1)
C(35)	4317(1)	3784(2)	3955(1)	34(1)
C(36)	3751(1)	3688(2)	3549(1)	30(1)

Table 3. Bond lengths [Å] and angles [°] for jsdmso.

N(1)-N(3)	1.3356(13)	C(15)-C(16)	1.3880(16)
N(1)-C(1)	1.3387(14)	C(21)-C(22)	1.3960(15)
C(1)-C(2)	1.4171(14)	C(21)-C(26)	1.3981(15)
C(1)-C(11)	1.4757(15)	C(22)-C(23)	1.3881(16)
C(2)-N(2)	1.3389(14)	C(23)-C(24)	1.3884(17)
C(2)-C(21)	1.4755(15)	C(24)-C(25)	1.3880(18)
N(2)-N(3)	1.3349(13)	C(25)-C(26)	1.3855(16)
N(3)-C(31)	1.4249(14)	C(31)-C(36)	1.3838(15)
C(11)-C(16)	1.3930(15)	C(31)-C(32)	1.3848(15)
C(11)-C(12)	1.3932(15)	C(32)-C(33)	1.3854(17)
C(12)-C(13)	1.3867(16)	C(33)-C(34)	1.3848(17)
C(13)-C(14)	1.3837(19)	C(34)-C(35)	1.3854(17)
C(14)-C(15)	1.3823(18)	C(35)-C(36)	1.3858(16)

N(3)-N(1)-C(1)	103.82(9)	C(22)-C(21)-C(26)	118.84(10)
N(1)-C(1)-C(2)	108.36(9)	C(22)-C(21)-C(2)	121.55(10)
N(1)-C(1)-C(11)	119.09(9)	C(26)-C(21)-C(2)	119.58(10)
C(2)-C(1)-C(11)	132.55(10)	C(23)-C(22)-C(21)	120.38(10)
N(2)-C(2)-C(1)	108.35(10)	C(22)-C(23)-C(24)	120.41(11)
N(2)-C(2)-C(21)	119.49(9)	C(25)-C(24)-C(23)	119.50(11)
C(1)-C(2)-C(21)	132.15(10)	C(26)-C(25)-C(24)	120.38(11)
N(3)-N(2)-C(2)	103.83(9)	C(25)-C(26)-C(21)	120.48(11)
N(2)-N(3)-N(1)	115.64(9)	C(36)-C(31)-C(32)	121.36(10)
N(2)-N(3)-C(31)	122.04(9)	C(36)-C(31)-N(3)	119.36(10)
N(1)-N(3)-C(31)	122.31(9)	C(32)-C(31)-N(3)	119.27(10)
C(16)-C(11)-C(12)	118.70(10)	C(31)-C(32)-C(33)	118.97(11)
C(16)-C(11)-C(1)	122.09(10)	C(34)-C(33)-C(32)	120.44(11)
C(12)-C(11)-C(1)	119.11(10)	C(33)-C(34)-C(35)	119.80(11)
C(13)-C(12)-C(11)	120.63(11)	C(34)-C(35)-C(36)	120.46(11)
C(14)-C(13)-C(12)	120.31(11)	C(31)-C(36)-C(35)	118.95(11
C(15)-C(14)-C(13)	119.43(11)		
C(14)-C(15)-C(16)	120.61(11)		
C(15)-C(16)-C(11)	120.31(11)		

Table 4. Anisotropic displacement parameters ($Å^2 x\ 10^3$) for jsdmso. The anisotropic displacement factor exponent takes the form: $-2\pi^2[\ h^2\ a^{*2}U^{11} + ...\ + 2\ h\ k\ a^*\ b^*\ U^{12}\ ]$

	U^{11}	U^{22}	U^{33}	U^{23}	U^{13}	U^{12}
N(1)	29(1)	32(1)	21(1)	0(1)	2(1)	2(1)
C(1)	26(1)	24(1)	24(1)	1(1)	2(1)	2(1)
C(2)	27(1)	24(1)	22(1)	0(1)	2(1)	1(1)
N(2)	26(1)	32(1)	24(1)	-1(1)	3(1)	0(1)
N(3)	25(1)	35(1)	22(1)	-1(1)	3(1)	1(1)
C(11)	25(1)	25(1)	22(1)	1(1)	3(1)	-2(1)
C(12)	31(1)	32(1)	28(1)	-1(1)	3(1)	5(1)
C(13)	39(1)	41(1)	30(1)	-9(1)	9(1)	-1(1)
C(14)	34(1)	53(1)	22(1)	-1(1)	2(1)	-11(1)
C(15)	27(1)	44(1)	28(1)	8(1)	-2(1)	-4(1)
C(16)	27(1)	30(1)	28(1)	3(1)	3(1)	2(1)
C(21)	26(1)	24(1)	23(1)	3(1)	2(1)	1(1)
C(22)	32(1)	25(1)	23(1)	2(1)	2(1)	0(1)
C(23)	30(1)	30(1)	31(1)	7(1)	-3(1)	-5(1)
C(24)	26(1)	37(1)	38(1)	9(1)	5(1)	1(1)
C(25)	34(1)	35(1)	32(1)	0(1)	9(1)	5(1)
C(26)	32(1)	28(1)	26(1)	-2(1)	2(1)	0(1)
C(31)	26(1)	29(1)	24(1)	-2(1)	1(1)	2(1)
C(32)	29(1)	45(1)	25(1)	0(1)	3(1)	-3(1)
C(33)	34(1)	47(1)	24(1)	0(1)	-1(1)	0(1)
C(34)	30(1)	36(1)	32(1)	-4(1)	-5(1)	0(1)
C(35)	27(1)	36(1)	38(1)	3(1)	2(1)	-3(1)
C(36)	30(1)	31(1)	27(1)	4(1)	3(1)	2(1)

Table 5. Hydrogen coordinates (x 10^4) and isotropic displacement parameters ($Å^2$x 10^3) for jsdmso.

	x	y	z	U(eq)
H(12)	2551	626	1678	37
H(13)	2369	276	551	44
H(14)	1528	1910	16	44
H(15)	870	3894	615	40
H(16)	1039	4234	1745	34
H(22)	533	1487	2387	32
H(23)	-645	1620	2537	36
H(24)	-1106	3234	3409	40
H(25)	-381	4751	4124	40
H(26)	796	4645	3974	35
H(32)	2685	2007	4614	40
H(33)	3642	2234	5297	42
H(34)	4668	3313	4881	39
H(35)	4735	4226	3786	41
H(36)	3776	4070	3104	35

A.5.2 6-Methoxycarbonyl-2,3a,4,6a-tetraphenyl-3,3a,4,6a-tetrahydropyrrolo[2,3-d]-[1,2,3]-triazol-2-ium-3-ide.

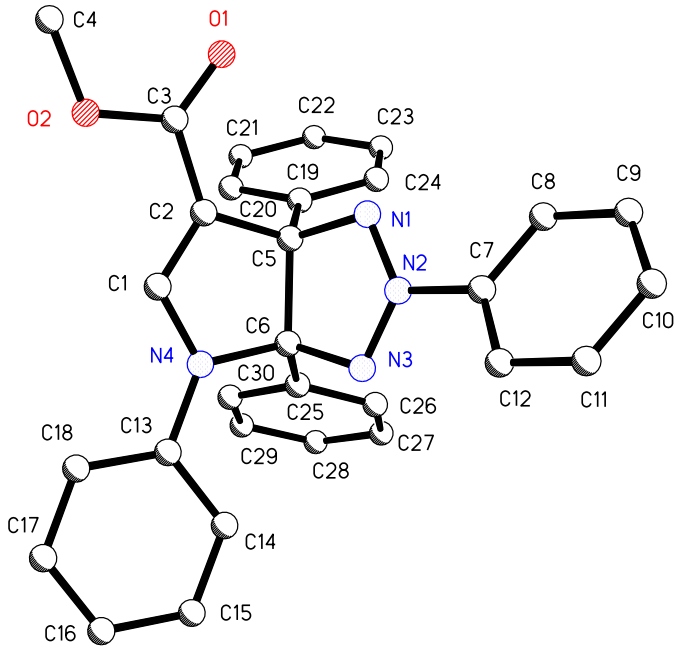

The data were collected at 150(2)K on a Bruker Apex II CCD diffractometer using MoK_α radiation (λ = 0.71073Å). The structure was solved by direct methods and refined on F^2 using all the reflections*. All the non-hydrogen atoms were refined using anisotropic atomic displacement parameters and hydrogen atoms were inserted at calculated positions using a riding model. Parameters for data collection and refinement are summarised in Table 1.

* G.M. Sheldrick, Acta Cryst. 2008, A64, 112-122.

Table 1. Crystal data and structure refinement for 6-Methoxycarbonyl-2,3a,4,6a-tetraphenyl-3,3a,4,6a-tetrahydropyrrolo[2,3-d]-[1,2,3]-triazol-2-ium-3-ide.

Identification code	dsm11	
Empirical formula	C30 H24 N4 O2	
Formula weight	472.53	
Temperature	150(2) K	
Wavelength	0.71073 Å	
Crystal system	Monoclinic	
Space group	P2(1)/c	
Unit cell dimensions	a = 13.3042(10) Å	α= 90°.
	b = 11.1369(8) Å	β= 112.495(1)°.
	c = 17.1804(13) Å	γ = 90°.
Volume	2351.9(3) $Å^3$	
Z	4	
Density (calculated)	1.335 Mg/m^3	
Absorption coefficient	0.086 mm^{-1}	
F(000)	992	
Crystal size	0.59 x 0.30 x 0.23 mm^3	
Crystal description	pale yellow block	
Theta range for data collection	2.23 to 28.33°.	
Index ranges	-17<=h<=17, -14<=k<=14, -22<=l<=22	
Reflections collected	23425	
Independent reflections	5845 [R(int) = 0.0259]	
Completeness to theta = 28.33°	99.8 %	
Absorption correction	Semi-empirical from equivalents	
Max. and min. transmission	0.9806 and 0.9512	
Refinement method	Full-matrix least-squares on F^2	
Data / restraints / parameters	5845 / 0 / 325	
Goodness-of-fit on F^2	1.037	
Final R indices [I>2sigma(I)]	R1 = 0.0416, wR2 = 0.1065	
R indices (all data)	R1 = 0.0516, wR2 = 0.1136	
Largest diff. peak and hole	0.388 and -0.213 $e.Å^{-3}$	

Table 2. Atomic coordinates (x 10^4) and equivalent isotropic displacement parameters ($Å^2$x 10^3) for dsm11. U(eq) is defined as one third of the trace of the orthogonalized U^{ij} tensor.

	x	y	z	U(eq)
C(1)	3240(1)	-761(1)	4075(1)	23(1)
C(2)	2202(1)	-390(1)	3706(1)	22(1)
C(3)	1351(1)	-557(1)	4035(1)	24(1)
O(1)	462(1)	-76(1)	3760(1)	32(1)
O(2)	1659(1)	-1331(1)	4690(1)	33(1)
C(4)	886(1)	-1516(2)	5081(1)	42(1)
C(5)	2035(1)	269(1)	2896(1)	21(1)
N(1)	1853(1)	1562(1)	2978(1)	22(1)
N(2)	2746(1)	2070(1)	3015(1)	20(1)
N(3)	3579(1)	1492(1)	2970(1)	22(1)
C(6)	3233(1)	228(1)	2871(1)	20(1)
N(4)	3873(1)	-485(1)	3635(1)	23(1)
C(7)	2815(1)	3369(1)	3101(1)	21(1)
C(8)	1858(1)	4027(1)	2783(1)	28(1)
C(9)	1921(1)	5267(1)	2881(1)	32(1)
C(10)	2923(1)	5815(1)	3295(1)	31(1)
C(11)	3867(1)	5139(1)	3597(1)	33(1)
C(12)	3821(1)	3899(1)	3496(1)	29(1)
C(13)	4991(1)	-752(1)	3887(1)	23(1)
C(14)	5612(1)	-205(1)	3488(1)	24(1)
C(15)	6699(1)	-496(1)	3721(1)	29(1)
C(16)	7196(1)	-1308(1)	4366(1)	32(1)
C(17)	6588(1)	-1842(1)	4768(1)	32(1)
C(18)	5491(1)	-1581(1)	4529(1)	27(1)
C(19)	1105(1)	-241(1)	2138(1)	22(1)
C(20)	871(1)	-1467(1)	2093(1)	26(1)
C(21)	20(1)	-1941(1)	1406(1)	31(1)
C(22)	-604(1)	-1193(1)	759(1)	35(1)
C(23)	-379(1)	23(1)	794(1)	36(1)
C(24)	474(1)	498(1)	1481(1)	30(1)

C(25)	3292(1)	-303(1)	2076(1)	21(1)
C(26)	3178(1)	435(1)	1392(1)	27(1)
C(27)	3155(1)	-58(1)	642(1)	32(1)
C(28)	3237(1)	-1285(1)	563(1)	32(1)
C(29)	3364(1)	-2024(1)	1242(1)	31(1)
C(30)	3395(1)	-1538(1)	1994(1)	26(1)

Table 3. Bond lengths [Å] and angles [°] for dsm11.

C(1)-C(2)	1.3455(17)	C(10)-C(11)	1.384(2)
C(1)-N(4)	1.3649(15)	C(11)-C(12)	1.3898(18)
C(2)-C(3)	1.4589(17)	C(13)-C(18)	1.3962(17)
C(2)-C(5)	1.5132(16)	C(13)-C(14)	1.3991(17)
C(3)-O(1)	1.2175(15)	C(14)-C(15)	1.3833(17)
C(3)-O(2)	1.3497(15)	C(15)-C(16)	1.386(2)
O(2)-C(4)	1.4436(16)	C(16)-C(17)	1.383(2)
C(5)-N(1)	1.4758(14)	C(17)-C(18)	1.3877(18)
C(5)-C(19)	1.5214(16)	C(19)-C(24)	1.3897(17)
C(5)-C(6)	1.6117(16)	C(19)-C(20)	1.3961(17)
N(1)-N(2)	1.2952(13)	C(20)-C(21)	1.3888(18)
N(2)-N(3)	1.3090(13)	C(21)-C(22)	1.383(2)
N(2)-C(7)	1.4538(14)	C(22)-C(23)	1.383(2)
N(3)-C(6)	1.4711(14)	C(23)-C(24)	1.3909(19)
C(6)-N(4)	1.4894(14)	C(25)-C(26)	1.3929(17)
C(6)-C(25)	1.5186(16)	C(25)-C(30)	1.3941(17)
N(4)-C(13)	1.4125(15)	C(26)-C(27)	1.3915(19)
C(7)-C(12)	1.3804(17)	C(27)-C(28)	1.382(2)
C(7)-C(8)	1.3862(17)	C(28)-C(29)	1.383(2)
C(8)-C(9)	1.3905(18)	C(29)-C(30)	1.3876(19)
C(9)-C(10)	1.389(2)		

C(2)-C(1)-N(4)	114.19(11)	N(1)-C(5)-C(6)	103.31(9)
C(1)-C(2)-C(3)	125.98(11)	C(2)-C(5)-C(6)	102.19(9)
C(1)-C(2)-C(5)	110.19(10)	C(19)-C(5)-C(6)	117.10(9)
C(3)-C(2)-C(5)	123.81(10)	N(2)-N(1)-C(5)	104.50(9)
O(1)-C(3)-O(2)	123.08(11)	N(1)-N(2)-N(3)	124.29(10)
O(1)-C(3)-C(2)	125.17(11)	N(1)-N(2)-C(7)	117.40(9)
O(2)-C(3)-C(2)	111.75(10)	N(3)-N(2)-C(7)	118.31(9)
C(3)-O(2)-C(4)	115.78(10)	N(2)-N(3)-C(6)	104.08(9)
N(1)-C(5)-C(2)	110.93(9)	N(3)-C(6)-N(4)	111.10(9)
N(1)-C(5)-C(19)	109.69(9)	N(3)-C(6)-C(25)	110.80(9)
C(2)-C(5)-C(19)	113.04(9)	N(4)-C(6)-C(25)	112.11(9)

N(3)-C(6)-C(5)	103.79(9)	C(27)-C(28)-C(29)	119.70(12)
N(4)-C(6)-C(5)	103.32(9)	C(28)-C(29)-C(30)	120.21(12)
C(25)-C(6)-C(5)	115.23(9)	C(29)-C(30)-C(25)	120.64(12)
C(1)-N(4)-C(13)	125.63(10)		
C(1)-N(4)-C(6)	109.99(9)		
C(13)-N(4)-C(6)	124.23(10)		
C(12)-C(7)-C(8)	122.64(11)		
C(12)-C(7)-N(2)	119.14(10)		
C(8)-C(7)-N(2)	118.22(10)		
C(7)-C(8)-C(9)	118.22(12)		
C(10)-C(9)-C(8)	120.03(12)		
C(11)-C(10)-C(9)	120.52(12)		
C(10)-C(11)-C(12)	120.23(13)		
C(7)-C(12)-C(11)	118.32(12)		
C(18)-C(13)-C(14)	118.84(11)		
C(18)-C(13)-N(4)	120.64(11)		
C(14)-C(13)-N(4)	120.51(11)		
C(15)-C(14)-C(13)	120.29(12)		
C(14)-C(15)-C(16)	120.71(13)		
C(17)-C(16)-C(15)	119.19(12)		
C(16)-C(17)-C(18)	120.84(12)		
C(17)-C(18)-C(13)	120.10(12)		
C(24)-C(19)-C(20)	118.76(12)		
C(24)-C(19)-C(5)	120.98(11)		
C(20)-C(19)-C(5)	120.26(11)		
C(21)-C(20)-C(19)	120.76(12)		
C(22)-C(21)-C(20)	119.80(13)		
C(23)-C(22)-C(21)	120.06(13)		
C(22)-C(23)-C(24)	120.16(13)		
C(19)-C(24)-C(23)	120.46(13)		
C(26)-C(25)-C(30)	118.71(11)		
C(26)-C(25)-C(6)	120.16(10)		
C(30)-C(25)-C(6)	121.02(10)		
C(27)-C(26)-C(25)	120.34(12)		
C(28)-C(27)-C(26)	120.38(12)		

Table 4. Anisotropic displacement parameters ($Å^2 x\ 10^3$) for dsm11. The anisotropic displacement factor exponent takes the form: $-2\pi^2[\ h^2\ a^{*2}U^{11} + ...\ + 2\ h\ k\ a^*\ b^*\ U^{12}\ ]$

	U^{11}	U^{22}	U^{33}	U^{23}	U^{13}	U^{12}
C(1)	26(1)	17(1)	23(1)	2(1)	8(1)	-1(1)
C(2)	23(1)	17(1)	24(1)	2(1)	8(1)	-1(1)
C(3)	25(1)	21(1)	27(1)	2(1)	9(1)	-2(1)
O(1)	26(1)	36(1)	37(1)	8(1)	13(1)	6(1)
O(2)	29(1)	36(1)	37(1)	15(1)	17(1)	4(1)
C(4)	36(1)	51(1)	47(1)	20(1)	24(1)	3(1)
C(5)	21(1)	16(1)	24(1)	2(1)	8(1)	0(1)
N(1)	21(1)	16(1)	28(1)	2(1)	9(1)	0(1)
N(2)	20(1)	16(1)	23(1)	1(1)	7(1)	1(1)
N(3)	20(1)	17(1)	29(1)	-1(1)	9(1)	1(1)
C(6)	19(1)	17(1)	23(1)	2(1)	6(1)	1(1)
N(4)	21(1)	22(1)	23(1)	4(1)	7(1)	3(1)
C(7)	25(1)	16(1)	24(1)	1(1)	11(1)	0(1)
C(8)	25(1)	21(1)	38(1)	4(1)	14(1)	1(1)
C(9)	34(1)	21(1)	45(1)	6(1)	21(1)	5(1)
C(10)	43(1)	17(1)	37(1)	0(1)	21(1)	-1(1)
C(11)	34(1)	24(1)	38(1)	-4(1)	10(1)	-7(1)
C(12)	26(1)	22(1)	35(1)	0(1)	8(1)	0(1)
C(13)	22(1)	20(1)	23(1)	-3(1)	6(1)	2(1)
C(14)	22(1)	22(1)	26(1)	1(1)	6(1)	1(1)
C(15)	24(1)	30(1)	33(1)	-5(1)	10(1)	-2(1)
C(16)	23(1)	32(1)	36(1)	-6(1)	6(1)	5(1)
C(17)	31(1)	30(1)	29(1)	1(1)	5(1)	9(1)
C(18)	28(1)	25(1)	26(1)	3(1)	8(1)	4(1)
C(19)	19(1)	23(1)	25(1)	0(1)	9(1)	-2(1)
C(20)	24(1)	23(1)	31(1)	-2(1)	12(1)	-1(1)
C(21)	28(1)	30(1)	40(1)	-11(1)	17(1)	-8(1)
C(22)	25(1)	47(1)	32(1)	-11(1)	9(1)	-8(1)
C(23)	29(1)	44(1)	28(1)	2(1)	4(1)	-1(1)
C(24)	27(1)	29(1)	29(1)	4(1)	6(1)	-3(1)

C(25)	17(1)	20(1)	24(1)	1(1)	6(1)	1(1)
C(26)	28(1)	23(1)	28(1)	4(1)	9(1)	4(1)
C(27)	33(1)	37(1)	26(1)	6(1)	10(1)	7(1)
C(28)	29(1)	39(1)	27(1)	-6(1)	8(1)	3(1)
C(29)	31(1)	24(1)	36(1)	-5(1)	11(1)	2(1)
C(30)	26(1)	21(1)	29(1)	2(1)	9(1)	1(1)

Table 5. Hydrogen coordinates (x 10^4) and isotropic displacement parameters ($Å^2$x 10^3) for dsm11.

	x	y	z	U(eq)
H(1)	3509	-1179	4596	27
H(4A)	1186	-2087	5547	63
H(4B)	207	-1837	4664	63
H(4C)	739	-749	5297	63
H(8)	1178	3640	2505	33
H(9)	1279	5740	2664	38
H(10)	2961	6661	3372	37
H(11)	4549	5523	3873	40
H(12)	4465	3429	3695	35
H(14)	5286	368	3055	29
H(15)	7109	-135	3437	35
H(16)	7946	-1496	4529	38
H(17)	6926	-2394	5213	38
H(18)	5079	-1967	4802	32
H(20)	1297	-1982	2537	31
H(21)	-132	-2777	1381	37
H(22)	-1187	-1515	289	42
H(23)	-809	535	349	43
H(24)	625	1334	1501	35
H(26)	3115	1279	1439	32
H(27)	3082	452	180	38
H(28)	3206	-1620	46	39
H(29)	3430	-2867	1192	37
H(30)	3487	-2051	2458	31

A.5.3 5-Methoxycarbonyl-5-(N-phenylimino(ethyl))-2,4,6-triphenyl-2,5-dihydro-1,2,3-triazine.

Table 1. Crystal data and structure refinement for 5-Methoxycarbonyl-5-(N-phenylimino(ethyl))-2,4,6-triphenyl-2,5-dihydro-1,2,3-triazine.

Identification code	triazine_me_coome	
Empirical formula	$C_{31}H_{26}N_4O_2$	
Formula weight	486.56	
Temperature	150.0(1) K	
Wavelength	0.71073 Å	
Crystal system	Monoclinic	
Space group	Cc	
Unit cell dimensions	a = 20.2852(7) Å	α= 90°.
	b = 8.5223(2) Å	β= 111.205(4)°.
	c = 15.7706(5) Å	γ = 90°.
Volume	2541.79(14) $Å^3$	
Z	4	
Density (calculated)	1.271 Mg/m^3	
Absorption coefficient	0.081 mm^{-1}	
F(000)	1024	
Crystal size	0.45 x 0.40 x 0.35 mm^3	
Theta range for data collection	3.142 to 25.350°.	
Index ranges	-24<=h<=23, -6<=k<=10, -18<=l<=18	
Reflections collected	4878	
Independent reflections	3330 [R(int) = 0.0143]	
Completeness to theta = 25.242°	99.7 %	
Absorption correction	Semi-empirical from equivalents	
Max. and min. transmission	1.00000 and 0.99352	
Refinement method	Full-matrix least-squares on F^2	
Data / restraints / parameters	3330 / 2 / 336	
Goodness-of-fit on F^2	1.021	
Final R indices [I>2sigma(I)]	R1 = 0.0294, wR2 = 0.0702	
R indices (all data)	R1 = 0.0319, wR2 = 0.0717	
Absolute structure parameter	1.9(8)	
Extinction coefficient	n/a	
Largest diff. peak and hole	0.146 and -0.174 e.$Å^{-3}$	

Table 2. Atomic coordinates (x 10^4) and equivalent isotropic displacement parameters ($Å^2$x 10^3) for triazine_me_coome. U(eq) is defined as one third of the trace of the orthogonalized U^{ij} tensor.

	x	y	z	U(eq)
N(3)	5403(1)	2775(2)	9680(1)	21(1)
N(2)	5313(1)	3230(2)	8812(1)	23(1)
N(4)	3123(1)	3761(2)	9638(1)	22(1)
N(1)	4684(1)	2978(2)	8103(1)	23(1)
O(1)	3857(1)	6087(2)	8670(1)	35(1)
O(2)	4458(1)	5726(2)	10163(1)	32(1)
C(1)	5929(1)	3118(3)	8570(2)	23(1)
C(2)	5924(1)	3955(3)	7809(2)	28(1)
C(3)	6518(2)	3910(3)	7573(2)	36(1)
C(4)	7107(1)	3054(3)	8080(2)	35(1)
C(5)	7099(1)	2211(3)	8827(2)	32(1)
C(6)	6509(1)	2239(3)	9075(2)	26(1)
C(7)	5403(1)	868(3)	11141(2)	24(1)
C(8)	5536(1)	270(3)	12005(2)	31(1)
C(9)	5213(1)	922(3)	12551(2)	33(1)
C(10)	4758(1)	2180(3)	12244(2)	32(1)
C(11)	4625(1)	2791(3)	11381(2)	26(1)
C(12)	4952(1)	2145(3)	10821(2)	22(1)
C(13)	4852(1)	2780(3)	9905(2)	20(1)
C(14)	4150(1)	3434(3)	9251(2)	21(1)
C(15)	4121(1)	2971(3)	8303(1)	22(1)
C(16)	3457(1)	2467(3)	7576(2)	24(1)
C(17)	2815(1)	3226(3)	7425(2)	28(1)
C(18)	2202(1)	2682(4)	6763(2)	35(1)
C(19)	2214(1)	1382(4)	6248(2)	36(1)
C(20)	2844(2)	620(4)	6388(2)	38(1)
C(21)	3464(1)	1167(3)	7045(2)	32(1)
C(22)	4130(1)	5241(3)	9310(2)	24(1)
C(23)	4379(2)	7373(3)	10330(2)	47(1)
C(24)	3517(1)	2770(3)	9454(1)	21(1)

C(25)	3447(1)	1011(3)	9429(2)	25(1)
C(26)	2525(1)	3282(3)	9844(2)	24(1)
C(27)	1961(1)	2457(3)	9238(2)	28(1)
C(28)	1382(1)	2094(3)	9470(2)	33(1)
C(29)	1362(2)	2549(3)	10301(2)	34(1)
C(30)	1916(1)	3396(3)	10893(2)	34(1)
C(31)	2493(1)	3782(3)	10666(2)	29(1)

Table 3. Bond lengths [Å] and angles [°] for triazine_me_coome.

N(3)-C(13)	1.288(3)
N(3)-N(2)	1.370(3)
N(2)-N(1)	1.376(3)
N(2)-C(1)	1.436(3)
N(4)-C(24)	1.267(3)
N(4)-C(26)	1.424(3)
N(1)-C(15)	1.290(3)
O(1)-C(22)	1.200(3)
O(2)-C(22)	1.333(3)
O(2)-C(23)	1.447(3)
C(1)-C(6)	1.380(3)
C(1)-C(2)	1.393(3)
C(2)-C(3)	1.383(3)
C(2)-H(2)	0.9300
C(3)-C(4)	1.382(4)
C(3)-H(3)	0.9300
C(4)-C(5)	1.384(4)
C(4)-H(4)	0.9300
C(5)-C(6)	1.387(3)
C(5)-H(5)	0.9300
C(6)-H(6)	0.9300
C(7)-C(8)	1.386(3)
C(7)-C(12)	1.393(3)
C(7)-H(7)	0.9300
C(8)-C(9)	1.376(4)
C(8)-H(8)	0.9300
C(9)-C(10)	1.383(4)
C(9)-H(9)	0.9300
C(10)-C(11)	1.389(3)
C(10)-H(10)	0.9300
C(11)-C(12)	1.396(3)
C(11)-H(11)	0.9300
C(12)-C(13)	1.487(3)

C(13)-C(14)	1.530(3)
C(14)-C(15)	1.526(3)
C(14)-C(24)	1.538(3)
C(14)-C(22)	1.544(3)
C(15)-C(16)	1.482(3)
C(16)-C(21)	1.392(4)
C(16)-C(17)	1.395(3)
C(17)-C(18)	1.383(4)
C(17)-H(17)	0.9300
C(18)-C(19)	1.379(4)
C(18)-H(18)	0.9300
C(19)-C(20)	1.379(4)
C(19)-H(19)	0.9300
C(20)-C(21)	1.389(4)
C(20)-H(20)	0.9300
C(21)-H(21)	0.9300
C(23)-H(23A)	0.9600
C(23)-H(23B)	0.9600
C(23)-H(23C)	0.9600
C(24)-C(25)	1.505(3)
C(25)-H(25A)	0.9600
C(25)-H(25B)	0.9600
C(25)-H(25C)	0.9600
C(26)-C(27)	1.388(4)
C(26)-C(31)	1.389(3)
C(27)-C(28)	1.386(3)
C(27)-H(27)	0.9300
C(28)-C(29)	1.381(4)
C(28)-H(28)	0.9300
C(29)-C(30)	1.378(4)
C(29)-H(29)	0.9300
C(30)-C(31)	1.382(4)
C(30)-H(30)	0.9300
C(31)-H(31)	0.9300

C(13)-N(3)-N(2)	117.30(19)
N(3)-N(2)-N(1)	121.12(17)
N(3)-N(2)-C(1)	115.65(18)
N(1)-N(2)-C(1)	114.46(17)
C(24)-N(4)-C(26)	121.4(2)
C(15)-N(1)-N(2)	116.42(18)
C(22)-O(2)-C(23)	115.9(2)
C(6)-C(1)-C(2)	120.9(2)
C(6)-C(1)-N(2)	121.7(2)
C(2)-C(1)-N(2)	117.4(2)
C(3)-C(2)-C(1)	118.9(2)
C(3)-C(2)-H(2)	120.6
C(1)-C(2)-H(2)	120.6
C(4)-C(3)-C(2)	120.9(2)
C(4)-C(3)-H(3)	119.6
C(2)-C(3)-H(3)	119.6
C(3)-C(4)-C(5)	119.6(2)
C(3)-C(4)-H(4)	120.2
C(5)-C(4)-H(4)	120.2
C(4)-C(5)-C(6)	120.5(2)
C(4)-C(5)-H(5)	119.8
C(6)-C(5)-H(5)	119.8
C(1)-C(6)-C(5)	119.3(2)
C(1)-C(6)-H(6)	120.4
C(5)-C(6)-H(6)	120.4
C(8)-C(7)-C(12)	120.9(2)
C(8)-C(7)-H(7)	119.6
C(12)-C(7)-H(7)	119.6
C(9)-C(8)-C(7)	119.9(2)
C(9)-C(8)-H(8)	120.0
C(7)-C(8)-H(8)	120.0
C(8)-C(9)-C(10)	120.2(2)
C(8)-C(9)-H(9)	119.9
C(10)-C(9)-H(9)	119.9
C(9)-C(10)-C(11)	120.2(2)

C(9)-C(10)-H(10)	119.9
C(11)-C(10)-H(10)	119.9
C(10)-C(11)-C(12)	120.2(2)
C(10)-C(11)-H(11)	119.9
C(12)-C(11)-H(11)	119.9
C(7)-C(12)-C(11)	118.6(2)
C(7)-C(12)-C(13)	118.6(2)
C(11)-C(12)-C(13)	122.9(2)
N(3)-C(13)-C(12)	116.1(2)
N(3)-C(13)-C(14)	120.34(19)
C(12)-C(13)-C(14)	123.60(18)
C(15)-C(14)-C(13)	105.17(17)
C(15)-C(14)-C(24)	111.63(19)
C(13)-C(14)-C(24)	111.74(18)
C(15)-C(14)-C(22)	108.91(18)
C(13)-C(14)-C(22)	111.1(2)
C(24)-C(14)-C(22)	108.24(18)
N(1)-C(15)-C(16)	116.7(2)
N(1)-C(15)-C(14)	121.0(2)
C(16)-C(15)-C(14)	122.34(19)
C(21)-C(16)-C(17)	118.5(2)
C(21)-C(16)-C(15)	119.5(2)
C(17)-C(16)-C(15)	121.9(2)
C(18)-C(17)-C(16)	120.2(3)
C(18)-C(17)-H(17)	119.9
C(16)-C(17)-H(17)	119.9
C(19)-C(18)-C(17)	120.8(3)
C(19)-C(18)-H(18)	119.6
C(17)-C(18)-H(18)	119.6
C(18)-C(19)-C(20)	119.8(2)
C(18)-C(19)-H(19)	120.1
C(20)-C(19)-H(19)	120.1
C(19)-C(20)-C(21)	119.9(3)
C(19)-C(20)-H(20)	120.1
C(21)-C(20)-H(20)	120.1

C(20)-C(21)-C(16)	120.8(2)
C(20)-C(21)-H(21)	119.6
C(16)-C(21)-H(21)	119.6
O(1)-C(22)-O(2)	124.9(2)
O(1)-C(22)-C(14)	124.2(2)
O(2)-C(22)-C(14)	110.8(2)
O(2)-C(23)-H(23A)	109.5
O(2)-C(23)-H(23B)	109.5
H(23A)-C(23)-H(23B)	109.5
O(2)-C(23)-H(23C)	109.5
H(23A)-C(23)-H(23C)	109.5
H(23B)-C(23)-H(23C)	109.5
N(4)-C(24)-C(25)	127.5(2)
N(4)-C(24)-C(14)	116.5(2)
C(25)-C(24)-C(14)	116.03(19)
C(24)-C(25)-H(25A)	109.5
C(24)-C(25)-H(25B)	109.5
H(25A)-C(25)-H(25B)	109.5
C(24)-C(25)-H(25C)	109.5
H(25A)-C(25)-H(25C)	109.5
H(25B)-C(25)-H(25C)	109.5
C(27)-C(26)-C(31)	119.5(2)
C(27)-C(26)-N(4)	123.2(2)
C(31)-C(26)-N(4)	117.1(2)
C(28)-C(27)-C(26)	119.8(2)
C(28)-C(27)-H(27)	120.1
C(26)-C(27)-H(27)	120.1
C(29)-C(28)-C(27)	120.5(3)
C(29)-C(28)-H(28)	119.8
C(27)-C(28)-H(28)	119.8
C(30)-C(29)-C(28)	119.6(2)
C(30)-C(29)-H(29)	120.2
C(28)-C(29)-H(29)	120.2
C(29)-C(30)-C(31)	120.6(2)
C(29)-C(30)-H(30)	119.7

C(31)-C(30)-H(30)	119.7
C(30)-C(31)-C(26)	120.0(2)
C(30)-C(31)-H(31)	120.0
C(26)-C(31)-H(31)	120.0

Table 4. Anisotropic displacement parameters ($Å^2 x\ 10^3$) for triazine_me_coome. The anisotropic displacement factor exponent takes the form: $-2\pi^2[\ h^2\ a^{*2}U^{11} + ...\ + 2\ h\ k\ a^*\ b^*\ U^{12}\ ]$

	U^{11}	U^{22}	U^{33}	U^{23}	U^{13}	U^{12}
N(3)	22(1)	22(1)	21(1)	0(1)	9(1)	1(1)
N(2)	21(1)	31(1)	20(1)	3(1)	9(1)	1(1)
N(4)	21(1)	24(1)	23(1)	-1(1)	10(1)	2(1)
N(1)	21(1)	25(1)	21(1)	1(1)	7(1)	3(1)
O(1)	40(1)	25(1)	42(1)	10(1)	15(1)	6(1)
O(2)	33(1)	20(1)	39(1)	-5(1)	10(1)	0(1)
C(1)	22(1)	23(1)	26(1)	-7(1)	12(1)	-4(1)
C(2)	29(1)	25(1)	31(1)	0(1)	14(1)	-1(1)
C(3)	44(2)	36(2)	36(1)	-3(1)	25(1)	-11(1)
C(4)	28(1)	43(2)	42(2)	-14(1)	21(1)	-11(1)
C(5)	22(1)	39(2)	37(1)	-10(1)	11(1)	1(1)
C(6)	24(1)	31(1)	24(1)	-4(1)	9(1)	-2(1)
C(7)	20(1)	25(1)	27(1)	1(1)	8(1)	-2(1)
C(8)	26(1)	29(1)	35(1)	6(1)	8(1)	-3(1)
C(9)	35(1)	38(2)	23(1)	4(1)	7(1)	-12(1)
C(10)	36(2)	40(2)	25(1)	-6(1)	15(1)	-8(1)
C(11)	25(1)	28(1)	25(1)	-4(1)	9(1)	-2(1)
C(12)	18(1)	24(1)	22(1)	-1(1)	6(1)	-3(1)
C(13)	20(1)	19(1)	23(1)	-2(1)	9(1)	0(1)
C(14)	22(1)	19(1)	23(1)	1(1)	9(1)	2(1)
C(15)	22(1)	22(1)	22(1)	4(1)	9(1)	6(1)
C(16)	22(1)	31(1)	21(1)	5(1)	8(1)	1(1)
C(17)	25(1)	33(1)	27(1)	8(1)	10(1)	4(1)
C(18)	23(1)	44(2)	34(1)	17(1)	8(1)	2(1)
C(19)	30(2)	51(2)	24(1)	9(1)	3(1)	-14(1)
C(20)	40(2)	47(2)	28(1)	-8(1)	13(1)	-9(1)
C(21)	28(1)	42(2)	30(1)	-3(1)	15(1)	1(1)
C(22)	19(1)	23(1)	33(1)	2(1)	12(1)	-1(1)
C(23)	47(2)	23(1)	66(2)	-14(1)	13(2)	0(1)
C(24)	21(1)	22(1)	19(1)	1(1)	6(1)	2(1)

C(25)	24(1)	21(1)	32(1)	0(1)	11(1)	1(1)
C(26)	23(1)	21(1)	30(1)	4(1)	13(1)	6(1)
C(27)	25(1)	33(1)	29(1)	-3(1)	12(1)	2(1)
C(28)	23(1)	32(1)	42(2)	0(1)	10(1)	1(1)
C(29)	30(2)	29(1)	51(2)	7(1)	24(1)	4(1)
C(30)	38(2)	36(2)	34(1)	1(1)	22(1)	6(1)
C(31)	30(1)	28(1)	32(1)	-4(1)	13(1)	2(1)

Table 5. Hydrogen coordinates (x 10^4) and isotropic displacement parameters ($Å^2$x 10^{3}) for triazine_me_coome.

	x	y	z	U(eq)
H(2)	5529	4535	7466	36
H(3)	6520	4463	7065	46
H(4)	7506	3045	7922	46
H(5)	7492	1622	9164	42
H(6)	6505	1671	9576	34
H(7)	5616	410	10771	32
H(8)	5845	-571	12215	41
H(9)	5300	515	13129	43
H(10)	4541	2619	12616	42
H(11)	4316	3633	11175	34
H(17)	2799	4101	7769	37
H(18)	1777	3199	6664	45
H(19)	1798	1019	5808	48
H(20)	2854	-259	6044	49
H(21)	3889	659	7130	42
H(23A)	3887	7617	10168	61
H(23B)	4574	7996	9971	61
H(23C)	4625	7598	10963	61
H(25A)	3052	707	8900	33
H(25B)	3374	657	9966	33
H(25C)	3871	548	9404	33
H(27)	1971	2150	8677	37
H(28)	1005	1540	9064	43
H(29)	977	2285	10460	44
H(30)	1902	3711	11451	44
H(31)	2859	4376	11063	38

A.5.4 5-Methoxycarbonyl-5-(2-methoxy-2-oxo-1-(phenylimino(ethyl)))-2,4,6-triphenyl-2,5-dihydro-1,2,3-triazine.

Table 1. Crystal data and structure refinement for 5-Methoxycarbonyl-5-(2-methoxy-2-oxo-1-(phenylimino(ethyl)))-2,4,6-triphenyl-2,5-dihydro-1,2,3-triazine.

Identification code	triazine_2_coome	
Empirical formula	$C_{32}H_{26}N_4O_4$	
Formula weight	530.57	
Temperature	150.1(1) K	
Wavelength	0.71073 Å	
Crystal system	Monoclinic	
Space group	$P2_1/c$	
Unit cell dimensions	a = 10.8071(4) Å	α= 90°.
	b = 29.5422(8) Å	β= 114.159(4)°.
	c = 9.1786(3) Å	γ = 90°.
Volume	2673.73(17) $Å^3$	
Z	4	
Density (calculated)	1.318 Mg/m^3	
Absorption coefficient	0.089 mm^{-1}	
F(000)	1112	
Crystal size	0.40 x 0.30 x 0.30 mm^3	
Theta range for data collection	2.923 to 29.218°.	
Index ranges	-14<=h<=7, -38<=k<=39, -11<=l<=12	
Reflections collected	12187	
Independent reflections	6190 [R(int) = 0.0243]	
Completeness to theta = 25.242°	99.8 %	
Absorption correction	Semi-empirical from equivalents	
Max. and min. transmission	1.00000 and 0.97027	
Refinement method	Full-matrix least-squares on F^2	
Data / restraints / parameters	6190 / 0 / 363	
Goodness-of-fit on F^2	1.043	
Final R indices [I>2sigma(I)]	R1 = 0.0539, wR2 = 0.1142	
R indices (all data)	R1 = 0.0756, wR2 = 0.1261	
Extinction coefficient	n/a	
Largest diff. peak and hole	0.681 and -0.360 $e.Å^{-3}$	

Table 2. Atomic coordinates (x 10^4) and equivalent isotropic displacement parameters ($Å^2$x 10^3) for triazine_2_coome. U(eq) is defined as one third of the trace of the orthogonalized U^{ij} tensor.

	x	y	z	U(eq)
O(1)	2348(1)	1800(1)	8835(2)	29(1)
N(1)	-453(2)	1312(1)	6664(2)	20(1)
O(2)	3757(1)	1208(1)	9306(1)	25(1)
O(3)	837(1)	893(1)	3620(2)	32(1)
N(3)	729(2)	616(1)	7625(2)	21(1)
N(2)	-79(2)	959(1)	7741(2)	22(1)
N(4)	3457(2)	1613(1)	6121(2)	20(1)
O(4)	2784(2)	1041(1)	3390(2)	39(1)
C(1)	-1031(2)	851(1)	8398(2)	22(1)
C(2)	-1795(2)	1197(1)	8640(2)	31(1)
C(3)	-2684(2)	1100(1)	9340(3)	34(1)
C(4)	-2785(2)	670(1)	9845(2)	32(1)
C(5)	-1997(2)	331(1)	9637(3)	34(1)
C(6)	-1133(2)	417(1)	8895(2)	31(1)
C(7)	1785(2)	-79(1)	6320(2)	25(1)
C(8)	2477(2)	-430(1)	5990(2)	31(1)
C(9)	3794(2)	-366(1)	6127(2)	33(1)
C(10)	4420(2)	46(1)	6625(2)	30(1)
C(11)	3731(2)	401(1)	6953(2)	24(1)
C(12)	2396(2)	344(1)	6783(2)	20(1)
C(13)	1614(2)	720(1)	7070(2)	18(1)
C(14)	1835(2)	1219(1)	6799(2)	17(1)
C(15)	417(2)	1429(1)	6116(2)	19(1)
C(16)	-13(2)	1796(1)	4890(2)	21(1)
C(17)	571(2)	2222(1)	5278(3)	28(1)
C(18)	79(2)	2578(1)	4202(3)	35(1)
C(19)	-967(2)	2506(1)	2731(3)	37(1)
C(20)	-1531(2)	2081(1)	2323(3)	38(1)
C(21)	-1056(2)	1725(1)	3398(2)	30(1)
C(22)	2666(2)	1450(1)	8426(2)	20(1)

C(23)	4621(2)	1421(1)	10807(2)	33(1)
C(24)	2541(2)	1315(1)	5689(2)	17(1)
C(25)	1931(2)	1064(1)	4103(2)	22(1)
C(26)	2258(3)	794(1)	1894(3)	66(1)
C(27)	4153(2)	1784(1)	5210(2)	19(1)
C(28)	5389(2)	1601(1)	5404(2)	28(1)
C(29)	6146(2)	1806(1)	4683(2)	32(1)
C(30)	5680(2)	2192(1)	3779(2)	32(1)
C(31)	4451(2)	2371(1)	3587(3)	38(1)
C(32)	3684(2)	2171(1)	4313(3)	32(1)

Table 3. Bond lengths [Å] and angles [°] for triazine_2_coome.

O(1)-C(22)	1.196(2)
N(1)-C(15)	1.283(2)
N(1)-N(2)	1.3793(19)
O(2)-C(22)	1.333(2)
O(2)-C(23)	1.454(2)
O(3)-C(25)	1.192(2)
N(3)-C(13)	1.291(2)
N(3)-N(2)	1.370(2)
N(2)-C(1)	1.425(2)
N(4)-C(24)	1.262(2)
N(4)-C(27)	1.426(2)
O(4)-C(25)	1.333(2)
O(4)-C(26)	1.449(3)
C(1)-C(6)	1.380(3)
C(1)-C(2)	1.388(3)
C(2)-C(3)	1.387(3)
C(2)-H(2)	0.9300
C(3)-C(4)	1.371(3)
C(3)-H(3)	0.9300
C(4)-C(5)	1.379(3)
C(4)-H(4)	0.9300
C(5)-C(6)	1.386(3)
C(5)-H(5)	0.9300
C(6)-H(6)	0.9300
C(7)-C(8)	1.381(3)
C(7)-C(12)	1.397(2)
C(7)-H(7)	0.9300
C(8)-C(9)	1.389(3)
C(8)-H(8)	0.9300
C(9)-C(10)	1.377(3)
C(9)-H(9)	0.9300
C(10)-C(11)	1.389(3)
C(10)-H(10)	0.9300

C(11)-C(12)	1.396(3)
C(11)-H(11)	0.9300
C(12)-C(13)	1.483(2)
C(13)-C(14)	1.529(2)
C(14)-C(24)	1.529(2)
C(14)-C(15)	1.530(2)
C(14)-C(22)	1.551(2)
C(15)-C(16)	1.493(2)
C(16)-C(21)	1.388(3)
C(16)-C(17)	1.389(3)
C(17)-C(18)	1.390(3)
C(17)-H(17)	0.9300
C(18)-C(19)	1.378(3)
C(18)-H(18)	0.9300
C(19)-C(20)	1.379(3)
C(19)-H(19)	0.9300
C(20)-C(21)	1.388(3)
C(20)-H(20)	0.9300
C(21)-H(21)	0.9300
C(23)-H(23A)	0.9600
C(23)-H(23B)	0.9600
C(23)-H(23C)	0.9600
C(24)-C(25)	1.522(2)
C(26)-H(26A)	0.9600
C(26)-H(26B)	0.9600
C(26)-H(26C)	0.9600
C(27)-C(32)	1.380(3)
C(27)-C(28)	1.383(3)
C(28)-C(29)	1.385(3)
C(28)-H(28)	0.9300
C(29)-C(30)	1.379(3)
C(29)-H(29)	0.9300
C(30)-C(31)	1.372(3)
C(30)-H(30)	0.9300
C(31)-C(32)	1.389(3)

C(31)-H(31)	0.9300
C(32)-H(32)	0.9300
C(15)-N(1)-N(2)	115.97(14)
C(22)-O(2)-C(23)	114.01(14)
C(13)-N(3)-N(2)	116.95(14)
N(3)-N(2)-N(1)	120.90(13)
N(3)-N(2)-C(1)	117.44(14)
N(1)-N(2)-C(1)	114.97(14)
C(24)-N(4)-C(27)	126.63(15)
C(25)-O(4)-C(26)	114.11(16)
C(6)-C(1)-C(2)	119.87(17)
C(6)-C(1)-N(2)	121.12(16)
C(2)-C(1)-N(2)	118.86(16)
C(3)-C(2)-C(1)	119.51(19)
C(3)-C(2)-H(2)	120.2
C(1)-C(2)-H(2)	120.2
C(4)-C(3)-C(2)	120.91(19)
C(4)-C(3)-H(3)	119.5
C(2)-C(3)-H(3)	119.5
C(3)-C(4)-C(5)	119.19(18)
C(3)-C(4)-H(4)	120.4
C(5)-C(4)-H(4)	120.4
C(4)-C(5)-C(6)	120.84(19)
C(4)-C(5)-H(5)	119.6
C(6)-C(5)-H(5)	119.6
C(1)-C(6)-C(5)	119.64(19)
C(1)-C(6)-H(6)	120.2
C(5)-C(6)-H(6)	120.2
C(8)-C(7)-C(12)	120.43(18)
C(8)-C(7)-H(7)	119.8
C(12)-C(7)-H(7)	119.8
C(7)-C(8)-C(9)	120.41(18)
C(7)-C(8)-H(8)	119.8
C(9)-C(8)-H(8)	119.8

C(10)-C(9)-C(8)	119.67(18)
C(10)-C(9)-H(9)	120.2
C(8)-C(9)-H(9)	120.2
C(9)-C(10)-C(11)	120.38(19)
C(9)-C(10)-H(10)	119.8
C(11)-C(10)-H(10)	119.8
C(10)-C(11)-C(12)	120.40(18)
C(10)-C(11)-H(11)	119.8
C(12)-C(11)-H(11)	119.8
C(11)-C(12)-C(7)	118.67(17)
C(11)-C(12)-C(13)	121.88(16)
C(7)-C(12)-C(13)	119.45(16)
N(3)-C(13)-C(12)	117.40(15)
N(3)-C(13)-C(14)	118.93(15)
C(12)-C(13)-C(14)	123.63(15)
C(24)-C(14)-C(13)	116.19(14)
C(24)-C(14)-C(15)	109.89(13)
C(13)-C(14)-C(15)	105.12(13)
C(24)-C(14)-C(22)	108.01(13)
C(13)-C(14)-C(22)	109.66(13)
C(15)-C(14)-C(22)	107.68(13)
N(1)-C(15)-C(16)	116.02(15)
N(1)-C(15)-C(14)	120.13(15)
C(16)-C(15)-C(14)	123.71(14)
C(21)-C(16)-C(17)	119.33(17)
C(21)-C(16)-C(15)	120.73(16)
C(17)-C(16)-C(15)	119.79(17)
C(16)-C(17)-C(18)	120.12(19)
C(16)-C(17)-H(17)	119.9
C(18)-C(17)-H(17)	119.9
C(19)-C(18)-C(17)	120.1(2)
C(19)-C(18)-H(18)	120.0
C(17)-C(18)-H(18)	120.0
C(18)-C(19)-C(20)	120.11(19)
C(18)-C(19)-H(19)	119.9

C(20)-C(19)-H(19)	119.9
C(19)-C(20)-C(21)	120.1(2)
C(19)-C(20)-H(20)	119.9
C(21)-C(20)-H(20)	119.9
C(20)-C(21)-C(16)	120.18(19)
C(20)-C(21)-H(21)	119.9
C(16)-C(21)-H(21)	119.9
O(1)-C(22)-O(2)	124.80(17)
O(1)-C(22)-C(14)	123.73(16)
O(2)-C(22)-C(14)	111.46(14)
O(2)-C(23)-H(23A)	109.5
O(2)-C(23)-H(23B)	109.5
H(23A)-C(23)-H(23B)	109.5
O(2)-C(23)-H(23C)	109.5
H(23A)-C(23)-H(23C)	109.5
H(23B)-C(23)-H(23C)	109.5
N(4)-C(24)-C(25)	128.14(15)
N(4)-C(24)-C(14)	117.50(15)
C(25)-C(24)-C(14)	114.06(14)
O(3)-C(25)-O(4)	125.18(17)
O(3)-C(25)-C(24)	122.51(16)
O(4)-C(25)-C(24)	112.22(15)
O(4)-C(26)-H(26A)	109.5
O(4)-C(26)-H(26B)	109.5
H(26A)-C(26)-H(26B)	109.5
O(4)-C(26)-H(26C)	109.5
H(26A)-C(26)-H(26C)	109.5
H(26B)-C(26)-H(26C)	109.5
C(32)-C(27)-C(28)	120.04(17)
C(32)-C(27)-N(4)	119.32(16)
C(28)-C(27)-N(4)	119.99(16)
C(27)-C(28)-C(29)	119.71(18)
C(27)-C(28)-H(28)	120.1
C(29)-C(28)-H(28)	120.1
C(30)-C(29)-C(28)	120.51(19)

C(30)-C(29)-H(29)	119.7
C(28)-C(29)-H(29)	119.7
C(31)-C(30)-C(29)	119.44(18)
C(31)-C(30)-H(30)	120.3
C(29)-C(30)-H(30)	120.3
C(30)-C(31)-C(32)	120.76(19)
C(30)-C(31)-H(31)	119.6
C(32)-C(31)-H(31)	119.6
C(27)-C(32)-C(31)	119.52(18)
C(27)-C(32)-H(32)	120.2
C(31)-C(32)-H(32)	120.2

Table 4. Anisotropic displacement parameters ($Å^2 x\ 10^3$) for triazine_2_coome. The anisotropic displacement factor exponent takes the form: $-2\pi^2[\ h^2\ a^{*2}U^{11} + ... + 2\ h\ k\ a^*\ b^*\ U^{12}\ ]$

	U^{11}	U^{22}	U^{33}	U^{23}	U^{13}	U^{12}
O(1)	32(1)	26(1)	31(1)	-8(1)	13(1)	2(1)
N(1)	21(1)	18(1)	22(1)	5(1)	9(1)	2(1)
O(2)	25(1)	27(1)	20(1)	-3(1)	5(1)	3(1)
O(3)	26(1)	39(1)	30(1)	-10(1)	11(1)	-9(1)
N(3)	20(1)	19(1)	24(1)	4(1)	9(1)	4(1)
N(2)	21(1)	20(1)	27(1)	8(1)	14(1)	4(1)
N(4)	21(1)	18(1)	22(1)	-1(1)	11(1)	-1(1)
O(4)	45(1)	50(1)	32(1)	-19(1)	25(1)	-23(1)
C(1)	19(1)	27(1)	20(1)	5(1)	8(1)	0(1)
C(2)	34(1)	28(1)	38(1)	5(1)	23(1)	2(1)
C(3)	37(1)	36(1)	38(1)	3(1)	24(1)	6(1)
C(4)	28(1)	44(1)	28(1)	6(1)	18(1)	0(1)
C(5)	37(1)	30(1)	42(1)	12(1)	23(1)	2(1)
C(6)	32(1)	26(1)	40(1)	10(1)	21(1)	5(1)
C(7)	26(1)	21(1)	26(1)	3(1)	7(1)	-1(1)
C(8)	41(1)	18(1)	28(1)	-2(1)	9(1)	1(1)
C(9)	43(1)	26(1)	33(1)	-2(1)	18(1)	11(1)
C(10)	29(1)	29(1)	34(1)	2(1)	16(1)	7(1)
C(11)	25(1)	19(1)	28(1)	1(1)	12(1)	1(1)
C(12)	22(1)	18(1)	19(1)	2(1)	7(1)	1(1)
C(13)	18(1)	17(1)	19(1)	3(1)	6(1)	0(1)
C(14)	19(1)	16(1)	19(1)	1(1)	10(1)	0(1)
C(15)	19(1)	17(1)	22(1)	-1(1)	9(1)	0(1)
C(16)	19(1)	21(1)	26(1)	6(1)	14(1)	4(1)
C(17)	25(1)	22(1)	40(1)	4(1)	16(1)	1(1)
C(18)	34(1)	24(1)	55(1)	11(1)	28(1)	2(1)
C(19)	40(1)	35(1)	48(1)	24(1)	29(1)	15(1)
C(20)	39(1)	43(1)	31(1)	14(1)	12(1)	9(1)
C(21)	30(1)	28(1)	29(1)	6(1)	10(1)	1(1)
C(22)	21(1)	22(1)	21(1)	0(1)	13(1)	-3(1)

C(23)	29(1)	42(1)	23(1)	-6(1)	5(1)	-1(1)
C(24)	19(1)	16(1)	18(1)	2(1)	8(1)	3(1)
C(25)	23(1)	21(1)	20(1)	1(1)	8(1)	-1(1)
C(26)	74(2)	93(2)	46(2)	-44(2)	38(2)	-42(2)
C(27)	21(1)	19(1)	20(1)	-4(1)	10(1)	-6(1)
C(28)	24(1)	32(1)	28(1)	2(1)	11(1)	1(1)
C(29)	21(1)	46(1)	33(1)	-5(1)	15(1)	-4(1)
C(30)	38(1)	32(1)	35(1)	-6(1)	25(1)	-13(1)
C(31)	55(1)	27(1)	42(1)	8(1)	33(1)	3(1)
C(32)	34(1)	30(1)	41(1)	9(1)	25(1)	9(1)

Table 5. Hydrogen coordinates (x 10^4) and isotropic displacement parameters ($Å^2$x 10^{3}) for triazine_2_coome.

	x	y	z	U(eq)
H(2)	-1711	1492	8334	40
H(3)	-3219	1330	9470	44
H(4)	-3378	609	10321	41
H(5)	-2046	40	9998	44
H(6)	-625	184	8733	40
H(7)	906	-126	6233	33
H(8)	2059	-710	5673	40
H(9)	4251	-601	5885	43
H(10)	5309	87	6741	39
H(11)	4161	678	7288	31
H(17)	1293	2270	6260	37
H(18)	457	2865	4475	45
H(19)	-1294	2744	2012	48
H(20)	-2231	2032	1325	50
H(21)	-1439	1439	3118	39
H(23A)	4960	1702	10596	43
H(23B)	5368	1224	11390	43
H(23C)	4106	1476	11428	43
H(26A)	1926	505	2048	86
H(26B)	2967	752	1533	86
H(26C)	1531	963	1109	86
H(28)	5710	1341	6016	36
H(29)	6976	1682	4810	41
H(30)	6194	2330	3302	41
H(31)	4128	2628	2965	49
H(32)	2860	2298	4195	41

A.6 COMPUTATION.

In all cases for the computation study, the HOMO is symmetric and concentrated over the triphenyl triazine π system, while the HOMO-1 is asymmetric and concentrated on the phenylimine. The LUMO is asymmetric and concentrated on the triazine-ester-imine, while the LUMO+1 is also asymmetric but more concentrated on the imine π systems.

For N=C-H triazine (Figure A.6.1 and A.6.2), the **g0** and **g1** structures resemble **g2**, due to the resemblance of the two highest occupied (HOMO and HOMO-1) and two lowest unoccupied molecular orbitals (LUMO and LUMO+1).

Figure A.6.1 shows the HOMO for **g0** is concentrated on the N-2 phenyl ring of the triazine for N=C-H. The larger shift of electron density out of the triazine π system onto the imine C=N in the LUMO+1 (S_2) compared to the LUMO (S_1) is an indication of the higher dipole moment of S_2 compared to S_1.

In N=C-CH_3 triazine (Figure A.6.3), the different S_0 (**g0**) geometry leads to a vertical transition to S_1 (**g0**) through S_3 (**g0**). However for N=C-CH_3 triazine, S_0 (**g0**) does not necessarily have similar covalent/zwitterionic properties as in S_2 (**g2**) or S_1 (**g1**).

For both N=C-H and N=C-CH_3 triazine, the S_1 (**g1**) state structurally resembles the S_2 (**g2**) and leads to similar dipole moments for S_1 (**g1**) and S_2 (**g2**).

S_1 (**g2**) and S_2 (**g2**) are both asymmetric A" states, and S_3 (**g2**) is symmetric'. The imine and ester combine symmetrically and anti-symmetrically to form a covalent and zwitterionic pair within each symmetric and asymmetric ES. Thus, S_1 (**g2**) is asymmetric and covalent, having a dipole moment not very different from the S_0 (**g2**).

However, the S_2 states (**g0**, **g1**, **g2**) are asymmetric zwitterionic with large dipole moments, *ca.* 12 D, showing charge transfer from the triazine to the phenylimine group.

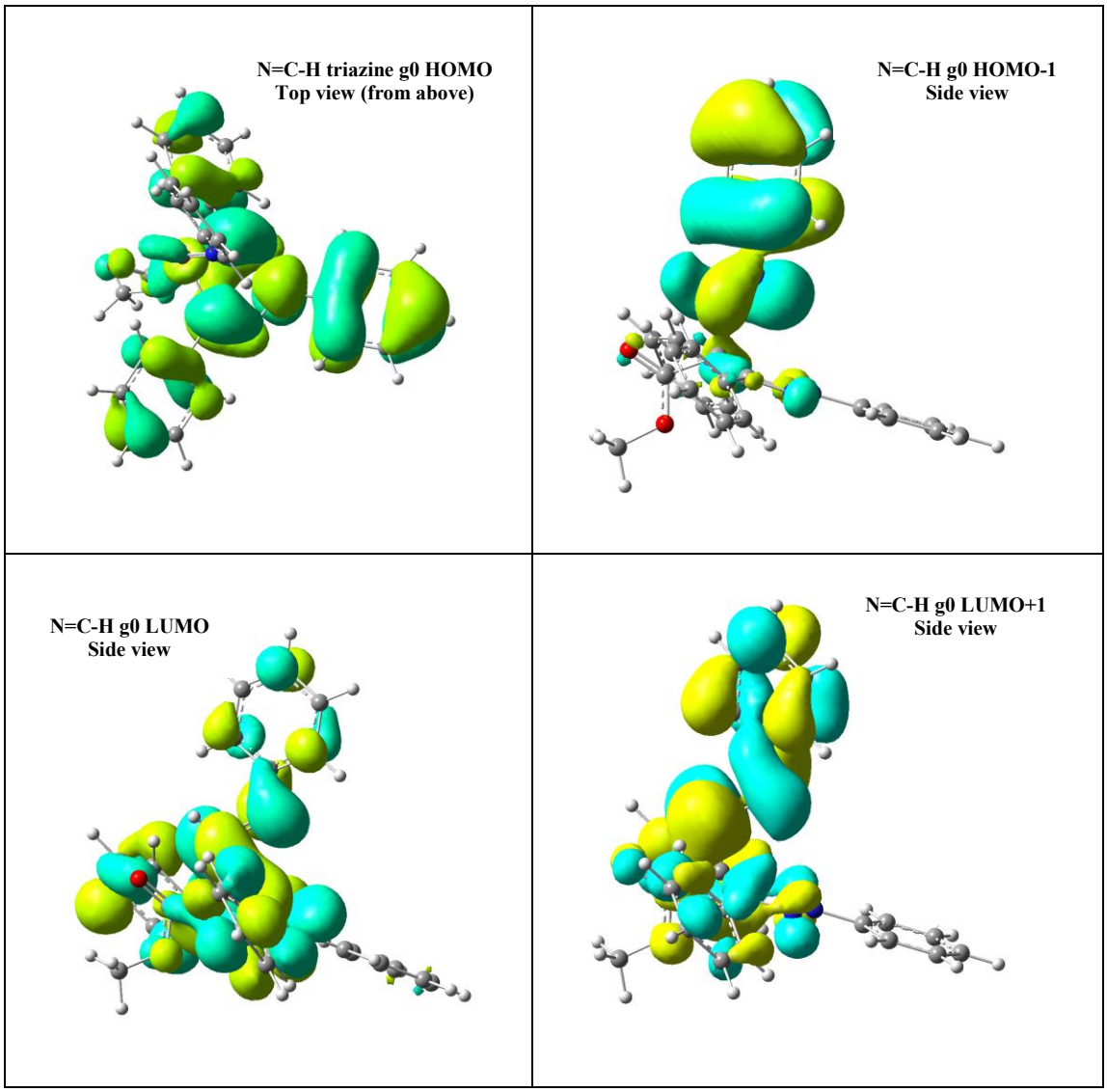

Figure A.6.1. MO plots of the structures of N=C-H triazine for the **g0** geometry (i.e., optimized for S_0) showing the HOMO, HOMO-1, LUMO and LUMO+1.

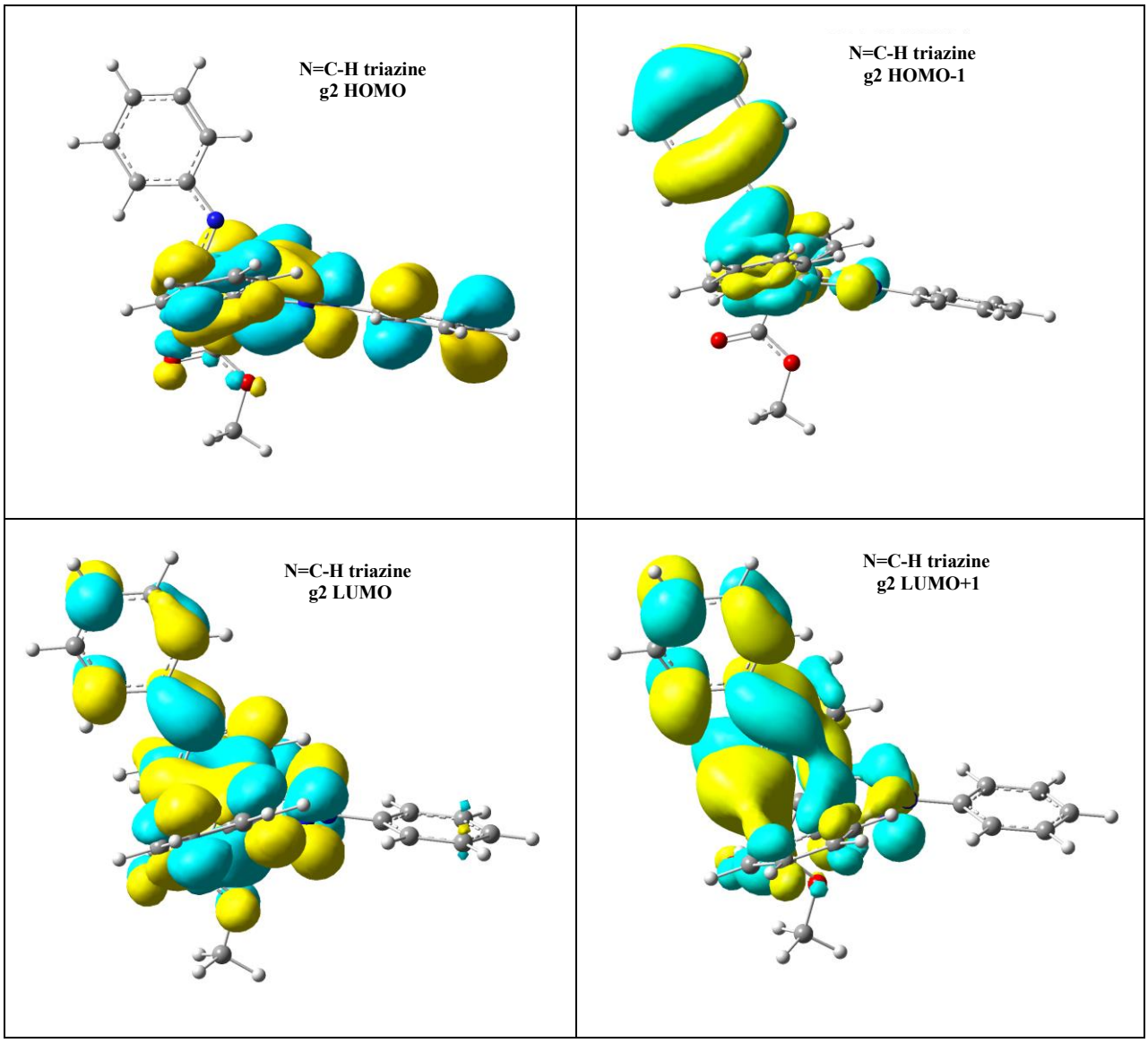

Figure A.6.2. MO plots of the structures of N=C-H triazine with **g2** geometries (optimized for the S_2 state) showing the HOMO, HOMO-1, LUMO and LUMO+1.

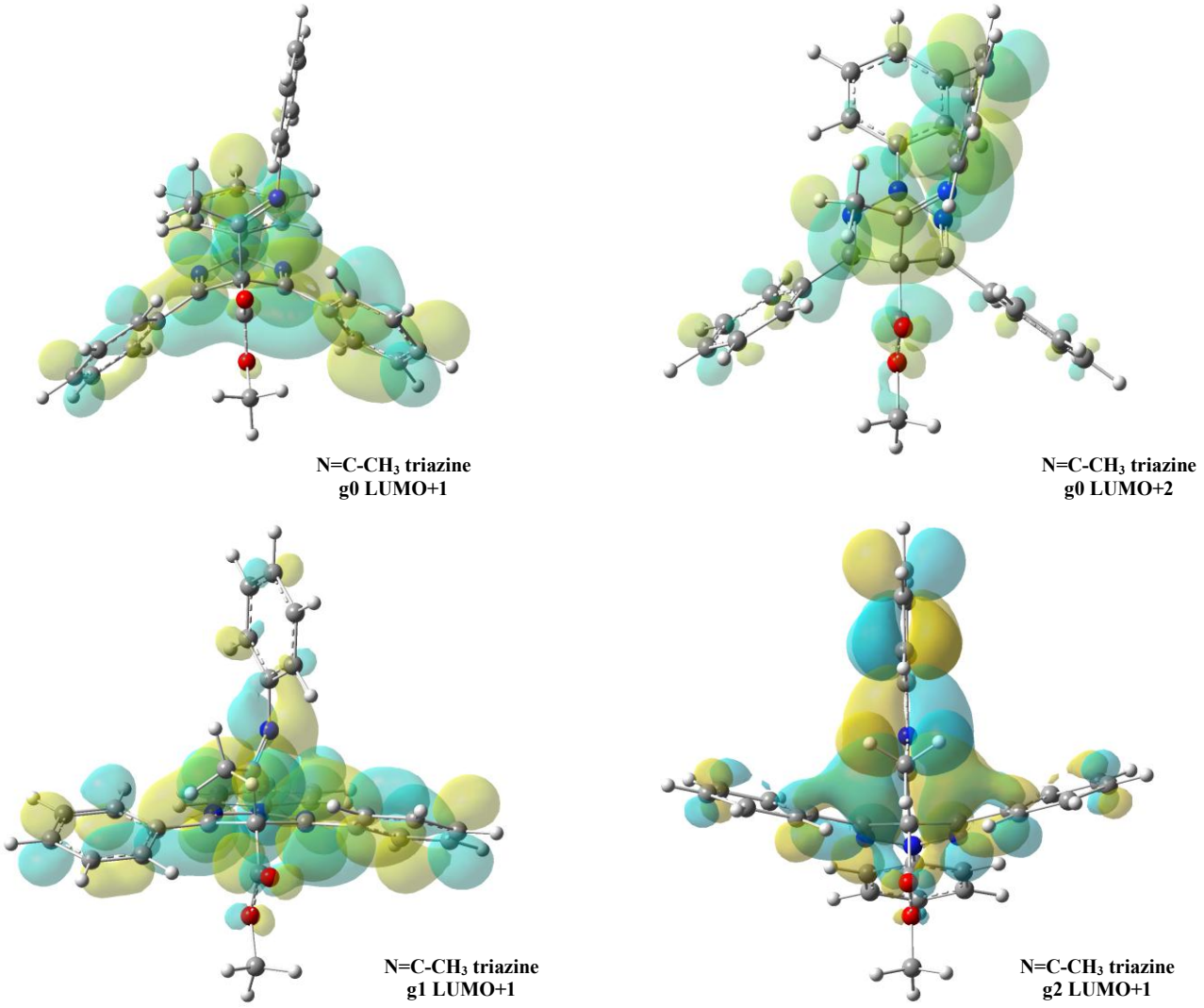

Figure A.6.3. N=C-CH_3 triazine structures showing **g0** geometry LUMO+1, **g0** geometry LUMO+2, **g1** geometry LUMO+1, and **g2** geometry LUMO+1.

A.7 2,5-DIHYDRO-1,2,3-TRIAZINE STRUCTURE SUMMARY.

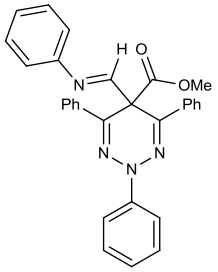

3a

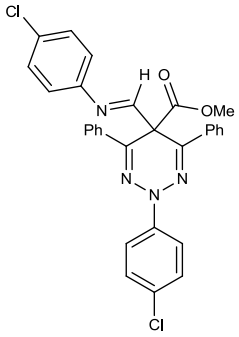

6a

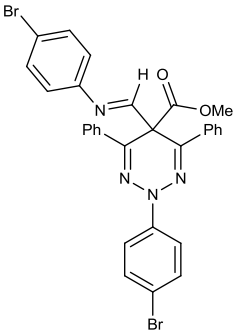

9a

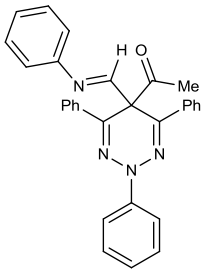

10a

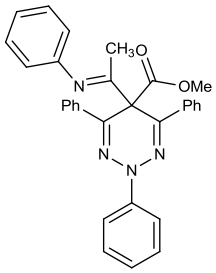

11a

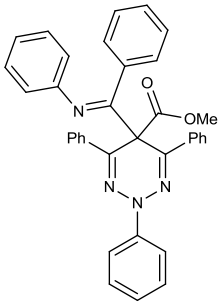

12

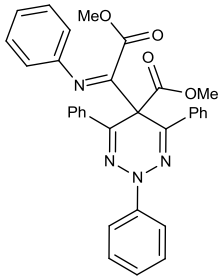

13

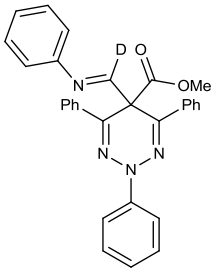

15

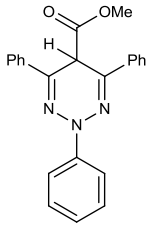

16

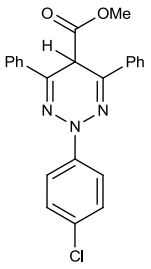

17

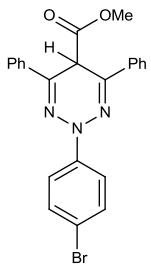

18

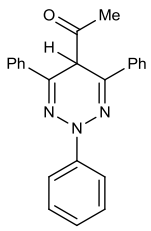

19

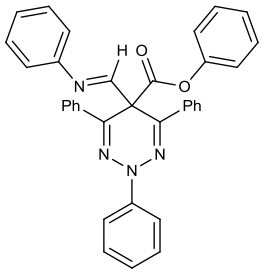

21

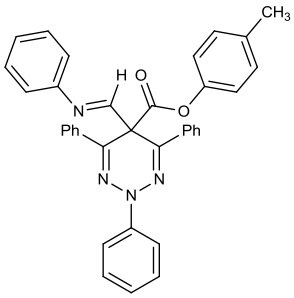

23

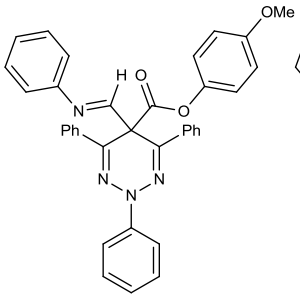

25

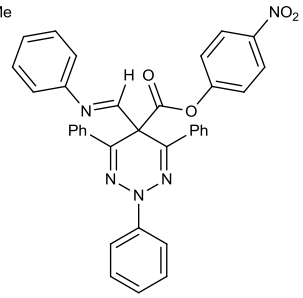

27

A.8 LIST OF PRESENTATIONS / PUBLICATIONS.

1. D. St. Mart, D. M. Togashi, A. G. Ryder and J. C. Stephens.
   "A Novel Organic Fluorophore and its Potential Application as a Biological Probe".
   Poster presentation at the Centre for Synthesis and Chemical Biology "Recent Advances in Synthesis and Chemical Biology IX", O'Callaghan Davenport Hotel, Friday, 10th December, 2010.

2. D. St. Mart, D. M. Togashi, A. G. Ryder and J. C. Stephens.
   "Synthesis and Photophysics of a New Heterocyclic Fluorophore".
   Poster presentation at the Royal Society of Chemistry Photochemistry Group "Photochemistry and Photochemical Techniques", University College Dublin, Monday to Wednesday, 16th to 18th May 2011.

3. D. St. Mart, D. M. Togashi, L. A. Burke, A. G. Ryder and J. C. Stephens.
   "2,5-dihydro-1,2,3-triazines. A novel class of fluorophore".
   Presentation lecture at the 65th Irish Universities Chemistry Research Colloquium 2013, TCD School of Chemistry, Thursday 27th June 2013.

4. D. St. Mart, D. M. Togashi, L. A. Burke, A. G. Ryder and J. C. Stephens.
   Paper on the photophysical model of the 2,5-dihydro-1,2,3-triazine fluorophore in preparation.

5. D. St. Mart, D. M. Togashi, L. A. Burke, A. G. Ryder and J. C. Stephens.
   Paper on solvatochromism of the 2,5-dihydro-1,2,3-triazine fluorophores in preparation.

References

1. Gore, M. G., *Spectrophotometry & Spectrofluorimetry*. Oxford University Press: **2005.**
2. Valeur, B., *Molecular Fluorescence: Principles and Applications*. Wiley: **2002.**
3. Lakowicz, J. R., *Introduction to fluorescence. Principles in Fluorescence Spectroscopy*. New York:Kluwer Academic/Plenum Publishers: **1999**; p 1-23.
4. Lakowicz, J. R., *Instrumentation for fluorescence spectroscopy. Principles in Fluorescence Spectroscopy*. New York:Kluwer Academic/Plenum Publishers: **1999**; p 25-61.
5. Suppan, P., *Chemistry and Light*. Royal Society of Chemistry: **1994**; p 56.
6. Lakowicz, J. R., *Time-domain lifetime measurements. Principles in Fluorescence Spectroscopy*. New York:Kluwer Academic/Plenum Publishers: **1999**; p 95-141.
7. Lakowicz, J. R., *Fluorophores. Principles in Fluorescence Spectroscopy*. New York:Kluwer Academic/Plenum Publishers: **1999**; p 63-95.
8. Invitrogen, L. T., *The Molecular Probes Handbook*. Life Technologies Corporation: **2010**.
9. Goncalves, M. S. T., *Chemical Reviews* **2008,** *109* (1), 190-212.
10. Lakowicz, J. R., *Solvent and environmental effects. Principles in Fluorescence Spectroscopy*. New York:Kluwer Academic/Plenum Publishers: **1999**; p 205-235.
11. Muller, P., *Pure and Applied Chemistry* **1994,** *66*, 1077-1184.
12. Dimroth, K.; Reichardt, C.; Siepmann, T.; Bohlmann, F., *Justus Liebigs Annalen der Chemie* **1963,** *661* (1), 1-37.
13. Kamlet, M. J.; Taft, R. W., *Journal of the American Chemical Society* **1976,** *98*, 377-83.
14. Taft, R. W.; Kamlet, M. J., *Journal of the American Chemical Society* **1976,** *98*, 2886-94.
15. Kamlet, M. J.; Abboud, J. L. M.; Abraham, M. H.; Taft, R. W., *Journal of Organic Chemistry* **1983,** *48*, 2877-87.
16. Kamlet, M. J.; Abboud, J. L.; Taft, R. W., *Journal of the American Chemical Society* **1977,** *99*, 6027-38.
17. Catalán, J.; López, V.; Pérez, P., *Liebigs Annalen* **1995,** *1995* (5), 793-795.

18. Catalan, J., *The Journal of Organic Chemistry* **1997,** *62* (23), 8231-8234.
19. Catalán, J.; Díaz, C., *European Journal of Organic Chemistry* **1999,** *1999* (4), 885-891.
20. Reichardt, C., *Chemical Reviews* **1994,** *94*, 2319-58.
21. Huisgen, R., *1,3-Dipolar Cycloadditions - Introduction, survey and mechanism*. Wiley: **1984**; p 2-5.
22. Jorgensen, K. A.; Gothelf, K. V., *Chemical Reviews* **1998,** *98* (2), 863-910.
23. Huisgen, R., *Angewandte Chemie International Edition in English* **1963,** *2* (10), 565-598.
24. Huisgen, R., *Journal of Organic Chemistry* **1968,** *33*, 2291-7.
25. Firestone, R. A., *Jounral of Organic Chemistry* **1968,** *33*, 2285-90.
26. Woodward, R. B.; Wintner, C., *Tetrahedron Letters* **1969,** *10* (32), 2697-2700.
27. Butler, R. N.; James, J. P., *Journal of the Chemical Society, Chemical Communications* **1983,** *0* (11), 627-629.
28. Angadiyavar, C. S.; Sukumaran, K. B.; George, M. V., *Tetrahedron Letters* **1971,** *12* (7), 633-636.
29. Sukumaran, K. B.; Angadiyavar, C. S.; George, M. V., *Tetrahedron* **1972,** *28* (14), 3987-3998.
30. Sukumaran, K. B.; Satish, S.; George, M. V., *Tetrahedron* **1974,** *30* (3), 445-450.
31. Butler, R. N.; Gillan, A. M.; Collier, S.; James, J. P., *J. Chem Research (S)* **1987**, 332-333.
32. Butler, R. N.; Evans, A. M.; Gillan, A. M.; James, J. P.; McNeela, E. M.; Cunningham, D.; McArdle, P., *Journal of the Chemical Society, Perkin Transactions 1* **1990,** *0* (9), 2537-2544.
33. Butler, R. N.; Colleran, D. M., *Journal of the Chemical Society, Perkin Transactions 1* **1992,** *0* (17), 2159-2161.
34. Butler, R. N.; O'Shea, D. F., *Journal of the Chemical Society, Perkin Transactions 1* **1994,** *0* (19), 2797-2800.
35. Butler, R. N.; O'Shea, D. F, *Heterocycles* **1994,** *37*, 571-584.
36. Rodina, L. L.; Kolberg, A.; Schulze, B., *Heterocycles* **1998,** *49*, 587-618.
37. Bann, B.; Miller, S. A., *Chemical Reviews* **1958,** *58* (1), 131-172.

38. Simons, J. K.; Saxton, M. R., *Benzoguanamine; 2,4-diamino-6-phenyl-1,3,5-triazine*. **1963**; Vol. 4.

39. Cossy, J.; Pete, J. P., *Tetrahedron Letters* **1986,** *27* (21), 2369-2370.

40. Qi, X.; Kim, S. K.; Han, S. J.; Xu, L.; Jee, A. Y.; Kim, H. N.; Lee, C.; Kim, Y.; Lee, M.; Kim, S.-J.; Yoon, J., *Tetrahedron Letters* **2008,** *49* (2), 261-264.

41. Kuplich, M. D.; Grasel, F. S.; Campo, L. F.; Rodembusch, F. S.; Stefani, V., *J. Braz. Chem. Soc.* **2012,** *23* (1), 25-31.

42. Keck, J.; Stüber, G. J.; Kramer, H. E. A., *Die Angewandte Makromolekulare Chemie* **2003,** *252* (1), 119-138.

43. Congreve, M.; Andrews, S. P.; Doré, A. S.; Hollenstein, K.; Hurrell, E.; Langmead, C. J.; Mason, J. S.; Ng, I. W.; Tehan, B.; Zhukov, A.; Weir, M.; Marshall, F. H., *Journal of Medicinal Chemistry* **2012,** *55* (5), 1898-1903.

44. Thirumurugan, P.; Perumal, P. T., *Dyes and Pigments* **2011,** *88* (3), 403-412.

45. Laakso, P. V.; Robinson, R.; Vandrewala, H. P., *Tetrahedron* **1957,** *1* (1–2), 103-118.

46. Sun, Y.-F.; Huang, W.; Lu, C.-G.; Cui, Y.-P., *Dyes and Pigments* **2009,** *81* (1), 10-17.

47. Sun, Y.-F.; Pan, W.-L.; Wu, R.-T.; Song, H.-C., *Chin. J. Org. Chem.* **2006,** *26* (08), 1079-1082.

48. Singh, K.; Kumar, Y.; Puri, P.; Sharma, C.; Aneja, K. R., *International Journal of Inorganic Chemistry 2012*, 9.

49. Ohsawa, A.; Arai, H.; Ohnishi, H.; Igeta, H., *Journal of the Chemical Society, Chemical Communications* **1981,** *0* (22), 1174-1174.

50. Henrikse.L; Autrup, H., *Acta Chemica Scandinavica* **1972,** *26* (8), 3342-3346.

51. Ferrand, G.; Dumas, H.; Depin, J.-C.; Chavernac, G., *European Journal of Medicinal Chemistry* **1987,** *22* (4), 337-345.

52. Zhu, L. J.; Becker, H. C.; Henriksen, L.; Kilsa, K., *Spectrochimica Acta Part A-Molecular And Biomolecular Spectroscopy* **2009,** *73* (4), 757-763.

53. Perspicace, E.; Jouan-Hureaux, V.; Ragno, R.; Ballante, F.; Sartini, S.; La Motta, C.; Da Settimo, F.; Chen, B.; Kirsch, G.; Schneider, S.; Faivre, B.; Hesse, S., *European Journal of Medicinal Chemistry* **2013,** *63* (0), 765-781; Viswanatha, G.

L.; B, J. P.; Hanumanthappa, S.; Rangappa, S.; Janardhanan, S., *Oman Med J* **2012,** *27* (5), 388-395.

54. Butler, R. N.; Fahy, A. M.; Fox, A.; Stephens, J. C.; McArdle, P.; Cunningham, D.; Ryder, A., *The Journal of Organic Chemistry* **2006,** *71* (15), 5679-5687.
55. Williams, D. B. G.; Lawton, M., *The Journal of Organic Chemistry* **2010,** *75* (24), 8351-8354.
56. El Khadem, H.; El-Shafei, Z. M.; Hashem, M. M., *Journal of the Chemical Society C: Organic* **1968,** *0* (0), 949-951.
57. Butler, R. N.; Colleran, D. M.; Lysaght, F. A.; O'Shea, D. F., *Journal of Chemical Research, Synopses* **1993**, 78-79.
58. Alan Aitken, R.; J. Blake, A.; Gosney, I.; O. Gould, R.; Lloyd, D.; A. Ormiston, R., *Journal of the Chemical Society, Perkin Transactions 1* **1998,** *0* (11), 1801-1806.
59. Bialecka-Florjańczyk, E., *Synthetic Communications* **2000,** *30* (24), 4417-4424.
60. Katritzky, A. R.; Zhang, Y.; Singh, S. K., *Synthesis* **2003,** *2003* (EFirst), 2795-2798.
61. Narayanan, N.; Patonay, G., *The Journal of Organic Chemistry* **1995,** *60* (8), 2391-2395.
62. Arbeloa, T. L., **1992,** *160* (1), 123–130.
63. Boonacker, E.; Van Noorden, C. J. F., *Journal of Histochemistry & Cytochemistry* **2001,** *49* (12), 1473-1486.
64. Ohsawa, A.; Itoh, T., 6.10 - 1,2,3-Triazines and their Benzo Derivatives. In *Comprehensive Heterocyclic Chemistry II*, Pergamon: Oxford, 1996; pp 483-505.
65. Klimova, E. I.; Klimova, T.; Álamo, M. F.; Iturbide, D. M.; García, M. M., *Journal of Heterocyclic Chemistry* **2009,** *46* (3), 477-483.
66. Butler, R. N.; Lysaght, F. A.; Burke, L. A., *Journal of the Chemical Society, Perkin Transactions 2* **1992,** *0* (7), 1103-1106.
67. Butler, R. N.; Cunningham, D.; James, J. P.; McArdle, P., *Journal of the Chemical Society, Chemical Communications* **1983,** *0* (14), 762-763.
68. Butler, R. N.; Cunningham, D.; Marren, E. G.; McArdle, P., *Journal of the Chemical Society, Chemical Communications* **1987,** *0* (10), 706-708.
69. Mazzarello, A. J.; Szatyłowicz, H.; Krygowsk, T. M., *Journal of Molecular Modeling* **2013,** *18* (1), 127-135.

70. Bhatnagar, I.; George, M. V., *The Journal of Organic Chemistry* **1967,** *32* (7), 2252-2256.

71. Balachandran, K. S.; Bhatnagar, I.; George, M. V., *The Journal of Organic Chemistry* **1968,** *33* (10), 3891-3895.

72. Tsien, R. Y.; Rink, T. J.; Poenie, M., *Cell Calcium* **1985,** *6* (1–2), 145-157.

73. Kermis, H. R.; Kostov, Y.; Harms, P.; Rao, G., *Biotechnology Progress 18* (5), 1047-1053.

74. Anastas, P.; Warner, J., *Twelve Principles of Green Chemistry. Green Chemistry: Theory and Practice*. Oxford University Press: 1998.

75. Attenburrow, J.; Cameron, A. F. B.; Chapman, J. H.; Evans, R. M.; Hems, B. A.; Jansen, A. B. A.; Walker, T., *Journal of the Chemical Society (Resumed)* **1952,** *0* (0), 1094-1111.

76. Zazza, C.; Amadei, A.; Sanna, N.; Grandi, A.; Chillemi, G.; Di Nola, A.; D'Abramo, M.; Aschi, M., *Physical Chemistry Chemical Physics* **2006,** *8* (12), 1385-1393; Fischer, G.; Smith, D. M.; Nwankwoala, A. U., *Chemical Physics* **1997,** *221* (1-2), 11-21.

77. Velapoldi, R. A.; Mielenz, K. D., *Section VI. Quinine Sulfate. C. Stability. A Fluorescence Standard Reference Material: Qunine Sulfate Dihydrate.* U.S Department of Commerce, National Bureau of Standards: **1980**; p 1-120.

78. Prescott, D. M.; Charles, H. C.; Poulson, J. M.; Page, R. L.; Thrall, D. E.; Vujaskovic, Z.; Dewhirst, M. W., *Clinical Cancer Research* **2000,** *6* (6), 2501-2505.

79. Clayden, J.; Greeves, N.; Warren, S., *Chapter 14 Nucleophilic substitution at C=O with loss of carbonyl oxygen*. Oxford University Press: 2001; Vol. 1, p 1264.

80. Butler, R. N.; Cunningham, D.; Marren, E. G.; McArdle, P., *Journal of the Chemical Society, Perkin Transactions 1* **1990,** *0* (12), 3321-3326.

81. Cohen, B. E.; Pralle, A.; Yao, X.; Swaminath, G.; Gandhi, C. S.; Jan, Y. N.; Kobilka, B. K.; Isacoff, E. Y.; Jan, L. Y., **2005**.

82. Katritzky, A. R.; Narindoshvili, T.; Angrish, P., *Synthesis* **2008,** 2013-2022.

83. Invitrogen, L. T., *1.1 Introduction to Amine Modification. Fluorophores and their amine reactive deriviative.* Life Technologies Corporation: 2010; p 15-21.

84. El-Faham, A.; Albericio, F., *Chemical Reviews* **2011,** *111* (11), 6557-6602.

85. Dubey, I.; Pratviel, G.; Meunier, B., *Bioconjugate Chemistry* **1998,** *9* (5), 627-632.

86. Van Loock, E., *Industrie Chimique Belge* **1974,** *39* (7), 661-686.

87. Cryan, S.-A.; Devocelle, M.; Moran, P. J.; Hickey, A. J.; Kelly, J. G., *Mol. Pharm* **2006,** *3* (2), 104-112.

88. Lide, D. R., *Laboratory Solvents and Other Liquid Reagents. CRC Handbook of Chemistry and Physics*. 90th ed.; National Institute of Standards and Technology: **2010**; p 15-13-15-22.

89. Marcus, Y., *The Journal of Organic Chemistry* **1990,** *55* (7), 2224-2226.

90. Marcus, Y., *Chemical Society Reviews* **1993,** *22* (6), 409-416.

91. Chitra, R.; Smith, P. E., *The Journal of Chemical Physics* **2001,** *114* (1), 426-435.

92. Albuquerque, L. M. P. C.; Moita, M. L. C. J.; Gonçalves, R. M. C., *Journal of Physical Organic Chemistry 14* (3), 139-145.

Design, synthesis and fluorescent characterisation of 2,5-dihydro-1,2,3-triazines.

NUI MAYNOOTH

Ollscoil na hÉireann Má Nuad

PhD. Thesis – Appendix of Results

Presented to the Department of Chemistry,
Faculty of Science and Engineering,
National University of Ireland Maynooth,
Maynooth,
Co. Kildare,
Ireland.
in requirements for the Degree of:

MHE02 Philosophiae Doctor Research Degree in Chemistry

By

Dean Edward St. Mart BSc.

October 2013

Supervisor / Head of Department: Dr. John C. Stephens

Table of Contents

Appendix 1: 2,5-dihydro-1,2,3-triazines with substituted aryl groups.

1.1 COMPOUND 3A

1.1.1 Quantum Yield Summary.

Solvent	abs (310 nm)	$\lambda_{ems\ (max)}$	$\Phi_{310\ nm}$	abs (400 nm)	$\lambda_{ems\ (max)}$	$\Phi_{400\ nm}$
Toluene	0.07	510.00	0.76	0.02	508.95	0.79
1,4-Dioxane	0.09	511.96	0.60	0.02	511.06	0.64
Ethyl acetate	0.10	513.03	0.53	0.02	508.05	0.55
Chloroform	0.07	516.96	0.66	0.02	511.96	0.67
2-Methyl-2-butanol	0.04	511.96	0.55	0.01	511.06	0.52
N,N-dimethylformamide	0.10	518.03	0.58	0.03	513.03	0.64
Acetonitrile	0.07	516.96	0.54	0.02	511.06	0.54
Propylene Carbonate	0.13	516.96	0.13	0.03	507.01	0.61
1-Octanol	0.05	513.93	0.63	0.01	508.05	0.61
1-Hexanol	0.08	516.96	0.56	0.02	508.95	0.56
1-Butanol	0.04	516.06	0.56	0.01	505.97	0.52
1-Pentanol	0.07	516.06	0.59	0.02	508.95	0.56
1-propanol	0.07	518.03	0.51	0.02	510.00	0.49
Acetic acid	0.09	505.07	0.02	0.02	481.06	0.03
1,5-Pentanediol	0.05	515.00	0.53	0.01	505.07	0.50
Ethanol	0.02	516.96	0.66	0.01	507.01	0.64
1,3-Butanediol	0.03	516.06	0.60	0.01	508.95	0.48
1,4-Butanediol	0.03	513.03	0.66	0.01	510.00	0.57
1,3-Propanediol	0.02	516.06	0.62	0.01	508.95	0.55
Methanol	0.10	518.93	0.35	0.03	504.02	0.32
Ethylene Glycol	0.08	521.04	0.46	0.02	511.06	0.43
2,2,2-Trifluoroethanol	0.09	546.02	0.03	0.02	521.94	0.01
Ethanol-d	0.07	513.93	0.54	0.02	508.05	0.51
Methanol-d	0.06	518.93	0.44	0.01	508.05	0.42

Table 1.1.1. Summary of ultraviolet-visible absorbance values at 310 nm and 400 nm, emission maxima and quantum yield (Φ) of **3a** at 310 nm and 400 nm excitation.

1.1.2 310 nm excitation Gaussian band fit summaries.

Solvent	λ max$_{em}$ Band 1 (cm^{-1})	λ max$_{em}$ Band 1 (nm)	λ max$_{em}$ Band 2 (cm^{-1})	λ max$_{em}$ Band 2 (nm)	λ max$_{em}$ Band 3 (cm^{-1})	λ max$_{em}$ Band 3 (nm)
Toluene	18699.53	534.77	19787.50	505.37	21191.30	471.89
1,4-Dioxane	18609.20	537.37	19776.83	505.64	21220.91	471.23
Ethyl acetate	18560.15	538.79	19828.66	504.32	21291.51	469.67
Chloroform	18479.36	541.14	19602.80	510.13	21042.17	475.24
2-Methyl-2-butanol	18757.35	533.12	19854.54	503.66	21358.16	468.21
N,N-dimethylformamide	18270.31	547.34	19607.85	510.00	21023.55	475.66
Acetonitrile	18237.96	548.31	19597.51	510.27	21072.79	474.55
Propylene carbonate	18240.20	548.24	19579.54	510.74	21010.91	475.94
1-Octanol	18469.28	541.44	19710.40	507.35	21195.24	471.80
1-Hexanol	18415.30	543.03	19679.60	508.14	21181.46	472.11
1-Butanol	18354.09	544.84	19660.01	508.65	21151.45	472.78
1-Pentanol	18401.11	543.45	19668.91	508.42	21164.43	472.49
1-Propanol	18329.40	545.57	19651.50	508.87	21128.43	473.30
Acetic acid	18757.69	533.11	19947.18	501.32	21162.90	472.52
Ethanol	18317.79	545.92	19666.15	508.49	21125.49	473.36
1,5-Pentanediol	18340.52	545.24	19634.11	509.32	20989.65	476.43
1,3-Butanediol	18507.43	540.32	19620.65	509.67	20987.77	476.47
1,4-Butanediol	18529.81	539.67	19632.87	509.35	20951.13	477.30
1,3-Propanediol	18187.12	549.84	19495.87	512.93	20874.87	479.04
Methanol	18181.41	550.01	19552.86	511.43	21080.38	474.37
1,2-Ethanediol	18039.29	554.35	19416.23	515.03	20862.17	479.34
2,2,2-Trifluoroethanol	17980.12	556.17	18557.27	538.87	-	-
Ethanol-d	18329.14	545.58	19679.56	508.14	21143.94	472.95
Methanol-d	18202.11	549.39	19581.38	510.69	21082.16	474.33

Solvent	λ max$_{em}$ Band 4 (cm^{-1})	λ max$_{em}$ Band 4 (nm)	λ max$_{em}$ Band 5 (cm^{-1})	λ max$_{em}$ Band 5 (nm)
Toluene	-	-	-	-
1,4-Dioxane	-	-	-	-
Ethyl acetate	-	-	-	-
Chloroform	-	-	-	-
2-Methyl-2-butanol	-	-	-	-
N,N-dimethylformamide	-	-	-	-
Acetonitrile	-	-	-	-
Propylene carbonate	-	-	-	-
1-Octanol	-	-	-	-
1-Hexanol	-	-	-	-
1-Butanol	-	-	-	-
1-Pentanol	-	-	-	-
1-Propanol	-	-	-	-
Acetic acid	28082.88	356.09	-	-
Ethanol	-	-	-	-
1,5-Pentanediol	-	-	-	-
1,3-Butanediol	27832.59	359.29	29356.02	340.65
1,4-Butanediol	26296.72	380.28	28326.21	353.03
1,3-Propanediol	29071.80	343.98	29558.45	338.31
Methanol	-	-	-	-
1,2-Ethanediol	-	-	-	-
2,2,2-Trifluoroethanol	26860.88	372.29	-	-
Ethanol-d	-	-	-	-
Methanol-d	-	-	-	-

Table 1.1.2. Summary of band maxima of 5 band fit using Gaussian model for normalised **3a** emission spectra recorded at 310 nm excitation.

(a)

Solvent	Width Band 1 (cm^{-1})	Width Band 2 (cm^{-1})	Width Band 3 (cm^{-1})	Width Band 4 (cm^{-1})	Width Band 5 (cm^{-1})
Toluene	3089.34	1807.45	930.43	-	-
1,4-Dioxane	3127.46	1967.64	932.20	-	-
Ethyl acetate	3166.47	2115.98	973.63	-	-
Chloroform	3142.97	1937.46	985.29	-	-
2-Methyl-2-butanol	3171.41	1908.75	946.50	-	-
N,N-dimethylformamide	3218.06	2252.04	1088.68	-	-
Acetonitrile	3231.96	2307.94	1096.82	-	-
Propylene carbonate	3245.49	2264.47	1107.58	-	-
1-Octanol	3185.65	2096.31	979.02	-	-
1-Hexanol	3190.19	2127.17	992.76	-	-
1-Butanol	3206.92	2180.27	998.96	-	-
1-Pentanol	3197.93	2138.94	996.66	-	-
1-Propanol	3193.50	2190.25	1016.45	-	-
Acetic acid	3425.50	2223.64	1027.11	4114.06	-
Ethanol	3195.23	2214.25	1022.22	-	-
1,5-Pentanediol	3245.77	2199.33	1064.22	-	-
1,3-Butanediol	3387.79	2209.70	1080.63	3706.60	2541.28
1,4-Butanediol	3398.85	2224.27	1043.68	4815.69	3543.18
1,3-Propanediol	3289.12	2274.22	1085.48	5313.95	2323.26
Methanol	3242.72	2296.54	1056.70	-	-
1,2-Ethanediol	3231.28	2272.46	1098.41	-	-
2,2,2-Trifluoroethanol	3875.14	2341.41	-	5563.76	-
Ethanol-d	3199.84	2221.11	1016.24	-	-
Methanol-d	3244.65	2288.87	1071.98	-	-

(b)

Solvent	Area Band 1 (cm^{-1})	Area Band 2 (cm^{-1})	Area Band 3 (cm^{-1})	Area Band 4 (cm^{-1})	Area Band 5 (cm^{-1})
Toluene	2102.83	1222.98	303.17	-	-
1,4-Dioxane	2030.24	1394.30	260.44	-	-
Ethyl acetate	1934.54	1618.27	272.82	-	-
Chloroform	2056.60	1347.99	302.82	-	-
2-Methyl-2-butanol	2187.67	1242.59	261.19	-	-
N,N-dimethylformamide	1843.32	1816.09	323.93	-	-
Acetonitrile	1852.88	1844.49	275.09	-	-
Propylene carbonate	1894.13	1795.91	326.78	-	-
1-Octanol	1977.84	1557.50	287.46	-	-
1-Hexanol	1949.70	1596.44	278.81	-	-
1-Butanol	1897.38	1709.97	277.82	-	-
1-Pentanol	1938.56	1610.33	281.50	-	-
1-Propanol	1879.81	1725.65	284.93	-	-
Acetic acid	1788.94	1752.73	310.94	256.28	-
Ethanol	1875.27	1758.95	291.13	-	-
1,5-Pentanediol	1877.51	1739.10	330.24	-	-
1,3-Butanediol	2101.88	1582.56	318.38	876.85	910.57
1,4-Butanediol	2128.59	1561.50	303.94	753.82	514.06
1,3-Propanediol	1850.63	1817.46	322.52	376.37	159.37
Methanol	1929.13	1802.42	267.91	-	-
1,2-Ethanediol	1888.13	1817.93	309.47	-	-
2,2,2-Trifluoroethanol	2581.37	1355.52	-	243.35	-
Ethanol-d	1897.20	1767.54	272.53		-
Methanol-d	1902.82	1830.90	288.30	-	-

(c)

Solvent	fwhm Band 1 (nm)	fwhm Band 2 (nm)	fwhm Band 3 (nm)	fwhm Band 4 (nm)	fwhm Band 5 (nm)
Toluene	104.37	53.33	25.27	-	-
1,4-Dioxane	111.11	63.10	25.27	-	-
Ethyl acetate	111.11	86.84	25.27	-	-
Chloroform	106.54	64.33	25.73	-	-
2-Methyl-2-butanol	108.85	57.66	24.83	-	-
N,N-dimethylformamide	120.50	74.32	34.33	-	-
Acetonitrile	120.50	74.32	29.76	-	-
Propylene carbonate	115.84	74.32	30.30	-	-
1-Octanol	118.01	68.65	25.27	-	-
1-Hexanol	113.44	68.65	20.87	-	-
1-Butanol	113.44	68.65	29.76	-	-
1-Pentanol	113.44	64.33	25.27	-	-
1-Propanol	113.44	64.33	29.76	-	-
Acetic acid	115.60	61.90	33.72	63.16	-
Ethanol	113.44	68.65	29.76	-	-
1,5-Pentanediol	113.44	68.65	30.30	-	-
1,3-Butanediol	118.01	64.33	30.30	54.06	35.26
1,4-Butanediol	122.49	68.65	30.30	82.95	54.66
1,3-Propanediol	115.84	70.00	30.30	74.81	30.44
Methanol	115.84	70.00	29.76	-	-
1,2-Ethanediol	118.32	75.79	30.30	-	-
2,2,2-Trifluoroethanol	142.69	32.83	-	6.17	-
Ethanol-d	113.44	68.65	29.76	-	-
Methanol-d	115.84	74.32	29.76	-	-

Tables 1.1.3 (a), (b) and (c). Summary band width, band area, full width half maximum of 5 band fit using Gaussian model for normalised **3a** emission spectra recorded at 310 nm excitation.

Solvent	Band 1 Area Percentage (%)	Band 2 Area Percentage (%)	Band 3 Area Percentage (%)	Band 4 Area Percentage (%)	Band 5 Area Percentage (%)
Toluene	57.95	33.70	8.35	-	-
1,4-Dioxane	55.10	37.84	7.07	-	-
Ethyl acetate	50.57	42.30	7.13	-	-
Chloroform	55.47	36.36	8.17	-	-
2-Methyl-2-butanol	59.26	33.66	7.08	-	-
N,N-dimethylformamide	46.28	45.59	8.13	-	-
Acetonitrile	46.64	46.43	6.92	-	-
Propylene carbonate	47.15	44.71	8.14	-	-
1-Octanol	51.74	40.74	7.52	-	-
1-Hexanol	50.97	41.74	7.29	-	-
1-Butanol	48.84	44.01	7.15	-	-
1-Pentanol	50.61	42.04	7.35	-	-
1-Propanol	48.32	44.36	7.32	-	-
Acetic acid	43.54	42.66	7.57	6.24	-
Ethanol	47.77	44.81	7.42	-	-
1,5-Pentanediol	47.57	44.06	8.37	-	-
1,3-Butanediol	36.30	27.33	5.50	15.14	15.73
1,4-Butanediol	40.45	29.68	5.78	14.33	9.77
1,3-Propanediol	40.89	40.15	7.13	8.32	3.52
Methanol	48.23	45.07	6.70	-	-
1,2-Ethanediol	47.02	45.27	7.71	-	-
2,2,2-Trifluoroethanol	61.75	32.43	-	5.82	-
Ethanol-d	48.19	44.89	6.92	-	-
Methanol-d	47.31	45.52	7.17	-	-

Table 1.1.4. Total Area Percentages of 5 band fit using Gaussian model for normalised **3a** emission spectra recorded at 310 nm excitation.

Solvent	Area Ratio Band 1/2 (310 nm ex)	Area Ratio Band 1/3 (310 nm ex)	Area Ratio Band 1/4 (310 nm ex)	Area Ratio Band 1/5 (310 nm ex)
Toluene	1.72	6.94	-	-
1,4-Dioxane	1.46	7.80	-	-
Ethyl acetate	1.20	7.09	-	-
Chloroform	1.53	6.79	-	-
2-Methyl-2-butanol	1.76	8.38	-	-
N,N-dimethylformamide	1.01	5.69	-	-
Acetonitrile	1.00	6.74	-	-
Propylene carbonate	1.05	5.80	-	-
1-Octanol	1.27	6.88	-	-
1-Hexanol	1.22	6.99	-	-
1-Butanol	1.11	6.83	-	-
1-Pentanol	1.20	6.89	-	-
1-Propanol	1.09	6.60	-	-
Acetic acid	1.02	5.75	6.98	-
Ethanol	1.07	6.44	-	-
1,5-Pentanediol	1.08	5.69	-	-
1,3-Butanediol	1.33	6.60	2.40	2.31
1,4-Butanediol	1.36	7.00	2.82	4.14
1,3-Propanediol	1.02	5.74	4.92	11.61
Methanol	1.07	7.20	-	-
1,2-Ethanediol	1.04	6.10	-	-
2,2,2-Trifluoroethanol	1.90	-	10.61	-
Ethanol-d	1.07	6.96	-	-
Methanol-d	1.04	6.60	-	-

Solvent	Area Ratio Band 2/3 (310 nm ex)	Area Ratio Band 2/4 (310 nm ex)	Area atio Band 2/5 (310 nm ex)	Area Ratio Band 3/4 (310 nm ex)	Area Ratio Band 3/5 (310 nm ex)	Area Ratio Band 4/5 (310 nm ex)
Toluene	4.03	-	-	-	-	-
1,4-Dioxane	5.35	-	-	-	-	-
Ethyl acetate	5.93	-	-	-	-	-
Chloroform	4.45	-	-	-	-	-
2-Methyl-2-butanol	4.76	-	-	-	-	-
N,N-dimethylformamide	5.61	-	-	-	-	-
Acetonitrile	6.71	-	-	-	-	-
Propylene carbonate	5.50	-	-	-	-	-
1-Octanol	5.42	-	-	-	-	-
1-Hexanol	5.73	-	-	-	-	-
1-Butanol	6.15	-	-	-	-	-
1-Pentanol	5.72	-	-	-	-	-
1-Propanol	6.06	-	-	-	-	-
Acetic acid	5.64	6.84	-	1.21	-	-
Ethanol	6.04	-	-	-	-	-
1,5-Pentanediol	5.27	-	-	-	-	-
1,3-Butanediol	4.97	1.80	1.74	0.36	0.35	0.96
1,4-Butanediol	5.14	2.07	3.04	0.40	0.59	1.47
1,3-Propanediol	5.64	4.83	11.40	0.86	2.02	2.36
Methanol	6.73	-	-	-	-	-
1,2-Ethanediol	5.87	-	-	-	-	-
2,2,2-Trifluoroethanol	-	5.57	-	-	-	-
Ethanol-d	6.49	-	-	-	-	-
Methanol-d	-	-	-	-	-	-

Table 1.1.5. Area Ratios of 5 band fit using Gaussian model for normalised **3a** emission spectra recorded at 310 nm excitation.

1.1.3 400 nm excitation Gaussian band fit summaries.

Solvent	λ max$_{em}$ Band 1 (cm^{-1})	λ max$_{em}$ Band 1 (nm)	λ max$_{em}$ Band 2 (cm^{-1})	λ max$_{em}$ Band 2 (nm)	λ max$_{em}$ Band 3 (cm^{-1})	λ max$_{em}$ Band 3 (nm)
Toluene	18722.95	534.10	19885.03	502.89	21175.04	472.25
1,4-Dioxane	18603.61	537.53	19866.41	503.36	21177.96	472.19
Ethyl acetate	18643.51	536.38	19950.49	501.24	21243.47	470.73
Chloroform	18475.71	541.25	19724.23	506.99	21008.89	475.99
2-Methyl-2-butanol	18721.94	534.13	19979.37	500.52	21320.50	469.03
N,N-dimethylformamide	18398.49	543.52	19725.12	506.97	20992.14	476.37
Acetonitrile	18376.96	544.16	19729.53	506.85	21010.86	475.94
Propylene carbonate	18365.62	544.50	19718.97	507.13	20967.89	476.92
1-Octanol	18525.48	539.80	19853.56	503.69	21150.26	472.81
1-Hexanol	18487.34	540.91	19835.17	504.16	21123.31	473.41
1-Butanol	18489.30	540.85	19831.52	504.25	21096.49	474.01
1-Pentanol	18506.19	540.36	19842.70	503.96	21109.90	473.71
1-Propanol	18491.90	540.78	19818.03	504.59	21073.29	474.53
Acetic acid	19742.01	506.53	19851.35	503.74	21064.80	474.73
Ethanol	18535.59	539.50	19863.53	503.44	21084.58	474.28
1,5-Pentanediol	18418.50	542.93	19729.27	506.86	20947.94	477.37
1,3-Butanediol	18378.18	544.12	19638.43	509.21	20836.89	479.92
1,4-Butanediol	18490.80	540.81	19705.73	507.47	20900.20	478.46
1,3-Propanediol	18378.18	544.12	19638.43	509.21	20836.89	479.92
Methanol	18443.02	542.21	19793.25	505.22	21014.88	475.85
1,2-Ethanediol	18245.90	548.07	19592.29	510.40	20817.99	480.35
2,2,2-Trifluoroethanol	17327.68	577.11	19171.97	521.59	20611.51	485.17
Ethanol-d	18481.97	541.07	19828.55	504.32	21084.08	474.29
Methanol-d	18446.93	542.10	19796.09	505.15	21016.57	475.82

Table 1.1.6. Summary of band maxima of 3 band fit using Gaussian model for normalised **3a** emission spectra recorded at 400 nm excitation.

Solvent	fwhm Band 1 (nm)	fwhm Band 2 (nm)	fwhm Band 3 (nm)	Width Band 1 (cm^{-1})	Width Band 2 (cm^{-1})	Width Band 3 (cm^{-1})
Toluene	103.49	57.89	26.88	3059.86	1885.77	956.62
1,4-Dioxane	109.12	64.03	26.88	3080.82	2021.46	987.48
Ethyl acetate	104.85	60.59	26.57	3107.31	2076.64	1049.99
Chloroform	106.22	62.09	27.19	3096.86	2025.27	1023.96
2-Methyl-2-butanol	110.54	60.59	26.57	3120.72	2037.61	1016.78
N,N-dimethylformamide	110.56	68.35	32.63	3174.62	2169.25	1155.97
Acetonitrile	107.63	68.35	32.63	3166.06	2176.37	1223.28
Propylene carbonate	114.96	68.35	35.56	3130.18	2139.79	1187.86
1-Octanol	109.12	64.03	26.88	3101.92	2083.80	1049.14
1-Hexanol	106.22	61.33	29.74	3107.72	2098.77	1076.06
1-Butanol	110.56	61.33	29.74	3123.66	2117.66	1095.18
1-Pentanol	106.22	64.03	29.74	3103.86	2085.41	1085.58
1-Propanol	106.22	61.33	29.74	3112.78	2078.09	1122.22
Acetic acid	134.48	64.03	29.74	4410.81	2169.00	1076.26
Ethanol	109.12	61.33	29.74	3075.49	2048.77	1130.86
1,5-Pentanediol	110.56	64.82	30.08	3152.27	2121.42	1139.46
1,3-Butanediol	114.96	65.62	30.43	3203.55	2113.51	1169.34
1,4-Butanediol	113.46	68.35	33.01	3294.71	2191.51	1161.92
1,3-Propanediol	114.96	65.62	30.43	3203.55	2113.51	1169.34
Methanol	110.56	64.82	32.63	3124.89	2106.48	1195.75
1,2-Ethanediol	116.49	62.85	33.39	3146.65	2118.93	1179.37
2,2,2-Trifluoroethanol	113.38	68.96	48.20	2386.72	2086.97	1466.78
Ethanol-d	110.56	61.33	29.74	3113.73	2104.40	1141.30
Methanol-d	110.56	64.82	32.63	3131.92	2118.35	1195.76

Table 1.1.7. Summary of full width half maximum (fwhm) and band width of 3 band fit using Gaussian model for normalised **3a** emission spectra recorded at 400 nm excitation.

Solvent	Area Band 1 (cm^{-1})	Area Band 2 (cm^{-1})	Area Band 3 (cm^{-1})	Area Ratio Band 1/2 (400 nm ex)	Area Ratio Band 1/3 (400 nm ex)	Area Ratio Band 2/3 (400 nm ex)
Toluene	1852.60	1421.18	380.16	1.30	4.87	3.74
1,4-Dioxane	1770.19	1622.03	352.83	1.09	5.02	4.60
Ethyl acetate	1721.97	1702.84	398.22	1.01	4.32	4.28
Chloroform	1711.16	1627.26	391.48	1.05	4.37	4.16
2-Methyl-2-butanol	1796.23	1605.80	361.44	1.12	4.97	4.44
N,N-dimethylformamide	1676.14	1798.61	435.55	0.93	3.85	4.13
Acetonitrile	1592.51	1821.86	474.06	0.87	3.36	3.84
Propylene carbonate	1623.80	1791.05	475.80	0.91	3.41	3.76
1-Octanol	1667.78	1710.15	408.63	0.98	4.08	4.19
1-Hexanol	1647.48	1765.80	426.82	0.93	3.86	4.14
1-Butanol	1599.66	1783.50	436.60	0.90	3.66	4.08
1-Pentanol	1652.10	1751.79	435.37	0.94	3.79	4.02
1-Propanol	1609.76	1763.05	474.84	0.91	3.39	3.71
Acetic acid	1958.70	1534.09	401.82	1.28	4.87	3.82
Ethanol	1613.81	1697.43	479.40	0.95	3.37	3.54
1,5-Pentanediol	1572.25	1779.61	461.75	0.88	3.41	3.85
1,3-Butanediol	1626.49	1726.54	475.17	0.94	3.42	3.63
1,4-Butanediol	1598.41	1776.23	452.19	0.90	3.53	3.93
1,3-Propanediol	1626.49	1726.54	475.17	0.94	3.42	3.63
Methanol	1566.78	1767.89	517.53	0.89	3.03	3.42
1,2-Ethanediol	1567.77	1781.03	486.20	0.88	3.22	3.66
2,2,2-Trifluoroethanol	726.74	1997.55	743.02	0.36	0.98	2.69
Ethanol-d	1595.80	1791.58	476.57	0.89	3.35	3.76
Methanol-d	1537.58	1787.38	517.79	0.86	2.97	3.45

Solvent	Band 1 Area Percentage (%)	Band 2 Area Percentage (%)	Band 3 Area Percentage (%)
Toluene	50.70	38.89	10.40
1,4-Dioxane	47.27	43.31	9.42
Ethyl acetate	45.04	44.54	10.42
Chloroform	45.88	43.63	10.50
2-Methyl-2-butanol	47.73	42.67	9.60
N,N-dimethylformamide	42.86	46.00	11.14
Acetonitrile	40.96	46.85	12.19
Propylene carbonate	41.74	46.03	12.23
1-Octanol	44.04	45.16	10.79
1-Hexanol	42.90	45.98	11.11
1-Butanol	41.88	46.69	11.43
1-Pentanol	43.03	45.63	11.34
1-Propanol	41.84	45.82	12.34
Acetic acid	50.29	39.39	10.32
Ethanol	42.57	44.78	12.65
1,5-Pentanediol	41.23	46.66	12.11
1,3-Butanediol	42.49	45.10	12.41
1,4-Butanediol	41.77	46.42	11.82
1,3-Propanediol	42.49	45.10	12.41
Methanol	40.67	45.89	13.43
1,2-Ethanediol	40.88	46.44	12.68
2,2,2-Trifluoroethanol	20.96	57.61	21.43
Ethanol-d	41.30	46.37	12.33
Methanol-d	40.01	46.51	13.47

Table 1.1.8. Band area, area Ratios and total area percentage of 3 band fit using Gaussian model for normalised **3a** emission spectra recorded at 400 nm excitation.

1.1.4 310 nm Gaussian band fit - Solvatochromic analysis.

1.1.4.1 E_T^N.

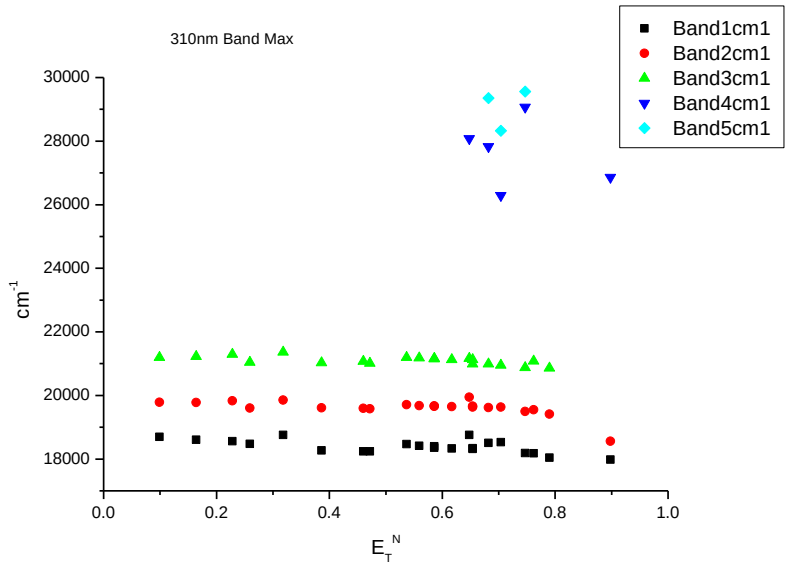

Figure 1.1.1. Band maxima from Gaussian model fit of the normalised fluorescence emission spectra of **3a** recorded at 310 nm excitation against E_T^N.

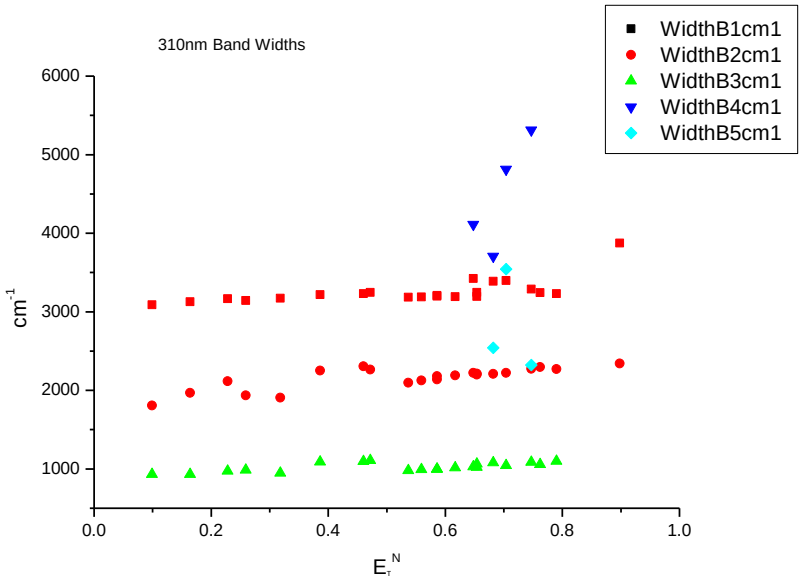

Figure 1.1.2. Band widths from Gaussian model fit of the normalised fluorescence emission spectra of **3a** recorded at 310 nm excitation against E_T^N.

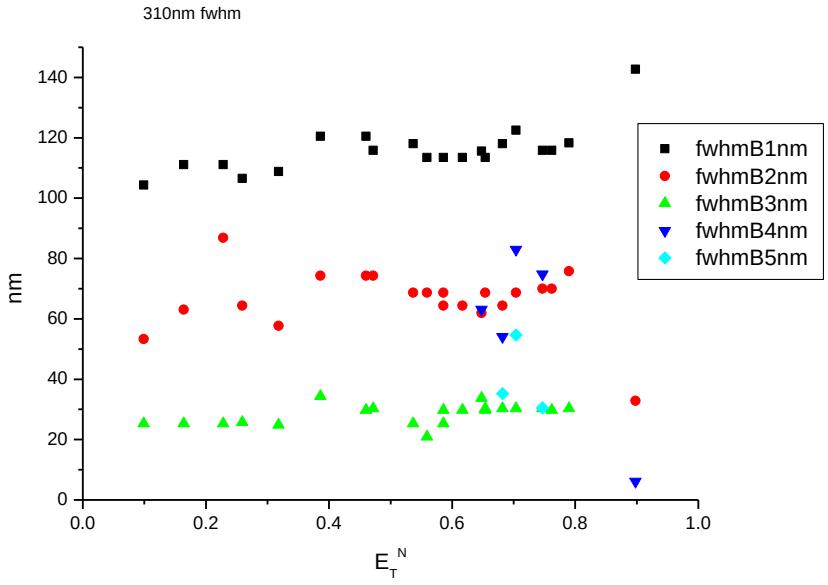

Figure 1.1.3. Full width half maxima of each band from Gaussian model fit of the normalised fluorescence emission spectra of **3a** recorded at 310 nm excitation against E_T^N.

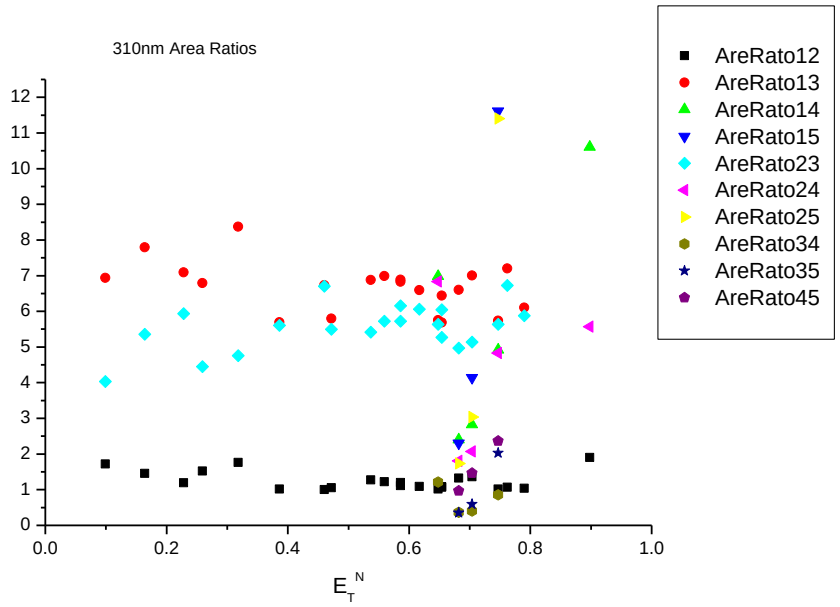

Figure 1.1.4. Area ratios from Gaussian model fit of the normalised fluorescence emission spectra of **3a** recorded at 310 nm excitation against E_T^N.

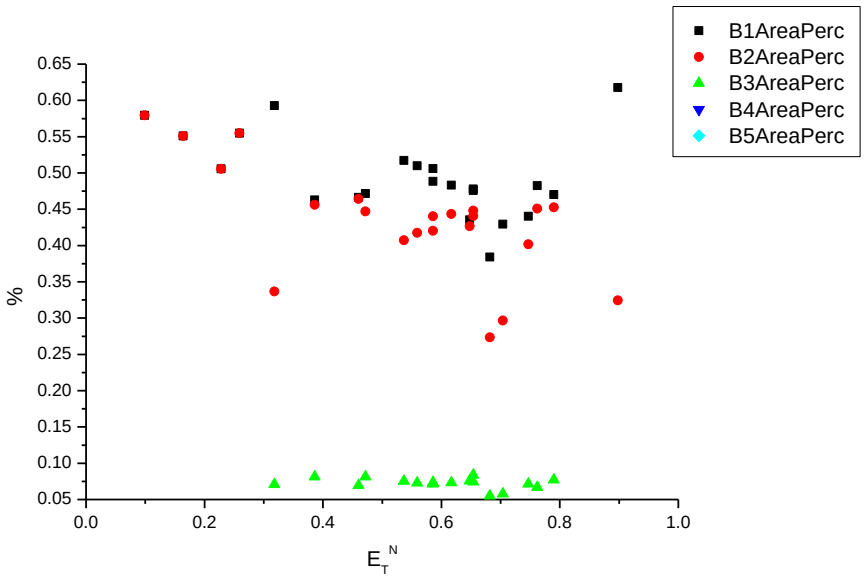

Figure 1.1.5. Area percentages from Gaussian model fit of the normalised fluorescence emission spectra of **3a** recorded at 310 nm excitation against E_T^N.

1.1.4.2 α

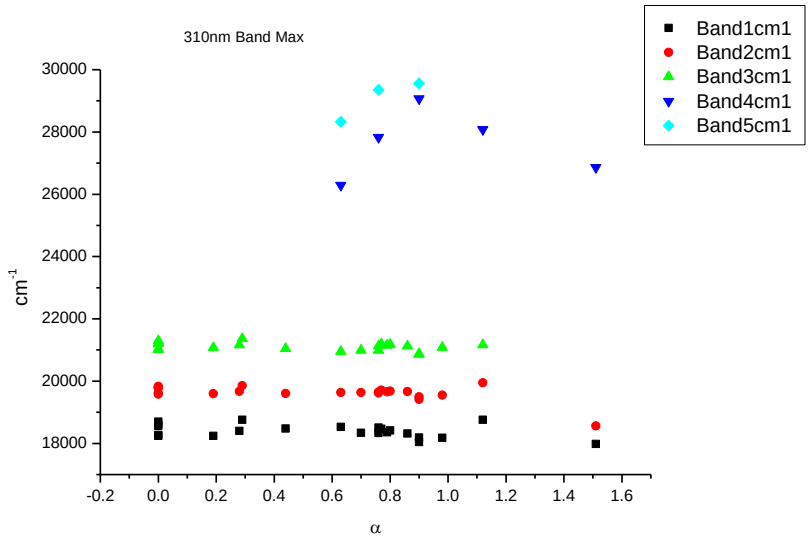

Figure 1.1.6. Band maxima from Gaussian model fit of the normalised fluorescence emission spectra of **3a** recorded at 310 nm excitation against α.

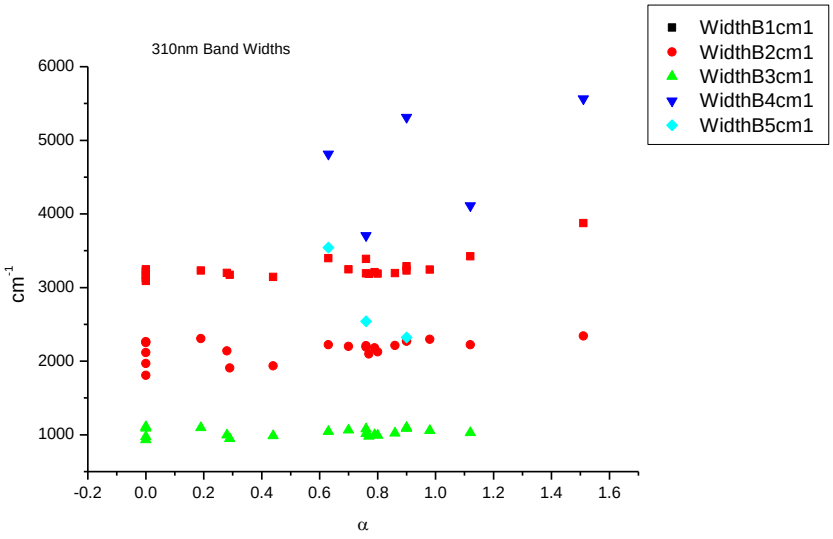

Figure 1.1.7. Band widths from Gaussian model fit of the normalised fluorescence emission spectra of **3a** recorded at 310 nm excitation against α.

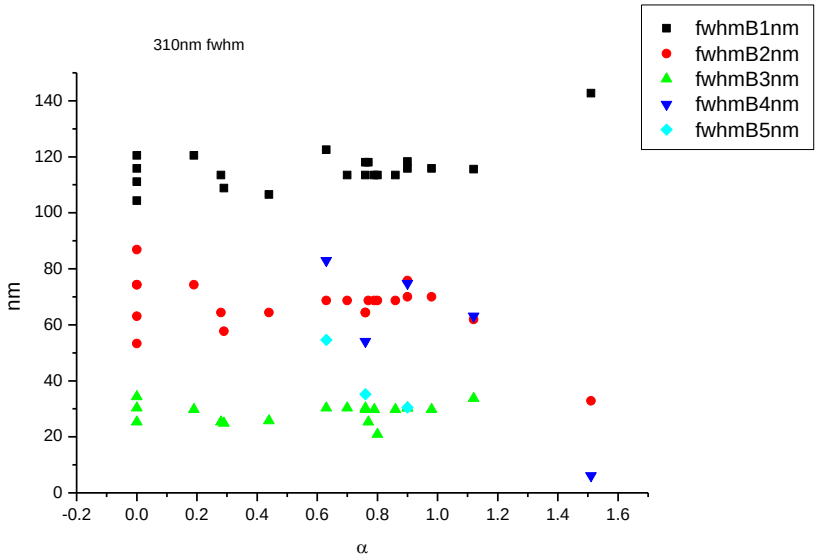

Figure 1.1.8. Full width half maxima from Gaussian model fit of the normalised fluorescence emission spectra of **3a** recorded at 310 nm excitation against α.

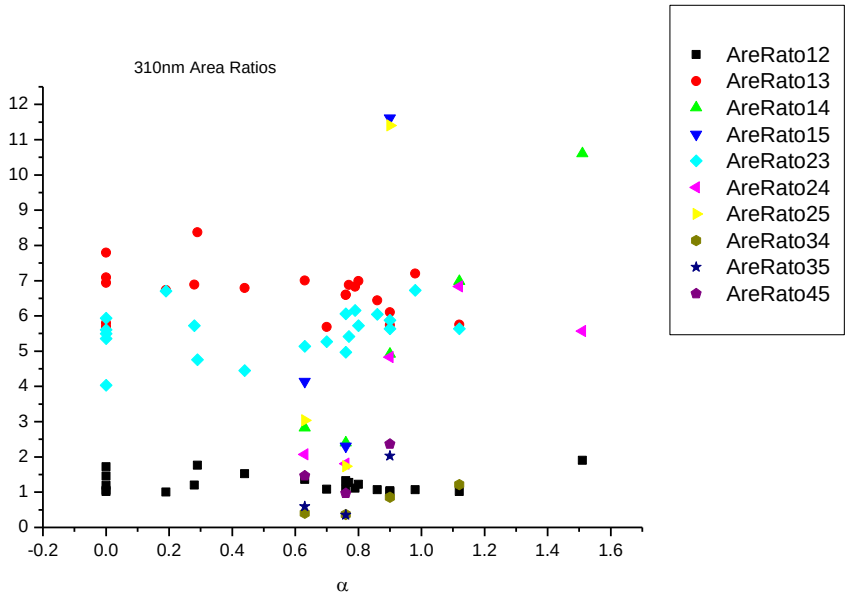

Figure 1.1.9. Area Ratios from Gaussian model fit of the normalised fluorescence emission spectra of **3a** recorded at 310 nm excitation against α.

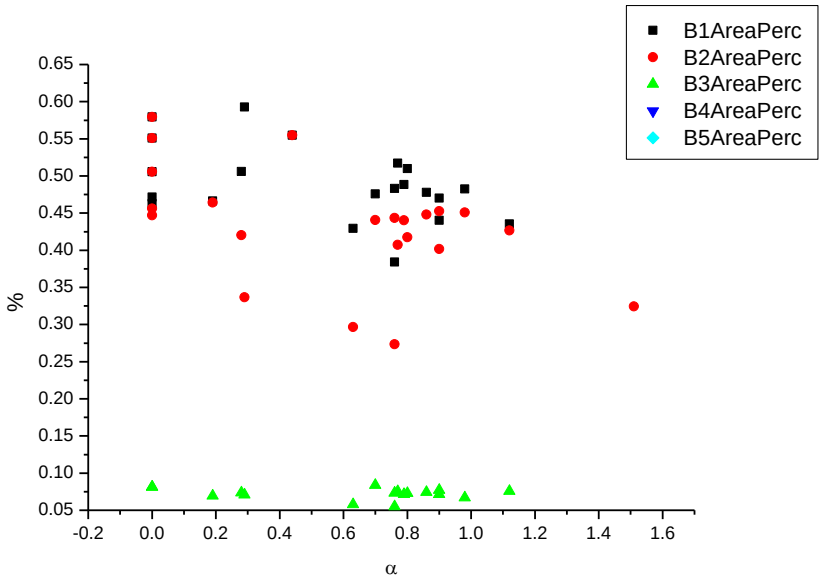

Figure 1.1.10. Area percentages from Gaussian model fit of the normalised fluorescence emission spectra of **3a** recorded at 310 nm excitation against α.

1.1.4.3 β.

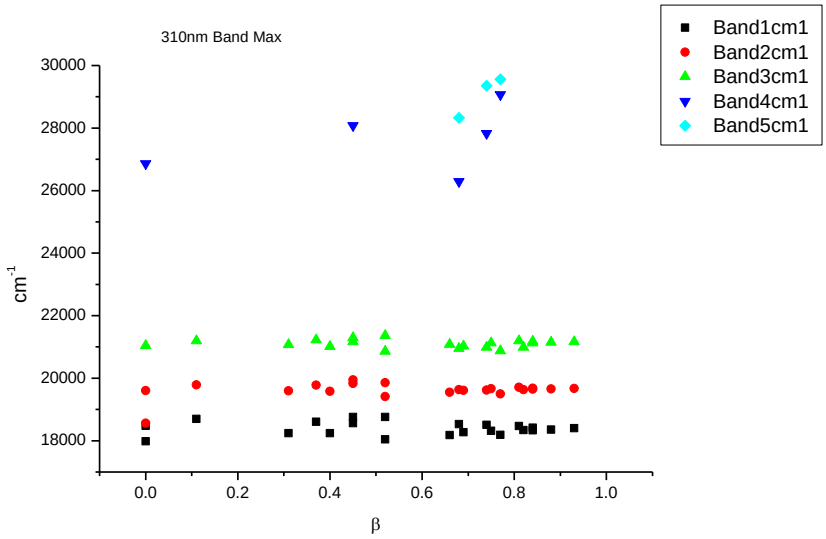

Figure 1.1.11. Band maxima from Gaussian model fit of the normalised fluorescence emission spectra of **3a** recorded at 310 nm excitation against β.

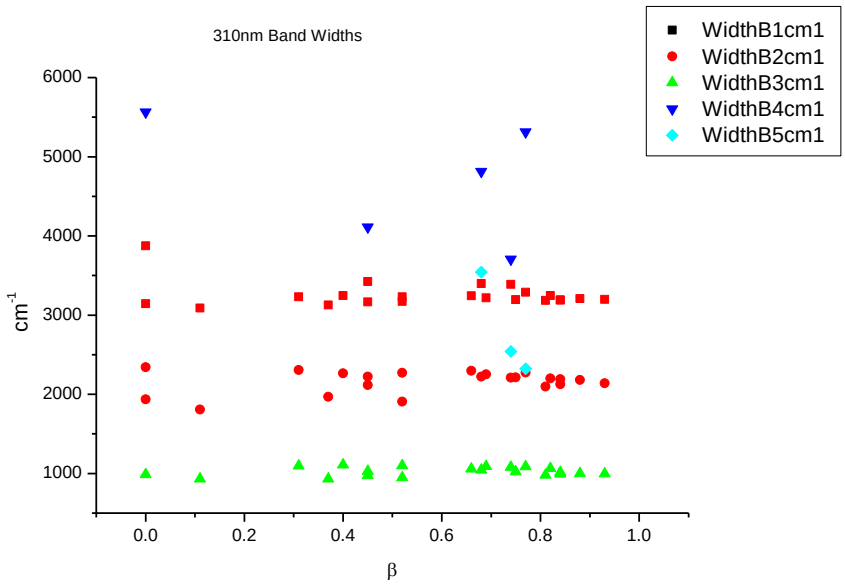

Figure 1.1.12. Band widths from Gaussian model fit of the normalised fluorescence emission spectra of **3a** recorded at 310 nm excitation against β.

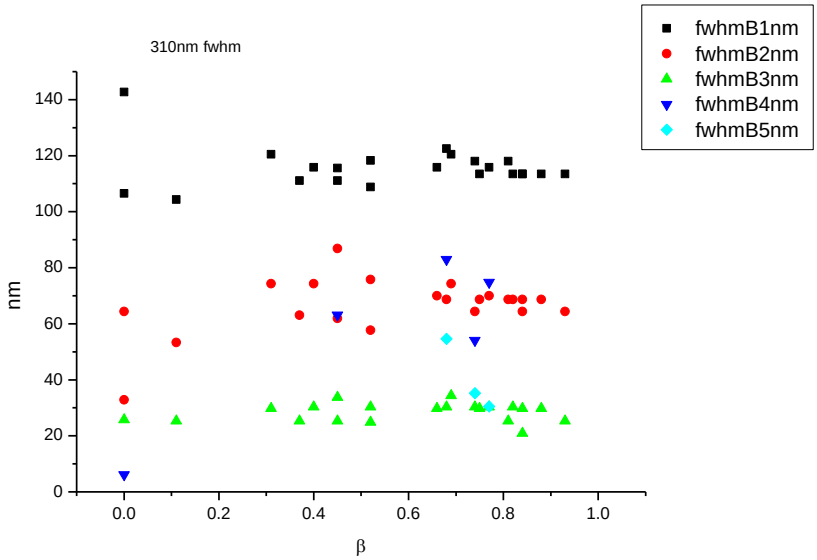

Figure 1.1.13. Full width half maxima from Gaussian model fit of the normalised fluorescence emission spectra of **3a** recorded at 310 nm excitation against β.

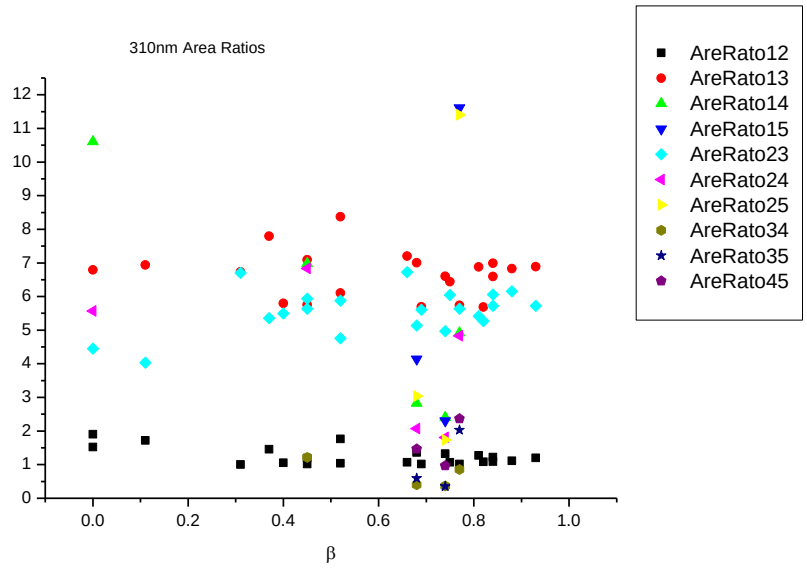

Figure 1.1.14. Area ratios from Gaussian model fit of the normalised fluorescence emission spectra of **3a** recorded at 310 nm excitation against β.

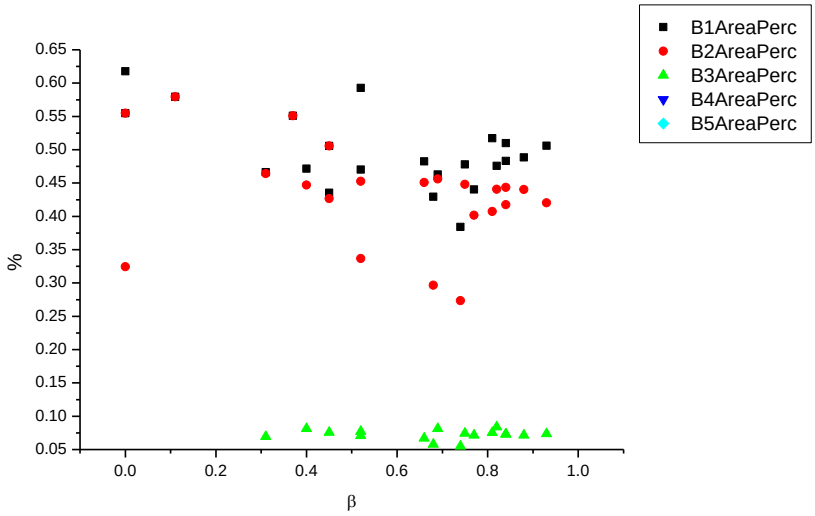

Figure 1.1.15. Area percentages from Gaussian model fit of the normalised fluorescence emission spectra of **3a** recorded at 310 nm excitation against β.

1.1.4.4 π.*

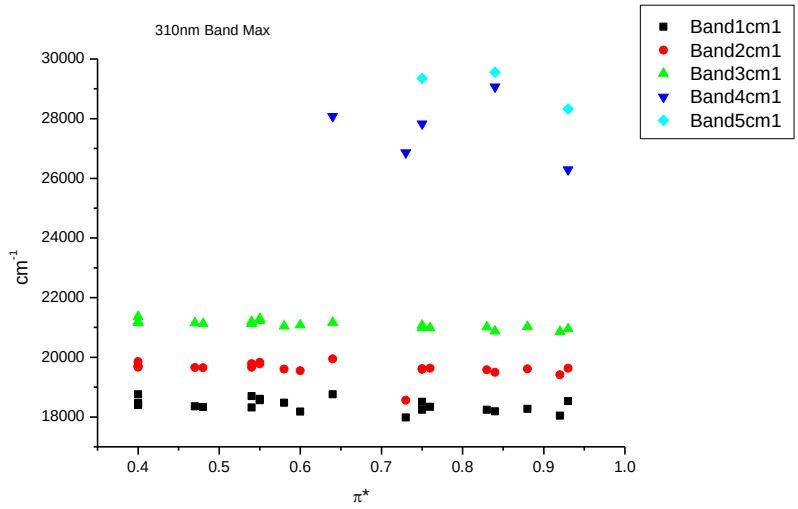

Figure 1.1.16. Band maxima from Gaussian model fit of the normalised fluorescence emission spectra of **3a** recorded at 310 nm excitation against π*.

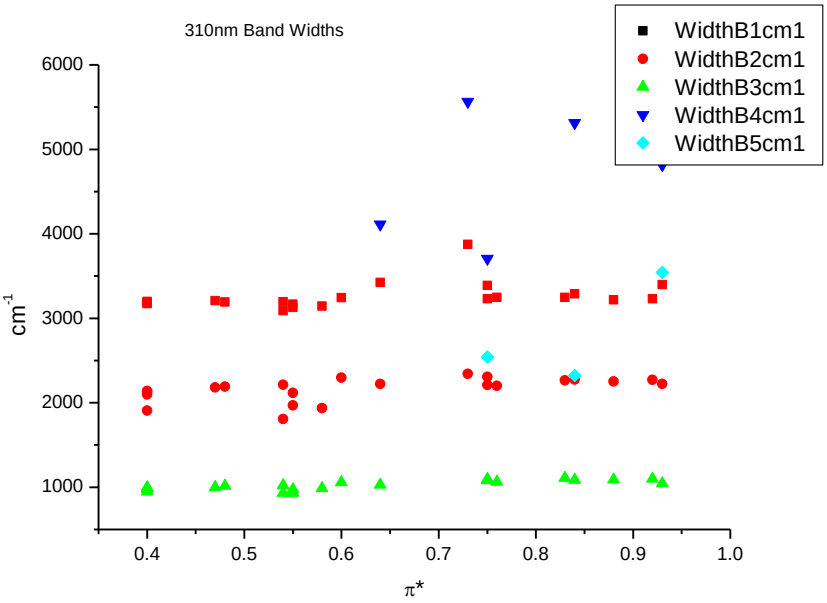

Figure 1.1.17. Band widths from Gaussian model fit of the normalised fluorescence emission spectra of **3a** recorded at 310 nm excitation against π*.

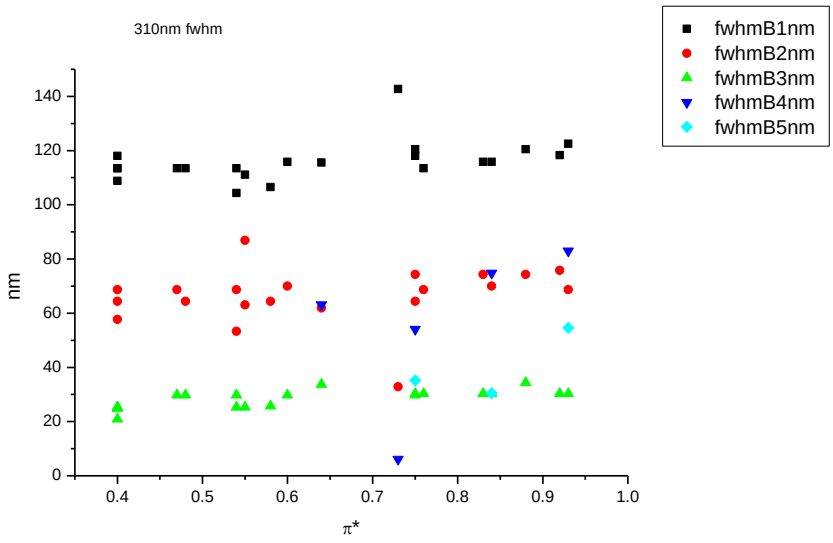

Figure 1.1.18. Full width half maxima from Gaussian model fit of the normalised fluorescence emission spectra of **3a** recorded at 310 nm excitation against π*.

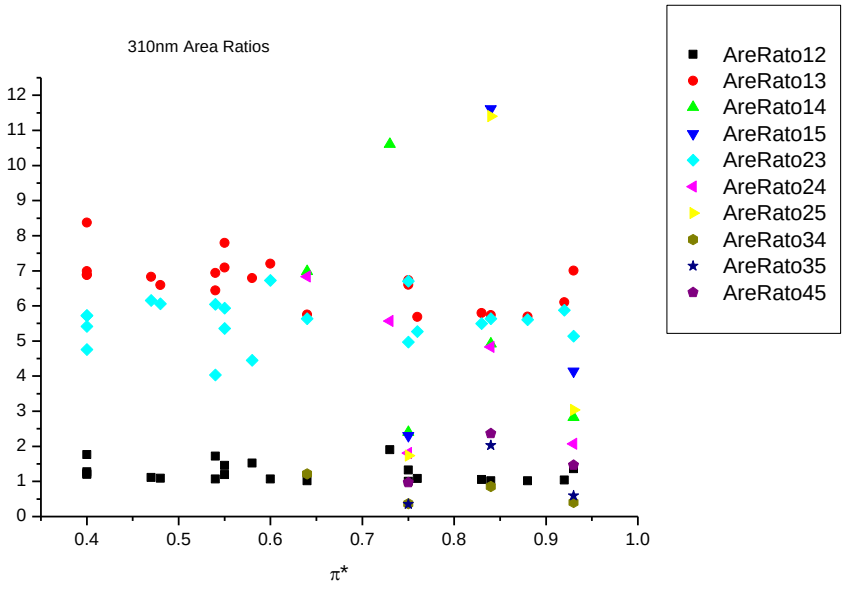

Figure 1.1.19. Area ratios from Gaussian model fit of the normalised fluorescence emission spectra of **3a** recorded at 310 nm excitation against π*.

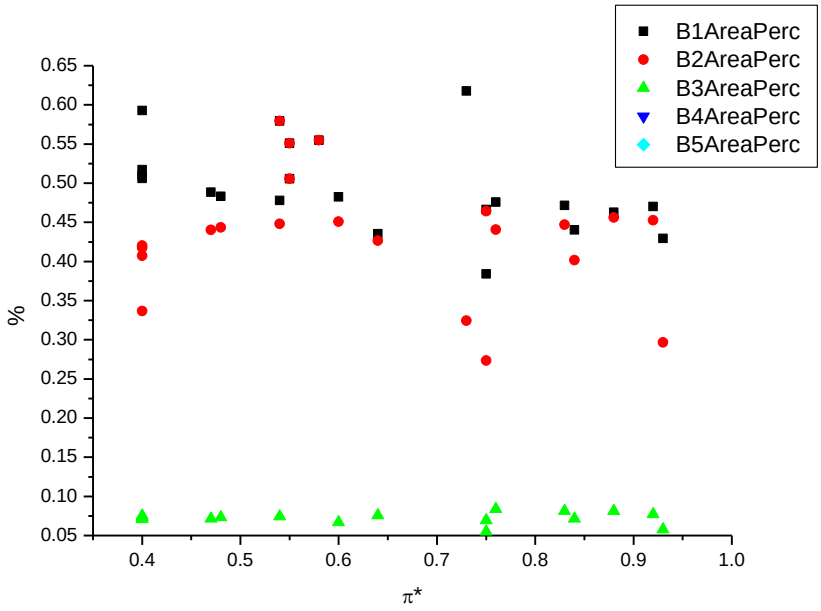

Figure 1.1.20. Area percentages from Gaussian model fit of the normalised fluorescence emission spectra of **3a** recorded at 310 nm excitation against π*.

1.1.4.5 μ(D).

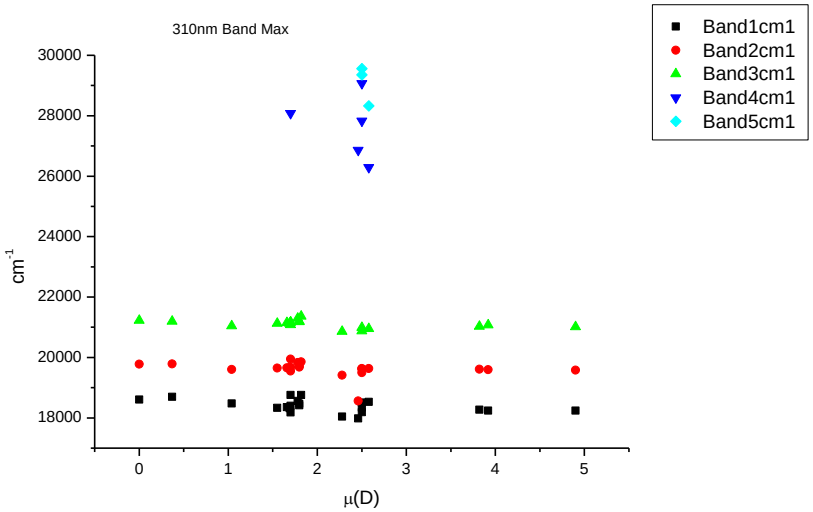

Figure 1.1.21. Band maxima from Gaussian model fit of the normalised fluorescence emission spectra of **3a** recorded at 310 nm excitation against μ(D).

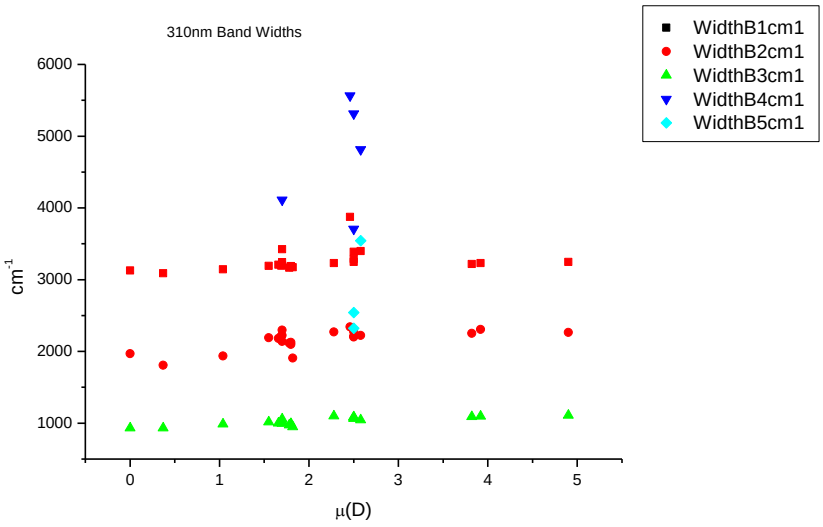

Figure 1.1.22. Band widths from Gaussian model fit of the normalised fluorescence emission spectra of **3a** recorded at 310 nm excitation against μ(D).

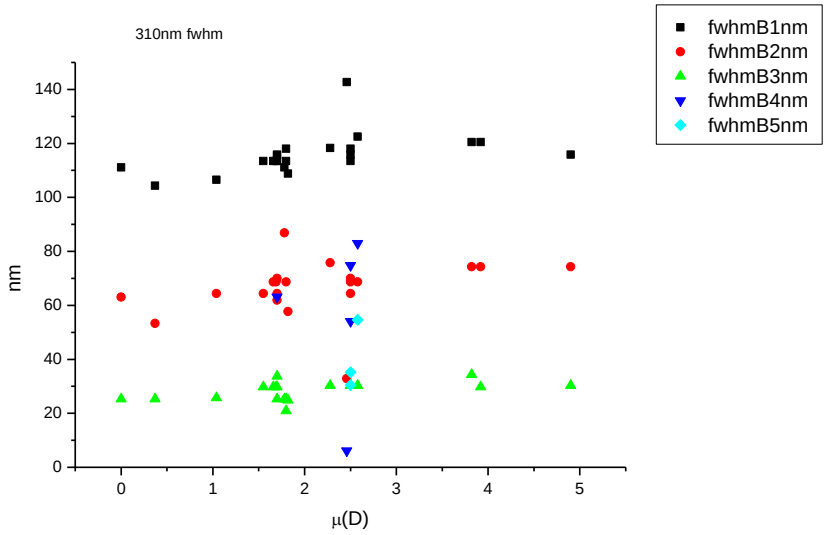

Figure 1.1.23. Full width half maxima from Gaussian model fit of the normalised fluorescence emission spectra of **3a** recorded at 310 nm excitation against μ(D).

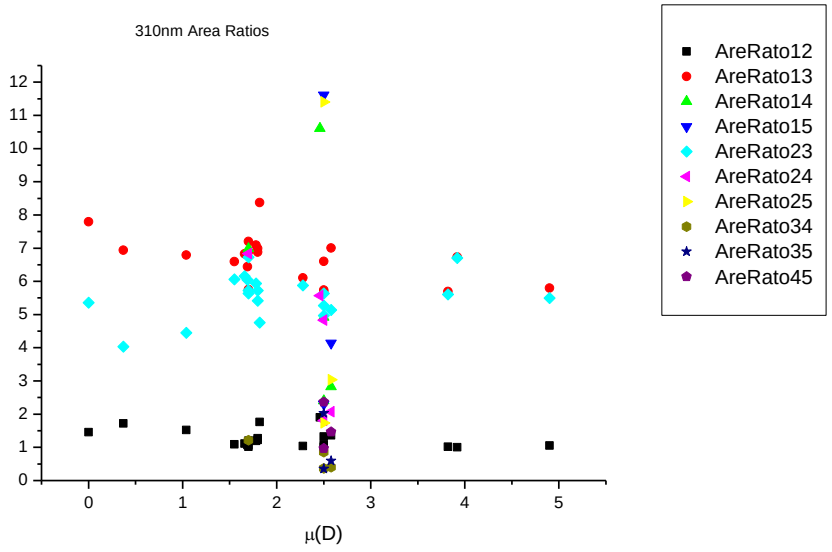

Figure 1.1.24. Area ratios from Gaussian model fit of the normalised fluorescence emission spectra of **3a** recorded at 310 nm excitation against μ(D).

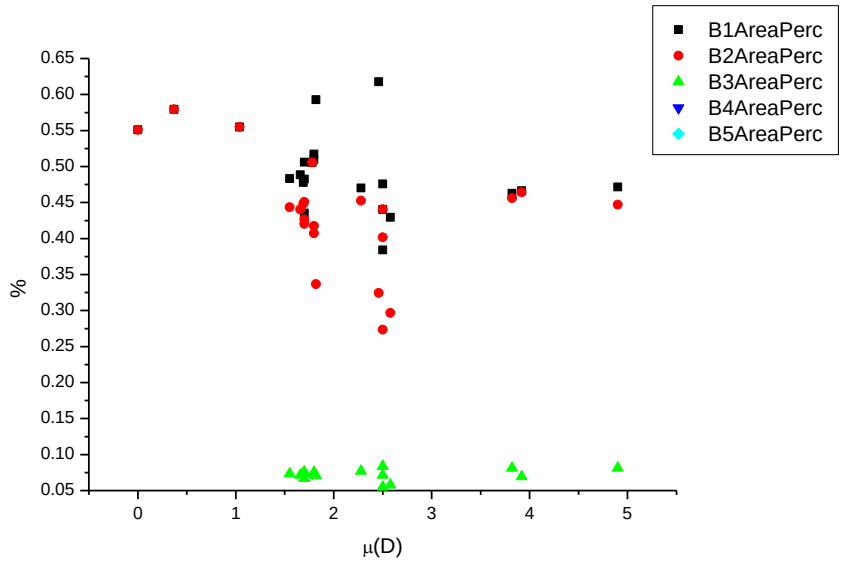

Figure 1.1.25. Area percentages from Gaussian model fit of the normalised fluorescence emission spectra of **3a** recorded at 310 nm excitation against μ(D).

1.1.4.6 η(Cp).

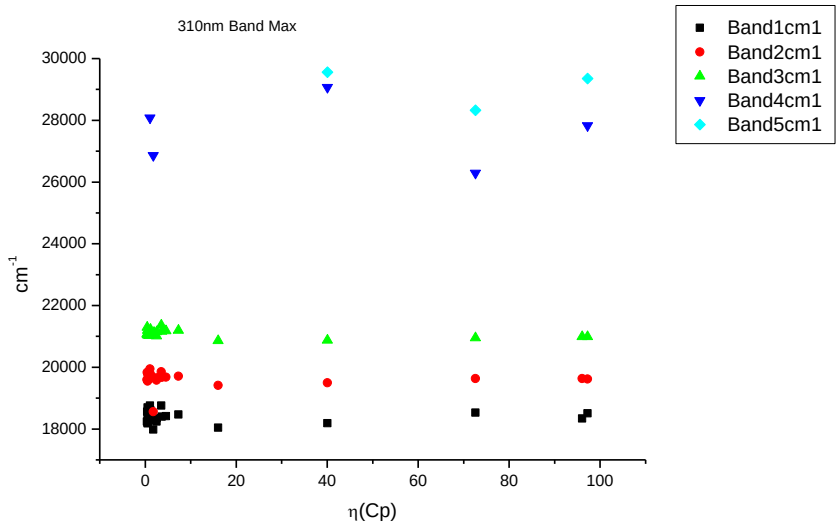

Figure 1.1.26. Band maxima from Gaussian model fit of the normalised fluorescence emission spectra of **3a** recorded at 310 nm excitation against η(Cp).

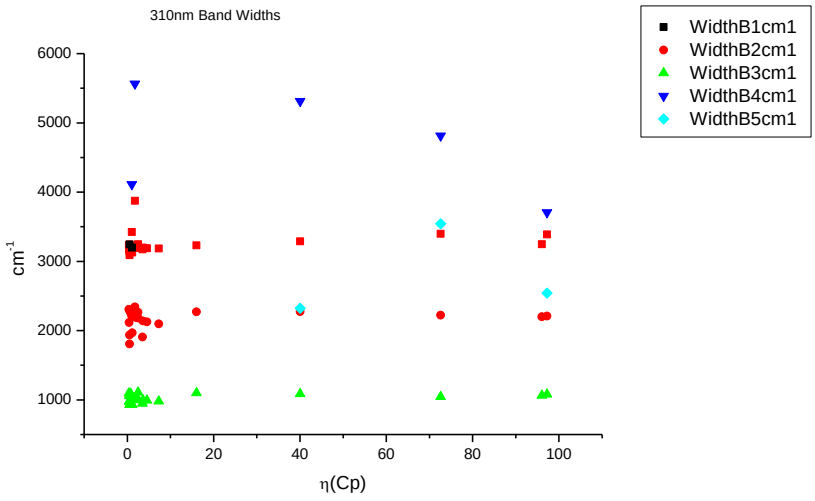

Figure 1.1.27. Band widths from Gaussian model fit of the normalised fluorescence emission spectra of **3a** recorded at 310 nm excitation against η(Cp).

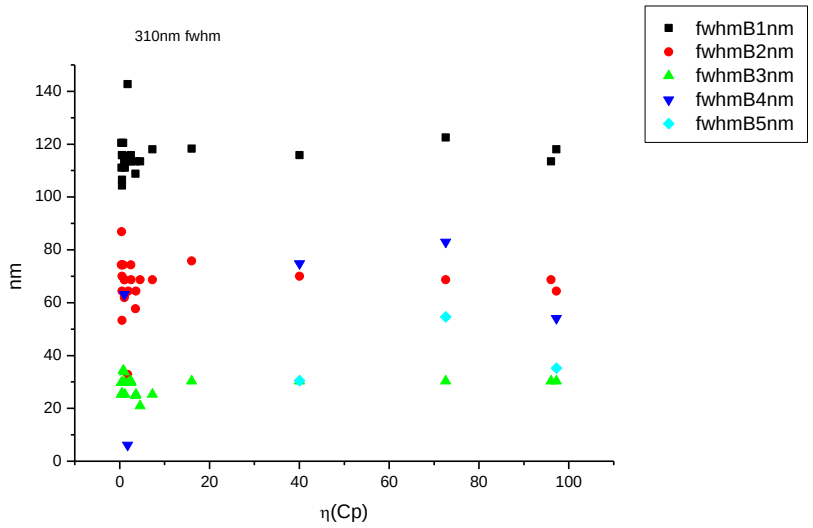

Figure 1.1.28. Full width half maxima from Gaussian model fit of the normalised fluorescence emission spectra of **3a** recorded at 310 nm excitation against η(Cp).

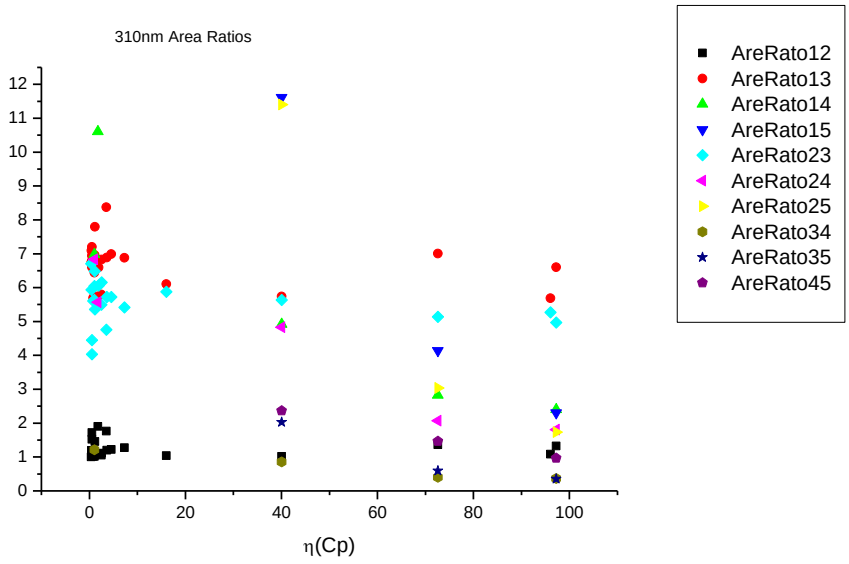

Figure 1.1.29. Area ratios from Gaussian model fit of the normalised fluorescence emission spectra of **3a** recorded at 310 nm excitation against η(Cp).

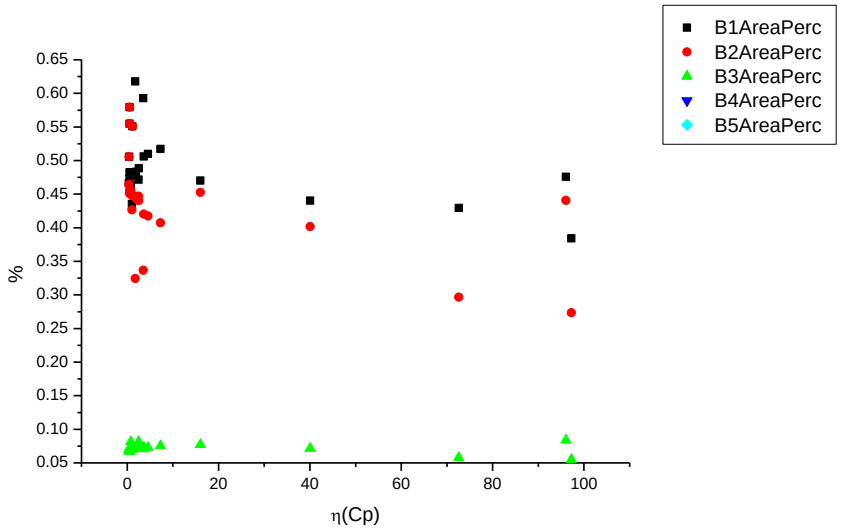

Figure 1.1.30. Area percentages from Gaussian model fit of the normalised fluorescence emission spectra of **3a** recorded at 310 nm excitation against η(Cp).

1.1.5 400 nm Gaussian band fit - Solvatochromic analysis.

1.1.5.1 E_T^N.

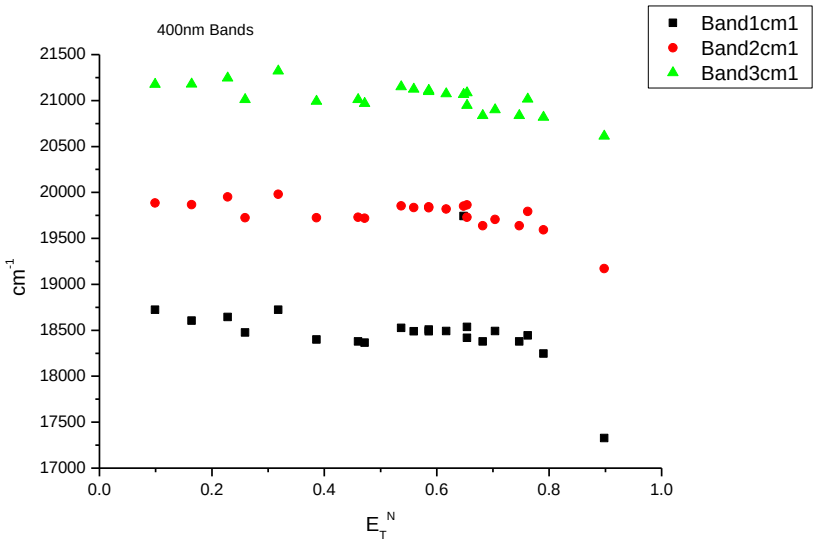

Figure 1.1.31. Band maxima from Gaussian model fit of the normalised fluorescence emission spectra of **3a** recorded at 400 nm excitation against E_T^N.

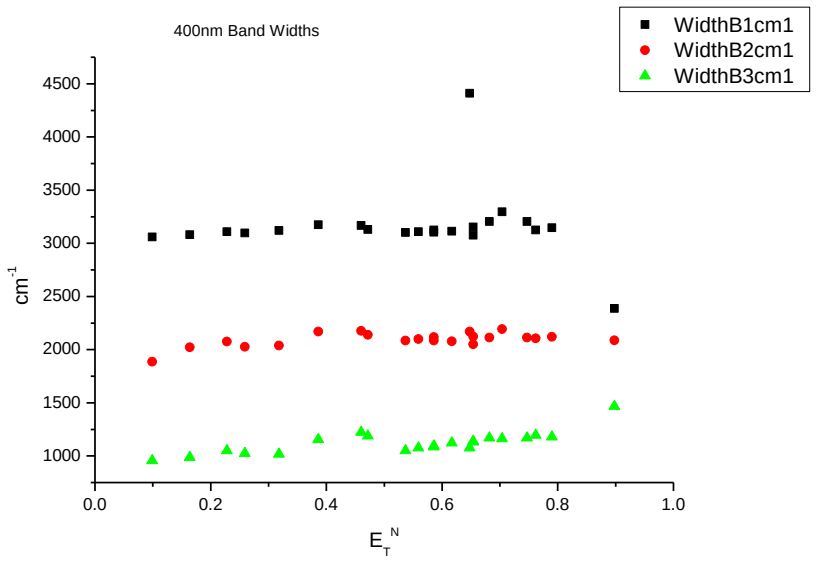

Figure 1.1.32. Band widths from Gaussian model fit of the normalised fluorescence emission spectra of **3a** recorded at 400 nm excitation against E_T^N.

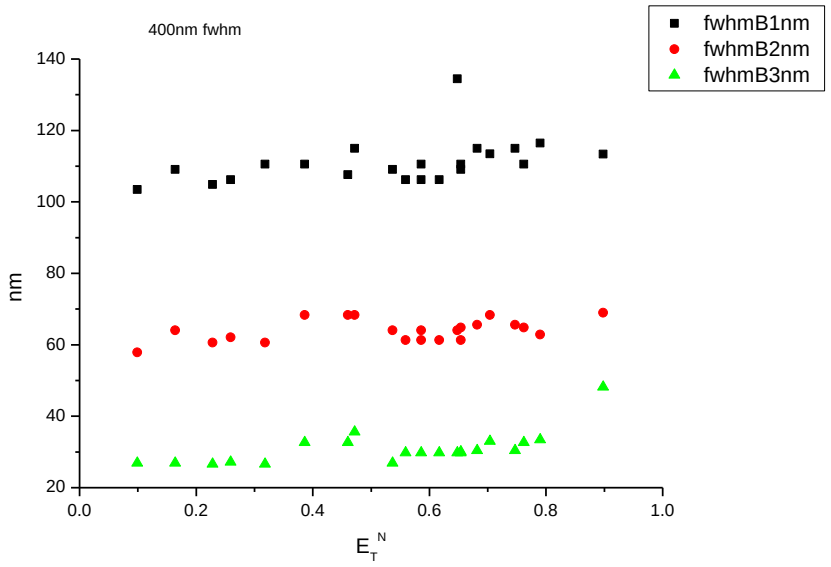

Figure 1.1.33. Full width half maxima from Gaussian model fit of the normalised fluorescence emission spectra of **3a** recorded at 400 nm excitation against E_T^N.

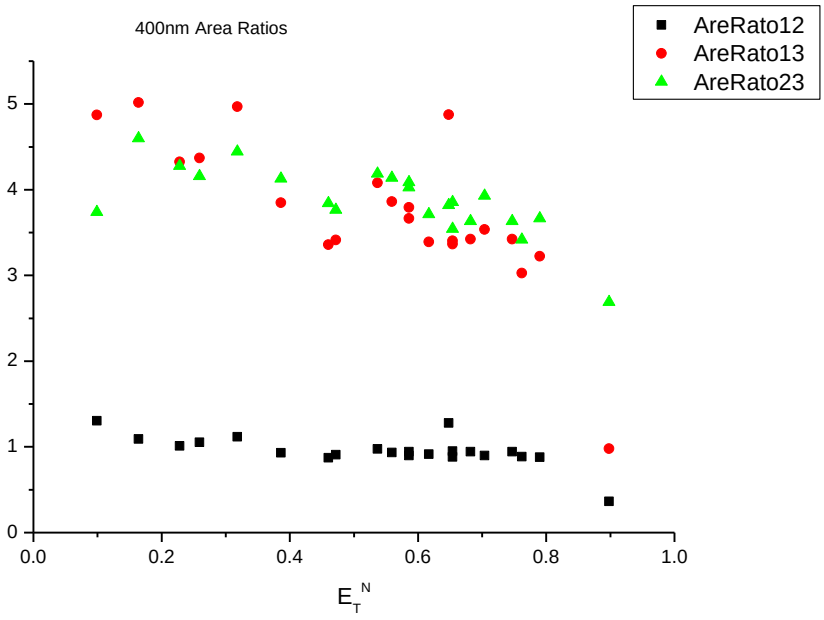

Figure 1.1.34. Area ratios from Gaussian model fit of the normalised fluorescence emission spectra of **3a** recorded at 400 nm excitation against E_T^N.

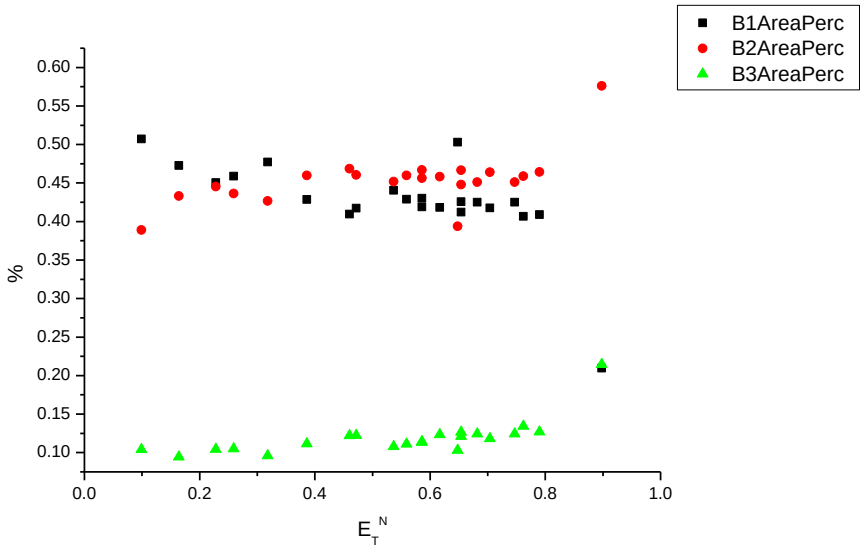

Figure 1.1.35. Area percentages from Gaussian model fit of the normalised fluorescence emission spectra of **3a** recorded at 400 nm excitation against E_T^N.

1.1.5.2 α.

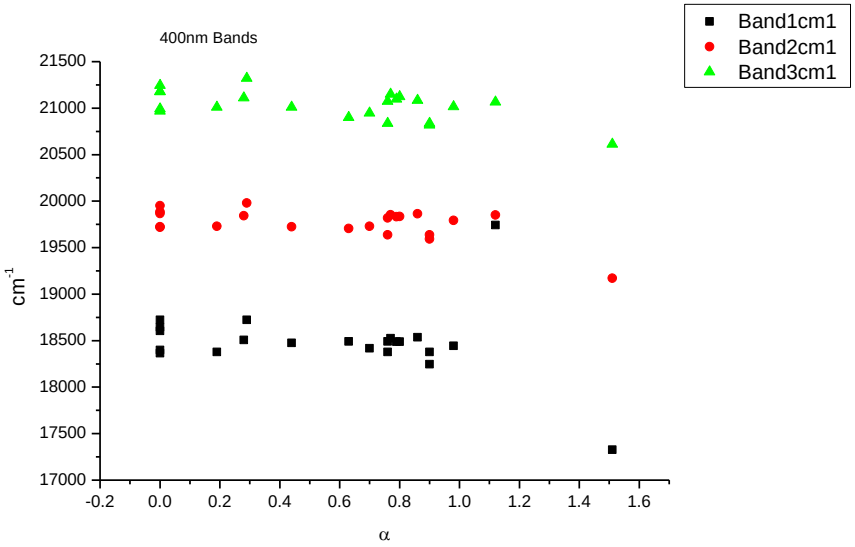

Figure 1.1.36. Band maxima from Gaussian model fit of the normalised fluorescence emission spectra of **3a** recorded at 400 nm excitation against α.

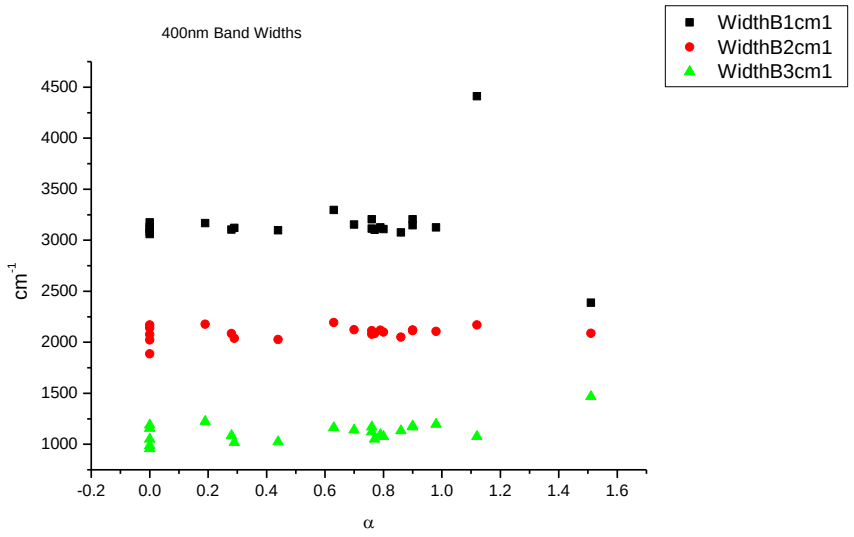

Figure 1.1.37. Band widths from Gaussian model fit of the normalised fluorescence emission spectra of **3a** recorded at 400 nm excitation against α.

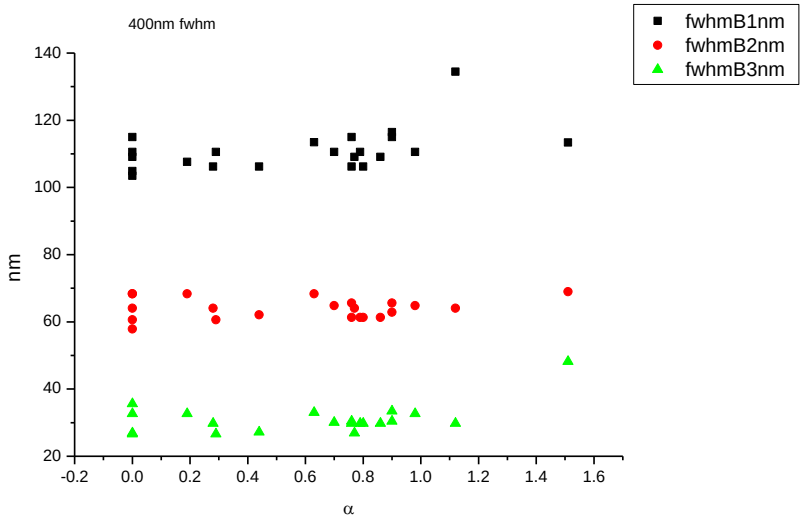

Figure 1.1.38. Full width half maxima from Gaussian model fit of the normalised fluorescence emission spectra of **3a** recorded at 400 nm excitation against α.

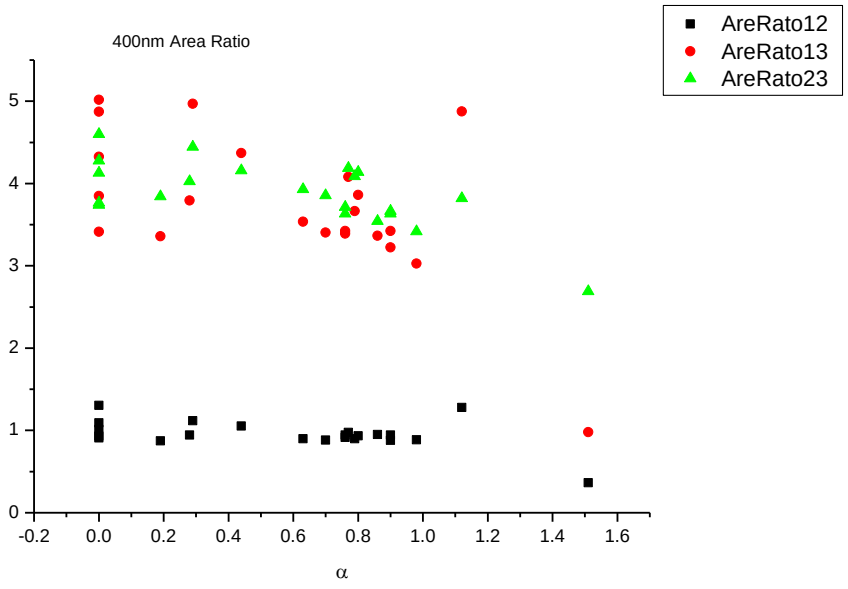

Figure 1.1.39. Area ratios from Gaussian model fit of the normalised fluorescence emission spectra of **3a** recorded at 400 nm excitation against α.

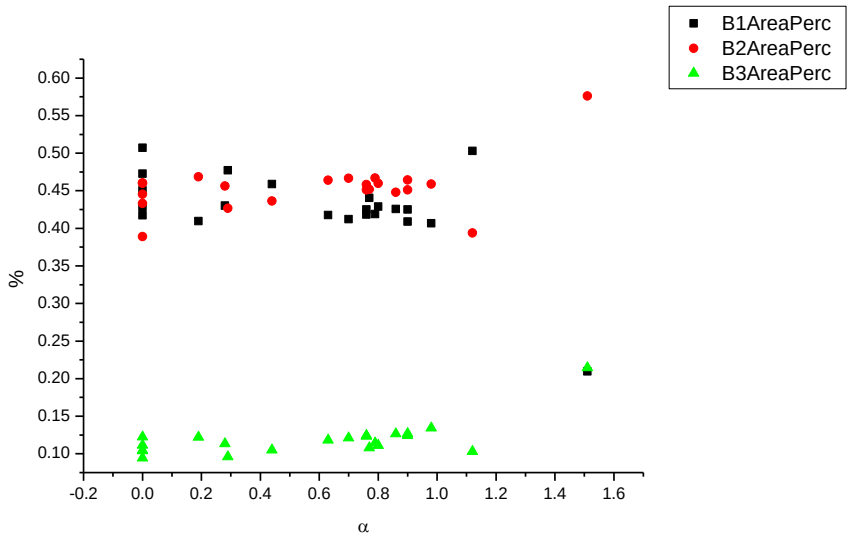

Figure 1.1.40. Area percentages from Gaussian model fit of the normalised fluorescence emission spectra of **3a** recorded at 400 nm excitation against α.

1.1.5.3 β.

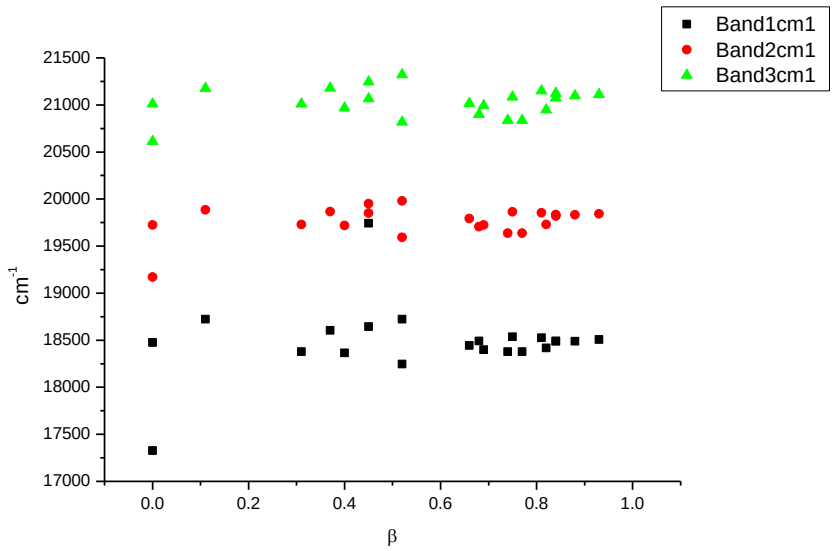

Figure 1.1.41. Band maxima from Gaussian model fit of the normalised fluorescence emission spectra of **3a** recorded at 400 nm excitation against β.

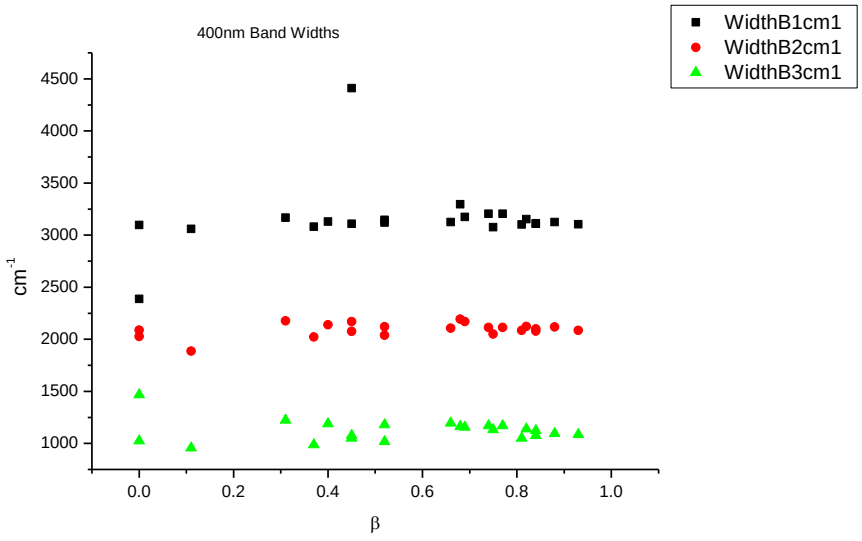

Figure 1.1.42. Band widths from Gaussian model fit of the normalised fluorescence emission spectra of **3a** recorded at 400 nm excitation against β.

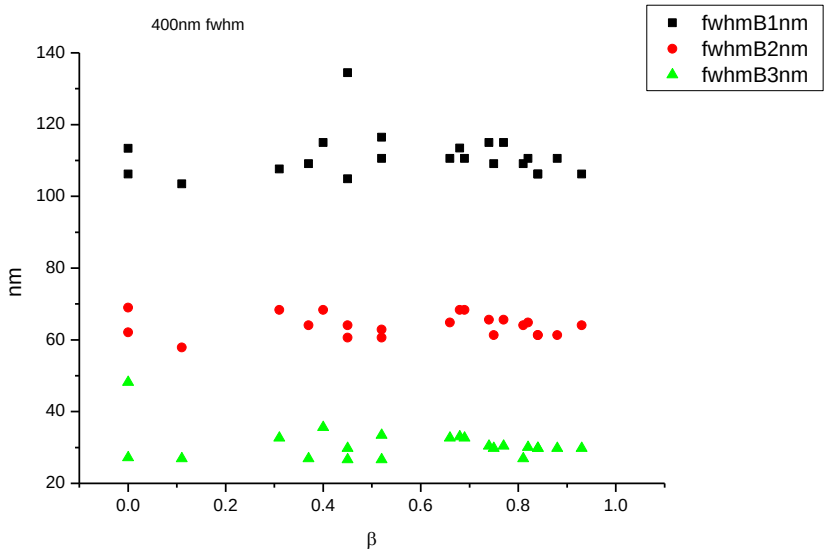

Figure 1.1.43. Full width half maxima from Gaussian model fit of the normalised fluorescence emission spectra of **3a** recorded at 400 nm excitation against β.

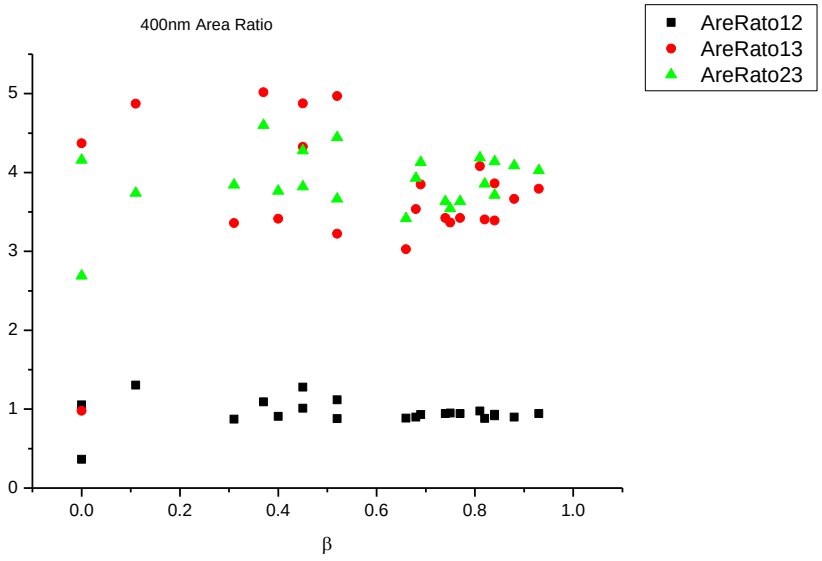

Figure 1.1.44. Area ratios from Gaussian model fit of the normalised fluorescence emission spectra of **3a** recorded at 400 nm excitation against β.

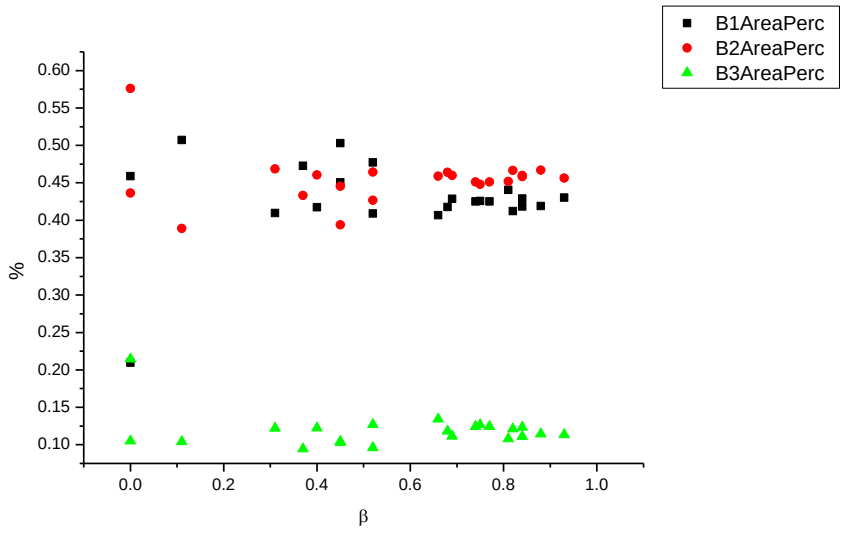

Figure 1.1.45. Area percentages from Gaussian model fit of the normalised fluorescence emission spectra of **3a** recorded at 400 nm excitation against β.

1.1.5.4 π.*

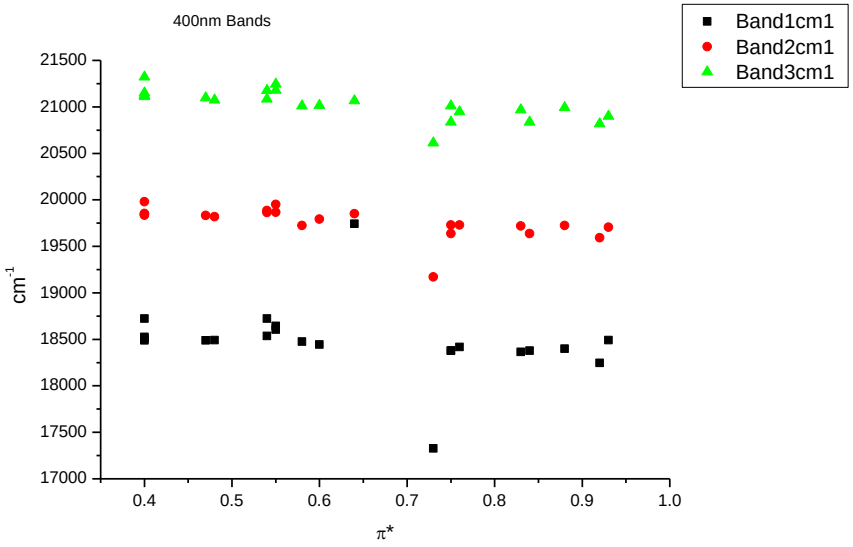

Figure 1.1.46. Band maxima from Gaussian model fit of the normalised fluorescence emission spectra of **3a** recorded at 400 nm excitation against π*.

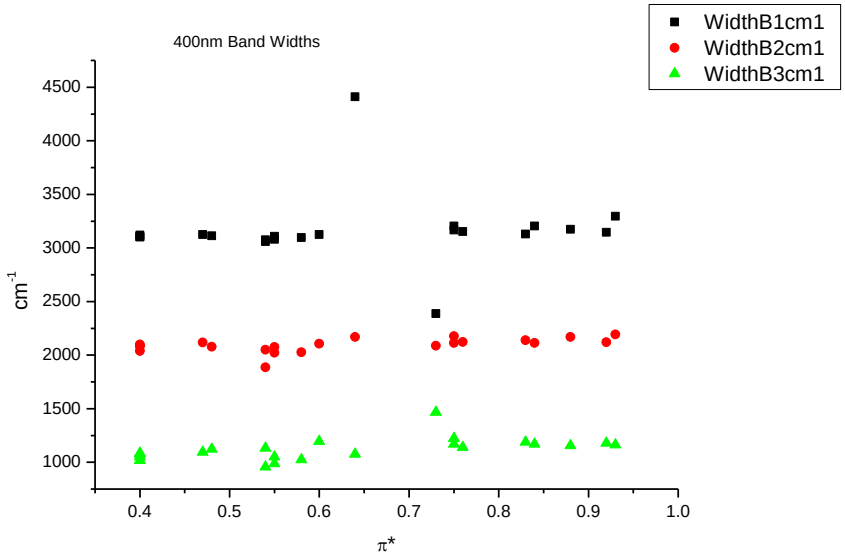

Figure 1.1.47. Band widths from Gaussian model fit of the normalised fluorescence emission spectra of **3a** recorded at 400 nm excitation against π*.

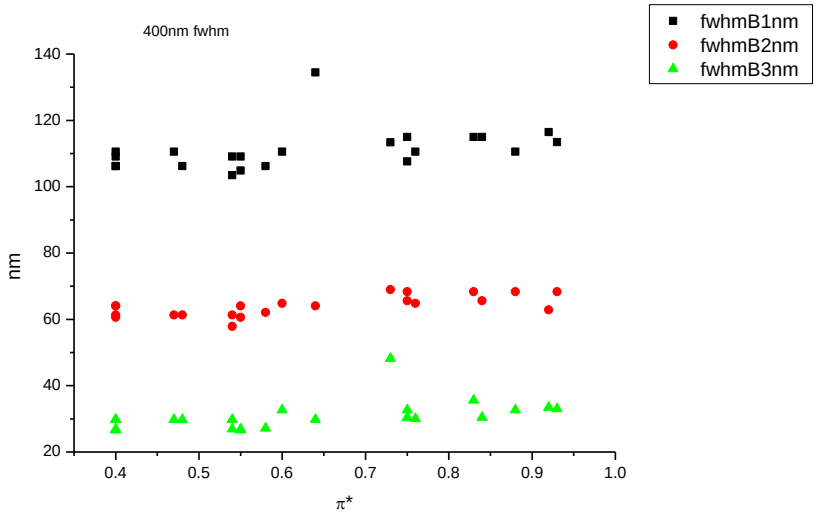

Figure 1.1.48. Full width half maxima from Gaussian model fit of the normalised fluorescence emission spectra of **3a** recorded at 400 nm excitation against π*.

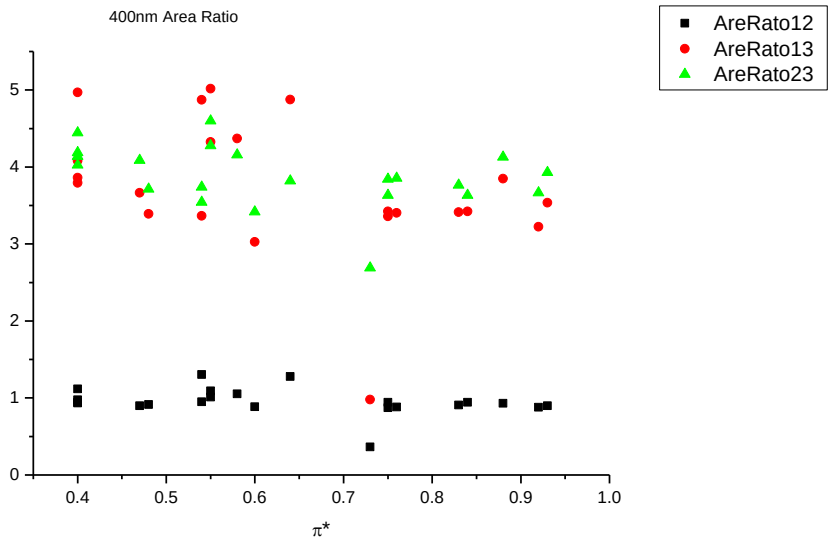

Figure 1.1.49. Area ratios from Gaussian model fit of the normalised fluorescence emission spectra of **3a** recorded at 400 nm excitation against π*.

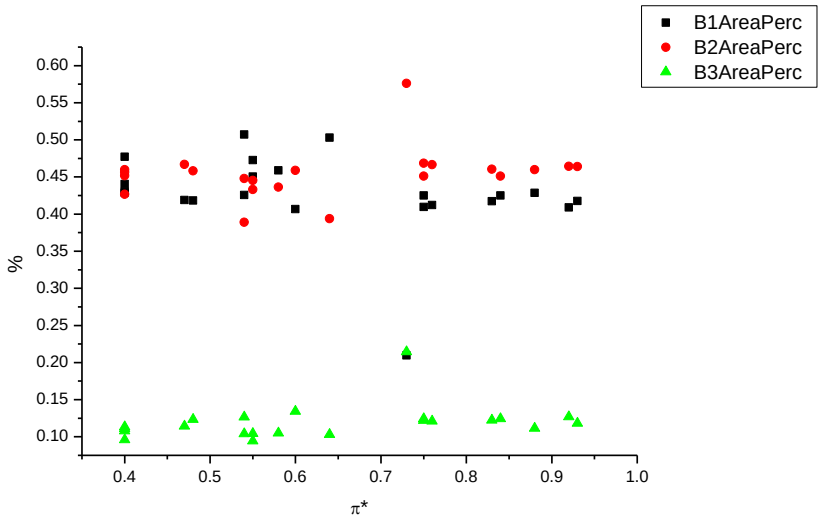

Figure 1.1.50. Area percentages from Gaussian model fit of the normalised fluorescence emission spectra of **3a** recorded at 400 nm excitation against π*.

1.1.5.5 μ(D).

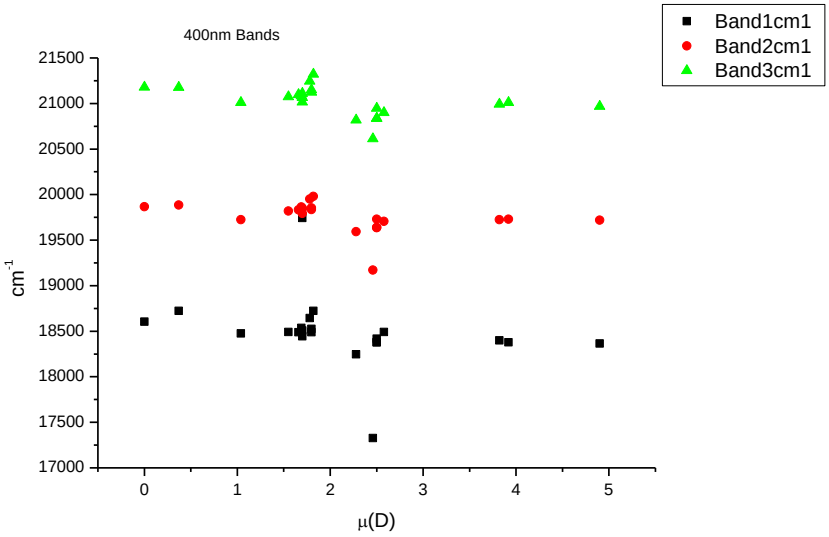

Figure 1.1.51. Band maxima from Gaussian model fit of the normalised fluorescence emission spectra of **3a** recorded at 400 nm excitation against μ(D).

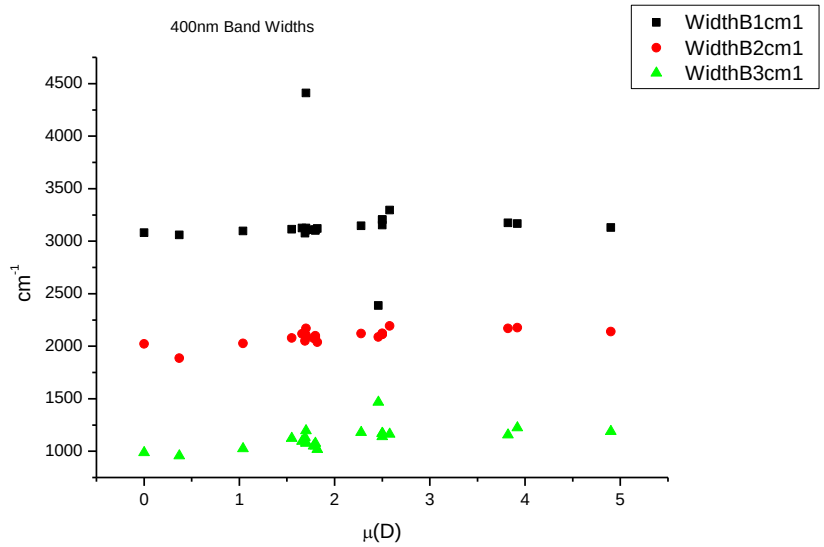

Figure 1.1.52. Band widths from Gaussian model fit of the normalised fluorescence emission spectra of **3a** recorded at 400 nm excitation against μ(D).

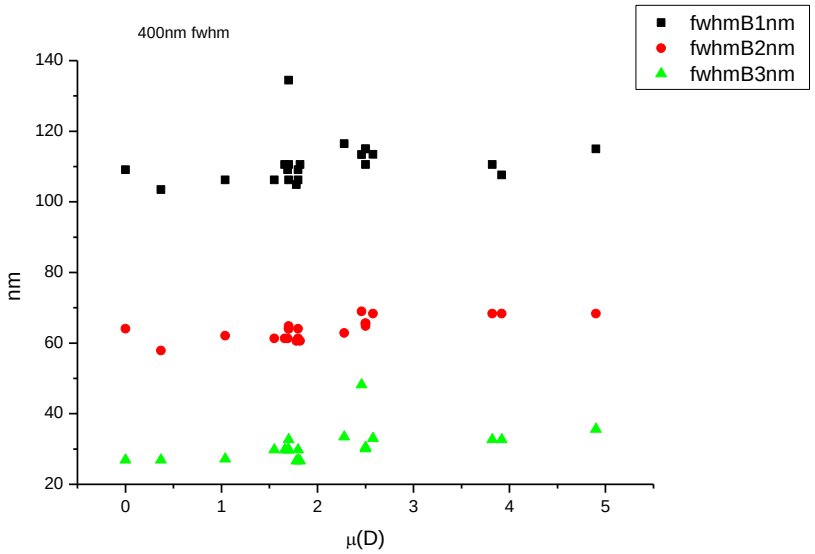

Figure 1.1.53. Full width half maxima from Gaussian model fit of the normalised fluorescence emission spectra of **3a** recorded at 400 nm excitation against μ(D).

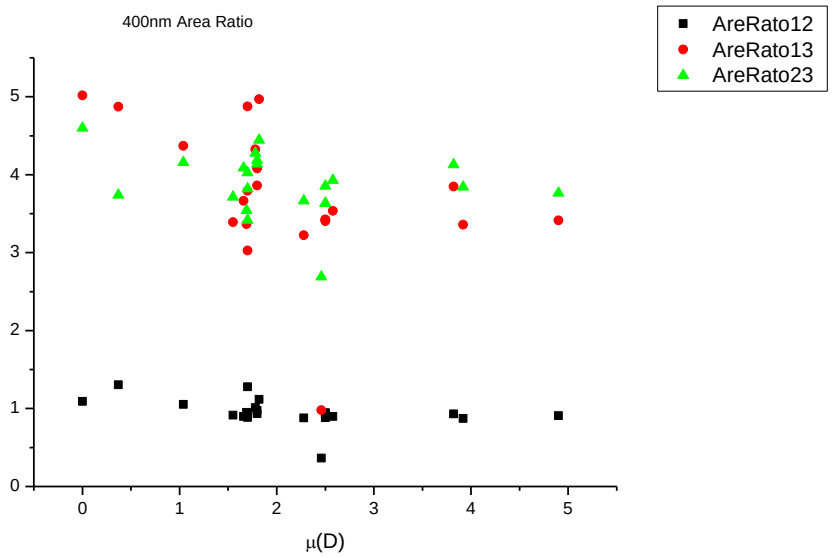

Figure 1.1.54. Area ratios from Gaussian model fit of the normalised fluorescence emission spectra of **3a** recorded at 400 nm excitation against μ(D).

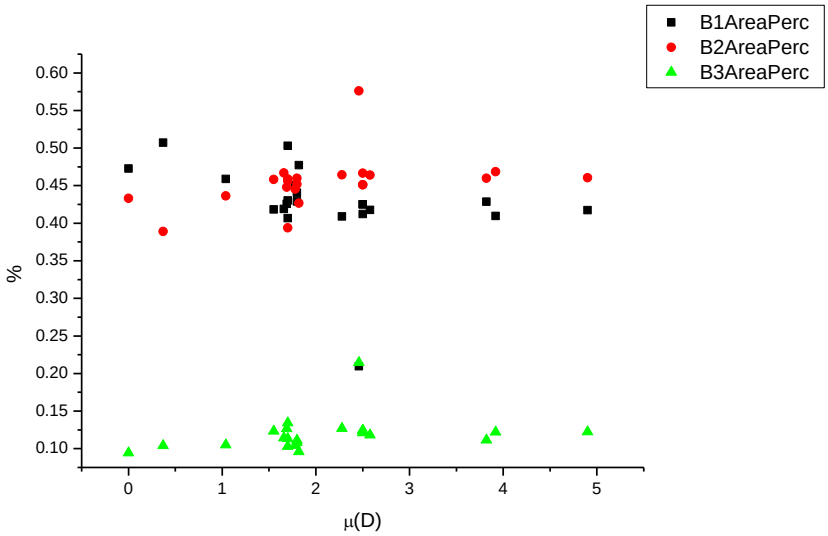

Figure 1.1.55. Area percentages from Gaussian model fit of the normalised fluorescence emission spectra of **3a** recorded at 400 nm excitation against μ(D).

1.1.5.6 η(Cp).

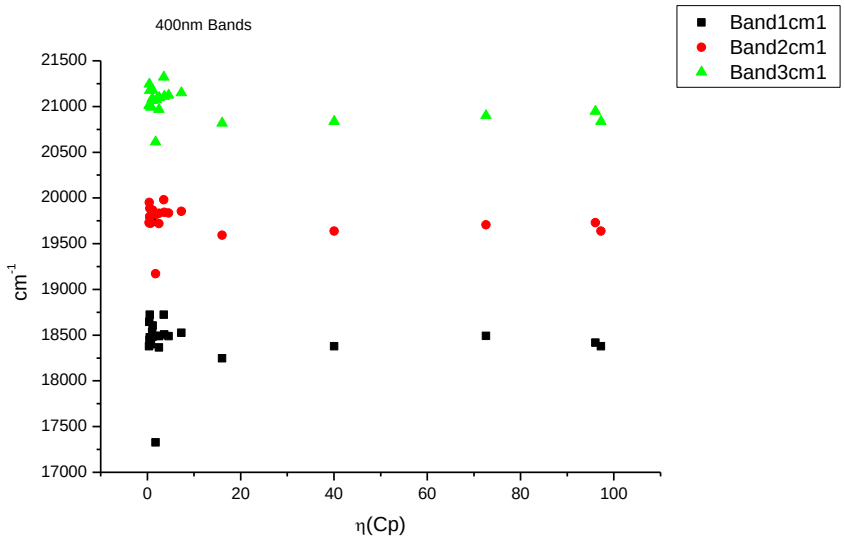

Figure 1.1.56. Band maxima from Gaussian model fit of the normalised fluorescence emission spectra of **3a** recorded at 400 nm excitation against η(Cp).

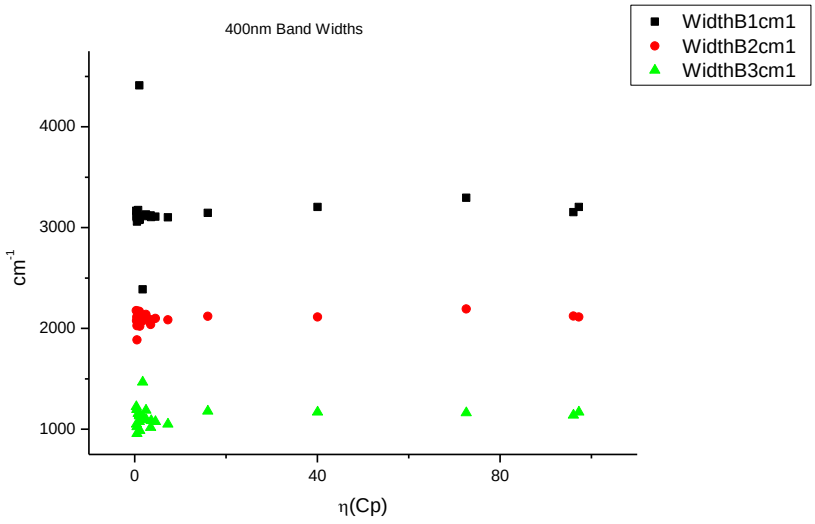

Figure 1.1.57. Band widths from Gaussian model fit of the normalised fluorescence emission spectra of **3a** recorded at 400 nm excitation against η(Cp).

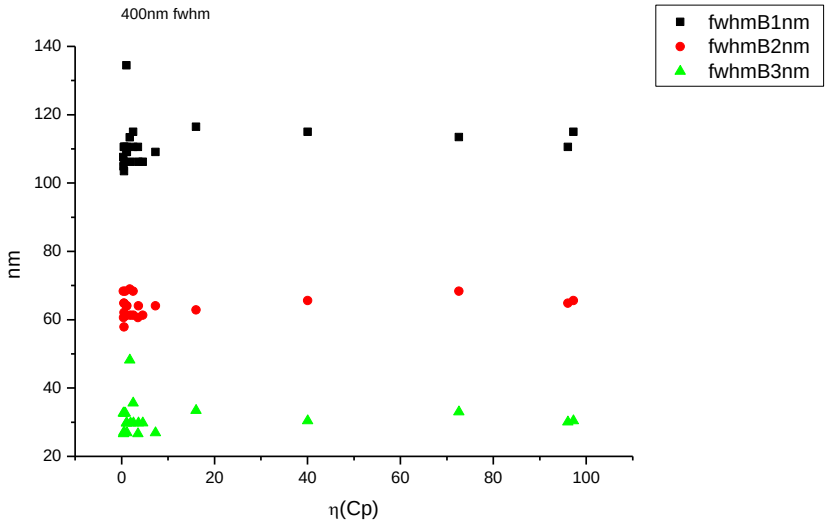

Figure 1.1.58. Full width half maxima from Gaussian model fit of the normalised fluorescence emission spectra of **3a** recorded at 400 nm excitation against η(Cp).

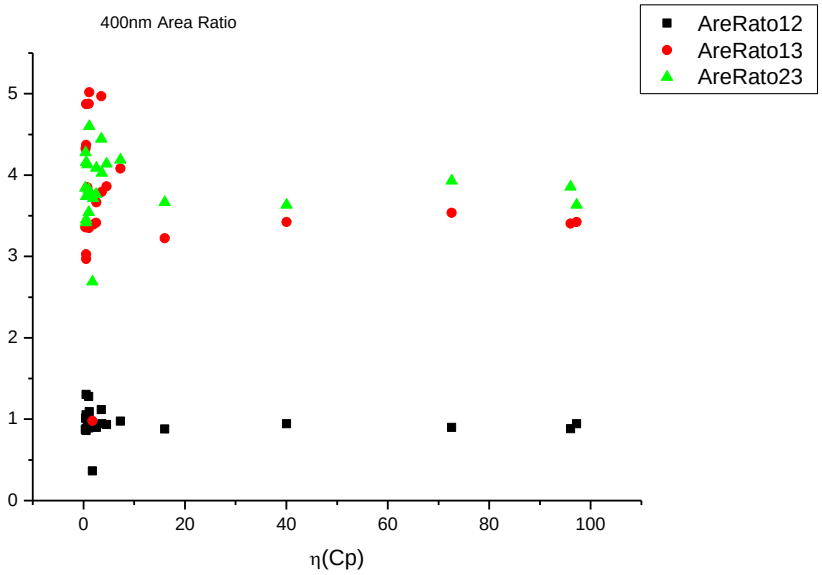

Figure 1.1.59. Area ratios from Gaussian model fit of the normalised fluorescence emission spectra of **3a** recorded at 400 nm excitation against η(Cp).

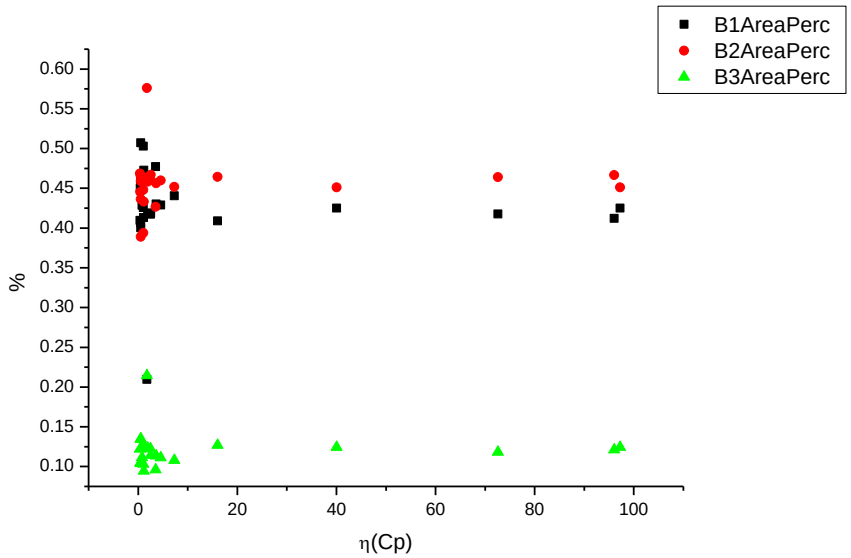

Figure 1.1.60. Area percentages from Gaussian model fit of the normalised fluorescence emission spectra of **3a** recorded at 400 nm excitation against η(Cp).

1.1.6 400 nm fluorescent lifetime results.

1.1.6.1 Intensity weighted.

Wavelength (nm)	Solvent	τ_1 (ns)	A_1 (%)	τ_2 (ns)	A_2 (%)	τ_3 (ns)	A_3 (%)	τ_f (ns) (Intensity Weighted)	$1/\tau_f$	χ^2
470	Toluene	-	-	3.88	64.35	9.15	35.65	5.76	0.17	1.08
470	1,4-Dioxane	0.33	3.30	3.35	72.12	8.10	24.58	4.42	0.23	1.12
470	Ethyl acetate	-	-	4.73	73.15	10.19	26.85	6.19	0.16	1.10
470	Chloroform	-	-	4.99	70.84	10.59	29.16	6.62	0.15	1.07
470	2-Methyl-2-butanol	0.40	2.70	4.28	71.98	10.23	25.31	5.68	0.18	1.13
470	N,N-dimethylformamide	0.24	0.97	5.50	72.12	10.36	26.92	6.75	0.15	1.10
470	Acetonitrile	-	-	4.78	68.38	9.60	31.62	6.30	0.16	1.19
470	Propylene carbonate	0.37	1.14	5.53	70.78	10.53	28.08	6.87	0.15	1.12
470	1-Octanol	0.60	4.69	5.16	76.63	10.57	18.68	5.96	0.17	1.11
470	1-Hexanol	0.41	3.58	5.13	80.46	10.25	15.95	5.78	0.17	1.06
470	1-Butanol	0.32	2.79	4.98	82.67	9.77	14.54	5.54	0.18	1.07
470	1-Pentanol	0.33	2.63	5.18	80.89	9.69	16.48	5.80	0.17	1.10
470	1-Propanol	0.20	1.96	4.88	79.76	8.56	18.28	5.46	0.18	1.04
470	Acetic acid	0.37	90.61	1.19	9.39	-	-	0.45	2.23	0.94
470	Ethanol	0.44	4.51	4.72	37.24	7.99	58.25	6.43	0.16	1.10
470	1,5-Pentanediol	-	-	4.74	72.19	7.75	27.81	5.57	0.18	1.14
470	1,3-Butanediol	0.42	3.93	4.23	33.60	7.57	62.47	6.17	0.16	1.12
470	1,4-Butanediol	0.32	4.56	3.10	34.16	6.61	61.28	5.12	0.20	1.19
470	1,3-Propanediol	0.39	2.16	3.78	25.75	6.78	72.09	5.87	0.17	1.07
470	Methanol	-	-	3.09	35.61	4.76	64.39	4.16	0.24	1.11
470	1,2-Ethanediol	-	-	2.05	12.27	5.55	87.73	5.12	0.20	1.14
470	2,2,2-Trifluoroethanol	0.19	85.52	0.41	14.48	-	-	0.22	4.47	1.40
470	Ethanol-d	-	-	4.88	70.23	8.16	29.77	5.85	0.17	1.11
470	Methanol-d	-	-	4.49	78.18	7.10	21.82	5.06	0.20	1.10

Table 1.1.9[1]. Summary of Time Correlated Single Photon Counting (TCSPC) fluorescent lifetimes (intensity weighted) of **3a** recorded at 470 nm.

[1] A_i represents the fractional intensities, τ_i represents the individual lifetime components, and τ_f is the intensity-averaged lifetime.

Wavelength (nm)	Solvent	τ_1 (ns)	A_1 (%)	τ_2 (ns)	A_2 (%)	τ_3 (ns)	A_3 (%)	τ_f (ns) (Intensity Weighted)	$1/\tau_f$	χ^2
490	Toluene	-	-	3.95	51.94	9.43	48.06	6.58	0.15	1.09
490	1,4-Dioxane	0.34	2.75	3.29	66.47	8.66	30.79	4.86	0.21	1.13
490	Ethyl acetate	-	-	4.67	61.81	10.79	38.19	7.01	0.14	1.15
490	Chloroform	-	-	5.13	63.86	11.36	36.14	7.38	0.14	1.10
490	2-Methyl-2-butanol	0.37	1.76	4.29	55.62	10.72	42.62	6.96	0.14	1.06
490	N,N-dimethylformamide	0.22	0.97	5.65	69.75	11.08	29.28	7.19	0.14	1.11
490	Acetonitrile	-	-	4.95	64.67	10.56	35.33	6.93	0.14	1.04
490	Propylene carbonate	0.39	0.78	5.64	68.78	11.68	30.44	7.44	0.13	1.09
490	1-Octanol	0.64	2.95	5.26	67.86	11.44	29.19	6.93	0.14	1.12
490	1-Hexanol	0.44	2.34	5.20	73.52	11.73	24.14	6.67	0.15	1.07
490	1-Butanol	0.33	1.74	5.04	76.50	11.19	21.76	6.30	0.16	1.06
490	1-Pentanol	0.39	1.86	5.33	77.43	11.49	20.71	6.52	0.15	1.07
490	1-Propanol	-	-	4.87	76.72	9.86	23.28	6.03	0.17	1.08
490	Acetic acid	0.38	93.29	1.31	6.71	-	-	0.45	2.24	1.14
490	Ethanol	0.43	2.17	5.59	61.30	9.81	36.53	7.02	0.14	1.14
490	1,5-Pentanediol	-	-	4.93	75.99	9.98	24.01	6.14	0.16	1.18
490	1,3-Butanediol	0.51	2.01	5.08	55.69	9.07	42.30	6.67	0.15	1.13
490	1,4-Butanediol	0.43	2.99	3.65	44.82	7.66	52.19	5.65	0.18	1.09
490	1,3-Propanediol	0.43	0.67	4.25	37.10	7.47	62.23	6.23	0.16	1.08
490	Methanol	-	-	3.85	84.77	8.06	15.23	4.49	0.22	1.21
490	1,2-Ethanediol	1.19	3.95	4.60	62.63	7.38	33.41	5.39	0.19	1.11
490	2,2,2-Trifluoroethanol	0.20	91.33	0.68	8.67	-	-	0.24	4.22	1.15
490	Ethanol-d	-	-	5.12	74.32	10.36	25.68	6.47	0.15	1.08
490	Methanol-d	-	-	4.67	84.48	9.49	15.52	5.42	0.18	1.05

Table 1.1.10. Summary of Time Correlated Single Photon Counting (TCSPC) fluorescent lifetimes (intensity weighted) of **3a** recorded at 490 nm.

Wavelength (nm)	Solvent	τ_1 (ns)	A_1 (%)	τ_2 (ns)	A_2 (%)	τ_3 (ns)	A_3 (%)	τ_f (ns) (Intensity Weighted)	$1/\tau_f$	χ^2
520	Toluene	-	-	3.86	25.26	9.56	74.74	8.12	0.12	1.06
520	1,4-Dioxane	0.23	0.83	4.46	26.40	11.15	72.77	9.32	0.11	1.07
520	Ethyl acetate	-	-	4.71	37.85	11.22	62.15	8.75	0.11	1.05
520	Chloroform	-	-	5.16	36.98	11.86	63.02	9.38	0.11	1.10
520	2-Methyl-2-butanol	0.38	1.11	4.20	31.98	10.85	66.91	8.61	0.12	1.07
520	N,N-dimethylformamide	0.26	0.74	5.80	51.58	12.33	47.68	8.87	0.11	1.05
520	Acetonitrile	-	-	5.13	49.74	12.29	50.26	8.73	0.11	1.06
520	Propylene carbonate	0.39	0.66	5.63	47.94	12.48	51.40	9.12	0.11	1.12
520	1-Octanol	0.66	1.66	5.33	44.97	12.34	53.36	8.99	0.11	1.08
520	1-Hexanol	0.47	1.35	5.25	51.64	12.50	47.01	8.59	0.12	1.07
520	1-Butanol	0.36	0.90	5.04	76.50	11.19	21.76	7.96	0.13	1.05
520	1-Pentanol	0.36	1.13	5.38	57.46	12.54	41.41	8.28	0.12	1.10
520	1-Propanol	-	-	4.92	61.62	11.79	38.38	7.56	0.13	1.14
520	Acetic acid	0.37	89.57	0.89	10.43	-	-	0.42	2.38	0.87
520	Ethanol	0.37	0.74	6.05	60.29	12.32	38.97	8.45	0.12	1.11
520	1,5-Pentanediol	-	-	5.10	64.73	12.26	35.27	7.62	0.13	1.10
520	1,3-Butanediol	-	-	5.36	55.84	11.67	44.16	8.14	0.12	1.11
520	1,4-Butanediol	0.49	2.03	4.25	55.10	10.38	42.86	6.80	0.15	1.19
520	1,3-Propanediol	-	-	4.95	57.82	10.25	42.18	7.19	0.14	1.10
520	Methanol	-	-	3.91	76.66	11.29	23.34	5.63	0.18	1.00
520	1,2-Ethanediol	1.86	7.29	5.26	70.75	11.52	21.96	6.38	0.16	1.12
520	2,2,2-Trifluoroethanol	0.20	86.19	1.60	13.81	-	-	0.39	2.56	0.97
520	Ethanol-d	-	-	5.30	61.80	12.40	38.20	8.01	0.12	1.11
520	Methanol-d	-	-	4.75	76.13	12.61	23.87	6.62	0.15	1.06

Table 1.1.11. Summary of Time Correlated Single Photon Counting (TCSPC) fluorescent lifetimes (intensity weighted) of **3a** recorded at 520 nm.

Wavelength (nm)	Solvent	τ_1 (ns)	A_1 (%)	τ_2 (ns)	A_2 (%)	τ_3 (ns)	A_3 (%)	τ_f (ns) (Intensity Weighted)	$1/\tau_f$	χ^2
540	Toluene	-	-	4.04	19.06	9.70	80.94	8.62	0.12	0.98
540	1,4-Dioxane	-	-	4.32	16.34	11.11	83.66	10.00	0.10	1.09
540	Ethyl acetate	-	-	4.77	29.19	11.35	70.81	9.43	0.11	1.09
540	Chloroform	-	-	5.04	25.57	11.79	74.43	10.07	0.10	1.07
540	2-Methyl-2-butanol	0.40	0.98	4.28	23.87	10.92	75.15	9.23	0.11	1.02
540	N,N-dimethylformamide	0.27	0.66	5.81	38.86	12.35	60.48	9.73	0.10	1.07
540	Acetonitrile	-	-	5.21	40.35	12.61	59.65	9.63	0.10	1.09
540	Propylene carbonate	-	-	5.47	36.22	12.59	63.78	10.01	0.10	1.16
540	1-Octanol	0.81	1.34	5.26	34.36	12.36	64.30	9.77	0.10	1.07
540	1-Hexanol	0.36	0.81	5.16	40.81	12.44	58.38	9.37	0.11	1.03
540	1-Butanol	0.36	0.85	5.14	50.21	12.46	48.95	8.68	0.12	1.15
540	1-Pentanol	0.41	0.69	5.31	47.45	12.56	51.86	9.03	0.11	1.10
540	1-Propanol	-	-	5.01	55.15	12.32	44.85	8.29	0.12	1.12
540	Acetic acid	0.36	86.19	0.78	13.81	-	-	0.42	2.40	1.14
540	Ethanol	-	-	6.22	55.84	13.03	44.16	9.23	0.11	1.12
540	1,5-Pentanediol	-	-	5.09	56.14	12.43	43.86	8.31	0.12	1.05
540	1,3-Butanediol	-	-	5.67	53.24	12.62	46.76	8.92	0.11	1.12
540	1,4-Butanediol	0.59	1.51	4.36	52.21	11.21	46.28	7.47	0.13	1.18
540	1,3-Propanediol	-	-	5.14	57.78	11.45	42.22	7.80	0.13	1.12
540	Methanol	-	-	3.92	70.73	11.94	29.27	6.26	0.16	1.02
540	1,2-Ethanediol	1.87	6.45	5.32	66.68	12.67	26.88	7.07	0.14	1.08
540	2,2,2-Trifluoroethanol	0.21	81.81	2.06	18.19	-	-	0.55	1.83	1.07
540	Ethanol-d	-	-	5.22	52.05	12.48	47.95	8.70	0.11	1.12
540	Methanol-d	-	-	4.79	70.10	13.25	29.90	7.32	0.14	1.08

Table 1.1.12. Summary of Time Correlated Single Photon Counting (TCSPC) fluorescent lifetimes (intensity weighted) of **3a** recorded at 540 nm.

Wavelength (nm)	Solvent	τ_1 (ns)	A_1 (%)	τ_2 (ns)	A_2 (%)	τ_3 (ns)	A_3 (%)	τ_f (ns) (Intensity Weighted)	$1/\tau_f$	χ^2
570	Toluene	-	-	3.78	6.20	9.67	93.80	9.31	0.11	1.09
570	1,4-Dioxane	-	-	3.82	4.33	11.12	95.67	10.80	0.09	1.06
570	Ethyl acetate	-	-	4.90	16.92	11.44	83.08	10.34	0.10	1.10
570	Chloroform	-	-	5.43	15.48	12.04	84.52	11.02	0.09	1.01
570	2-Methyl-2-butanol	-	-	3.67	11.62	10.87	88.38	10.03	0.10	1.10
570	N,N-dimethylformamide	0.14	0.82	5.44	20.47	12.27	78.71	10.77	0.09	1.04
570	Acetonitrile	-	-	5.33	28.72	12.88	71.28	10.71	0.09	1.10
570	Propylene carbonate	-	-	5.32	22.60	12.77	77.40	11.09	0.09	1.10
570	1-Octanol	0.76	0.80	5.27	21.87	12.50	77.34	10.83	0.09	1.06
570	1-Hexanol	0.36	0.82	5.27	29.54	12.64	69.64	10.36	0.10	1.07
570	1-Butanol	0.40	0.96	5.11	37.81	12.49	61.23	9.58	0.10	1.08
570	1-Pentanol	0.44	0.44	5.40	36.47	12.74	63.10	10.01	0.10	1.10
570	1-Propanol	-	-	4.97	43.66	12.47	56.34	9.20	0.11	1.10
570	Acetic acid	0.31	64.79	0.59	35.21	-	-	0.41	2.46	1.40
570	Ethanol	-	-	6.56	48.04	13.45	51.96	10.14	0.10	1.13
570	1,5-Pentanediol	-	-	5.12	46.53	12.77	53.47	9.21	0.11	1.06
570	1,3-Butanediol	-	-	6.09	48.30	13.50	51.70	9.92	0.10	1.18
570	1,4-Butanediol	2.84	13.58	5.79	45.15	13.20	41.26	8.45	0.12	1.09
570	1,3-Propanediol	-	-	5.35	54.42	12.44	45.58	8.58	0.12	1.16
570	Methanol	-	-	3.93	62.79	12.57	37.21	7.15	0.14	1.05
570	1,2-Ethanediol	2.16	7.63	5.43	56.21	12.93	36.17	7.89	0.13	1.10
570	2,2,2-Trifluoroethanol	0.22	74.67	2.32	25.33	-	-	0.76	1.32	1.30
570	Ethanol-d	-	-	5.22	41.02	12.71	58.98	9.64	0.10	1.13
570	Methanol-d	-	-	4.84	61.63	13.59	38.37	8.20	0.12	1.09

Table 1.1.13. Summary of Time Correlated Single Photon Counting (TCSPC) fluorescent lifetimes (intensity weighted) of **3a** recorded at 570 nm.

1.1.6.2 Amplitude weighted.

Wavelength (nm)	Solvent	τ_1 (ns)	A_1 (%)	τ_2 (ns)	A_2 (%)	τ_3 (ns)	A_3 (%)	τ_f (ns) (Amplitude Weighted)	$1/\tau_f$	χ^2
470	Toluene	-	-	3.88	80.97	9.15	19.03	4.88	0.20	1.08
470	1,4-Dioxane	0.33	28.08	3.35	63.04	8.10	8.88	2.30	0.44	1.12
470	Ethyl acetate	-	-	4.73	85.45	10.19	14.55	5.52	0.18	1.10
470	Chloroform	-	-	4.99	83.77	10.59	16.23	5.90	0.17	1.07
470	2-Methyl-2-butanol	0.40	25.73	4.28	64.75	10.23	9.52	3.85	0.26	1.13
470	N,N-dimethylformamide	0.24	20.49	5.50	66.37	10.36	13.14	5.06	0.20	1.10
470	Acetonitrile	-	-	4.78	81.29	9.60	18.71	5.68	0.18	1.19
470	Propylene carbonate	0.37	16.55	5.53	69.08	10.53	14.38	5.39	0.19	1.12
470	1-Octanol	0.60	31.96	5.16	60.90	10.57	7.24	4.09	0.24	1.11
470	1-Hexanol	0.41	33.73	5.13	60.29	10.25	5.98	3.84	0.26	1.06
470	1-Butanol	0.32	32.61	4.98	61.84	9.77	5.54	3.72	0.27	1.07
470	1-Pentanol	0.33	31.25	5.18	62.00	9.69	6.75	3.97	0.25	1.10
470	1-Propanol	0.20	35.06	4.88	57.44	8.56	7.50	3.51	0.28	1.04
470	Acetic acid	0.37	96.87	1.19	3.13	-	-	0.40	2.52	0.94
470	Ethanol	0.44	40.54	4.72	30.91	7.99	28.56	3.92	0.26	1.10
470	1,5-Pentanediol	-	-	4.74	80.94	7.75	19.06	5.31	0.19	1.14
470	1,3-Butanediol	0.42	36.49	4.23	31.14	7.57	32.37	3.92	0.25	1.12
470	1,4-Butanediol	0.32	41.49	3.10	31.75	6.61	26.76	2.89	0.35	1.19
470	1,3-Propanediol	0.39	24.33	3.78	29.57	6.78	46.11	4.34	0.23	1.07
470	Methanol	-	-	3.09	46.05	4.76	53.95	3.99	0.25	1.11
470	1,2-Ethanediol	-	-	2.05	27.49	5.55	72.51	4.59	0.22	1.14
470	2,2,2-Trifluoroethanol	0.19	92.57	0.41	7.43	-	-	0.21	4.80	1.40
470	Ethanol-d	-	-	4.88	79.79	8.16	20.21	5.54	0.18	1.11
470	Methanol-d	-	-	4.49	84.99	7.10	15.01	4.89	0.20	1.10

Table 1.1.14[2]. Summary of Time Correlated Single Photon Counting (TCSPC) fluorescent lifetimes (amplitude weighted) of **3a** recorded at 470 nm.

[2] A_i represents the fractional intensities, τ_i represents the individual lifetime components, and τ_f is the amplitude-averaged lifetime.

Wavelength (nm)	Solvent	τ_1 (ns)	A_1 (%)	τ_2 (ns)	A_2 (%)	τ_3 (ns)	A_3 (%)	τ_f (ns) (Amplitude Weighted)	$1/\tau_f$	χ^2
490	Toluene	-	-	3.95	72.06	9.43	27.94	5.48	0.18	1.09
490	1,4-Dioxane	0.34	25.48	3.29	63.39	8.66	11.13	3.13	0.32	1.13
490	Ethyl acetate	-	-	4.67	78.89	10.79	21.11	5.97	0.17	1.15
490	Chloroform	-	-	5.13	79.65	11.36	20.35	6.40	0.16	1.10
490	2-Methyl-2-butanol	0.37	21.93	4.29	59.76	10.72	18.32	4.61	0.22	1.06
490	N,N-dimethylformamide	0.22	22.78	5.65	63.60	11.08	13.62	5.15	0.19	1.11
490	Acetonitrile	-	-	4.95	79.63	10.56	20.37	6.09	0.16	1.04
490	Propylene carbonate	0.39	11.96	5.64	72.55	11.68	15.49	5.95	0.17	1.09
490	1-Octanol	0.64	23.04	5.26	64.25	11.44	12.71	4.98	0.20	1.12
490	1-Hexanol	0.44	24.92	5.20	65.54	11.73	9.54	4.64	0.22	1.07
490	1-Butanol	0.33	23.68	5.04	67.66	11.19	8.66	4.46	0.22	1.06
490	1-Pentanol	0.39	22.56	5.33	68.89	11.49	8.55	4.75	0.21	1.07
490	1-Propanol	-	-	4.87	86.97	9.86	13.03	5.52	0.18	1.08
490	Acetic acid	0.38	97.93	1.31	2.07	-	-	0.40	2.48	1.14
490	Ethanol	0.43	25.74	5.59	55.44	9.81	18.82	5.06	0.20	1.14
490	1,5-Pentanediol	-	-	4.93	86.52	9.98	13.48	5.61	0.18	1.18
490	1,3-Butanediol	0.51	20.28	5.08	55.94	9.07	23.78	5.10	0.20	1.13
490	1,4-Butanediol	0.43	26.73	3.65	47.15	7.66	26.12	3.84	0.26	1.09
490	1,3-Propanediol	0.43	8.46	4.25	46.81	7.47	44.73	5.37	0.19	1.08
490	Methanol	-	-	3.85	92.10	8.06	7.90	4.18	0.24	1.21
490	1,2-Ethanediol	1.19	15.42	4.60	63.48	7.38	21.09	4.66	0.21	1.11
490	2,2,2-Trifluoroethanol	0.20	97.34	0.68	2.66	-	-	0.21	4.81	1.15
490	Ethanol-d	-	-	5.12	85.41	10.36	14.59	5.89	0.17	1.08
490	Methanol-d	-	-	4.67	91.71	9.49	8.29	5.07	0.20	1.05

Table 1.1.15. Summary of Time Correlated Single Photon Counting (TCSPC) fluorescent lifetimes (amplitude weighted) of **3a** recorded at 490 nm.

Wavelength (nm)	Solvent	τ_1 (ns)	A_1 (%)	τ_2 (ns)	A_2 (%)	τ_3 (ns)	A_3 (%)	τ_f (ns) (Amplitude Weighted)	$1/\tau_f$	χ^2
520	Toluene	-	-	3.86	45.56	9.56	54.44	6.96	0.14	1.06
520	1,4-Dioxane	0.23	22.40	4.46	36.53	11.15	41.07	6.29	0.16	1.07
520	Ethyl acetate	-	-	4.71	59.22	11.22	40.78	7.36	0.14	1.05
520	Chloroform	-	-	5.16	57.46	11.86	42.54	8.01	0.12	1.10
520	2-Methyl-2-butanol	0.38	17.63	4.20	45.50	10.85	36.87	5.98	0.17	1.07
520	N,N-dimethylformamide	0.26	18.14	5.80	57.06	12.33	24.80	6.42	0.16	1.05
520	Acetonitrile	--	-	5.13	70.33	12.29	29.67	7.25	0.14	1.06
520	Propylene carbonate	0.39	11.92	5.63	59.35	12.48	28.73	6.98	0.14	1.12
520	1-Octanol	0.66	16.51	5.33	55.22	12.34	28.27	6.54	0.15	1.08
520	1-Hexanol	0.47	17.41	5.25	59.74	12.50	22.85	6.07	0.16	1.07
520	1-Butanol	0.36	14.35	5.04	65.89	11.19	19.76	5.78	0.17	1.05
520	1-Pentanol	0.36	18.27	5.38	62.44	12.54	19.29	5.84	0.17	1.10
520	1-Propanol	-	-	4.92	79.36	11.79	20.64	6.34	0.16	1.14
520	Acetic acid	0.37	95.45	0.89	4.55	-	-	0.39	2.57	0.87
520	Ethanol	0.37	13.39	6.05	65.75	12.32	20.86	6.59	0.15	1.11
520	1,5-Pentanediol	-	-	5.10	81.52	12.26	18.48	6.42	0.16	1.10
520	1,3-Butanediol	-	-	5.36	73.36	11.67	26.64	7.04	0.14	1.11
520	1,4-Butanediol	0.49	19.41	4.25	61.12	10.38	19.48	4.71	0.21	1.19
520	1,3-Propanediol	-	-	4.95	73.97	10.25	26.03	6.33	0.16	1.10
520	Methanol	-	-	3.91	90.46	11.29	9.54	4.61	0.22	1.00
520	1,2-Ethanediol	1.86	20.34	5.26	69.78	11.52	9.88	5.18	0.19	1.12
520	2,2,2-Trifluoroethanol	0.20	98.09	1.60	1.91	-	-	0.22	4.50	0.97
520	Ethanol-d	-	-	5.30	79.10	12.40	20.90	6.78	0.15	1.11
520	Methanol-d	-	-	4.75	89.44	12.61	10.56	5.58	0.18	1.06

Table 1.1.16. Summary of Time Correlated Single Photon Counting (TCSPC) fluorescent lifetimes (amplitude weighted) of **3a** recorded at 520 nm.

Wavelength (nm)	Solvent	τ_1 (ns)	A_1 (%)	τ_2 (ns)	A_2 (%)	τ_3 (ns)	A_3 (%)	τ_f (ns) (Amplitude Weighted)	$1/\tau_f$	χ^2
540	Toluene	-	-	4.04	36.08	9.70	63.92	7.66	0.13	0.98
540	1,4-Dioxane	-	-	4.32	33.41	11.11	66.59	8.84	0.11	1.09
540	Ethyl acetate	-	-	4.77	49.53	11.35	50.47	8.09	0.12	1.09
540	Chloroform	-	-	5.04	44.58	11.79	55.42	8.78	0.11	1.07
540	2-Methyl-2-butanol	0.40	16.41	4.28	37.41	10.92	46.18	6.71	0.15	1.02
540	N,N-dimethylformamide	0.27	17.46	5.81	47.64	12.35	34.90	7.13	0.14	1.07
540	Acetonitrile	-	-	5.21	62.07	12.61	37.93	8.02	0.12	1.09
540	Propylene carbonate	-		5.47	56.65	12.59	43.35	8.56	0.12	1.16
540	1-Octanol	0.81	12.31	5.26	48.83	12.36	38.87	7.47	0.13	1.07
540	1-Hexanol	0.36	15.02	5.16	53.35	12.44	31.64	6.74	0.15	1.03
540	1-Butanol	0.36	14.51	5.14	60.98	12.46	24.51	6.24	0.16	1.15
540	1-Pentanol	0.41	11.41	5.31	60.59	12.56	28.01	6.78	0.15	1.10
540	1-Propanol	-	-	5.01	75.14	12.32	24.86	6.83	0.15	1.12
540	Acetic acid	0.36	93.11	0.78	6.89	-	-	0.39	2.58	1.14
540	Ethanol	-	-	6.22	72.61	13.03	27.39	8.08	0.12	1.12
540	1,5-Pentanediol	-	-	5.09	75.74	12.43	24.26	6.87	0.15	1.05
540	1,3-Butanediol	-	-	5.67	71.72	12.62	28.28	7.63	0.13	1.12
540	1,4-Butanediol	0.59	13.73	4.36	64.18	11.21	22.09	5.35	0.19	1.18
540	1,3-Propanediol	-	-	5.14	75.30	11.45	24.70	6.70	0.15	1.12
540	Methanol	-	-	3.92	88.04	11.94	11.96	4.88	0.20	1.02
540	1,2-Ethanediol	1.87	19.02	5.32	69.36	12.67	11.72	5.53	0.18	1.08
540	2,2,2-Trifluoroethanol	0.21	81.81	2.06	18.19	-	-	0.25	4.00	1.07
540	Ethanol-d	-	-	5.22	72.21	12.48	27.79	7.24	0.14	1.12
540	Methanol-d	-	-	4.79	86.62	13.25	13.38	5.92	0.17	1.08

Table 1.1.17. Summary of Time Correlated Single Photon Counting (TCSPC) fluorescent lifetimes (amplitude weighted) of **3a** recorded at 540 nm.

Wavelength (nm)	Solvent	τ_1 (ns)	A_1 (%)	τ_2 (ns)	A_2 (%)	τ_3 (ns)	A_3 (%)	τ_f (ns) (Amplitude Weighted)	$1/\tau_f$	χ^2
570	Toluene	-	-	3.78	14.47	9.67	85.53	8.82	0.11	1.09
570	1,4-Dioxane	-	-	3.82	11.62	11.12	88.38	10.27	0.10	1.06
570	Ethyl acetate	-	-	4.90	16.92	11.44	83.08	9.33	0.11	1.10
570	Chloroform	-	-	5.43	28.88	12.04	71.12	10.13	0.10	1.01
570	2-Methyl-2-butanol	-	-	3.67	28.03	10.87	71.97	8.85	0.11	1.10
570	N,N-dimethylformamide	0.14	37.12	5.44	23.23	12.27	39.65	6.18	0.16	1.04
570	Acetonitrile	-	-	5.33	49.32	12.88	50.68	9.16	0.11	1.10
570	Propylene carbonate	-	-	5.32	41.22	12.77	58.78	9.70	0.10	1.10
570	1-Octanol	0.76	9.19	5.27	36.45	12.50	54.36	8.79	0.11	1.06
570	1-Hexanol	0.36	17.00	5.27	41.85	12.64	41.14	7.47	0.13	1.07
570	1-Butanol	0.40	16.38	5.11	50.31	12.49	33.31	6.79	0.15	1.08
570	1-Pentanol	0.44	7.85	5.40	53.17	12.74	38.98	7.87	0.13	1.10
570	1-Propanol	-	-	4.97	66.06	12.47	33.94	7.51	0.13	1.10
570	Acetic acid	0.31	77.88	0.59	22.12	-	-	0.37	2.71	1.40
570	Ethanol	-	-	6.56	65.48	13.45	34.52	8.94	0.11	1.13
570	1,5-Pentanediol	-	-	5.12	68.47	12.77	31.53	7.53	0.13	1.06
570	1,3-Butanediol	-	-	6.09	67.43	13.50	32.57	8.50	0.12	1.18
570	1,4-Butanediol	2.84	30.43	5.79	49.66	13.20	19.91	6.37	0.16	1.09
570	1,3-Propanediol	-	-	5.35	73.51	12.44	26.49	7.23	0.14	1.16
570	Methanol	-	-	3.93	84.36	12.57	15.64	5.29	0.19	1.05
570	1,2-Ethanediol	2.16	21.18	5.43	62.06	12.93	16.77	6.00	0.17	1.10
570	2,2,2-Trifluoroethanol	0.22	74.67	2.32	25.33	-	-	0.29	3.45	1.30
570	Ethanol-d	-	-	5.22	62.88	12.71	37.12	8.00	0.13	1.13
570	Methanol-d	-	-	4.84	81.86	13.59	18.14	6.43	0.16	1.09

Table 1.1.18. Summary of Time Correlated Single Photon Counting (TCSPC) fluorescent lifetimes (amplitude weighted) of **3a** recorded at 570 nm.

1.1.7 Average fluorescent lifetimes - Solvatochromic analysis.

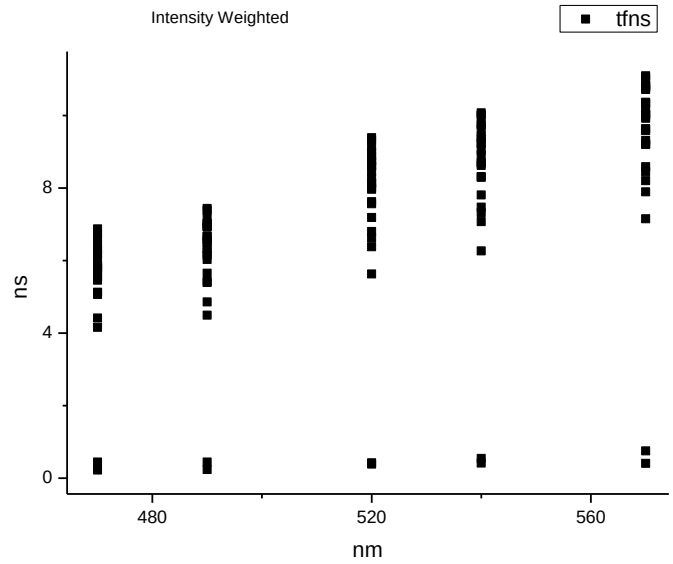

Figure 1.1.61. Intensity weighted average lifetime (τ_f) of **3a** versus wavelength (nm).

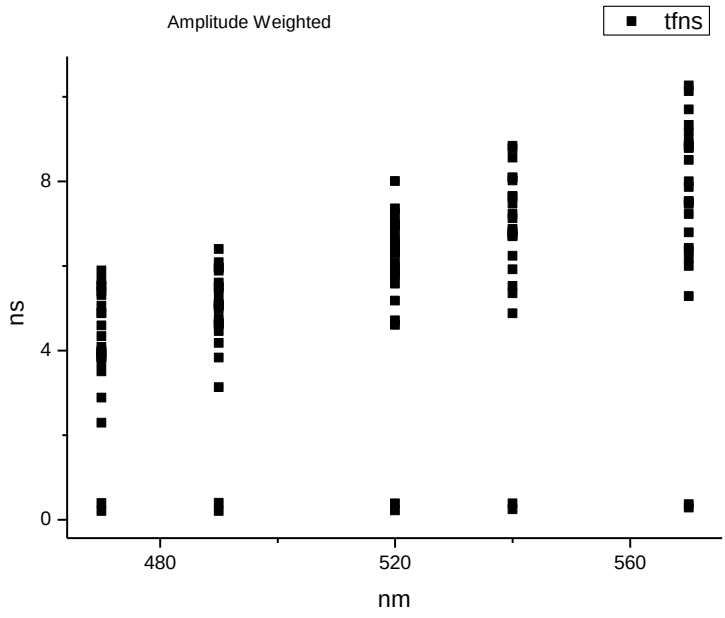

Figure 1.1.62. Amplitude weighted average lifetime (τ_f) of **3a** versus wavelength (nm).

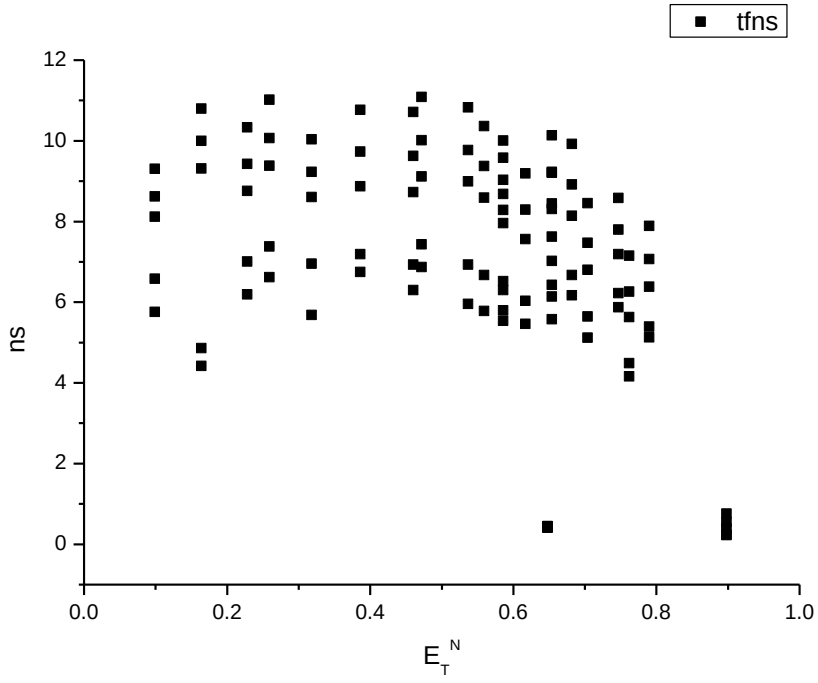

Figure 1.1.63. Intensity weighted average lifetime (τ_f) of **3a** versus E_T^N.

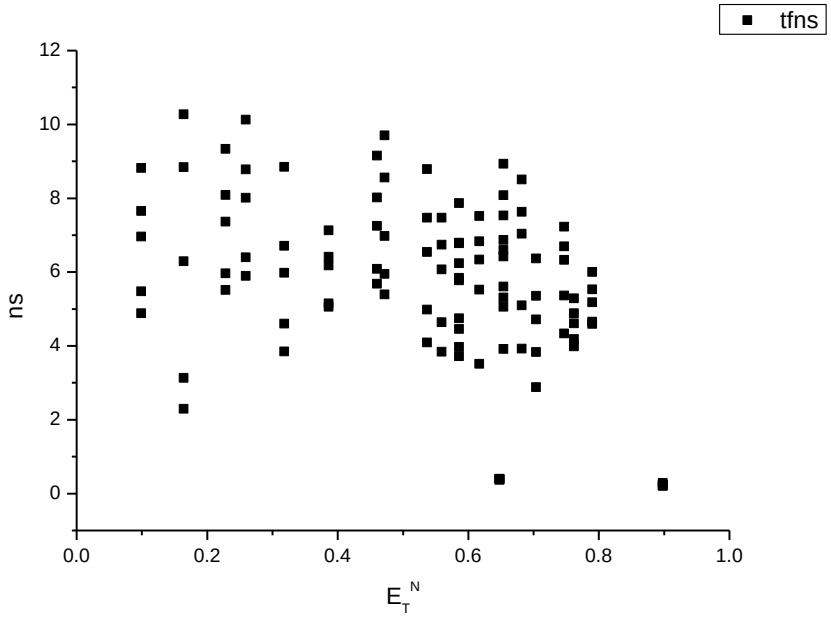

Figure 1.1.64. Amplitude weighted average lifetime (τ_f) of **3a** versus E_T^N.

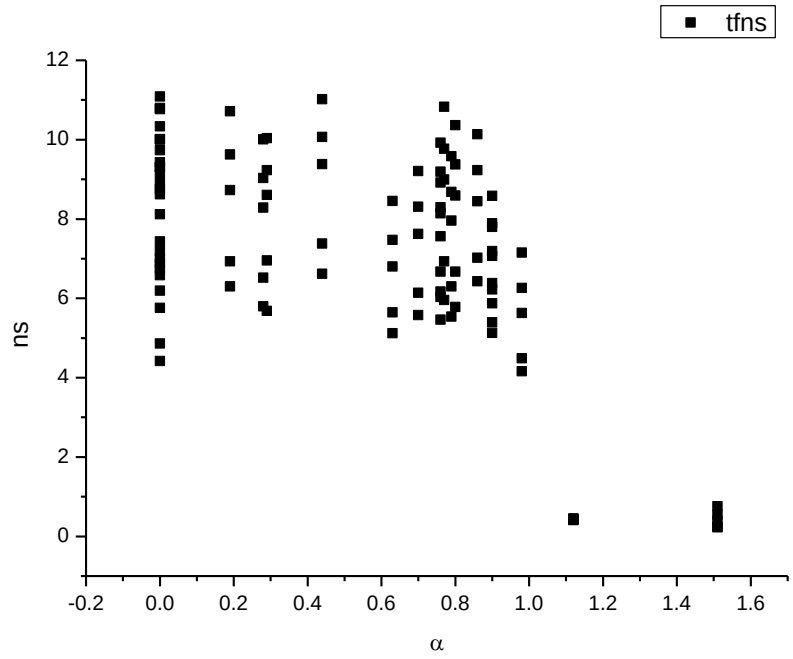

Figure 1.1.65. Intensity weighted average lifetime (τ_f) of **3a** versus α.

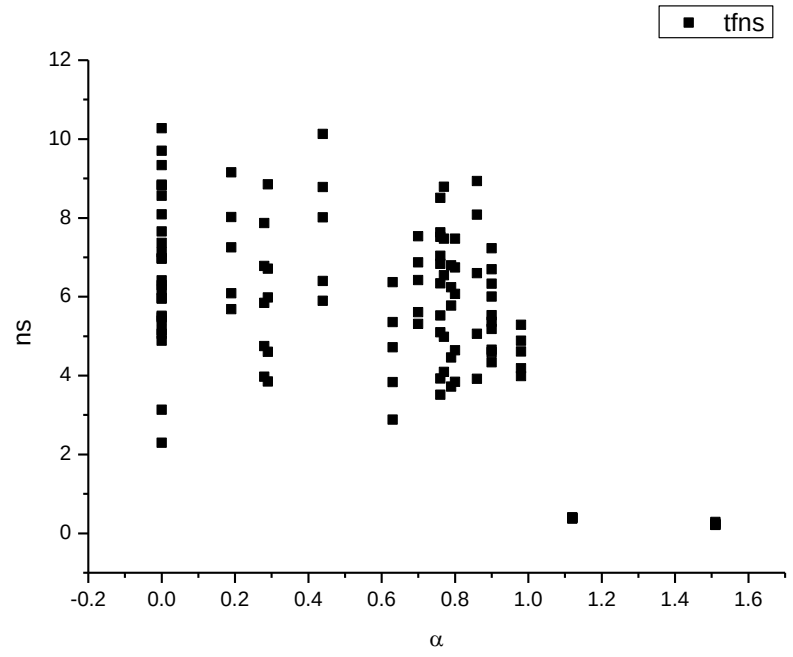

Figure 1.1.66. Amplitude weighted average lifetime (τ_f) of **3a** versus α.

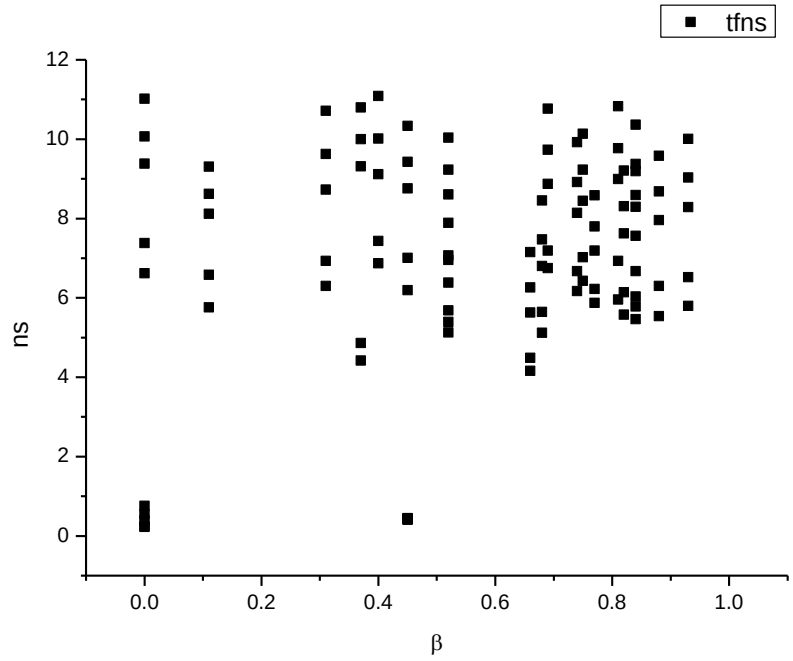

Figure 1.1.67. Intensity weighted average lifetime (τ_f) of **3a** versus β.

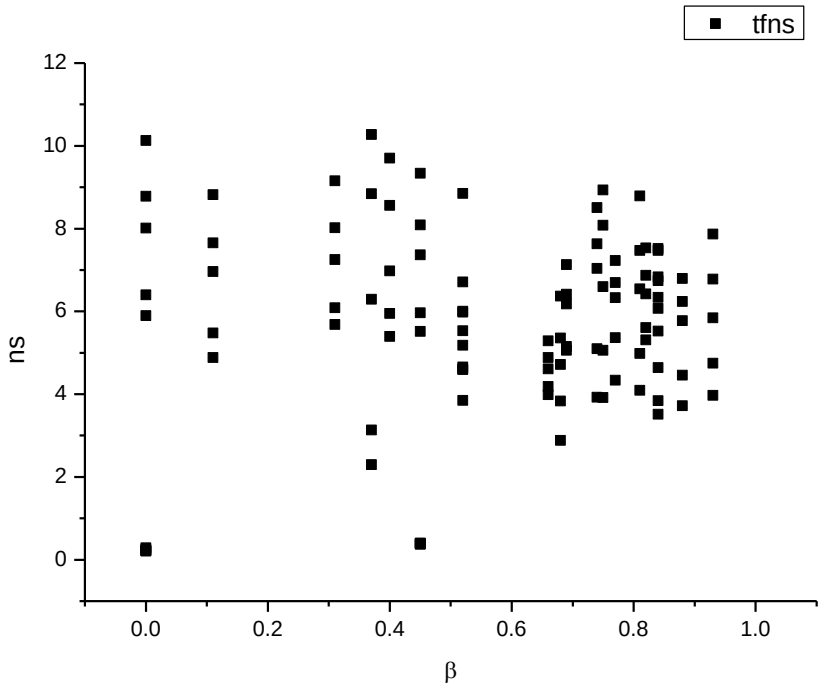

Figure 1.1.68. Amplitude weighted average lifetime (τ_f) of **3a** versus β.

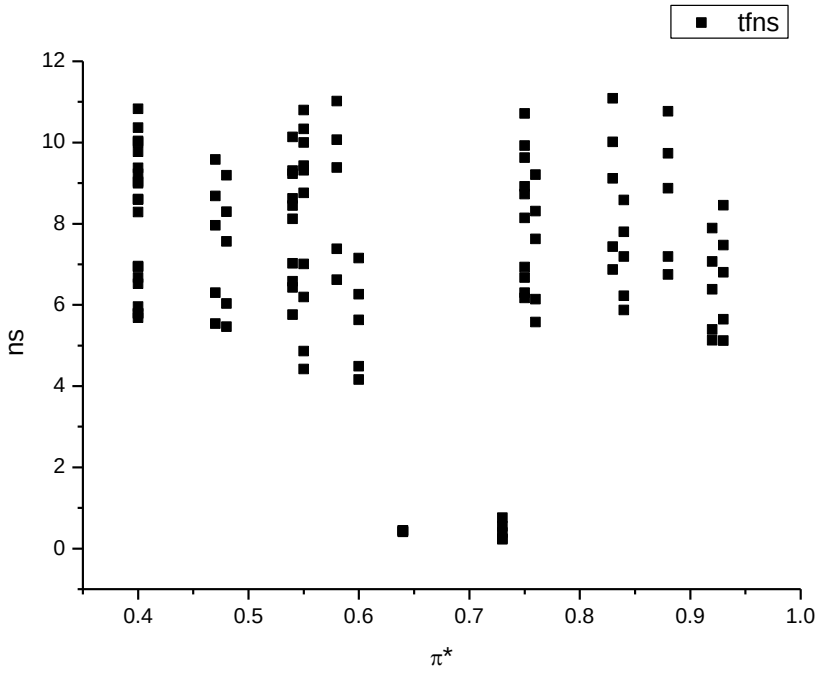

Figure 1.1.69. Intensity weighted average lifetime (τ_f) of **3a** versus π^*.

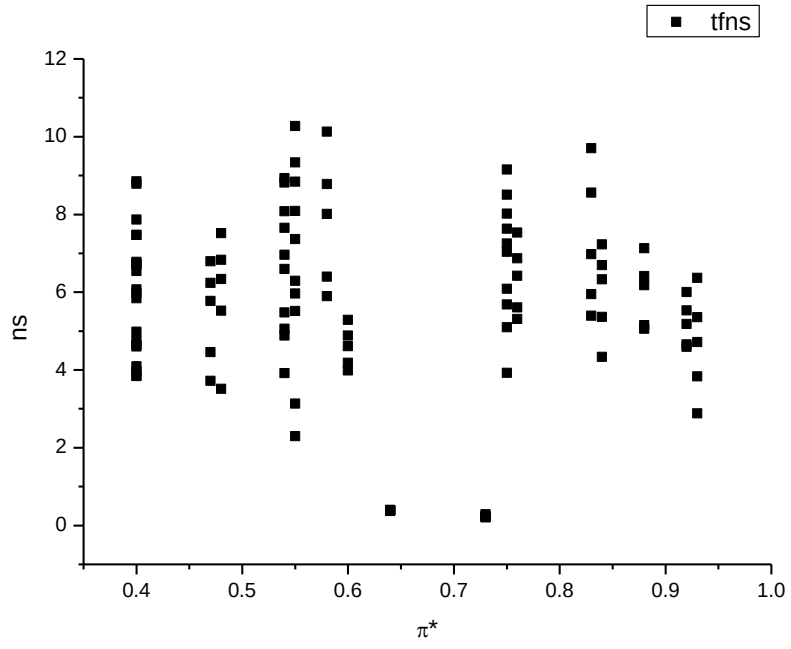

Figure 1.1.70. Amplitude weighted average lifetime (τ_f) of **3a** versus π^*.

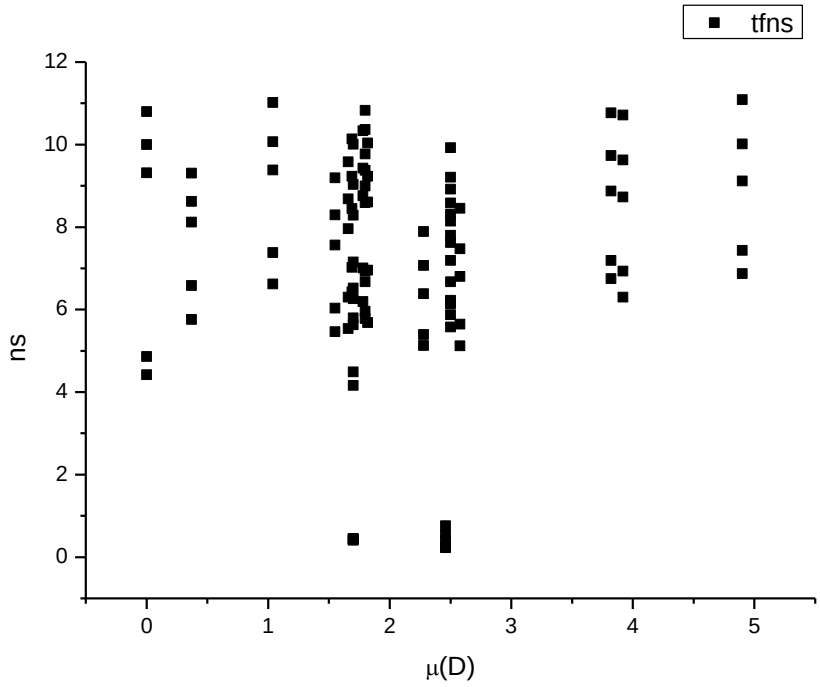

Figure 1.1.71. Intensity weighted average lifetime (τ_f) of **3a** versus μ(D).

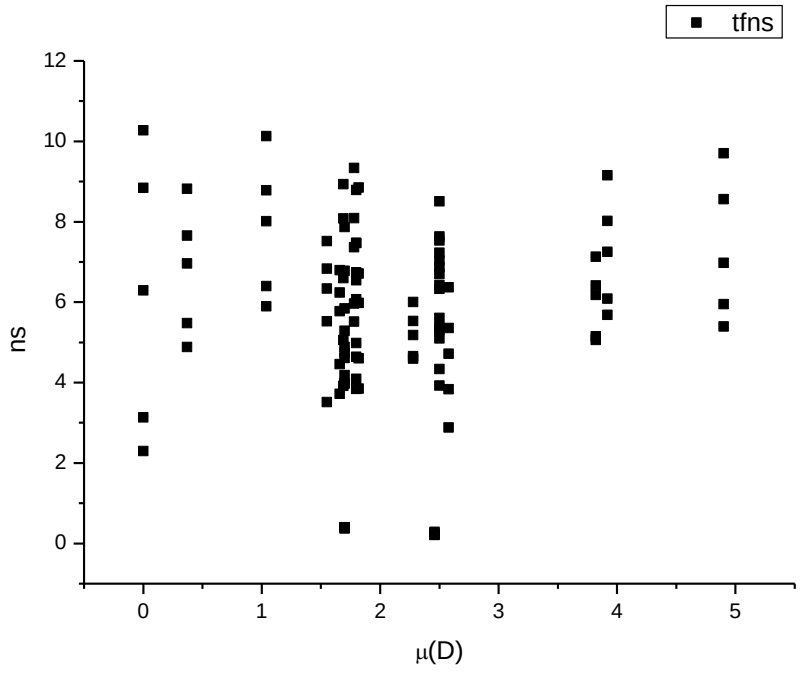

Figure 1.1.72. Amplitude weighted average lifetime (τ_f) of **3a** versus μ(D).

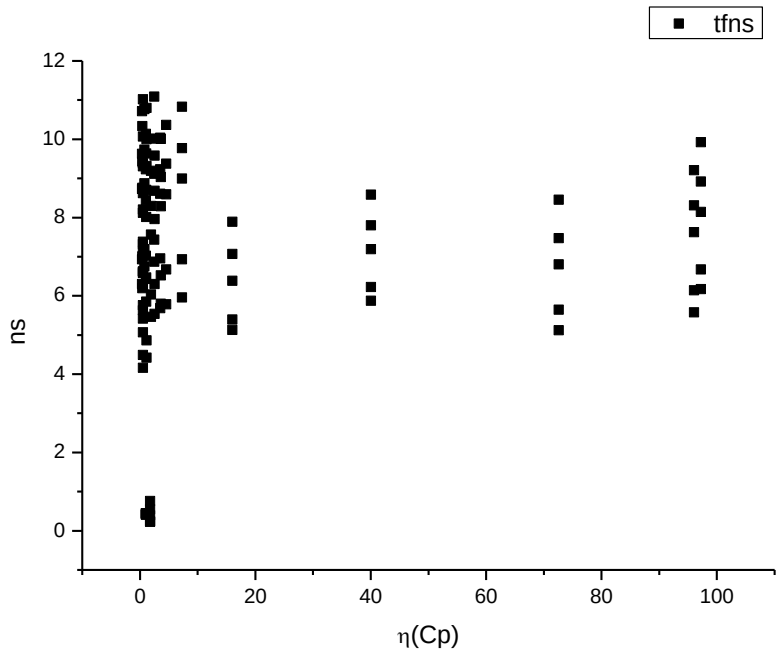

Figure 1.1.73. Intensity weighted average lifetime (τ_f) of **3a** versus η(Cp).

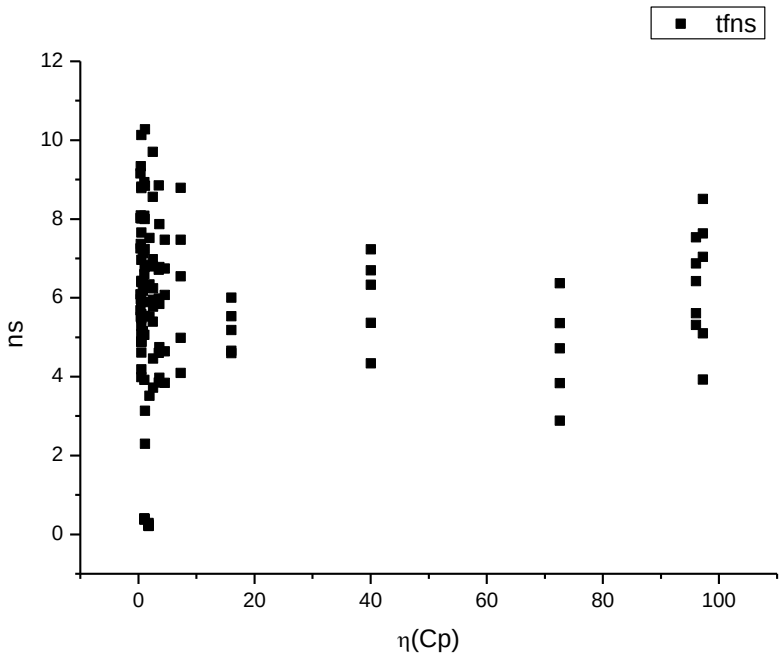

Figure 1.1.74. Amplitude weighted average lifetime (τ_f) of **3a** versus η(Cp).

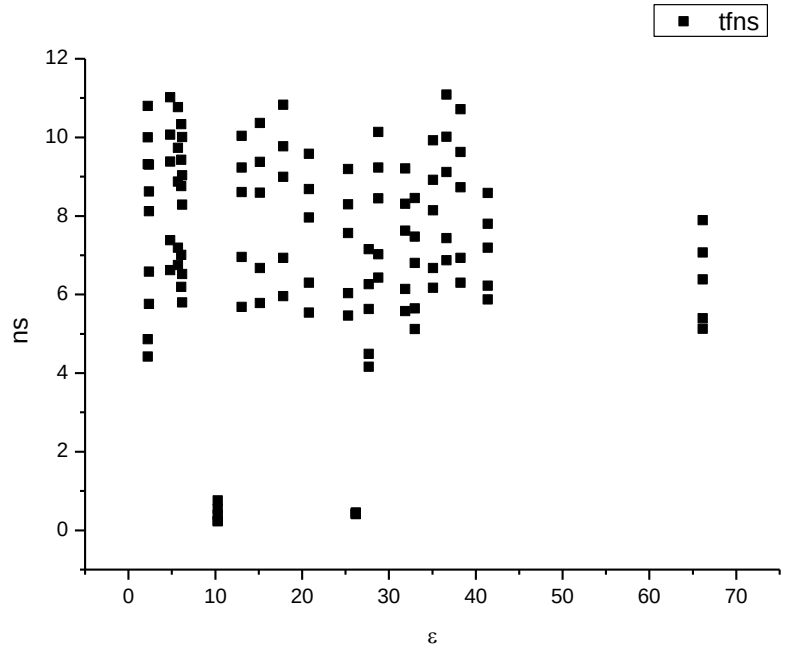

Figure 1.1.75. Intensity weighted average lifetime (τ_f) of **3a** versus ε.

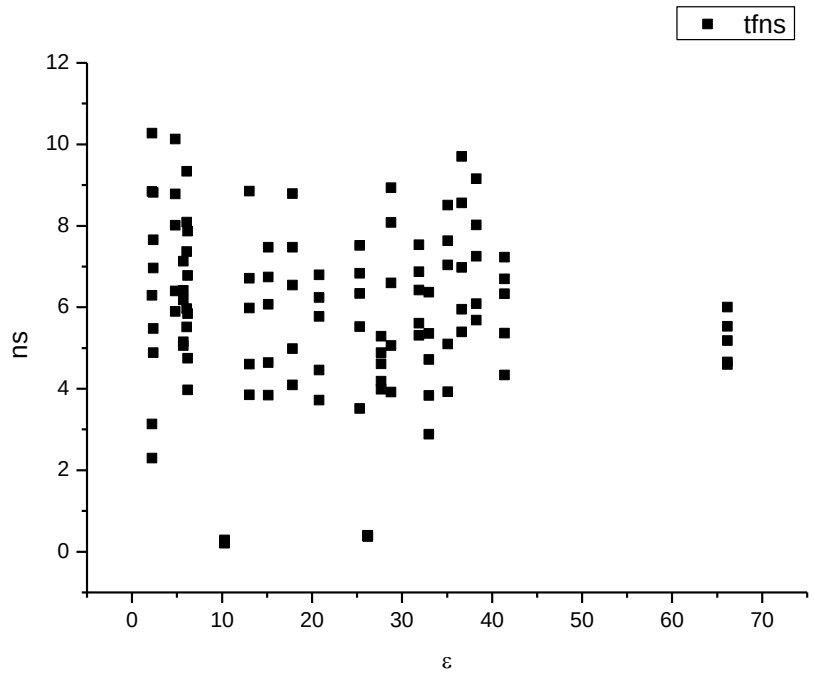

Figure 1.1.76. Amplitude weighted average lifetime (τ_f) of **3a** versus ε.

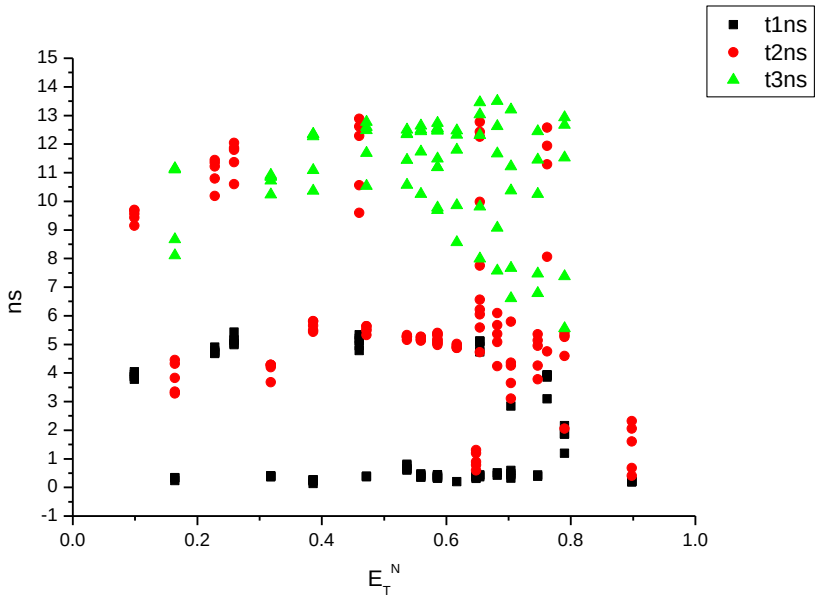

Figure 1.1.77. Intensity weighted components of TCSPC lifetime decay of **3a** (470 nm to 570 nm) versus E_T^N.

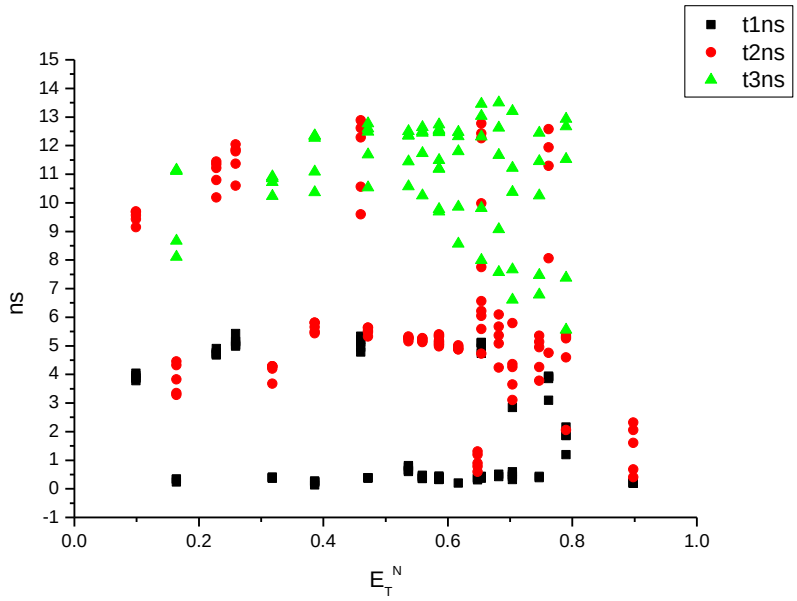

Figure 1.1.78. Amplitude weighted components of TCSPC lifetime decay of **3a** (470 nm to 570 nm) versus E_T^N.

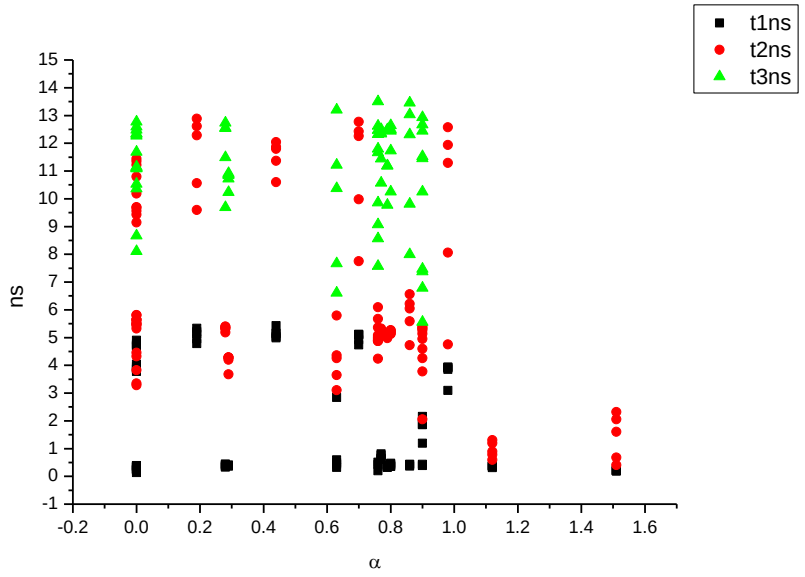

Figure 1.1.79. Intensity weighted components of TCSPC lifetime decay of **3a** (470 nm to 570 nm) versus α.

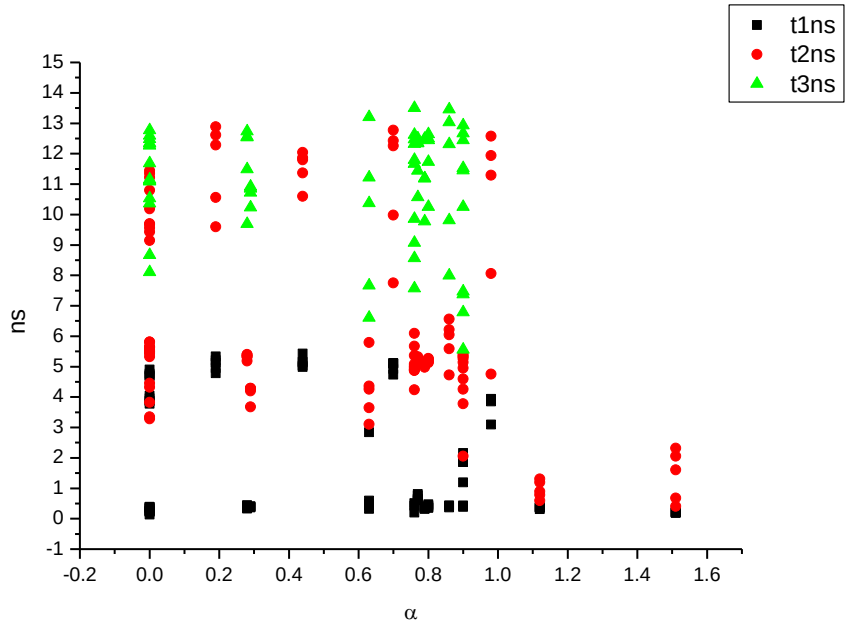

Figure 1.1.80. Amplitude weighted components of TCSPC lifetime decay of **3a** (470 nm to 570 nm) versus α.

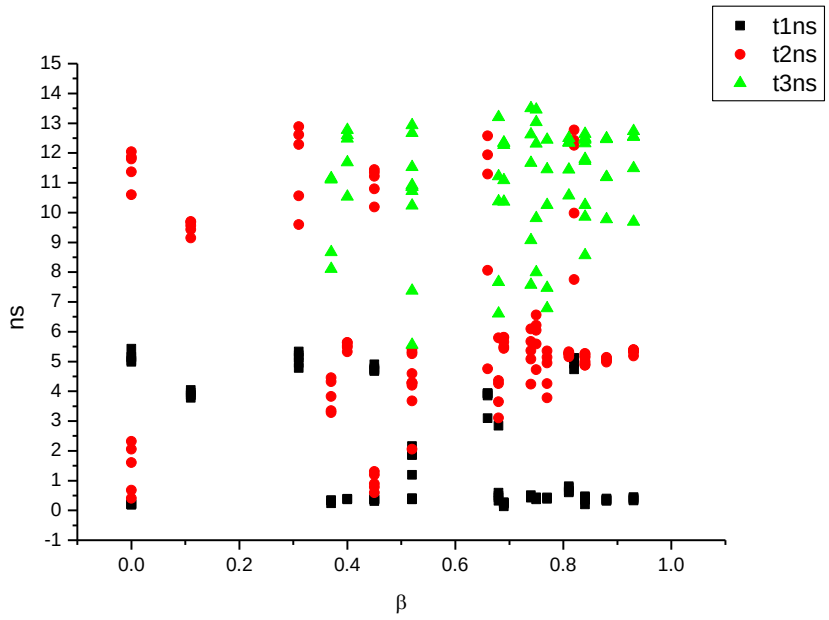

Figure 1.1.81. Intensity weighted components of TCSPC lifetime decay of **3a** (470 nm to 570 nm) versus β.

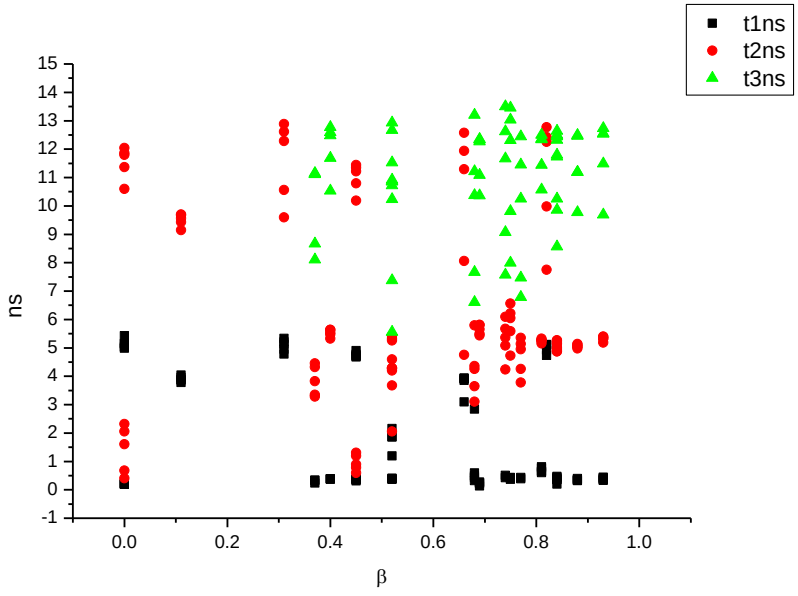

Figure 1.1.82. Amplitude weighted components of TCSPC lifetime decay of **3a** (470 nm to 570 nm) versus β.

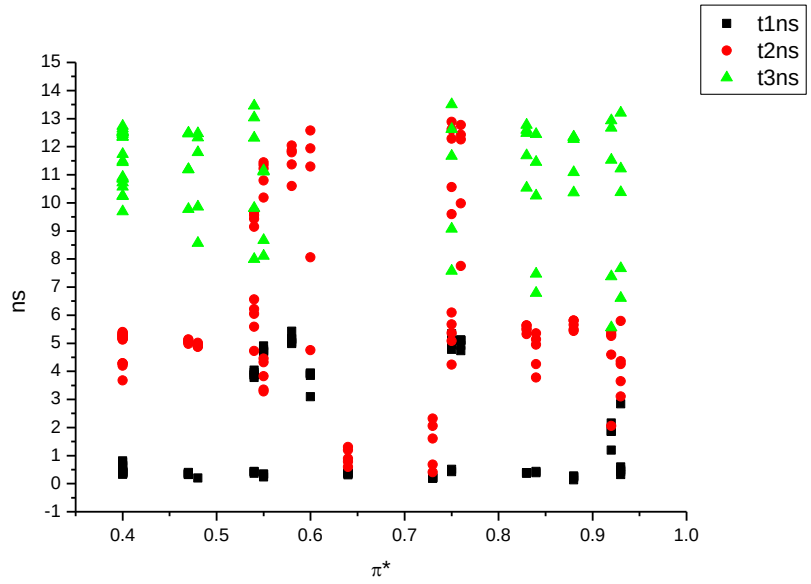

Figure 1.1.83. Intensity weighted components of TCSPC lifetime decay of **3a** (470 nm to 570 nm) versus π*.

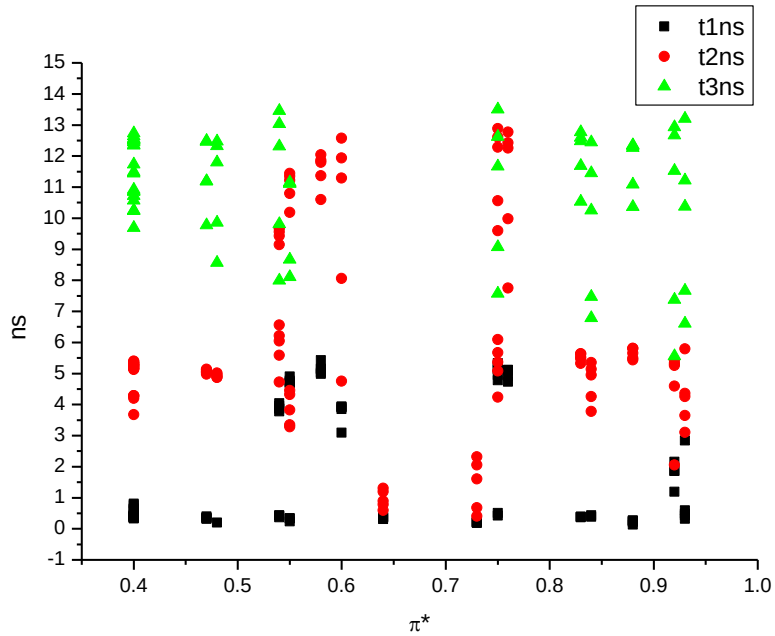

Figure 1.1.84. Amplitude weighted components of TCSPC lifetime decay of **3a** (470 nm to 570 nm) versus π*.

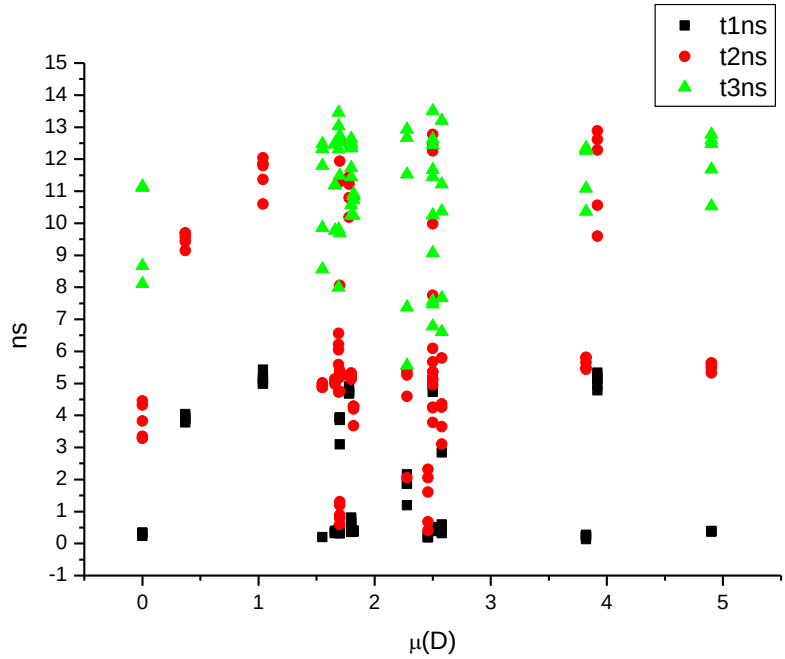

Figure 1.1.85. Intensity weighted components of TCSPC lifetime decay of **3a** (470 nm to 570 nm) versus μ(D).

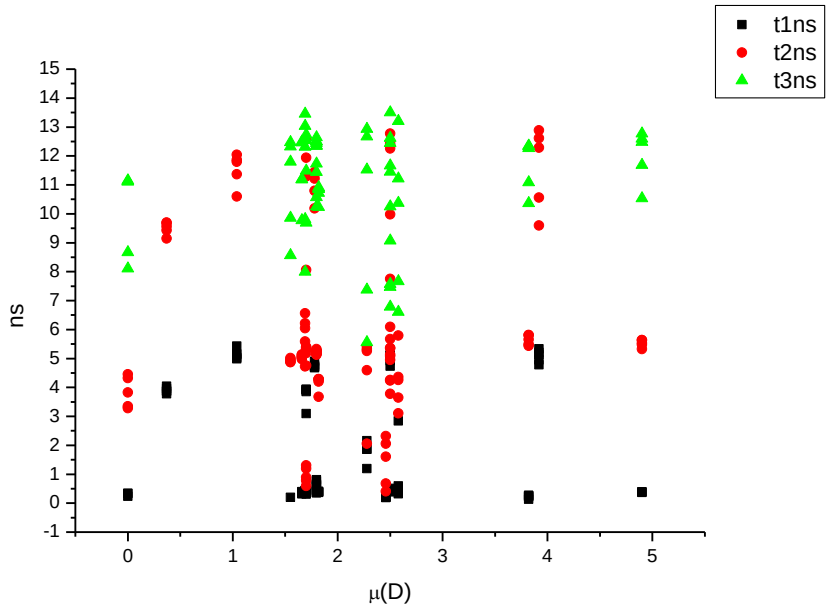

Figure 1.1.86. Amplitude weighted components of TCSPC lifetime decay of **3a** (470 nm to 570 nm) versus μ(D).

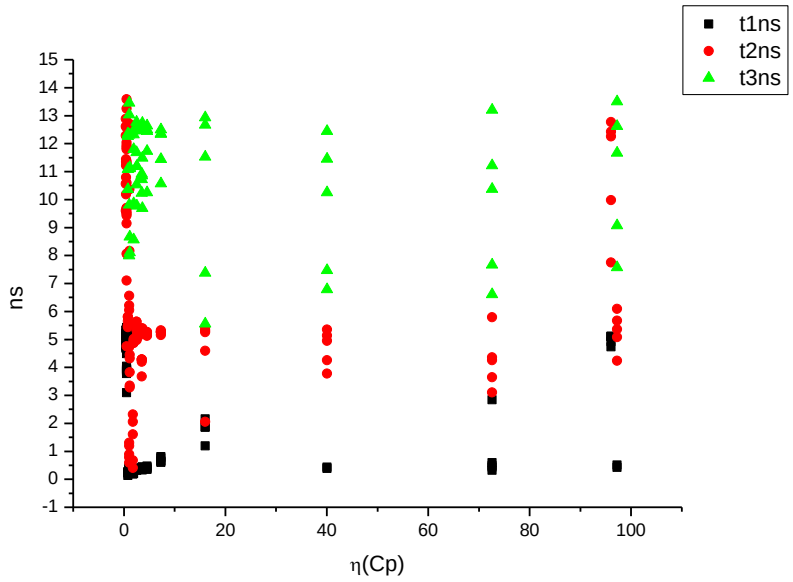

Figure 1.1.87. Intensity weighted components of TCSPC lifetime decay of **3a** (470 nm to 570 nm) versus η(Cp).

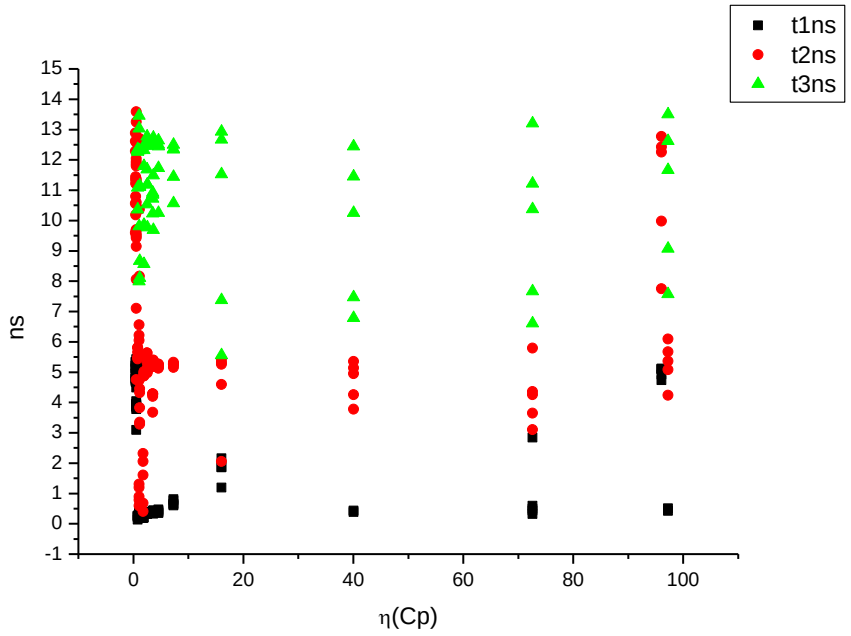

Figure 1.1.88. Amplitude weighted components of TCSPC lifetime decay of **3a** (470 nm to 570 nm) versus η(Cp).

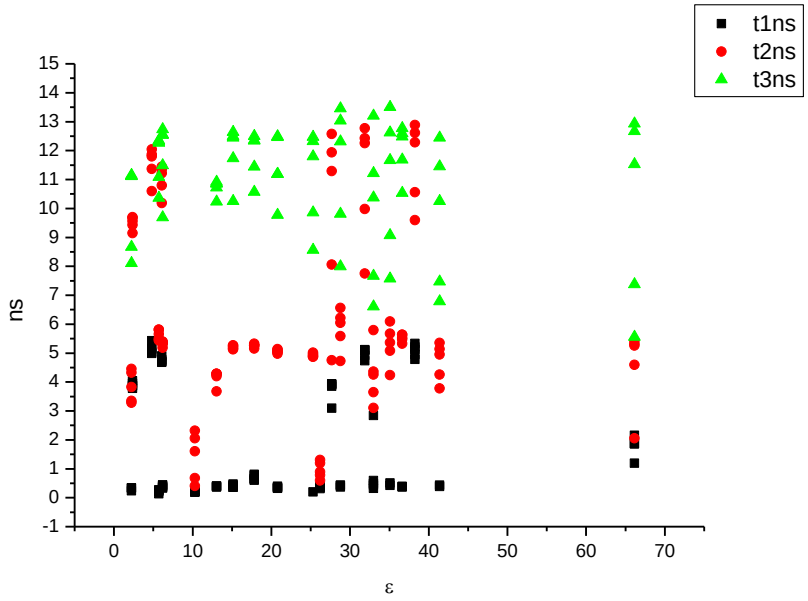

Figure 1.1.89. Intensity weighted components of TCSPC lifetime decay of **3a** (470 nm to 570 nm) versus ε.

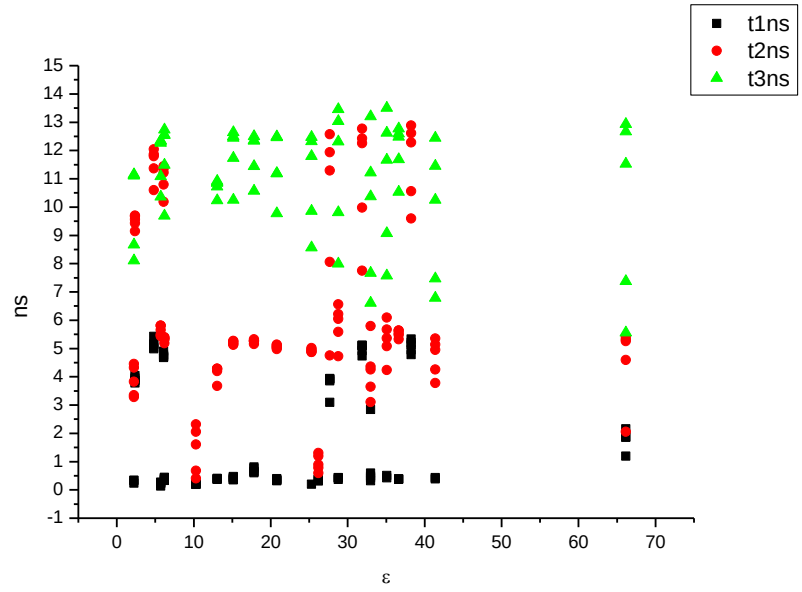

Figure 1.1.90. Amplitude weighted components of TCSPC lifetime decay of **3a** (470 nm to 570 nm) versus ε.

1.1.7.1 470 nm Lifetime – Solvatochromic analysis.

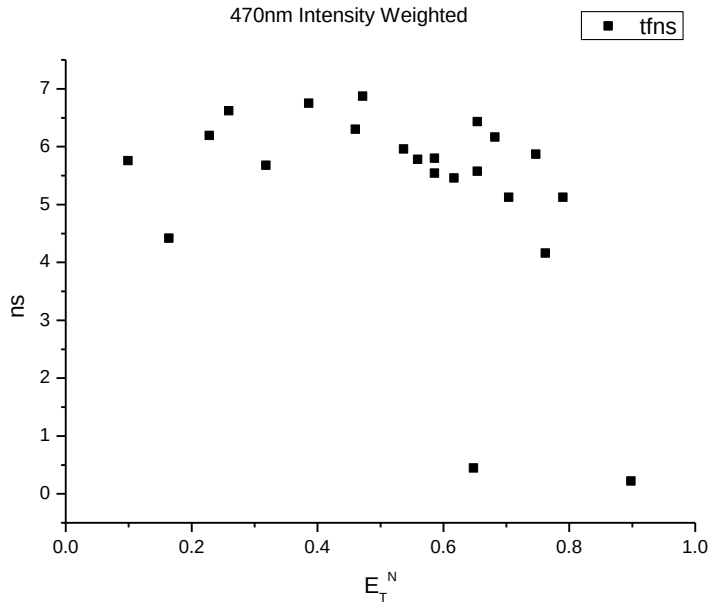

Figure 1.1.91. Intensity weighted average lifetime (τ_f) of **3a** at 470 nm versus E_T^N.

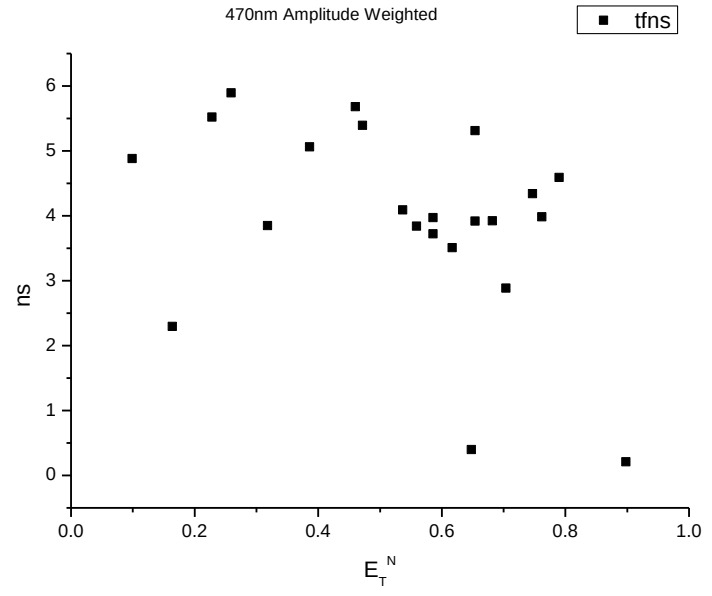

Figure 1.1.92. Amplitude weighted average lifetime (τ_f) of **3a** at 470 nm versus E_T^N.

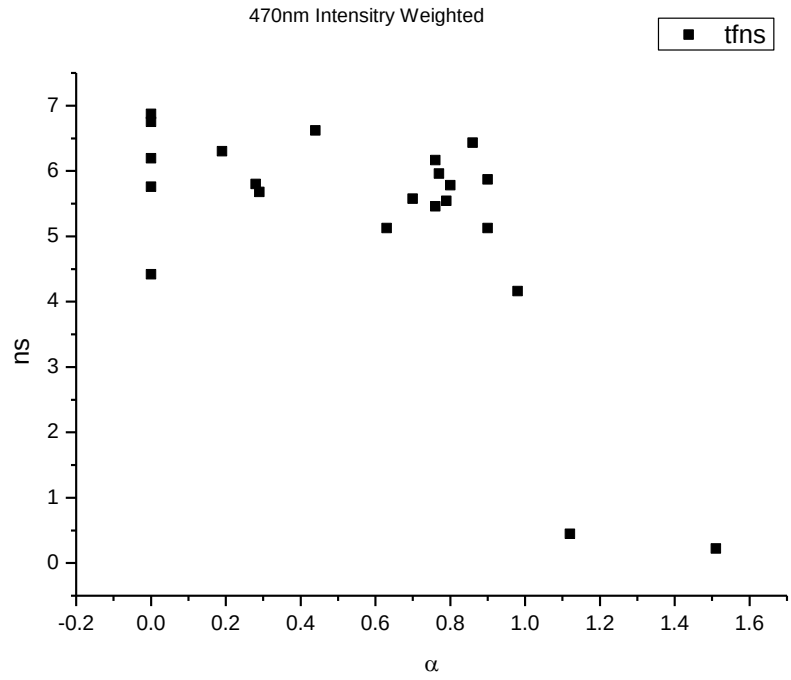

Figure 1.1.93. Intensity weighted average lifetime (τ_f) of **3a** at 470 nm versus α.

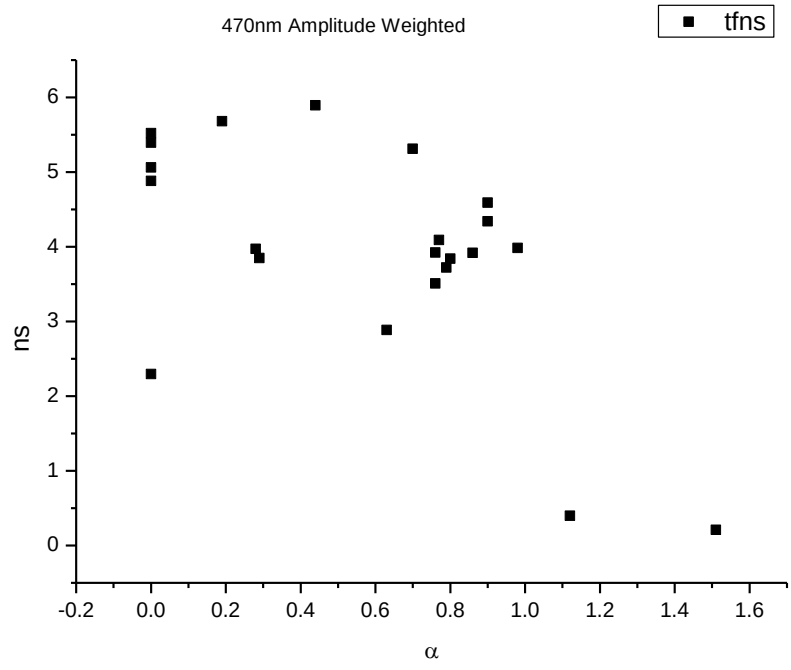

Figure 1.1.94. Amplitude weighted average lifetime (τ_f) of **3a** at 470 nm versus α.

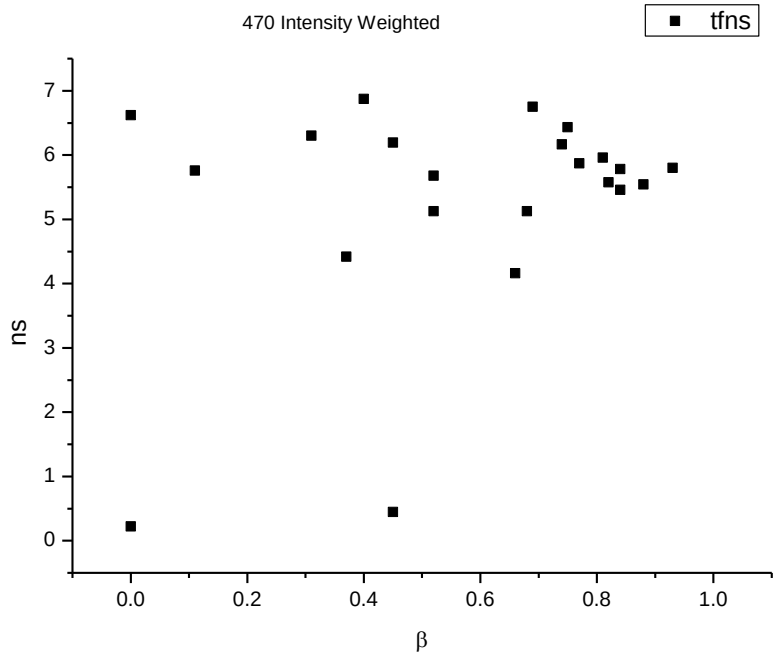

Figure 1.1.95. Intensity weighted average lifetime (τ_f) of **3a** at 470 nm versus β.

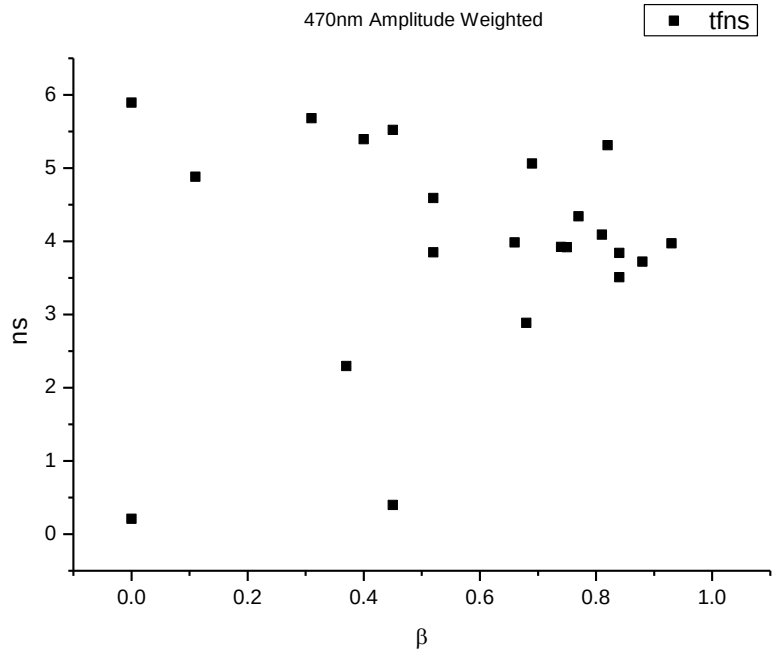

Figure 1.1.96. Amplitude weighted average lifetime (τ_f) of **3a** at 470 nm versus β.

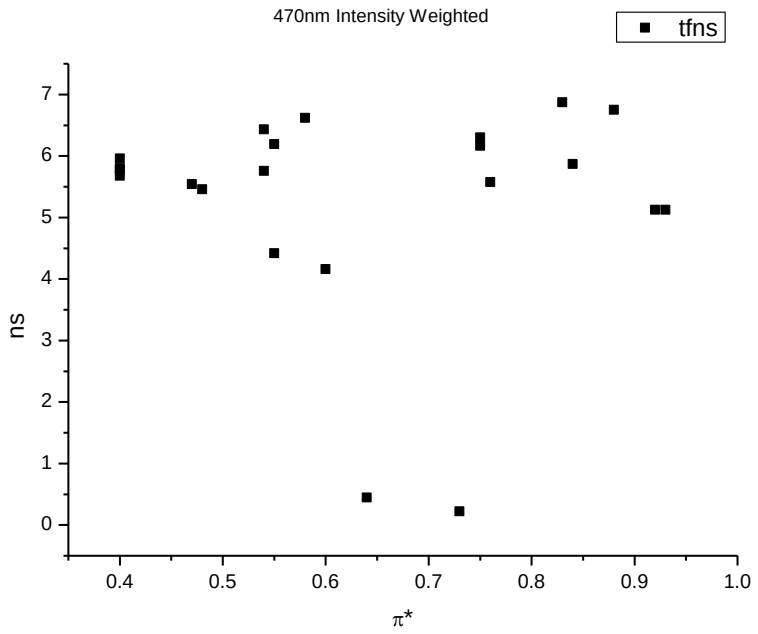

Figure 1.1.97. Intensity weighted average lifetime (τ_f) of **3a** at 470 nm versus π*.

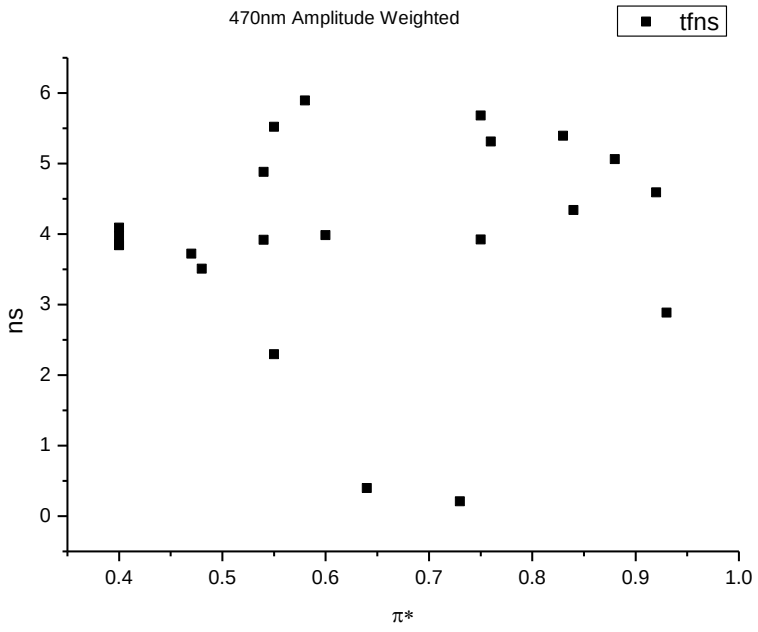

Figure 1.1.98. Amplitude weighted average lifetime (τ_f) of **3a** at 470 nm versus π*.

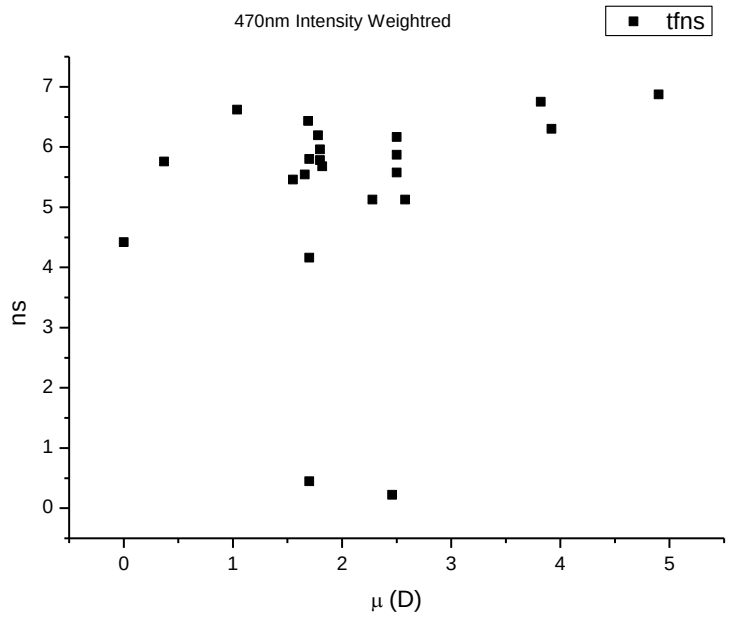

Figure 1.1.99. Intensity weighted average lifetime (τ_f) of **3a** at 470 nm versus μ(D).

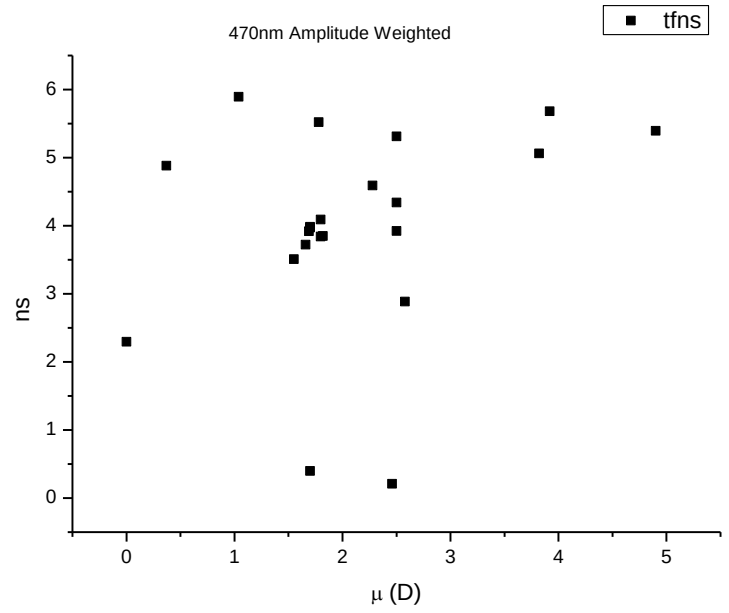

Figure 1.1.100. Amplitude weighted average lifetime (τ_f) of **3a** at 470 nm versus μ(D).

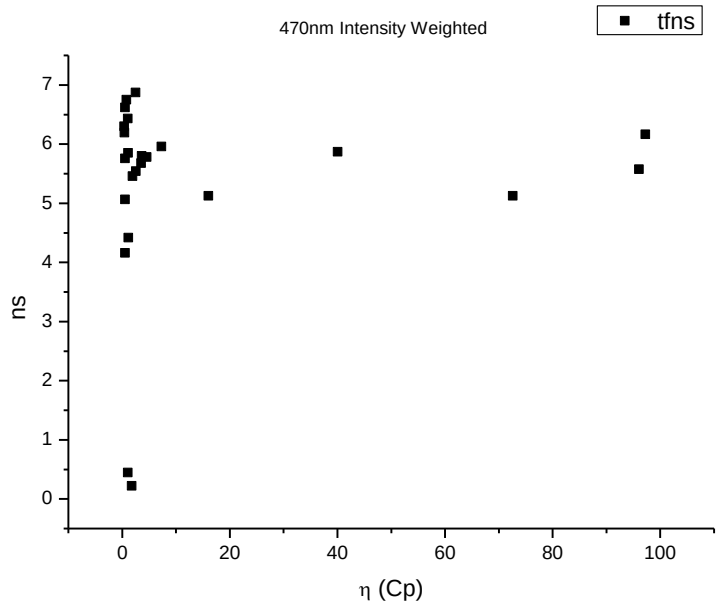

Figure 1.1.111. Intensity weighted average lifetime (τ_f) of **3a** at 470 nm versus η(Cp).

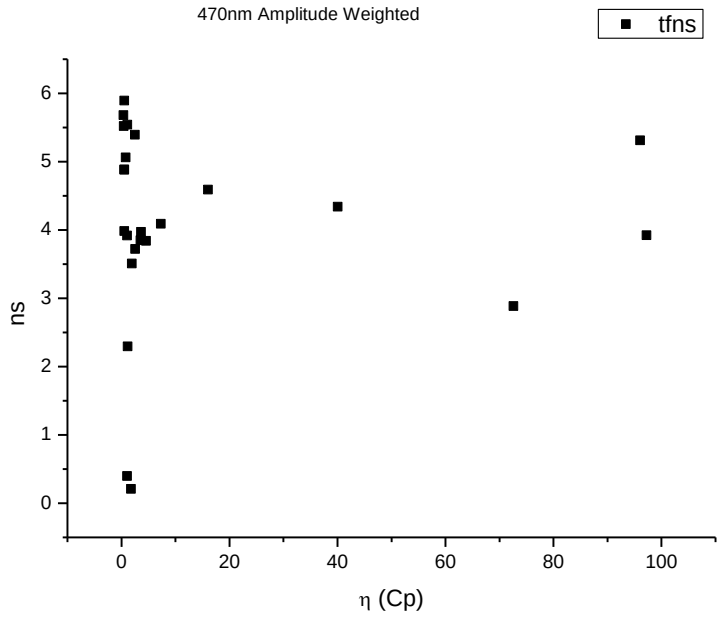

Figure 1.1.112. Amplitude weighted average lifetime (τ_f) of **3a** at 470 nm versus η(Cp).

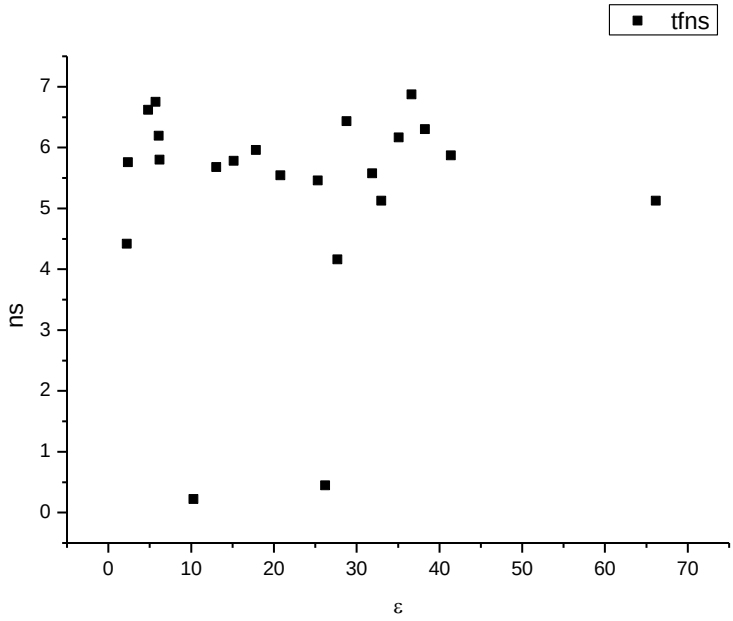

Figure 1.1.113. Intensity weighted average lifetime (τ_f) of **3a** at 470 nm versus ε.

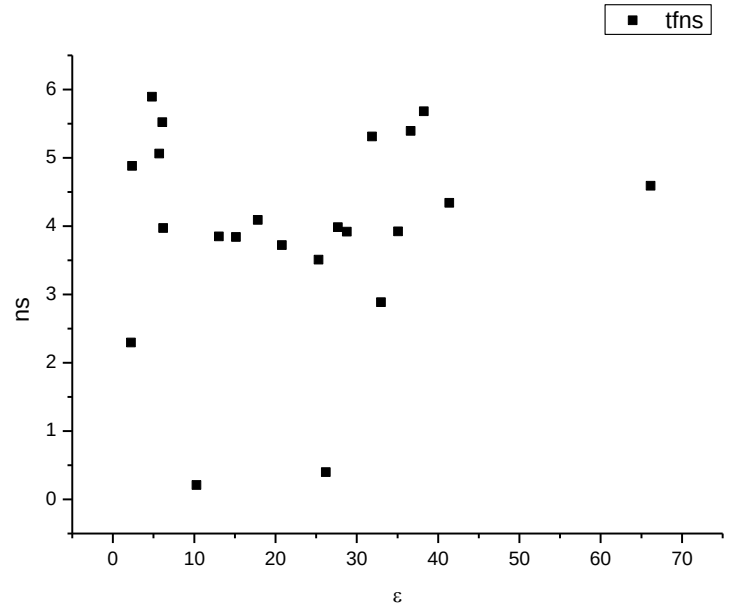

Figure 1.1.114. Amplitude weighted average lifetime (τ_f) of **3a** at 470 nm versus ε.

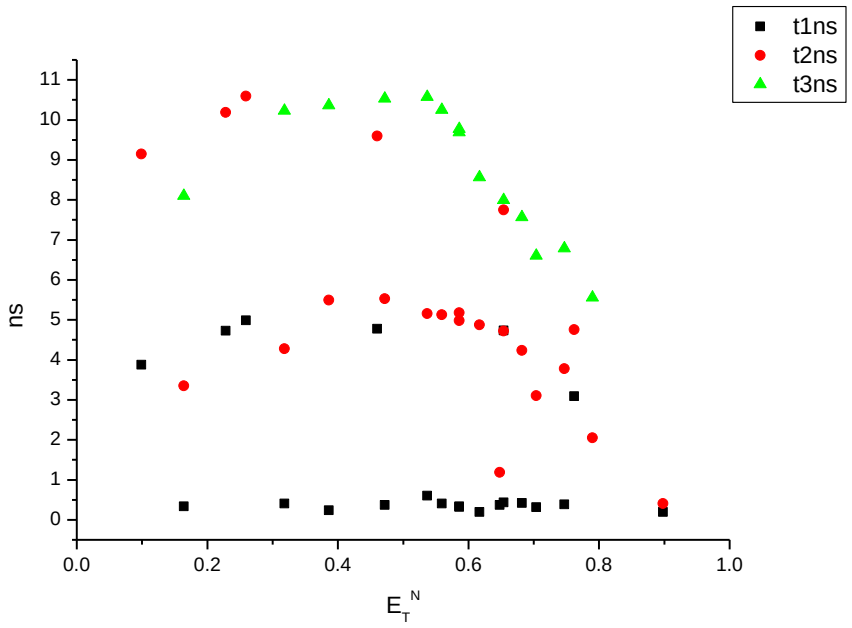

Figure 1.1.115. Intensity weighted components of TCSPC lifetime decay of **3a** (470 nm) versus E_T^N.

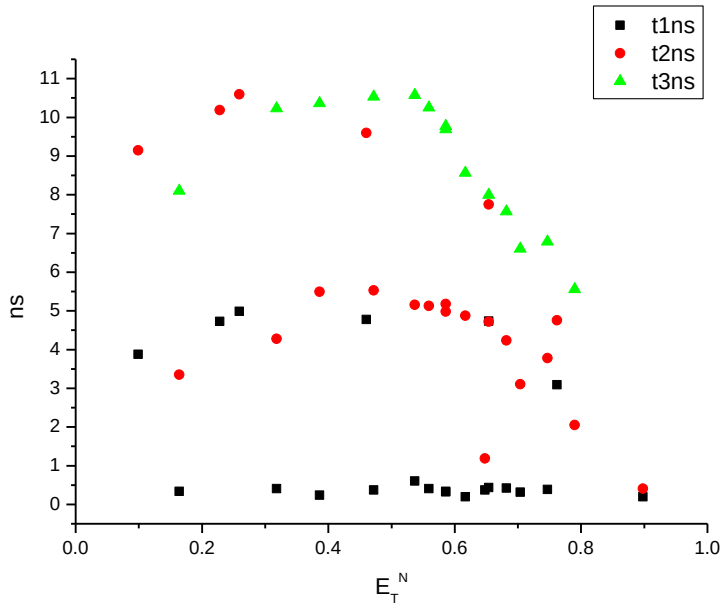

Figure 1.1.116. Amplitude weighted components of TCSPC lifetime decay of **3a** (470 nm) versus E_T^N.

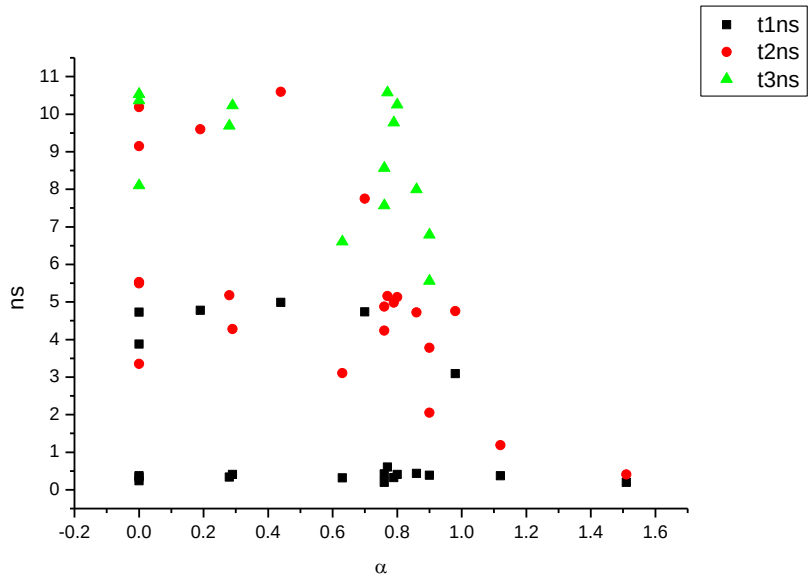

Figure 1.1.117. Intensity weighted components of TCSPC lifetime decay of **3a** (470 nm) versus α.

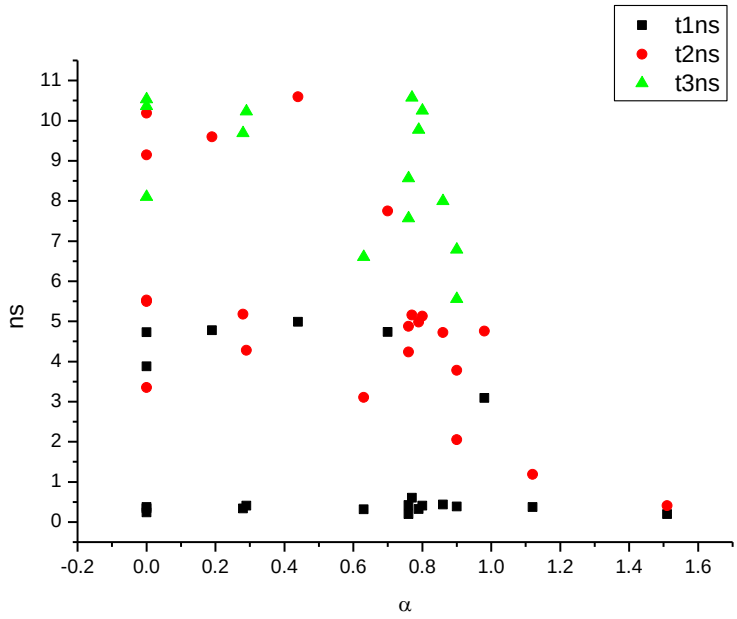

Figure 1.1.118. Amplitude weighted components of TCSPC lifetime decay of **3a** (470 nm) versus α.

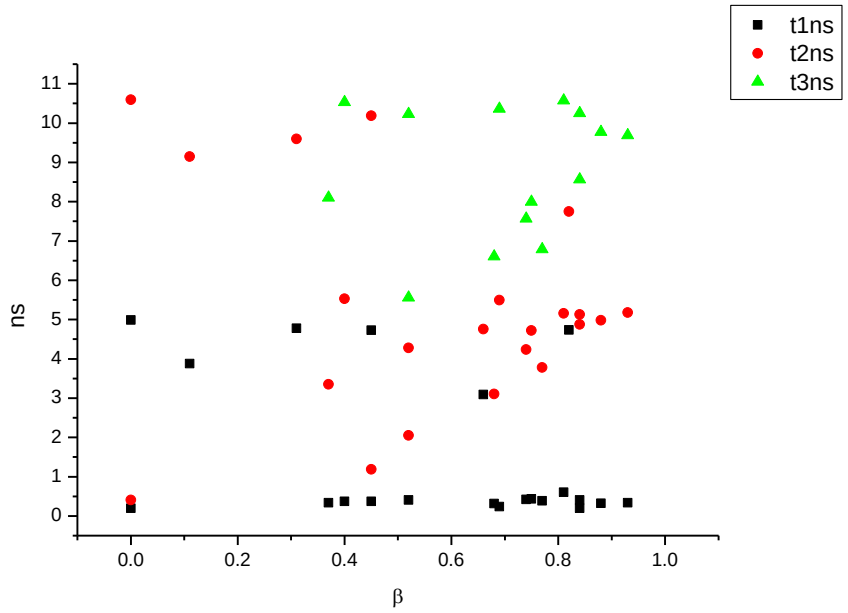

Figure 1.1.119. Intensity weighted components of TCSPC lifetime decay of **3a** (470 nm) versus β.

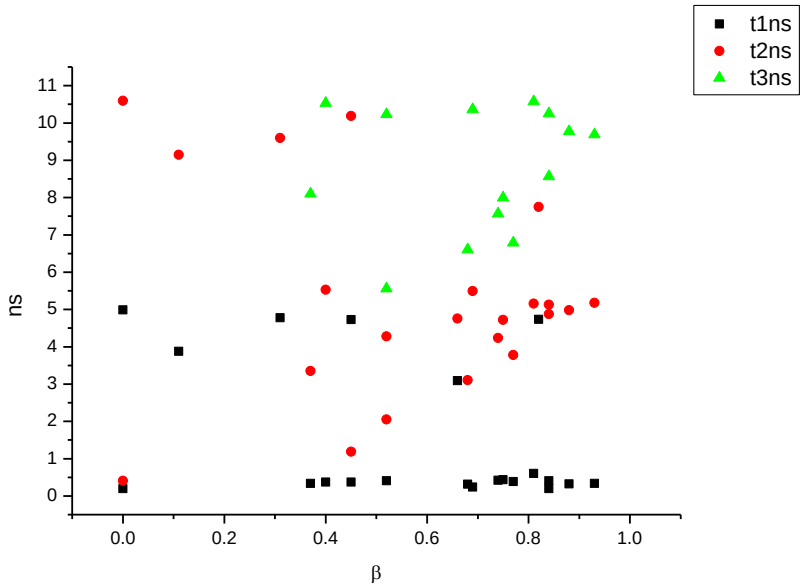

Figure 1.1.120. Amplitude weighted components of TCSPC lifetime decay of **3a** (470 nm) versus β.

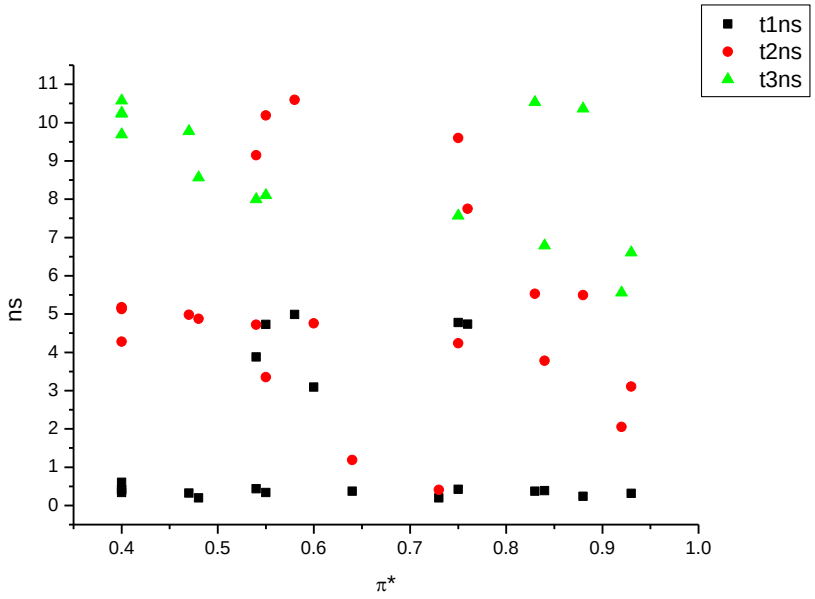

Figure 1.1.121. Intensity weighted components of TCSPC lifetime decay of **3a** (470 nm) versus π*.

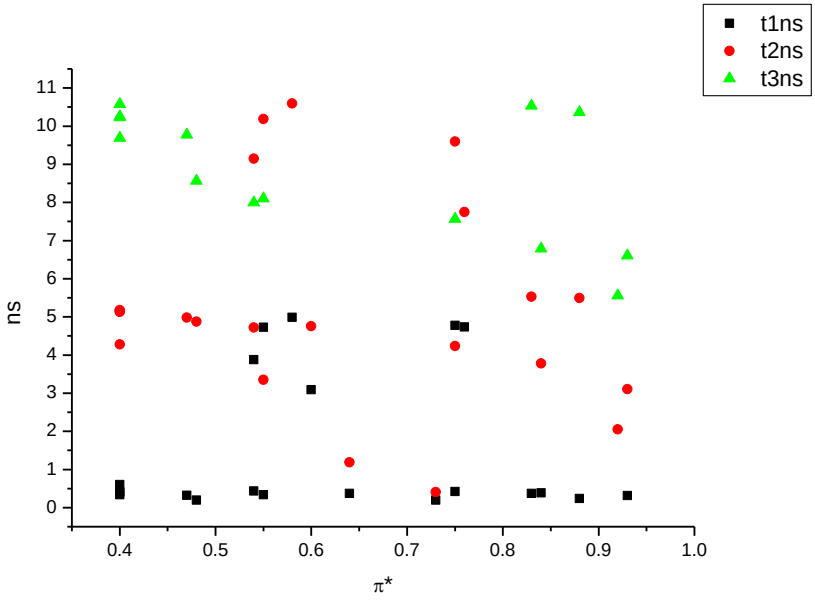

Figure 1.1.122. Amplitude weighted components of TCSPC lifetime decay of **3a** (470 nm) versus π*.

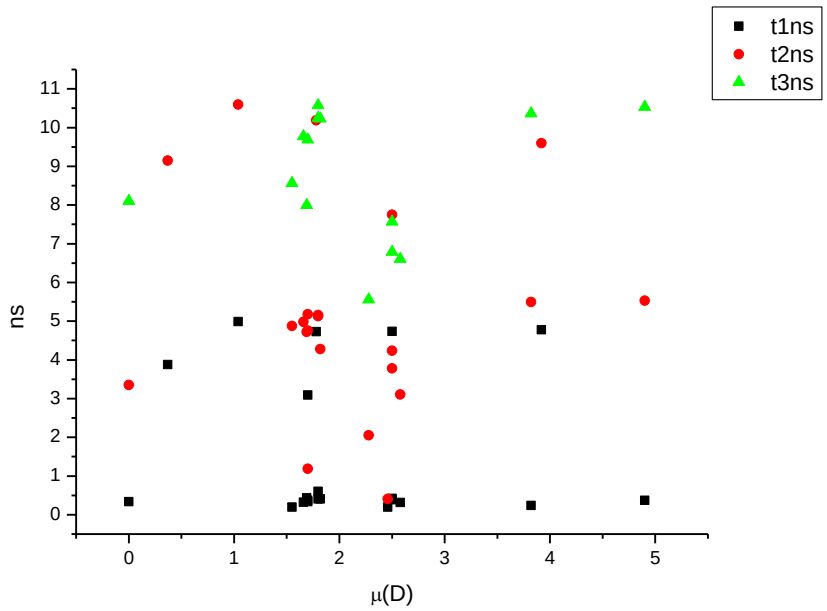

Figure 1.1.123. Intensity weighted components of TCSPC lifetime decay of **3a** (470 nm) versus μ(D).

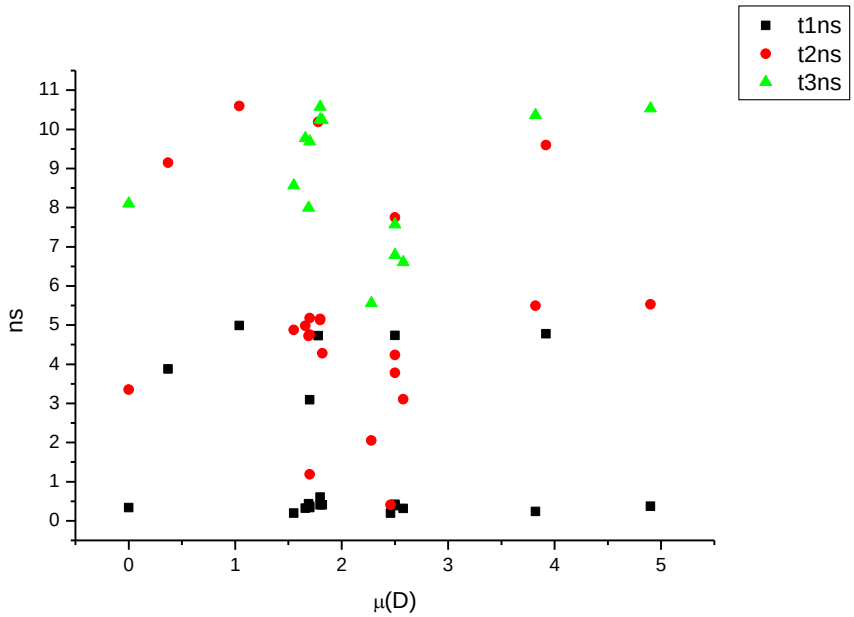

Figure 1.1.124. Amplitude weighted components of TCSPC lifetime decay of **3a** (470 nm) versus μ(D).

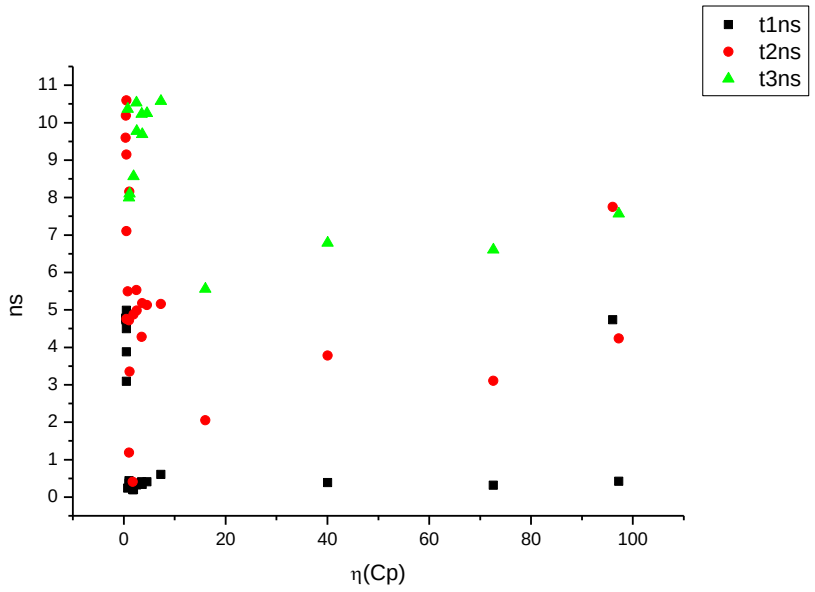

Figure 1.1.125. Intensity weighted components of TCSPC lifetime decay of **3a** (470 nm) versus η(Cp).

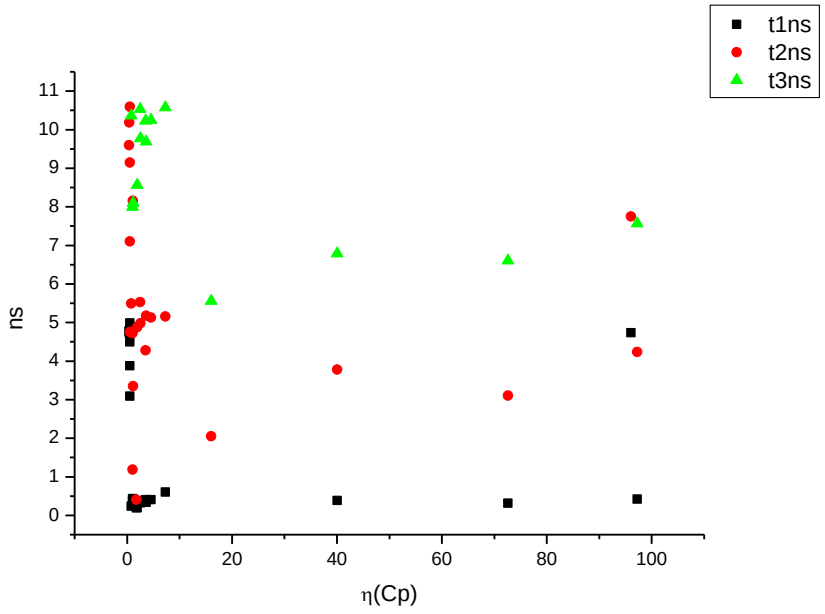

Figure 1.1.126. Amplitude weighted components of TCSPC lifetime decay of **3a** (470 nm) versus η(Cp).

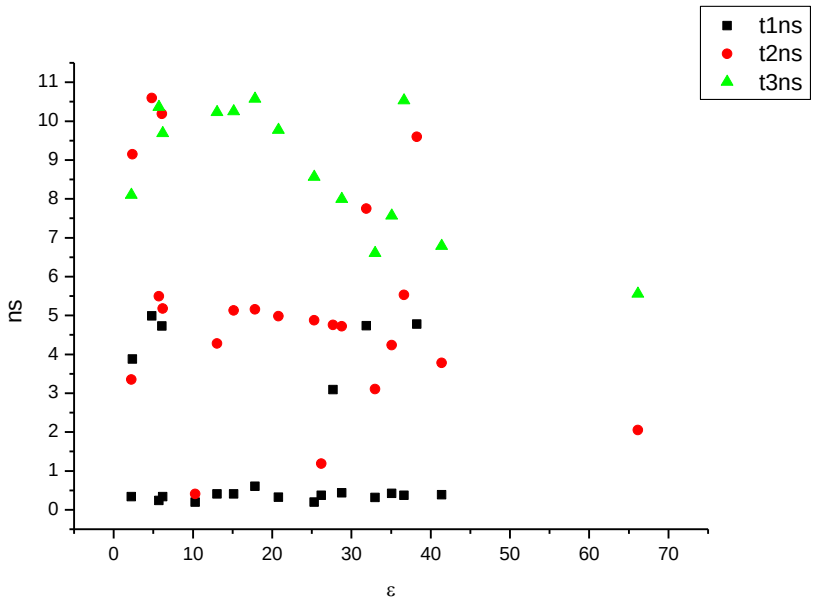

Figure 1.1.127. Intensity weighted components of TCSPC lifetime decay of **3a** (470 nm) versus ε.

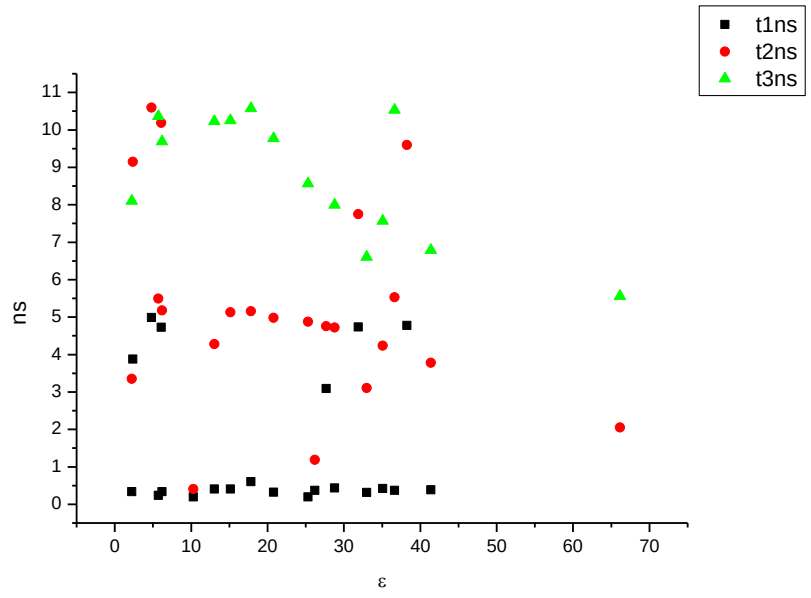

Figure 1.1.128. Amplitude weighted components of TCSPC lifetime decay of **3a** (470 nm) versus ε.

1.1.7.2 570 nm Lifetime – Solvatochromic analysis.

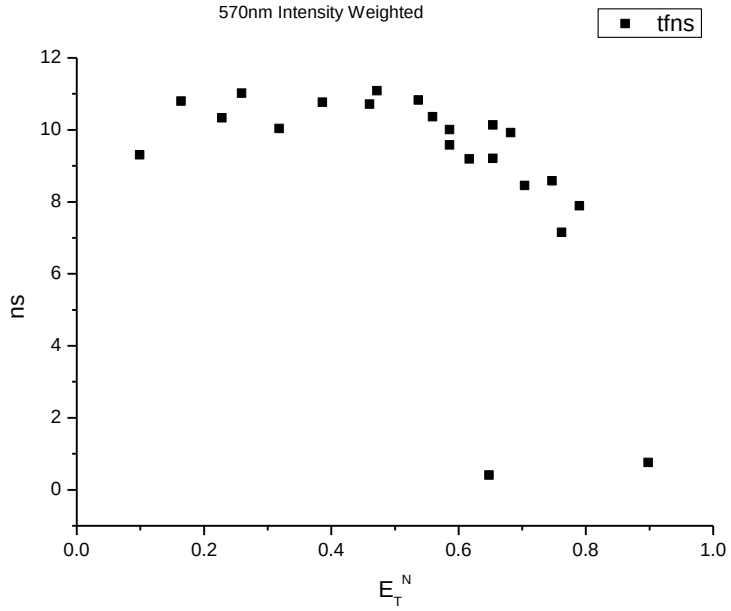

Figure 1.1.129. Intensity weighted average lifetime (τ_f) of **3a** at 570 nm versus E_T^N.

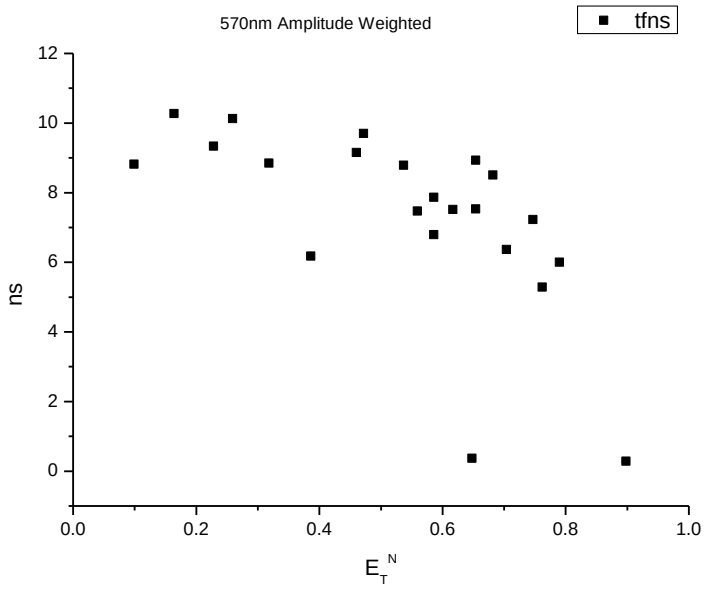

Figure 1.1.130. Amplitude weighted average lifetime (τ_f) of **3a** at 570 nm versus E_T^N.

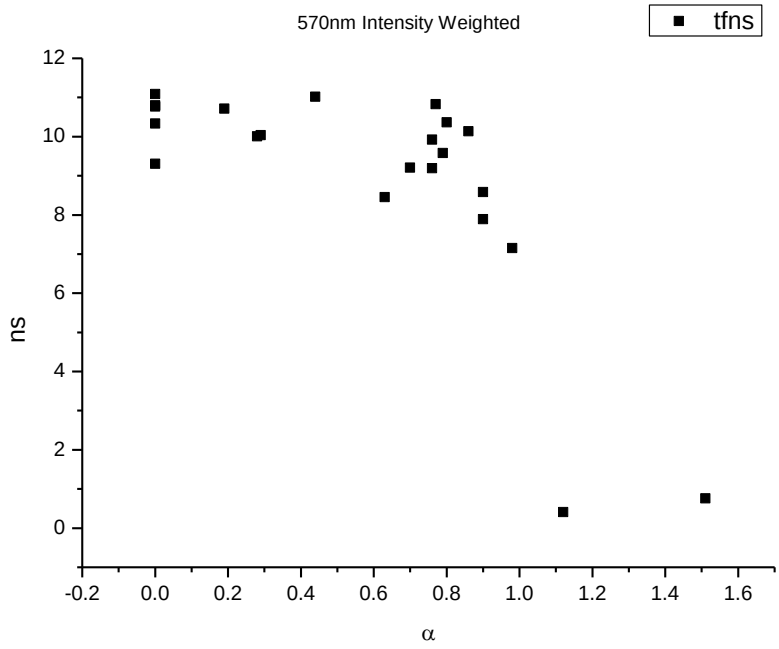

Figure 1.1.131. Intensity weighted average lifetime (τ_f) of **3a** at 570 nm versus α.

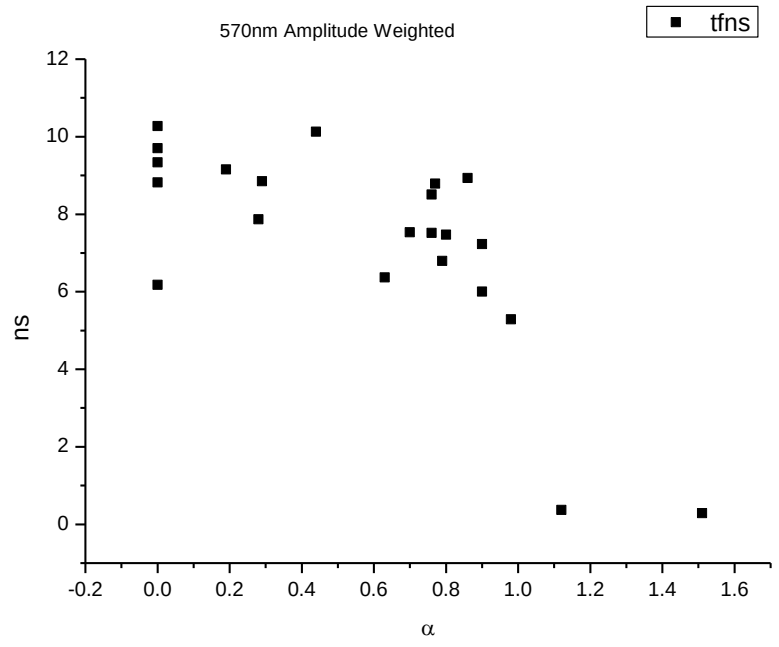

Figure 1.1.132. Amplitude weighted average lifetime (τ_f) of **3a** at 570 nm versus α.

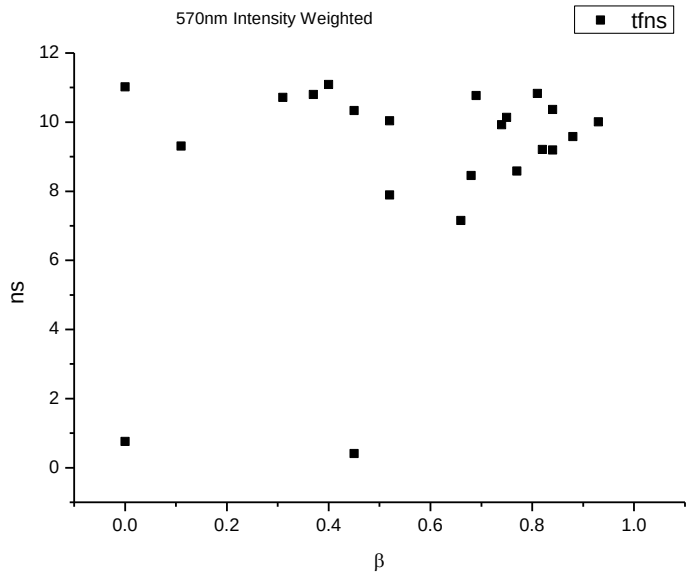

Figure 1.1.133. Intensity weighted average lifetime (τ_f) of **3a** at 570 nm versus β.

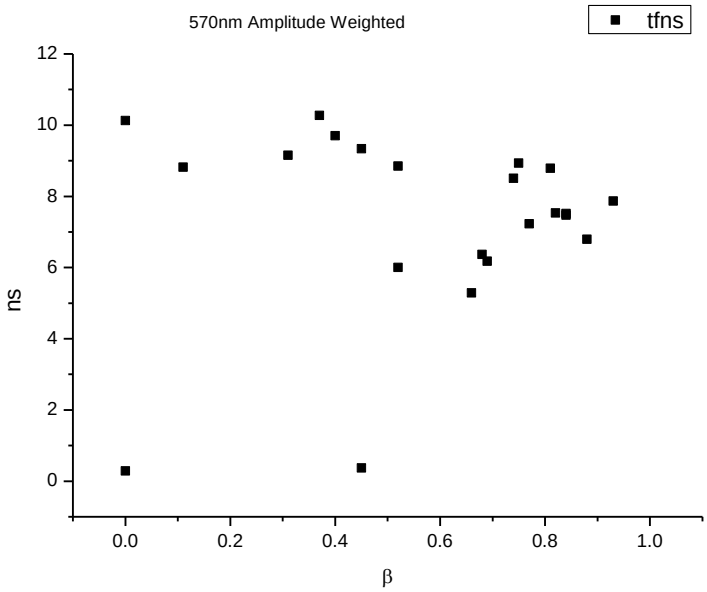

Figure 1.1.134. Amplitude weighted average lifetime (τ_f) of **3a** at 570 nm versus β.

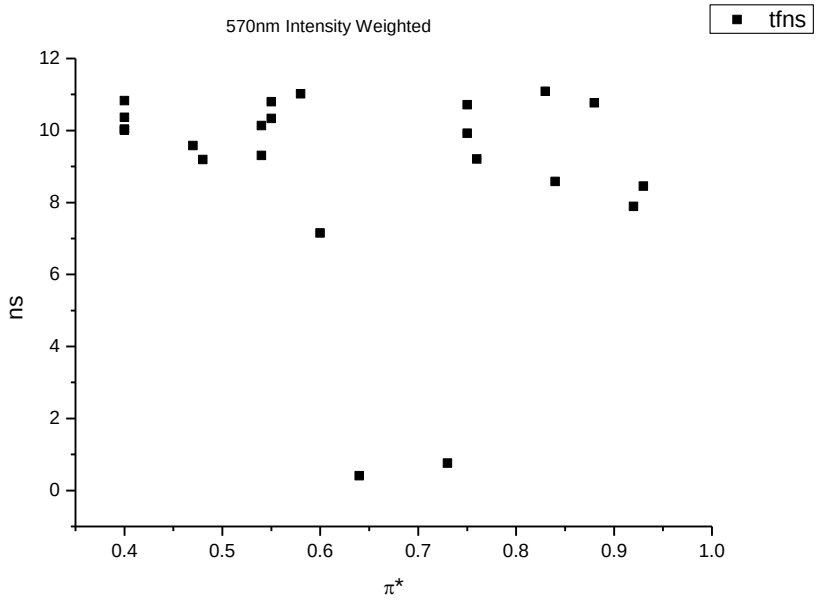

Figure 1.1.135. Intensity weighted average lifetime (τ_f) of **3a** at 570 nm versus π*.

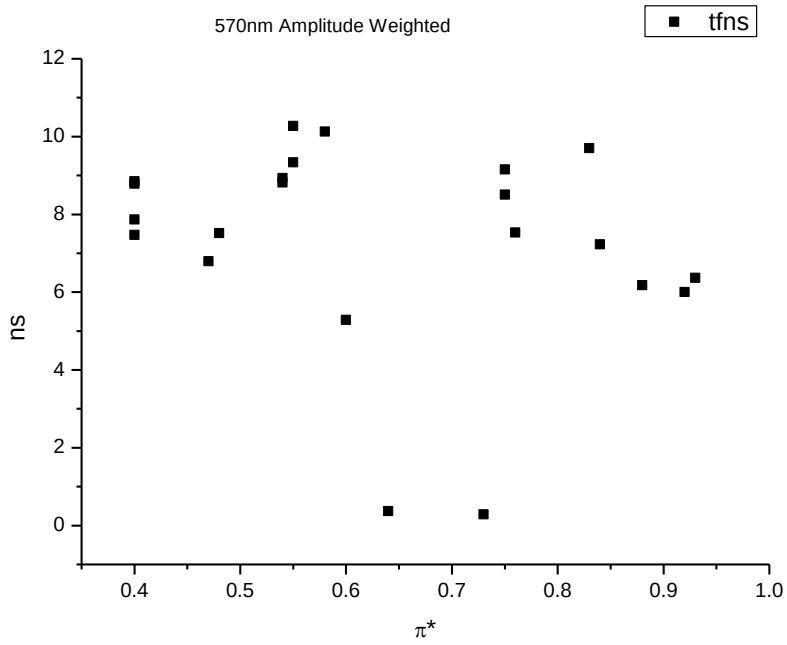

Figure 1.1.136. Amplitude weighted average lifetime (τ_f) of **3a** at 570 nm versus π*.

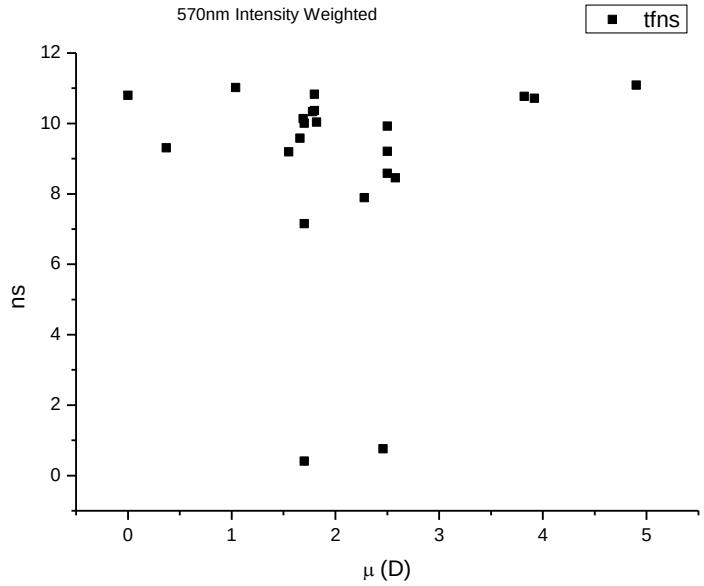

Figure 1.1.137. Intensity weighted average lifetime (τ_f) of **3a** at 570 nm versus μ(D).

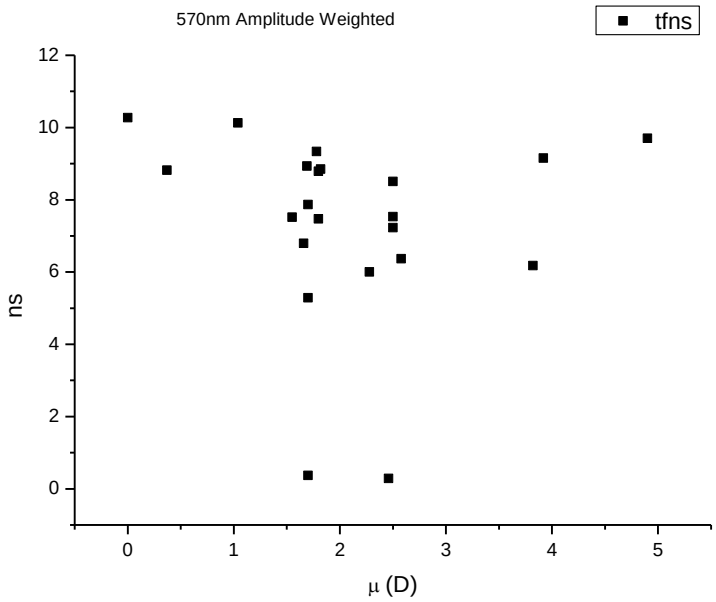

Figure 1.1.138. Amplitude weighted average lifetime (τ_f) of **3a** at 570 nm versus μ(D).

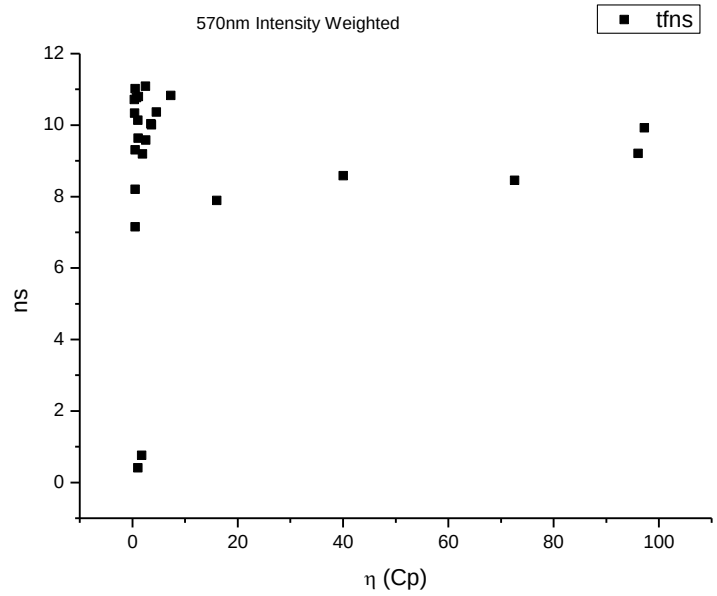

Figure 1.1.139. Intensity weighted average lifetime (τ_f) of **3a** at 570 nm versus η(Cp).

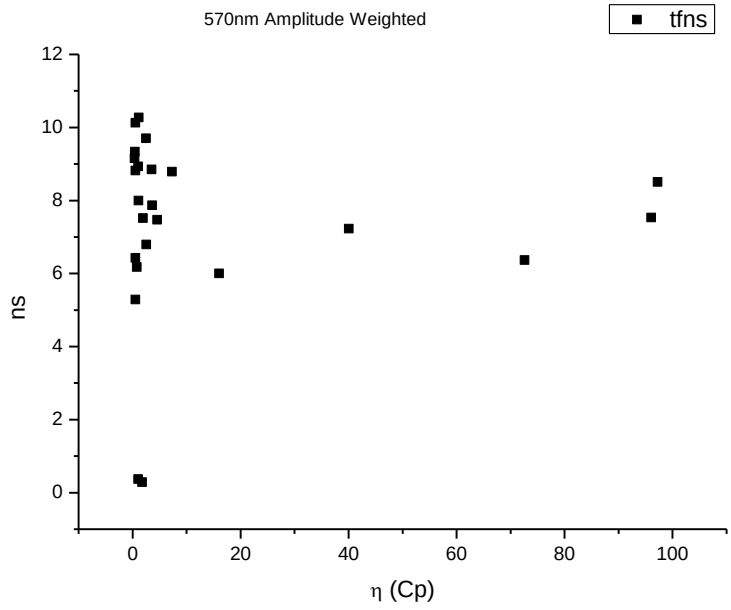

Figure 1.1.140. Amplitude weighted average lifetime (τ_f) of **3a** at 570 nm versus η(Cp).

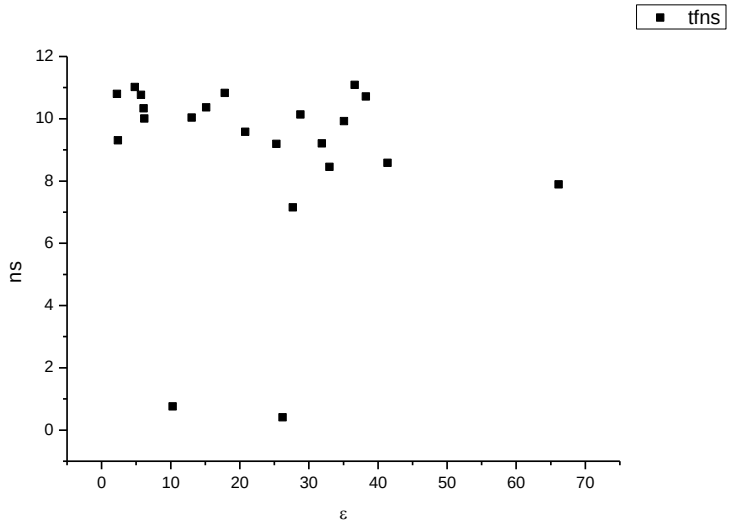

Figure 1.1.141. Intensity weighted average lifetime (τ_f) of **3a** at 570 nm versus ε.

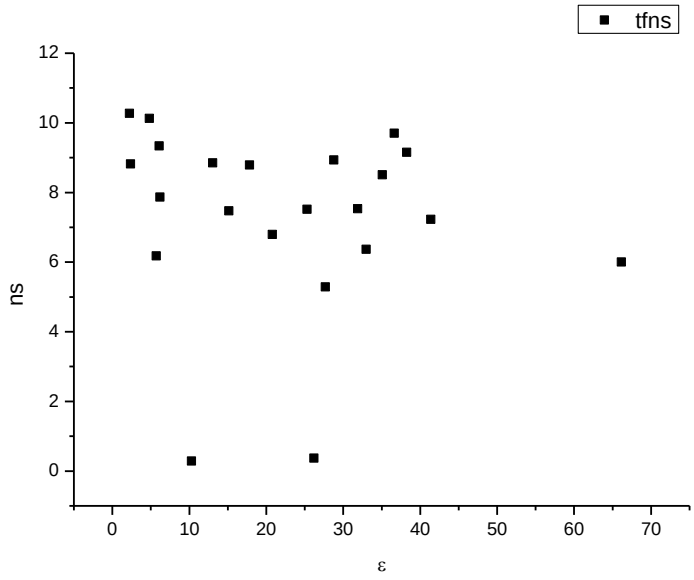

Figure 1.1.142. Amplitude weighted average lifetime (τ_f) of **3a** at 570 nm versus ε.

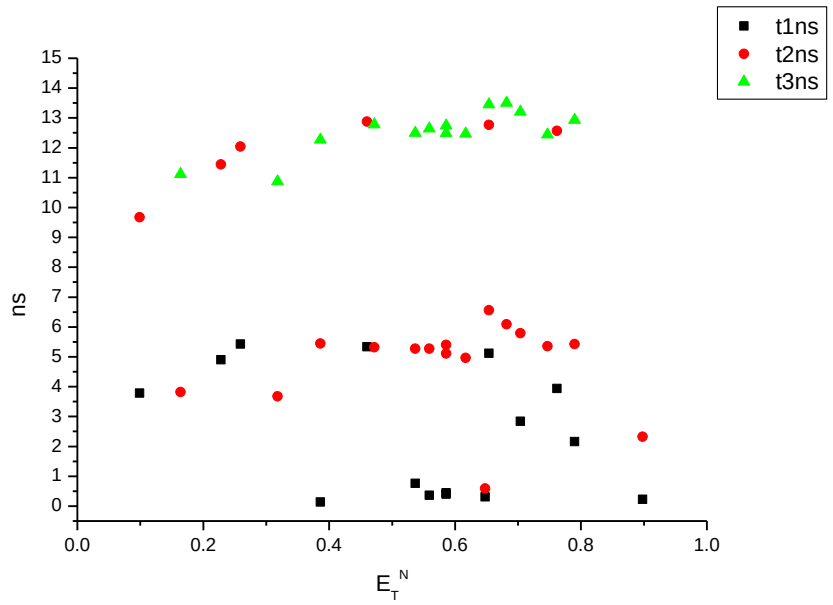

Figure 1.1.143. Intensity weighted components of TCSPC lifetime decay of **3a** (570 nm) versus E_T^N.

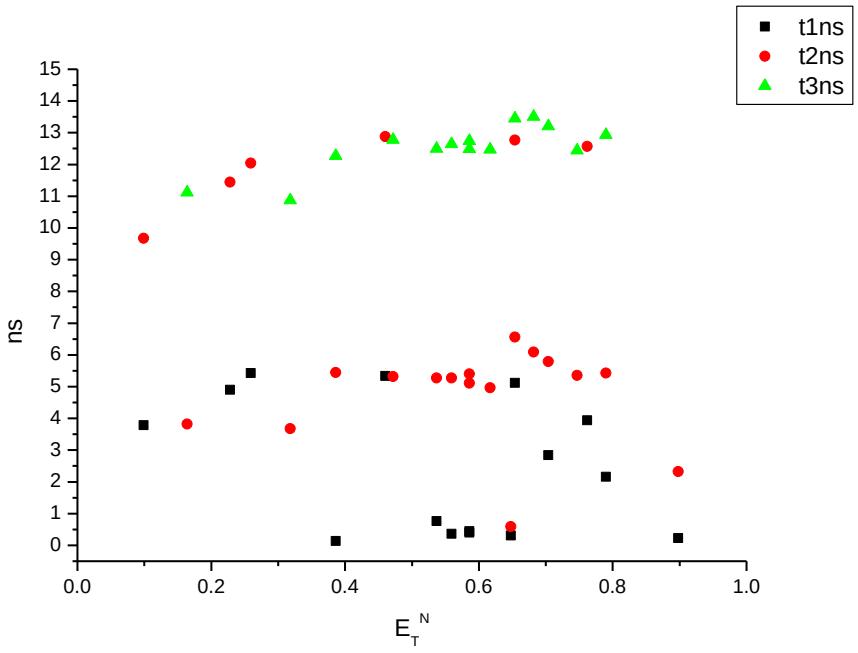

Figure 1.1.144. Amplitude weighted components of TCSPC lifetime decay of **3a** (570 nm) versus E_T^N.

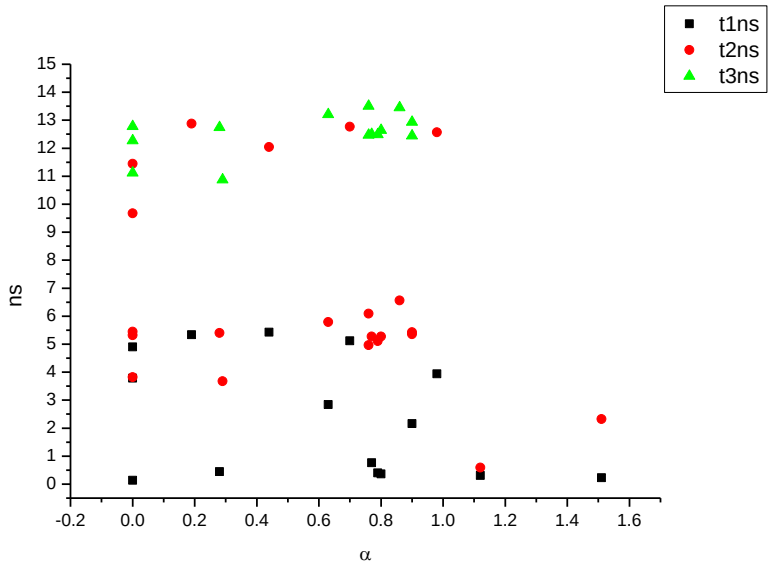

Figure 1.1.145. Intensity weighted components of TCSPC lifetime decay of **3a** (570 nm) versus α.

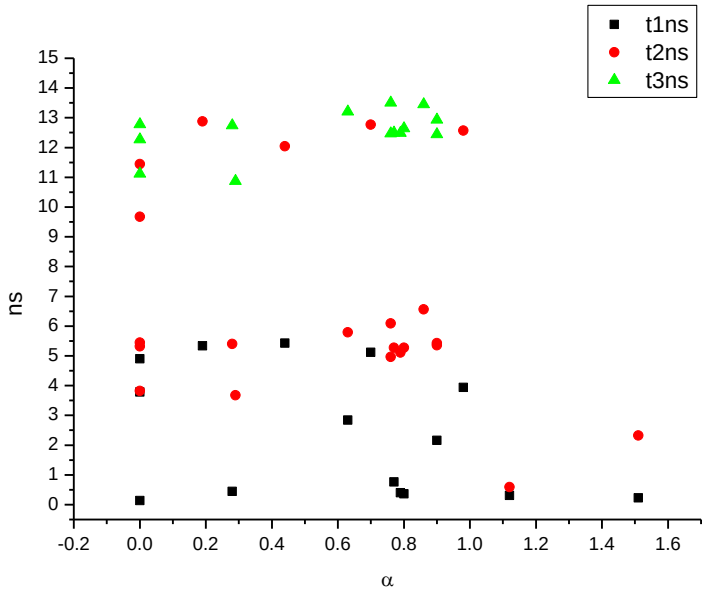

Figure 1.1.146. Amplitude weighted components of TCSPC lifetime decay of **3a** (570 nm) versus α.

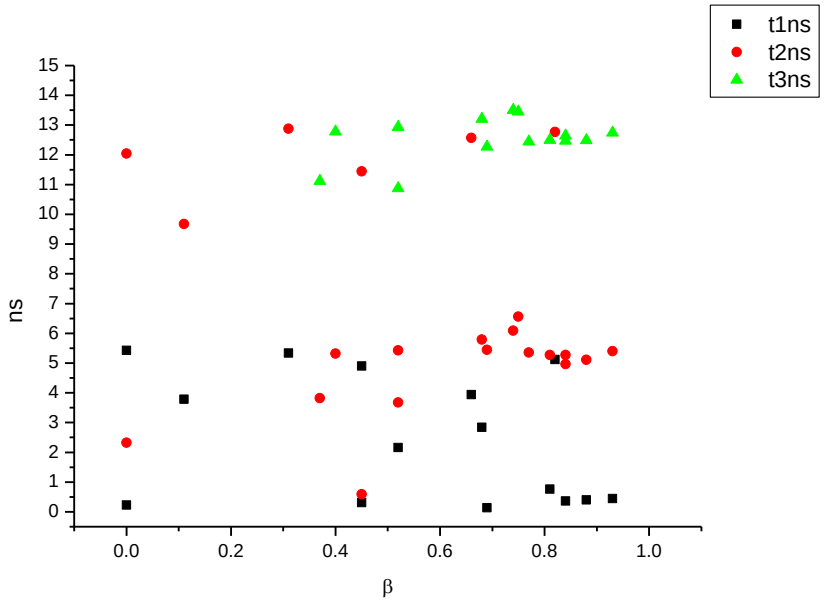

Figure 1.1.147. Intensity weighted components of TCSPC lifetime decay of **3a** (570 nm) versus β.

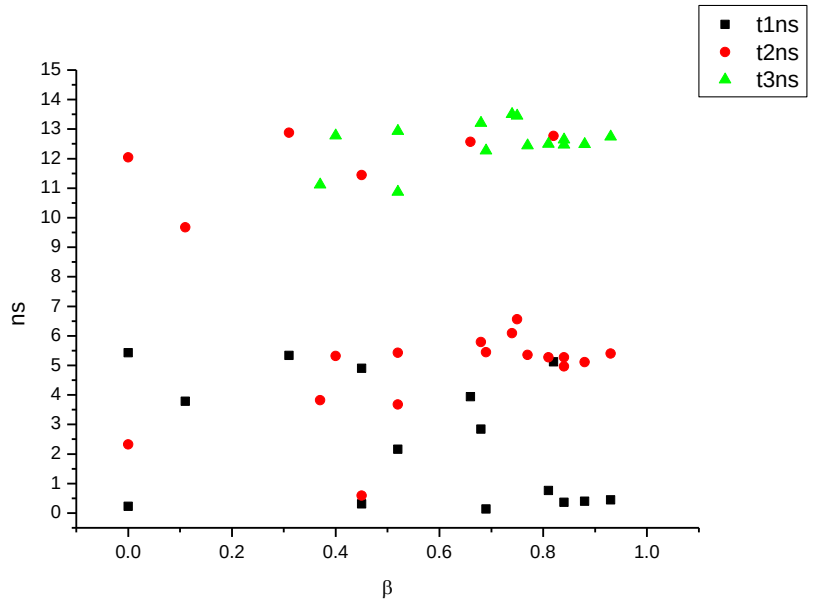

Figure 1.1.148. Amplitude weighted components of TCSPC lifetime decay of **3a** (570 nm) versus β.

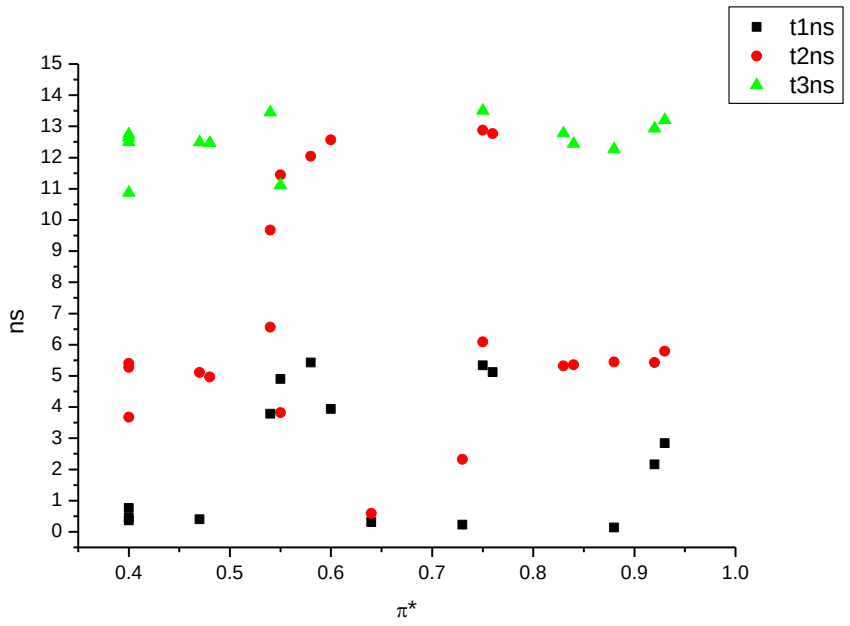

Figure 1.1.149. Intensity weighted components of TCSPC lifetime decay of **3a** (570 nm) versus π*.

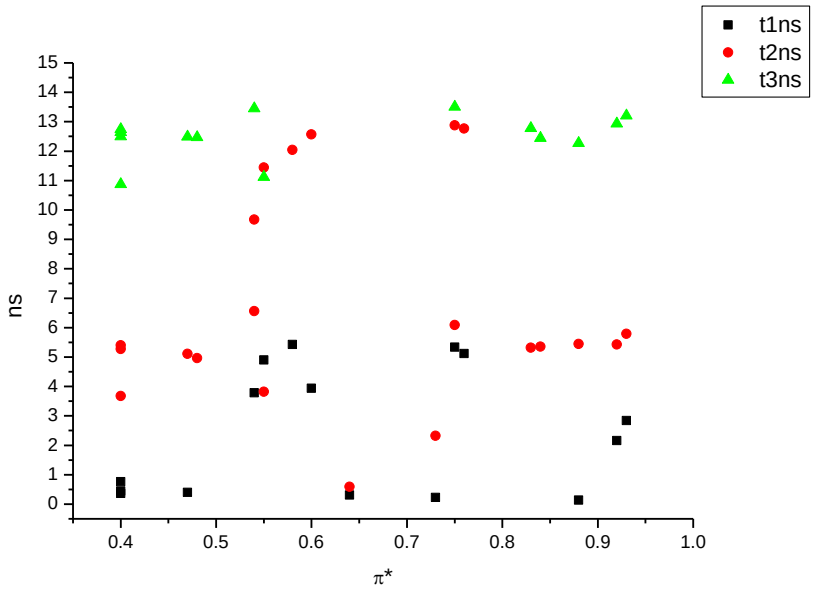

Figure 1.1.150. Amplitude weighted components of TCSPC lifetime decay of **3a** (570 nm) versus π*.

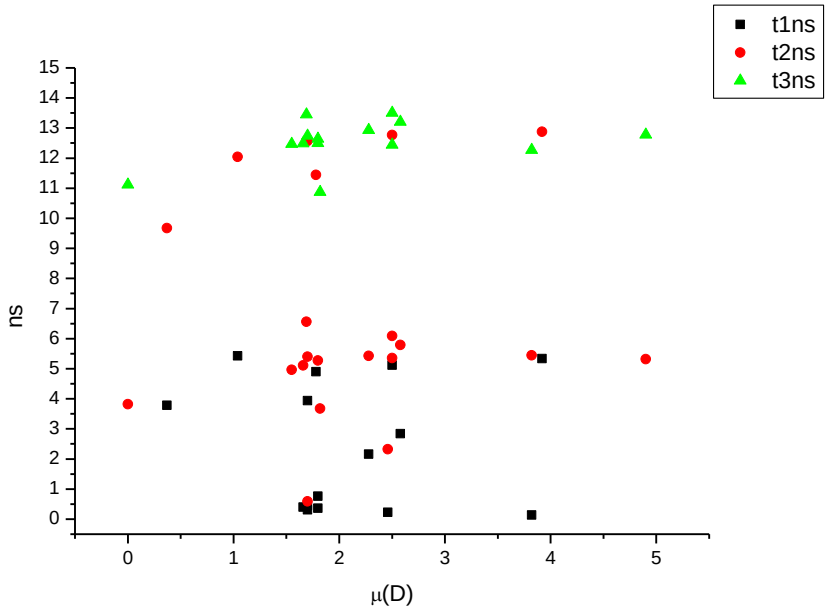

Figure 1.1.151. Intensity weighted components of TCSPC lifetime decay of **3a** (570 nm) versus μ(D).

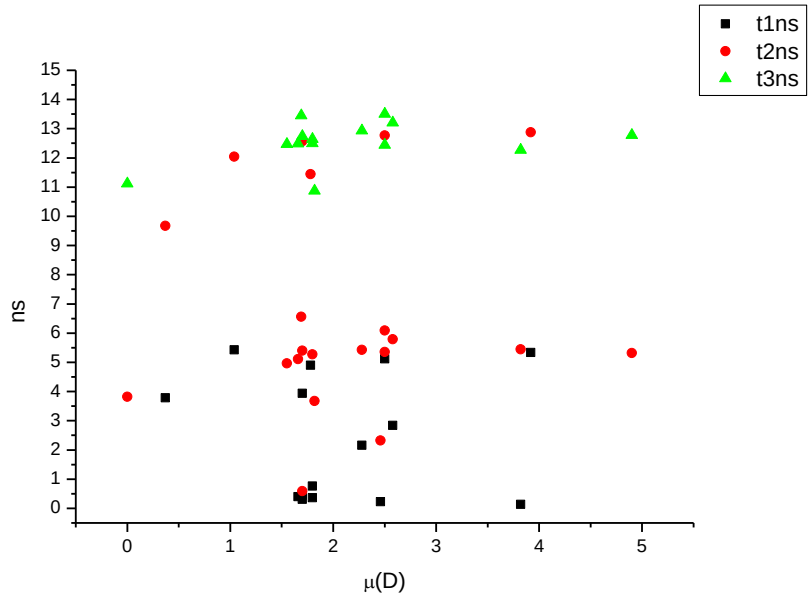

Figure 1.1.152. Amplitude weighted components of TCSPC lifetime decay of **3a** (570 nm) versus μ(D).

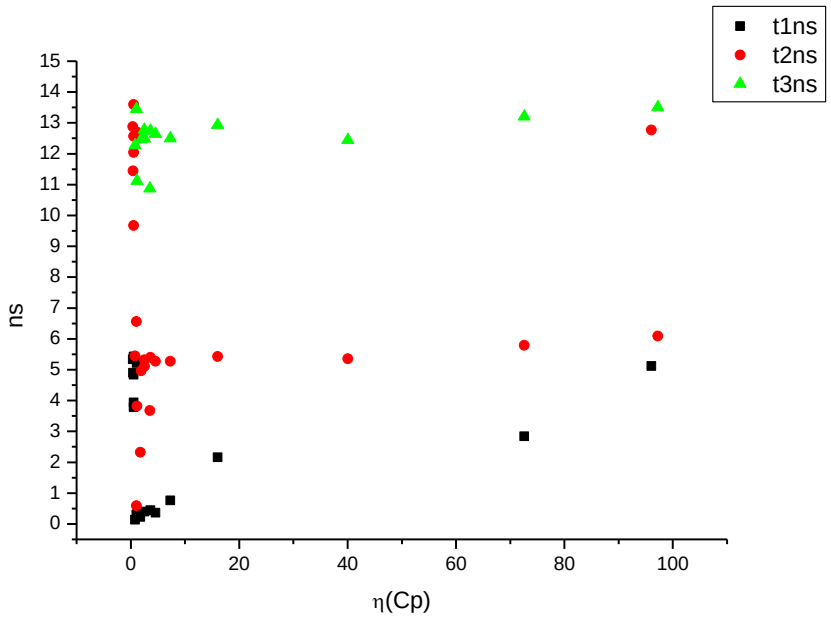

Figure 1.1.153. Intensity weighted components of TCSPC lifetime decay of **3a** (570 nm) versus η(Cp).

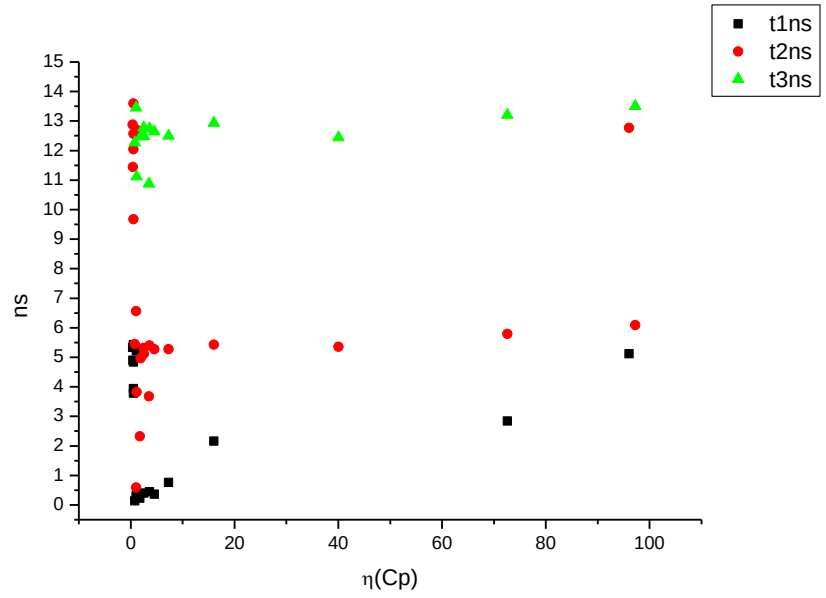

Figure 1.1.154. Amplitude weighted components of TCSPC lifetime decay of **3a** (570 nm) versus η(Cp).

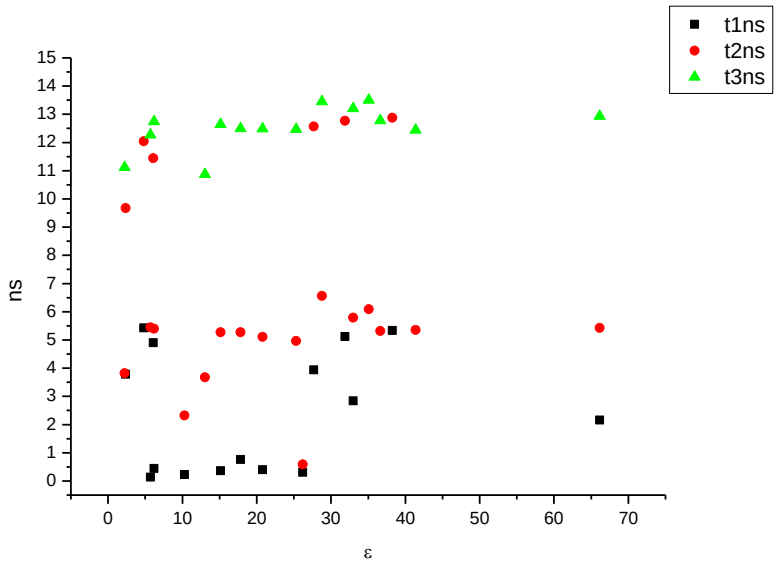

Figure 1.1.155. Intensity weighted components of TCSPC lifetime decay of **3a** (570 nm) versus ε.

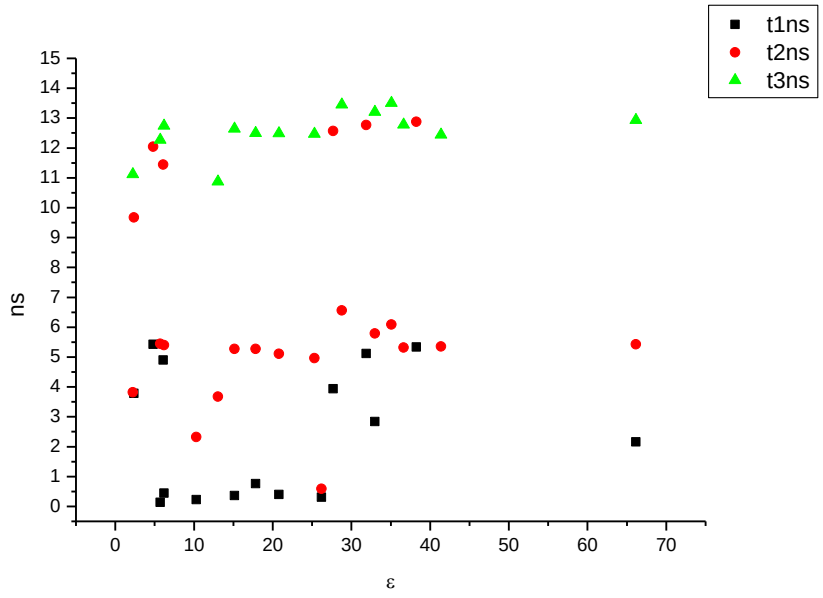

Figure 1.1.156. Amplitude weighted components of TCSPC lifetime decay of **3a** (570 nm) versus ε.

1.1.8 Ultraviolet-visible absorption spectra.

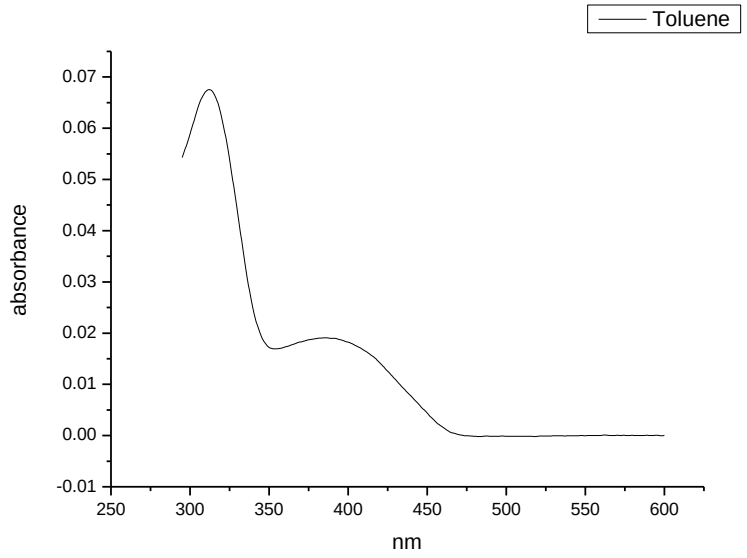

Figure 1.1.157. Ultraviolet-Visible absorption spectrum of **3a** recorded in Toluene.

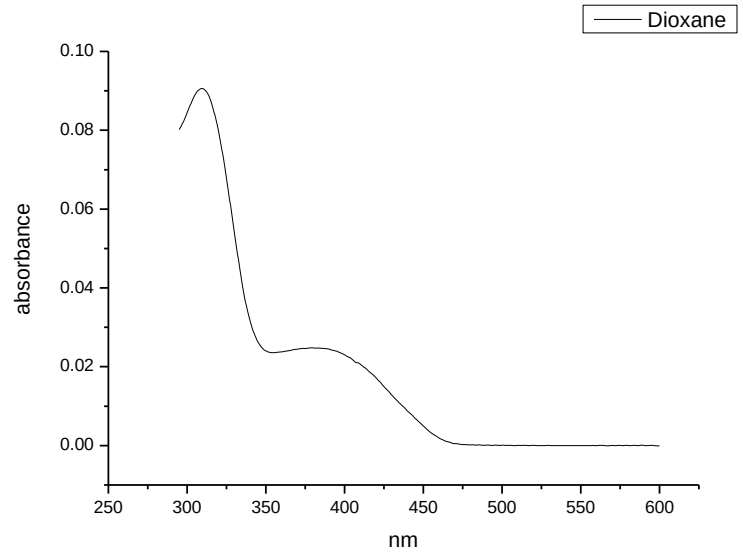

Figure 1.1.158. Ultraviolet-Visible absorption spectrum of **3a** recorded in 1,4-dioxane.

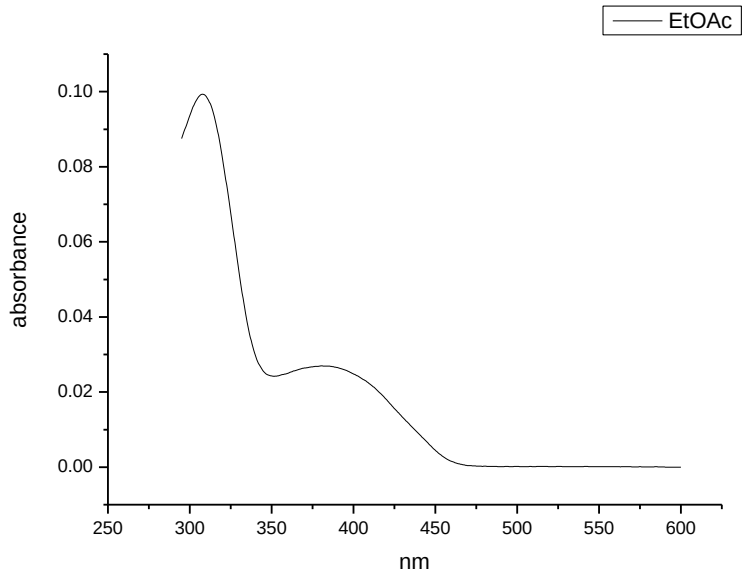

Figure 1.1.159. Ultraviolet-Visible absorption spectrum of **3a** recorded in Ethyl Acetate.

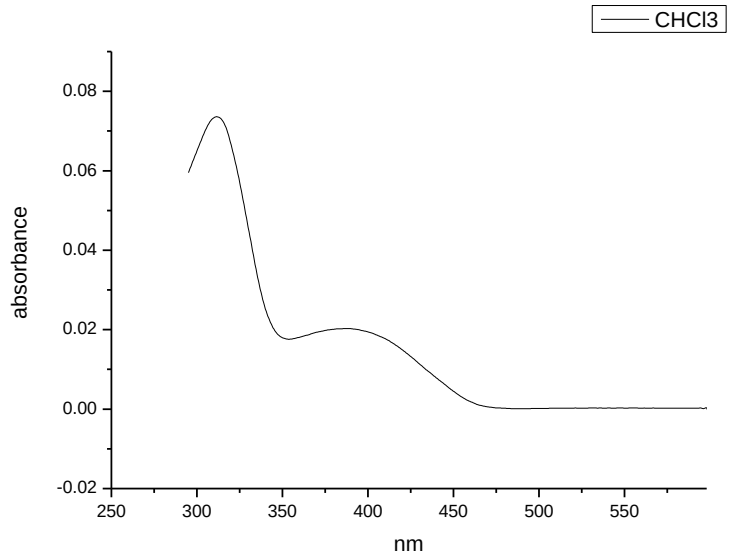

Figure 1.1.160. Ultraviolet-Visible absorption spectrum of **3a** recorded in Chloroform.

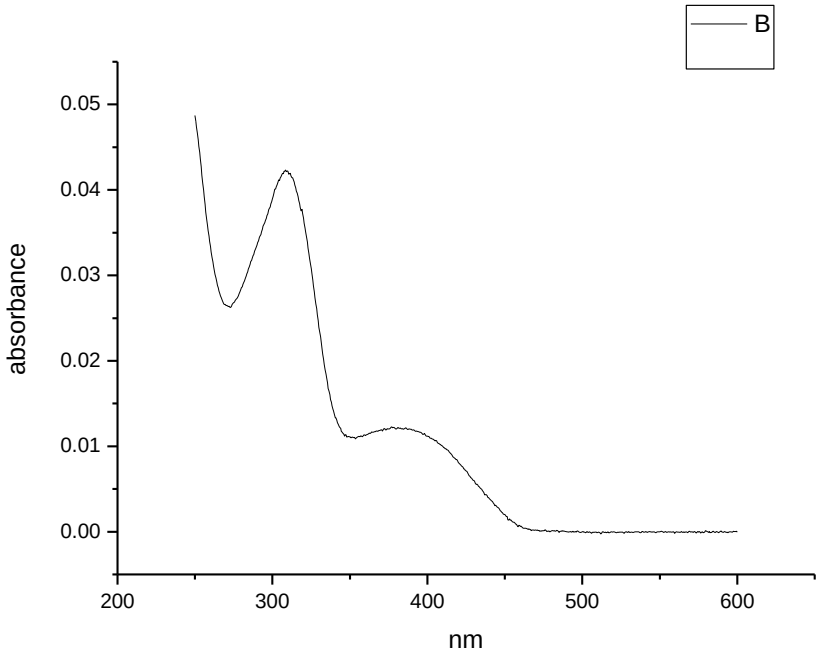

Figure 1.1.161. Ultraviolet-Visible absorption spectrum of **3a** recorded in 2-methyl-butanol.

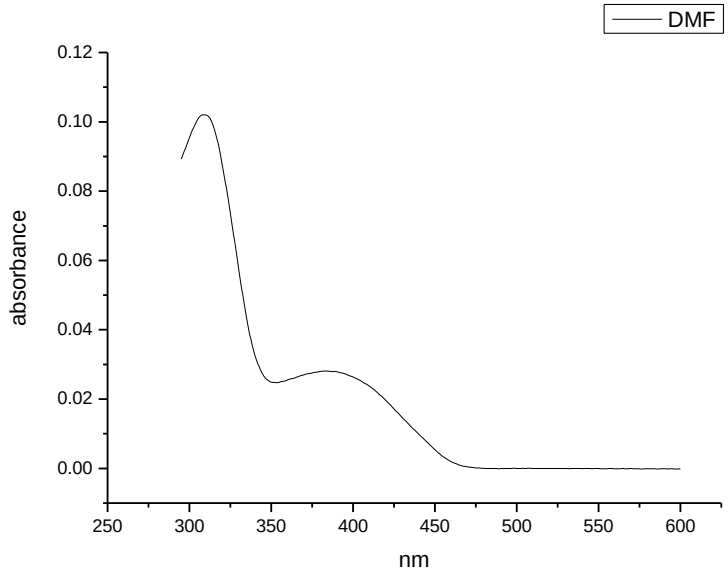

Figure 1.1.162. Ultraviolet-Visible absorption spectrum of **3a** recorded in N,N-dimethylformamide.

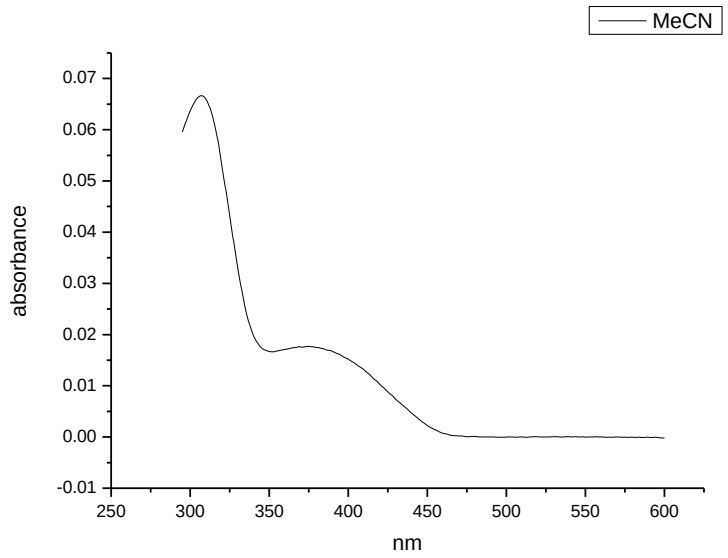

Figure 1.1.163. Ultraviolet-Visible absorption spectrum of **3a** recorded in Acetonitrile.

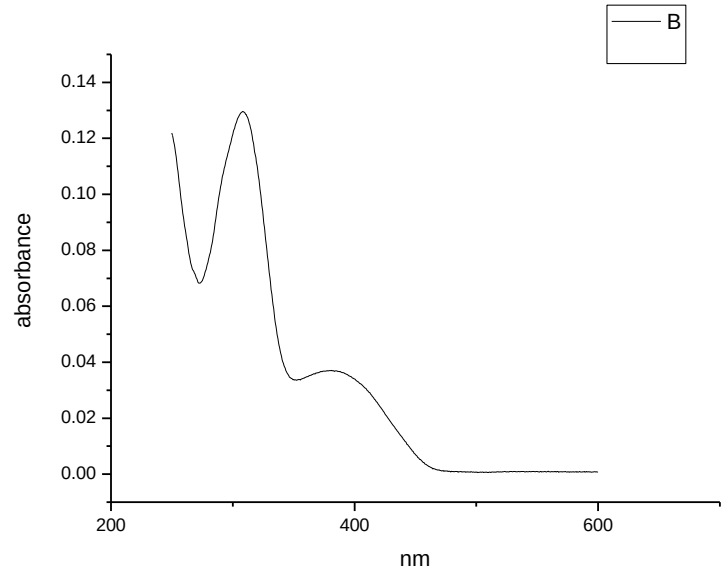

Figure 1.1.164. Ultraviolet-Visible absorption spectrum of **3a** recorded in Propylene Carbonate.

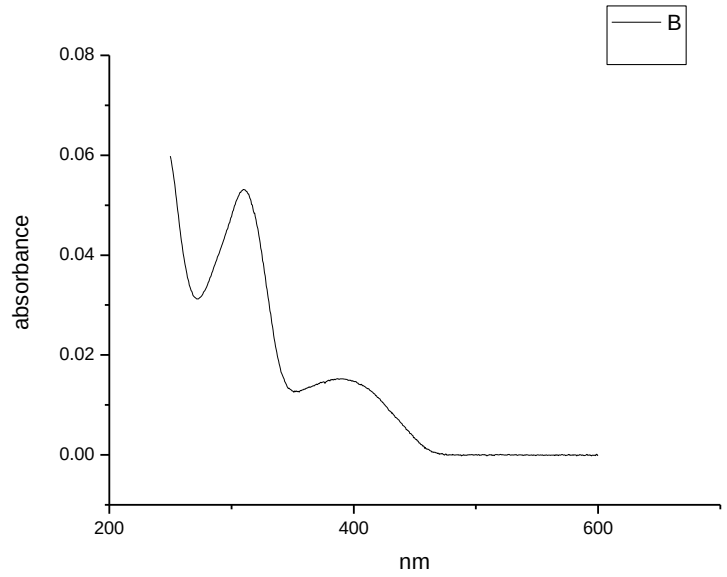

Figure 1.1.165. Ultraviolet-Visible absorption spectrum of **3a** recorded in 1-octanol.

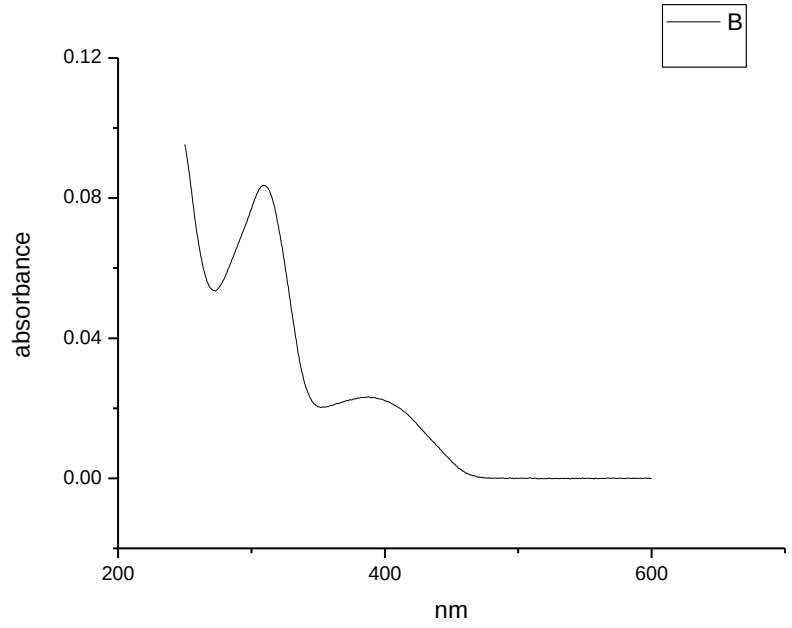

Figure 1.1.166. Ultraviolet-Visible absorption spectrum of **3a** recorded in 1-hexanol.

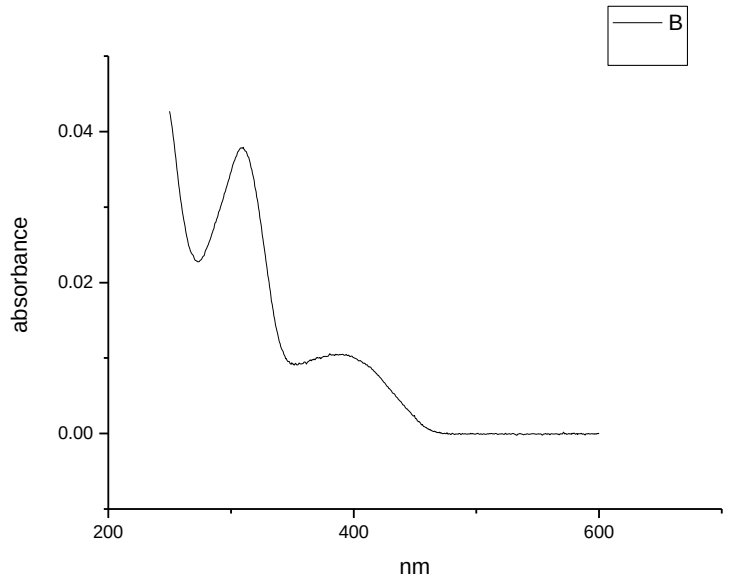

Figure 1.1.167. Ultraviolet-Visible absorption spectrum of **3a** recorded in 1-butanol.

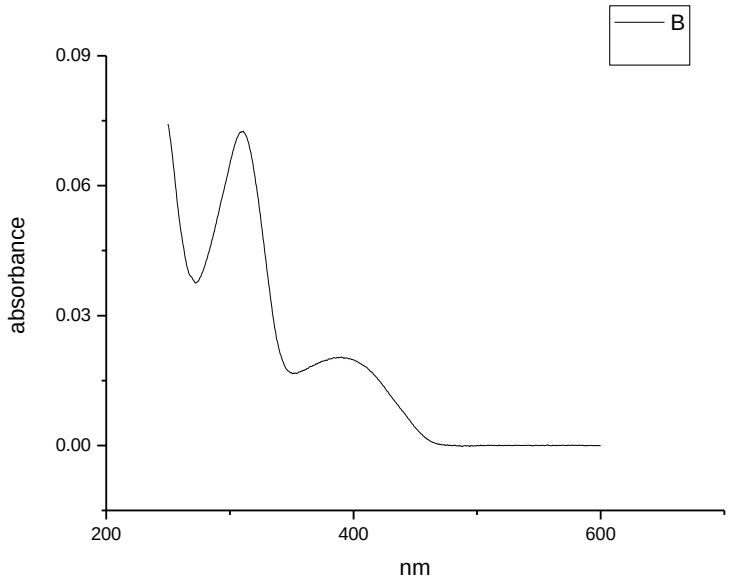

Figure 1.1.168. Ultraviolet-Visible absorption spectrum of **3a** recorded in 1-pentanol.

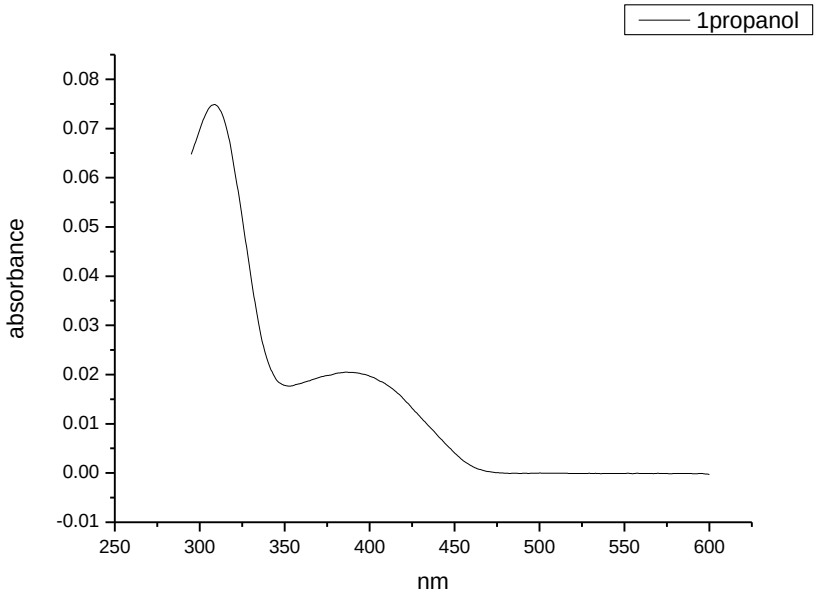

Figure 1.1.169. Ultraviolet-Visible absorption spectrum of **3a** recorded in 1-propanol.

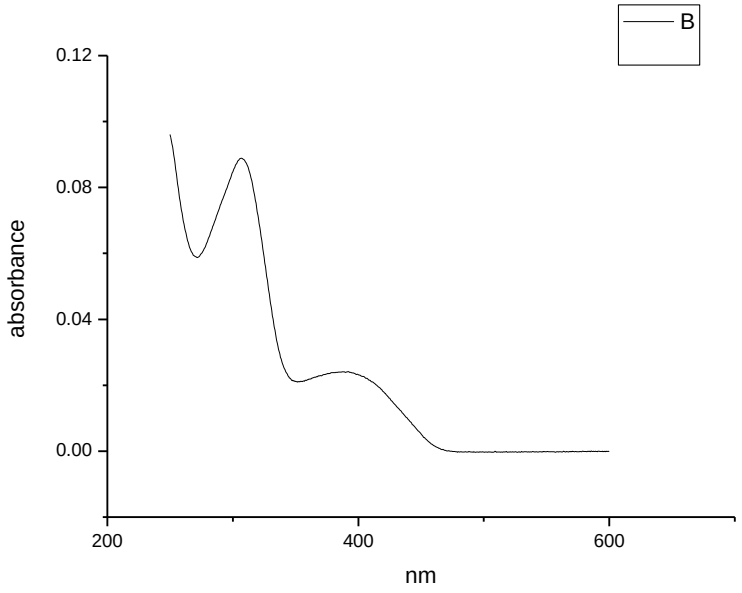

Figure 1.1.170. Ultraviolet-Visible absorption spectrum of **3a** recorded in Acetic Acid.

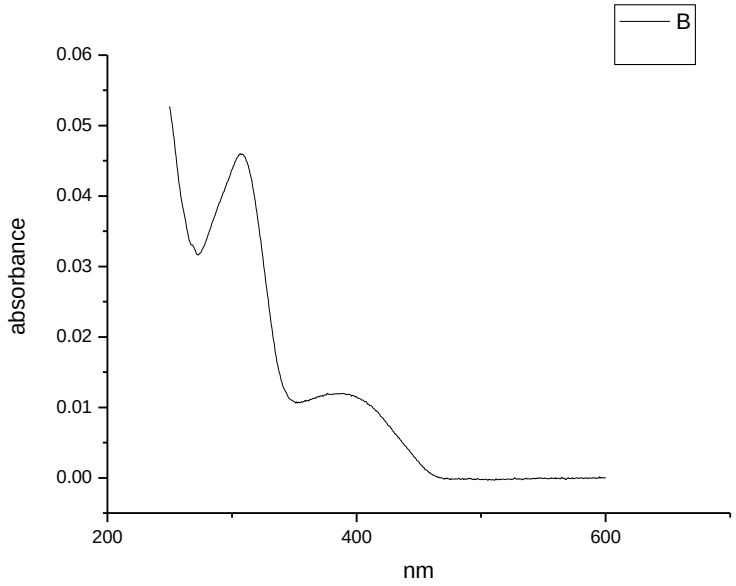

Figure 1.1.171. Ultraviolet-Visible absorption spectrum of **3a** recorded in Ethanol.

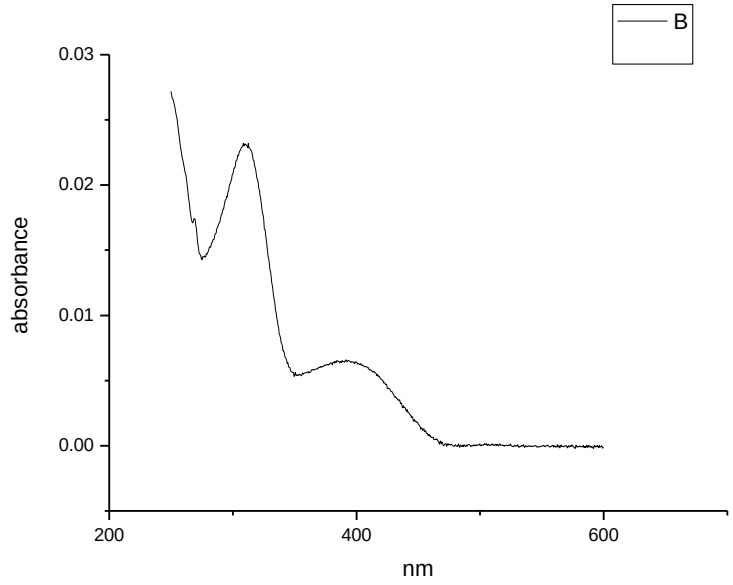

Figure 1.1.172. Ultraviolet-Visible absorption spectrum of **3a** recorded in 1,5-pentanediol.

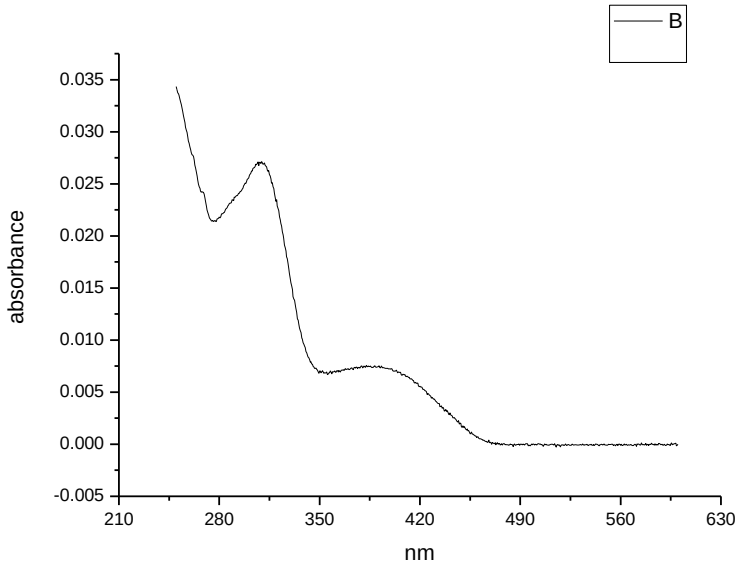

Figure 1.1.173. Ultraviolet-Visible absorption spectrum of **3a** recorded in 1,3-butanediol.

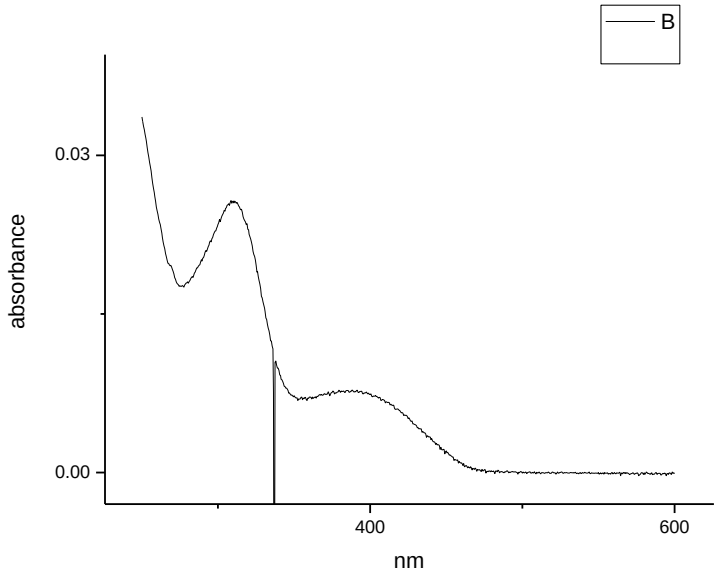

Figure 1.1.174. Ultraviolet-Visible absorption spectrum of **3a** recorded in 1,4-butanediol.

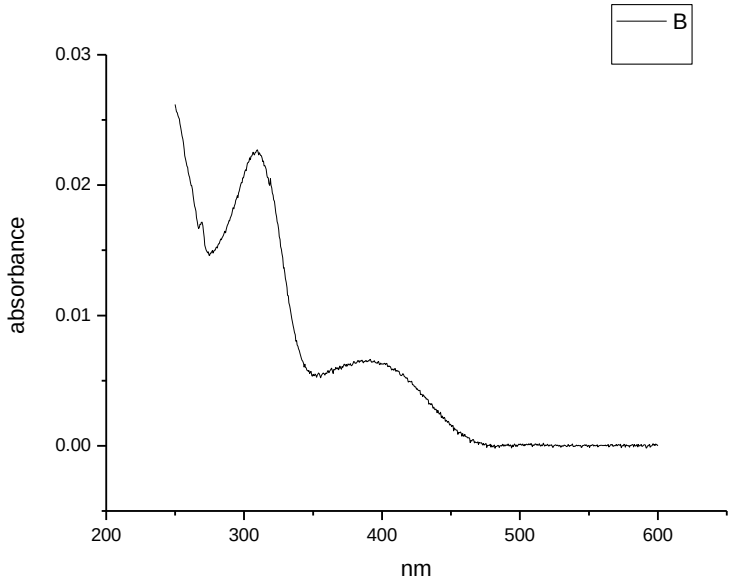

Figure 1.1.175. Ultraviolet-Visible absorption spectrum of **3a** recorded in 1,3-propanediol.

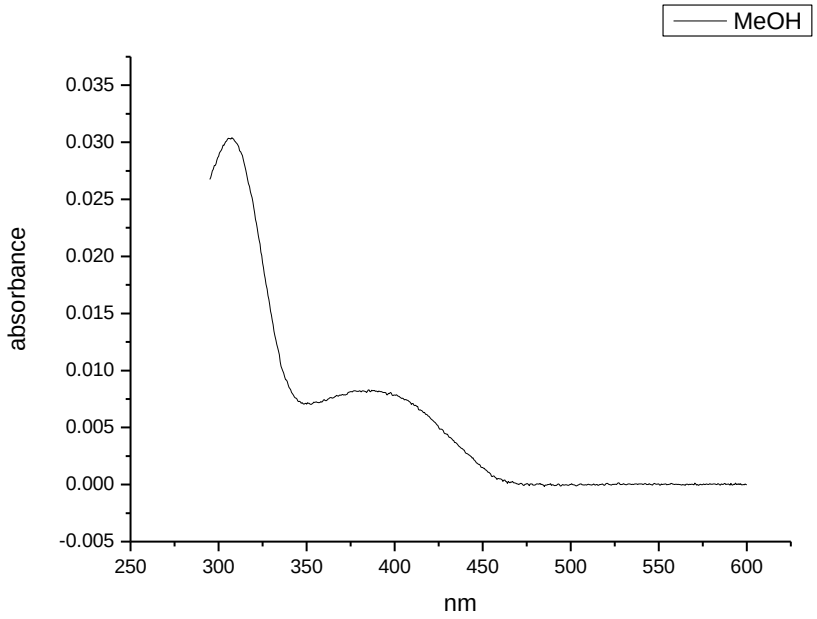

Figure 1.1.176. Ultraviolet-Visible absorption spectrum of **3a** recorded in Methanol.

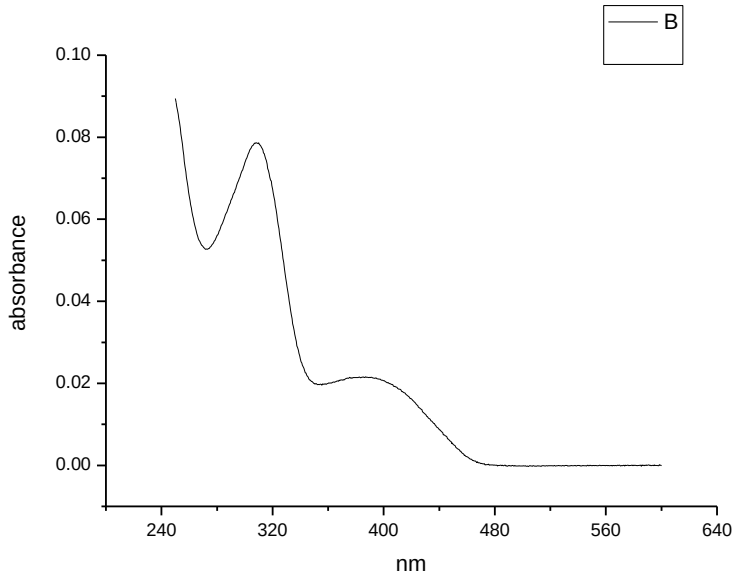

Figure 1.1.177. Ultraviolet-Visible absorption spectrum of **3a** recorded in 1,2-ethanediol.

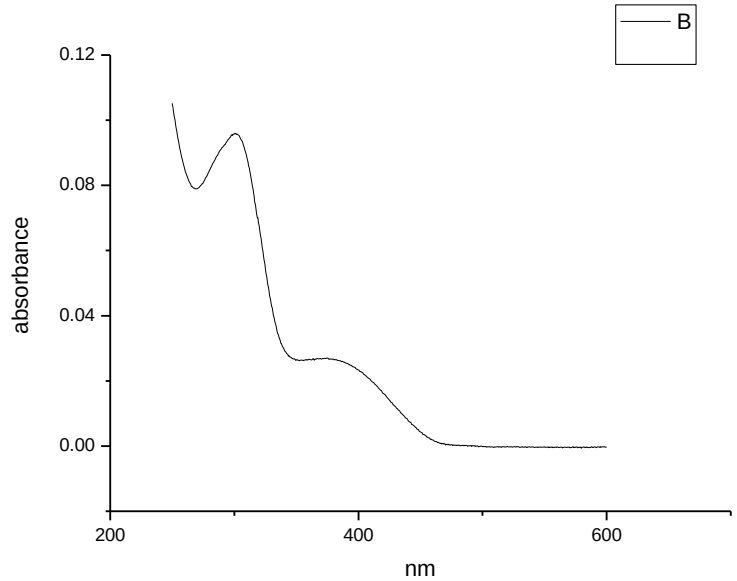

Figure 1.1.178. Ultraviolet-Visible absorption spectrum of **3a** recorded in 2,2,2-trifluoroethanol.

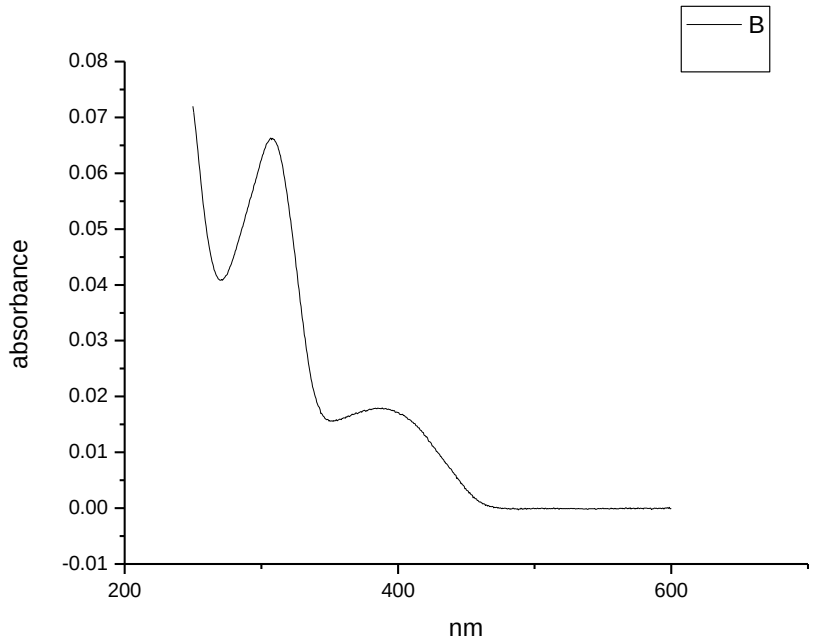

Figure 1.1.179. Ultraviolet-Visible absorption spectrum of **3a** recorded in Ethanol-d_1 (EtOD).

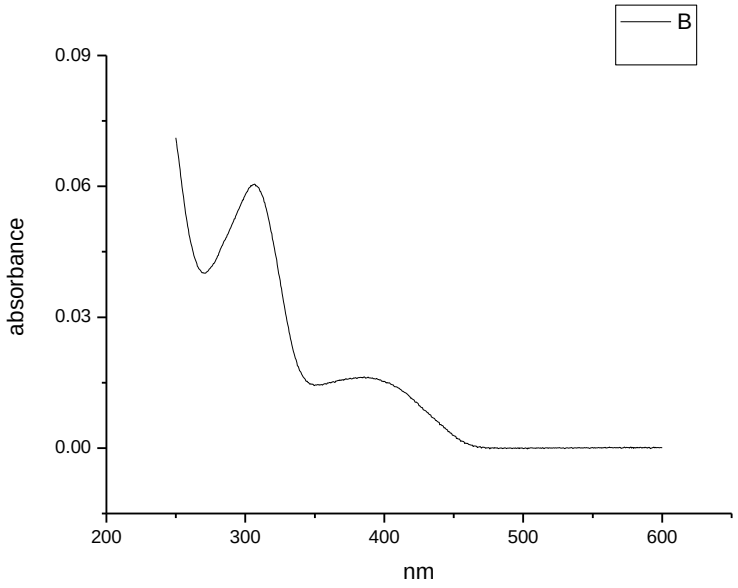

Figure 1.1.180. Ultraviolet-Visible absorption spectrum of **3a** recorded in Methanol-d_1 (MeOD).

1.1.9 Fluorescence Emission spectra.

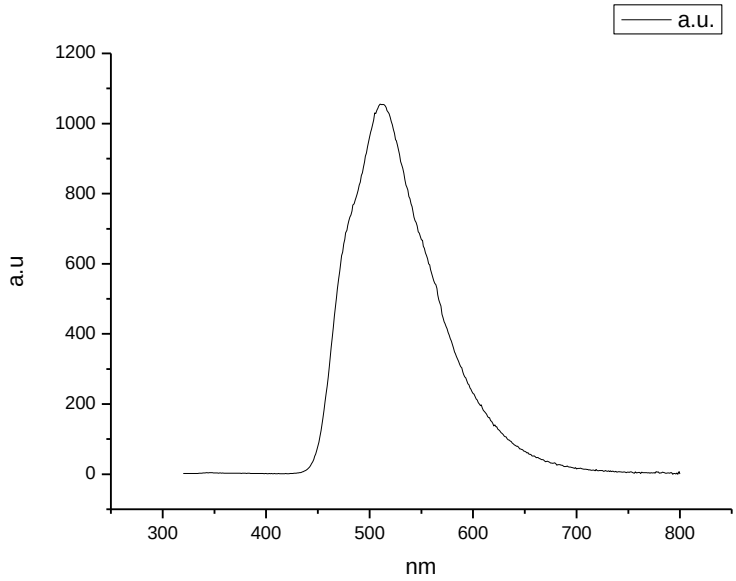

Figure 1.1.181. Fluorescence emission spectrum of **3a** recorded in Toluene at 310 nm excitation.

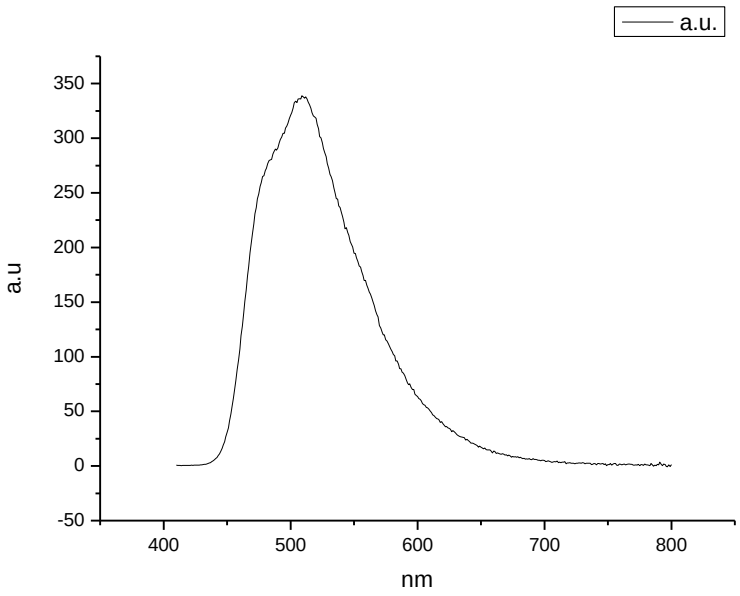

Figure 1.1.182. Fluorescence emission spectrum of **3a** recorded in Toluene at 400 nm excitation.

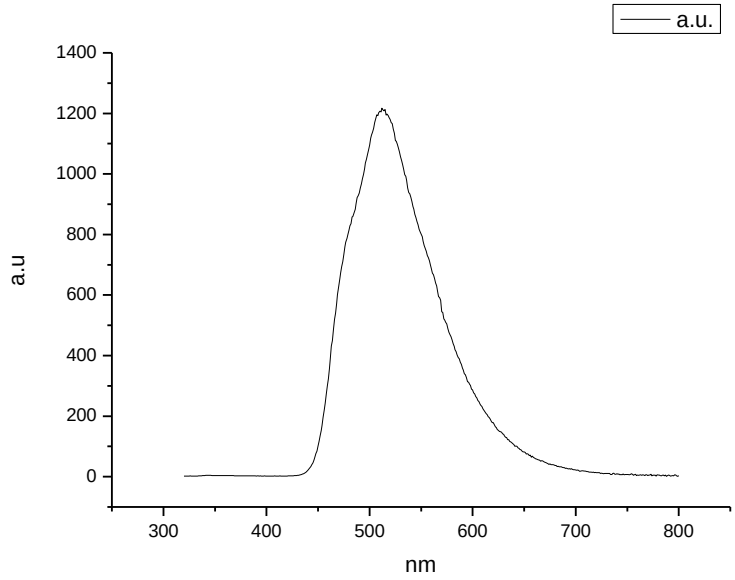

Figure 1.1.183. Fluorescence emission spectrum of **3a** recorded in 1,4-dioxane at 310 nm excitation.

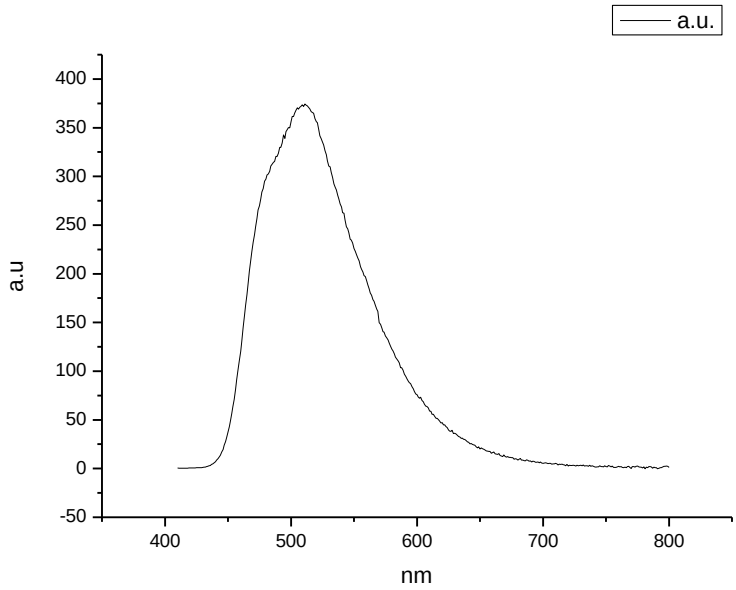

Figure 1.1.184. Fluorescence emission spectrum of **3a** recorded in 1,4-dioxane at 400 nm excitation.

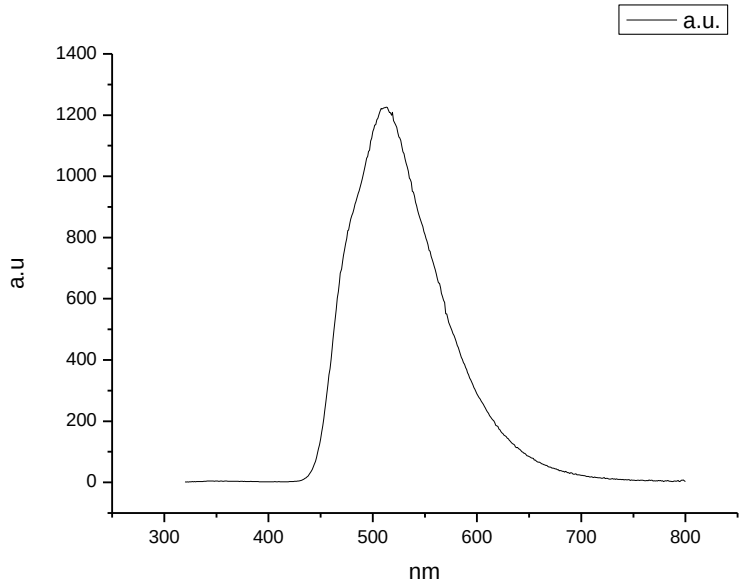

Figure 1.1.185. Fluorescence emission spectrum of **3a** recorded in Ethyl Acetate at 310 nm excitation.

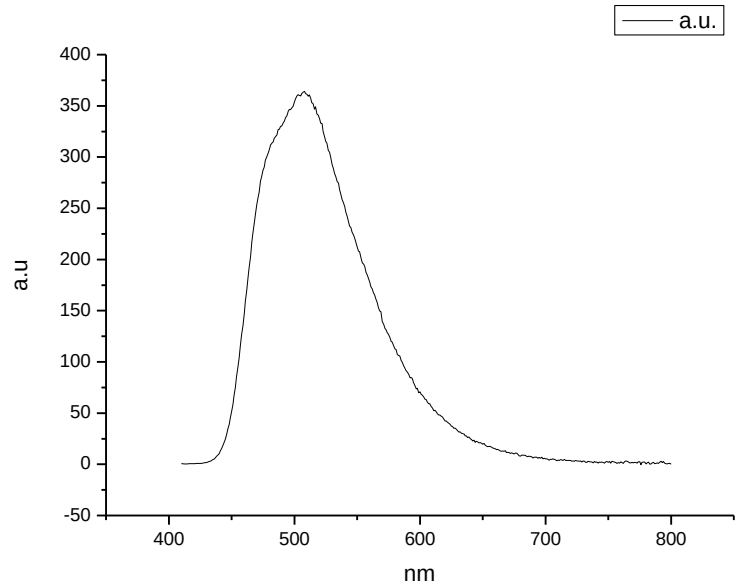

Figure 1.1.186. Fluorescence emission spectrum of **3a** recorded in Ethyl Acetate at 400 nm excitation.

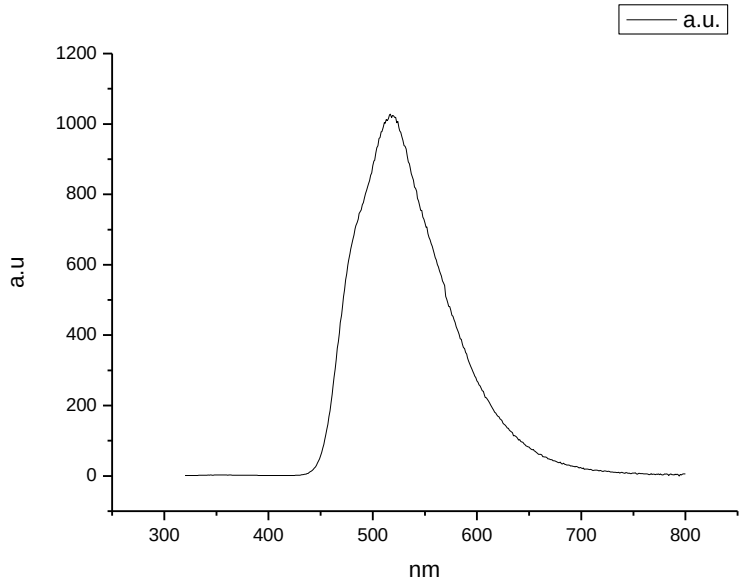

Figure 1.1.187. Fluorescence emission spectrum of **3a** recorded in Chloroform at 310 nm excitation.

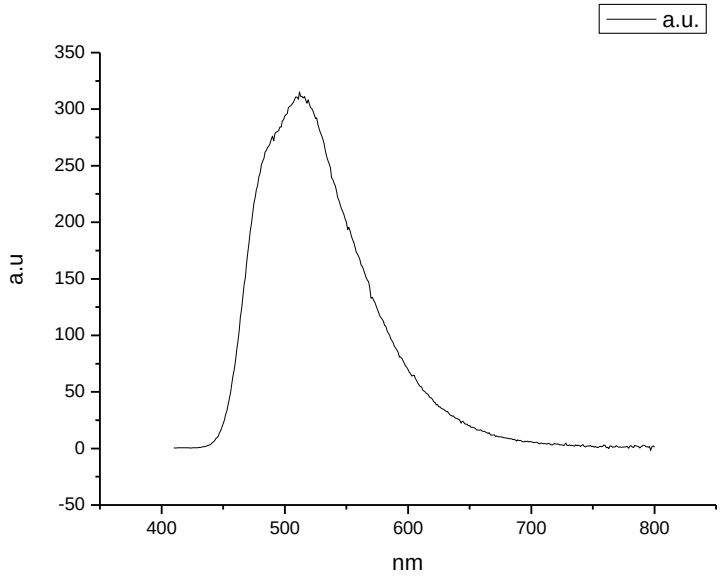

Figure 1.1.188. Fluorescence emission spectrum of **3a** recorded in Chloroform at 400 nm excitation.

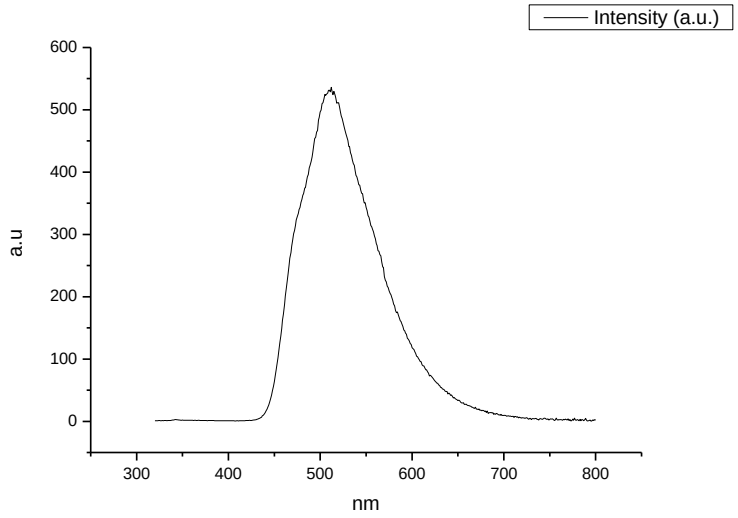

Figure 1.1.189. Fluorescence emission spectrum of **3a** recorded in 2-methyl-2-butanol at 310 nm excitation.

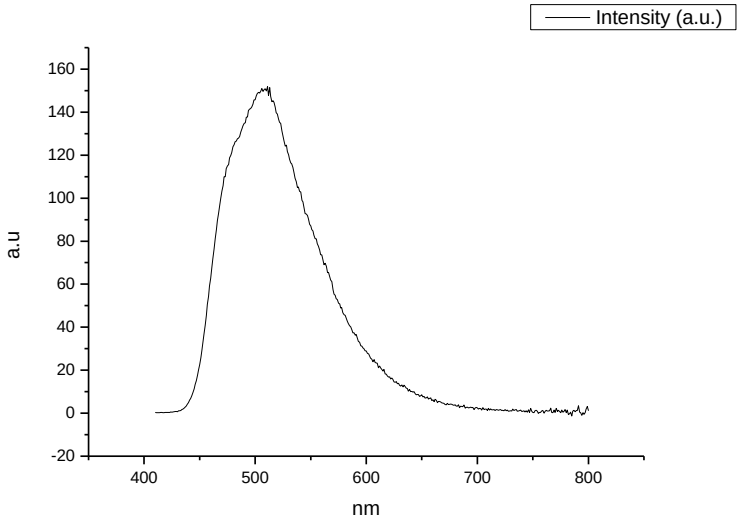

Figure 1.1.190. Fluorescence emission spectrum of **3a** recorded in 2-methyl-2-butanol at 400 nm excitation.

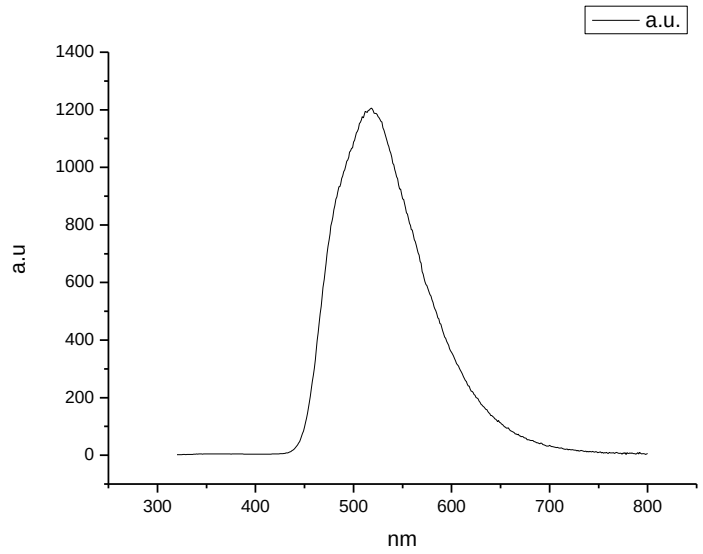

Figure 1.1.191. Fluorescence emission spectrum of **3a** recorded in N,N-dimethylformamide at 310 nm excitation.

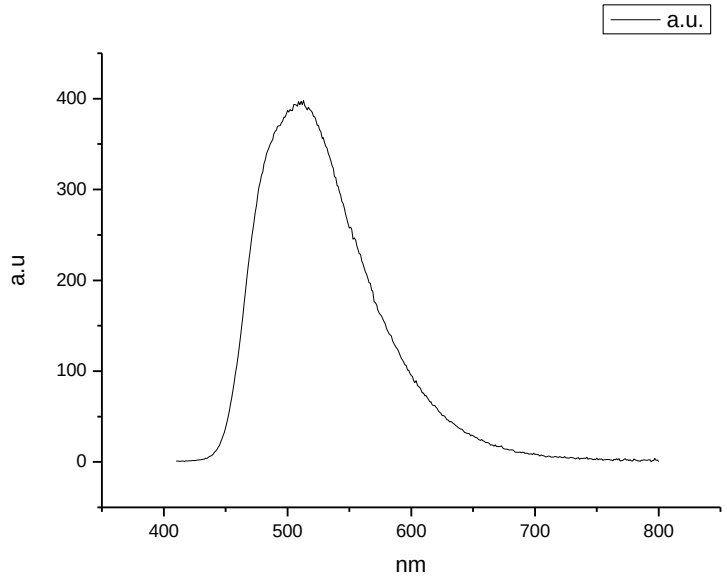

Figure 1.1.192. Fluorescence emission spectrum of **3a** recorded in N,N-dimethylformamide at 400 nm excitation.

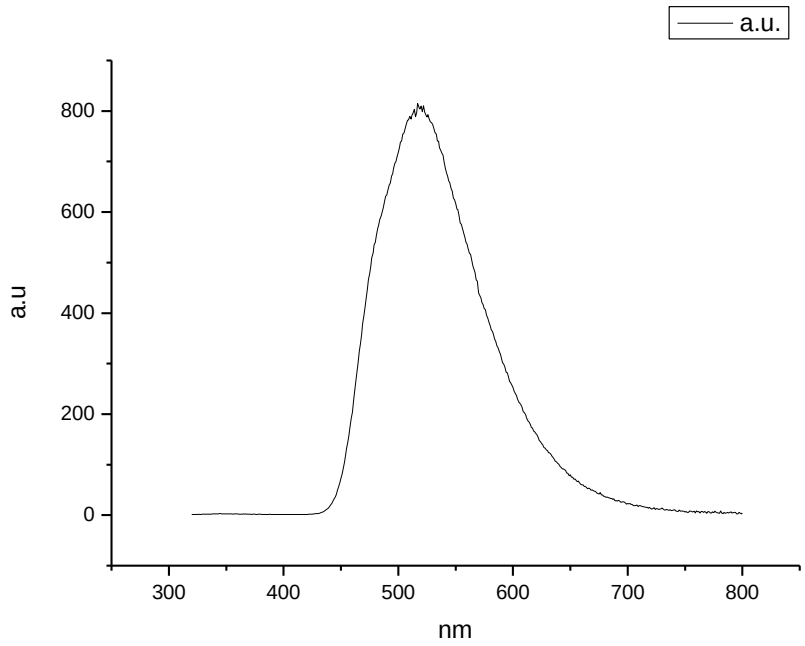

Figure 1.1.193. Fluorescence emission spectrum of **3a** recorded in Acetonitrile at 310 nm excitation.

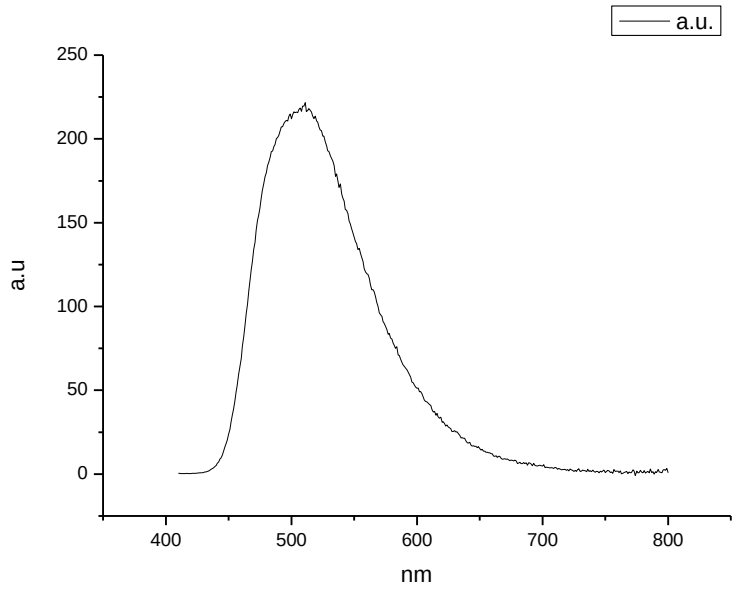

Figure 1.1.194. Fluorescence emission spectrum of **3a** recorded in Acetonitrile at 400 nm excitation.

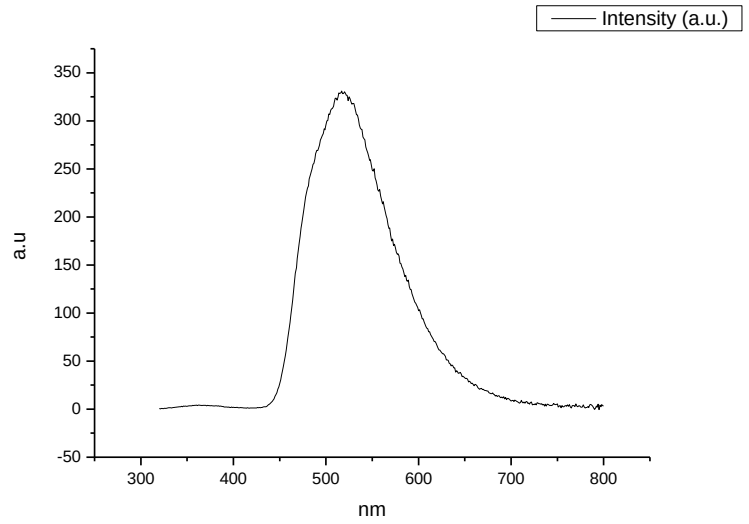

Figure 1.1.195. Fluorescence emission spectrum of **3a** recorded in Propylene Carbonate at 310 nm excitation.

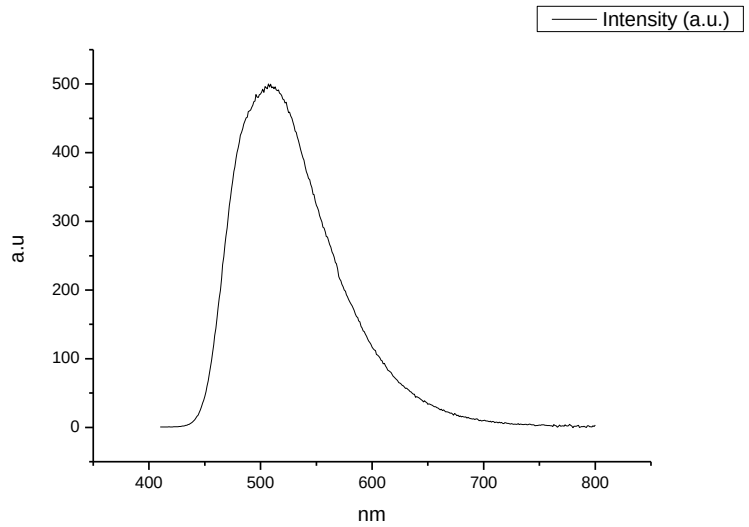

Figure 1.1.196. Fluorescence emission spectrum of **3a** recorded in Propylene Carbonate at 400 nm excitation.

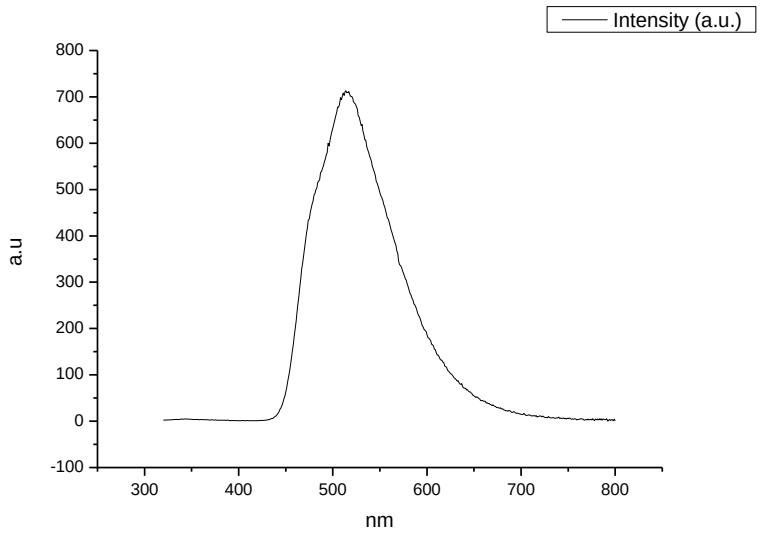

Figure 1.1.197. Fluorescence emission spectrum of **3a** recorded in 1-octanol at 310 nm excitation.

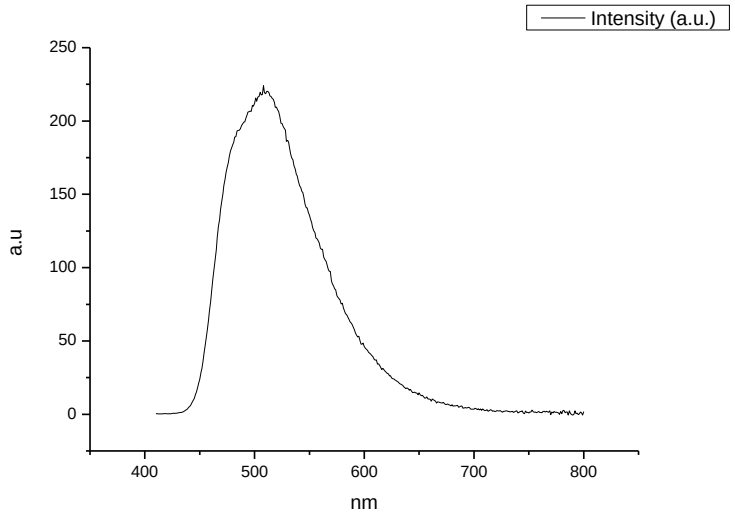

Figure 1.1.198. Fluorescence emission spectrum of **3a** recorded in 1-octanol at 400 nm excitation.

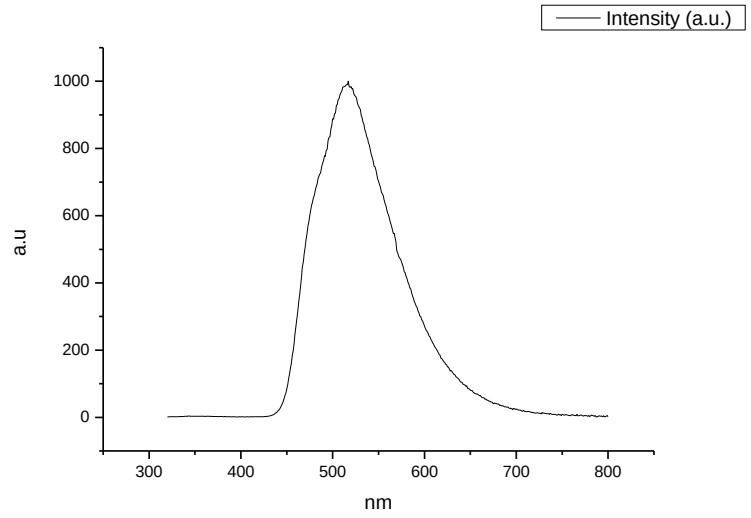

Figure 1.1.199. Fluorescence emission spectrum of **3a** recorded in 1-hexanol at 310 nm excitation.

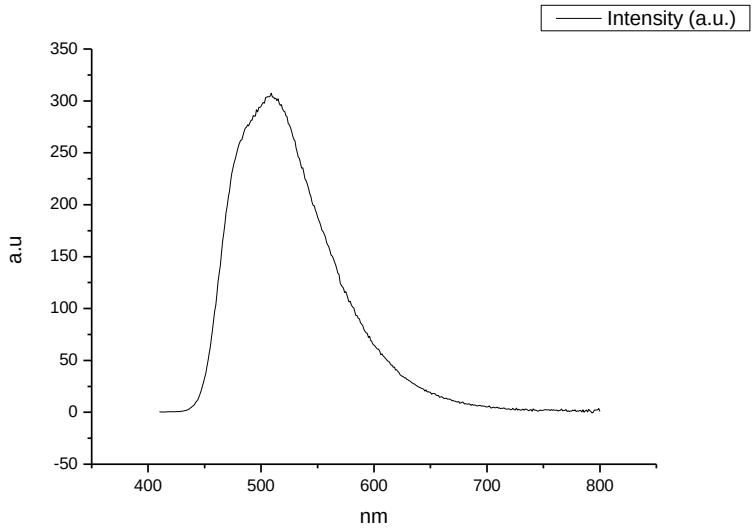

Figure 1.1.200. Fluorescence emission spectrum of **3a** recorded in 1-hexanol at 400 nm excitation.

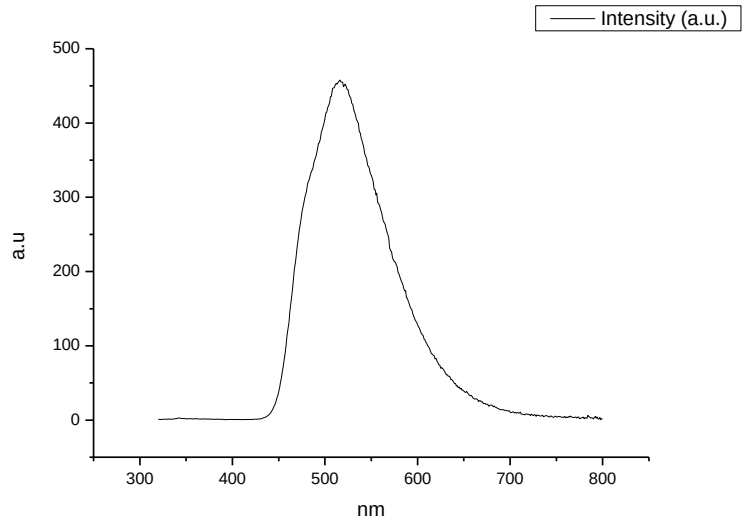

Figure 1.1.201. Fluorescence emission spectrum of **3a** recorded in 1-butanol at 310 nm excitation.

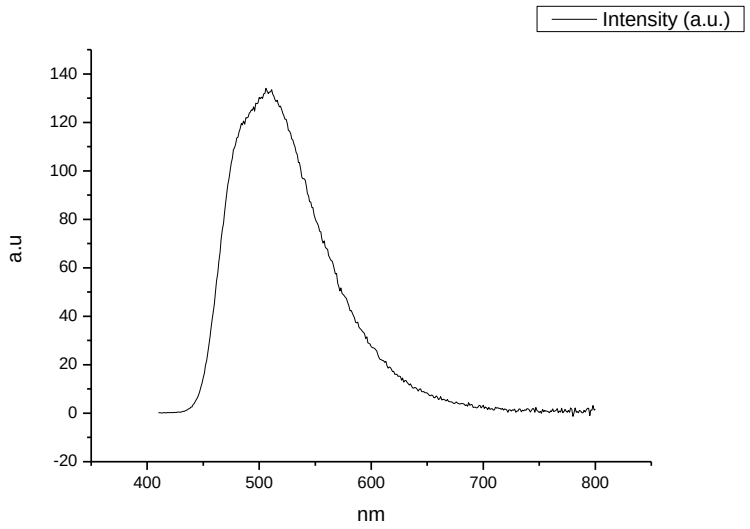

Figure 1.1.202. Fluorescence emission spectrum of **3a** recorded in 1-butanol at 400 nm excitation.

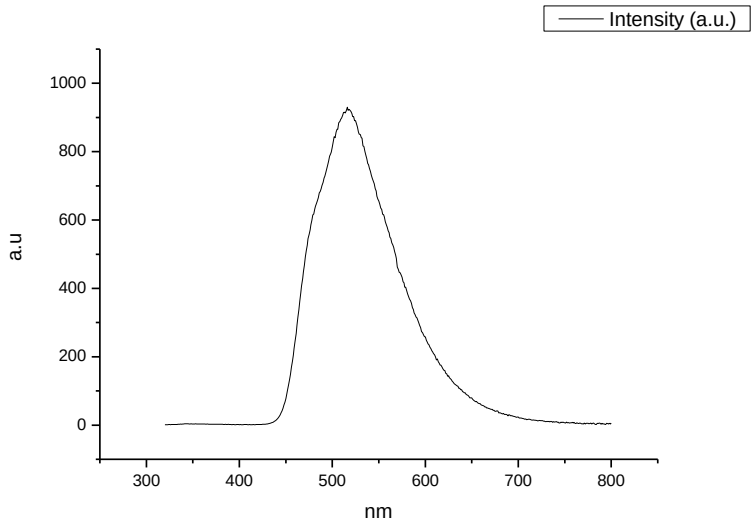

Figure 1.1.203. Fluorescence emission spectrum of **3a** recorded in 1-pentanol at 310 nm excitation.

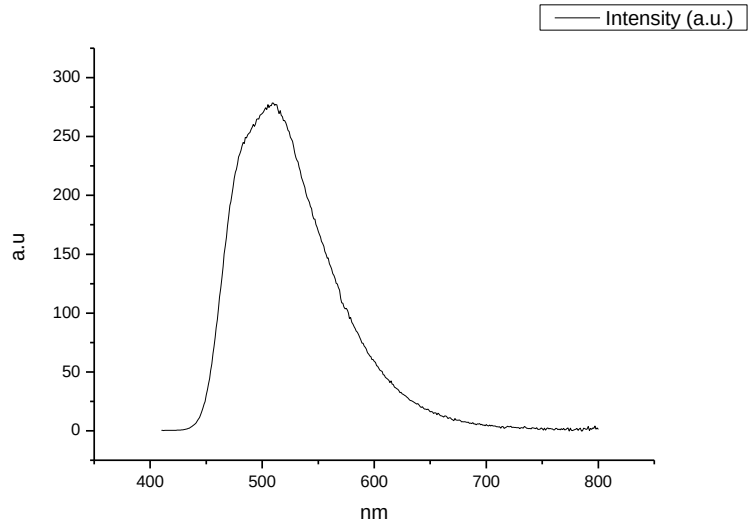

Figure 1.1.204. Fluorescence emission spectrum of **3a** recorded in 1-pentanol at 400 nm excitation.

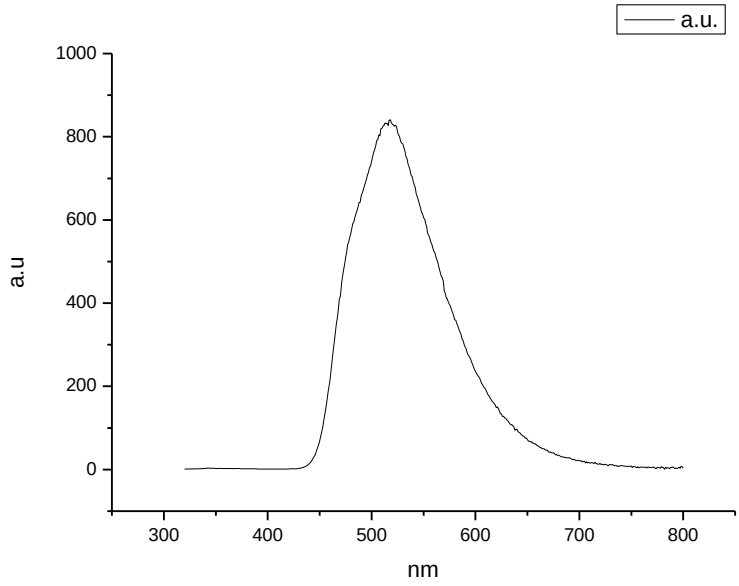

Figure 1.1.205. Fluorescence emission spectrum of **3a** recorded in 1-propanol at 310 nm excitation.

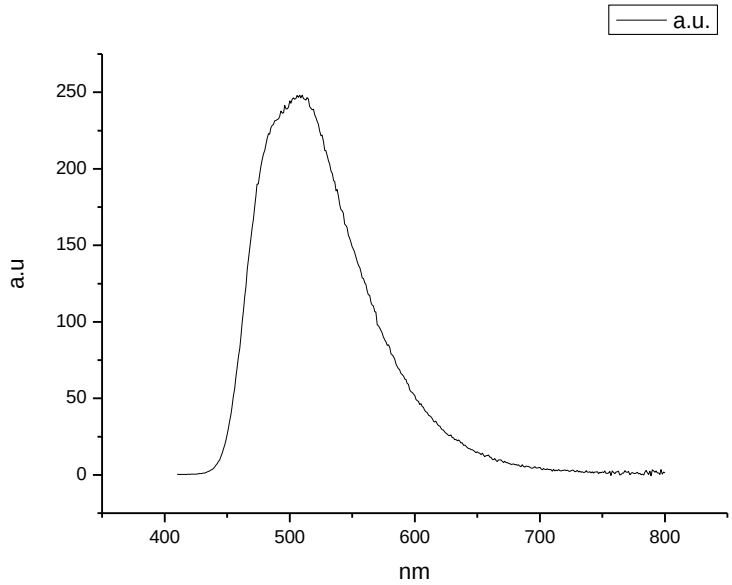

Figure 1.1.206. Fluorescence emission spectrum of **3a** recorded in 1-propanol at 400 nm excitation.

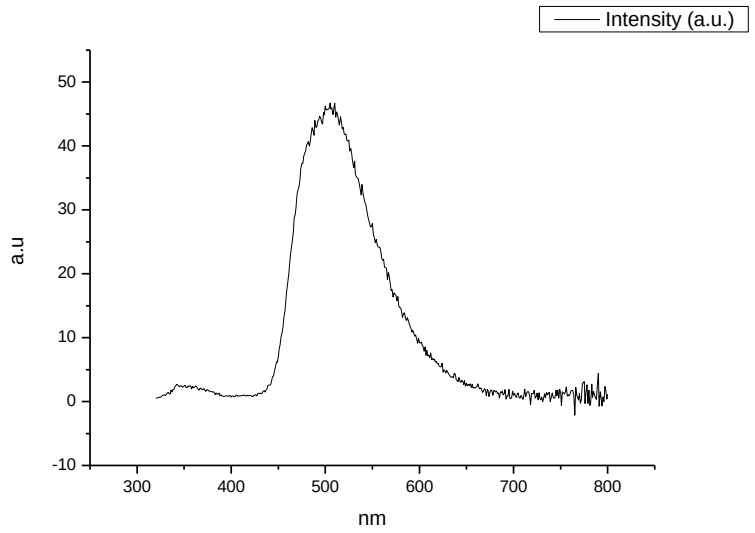

Figure 1.1.207. Fluorescence emission spectrum of **3a** recorded in Acetic Acid at 310 nm excitation.

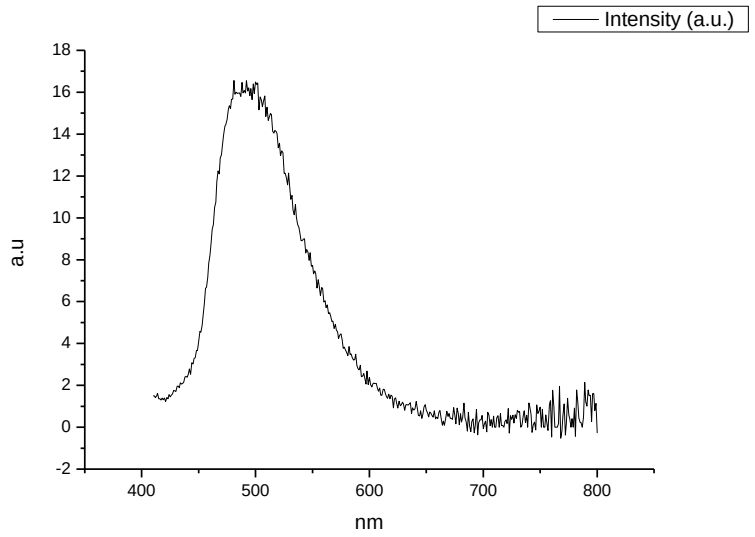

Figure 1.1.208. Fluorescence emission spectrum of **3a** recorded in Acetic Acid at 400 nm excitation.

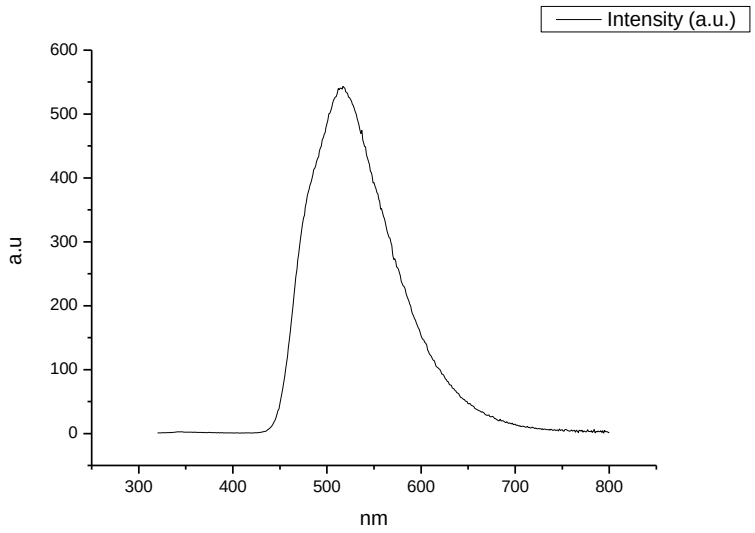

Figure 1.1.209. Fluorescence emission spectrum of **3a** recorded in Ethanol at 310 nm excitation.

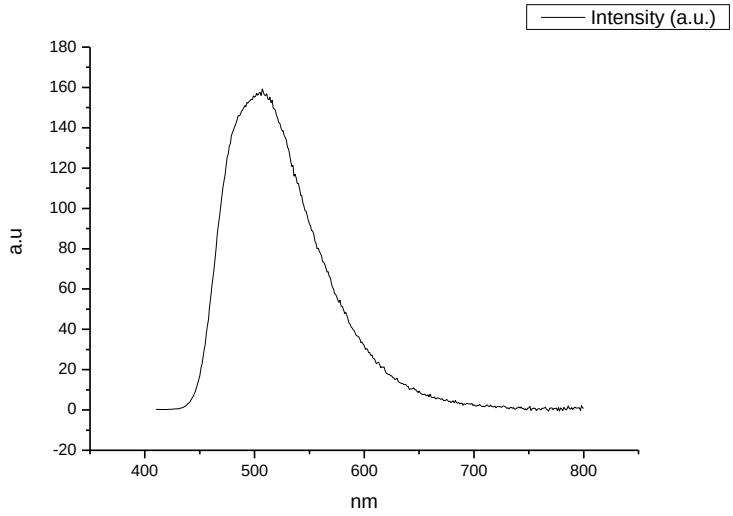

Figure 1.1.210. Fluorescence emission spectrum of **3a** recorded in Ethanol at 400 nm excitation.

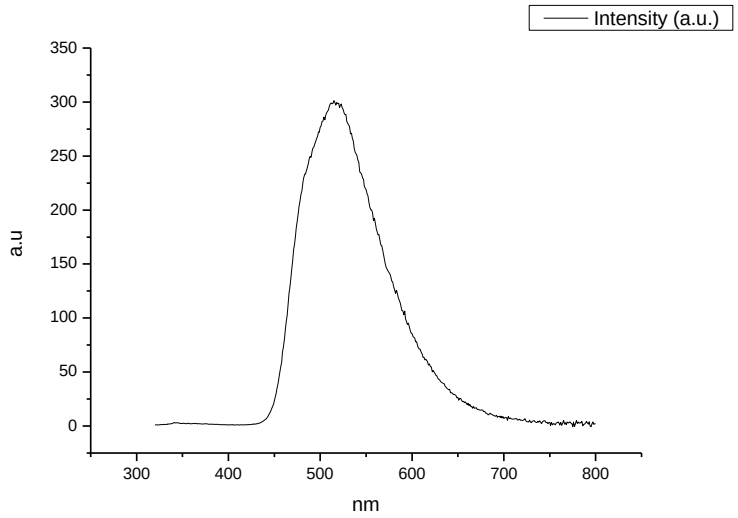

Figure 1.1.211. Fluorescence emission spectrum of **3a** recorded in 1,5-pentanediol at 310 nm excitation.

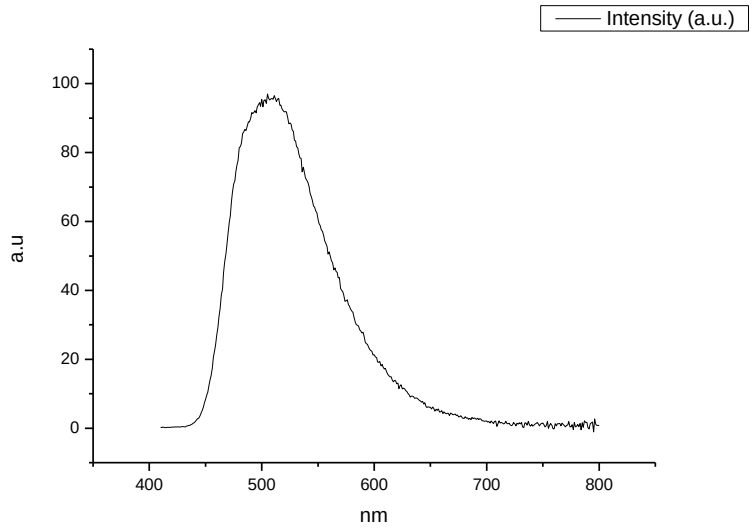

Figure 1.1.212. Fluorescence emission spectrum of **3a** recorded in 1,5-pentanediol at 400 nm excitation.

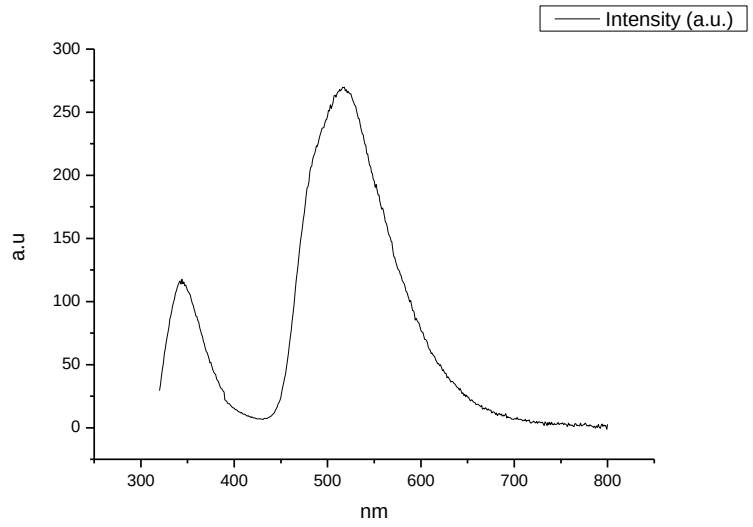

Figure 1.1.213. Fluorescence emission spectrum of **3a** recorded in 1,3-butanediol at 310 nm excitation.

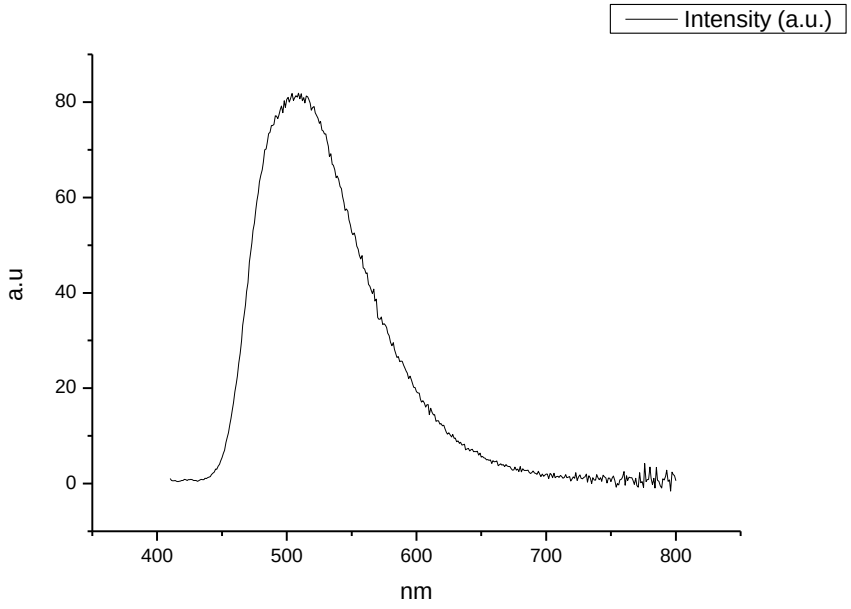

Figure 1.1.214. Fluorescence emission spectrum of **3a** recorded in 1,3-butanediol at 400 nm excitation.

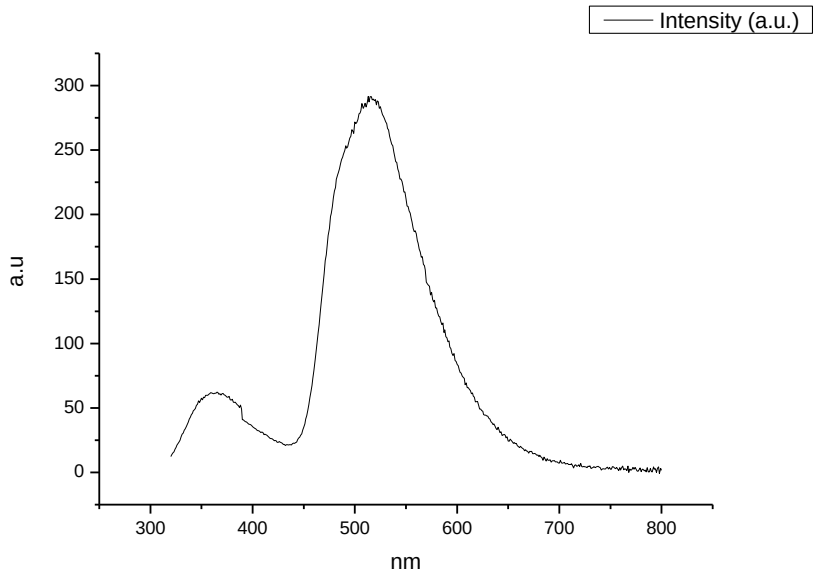

Figure 1.1.215. Fluorescence emission spectrum of **3a** recorded in 1,4-butanediol at 310 nm excitation.

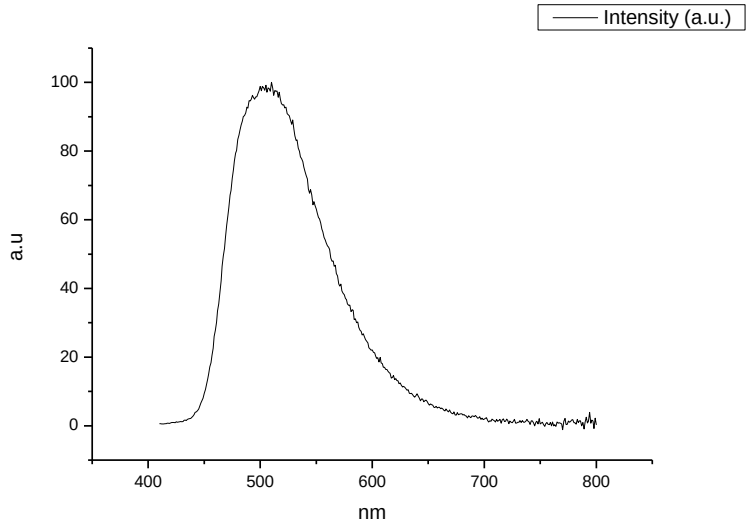

Figure 1.1.216. Fluorescence emission spectrum of **3a** recorded in 1,4-butanediol at 400 nm excitation.

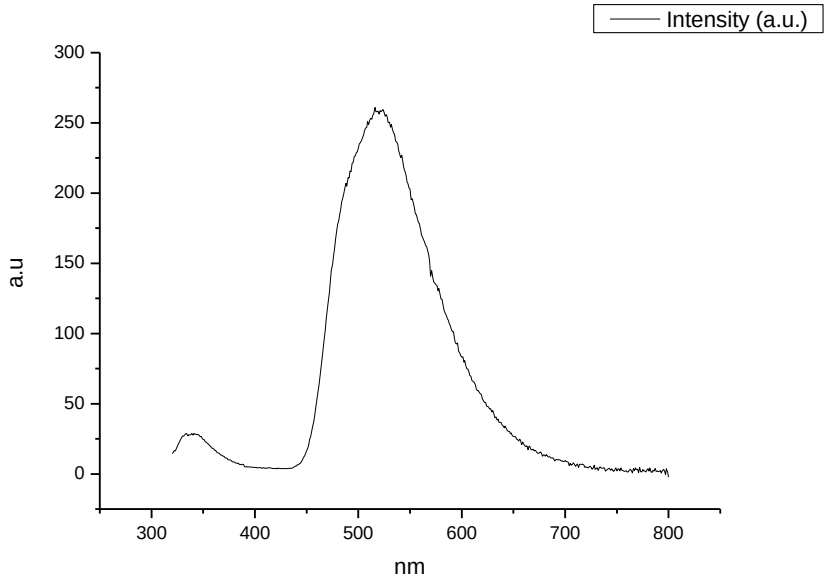

Figure 1.1.217. Fluorescence emission spectrum of **3a** recorded in 1,3-propanediol at 310 nm excitation.

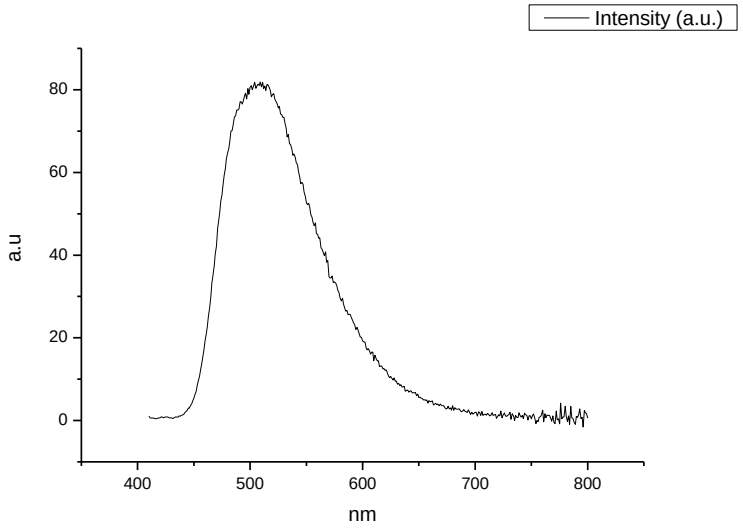

Figure 1.1.218. Fluorescence emission spectrum of **3a** recorded in 1,3-propanediol at 400 nm excitation.

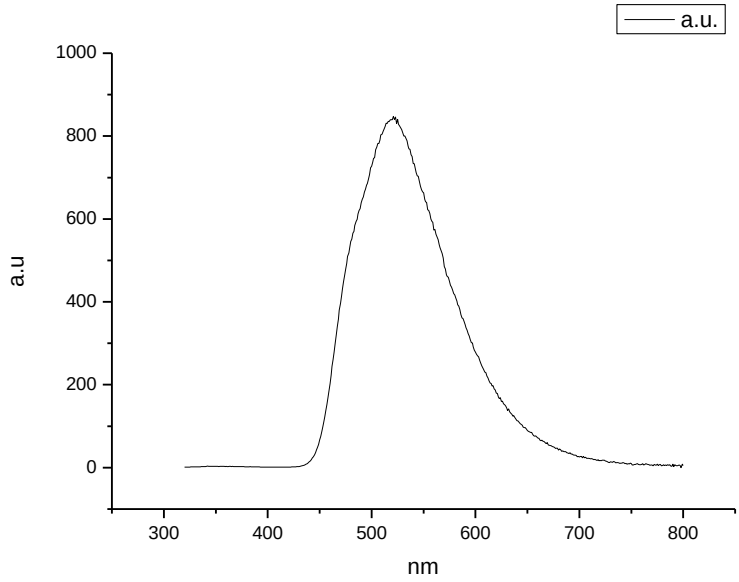

Figure 1.1.219. Fluorescence emission spectrum of **3a** recorded in Methanol at 310 nm excitation.

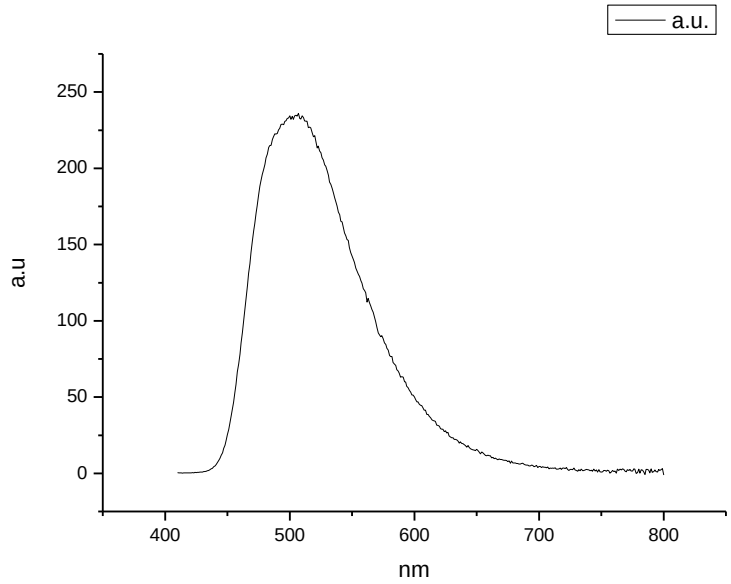

Figure 1.1.220. Fluorescence emission spectrum of **3a** recorded in Methanol at 400 nm excitation.

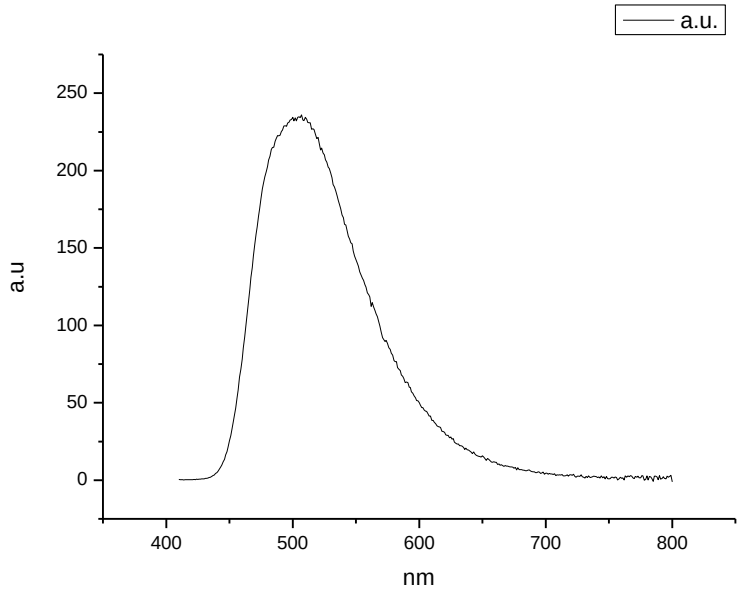

Figure 1.1.221. Fluorescence emission spectrum of **3a** recorded in 1,2-ethanediol at 310 nm excitation.

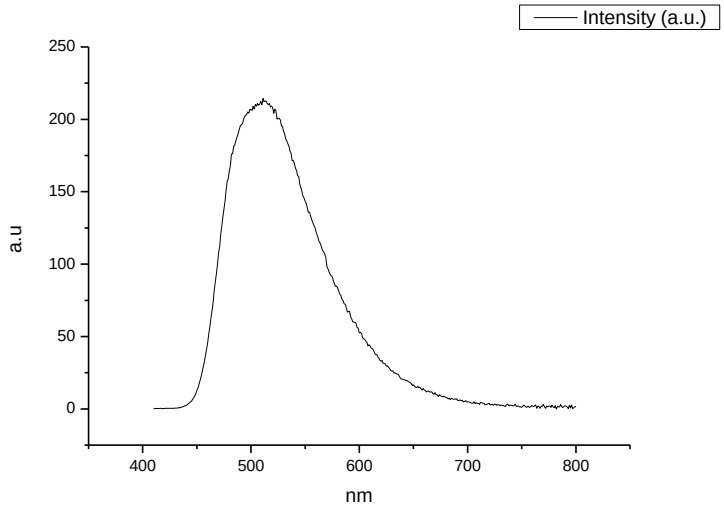

Figure 1.1.222. Fluorescence emission spectrum of **3a** recorded in 1,2-ethanediol at 400 nm excitation.

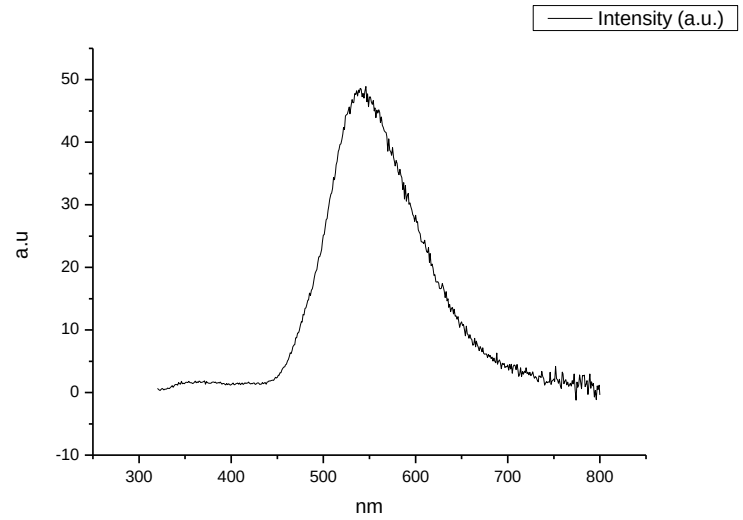

Figure 1.1.223. Fluorescence emission spectrum of **3a** recorded in 2,2,2-trifluoroethanol at 310 nm excitation.

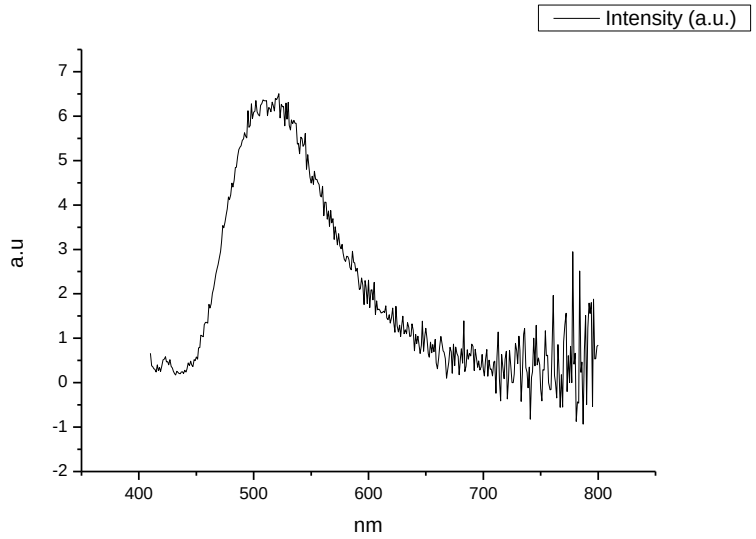

Figure 1.1.224 Fluorescence emission spectrum of **3a** recorded in 2,2,2-trifluoroethanol at 400 nm excitation.

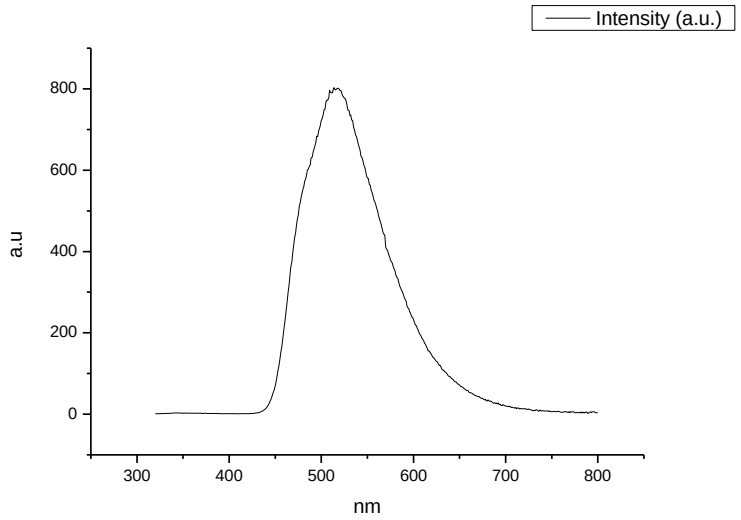

Figure 1.1.225. Fluorescence emission spectrum of **3a** recorded in ethanol-d_1 (EtOD) at 310 nm excitation.

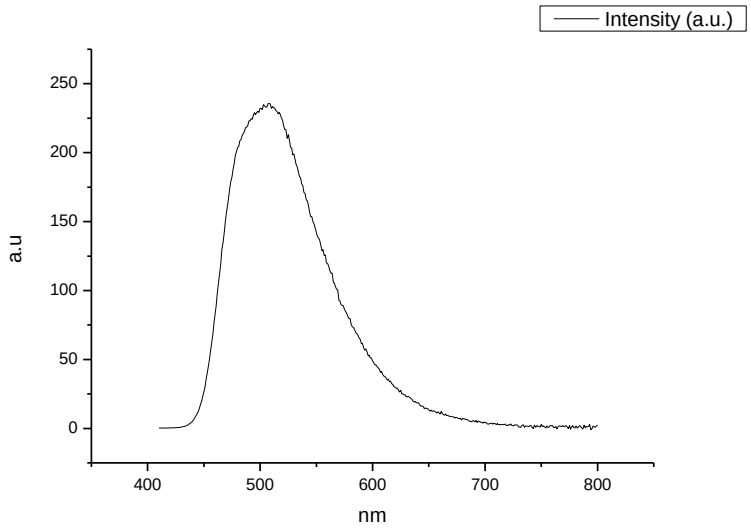

Figure 1.1.226. Fluorescence emission spectrum of **3a** recorded in ethanol-d_1 (EtOD) at 400 nm excitation.

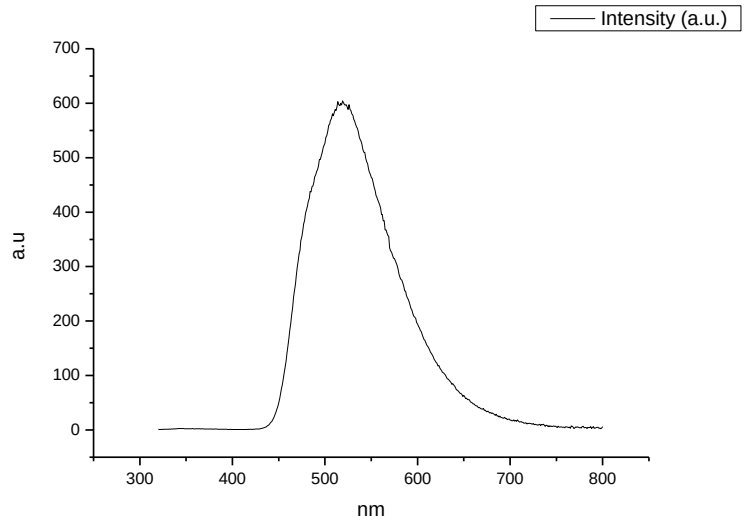

Figure 1.1.227. Fluorescence emission spectrum of **3a** recorded in methanol-d_1 (MeOD) at 310 nm excitation.

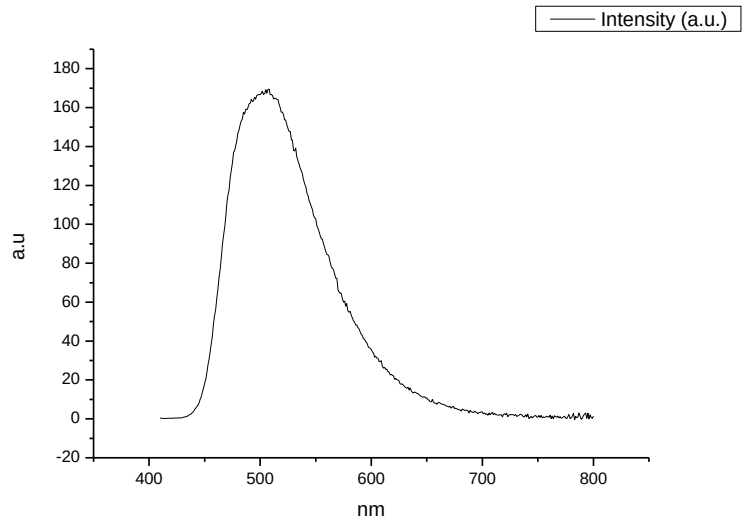

Figure 1.1.228. Fluorescence emission spectrum of **3a** recorded in methanol-d_1 (MeOD) at 400 nm excitation.

1.1.10 Normalised Fluorescence Emission spectra (Gaussian fitted).

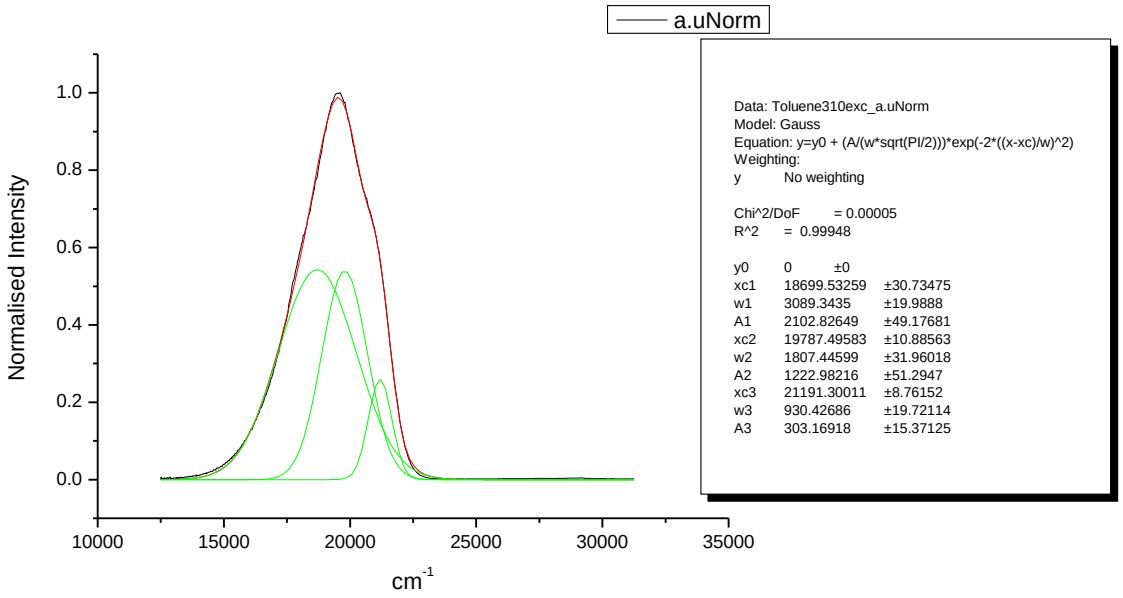

Figure 1.1.229. Gaussian model fit of the normalised fluorescence emission spectrum of **3a** recorded in Toluene at 310 nm excitation.

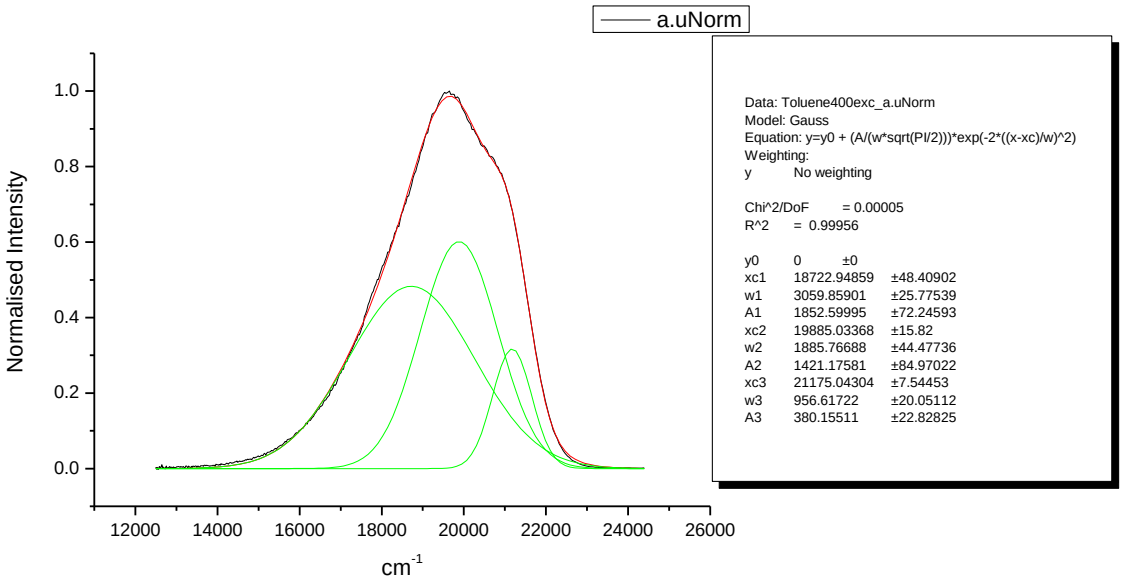

Figure 1.1.230. Gaussian model fit of the normalised fluorescence emission spectrum of **3a** recorded in Toluene at 400 nm excitation.

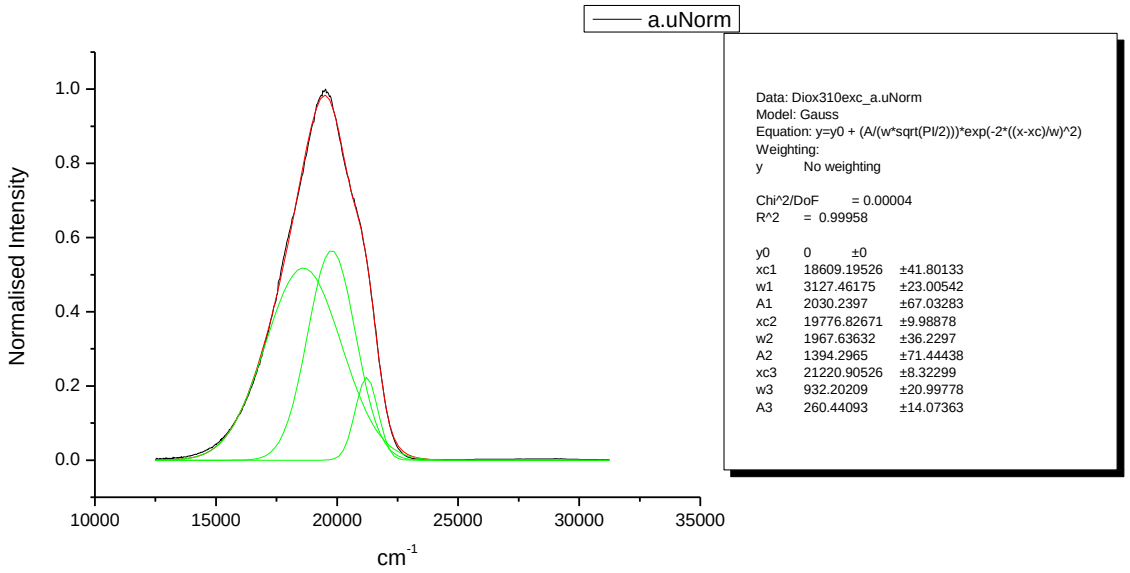

Figure 1.1.231. Gaussian model fit of the normalised fluorescence emission spectrum of **3a** recorded in 1,4-dioxane at 310 nm excitation.

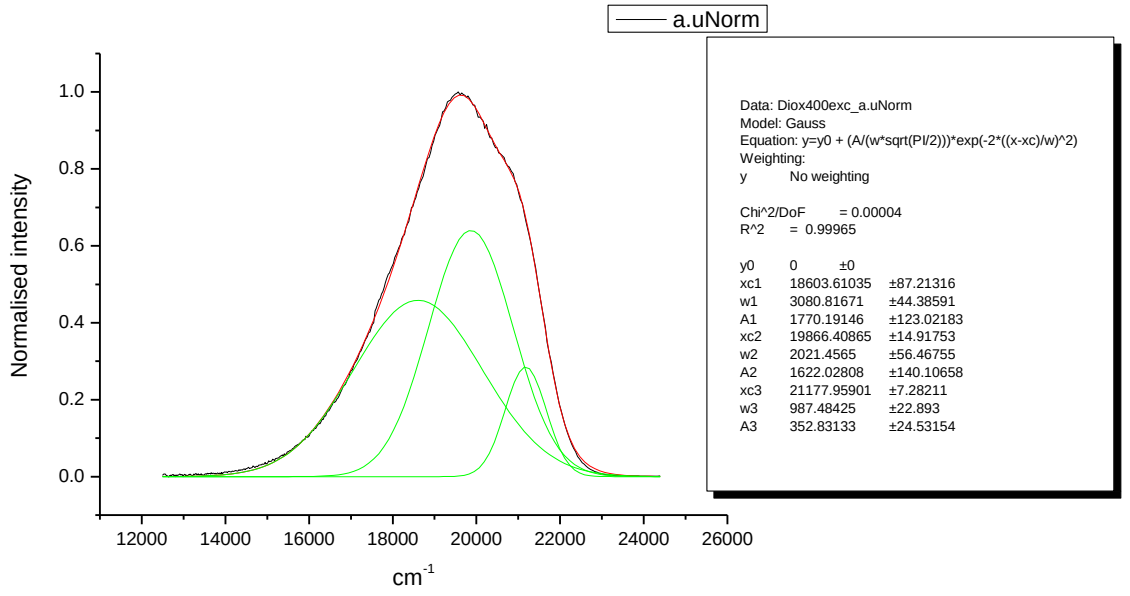

Figure 1.1.232. Gaussian model fit of the normalised fluorescence emission spectrum of **3a** recorded in 1,4-dioxane at 400 nm excitation.

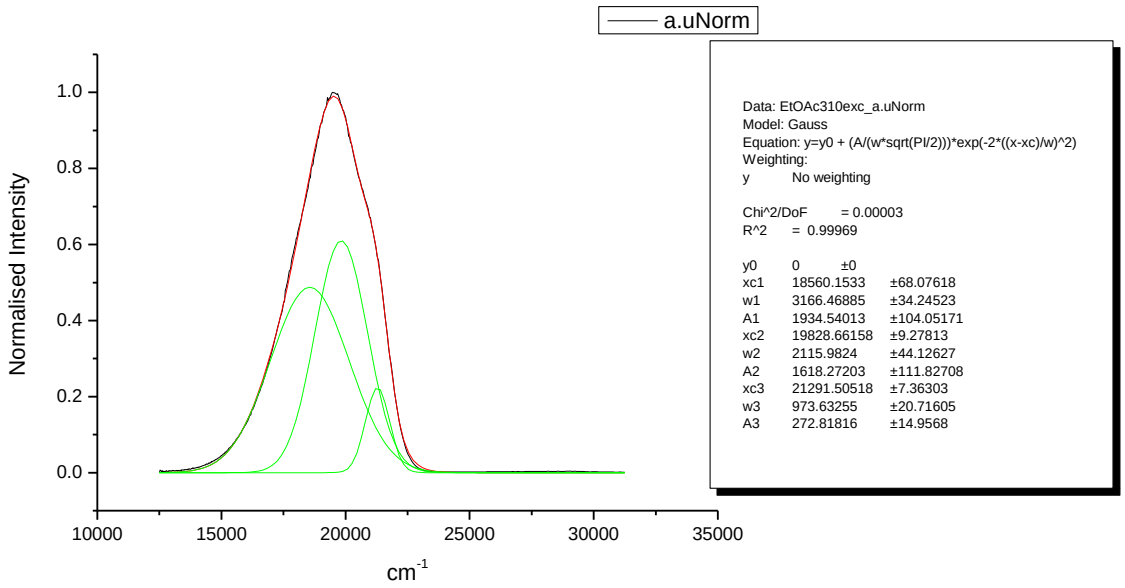

Figure 1.1.233. Gaussian model fit of the normalised fluorescence emission spectrum of **3a** recorded in Ethyl Acetate at 310 nm excitation.

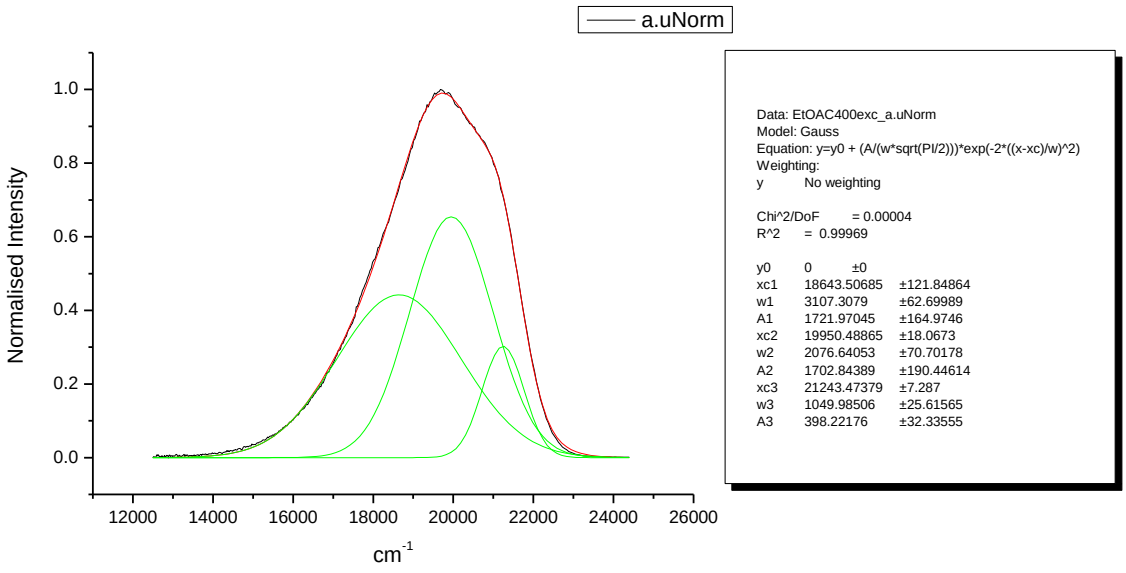

Figure 1.1.234. Gaussian model fit of the normalised fluorescence emission spectrum of **3a** recorded in Ethyl Acetate at 400 nm excitation.

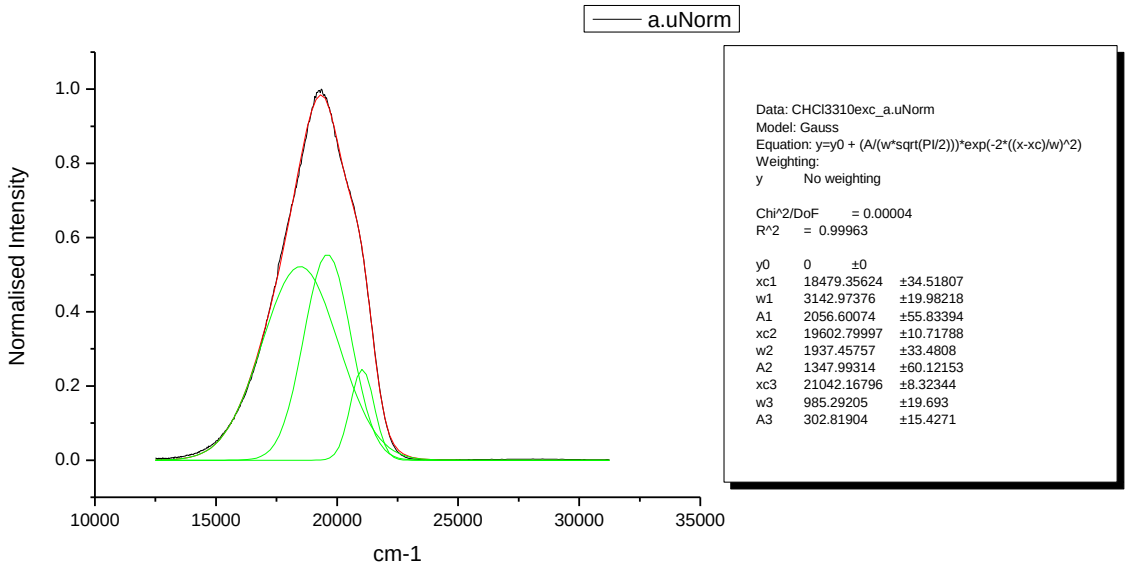

Figure 1.1.235. Gaussian model fit of the normalised fluorescence emission spectrum of **3a** recorded in Chloroform at 310 nm excitation.

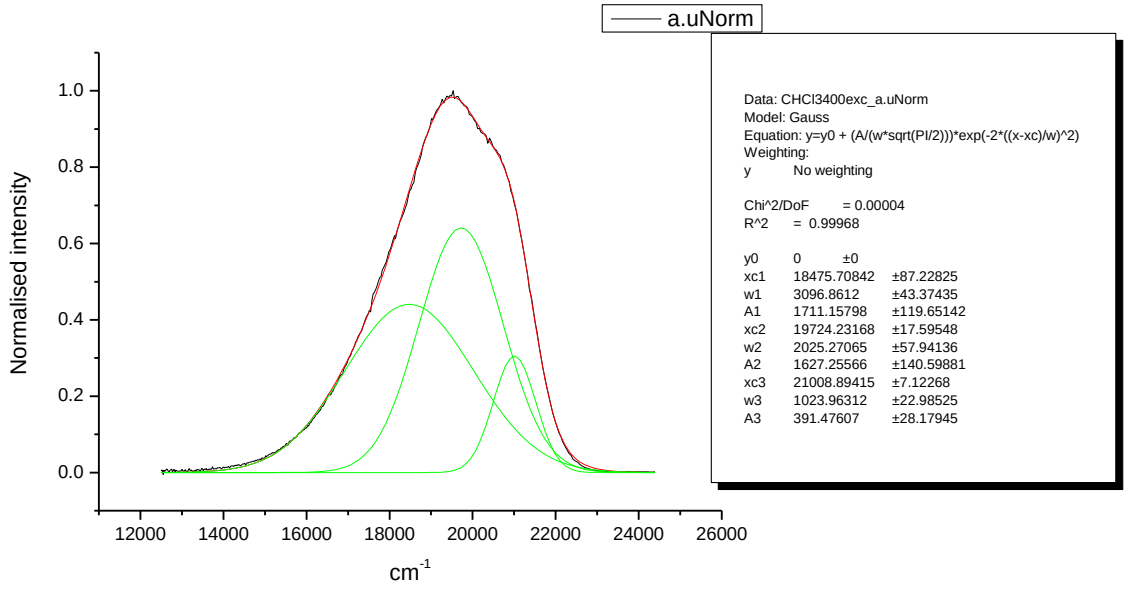

Figure 1.1.236. Gaussian model fit of the normalised fluorescence emission spectrum of **3a** recorded in Chloroform at 400 nm excitation.

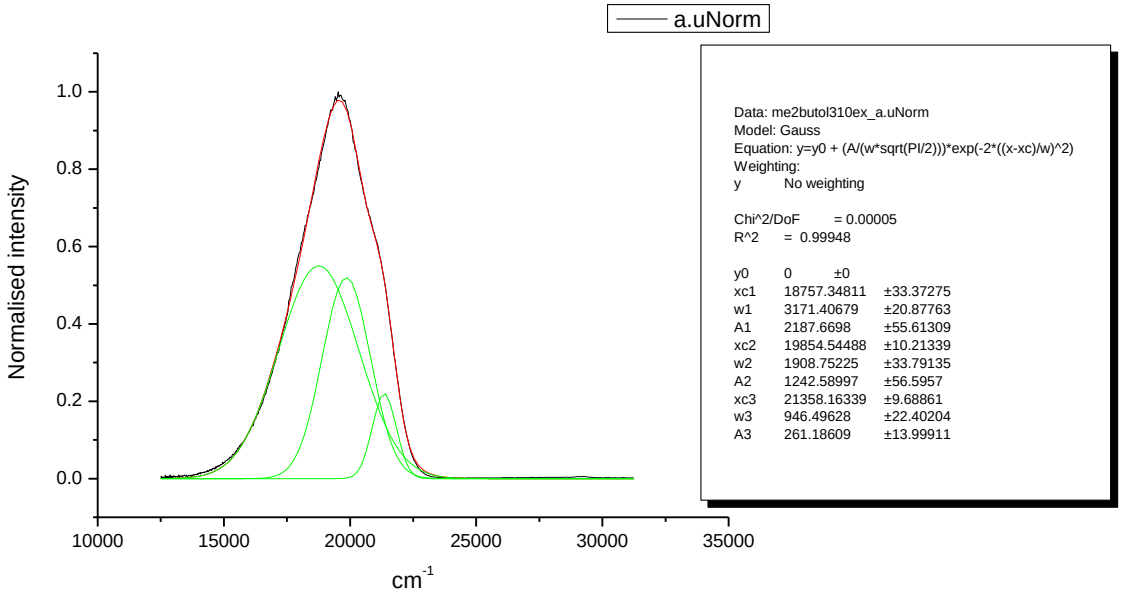

Figure 1.1.237. Gaussian model fit of the normalised fluorescence emission spectrum of **3a** recorded in 2-methyl-2-butanol at 310 nm excitation.

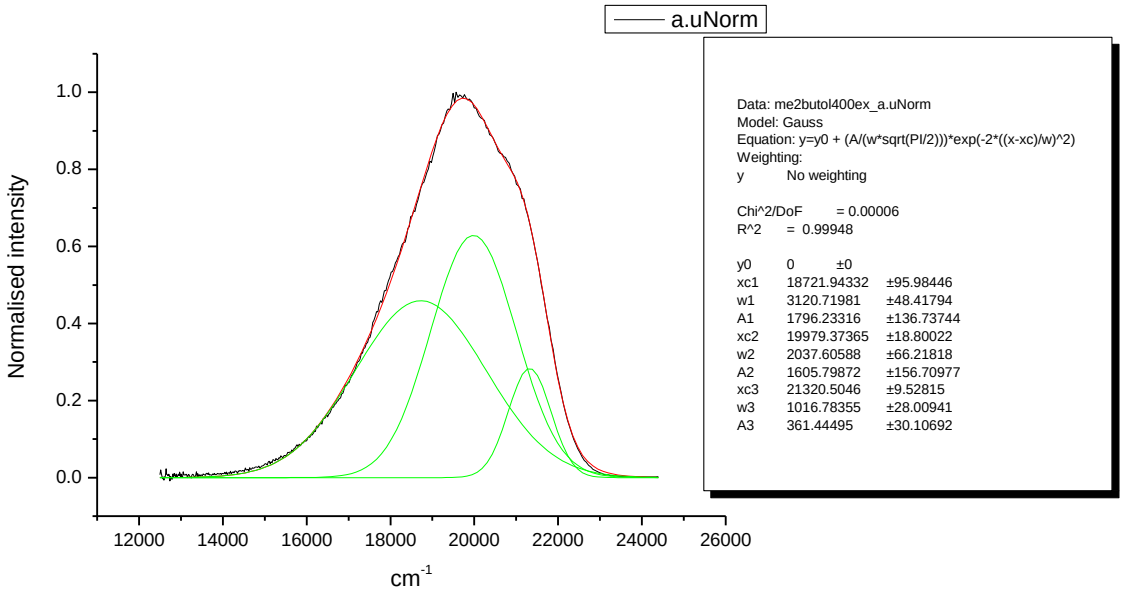

Figure 1.1.238. Gaussian model fit of the normalised fluorescence emission spectrum of **3a** recorded in 2-methyl-2-butanol at 400 nm excitation.

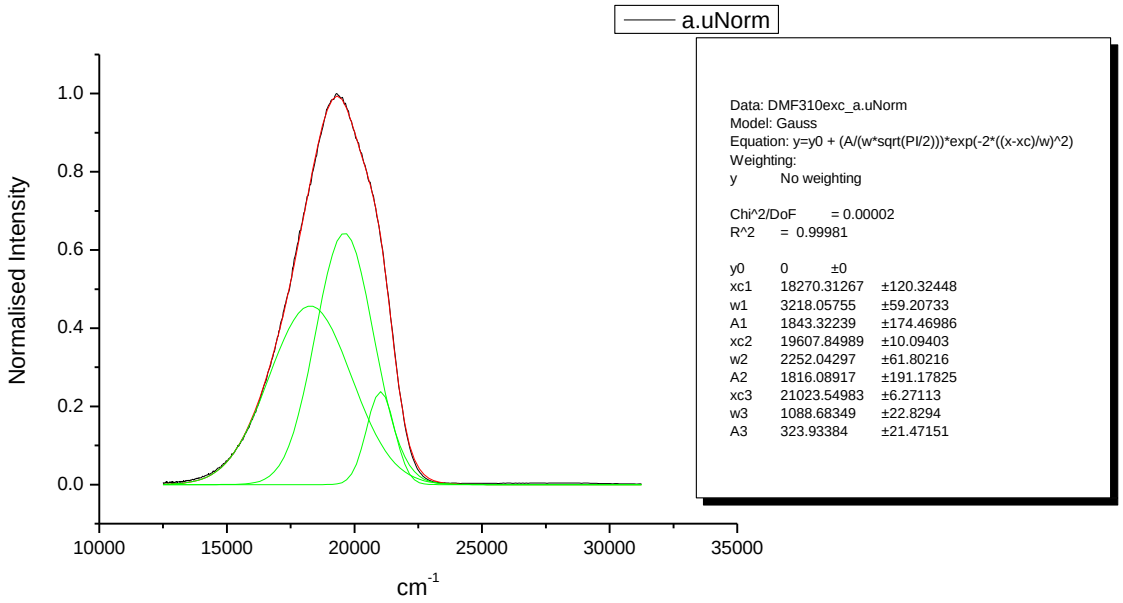

Figure 1.1.239. Gaussian model fit of the normalised fluorescence emission spectrum of **3a** recorded in N,N-dimethylformamide at 310 nm excitation.

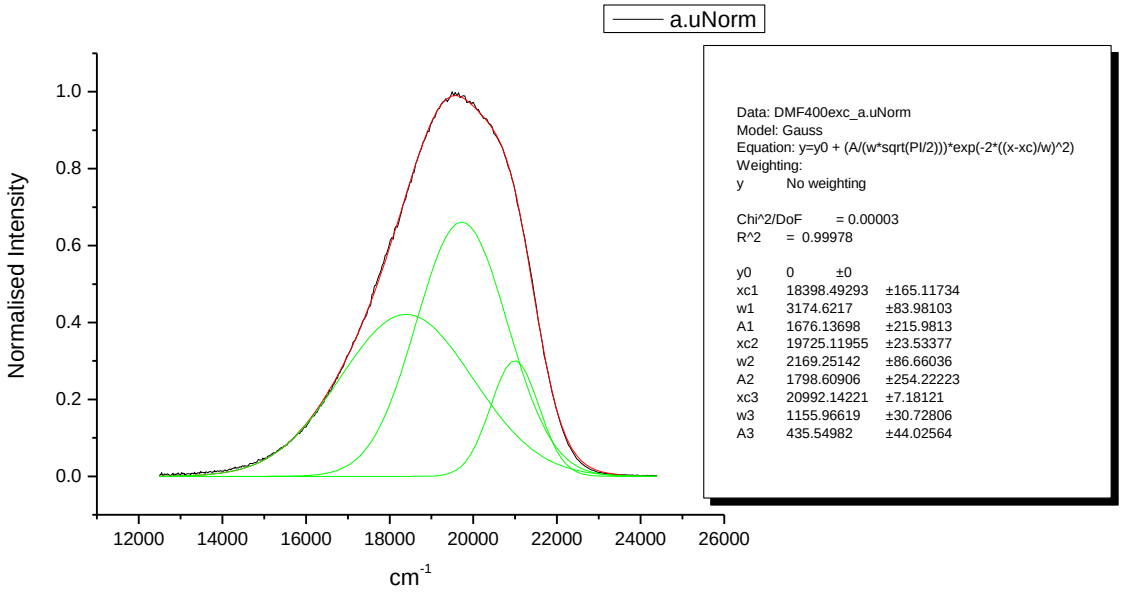

Figure 1.1.240. Gaussian model fit of the normalised fluorescence emission spectrum of **3a** recorded in N,N-dimethylformamide at 400 nm excitation.

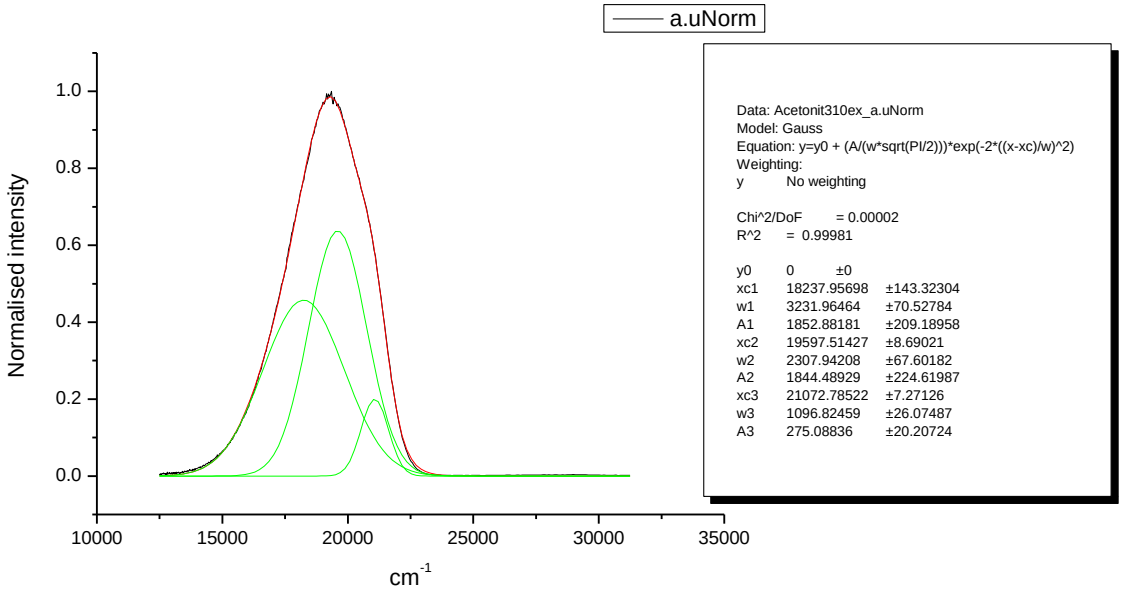

Figure 1.1.241. Gaussian model fit of the normalised fluorescence emission spectrum of **3a** recorded in Acetonitrile at 310 nm excitation.

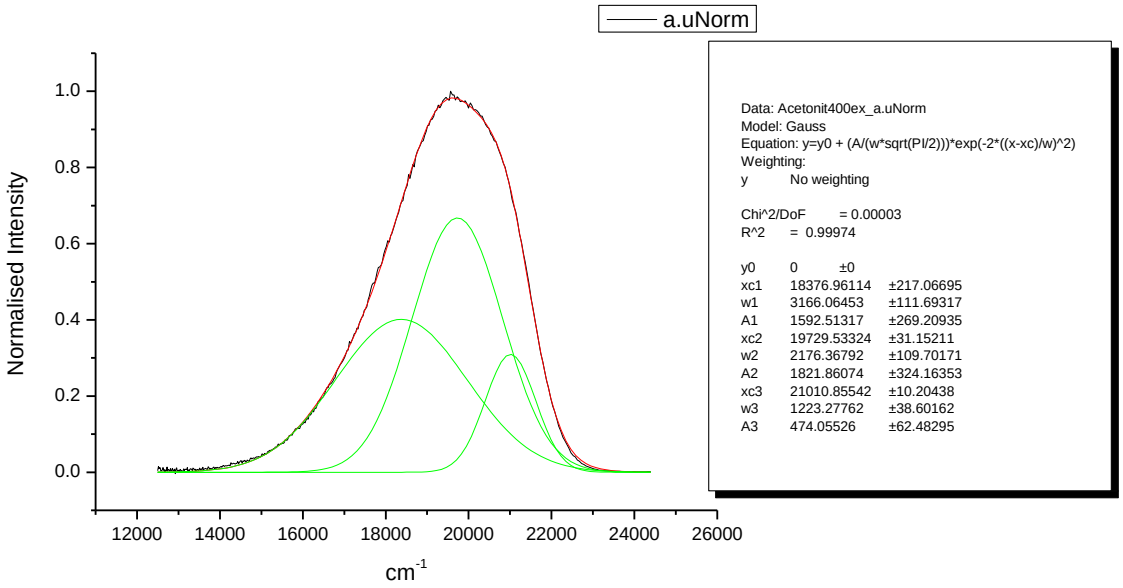

Figure 1.1.242. Gaussian model fit of the normalised fluorescence emission spectrum of **3a** recorded in Acetonitrile at 400 nm excitation.

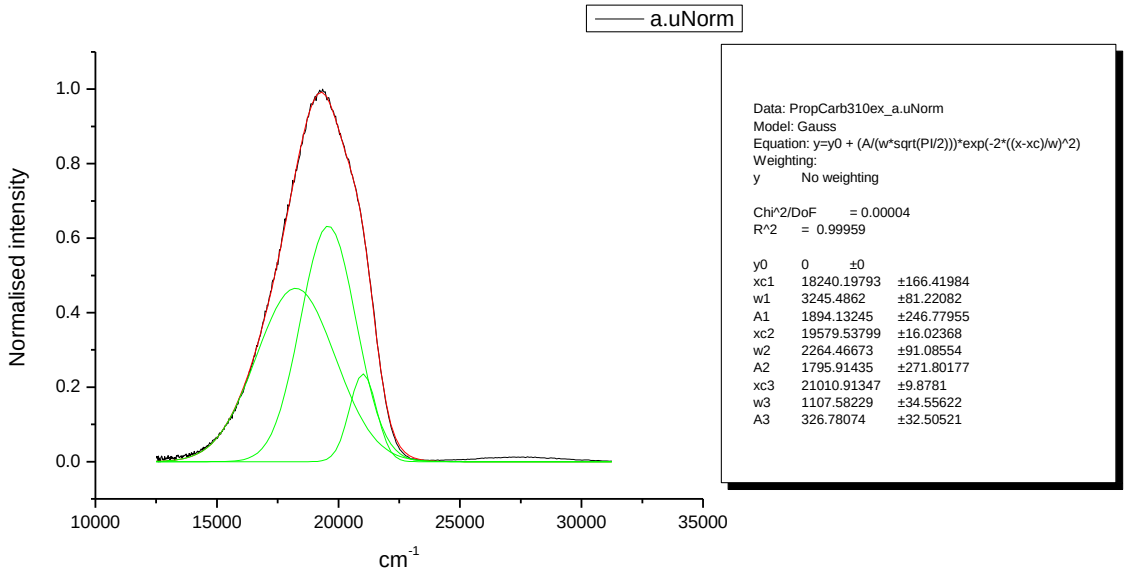

Figure 1.1.243. Gaussian model fit of the normalised fluorescence emission spectrum of **3a** recorded in Propylene Carbonate at 310 nm excitation.

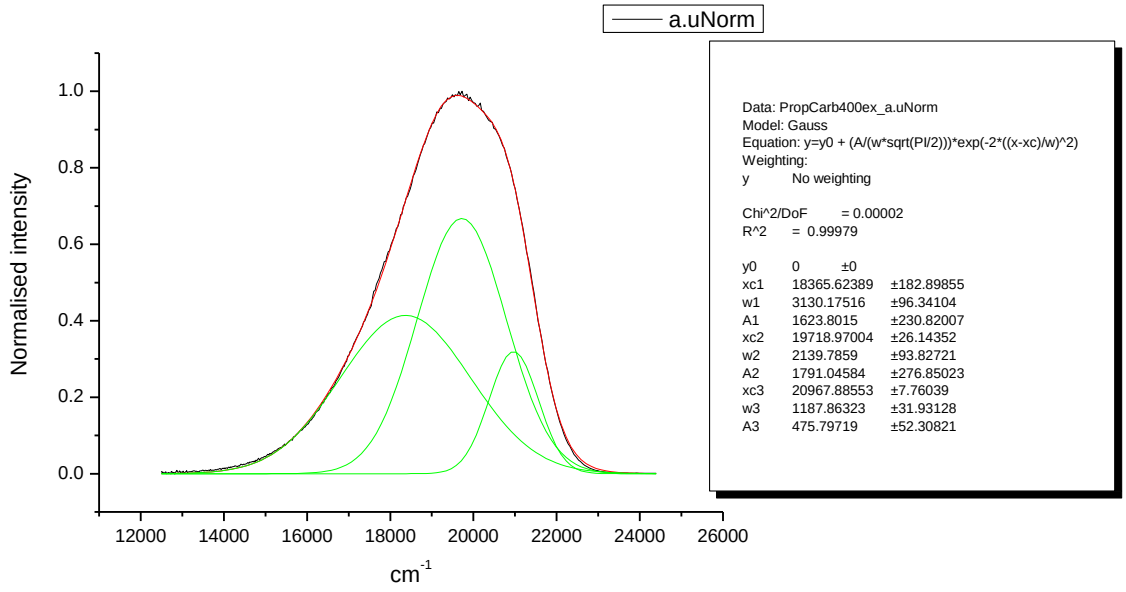

Figure 1.1.244. Gaussian model fit of the normalised fluorescence emission spectrum of **3a** recorded in Propylene Carbonate at 400 nm excitation.

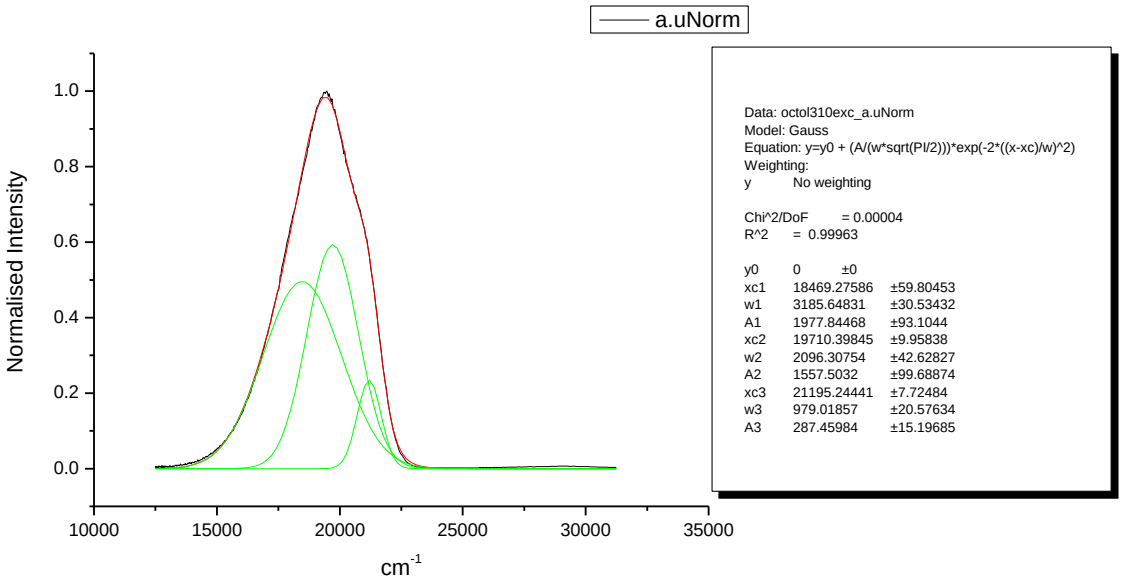

Figure 1.1.245. Gaussian model fit of the normalised fluorescence emission spectrum of **3a** recorded in 1-octanol at 310 nm excitation.

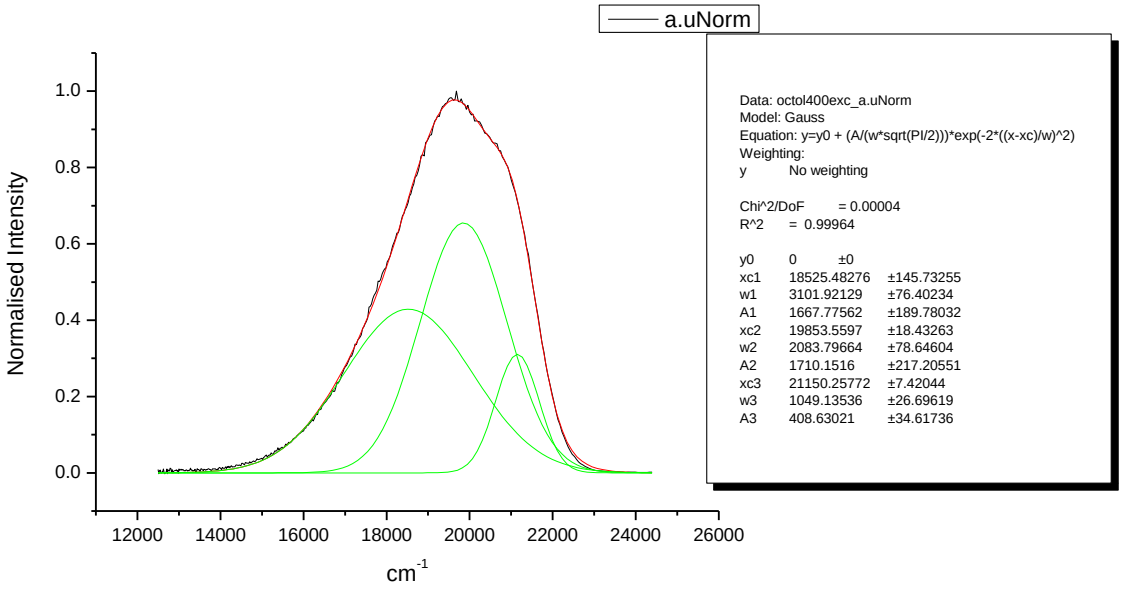

Figure 1.1.246. Gaussian model fit of the normalised fluorescence emission spectrum of **3a** recorded in 1-octanol at 400 nm excitation.

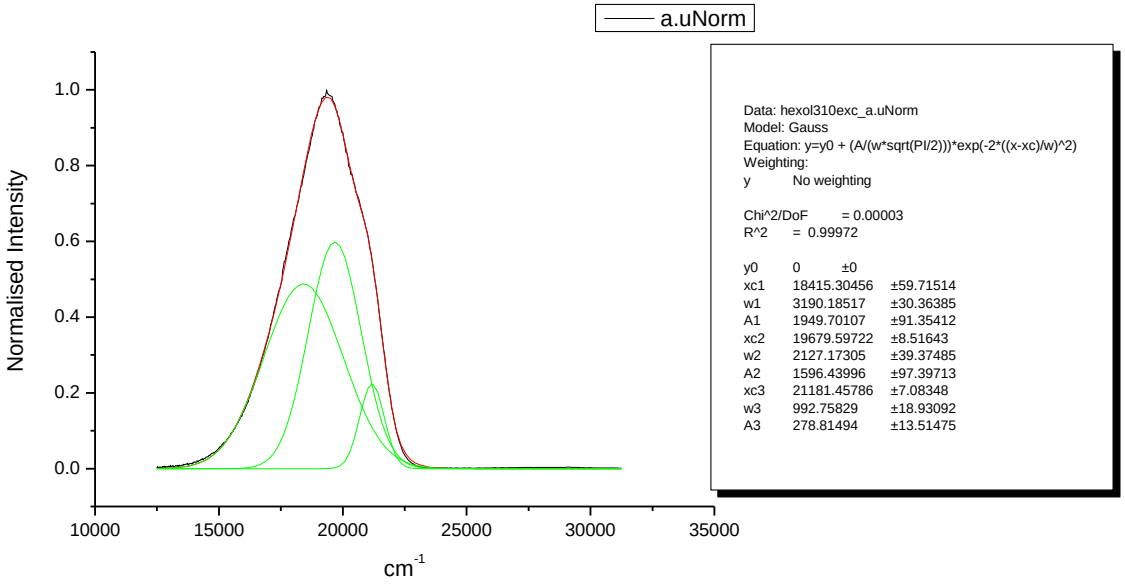

Figure 1.1.247. Gaussian model fit of the normalised fluorescence emission spectrum of **3a** recorded in 1-hexanol at 310 nm excitation.

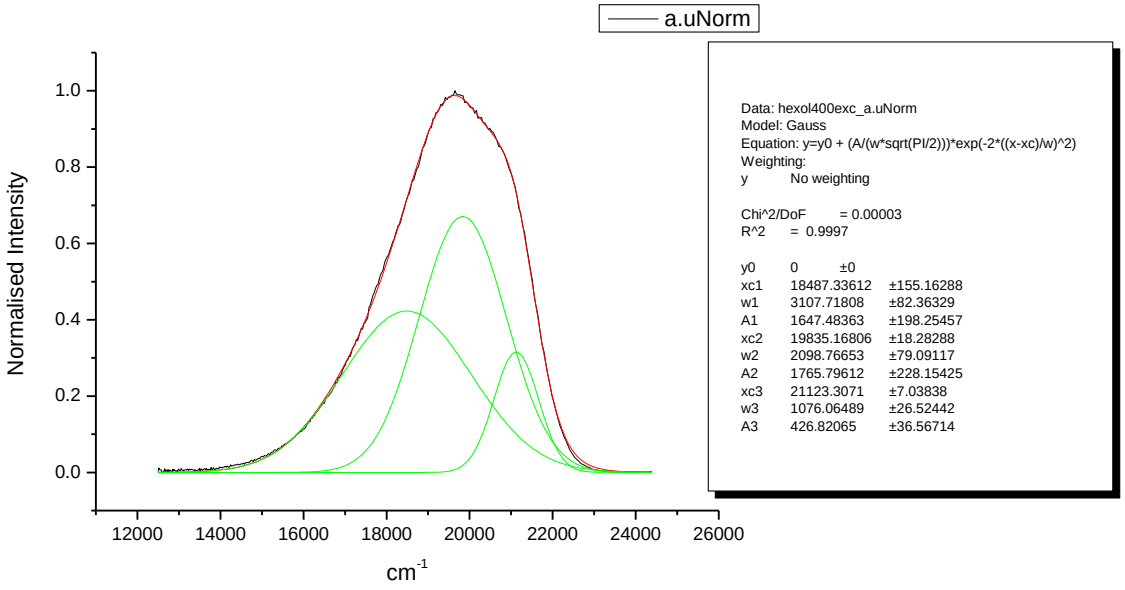

Figure 1.1.248. Gaussian model fit of the normalised fluorescence emission spectrum of **3a** recorded in 1-hexanol at 400 nm excitation.

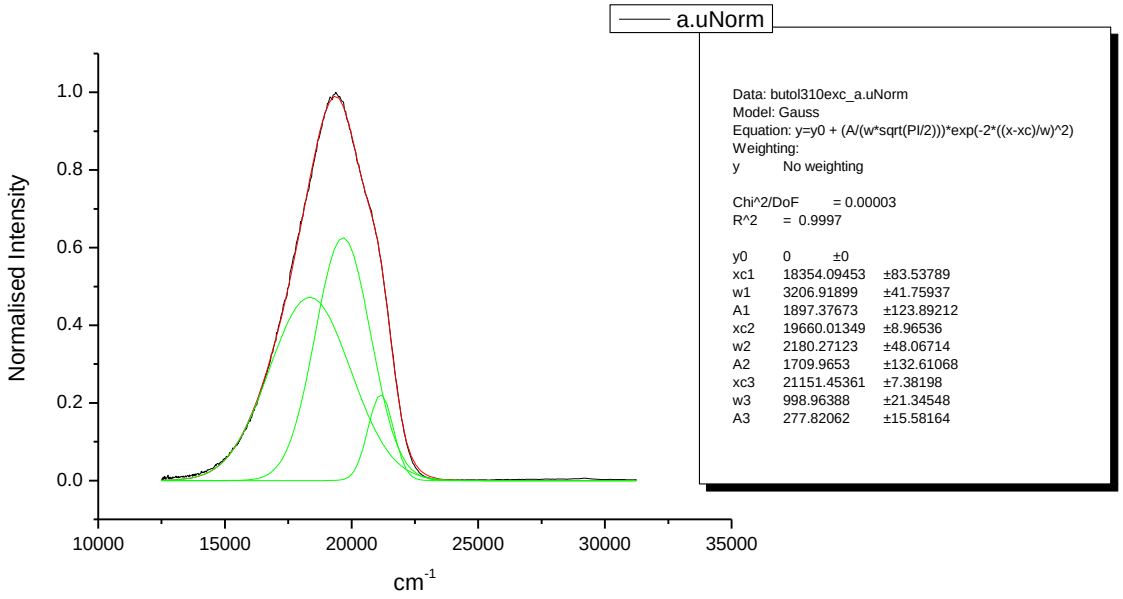

Figure 1.1.249. Gaussian model fit of the normalised fluorescence emission spectrum of **3a** recorded in 1-butanol at 310 nm excitation.

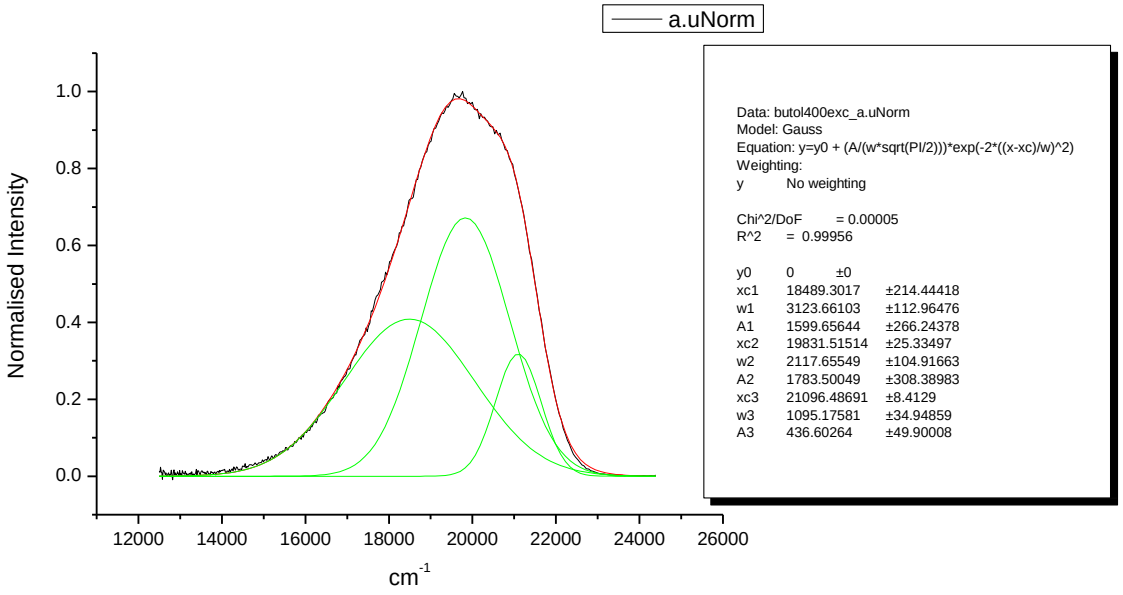

Figure 1.1.250. Gaussian model fit of the normalised fluorescence emission spectrum of **3a** recorded in 1-butanol at 400 nm excitation.

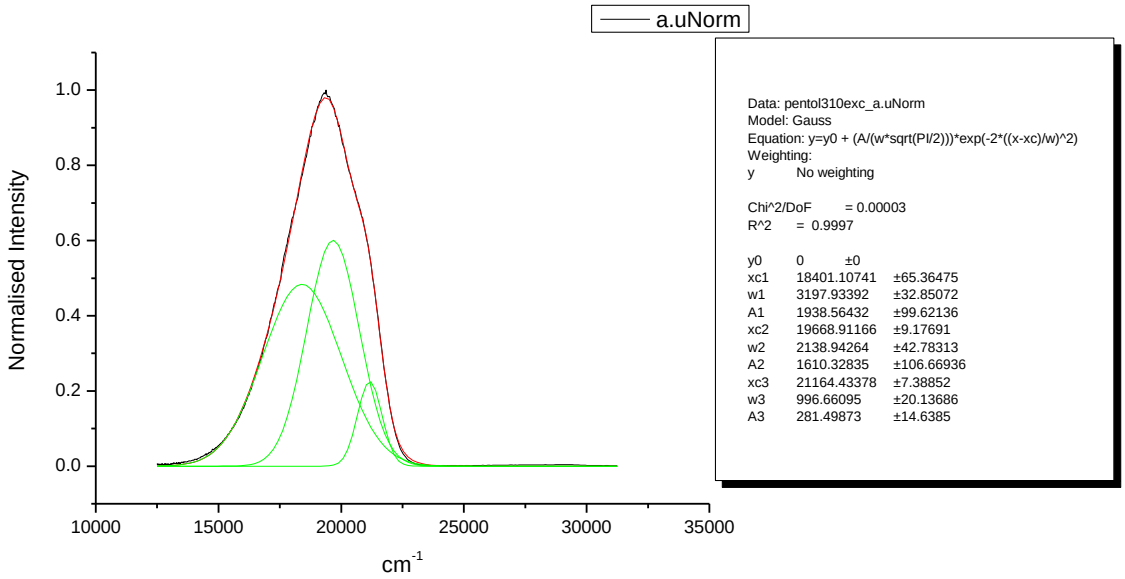

Figure 1.1.251. Gaussian model fit of the normalised fluorescence emission spectrum of **3a** recorded in 1-pentanol at 310 nm excitation.

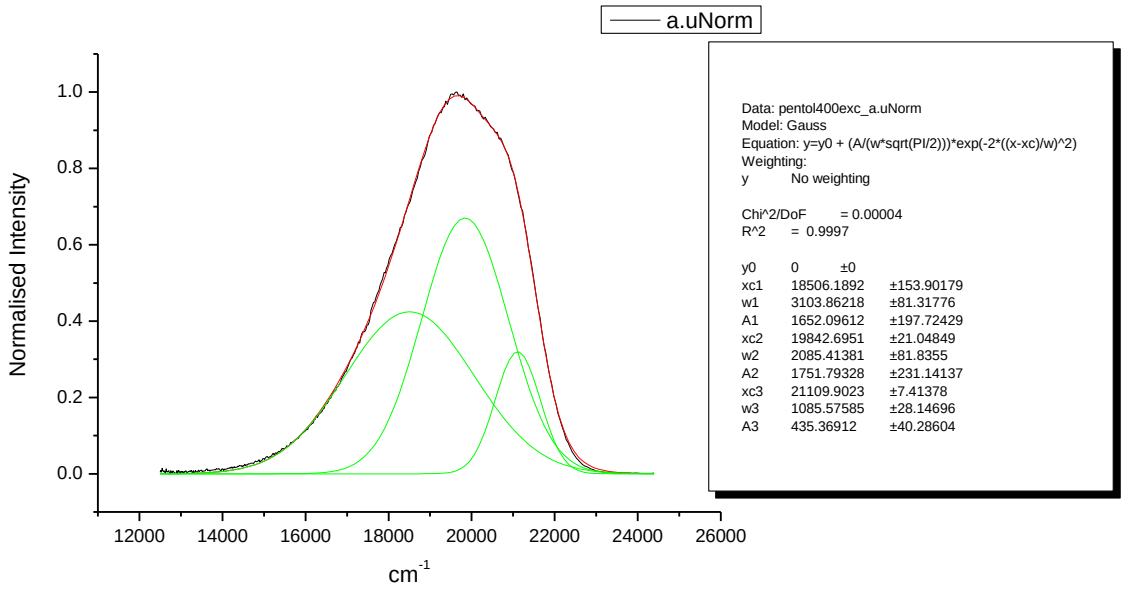

Figure 1.1.252. Gaussian model fit of the normalised fluorescence emission spectrum of **3a** recorded in 1-pentanol at 400 nm excitation.

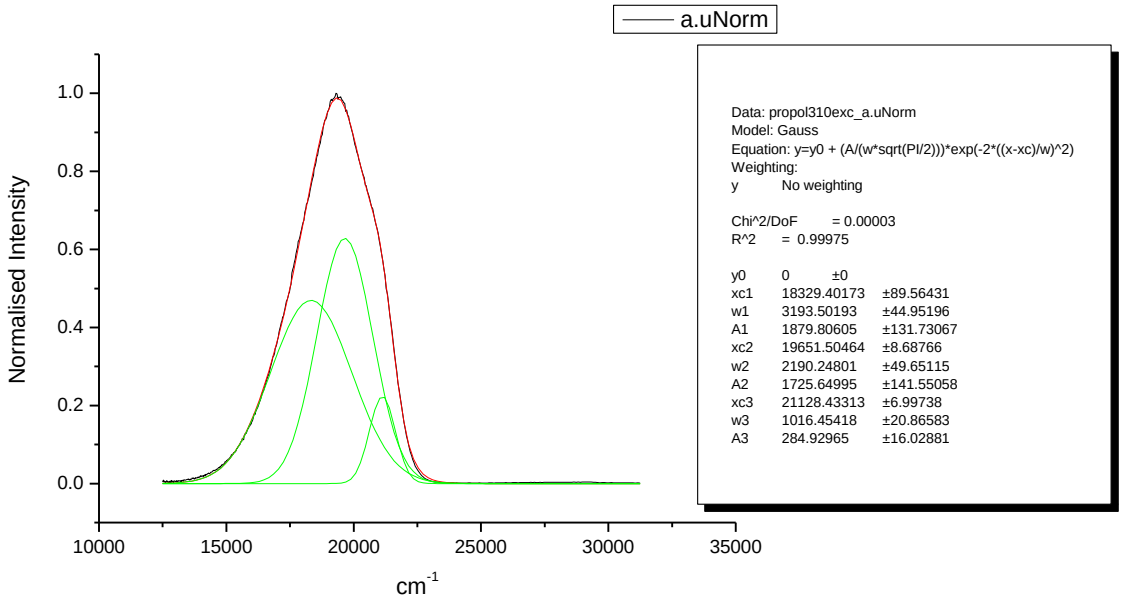

Figure 1.1.253. Gaussian model fit of the normalised fluorescence emission spectrum of **3a** recorded in 1-propanol at 310 nm excitation.

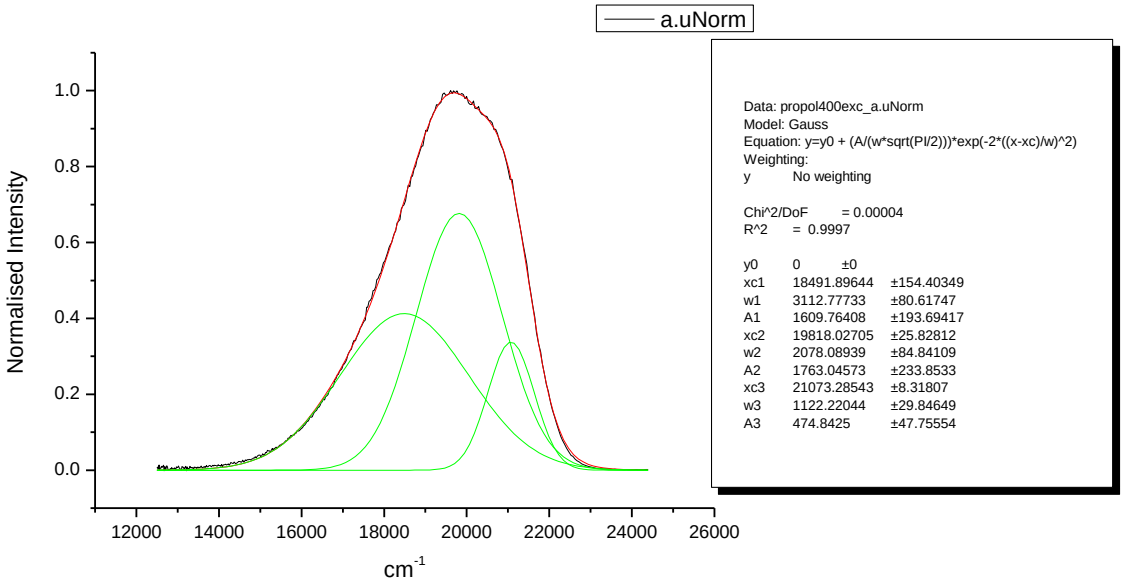

Figure 1.1.254. Gaussian model fit of the normalised fluorescence emission spectrum of **3a** recorded in 1-propanol at 400 nm excitation.

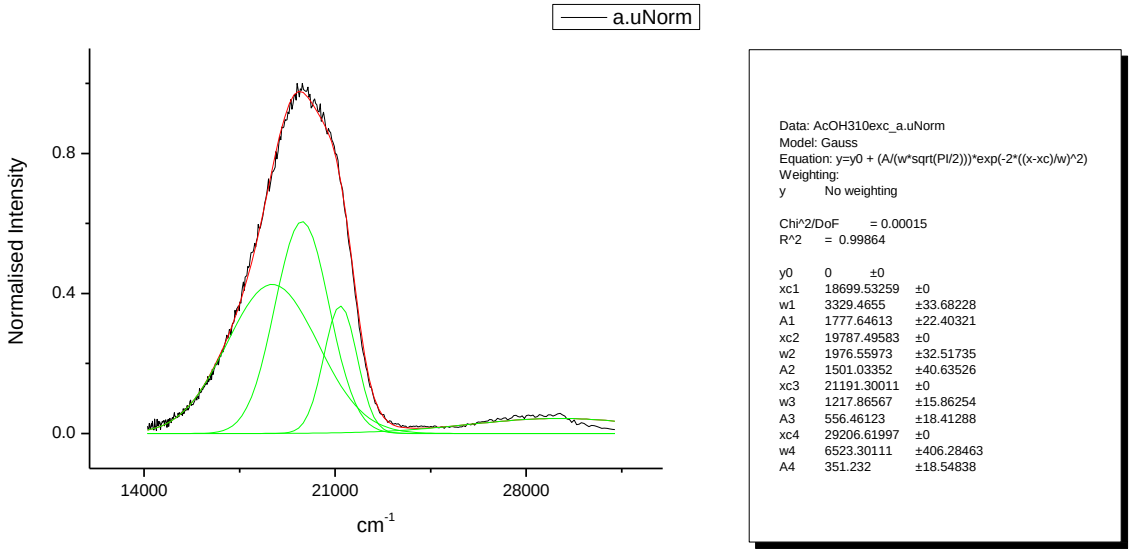

Figure 1.1.255. Gaussian model fit of the normalised fluorescence emission spectrum of **3a** recorded in Acetic Acid at 310 nm excitation.

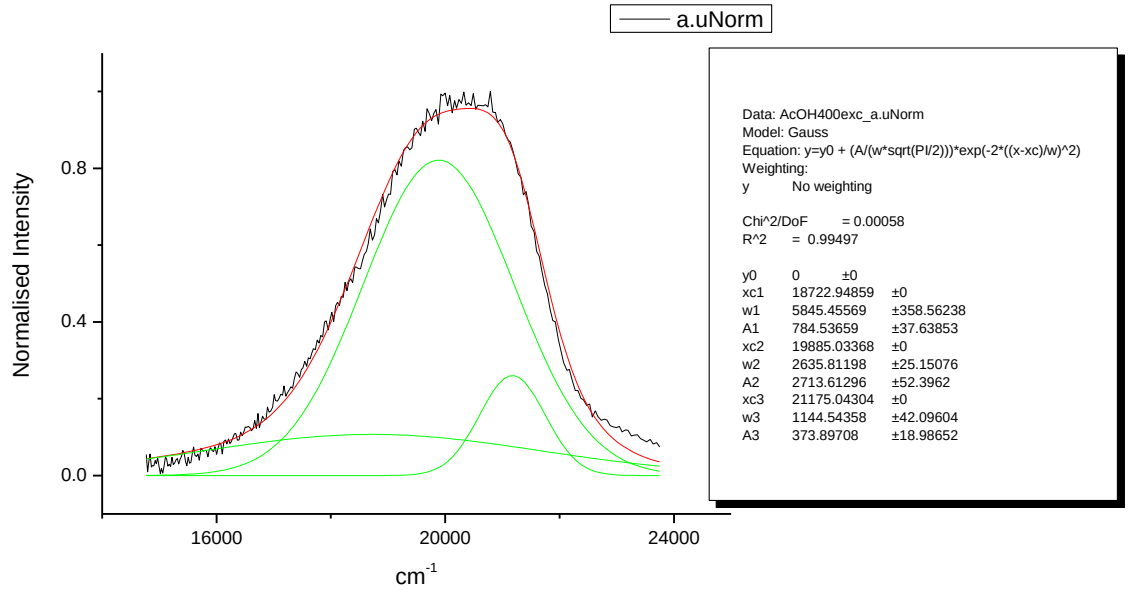

Figure 1.1.256. Gaussian model fit of the normalised fluorescence emission spectrum of **3a** recorded in Acetic Acid at 400 nm excitation.

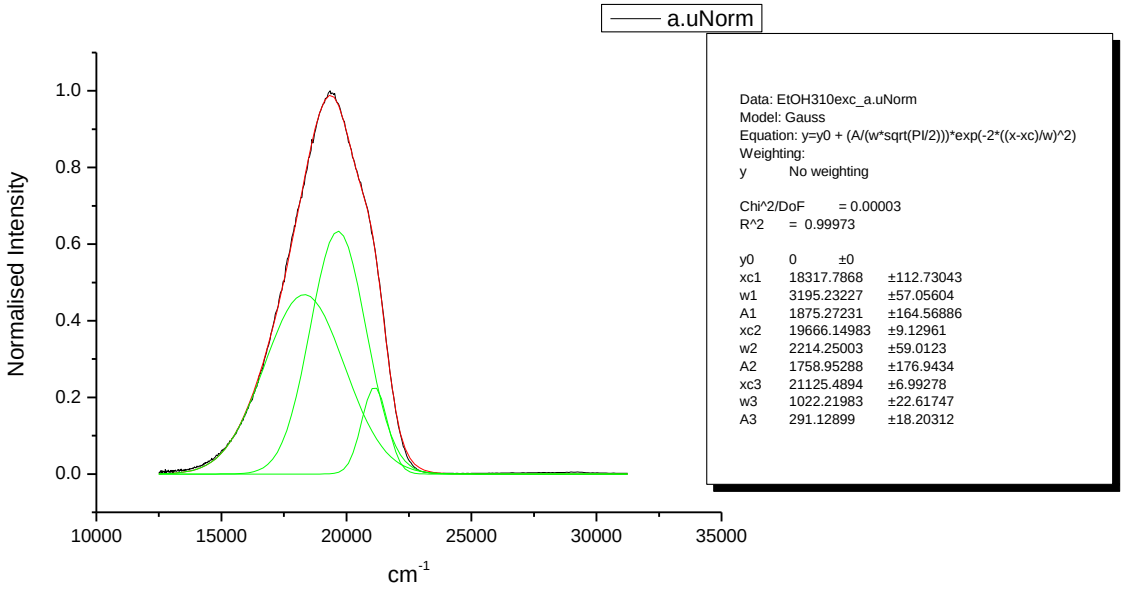

Figure 1.1.257. Gaussian model fit of the normalised fluorescence emission spectrum of **3a** recorded in Ethanol at 310 nm excitation.

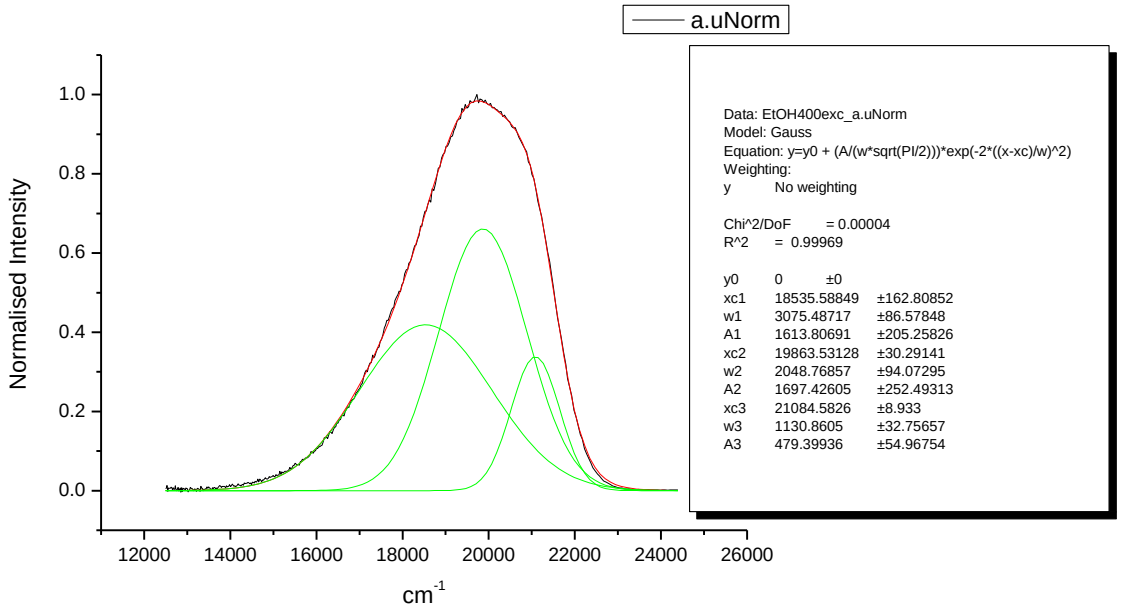

Figure 1.1.258. Gaussian model fit of the normalised fluorescence emission spectrum of **3a** recorded in Ethanol at 400 nm excitation.

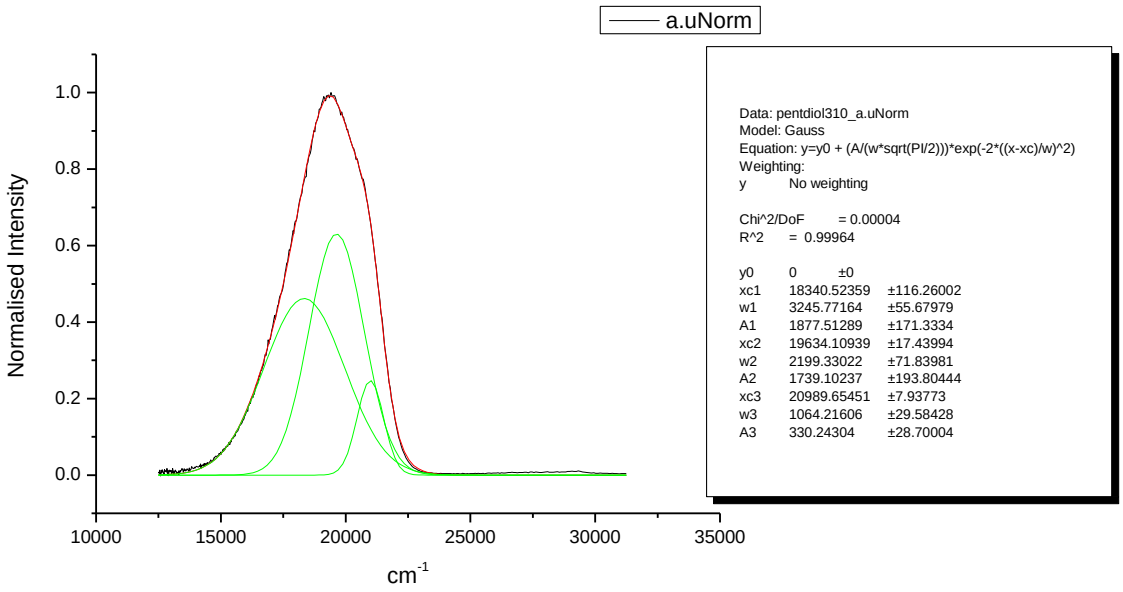

Figure 1.1.259. Gaussian model fit of the normalised fluorescence emission spectrum of **3a** recorded in 1,5-pentanediol at 310 nm excitation.

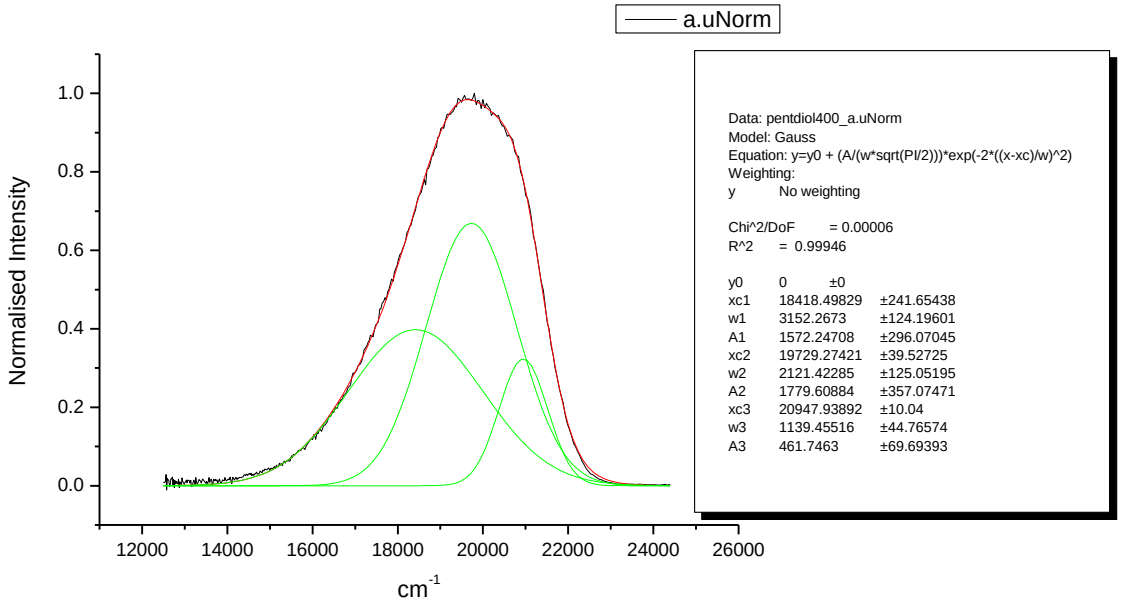

Figure 1.1.260. Gaussian model fit of the normalised fluorescence emission spectrum of **3a** recorded in 1,5-pentanediol at 400 nm excitation.

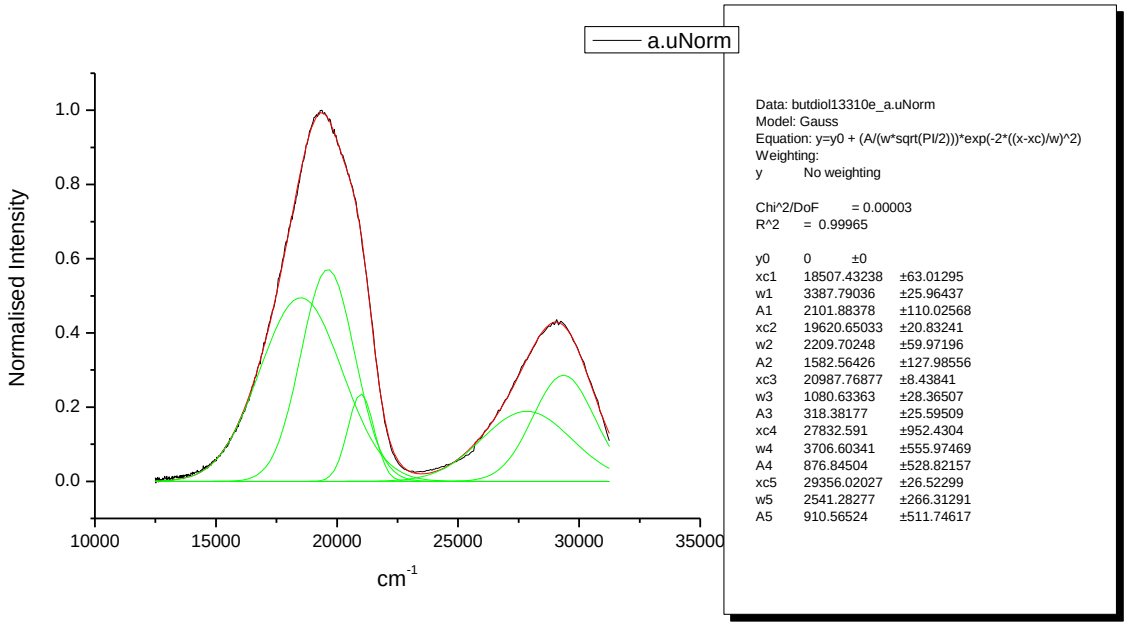

Figure 1.1.261. Gaussian model fit of the normalised fluorescence emission spectrum of **3a** recorded in 1,3-butanediol at 310 nm excitation.

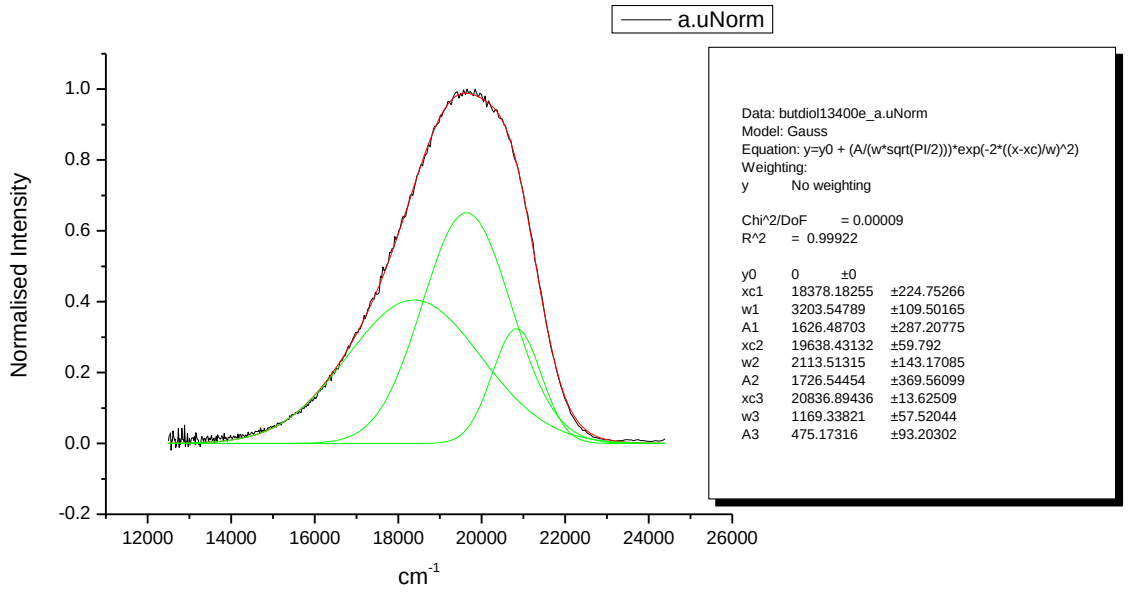

Figure 1.1.262. Gaussian model fit of the normalised fluorescence emission spectrum of **3a** recorded in 1,3-butanediol at 400 nm excitation.

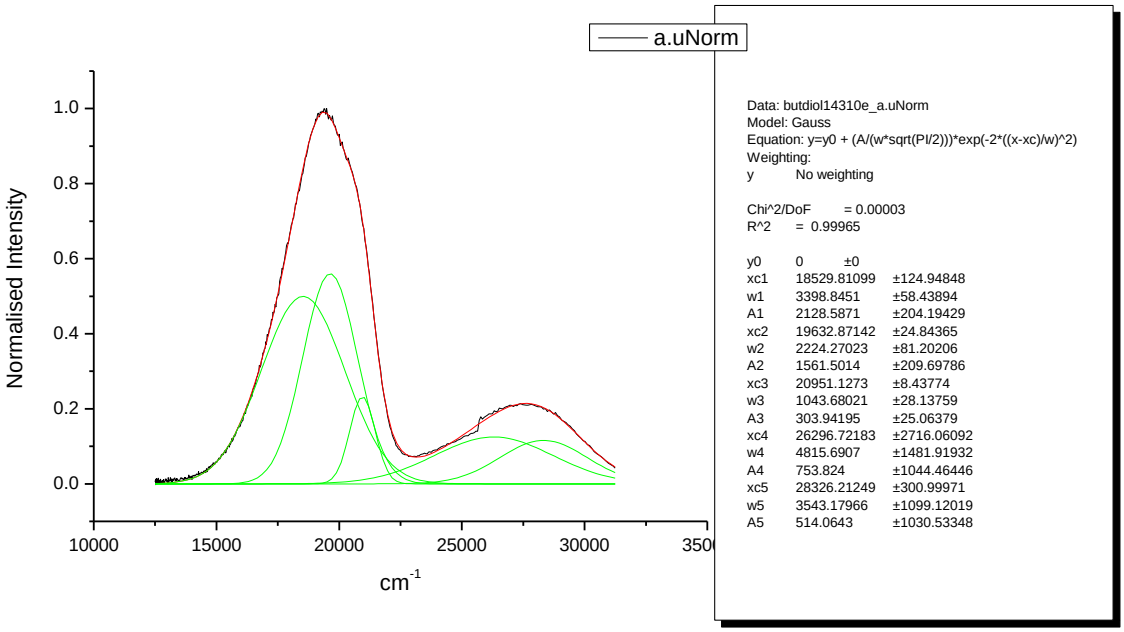

Figure 1.1.263. Gaussian model fit of the normalised fluorescence emission spectrum of **3a** recorded in 1,4-butanediol at 310 nm excitation.

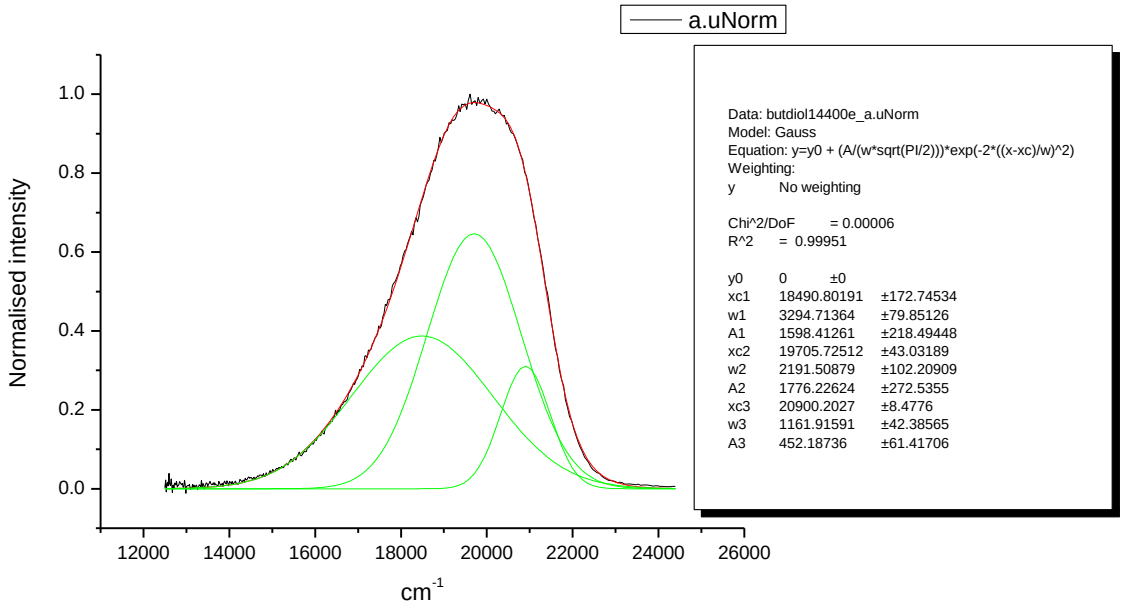

Figure 1.1.264. Gaussian model fit of the normalised fluorescence emission spectrum of **3a** recorded in 1,4-butanediol at 400 nm excitation.

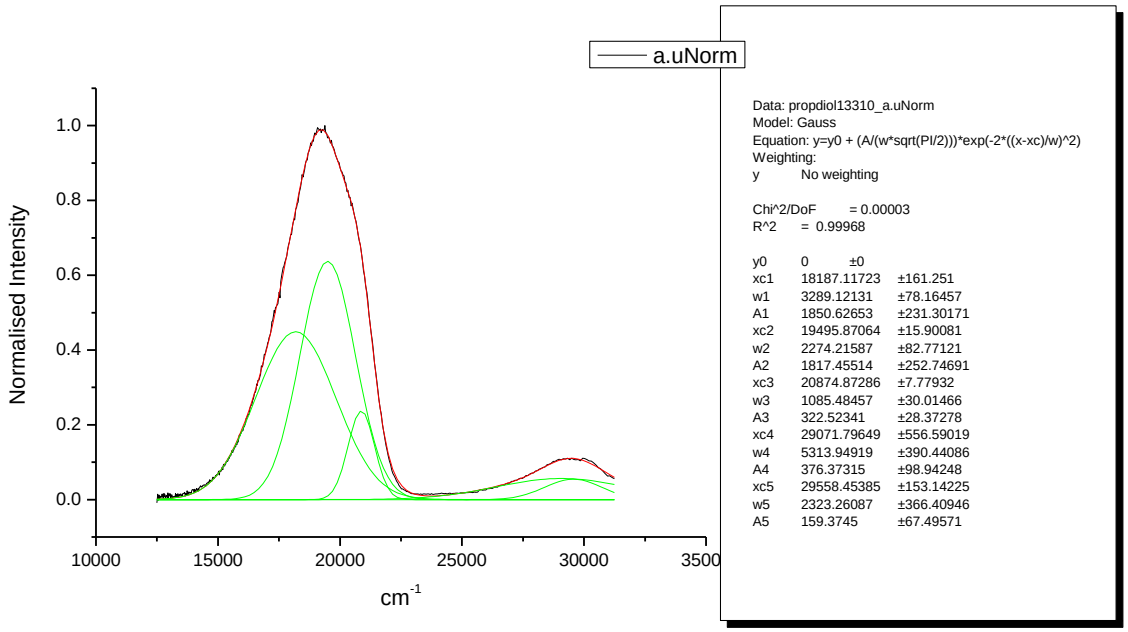

Figure 1.1.265. Gaussian model fit of the normalised fluorescence emission spectrum of **3a** recorded in 1,3-propanediol at 310 nm excitation.

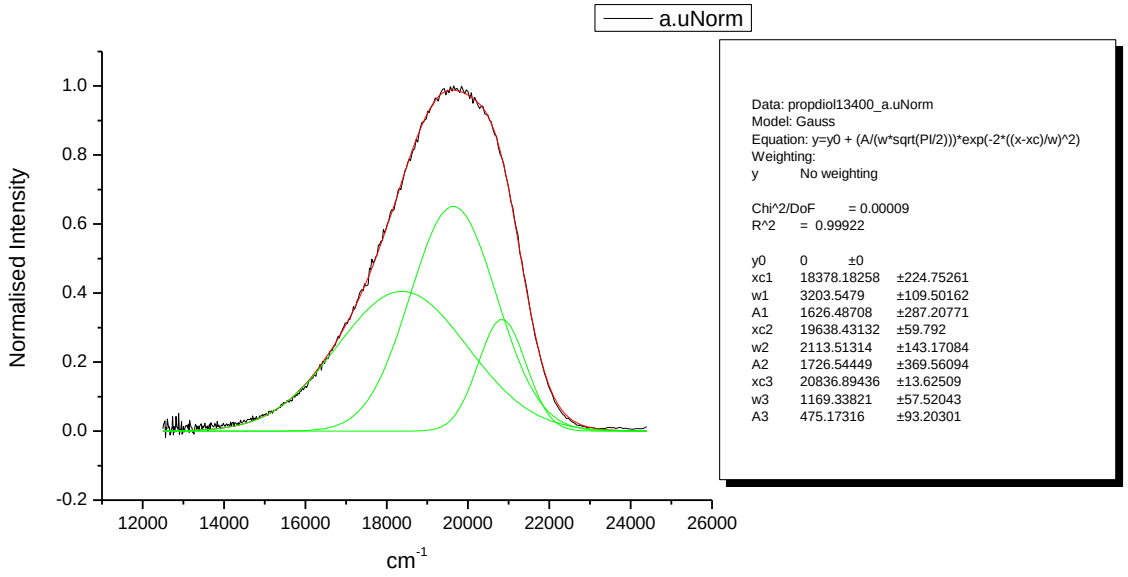

Figure 1.1.266. Gaussian model fit of the normalised fluorescence emission spectrum of **3a** recorded in 1,3-propanediol at 400 nm excitation.

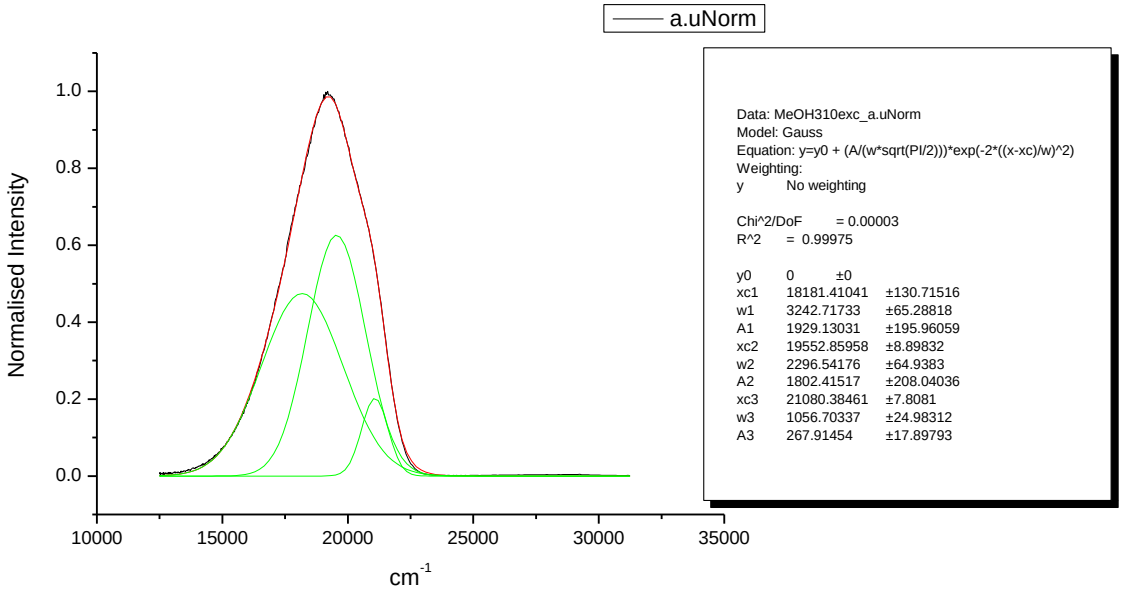

Figure 1.1.267. Gaussian model fit of the normalised fluorescence emission spectrum of **3a** recorded in Methanol at 310 nm excitation.

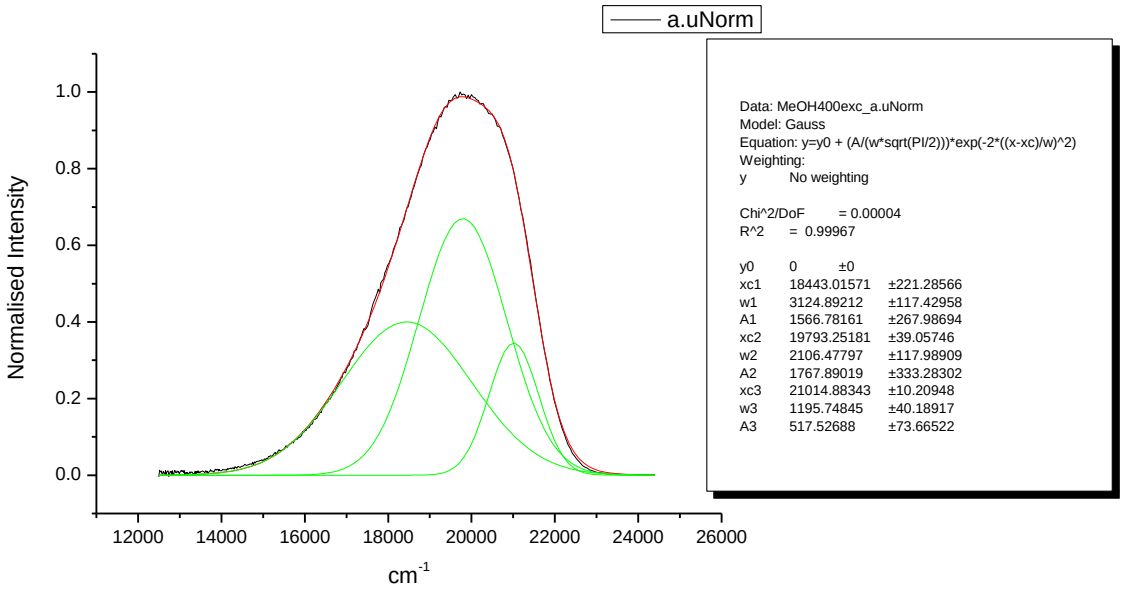

Figure 1.1.268. Gaussian model fit of the normalised fluorescence emission spectrum of **3a** recorded in Methanol at 400 nm excitation.

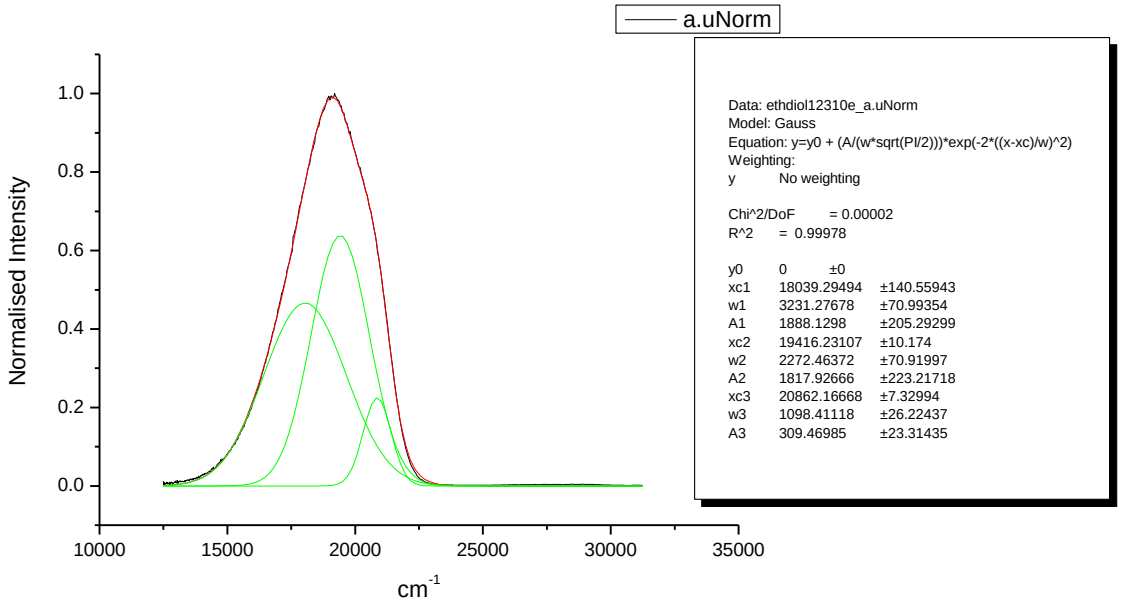

Figure 1.1.269. Gaussian model fit of the normalised fluorescence emission spectrum of **3a** recorded in 1,2-ethanediol at 310 nm excitation.

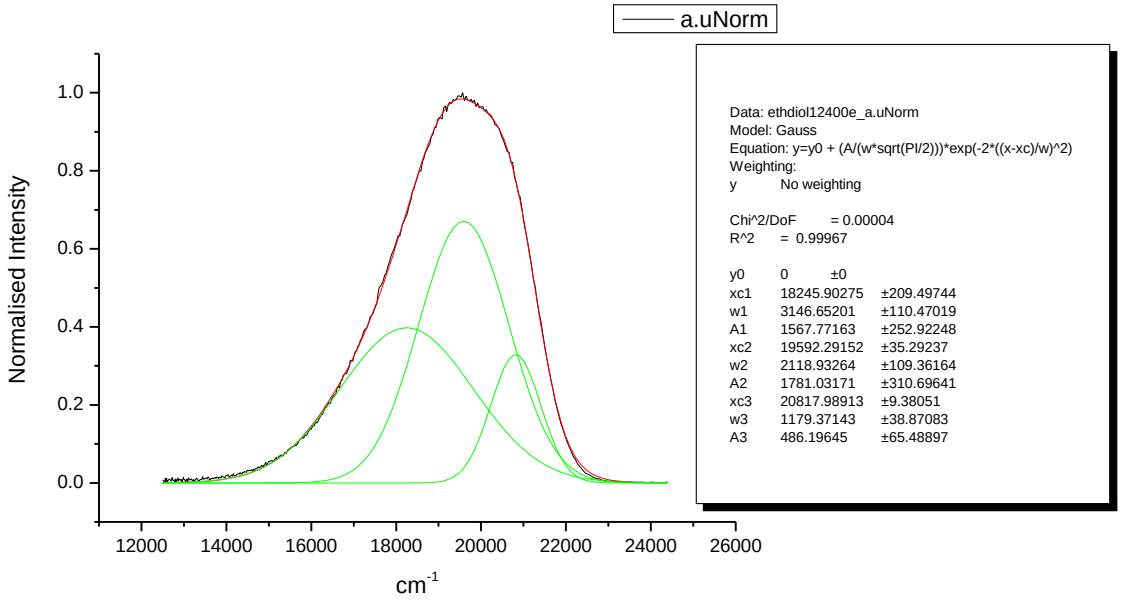

Figure 1.1.270. Gaussian model fit of the normalised fluorescence emission spectrum of **3a** recorded in 1,2-ethanediol at 400 nm excitation.

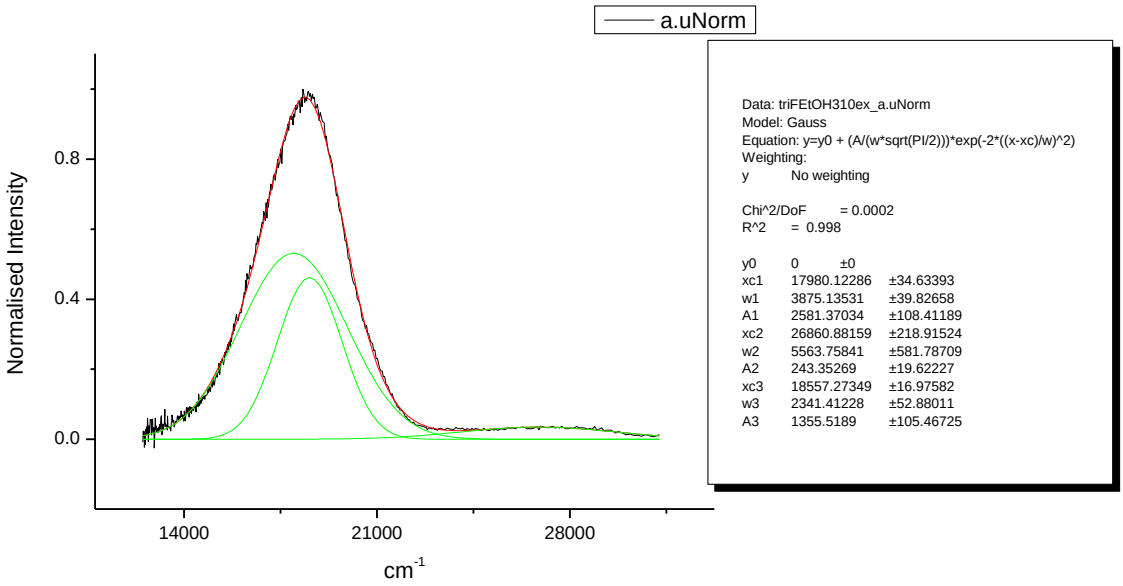

Figure 1.1.271. Gaussian model fit of the normalised fluorescence emission spectrum of **3a** recorded in 2,2,2-trifluoroethanol at 310 nm excitation.

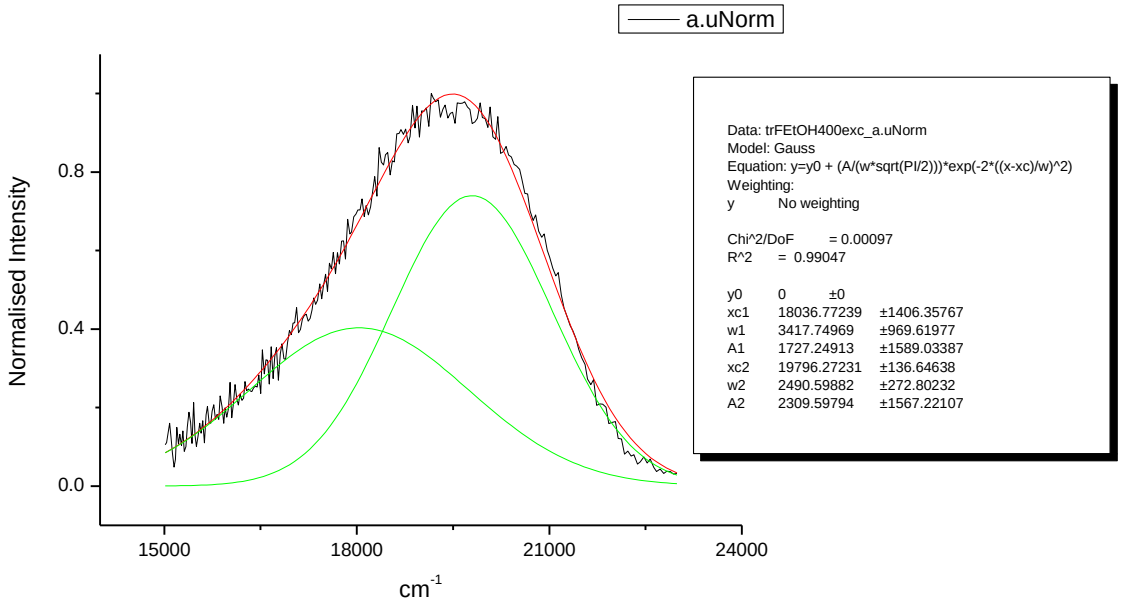

Figure 1.1.272. Gaussian model fit of the normalised fluorescence emission spectrum of **3a** recorded in 2,2,2-trifluoroethanol at 400 nm excitation.

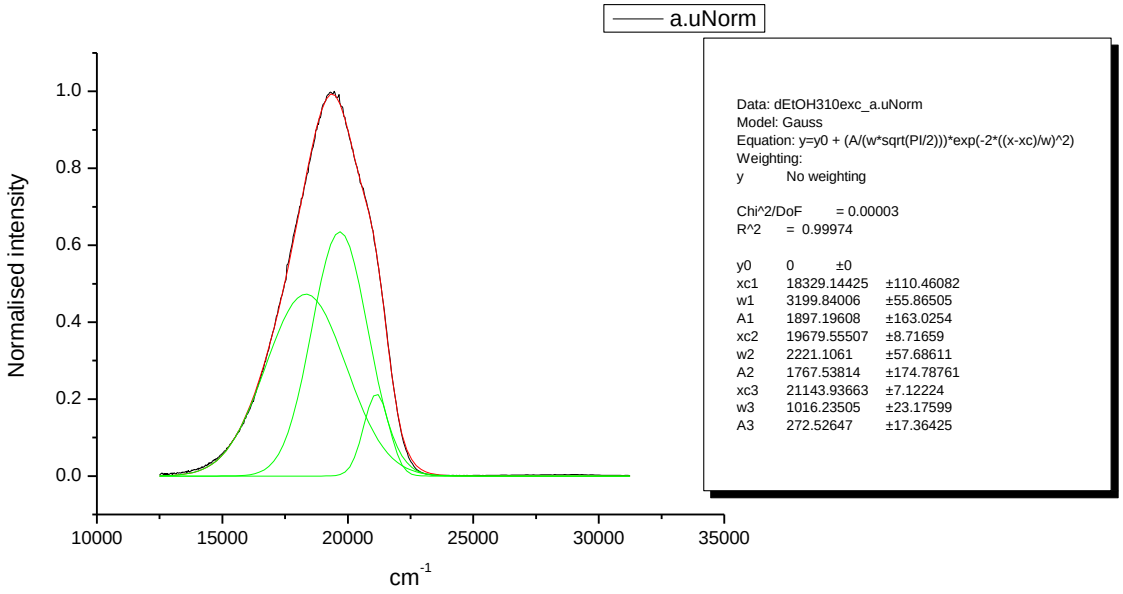

Figure 1.1.273. Gaussian model fit of the normalised fluorescence emission spectrum of **3a** recorded in ethanol-d_1 (EtOD) at 310 nm excitation.

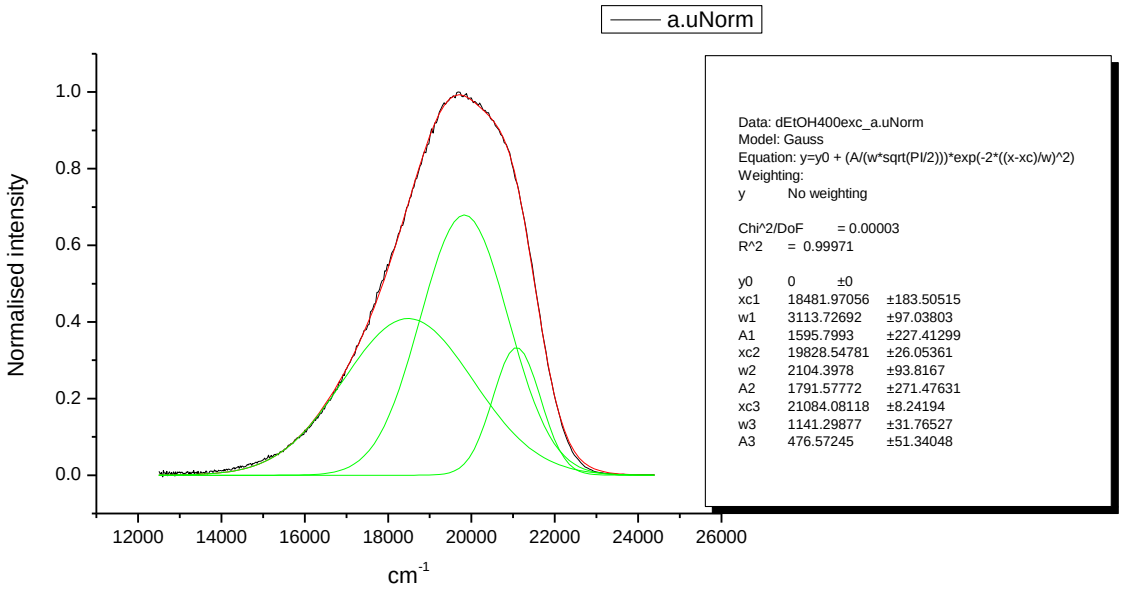

Figure 1.1.274. Gaussian model fit of the normalised fluorescence emission spectrum of **3a** recorded in ethanol-d_1 (EtOD) at 400 nm excitation.

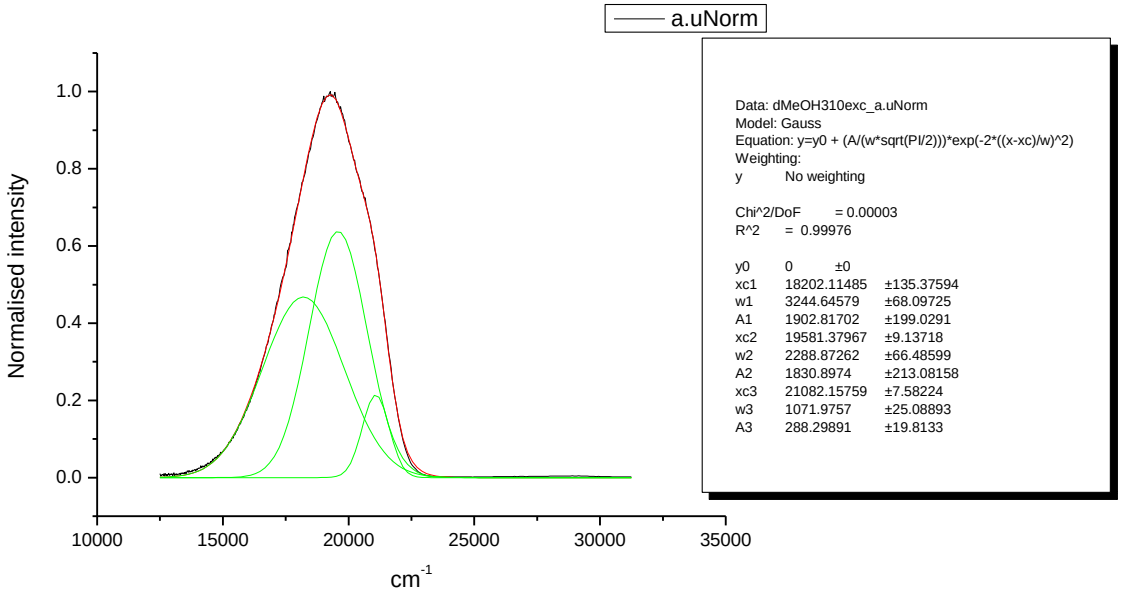

Figure 1.1.275. Gaussian model fit of the normalised fluorescence emission spectrum of **3a** recorded in methanol-d_1 (MeOD) at 310 nm excitation.

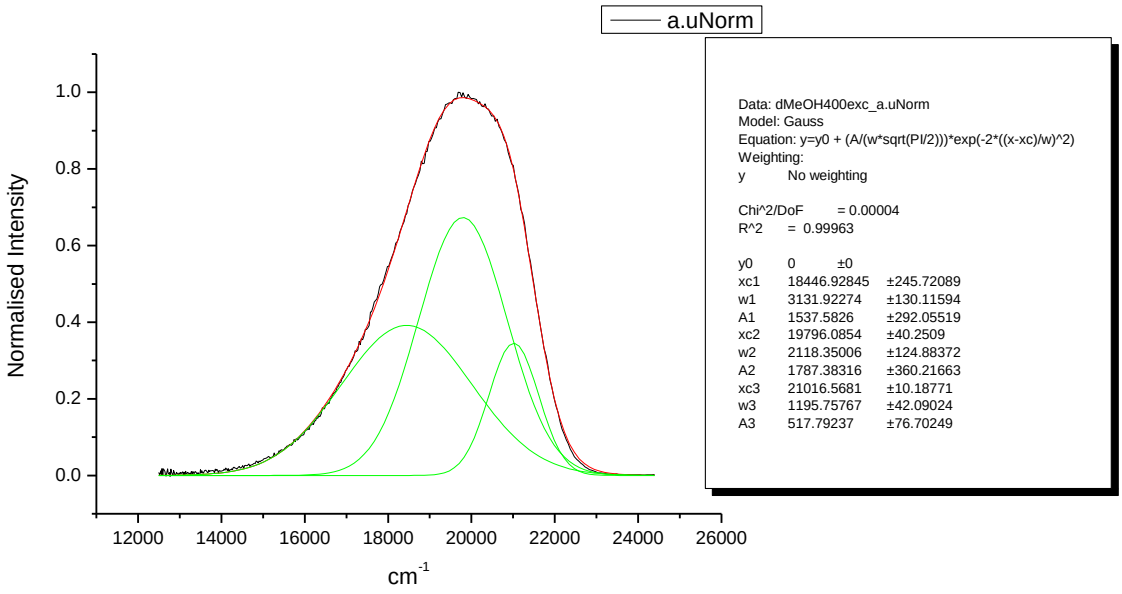

Figure 1.1.276. Gaussian model fit of the normalised fluorescence emission spectrum of **3a** recorded in methanol-d_1 (MeOD) at 400 nm excitation.

1.1.11 Fluorescence Excitation spectra.

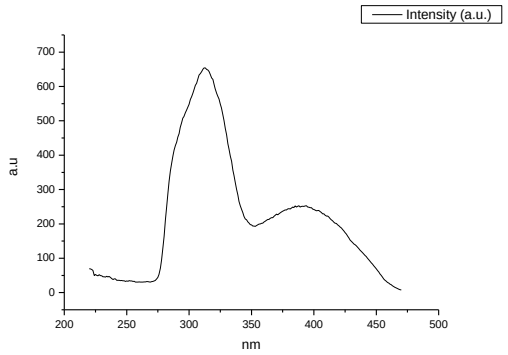

Figure 1.1.277. Fluorescence excitation spectrum of **3a** recorded in Toluene with emission fixed at 480 nm.

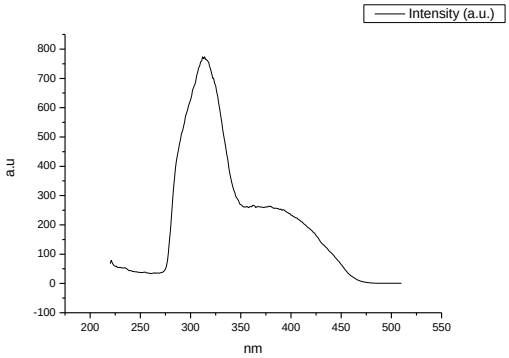

Figure 1.1.278. Fluorescence excitation spectrum of **3a** recorded in Toluene with emission fixed at 520 nm.

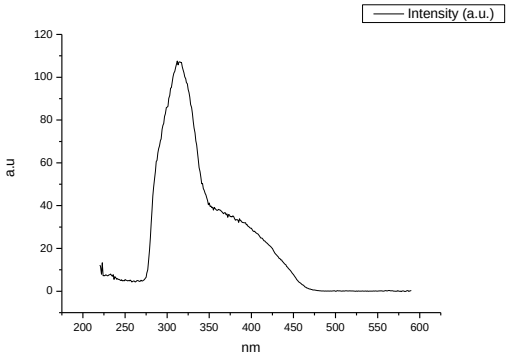

Figure 1.1.279. Fluorescence excitation spectrum of **3a** recorded in Toluene with emission fixed at 600 nm.

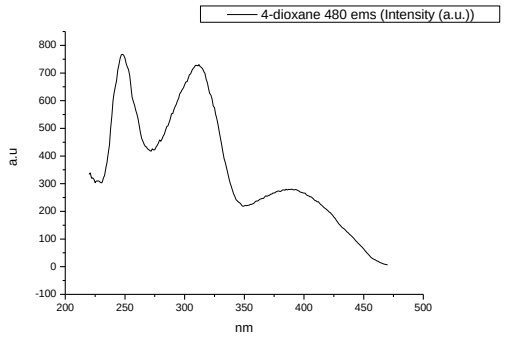

Figure 1.1.280. Fluorescence excitation spectrum of **3a** recorded in 1,4-dioxane with emission fixed at 480 nm.

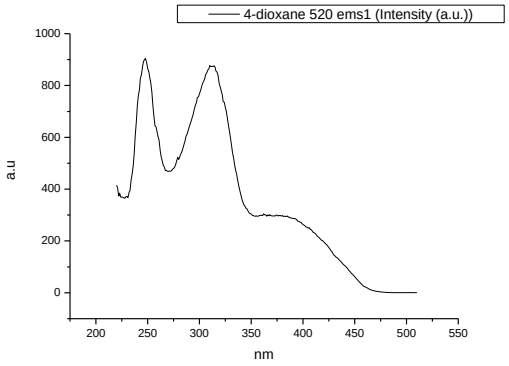

Figure 1.1.281. Fluorescence excitation spectrum of **3a** recorded in 1,4-dioxane with emission fixed at 520 nm.

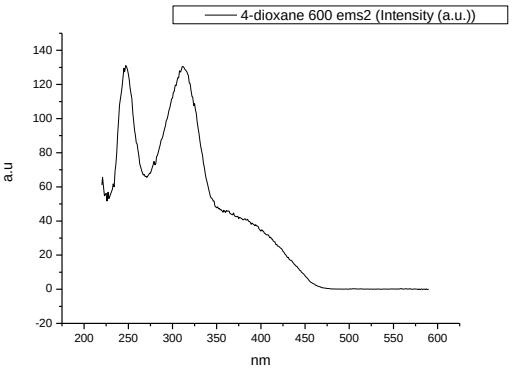

Figure 1.1.282. Fluorescence excitation spectrum of **3a** recorded in 1,4-dioxane with emission fixed at 600 nm.

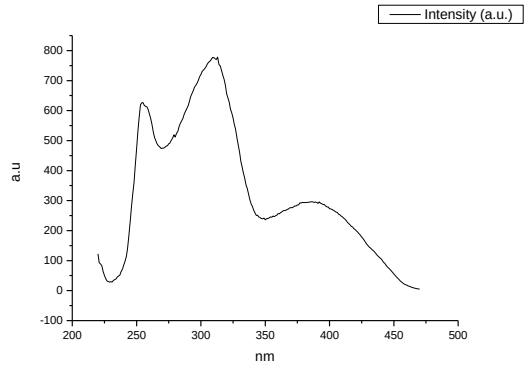

Figure 1.1.283. Fluorescence excitation spectrum of **3a** recorded in Ethyl Acetate with emission fixed at 480 nm.

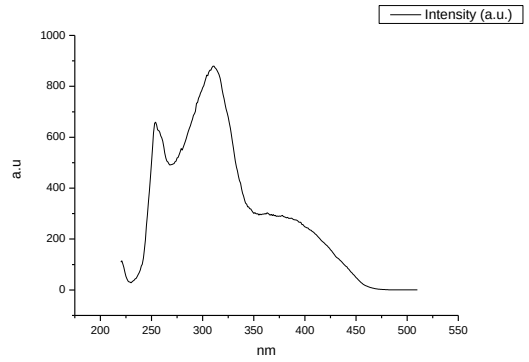

Figure 1.1.284. Fluorescence excitation spectrum of **3a** recorded in Ethyl Acetate with emission fixed at 520 nm.

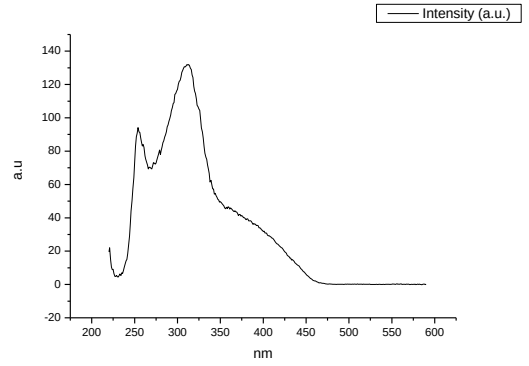

Figure 1.1.285. Fluorescence excitation spectrum of **3a** recorded in Ethyl Acetate with emission fixed at 600 nm.

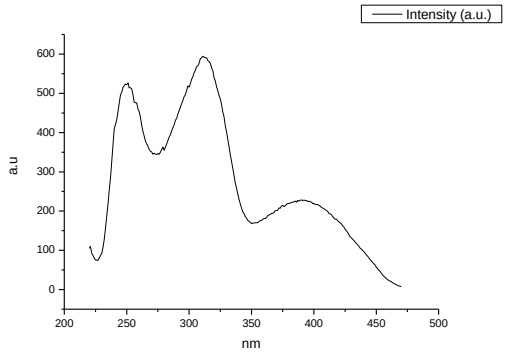

Figure 1.1.286. Fluorescence excitation spectrum of **3a** recorded in Chloroform with emission fixed at 480 nm.

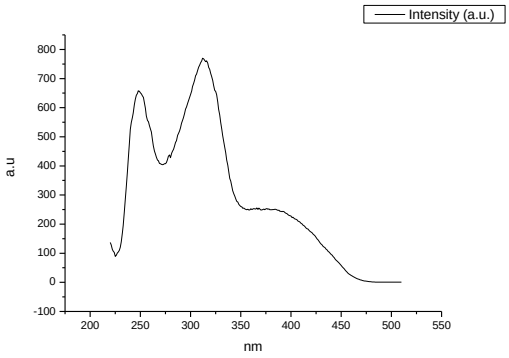

Figure 1.1.287. Fluorescence excitation spectrum of **3a** recorded in Chloroform with emission fixed at 520 nm.

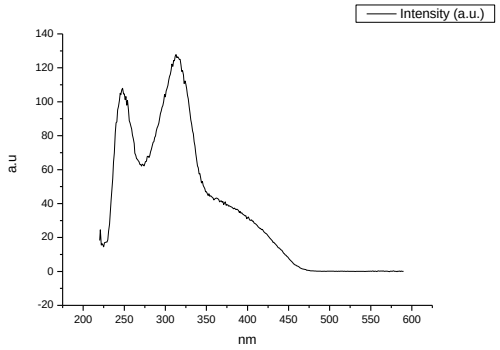

Figure 1.1.288. Fluorescence excitation spectrum of **3a** recorded in Chloroform with emission fixed at 600 nm.

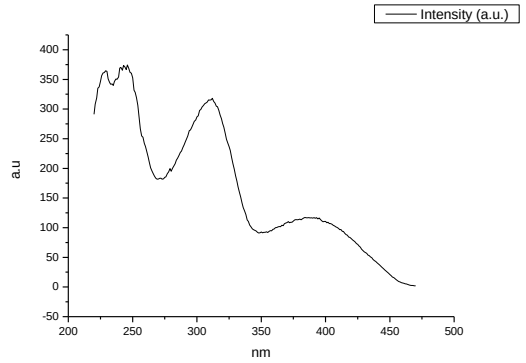

Figure 1.1.289. Fluorescence excitation spectrum of **3a** recorded in 2-methyl-2-butanol with emission fixed at 480 nm.

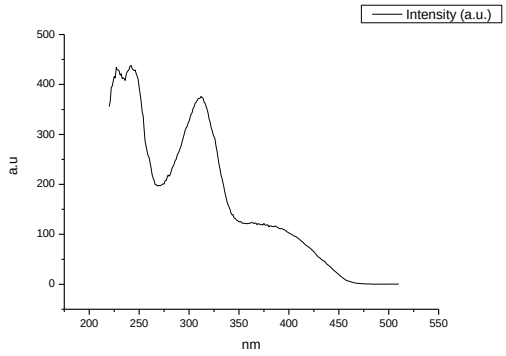

Figure 1.1.290. Fluorescence excitation spectrum of **3a** recorded in 2-methyl-2-butanol with emission fixed at 520 nm.

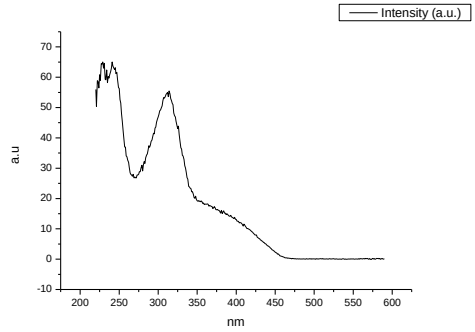

Figure 1.1.291. Fluorescence excitation spectrum of **3a** recorded in 2-methyl-2-butanol with emission fixed at 600 nm.

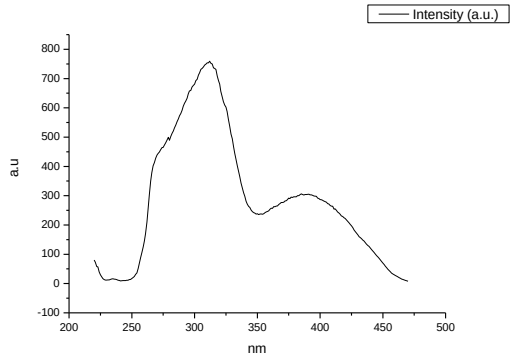

Figure 1.1.292. Fluorescence excitation spectrum of **3a** recorded in N,N-dimethylformamide with emission fixed at 480 nm.

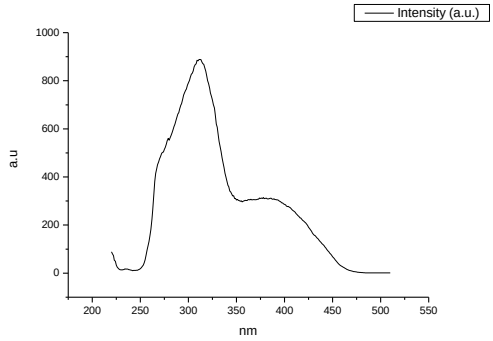

Figure 1.1.293. Fluorescence excitation spectrum of **3a** recorded in N,N-dimethylformamide with emission fixed at 520 nm.

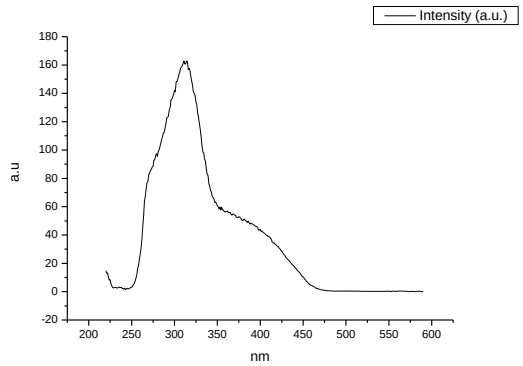

Figure 1.1.294. Fluorescence excitation spectrum of **3a** recorded in N,N-dimethylformamide with emission fixed at 600 nm.

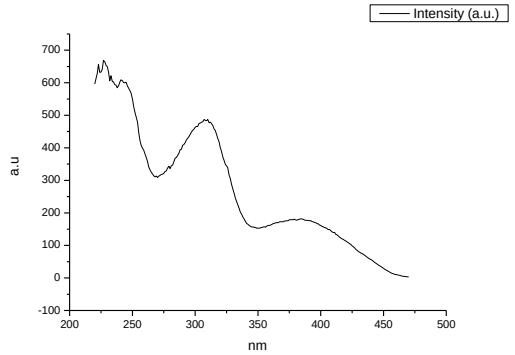

Figure 1.1.295. Fluorescence excitation spectrum of **3a** recorded in Acetonitrile with emission fixed at 480 nm.

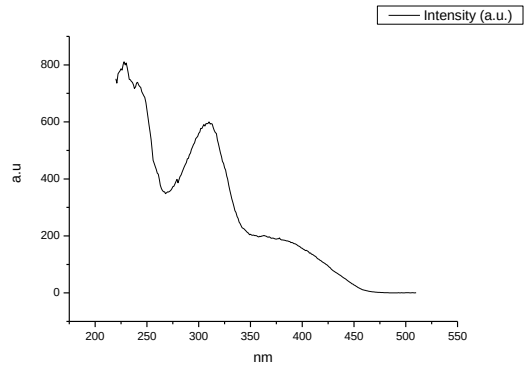

Figure 1.1.296. Fluorescence excitation spectrum of **3a** recorded in Acetonitrile with emission fixed at 520 nm.

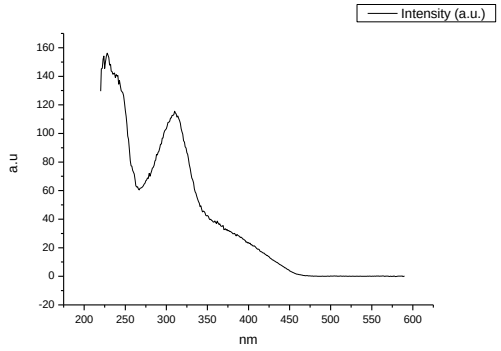

Figure 1.1.297. Fluorescence excitation spectrum of **3a** recorded in Acetonitrile with emission fixed at 600 nm.

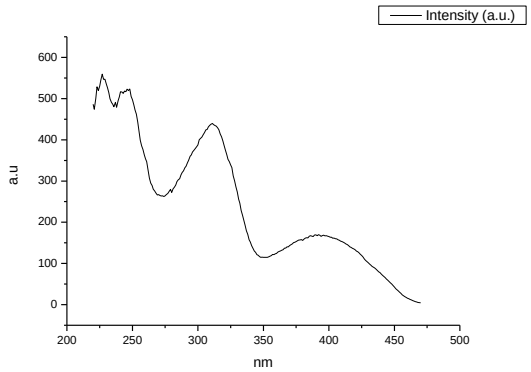

Figure 1.1.298. Fluorescence excitation spectrum of **3a** recorded in 1-octanol with emission fixed at 480 nm.

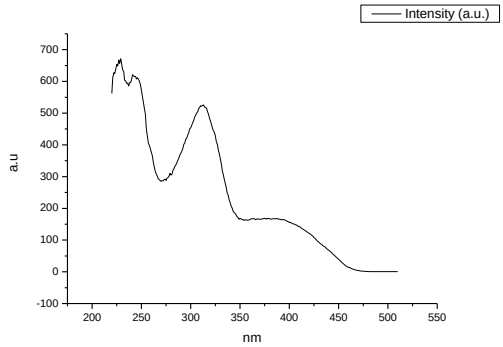

Figure 1.1.299. Fluorescence excitation spectrum of **3a** recorded in 1-octanol with emission fixed at 520 nm.

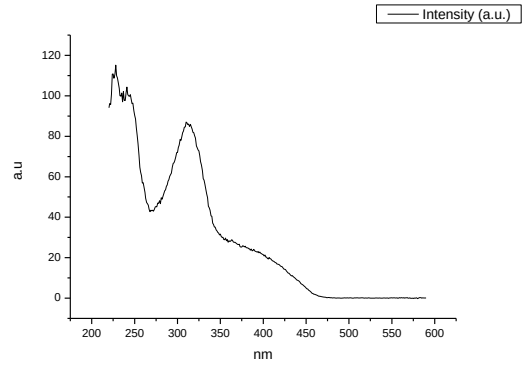

Figure 1.1.300. Fluorescence excitation spectrum of **3a** recorded in 1-octanol with emission fixed at 600 nm.

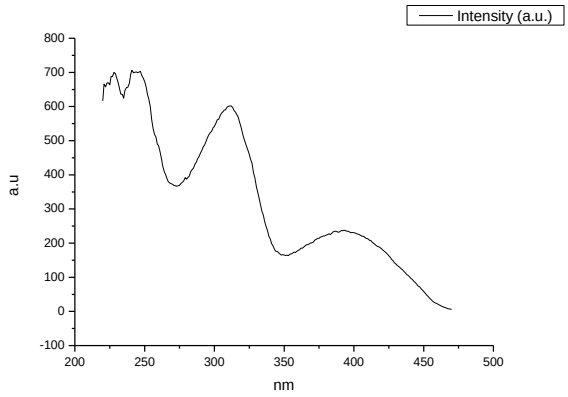

Figure 1.1.301. Fluorescence excitation spectrum of **3a** recorded in 1-hexanol with emission fixed at 480 nm.

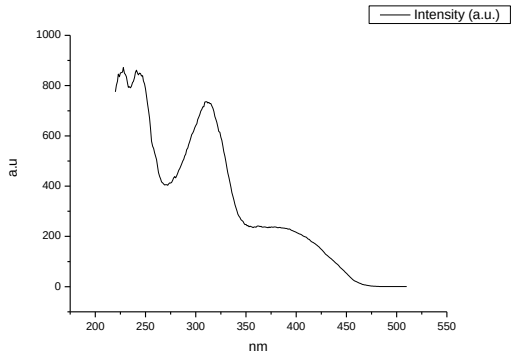

Figure 1.1.302. Fluorescence excitation spectrum of **3a** recorded in 1-hexanol with emission fixed at 520 nm.

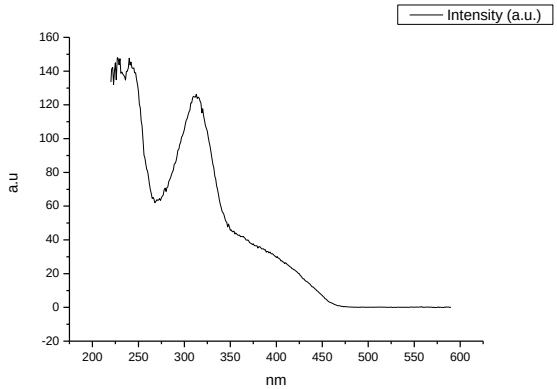

Figure 1.1.303. Fluorescence excitation spectrum of **3a** recorded in 1-hexanol with emission fixed at 600 nm.

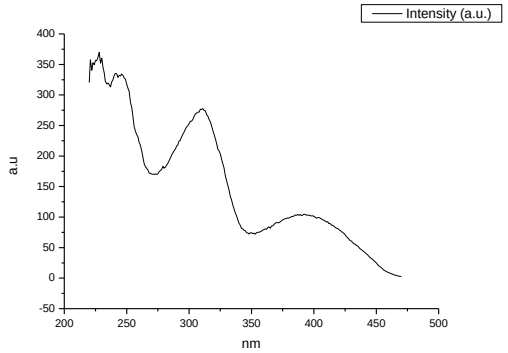

Figure 1.1.304. Fluorescence excitation spectrum of **3a** recorded in 1-butanol with emission fixed at 480 nm.

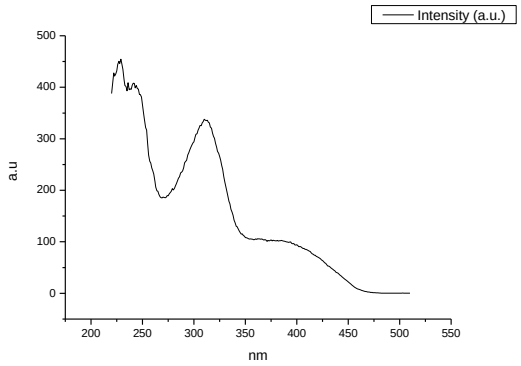

Figure 1.1.305. Fluorescence excitation spectrum of **3a** recorded in 1-butanol with emission fixed at 520 nm.

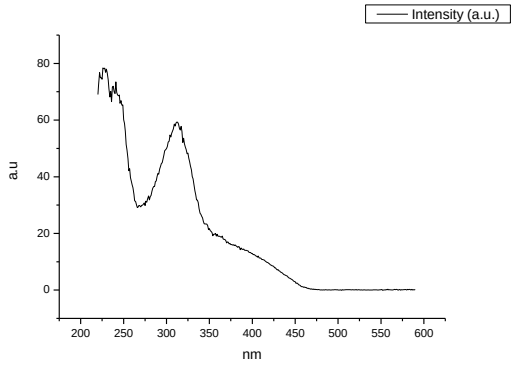

Figure 1.1.306. Fluorescence excitation spectrum of **3a** recorded in 1-butanol with emission fixed at 600 nm.

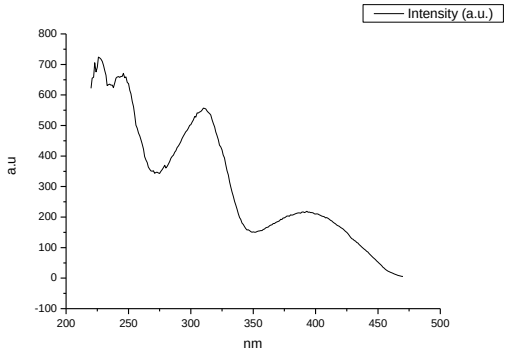

Figure 1.1.307. Fluorescence excitation spectrum of **3a** recorded in 1-pentanol with emission fixed at 480 nm.

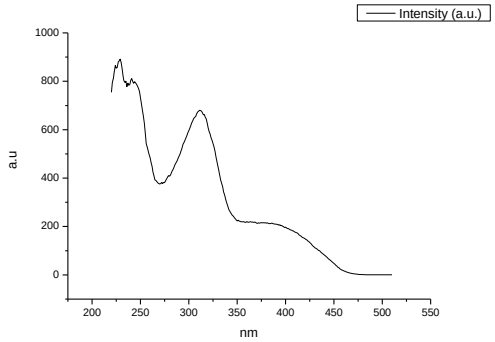

Figure 1.1.308. Fluorescence excitation spectrum of **3a** recorded in 1-pentanol with emission fixed at 520 nm.

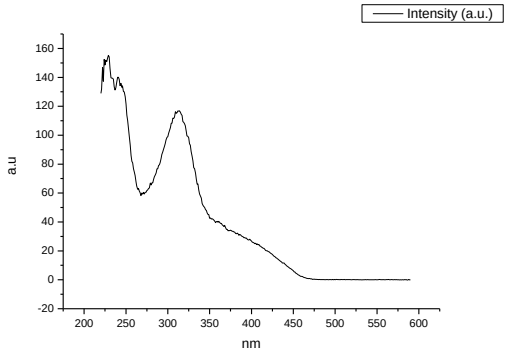

Figure 1.1.309. Fluorescence excitation spectrum of **3a** recorded in 1-pentanol with emission fixed at 600 nm.

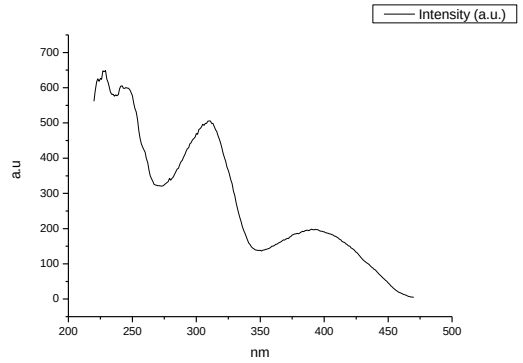

Figure 1.1.310. Fluorescence excitation spectrum of **3a** recorded in 1-propanol with emission fixed at 480 nm.

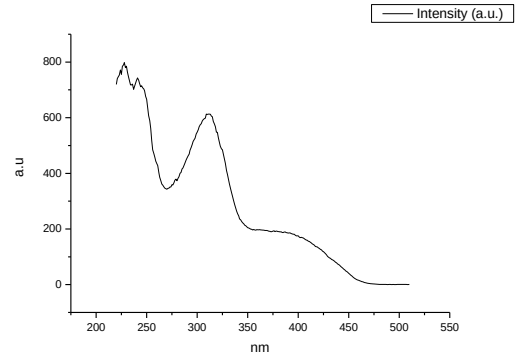

Figure 1.1.311. Fluorescence excitation spectrum of **3a** recorded in 1-propanol with emission fixed at 520 nm.

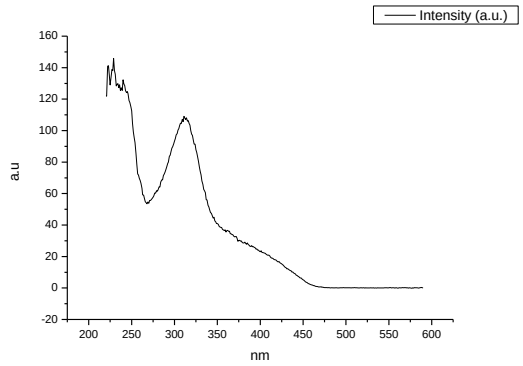

Figure 1.1.312. Fluorescence excitation spectrum of **3a** recorded in 1-propanol with emission fixed at 600 nm.

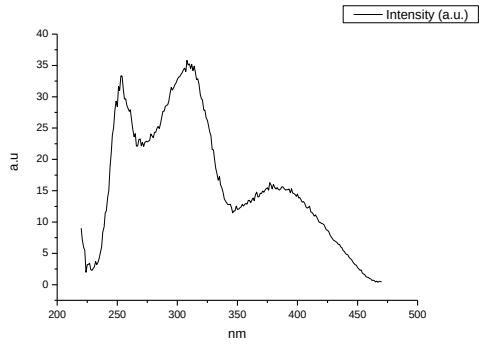

Figure 1.1.313. Fluorescence excitation spectrum of **3a** recorded in 1-propanol with emission fixed at 480 nm.

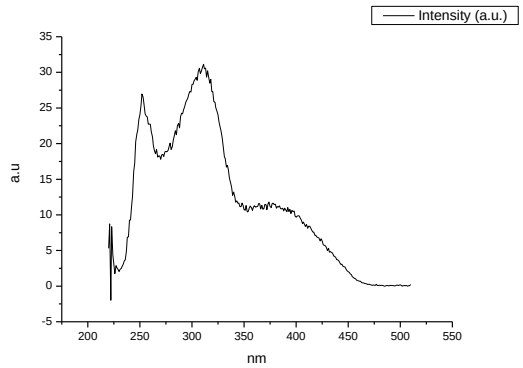

Figure 1.1.314. Fluorescence excitation spectrum of **3a** recorded in 1-propanol with emission fixed at 520 nm.

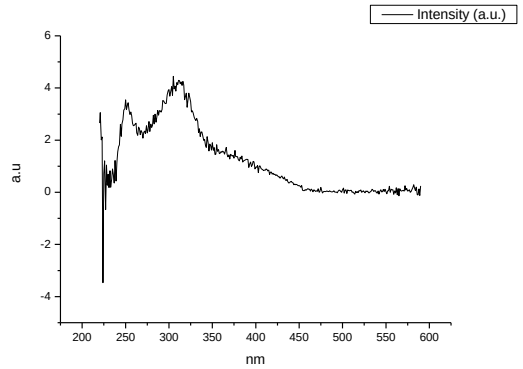

Figure 1.1.315. Fluorescence excitation spectrum of **3a** recorded in 1-propanol with emission fixed at 600 nm.

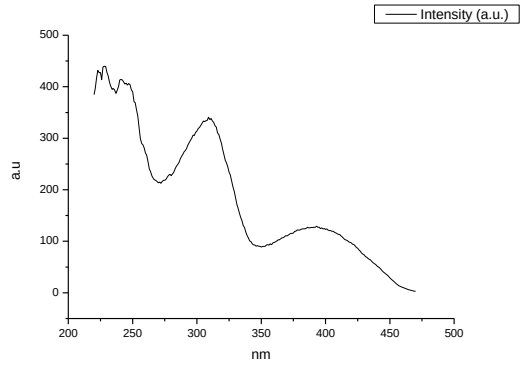

Figure 1.1.316. Fluorescence excitation spectrum of **3a** recorded in Ethanol with emission fixed at 480 nm.

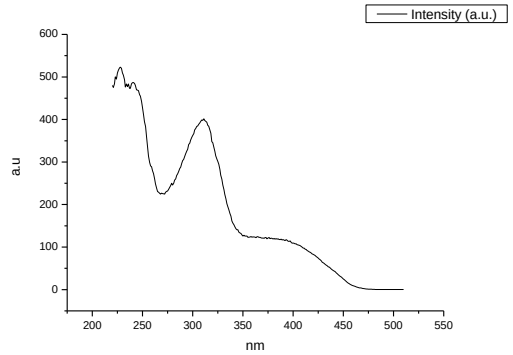

Figure 1.1.317. Fluorescence excitation spectrum of **3a** recorded in Ethanol with emission fixed at 520 nm.

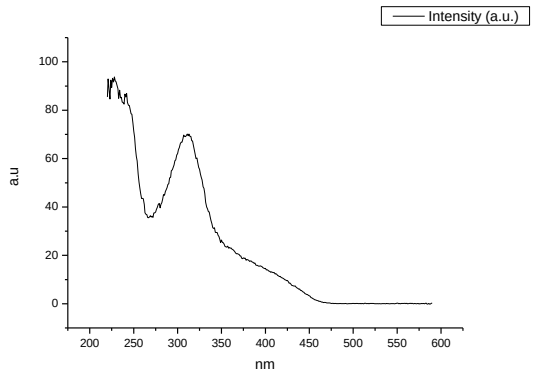

Figure 1.1.318. Fluorescence excitation spectrum of **3a** recorded in Ethanol with emission fixed at 600 nm.

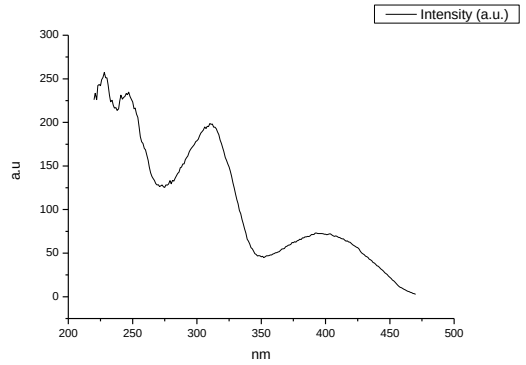

Figure 1.1.319. Fluorescence excitation spectrum of **3a** recorded in 1,5-pentanediol with emission fixed at 480 nm.

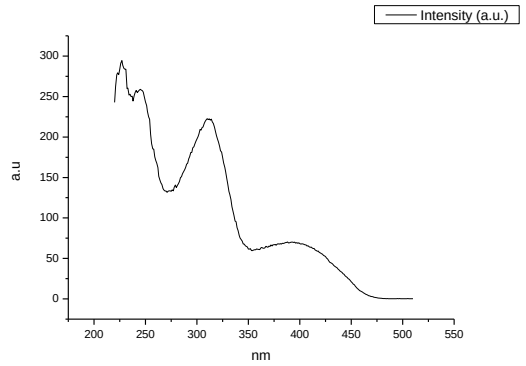

Figure 1.1.320. Fluorescence excitation spectrum of **3a** recorded in 1,5-pentanediol with emission fixed at 520 nm.

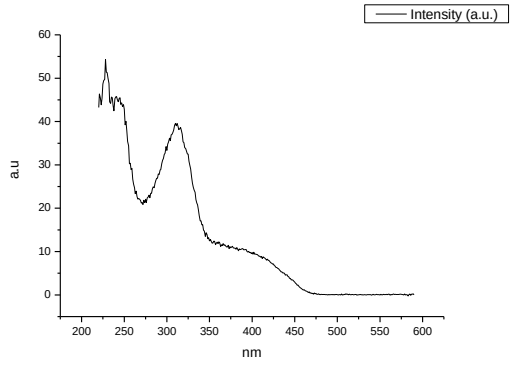

Figure 1.1.321. Fluorescence excitation spectrum of **3a** recorded in 1,5-pentanediol with emission fixed at 600 nm.

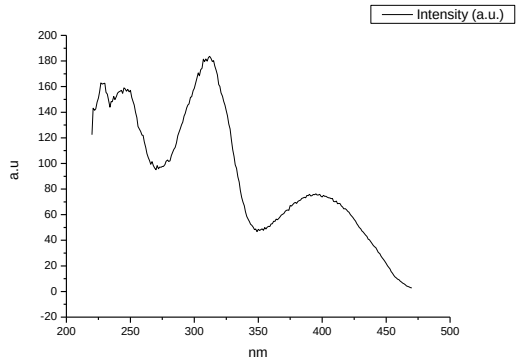

Figure 1.1.322. Fluorescence excitation spectrum of **3a** recorded in 1,3-butanediol with emission fixed at 480 nm.

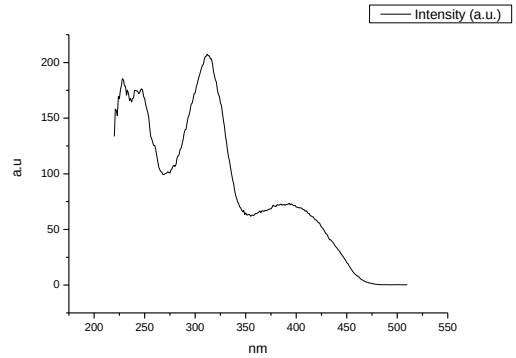

Figure 1.1.323. Fluorescence excitation spectrum of **3a** recorded in 1,3-butanediol with emission fixed at 520 nm.

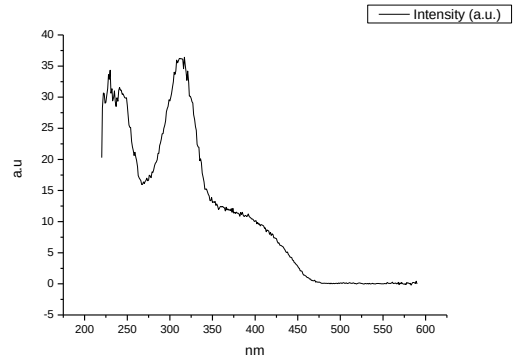

Figure 1.1.324. Fluorescence excitation spectrum of **3a** recorded in 1,3-butanediol with emission fixed at 600 nm.

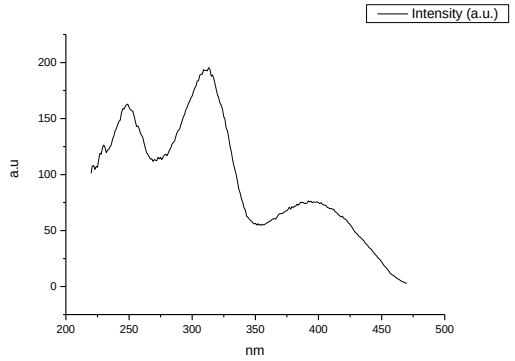

Figure 1.1.325. Fluorescence excitation spectrum of **3a** recorded in 1,4-butanediol with emission fixed at 480 nm.

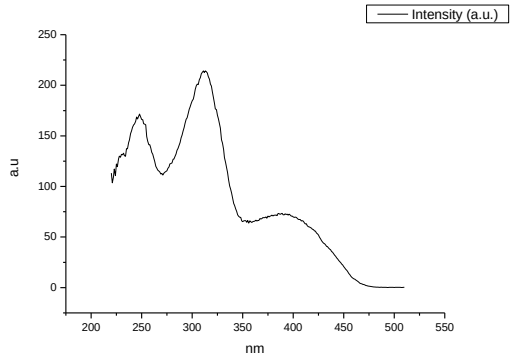

Figure 1.1.326. Fluorescence excitation spectrum of **3a** recorded in 1,4-butanediol with emission fixed at 520 nm.

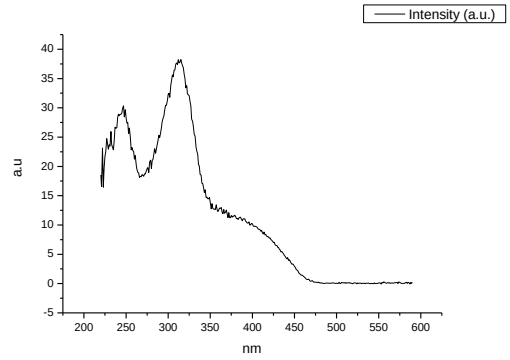

Figure 1.1.327. Fluorescence excitation spectrum of **3a** recorded in 1,4-butanediol with emission fixed at 600 nm.

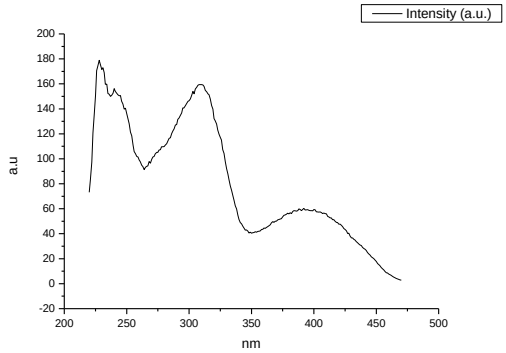

Figure 1.1.328. Fluorescence excitation spectrum of **3a** recorded in 1,3-propanediol with emission fixed at 480 nm.

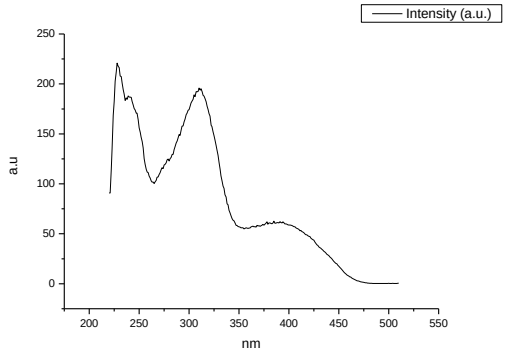

Figure 1.1.329. Fluorescence excitation spectrum of **3a** recorded in 1,3-propanediol with emission fixed at 520 nm.

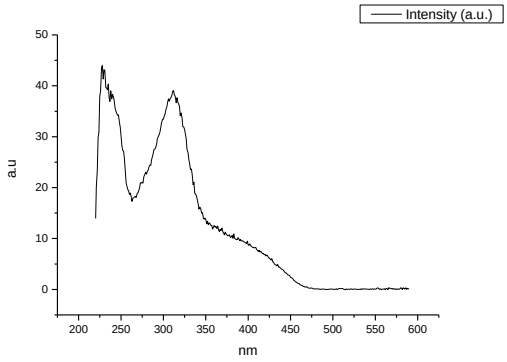

Figure 1.1.330. Fluorescence excitation spectrum of **3a** recorded in 1,3-propanediol with emission fixed at 600 nm.

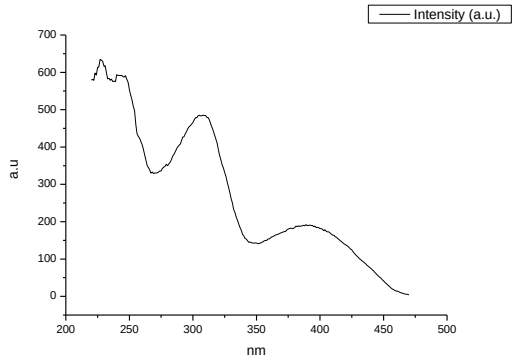

Figure 1.1.331. Fluorescence excitation spectrum of **3a** recorded in Methanol with emission fixed at 480 nm.

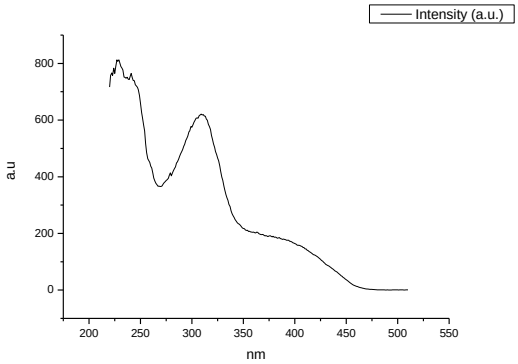

Figure 1.1.332. Fluorescence excitation spectrum of **3a** recorded in Methanol with emission fixed at 520 nm.

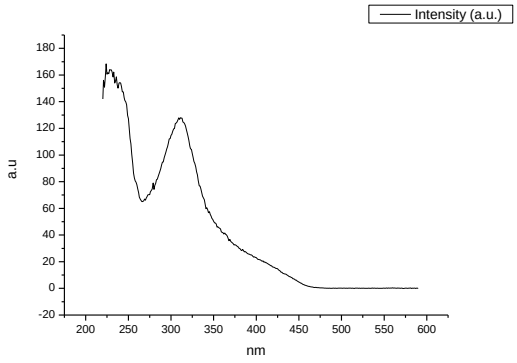

Figure 1.1.333. Fluorescence excitation spectrum of **3a** recorded in Methanol with emission fixed at 600 nm.

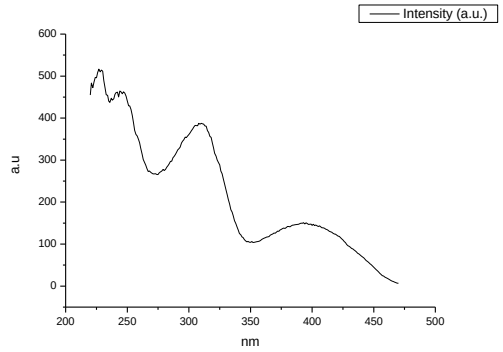

Figure 1.1.334. Fluorescence excitation spectrum of **3a** recorded in 1,2-ethanediol with emission fixed at 480 nm.

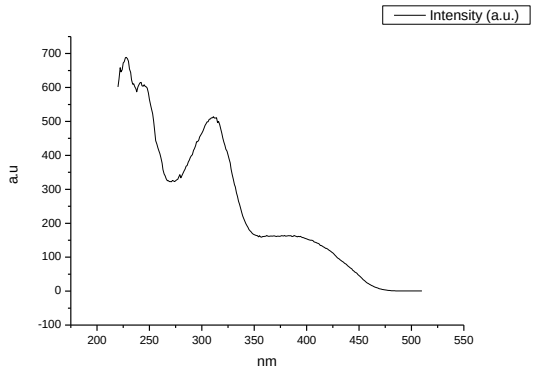

Figure 1.1.335. Fluorescence excitation spectrum of **3a** recorded in 1,2-ethanediol with emission fixed at 520 nm.

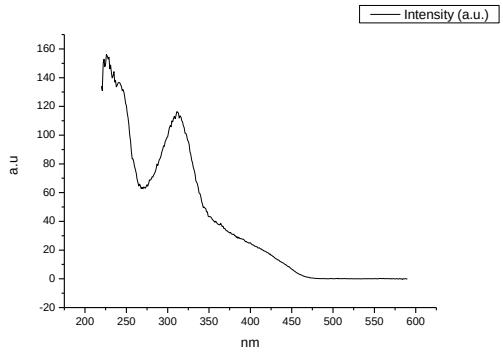

Figure 1.1.336. Fluorescence excitation spectrum of **3a** recorded in 1,2-ethanediol with emission fixed at 600 nm.

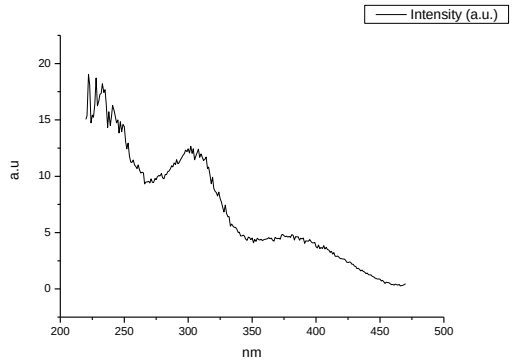

Figure 1.1.337. Fluorescence excitation spectrum of **3a** recorded in 2,2,2-trifluoroethanol with emission fixed at 480 nm.

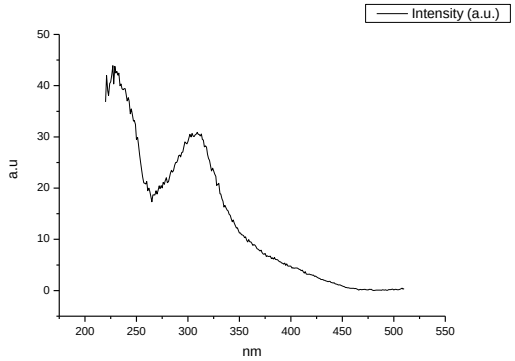

Figure 1.1.338. Fluorescence excitation spectrum of **3a** recorded in 2,2,2-trifluoroethanol with emission fixed at 520 nm.

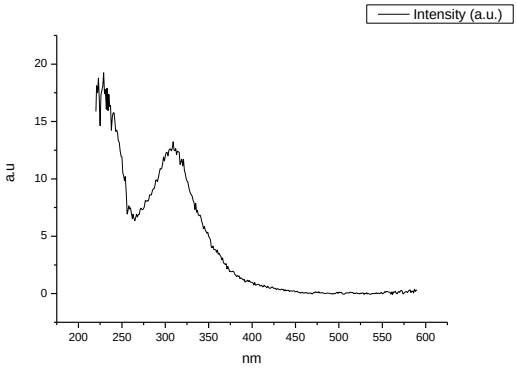

Figure 1.1.339. Fluorescence excitation spectrum of **3a** recorded in 2,2,2-trifluoroethanol with emission fixed at 600 nm.

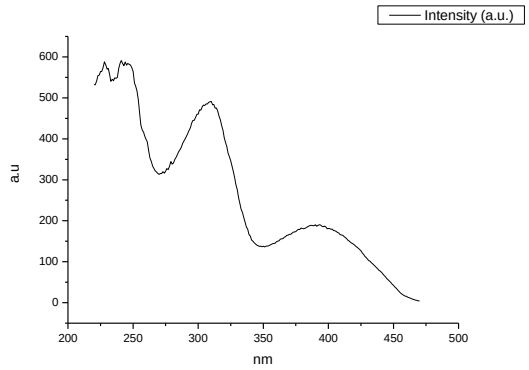

Figure 1.1.340. Fluorescence excitation spectrum of **3a** recorded in Ethanol-d_1 (EtOD) with emission fixed at 480 nm.

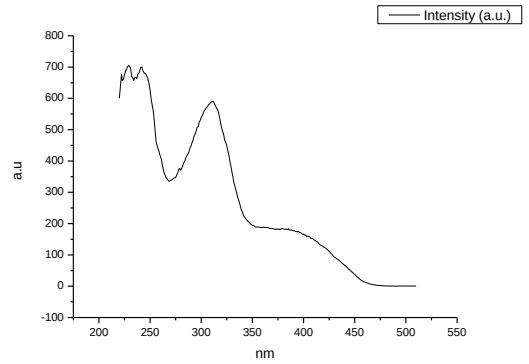

Figure 1.1.341. Fluorescence excitation spectrum of **3a** recorded in Ethanol-d_1 (EtOD) with emission fixed at 520 nm.

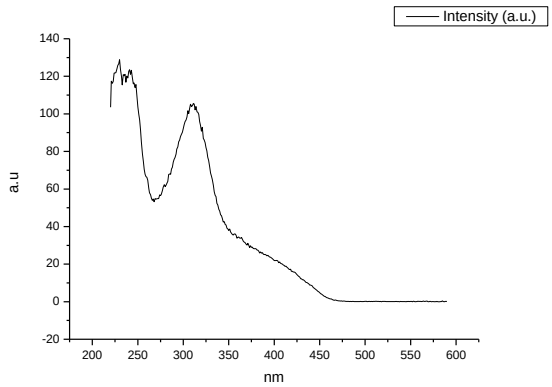

Figure 1.1.342. Fluorescence excitation spectrum of **3a** recorded in Ethanol-d_1 (EtOD) with emission fixed at 600 nm.

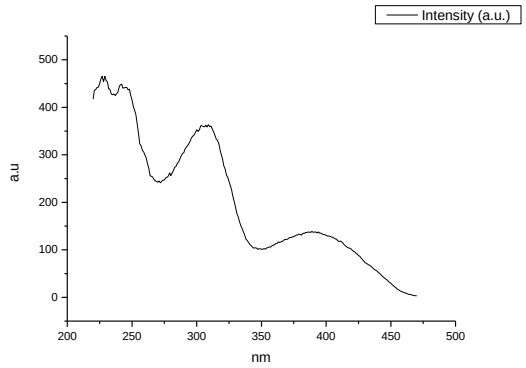

Figure 1.1.343. Fluorescence excitation spectrum of **3a** recorded in Methanol-d_1 (MeOD) with emission fixed at 480 nm.

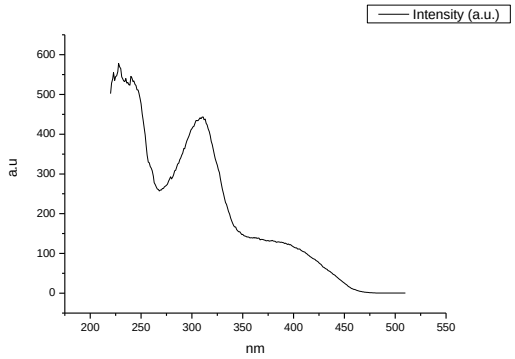

Figure 1.1.344. Fluorescence excitation spectrum of **3a** recorded in Methanol-d_1 (MeOD) with emission fixed at 520 nm.

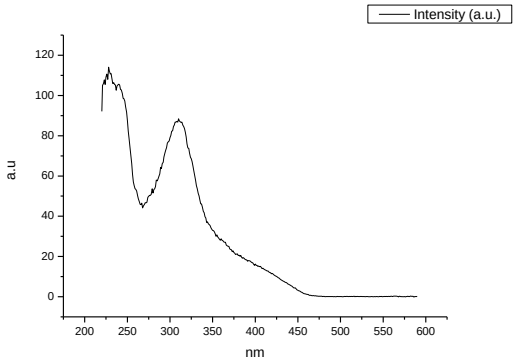

Figure 1.1.345. Fluorescence excitation spectrum of **3a** recorded in Methanol-d_1 (MeOD) with emission fixed at 600 nm.

1.2 COMPOUND 6A

1.2.1 Quantum Yield Summary.

Solvent	abs (310 nm)	$\lambda_{ems\ (max)}$	$\Phi_{310\ nm}$	abs (400 nm)	$\lambda_{ems\ (max)}$	$\Phi_{400\ nm}$
Toluene	0.06	515.00	0.65	0.01	511.96	0.64
1,4-dioxane	0.11	513.03	0.45	0.02	511.96	0.48
Ethyl acetate	0.04	511.06	0.43	0.01	504.02	0.38
Chloroform	0.08	518.93	0.51	0.02	515.00	0.51
2-methyl-2-butanol	0.04	511.96	0.39	0.01	505.97	0.35
N,N-dimethylformamide	0.12	518.03	0.44	0.02	507.01	0.48
Acetonitrile	0.07	520.00	0.42	0.01	507.01	0.39
Propylene Carbonate	0.05	516.96	0.46	0.01	521.04	0.41
1-Octanol	0.03	516.06	0.73	0.01	505.97	0.71
1-Hexanol	0.03	515.00	0.49	0.01	505.97	0.47
1-Butanol	0.04	518.03	0.46	0.01	504.02	0.41
1-Pentanol	0.05	516.06	0.53	0.01	505.97	0.47
1-Propanol	0.09	516.06	0.42	0.02	504.02	0.41
Acetic acid	0.06	505.07	0.03	0.01	495.07	0.03
1,5-Pentanediol	0.04	513.93	0.45	0.01	508.95	0.41
Ethanol	0.05	516.06	0.58	0.01	498.05	0.61
1,3-Butanediol	0.07	515.00	0.50	0.01	508.05	0.55
1,4-Butanediol	0.05	513.93	0.54	0.01	510.00	0.51
1,3-Propanediol	0.05	515.00	0.53	0.01	513.93	0.50
Methanol	0.05	518.93	0.35	0.01	505.97	0.30
Ethylene Glycol	0.05	521.04	0.75	0.01	511.06	0.93
2,2,2-Trifluoroethanol	0.04	543.97	0.04	0.01	-	0.16
Ethanol-d	0.04	513.03	0.45	0.01	511.06	0.41
Methanol-d	0.04	518.93	0.64	0.01	508.05	0.76

Table 1.2.1. Summary of ultraviolet-visible absorbance values at 310 nm and 400 nm, emission maxima and quantum yield (Φ) of **6a** at 310 nm and 400 nm excitation.

1.2.2 310 nm excitation Gaussian band fit summaries.

Solvent	λ max$_{em}$ Band 1 (cm^{-1})	λ max$_{em}$ Band 1 (nm)	λ max$_{em}$ Band 2 (cm^{-1})	λ max$_{em}$ Band 2 (nm)	λ max$_{em}$ Band 3 (cm^{-1})	λ max$_{em}$ Band 3 (nm)
Toluene	18640.84	536.46	19740.64	506.57	21145.70	472.91
1,4-Dioxane	18566.12	538.62	19733.60	506.75	21186.98	471.99
Ethyl acetate	18523.61	539.85	19798.24	505.10	21304.14	469.39
Chloroform	18464.37	541.58	19585.41	510.58	21048.43	475.09
2-Methyl-2-butanol	18714.37	534.35	19806.29	504.89	21359.38	468.18
N,N-dimethylformamide	18229.03	548.58	19584.95	510.60	21044.12	475.19
Acetonitrile	18178.36	550.10	19537.97	511.82	21077.52	474.44
Propylene carbonate	18200.51	549.44	19534.82	511.91	21000.18	476.19
1-Octanol	18413.27	543.09	19699.65	507.62	21193.53	471.84
1-Hexanol	18344.93	545.11	19662.44	508.58	21184.04	472.05
1-Butanol	18337.59	545.33	19648.51	508.94	21165.26	472.47
1-Pentanol	18328.43	545.60	19662.44	508.58	21175.19	472.25
1-Propanol	18288.99	546.78	19641.76	509.12	21151.14	472.79
Acetic acid	19276.55	518.77	20017.15	499.57	21143.88	472.95
Ethanol	18300.02	546.45	19656.05	508.75	21148.48	472.85
1,5-Pentanediol	18302.39	546.38	19648.89	508.93	21001.94	476.15
1,3-Butanediol	18372.78	544.28	19675.84	508.24	21020.75	475.72
1,4-Butanediol	18449.73	542.01	19658.42	508.69	20974.52	476.77
1,3-Propanediol	18209.34	549.17	19535.38	511.89	20883.48	478.85
Methanol	18176.61	550.16	19572.69	510.92	21101.99	473.89
1,2-Ethanediol	18039.29	554.35	19416.23	515.03	20862.17	479.34
2,2,2-Trifluoroethanol	16271.41	614.57	18418.16	542.94	-	-
Ethanol-d	18314.13	546.03	19663.35	508.56	21169.68	472.37
Methanol-d	18202.11	549.39	19581.38	510.69	21082.16	474.33

Solvent	λ max$_{em}$ Band 4 (cm^{-1})	λ max$_{em}$ Band 4 (nm)	λ max$_{em}$ Band 5 (cm^{-1})	λ max$_{em}$ Band 5 (nm)
Toluene	28037.87	356.66	-	-
1,4-Dioxane	28033.30	356.72	-	-
Ethyl acetate	28213.88	354.44	-	-
Chloroform	27854.45	359.01	-	-
2-Methyl-2-butanol	28143.87	355.32	-	-
N,N-dimethylformamide	27833.83	359.28	-	-
Acetonitrile	28142.32	355.34	-	-
Propylene carbonate	27627.91	361.95	-	-
1-Octanol	28126.97	355.53	-	-
1-Hexanol	28083.47	356.08	-	-
1-Butanol	28061.97	356.35	-	-
1-Pentanol	28050.94	356.49	-	-
1-Propanol	28036.29	356.68	-	-
Acetic acid	27215.31	367.44	28772.20	347.56
Ethanol	28127.93	355.52	-	-
1,5-Pentanediol	27874.10	358.76	-	-
1,3-Butanediol	27493.96	363.72	29095.73	343.69
1,4-Butanediol	25554.66	391.32	28185.74	354.79
1,3-Propanediol	28519.73	350.63	-	-
Methanol	28078.58	356.14	-	-
1,2-Ethanediol	-	-	-	-
2,2,2-Trifluoroethanol	25443.78	393.02	27756.70	360.27
Ethanol-d	28129.16	355.50	-	-
Methanol-d	-	-	-	-

Table 1.2.2. Summary of band maxima of 5 band fit using Gaussian model for normalised **6a** emission spectra recorded at 310 nm excitation.

(a)

Solvent	Width Band 1 (cm^{-1})	Width Band 2 (cm^{-1})	Width Band 3 (cm^{-1})	Width Band 4 (cm^{-1})	Width Band 5 (cm^{-1})
Toluene	3127.96	1863.06	957.25	3098.52	-
1,4-Dioxane	3168.12	2000.57	974.49	3096.13	-
Ethyl acetate	3226.99	2178.67	983.99	3209.40	-
Chloroform	3185.75	1965.93	1000.90	3087.44	-
2-Methyl-2-butanol	3241.28	1987.53	970.42	3159.74	-
N,N-dimethylformamide	3266.61	2309.36	1105.78	3197.15	-
Acetonitrile	3288.65	2370.99	1114.62	3147.03	-
Propylene carbonate	3299.30	2328.61	1141.05	3449.41	-
1-Octanol	3229.18	2179.26	1022.75	3238.99	-
1-Hexanol	3253.58	2249.90	1023.71	3192.40	-
1-Butanol	3248.33	2228.49	1057.80	3178.07	-
1-Pentanol	3243.07	2256.27	1024.37	3145.18	-
1-Propanol	3245.84	2276.52	1051.25	3130.01	-
Acetic acid	3309.40	1832.88	1018.02	3158.34	2100.77
Ethanol	3253.88	2274.37	1081.36	3188.16	-
1,5-Pentanediol	3247.11	2253.11	1142.55	3236.83	-
1,3-Butanediol	3297.84	2265.08	1116.93	3552.08	2585.44
1,4-Butanediol	3379.06	2282.70	1106.68	3763.17	3226.75
1,3-Propanediol	3290.28	2265.68	1144.93	3915.15	-
Methanol	3311.37	2373.65	1093.80	3211.24	-
1,2-Ethanediol	3231.28	2272.46	1098.41	-	-
2,2,2-Trifluoroethanol	2320.53	2557.16	-	4094.17	2701.87
Ethanol-d	3265.82	2285.32	1066.41	3187.62	-
Methanol-d	3244.65	2288.87	1071.98	-	-

(b)

Solvent	Area Band 1 (cm^{-1})	Area Band 2 (cm^{-1})	Area Band 3 (cm^{-1})	Area Band 4 (cm^{-1})	Area Band 5 (cm^{-1})
Toluene	2082.63	1278.15	330.83	166.26	-
1,4-Dioxane	2043.62	1430.53	287.43	155.53	-
Ethyl acetate	1983.62	1627.06	254.03	210.71	-
Chloroform	2086.05	1367.26	318.46	144.32	-
2-Methyl-2-butanol	2208.55	1309.89	267.72	212.35	-
N,N-dimethylformamide	1875.59	1864.81	305.63	153.87	-
Acetonitrile	1911.48	1888.49	256.57	194.44	-
Propylene carbonate	1922.12	1839.35	310.01	347.92	-
1-Octanol	1921.76	1675.49	303.90	194.23	-
1-Hexanol	1903.07	1780.67	280.52	198.92	-
1-Butanol	1953.68	1711.48	290.03	203.74	-
1-Pentanol	1911.29	1778.10	274.92	194.31	-
1-Propanol	1890.21	1822.71	280.66	189.90	-
Acetic acid	2582.87	827.61	322.23	1832.90	1087.42
Ethanol	1905.87	1802.83	303.87	200.35	-
1,5-Pentanediol	1799.00	1848.55	362.90	160.06	-
1,3-Butanediol	1900.68	1779.62	331.07	378.59	437.23
1,4-Butanediol	2003.39	1701.85	317.33	333.68	538.27
1,3-Propanediol	1913.61	1803.69	345.63	382.62	-
Methanol	1961.99	1889.25	268.59	240.70	-
1,2-Ethanediol	1888.13	1817.93	309.47	-	-
2,2,2-Trifluoroethanol	590.40	2855.46	-	531.53	1475.84
Ethanol-d	1940.12	1798.20	279.67	204.69	-
Methanol-d	1902.82	1830.90	288.30	-	-

(c)

Solvent	fwhm Band 1 (nm)	fwhm Band 2 (nm)	fwhm Band 3 (nm)	fwhm Band 4 (nm)	fwhm Band 5 (nm)
Toluene	104.37	58.78	25.27	48.43	-
1,4-Dioxane	111.11	58.78	25.27	43.55	-
Ethyl acetate	111.11	63.10	25.27	47.78	-
Chloroform	106.54	64.33	25.73	49.10	-
2-Methyl-2-butanol	108.85	63.10	24.83	47.78	-
N,N-dimethylformamide	120.50	74.32	29.76	49.10	-
Acetonitrile	115.84	70.00	29.76	45.68	-
Propylene carbonate	115.84	70.00	30.30	49.77	-
1-Octanol	113.44	68.65	25.27	50.53	-
1-Hexanol	113.44	68.65	25.27	48.43	-
1-Butanol	113.44	68.65	25.27	48.43	-
1-Pentanol	113.44	68.65	25.27	48.43	-
1-Propanol	113.44	74.32	29.76	48.43	-
Acetic acid	108.79	56.57	29.76	51.17	32.06
Ethanol	113.44	68.65	29.76	45.68	-
1,5-Pentanediol	113.44	68.65	34.33	49.10	-
1,3-Butanediol	113.44	68.65	34.33	55.57	35.72
1,4-Butanediol	118.01	68.65	30.30	70.08	47.78
1,3-Propanediol	115.84	70.00	30.30	58.68	-
Methanol	115.84	74.32	29.76	48.43	-
1,2-Ethanediol	118.32	75.79	30.30	-	-
2,2,2-Trifluoroethanol	115.22	95.15	-	101.61	44.15
Ethanol-d	120.50	68.65	25.27	45.68	-
Methanol-d	115.84	74.32	29.76	-	-

Tables 1.2.3 (a), (b) and (c). Summary band width, band area, full width half maximum of 5 band fit using Gaussian model for normalised **6a** emission spectra recorded at 310 nm excitation.

Solvent	Band 1 Area Percentage (%)	Band 2 Area Percentage (%)	Band 3 Area Percentage (%)	Band 4 Area Percentage(%)	Band 5 Area Percentage (%)
Toluene	53.98	33.13	8.58	4.31	-
1,4-Dioxane	52.17	36.52	7.34	3.97	-
Ethyl acetate	48.67	39.92	6.23	5.17	-
Chloroform	53.27	34.91	8.13	3.69	-
2-Methyl-2-butanol	55.23	32.76	6.70	5.31	-
N,N-dimethylformamide	44.66	44.40	7.28	3.66	-
Acetonitrile	44.97	44.42	6.04	4.57	-
Propylene carbonate	43.49	41.62	7.01	7.87	-
1-Octanol	46.93	40.91	7.42	4.74	-
1-Hexanol	45.71	42.77	6.74	4.78	-
1-Butanol	46.98	41.15	6.97	4.90	-
1-Pentanol	45.96	42.76	6.61	4.67	-
1-Propanol	45.18	43.57	6.71	4.54	-
Acetic acid	38.82	12.44	4.84	27.55	16.34
Ethanol	45.24	42.79	7.21	4.76	-
1,5-Pentanediol	43.14	44.32	8.70	3.84	-
1,3-Butanediol	39.37	36.87	6.86	7.84	9.06
1,4-Butanediol	40.93	34.77	6.48	6.82	11.00
1,3-Propanediol	43.05	40.57	7.77	8.61	-
Methanol	44.99	43.33	6.16	5.52	-
1,2-Ethanediol	47.02	45.27	7.71	-	-
2,2,2-Trifluoroethanol	10.83	52.36	-	9.75	27.06
Ethanol-d	45.95	42.58	6.62	4.85	-
Methanol-d	47.31	45.52	7.17	-	-

Table 1.2.4. Total Area Percentages of 5 band fit using Gaussian model for normalised **6a** emission spectra recorded at 310 nm excitation.

Solvent	Area Ratio Band 1/2 (310 nm ex)	Area Ratio Band 1/3 (310 nm ex)	Area Ratio Band 1/4 (310 nm ex)	Area Ratio Band 1/5 (310 nm ex)
Toluene	1.63	6.30	12.53	-
1,4-Dioxane	1.43	7.11	13.14	-
Ethyl acetate	1.22	7.81	9.41	-
Chloroform	1.53	6.55	14.45	-
2-Methyl-2-butanol	1.69	8.25	10.40	-
N,N-dimethylformamide	1.01	6.14	12.19	-
Acetonitrile	1.01	7.45	9.83	-
Propylene carbonate	1.05	6.20	5.52	-
1-Octanol	1.15	6.32	9.89	-
1-Hexanol	1.07	6.78	9.57	-
1-Butanol	1.14	6.74	9.59	-
1-Pentanol	1.07	6.95	9.84	-
1-Propanol	1.04	6.73	9.95	-
Acetic acid	3.12	8.02	1.41	2.38
Ethanol	1.06	6.27	9.51	-
1,5-Pentanediol	0.97	4.96	11.24	-
1,3-Butanediol	1.07	5.74	5.02	4.35
1,4-Butanediol	1.18	6.31	6.00	3.72
1,3-Propanediol	1.06	5.54	5.00	-
Methanol	1.04	7.30	8.15	-
1,2-Ethanediol	1.04	6.10	-	-
2,2,2-Trifluoroethanol	-	-	1.11	0.40
Ethanol-d	1.08	6.94	9.48	-
Methanol-d	1.04	6.60	-	-

Solvent	Area Ratio Band 2/3 (310 nm ex)	Area Ratio Band 2/4 (310 nm ex)	Area Ratio Band 2/5 (310 nm ex)	Area Ratio Band ¾ (310 nm ex)	Area Ratio Band 3/5 (310 nm ex)	Area Ratio Band 4/5 (310 nm ex)
Toluene	3.86	7.69	-	1.99	-	-
1,4-Dioxane	4.98	9.20	-	1.85	-	-
Ethyl acetate	6.40	7.72	-	1.21	-	-
Chloroform	4.29	9.47	-	2.21	-	-
2-Methyl-2-butanol	4.89	6.17	-	1.26	-	-
N,N-dimethylformamide	6.10	12.12	-	1.99	-	-
Acetonitrile	7.36	9.71	-	1.32	-	-
Propylene carbonate	5.93	5.29	-	0.89	-	-
1-Octanol	5.51	8.63	-	1.56	-	-
1-Hexanol	6.35	8.95	-	1.41	-	-
1-Butanol	5.90	8.40	-	1.42	-	-
1-Pentanol	6.47	9.15	-	1.41	-	-
1-Propanol	6.49	9.60	-	1.48	-	-
Acetic acid	2.57	0.45	0.76	0.18	0.30	1.69
Ethanol	5.93	9.00	-	1.52	-	-
1,5-Pentanediol	5.09	11.55	-	2.27	-	-
1,3-Butanediol	5.38	4.70	4.07	0.87	0.76	0.87
1,4-Butanediol	5.36	5.10	3.16	0.95	0.59	0.62
1,3-Propanediol	5.22	4.71	-	0.90	-	-
Methanol	7.03	7.85	-	1.12	-	-
1,2-Ethanediol	5.87	-	-	-	-	-
2,2,2-Trifluoroethanol	-	5.37	1.93	-	-	0.36
Ethanol-d	6.43	8.78	-	1.37	-	-
Methanol-d	6.35	-	-	-	-	-

Table 1.2.5. Area Ratios of 5 band fit using Gaussian model for normalised **6a** emission spectra recorded at 310 nm excitation.

1.2.3 400 nm excitation Gaussian band fit summaries.

Solvent	λ max$_{em}$ Band 1 (cm^{-1})	λ max$_{em}$ Band 1nm)	λ max$_{em}$ Band 2 (cm^{-1})	λ max$_{em}$ Band 2 (nm)	λ max$_{em}$ Band 3 (cm^{-1})	λ max$_{em}$ Band 3 (nm)
Toluene	18656.36	536.01	19839.39	504.05	21120.63	473.47
1,4-Dioxane	18572.75	538.42	19865.17	503.39	21149.14	472.83
Ethyl acetate	18598.67	537.67	19947.75	501.31	21252.45	470.53
Chloroform	18467.31	541.50	19726.87	506.92	21020.26	475.73
2-Methyl-2-butanol	18694.65	534.91	19999.62	500.01	21323.65	468.96
N,N-dimethylformamide	18404.22	543.35	19732.77	506.77	21004.09	476.10
Acetonitrile	18344.10	545.13	19709.87	507.36	20996.60	476.27
Propylene carbonate	18368.96	544.40	19708.11	507.41	20968.58	476.90
1-Octanol	18518.96	539.99	19866.74	503.35	21155.22	472.70
1-Hexanol	18494.14	540.71	19843.88	503.93	21133.37	473.19
1-Butanol	18482.72	541.05	19838.40	504.07	21108.16	473.75
1-Pentanol	18487.79	540.90	19840.52	504.02	21126.87	473.33
1-Propanol	18456.60	541.81	19818.29	504.58	21092.71	474.10
Acetic acid	19817.89	504.59	20942.08	477.51	25133.87	397.87
Ethanol	18493.83	540.72	19855.44	503.64	21098.88	473.96
1,5-Pentanediol	18362.78	544.58	19709.47	507.37	20954.93	477.21
1,3-Butanediol	18398.04	543.54	19741.45	506.55	20981.26	476.62
1,4-Butanediol	18453.37	541.91	19726.97	506.92	20939.42	477.57
1,3-Propanediol	18285.03	546.90	19622.46	509.62	20847.23	479.68
Methanol	18397.72	543.55	19752.82	506.26	21013.66	475.88
1,2-Ethanediol	18245.90	548.07	19592.29	510.40	20817.99	480.35
2,2,2-Trifluoroethanol	17150.39	583.08	18921.62	528.50	20474.76	488.41
Ethanol-d	18499.93	540.54	19862.62	503.46	21123.45	473.41
Methanol-d	18446.93	542.10	19796.09	505.15	21016.57	475.82

Table 1.2.6. Summary of band maxima of 3 band fit using Gaussian model for normalised **6a** emission spectra recorded at 400 nm excitation.

Solvent	fwhm Band 1 (nm)	fwhm Band 2 (nm)	Fwhm Band 3 (nm)	Width Band 1 (cm^{-1})	Width Band 2 (cm^{-1})	Width Band 3 (cm^{-1})
Toluene	104.85	57.89	26.88	3084.01	1928.31	1010.74
1,4-Dioxane	109.12	64.03	26.88	3097.21	2050.13	1025.65
Ethyl acetate	192.80	66.70	29.40	3174.80	2139.37	1069.76
Chloroform	110.56	62.09	27.19	3119.41	2038.37	1038.95
2-Methyl-2-butanol	107.71	63.26	29.07	3167.01	2102.85	1036.58
N,N-dimethylformamide	114.96	68.35	32.63	3225.75	2202.41	1193.92
Acetonitrile	114.96	68.35	35.56	3219.13	2229.55	1263.53
Propylene carbonate	114.96	68.35	35.56	3211.23	2188.68	1207.29
1-Octanol	109.12	64.03	29.40	3130.93	2109.69	1088.24
1-Hexanol	113.46	64.03	32.26	3165.09	2132.69	1144.88
1-Butanol	110.56	67.52	29.74	3170.49	2147.30	1153.04
1-Pentanol	113.46	64.03	32.26	3139.72	2128.11	1140.05
1-Propanol	110.56	64.82	29.74	3146.29	2141.68	1173.02
Acetic acid	92.43	41.05	97.20	2954.37	1297.19	5966.89
Ethanol	110.56	64.03	35.16	3135.53	2130.05	1188.00
1,5-Pentanediol	107.63	68.35	35.56	3153.16	2155.55	1238.79
1,3-Butanediol	110.56	64.82	35.56	3166.73	2156.78	1209.20
1,4-Butanediol	110.56	68.35	35.56	3266.08	2202.21	1204.73
1,3-Propanediol	112.03	65.62	35.98	3186.07	2156.75	1229.08
Methanol	107.63	64.82	35.56	3209.04	2192.65	1288.04
1,2-Ethanediol	109.06	65.62	33.39	3146.65	2118.93	1179.37
2,2,2-Trifluoroethanol	86.48	77.54	54.54	1296.46	1922.45	1264.56
Ethanol-d	106.22	64.03	32.26	3131.52	2142.00	1172.12
Methanol-d	110.56	64.82	32.63	3131.92	2118.35	1195.76

Table 1.2.7. Summary of full width half maximum (fwhm) and band width of 3 band fit using Gaussian model for normalised **6a** emission spectra recorded at 400 nm excitation.

Solvent	Area Band 1 (cm^{-1})	Area Band 2 (cm^{-1})	Area Band 3 (cm^{-1})	Area Ratio Band 1/2 (400 nm ex)	Area Ratio Band 1/3 (400 nm ex)	Area Ratio Band 2/3 (400 nm ex)
Toluene	1794.42	1503.12	434.16	1.19	4.13	3.46
1,4-Dioxane	1725.92	1673.24	378.99	1.03	4.55	4.41
Ethyl acetate	1670.70	1807.19	394.84	0.92	4.23	4.58
Chloroform	1717.93	1656.28	409.20	1.04	4.20	4.05
2-Methyl-2-butanol	1754.70	1693.92	364.41	1.04	4.82	4.65
N,N-dimethylformamide	1692.33	1826.98	437.09	0.93	3.87	4.18
Acetonitrile	1599.78	1874.45	466.89	0.85	3.43	4.01
Propylene carbonate	1654.55	1819.23	448.88	0.91	3.69	4.05
1-Octanol	1657.53	1753.48	426.98	0.95	3.88	4.11
1-Hexanol	1651.19	1775.89	435.89	0.93	3.79	4.07
1-Butanol	1627.25	1809.58	439.97	0.90	3.70	4.11
1-Pentanol	1635.15	1802.32	448.32	0.91	3.65	4.02
1-Propanol	1602.23	1826.13	473.77	0.88	3.38	3.85
Acetic acid	2889.95	405.04	1055.93	7.14	2.74	0.38
Ethanol	1611.58	1801.81	477.86	0.89	3.37	3.77
1,5-Pentanediol	1520.19	2155.55	515.72	0.71	2.95	4.18
1,3-Butanediol	1567.66	1817.05	487.64	0.86	3.21	3.73
1,4-Butanediol	1633.64	1798.82	446.60	0.91	3.66	4.03
1,3-Propanediol	1550.98	1792.65	479.53	0.87	3.23	3.74
Methanol	1539.20	1842.25	534.83	0.84	2.88	3.44
1,2-Ethanediol	1567.77	1781.03	486.20	0.88	3.22	3.66
2,2,2-Trifluoroethanol	259.45	1423.36	492.00	0.18	0.53	2.89
Ethanol-d	1658.97	1782.78	452.65	0.93	3.67	3.94
Methanol-d	1537.58	1787.38	517.79	0.86	2.97	3.45

Solvent	Band 1 Area Percentage (%)	Band 2 Area Percentage (%)	Band 3 Area Percentage (%)
Toluene	48.09	40.28	11.63
1,4-Dioxane	45.68	44.29	10.03
Ethyl acetate	43.14	46.66	10.20
Chloroform	45.41	43.78	10.82
2-Methyl-2-butanol	46.02	44.42	9.56
N,N-dimethylformamide	42.77	46.18	11.05
Acetonitrile	40.59	47.56	11.85
Propylene carbonate	42.18	46.38	11.44
1-Octanol	43.19	45.88	11.13
1-Hexanol	42.74	45.97	11.28
1-Butanol	41.97	46.68	11.35
1-Pentanol	42.08	46.38	11.54
1-Propanol	41.06	46.80	12.14
Acetic acid	66.42	9.31	24.27
Ethanol	41.42	46.30	12.28
1,5-Pentanediol	36.27	51.43	12.30
1,3-Butanediol	40.48	46.92	12.59
1,4-Butanediol	42.11	46.37	11.51
1,3-Propanediol	40.57	46.89	12.54
Methanol	39.30	47.04	13.66
1,2-Ethanediol	40.88	46.44	12.68
2,2,2-Trifluoroethanol	11.93	65.45	22.62
Ethanol-d	42.60	45.78	11.62
Methanol-d	40.01	46.51	13.47

Table 1.2.8. Band area, area ratios and total area percentage of 3 band fit using Gaussian model for normalised **6a** emission spectra recorded at 400 nm excitation.

1.2.4 310 nm Gaussian band fit - Solvatochromic analysis.

1.2.4.1 E_T^N.

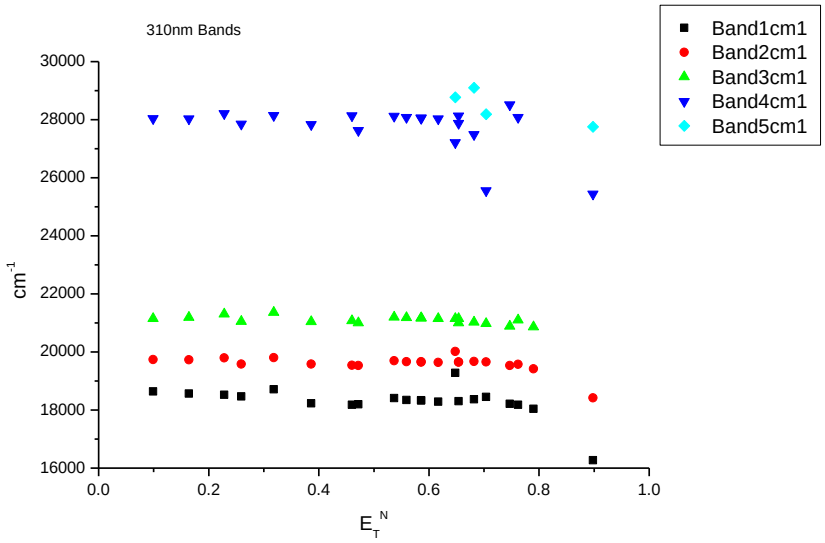

Figure 1.2.1. Band maxima from Gaussian model fit of the normalised fluorescence emission spectra of **6a** recorded at 310 nm excitation against E_T^N.

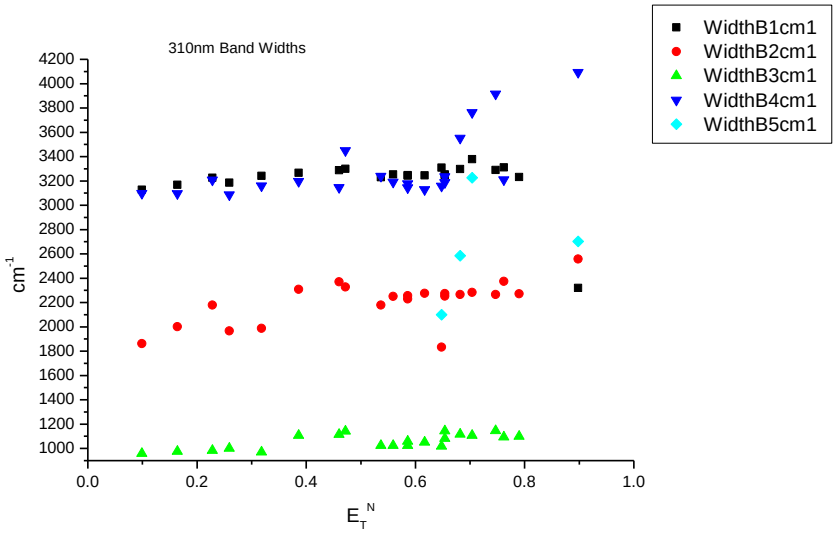

Figure 1.2.2. Band widths from Gaussian model fit of the normalised fluorescence emission spectra of **6a** recorded at 310 nm excitation against E_T^N.

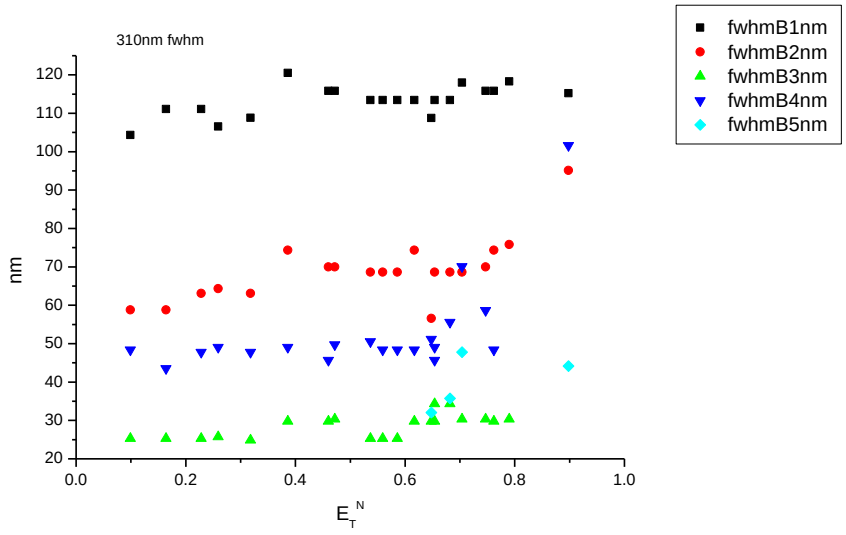

Figure 1.2.3. Full width half maxima of each band from Gaussian model fit of the normalised fluorescence emission spectra of **6a** recorded at 310 nm excitation against E_T^N.

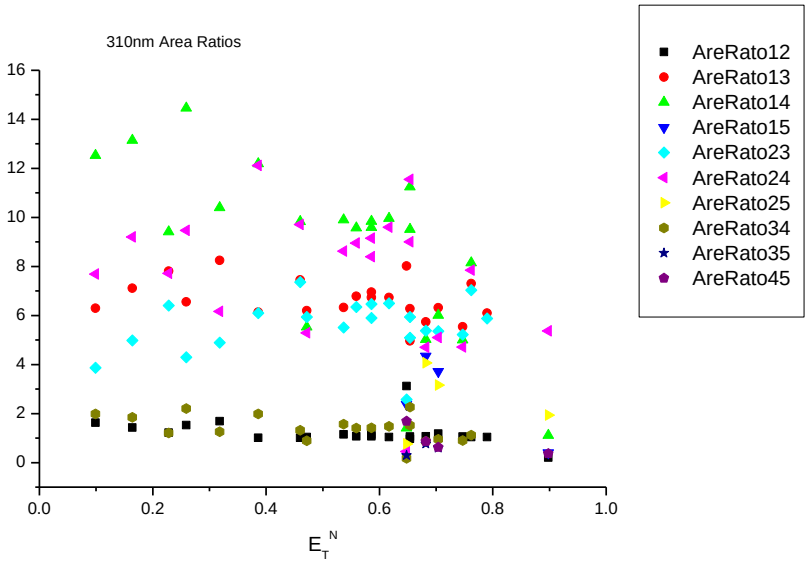

Figure 1.2.4. Area ratios from Gaussian model fit of the normalised fluorescence emission spectra of **6a** recorded at 310 nm excitation against E_T^N.

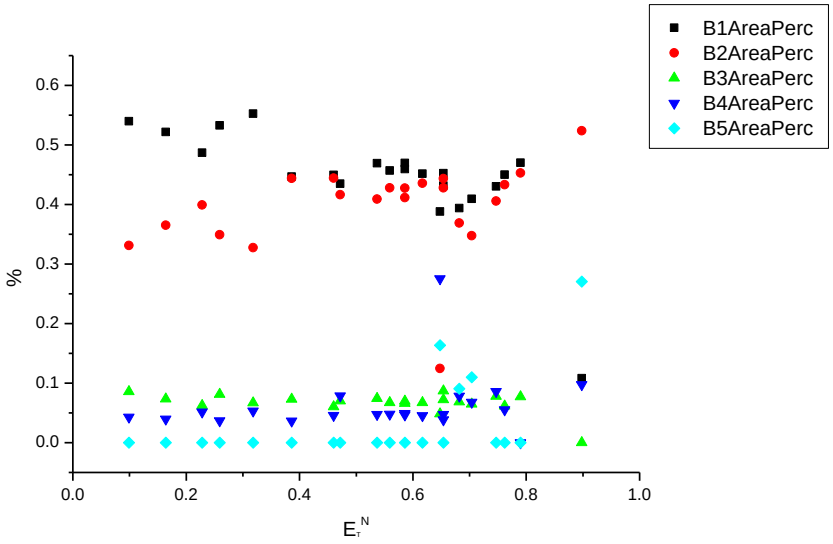

Figure 1.2.5. Area percentages from Gaussian model fit of the normalised fluorescence emission spectra of **6a** recorded at 310 nm excitation against E_T^N.

1.2.4.2 α

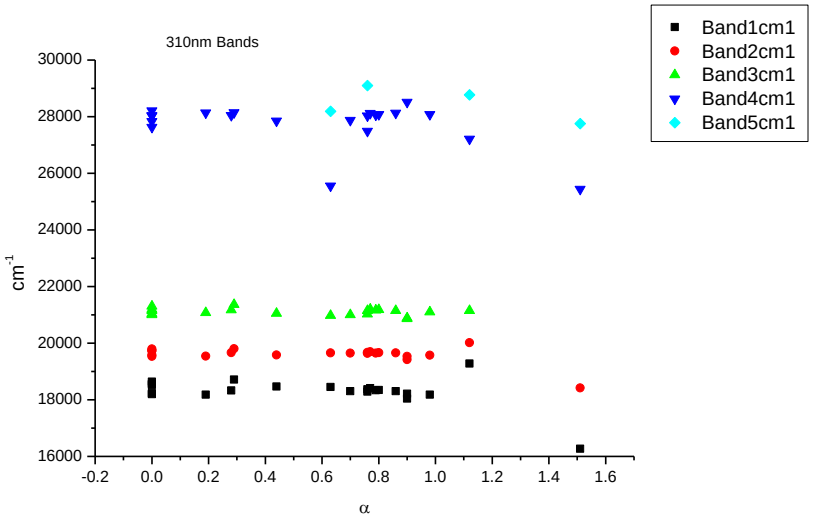

Figure 1.2.6. Band maxima from Gaussian model fit of the normalised fluorescence emission spectra of **6a** recorded at 310 nm excitation against α.

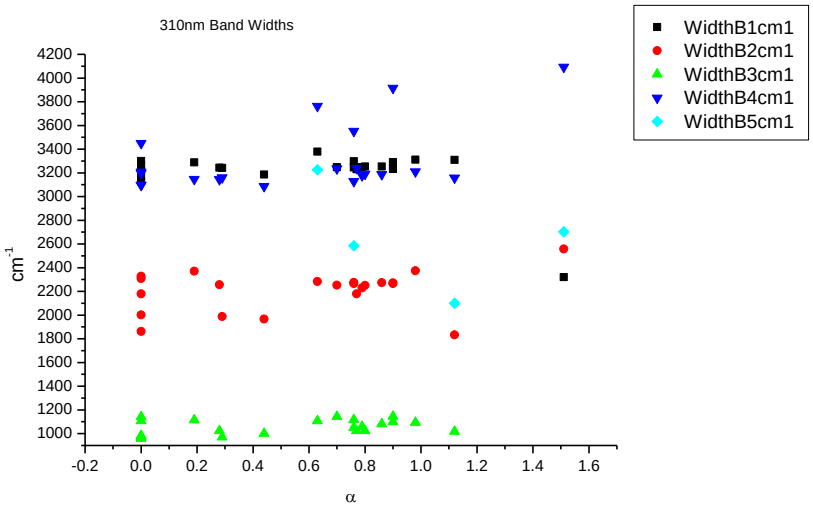

Figure 1.2.7. Band widths from Gaussian model fit of the normalised fluorescence emission spectra of **6a** recorded at 310 nm excitation against α.

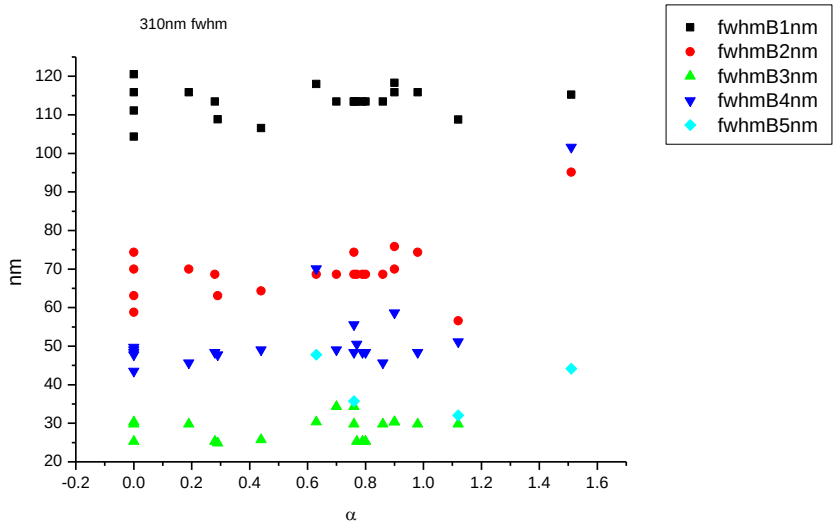

Figure 1.2.8. Full width half maxima from Gaussian model fit of the normalised fluorescence emission spectra of **6a** recorded at 310 nm excitation against α.

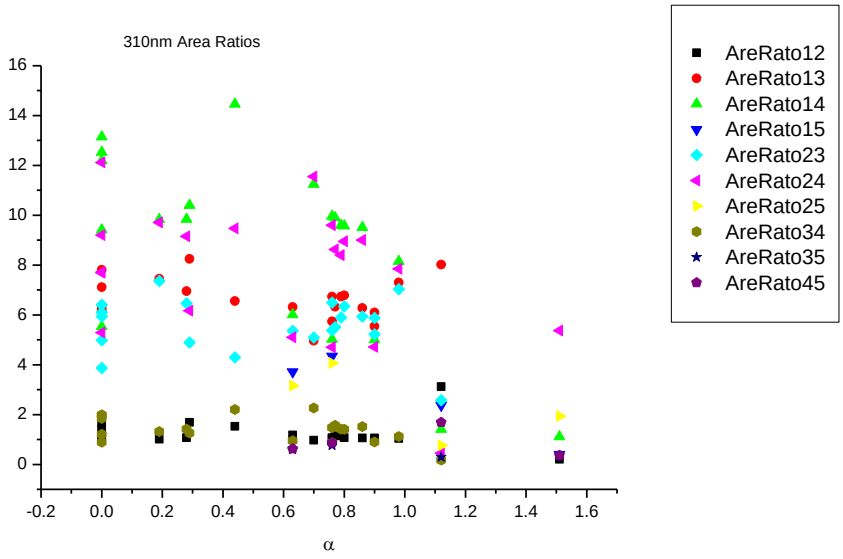

Figure 1.2.9. Area Ratios from Gaussian model fit of the normalised fluorescence emission spectra of **6a** recorded at 310 nm excitation against α.

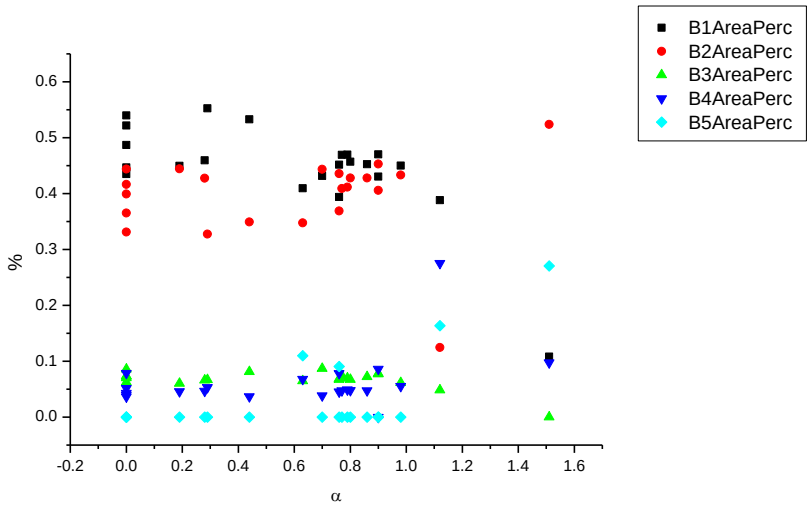

Figure 1.2.10. Area percentages from Gaussian model fit of the normalised fluorescence emission spectra of **6a** recorded at 310 nm excitation against α.

1.2.4.3 β.

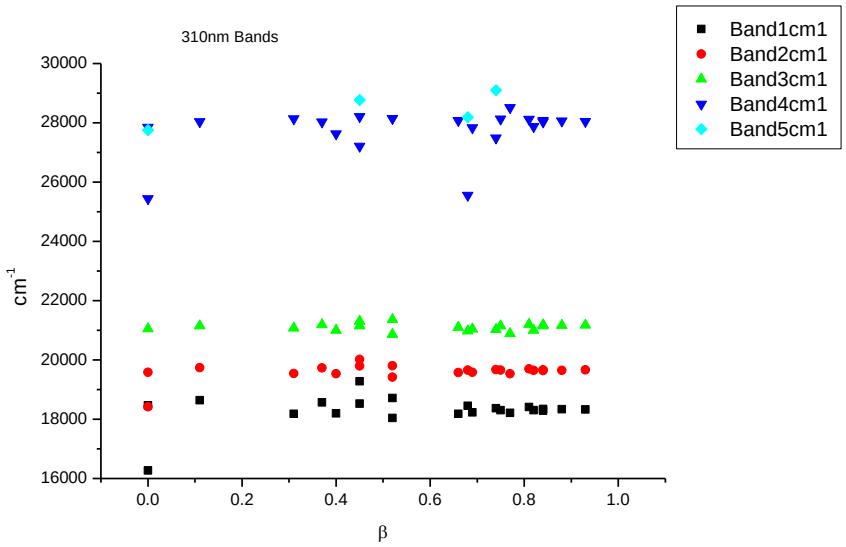

Figure 1.2.11. Band maxima from Gaussian model fit of the normalised fluorescence emission spectra of **6a** recorded at 310 nm excitation against β.

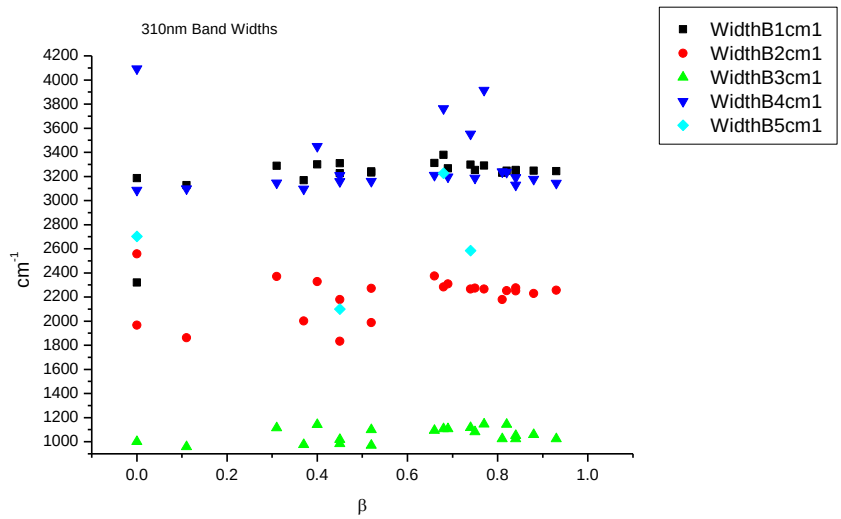

Figure 1.2.12. Band widths from Gaussian model fit of the normalised fluorescence emission spectra of **6a** recorded at 310 nm excitation against β.

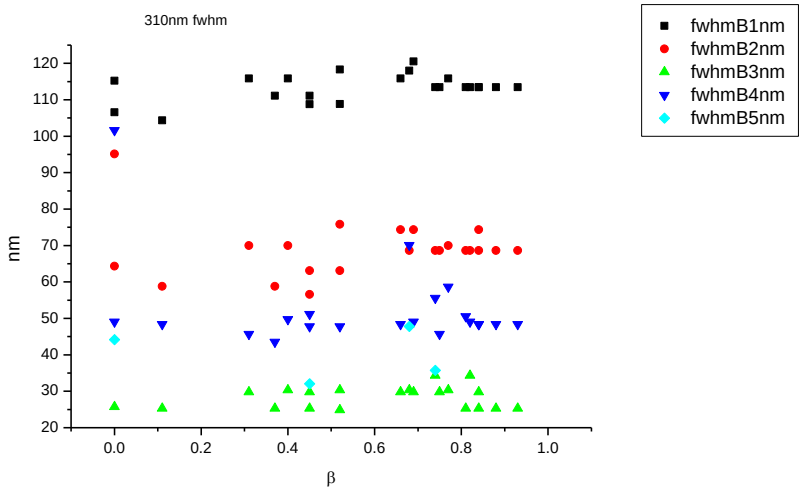

Figure 1.2.13. Full width half maxima from Gaussian model fit of the normalised fluorescence emission spectra of **6a** recorded at 310 nm excitation against β.

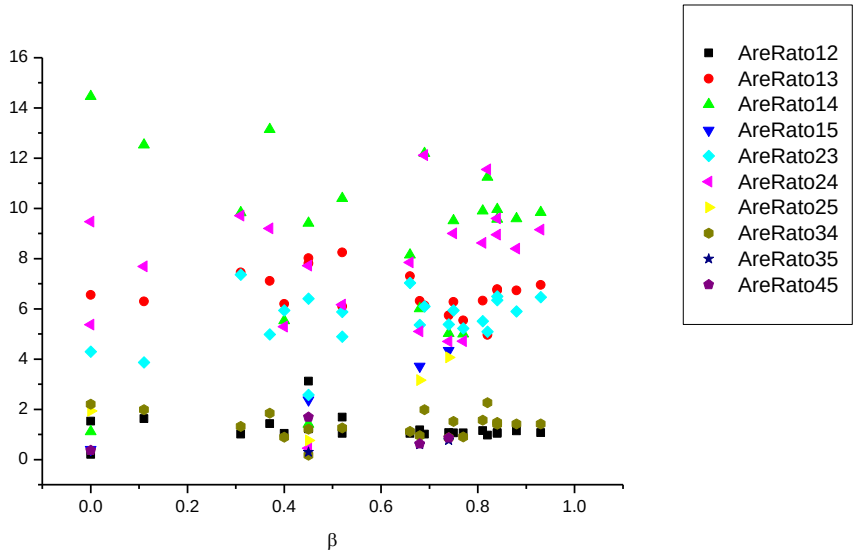

Figure 1.2.14. Area ratios from Gaussian model fit of the normalised fluorescence emission spectra of **6a** recorded at 310 nm excitation against β.

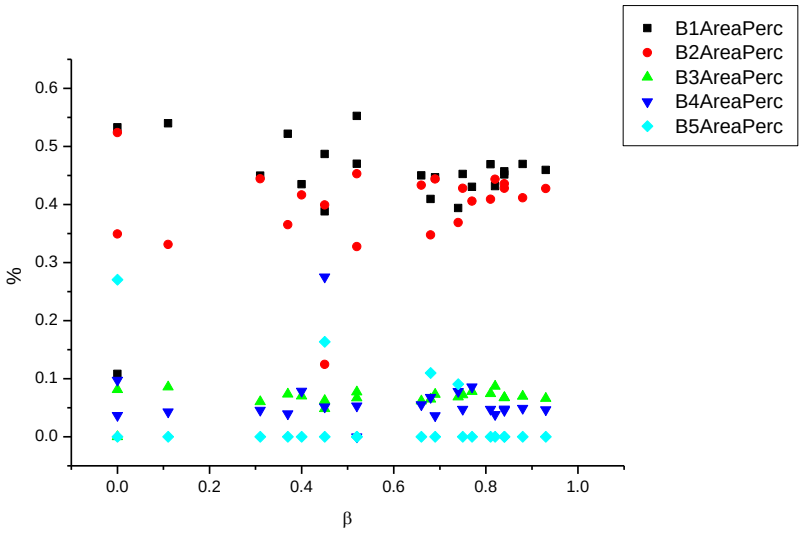

Figure 1.2.15. Area percentages from Gaussian model fit of the normalised fluorescence emission spectra of **6a** recorded at 310 nm excitation against β.

1.2.4.4 π.*

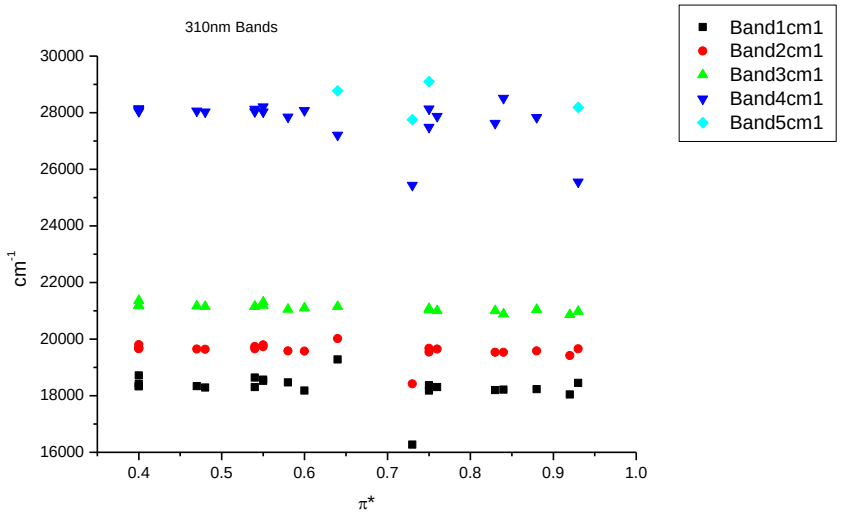

Figure 1.2.16. Band maxima from Gaussian model fit of the normalised fluorescence emission spectra of **6a** recorded at 310 nm excitation against π*.

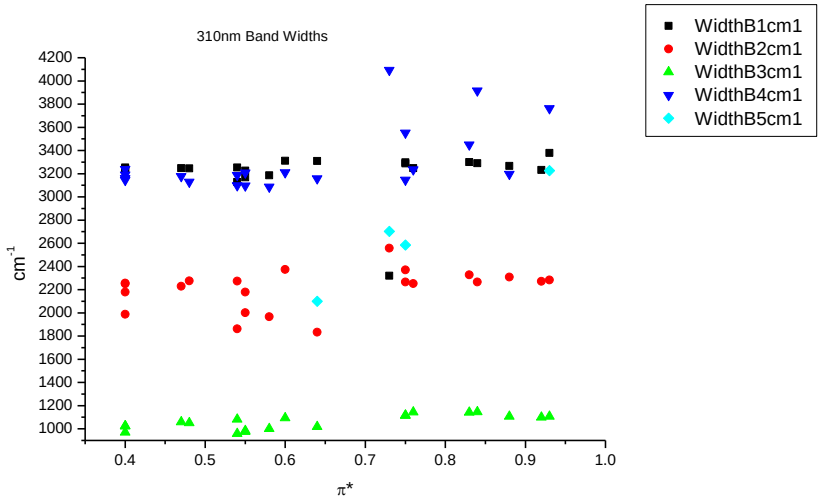

Figure 1.2.17. Band widths from Gaussian model fit of the normalised fluorescence emission spectra of **6a** recorded at 310 nm excitation against π*.

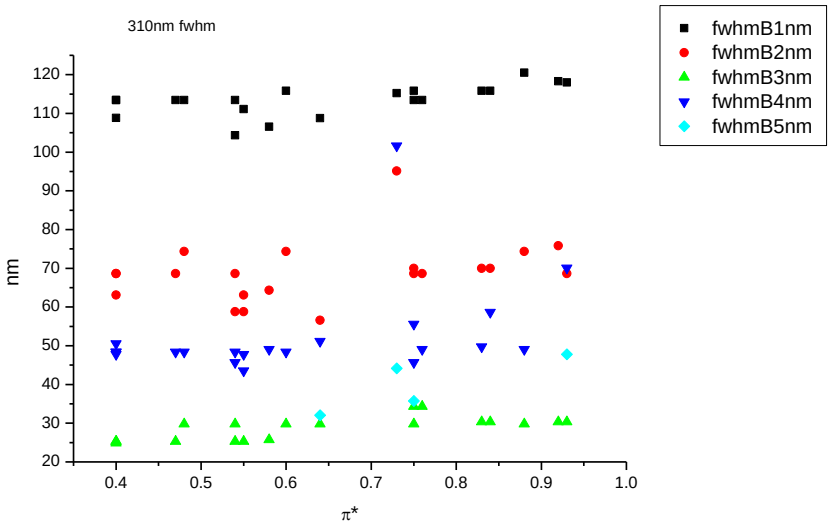

Figure 1.2.18. Full width half maxima from Gaussian model fit of the normalised fluorescence emission spectra of **6a** recorded at 310 nm excitation against π*.

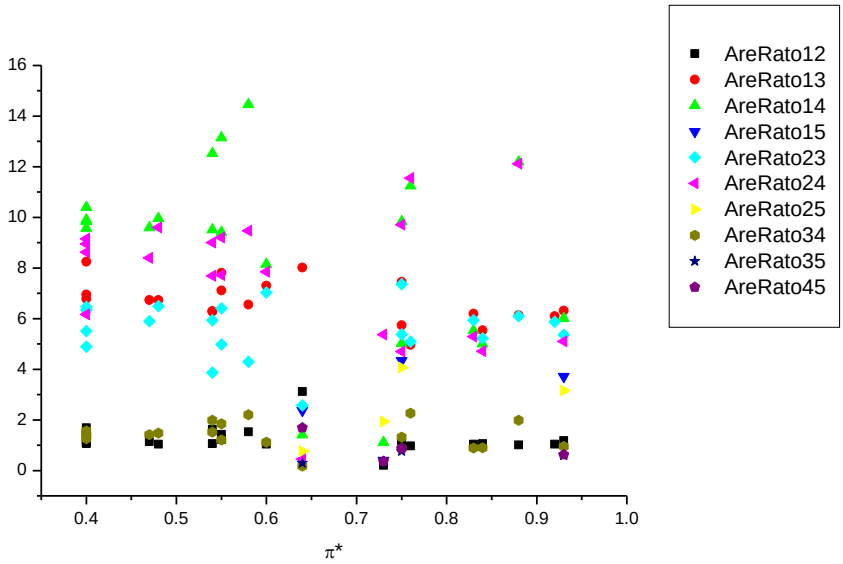

Figure 1.2.19. Area ratios from Gaussian model fit of the normalised fluorescence emission spectra of **6a** recorded at 310 nm excitation against π*.

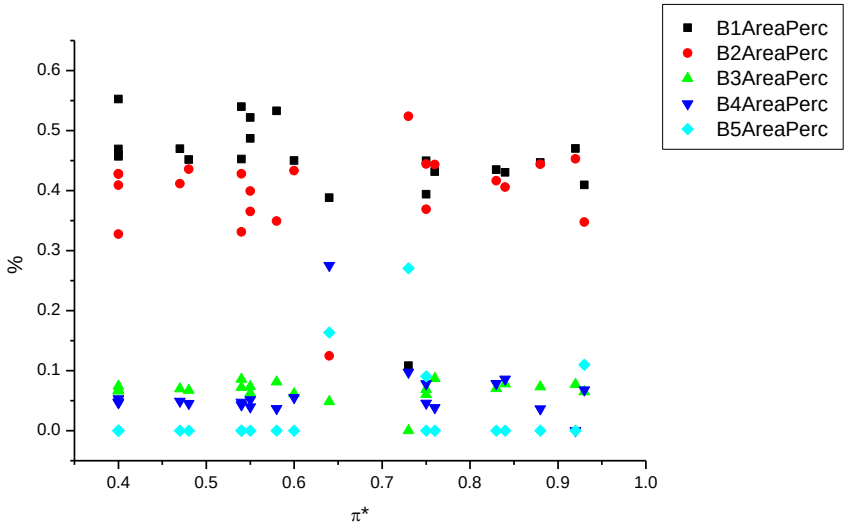

Figure 1.2.20. Area percentages from Gaussian model fit of the normalised fluorescence emission spectra of **6a** recorded at 310 nm excitation against π*.

1.2.4.5 μ(D).

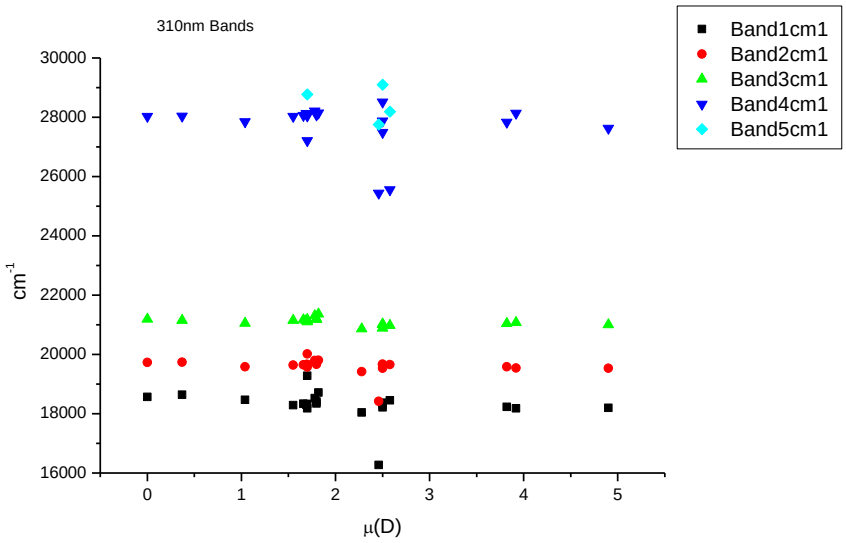

Figure 1.2.21. Band maxima from Gaussian model fit of the normalised fluorescence emission spectra of **6a** recorded at 310 nm excitation against μ(D).

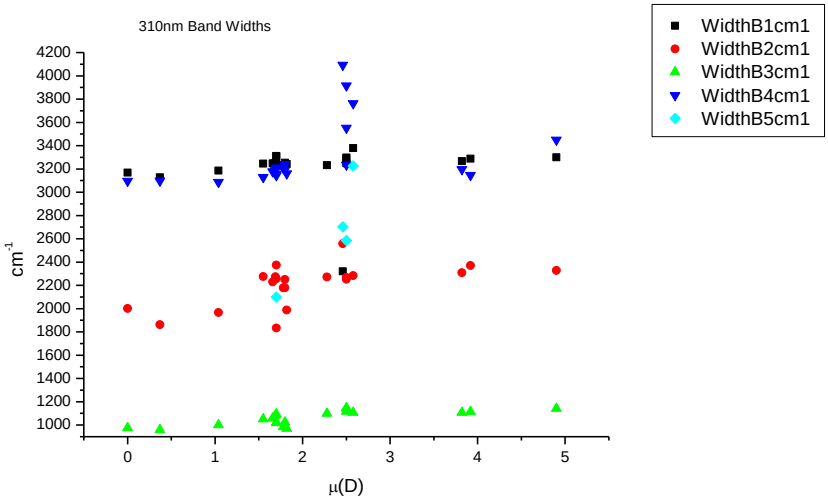

Figure 1.2.22. Band widths from Gaussian model fit of the normalised fluorescence emission spectra of **6a** recorded at 310 nm excitation against μ(D).

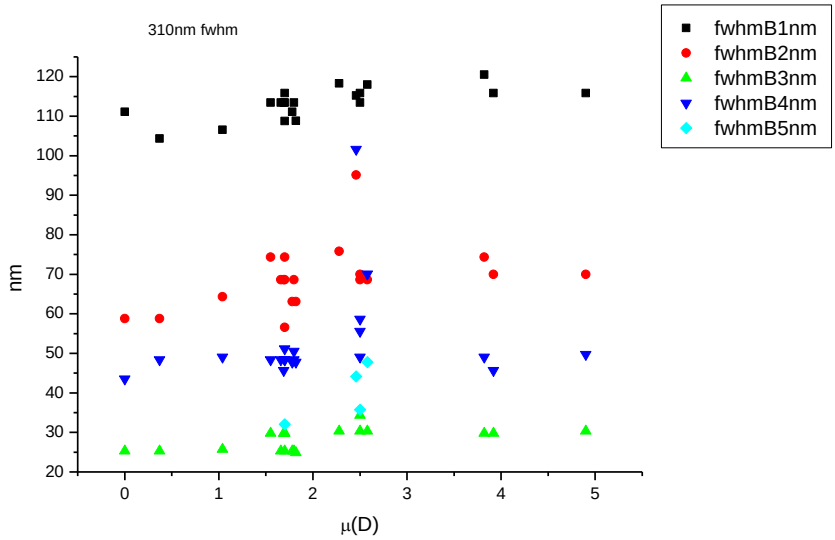

Figure 1.2.23. Full width half maxima from Gaussian model fit of the normalised fluorescence emission spectra of **6a** recorded at 310 nm excitation against μ(D).

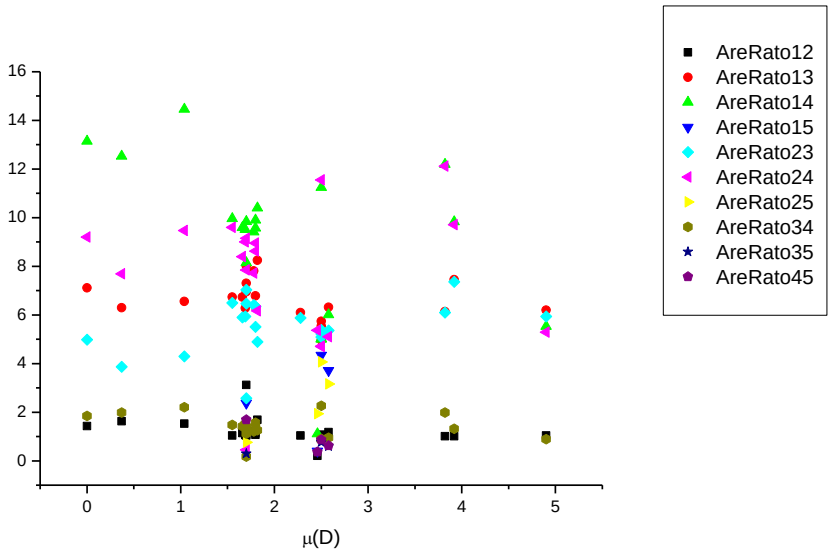

Figure 1.2.24. Area ratios from Gaussian model fit of the normalised fluorescence emission spectra of **6a** recorded at 310 nm excitation against μ(D).

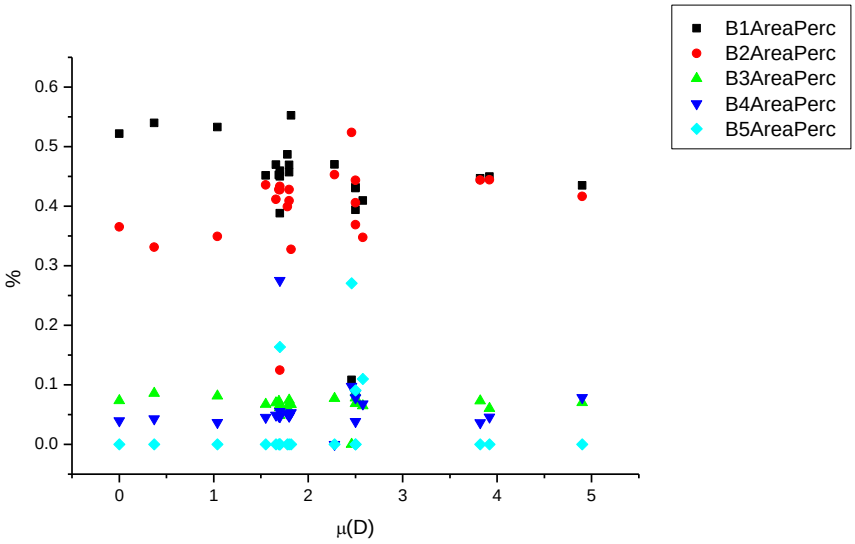

Figure 1.2.25. Area percentages from Gaussian model fit of the normalised fluorescence emission spectra of **6a** recorded at 310 nm excitation against μ(D).

1.2.4.6 η(Cp).

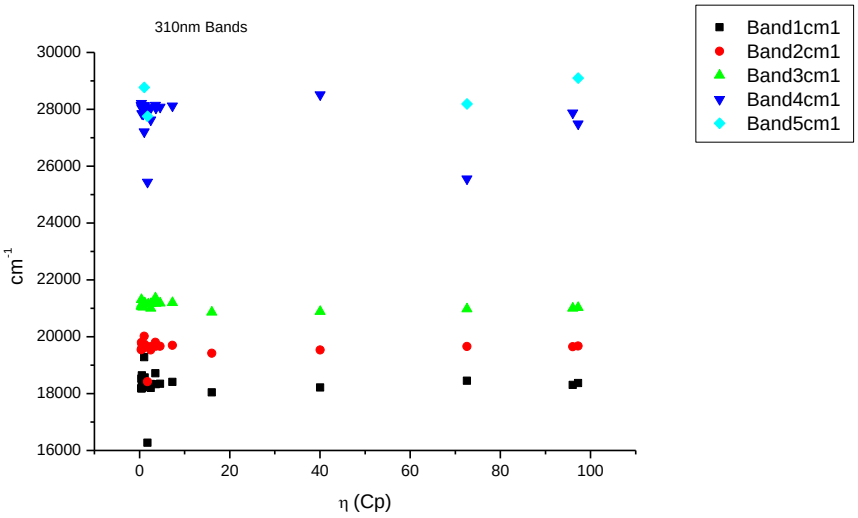

Figure 1.2.26. Band maxima from Gaussian model fit of the normalised fluorescence emission spectra of **6a** recorded at 310 nm excitation against η(Cp).

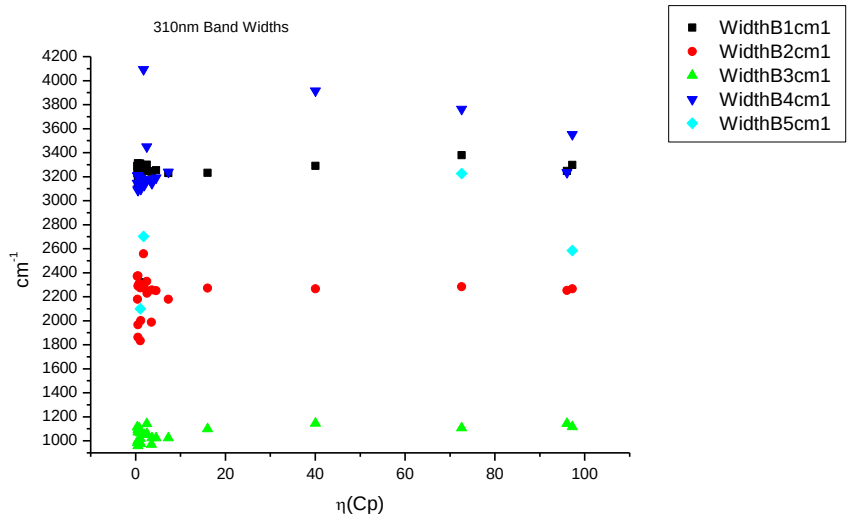

Figure 1.2.27. Band widths from Gaussian model fit of the normalised fluorescence emission spectra of **6a** recorded at 310 nm excitation against η(Cp).

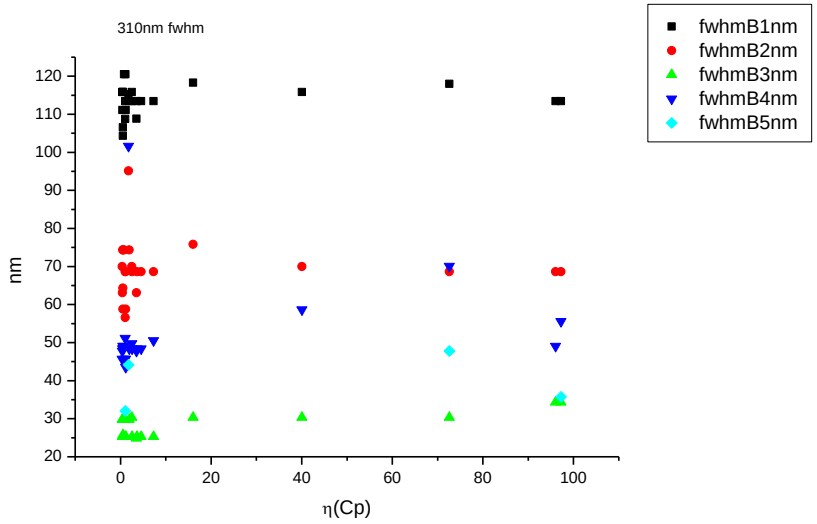

Figure 1.2.28. Full width half maxima from Gaussian model fit of the normalised fluorescence emission spectra of **6a** recorded at 310 nm excitation against η(Cp).

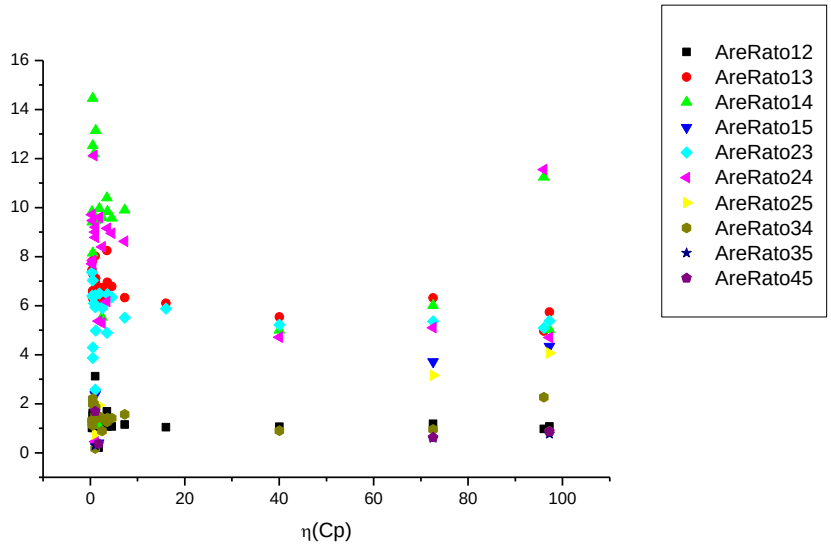

Figure 1.2.29. Area ratios from Gaussian model fit of the normalised fluorescence emission spectra of **6a** recorded at 310 nm excitation against η(Cp).

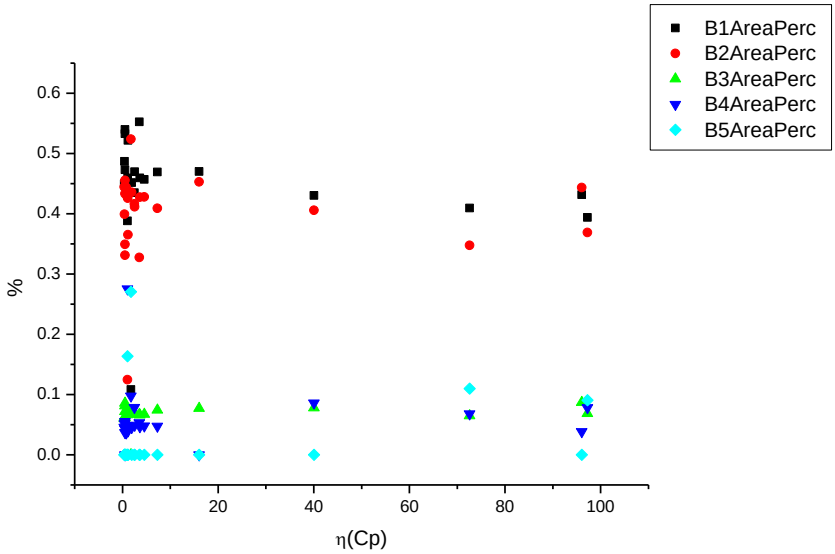

Figure 1.2.30. Area percentages from Gaussian model fit of the normalised fluorescence emission spectra of **6a** recorded at 310 nm excitation against η(Cp).

1.2.5 400 nm Gaussian band fit - Solvatochromic analysis.

1.2.5.1 E_T^N.

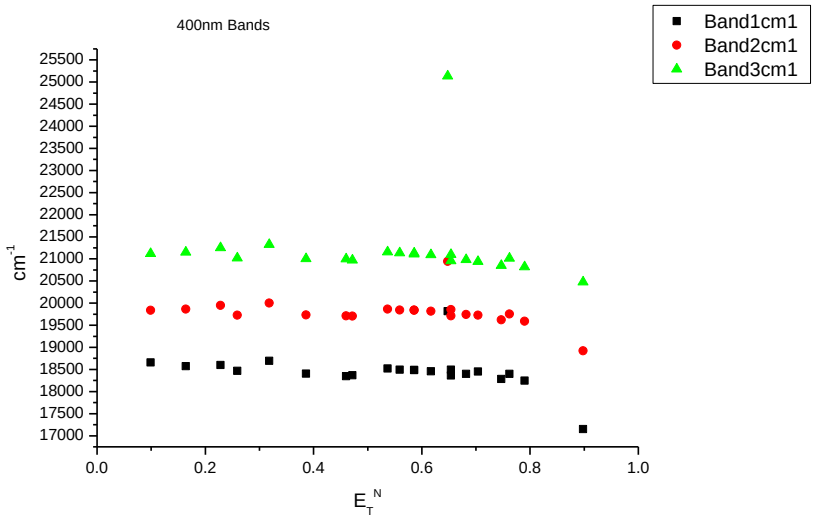

Figure 1.2.31. Band maxima from Gaussian model fit of the normalised fluorescence emission spectra of **6a** recorded at 400 nm excitation against E_T^N.

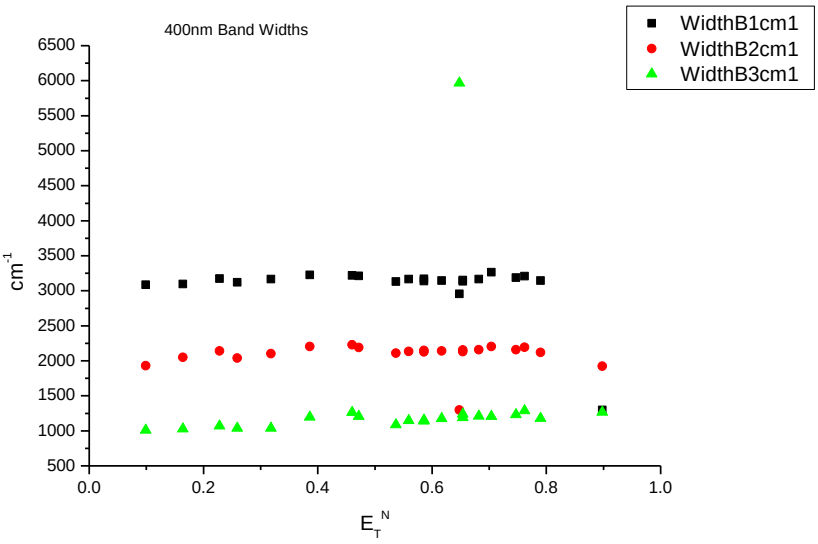

Figure 1.2.32. Band widths from Gaussian model fit of the normalised fluorescence emission spectra of **6a** recorded at 400 nm excitation against E_T^N.

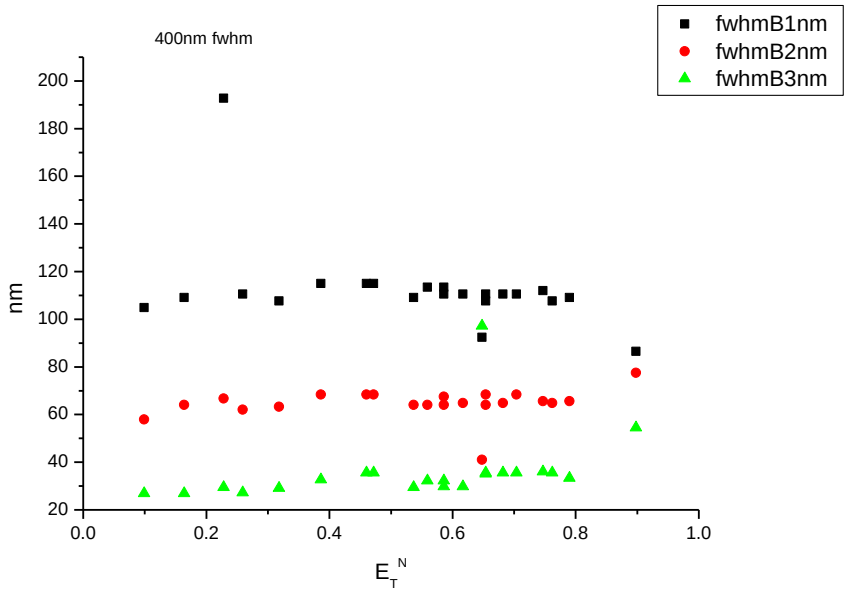

Figure 1.2.33. Full width half maxima from Gaussian model fit of the normalised fluorescence emission spectra of **6a** recorded at 400 nm excitation against E_T^N.

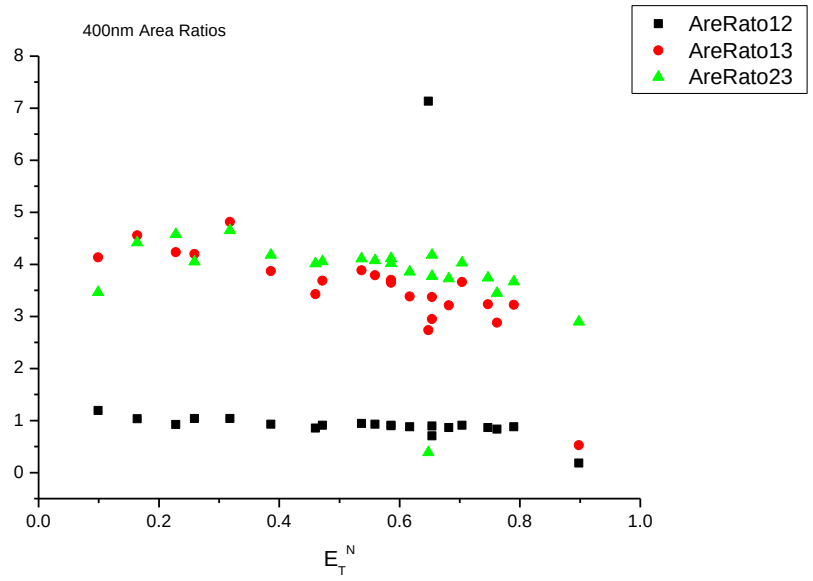

Figure 1.2.34. Area ratios from Gaussian model fit of the normalised fluorescence emission spectra of **6a** recorded at 400 nm excitation against E_T^N.

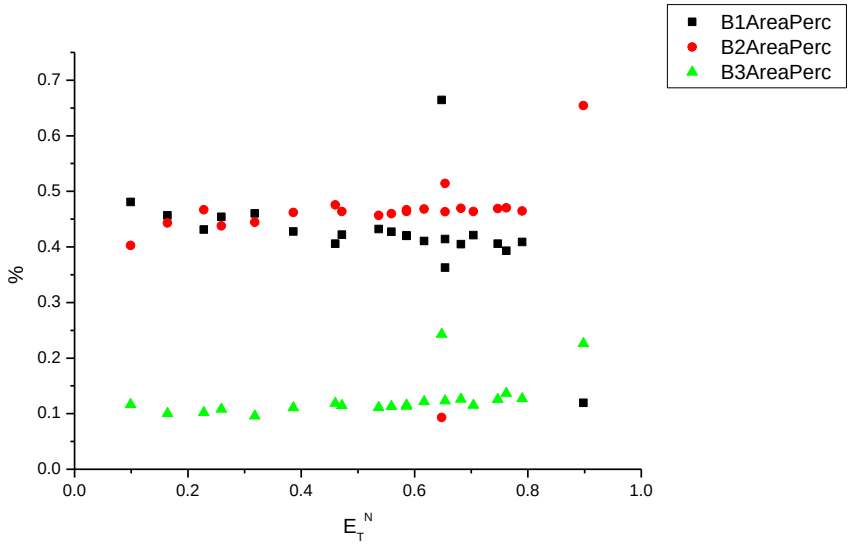

Figure 1.2.35. Area percentages from Gaussian model fit of the normalised fluorescence emission spectra of **6a** recorded at 400 nm excitation against E_T^N.

1.2.5.2 α

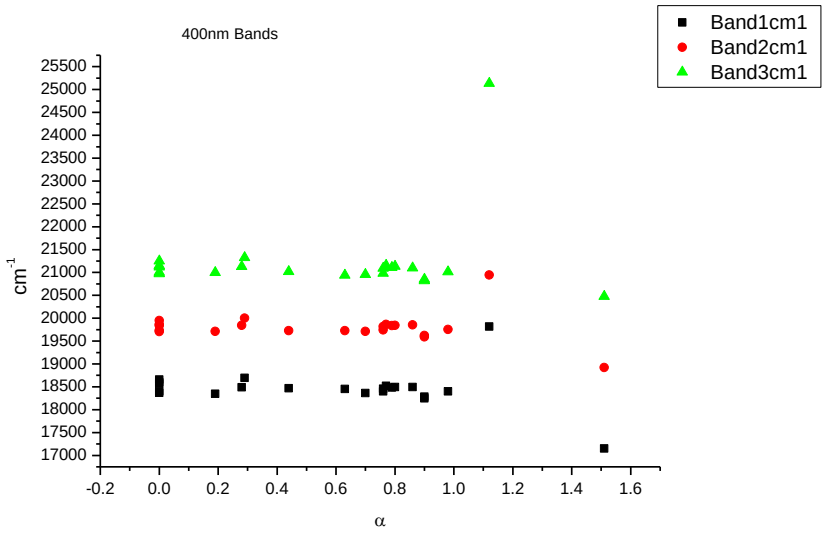

Figure 1.2.36. Band maxima from Gaussian model fit of the normalised fluorescence emission spectra of **6a** recorded at 400 nm excitation against α.

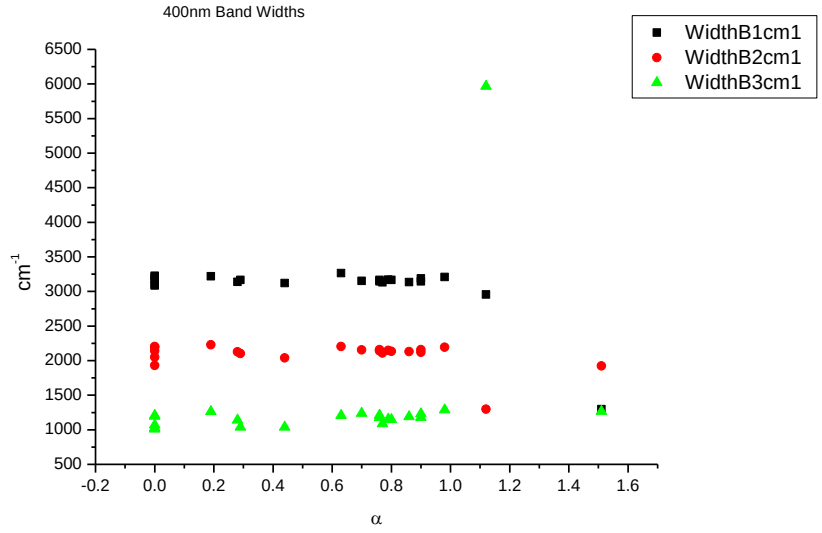

Figure 1.2.37. Band widths from Gaussian model fit of the normalised fluorescence emission spectra of **6a** recorded at 400 nm excitation against α.

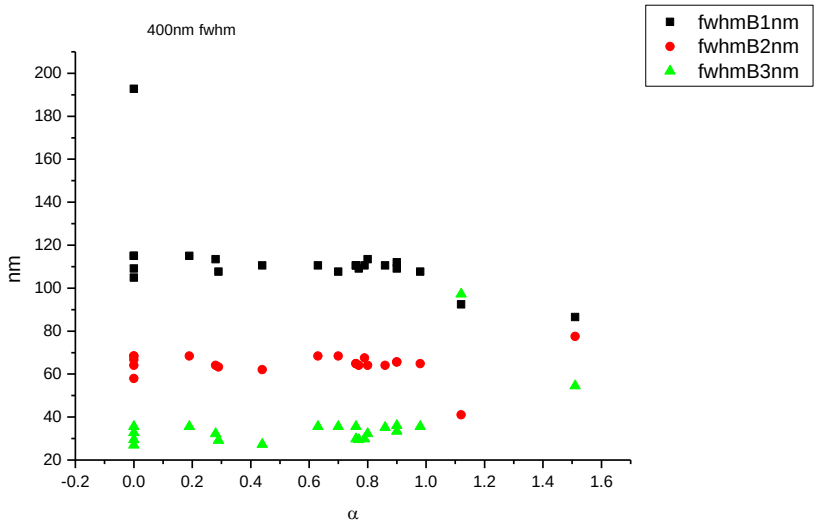

Figure 1.2.38. Full width half maxima from Gaussian model fit of the normalised fluorescence emission spectra of **6a** recorded at 400 nm excitation against α.

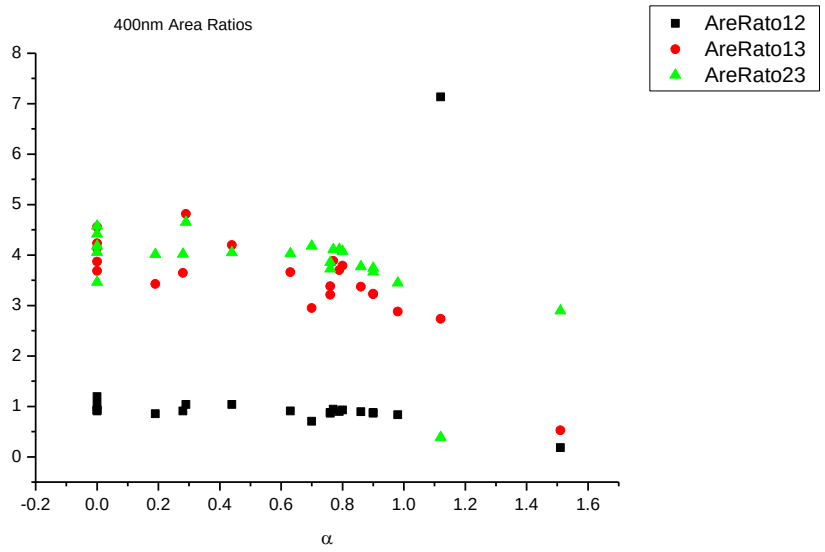

Figure 1.2.39. Area ratios from Gaussian model fit of the normalised fluorescence emission spectra of **6a** recorded at 400 nm excitation against α.

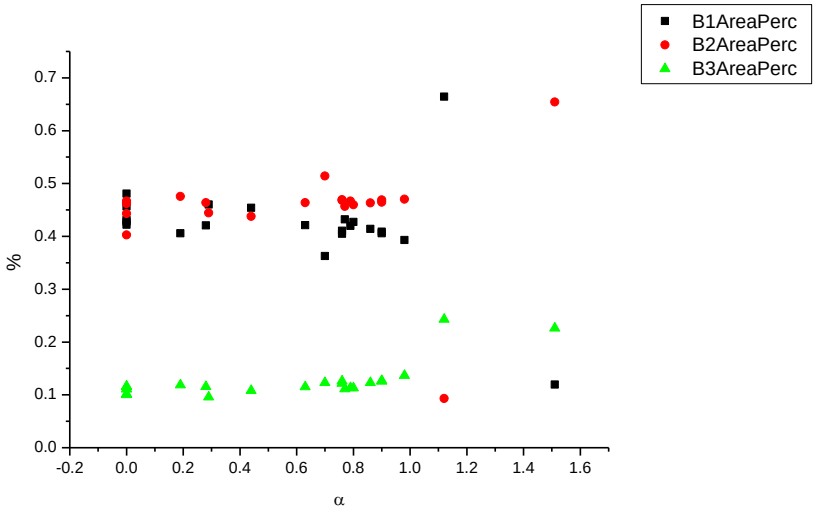

Figure 1.2.40. Area percentages from Gaussian model fit of the normalised fluorescence emission spectra of **6a** recorded at 400 nm excitation against α.

1.2.5.3 β.

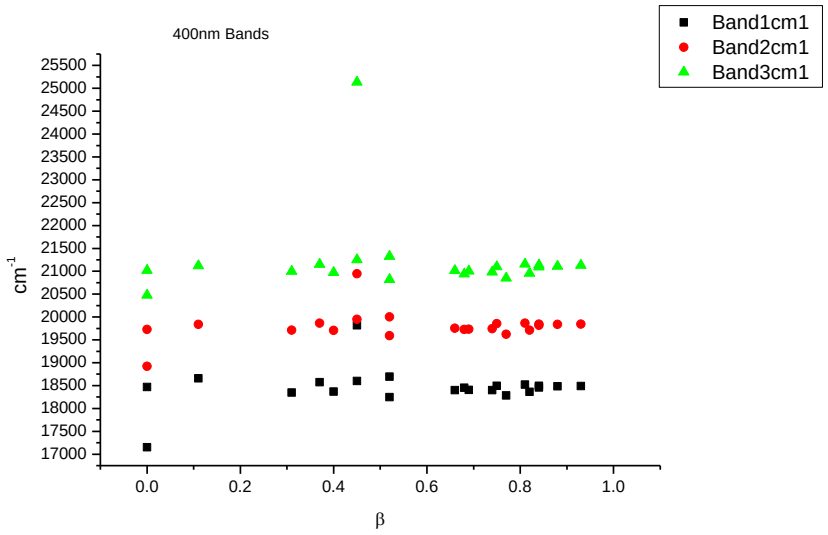

Figure 1.2.41. Band maxima from Gaussian model fit of the normalised fluorescence emission spectra of **6a** recorded at 400 nm excitation against β.

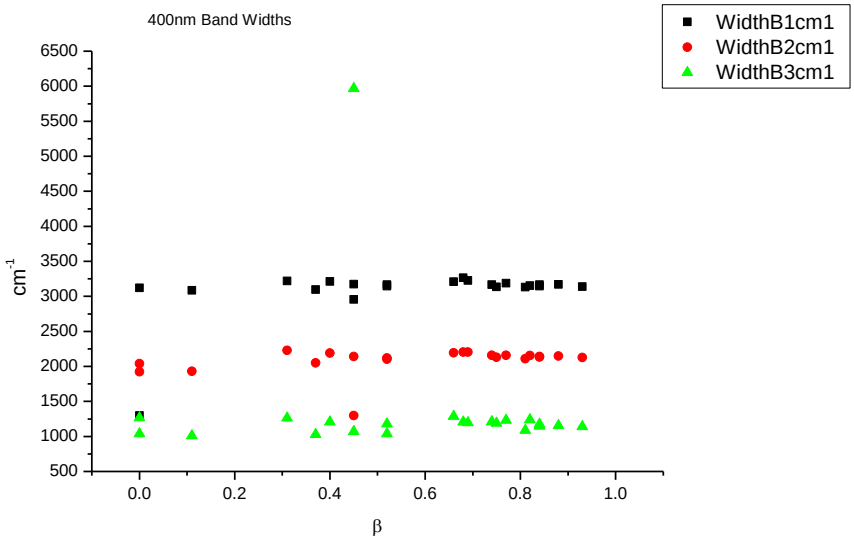

Figure 1.2.42. Band widths from Gaussian model fit of the normalised fluorescence emission spectra of **6a** recorded at 400 nm excitation against β.

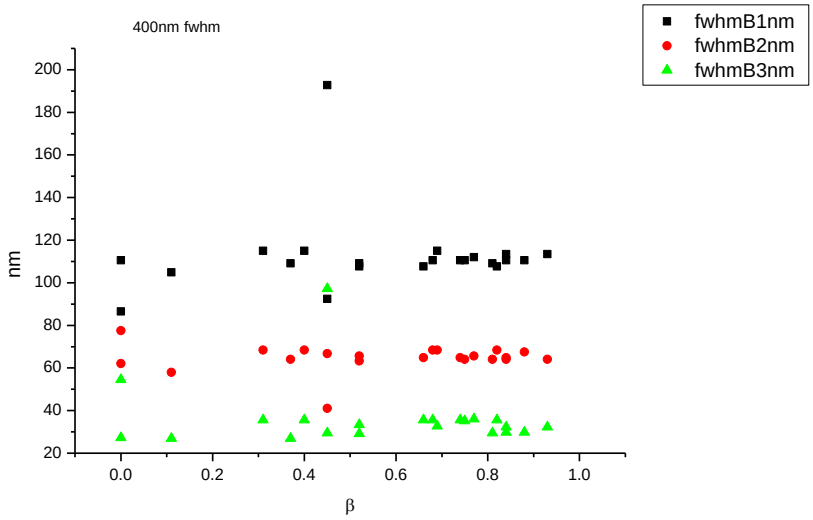

Figure 1.2.43. Full width half maxima from Gaussian model fit of the normalised fluorescence emission spectra of **6a** recorded at 400 nm excitation against β.

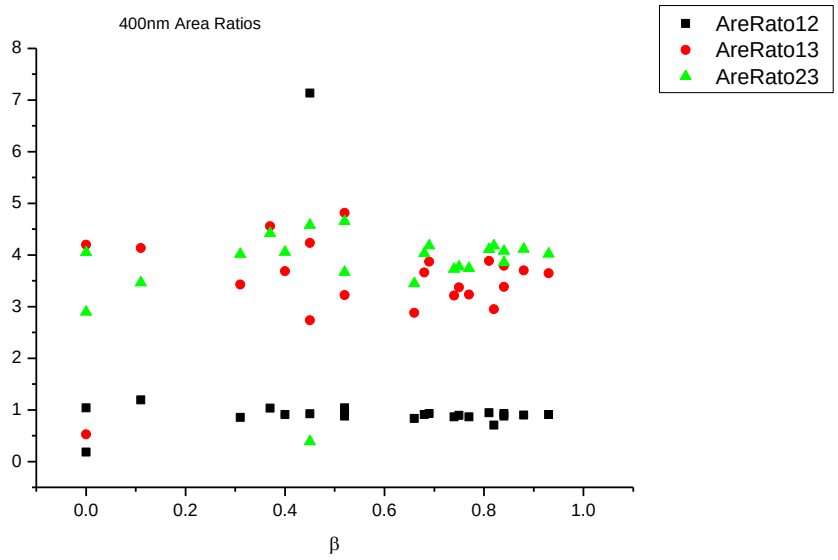

Figure 1.2.44. Area ratios from Gaussian model fit of the normalised fluorescence emission spectra of **6a** recorded at 400 nm excitation against β.

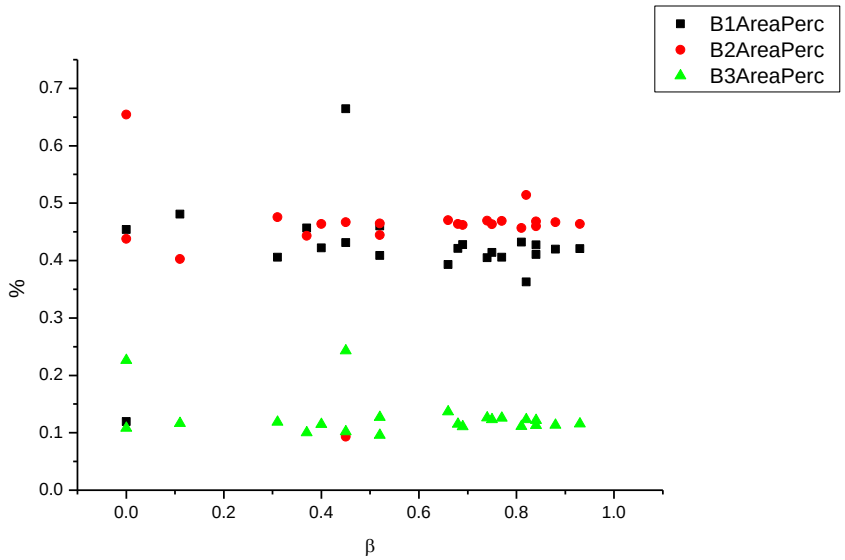

Figure 1.2.45. Area percentages from Gaussian model fit of the normalised fluorescence emission spectra of **6a** recorded at 400 nm excitation against β.

1.2.5.4 π.*

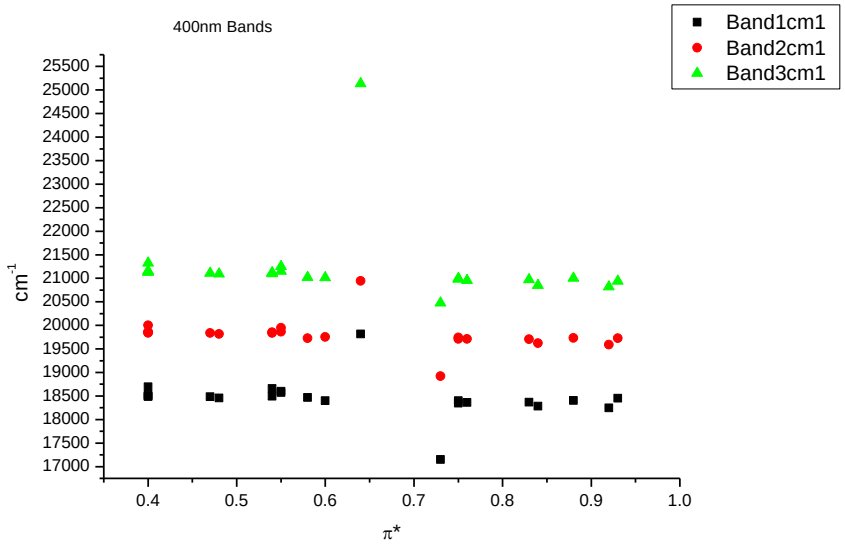

Figure 1.2.46. Band maxima from Gaussian model fit of the normalised fluorescence emission spectra of **6a** recorded at 400 nm excitation against π*.

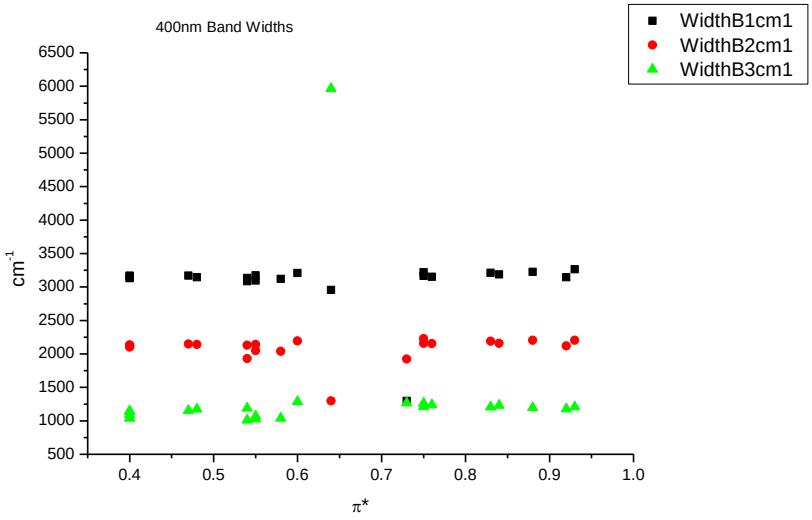

Figure 1.2.47. Band widths from Gaussian model fit of the normalised fluorescence emission spectra of **6a** recorded at 400 nm excitation against π*.

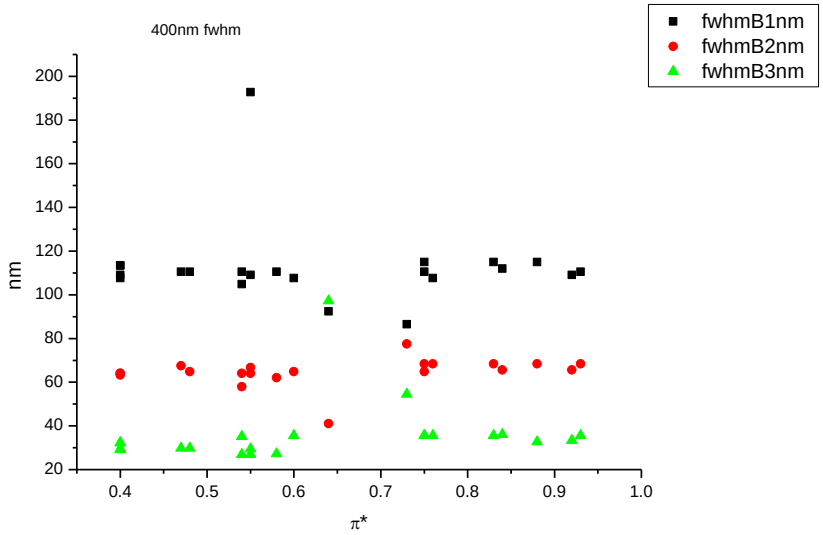

Figure 1.2.48. Full width half maxima from Gaussian model fit of the normalised fluorescence emission spectra of **6a** recorded at 400 nm excitation against π*.

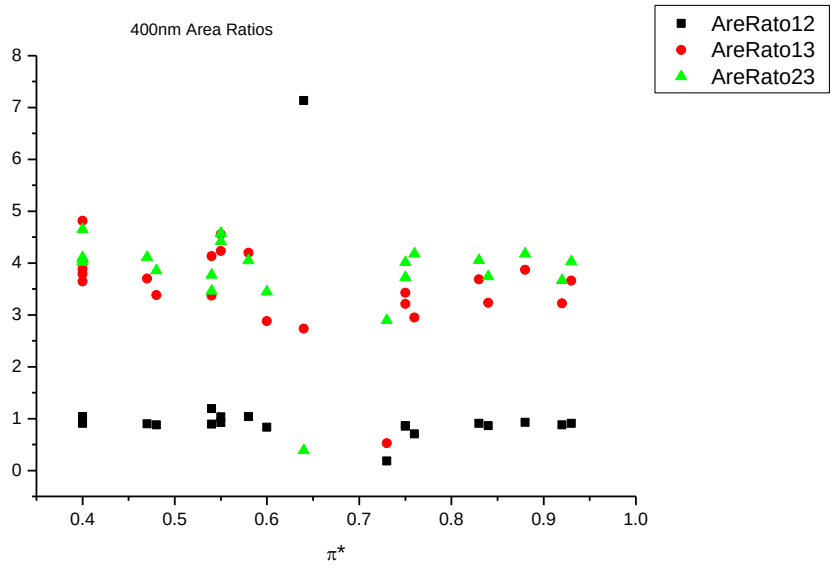

Figure 1.2.49. Area ratios from Gaussian model fit of the normalised fluorescence emission spectra of **6a** recorded at 400 nm excitation against π*.

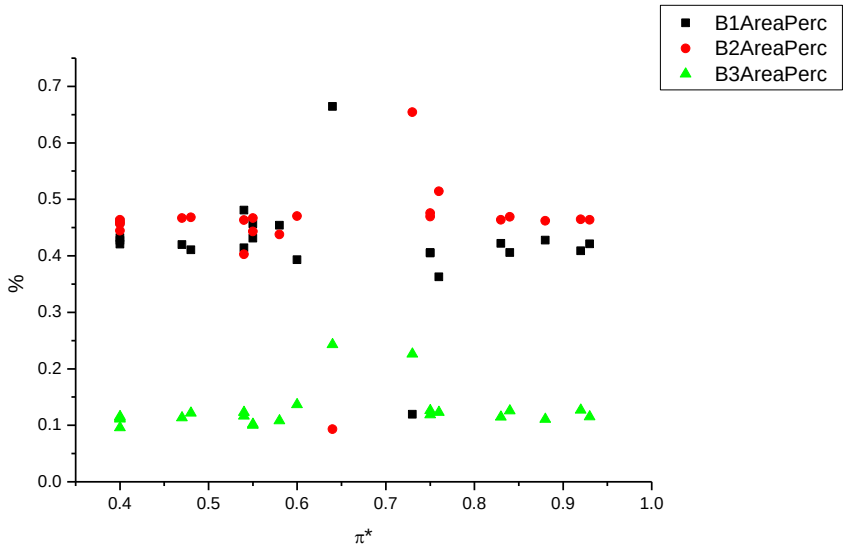

Figure 1.2.50. Area percentages from Gaussian model fit of the normalised fluorescence emission spectra of **6a** recorded at 400 nm excitation against π*.

1.2.5.5 μ(D).

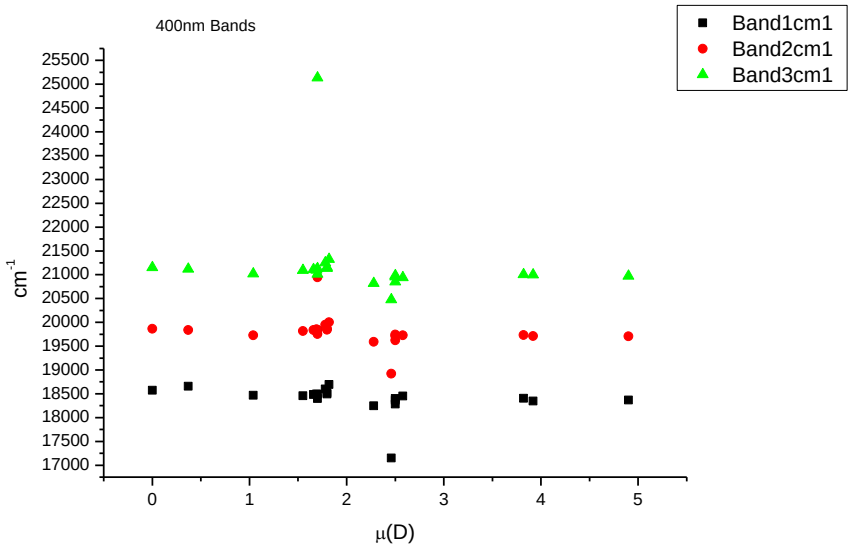

Figure 1.2.51. Band maxima from Gaussian model fit of the normalised fluorescence emission spectra of **6a** recorded at 400 nm excitation against μ(D).

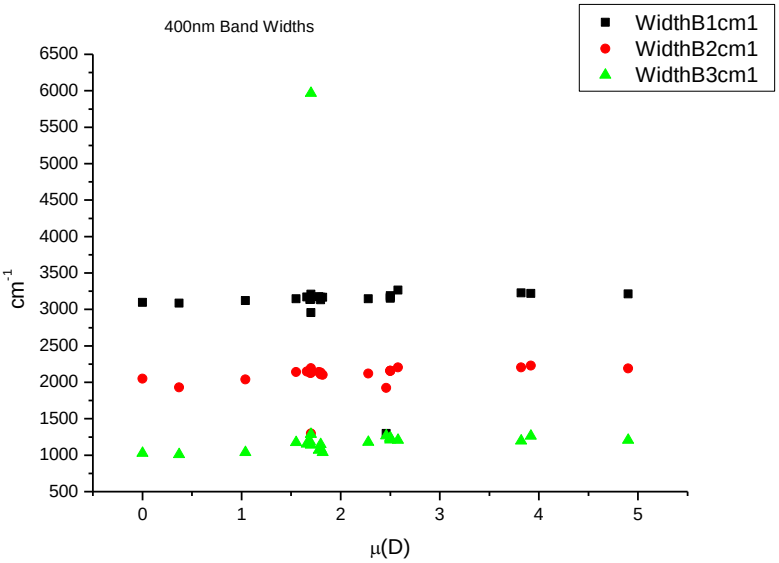

Figure 1.2.52. Band widths from Gaussian model fit of the normalised fluorescence emission spectra of **6a** recorded at 400 nm excitation against μ(D).

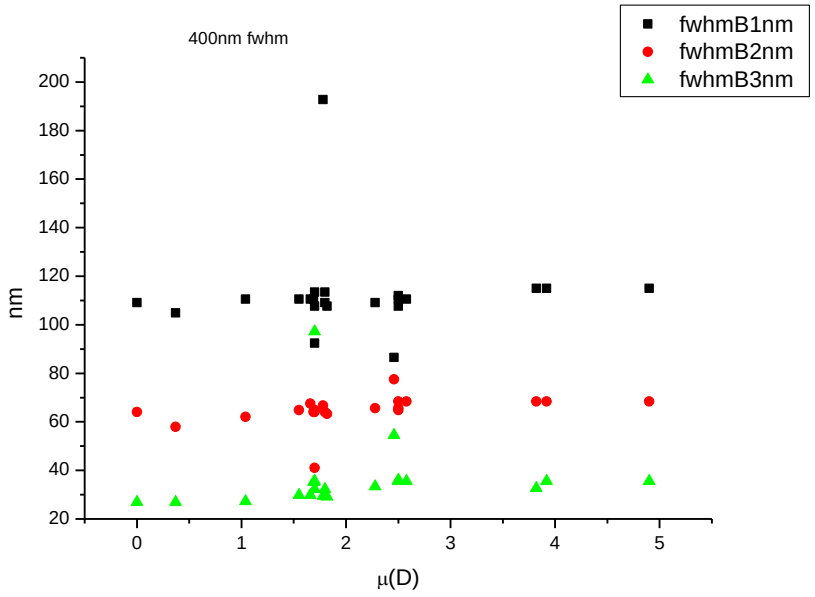

Figure 1.2.53. Full width half maxima from Gaussian model fit of the normalised fluorescence emission spectra of **6a** recorded at 400 nm excitation against μ(D).

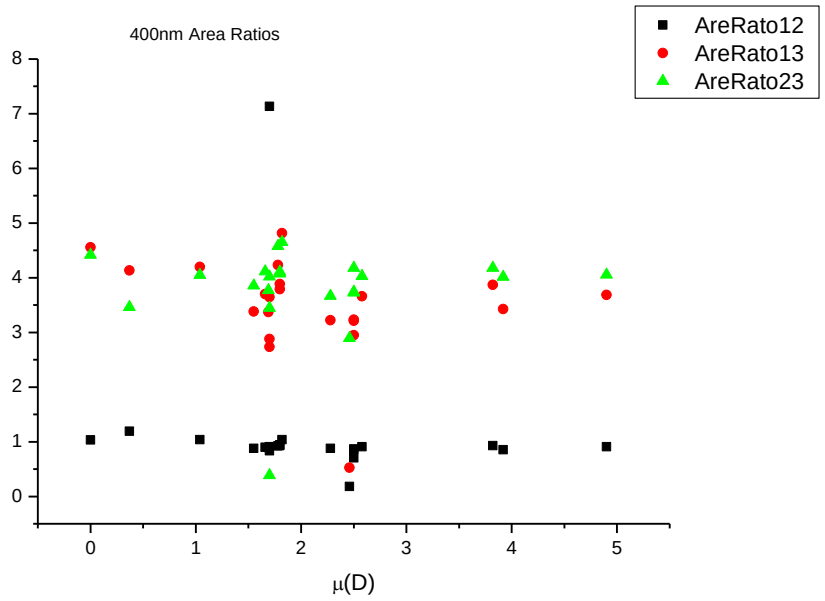

Figure 1.2.54. Area ratios from Gaussian model fit of the normalised fluorescence emission spectra of **6a** recorded at 400 nm excitation against μ(D).

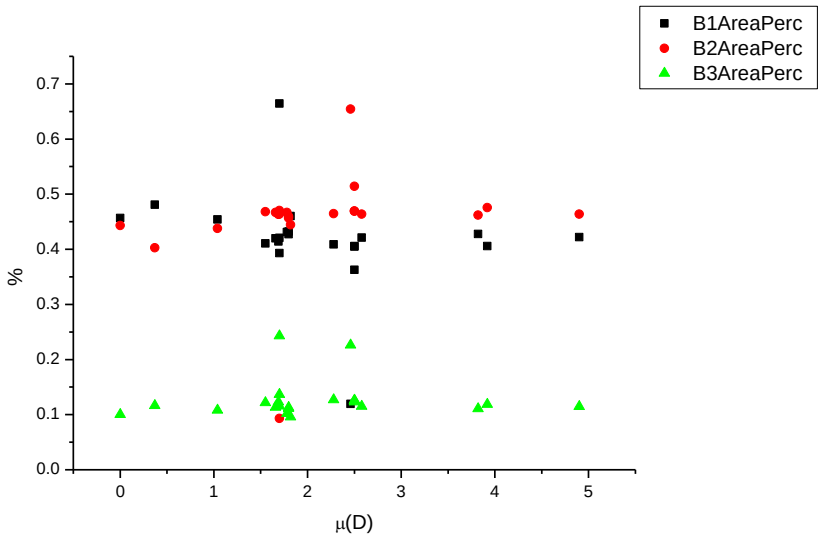

Figure 1.2.55. Area percentages from Gaussian model fit of the normalised fluorescence emission spectra of **6a** recorded at 400 nm excitation against μ(D).

1.2.5.6 η(Cp).

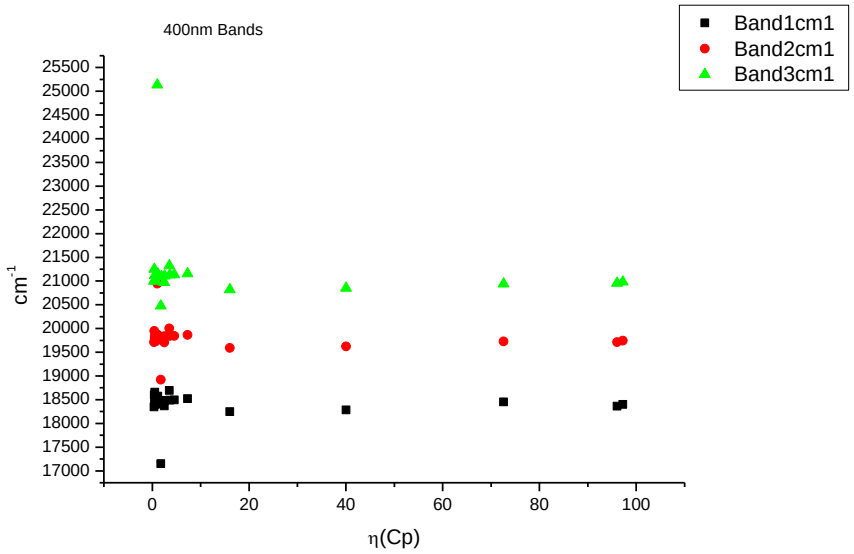

Figure 1.2.56. Band maxima from Gaussian model fit of the normalised fluorescence emission spectra of **6a** recorded at 400 nm excitation against η(Cp).

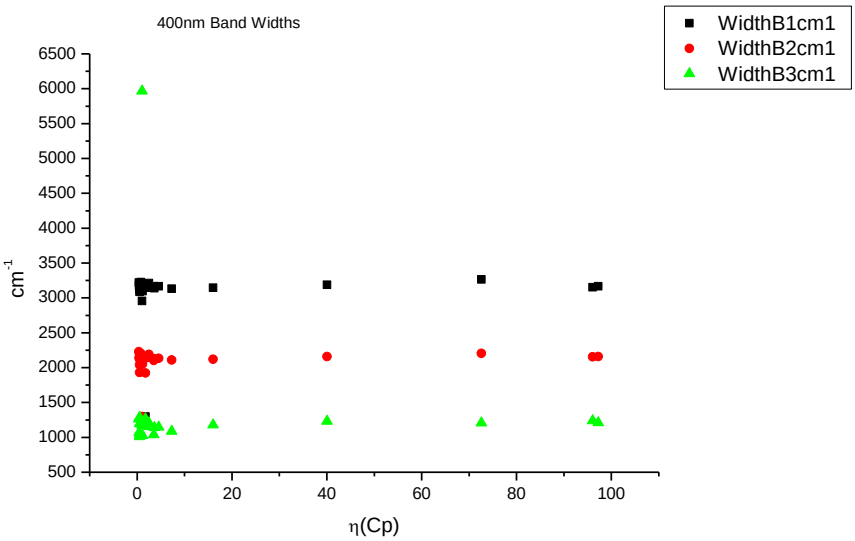

Figure 1.2.57. Band widths from Gaussian model fit of the normalised fluorescence emission spectra of **6a** recorded at 400 nm excitation against η(Cp).

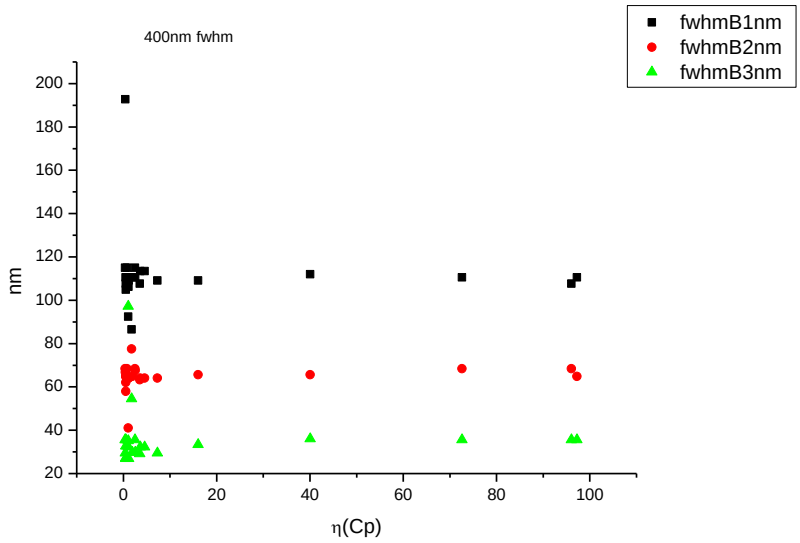

Figure 1.2.58. Full width half maxima from Gaussian model fit of the normalised fluorescence emission spectra of **6a** recorded at 400 nm excitation against η(Cp).

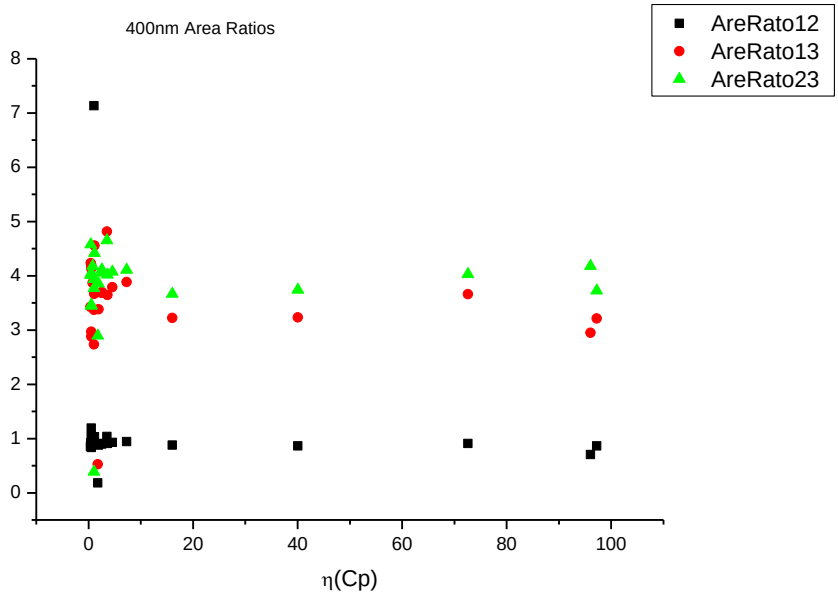

Figure 1.2.59. Area ratios from Gaussian model fit of the normalised fluorescence emission spectra of **6a** recorded at 400 nm excitation against η(Cp).

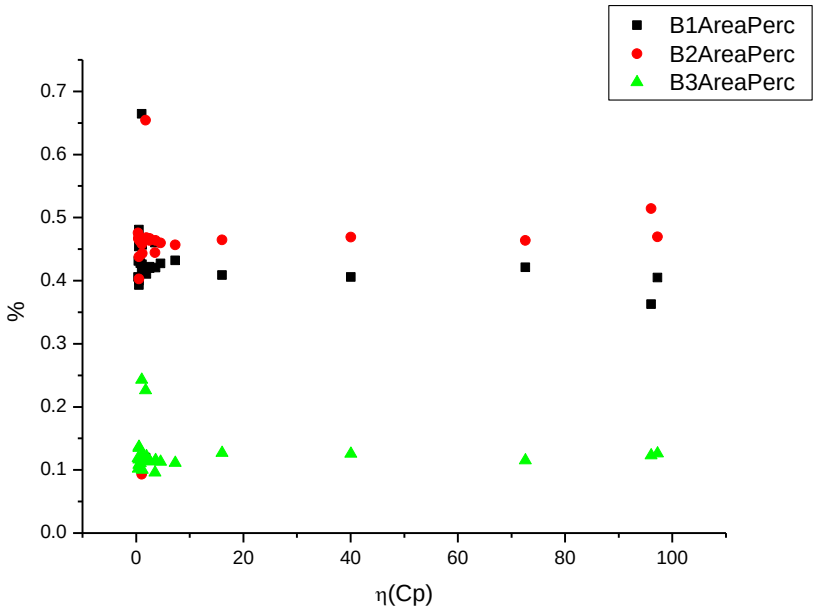

Figure 1.2.60. Area percentages from Gaussian model fit of the normalised fluorescence emission spectra of **6a** recorded at 400 nm excitation against η(Cp).

1.2.6 400 nm fluorescent lifetime results.

1.2.6.1 Intensity weighted.

Wavelength (nm)	Solvent	τ_1 (ns)	A_1 (%)	τ_2 (ns)	A_2 (%)	τ_3 (ns)	A_3 (%)	τ_f (ns) (Intensity Weighted)	$1/\tau_f$	χ^2
470	Toluene	-	-	4.09	78.35	9.16	21.65	5.18	0.19	1.09
470	1,4-Dioxane	0.27	1.75	4.39	77.65	9.37	20.59	5.34	0.19	1.04
470	Ethyl acetate	0.33	1.35	3.99	84.42	8.72	14.23	4.61	0.22	1.03
470	Chloroform	-	-	4.51	78.31	8.93	21.69	5.47	0.18	1.10
470	2-Methyl-2-butanol	0.42	3.39	3.48	83.21	9.32	13.40	4.16	0.24	1.06
470	N,N-dimethylformamide	0.30	1.22	4.69	68.10	8.12	30.68	5.69	0.18	1.10
470	Acetonitrile	0.36	1.27	4.25	69.40	7.61	29.33	5.19	0.19	1.05
470	Propylene carbonate	0.42	1.54	4.66	68.66	8.37	29.79	5.70	0.18	1.06
470	1-Octanol	0.59	6.58	4.82	74.40	8.79	19.02	5.30	0.19	1.08
470	1-Hexanol	0.43	5.61	4.95	85.71	10.84	8.68	5.21	0.19	1.09
470	1-Butanol	0.29	5.33	4.78	77.73	7.59	16.94	5.01	0.20	1.08
470	1-Pentanol	0.37	4.41	4.84	87.25	10.32	8.33	5.10	0.20	1.05
470	1-Propanol	0.22	2.80	4.44	83.87	7.93	13.33	4.79	0.21	1.09
470	Acetic acid	0.32	25.76	1.08	60.97	2.30	13.28	1.04	0.96	1.07
470	Ethanol	0.42	5.58	4.64	26.11	8.01	68.31	6.70	0.15	1.13
470	1,5-Pentanediol	-	-	3.96	55.14	6.05	44.86	4.89	0.20	1.19
470	1,3-Butanediol	0.54	3.79	4.10	19.67	7.61	76.55	6.65	0.15	1.07
470	1,4-Butanediol	0.38	4.23	2.86	17.09	7.51	78.69	6.41	0.16	1.12
470	1,3-Propanediol	0.41	2.26	3.83	19.34	7.31	78.40	6.48	0.15	1.05
470	Methanol	0.29	2.25	4.20	89.99	7.98	7.77	4.41	0.23	1.01
470	1,2-Ethanediol	0.44	1.26	3.02	17.67	6.44	81.07	5.76	0.17	1.04
470	2,2,2-Trifluoroethanol	0.17	87.71	1.26	12.29	-	-	0.30	3.29	1.00
470	Ethanol-d	-	-	4.38	63.03	6.62	36.97	5.20	0.19	1.08
470	Methanol-d	-	-	4.55	84.65	7.46	15.35	5.00	0.20	1.01

Table 1.2.9. Summary of Time Correlated Single Photon Counting (TCSPC) fluorescent lifetimes (intensity weighted) of **6a** recorded at 470 nm.

Wavelength (nm)	Solvent	τ_1 (ns)	A_1 (%)	τ_2 (ns)	A_2 (%)	τ_3 (ns)	A_3 (%)	τ_f (ns) (Intensity Weighted)	$1/\tau_f$	χ^2
490	Toluene	-	-	4.05	66.71	9.23	33.29	5.78	0.17	1.06
490	1,4-Dioxane	0.30	1.63	4.50	71.03	10.86	27.35	6.17	0.16	1.12
490	Ethyl acetate	-	-	4.00	75.53	9.82	24.47	5.43	0.18	1.16
490	Chloroform	-	-	4.71	74.75	10.61	25.25	6.20	0.16	1.06
490	2-Methyl-2-butanol	0.42	2.62	3.63	70.27	10.69	27.10	5.46	0.18	1.06
490	N,N-dimethylformamide	0.23	1.14	4.98	74.95	9.99	23.91	6.12	0.16	1.08
490	Acetonitrile	0.39	1.25	4.41	71.65	9.11	27.09	5.63	0.18	1.09
490	Propylene carbonate	0.42	1.23	4.85	69.33	9.74	29.44	6.23	0.16	1.09
490	1-Octanol	0.66	4.65	5.14	76.06	11.57	19.29	6.18	0.16	1.12
490	1-Hexanol	0.43	3.42	5.01	80.94	12.27	15.64	5.99	0.17	1.08
490	1-Butanol	0.33	3.29	4.96	81.02	10.79	15.69	5.72	0.17	1.06
490	1-Pentanol	0.41	2.74	4.87	81.84	11.14	15.42	5.71	0.18	1.10
490	1-Propanol	0.20	2.26	4.59	85.61	11.56	12.13	5.34	0.19	1.10
490	Acetic acid	0.23	29.65	0.91	50.99	1.87	19.35	0.89	1.12	0.91
490	Ethanol	0.40	3.11	5.61	47.67	9.26	49.22	7.24	0.14	1.14
490	1,5-Pentanediol	-	-	4.45	79.28	9.31	20.72	5.46	0.18	1.15
490	1,3-Butanediol	0.45	2.10	5.14	41.39	8.80	56.51	7.11	0.14	1.11
490	1,4-Butanediol	0.53	3.12	4.02	27.44	8.27	69.44	6.86	0.15	1.12
490	1,3-Propanediol	0.63	1.22	4.96	39.16	8.20	59.62	6.84	0.15	1.08
490	Methanol	-	-	3.72	63.84	6.25	36.16	4.63	0.22	1.15
490	1,2-Ethanediol	1.65	4.76	5.08	53.37	7.91	41.87	6.10	0.16	1.04
490	2,2,2-Trifluoroethanol	0.17	87.71	1.31	12.29	-	-	0.31	3.19	1.17
490	Ethanol-d	-	-	4.81	80.71	9.92	19.29	5.80	0.17	1.16
490	Methanol-d	-	-	4.74	87.95	10.73	12.05	5.46	0.18	1.05

Table 1.2.10. Summary of Time Correlated Single Photon Counting (TCSPC) fluorescent lifetimes (intensity weighted) of **6a** recorded at 490 nm.

Wavelength (nm)	Solvent	τ_1 (ns)	A_1 (%)	τ_2 (ns)	A_2 (%)	τ_3 (ns)	A_3 (%)	τ_f (ns) (Intensity Weighted)	$1/\tau_f$	χ^2
520	Toluene	-	-	4.14	44.56	9.83	55.44	7.29	0.14	1.01
520	1,4-Dioxane	0.23	1.39	4.58	47.77	11.44	50.84	8.01	0.12	1.14
520	Ethyl acetate	-	-	4.11	57.46	11.44	42.54	7.23	0.14	1.08
520	Chloroform	-	-	4.77	51.22	11.74	48.78	8.17	0.12	1.06
520	2-Methyl-2-butanol	0.42	1.74	3.64	49.39	10.95	48.87	7.16	0.14	1.06
520	N,N-dimethylformamide	0.28	0.89	5.08	60.83	12.11	38.27	7.73	0.13	1.10
520	Acetonitrile	0.56	1.04	4.64	63.29	12.33	35.67	7.34	0.14	1.07
520	Propylene carbonate	0.50	1.31	5.14	60.77	12.65	37.92	7.93	0.13	1.13
520	1-Octanol	0.78	2.38	5.24	57.96	12.87	39.66	8.16	0.12	1.12
520	1-Hexanol	0.44	2.07	5.03	62.32	12.92	35.61	7.74	0.13	1.13
520	1-Butanol	0.33	2.07	4.99	67.14	12.70	30.80	7.27	0.14	1.09
520	1-Pentanol	0.50	1.82	5.01	66.96	13.01	31.22	7.43	0.13	1.12
520	1-Propanol	-	-	4.49	67.83	12.27	32.17	7.00	0.14	1.08
520	Acetic acid	0.20	39.01	0.74	34.81	1.61	26.18	0.76	1.32	1.10
520	Ethanol	0.45	1.40	6.63	64.66	13.15	33.94	8.76	0.11	1.10
520	1,5-Pentanediol	-	-	4.60	68.68	12.29	31.32	7.01	0.14	1.10
520	1,3-Butanediol	0.60	0.98	6.33	64.04	13.22	34.97	8.68	0.12	1.08
520	1,4-Butanediol	1.23	3.24	5.85	56.52	11.86	40.24	8.12	0.12	1.16
520	1,3-Propanediol	-	-	5.27	51.35	10.45	48.65	7.79	0.13	1.10
520	Methanol	-	-	4.17	78.70	11.71	21.30	5.77	0.17	1.19
520	1,2-Ethanediol	2.13	6.01	5.78	69.52	12.18	24.47	7.13	0.14	1.08
520	2,2,2-Trifluoroethanol	0.81	11.98	0.18	73.95	3.72	14.07	0.75	1.33	0.95
520	Ethanol-d	-	-	4.91	68.43	12.49	31.57	7.30	0.14	1.12
520	Methanol-d	-	-	4.84	79.20	13.49	20.80	6.64	0.15	1.11

Table 1.2.11. Summary of Time Correlated Single Photon Counting (TCSPC) fluorescent lifetimes (intensity weighted) of **6a** recorded at 520 nm.

Wavelength (nm)	Solvent	τ_1 (ns)	A_1 (%)	τ_2 (ns)	A_2 (%)	τ_3 (ns)	A_3 (%)	τ_f (ns) (Intensity Weighted)	$1/\tau_f$	χ^2
540	Toluene	-	-	4.20	36.93	9.95	63.07	7.83	0.13	1.05
540	1,4-Dioxane	-	-	4.42	37.87	11.42	62.13	8.77	0.11	1.13
540	Ethyl acetate	-	-	4.13	48.32	11.58	51.68	7.98	0.13	1.10
540	Chloroform	-	-	4.87	44.19	12.14	55.81	8.93	0.11	1.03
540	2-Methyl-2-butanol	0.44	1.33	3.72	42.17	11.09	56.50	7.84	0.13	1.13
540	N,N-dimethylformamide	0.32	0.98	5.03	50.45	12.47	48.57	8.60	0.12	1.09
540	Acetonitrile	0.37	0.74	4.53	51.61	12.19	47.66	8.15	0.12	1.12
540	Propylene carbonate	0.47	0.98	5.05	49.75	12.79	49.27	8.82	0.11	1.13
540	1-Octanol	0.74	1.72	5.16	47.74	12.76	50.54	8.92	0.11	1.09
540	1-Hexanol	0.49	1.61	5.03	53.45	12.89	44.94	8.49	0.12	1.11
540	1-Butanol	0.36	1.35	5.05	60.47	13.04	38.19	8.04	0.12	1.14
540	1-Pentanol	0.52	1.46	5.04	58.63	13.08	39.91	8.18	0.12	1.09
540	1-Propanol	-	-	4.52	59.85	12.76	40.15	7.83	0.13	1.14
540	Acetic acid	0.20	42.90	0.82	40.10	1.81	17.00	0.72	1.39	1.03
540	Ethanol	-	-	6.15	50.74	13.03	49.26	9.54	0.10	1.14
540	1,5-Pentanediol	-	-	4.61	61.64	12.69	38.36	7.71	0.13	1.09
540	1,3-Butanediol	-	-	6.30	55.02	13.36	44.98	9.48	0.11	1.09
540	1,4-Butanediol	2.20	5.36	6.70	60.59	13.94	34.05	8.92	0.11	1.14
540	1,3-Propanediol	-	-	5.69	56.44	12.05	43.56	8.46	0.12	1.11
540	Methanol	-	-	4.11	70.46	11.90	29.54	6.41	0.16	1.04
540	1,2-Ethanediol	2.69	9.77	6.36	67.10	14.27	23.13	7.83	0.13	1.12
540	2,2,2-Trifluoroethanol	0.98	13.11	0.19	66.94	4.12	19.95	1.08	0.92	1.02
540	Ethanol-d	-	-	4.97	61.47	12.87	38.53	8.02	0.12	1.10
540	Methanol-d	-	-	4.86	72.45	13.65	27.55	7.29	0.14	1.10

Table 1.2.12. Summary of Time Correlated Single Photon Counting (TCSPC) fluorescent lifetimes (intensity weighted) of **6a** recorded at 540 nm.

Wavelength (nm)	Solvent	τ_1 (ns)	A_1 (%)	τ_2 (ns)	A_2 (%)	τ_3 (ns)	A_3 (%)	τ_f (ns) (Intensity Weighted)	$1/\tau_f$	χ^2
570	Toluene	-	-	4.11	23.38	9.97	76.62	8.60	0.12	1.03
570	1,4-Dioxane	-	-	4.35	24.89	11.45	75.11	9.68	0.10	1.10
570	Ethyl acetate	-	-	4.20	37.78	11.89	62.22	8.99	0.11	1.11
570	Chloroform	-	-	4.82	31.03	12.15	68.97	9.88	0.10	1.07
570	2-Methyl-2-butanol	0.46	1.59	3.73	30.75	11.09	67.66	8.66	0.12	1.09
570	N,N-dimethylformamide	-	-	4.88	37.22	12.59	62.78	9.72	0.10	1.09
570	Acetonitrile	2.43	5.55	5.41	43.36	13.74	51.09	9.50	0.11	1.10
570	Propylene carbonate	0.62	0.89	5.08	37.96	13.08	61.15	9.93	0.10	1.08
570	1-Octanol	0.68	1.41	5.33	37.68	13.02	60.91	9.95	0.10	1.08
570	1-Hexanol	0.42	1.26	5.01	41.82	13.05	56.92	9.53	0.10	1.06
570	1-Butanol	0.32	1.58	5.02	49.83	13.13	48.59	8.89	0.11	1.08
570	1-Pentanol	0.45	1.09	5.01	47.48	13.24	51.33	9.18	0.11	1.02
570	1-Propanol	-	-	4.55	49.88	13.14	50.12	8.85	0.11	1.11
570	Acetic acid	0.19	48.35	0.86	42.83	2.42	8.82	0.67	1.49	1.31
570	Ethanol	-	-	7.12	51.21	14.45	48.79	10.69	0.09	1.13
570	1,5-Pentanediol	-	-	4.64	52.09	13.08	47.91	8.69	0.12	1.11
570	1,3-Butanediol	-	-	6.88	52.29	14.59	47.71	10.56	0.09	1.12
570	1,4-Butanediol	2.99	8.18	7.16	51.57	14.56	40.25	9.80	0.10	1.08
570	1,3-Propanediol	-	-	5.84	52.07	13.01	47.93	9.28	0.11	1.08
570	Methanol	-	-	4.15	63.38	12.75	36.62	7.30	0.14	1.11
570	1,2-Ethanediol	2.80	7.26	5.93	53.59	13.23	39.14	8.56	0.12	1.19
570	2,2,2-Trifluoroethanol	0.93	12.81	0.20	58.32	3.87	28.87	1.36	0.74	1.08
570	Ethanol-d	-	-	4.94	51.50	13.28	48.50	8.99	0.11	1.06
570	Methanol-d	-	-	4.89	64.46	14.15	35.54	8.18	0.12	1.15

Table 1.2.13. Summary of Time Correlated Single Photon Counting (TCSPC) fluorescent lifetimes (intensity weighted) of **6a** recorded at 570 nm.

1.2.6.2 Amplitude weighted.

Wavelength (nm)	Solvent	τ_1 (ns)	A_1 (%)	τ_2 (ns)	A_2 (%)	τ_3 (ns)	A_3 (%)	τ_f (ns) (Amplitude Weighted)	$1/\tau_f$	χ^2
470	Toluene	-	-	4.09	89.03	9.16	10.97	4.64	0.22	1.09
470	1,4-Dioxane	0.27	24.58	4.39	67.08	9.37	8.33	3.79	0.26	1.04
470	Ethyl acetate	0.33	15.18	3.99	78.75	8.72	6.07	3.72	0.27	1.03
470	Chloroform	4.51	87.72	8.93	12.28	-	-	5.06	0.20	1.10
470	2-Methyl-2-butanol	0.42	23.99	3.48	71.70	9.32	4.31	3.00	0.33	1.06
470	N,N-dimethylformamide	0.30	18.32	4.69	64.82	8.12	16.86	4.46	0.22	1.10
470	Acetonitrile	0.36	14.82	4.25	68.92	7.61	16.26	4.22	0.24	1.05
470	Propylene carbonate	0.42	16.65	4.66	67.13	8.37	16.22	4.56	0.22	1.06
470	1-Octanol	0.59	38.96	4.82	53.54	8.79	7.51	3.47	0.29	1.08
470	1-Hexanol	0.43	41.89	4.95	55.54	10.84	2.57	3.21	0.31	1.09
470	1-Butanol	0.29	49.48	4.78	44.42	7.59	6.09	2.73	0.37	1.08
470	1-Pentanol	0.37	38.96	4.84	58.42	10.32	2.62	3.24	0.31	1.05
470	1-Propanol	0.22	38.60	4.44	56.38	7.93	5.02	2.99	0.33	1.09
470	Acetic acid	0.32	56.94	1.08	39.08	2.30	3.97	0.69	1.45	1.07
470	Ethanol	0.42	48.25	4.64	20.57	8.01	31.17	3.65	0.27	1.13
470	1,5-Pentanediol	-	-	3.96	65.26	6.05	34.74	4.68	0.21	1.19
470	1,3-Butanediol	0.54	32.29	4.10	21.85	7.61	45.86	4.56	0.22	1.07
470	1,4-Butanediol	0.38	40.26	2.86	21.70	7.51	38.03	3.63	0.28	1.12
470	1,3-Propanediol	0.41	26.04	3.83	23.67	7.31	50.29	4.69	0.21	1.05
470	Methanol	0.29	25.74	4.20	71.03	7.98	3.22	3.32	0.30	1.01
470	1,2-Ethanediol	0.44	13.58	3.02	27.41	6.44	59.01	4.69	0.21	1.04
470	2,2,2-Trifluoroethanol	0.17	98.14	1.26	1.86	-	-	0.19	5.24	1.00
470	Ethanol-d	-	-	4.38	72.06	6.62	27.94	5.00	0.20	1.08
470	Methanol-d	-	-	4.55	90.04	7.46	9.96	4.84	0.21	1.01

Table 1.2.14. Summary of Time Correlated Single Photon Counting (TCSPC) fluorescent lifetimes (amplitude weighted) of **6a** recorded at 470 nm.

Wavelength (nm)	Solvent	τ_1 (ns)	A_1 (%)	τ_2 (ns)	A_2 (%)	τ_3 (ns)	A_3 (%)	τ_f (ns) (Amplitude Weighted)	$1/\tau_f$	χ^2
490	Toluene	-	-	4.05	82.03	9.23	17.97	4.98	0.20	1.06
490	1,4-Dioxane	0.30	23.13	4.50	66.30	10.86	10.57	4.20	0.24	1.12
490	Ethyl acetate	-	-	4.00	88.34	9.82	11.66	4.68	0.21	1.16
490	Chloroform	-	-	4.71	86.95	10.61	13.05	5.48	0.18	1.06
490	2-Methyl-2-butanol	0.42	22.13	3.63	68.85	10.69	9.02	3.56	0.28	1.06
490	N,N-dimethylformamide	0.23	22.09	4.98	67.22	9.99	10.69	4.46	0.22	1.08
490	Acetonitrile	0.39	14.23	4.41	72.51	9.11	13.26	4.46	0.22	1.09
490	Propylene carbonate	0.42	14.44	4.85	70.62	9.74	14.94	4.94	0.20	1.09
490	1-Octanol	0.66	29.95	5.14	62.96	11.57	7.10	4.26	0.23	1.12
490	1-Hexanol	0.43	31.37	5.01	63.62	12.27	5.01	3.93	0.25	1.08
490	1-Butanol	0.33	36.01	4.96	58.76	10.79	5.23	3.60	0.28	1.06
490	1-Pentanol	0.41	27.10	4.87	67.36	11.14	5.54	4.00	0.25	1.10
490	1-Propanol	0.20	36.19	4.59	60.41	11.56	3.40	3.24	0.31	1.10
490	Acetic acid	0.23	65.47	0.91	29.16	1.87	5.37	0.52	1.93	0.91
490	Ethanol	0.40	35.85	5.61	39.47	9.26	24.68	4.64	0.22	1.14
490	1,5-Pentanediol	-	-	4.45	88.89	9.31	11.11	4.99	0.20	1.15
490	1,3-Butanediol	0.45	24.58	5.14	41.98	8.80	33.44	5.21	0.19	1.11
490	1,4-Butanediol	0.53	27.71	4.02	32.41	8.27	39.88	4.75	0.21	1.12
490	1,3-Propanediol	0.63	11.35	4.96	46.14	8.20	42.51	5.84	0.17	1.08
490	Methanol	-	-	3.72	74.81	6.25	25.19	4.36	0.23	1.15
490	1,2-Ethanediol	1.65	15.46	5.08	56.20	7.91	28.33	5.35	0.19	1.04
490	2,2,2-Trifluoroethanol	0.17	98.17	1.31	1.83	-	-	0.20	5.13	1.17
490	Ethanol-d	-	-	4.81	89.61	9.92	10.39	5.34	0.19	1.16
490	Methanol-d	-	-	4.74	94.29	10.73	5.71	5.08	0.20	1.05

Table 1.2.15. Summary of Time Correlated Single Photon Counting (TCSPC) fluorescent lifetimes (amplitude weighted) of **6a** recorded at 490 nm.

Wavelength (nm)	Solvent	τ_1 (ns)	A_1 (%)	τ_2 (ns)	A_2 (%)	τ_3 (ns)	A_3 (%)	τ_f (ns) (Amplitude Weighted)	$1/\tau_f$	χ^2
520	Toluene	-	-	4.14	65.62	9.83	34.38	6.10	0.16	1.01
520	1,4-Dioxane	0.23	28.49	4.58	50.16	11.44	21.35	4.80	0.21	1.14
520	Ethyl acetate	-	-	4.11	78.99	11.44	21.01	5.65	0.18	1.08
520	Chloroform	-	-	4.77	72.10	11.74	27.90	6.72	0.15	1.06
520	2-Methyl-2-butanol	0.42	18.72	3.64	61.14	10.95	20.13	4.51	0.22	1.06
520	N,N-dimethylformamide	0.28	17.59	5.08	65.19	12.11	17.22	5.45	0.18	1.10
520	Acetonitrile	0.56	10.13	4.64	74.16	12.33	15.71	5.43	0.18	1.07
520	Propylene carbonate	0.50	15.11	5.14	67.73	12.65	17.16	5.73	0.17	1.13
520	1-Octanol	0.78	17.78	5.24	64.31	12.87	17.91	5.81	0.17	1.12
520	1-Hexanol	0.44	23.87	5.03	62.28	12.92	13.85	5.03	0.20	1.13
520	1-Butanol	0.33	28.42	4.99	60.65	12.70	10.93	4.51	0.22	1.09
520	1-Pentanol	0.50	18.88	5.01	68.77	13.01	12.35	5.15	0.19	1.12
520	1-Propanol	-	-	4.49	85.21	12.27	14.79	5.64	0.18	1.08
520	Acetic acid	0.20	75.57	0.74	18.16	1.61	6.27	0.39	2.60	1.10
520	Ethanol	0.45	20.31	6.63	63.02	13.15	16.68	6.46	0.15	1.10
520	1,5-Pentanediol	-	-	4.60	85.43	12.29	14.57	5.72	0.17	1.10
520	1,3-Butanediol	0.60	11.41	6.33	70.24	13.22	18.35	6.94	0.14	1.08
520	1,4-Butanediol	1.23	16.85	5.85	61.54	11.86	21.62	6.37	0.16	1.16
520	1,3-Propanediol	-	-	5.27	67.68	10.45	32.32	6.94	0.14	1.10
520	Methanol	-	-	4.17	91.22	11.71	8.78	4.83	0.21	1.19
520	1,2-Ethanediol	2.13	16.75	5.78	71.33	12.18	11.92	5.93	0.17	1.08
520	2,2,2-Trifluoroethanol	0.18	95.67	0.81	3.45	3.72	0.88	0.23	4.31	0.95
520	Ethanol-d	-	-	4.91	84.65	12.49	15.35	6.07	0.16	1.12
520	Methanol-d	-	-	4.84	91.39	13.49	8.61	5.59	0.18	1.11

Table 1.2.16. Summary of Time Correlated Single Photon Counting (TCSPC) fluorescent lifetimes (amplitude weighted) of **6a** recorded at 520 nm.

Wavelength (nm)	Solvent	τ_1 (ns)	A_1 (%)	τ_2 (ns)	A_2 (%)	τ_3 (ns)	A_3 (%)	τ_f (ns) (Amplitude Weighted)	$1/\tau_f$	χ^2
540	Toluene	-	-	4.20	58.09	9.95	41.91	6.61	0.15	1.05
540	1,4-Dioxane	-	-	4.42	61.15	11.42	38.85	7.14	0.14	1.13
540	Ethyl acetate	-	-	4.13	72.40	11.58	27.60	6.19	0.16	1.10
540	Chloroform	-	-	4.87	66.39	12.14	33.61	7.31	0.14	1.03
540	2-Methyl-2-butanol	0.44	15.66	3.72	58.21	11.09	26.13	5.13	0.19	1.13
540	N,N-dimethylformamide	0.32	18.19	5.03	58.94	12.47	22.87	5.87	0.17	1.09
540	Acetonitrile	0.37	11.43	4.53	65.95	12.19	22.62	5.79	0.17	1.12
540	Propylene carbonate	0.47	13.17	5.05	62.44	12.79	24.39	6.33	0.16	1.13
540	1-Octanol	0.74	14.86	5.16	59.62	12.76	25.53	6.44	0.16	1.09
540	1-Hexanol	0.49	18.97	5.03	61.02	12.89	20.01	5.74	0.17	1.11
540	1-Butanol	0.36	20.14	5.05	64.16	13.04	15.70	5.36	0.19	1.14
540	1-Pentanol	0.52	15.99	5.04	66.56	13.08	17.45	5.72	0.17	1.09
540	1-Propanol	-	-	4.52	80.80	12.76	19.20	6.10	0.16	1.14
540	Acetic acid	0.20	78.82	0.82	17.76	1.81	3.42	0.36	2.75	1.03
540	Ethanol	-	-	6.15	68.58	13.03	31.42	8.31	0.12	1.14
540	1,5-Pentanediol	-	-	4.61	81.55	12.69	18.45	6.10	0.16	1.09
540	1,3-Butanediol	-	-	6.30	72.17	13.36	27.83	8.27	0.12	1.09
540	1,4-Butanediol	2.20	17.52	6.70	64.95	13.94	17.53	7.18	0.14	1.14
540	1,3-Propanediol	-	-	5.69	73.28	12.05	26.72	7.39	0.14	1.11
540	Methanol	-	-	4.11	87.36	11.90	12.64	5.09	0.20	1.04
540	1,2-Ethanediol	2.69	22.95	6.36	66.78	14.27	10.27	6.33	0.16	1.12
540	2,2,2-Trifluoroethanol	0.19	94.96	0.98	3.70	4.12	1.34	0.28	3.62	1.02
540	Ethanol-d	-	-	4.97	80.51	12.87	19.49	6.51	0.15	1.10
540	Methanol-d	-	-	4.86	88.07	13.65	11.93	5.91	0.17	1.10

Table 1.2.17. Summary of Time Correlated Single Photon Counting (TCSPC) fluorescent lifetimes (amplitude weighted) of **6a** recorded at 540 nm.

Wavelength (nm)	Solvent	τ_1 (ns)	A_1 (%)	τ_2 (ns)	A_2 (%)	τ_3 (ns)	A_3 (%)	τ_f (ns) (Amplitude Weighted)	$1/\tau_f$	χ^2
570	Toluene	-	-	4.11	42.56	9.97	57.44	7.47	0.13	1.03
570	1,4-Dioxane	-	-	4.35	46.60	11.45	53.40	8.14	0.12	1.10
570	Ethyl acetate	-	-	4.20	63.23	11.89	36.77	7.03	0.14	1.11
570	Chloroform	-	-	4.82	53.15	12.15	46.85	8.26	0.12	1.07
570	2-Methyl-2-butanol	0.46	19.35	3.73	46.33	11.09	34.31	5.62	0.18	1.09
570	N,N-dimethylformamide	-	-	4.88	60.47	12.59	39.53	7.93	0.13	1.09
570	Acetonitrile	2.43	16.28	5.41	57.18	13.74	26.54	7.14	0.14	1.10
570	Propylene carbonate	0.62	10.63	5.08	54.99	13.08	34.38	7.35	0.14	1.08
570	1-Octanol	0.68	14.96	5.33	51.16	13.02	33.88	7.24	0.14	1.08
570	1-Hexanol	0.42	18.96	5.01	53.23	13.05	27.81	6.38	0.16	1.06
570	1-Butanol	0.32	26.54	5.02	53.49	13.13	19.96	5.39	0.19	1.08
570	1-Pentanol	0.45	15.43	5.01	60.05	13.24	24.52	6.32	0.16	1.02
570	1-Propanol	-	-	4.55	74.20	13.14	25.80	6.76	0.15	1.11
570	Acetic acid	0.19	82.74	0.86	16.09	2.42	1.18	0.32	3.10	1.31
570	Ethanol	-	-	7.12	68.06	14.45	31.94	9.46	0.11	1.13
570	1,5-Pentanediol	-	-	4.64	75.40	13.08	24.60	6.72	0.15	1.11
570	1,3-Butanediol	-	-	6.88	69.91	14.59	30.09	9.20	0.11	1.12
570	1,4-Butanediol	2.99	21.55	7.16	56.69	14.56	21.76	7.87	0.13	1.08
570	1,3-Propanediol	-	-	5.84	52.07	13.01	47.93	7.94	0.13	1.08
570	Methanol	-	-	4.15	84.17	12.75	15.83	5.51	0.18	1.11
570	1,2-Ethanediol	2.80	17.76	5.93	61.95	13.23	20.29	6.86	0.15	1.19
570	2,2,2-Trifluoroethanol	0.20	58.32	0.93	12.81	3.87	28.87	0.33	3.07	1.08
570	Ethanol-d	-	-	4.94	74.06	13.28	25.94	7.10	0.14	1.06
570	Methanol-d	-	-	4.89	83.99	14.15	16.01	6.37	0.16	1.15

Table 1.2.18. Summary of Time Correlated Single Photon Counting (TCSPC) fluorescent lifetimes (amplitude weighted) of **6a** recorded at 570 nm.

1.2.7 Average fluorescent lifetimes - Solvatochromic analysis.

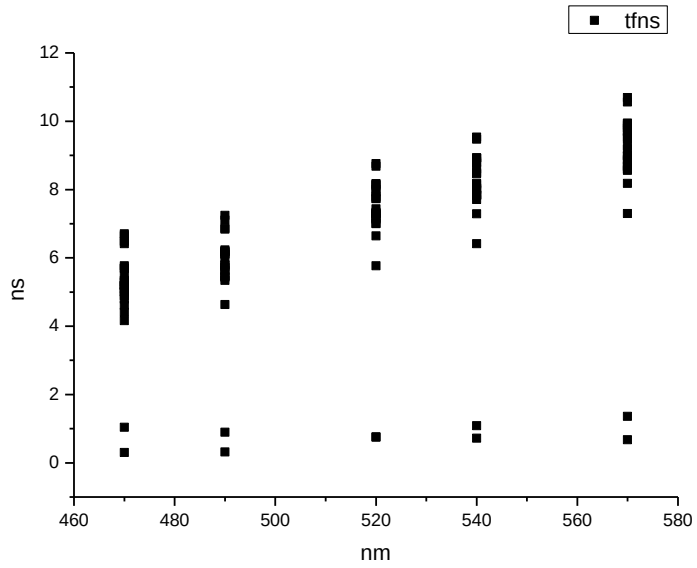

Figure 1.2.61. Intensity weighted average lifetime (τ_f) of **6a** versus wavelength (nm).

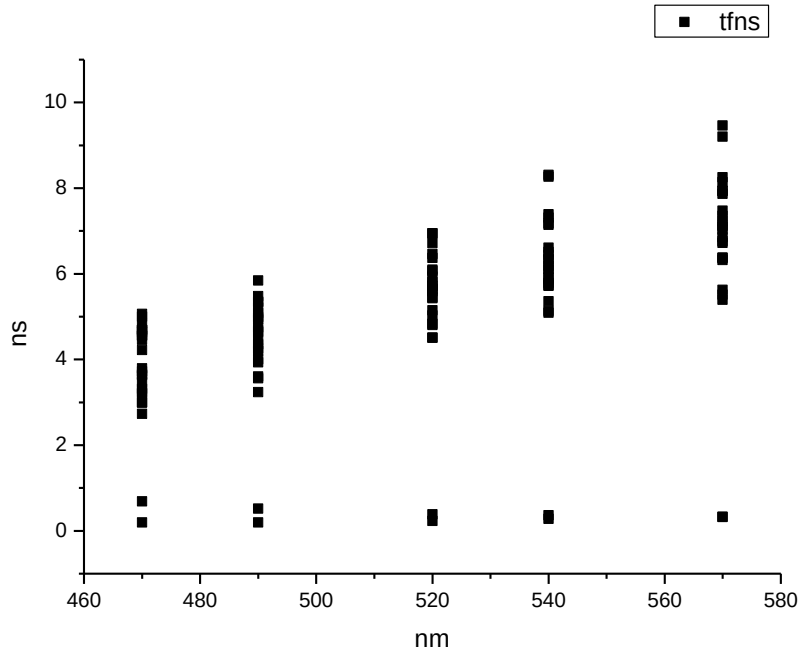

Figure 1.2.62. Amplitude weighted average lifetime (τ_f) of **6a** versus wavelength (nm).

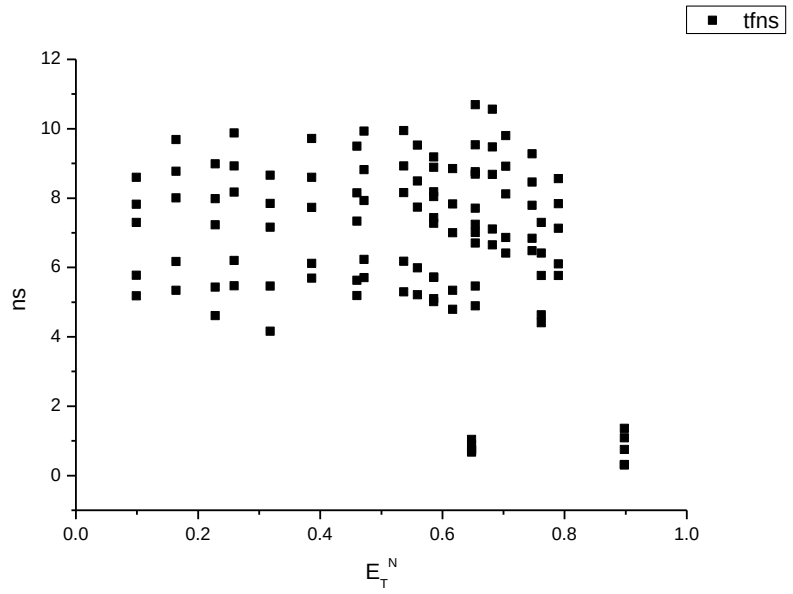

Figure 1.2.63. Intensity weighted average lifetime (τ_f) of **6a** versus E_T^N.

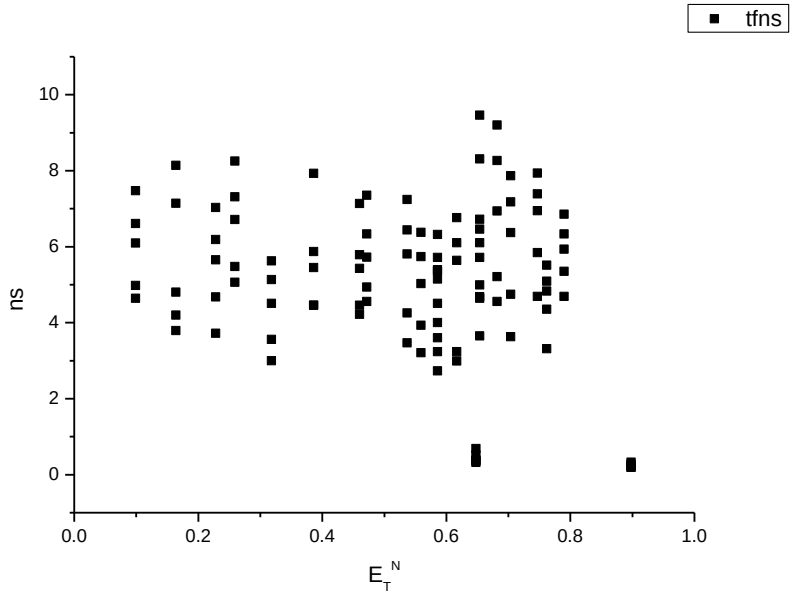

Figure 1.2.64. Amplitude weighted average lifetime (τ_f) of **6a** versus E_T^N.

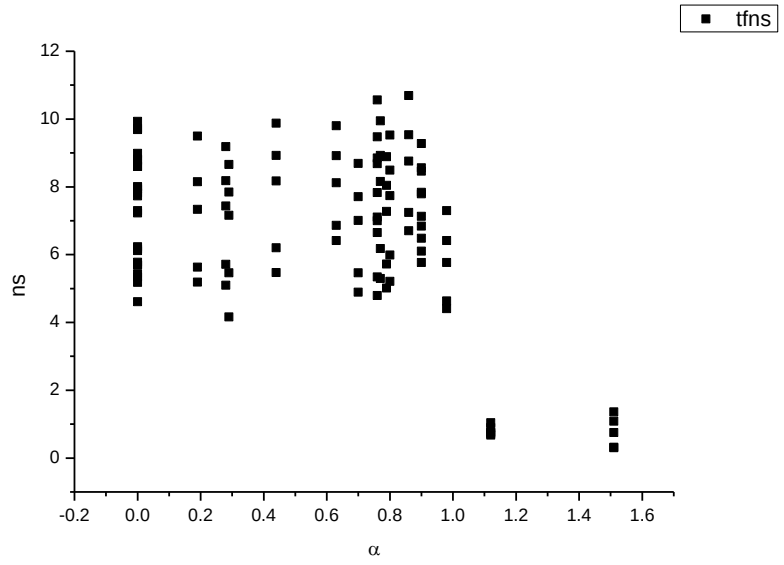

Figure 1.2.65. Intensity weighted average lifetime (τ_f) of **6a** versus α.

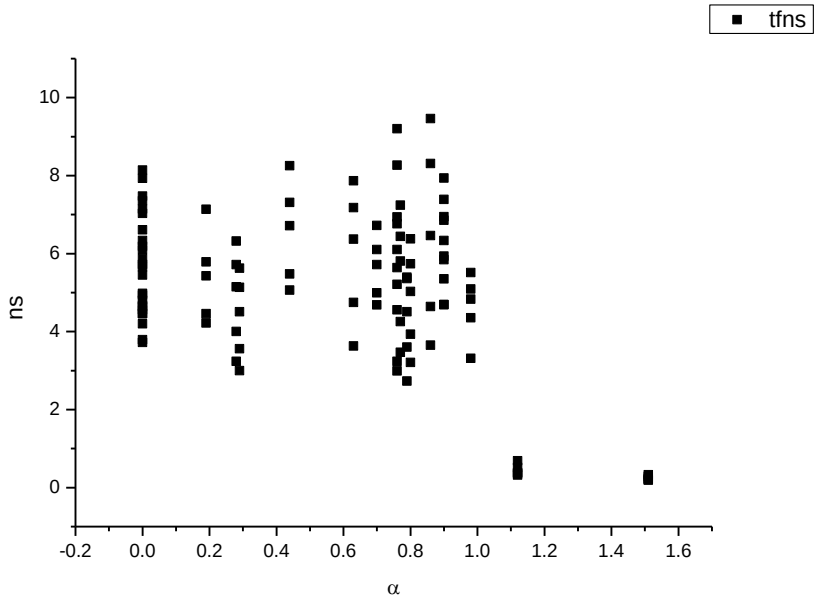

Figure 1.2.66. Amplitude weighted average lifetime (τ_f) of **6a** versus α.

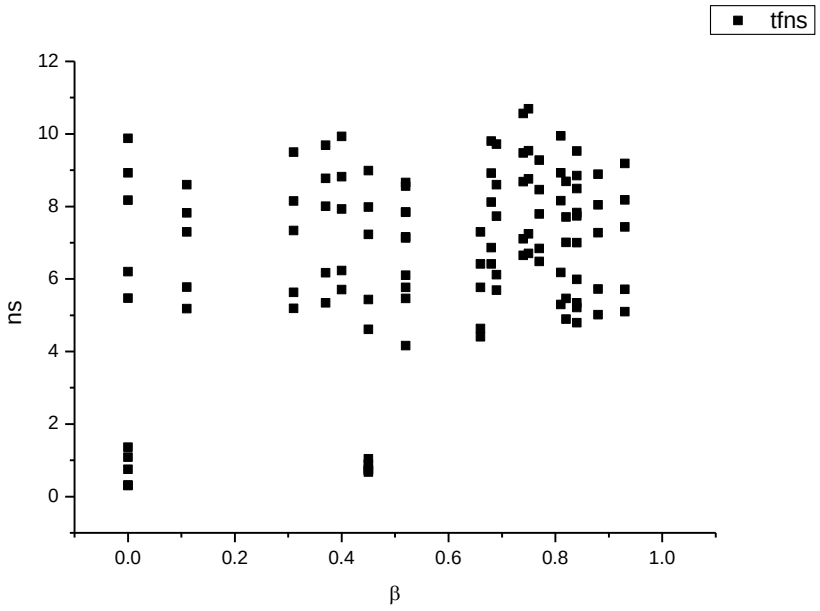

Figure 1.2.67. Intensity weighted average lifetime (τ_f) of **6a** versus β.

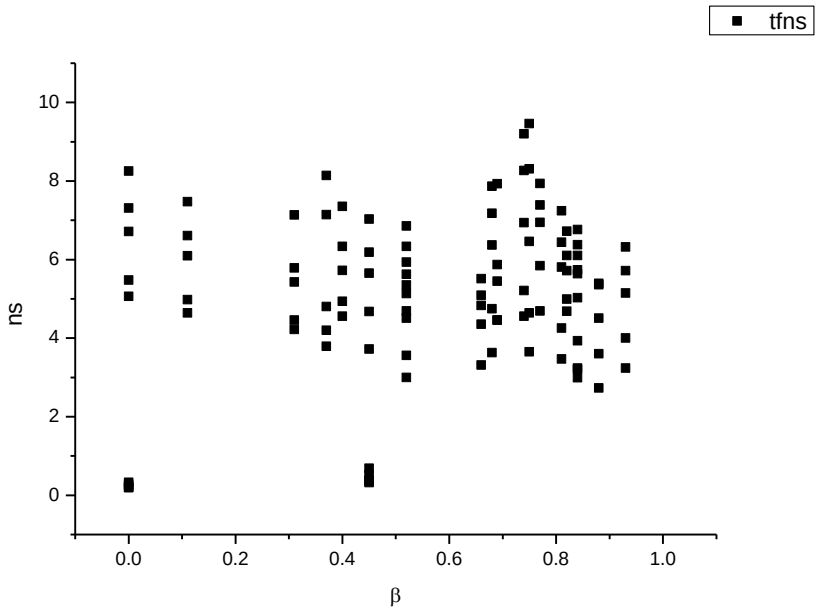

Figure 1.2.68. Amplitude weighted average lifetime (τ_f) of **6a** versus β.

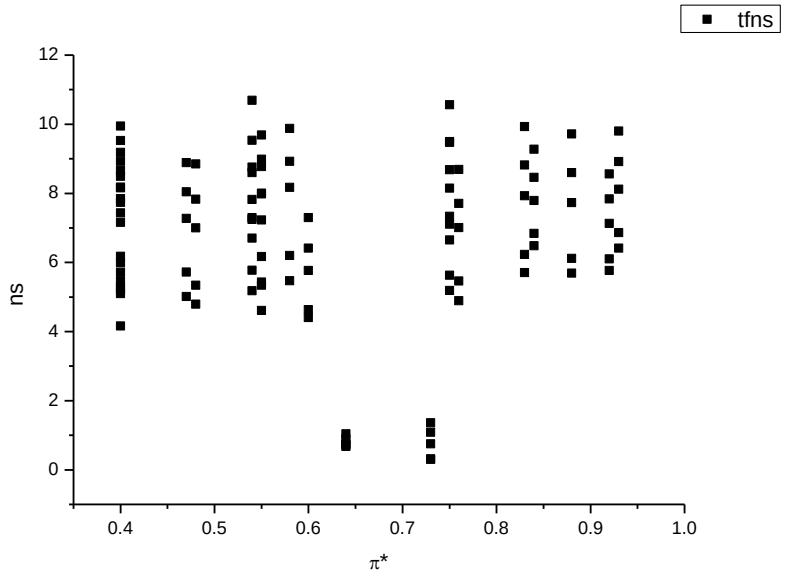

Figure 1.2.69. Intensity weighted average lifetime (τ_f) of **6a** versus π^*.

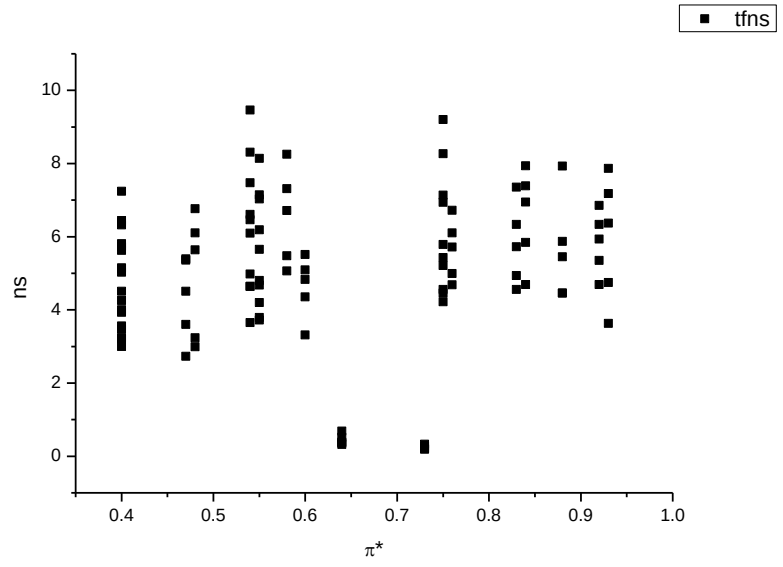

Figure 1.2.70. Amplitude weighted average lifetime (τ_f) of **6a** versus π^*.

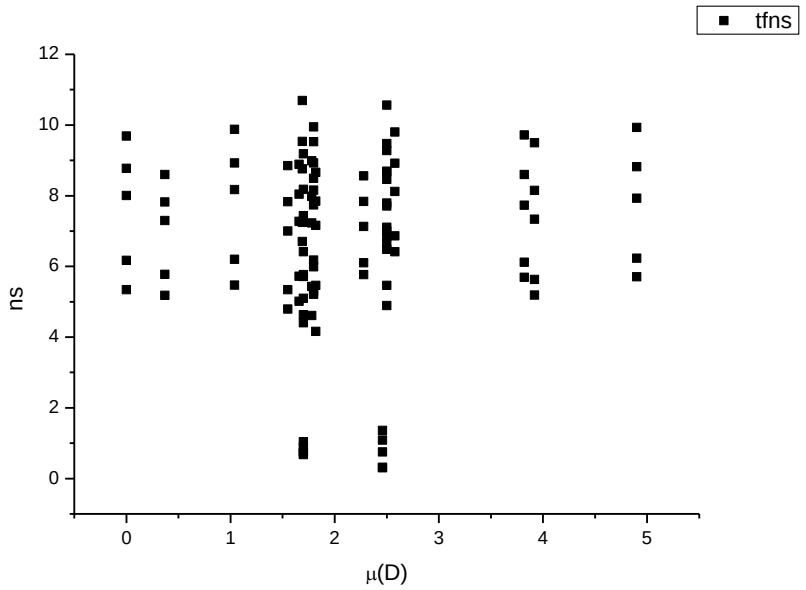

Figure 1.2.71. Intensity weighted average lifetime (τ_f) of **6a** versus μ(D).

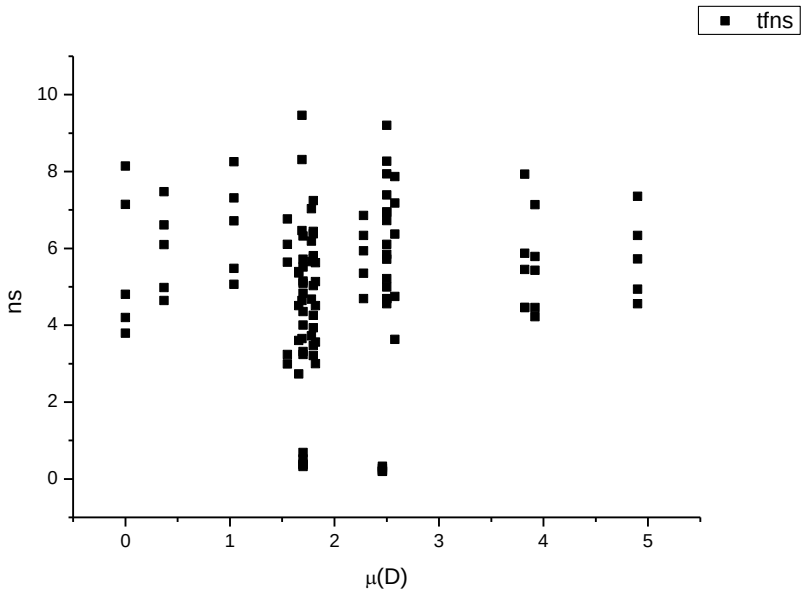

Figure 1.2.72. Amplitude weighted average lifetime (τ_f) of **6a** versus μ(D).

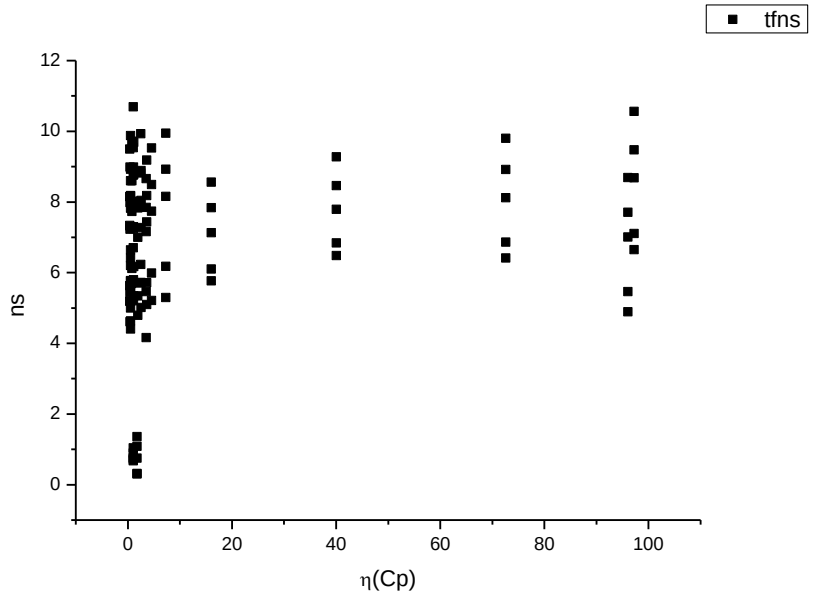

Figure 1.2.73. Intensity weighted average lifetime (τ_f) of **6a** versus η(Cp).

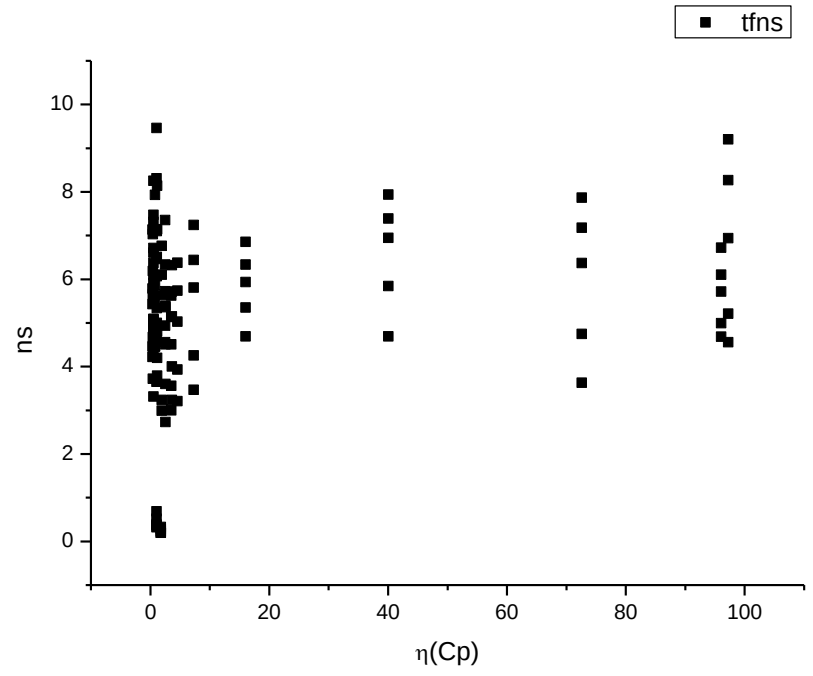

Figure 1.2.74. Amplitude weighted average lifetime (τ_f) of **6a** versus η(Cp).

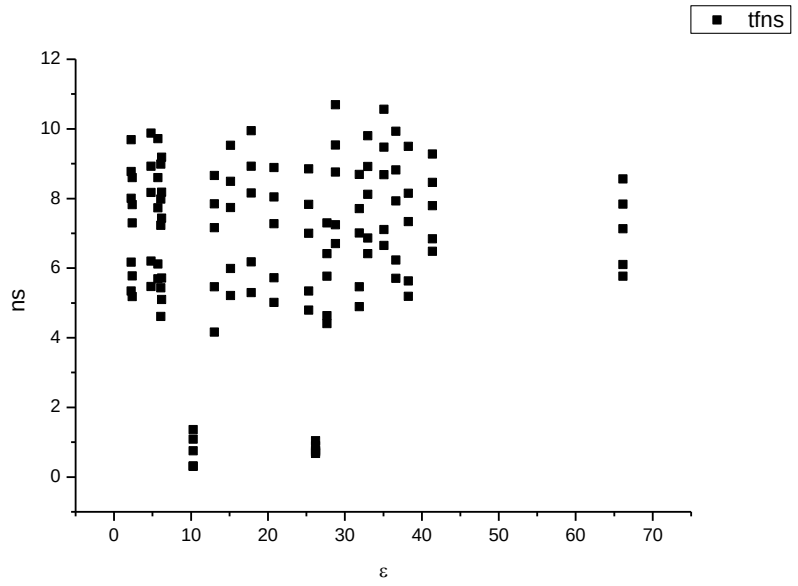

Figure 1.2.75. Intensity weighted average lifetime (τ_f) of **6a** versus ε.

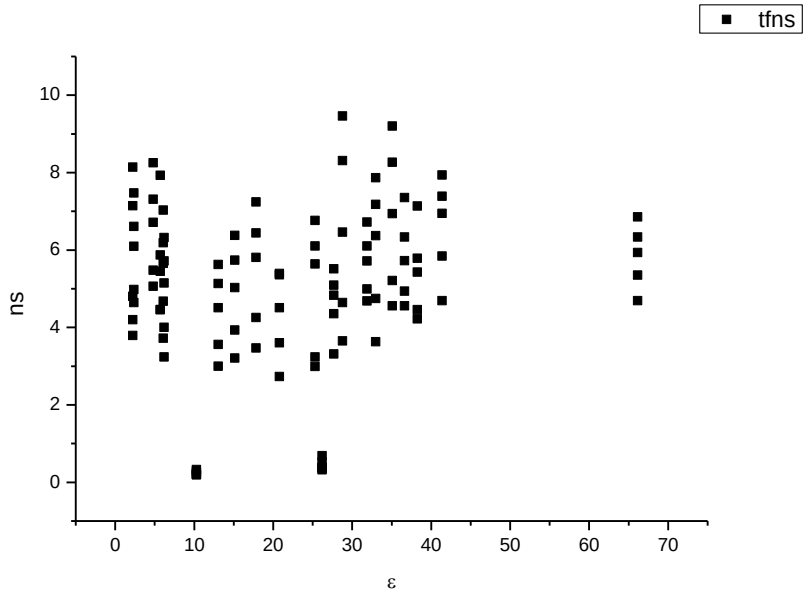

Figure 1.2.76. Amplitude weighted average lifetime (τ_f) of **6a** versus ε.

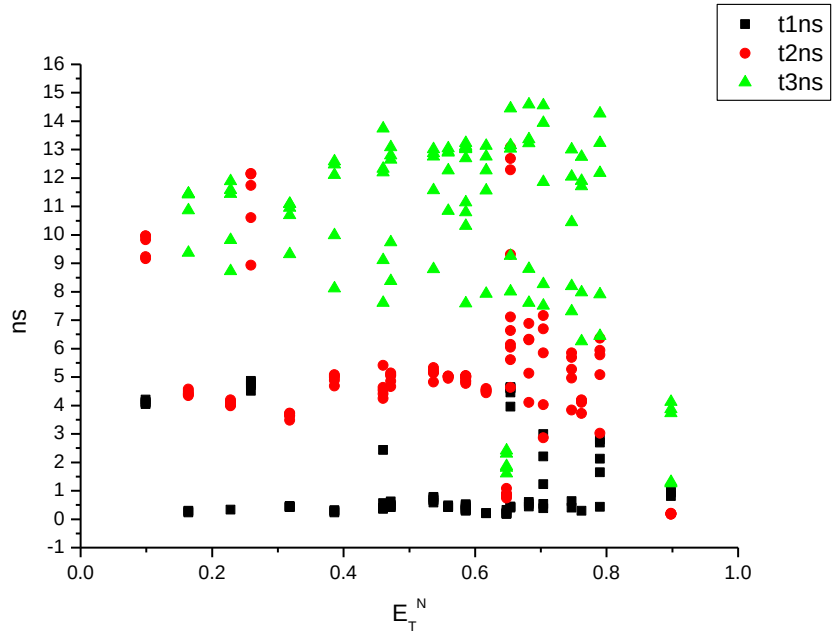

Figure 1.2.77. Intensity weighted components of TCSPC lifetime decay of **6a** (470 nm to 570 nm) versus E_T^N.

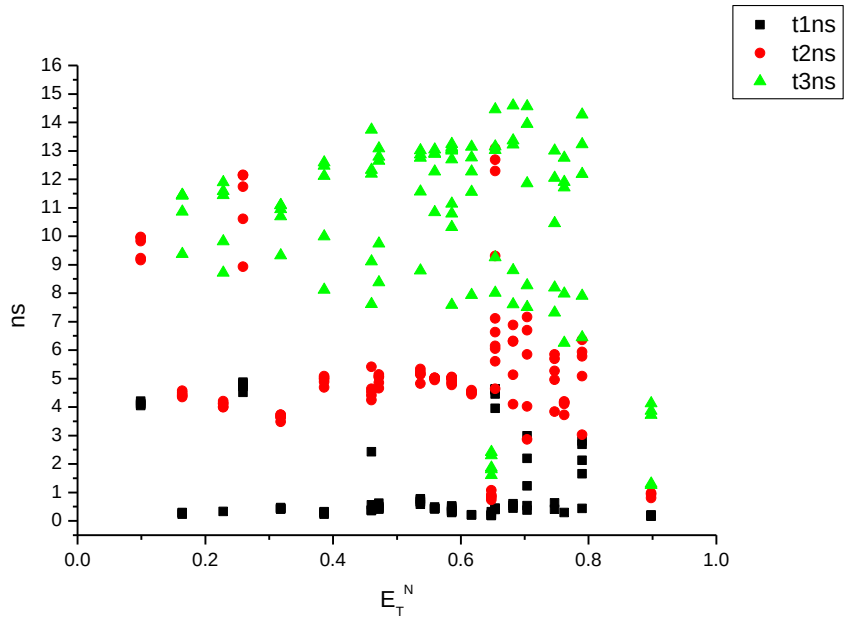

Figure 1.2.78. Amplitude weighted components of TCSPC lifetime decay of **6a** (470 nm to 570 nm) versus E_T^N.

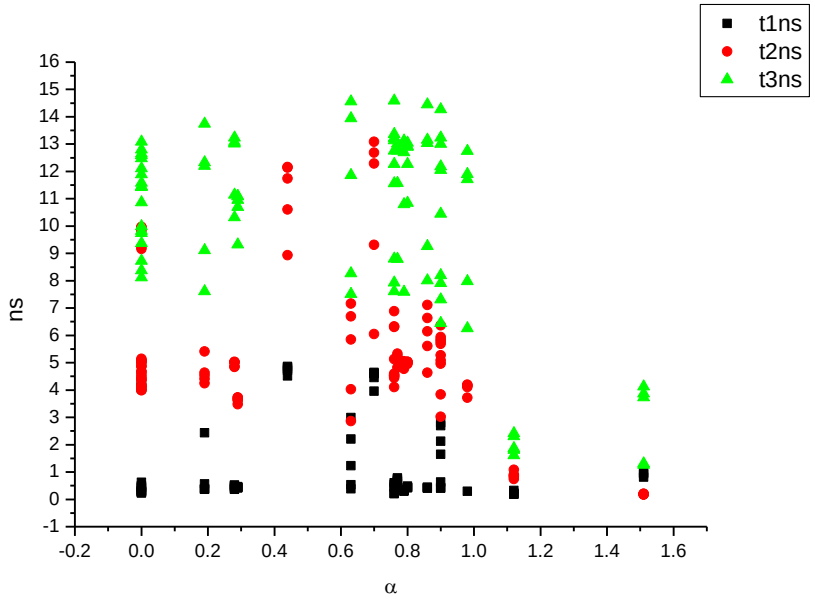

Figure 1.2.79. Intensity weighted components of TCSPC lifetime decay of **6a** (470 nm to 570 nm) versus α.

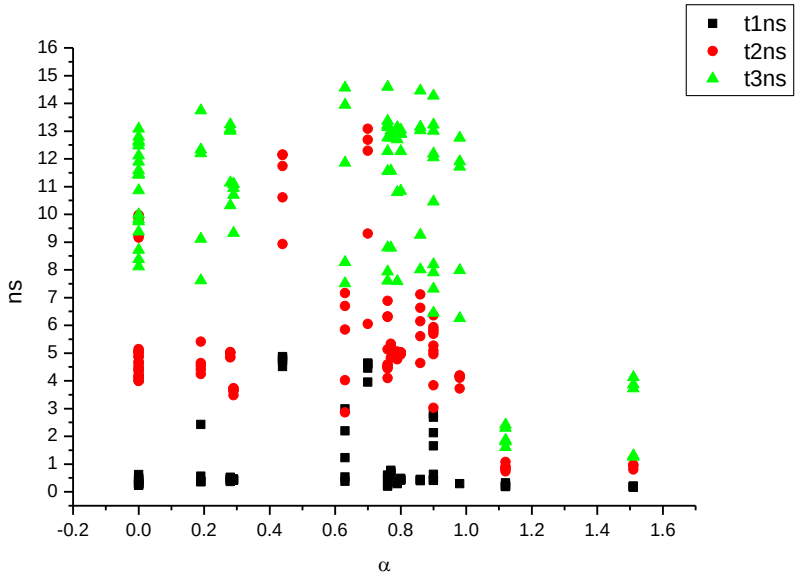

Figure 1.2.80. Amplitude weighted components of TCSPC lifetime decay of **6a** (470 nm to 570 nm) versus α.

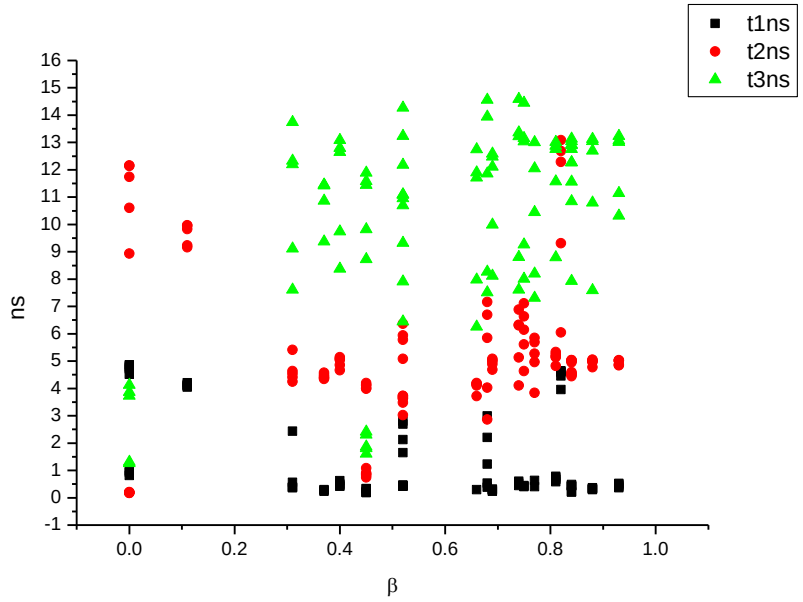

Figure 1.2.81. Intensity weighted components of TCSPC lifetime decay of **6a** (470 nm to 570 nm) versus β.

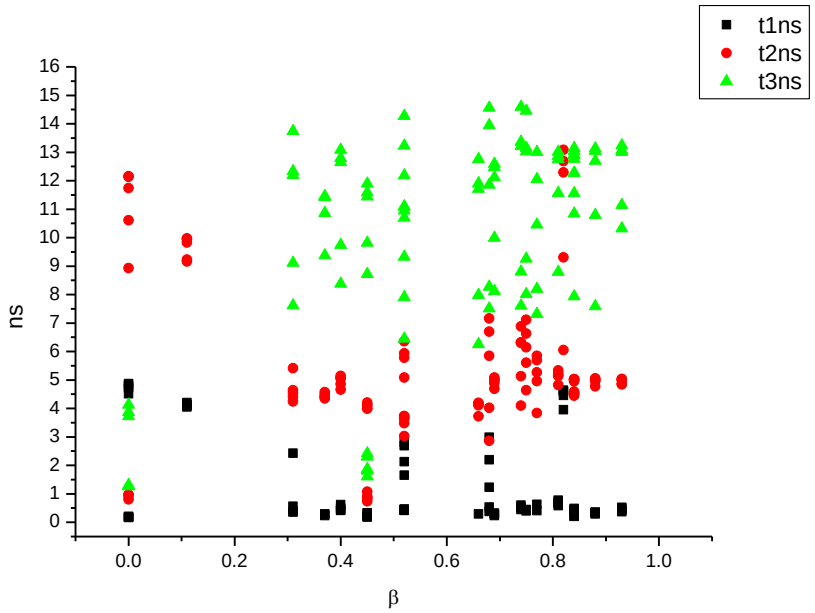

Figure 1.2.82. Amplitude weighted components of TCSPC lifetime decay of **6a** (470 nm to 570 nm) versus β.

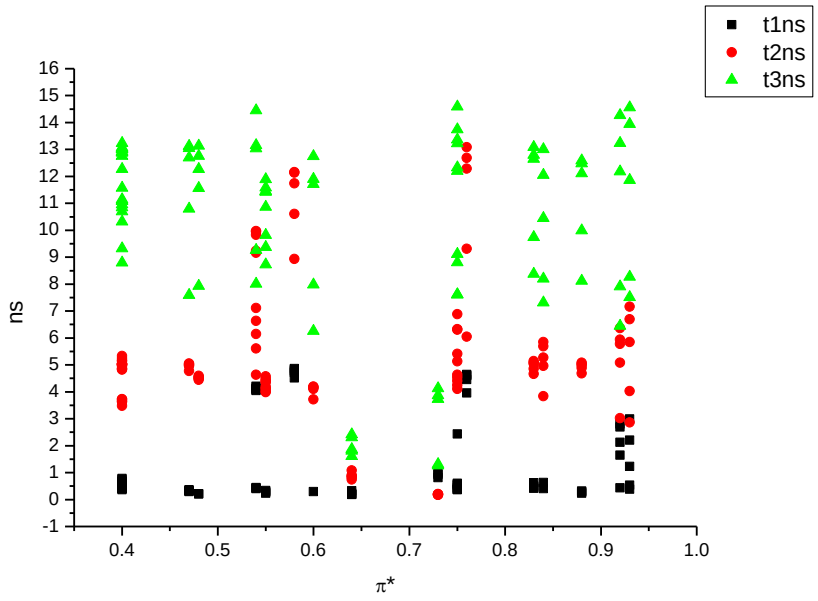

Figure 1.2.83. Intensity weighted components of TCSPC lifetime decay of **6a** (470 nm to 570 nm) versus π*.

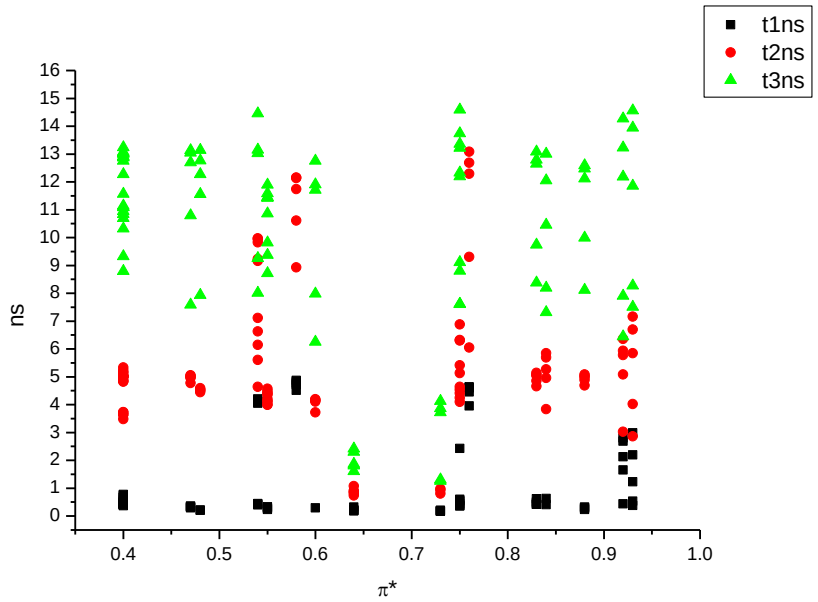

Figure 1.2.84. Amplitude weighted components of TCSPC lifetime decay of **6a** (470 nm to 570 nm) versus π*.

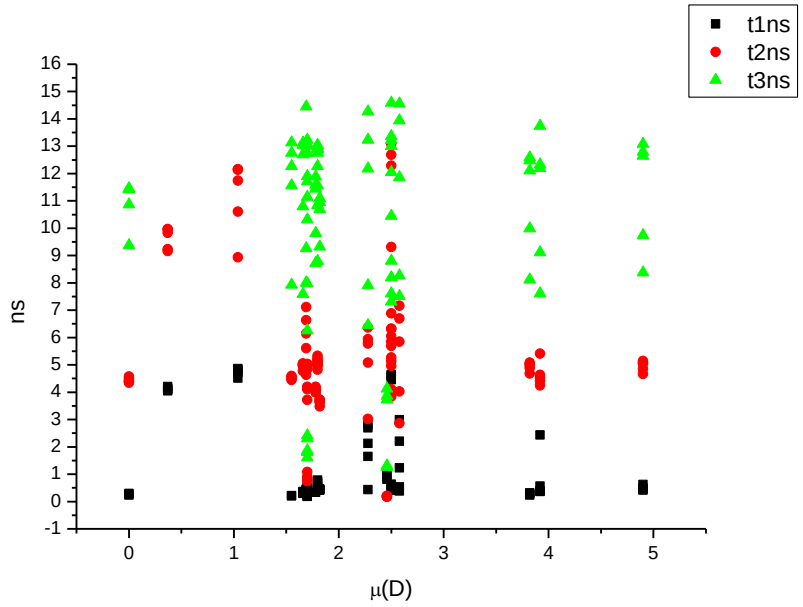

Figure 1.2.85. Intensity weighted components of TCSPC lifetime decay of **6a** (470 nm to 570 nm) versus μ(D).

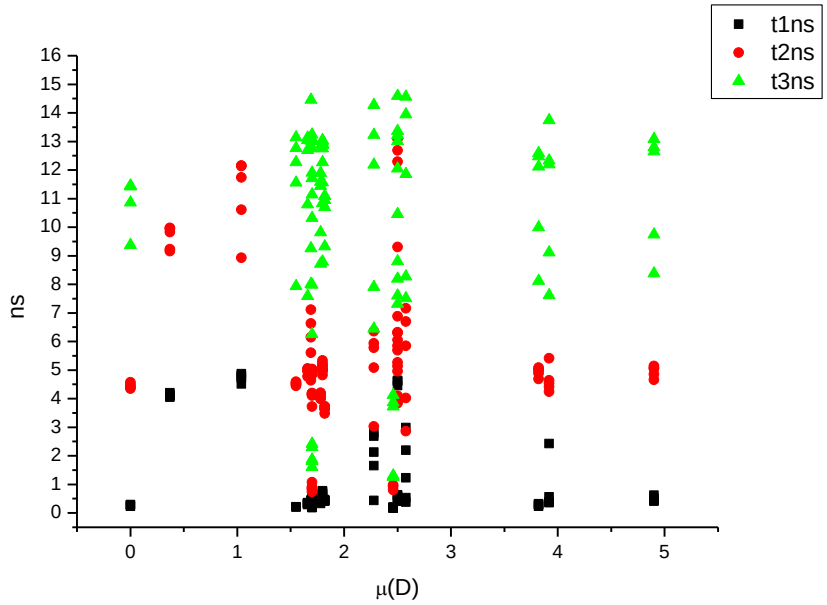

Figure 1.2.86. Amplitude weighted components of TCSPC lifetime decay of **6a** (470 nm to 570 nm) versus μ(D).

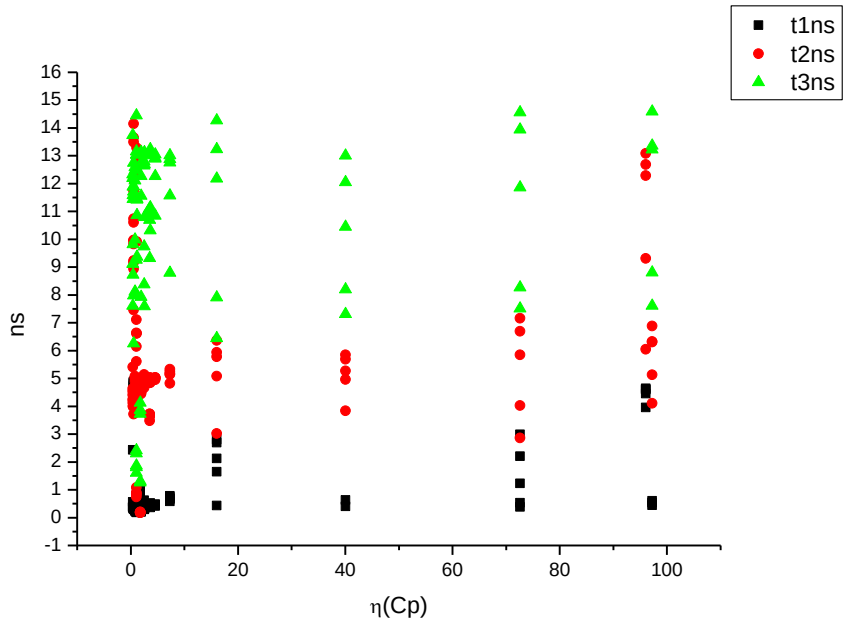

Figure 1.2.87. Intensity weighted components of TCSPC lifetime decay of **6a** (470 nm to 570 nm) versus η(Cp).

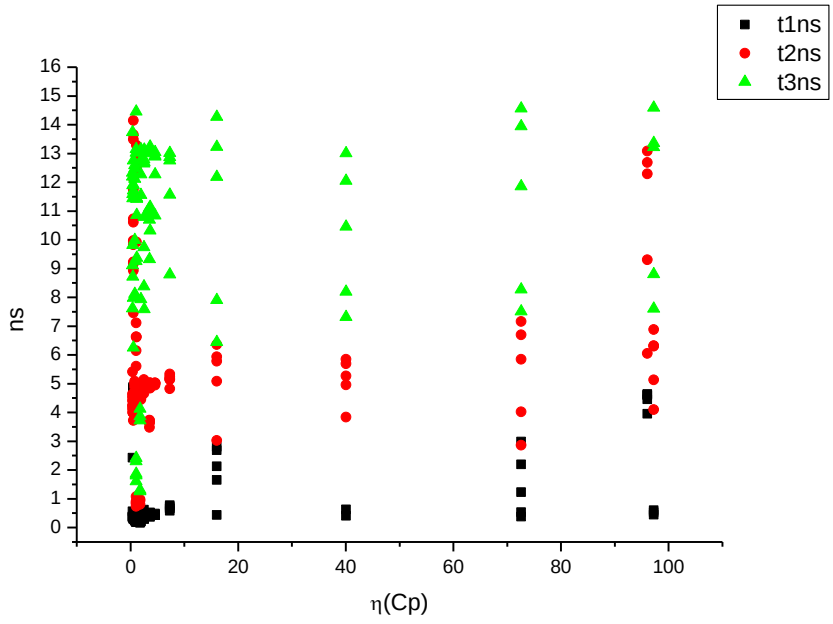

Figure 1.2.88. Amplitude weighted components of TCSPC lifetime decay of **6a** (470 nm to 570 nm) versus η(Cp).

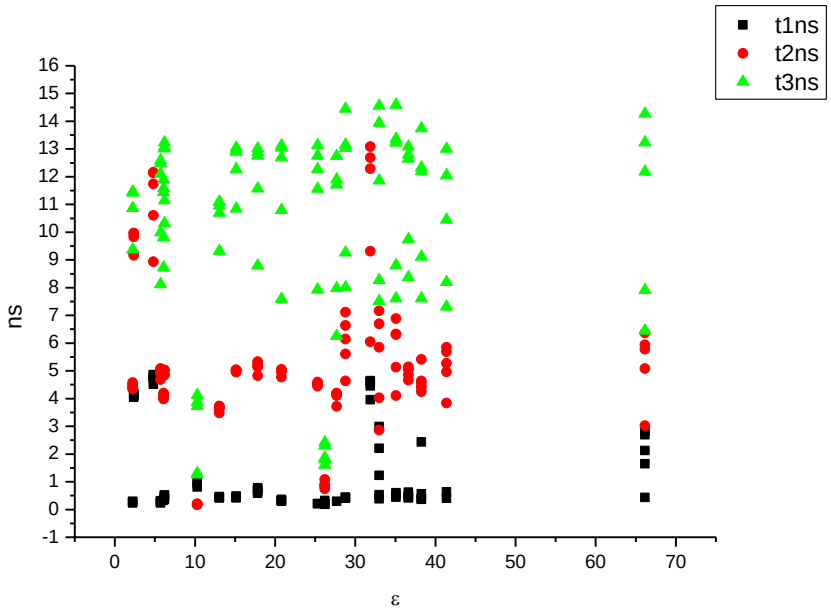

Figure 1.2.89. Intensity weighted components of TCSPC lifetime decay of **6a** (470 nm to 570 nm) versus ε.

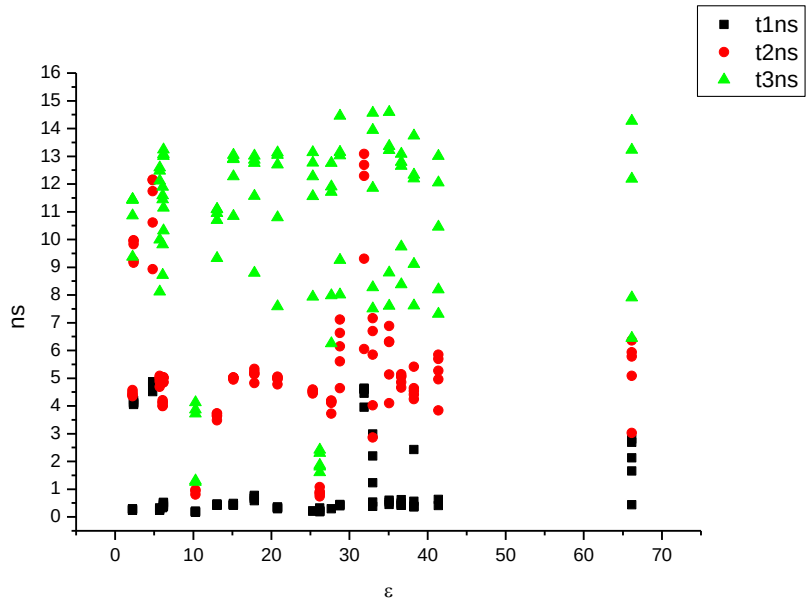

Figure 1.2.90. Amplitude weighted components of TCSPC lifetime decay of **6a** (470 nm to 570 nm) versus ε.

1.2.7.1 470 nm Lifetime – Solvatochromic analysis.

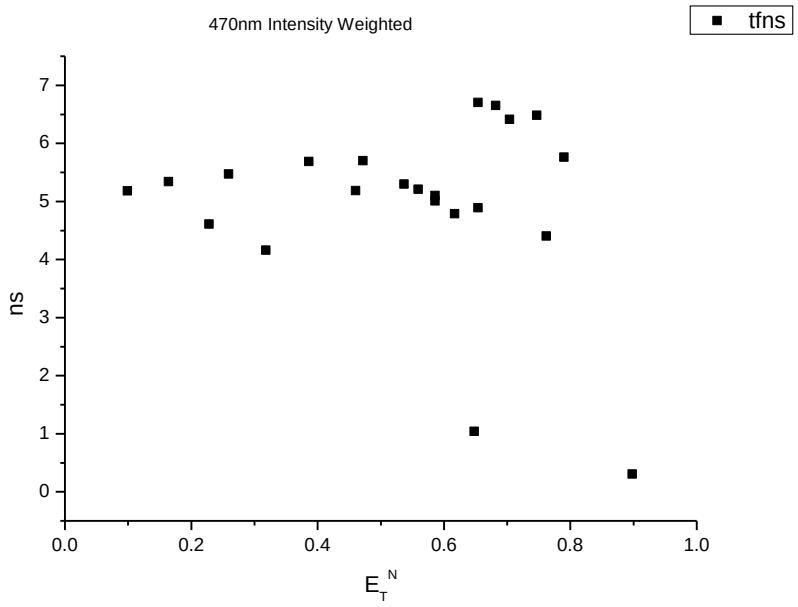

Figure 1.2.91. Intensity weighted average lifetime (τ_f) of **6a** at 470 nm versus E_T^N.

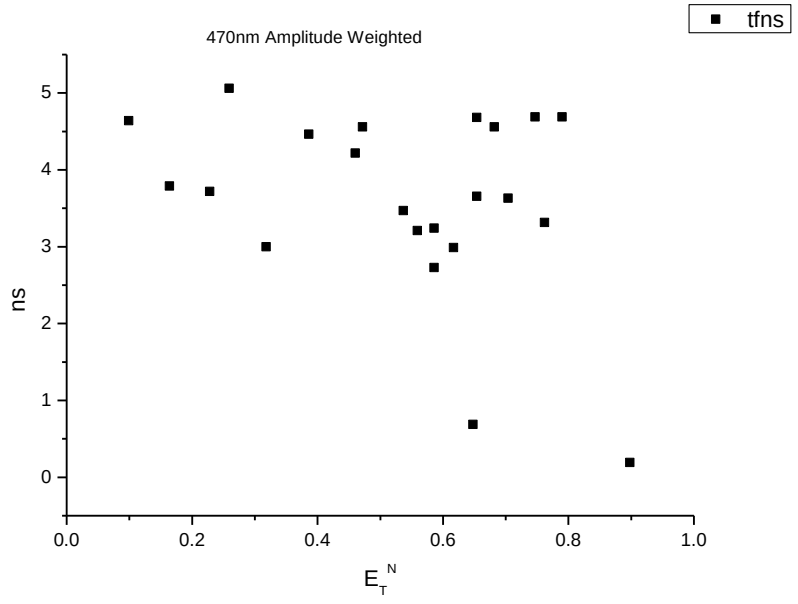

Figure 1.2.92. Amplitude weighted average lifetime (τ_f) of **6a** at 470 nm versus E_T^N.

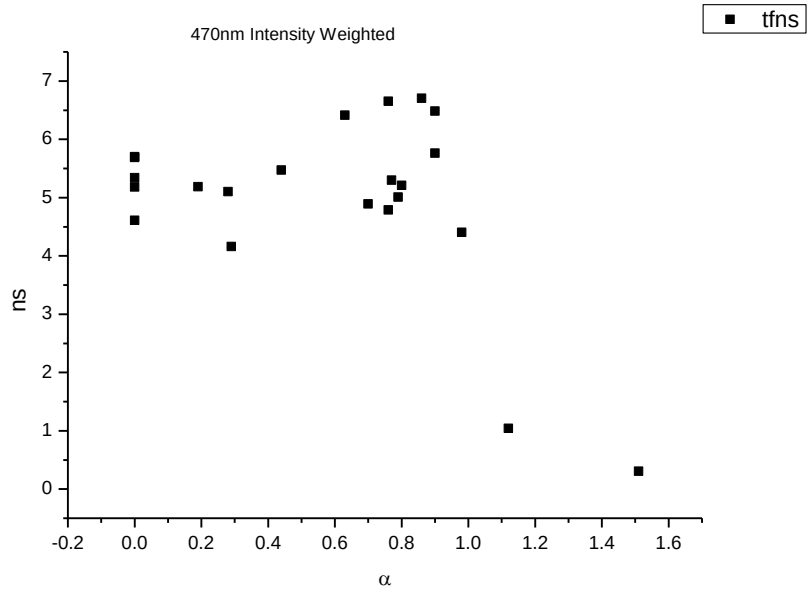

Figure 1.2.93. Intensity weighted average lifetime (τ_f) of **6a** at 470 nm versus α.

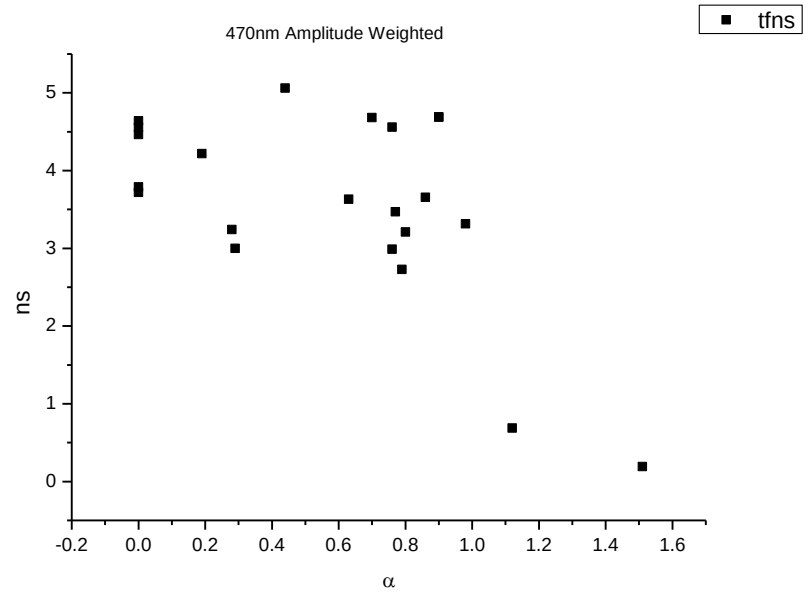

Figure 1.2.94. Amplitude weighted average lifetime (τ_f) of **6a** at 470 nm versus α.

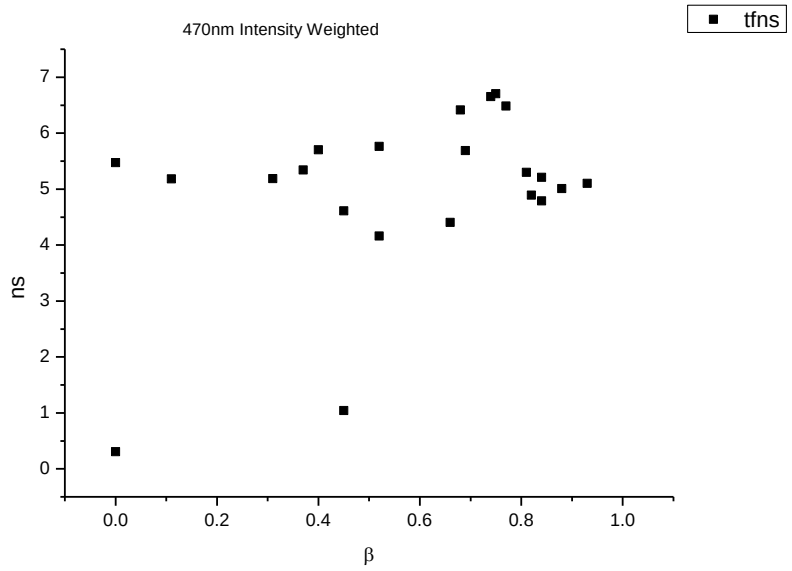

Figure 1.2.95. Intensity weighted average lifetime (τ_f) of **6a** at 470 nm versus β.

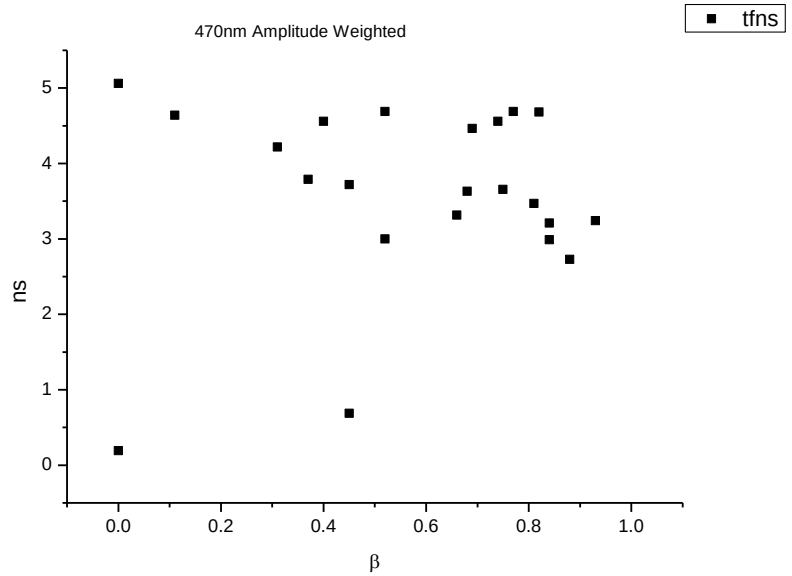

Figure 1.2.96. Amplitude weighted average lifetime (τ_f) of **6a** at 470 nm versus β.

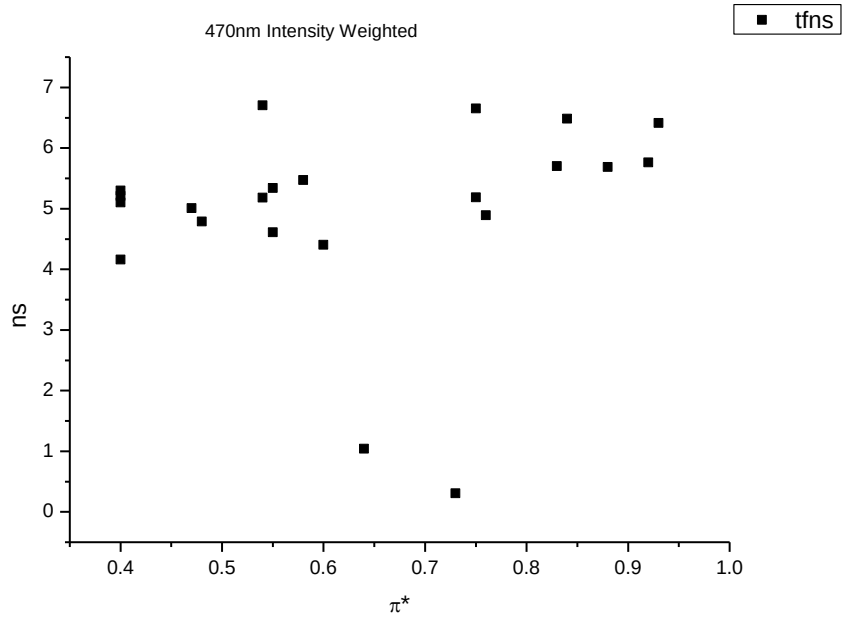

Figure 1.2.97. Intensity weighted average lifetime (τ_f) of **6a** at 470 nm versus π*.

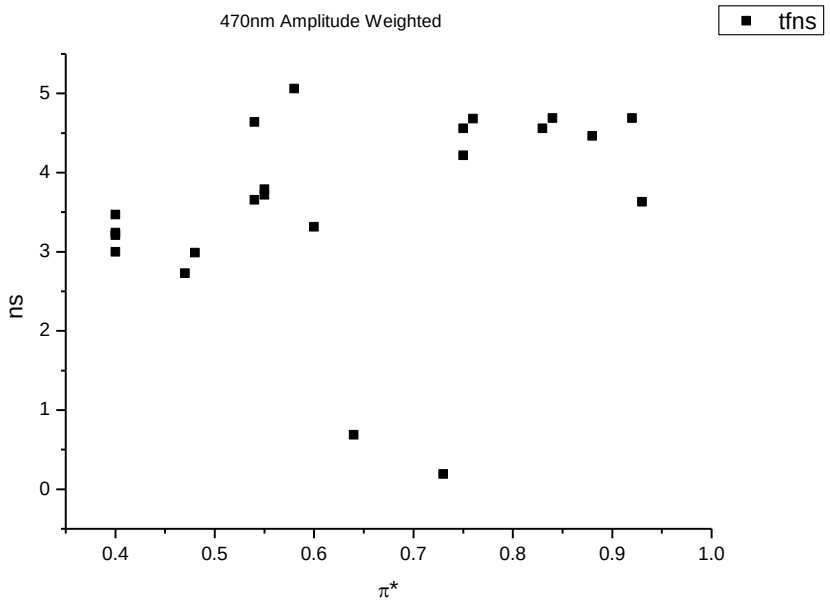

Figure 1.2.98. Amplitude weighted average lifetime (τ_f) of **6a** at 470 nm versus π*.

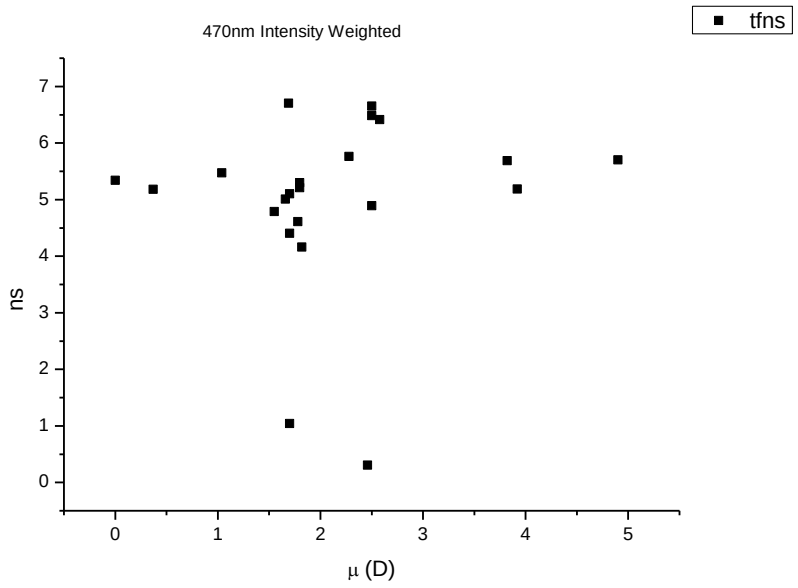

Figure 1.2.99. Intensity weighted average lifetime (τ_f) of **6a** at 470 nm versus μ(D).

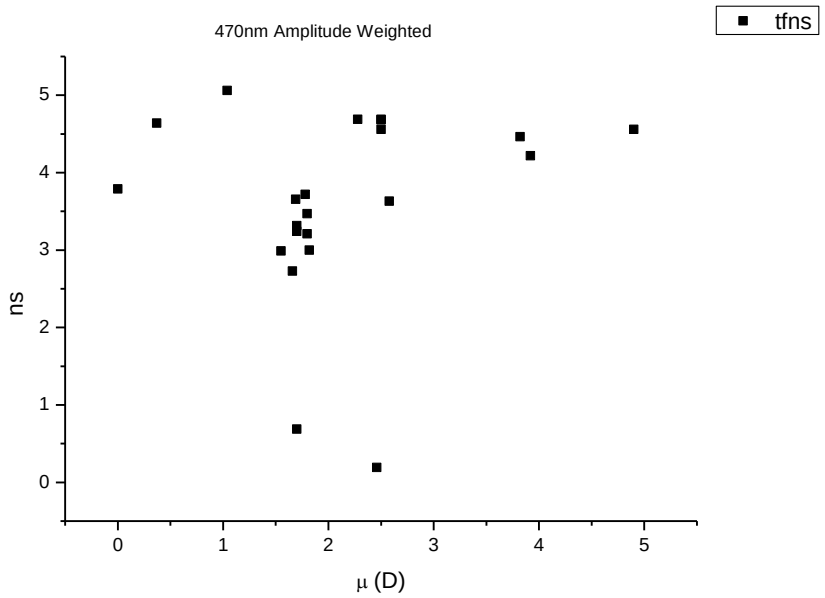

Figure 1.2.100. Amplitude weighted average lifetime (τ_f) of **6a** at 470 nm versus μ(D).

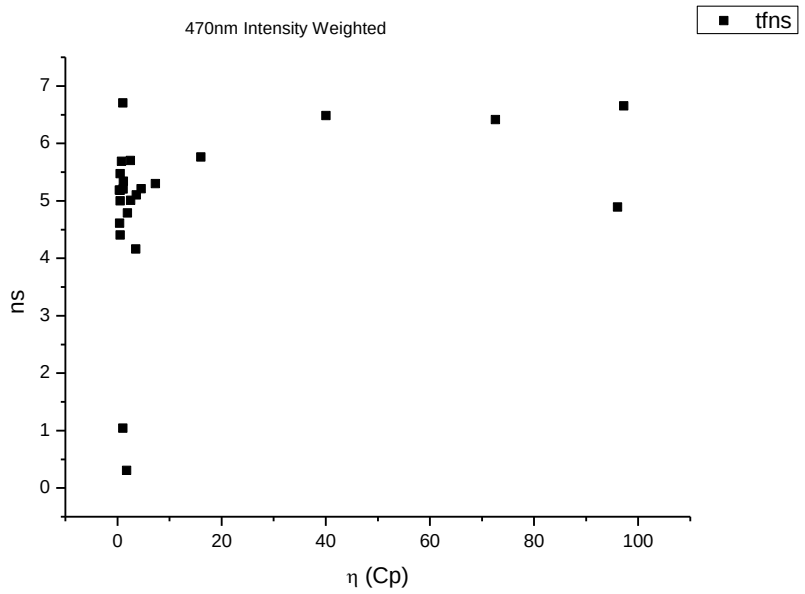

Figure 1.2.101. Intensity weighted average lifetime (τ_f) of **6a** at 470 nm versus η(Cp).

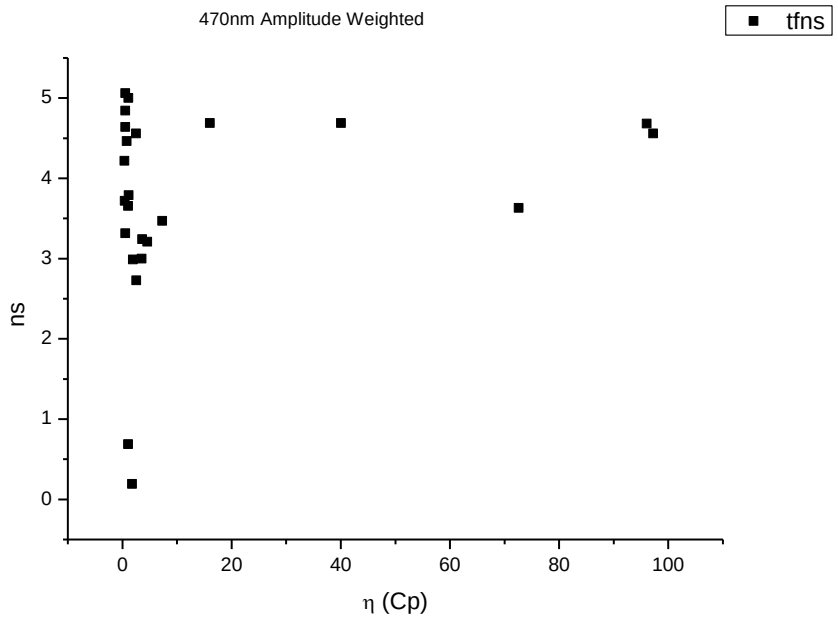

Figure 1.2.102. Amplitude weighted average lifetime (τ_f) of **6a** at 470 nm versus η(Cp).

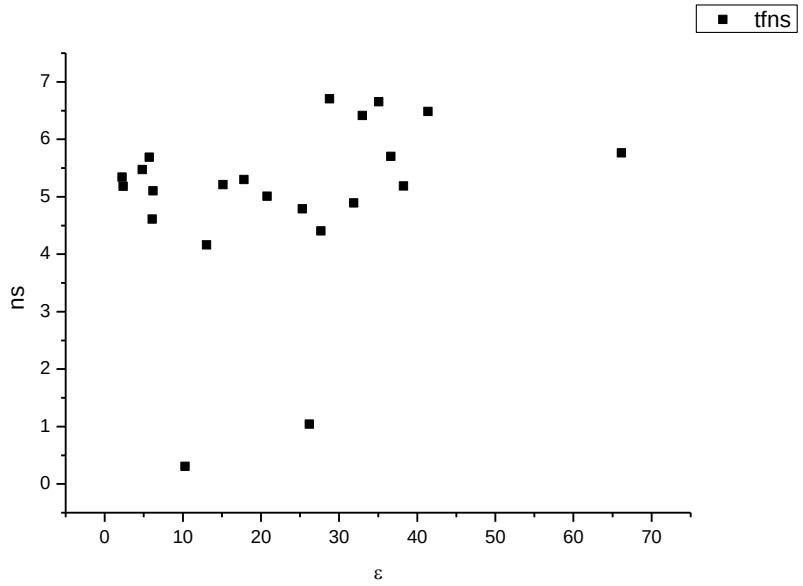

Figure 1.2.103. Intensity weighted average lifetime (τ_f) of **6a** at 470 nm versus ε.

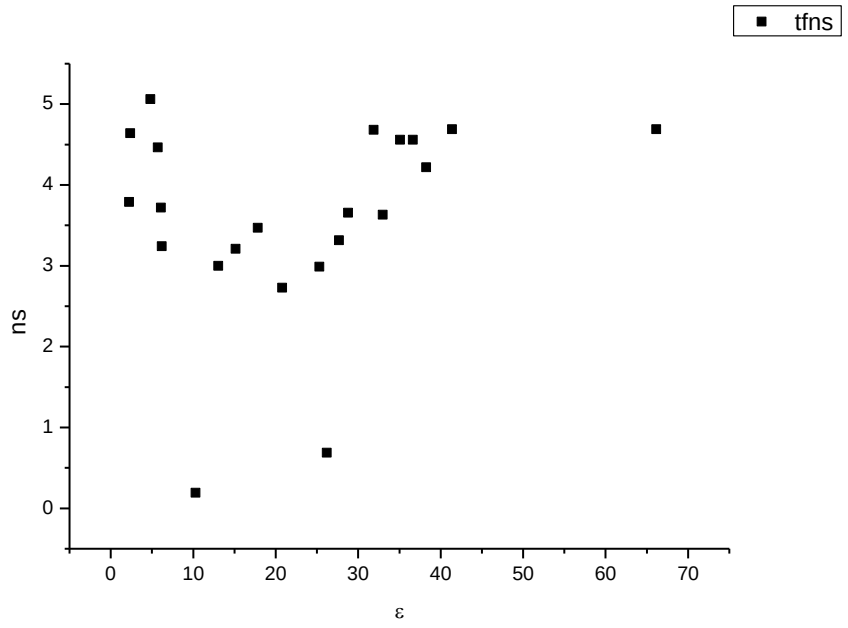

Figure 1.2.104. Amplitude weighted average lifetime (τ_f) of **6a** at 470 nm versus ε.

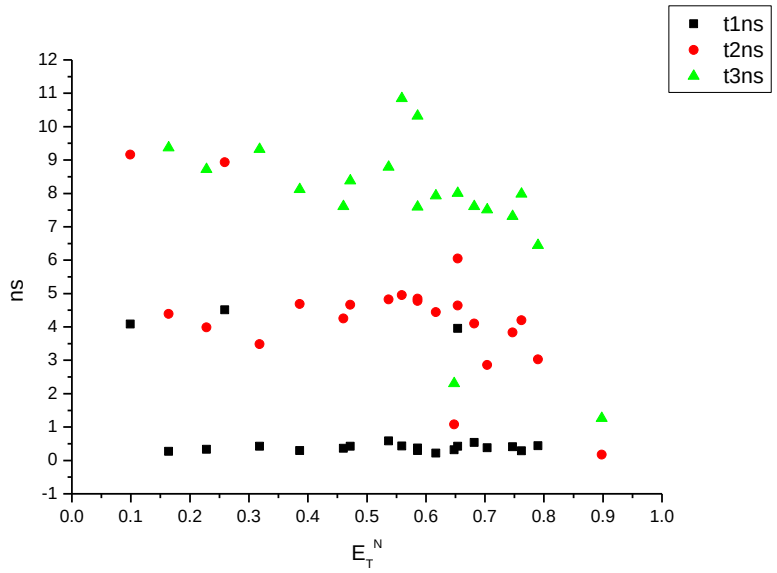

Figure 1.2.105. Intensity weighted components of TCSPC lifetime decay of **6a** (470 nm) versus E_T^N.

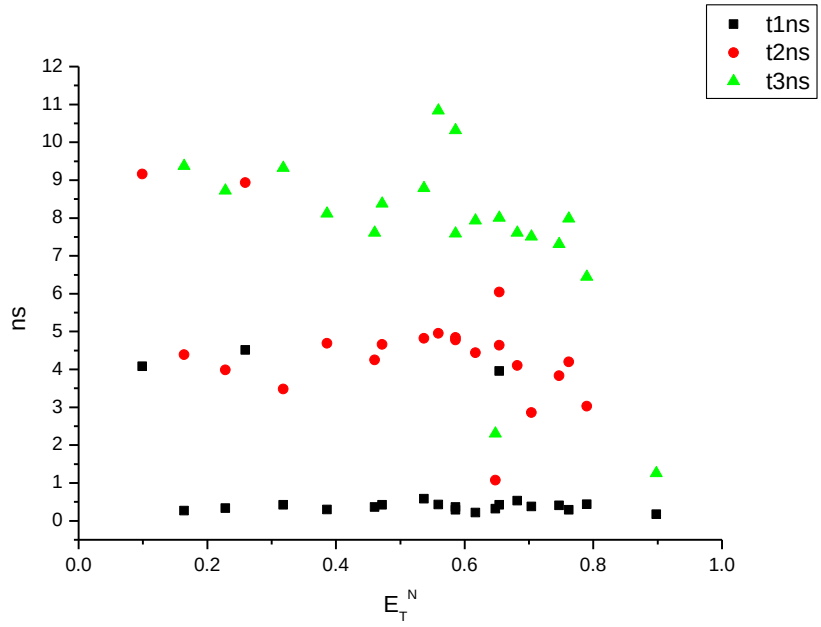

Figure 1.2.106. Amplitude weighted components of TCSPC lifetime decay of **6a** (470 nm) versus E_T^N.

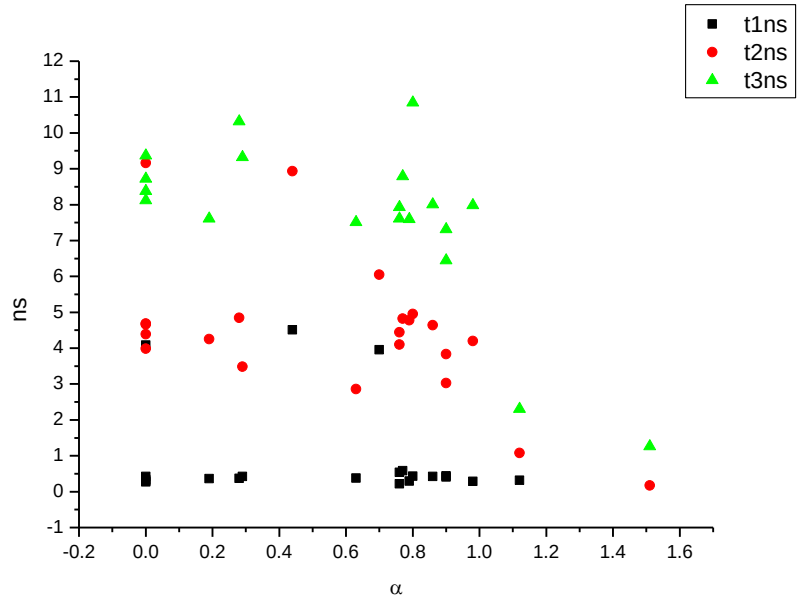

Figure 1.2.107. Intensity weighted components of TCSPC lifetime decay of **6a** (470 nm) versus α.

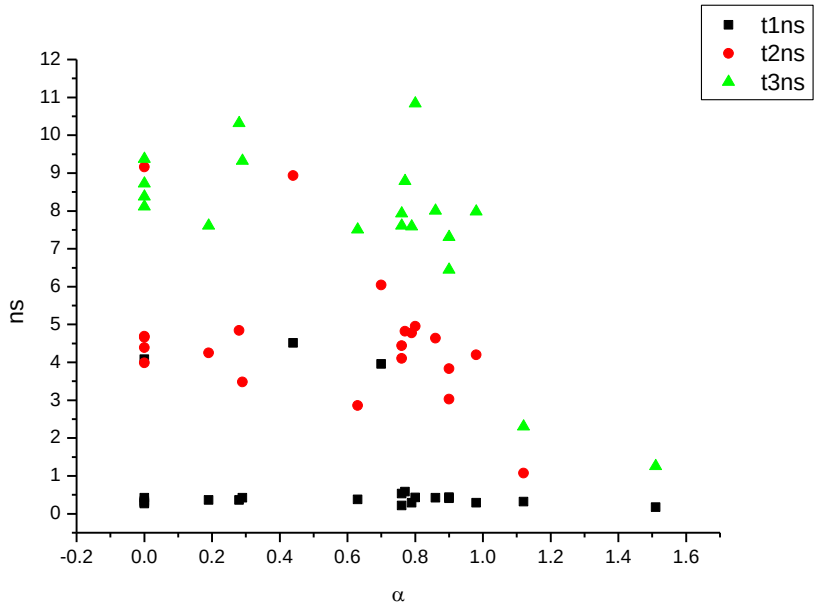

Figure 1.2.108. Amplitude weighted components of TCSPC lifetime decay of **6a** (470 nm) versus α.

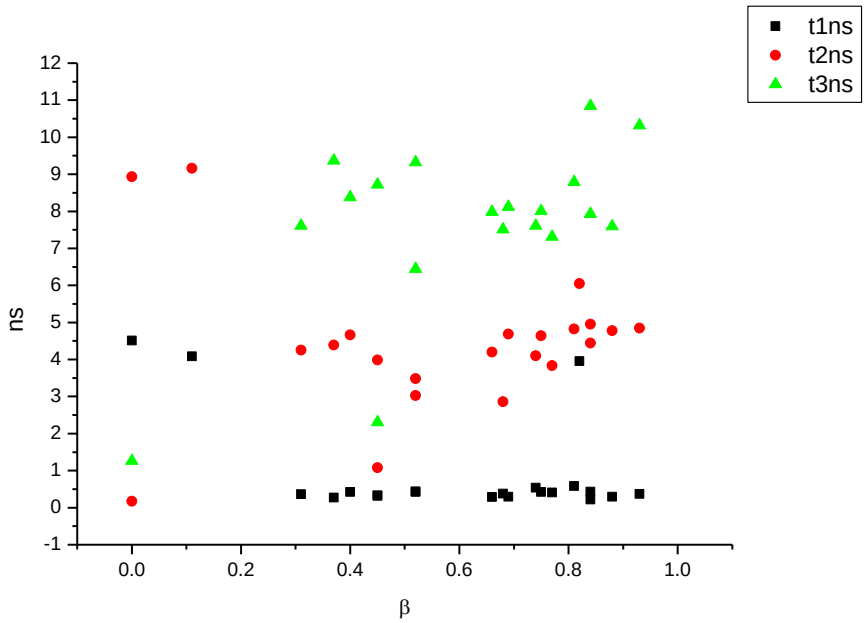

Figure 1.2.109. Intensity weighted components of TCSPC lifetime decay of **6a** (470 nm) versus β.

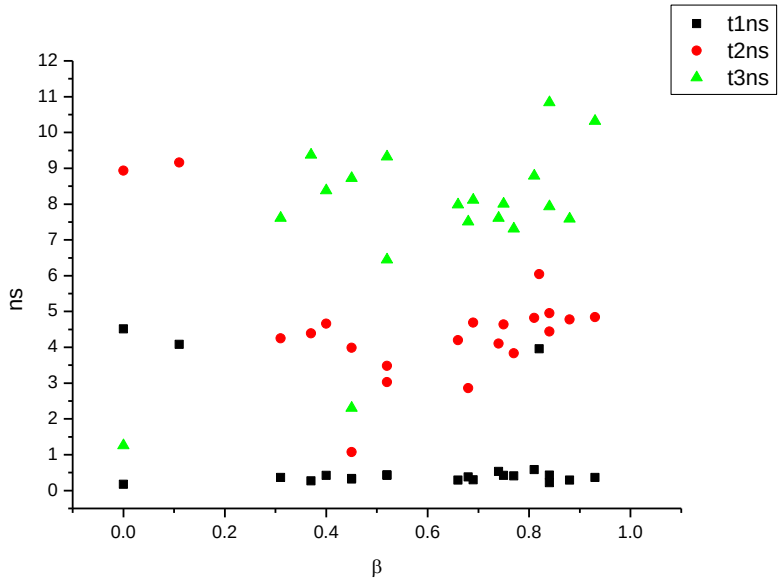

Figure 1.2.110. Amplitude weighted components of TCSPC lifetime decay of **6a** (470 nm) versus β.

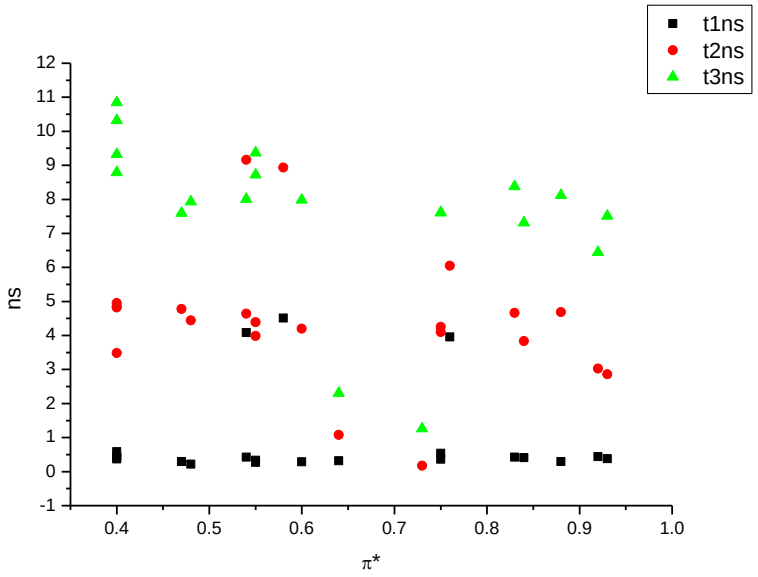

Figure 1.2.111. Intensity weighted components of TCSPC lifetime decay of **6a** (470 nm) versus π*.

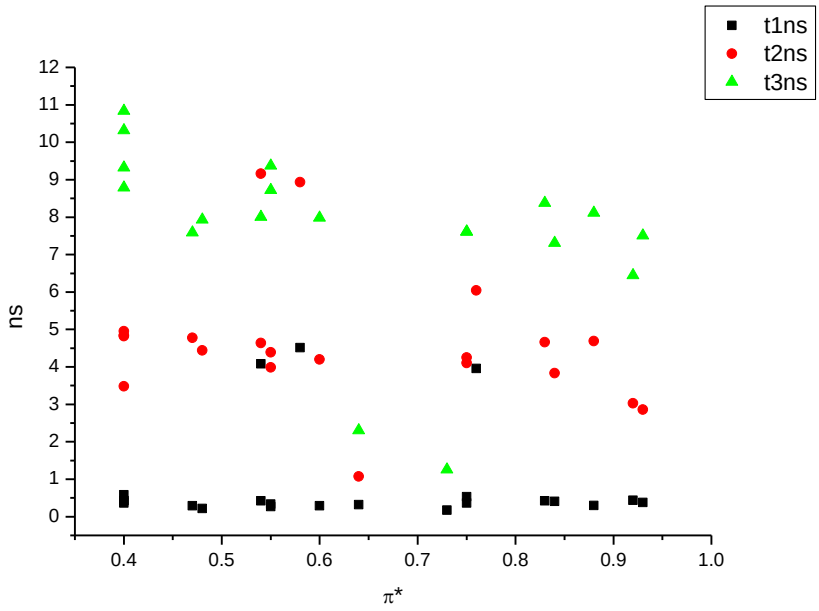

Figure 1.2.112. Amplitude weighted components of TCSPC lifetime decay of **6a** (470 nm) versus π*.

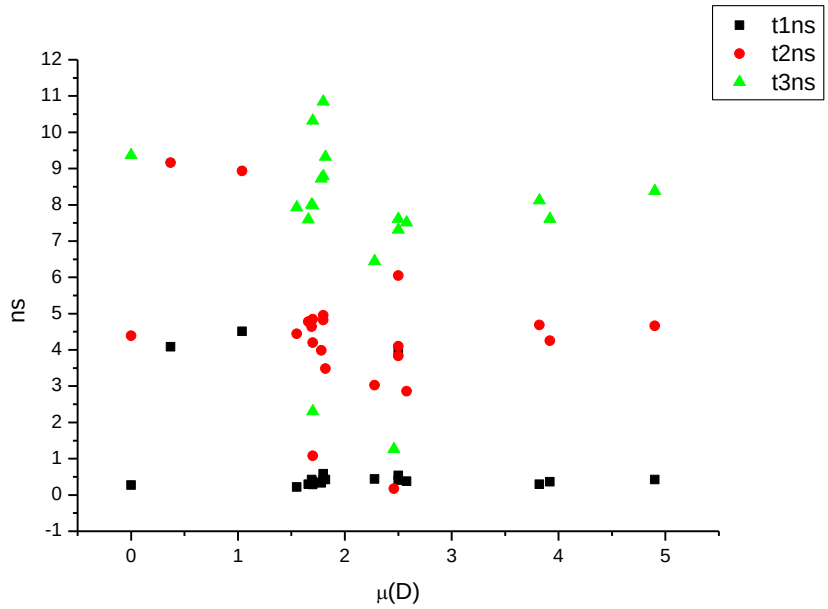

Figure 1.2.113. Intensity weighted components of TCSPC lifetime decay of **6a** (470 nm) versus μ(D).

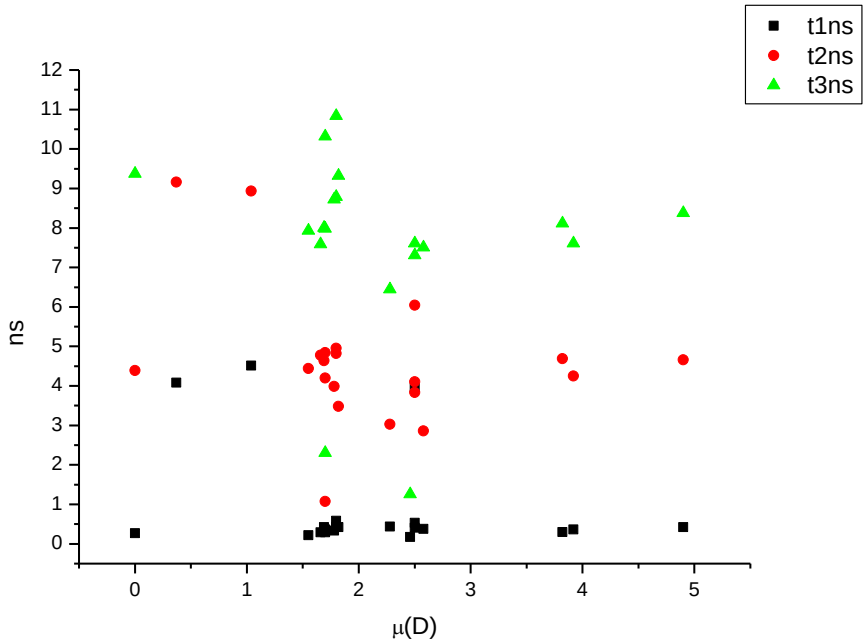

Figure 1.2.114. Amplitude weighted components of TCSPC lifetime decay of **6a** (470 nm) versus μ(D).

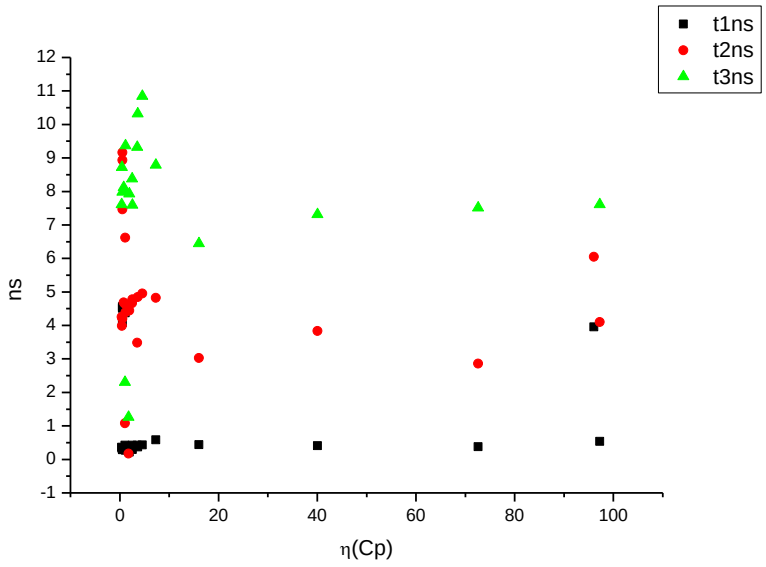

Figure 1.2.115. Intensity weighted components of TCSPC lifetime decay of **6a** (470 nm) versus η(Cp).

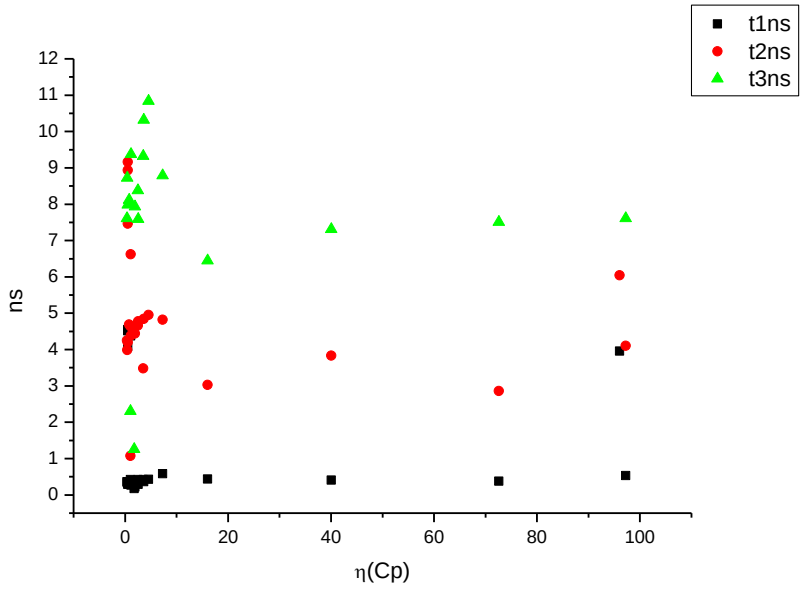

Figure 1.2.116. Amplitude weighted components of TCSPC lifetime decay of **6a** (470 nm) versus η(Cp).

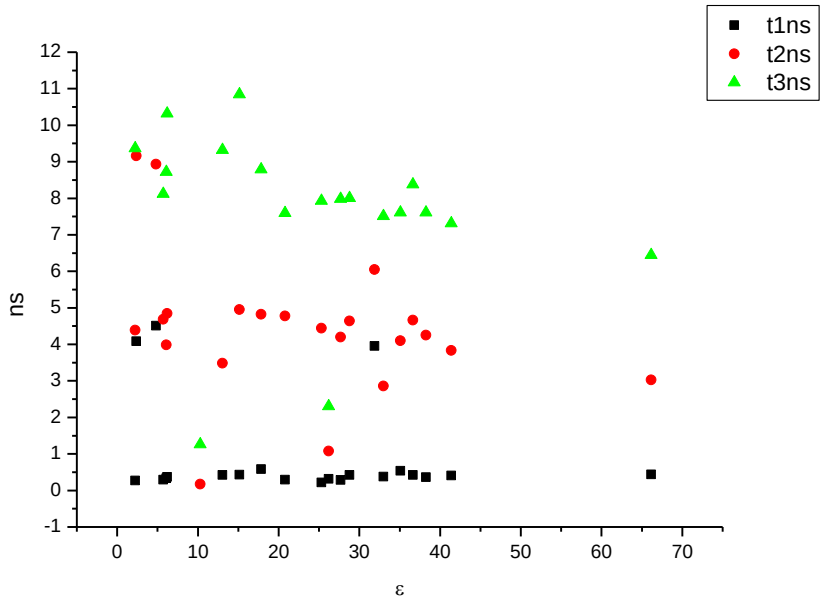

Figure 1.2.117. Intensity weighted components of TCSPC lifetime decay of **6a** (470 nm) versus ε.

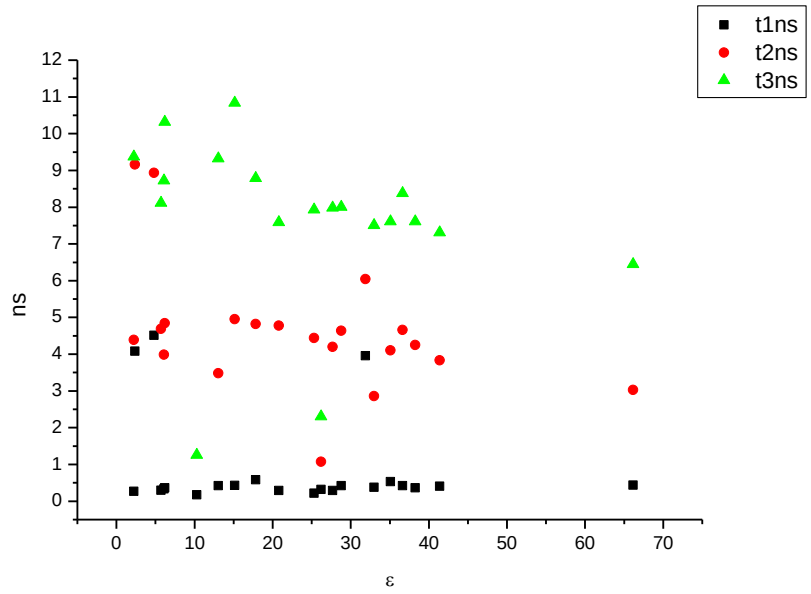

Figure 1.2.118. Amplitude weighted components of TCSPC lifetime decay of **6a** (470 nm) versus ε.

1.2.7.2 6a 570 nm Lifetime – Solvatochromic analysis.

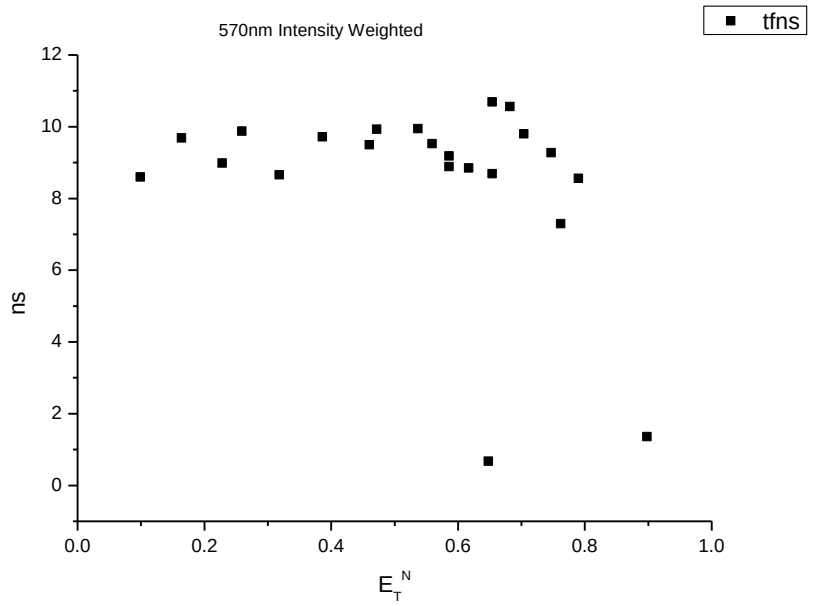

Figure 1.2.119. Intensity weighted average lifetime (τ_f) of **6a** at 570 nm versus E_T^N.

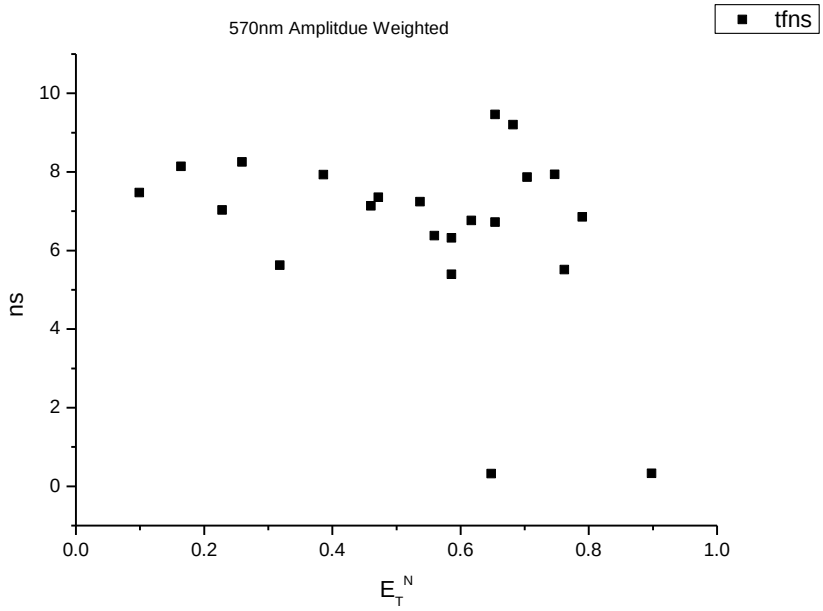

Figure 1.2.120. Amplitude weighted average lifetime (τ_f) of **6a** at 570 nm versus E_T^N.

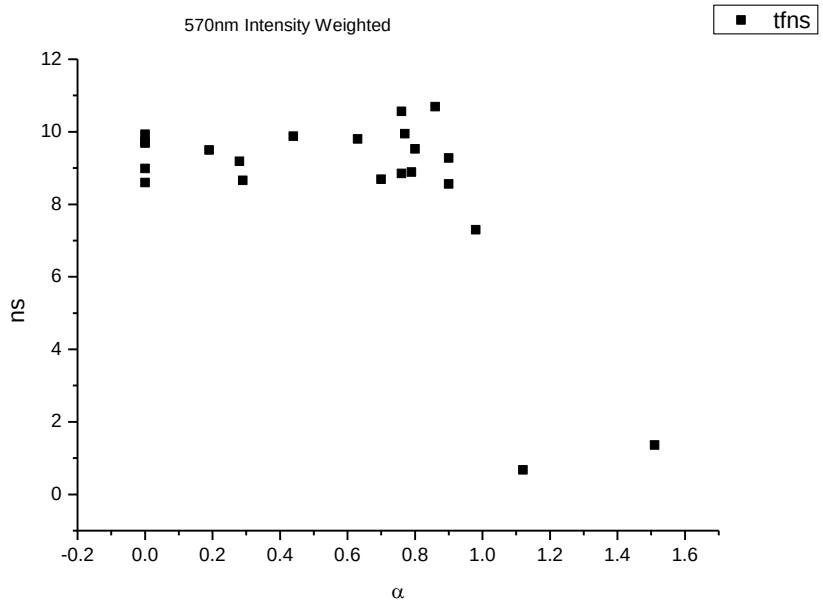

Figure 1.2.121. Intensity weighted average lifetime (τ_f) of **6a** at 570 nm versus α.

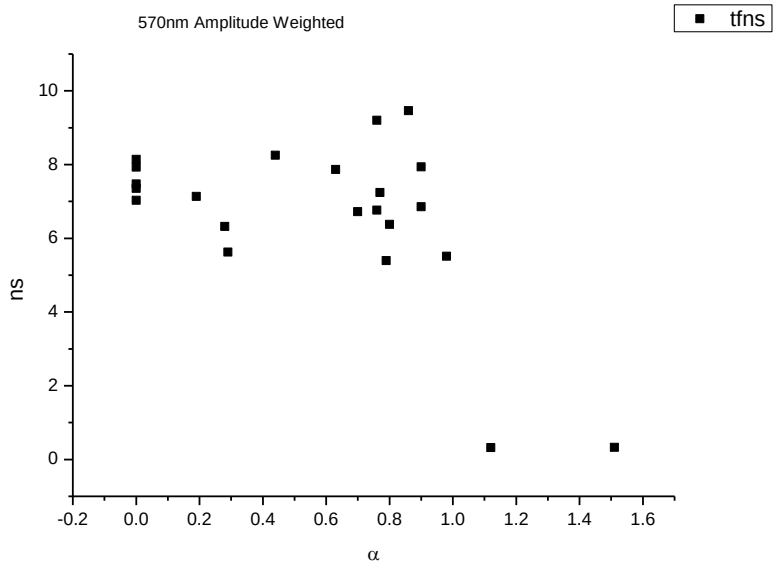

Figure 1.2.122. Amplitude weighted average lifetime (τ_f) of **6a** at 570 nm versus α.

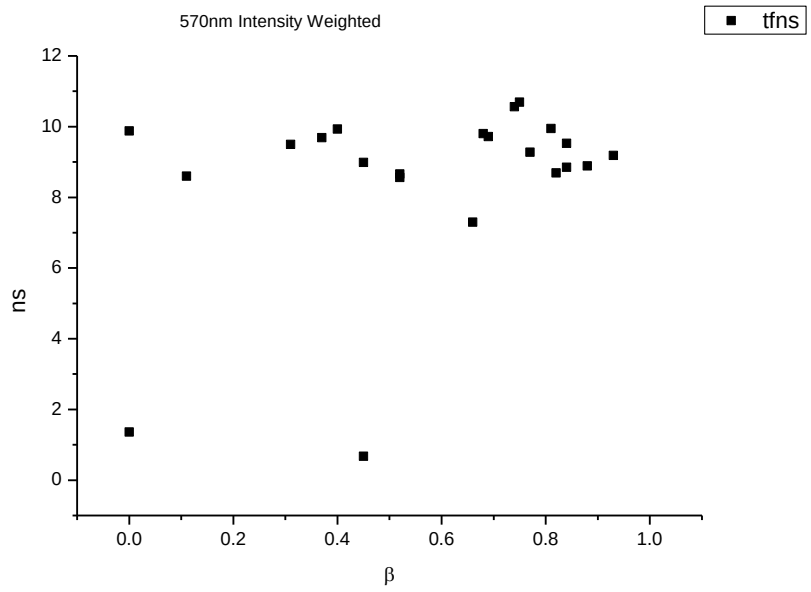

Figure 1.2.123. Intensity weighted average lifetime (τ_f) of **6a** at 570 nm versus β.

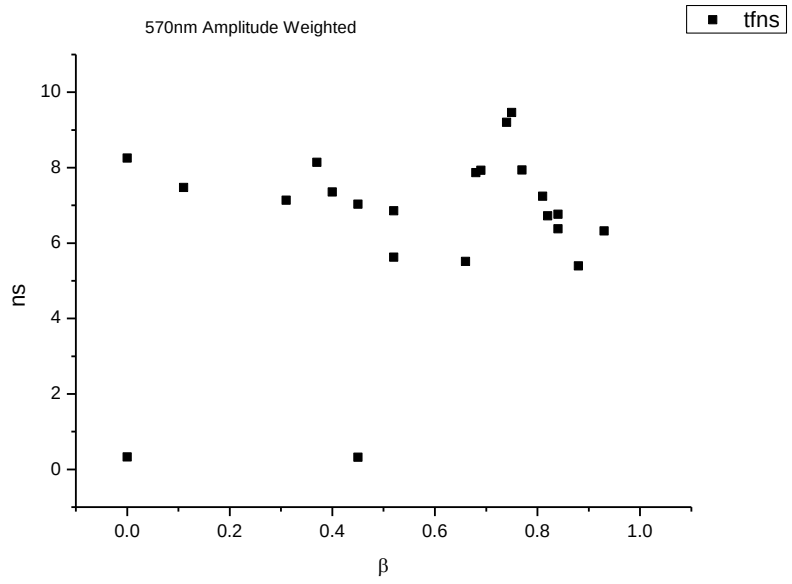

Figure 1.2.124. Amplitude weighted average lifetime (τ_f) of **6a** at 570 nm versus β.

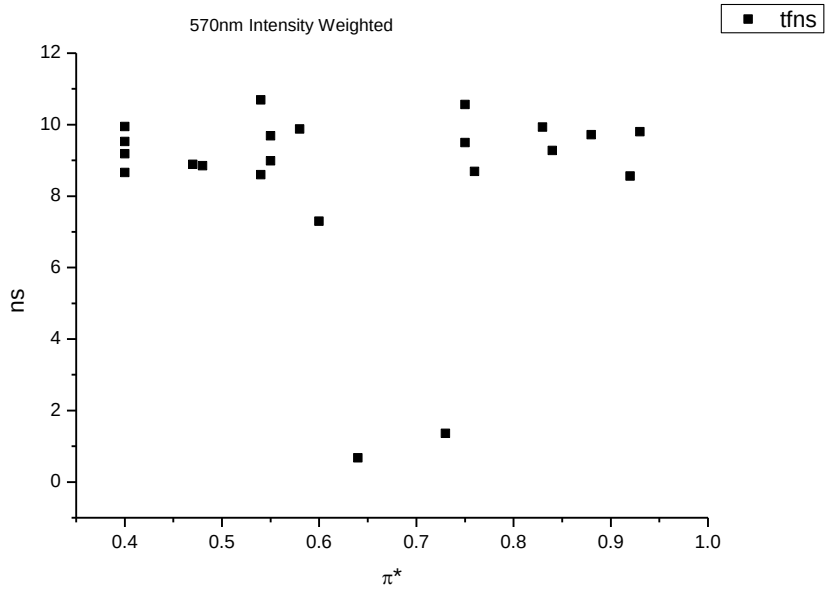

Figure 1.2.125. Intensity weighted average lifetime (τ_f) of **6a** at 570 nm versus π*.

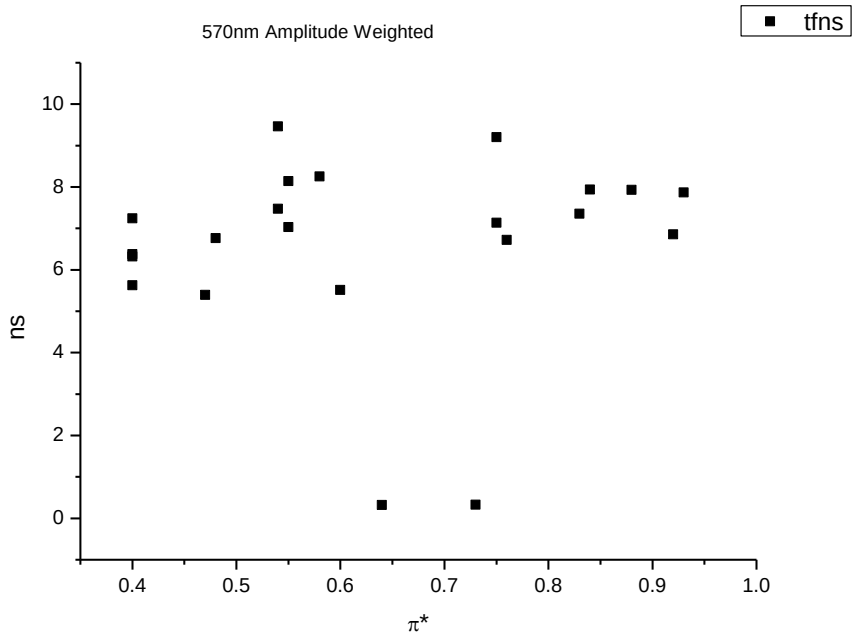

Figure 1.2.126. Amplitude weighted average lifetime (τ_f) of **6a** at 570 nm versus π*.

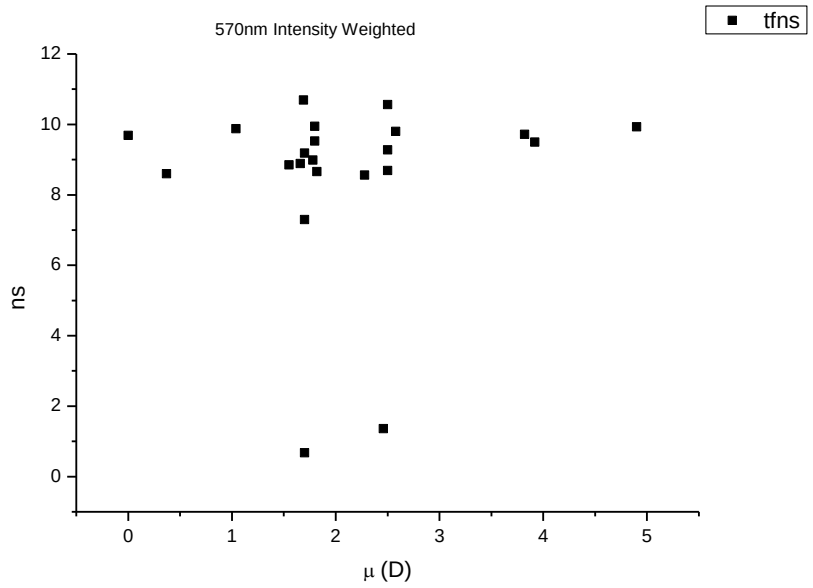

Figure 1.2.127. Intensity weighted average lifetime (τ_f) of **6a** at 570 nm versus μ(D).

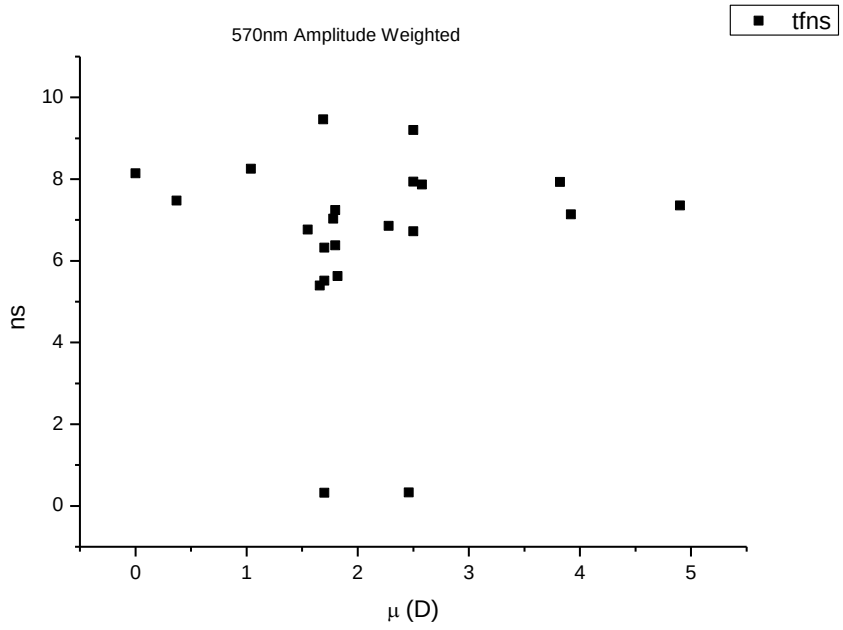

Figure 1.2.128. Amplitude weighted average lifetime (τ_f) of **6a** at 570 nm versus μ(D).

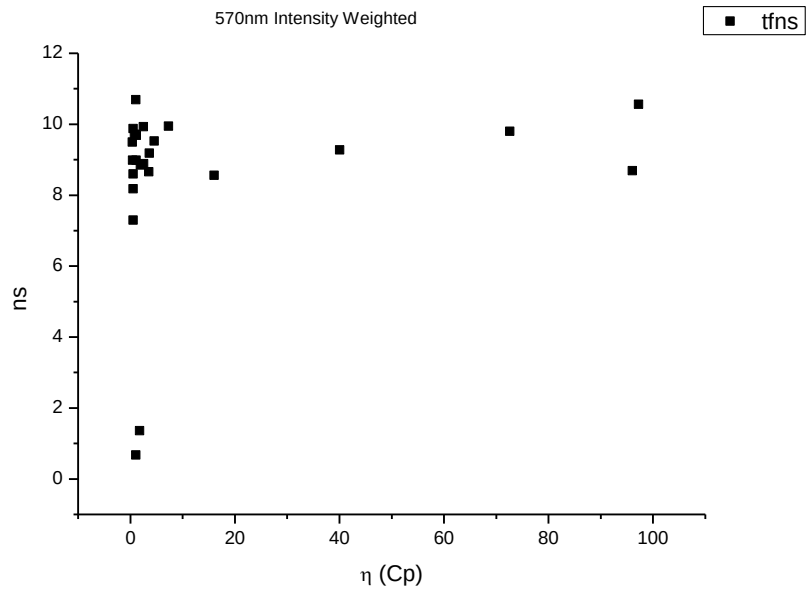

Figure 1.2.129. Intensity weighted average lifetime (τ_f) of **6a** at 570 nm versus η(Cp).

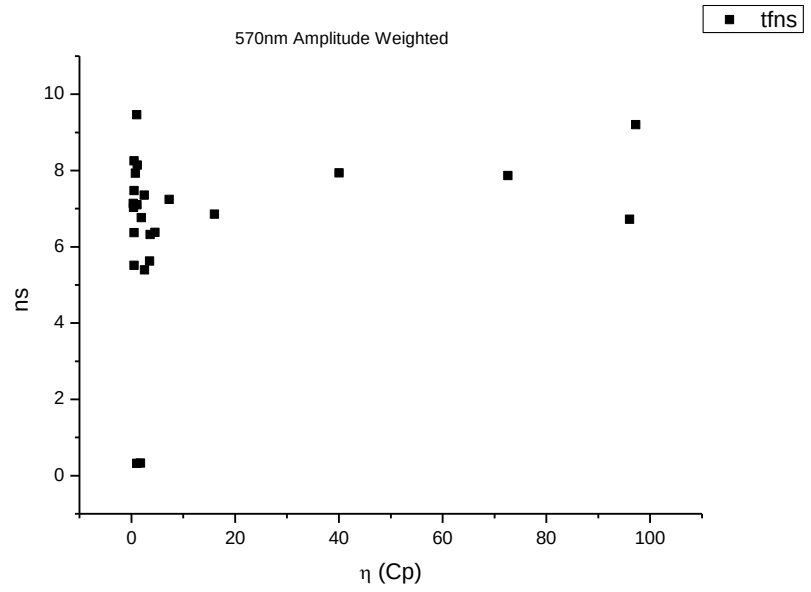

Figure 1.2.130. Amplitude weighted average lifetime (τ_f) of **6a** at 570 nm versus η(Cp).

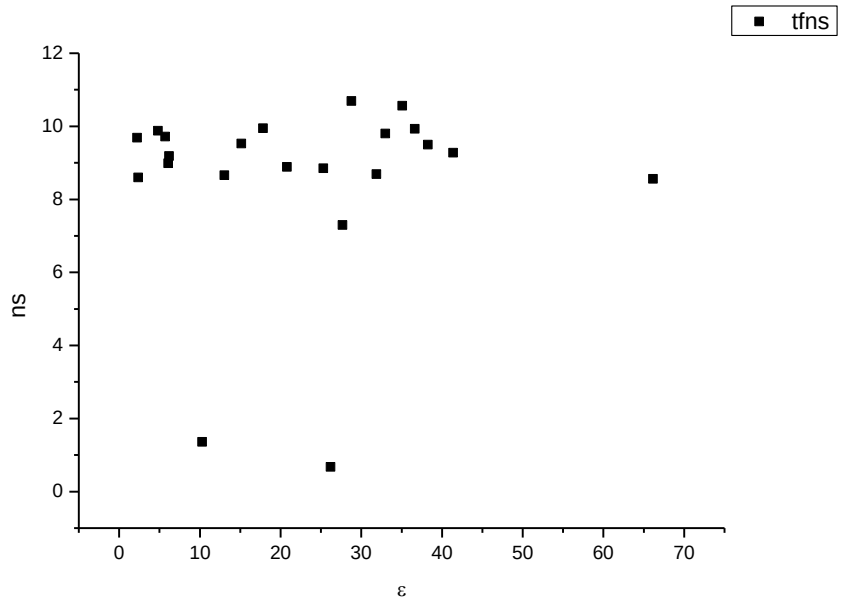

Figure 1.2.131. Intensity weighted average lifetime (τ_f) of **6a** at 570 nm versus ε.

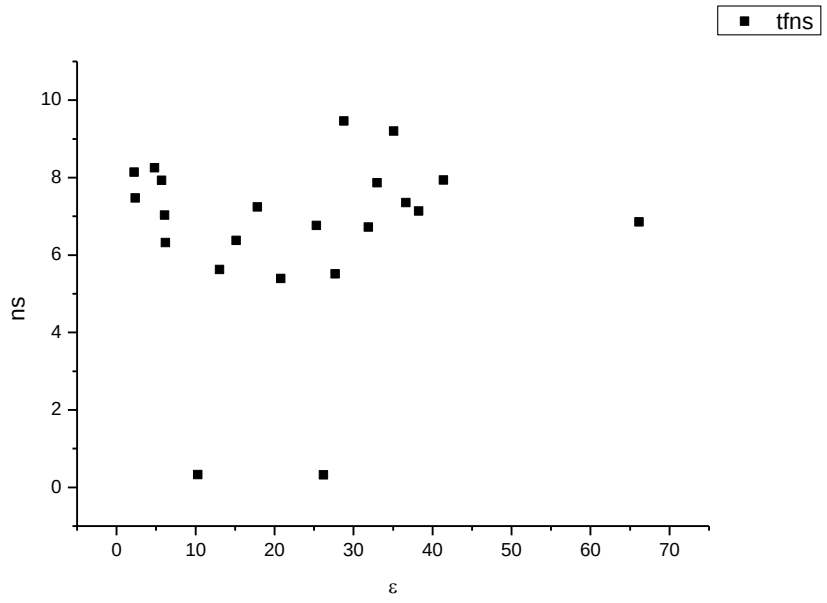

Figure 1.2.132. Amplitude weighted average lifetime (τ_f) of **6a** at 570 nm versus ε.

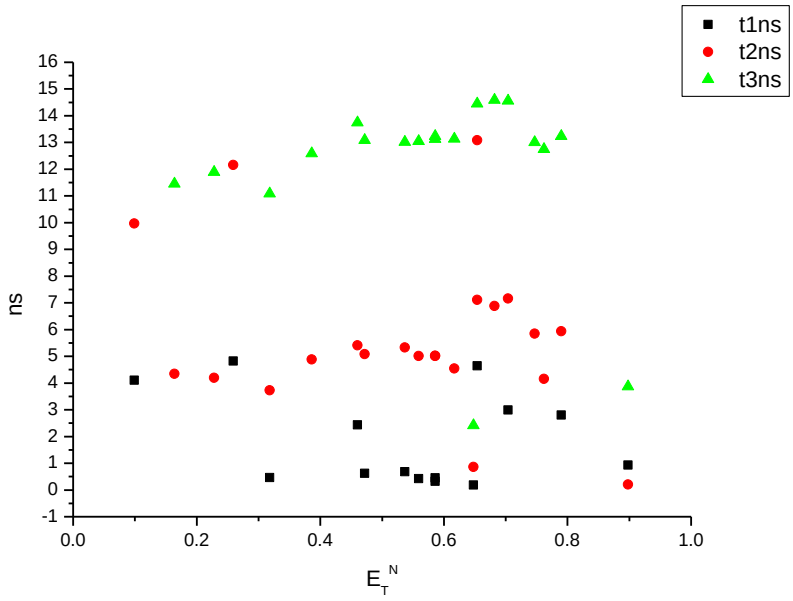

Figure 1.2.133. Intensity weighted components of TCSPC lifetime decay of **6a** (570 nm) versus E_T^N.

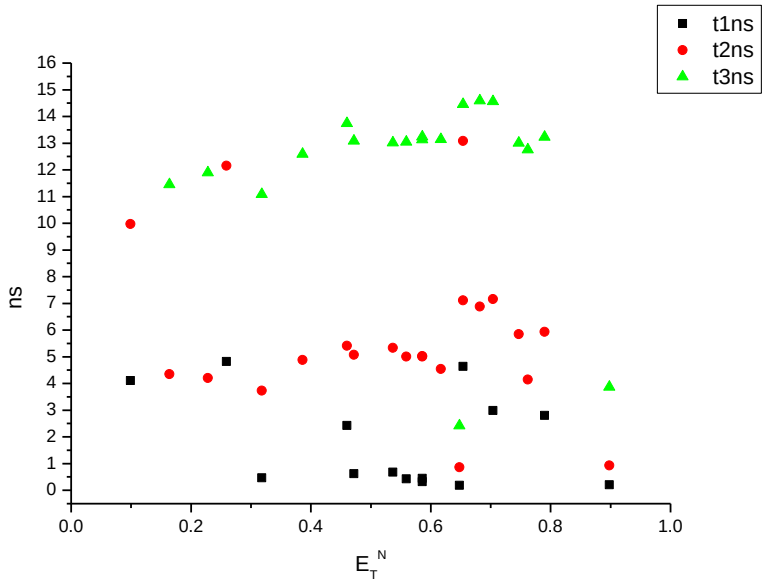

Figure 1.2.134. Amplitude weighted components of TCSPC lifetime decay of **6a** (570 nm) versus E_T^N.

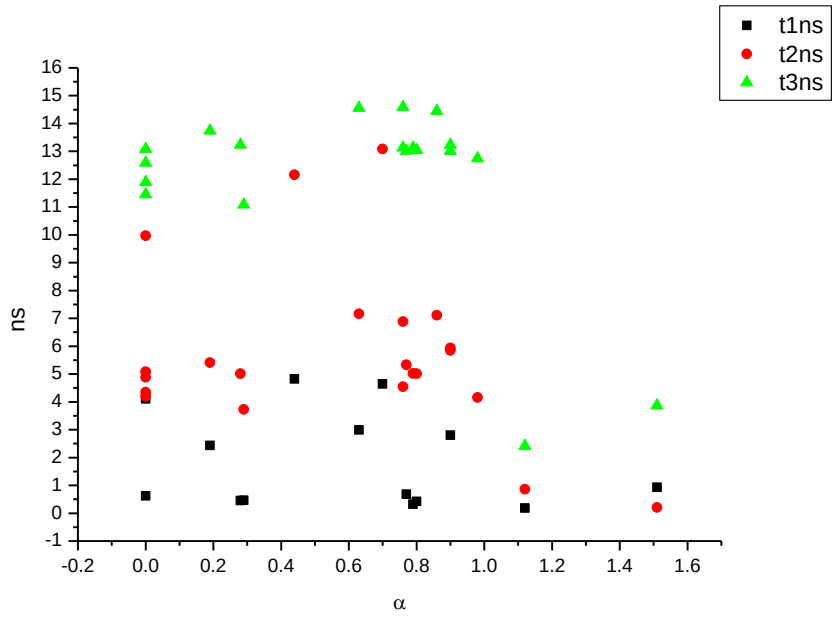

Figure 1.2.135. Intensity weighted components of TCSPC lifetime decay of **6a** (570 nm) versus α.

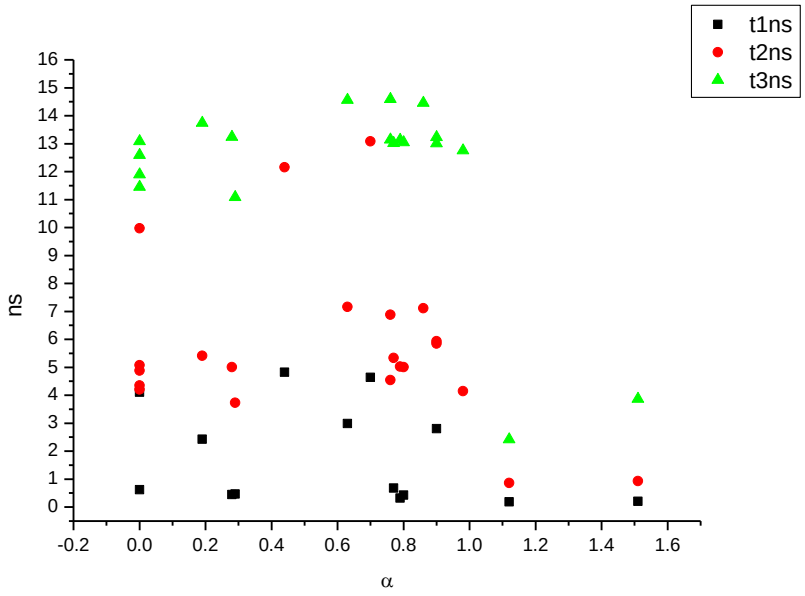

Figure 1.2.136. Amplitude weighted components of TCSPC lifetime decay of **6a** (570 nm) versus α.

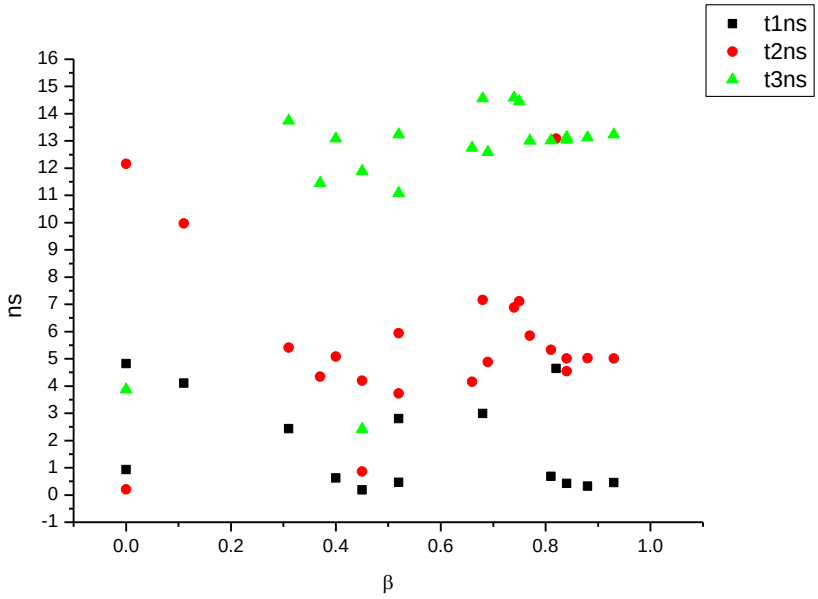

Figure 1.2.137. Intensity weighted components of TCSPC lifetime decay of **6a** (570 nm) versus β.

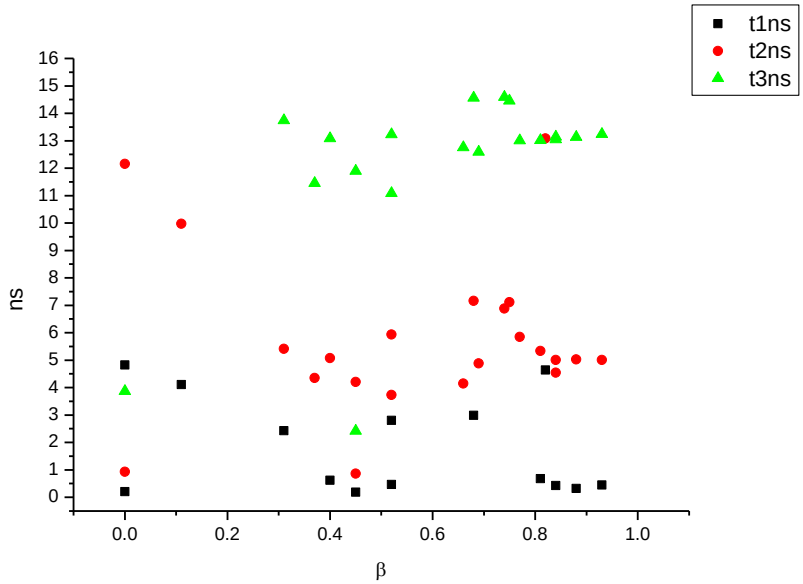

Figure 1.2.138. Amplitude weighted components of TCSPC lifetime decay of **6a** (570 nm) versus β.

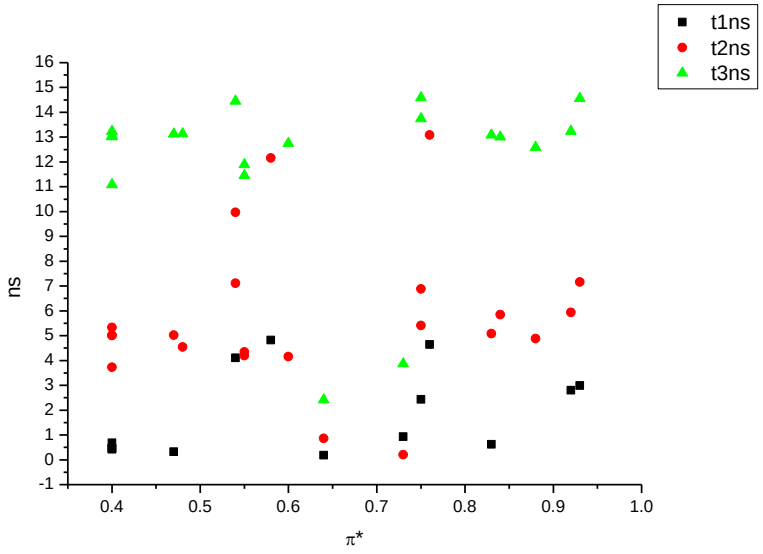

Figure 1.2.139. Intensity weighted components of TCSPC lifetime decay of **6a** (570 nm) versus π*.

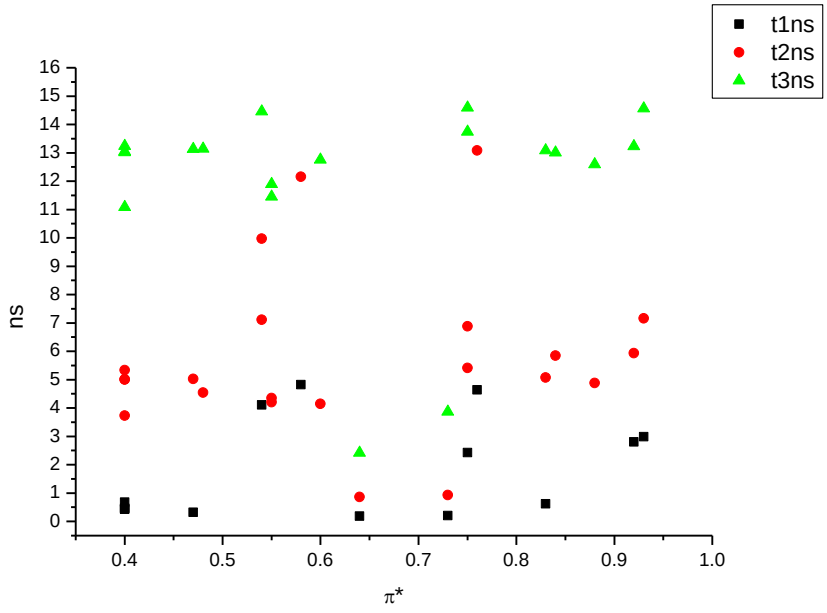

Figure 1.2.140. Amplitude weighted components of TCSPC lifetime decay of **6a** (570 nm) versus π*.

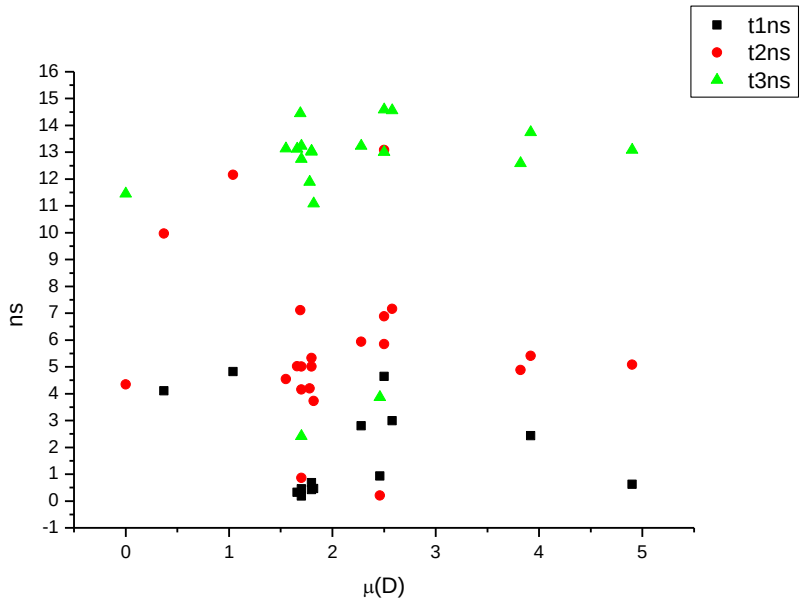

Figure 1.2.141. Intensity weighted components of TCSPC lifetime decay of **6a** (570 nm) versus μ(D).

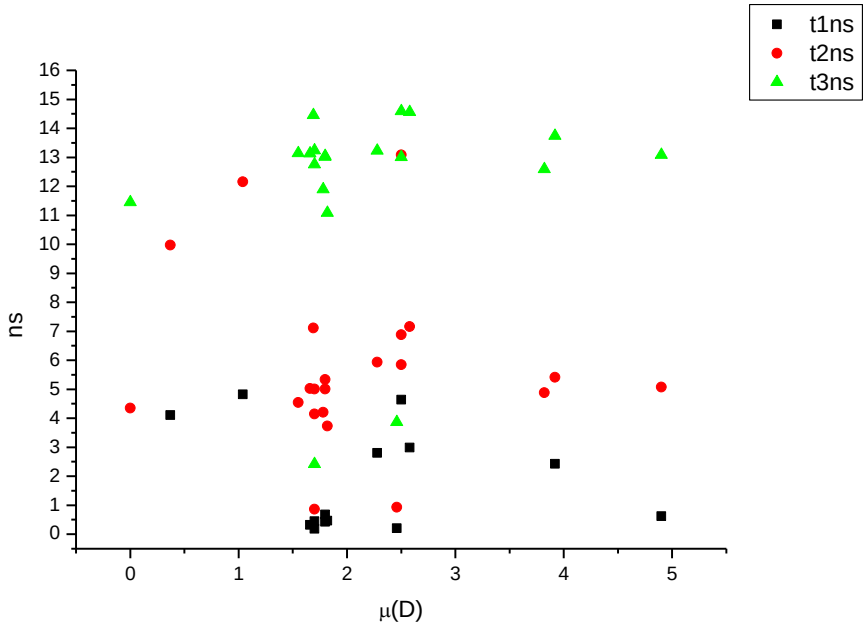

Figure 1.2.142. Amplitude weighted components of TCSPC lifetime decay of **6a** (570 nm) versus μ(D).

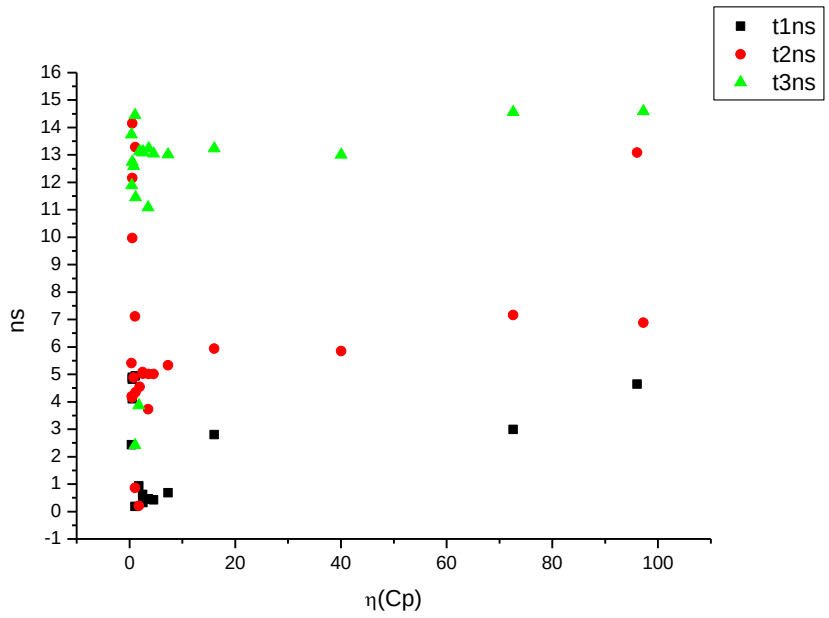

Figure 1.2.143. Intensity weighted components of TCSPC lifetime decay of **6a** (570 nm) versus η(Cp).

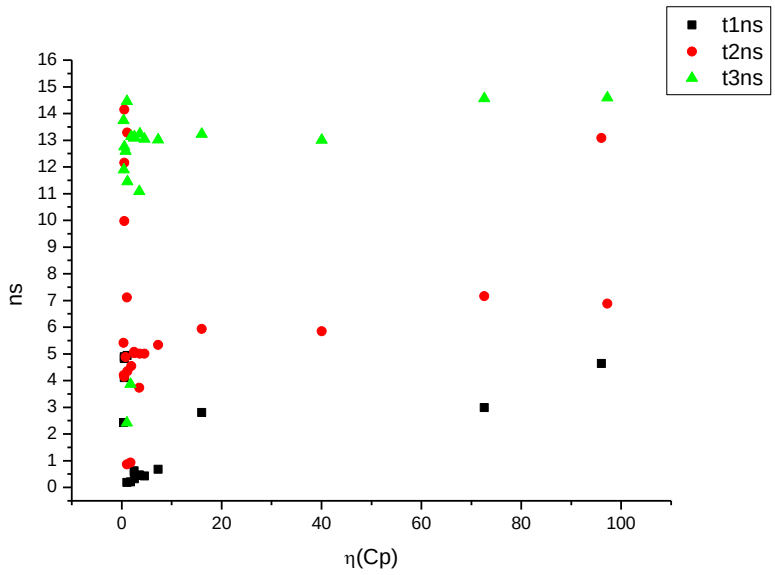

Figure 1.2.144. Amplitude weighted components of TCSPC lifetime decay of **6a** (570 nm) versus η(Cp).

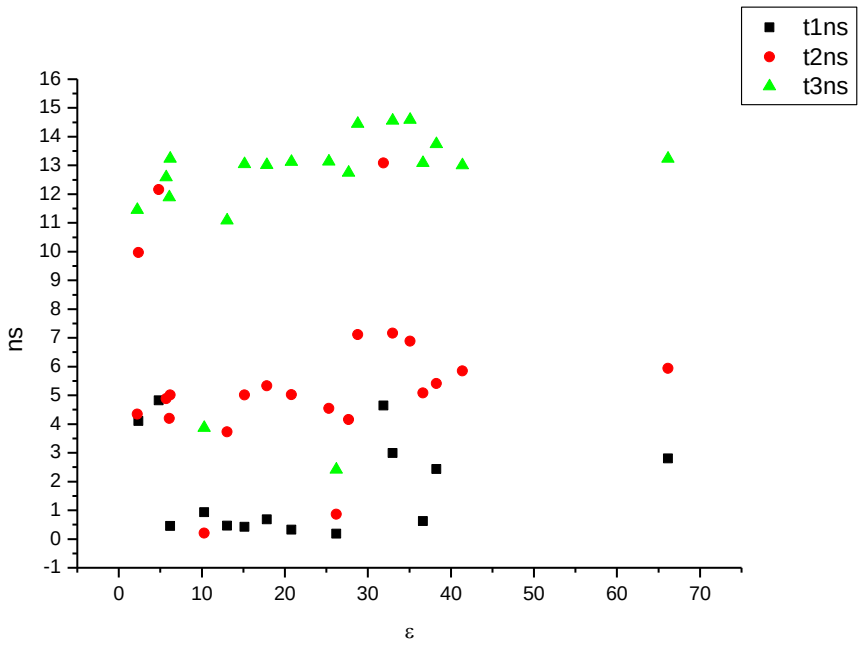

Figure 1.2.145. Intensity weighted components of TCSPC lifetime decay of **6a** (570 nm) versus ε.

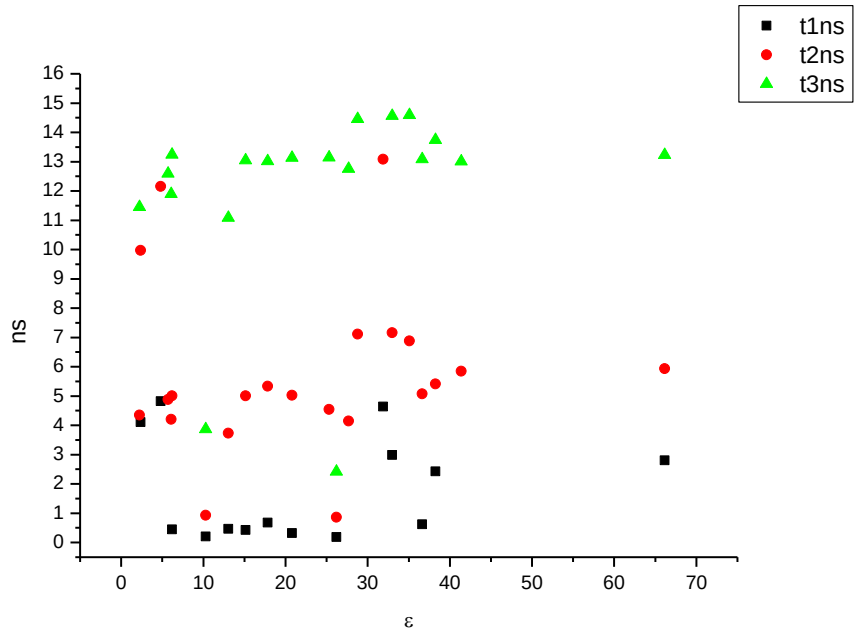

Figure 1.2.146. Amplitude weighted components of TCSPC lifetime decay of **6a** (570 nm) versus ε.

1.2.8 Ultraviolet-visible absorption spectra.

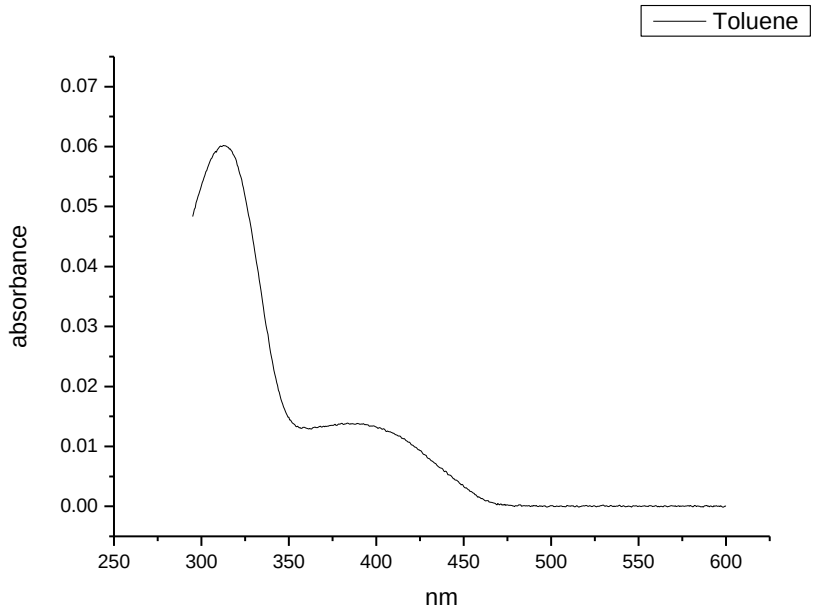

Figure 1.2.147. Ultraviolet-Visible absorption spectrum of **6a** recorded in Toluene.

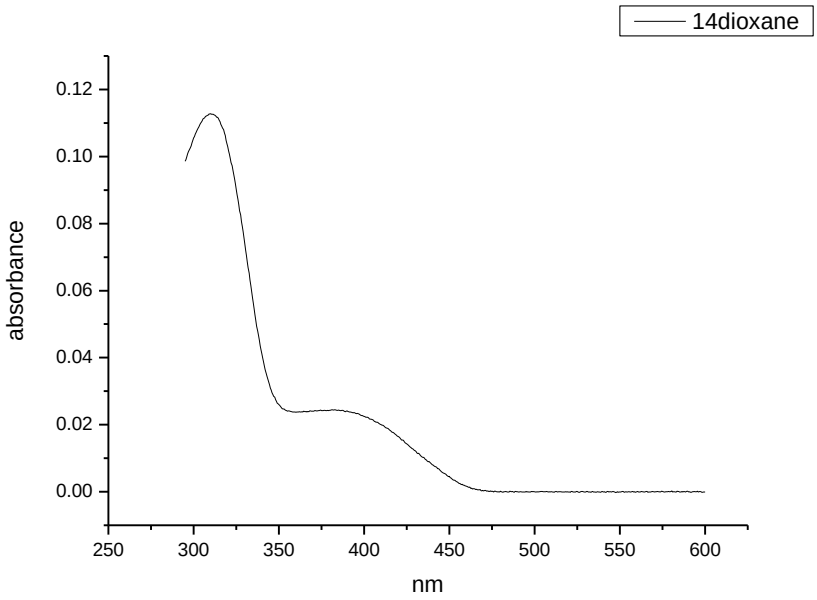

Figure 1.2.148. Ultraviolet-Visible absorption spectrum of **6a** recorded in 1,4-dioxane.

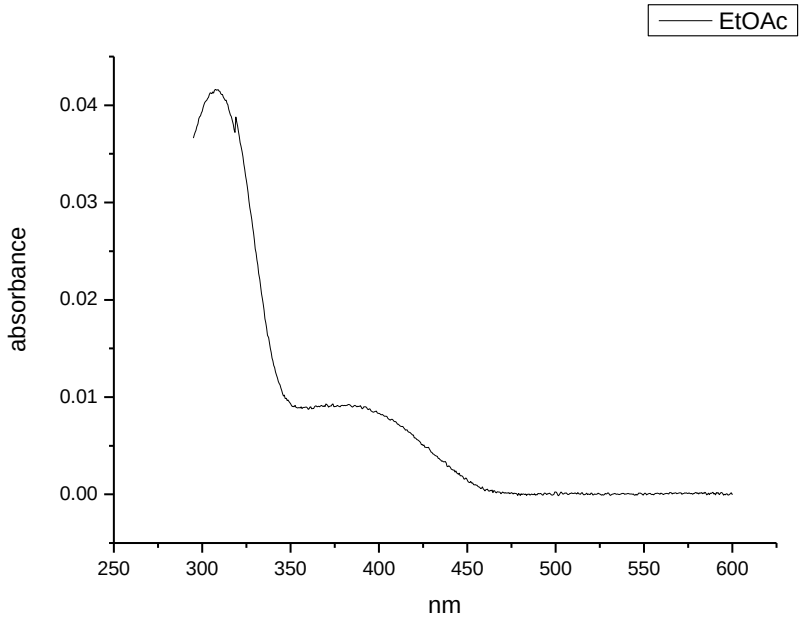

Figure 1.2.149. Ultraviolet-Visible absorption spectrum of **6a** recorded in Ethyl Acetate.

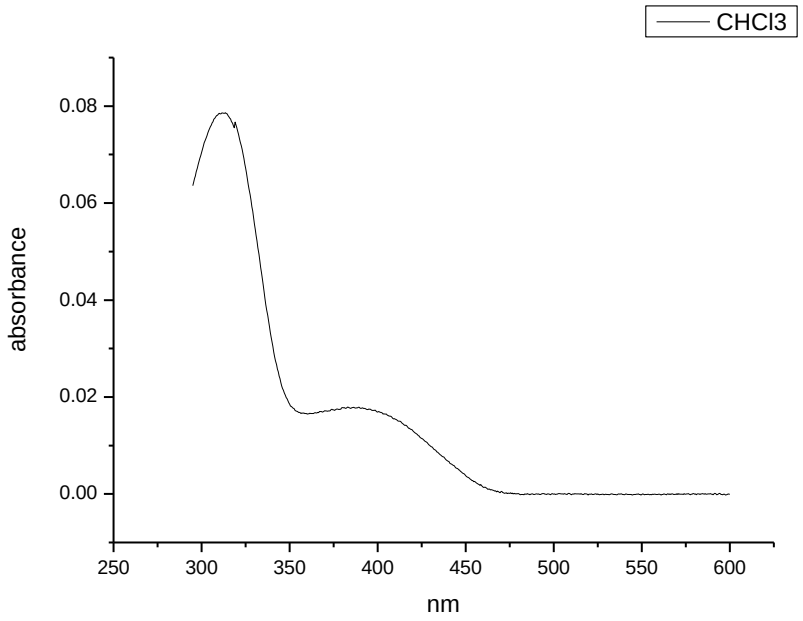

Figure 1.2.150. Ultraviolet-Visible absorption spectrum of **6a** recorded in Chloroform.

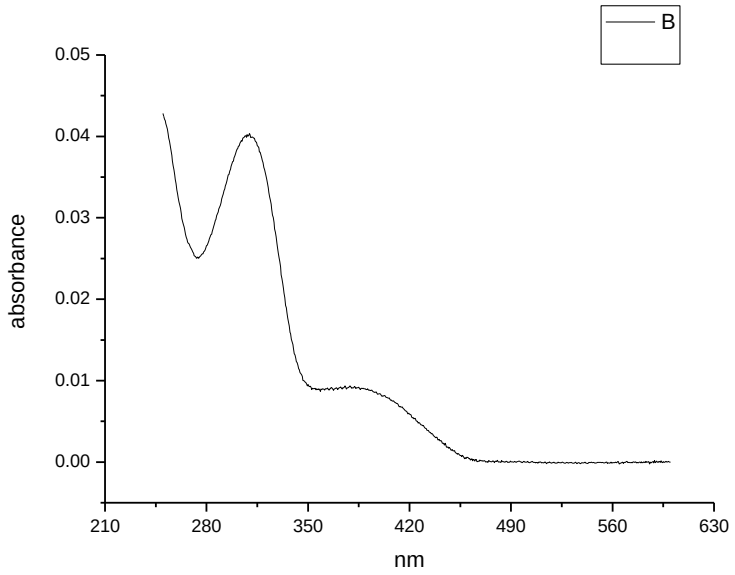

Figure 1.2.151. Ultraviolet-Visible absorption spectrum of **6a** recorded in 2-methyl-2-butanol.

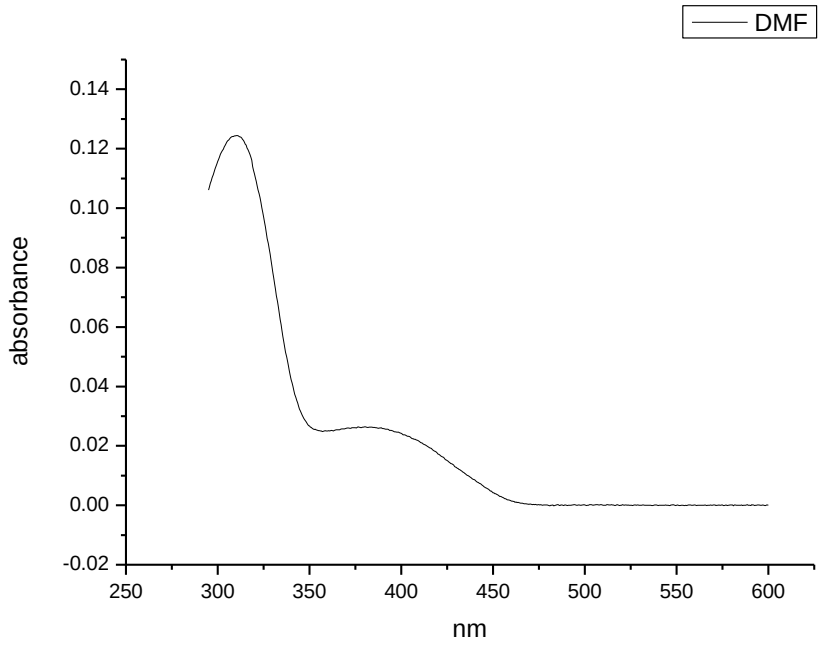

Figure 1.2.152. Ultraviolet-Visible absorption spectrum of **6a** recorded in N,N-dimethylformamide.

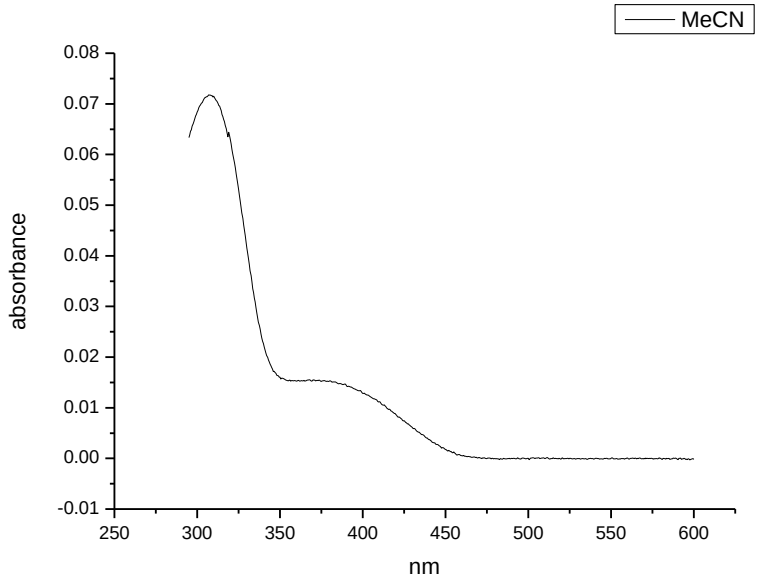

Figure 1.2.153. Ultraviolet-Visible absorption spectrum of **6a** recorded in Acetonitrile.

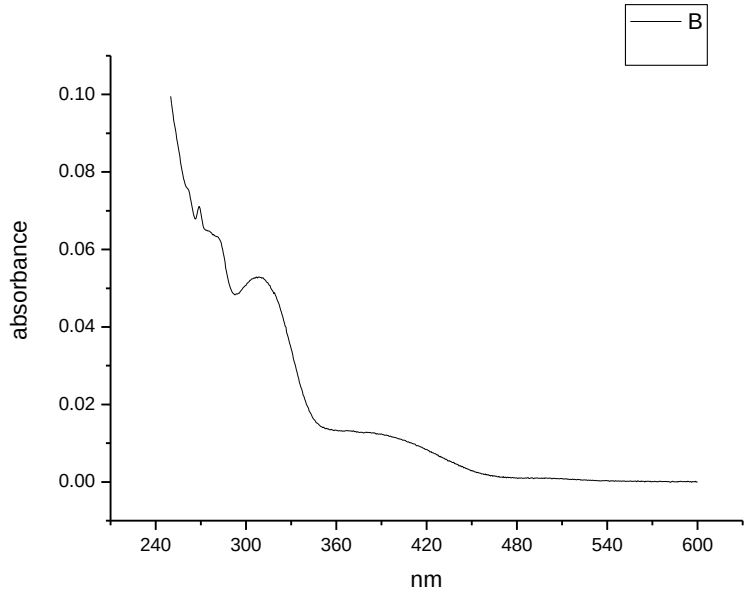

Figure 1.2.154. Ultraviolet-Visible absorption spectrum of **6a** recorded in Propylene Carbonate.

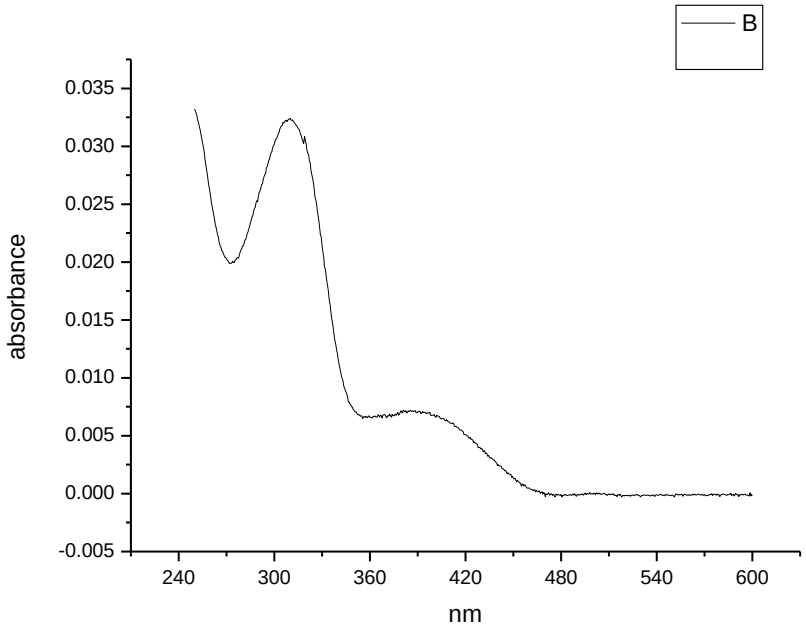

Figure 1.2.155. Ultraviolet-Visible absorption spectrum of **6a** recorded in 1-octanol.

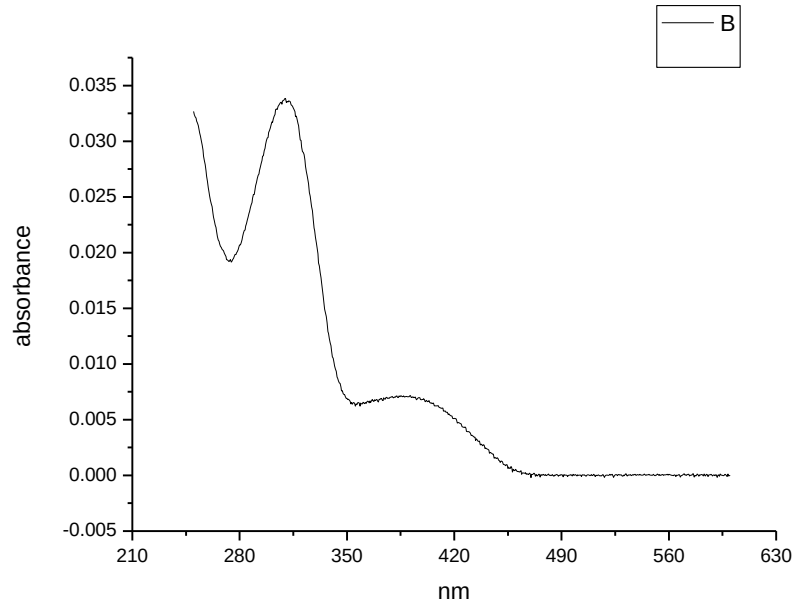

Figure 1.2.156. Ultraviolet-Visible absorption spectrum of **6a** recorded in 1-hexanol.

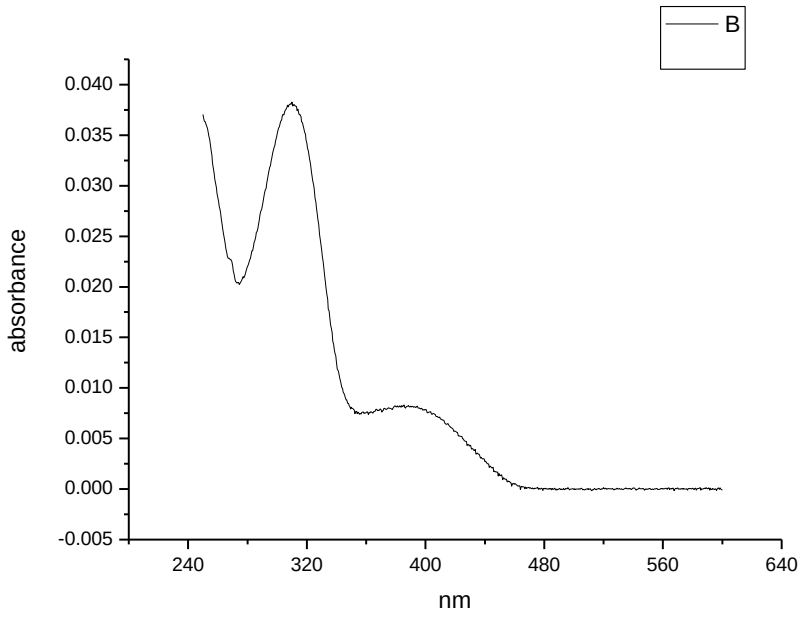

Figure 1.2.157. Ultraviolet-Visible absorption spectrum of **6a** recorded in 1-butanol.

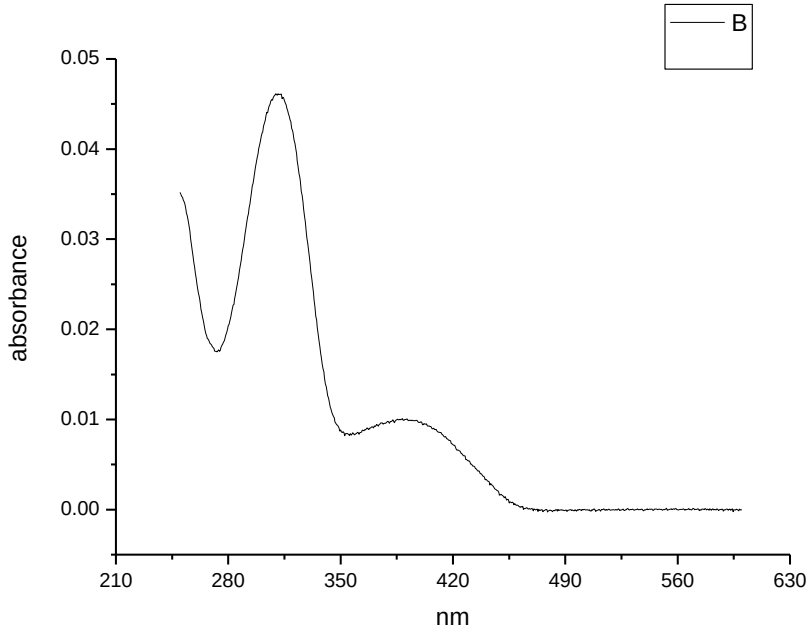

Figure 1.2.158. Ultraviolet-Visible absorption spectrum of **6a** recorded in 1-pentanol.

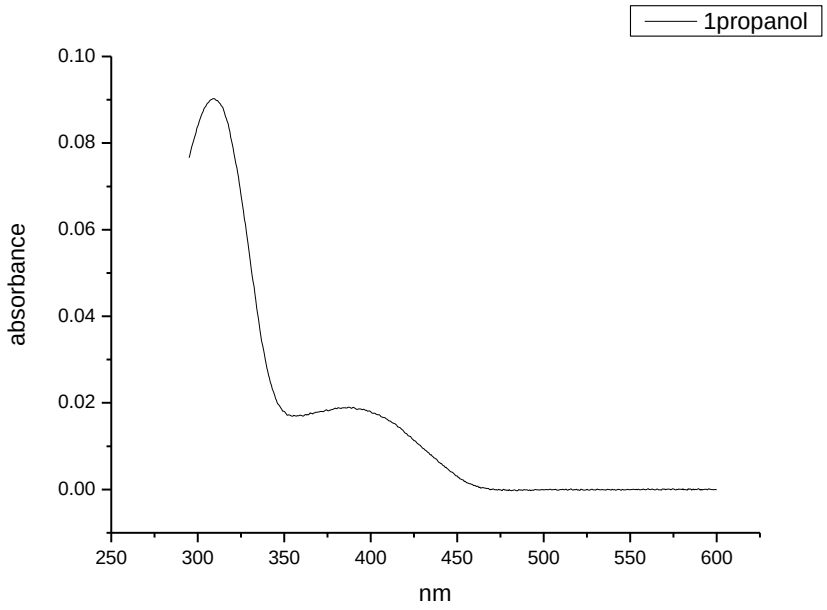

Figure 1.2.159. Ultraviolet-Visible absorption spectrum of **6a** recorded in 1-propanol.

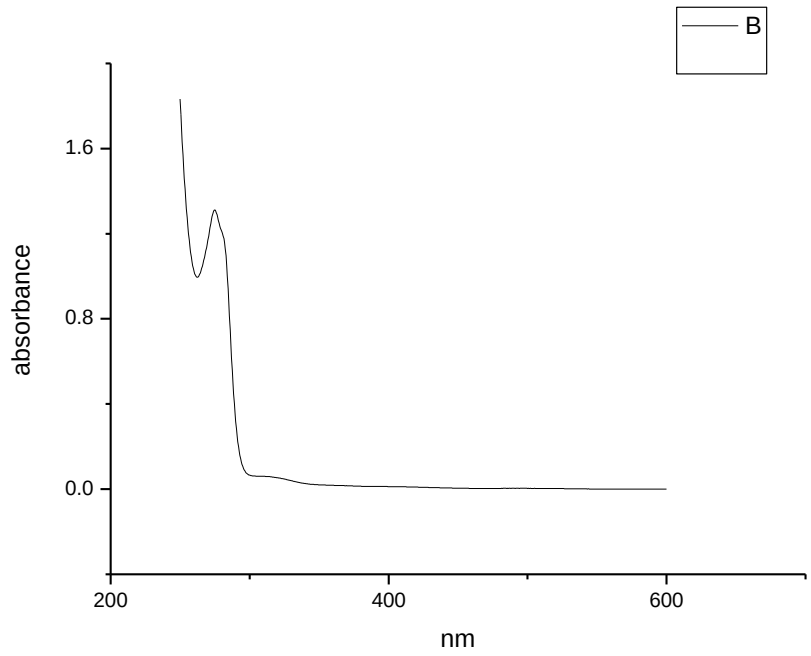

Figure 1.2.160. Ultraviolet-Visible absorption spectrum of **6a** recorded in Acetic Acid.

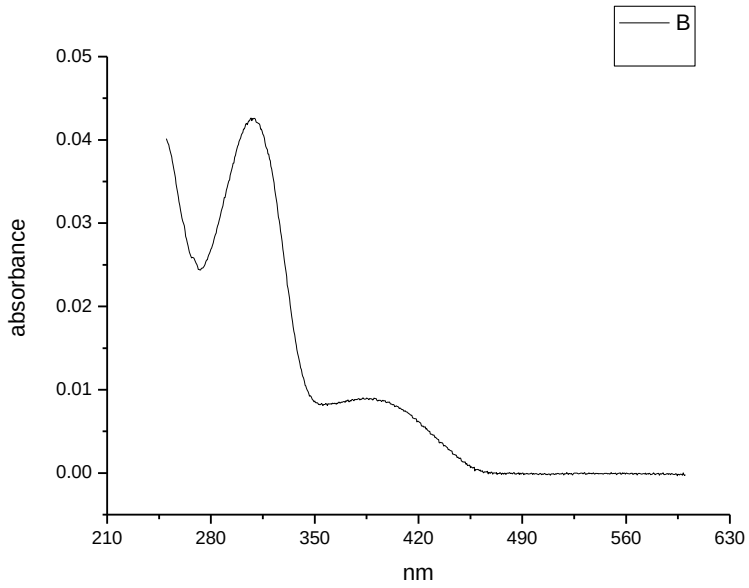

Figure 1.2.161. Ultraviolet-Visible absorption spectrum of **6a** recorded in Ethanol

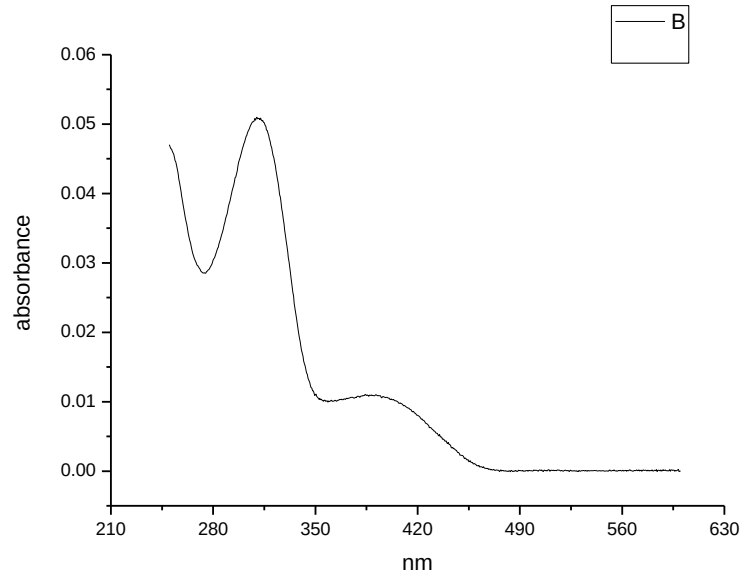

Figure 1.2.162. Ultraviolet-Visible absorption spectrum of **6a** recorded in 1,5-pentanediol.

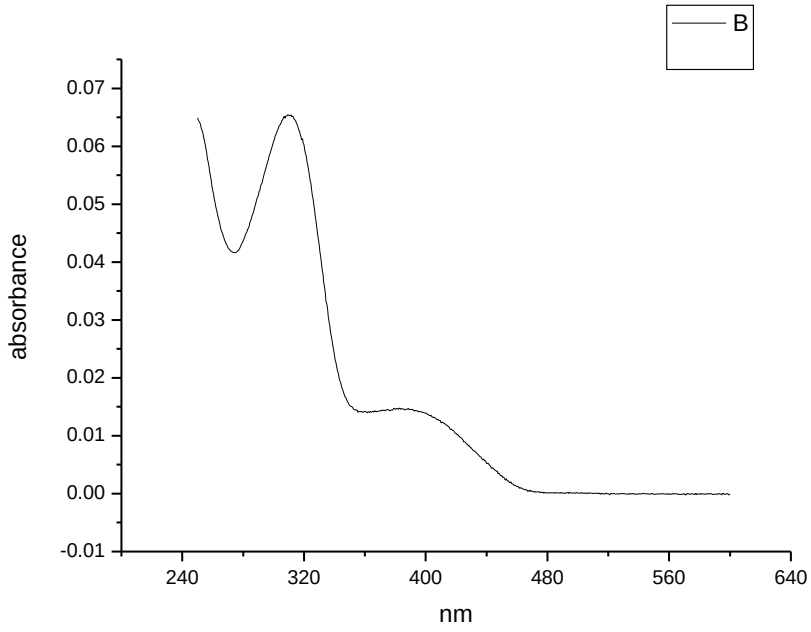

Figure 1.2.163. Ultraviolet-Visible absorption spectrum of **6a** recorded in 1,3-butanediol.

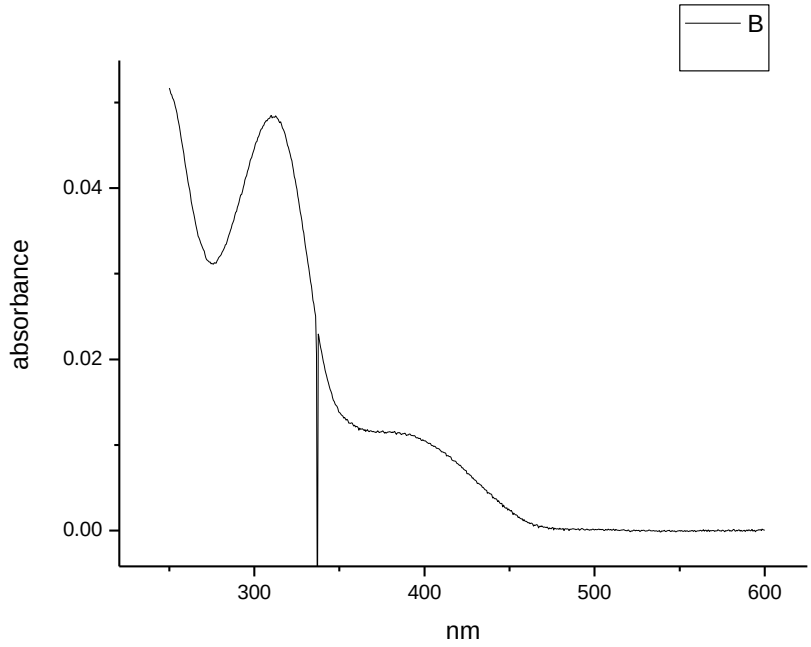

Figure 1.2.164. Ultraviolet-Visible absorption spectrum of **6a** recorded in 1,4-butanediol.

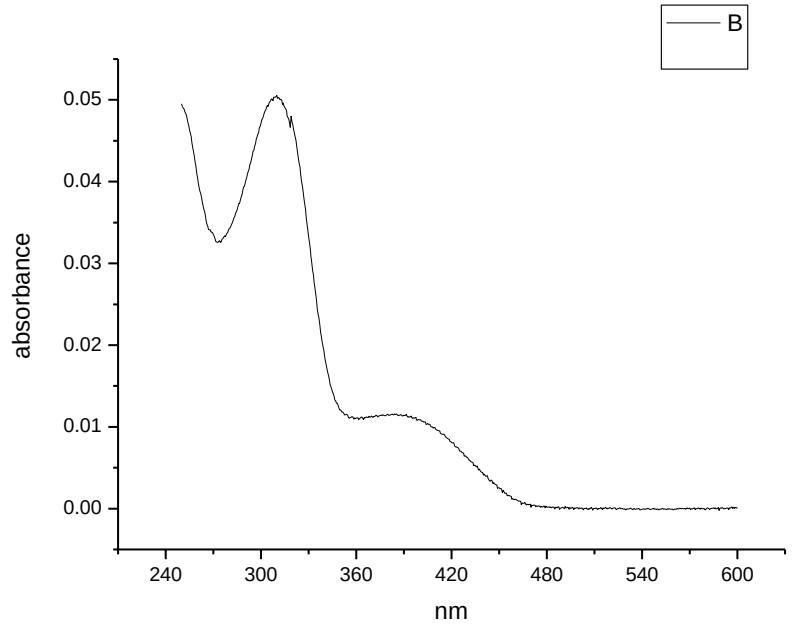

Figure 1.2.165. Ultraviolet-Visible absorption spectrum of **6a** recorded in 1,3-propanediol.

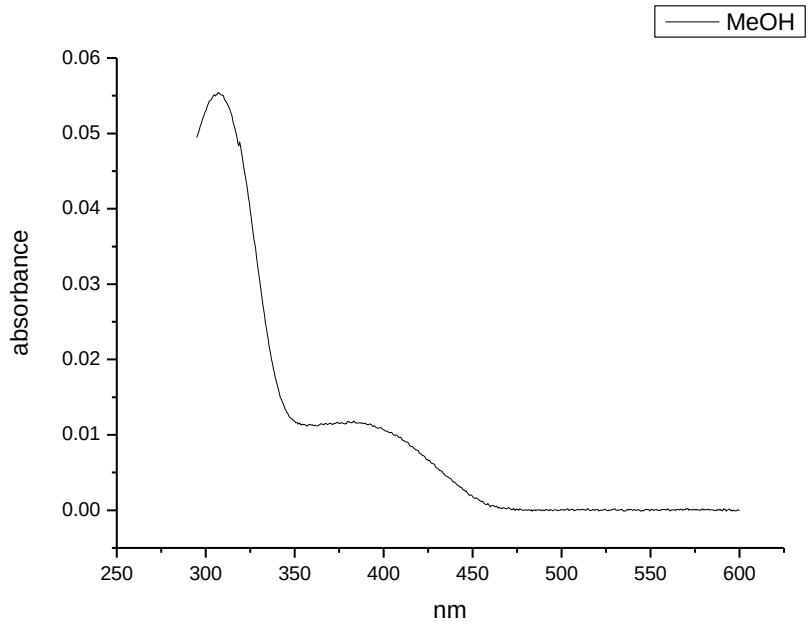

Figure 1.2.166. Ultraviolet-Visible absorption spectrum of **6a** recorded in Methanol.

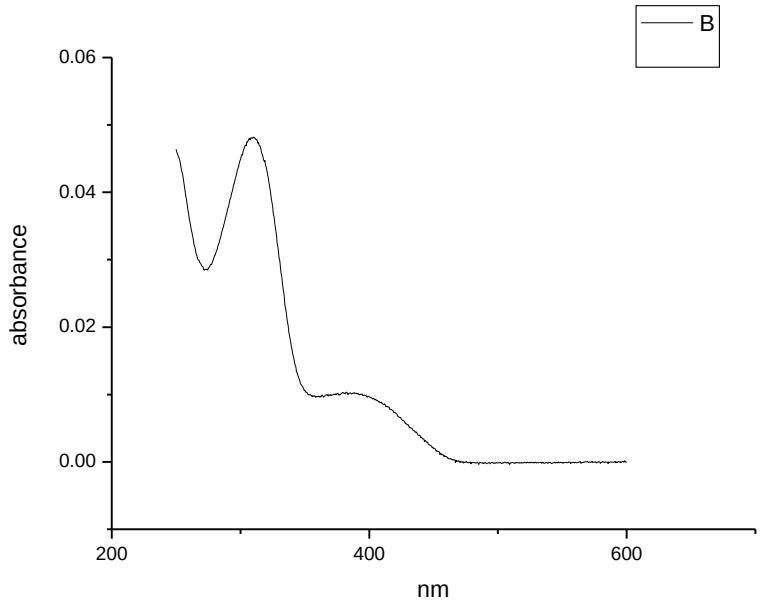

Figure 1.2.167. Ultraviolet-Visible absorption spectrum of **6a** recorded in 1,2-ethanediol.

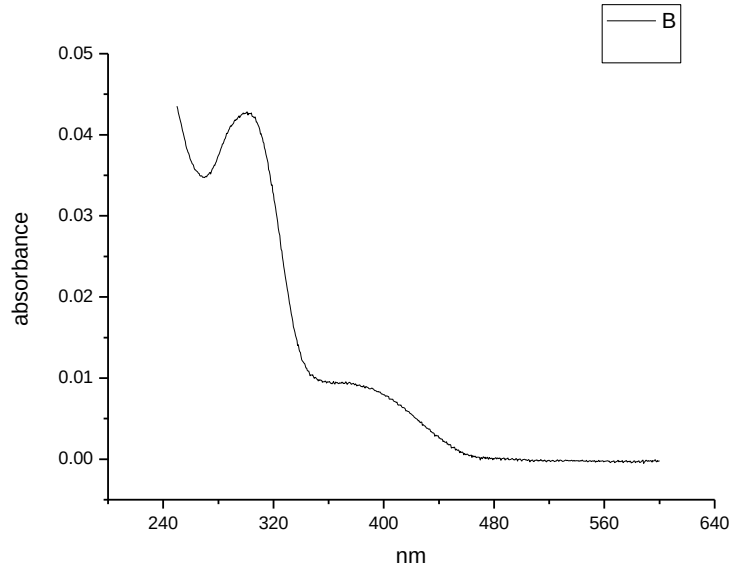

Figure 1.2.168. Ultraviolet-Visible absorption spectrum of **6a** recorded in 2,2,2-trifluoroethanol.

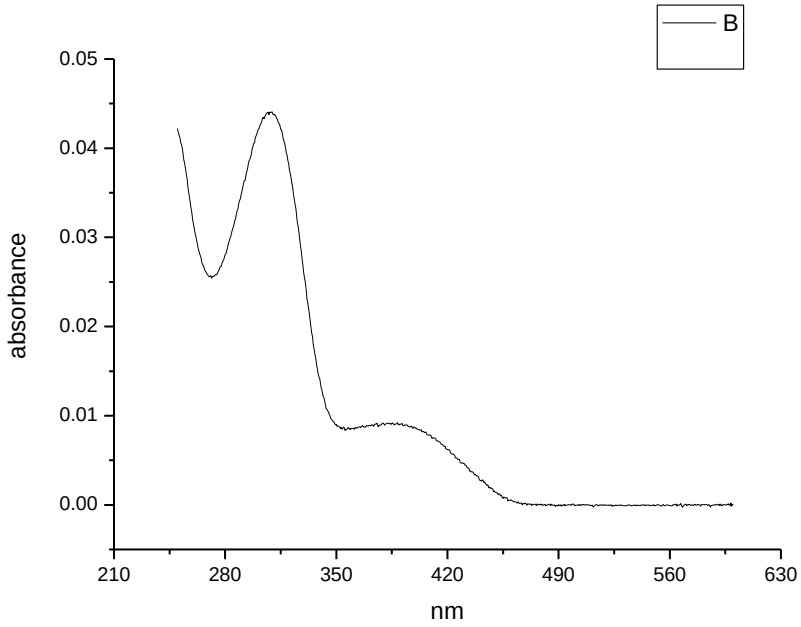

Figure 1.2.169. Ultraviolet-Visible absorption spectrum of **6a** recorded in Ethanol-d_1 (EtOD).

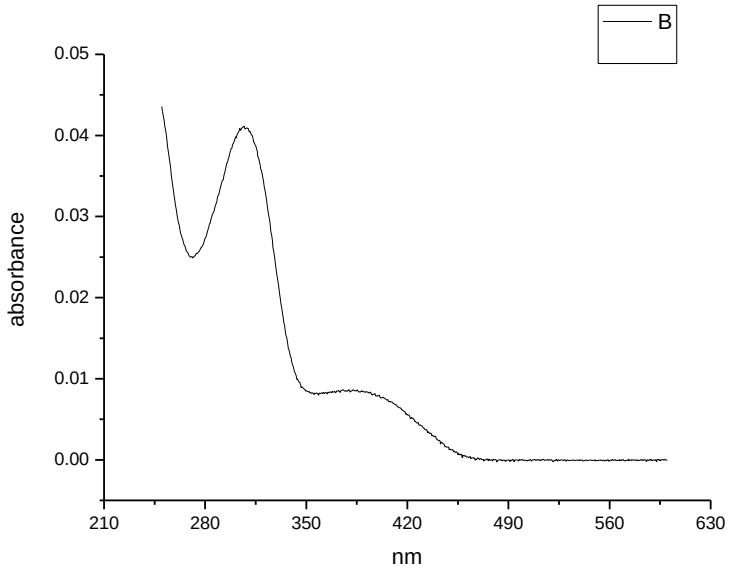

Figure 1.2.170. Ultraviolet-Visible absorption spectrum of **6a** recorded in Methanol-d_1 (MeOD).

1.2.9 Fluorescence Emission spectra.

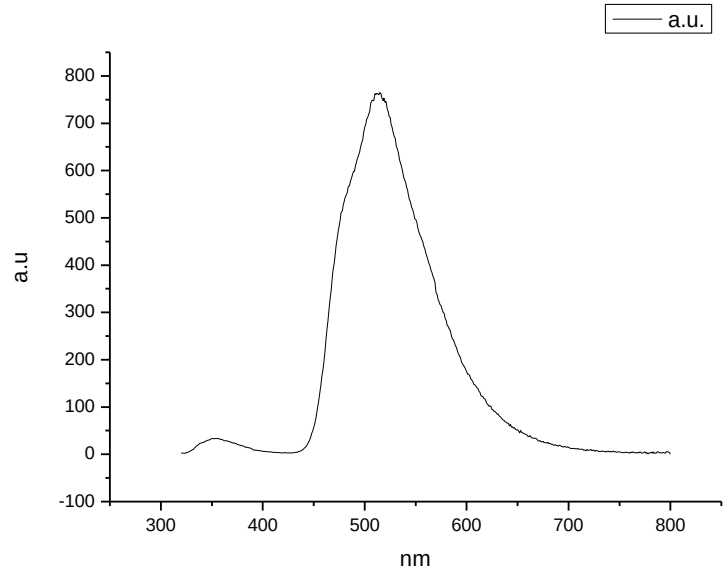

Figure 1.2.171. Fluorescence emission spectrum of **6a** recorded in Toluene at 310 nm excitation.

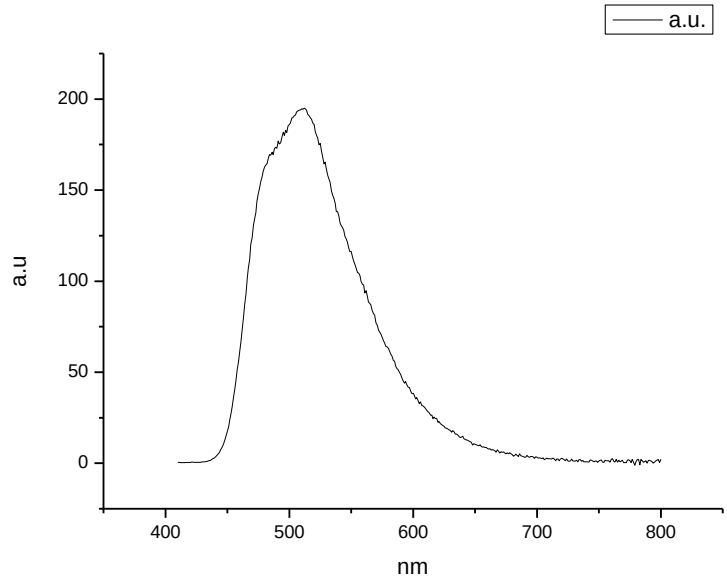

Figure 1.2.172. Fluorescence emission spectrum of **6a** recorded in Toluene at 400 nm excitation.

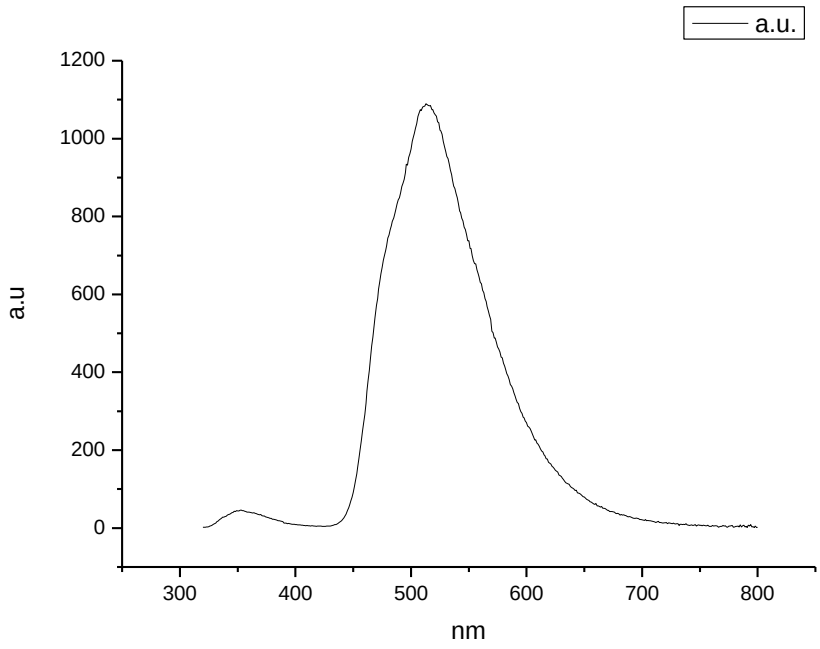

Figure 1.2.173. Fluorescence emission spectrum of **6a** recorded in 1,4-dioxane at 310 nm excitation.

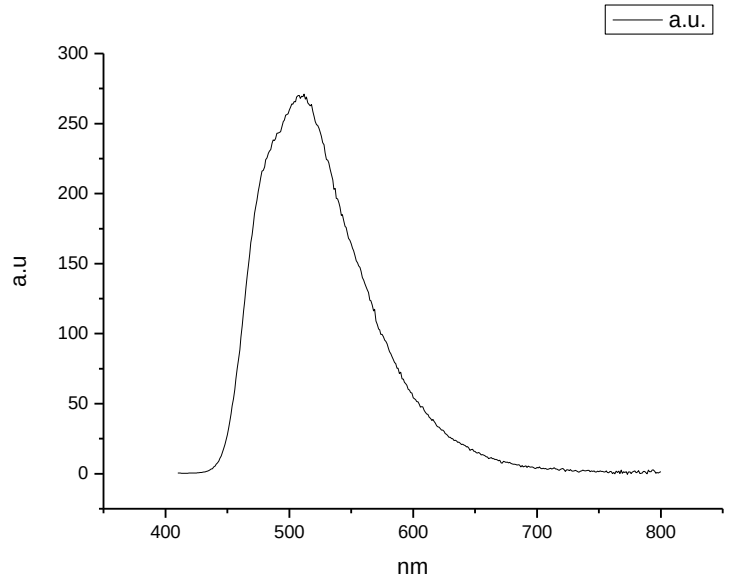

Figure 1.2.174. Fluorescence emission spectrum of **6a** recorded in 1,4-dioxane at 400 nm excitation.

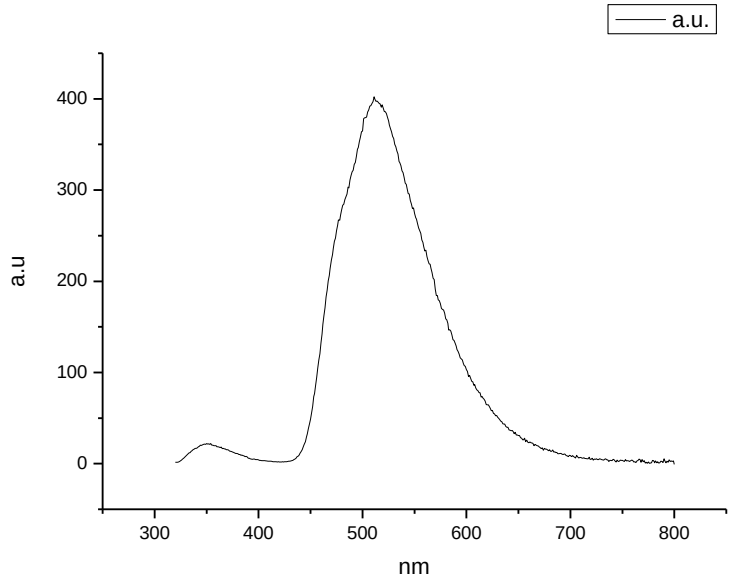

Figure 1.2.175. Fluorescence emission spectrum of **6a** recorded in Ethyl Acetate at 310 nm excitation.

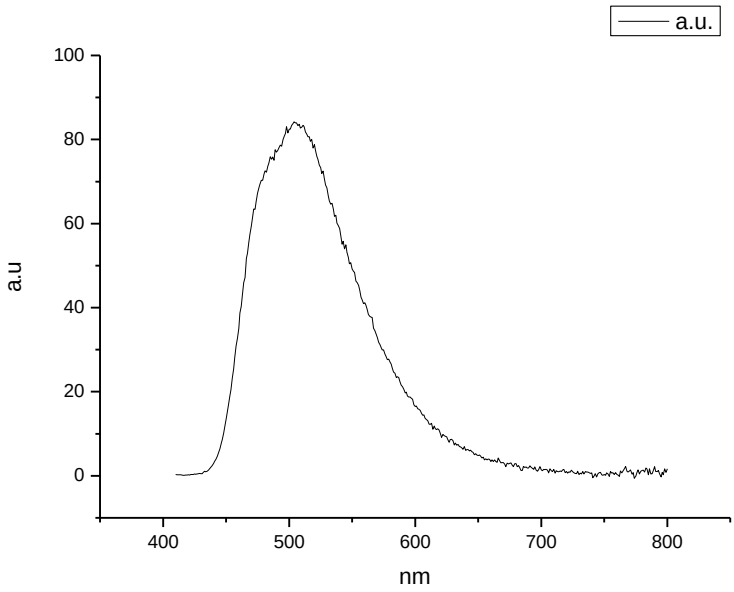

Figure 1.2.176. Fluorescence emission spectrum of **6a** recorded in Ethyl Acetate at 400 nm excitation.

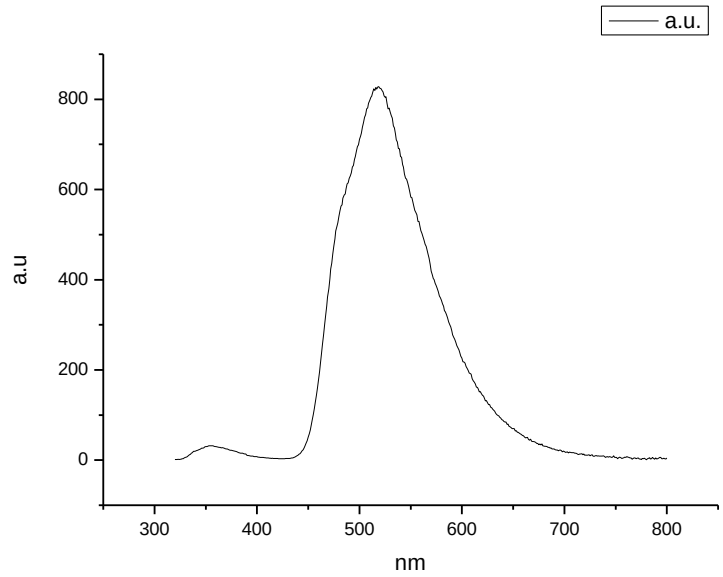

Figure 1.2.177. Fluorescence emission spectrum of **6a** recorded in Chloroform at 310 nm excitation.

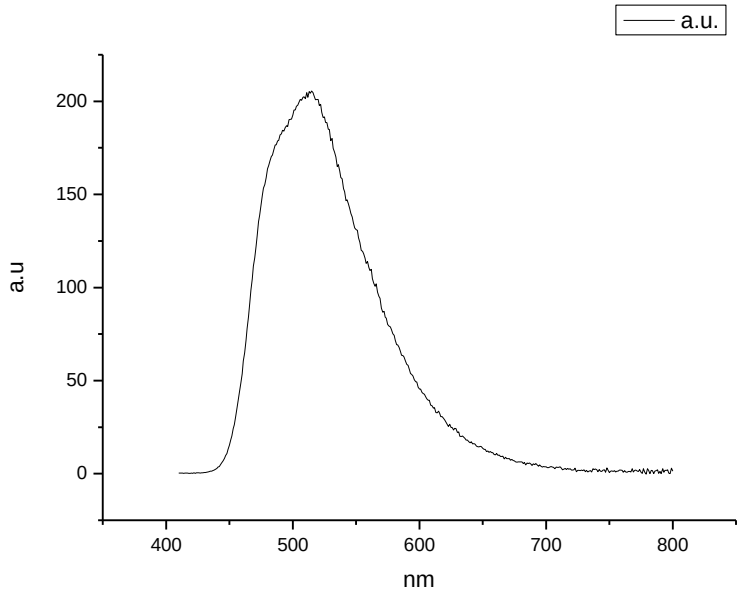

Figure 1.2.178. Fluorescence emission spectrum of **6a** recorded in Chloroform at 400 nm excitation.

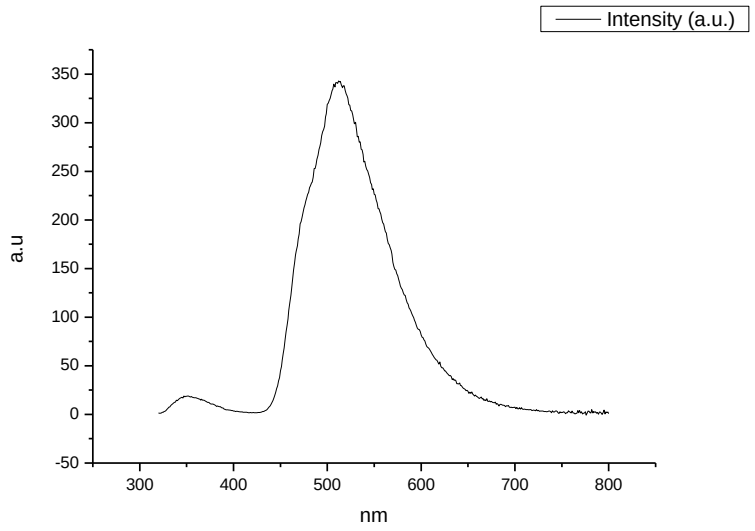

Figure 1.2.179. Fluorescence emission spectrum of **6a** recorded in 2-methyl-2-butanol at 310 nm excitation.

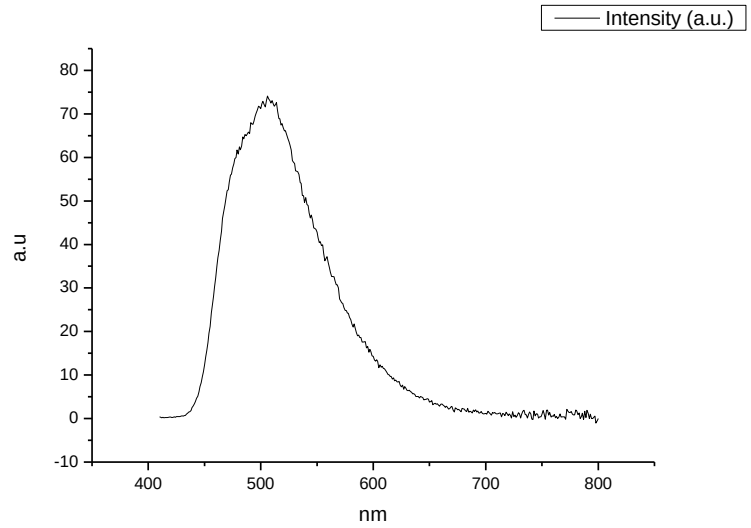

Figure 1.2.180. Fluorescence emission spectrum of **6a** recorded in 2-methyl-2-butanol at 400 nm excitation.

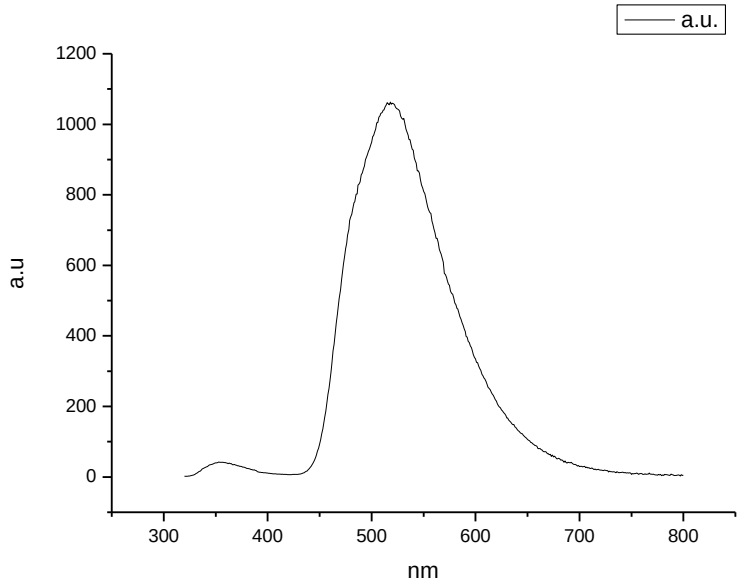

Figure 1.2.181. Fluorescence emission spectrum of **6a** recorded in N,N-dimethylformamide at 310 nm excitation.

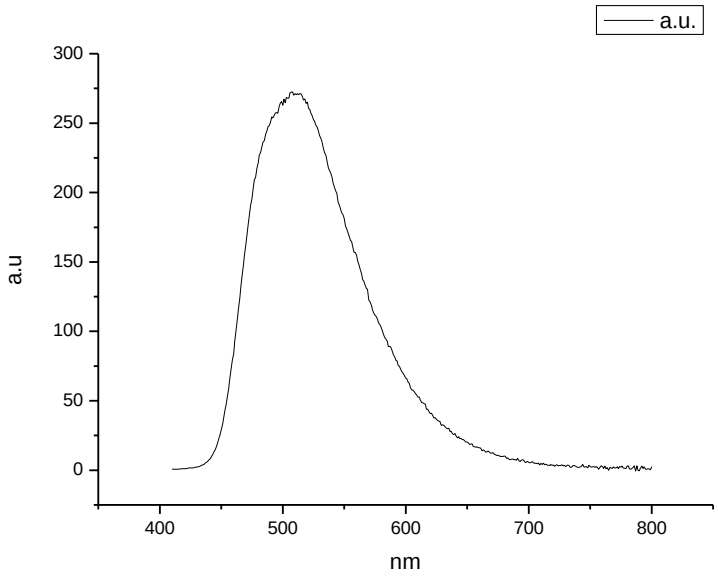

Figure 1.2.182. Fluorescence emission spectrum of **6a** recorded in N,N-dimethylformamide at 400 nm excitation.

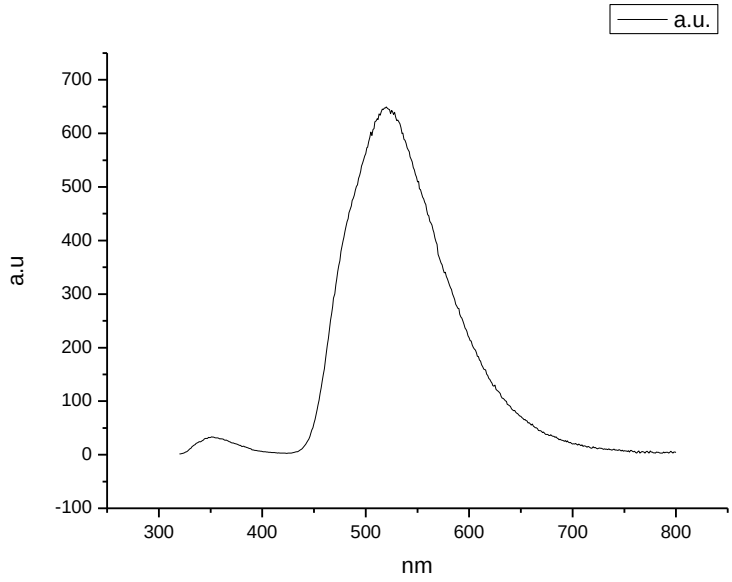

Figure 1.2.183. Fluorescence emission spectrum of **6a** recorded in Acetonitrile at 310 nm excitation.

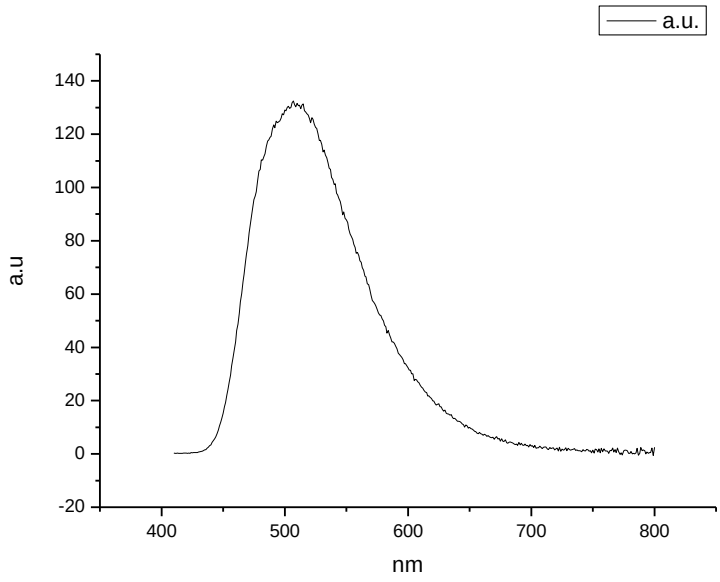

Figure 1.2.184. Fluorescence emission spectrum of **6a** recorded in Acetonitrile at 400 nm excitation.

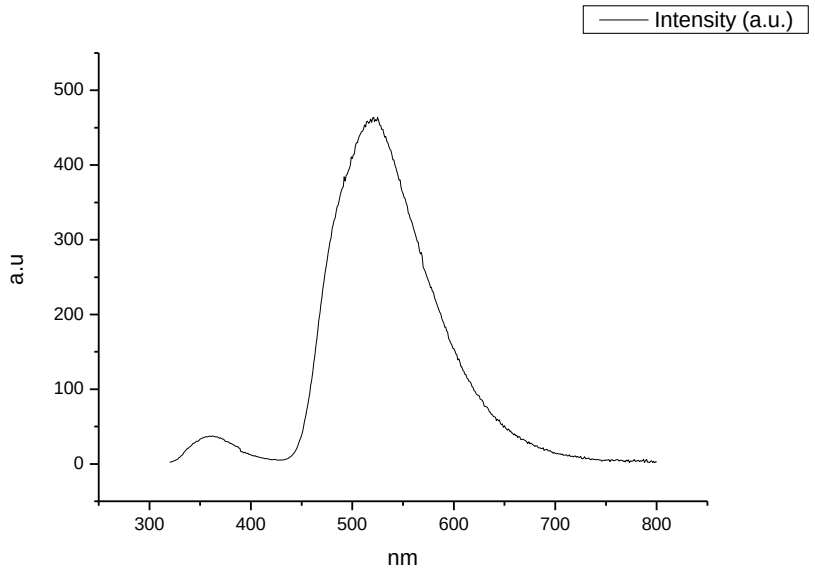

Figure 1.2.185. Fluorescence emission spectrum of **6a** recorded in Propylene Carbonate at 310 nm excitation.

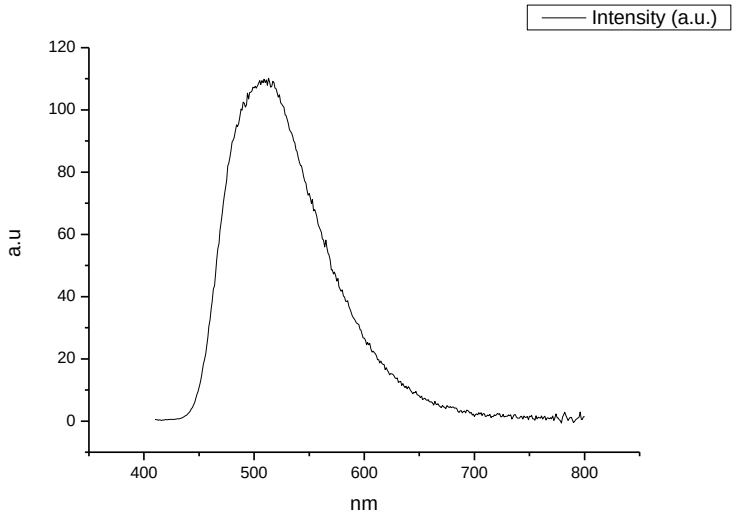

Figure 1.2.186. Fluorescence emission spectrum of **6a** recorded in Propylene Carbonate at 400 nm excitation.

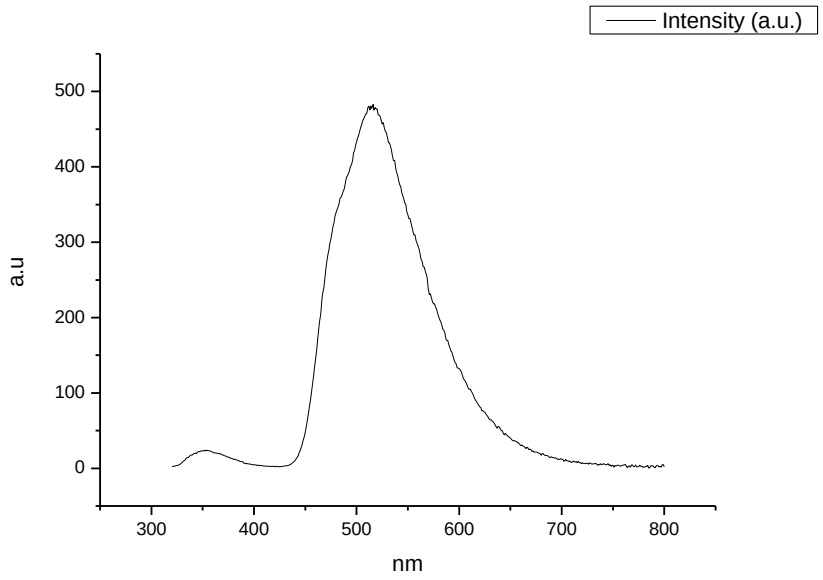

Figure 1.2.187. Fluorescence emission spectrum of **6a** recorded in 1-octanol at 310 nm excitation.

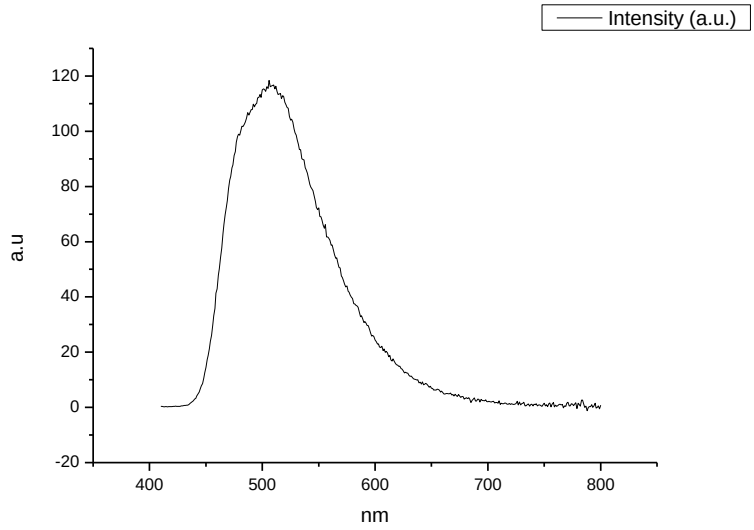

Figure 1.2.188. Fluorescence emission spectrum of **6a** recorded in 1-octanol at 400 nm excitation.

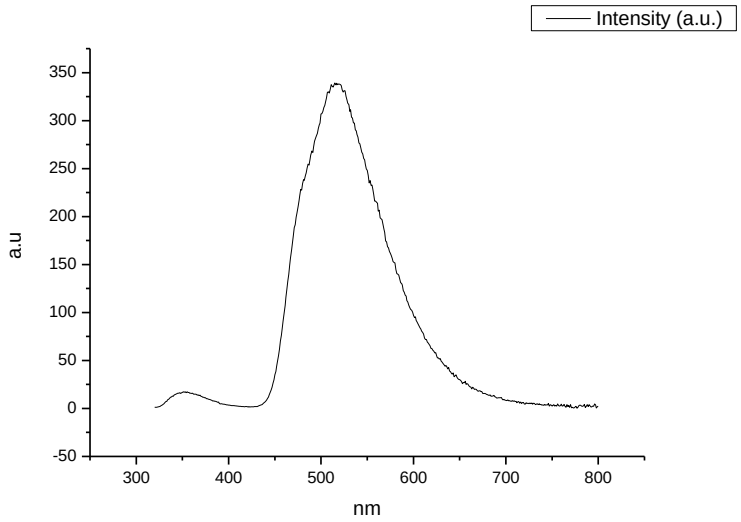

Figure 1.2.189. Fluorescence emission spectrum of **6a** recorded in 1-hexanol at 310 nm excitation.

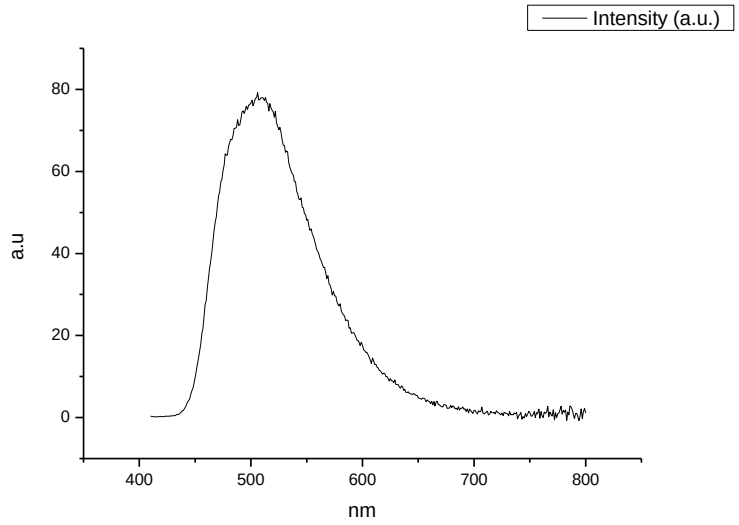

Figure 1.2.190. Fluorescence emission spectrum of **6a** recorded in 1-hexanol at 400 nm excitation.

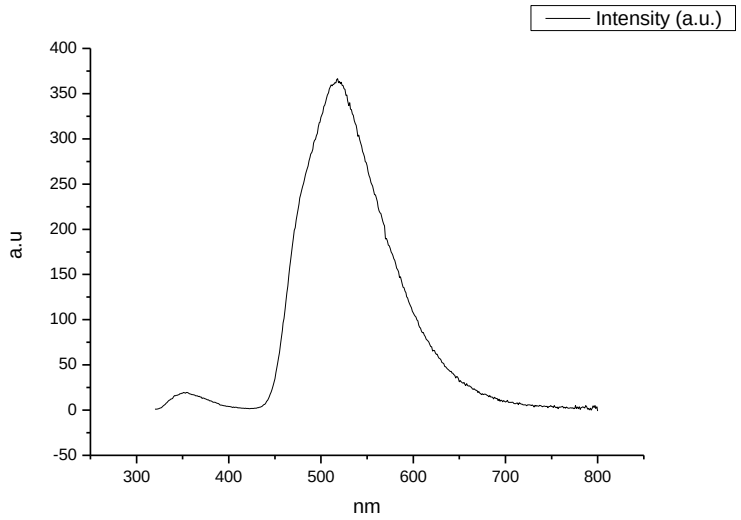

Figure 1.2.191. Fluorescence emission spectrum of **6a** recorded in 1-butanol at 310 nm excitation.

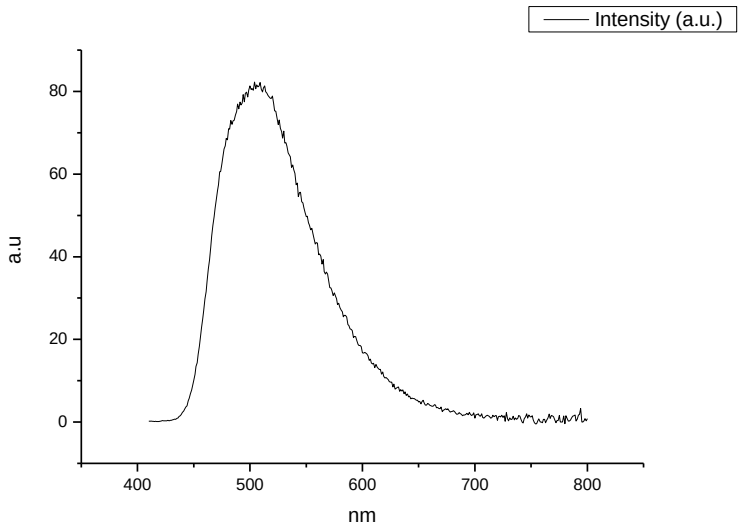

Figure 1.2.192. Fluorescence emission spectrum of **6a** recorded in 1-butanol at 400 nm excitation.

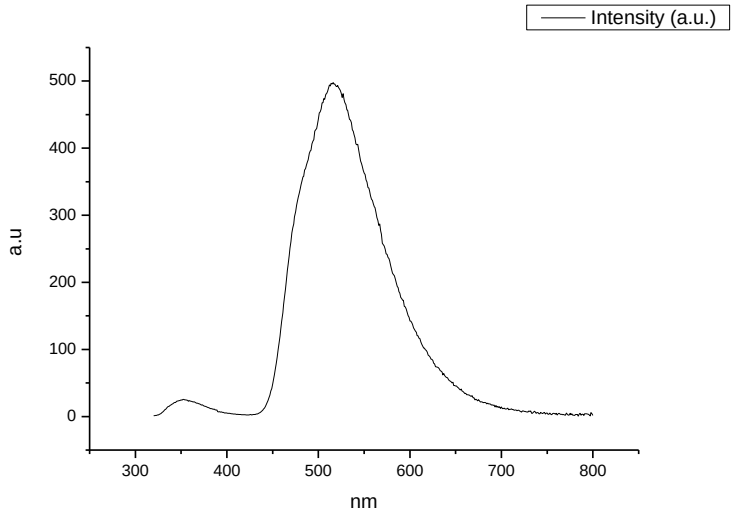

Figure 1.2.193. Fluorescence emission spectrum of **6a** recorded in 1-pentanol at 310 nm excitation.

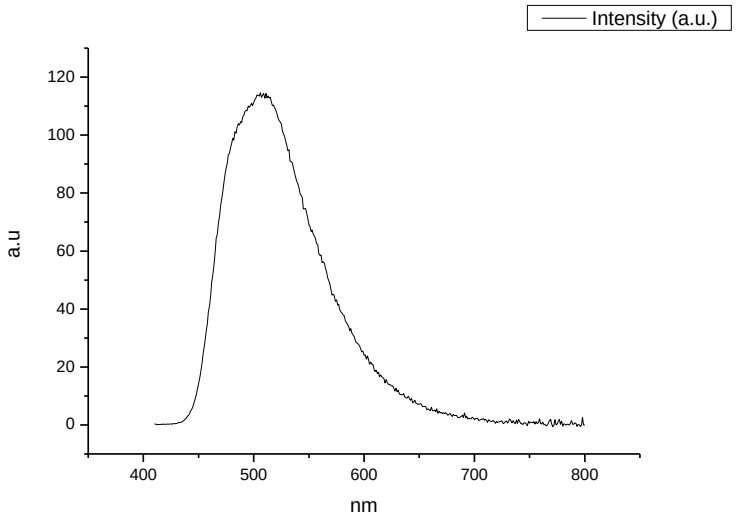

Figure 1.2.194. Fluorescence emission spectrum of **6a** recorded in 1-pentanol at 400 nm excitation.

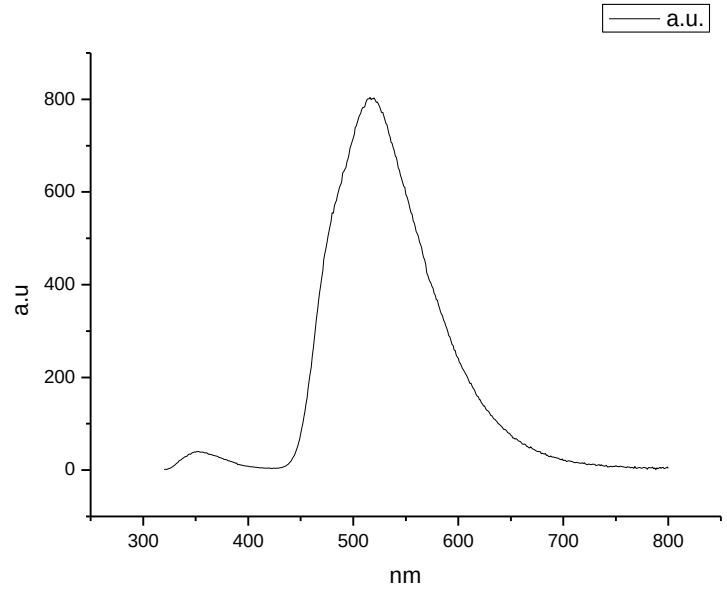

Figure 1.2.195. Fluorescence emission spectrum of **6a** recorded in 1-propanol at 310 nm excitation.

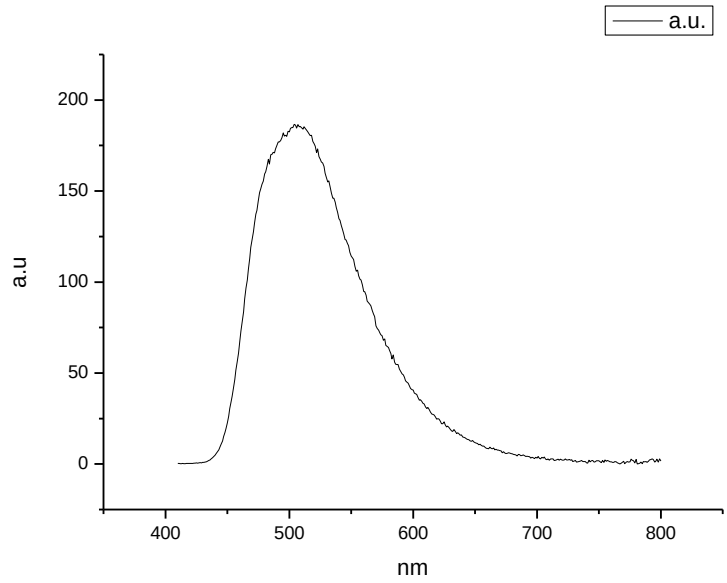

Figure 1.2.196. Fluorescence emission spectrum of **6a** recorded in 1-propanol at 400 nm excitation.

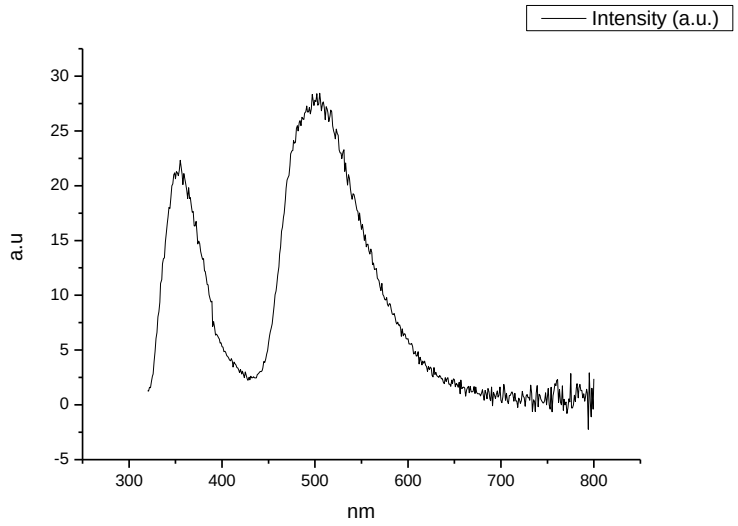

Figure 1.2.197. Fluorescence emission spectrum of **6a** recorded in Acetic Acid at 310 nm excitation.

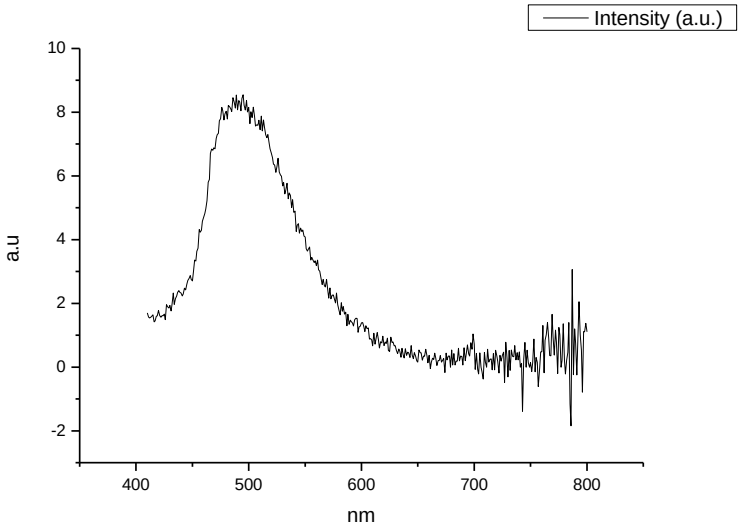

Figure 1.2.198. Fluorescence emission spectrum of **6a** recorded in Acetic Acid at 400 nm excitation.

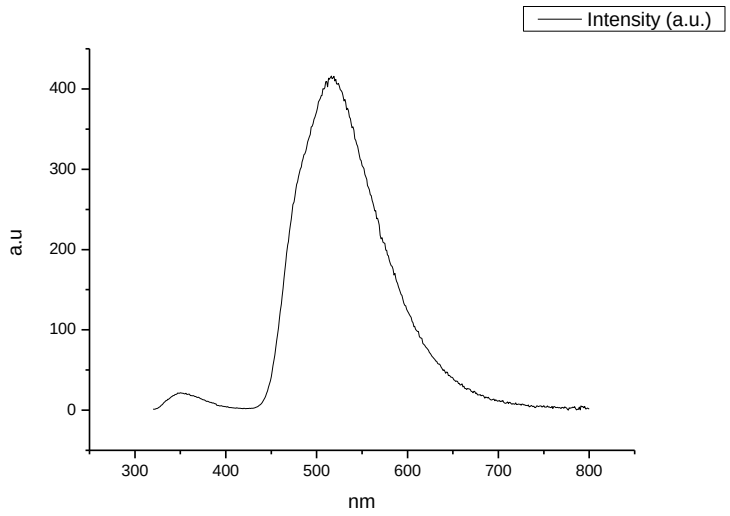

Figure 1.2.199. Fluorescence emission spectrum of **6a** recorded in Ethanol at 310 nm excitation.

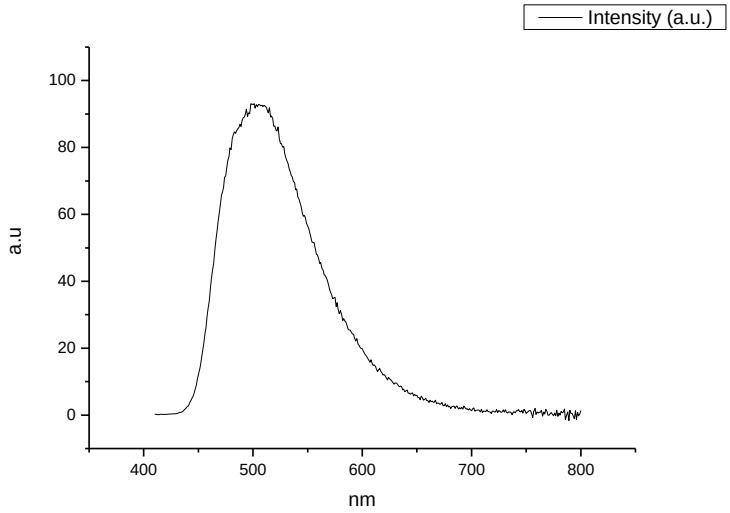

Figure 1.2.200. Fluorescence emission spectrum of **6a** recorded in Ethanol at 400 nm excitation.

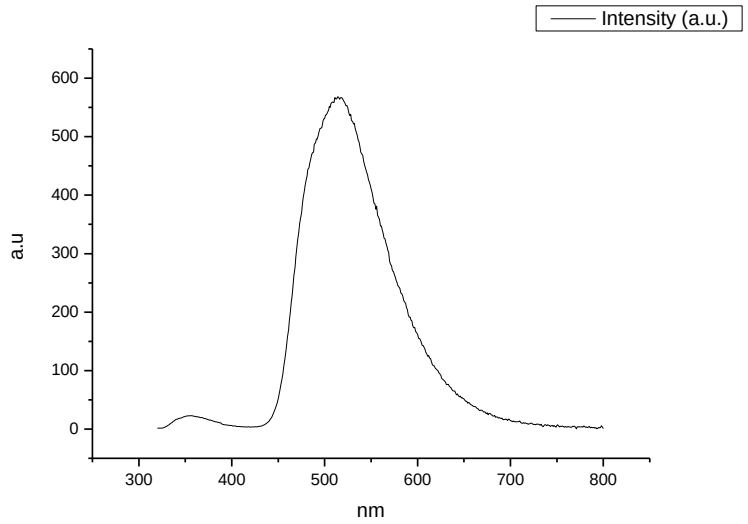

Figure 1.2.201. Fluorescence emission spectrum of **6a** recorded in 1,5-pentanediol at 310 nm excitation.

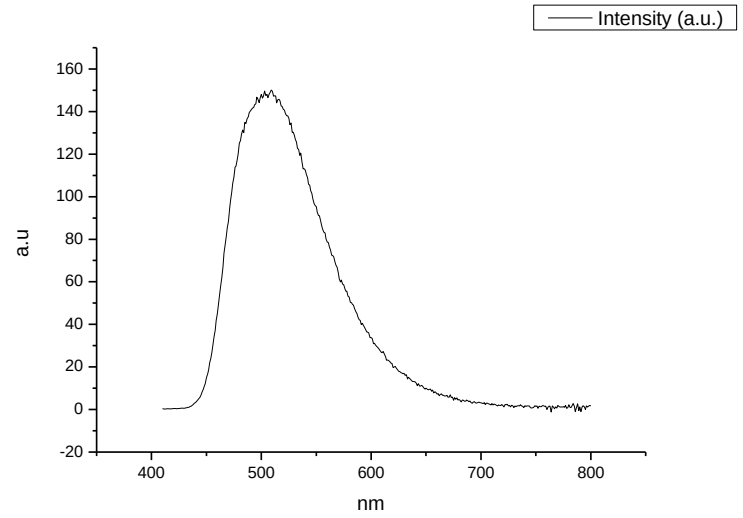

Figure 1.2.202. Fluorescence emission spectrum of **6a** recorded in 1,5-pentanediol at 400 nm excitation.

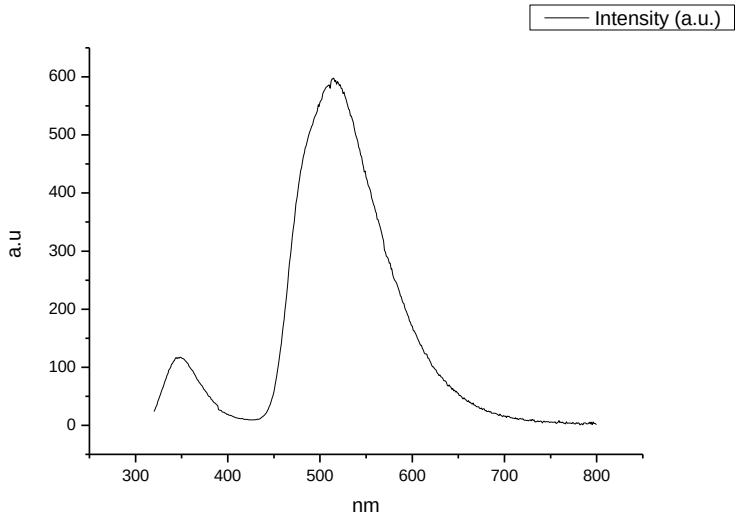

Figure 1.2.203. Fluorescence emission spectrum of **6a** recorded in 1,3-butanediol at 310 nm excitation.

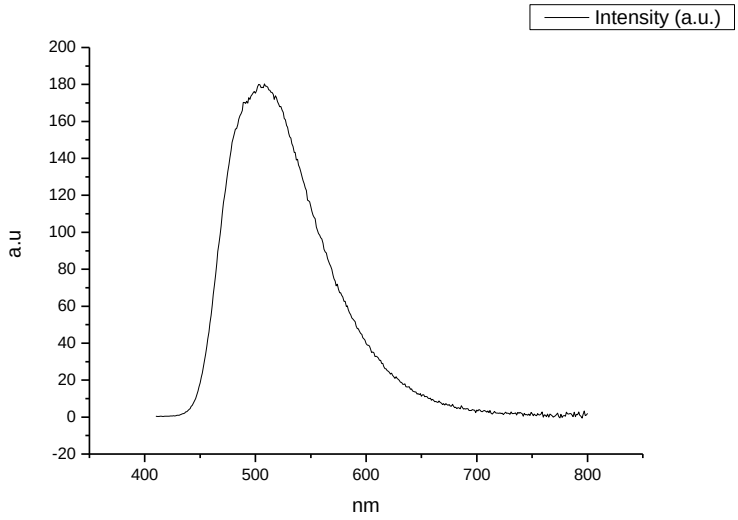

Figure 1.2.204. Fluorescence emission spectrum of **6a** recorded in 1,3-butanediol at 400 nm excitation.

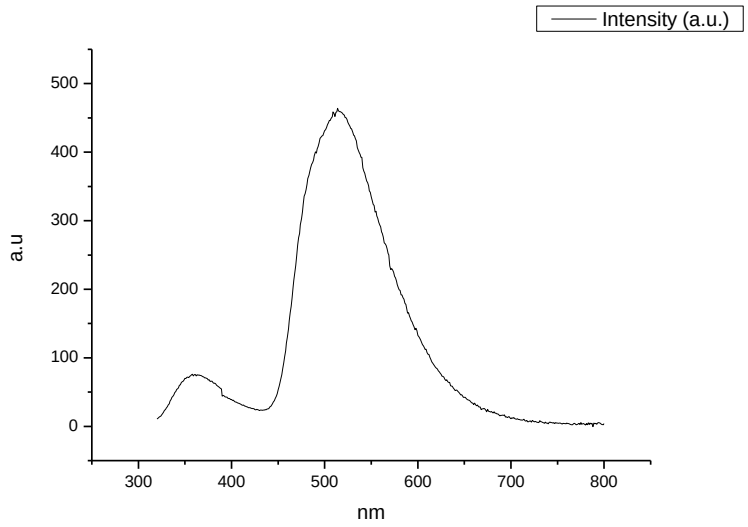

Figure 1.2.205. Fluorescence emission spectrum of **6a** recorded in 1,4-butanediol at 310 nm excitation.

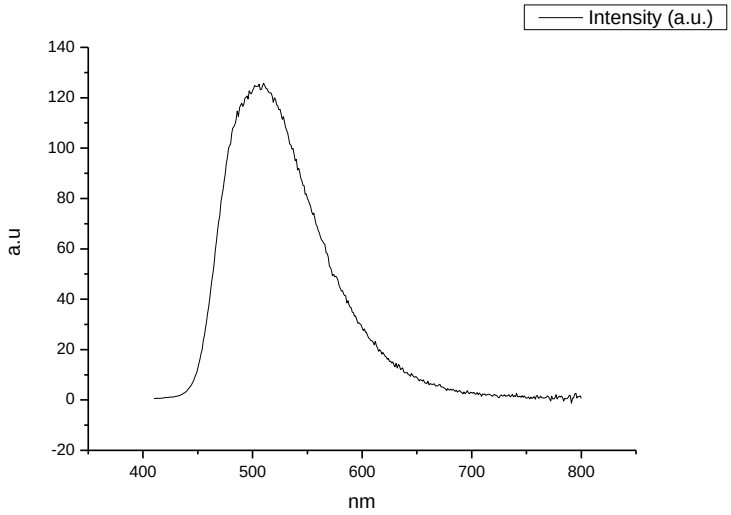

Figure 1.2.206. Fluorescence emission spectrum of **6a** recorded in 1,4-butanediol at 400 nm excitation.

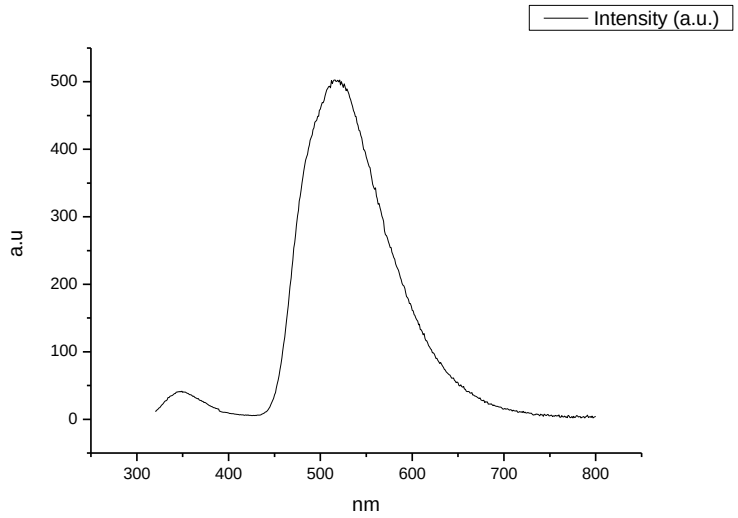

Figure 1.2.207. Fluorescence emission spectrum of **6a** recorded in 1,3-propanediol at 310 nm excitation.

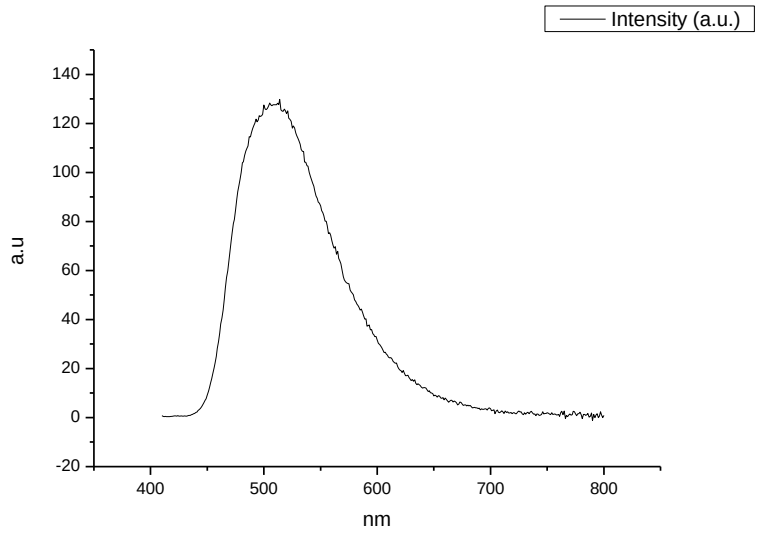

Figure 1.2.208. Fluorescence emission spectrum of **6a** recorded in 1,3-propanediol at 400 nm excitation.

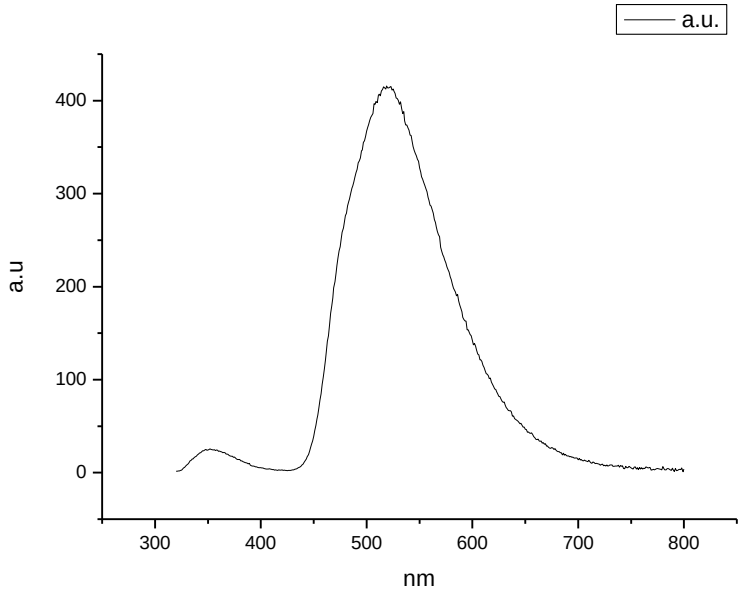

Figure 1.2.209. Fluorescence emission spectrum of **6a** recorded in Methanol at 310 nm excitation.

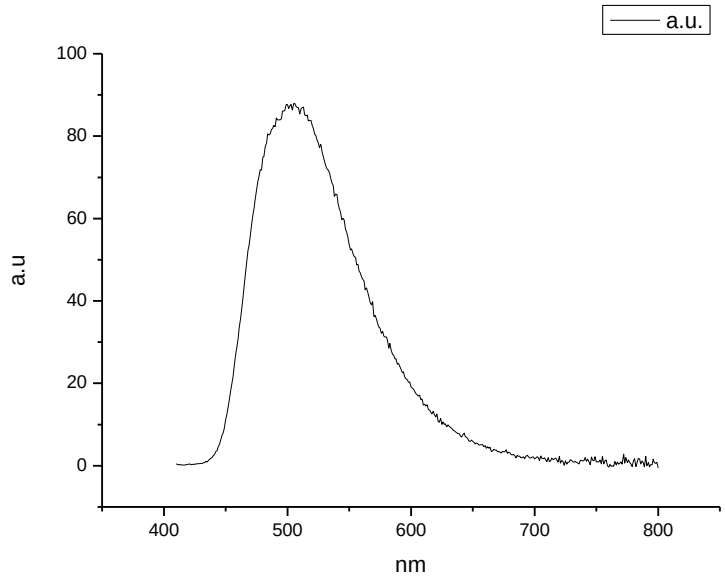

Figure 1.2.210. Fluorescence emission spectrum of **6a** recorded in Methanol at 400 nm excitation.

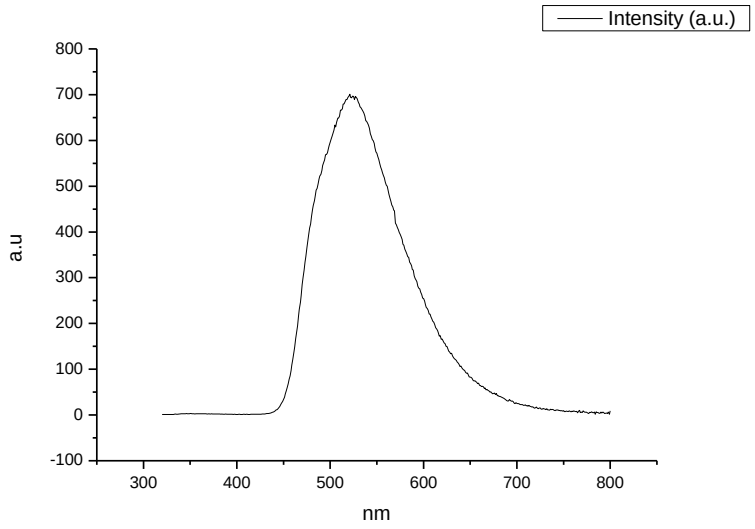

Figure 1.2.211. Fluorescence emission spectrum of **6a** recorded in 1,2-ethanediol at 310 nm excitation.

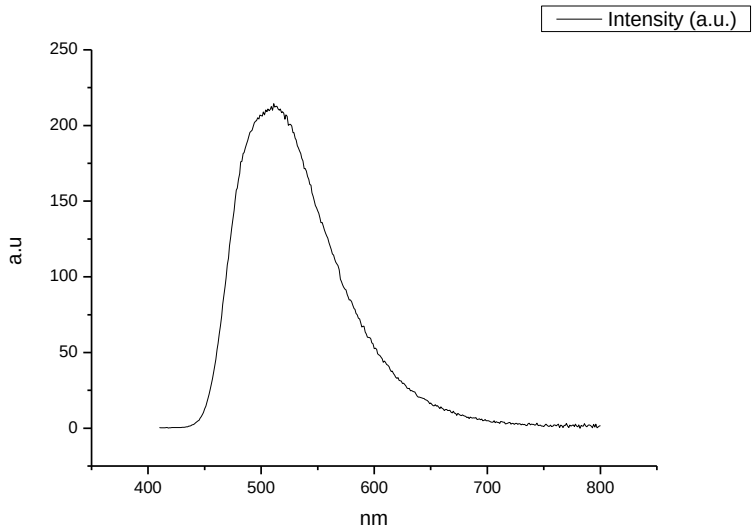

Figure 1.2.212. Fluorescence emission spectrum of **6a** recorded in 1,2-ethanediol at 400 nm excitation.

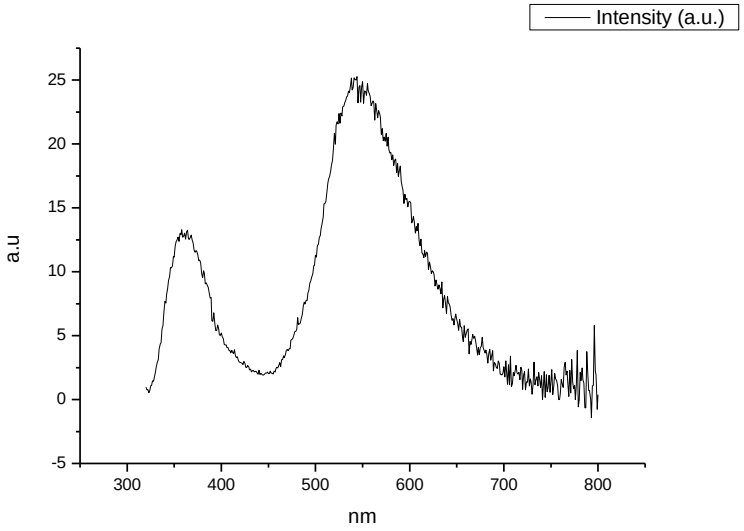

Figure 1.2.213. Fluorescence emission spectrum of **6a** recorded in 2,2,2-trifluoroethanol at 310 nm excitation.

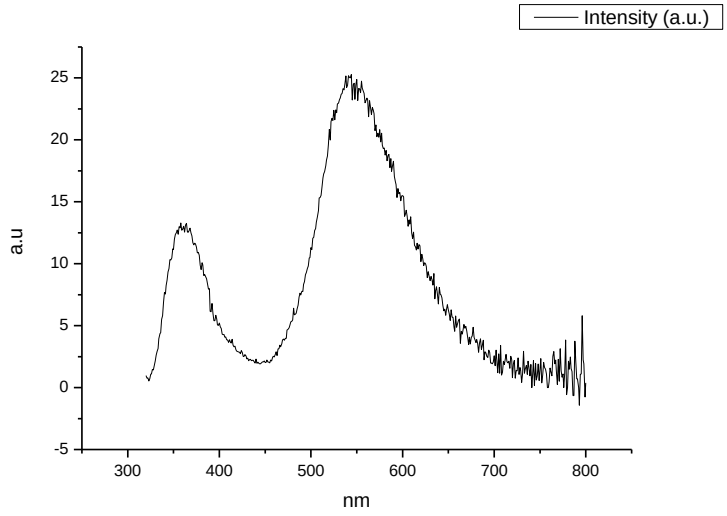

Figure 1.2.214. Fluorescence emission spectrum of **6a** recorded in 2,2,2-trifluoroethanol at 400 nm excitation.

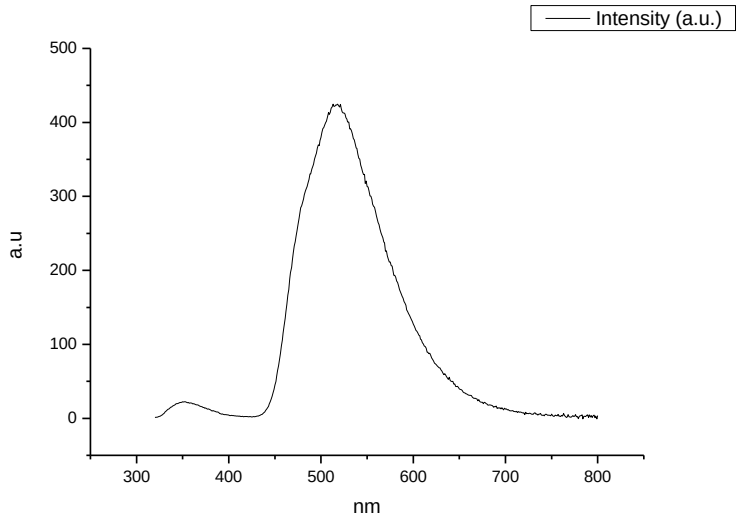

Figure 1.2.215. Fluorescence emission spectrum of **6a** recorded in ethanol-d_1 (EtOD) at 310 nm excitation.

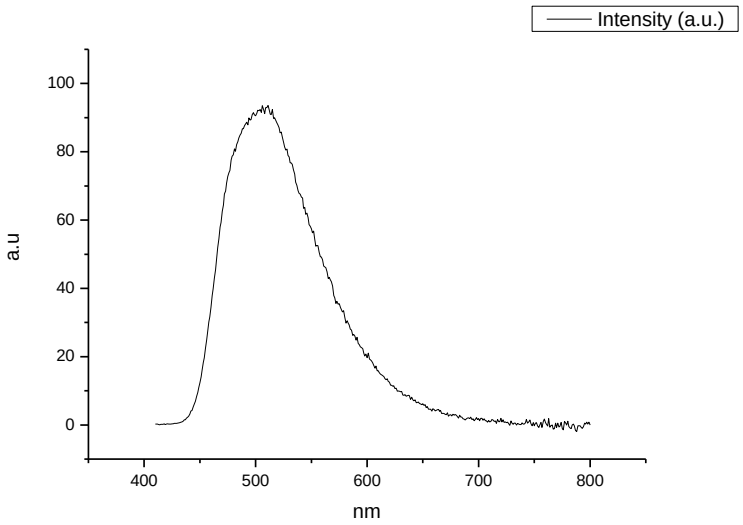

Figure 1.2.216. Fluorescence emission spectrum of **6a** recorded in ethanol-d_1 (EtOD) at 400 nm excitation.

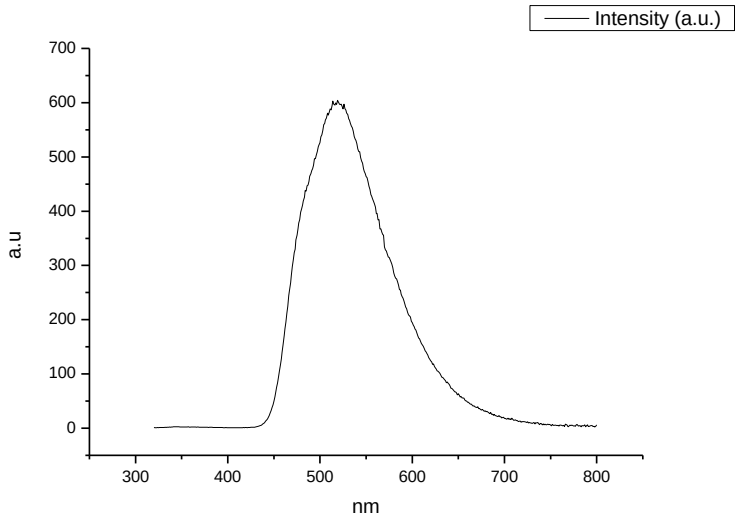

Figure 1.2.217. Fluorescence emission spectrum of **6a** recorded in methanol-d_1 (MeOD) at 310 nm excitation.

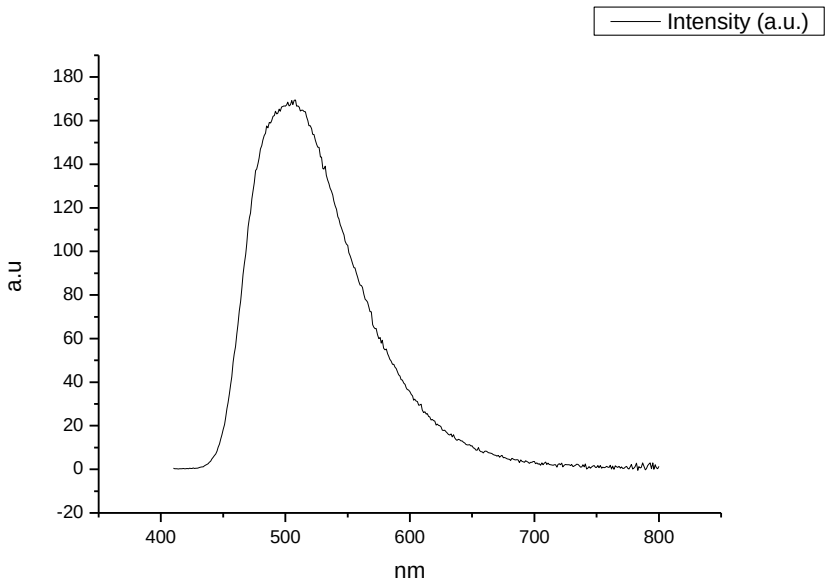

Figure 1.2.218. Fluorescence emission spectrum of **6a** recorded in methanol-d_1 (MeOD) at 400 nm excitation.

1.2.10 Normalised Fluorescence Emission spectra (Gaussian fitted).

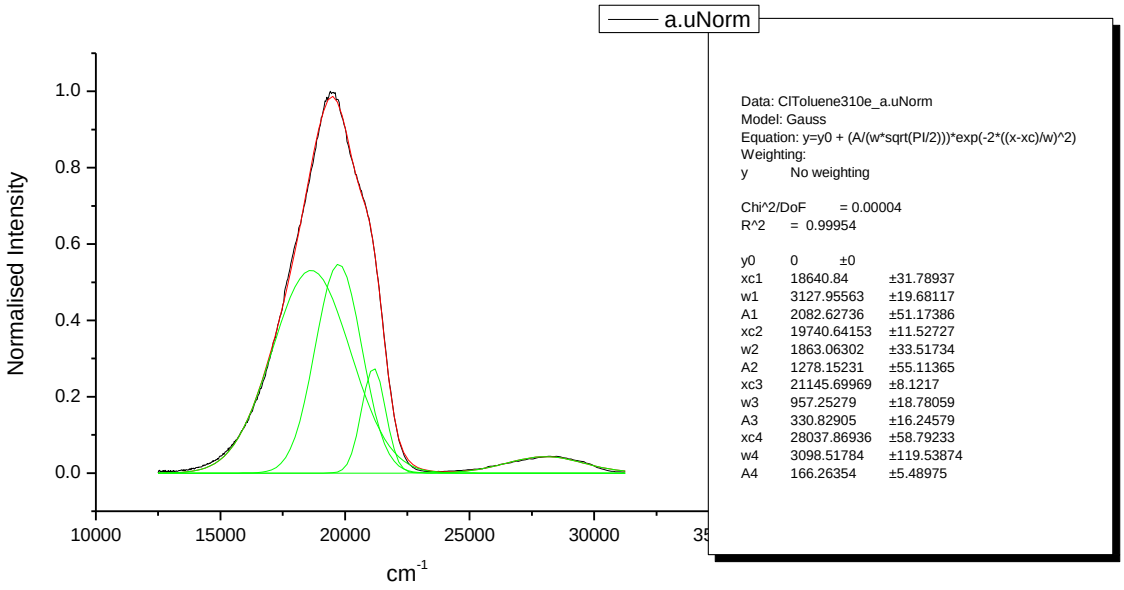

Figure 1.2.219. Gaussian model fit of the normalised fluorescence emission spectrum of **6a** recorded in Toluene at 310 nm excitation.

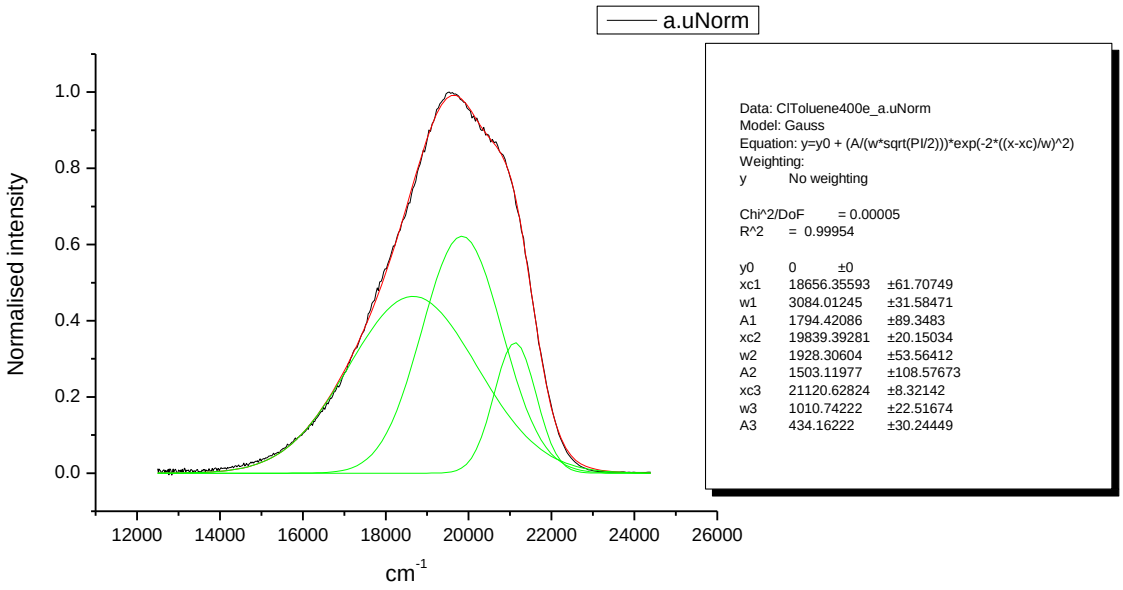

Figure 1.2.220. Gaussian model fit of the normalised fluorescence emission spectrum of **6a** recorded in Toluene at 400 nm excitation.

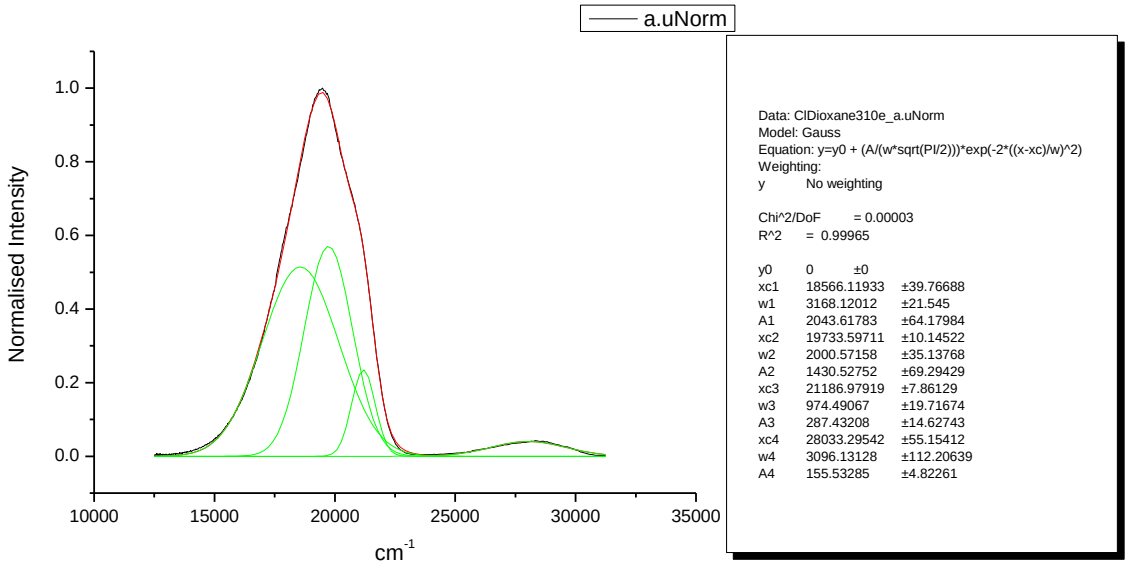

Figure 1.2.221. Gaussian model fit of the normalised fluorescence emission spectrum of **6a** recorded in 1,4-dioxane at 310 nm excitation.

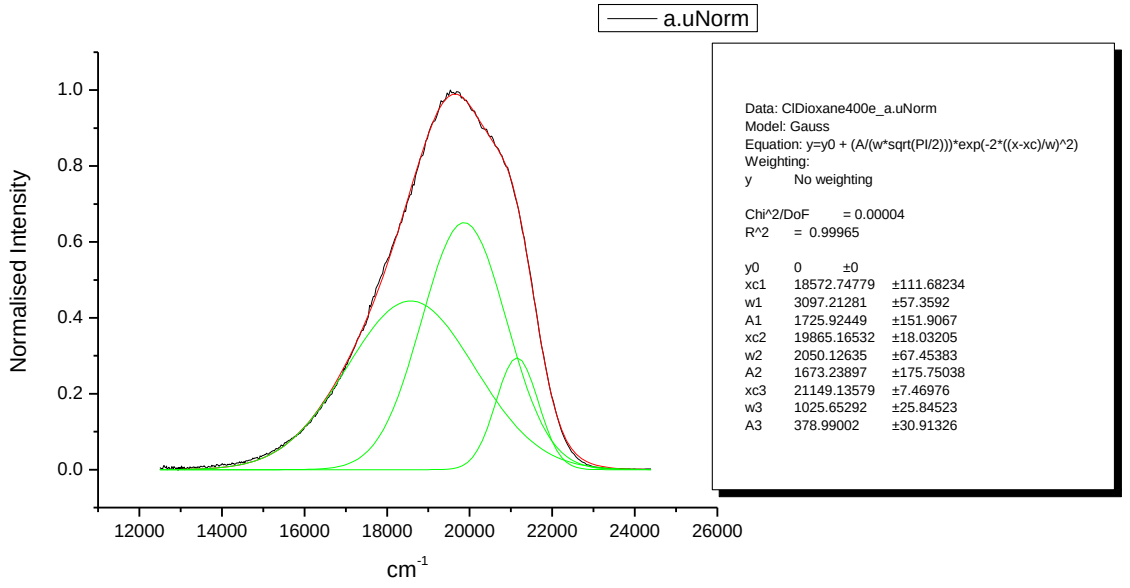

Figure 1.2.222. Gaussian model fit of the normalised fluorescence emission spectrum of **6a** recorded in 1,4-dioxane at 400 nm excitation.

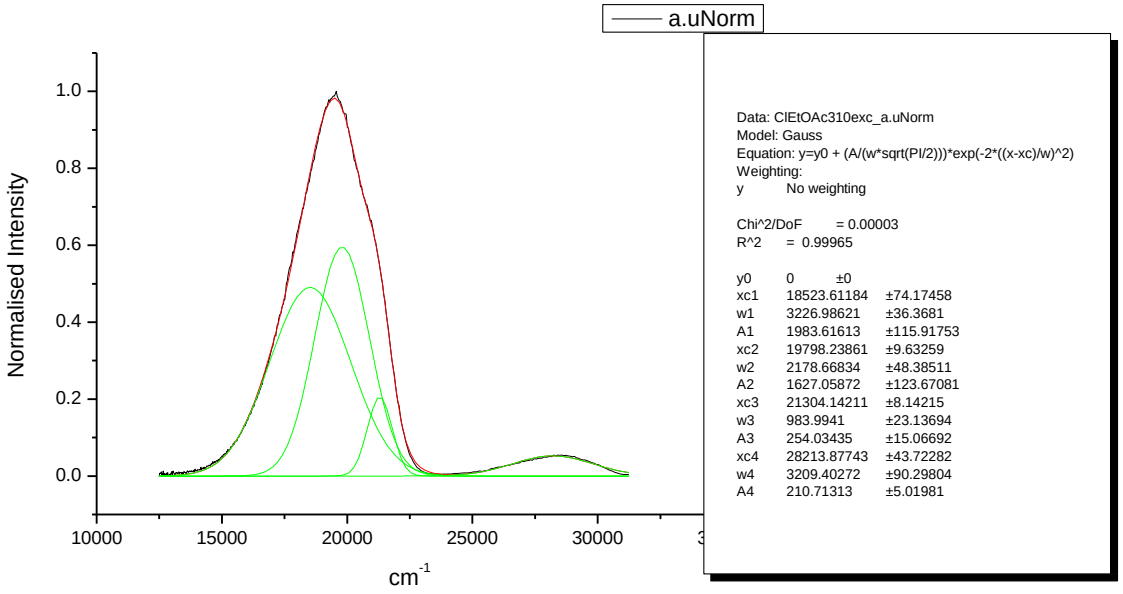

Figure 1.2.223. Gaussian model fit of the normalised fluorescence emission spectrum of **6a** recorded in Ethyl Acetate at 310 nm excitation.

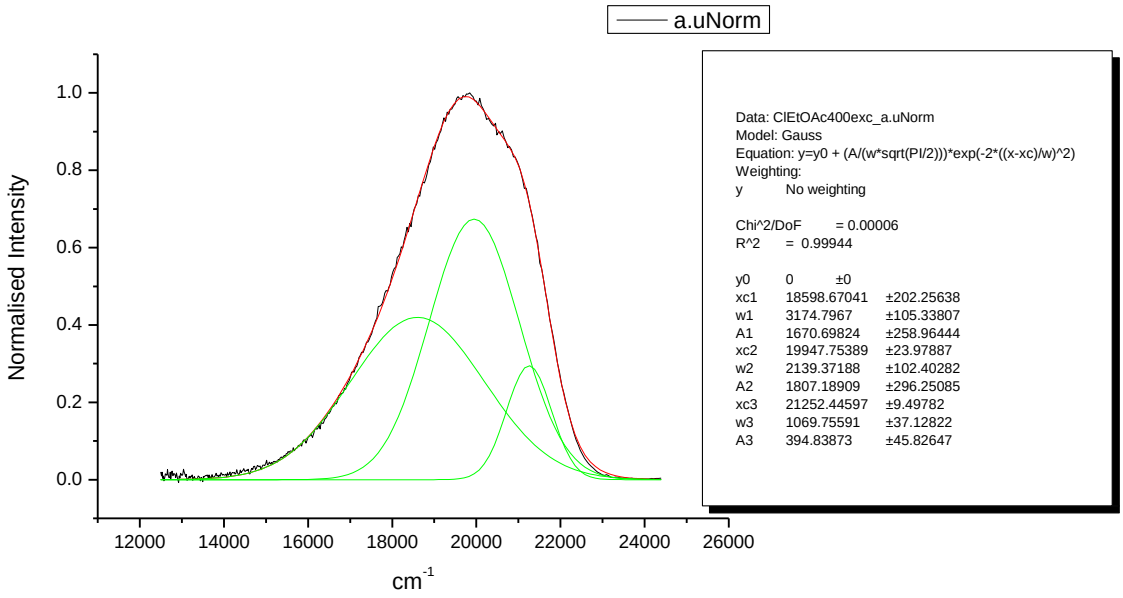

Figure 1.2.224. Gaussian model fit of the normalised fluorescence emission spectrum of **6a** recorded in Ethyl Acetate at 400 nm excitation.

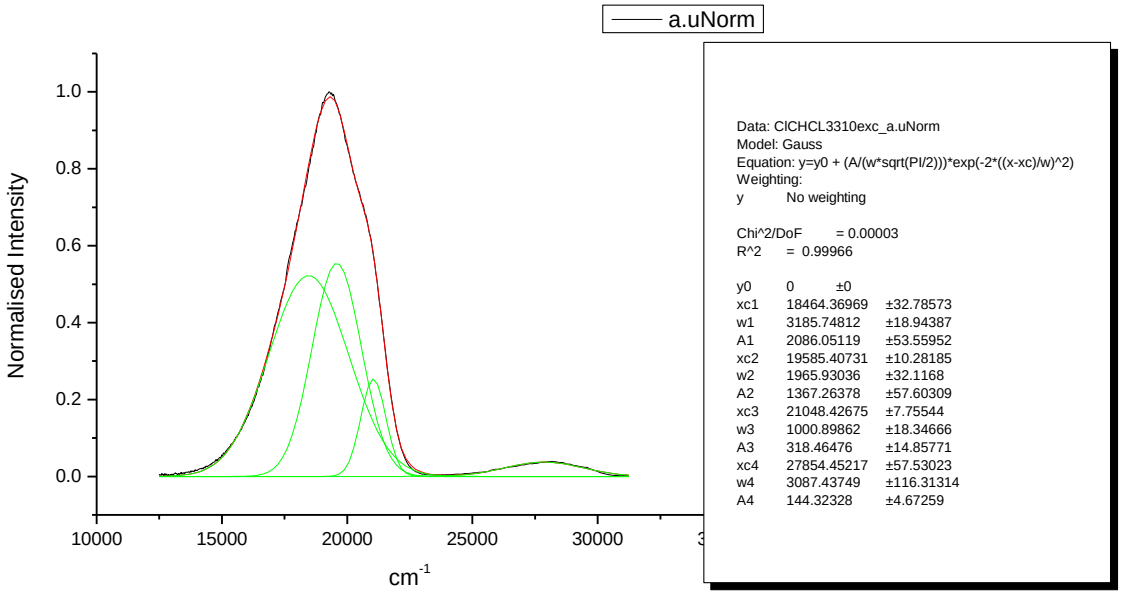

Figure 1.2.225. Gaussian model fit of the normalised fluorescence emission spectrum of **6a** recorded in Chloroform at 310 nm excitation.

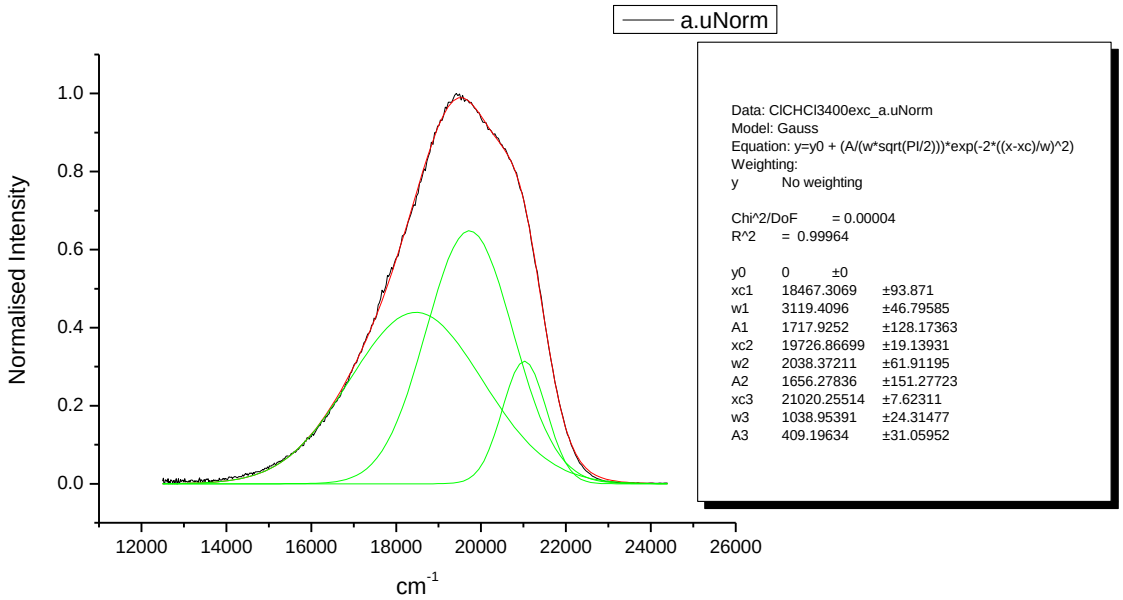

Figure 1.2.226. Gaussian model fit of the normalised fluorescence emission spectrum of **6a** recorded in Chloroform at 400 nm excitation.

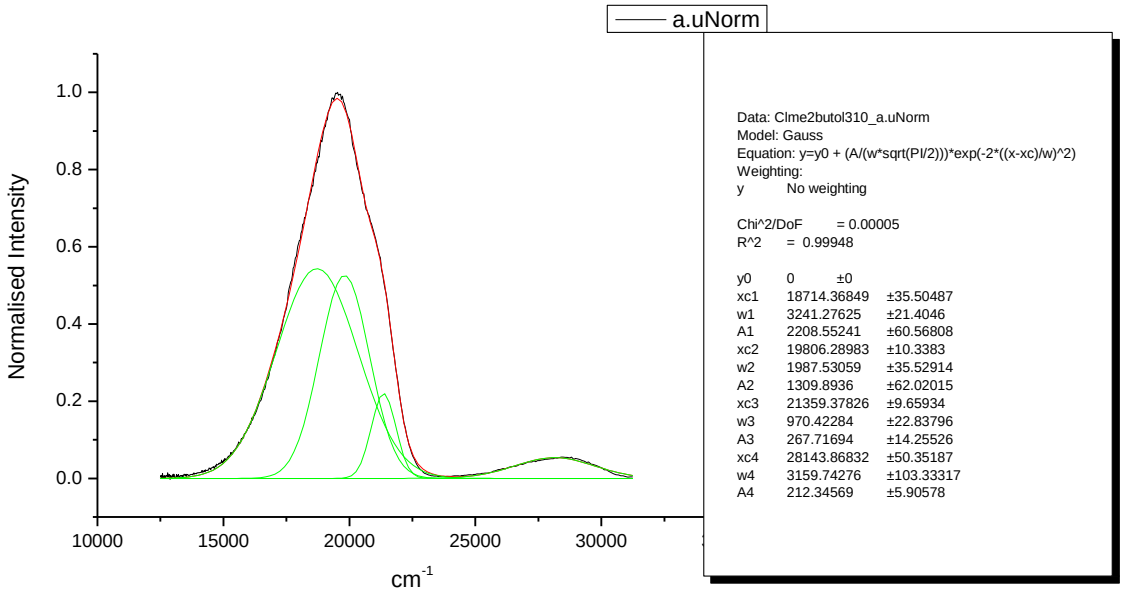

Figure 1.2.227. Gaussian model fit of the normalised fluorescence emission spectrum of **6a** recorded in 2-methyl-2-butanol at 310 nm excitation.

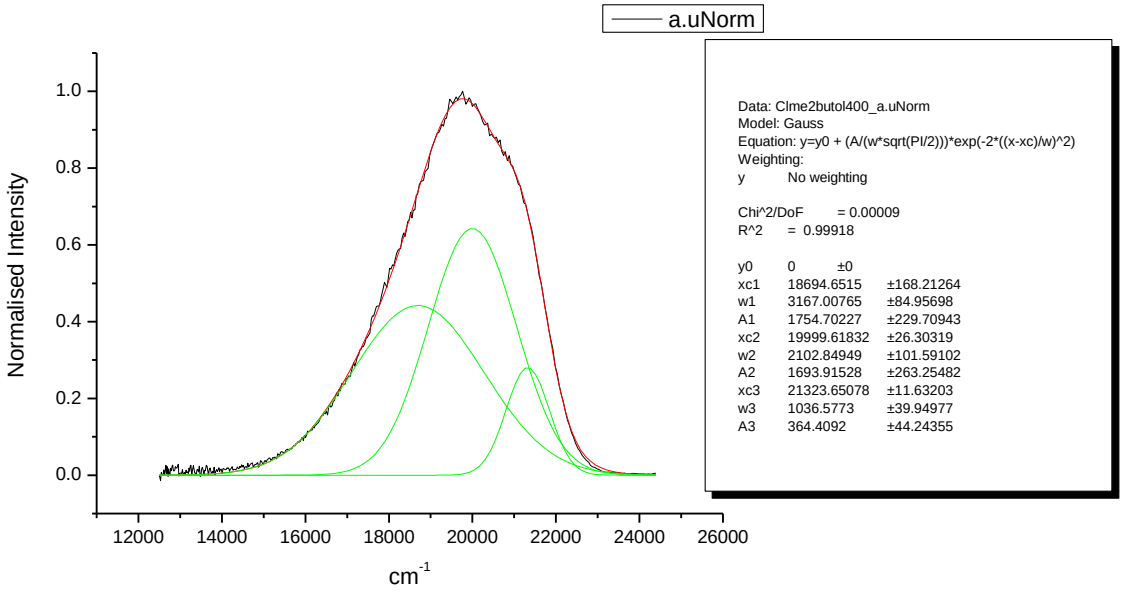

Figure 1.2.228. Gaussian model fit of the normalised fluorescence emission spectrum of **6a** recorded in 2-methyl-2-butanol at 400 nm excitation.

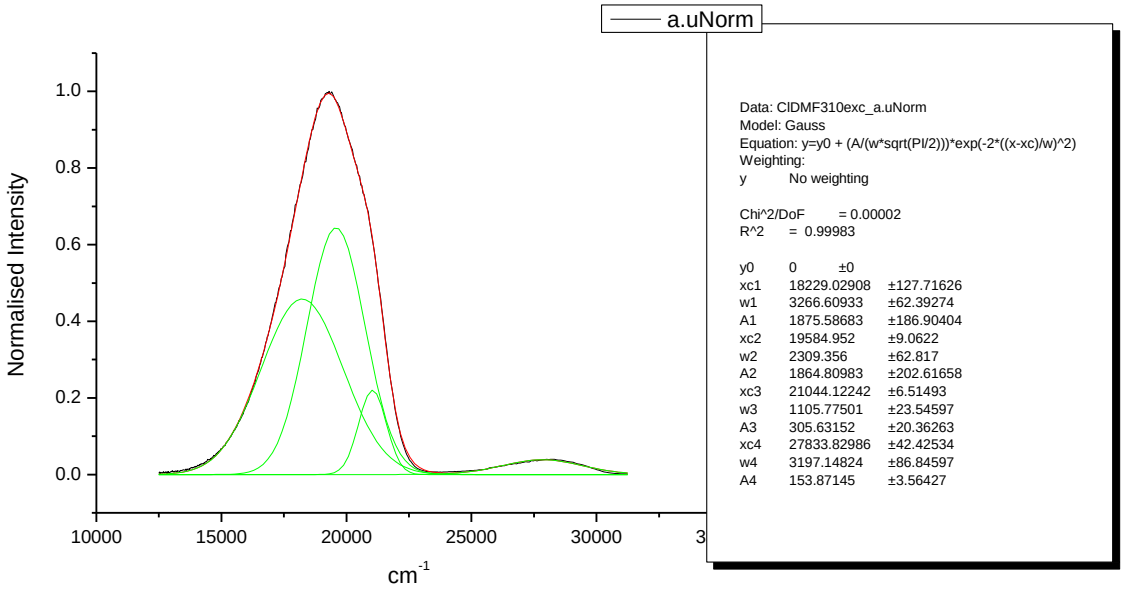

Figure 1.2.229. Gaussian model fit of the normalised fluorescence emission spectrum of **6a** recorded in N,N-dimethylformamide at 310 nm excitation.

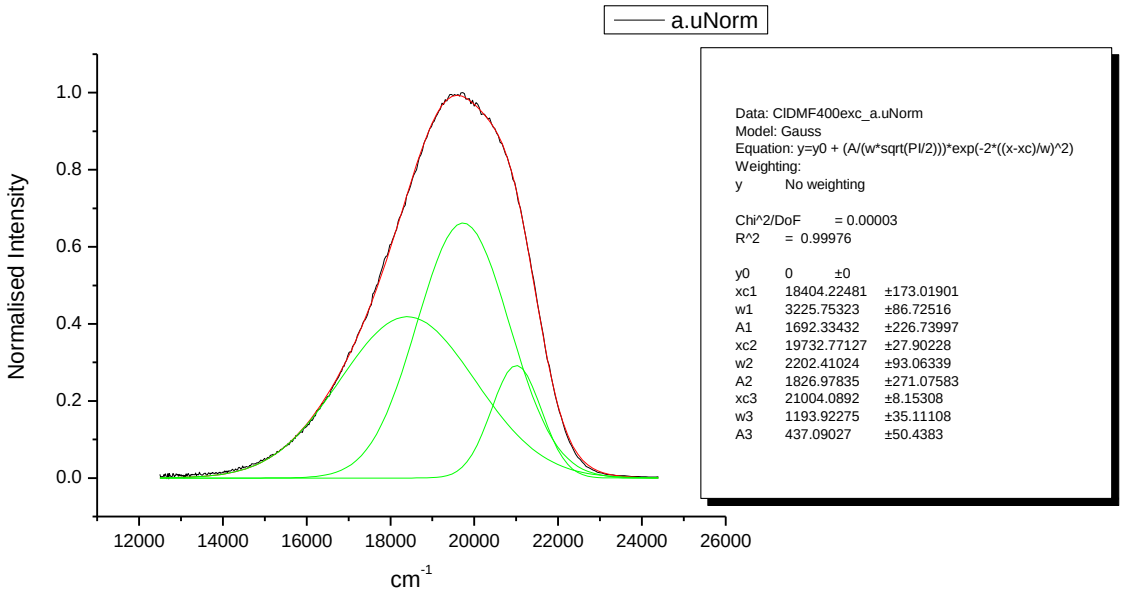

Figure 1.2.230. Gaussian model fit of the normalised fluorescence emission spectrum of **6a** recorded in N,N-dimethylformamide at 400 nm excitation.

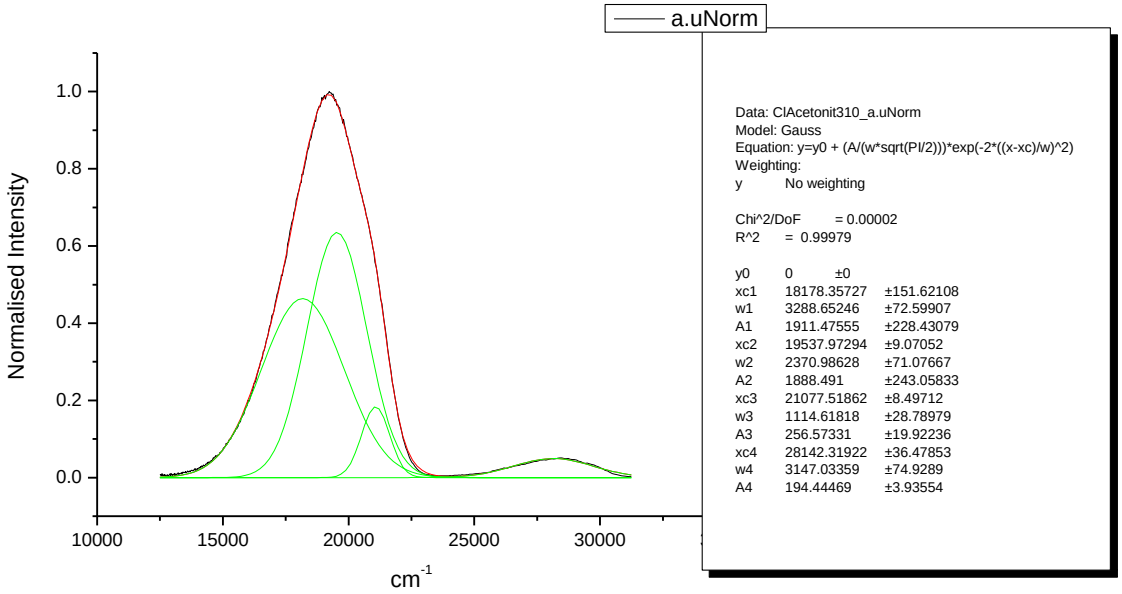

Figure 1.2.231. Gaussian model fit of the normalised fluorescence emission spectrum of **6a** recorded in Acetonitrile at 310 nm excitation.

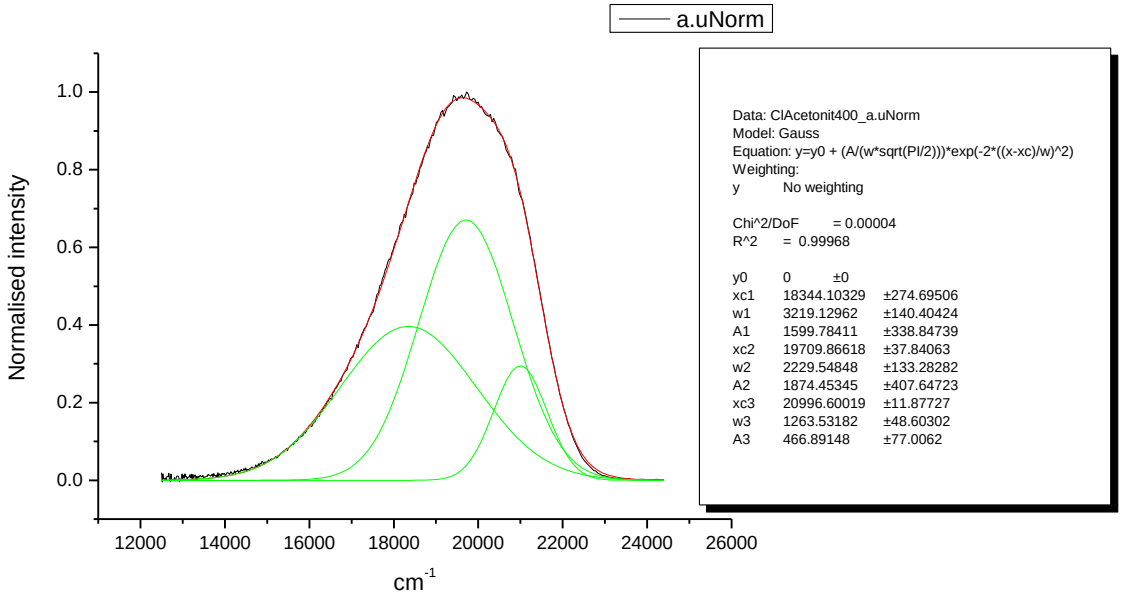

Figure 1.2.232. Gaussian model fit of the normalised fluorescence emission spectrum of **6a** recorded in Acetonitrile at 400 nm excitation.

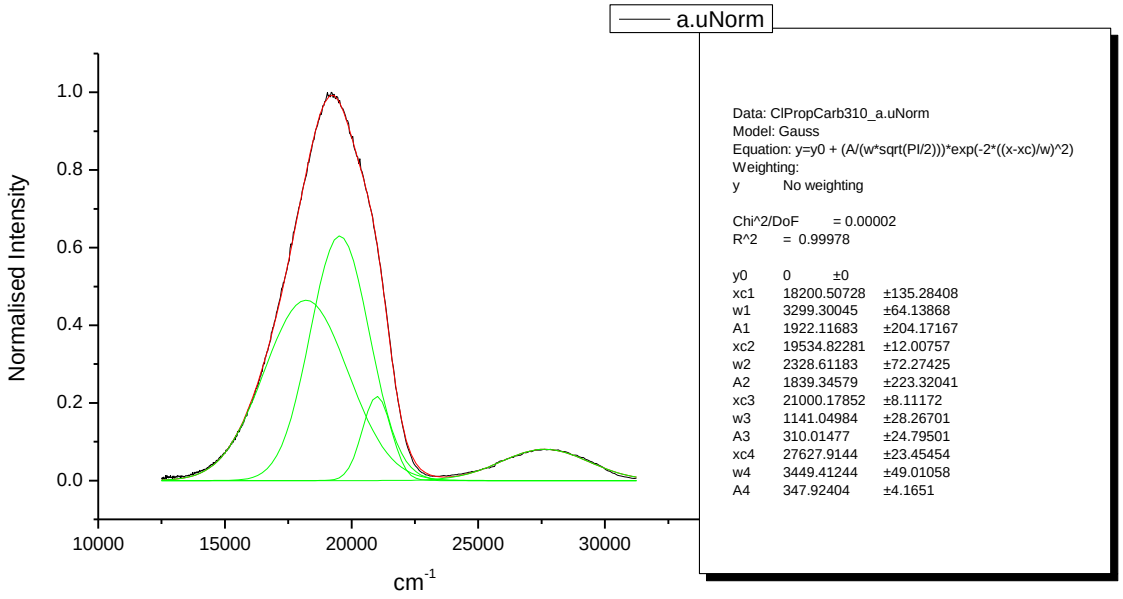

Figure 1.2.233. Gaussian model fit of the normalised fluorescence emission spectrum of **6a** recorded in Propylene Carbonate at 310 nm excitation.

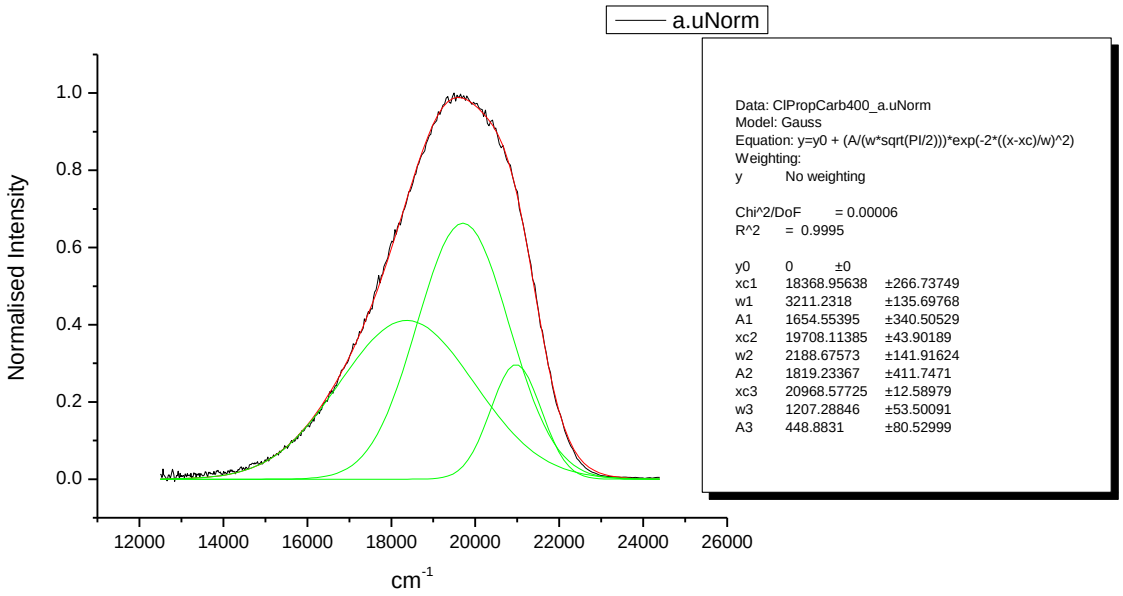

Figure 1.2.234. Gaussian model fit of the normalised fluorescence emission spectrum of **6a** recorded in Propylene Carbonate at 400 nm excitation.

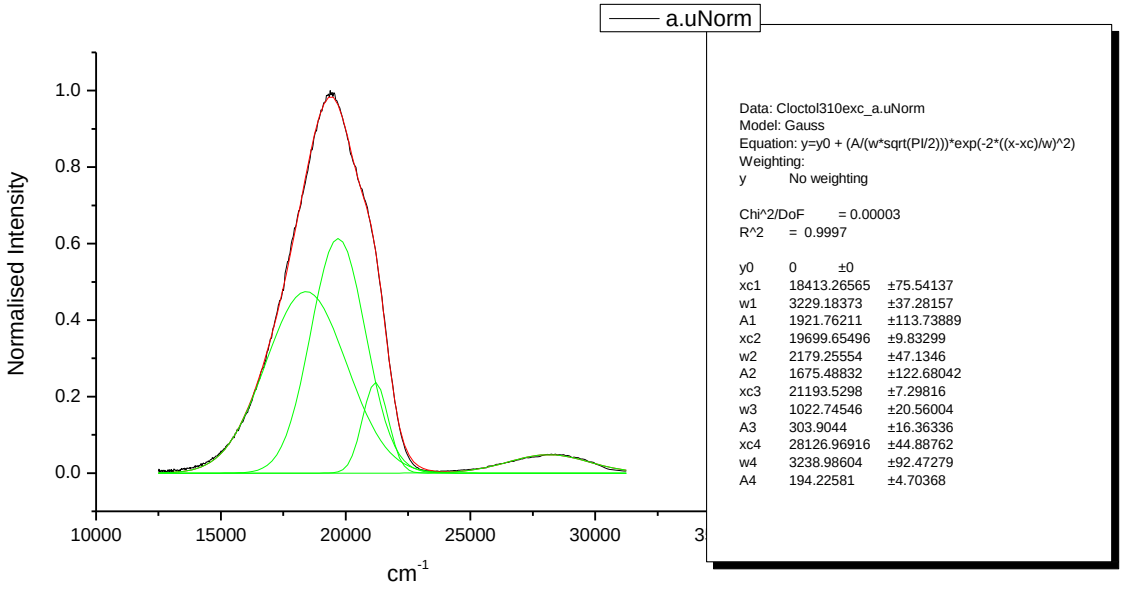

Figure 1.2.235. Gaussian model fit of the normalised fluorescence emission spectrum of **6a** recorded in 1-octanol at 310 nm excitation.

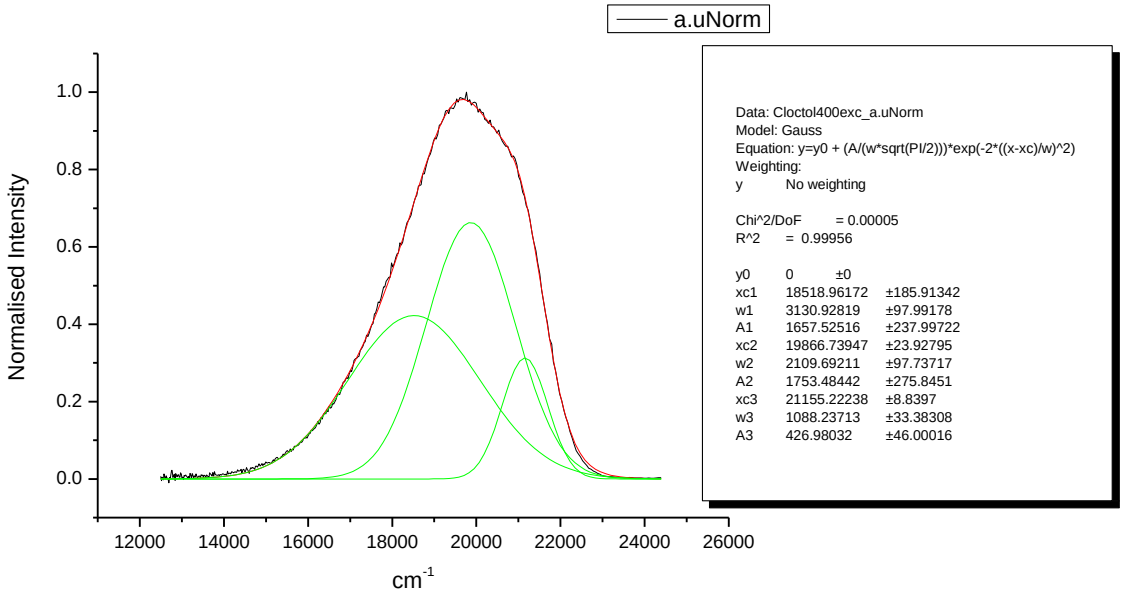

Figure 1.2.236. Gaussian model fit of the normalised fluorescence emission spectrum of **6a** recorded in 1-octanol at 400 nm excitation.

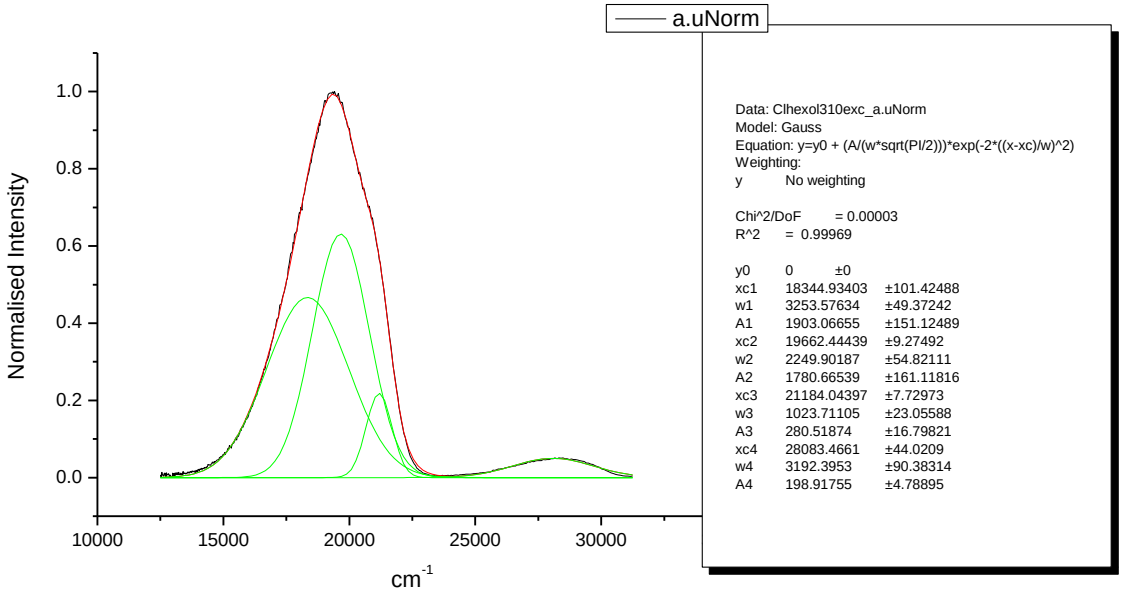

Figure 1.2.237. Gaussian model fit of the normalised fluorescence emission spectrum of **6a** recorded in 1-hexanol at 310 nm excitation.

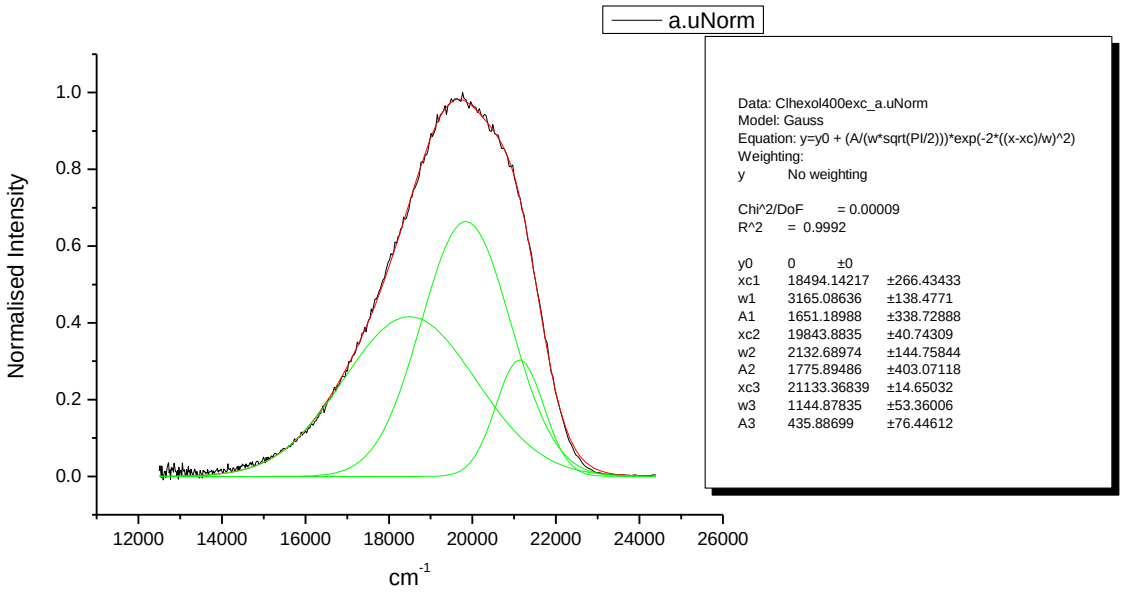

Figure 1.2.238. Gaussian model fit of the normalised fluorescence emission spectrum of **6a** recorded in 1-hexanol at 400 nm excitation.

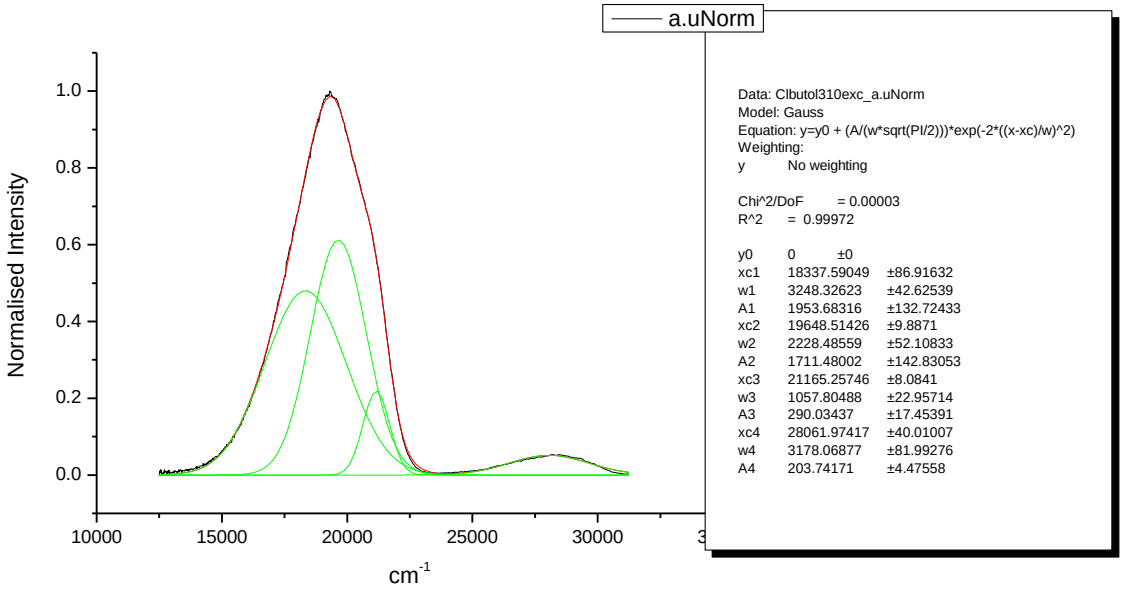

Figure 1.2.239. Gaussian model fit of the normalised fluorescence emission spectrum of **6a** recorded in 1-butanol at 310 nm excitation.

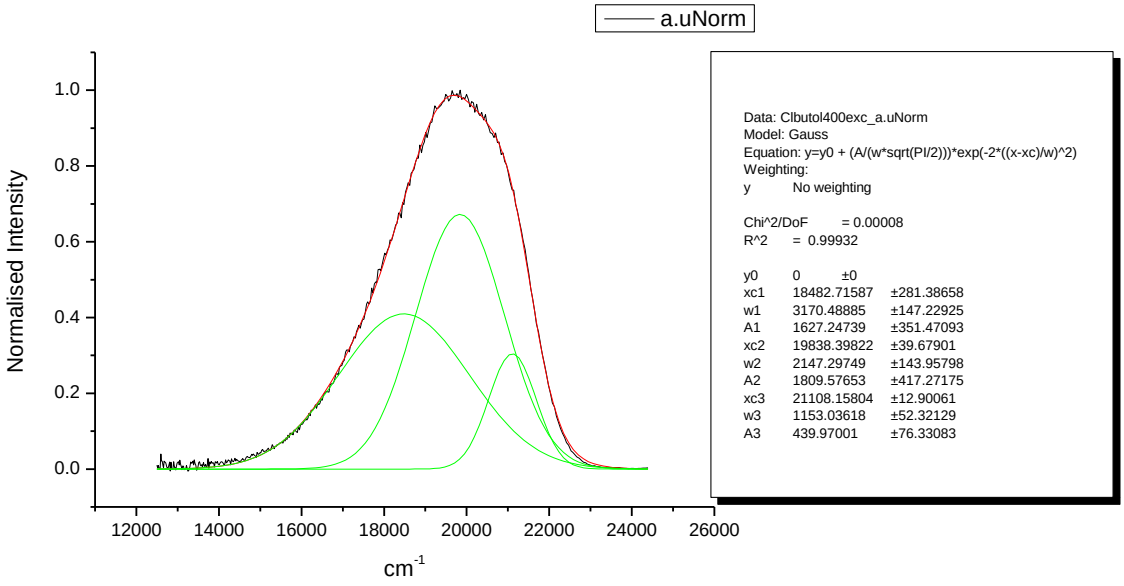

Figure 1.2.240. Gaussian model fit of the normalised fluorescence emission spectrum of **6a** recorded in 1-butanol at 400 nm excitation.

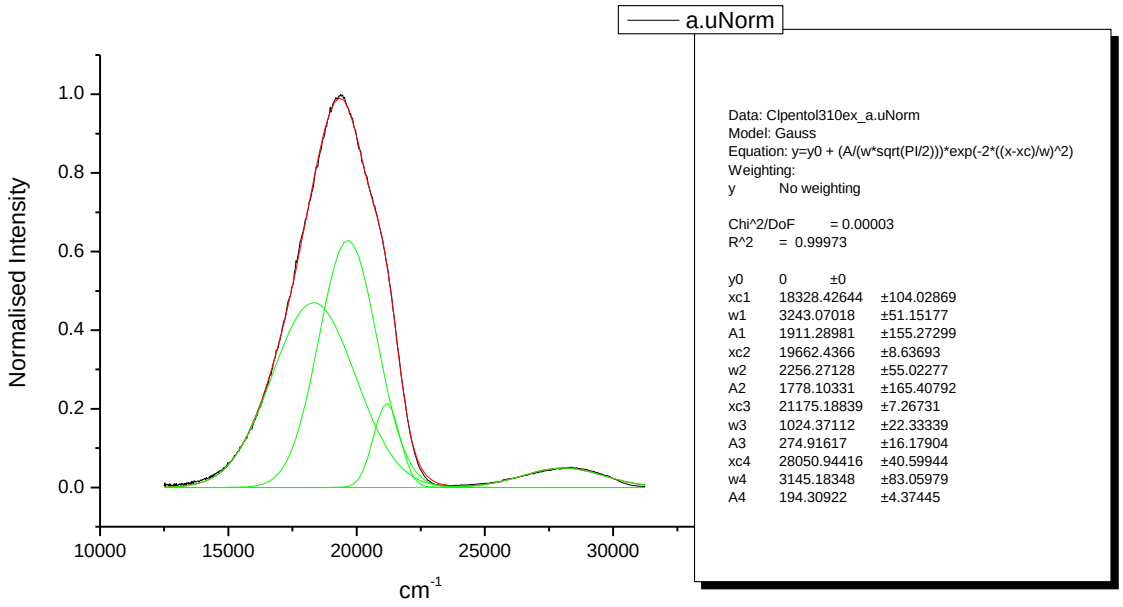

Figure 1.2.241. Gaussian model fit of the normalised fluorescence emission spectrum of **6a** recorded in 1-pentanol at 310 nm excitation.

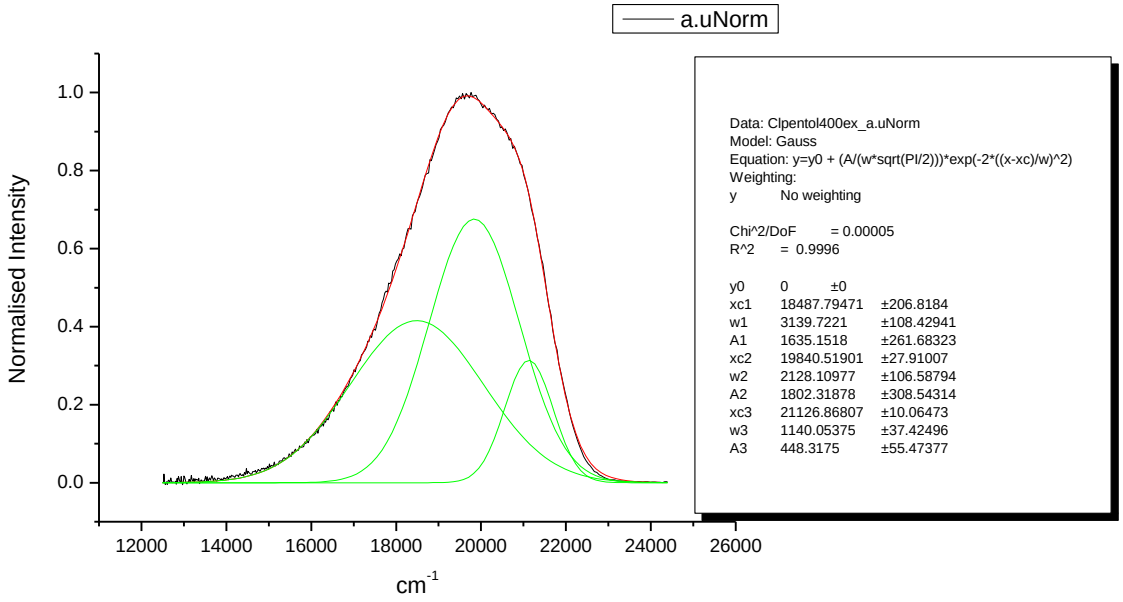

Figure 1.2.242. Gaussian model fit of the normalised fluorescence emission spectrum of **6a** recorded in 1-pentanol at 400 nm excitation.

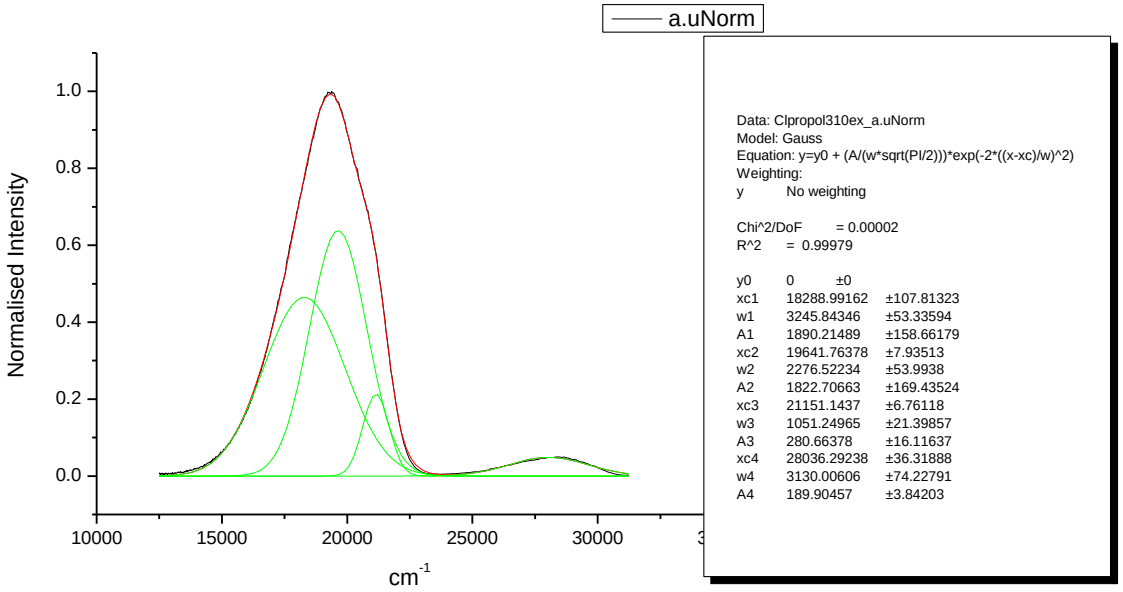

Figure 1.2.243. Gaussian model fit of the normalised fluorescence emission spectrum of **6a** recorded in 1-propanol at 310 nm excitation.

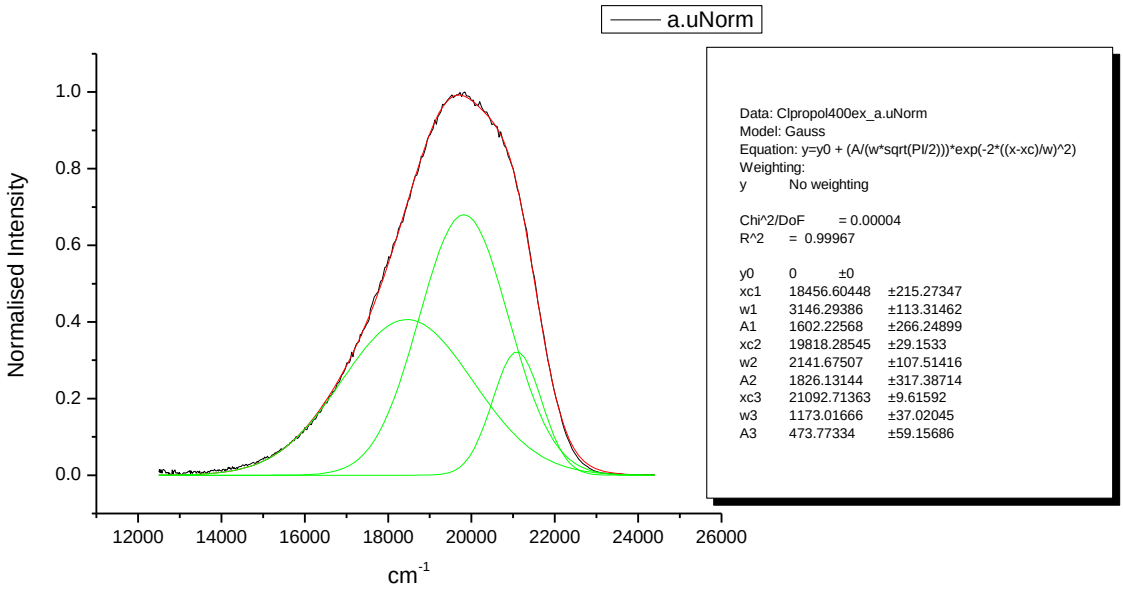

Figure 1.2.244. Gaussian model fit of the normalised fluorescence emission spectrum of **6a** recorded in 1-propanol at 400 nm excitation.

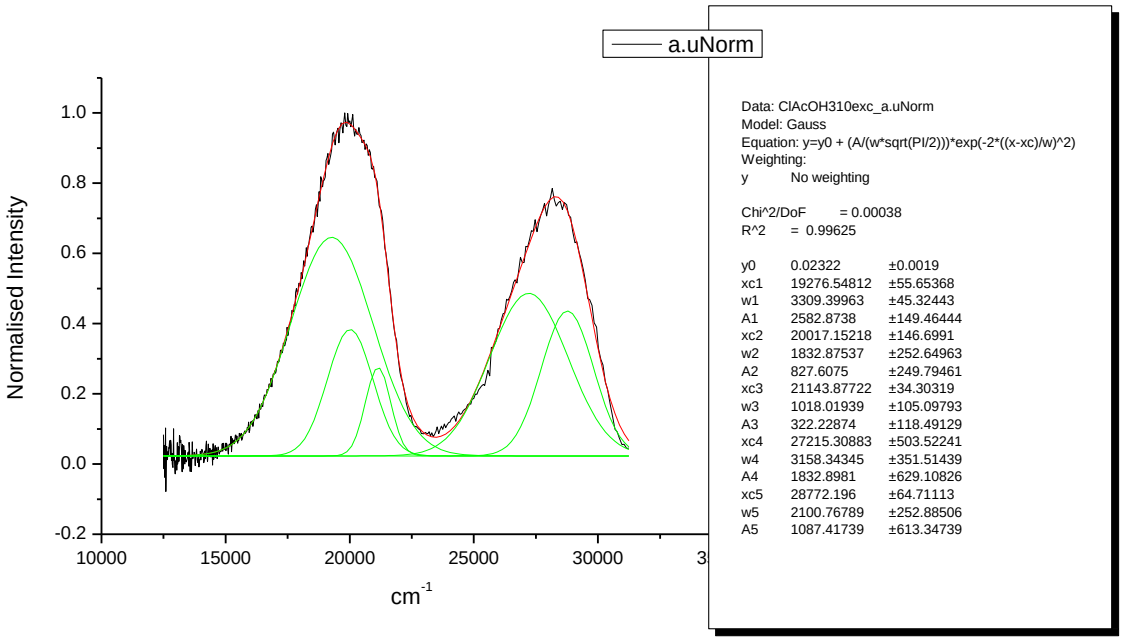

Figure 1.2.245. Gaussian model fit of the normalised fluorescence emission spectrum of **6a** recorded in Acetic Acid at 310 nm excitation.

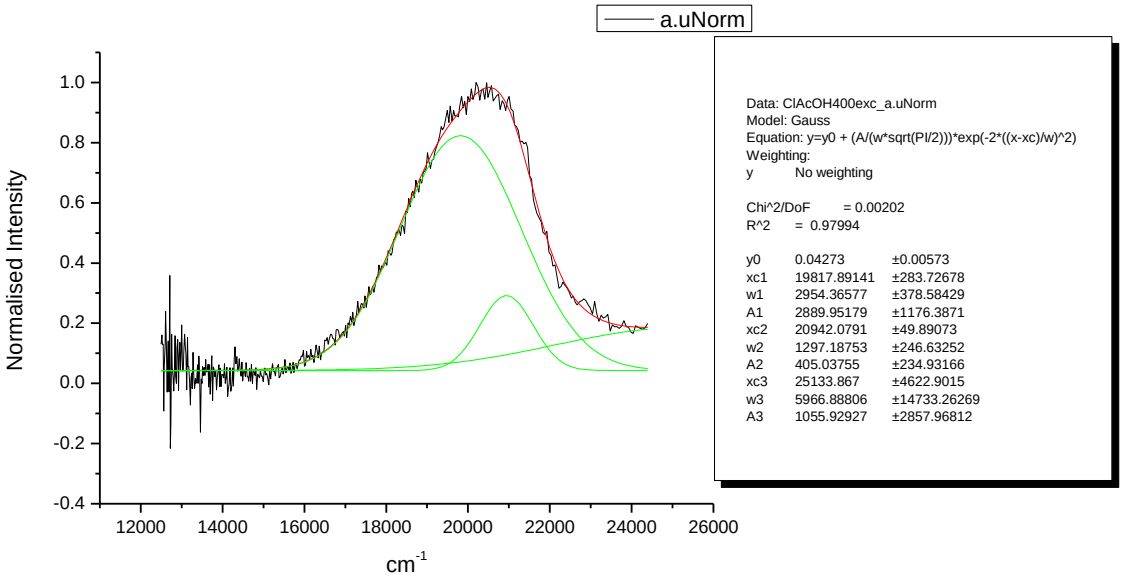

Figure 1.2.246. Gaussian model fit of the normalised fluorescence emission spectrum of **6a** recorded in Acetic Acid at 400 nm excitation.

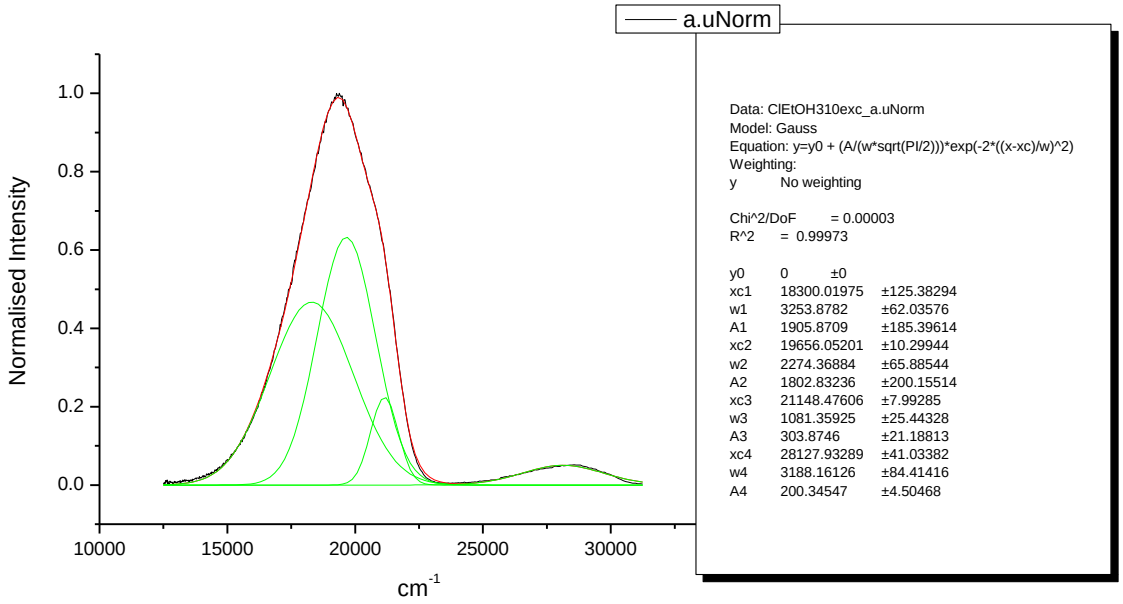

Figure 1.2.247. Gaussian model fit of the normalised fluorescence emission spectrum of **6a** recorded in Ethanol at 310 nm excitation.

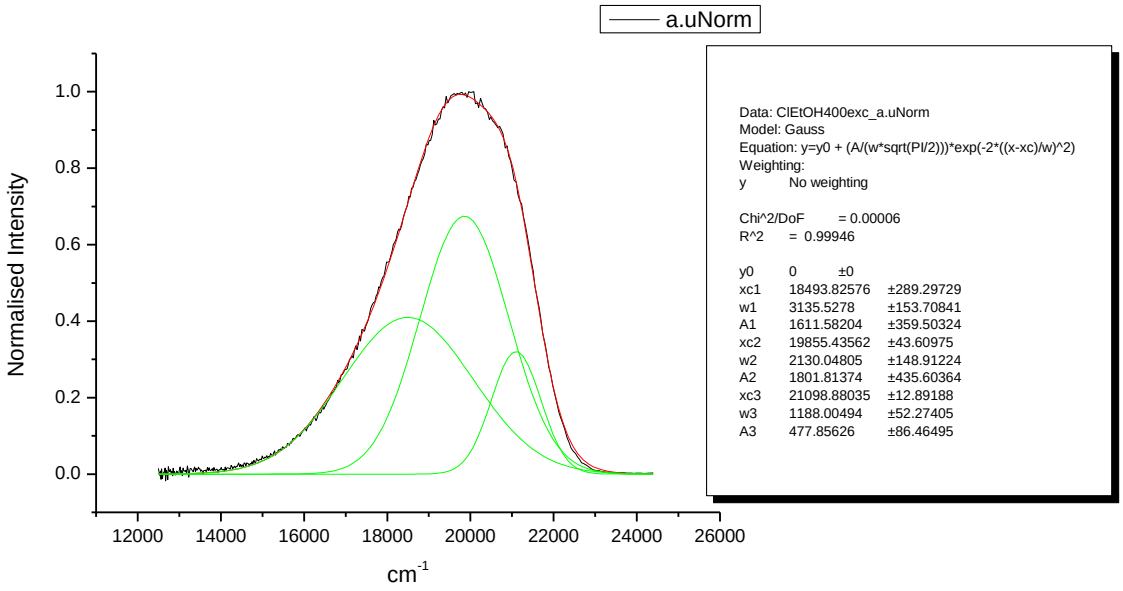

Figure 1.2.248. Gaussian model fit of the normalised fluorescence emission spectrum of **6a** recorded in Ethanol at 400 nm excitation.

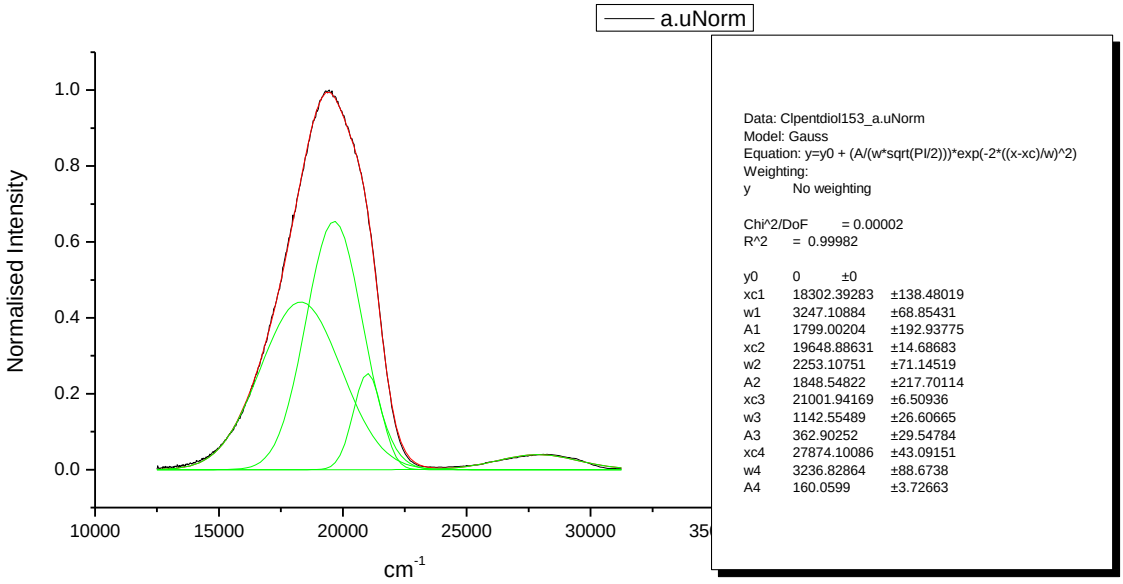

Figure 1.2.249. Gaussian model fit of the normalised fluorescence emission spectrum of **6a** recorded in 1,5-pentanediol at 310 nm excitation.

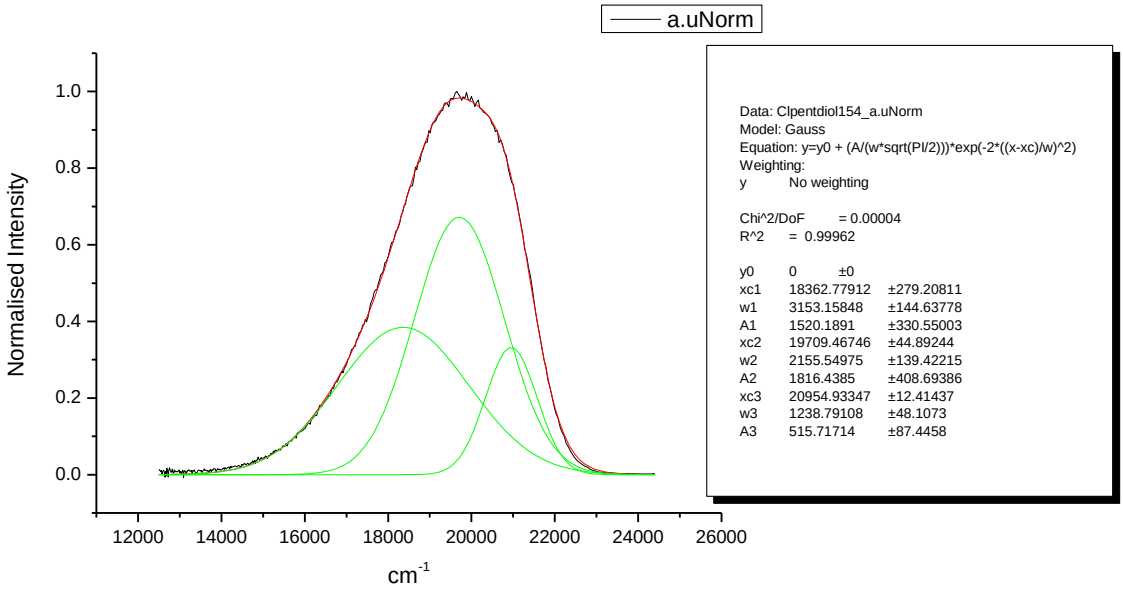

Figure 1.2.250. Gaussian model fit of the normalised fluorescence emission spectrum of **6a** recorded in 1,5-pentanediol at 400 nm excitation.

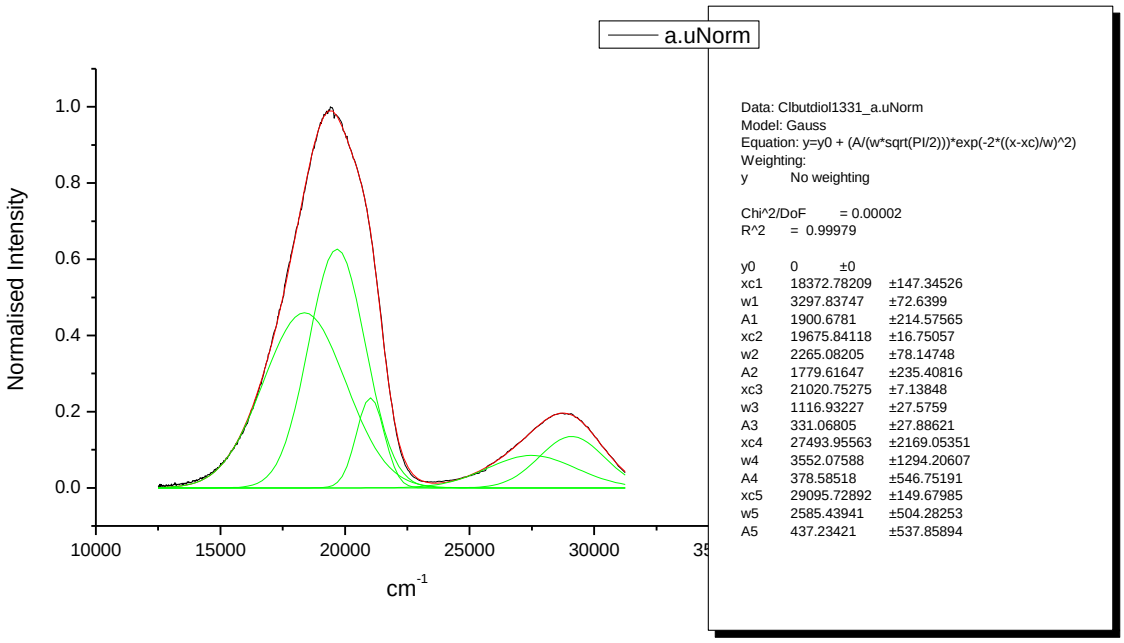

Figure 1.2.251. Gaussian model fit of the normalised fluorescence emission spectrum of **6a** recorded in 1,3-butanediol at 310 nm excitation.

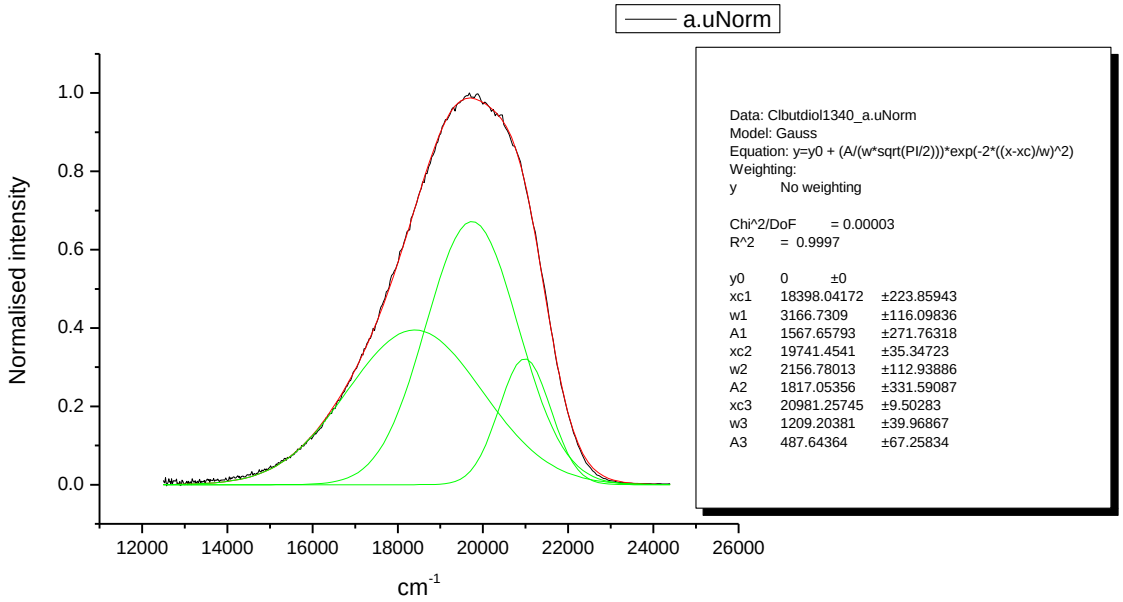

Figure 1.2.252. Gaussian model fit of the normalised fluorescence emission spectrum of **6a** recorded in 1,3-butanediol at 400 nm excitation.

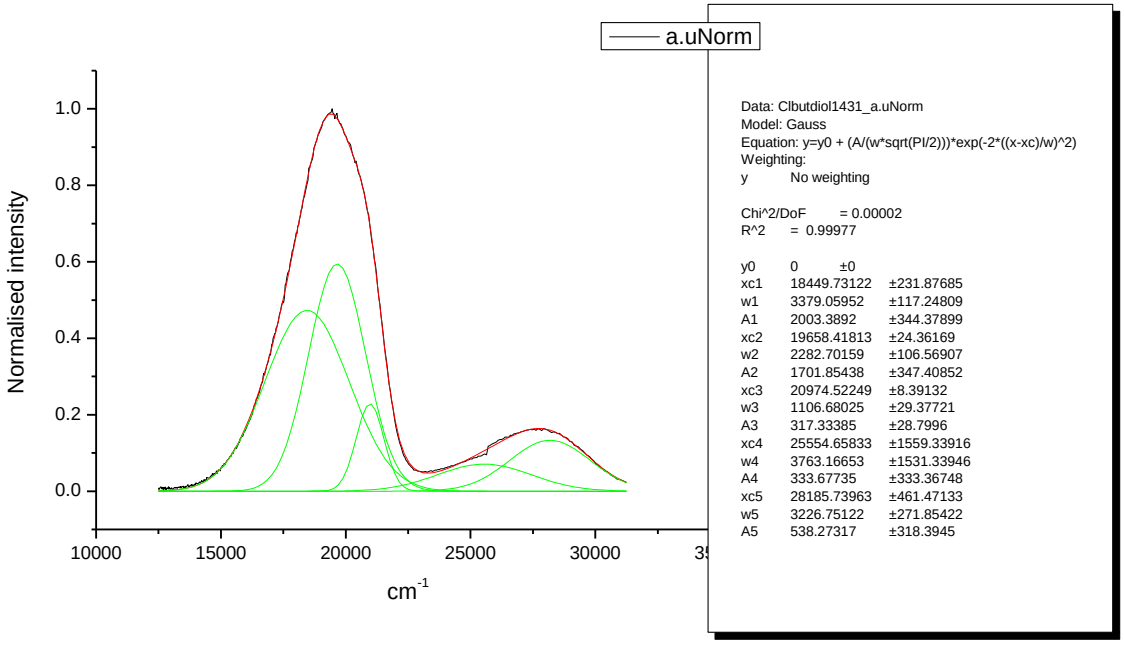

Figure 1.2.253. Gaussian model fit of the normalised fluorescence emission spectrum of **6a** recorded in 1,4-butanediol at 310 nm excitation.

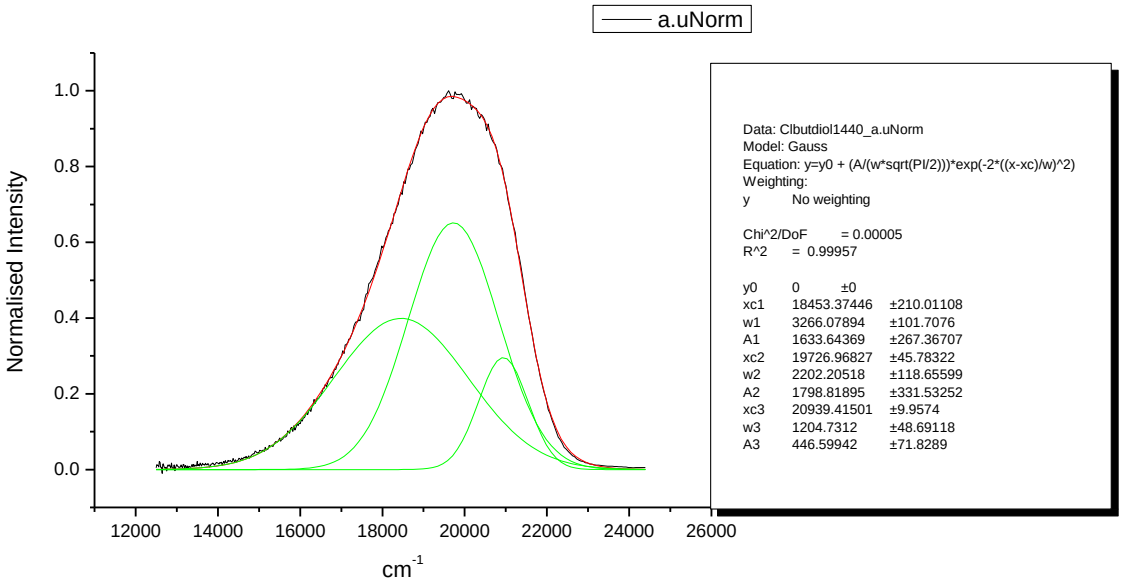

Figure 1.2.254. Gaussian model fit of the normalised fluorescence emission spectrum of **6a** recorded in 1,4-butanediol at 400 nm excitation.

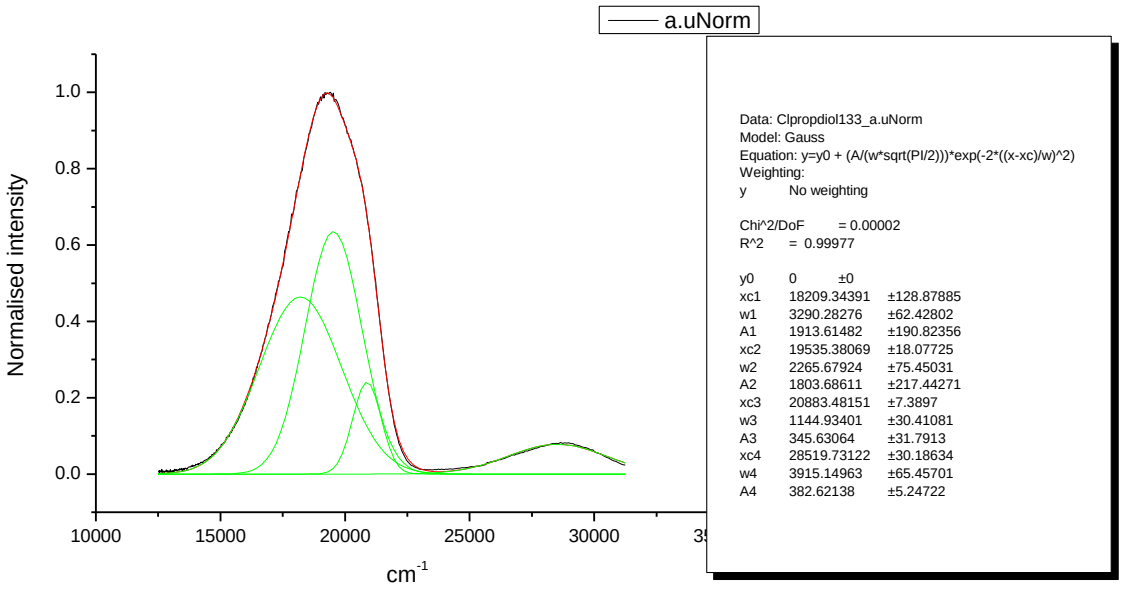

Figure 1.2.255. Gaussian model fit of the normalised fluorescence emission spectrum of **6a** recorded in 1,3-propanediol at 310 nm excitation.

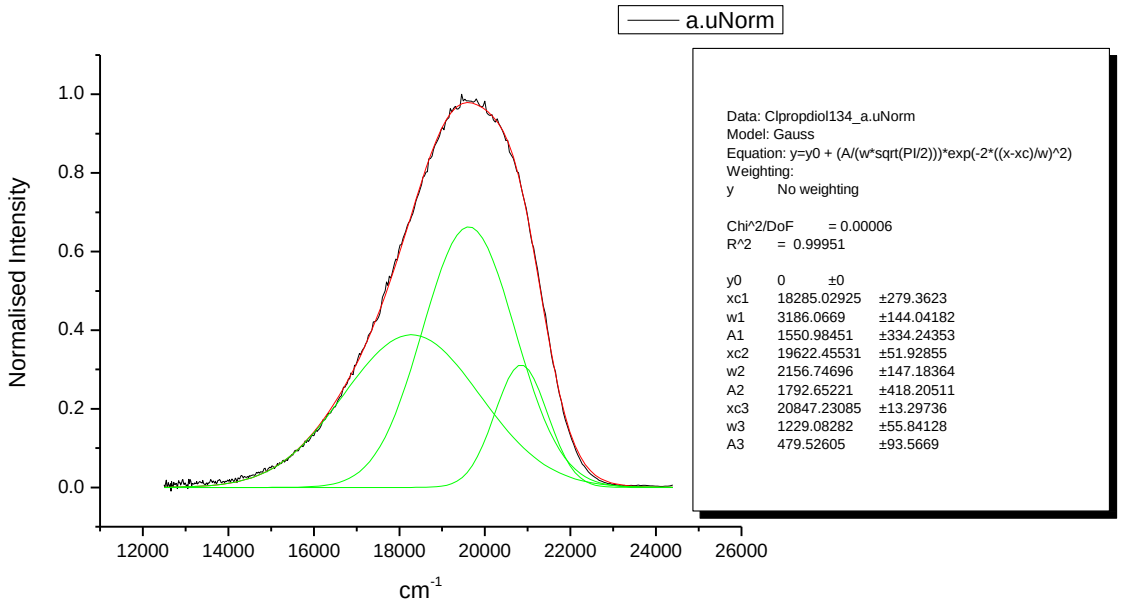

Figure 1.2.256. Gaussian model fit of the normalised fluorescence emission spectrum of **6a** recorded in 1,3-propanediol at 400 nm excitation.

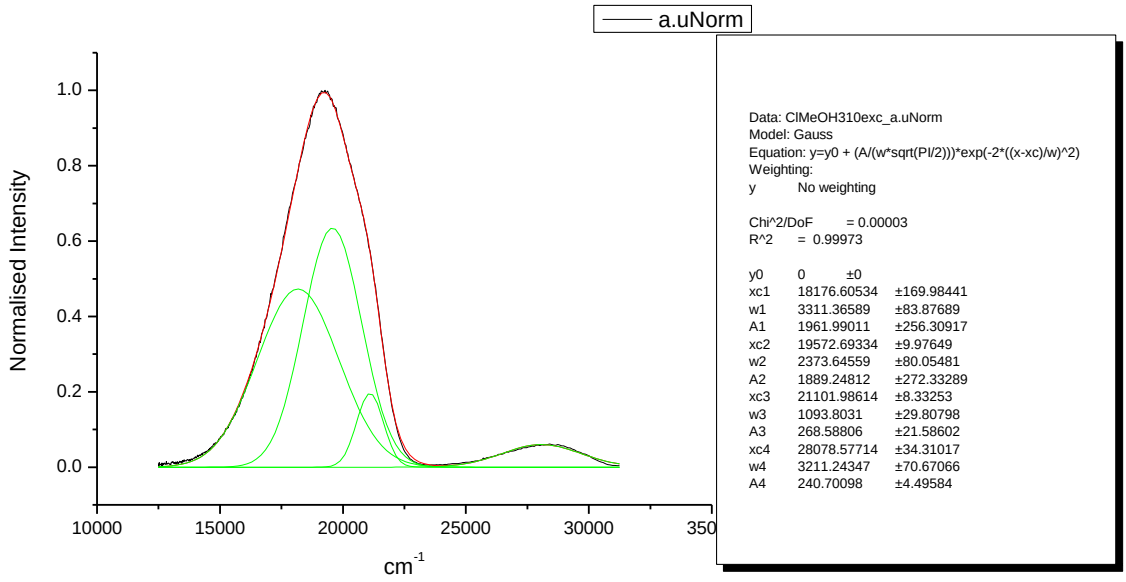

Figure 1.2.257. Gaussian model fit of the normalised fluorescence emission spectrum of **6a** recorded in Methanol at 310 nm excitation.

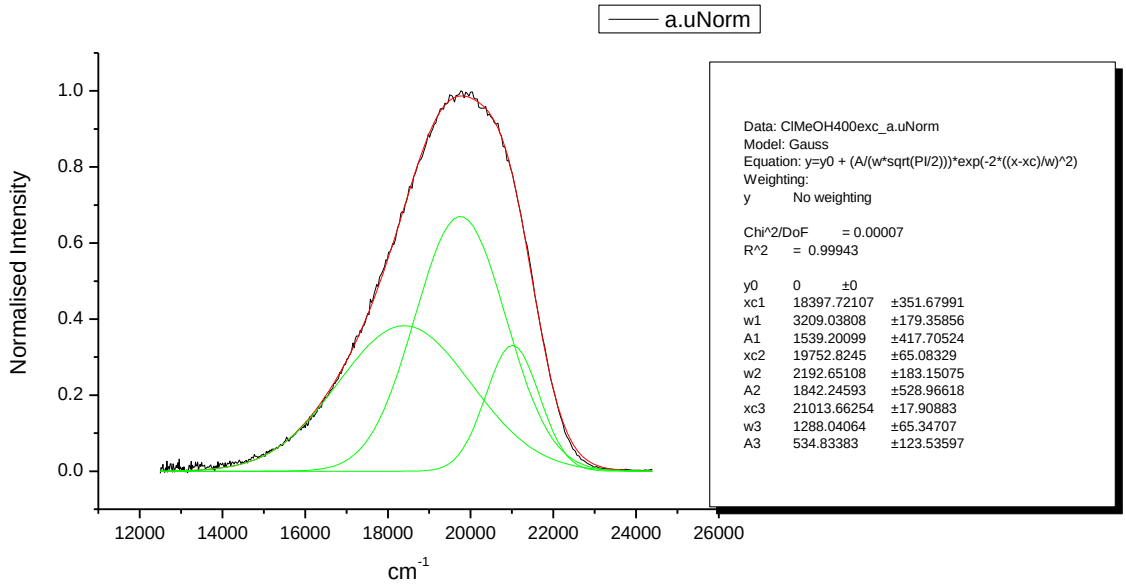

Figure 1.2.258. Gaussian model fit of the normalised fluorescence emission spectrum of **6a** recorded in Methanol at 400 nm excitation.

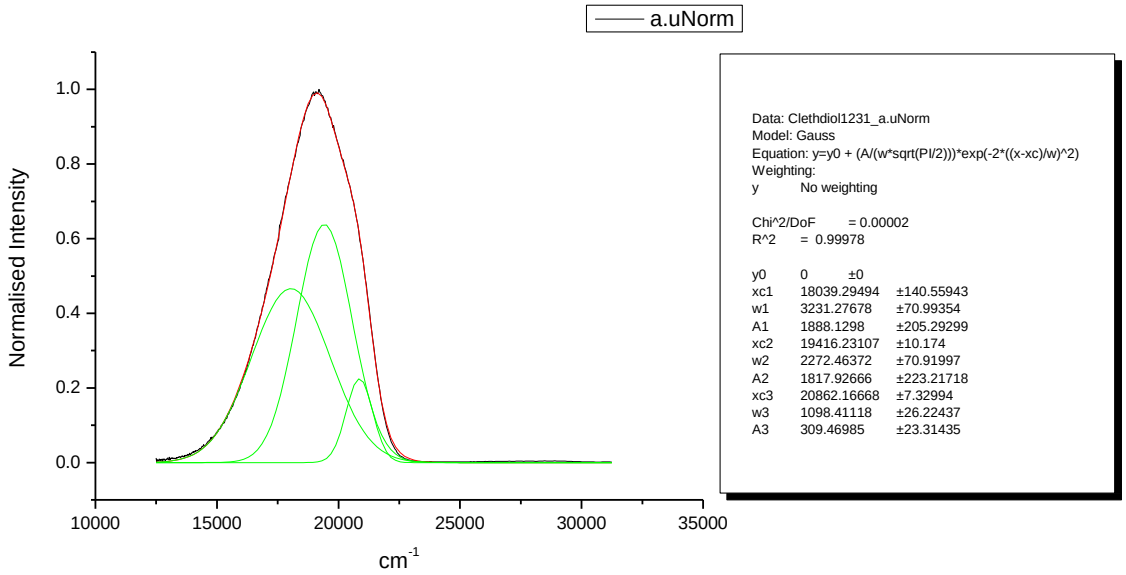

Figure 1.2.259. Gaussian model fit of the normalised fluorescence emission spectrum of **6a** recorded in 1,2-ethanediol at 310 nm excitation.

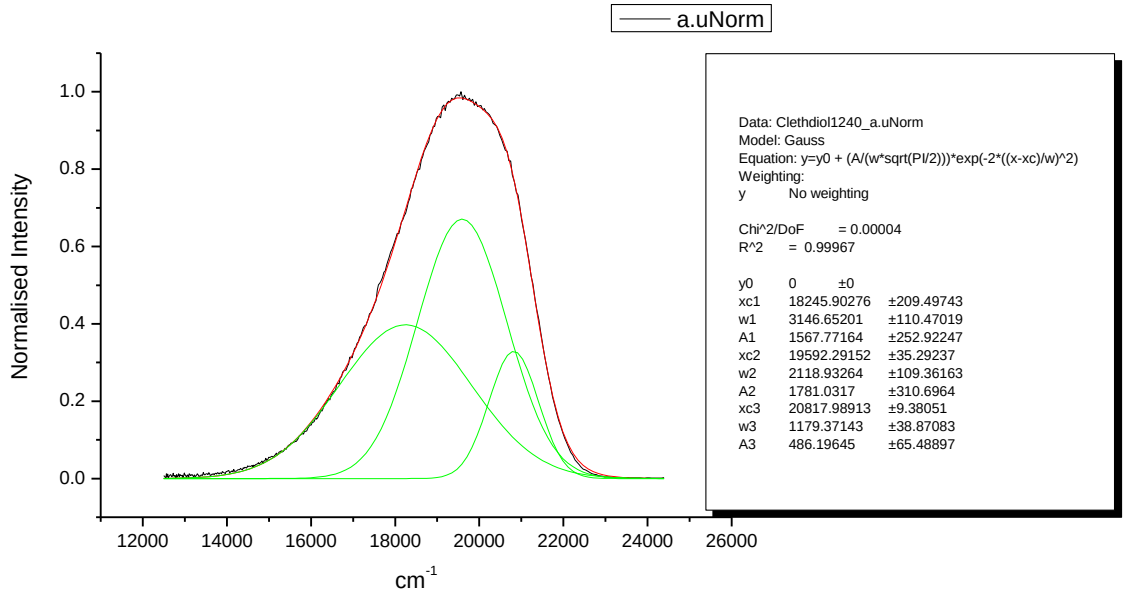

Figure 1.2.260. Gaussian model fit of the normalised fluorescence emission spectrum of **6a** recorded in 1,2-ethanediol at 400 nm excitation.

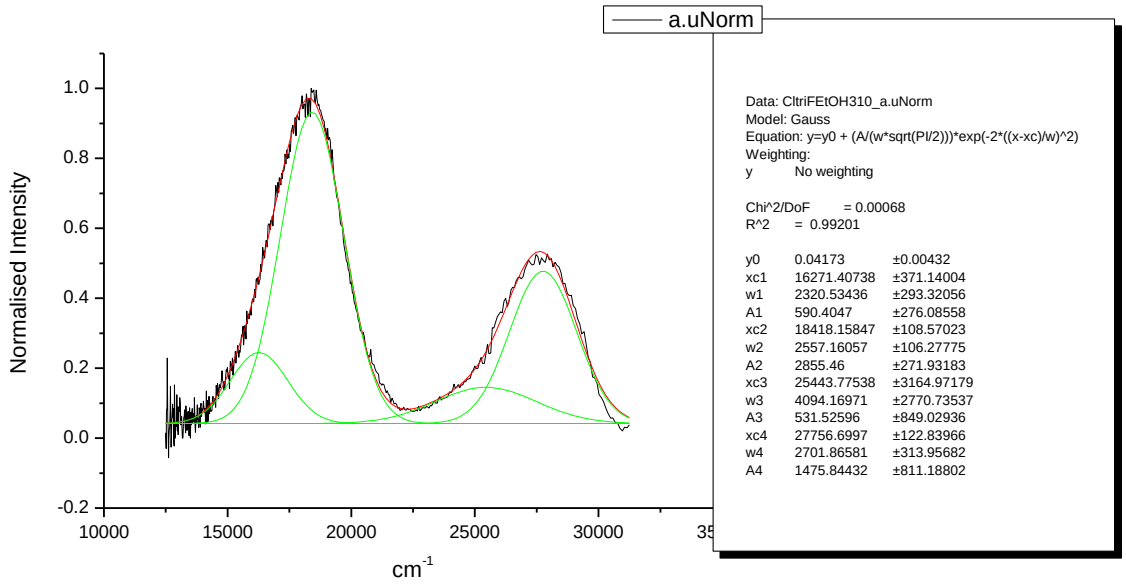

Figure 1.2.261. Gaussian model fit of the normalised fluorescence emission spectrum of **6a** recorded in 2,2,2-trifluoroethanol at 310 nm excitation.

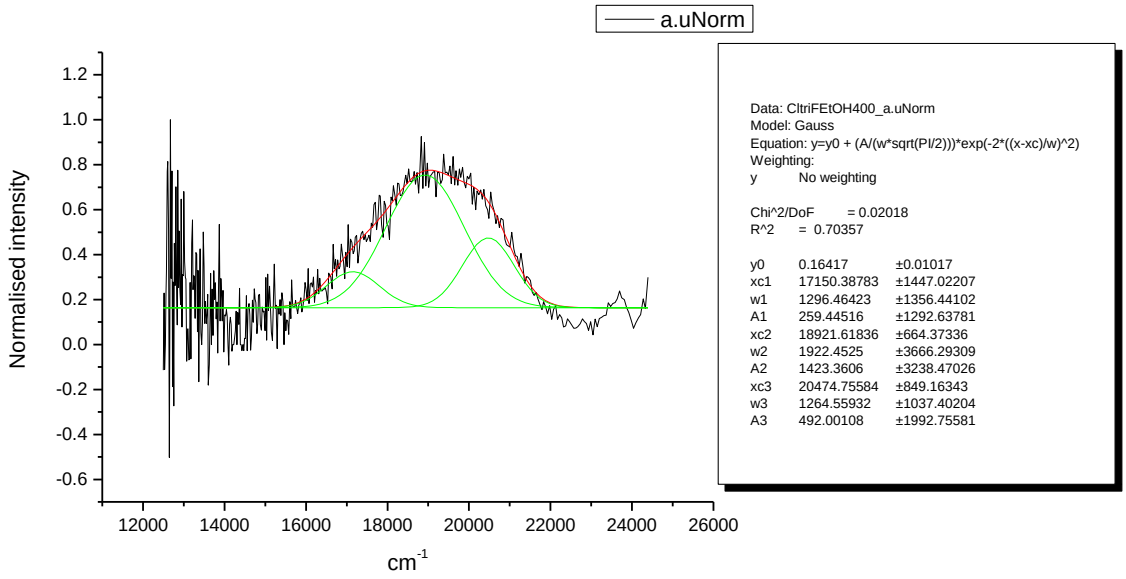

Figure 1.2.262. Gaussian model fit of the normalised fluorescence emission spectrum of **6a** recorded in 2,2,2-trifluoroethanol at 400 nm excitation.

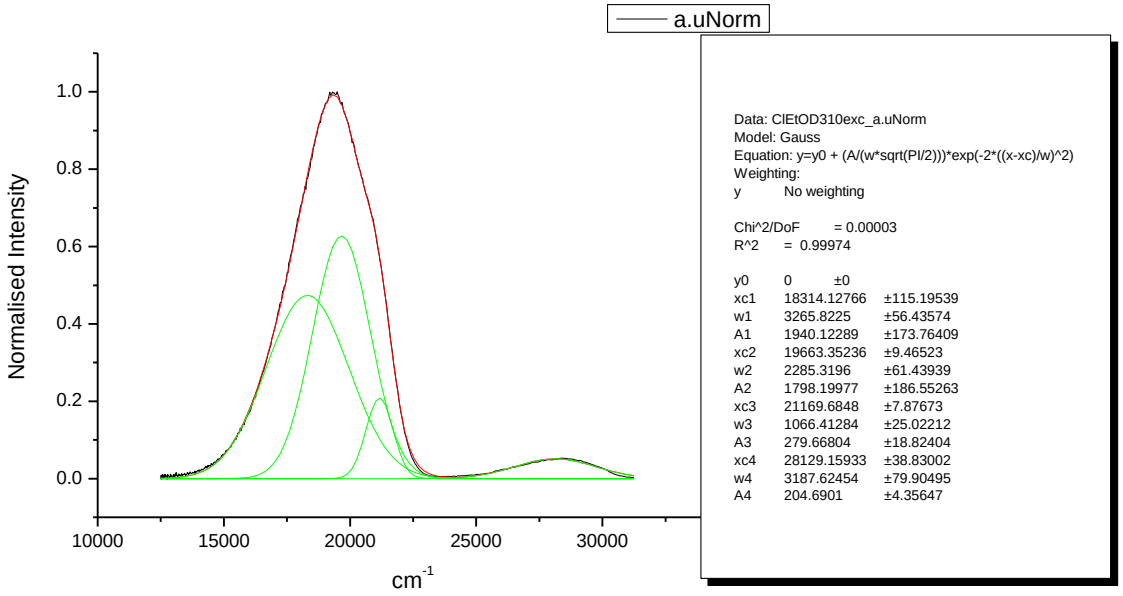

Figure 1.2.263. Gaussian model fit of the normalised fluorescence emission spectrum of **6a** recorded in ethanol-d_1 (EtOD) at 310 nm excitation.

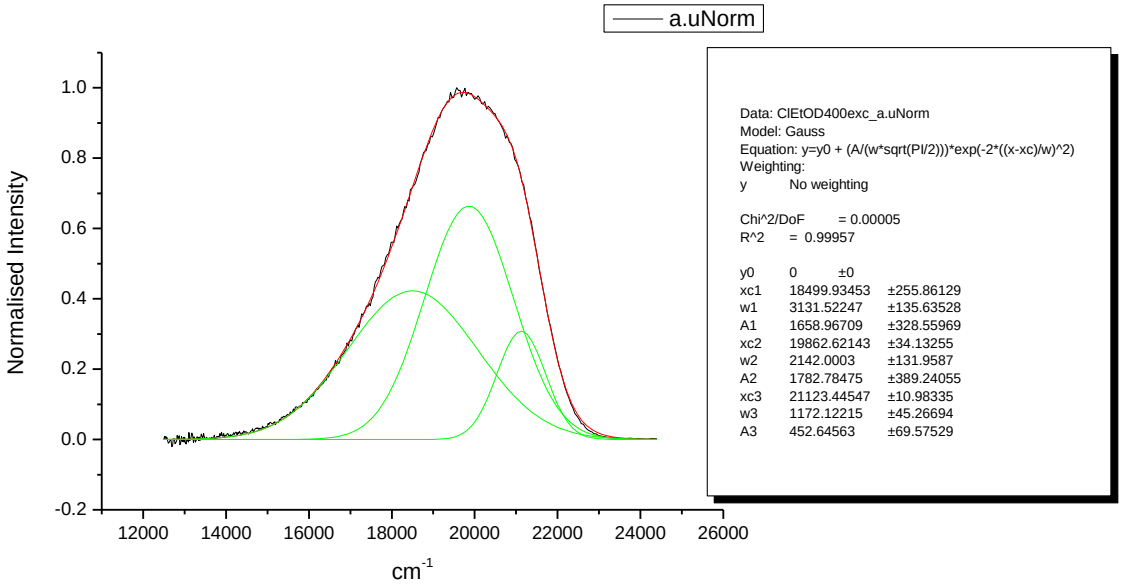

Figure 1.2.264. Gaussian model fit of the normalised fluorescence emission spectrum of **6a** recorded in ethanol-d_1 (EtOD) at 400 nm excitation.

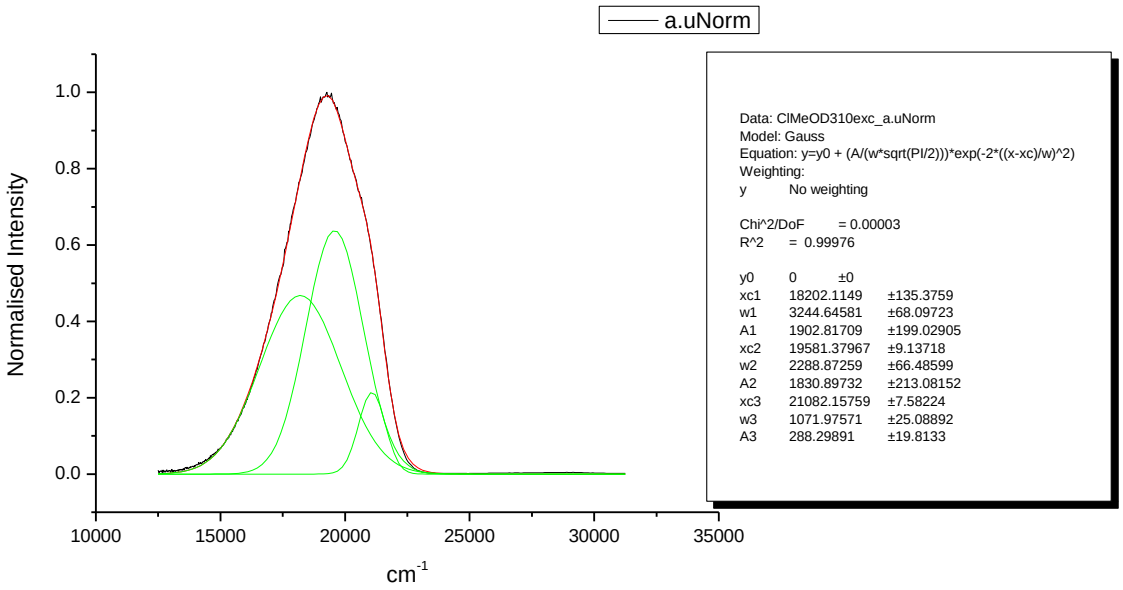

Figure 1.2.265. Gaussian model fit of the normalised fluorescence emission spectrum of **6a** recorded in methanol-d_1 (MeOD) at 310 nm excitation.

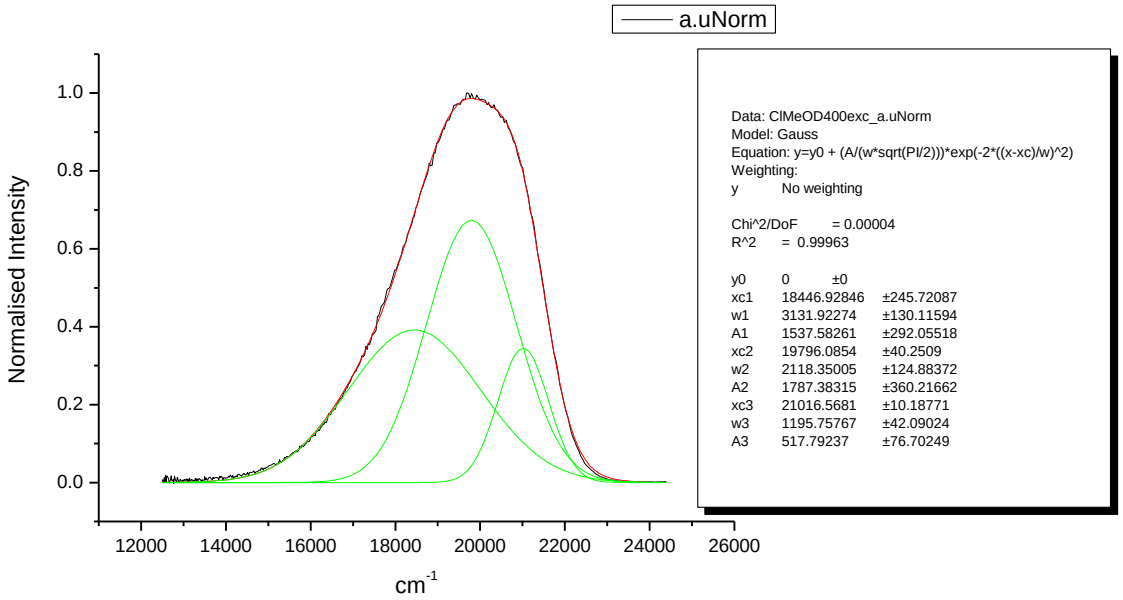

Figure 1.2.266. Gaussian model fit of the normalised fluorescence emission spectrum of **6a** recorded in methanol-d_1 (MeOD) at 400 nm excitation.

1.2.11 Fluorescence Excitation spectra.

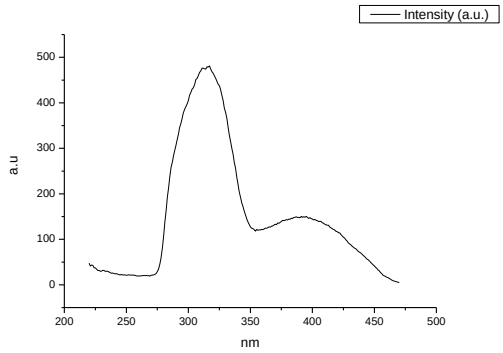

Figure 1.2.267. Fluorescence excitation spectrum of **6a** recorded in Toluene with emission fixed at 480 nm.

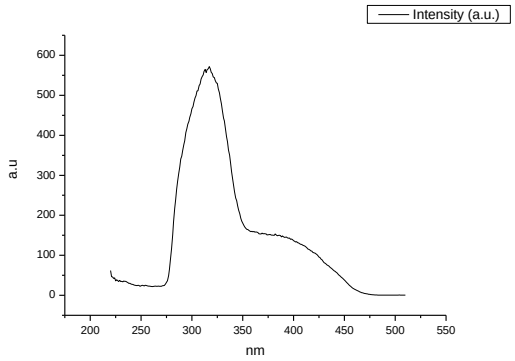

Figure 1.2.268. Fluorescence excitation spectrum of **6a** recorded in Toluene with emission fixed at 520 nm.

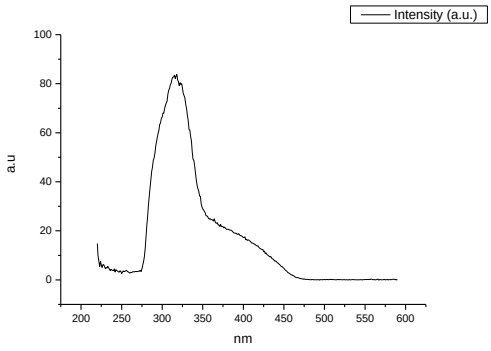

Figure 1.2.269. Fluorescence excitation spectrum of **6a** recorded in Toluene with emission fixed at 600 nm.

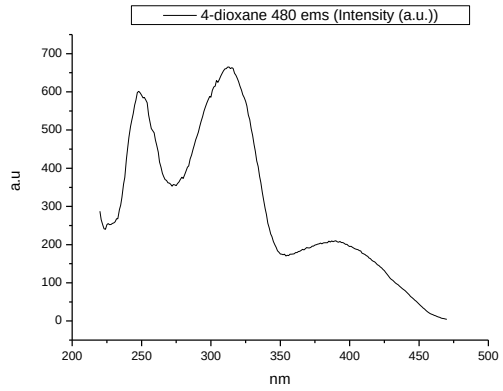

Figure 1.2.270. Fluorescence excitation spectrum of **6a** recorded in 1,4-dioxane with emission fixed at 480 nm.

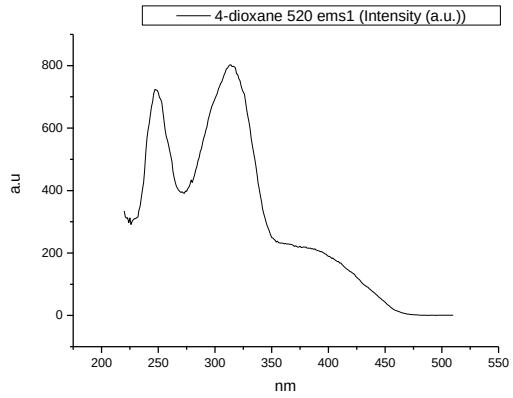

Figure 1.2.271. Fluorescence excitation spectrum of **6a** recorded in 1,4-dioxane with emission fixed at 520 nm.

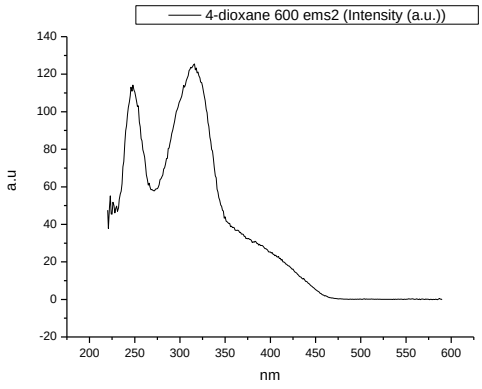

Figure 1.2.272. Fluorescence excitation spectrum of **6a** recorded in 1,4-dioxane with emission fixed at 600 nm.

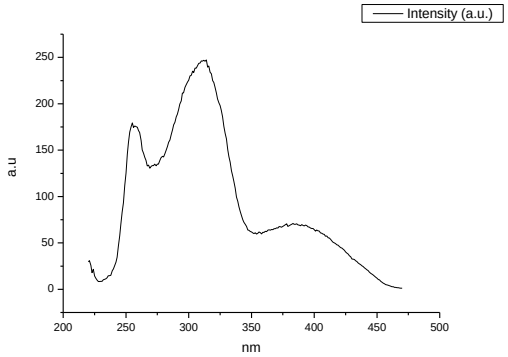

Figure 1.2.273. Fluorescence excitation spectrum of **6a** recorded in Ethyl Acetate with emission fixed at 480 nm.

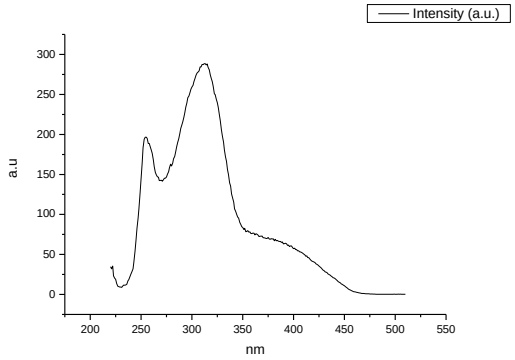

Figure 1.2.274. Fluorescence excitation spectrum of **6a** recorded in Ethyl Acetate with emission fixed at 520 nm.

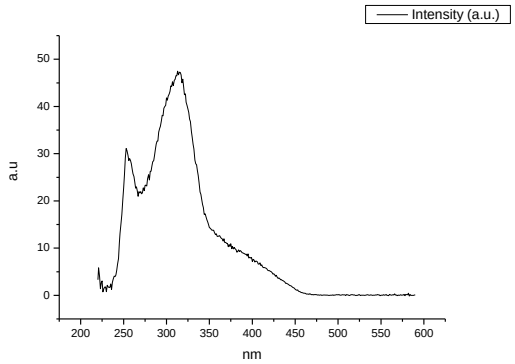

Figure 1.2.275. Fluorescence excitation spectrum of **6a** recorded in Ethyl Acetate with emission fixed at 600 nm.

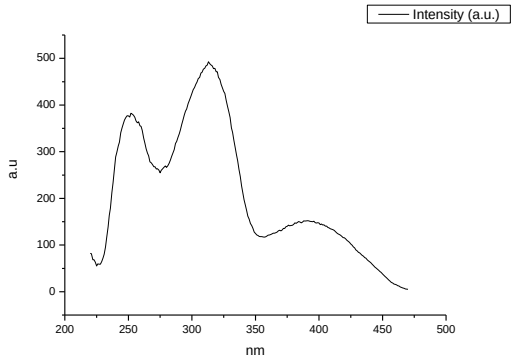

Figure 1.2.276. Fluorescence excitation spectrum of **6a** recorded in Chloroform with emission fixed at 480 nm.

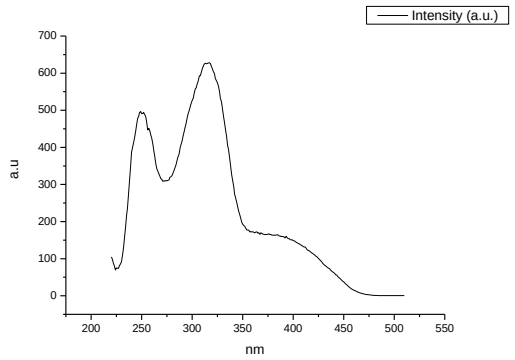

Figure 1.2.277. Fluorescence excitation spectrum of **6a** recorded in Chloroform with emission fixed at 520 nm.

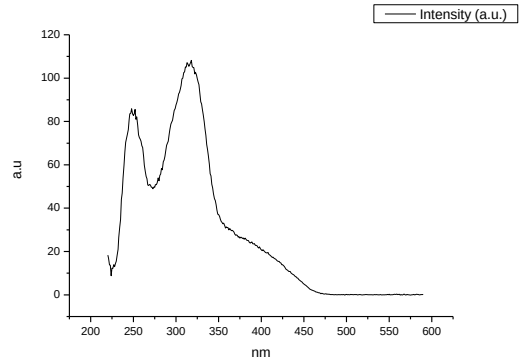

Figure 1.2.278. Fluorescence excitation spectrum of **6a** recorded in Chloroform with emission fixed at 600 nm.

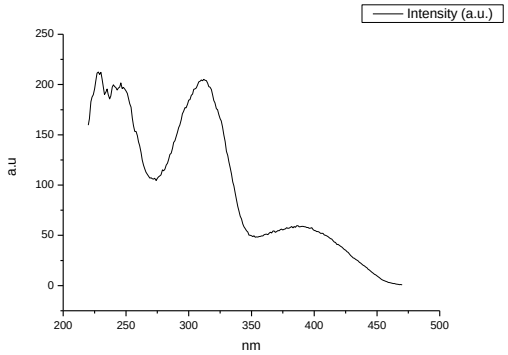

Figure 1.2.279. Fluorescence excitation spectrum of **6a** recorded in 2-methyl-2-butanol with emission fixed at 480 nm.

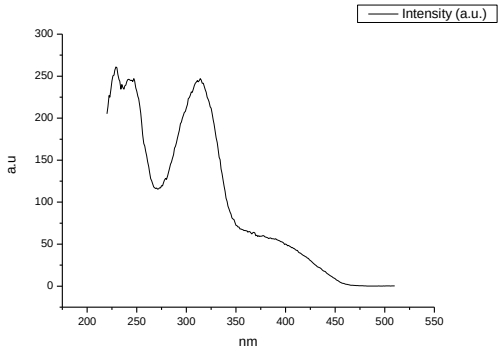

Figure 1.2.280. Fluorescence excitation spectrum of **6a** recorded in 2-methyl-2-butanol with emission fixed at 520 nm.

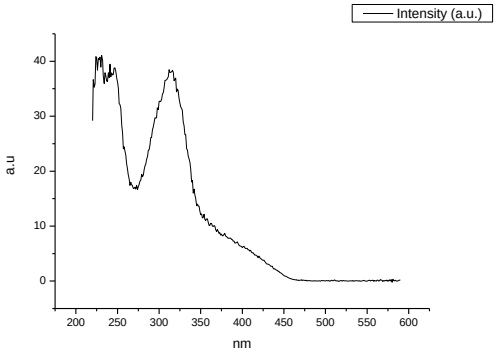

Figure 1.2.281. Fluorescence excitation spectrum of **6a** recorded in 2-methyl-2-butanol with emission fixed at 600 nm.

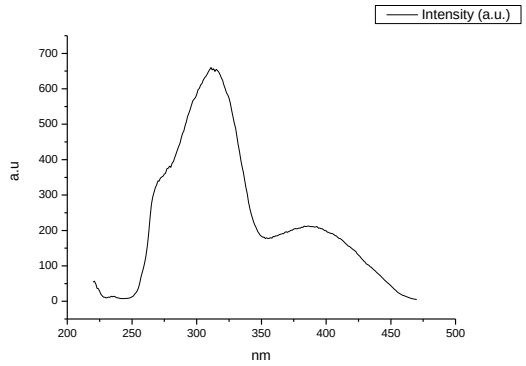

Figure 1.2.282. Fluorescence excitation spectrum of **6a** recorded in N,N-dimethylformamide with emission fixed at 480 nm.

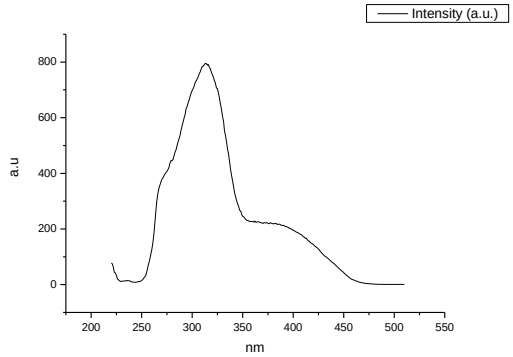

Figure 1.2.283. Fluorescence excitation spectrum of **6a** recorded in N,N-dimethylformamide with emission fixed at 520 nm.

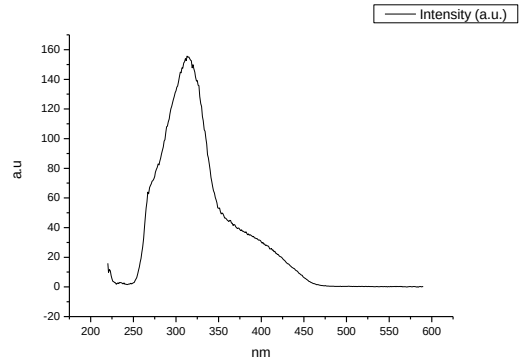

Figure 1.2.284. Fluorescence excitation spectrum of **6a** recorded in N,N-dimethylformamide with emission fixed at 600 nm.

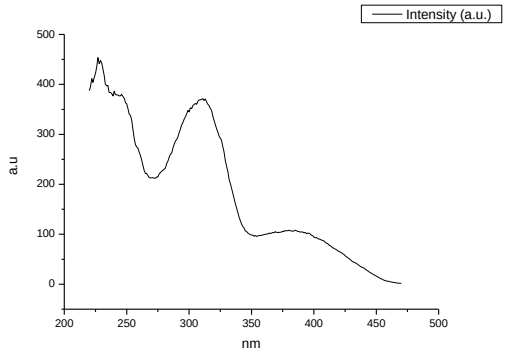

Figure 1.2.285. Fluorescence excitation spectrum of **6a** recorded in Acetonitrile with emission fixed at 480 nm.

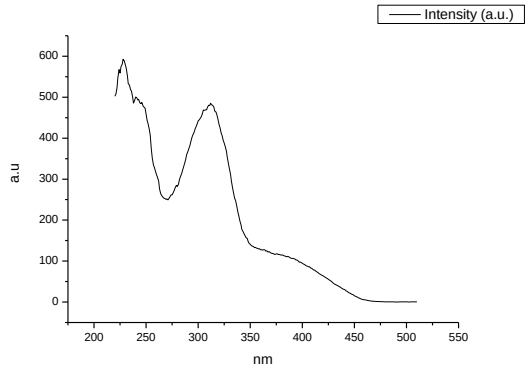

Figure 1.2.286. Fluorescence excitation spectrum of **6a** recorded in Acetonitrile with emission fixed at 520 nm.

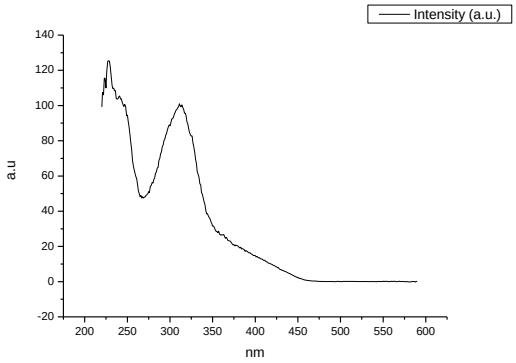

Figure 1.2.287. Fluorescence excitation spectrum of **6a** recorded in Acetonitrile with emission fixed at 600 nm.

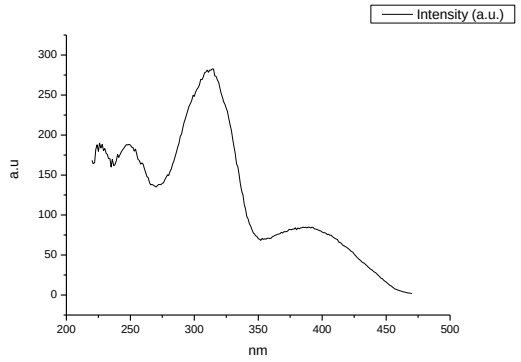

Figure 1.2.288. Fluorescence excitation spectrum of **6a** recorded in Propylene Carbonate with emission fixed at 480 nm.

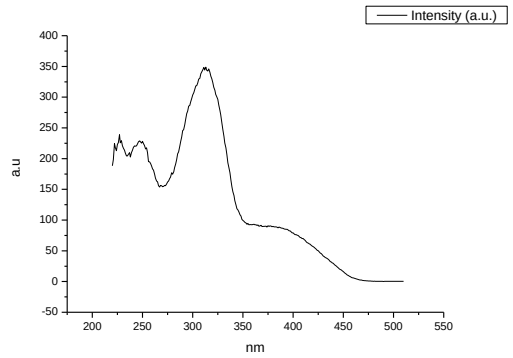

Figure 1.2.289. Fluorescence excitation spectrum of **6a** recorded in Propylene Carbonate with emission fixed at 520 nm.

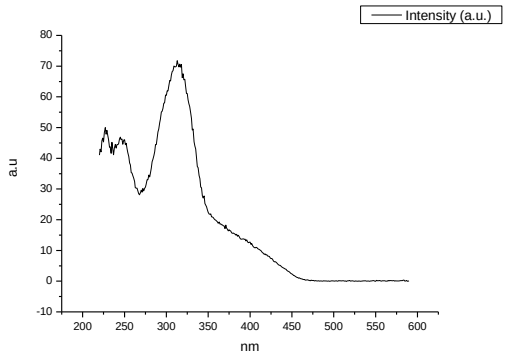

Figure 1.2.290. Fluorescence excitation spectrum of **6a** recorded in Propylene Carbonate with emission fixed at 600 nm.

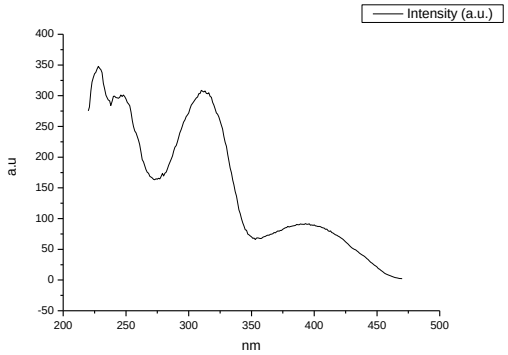

Figure 1.2.291. Fluorescence excitation spectrum of **6a** recorded in 1-octanol with emission fixed at 480 nm.

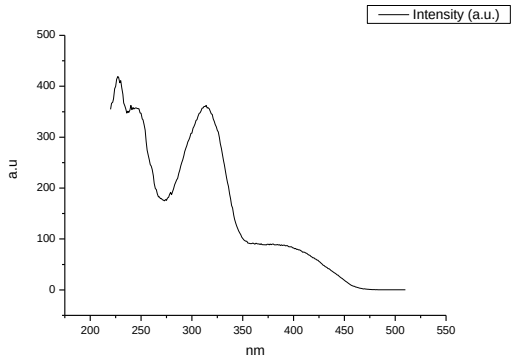

Figure 1.2.292. Fluorescence excitation spectrum of **6a** recorded in 1-octanol with emission fixed at 520 nm.

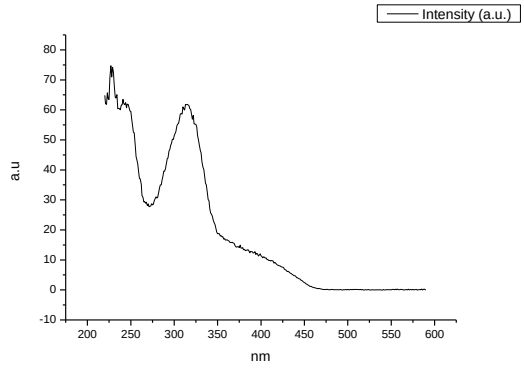

Figure 1.2.293. Fluorescence excitation spectrum of **6a** recorded in 1-octanol with emission fixed at 600 nm.

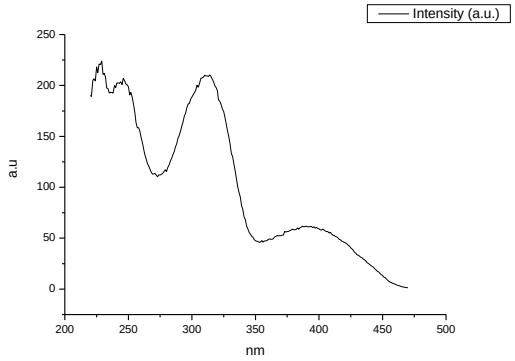

Figure 1.2.294. Fluorescence excitation spectrum of **6a** recorded in 1-hexanol with emission fixed at 480 nm.

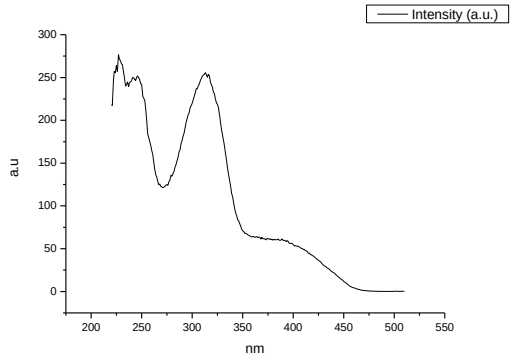

Figure 1.2.295. Fluorescence excitation spectrum of **6a** recorded in 1-hexanol with emission fixed at 520 nm.

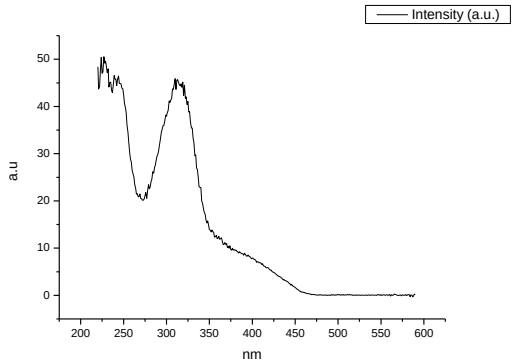

Figure 1.2.296. Fluorescence excitation spectrum of **6a** recorded in 1-hexanol with emission fixed at 600 nm.

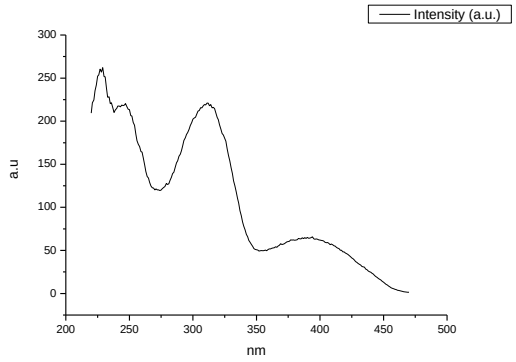

Figure 1.2.297. Fluorescence excitation spectrum of **6a** recorded in 1-butanol with emission fixed at 480 nm.

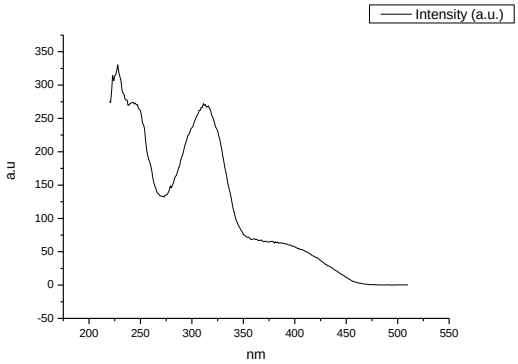

Figure 1.2.298. Fluorescence excitation spectrum of **6a** recorded in 1-butanol with emission fixed at 520 nm.

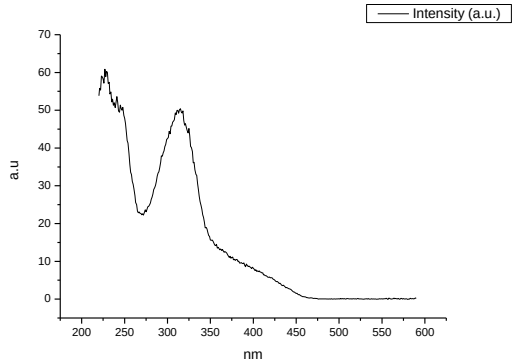

Figure 1.2.299. Fluorescence excitation spectrum of **6a** recorded in 1-butanol with emission fixed at 600 nm.

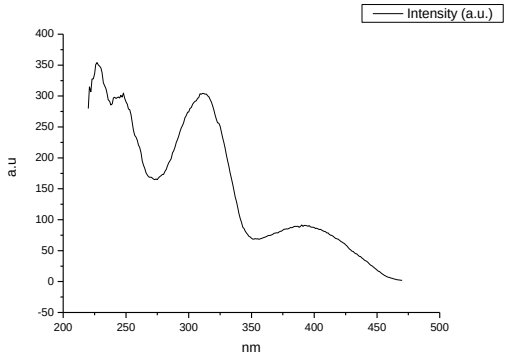

Figure 1.2.300. Fluorescence excitation spectrum of **6a** recorded in 1-pentanol with emission fixed at 480 nm.

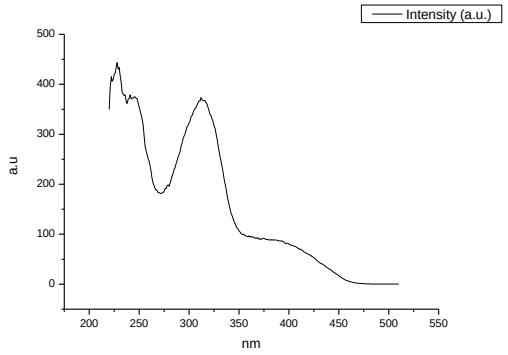

Figure 1.2.301. Fluorescence excitation spectrum of **6a** recorded in 1-pentanol with emission fixed at 520 nm.

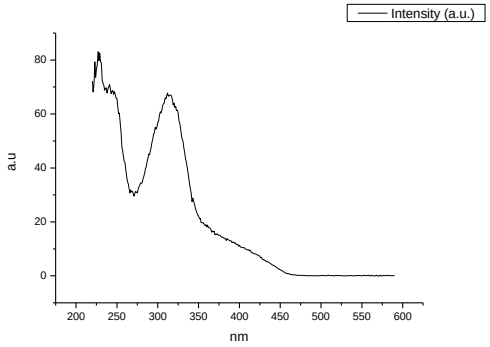

Figure 1.2.302. Fluorescence excitation spectrum of **6a** recorded in 1-pentanol with emission fixed at 600 nm.

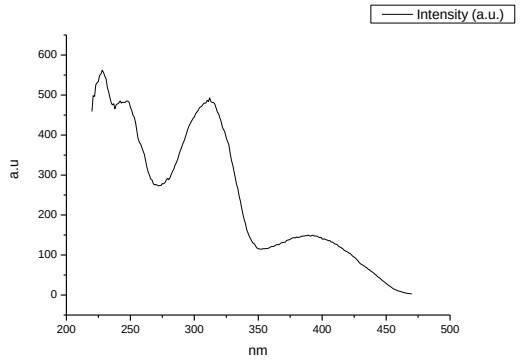

Figure 1.2.303. Fluorescence excitation spectrum of **6a** recorded in 1-propanol with emission fixed at 480 nm.

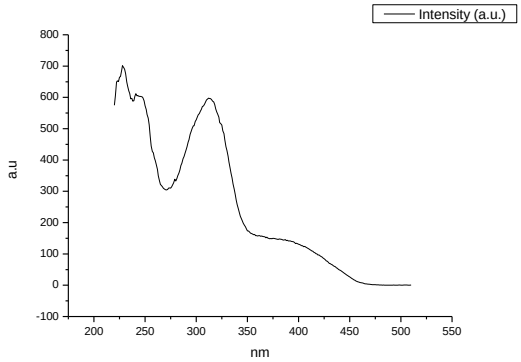

Figure 1.2.304. Fluorescence excitation spectrum of **6a** recorded in 1-propanol with emission fixed at 520 nm.

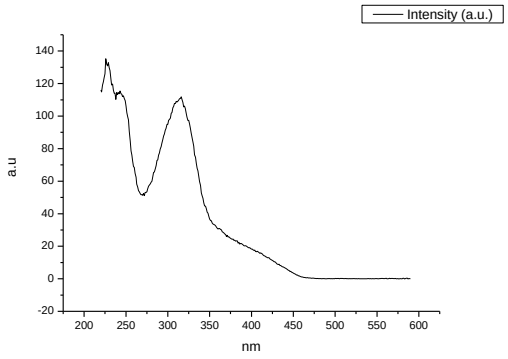

Figure 1.2.305. Fluorescence excitation spectrum of **6a** recorded in 1-propanol with emission fixed at 600 nm.

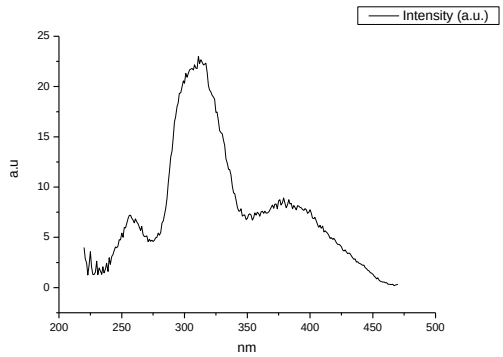

Figure 1.2.306. Fluorescence excitation spectrum of **6a** recorded in Acetic Acid with emission fixed at 480 nm.

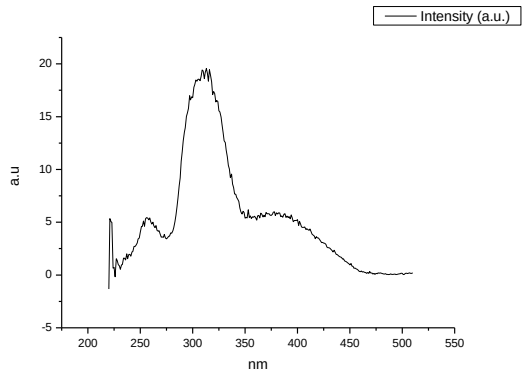

Figure 1.2.307. Fluorescence excitation spectrum of **6a** recorded in Acetic Acid with emission fixed at 520 nm.

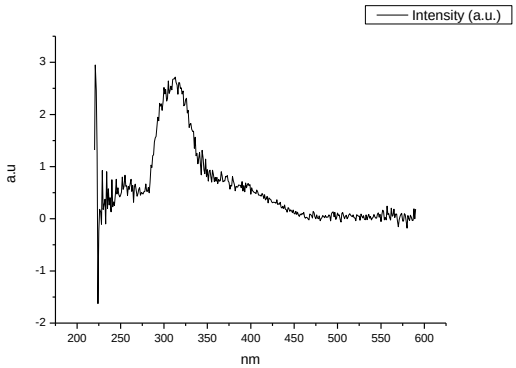

Figure 1.2.308. Fluorescence excitation spectrum of **6a** recorded in Acetic Acid with emission fixed at 600 nm.

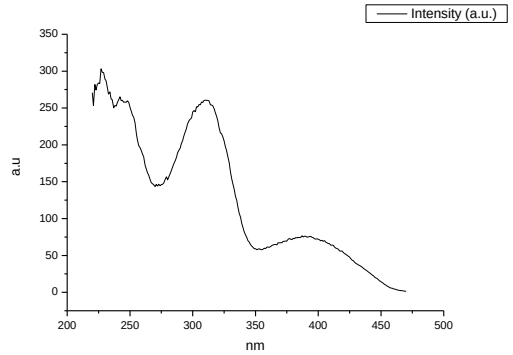

Figure 1.2.309. Fluorescence excitation spectrum of **6a** recorded in Ethanol with emission fixed at 480 nm.

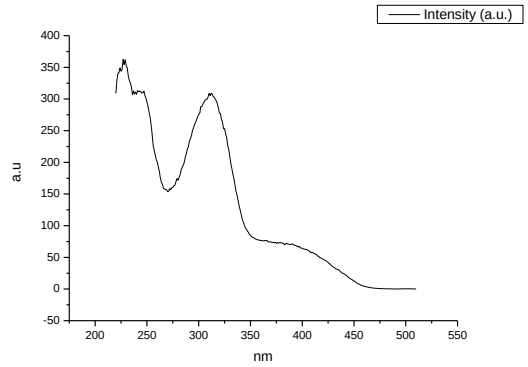

Figure 1.2.310. Fluorescence excitation spectrum of **6a** recorded in Ethanol with emission fixed at 520 nm.

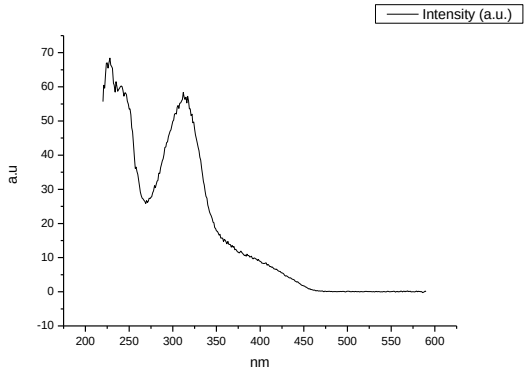

Figure 1.2.311. Fluorescence excitation spectrum of **6a** recorded in Ethanol with emission fixed at 600 nm.

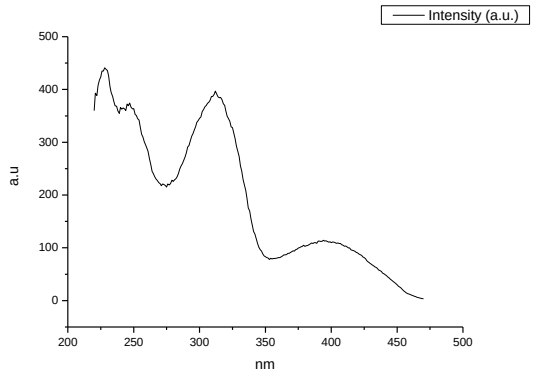

Figure 1.2.312. Fluorescence excitation spectrum of **6a** recorded in 1,5-pentanediol with emission fixed at 480 nm.

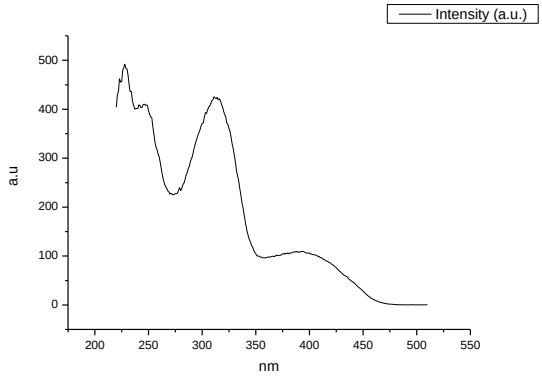

Figure 1.2.313. Fluorescence excitation spectrum of **6a** recorded in 1,5-pentanediol with emission fixed at 520 nm.

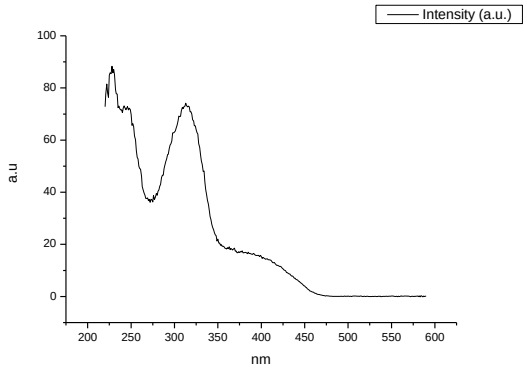

Figure 1.2.314. Fluorescence excitation spectrum of **6a** recorded in 1,5-pentanediol with emission fixed at 600 nm.

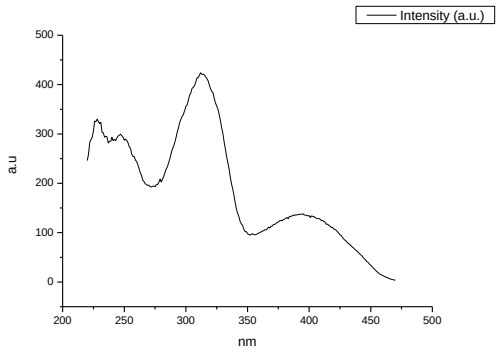

Figure 1.2.315. Fluorescence excitation spectrum of **6a** recorded in 1,3-butanediol with emission fixed at 480 nm.

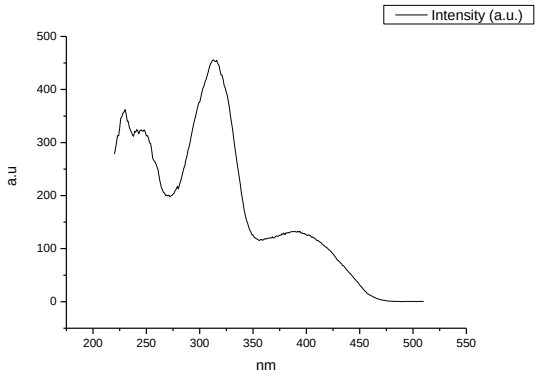

Figure 1.2.316. Fluorescence excitation spectrum of **6a** recorded in 1,3-butanediol with emission fixed at 520 nm.

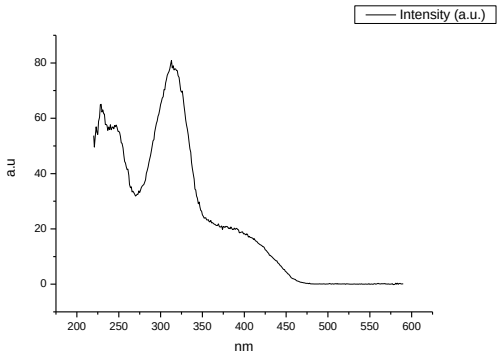

Figure 1.2.317. Fluorescence excitation spectrum of **6a** recorded in 1,3-butanediol with emission fixed at 600 nm.

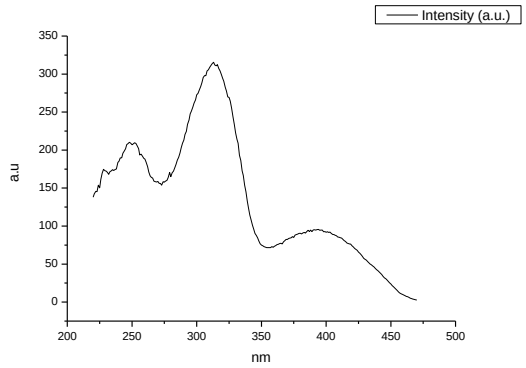

Figure 1.2.318. Fluorescence excitation spectrum of **6a** recorded in 1,4-butanediol with emission fixed at 480 nm.

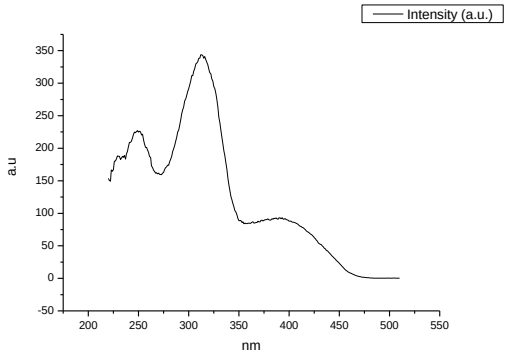

Figure 1.2.319. Fluorescence excitation spectrum of **6a** recorded in 1,4-butanediol with emission fixed at 520 nm.

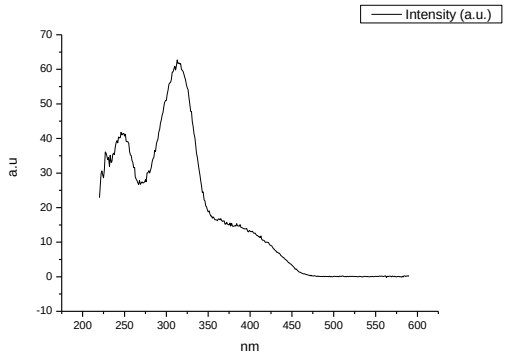

Figure 1.2.320. Fluorescence excitation spectrum of **6a** recorded in 1,4-butanediol with emission fixed at 600 nm.

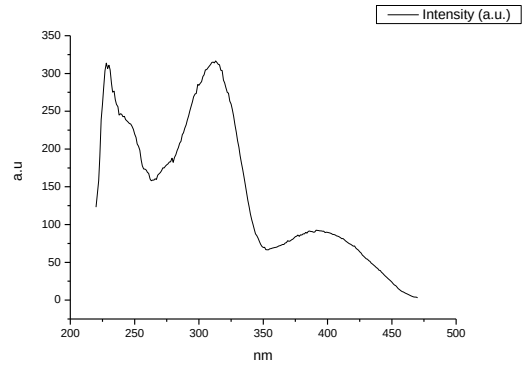

Figure 1.2.321. Fluorescence excitation spectrum of **6a** recorded in 1,4-butanediol with emission fixed at 480 nm.

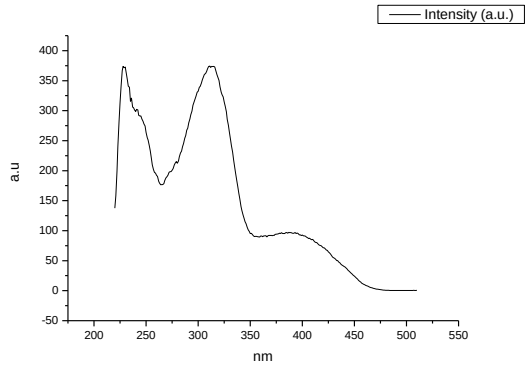

Figure 1.2.322. Fluorescence excitation spectrum of **6a** recorded in 1,4-butanediol with emission fixed at 520 nm.

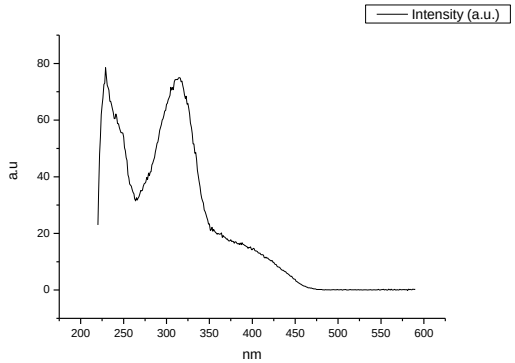

Figure 1.2.323. Fluorescence excitation spectrum of **6a** recorded in 1,4-butanediol with emission fixed at 600 nm.

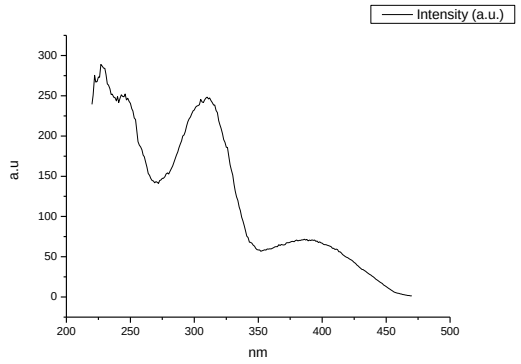

Figure 1.2.324. Fluorescence excitation spectrum of **6a** recorded in Methanol with emission fixed at 480 nm.

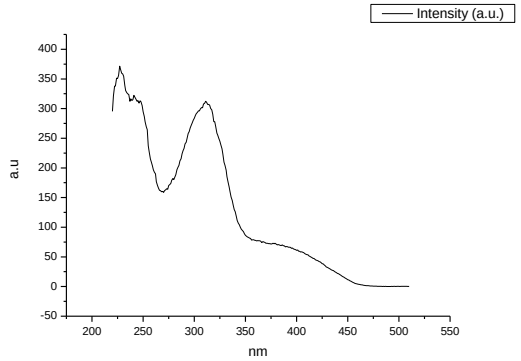

Figure 1.2.325. Fluorescence excitation spectrum of **6a** recorded in Methanol with emission fixed at 520 nm.

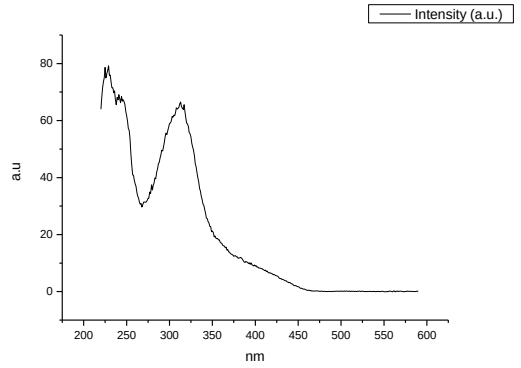

Figure 1.2.326. Fluorescence excitation spectrum of **6a** recorded in Methanol with emission fixed at 600 nm.

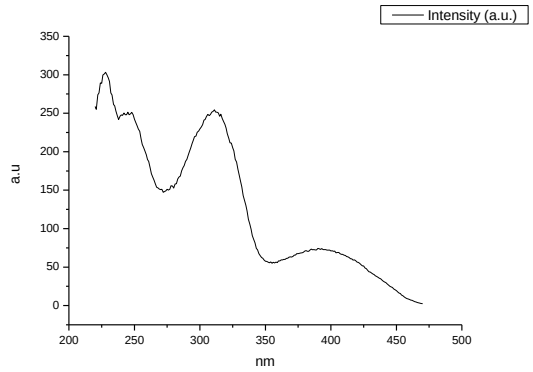

Figure 1.2.327. Fluorescence excitation spectrum of **6a** recorded in 1,2-ethanediol with emission fixed at 480 nm.

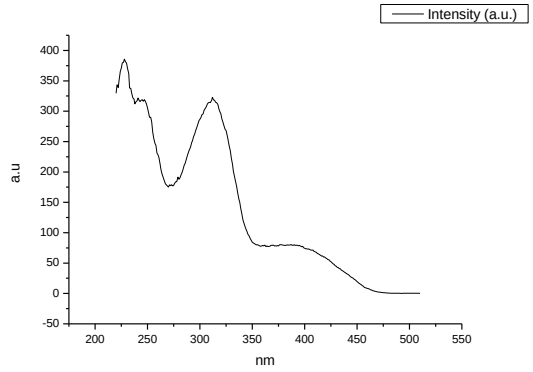

Figure 1.2.328. Fluorescence excitation spectrum of **6a** recorded in 1,2-ethanediol with emission fixed at 520 nm.

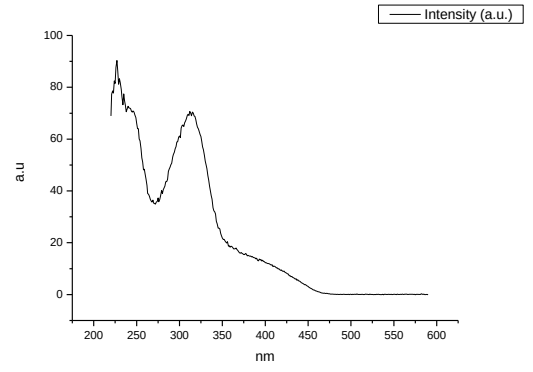

Figure 1.2.329. Fluorescence excitation spectrum of **6a** recorded in 1,2-ethanediol with emission fixed at 600 nm.

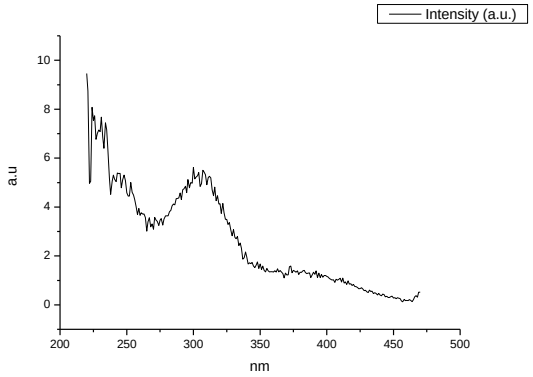

Figure 1.2.330. Fluorescence excitation spectrum of **6a** recorded in 2,2,2-trifluoroethanol with emission fixed at 480 nm.

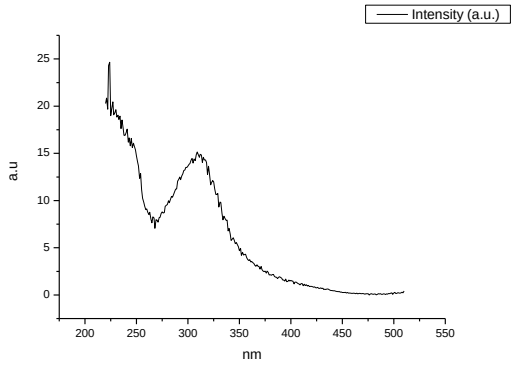

Figure 1.2.331. Fluorescence excitation spectrum of **6a** recorded in 2,2,2-trifluoroethanol with emission fixed at 520 nm.

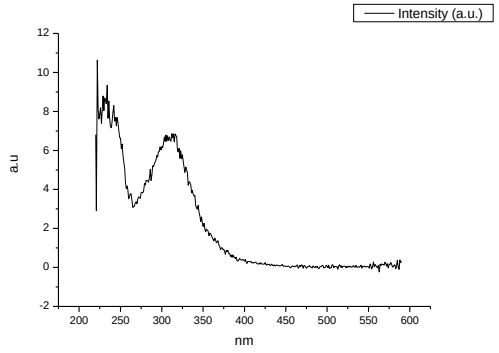

Figure 1.2.332. Fluorescence excitation spectrum of **6a** recorded in 2,2,2-trifluoroethanol with emission fixed at 600 nm.

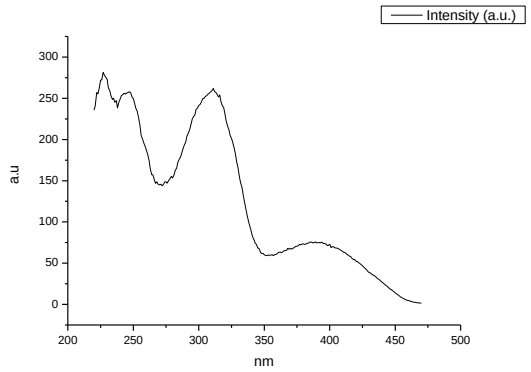

Figure 1.2.333. Fluorescence excitation spectrum of **6a** recorded in Ethanol-d_1 (EtOD) with emission fixed at 480 nm.

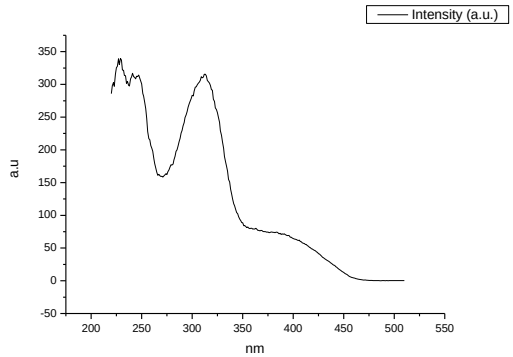

Figure 1.2.334. Fluorescence excitation spectrum of **6a** recorded in Ethanol-d_1 (EtOD) with emission fixed at 520 nm.

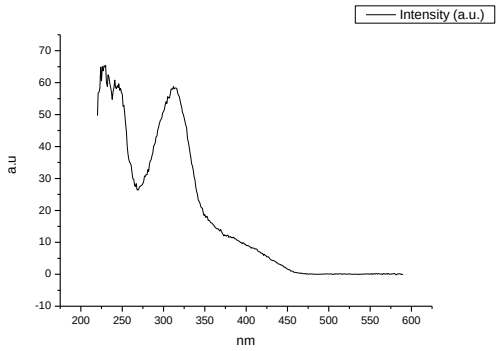

Figure 1.2.335. Fluorescence excitation spectrum of **6a** recorded in Ethanol-d_1 (EtOD) with emission fixed at 600 nm.

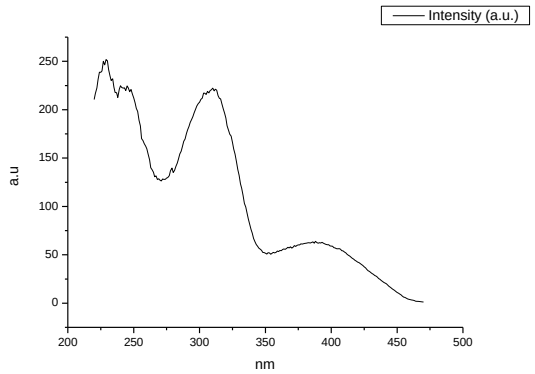

Figure 1.2.336. Fluorescence excitation spectrum of **6a** recorded in Methanol-d_1 (MeOD) with emission fixed at 480 nm.

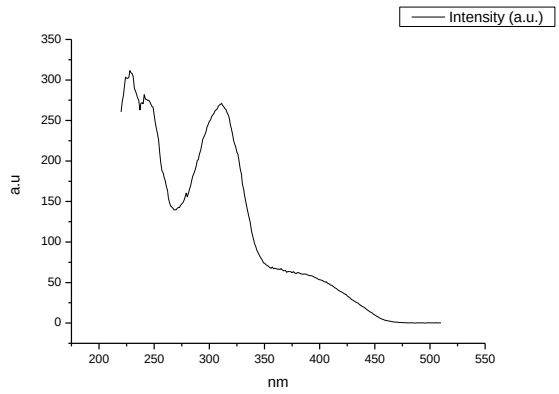

Figure 1.2.337. Fluorescence excitation spectrum of **6a** recorded in Methanol-d_1 (MeOD) with emission fixed at 520 nm.

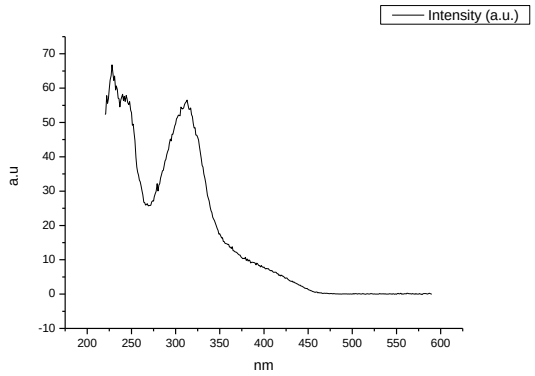

Figure 1.2.338. Fluorescence excitation spectrum of **6a** recorded in Methanol-d_1 (MeOD) with emission fixed at 600 nm.

1.3 COMPOUND 9A

1.3.1 Quantum Yield Summary.

Solvent	abs (310 nm)	$\lambda_{ems\ (max)}$	$\Phi_{310\ nm}$	abs (400 nm)	$\lambda_{ems\ (max)}$	$\Phi_{400\ nm}$
Toluene	0.07	510.00	0.57	0.01	507.01	0.63
1,4-Dioxane	0.12	513.93	0.40	0.02	508.95	0.45
Ethyl acetate	0.10	511.06	0.37	0.02	505.07	0.37
Chloroform	0.11	515.00	0.46	0.02	515.00	0.50
2-Methyl-2-butanol	0.05	510.00	0.34	0.01	505.07	0.29
N,N-dimethylformamide	0.11	518.03	0.45	0.02	508.95	0.52
Acetonitrile	0.09	518.03	0.38	0.02	511.06	0.39
Propylene carbonate	0.07	520.00	0.44	0.01	511.96	0.43
1-Octanol	0.05	516.06	0.61	0.01	502.98	0.60
1-Hexanol	0.06	511.96	0.44	0.01	504.02	0.43
1-Butanol	0.05	516.96	0.40	0.01	505.97	0.37
1-Pentanol	0.06	518.03	0.46	0.01	508.95	0.42
1-Propanol	0.13	515.00	0.36	0.02	505.07	0.37
Acetic acid	0.07	498.95	0.03	0.01	498.95	0.03
Ethanol	0.04	516.96	0.54	0.01	508.95	0.48
1,5-Pentanediol	0.09	516.06	0.46	0.02	505.07	0.51
1,3-Butanediol	0.11	513.03	0.43	0.02	505.07	0.50
1,4-Butanediol	0.09	511.96	0.39	0.02	507.01	0.32
1,3-Propanediol	0.08	516.06	0.44	0.01	508.05	0.46
Methanol	0.10	518.03	0.33	0.02	508.95	0.32
1,2-Ethanediol	0.06	518.93	0.44	0.01	508.95	0.44
2,2,2-Trifluoroethanol	0.05	537.01	0.03	0.01	-	0.01
Ethanol-d	0.06	513.93	0.34	0.01	504.02	0.28
Methanol-d	0.05	516.06	0.35	0.01	504.02	0.32

Table 1.3.1. Summary of ultraviolet-visible absorbance values at 310 nm and 400 nm, emission maxima and quantum yield (Φ) of **9a** at 310 nm and 400 nm excitation.

1.3.2 310 nm excitation Gaussian band fit summaries.

Solvent	λ max$_{em}$ Band 1 (cm^{-1})	λ max$_{em}$ Band 1 (nm)	λ max$_{em}$ Band 2 (cm^{-1})	λ max$_{em}$ Band 2 (nm)	λ max$_{em}$ Band 3 (cm^{-1})	λ max$_{em}$ Band 3 (nm)
Toluene	18635.09	536.62	19754.22	506.22	21174.43	472.27
1,4-Dioxane	18555.15	538.93	19756.33	506.17	21222.59	471.20
Ethyl acetate	18490.15	540.83	19798.20	505.10	21311.83	469.22
Chloroform	18499.99	540.54	19598.56	510.24	21058.87	474.86
2-Methyl-2-butanol	18751.79	533.28	19832.30	504.23	21393.47	467.43
N,N-dimethylformamide	18308.51	546.19	19605.30	510.07	21054.70	474.95
Acetonitrile	18183.36	549.95	19555.68	511.36	21091.87	474.12
Propylene carbonate	18192.18	549.69	19554.80	511.38	21034.04	475.42
1-Octanol	18417.86	542.95	19727.16	506.92	21240.61	470.80
1-Hexanol	18377.26	544.15	19699.50	507.63	21220.12	471.25
1-Butanol	18323.54	545.75	19669.44	508.40	21203.23	471.63
1-Pentanol	18325.68	545.68	19682.26	508.07	21212.33	471.42
1-Propanol	18306.72	546.25	19661.88	508.60	21188.63	471.95
Acetic acid	18793.71	532.09	19916.56	502.09	21133.18	473.19
Ethanol	18295.96	546.57	19681.01	508.10	21185.79	472.01
1,5-Pentanediol	18327.68	545.62	19683.67	508.04	21032.05	475.46
1,3-Butanediol	18377.75	544.14	19716.25	507.20	21049.79	475.06
1,4-Butanediol	18552.28	539.02	19692.08	507.82	21006.79	476.04
1,3-Propanediol	18204.68	549.31	19553.34	511.42	20906.13	478.33
Methanol	18196.41	549.56	19606.85	510.03	21110.58	473.70
1,2-Ethanediol	18104.06	552.36	19491.89	513.03	20894.76	478.59
2,2,2-Trifluoroethanol	18101.55	552.44	17823.06	561.07	18783.08	532.39
Ethanol-d	18299.47	546.46	19673.40	508.30	21199.48	471.71
Methanol-d	18181.55	550.01	19592.90	510.39	21117.02	473.55

Solvent	λ max$_{em}$ Band 4 (cm^{-1})	λ max$_{em}$ Band 4 (nm)	λ max$_{em}$ Band 5 (cm^{-1})	λ max$_{em}$ Band 5 (nm)
Toluene	28034.39	356.70	-	-
1,4-Dioxane	27957.30	357.69	-	-
Ethyl acetate	28071.82	356.23	-	-
Chloroform	27764.27	360.18	-	-
2-Methyl-2-butanol	28061.22	356.36	-	-
N,N-dimethylformamide	27184.25	367.86	-	-
Acetonitrile	28021.29	356.87	-	-
Propylene carbonate	27497.41	363.67	-	-
1-Octanol	28090.92	355.99	-	-
1-Hexanol	27985.41	357.33	-	-
1-Butanol	27980.17	357.40	-	-
1-Pentanol	27967.49	357.56	-	-
1-Propanol	27906.54	358.34	-	-
Acetic acid	26896.06	371.80	28590.19	349.77
Ethanol	28010.60	357.01	-	-
1,5-Pentanediol	27767.89	360.13	-	-
1,3-Butanediol	26715.60	374.31	28901.56	346.00
1,4-Butanediol	27261.54	366.82	-	-
1,3-Propanediol	28592.34	349.74	-	-
Methanol	27952.44	357.75	-	-
1,2-Ethanediol	27669.61	361.41	-	-
2,2,2-Trifluoroethanol	25959.87	385.21	27966.28	357.57
Ethanol-d	28047.10	356.54	-	-
Methanol-d	27990.24	357.27	-	-

Table 1.3.2. Summary of band maxima of 5 band fit using Gaussian model for normalised **9a** emission spectra recorded at 310 nm excitation.

(a)

Solvent	Width Band 1 (cm^{-1})	Width Band 2 (cm^{-1})	Width Band 3 (cm^{-1})	Width Band 4 (cm^{-1})	Width Band 5 (cm^{-1})
Toluene	3127.94	1879.73	964.65	3163.59	-
1,4-Dioxane	3168.66	2044.52	950.15	3113.34	-
Ethyl acetate	3206.42	2196.43	991.78	3146.59	-
Chloroform	3171.29	1911.83	1018.31	3041.12	-
2-Methyl-2-butanol	3220.17	1927.15	998.18	3156.45	-
N,N-dimethylformamide	3321.61	2319.63	1092.86	4055.62	-
Acetonitrile	3271.51	2361.67	1112.06	3162.08	-
Propylene carbonate	3283.74	2340.47	1122.94	3394.23	-
1-Octanol	3219.73	2203.31	1017.39	3310.53	-
1-Hexanol	3236.14	2239.23	1023.39	3189.42	-
1-Butanol	3243.93	2276.55	1045.30	3196.81	-
1-Pentanol	3234.55	2271.83	1024.89	3184.39	-
1-Propanol	3241.72	2276.63	1053.22	3121.76	-
Acetic acid	3639.24	2344.77	1134.84	3354.25	2283.39
Ethanol	3247.73	2296.23	1062.03	3200.47	-
1,5-Pentanediol	3237.02	2254.00	1143.96	3324.17	-
1,3-Butanediol	3266.01	2252.49	1127.06	3055.46	2629.89
1,4-Butanediol	3408.23	2246.76	1094.61	4248.07	-
1,3-Propanediol	3281.35	2282.00	1152.88	4025.01	-
Methanol	3277.11	2337.44	1116.10	3204.77	-
1,2-Ethanediol	3268.15	2290.84	1174.56	3241.49	-
2,2,2-Trifluoroethanol	3063.65	7875.03	1329.21	3542.24	2795.43
Ethanol-d	3264.67	2307.54	1066.73	3199.57	-
Methanol-d	3301.25	2372.28	1145.27	3267.12	-

(b)

Solvent	Area Band 1 (cm^{-1})	Area Band 2 (cm^{-1})	Area Band 3 (cm^{-1})	Area Band 4 (cm^{-1})	Area Band 5 (cm^{-1})
Toluene	2056.98	1307.42	332.43	92.08	-
1,4-Dioxane	1982.85	1474.05	264.97	82.79	-
Ethyl acetate	1927.25	1702.15	261.65	95.60	-
Chloroform	2097.89	1307.91	353.04	67.65	-
2-Methyl-2-butanol	2270.12	1226.74	288.36	109.38	-
N,N-dimethylformamide	1986.19	1795.55	294.30	107.35	-
Acetonitrile	1892.46	1893.78	259.24	94.49	-
Propylene carbonate	1901.30	1865.51	294.82	209.19	-
1-Octanol	1896.58	1723.93	291.85	102.91	-
1-Hexanol	1915.04	1752.30	279.64	95.81	-
1-Butanol	1887.09	1804.54	269.73	106.13	-
1-Pentanol	1873.21	1820.93	270.71	97.91	-
1-Propanol	1894.37	1819.54	279.71	94.86	-
Acetic acid	1676.51	1904.15	359.34	699.50	624.58
Ethanol	1873.65	1857.66	287.53	103.55	-
1,5-Pentanediol	1773.17	1855.77	365.53	81.55	-
1,3-Butanediol	1824.14	1810.38	349.14	124.67	307.41
1,4-Butanediol	2147.27	1608.93	315.61	523.33	-
1,3-Propanediol	1841.47	1846.81	354.62	244.44	-
Methanol	1931.02	1873.00	299.21	105.30	-
1,2-Ethanediol	1896.37	1836.97	349.91	89.07	-
2,2,2-Trifluoroethanol	2916.63	963.21	277.57	375.53	649.01
Ethanol-d	1897.52	1855.50	272.65	104.17	-
Methanol-d	1889.41	1934.67	302.80	108.56	-

(c)

Solvent	fwhm Band 1 (nm)	fwhm Band 2 (nm)	fwhm Band 3 (nm)	fwhm Band 4 (nm)	fwhm Band 5 (nm)
Toluene	104.37	58.78	38.29	48.43	-
1,4-Dioxane	111.11	63.10	25.27	48.43	-
Ethyl acetate	118.01	63.10	29.23	50.53	-
Chloroform	111.11	54.37	29.76	46.94	-
2-Methyl-2-butanol	108.85	57.66	24.83	48.43	-
N,N-dimethylformamide	120.50	74.32	48.56	64.59	-
Acetonitrile	115.84	74.32	29.76	48.43	-
Propylene carbonate	115.84	74.32	25.73	52.65	-
1-Octanol	113.44	68.65	25.27	50.53	-
1-Hexanol	113.44	68.65	25.27	51.22	-
1-Butanol	113.44	68.65	25.27	48.43	-
1-Pentanol	113.44	68.65	25.27	51.22	-
1-Propanol	113.44	68.65	29.76	46.30	-
Acetic acid	124.32	71.52	29.76	54.90	32.49
Ethanol	120.50	68.65	42.18	51.22	-
1,5-Pentanediol	113.44	68.65	34.33	51.93	-
1,3-Butanediol	113.44	68.65	34.33	53.38	38.72
1,4-Butanediol	122.49	68.65	34.33	66.75	-
1,3-Propanediol	125.06	70.00	30.30	55.93	-
Methanol	115.84	74.32	29.76	48.43	-
1,2-Ethanediol	115.84	70.00	34.96	49.77	-
2,2,2-Trifluoroethanol	111.10	292.38	48.10	56.56	43.55
Ethanol-d	113.44	68.65	25.27	48.43	-
Methanol-d	120.50	74.32	29.76	48.43	-

Tables 1.3.3 (a), (b) and (c). Summary band width, band area, full width half maximum of 5 band fit using Gaussian model for normalised **9a** emission spectra recorded at 310 nm excitation.

Solvent	Band 1 Area Percentage (%)	Band 2 Area Percentage (%)	Band 3 Area Percentage (%)	Band 4 Area Percentage (%)	Band 5 Area Percentage (%)
Toluene	54.29	34.51	8.77	2.43	-
1,4-Dioxane	52.12	38.74	6.96	2.18	-
Ethyl acetate	48.34	42.70	6.56	2.40	-
Chloroform	54.83	34.18	9.23	1.77	-
2-Methyl-2-butanol	58.29	31.50	7.40	2.81	-
N,N-dimethylformamide	47.48	42.92	7.04	2.57	-
Acetonitrile	45.71	45.74	6.26	2.28	-
Propylene carbonate	44.52	43.68	6.90	4.90	-
1-Octanol	47.23	42.93	7.27	2.56	-
1-Hexanol	47.37	43.34	6.92	2.37	-
1-Butanol	46.39	44.36	6.63	2.61	-
1-Pentanol	46.11	44.82	6.66	2.41	-
1-Propanol	46.33	44.50	6.84	2.32	-
Acetic acid	31.85	36.17	6.83	13.29	11.87
Ethanol	45.45	45.06	6.97	2.51	-
1,5-Pentanediol	43.50	45.53	8.97	2.00	-
1,3-Butanediol	41.31	41.00	7.91	2.82	6.96
1,4-Butanediol	46.73	35.01	6.87	11.39	-
1,3-Propanediol	42.95	43.08	8.27	5.70	-
Methanol	45.88	44.50	7.11	2.50	-
1,2-Ethanediol	45.45	44.03	8.39	2.13	-
2,2,2-Trifluoroethanol	56.28	18.59	5.36	7.25	12.52
Ethanol-d	45.95	44.93	6.60	2.52	-
Methanol-d	44.61	45.68	7.15	2.56	-

Table 1.3.4. Total Area Percentages of 5 band fit using Gaussian model for normalised **9a** emission spectra recorded at 310 nm excitation.

Solvent	Area Ratio Band 1/2 (310 nm ex)	Area Ratio Band 1/3 (310 nm ex)	Area Ratio Band 1/4 (310 nm ex)	Area Ratio Band 1/5 (310 nm ex)
Toluene	1.57	6.19	22.34	-
1,4-Dioxane	1.35	7.48	23.95	-
Ethyl acetate	1.13	7.37	20.16	-
Chloroform	1.60	5.94	31.01	-
2-Methyl-2-butanol	1.85	7.87	20.76	-
N,N-dimethylformamide	1.11	6.75	18.50	-
Acetonitrile	1.00	7.30	20.03	-
Propylene carbonate	1.02	6.45	9.09	-
1-Octanol	1.10	6.50	18.43	-
1-Hexanol	1.09	6.85	19.99	-
1-Butanol	1.05	7.00	17.78	-
1-Pentanol	1.03	6.92	19.13	-
1-Propanol	1.04	6.77	19.97	-
Acetic acid	0.88	4.67	2.40	2.68
Ethanol	1.01	6.52	18.09	-
1,5-Pentanediol	0.96	4.85	21.74	-
1,3-Butanediol	1.01	5.22	14.63	5.93
1,4-Butanediol	1.33	6.80	4.10	-
1,3-Propanediol	1.00	5.19	7.53	-
Methanol	1.03	6.45	18.34	-
1,2-Ethanediol	1.03	5.42	21.29	-
2,2,2-Trifluoroethanol	3.03	10.51	7.77	4.49
Ethanol-d	1.02	6.96	18.22	-
Methanol-d	0.98	6.24	17.40	-

Solvent	Area Ratio Band 2/3 (310 nm ex)	Area Ratio Band 2/4 (310 nm ex)	Area Ratio Band 2/5 (310 nm ex)	Area Ratio Band 3/4 (310 nm ex)	Area Ratio Band 3/5 (310 nm ex)	Area Ratio Band 4/5 (310 nm ex)
Toluene	3.93	14.20	-	3.61	-	-
1,4-Dioxane	5.56	17.80	-	3.20	-	-
Ethyl acetate	6.51	17.80	-	2.74	-	-
Chloroform	3.70	19.33	-	5.22	-	-
2-Methyl-2-butanol	4.25	11.22	-	2.64	-	-
N,N-dimethylformamide	6.10	16.73	-	2.74	-	-
Acetonitrile	7.31	20.04	-	2.74	-	-
Propylene carbonate	6.33	8.92	-	1.41	-	-
1-Octanol	5.91	16.75	-	2.84	-	-
1-Hexanol	6.27	18.29	-	2.92	-	-
1-Butanol	6.69	17.00	-	2.54	-	-
1-Pentanol	6.73	18.60	-	2.76	-	-
1-Propanol	6.51	19.18	-	2.95	-	-
Acetic acid	5.30	2.72	3.05	0.51	0.58	1.12
Ethanol	6.46	17.94	-	2.78	-	-
1,5-Pentanediol	5.08	22.76	-	4.48	-	-
1,3-Butanediol	5.19	14.52	5.89	2.80	1.14	0.41
1,4-Butanediol	5.10	3.07	-	0.60	-	-
1,3-Propanediol	5.21	7.56	-	1.45	-	-
Methanol	6.26	17.79	-	2.84	-	-
1,2-Ethanediol	5.25	20.62	-	3.93	-	-
2,2,2-Trifluoroethanol	3.47	2.56	1.48	0.74	0.43	0.58
Ethanol-d	6.81	17.81	-	2.62	-	-
Methanol-d	6.39	17.82	-	2.79	-	-

Table 1.3.5. Area Ratios of 5 band fit using Gaussian model for normalised **9a** emission spectra recorded at 310 nm excitation.

1.3.3 400 nm excitation Gaussian band fit summaries.

Solvent	λ max$_{em}$ Band 1 (cm^{-1})	λ max$_{em}$ Band 1 (nm)	λ max$_{em}$ Band 2 (cm^{-1})	λ max$_{em}$ Band 2 (nm)	λ max$_{em}$ Band 3 (cm^{-1})	λ max$_{em}$ Band 3 (nm)
Toluene	18563.08	538.70	19869.97	503.27	21138.26	473.08
1,4-Dioxane	18534.76	539.53	19869.19	503.29	21161.33	472.56
Ethyl acetate	18593.86	537.81	19958.28	501.05	21242.94	470.74
Chloroform	18429.98	542.59	19746.22	506.43	21029.23	475.53
2-Methyl-2-butanol	18740.72	533.60	20038.95	499.03	21350.72	468.37
N,N-dimethylformamide	18556.68	538.89	19771.09	505.79	20993.04	476.35
Acetonitrile	18330.89	545.53	19728.75	506.87	21003.55	476.11
Propylene carbonate	18373.83	544.25	19729.09	506.87	20991.81	476.38
1-Octanol	18560.78	538.77	19902.07	502.46	21177.86	472.19
1-Hexanol	18507.22	540.33	19871.49	503.23	21153.40	472.74
1-Butanol	18511.99	540.19	19871.39	503.24	21146.73	472.89
1-Pentanol	18512.80	540.17	19870.24	503.27	21151.39	472.78
1-Propanol	18451.35	541.97	19847.10	503.85	21113.51	473.63
Acetic acid	17836.36	560.65	18938.15	528.03	20404.35	490.09
Ethanol	18506.22	540.36	19873.46	503.18	21128.70	473.29
1,5-Pentanediol	18444.64	542.16	19777.92	505.61	21003.46	476.11
1,3-Butanediol	18425.27	542.73	19778.12	505.61	21007.57	476.02
1,4-Butanediol	18474.56	541.28	19768.81	505.85	20970.85	476.85
1,3-Propanediol	18303.73	546.34	19646.75	508.99	20869.97	479.16
Methanol	18356.71	544.76	19766.46	505.91	21019.57	475.75
1,2-Ethanediol	18227.45	548.62	19596.86	510.29	20848.30	479.66
2,2,2-Trifluoroethanol	16977.07	589.03	18866.56	530.04	20486.20	488.13
Ethanol-d	18533.52	539.56	19891.10	502.74	21147.74	472.86
Methanol-d	18422.36	542.82	19783.68	505.47	21044.29	475.19

Table 1.3.6. Summary of band maxima of 3 band fit using Gaussian model for normalised **9a** emission spectra recorded at 400 nm excitation.

Solvent	fwhm Band 1 (nm)	fwhm Band 2 (nm)	fwhm Band 3 (nm)	Width Band 1 (cm^{-1})	Width Band 2 (cm^{-1})	Width Band 3 (cm^{-1})
Toluene	109.12	64.03	26.88	3100.95	2036.17	967.41
1,4-Dioxane	109.12	64.03	26.88	3132.57	2096.06	1007.05
Ethyl acetate	111.98	63.26	29.40	3158.93	2130.30	1066.83
Chloroform	110.56	64.82	27.19	3119.55	2059.77	1034.79
2-Methyl-2-butanol	110.54	63.26	29.07	3161.31	2097.11	1048.73
N,N-dimethylformamide	123.55	71.05	32.63	3430.87	2271.90	1147.14
Acetonitrile	114.96	68.35	35.56	3218.50	2211.87	1239.75
Propylene carbonate	107.63	68.35	35.56	3195.55	2177.42	1217.35
1-Octanol	109.12	64.03	29.40	3126.12	2108.97	1109.62
1-Hexanol	113.46	64.03	32.26	3143.33	2144.64	1155.09
1-Butanol	109.12	64.03	32.26	3169.94	2149.32	1145.43
1-Pentanol	113.46	64.03	32.26	3138.80	2131.90	1150.40
1-Propanol	110.56	64.03	29.74	3174.10	2158.39	1154.00
Acetic acid	84.00	43.67	72.78	1825.92	1086.10	2498.30
Ethanol	106.22	64.03	32.26	3138.61	2131.24	1205.22
1,5-Pentanediol	110.56	64.82	32.63	3159.55	2144.09	1191.71
1,3-Butanediol	110.56	64.82	32.63	3150.61	2150.38	1204.63
1,4-Butanediol	113.46	64.82	30.08	3213.11	2160.37	1208.82
1,3-Propanediol	112.03	65.62	35.98	3165.63	2147.94	1241.42
Methanol	112.03	64.82	32.63	3189.35	2176.94	1263.85
1,2-Ethanediol	113.53	69.19	35.98	3193.29	2179.75	1269.08
2,2,2-Trifluoroethanol	82.91	81.47	54.54	1374.03	2047.59	1373.87
Ethanol-d	113.46	64.03	32.26	3176.53	2155.76	1177.26
Methanol-d	110.56	64.82	32.63	3216.02	2193.81	1290.18

Table 1.3.7. Summary of full width half maximum (fwhm), band width, and band area of 3 band fit using Gaussian model for normalised **9a** emission spectra recorded at 400 nm excitation.

Solvent	Area Band 1 (cm^{-1})	Area Band 2 (cm^{-1})	Area Band 3 (cm^{-1})	Area Ratio Band 1/2 (400 nm ex)	Area Ratio Band 1/3 (400 nm ex)	Area Ratio Band 2/3 (400 nm ex)
Toluene	1644.60	1713.76	388.80	0.96	4.23	4.41
1,4-Dioxane	1670.33	1765.79	366.17	0.95	4.56	4.82
Ethyl acetate	1642.29	1809.71	407.68	0.91	4.03	4.44
Chloroform	1612.39	1744.83	427.38	0.92	3.77	4.08
2-Methyl-2-butanol	1737.19	1686.76	381.00	1.03	4.56	4.43
N,N-dimethylformamide	1827.90	1782.22	369.21	1.03	4.95	4.83
Acetonitrile	1549.60	1890.09	463.98	0.82	3.34	4.07
Propylene carbonate	1613.13	1816.09	457.37	0.89	3.53	3.97
1-Octanol	1672.16	1767.63	450.08	0.95	3.72	3.93
1-Hexanol	1609.58	1823.30	456.19	0.88	3.53	4.00
1-Butanol	1609.17	1816.90	439.39	0.89	3.66	4.14
1-Pentanol	1599.88	1792.33	456.81	0.89	3.50	3.92
1-Propanol	1579.41	1860.97	446.04	0.85	3.54	4.17
Acetic acid	409.03	133.50	2963.80	3.06	0.14	0.05
Ethanol	1578.78	1800.73	487.60	0.88	3.24	3.69
1,5-Pentanediol	1589.36	1800.57	471.80	0.88	3.37	3.82
1,3-Butanediol	1543.08	1816.74	483.19	0.85	3.19	3.76
1,4-Butanediol	1627.34	1760.69	457.04	0.92	3.56	3.85
1,3-Propanediol	1539.13	1796.71	498.09	0.86	3.09	3.61
Methanol	1473.52	1886.04	537.90	0.78	2.74	3.51
1,2-Ethanediol	1539.24	1832.94	515.50	0.84	2.99	3.56
2,2,2-Trifluoroethanol	159.84	1395.96	530.13	0.11	0.30	2.63
Ethanol-d	1658.05	1803.36	445.16	0.92	3.72	4.05
Methanol-d	1481.18	1827.21	524.06	0.81	2.83	3.49

Solvent	Band 1 Area Percentage (%)	Band 2 Area Percentage (%)	Band 3 Area Percentage (%)
Toluene	43.89	45.74	10.38
1,4-Dioxane	43.93	46.44	9.63
Ethyl acetate	42.55	46.89	10.56
Chloroform	42.60	46.10	11.29
2-Methyl-2-butanol	45.66	44.33	10.01
N,N-dimethylformamide	45.93	44.79	9.28
Acetonitrile	39.70	48.42	11.89
Propylene carbonate	41.50	46.73	11.77
1-Octanol	42.99	45.44	11.57
1-Hexanol	41.39	46.88	11.73
1-Butanol	41.63	47.00	11.37
1-Pentanol	41.57	46.57	11.87
1-Propanol	40.64	47.88	11.48
Acetic acid	11.67	3.81	84.53
Ethanol	40.83	46.57	12.61
1,5-Pentanediol	41.16	46.63	12.22
1,3-Butanediol	40.15	47.27	12.57
1,4-Butanediol	42.32	45.79	11.89
1,3-Propanediol	40.14	46.86	12.99
Methanol	37.81	48.39	13.80
1,2-Ethanediol	39.59	47.15	13.26
2,2,2-Trifluoroethanol	7.66	66.92	25.41
Ethanol-d	42.44	46.16	11.40
Methanol-d	38.65	47.68	13.67

Table 1.3.8. Band areas, area ratios and total area percentage of 3 band fit using Gaussian model for normalised **9a** emission spectra recorded at 400 nm excitation.

1.3.4 310 nm Gaussian band fit - Solvatochromic analysis.

1.3.4.1 E_T^N.

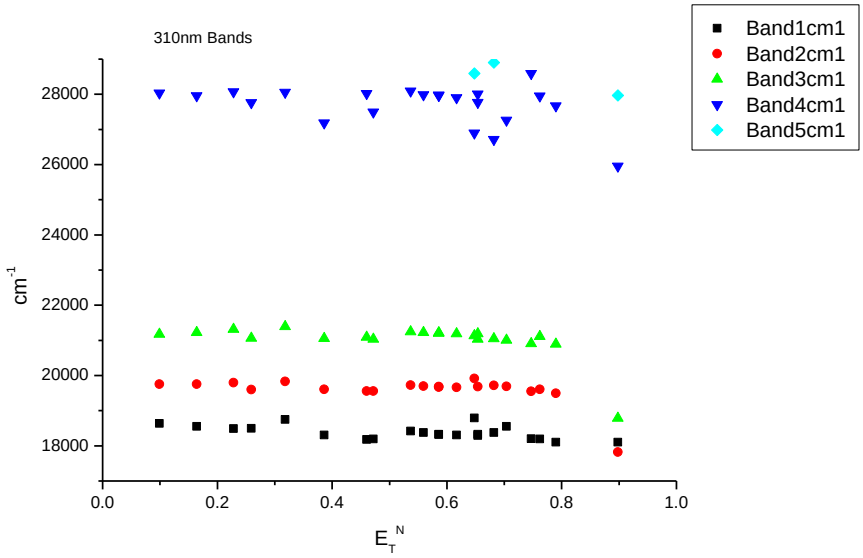

Figure 1.3.1. Band maxima from Gaussian model fit of the normalised fluorescence emission spectra of **9a** recorded at 310 nm excitation against E_T^N.

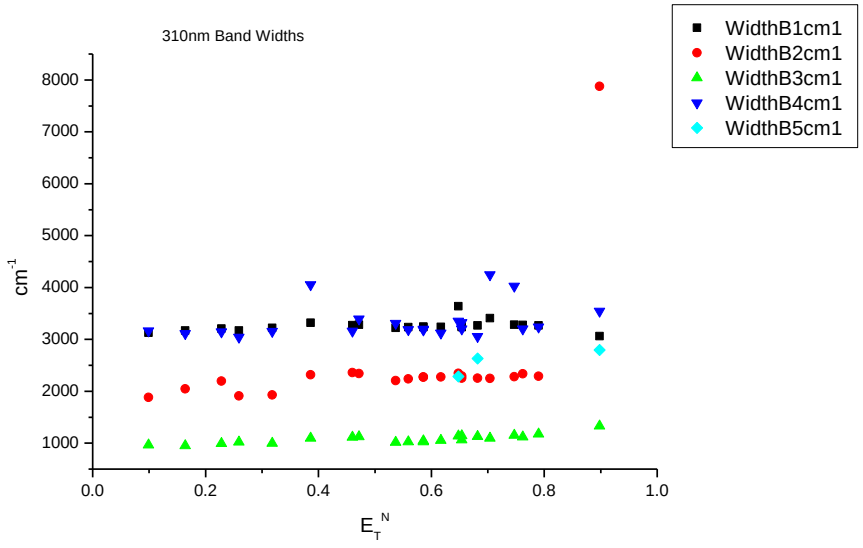

Figure 1.3.2. Band widths from Gaussian model fit of the normalised fluorescence emission spectra of **9a** recorded at 310 nm excitation against E_T^N.

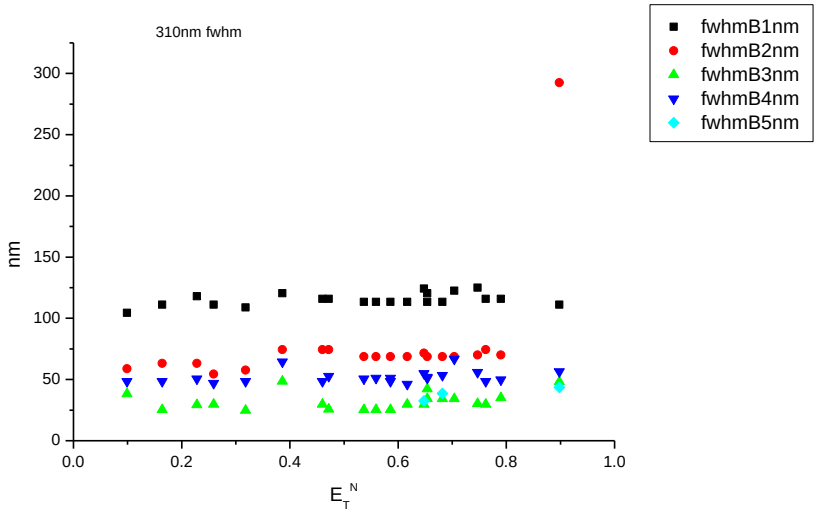

Figure 1.3.3. Full width half maxima of each band from Gaussian model fit of the normalised fluorescence emission spectra of **9a** recorded at 310 nm excitation against E_T^N.

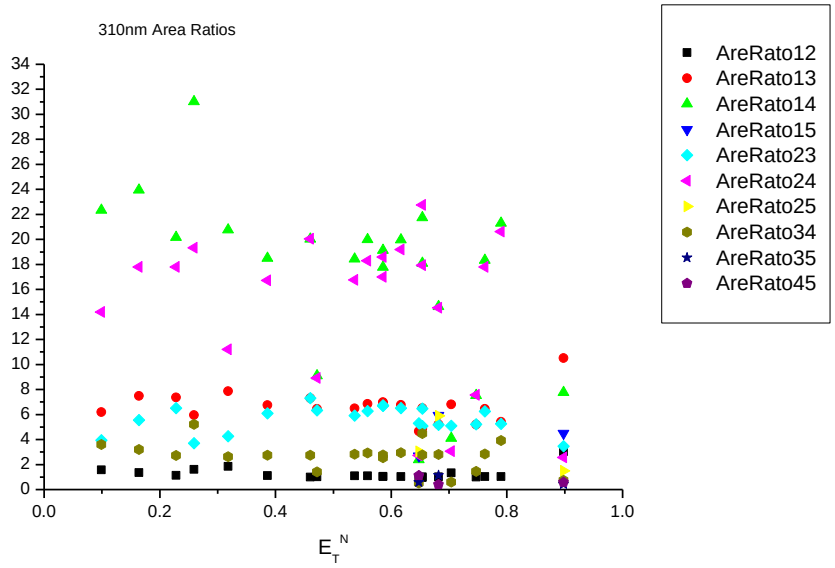

Figure 1.3.4. Area ratios from Gaussian model fit of the normalised fluorescence emission spectra of **9a** recorded at 310 nm excitation against E_T^N.

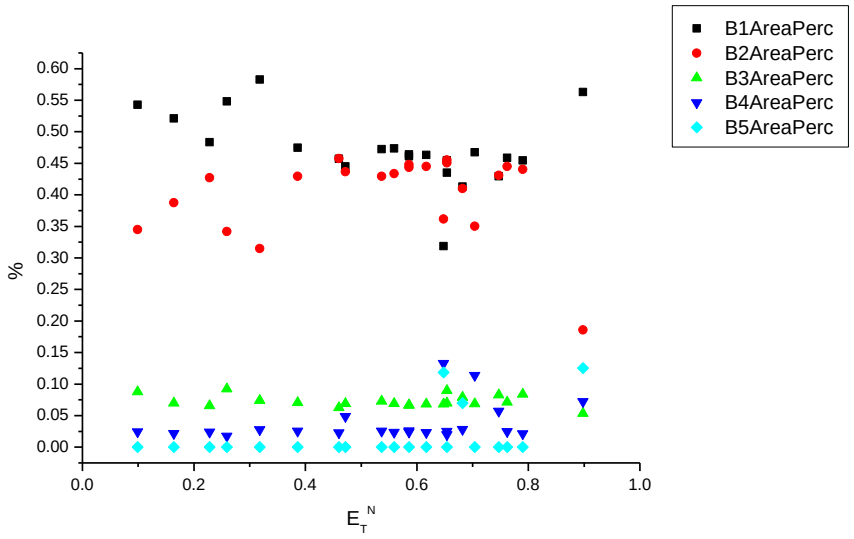

Figure 1.3.5. Area percentages from Gaussian model fit of the normalised fluorescence emission spectra of **9a** recorded at 310 nm excitation against E_T^N.

1.3.4.2 α

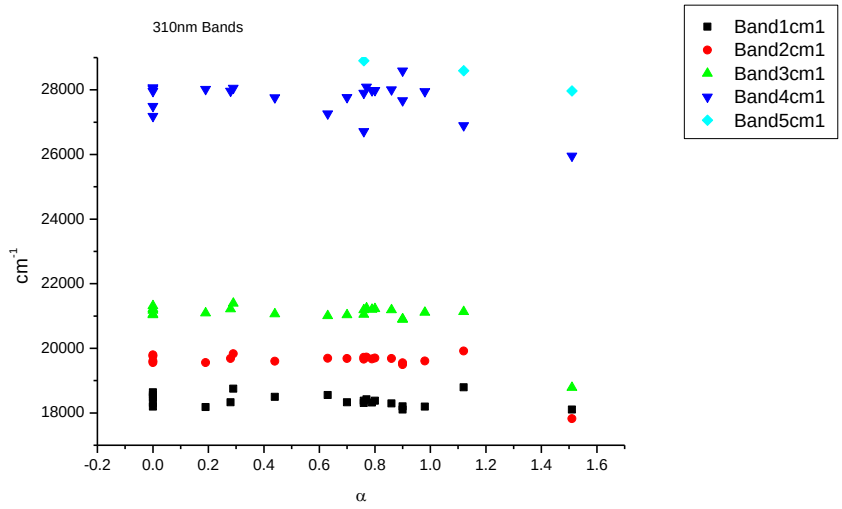

Figure 1.3.6. Band maxima from Gaussian model fit of the normalised fluorescence emission spectra of **9a** recorded at 310 nm excitation against α.

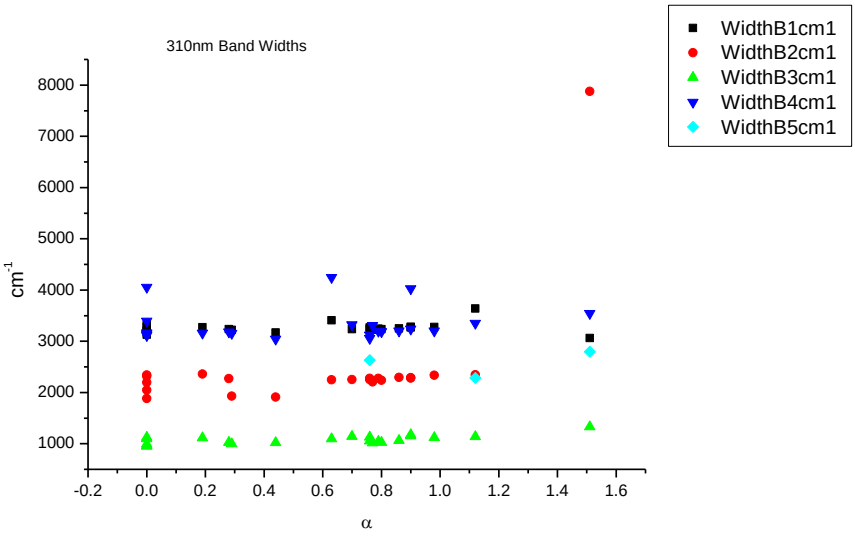

Figure 1.3.7. Band widths from Gaussian model fit of the normalised fluorescence emission spectra of **9a** recorded at 310 nm excitation against α.

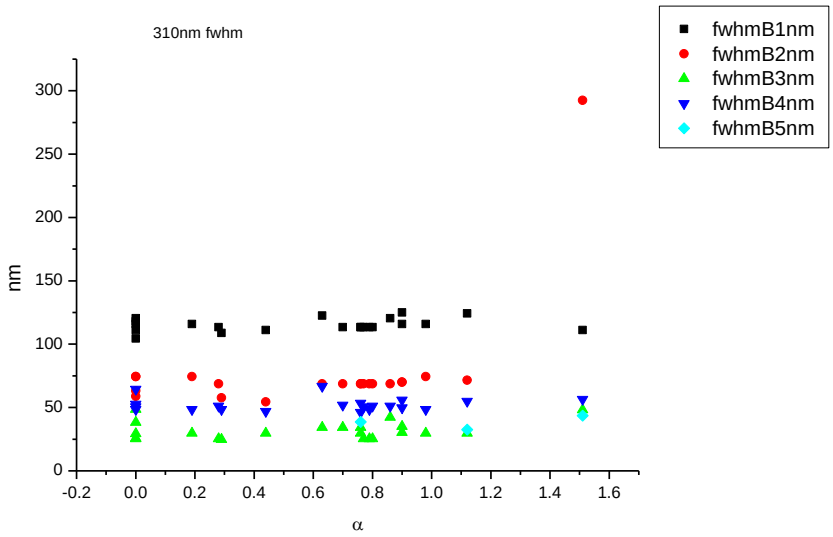

Figure 1.3.8. Full width half maxima from Gaussian model fit of the normalised fluorescence emission spectra of **9a** recorded at 310 nm excitation against α.

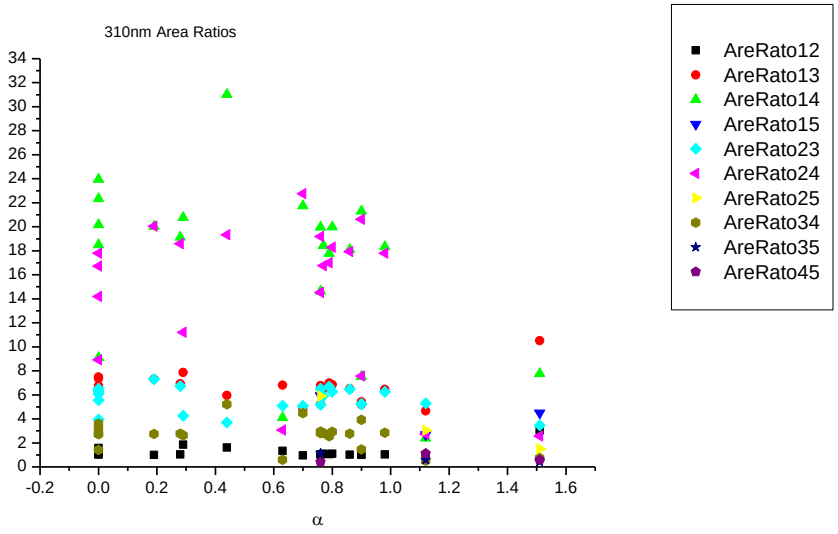

Figure 1.3.9. Area Ratios from Gaussian model fit of the normalised fluorescence emission spectra of **9a** recorded at 310 nm excitation against α.

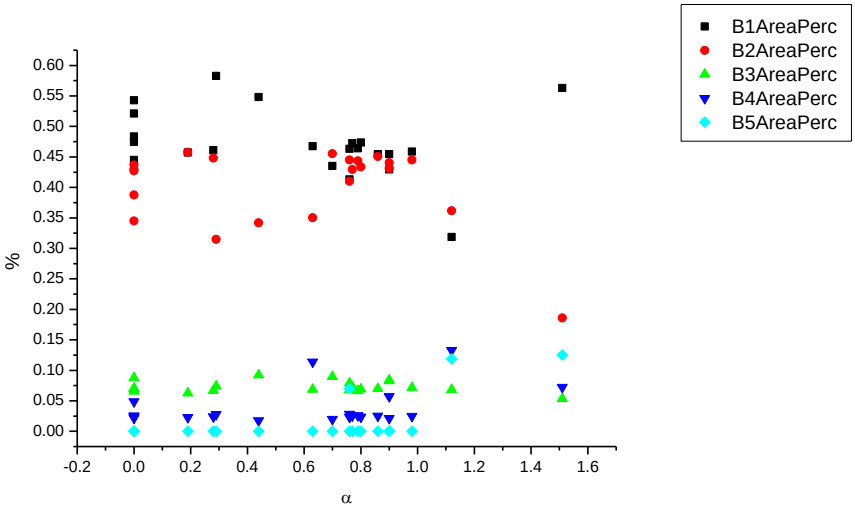

Figure 1.3.10. Area percentages from Gaussian model fit of the normalised fluorescence emission spectra of **9a** recorded at 310 nm excitation against α.

1.3.4.3 β.

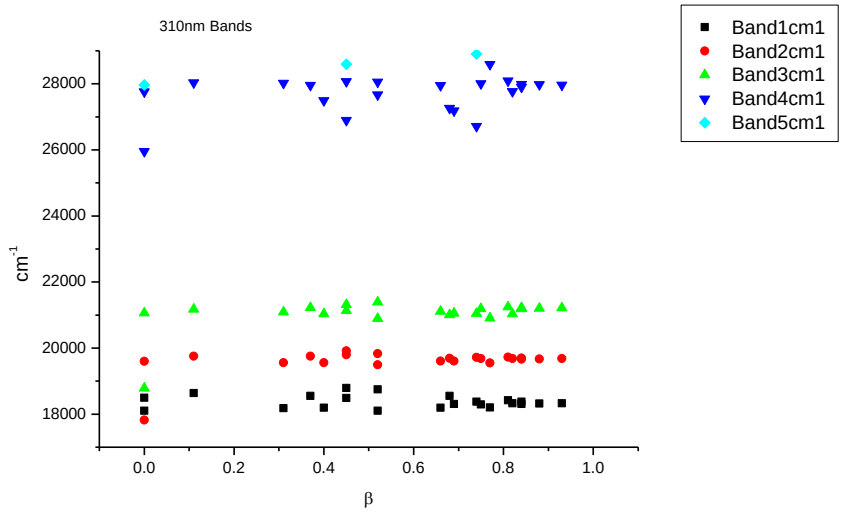

Figure 1.3.11. Band maxima from Gaussian model fit of the normalised fluorescence emission spectra of **9a** recorded at 310 nm excitation against β.

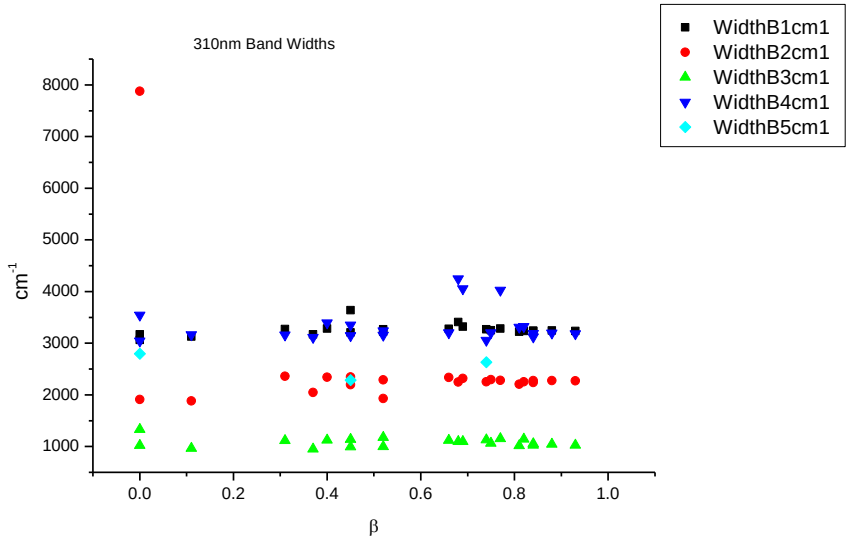

Figure 1.3.12. Band widths from Gaussian model fit of the normalised fluorescence emission spectra of **9a** recorded at 310 nm excitation against β.

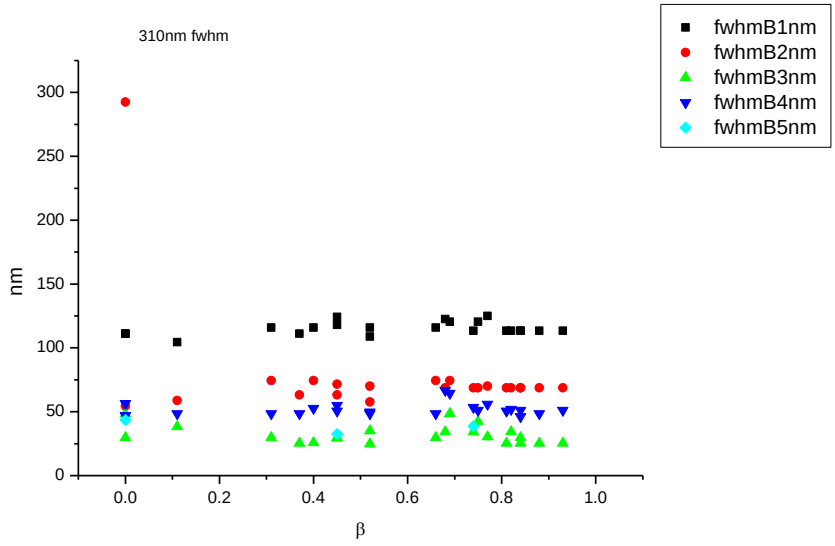

Figure 1.3.13. Full width half maxima from Gaussian model fit of the normalised fluorescence emission spectra of **9a** recorded at 310 nm excitation against β.

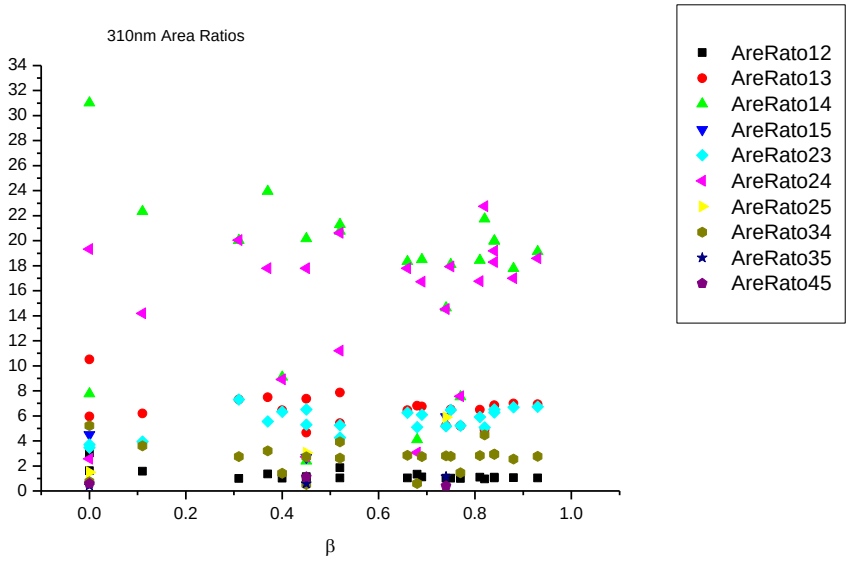

Figure 1.3.14. Area ratios from Gaussian model fit of the normalised fluorescence emission spectra of **9a** recorded at 310 nm excitation against β.

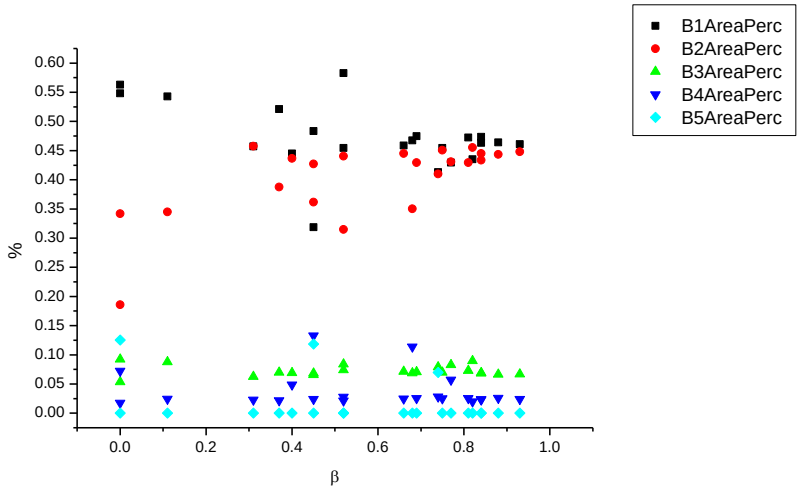

Figure 1.3.15. Area percentages from Gaussian model fit of the normalised fluorescence emission spectra of **9a** recorded at 310 nm excitation against β.

1.3.4.4 π.*

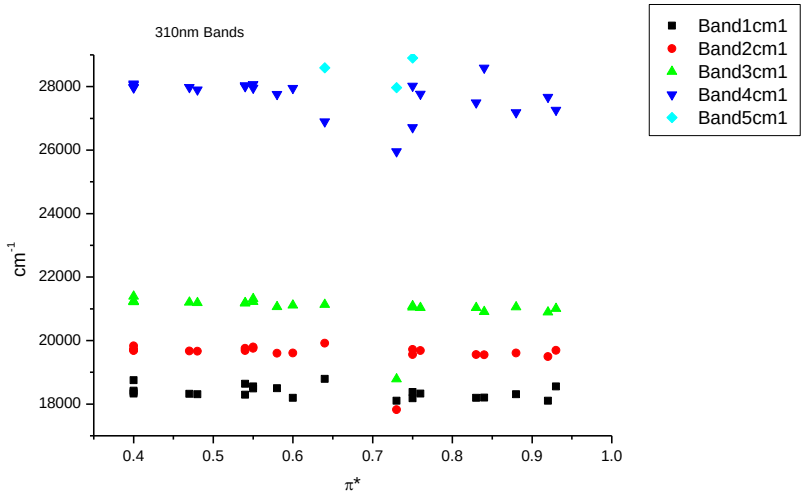

Figure 1.3.16. Band maxima from Gaussian model fit of the normalised fluorescence emission spectra of **9a** recorded at 310 nm excitation against π*.

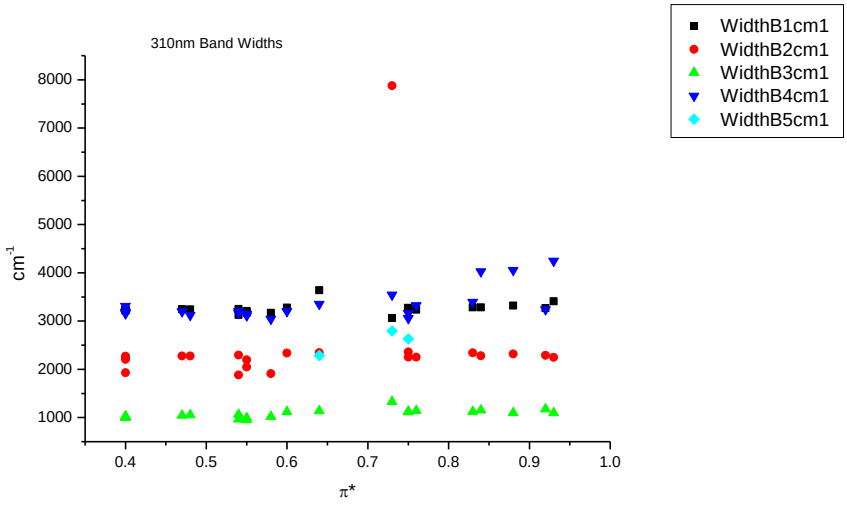

Figure 1.3.17. Band widths from Gaussian model fit of the normalised fluorescence emission spectra of **9a** recorded at 310 nm excitation against π*.

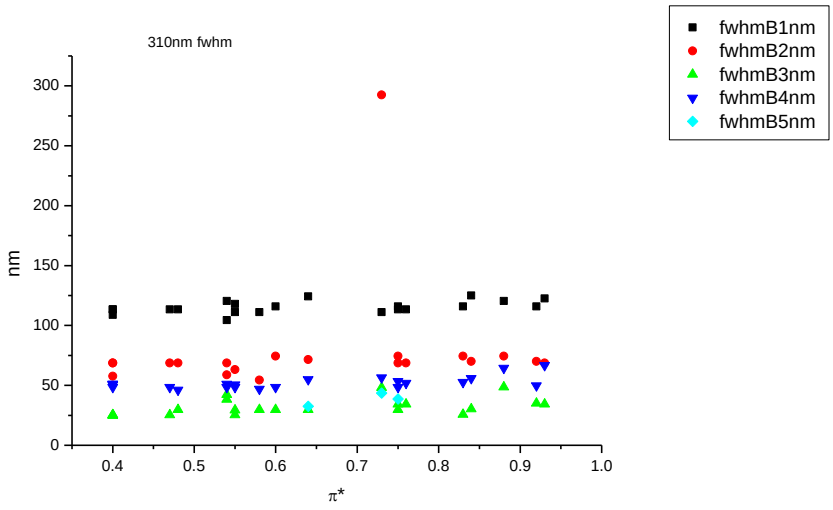

Figure 1.3.18. Full width half maxima from Gaussian model fit of the normalised fluorescence emission spectra of **9a** recorded at 310 nm excitation against π*.

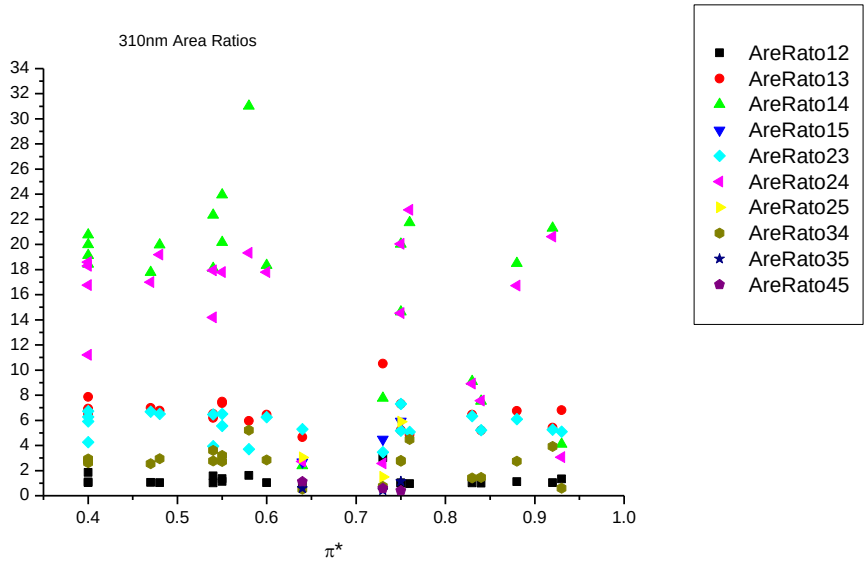

Figure 1.3.19. Area ratios from Gaussian model fit of the normalised fluorescence emission spectra of **9a** recorded at 310 nm excitation against π*.

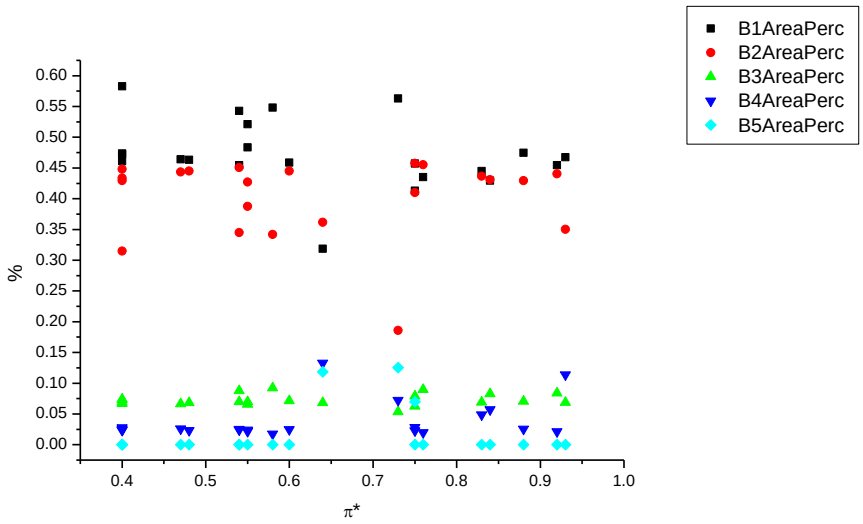

Figure 1.3.20. Area percentages from Gaussian model fit of the normalised fluorescence emission spectra of **9a** recorded at 310 nm excitation against π*.

1.3.4.5 μ(D).

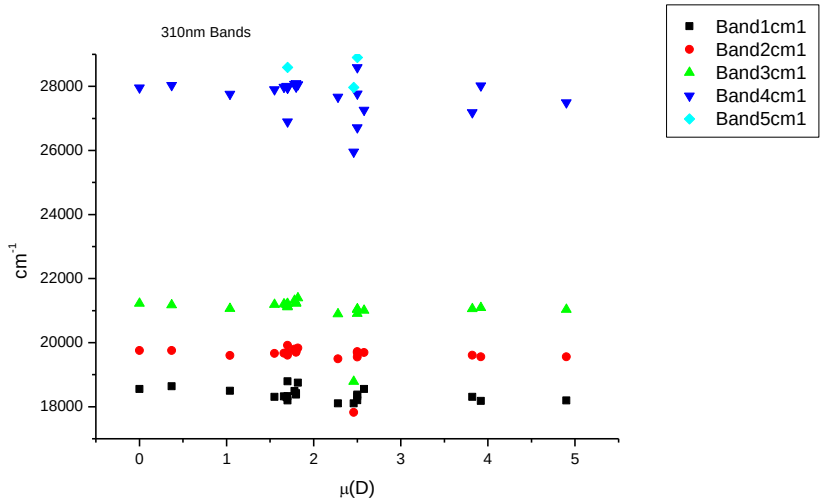

Figure 1.3.21. Band maxima from Gaussian model fit of the normalised fluorescence emission spectra of **9a** recorded at 310 nm excitation against μ(D).

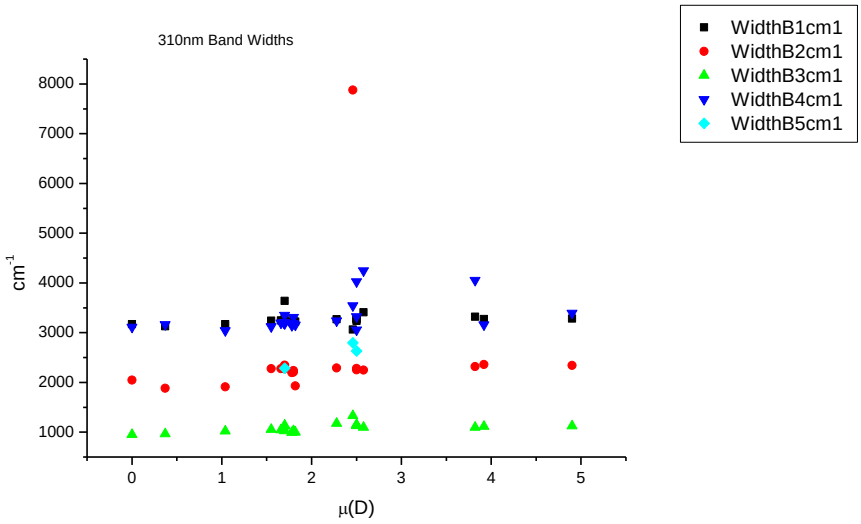

Figure 1.3.22. Band widths from Gaussian model fit of the normalised fluorescence emission spectra of **9a** recorded at 310 nm excitation against μ(D).

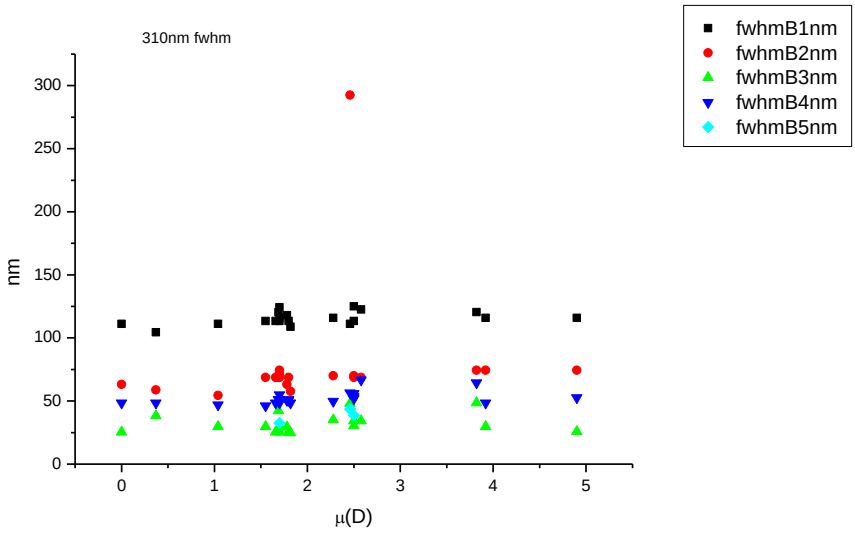

Figure 1.3.23. Full width half maxima from Gaussian model fit of the normalised fluorescence emission spectra of **9a** recorded at 310 nm excitation against μ(D).

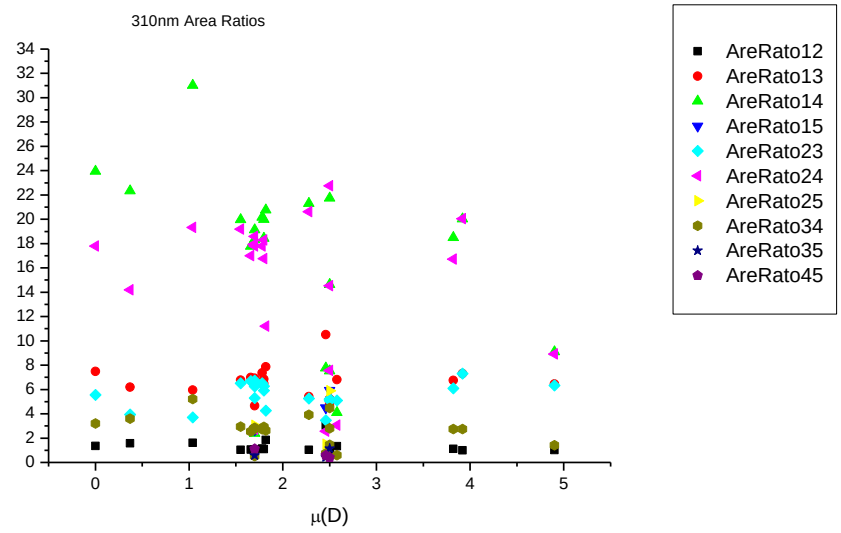

Figure 1.3.24. Area ratios from Gaussian model fit of the normalised fluorescence emission spectra of **9a** recorded at 310 nm excitation against μ(D).

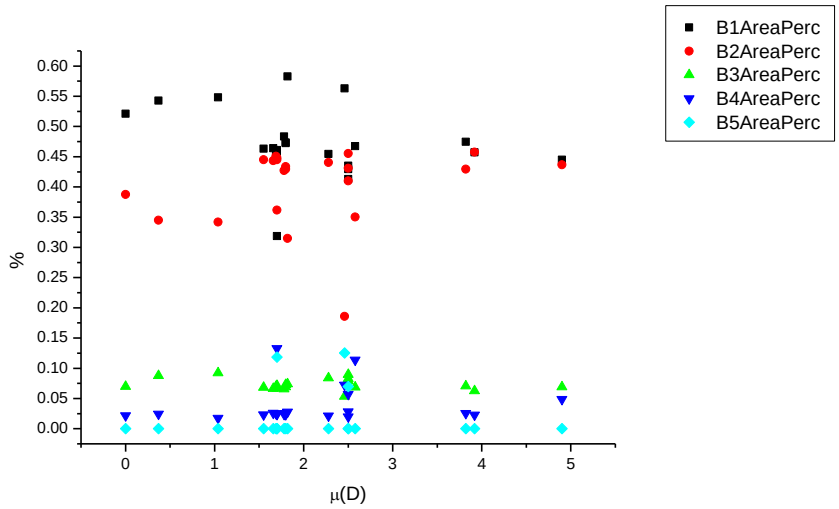

Figure 1.3.25. Area percentages from Gaussian model fit of the normalised fluorescence emission spectra of **9a** recorded at 310 nm excitation against μ(D).

1.3.4.6 η(Cp).

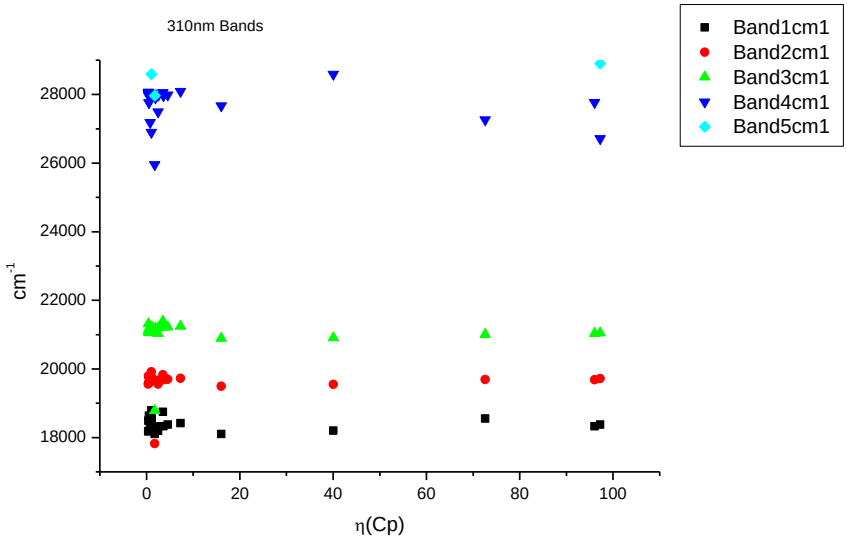

Figure 1.3.26. Band maxima from Gaussian model fit of the normalised fluorescence emission spectra of **9a** recorded at 310 nm excitation against η(Cp).

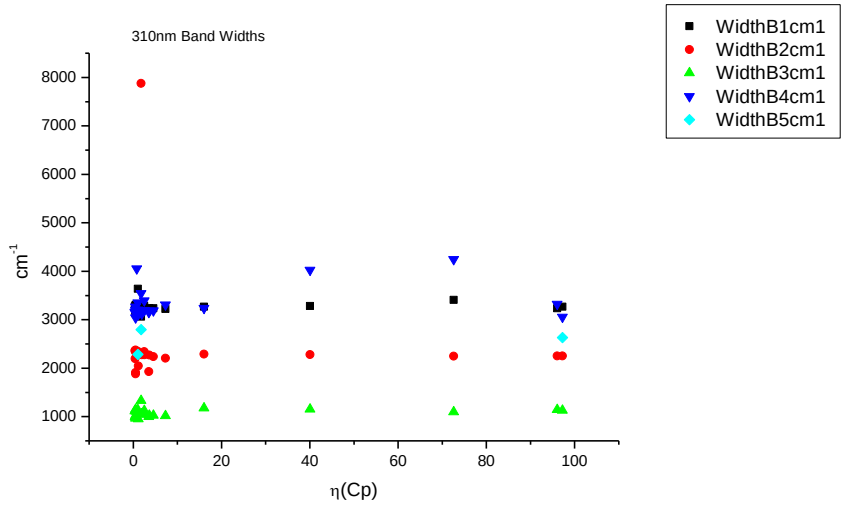

Figure 1.3.27. Band widths from Gaussian model fit of the normalised fluorescence emission spectra of **9a** recorded at 310 nm excitation against η(Cp).

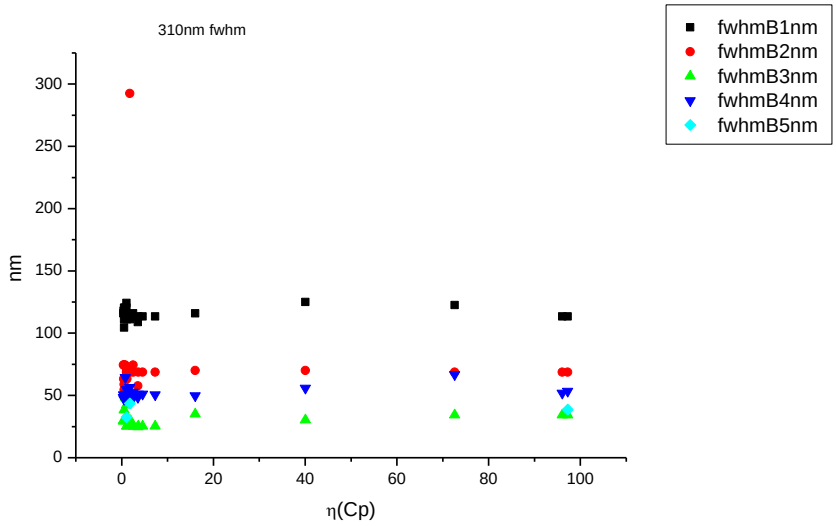

Figure 1.3.28. Full width half maxima from Gaussian model fit of the normalised fluorescence emission spectra of **9a** recorded at 310 nm excitation against η(Cp).

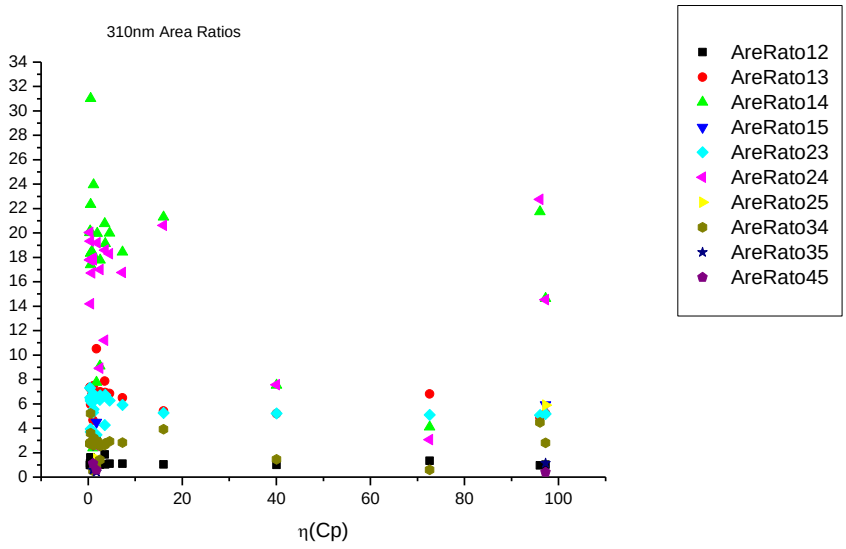

Figure 1.3.29. Area ratios from Gaussian model fit of the normalised fluorescence emission spectra of **9a** recorded at 310 nm excitation against η(Cp).

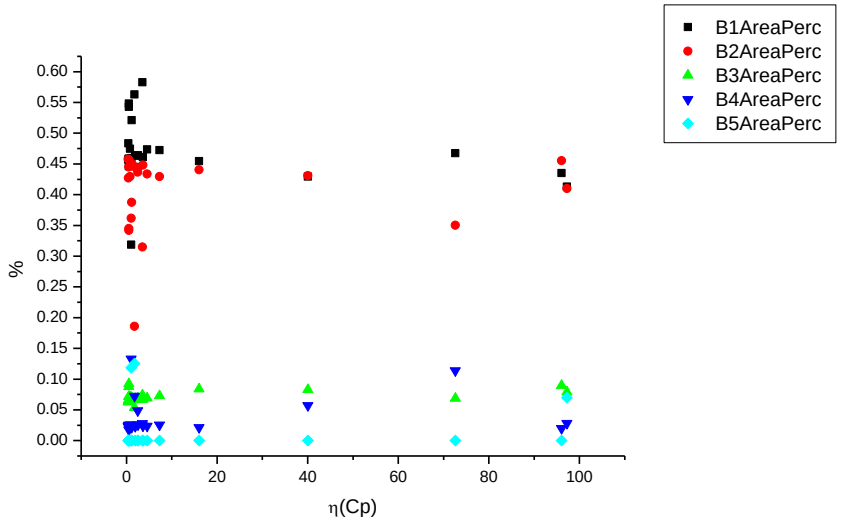

Figure 1.3.30. Area percentages from Gaussian model fit of the normalised fluorescence emission spectra of **9a** recorded at 310 nm excitation against η(Cp).

1.3.5 400 nm Gaussian band fit - Solvatochromic analysis.

1.3.5.1 E_T^N.

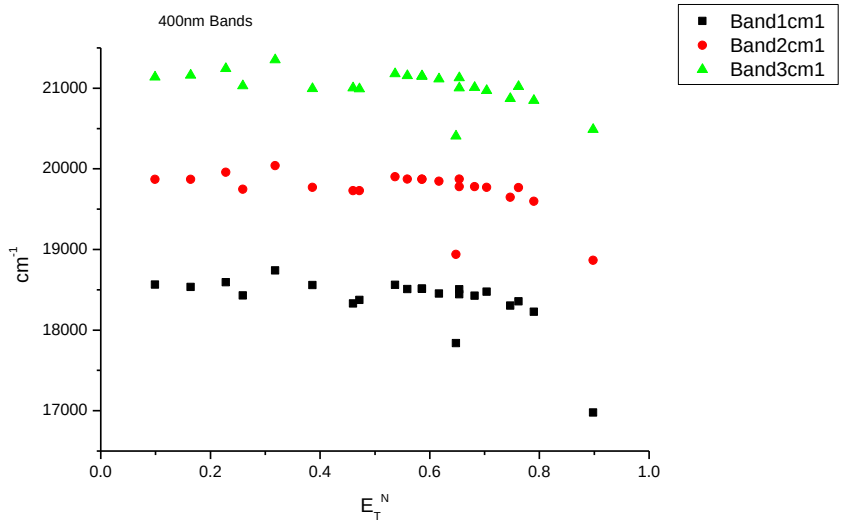

Figure 1.3.31. Band maxima from Gaussian model fit of the normalised fluorescence emission spectra of **9a** recorded at 400 nm excitation against E_T^N.

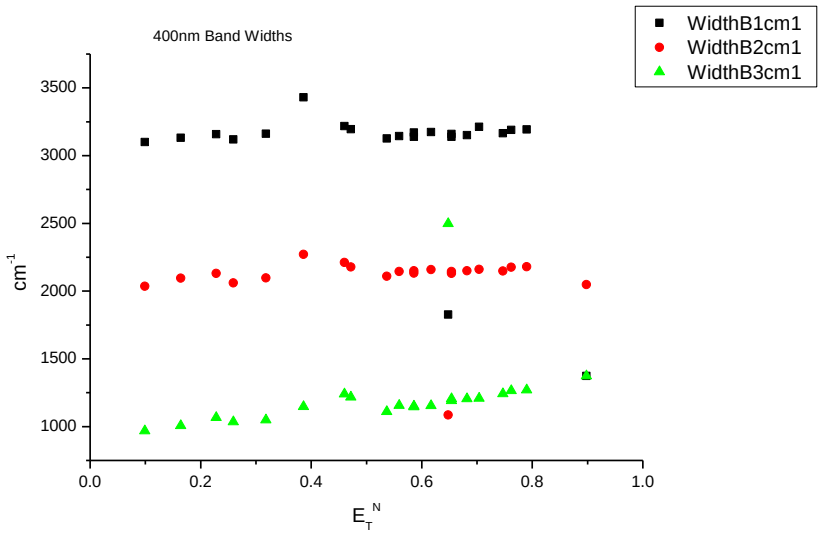

Figure 1.3.32. Band widths from Gaussian model fit of the normalised fluorescence emission spectra of **9a** recorded at 400 nm excitation against E_T^N.

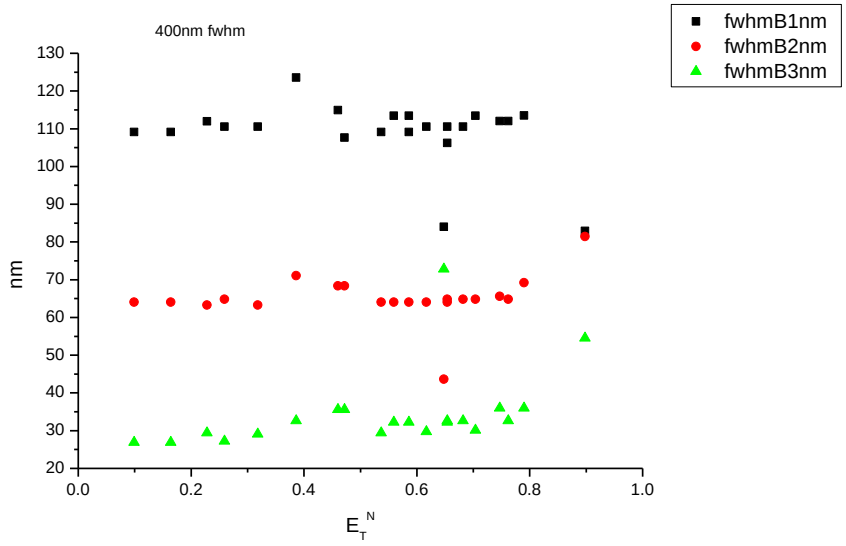

Figure 1.3.33. Full width half maxima from Gaussian model fit of the normalised fluorescence emission spectra of **9a** recorded at 400 nm excitation against E_T^N.

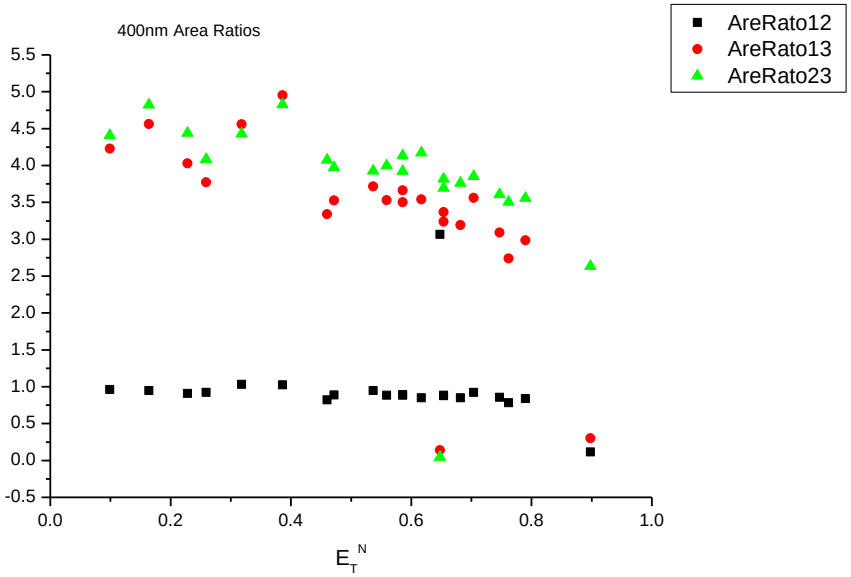

Figure 1.3.34. Area ratios from Gaussian model fit of the normalised fluorescence emission spectra of **9a** recorded at 400 nm excitation against E_T^N.

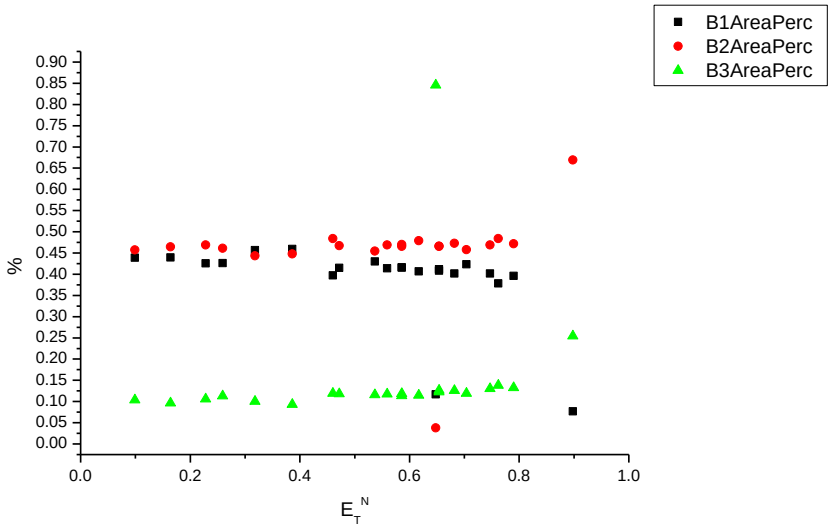

Figure 1.3.35. Area percentages from Gaussian model fit of the normalised fluorescence emission spectra of **9a** recorded at 400 nm excitation against E_T^N.

1.3.5.2 α

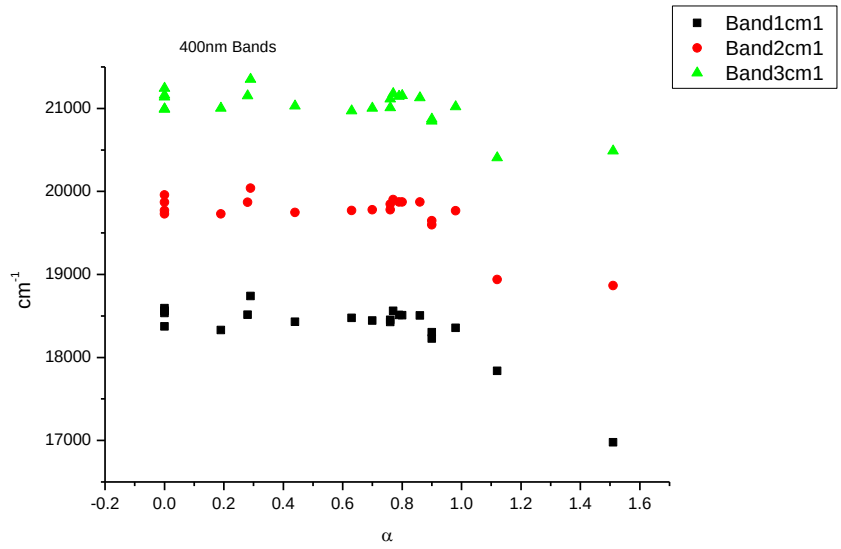

Figure 1.3.36. Band maxima from Gaussian model fit of the normalised fluorescence emission spectra of **9a** recorded at 400 nm excitation against α.

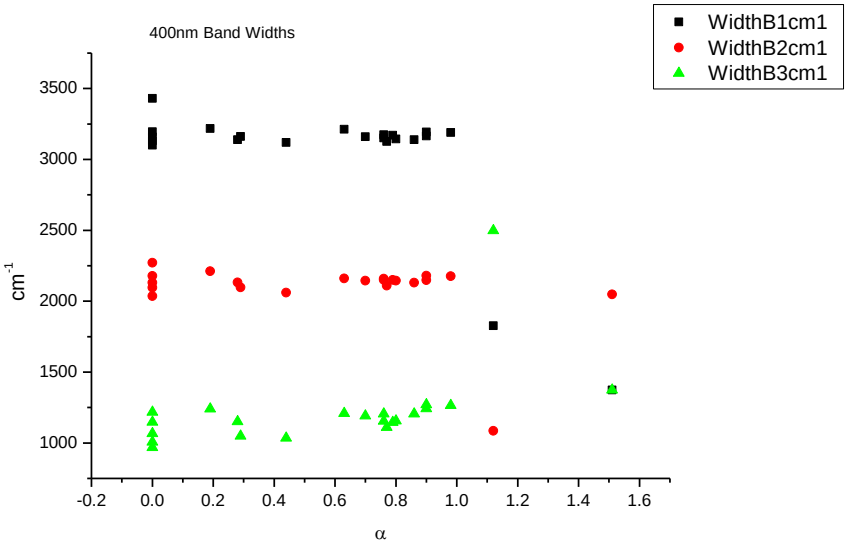

Figure 1.3.37. Band widths from Gaussian model fit of the normalised fluorescence emission spectra of **9a** recorded at 400 nm excitation against α.

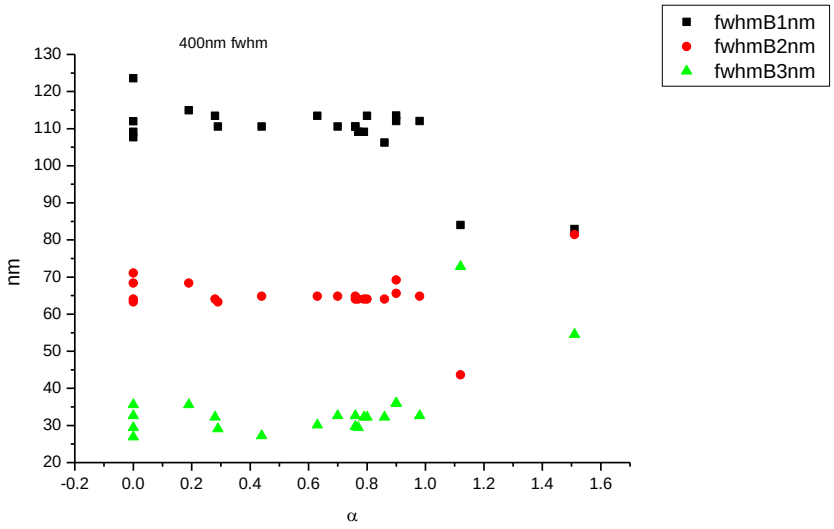

Figure 1.3.38. Full width half maxima from Gaussian model fit of the normalised fluorescence emission spectra of **9a** recorded at 400 nm excitation against α.

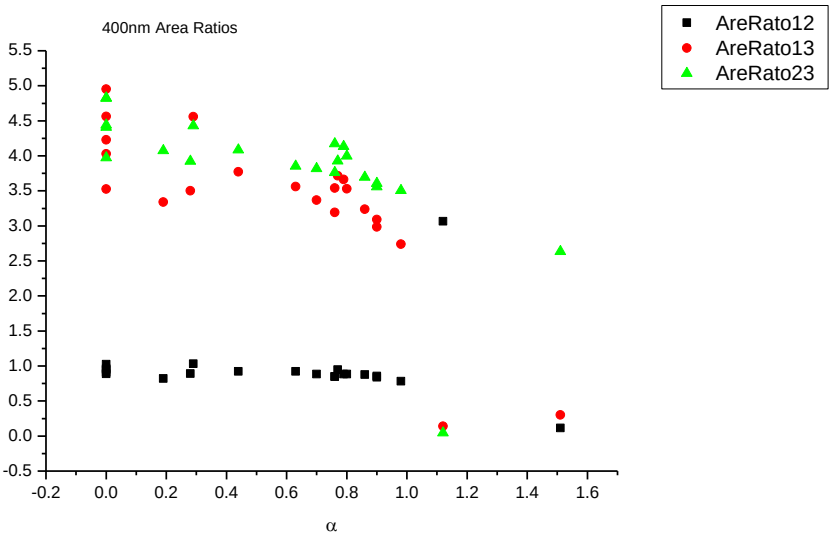

Figure 1.3.39. Area ratios from Gaussian model fit of the normalised fluorescence emission spectra of **9a** recorded at 400 nm excitation against α.

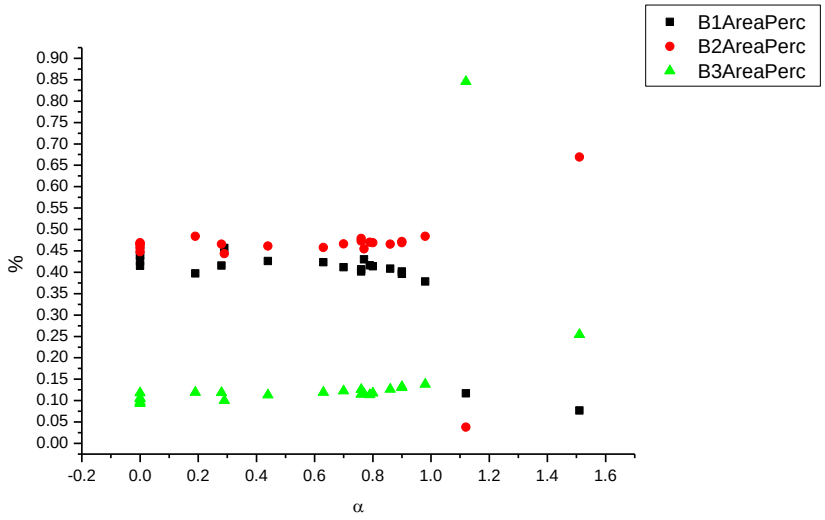

Figure 1.3.40. Area percentages from Gaussian model fit of the normalised fluorescence emission spectra of **9a** recorded at 400 nm excitation against α.

1.3.5.3 β.

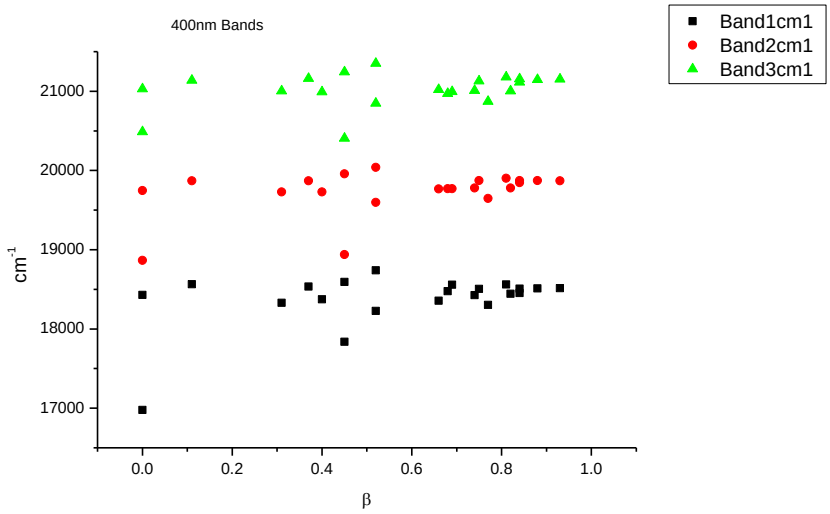

Figure 1.3.41. Band maxima from Gaussian model fit of the normalised fluorescence emission spectra of **9a** recorded at 400 nm excitation against β.

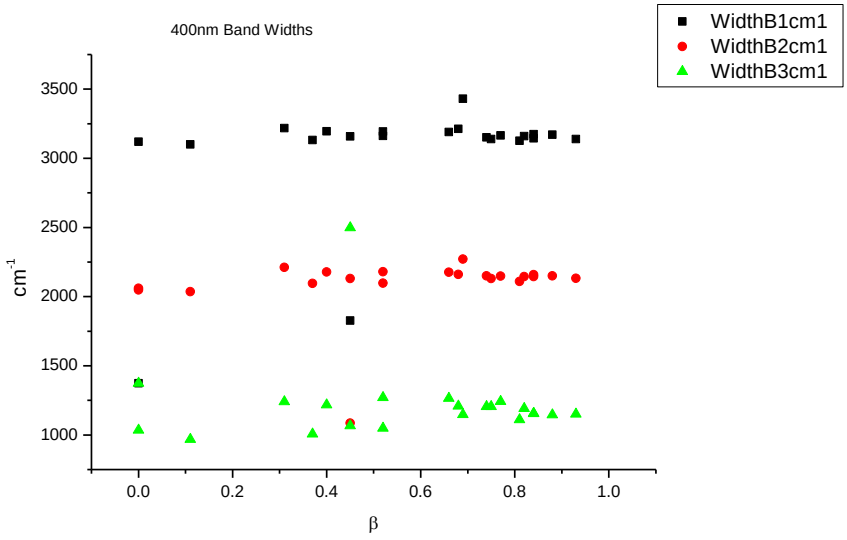

Figure 1.3.42. Band widths from Gaussian model fit of the normalised fluorescence emission spectra of **9a** recorded at 400 nm excitation against β.

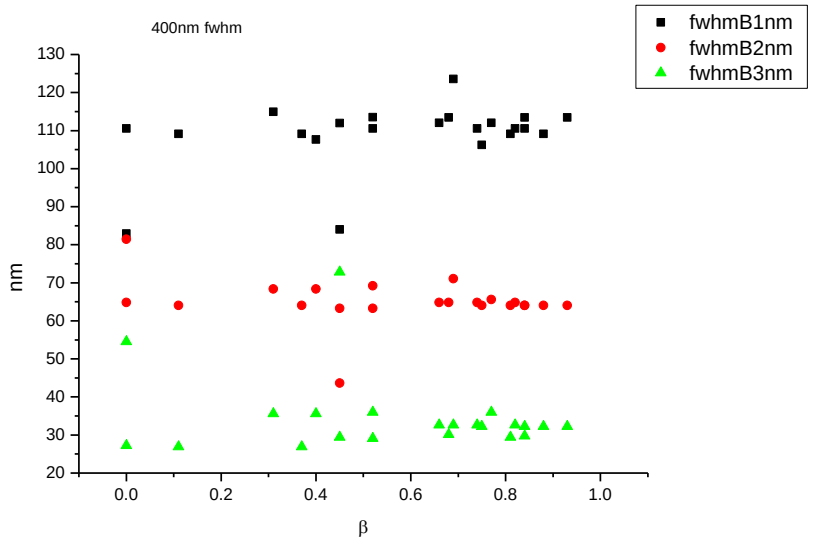

Figure 1.3.43. Full width half maxima from Gaussian model fit of the normalised fluorescence emission spectra of **9a** recorded at 400 nm excitation against β.

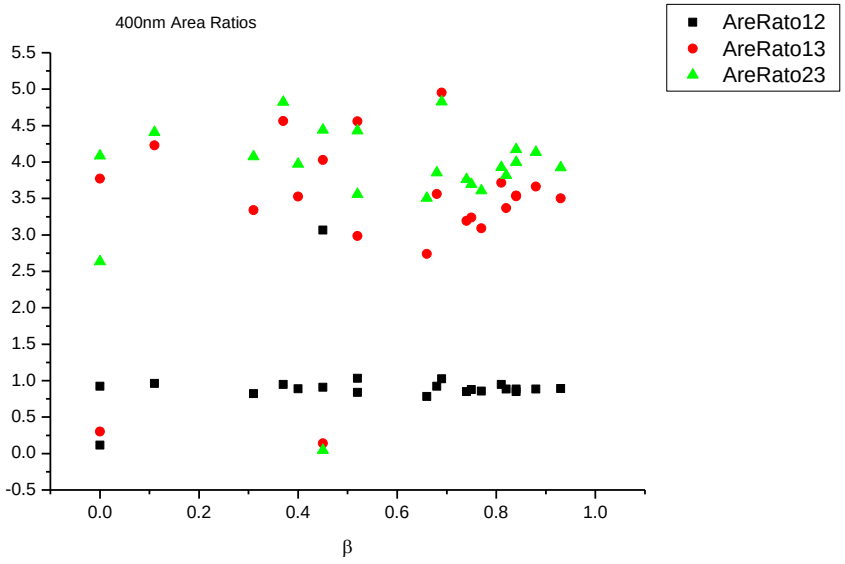

Figure 1.3.44. Area ratios from Gaussian model fit of the normalised fluorescence emission spectra of **9a** recorded at 400 nm excitation against β.

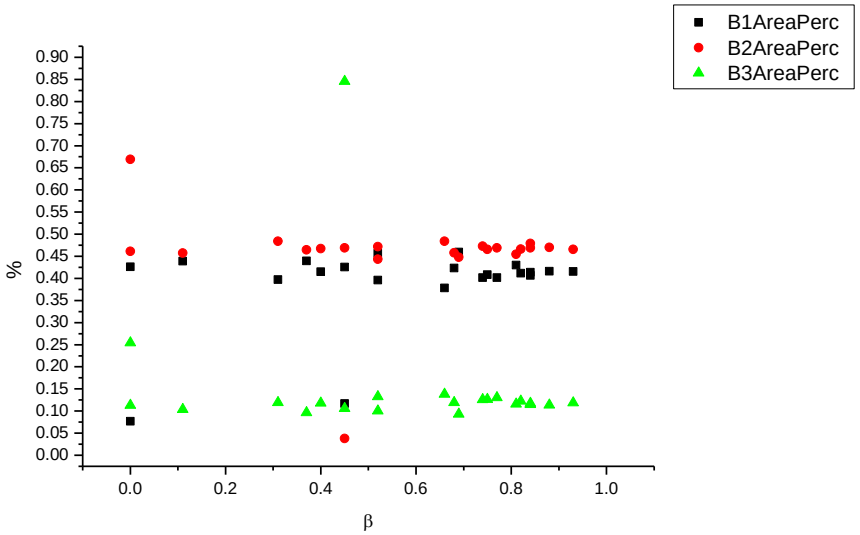

Figure 1.3.45. Area percentages from Gaussian model fit of the normalised fluorescence emission spectra of **9a** recorded at 400 nm excitation against β.

1.3.5.4 π.*

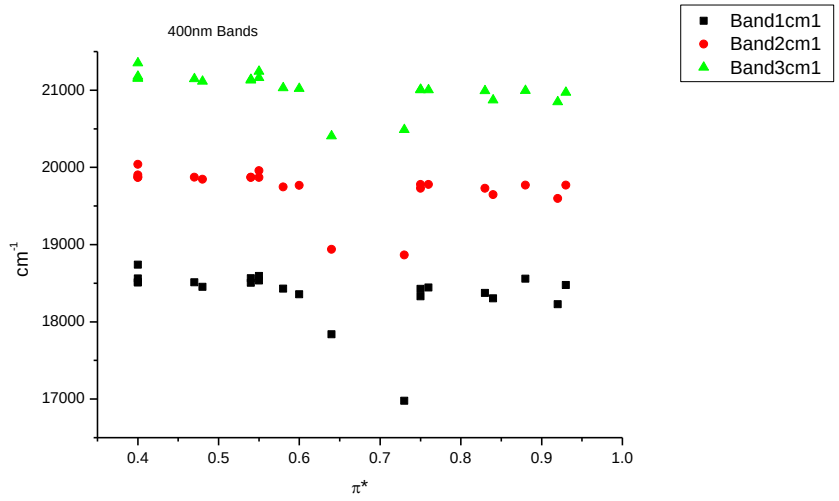

Figure 1.3.46. Band maxima from Gaussian model fit of the normalised fluorescence emission spectra of **9a** recorded at 400 nm excitation against π*.

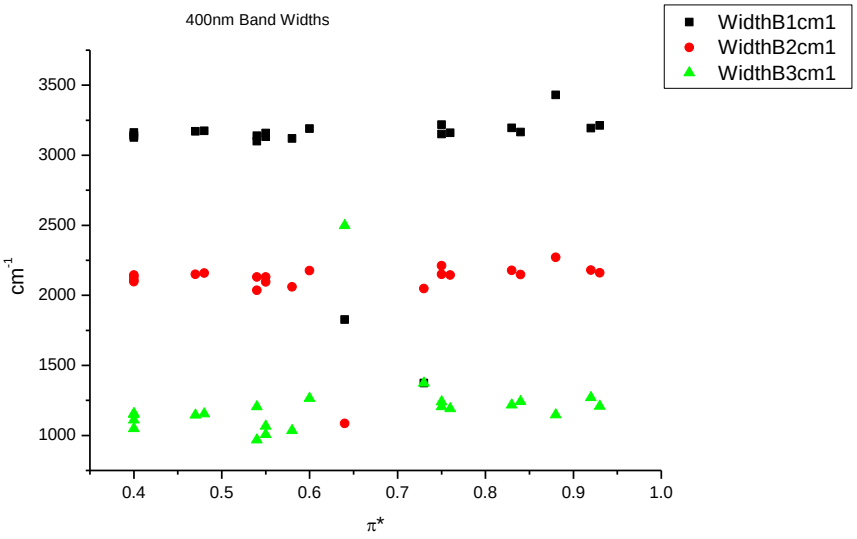

Figure 1.3.47. Band widths from Gaussian model fit of the normalised fluorescence emission spectra of **9a** recorded at 400 nm excitation against π*.

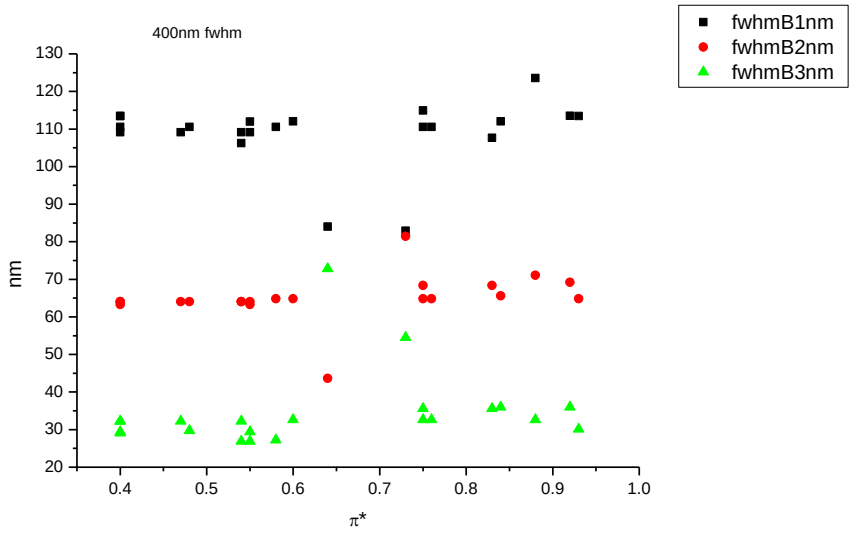

Figure 1.3.48. Full width half maxima from Gaussian model fit of the normalised fluorescence emission spectra of **9a** recorded at 400 nm excitation against π*.

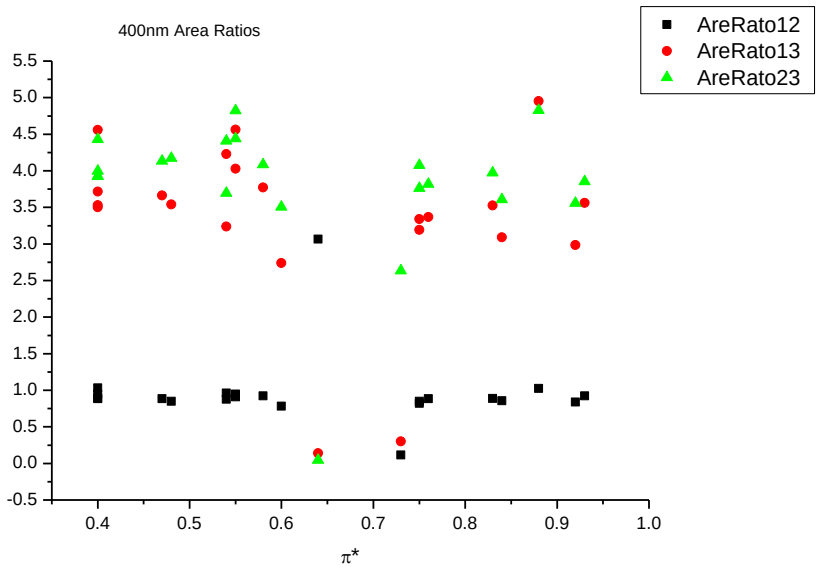

Figure 1.3.49. Area ratios from Gaussian model fit of the normalised fluorescence emission spectra of **9a** recorded at 400 nm excitation against π*.

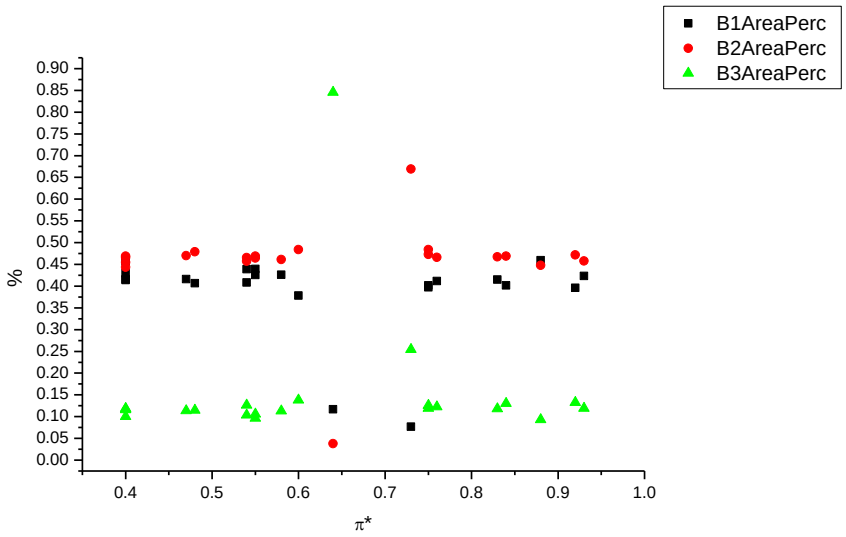

Figure 1.3.50. Area percentages from Gaussian model fit of the normalised fluorescence emission spectra of **9a** recorded at 400 nm excitation against π*.

1.3.5.5 μ(D).

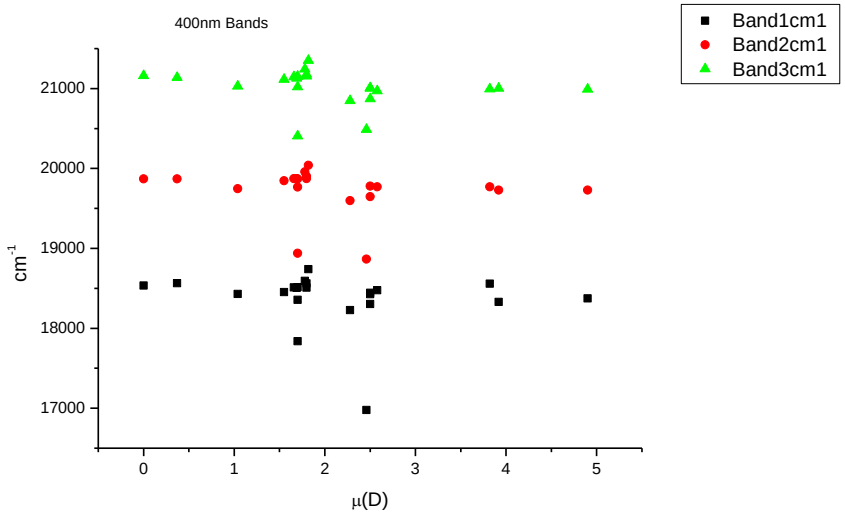

Figure 1.3.51. Band maxima from Gaussian model fit of the normalised fluorescence emission spectra of **9a** recorded at 400 nm excitation against μ(D).

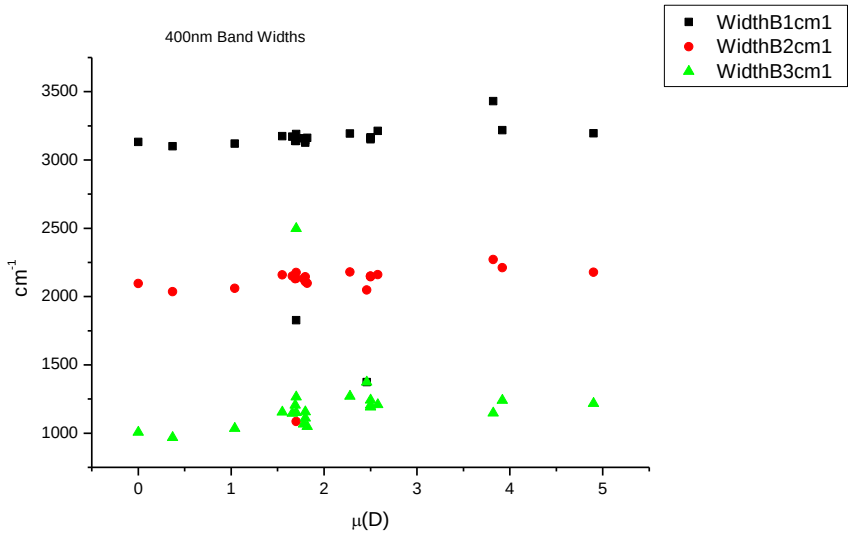

Figure 1.3.52. Band widths from Gaussian model fit of the normalised fluorescence emission spectra of **9a** recorded at 400 nm excitation against μ(D).

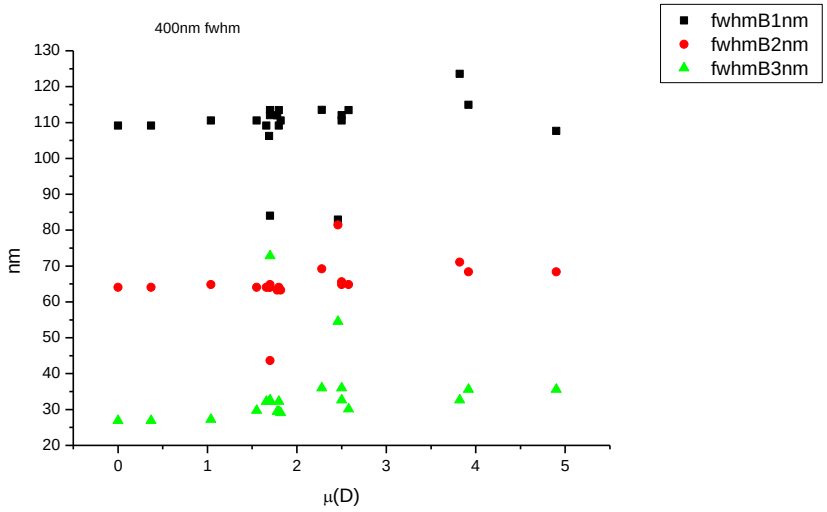

Figure 1.3.53. Full width half maxima from Gaussian model fit of the normalised fluorescence emission spectra of **9a** recorded at 400 nm excitation against μ(D).

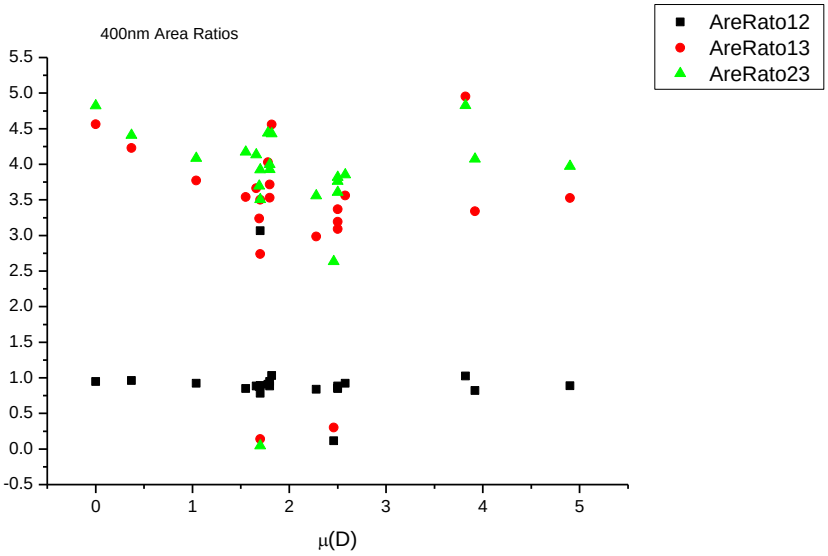

Figure 1.3.54. Area ratios from Gaussian model fit of the normalised fluorescence emission spectra of **9a** recorded at 400 nm excitation against μ(D).

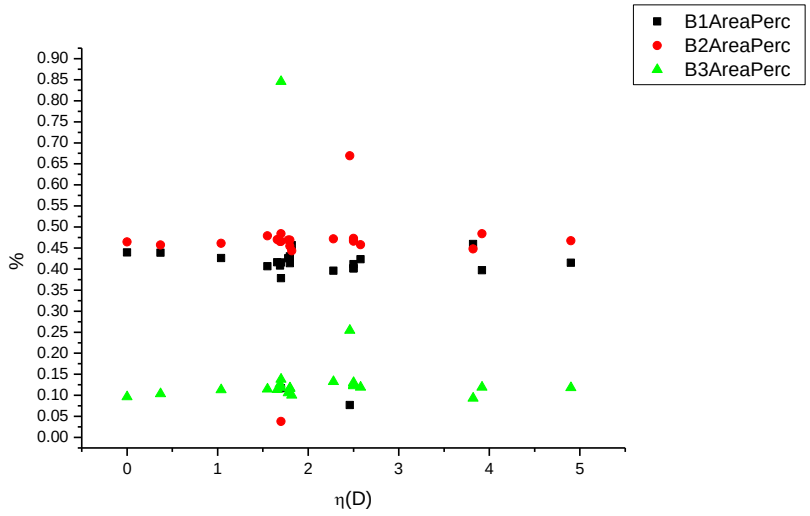

Figure 1.3.55. Area percentages from Gaussian model fit of the normalised fluorescence emission spectra of **9a** recorded at 400 nm excitation against μ(D).

1.3.5.6 η(Cp).

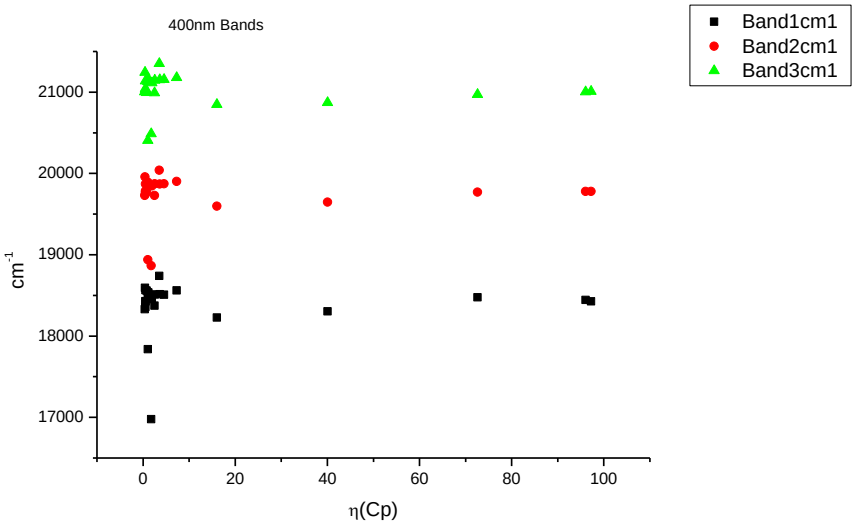

Figure 1.3.56. Band maxima from Gaussian model fit of the normalised fluorescence emission spectra of **9a** recorded at 400 nm excitation against η(Cp).

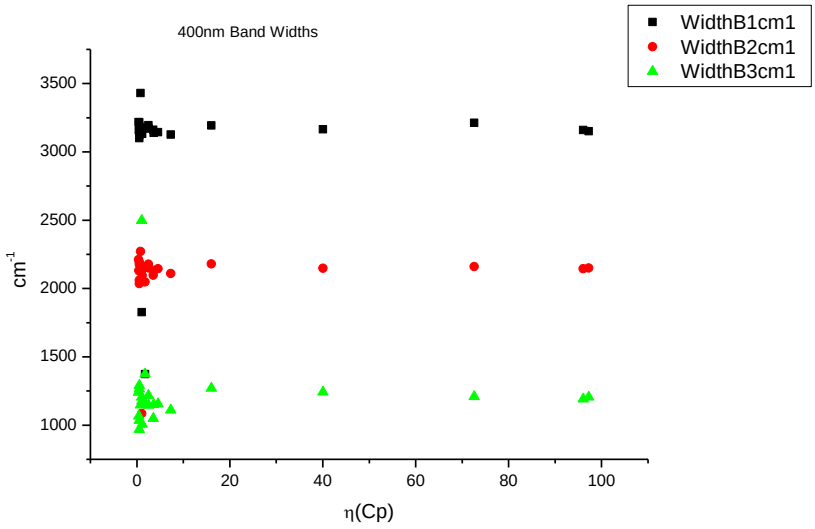

Figure 1.3.57. Band widths from Gaussian model fit of the normalised fluorescence emission spectra of **9a** recorded at 400 nm excitation against η(Cp).

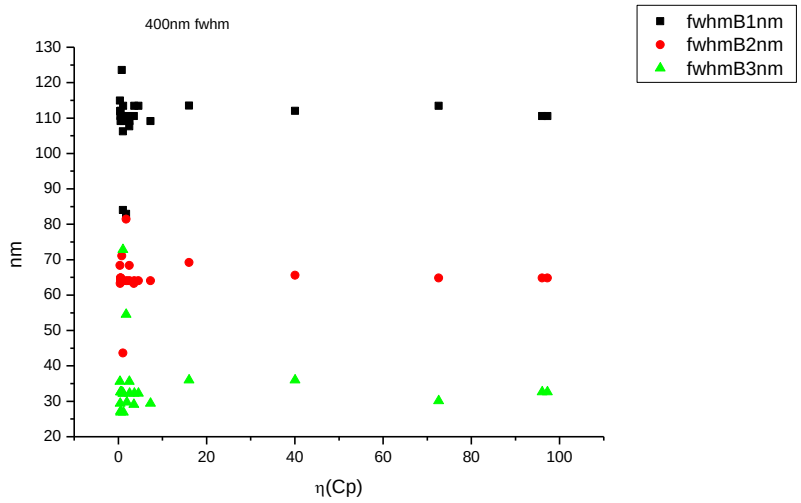

Figure 1.3.58. Full width half maxima from Gaussian model fit of the normalised fluorescence emission spectra of **9a** recorded at 400 nm excitation against η(Cp).

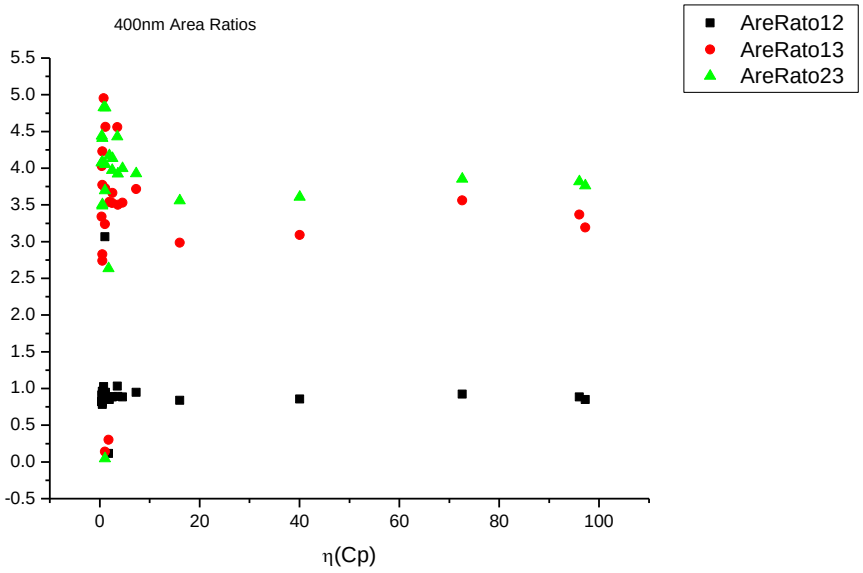

Figure 1.3.59. Area ratios from Gaussian model fit of the normalised fluorescence emission spectra of **9a** recorded at 400 nm excitation against η(Cp).

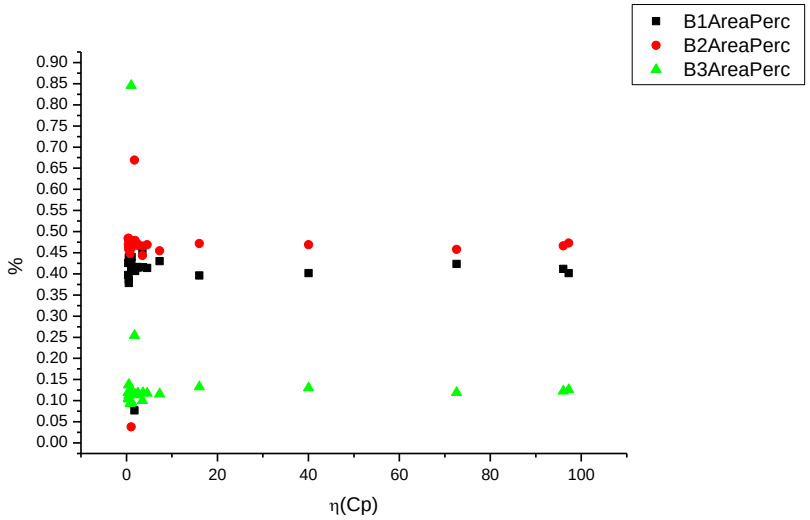

Figure 1.3.60. Area percentages from Gaussian model fit of the normalised fluorescence emission spectra of **9a** recorded at 400 nm excitation against η(Cp).

1.3.6 400 nm fluorescent lifetime results.

1.3.6.1 Intensity weighted.

Wavelength (nm)	Solvent	τ_1 (ns)	A_1 (%)	τ_2 (ns)	A_2 (%)	τ_3 (ns)	A_3 (%)	τ_f (ns) (Intensity Weighted)	$1/\tau_f$	χ^2
470	Toluene	0.30	1.17	4.04	82.96	8.99	15.87	4.78	0.21	1.05
470	1,4-Dioxane	0.29	2.12	3.87	81.13	8.90	16.75	4.64	0.22	1.05
470	Ethyl acetate	0.34	1.74	3.55	87.77	8.84	10.49	4.05	0.25	1.10
470	Chloroform	-	-	4.12	72.95	7.32	27.05	4.99	0.20	1.08
470	2-Methyl-2-butanol	0.45	4.60	3.30	85.77	10.49	9.62	3.86	0.26	1.15
470	N,N-dimethylformamide	0.31	2.26	3.97	54.86	6.76	42.88	5.08	0.20	1.04
470	Acetonitrile	0.32	1.34	3.69	64.74	6.53	33.92	4.61	0.22	1.13
470	Propylene carbonate	0.41	1.64	4.12	62.34	7.26	36.02	5.19	0.19	1.12
470	1-Octanol	0.61	7.62	4.29	58.61	7.03	33.77	4.93	0.20	1.07
470	1-Hexanol	0.40	7.27	4.47	83.34	9.02	9.39	4.60	0.22	1.06
470	1-Butanol	0.33	3.74	4.05	60.84	5.79	35.42	4.53	0.22	1.06
470	1-Pentanol	0.39	4.85	4.38	80.49	7.44	14.65	4.64	0.22	1.12
470	1-Propanol	0.22	3.32	4.16	88.83	8.75	7.85	4.39	0.23	1.09
470	Acetic acid	0.33	31.63	1.08	59.20	2.89	9.17	1.01	0.99	0.93
470	Ethanol	0.49	4.55	3.86	18.54	7.78	76.91	6.72	0.15	1.11
470	1,5-Pentanediol	0.36	1.92	4.23	89.89	8.97	8.19	4.55	0.22	1.12
470	1,3-Butanediol	0.45	4.60	3.69	17.72	7.26	77.68	6.31	0.16	1.09
470	1,4-Butanediol	0.42	4.31	3.11	21.79	7.35	73.90	6.13	0.16	1.02
470	1,3-Propanediol	0.44	2.42	3.63	19.69	7.01	77.89	6.18	0.16	1.06
470	Methanol	0.32	1.97	4.08	89.30	7.40	8.73	4.29	0.23	1.08
470	1,2-Ethanediol	0.47	1.51	3.11	17.42	6.35	81.07	5.69	0.18	1.05
470	2,2,2-Trifluoroethanol	0.17	81.49	0.88	14.62	3.61	3.89	0.41	2.44	1.19
470	Ethanol-d	-	-	4.22	82.87	7.42	17.13	4.77	0.21	1.13
470	Methanol-d	-	-	4.05	65.22	5.96	34.78	4.71	0.21	1.11

Table 1.3.9. Summary of Time Correlated Single Photon Counting (TCSPC) fluorescent lifetimes (intensity weighted) of **9a** recorded at 470 nm.

Wavelength (nm)	Solvent	τ_1 (ns)	A_1 (%)	τ_2 (ns)	A_2 (%)	τ_3 (ns)	A_3 (%)	τ_f (ns) (Intensity Weighted)	$1/\tau_f$	χ^2
490	Toluene	-	-	3.98	72.12	8.95	27.88	5.37	0.19	1.09
490	1,4-Dioxane	0.29	1.82	4.09	74.22	10.30	23.96	5.51	0.18	1.03
490	Ethyl acetate	0.23	1.61	3.57	78.62	9.62	19.78	4.71	0.21	1.07
490	Chloroform	-	-	4.29	74.37	9.15	25.63	5.54	0.18	1.08
490	2-Methyl-2-butanol	0.42	3.29	3.30	71.35	10.21	25.36	4.96	0.20	1.10
490	N,N-dimethylformamide	0.42	1.66	4.37	68.79	8.31	29.55	5.47	0.18	1.09
490	Acetonitrile	0.27	1.28	3.86	68.29	7.89	30.43	5.04	0.20	1.12
490	Propylene carbonate	0.53	1.67	4.52	73.41	9.60	24.93	5.72	0.17	1.08
490	1-Octanol	0.77	4.82	4.74	72.91	10.14	22.27	5.75	0.17	1.09
490	1-Hexanol	0.45	4.91	4.60	79.37	10.76	15.72	5.37	0.19	1.11
490	1-Butanol	0.37	2.80	4.34	76.03	8.35	21.17	5.08	0.20	1.03
490	1-Pentanol	0.39	3.07	4.44	78.54	9.59	18.39	5.26	0.19	1.08
490	1-Propanol	0.26	2.78	4.16	82.44	9.38	14.78	4.83	0.21	1.05
490	Acetic acid	0.25	34.84	0.97	54.44	2.50	10.72	0.89	1.13	1.17
490	Ethanol	0.52	2.90	5.34	42.73	8.98	54.37	7.18	0.14	1.14
490	1,5-Pentanediol	-	-	4.15	81.87	9.30	18.13	5.08	0.20	1.15
490	1,3-Butanediol	0.45	2.52	4.47	27.66	7.89	69.82	6.76	0.15	1.13
490	1,4-Butanediol	0.49	2.76	3.63	25.17	7.85	72.07	6.59	0.15	1.09
490	1,3-Propanediol	0.70	1.77	4.55	34.89	7.83	63.34	6.56	0.15	1.03
490	Methanol	-	-	3.45	47.46	5.69	52.54	4.62	0.22	1.17
490	1,2-Ethanediol	1.69	5.65	5.62	78.04	9.52	16.31	6.04	0.17	1.10
490	2,2,2-Trifluoroethanol	0.18	78.33	0.82	16.61	4.79	5.05	0.52	1.92	0.88
490	Ethanol-d	-	-	4.39	81.03	9.31	18.97	5.32	0.19	1.12
490	Methanol-d	-	-	4.33	82.56	8.56	17.44	5.07	0.20	1.16

Table 1.3.10. Summary of Time Correlated Single Photon Counting (TCSPC) fluorescent lifetimes (intensity weighted) of **9a** recorded at 490 nm.

Wavelength (nm)	Solvent	τ_1 (ns)	A_1 (%)	τ_2 (ns)	A_2 (%)	τ_3 (ns)	A_3 (%)	τ_f (ns) (Intensity Weighted)	$1/\tau_f$	χ^2
520	Toluene	-	-	4.07	50.79	9.74	49.21	6.86	0.15	1.11
520	1,4-Dioxane	0.22	1.70	4.05	49.83	10.78	48.47	7.25	0.14	1.06
520	Ethyl acetate	0.47	0.90	3.65	60.44	11.08	38.66	6.49	0.15	1.07
520	Chloroform	-	-	4.31	53.69	11.24	46.31	7.52	0.13	1.26
520	2-Methyl-2-butanol	0.40	2.12	3.30	52.48	10.58	45.40	6.55	0.15	1.04
520	N,N-dimethylformamide	0.30	1.36	4.58	62.98	11.36	35.67	6.94	0.14	1.09
520	Acetonitrile	1.92	6.51	4.64	65.10	12.65	28.39	6.74	0.15	1.11
520	Propylene carbonate	0.52	1.47	4.59	60.66	11.71	37.87	7.23	0.14	1.03
520	1-Octanol	0.74	2.83	4.87	59.01	12.30	38.16	7.59	0.13	1.06
520	1-Hexanol	0.49	3.06	4.71	64.80	12.48	32.14	7.08	0.14	1.07
520	1-Butanol	0.34	1.81	4.49	68.55	12.05	29.65	6.66	0.15	1.11
520	1-Pentanol	0.47	1.82	4.57	66.35	12.03	31.83	6.87	0.15	1.09
520	1-Propanol	0.26	1.60	4.18	69.75	11.85	28.65	6.32	0.16	1.03
520	Acetic acid	0.20	37.09	0.74	39.97	1.72	22.94	0.77	1.31	0.98
520	Ethanol	0.52	1.20	6.20	57.69	11.95	41.11	8.50	0.12	1.15
520	1,5-Pentanediol	-	-	4.24	70.49	11.78	29.51	6.47	0.15	1.14
520	1,3-Butanediol	0.59	1.47	6.00	62.61	12.13	35.92	8.12	0.12	1.14
520	1,4-Butanediol	1.35	4.03	5.72	56.83	11.51	39.14	7.81	0.13	1.12
520	1,3-Propanediol	2.57	5.82	6.38	71.67	12.93	22.51	7.63	0.13	1.05
520	Methanol	-	-	4.07	75.79	10.14	24.41	5.56	0.18	1.10
520	1,2-Ethanediol	2.39	9.11	6.20	75.87	14.37	15.02	7.08	0.14	1.08
520	2,2,2-Trifluoroethanol	0.19	70.74	0.87	15.89	4.29	13.37	0.84	1.19	0.96
520	Ethanol-d	-	-	4.47	69.35	11.81	30.65	6.72	0.15	1.07
520	Methanol-d	-	-	4.45	77.07	11.84	22.93	6.15	0.16	1.12

Table 1.3.11. Summary of Time Correlated Single Photon Counting (TCSPC) fluorescent lifetimes (intensity weighted) of **9a** recorded at 520 nm.

Wavelength (nm)	Solvent	τ_1 (ns)	A_1 (%)	τ_2 (ns)	A_2 (%)	τ_3 (ns)	A_3 (%)	τ_f (ns) (Intensity Weighted)	$1/\tau_f$	χ^2
540	Toluene	-	-	4.00	41.11	9.69	58.89	7.35	0.14	1.10
540	1,4-Dioxane	0.26	1.14	4.06	41.52	10.88	57.35	7.93	0.13	1.02
540	Ethyl acetate	-	-	3.57	51.28	11.02	48.72	7.20	0.14	1.07
540	Chloroform	-	-	4.04	45.15	11.32	54.85	8.03	0.12	1.08
540	2-Methyl-2-butanol	0.40	1.62	3.30	44.16	10.54	54.22	7.18	0.14	0.97
540	N,N-dimethylformamide	0.33	0.96	4.55	52.85	11.69	46.19	7.81	0.13	1.09
540	Acetonitrile	0.37	1.16	4.24	57.66	12.38	41.19	7.55	0.13	1.08
540	Propylene carbonate	0.62	1.51	4.71	54.16	12.57	44.32	8.13	0.12	1.09
540	1-Octanol	0.75	2.18	4.86	49.83	12.25	47.99	8.32	0.12	1.07
540	1-Hexanol	0.45	2.45	4.66	56.58	12.51	40.97	7.77	0.13	1.10
540	1-Butanol	0.40	1.67	4.57	62.06	12.38	36.27	7.33	0.14	1.07
540	1-Pentanol	0.52	1.55	4.62	59.68	12.55	38.77	7.63	0.13	1.16
540	1-Propanol	0.25	1.36	4.24	63.39	12.33	35.24	7.03	0.14	1.06
540	Acetic acid	0.23	43.93	0.93	44.90	2.20	11.18	0.77	1.31	1.19
540	Ethanol	-	-	6.13	49.22	12.24	50.78	9.23	0.11	1.22
540	1,5-Pentanediol	-	-	4.22	63.06	12.13	36.94	7.14	0.14	1.06
540	1,3-Butanediol	1.21	1.18	6.51	63.44	13.84	35.38	9.04	0.11	1.07
540	1,4-Butanediol	2.20	6.42	6.54	60.11	13.38	33.47	8.55	0.12	1.14
540	1,3-Propanediol	3.47	9.73	6.69	63.35	13.44	26.93	8.19	0.12	1.10
540	Methanol	0.36	1.11	4.24	72.86	11.79	26.03	6.16	0.16	1.08
540	1,2-Ethanediol	2.66	10.82	6.35	66.80	13.83	22.38	7.62	0.13	1.14
540	2,2,2-Trifluoroethanol	0.20	65.96	1.05	15.92	4.44	18.14	1.10	0.91	1.06
540	Ethanol-d	-	-	4.52	63.86	12.54	36.14	7.42	0.13	1.09
540	Methanol-d	-	-	4.52	72.68	12.91	27.32	6.81	0.15	1.09

Table 1.3.12. Summary of Time Correlated Single Photon Counting (TCSPC) fluorescent lifetimes (intensity weighted) of **9a** recorded at 540 nm.

Wavelength (nm)	Solvent	τ_1 (ns)	A_1 (%)	τ_2 (ns)	A_2 (%)	τ_3 (ns)	A_3 (%)	τ_f (ns) (Intensity Weighted)	$1/\tau_f$	χ^2
570	Toluene	-	-	3.93	27.94	9.71	72.06	8.10	0.12	1.08
570	1,4-Dioxane	0.22	1.16	4.11	30.30	11.06	68.54	8.83	0.11	1.07
570	Ethyl acetate	0.26	1.11	3.67	40.43	11.28	58.46	8.08	0.12	1.05
570	Chloroform	-	-	4.42	36.13	11.80	63.87	9.13	0.11	1.07
570	2-Methyl-2-butanol	0.43	2.09	3.34	34.01	10.67	63.90	7.96	0.13	1.07
570	N,N-dimethylformamide	0.43	1.38	4.66	43.31	12.35	55.32	8.85	0.11	1.03
570	Acetonitrile	0.75	1.32	4.32	47.52	12.83	51.16	8.63	0.12	1.11
570	Propylene carbonate	0.59	1.36	4.76	43.54	12.86	55.10	9.16	0.11	1.08
570	1-Octanol	0.98	1.98	4.99	39.54	12.59	58.47	9.35	0.11	1.06
570	1-Hexanol	0.28	3.58	4.52	42.95	12.30	53.47	8.53	0.12	1.07
570	1-Butanol	0.37	1.42	4.57	52.16	12.60	46.42	8.24	0.12	1.10
570	1-Pentanol	0.48	1.26	4.58	48.49	12.54	50.24	8.53	0.12	1.07
570	1-Propanol	-	-	4.11	52.55	12.34	47.45	8.02	0.12	1.16
570	Acetic acid	0.19	43.22	0.76	39.54	1.76	17.24	0.69	1.46	1.09
570	Ethanol	-	-	6.90	51.21	13.66	48.79	10.20	0.10	1.12
570	1,5-Pentanediol	-	-	4.20	53.63	12.52	46.37	8.06	0.12	1.13
570	1,3-Butanediol	-	-	6.50	52.94	13.86	47.06	9.96	0.10	1.10
570	1,4-Butanediol	3.06	9.01	7.04	52.66	14.16	38.33	9.41	0.11	1.14
570	1,3-Propanediol	3.95	8.27	6.52	53.90	13.43	37.82	8.92	0.11	1.13
570	Methanol	0.24	1.24	4.27	66.84	12.68	31.93	6.90	0.14	1.09
570	1,2-Ethanediol	2.91	10.96	6.38	56.91	13.64	32.13	8.34	0.12	1.10
570	2,2,2-Trifluoroethanol	0.21	57.34	0.99	16.04	4.30	26.62	1.43	0.70	1.05
570	Ethanol-d	-	-	4.53	54.98	12.92	45.02	8.31	0.12	1.10
570	Methanol-d	-	-	4.57	65.69	13.59	34.31	7.66	0.13	1.09

Table 1.3.13. Summary of Time Correlated Single Photon Counting (TCSPC) fluorescent lifetimes (intensity weighted) of **9a** recorded at 570 nm.

1.3.6.2 Amplitude weighted.

Wavelength (nm)	Solvent	τ_1 (ns)	A_1 (%)	τ_2 (ns)	A_2 (%)	τ_3 (ns)	A_3 (%)	τ_f (ns) (Amplitude Weighted)	$1/\tau_f$	χ^2
470	Toluene	0.30	15.03	4.04	78.25	8.99	6.72	3.81	0.26	1.05
470	1,4-Dioxane	0.29	24.28	3.87	69.48	8.90	6.24	3.32	0.30	1.05
470	Ethyl acetate	0.34	16.51	3.55	79.66	8.84	3.83	3.22	0.31	1.10
470	Chloroform	-	-	4.12	82.73	7.32	17.27	4.67	0.21	1.08
470	2-Methyl-2-butanol	0.45	27.58	3.30	69.95	10.49	2.47	2.69	0.37	1.15
470	N,N-dimethylformamide	0.31	26.37	3.97	50.46	6.76	23.16	3.65	0.27	1.04
470	Acetonitrile	0.32	15.62	3.69	65.07	6.53	19.30	3.71	0.27	1.13
470	Propylene carbonate	0.41	16.49	4.12	62.87	7.26	20.65	4.16	0.24	1.12
470	1-Octanol	0.61	40.30	4.29	44.18	7.03	15.52	3.23	0.31	1.07
470	1-Hexanol	0.40	48.27	4.47	48.99	9.02	2.74	2.63	0.38	1.06
470	1-Butanol	0.33	35.25	4.38	56.16	7.44	6.02	3.06	0.33	1.12
470	1-Pentanol	0.39	37.82	4.05	46.04	5.79	18.72	3.06	0.33	1.06
470	1-Propanol	0.22	40.36	4.16	57.23	8.75	2.41	2.68	0.37	1.09
470	Acetic acid	0.33	62.54	1.08	35.41	2.89	2.06	0.65	1.54	0.93
470	Ethanol	0.49	38.81	3.86	20.01	7.78	41.18	4.16	0.24	1.11
470	1,5-Pentanediol	0.36	19.37	4.23	77.31	8.97	3.32	3.64	0.27	1.12
470	1,3-Butanediol	0.45	39.67	3.69	18.68	7.26	41.64	3.89	0.26	1.09
470	1,4-Butanediol	0.42	37.43	3.11	25.59	7.35	36.88	3.67	0.27	1.02
470	1,3-Propanediol	0.44	25.19	3.63	24.53	7.01	50.29	4.52	0.22	1.06
470	Methanol	0.32	21.13	4.08	74.48	7.40	4.03	3.42	0.29	1.08
470	1,2-Ethanediol	0.47	14.91	3.11	25.95	6.35	59.14	4.63	0.22	1.05
470	2,2,2-Trifluoroethanol	0.17	96.32	0.88	3.45	3.61	0.22	0.21	4.76	1.19
470	Ethanol-d	-	-	4.22	89.49	7.42	10.51	4.56	0.22	1.13
470	Methanol-d	-	-	4.05	73.42	5.96	26.58	4.56	0.22	1.11

Table 1.3.14. Summary of Time Correlated Single Photon Counting (TCSPC) fluorescent lifetimes (amplitude weighted) of **9a** recorded at 470 nm.

Wavelength (nm)	Solvent	τ_1 (ns)	A_1 (%)	τ_2 (ns)	A_2 (%)	τ_3 (ns)	A_3 (%)	τ_f (ns) (Amplitude Weighted)	$1/\tau_f$	χ^2
490	Toluene	-	-	3.98	85.33	8.95	14.67	4.71	0.21	1.09
490	1,4-Dioxane	0.29	23.22	4.09	68.07	10.30	8.71	3.75	0.27	1.03
490	Ethyl acetate	0.23	22.15	3.57	71.20	9.62	6.65	3.23	0.31	1.07
490	Chloroform	-	-	4.29	86.10	9.15	13.90	4.96	0.20	1.08
490	2-Methyl-2-butanol	0.42	24.40	3.30	67.81	10.21	7.79	3.13	0.32	1.10
490	N,N-dimethylformamide	0.42	16.96	4.37	67.74	8.31	15.29	4.30	0.23	1.09
490	Acetonitrile	0.27	17.82	3.86	67.48	7.89	14.70	3.81	0.26	1.12
490	Propylene carbonate	0.53	14.20	4.52	73.98	9.60	11.83	4.55	0.22	1.08
490	1-Octanol	0.77	26.31	4.74	64.49	10.14	9.20	4.19	0.24	1.09
490	1-Hexanol	0.45	36.97	4.60	58.11	10.76	4.92	3.37	0.30	1.11
490	1-Butanol	0.37	27.22	4.44	64.37	9.59	6.97	3.64	0.27	1.08
490	1-Pentanol	0.39	28.66	4.34	63.58	8.35	9.21	3.63	0.28	1.03
490	1-Propanol	0.26	33.18	4.16	61.89	9.38	4.93	3.13	0.32	1.05
490	Acetic acid	0.25	69.69	0.97	28.15	2.50	2.16	0.50	1.99	1.17
490	Ethanol	0.52	28.57	5.34	40.65	8.98	30.78	5.08	0.20	1.14
490	1,5-Pentanediol	-	-	4.15	91.02	9.30	8.98	4.61	0.22	1.15
490	1,3-Butanediol	0.45	27.25	4.47	29.94	7.89	42.81	4.84	0.21	1.13
490	1,4-Butanediol	0.49	25.90	3.63	31.92	7.85	42.18	4.60	0.22	1.09
490	1,3-Propanediol	0.70	13.82	4.55	41.93	7.83	44.25	5.47	0.18	1.03
490	Methanol	-	-	3.45	59.86	5.69	40.14	4.34	0.23	1.17
490	1,2-Ethanediol	1.69	17.65	5.62	73.30	9.52	9.04	5.28	0.19	1.10
490	2,2,2-Trifluoroethanol	0.18	95.26	0.82	4.50	4.79	0.23	0.22	4.50	0.88
490	Ethanol-d	-	-	4.39	90.07	9.31	9.93	4.88	0.20	1.12
490	Methanol-d	-	-	4.33	90.34	8.56	9.66	4.74	0.21	1.16

Table 1.3.15. Summary of Time Correlated Single Photon Counting (TCSPC) fluorescent lifetimes (amplitude weighted) of **9a** recorded at 490 nm.

Wavelength (nm)	Solvent	τ_1 (ns)	A_1 (%)	τ_2 (ns)	A_2 (%)	τ_3 (ns)	A_3 (%)	τ_f (ns) (Amplitude Weighted)	$1/\tau_f$	χ^2
520	Toluene	-	-	4.07	71.16	9.74	28.84	5.71	0.18	1.11
520	1,4-Dioxane	0.22	31.91	4.05	49.86	10.78	18.23	4.05	0.25	1.06
520	Ethyl acetate	0.47	8.83	3.65	75.30	11.08	15.87	4.55	0.22	1.07
520	Chloroform	-	-	4.31	75.13	11.24	24.87	6.04	0.17	1.26
520	2-Methyl-2-butanol	0.40	20.78	3.30	62.38	10.58	16.85	3.93	0.25	1.04
520	N,N-dimethylformamide	0.30	21.22	4.58	64.13	11.36	14.65	4.66	0.21	1.09
520	Acetonitrile	1.92	17.27	4.64	71.32	12.65	11.41	5.09	0.20	1.11
520	Propylene carbonate	0.52	14.57	4.59	68.62	11.71	16.81	5.19	0.19	1.03
520	1-Octanol	0.74	20.02	4.87	63.37	12.30	16.31	5.26	0.19	1.06
520	1-Hexanol	0.49	27.67	4.71	60.94	12.48	11.40	4.43	0.23	1.07
520	1-Butanol	0.34	23.06	4.57	68.91	12.03	12.54	4.74	0.21	1.09
520	1-Pentanol	0.47	18.54	4.49	66.26	12.05	10.68	4.34	0.23	1.11
520	1-Propanol	0.26	24.14	4.18	66.26	11.85	9.60	3.97	0.25	1.03
520	Acetic acid	0.20	73.33	0.74	21.36	1.72	5.31	0.40	2.52	0.98
520	Ethanol	0.52	15.42	6.20	61.74	11.95	22.84	6.64	0.15	1.15
520	1,5-Pentanediol	-	-	4.24	86.89	11.78	13.11	5.23	0.19	1.14
520	1,3-Butanediol	0.59	15.72	6.00	65.66	12.13	18.62	6.29	0.16	1.14
520	1,4-Butanediol	1.35	18.29	5.72	60.89	11.51	20.83	6.13	0.16	1.12
520	1,3-Propanediol	2.57	14.86	6.38	73.72	12.93	11.42	6.56	0.15	1.05
520	Methanol	-	-	4.07	88.51	10.14	11.49	4.77	0.21	1.10
520	1,2-Ethanediol	2.39	22.33	6.20	71.56	14.37	6.12	5.85	0.17	1.08
520	2,2,2-Trifluoroethanol	0.19	94.66	0.87	4.56	4.29	0.78	0.25	4.00	0.96
520	Ethanol-d	-	-	4.47	85.67	11.81	14.33	5.52	0.18	1.07
520	Methanol-d	-	-	4.45	89.93	11.84	10.07	5.20	0.19	1.12

Table 1.3.16. Summary of Time Correlated Single Photon Counting (TCSPC) fluorescent lifetimes (amplitude weighted) of **9a** recorded at 520 nm.

Wavelength (nm)	Solvent	τ_1 (ns)	A_1 (%)	τ_2 (ns)	A_2 (%)	τ_3 (ns)	A_3 (%)	τ_f (ns) (Amplitude Weighted)	$1/\tau_f$	χ^2
540	Toluene	-	-	4.00	62.84	9.69	37.16	6.12	0.16	1.10
540	1,4-Dioxane	0.26	21.95	4.06	51.52	10.88	26.53	5.03	0.20	1.02
540	Ethyl acetate	-	-	3.57	76.44	11.02	23.56	5.33	0.19	1.07
540	Chloroform	-	-	4.04	69.76	11.32	30.24	6.24	0.16	1.08
540	2-Methyl-2-butanol	0.40	17.89	3.30	59.32	10.54	22.79	4.43	0.23	0.97
540	N,N-dimethylformamide	0.33	15.83	4.55	62.82	11.69	21.36	5.40	0.19	1.09
540	Acetonitrile	0.37	15.65	4.24	67.78	12.38	16.58	4.98	0.20	1.08
540	Propylene carbonate	0.62	13.99	4.71	65.81	12.57	20.20	5.73	0.17	1.09
540	1-Octanol	0.75	17.05	4.86	60.01	12.25	22.93	5.85	0.17	1.07
540	1-Hexanol	0.45	26.03	4.66	58.28	12.51	15.70	4.79	0.21	1.10
540	1-Butanol	0.40	20.16	4.62	68.00	12.55	16.25	5.26	0.19	1.16
540	1-Pentanol	0.52	15.75	4.57	65.68	12.38	14.16	4.83	0.21	1.07
540	1-Propanol	0.25	23.31	4.24	64.39	12.33	12.30	4.30	0.23	1.06
540	Acetic acid	0.23	77.91	0.93	20.00	2.20	2.09	0.41	2.42	1.19
540	Ethanol	-	-	6.13	65.94	12.24	34.06	8.21	0.12	1.22
540	1,5-Pentanediol	-	-	4.22	83.06	12.13	16.94	5.56	0.18	1.06
540	1,3-Butanediol	1.21	7.33	6.51	73.43	13.84	19.24	7.53	0.13	1.07
540	1,4-Butanediol	2.20	19.98	6.54	62.89	13.38	17.13	6.85	0.15	1.14
540	1,3-Propanediol	3.47	19.64	6.69	66.33	13.44	14.03	7.01	0.14	1.10
540	Methanol	0.36	13.86	4.24	76.34	11.79	9.79	4.44	0.23	1.08
540	1,2-Ethanediol	2.66	25.08	6.35	64.93	13.83	9.99	6.17	0.16	1.14
540	2,2,2-Trifluoroethanol	0.20	94.54	1.05	4.30	4.44	1.16	0.28	3.52	1.06
540	Ethanol-d	-	-	4.52	83.08	12.54	16.92	5.87	0.17	1.09
540	Methanol-d	-	-	4.52	88.37	12.91	11.63	5.50	0.18	1.09

Table 1.3.17. Summary of Time Correlated Single Photon Counting (TCSPC) fluorescent lifetimes (amplitude weighted) of **9a** recorded at 540 nm.

Wavelength (nm)	Solvent	τ_1 (ns)	A_1 (%)	τ_2 (ns)	A_2 (%)	τ_3 (ns)	A_3 (%)	τ_f (ns) (Amplitude Weighted)	$1/\tau_f$	χ^2
570	Toluene	-	-	3.93	48.93	9.71	51.07	6.88	0.15	1.08
570	1,4-Dioxane	0.22	28.12	4.11	39.04	11.06	32.84	5.30	0.19	1.07
570	Ethyl acetate	0.26	20.70	3.67	53.96	11.28	25.35	4.89	0.20	1.05
570	Chloroform	-	-	4.42	60.14	11.80	39.86	7.36	0.14	1.07
570	2-Methyl-2-butanol	0.43	23.15	3.34	48.37	10.67	28.48	4.75	0.21	1.07
570	N,N-dimethylformamide	0.43	18.75	4.66	54.84	12.35	26.41	5.90	0.17	1.03
570	Acetonitrile	0.75	10.42	4.32	65.74	12.83	23.84	5.98	0.17	1.11
570	Propylene carbonate	0.59	14.57	4.76	58.20	12.86	27.23	6.36	0.16	1.08
570	1-Octanol	0.98	13.90	4.99	54.28	12.59	31.83	6.85	0.15	1.06
570	1-Hexanol	0.28	48.40	4.52	35.40	12.30	16.20	3.73	0.27	1.07
570	1-Butanol	0.37	20.24	4.58	61.46	12.54	23.24	5.80	0.17	1.07
570	1-Pentanol	0.48	15.30	4.57	60.29	12.60	19.48	5.29	0.19	1.10
570	1-Propanol	-	-	4.11	76.87	12.34	23.13	6.01	0.17	1.16
570	Acetic acid	0.19	78.67	0.76	17.94	1.76	3.38	0.35	2.89	1.09
570	Ethanol	-	-	6.90	67.53	13.66	32.47	9.09	0.11	1.12
570	1,5-Pentanediol	-	-	4.20	77.50	12.52	22.50	6.07	0.16	1.13
570	1,3-Butanediol	-	-	6.50	70.60	13.86	29.40	8.67	0.12	1.10
570	1,4-Butanediol	3.06	22.45	7.04	56.94	14.16	20.61	7.61	0.13	1.14
570	1,3-Propanediol	3.95	15.88	6.52	62.76	13.43	21.36	7.59	0.13	1.13
570	Methanol	0.24	22.11	4.27	67.11	12.68	10.78	4.28	0.23	1.09
570	1,2-Ethanediol	2.91	25.09	6.38	59.26	13.64	15.65	6.65	0.15	1.10
570	2,2,2-Trifluoroethanol	0.21	92.33	0.99	5.55	4.30	2.12	0.34	2.92	1.05
570	Ethanol-d	-	-	4.53	77.69	12.92	22.31	6.40	0.16	1.10
570	Methanol-d	-	-	4.57	85.07	13.59	14.93	5.91	0.17	1.09

Table 1.3.18. Summary of Time Correlated Single Photon Counting (TCSPC) fluorescent lifetimes (amplitude weighted) of **9a** recorded at 570 nm.

1.3.7 Average fluorescent lifetimes - Solvatochromic analysis.

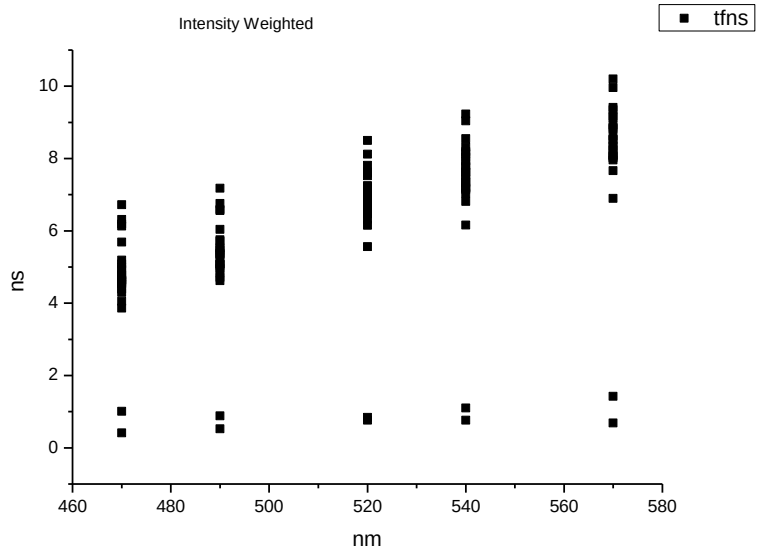

Figure 1.3.61. Intensity weighted average lifetime (τ_f) of **9a** versus wavelength (nm).

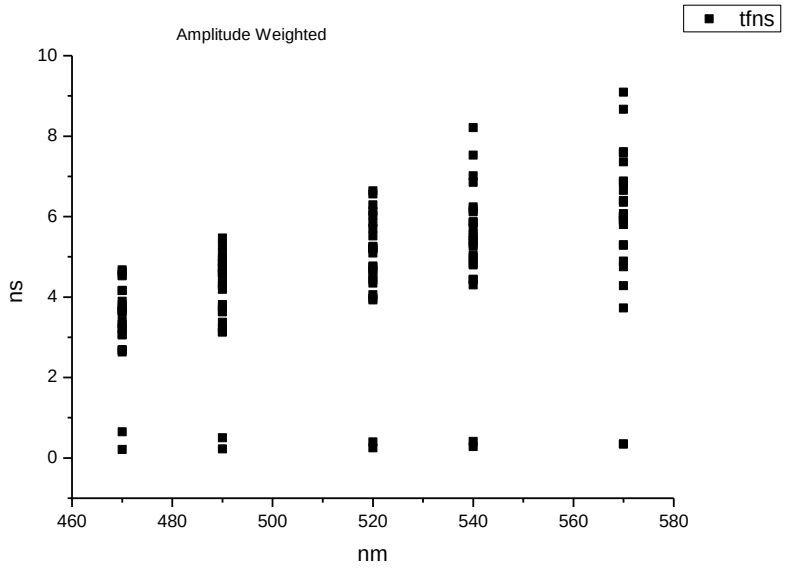

Figure 1.3.62. Amplitude weighted average lifetime (τ_f) of **9a** versus wavelength (nm).

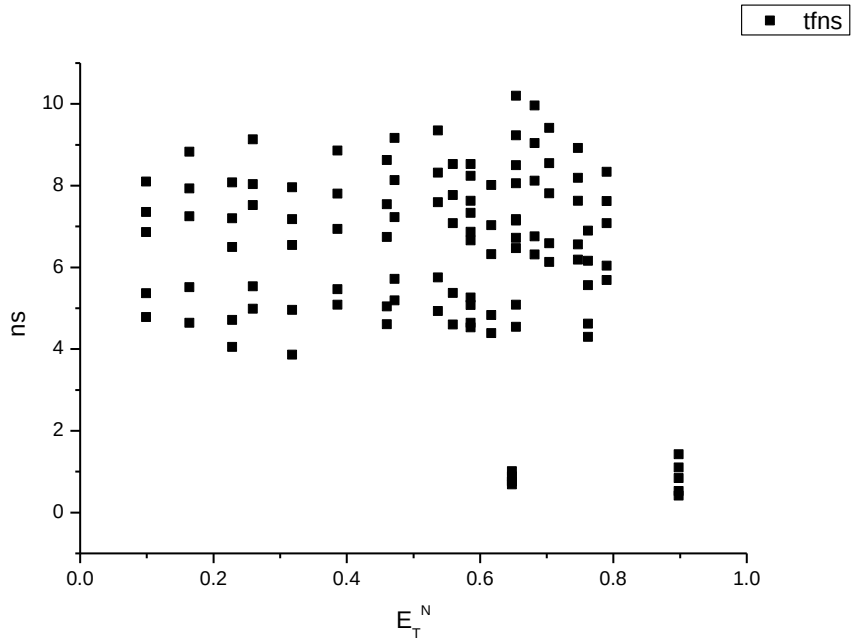

Figure 1.3.63. Intensity weighted average lifetime (τ_f) of **9a** versus E_T^N.

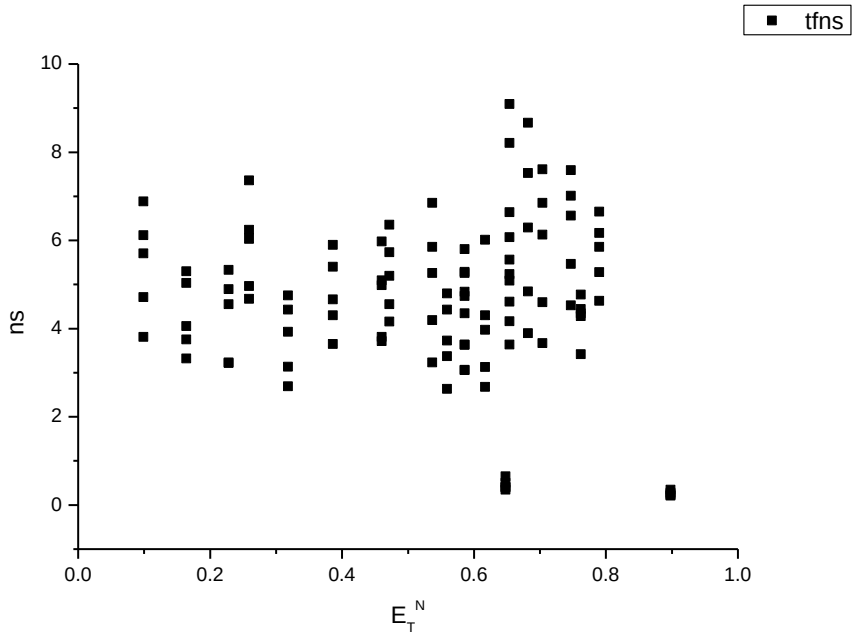

Figure 1.3.64. Amplitude weighted average lifetime (τ_f) of **9a** versus E_T^N.

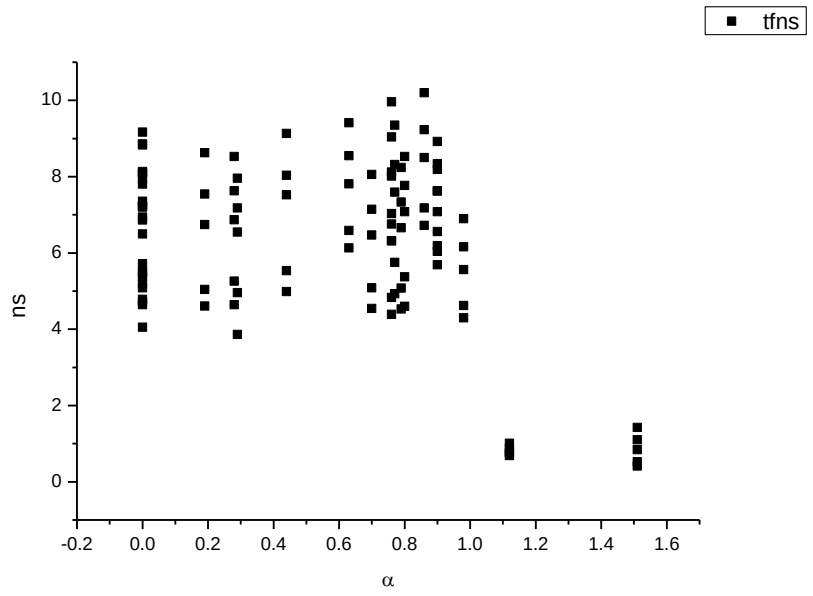

Figure 1.3.65. Intensity weighted average lifetime (τ_f) of **9a** versus α.

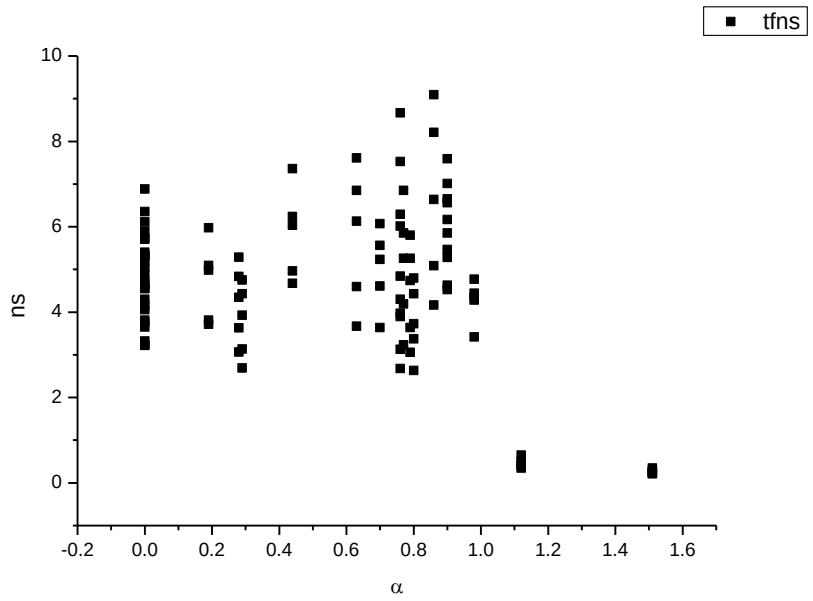

Figure 1.3.66. Amplitude weighted average lifetime (τ_f) of **9a** versus α.

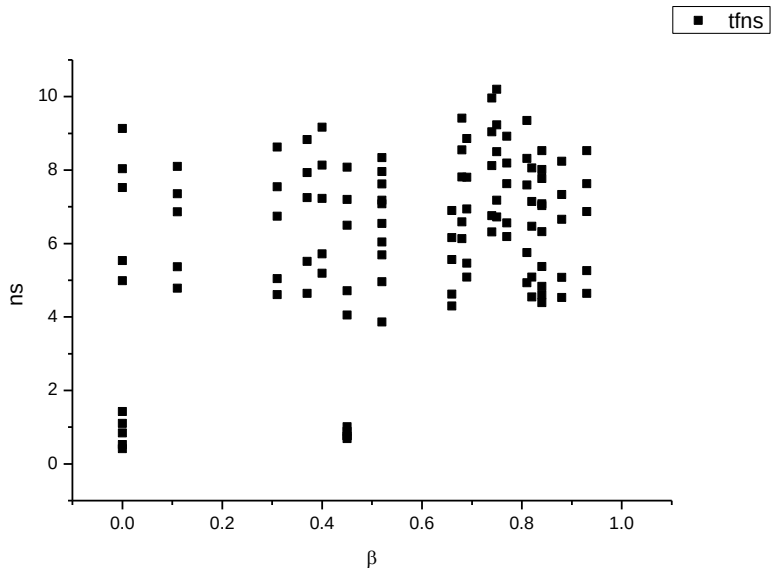

Figure 1.3.67. Intensity weighted average lifetime (τ_f) of **9a** versus β.

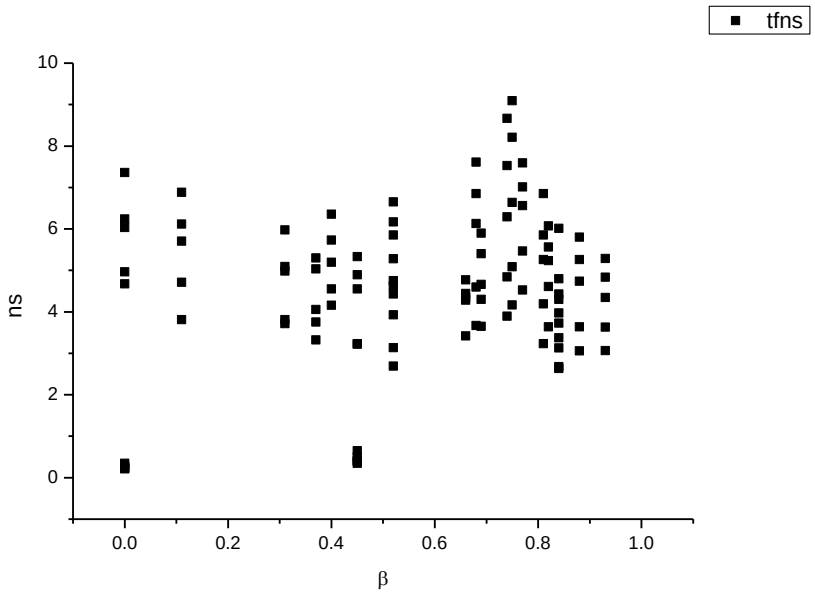

Figure 1.3.68. Amplitude weighted average lifetime (τ_f) of **9a** versus β.

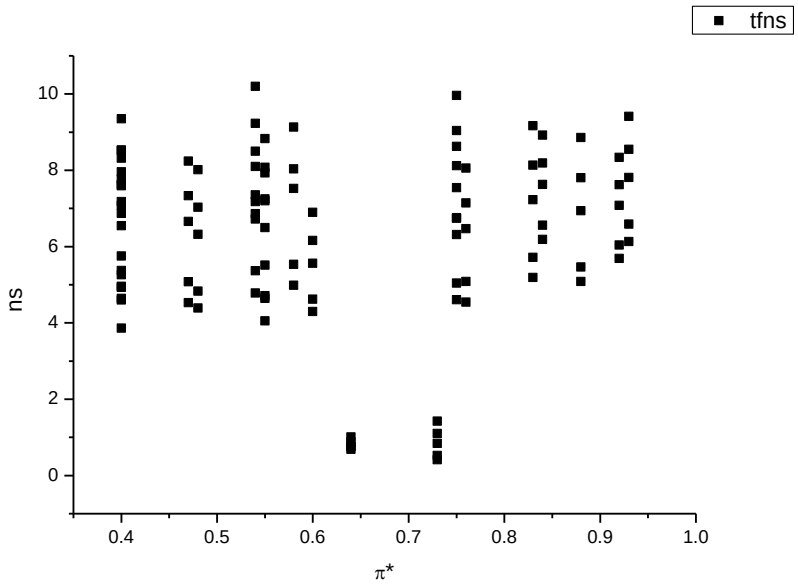

Figure 1.3.69. Intensity weighted average lifetime (τ_f) of **9a** versus π^*.

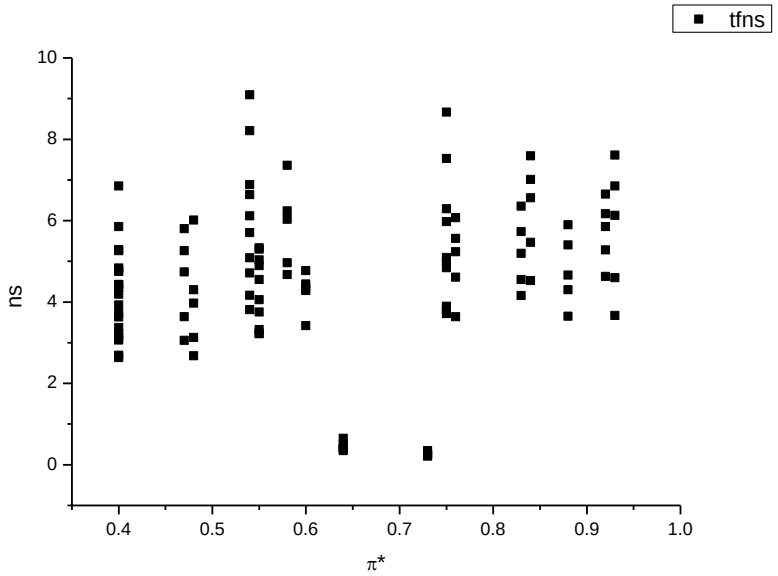

Figure 1.3.70. Amplitude weighted average lifetime (τ_f) of **9a** versus π^*.

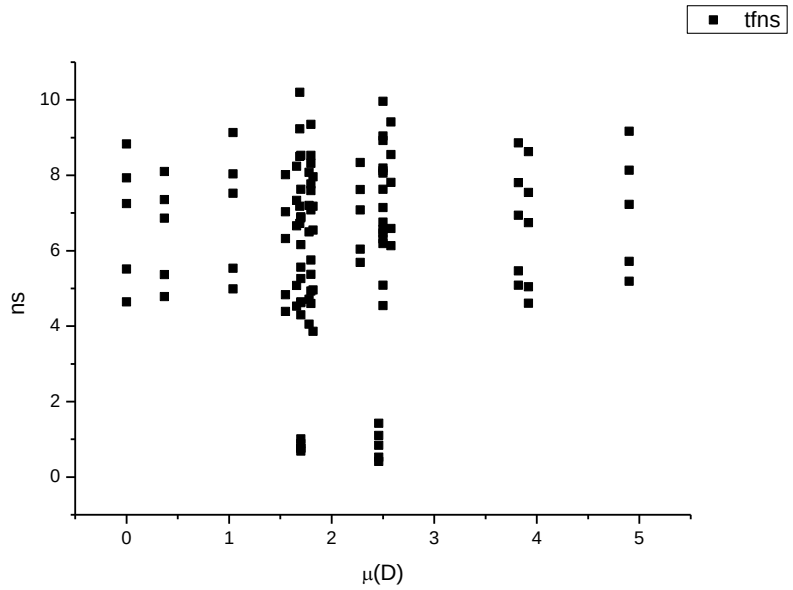

Figure 1.3.71. Intensity weighted average lifetime (τ_f) of **9a** versus μ(D).

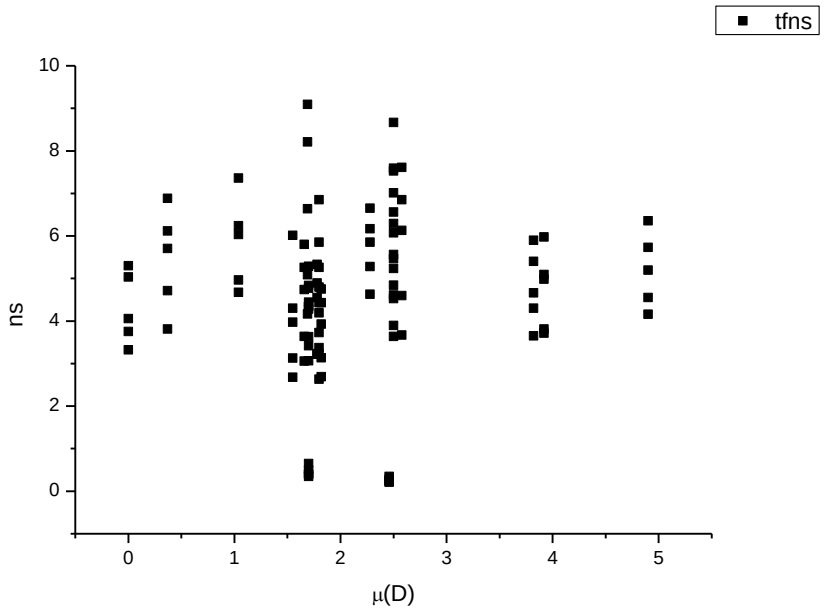

Figure 1.3.72. Amplitude weighted average lifetime (τ_f) of **9a** versus μ(D).

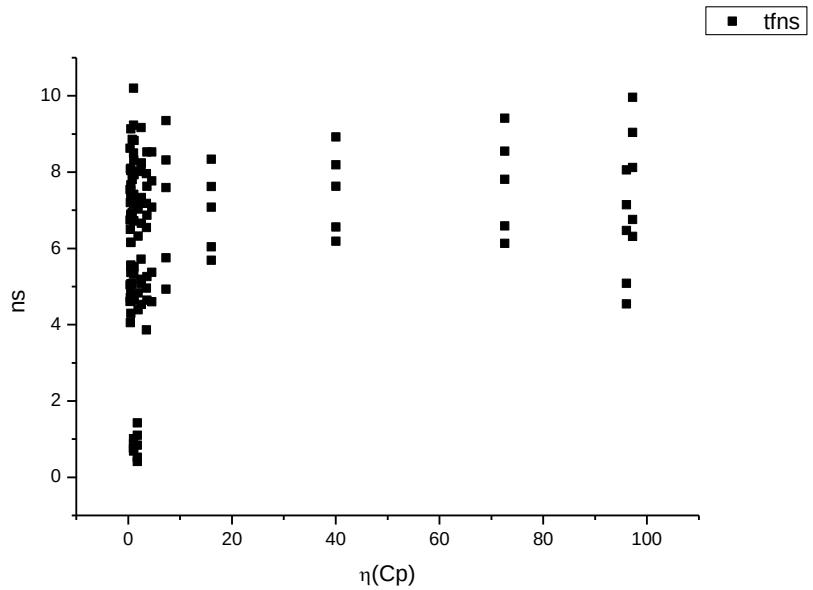

Figure 1.3.73. Intensity weighted average lifetime (τ_f) of **9a** versus η(Cp).

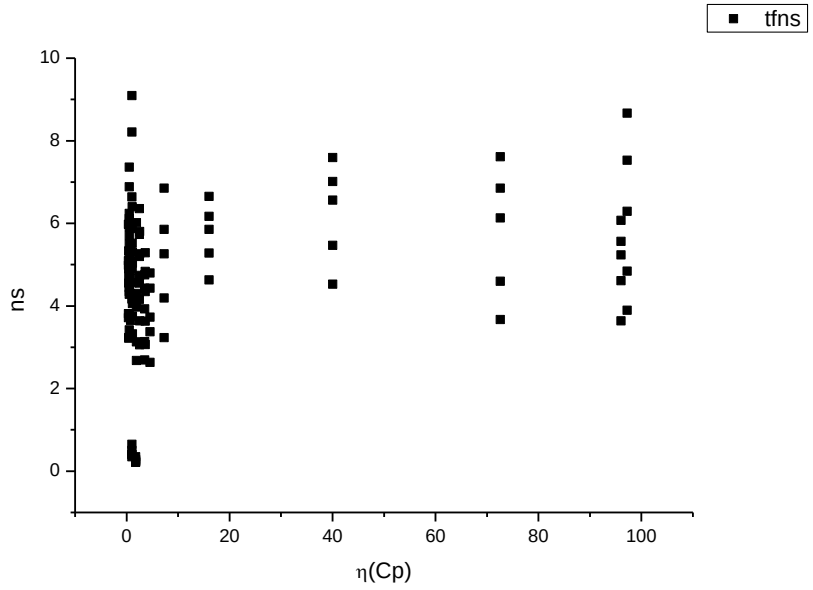

Figure 1.3.74. Amplitude weighted average lifetime (τ_f) of **9a** versus η(Cp).

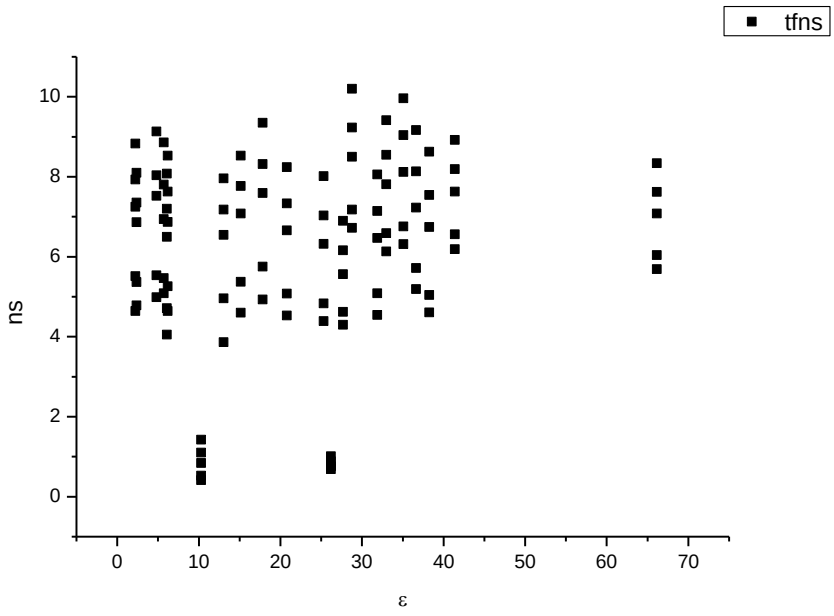

Figure 1.3.75. Intensity weighted average lifetime (τ_f) of **9a** versus ε.

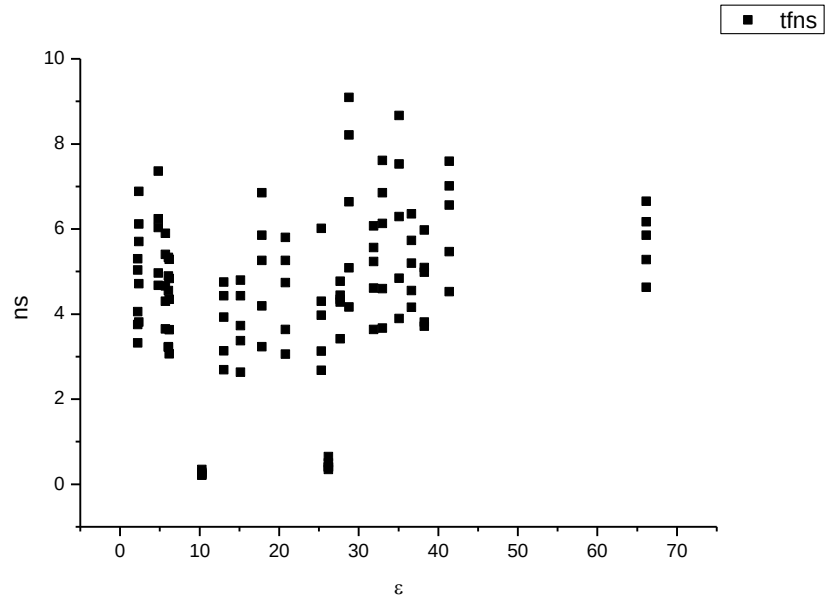

Figure 1.3.76. Amplitude weighted average lifetime (τ_f) of **9a** versus ε.

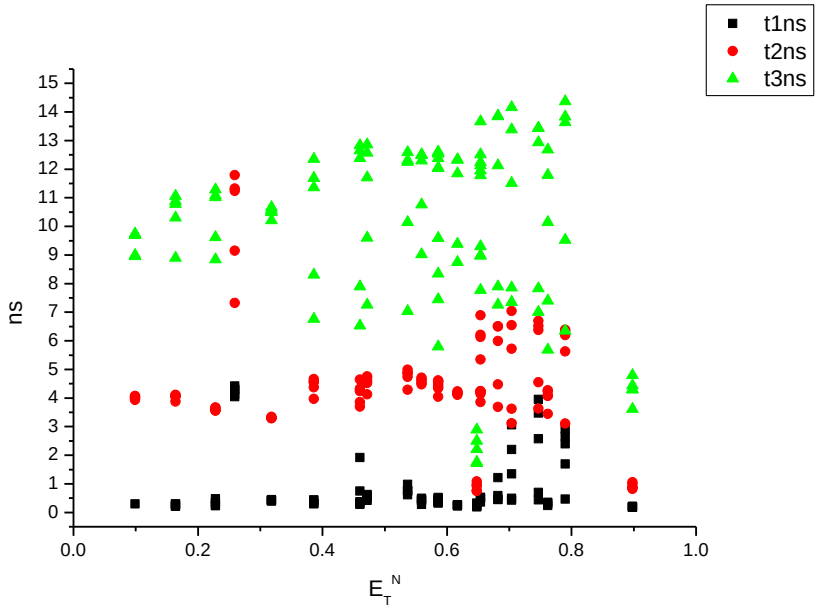

Figure 1.3.77. Intensity weighted components of TCSPC lifetime decay of **9a** (470 nm to 570 nm) versus E_T^N.

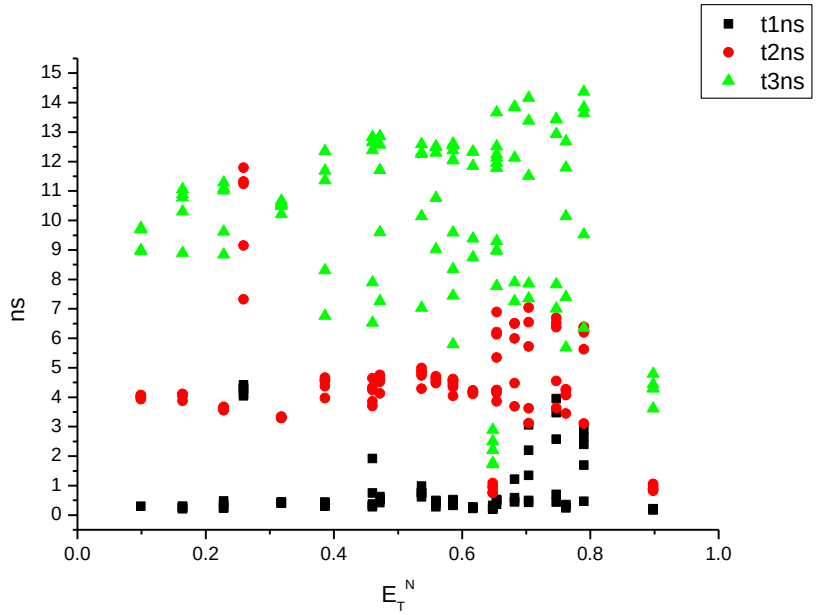

Figure 1.3.78. Amplitude weighted components of TCSPC lifetime decay of **9a** (470 nm to 570 nm) versus E_T^N.

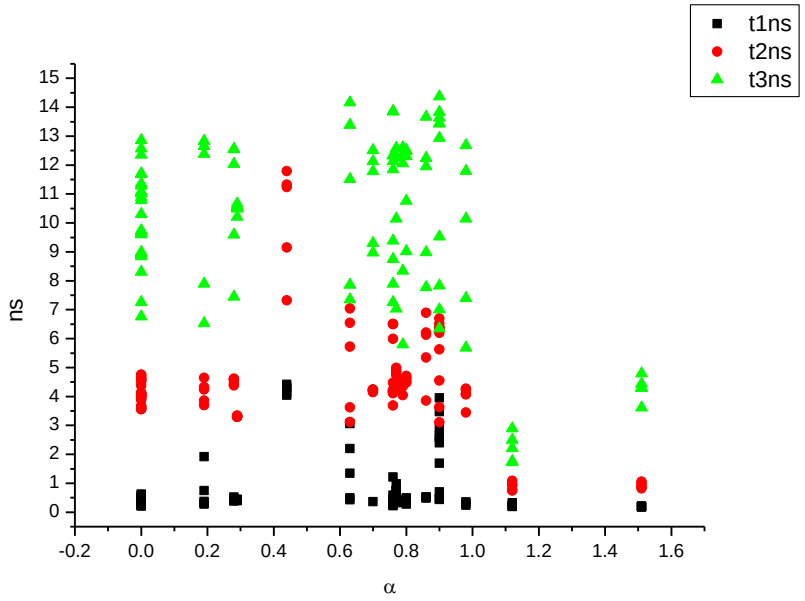

Figure 1.3.79. Intensity weighted components of TCSPC lifetime decay of **9a** (470 nm to 570 nm) versus α.

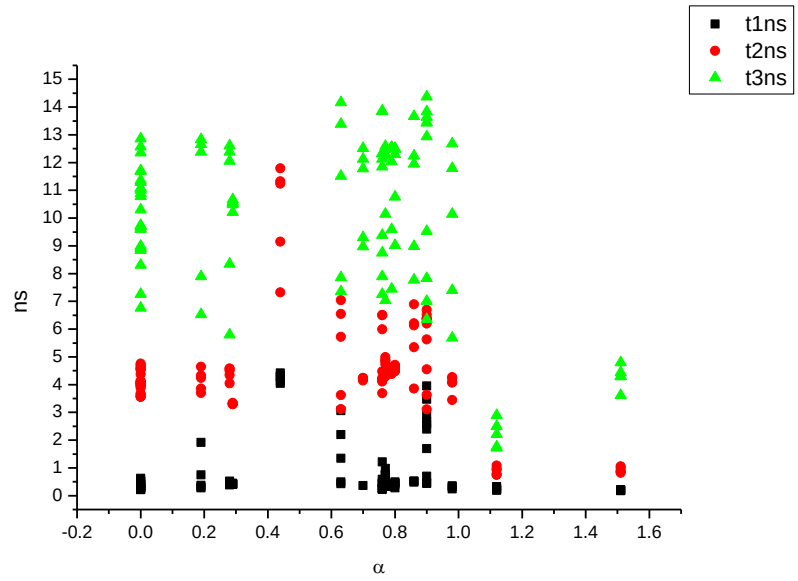

Figure 1.3.80. Amplitude weighted components of TCSPC lifetime decay of **9a** (470 nm to 570 nm) versus α.

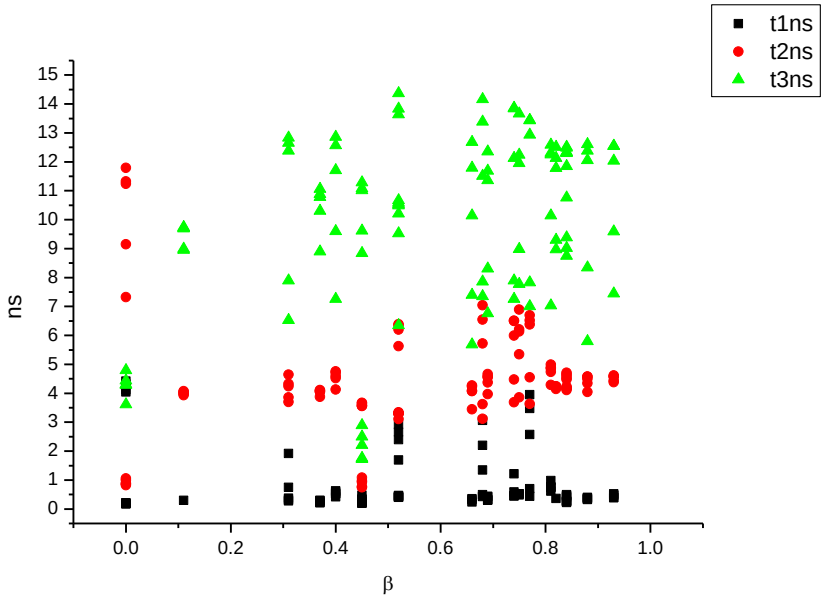

Figure 1.3.81. Intensity weighted components of TCSPC lifetime decay of **9a** (470 nm to 570 nm) versus β.

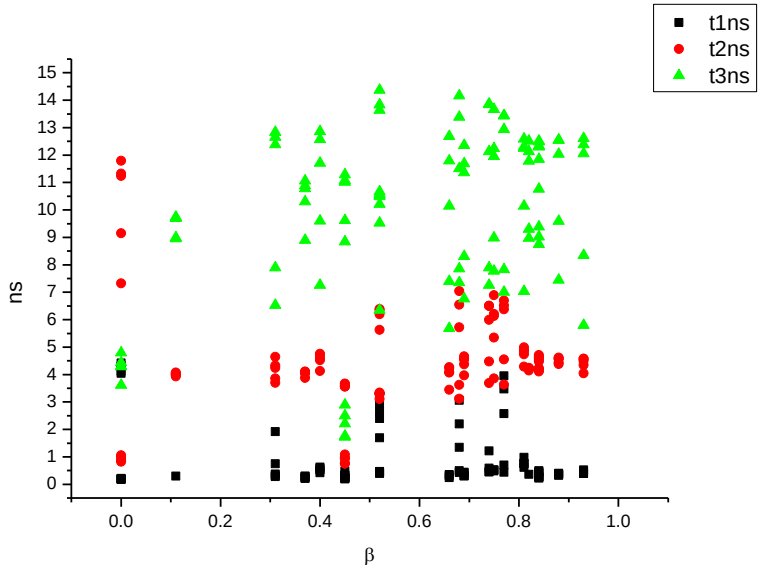

Figure 1.3.82. Amplitude weighted components of TCSPC lifetime decay of **9a** (470 nm to 570 nm) versus β.

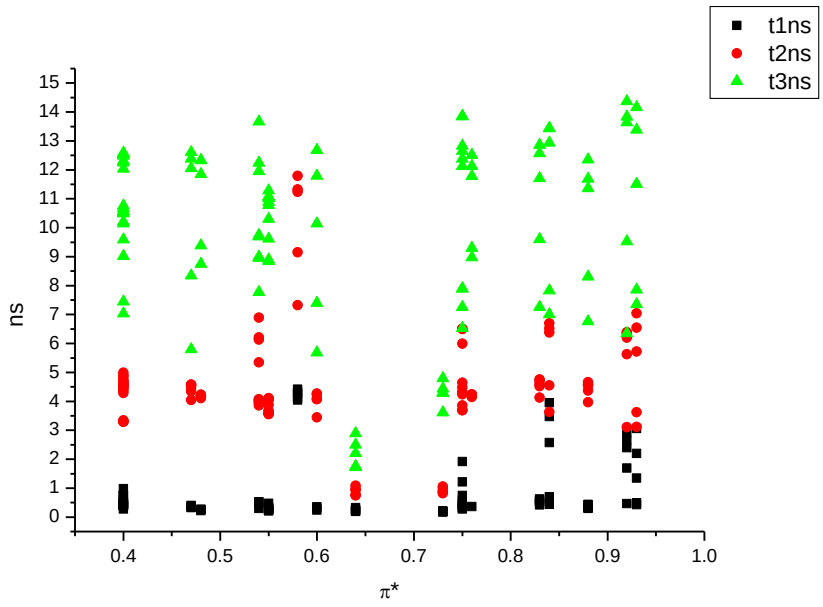

Figure 1.3.83. Intensity weighted components of TCSPC lifetime decay of **9a** (470 nm to 570 nm) versus π*.

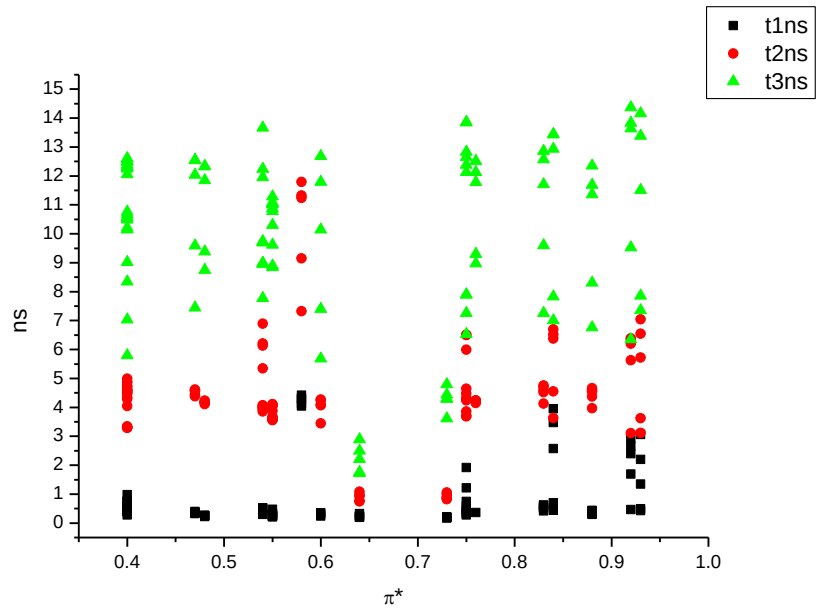

Figure 1.3.84. Amplitude weighted components of TCSPC lifetime decay of **9a** (470 nm to 570 nm) versus π*.

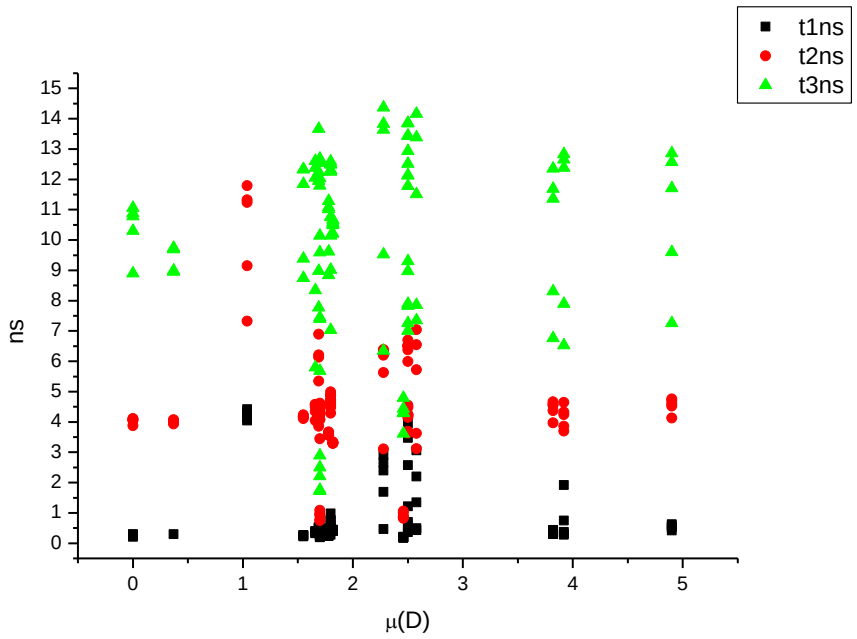

Figure 1.3.85. Intensity weighted components of TCSPC lifetime decay of **9a** (470 nm to 570 nm) versus μ(D).

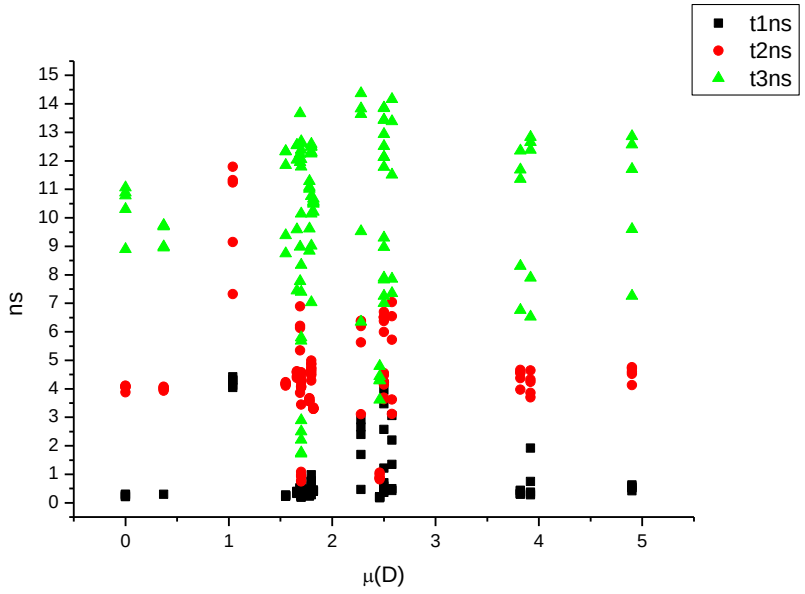

Figure 1.3.86. Amplitude weighted components of TCSPC lifetime decay of **9a** (470 nm to 570 nm) versus μ(D).

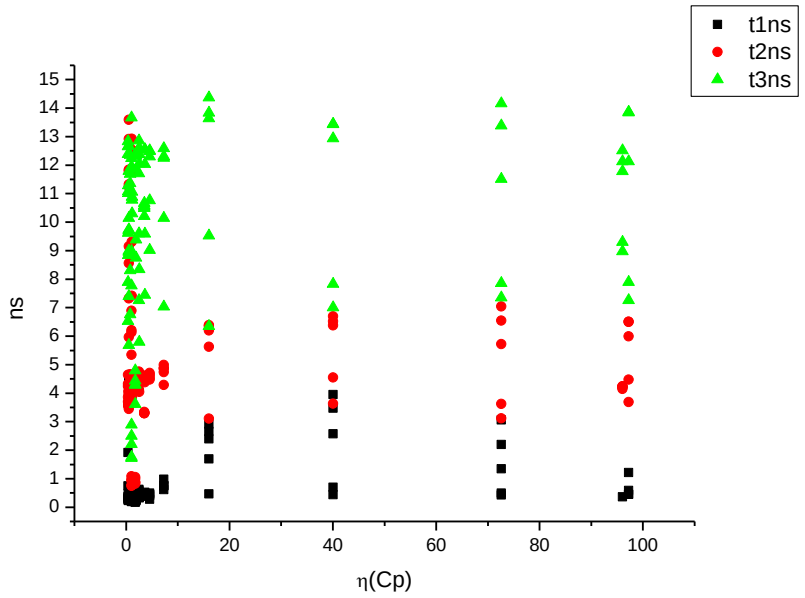

Figure 1.3.87. Intensity weighted components of TCSPC lifetime decay of **9a** (470 nm to 570 nm) versus η(Cp).

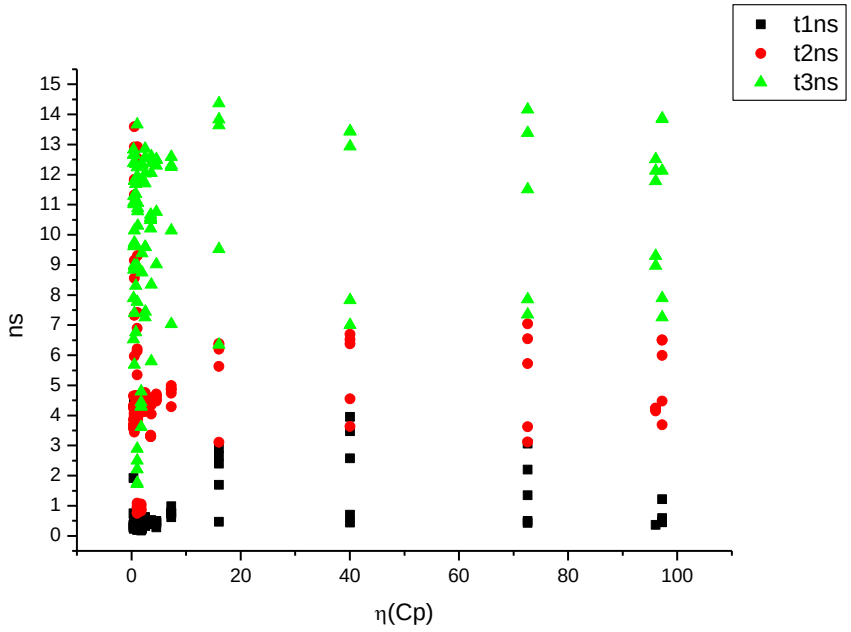

Figure 1.3.88. Amplitude weighted components of TCSPC lifetime decay of **9a** (470 nm to 570 nm) versus η(Cp).

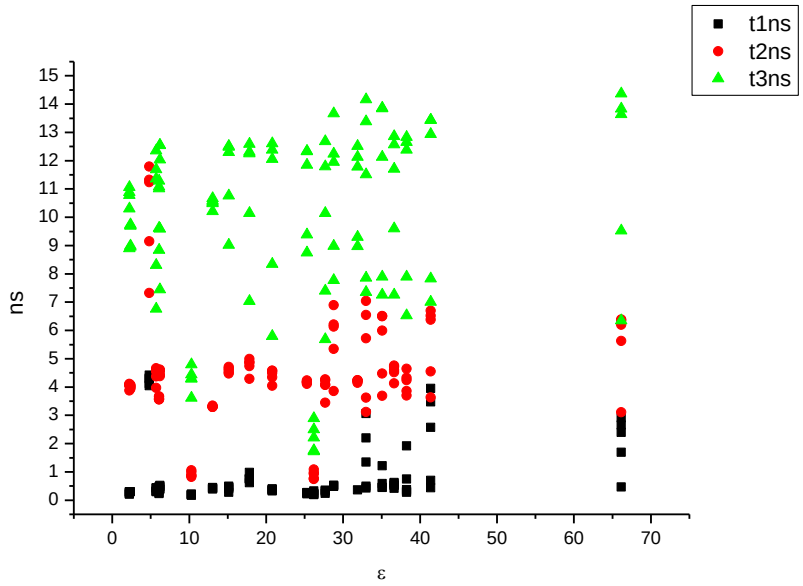

Figure 1.3.89. Intensity weighted components of TCSPC lifetime decay of **9a** (470 nm to 570 nm) versus ε.

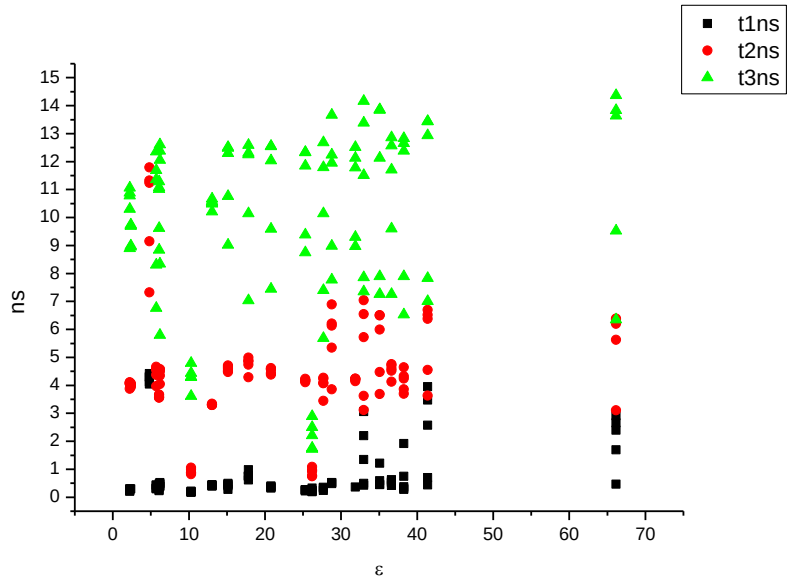

Figure 1.3.90. Amplitude weighted components of TCSPC lifetime decay of **9a** (470 nm to 570 nm) versus ε.

1.3.7.1 470 nm Lifetime – Solvatochromic analysis.

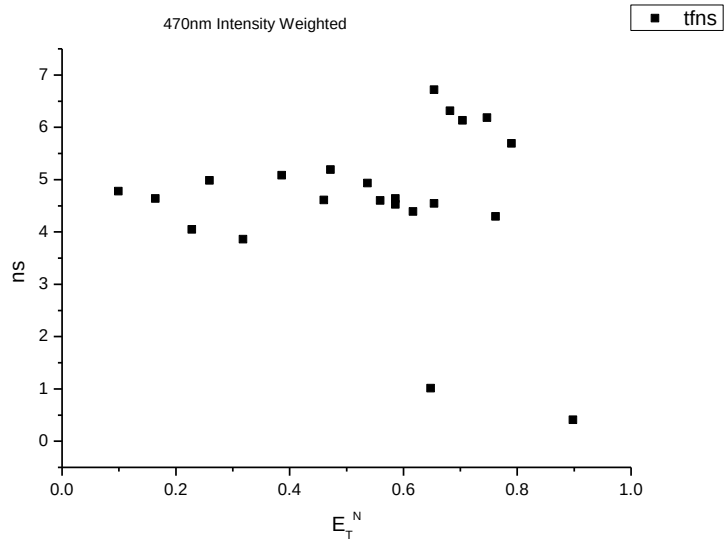

Figure 1.3.91. Intensity weighted average lifetime (τ_f) of **9a** at 470 nm versus E_T^N.

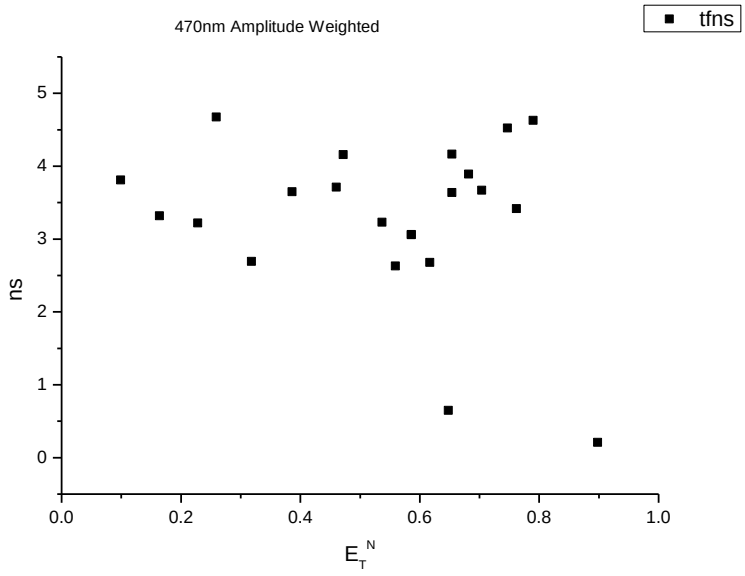

Figure 1.3.92. Amplitude weighted average lifetime (τ_f) of **9a** at 470 nm versus E_T^N.

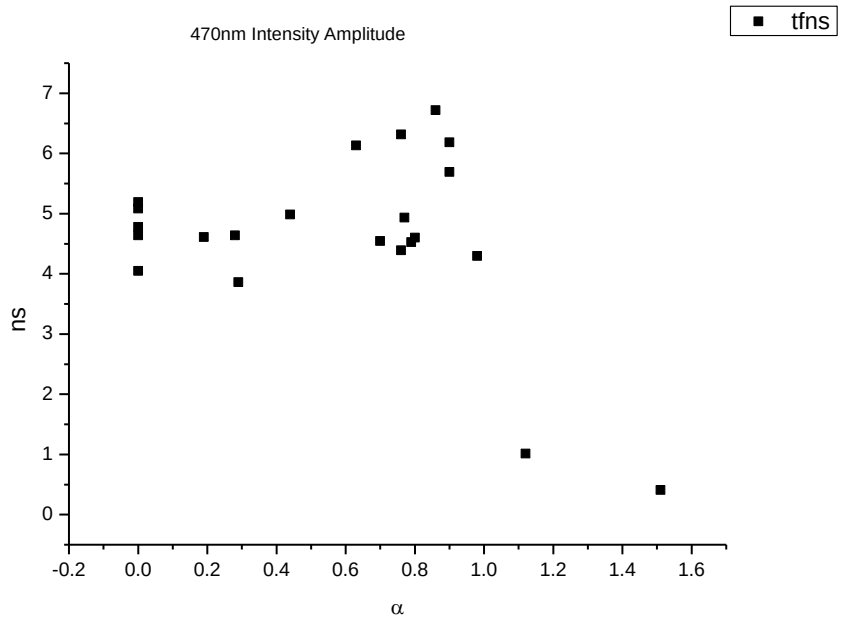

Figure 1.3.93. Intensity weighted average lifetime (τ_f) of **9a** at 470 nm versus α.

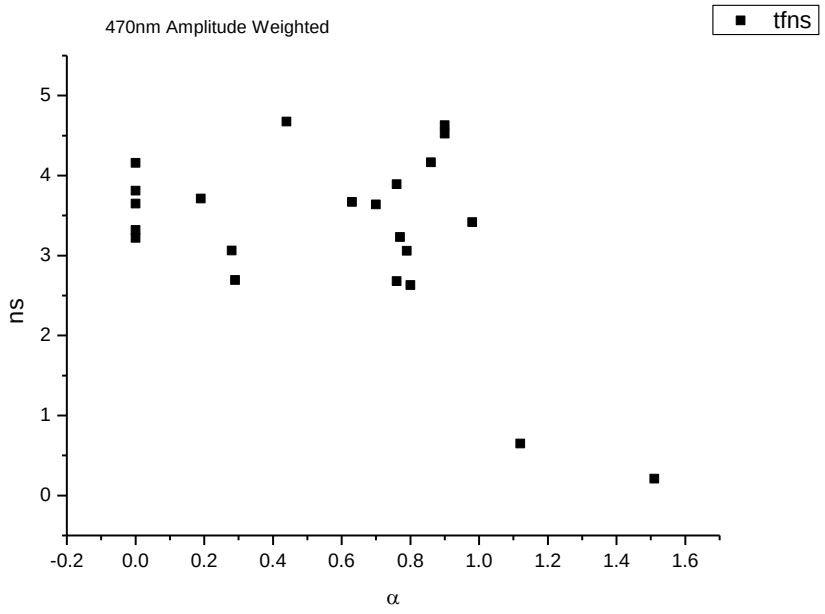

Figure 1.3.94. Amplitude weighted average lifetime (τ_f) of **9a** at 470 nm versus α.

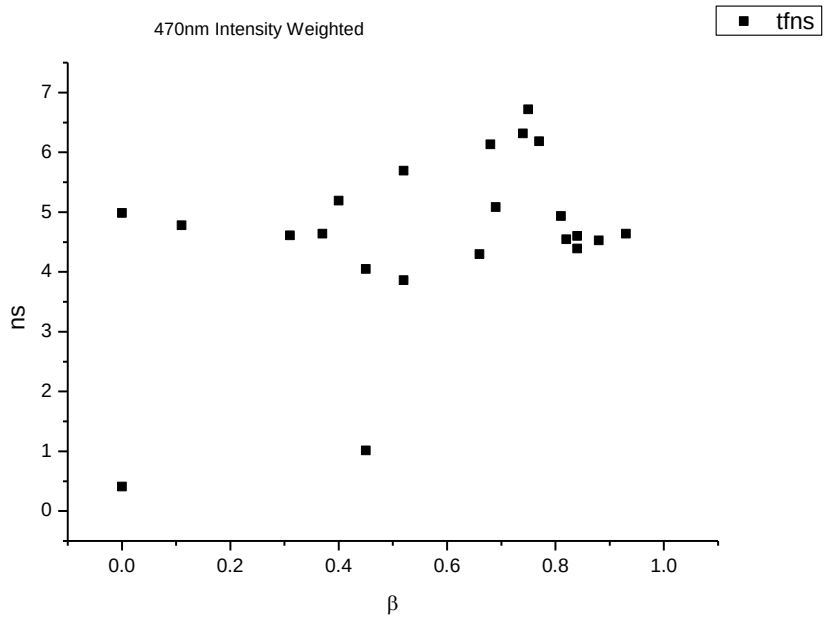

Figure 1.3.95. Intensity weighted average lifetime (τ_f) of **9a** at 470 nm versus β.

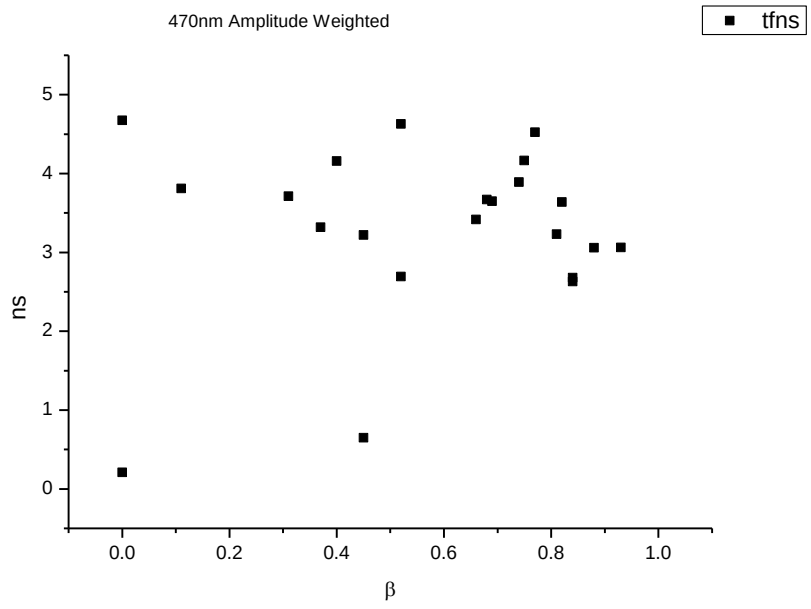

Figure 1.3.96. Amplitude weighted average lifetime (τ_f) of **9a** at 470 nm versus β.

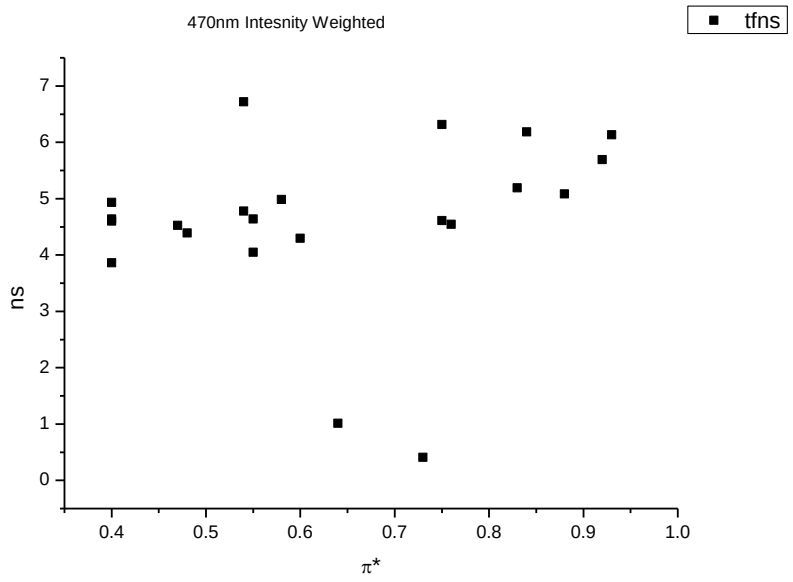

Figure 1.3.97. Intensity weighted average lifetime (τ_f) of **9a** at 470 nm versus π^*.

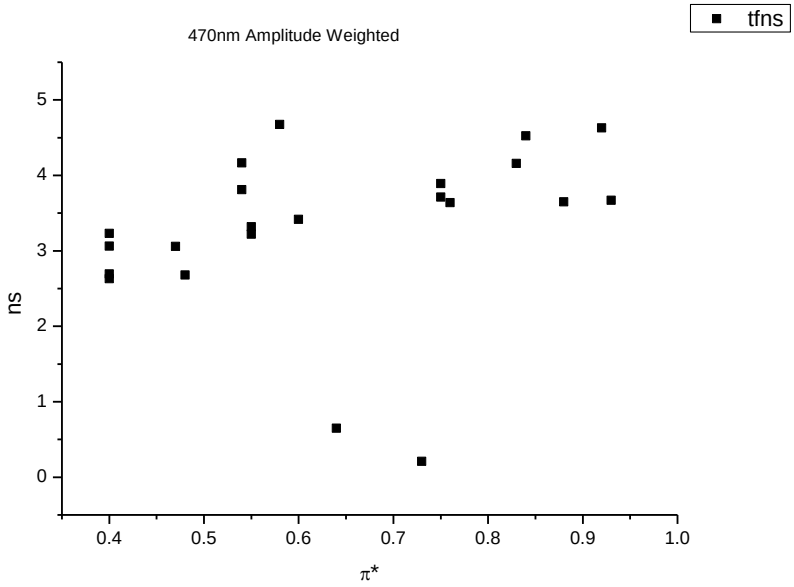

Figure 1.3.98. Amplitude weighted average lifetime (τ_f) of **9a** at 470 nm versus π^*.

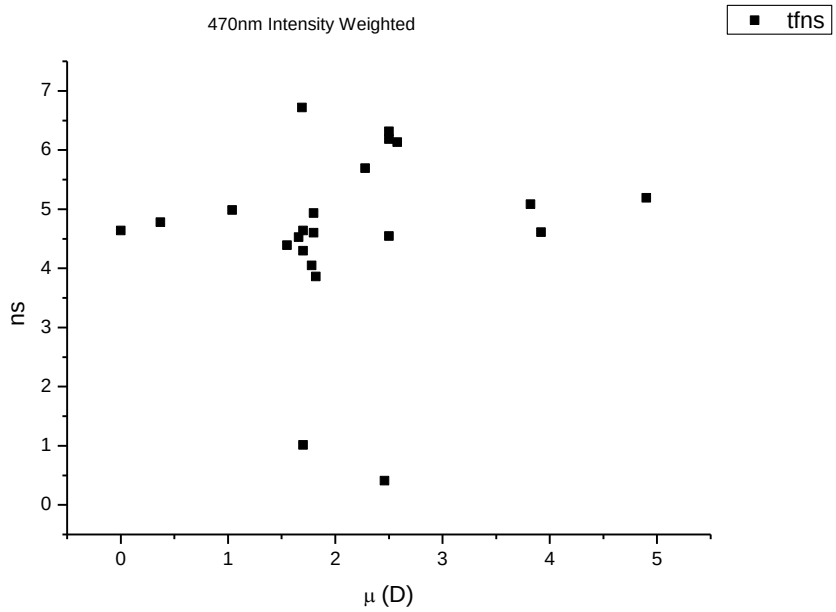

Figure 1.3.99. Intensity weighted average lifetime (τ_f) of **9a** at 470 nm versus μ(D).

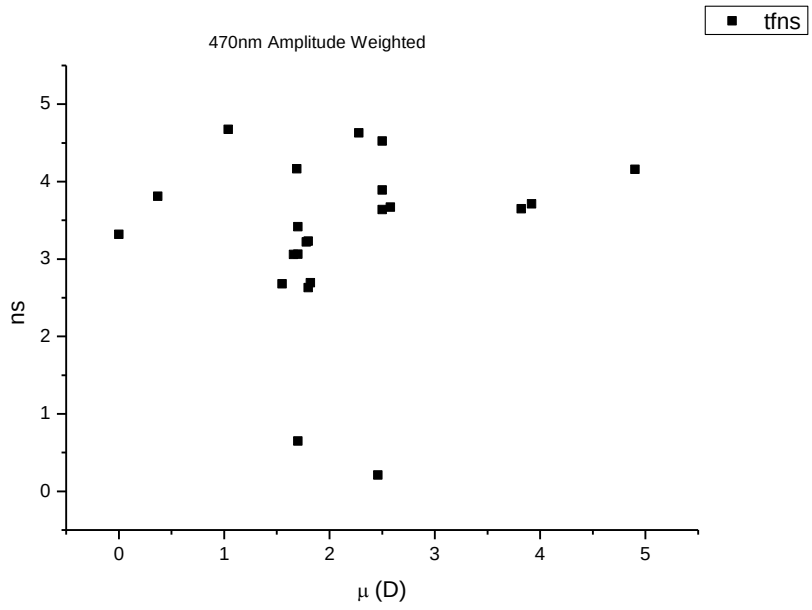

Figure 1.3.100. Amplitude weighted average lifetime (τ_f) of **9a** at 470 nm versus μ(D).

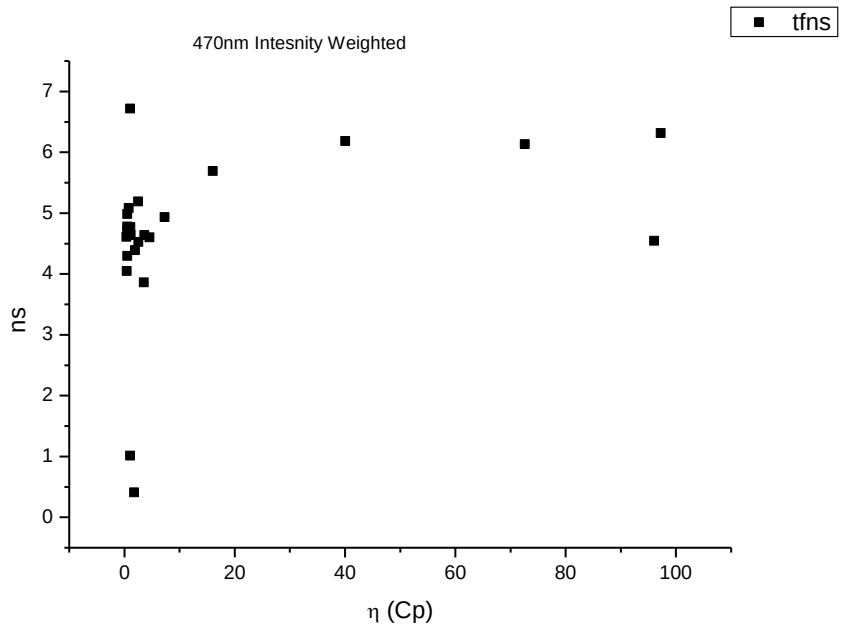

Figure 1.3.101. Intensity weighted average lifetime (τ_f) of **9a** at 470 nm versus η(Cp).

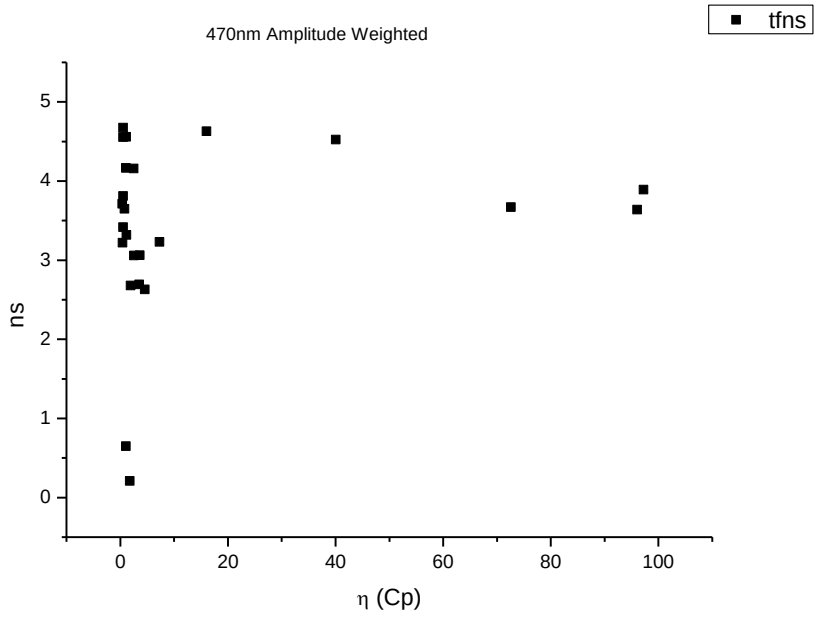

Figure 1.3.102. Amplitude weighted average lifetime (τ_f) of **9a** at 470 nm versus η(Cp).

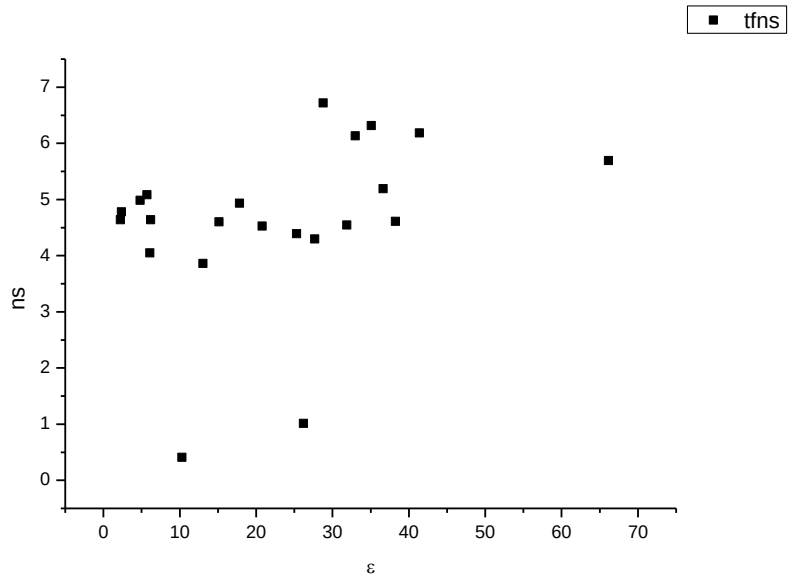

Figure 1.3.103. Intensity weighted average lifetime (τ_f) of **9a** at 470 nm versus ε.

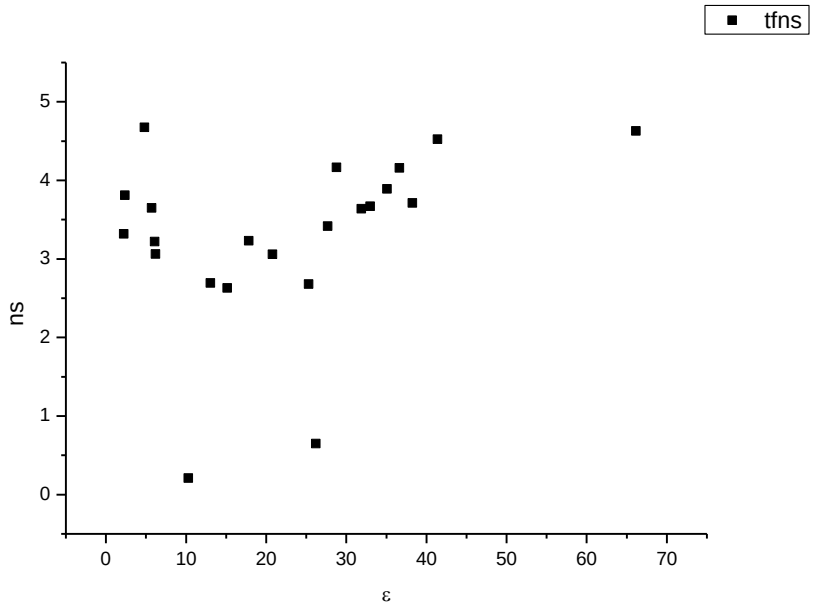

Figure 1.3.104. Amplitude weighted average lifetime (τ_f) of **9a** at 470 nm versus ε.

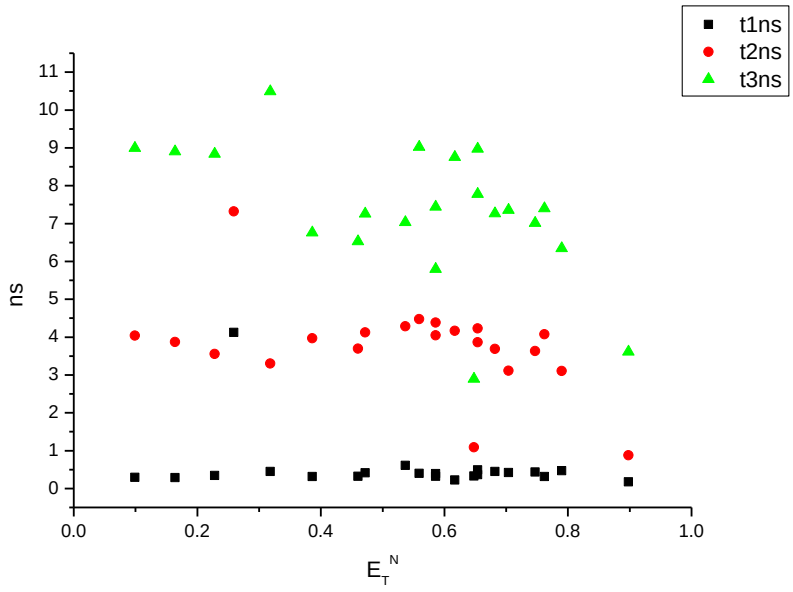

Figure 1.3.105. Intensity weighted components of TCSPC lifetime decay of **9a** (470 nm) versus E_T^N.

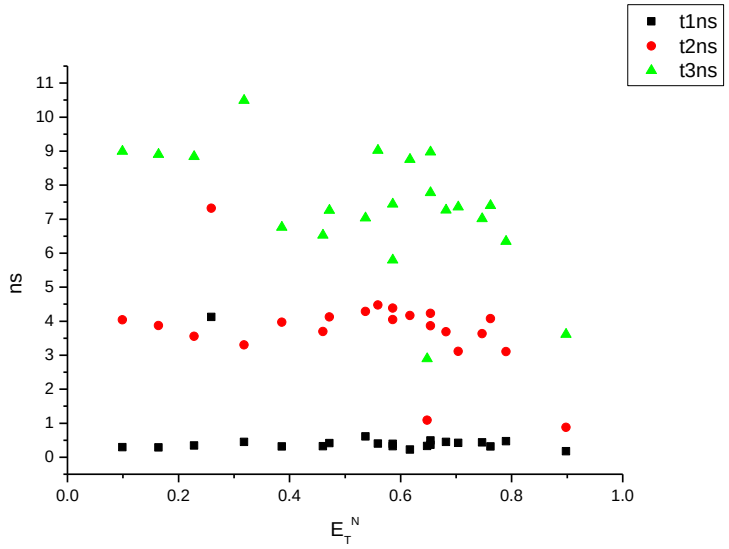

Figure 1.3.106. Amplitude weighted components of TCSPC lifetime decay of **9a** (470 nm) versus E_T^N.

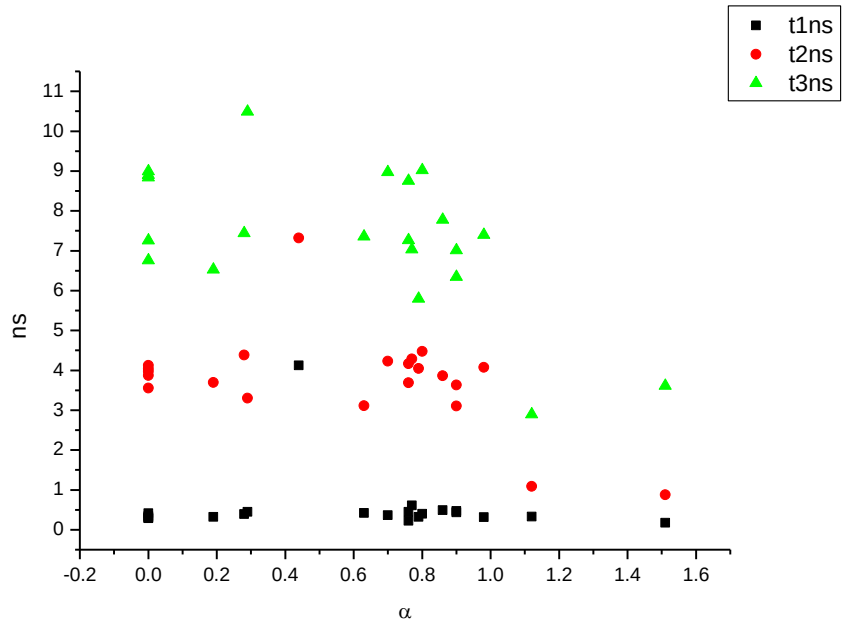

Figure 1.3.107. Intensity weighted components of TCSPC lifetime decay of **9a** (470 nm) versus α.

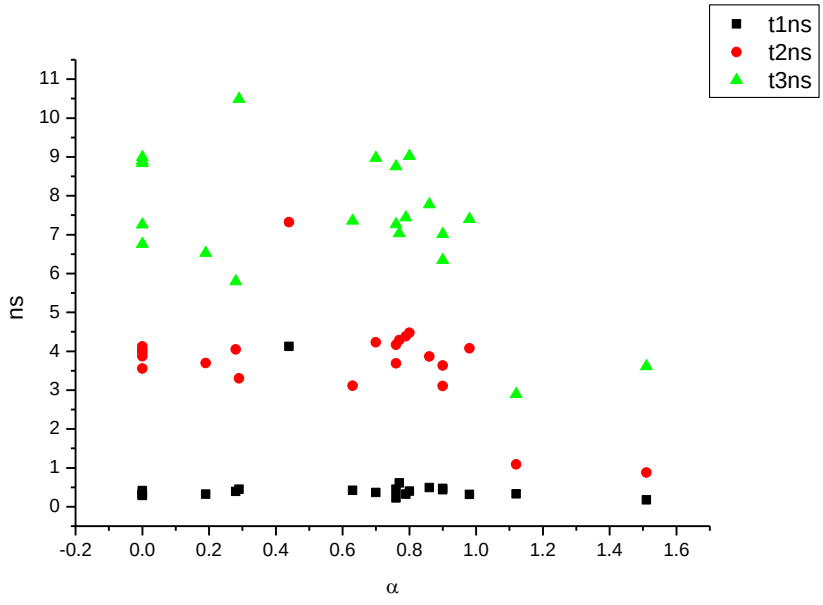

Figure 1.3.108. Amplitude weighted components of TCSPC lifetime decay of **9a** (470 nm) versus α.

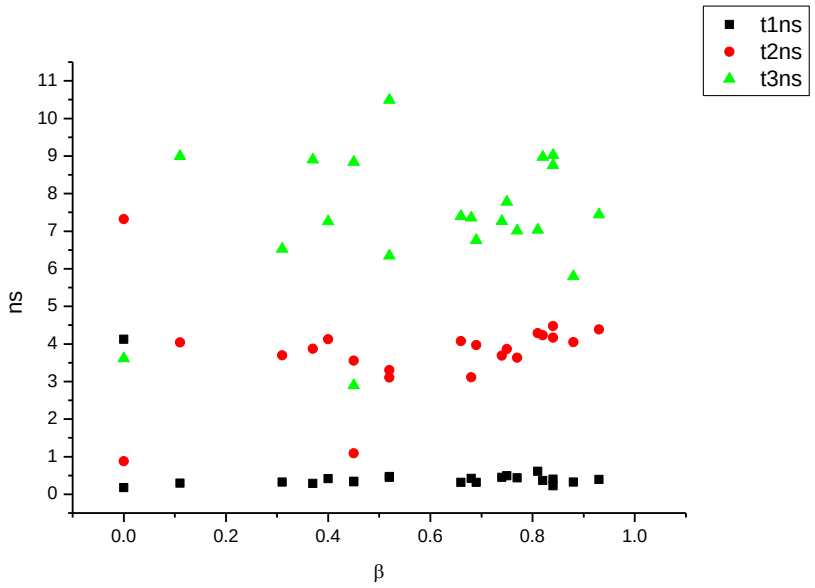

Figure 1.3.109. Intensity weighted components of TCSPC lifetime decay of **9a** (470 nm) versus β.

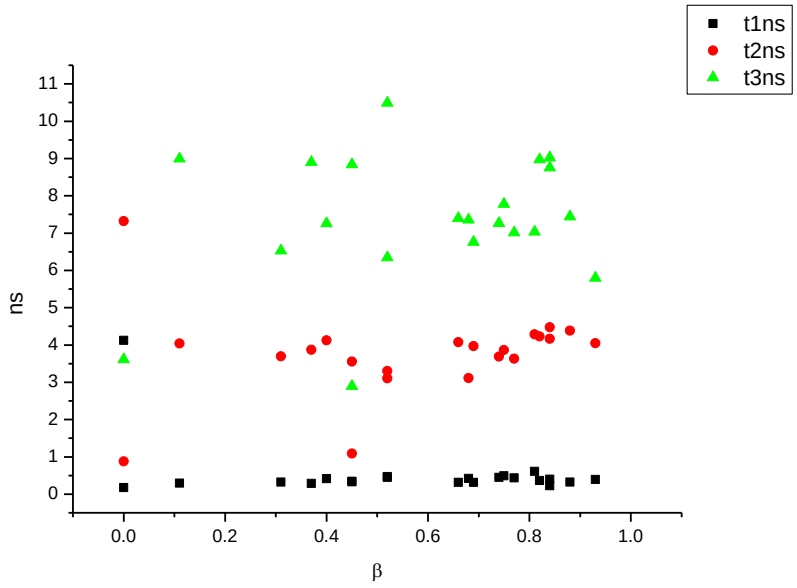

Figure 1.3.110. Amplitude weighted components of TCSPC lifetime decay of **9a** (470 nm) versus β.

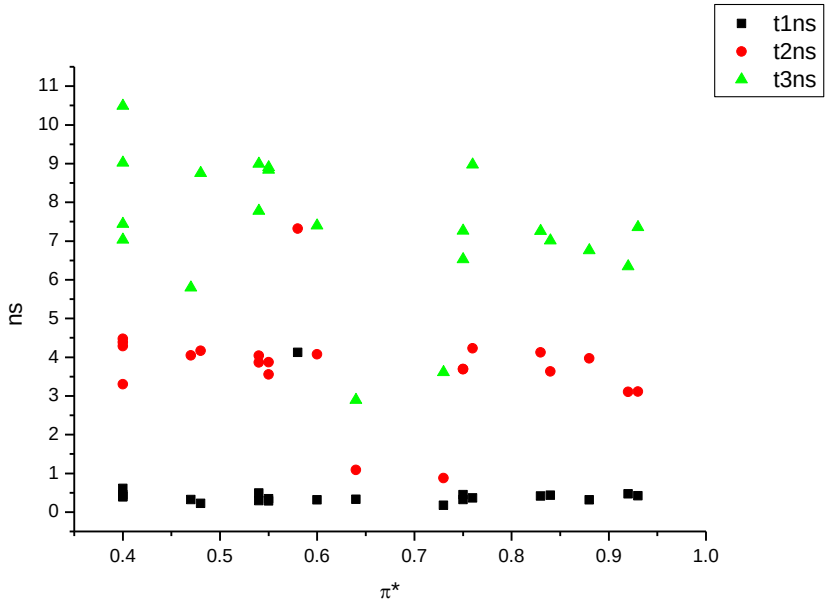

Figure 1.3.111. Intensity weighted components of TCSPC lifetime decay of **9a** (470 nm) versus π*.

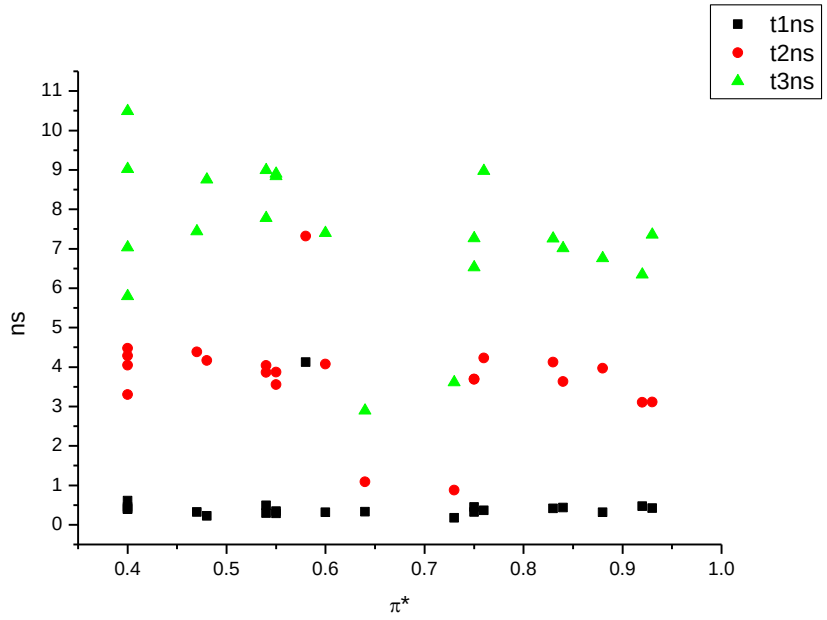

Figure 1.3.112. Amplitude weighted components of TCSPC lifetime decay of **9a** (470 nm) versus π*.

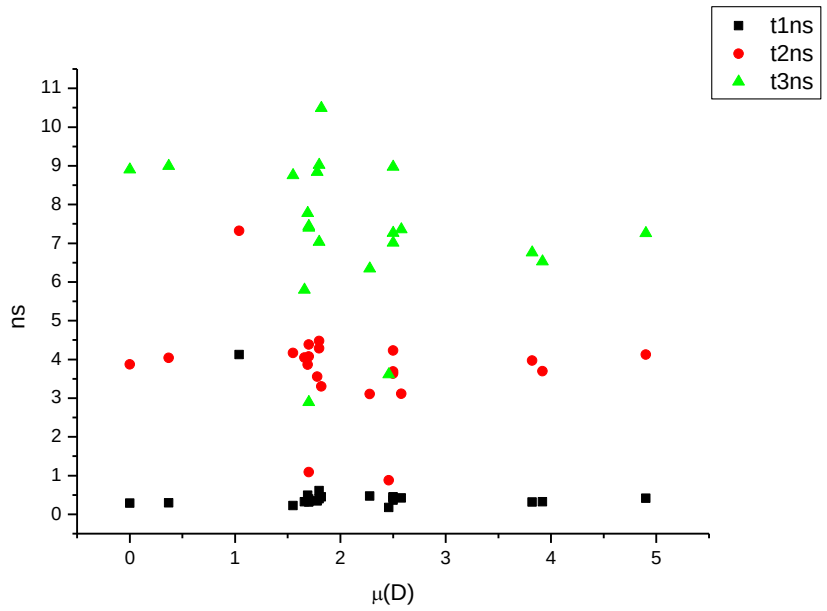

Figure 1.3.113. Intensity weighted components of TCSPC lifetime decay of **9a** (470 nm) versus μ(D).

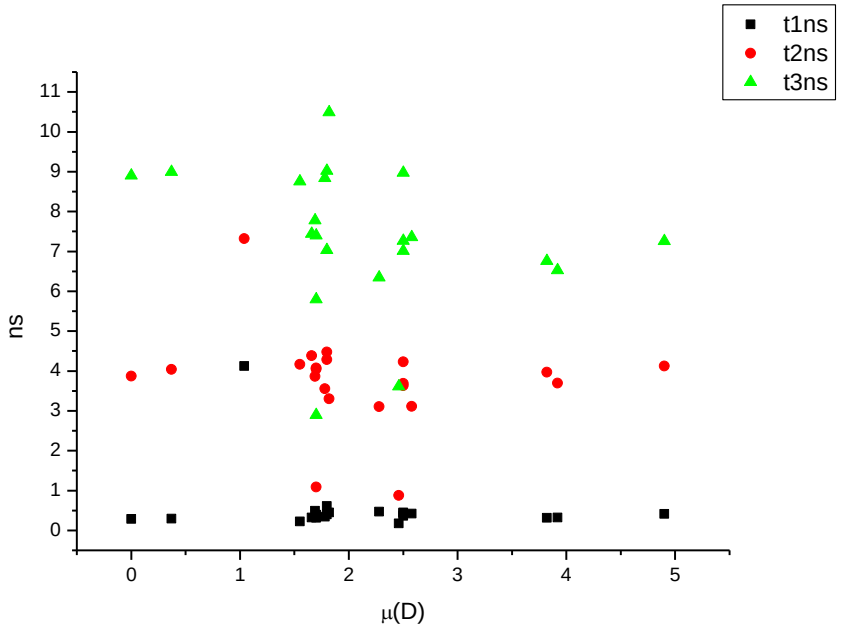

Figure 1.3.114. Amplitude weighted components of TCSPC lifetime decay of **9a** (470 nm) versus μ(D).

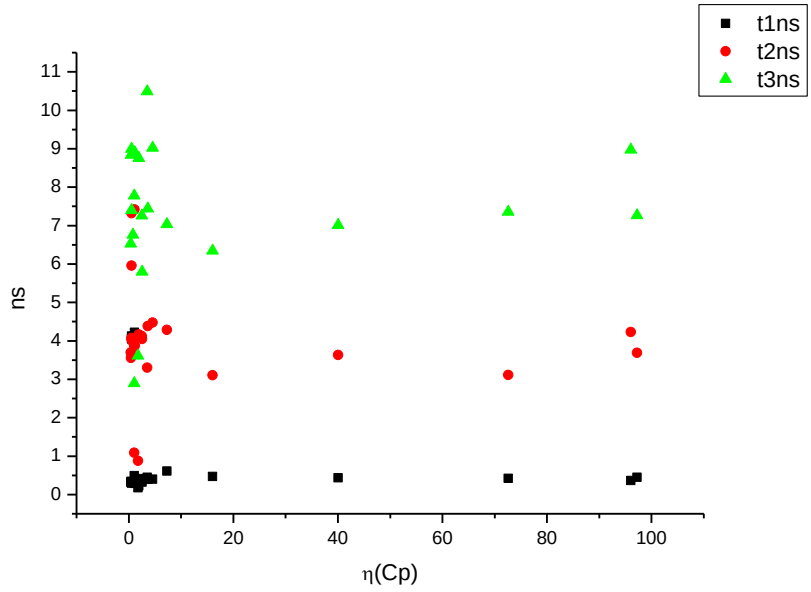

Figure 1.3.115. Intensity weighted components of TCSPC lifetime decay of **9a** (470 nm) versus η(Cp).

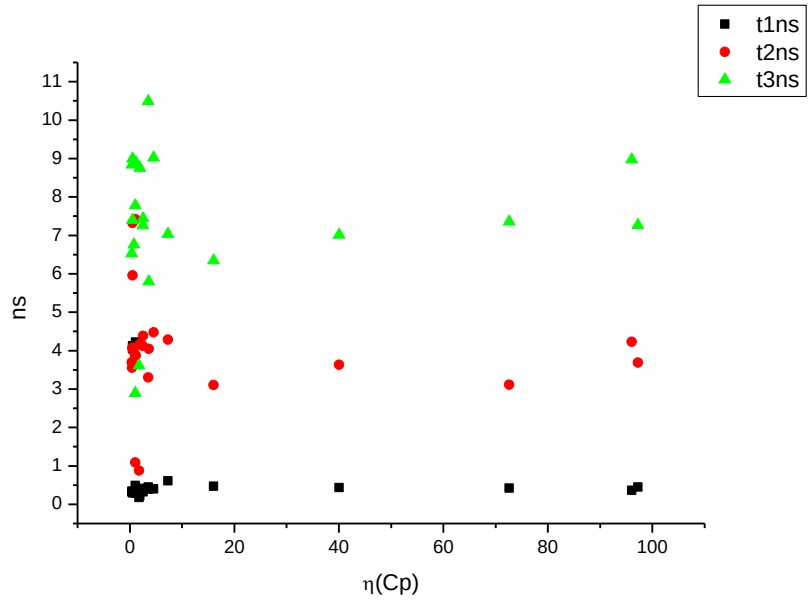

Figure 1.3.116. Amplitude weighted components of TCSPC lifetime decay of **9a** (470 nm) versus η(Cp).

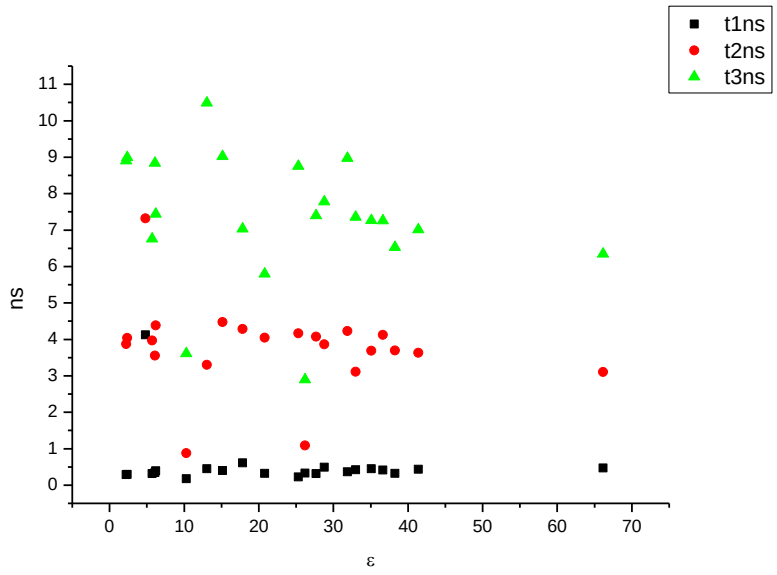

Figure 1.3.117. Intensity weighted components of TCSPC lifetime decay of **9a** (470 nm) versus ε.

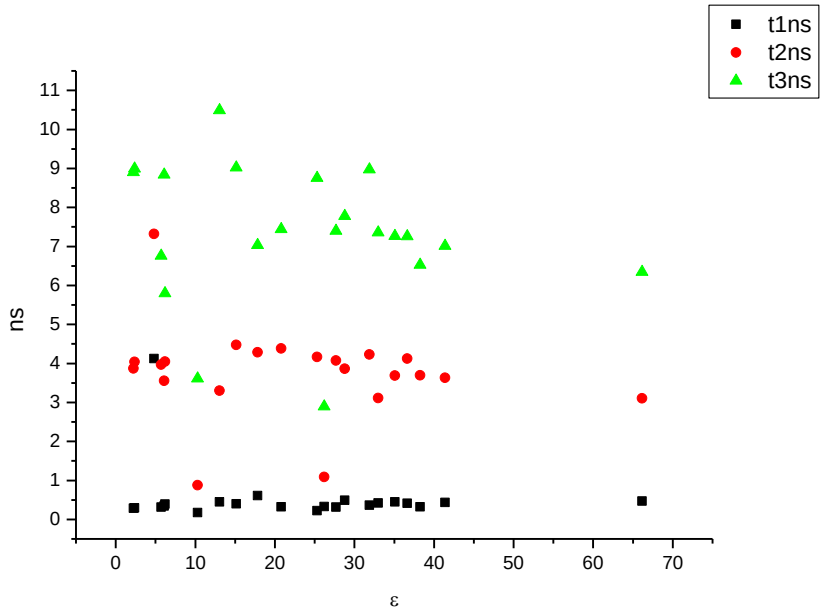

Figure 1.3.118. Amplitude weighted components of TCSPC lifetime decay of **9a** (470 nm) versus ε.

1.3.7.2 570 nm Lifetime – Solvatochromic analysis.

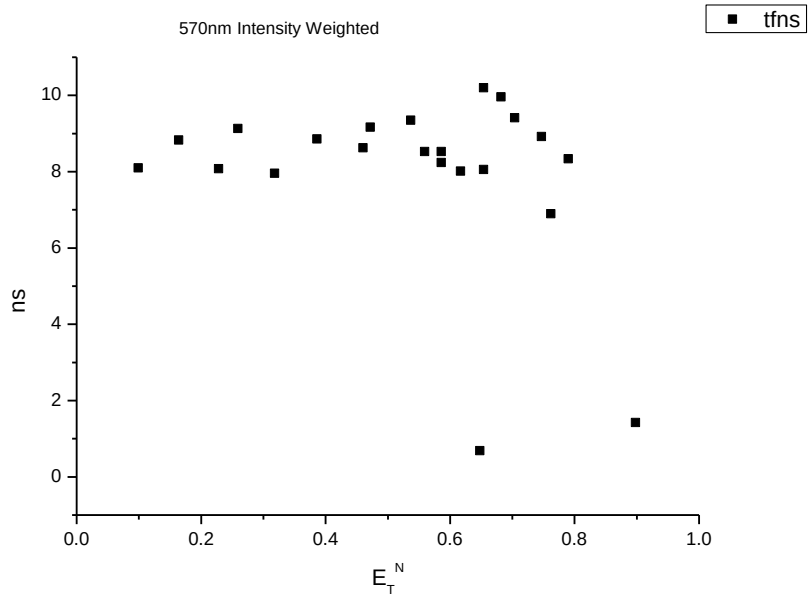

Figure 1.3.119. Intensity weighted average lifetime (τ_f) of **9a** at 570 nm versus E_T^N.

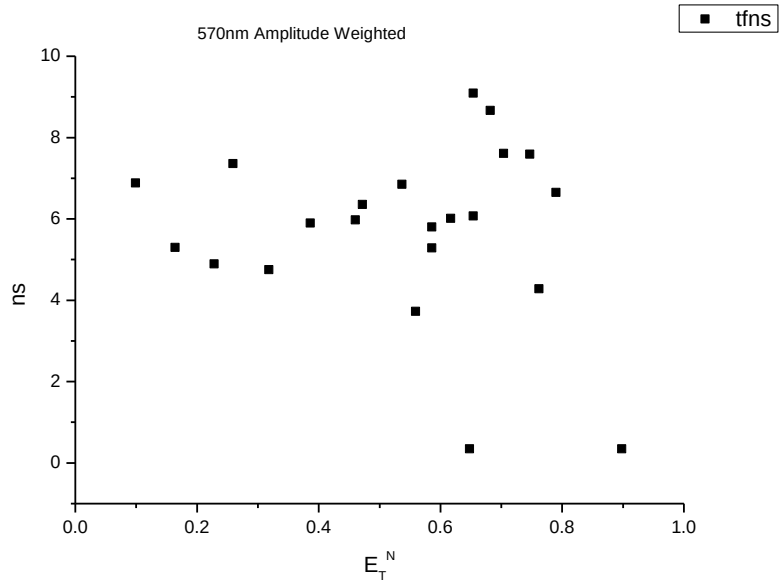

Figure 1.3.120. Amplitude weighted average lifetime (τ_f) of **9a** at 570 nm versus E_T^N.

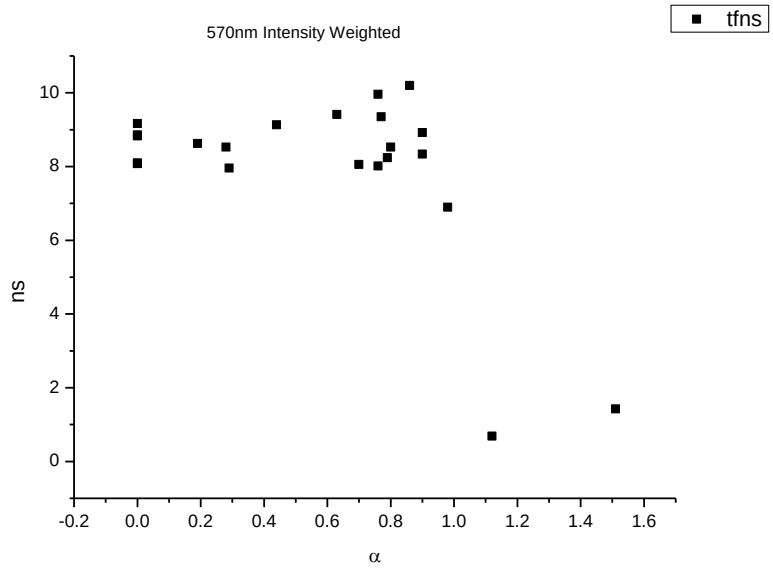

Figure 1.3.121. Intensity weighted average lifetime (τ_f) of **9a** at 570 nm versus α.

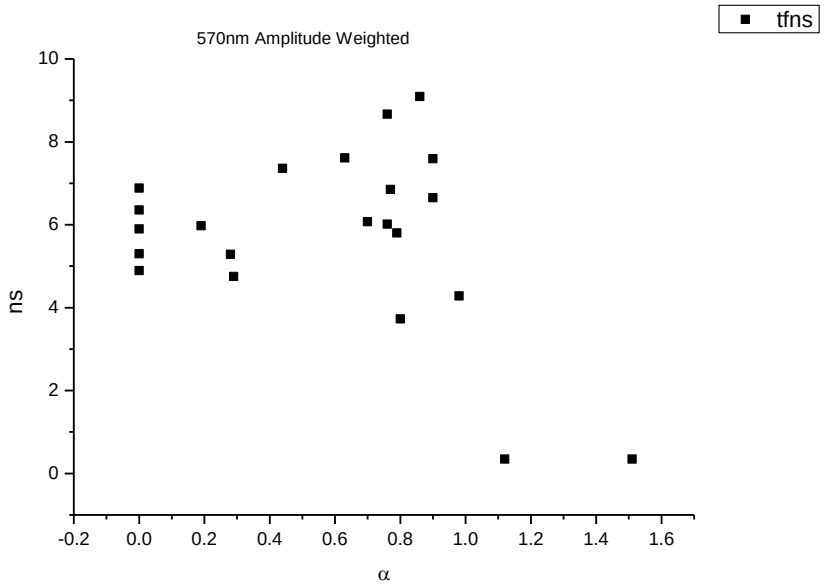

Figure 1.3.122. Amplitude weighted average lifetime (τ_f) of **9a** at 570 nm versus α.

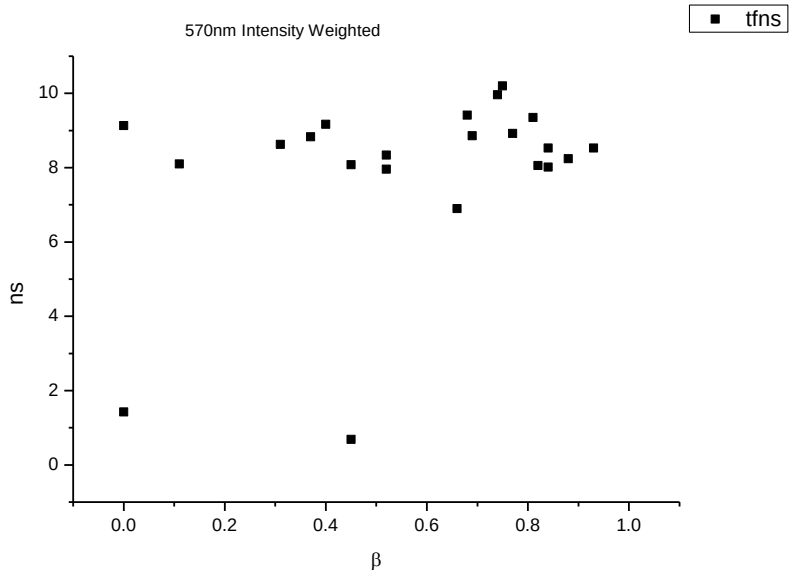

Figure 1.3.123. Intensity weighted average lifetime (τ_f) of **9a** at 570 nm versus β.

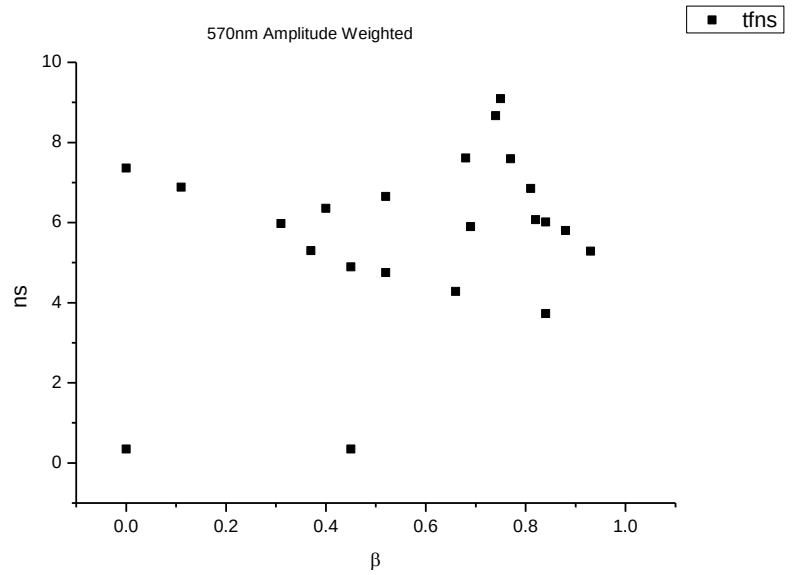

Figure 1.3.124. Amplitude weighted average lifetime (τ_f) of **9a** at 570 nm versus β.

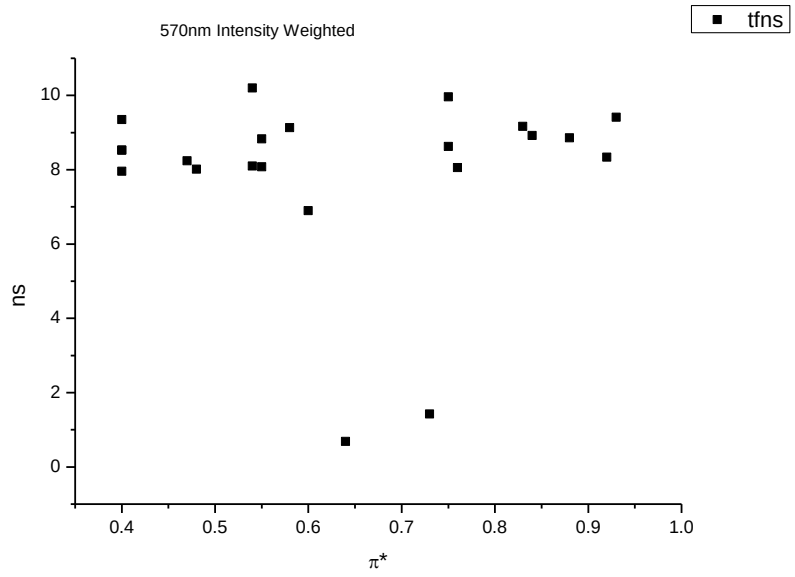

Figure 1.3.125. Intensity weighted average lifetime (τ_f) of **9a** at 570 nm versus π*.

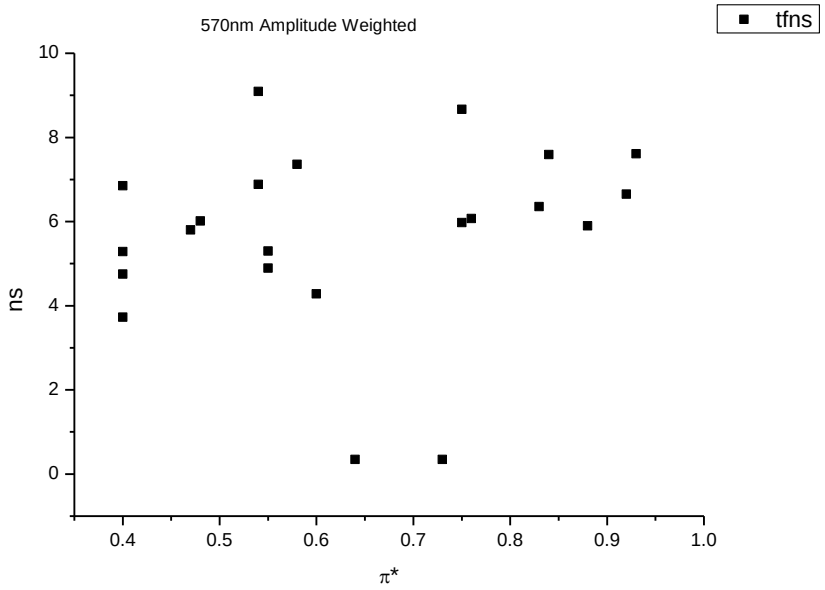

Figure 1.3.126. Amplitude weighted average lifetime (τ_f) of **9a** at 570 nm versus π*.

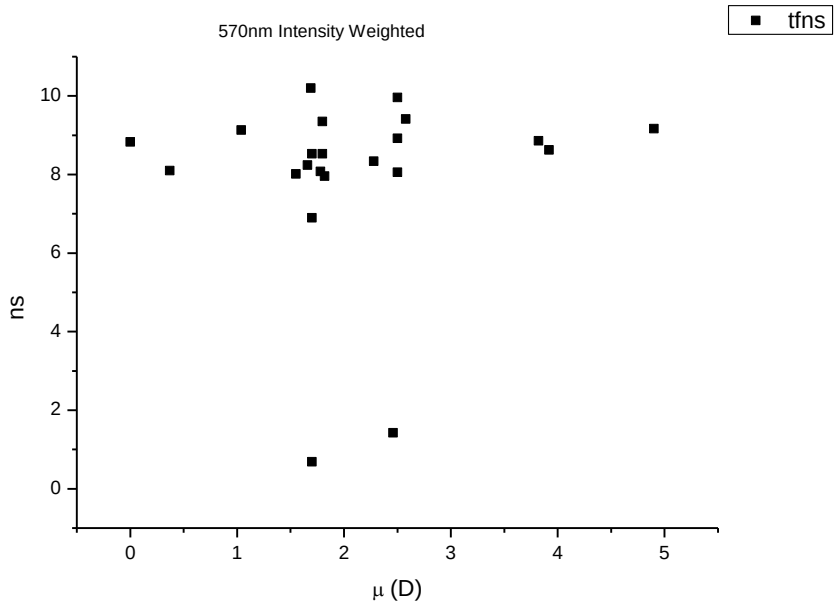

Figure 1.3.127. Intensity weighted average lifetime (τ_f) of **9a** at 570 nm versus μ(D).

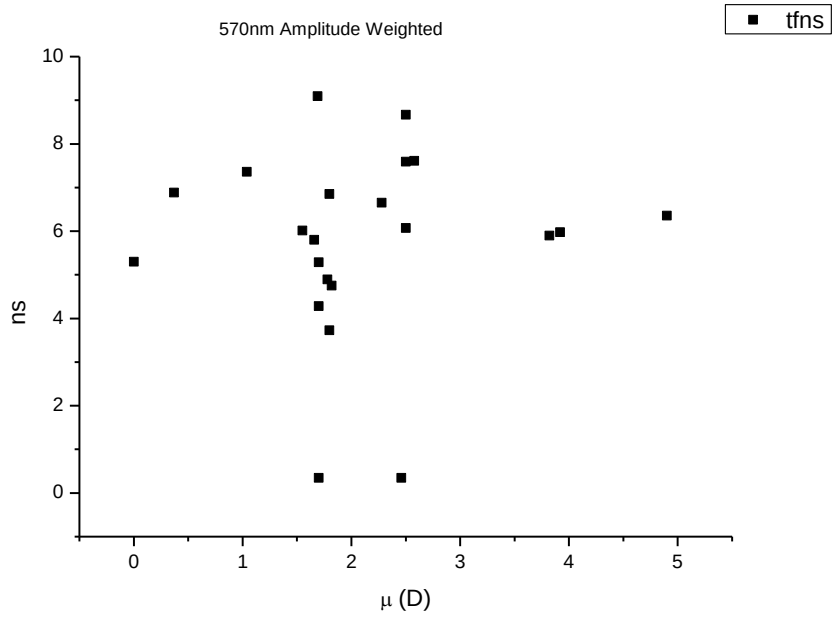

Figure 1.3.128. Amplitude weighted average lifetime (τ_f) of **9a** at 570 nm versus μ(D).

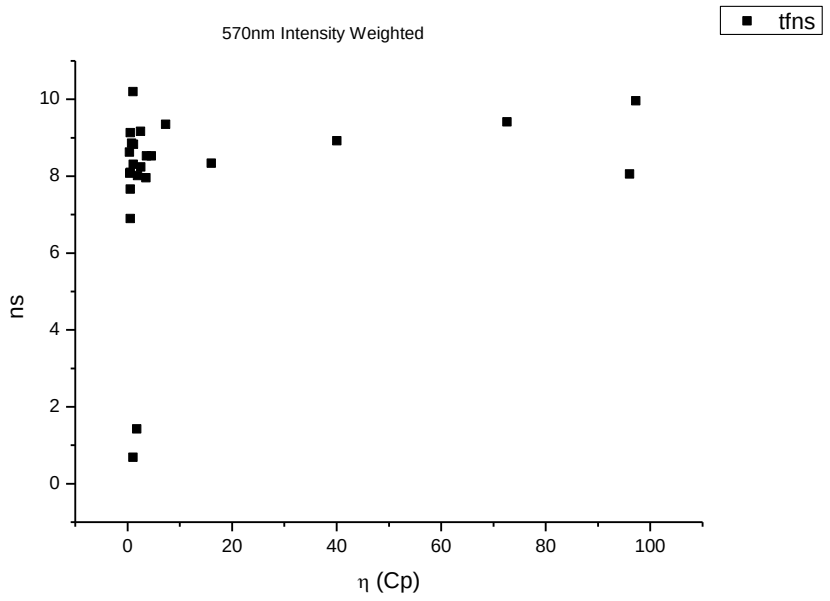

Figure 1.3.129. Intensity weighted average lifetime (τ_f) of **9a** at 570 nm versus η(Cp).

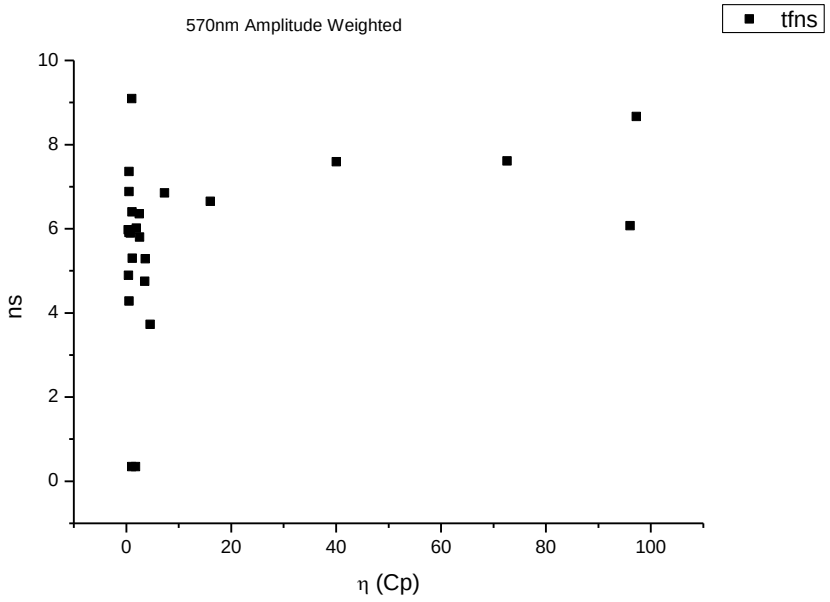

Figure 1.3.130. Amplitude weighted average lifetime (τ_f) of **9a** at 570 nm versus η(Cp).

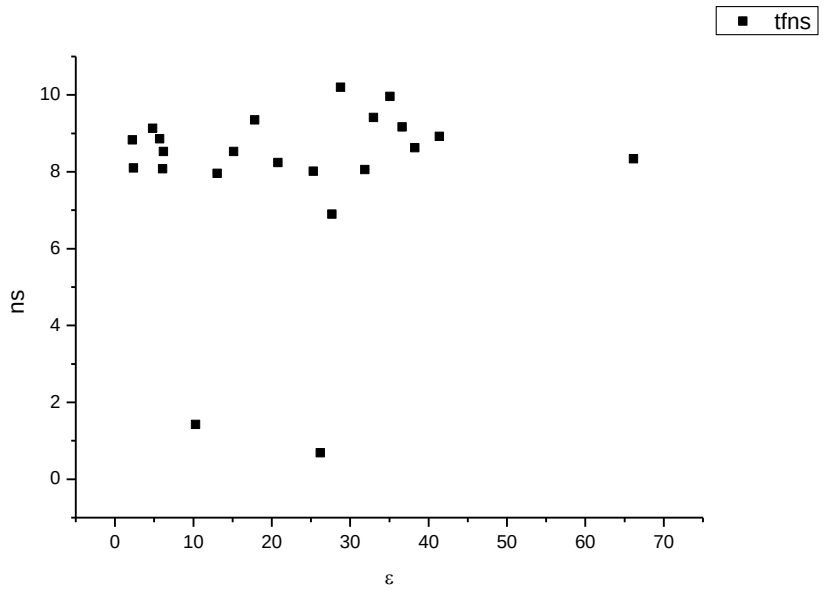

Figure 1.3.131. Intensity weighted average lifetime (τ_f) of **9a** at 570 nm versus ε.

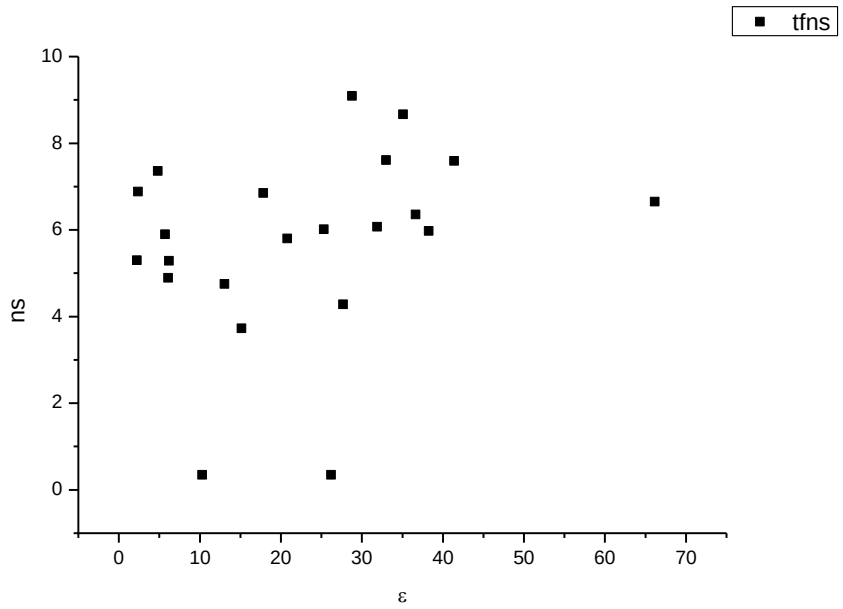

Figure 1.3.132. Amplitude weighted average lifetime (τ_f) of **9a** at 570 nm versus ε.

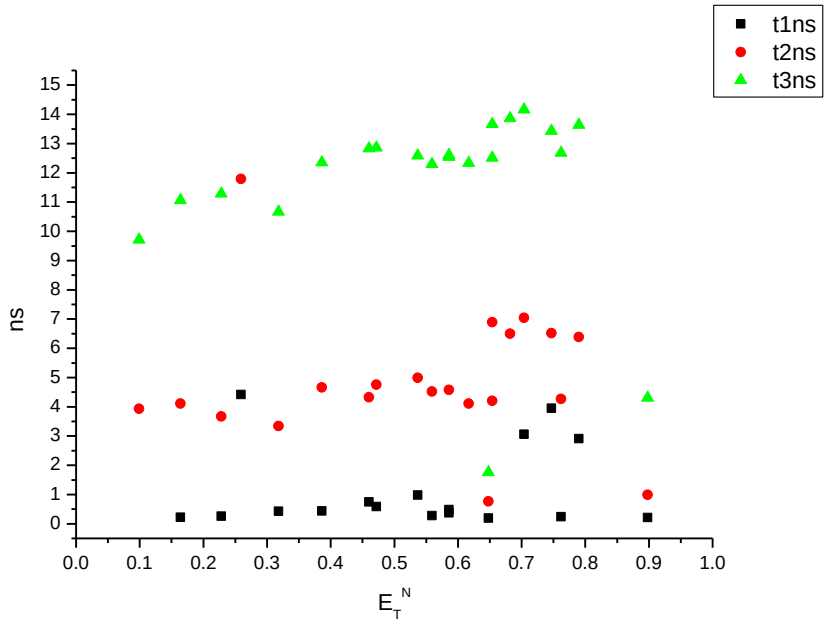

Figure 1.3.133. Intensity weighted components of TCSPC lifetime decay of **9a** (570 nm) versus E_T^N.

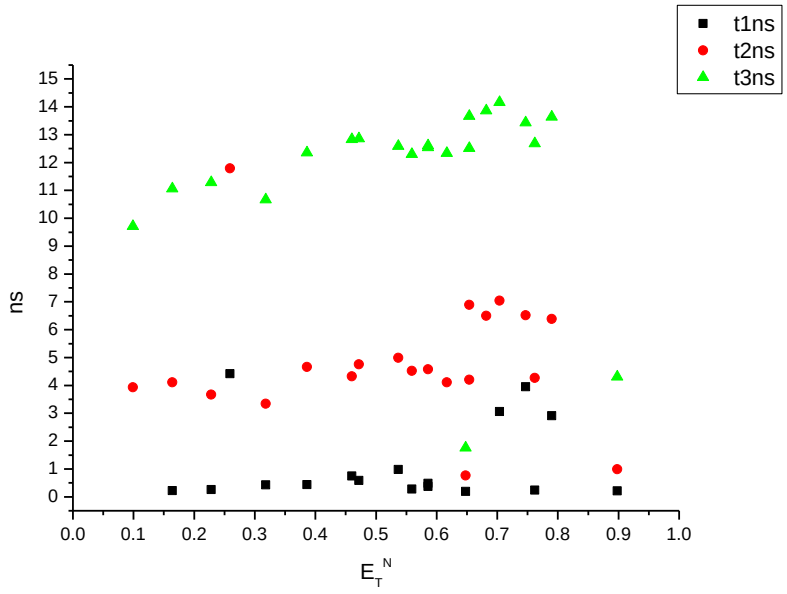

Figure 1.3.134. Amplitude weighted components of TCSPC lifetime decay of **9a** (570 nm) versus E_T^N.

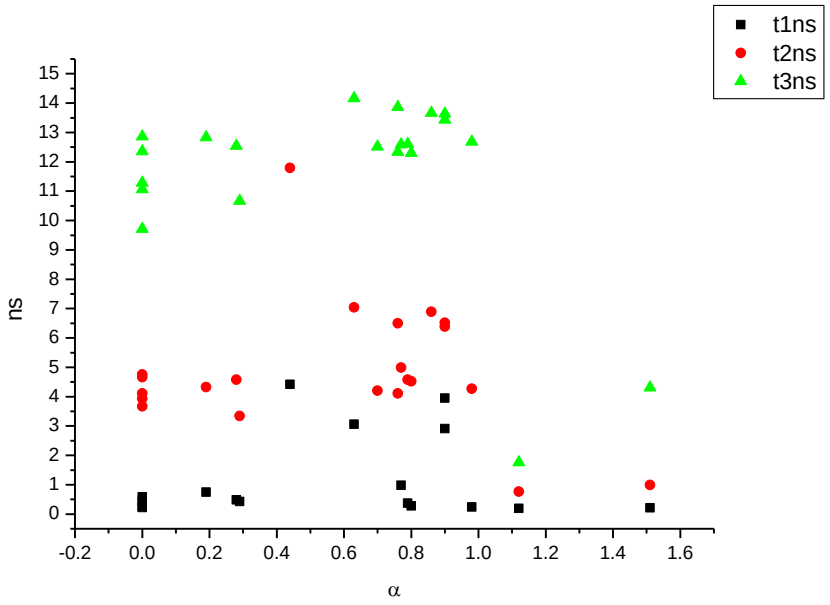

Figure 1.3.135. Intensity weighted components of TCSPC lifetime decay of **9a** (570 nm) versus α.

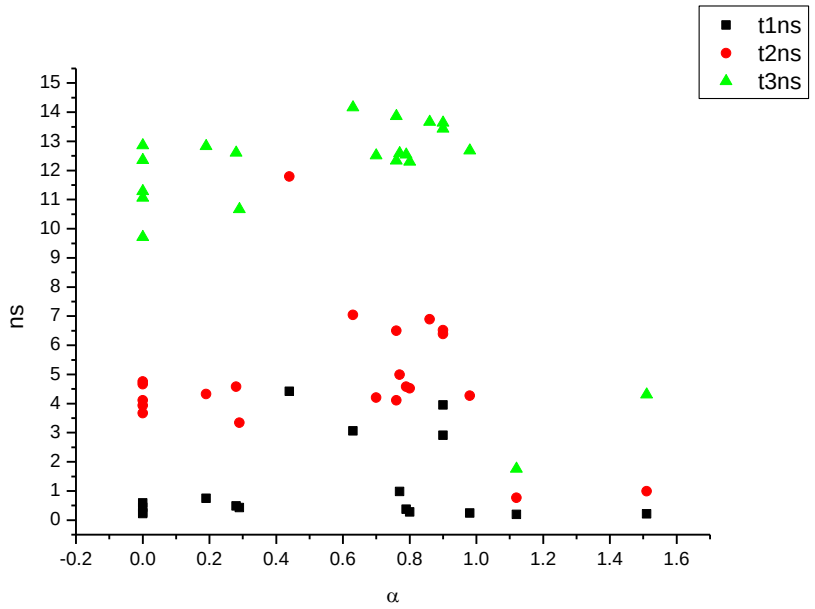

Figure 1.3.136. Amplitude weighted components of TCSPC lifetime decay of **9a** (570 nm) versus α.

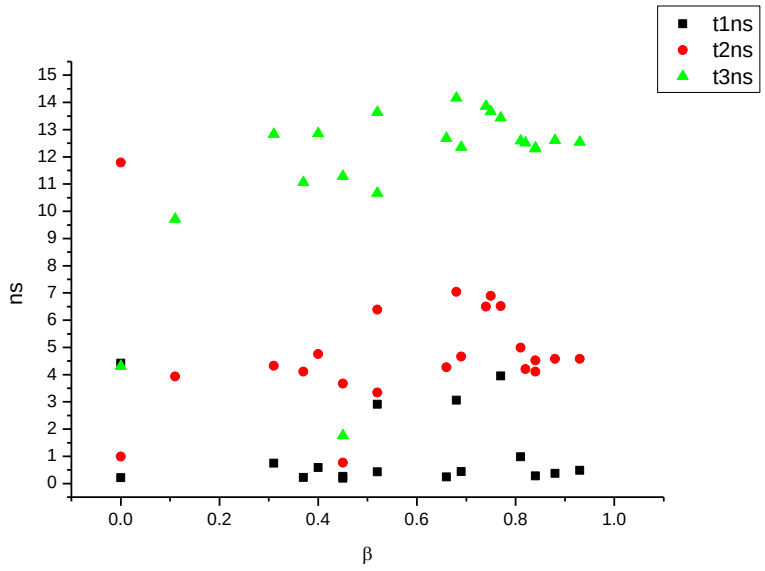

Figure 1.3.137. Intensity weighted components of TCSPC lifetime decay of **9a** (570 nm) versus β.

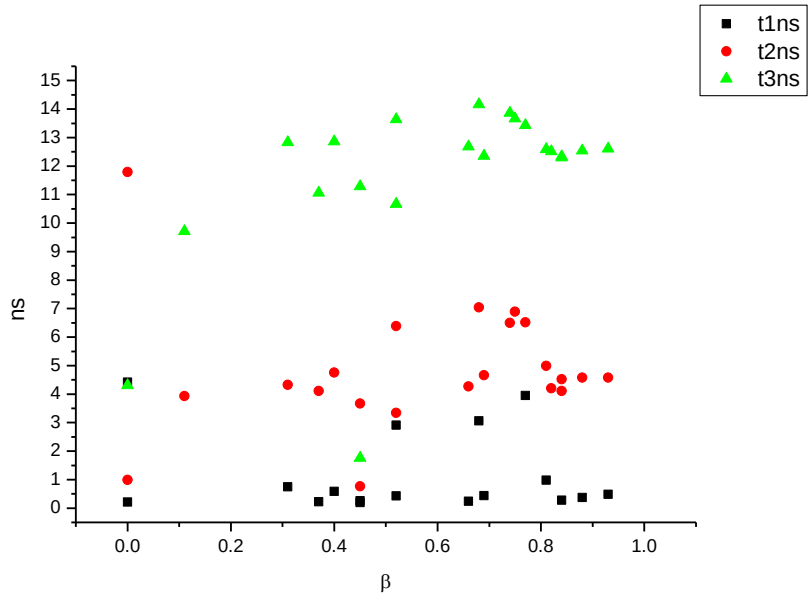

Figure 1.3.138. Amplitude weighted components of TCSPC lifetime decay of **9a** (570 nm) versus β.

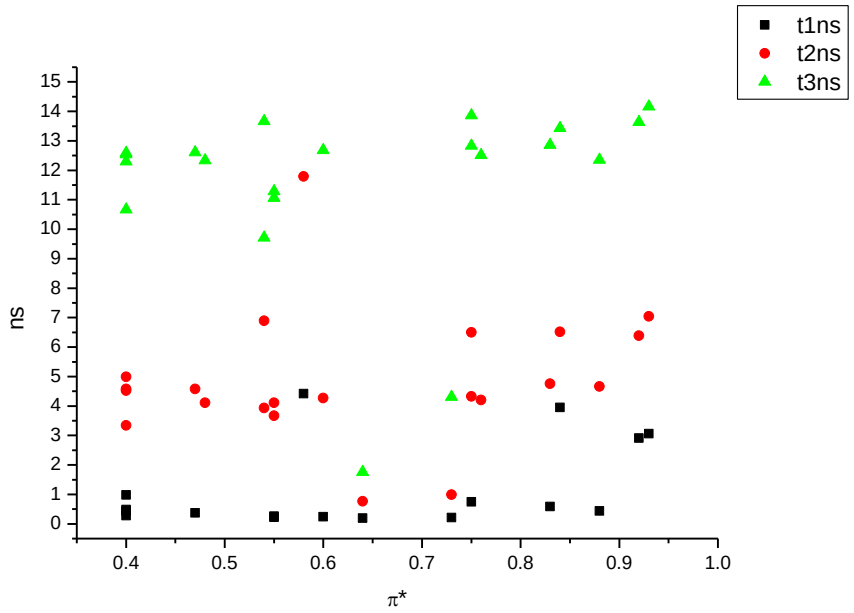

Figure 1.3.139. Intensity weighted components of TCSPC lifetime decay of **9a** (570 nm) versus π*.

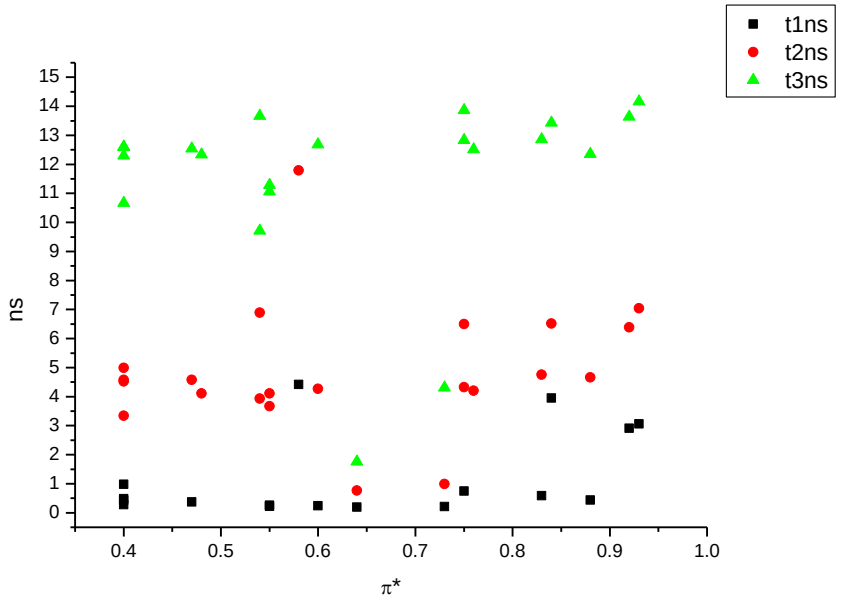

Figure 1.3.140. Amplitude weighted components of TCSPC lifetime decay of **9a** (570 nm) versus π*.

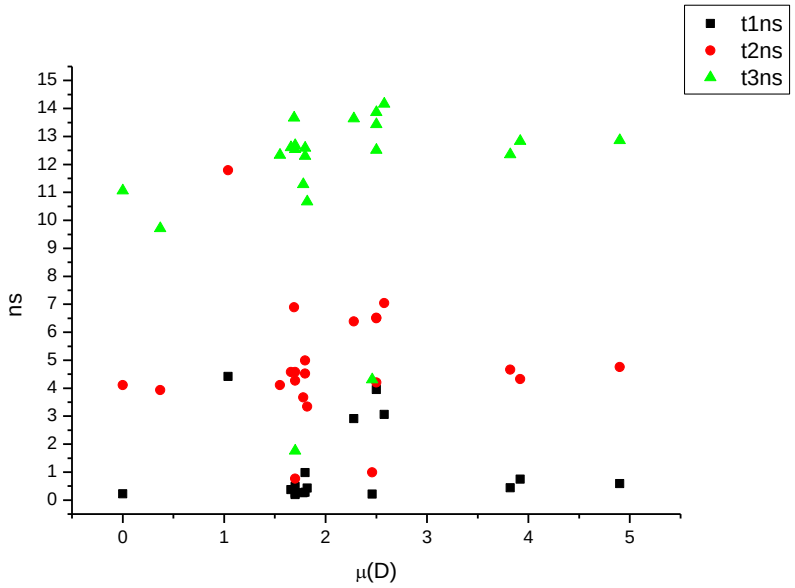

Figure 1.3.141. Intensity weighted components of TCSPC lifetime decay of **9a** (570 nm) versus μ(D).

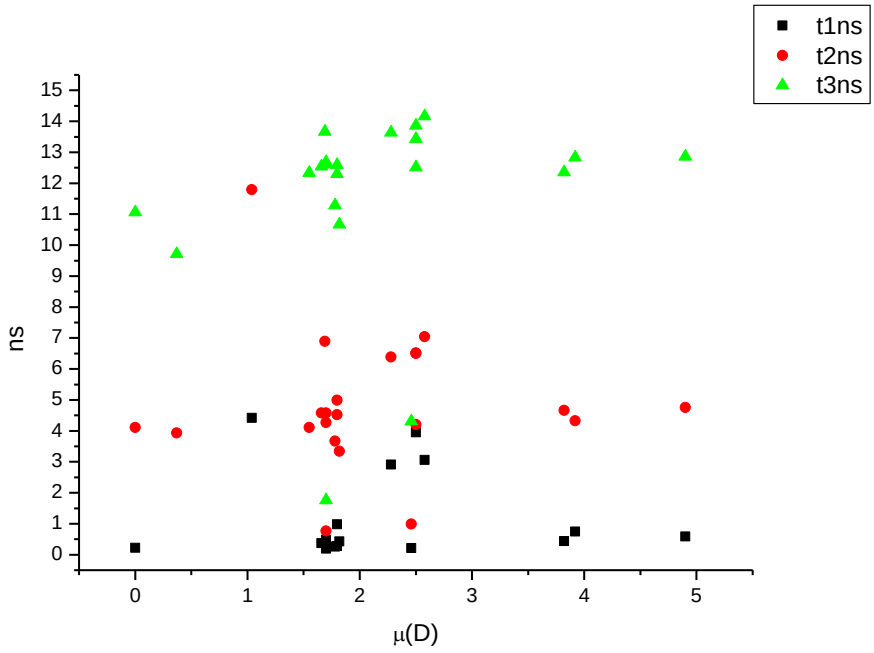

Figure 1.3.142. Amplitude weighted components of TCSPC lifetime decay of **9a** (570 nm) versus μ(D).

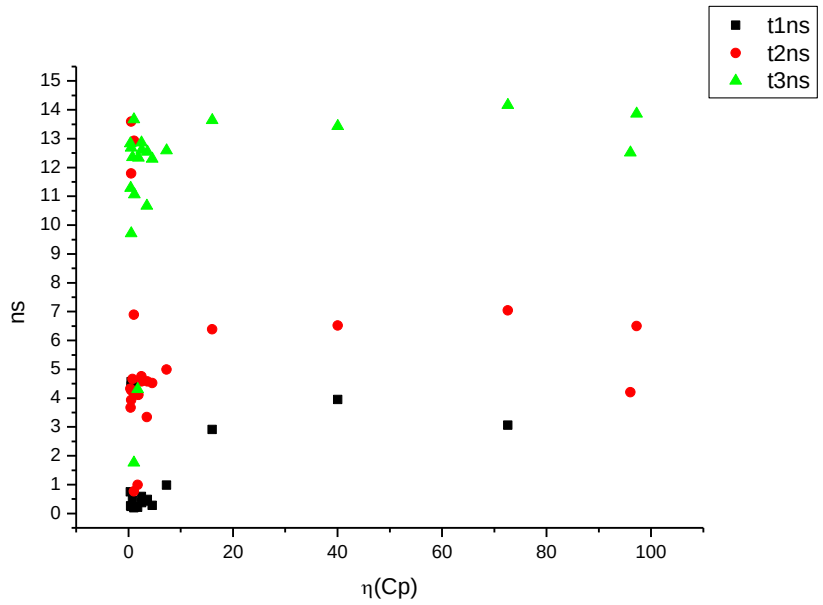

Figure 1.3.143. Intensity weighted components of TCSPC lifetime decay of **9a** (570 nm) versus η(Cp).

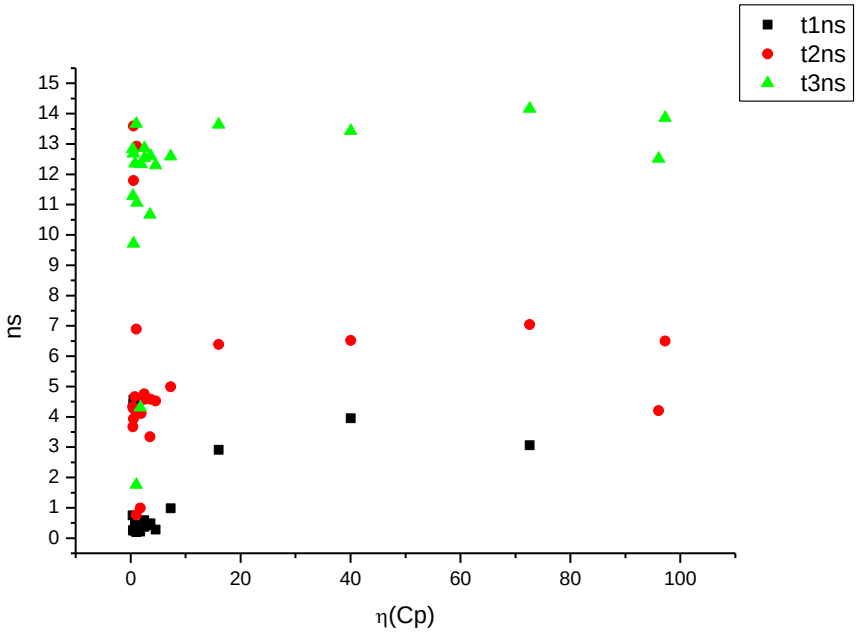

Figure 1.3.144. Amplitude weighted components of TCSPC lifetime decay of **9a** (570 nm) versus η(Cp).

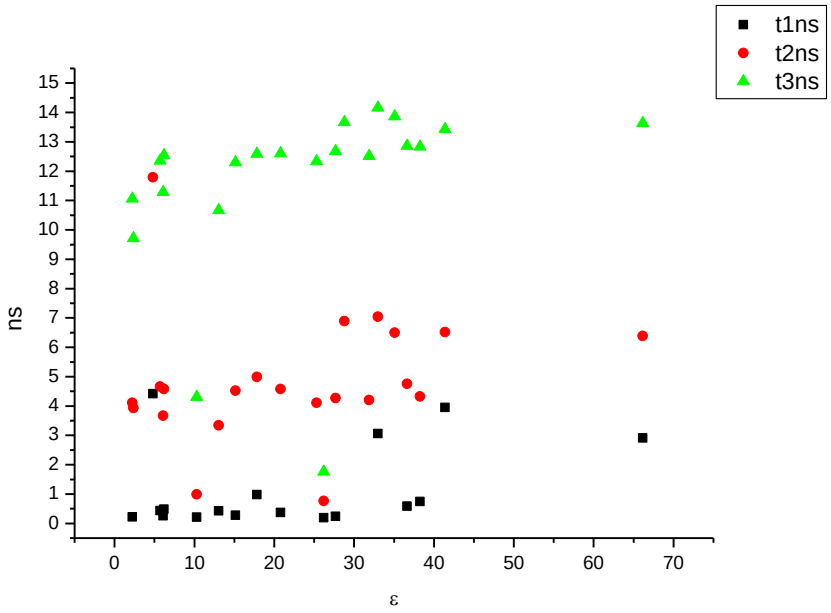

Figure 1.3.145. Intensity weighted components of TCSPC lifetime decay of **9a** (570 nm) versus ε.

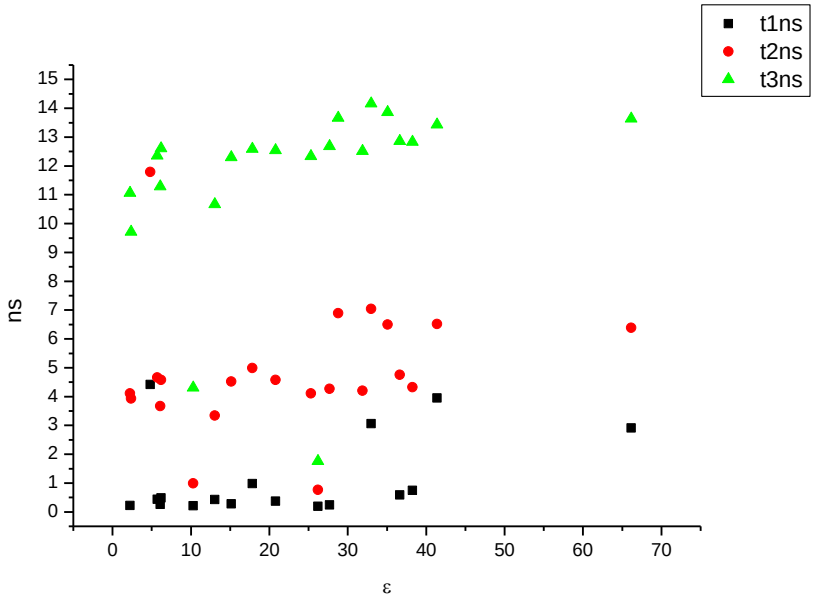

Figure 1.3.146. Amplitude weighted components of TCSPC lifetime decay of **9a** (570 nm) versus ε.

1.3.8 Ultraviolet-visible absorption spectra.

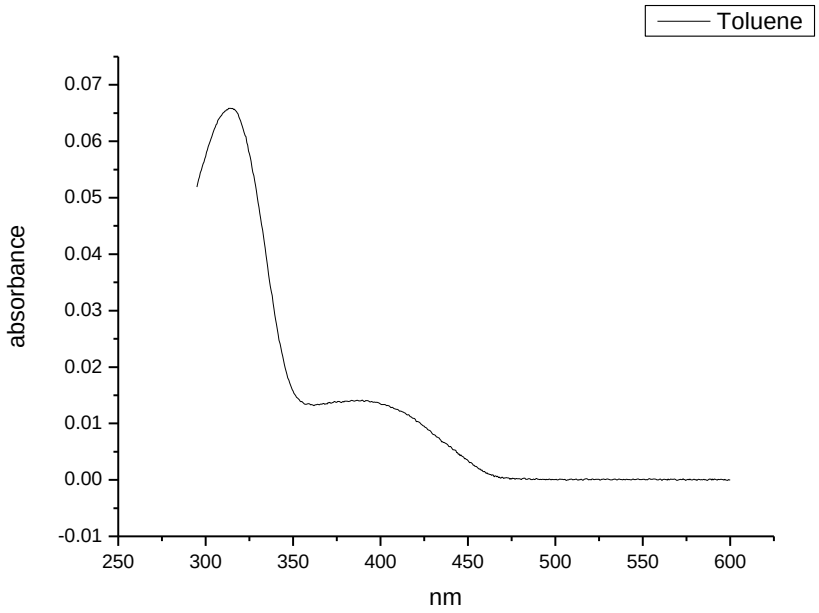

Figure 1.3.147. Ultraviolet-Visible absorption spectrum of **9a** recorded in Toluene.

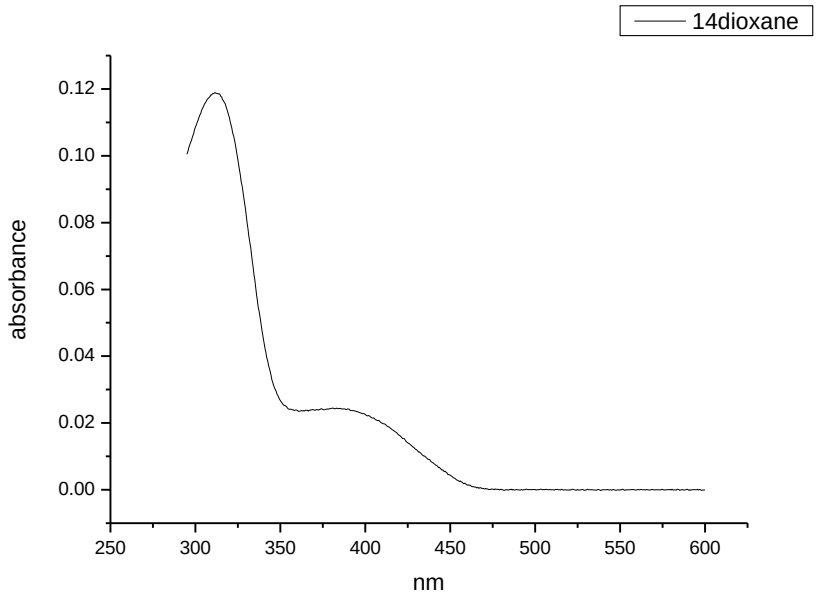

Figure 1.3.148. Ultraviolet-Visible absorption spectrum of **9a** recorded in 1,4-dioxane.

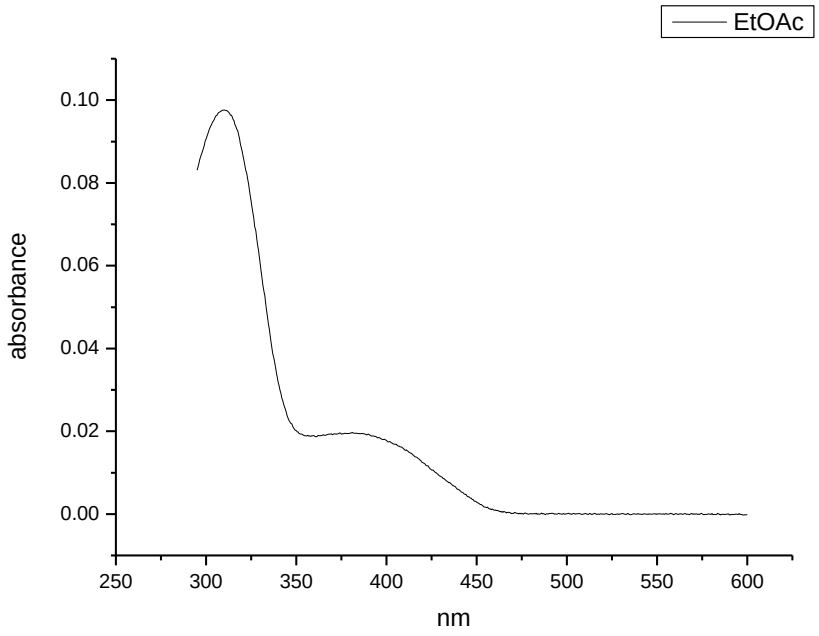

Figure 1.3.149. Ultraviolet-Visible absorption spectrum of **9a** recorded in Ethyl Acetate.

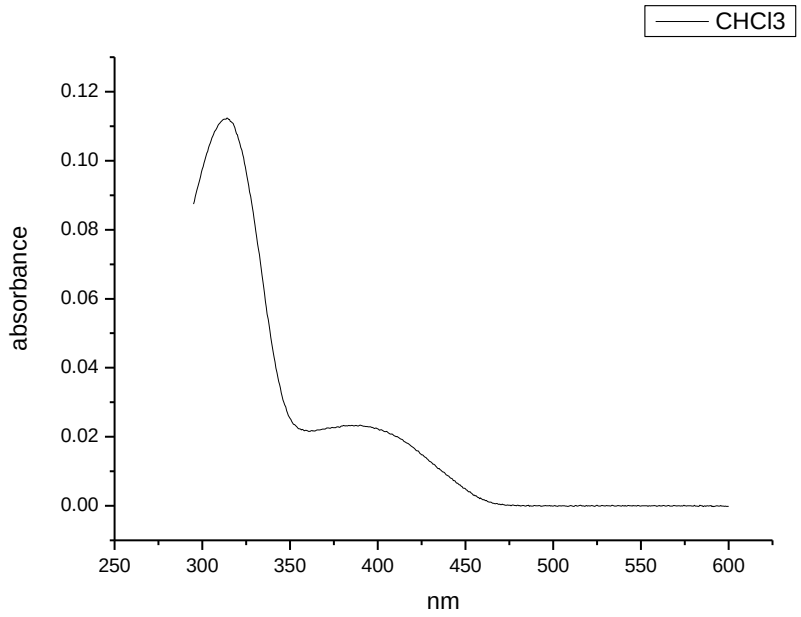

Figure 1.3.150. Ultraviolet-Visible absorption spectrum of **9a** recorded in Chloroform.

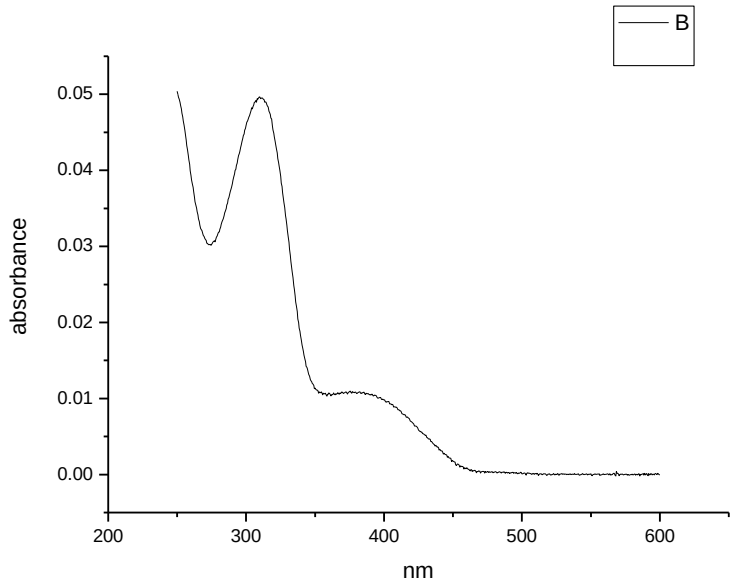

Figure 1.3.151. Ultraviolet-Visible absorption spectrum of **9a** recorded in 2-methyl-2-butanol.

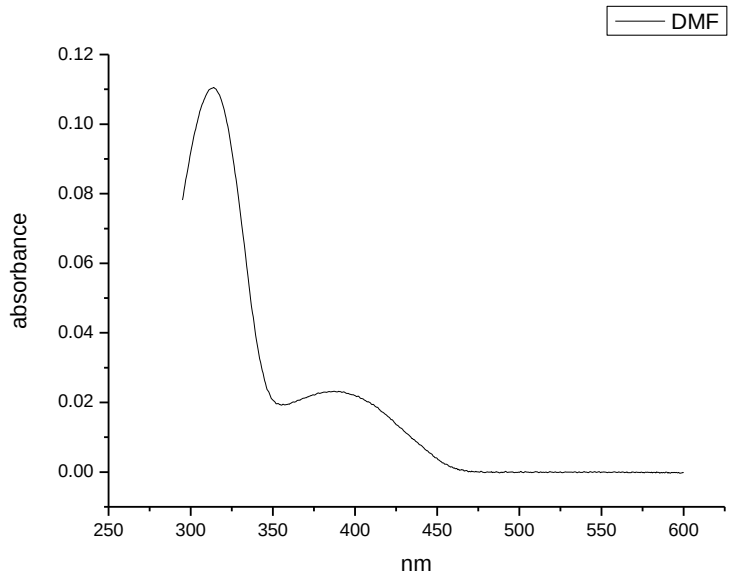

Figure 1.3.152. Ultraviolet-Visible absorption spectrum of **9a** recorded in N,N-dimethylformamide.

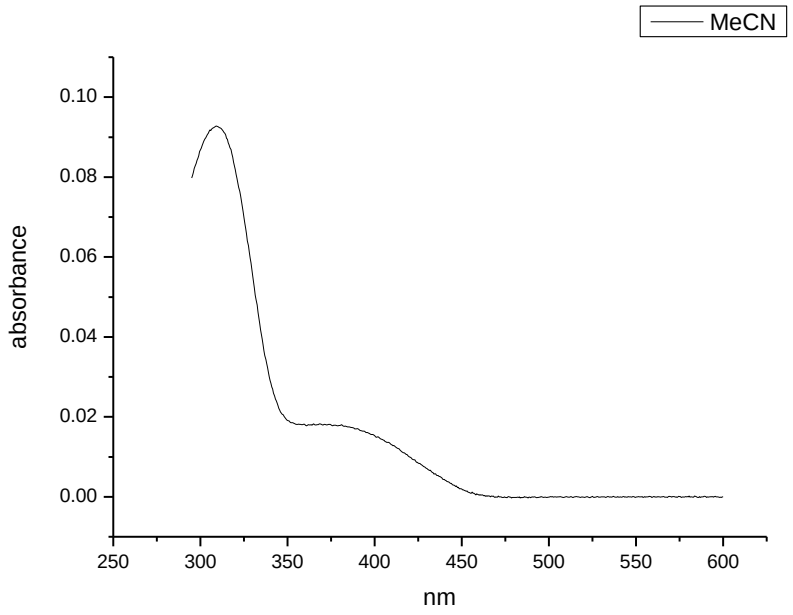

Figure 1.3.153. Ultraviolet-Visible absorption spectrum of **9a** recorded in Acetonitrile.

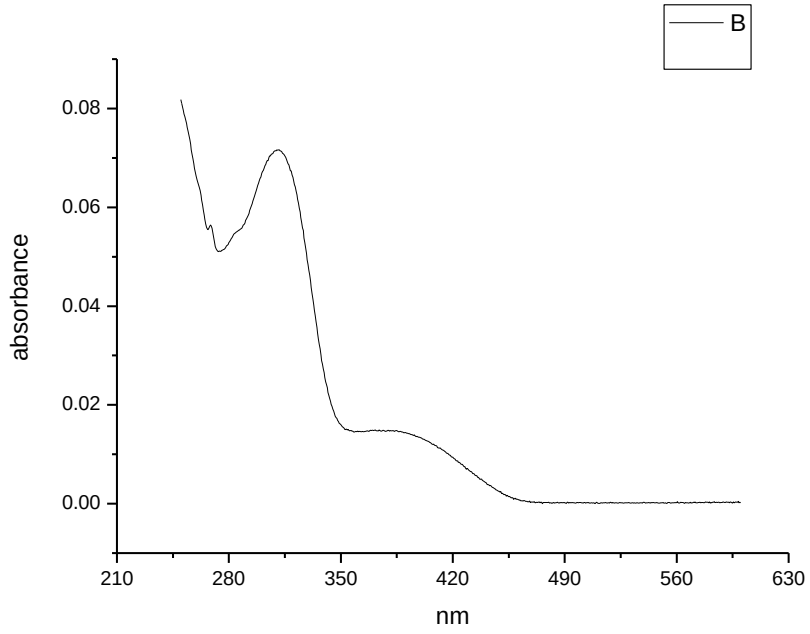

Figure 1.3.154. Ultraviolet-Visible absorption spectrum of **9a** recorded in Propylene Carbonate.

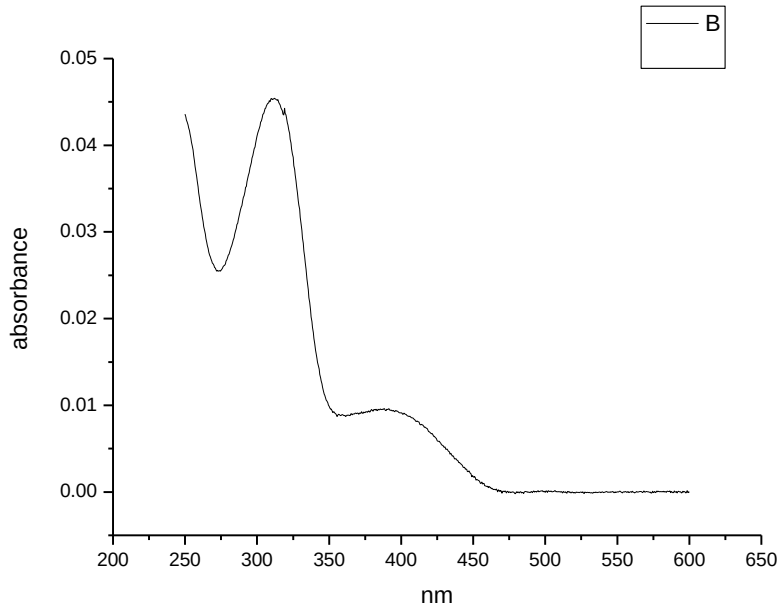

Figure 1.3.155. Ultraviolet-Visible absorption spectrum of **9a** recorded in 1-octanol.

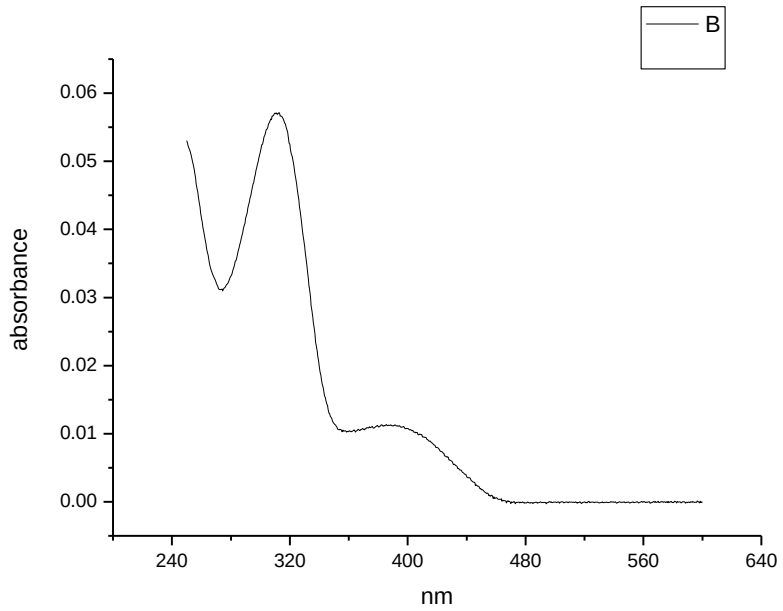

Figure 1.3.156. Ultraviolet-Visible absorption spectrum of **9a** recorded in 1-hexanol.

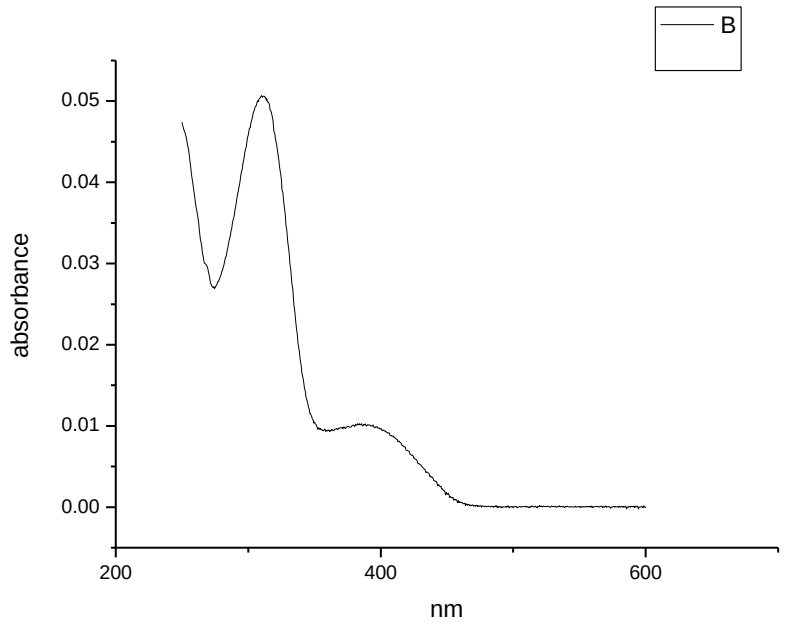

Figure 1.3.157. Ultraviolet-Visible absorption spectrum of **9a** recorded in 1-butanol.

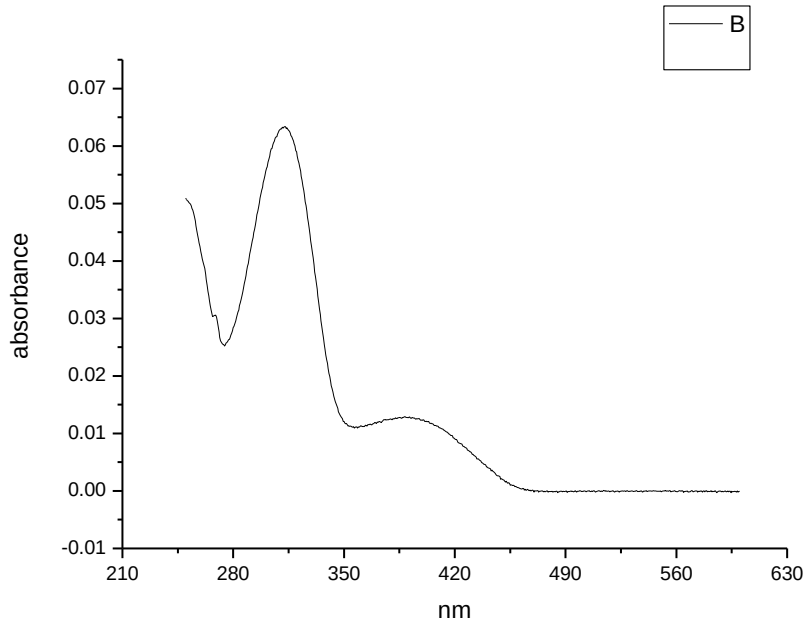

Figure 1.3.158. Ultraviolet-Visible absorption spectrum of **9a** recorded in 1-pentanol.

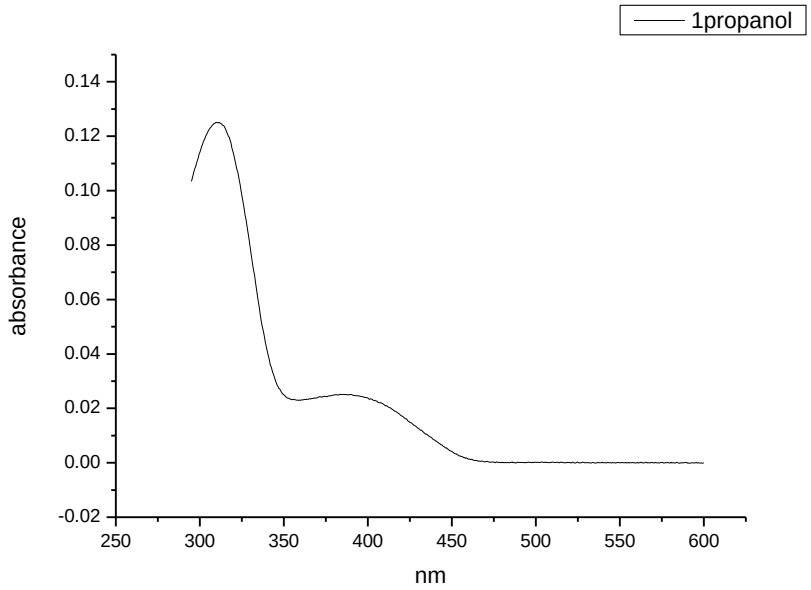

Figure 1.3.159. Ultraviolet-Visible absorption spectrum of **9a** recorded in 1-propanol.

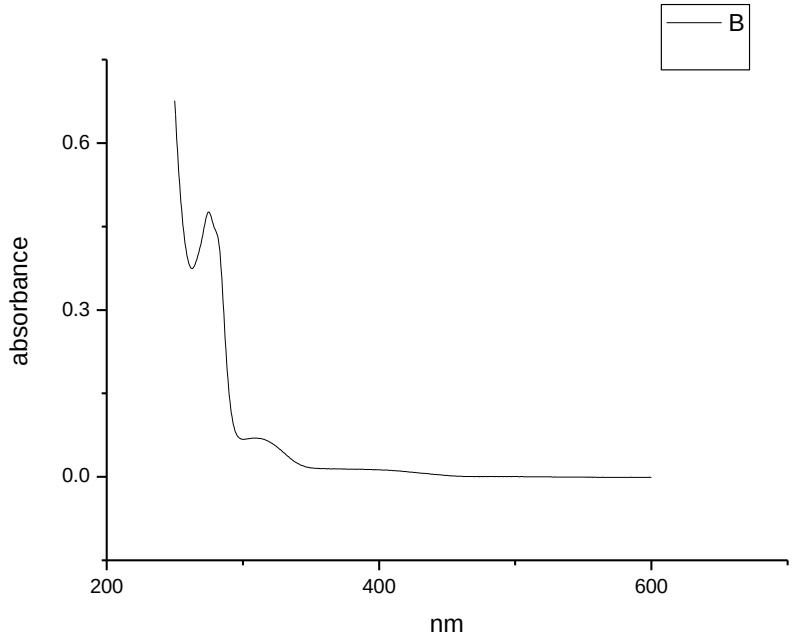

Figure 1.3.160. Ultraviolet-Visible absorption spectrum of **9a** recorded in Acetic Acid.

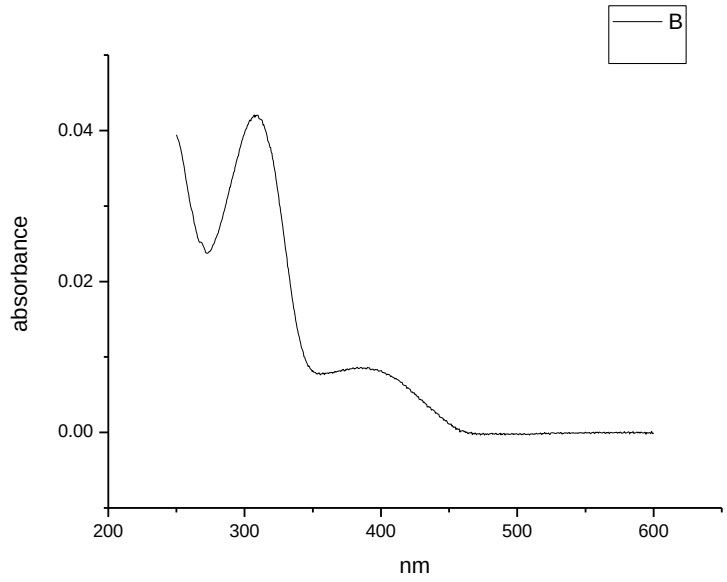

Figure 1.3.161. Ultraviolet-Visible absorption spectrum of **9a** recorded in Ethanol.

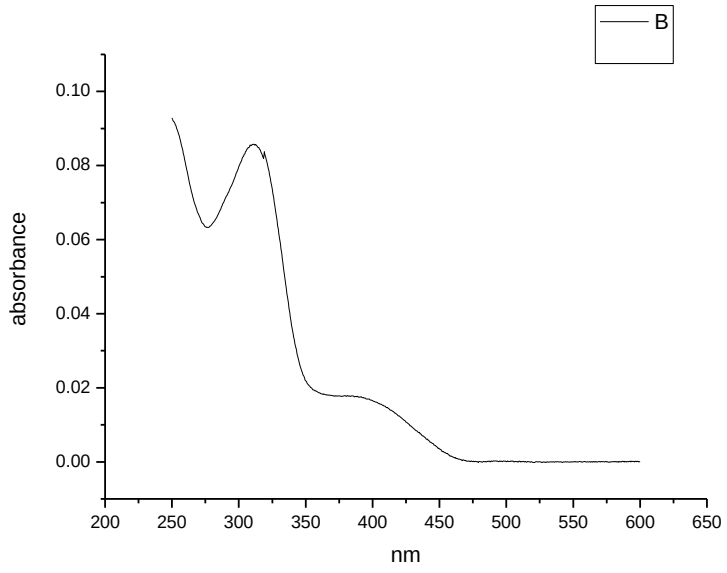

Figure 1.3.162. Ultraviolet-Visible absorption spectrum of **9a** recorded in 1,5-pentanediol.

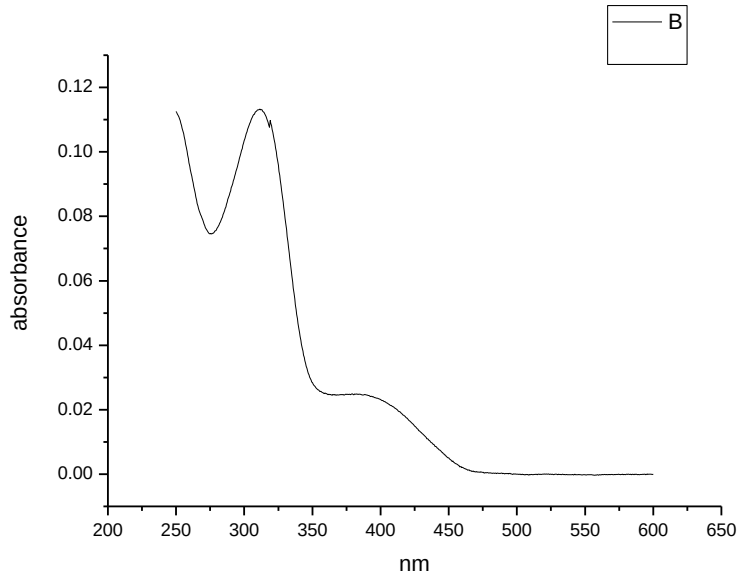

Figure 1.3.163. Ultraviolet-Visible absorption spectrum of **9a** recorded in 1,3-buttanediol.

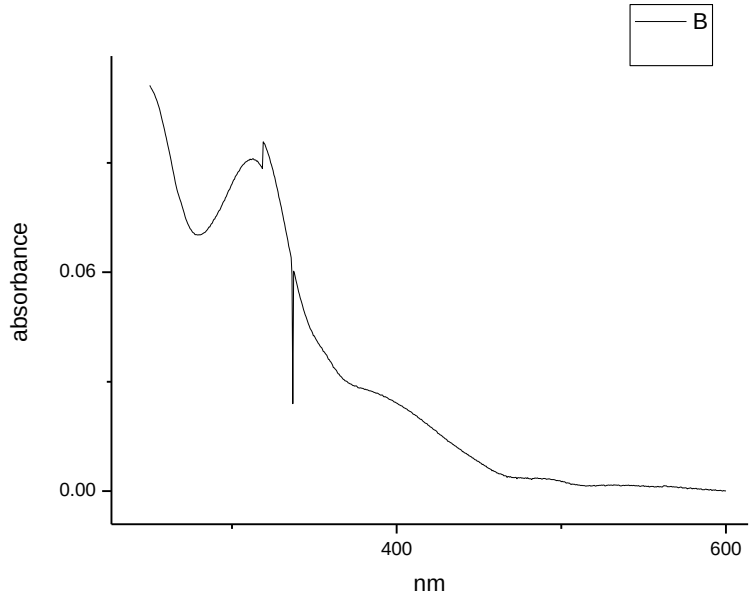

Figure 1.3.164. Ultraviolet-Visible absorption spectrum of **9a** recorded in 1,4-buttanediol.

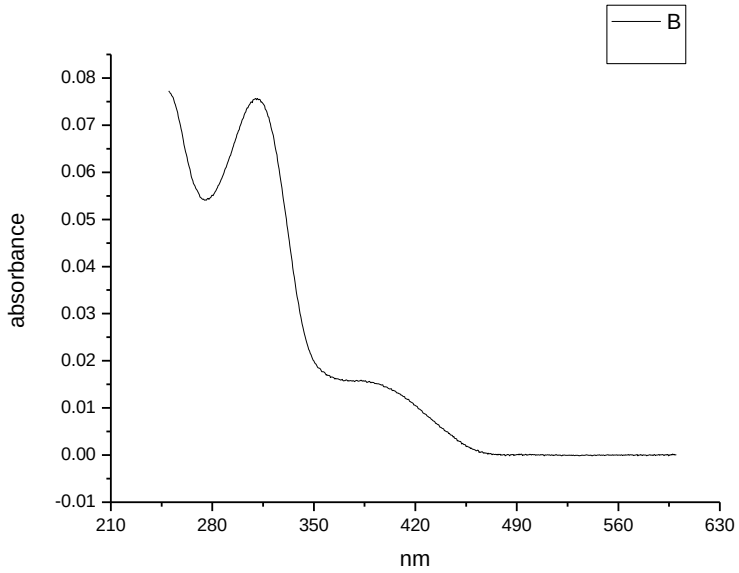

Figure 1.3.165. Ultraviolet-Visible absorption spectrum of **9a** recorded in 1,3-propanediol.

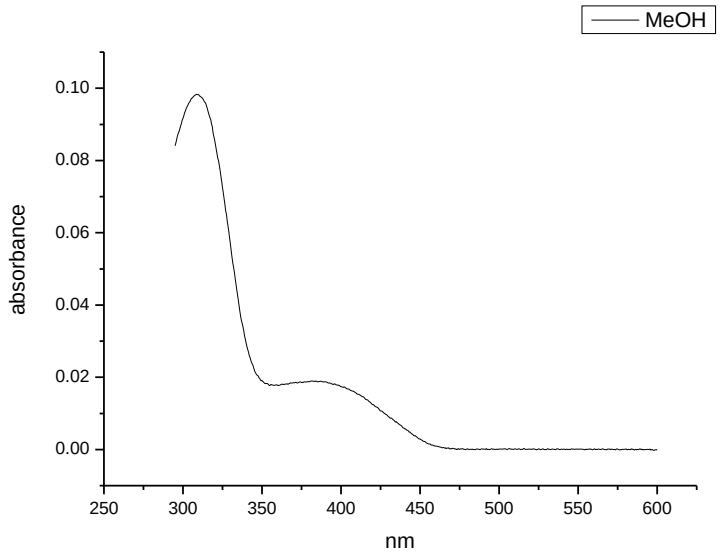

Figure 1.3.166. Ultraviolet-Visible absorption spectrum of **9a** recorded in Methanol.

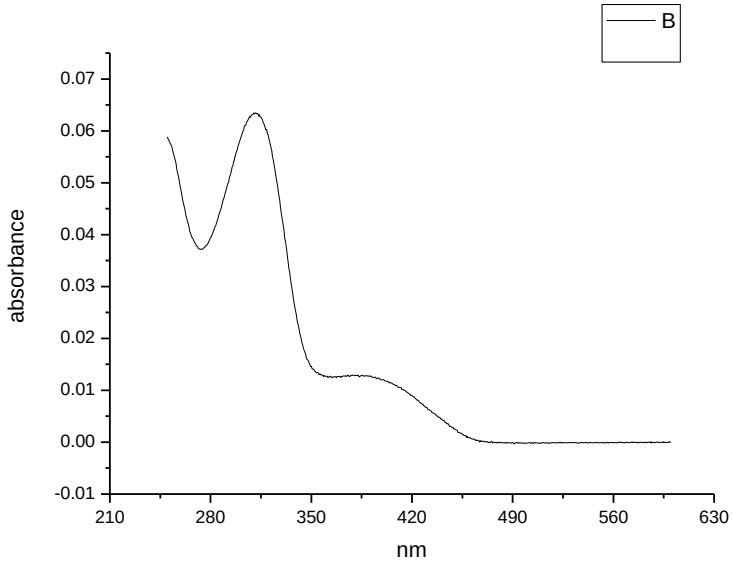

Figure 1.3.167. Ultraviolet-Visible absorption spectrum of **9a** recorded in 1,2-ethanediol.

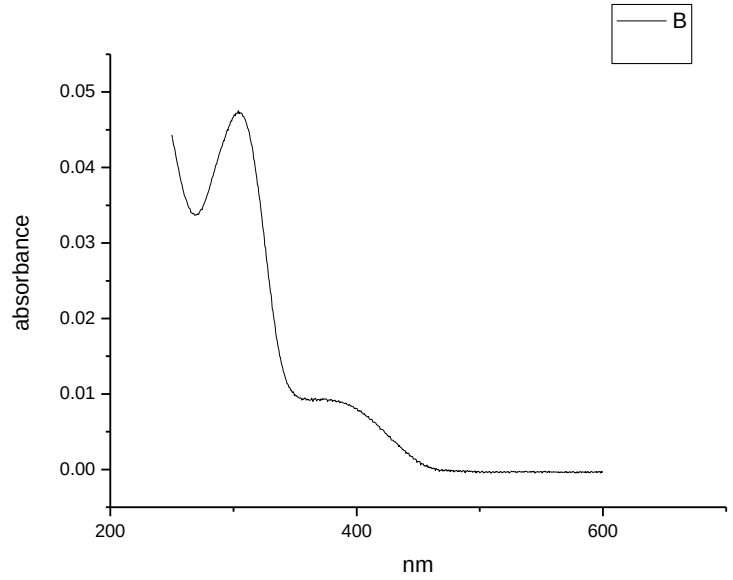

Figure 1.3.168. Ultraviolet-Visible absorption spectrum of **9a** recorded in 2,2,2-trifluoroethanol.

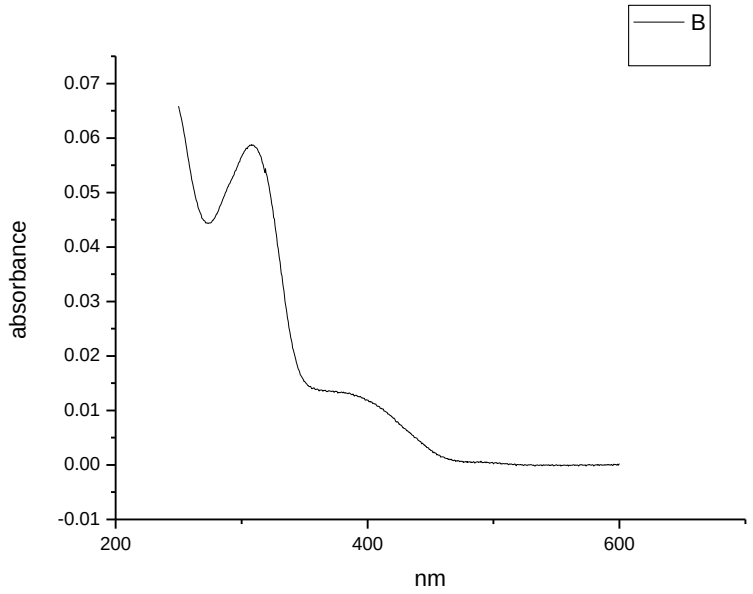

Figure 1.3.169. Ultraviolet-Visible absorption spectrum of **9a** recorded in Ethanol-d_1 (EtOD).

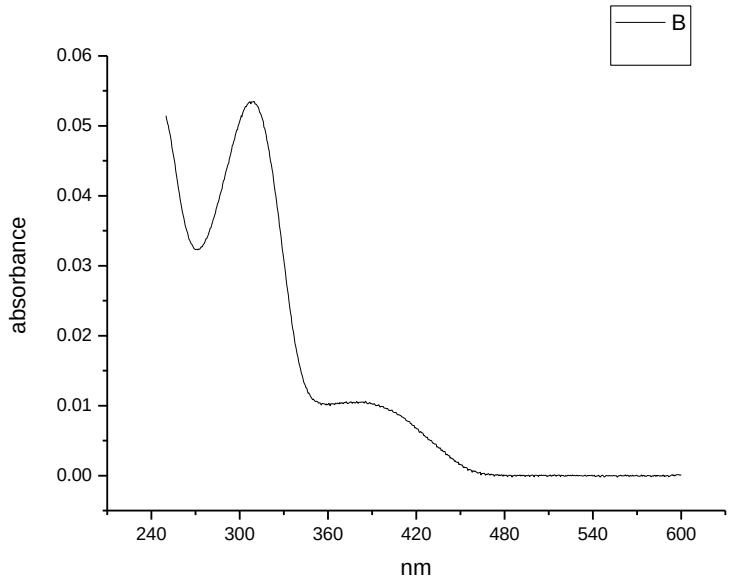

Figure 1.3.170. Ultraviolet-Visible absorption spectrum of **9a** recorded in Methanol-d_1 (MeOD).

1.3.9 Fluorescence Emission spectra.

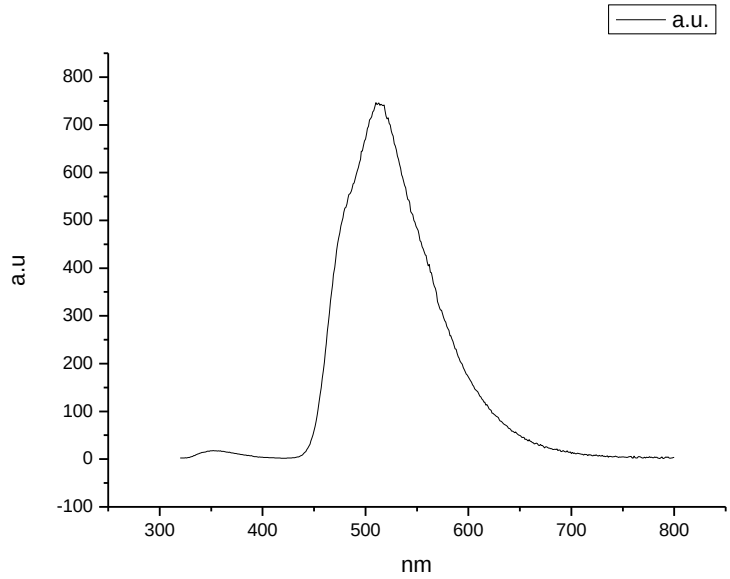

Figure 1.3.171. Fluorescence emission spectrum of **9a** recorded in Toluene at 310 nm excitation.

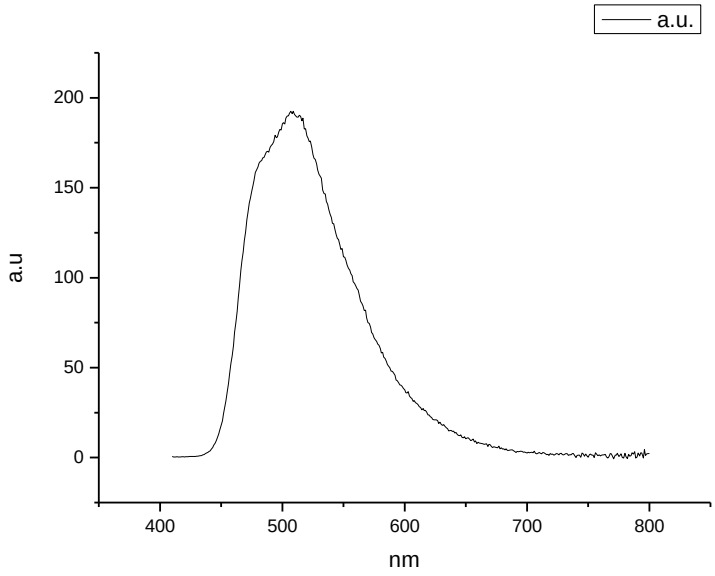

Figure 1.3.172. Fluorescence emission spectrum of **9a** recorded in Toluene at 400 nm excitation.

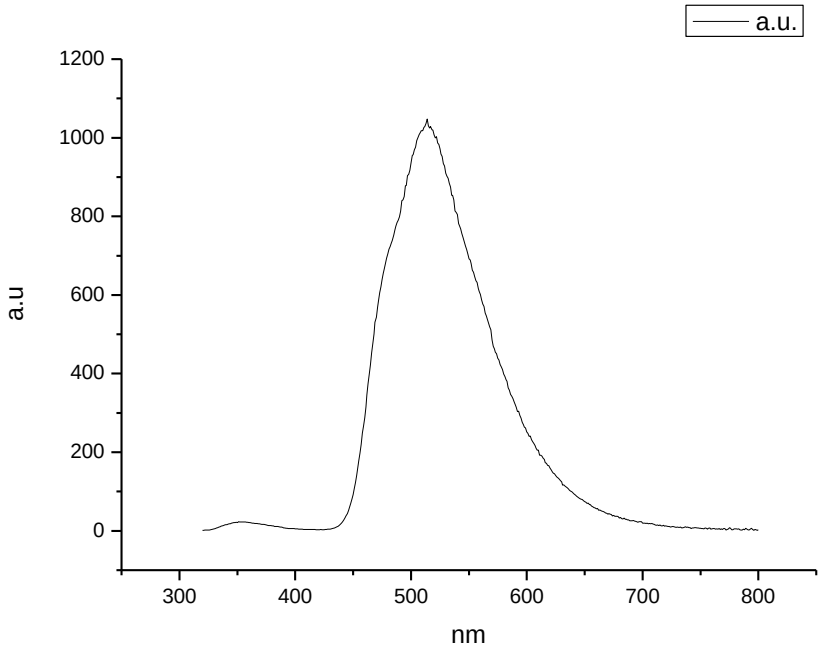

Figure 1.3.173. Fluorescence emission spectrum of **9a** recorded in 1,4-dioxane at 310 nm excitation.

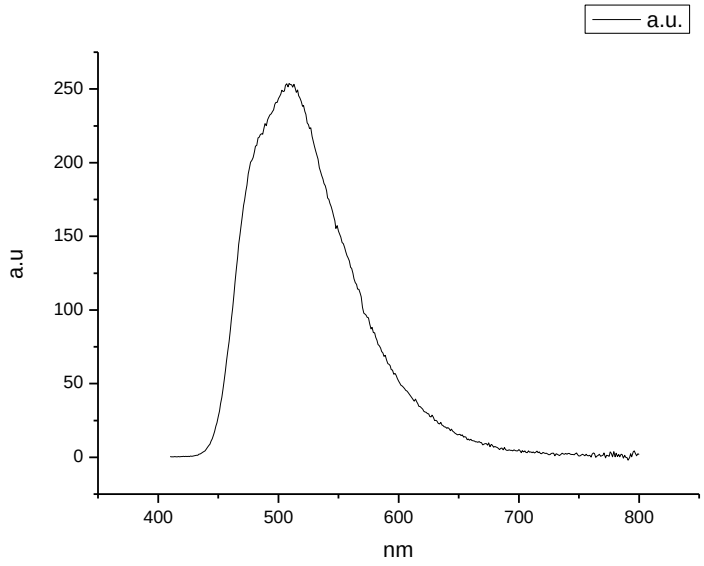

Figure 1.3.174. Fluorescence emission spectrum of **9a** recorded in 1,4-dioxane at 400 nm excitation.

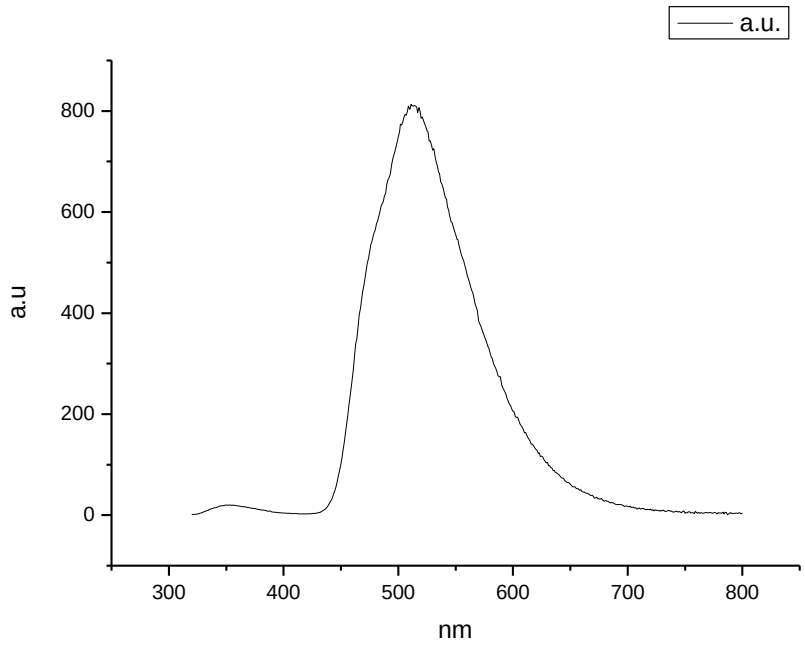

Figure 1.3.175. Fluorescence emission spectrum of **9a** recorded in Ethyl Acetate at 310 nm excitation.

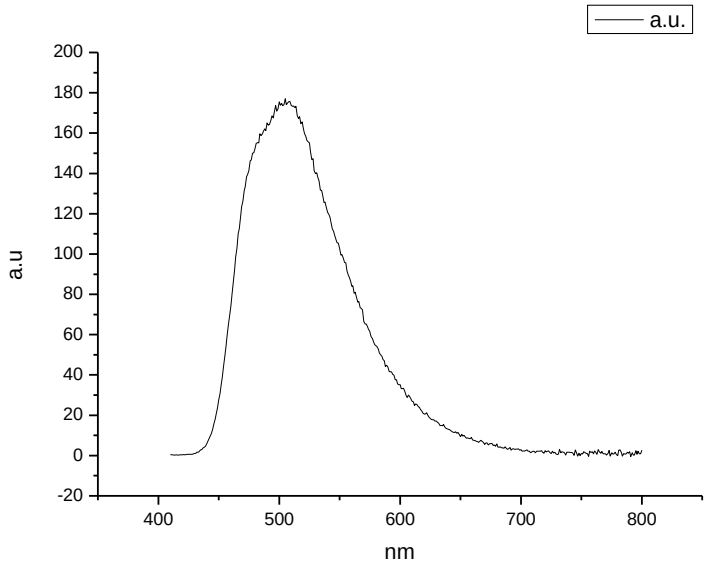

Figure 1.3.176. Fluorescence emission spectrum of **9a** recorded in Ethyl Acetate at 400 nm excitation.

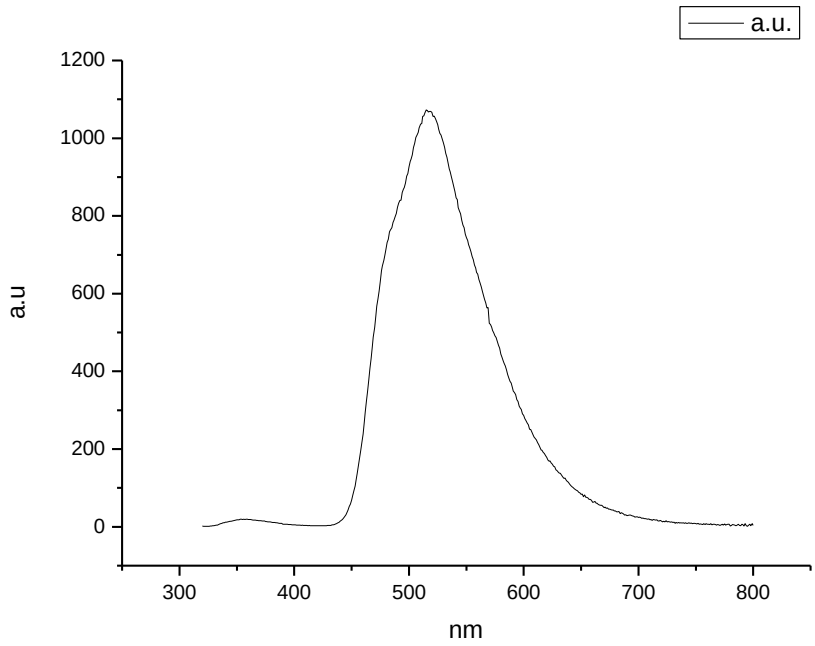

Figure 1.3.177. Fluorescence emission spectrum of **9a** recorded in Chloroform at 310 nm excitation.

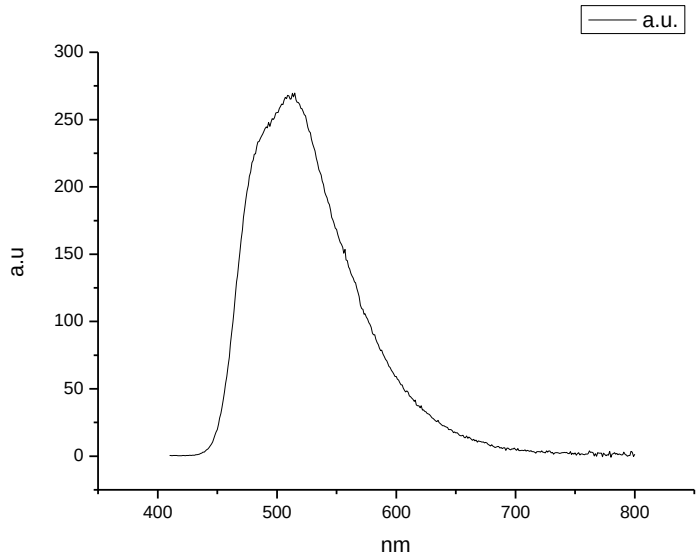

Figure 1.3.178. Fluorescence emission spectrum of **9a** recorded in Chloroform at 400 nm excitation.

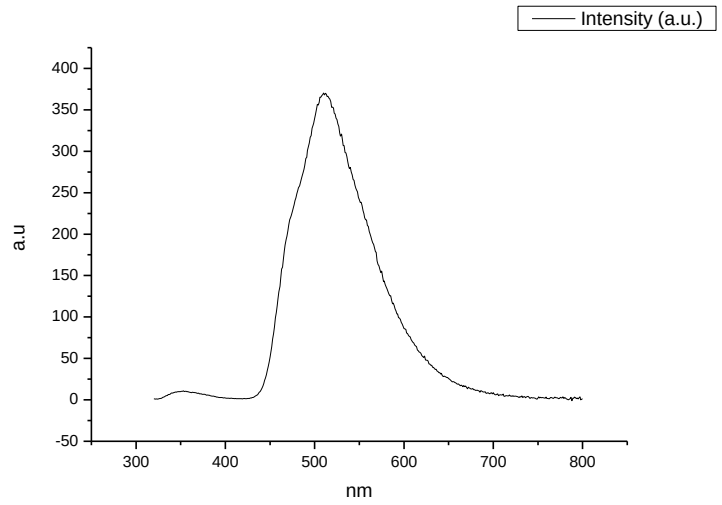

Figure 1.3.179. Fluorescence emission spectrum of **9a** recorded in 2-methyl-2-butanol at 310 nm excitation.

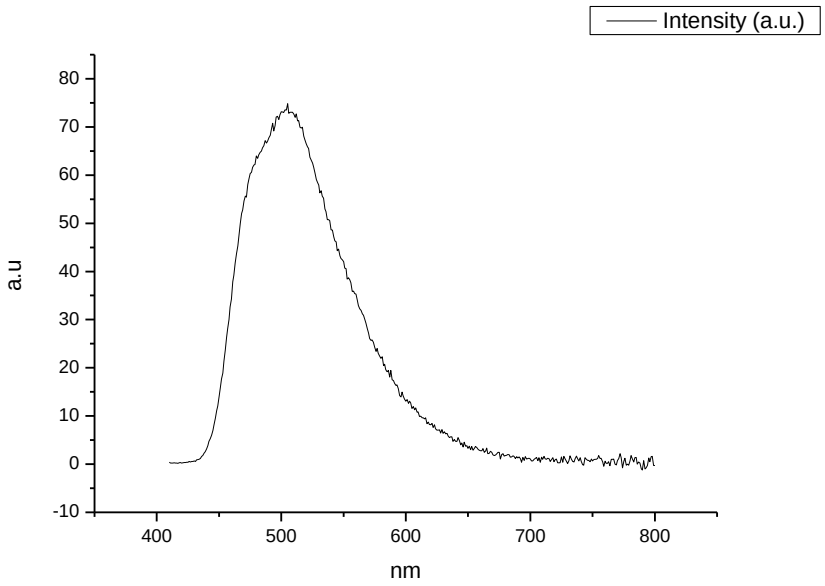

Figure 1.3.180. Fluorescence emission spectrum of **9a** recorded in 2-methyl-2-butanol at 400 nm excitation.

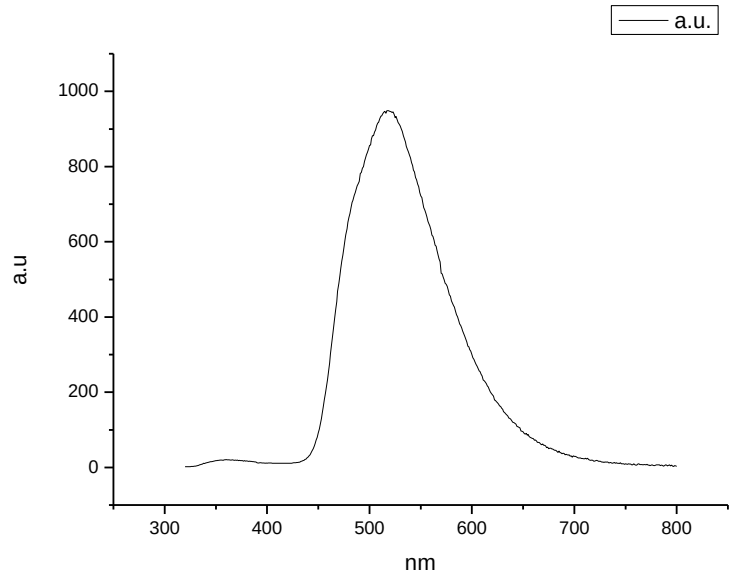

Figure 1.3.181. Fluorescence emission spectrum of **9a** recorded in N,N-dimethylformamide at 310 nm excitation.

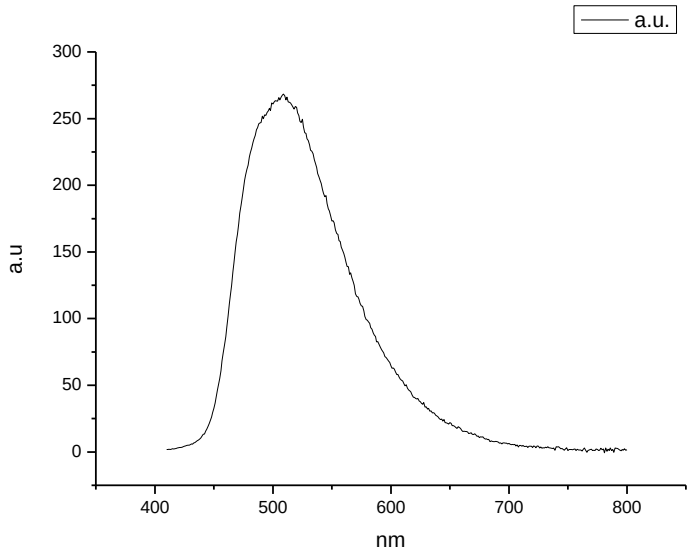

Figure 1.3.182. Fluorescence emission spectrum of **9a** recorded in N,N-dimethylformamide at 400 nm excitation.

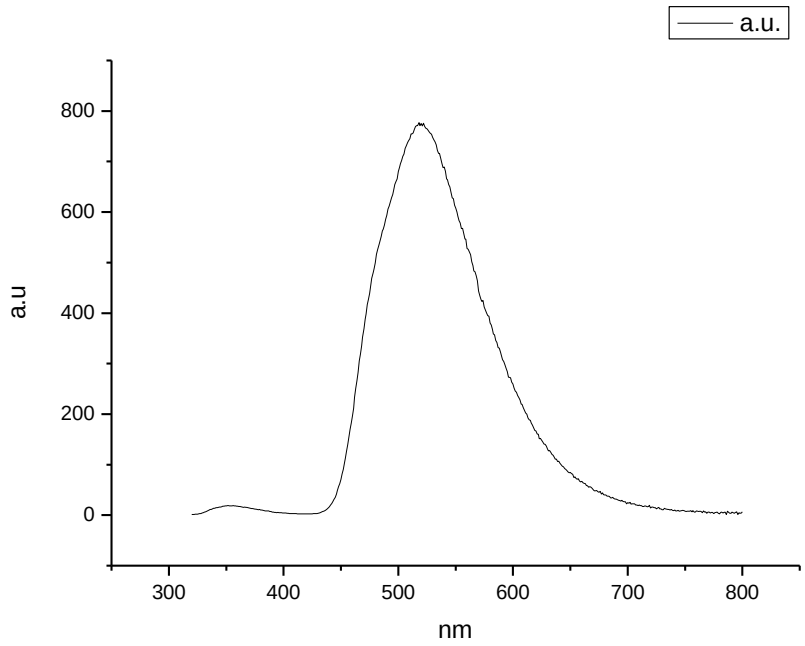

Figure 1.3.183. Fluorescence emission spectrum of **9a** recorded in Acetonitrile at 310 nm excitation.

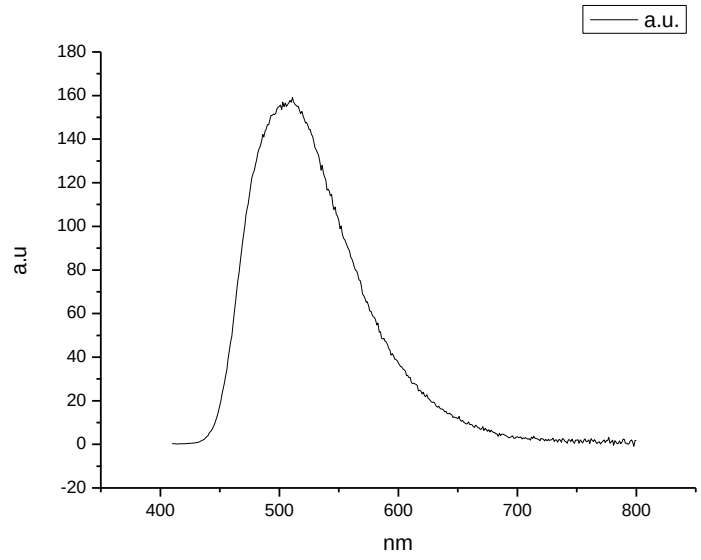

Figure 1.3.184. Fluorescence emission spectrum of **9a** recorded in Acetonitrile at 400 nm excitation.

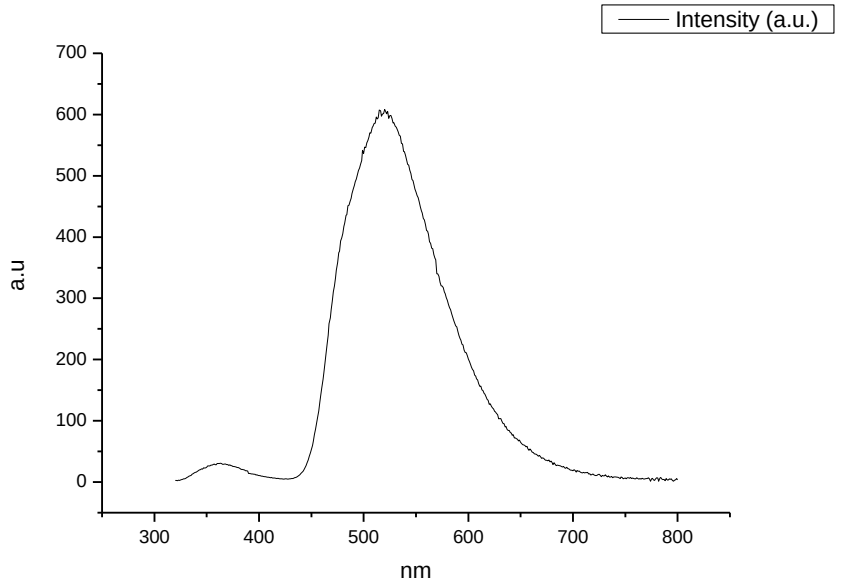

Figure 1.3.185. Fluorescence emission spectrum of **9a** recorded in Propylene Carbonate at 310 nm excitation.

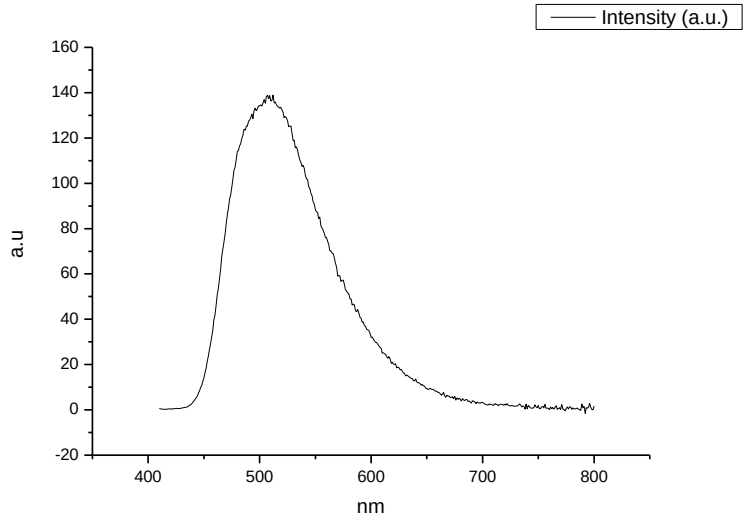

Figure 1.3.186. Fluorescence emission spectrum of **9a** recorded in Propylene Carbonate at 400 nm excitation.

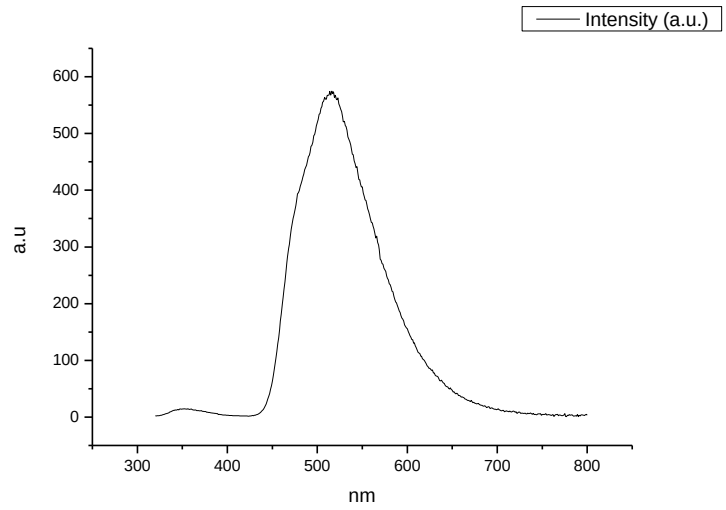

Figure 1.3.187. Fluorescence emission spectrum of **9a** recorded in 1-octanol at 310 nm excitation.

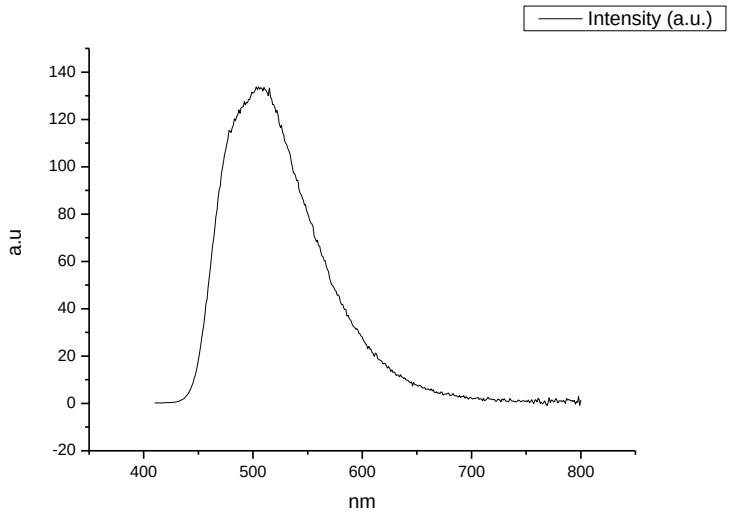

Figure 1.3.188. Fluorescence emission spectrum of **9a** recorded in 1-octanol at 400 nm excitation.

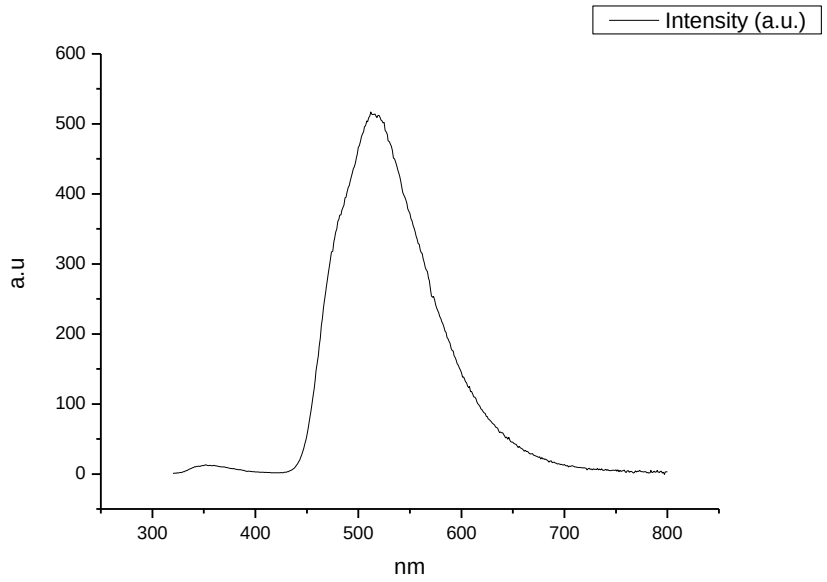

Figure 1.3.189. Fluorescence emission spectrum of **9a** recorded in 1-hexanol at 310 nm excitation.

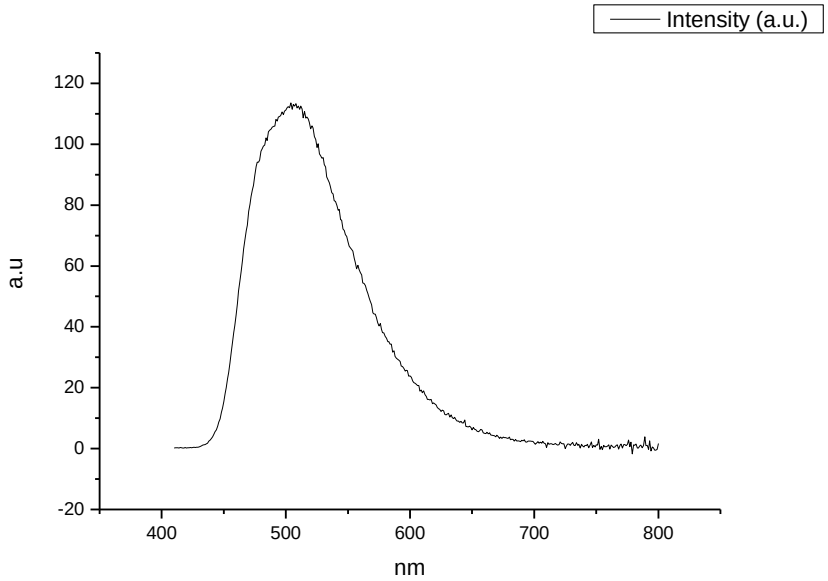

Figure 1.3.190. Fluorescence emission spectrum of **9a** recorded in 1-hexanol at 400 nm excitation.

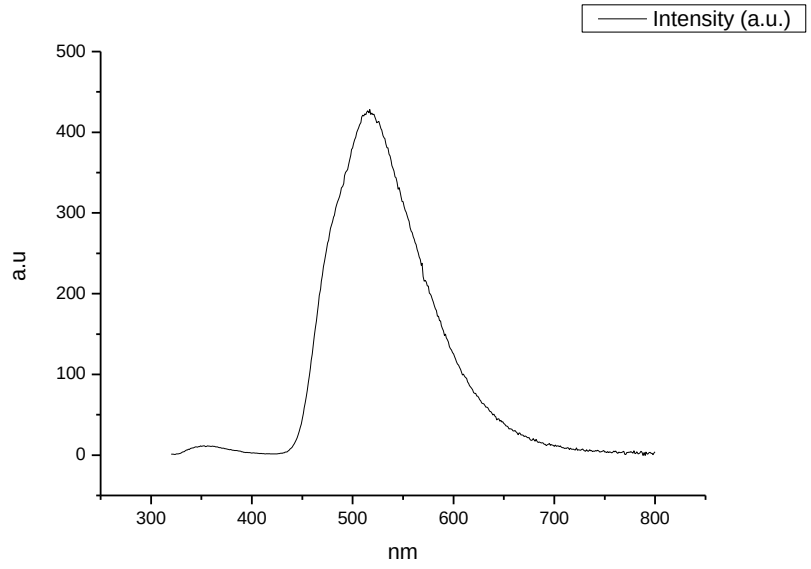

Figure 1.3.191. Fluorescence emission spectrum of **9a** recorded in 1-butanol at 310 nm excitation.

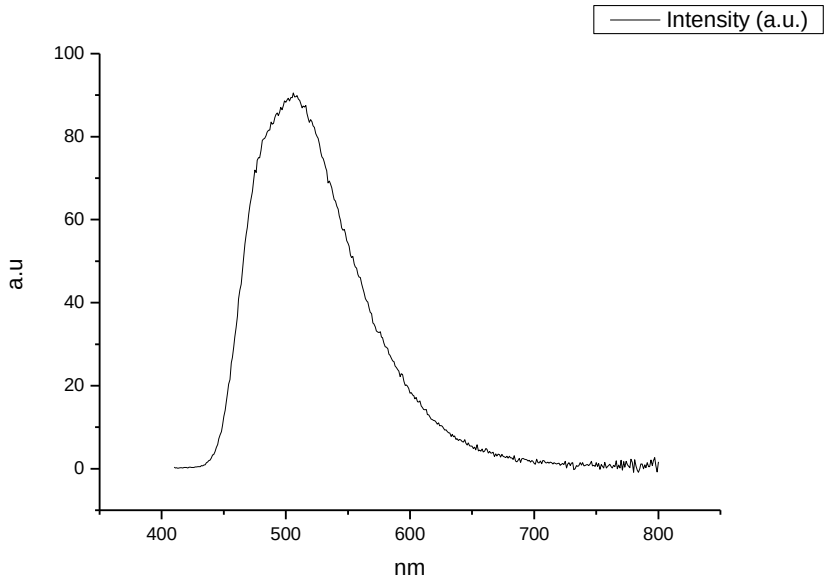

Figure 1.3.192. Fluorescence emission spectrum of **9a** recorded in 1-butanol at 400 nm excitation.

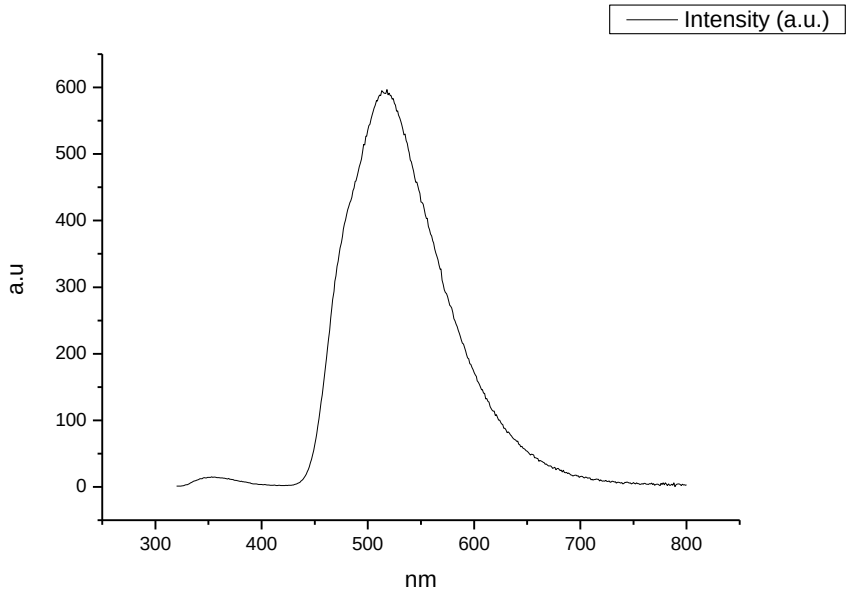

Figure 1.3.193. Fluorescence emission spectrum of **9a** recorded in 1-pentanol at 310 nm excitation.

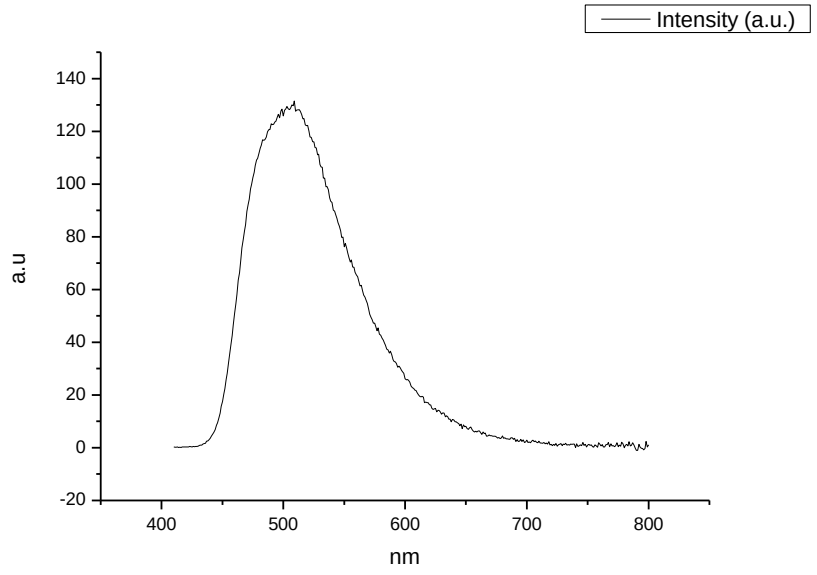

Figure 1.3.194. Fluorescence emission spectrum of **9a** recorded in 1-pentanol at 400 nm excitation.

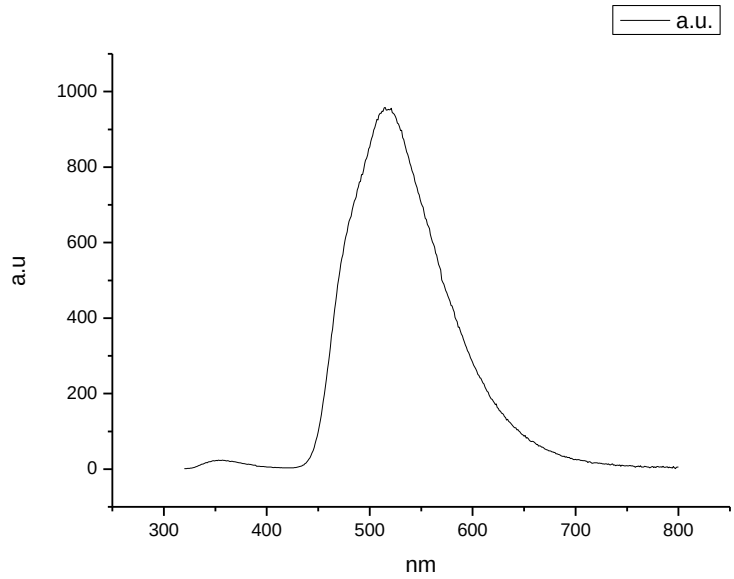

Figure 1.3.195. Fluorescence emission spectrum of **9a** recorded in 1-propanol at 310 nm excitation.

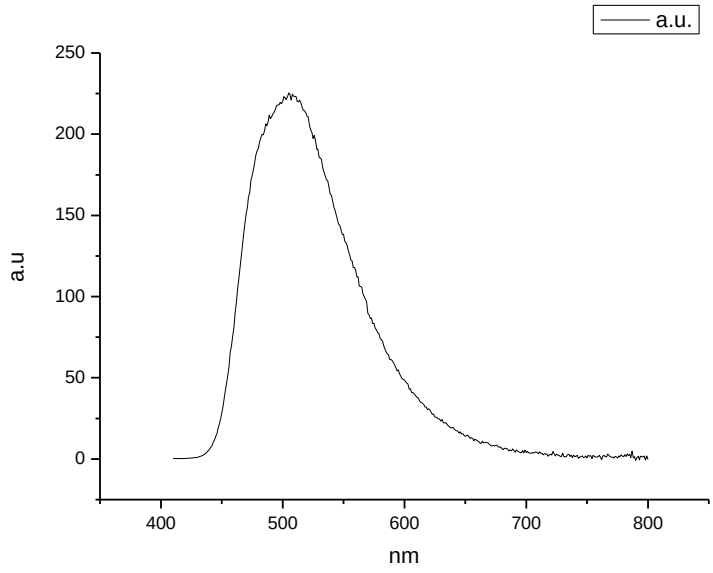

Figure 1.3.196. Fluorescence emission spectrum of **9a** recorded in 1-propanol at 400 nm excitation.

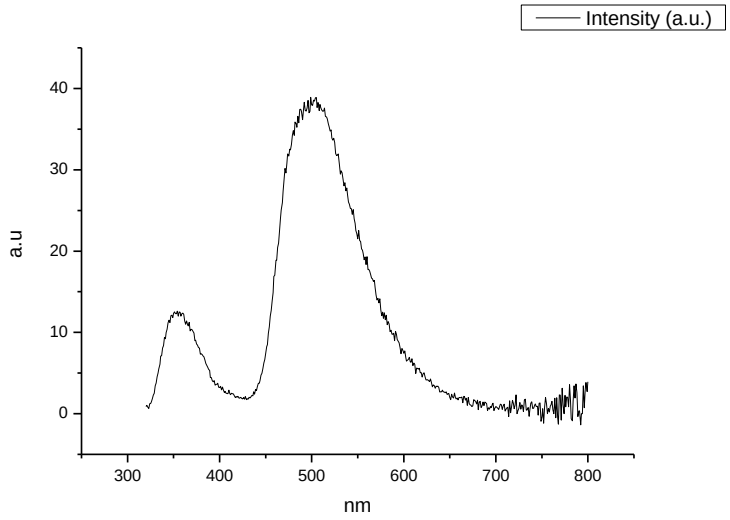

Figure 1.3.197. Fluorescence emission spectrum of **9a** recorded in Acetic Acid at 310 nm excitation.

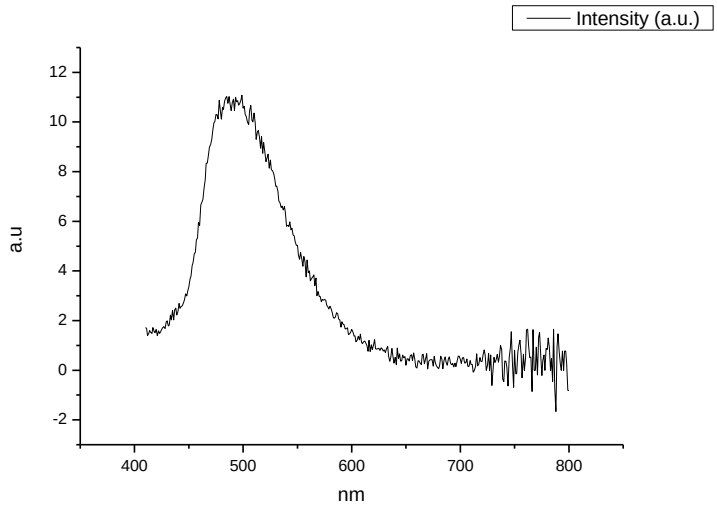

Figure 1.3.198. Fluorescence emission spectrum of **9a** recorded in Acetic Acid at 400 nm excitation.

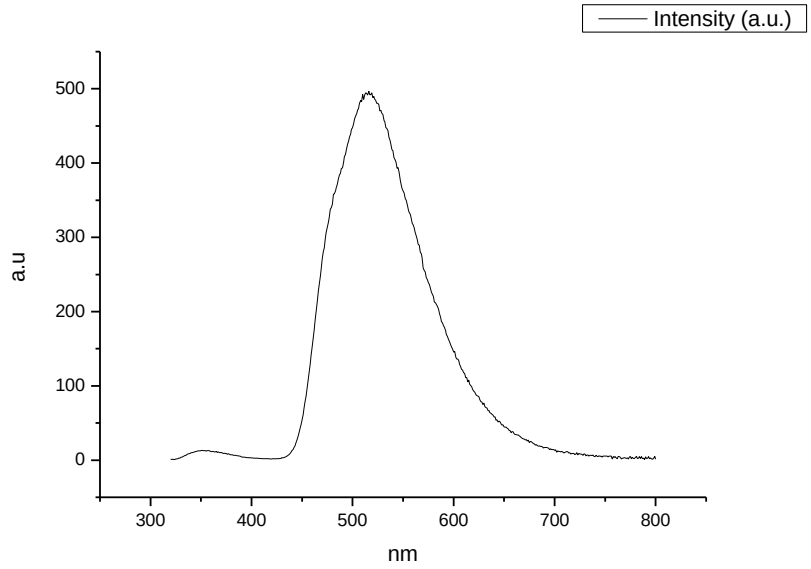

Figure 1.3.199. Fluorescence emission spectrum of **9a** recorded in Ethanol at 310 nm excitation.

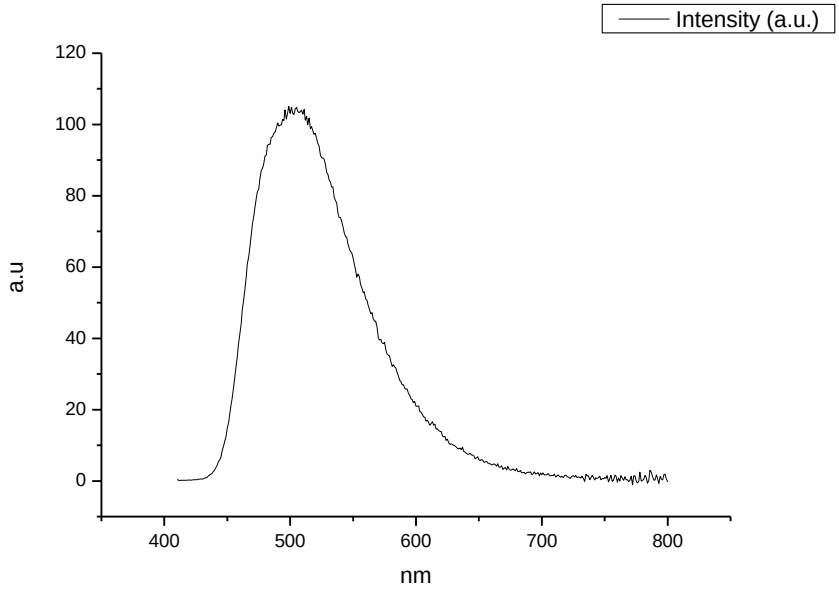

Figure 1.3.200. Fluorescence emission spectrum of **9a** recorded in Ethanol at 400 nm excitation.

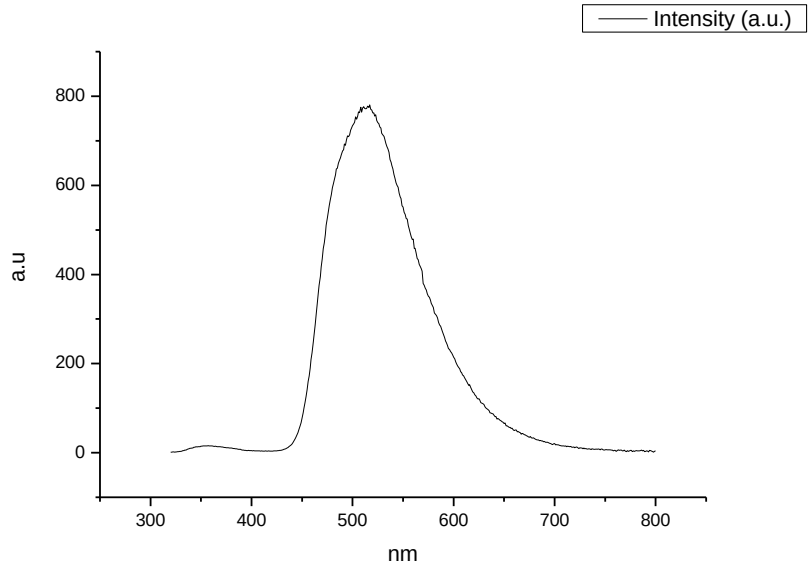

Figure 1.3.201. Fluorescence emission spectrum of **9a** recorded in 1,5-pentanediol at 310 nm excitation.

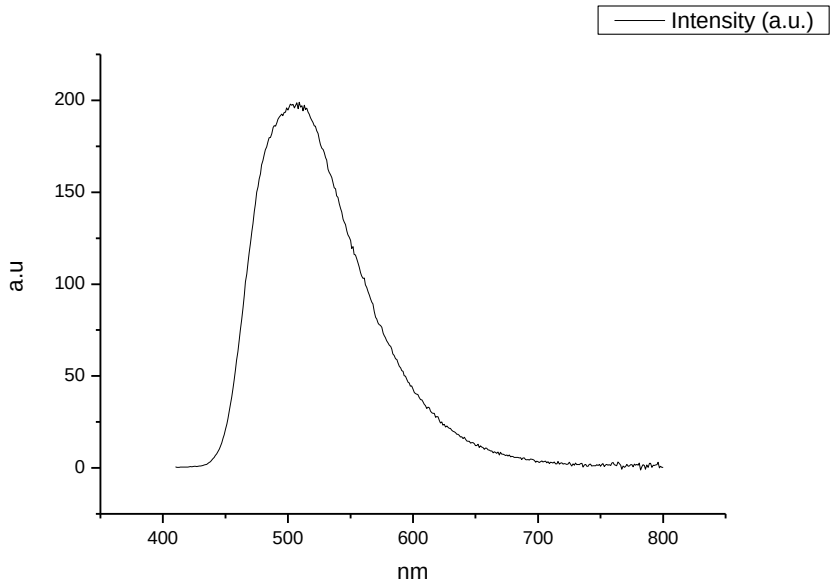

Figure 1.3.202. Fluorescence emission spectrum of **9a** recorded in 1,5-pentanediol at 400 nm excitation.

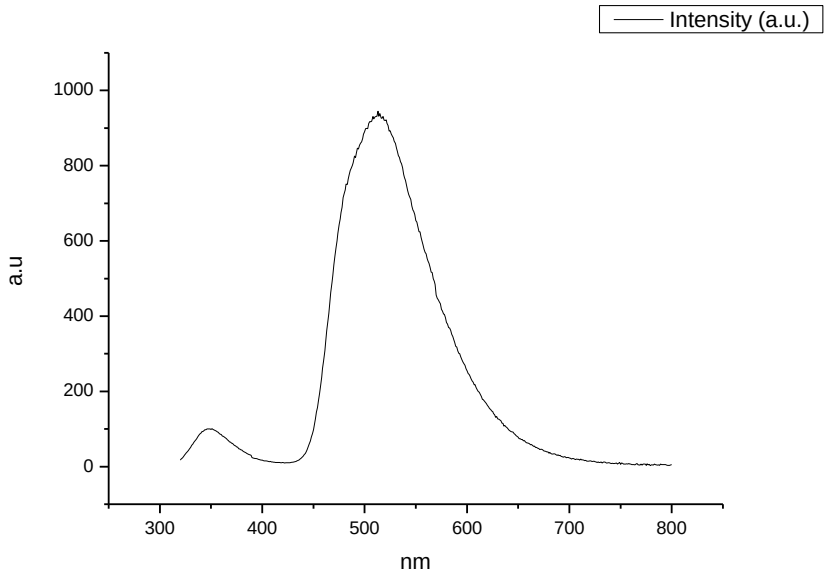

Figure 1.3.203. Fluorescence emission spectrum of **9a** recorded in 1,3-butanediol at 310 nm excitation.

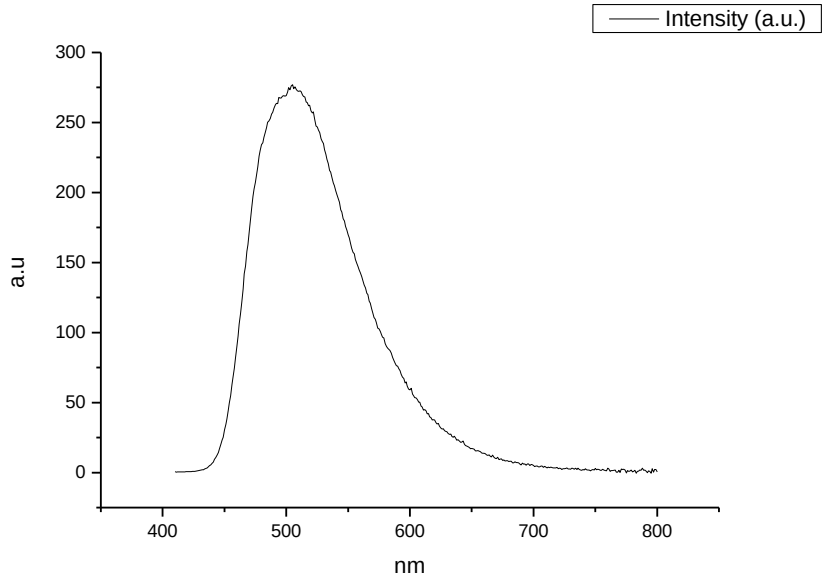

Figure 1.3.204. Fluorescence emission spectrum of **9a** recorded in 1,3-butanediol at 400 nm excitation.

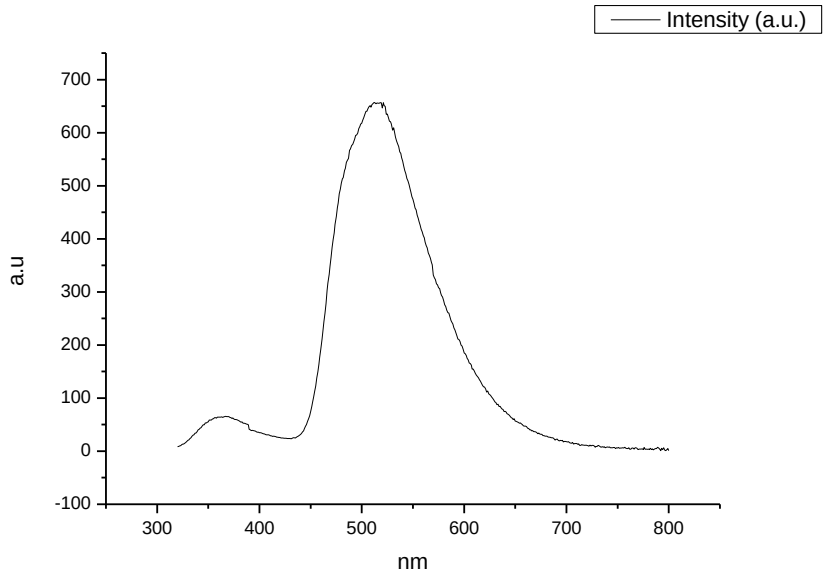

Figure 1.3.205. Fluorescence emission spectrum of **9a** recorded in 1,4-butanediol at 310 nm excitation.

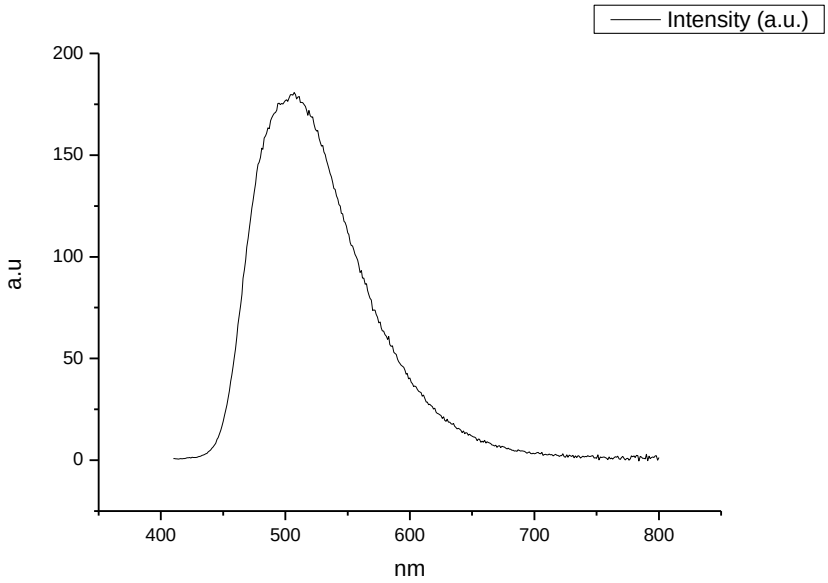

Figure 1.3.206. Fluorescence emission spectrum of **9a** recorded in 1,4-butanediol at 400 nm excitation.

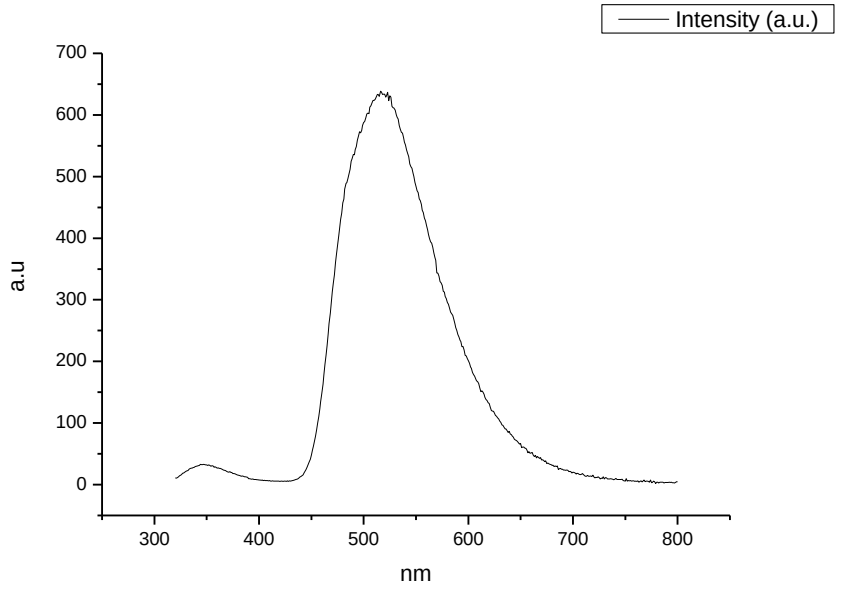

Figure 1.3.207. Fluorescence emission spectrum of **9a** recorded in 1,3-propanediol at 310 nm excitation.

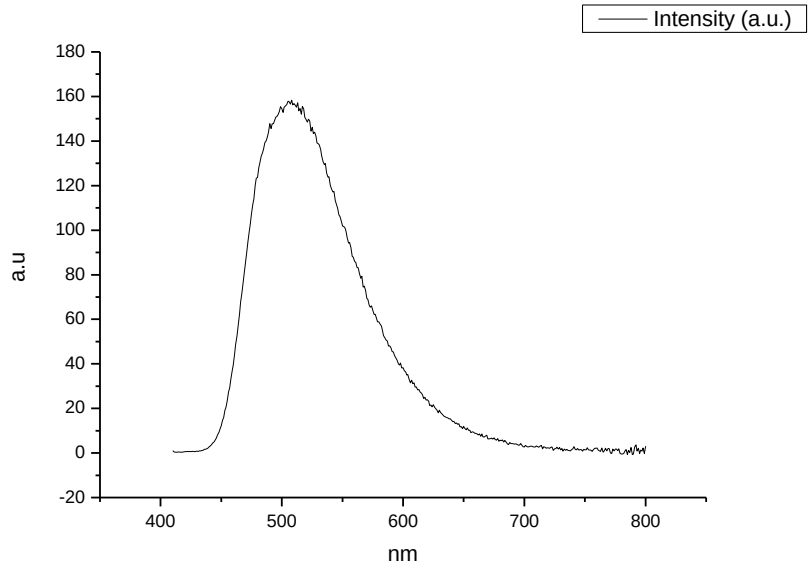

Figure 1.3.208. Fluorescence emission spectrum of **9a** recorded in 1,3-propanediol at 400 nm excitation.

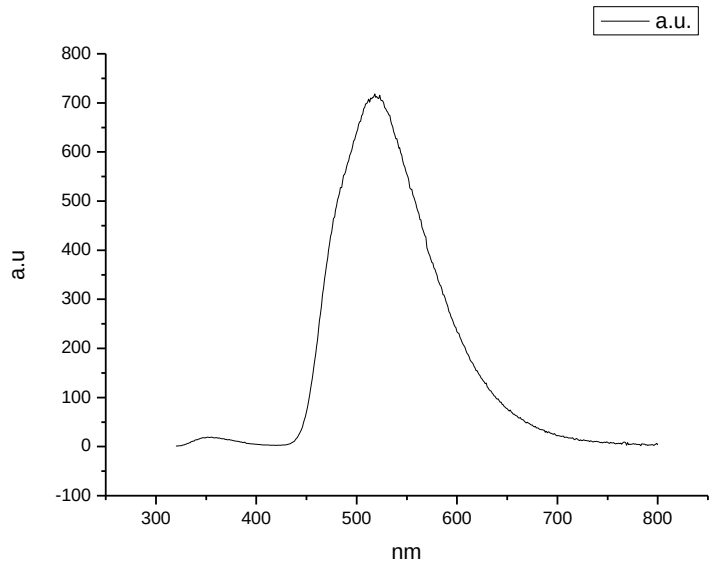

Figure 1.3.209. Fluorescence emission spectrum of **9a** recorded in Methanol at 310 nm excitation.

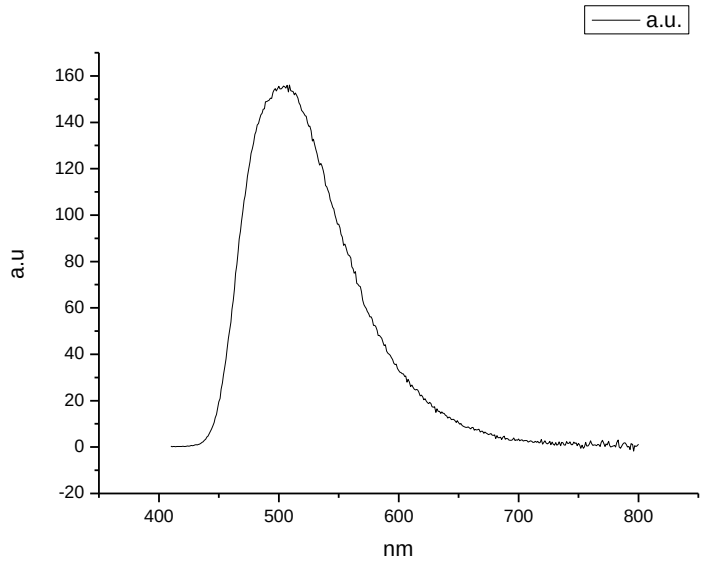

Figure 1.3.210. Fluorescence emission spectrum of **9a** recorded in Methanol at 400 nm excitation.

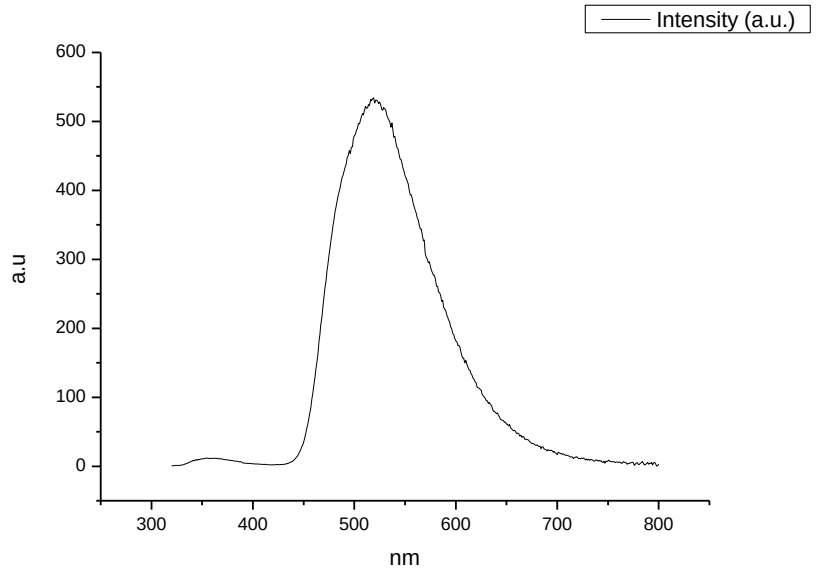

Figure 1.3.211. Fluorescence emission spectrum of **9a** recorded in 1,2-ethanediol at 310 nm excitation.

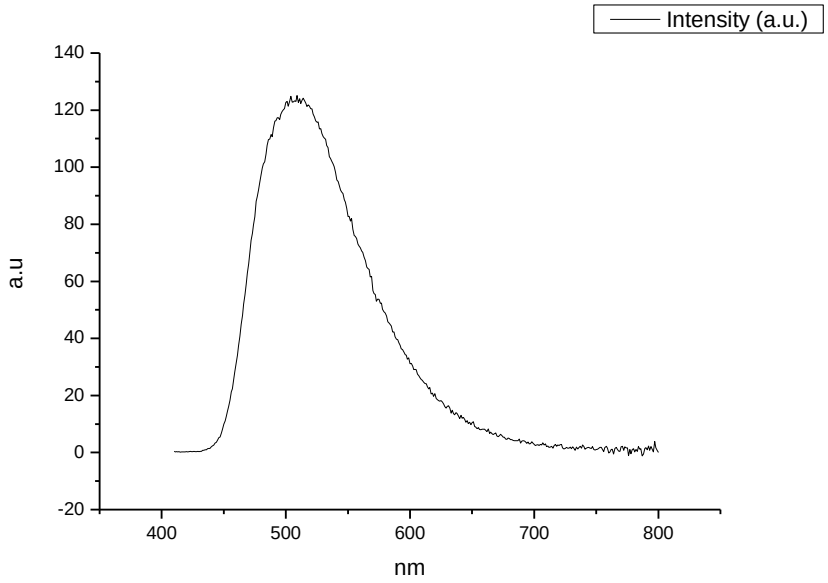

Figure 1.3.212. Fluorescence emission spectrum of **9a** recorded in 1,2-ethanediol at 400 nm excitation.

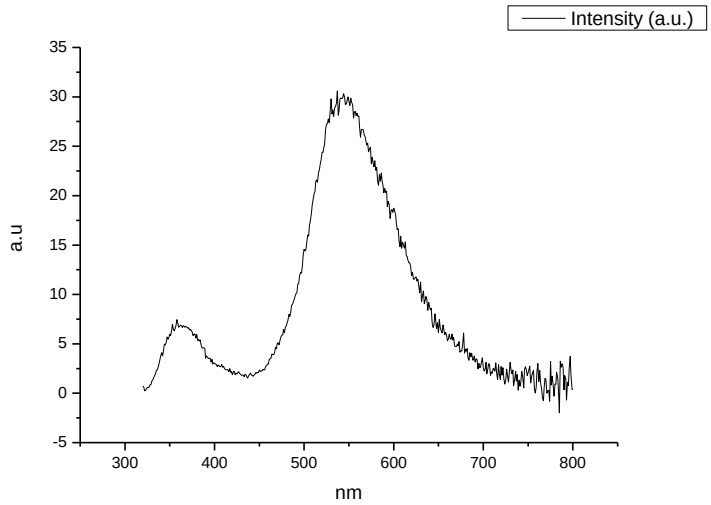

Figure 1.3.213. Fluorescence emission spectrum of **9a** recorded in 2,2,2-trifluoroethanol at 310 nm excitation.

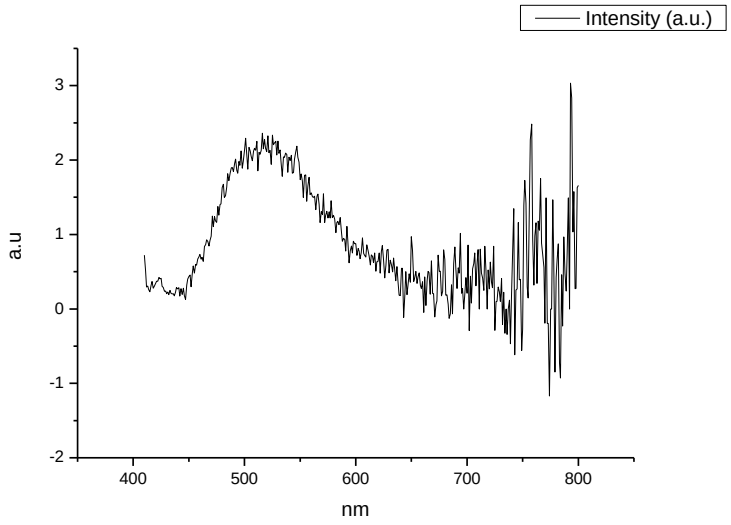

Figure 1.3.214. Fluorescence emission spectrum of **9a** recorded in 2,2,2-trifluoroethanol at 400 nm excitation.

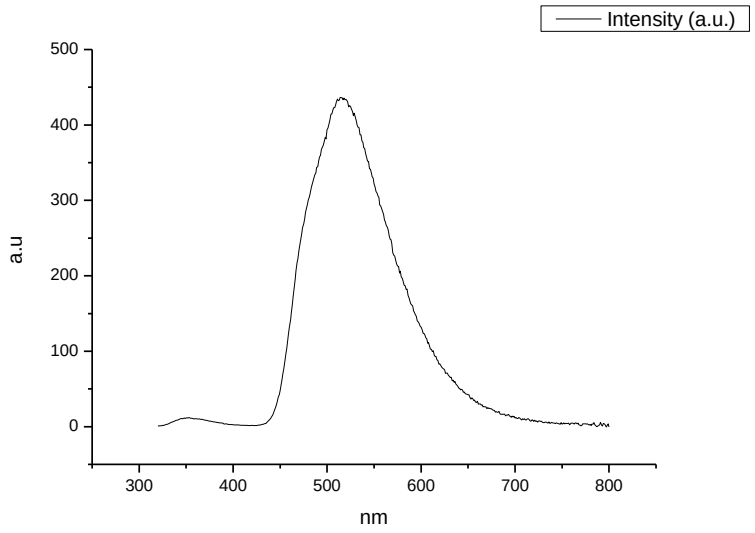

Figure 1.3.215. Fluorescence emission spectrum of **9a** recorded in ethanol-d_1 (EtOD) at 310 nm excitation.

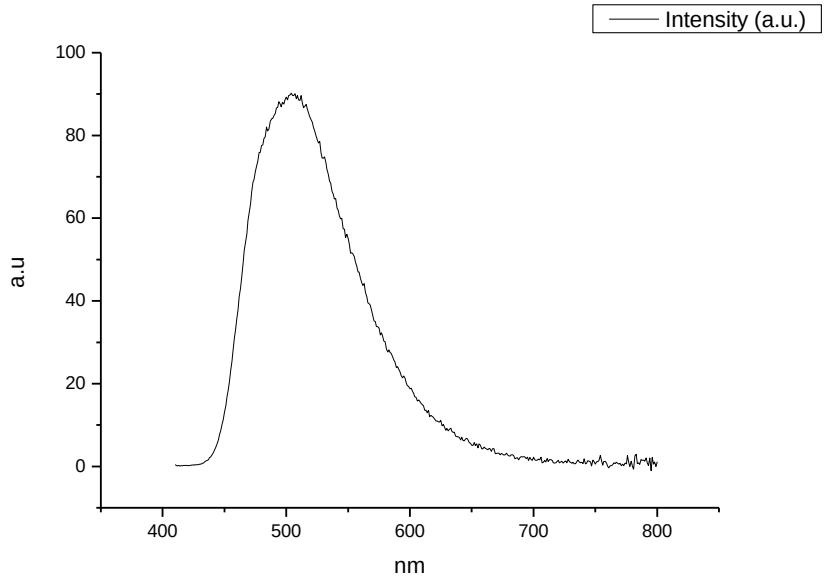

Figure 1.3.216. Fluorescence emission spectrum of **9a** recorded in ethanol-d_1 (EtOD) at 400 nm excitation.

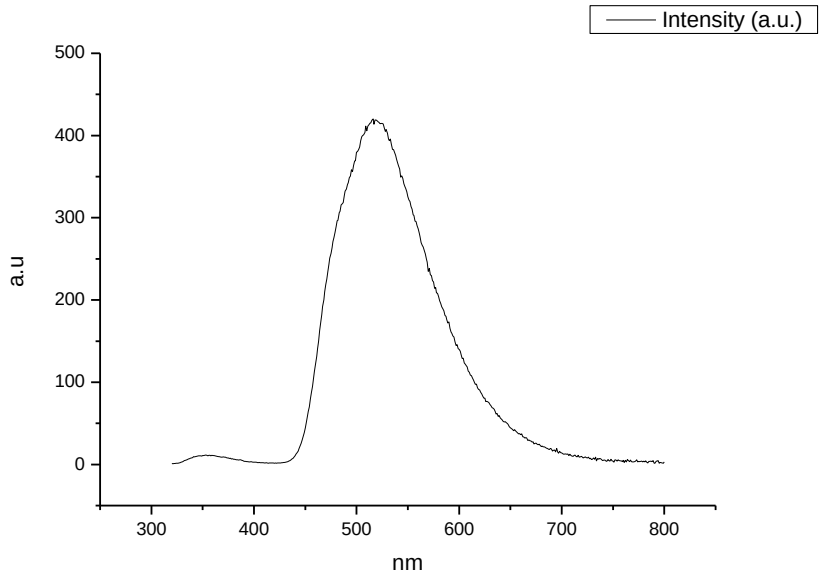

Figure 1.3.217. Fluorescence emission spectrum of **9a** recorded in methanol-d_1 (MeOD) at 310 nm excitation.

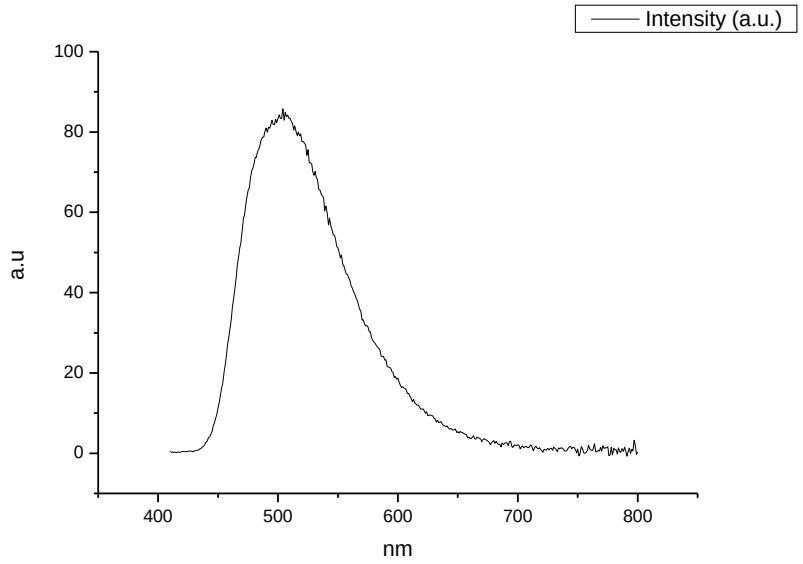

Figure 1.3.218. Fluorescence emission spectrum of **9a** recorded in methanol-d_1 (MeOD) at 400 nm excitation.

1.3.10 Normalised Fluorescence Emission spectra (Gaussian fitted).

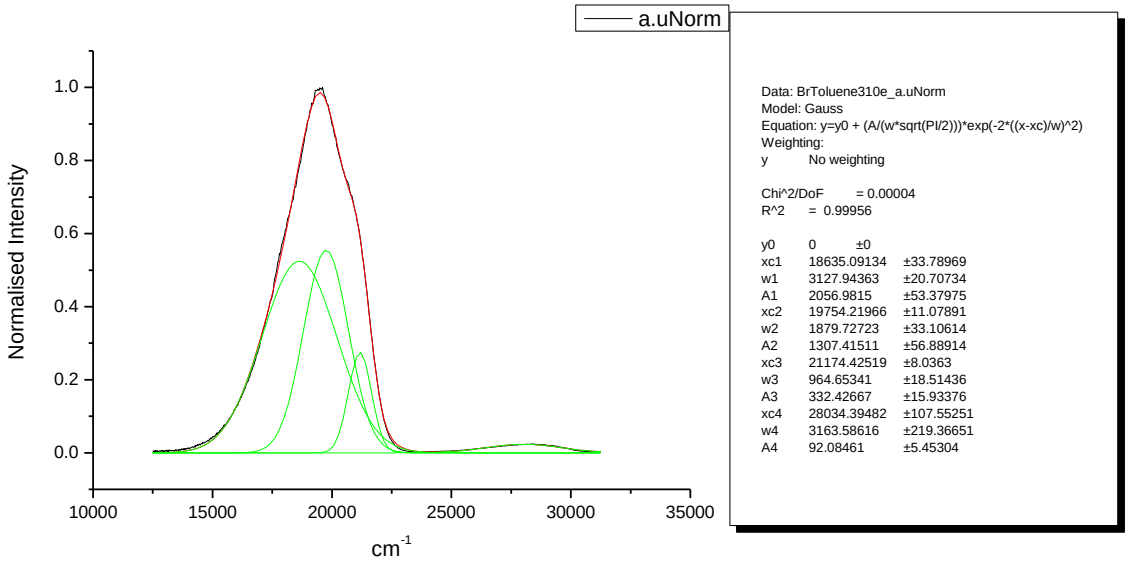

Figure 1.3.219. Gaussian model fit of the normalised fluorescence emission spectrum of **9a** recorded in Toluene at 310 nm excitation.

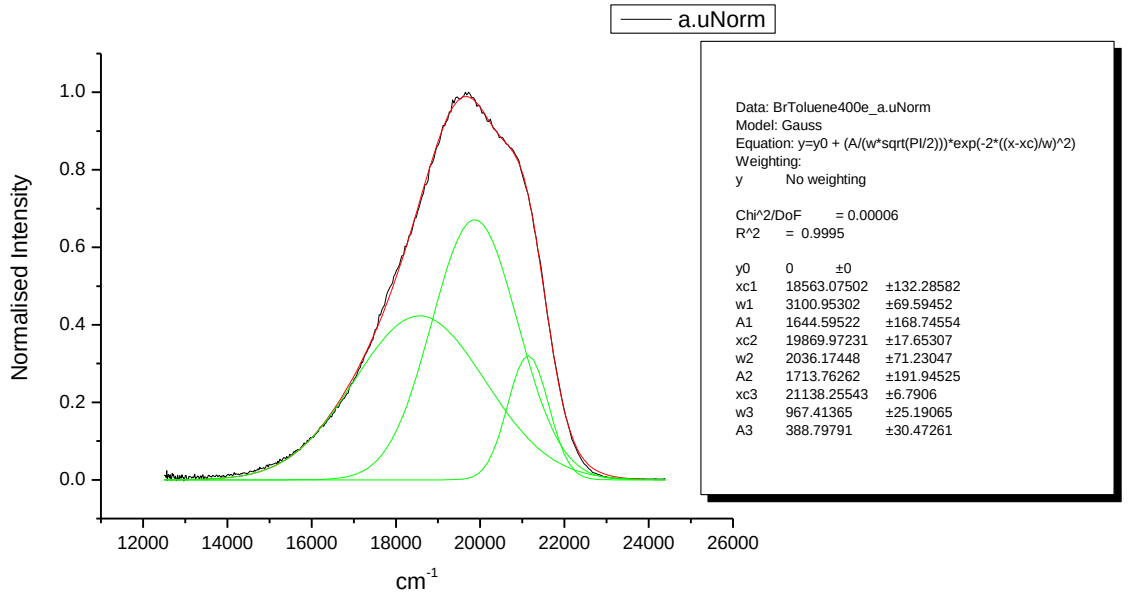

Figure 1.3.220. Gaussian model fit of the normalised fluorescence emission spectrum of **9a** recorded in Toluene at 400 nm excitation.

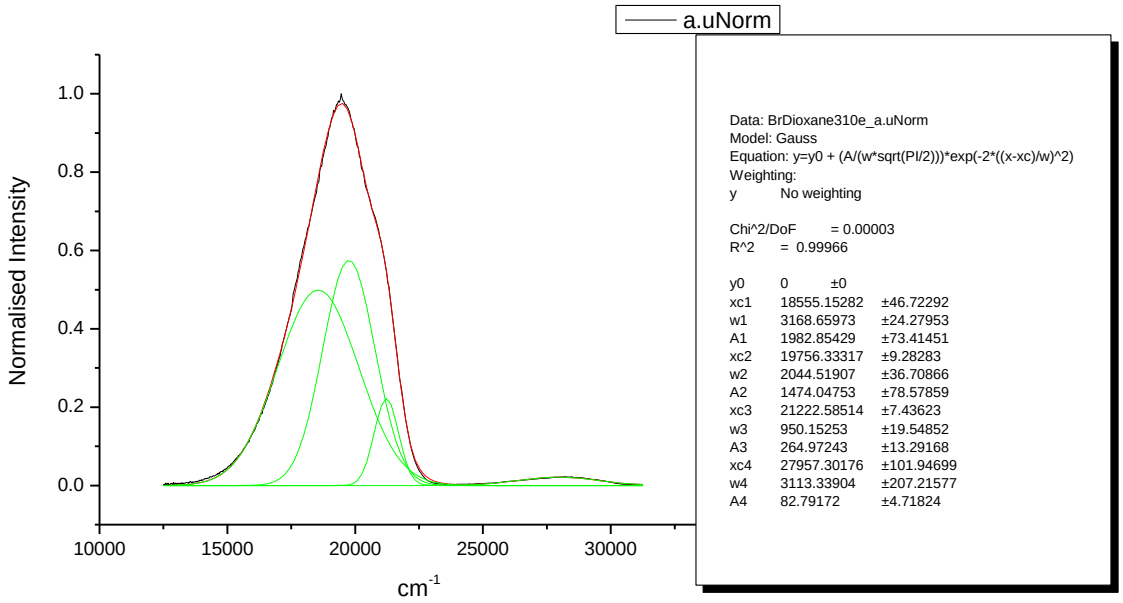

Figure 1.3.221. Gaussian model fit of the normalised fluorescence emission spectrum of **9a** recorded in 1,4-dioxane at 310 nm excitation.

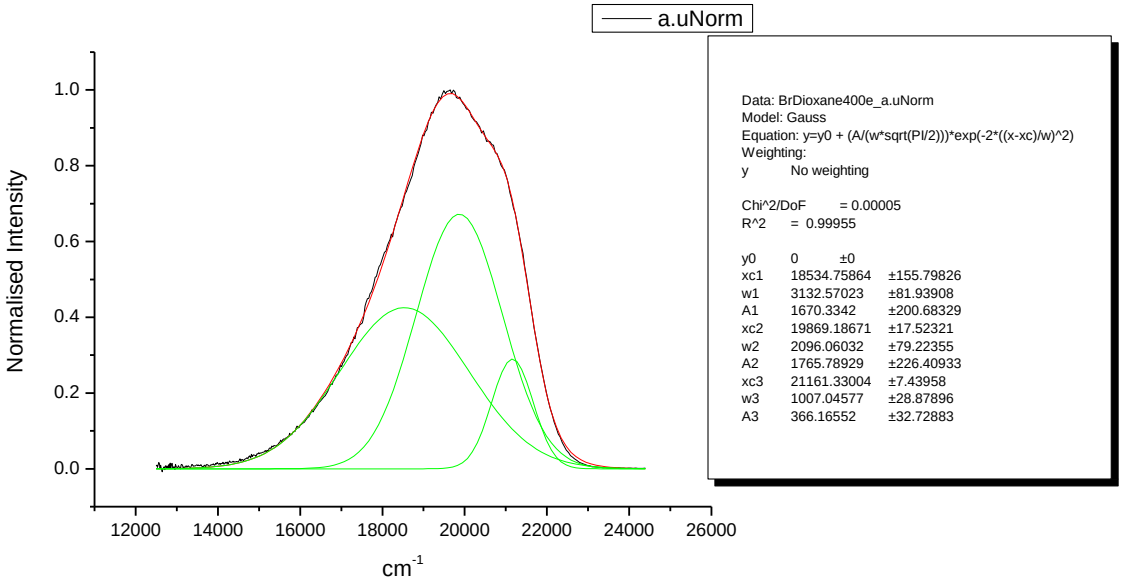

Figure 1.3.222. Gaussian model fit of the normalised fluorescence emission spectrum of **9a** recorded in 1,4-dioxane at 400 nm excitation.

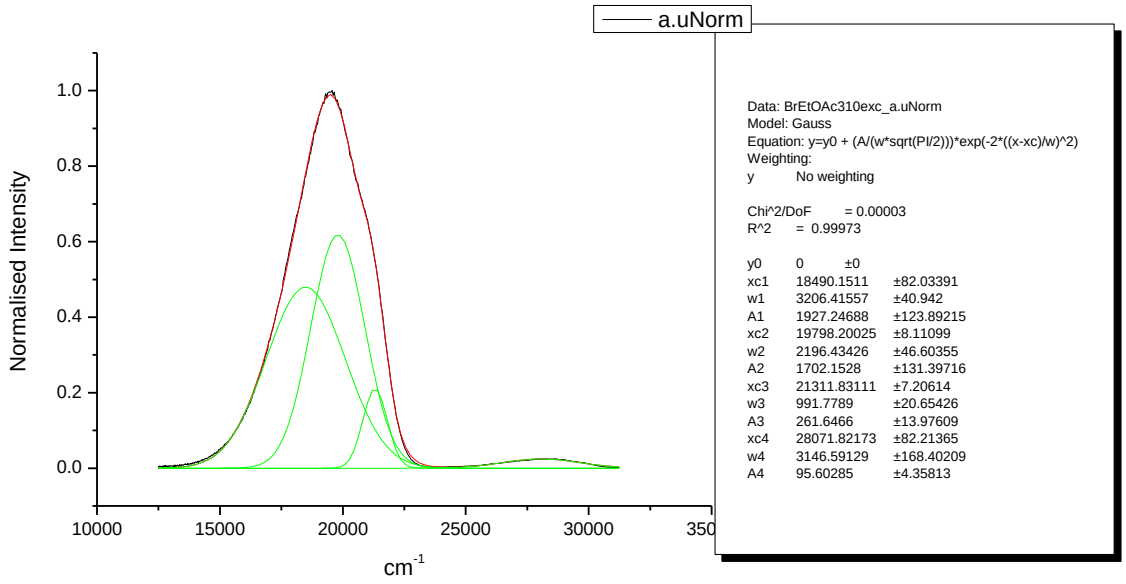

Figure 1.3.223. Gaussian model fit of the normalised fluorescence emission spectrum of **9a** recorded in Ethyl Acetate at 310 nm excitation.

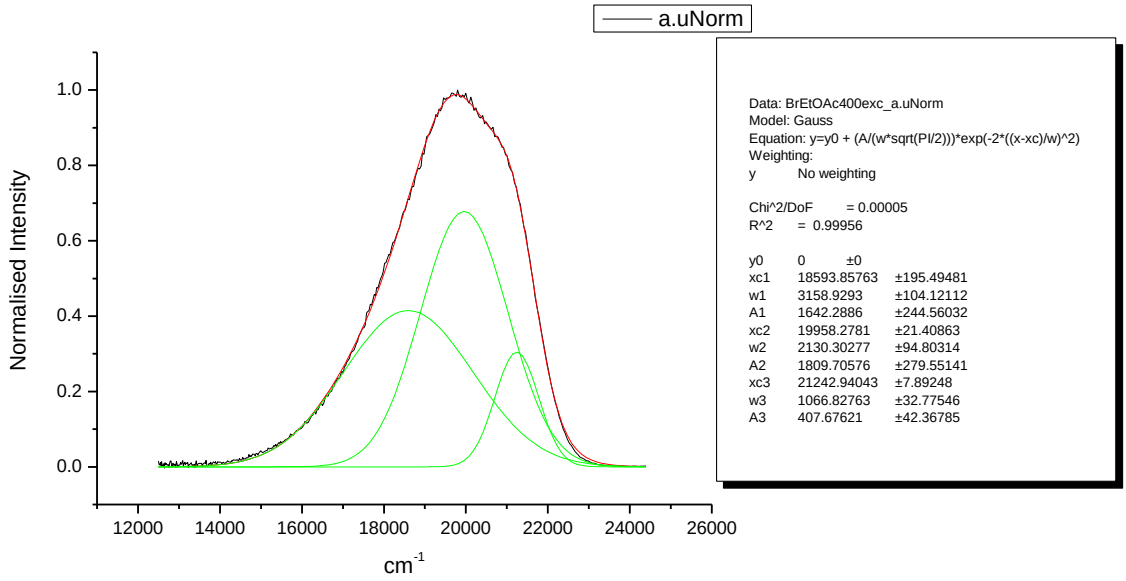

Figure 1.3.224. Gaussian model fit of the normalised fluorescence emission spectrum of **9a** recorded in Ethyl Acetate at 400 nm excitation.

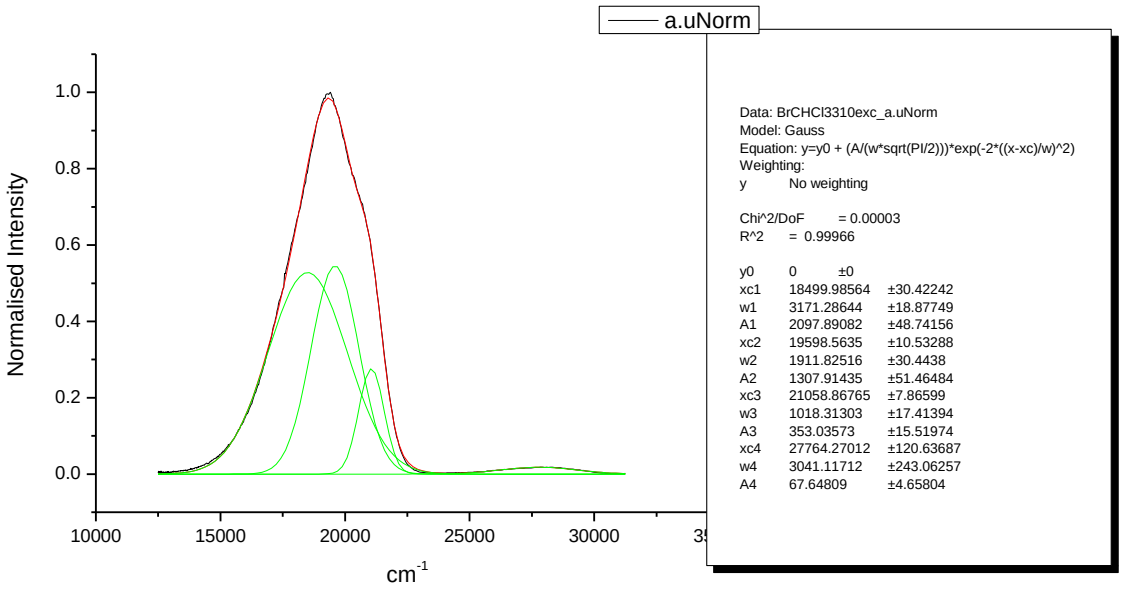

Figure 1.3.225. Gaussian model fit of the normalised fluorescence emission spectrum of **9a** recorded in Chloroform at 310 nm excitation.

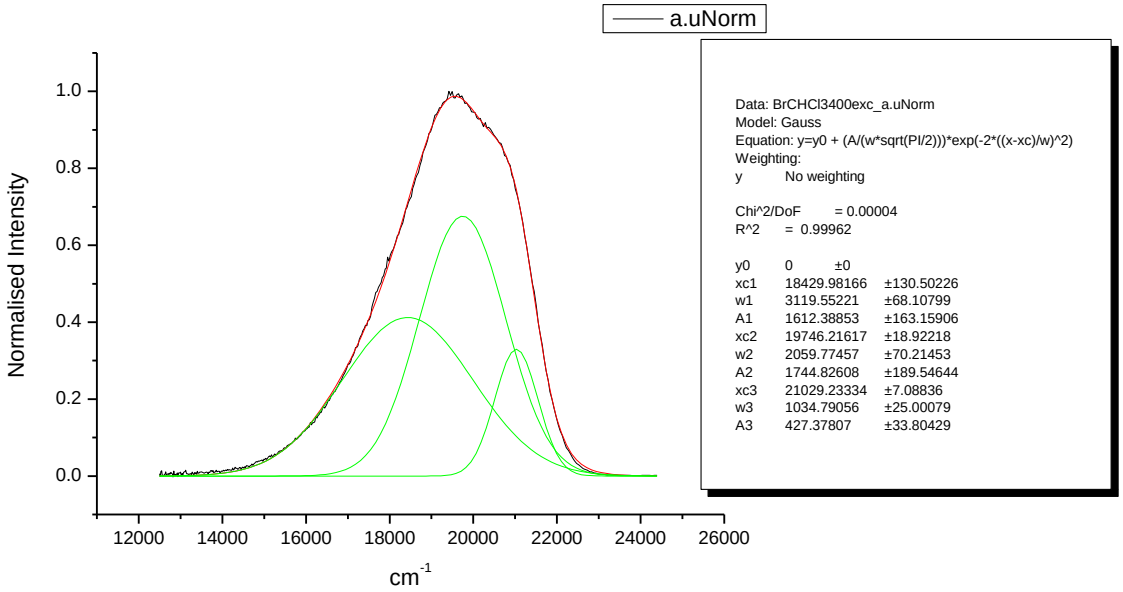

Figure 1.3.226. Gaussian model fit of the normalised fluorescence emission spectrum of **9a** recorded in Chloroform at 400 nm excitation.

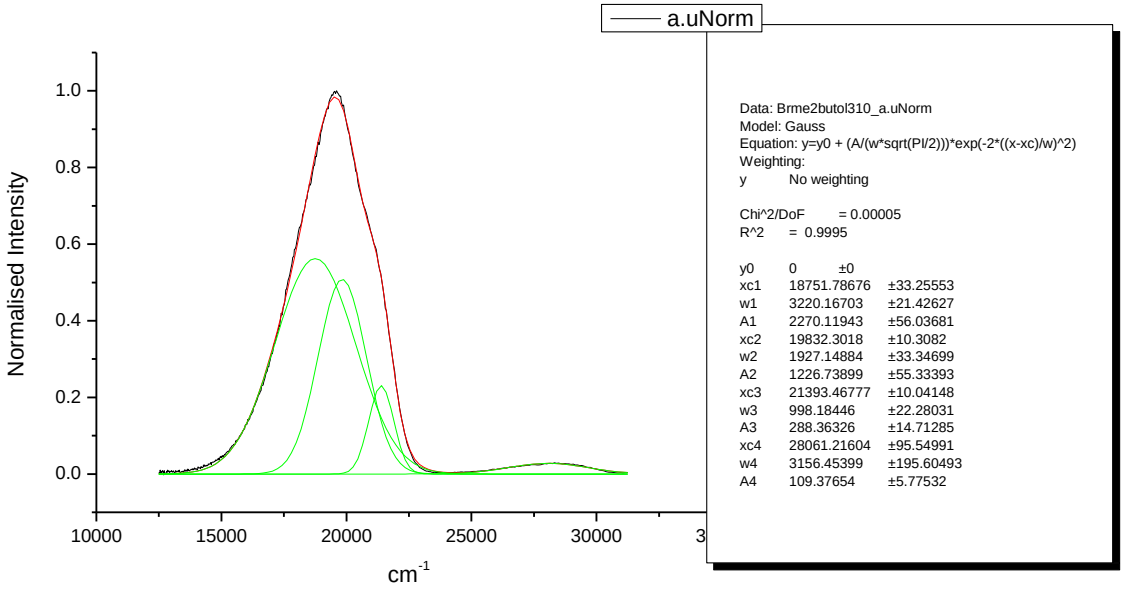

Figure 1.3.227. Gaussian model fit of the normalised fluorescence emission spectrum of **9a** recorded in 2-methyl-2-butanol at 310 nm excitation.

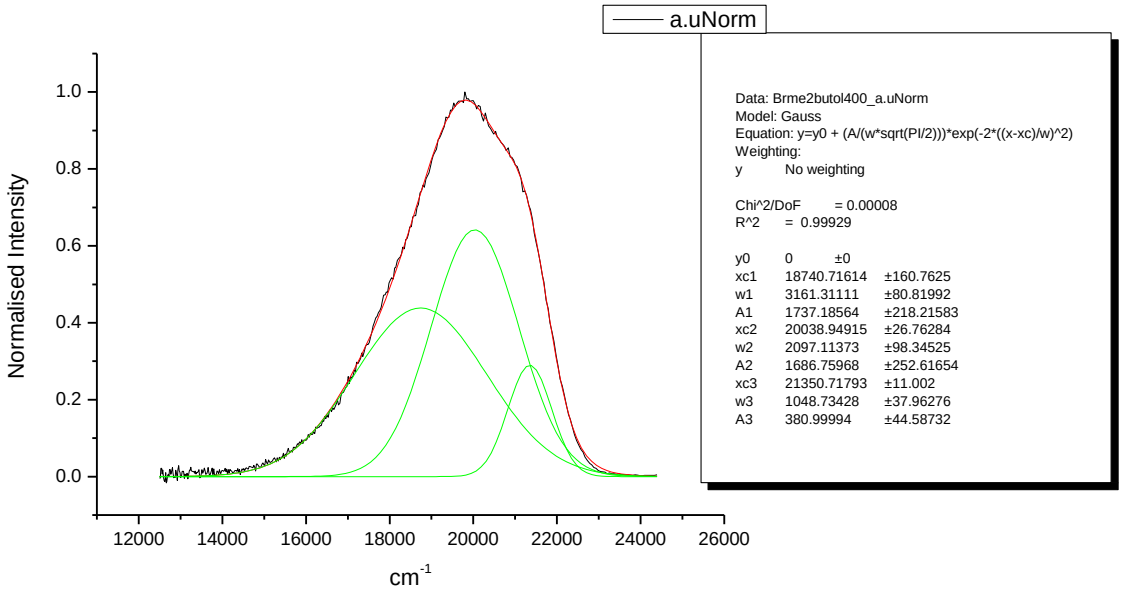

Figure 1.3.228. Gaussian model fit of the normalised fluorescence emission spectrum of **9a** recorded in 2-methyl-2-butanol at 400 nm excitation.

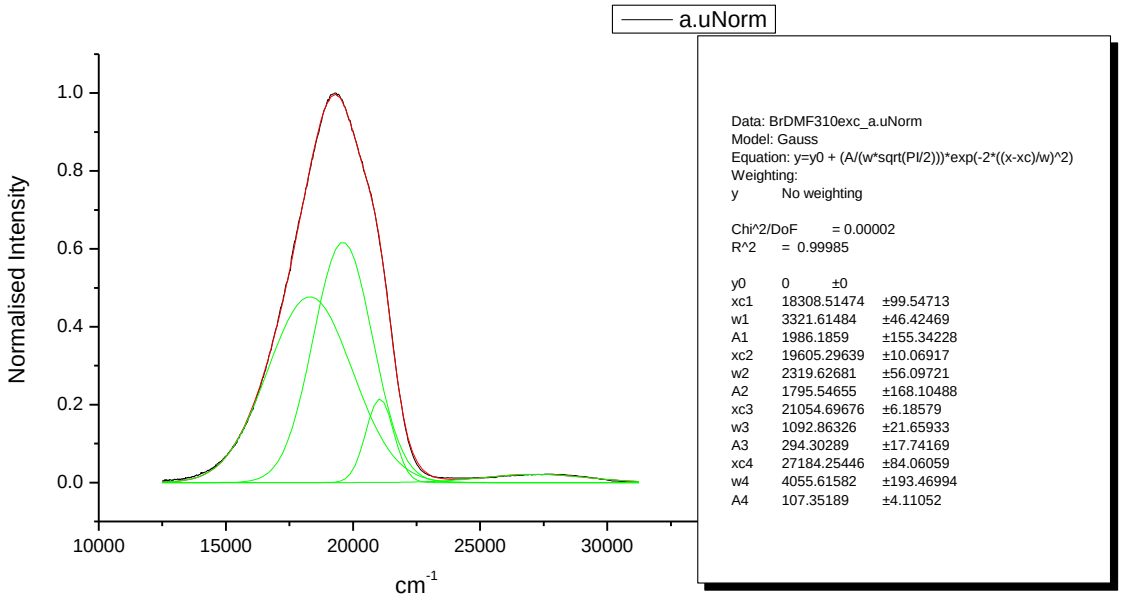

Figure 1.3.229. Gaussian model fit of the normalised fluorescence emission spectrum of **9a** recorded in N,N-dimethylformamide at 310 nm excitation.

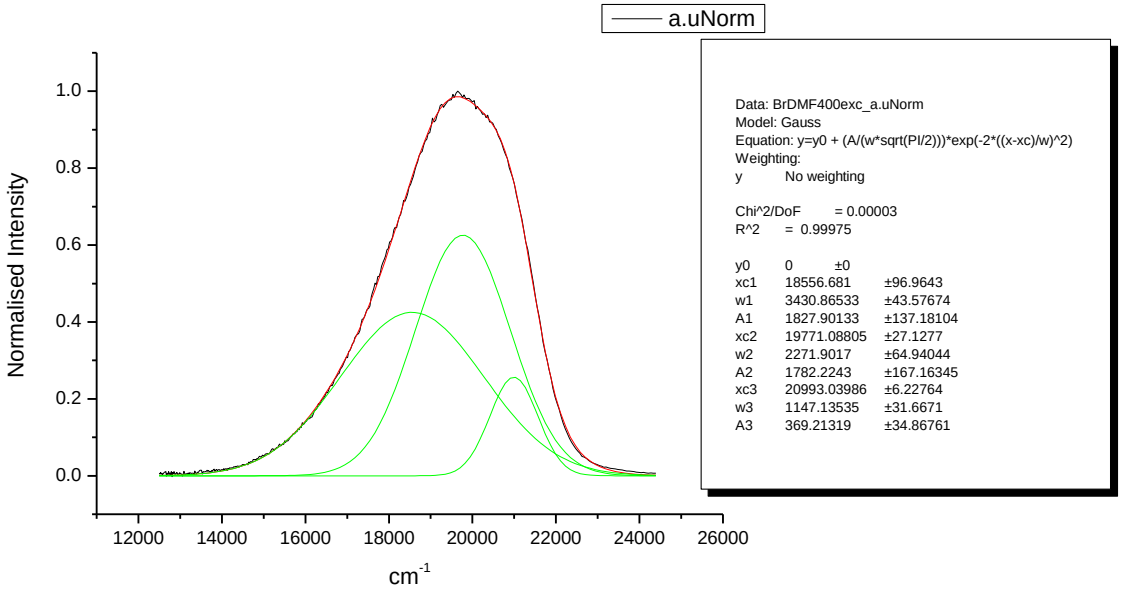

Figure 1.3.230. Gaussian model fit of the normalised fluorescence emission spectrum of **9a** recorded in N,N-dimethylformamide at 400 nm excitation.

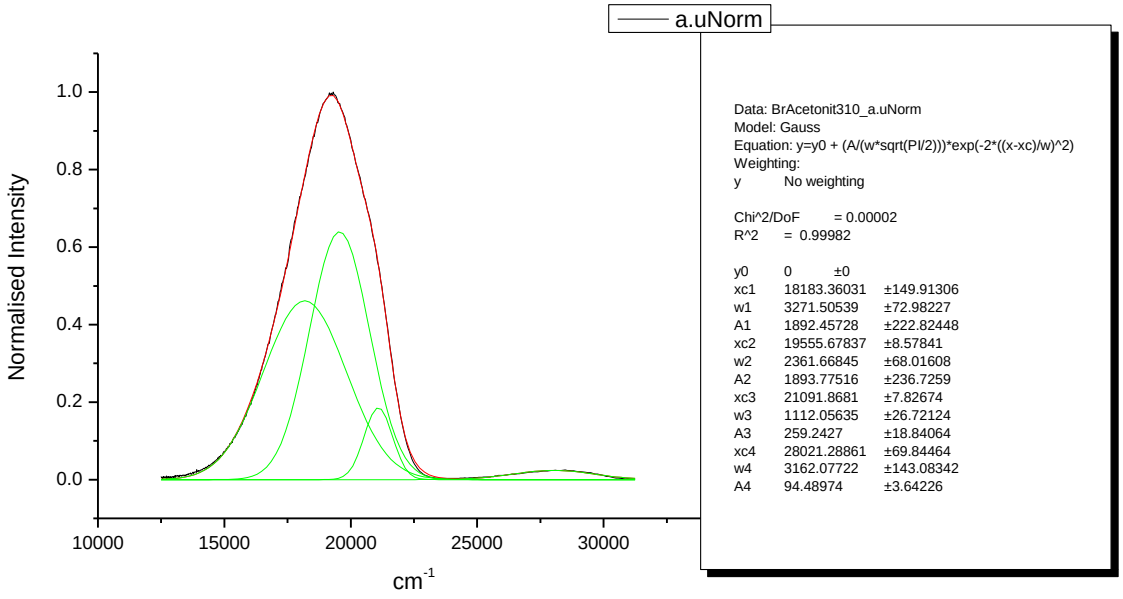

Figure 1.3.231. Gaussian model fit of the normalised fluorescence emission spectrum of **9a** recorded in Acetonitrile at 310 nm excitation.

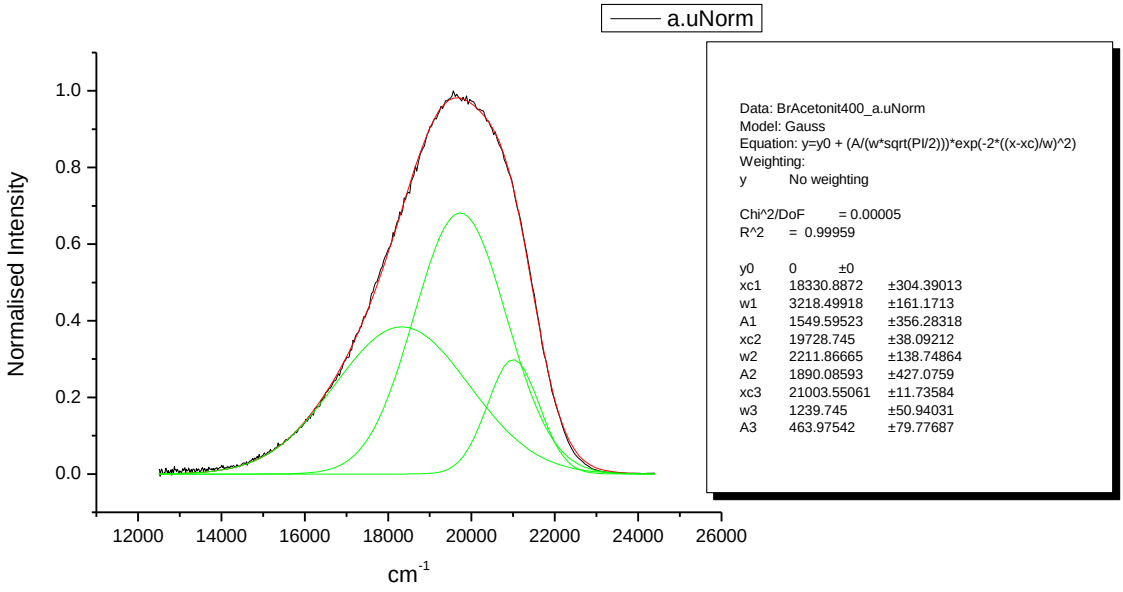

Figure 1.3.232. Gaussian model fit of the normalised fluorescence emission spectrum of **9a** recorded in Acetonitrile at 400 nm excitation.

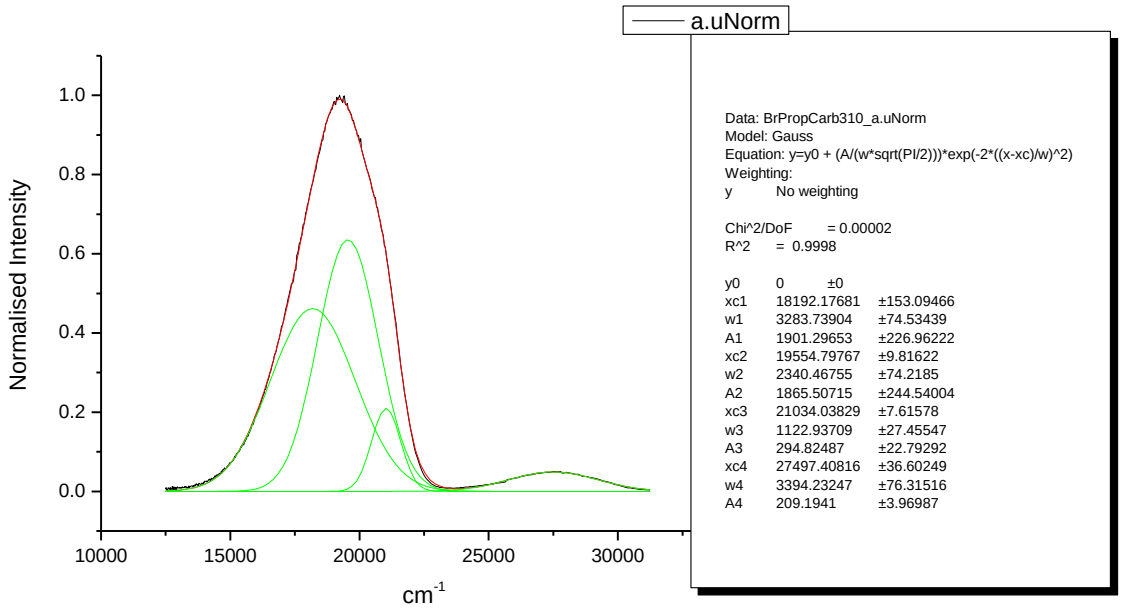

Figure 1.3.233. Gaussian model fit of the normalised fluorescence emission spectrum of **9a** recorded in Propylene Carbonate at 310 nm excitation.

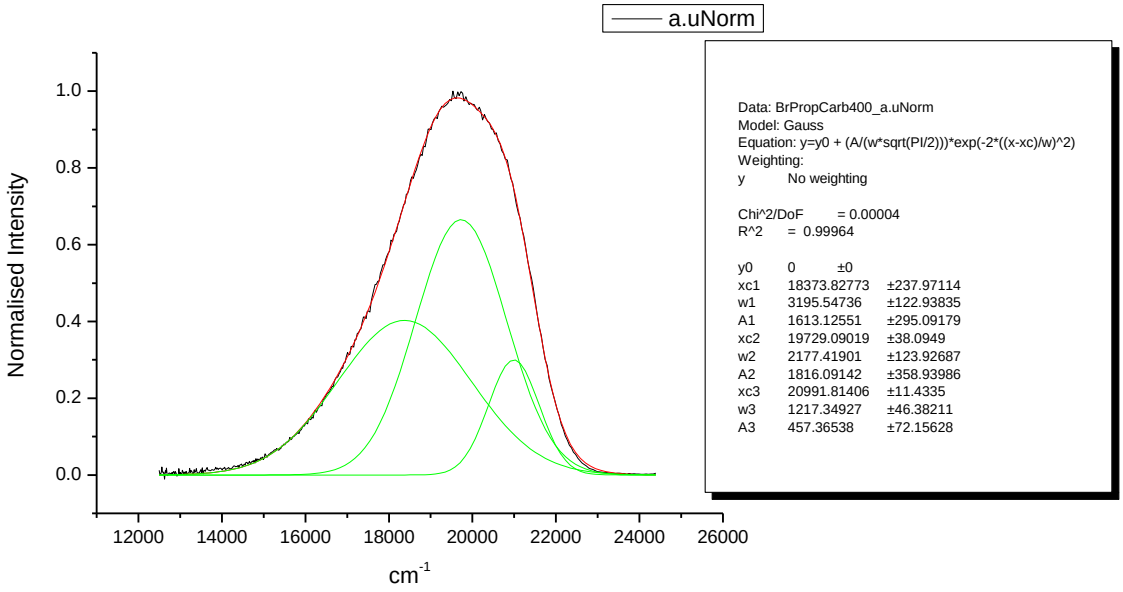

Figure 1.3.234. Gaussian model fit of the normalised fluorescence emission spectrum of **9a** recorded in Propylene Carbonate at 400 nm excitation.

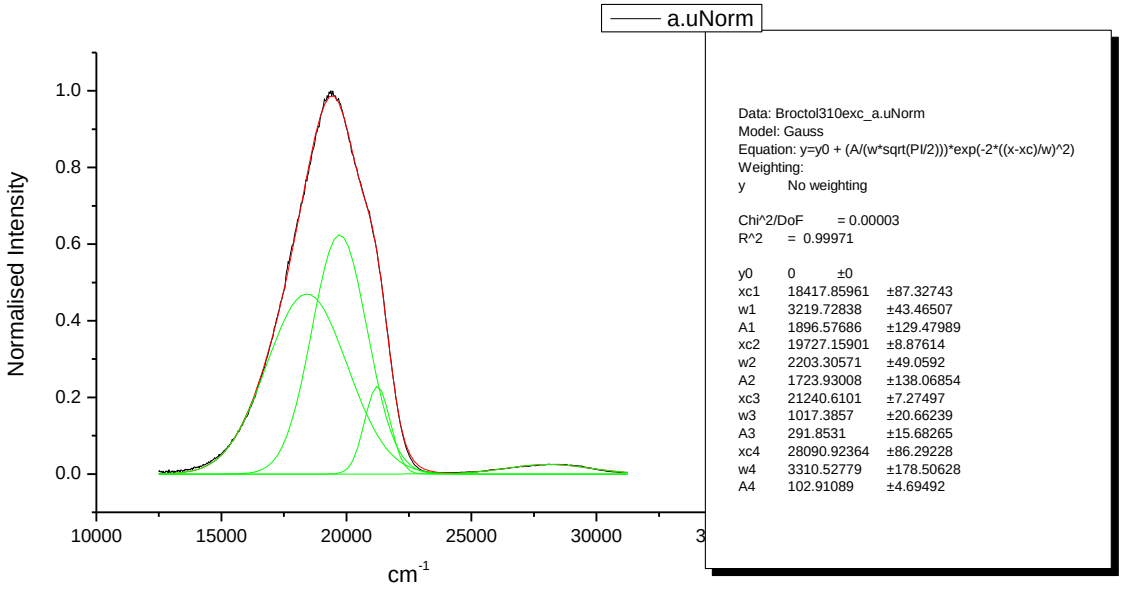

Figure 1.3.235. Gaussian model fit of the normalised fluorescence emission spectrum of **9a** recorded in 1-octanol at 310 nm excitation.

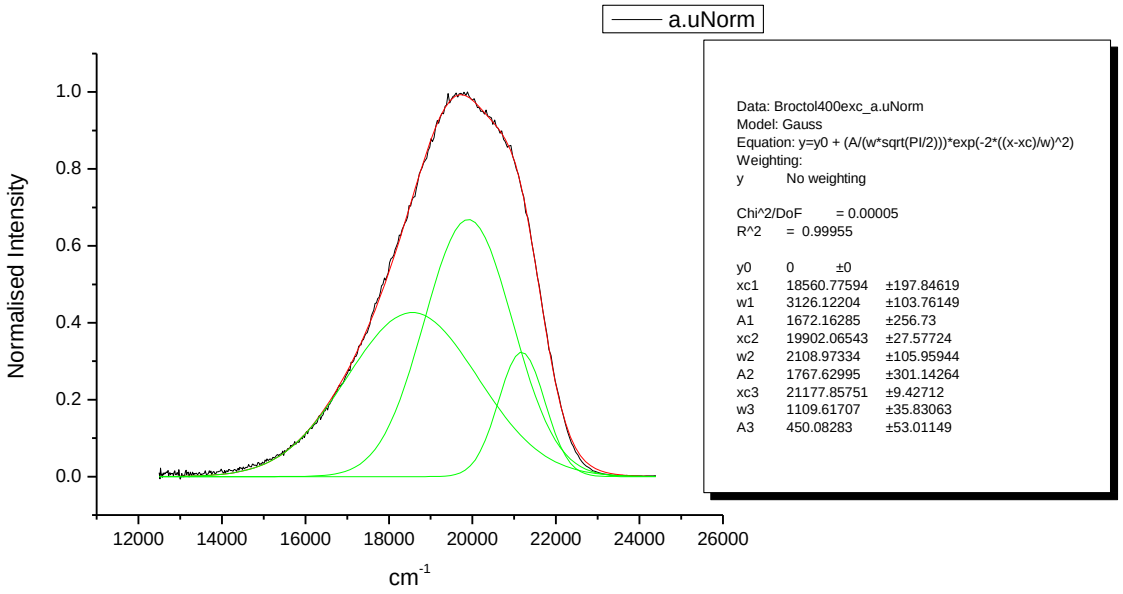

Figure 1.3.236. Gaussian model fit of the normalised fluorescence emission spectrum of **9a** recorded in 1-octanol at 400 nm excitation.

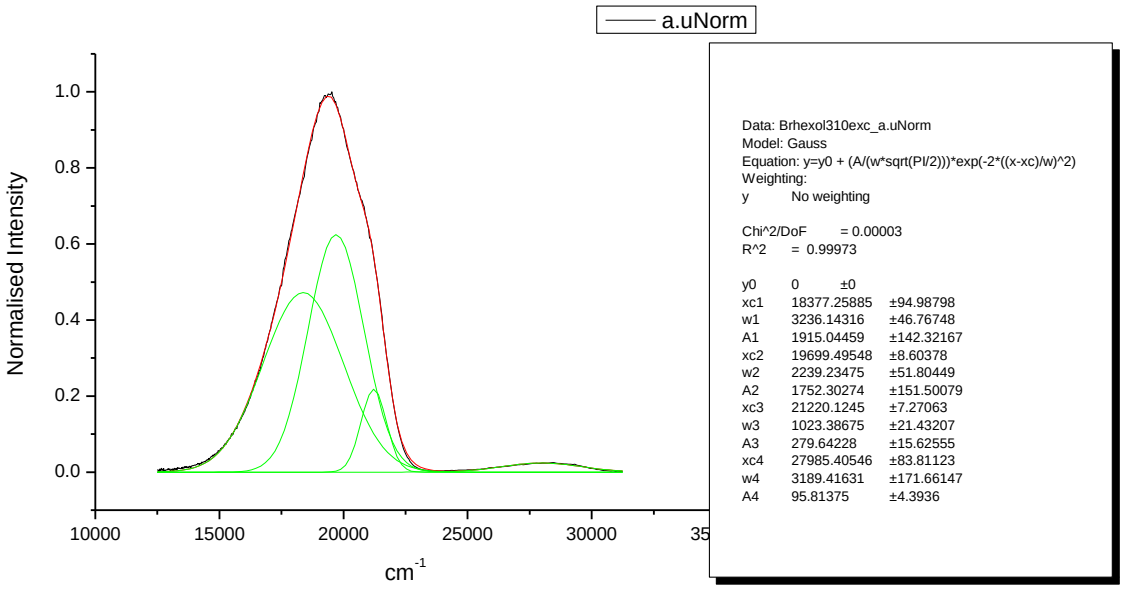

Figure 1.3.237. Gaussian model fit of the normalised fluorescence emission spectrum of **9a** recorded in 1-hexanol at 310 nm excitation.

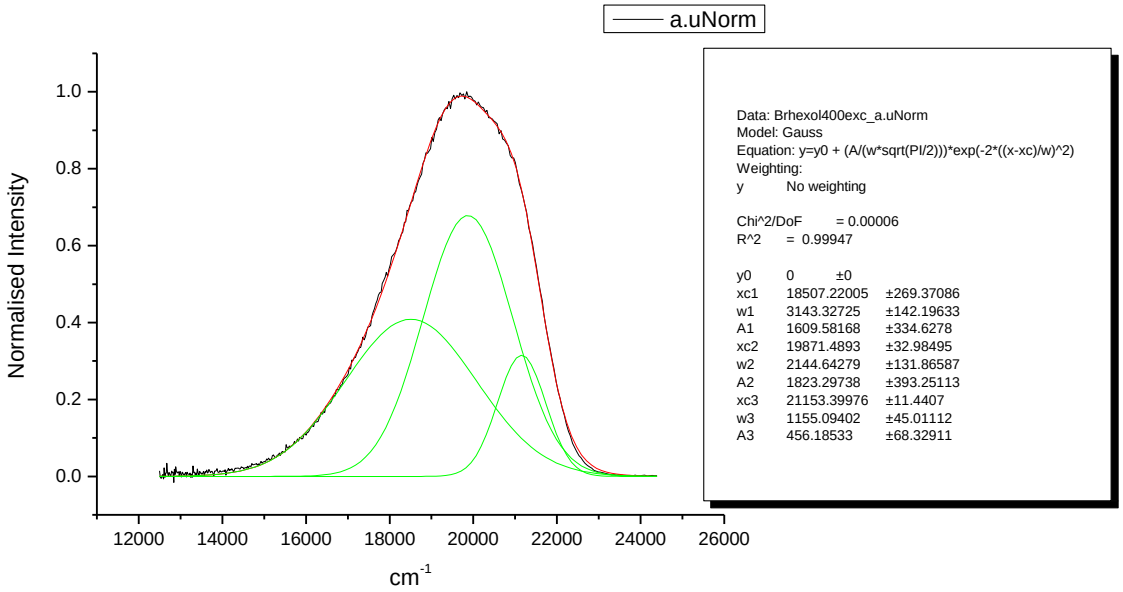

Figure 1.3.238. Gaussian model fit of the normalised fluorescence emission spectrum of **9a** recorded in 1-hexanol at 400 nm excitation.

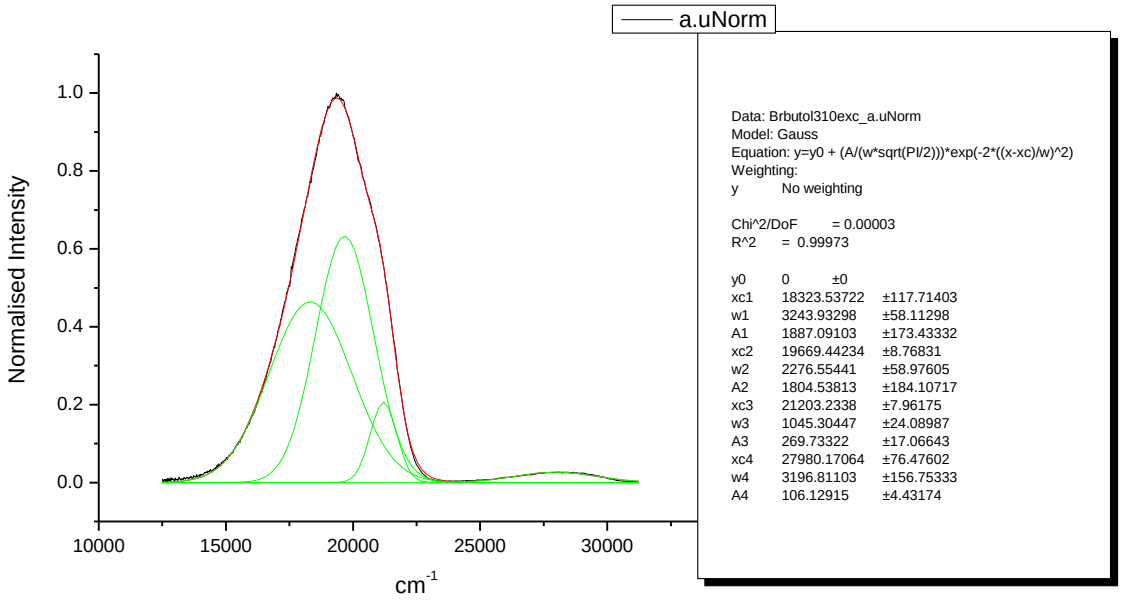

Figure 1.3.239. Gaussian model fit of the normalised fluorescence emission spectrum of **9a** recorded in 1-butanol at 310 nm excitation.

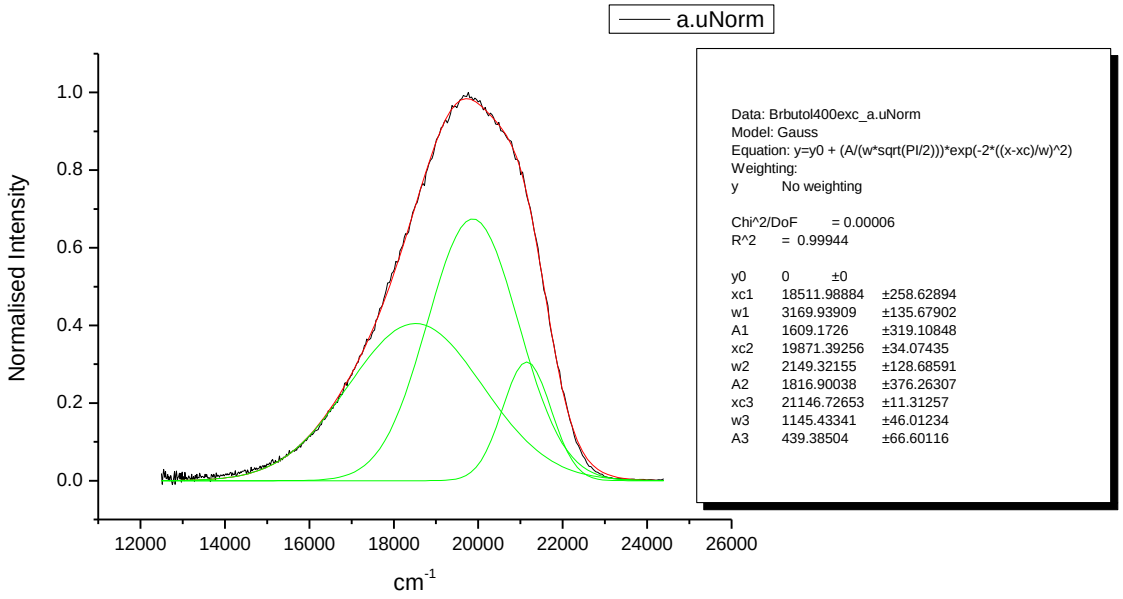

Figure 1.3.240. Gaussian model fit of the normalised fluorescence emission spectrum of **9a** recorded in 1-butanol at 400 nm excitation.

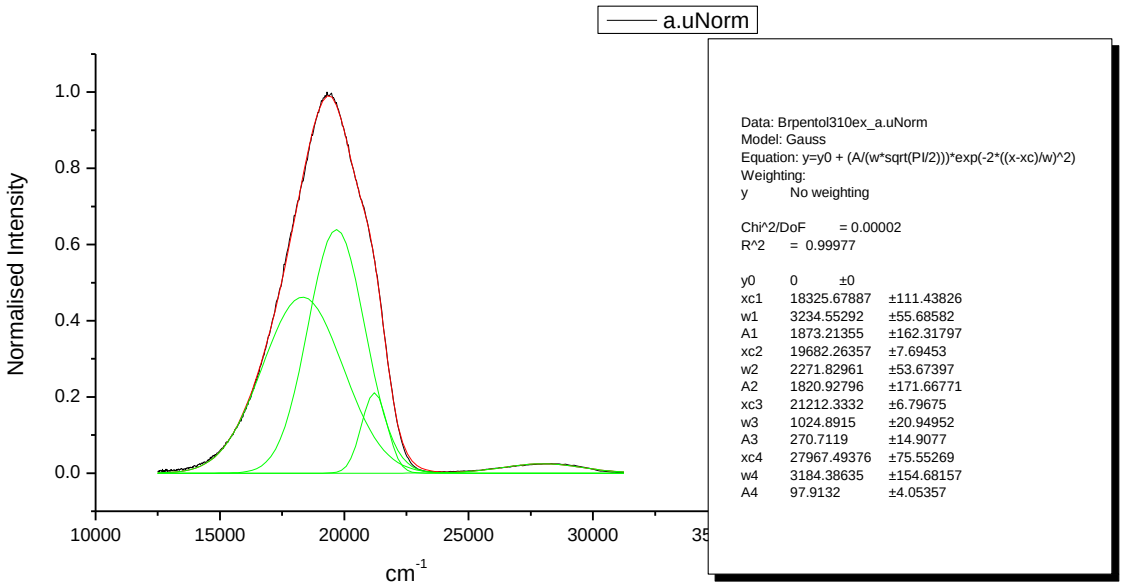

Figure 1.3.241. Gaussian model fit of the normalised fluorescence emission spectrum of **9a** recorded in 1-pentanol at 310 nm excitation.

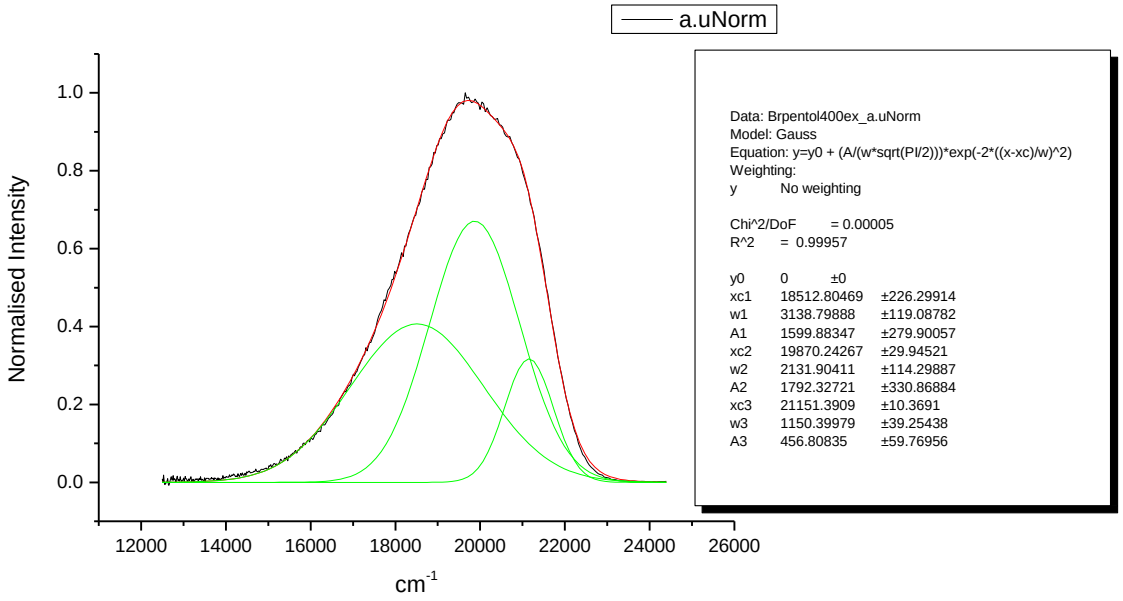

Figure 1.3.242. Gaussian model fit of the normalised fluorescence emission spectrum of **9a** recorded in 1-pentanol at 400 nm excitation.

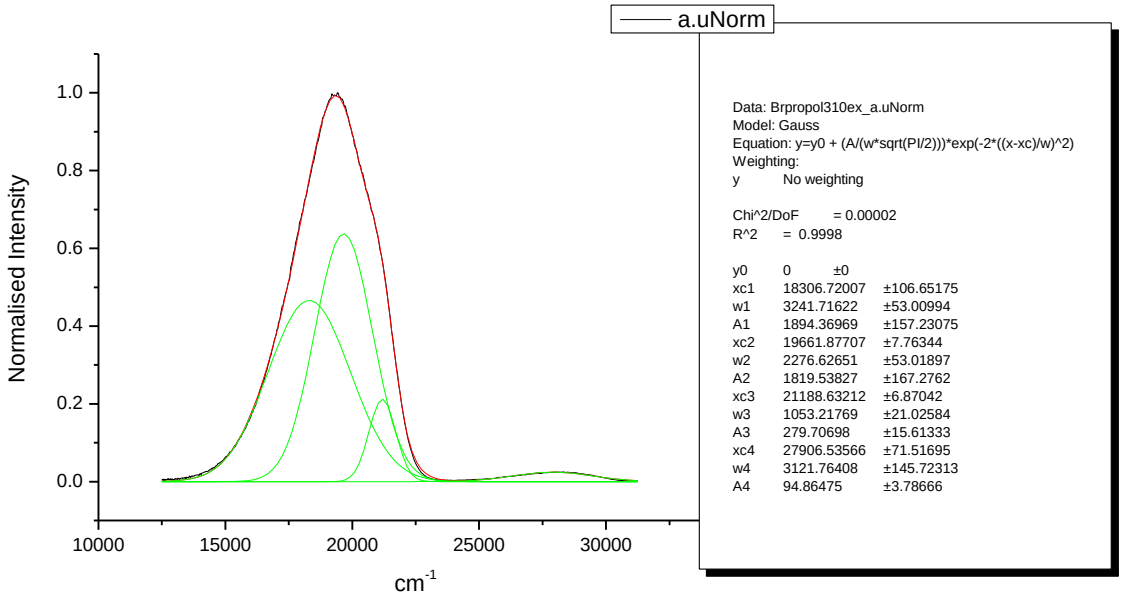

Figure 1.3.243. Gaussian model fit of the normalised fluorescence emission spectrum of **9a** recorded in 1-propanol at 310 nm excitation.

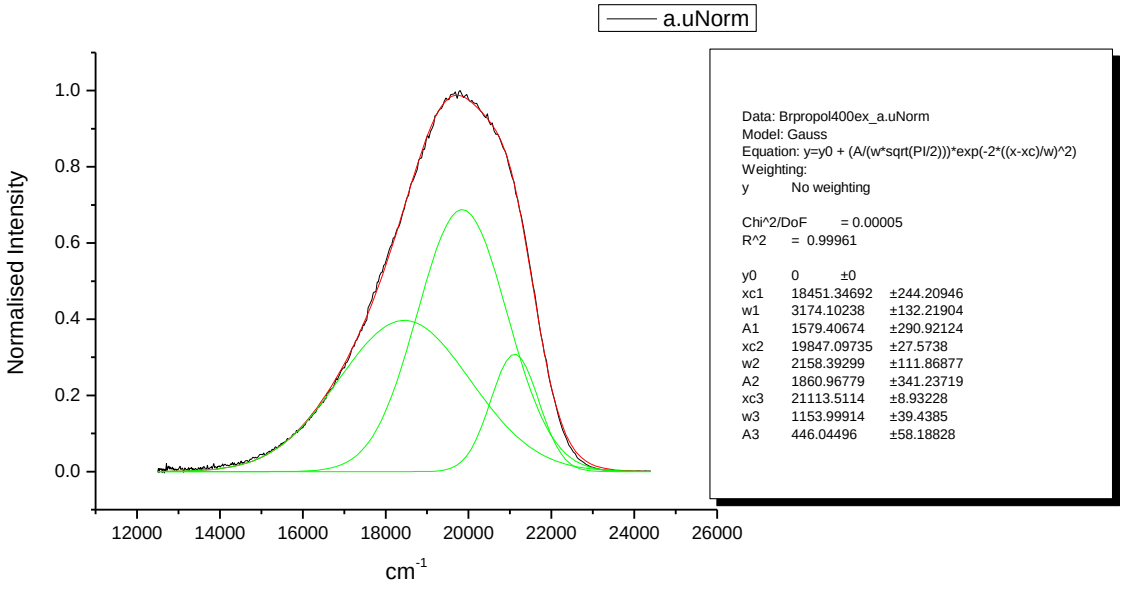

Figure 1.3.244. Gaussian model fit of the normalised fluorescence emission spectrum of **9a** recorded in 1-propanol at 400 nm excitation.

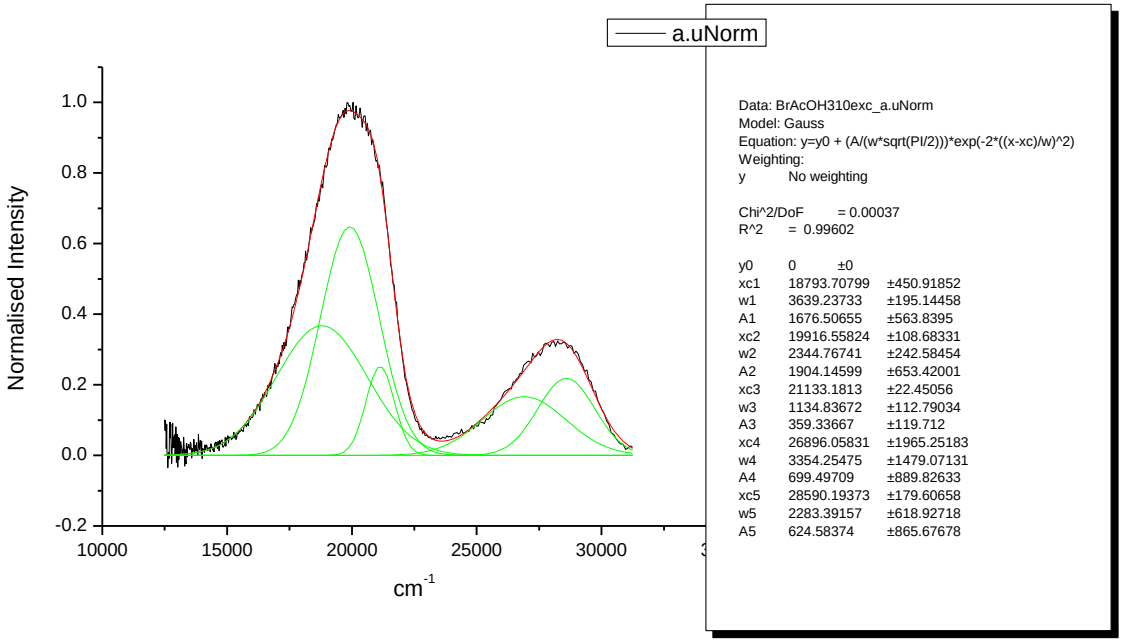

Figure 1.3.245. Gaussian model fit of the normalised fluorescence emission spectrum of **9a** recorded in Acetic Acid at 310 nm excitation.

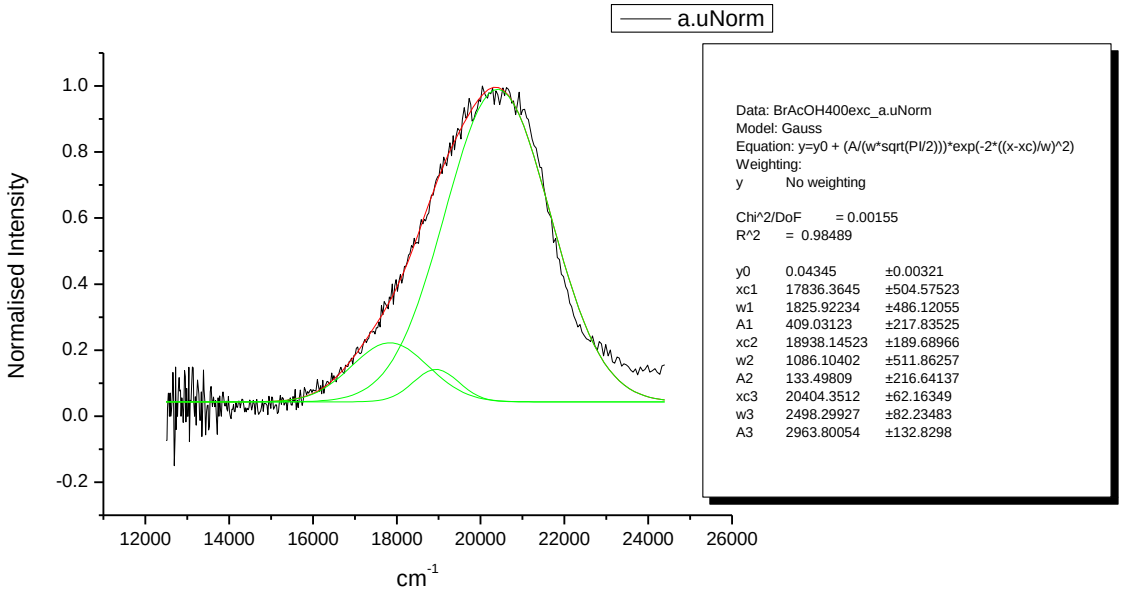

Figure 1.3.246. Gaussian model fit of the normalised fluorescence emission spectrum of **9a** recorded in Acetic Acid at 400 nm excitation.

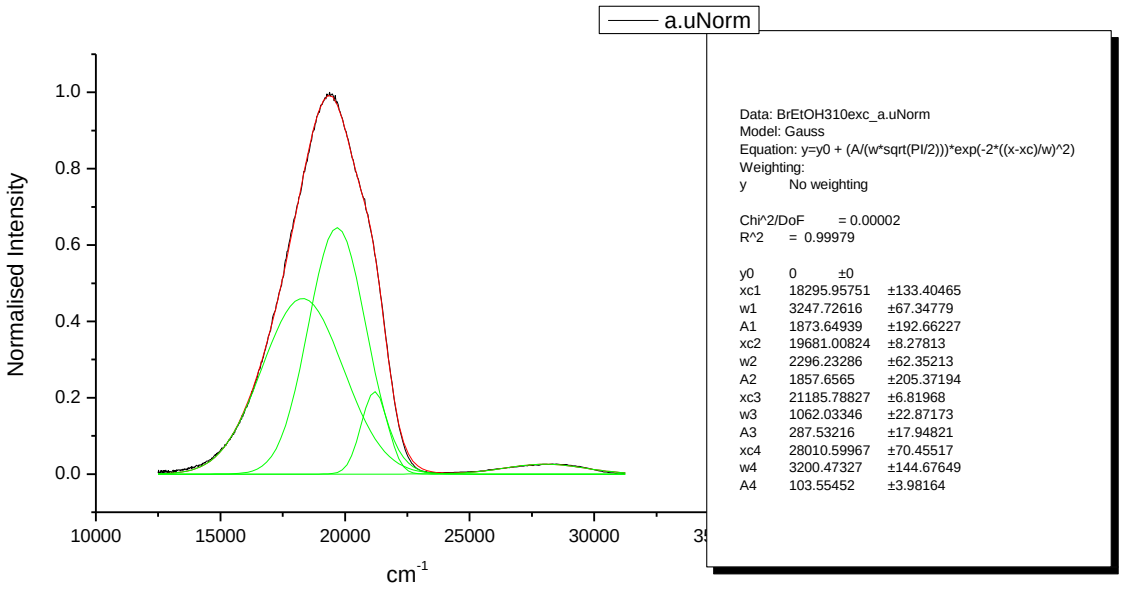

Figure 1.3.247. Gaussian model fit of the normalised fluorescence emission spectrum of **9a** recorded in Ethanol at 310 nm excitation.

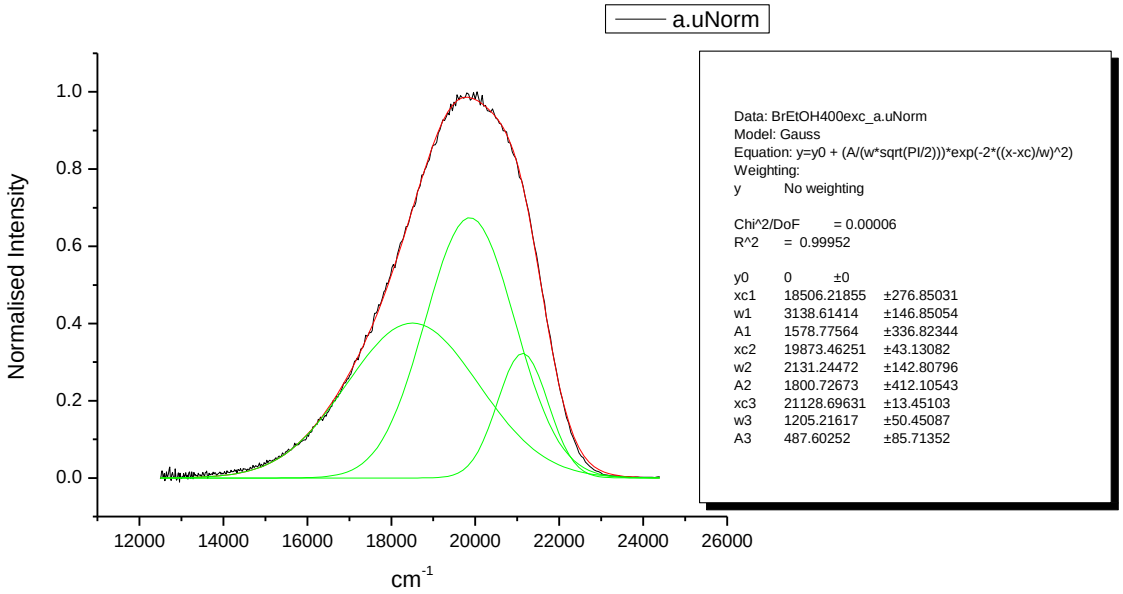

Figure 1.3.248. Gaussian model fit of the normalised fluorescence emission spectrum of **9a** recorded in Ethanol at 400 nm excitation.

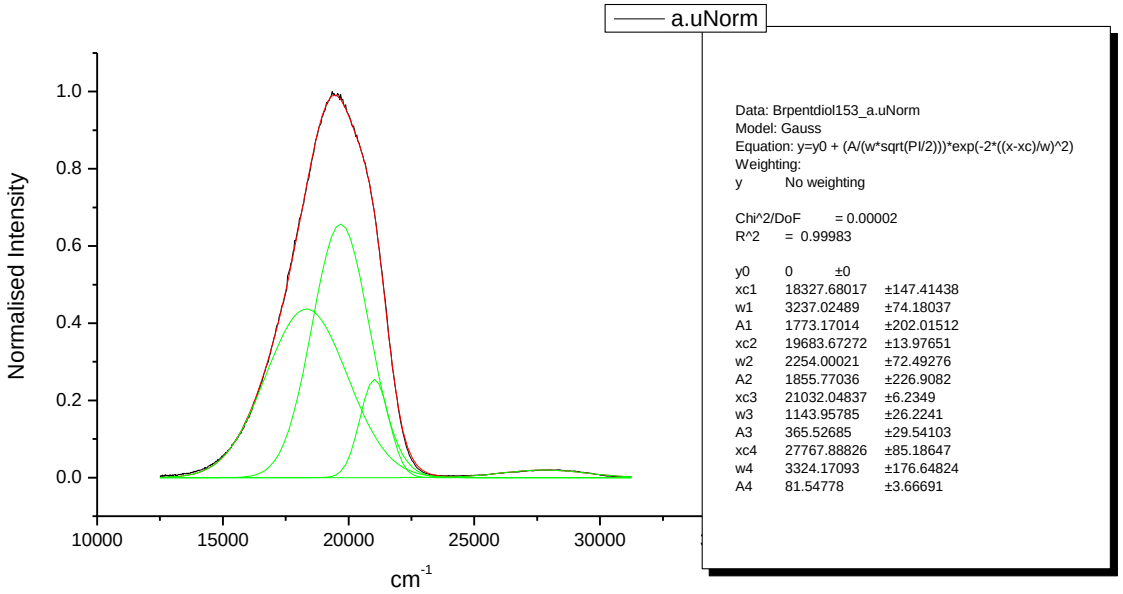

Figure 1.3.249. Gaussian model fit of the normalised fluorescence emission spectrum of **9a** recorded in 1,5-pentanediol at 310 nm excitation.

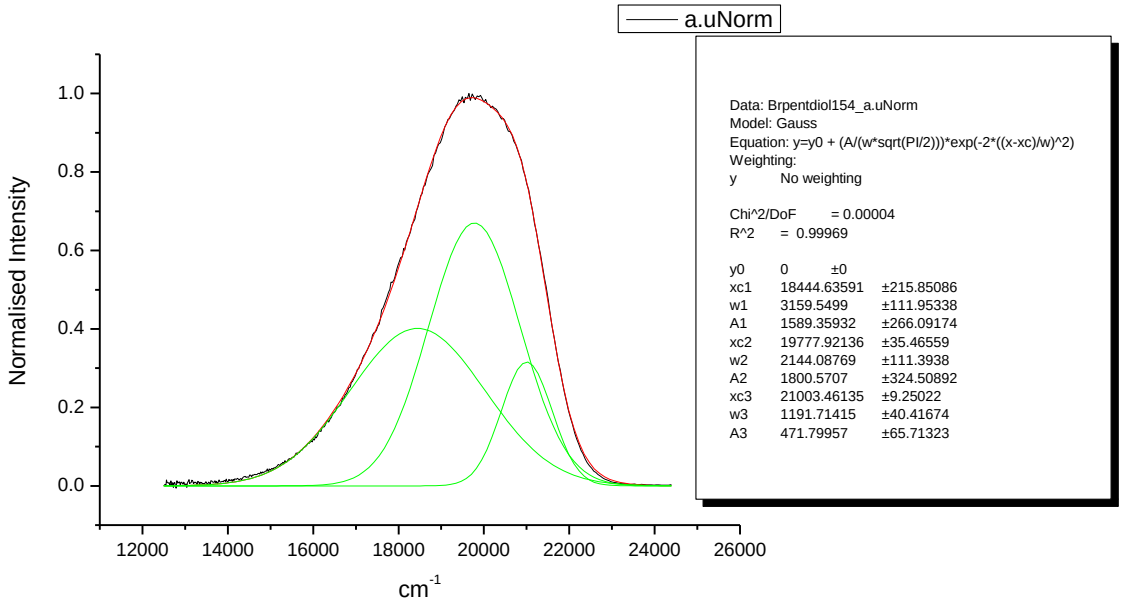

Figure 1.3.250. Gaussian model fit of the normalised fluorescence emission spectrum of **9a** recorded in 1,5-pentanediol at 400 nm excitation.

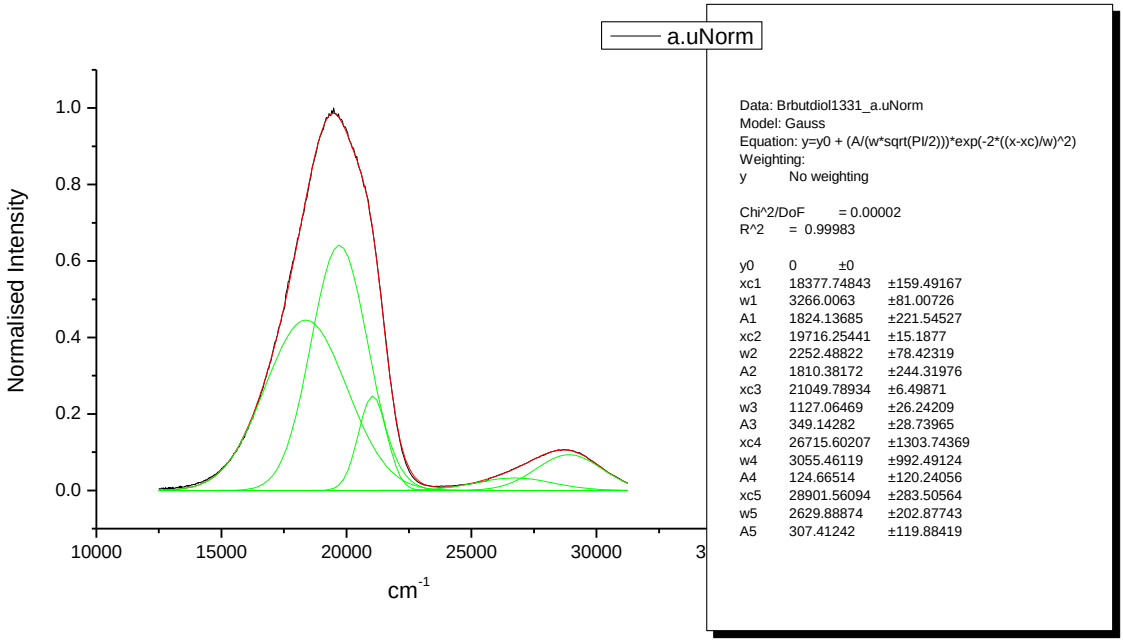

Figure 1.3.251. Gaussian model fit of the normalised fluorescence emission spectrum of **9a** recorded in 1,3-butanediol at 310 nm excitation.

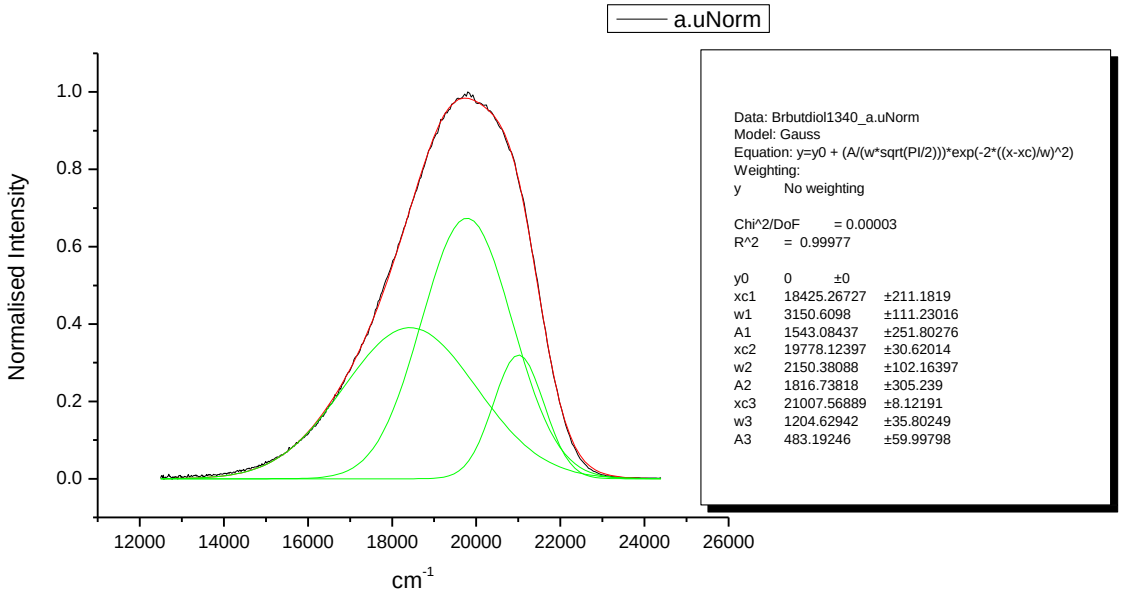

Figure 1.3.252. Gaussian model fit of the normalised fluorescence emission spectrum of **9a** recorded in 1,3-butanediol at 400 nm excitation.

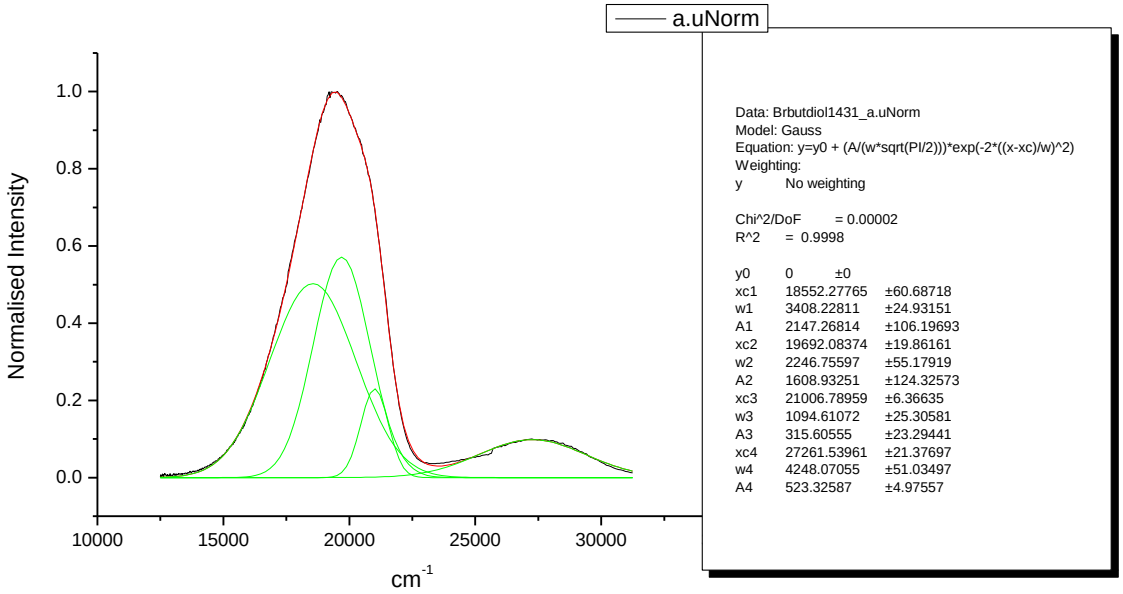

Figure 1.3.253. Gaussian model fit of the normalised fluorescence emission spectrum of **9a** recorded in 1,4-butanediol at 310 nm excitation.

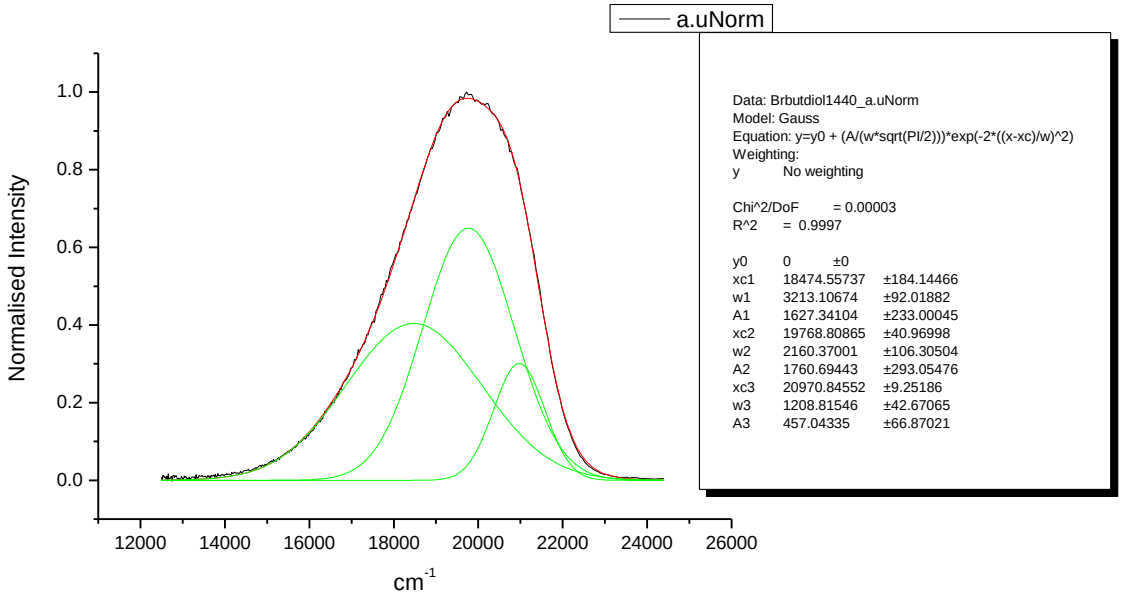

Figure 1.3.254. Gaussian model fit of the normalised fluorescence emission spectrum of **9a** recorded in 1,4-butanediol at 400 nm excitation.

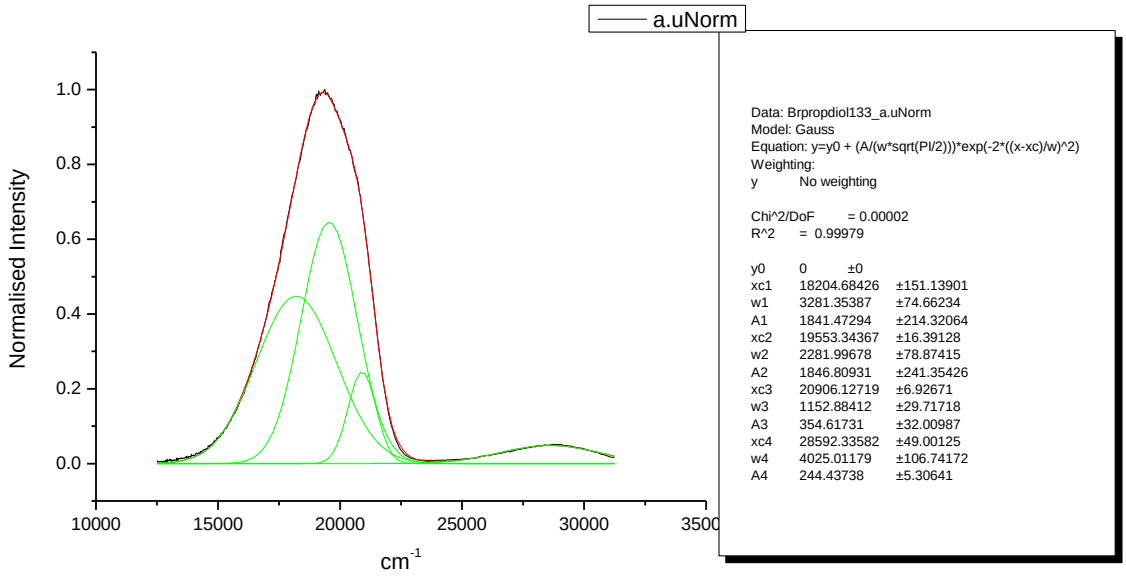

Figure 1.3.255. Gaussian model fit of the normalised fluorescence emission spectrum of **9a** recorded in 1,3-propanediol at 310 nm excitation.

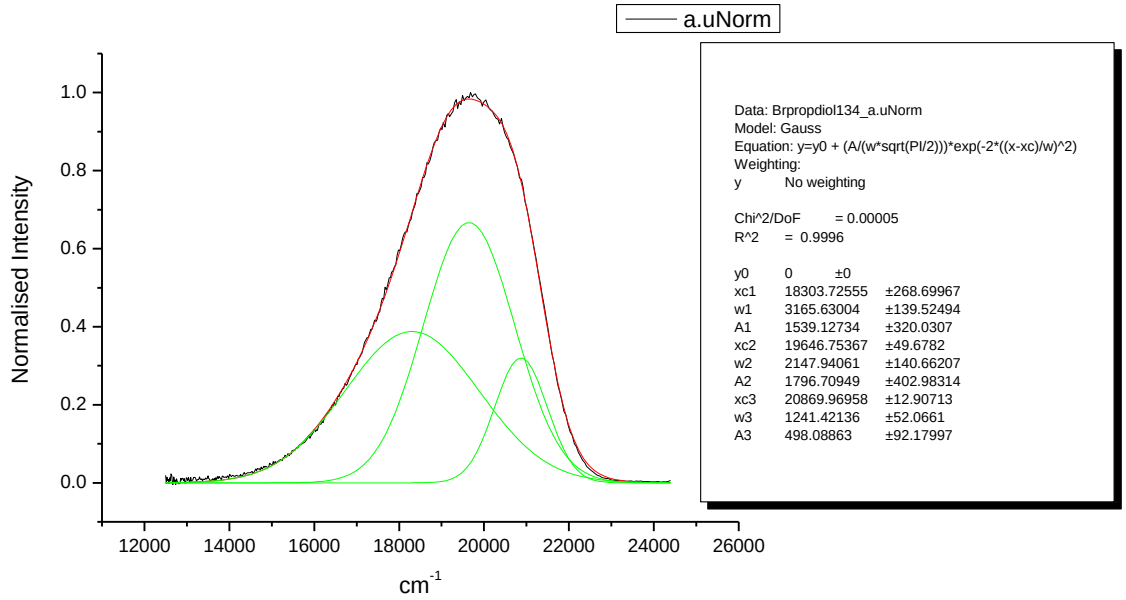

Figure 1.3.256. Gaussian model fit of the normalised fluorescence emission spectrum of **9a** recorded in 1,3-propanediol at 400 nm excitation.

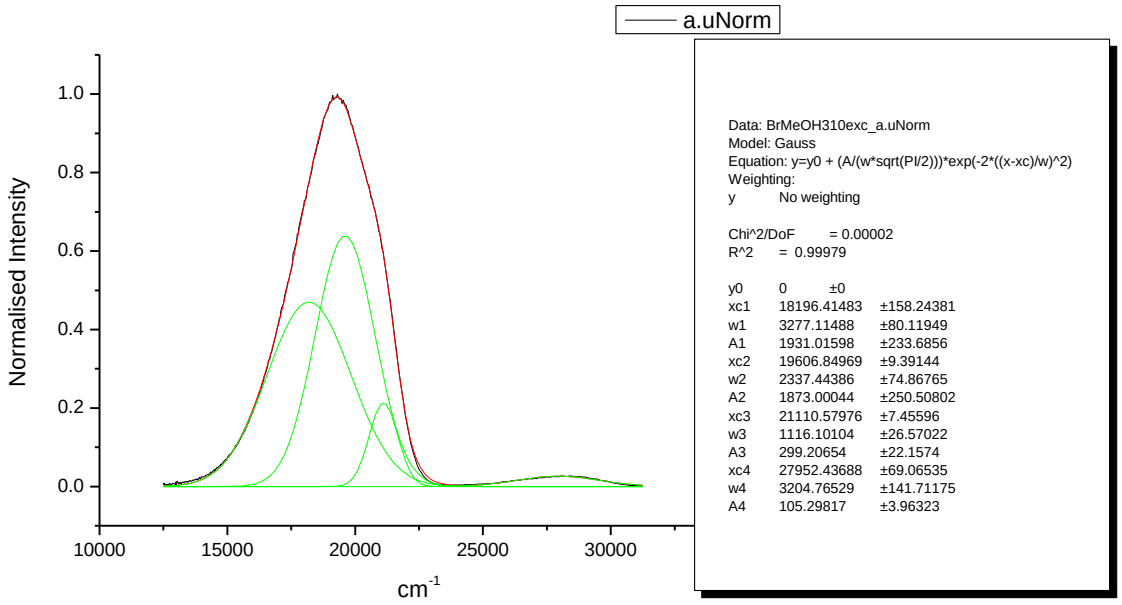

Figure 1.3.257. Gaussian model fit of the normalised fluorescence emission spectrum of **9a** recorded in Methanol at 310 nm excitation.

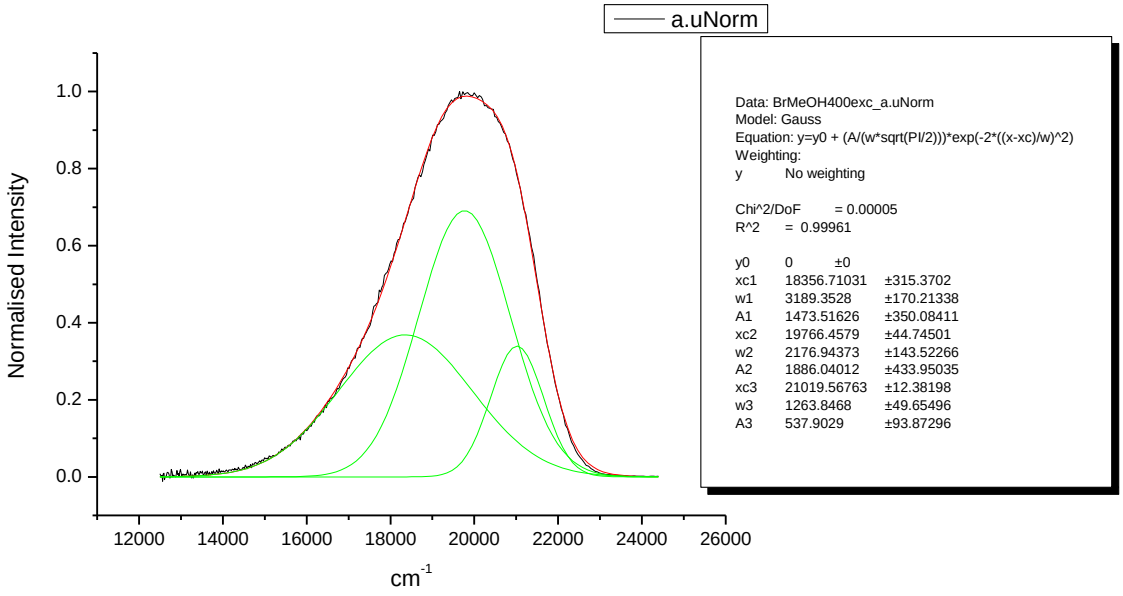

Figure 1.3.258. Gaussian model fit of the normalised fluorescence emission spectrum of **9a** recorded in Methanol at 400 nm excitation.

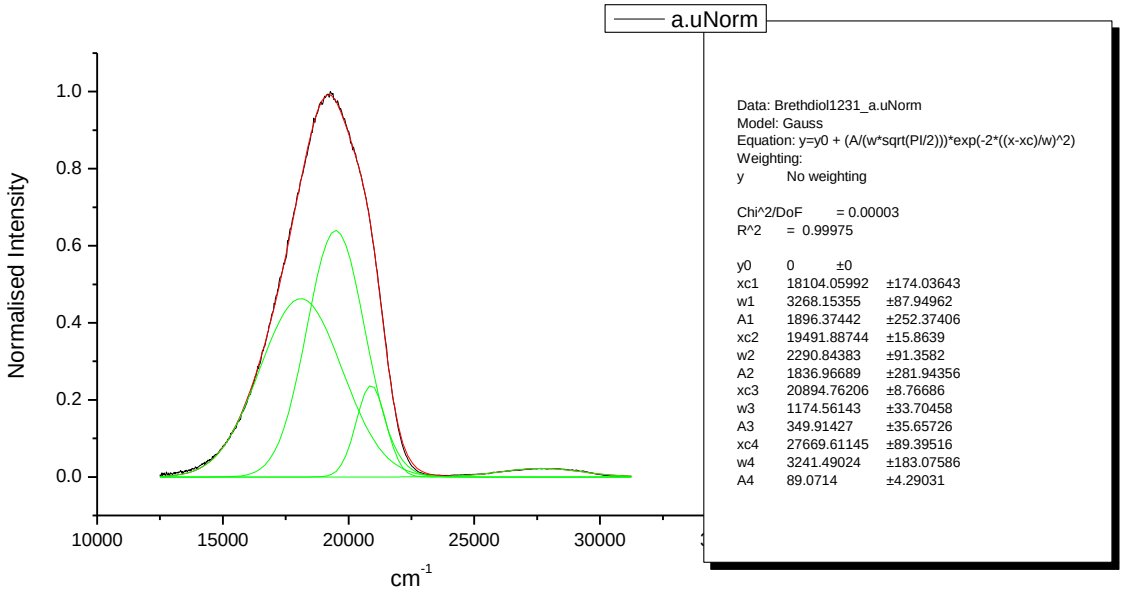

Figure 1.3.259. Gaussian model fit of the normalised fluorescence emission spectrum of **9a** recorded in 1,2-ethanediol at 310 nm excitation.

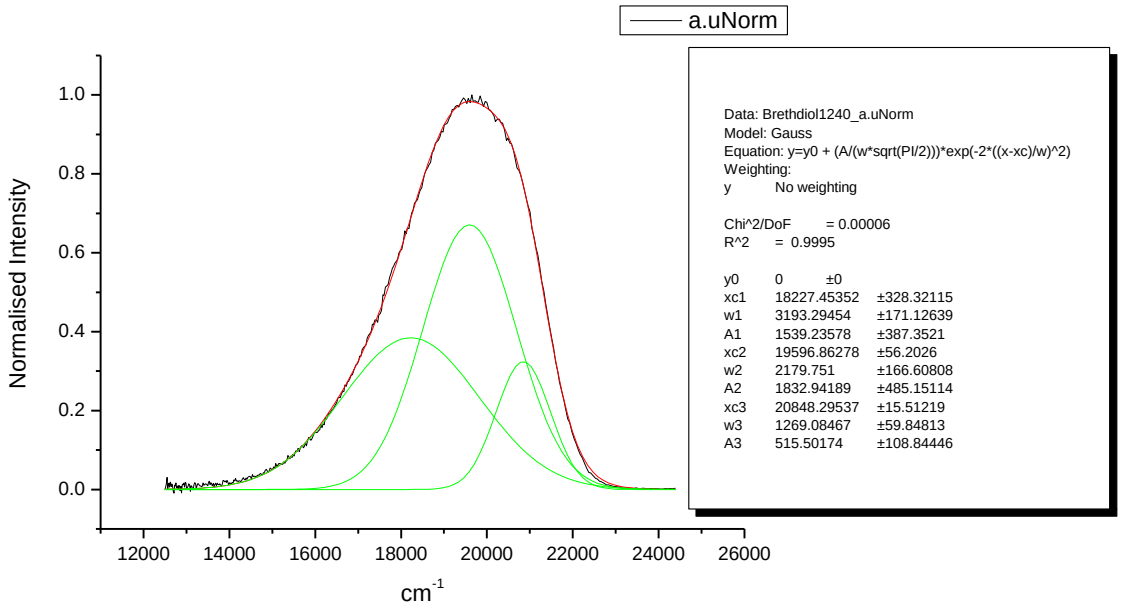

Figure 1.3.260. Gaussian model fit of the normalised fluorescence emission spectrum of **9a** recorded in 1,2-ethanediol at 400 nm excitation.

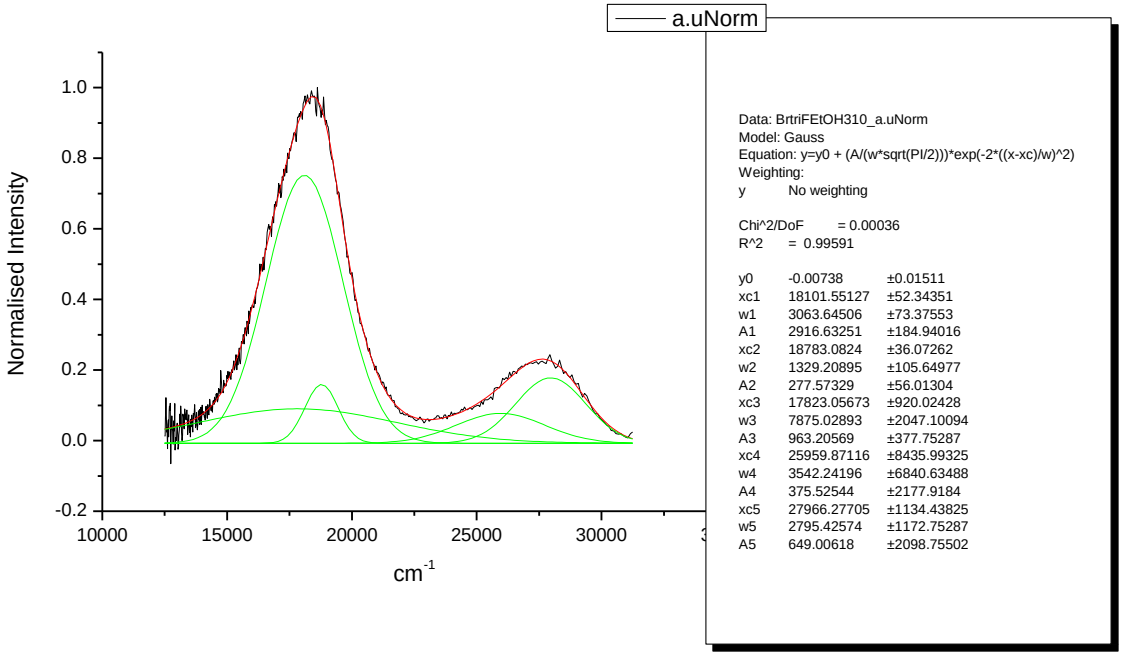

Figure 1.3.261. Gaussian model fit of the normalised fluorescence emission spectrum of **9a** recorded in 2,2,2-trifluoroethanol at 310 nm excitation.

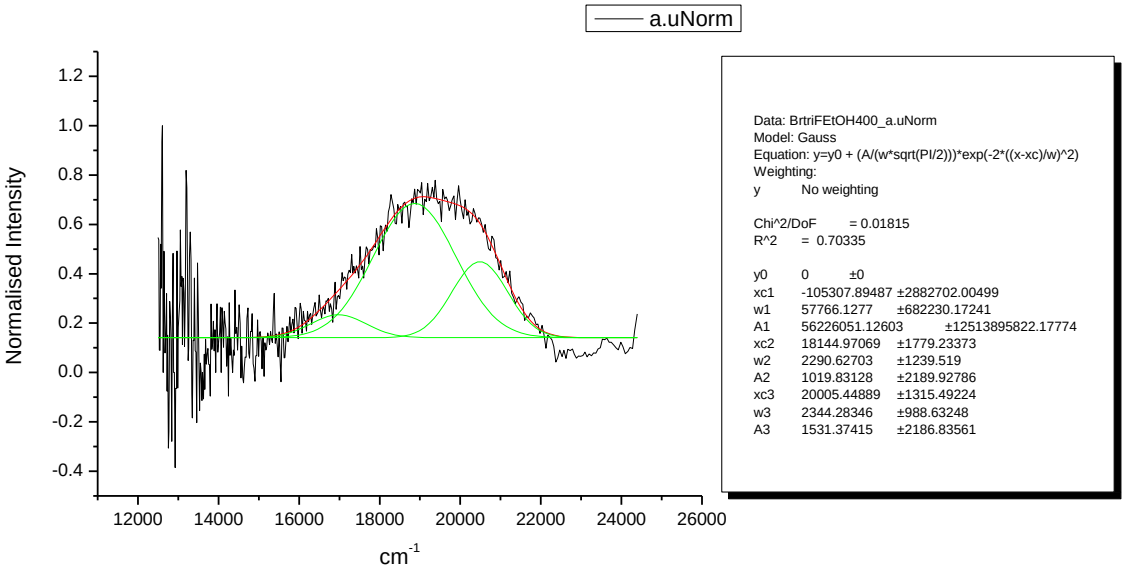

Figure 1.3.262. Gaussian model fit of the normalised fluorescence emission spectrum of **9a** recorded in 2,2,2-trifluoroethanol at 400 nm excitation.

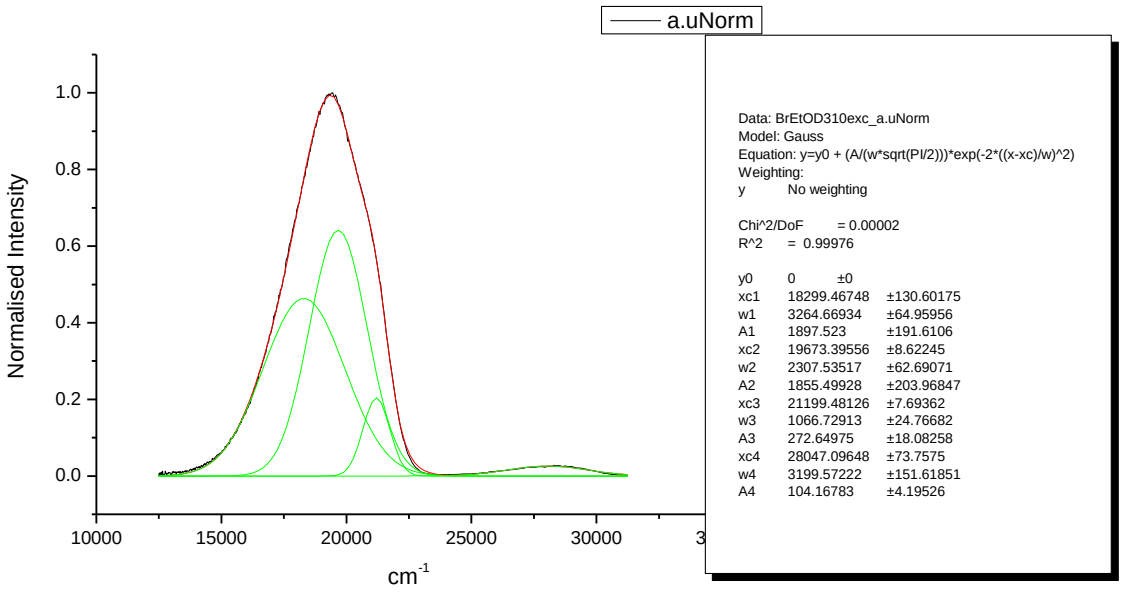

Figure 1.3.263. Gaussian model fit of the normalised fluorescence emission spectrum of **9a** recorded in ethanol-d_1 (EtOD) at 310 nm excitation.

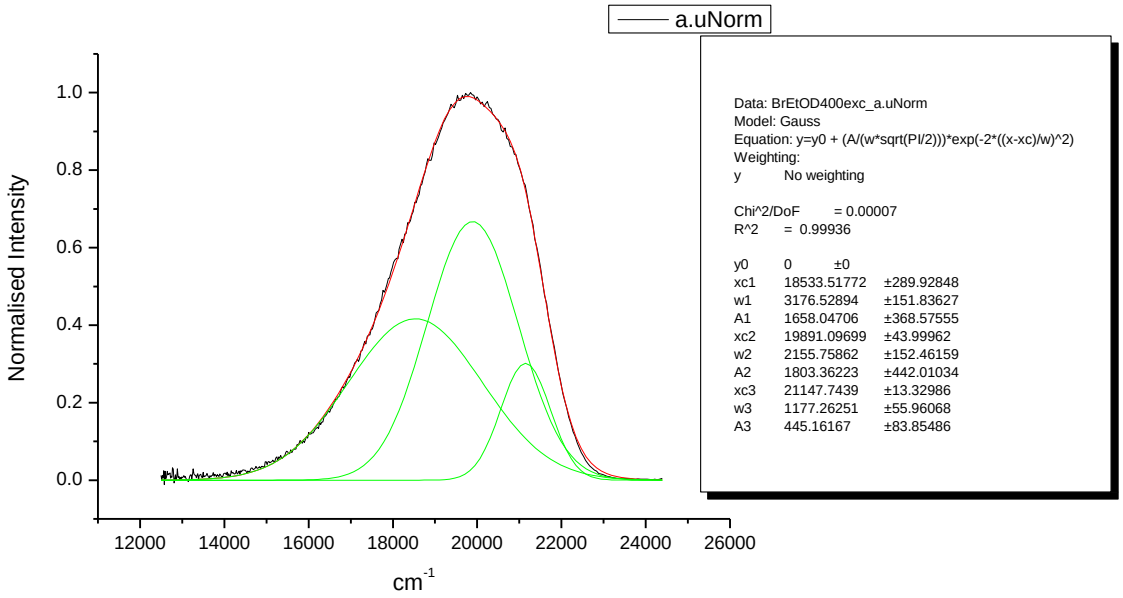

Figure 1.3.264. Gaussian model fit of the normalised fluorescence emission spectrum of **9a** recorded in ethanol-d_1 (EtOD) at 400 nm excitation.

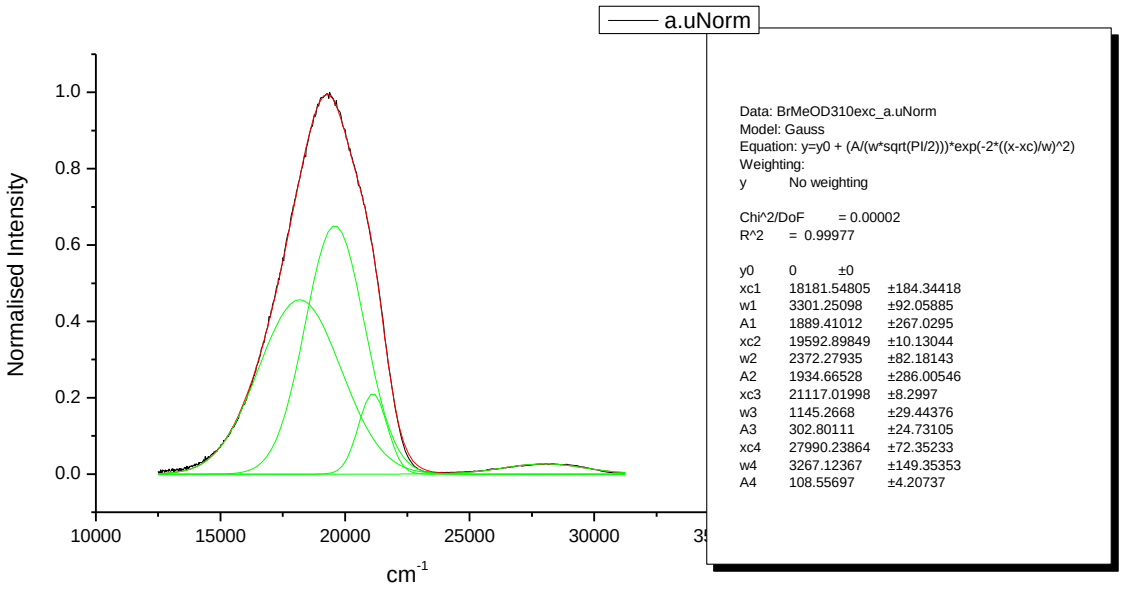

Figure 1.3.265. Gaussian model fit of the normalised fluorescence emission spectrum of **9a** recorded in methanol-d_1 (MeOD) at 310 nm excitation.

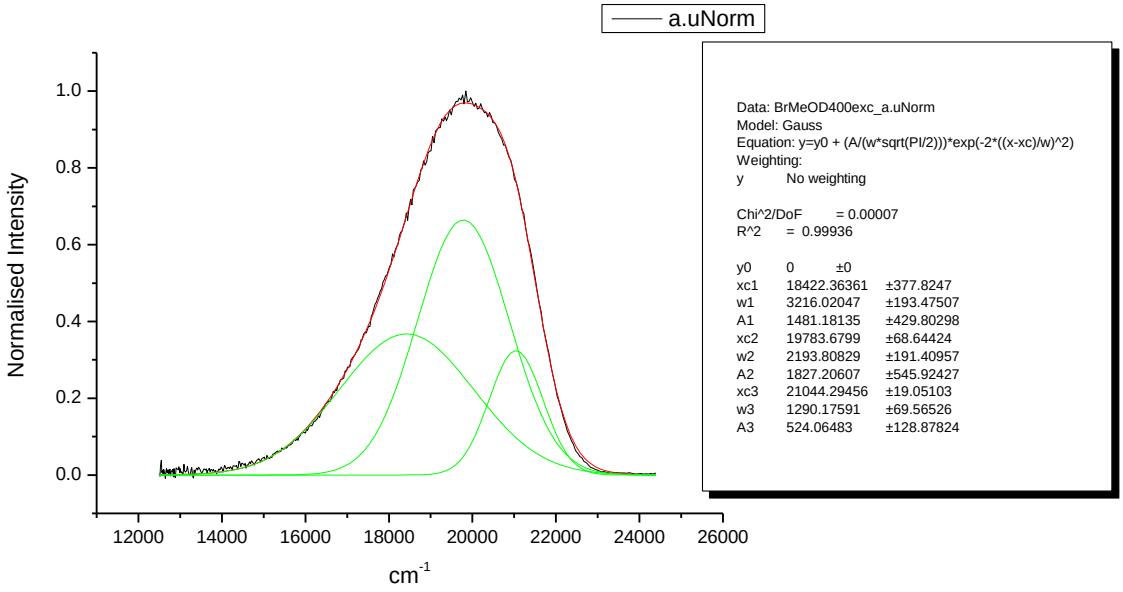

Figure 1.3.266. Gaussian model fit of the normalised fluorescence emission spectrum of **9a** recorded in methanol-d_1 (MeOD) at 400 nm excitation.

1.3.11 Fluorescence Excitation spectra.

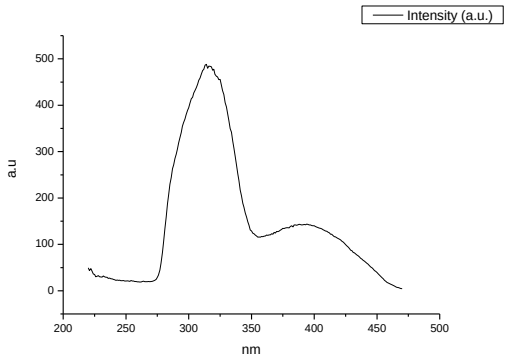

Figure 1.3.267. Fluorescence excitation spectrum of **9a** recorded in Toluene with emission fixed at 480 nm.

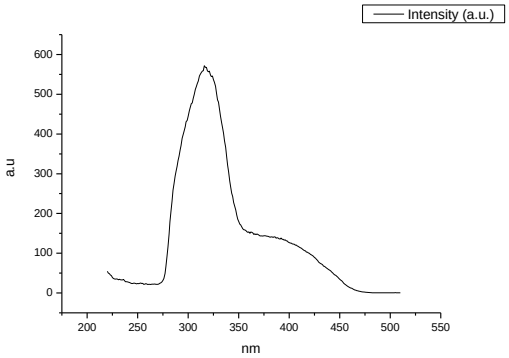

Figure 1.3.268. Fluorescence excitation spectrum of **9a** recorded in Toluene with emission fixed at 520 nm.

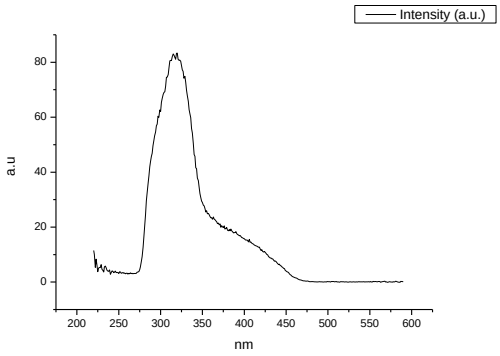

Figure 1.3.269. Fluorescence excitation spectrum of **9a** recorded in Toluene with emission fixed at 600 nm.

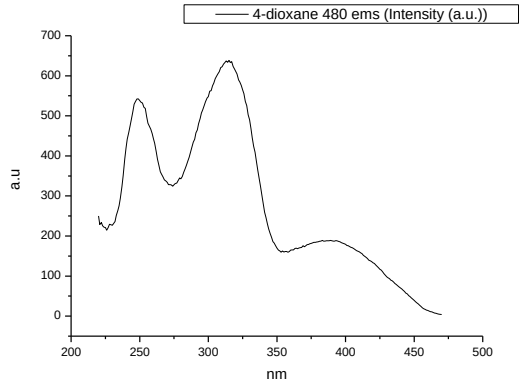

Figure 1.3.270. Fluorescence excitation spectrum of **9a** recorded in 1,4-dioxane with emission fixed at 480 nm.

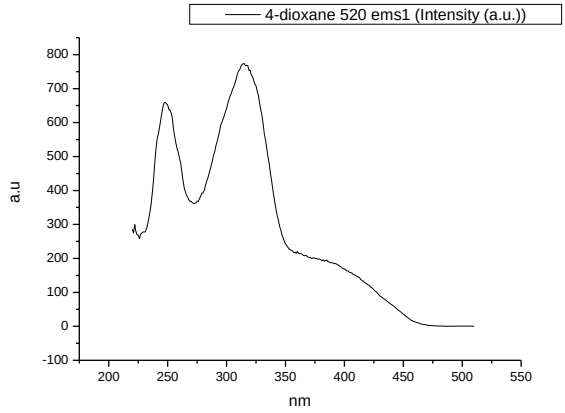

Figure 1.3.271. Fluorescence excitation spectrum of **9a** recorded in 1,4-dioxane with emission fixed at 520 nm.

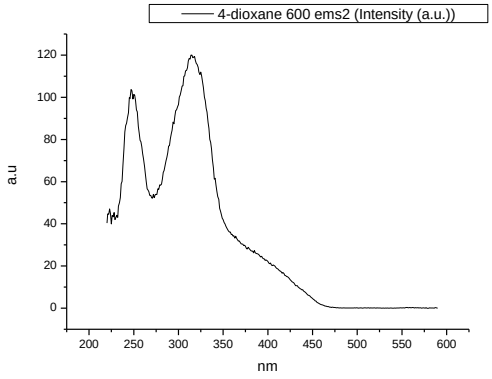

Figure 1.3.272. Fluorescence excitation spectrum of **9a** recorded in 1,4-dioxane with emission fixed at 600 nm.

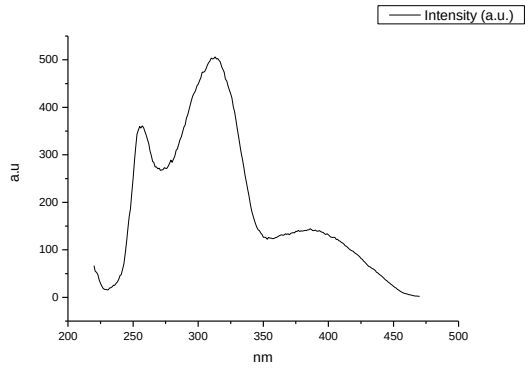

Figure 1.3.273. Fluorescence excitation spectrum of **9a** recorded in Ethyl Acetate with emission fixed at 480 nm.

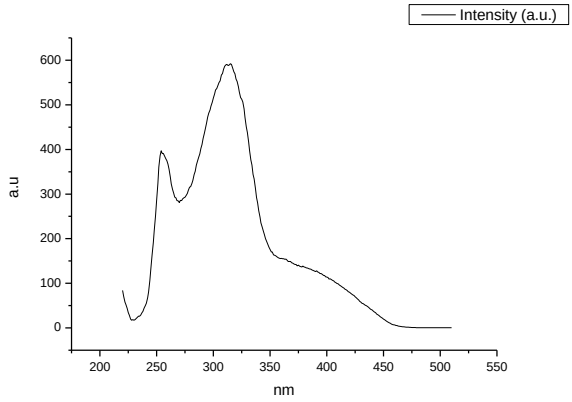

Figure 1.3.274. Fluorescence excitation spectrum of **9a** recorded in Ethyl Acetate with emission fixed at 520 nm.

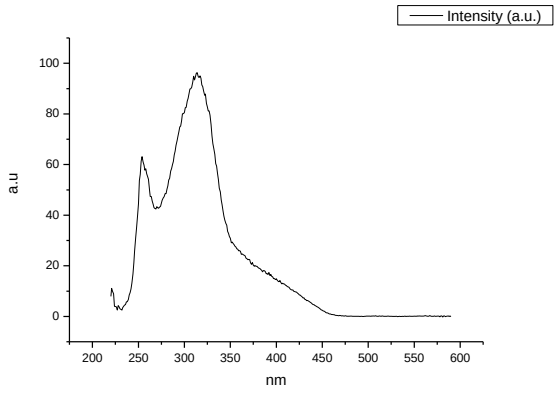

Figure 1.3.275. Fluorescence excitation spectrum of **9a** recorded in Ethyl Acetate with emission fixed at 600 nm.

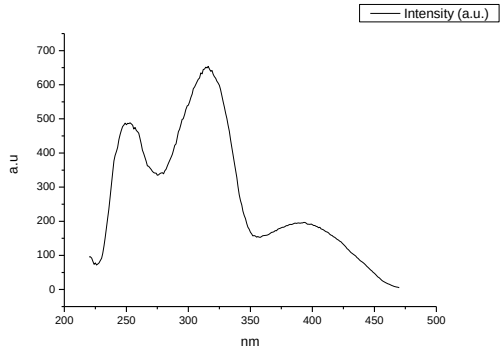

Figure 1.3.276. Fluorescence excitation spectrum of **9a** recorded in Chloroform with emission fixed at 480 nm.

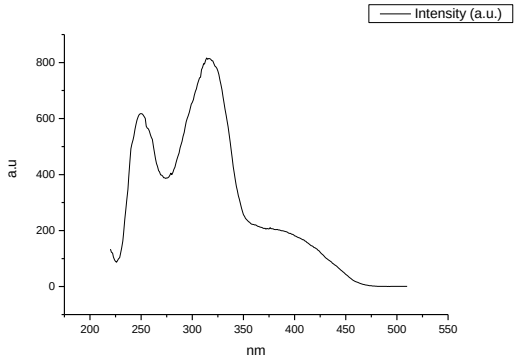

Figure 1.3.277. Fluorescence excitation spectrum of **9a** recorded in Chloroform with emission fixed at 520 nm.

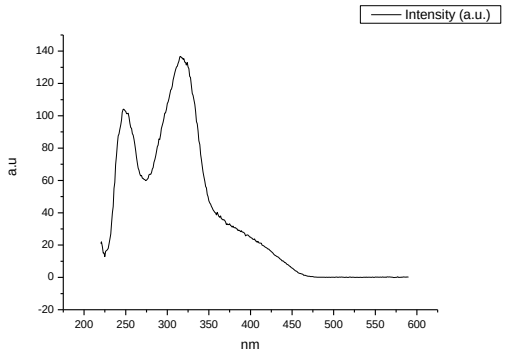

Figure 1.3.278. Fluorescence excitation spectrum of **9a** recorded in Chloroform with emission fixed at 600 nm.

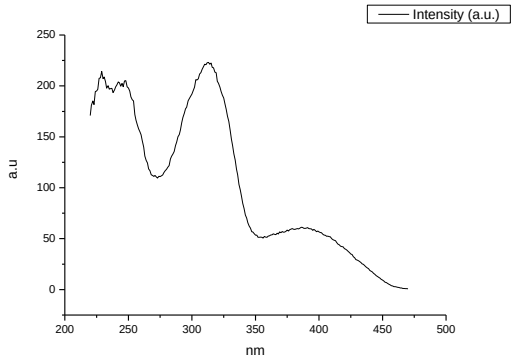

Figure 1.3.279. Fluorescence excitation spectrum of **9a** recorded in 2-methyl-2-butanol with emission fixed at 480 nm.

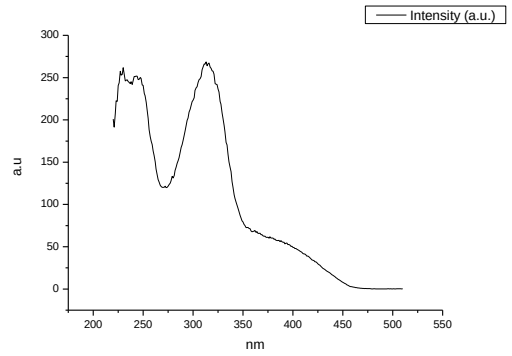

Figure 1.3.280. Fluorescence excitation spectrum of **9a** recorded in 2-methyl-2-butanol with emission fixed at 520 nm.

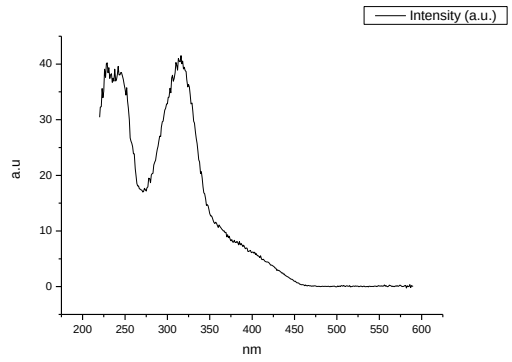

Figure 1.3.281. Fluorescence excitation spectrum of **9a** recorded in 2-methyl-2-butanol with emission fixed at 600 nm.

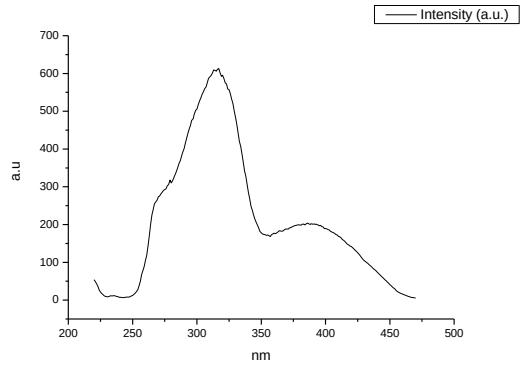

Figure 1.3.282. Fluorescence excitation spectrum of **9a** recorded in N,N-dimethylformamide with emission fixed at 480 nm.

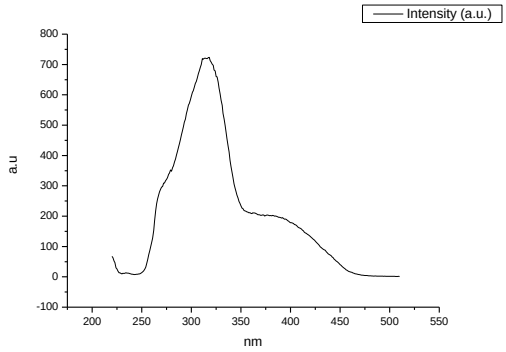

Figure 1.3.283. Fluorescence excitation spectrum of **9a** recorded in N,N-dimethylformamide with emission fixed at 520 nm.

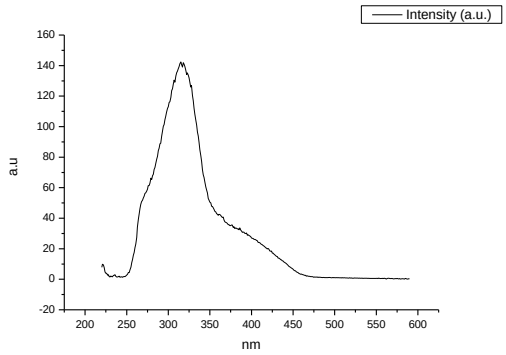

Figure 1.3.284. Fluorescence excitation spectrum of **9a** recorded in N,N-dimethylformamide with emission fixed at 600 nm.

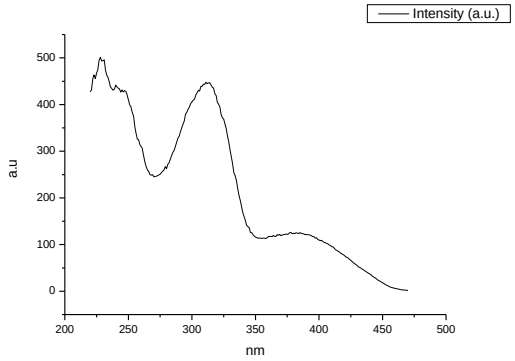

Figure 1.3.285. Fluorescence excitation spectrum of **9a** recorded in Acetonitrile with emission fixed at 480 nm.

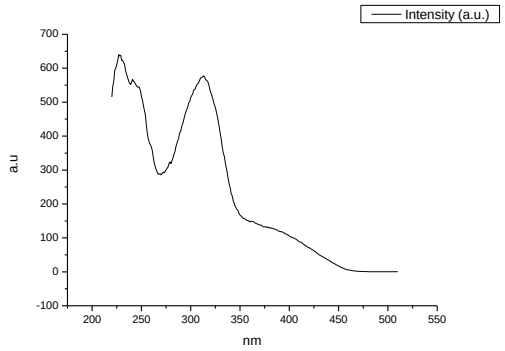

Figure 1.3.286. Fluorescence excitation spectrum of **9a** recorded in Acetonitrile with emission fixed at 520 nm.

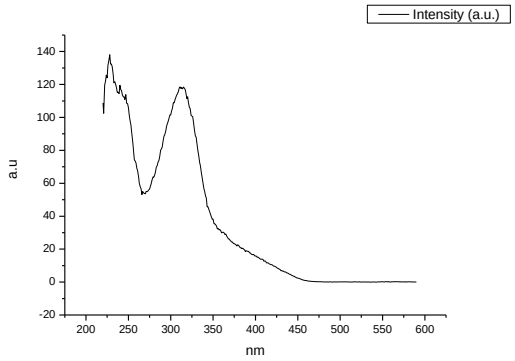

Figure 1.3.287. Fluorescence excitation spectrum of **9a** recorded in Acetonitrile with emission fixed at 600 nm.

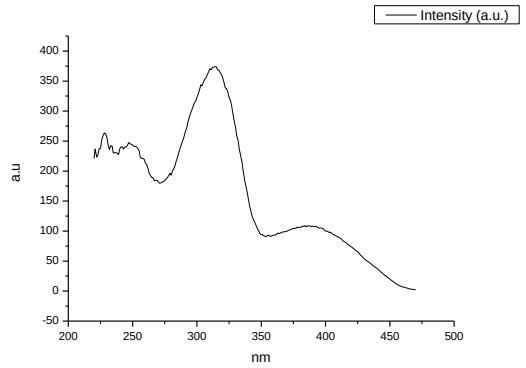

Figure 1.3.288. Fluorescence excitation spectrum of **9a** recorded in Propylene Carbonate with emission fixed at 480 nm.

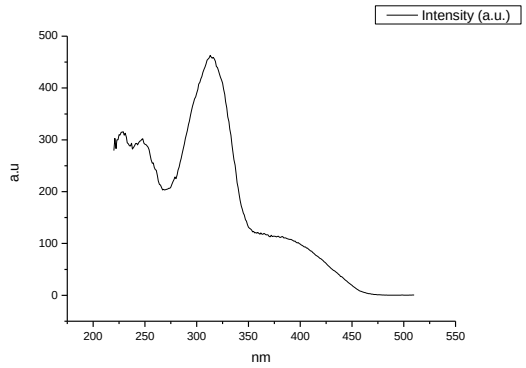

Figure 1.3.289. Fluorescence excitation spectrum of **9a** recorded in Propylene Carbonate with emission fixed at 520 nm.

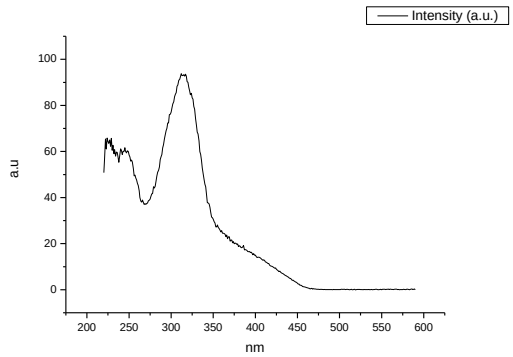

Figure 1.3.290. Fluorescence excitation spectrum of **9a** recorded in Propylene Carbonate with emission fixed at 600 nm.

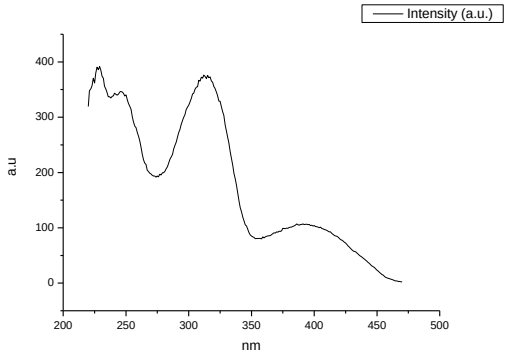

Figure 1.3.291. Fluorescence excitation spectrum of **9a** recorded in 1-octanol with emission fixed at 480 nm.

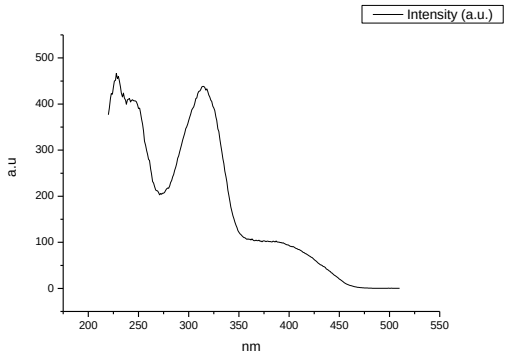

Figure 1.3.292. Fluorescence excitation spectrum of **9a** recorded in 1-octanol with emission fixed at 520 nm.

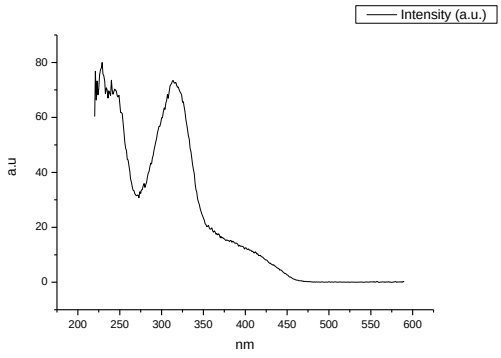

Figure 1.3.293. Fluorescence excitation spectrum of **9a** recorded in 1-octanol with emission fixed at 600 nm.

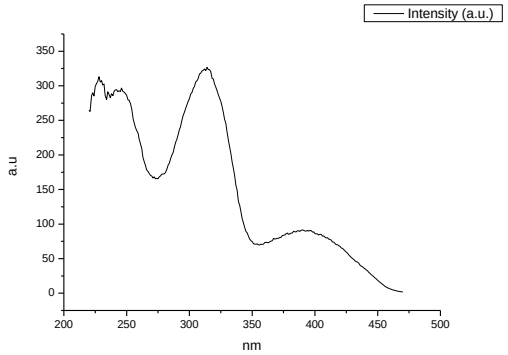

Figure 1.3.294. Fluorescence excitation spectrum of **9a** recorded in 1-hexanol with emission fixed at 480 nm.

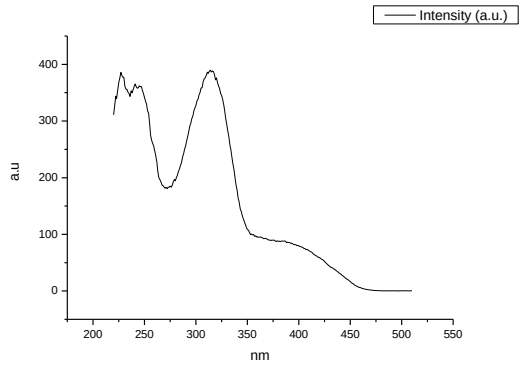

Figure 1.3.295. Fluorescence excitation spectrum of **9a** recorded in 1-hexanol with emission fixed at 520 nm.

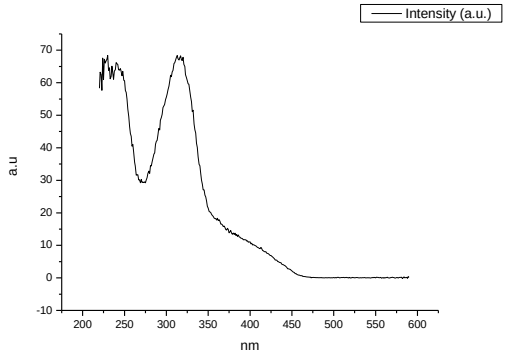

Figure 1.3.296. Fluorescence excitation spectrum of **9a** recorded in 1-hexanol with emission fixed at 600 nm.

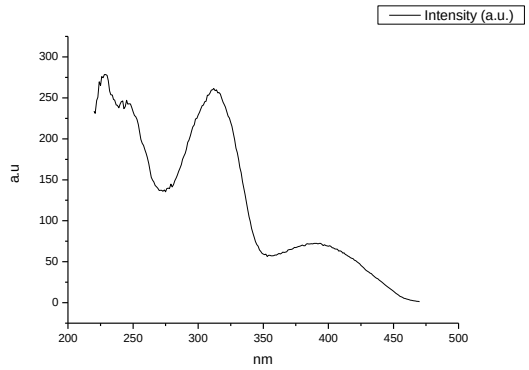

Figure 1.3.297. Fluorescence excitation spectrum of **9a** recorded in 1-butanol with emission fixed at 480 nm.

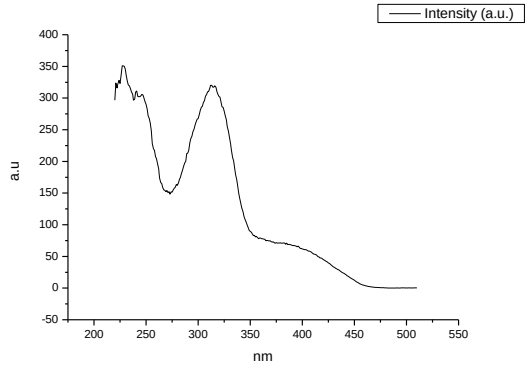

Figure 1.3.298. Fluorescence excitation spectrum of **9a** recorded in 1-butanol with emission fixed at 520 nm.

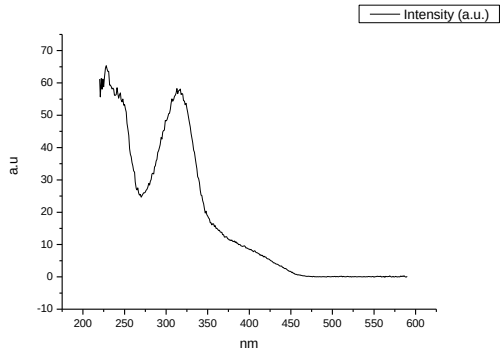

Figure 1.3.299. Fluorescence excitation spectrum of **9a** recorded in 1-butanol with emission fixed at 600 nm.

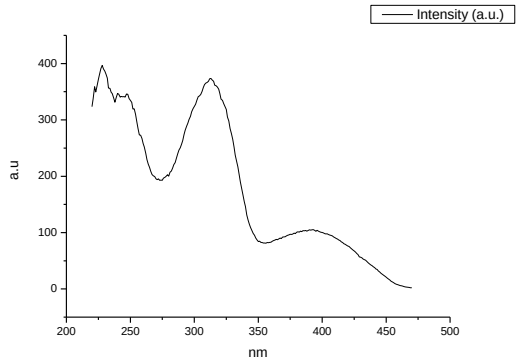

Figure 1.3.300. Fluorescence excitation spectrum of **9a** recorded in 1-pentanol with emission fixed at 480 nm.

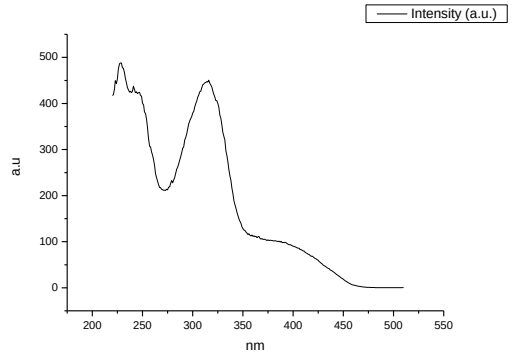

Figure 1.3.301. Fluorescence excitation spectrum of **9a** recorded in 1-pentanol with emission fixed at 520 nm.

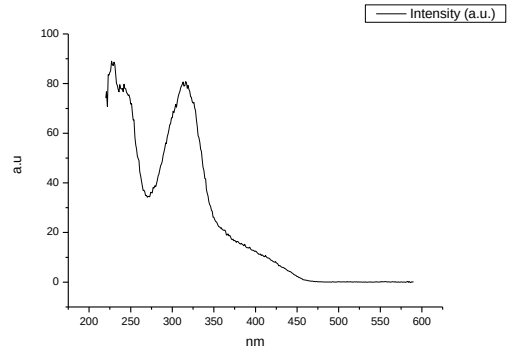

Figure 1.3.302. Fluorescence excitation spectrum of **9a** recorded in 1-pentanol with emission fixed at 600 nm.

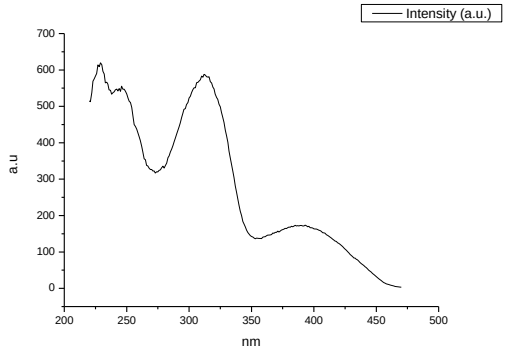

Figure 1.3.303. Fluorescence excitation spectrum of **9a** recorded in 1-propanol with emission fixed at 480 nm.

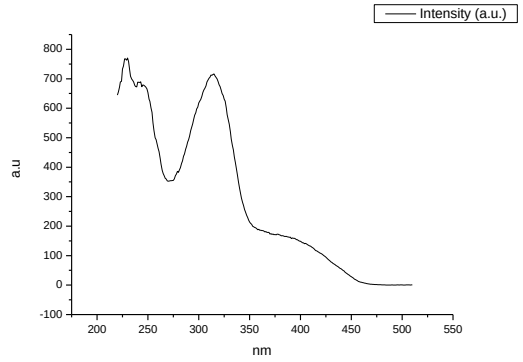

Figure 1.3.304. Fluorescence excitation spectrum of **9a** recorded in 1-propanol with emission fixed at 520 nm.

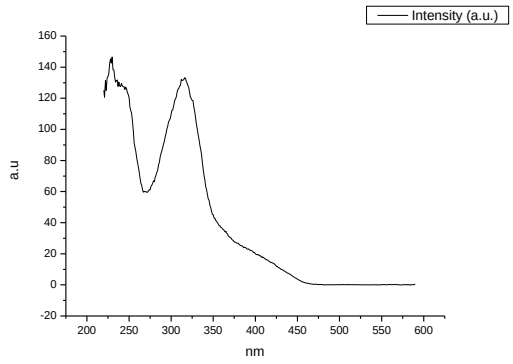

Figure 1.3.305. Fluorescence excitation spectrum of **9a** recorded in 1-propanol with emission fixed at 600 nm.

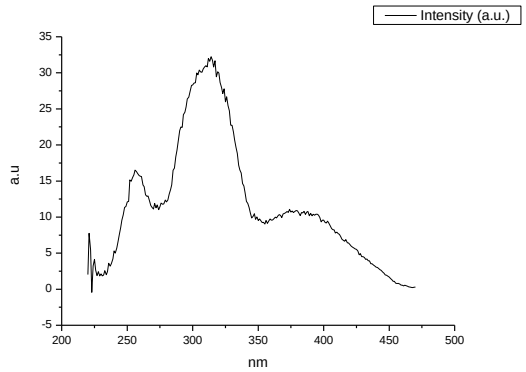

Figure 1.3.306. Fluorescence excitation spectrum of **9a** recorded in Acetic Acid with emission fixed at 480 nm.

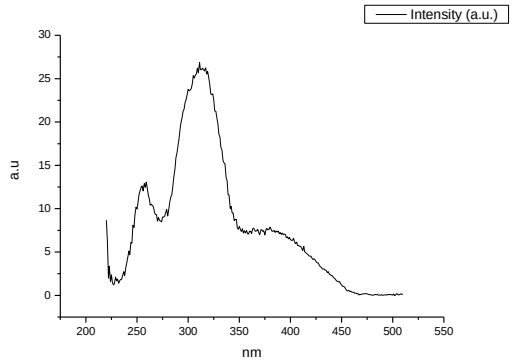

Figure 1.3.307. Fluorescence excitation spectrum of **9a** recorded in Acetic Acid with emission fixed at 520 nm.

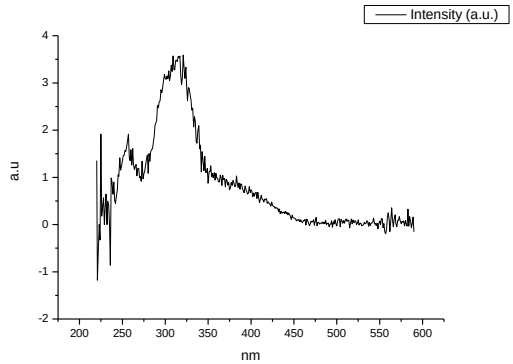

Figure 1.3.308. Fluorescence excitation spectrum of **9a** recorded in Acetic Acid with emission fixed at 600 nm.

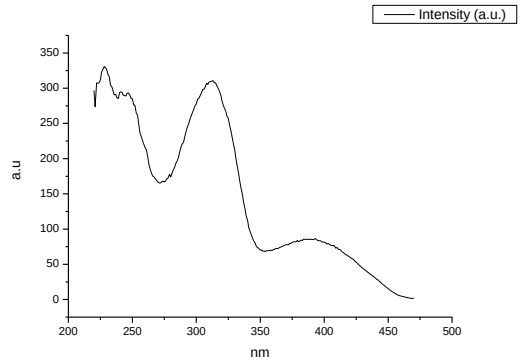

Figure 1.3.309. Fluorescence excitation spectrum of **9a** recorded in Ethanol with emission fixed at 480 nm.

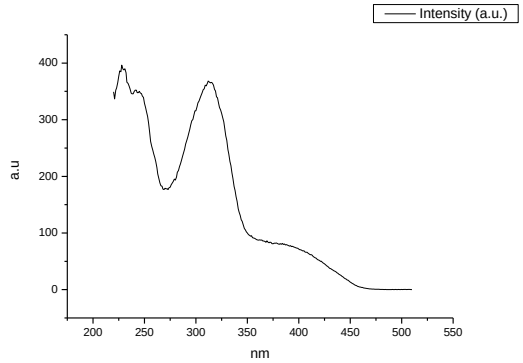

Figure 1.3.310. Fluorescence excitation spectrum of **9a** recorded in Ethanol with emission fixed at 520 nm.

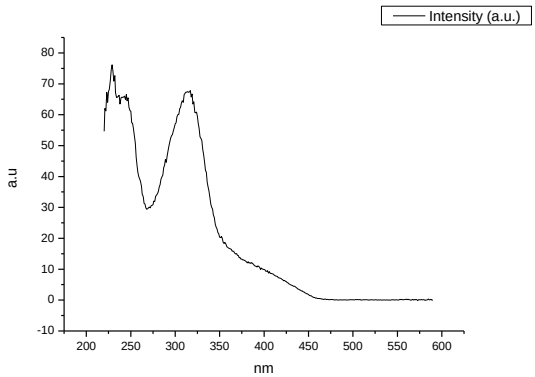

Figure 1.3.311. Fluorescence excitation spectrum of **9a** recorded in Ethanol with emission fixed at 600 nm.

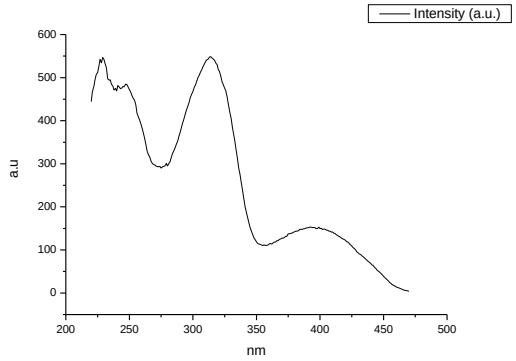

Figure 1.3.312. Fluorescence excitation spectrum of **9a** recorded in 1,5-pentanediol with emission fixed at 480 nm.

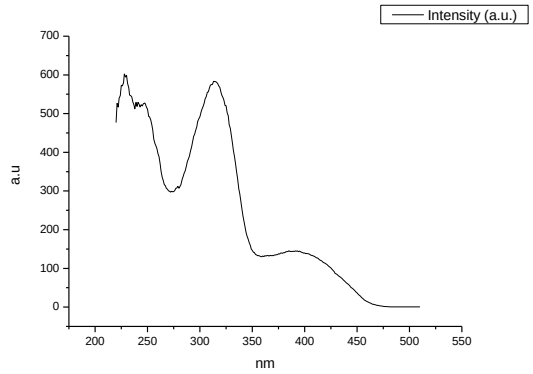

Figure 1.3.313. Fluorescence excitation spectrum of **9a** recorded in 1,5-pentanediol with emission fixed at 520 nm.

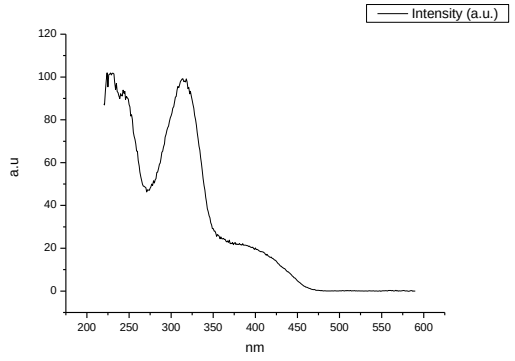

Figure 1.3.314. Fluorescence excitation spectrum of **9a** recorded in 1,5-pentanediol with emission fixed at 600 nm.

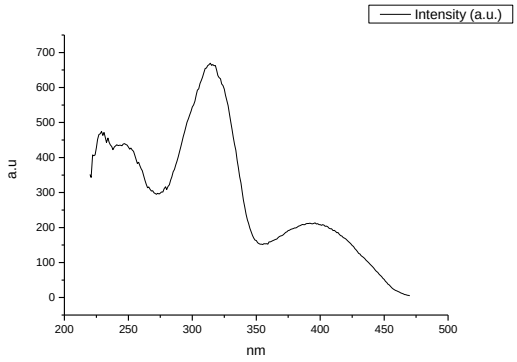

Figure 1.3.315. Fluorescence excitation spectrum of **9a** recorded in 1,3-butanediol with emission fixed at 480 nm.

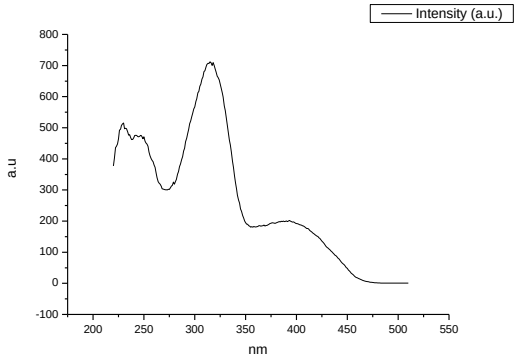

Figure 1.3.316. Fluorescence excitation spectrum of **9a** recorded in 1,3-butanediol with emission fixed at 520 nm.

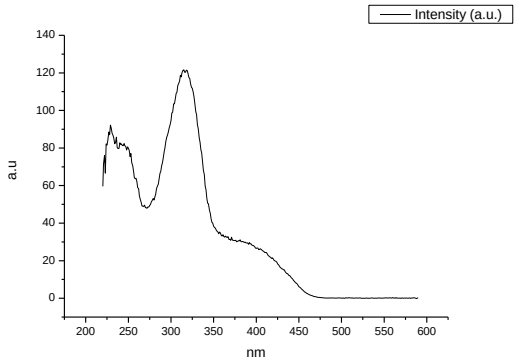

Figure 1.3.317. Fluorescence excitation spectrum of **9a** recorded in 1,3-butanediol with emission fixed at 600 nm.

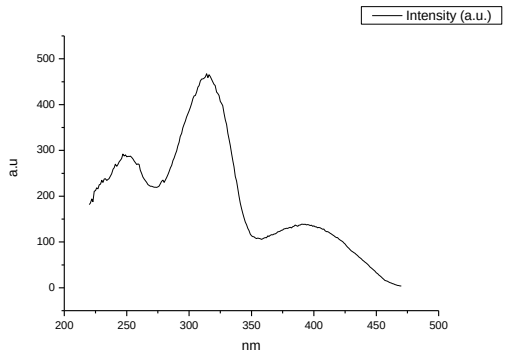

Figure 1.3.318. Fluorescence excitation spectrum of **9a** recorded in 1,4-butanediol with emission fixed at 480 nm.

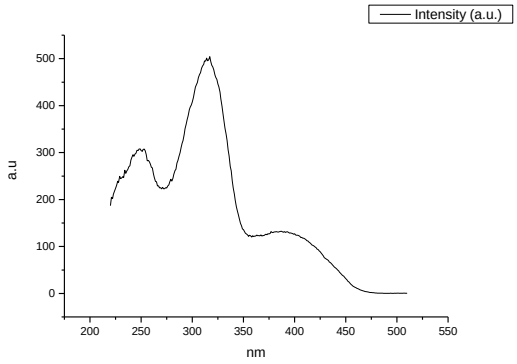

Figure 1.3.319. Fluorescence excitation spectrum of **9a** recorded in 1,4-butanediol with emission fixed at 520 nm.

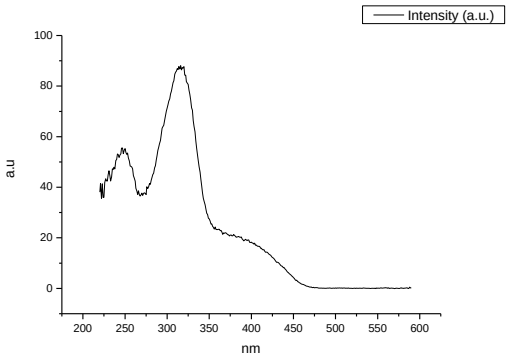

Figure 1.3.320. Fluorescence excitation spectrum of **9a** recorded in 1,4-butanediol with emission fixed at 600 nm.

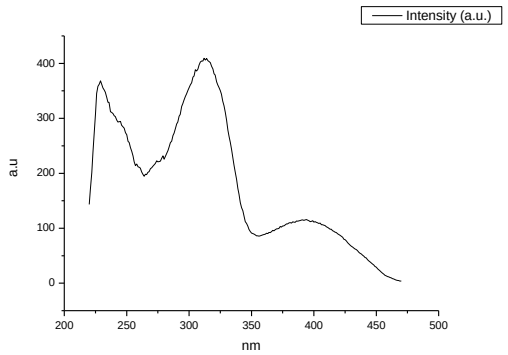

Figure 1.3.321. Fluorescence excitation spectrum of **9a** recorded in 1,3-propanediol with emission fixed at 480 nm.

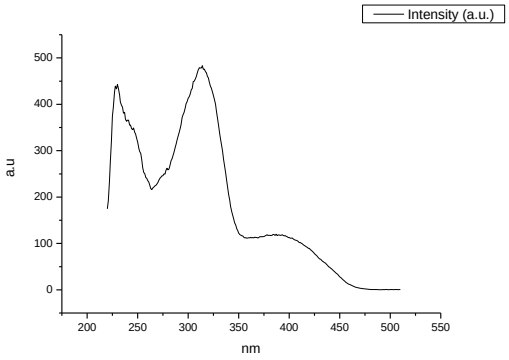

Figure 1.3.322. Fluorescence excitation spectrum of **9a** recorded in 1,3-propanediol with emission fixed at 520 nm.

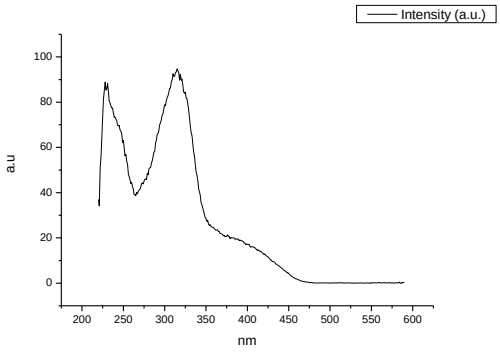

Figure 1.3.323. Fluorescence excitation spectrum of **9a** recorded in 1,3-propanediol with emission fixed at 600 nm.

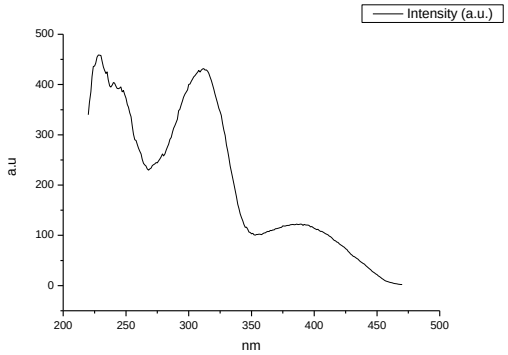

Figure 1.3.324. Fluorescence excitation spectrum of **9a** recorded in Methanol with emission fixed at 480 nm.

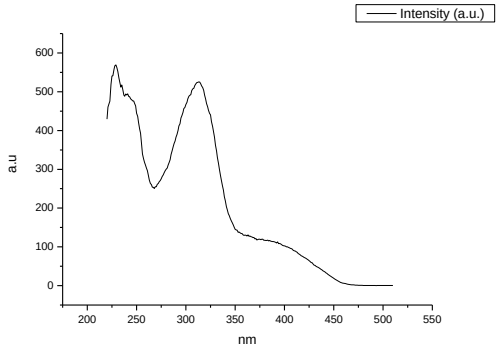

Figure 1.3.325. Fluorescence excitation spectrum of **9a** recorded in Methanol with emission fixed at 520 nm.

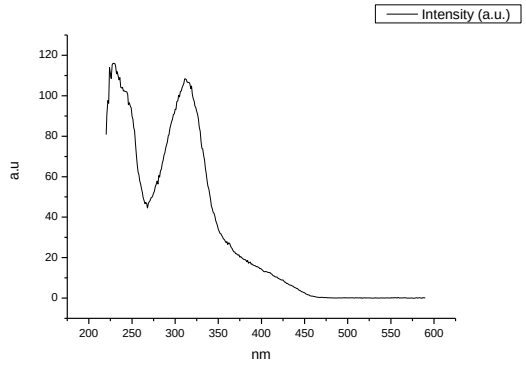

Figure 1.3.326. Fluorescence excitation spectrum of **9a** recorded in Methanol with emission fixed at 600 nm.

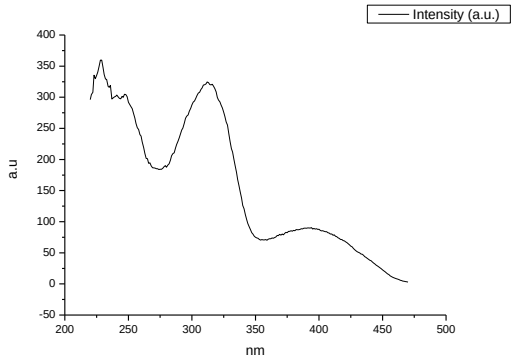

Figure 1.3.327. Fluorescence excitation spectrum of **9a** recorded in 1,2-ethanediol with emission fixed at 480 nm.

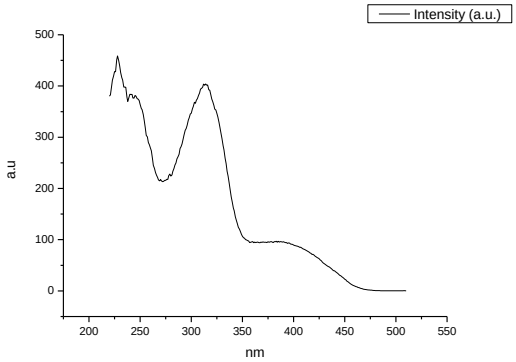

Figure 1.3.328. Fluorescence excitation spectrum of **9a** recorded in 1,2-ethanediol with emission fixed at 520 nm.

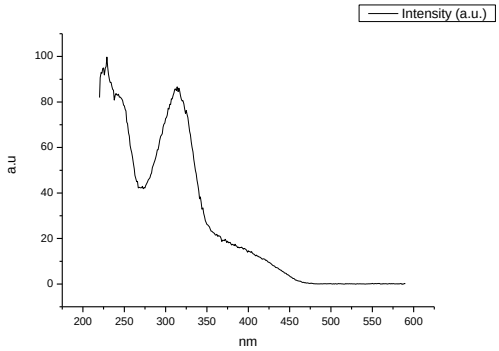

Figure 1.3.329. Fluorescence excitation spectrum of **9a** recorded in 1,2-ethanediol with emission fixed at 600 nm.

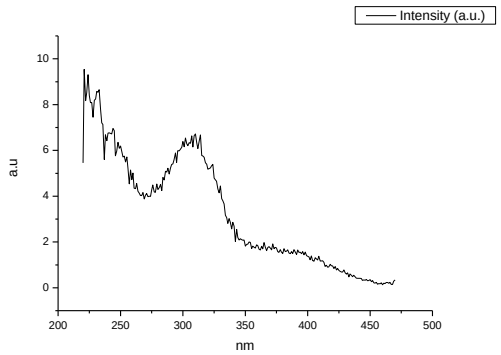

Figure 1.3.330. Fluorescence excitation spectrum of **9a** recorded in 2,2,2-trifluoroethanol with emission fixed at 480 nm.

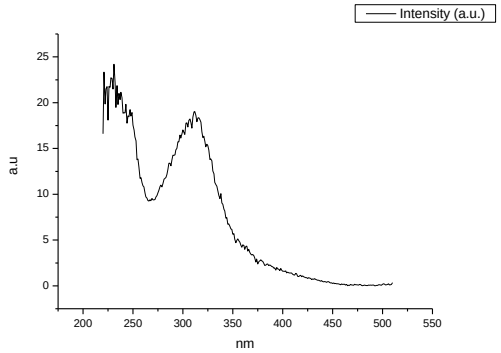

Figure 1.3.331. Fluorescence excitation spectrum of **9a** recorded in 2,2,2-trifluoroethanol with emission fixed at 520 nm.

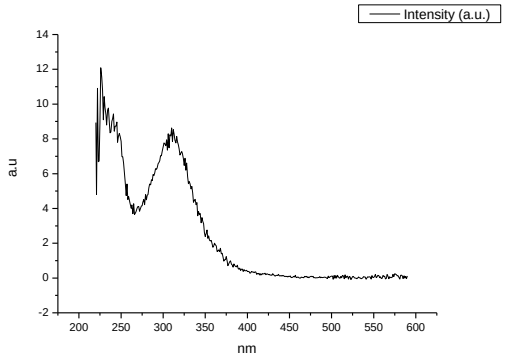

Figure 1.3.332. Fluorescence excitation spectrum of **9a** recorded in 2,2,2-trifluoroethanol with emission fixed at 600 nm.

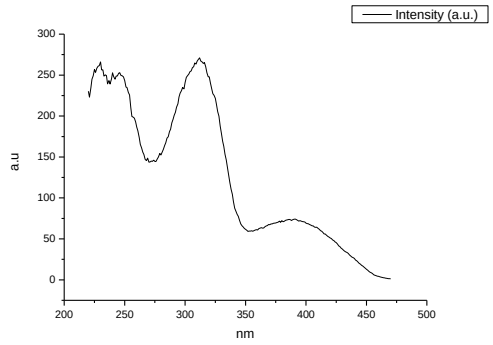

Figure 1.3.333. Fluorescence excitation spectrum of **9a** recorded in Ethanol-d_1 (EtOD) with emission fixed at 480 nm.

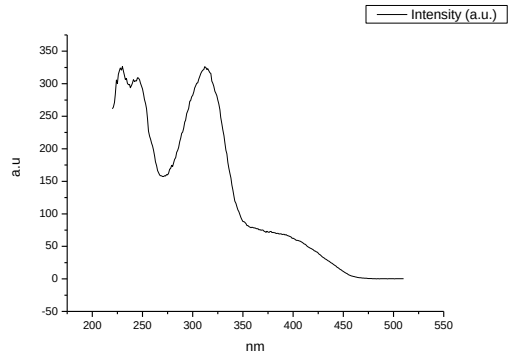

Figure 1.3.334. Fluorescence excitation spectrum of **9a** recorded in Ethanol-d_1 (EtOD) with emission fixed at 520 nm.

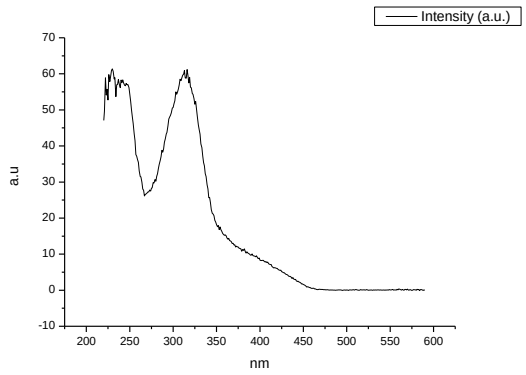

Figure 1.3.335. Fluorescence excitation spectrum of **9a** recorded in Ethanol-d_1 (EtOD) with emission fixed at 600 nm.

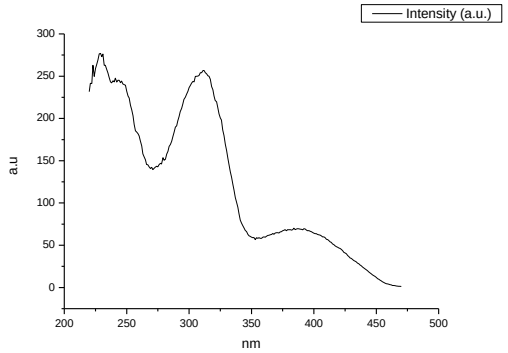

Figure 1.3.336. Fluorescence excitation spectrum of **9a** recorded in Methanol-d_1 (MeOD) with emission fixed at 480 nm.

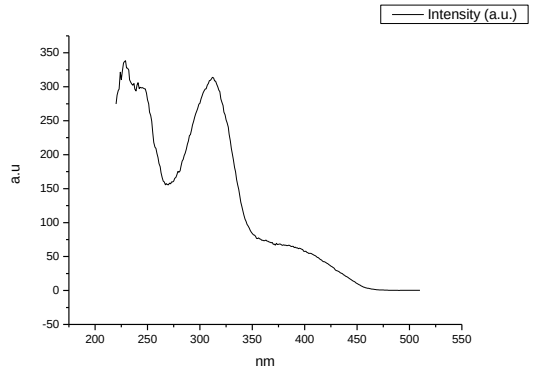

Figure 1.3.337. Fluorescence excitation spectrum of **9a** recorded in Methanol-d_1 (MeOD) with emission fixed at 520 nm.

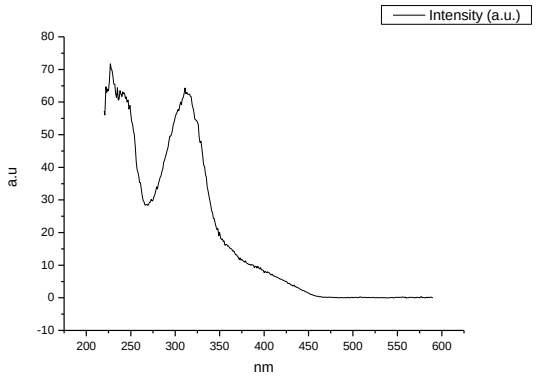

Figure 1.3.338. Fluorescence excitation spectrum of **9a** recorded in Methanol-d_1 (MeOD) with emission fixed at 600 nm.

1.4 COMPOUND 10A

1.4.1 Quantum Yield Summary.

Solvent	abs (310 nm)	$\lambda_{ems\ (max)}$	$\Phi_{310\ nm}$	abs (400 nm)	$\lambda_{ems\ (max)}$	$\Phi_{400\ nm}$
Toluene	0.08	530.00	0.83	0.02	532.98	0.75
1,4-Dioxane	0.06	531.94	0.65	0.01	531.94	0.69
Ethyl acetate	0.07	530.00	0.66	0.02	531.04	0.67
Chloroform	0.06	538.95	0.65	0.01	535.97	0.66
2-Methyl-2-butanol	0.03	537.01	0.57	0.01	540.00	0.58
N,N-dimethylformamide	0.09	542.94	0.59	0.02	542.94	0.61
Acetonitrile	0.07	542.05	0.64	0.01	542.05	0.64
Propylene carbonate	0.04	546.02	0.67	0.01	546.02	0.68
1-Octanol	0.05	538.95	0.62	0.01	541.02	0.64
1-Hexanol	0.03	542.05	0.64	0.01	546.02	0.70
1-Butanol	0.03	542.94	0.63	0.01	542.05	0.64
1-Pentanol	0.03	542.05	0.73	0.01	541.02	0.71
1-Propanol	0.06	545.00	0.59	0.01	546.02	0.59
Acetic acid	0.05	548.97	0.02	0.01	538.95	0.02
Ethanol	0.04	545.00	0.62	0.01	551.04	0.66
1,5-Pentanediol	0.04	546.02	0.60	0.01	546.02	0.61
1,3-Butanediol	0.07	552.98	0.53	0.01	550.00	0.57
1,4-Butanediol	0.05	551.94	0.56	0.01	552.98	0.57
1,3-Propanediol	0.04	551.04	0.56	0.01	550.00	0.51
Methanol	0.05	551.94	0.50	0.01	547.94	0.50
1,2-Ethanediol	0.04	555.97	0.48	0.01	555.07	0.47
2,2,2-Trifluoroethanol	0.02	564.02	0.10	0.01	567.01	0.10
Ethanol-d	0.03	548.97	0.58	0.01	547.05	0.57
Methanol-d	0.03	547.94	0.62	0.01	547.94	0.59

Table 1.4.1. Summary of ultraviolet-visible absorbance values at 310 nm and 400 nm, emission maxima and quantum yield (Φ) of **10a** at 310 nm and 400 nm excitation.

1.4.2 310 nm excitation Gaussian band fit summaries.

Solvent	λ max$_{em}$ Band 1 (cm^{-1})	λ max$_{em}$ Band 1 (nm)	λ max$_{em}$ Band 2 (cm^{-1})	λ max$_{em}$ Band 2 (nm)	λ max$_{em}$ Band 3 (cm^{-1})	λ max$_{em}$ Band 3 (nm)
Toluene	17178.69	582.12	18345.40	545.10	19392.72	515.66
1,4-Dioxane	17167.37	582.50	18322.99	545.76	19365.69	516.38
Ethyl acetate	17134.10	583.63	18312.77	546.07	19386.96	515.81
Chloroform	16872.10	592.69	18036.67	554.43	19114.13	523.17
2-Methyl-2-butanol	17013.02	587.79	18188.48	549.80	19255.43	519.33
N,N-dimethylformamide	16977.90	589.00	18060.13	553.71	19128.52	522.78
Acetonitrile	16843.61	593.70	18030.17	554.63	19146.47	522.29
Propylene carbonate	16830.73	594.15	17983.95	556.05	19092.76	523.76
1-Octanol	16922.25	590.94	18129.03	551.60	19217.06	520.37
1-Hexanol	16892.93	591.96	18082.39	553.02	19163.88	521.81
1-Butanol	16761.46	596.61	17976.93	556.27	19097.83	523.62
1-Pentanol	16758.64	596.71	17973.18	556.38	19102.48	523.49
1-Propanol	16750.40	597.00	17960.31	556.78	19079.00	524.14
Acetic acid	16953.28	589.86	18423.49	542.79		
Ethanol	16773.45	596.18	17982.27	556.10	19100.72	523.54
1,5-Pentanediol	16701.21	598.76	17852.90	560.13	18961.67	527.38
1,3-Butanediol	16642.14	600.88	17768.98	562.78	18903.66	529.00
1,4-Butanediol	16685.74	599.31	17818.32	561.22	18925.24	528.39
1,3-Propanediol	16546.74	604.35	17694.91	565.13	18835.65	530.91
Methanol	16664.15	600.09	17904.61	558.52	19047.61	525.00
1,2-Ethanediol	16403.54	609.62	17636.63	567.00	18811.27	531.60
2,2,2-Trifluoroethanol	16664.98	600.06	18049.80	554.02	-	-
Ethanol-d	17588.24	568.56	18140.88	551.24	19135.07	522.60
Methanol-d	16728.01	597.80	17921.99	557.97	19046.49	525.03

Solvent	λ max$_{em}$ Band 4 (cm^{-1})	λ max$_{em}$ Band 4 (nm)	λ max$_{em}$ Band 5 (cm^{-1})	λ max$_{em}$ Band 5 (nm)
Toluene	28178.69	354.88	-	-
1,4-Dioxane	28264.79	353.80	-	-
Ethyl acetate	28370.86	352.47	-	-
Chloroform	28087.89	356.03	-	-
2-Methyl-2-butanol	28390.85	352.23	-	-
N,N-dimethylformamide	27924.88	358.10	-	-
Acetonitrile	28347.21	352.77	-	-
Propylene carbonate	27579.42	362.59	-	-
1-Octanol	28368.90	352.50	-	-
1-Hexanol	28296.65	353.40	-	-
1-Butanol	28284.43	353.55	-	-
1-Pentanol	28268.64	353.75	-	-
1-Propanol	28252.71	353.95	-	-
Acetic acid	25635.49	390.08	28466.31	351.29
Ethanol	28322.33	353.08	-	-
1,5-Pentanediol	28060.78	356.37	-	-
1,3-Butanediol	26950.75	371.05	28895.45	346.08
1,4-Butanediol	23709.02	421.78	27776.58	360.02
1,3-Propanediol	28842.73	346.71	-	-
Methanol	28270.61	353.72	-	-
1,2-Ethanediol	27964.23	357.60	-	-
2,2,2-Trifluoroethanol	27397.17	365.00	-	-
Ethanol-d	28355.89	352.66	-	-
Methanol-d	28346.91	352.77	-	-

Table 1.4.2. Summary of band maxima of 5 band fit using Gaussian model for normalised **10a** emission spectra recorded at 310 nm excitation.

(a)

Solvent	Width Band 1 (cm^{-1})	Width Band 2 (cm^{-1})	Width Band 3 (cm^{-1})	Width Band 4 (cm^{-1})	Width Band 5 (cm^{-1})
Toluene	2920.49	1966.81	1180.61	3369.63	-
1,4-Dioxane	2963.63	2005.34	1222.63	3523.36	-
Ethyl acetate	2955.62	2026.34	1276.90	3547.94	-
Chloroform	2948.26	2045.68	1312.78	3345.32	-
2-Methyl-2-butanol	2984.10	2061.52	1330.16	3521.81	-
N,N-dimethylformamide	3060.72	2105.67	1374.10	3886.96	-
Acetonitrile	3014.65	2133.70	1437.99	3444.97	-
Propylene carbonate	3065.86	2151.00	1419.74	3738.46	-
1-Octanol	2964.46	2071.88	1389.50	3523.14	-
1-Hexanol	2969.32	2071.74	1383.15	3477.68	-
1-Butanol	2988.41	2114.96	1431.10	3466.13	-
1-Pentanol	2992.11	2118.87	1433.25	3431.26	-
1-Propanol	2978.95	2113.01	1441.66	3438.86	-
Acetic acid	3490.26	2371.24	-	4470.16	2943.82
Ethanol	2984.29	2105.57	1421.18	3464.61	-
1,5-Pentanediol	3051.48	2149.58	1470.95	3534.50	-
1,3-Butanediol	3135.35	2211.74	1512.84	4447.63	2898.78
1,4-Butanediol	3109.94	2202.42	1506.02	3925.96	3707.81
1,3-Propanediol	3103.48	2188.98	1495.45	4053.38	-
Methanol	2996.55	2139.84	1484.77	3490.30	-
1,2-Ethanediol	3100.07	2197.51	1509.28	3518.21	-
2,2,2-Trifluoroethanol	3007.64	2010.35	-	5031.97	-
Ethanol-d	3413.27	2074.95	1317.64	3437.09	-
Methanol-d	3071.82	2178.73	1492.29	3596.68	-

(b)

Solvent	Area Band 1 (cm^{-1})	Area Band 2 (cm^{-1})	Area Band 3 (cm^{-1})	Area Band 4 (cm^{-1})	Area Band 5 (cm^{-1})
Toluene	1196.67	1524.89	640.36	91.93	-
1,4-Dioxane	1230.59	1552.30	622.93	95.13	-
Ethyl acetate	1167.82	1558.43	673.57	88.54	-
Chloroform	1074.31	1545.62	743.84	85.39	-
2-Methyl-2-butanol	1165.59	1577.36	688.65	105.70	-
N,N-dimethylformamide	1251.78	1565.81	671.61	98.31	-
Acetonitrile	1074.94	1643.33	760.31	85.05	-
Propylene carbonate	1092.73	1663.46	731.54	241.91	-
1-Octanol	1183.29	1605.09	692.91	125.97	-
1-Hexanol	1194.11	1583.89	685.21	113.78	-
1-Butanol	1076.61	1650.07	764.12	110.85	-
1-Pentanol	1044.02	1652.71	785.05	111.83	-
1-Propanol	1084.77	1643.43	773.67	102.12	-
Acetic acid	1687.46	2058.47	-	773.80	2536.54
Ethanol	1105.96	1632.92	738.78	102.60	-
1,5-Pentanediol	1108.65	1628.32	762.75	122.04	-
1,3-Butanediol	1005.95	1657.96	807.50	212.62	581.77
1,4-Butanediol	1097.80	1661.01	763.73	157.45	592.49
1,3-Propanediol	1063.15	1682.49	777.70	367.64	-
Methanol	1082.13	1673.89	778.93	108.99	-
1,2-Ethanediol	979.13	1754.17	809.24	129.15	-
2,2,2-Trifluoroethanol	2040.52	1503.07	-	509.85	-
Ethanol-d	1986.93	1147.36	469.11	104.82	-
Methanol-d	1110.09	1683.63	749.15	103.59	-

(c)

Solvent	fwhm Band 1 (nm)	fwhm Band 2 (nm)	fwhm Band 3 (nm)	fwhm Band 4 (nm)	fwhm Band 5 (nm)
Toluene	115.90	67.60	35.22	52.61	-
1,4-Dioxane	123.85	67.60	35.22	54.66	-
Ethyl acetate	123.85	74.05	40.66	54.66	-
Chloroform	121.22	75.61	41.47	50.53	-
2-Methyl-2-butanol	126.67	69.02	40.66	51.91	-
N,N-dimethylformamide	126.67	75.61	41.47	56.16	-
Acetonitrile	129.58	75.61	46.22	49.86	-
Propylene carbonate	129.58	82.35	47.14	57.72	-
1-Octanol	126.67	75.61	46.22	51.91	-
1-Hexanol	121.22	75.61	46.22	49.86	-
1-Butanol	129.58	70.49	41.47	52.61	-
1-Pentanol	129.58	82.35	51.89	52.61	-
1-Propanol	129.58	77.23	47.14	52.61	-
Acetic acid	140.35	83.81	-	78.42	44.47
Ethanol	129.58	82.35	47.14	52.61	-
1,5-Pentanediol	129.58	77.23	47.14	55.40	-
1,3-Butanediol	138.15	84.12	52.93	70.84	43.30
1,4-Butanediol	138.15	84.12	52.93	86.03	56.93
1,3-Propanediol	141.38	78.90	48.10	57.14	-
Methanol	124.02	77.23	47.14	52.61	-
1,2-Ethanediol	141.38	85.95	48.10	54.06	-
2,2,2-Trifluoroethanol	124.02	75.61	-	79.30	-
Ethanol-d	136.21	75.61	41.47	49.86	-
Methanol-d	129.58	77.23	47.14	54.66	-

Tables 1.4.3 (a), (b) and (c). Summary band width, band area, full width half maximum of 5 band fit using Gaussian model for normalised **10a** emission spectra recorded at 310 nm excitation.

Solvent	Band 1 Area Percentage (%)	Band 2 Area Percentage (%)	Band 3 Area Percentage(%)	Band 4 Area Percentage(%)	Band 5 Area Percentage (%)
Toluene	34.65	44.15	18.54	2.66	-
1,4-Dioxane	35.15	44.34	17.79	2.72	-
Ethyl acetate	33.48	44.68	19.31	2.54	-
Chloroform	31.15	44.81	21.57	2.48	-
2-Methyl-2-butanol	32.95	44.59	19.47	2.99	-
N,N-dimethylformamide	34.89	43.65	18.72	2.74	-
Acetonitrile	30.16	46.11	21.34	2.39	-
Propylene carbonate	29.30	44.60	19.61	6.49	-
1-Octanol	32.80	44.50	19.21	3.49	-
1-Hexanol	33.38	44.28	19.16	3.18	-
1-Butanol	29.89	45.81	21.22	3.08	-
1-Pentanol	29.05	45.99	21.85	3.11	-
1-Propanol	30.10	45.60	21.47	2.83	-
Acetic acid	23.91	29.17	-	10.97	35.95
Ethanol	30.89	45.61	20.63	2.87	-
1,5-Pentanediol	30.61	44.96	21.06	3.37	-
1,3-Butanediol	23.58	38.87	18.93	4.98	13.64
1,4-Butanediol	25.69	38.88	17.88	3.69	13.87
1,3-Propanediol	27.32	43.24	19.99	9.45	-
Methanol	29.70	45.94	21.38	2.99	-
1,2-Ethanediol	26.67	47.78	22.04	3.52	-
2,2,2-Trifluoroethanol	50.34	37.08	-	12.58	-
Ethanol-d	53.58	30.94	12.65	2.83	-
Methanol-d	30.44	46.17	20.54	2.84	-

Table 1.4.4. Total Area Percentages of 5 band fit using Gaussian model for normalised **10a** emission spectra recorded at 310 nm excitation.

Solvent	Area Ratio Band 1/2 (310 nm ex)	Area Ratio Band 1/3 (310 nm ex)	Area Ratio Band 1/4 (310 nm ex)	Area Ratio Band 1/5 (310 nm ex)
Toluene	0.78	1.87	-	-
1,4-Dioxane	0.79	1.98	12.94	-
Ethyl acetate	0.75	1.73	13.19	-
Chloroform	0.70	1.44	12.58	-
2-Methyl-2-butanol	0.74	1.69	11.03	-
N,N-dimethylformamide	0.80	1.86	12.73	-
Acetonitrile	0.65	1.41	12.64	-
Propylene carbonate	0.66	1.49	4.52	-
1-Octanol	0.74	1.71	9.39	-
1-Hexanol	0.75	1.74	10.49	-
1-Butanol	0.65	1.41	9.71	-
1-Pentanol	0.63	1.33	9.34	-
1-Propanol	0.66	1.40	10.62	-
Acetic acid	0.82	-	2.18	0.67
Ethanol	0.68	1.50	10.78	
1,5-Pentanediol	0.68	1.45	9.08	
1,3-Butanediol	0.61	1.25	4.73	1.73
1,4-Butanediol	0.66	1.44	6.97	1.85
1,3-Propanediol	0.63	1.37	2.89	-
Methanol	0.65	1.39	9.93	-
1,2-Ethanediol	0.56	1.21	7.58	-
2,2,2-Trifluoroethanol	1.36	-	4.00	-
Ethanol-d	1.73	4.24	18.96	-
Methanol-d	0.66	1.48	10.72	-

Solvent	Area Ratio Band 2/3 (310 nm ex)	Area Ratio Band 2/4 (310 nm ex)	Area Ratio Band 2/5 (310 nm ex)	Area Ratio Band 3/4 (310 nm ex)	Area Ratio Band 3/5 (310 nm ex)	Area Ratio Band 4/5 (310 nm ex)
Toluene	2.38	-	-	-	-	-
1,4-Dioxane	2.49	16.32	-	6.55	-	-
Ethyl acetate	2.31	17.60	-	7.61	-	-
Chloroform	2.08	18.10	-	8.71	-	-
2-Methyl-2-butanol	2.29	14.92	-	6.52	-	-
N,N-dimethylformamide	2.33	15.93	-	6.83	-	-
Acetonitrile	2.16	19.32	-	8.94	-	-
Propylene carbonate	2.27	6.88	-	3.02	-	-
1-Octanol	2.32	12.74	-	5.50	-	-
1-Hexanol	2.31	13.92	-	6.02	-	-
1-Butanol	2.16	14.89	-	6.89	-	-
1-Pentanol	2.11	14.78	-	7.02	-	-
1-Propanol	2.12	16.09	-	7.58	-	-
Acetic acid	-	2.66	0.81	-	-	0.31
Ethanol	2.21	15.92	-	7.20	-	-
1,5-Pentanediol	2.13	13.34	-	6.25	-	-
1,3-Butanediol	2.05	7.80	2.85	3.80	1.39	0.37
1,4-Butanediol	2.17	10.55	2.80	4.85	1.29	0.27
1,3-Propanediol	2.16	4.58	-	2.12	-	-
Methanol	2.15	15.36	-	7.15	-	-
1,2-Ethanediol	2.17	13.58	-	6.27	-	-
2,2,2-Trifluoroethanol	-	2.95	-	-	-	-
Ethanol-d	2.45	10.95	-	4.48	-	-
Methanol-d	2.25	16.25	-	7.23	-	-

Table 1.4.5. Area Ratios of 5 band fit using Gaussian model for normalised **10a** emission spectra recorded at 310 nm excitation.

1.4.3 400 nm excitation Gaussian band fit summaries.

Solvent	λ max$_{em}$ Band 1 (cm^{-1})	λ max$_{em}$ Band 1 (nm)	λ max$_{em}$ Band 2 (cm^{-1})	λ max$_{em}$ Band 2 (nm)	λ max$_{em}$ Band 3 (cm^{-1})	λ max$_{em}$ Band 3 (nm)
Toluene	17158.41	582.80	18322.17	545.79	19379.19	516.02
1,4-Dioxane	17169.75	582.42	18308.24	546.20	19353.56	516.70
Ethyl acetate	17154.45	582.94	18321.10	545.82	19389.46	515.74
Chloroform	16798.65	595.29	18001.75	555.50	19111.72	523.24
2-Methyl-2-butanol	16919.59	591.03	18123.04	551.78	19222.55	520.22
N,N-dimethylformamide	17018.75	587.59	17964.96	556.64	19086.91	523.92
Acetonitrile	16641.60	600.90	17904.87	558.51	19099.56	523.57
Propylene carbonate	16862.01	593.05	18031.69	554.58	19120.14	523.01
1-Octanol	16805.00	595.06	18040.20	554.32	19183.45	521.28
1-Hexanol	16715.71	598.24	17956.22	556.91	19102.36	523.50
1-Butanol	16640.40	600.95	17895.98	558.78	19055.72	524.78
1-Pentanol	16683.46	599.40	17946.65	557.21	19085.99	523.94
1-Propanol	16503.28	605.94	17805.73	561.62	19025.61	525.61
Acetic acid	17797.84	561.87	19038.30	525.26	23414.08	427.09
Ethanol	16674.80	599.71	17916.10	558.16	19065.29	524.51
1,5-Pentanediol	16567.64	603.59	17793.39	562.01	18950.91	527.68
1,3-Butanediol	16638.75	601.01	17771.36	562.70	18906.85	528.91
1,4-Butanediol	17100.05	584.79	17844.68	560.39	18935.36	528.11
1,3-Propanediol	16385.51	610.30	17616.89	567.64	18799.64	531.92
Methanol	16417.82	609.09	17759.54	563.08	18991.85	526.54
1,2-Ethanediol	16425.19	608.82	17614.41	567.72	18785.08	532.34
2,2,2-Trifluoroethanol	15384.23	650.02	17265.46	579.19	18418.23	542.94
Ethanol-d	17590.35	568.49	17939.50	557.43	19030.17	525.48
Methanol-d	16632.00	601.25	17875.08	559.44	19017.76	525.82

Table 1.4.6. Summary of band maxima of 3 band fit using Gaussian model for normalised **10a** emission spectra recorded at 400 nm excitation.

Solvent	fwhm Band 1 (nm)	fwhm Band 2 (nm)	fwhm Band 3 (nm)	Width Band 1 (cm^{-1})	Width Band 2 (cm^{-1})	Width Band 3 (cm^{-1})
Toluene	114.99	68.22	38.56	2890.87	1982.57	1211.37
1,4-Dioxane	123.37	72.32	38.56	2955.97	2029.41	1239.22
Ethyl acetate	128.49	75.47	41.53	2939.21	2038.24	1259.81
Chloroform	125.29	78.54	46.15	2961.65	2086.34	1319.63
2-Methyl-2-butanol	123.50	73.28	45.58	2964.44	2075.30	1387.59
N,N-dimethylformamide	133.69	78.54	46.15	3227.23	2179.67	1409.87
Acetonitrile	127.13	82.87	49.78	2986.40	2183.63	1485.75
Propylene carbonate	128.78	74.26	46.15	3028.50	2101.66	1384.00
1-Octanol	128.78	77.49	49.15	3007.70	2137.10	1450.82
1-Hexanol	130.66	78.54	46.15	3045.03	2149.37	1448.81
1-Butanol	127.13	82.87	49.78	3031.29	2156.55	1472.75
1-Pentanol	136.11	78.54	46.15	3034.01	2142.17	1452.14
1-Propanol	129.00	84.00	49.78	3030.08	2191.51	1495.95
Acetic acid	107.28	56.45	83.47	2748.17	1552.10	3608.95
Ethanol	127.13	78.54	49.78	2992.86	2128.63	1456.51
1,5-Pentanediol	132.58	84.00	50.41	3126.46	2201.89	1482.90
1,3-Butanediol	136.11	84.00	50.41	3172.48	2217.25	1506.60
1,4-Butanediol	133.69	79.60	46.74	3361.45	2138.71	1425.68
1,3-Propanediol	140.18	89.69	51.06	3172.06	2243.04	1534.40
Methanol	130.92	84.00	53.45	3041.70	2209.81	1543.59
1,2-Ethanediol	140.18	81.80	51.06	3178.66	2227.07	1520.27
2,2,2-Trifluoroethanol	241.27	101.75	53.08	4102.33	2477.67	1506.99
Ethanol-d	137.60	82.87	46.74	3678.79	2256.07	1464.62
Methanol-d	136.11	82.87	49.78	3147.30	2226.87	1511.10

Table 1.4.7. Summary of full width half maximum (fwhm) and band width of 3 band fit using Gaussian model for normalised **10a** emission spectra recorded at 400 nm excitation.

Solvent	Area Band 1 (cm^{-1})	Area Band 2 (cm^{-1})	Area Band 3 (cm^{-1})	Area Ratio Band 1/2 (400 nm ex)	Area Ratio Band 1/3 (400 nm ex)	Area Ratio Band 2/3 (400 nm ex)
Toluene	1125.77	1526.70	681.64	0.74	1.65	2.24
1,4-Dioxane	1164.52	1556.85	643.37	0.75	1.81	2.42
Ethyl acetate	1149.06	1587.95	662.61	0.72	1.73	2.40
Chloroform	932.02	1643.70	759.70	0.57	1.23	2.16
2-Methyl-2-butanol	1059.99	1553.28	758.78	0.68	1.40	2.05
N,N-dimethylformamide	1126.67	1614.16	733.18	0.70	1.54	2.20
Acetonitrile	810.52	1741.76	897.61	0.47	0.90	1.94
Propylene carbonate	1187.73	1602.59	686.68	0.74	1.73	2.33
1-Octanol	1044.11	1675.33	783.42	0.62	1.33	2.14
1-Hexanol	987.56	1697.53	800.81	0.58	1.23	2.12
1-Butanol	953.04	1694.25	834.09	0.56	1.14	2.03
1-Pentanol	986.78	1696.52	784.54	0.58	1.26	2.16
1-Propanol	763.05	1784.65	909.82	0.43	0.84	1.96
Acetic acid	2238.23	720.94	3445.83	3.10	0.65	0.21
Ethanol	1005.24	1669.88	803.23	0.60	1.25	2.08
1,5-Pentanediol	970.52	1748.06	787.01	0.56	1.23	2.22
1,3-Butanediol	1035.07	1696.39	784.86	0.61	1.32	2.16
1,4-Butanediol	1532.12	1384.45	640.12	1.11	2.39	2.16
1,3-Propanediol	903.57	1777.91	839.37	0.51	1.08	2.12
Methanol	776.06	1804.30	915.20	0.43	0.85	1.97
1,2-Ethanediol	966.68	1722.07	809.62	0.56	1.19	2.13
2,2,2-Trifluoroethanol	617.36	2216.38	621.74	0.28	0.99	3.56
Ethanol-d	1683.64	1318.44	630.99	1.28	2.67	2.09
Methanol-d	996.39	1769.24	760.91	0.56	1.31	2.33

Solvent	Band 1 Area Percentage (%)	Band 2 Area Percentage (%)	Band 3 Area Percentage (%)
Toluene	33.77	45.79	20.44
1,4-Dioxane	34.61	46.27	19.12
Ethyl acetate	33.80	46.71	19.49
Chloroform	27.94	49.28	22.78
2-Methyl-2-butanol	31.43	46.06	22.50
N,N-dimethylformamide	32.43	46.46	21.10
Acetonitrile	23.49	50.49	26.02
Propylene carbonate	34.16	46.09	19.75
1-Octanol	29.81	47.83	22.37
1-Hexanol	28.33	48.70	22.97
1-Butanol	27.38	48.67	23.96
1-Pentanol	28.46	48.92	22.62
1-Propanol	22.07	51.62	26.31
Acetic acid	34.95	11.26	53.80
Ethanol	28.90	48.01	23.09
1,5-Pentanediol	27.68	49.86	22.45
1,3-Butanediol	29.44	48.24	22.32
1,4-Butanediol	43.08	38.93	18.00
1,3-Propanediol	25.66	50.50	23.84
Methanol	22.20	51.62	26.18
1,2-Ethanediol	27.63	49.22	23.14
2,2,2-Trifluoroethanol	17.87	64.14	17.99
Ethanol-d	46.34	36.29	17.37
Methanol-d	28.25	50.17	21.58

Table 1.4.8. Band area, area ratios and total area percentage of 3 band fit using Gaussian model for normalised **10a** emission spectra recorded at 400 nm excitation.

1.4.4 310 nm Gaussian band fit - Solvatochromic analysis.

1.4.4.1 E_T^N.

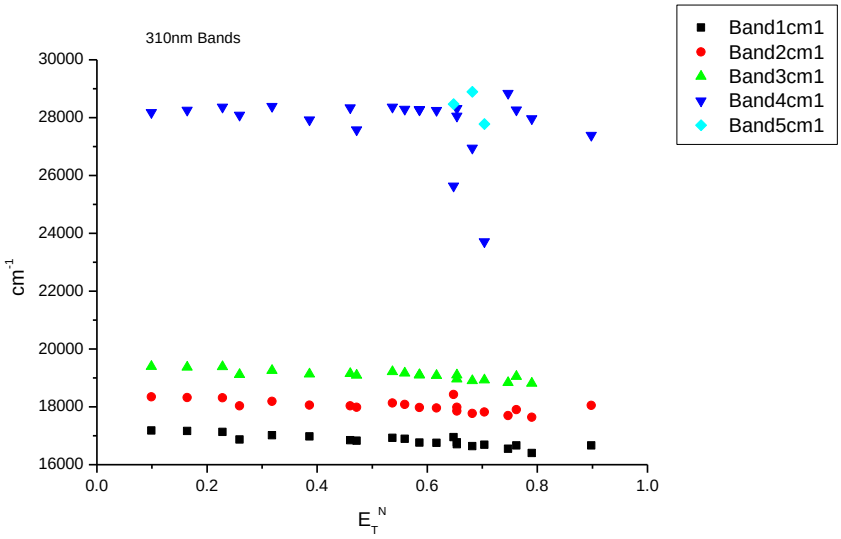

Figure 1.4.1. Band maxima from Gaussian model fit of the normalised fluorescence emission spectra of **10a** recorded at 310 nm excitation against E_T^N.

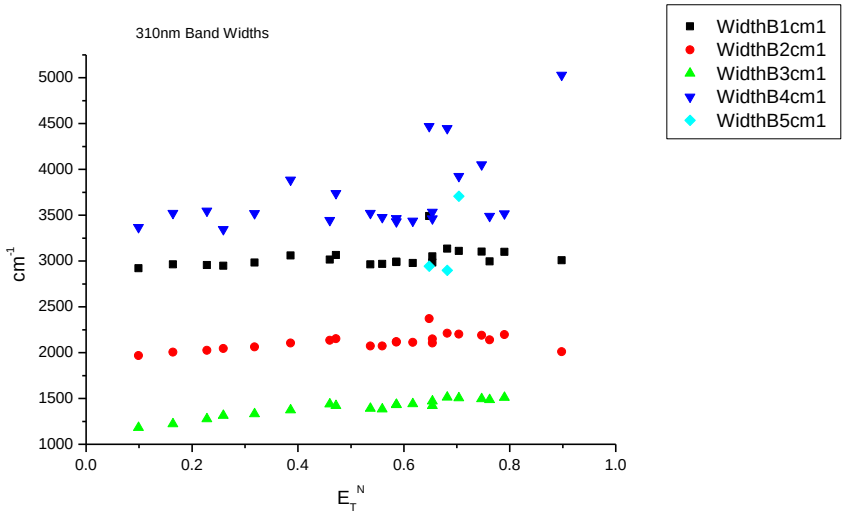

Figure 1.4.2. Band widths from Gaussian model fit of the normalised fluorescence emission spectra of **10a** recorded at 310 nm excitation against E_T^N.

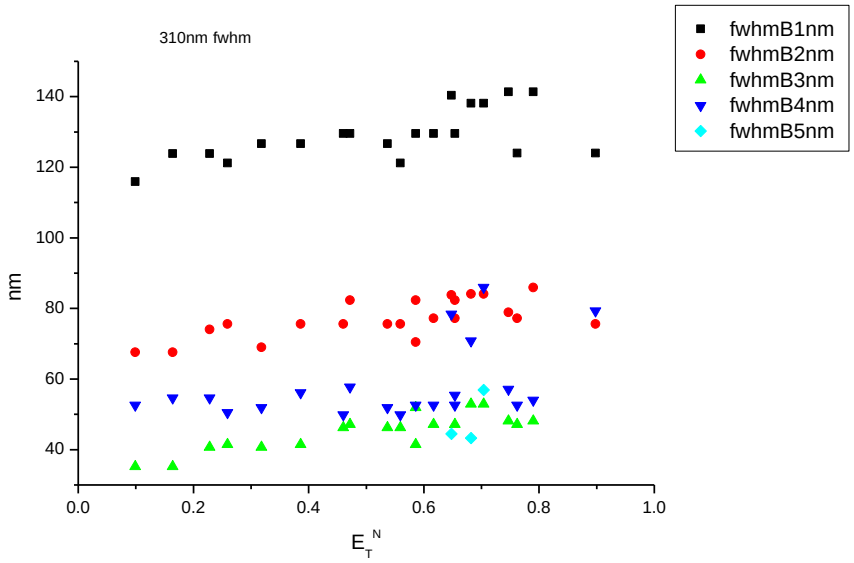

Figure 1.4.3. Full width half maxima of each band from Gaussian model fit of the normalised fluorescence emission spectra of **10a** recorded at 310 nm excitation against E_T^N.

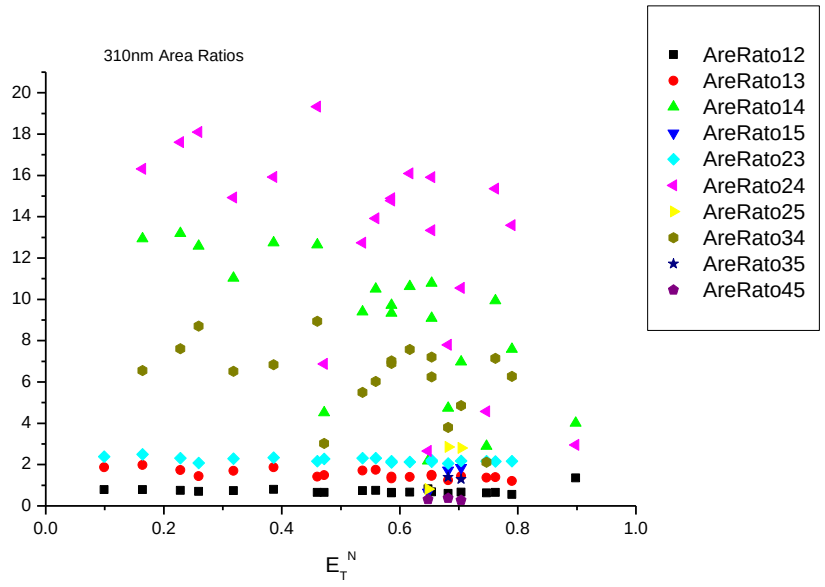

Figure 1.4.4. Area ratios from Gaussian model fit of the normalised fluorescence emission spectra of **10a** recorded at 310 nm excitation against E_T^N.

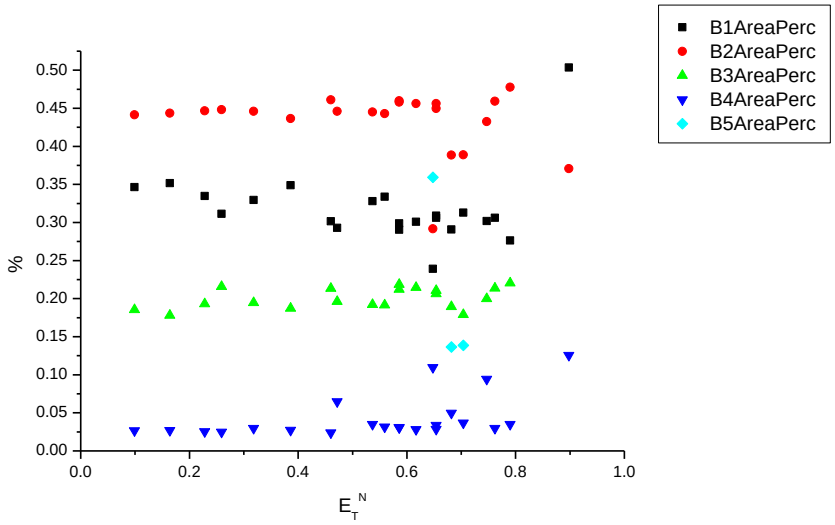

Figure 1.4.5. Area percentages from Gaussian model fit of the normalised fluorescence emission spectra of **10a** recorded at 310 nm excitation against E_T^N.

1.4.4.2 α

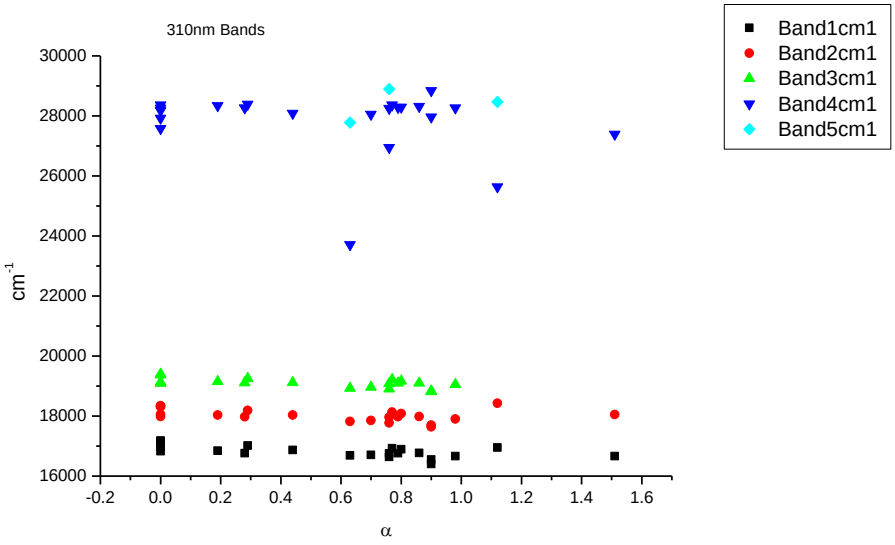

Figure 1.4.6. Band maxima from Gaussian model fit of the normalised fluorescence emission spectra of **10a** recorded at 310 nm excitation against α.

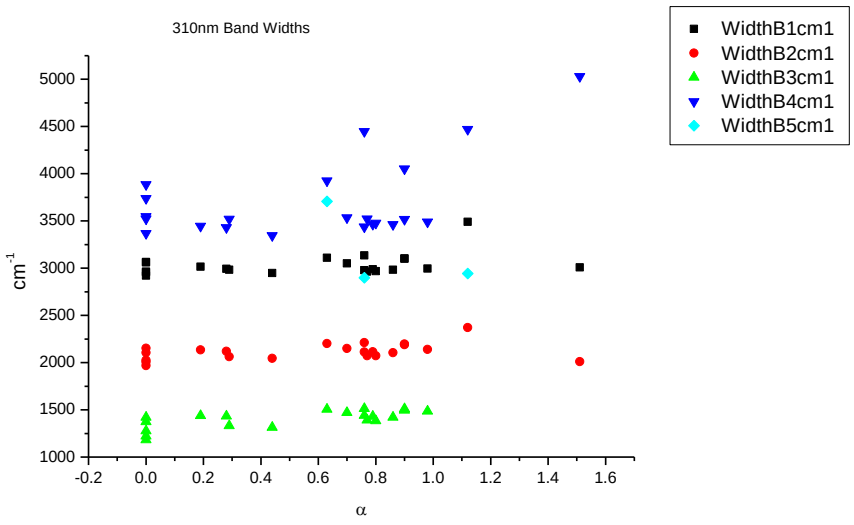

Figure 1.4.7. Band widths from Gaussian model fit of the normalised fluorescence emission spectra of **10a** recorded at 310 nm excitation against α.

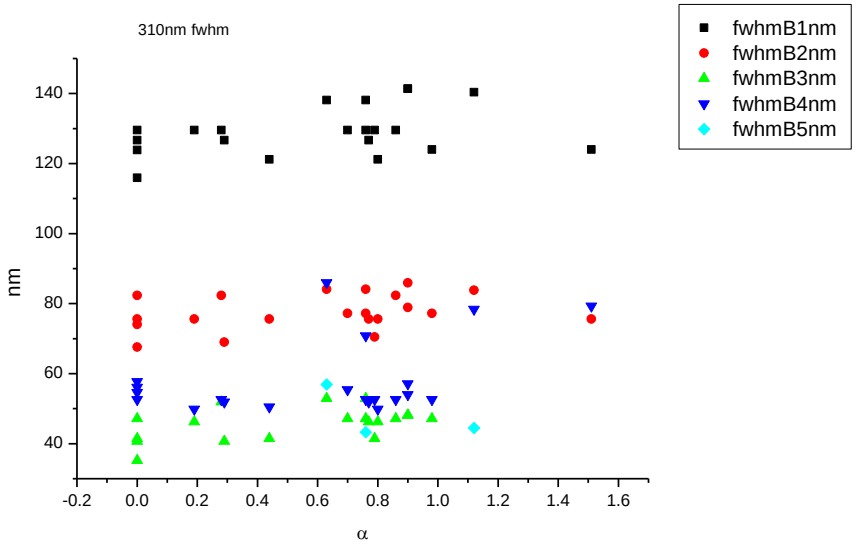

Figure 1.4.8. Full width half maxima from Gaussian model fit of the normalised fluorescence emission spectra of **10a** recorded at 310 nm excitation against α.

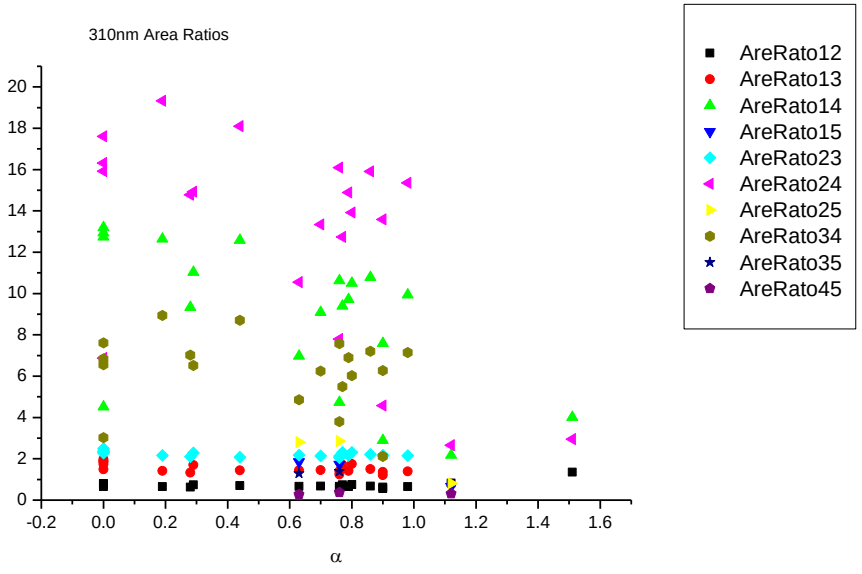

Figure 1.4.9. Area Ratios from Gaussian model fit of the normalised fluorescence emission spectra of **10a** recorded at 310 nm excitation against α.

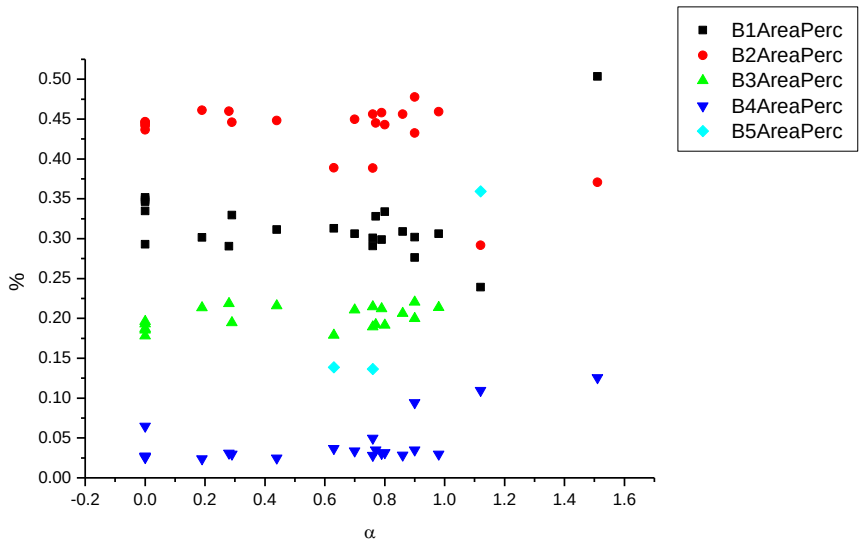

Figure 1.4.10. Area percentages from Gaussian model fit of the normalised fluorescence emission spectra of **10a** recorded at 310 nm excitation against α.

1.4.4.3 β.

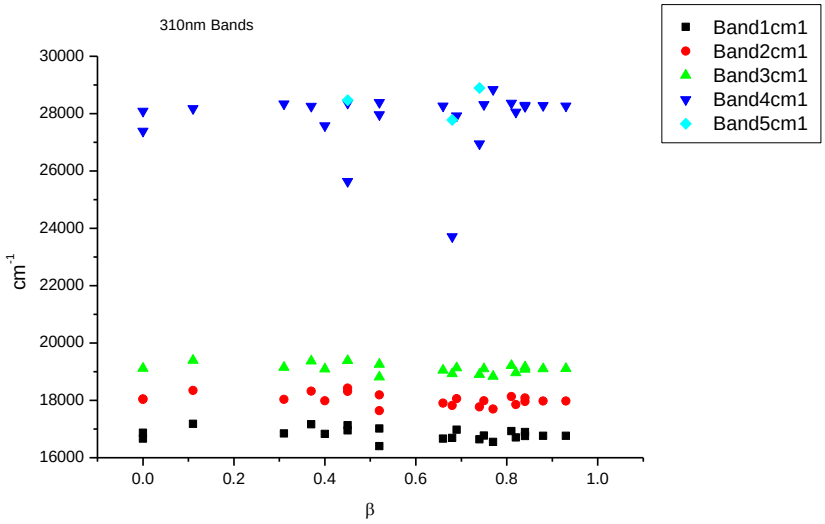

Figure 1.4.11. Band maxima from Gaussian model fit of the normalised fluorescence emission spectra of **10a** recorded at 310 nm excitation against β.

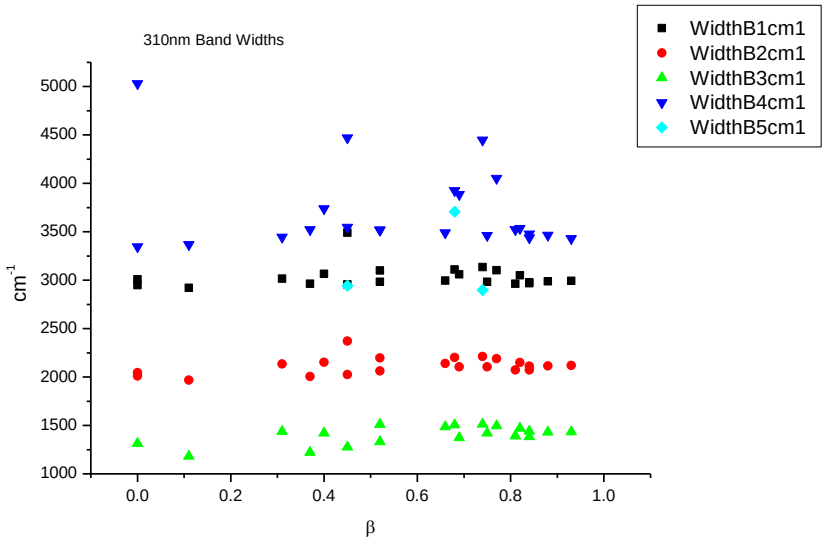

Figure 1.4.12. Band widths from Gaussian model fit of the normalised fluorescence emission spectra of **10a** recorded at 310 nm excitation against β.

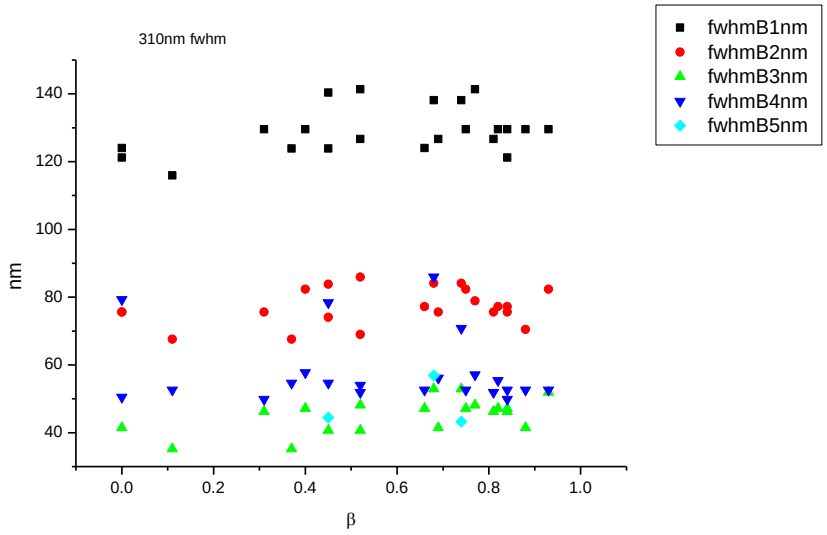

Figure 1.4.13. Full width half maxima from Gaussian model fit of the normalised fluorescence emission spectra of **10a** recorded at 310 nm excitation against β.

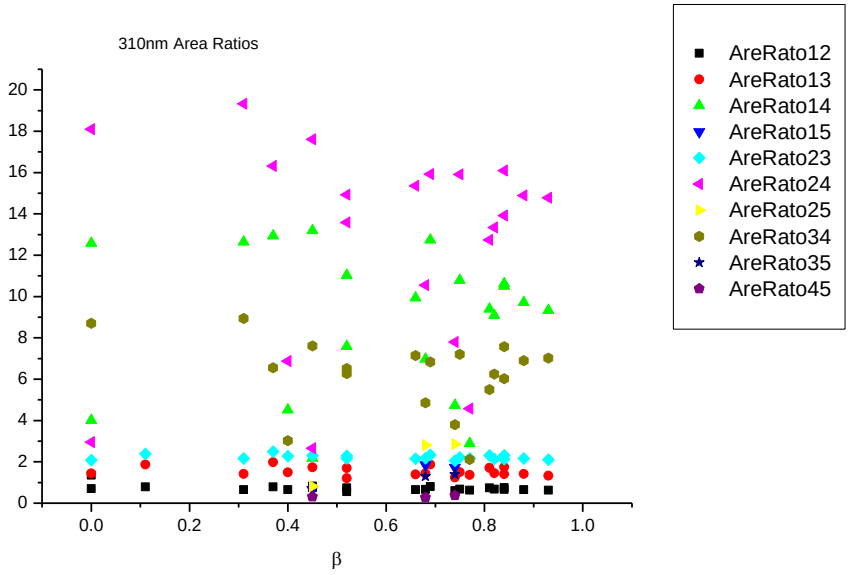

Figure 1.4.14. Area ratios from Gaussian model fit of the normalised fluorescence emission spectra of **10a** recorded at 310 nm excitation against β.

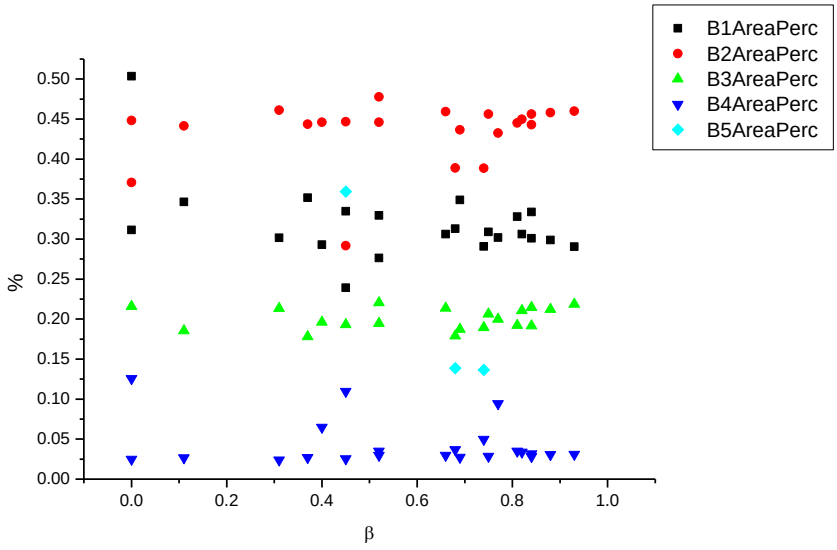

Figure 1.4.15. Area percentages from Gaussian model fit of the normalised fluorescence emission spectra of **10a** recorded at 310 nm excitation against β.

1.4.4.4 π.*

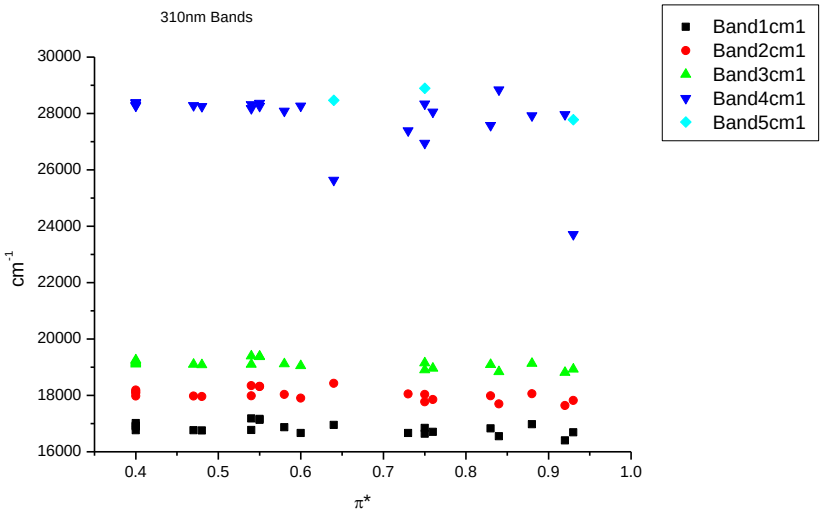

Figure 1.4.16. Band maxima from Gaussian model fit of the normalised fluorescence emission spectra of **10a** recorded at 310 nm excitation against π*.

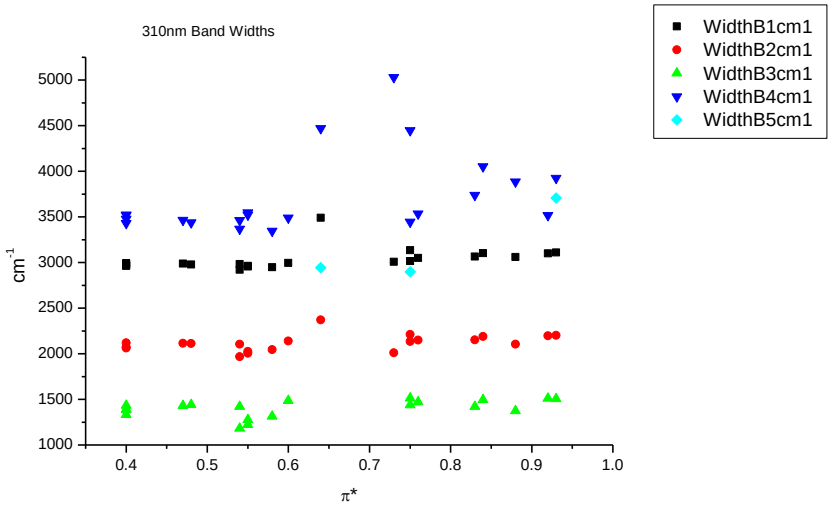

Figure 1.4.17. Band widths from Gaussian model fit of the normalised fluorescence emission spectra of **10a** recorded at 310 nm excitation against π*.

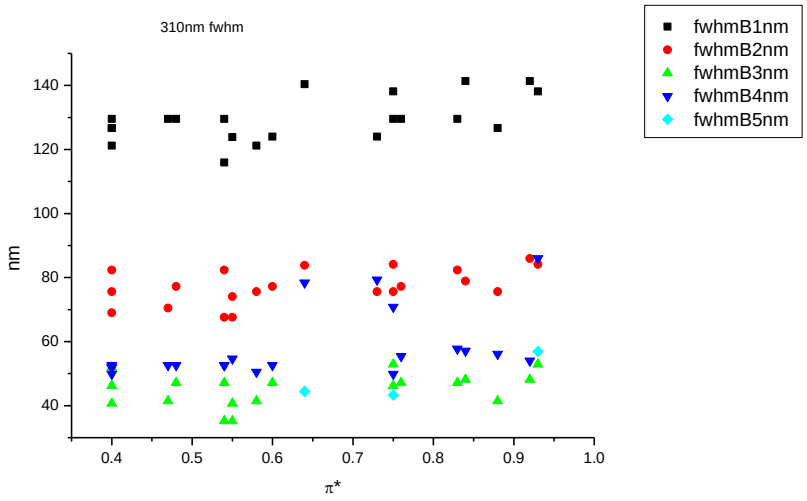

Figure 1.4.18. Full width half maxima from Gaussian model fit of the normalised fluorescence emission spectra of **10a** recorded at 310 nm excitation against π*.

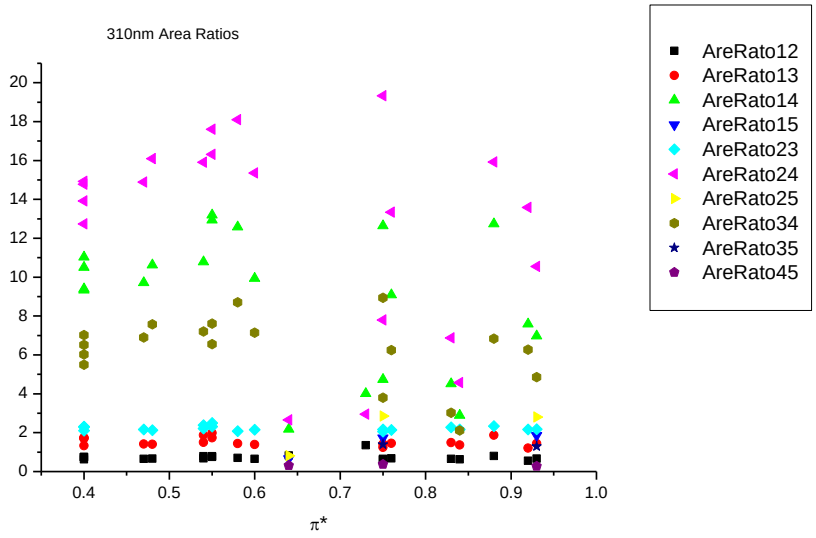

Figure 1.4.19. Area ratios from Gaussian model fit of the normalised fluorescence emission spectra of **3a** recorded at 310 nm excitation against π*.

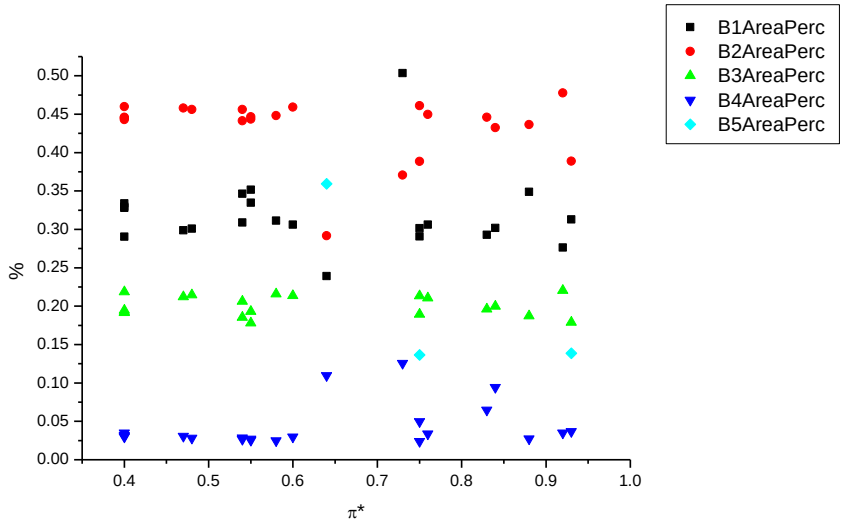

Figure 1.4.20. Area percentages from Gaussian model fit of the normalised fluorescence emission spectra of **10a** recorded at 310 nm excitation against π*.

1.4.4.5 μ(D).

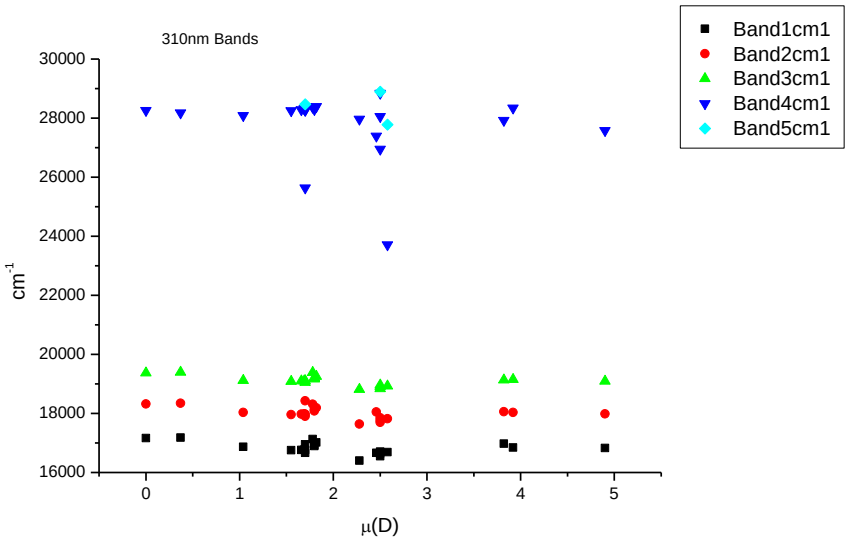

Figure 1.4.21. Band maxima from Gaussian model fit of the normalised fluorescence emission spectra of **10a** recorded at 310 nm excitation against μ(D).

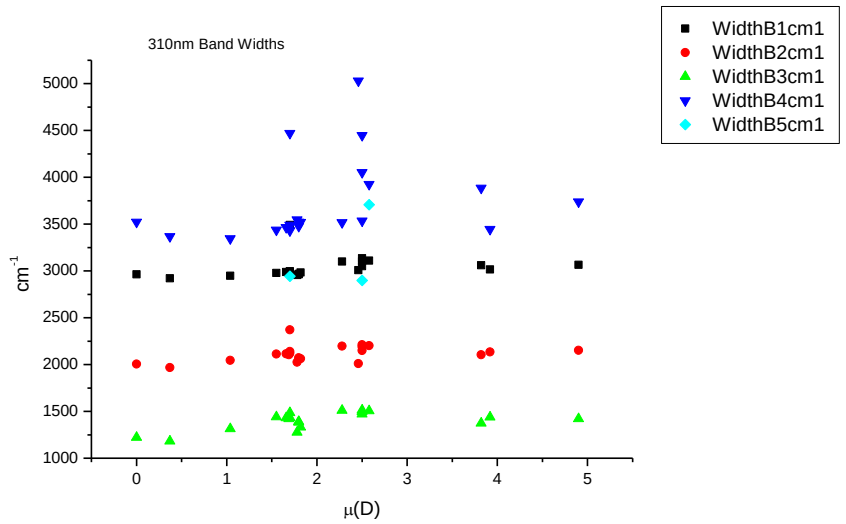

Figure 1.4.22. Band widths from Gaussian model fit of the normalised fluorescence emission spectra of **10a** recorded at 310 nm excitation against μ(D).

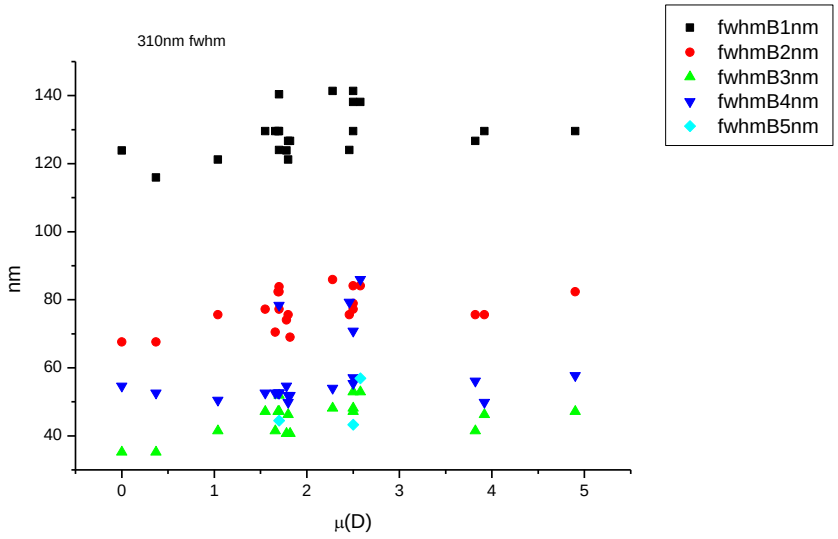

Figure 1.4.23. Full width half maxima from Gaussian model fit of the normalised fluorescence emission spectra of **10a** recorded at 310 nm excitation against μ(D).

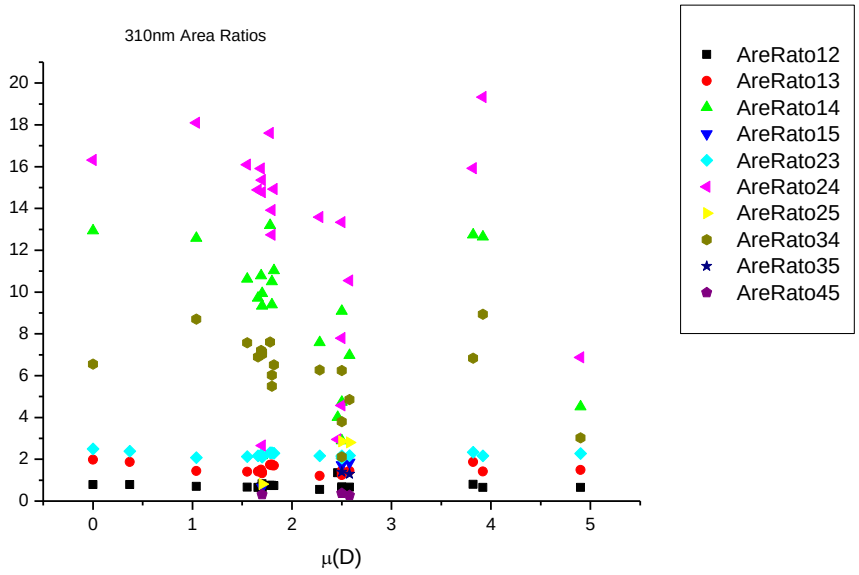

Figure 1.4.24. Area ratios from Gaussian model fit of the normalised fluorescence emission spectra of **10a** recorded at 310 nm excitation against μ(D).

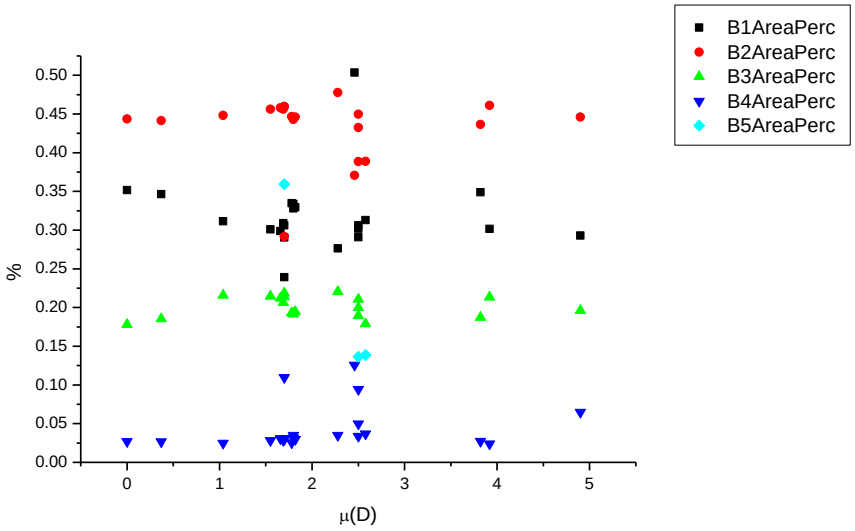

Figure 1.4.25. Area percentages from Gaussian model fit of the normalised fluorescence emission spectra of **10a** recorded at 310 nm excitation against μ(D).

1.4.4.6 η(Cp).

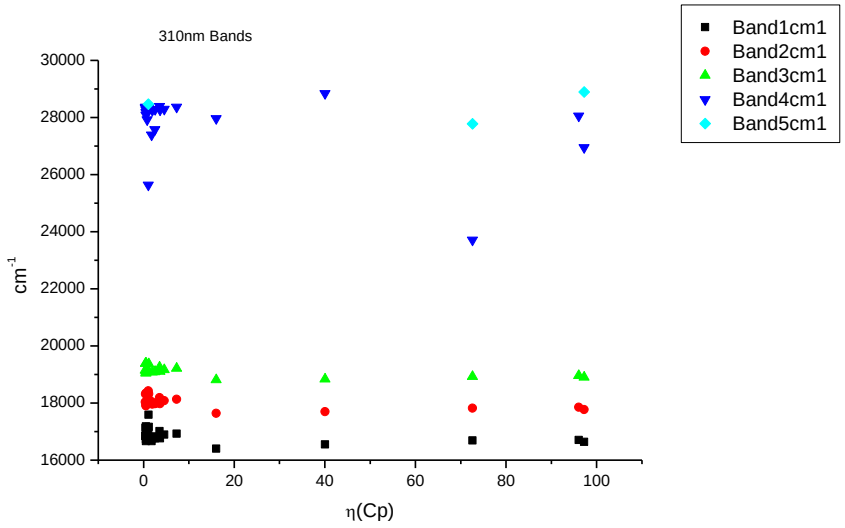

Figure 1.4.26. Band maxima from Gaussian model fit of the normalised fluorescence emission spectra of **10a** recorded at 310 nm excitation against η(Cp).

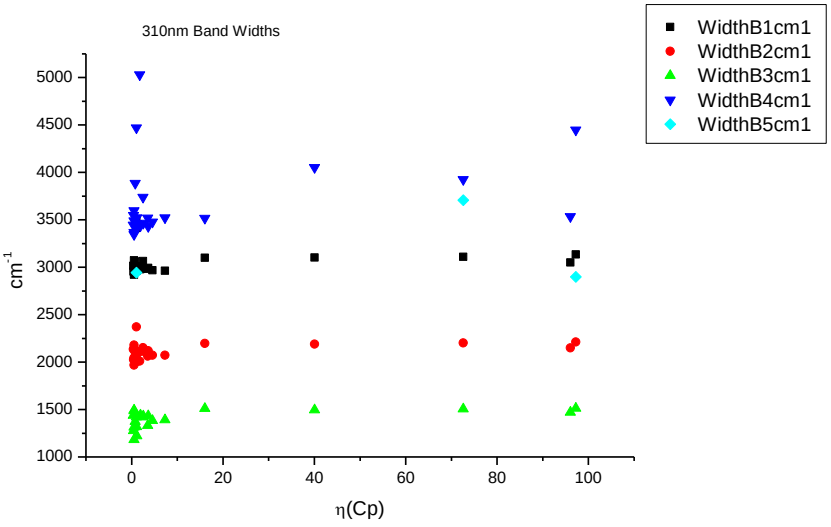

Figure 1.4.27. Band widths from Gaussian model fit of the normalised fluorescence emission spectra of **10a** recorded at 310 nm excitation against η(Cp).

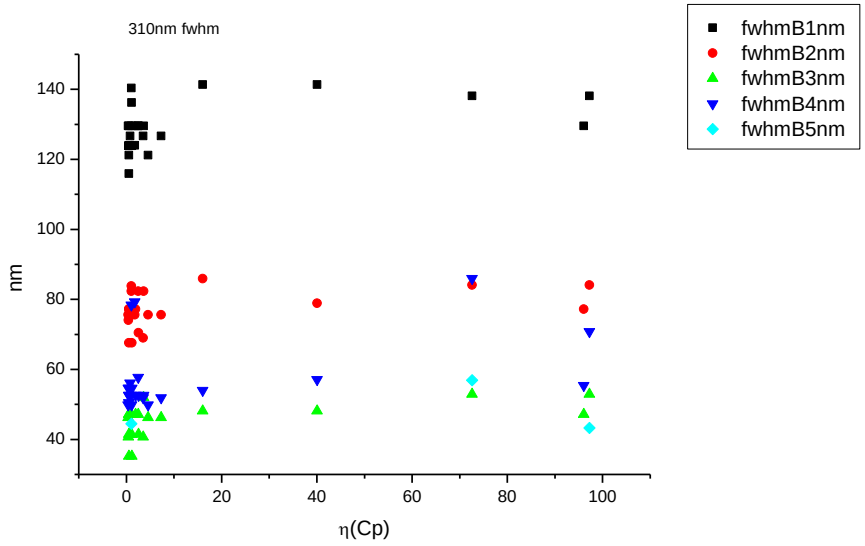

Figure 1.4.28. Full width half maxima from Gaussian model fit of the normalised fluorescence emission spectra of **10a** recorded at 310 nm excitation against η(Cp).

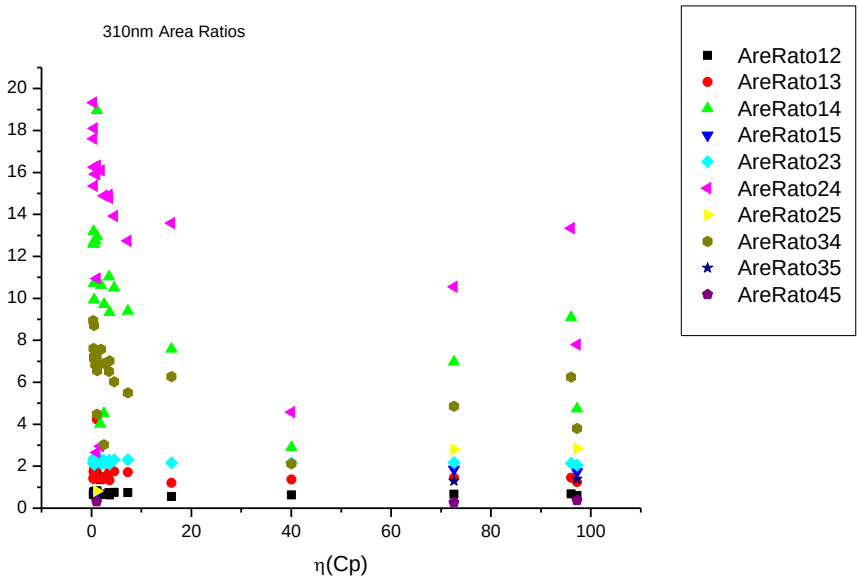

Figure 1.4.29. Area ratios from Gaussian model fit of the normalised fluorescence emission spectra of **10a** recorded at 310 nm excitation against η(Cp).

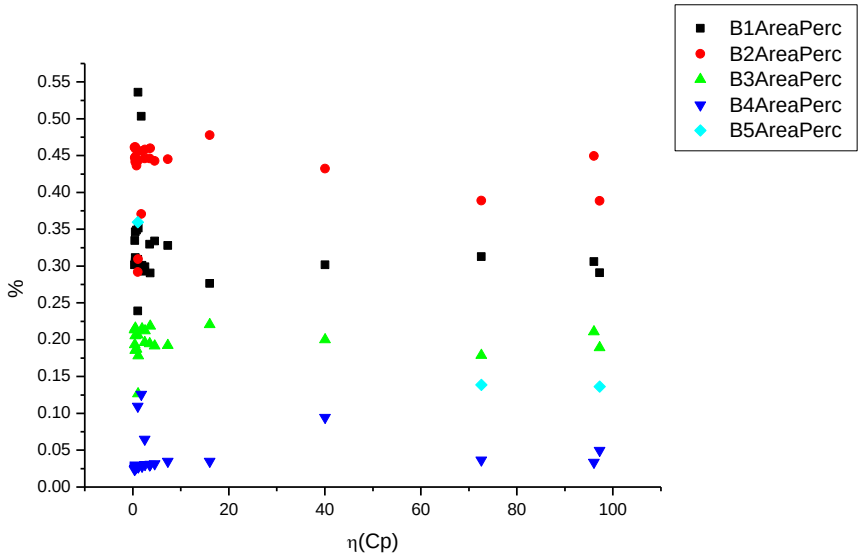

Figure 1.4.30. Area percentages from Gaussian model fit of the normalised fluorescence emission spectra of **10a** recorded at 310 nm excitation against η(Cp).

1.4.5 400 nm Gaussian band fit - Solvatochromic analysis.

1.4.5.1 E_T^N.

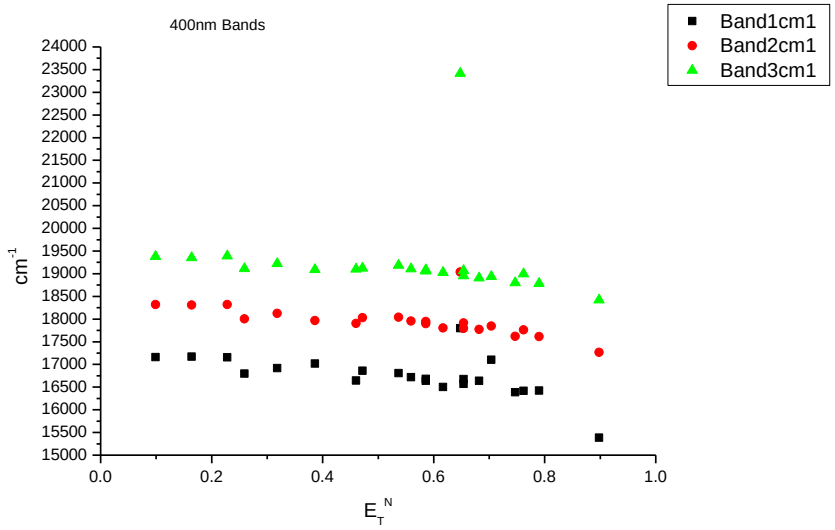

Figure 1.4.31. Band maxima from Gaussian model fit of the normalised fluorescence emission spectra of **10a** recorded at 400 nm excitation against E_T^N.

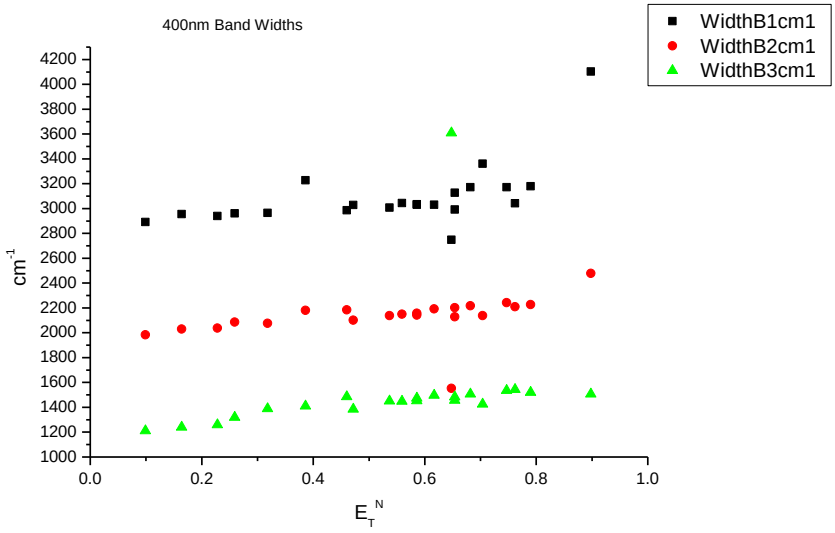

Figure 1.4.32. Band widths from Gaussian model fit of the normalised fluorescence emission spectra of **10a** recorded at 400 nm excitation against E_T^N.

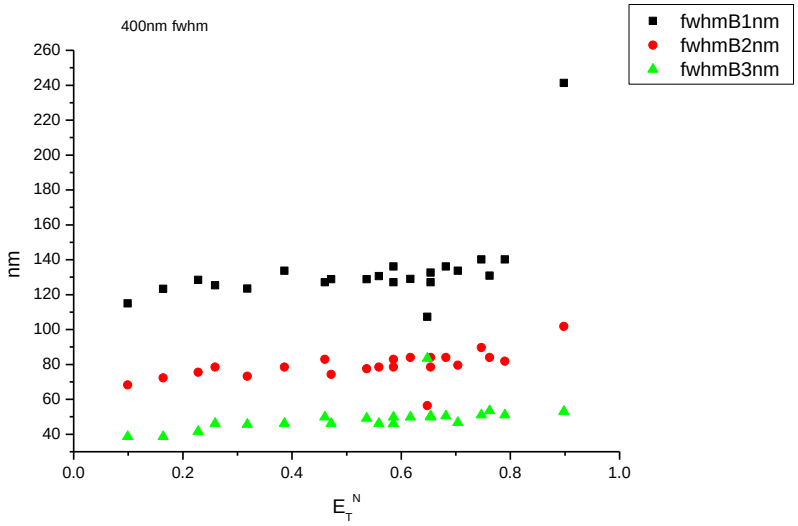

Figure 1.4.33. Full width half maxima from Gaussian model fit of the normalised fluorescence emission spectra of **10a** recorded at 400 nm excitation against E_T^N.

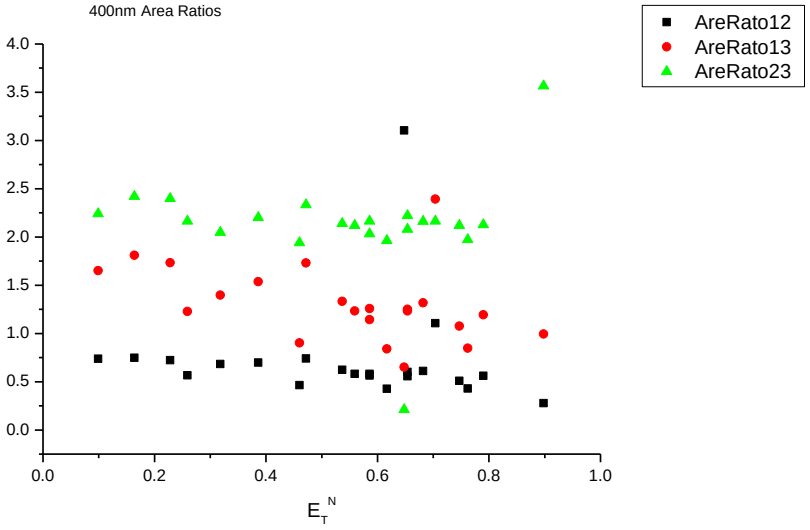

Figure 1.4.34. Area ratios from Gaussian model fit of the normalised fluorescence emission spectra of **10a** recorded at 400 nm excitation against E_T^N.

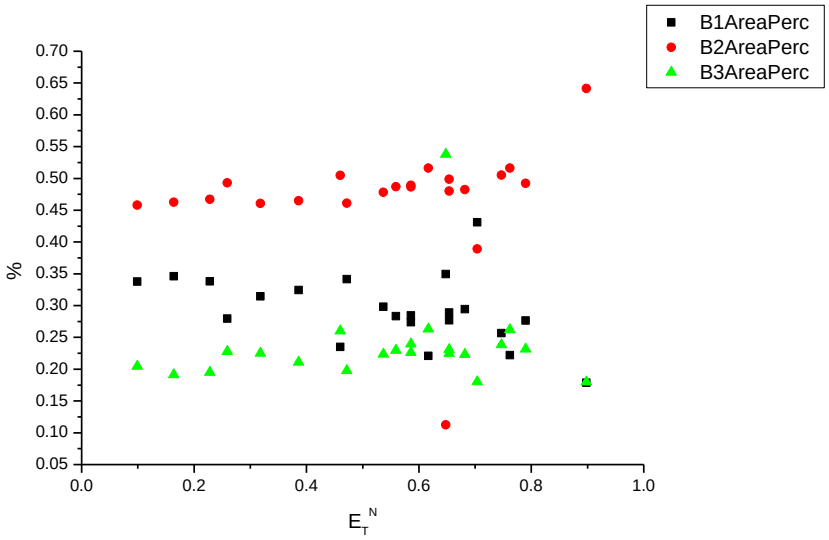

Figure 1.4.35. Area percentages from Gaussian model fit of the normalised fluorescence emission spectra of **10a** recorded at 400 nm excitation against E_T^N.

1.4.4.2 α

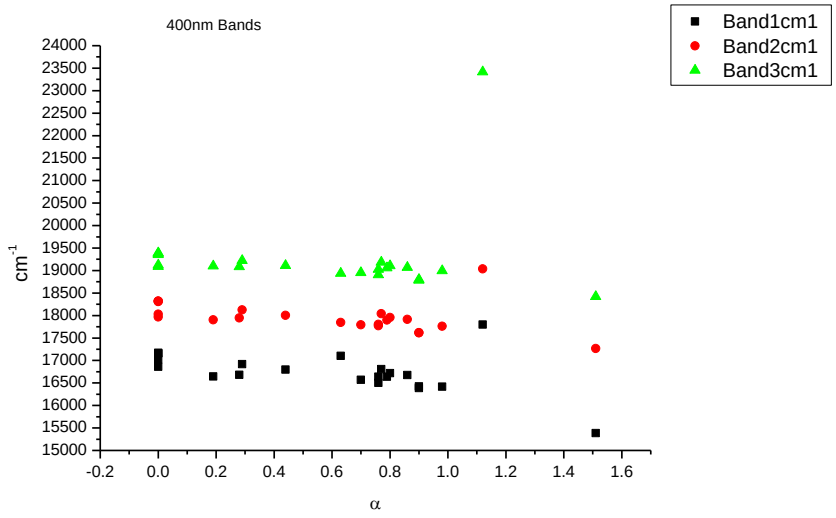

Figure 1.4.36. Band maxima from Gaussian model fit of the normalised fluorescence emission spectra of **10a** recorded at 400 nm excitation against α.

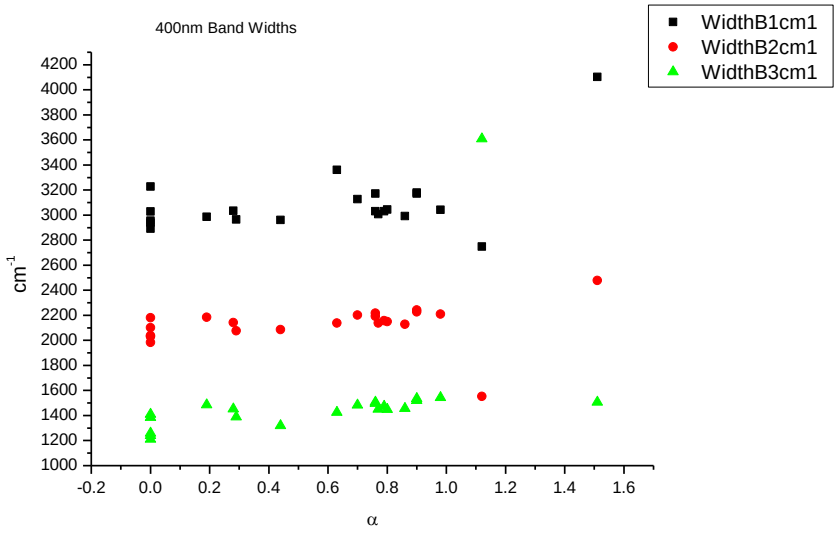

Figure 1.4.37. Band widths from Gaussian model fit of the normalised fluorescence emission spectra of **10a** recorded at 400 nm excitation against α.

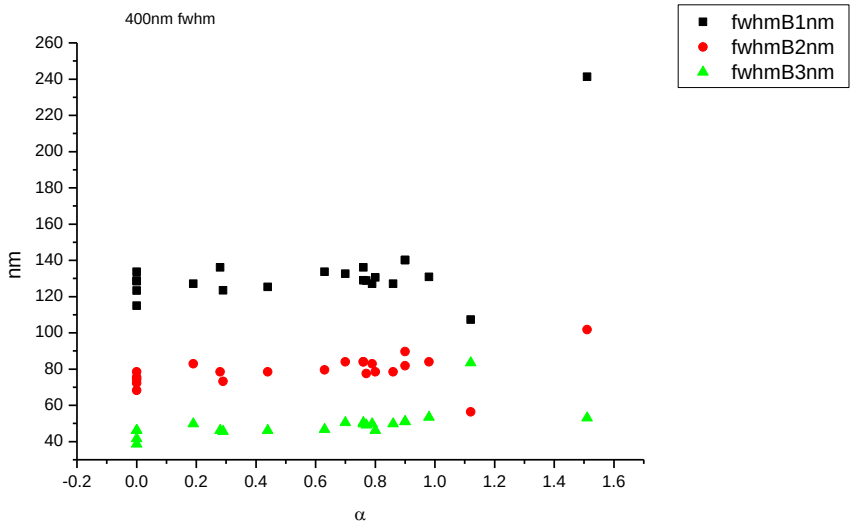

Figure 1.4.38. Full width half maxima from Gaussian model fit of the normalised fluorescence emission spectra of **10a** recorded at 400 nm excitation against α.

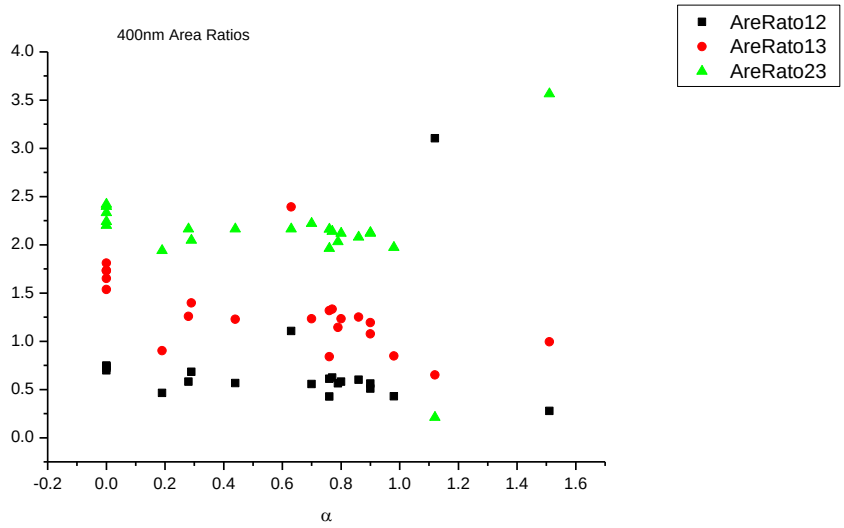

Figure 1.4.39. Area ratios from Gaussian model fit of the normalised fluorescence emission spectra of **10a** recorded at 400 nm excitation against α.

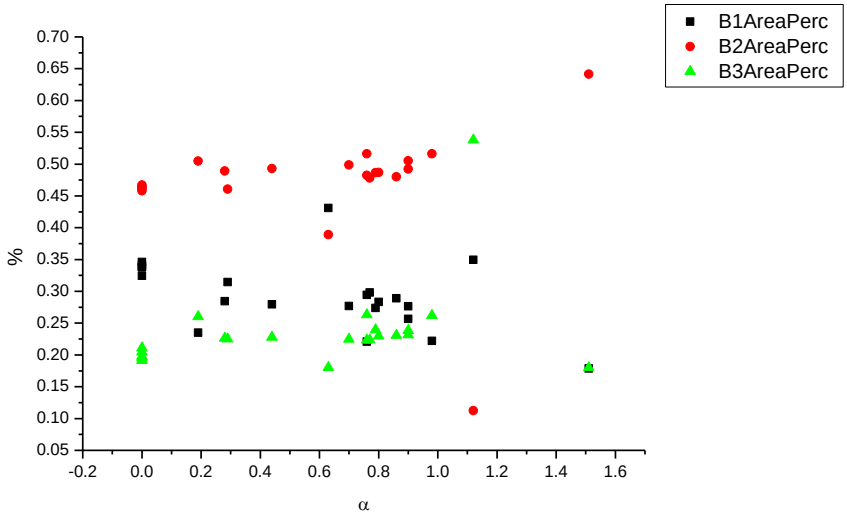

Figure 1.4.40. Area percentages from Gaussian model fit of the normalised fluorescence emission spectra of **10a** recorded at 400 nm excitation against α.

1.4.5.3 β.

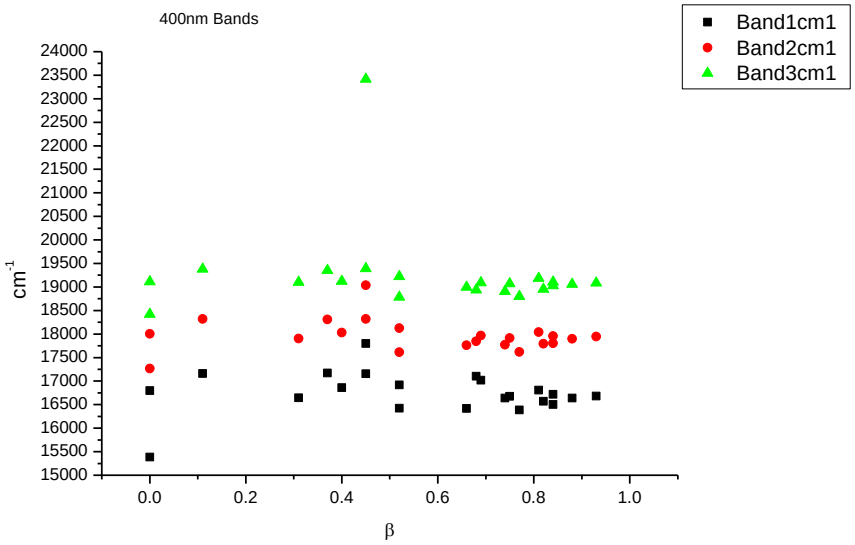

Figure 1.4.41. Band maxima from Gaussian model fit of the normalised fluorescence emission spectra of **10a** recorded at 400 nm excitation against β.

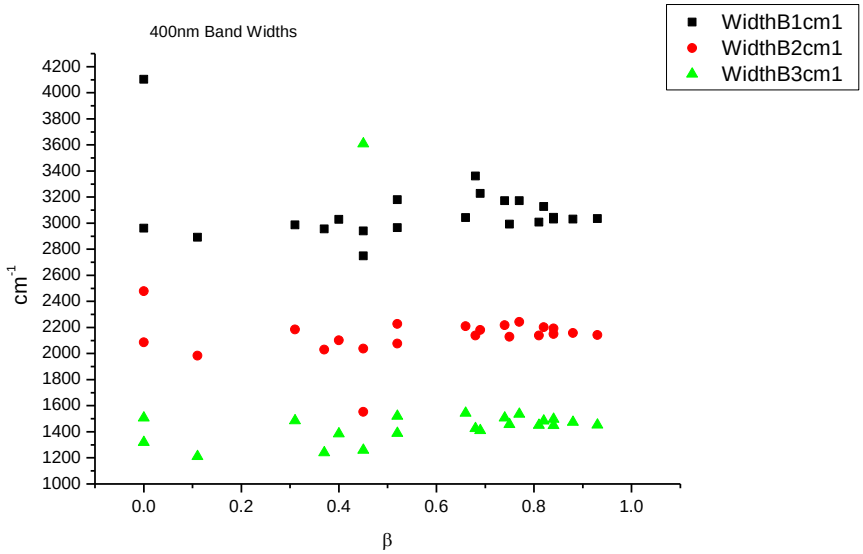

Figure 1.4.42. Band widths from Gaussian model fit of the normalised fluorescence emission spectra of **10a** recorded at 400 nm excitation against β.

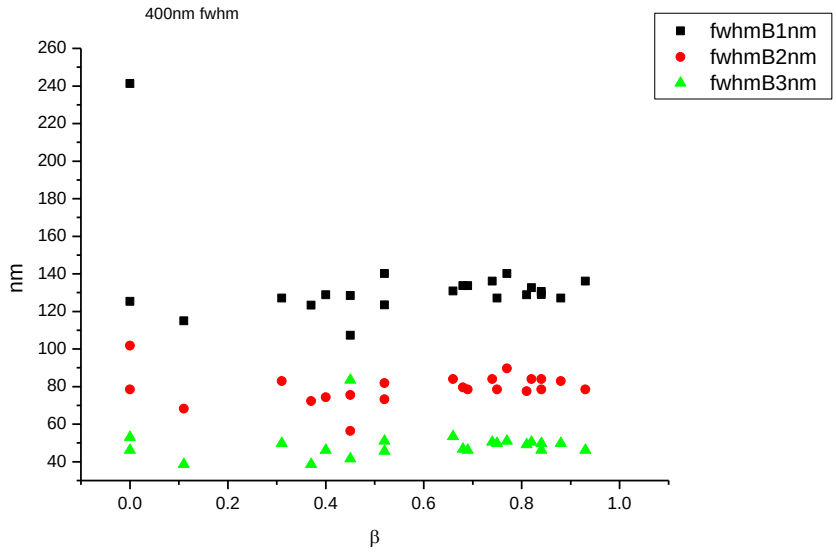

Figure 1.4.43. Full width half maxima from Gaussian model fit of the normalised fluorescence emission spectra of **10a** recorded at 400 nm excitation against β.

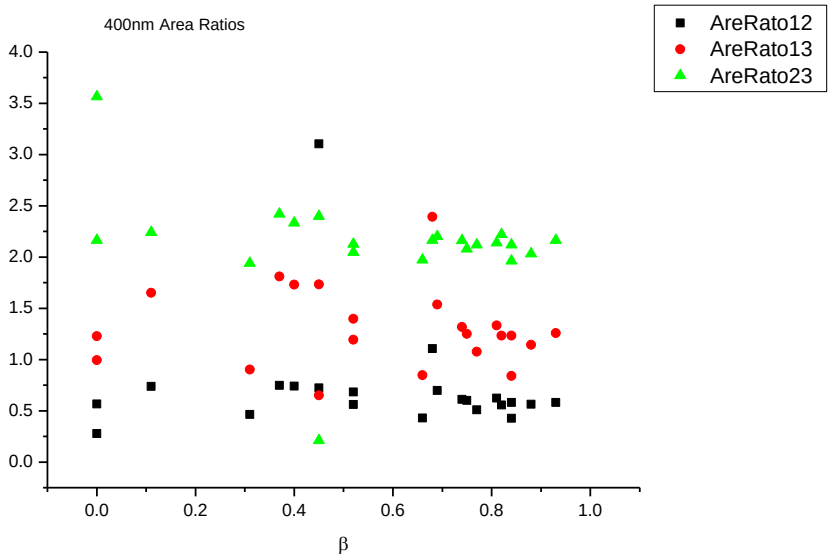

Figure 1.4.44. Area ratios from Gaussian model fit of the normalised fluorescence emission spectra of **10a** recorded at 400 nm excitation against β.

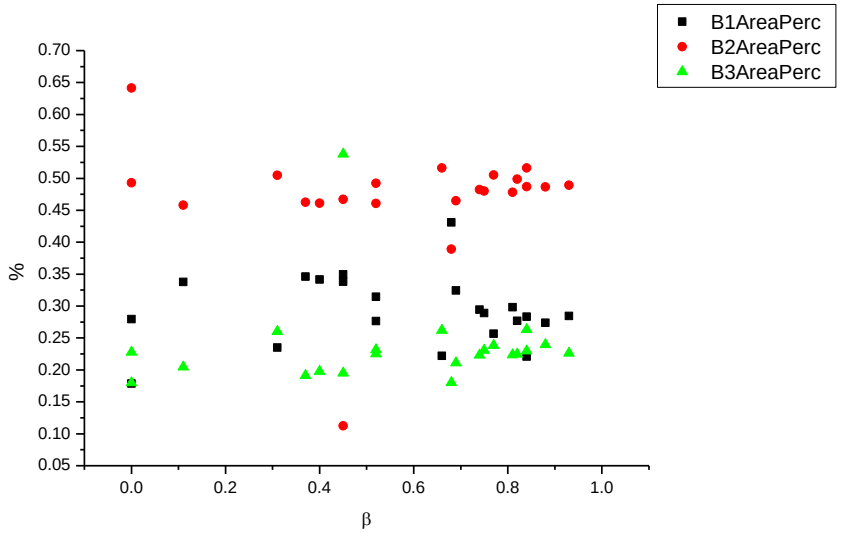

Figure 1.4.45. Area percentages from Gaussian model fit of the normalised fluorescence emission spectra of **10a** recorded at 400 nm excitation against β.

1.4.4.4 π.*

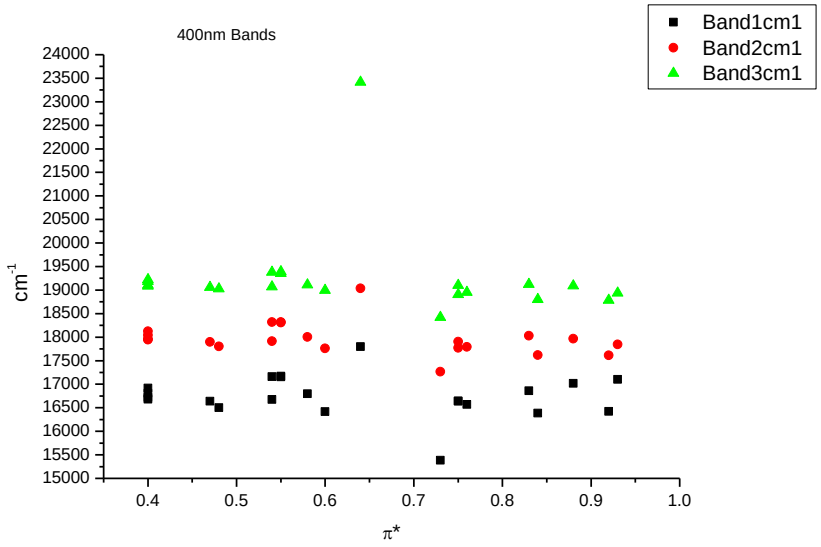

Figure 1.4.46. Band maxima from Gaussian model fit of the normalised fluorescence emission spectra of **10a** recorded at 400 nm excitation against π*.

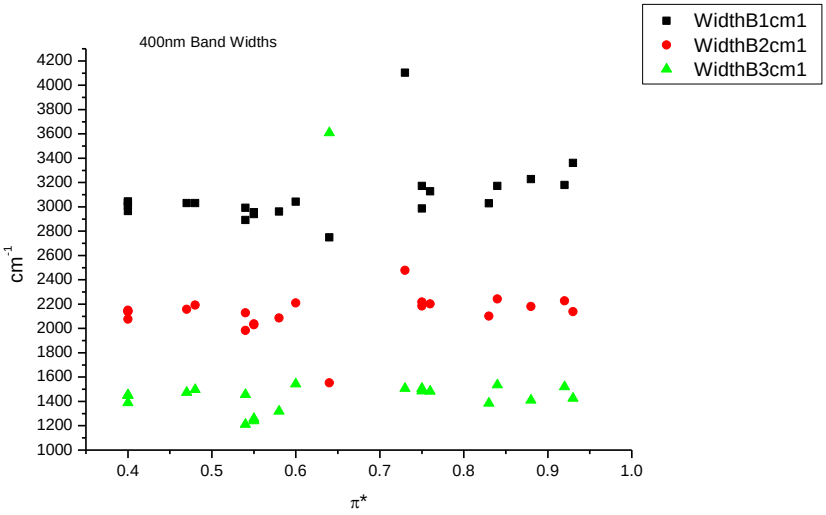

Figure 1.4.47. Band widths from Gaussian model fit of the normalised fluorescence emission spectra of **10a** recorded at 400 nm excitation against π*.

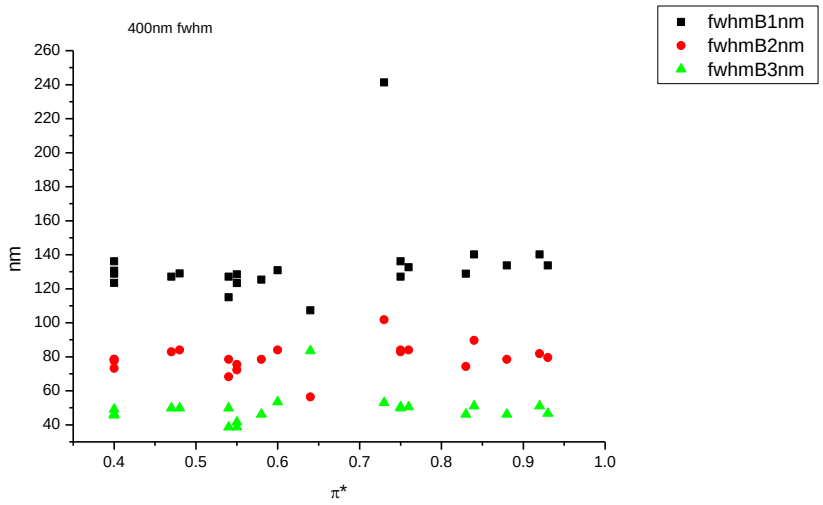

Figure 1.4.48. Full width half maxima from Gaussian model fit of the normalised fluorescence emission spectra of **10a** recorded at 400 nm excitation against π*.

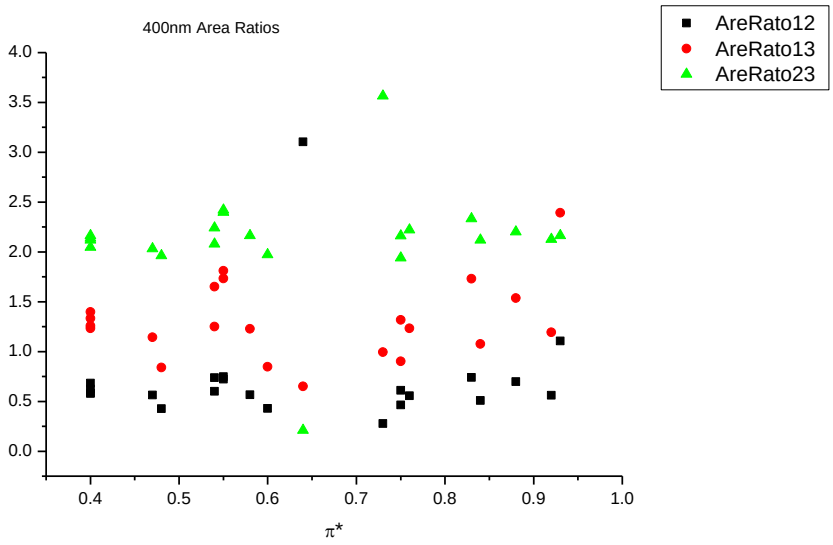

Figure 1.4.49. Area ratios from Gaussian model fit of the normalised fluorescence emission spectra of **10a** recorded at 400 nm excitation against π*.

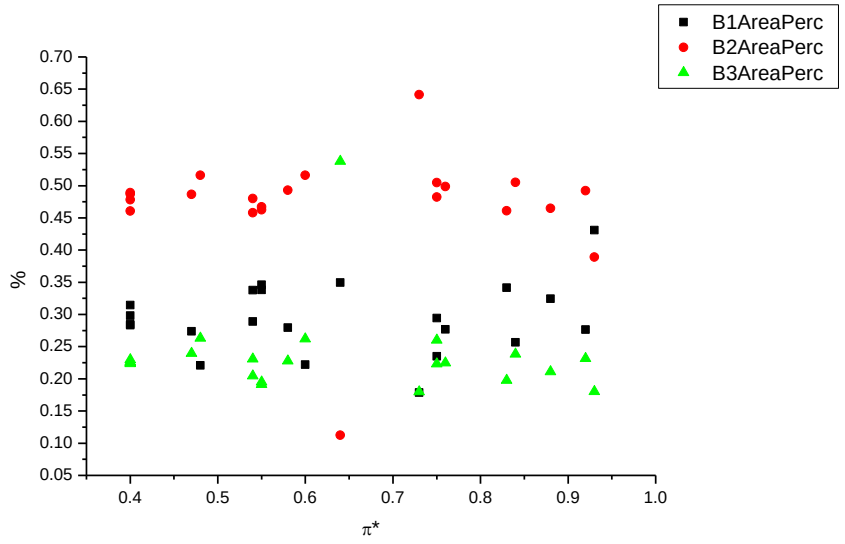

Figure 1.4.50. Area percentages from Gaussian model fit of the normalised fluorescence emission spectra of **10a** recorded at 400 nm excitation against π*.

1.4.4.5 μ(D).

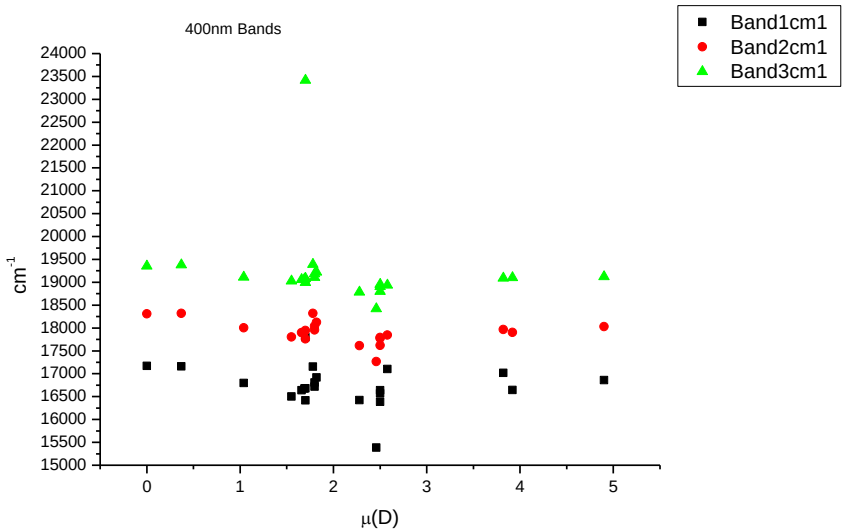

Figure 1.4.51. Band maxima from Gaussian model fit of the normalised fluorescence emission spectra of **10a** recorded at 400 nm excitation against μ(D).

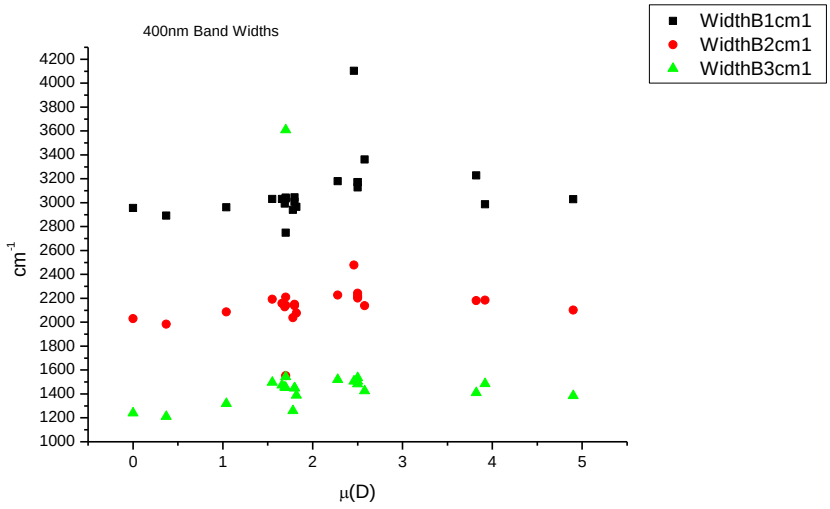

Figure 1.4.52. Band widths from Gaussian model fit of the normalised fluorescence emission spectra of **10a** recorded at 400 nm excitation against μ(D).

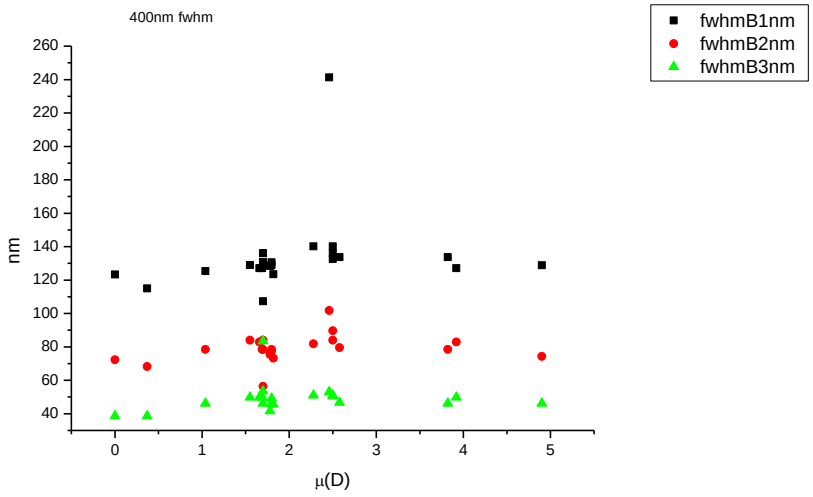

Figure 1.4.53. Full width half maxima from Gaussian model fit of the normalised fluorescence emission spectra of **10a** recorded at 400 nm excitation against μ(D).

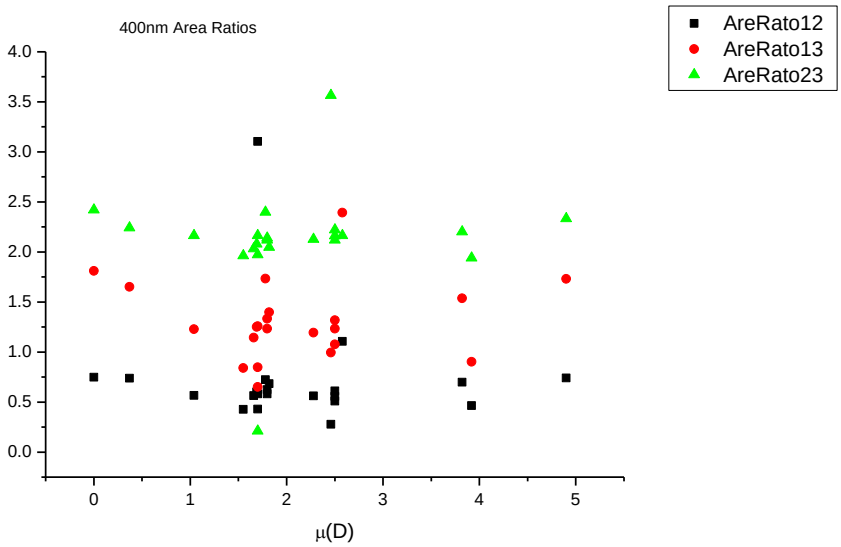

Figure 1.4.54. Area ratios from Gaussian model fit of the normalised fluorescence emission spectra of **10a** recorded at 400 nm excitation against μ(D).

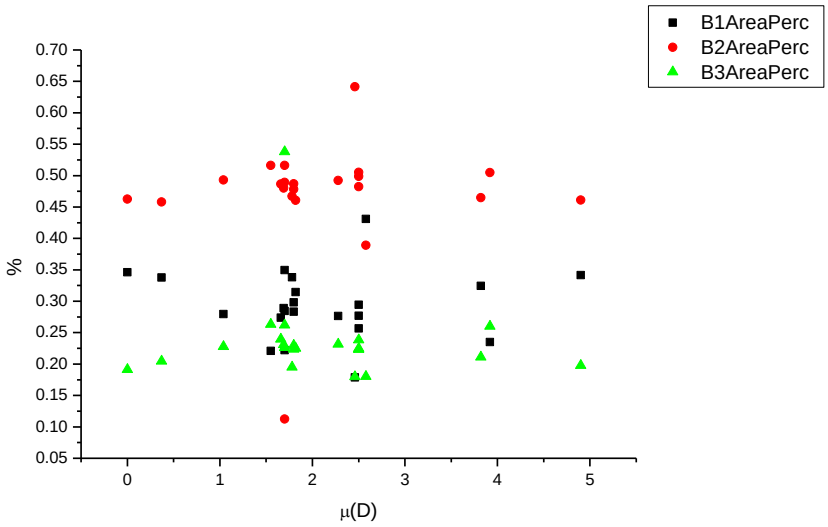

Figure 1.4.55. Area percentages from Gaussian model fit of the normalised fluorescence emission spectra of **10a** recorded at 400 nm excitation against μ(D).

1.4.4.6 η(Cp).

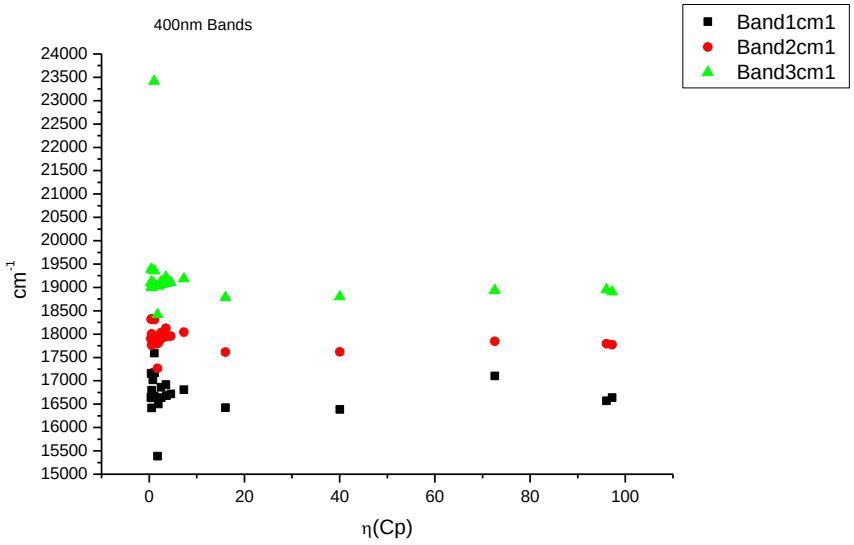

Figure 1.4.56. Band maxima from Gaussian model fit of the normalised fluorescence emission spectra of **10a** recorded at 400 nm excitation against η(Cp).

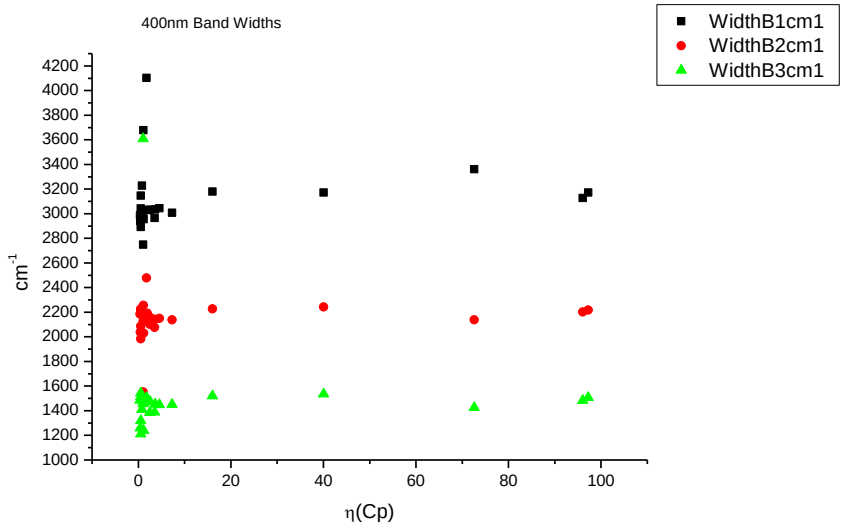

Figure 1.4.57. Band widths from Gaussian model fit of the normalised fluorescence emission spectra of **10a** recorded at 400 nm excitation against η(Cp).

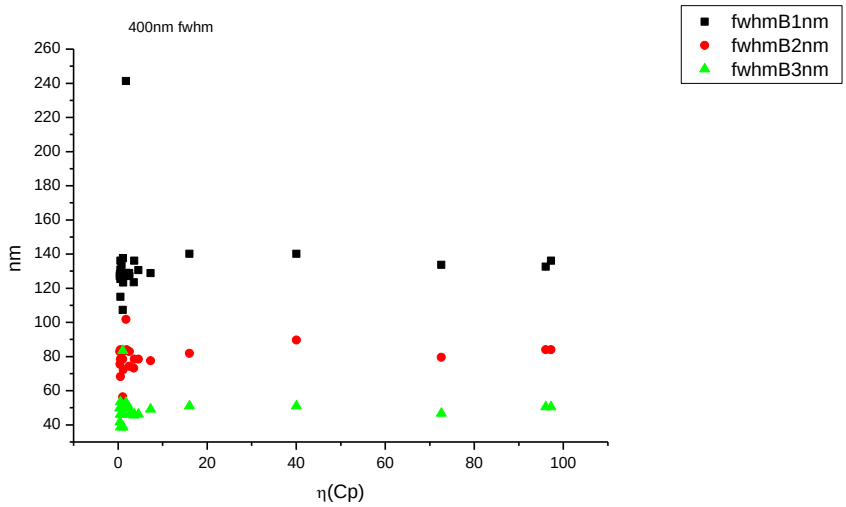

Figure 1.4.58. Full width half maxima from Gaussian model fit of the normalised fluorescence emission spectra of **10a** recorded at 400 nm excitation against η(Cp).

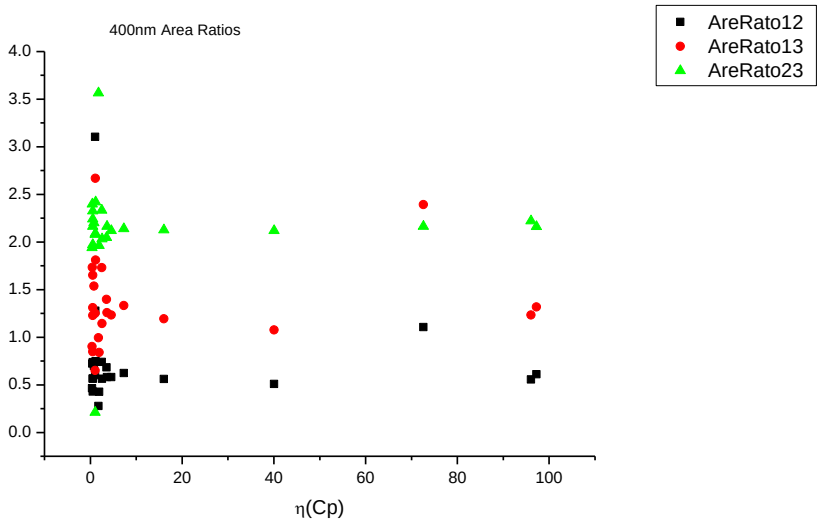

Figure 1.4.59. Area ratios from Gaussian model fit of the normalised fluorescence emission spectra of **10a** recorded at 400 nm excitation against η(Cp).

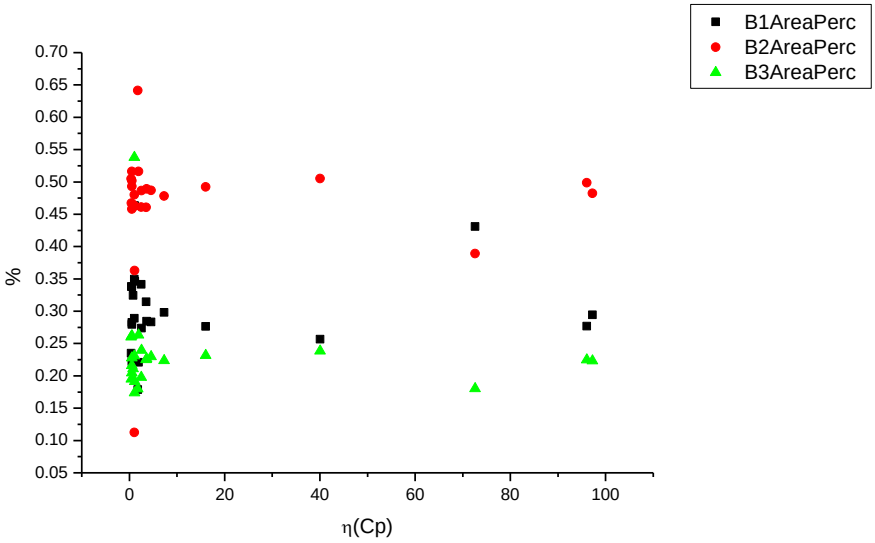

Figure 1.4.60. Area percentages from Gaussian model fit of the normalised fluorescence emission spectra of **10a** recorded at 400 nm excitation against η(Cp).

1.4.6 400 nm fluorescent lifetime results.

1.4.6.1 Intensity weighted.

Wavelength (nm)	Solvent	τ_1 (ns)	A_1 (%)	τ_2 (ns)	A_2 (%)	τ_3 (ns)	A_3 (%)	τ_f (ns) (Intensity Weighted)	$1/\tau_f$	χ^2
490	Toluene	-	-	1.12	1.10	12.55	98.90	12.42	0.08	1.12
490	1,4-Dioxane	0.22	0.54	2.15	0.75	13.69	98.71	13.53	0.07	1.09
490	Ethyl acetate	-	-	1.05	1.27	14.11	98.73	13.95	0.07	1.12
490	Chloroform	0.32	1.12	3.59	2.41	14.01	96.47	13.60	0.07	1.06
490	2-Methyl-2-butanol	0.40	3.03	-	-	14.06	96.97	13.64	0.07	1.05
490	N,N-dimethylformamide	0.34	1.84	3.40	7.67	13.43	90.49	12.42	0.08	1.07
490	Acetonitrile	0.34	1.82	3.32	2.98	14.68	95.21	14.08	0.07	1.10
490	Propylene carbonate	-	-	2.30	3.71	13.99	96.29	13.55	0.07	1.14
490	1-Octanol	0.38	4.84	2.08	2.53	13.83	92.62	12.88	0.08	1.07
490	1-Hexanol	0.33	4.67	3.01	2.53	13.82	92.80	12.92	0.08	1.02
490	1-Butanol	0.30	3.58	3.27	2.39	13.78	94.03	13.05	0.08	1.09
490	1-Pentanol	0.34	3.54	4.05	2.84	13.90	93.62	13.14	0.08	1.05
490	1-Propanol	0.26	2.25	4.68	9.32	13.86	88.43	12.70	0.08	1.07
490	Acetic acid	0.40	67.28	1.70	32.72	-	-	0.83	1.21	1.50
490	Ethanol	0.34	10.05	2.60	8.34	12.82	81.60	10.71	0.09	1.07
490	1,5-Pentanediol	0.35	6.58	-	-	13.68	93.42	12.80	0.08	1.13
490	1,3-Butanediol	0.41	10.82	3.28	9.83	12.99	79.34	10.67	0.09	1.05
490	1,4-Butanediol	0.31	8.38	3.51	13.32	12.25	78.30	10.08	0.10	1.08
490	1,3-Propanediol	0.26	6.44	3.37	11.93	12.32	81.63	10.47	0.10	1.01
490	Methanol	0.30	2.76	4.95	5.10	13.51	92.14	12.71	0.08	1.10
490	1,2-Ethanediol	0.24	2.38	2.70	9.13	12.01	88.49	10.88	0.09	1.08
490	2,2,2-Trifluoroethanol	0.74	8.66	3.40	91.34	-	-	3.17	0.32	1.13
490	Ethanol-d	-	-	4.71	19.36	14.18	80.64	12.35	0.08	1.09
490	Methanol-d	-	-	3.26	5.94	14.29	94.06	13.64	0.07	1.09

Table 1.4.9. Summary of Time Correlated Single Photon Counting (TCSPC) fluorescent lifetimes (intensity weighted) of **10a** recorded at 490 nm.

Wavelength (nm)	Solvent	τ_1 (ns)	A_1 (%)	τ_2 (ns)	A_2 (%)	τ_3 (ns)	A_3 (%)	τ_f (ns) (Intensity Weighted)	$1/\tau_f$	χ^2
520	Toluene	0.84	0.49	-	-	12.58	99.51	12.52	0.08	1.08
520	1,4-Dioxane	0.97	0.72	-	-	13.67	99.28	13.58	0.07	1.09
520	Ethyl acetate	-	-	1.74	0.69	14.22	99.31	14.13	0.07	1.11
520	Chloroform	0.40	1.25	-	-	13.82	98.75	13.66	0.07	1.14
520	2-Methyl-2-butanol	0.45	1.12	-	-	14.13	98.88	13.97	0.07	1.10
520	N,N-dimethylformamide	-	-	2.25	2.33	13.52	97.67	13.26	0.08	1.03
520	Acetonitrile	-	-	1.76	1.40	14.69	98.60	14.51	0.07	1.06
520	Propylene carbonate	-	-	1.81	1.89	14.06	98.11	13.82	0.07	1.06
520	1-Octanol	0.44	2.01	2.18	1.43	13.84	96.56	13.40	0.07	1.08
520	1-Hexanol	0.30	1.76	2.73	1.30	13.84	96.94	13.46	0.07	1.04
520	1-Butanol	0.30	0.90	3.10	0.99	13.80	98.11	13.57	0.07	1.10
520	1-Pentanol	0.30	1.19	2.75	1.22	13.85	97.59	13.55	0.07	1.11
520	1-Propanol	-	-	2.57	1.84	13.84	98.16	13.63	0.07	1.09
520	Acetic acid	0.44	82.74	1.48	17.26	-	-	0.62	1.61	1.02
520	Ethanol	0.43	2.90	4.49	8.62	13.12	88.47	12.00	0.08	1.07
520	1,5-Pentanediol	0.56	1.21	-	-	13.83	98.79	13.67	0.07	1.13
520	1,3-Butanediol	0.45	3.15	4.36	8.72	13.19	88.12	12.02	0.08	1.10
520	1,4-Butanediol	0.34	2.57	4.05	10.12	12.76	87.31	11.56	0.09	1.08
520	1,3-Propanediol	0.36	1.26	3.52	8.65	12.42	90.09	11.50	0.09	1.04
520	Methanol	-	-	2.95	2.27	13.37	97.73	13.13	0.08	1.09
520	1,2-Ethanediol	-	-	2.12	5.89	12.03	94.11	11.44	0.09	1.10
520	2,2,2-Trifluoroethanol	2.57	23.10	3.54	76.90	-	-	3.31	0.30	1.06
520	Ethanol-d	-	-	3.65	3.88	14.36	96.12	13.94	0.07	1.12
520	Methanol-d	-	-	3.98	2.57	14.43	97.43	14.16	0.07	1.10

Table 1.4.10. Summary of Time Correlated Single Photon Counting (TCSPC) fluorescent lifetimes (intensity weighted) of **10a** recorded at 520 nm.

Wavelength (nm)	Solvent	τ_1 (ns)	A_1 (%)	τ_2 (ns)	A_2 (%)	τ_3 (ns)	A_3 (%)	τ_f (ns) (Intensity Weighted)	$1/\tau_f$	χ^2
540	Toluene	-	-	-	-	12.55	100.00	12.55	0.08	1.08
540	1,4-Dioxane	-	-	-	-	13.65	100.00	13.65	0.07	1.14
540	Ethyl acetate	-	-	-	-	14.17	100.00	14.17	0.07	1.06
540	Chloroform	0.56	0.62	-	-	13.97	99.38	13.88	0.07	1.14
540	2-Methyl-2-butanol	0.48	0.73	-	-	14.14	99.27	14.04	0.07	1.08
540	N,N-dimethylformamide	2.53	1.67	-	-	13.55	98.33	13.37	0.07	1.07
540	Acetonitrile	2.65	0.96	-	-	14.71	99.04	14.60	0.07	1.11
540	Propylene carbonate	1.92	1.33	-	-	14.07	98.67	13.91	0.07	1.09
540	1-Octanol	0.72	1.65	-	-	13.81	98.35	13.59	0.07	1.07
540	1-Hexanol	0.57	1.07	-	-	13.79	98.93	13.65	0.07	1.09
540	1-Butanol	0.77	0.51	-	-	13.75	99.49	13.69	0.07	1.10
540	1-Pentanol	0.65	0.77	-	-	13.80	99.23	13.70	0.07	1.06
540	1-Propanol	-	-	2.81	1.05	13.86	98.95	13.74	0.07	1.11
540	Acetic acid	0.48	84.78	1.77	15.22	-	-	0.68	1.48	1.23
540	Ethanol	0.37	1.29	4.86	8.44	13.18	90.26	12.31	0.08	1.12
540	1,5-Pentanediol	0.43	0.70	-	-	13.84	99.30	13.74	0.07	1.11
540	1,3-Butanediol	0.46	1.20	4.42	7.70	13.17	91.10	12.35	0.08	1.14
540	1,4-Butanediol	0.40	1.41	4.62	10.06	12.88	88.53	11.88	0.08	1.14
540	1,3-Propanediol	-	-	3.16	7.26	12.40	92.74	11.73	0.09	1.08
540	Methanol	-	-	3.58	1.49	13.38	98.51	13.23	0.08	1.08
540	1,2-Ethanediol	-	-	2.11	4.86	12.05	95.14	11.57	0.09	1.04
540	2,2,2-Trifluoroethanol	3.08	60.99	3.71	39.01	-	-	3.33	0.30	1.10
540	Ethanol-d	-	-	3.94	2.57	14.44	97.43	14.17	0.07	1.07
540	Methanol-d	-	-	3.80	1.51	14.44	98.49	14.28	0.07	1.09

Table 1.4.11. Summary of Time Correlated Single Photon Counting (TCSPC) fluorescent lifetimes (intensity weighted) of **10a** recorded at 540 nm.

Wavelength (nm)	Solvent	τ_1 (ns)	A_1 (%)	τ_2 (ns)	A_2 (%)	τ_3 (ns)	A_3 (%)	τ_f (ns) (Intensity Weighted)	$1/\tau_f$	χ^2
570	Toluene	-	-	-	-	12.58	100.00	12.58	0.08	1.09
570	1,4-Dioxane	-	-	-	-	13.67	100.00	13.67	0.07	1.08
570	Ethyl acetate	-	-	-	-	14.19	100.00	14.19	0.07	1.08
570	Chloroform	-	-	-	-	14.00	100.00	14.00	0.07	1.14
570	2-Methyl-2-butanol	-	-	-	-	14.10	100.00	14.10	0.07	1.16
570	N,N-dimethylformamide	-	-	-	-	13.47	100.00	13.47	0.07	1.14
570	Acetonitrile	-	-	-	-	14.64	100.00	14.64	0.07	1.11
570	Propylene carbonate	-	-	-	-	14.02	100.00	14.02	0.07	1.16
570	1-Octanol	0.76	0.98	-	-	13.84	99.02	13.71	0.07	1.11
570	1-Hexanol	0.47	0.70	-	-	13.83	99.30	13.73	0.07	1.11
570	1-Butanol	-	-	-	-	13.78	100.00	13.78	0.07	1.10
570	1-Pentanol	0.50	0.50	-	-	13.84	99.50	13.78	0.07	1.09
570	1-Propanol	-	-	-	-	13.82	100.00	13.82	0.07	1.14
570	Acetic acid	0.50	76.13	2.17	23.87			0.90	1.11	1.22
570	Ethanol	-	-	5.29	7.67	13.17	92.33	12.56	0.08	1.07
570	1,5-Pentanediol	-	-	-	-	13.83	100.00	13.83	0.07	1.20
570	1,3-Butanediol	-	-	4.42	6.14	13.13	93.86	12.60	0.08	1.09
570	1,4-Butanediol	-	-	4.03	7.57	12.81	92.43	12.15	0.08	1.16
570	1,3-Propanediol	-	-	3.92	7.16	12.51	92.84	11.89	0.08	1.13
570	Methanol	-	-	-	-	13.32	100.00	13.32	0.08	1.07
570	1,2-Ethanediol	-	-	2.05	3.89	12.10	96.11	11.71	0.09	1.11
570	2,2,2-Trifluoroethanol	-	-	3.36	100.00	-	-	3.36	0.30	1.15
570	Ethanol-d	-	-	3.70	1.20	14.46	98.80	14.33	0.07	1.10
570	Methanol-d	-	-	5.20	1.20	14.46	98.80	14.35	0.07	1.11

Table 1.4.12. Summary of Time Correlated Single Photon Counting (TCSPC) fluorescent lifetimes (intensity weighted) of **10a** recorded at 570 nm.

Wavelength (nm)	Solvent	τ_1 (ns)	A_1 (%)	τ_2 (ns)	A_2 (%)	τ_3 (ns)	A_3 (%)	τ_f (ns) (Intensity Weighted)	$1/\tau_f$	χ^2
600	Toluene	-	-	-	-	12.59	100.00	12.59	0.08	1.13
600	1,4-Dioxane	-	-	-	-	13.70	100.00	13.70	0.07	1.06
600	Ethyl acetate	-	-	-	-	14.21	100.00	14.21	0.07	1.12
600	Chloroform	-	-	-	-	14.03	100.00	14.03	0.07	1.12
600	2-Methyl-2-butanol	-	-	-	-	14.10	100.00	14.10	0.07	1.20
600	N,N-dimethylformamide	-	-	-	-	13.52	100.00	13.52	0.07	1.16
600	Acetonitrile	-	-	-	-	14.69	100.00	14.69	0.07	1.10
600	Propylene carbonate	-	-	-	-	14.07	100.00	14.07	0.07	1.11
600	1-Octanol	0.64	0.96	-	-	13.82	99.04	13.69	0.07	1.06
600	1-Hexanol	0.36	0.90	-	-	13.84	99.10	13.71	0.07	1.11
600	1-Butanol	-	-	-	-	13.82	100.00	13.82	0.07	1.12
600	1-Pentanol	0.34	0.56	-	-	13.84	99.44	13.76	0.07	1.15
600	1-Propanol	-	-	-	-	13.86	100.00	13.86	0.07	1.12
600	Acetic acid	0.50	68.53	2.31	31.47	-	-	1.07	0.94	1.76
600	Ethanol	-	-	7.56	11.70	13.37	88.30	12.69	0.08	1.22
600	1,5-Pentanediol	-	-	-	-	13.86	100.00	13.86	0.07	1.14
600	1,3-Butanediol	-	-	7.30	13.61	13.50	86.39	12.66	0.08	1.22
600	1,4-Butanediol	-	-	4.63	7.58	12.87	92.42	12.25	0.08	1.16
600	1,3-Propanediol	-	-	4.48	7.25	12.60	92.75	12.01	0.08	1.13
600	Methanol	-	-	-	-	13.37	100.00	13.37	0.07	1.07
600	1,2-Ethanediol	-	-	2.35	3.67	12.15	96.33	11.79	0.08	1.11
600	2,2,2-Trifluoroethanol	-	-	3.38	100.00	-	-	3.38	0.30	1.24
600	Ethanol-d	-	-	-	-	14.40	100.00	14.40	0.07	1.12
600	Methanol-d	-	-	-	-	14.43	100.00	14.43	0.07	1.07

Table 1.4.13. Summary of Time Correlated Single Photon Counting (TCSPC) fluorescent lifetimes (intensity weighted) of **10a** recorded at 600 nm.

1.4.6.2 Amplitude weighted.

Wavelength (nm)	Solvent	τ_1 (ns)	A_1 (%)	τ_2 (ns)	A_2 (%)	τ_3 (ns)	A_3 (%)	τ_f (ns) (Amplitude Weighted)	$1/\tau_f$	χ^2
490	Toluene	-	-	1.12	11.07	12.55	88.93	11.28	0.09	1.12
490	1,4-Dioxane	0.22	24.27	2.15	3.49	13.69	72.24	10.02	0.10	1.09
490	Ethyl acetate	-	-	1.05	14.69	14.11	85.31	12.19	0.08	1.12
490	Chloroform	0.32	31.86	3.59	6.04	14.01	62.10	9.02	0.11	1.06
490	2-Methyl-2-butanol	0.40	52.11	-	-	14.06	47.89	6.94	0.14	1.05
490	N,N-dimethylformamide	0.34	37.61	3.40	15.64	13.43	46.75	6.94	0.14	1.07
490	Acetonitrile	0.34	41.83	3.32	7.07	14.68	51.10	7.88	0.13	1.10
490	Propylene carbonate	-	-	2.30	19.02	13.99	80.98	11.76	0.09	1.14
490	1-Octanol	0.38	62.02	2.08	5.85	13.83	31.12	4.80	0.21	1.07
490	1-Hexanol	0.33	65.28	3.01	3.86	13.82	30.87	4.60	0.22	1.02
490	1-Butanol	0.30	61.55	3.27	3.71	13.78	34.73	5.09	0.20	1.09
490	1-Pentanol	0.34	58.32	4.05	3.94	13.90	37.74	5.61	0.18	1.05
490	1-Propanol	0.26	50.95	4.68	11.68	13.86	37.38	5.86	0.17	1.07
490	Acetic acid	0.40	89.66	1.70	10.34	-	-	0.54	1.87	1.50
490	Ethanol	0.34	75.33	2.60	8.27	12.82	16.40	2.58	0.39	1.07
490	1,5-Pentanediol	0.35	75.53	-	-	13.68	26.47	3.88	0.26	1.13
490	1,3-Butanediol	0.41	74.58	3.28	8.37	12.99	17.05	2.79	0.36	1.05
490	1,4-Butanediol	0.31	72.44	3.51	10.27	12.25	17.29	2.70	0.37	1.08
490	1,3-Propanediol	0.26	70.94	3.37	10.12	12.32	18.94	2.86	0.35	1.01
490	Methanol	0.30	53.68	4.95	6.08	13.51	40.25	5.90	0.17	1.10
490	1,2-Ethanediol	0.24	47.90	2.70	16.40	12.01	35.70	4.85	0.21	1.08
490	2,2,2-Trifluoroethanol	0.74	30.40	3.40	69.60	-	-	2.59	0.39	1.13
490	Ethanol-d	-	-	4.71	41.97	14.18	58.03	10.21	0.10	1.09
490	Methanol-d	-	-	3.26	21.67	14.29	78.33	11.90	0.08	1.09

Table 1.4.14. Summary of Time Correlated Single Photon Counting (TCSPC) fluorescent lifetimes (amplitude weighted) of **10a** recorded at 490 nm.

Wavelength (nm)	Solvent	τ_1 (ns)	A_1 (%)	τ_2 (ns)	A_2 (%)	τ_3 (ns)	A_3 (%)	τ_f (ns) (Amplitude Weighted)	$1/\tau_f$	χ^2
520	Toluene	0.84	6.91	-	-	12.58	93.09	11.77	0.08	1.08
520	1,4-Dioxane	0.97	9.31	-	-	13.67	90.69	12.49	0.08	1.09
520	Ethyl acetate	-	-	1.74	5.36	14.22	94.64	13.55	0.07	1.11
520	Chloroform	0.40	30.57	-	-	13.82	69.43	9.72	0.10	1.14
520	2-Methyl-2-butanol	0.45	26.15	-	-	14.13	73.85	10.55	0.09	1.10
520	N,N-dimethylformamide	-	-	2.25	12.52	13.52	87.48	12.11	0.08	1.03
520	Acetonitrile	-	-	1.76	10.61	14.69	89.39	13.32	0.08	1.06
520	Propylene carbonate	-	-	1.81	13.01	14.06	86.99	12.46	0.08	1.06
520	1-Octanol	0.44	37.59	2.18	5.34	13.84	57.07	8.18	0.12	1.08
520	1-Hexanol	0.30	43.76	2.73	3.57	13.84	52.66	7.52	0.13	1.04
520	1-Butanol	0.30	28.71	3.10	3.07	13.80	68.22	9.60	0.10	1.10
520	1-Pentanol	0.30	1.19	2.75	1.22	13.85	97.59	8.77	0.11	1.11
520	1-Propanol	-	-	2.57	9.18	13.84	90.82	12.80	0.08	1.09
520	Acetic acid	0.44	94.09	1.48	5.91	-	-	0.51	1.98	1.02
520	Ethanol	0.43	44.10	4.49	12.39	13.12	43.51	6.45	0.16	1.07
520	1,5-Pentanediol	0.56	23.32	-	-	13.83	76.68	10.73	0.09	1.13
520	1,3-Butanediol	0.45	44.66	4.36	12.76	13.19	42.58	6.37	0.16	1.10
520	1,4-Butanediol	0.34	44.99	4.05	14.73	12.76	40.28	5.89	0.17	1.08
520	1,3-Propanediol	0.36	26.64	3.52	18.57	12.42	54.79	7.55	0.13	1.04
520	Methanol	-	-	2.95	9.54	13.37	90.46	12.38	0.08	1.09
520	1,2-Ethanediol	-	-	2.12	26.21	12.03	73.79	9.43	0.11	1.10
520	2,2,2-Trifluoroethanol	2.57	29.21	3.54	70.79	-	-	3.26	0.31	1.06
520	Ethanol-d	-	-	3.65	13.72	14.36	86.28	12.89	0.08	1.12
520	Methanol-d	-	-	3.98	8.72	14.43	91.28	13.52	0.07	1.10

Table 1.4.15. Summary of Time Correlated Single Photon Counting (TCSPC) fluorescent lifetimes (amplitude weighted) of **10a** recorded at 520 nm.

Wavelength (nm)	Solvent	τ_1 (ns)	A_1 (%)	τ_2 (ns)	A_2 (%)	τ_3 (ns)	A_3 (%)	τ_f (ns) (Amplitude Weighted)	$1/\tau_f$	χ^2
540	Toluene	-	-	-	-	12.55	100.00	12.55	0.08	1.08
540	1,4-Dioxane	-	-	-	-	13.65	100.00	13.65	0.07	1.14
540	Ethyl acetate	-	-	-	-	14.17	100.00	14.17	0.07	1.06
540	Chloroform	0.56	13.57	-	-	13.97	86.43	12.15	0.08	1.14
540	2-Methyl-2-butanol	0.48	17.88	-	-	14.14	82.12	11.69	0.09	1.08
540	N,N-dimethylformamide	-	-	2.53	8.35	13.55	91.65	12.63	0.08	1.07
540	Acetonitrile	-	-	2.65	5.08	14.71	94.92	14.10	0.07	1.11
540	Propylene carbonate	-	-	1.92	9.01	14.07	90.99	12.98	0.08	1.09
540	1-Octanol	0.72	24.42	-	-	13.81	75.58	10.61	0.09	1.07
540	1-Hexanol	0.57	20.81	-	-	13.79	79.19	11.04	0.09	1.09
540	1-Butanol	0.77	8.48	-	-	13.75	91.52	12.65	0.08	1.10
540	1-Pentanol	0.65	14.16	-	-	13.80	85.54	11.94	0.08	1.06
540	1-Propanol	-	-	2.81	4.99	13.86	95.01	13.31	0.08	1.11
540	Acetic acid	0.48	95.38	1.77	4.62	-	-	0.54	1.86	1.23
540	Ethanol	0.37	28.87	4.86	14.39	13.18	56.74	8.28	0.12	1.12
540	1,5-Pentanediol	0.43	18.44	-	-	13.84	81.56	11.36	0.09	1.11
540	1,3-Butanediol	0.46	23.04	4.42	15.49	13.17	61.48	8.89	0.11	1.14
540	1,4-Butanediol	0.40	28.28	4.62	17.26	12.88	54.46	7.92	0.13	1.14
540	1,3-Propanediol	-	-	3.16	23.51	12.40	76.49	10.23	0.10	1.08
540	Methanol	-	-	3.58	5.35	13.38	94.65	12.85	0.08	1.08
540	1,2-Ethanediol	-	-	2.11	22.58	12.05	77.42	9.81	0.10	1.04
540	2,2,2-Trifluoroethanol	3.08	65.32	3.71	34.68	-	-	3.30	0.30	1.10
540	Ethanol-d	-	-	3.94	8.84	14.44	91.16	13.52	0.07	1.07
540	Methanol-d	-	-	3.80	5.44	14.44	94.56	13.86	0.07	1.09

Table 1.4.16. Summary of Time Correlated Single Photon Counting (TCSPC) fluorescent lifetimes (amplitude weighted) of **10a** recorded at 540 nm.

Wavelength (nm)	Solvent	τ_1 (ns)	A_1 (%)	τ_2 (ns)	A_2 (%)	τ_3 (ns)	A_3 (%)	τ_f (ns) (Amplitude Weighted)	$1/\tau_f$	χ^2
570	Toluene	-	-	-	-	12.58	100.00	12.58	0.08	1.09
570	1,4-Dioxane	-	-	-	-	13.67	100.00	13.67	0.07	1.08
570	Ethyl acetate	-	-	-	-	14.19	100.00	14.19	0.07	1.08
570	Chloroform	-	-	-	-	14.00	100.00	14.00	0.07	1.14
570	2-Methyl-2-butanol	-	-	-	-	14.10	100.00	14.10	0.07	1.16
570	N,N-dimethylformamide	-	-	-	-	13.47	100.00	13.47	0.07	1.14
570	Acetonitrile	-	-	-	-	14.64	100.00	14.64	0.07	1.11
570	Propylene carbonate	-	-	-	-	14.02	100.00	14.02	0.07	1.16
570	1-Octanol	0.76	15.27	-	-	13.84	84.73	11.84	0.08	1.11
570	1-Hexanol	0.47	17.26	-	-	13.83	82.74	11.52	0.09	1.11
570	1-Butanol	-	-	-	-	13.78	100.00	13.78	0.07	1.10
570	1-Pentanol	0.50	12.30	-	-	13.84	87.70	12.20	0.08	1.09
570	1-Propanol	-	-	-	-	13.82	100.00	13.82	0.07	1.14
570	Acetic acid	0.50	93.30	2.17	6.70	-	-	0.61	1.64	1.22
570	Ethanol	-	-	5.29	17.15	13.17	82.85	11.82	0.08	1.07
570	1,5-Pentanediol	-	-	-	-	13.83	100.00	13.83	0.07	1.20
570	1,3-Butanediol	-	-	4.42	16.27	13.13	83.73	11.71	0.09	1.09
570	1,4-Butanediol	-	-	4.03	20.66	12.81	79.34	11.00	0.09	1.16
570	1,3-Propanediol	-	-	3.92	19.74	12.51	80.26	10.81	0.09	1.13
570	Methanol	-	-	-	-	13.32	100.00	13.32	0.08	1.07
570	1,2-Ethanediol	-	-	2.05	19.28	12.10	80.72	10.17	0.10	1.11
570	2,2,2-Trifluoroethanol	-	-	3.36	100.00	-	-	3.36	0.30	1.15
570	Ethanol-d	-	-	3.70	4.48	14.46	95.52	13.98	0.07	1.10
570	Methanol-d	-	-	5.20	3.29	14.46	96.71	14.15	0.07	1.11

Table 1.4.17. Summary of Time Correlated Single Photon Counting (TCSPC) fluorescent lifetimes (amplitude weighted) of **10a** recorded at 570 nm.

Wavelength (nm)	Solvent	τ_1 (ns)	A_1 (%)	τ_2 (ns)	A_2 (%)	τ_3 (ns)	A_3 (%)	τ_f (ns) (Amplitude Weighted)	$1/\tau_f$	χ^2
600	Toluene	-	-	-	-	12.59	100.00	12.59	0.08	1.13
600	1,4-Dioxane	-	-	-	-	13.70	100.00	13.70	0.07	1.06
600	Ethyl acetate	-	-	-	-	14.21	100.00	14.21	0.07	1.12
600	Chloroform	-	-	-	-	14.03	100.00	14.03	0.07	1.12
600	2-Methyl-2-butanol	-	-	-	-	14.10	100.00	14.10	0.07	1.20
600	N,N-dimethylformamide	-	-	-	-	13.52	100.00	13.52	0.07	1.16
600	Acetonitrile	-	-	-	-	14.69	100.00	14.69	0.07	1.10
600	Propylene carbonate	-	-	-	-	14.07	100.00	14.07	0.07	1.11
600	1-Octanol	0.64	17.33	-	-	13.82	82.67	11.53	0.09	1.06
600	1-Hexanol	0.36	25.98	-	-	13.84	74.02	10.33	0.10	1.11
600	1-Butanol	-	-	-	-	13.82	100.00	13.82	0.07	1.12
600	1-Pentanol	0.34	18.76	-	-	13.84	81.24	11.31	0.09	1.15
600	1-Propanol	-	-	-	-	13.86	100.00	13.86	0.07	1.12
600	Acetic acid	0.50	68.53	2.31	31.47	-	-	0.66	1.52	1.76
600	Ethanol	-	-	7.56	18.99	13.37	81.01	12.27	0.08	1.22
600	1,5-Pentanediol	-	-	-	-	13.86	100.00	13.86	0.07	1.14
600	1,3-Butanediol	-	-	7.30	22.58	13.50	77.42	12.10	0.08	1.22
600	1,4-Butanediol	-	-	4.63	18.57	12.87	81.43	11.34	0.09	1.16
600	1,3-Propanediol	-	-	4.48	18.02	12.60	81.98	11.14	0.09	1.13
600	Methanol	-	-	-	-	13.37	100.00	13.37	0.07	1.07
600	1,2-Ethanediol	-	-	2.35	16.45	12.15	83.55	10.54	0.09	1.11
600	2,2,2-Trifluoroethanol	-	-	3.38	100.00	-	-	3.38	0.30	1.24
600	Ethanol-d	-	-	-	-	14.40	100.00	14.40	0.07	1.12
600	Methanol-d	-	-	-	-	14.43	100.00	14.43	0.07	1.07

Table 1.4.18. Summary of Time Correlated Single Photon Counting (TCSPC) fluorescent lifetimes (amplitude weighted) of **10a** recorded at 600 nm.

1.4.7 Average fluorescent lifetimes - Solvatochromic analysis.

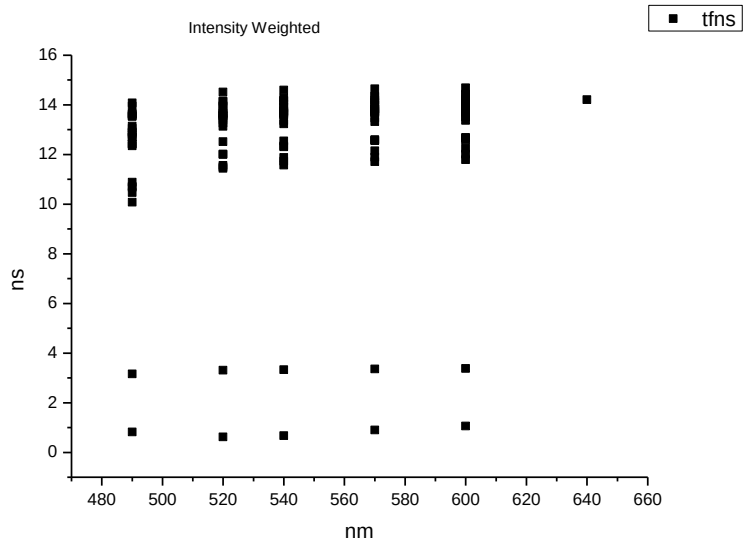

Figure 1.4.61. Intensity weighted average lifetime (τ_f) of **10a** versus wavelength (nm).

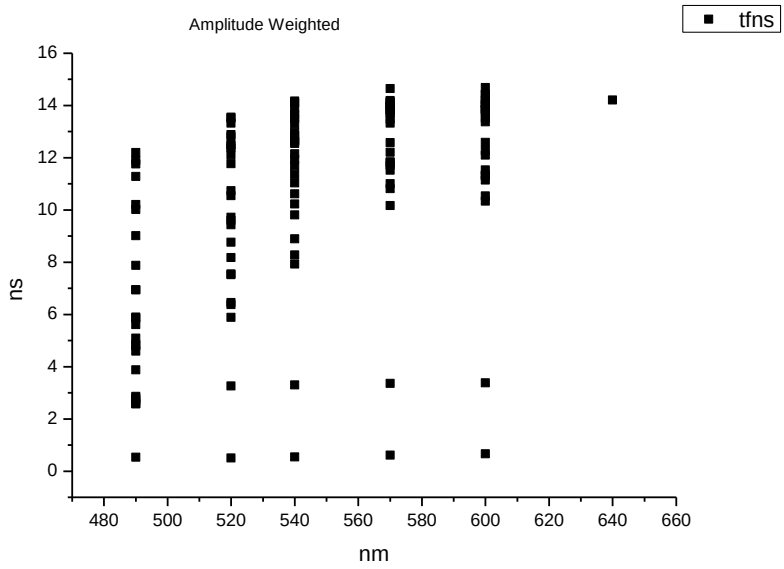

Figure 1.4.62. Amplitude weighted average lifetime (τ_f) of **10a** versus wavelength (nm).

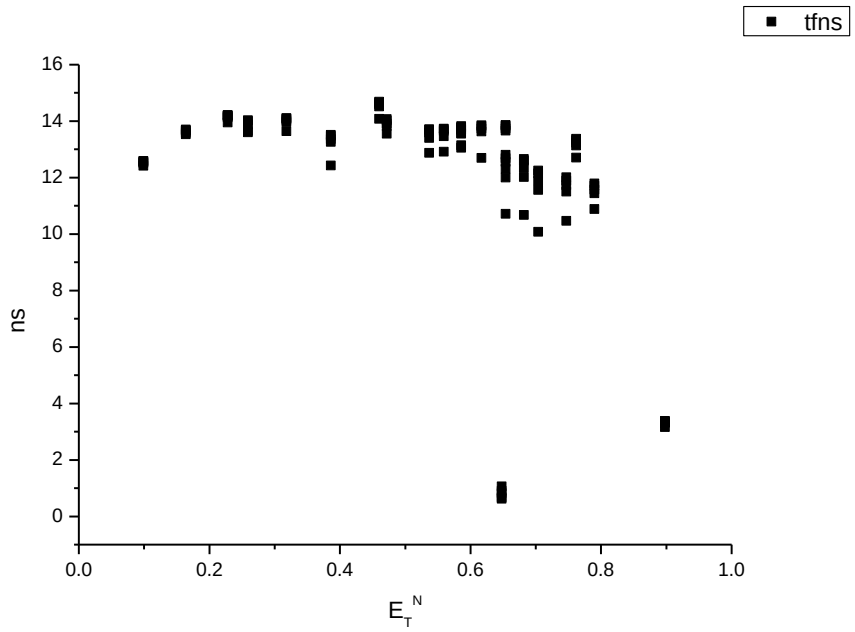

Figure 1.4.63. Intensity weighted average lifetime (τ_f) of **10a** versus E_T^N.

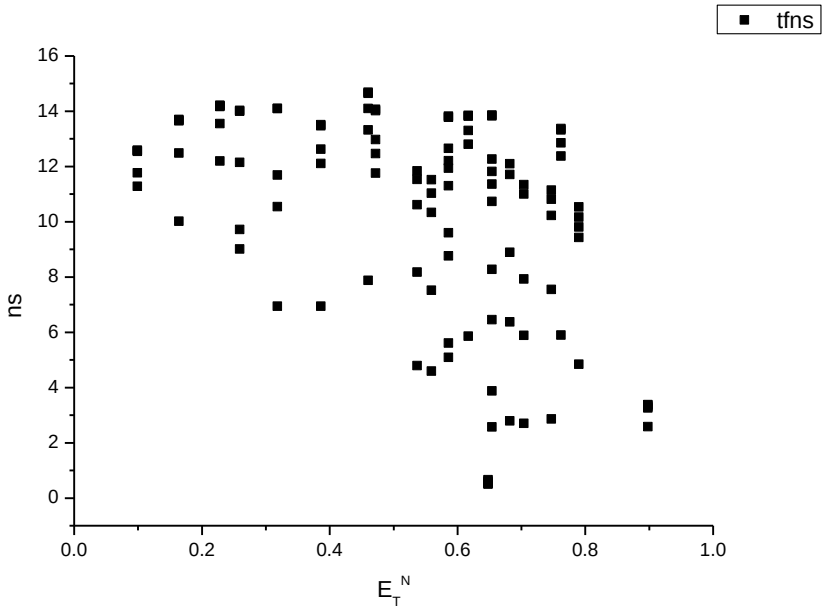

Figure 1.4.64. Amplitude weighted average lifetime (τ_f) of **10a** versus E_T^N.

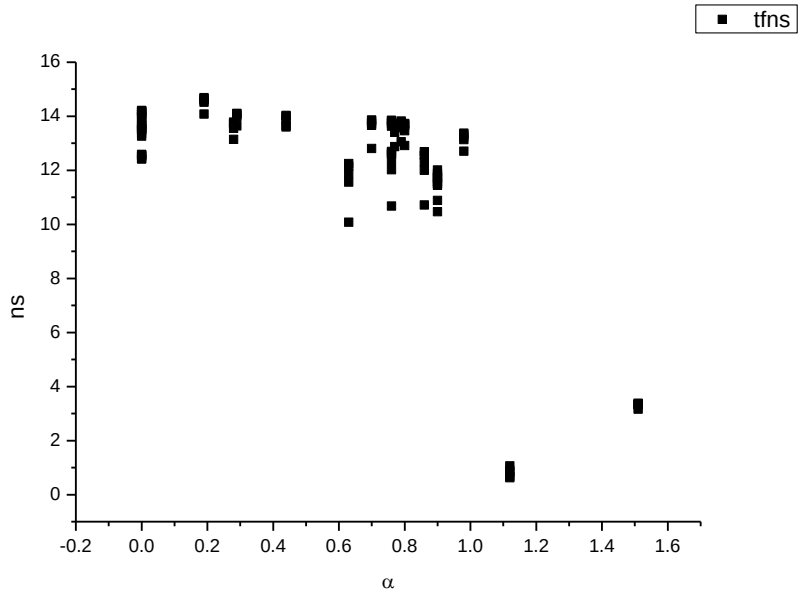

Figure 1.4.65. Intensity weighted average lifetime (τ_f) of **10a** versus α.

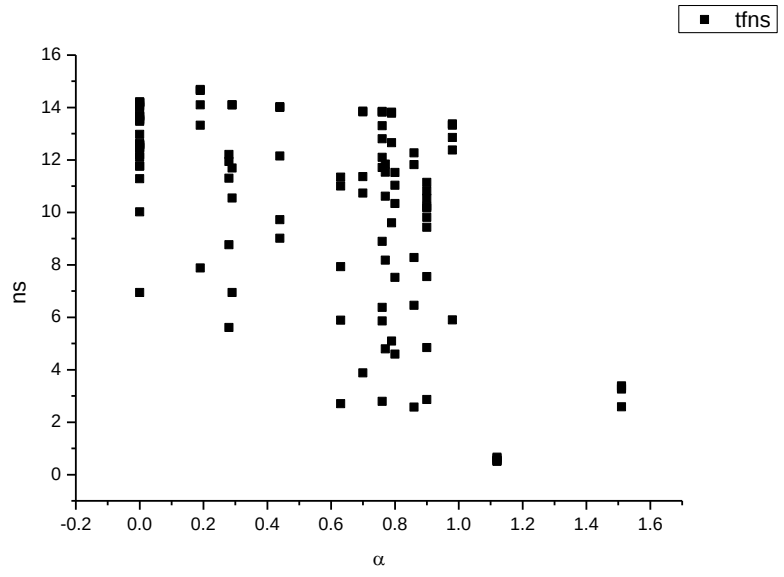

Figure 1.4.66. Amplitude weighted average lifetime (τ_f) of **10a** versus α.

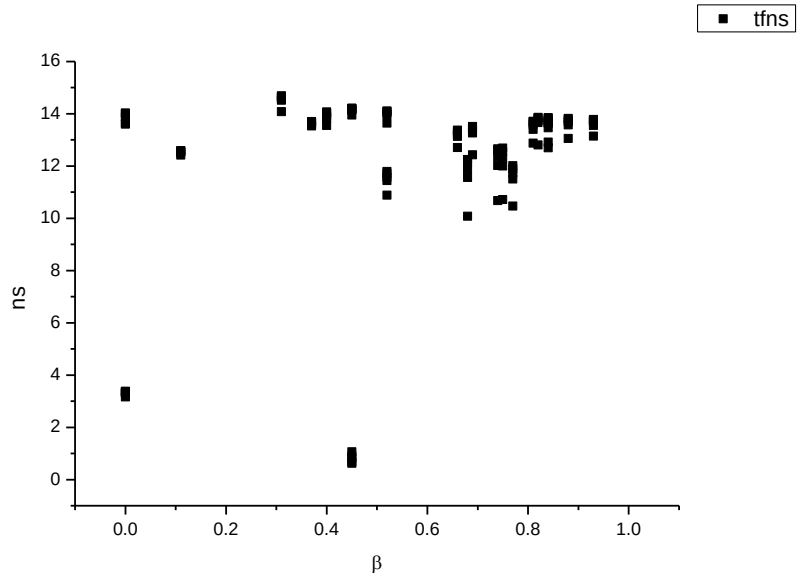

Figure 1.4.67. Intensity weighted average lifetime (τ_f) of **10a** versus β.

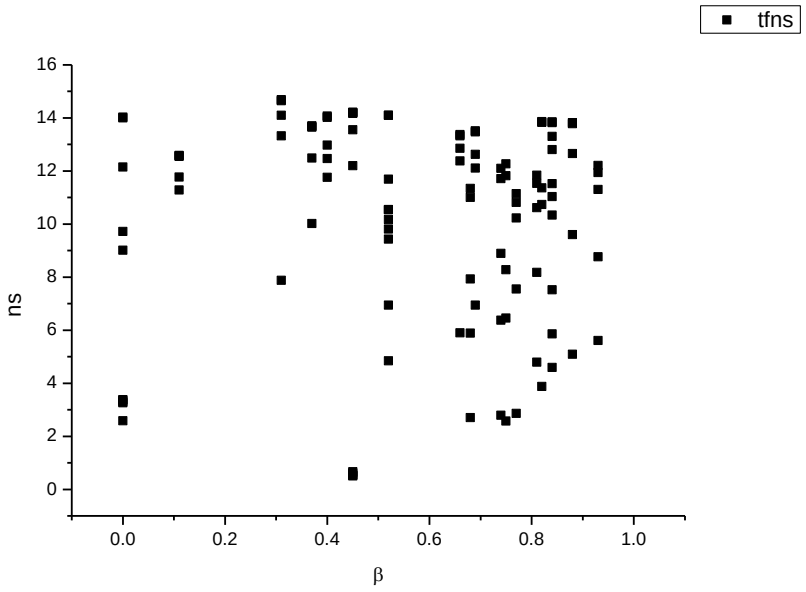

Figure 1.4.68. Amplitude weighted average lifetime (τ_f) of **10a** versus β.

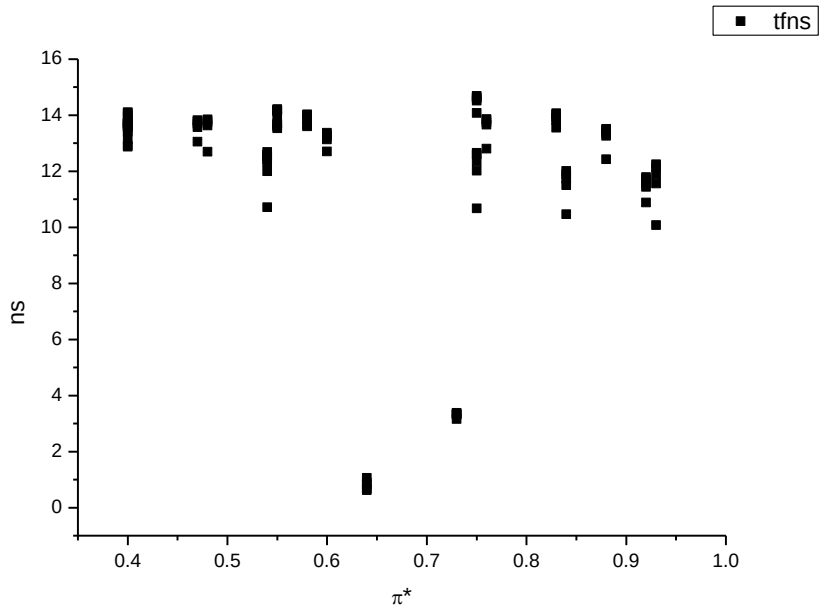

Figure 1.4.69. Intensity weighted average lifetime (τ_f) of **10a** versus π*.

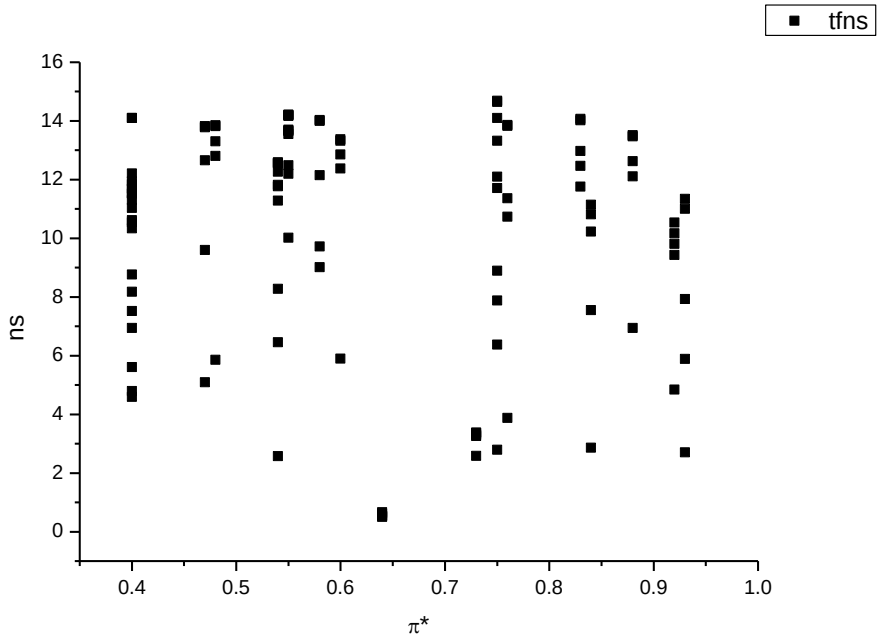

Figure 1.4.70. Amplitude weighted average lifetime (τ_f) of **10a** versus π*.

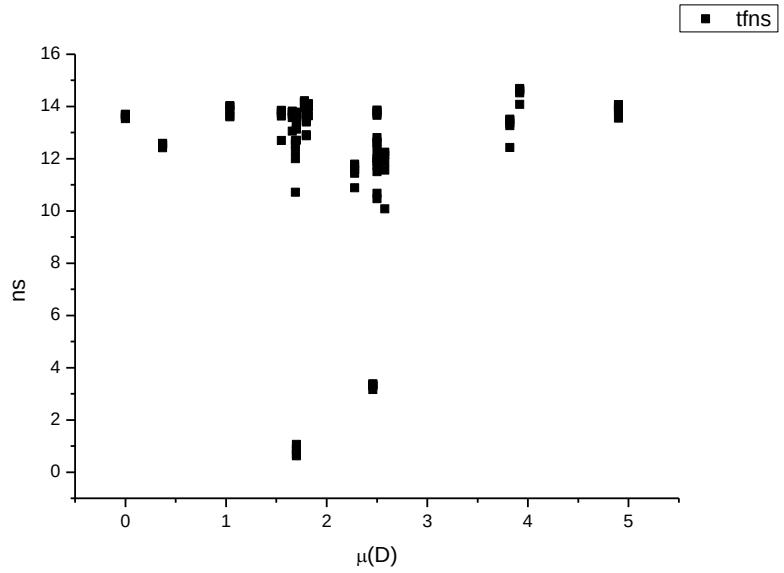

Figure 1.4.71. Intensity weighted average lifetime (τ_f) of **10a** versus μ(D).

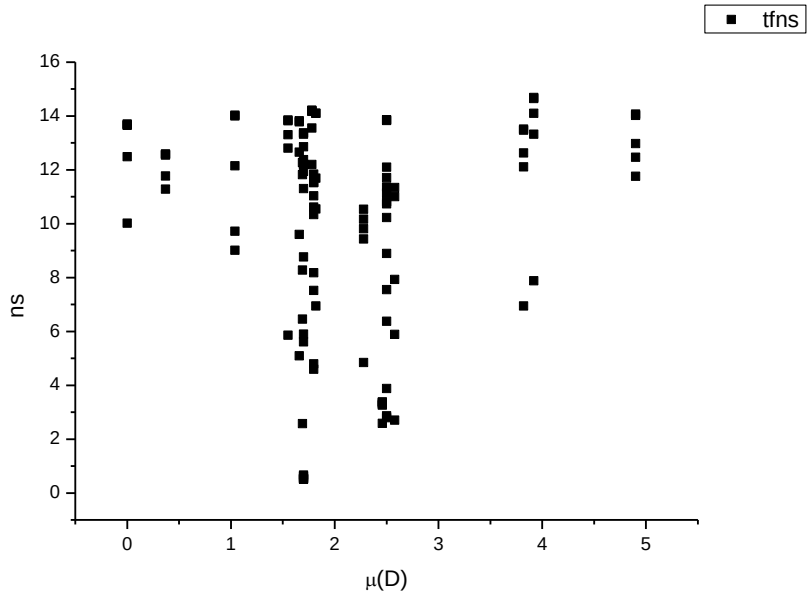

Figure 1.4.72. Amplitude weighted average lifetime (τ_f) of **10a** versus μ(D).

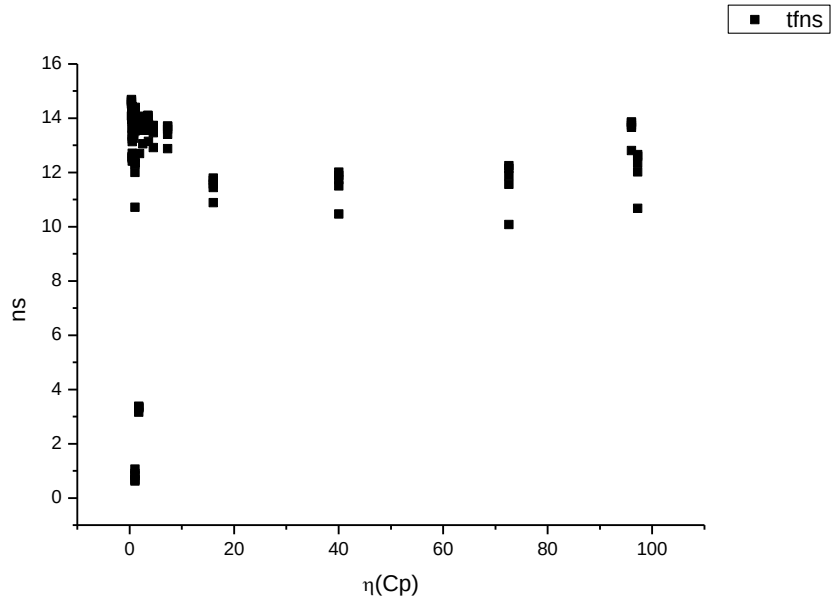

Figure 1.4.73. Intensity weighted average lifetime (τ_f) of **10a** versus η(Cp).

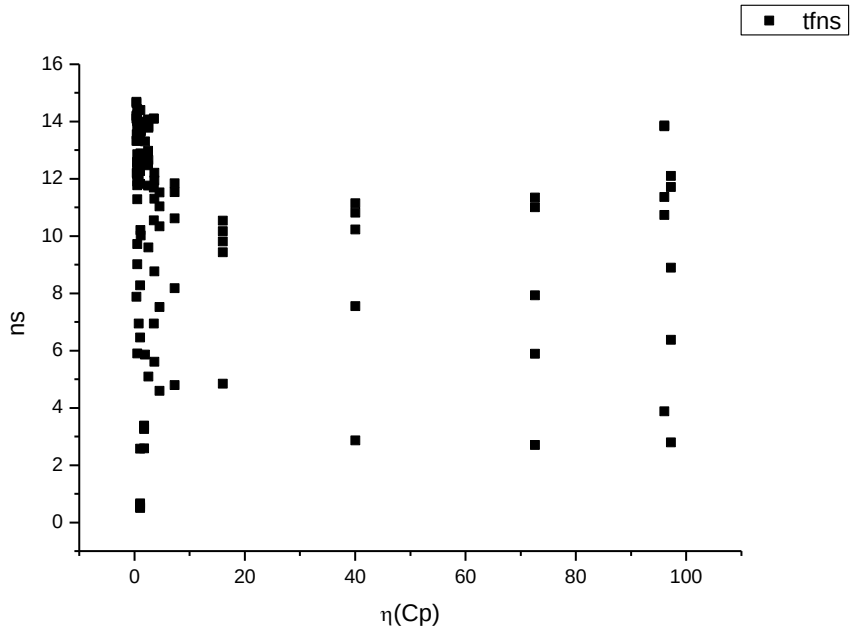

Figure 1.4.74. Amplitude weighted average lifetime (τ_f) of **10a** versus η(Cp).

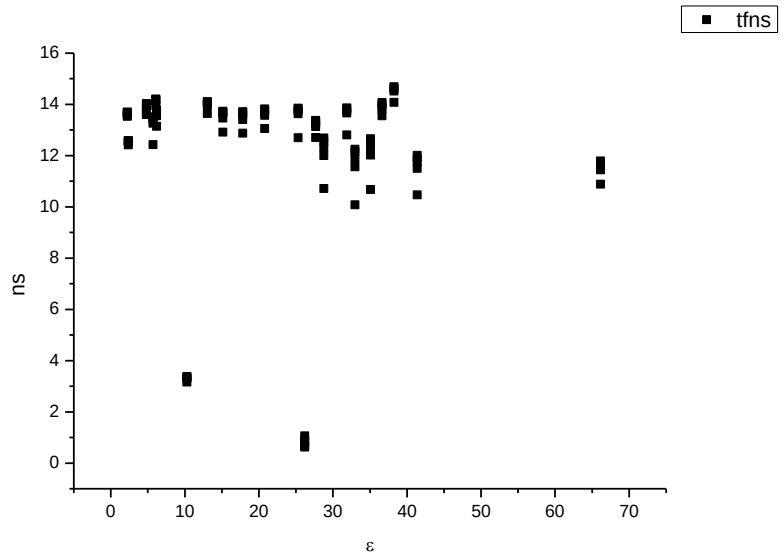

Figure 1.4.75. Intensity weighted average lifetime (τ_f) of **10a** versus ε.

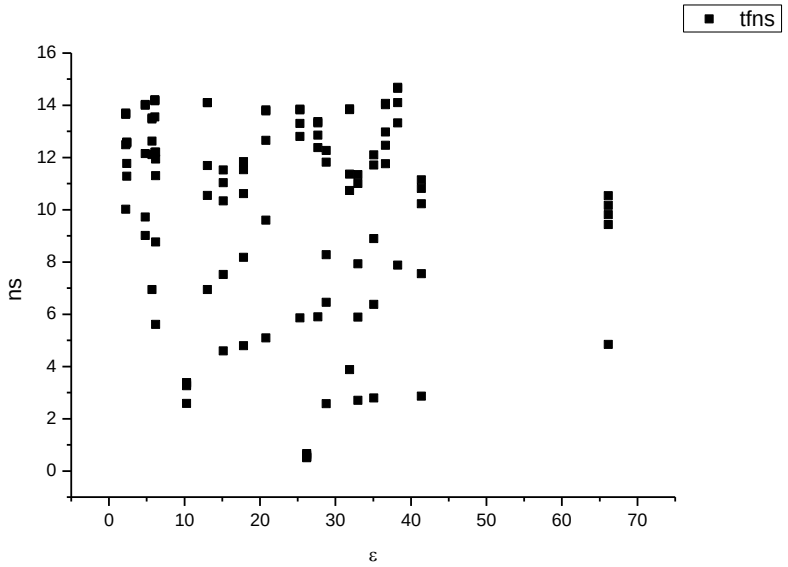

Figure 1.4.76. Amplitude weighted average lifetime (τ_f) of **10a** versus ε.

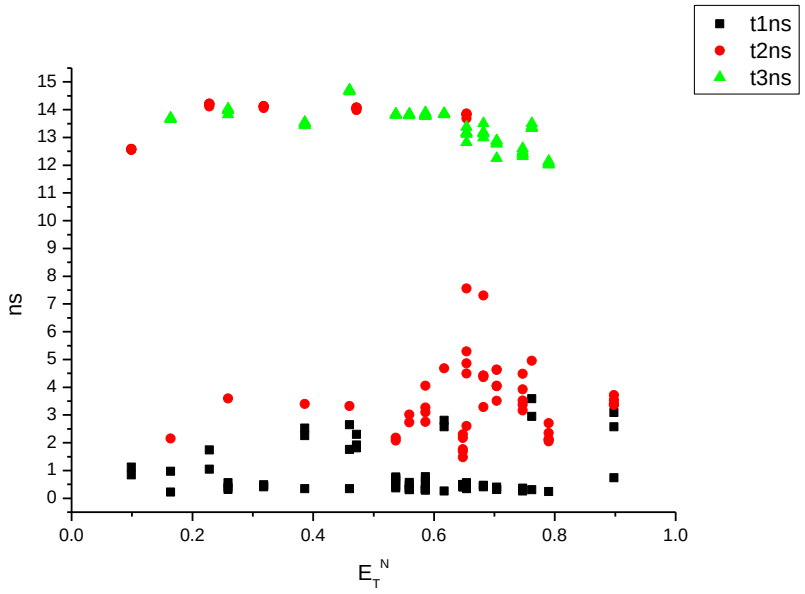

Figure 1.4.77. Intensity weighted components of TCSPC lifetime decay of **10a** (490 nm to 600 nm) versus E_T^N.

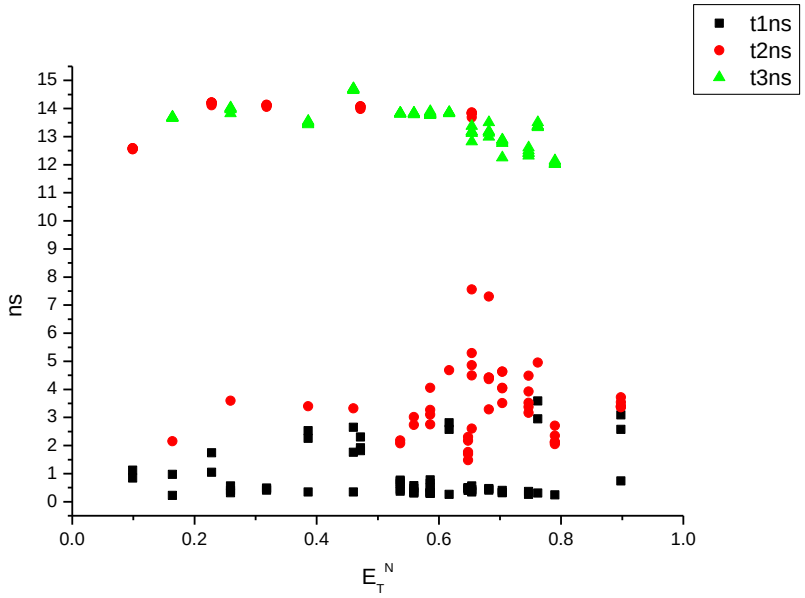

Figure 1.4.78. Amplitude weighted components of TCSPC lifetime decay of **10a** (490 nm to 600 nm) versus E_T^N.

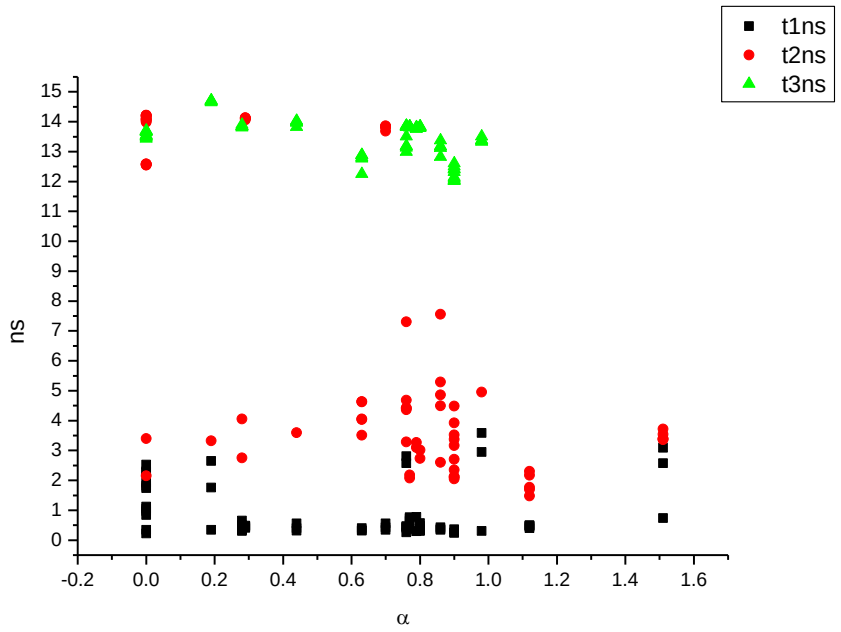

Figure 1.4.79. Intensity weighted components of TCSPC lifetime decay of **10a** (490 nm to 600 nm) versus α.

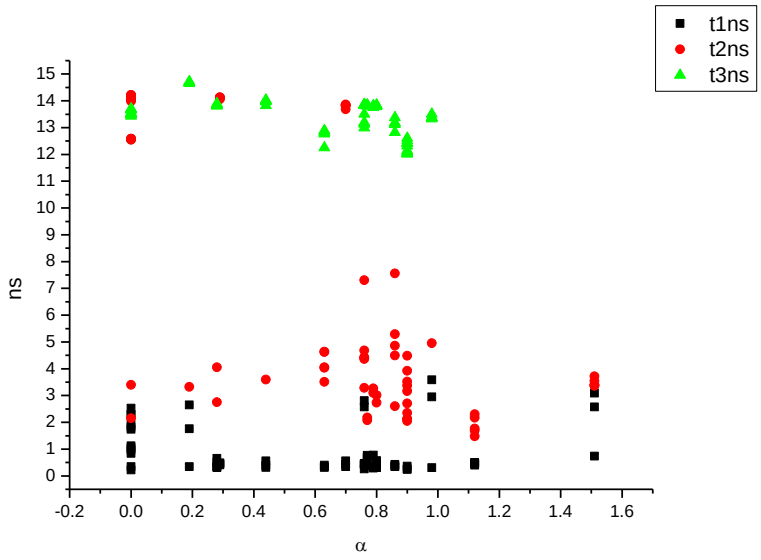

Figure 1.4.80. Amplitude weighted components of TCSPC lifetime decay of **10a** (490 nm to 600 nm) versus α.

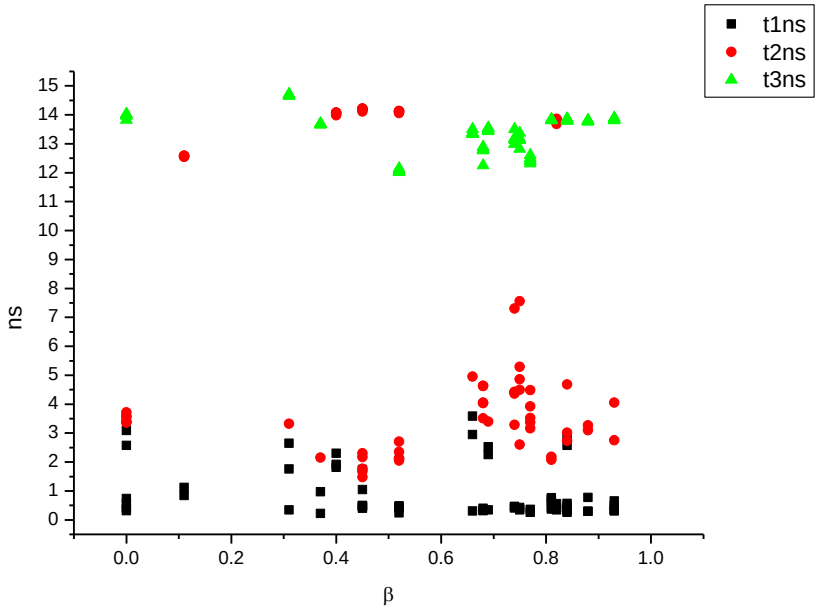

Figure 1.4.81. Intensity weighted components of TCSPC lifetime decay of **10a** (490 nm to 600 nm) versus β.

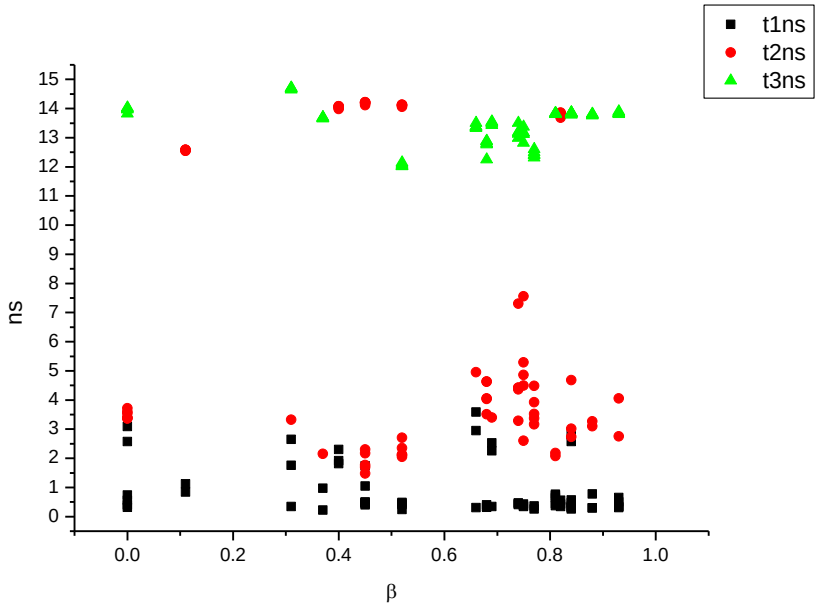

Figure 1.4.82. Amplitude weighted components of TCSPC lifetime decay of **10a** (490 nm to 600 nm) versus β.

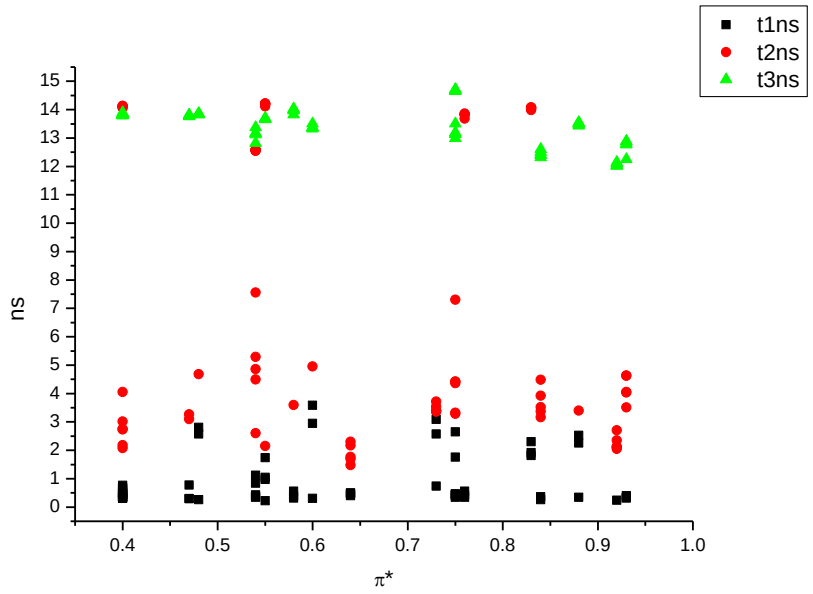

Figure 1.4.83. Intensity weighted components of TCSPC lifetime decay of **10a** (490 nm to 600 nm) versus π*.

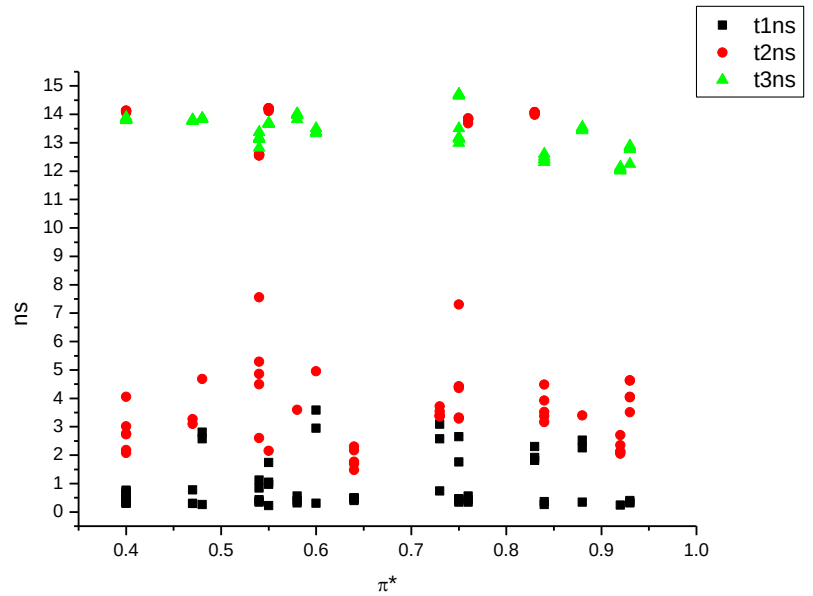

Figure 1.4.84. Amplitude weighted components of TCSPC lifetime decay of **10a** (490 nm to 600 nm) versus π*.

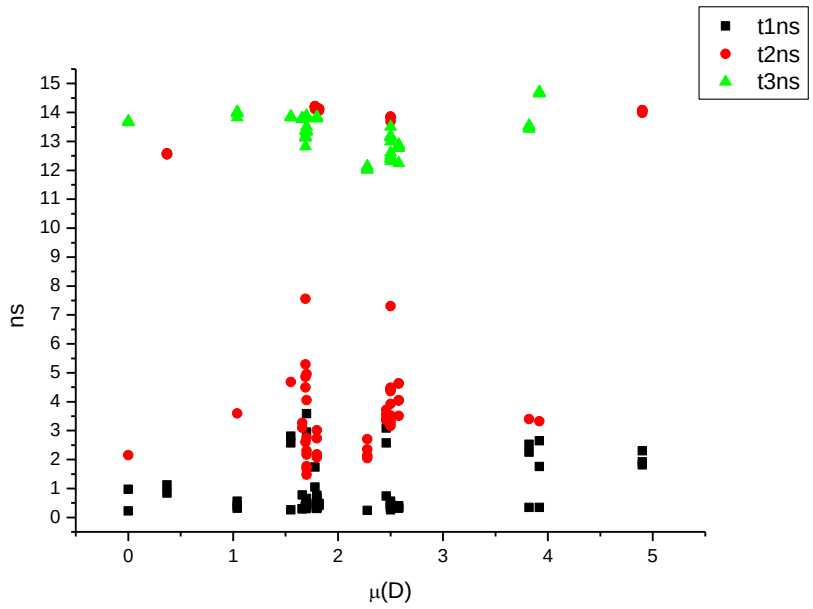

Figure 1.4.85. Intensity weighted components of TCSPC lifetime decay of **10a** (490 nm to 600 nm) versus μ(D).

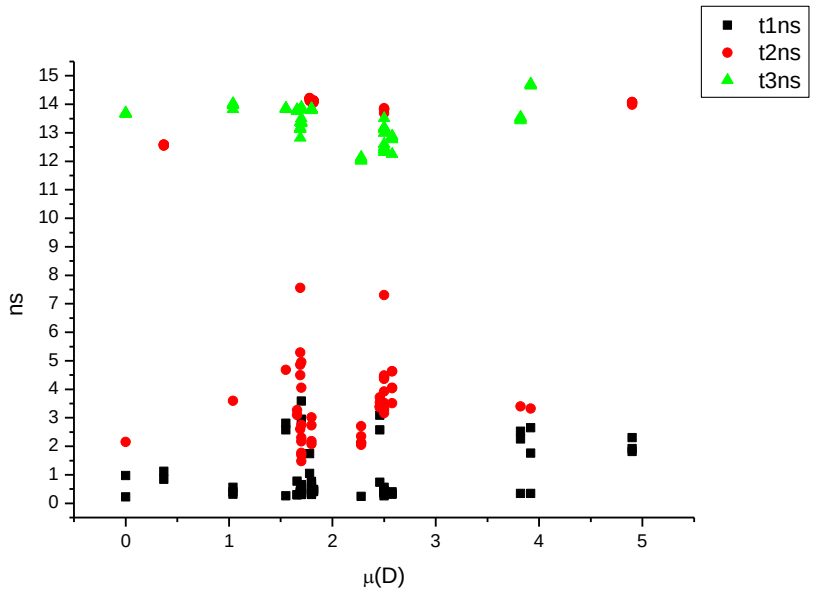

Figure 1.4.86. Amplitude weighted components of TCSPC lifetime decay of **10a** (490 nm to 600 nm) versus μ(D).

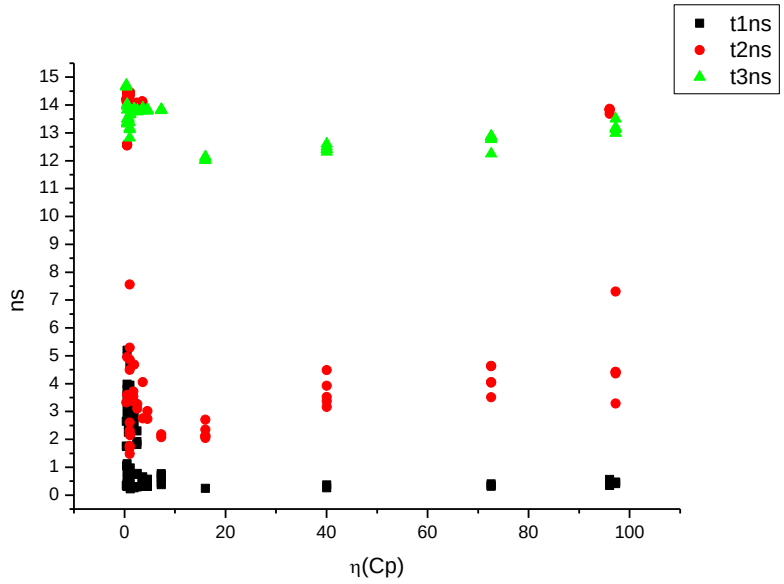

Figure 1.4.87. Intensity weighted components of TCSPC lifetime decay of **10a** (490 nm to 600 nm) versus η(Cp).

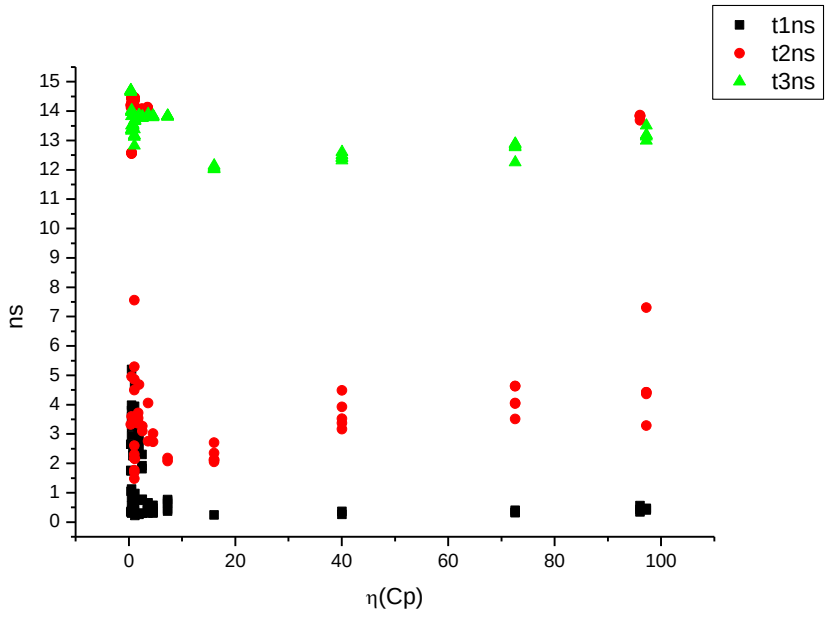

Figure 1.4.88. Amplitude weighted components of TCSPC lifetime decay of **10a** (490 nm to 600 nm) versus η(Cp).

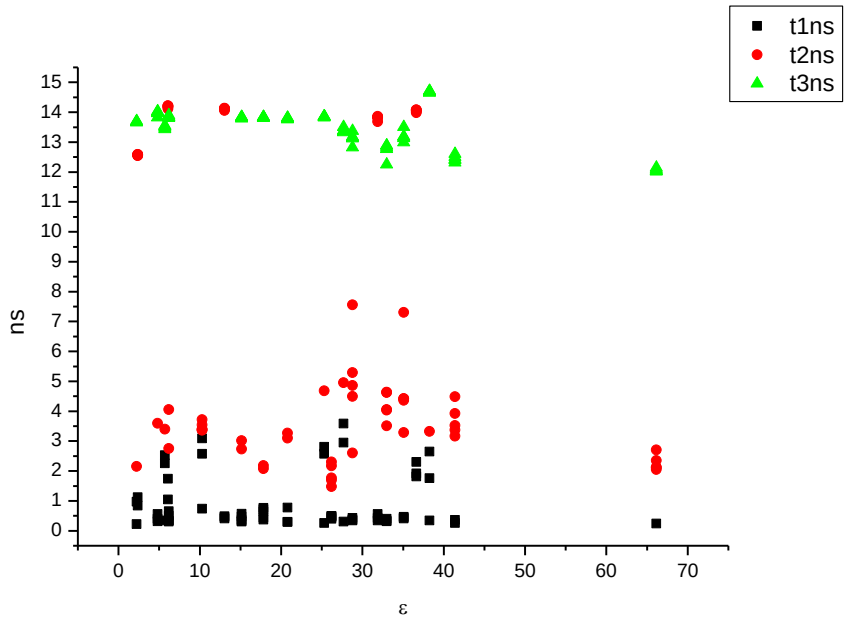

Figure 1.4.89. Intensity weighted components of TCSPC lifetime decay of **10a** (490 nm to 600 nm) versus ε.

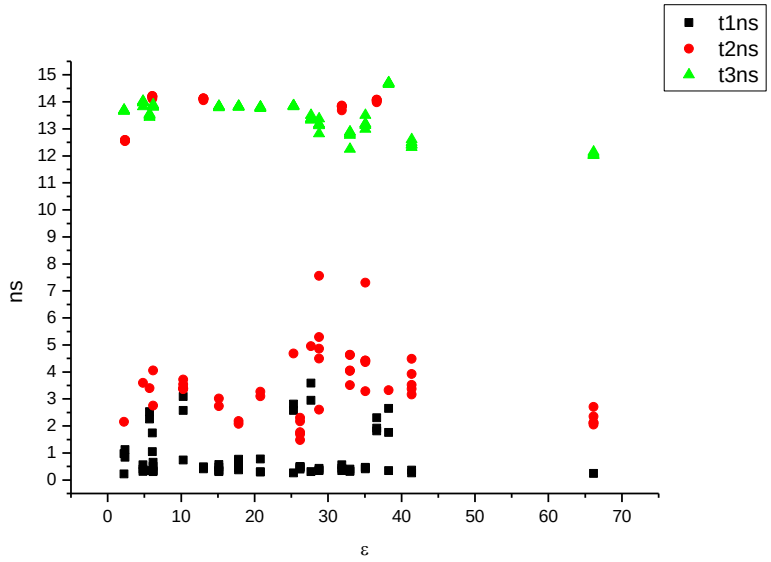

Figure 1.4.90. Amplitude weighted components of TCSPC lifetime decay of **10a** (490 nm to 600 nm) versus ε.

1.4.7.1 490 nm Lifetime – Solvatochromic analysis.

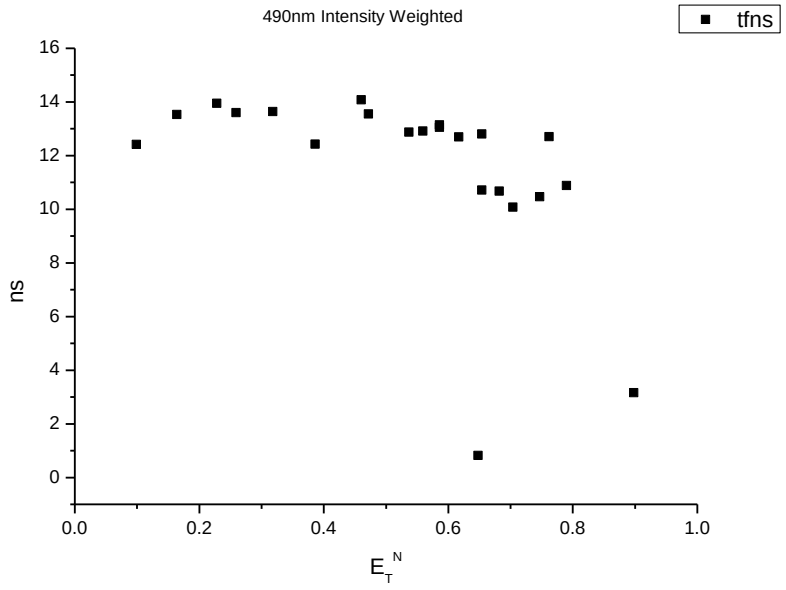

Figure 1.4.91. Intensity weighted average lifetime (τ_f) of **10a** at 490 nm versus E_T^N.

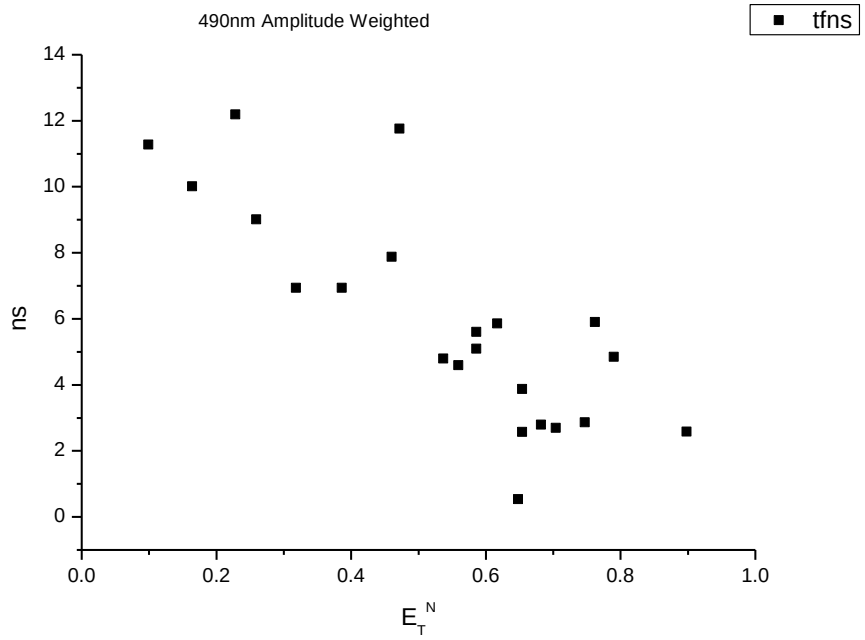

Figure 1.4.92. Amplitude weighted average lifetime (τ_f) of **10a** at 490 nm versus E_T^N.

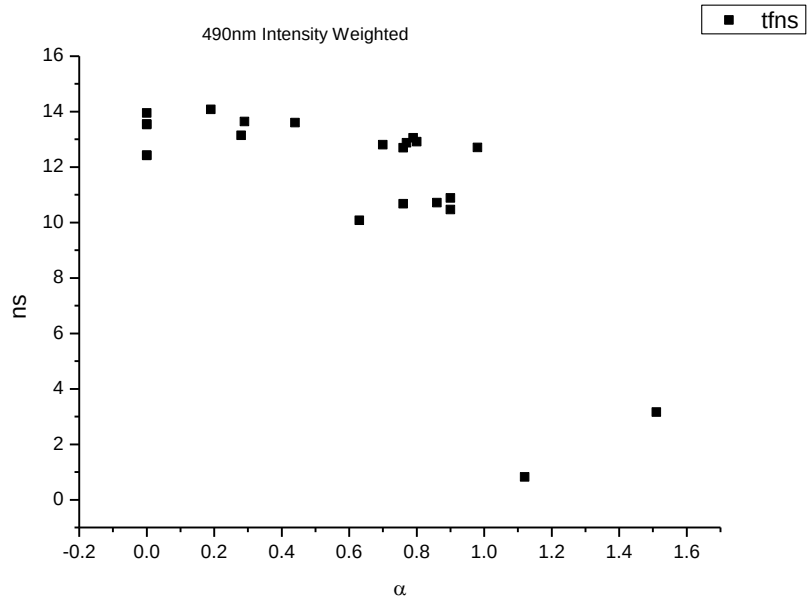

Figure 1.4.93. Intensity weighted average lifetime (τ_f) of **10a** at 490 nm versus α.

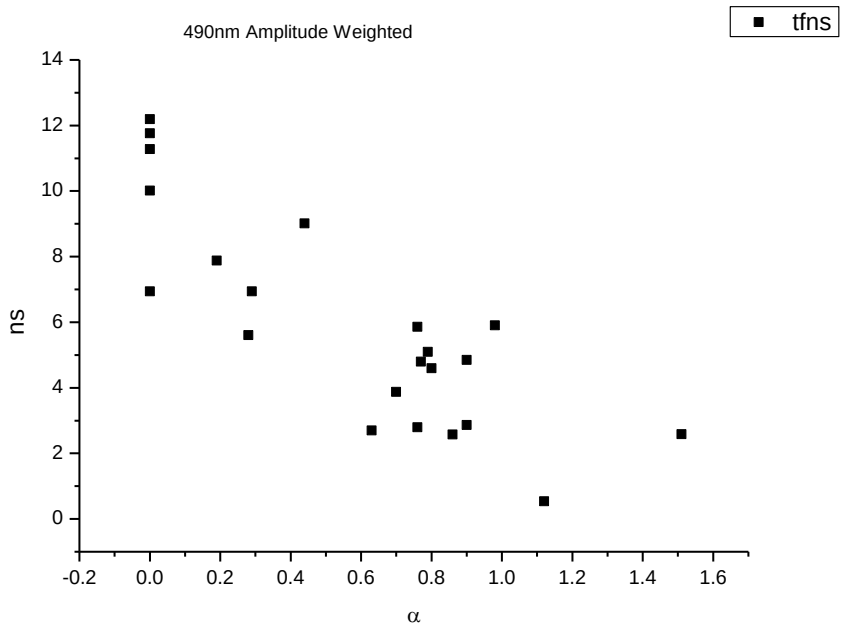

Figure 1.4.94. Amplitude weighted average lifetime (τ_f) of **10a** at 490 nm versus α.

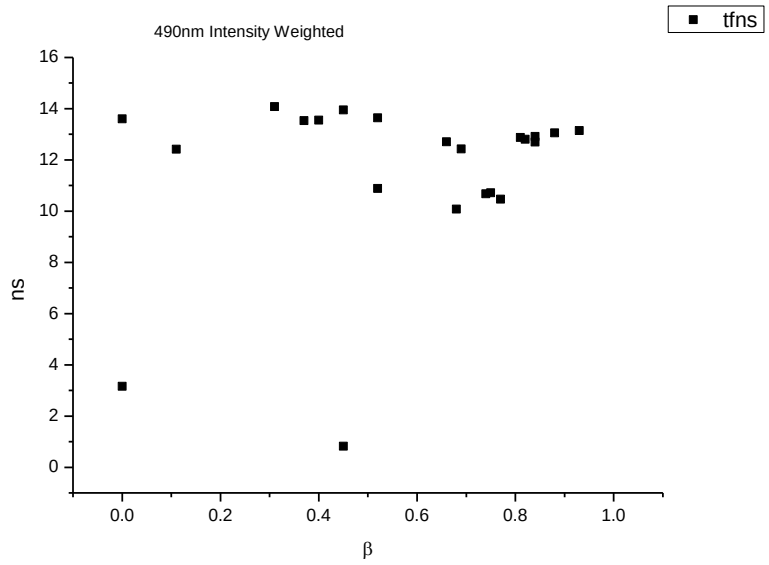

Figure 1.4.95. Intensity weighted average lifetime (τ_f) of **10a** at 490 nm versus β.

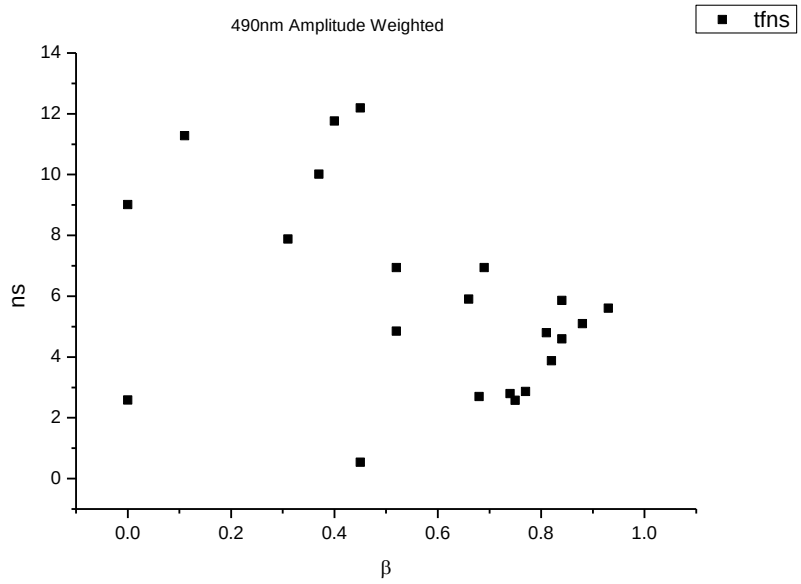

Figure 1.4.96. Amplitude weighted average lifetime (τ_f) of **9a** at 490 nm versus β.

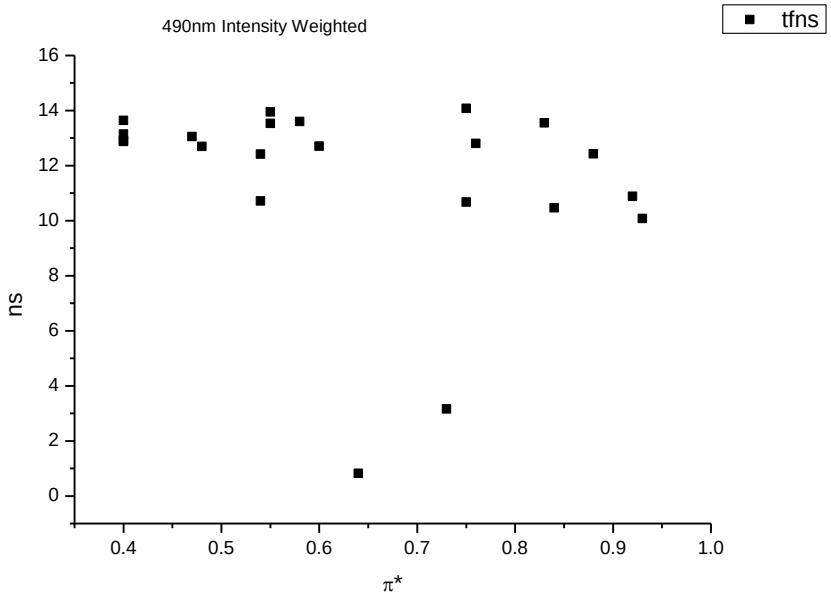

Figure 1.4.97. Intensity weighted average lifetime (τ_f) of **10a** at 490 nm versus π*.

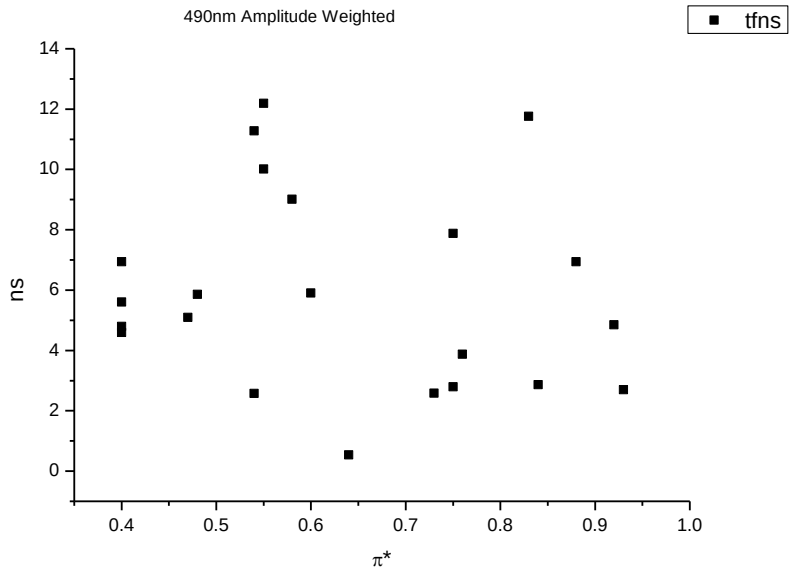

Figure 1.4.98. Amplitude weighted average lifetime (τ_f) of **10a** at 490 nm versus π*.

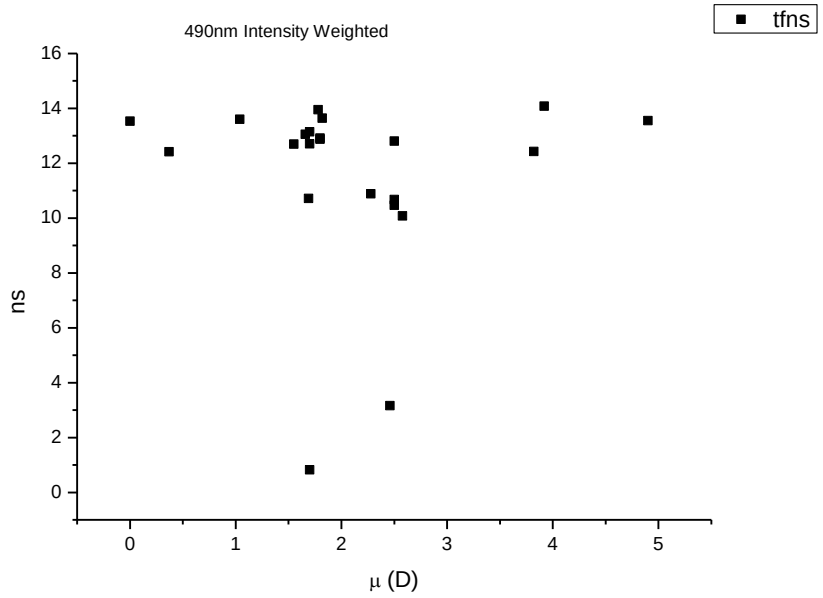

Figure 1.4.99. Intensity weighted average lifetime (τ_f) of **10a** at 490 nm versus μ(D).

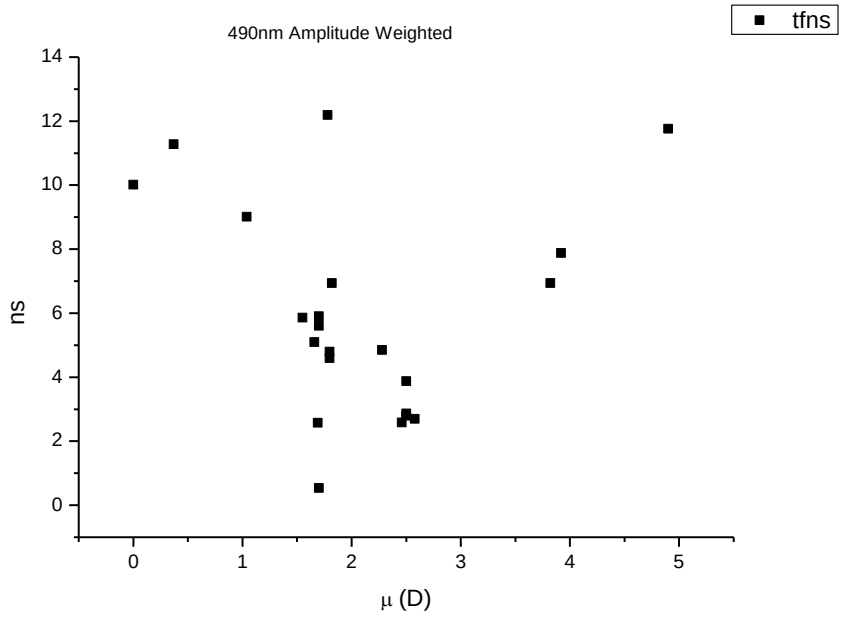

Figure 1.4.100. Amplitude weighted average lifetime (τ_f) of **10a** at 490 nm versus μ(D).

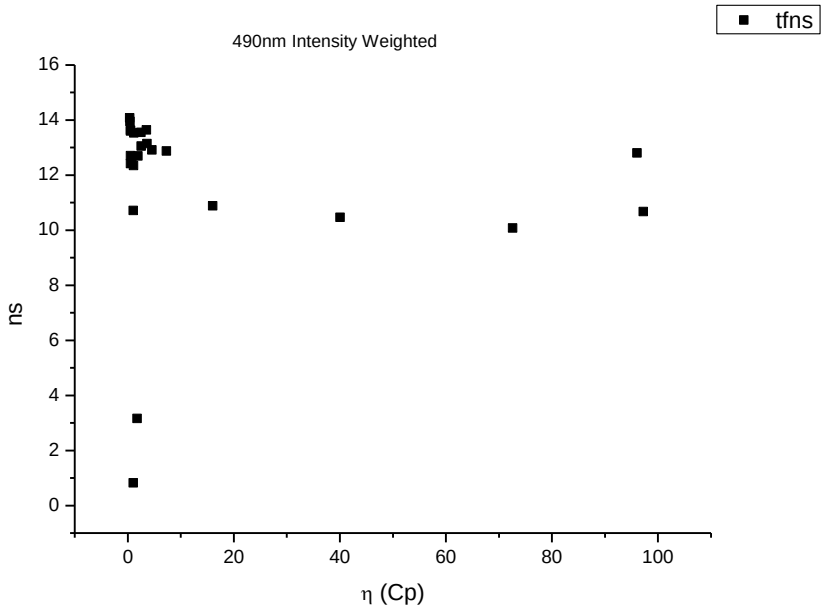

Figure 1.4.101. Intensity weighted average lifetime (τ_f) of **10a** at 490 nm versus η(Cp).

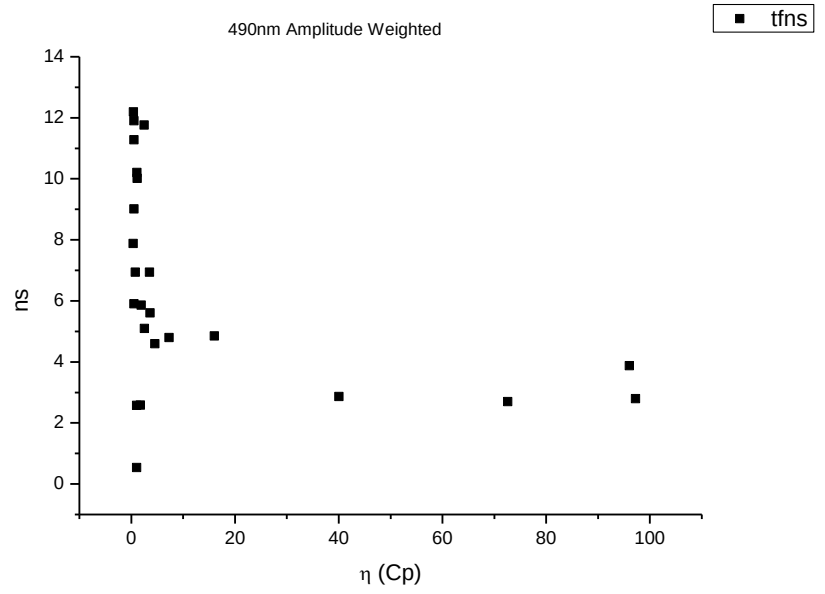

Figure 1.4.102. Amplitude weighted average lifetime (τ_f) of **10a** at 490 nm versus η(Cp).

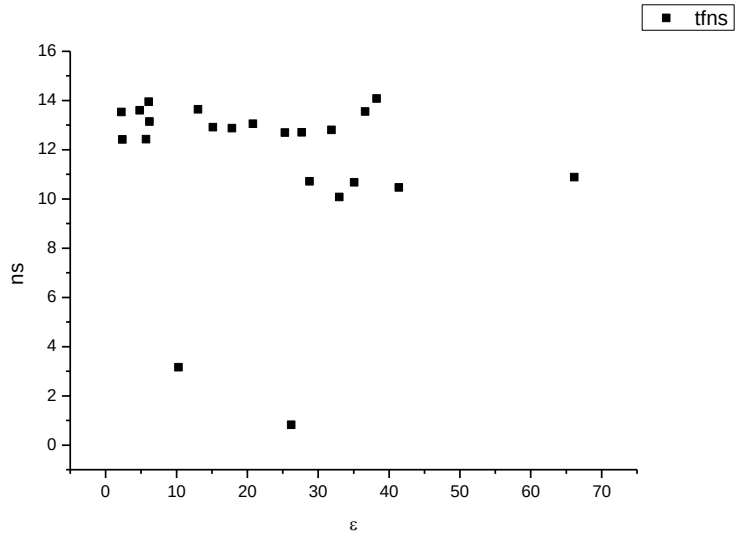

Figure 1.4.103. Intensity weighted average lifetime (τ_f) of **10a** at 490 nm versus ε.

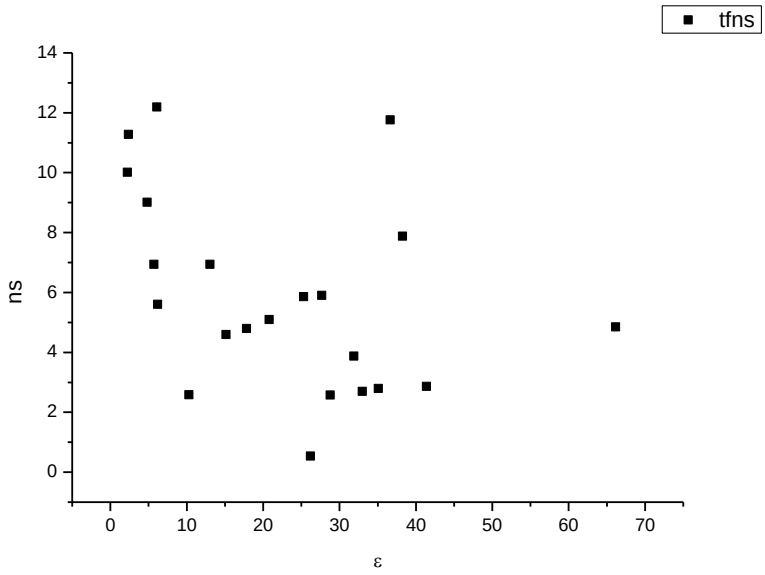

Figure 1.4.104. Amplitude weighted average lifetime (τ_f) of **10a** at 490 nm versus ε.

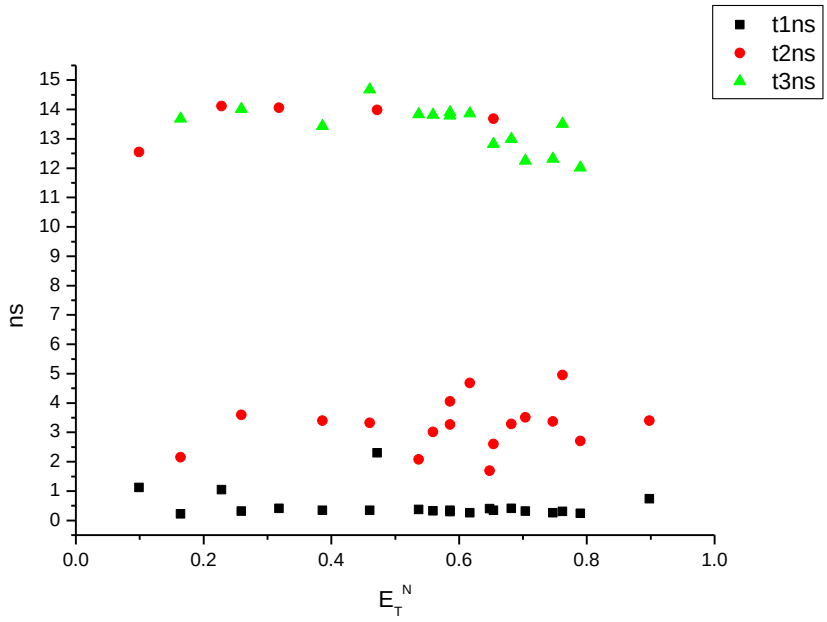

Figure 1.4.105. Intensity weighted components of TCSPC lifetime decay of **10a** (490 nm) versus E_T^N.

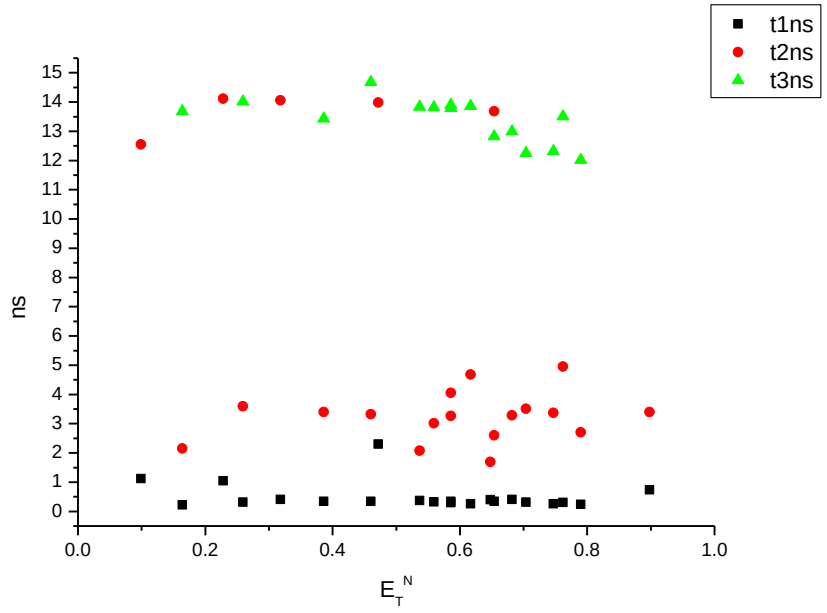

Figure 1.4.106. Amplitude weighted components of TCSPC lifetime decay of **10a** (490 nm) versus E_T^N.

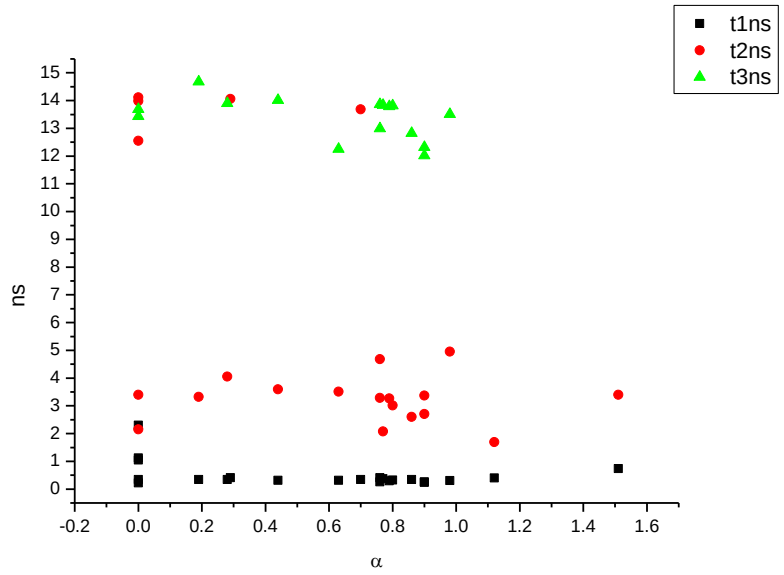

Figure 1.4.107. Intensity weighted components of TCSPC lifetime decay of **10a** (490 nm) versus α.

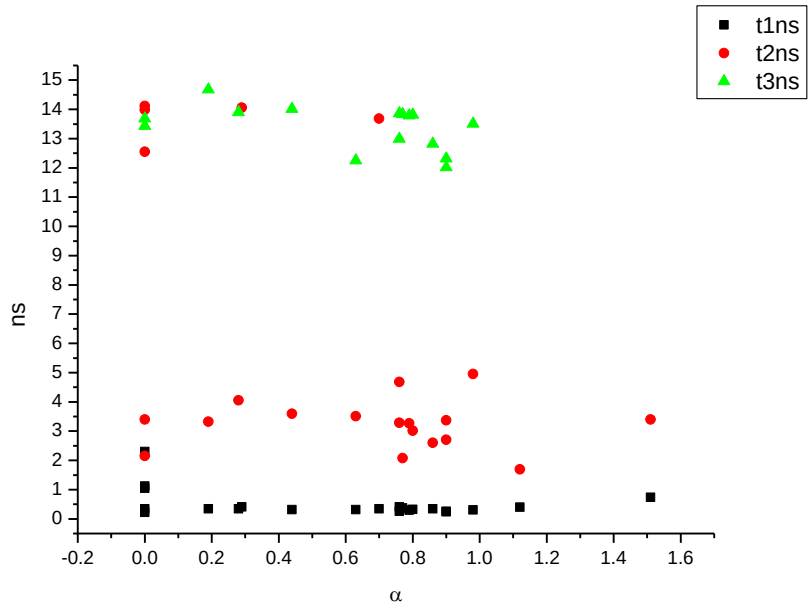

Figure 1.4.108. Amplitude weighted components of TCSPC lifetime decay of **10a** (490 nm) versus α.

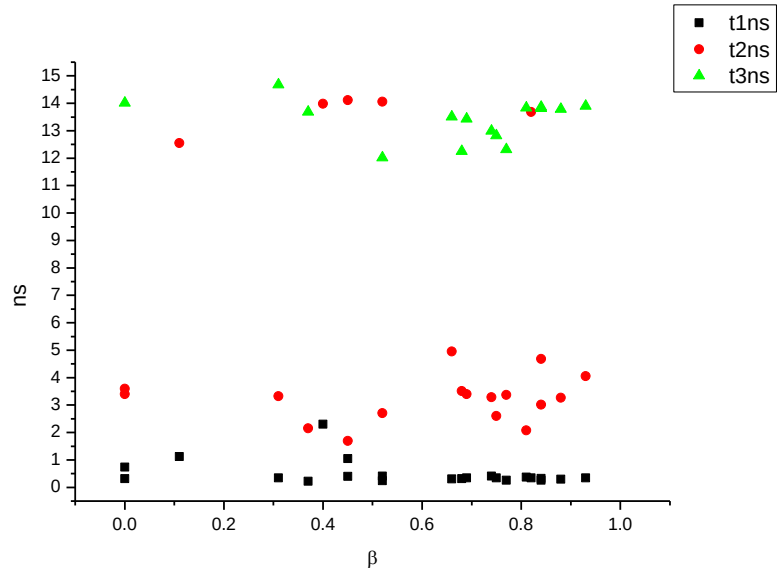

Figure 1.4.109. Intensity weighted components of TCSPC lifetime decay of **10a** (490 nm) versus β.

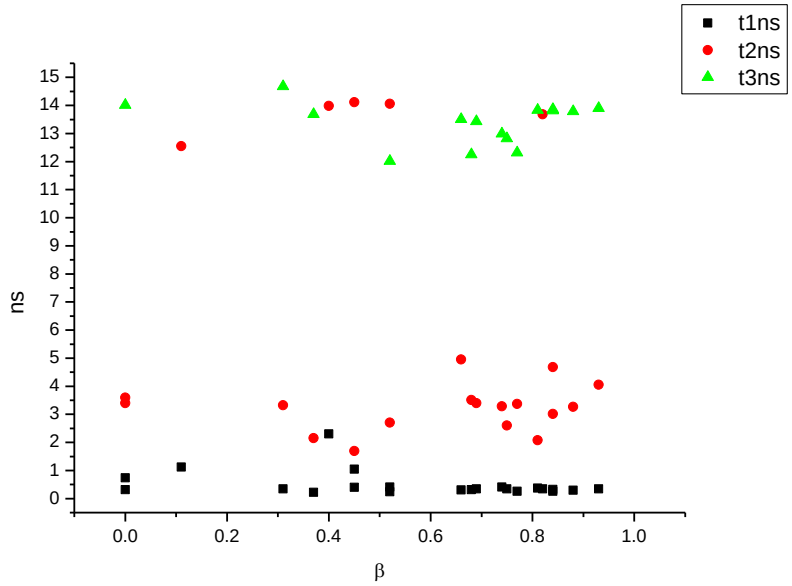

Figure 1.4.110. Amplitude weighted components of TCSPC lifetime decay of **10a** (490 nm) versus β.

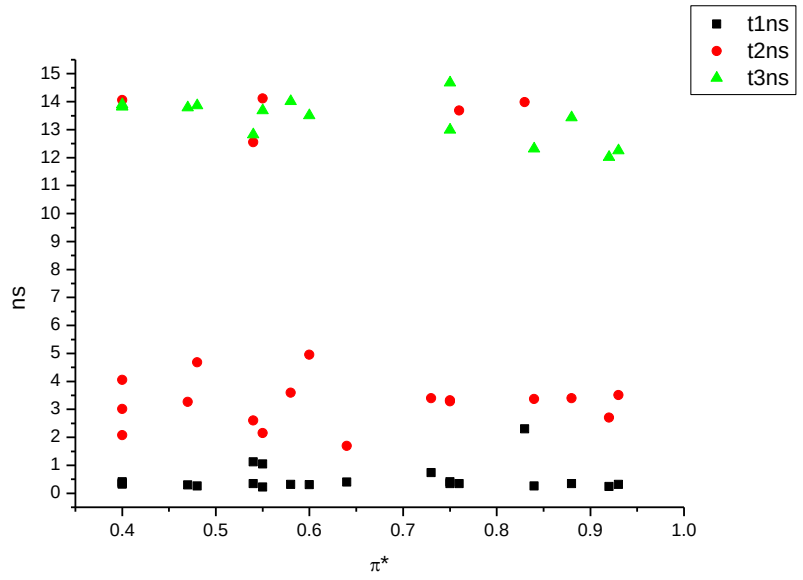

Figure 1.4.111. Intensity weighted components of TCSPC lifetime decay of **10a** (490 nm) versus π*.

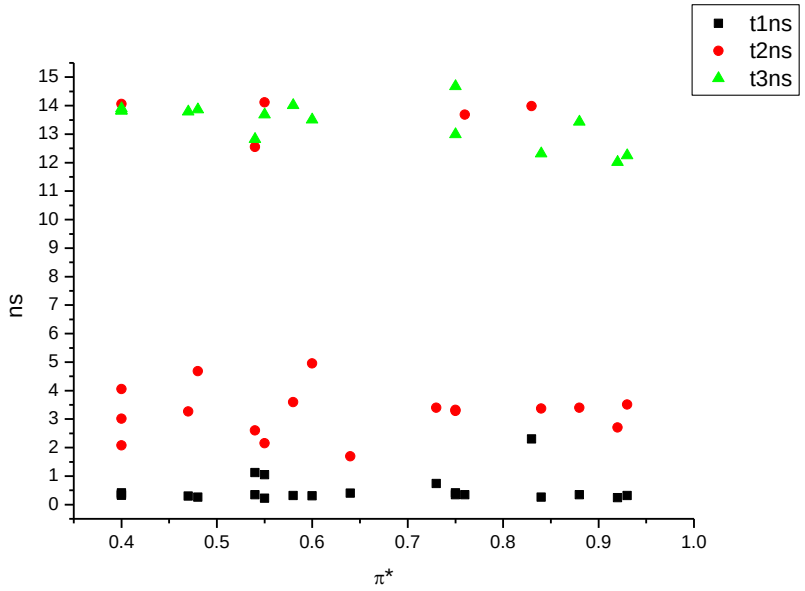

Figure 1.4.112. Amplitude weighted components of TCSPC lifetime decay of **10a** (490 nm) versus π*.

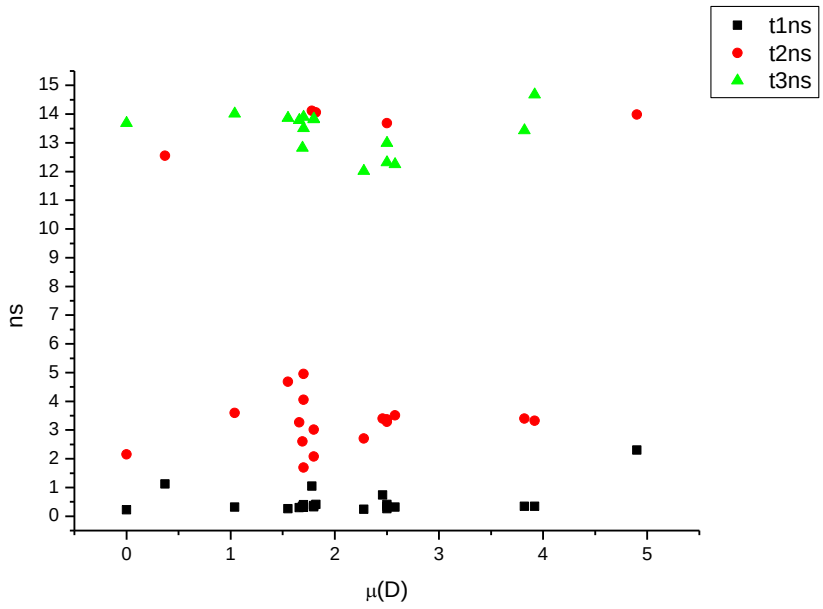

Figure 1.4.113. Intensity weighted components of TCSPC lifetime decay of **10a** (490 nm) versus μ(D).

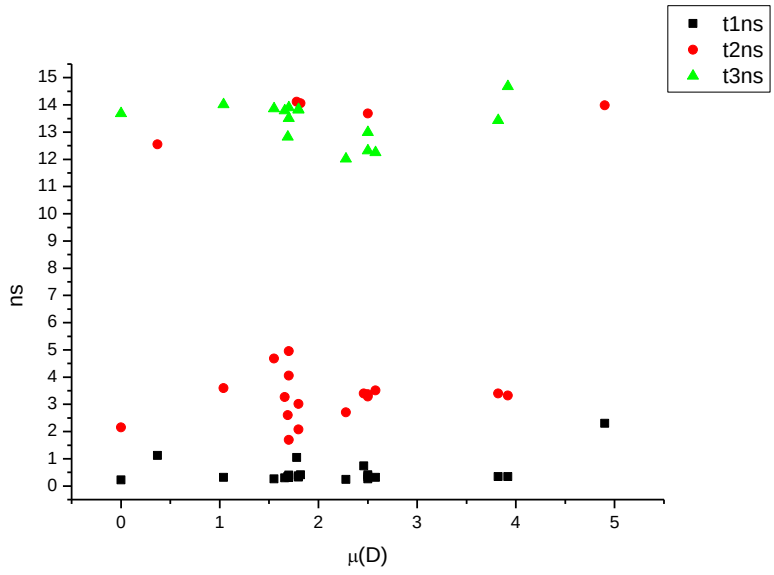

Figure 1.4.114. Amplitude weighted components of TCSPC lifetime decay of **10a** (490 nm) versus μ(D).

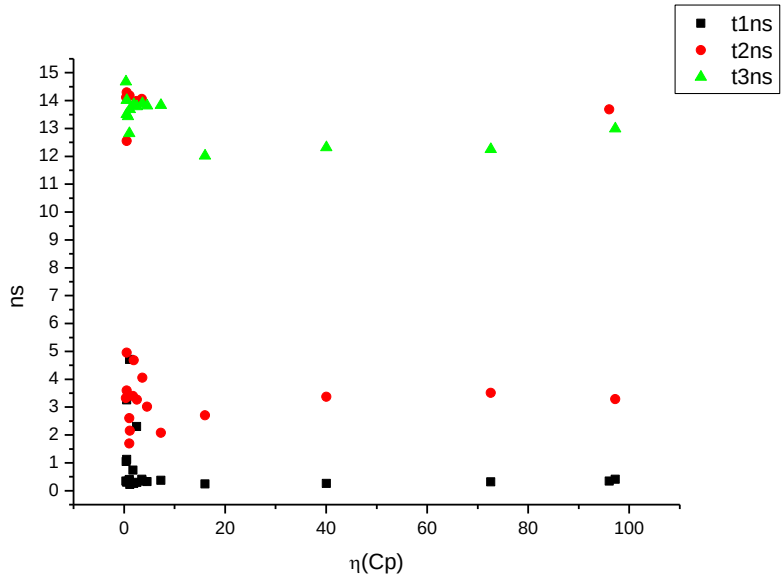

Figure 1.4.115. Intensity weighted components of TCSPC lifetime decay of **10a** (490 nm) versus η(Cp).

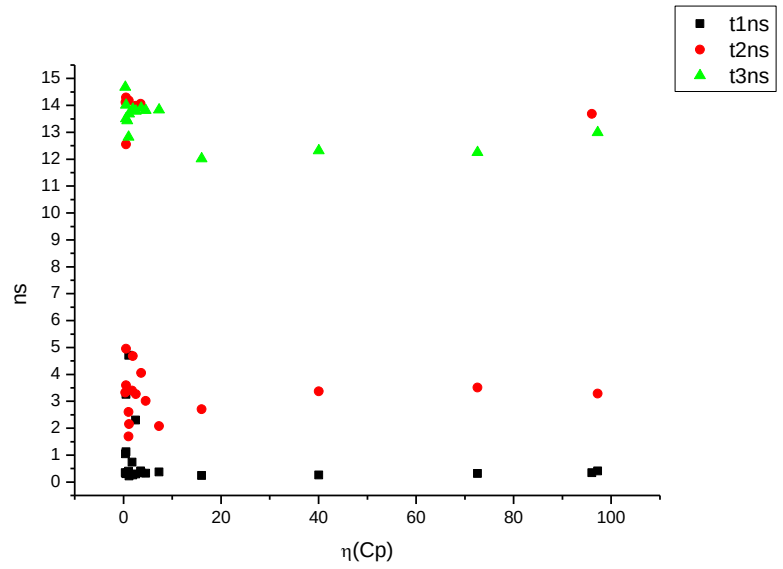

Figure 1.4.116. Amplitude weighted components of TCSPC lifetime decay of **10a** (490 nm) versus η(Cp).

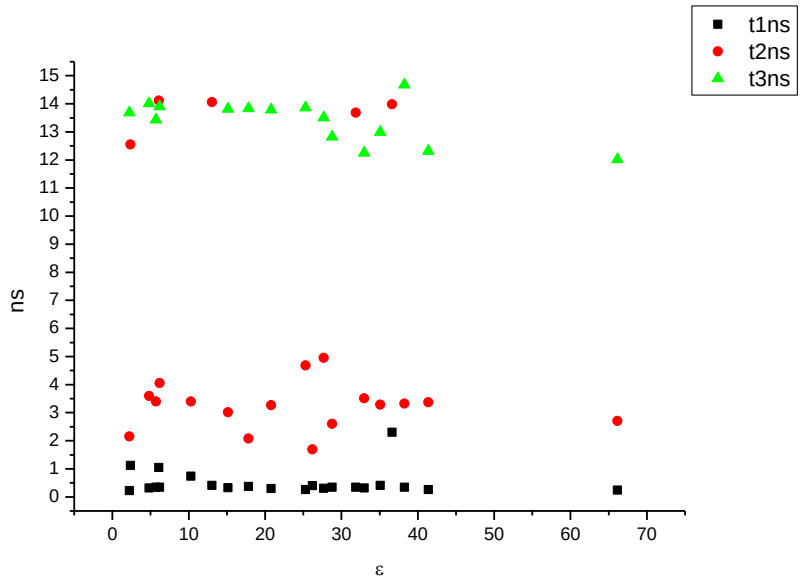

Figure 1.4.117. Intensity weighted components of TCSPC lifetime decay of **10a** (490 nm) versus ε.

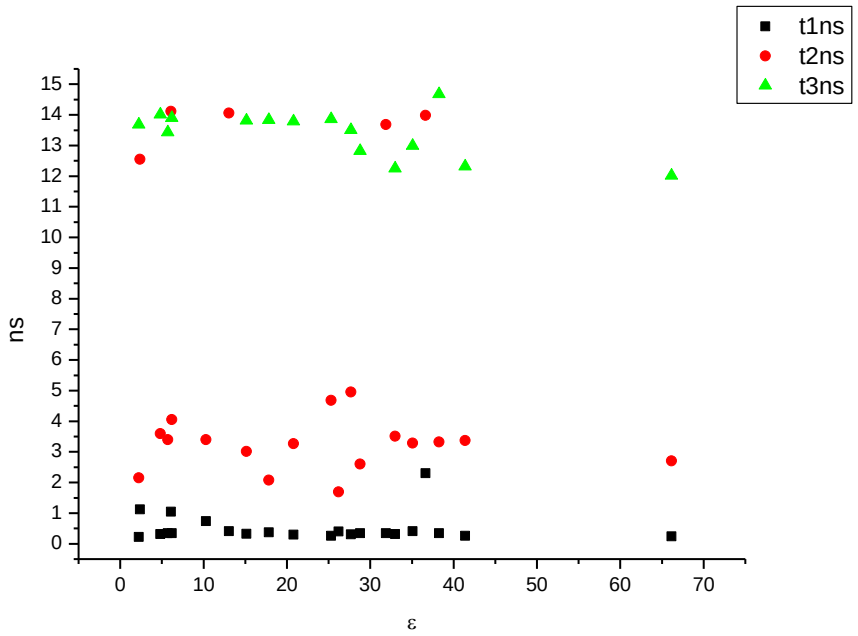

Figure 1.4.118. Amplitude weighted components of TCSPC lifetime decay of **10a** (490 nm) versus ε.

1.4.7.2 600 nm Lifetime – Solvatochromic analysis.

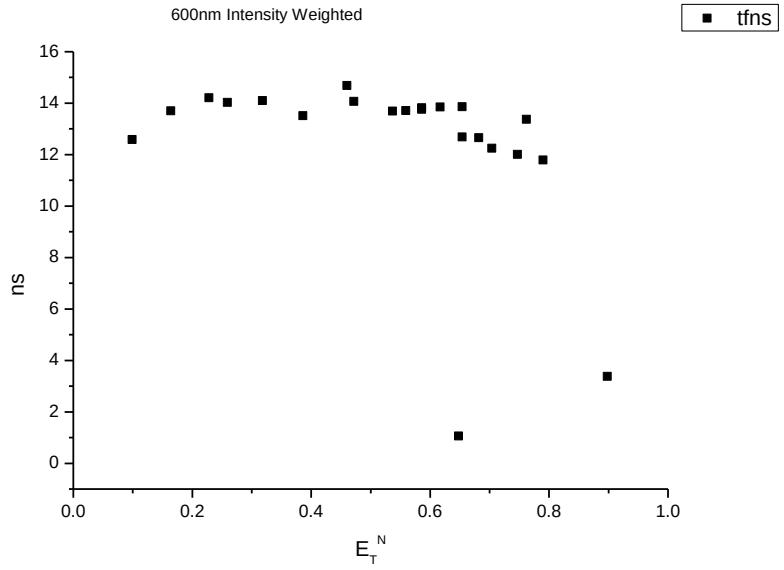

Figure 1.4.119. Intensity weighted average lifetime (τ_f) of **10a** at 600 nm versus E_T^N.

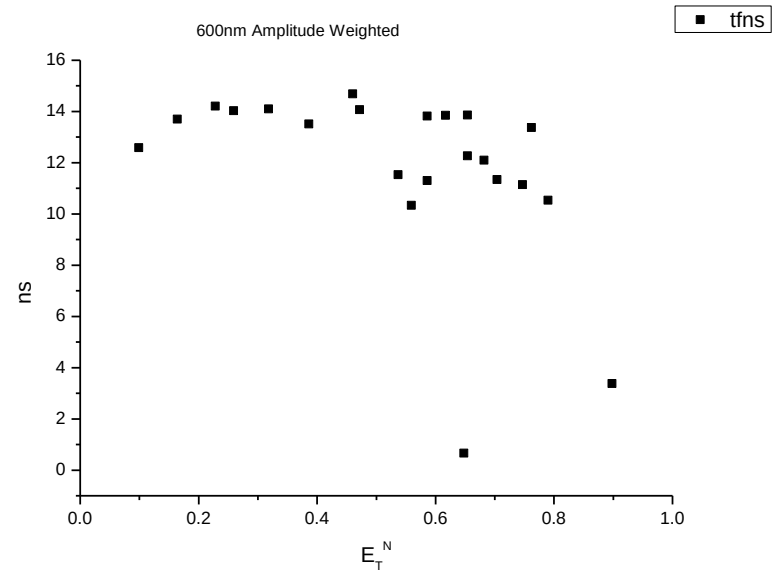

Figure 1.4.120. Amplitude weighted average lifetime (τ_f) of **10a** at 600 nm versus E_T^N.

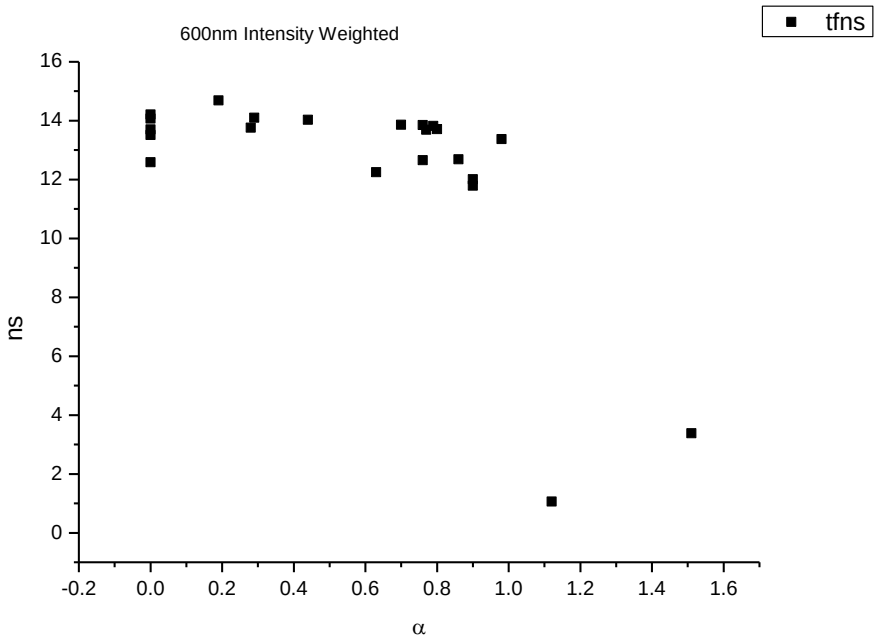

Figure 1.4.121. Intensity weighted average lifetime (τ_f) of **10a** at 600 nm versus α.

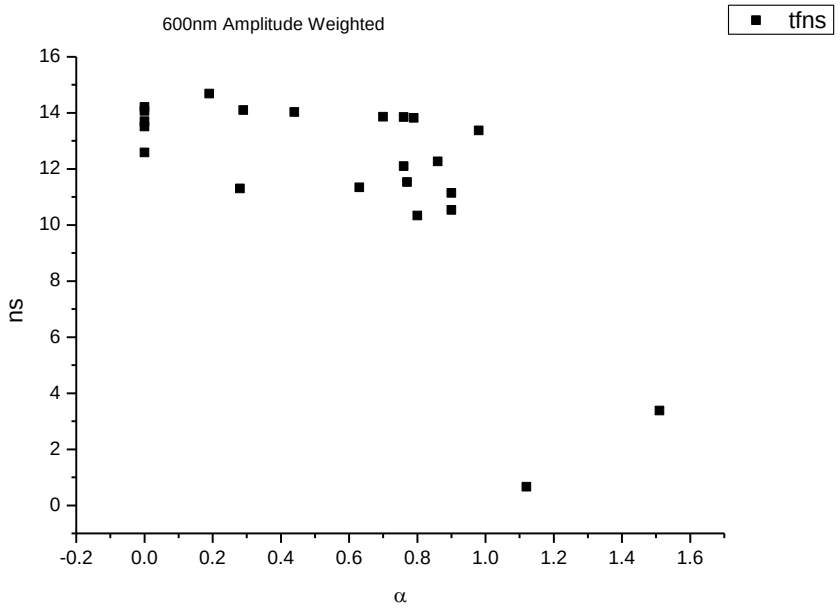

Figure 1.4.122. Amplitude weighted average lifetime (τ_f) of **10a** at 600 nm versus α.

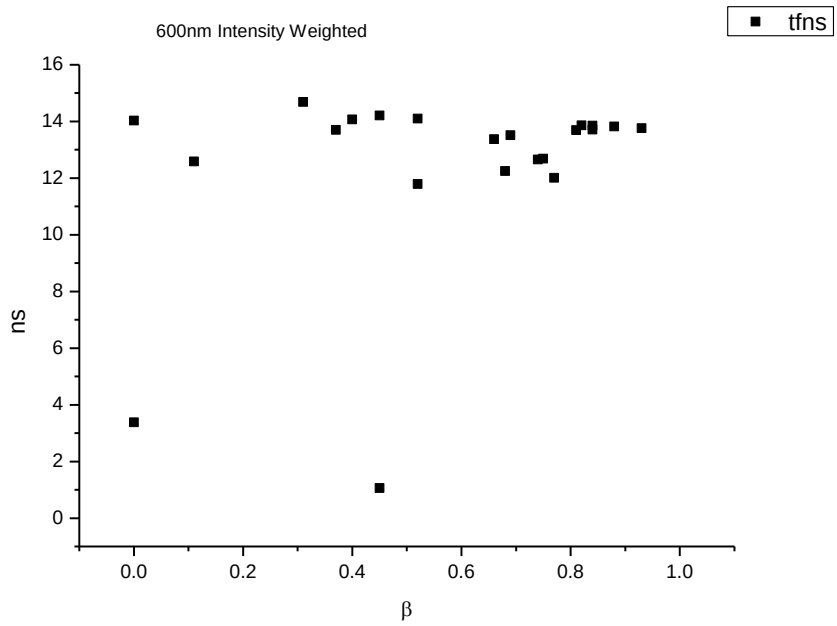

Figure 1.4.123. Intensity weighted average lifetime (τ_f) of **10a** at 600 nm versus β.

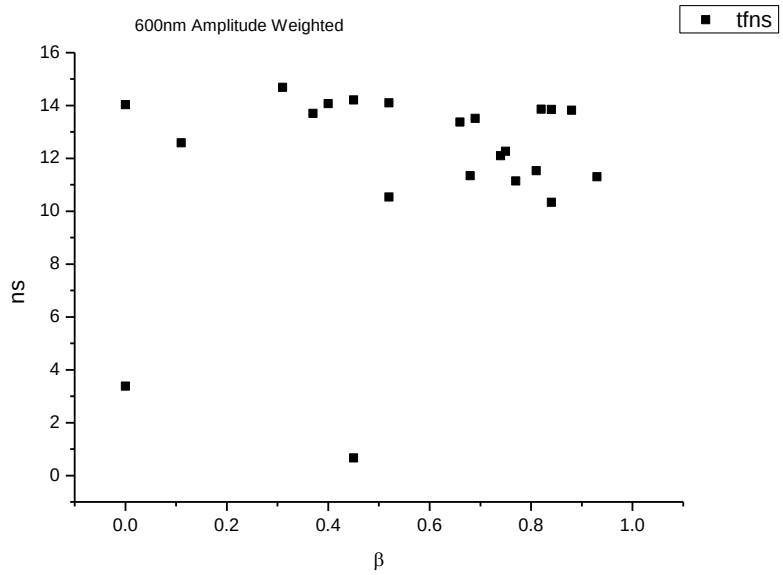

Figure 1.4.124. Amplitude weighted average lifetime (τ_f) of **10a** at 600 nm versus β.

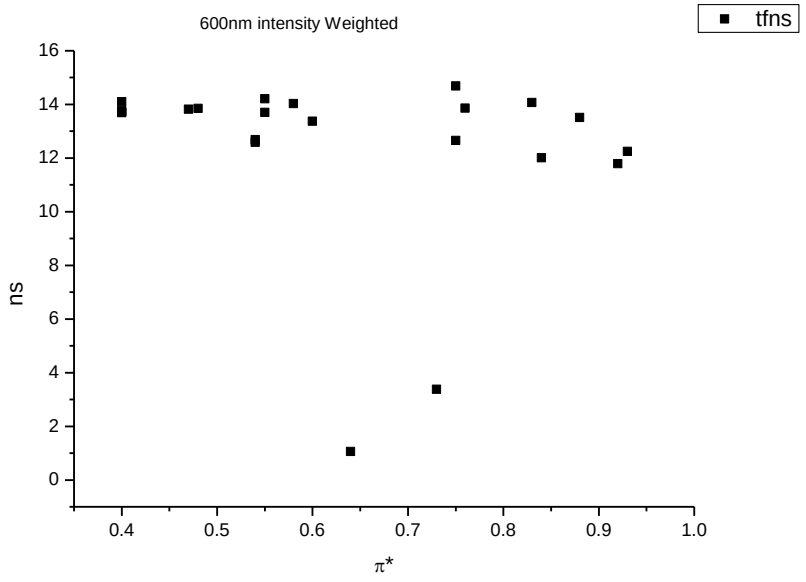

Figure 1.4.125. Intensity weighted average lifetime (τ_f) of **10a** at 600 nm versus π*.

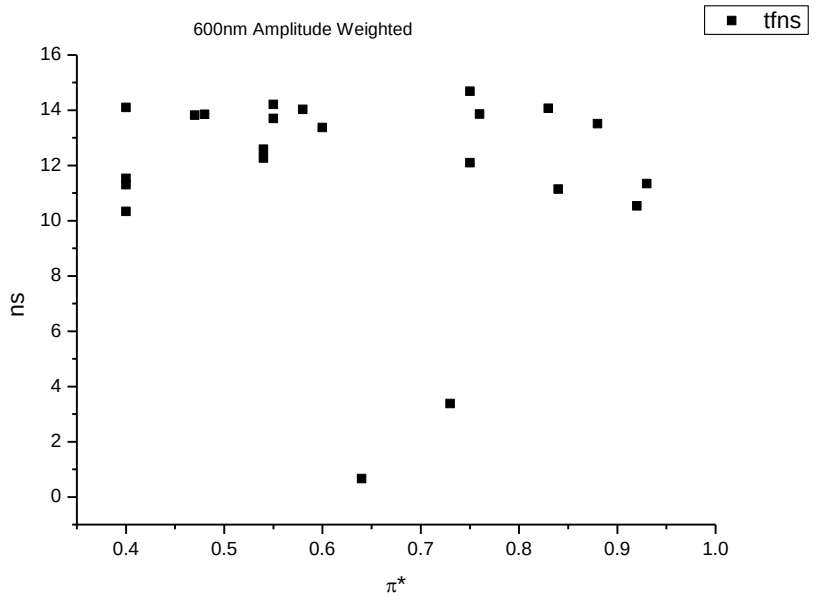

Figure 1.4.126. Amplitude weighted average lifetime (τ_f) of **10a** at 600 nm versus π*.

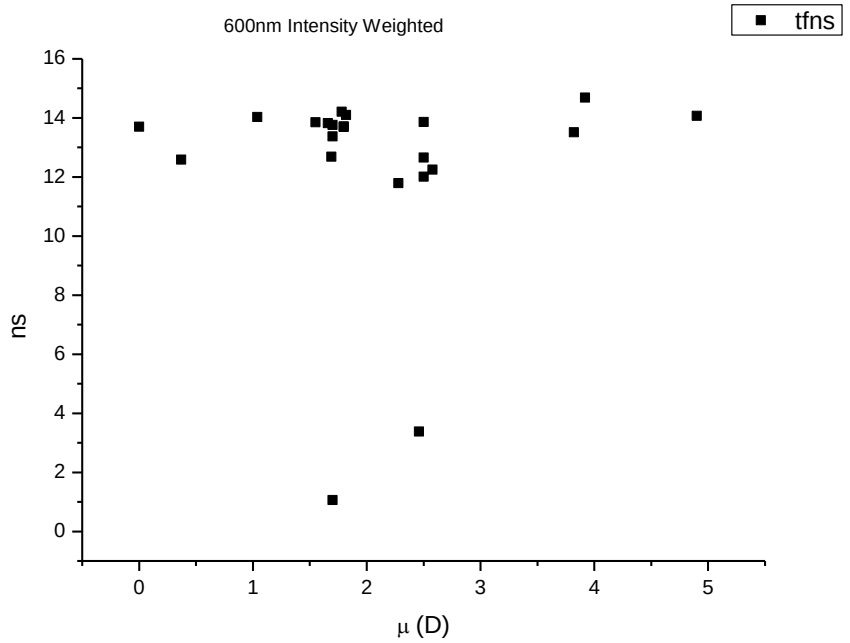

Figure 1.4.127. Intensity weighted average lifetime (τ_f) of **10a** at 600 nm versus μ(D).

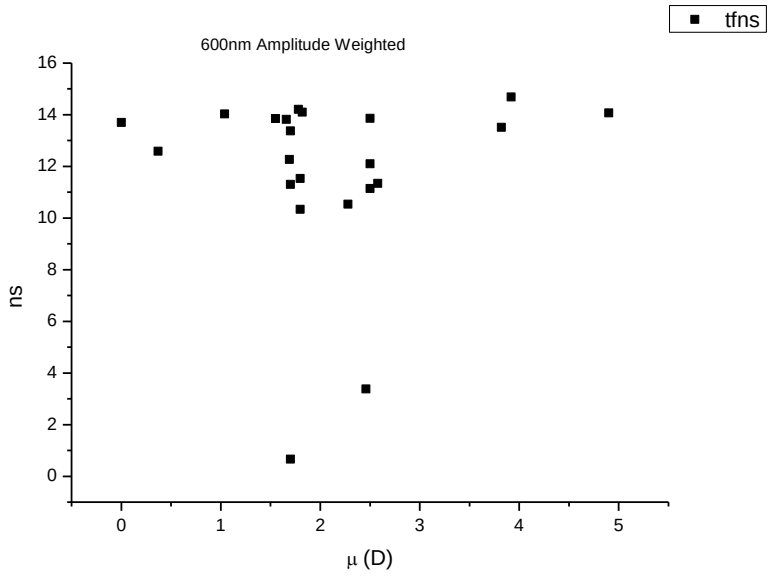

Figure 1.4.128. Amplitude weighted average lifetime (τ_f) of **10a** at 600 nm versus μ(D).

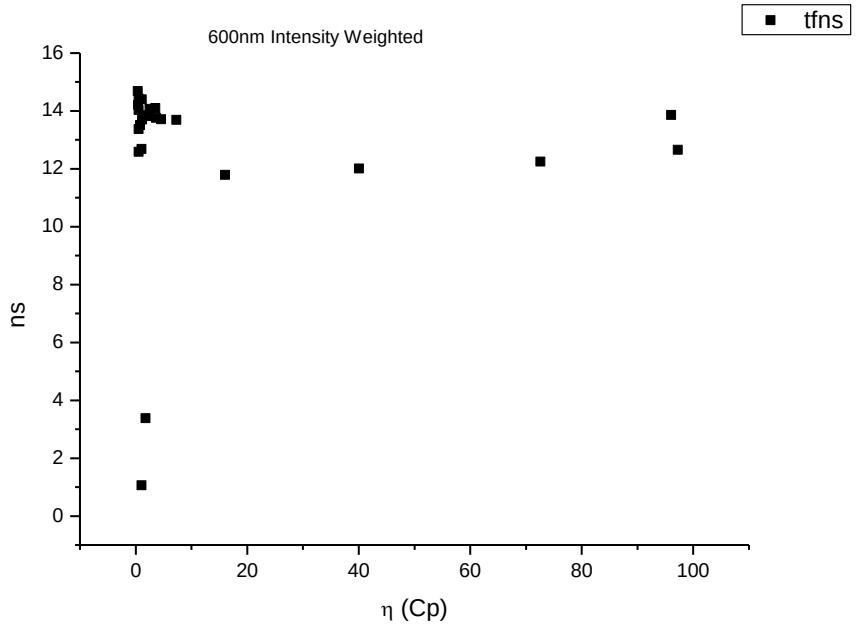

Figure 1.4.129. Intensity weighted average lifetime (τ_f) of **10a** at 600 nm versus η(Cp).

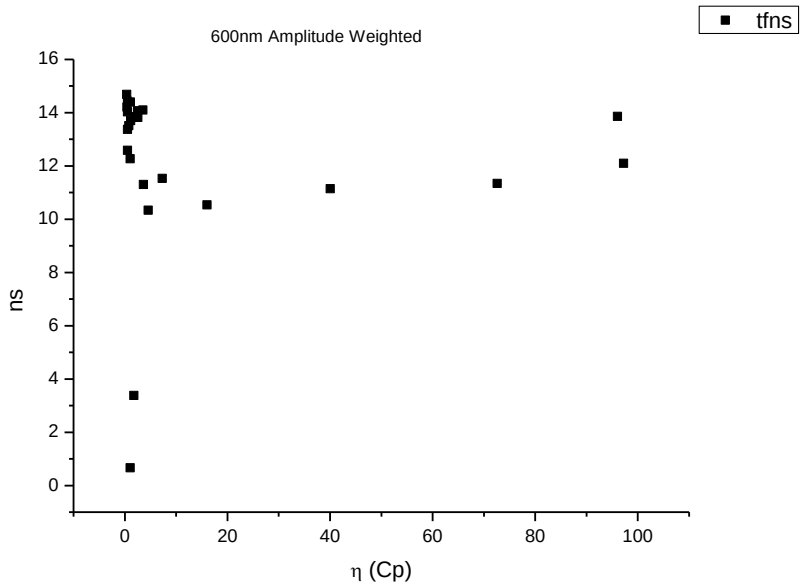

Figure 1.4.130. Amplitude weighted average lifetime (τ_f) of **10a** at 600 nm versus η(Cp).

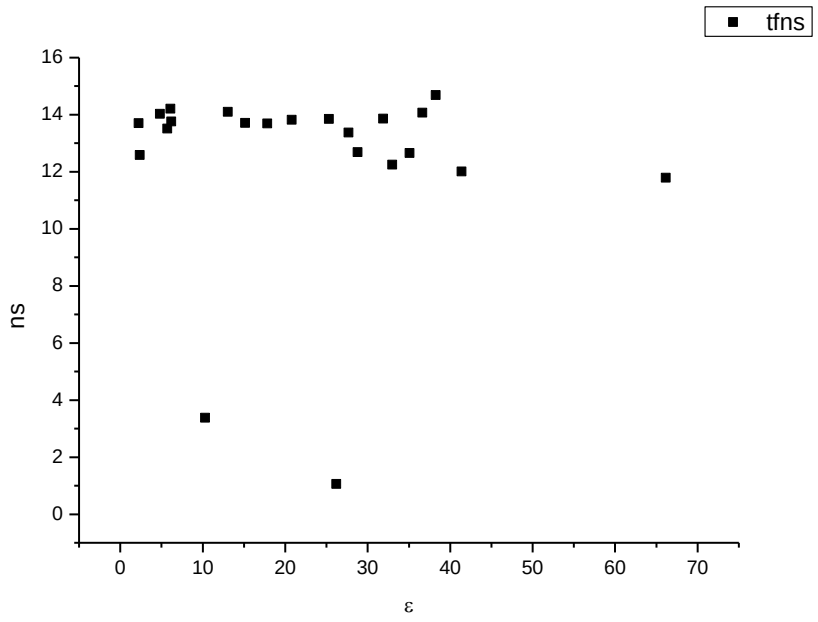

Figure 1.4.131. Intensity weighted average lifetime (τ_f) of **10a** at 600 nm versus ε.

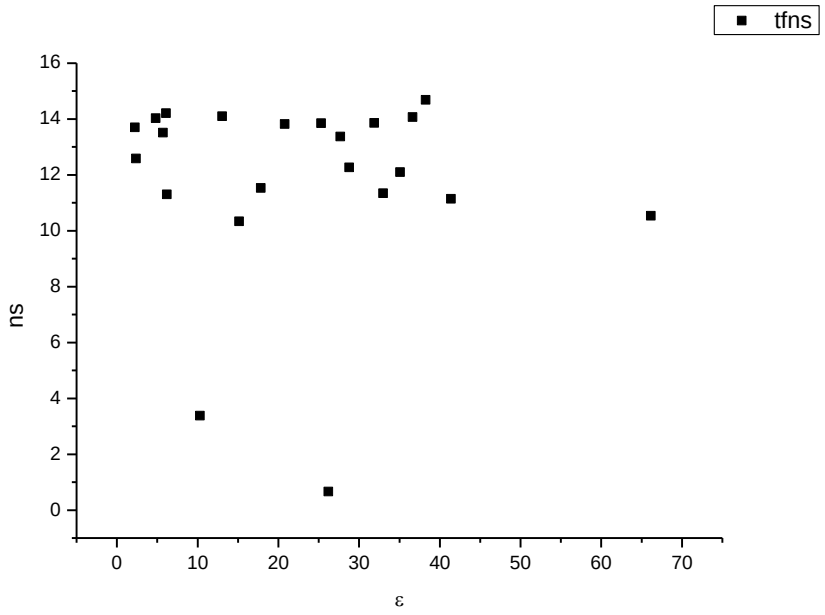

Figure 1.4.132. Amplitude weighted average lifetime (τ_f) of **10a** at 600 nm versus ε.

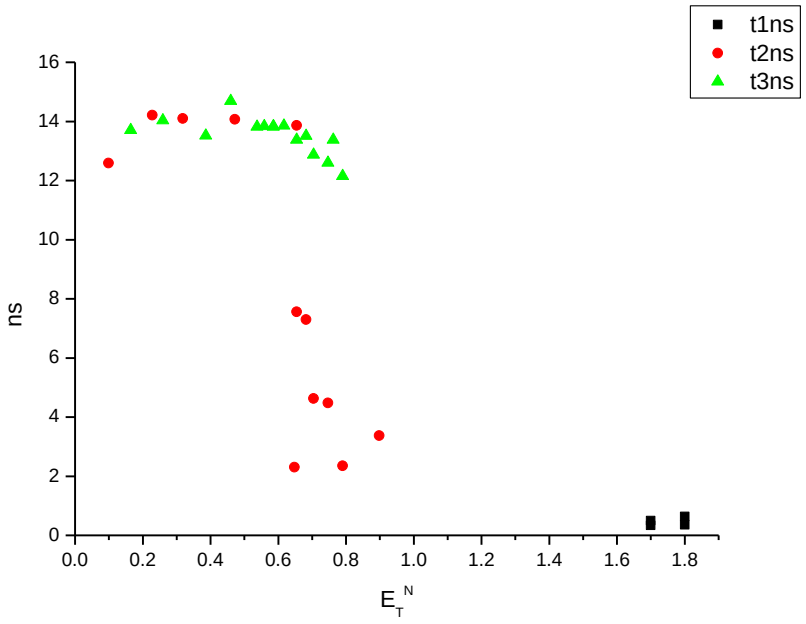

Figure 1.4.133. Intensity weighted components of TCSPC lifetime decay of **10a** (600 nm) versus E_T^N.

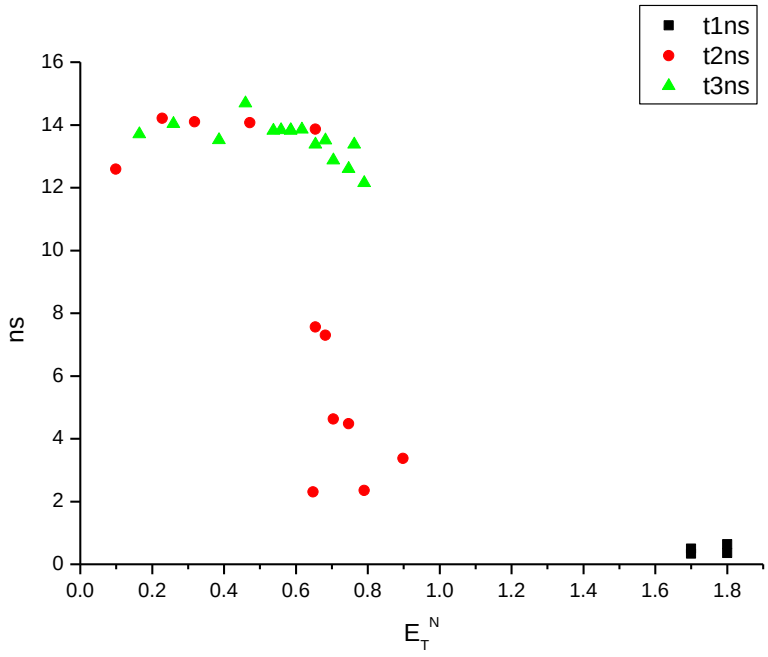

Figure 1.4.134. Amplitude weighted components of TCSPC lifetime decay of **10a** (600 nm) versus E_T^N.

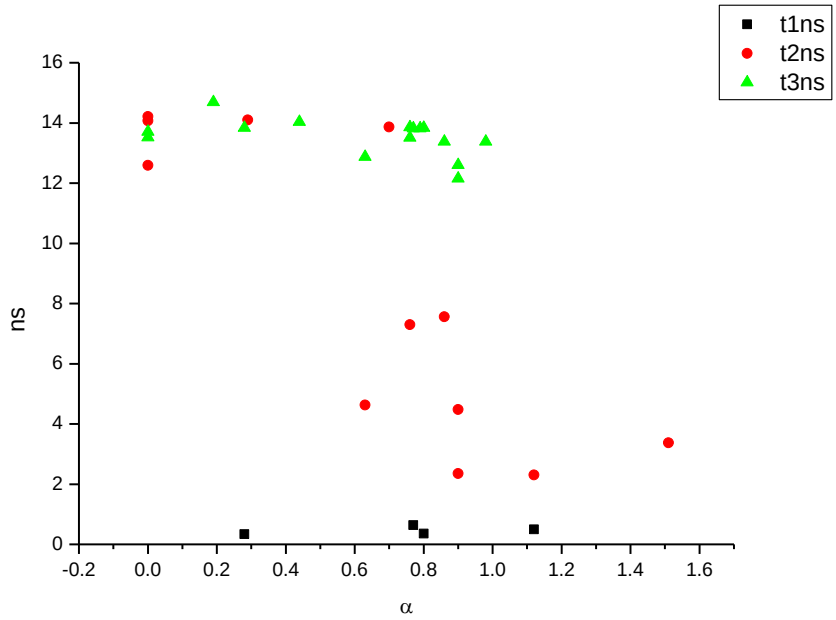

Figure 1.4.135. Intensity weighted components of TCSPC lifetime decay of **10a** (600 nm) versus α.

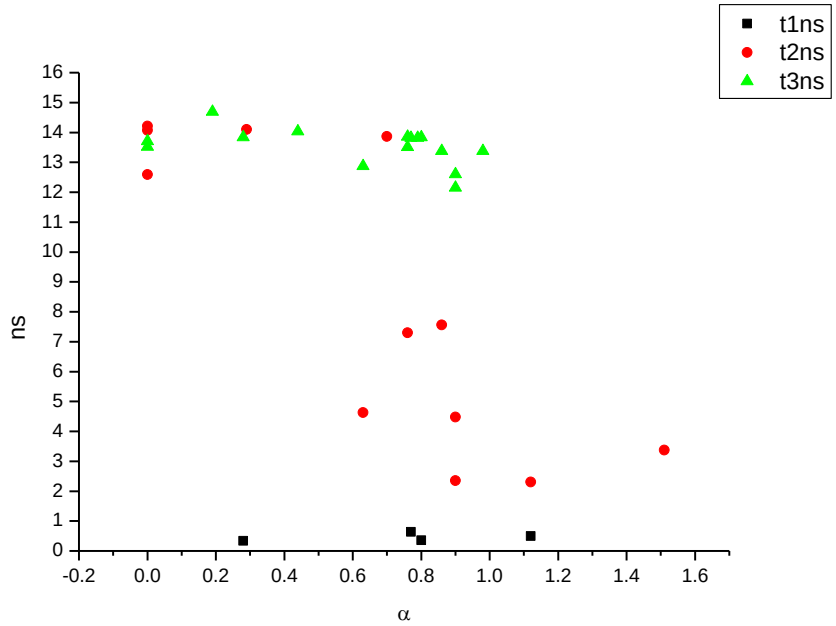

Figure 1.4.136. Amplitude weighted components of TCSPC lifetime decay of **10a** (600 nm) versus α.

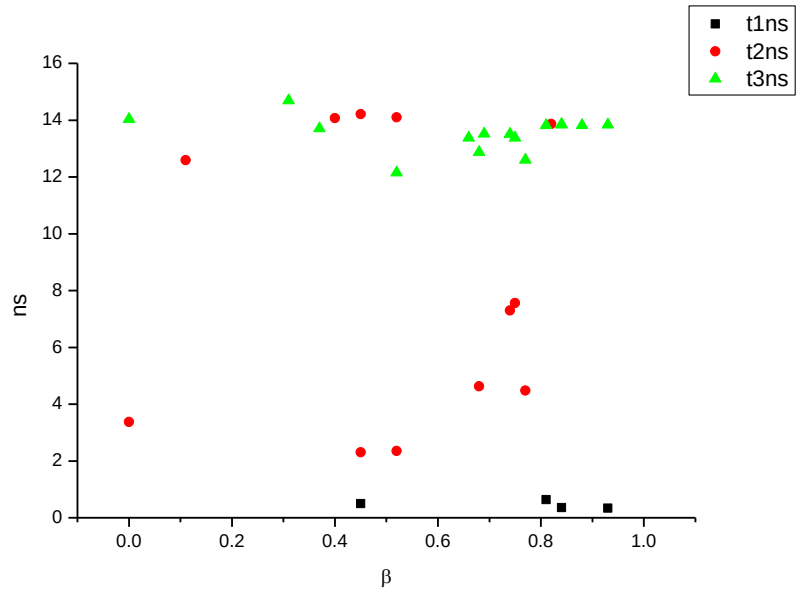

Figure 1.4.137. Intensity weighted components of TCSPC lifetime decay of **10a** (600 nm) versus β.

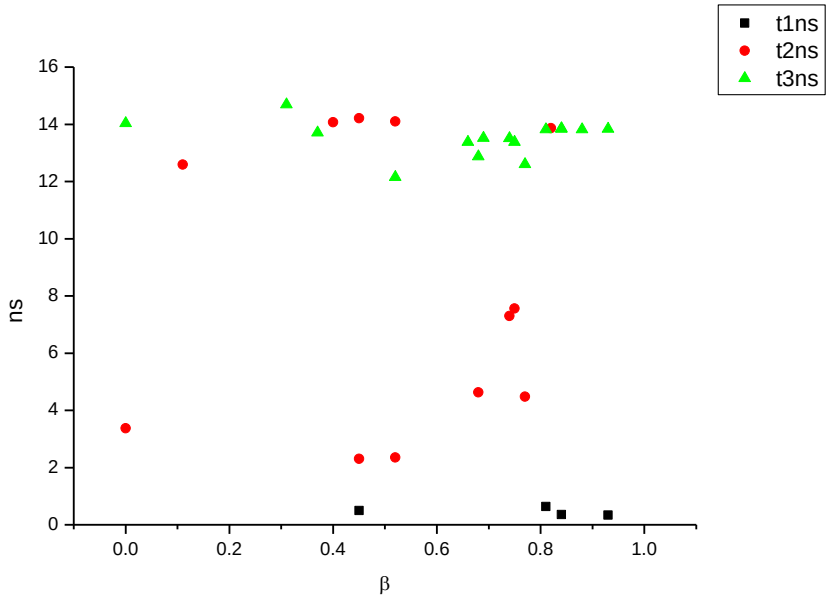

Figure 1.4.138. Amplitude weighted components of TCSPC lifetime decay of **10a** (600 nm) versus β.

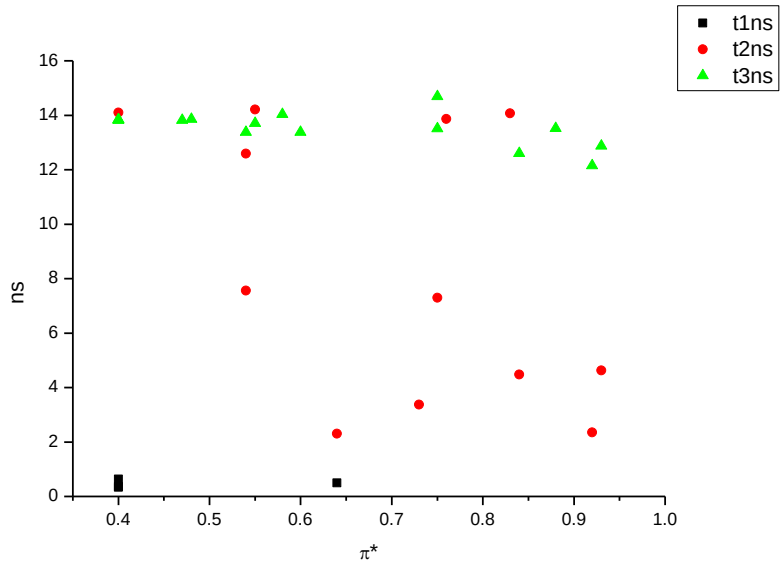

Figure 1.4.139. Intensity weighted components of TCSPC lifetime decay of **10a** (600 nm) versus π*.

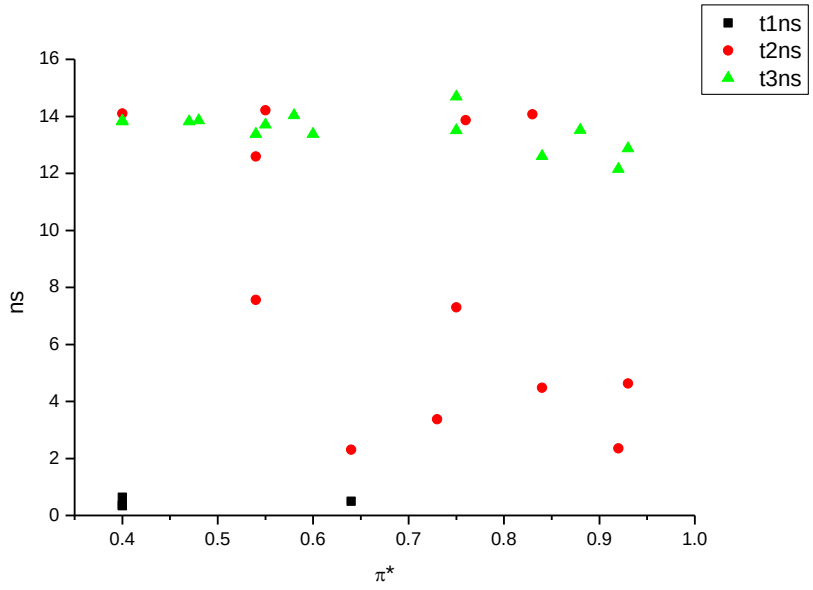

Figure 1.4.140. Amplitude weighted components of TCSPC lifetime decay of **10a** (600 nm) versus π*.

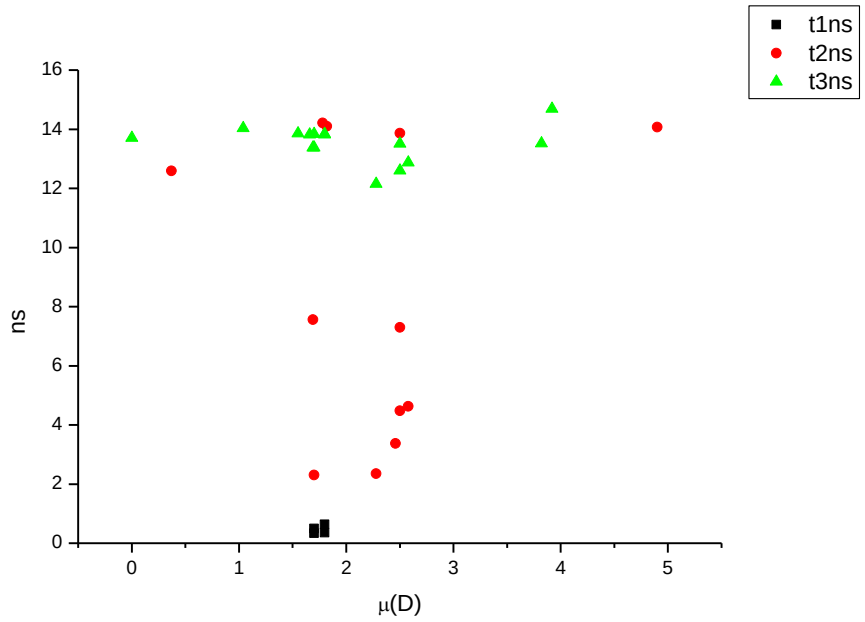

Figure 1.4.141. Intensity weighted components of TCSPC lifetime decay of **10a** (600 nm) versus μ(D).

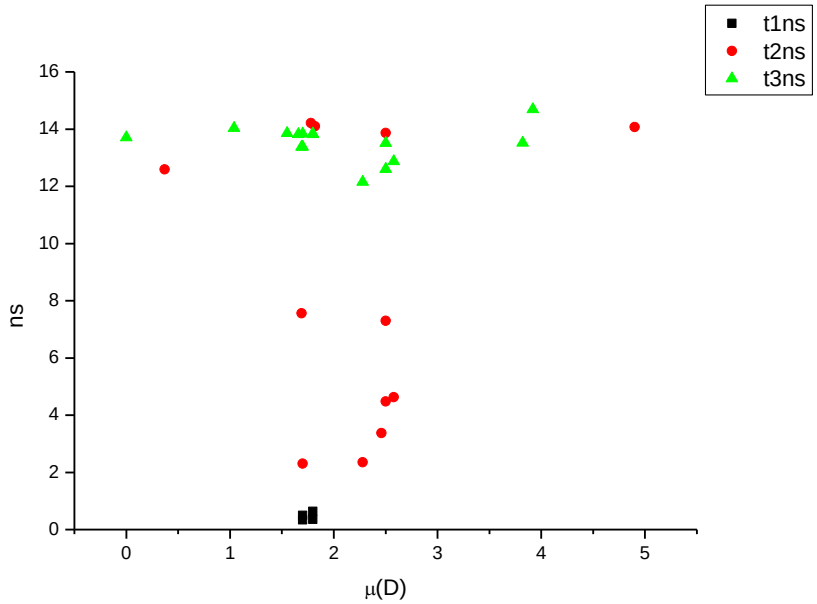

Figure 1.4.142. Amplitude weighted components of TCSPC lifetime decay of **10a** (600 nm) versus μ(D).

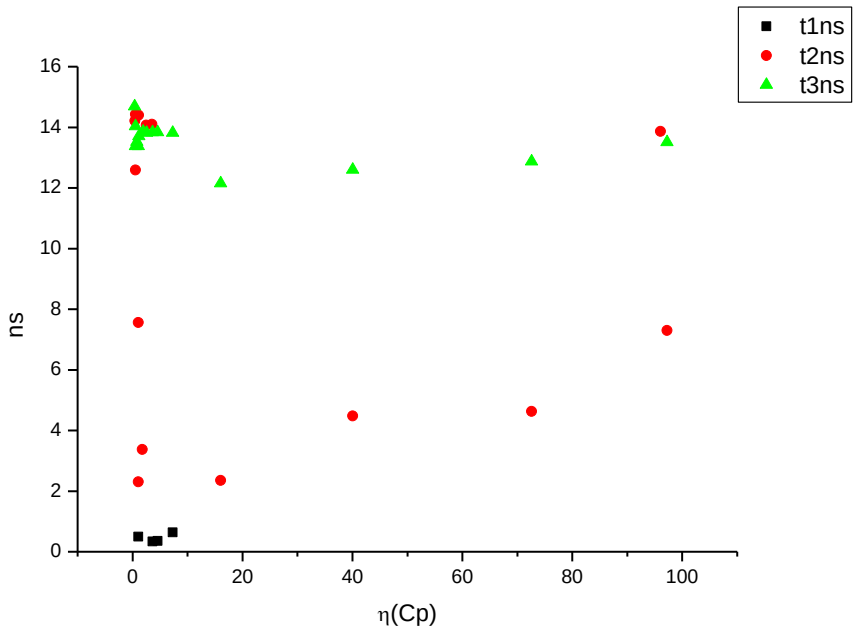

Figure 1.4.143. Intensity weighted components of TCSPC lifetime decay of **10a** (600 nm) versus η(Cp).

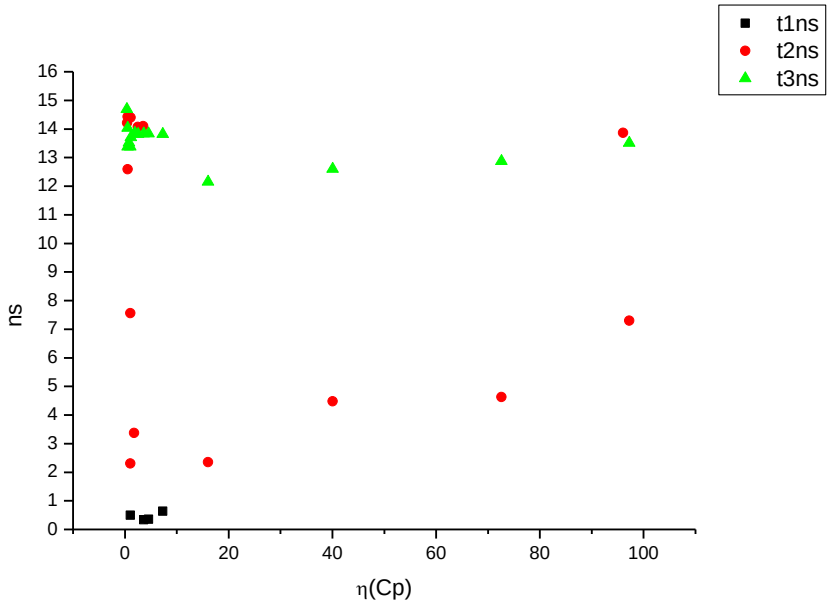

Figure 1.4.144. Amplitude weighted components of TCSPC lifetime decay of **10a** (600 nm) versus η(Cp).

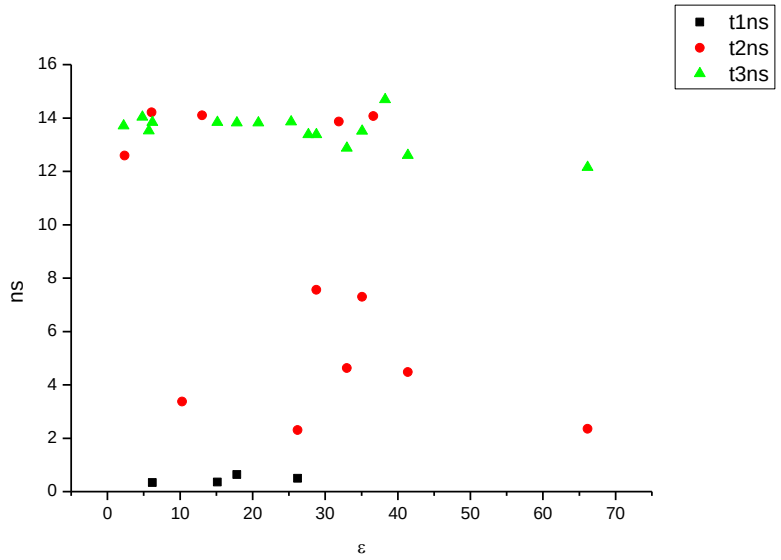

Figure 1.4.145. Intensity weighted components of TCSPC lifetime decay of **10a** (600 nm) versus ε.

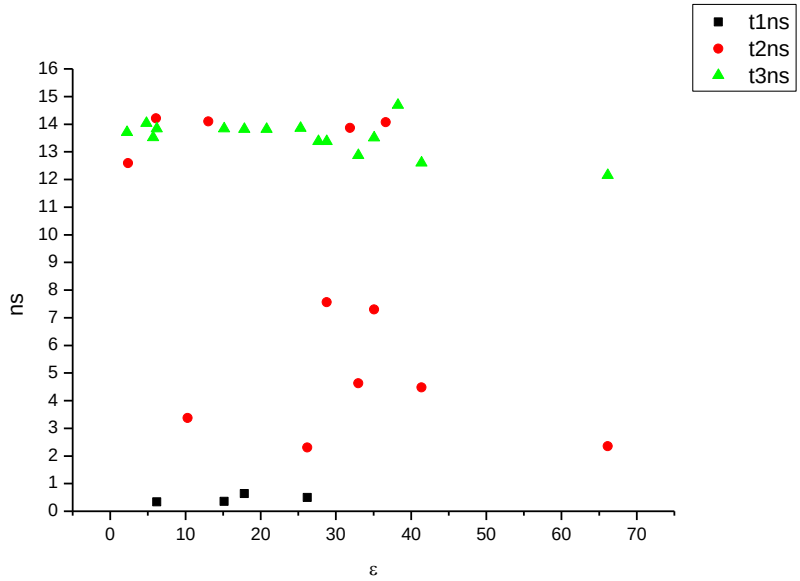

Figure 1.4.146. Amplitude weighted components of TCSPC lifetime decay of **10a** (600 nm) versus ε.

1.4.8 Ultraviolet-visible absorption spectra.

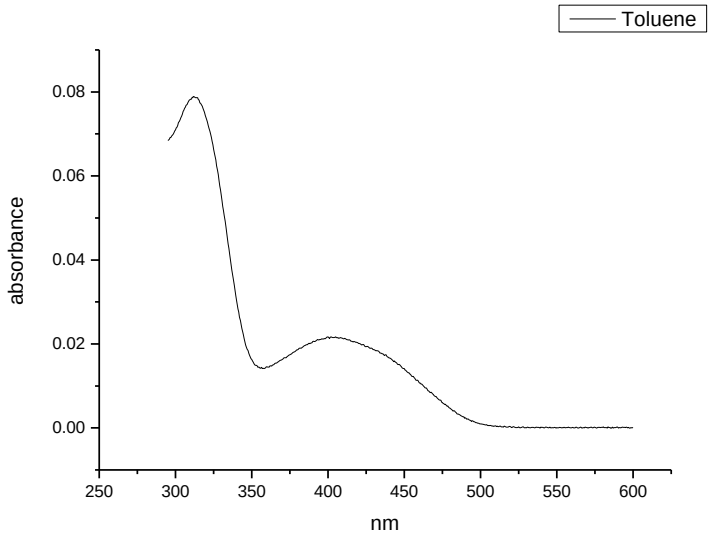

Figure 1.4.147. Ultraviolet-Visible absorption spectrum of **10a** recorded in Toluene.

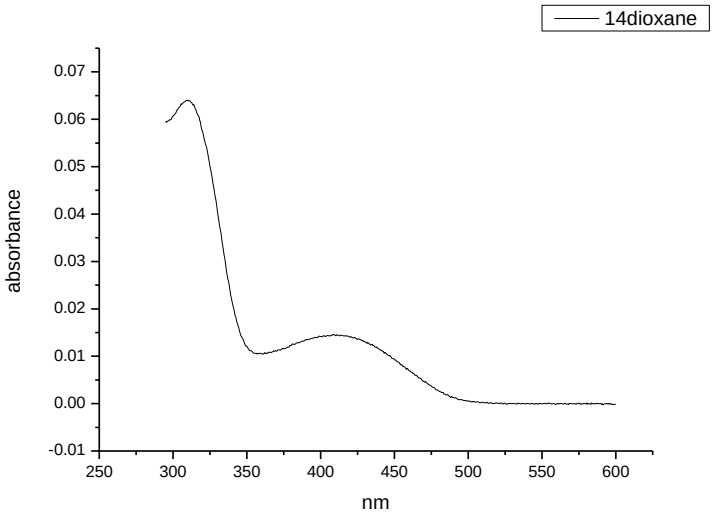

Figure 1.4.1.48. Ultraviolet-Visible absorption spectrum of **10a** recorded in 1,4-dioxane.

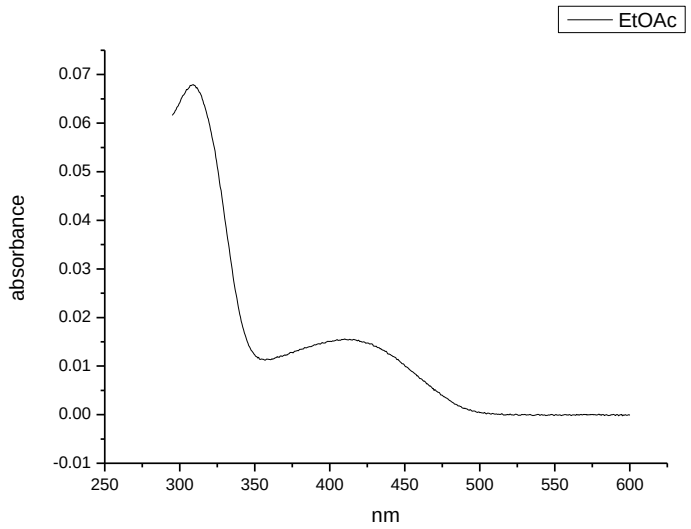

Figure 1.4.149. Ultraviolet-Visible absorption spectrum of **10a** recorded in Ethyl Acetate.

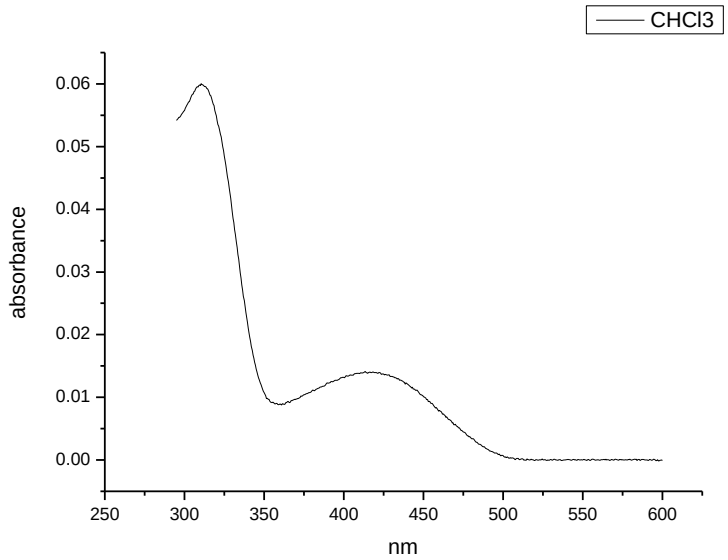

Figure 1.4.150. Ultraviolet-Visible absorption spectrum of **10a** recorded in Chloroform.

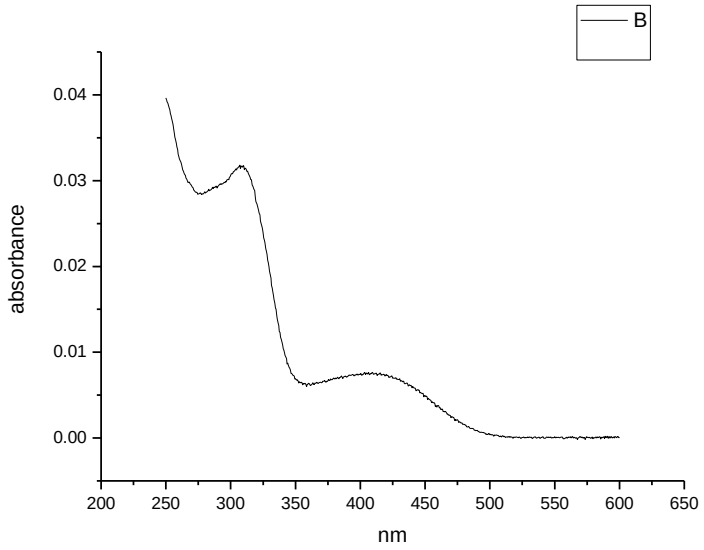

Figure 1.4.151. Ultraviolet-Visible absorption spectrum of **10a** recorded in 2-methyl-2-butanol.

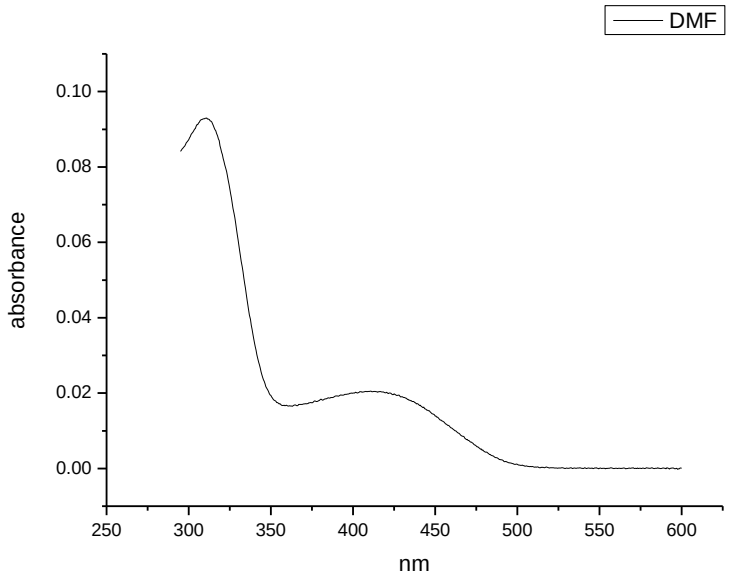

Figure 1.4.152. Ultraviolet-Visible absorption spectrum of **10a** recorded in N,N-dimethylformamide.

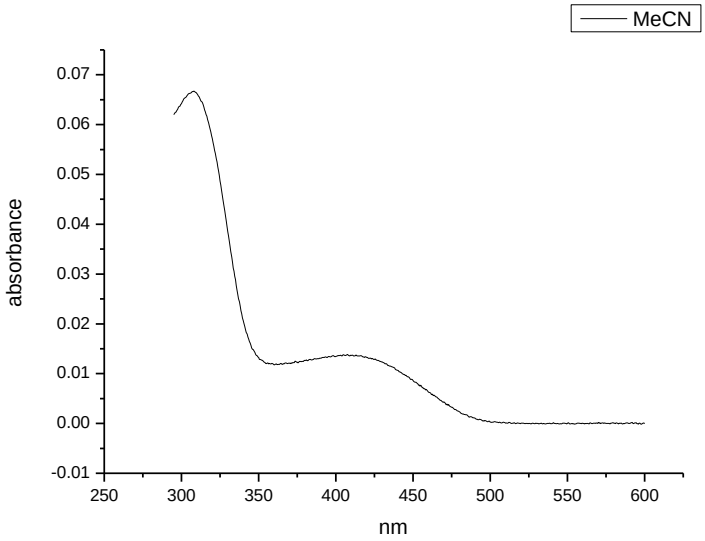

Figure 1.4.153. Ultraviolet-Visible absorption spectrum of **10a** recorded in Acetonitrile.

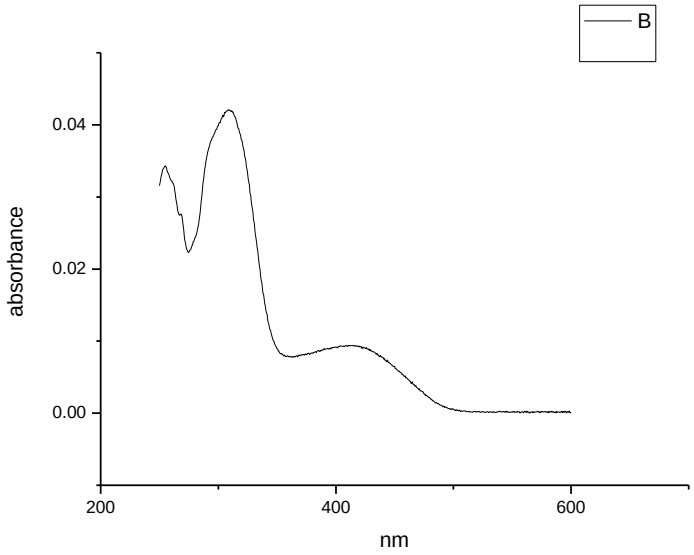

Figure 1.4.154. Ultraviolet-Visible absorption spectrum of **10a** recorded in Propylene Carbonate.

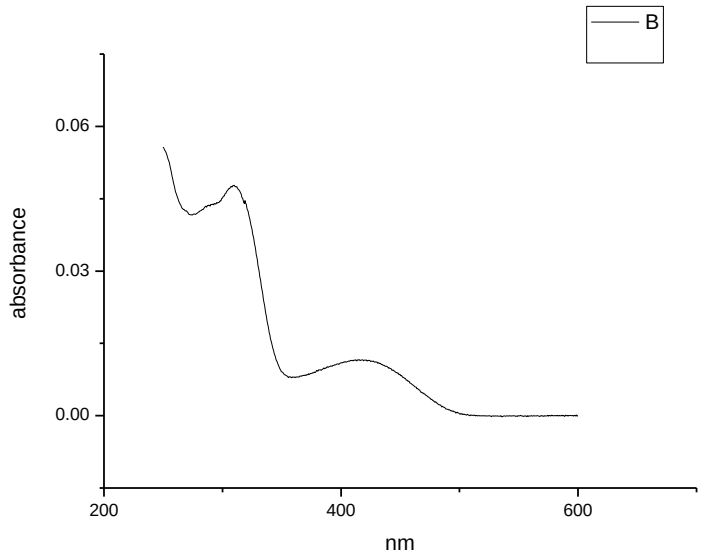

Figure 1.4.155. Ultraviolet-Visible absorption spectrum of **10a** recorded in 1-octanol.

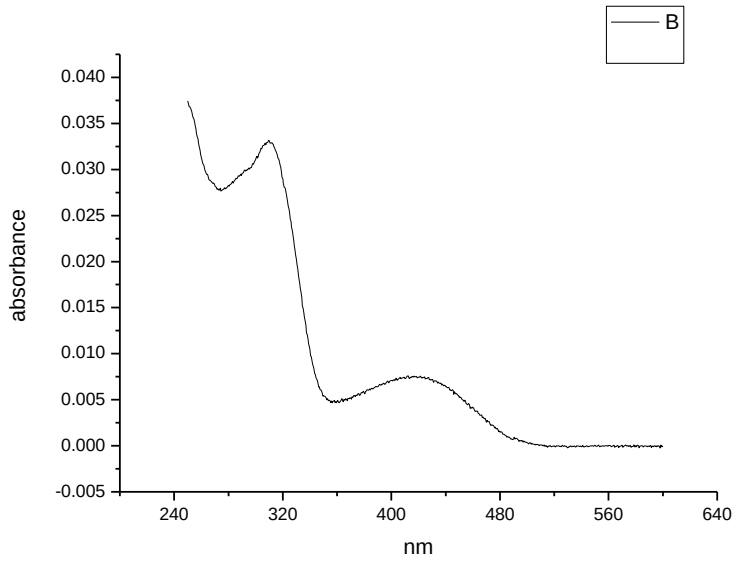

Figure 1.4.156. Ultraviolet-Visible absorption spectrum of **10a** recorded in 1-hexanol.

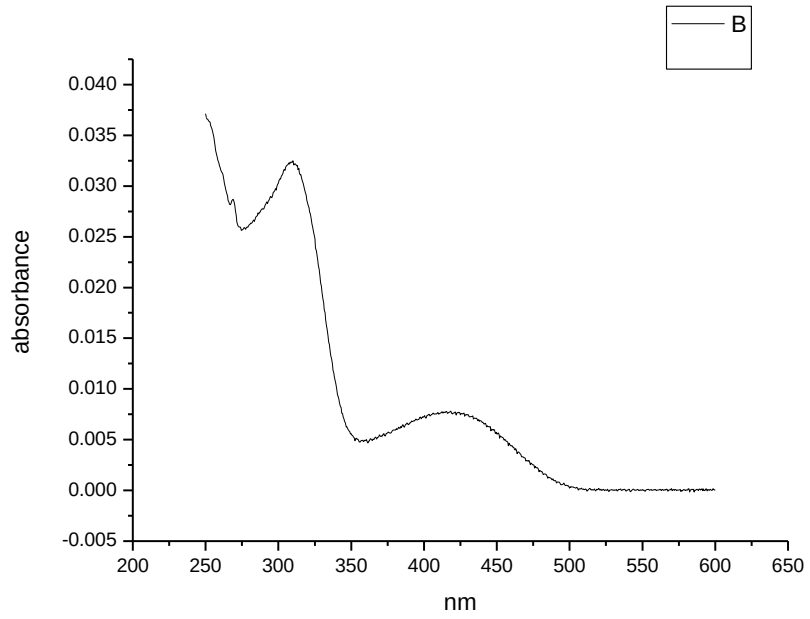

Figure 1.4.157. Ultraviolet-Visible absorption spectrum of **10a** recorded in 1-butanol.

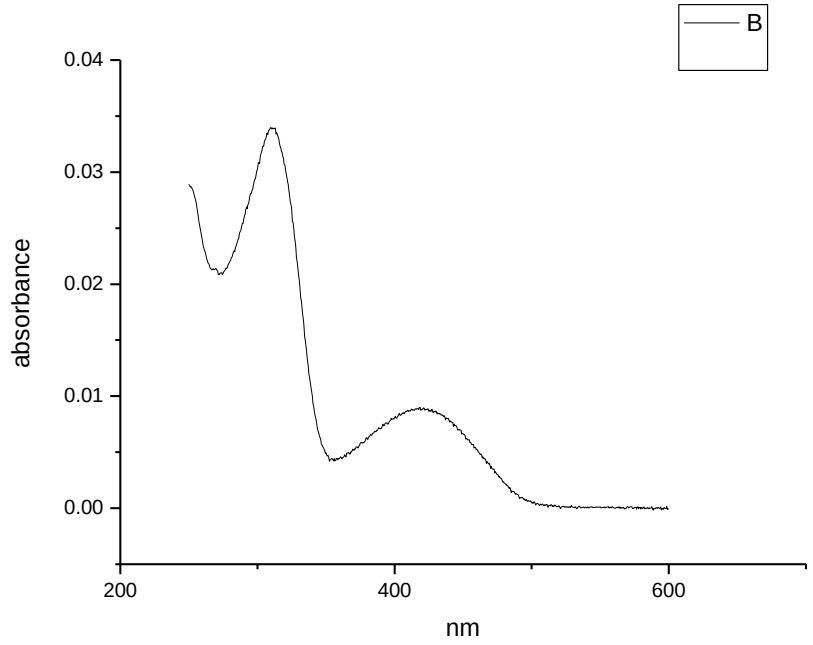

Figure 1.4.158. Ultraviolet-Visible absorption spectrum of **10a** recorded in 1-pentanol.

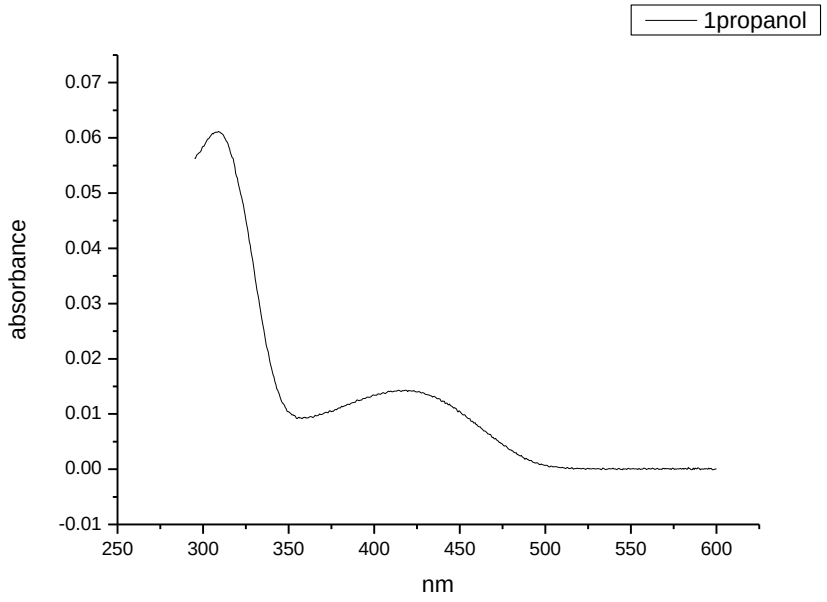

Figure 1.4.159. Ultraviolet-Visible absorption spectrum of **10a** recorded in 1-propanol.

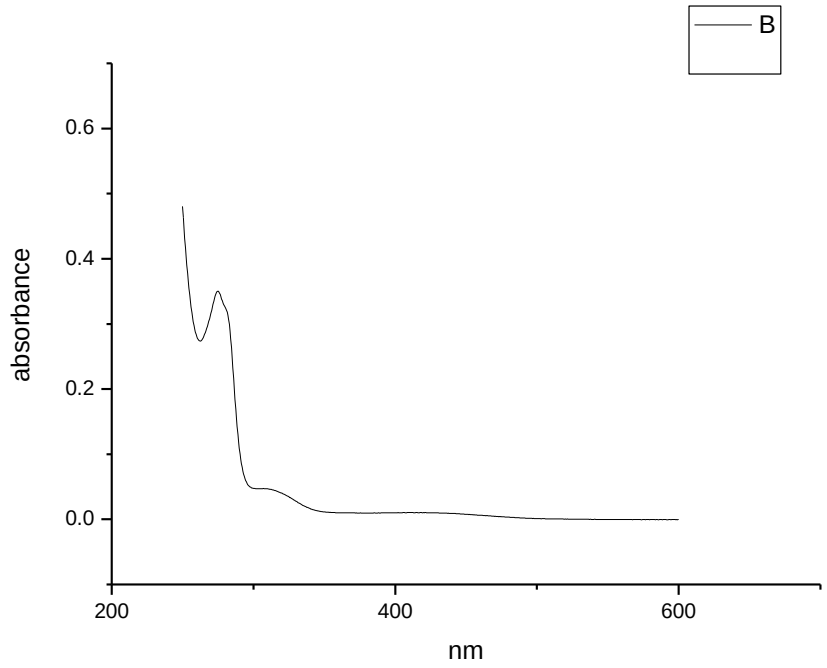

Figure 1.4.160. Ultraviolet-Visible absorption spectrum of **10a** recorded in Acetic Acid.

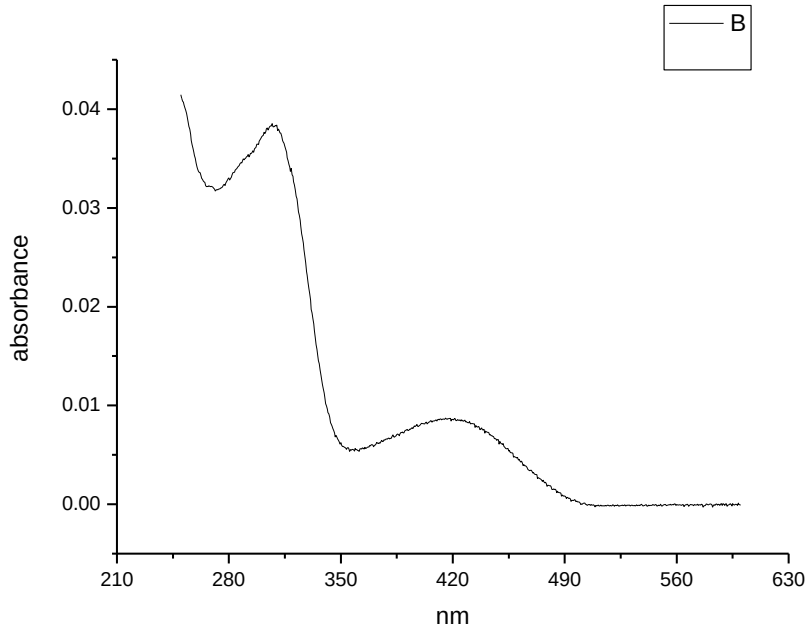

Figure 1.4.161. Ultraviolet-Visible absorption spectrum of **10a** recorded in Ethanol.

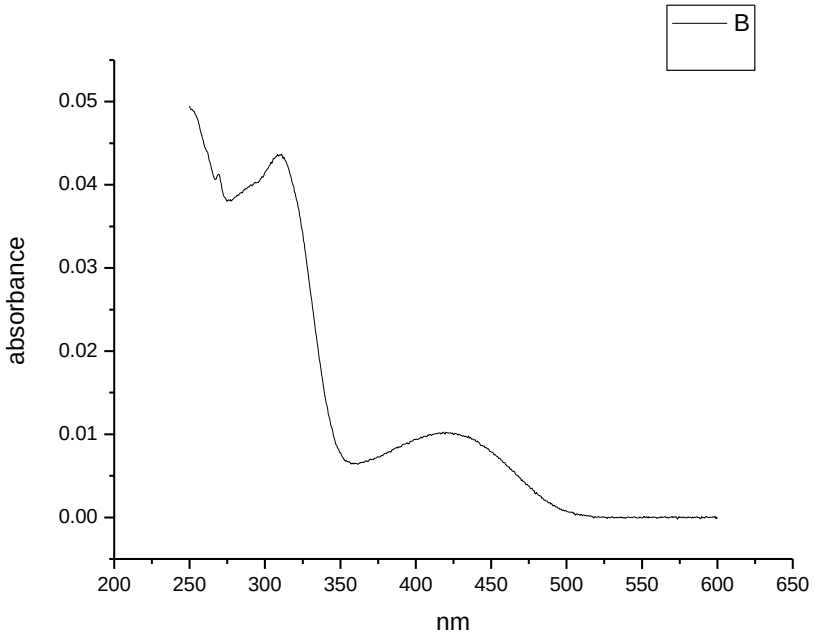

Figure 1.4.162. Ultraviolet-Visible absorption spectrum of **10a** recorded in 1,5-pentanediol.

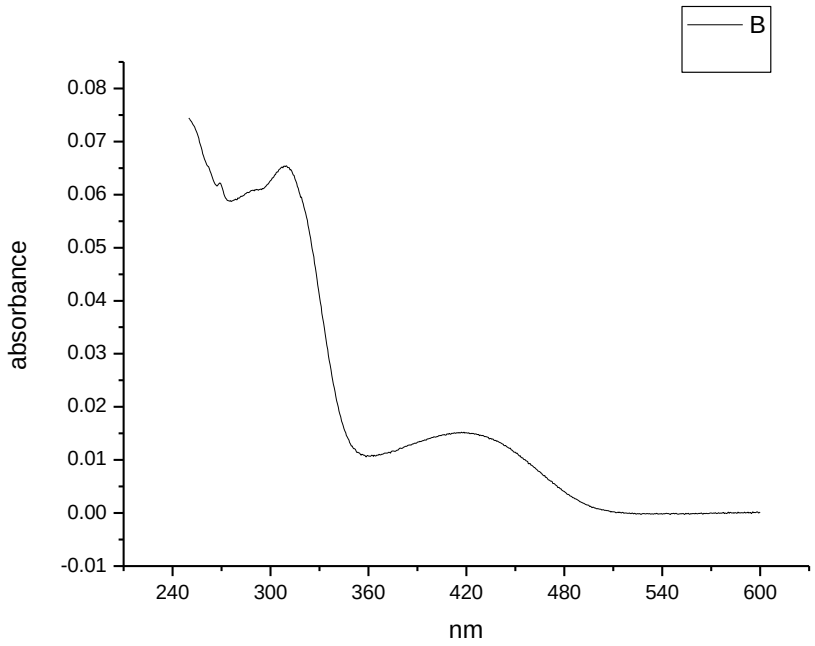

Figure 1.4.163. Ultraviolet-Visible absorption spectrum of **10a** recorded in 1,3-butanediol.

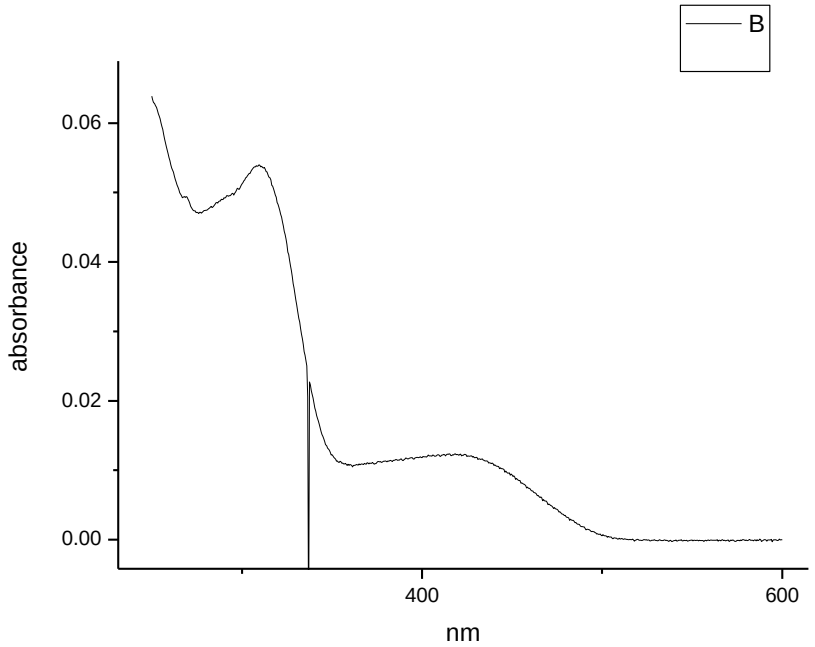

Figure 1.4.164. Ultraviolet-Visible absorption spectrum of **10a** recorded in 1,4-butanediol.

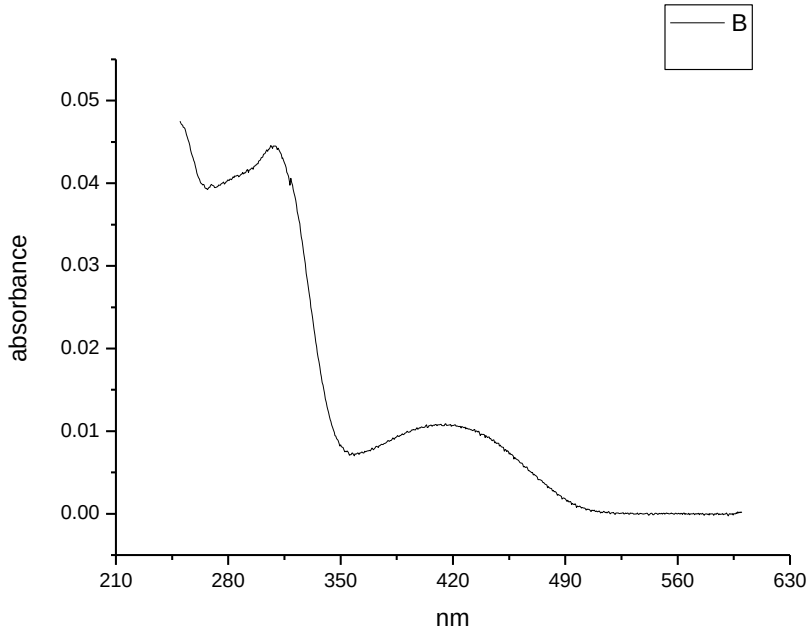

Figure 1.4.165. Ultraviolet-Visible absorption spectrum of **10a** recorded in 1,3-propanediol.

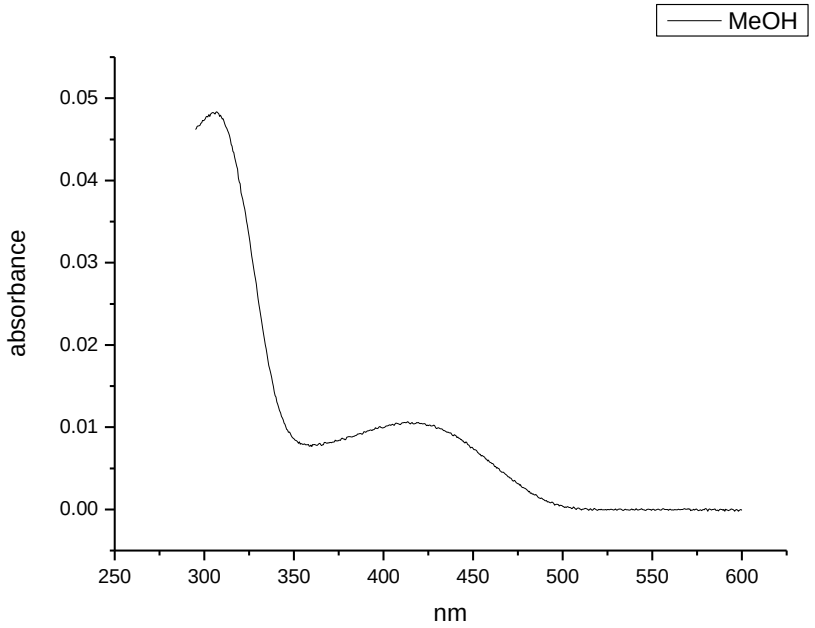

Figure 1.4.166. Ultraviolet-Visible absorption spectrum of **10a** recorded in Methanol.

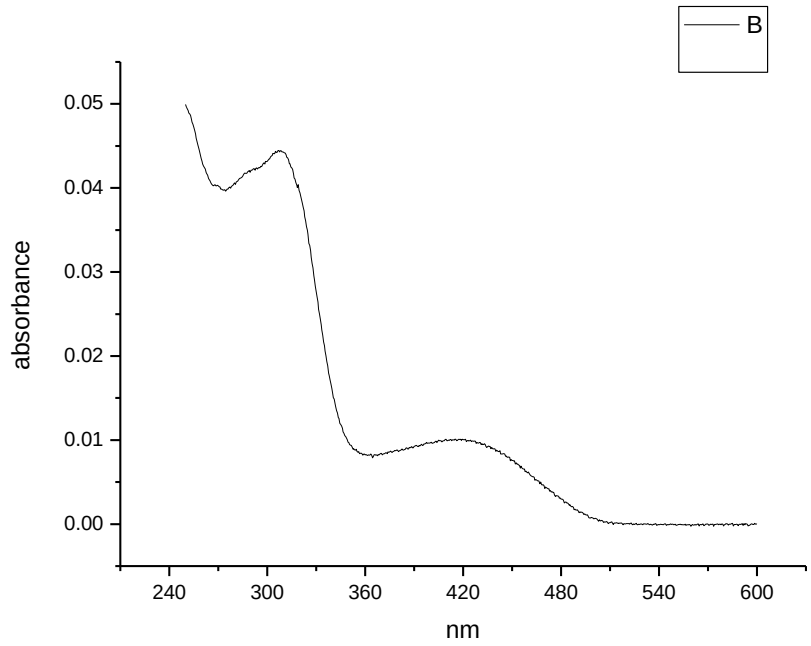

Figure 1.4.167. Ultraviolet-Visible absorption spectrum of **10a** recorded in 1,2-ethanediol.

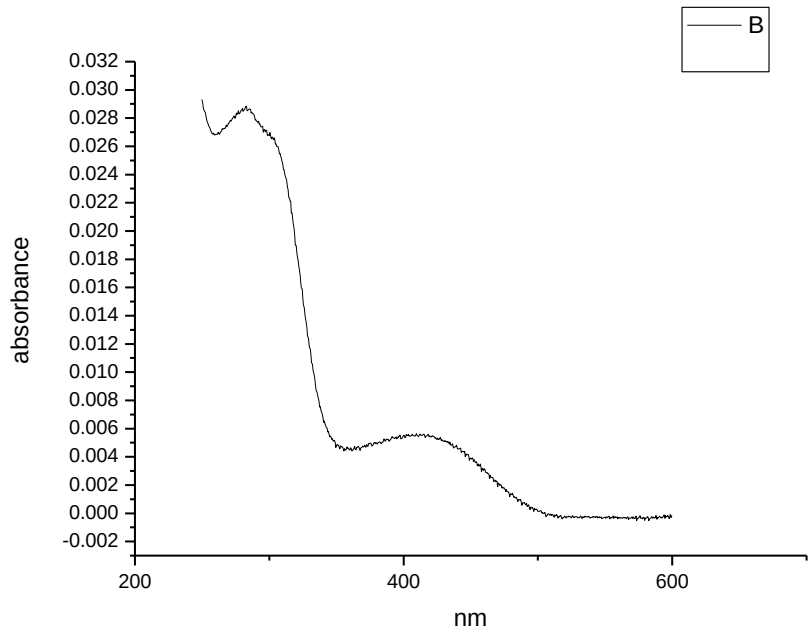

Figure 1.4.168. Ultraviolet-Visible absorption spectrum of **10a** recorded in 2,2,2-trifluoroethanol.

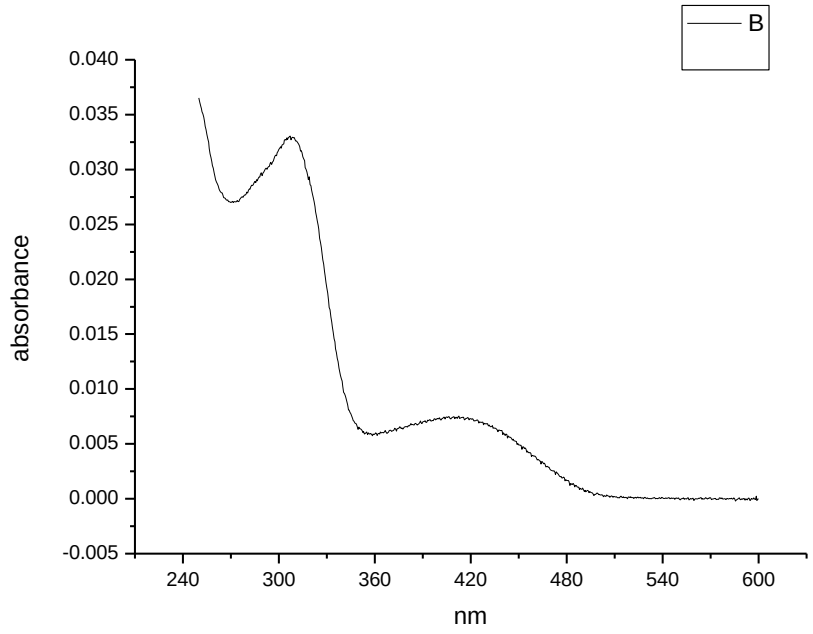

Figure 1.4.169. Ultraviolet-Visible absorption spectrum of **10a** recorded in Ethanol-d_1 (EtOD).

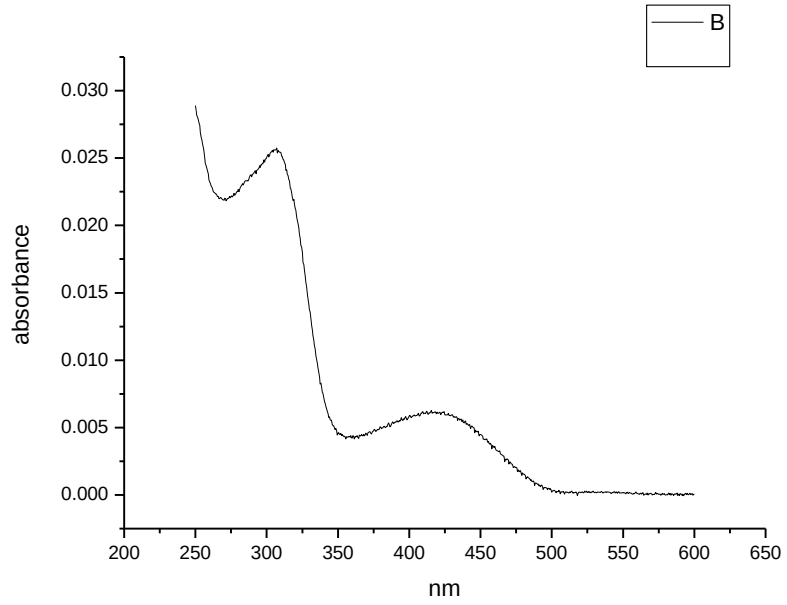

Figure 1.4.170. Ultraviolet-Visible absorption spectrum of **10a** recorded in Methanol-d_1 (MeOD).

1.4.9 Fluorescence Emission spectra.

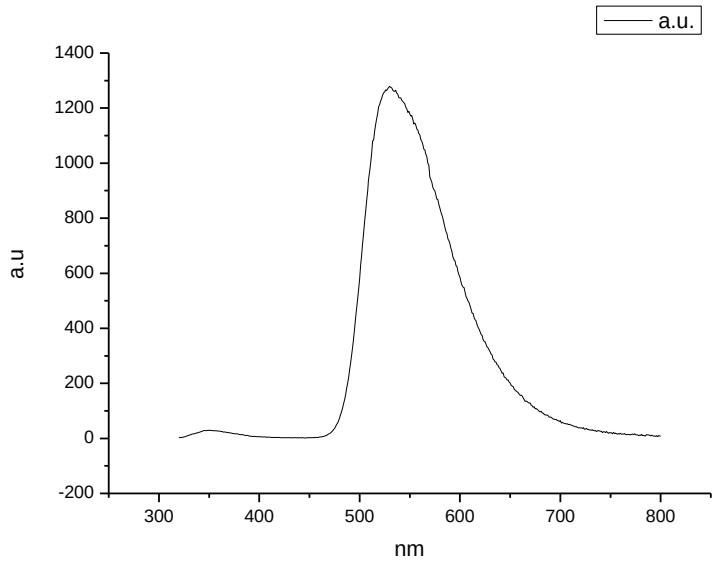

Figure 1.4.171. Fluorescence emission spectrum of **10a** recorded in Toluene at 310 nm excitation.

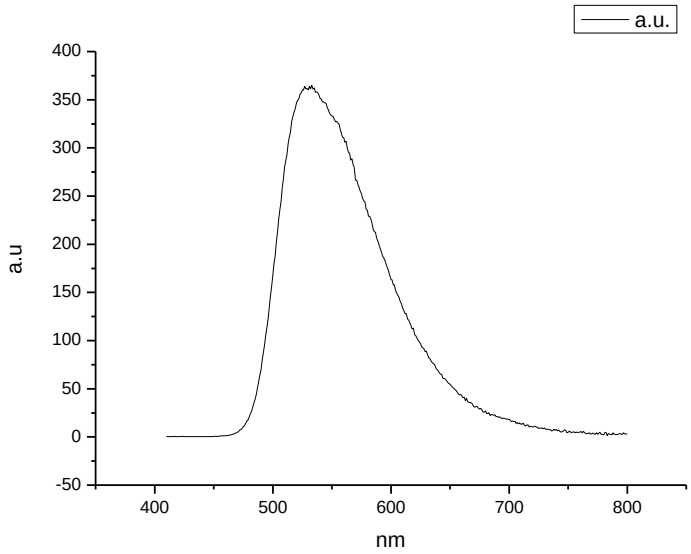

Figure 1.4.172. Fluorescence emission spectrum of **10a** recorded in Toluene at 400 nm excitation.

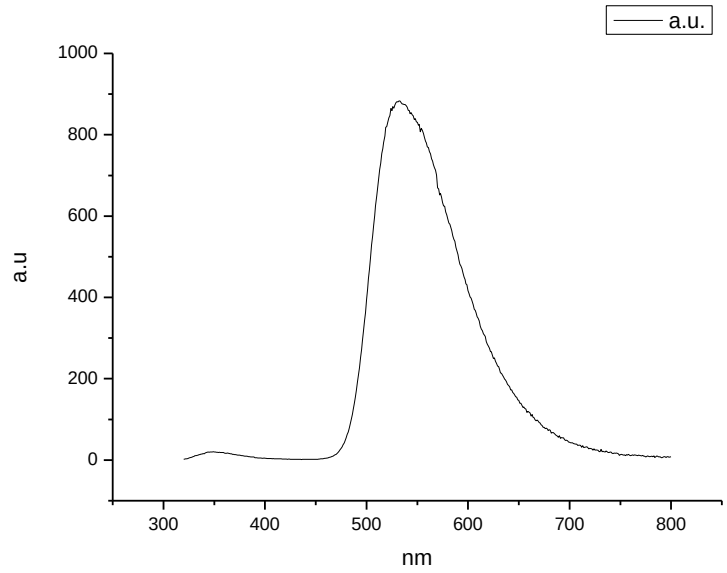

Figure 1.4.173. Fluorescence emission spectrum of **10a** recorded in 1,4-dioxane at 310 nm excitation.

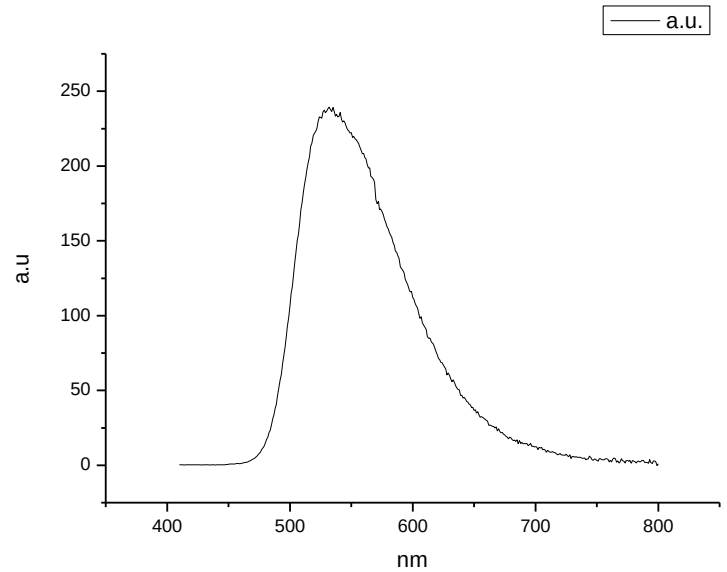

Figure 1.4.174. Fluorescence emission spectrum of **10a** recorded in 1,4-dioxane at 400 nm excitation.

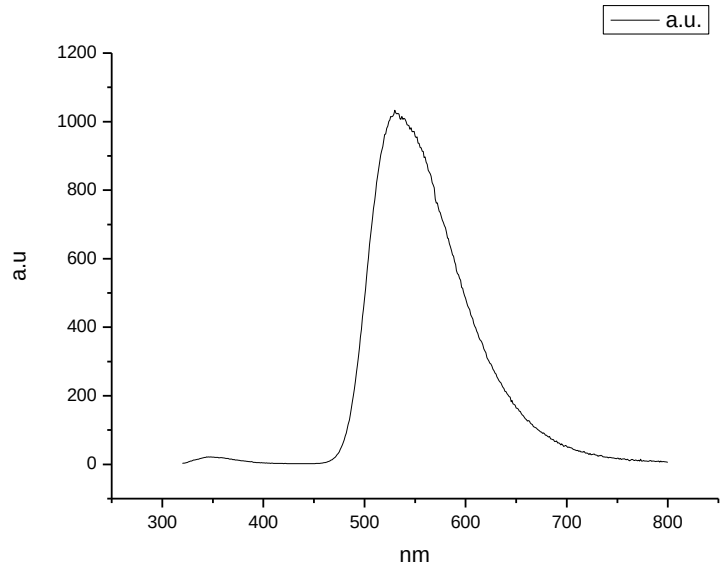

Figure 1.4.175. Fluorescence emission spectrum of **10a** recorded in Ethyl Acetate at 310 nm excitation.

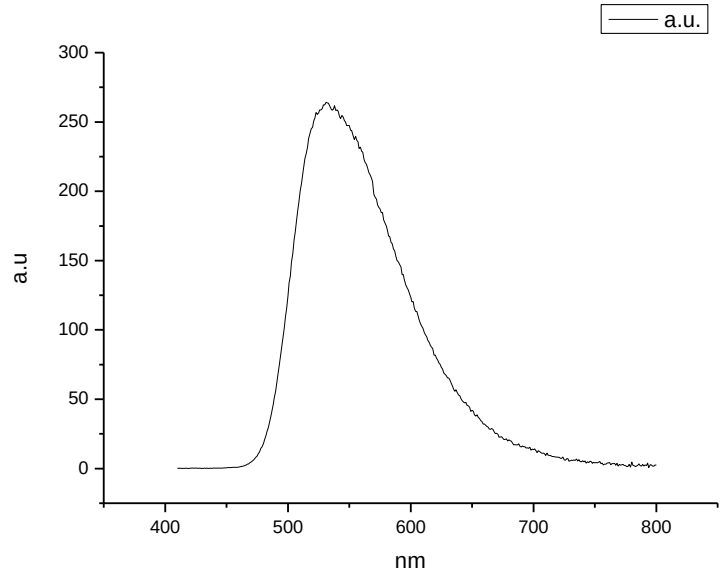

Figure 1.4.176. Fluorescence Emission spectrum of **10a** recorded in Ethyl Acetate at 400 nm excitation.

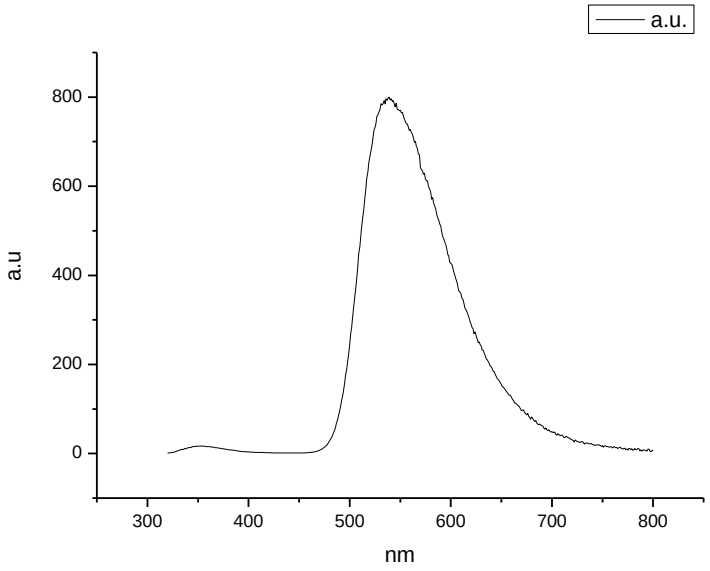

Figure 1.4.177. Fluorescence emission spectrum of **10a** recorded in Chloroform at 310 nm excitation.

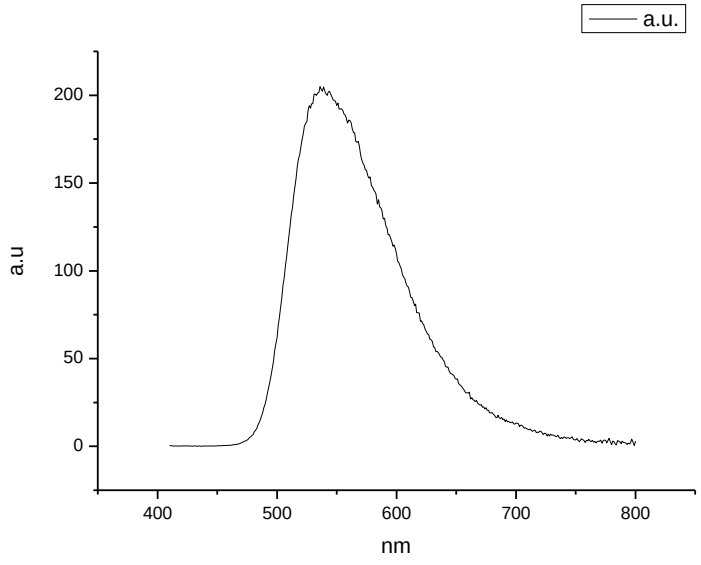

Figure 1.4.178. Fluorescence emission spectrum of **10a** recorded in Chloroform at 400 nm excitation.

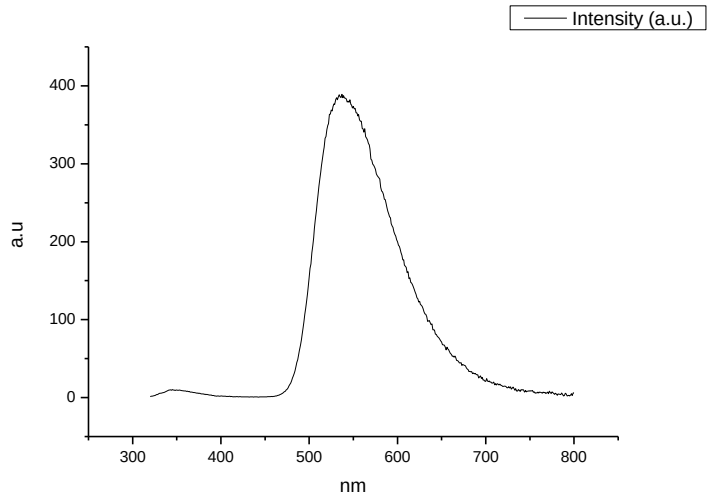

Figure 1.4.179. Fluorescence emission spectrum of **10a** recorded in 2-methyl-2-butanol at 310 nm excitation.

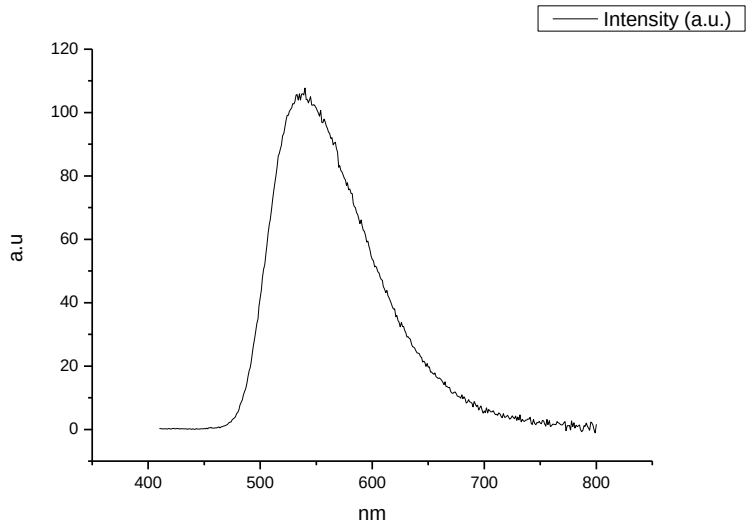

Figure 1.4.180. Fluorescence emission spectrum of **10a** recorded in 2-methyl-2-butanol at 400 nm excitation.

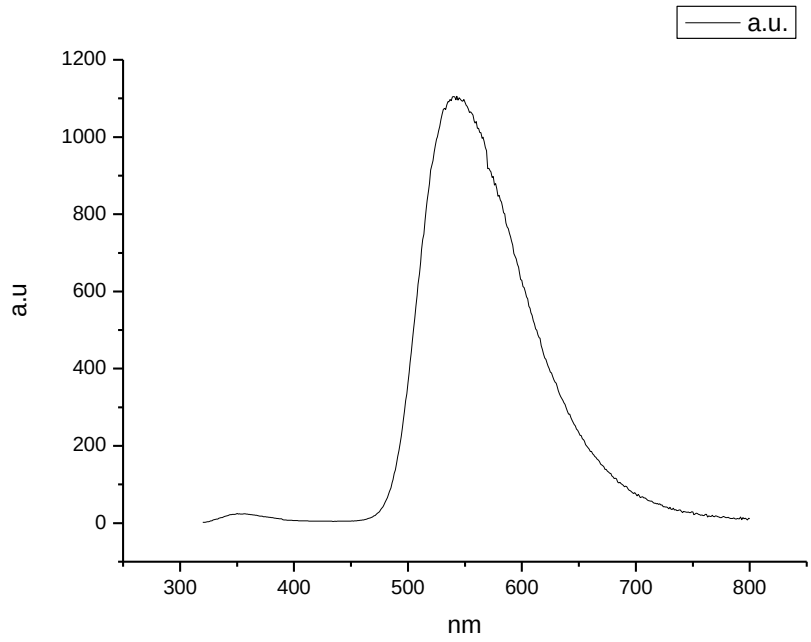

Figure 1.4.181. Fluorescence emission spectrum of **10a** recorded in N,N-dimethylformamide at 310 nm excitation.

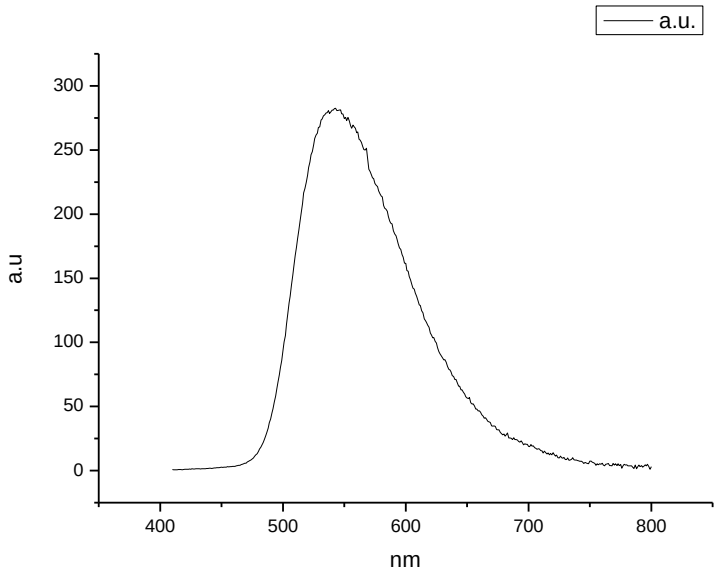

Figure 1.4.182. Fluorescence emission spectrum of **10a** recorded in N,N-dimethylformamide at 400 nm excitation.

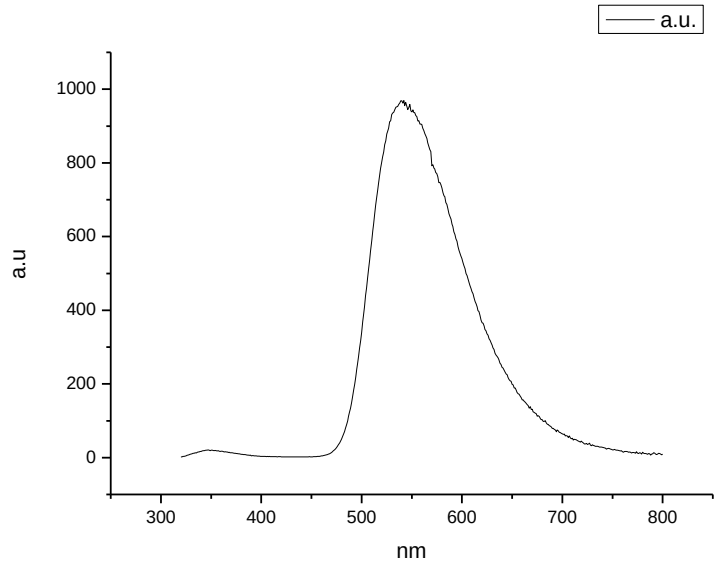

Figure 1.4.183. Fluorescence emission spectrum of **10a** recorded in Acetonitrile at 310 nm excitation.

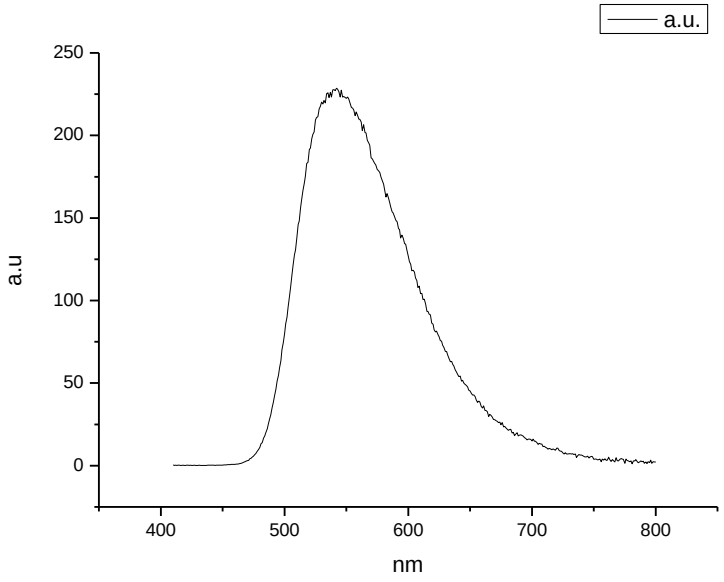

Figure 1.4.184. Fluorescence emission spectrum of **10a** recorded in Acetonitrile at 400 nm excitation.

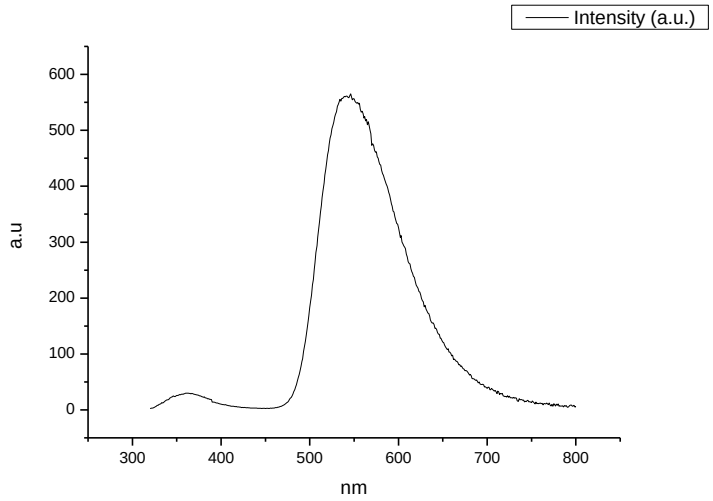

Figure 1.4.185. Fluorescence emission spectrum of **10a** recorded in Propylene Carbonate at 310 nm excitation.

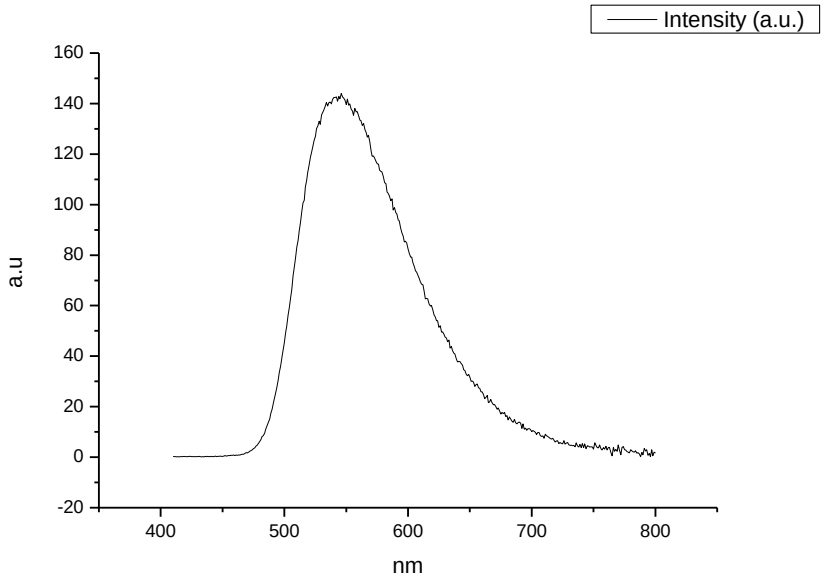

Figure 1.4.186. Fluorescence emission spectrum of **10a** recorded in Propylene Carbonate at 400 nm excitation.

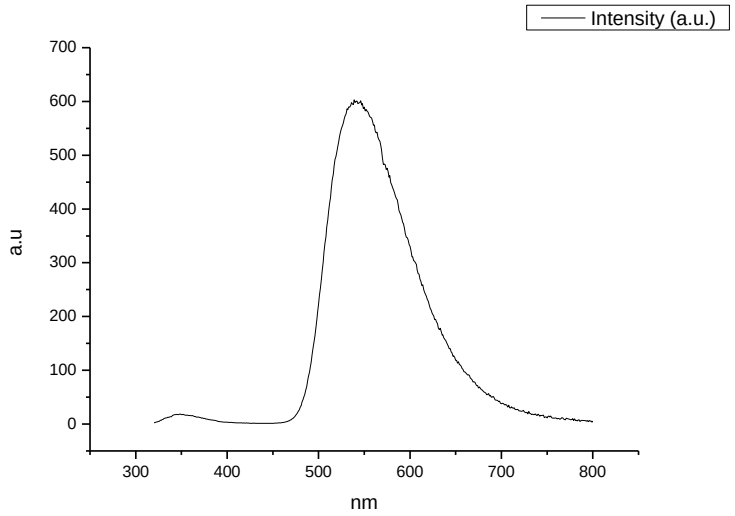

Figure 1.4.187. Fluorescence emission spectrum of **10a** recorded in 1-octanol at 310 nm excitation.

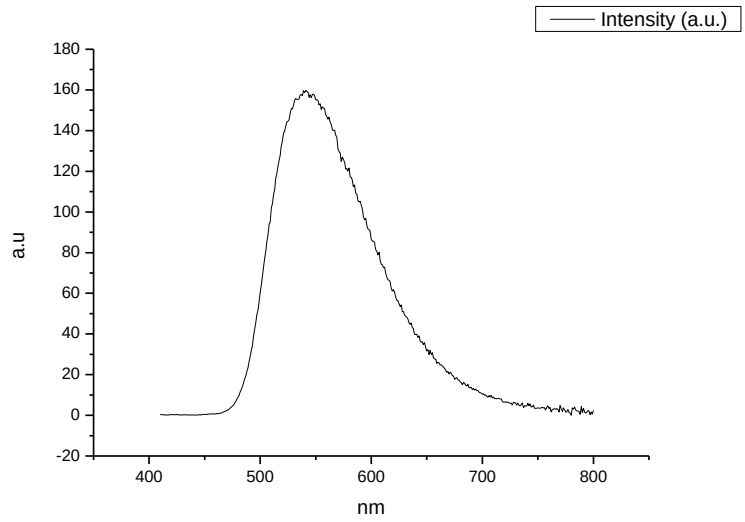

Figure 1.4.188. Fluorescence emission spectrum of **10a** recorded in 1-octanol at 400 nm excitation.

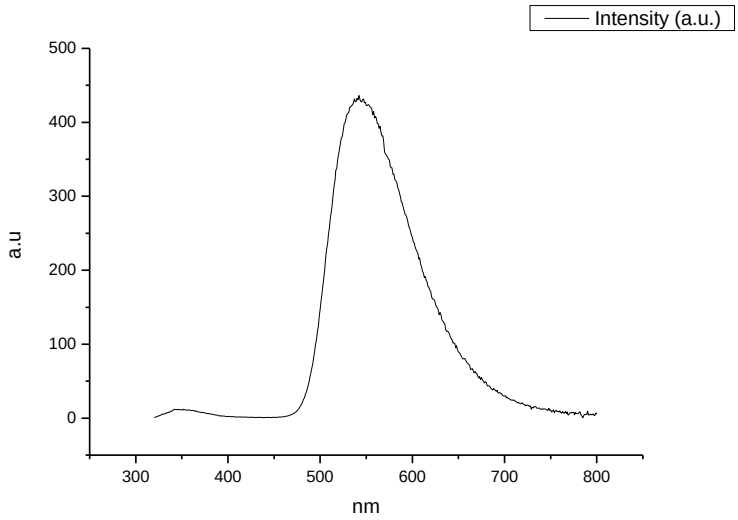

Figure 1.4.189. Fluorescence emission spectrum of **10a** recorded in 1-hexanol at 310 nm excitation.

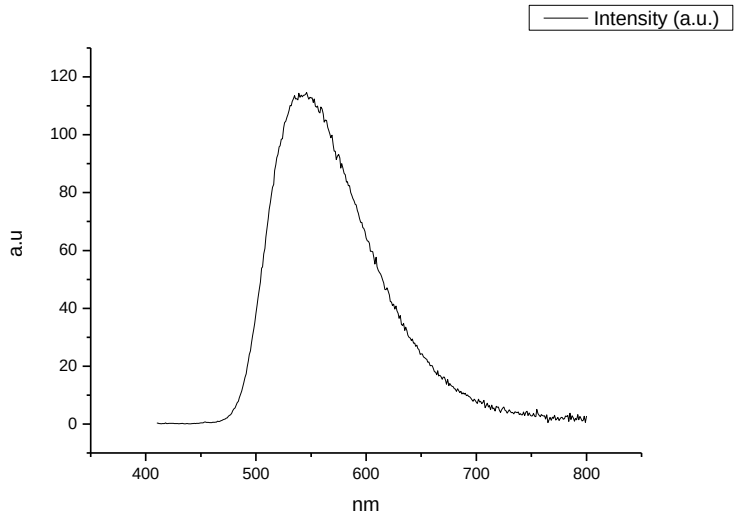

Figure 1.4.190. Fluorescence emission spectrum of **10a** recorded in 1-hexanol at 400 nm excitation.

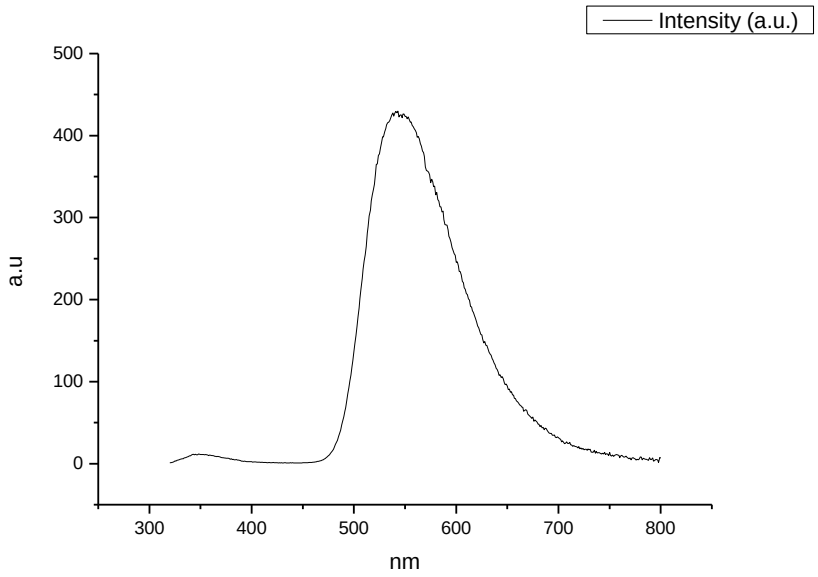

Figure 1.4.191. Fluorescence emission spectrum of **10a** recorded in 1-butanol at 310 nm excitation.

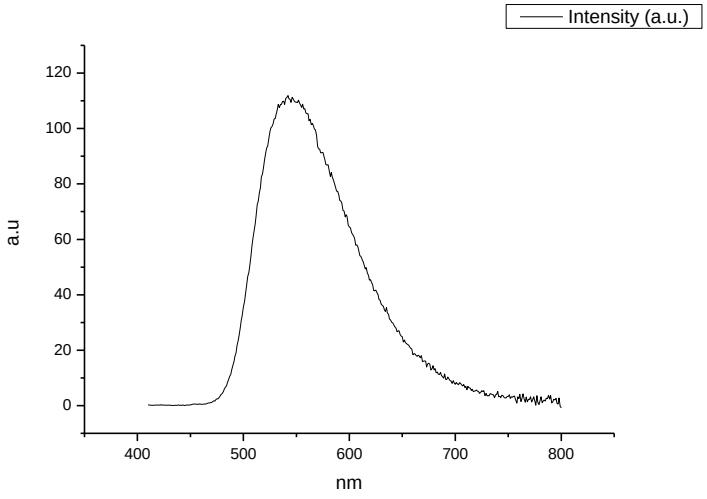

Figure 1.4.192. Fluorescence emission spectrum of **10a** recorded in 1-butanol at 400 nm excitation.

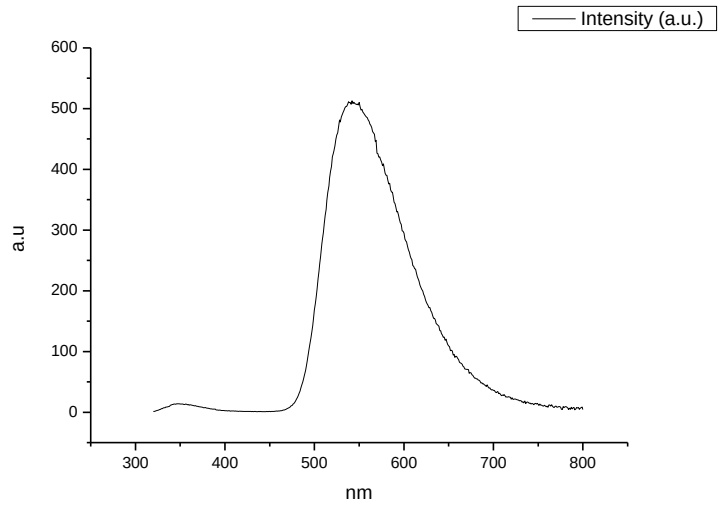

Figure 1.4.193. Fluorescence emission spectrum of **10a** recorded in 1-pentanol at 310 nm excitation.

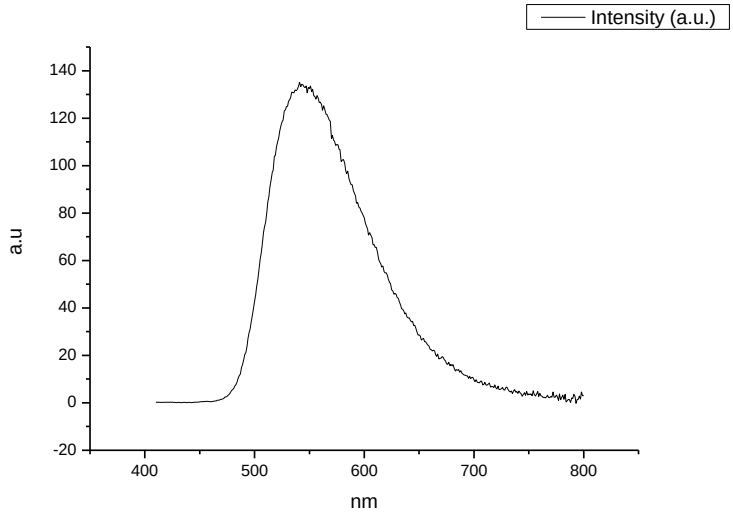

Figure 1.4.194. Fluorescence emission spectrum of **10a** recorded in 1-pentanol at 400 nm excitation.

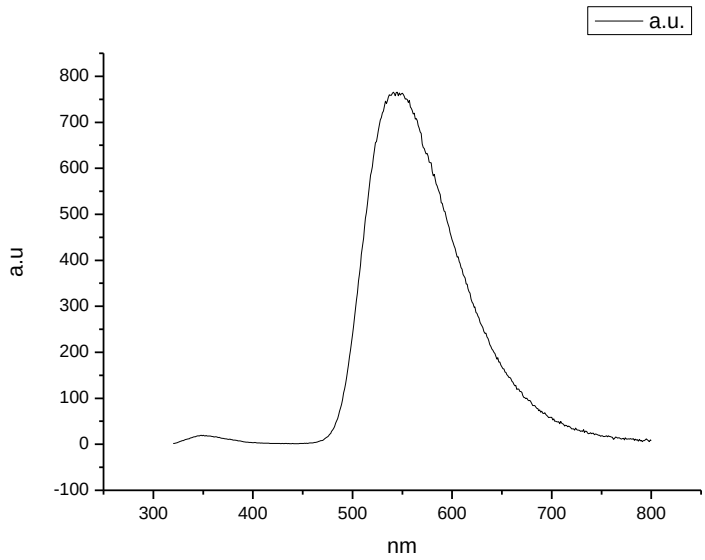

Figure 1.4.195. Fluorescence emission spectrum of **10a** recorded in 1-propanol at 310 nm excitation.

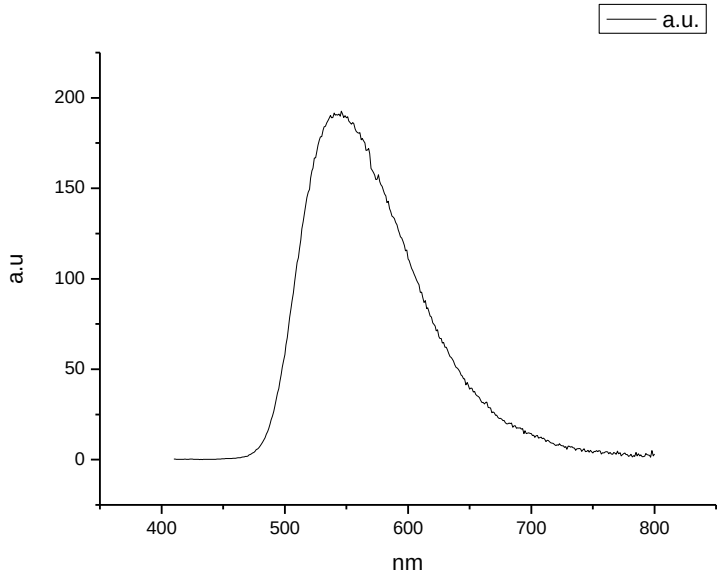

Figure 1.4.196. Fluorescence emission spectrum of **10a** recorded in 1-propanol at 400 nm excitation.

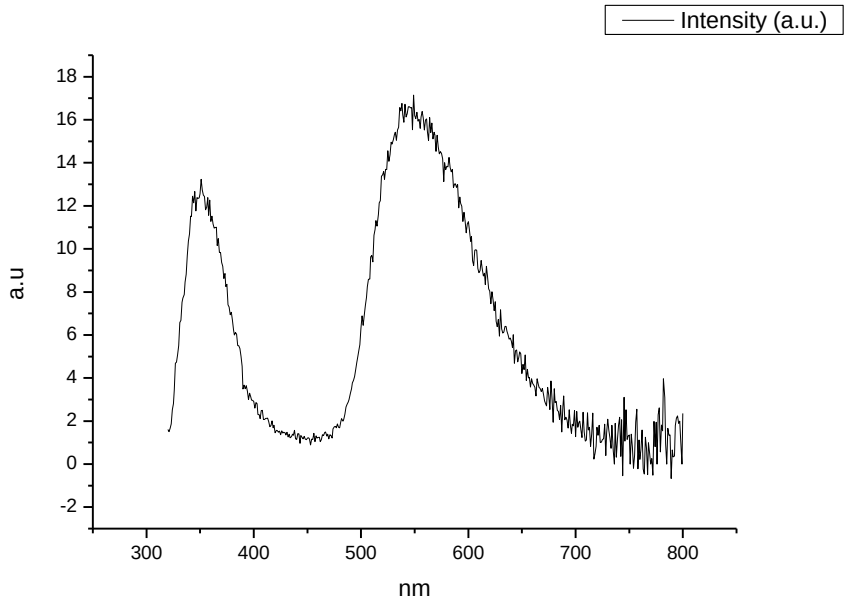

Figure 1.4.197. Fluorescence emission spectrum of **10a** recorded in Acetic Acid at 310 nm excitation.

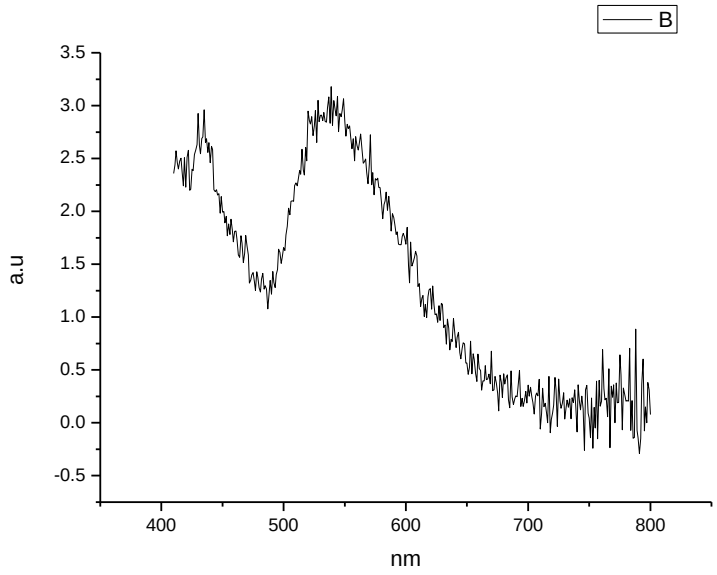

Figure 1.4.198. Fluorescence emission spectrum of **10a** recorded in Acetic Acid at 400 nm excitation.

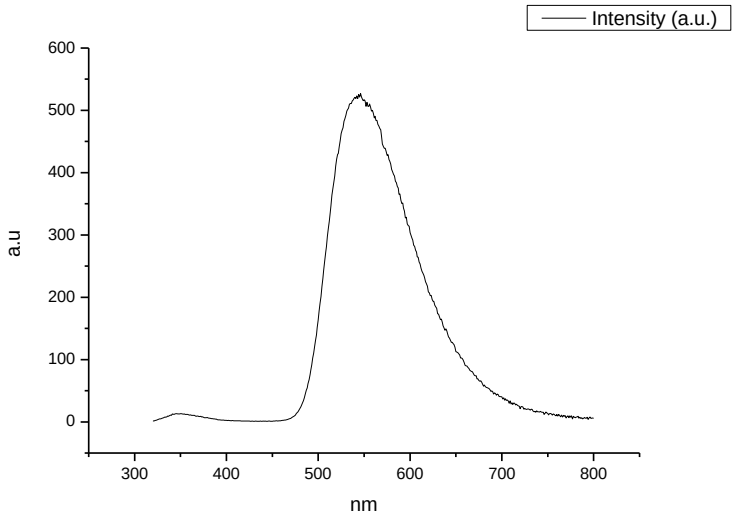

Figure 1.4.199. Fluorescence emission spectrum of **10a** recorded in Ethanol at 310 nm excitation.

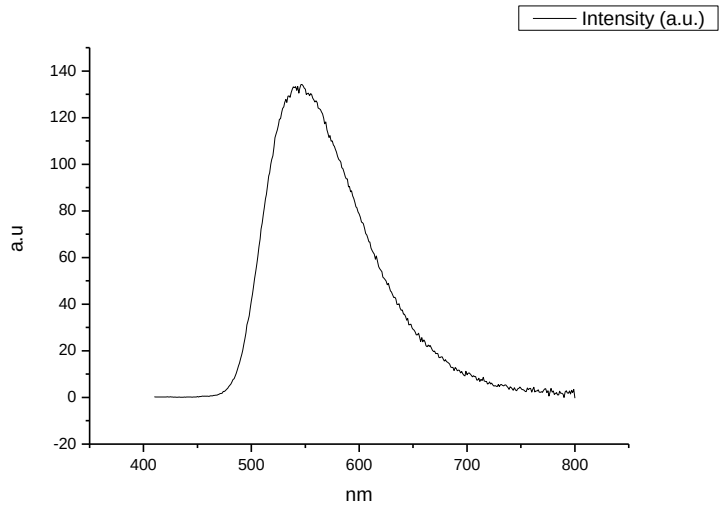

Figure 1.4.200. Fluorescence emission spectrum of **10a** recorded in Ethanol at 400 nm excitation.

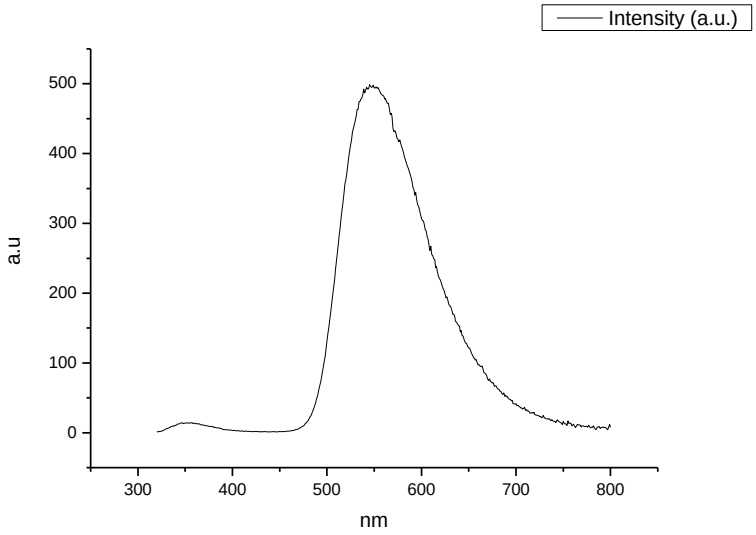

Figure 1.4.201. Fluorescence emission spectrum of **10a** recorded in 1,5-propanediol at 310 nm excitation.

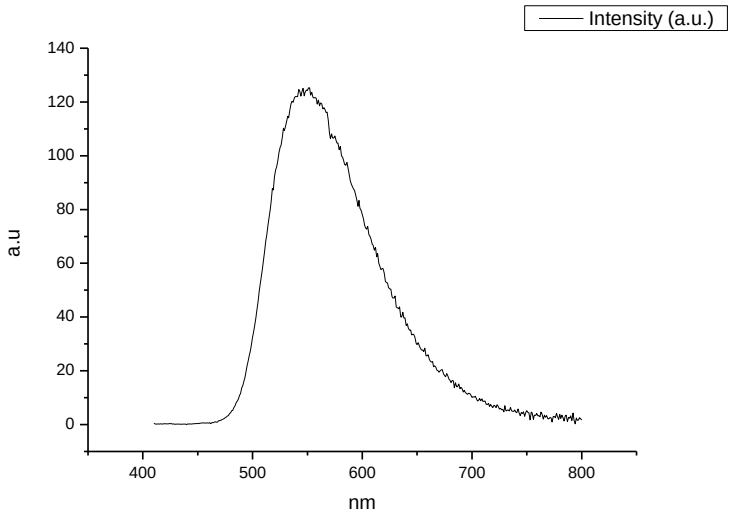

Figure 1.4.202. Fluorescence emission spectrum of **10a** recorded in 1,5-propanediol at 400 nm excitation.

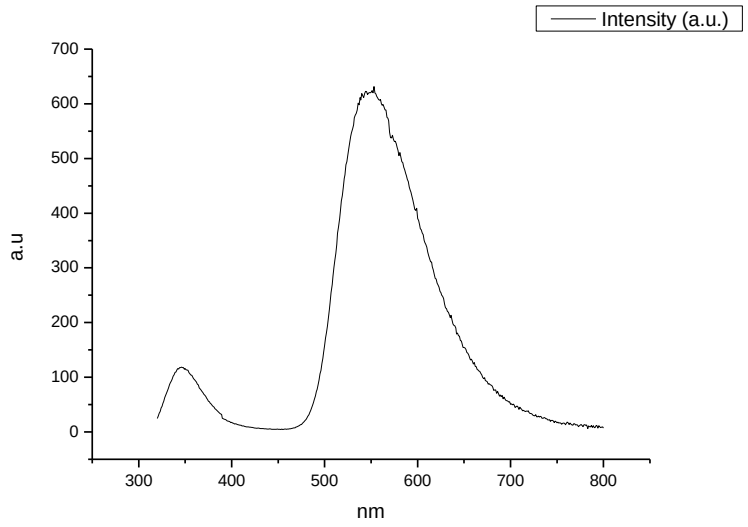

Figure 1.4.203. Fluorescence emission spectrum of **10a** recorded in 1,3-butanediol at 310 nm excitation.

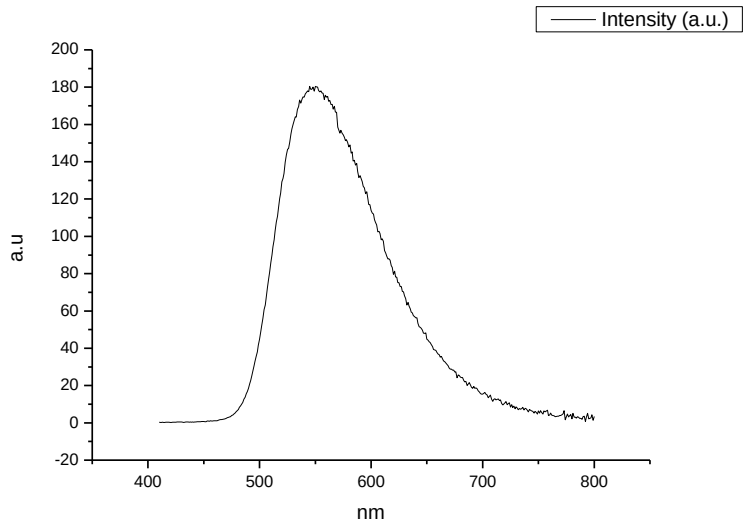

Figure 1.4.204. Fluorescence emission spectrum of **10a** recorded in 1,3-butanediol at 400 nm excitation.

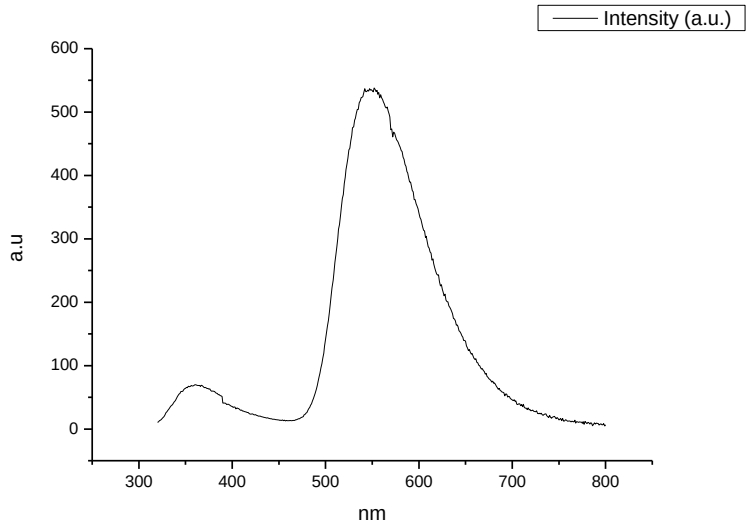

Figure 1.4.205. Fluorescence emission spectrum of **10a** recorded in 1,4-butanediol at 310 nm excitation.

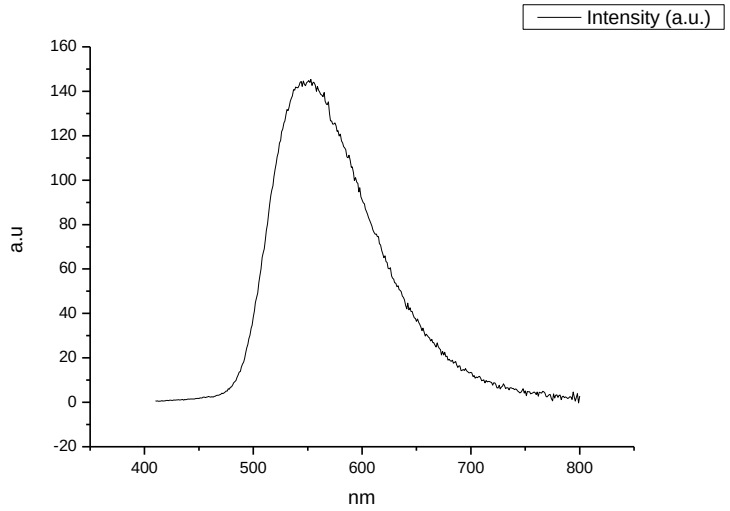

Figure 1.4.206. Fluorescence emission spectrum of **10a** recorded in 1,4-butanediol at 400 nm excitation.

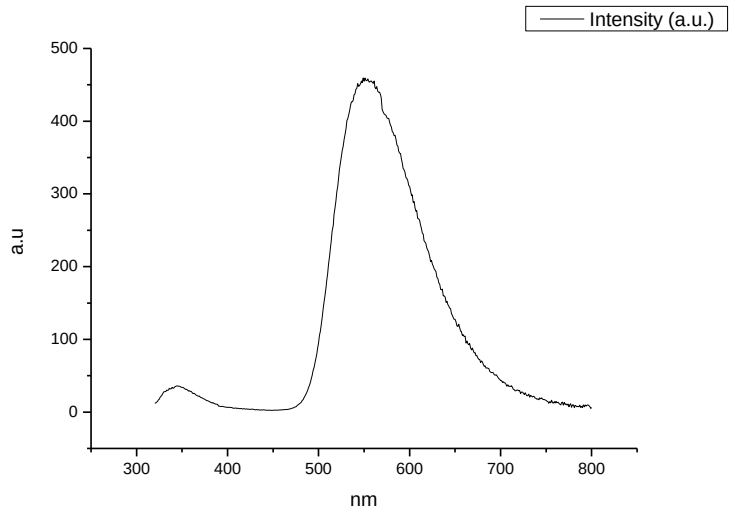

Figure 1.4.207. Fluorescence emission spectrum of **10a** recorded in 1,3-propanediol at 310 nm excitation.

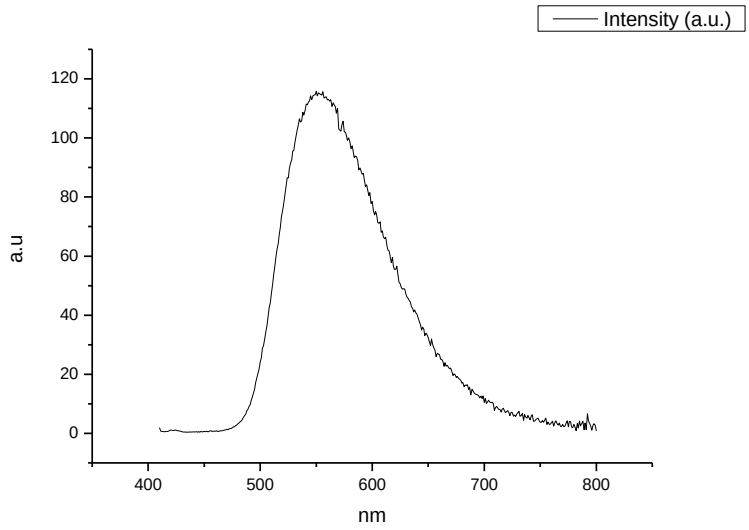

Figure 1.4.208. Fluorescence emission spectrum of **10a** recorded in 1,3-propanediol at 400 nm excitation.

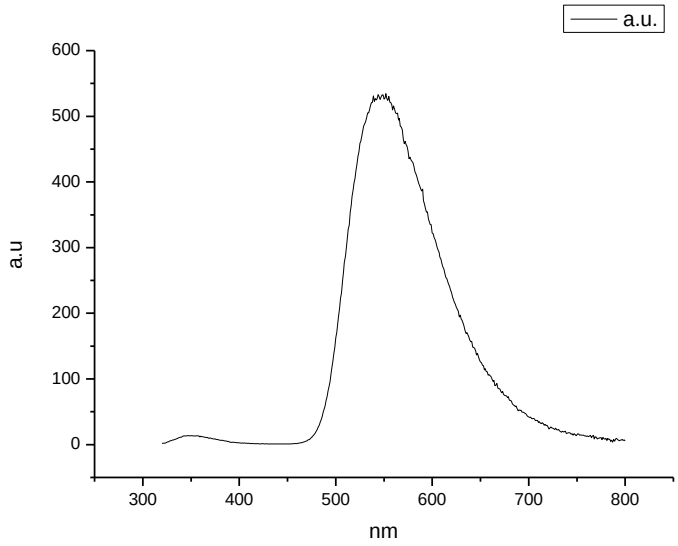

Figure 1.4.209. Fluorescence emission spectrum of **10a** recorded in Methanol at 310 nm excitation.

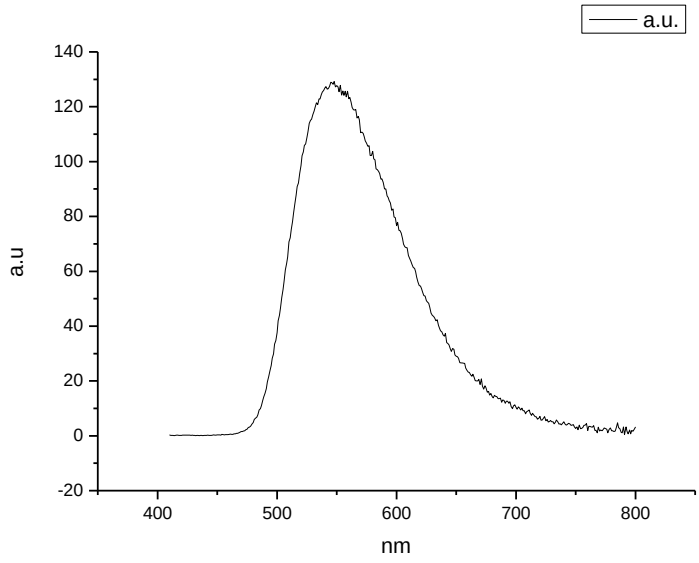

Figure 1.4.210. Fluorescence emission spectrum of **10a** recorded in Methanol at 400 nm excitation.

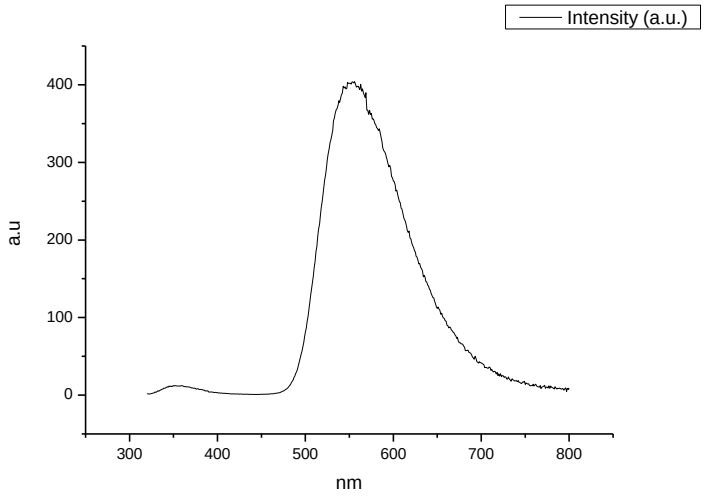

Figure 1.4.211. Fluorescence emission spectrum of **10a** recorded in 1,2-ethanediol at 310 nm excitation.

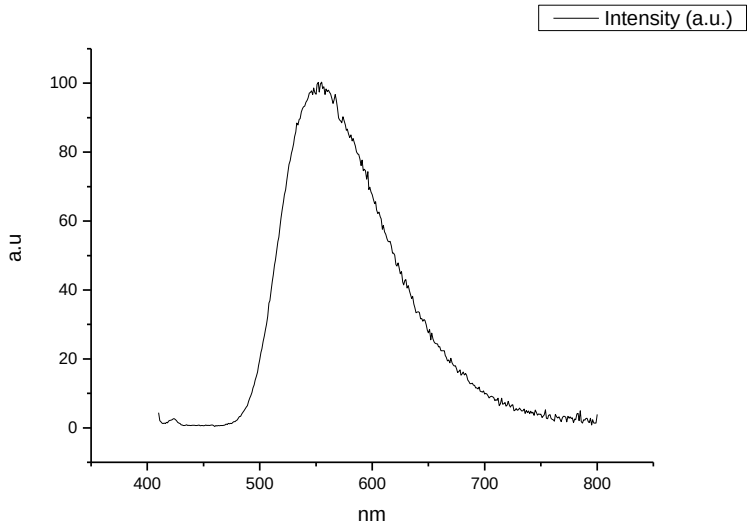

Figure 1.4.212. Fluorescence emission spectrum of **10a** recorded in 1,2-ethanediol at 400 nm excitation.

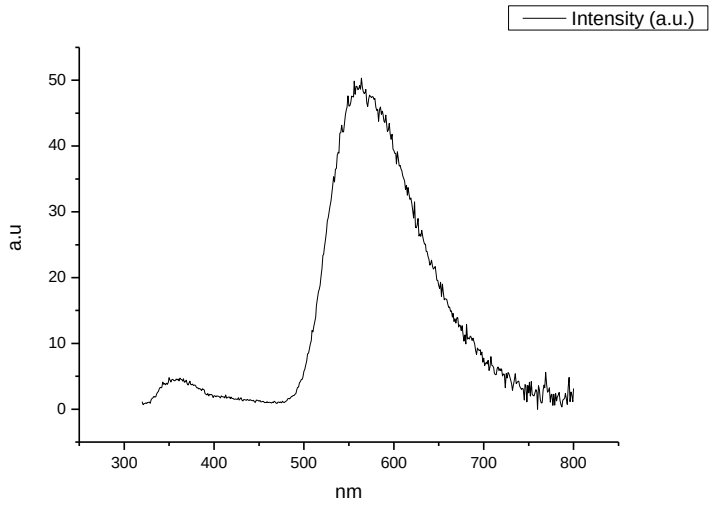

Figure 1.4.213. Fluorescence emission spectrum of **10a** recorded in 2,2,2-trifluoroethanol at 310 nm excitation.

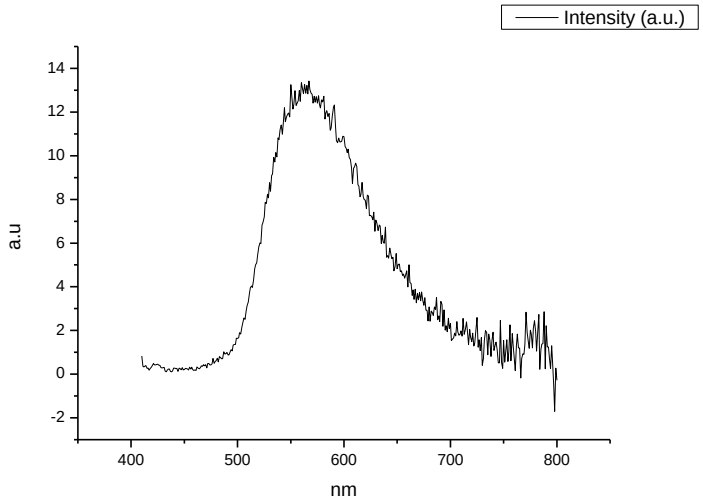

Figure 1.4.214. Fluorescence emission spectrum of **10a** recorded in 2,2,2-trifluoroethanol at 400 nm excitation.

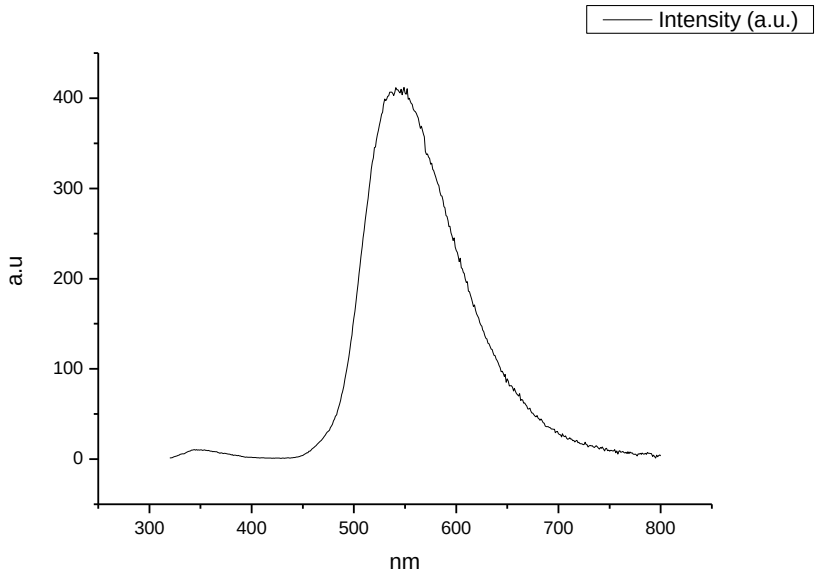

Figure 1.4.215. Fluorescence emission spectrum of **10a** recorded in ethanol-d_1 (EtOD) at 310 nm excitation.

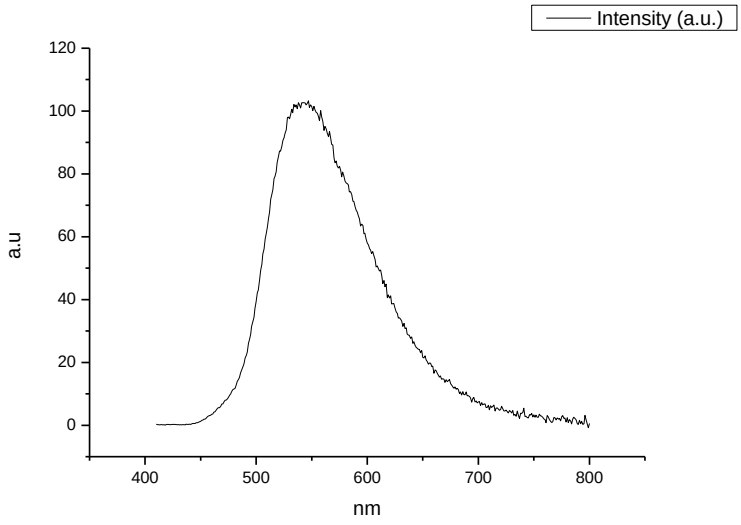

Figure 1.4.216. Fluorescence emission spectrum of **10a** recorded in ethanol-d_1 (EtOD) at 400 nm excitation.

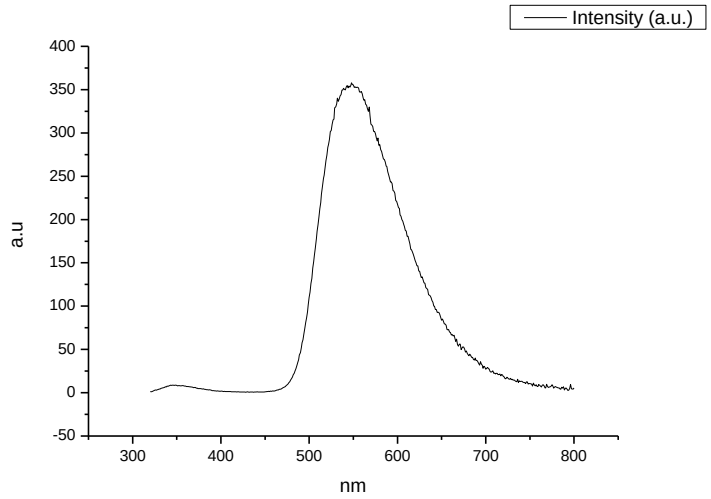

Figure 1.4.217. Fluorescence emission spectrum of **10a** recorded in methanol-d_1 (MeOD) at 310 nm excitation.

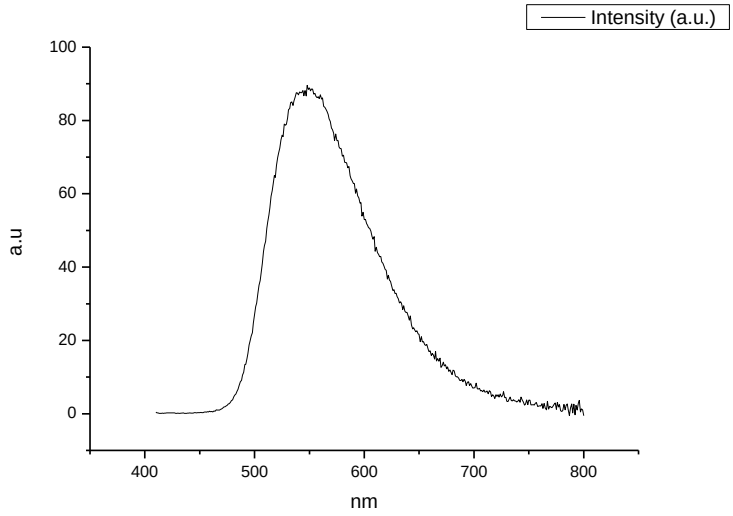

Figure 1.4.218. Fluorescence emission spectrum of **10a** recorded in methanol-d_1 (MeOD) at 400 nm excitation.

1.4.10 Normalised Fluorescence Emission spectra (Gaussian fitted).

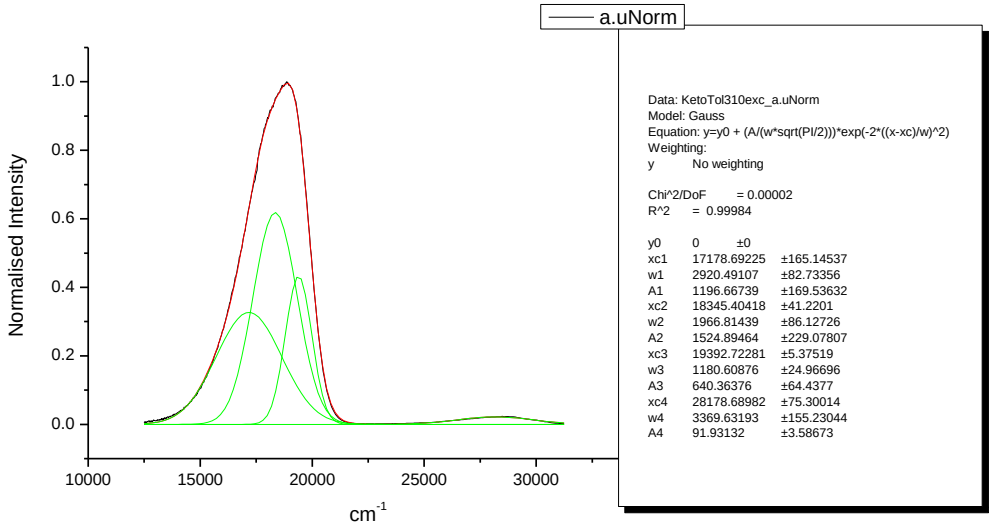

Figure 1.4.219. Gaussian model fit of the normalised fluorescence emission spectrum of **10a** recorded in Toluene at 310 nm excitation.

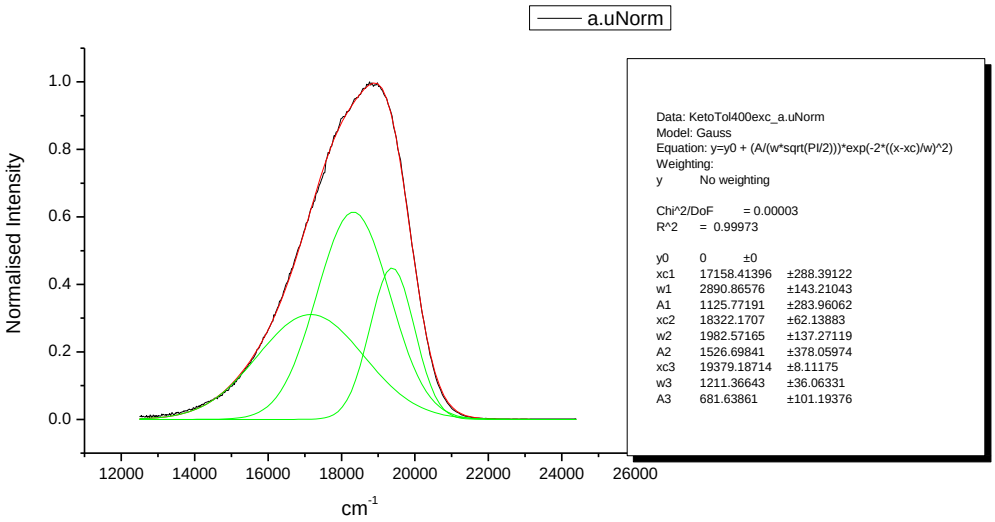

Figure 1.4.220. Gaussian model fit of the normalised fluorescence emission spectrum of **10a** recorded in Toluene at 400 nm excitation.

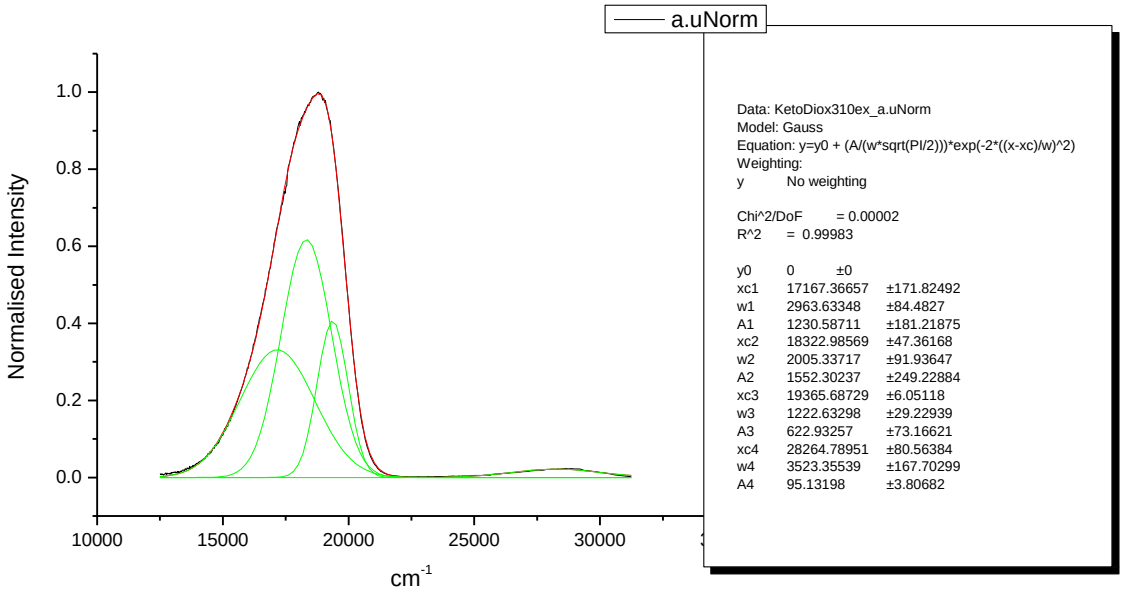

Figure 1.4.221. Gaussian model fit of the normalised fluorescence emission spectrum of **10a** recorded in 1,4-dioxane at 310 nm excitation.

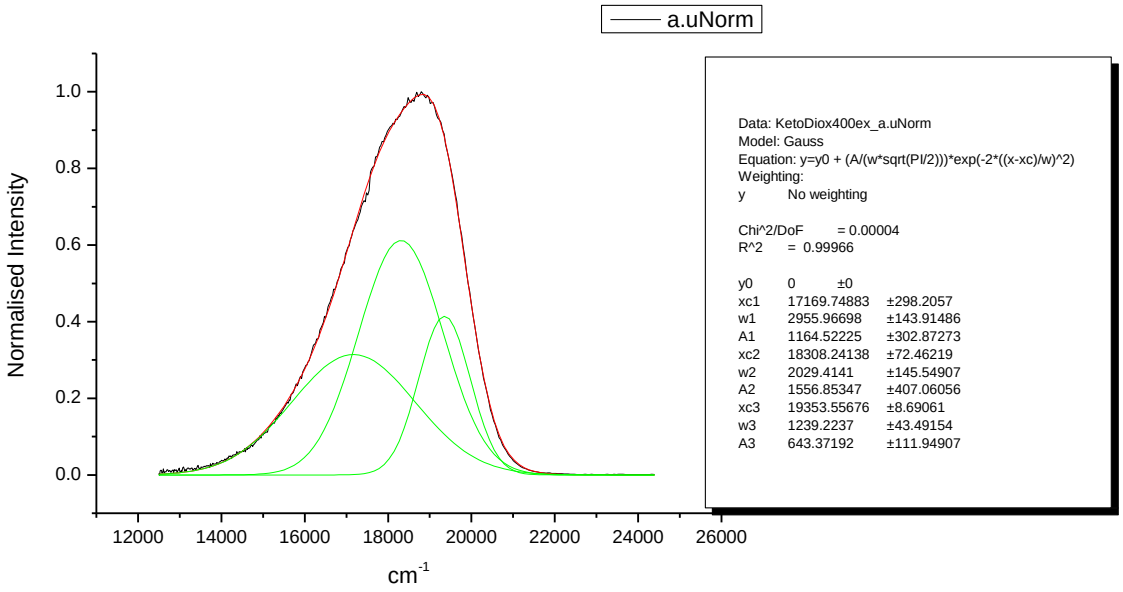

Figure 1.4.222. Gaussian model fit of the normalised fluorescence emission spectrum of **10a** recorded in 1,4-dioxane at 400 nm excitation.

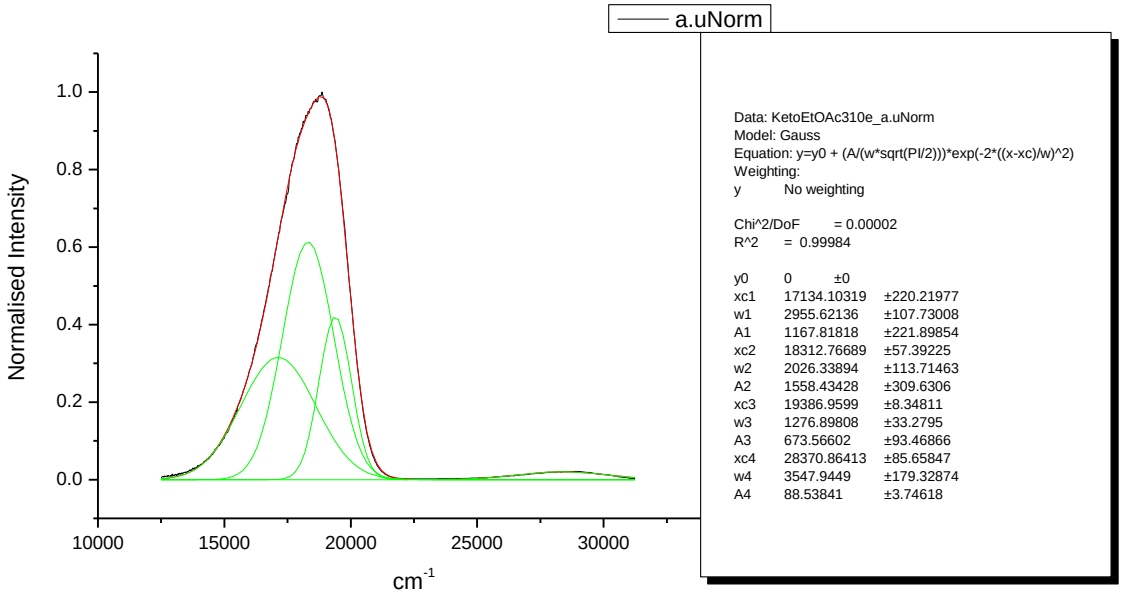

Figure 1.4.223. Gaussian model fit of the normalised fluorescence emission spectrum of **10a** recorded in Ethyl Acetate at 310 nm excitation.

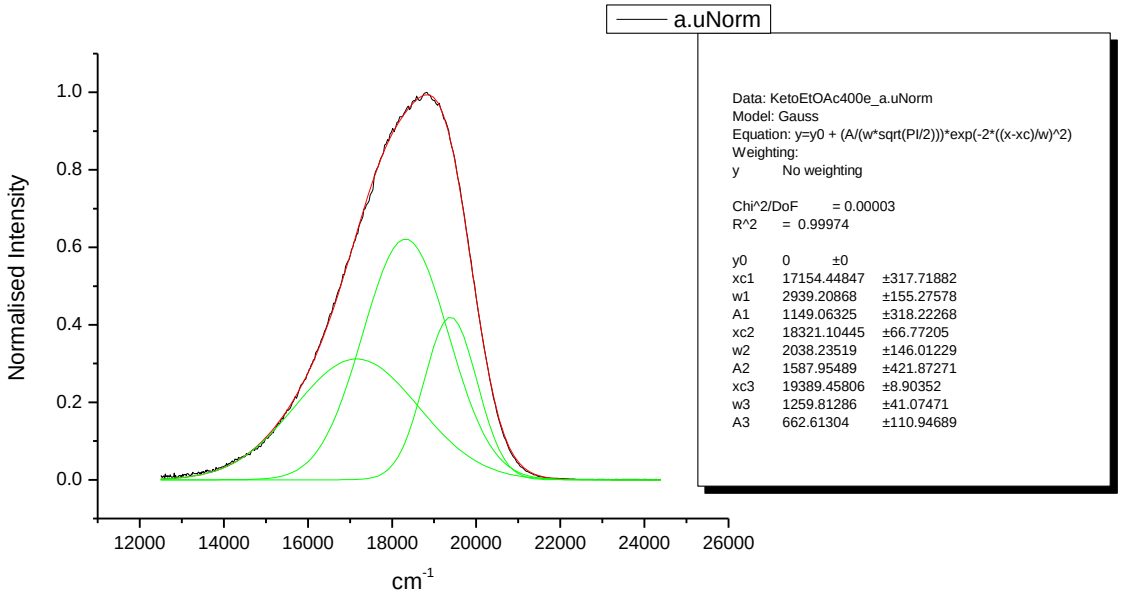

Figure 1.4.224. Gaussian model fit of the normalised fluorescence emission spectrum of **10a** recorded in Ethyl Acetate at 400 nm excitation.

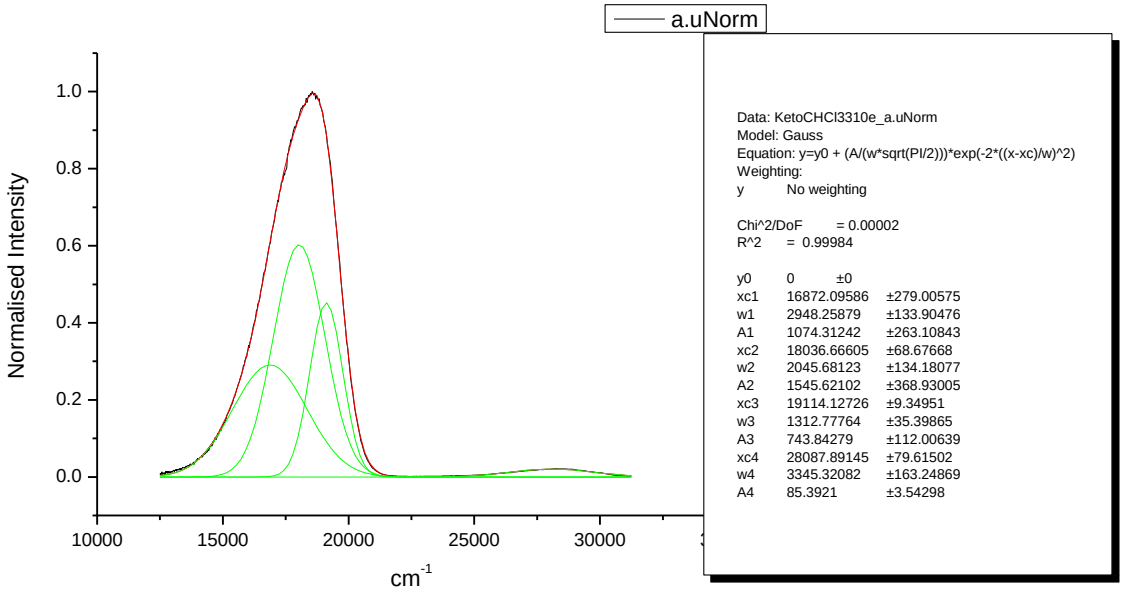

Figure 1.4.225. Gaussian model fit of the normalised fluorescence emission spectrum of **10a** recorded in Chloroform at 310 nm excitation.

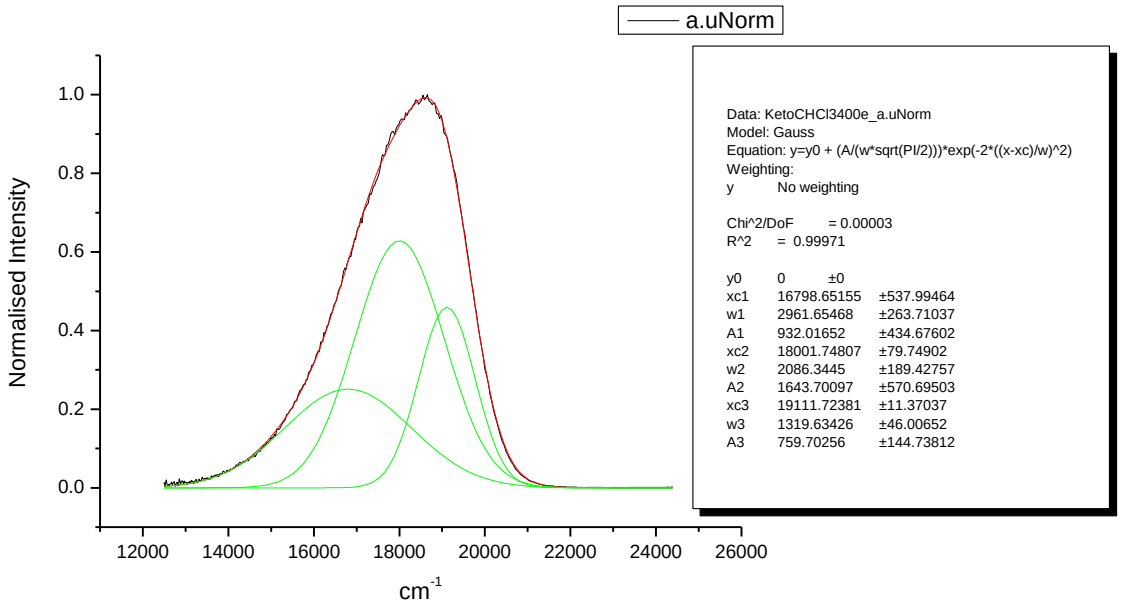

Figure 1.4.226. Gaussian model fit of the normalised fluorescence emission spectrum of **10a** recorded in Chloroform at 400 nm excitation.

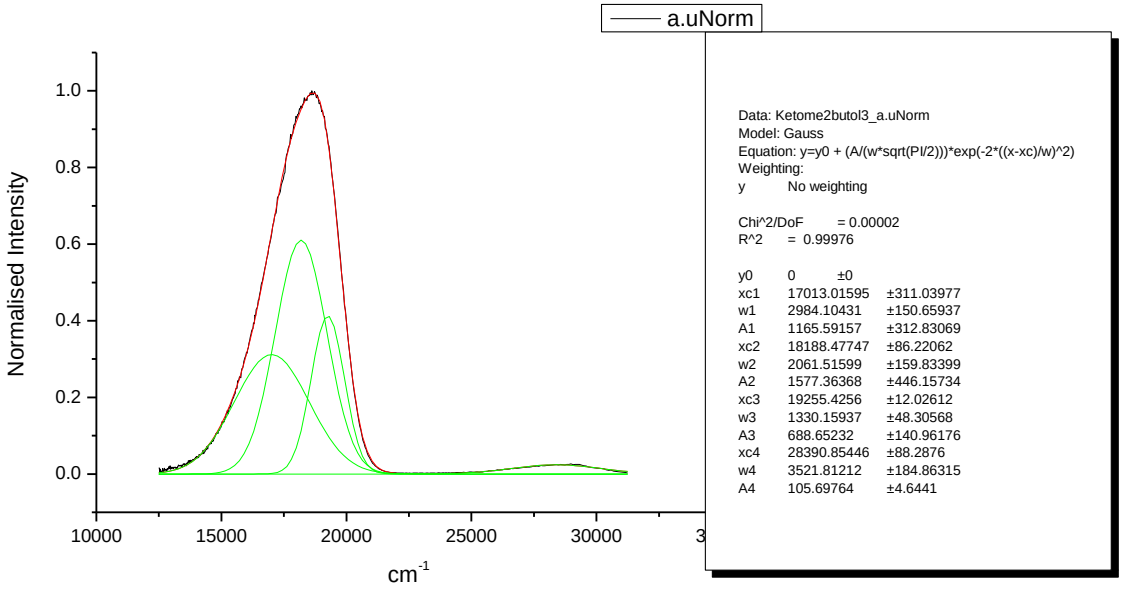

Figure 1.4.227. Gaussian model fit of the normalised fluorescence emission spectrum of **10a** recorded in 2-methyl-2-butanol at 310 nm excitation.

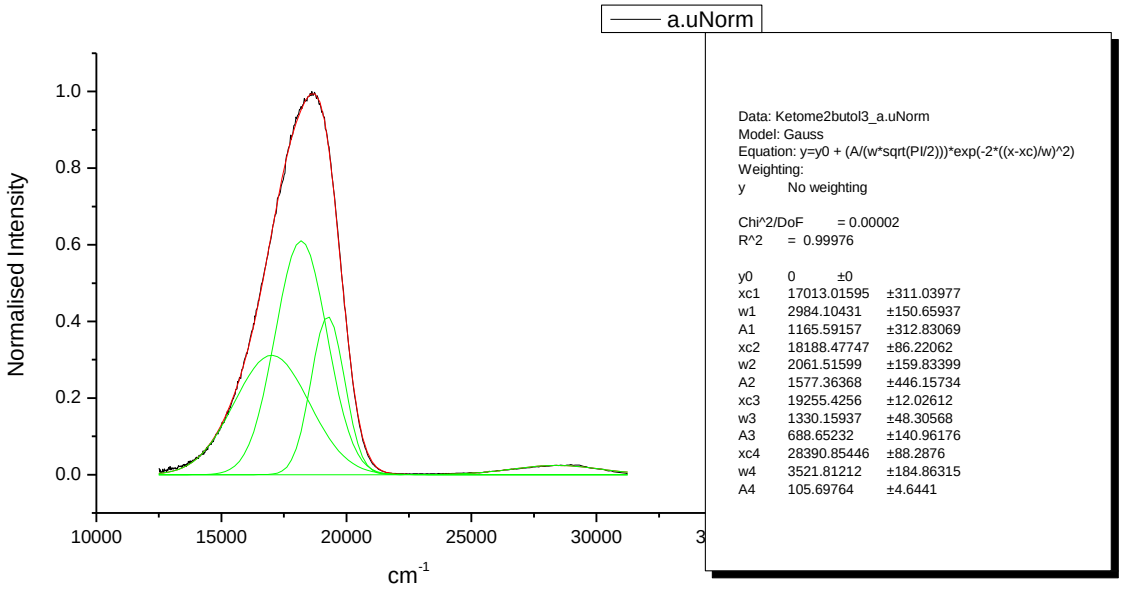

Figure 1.4.228. Gaussian model fit of the normalised fluorescence emission spectrum of **10a** recorded in 2-methyl-2-butanol at 400 nm excitation.

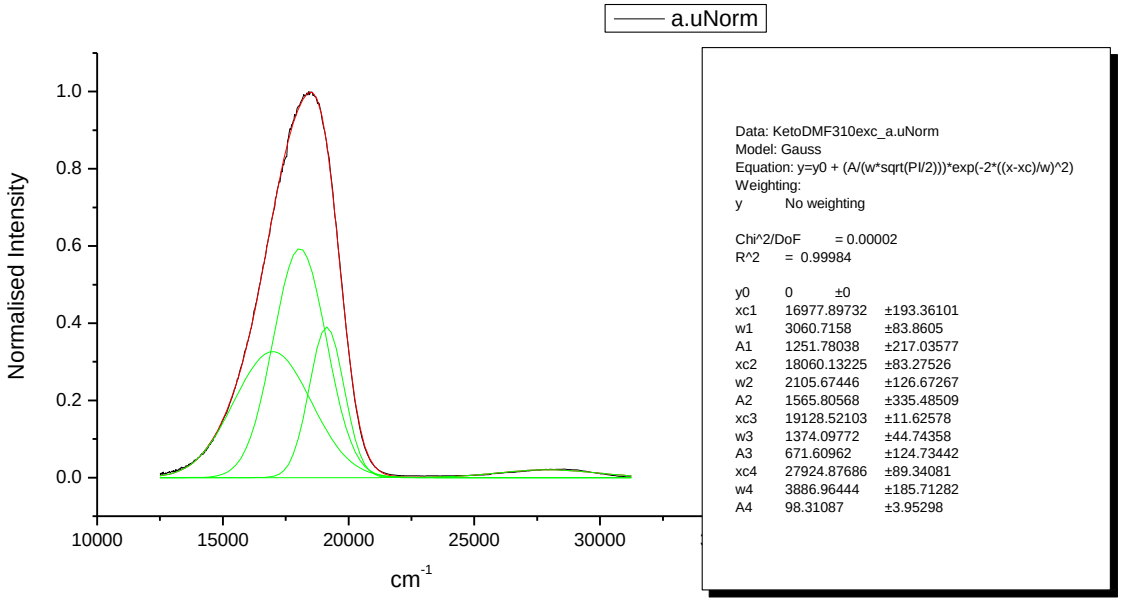

Figure 1.4.229. Gaussian model fit of the normalised fluorescence emission spectrum of **10a** recorded in N,N-dimethylformamide at 310 nm excitation.

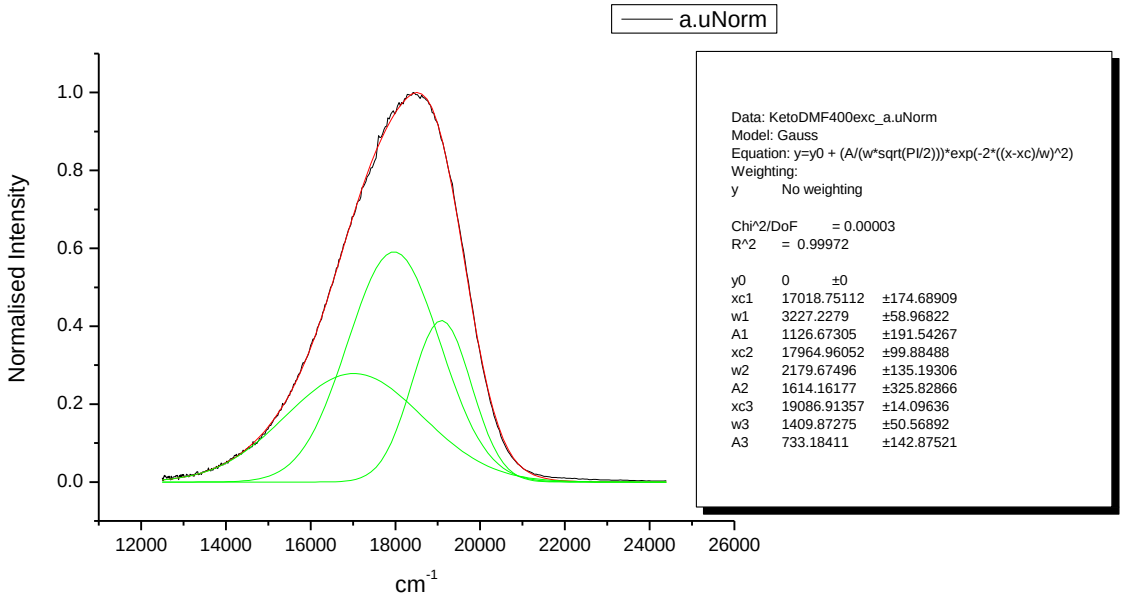

Figure 1.4.230. Gaussian model fit of the normalised fluorescence emission spectrum of **10a** recorded in N,N-dimethylformamide at 400 nm excitation.

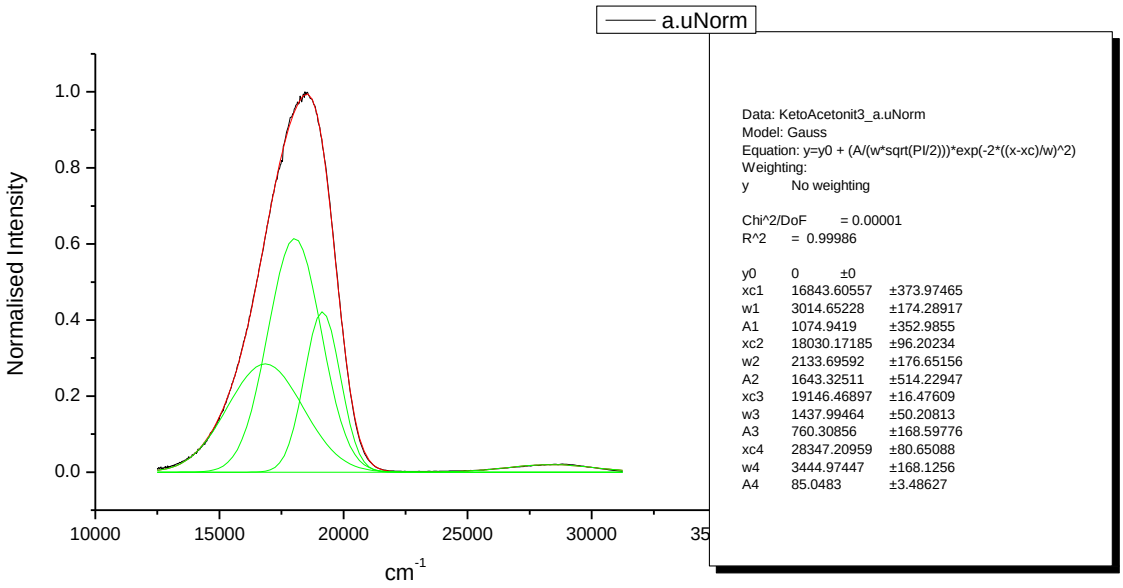

Figure 1.4.231. Gaussian model fit of the normalised fluorescence emission spectrum of **10a** recorded in Acetonitrile at 310 nm excitation.

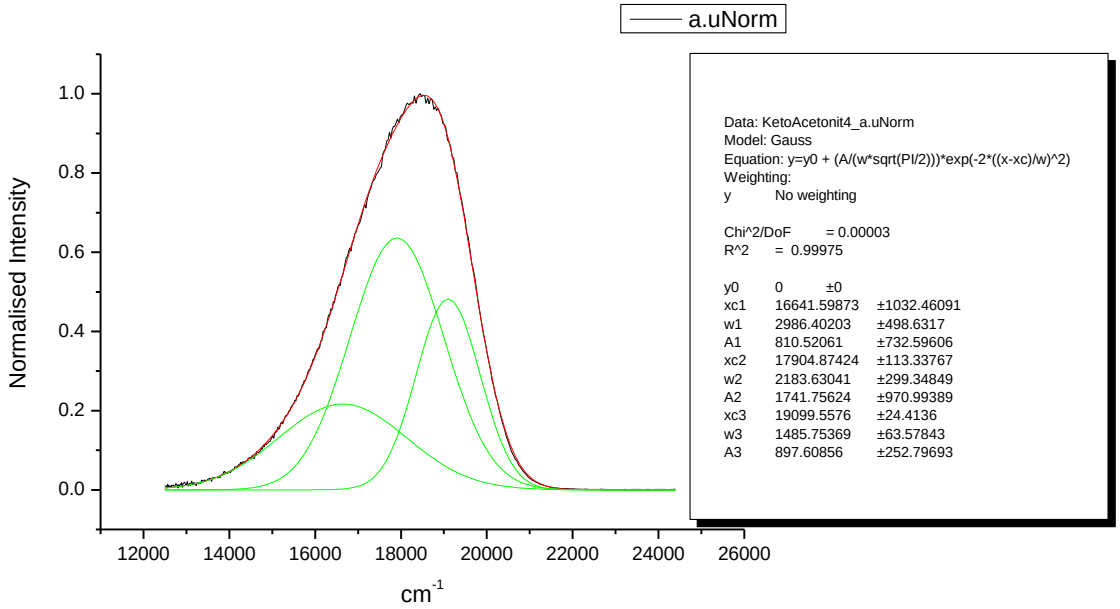

Figure 1.4.232. Gaussian model fit of the normalised fluorescence emission spectrum of **10a** recorded in Acetonitrile at 400 nm excitation.

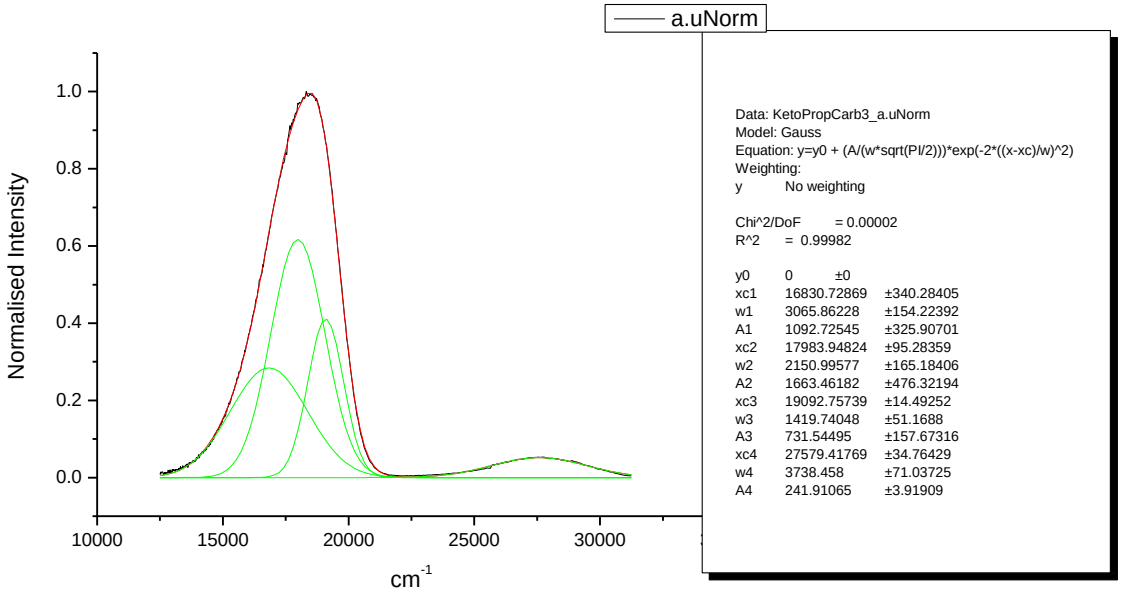

Figure 1.4.233. Gaussian model fit of the normalised fluorescence emission spectrum of **10a** recorded in Propylene Carbonate at 310 nm excitation.

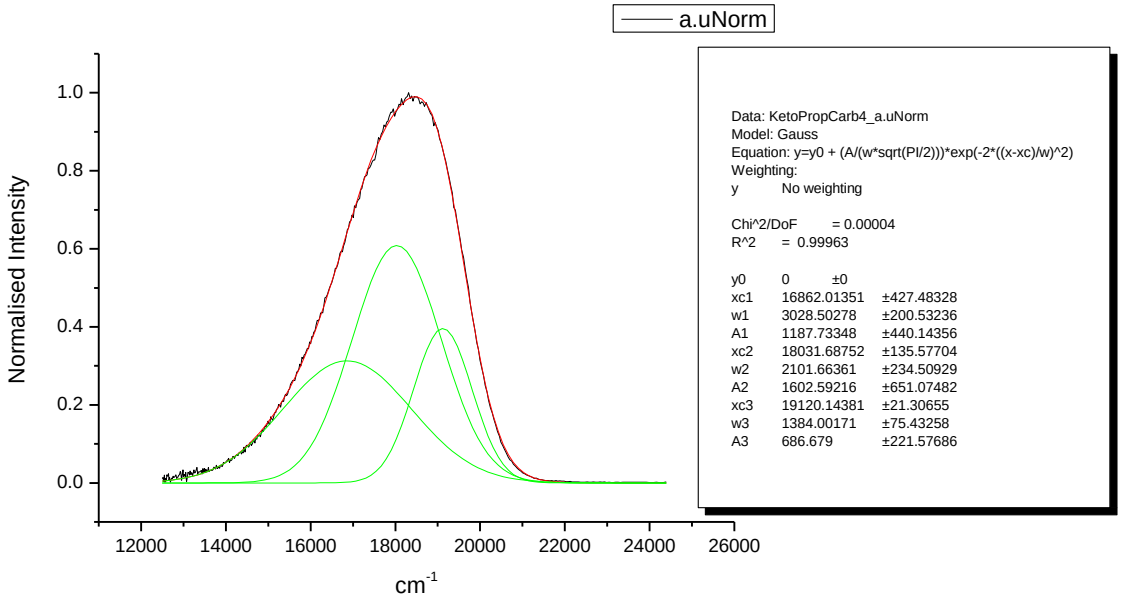

Figure 1.4.234. Gaussian model fit of the normalised fluorescence emission spectrum of **10a** recorded in Propylene Carbonate at 400 nm excitation.

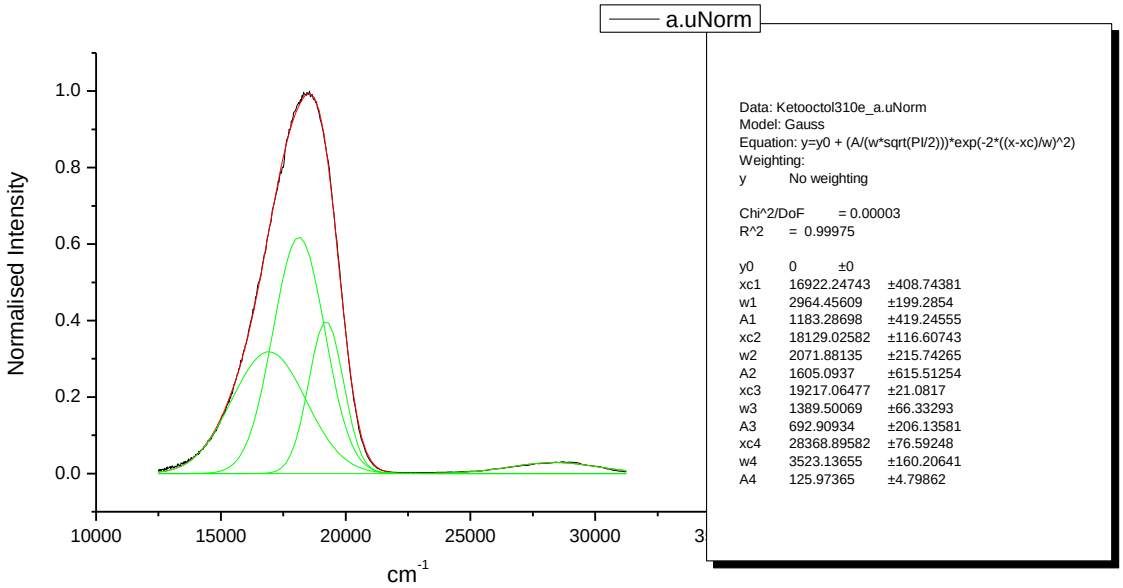

Figure 1.4.235. Gaussian model fit of the normalised fluorescence emission spectrum of **10a** recorded in 1-octanol at 310 nm excitation.

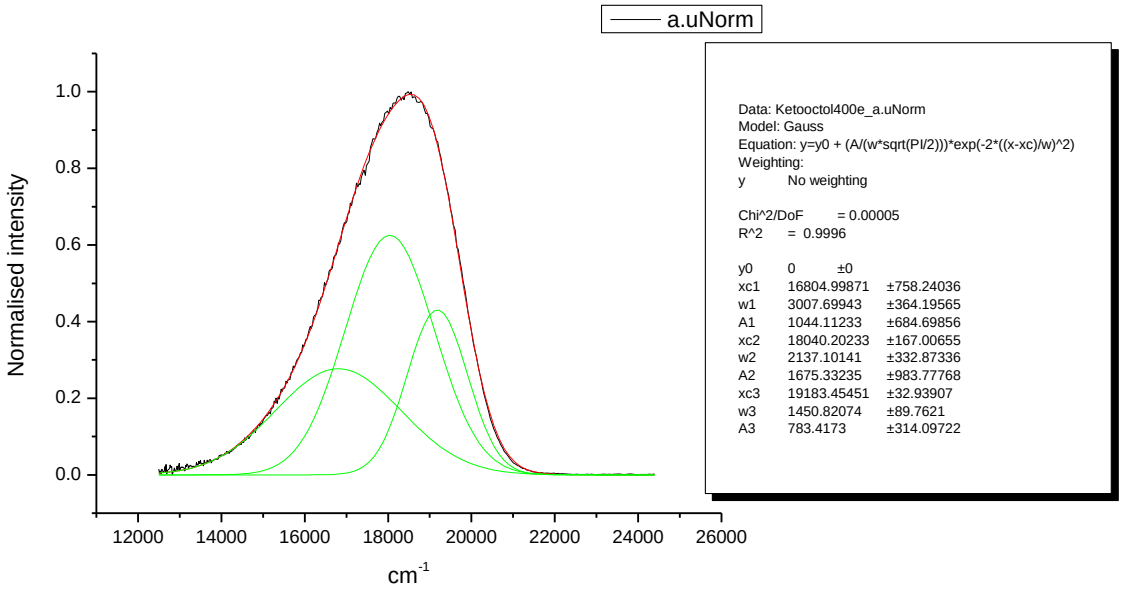

Figure 1.4.236. Gaussian model fit of the normalised fluorescence emission spectrum of **10a** recorded in 1-octanol at 400 nm excitation.

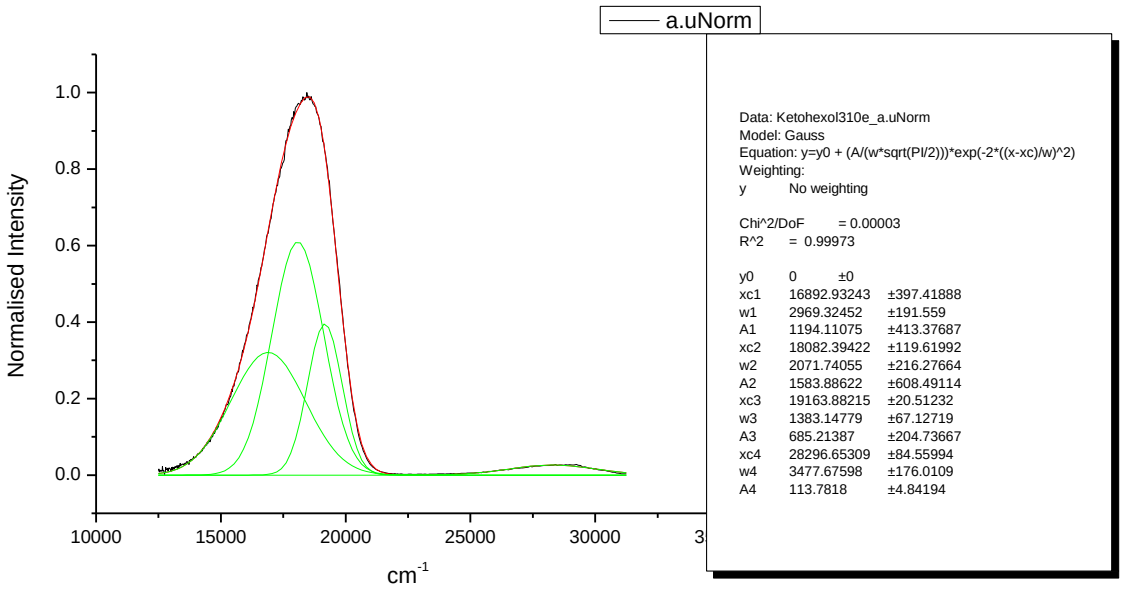

Figure 1.4.237. Gaussian model fit of the normalised fluorescence emission spectrum of **10a** recorded in 1-hexanol at 310 nm excitation.

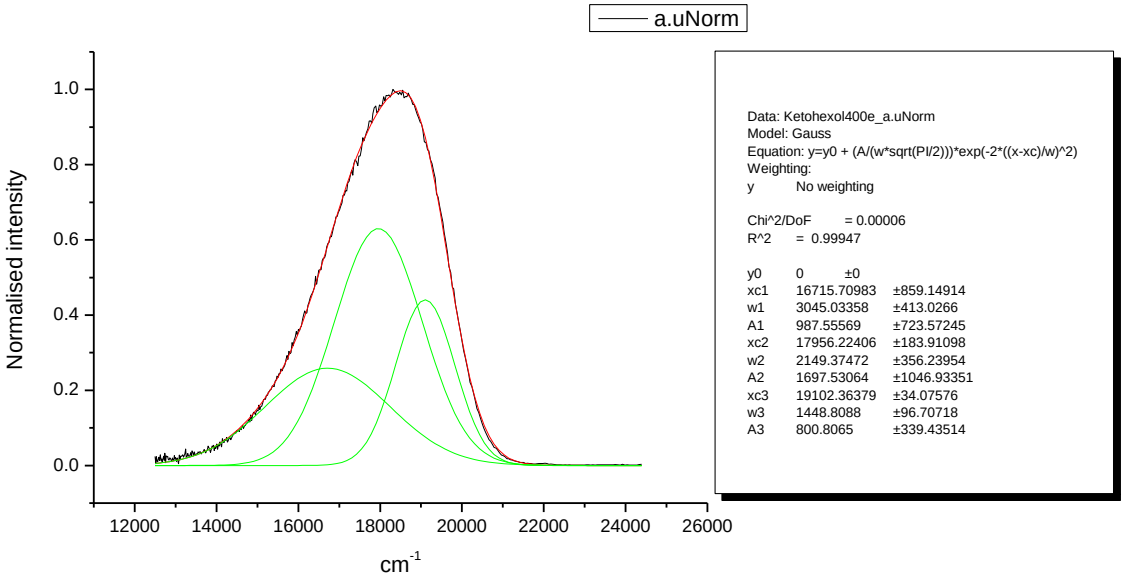

Figure 1.4.238. Gaussian model fit of the normalised fluorescence emission spectrum of **10a** recorded in 1-hexanol at 400 nm excitation.

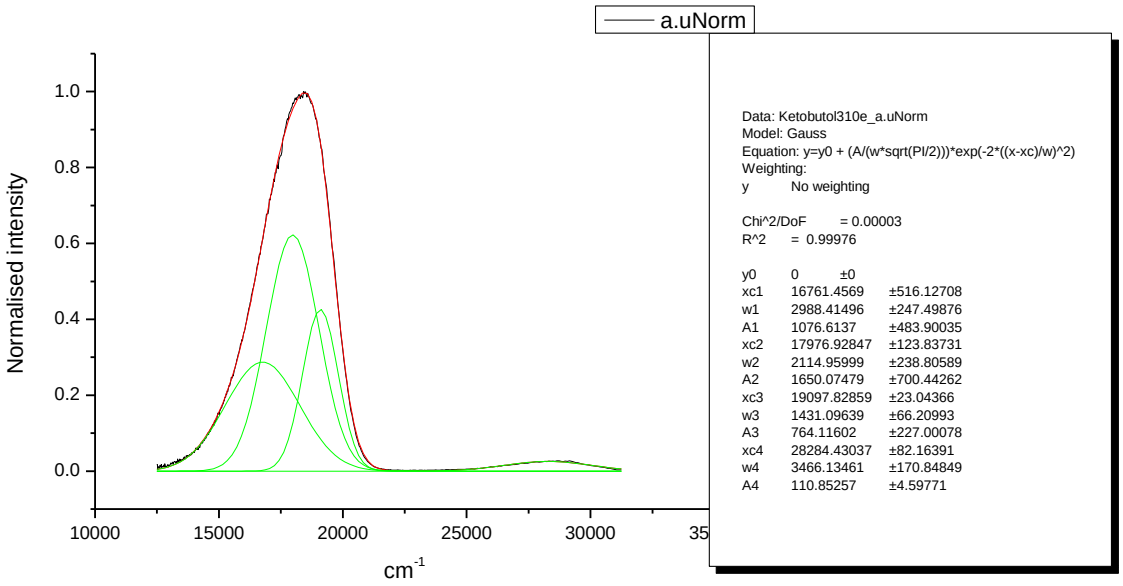

Figure 1.4.239. Gaussian model fit of the normalised fluorescence emission spectrum of **10a** recorded in 1-butanol at 310 nm excitation.

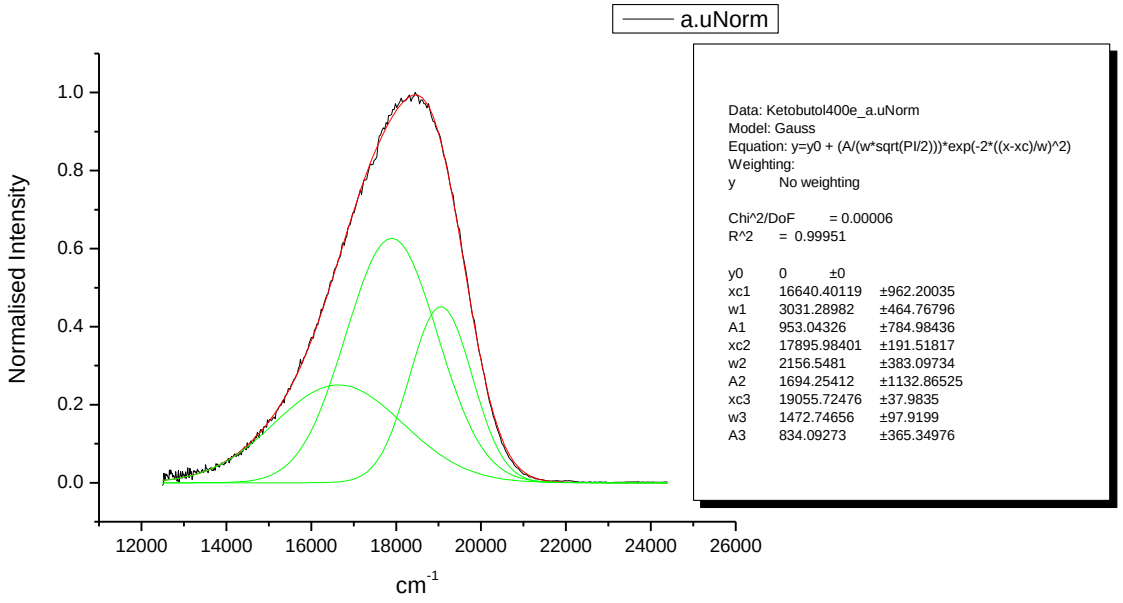

Figure 1.4.240. Gaussian model fit of the normalised fluorescence emission spectrum of **10a** recorded in 1-butanol at 400 nm excitation.

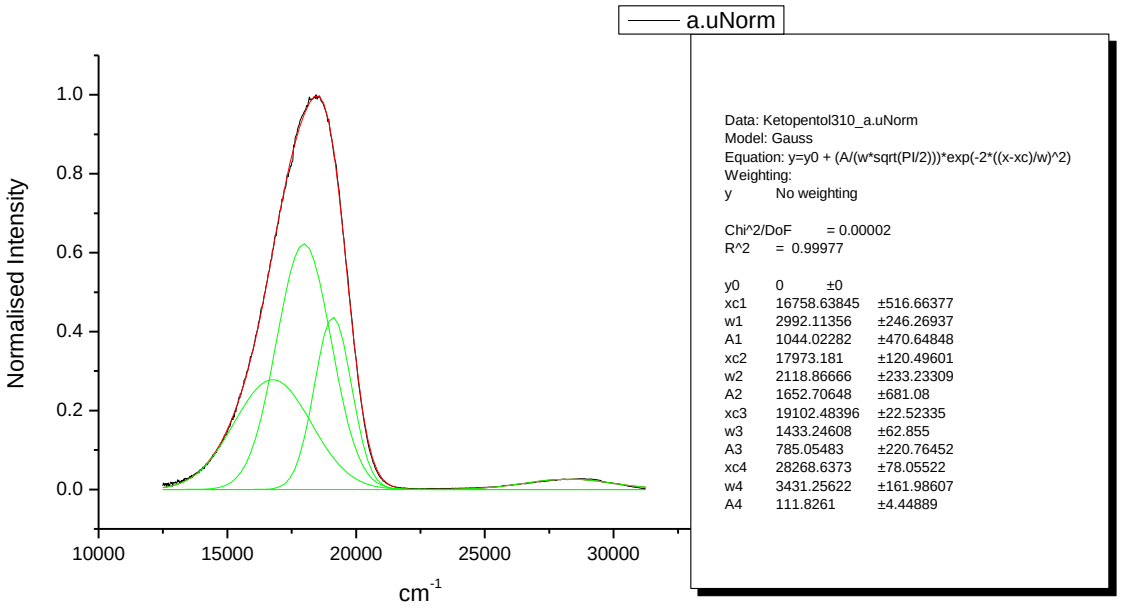

Figure 1.4.241. Gaussian model fit of the normalised fluorescence emission spectrum of **10a** recorded in 1-pentanol at 310 nm excitation.

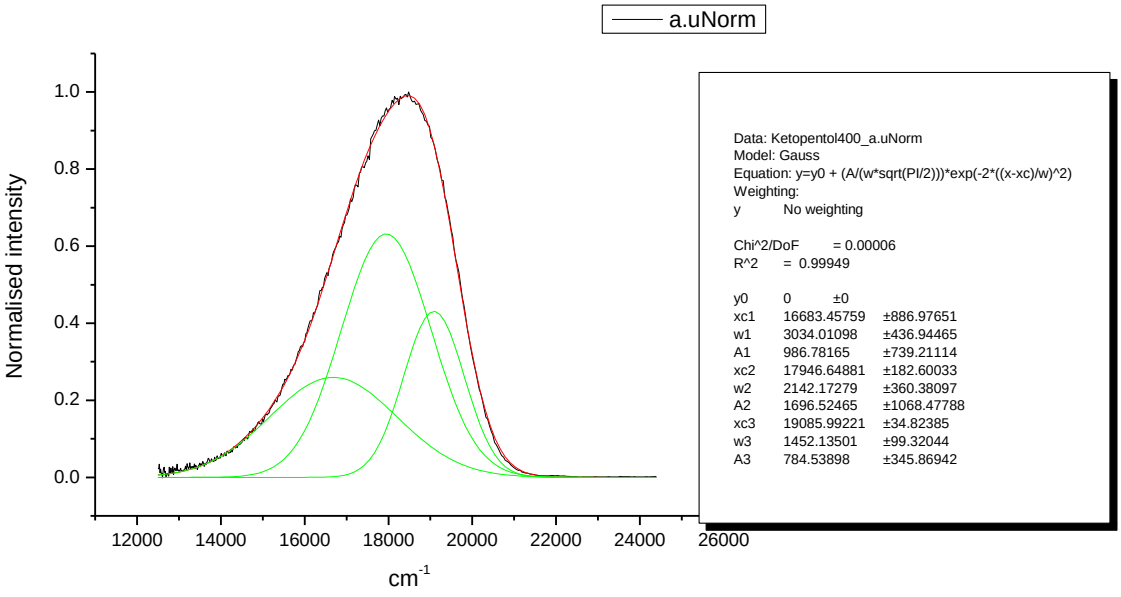

Figure 1.4.242. Gaussian model fit of the normalised fluorescence emission spectrum of **10a** recorded in 1-pentanol at 400 nm excitation.

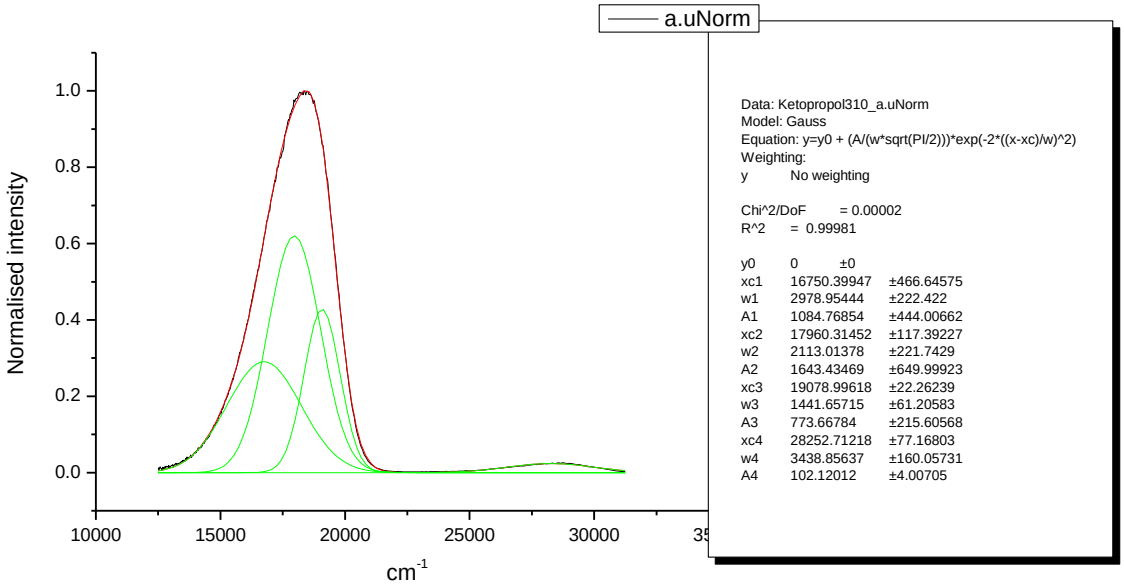

Figure 1.4.243. Gaussian model fit of the normalised fluorescence emission spectrum of **10a** recorded in 1-propanol at 310 nm excitation.

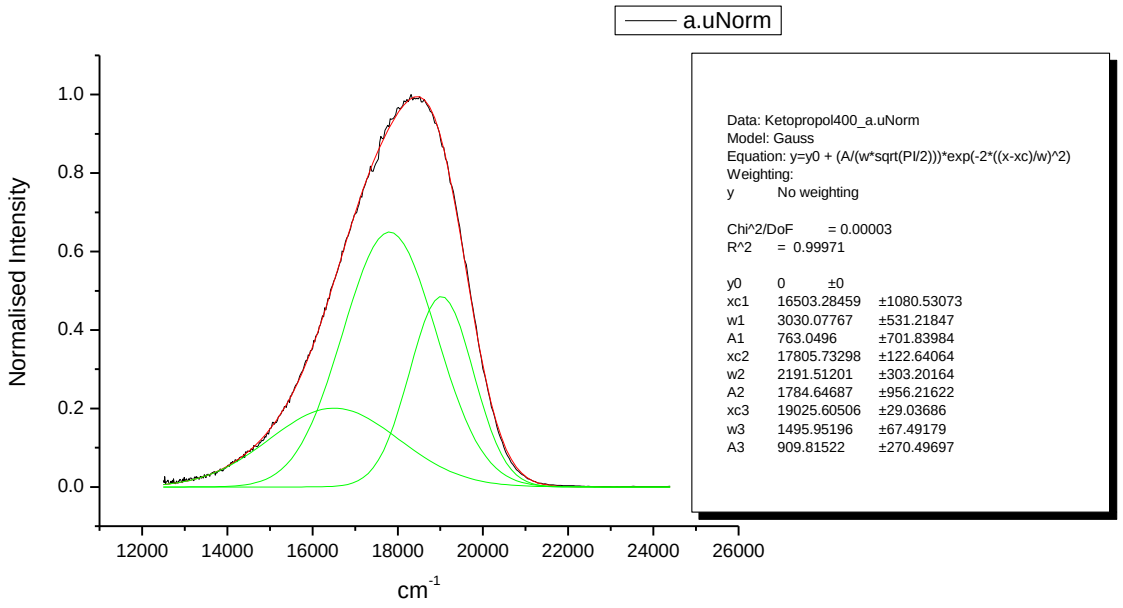

Figure 1.4.244. Gaussian model fit of the normalised fluorescence emission spectrum of **10a** recorded in 1-propanol at 400 nm excitation.

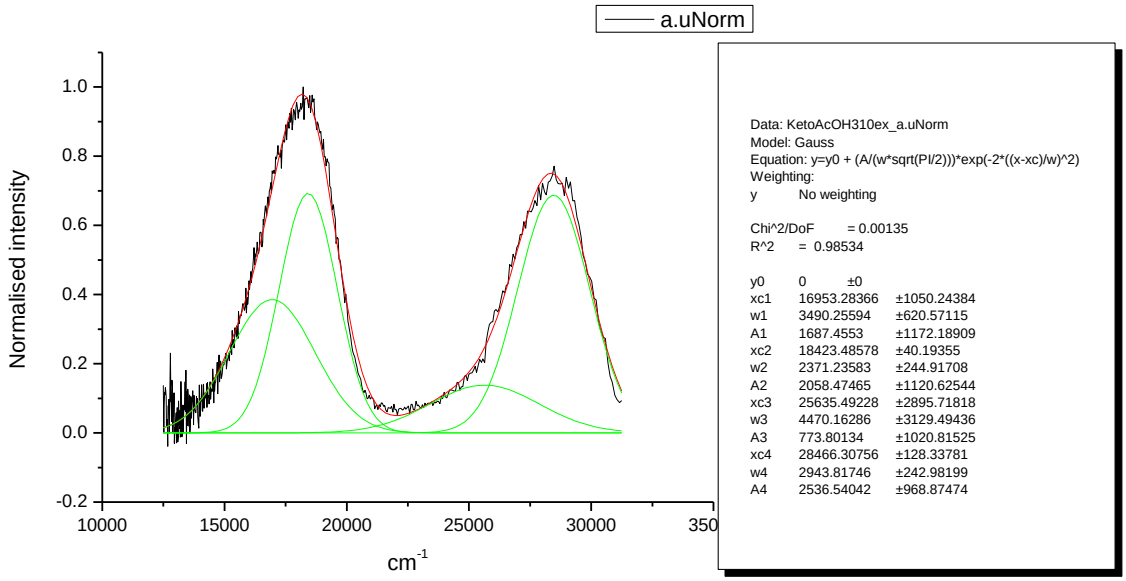

Figure 1.4.245. Gaussian model fit of the normalised fluorescence emission spectrum of **10a** recorded in Acetic Acid at 310 nm excitation.

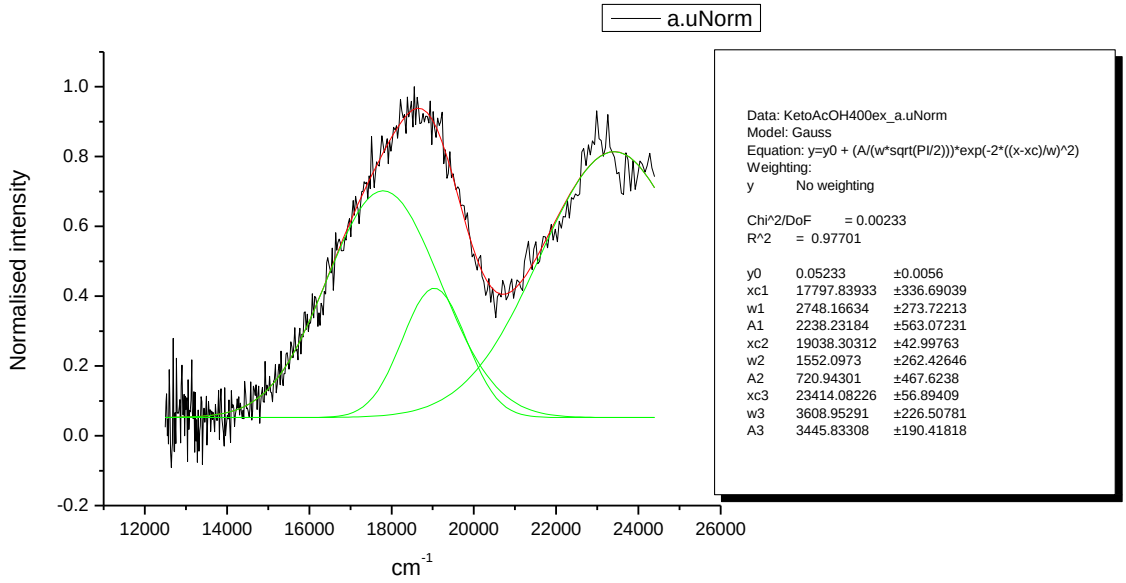

Figure 1.4.246. Gaussian model fit of the normalised fluorescence emission spectrum of **10a** recorded in Acetic Acid at 400 nm excitation.

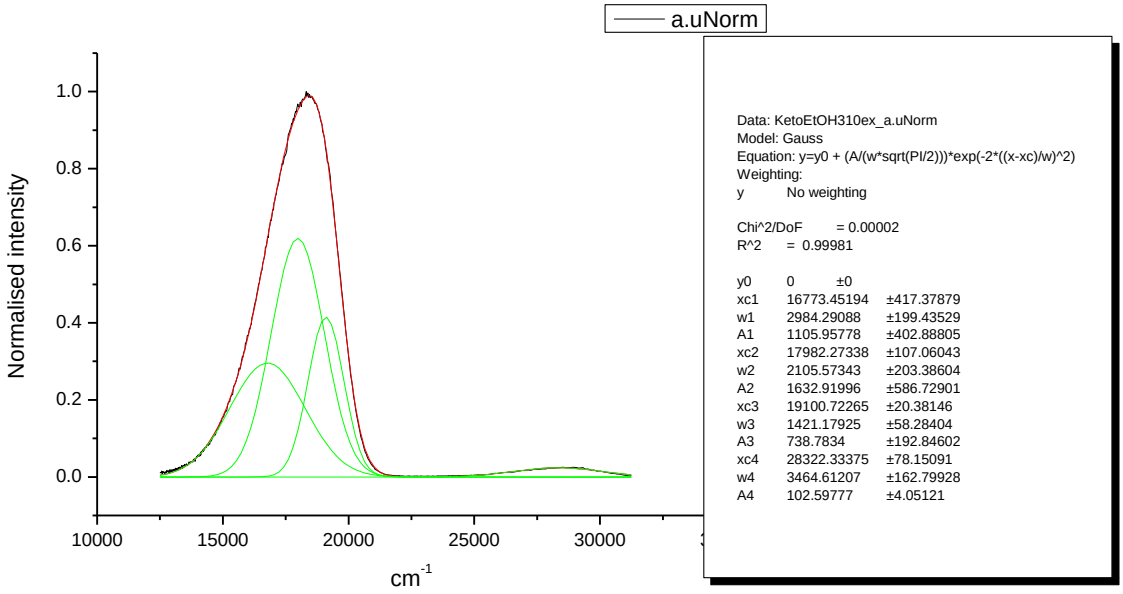

Figure 1.4.247. Gaussian model fit of the normalised fluorescence emission spectrum of **10a** recorded in Ethanol at 310 nm excitation.

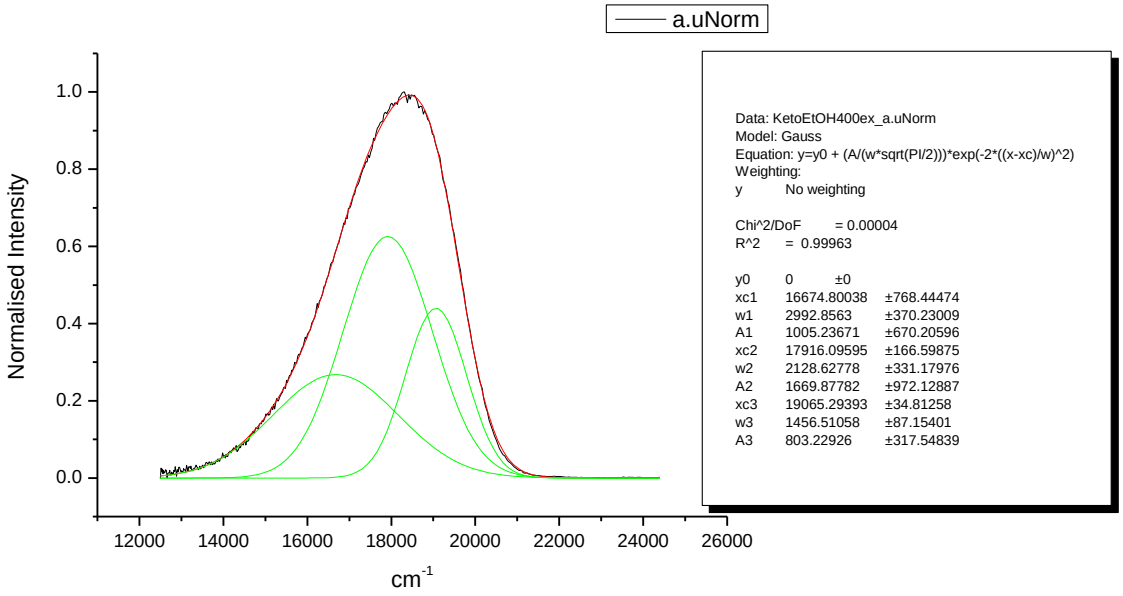

Figure 1.4.248. Gaussian model fit of the normalised fluorescence emission spectrum of **10a** recorded in Ethanol at 400 nm excitation.

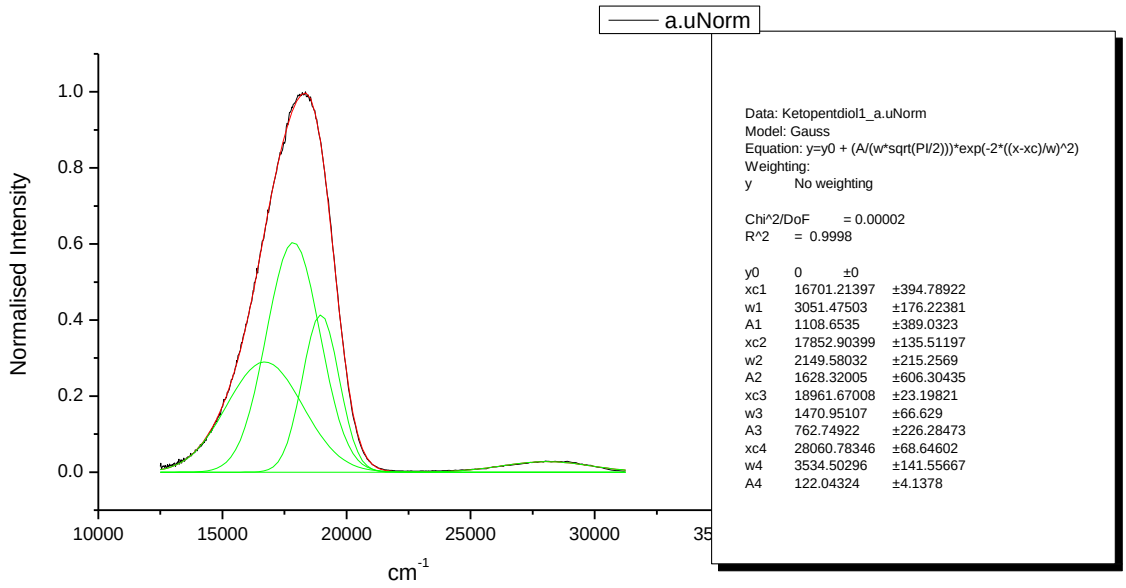

Figure 1.4.249. Gaussian model fit of the normalised fluorescence emission spectrum of **10a** recorded in 1,5-propanediol at 310 nm excitation.

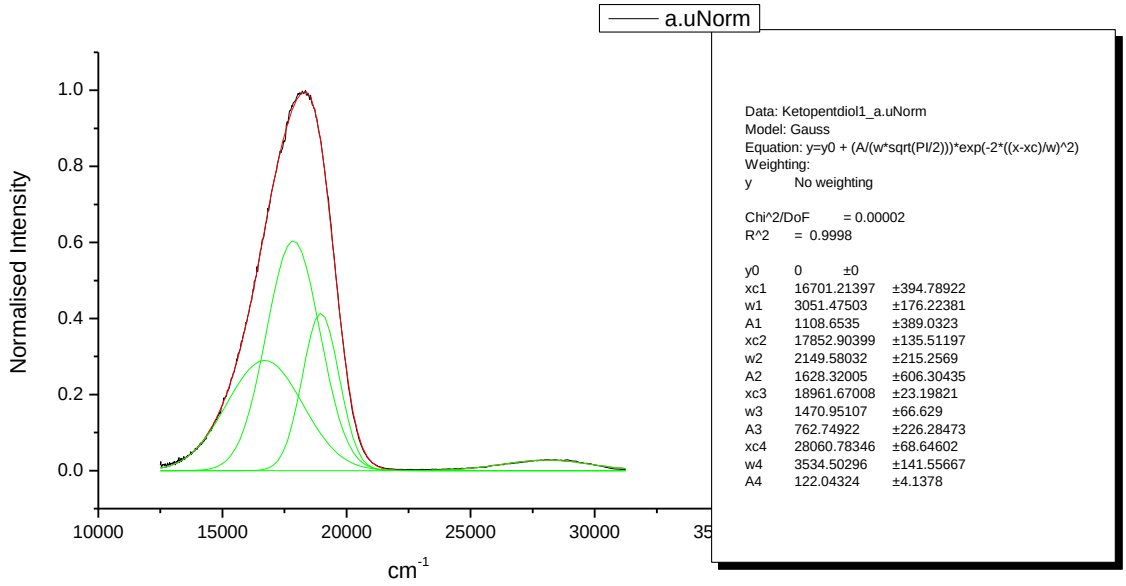

Figure 1.4.250. Gaussian model fit of the normalised fluorescence emission spectrum of **10a** recorded in 1,5-propanediol at 400 nm excitation.

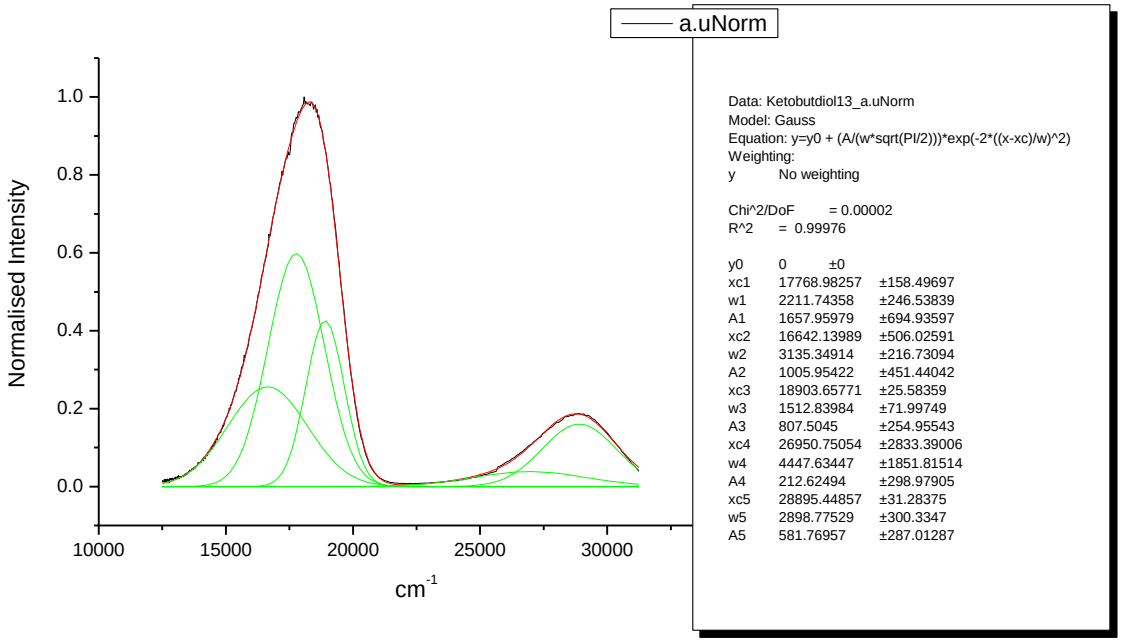

Figure 1.4.251. Gaussian model fit of the normalised fluorescence emission spectrum of **10a** recorded in 1,3-butanediol at 310 nm excitation.

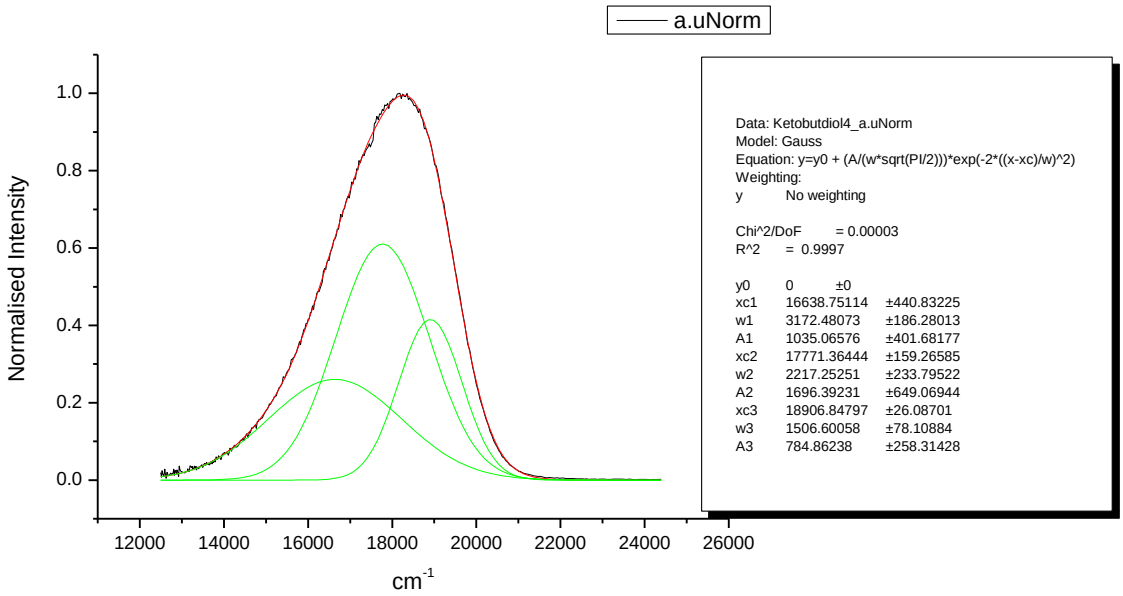

Figure 1.4.252. Gaussian model fit of the normalised fluorescence emission spectrum of **10a** recorded in 1,3-butanediol at 400 nm excitation.

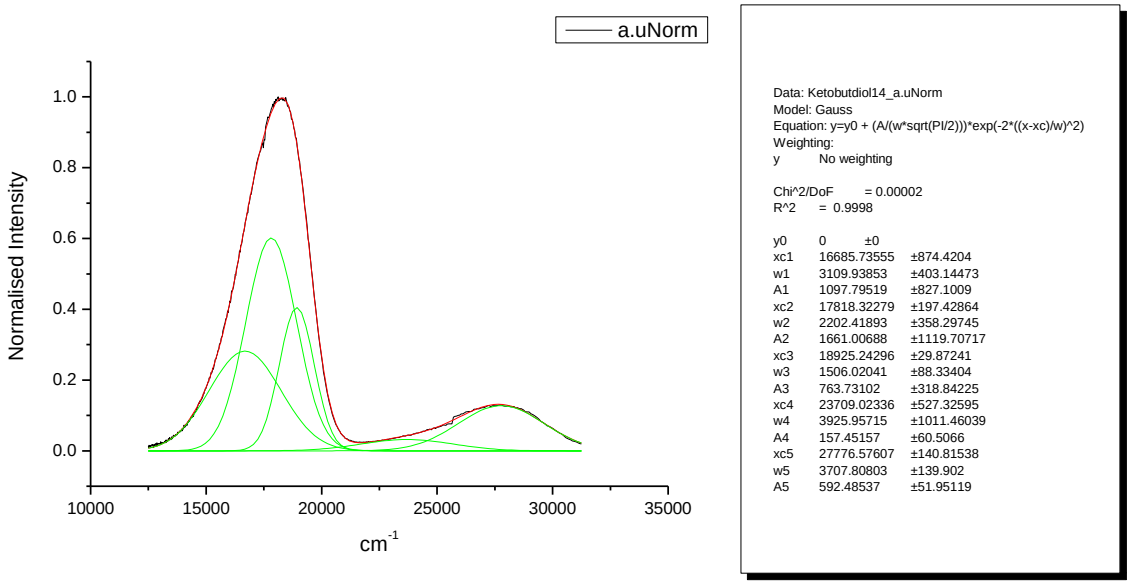

Figure 1.4.253. Gaussian model fit of the normalised fluorescence emission spectrum of **10a** recorded in 1,4-butanediol at 310 nm excitation.

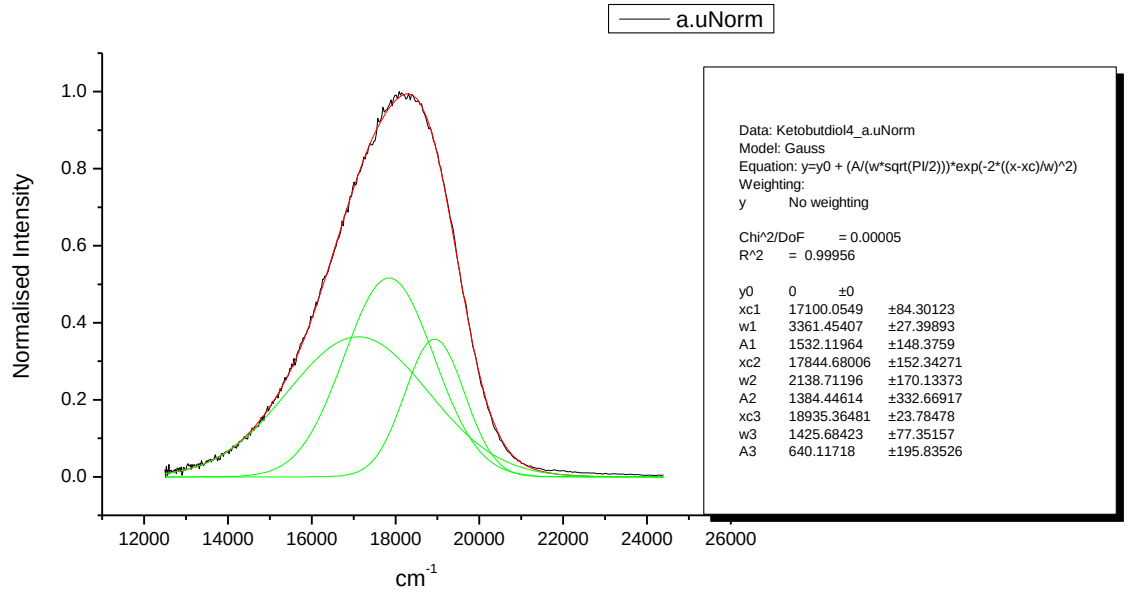

Figure 1.4.254. Gaussian model fit of the normalised fluorescence emission spectrum of **10a** recorded in 1,4-butanediol at 400 nm excitation.

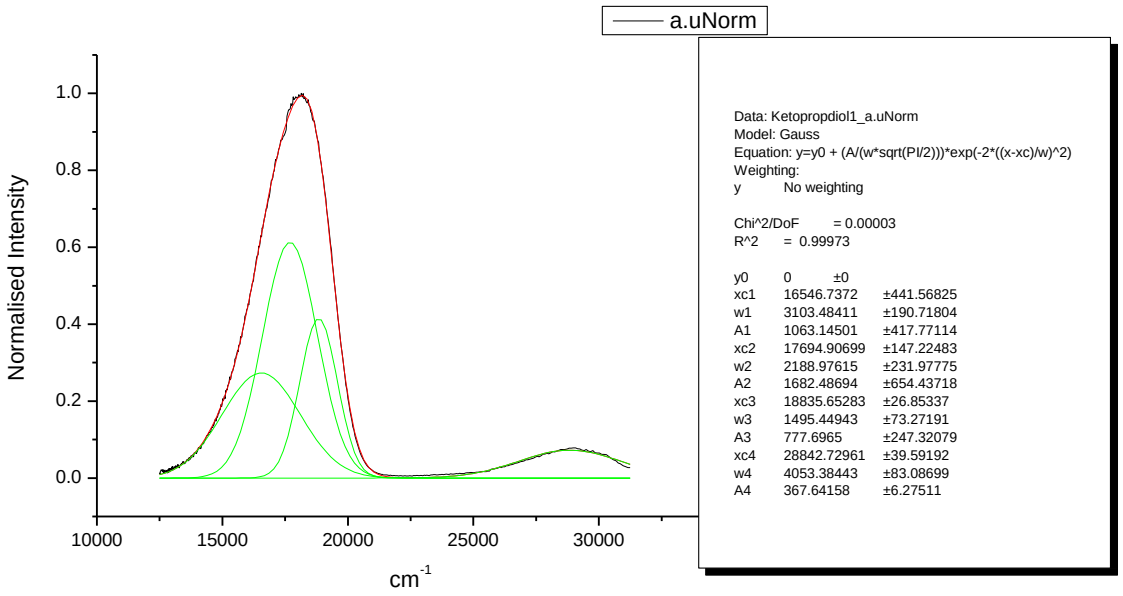

Figure 1.4.255. Gaussian model fit of the normalised fluorescence emission spectrum of **10a** recorded in 1,3-propanediol at 310 nm excitation.

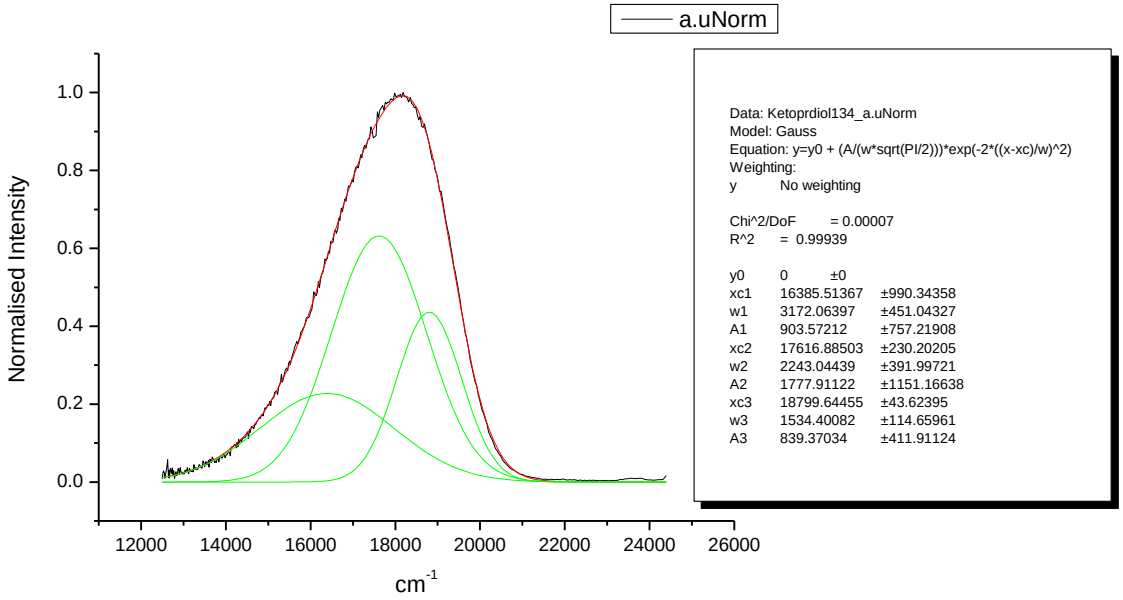

Figure 1.4.256. Gaussian model fit of the normalised fluorescence emission spectrum of **10a** recorded in 1,3-propanediol at 400 nm excitation.

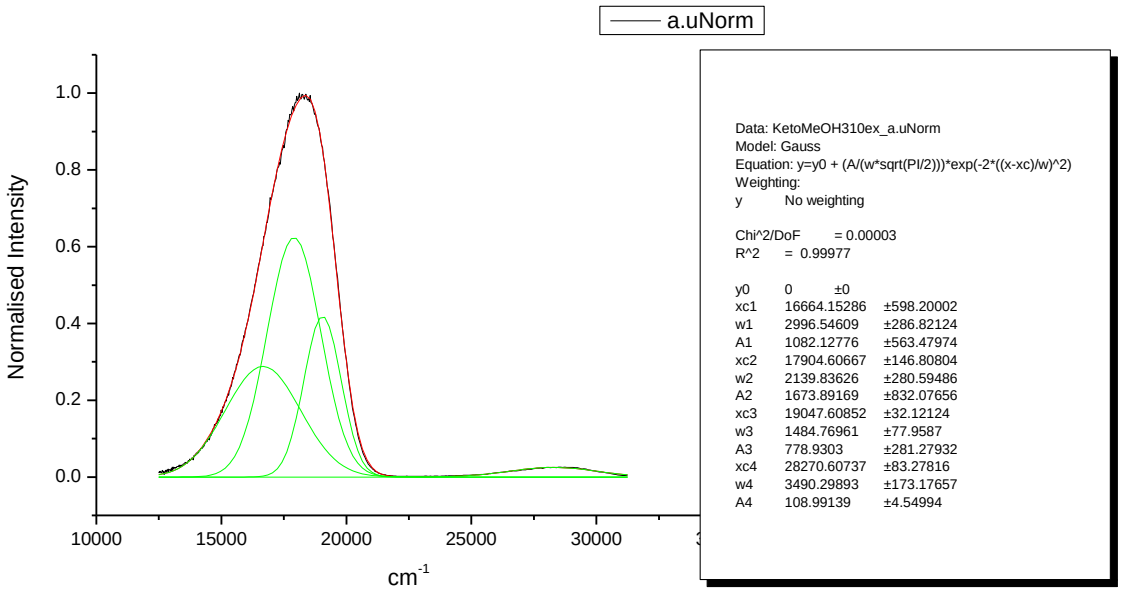

Figure 1.4.257. Gaussian model fit of the normalised fluorescence emission spectrum of **10a** recorded in Methanol at 310 nm excitation.

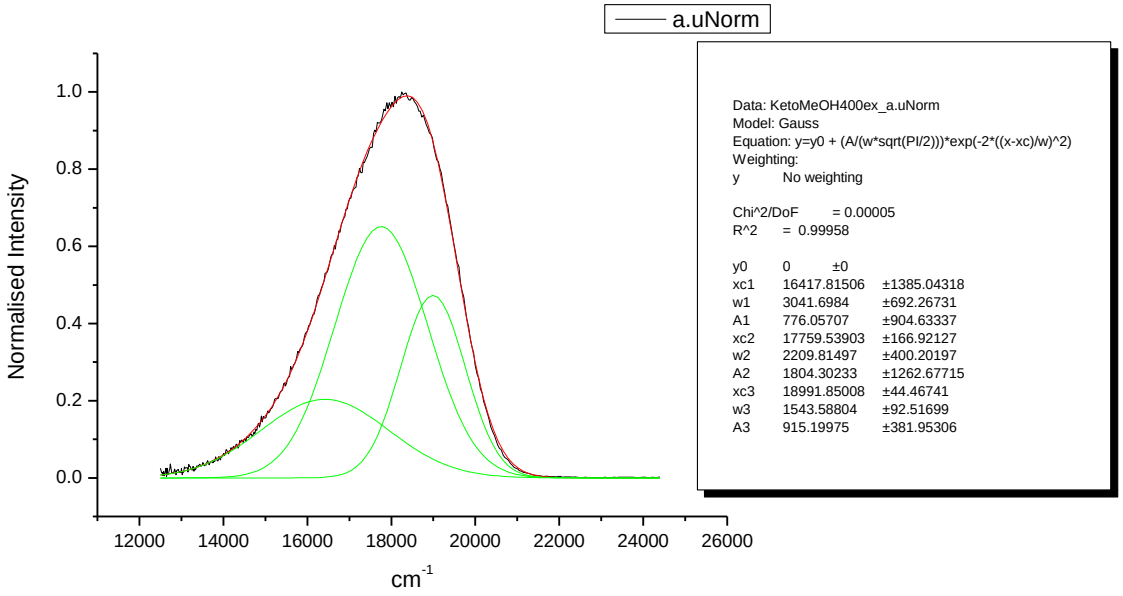

Figure 1.4.258. Gaussian model fit of the normalised fluorescence emission spectrum of **10a** recorded in Methanol at 400 nm excitation.

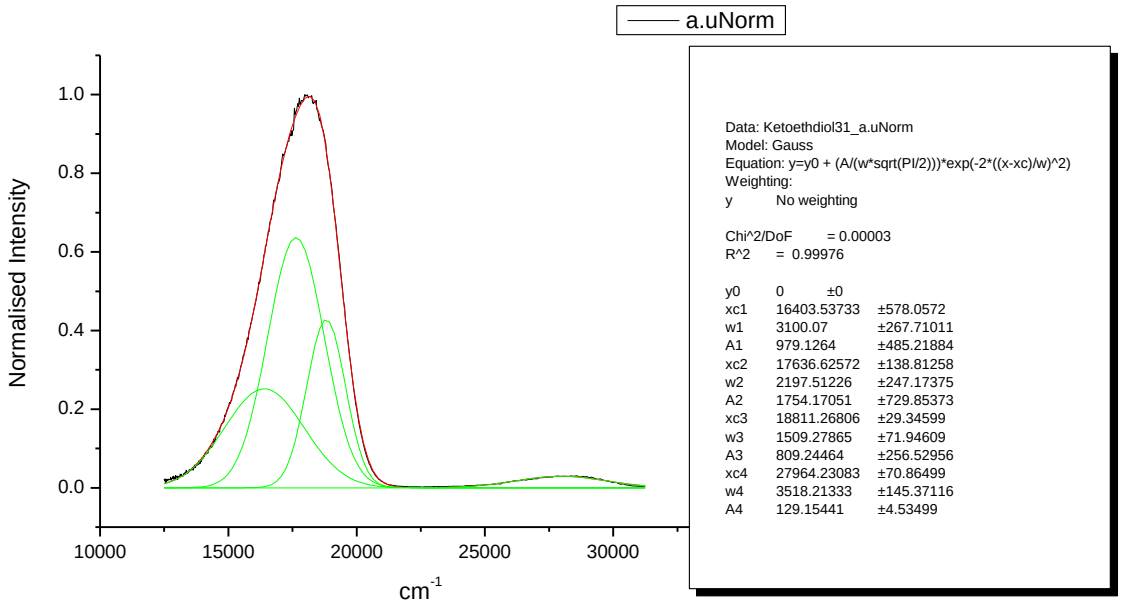

Figure 1.4.259. Gaussian model fit of the normalised fluorescence emission spectrum of **10a** recorded in 1,2-ethanediol at 310 nm excitation.

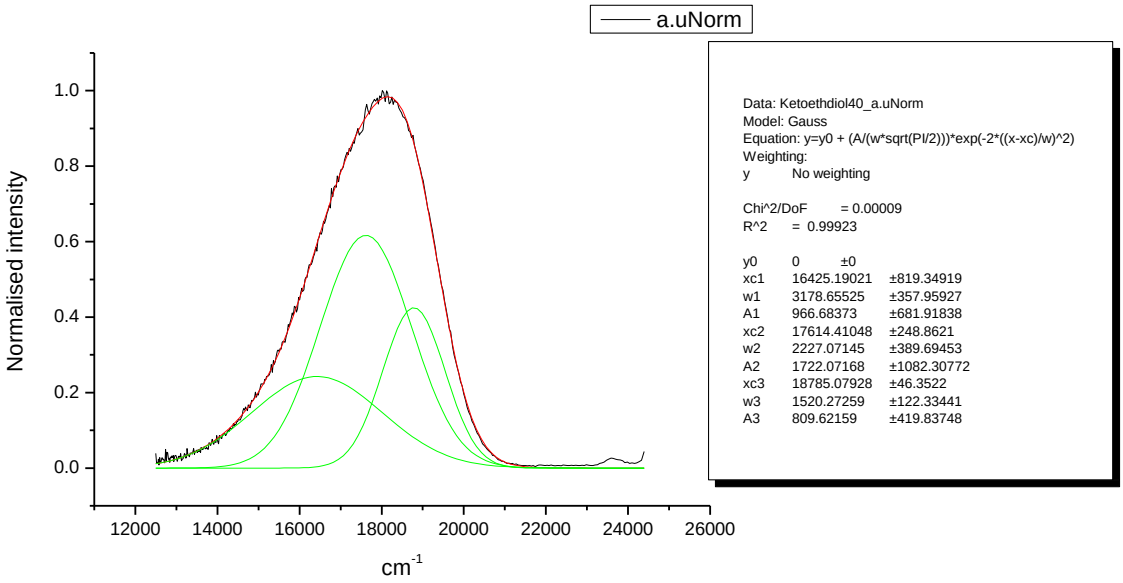

Figure 1.4.260. Gaussian model fit of the normalised fluorescence emission spectrum of **10a** recorded in 1,2-ethanediol at 400 nm excitation.

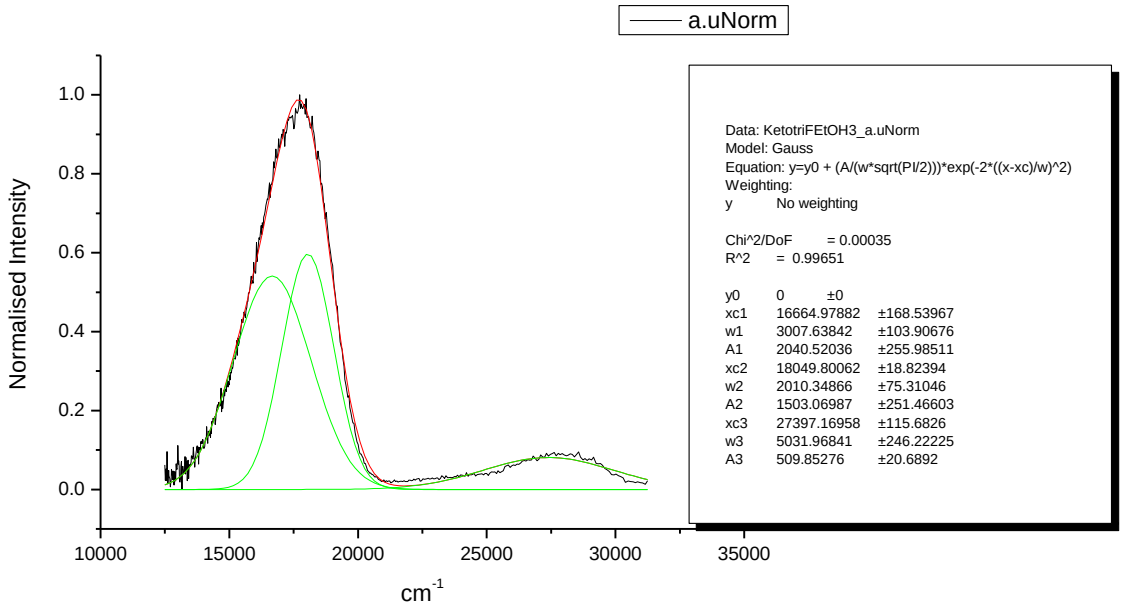

Figure 1.4.261. Gaussian model fit of the normalised fluorescence emission spectrum of **10a** recorded in 2,2,2-trifluoroethanol at 310 nm excitation.

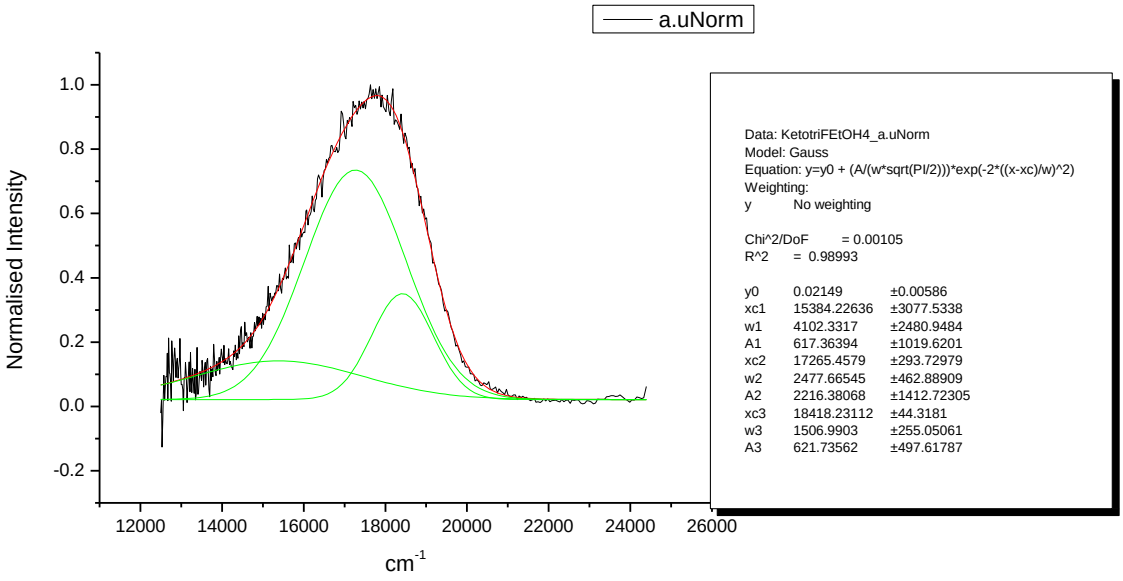

Figure 1.4.262. Gaussian model fit of the normalised fluorescence emission spectrum of **10a** recorded in 2,2,2-trifluoroethanol at 400 nm excitation.

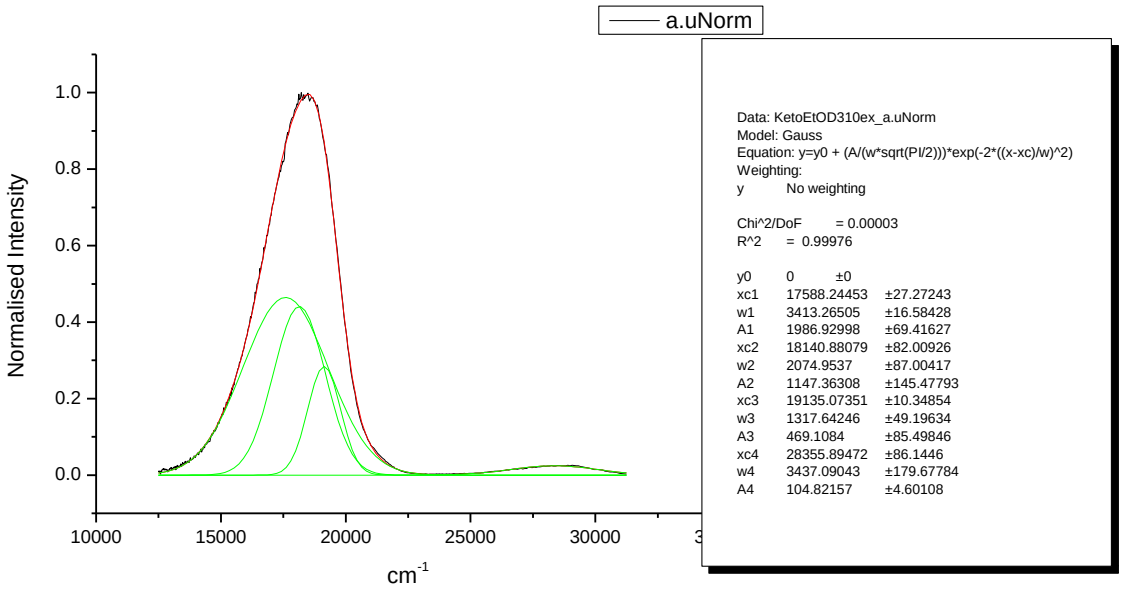

Figure 1.4.263. Gaussian model fit of the normalised fluorescence emission spectrum of **10a** recorded in ethanol-d_1 (EtOD) at 310 nm excitation.

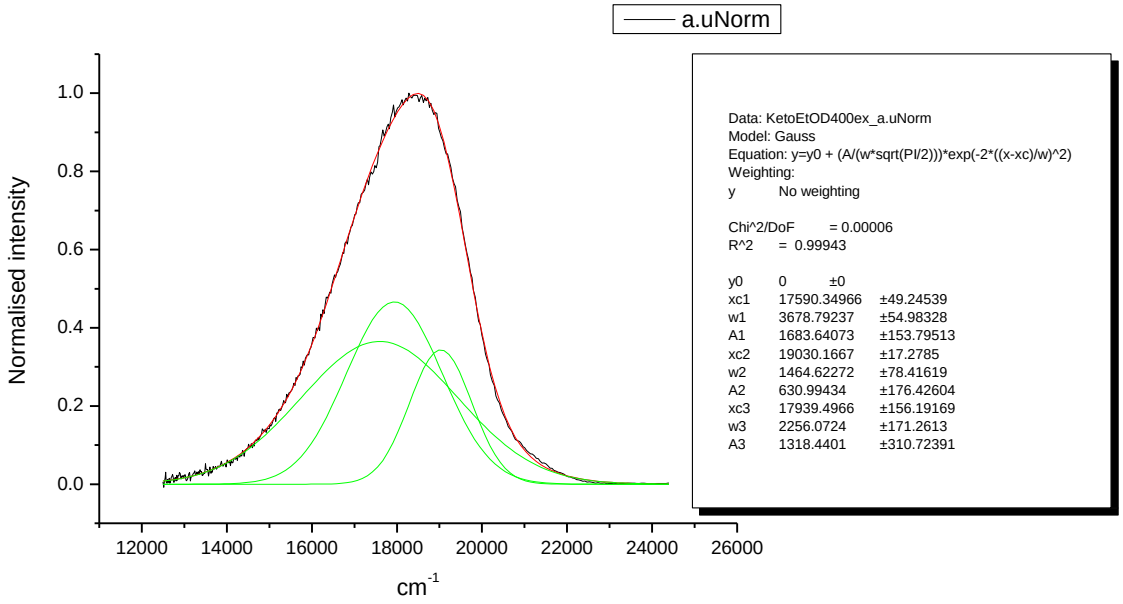

Figure 1.4.264. Gaussian model fit of the normalised fluorescence emission spectrum of **10a** recorded in ethanol-d_1 (EtOD) at 400 nm excitation.

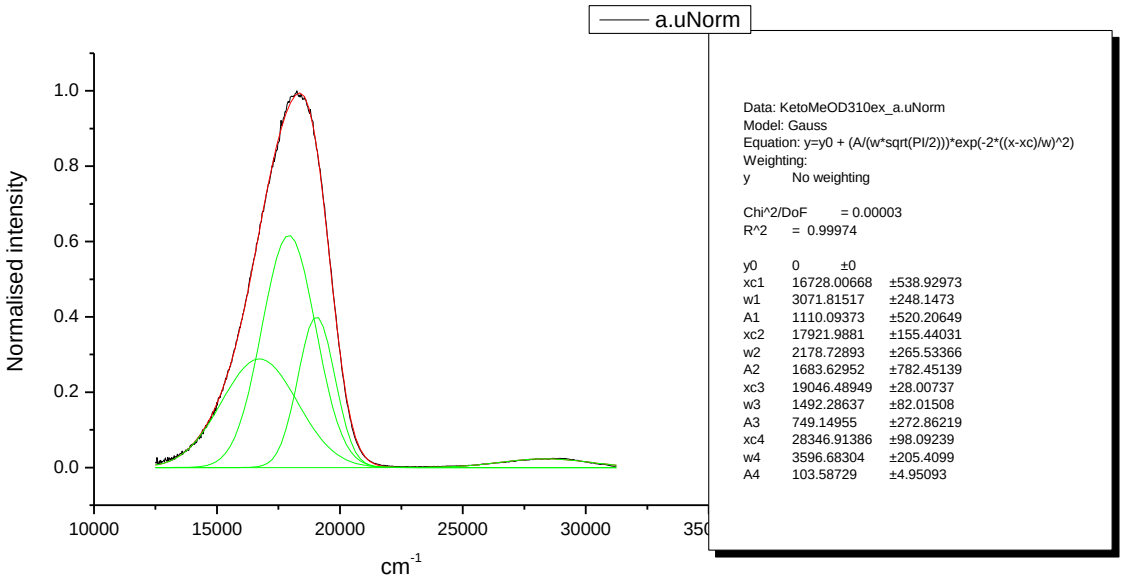

Figure 1.4.265. Gaussian model fit of the normalised fluorescence emission spectrum of **10a** recorded in methanol-d_1 (MeOD) at 310 nm excitation.

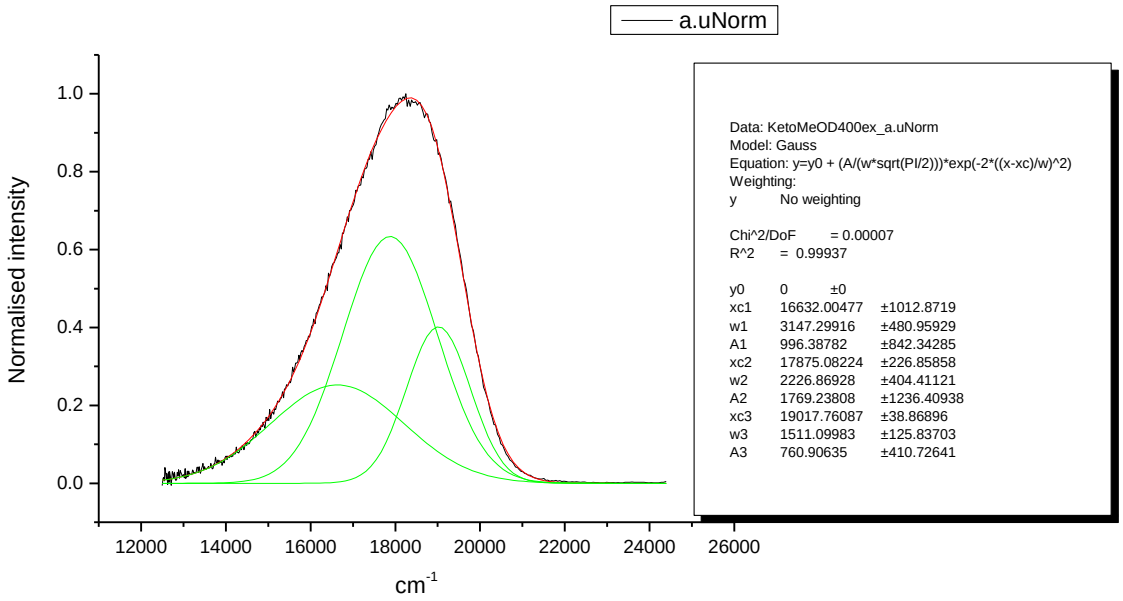

Figure 1.4.266. Gaussian model fit of the normalised fluorescence emission spectrum of **10a** recorded in methanol-d_1 (MeOD) at 400 nm excitation.

1.4.11 Fluorescence Excitation spectra.

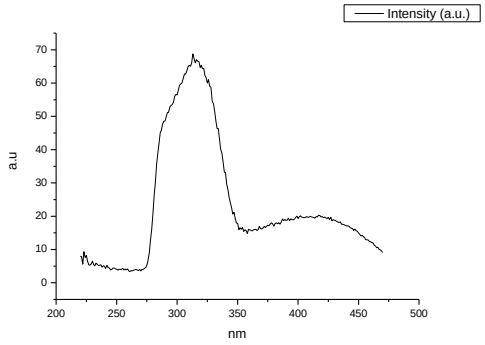

Figure 1.4.267. Fluorescence excitation spectrum of **10a** recorded in Toluene with emission fixed at 480 nm.

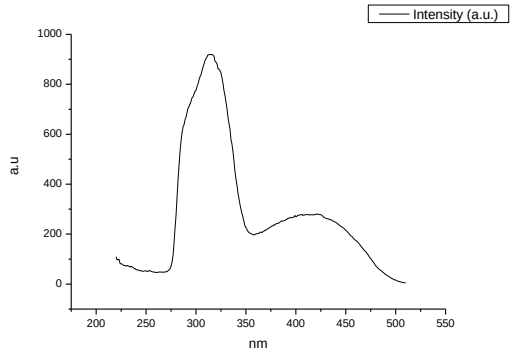

Figure 1.4.268. Fluorescence excitation spectrum of **10a** recorded in Toluene with emission fixed at 520 nm.

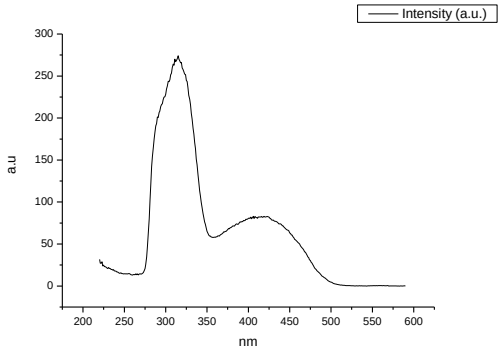

Figure 1.4.269. Fluorescence excitation spectrum of **10a** recorded in Toluene with emission fixed at 600 nm.

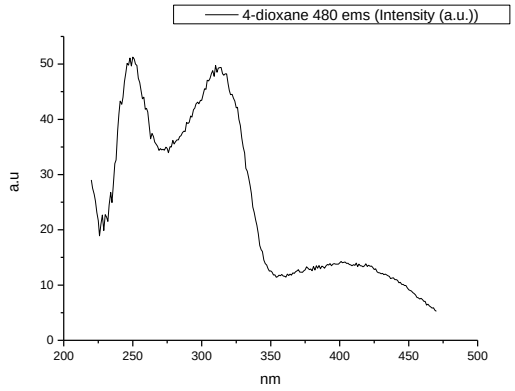

Figure 1.4.270. Fluorescence excitation spectrum of **10a** recorded in 1,4-dioxane with emission fixed at 480 nm.

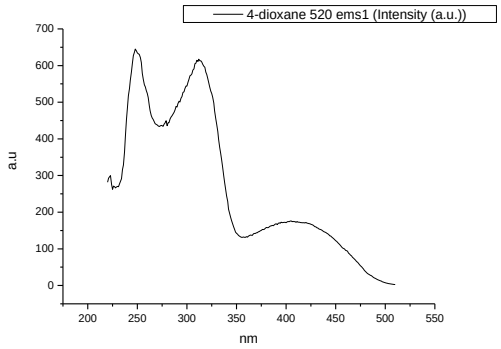

Figure 1.4.271. Fluorescence excitation spectrum of **10a** recorded in 1,4-dioxane with emission fixed at 520 nm.

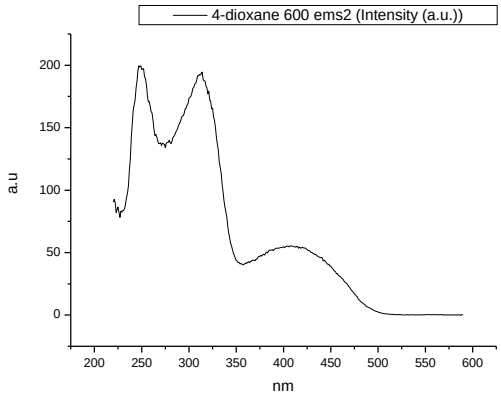

Figure 1.4.272. Fluorescence excitation spectrum of **10a** recorded in 1,4-dioxane with emission fixed at 600 nm.

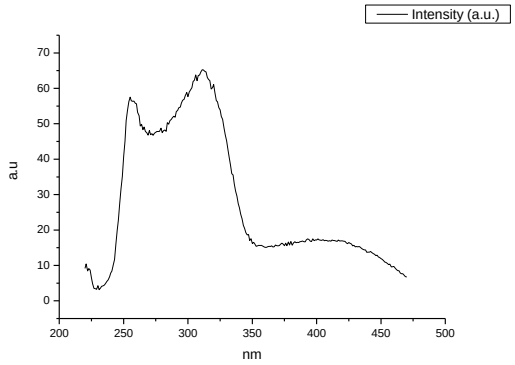

Figure 1.4.273. Fluorescence excitation spectrum of **10a** recorded in Ethyl Acetate with emission fixed at 480 nm.

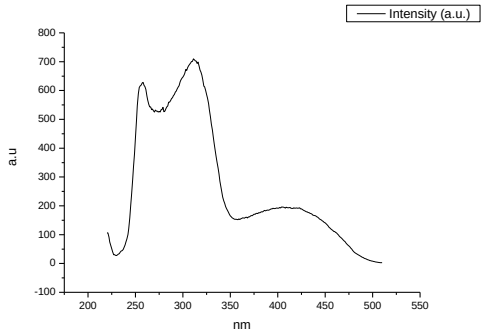

Figure 1.4.274. Fluorescence excitation spectrum of **10a** recorded in Ethyl Acetate with emission fixed at 520 nm.

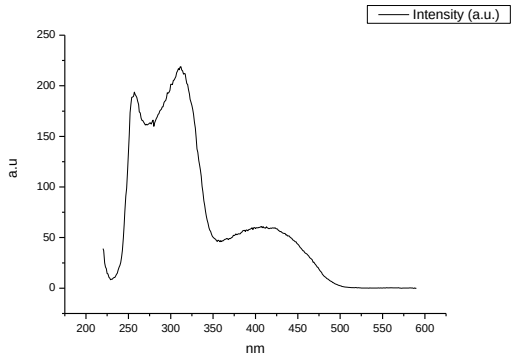

Figure 1.4.275. Fluorescence excitation spectrum of **10a** recorded in Ethyl Acetate with emission fixed at 600 nm.

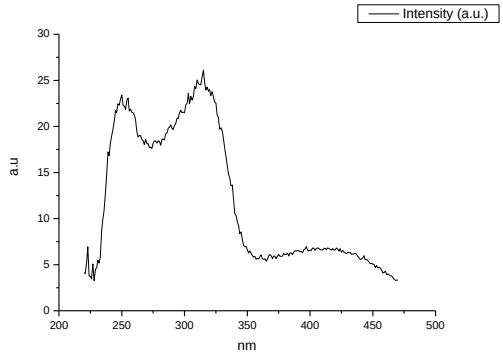

Figure 1.4.276. Fluorescence excitation spectrum of **10a** recorded in Chloroform with emission fixed at 480 nm.

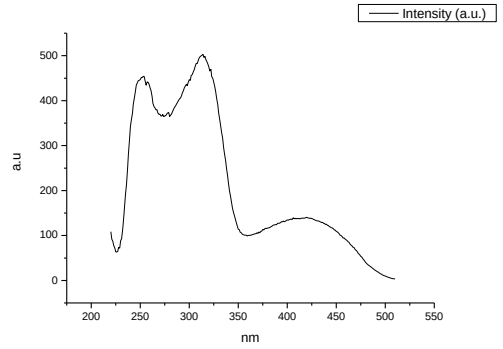

Figure 1.4.277. Fluorescence excitation spectrum of **10a** recorded in Chloroform with emission fixed at 520 nm.

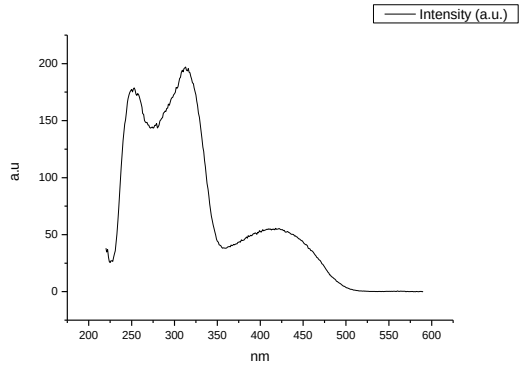

Figure 1.4.278. Fluorescence excitation spectrum of **10a** recorded in Chloroform with emission fixed at 600 nm.

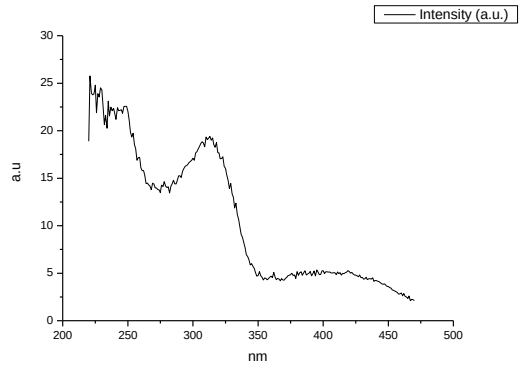

Figure 1.4.279. Fluorescence excitation spectrum of **10a** recorded in 2-methyl-2-butanol with emission fixed at 480 nm.

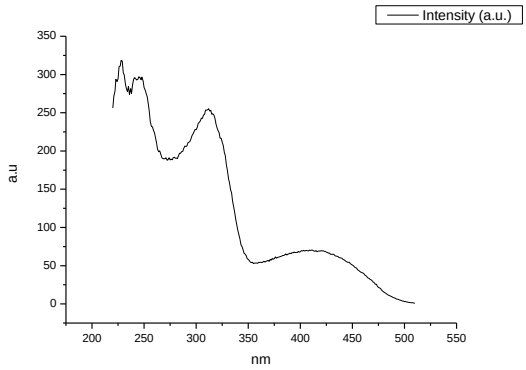

Figure 1.4.280. Fluorescence excitation spectrum of **10a** recorded in 2-methyl-2-butanol with emission fixed at 520 nm.

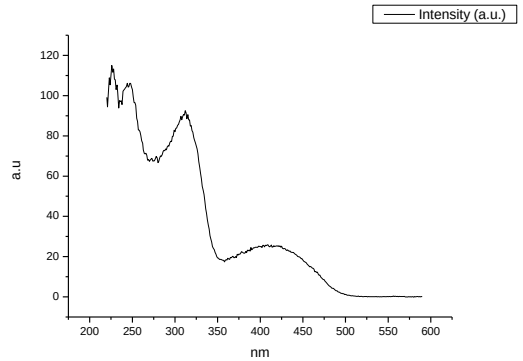

Figure 1.4.281. Fluorescence excitation spectrum of **10a** recorded in 2-methyl-2-butanol with emission fixed at 600 nm.

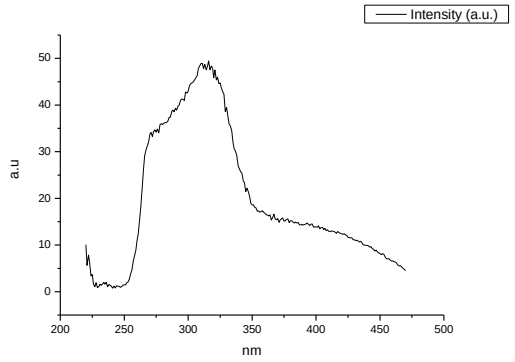

Figure 1.4.282. Fluorescence excitation spectrum of **10a** recorded in N,N-dimethylformamide with emission fixed at 480 nm.

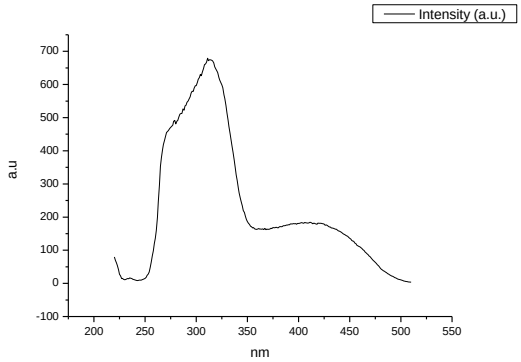

Figure 1.4.283. Fluorescence excitation spectrum of **10a** recorded in N,N-dimethylformamide with emission fixed at 520 nm.

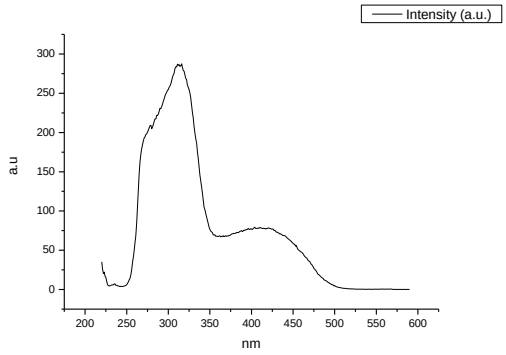

Figure 1.4.284. Fluorescence excitation spectrum of **10a** recorded in N,N-dimethylformamide with emission fixed at 600 nm.

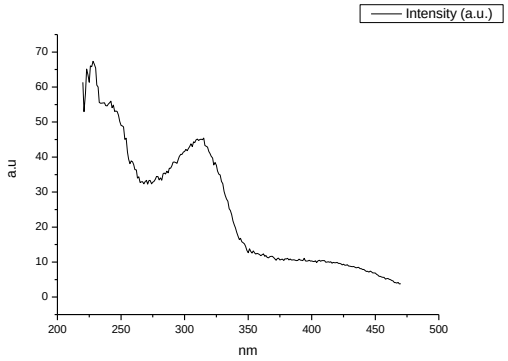

Figure 1.4.285. Fluorescence excitation spectrum of **10a** recorded in Acetonitrile with emission fixed at 480 nm.

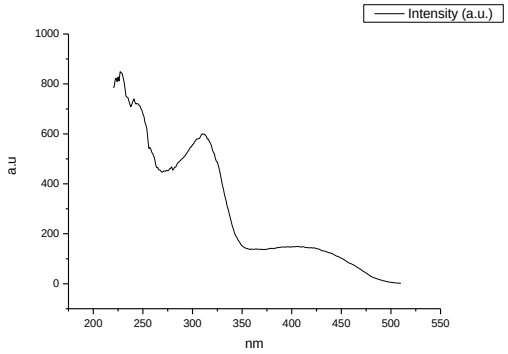

Figure 1.4.286. Fluorescence excitation spectrum of **10a** recorded in Acetonitrile with emission fixed at 520 nm.

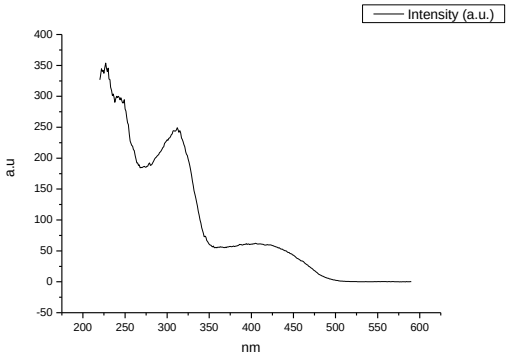

Figure 1.4.287. Fluorescence excitation spectrum of **10a** recorded in Acetonitrile with emission fixed at 600 nm.

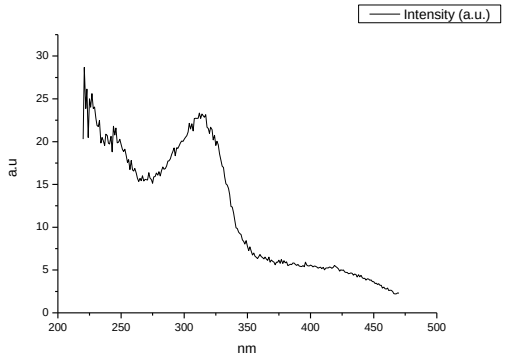

Figure 1.4.288. Fluorescence excitation spectrum of **10a** recorded in Propylene Carbonate with emission fixed at 480 nm.

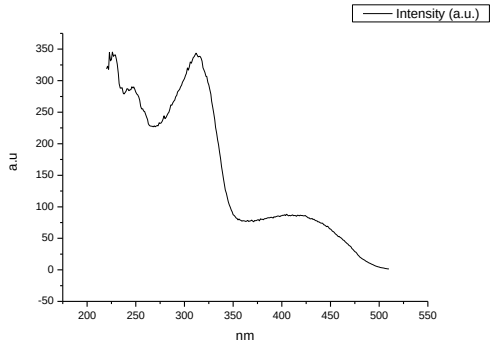

Figure 1.4.289. Fluorescence excitation spectrum of **10a** recorded in Propylene Carbonate with emission fixed at 520 nm.

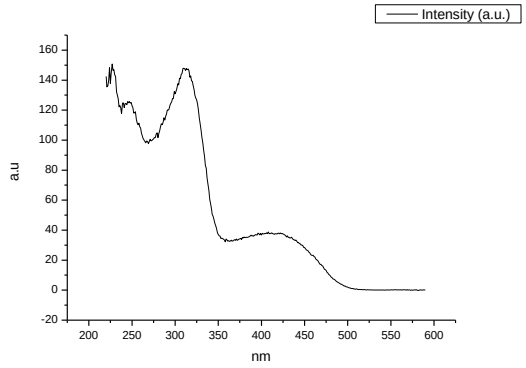

Figure 1.4.290. Fluorescence excitation spectrum of **10a** recorded in Propylene Carbonate with emission fixed at 600 nm.

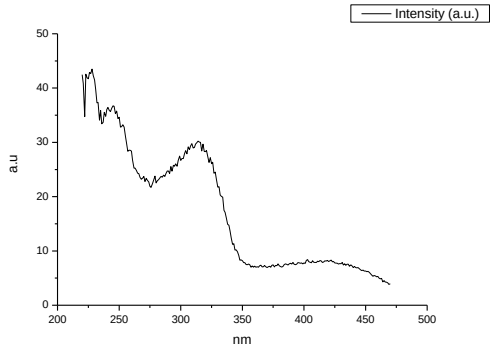

Figure 1.4.291. Fluorescence excitation spectrum of **10a** recorded in 1-octanol with emission fixed at 480 nm.

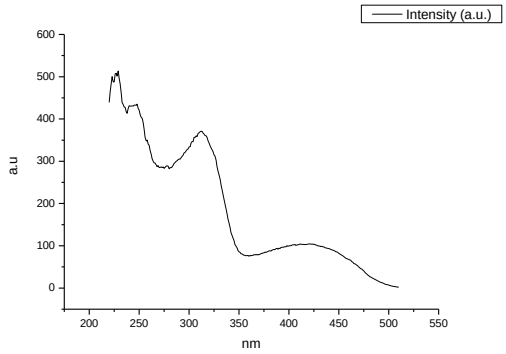

Figure 1.4.292. Fluorescence excitation spectrum of **10a** recorded in 1-octanol with emission fixed at 520 nm.

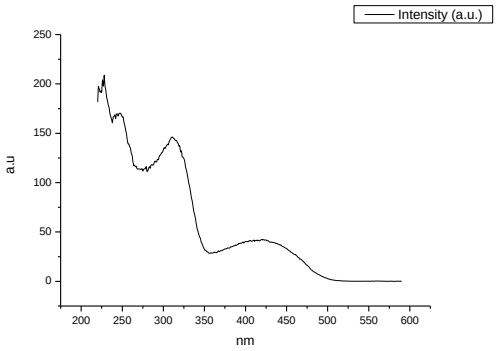

Figure 1.4.293. Fluorescence excitation spectrum of **10a** recorded in 1-octanol with emission fixed at 600 nm.

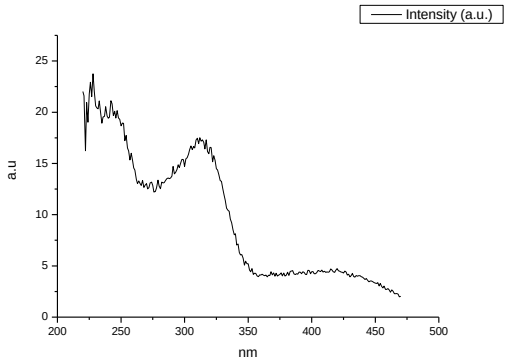

Figure 1.4.294. Fluorescence excitation spectrum of **10a** recorded in 1-hexanol with emission fixed at 480 nm.

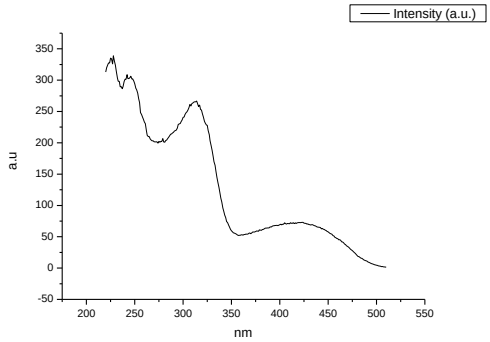

Figure 1.4.295. Fluorescence excitation spectrum of **10a** recorded in 1-hexanol with emission fixed at 520 nm.

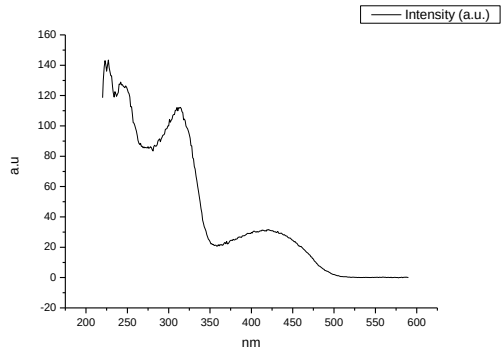

Figure 1.4.296. Fluorescence excitation spectrum of **10a** recorded in 1-hexanol with emission fixed at 600 nm.

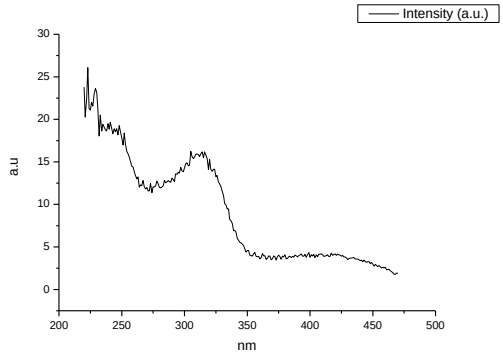

Figure 1.4.297. Fluorescence excitation spectrum of **10a** recorded in 1-butanol with emission fixed at 480 nm.

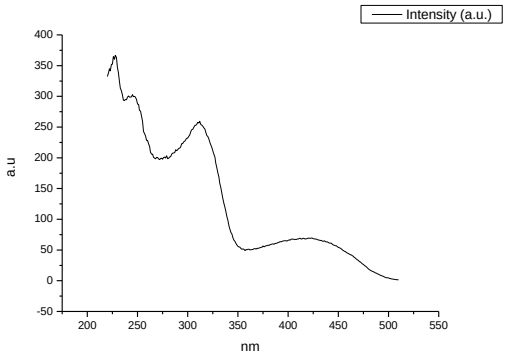

Figure 1.4.298. Fluorescence excitation spectrum of **10a** recorded in 1-butanol with emission fixed at 520 nm.

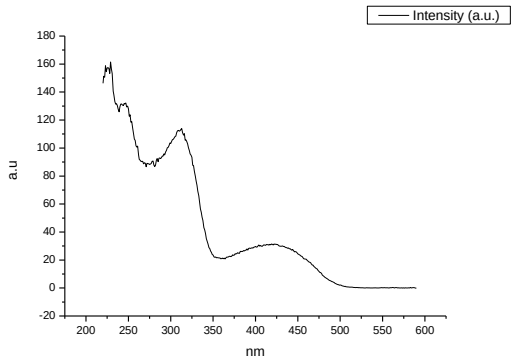

Figure 1.4.299. Fluorescence excitation spectrum of **10a** recorded in 1-butanol with emission fixed at 600 nm.

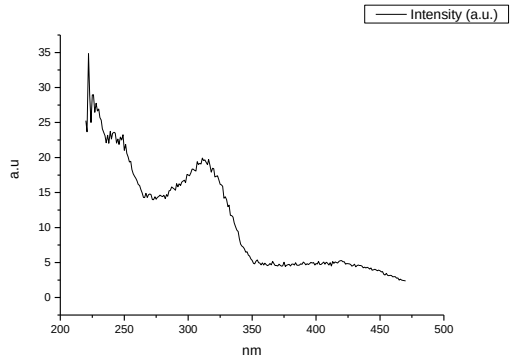

Figure 1.4.300. Fluorescence excitation spectrum of **10a** recorded in 1-pentanol with emission fixed at 480 nm.

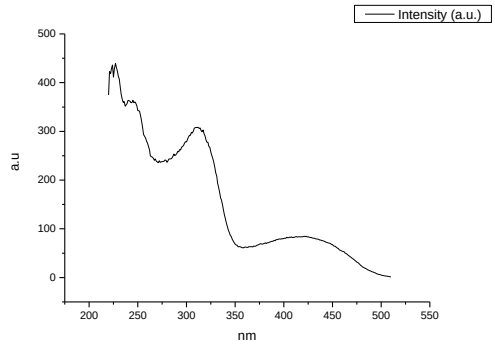

Figure 1.4.301. Fluorescence excitation spectrum of **10a** recorded in 1-pentanol with emission fixed at 520 nm.

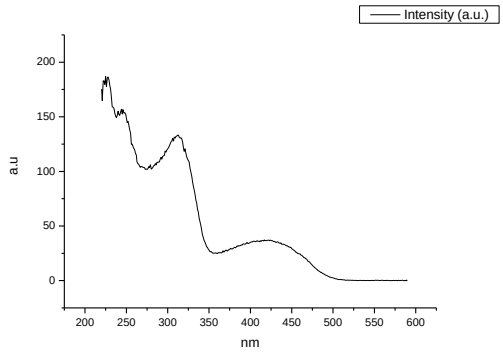

Figure 1.4.302. Fluorescence excitation spectrum of **10a** recorded in 1-pentanol with emission fixed at 600 nm.

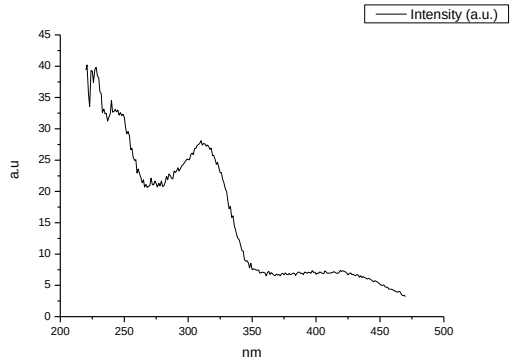

Figure 1.4.303. Fluorescence excitation spectrum of **10a** recorded in 1-propanol with emission fixed at 480 nm.

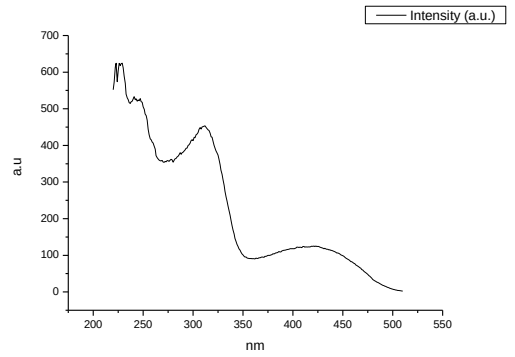

Figure 1.4.304. Fluorescence excitation spectrum of **10a** recorded in 1-propanol with emission fixed at 520 nm.

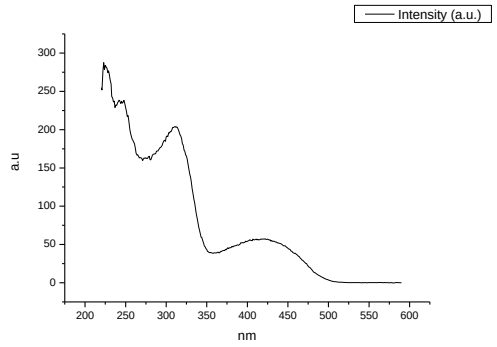

Figure 1.4.305. Fluorescence excitation spectrum of **10a** recorded in 1-propanol with emission fixed at 600 nm.

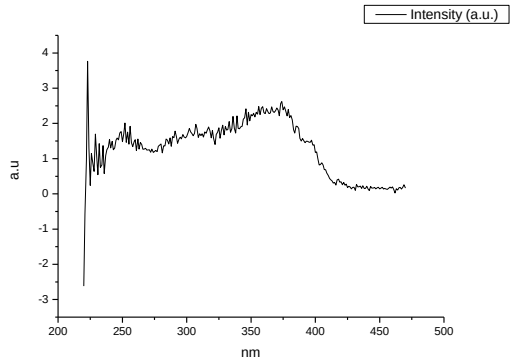

Figure 1.4.306. Fluorescence excitation spectrum of **10a** recorded in Acetic Acid with emission fixed at 480 nm.

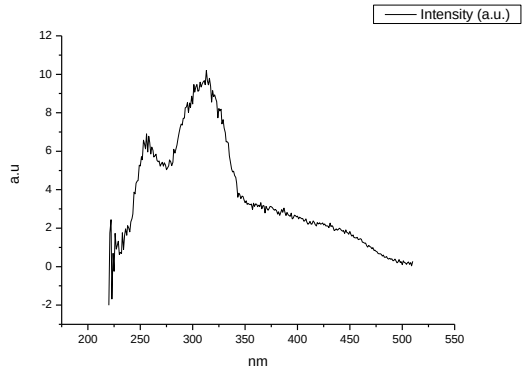

Figure 1.4.307. Fluorescence excitation spectrum of **10a** recorded in Acetic Acid with emission fixed at 520 nm.

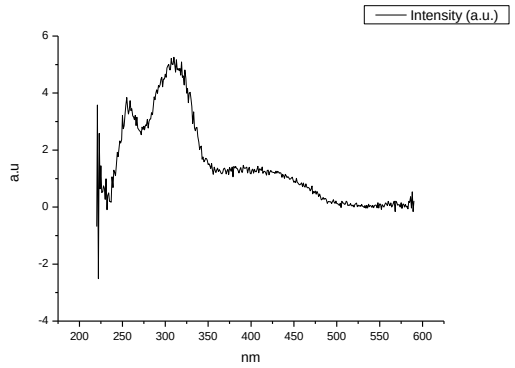

Figure 1.4.308. Fluorescence excitation spectrum of **10a** recorded in Acetic Acid with emission fixed at 600 nm.

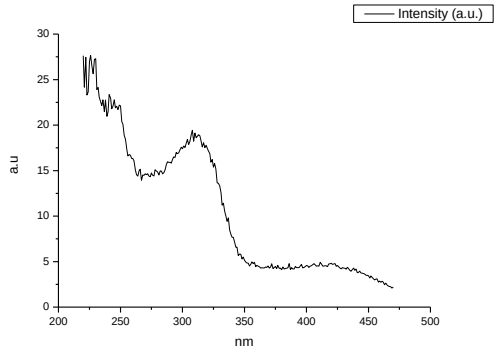

Figure 1.4.309. Fluorescence excitation spectrum of **10a** recorded in Ethanol with emission fixed at 480 nm.

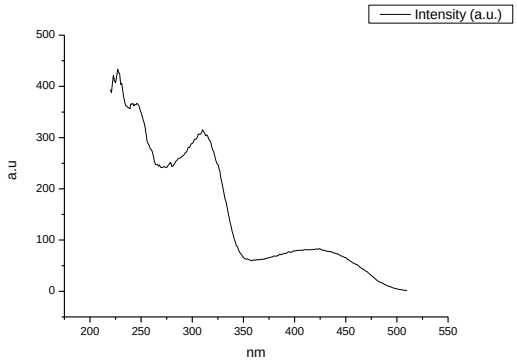

Figure 1.4.310. Fluorescence excitation spectrum of **10a** recorded in Ethanol with emission fixed at 520 nm.

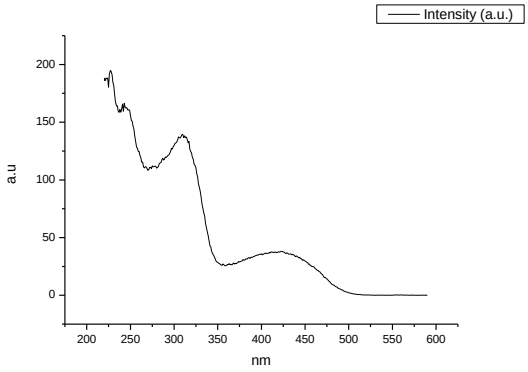

Figure 1.4.311. Fluorescence excitation spectrum of **10a** recorded in Ethanol with emission fixed at 600 nm.

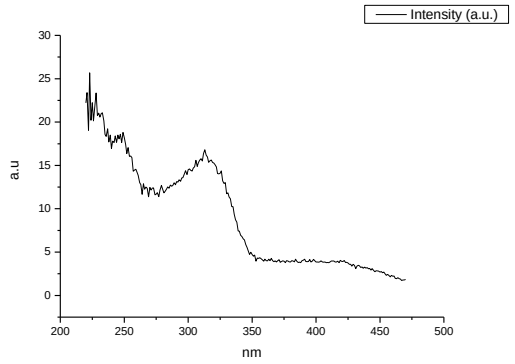

Figure 1.4.312. Fluorescence excitation spectrum of **10a** recorded in 1,5-pentanediol with emission fixed at 480 nm.

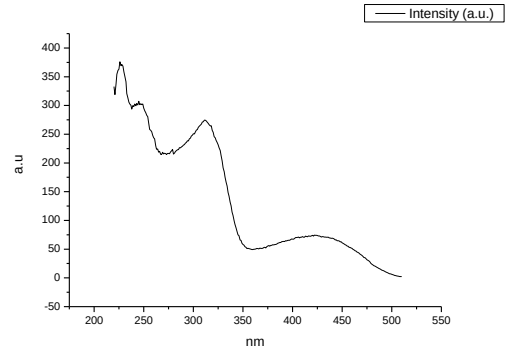

Figure 1.4.313. Fluorescence excitation spectrum of **10a** recorded in 1,5-pentanediol with emission fixed at 520 nm.

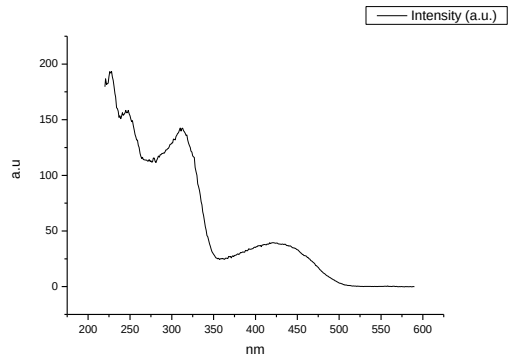

Figure 1.4.314. Fluorescence excitation spectrum of **10a** recorded in 1,5-pentanediol with emission fixed at 600 nm.

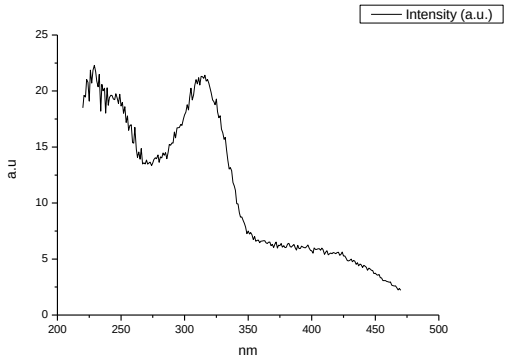

Figure 1.4.315. Fluorescence excitation spectrum of **10a** recorded in 1,3-butanediol with emission fixed at 480 nm.

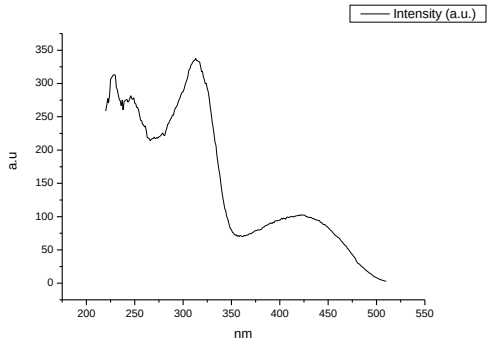

Figure 1.4.316. Fluorescence excitation spectrum of **10a** recorded in 1,3-butanediol with emission fixed at 520 nm.

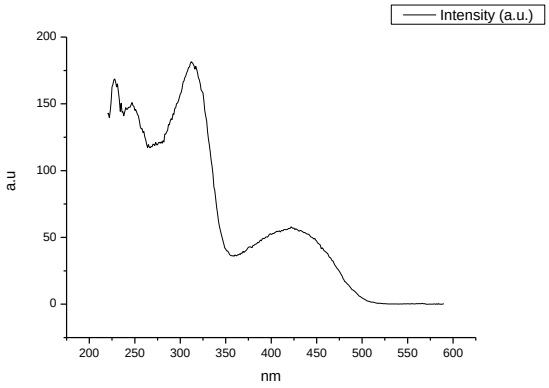

Figure 1.4.317. Fluorescence excitation spectrum of **10a** recorded in 1,3-butanediol with emission fixed at 600 nm.

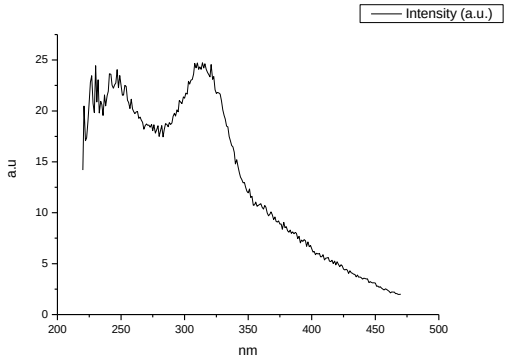

Figure 1.4.318. Fluorescence excitation spectrum of **10a** recorded in 1,4-butanediol with emission fixed at 480 nm.

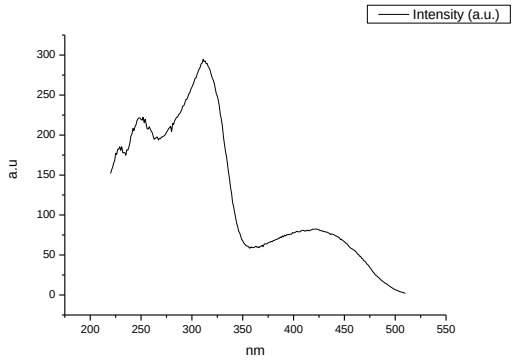

Figure 1.4.319. Fluorescence excitation spectrum of **10a** recorded in 1,4-butanediol with emission fixed at 520 nm.

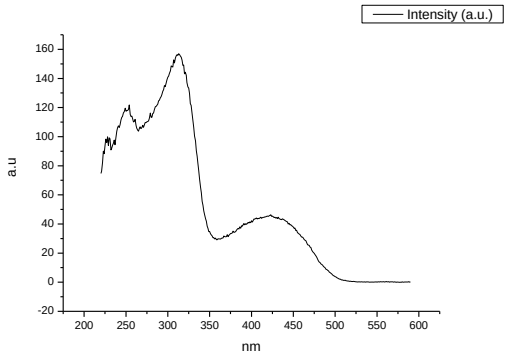

Figure 1.4.320. Fluorescence excitation spectrum of **10a** recorded in 1,4-butanediol with emission fixed at 600 nm.

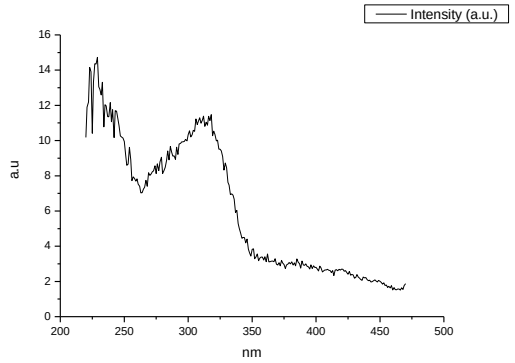

Figure 1.4.321. Fluorescence excitation spectrum of **10a** recorded in 1,3-propanediol with emission fixed at 480 nm.

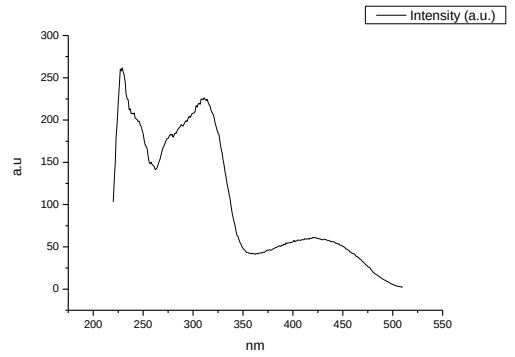

Figure 1.4.322. Fluorescence excitation spectrum of **10a** recorded in 1,3-propanediol with emission fixed at 520 nm.

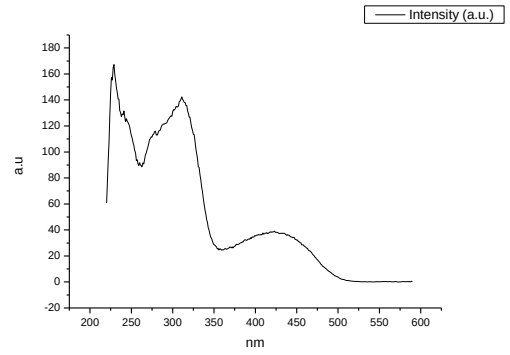

Figure 1.4.323. Fluorescence excitation spectrum of **10a** recorded in 1,3-propanediol with emission fixed at 600 nm.

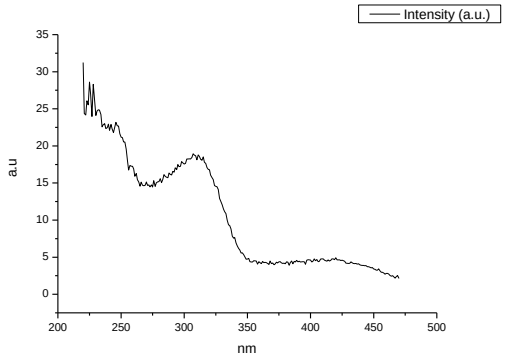

Figure 1.4.324. Fluorescence excitation spectrum of **10a** recorded in Methanol with emission fixed at 480 nm.

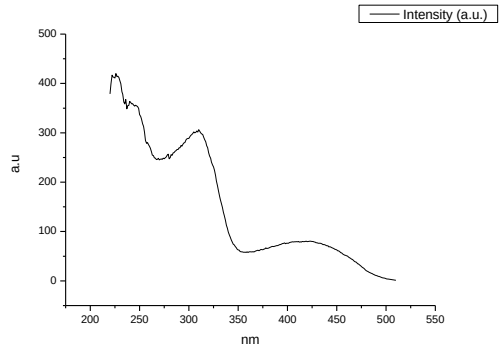

Figure 1.4.325. Fluorescence excitation spectrum of **10a** recorded in Methanol with emission fixed at 520 nm.

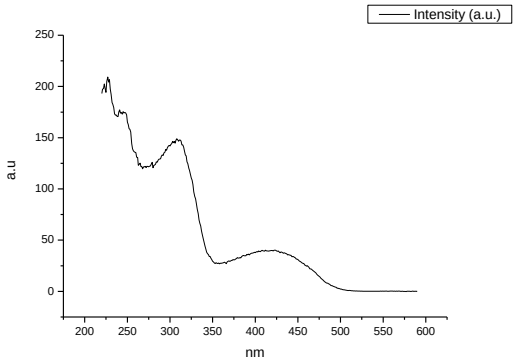

Figure 1.4.326. Fluorescence excitation spectrum of **10a** recorded in Methanol with emission fixed at 600 nm.

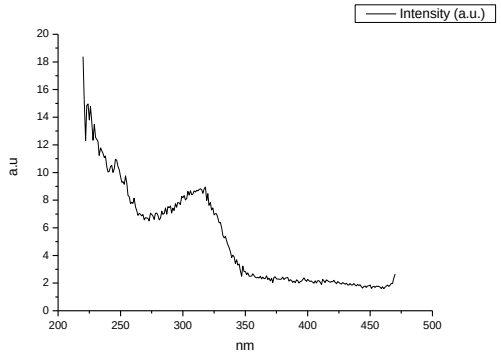

Figure 1.4.327. Fluorescence excitation spectrum of **10a** recorded in 1,2-ethanediol with emission fixed at 480 nm.

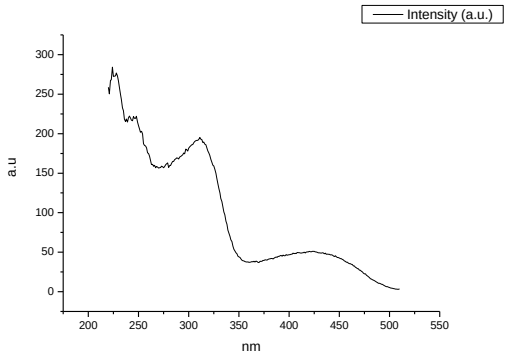

Figure 1.4.328. Fluorescence excitation spectrum of **10a** recorded in 1,2-ethanediol with emission fixed at 520 nm.

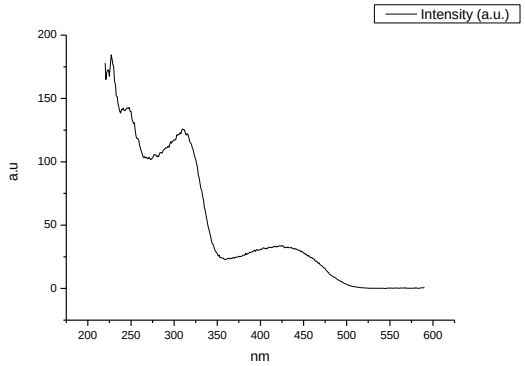

Figure 1.4.329. Fluorescence excitation spectrum of **10a** recorded in 1,2-ethanediol with emission fixed at 600 nm.

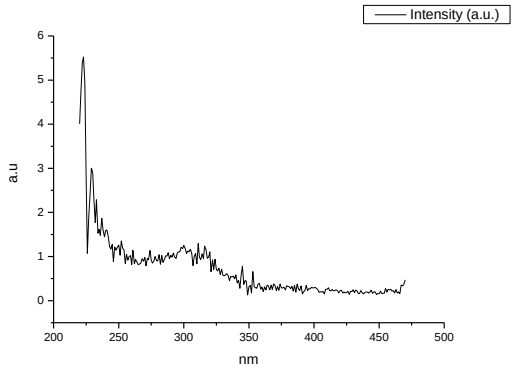

Figure 1.4.330. Fluorescence excitation spectrum of **10a** recorded in 2,2,2-trifluoroethanol with emission fixed at 480 nm.

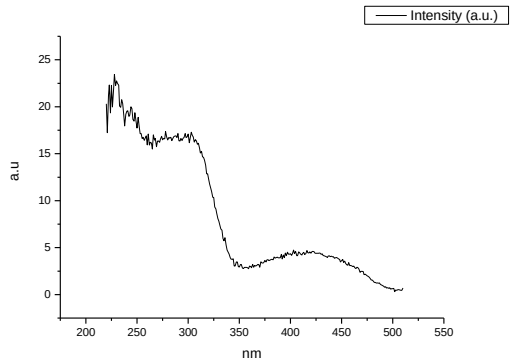

Figure 1.4.331. Fluorescence excitation spectrum of **10a** recorded in 2,2,2-trifluoroethanol with emission fixed at 520 nm.

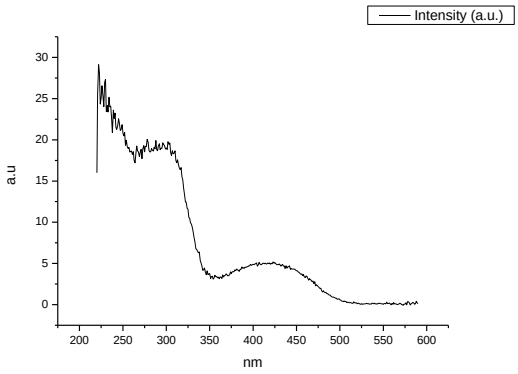

Figure 1.4.332. Fluorescence excitation spectrum of **10a** recorded in 2,2,2-trifluoroethanol with emission fixed at 600 nm.

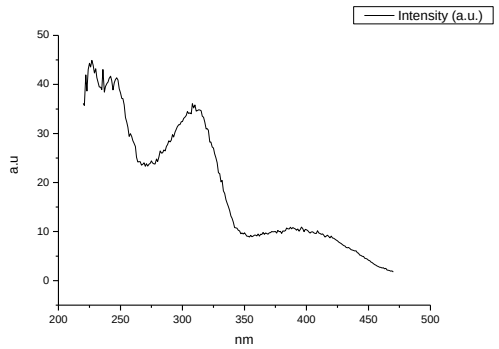

Figure 1.4.333. Fluorescence excitation spectrum of **10a** recorded in Ethanol-d_1 (EtOD) with emission fixed at 480 nm.

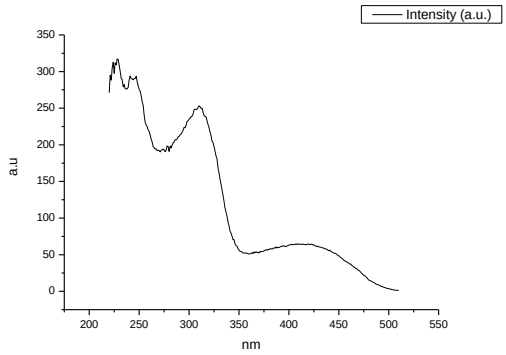

Figure 1.4.334. Fluorescence excitation spectrum of **10a** recorded in Ethanol-d_1 (EtOD) with emission fixed at 520 nm.

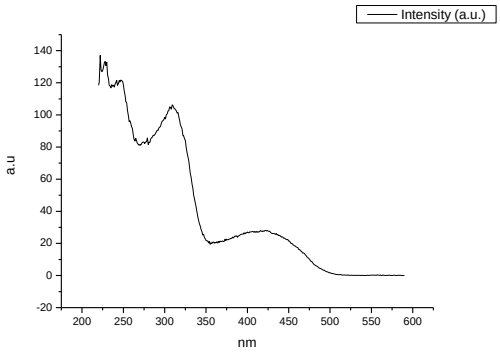

Figure 1.4.335. Fluorescence excitation spectrum of **10a** recorded in Ethanol-d_1 (EtOD) with emission fixed at 600 nm.

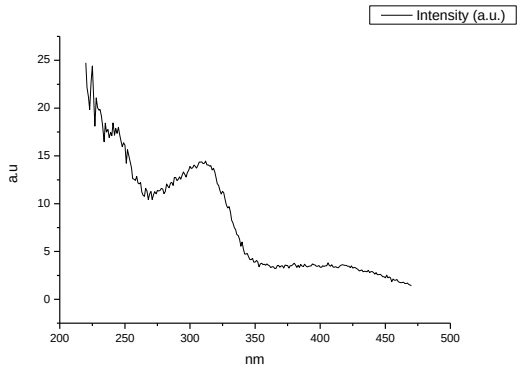

Figure 1.4.336. Fluorescence excitation spectrum of **10a** recorded in Methanol-d_1 (MeOD) with emission fixed at 480 nm.

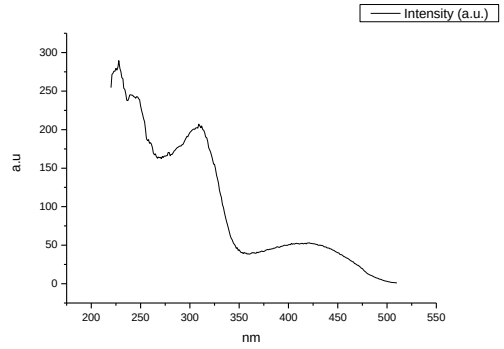

Figure 1.4.337. Fluorescence excitation spectrum of **10a** recorded in Methanol-d_1 (MeOD) with emission fixed at 520 nm.

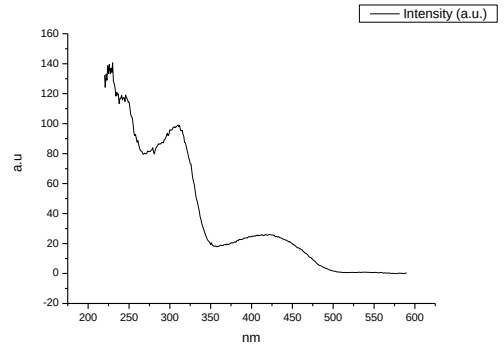

Figure 1.4.338. Fluorescence excitation spectrum of **10a** recorded in Methanol-d_1 (MeOD) with emission fixed at 600 nm.

Appendix 2: Imine substituted (N=C-Z) 2,5-dihydro-1,2,3-triazines.

2.1 COMPOUND 11A

2.1.1 Quantum Yield Summary.

Solvent	abs (310 nm)	$\lambda_{ems\ (max)}$	$\Phi_{310\ nm}$	abs (400 nm)	$\lambda_{ems\ (max)}$	$\Phi_{400\ nm}$
Toluene	0.08	348.00	0.14	0.04	508.33	0.07
1,4-Dioxane	0.07	347.07	0.18	0.00	507.09	0.03
Chloroform	0.06	352.00	0.17	0.00	522.57	0.03
Acetonitrile	0.04	346.00	0.18	0.00	523.81	0.02
1-Octanol	0.03	347.07	0.21	0.00	512.19	0.05
1-Hexanol	0.03	349.07	0.22	0.00	512.21	0.06
1-Butanol	0.06	347.07	0.19	0.00	515.84	0.03
1-Pentanol	0.05	346.00	0.18	0.00	506.93	0.02
1-Propanol	0.05	349.07	0.19	0.00	508.09	0.03
Acetic acid	0.04	348.00	0.14	0.00	-	0.01
Methanol	0.05	349.07	0.18	0.00	515.93	0.02
2,2,2-Trifluoroethanol	0.03	355.07	0.09	0.00	-	0.01

Table 2.1.1. Summary of ultraviolet-visible absorbance values at 310 nm and 400 nm, emission maxima and quantum yield (Φ) of **11a** at 310 nm and 400 nm excitation.

2.1.2 310 nm excitation Gaussian band fit summaries.

Solvent	λ max$_{em}$ Band 1 (cm^{-1})	λ max$_{em}$ Band 1 (nm)	λ max$_{em}$ Band 2 (cm^{-1})	λ max$_{em}$ Band 2 (nm)	λ max$_{em}$ Band 3 (cm^{-1})	λ max$_{em}$ Band 3 (nm)
Toluene	-	-	19332.31	517.27	25949.81	385.36
1,4-Dioxane	-	-	19379.49	516.01	25566.71	391.13
Chloroform	-	-	19203.96	520.73	25444.06	393.02
Acetonitrile	-	-	19082.66	524.04	25648.40	389.89
1-Octanol	-	-	19201.30	520.80	25731.37	388.63
1-Hexanol	-	-	19163.87	521.82	25665.67	389.63
1-Butanol	-	-	19132.00	522.68	25113.07	398.20
1-Pentanol	-	-	19146.48	522.29	24779.97	403.55
1-Propanol	-	-	19114.98	523.15	25189.32	396.99
Acetic acid	-	-	-	-	25872.54	386.51
Methanol	-	-	18984.72	526.74	24350.24	410.67
2,2,2-Trifluoroethanol	-	-	-	-	25639.74	390.02

Solvent	λ max$_{em}$ Band 4 (cm^{-1})	λ max$_{em}$ Band 4 (nm)	λ max$_{em}$ Band 5 (cm^{-1})	λ max$_{em}$ Band 5 (nm)
Toluene	27886.57	358.60	29400.47	340.13
1,4-Dioxane	27864.21	358.88	29434.20	339.74
Chloroform	27695.57	361.07	29273.25	341.61
Acetonitrile	27870.94	358.80	29450.31	339.55
1-Octanol	27851.27	359.05	29430.13	339.79
1-Hexanol	27842.19	359.17	29422.59	339.87
1-Butanol	27745.80	360.41	29376.60	340.41
1-Pentanol	27675.74	361.33	29341.88	340.81
1-Propanol	27774.66	360.04	29396.79	340.17
Acetic acid	27760.31	360.23	29361.46	340.58
Methanol	27639.16	361.81	29340.16	340.83
2,2,2-Trifluoroethanol	27491.85	363.74	29069.88	344.00

Table 2.1.2. Summary of band maxima of 5 band fit using Gaussian model for normalised **11a** emission spectra recorded at 310 nm excitation.

(a)

Solvent	Width Band 1 (cm^{-1})	Width Band 2 (cm^{-1})	Width Band 3 (cm^{-1})	Width Band 4 (cm^{-1})	Width Band 5 (cm^{-1})
Toluene	-	3221.75	3455.81	2539.29	1857.27
1,4-Dioxane	-	3209.45	3610.24	2622.37	1922.47
Chloroform	-	3112.98	3479.51	2557.91	1840.61
Acetonitrile	-	3166.96	3607.44	2686.22	1977.50
1-Octanol	-	3074.02	3393.58	2616.86	1927.99
1-Hexanol	-	3025.38	3372.18	2630.31	1938.58
1-Butanol	-	2992.82	2999.97	2668.22	1970.14
1-Pentanol	-	3034.23	2764.87	2681.89	1981.34
1-Propanol	-	3035.79	3071.60	2680.12	1976.21
Acetic acid	-	-	4112.05	2729.51	1972.76
Methanol	-	3022.22	2315.93	2802.12	2057.64
2,2,2-Trifluoroethanol	-	-	4790.18	2801.61	1895.89

(b)

Solvent	Area Band 1 (cm^{-1})	Area Band 2 (cm^{-1})	Area Band 3 (cm^{-1})	Area Band 4 (cm^{-1})	Area Band 5 (cm^{-1})
Toluene	-	158.77	498.72	2150.59	1213.31
1,4-Dioxane	-	186.70	405.77	2218.51	1288.55
Chloroform	-	244.86	451.98	2308.09	1209.10
Acetonitrile	-	208.72	365.94	2239.51	1375.28
1-Octanol	-	196.40	420.15	2220.30	1285.33
1-Hexanol	-	204.34	434.00	2315.76	1280.91
1-Butanol	-	233.48	288.12	2361.91	1370.23
1-Pentanol	-	216.12	226.75	2339.20	1413.77
1-Propanol	-	234.73	308.08	2391.82	1345.54
Acetic acid	-	-	510.48	2359.10	1276.08
Methanol	-	245.29	152.64	2445.30	1466.37
2,2,2-Trifluoroethanol	-	-	765.91	2638.42	929.26

Tables 2.1.3 (a) and (b). Summary band width and band area of 5 band fit using Gaussian model for normalised **11a** emission spectra recorded at 310 nm excitation.

Solvent	Band 1 Area Percentage (%)	Band 2 Area Percentage(%)	Band 3 Area Percentage (%)	Band 4 Area Percentage(%)	Band 5 Area Percentage (%)
Toluene	-	3.95	12.40	53.48	30.17
1,4-Dioxane	-	4.55	9.90	54.12	31.43
Chloroform	-	5.81	10.73	54.77	28.69
Acetonitrile	-	4.98	8.73	53.46	32.83
1-Octanol	-	4.76	10.19	53.86	31.18
1-Hexanol	-	4.82	10.25	54.68	30.25
1-Butanol	-	5.49	6.77	55.53	32.21
1-Pentanol	-	5.15	5.40	55.75	33.69
1-Propanol	-	5.48	7.20	55.88	31.44
Acetic acid	-	-	12.31	56.91	30.78
Methanol	-	5.69	3.54	56.74	34.03
2,2,2-Trifluoroethanol	-	-	17.67	60.88	21.44

Table 2.1.4. Total Area Percentages of 5 band fit using Gaussian model for normalised **11a** emission spectra recorded at 310 nm excitation.

Solvent	Area Ratio Band 1/2 (310 nm ex)	Area Ratio Band 1/3 (310 nm ex)	Area Ratio Band 1/4 (310 nm ex)	Area Ratio Band 1/5 (310 nm ex)
Toluene	-	-	-	-
1,4-Dioxane	-	-	-	-
Chloroform	-	-	-	-
Acetonitrile	-	-	-	-
1-Octanol	-	-	-	-
1-Hexanol	-	-	-	-
1-Butanol	-	-	-	-
1-Pentanol	-	-	-	-
1-Propanol	-	-	-	-
Acetic acid	-	-	-	-
Methanol	-	-	-	-
2,2,2-Trifluoroethanol	-	-	-	-

Solvent	Area Ratio Band 2/3 (310 nm ex)	Area Ratio Band 2/4 (310 nm ex)	Area Ratio Band 2/5 (310 nm ex)	Area Ratio Band 3/4 (310 nm ex)	Area Ratio Band 3/5 (310 nm ex)	Area Ratio Band 4/5 (310 nm ex)
Toluene	0.32	0.07	0.13	0.23	0.41	1.77
1,4-Dioxane	0.46	0.08	0.14	0.18	0.31	1.72
Chloroform	0.54	0.11	0.20	0.20	0.37	1.91
Acetonitrile	0.57	0.09	0.15	0.16	0.27	1.63
1-Octanol	0.47	0.09	0.15	0.19	0.33	1.73
1-Hexanol	0.47	0.09	0.16	0.19	0.34	1.81
1-Butanol	0.81	0.10	0.17	0.12	0.21	1.72
1-Pentanol	0.95	0.09	0.15	0.10	0.16	1.65
1-Propanol	0.76	0.10	0.17	0.13	0.23	1.78
Acetic acid	-	-	-	0.22	0.40	1.85
Methanol	1.61	0.10	0.17	0.06	0.10	1.67
2,2,2-Trifluoroethanol	-	-	-	0.29	0.82	2.84

Table 2.1.5. Area Ratios of 5 band fit using Gaussian model for normalised **11a** emission spectra recorded at 310 nm excitation.

2.1.3 400 nm excitation Gaussian band fit summaries.

Solvent	λ max$_{em}$ Band 1 (cm^{-1})	λ max$_{em}$ Band 1 (nm)	λ max$_{em}$ Band 2 (cm^{-1})	λ max$_{em}$ Band 2 (nm)	λmax$_{em}$ Band 3 (cm^{-1})	λmax$_{em}$ Band 3 (nm)
Toluene	-	-	19004.05	526.20	-	-
1,4-Dioxane	-	-	19525.51	512.15	-	-
Chloroform	-	-	19165.12	521.78	-	-
Acetonitrile	-	-	19197.83	520.89	-	-
1-Octanol	-	-	19266.32	519.04	-	-
1-Hexanol	-	-	19315.74	517.71	-	-
1-Butanol	-	-	19187.95	521.16	-	-
1-Pentanol	-	-	19215.38	520.42	-	-
1-Propanol	-	-	19160.60	521.90	-	-
Acetic acid	-	-	19359.24	516.55	-	-
Methanol	-	-	19049.14	524.96	-	-
2,2,2-Trifluoroethanol	-	-	-	-	-	-

Table 2.1.6. Summary of band maxima of 3 band fit using Gaussian model for normalised **11a** emission spectra recorded at 400 nm excitation.

Solvent	Width Band 1 (cm^{-1})	Width Band 2 (cm^{-1})	Width Band 3 (cm^{-1})
Toluene	-	3013.49	-
1,4-Dioxane	-	2867.18	-
Chloroform	-	2525.26	-
Acetonitrile	-	2422.88	-
1-Octanol	-	3116.84	-
1-Hexanol	-	2598.36	-
1-Butanol	-	2794.88	-
1-Pentanol	-	2571.22	-
1-Propanol	-	2619.20	-
Acetic acid	-	4531.50	-
Methanol	-	2439.01	-
2,2,2-Trifluoroethanol	-	-	-

Table 2.1.7. Summary of band width of 3 band fit using Gaussian model for normalised **11a** emission spectra recorded at 400 nm excitation.

Solvent	Area Band 1 (cm^{-1})	Area Band 2 (cm^{-1})	Area Band 3 (cm^{-1})	Area Ratio Band 1/2 (400 nm ex)	Area Ratio Band 1/3 (400 nm ex)	Area Ratio Band 2/3 (400 nm ex)
Toluene	-	42.97	-	-	-	-
1,4-Dioxane	-	2791.89	-	-	-	-
Chloroform	-	1645.04	-	-	-	-
Acetonitrile	-	599.27	-	-	-	-
1-Octanol	-	1347.14	-	-	-	-
1-Hexanol	-	1047.56	-	-	-	-
1-Butanol	-	2497.20	-	-	-	-
1-Pentanol	-	1714.21	-	-	-	-
1-Propanol	-	1880.34	-	-	-	-
Acetic acid	-	451.17	-	-	-	-
Methanol	-	1095.86	-	-	-	-
2,2,2-Trifluoroethanol	-	-	-	-	-	-

Solvent	Band 1 Area Percentage(%)	Band 2 Area Percentage (%)	Band 3 Area Percentage (%)
Toluene	-	100	-
1,4-Dioxane	-	100	-
Chloroform	-	100	-
Acetonitrile	-	100	-
1-Octanol	-	100	-
1-Hexanol	-	100	-
1-Butanol	-	100	-
1-Pentanol	-	100	-
1-Propanol	-	100	-
Acetic acid	-	100	-
Methanol	-	100	-
2,2,2-Trifluoroethanol	-	-	-

Table 2.1.8. Band area, area ratios and total area percentage of 3 band fit using Gaussian model for normalised **11a** emission spectra recorded at 400 nm excitation.

2.1.4 310 nm Gaussian band fit - Solvatochromic analysis.

2.1.4.1 E_T^N.

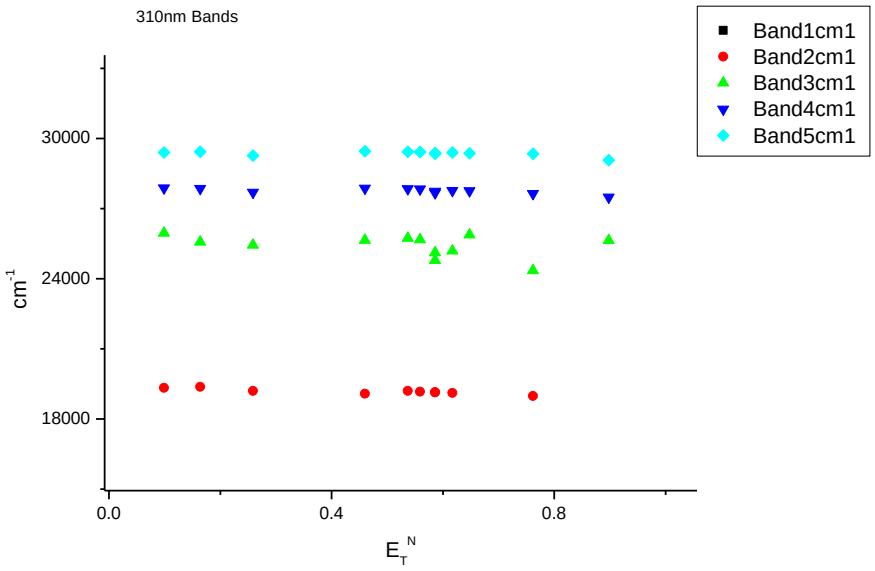

Figure 2.1.1. Band maxima from Gaussian model fit of the normalised fluorescence emission spectra of **11a** recorded at 310 nm excitation against E_T^N.

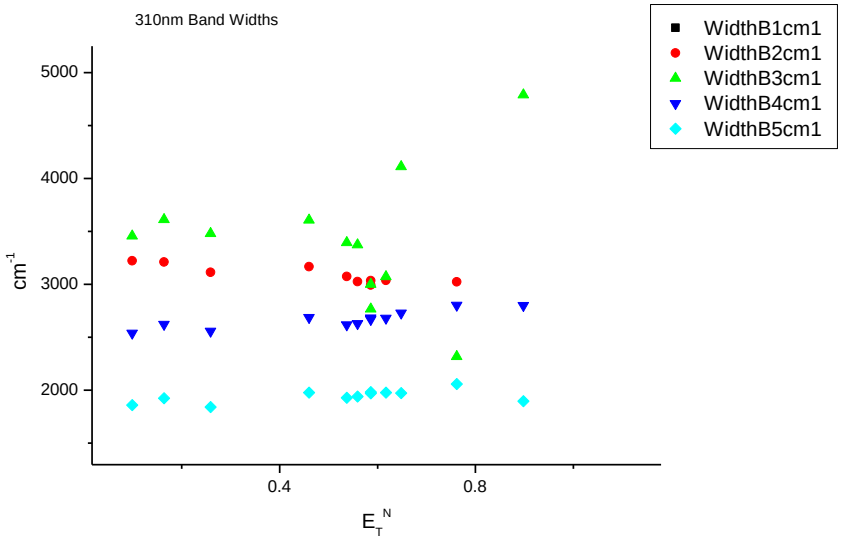

Figure 2.1.2. Band widths from Gaussian model fit of the normalised fluorescence emission spectra of **11a** recorded at 310 nm excitation against E_T^N.

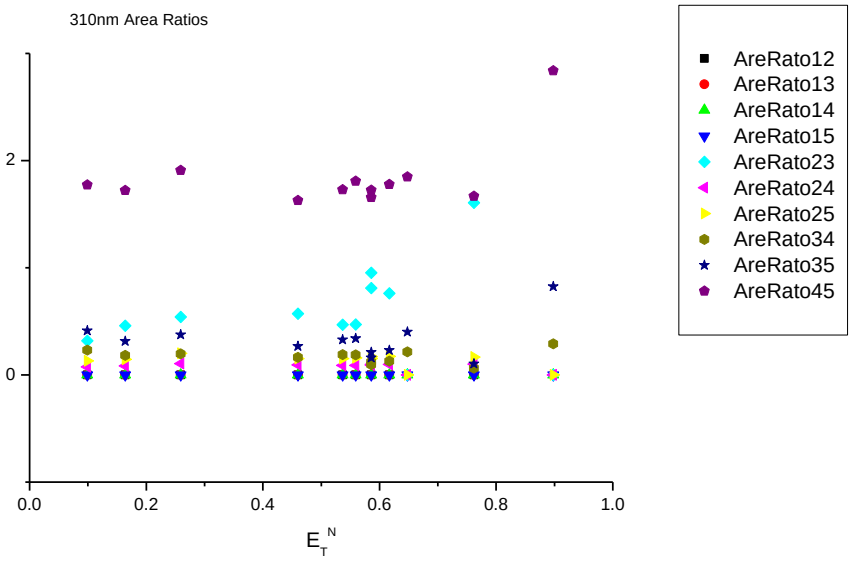

Figure 2.1.3. Area ratios from Gaussian model fit of the normalised fluorescence emission spectra of **11a** recorded at 310 nm excitation against E_T^N.

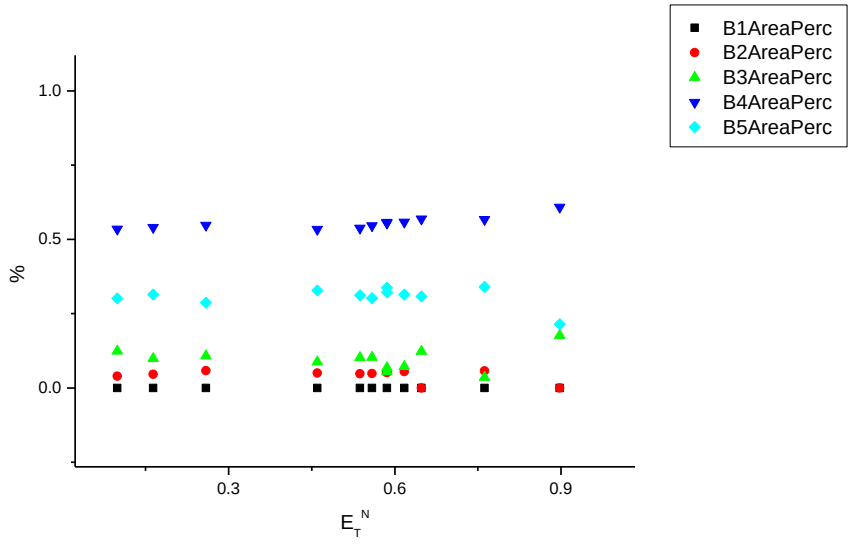

Figure 2.1.4. Area percentages from Gaussian model fit of the normalised fluorescence emission spectra of **11a** recorded at 310 nm excitation against E_T^N.

2.1.4.2 *α*

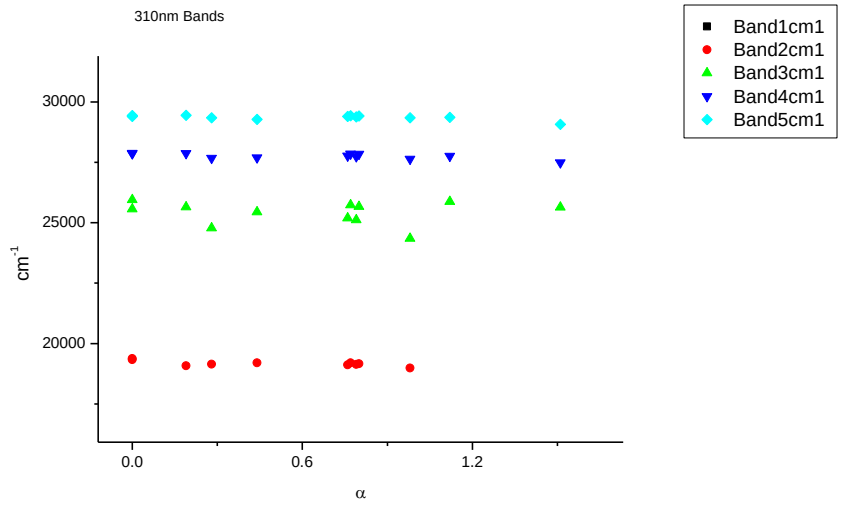

Figure 2.1.5. Band maxima from Gaussian model fit of the normalised fluorescence emission spectra of **11a** recorded at 310 nm excitation against α.

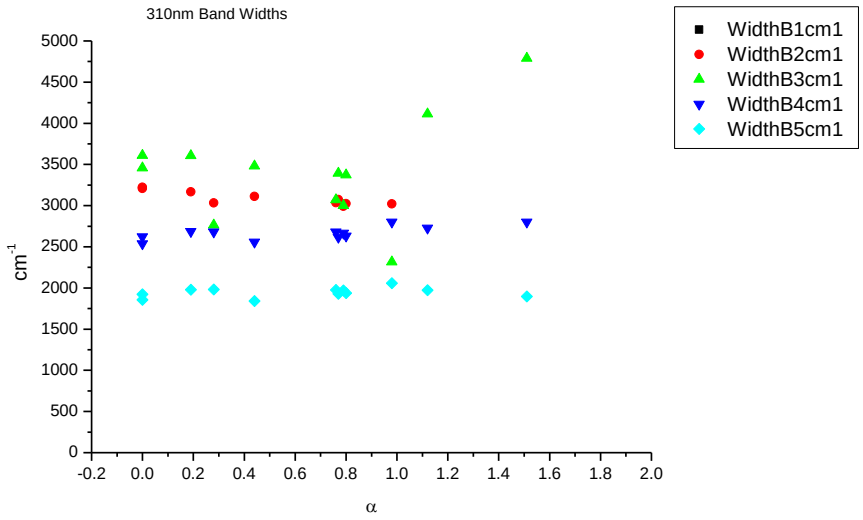

Figure 2.1.6. Band widths from Gaussian model fit of the normalised fluorescence emission spectra of **11a** recorded at 310 nm excitation against α.

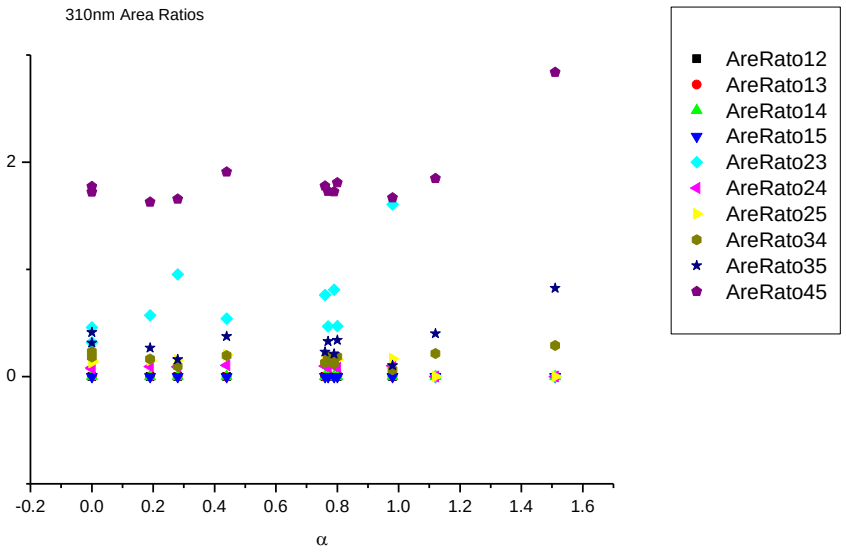

Figure 2.1.7. Area Ratios from Gaussian model fit of the normalised fluorescence emission spectra of **11a** recorded at 310 nm excitation against α.

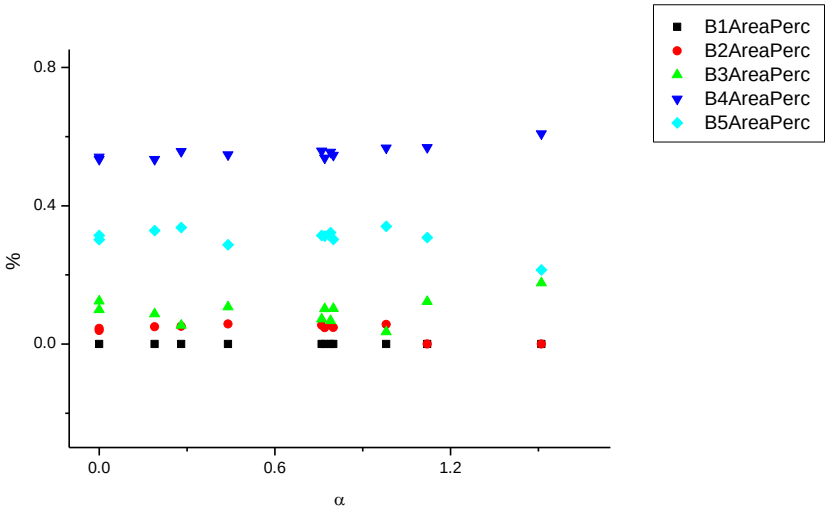

Figure 2.1.8. Area percentages from Gaussian model fit of the normalised fluorescence emission spectra of **11a** recorded at 310 nm excitation against α.

2.1.4.3 β.

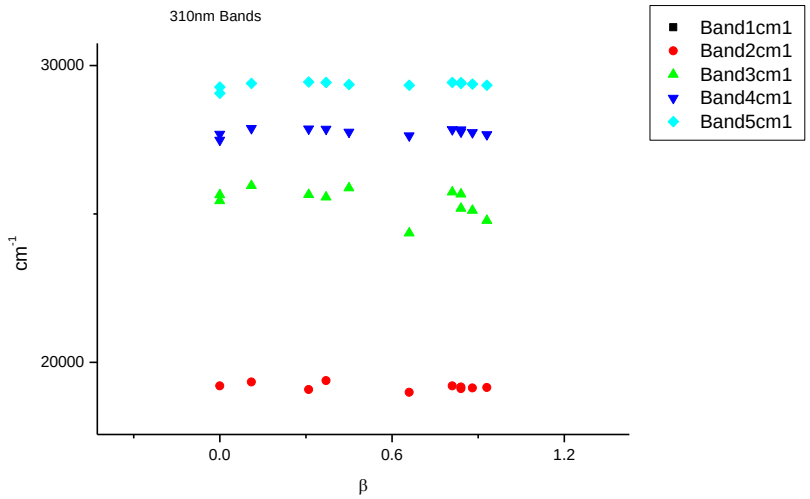

Figure 2.1.9. Band maxima from Gaussian model fit of the normalised fluorescence emission spectra of **11a** recorded at 310 nm excitation against β.

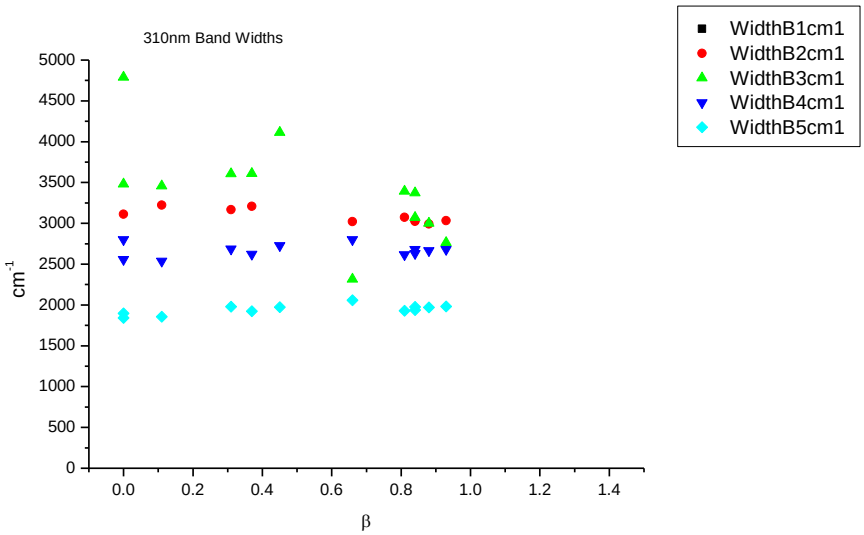

Figure 2.1.10. Band widths from Gaussian model fit of the normalised fluorescence emission spectra of **11a** recorded at 310 nm excitation against β.

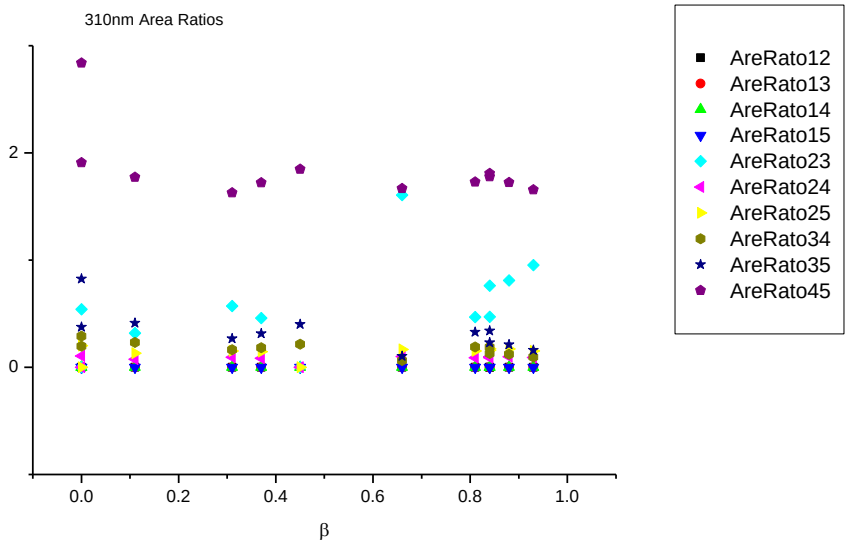

Figure 2.1.11. Area ratios from Gaussian model fit of the normalised fluorescence emission spectra of **11a** recorded at 310 nm excitation against β.

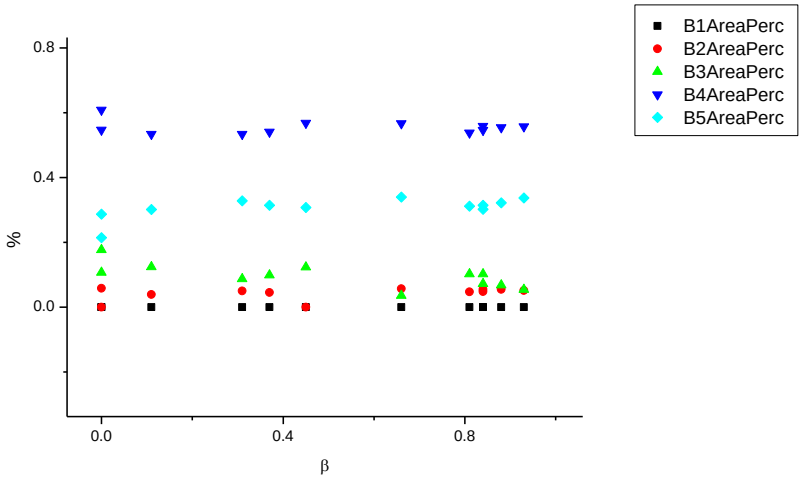

Figure 2.1.12. Area percentages from Gaussian model fit of the normalised fluorescence emission spectra of **11a** recorded at 310 nm excitation against β.

2.1.4.3 π.*

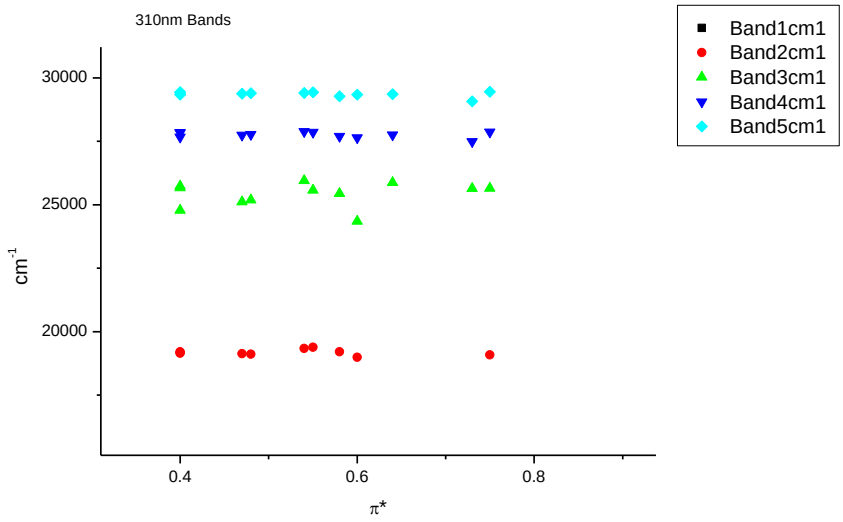

Figure 2.1.13. Band maxima from Gaussian model fit of the normalised fluorescence emission spectra of **11a** recorded at 310 nm excitation against π*.

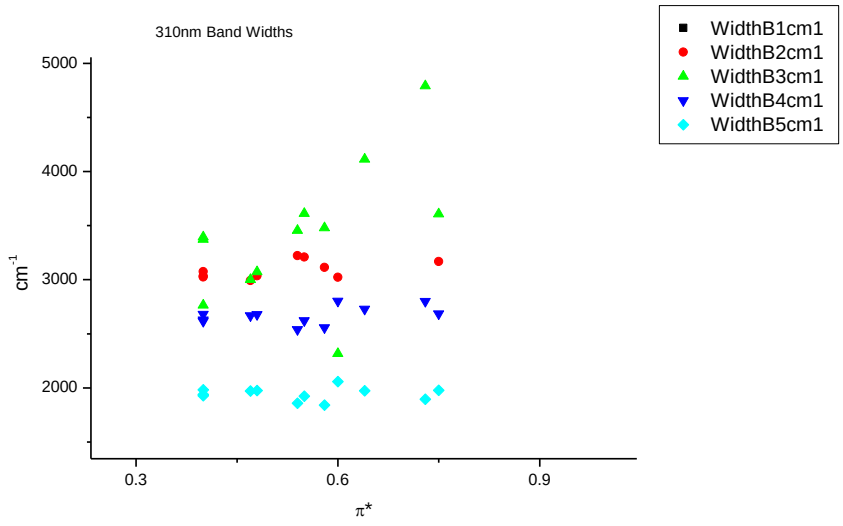

Figure 2.1.14. Band widths from Gaussian model fit of the normalised fluorescence emission spectra of **11a** recorded at 310 nm excitation against π*.

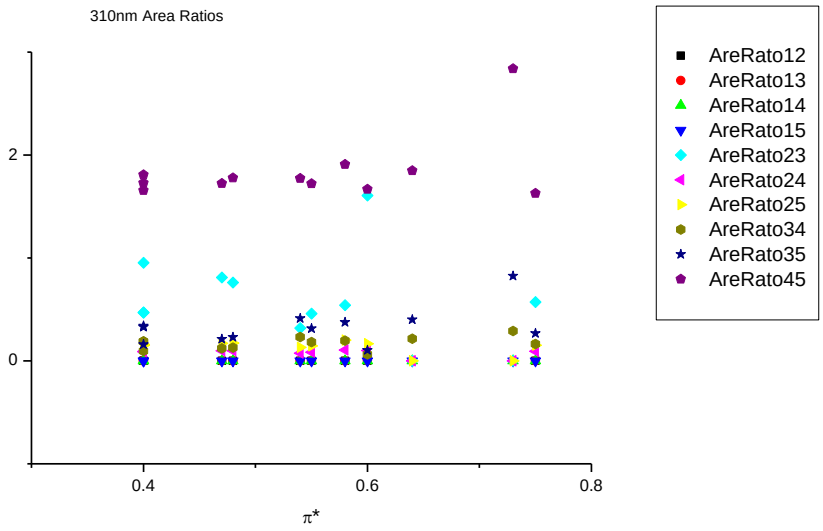

Figure 2.1.15. Area ratios from Gaussian model fit of the normalised fluorescence emission spectra of **11a** recorded at 310 nm excitation against π*.

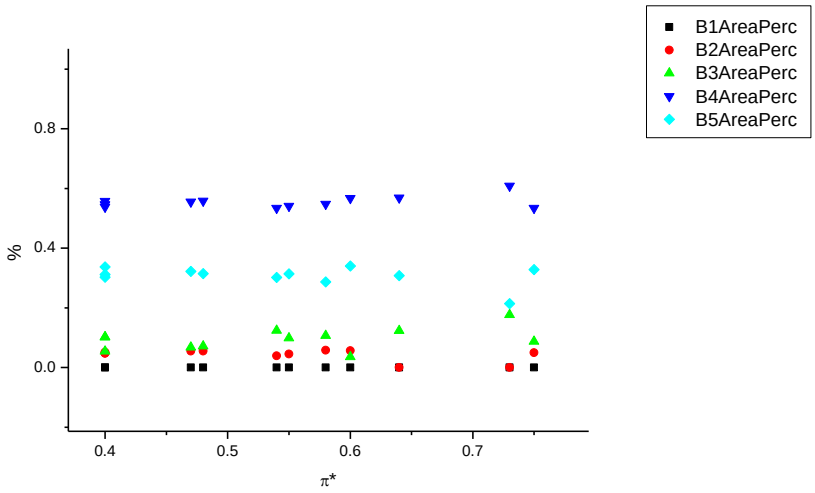

Figure 2.1.16. Area percentages from Gaussian model fit of the normalised fluorescence emission spectra of **11a** recorded at 310 nm excitation against π*.

2.1.4.5 μ(D).

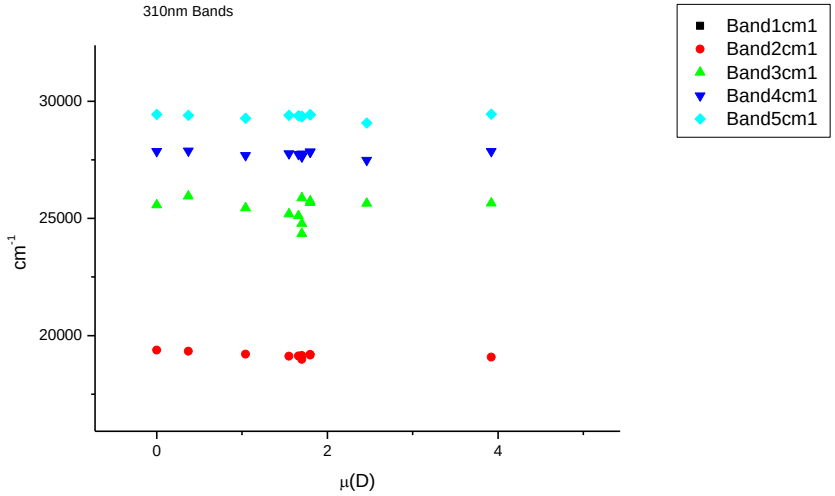

Figure 2.1.17. Band maxima from Gaussian model fit of the normalised fluorescence emission spectra of **11a** recorded at 310 nm excitation against μ(D).

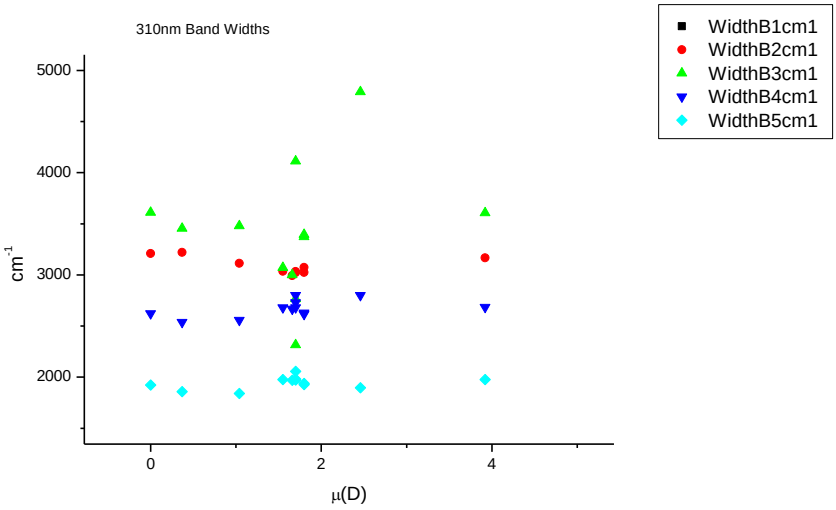

Figure 2.1.18. Band widths from Gaussian model fit of the normalised fluorescence emission spectra of **11a** recorded at 310 nm excitation against μ(D).

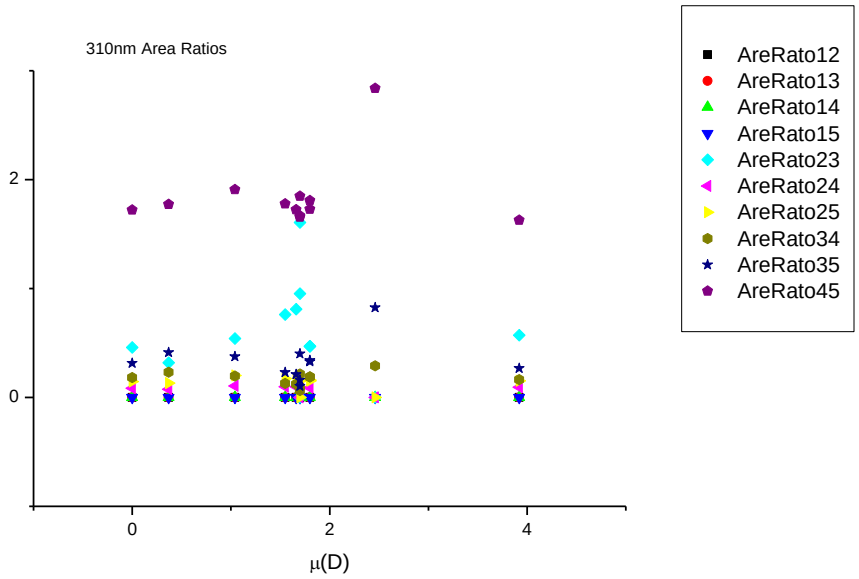

Figure 2.1.19. Area ratios from Gaussian model fit of the normalised fluorescence emission spectra of **11a** recorded at 310 nm excitation against μ(D).

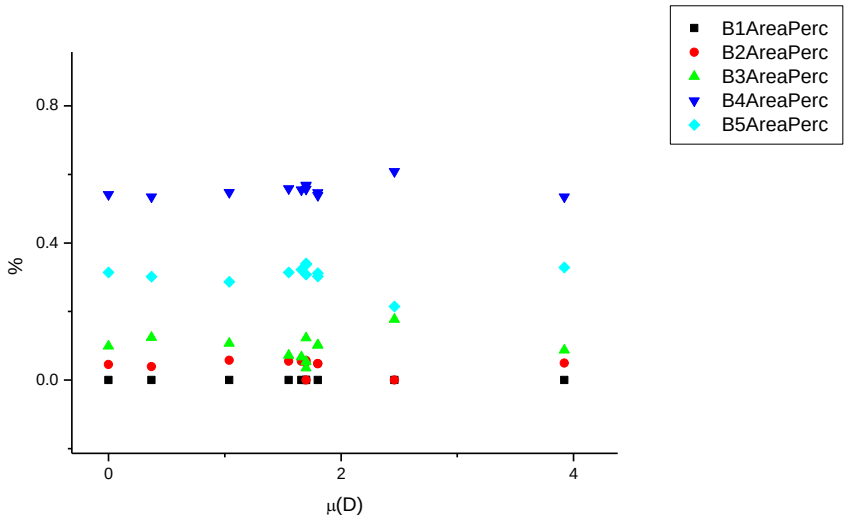

Figure 2.1.20. Area percentages from Gaussian model fit of the normalised fluorescence emission spectra of **11a** recorded at 310 nm excitation against μ(D).

2.1.4.6 η(Cp).

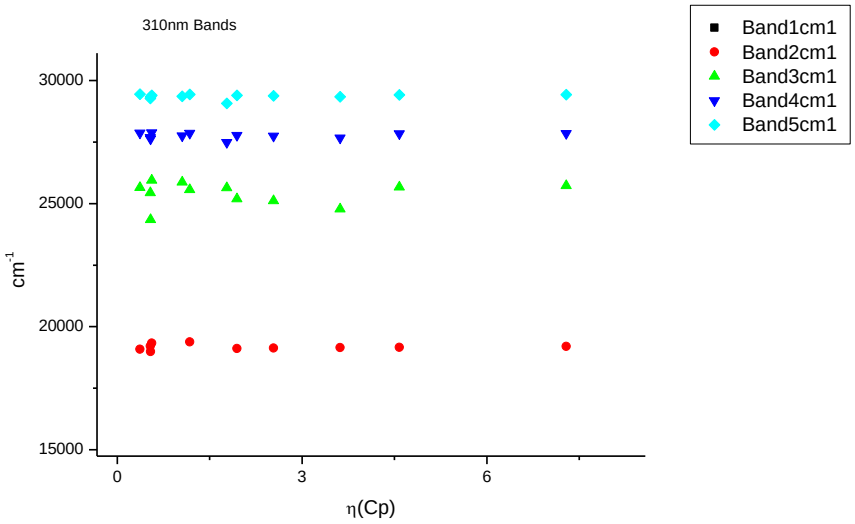

Figure 2.1.21. Band maxima from Gaussian model fit of the normalised fluorescence emission spectra of **11a** recorded at 310 nm excitation against η(Cp).

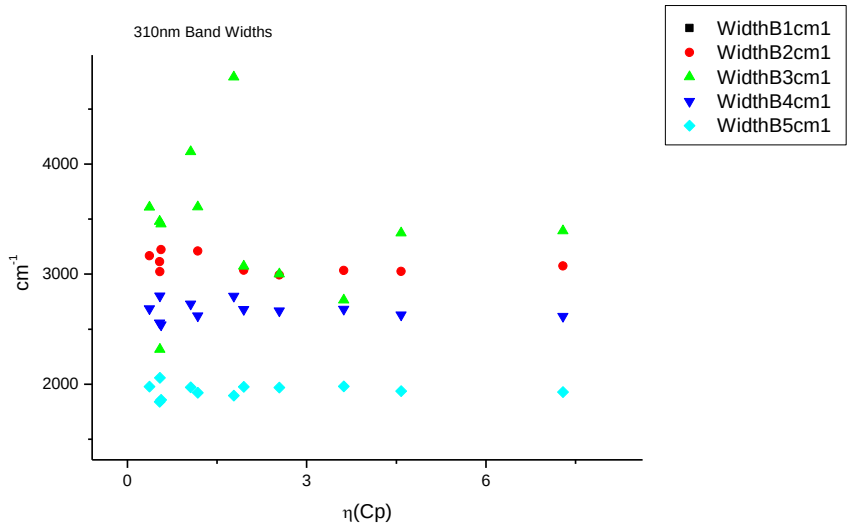

Figure 2.1.22. Band widths from Gaussian model fit of the normalised fluorescence emission spectra of **11a** recorded at 310 nm excitation against η(Cp).

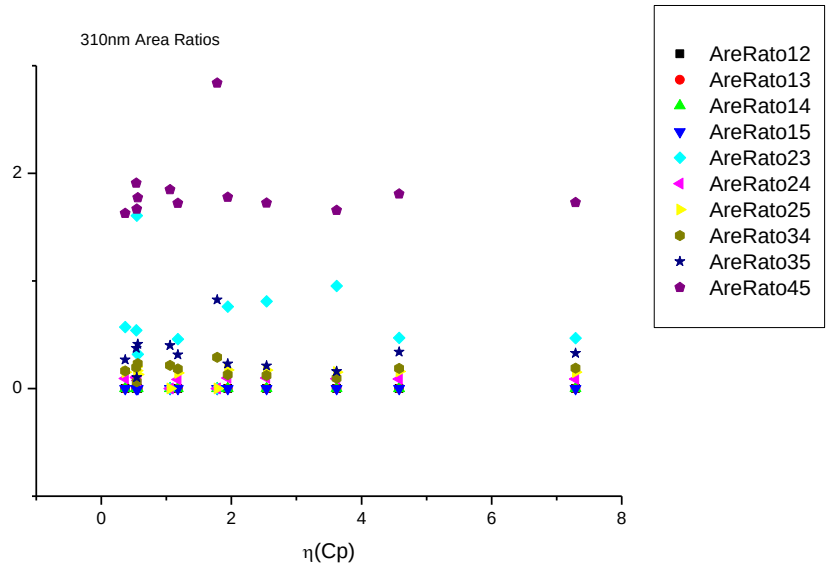

Figure 2.1.23. Area ratios from Gaussian model fit of the normalised fluorescence emission spectra of **11a** recorded at 310 nm excitation against η(Cp).

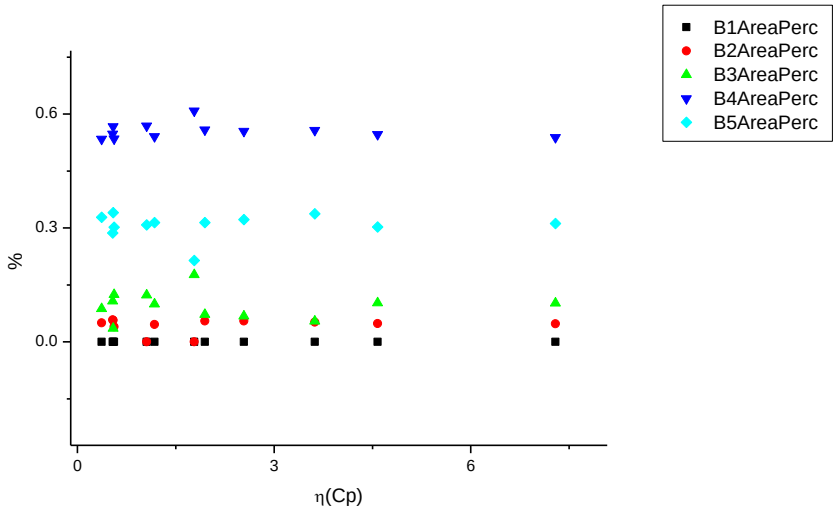

Figure 2.1.24. Area percentages from Gaussian model fit of the normalised fluorescence emission spectra of **11a** recorded at 310 nm excitation against η(Cp).

2.1.5 400 nm Gaussian band fit - Solvatochromic analysis.

2.1.5.1 E_T^N.

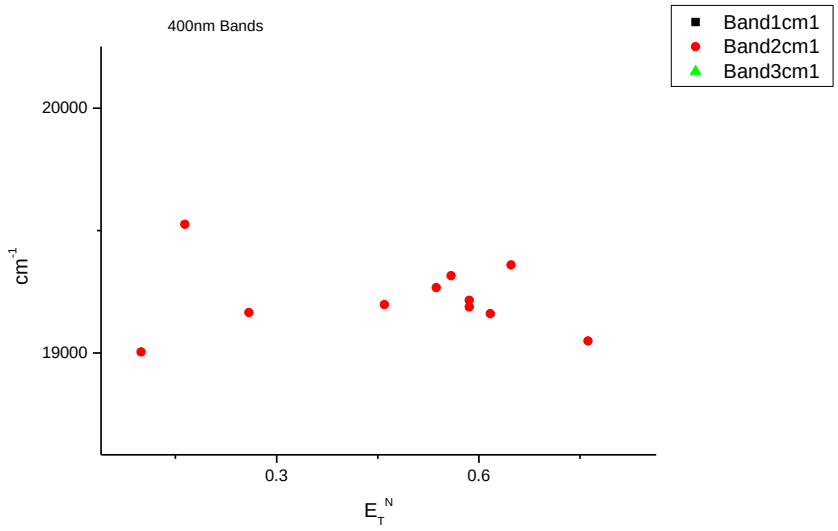

Figure 2.1.25. Band maxima from Gaussian model fit of the normalised fluorescence emission spectra of **11a** recorded at 400 nm excitation against E_T^N.

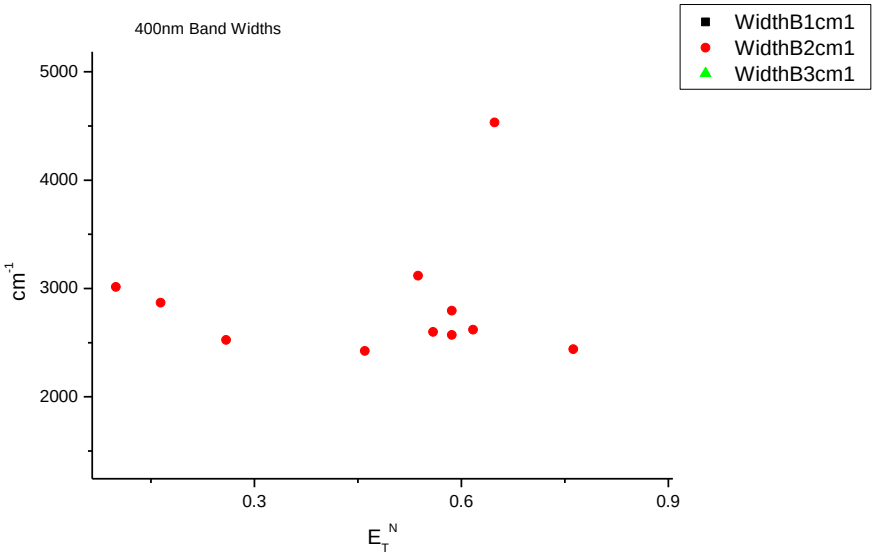

Figure 2.1.26. Band widths from Gaussian model fit of the normalised fluorescence emission spectra of **11a** recorded at 400 nm excitation against E_T^N.

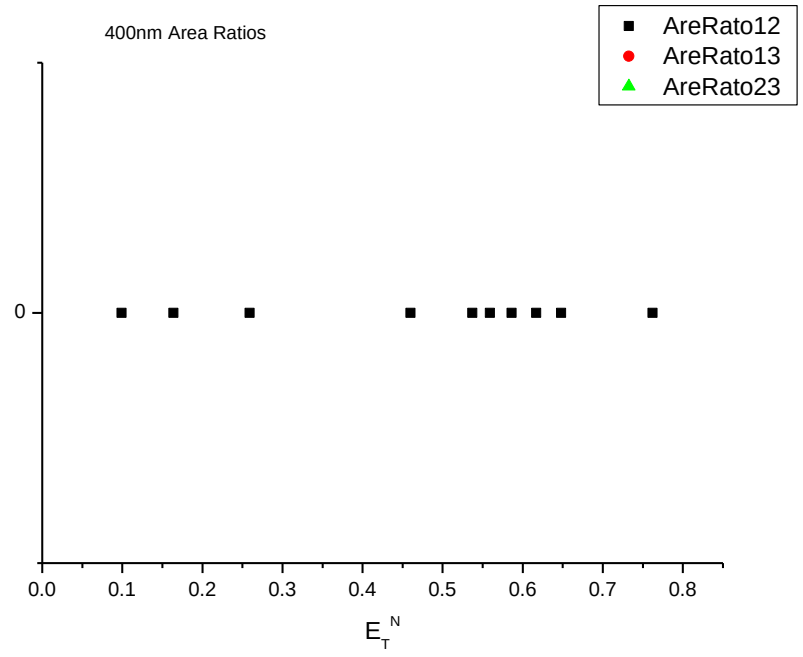

Figure 2.1.27. Area ratios from Gaussian model fit of the normalised fluorescence emission spectra of **11a** recorded at 400 nm excitation against E_T^N.

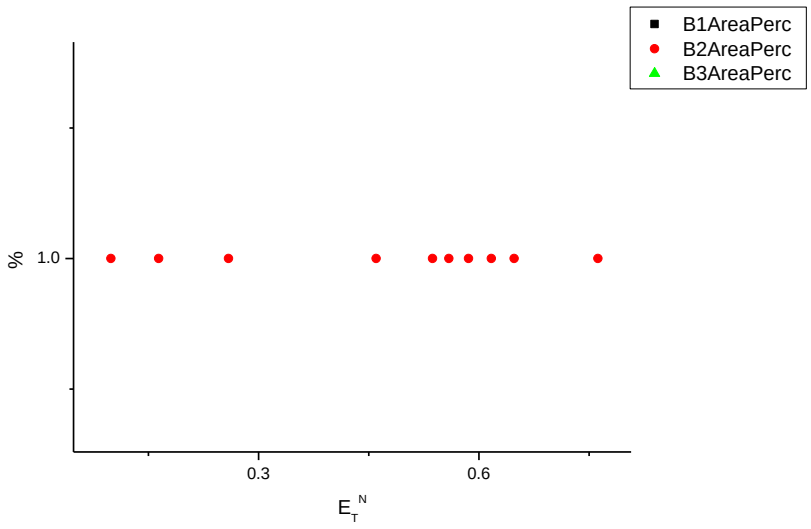

Figure 2.1.28. Area percentages from Gaussian model fit of the normalised fluorescence emission spectra of **11a** recorded at 400 nm excitation against E_T^N.

2.1.5.2 α.

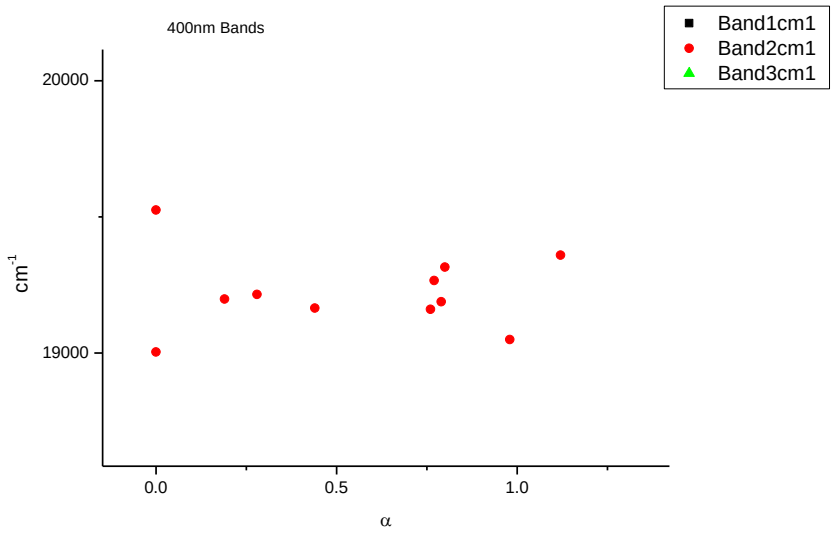

Figure 2.1.29. Band maxima from Gaussian model fit of the normalised fluorescence emission spectra of **11a** recorded at 400 nm excitation against α.

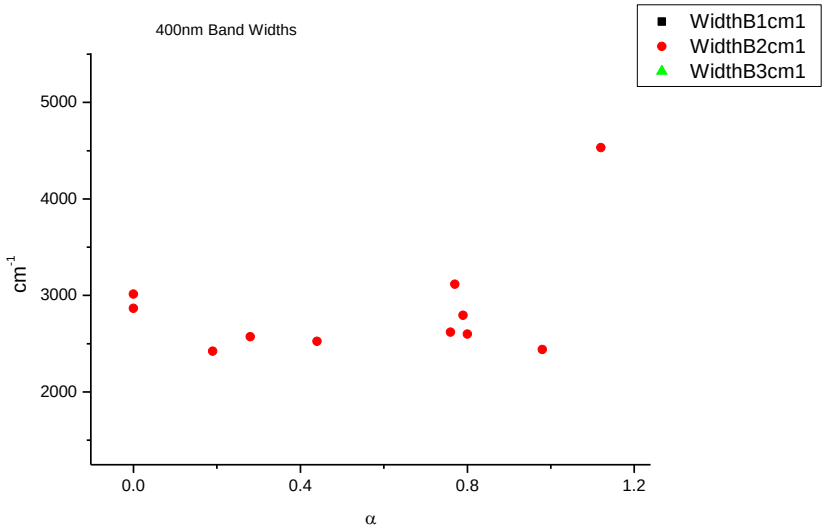

Figure 2.1.30. Band widths from Gaussian model fit of the normalised fluorescence emission spectra of **11a** recorded at 400 nm excitation against α.

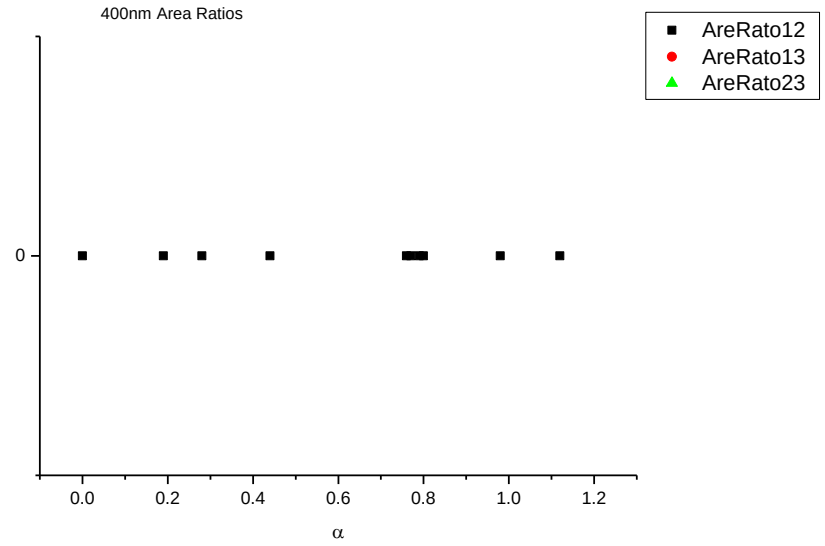

Figure 2.1.31. Area ratios from Gaussian model fit of the normalised fluorescence emission spectra of **11a** recorded at 400 nm excitation against α.

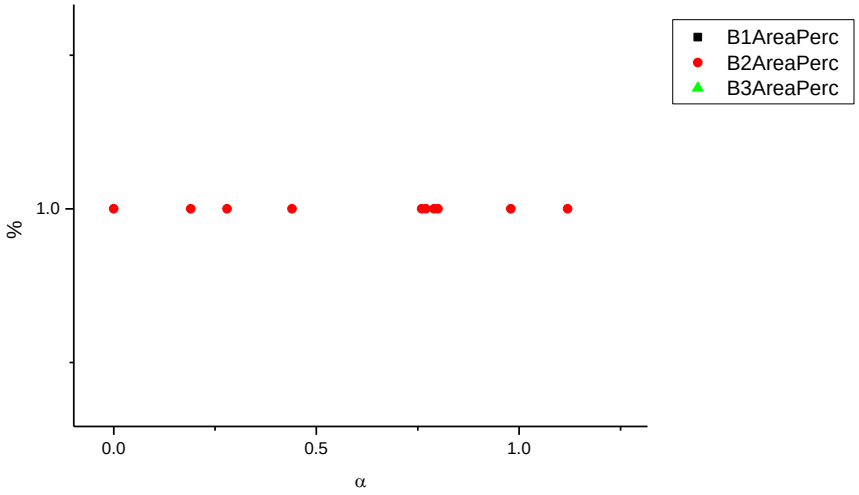

Figure 2.1.32. Area percentages from Gaussian model fit of the normalised fluorescence emission spectra of **11a** recorded at 400 nm excitation against α.

2.1.5.3 β.

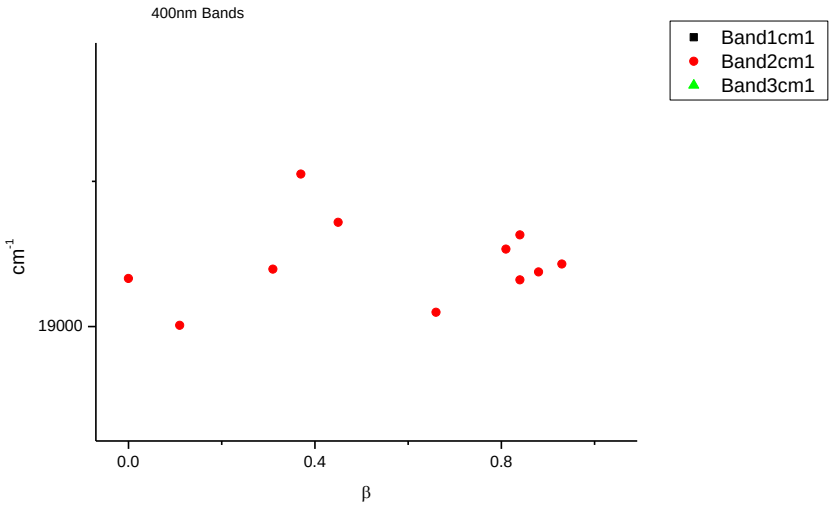

Figure 2.1.33. Band maxima from Gaussian model fit of the normalised fluorescence emission spectra of **11a** recorded at 400 nm excitation against β.

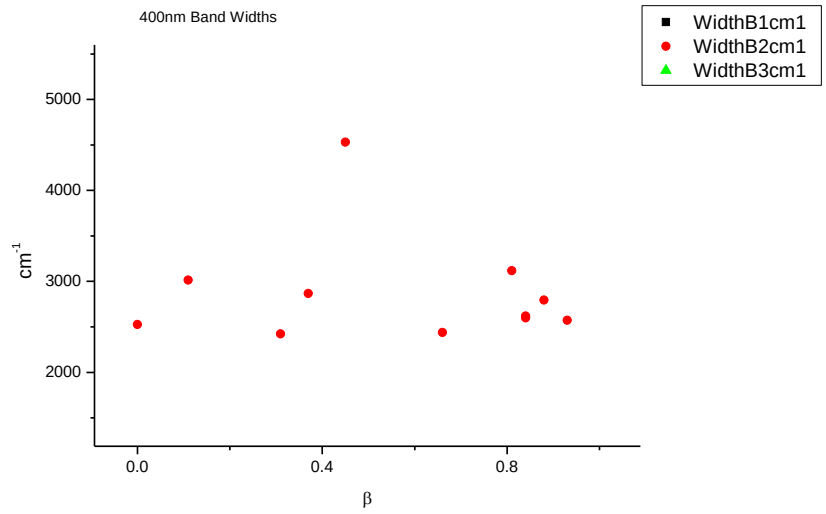

Figure 2.1.34. Band widths from Gaussian model fit of the normalised fluorescence emission spectra of **11a** recorded at 400 nm excitation against β.

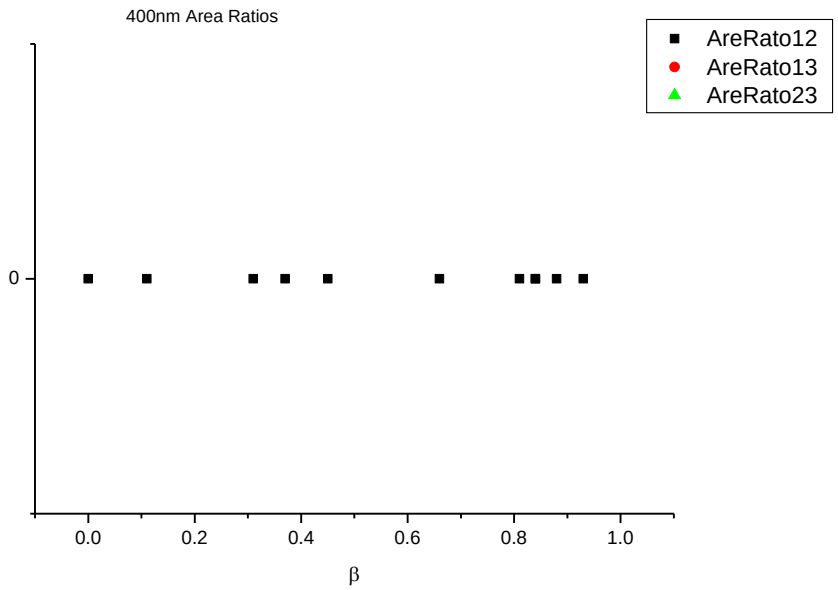

Figure 2.1.35. Area ratios from Gaussian model fit of the normalised fluorescence emission spectra of **11a** recorded at 400 nm excitation against β.

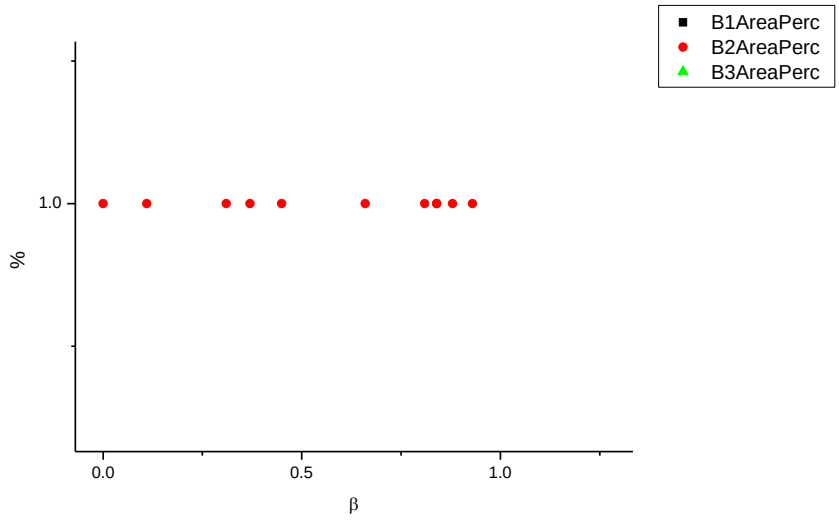

Figure 2.1.36. Area percentages from Gaussian model fit of the normalised fluorescence emission spectra of **11a** recorded at 400 nm excitation against β.

2.1.5.4 π.*

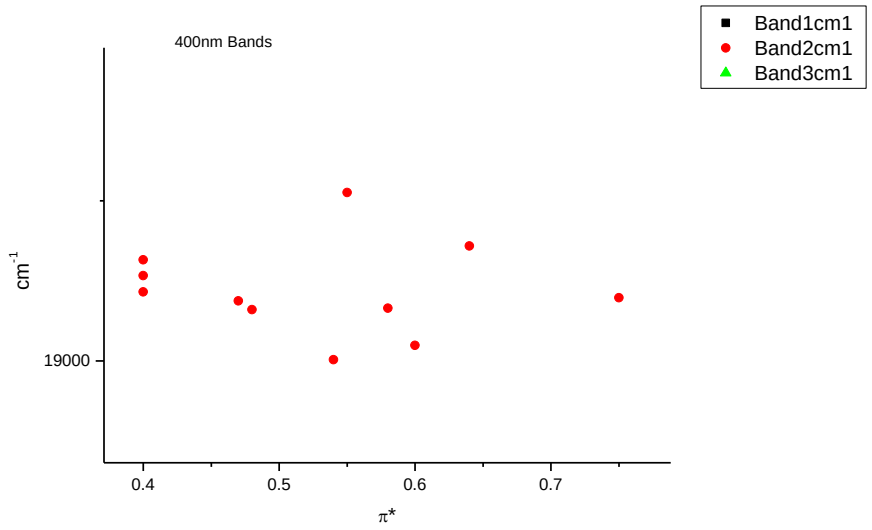

Figure 2.1.37. Band maxima from Gaussian model fit of the normalised fluorescence emission spectra of **11a** recorded at 400 nm excitation against π*.

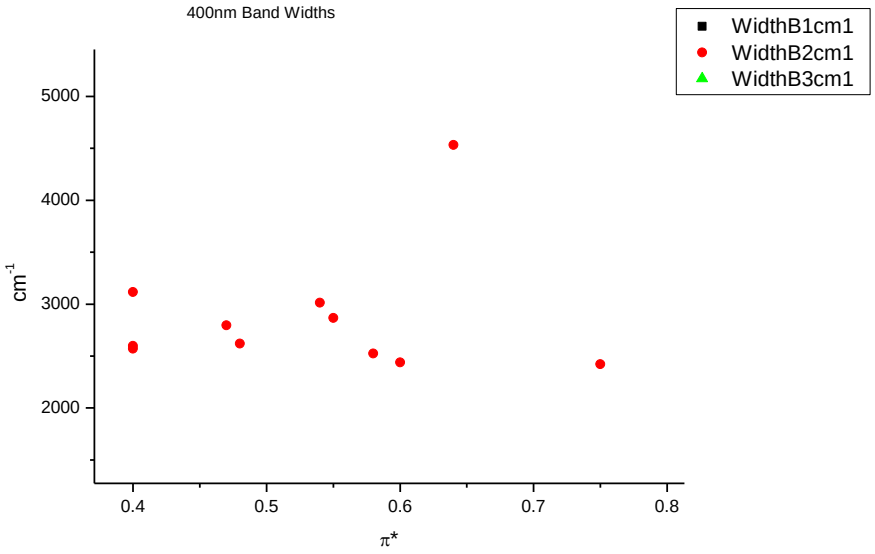

Figure 2.1.38. Band widths from Gaussian model fit of the normalised fluorescence emission spectra of **11a** recorded at 400 nm excitation against π*.

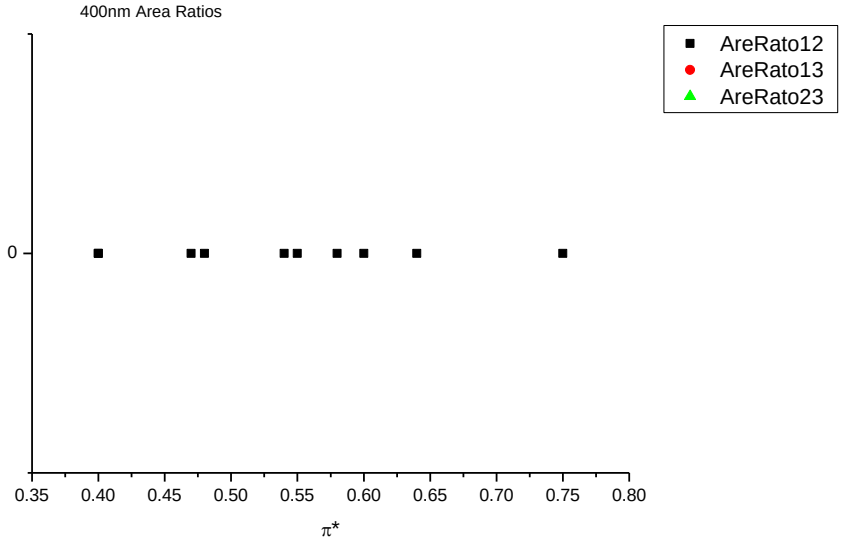

Figure 2.1.39. Area ratios from Gaussian model fit of the normalised fluorescence emission spectra of **11a** recorded at 400 nm excitation against π*.

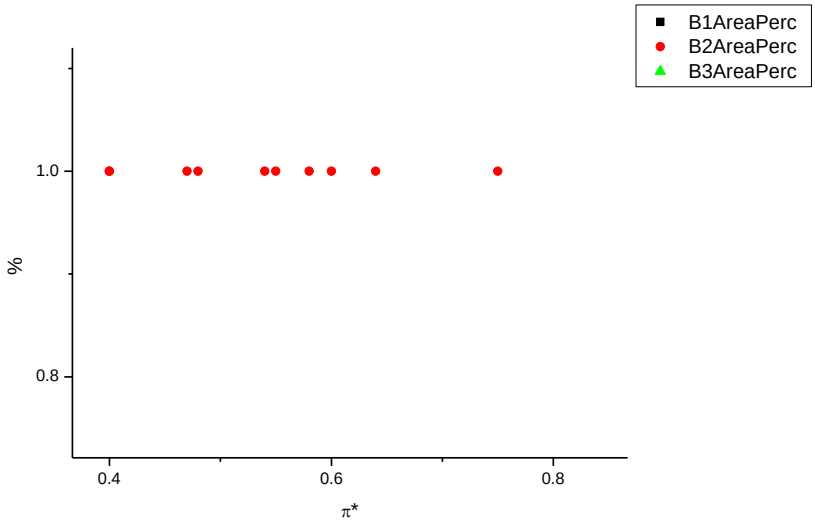

Figure 2.1.40. Area percentages from Gaussian model fit of the normalised fluorescence emission spectra of **11a** recorded at 400 nm excitation against π*.

2.1.5.5 μ(D).

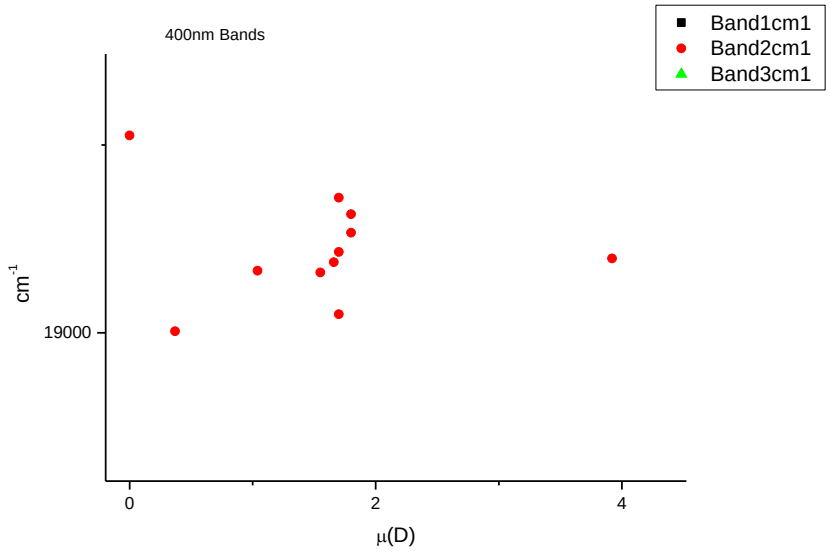

Figure 2.1.41. Band maxima from Gaussian model fit of the normalised fluorescence emission spectra of **11a** recorded at 400 nm excitation against μ(D).

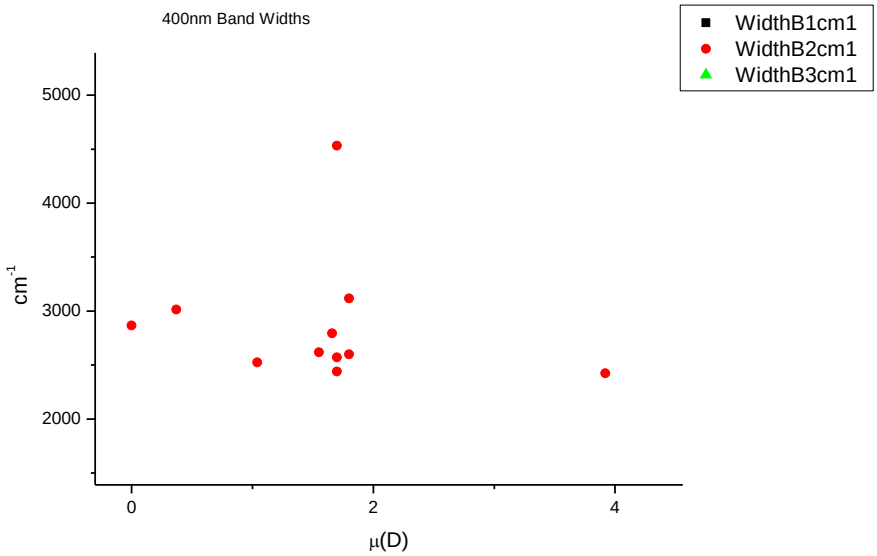

Figure 2.1.42. Band widths from Gaussian model fit of the normalised fluorescence emission spectra of **11a** recorded at 400 nm excitation against μ(D).

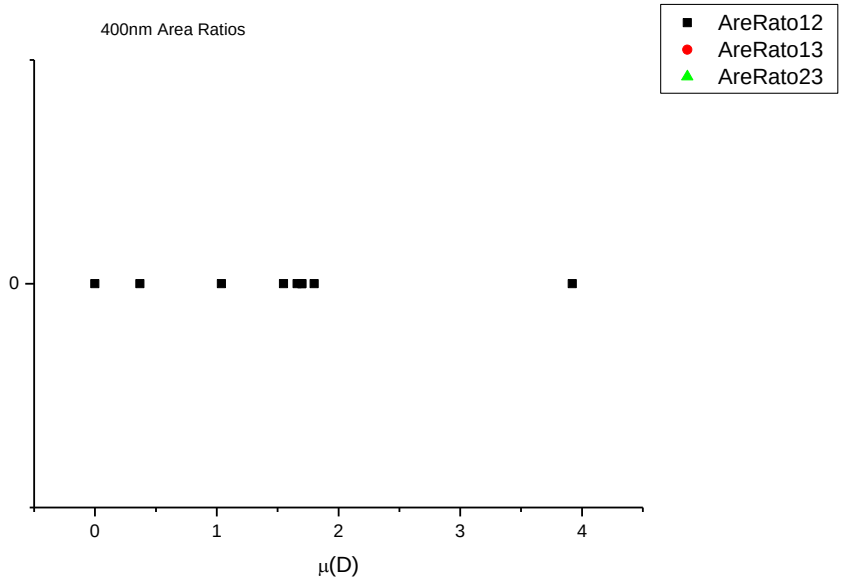

Figure 2.1.43. Area ratios from Gaussian model fit of the normalised fluorescence emission spectra of **11a** recorded at 400 nm excitation against μ(D).

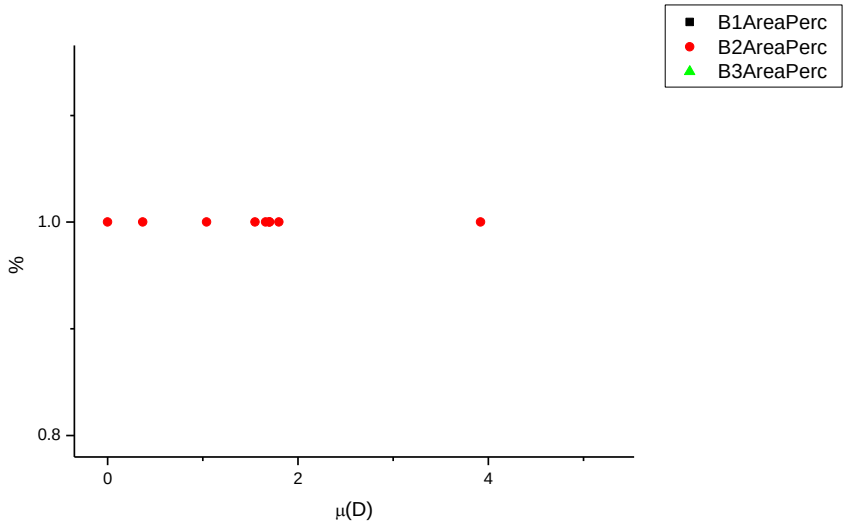

Figure 2.1.44. Area percentages from Gaussian model fit of the normalised fluorescence emission spectra of **11a** recorded at 400 nm excitation against μ(D).

2.1.5.6 η(Cp).

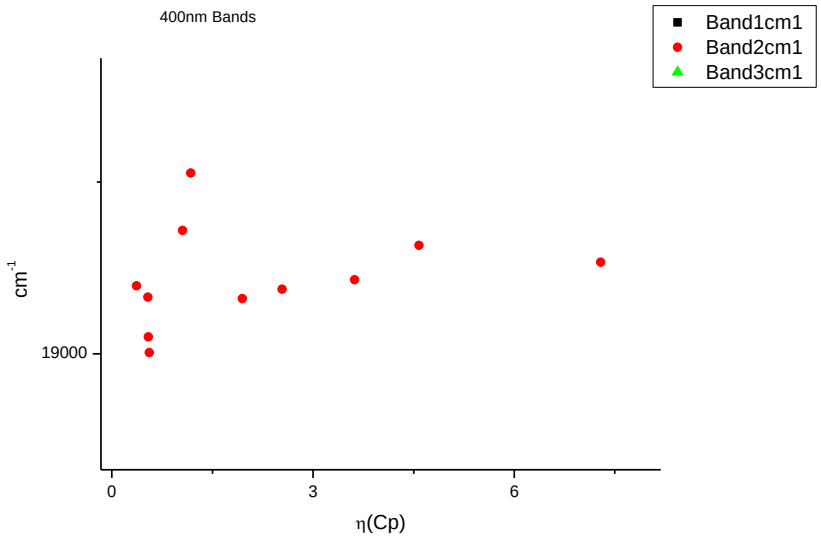

Figure 2.1.45. Band maxima from Gaussian model fit of the normalised fluorescence emission spectra of **11a** recorded at 400 nm excitation against η(Cp).

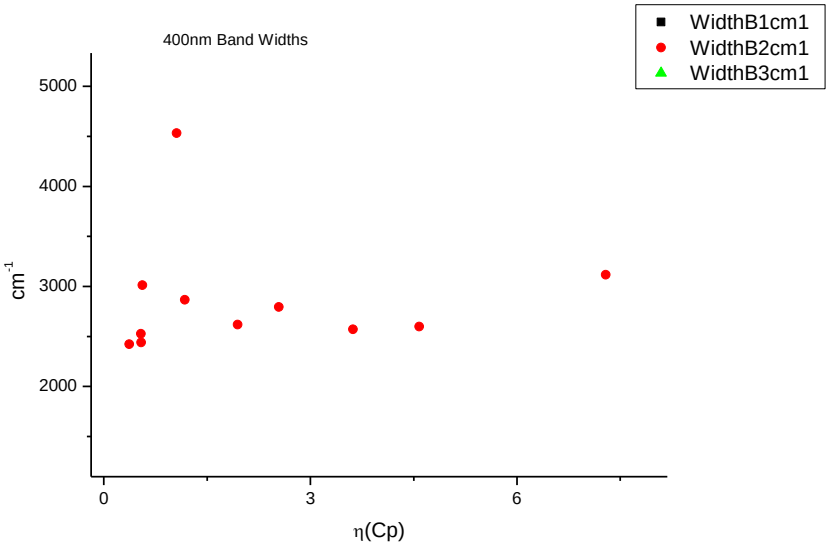

Figure 2.1.46. Band widths from Gaussian model fit of the normalised fluorescence emission spectra of **11a** recorded at 400 nm excitation against η(Cp).

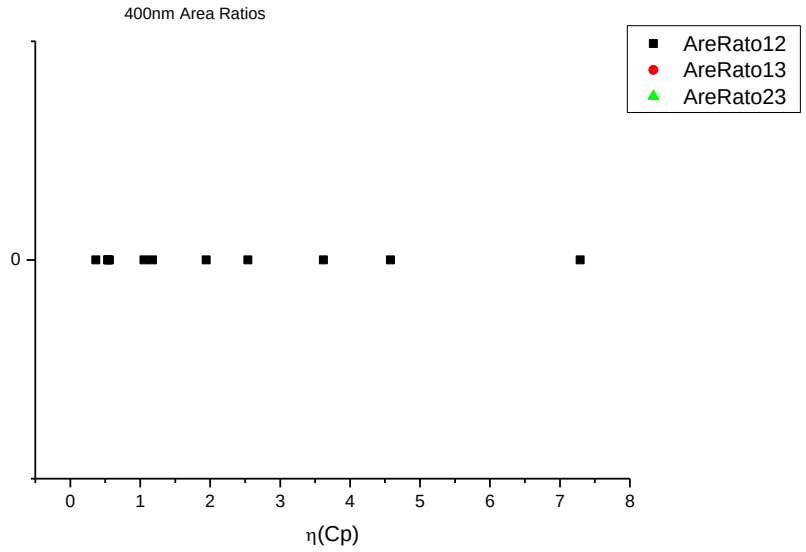

Figure 2.1.47. Area ratios from Gaussian model fit of the normalised fluorescence emission spectra of **11a** recorded at 400 nm excitation against η(Cp).

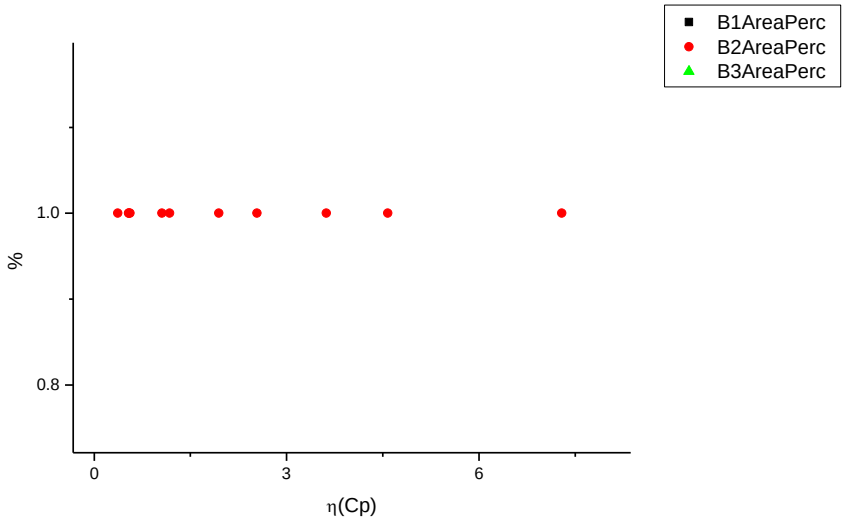

Figure 2.1.48. Area percentages from Gaussian model fit of the normalised fluorescence emission spectra of **11a** recorded at 400 nm excitation against η(Cp).

2.1.6 295 nm (LED) fluorescent lifetime results.

2.1.6.1 Intensity weighted.

Wavelength (nm)	Solvent	τ_1 (ns)	A_1 (%)	τ_2 (ns)	A_2 (%)	τ_3 (ns)	A_3 (%)	τ_f (ns) (Intensity Weighted)	$1/\tau_f$	χ^2
330	Toluene	1.02	97.96	6.69	2.04	-	-	1.14	0.88	1.20
330	1,4-Dioxane	1.08	98.29	7.31	1.71	-	-	1.19	0.84	1.34
330	Chloroform	1.02	98.74	6.77	1.26	-	-	1.09	0.92	1.19
330	Acetonitrile	1.15	92.22	7.83	7.78	-	-	1.67	0.60	1.24
330	1-Octanol	1.16	92.38	5.56	7.62	-	-	1.50	0.67	1.19
330	1-Hexanol	1.15	89.96	7.66	10.04	-	-	1.80	0.55	1.18
330	1-Butanol	1.12	97.08	8.14	2.92	-	-	1.33	0.75	1.22
330	1-Pentanol	1.13	96.70	5.60	3.30	-	-	1.28	0.78	1.26
330	1-Propanol	1.11	98.57	7.58	1.43	-	-	1.21	0.83	1.30
330	Acetic acid	1.16	91.40	7.97	8.60	-	-	1.75	0.57	1.34
330	Methanol	1.13	99.12	5.05	0.88	-	-	1.16	0.86	1.13
330	2,2,2-Trifluoroethanol	1.29	82.72	8.18	17.82	-	-	2.48	0.40	1.27

Wavelength (nm)	Solvent	τ_1 (ns)	A_1 (%)	τ_2 (ns)	A_2 (%)	τ_3 (ns)	A_3 (%)	τ_f (ns) (Intensity Weighted)	$1/\tau_f$	χ^2
350	Toluene	1.00	98.21	5.33	1.79	-	-	1.08	0.93	1.17
350	1,4-Dioxane	1.07	98.39	6.29	1.61	-	-	1.16	0.86	1.20
350	Chloroform	1.01	98.78	5.48	1.22	-	-	1.07	0.94	1.19
350	Acetonitrile	1.12	93.85	6.82	6.15	-	-	1.46	0.68	1.25
350	1-Octanol	1.12	89.86	3.81	10.14	-	-	1.39	0.72	1.38
350	1-Hexanol	1.11	93.89	7.97	6.11	-	-	1.52	0.66	1.43
350	1-Butanol	1.10	97.69	6.63	2.31	-	-	1.23	0.82	1.38
350	1-Pentanol	1.10	97.68	5.60	2.32	-	-	1.20	0.83	1.25
350	1-Propanol	1.09	99.13	6.79	0.87	-	-	1.14	0.87	1.17
350	Acetic acid	1.12	93.47	7.03	6.53	-	-	1.51	0.66	1.34
350	Methanol	1.11	99.07	3.67	0.93	-	-	1.13	0.88	1.13
350	2,2,2-Trifluoroethanol	1.08	79.93	3.42	12.55	14.01	7.52	2.35	0.43	1.25

Table 2.1.9. Summary of Time Correlated Single Photon Counting (TCSPC) fluorescent lifetimes (intensity weighted) of **11a** at (a.) 330 nm and (b.) 350 nm, recorded using a 295 nm Laser Emitting Diode (LED) Laser source.

2.1.6.2 Amplitude weighted.

Wavelength (nm)	Solvent	τ_1 (ns)	A_1 (%)	τ_2 (ns)	A_2 (%)	τ_3 (ns)	A_3 (%)	τ_f (ns) (Amplitude Weighted)	$1/\tau_f$	χ^2
330	Toluene	1.02	99.68	6.69	0.32	-	-	1.04	0.96	1.20
330	1,4-Dioxane	1.08	99.74	7.31	0.26	-	-	1.10	0.91	1.34
330	Chloroform	1.02	99.81	6.77	0.19	-	-	1.03	0.97	1.19
330	Acetonitrile	1.15	98.78	7.83	1.22	-	-	1.23	0.81	1.24
330	1-Octanol	1.16	98.30	5.56	1.70	-	-	1.24	0.81	1.19
330	1-Hexanol	1.15	98.35	7.66	1.65	-	-	1.26	0.80	1.18
330	1-Butanol	1.12	99.59	8.14	0.41	-	-	1.52	0.66	1.22
330	1-Pentanol	1.13	99.32	5.60	0.68	-	-	1.16	0.86	1.26
330	1-Propanol	1.11	99.79	7.58	0.21	-	-	1.13	0.89	1.30
330	Acetic acid	1.16	98.65	7.97	1.35	-	-	1.25	0.80	1.34
330	Methanol	1.13	99.80	5.05	0.20	-	-	1.13	0.88	1.13
330	2,2,2-Trifluoroethanol	1.29	96.81	8.18	3.19	-	-	1.51	0.66	1.27

Wavelength (nm)	Solvent	τ_1 (ns)	A_1 (%)	τ_2 (ns)	A_2 (%)	τ_3 (ns)	A_3 (%)	τ_f (ns) (Amplitude Weighted)	$1/\tau_f$	χ^2
350	Toluene	1.00	99.66	5.33	0.34	-	-	1.01	0.99	1.17
350	1,4-Dioxane	1.07	99.72	6.29	0.28	-	-	1.09	0.92	1.20
350	Chloroform	1.01	99.77	5.48	0.23	-	-	1.02	0.98	1.19
350	Acetonitrile	1.12	98.94	6.82	1.06	-	-	1.17	0.85	1.25
350	1-Octanol	1.12	96.79	3.81	3.21	-	-	1.38	0.72	1.38
350	1-Hexanol	1.11	99.11	7.97	0.89	-	-	1.17	0.86	1.43
350	1-Butanol	1.10	99.61	6.63	0.39	-	-	1.12	0.89	1.38
350	1-Pentanol	1.10	99.54	5.60	0.46	-	-	1.12	0.89	1.25
350	1-Propanol	1.09	99.86	6.79	0.14	-	-	1.10	0.91	1.17
350	Acetic acid	1.12	98.90	7.03	1.10	-	-	1.19	0.84	1.34
350	Methanol	1.11	99.72	3.67	0.28	-	-	1.11	0.90	1.13
350	2,2,2-Trifluoroethanol	1.08	94.60	3.42	4.71	14.01	0.69	1.28	0.78	1.25

Table 2.1.10. Summary of Time Correlated Single Photon Counting (TCSPC) fluorescent lifetimes (amplitude weighted) of **11a** at (a.) 330 nm and (b.) 350 nm, recorded using a 295 nm Laser Emitting Diode (LED) Laser source.

2.1.7 400 nm fluorescent lifetime results.

2.1.7.1 Intensity weighted.

Wavelength (nm)	Solvent	τ_1 (ns)	A_1 (%)	τ_2 (ns)	A_2 (%)	τ_3 (ns)	A_3 (%)	τ_f (ns) (Intensity Weighted)	$1/\tau_f$	χ^2
500	Toluene	-	-	-	-	-	-	-	-	-
500	1,4-Dioxane	0.30	22.53	3.57	56.51	8.56	20.96	3.88	0.26	1.36
500	Chloroform	0.62	7.82	1.51	65.28	6.53	27.40	2.82	0.36	1.14
500	Acetonitrile	-	-	-	-	-	-	-	-	-
500	1-Octanol	-	-	-	-	-	-	-	-	-
500	1-Hexanol	-	-	-	-	-	-	-	-	-
500	1-Butanol	-	-	-	-	-	-	-	-	-
500	1-Pentanol	-	-	-	-	-	-	-	-	-
500	1-Propanol	-	-	-	-	-	-	-	-	-
500	Acetic acid	-	-	-	-	-	-	-	-	-
500	Methanol	-	-	-	-	-	-	-	-	-
500	2,2,2-Trifluoroethanol	-	-	-	-	-	-	-	-	-

Table 2.1.11. Summary of Time Correlated Single Photon Counting (TCSPC) fluorescent lifetimes (intensity weighted) of **11a** at 500 nm, recorded using a 405 nm laser source.

2.1.7.2 Amplitude weighted.

Wavelength (nm)	Solvent	τ_1 (ns)	A_1 (%)	τ_2 (ns)	A_2 (%)	τ_3 (ns)	A_3 (%)	τ_f (ns) (Amplitude Weighted)	$1/\tau_f$	χ^2
500	Toluene	-	-	-	-	-	-	-	-	-
500	1,4-Dioxane	0.30	80.54	3.57	16.85	8.56	2.61	1.07	0.94	1.36
500	Chloroform	0.62	20.02	1.51	71.92	6.53	7.06	1.68	0.59	1.14
500	Acetonitrile	-	-	-	-	-	-	-	-	-
500	1-Octanol	-	-	-	-	-	-	-	-	-
500	1-Hexanol	-	-	-	-	-	-	-	-	-
500	1-Butanol	-	-	-	-	-	-	-	-	-
500	1-Pentanol	-	-	-	-	-	-	-	-	-
500	1-Propanol	-	-	-	-	-	-	-	-	-
500	Acetic acid	-	-	-	-	-	-	-	-	-
500	Methanol	-	-	-	-	-	-	-	-	-
500	2,2,2-Trifluoroethanol	-	-	-	-	-	-	-	-	-

Table 2.1.12. Summary of Time Correlated Single Photon Counting (TCSPC) fluorescent lifetimes (amplitude weighted) of **11a** at 500 nm, recorded using a 405 nm laser source.

2.1.8 400 nm average fluorescent lifetimes - Solvatochromic analysis.

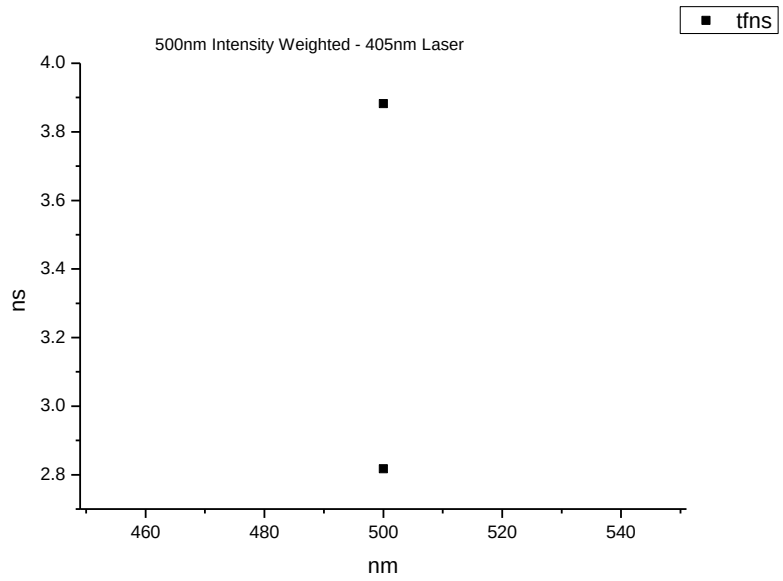

Figure 2.1.49. Intensity weighted average lifetime (τ_f) of **11a** versus wavelength (nm).

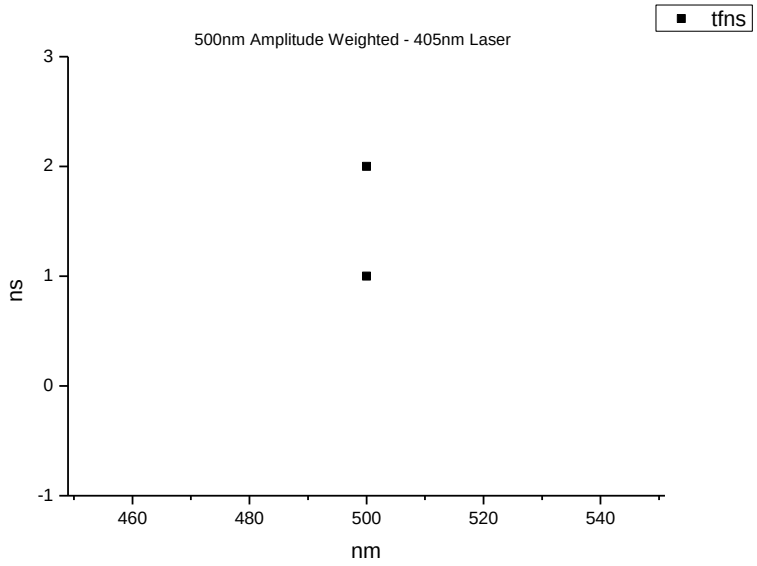

Figure 2.1.50. Amplitude weighted average lifetime (τ_f) of **11a** versus wavelength (nm).

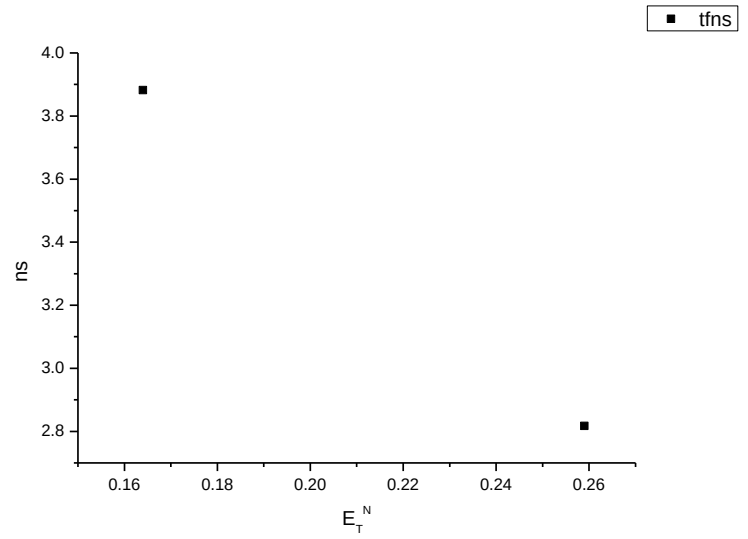

Figure 2.1.51. Intensity weighted average lifetime (τ_f) of **11a** versus E_T^N.

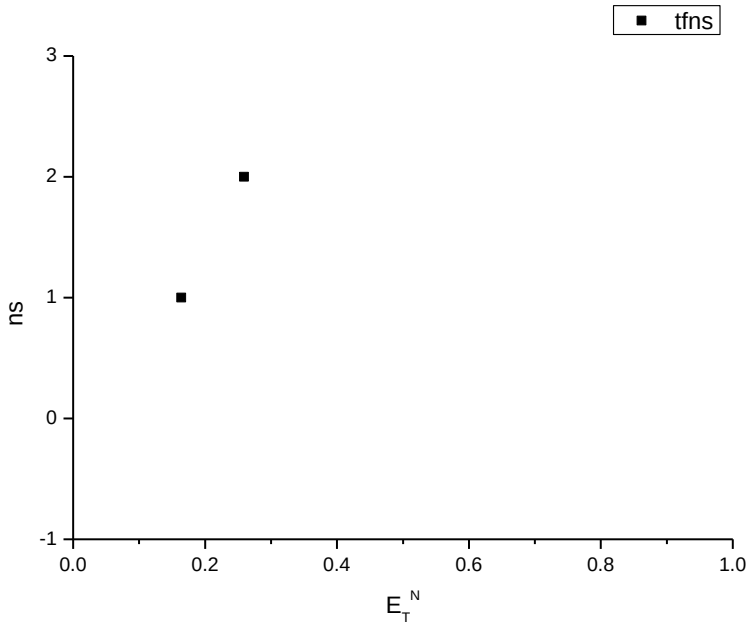

Figure 2.1.52. Amplitude weighted average lifetime (τ_f) of **11a** versus E_T^N.

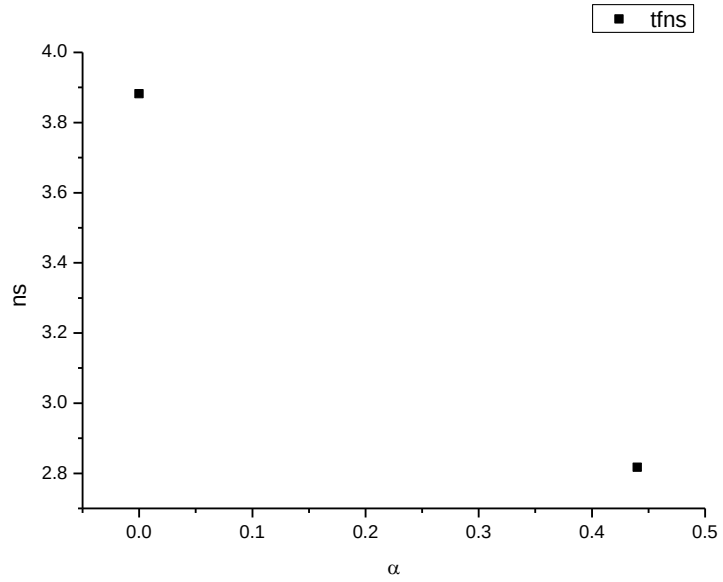

Figure 2.1.53. Intensity weighted average lifetime (τ_f) of **11a** versus α.

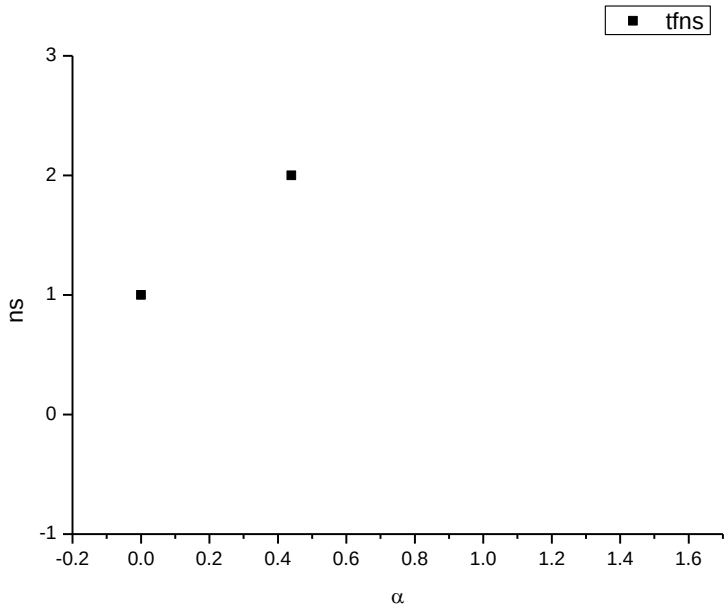

Figure 2.1.54. Amplitude weighted average lifetime (τ_f) of **11a** versus α.

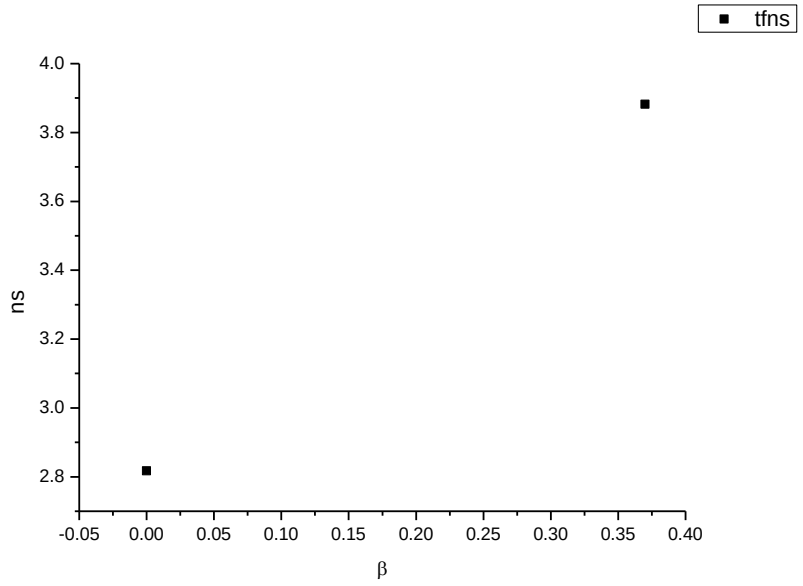

Figure 2.1.55. Intensity weighted average lifetime (τ_f) of **11a** versus β.

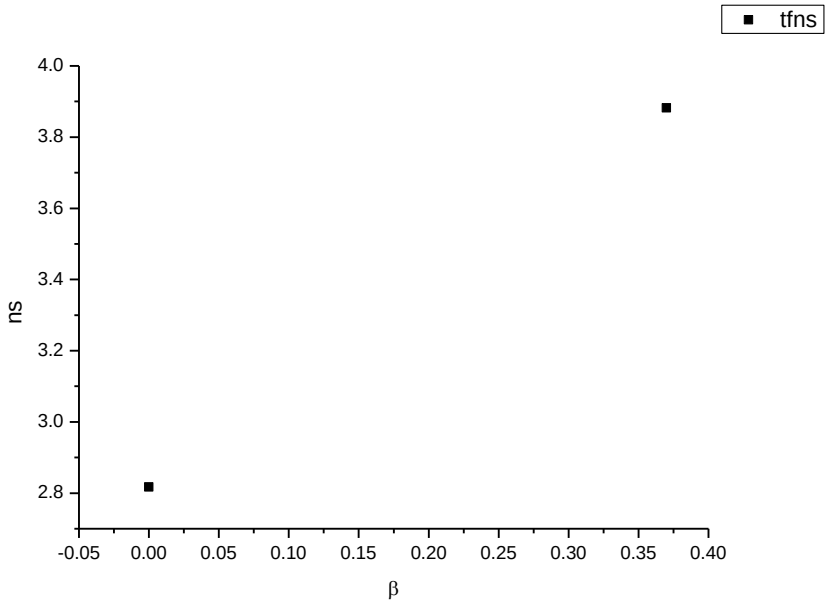

Figure 2.1.56. Amplitude weighted average lifetime (τ_f) of **11a** versus β.

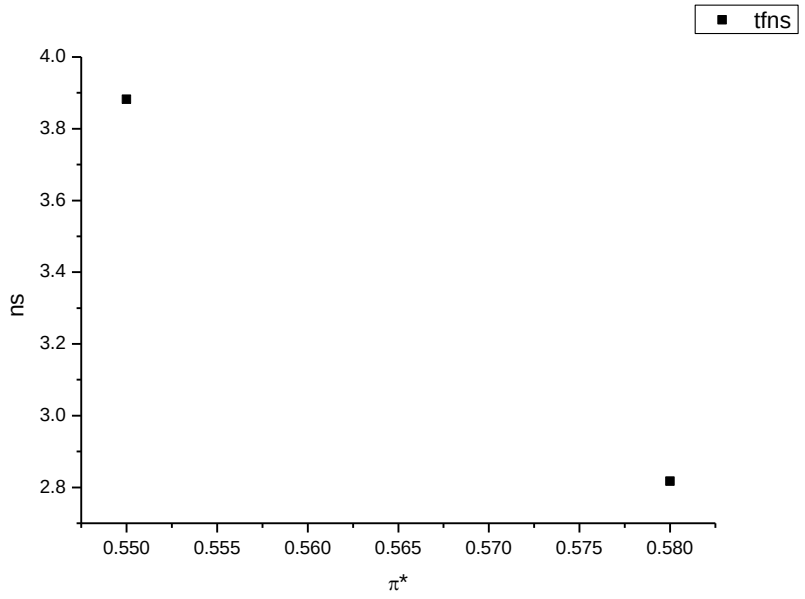

Figure 2.1.57. Intensity weighted average lifetime (τ_f) of **11a** versus π*.

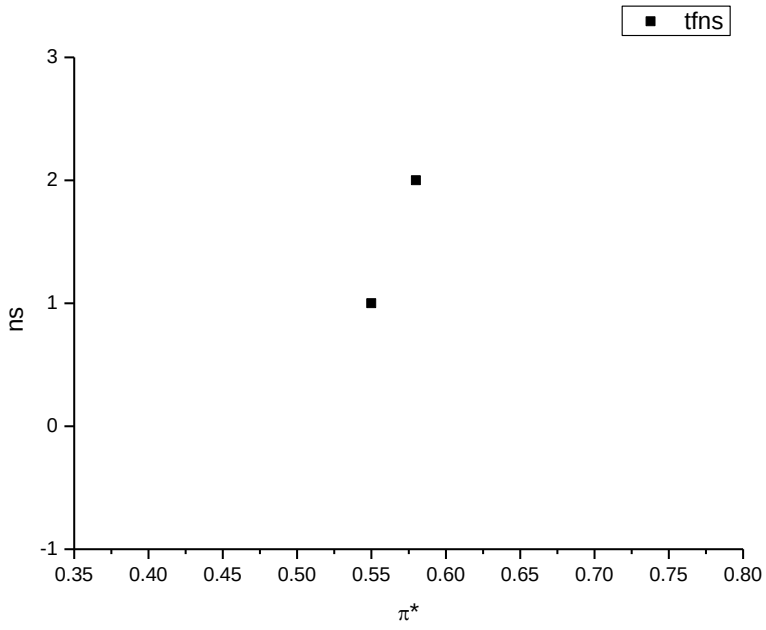

Figure 2.1.58. Amplitude weighted average lifetime (τ_f) of **11a** versus π*.

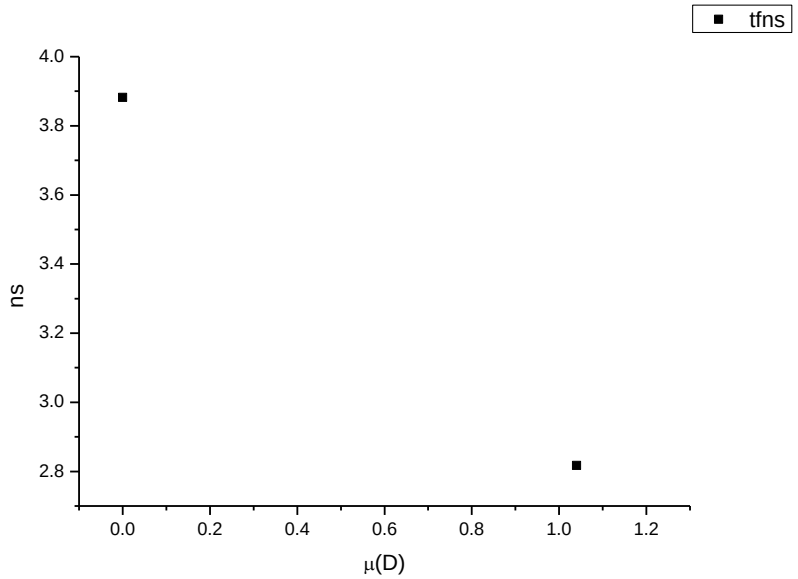

Figure 2.1.59. Intensity weighted average lifetime (τ_f) of **11a** versus μ(D).

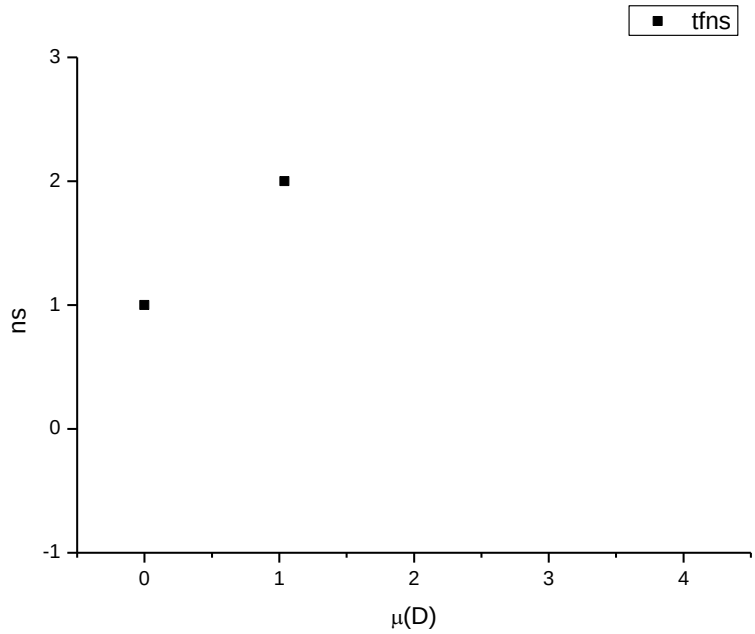

Figure 2.1.60. Amplitude weighted average lifetime (τ_f) of **11a** versus μ(D).

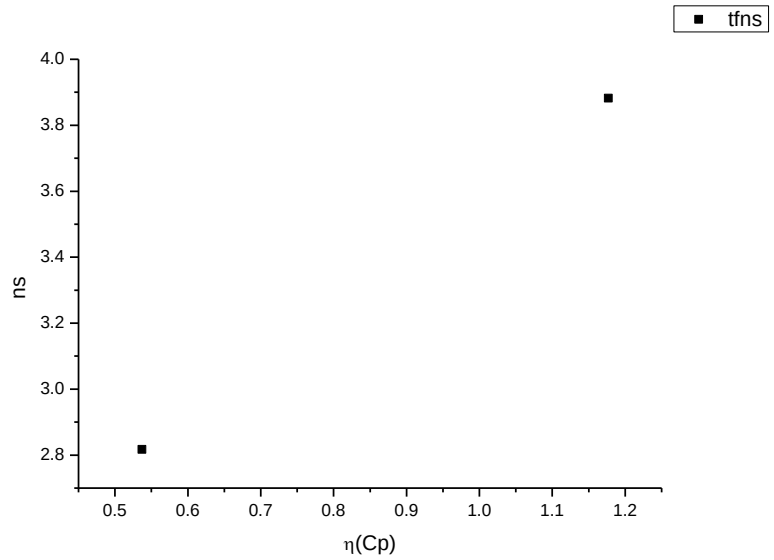

Figure 2.1.61. Intensity weighted average lifetime (τ_f) of **11a** versus η(Cp).

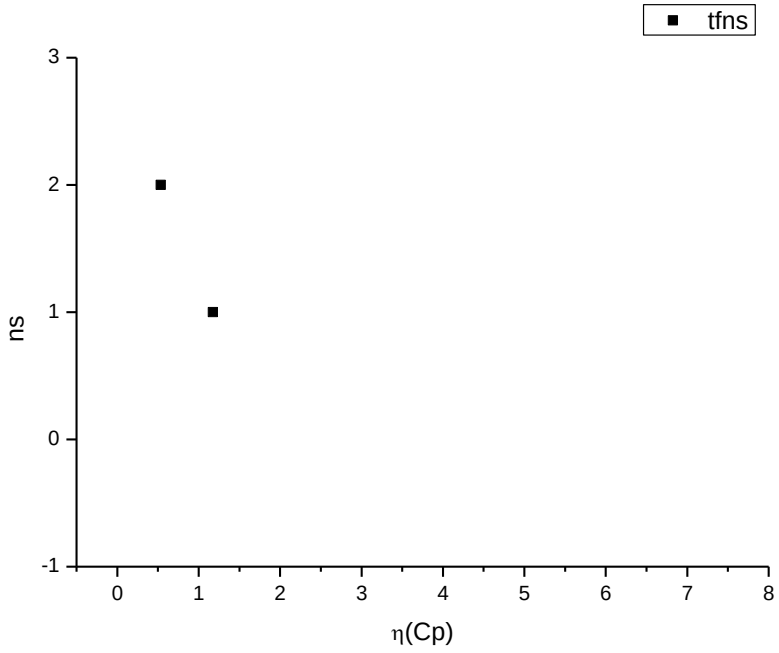

Figure 2.1.62. Amplitude weighted average lifetime (τ_f) of **11a** versus η(Cp).

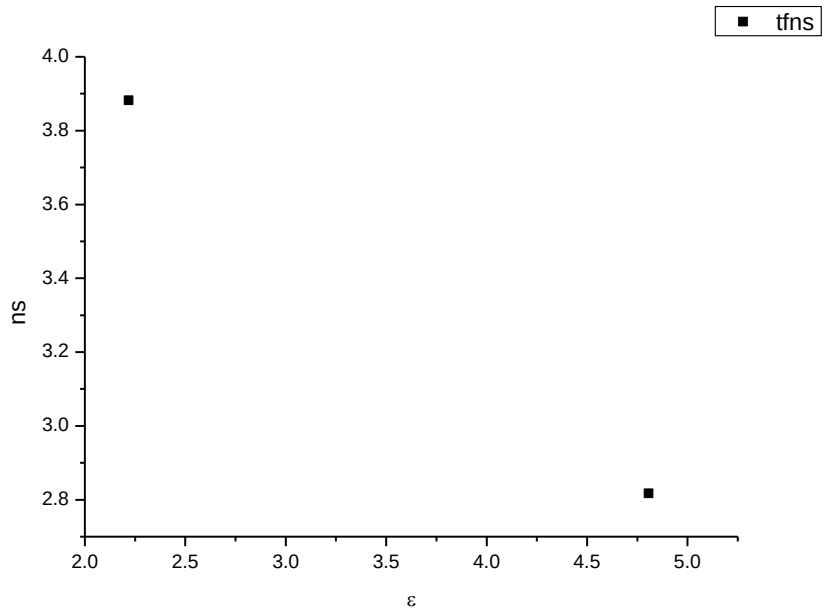

Figure 2.1.63. Intensity weighted average lifetime (τ_f) of **11a** versus ε.

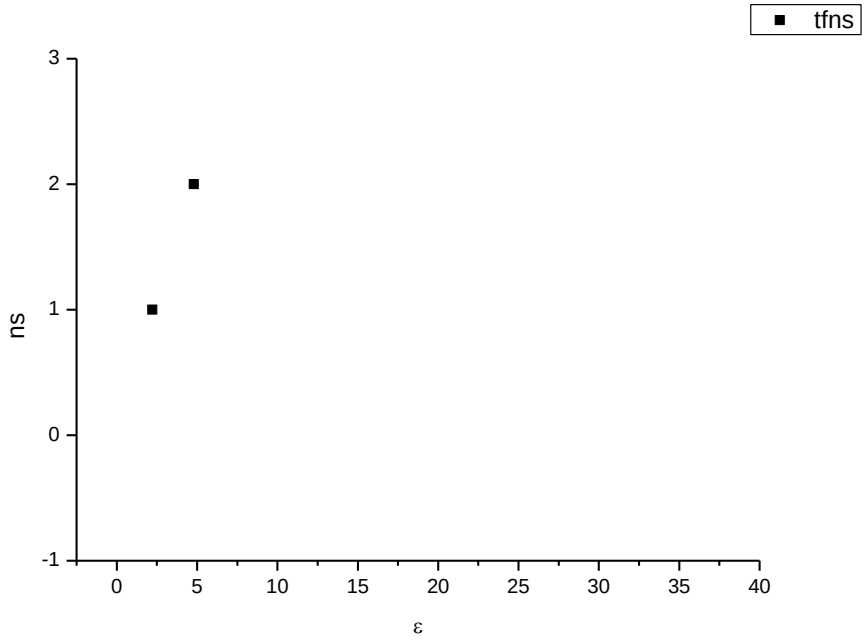

Figure 2.1.64. Amplitude weighted average lifetime (τ_f) of **11a** versus ε.

2.1.8.1 500 nm Lifetime – Solvatochromic analysis.

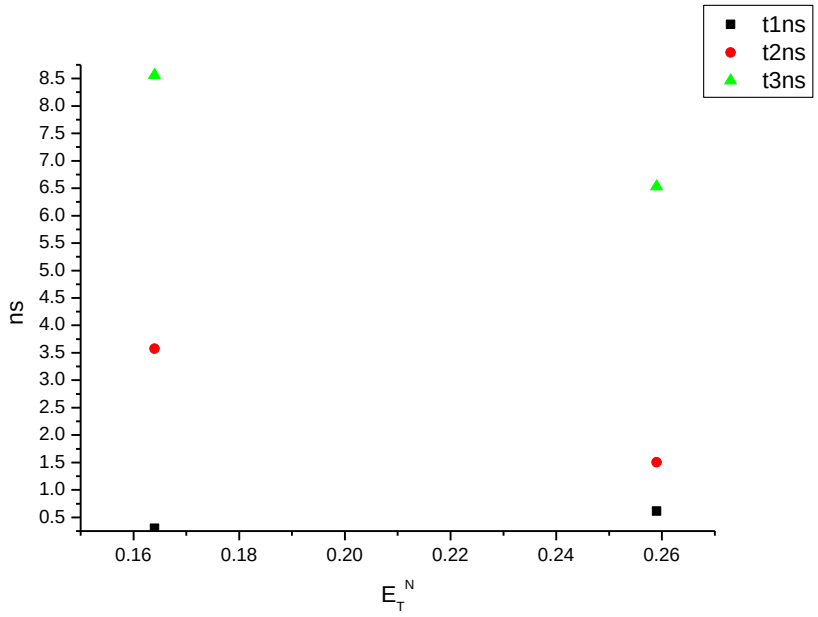

Figure 2.1.65. Intensity weighted components of TCSPC lifetime decay of **11a** (500 nm) versus E_T^N.

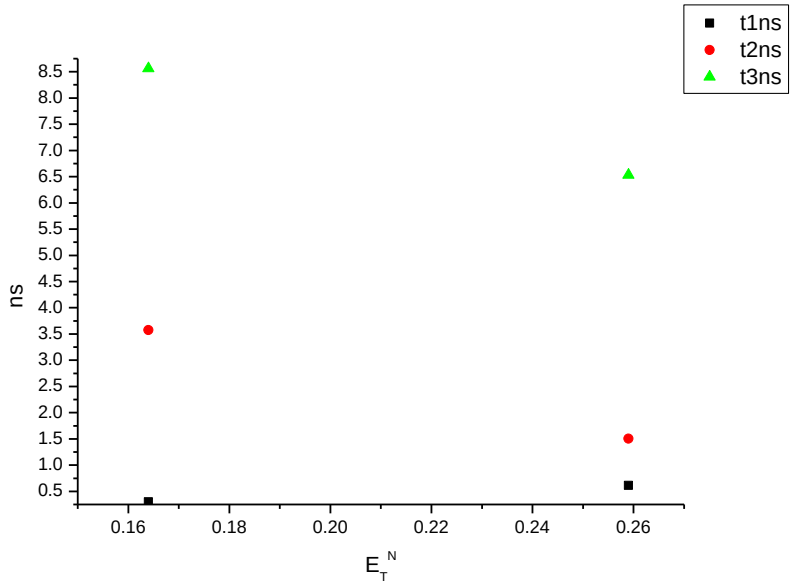

Figure 2.1.66. Amplitude weighted components of TCSPC lifetime decay of **11a** (500 nm) versus E_T^N.

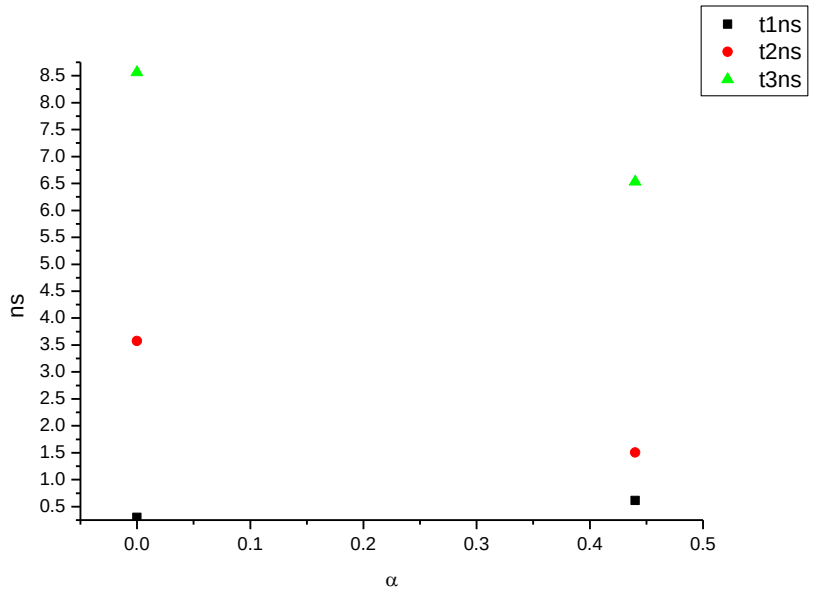

Figure 2.1.67. Intensity weighted components of TCSPC lifetime decay of **11a** (500 nm) versus α.

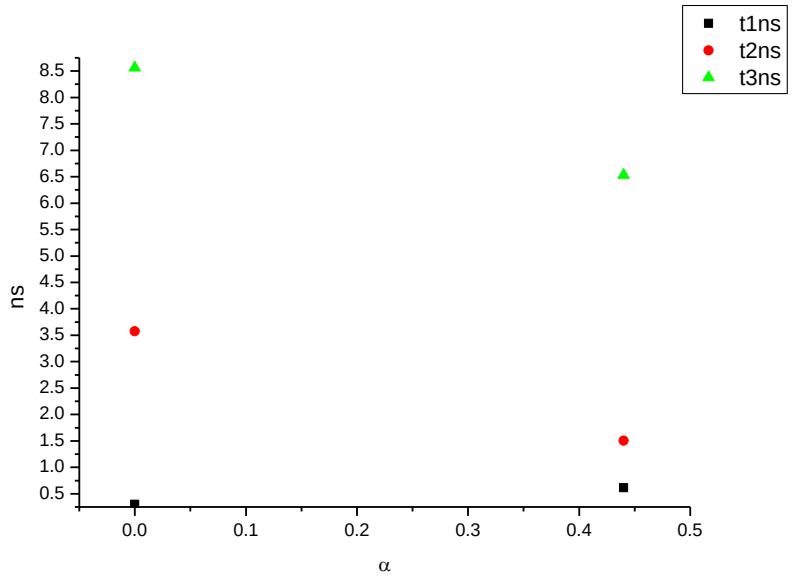

Figure 2.1.68. Amplitude weighted components of TCSPC lifetime decay of **11a** (500 nm) versus α.

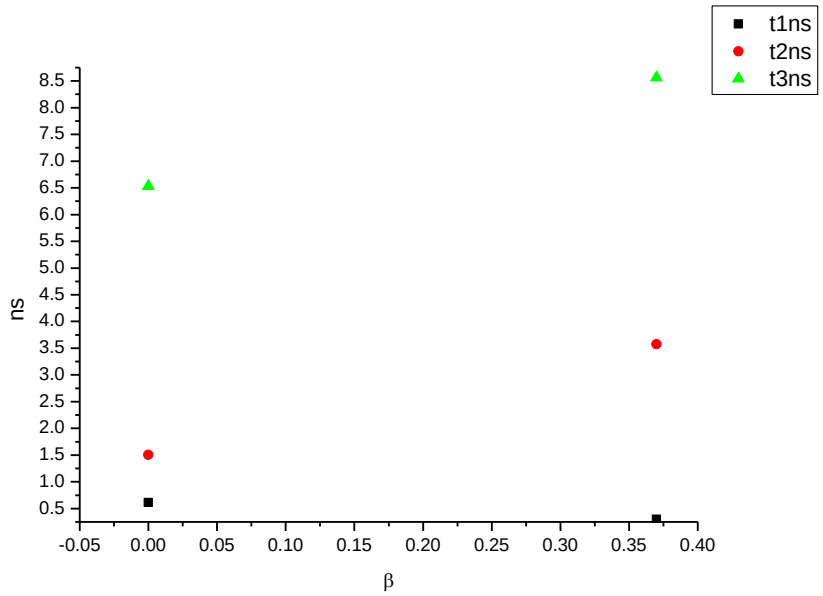

Figure 2.1.69. Intensity weighted components of TCSPC lifetime decay of **11a** (500 nm) versus β.

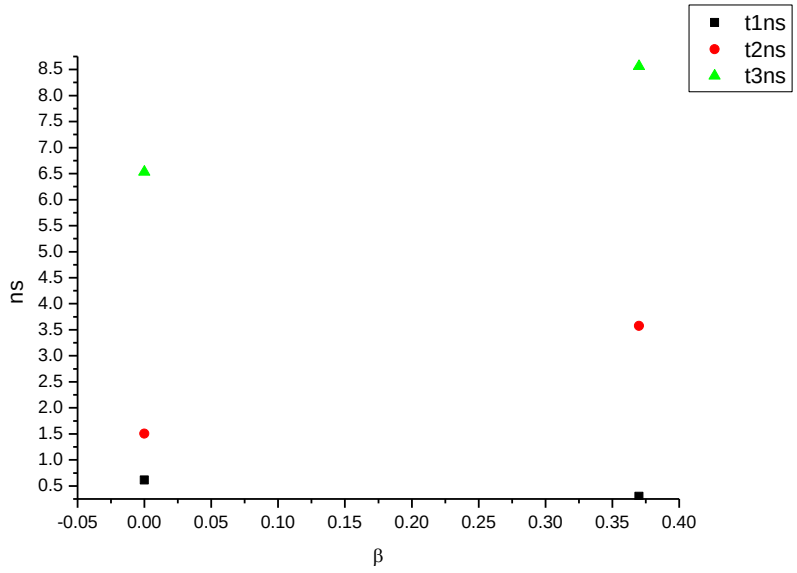

Figure 2.1.70. Amplitude weighted components of TCSPC lifetime decay of **11a** (500 nm) versus β.

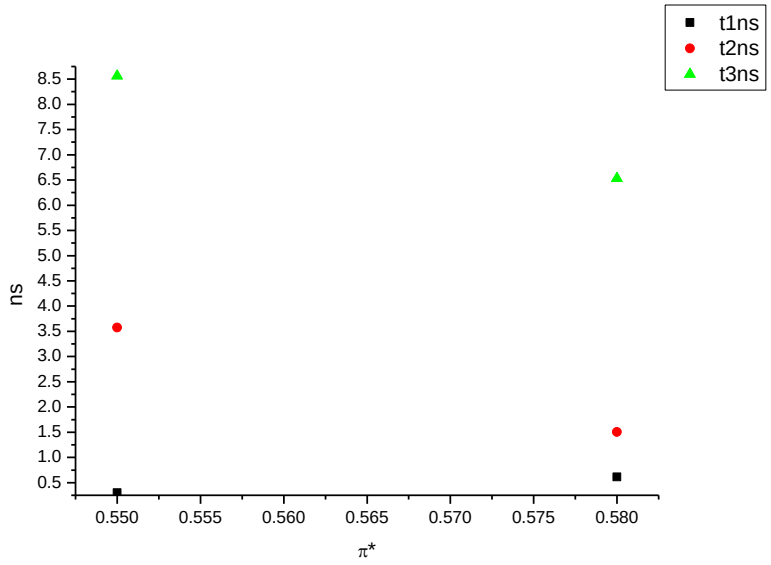

Figure 2.1.71. Intensity weighted components of TCSPC lifetime decay of **11a** (500 nm) versus π*.

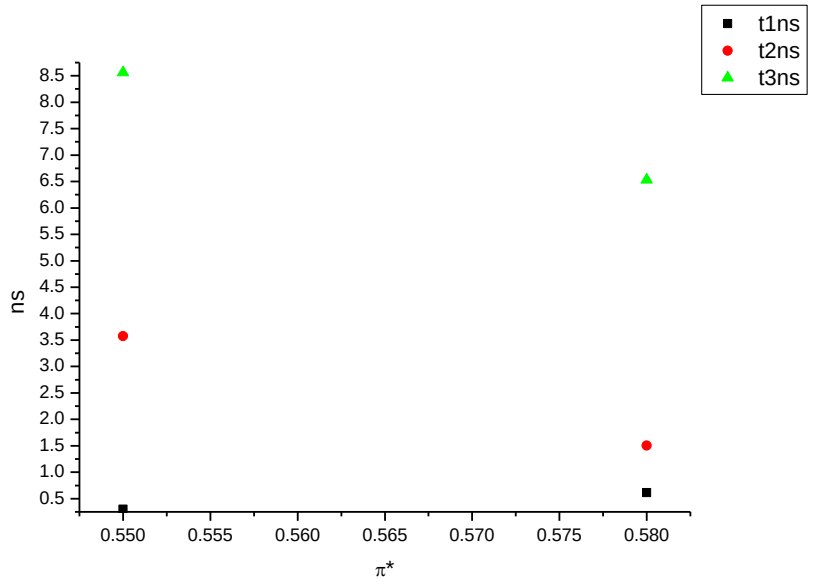

Figure 2.1.72. Amplitude weighted components of TCSPC lifetime decay of **11a** (500 nm) versus π*.

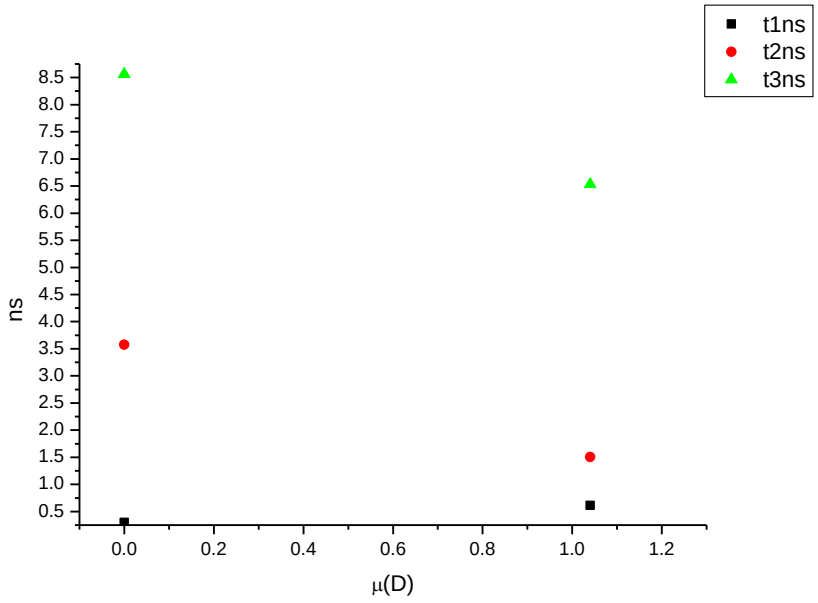

Figure 2.1.73. Intensity weighted components of TCSPC lifetime decay of **11a** (500 nm) versus μ(D).

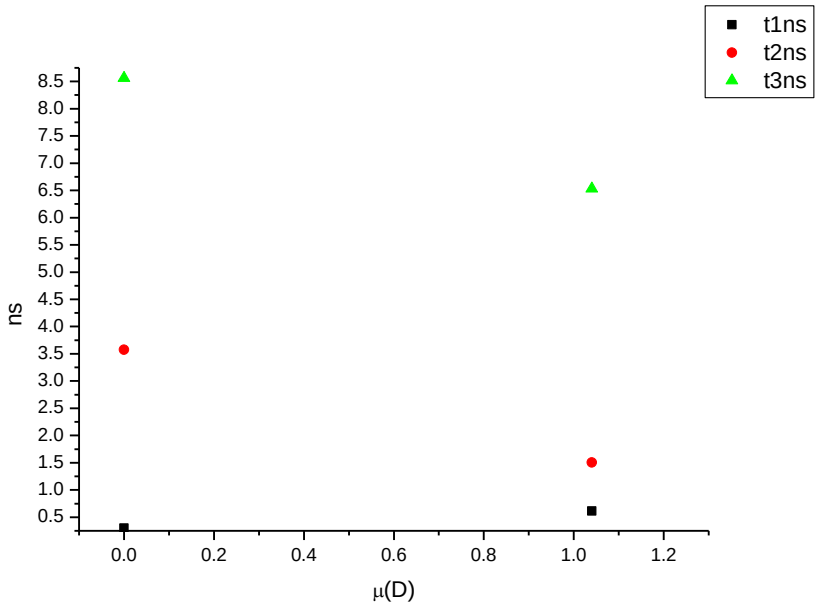

Figure 2.1.74. Amplitude weighted components of TCSPC lifetime decay of **11a** (500 nm) versus μ(D).

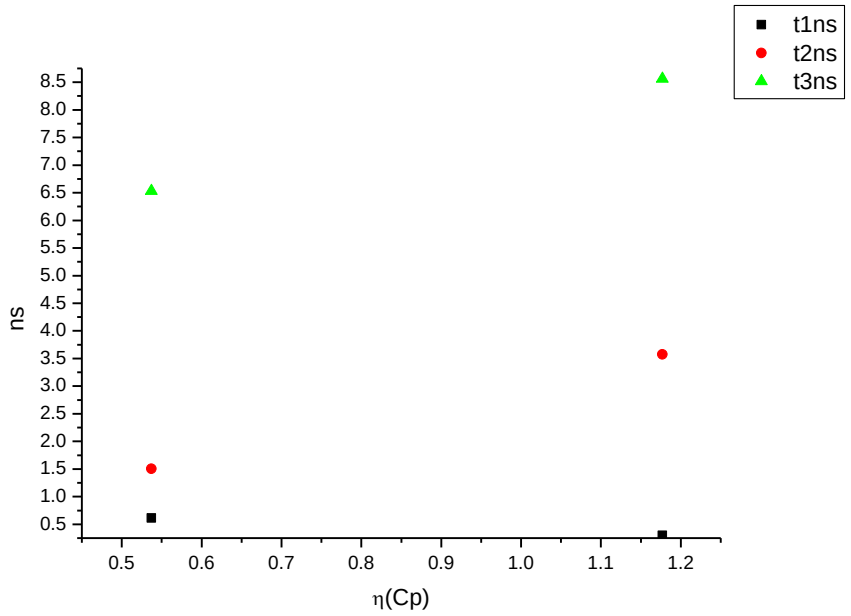

Figure 2.1.75. Intensity weighted components of TCSPC lifetime decay of **11a** (500 nm) versus η(Cp).

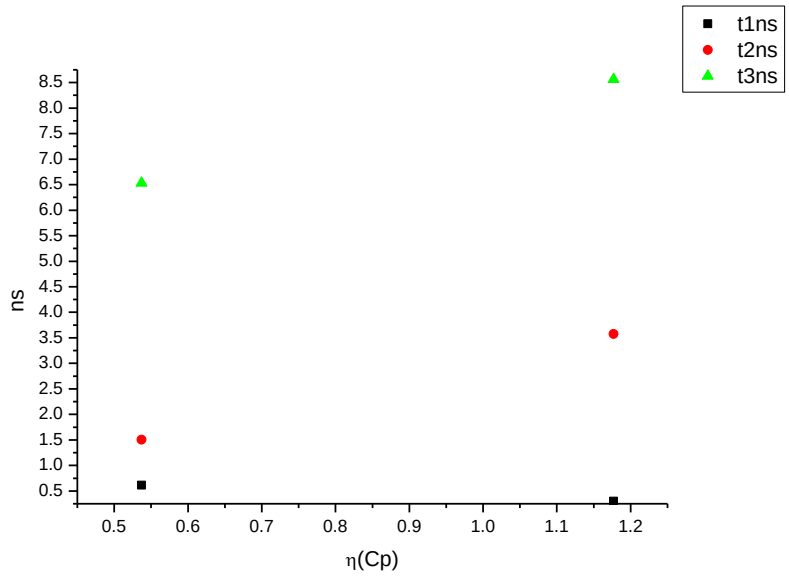

Figure 2.1.76. Amplitude weighted components of TCSPC lifetime decay of **11a** (500 nm) versus η(Cp).

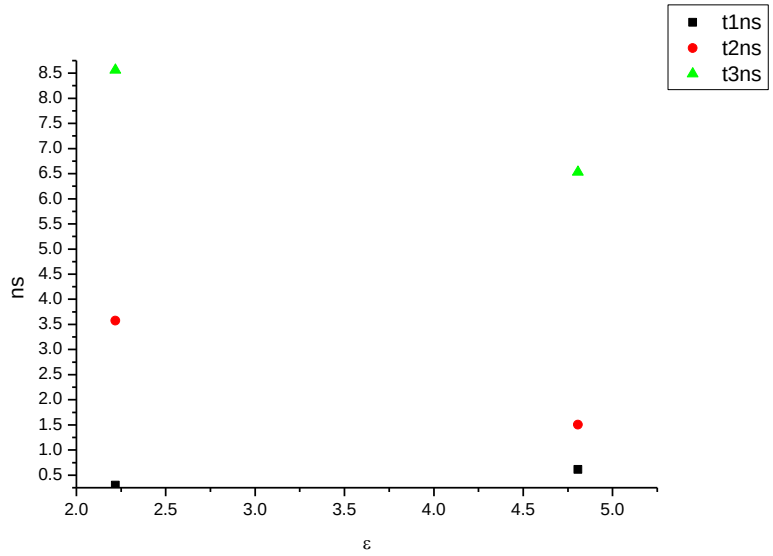

Figure 2.1.77. Intensity weighted components of TCSPC lifetime decay of **11a** (500 nm) versus ε.

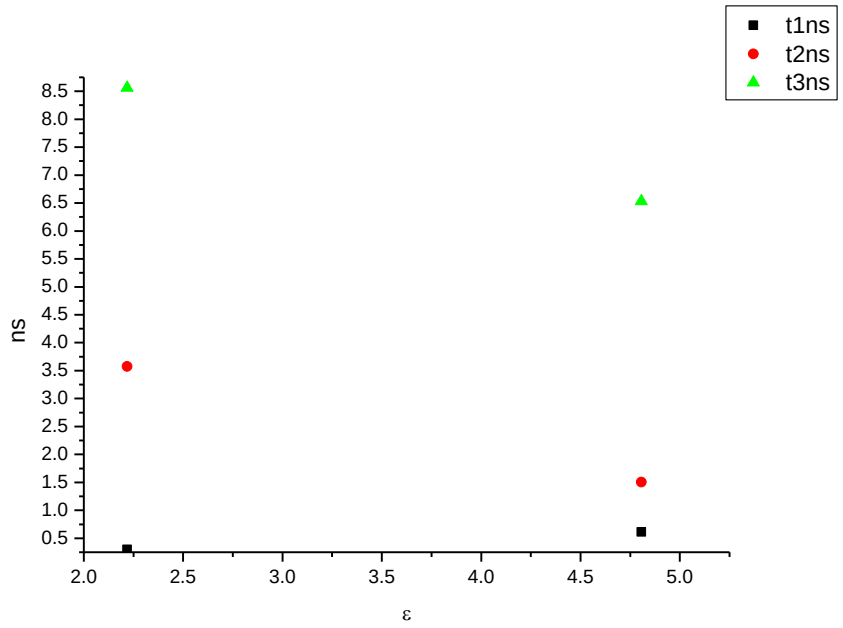

Figure 2.1.78. Amplitude weighted components of TCSPC lifetime decay of **11a** (500 nm) versus ε.

2.1.9 295 nm (LED) average fluorescent lifetimes - Solvatochromic analysis.

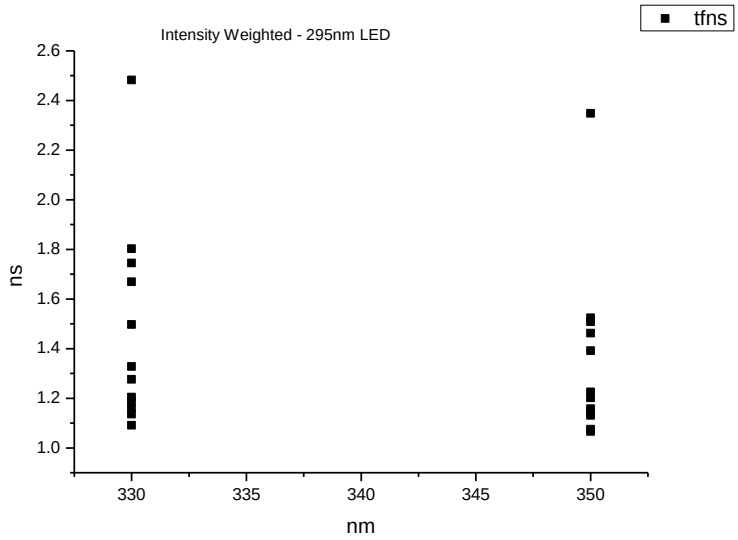

Figure 2.1.79. Intensity weighted average lifetime (τ_f) of **11a** versus wavelength (nm).

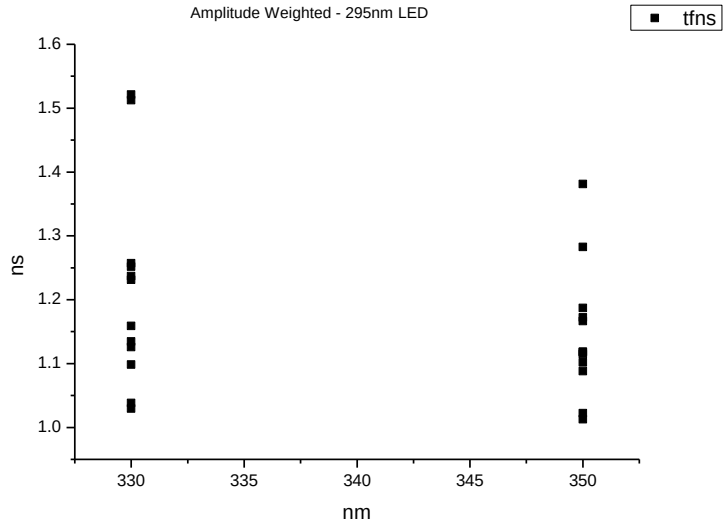

Figure 2.1.80. Amplitude weighted average lifetime (τ_f) of **11a** versus wavelength (nm).

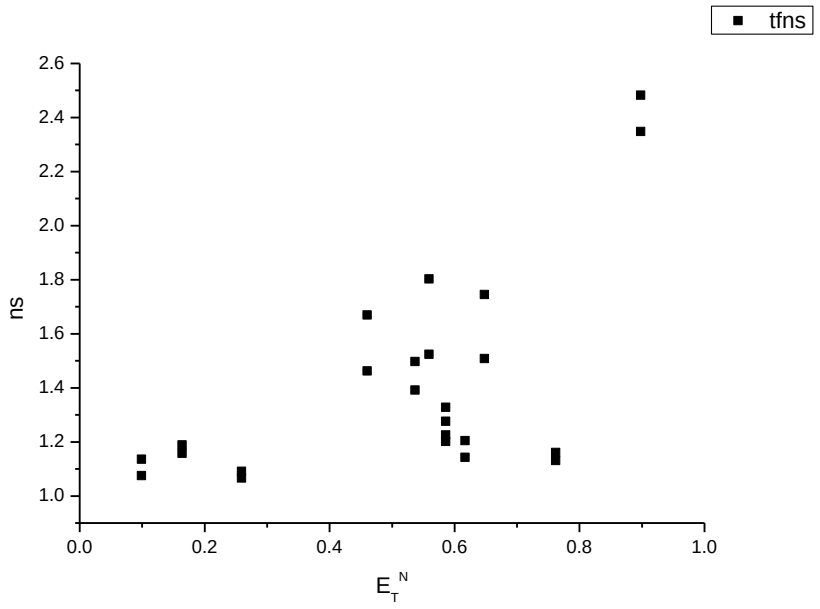

Figure 2.1.81. Intensity weighted average lifetime (τ_f) of **11a** versus E_T^N.

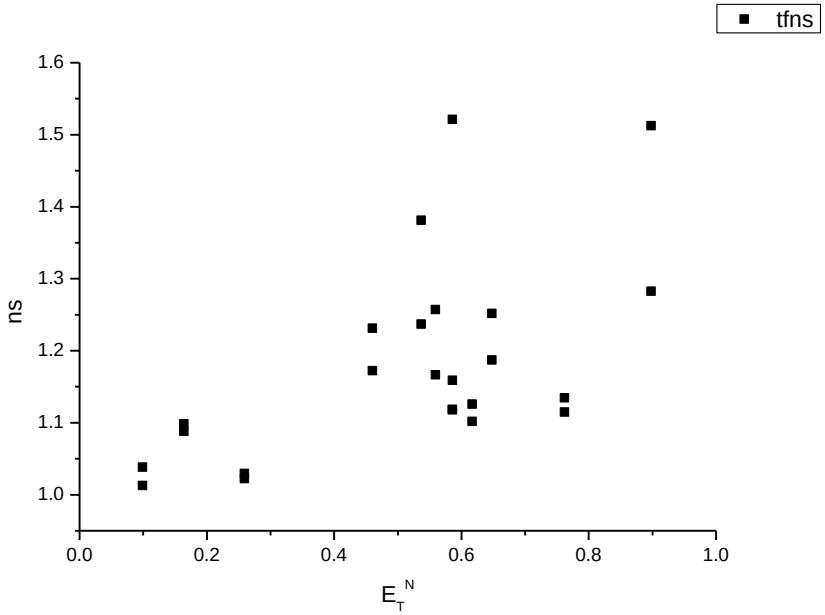

Figure 2.1.82. Amplitude weighted average lifetime (τ_f) of **11a** versus E_T^N.

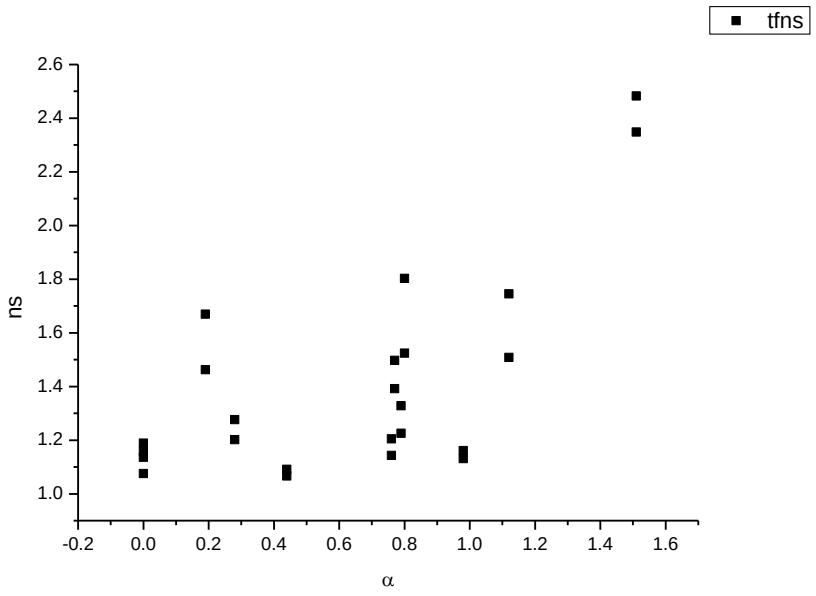

Figure 2.1.83. Intensity weighted average lifetime (τ_f) of **11a** versus α.

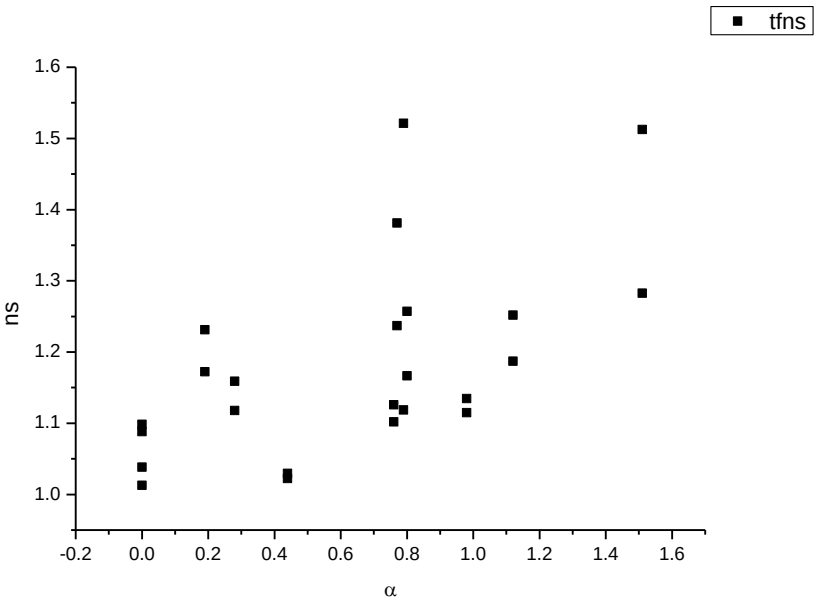

Figure 2.1.84. Amplitude weighted average lifetime (τ_f) of **11a** versus α.

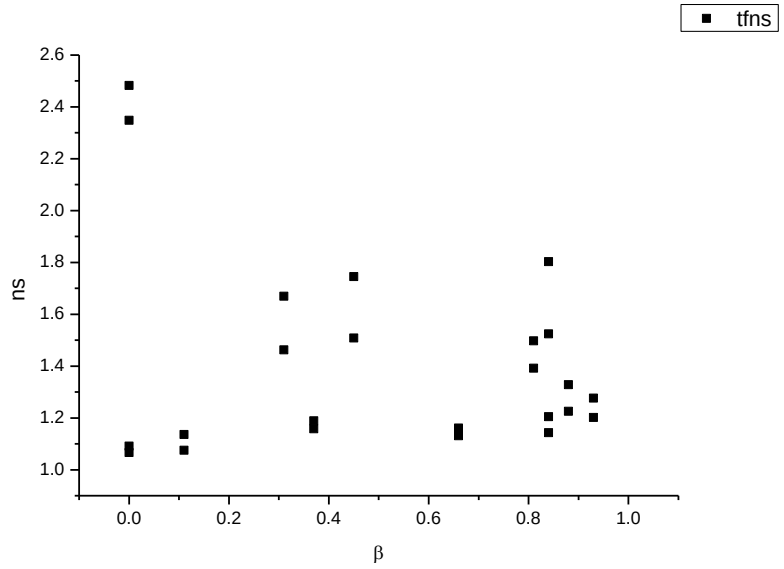

Figure 2.1.85. Intensity weighted average lifetime (τ_f) of **11a** versus β.

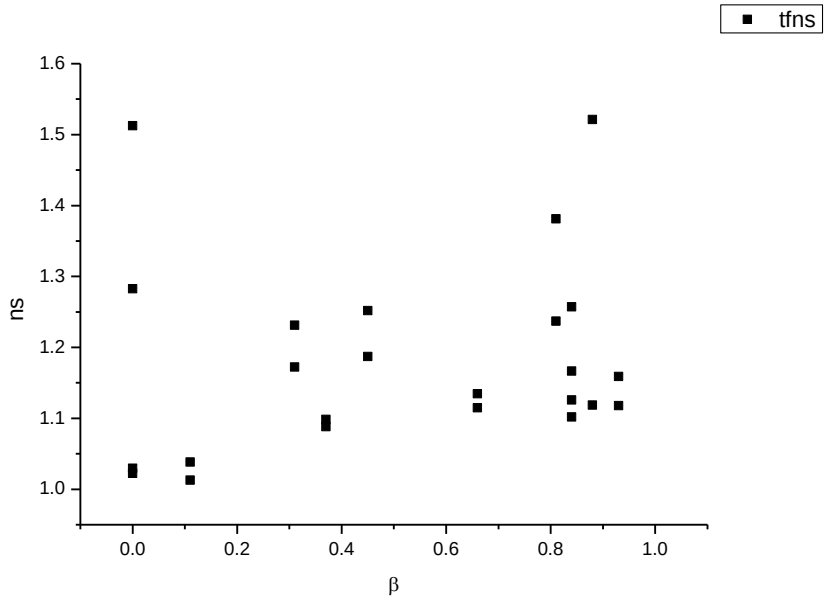

Figure 2.1.86. Amplitude weighted average lifetime (τ_f) of **11a** versus β.

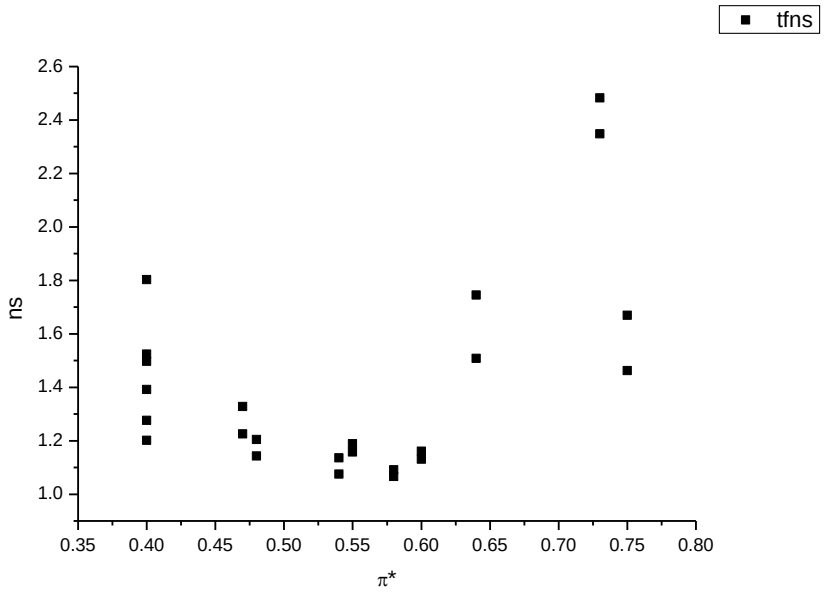

Figure 2.1.87. Intensity weighted average lifetime (τ_f) of **11a** versus π*.

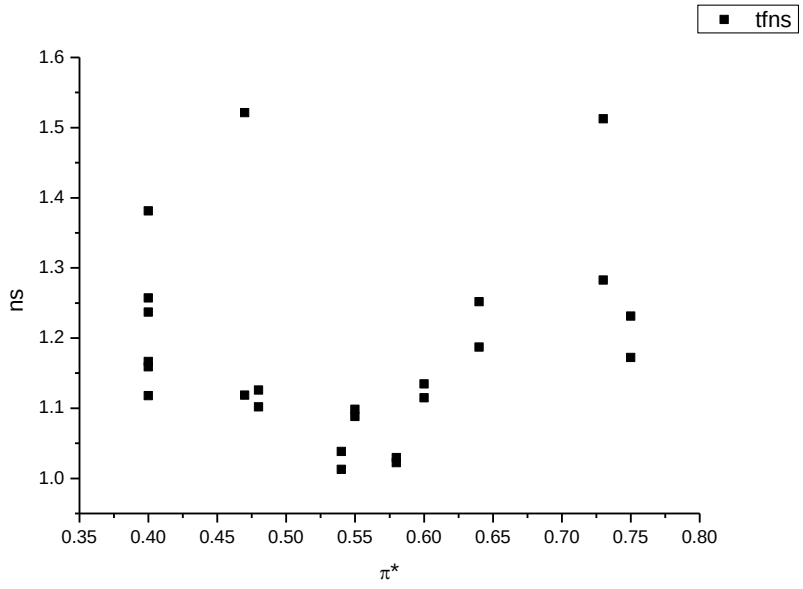

Figure 2.1.88. Amplitude weighted average lifetime (τ_f) of **11a** versus π*.

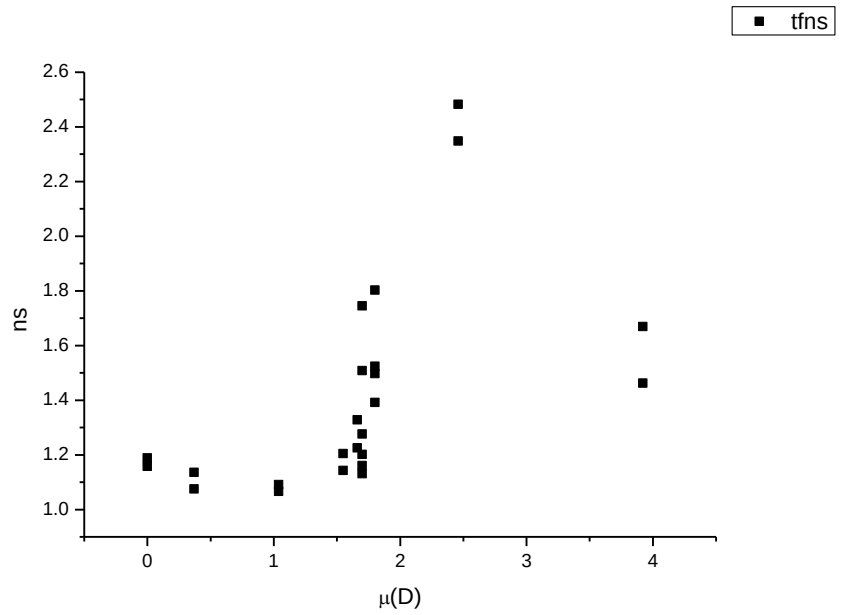

Figure 2.1.89. Intensity weighted average lifetime (τ_f) of **11a** versus μ(D).

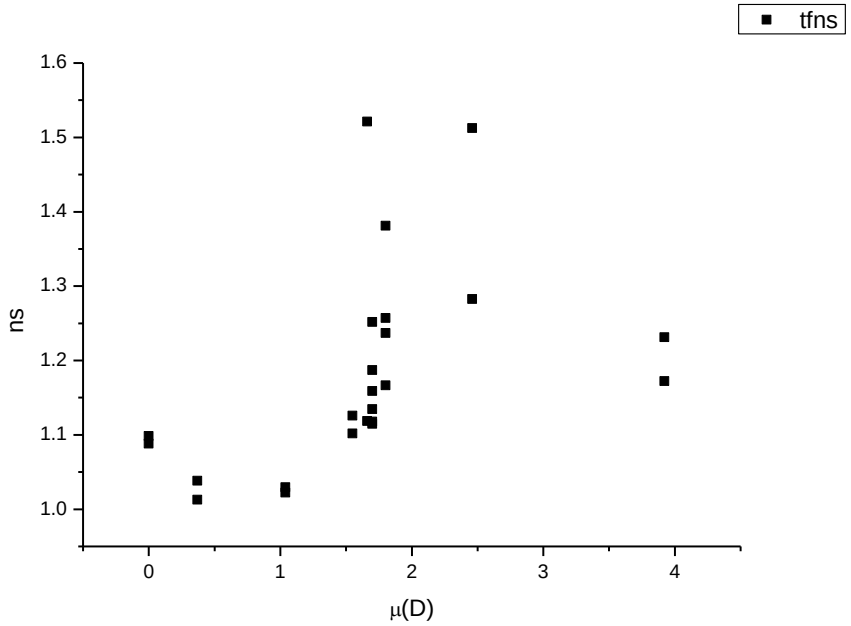

Figure 2.1.90. Amplitude weighted average lifetime (τ_f) of **11a** versus μ(D).

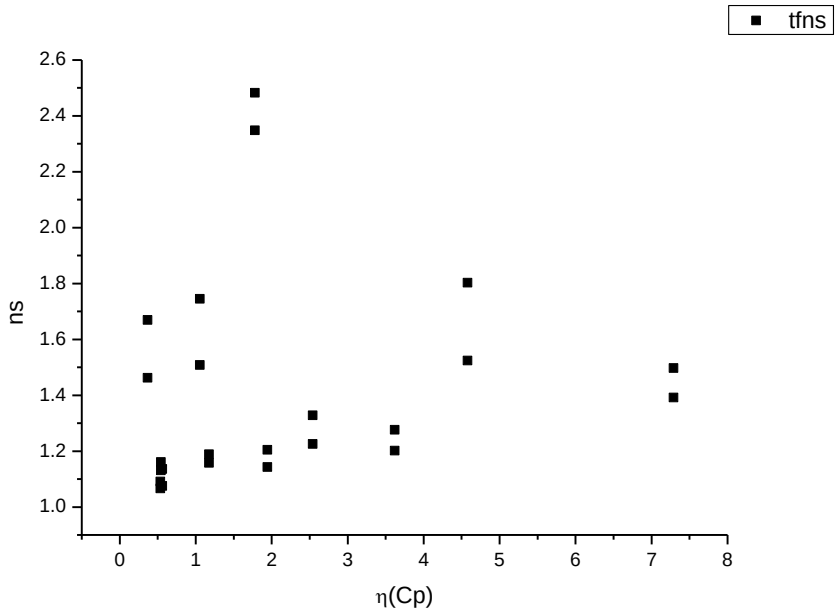

Figure 2.1.91. Intensity weighted average lifetime (τ_f) of **11a** versus η(Cp).

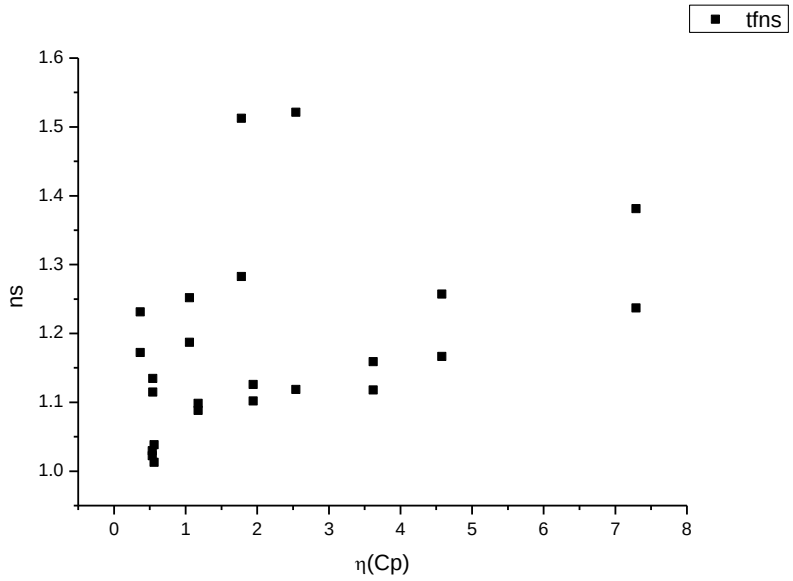

Figure 2.1.92. Amplitude weighted average lifetime (τ_f) of **11a** versus η(Cp).

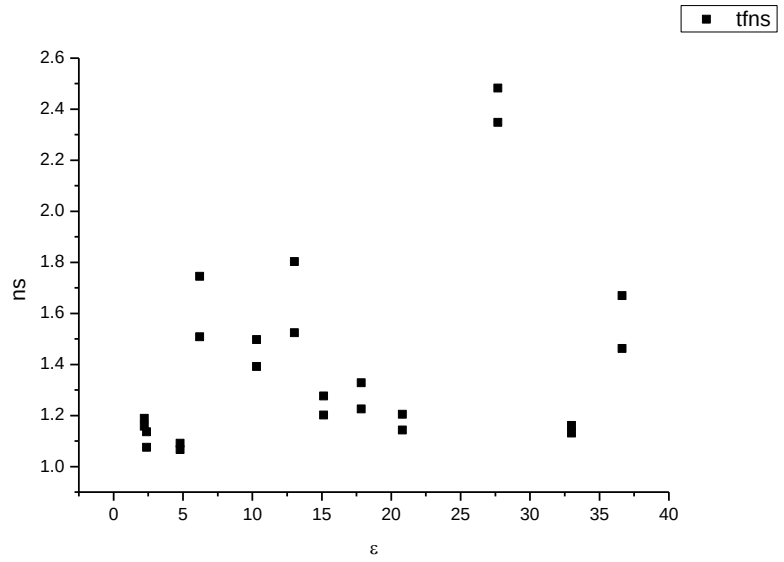

Figure 2.1.93. Intensity weighted average lifetime (τ_f) of **11a** versus ε.

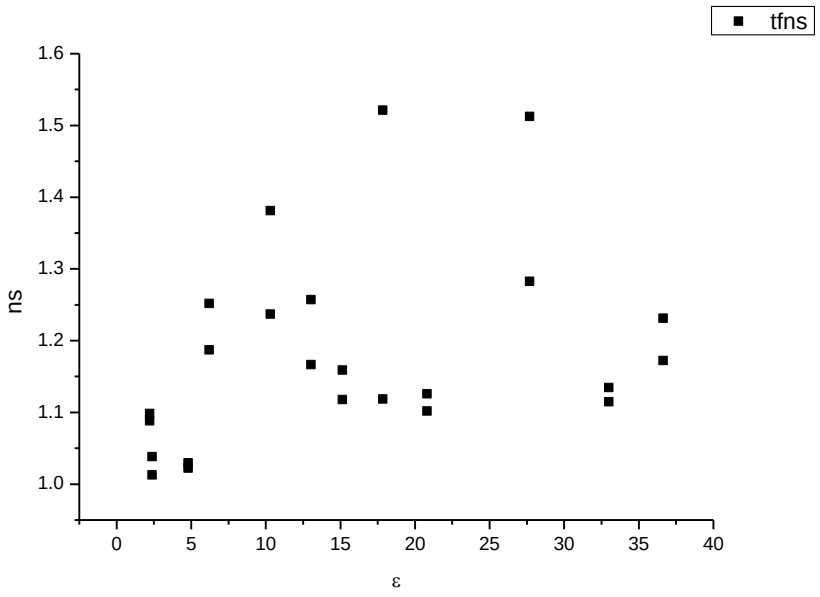

Figure 2.1.94. Amplitude weighted average lifetime (τ_f) of **11a** versus ε.

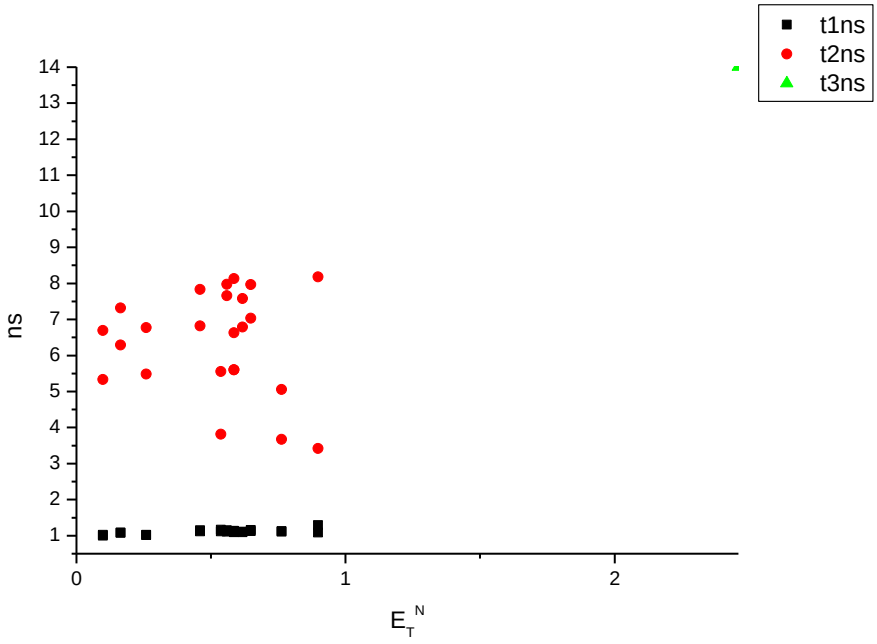

Figure 2.1.95. Intensity weighted components of TCSPC lifetime decay of **11a** (330 to 350 nm) versus E_T^N.

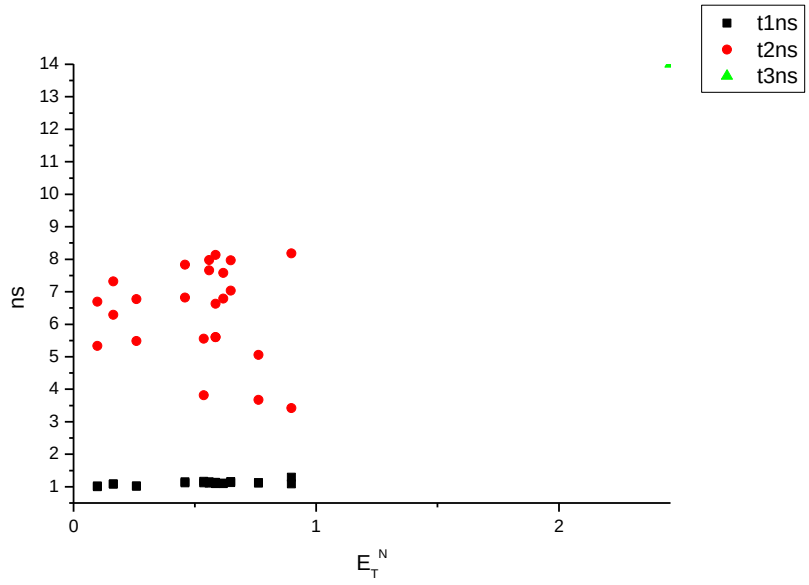

Figure 2.1.96. Amplitude weighted components of TCSPC lifetime decay of **11a** (330 to 350 nm) versus E_T^N.

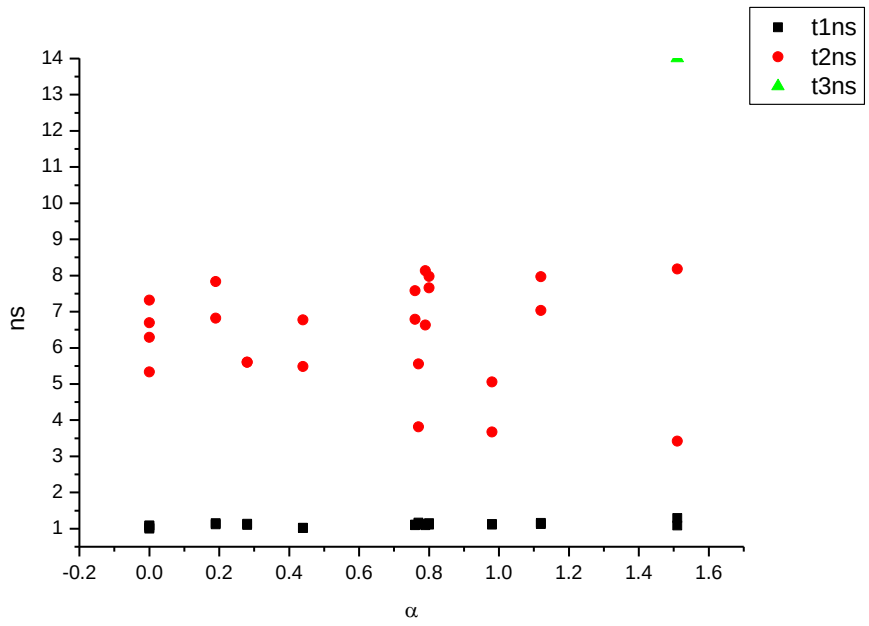

Figure 2.1.97. Intensity weighted components of TCSPC lifetime decay of **11a** (330 to 350 nm) versus α.

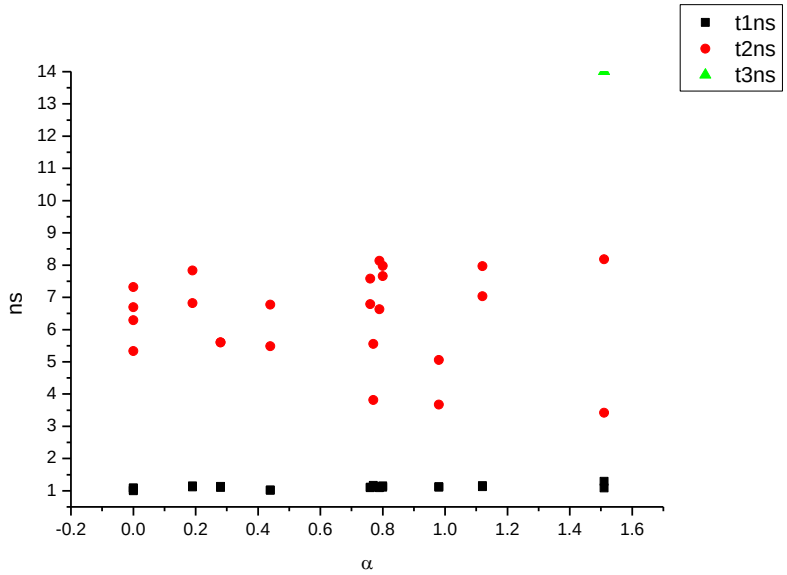

Figure 2.1.98. Amplitude weighted components of TCSPC lifetime decay of **11a** (330 to 350 nm) versus α.

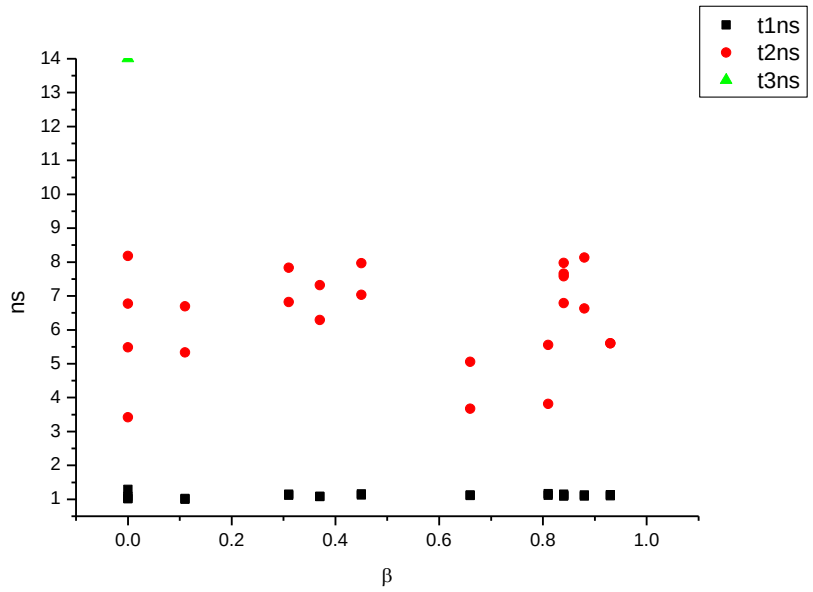

Figure 2.1.99. Intensity weighted components of TCSPC lifetime decay of **11a** (330 to 350 nm) versus β.

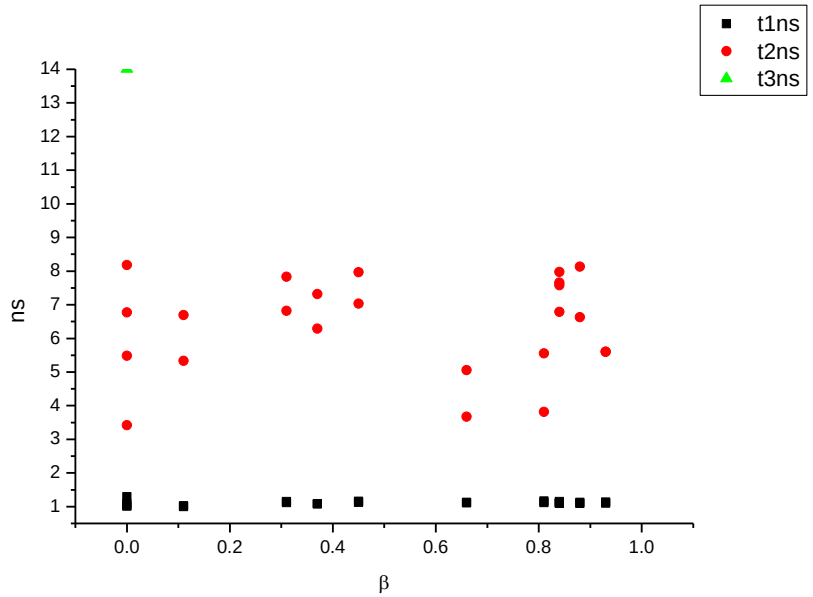

Figure 2.1.100. Amplitude weighted components of TCSPC lifetime decay of **11a** (350 to 350 nm) versus β.

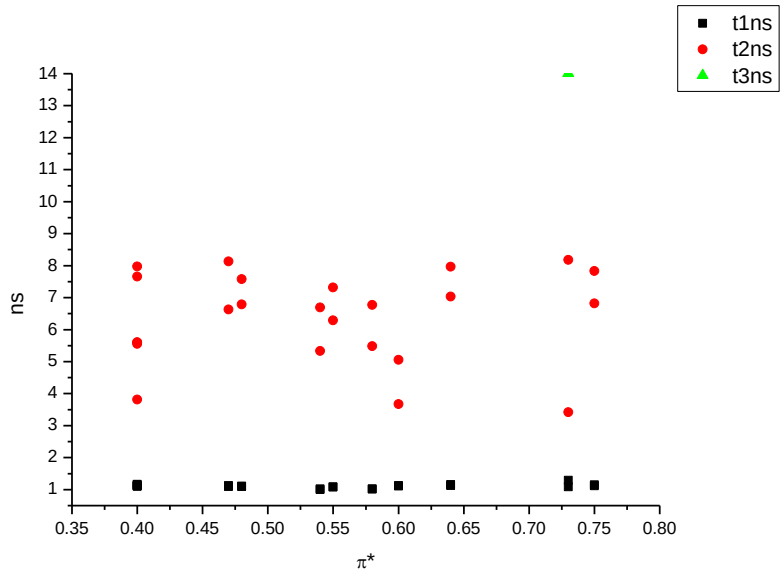

Figure 2.1.101. Intensity weighted components of TCSPC lifetime decay of **11a** (330 to 350 nm) versus π*.

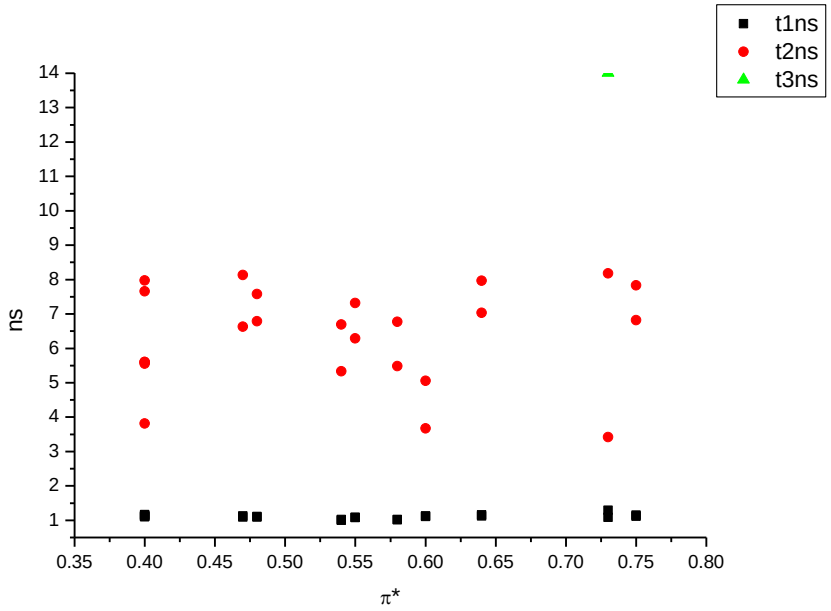

Figure 2.1.102. Amplitude weighted components of TCSPC lifetime decay of **11a** (330 to 350 nm) versus π*.

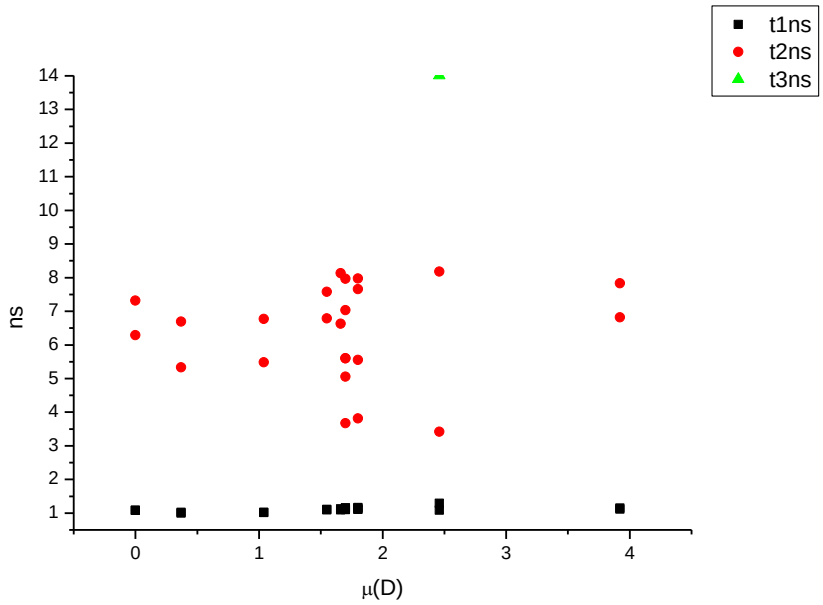

Figure 2.1.103. Intensity weighted components of TCSPC lifetime decay of **11a** (330 to 350 nm) versus μ(D).

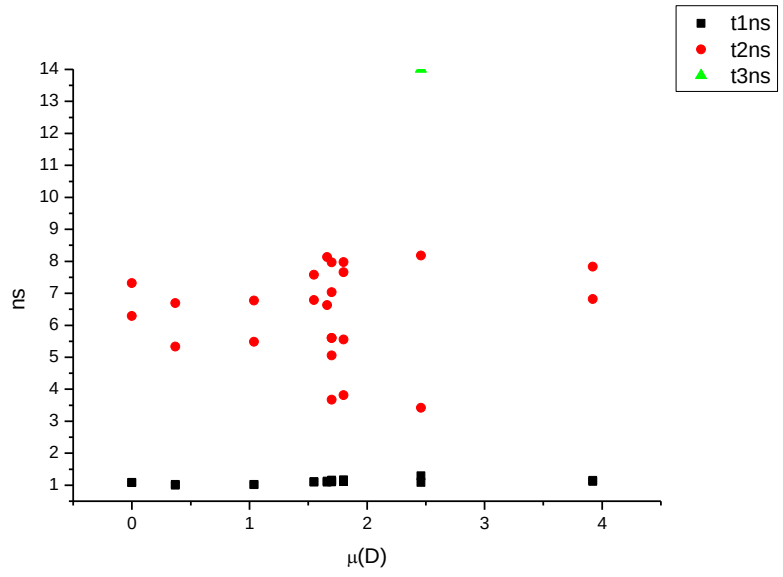

Figure 2.1.104. Amplitude weighted components of TCSPC lifetime decay of **11a** (330 to 350 nm) versus μ(D).

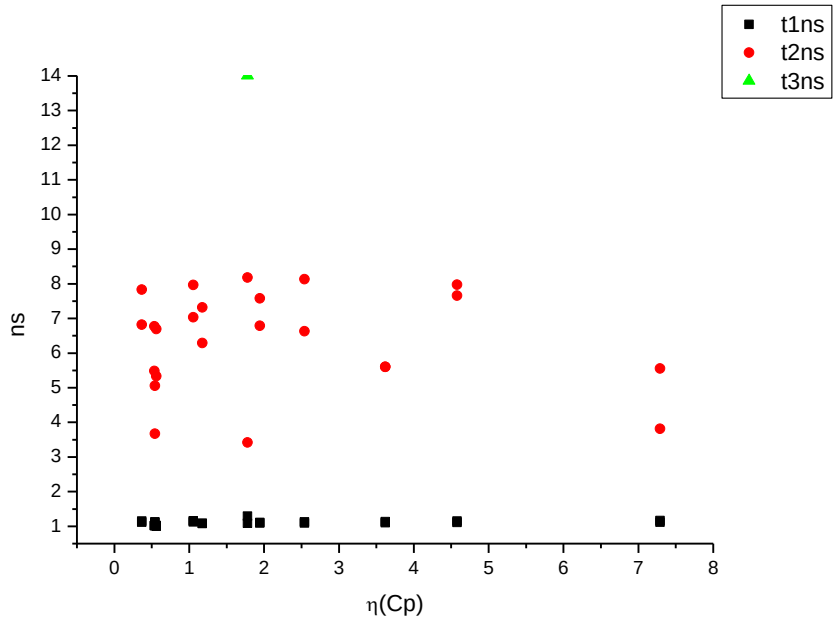

Figure 2.1.105. Intensity weighted components of TCSPC lifetime decay of **11a** (330 to 350 nm) versus η(Cp).

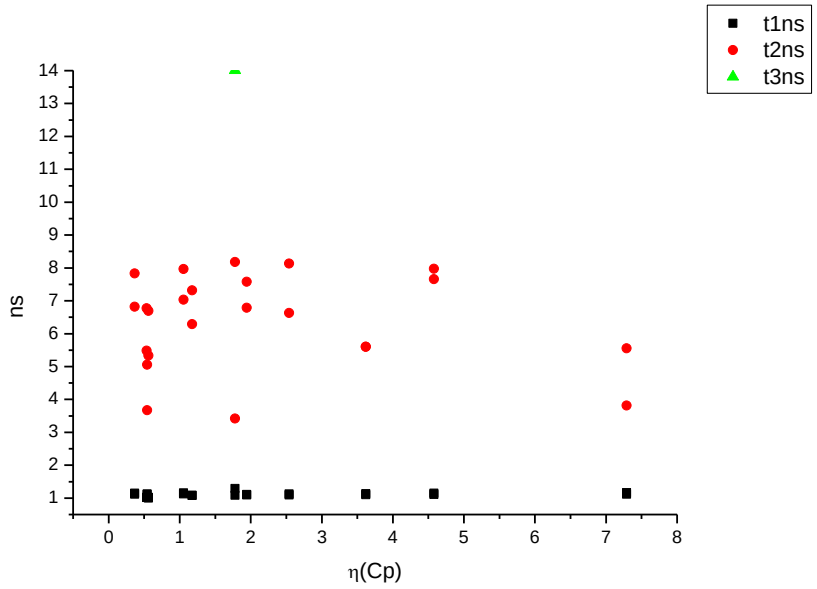

Figure 2.1.106. Amplitude weighted components of TCSPC lifetime decay of **11a** (330 to 350 nm) versus η(Cp).

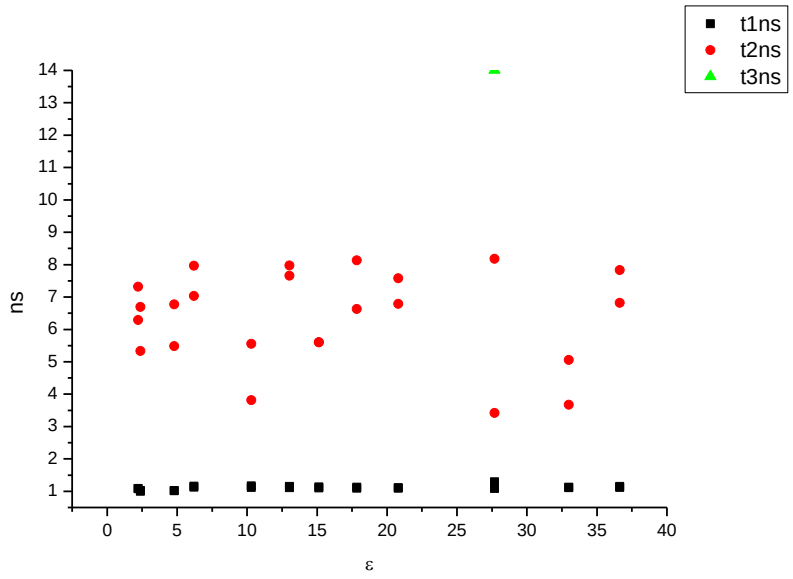

Figure 2.1.107. Intensity weighted components of TCSPC lifetime decay of **11a** (330 to 350 nm) versus ε.

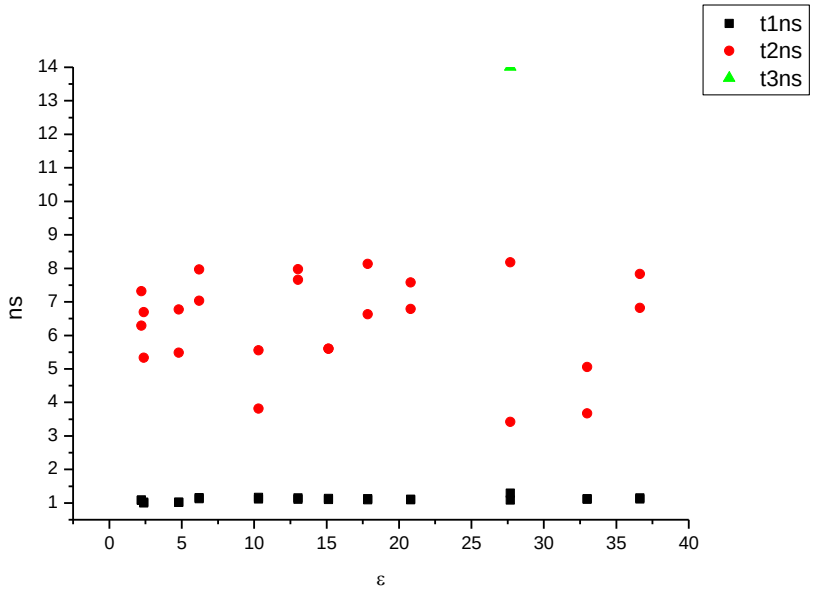

Figure 2.1.108. Amplitude weighted components of TCSPC lifetime decay of **11a** (330 to 350 nm) versus ε.

2.1.9.1 11a 330 nm (LED) Lifetime – Solvatochromic analysis.

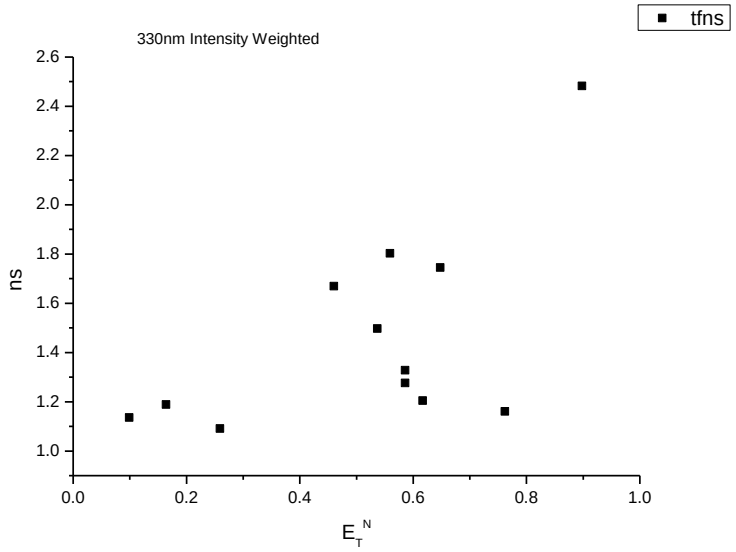

Figure 2.1.109. Intensity weighted average lifetime (τ_f) of **11a** at 330 nm versus E_T^N.

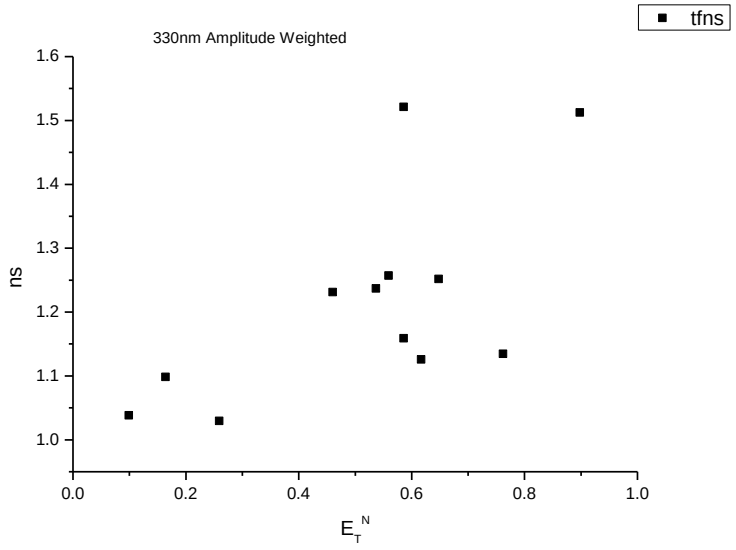

Figure 2.1.110. Amplitude weighted average lifetime (τ_f) of **11a** at 330 nm versus E_T^N.

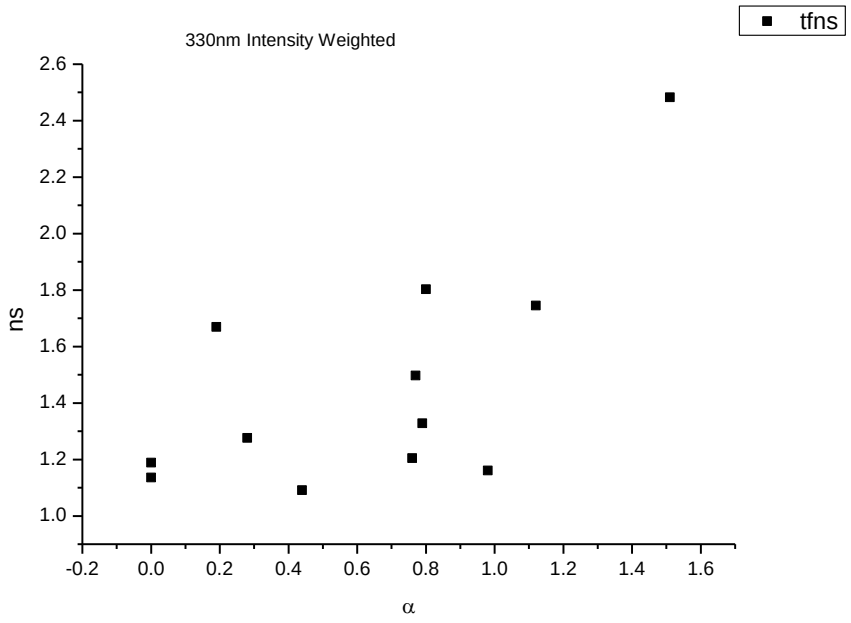

Figure 2.1.111. Intensity weighted average lifetime (τ_f) of **11a** at 330 nm versus α.

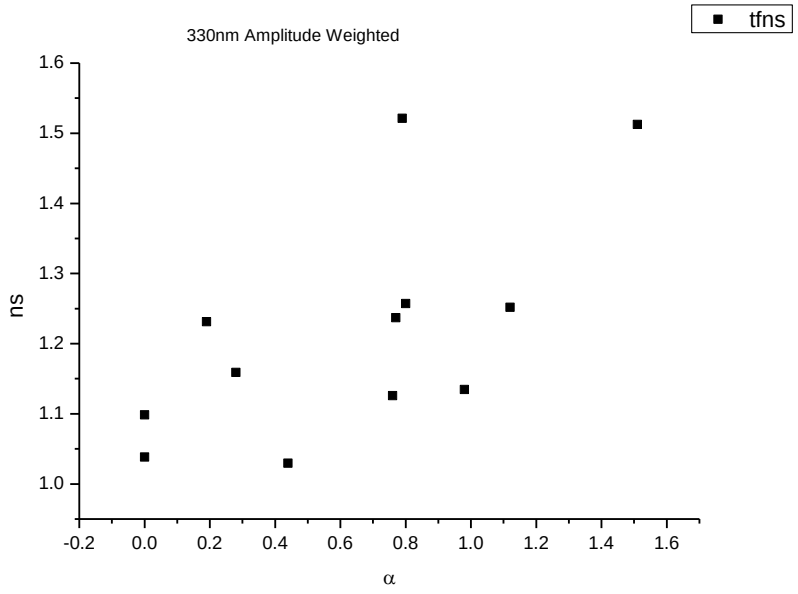

Figure 2.1.112. Amplitude weighted average lifetime (τ_f) of **11a** at 330 nm versus α.

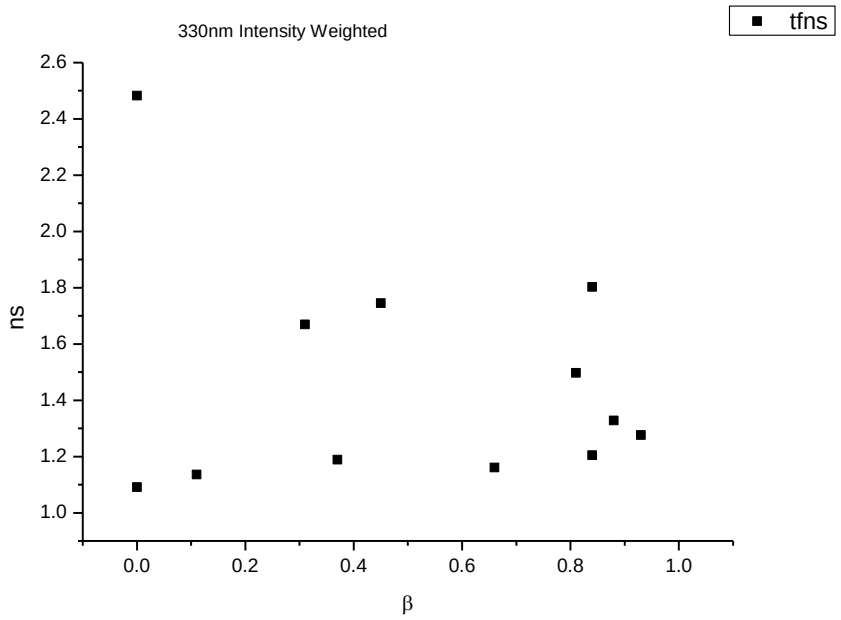

Figure 2.1.113. Intensity weighted average lifetime (τ_f) of **11a** at 330 nm versus β.

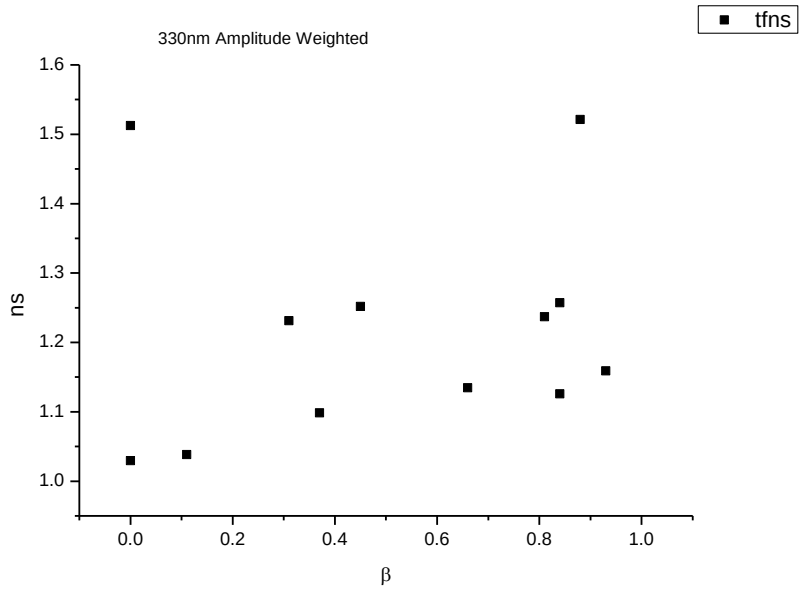

Figure 2.1.114. Amplitude weighted average lifetime (τ_f) of **11a** at 330 nm versus β.

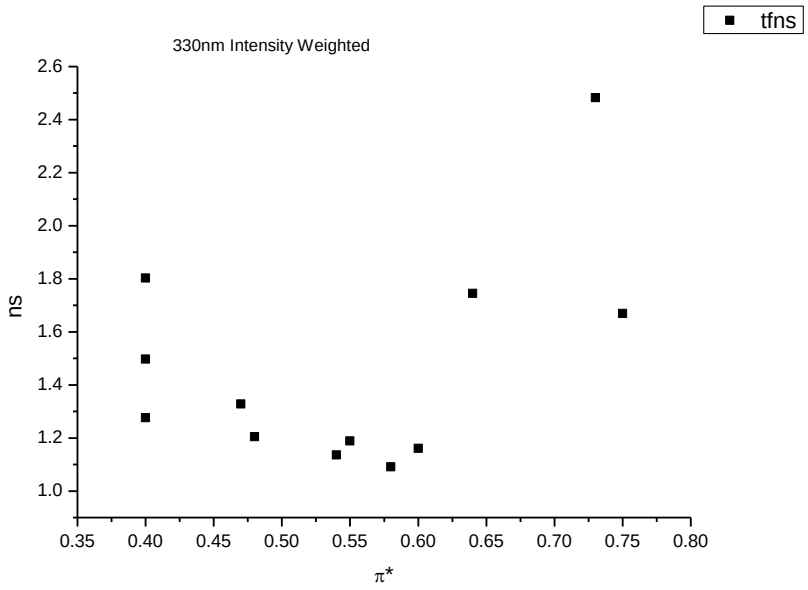

Figure 2.1.115. Intensity weighted average lifetime (τ_f) of **11a** at 330 nm versus π*.

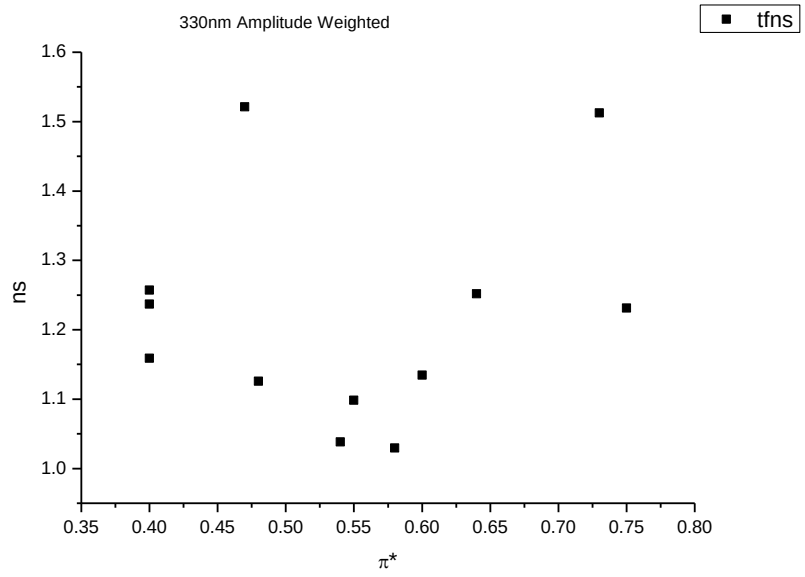

Figure 2.1.116. Amplitude weighted average lifetime (τ_f) of **11a** at 330 nm versus π*.

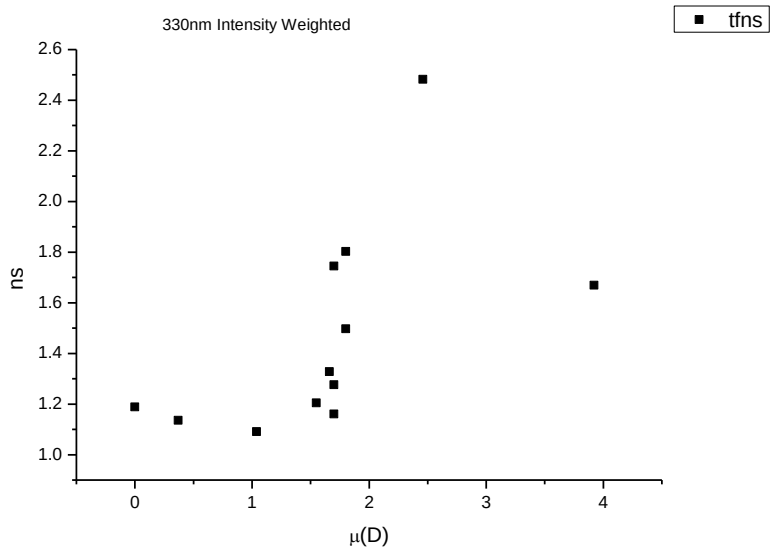

Figure 2.1.117. Intensity weighted average lifetime (τ_f) of **11a** at 330 nm versus μ(D).

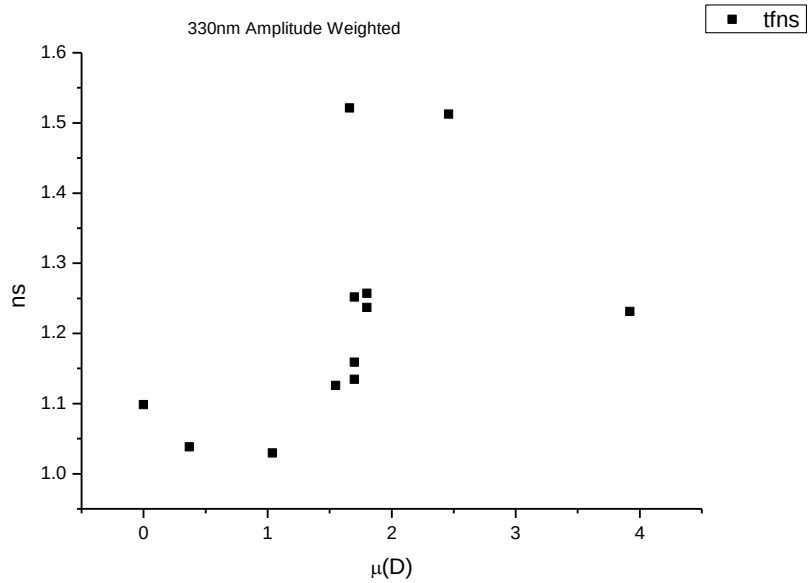

Figure 2.1.118. Amplitude weighted average lifetime (τ_f) of **11a** at 330 nm versus μ(D).

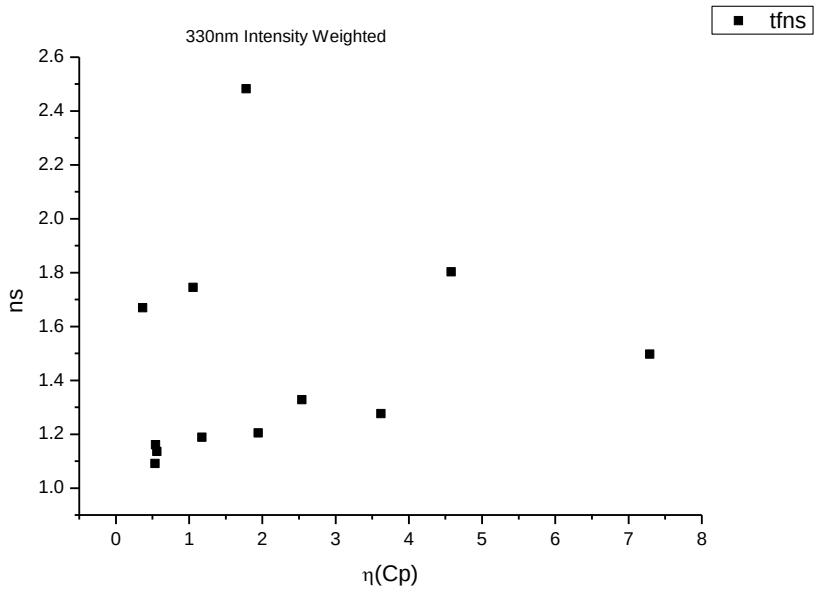

Figure 2.1.119. Intensity weighted average lifetime (τ_f) of **11a** at 330 nm versus η(Cp).

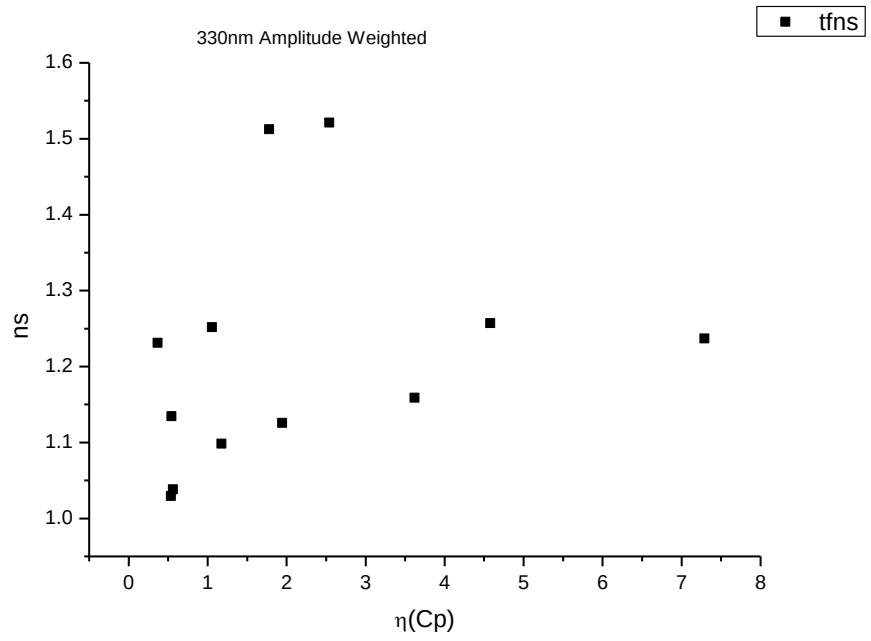

Figure 2.1.120. Amplitude weighted average lifetime (τ_f) of **11a** at 330 nm versus η(Cp).

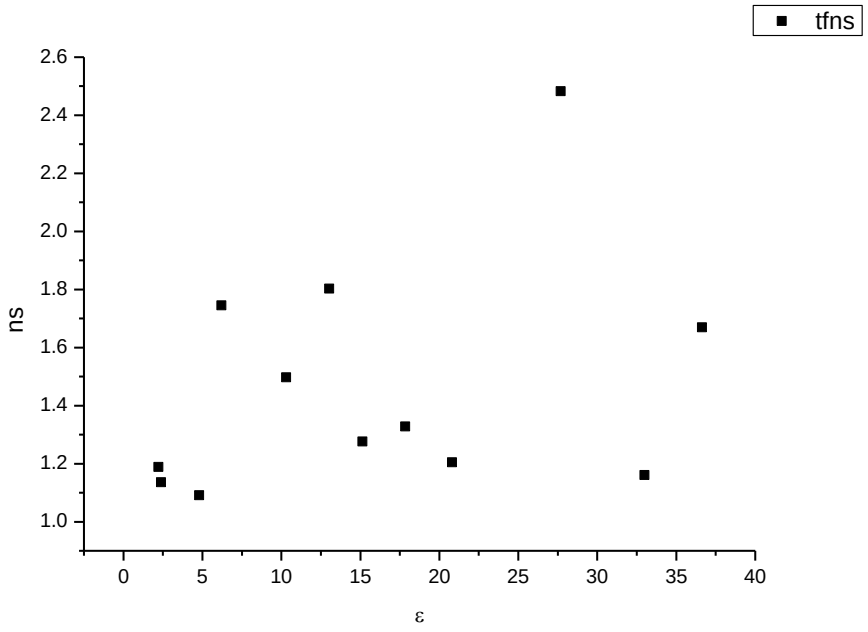

Figure 2.1.121. Intensity weighted average lifetime (τ_f) of **11a** at 330 nm versus ε.

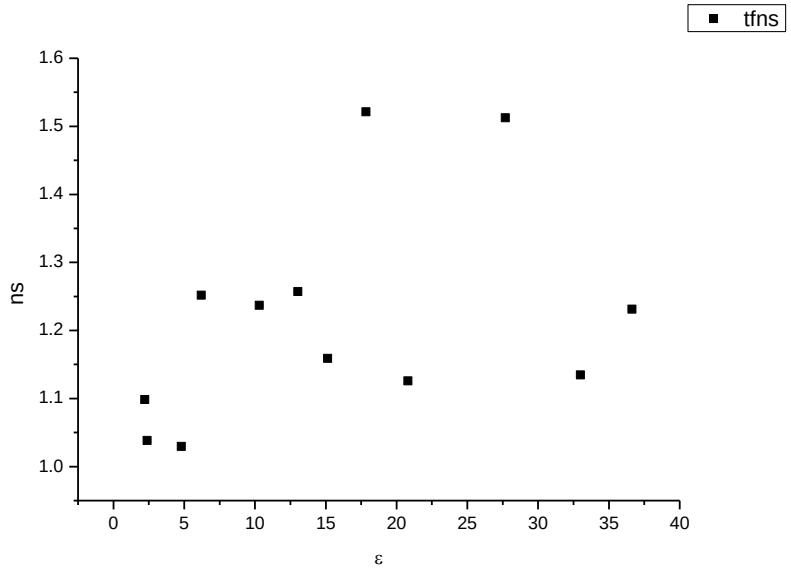

Figure 2.1.122. Amplitude weighted average lifetime (τ_f) of **11a** at 330 nm versus ε.

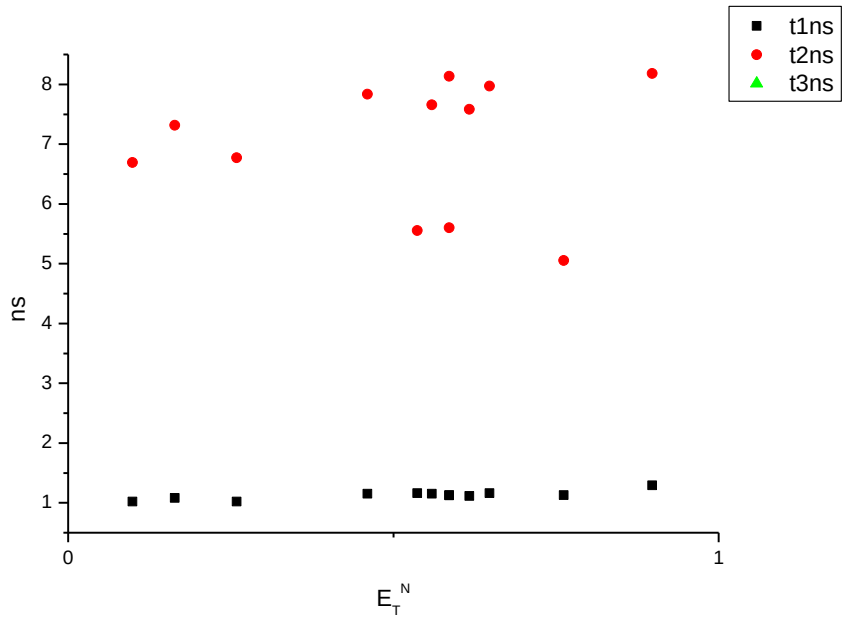

Figure 2.1.123. Intensity weighted components of TCSPC lifetime decay of **11a** (330 nm) versus E_T^N.

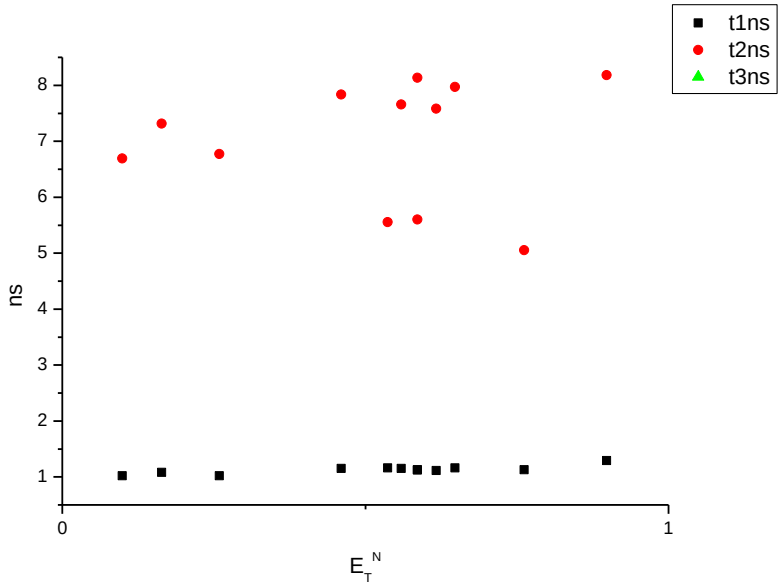

Figure 2.1.124. Amplitude weighted components of TCSPC lifetime decay of **11a** (330 nm) versus E_T^N.

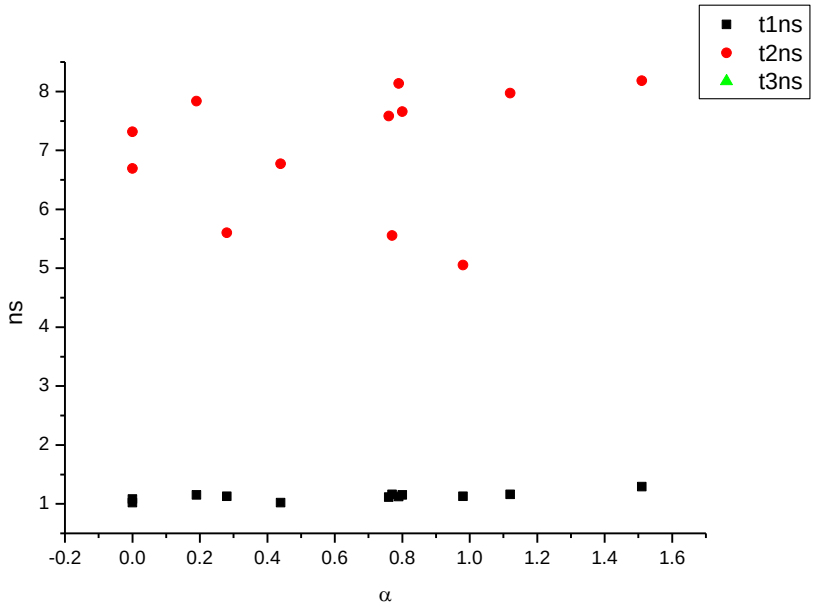

Figure 2.1.125. Intensity weighted components of TCSPC lifetime decay of **11a** (330 nm) versus α.

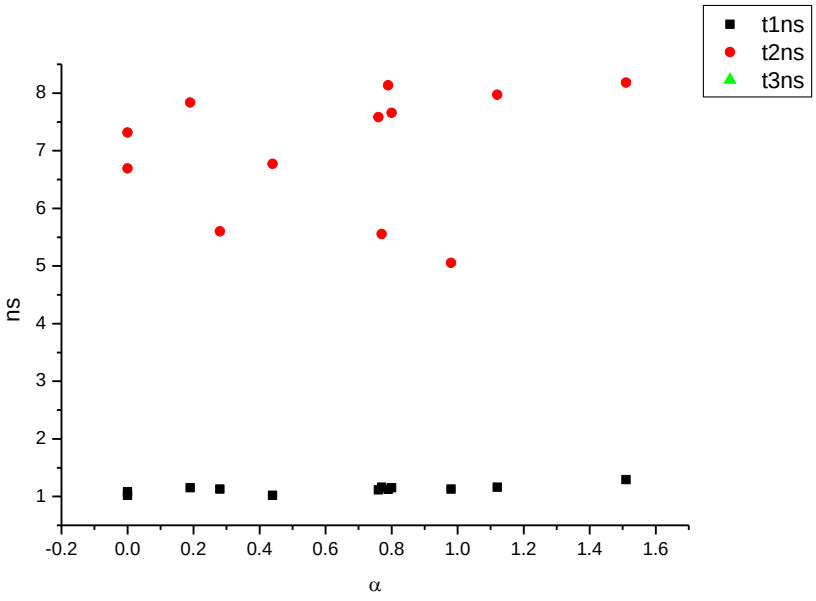

Figure 2.1.126. Amplitude weighted components of TCSPC lifetime decay of **11a** (330 nm) versus α.

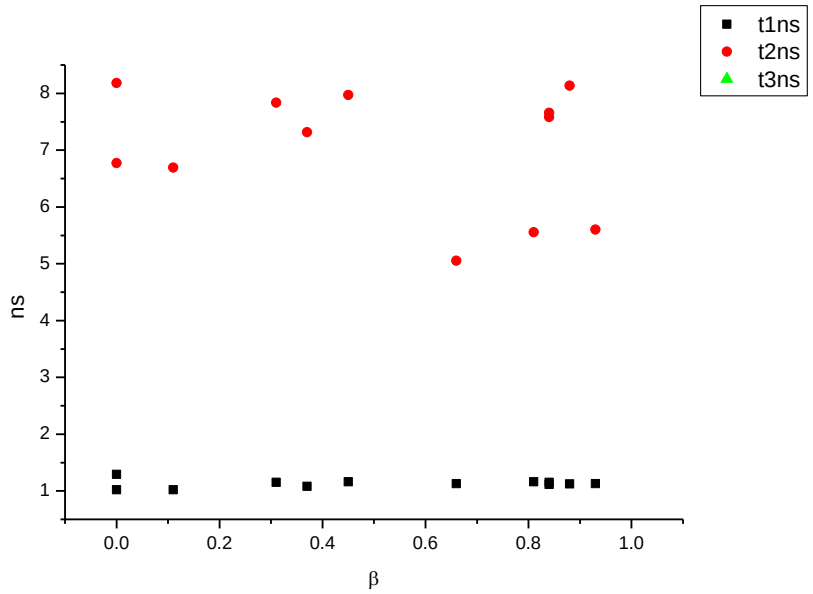

Figure 2.1.127. Intensity weighted components of TCSPC lifetime decay of **11a** (330 nm) versus β.

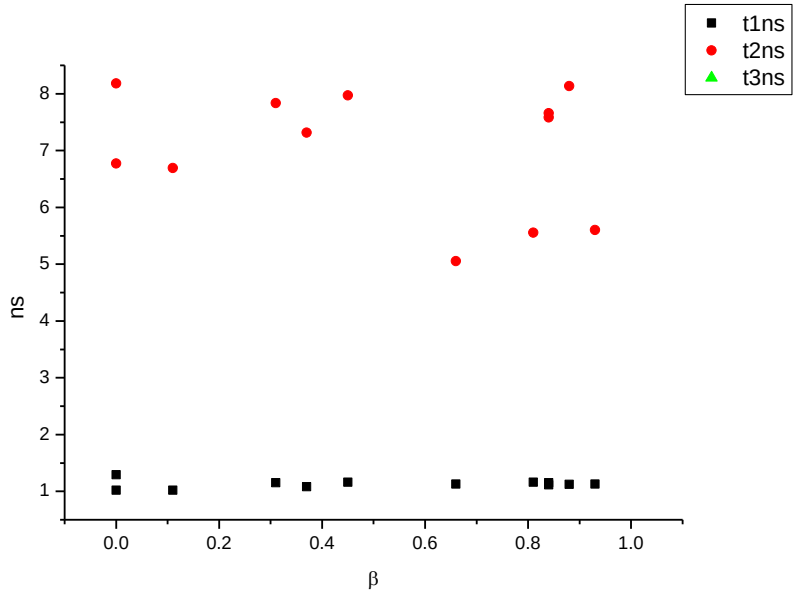

Figure 2.1.128. Amplitude weighted components of TCSPC lifetime decay of **11a** (330 nm) versus β.

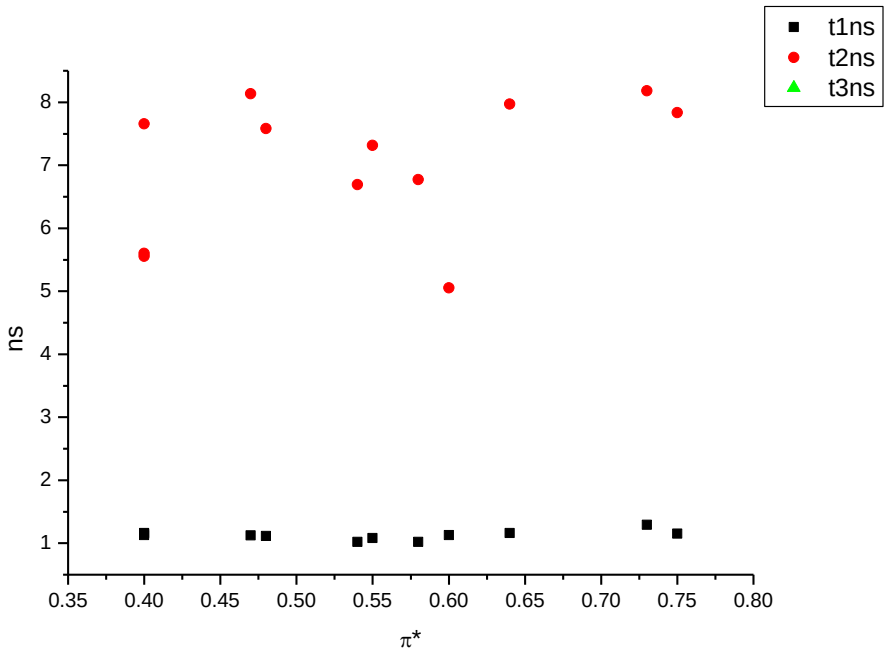

Figure 2.1.129. Intensity weighted components of TCSPC lifetime decay of **11a** (330 nm) versus π*.

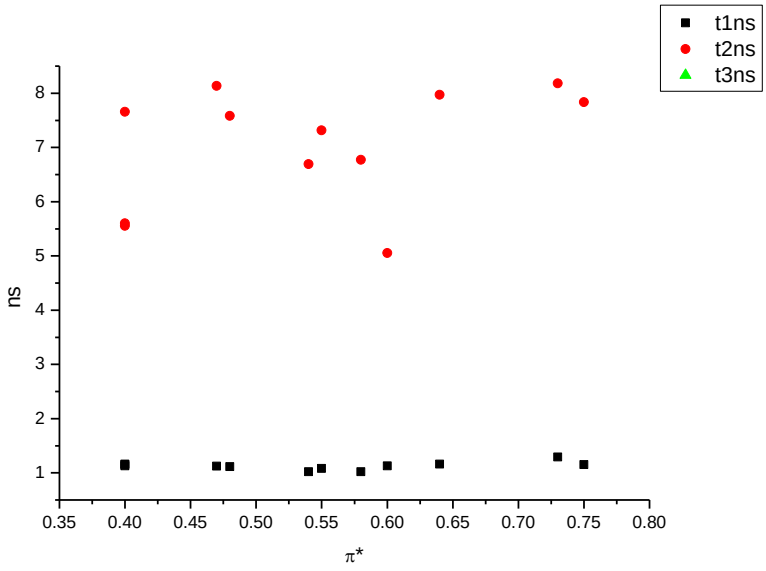

Figure 2.1.130. Amplitude weighted components of TCSPC lifetime decay of **11a** (330 nm) versus π*.

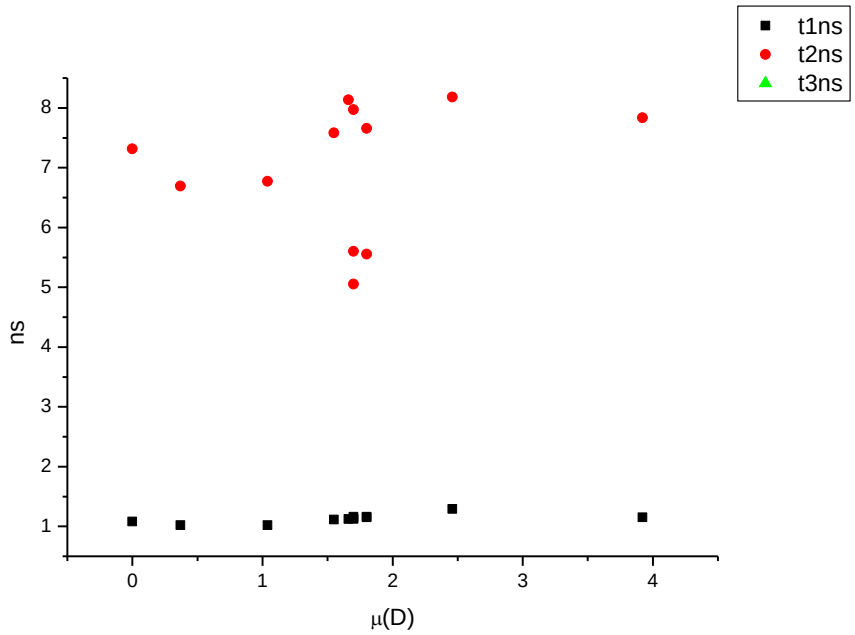

Figure 2.1.131. Intensity weighted components of TCSPC lifetime decay of **11a** (330 nm) versus μ(D).

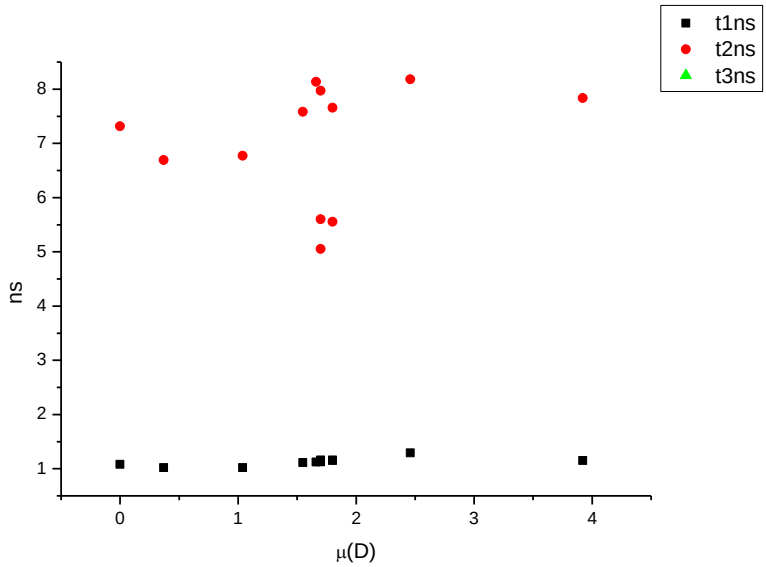

Figure 2.1.132. Amplitude weighted components of TCSPC lifetime decay of **11a** (330 nm) versus μ(D).

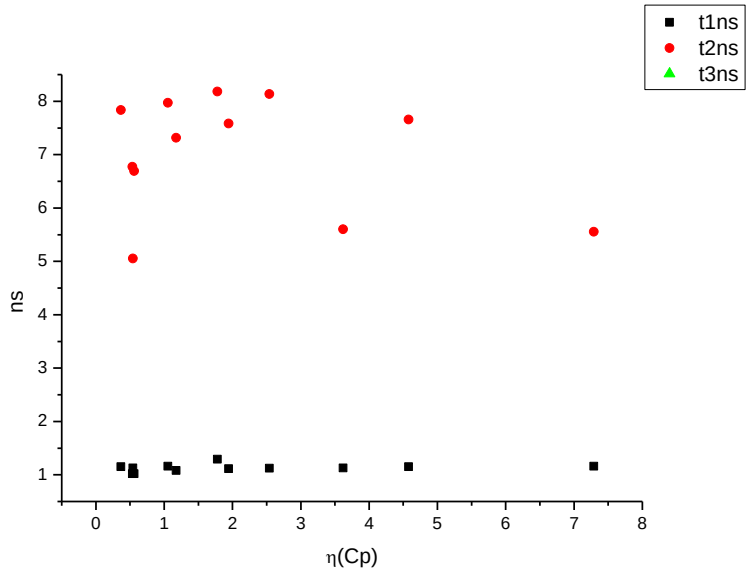

Figure 2.1.133. Intensity weighted components of TCSPC lifetime decay of **11a** (330 nm) versus η(Cp).

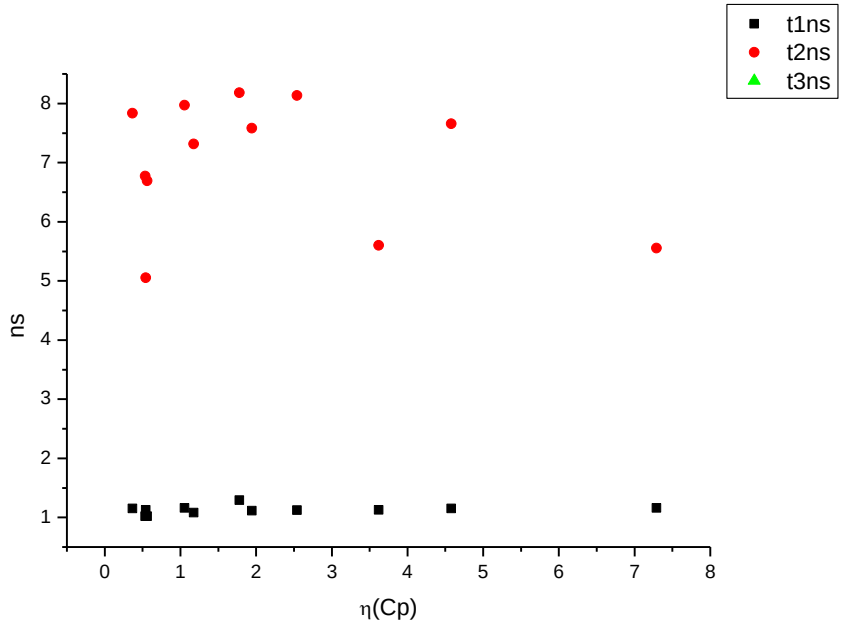

Figure 2.1.134. Amplitude weighted components of TCSPC lifetime decay of **11a** (330 nm) versus η(Cp).

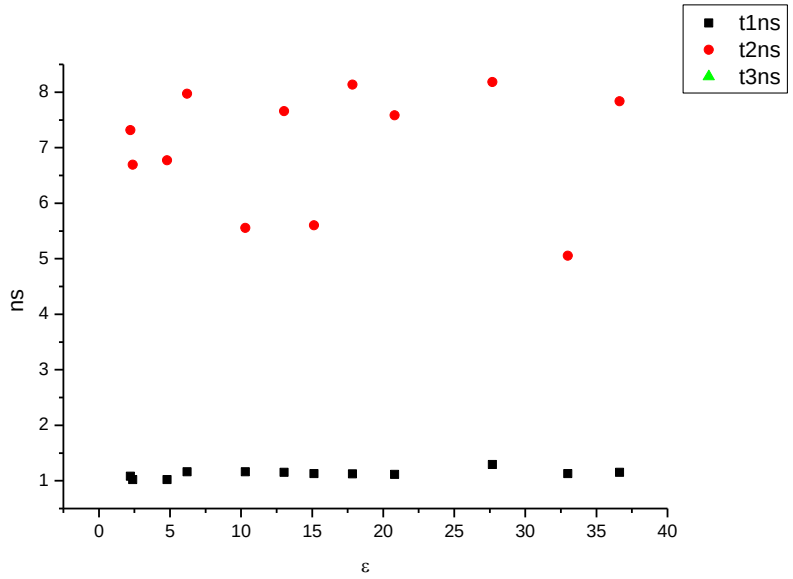

Figure 2.1.135. Intensity weighted components of TCSPC lifetime decay of **11a** (330 nm) versus ε.

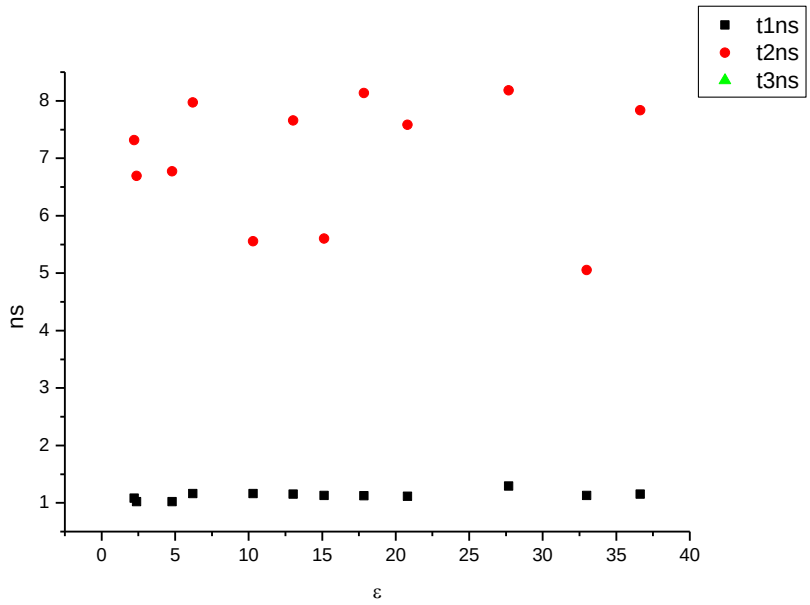

Figure 2.1.136. Amplitude weighted components of TCSPC lifetime decay of **11a** (330 nm) versus ε.

2.1.9.2 350 nm (LED) Lifetime – Solvatochromic analysis.

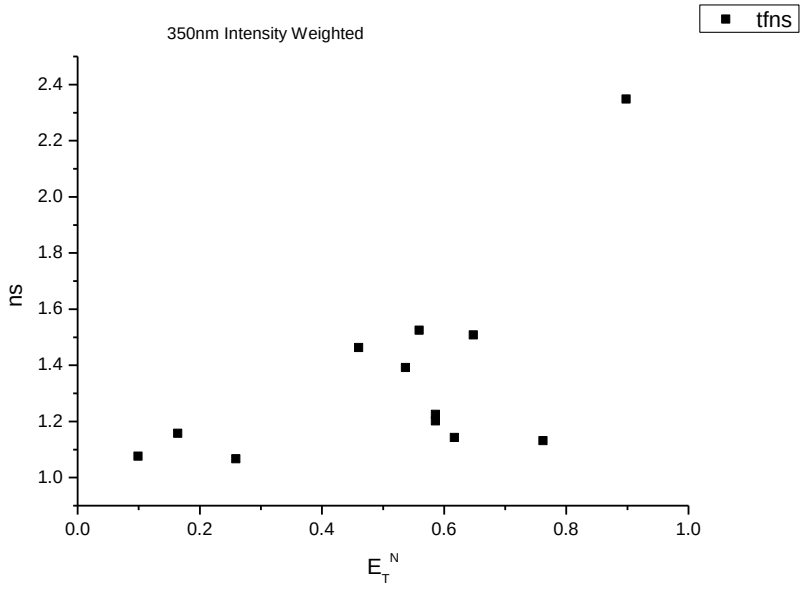

Figure 2.1.137. Intensity weighted average lifetime (τ_f) of **11a** at 350 nm versus E_T^N.

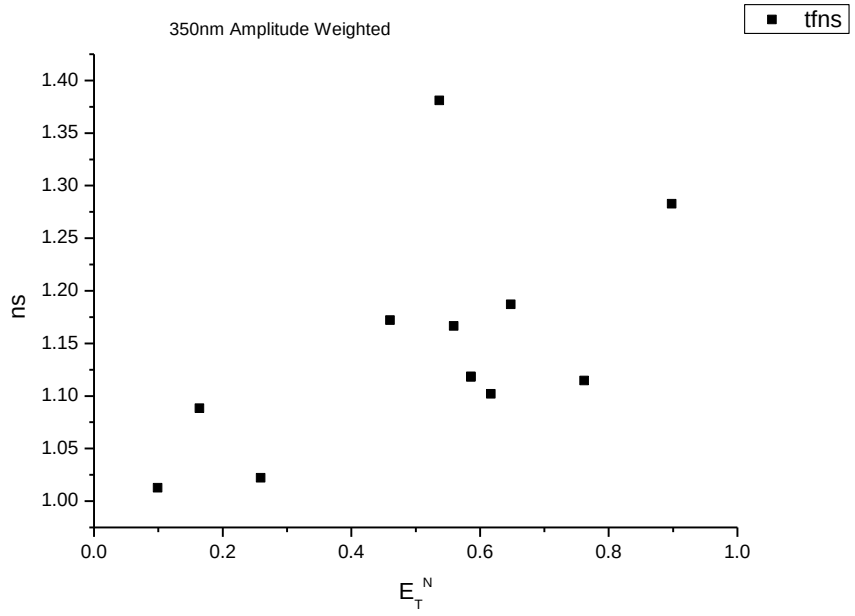

Figure 2.1.138. Amplitude weighted average lifetime (τ_f) of **11a** at 350 nm versus E_T^N.

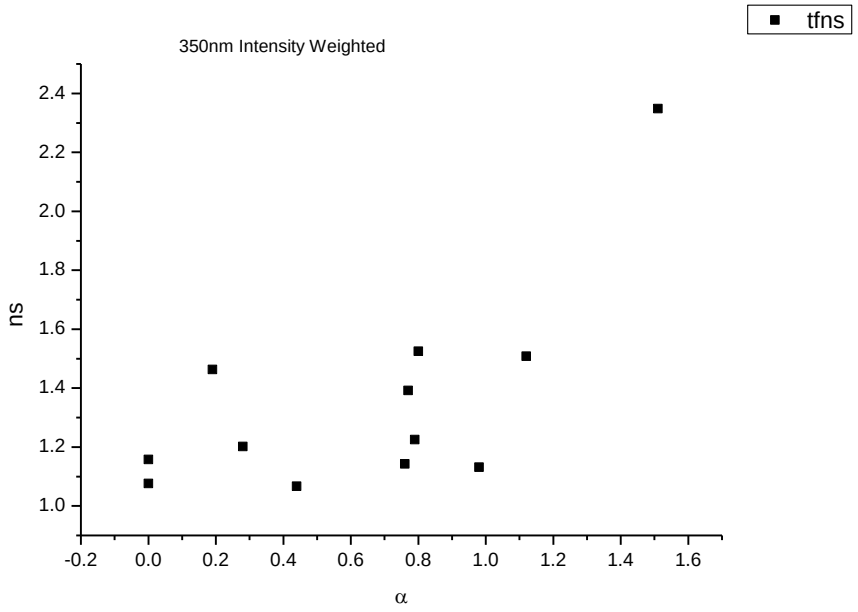

Figure 2.1.139. Intensity weighted average lifetime (τ_f) of **11a** at 350 nm versus α.

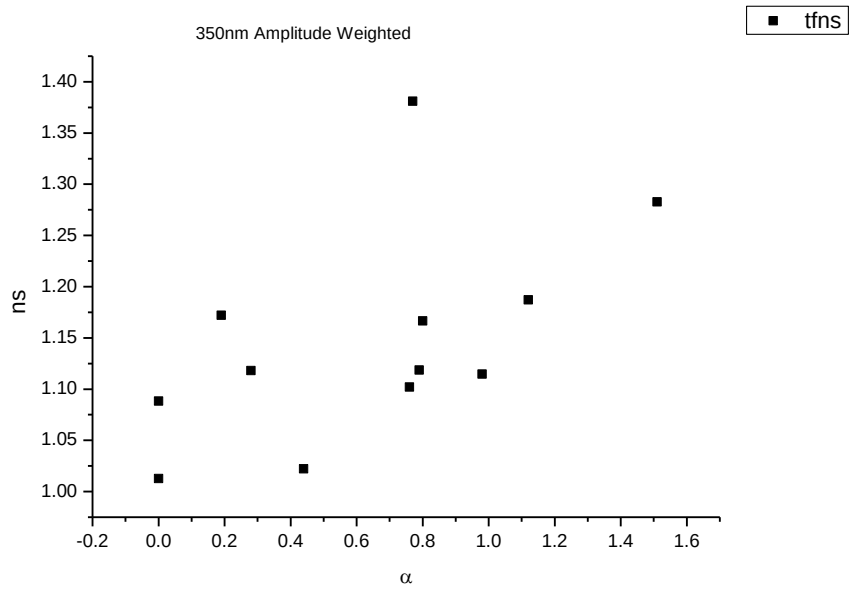

Figure 2.1.140. Amplitude weighted average lifetime (τ_f) of **11a** at 350 nm versus α.

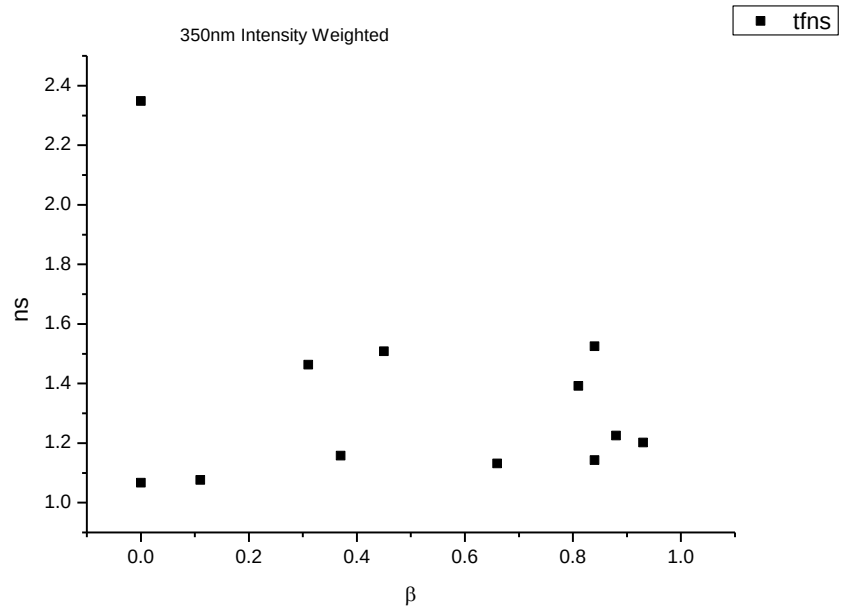

Figure 2.1.141. Intensity weighted average lifetime (τ_f) of **11a** at 350 nm versus β.

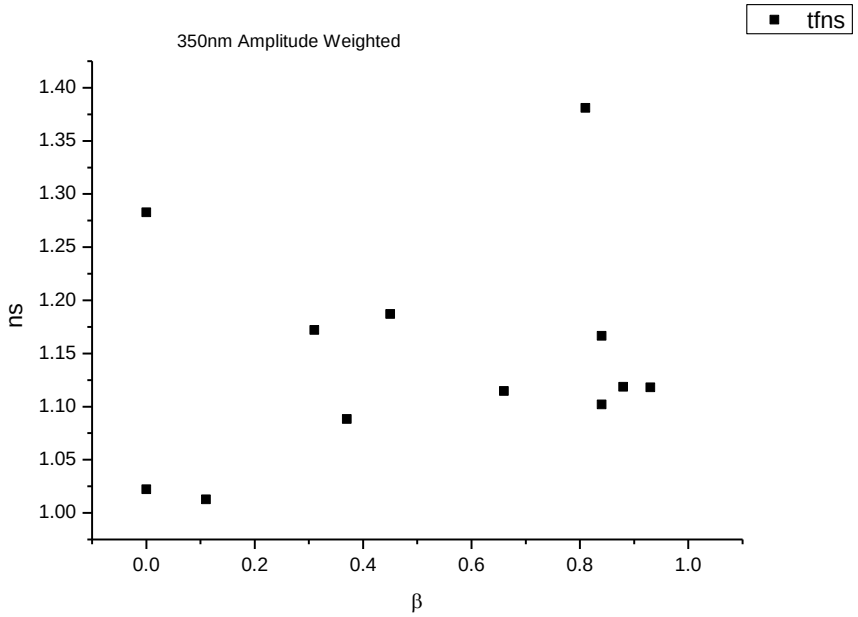

Figure 2.1.142. Amplitude weighted average lifetime (τ_f) of **11a** at 350 nm versus β.

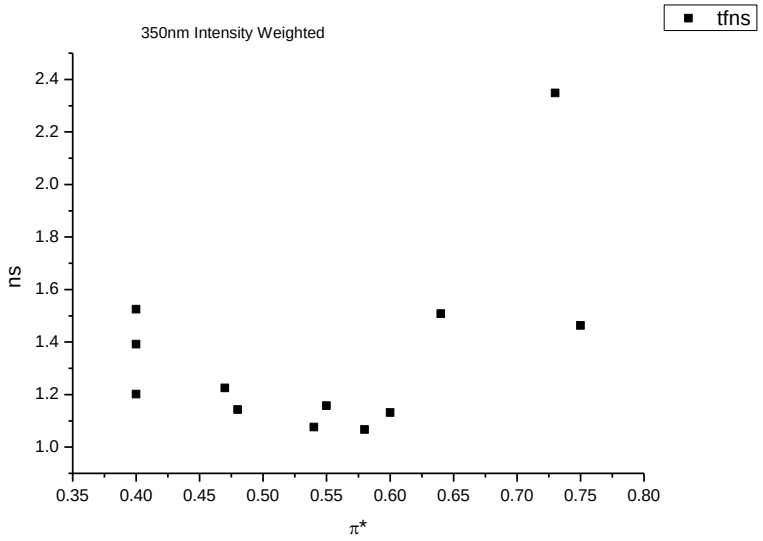

Figure 2.1.143. Intensity weighted average lifetime (τ_f) of **11a** at 350 nm versus π*.

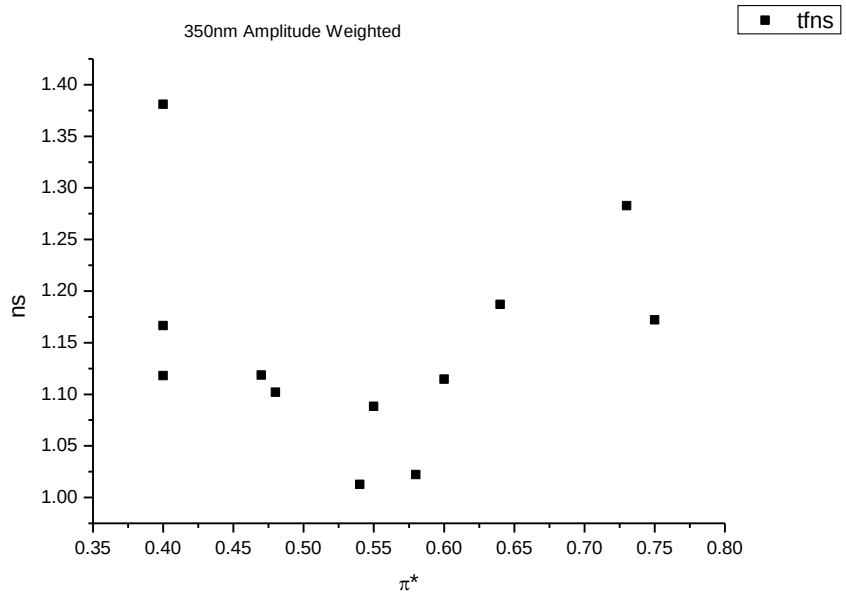

Figure 2.1.144. Amplitude weighted average lifetime (τ_f) of **11a** at 350 nm versus π*.

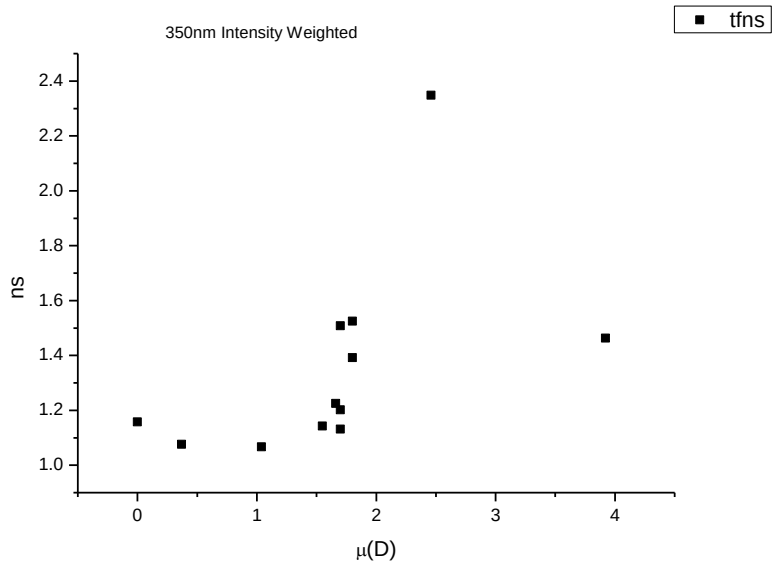

Figure 2.1.145. Intensity weighted average lifetime (τ_f) of **11a** at 350 nm versus μ(D).

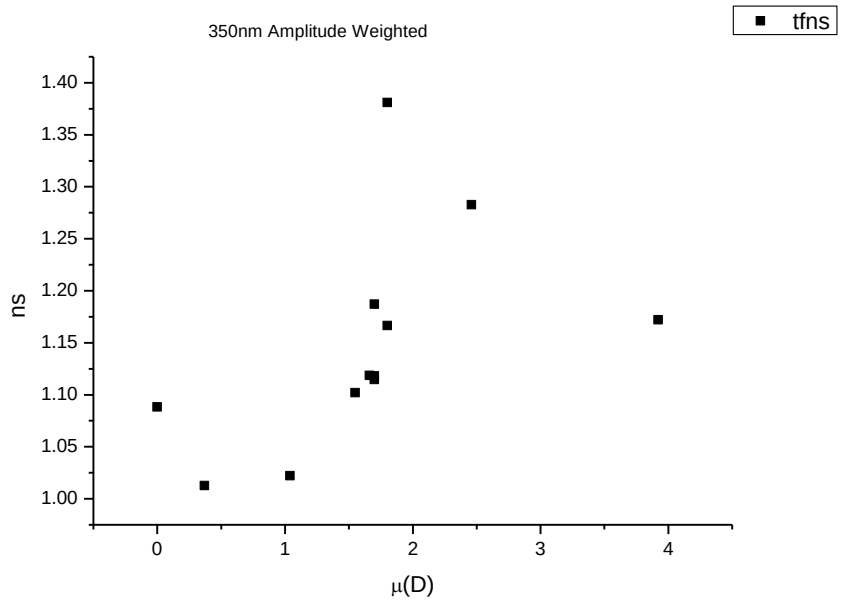

Figure 2.1.146. Amplitude weighted average lifetime (τ_f) of **11a** at 350 nm versus μ(D).

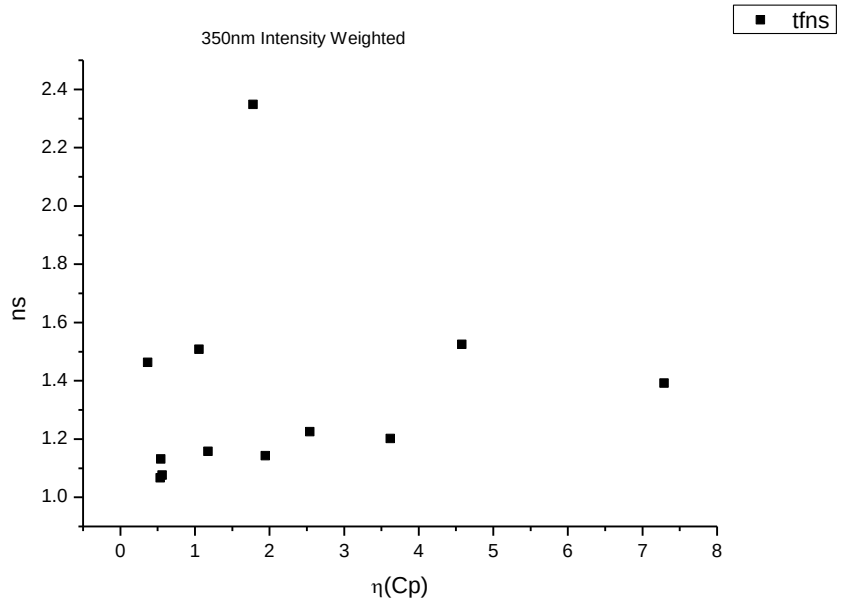

Figure 2.1.147. Intensity weighted average lifetime (τ_f) of **11a** at 350 nm versus η(Cp).

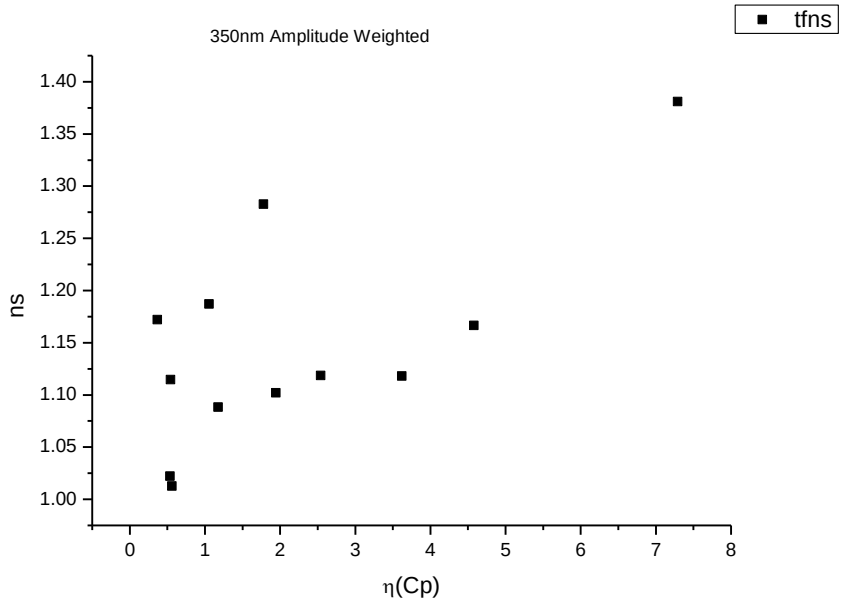

Figure 2.1.148. Amplitude weighted average lifetime (τ_f) of **11a** at 350 nm versus η(Cp).

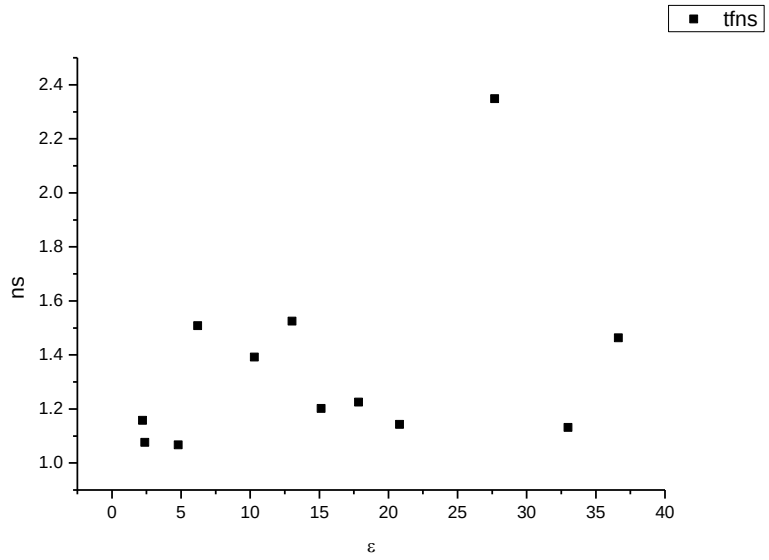

Figure 2.1.149. Intensity weighted average lifetime (τ_f) of **11a** at 350 nm versus ε.

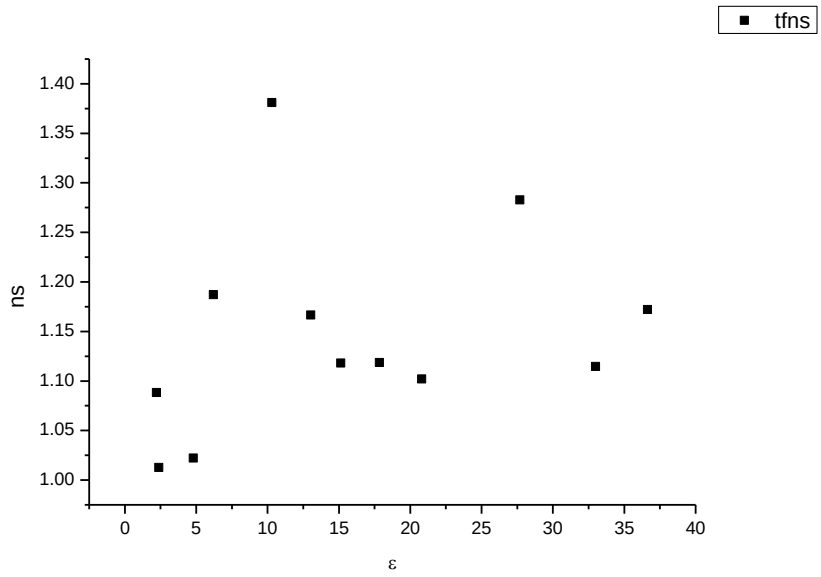

Figure 2.1.150. Amplitude weighted average lifetime (τ_f) of **11a** at 350 nm versus ε.

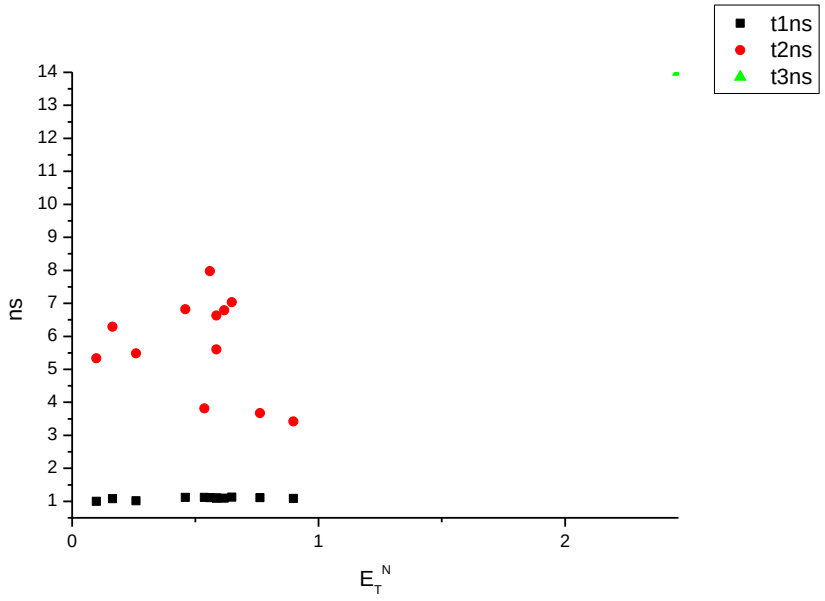

Figure 2.1.151. Intensity weighted components of TCSPC lifetime decay of **11a** (350 nm) versus E_T^N.

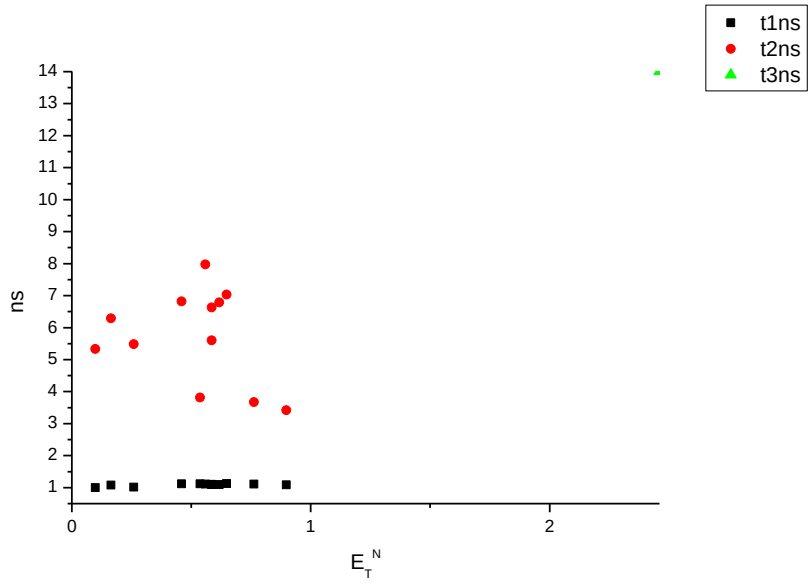

Figure 2.1.152. Amplitude weighted components of TCSPC lifetime decay of **11a** (350 nm) versus E_T^N.

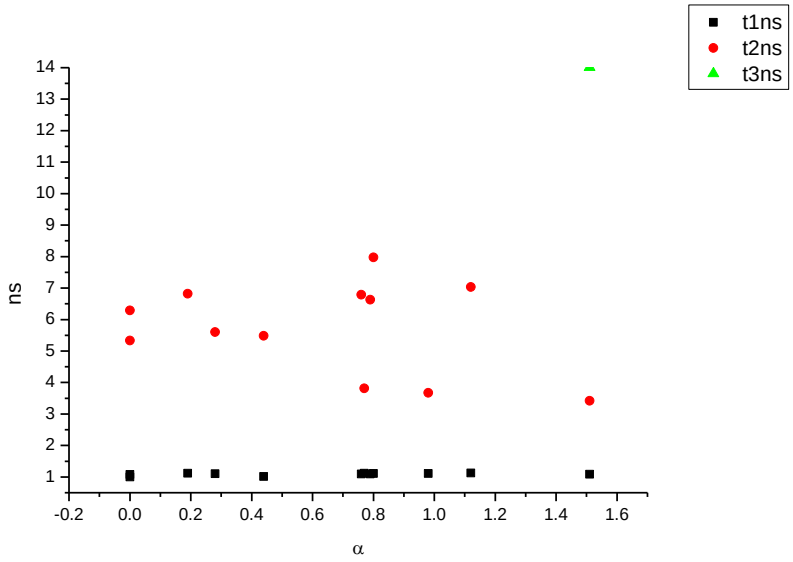

Figure 2.1.153. Intensity weighted components of TCSPC lifetime decay of **11a** (350 nm) versus α.

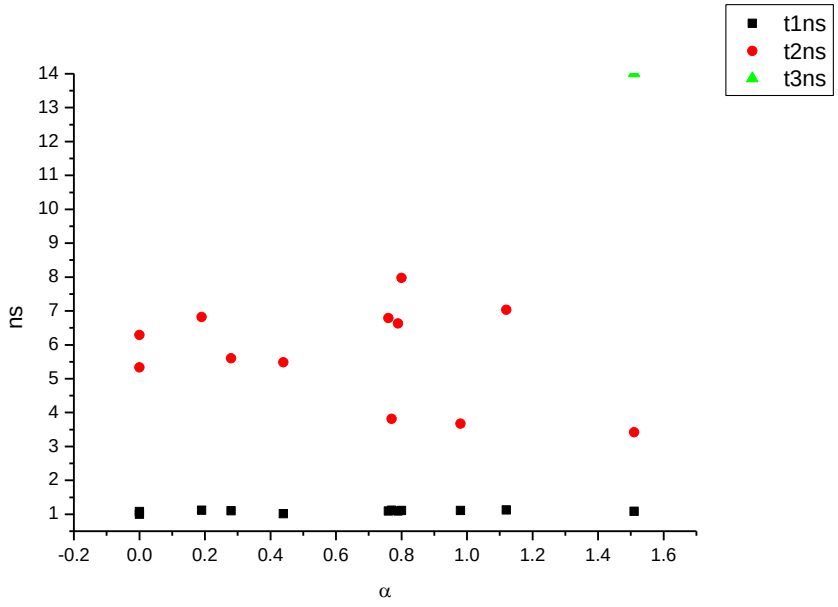

Figure 2.1.154. Amplitude weighted components of TCSPC lifetime decay of **11a** (350 nm) versus α.

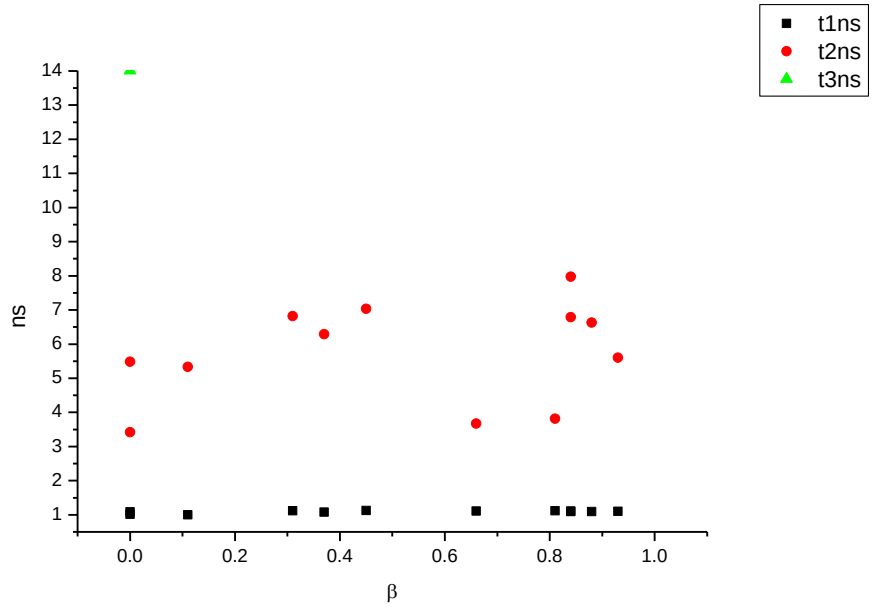

Figure 2.1.155. Intensity weighted components of TCSPC lifetime decay of **11a** (350 nm) versus β.

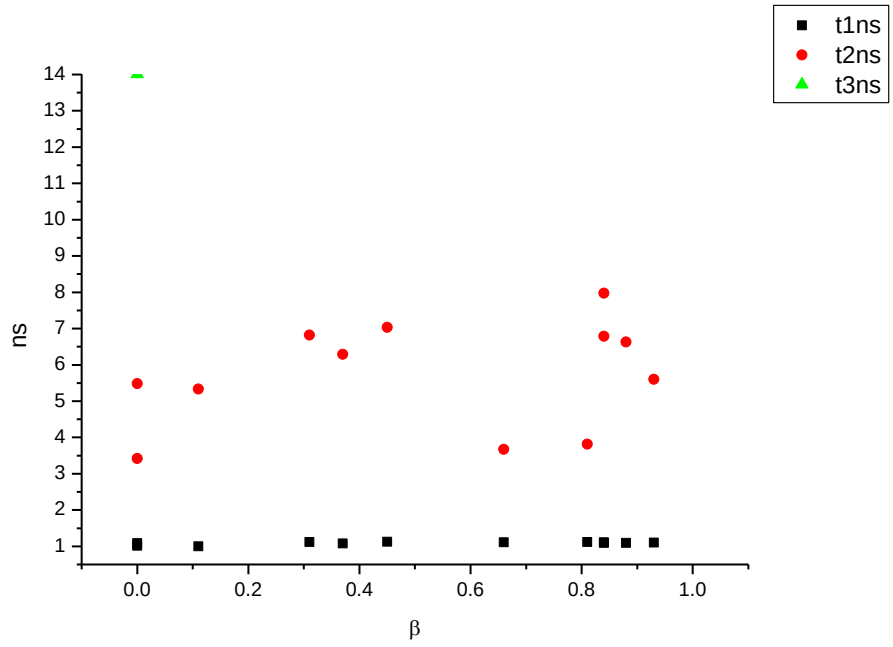

Figure 2.1.156. Amplitude weighted components of TCSPC lifetime decay of **11a** (350 nm) versus β.

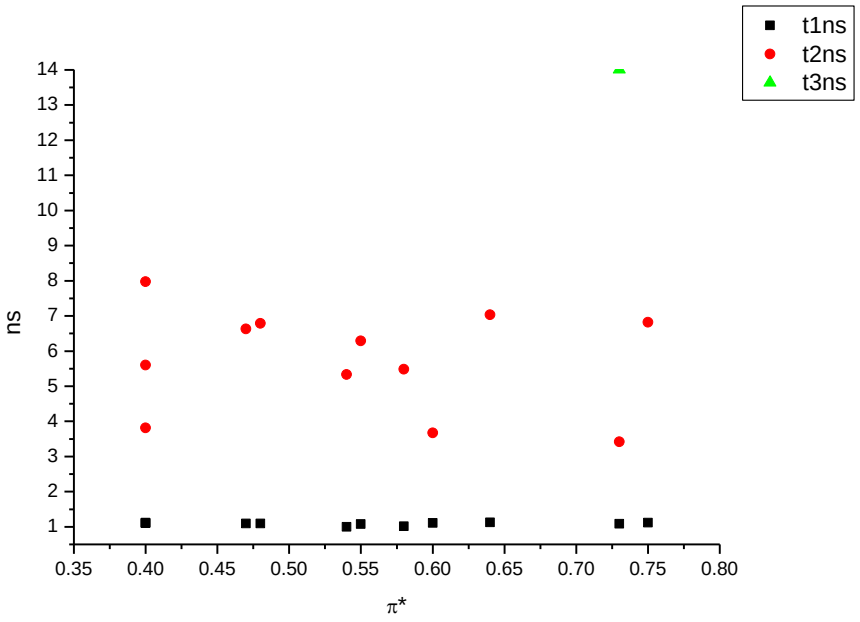

Figure 2.1.157. Intensity weighted components of TCSPC lifetime decay of **11a** (350 nm) versus π*.

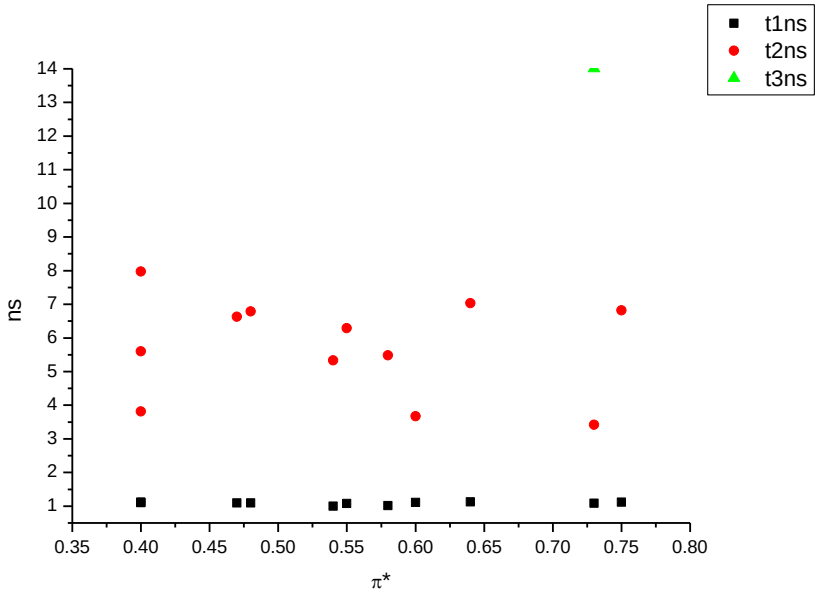

Figure 2.1.158. Amplitude weighted components of TCSPC lifetime decay of **11a** (350 nm) versus π*.

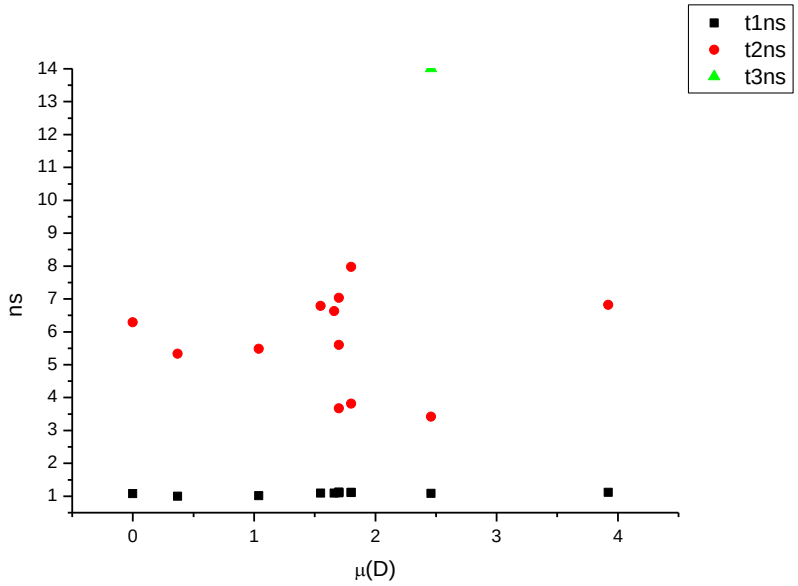

Figure 2.1.159. Intensity weighted components of TCSPC lifetime decay of **11a** (350 nm) versus μ(D).

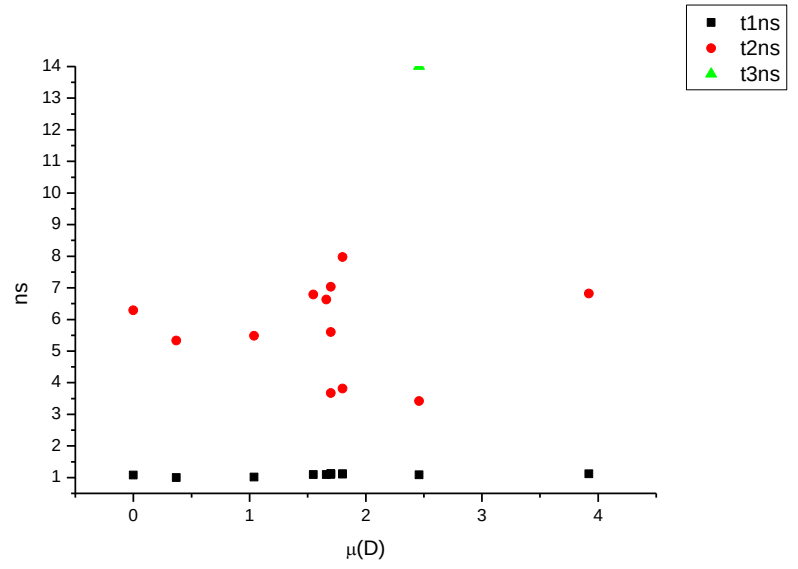

Figure 2.1.160. Amplitude weighted components of TCSPC lifetime decay of **11a** (350 nm) versus μ(D).

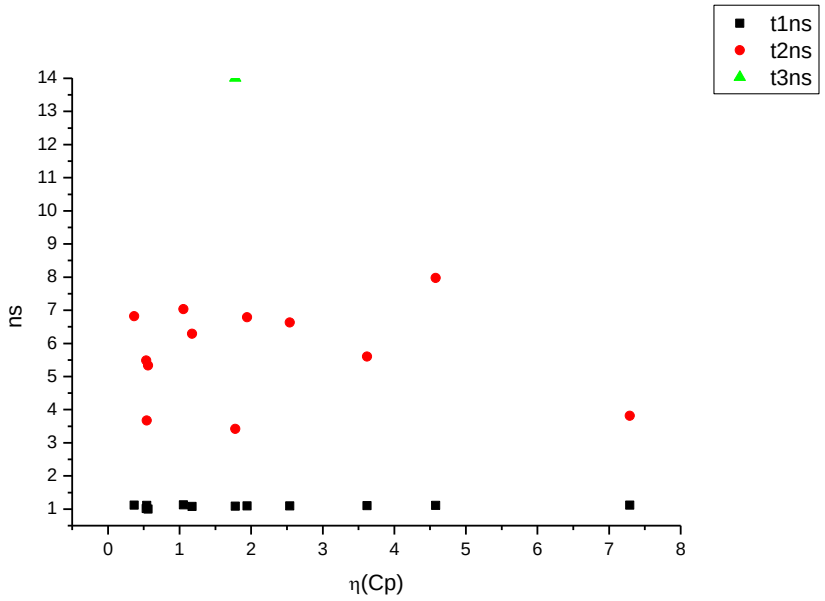

Figure 2.1.161. Intensity weighted components of TCSPC lifetime decay of **11a** (350 nm) versus η(Cp).

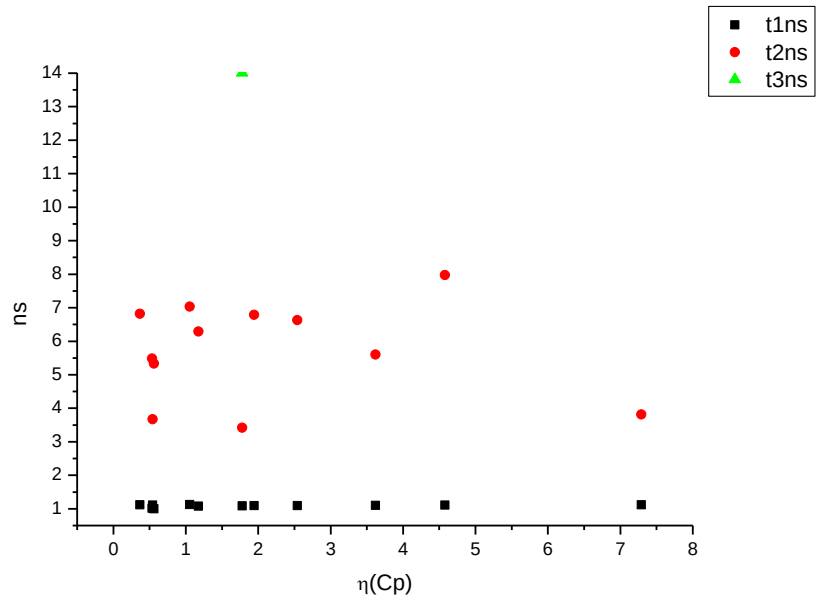

Figure 2.1.162. Amplitude weighted components of TCSPC lifetime decay of **11a** (350 nm) versus η(Cp).

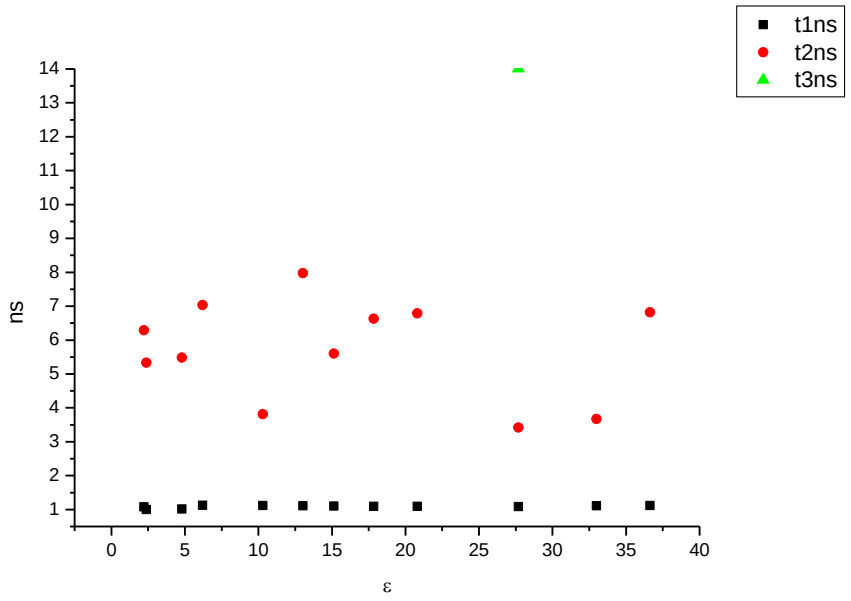

Figure 2.1.163. Intensity weighted components of TCSPC lifetime decay of **11a** (350 nm) versus ε.

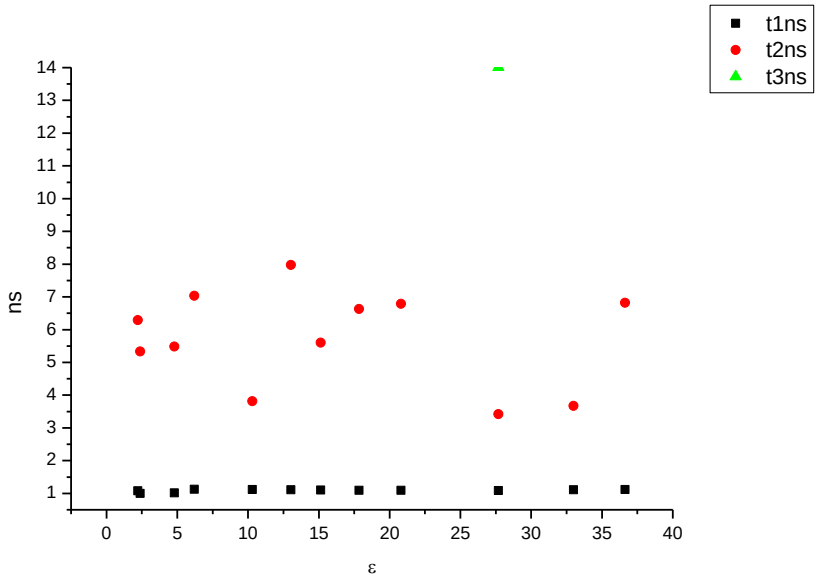

Figure 2.1.164. Amplitude weighted components of TCSPC lifetime decay of **11a** (350 nm) versus ε.

2.1.10 Ultraviolet-visible absorption spectra.

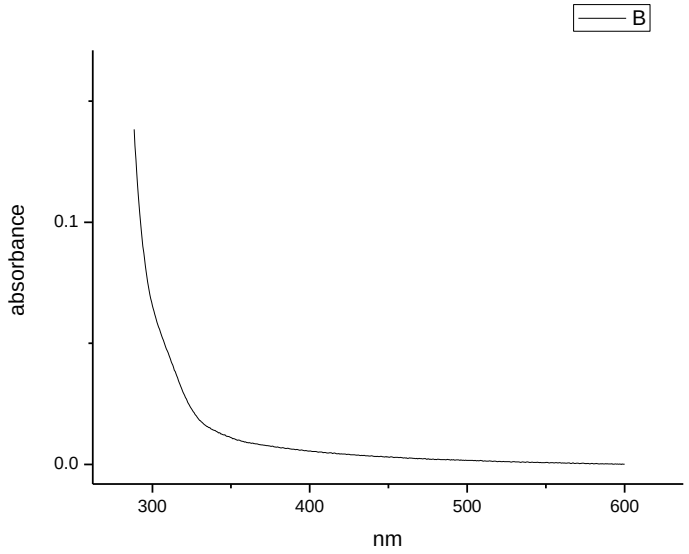

Figure 2.1.165. Ultraviolet-Visible absorption spectrum of **11a** recorded in Toluene.

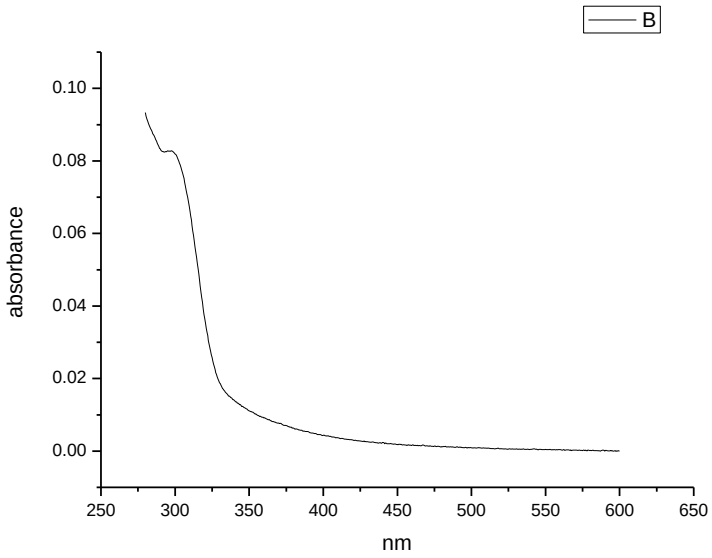

Figure 2.1.166. Ultraviolet-Visible absorption spectrum of **11a** recorded in 1,4-dioxane.

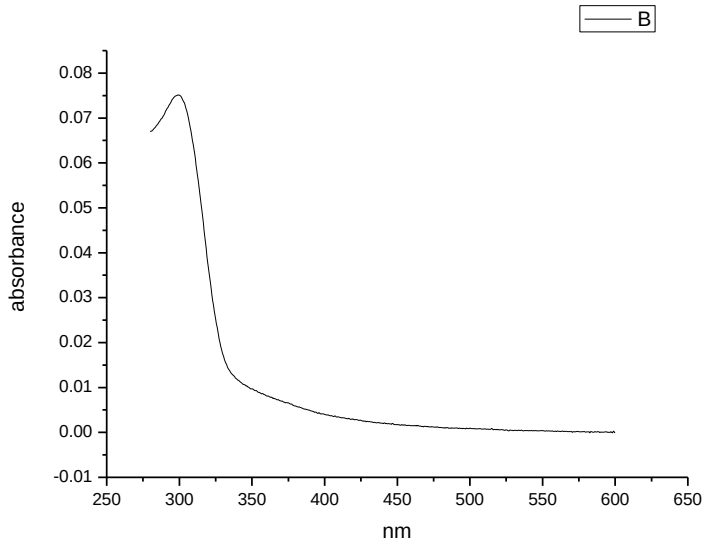

Figure 2.1.167. Ultraviolet-Visible absorption spectrum of **11a** recorded in Chloroform.

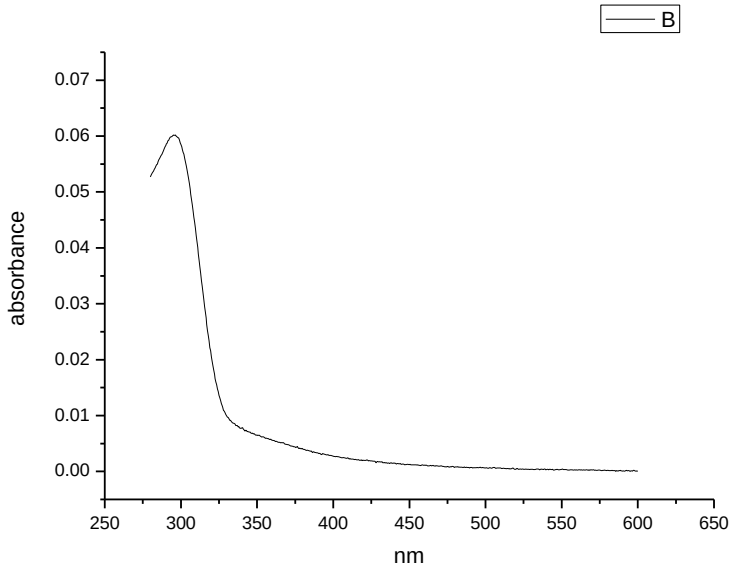

Figure 2.1.168. Ultraviolet-Visible absorption spectrum of **11a** recorded in Acetonitrile.

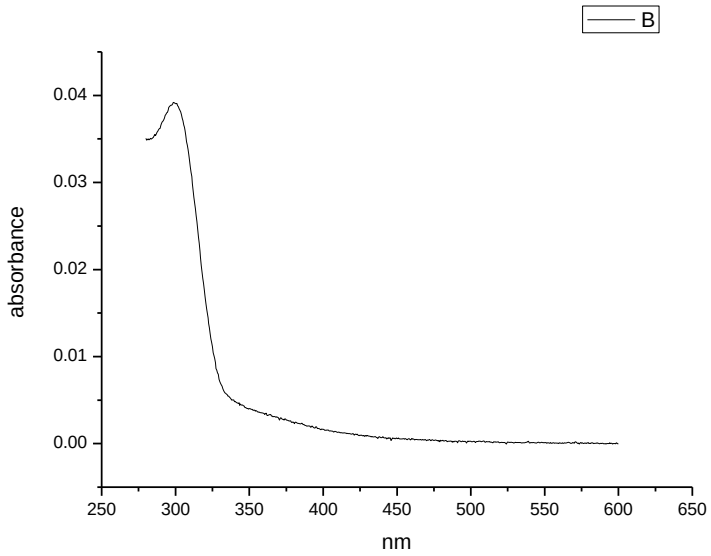

Figure 2.1.169. Ultraviolet-Visible absorption spectrum of **11a** recorded in 1-octanol.

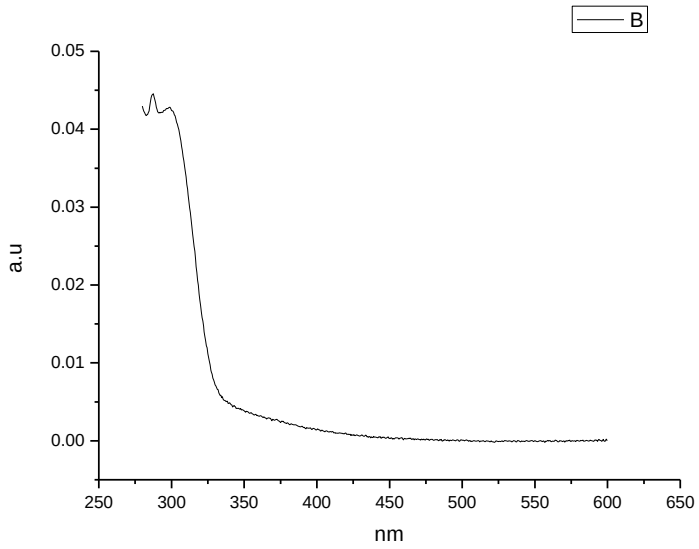

Figure 2.1.170. Ultraviolet-Visible absorption spectrum of **11a** recorded in 1-hexanol.

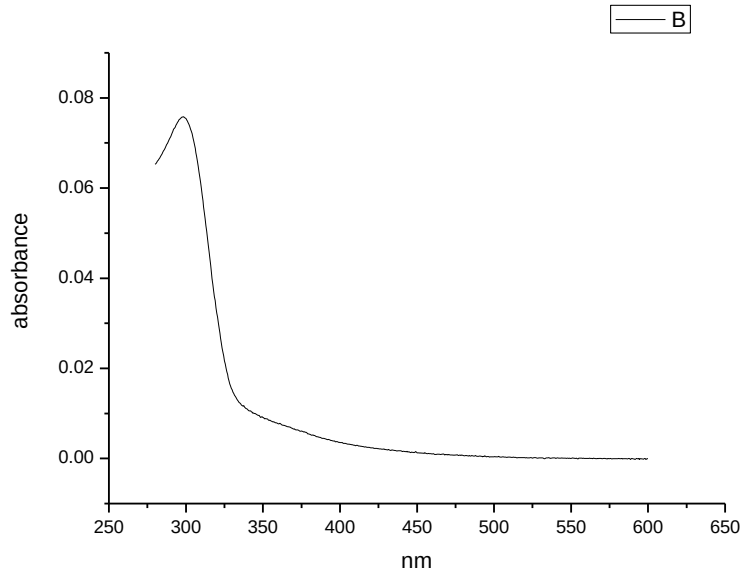

Figure 2.1.171. Ultraviolet-Visible absorption spectrum of **11a** recorded in 1-butanol.

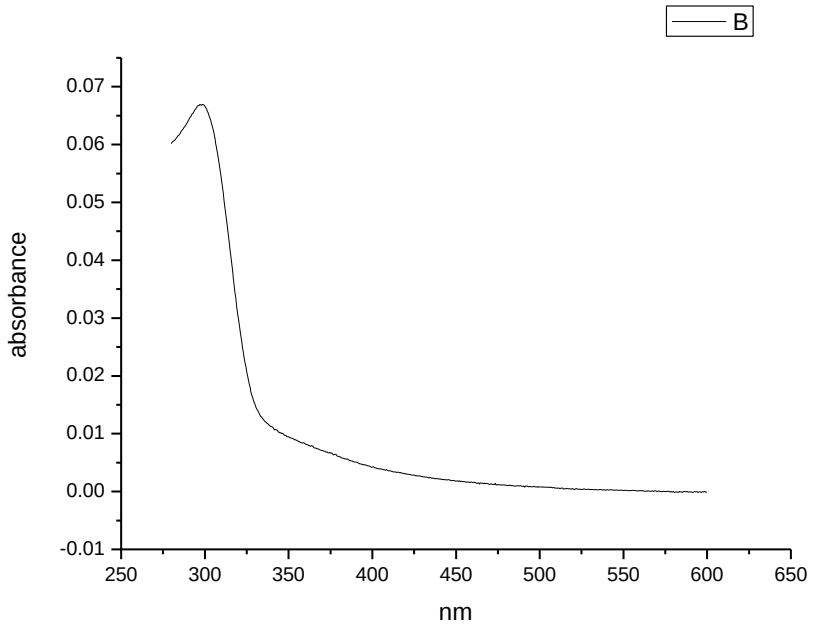

Figure 2.1.172. Ultraviolet-Visible absorption spectrum of **11a** recorded in 1-pentanol.

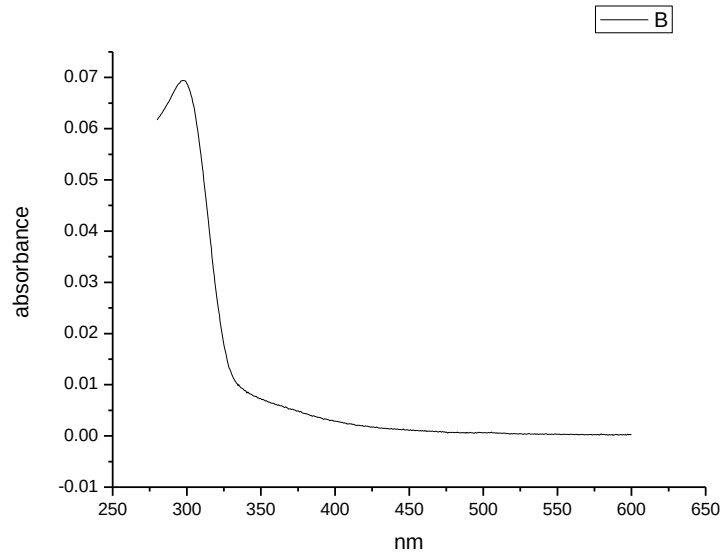

Figure 2.1.173. Ultraviolet-Visible absorption spectrum of **11a** recorded in 1-propanol.

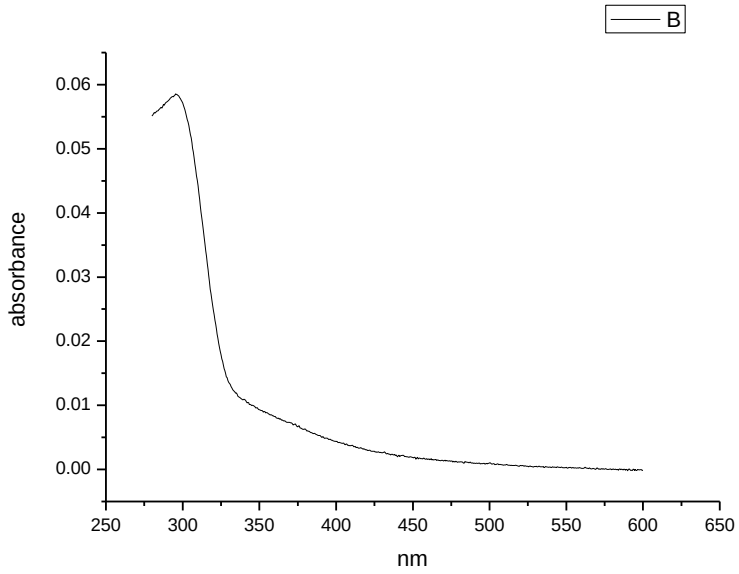

Figure 2.1.174. Ultraviolet-Visible absorption spectrum of **11a** recorded in Acetic Acid.

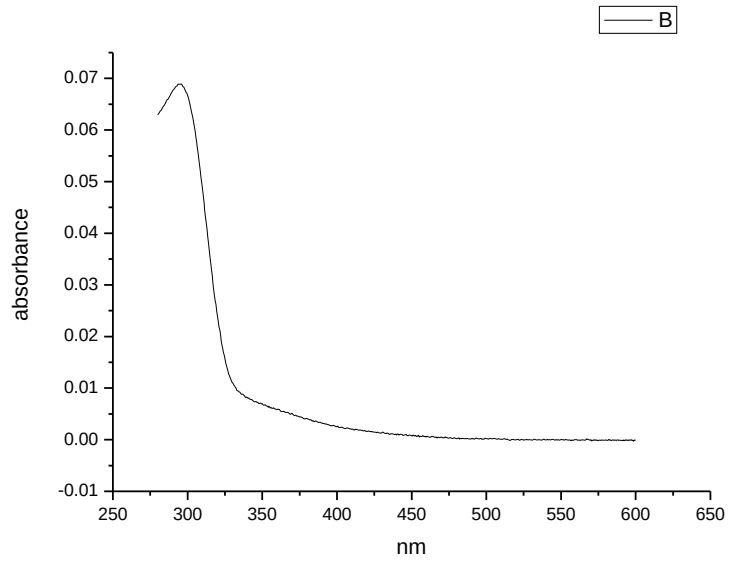

Figure 2.1.175. Ultraviolet-Visible absorption spectrum of **11a** recorded in Methanol

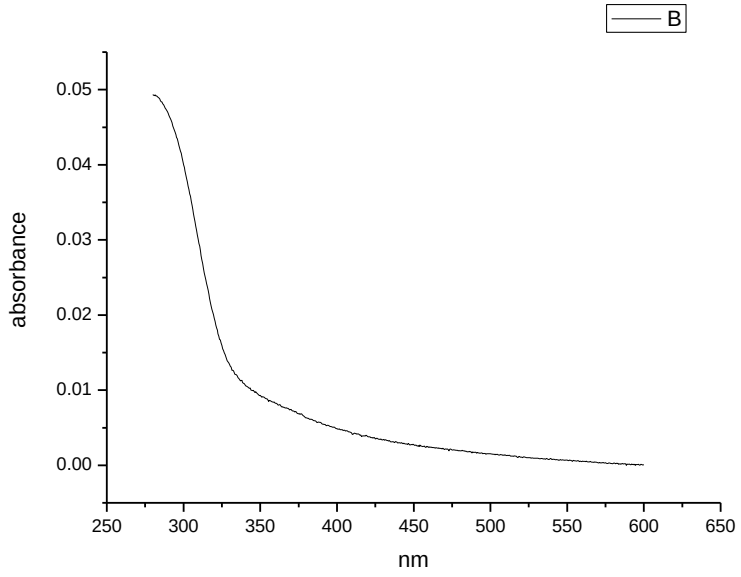

Figure 2.1.176. Ultraviolet-Visible absorption spectrum of **11a** recorded in 2,2,2-trifluoroethanol.

2.1.11 Fluorescence Emission spectra.

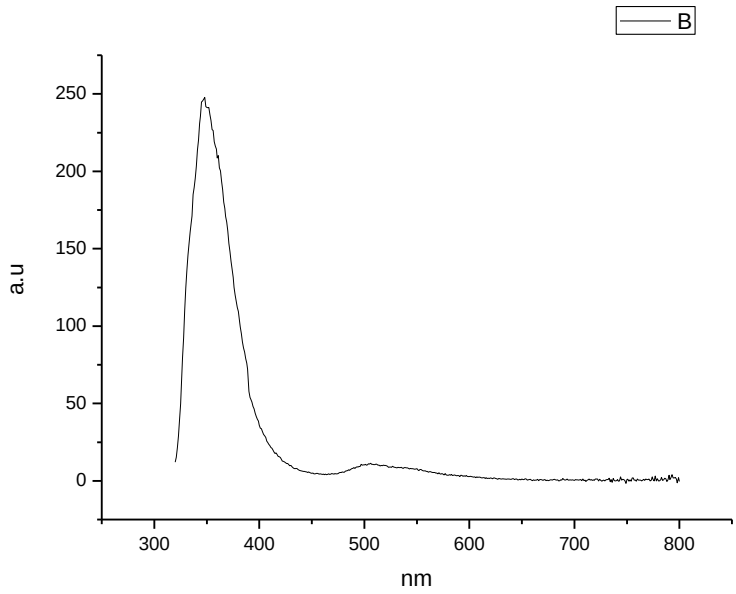

Figure 2.1.177. Fluorescence emission spectrum of **11a** recorded in Toluene at 310 nm excitation.

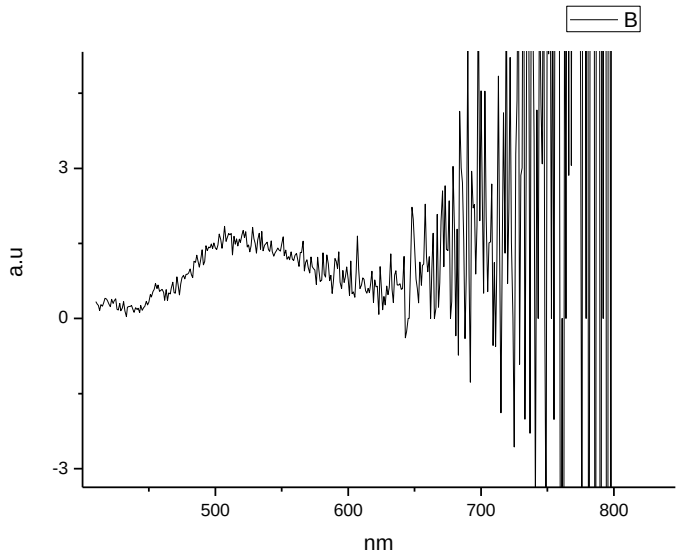

Figure 2.1.178. Fluorescence emission spectrum of **11a** recorded in Toluene at 400 nm excitation.

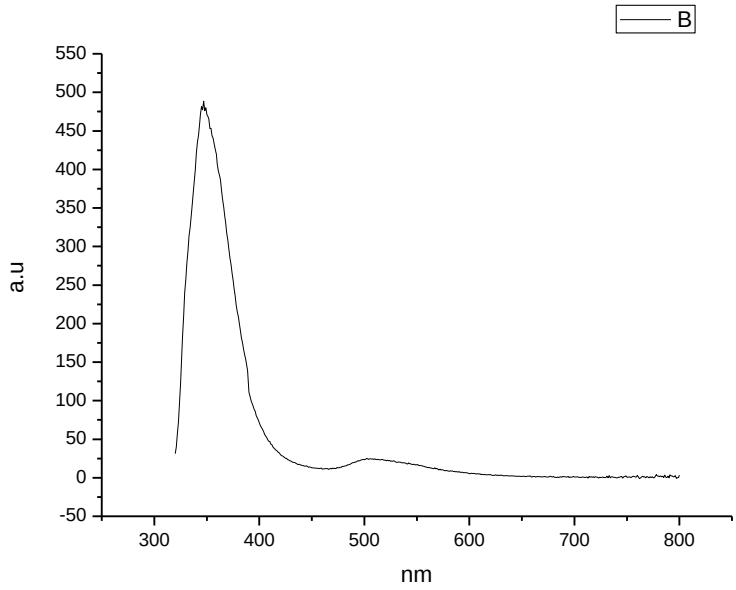

Figure 2.1.179. Fluorescence emission spectrum of **11a** recorded in 1,4-dioxane at 310 nm excitation.

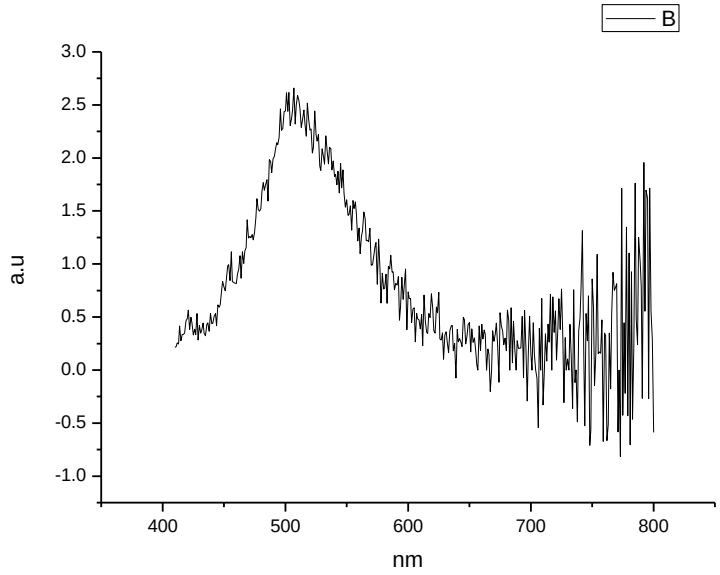

Figure 2.1.180. Fluorescence emission spectrum of **11a** recorded in 1,4-dioxane at 400 nm excitation.

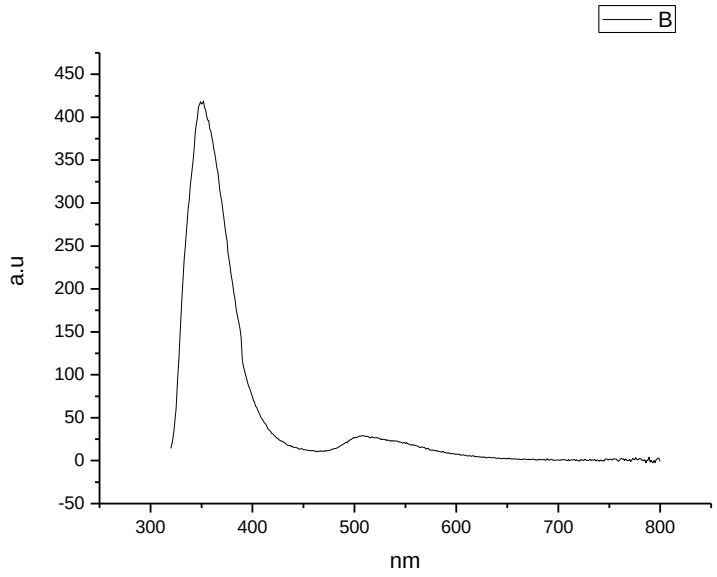

Figure 2.1.181. Fluorescence emission spectrum of **11a** recorded in Chloroform at 310 nm excitation.

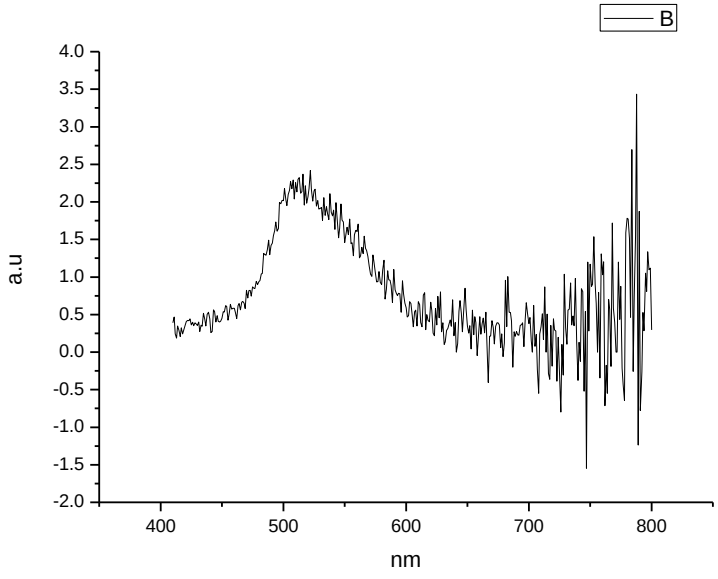

Figure 2.1.182. Fluorescence emission spectrum of **11a** recorded in Chloroform at 400 nm excitation.

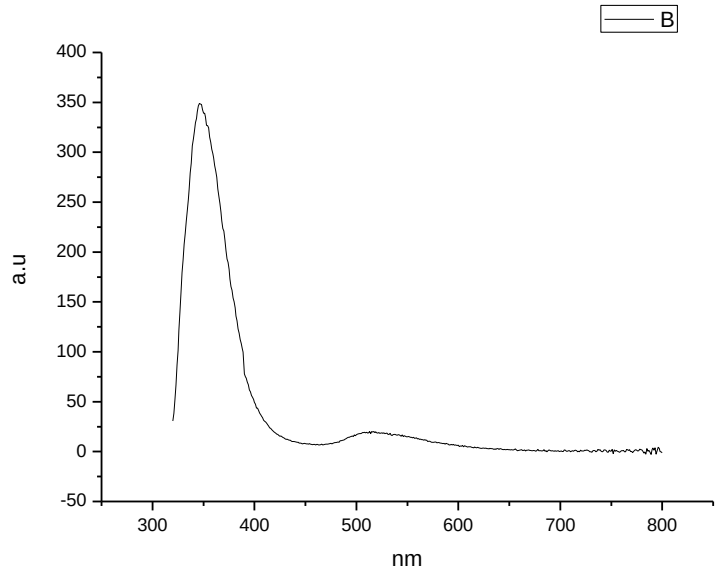

Figure 2.1.183. Fluorescence emission spectrum of **11a** recorded in Acetonitrile at 310 nm excitation.

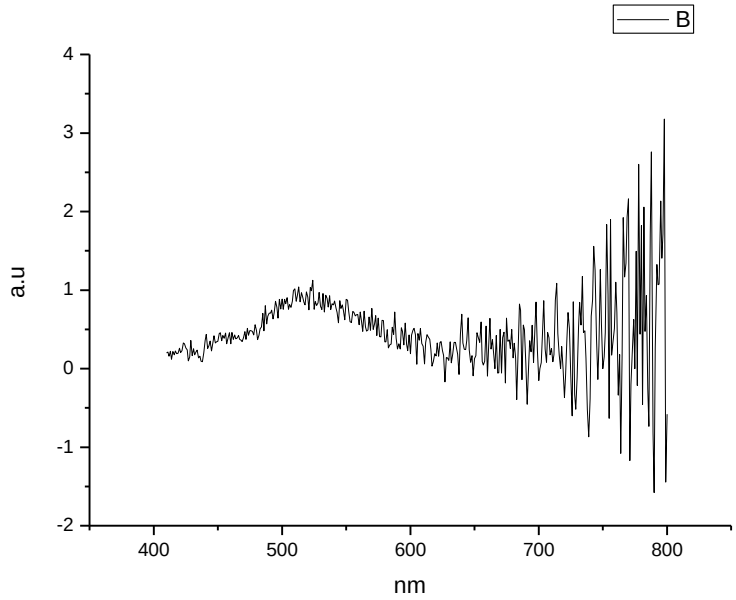

Figure 2.1.184. Fluorescence emission spectrum of **11a** recorded in Acetonitrile at 400 nm excitation.

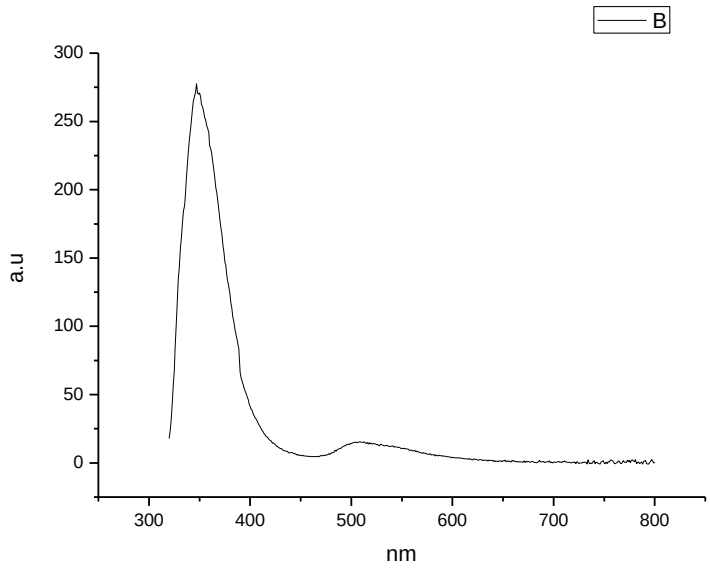

Figure 2.1.185. Fluorescence emission spectrum of **11a** recorded in 1-octanol at 310 nm excitation.

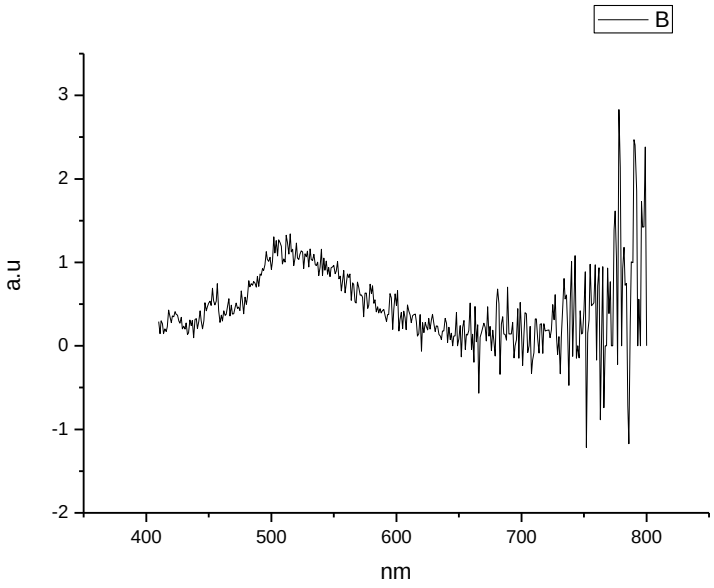

Figure 2.1.186. Fluorescence emission spectrum of **11a** recorded in 1-octanol at 400 nm excitation.

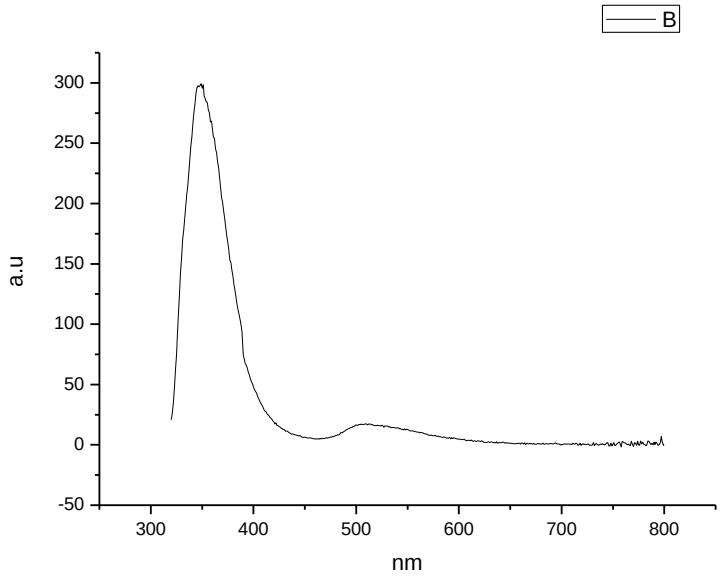

Figure 2.1.187. Fluorescence emission spectrum of **11a** recorded in 1-hexanol at 310 nm excitation.

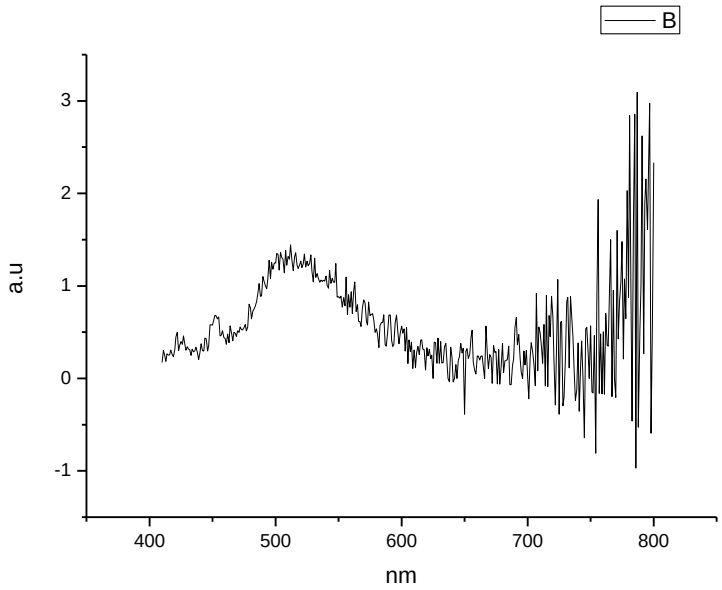

Figure 2.1.188. Fluorescence emission spectrum of **11a** recorded in 1-hexanol at 400 nm excitation.

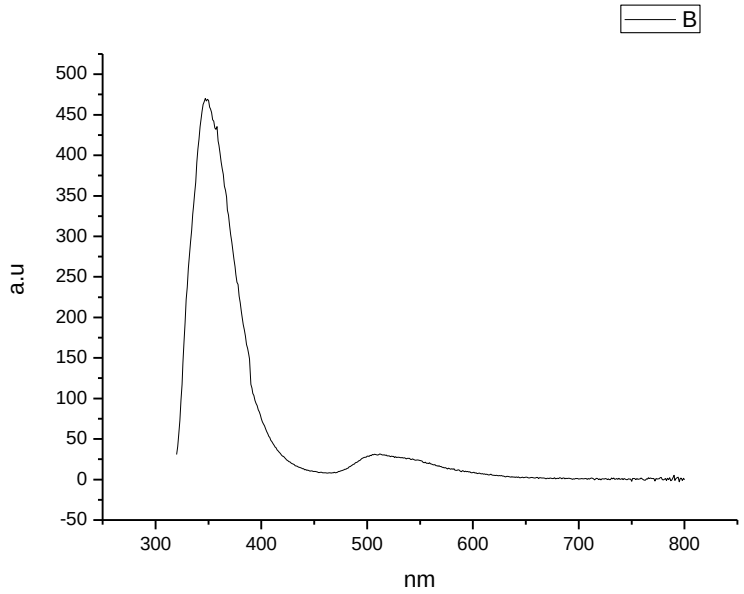

Figure 2.1.189. Fluorescence emission spectrum of **11a** recorded in 1-butanol at 310 nm excitation.

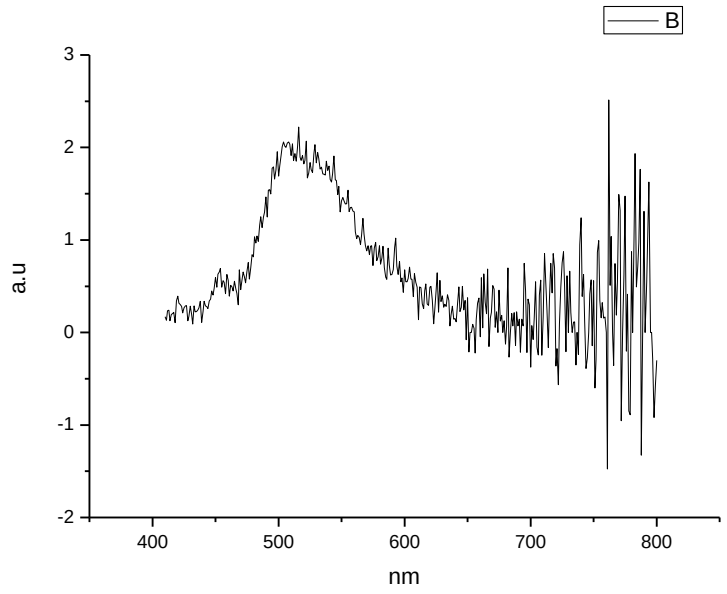

Figure 2.1.190. Fluorescence emission spectrum of **11a** recorded in 1-butanol at 400 nm excitation.

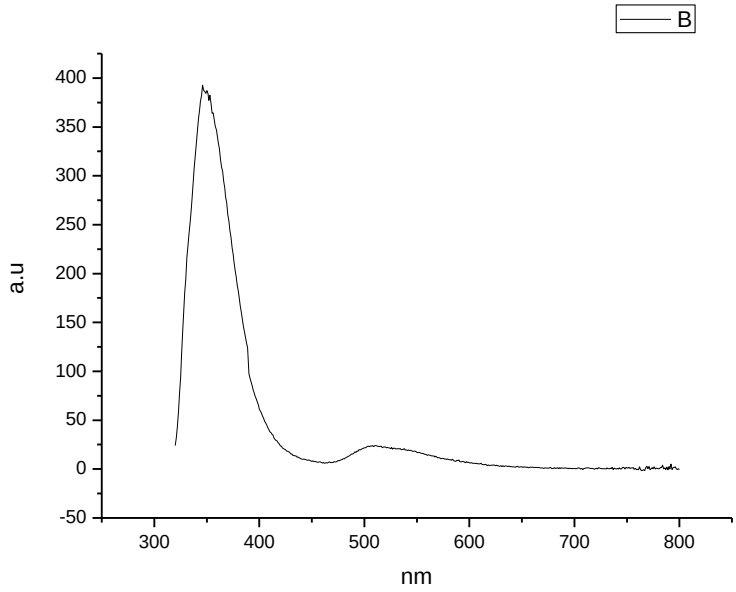

Figure 2.1.191. Fluorescence emission spectrum of **11a** recorded in 1-pentanol at 310 nm excitation.

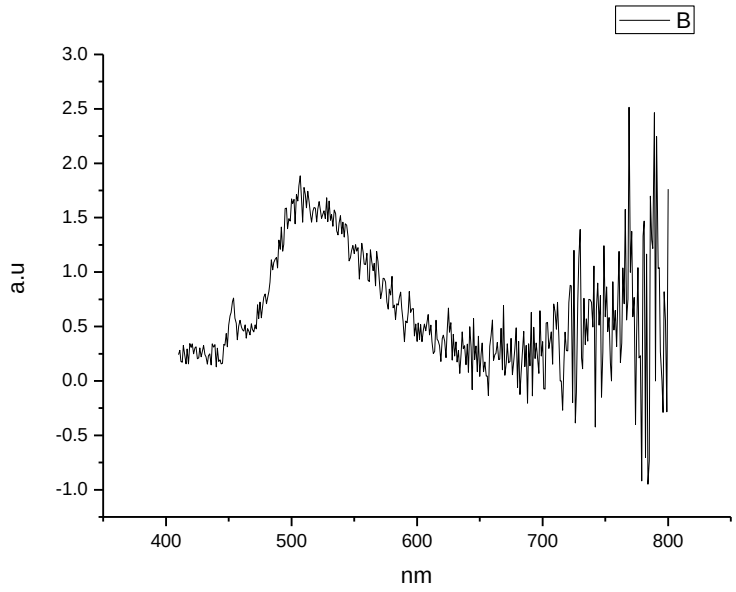

Figure 2.1.192. Fluorescence emission spectrum of **11a** recorded in 1-pentanol at 400 nm excitation.

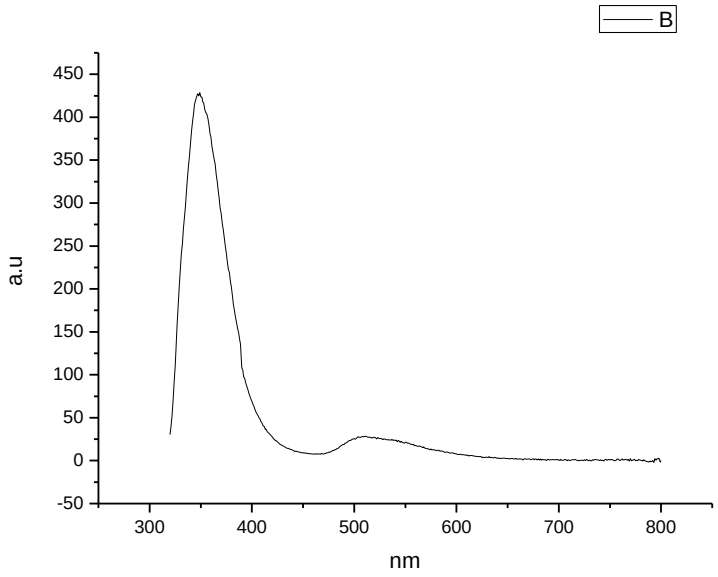

Figure 2.1.193. Fluorescence emission spectrum of **11a** recorded in 1-propanol at 310 nm excitation.

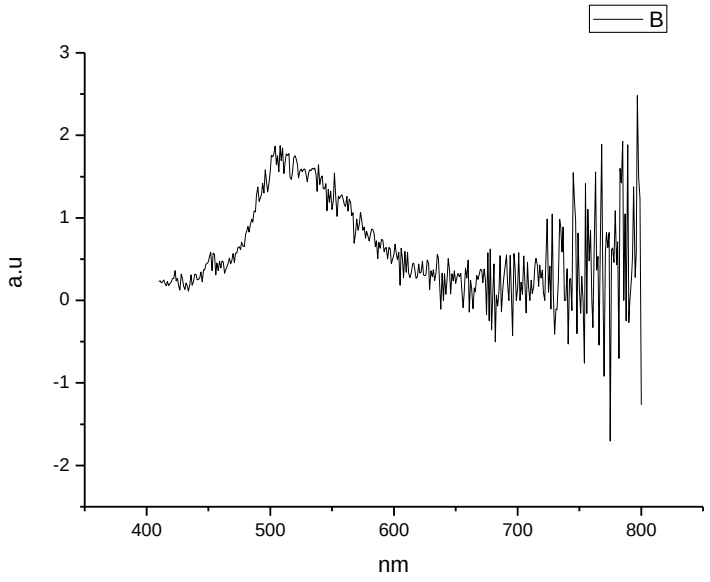

Figure 2.1.194. Fluorescence emission spectrum of **11a** recorded in 1-propanol at 400 nm excitation.

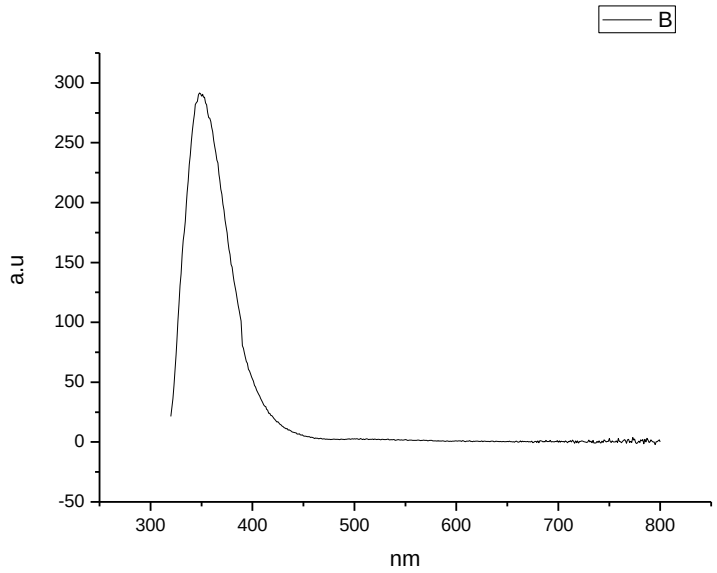

Figure 2.1.195. Fluorescence emission spectrum of **11a** recorded in Acetic Acid at 310 nm excitation.

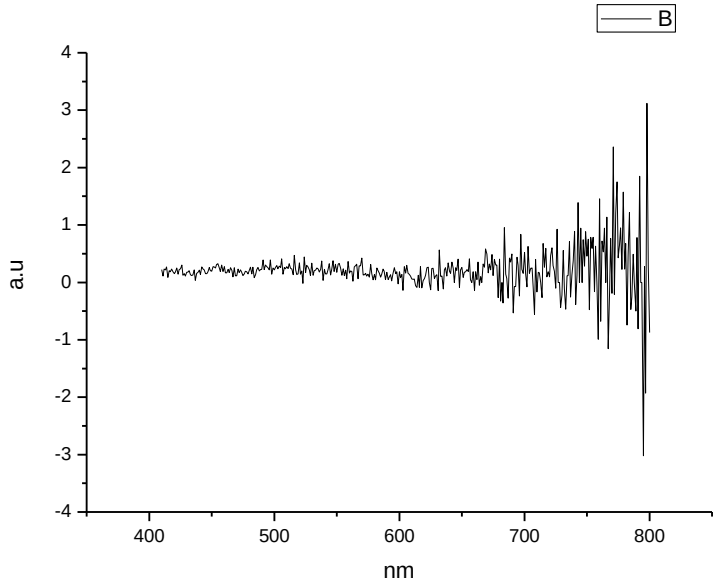

Figure 2.1.196. Fluorescence emission spectrum of **11a** recorded in Acetic Acid at 400 nm excitation.

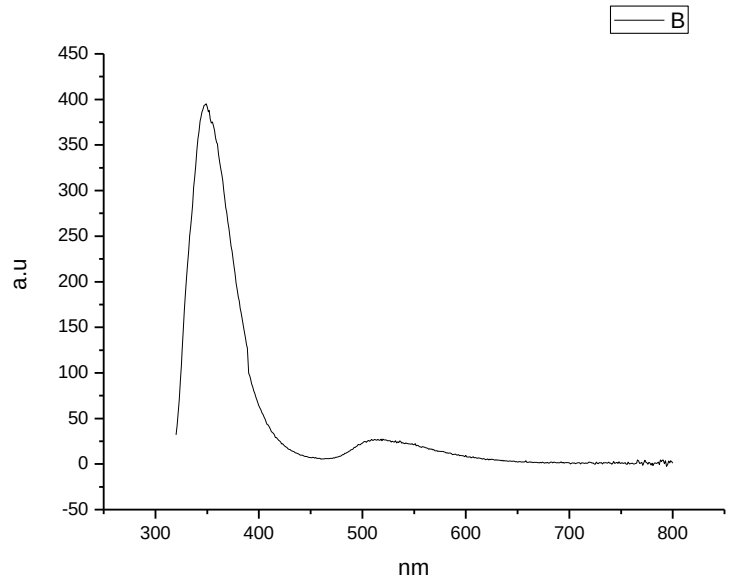

Figure 2.1.197. Fluorescence emission spectrum of **11a** recorded in Methanol at 310 nm excitation.

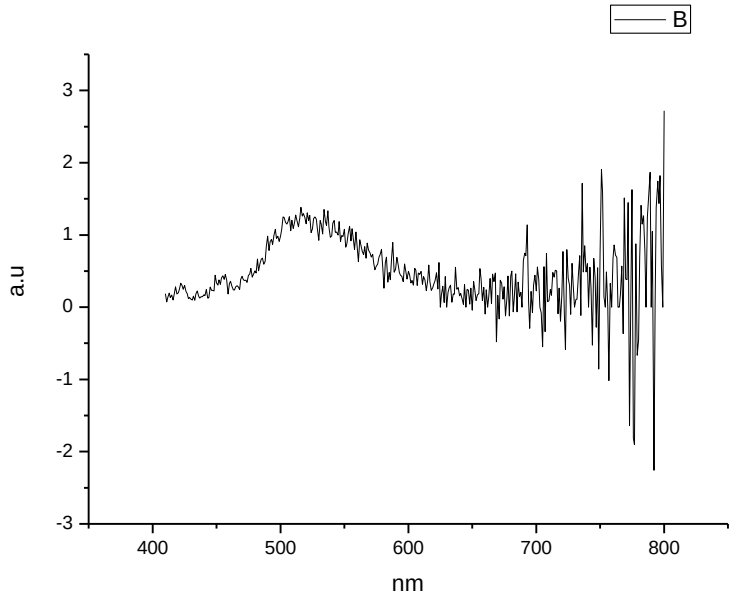

Figure 2.1.198. Fluorescence emission spectrum of **11a** recorded in Methanol at 400 nm excitation.

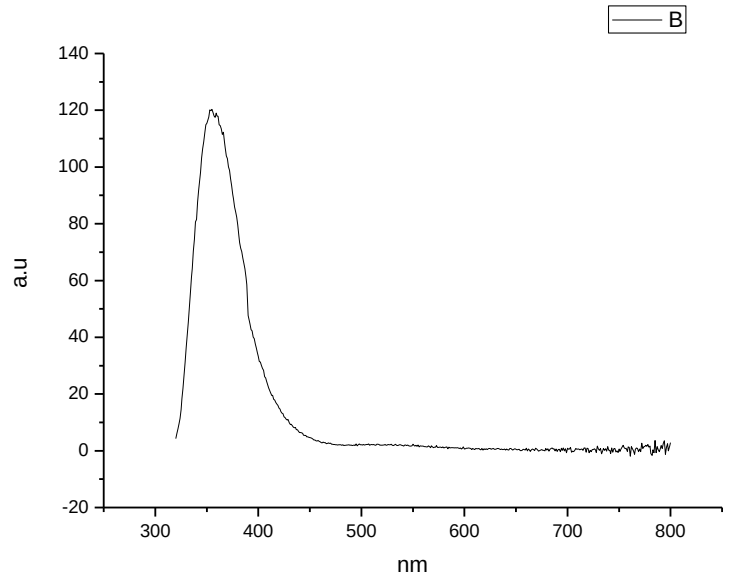

Figure 2.1.199. Fluorescence emission spectrum of **11a** recorded in 2,2,2-trifluoroethanol at 310 nm excitation.

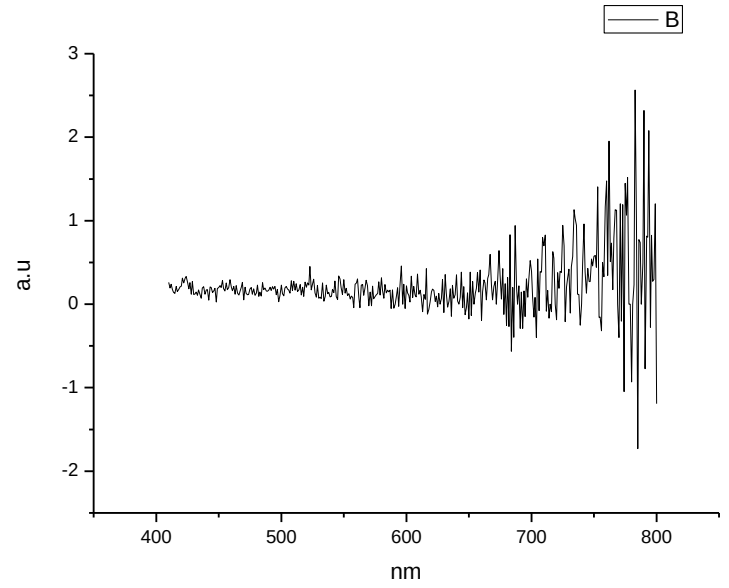

Figure 2.1.200. Fluorescence emission spectrum of **11a** recorded in 2,2,2-trifluoroethanol at 400 nm excitation.

2.1.12 Normalised Fluorescence Emission spectra (Gaussian fitted).

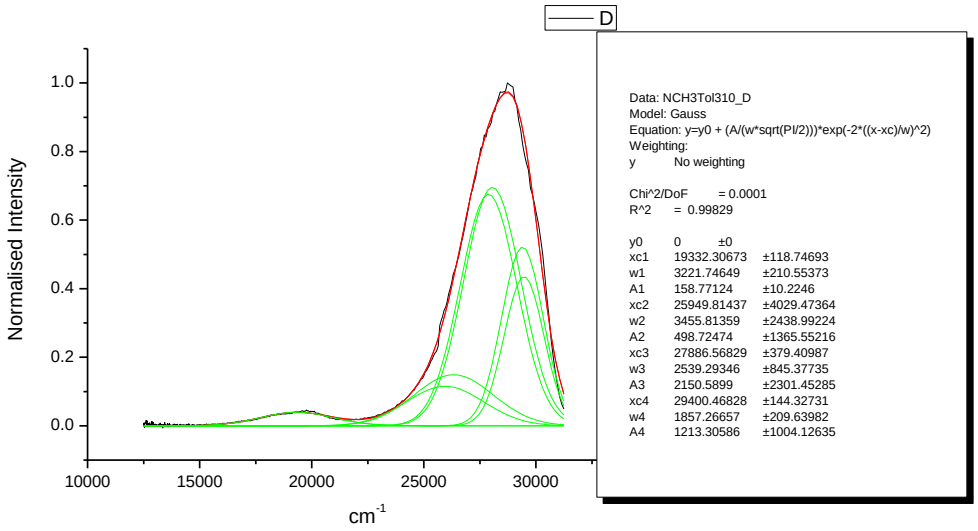

Figure 2.1.201. Gaussian model fit of the normalised fluorescence emission spectrum of **11a** recorded in Toluene at 310 nm excitation.

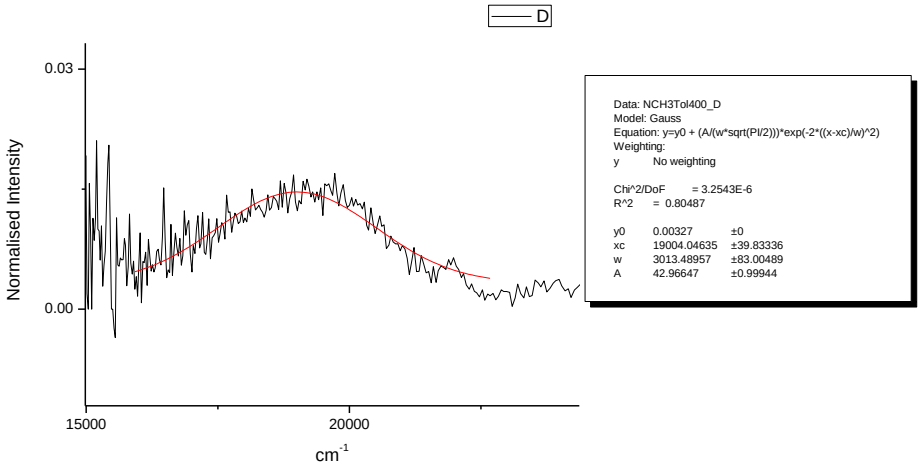

Figure 2.1.202. Gaussian model fit of the normalised fluorescence emission spectrum of **11a** recorded in Toluene at 400 nm excitation.

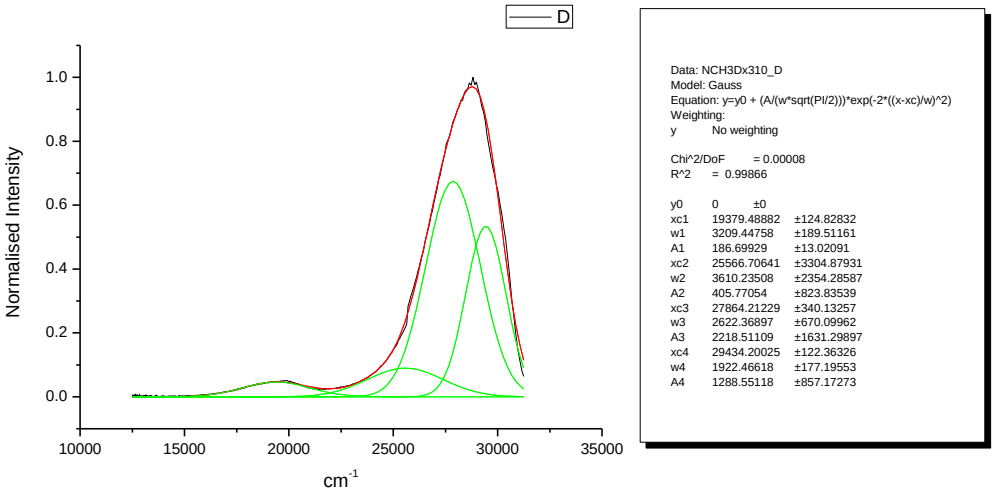

Figure 2.1.203. Gaussian model fit of the normalised fluorescence emission spectrum of **11a** recorded in 1,4-dioxane at 310 nm excitation.

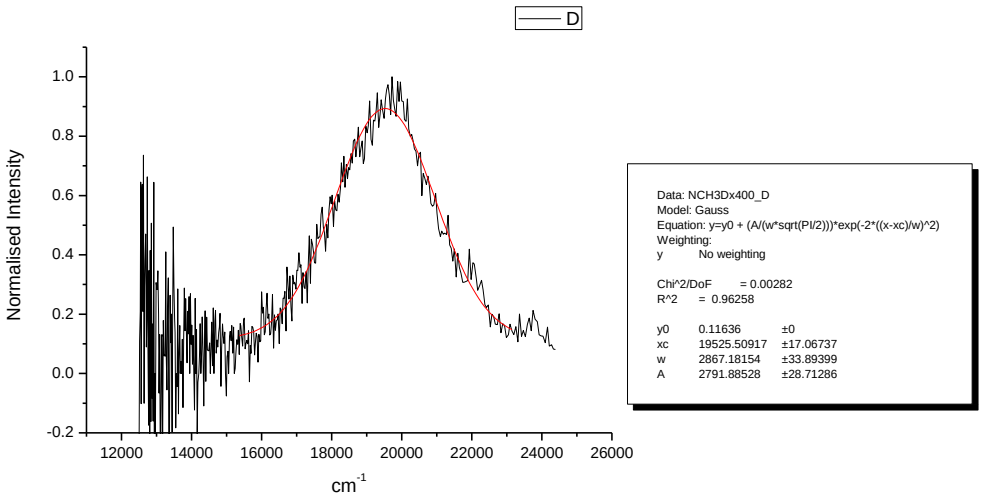

Figure 2.1.204. Gaussian model fit of the normalised fluorescence emission spectrum of **11a** recorded in 1,4-dioxane at 400 nm excitation.

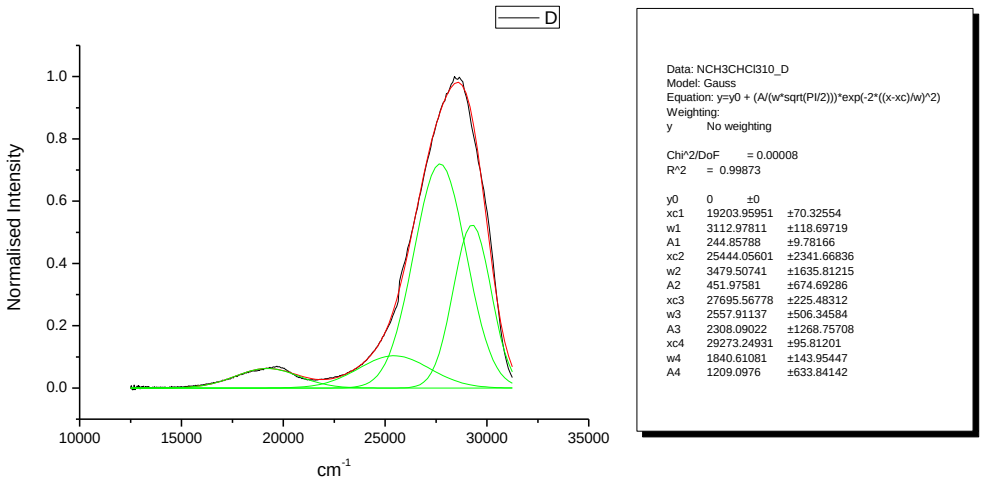

Figure 2.1.205. Gaussian model fit of the normalised fluorescence emission spectrum of **11a** recorded in Chloroform at 310 nm excitation.

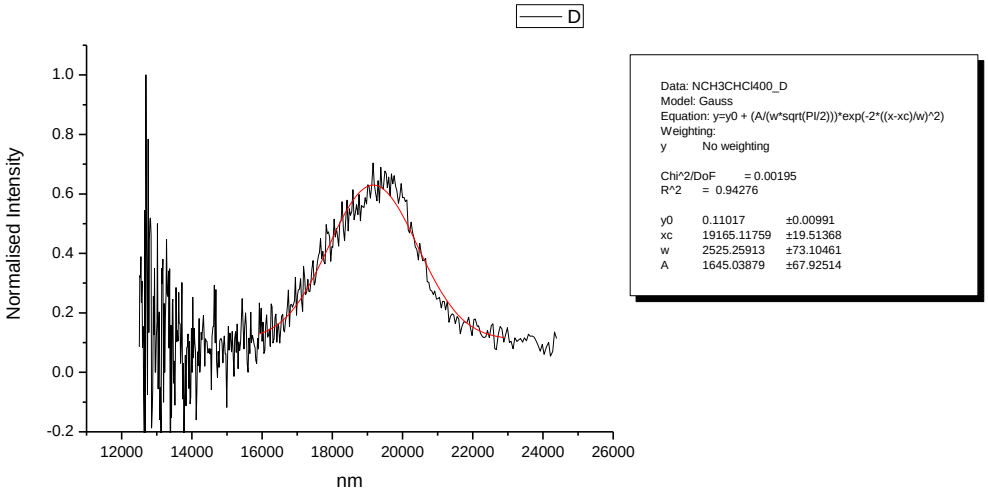

Figure 2.1.206. Gaussian model fit of the normalised fluorescence emission spectrum of **11a** recorded in Chloroform at 400 nm excitation.

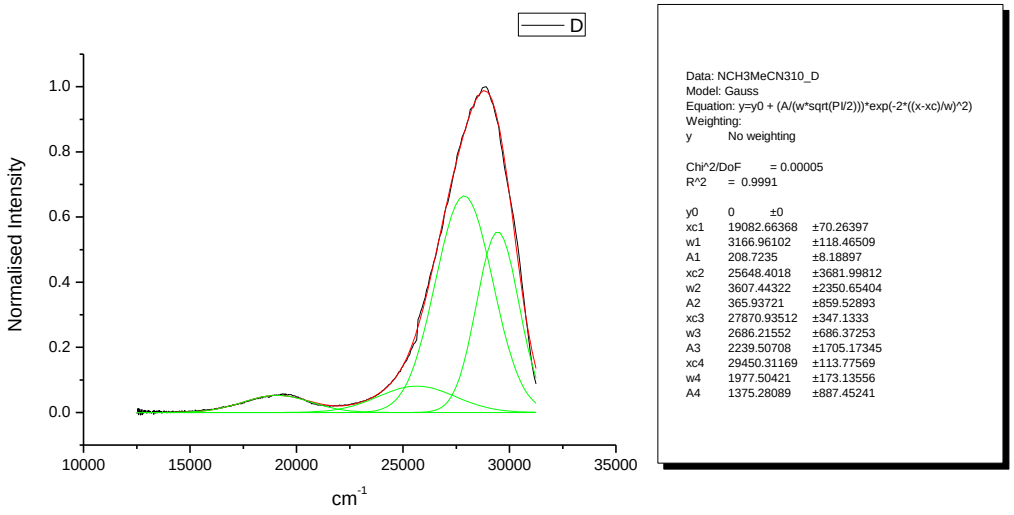

Figure 2.1.207. Gaussian model fit of the normalised fluorescence emission spectrum of **11a** recorded in Acetonitrile at 310 nm excitation.

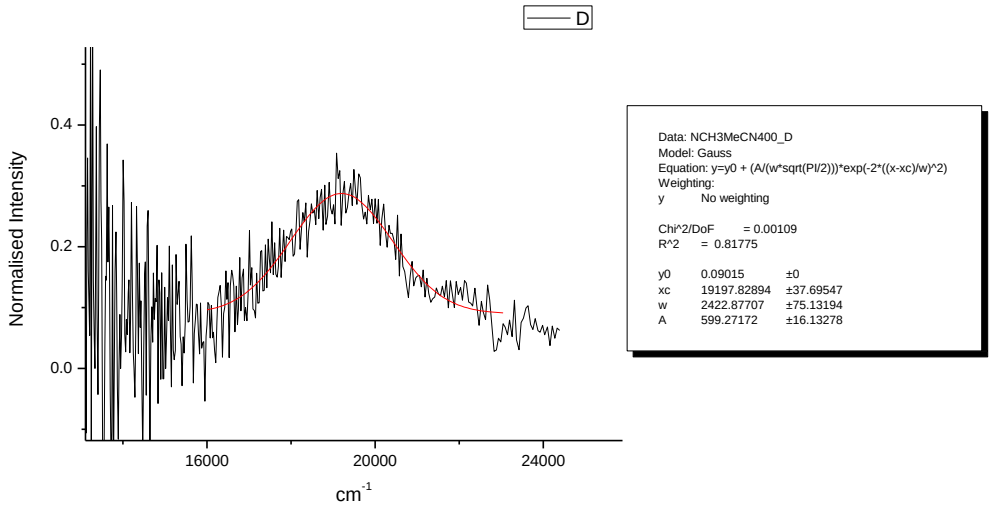

Figure 2.1.208. Gaussian model fit of the normalised fluorescence emission spectrum of **11a** recorded in Acetonitrile at 400 nm excitation.

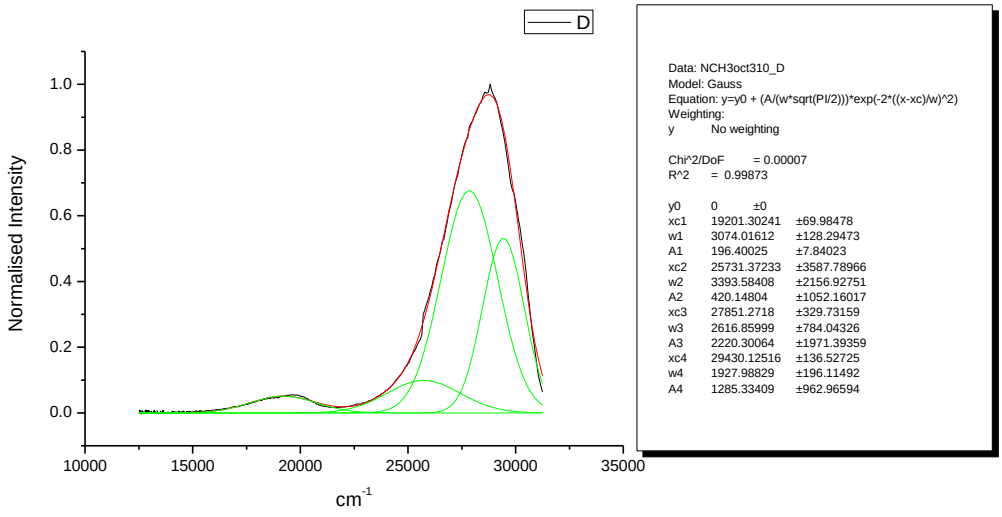

Figure 2.1.209. Gaussian model fit of the normalised fluorescence emission spectrum of **11a** recorded in 1-octanol at 310 nm excitation.

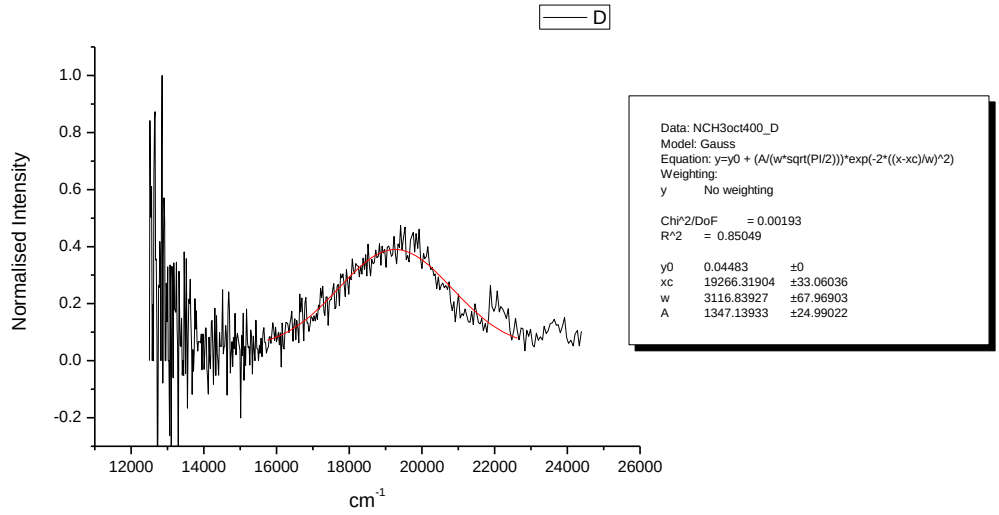

Figure 2.1.210. Gaussian model fit of the normalised fluorescence emission spectrum of **11a** recorded in 1-octanol at 400 nm excitation.

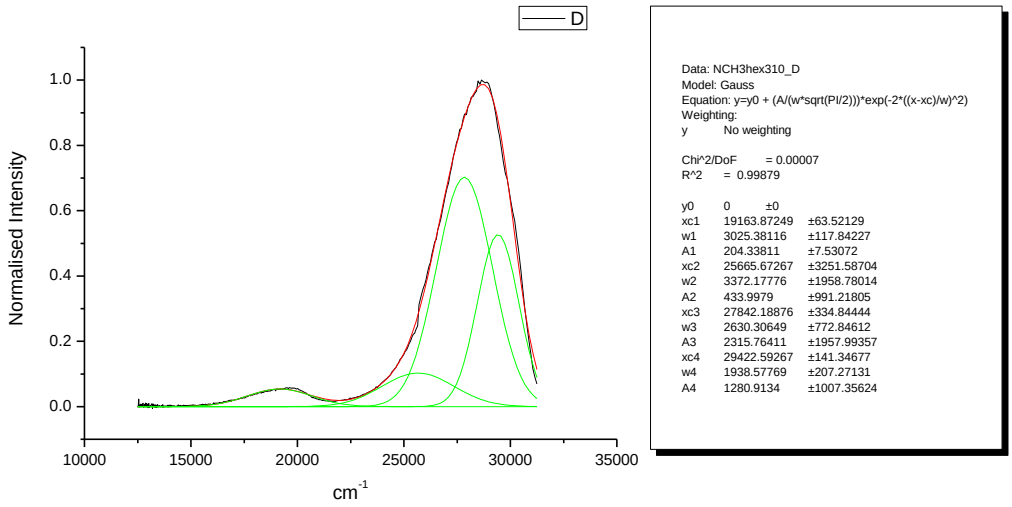

Figure 2.1.211. Gaussian model fit of the normalised fluorescence emission spectrum of **11a** recorded in 1-hexanol at 310 nm excitation.

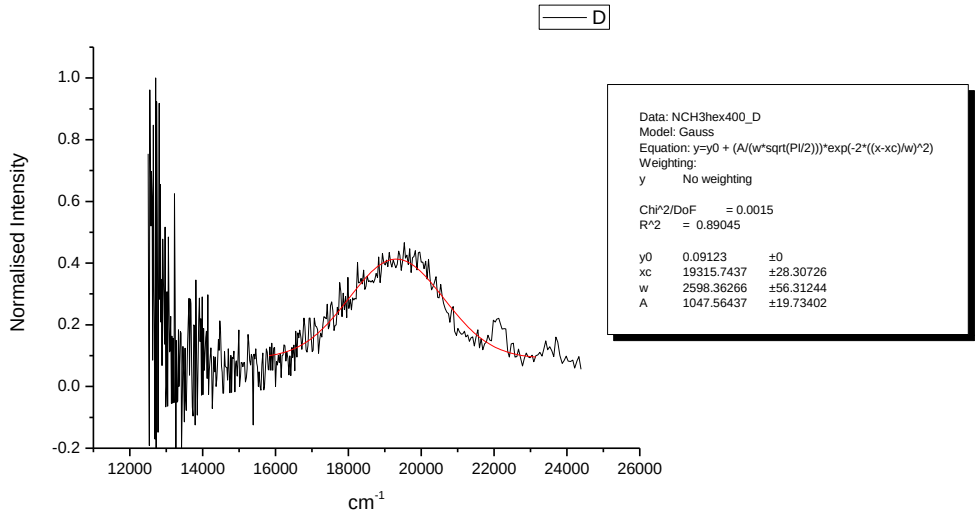

Figure 2.1.212. Gaussian model fit of the normalised fluorescence emission spectrum of **11a** recorded in 1-hexanol at 400 nm excitation.

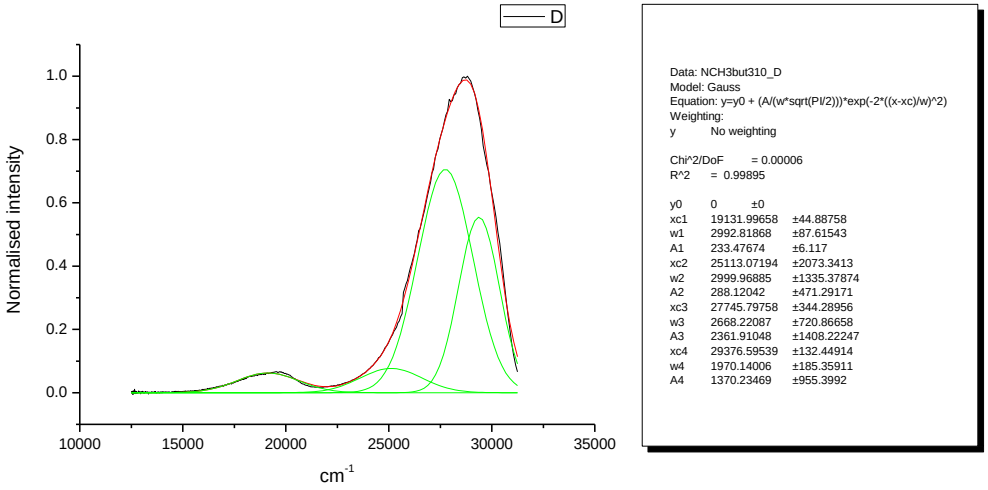

Figure 2.1.213. Gaussian model fit of the normalised fluorescence emission spectrum of **11a** recorded in 1-butanol at 310 nm excitation.

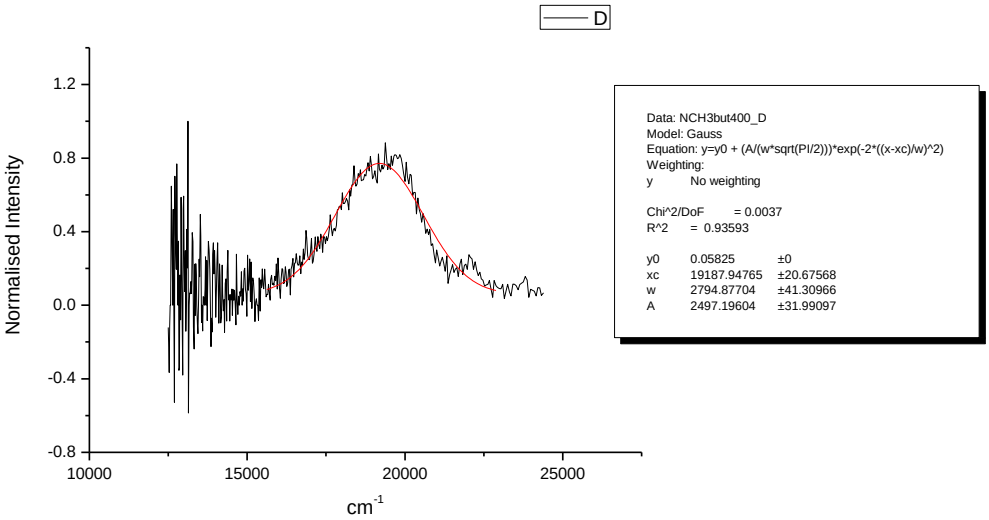

Figure 2.1.214. Gaussian model fit of the normalised fluorescence emission spectrum of **11a** recorded in 1-butanol at 400 nm excitation.

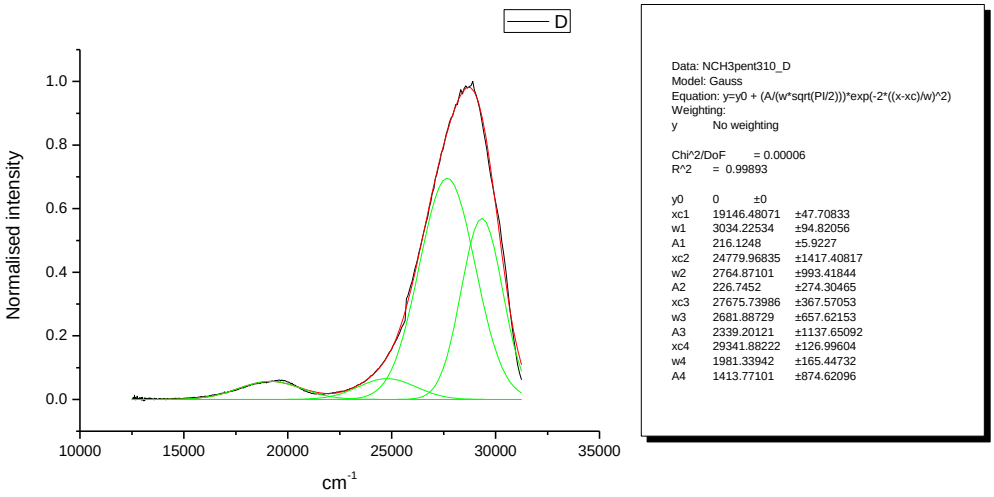

Figure 2.1.215. Gaussian model fit of the normalised fluorescence emission spectrum of **11a** recorded in 1-pentanol at 310 nm excitation.

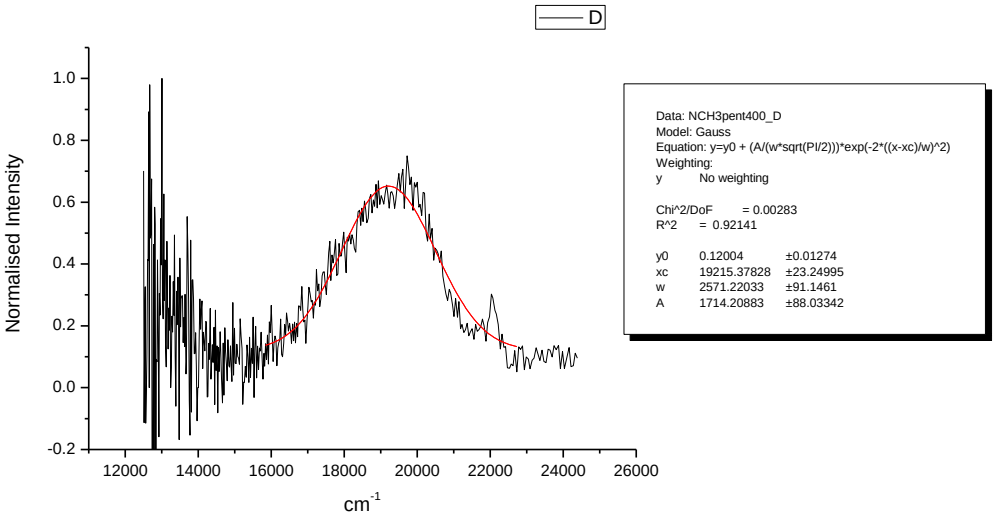

Figure 2.1.216. Gaussian model fit of the normalised fluorescence emission spectrum of **11a** recorded in 1-pentanol at 400 nm excitation.

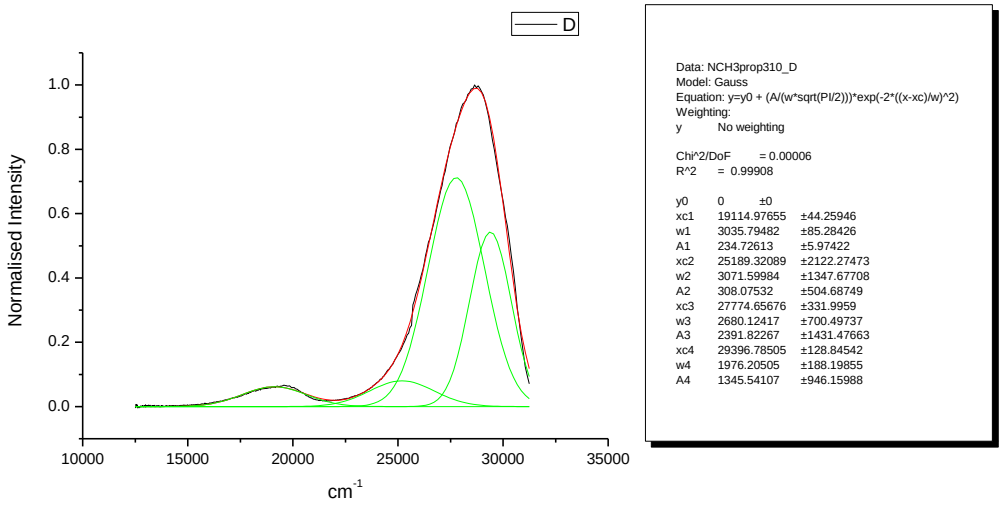

Figure 2.1.217. Gaussian model fit of the normalised fluorescence emission spectrum of **11a** recorded in 1-propanol at 310 nm excitation.

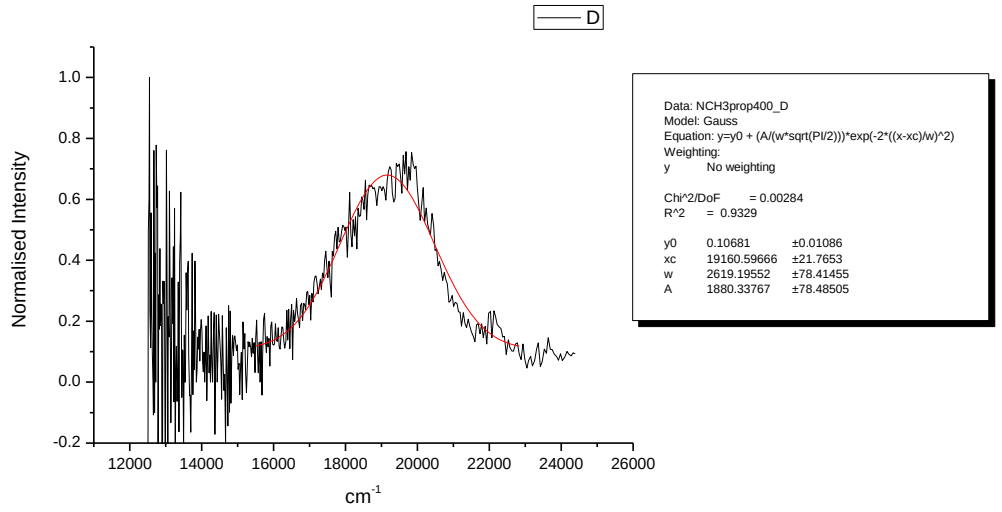

Figure 2.1.218. Gaussian model fit of the normalised fluorescence emission spectrum of **11a** recorded in 1-propanol at 400 nm excitation.

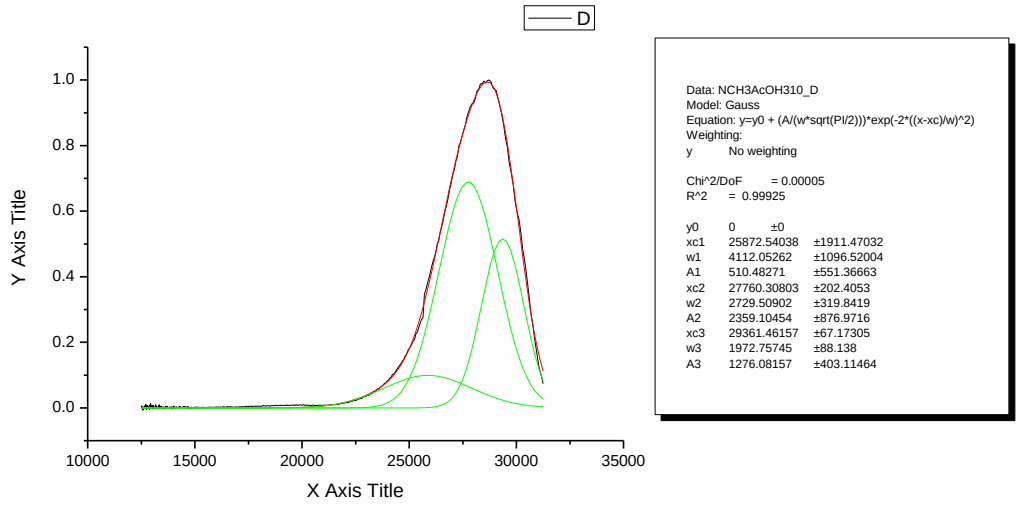

Figure 2.1.219. Gaussian model fit of the normalised fluorescence emission spectrum of **11a** recorded in Acetic Acid at 310 nm excitation.

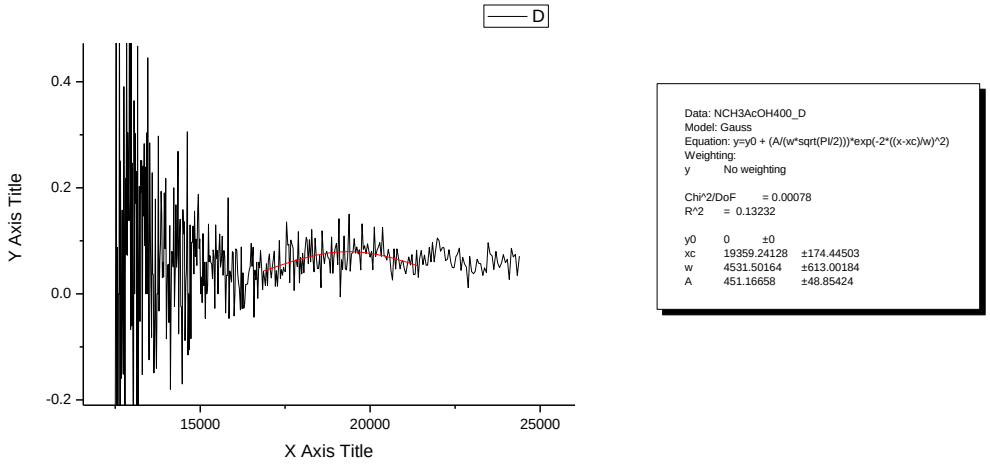

Figure 2.1.220. Gaussian model fit of the normalised fluorescence emission spectrum of **11a** recorded in Acetic Acid at 400 nm excitation.

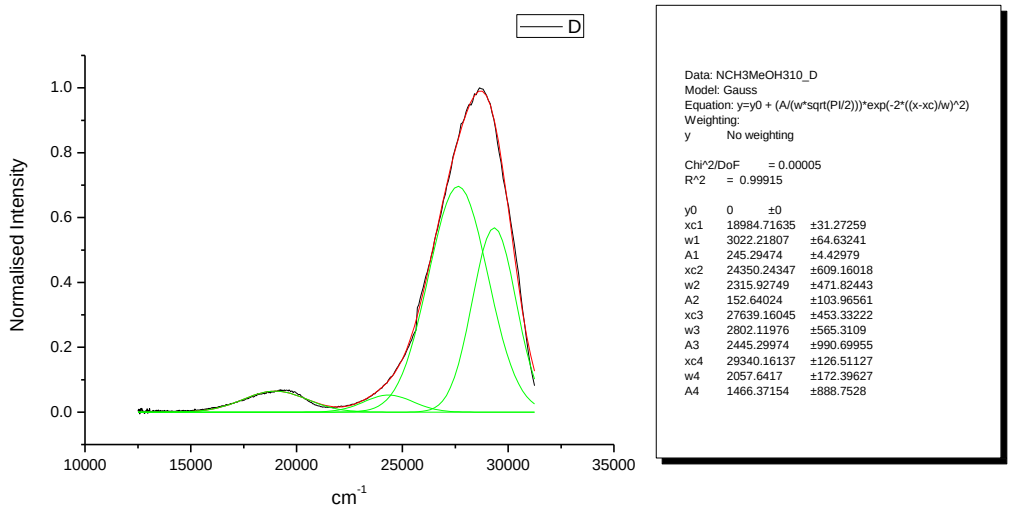

Figure 2.1.221. Gaussian model fit of the normalised fluorescence emission spectrum of **11a** recorded in Methanol at 310 nm excitation.

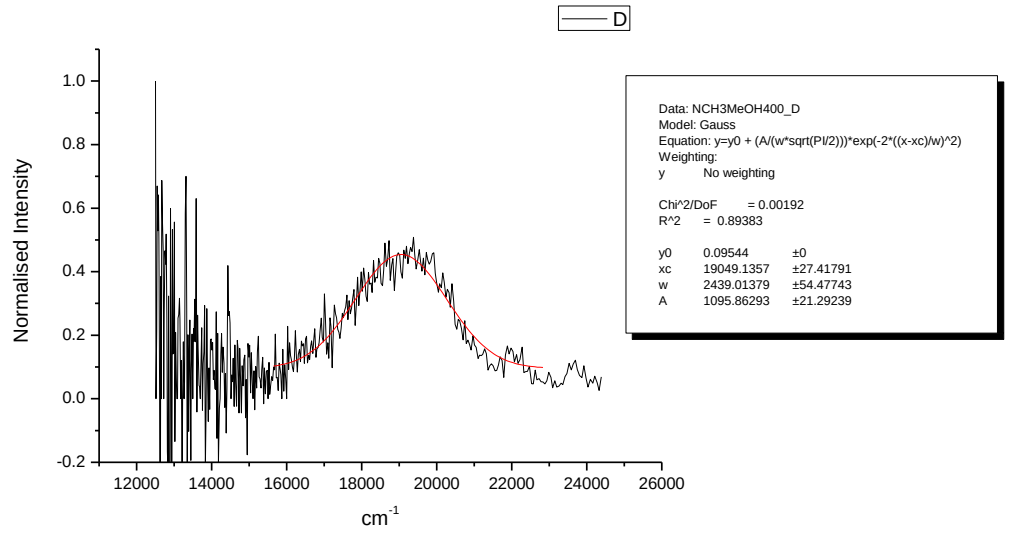

Figure 2.1.222. Gaussian model fit of the normalised fluorescence emission spectrum of **11a** recorded in Methanol at 400 nm excitation.

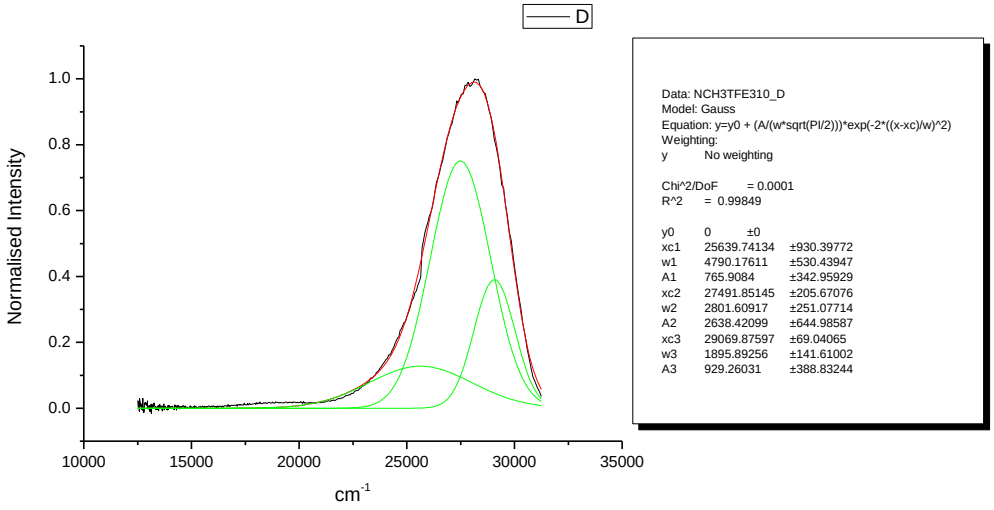

Figure 2.1.223. Gaussian model fit of the normalised fluorescence emission spectrum of **11a** recorded in 2,2,2-trifluoroethanol at 310 nm excitation.

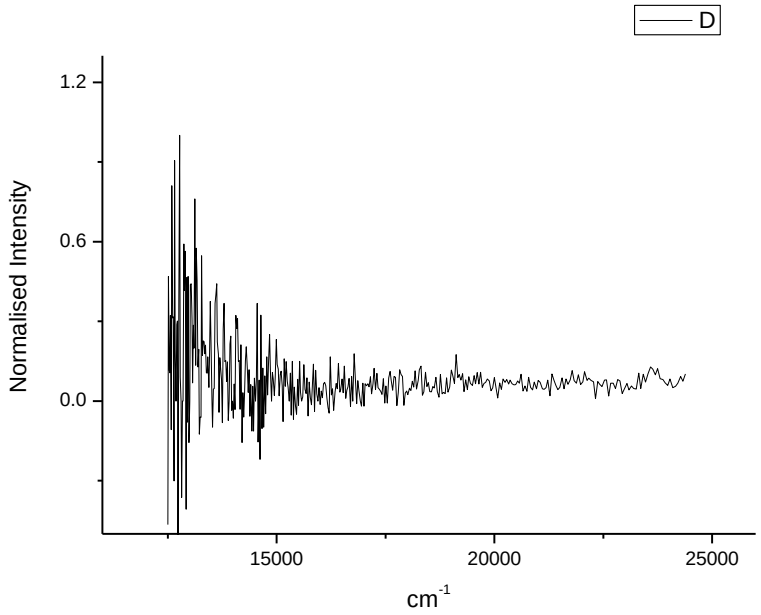

Figure 2.1.224. Attempted gaussian model fit of the normalised fluorescence emission spectrum of **11a** recorded in 2,2,2-trifluoroethanol at 400 nm excitation.

2.1.13 Fluorescence Excitation spectra.

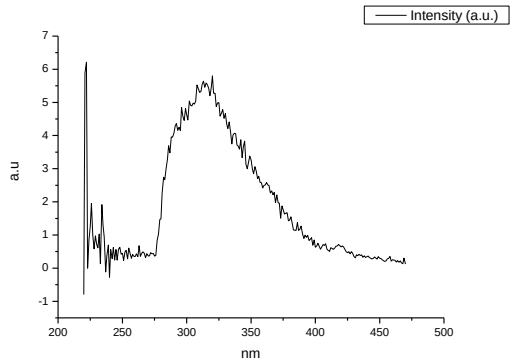

Figure 2.1.225. Fluorescence excitation spectrum of **11a** recorded in Toluene with emission fixed at 480 nm.

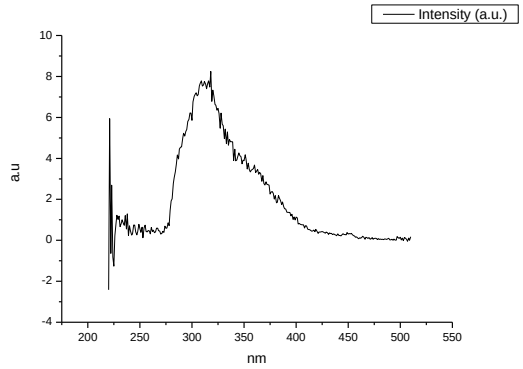

Figure 2.1.226. Fluorescence excitation spectrum of **11a** recorded in Toluene with emission fixed at 520 nm.

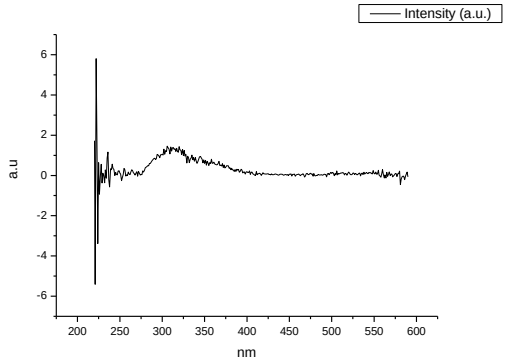

Figure 2.1.227. Fluorescence excitation spectrum of **11a** recorded in Toluene with emission fixed at 600 nm.

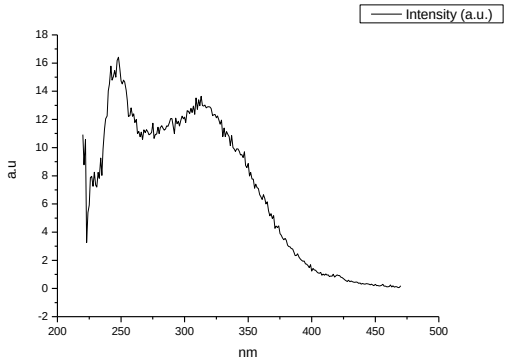

Figure 2.1.228. Fluorescence excitation spectrum of **11a** recorded in 1,4-dioxane with emission fixed at 480 nm.

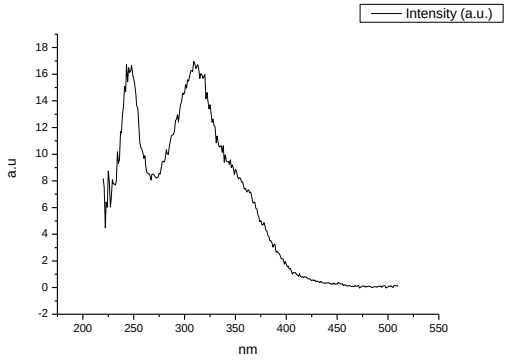

Figure 2.1.229. Fluorescence excitation spectrum of **11a** recorded in 1,4-dioxane with emission fixed at 520 nm.

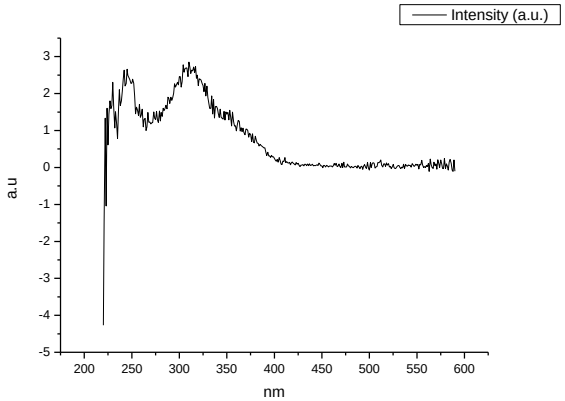

Figure 2.1.230. Fluorescence excitation spectrum of **11a** recorded in 1,4-dioxane with emission fixed at 600 nm.

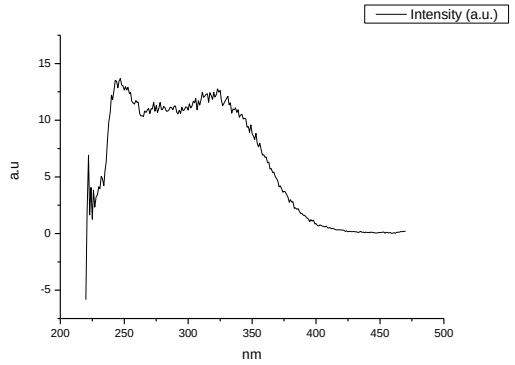

Figure 2.1.231. Fluorescence excitation spectrum of **11a** recorded in Chloroform with emission fixed at 480 nm.

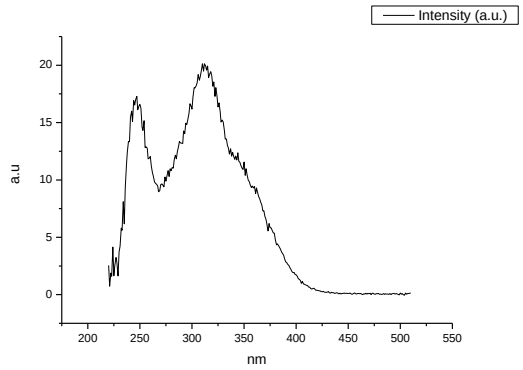

Figure 2.1.232. Fluorescence excitation spectrum of **11a** recorded in Chloroform with emission fixed at 520 nm.

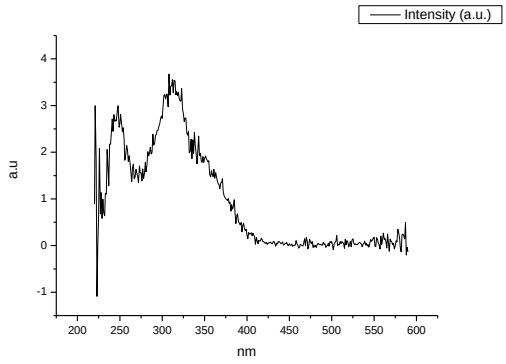

Figure 2.1.233. Fluorescence excitation spectrum of **11a** recorded in Chloroform with emission fixed at 600 nm.

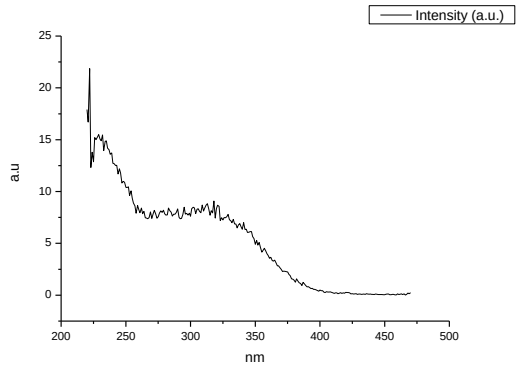

Figure 2.1.234. Fluorescence excitation spectrum of **11a** recorded in Acetonitrile with emission fixed at 480 nm.

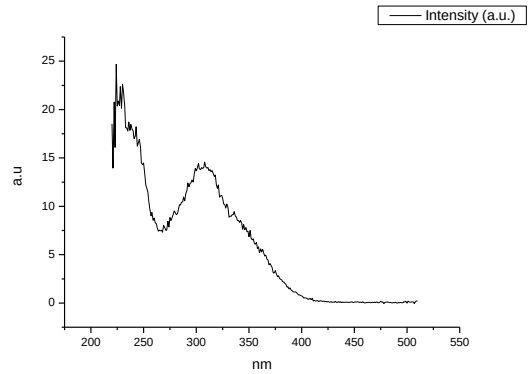

Figure 2.1.235. Fluorescence excitation spectrum of **11a** recorded in Acetonitrile with emission fixed at 520 nm.

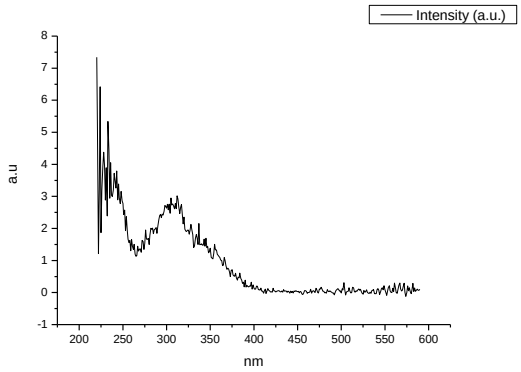

Figure 2.1.236. Fluorescence excitation spectrum of **11a** recorded in Acetonitrile with emission fixed at 600 nm.

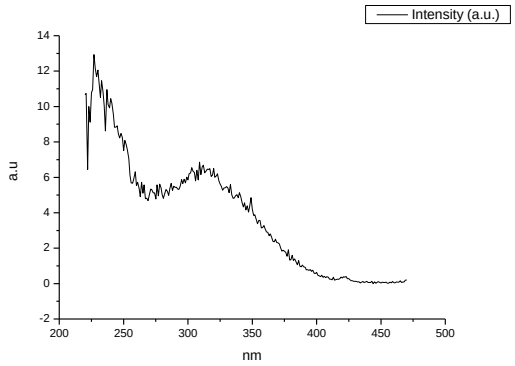

Figure 2.1.237. Fluorescence excitation spectrum of **11a** recorded in 1-octanol with emission fixed at 480 nm.

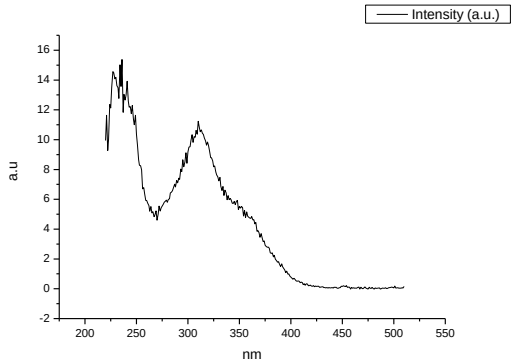

Figure 2.1.238. Fluorescence excitation spectrum of **11a** recorded in 1-octanol with emission fixed at 520 nm.

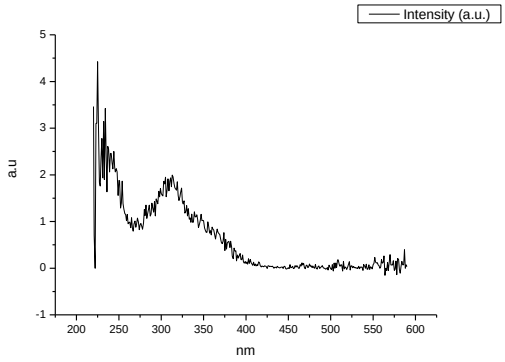

Figure 2.1.239. Fluorescence excitation spectrum of **11a** recorded in 1-octanol with emission fixed at 600 nm.

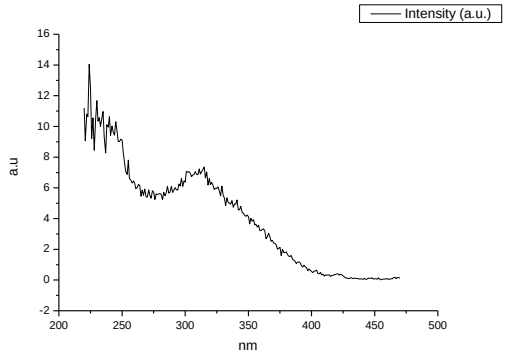

Figure 2.1.240. Fluorescence excitation spectrum of **11a** recorded in 1-hexanol with emission fixed at 480 nm.

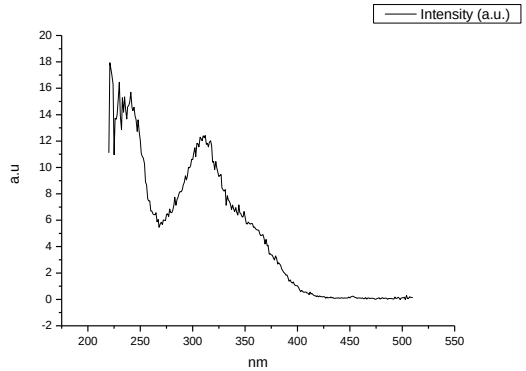

Figure 2.1.241. Fluorescence excitation spectrum of **11a** recorded in 1-hexanol with emission fixed at 520 nm.

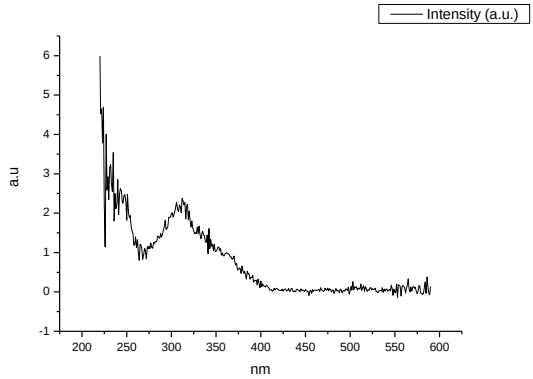

Figure 2.1.242. Fluorescence excitation spectrum of **11a** recorded in 1-hexanol with emission fixed at 600 nm.

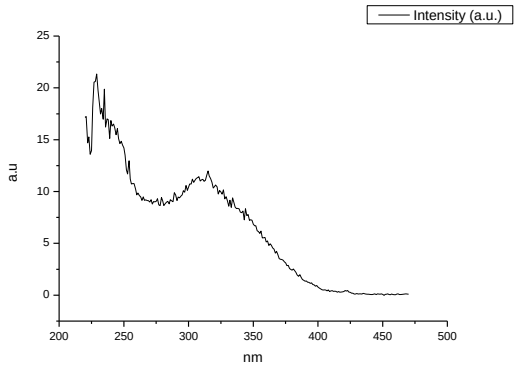

Figure 2.1.243. Fluorescence excitation spectrum of **11a** recorded in 1-butanol with emission fixed at 480 nm.

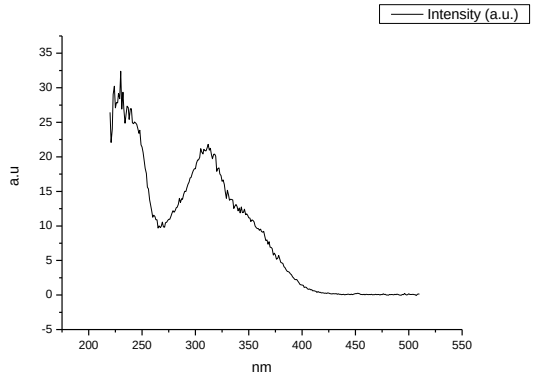

Figure 2.1.244. Fluorescence excitation spectrum of **11a** recorded in 1-butanol with emission fixed at 520 nm.

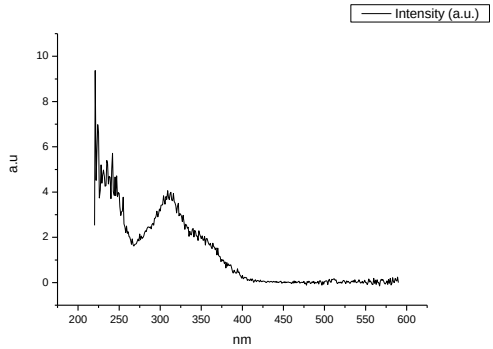

Figure 2.1.245. Fluorescence excitation spectrum of **11a** recorded in 1-butanol with emission fixed at 600 nm.

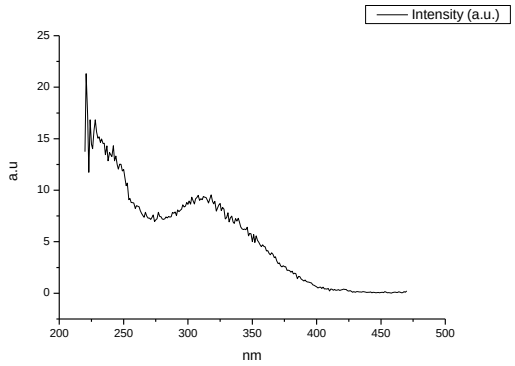

Figure 2.1.246. Fluorescence excitation spectrum of **11a** recorded in 1-pentanol with emission fixed at 480 nm.

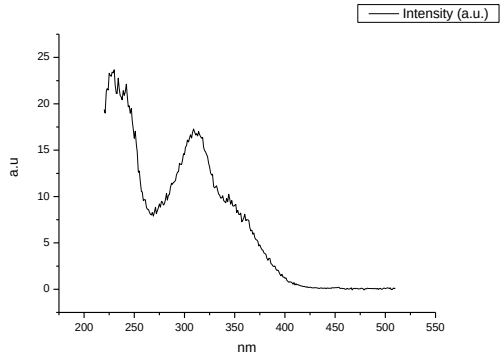

Figure 2.1.247. Fluorescence excitation spectrum of **11a** recorded in 1-pentanol with emission fixed at 520 nm.

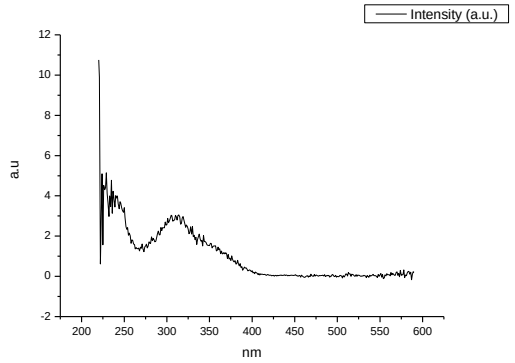

Figure 2.1.248. Fluorescence excitation spectrum of **11a** recorded in 1-pentanol with emission fixed at 600 nm.

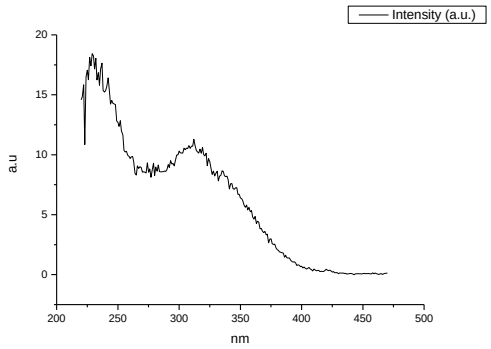

Figure 2.1.249. Fluorescence excitation spectrum of **11a** recorded in 1-propanol with emission fixed at 480 nm.

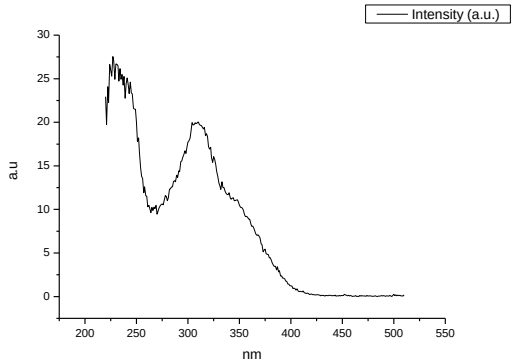

Figure 2.1.250. Fluorescence excitation spectrum of **11a** recorded in 1-propanol with emission fixed at 520 nm.

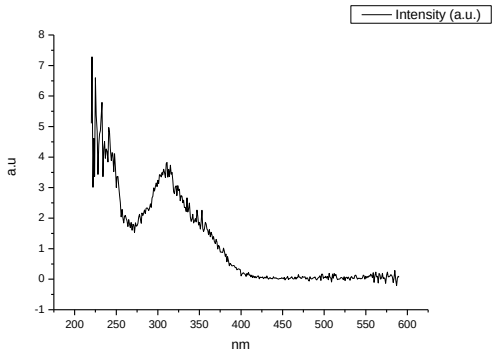

Figure 2.1.251. Fluorescence excitation spectrum of **11a** recorded in 1-propanol with emission fixed at 600 nm.

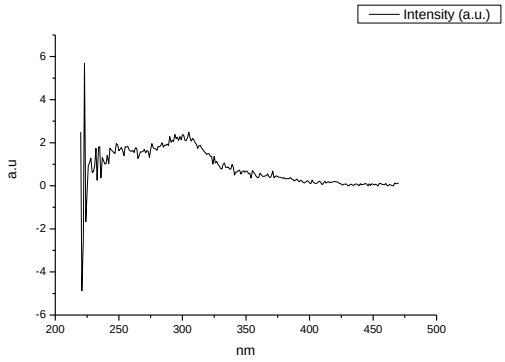

Figure 2.1.252. Fluorescence excitation spectrum of **11a** recorded in Acetic Acid with emission fixed at 480 nm.

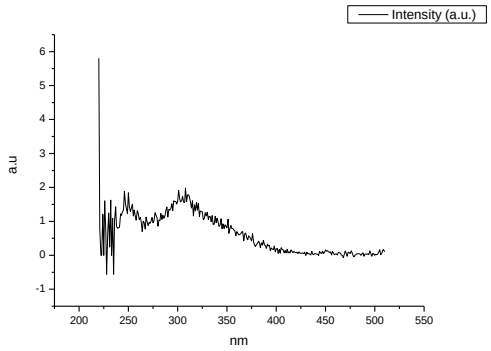

Figure 2.1.253. Fluorescence excitation spectrum of **11a** recorded in Acetic Acid with emission fixed at 520 nm.

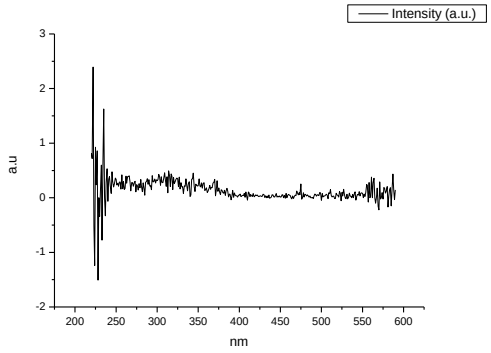

Figure 2.1.254. Fluorescence excitation spectrum of **11a** recorded in Acetic Acid with emission fixed at 600 nm.

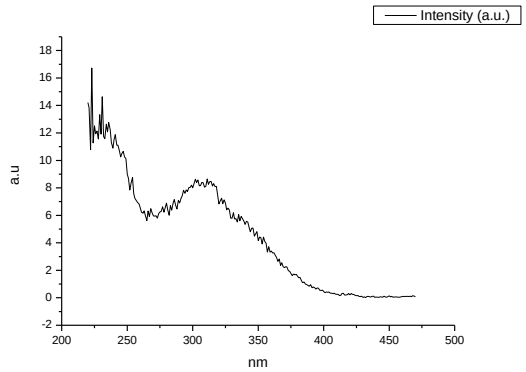

Figure 2.1.255. Fluorescence excitation spectrum of **11a** recorded in Methanol with emission fixed at 480 nm.

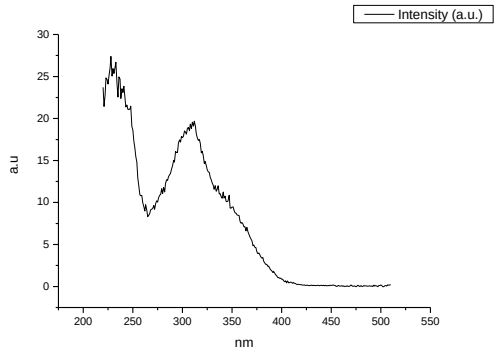

Figure 2.1.256. Fluorescence excitation spectrum of **11a** recorded in Methanol with emission fixed at 520 nm.

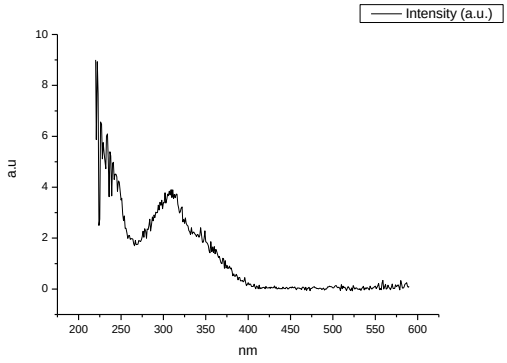

Figure 2.1.257. Fluorescence excitation spectrum of **11a** recorded in Methanol with emission fixed at 600 nm.

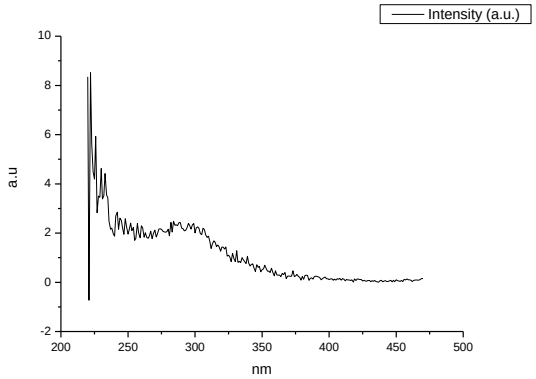

Figure 2.1.258. Fluorescence excitation spectrum of **11a** recorded in 2,2,2-trifluoroethanol with emission fixed at 480 nm.

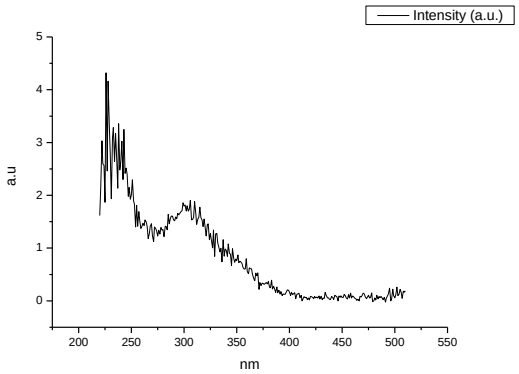

Figure 2.1.259. Fluorescence excitation spectrum of **11a** recorded in 2,2,2-trifluoroethanol with emission fixed at 520 nm.

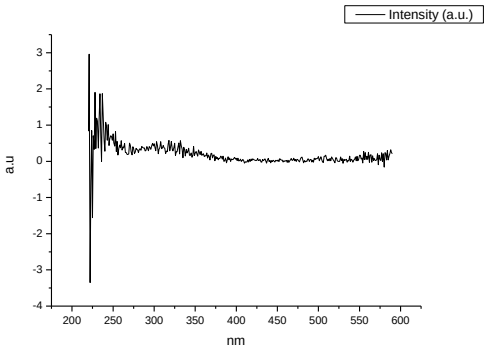

Figure 2.1.260. Fluorescence excitation spectrum of **11a** recorded in 2,2,2-trifluoroethanol with emission fixed at 600 nm.

2.2 COMPOUND 12

2.2.1 Quantum Yield Summary.

Solvent	abs (310 nm)	$\lambda_{ems\ (max)}$	$\Phi_{310\ nm}$	abs (400 nm)	$\lambda_{ems\ (max)}$	$\Phi_{400\ nm}$
Toluene	0.09	501.04	0.01	0.04	509.94	0.00
1,4-Dioxane	0.07	485.07	0.01	0.01	504.24	0.01
Chloroform	0.08	515.07	0.01	0.01	-	0.02
Acetonitrile	0.06	508.95	0.01	0.01	519.58	0.01
1-Octanol	0.04	504.02	0.01	0.01	519.42	0.02
1-Hexanol	0.03	339.07	0.05	0.00	-	0.02
1-Butanol	0.07	510.00	0.01	0.01	511.81	0.01
1-Pentanol	0.05	501.94	0.01	0.01	510.23	0.01
1-Propanol	0.07	508.95	0.01	0.01	506.27	0.01
Acetic acid	0.06	793.01	0.00	0.01	520.48	0.01
Methanol	0.07	511.94	0.01	0.01	523.49	0.01
2,2,2-Trifluoroethanol	0.04	535.07	0.01	0.01	528.25	0.01

Table 2.2.1. Summary of ultraviolet-visible absorbance values at 310 nm and 400 nm, emission maxima and quantum yield (Φ) of **12** at 310 nm and 400 nm excitation.

2.2.2 310 nm excitation Gaussian band fit summaries.

Solvent	λ max$_{em}$ Band 1 (cm^{-1})	λ max$_{em}$ Band 1 (nm)	λ max$_{em}$ Band 2 (cm^{-1})	λ max$_{em}$ Band 2 (nm)	λ max$_{em}$ Band 3 (cm^{-1})	λ max$_{em}$ Band 3 (nm)
Toluene	19608.14	509.99	20171.70	495.74	29542.89	338.49
1,4-Dioxane	19978.01	500.55	21000.86	476.17	29012.36	344.68
Chloroform	19507.76	512.62	19821.79	504.50	28090.77	355.99
Acetonitrile	19303.10	518.05	19783.22	505.48	28796.43	347.27
1-Octanol	19979.71	500.51	22019.65	454.14	29613.66	337.68
1-Hexanol	-	-	20077.22	498.08	27795.97	359.76
1-Butanol	19716.77	507.18	19954.37	501.14	28800.90	347.21
1-Pentanol	19817.32	504.61	19823.67	504.45	28634.79	349.23
1-Propanol	19523.57	512.20	19673.95	508.29	28803.29	347.18
Acetic acid	19979.05	500.52	-	-	28792.84	347.31
Methanol	19362.01	516.48	-	-	28429.23	351.75
2,2,2-Trifluoroethanol	19016.84	525.85	21805.82	458.59	23280.37	429.55

Solvent	λ max$_{em}$ Band 4 (cm^{-1})	λ max$_{em}$ Band 4 (nm)	λ max$_{em}$ Band 5 (cm^{-1})	λ max$_{em}$ Band 5 (nm)
Toluene	-	-	-	-
1,4-Dioxane	-	-	-	-
Chloroform	-	-	-	-
Acetonitrile	-	-	-	-
1-Octanol	-	-	-	-
1-Hexanol	30153.45	331.64	-	-
1-Butanol	-	-	-	-
1-Pentanol	-	-	-	-
1-Propanol	-	-	-	-
Acetic acid	-	-	-	-
Methanol	-	-	-	-
2,2,2-Trifluoroethanol	-	-	-	-

Table 2.2.1. Summary of band maxima of 5 band fit using Gaussian model for normalised **12** emission spectra recorded at 310 nm excitation.

(a)

Solvent	Width Band 1 (cm^{-1})	Width Band 2 (cm^{-1})	Width Band 3 (cm^{-1})	Width Band 4 (cm^{-1})	Width Band 5 (cm^{-1})
Toluene	3959.15	2221.07	5011.98	-	-
1,4-Dioxane	3001.79	9122.03	3061.89	-	-
Chloroform	4730.85	2597.76	5119.19	-	-
Acetonitrile	4818.74	2754.67	3757.45	-	-
1-Octanol	3324.99	8388.32	3473.76	-	-
1-Hexanol	-	4660.17	3882.76	2268.56	-
1-Butanol	3188.13	10950.42	2988.43	-	-
1-Pentanol	4347.28	2414.85	4010.26	-	-
1-Propanol	6818.83	3047.51	3110.57	-	-
Acetic acid	3254.11	-	3634.52	-	-
Methanol	3411.75	-	4322.83	-	-
2,2,2-Trifluoroethanol	2999.58	14457.83	3067.98	-	-

(b)

Solvent	Area Band 1 (cm^{-1})	Area Band 2 (cm^{-1})	Area Band 3 (cm^{-1})	Area Band 4 (cm^{-1})	Area Band 5 (cm^{-1})
Toluene	2665.34	1154.52	1844.63	-	-
1,4-Dioxane	3051.66	1744.23	722.22	-	-
Chloroform	2218.87	1850.86	577.61	-	-
Acetonitrile	2063.64	2075.89	751.62	-	-
1-Octanol	3234.59	1716.60	2531.55	-	-
1-Hexanol	-	617.12	3914.64	1171.35	-
1-Butanol	3443.63	1262.93	617.62	-	-
1-Pentanol	3027.74	1129.00	870.44	-	-
1-Propanol	1420.96	2927.15	668.16	-	-
Acetic acid	2627.34	-	655.10	-	-
Methanol	3898.26	-	806.30	-	-
2,2,2-Trifluoroethanol	2786.57	3252.22	786.45	-	-

Tables 2.2.2 (a) and (b). Summary band width and band area of 5 band fit using Gaussian model for normalised **12** emission spectra recorded at 310 nm excitation.

Solvent	Band 1 Area Percentage (%)	Band 2 Area Percentage (%)	Band 3 Area Percentage (%)	Band 4 Area Percentage (%)	Band 5 Area Percentage (%)
Toluene	47.05	20.38	32.56	-	-
1,4-Dioxane	55.30	31.61	13.09	-	-
Chloroform	47.74	39.83	12.43	-	-
Acetonitrile	42.19	42.44	15.37	-	-
1-Octanol	43.23	22.94	33.83	-	-
1-Hexanol	-	10.82	68.64	20.54	-
1-Butanol	64.68	23.72	11.60	-	-
1-Pentanol	60.23	22.46	17.31	-	-
1-Propanol	28.33	58.35	13.32	-	-
Acetic acid	80.04	-	19.96	-	-
Methanol	82.86	-	17.14	-	-
2,2,2-Trifluoroethanol	40.83	47.65	11.52	-	-

Table 2.2.3. Total Area Percentages of 5 band fit using Gaussian model for normalised N=C- **3a** emission spectra recorded at 310 nm excitation.

Solvent	Area Ratio Band 1/2 (310 nm ex)	Area Ratio Band 1/3 (310 nm ex)	Area Ratio Band 1/4 (310 nm ex)	Area Ratio Band 1/5 (310 nm ex)
Toluene	2.31	1.44	-	-
1,4-Dioxane	1.75	4.23	-	-
Chloroform	1.20	3.84	-	-
Acetonitrile	0.99	2.75	-	-
1-Octanol	1.88	1.28	-	-
1-Hexanol	-	-	-	-
1-Butanol	2.73	5.58	-	-
1-Pentanol	2.68	3.48	-	-
1-Propanol	0.49	2.13	-	-
Acetic acid	-	4.01	-	-
Methanol	-	4.83	-	-
2,2,2-Trifluoroethanol	0.86	3.54	-	-

Solvent	Area Ratio Band 2/3 (310 nm ex)	Area Ratio Band 2/4 (310 nm ex)	Area Ratio Band 2/5 (310 nm ex)	Area Ratio Band 3/4 (310 nm ex)	Area Ratio Band 3/5 (310 nm ex)	Area Ratio Band 4/5 (310 nm ex)
Toluene	0.63	-	-	-	-	-
1,4-Dioxane	2.42	-	-	-	-	-
Chloroform	3.20	-	-	-	-	-
Acetonitrile	2.76	-	-	-	-	-
1-Octanol	0.68	-	-	-	-	-
1-Hexanol	0.16	0.53	-	3.34	-	-
1-Butanol	2.04	-	-	-	-	-
1-Pentanol	1.30	-	-	-	-	-
1-Propanol	4.38	-	-	-	-	-
Acetic acid	-	-	-	-	-	-
Methanol	-	-	-	-	-	-
2,2,2-Trifluoroethanol	4.14	-	-	-	-	-

Table 2.2.4. Area Ratios of 5 band fit using Gaussian model for normalised **12** emission spectra recorded at 310 nm excitation.

2.2.3 400 nm excitation Gaussian band fit summaries.

Solvent	λ max_{em} Band 1 (cm^{-1})	λ max_{em} Band 1 (nm)	λ max_{em} Band 2 (cm^{-1})	λ max_{em} Band 2 (nm)	λmax_{em} Band 3 (cm^{-1})	λmax_{em} Band 3 (nm)
Toluene	-	-	19675.15	508.26	-	-
1,4-Dioxane	-	-	19816.42	504.63	-	-
Chloroform	-	-	22864.71	437.36	-	-
Acetonitrile	-	-	19490.70	513.07	-	-
1-Octanol	-	-	19819.35	504.56	-	-
1-Hexanol	-	-	-	-	-	-
1-Butanol	-	-	19364.11	516.42	-	-
1-Pentanol	-	-	19450.98	514.11	-	-
1-Propanol	-	-	19263.96	519.10	-	-
Acetic acid	-	-	-	-	-	-
Methanol	-	-	19049.66	524.94	-	-
2,2,2-Trifluoroethanol	-	-	18581.50	538.17	-	-

Table 2.2.5. Summary of band maxima of 3 band fit using Gaussian model for normalised **12** emission spectra recorded at 400 nm excitation.

Solvent	Width Band 1 (cm^{-1})	Width Band 2 (cm^{-1})	Width Band 3 (cm^{-1})
Toluene	-	2355.72	-
1,4-Dioxane	-	3207.37	-
Chloroform	-	6407.84	-
Acetonitrile	-	3325.11	-
1-Octanol	-	3290.55	-
1-Hexanol	-	-	-
1-Butanol	-	3247.66	-
1-Pentanol	-	2804.96	-
1-Propanol	-	2525.01	-
Acetic acid	-	-	-
Methanol	-	2488.12	-
2,2,2-Trifluoroethanol	-	2000.25	-

Table 2.2.6. Summary of band width of 3 band fit using Gaussian model for normalised **12** emission spectra recorded at 400 nm excitation.

Solvent	Area Band 1 (cm^{-1})	Area Band 2 (cm^{-1})	Area Band 3 (cm^{-1})	Area Ratio Band 1/2 (400 nm ex)	Area Ratio Band 1/3 (400 nm ex)	Area Ratio Band 2/3 (400 nm ex)
Toluene	-	489.29	-	-	-	-
1,4-Dioxane	-	1051.24	-	-	-	-
Chloroform	-	5974.33	-	-	-	-
Acetonitrile	-	456.51	-	-	-	-
1-Octanol	-	611.15	-	-	-	-
1-Hexanol	-	-	-	-	-	-
1-Butanol	-	768.55	-	-	-	-
1-Pentanol	-	498.43	-	-	-	-
1-Propanol	-	803.23	-	-	-	-
Acetic acid	-	-	-	-	-	-
Methanol	-	604.53	-	-	-	-
2,2,2-Trifluoroethanol	-	232.80	-	-	-	-

Solvent	Band 1 Area Percentage (%)	Band 2 Area Percentage (%)	Band 3 Area Percentage (%)
Toluene	-	100	-
1,4-Dioxane	-	100	-
Chloroform	-	100	-
Acetonitrile	-	100	-
1-Octanol	-	100	-
1-Hexanol	-	-	-
1-Butanol	-	100	-
1-Pentanol	-	100	-
1-Propanol	-	100	-
Acetic acid	-	-	-
Methanol	-	100	-
2,2,2-Trifluoroethanol	-	100	-

Table 2.2.7. Band area, area ratios and total area percentage of 3 band fit using Gaussian model for normalised **12** emission spectra recorded at 400 nm excitation.

2.2.4 310 nm Gaussian band fit - Solvatochromic analysis.

2.2.4.1 E_T^N.

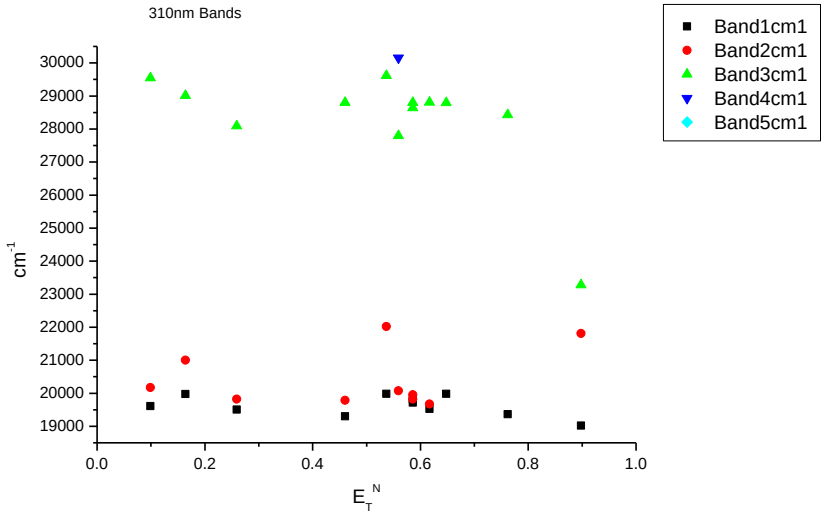

Figure 2.2.1. Band maxima from Gaussian model fit of the normalised fluorescence emission spectra of **12** recorded at 310 nm excitation against E_T^N.

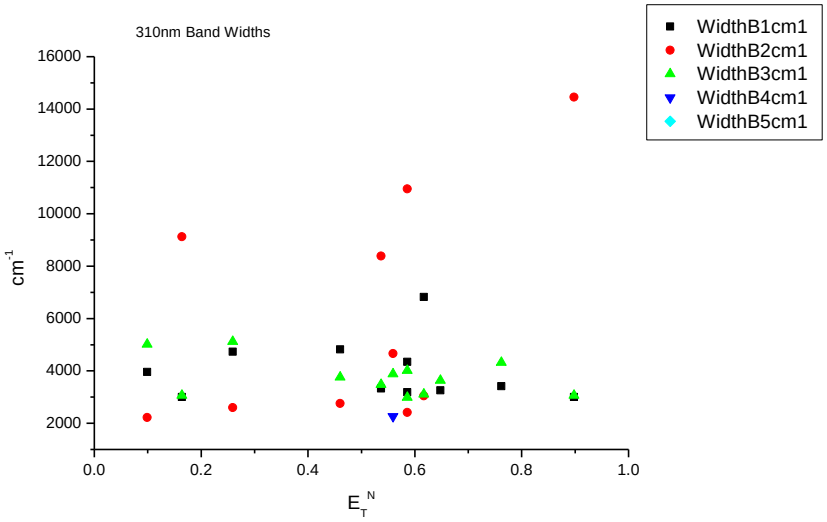

Figure 2.2.2. Band widths from Gaussian model fit of the normalised fluorescence emission spectra of **12** recorded at 310 nm excitation against E_T^N.

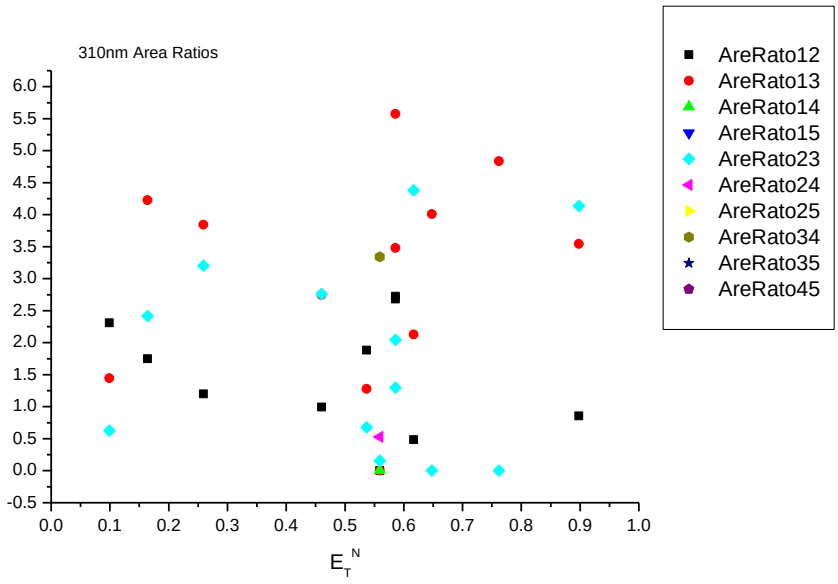

Figure 2.2.3. Area ratios from Gaussian model fit of the normalised fluorescence emission spectra of **12** recorded at 310 nm excitation against E_T^N.

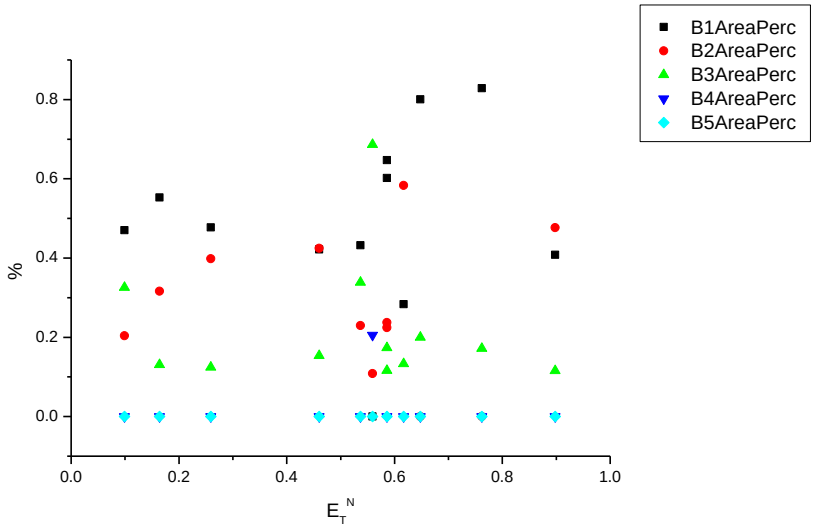

Figure 2.2.4. Area percentages from Gaussian model fit of the normalised fluorescence emission spectra of **12** recorded at 310 nm excitation against E_T^N.

2.2.4.2 α

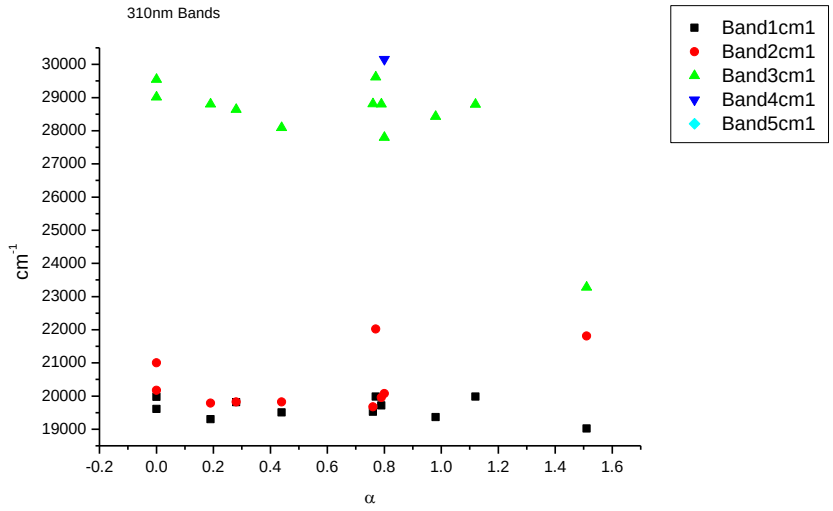

Figure 2.2.5. Band maxima from Gaussian model fit of the normalised fluorescence emission spectra of **12** recorded at 310 nm excitation against α.

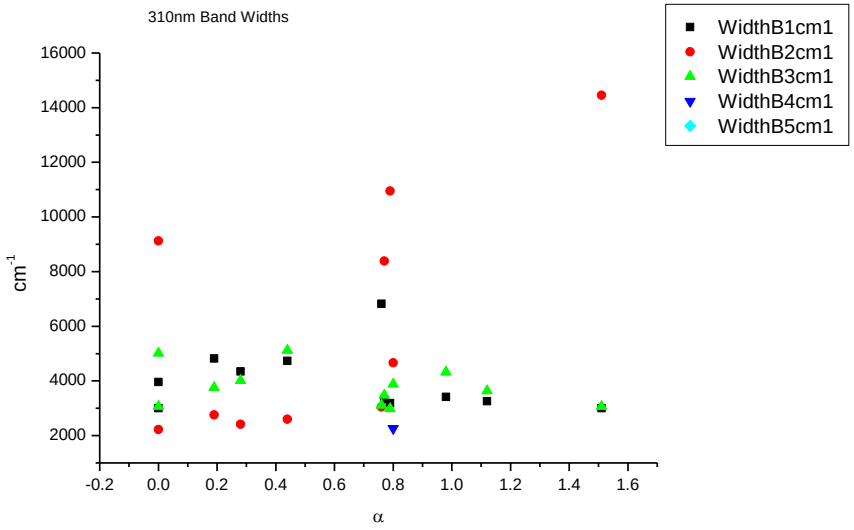

Figure 2.2.6. Band widths from Gaussian model fit of the normalised fluorescence emission spectra of **12** recorded at 310 nm excitation against α.

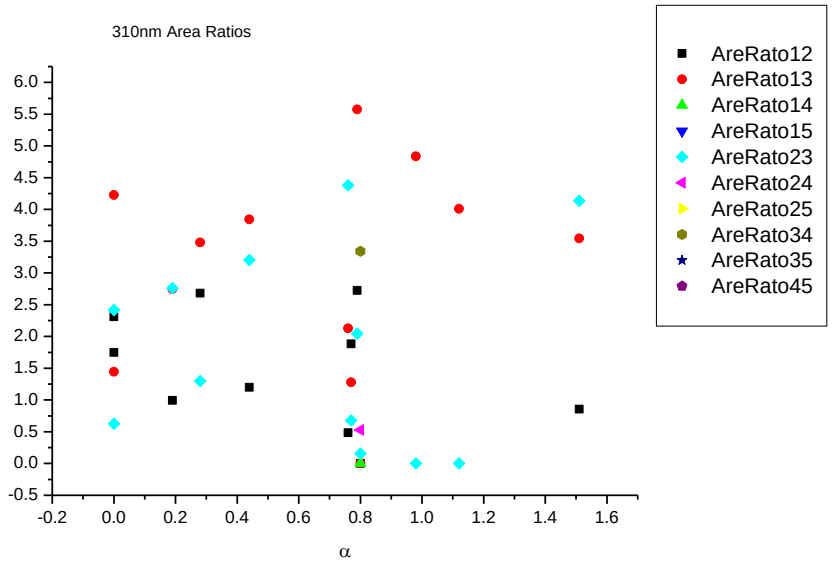

Figure 2.2.7. Area Ratios from Gaussian model fit of the normalised fluorescence emission spectra of **12** recorded at 310 nm excitation against α.

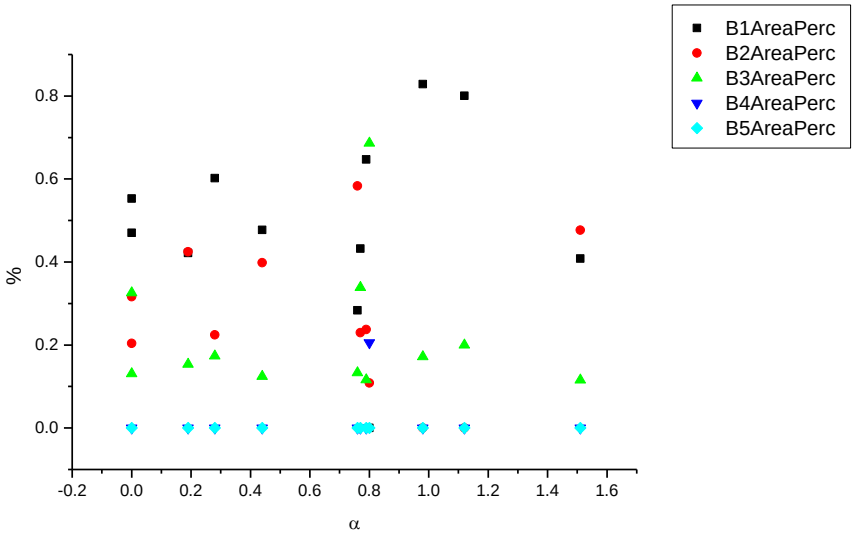

Figure 2.2.8. Area percentages from Gaussian model fit of the normalised fluorescence emission spectra of **12** recorded at 310 nm excitation against α.

2.2.4.3 β.

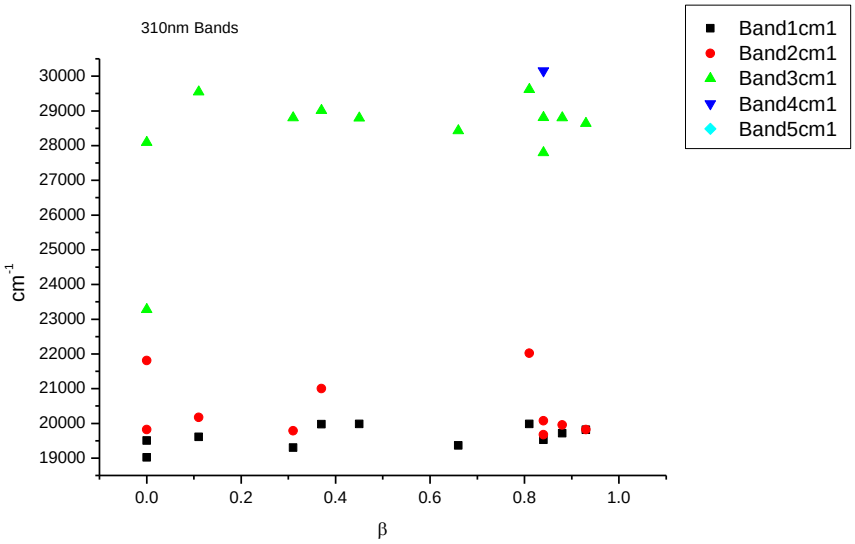

Figure 2.2.9. Band maxima from Gaussian model fit of the normalised fluorescence emission spectra of **12** recorded at 310 nm excitation against β.

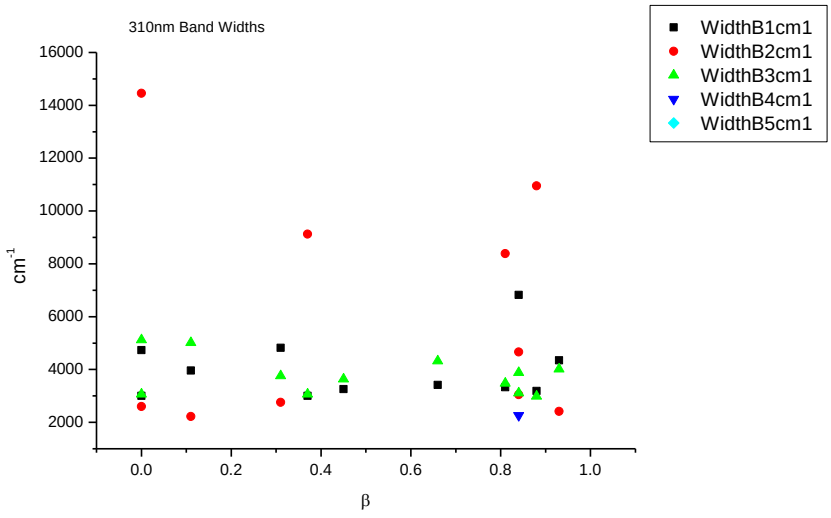

Figure 2.2.10. Band widths from Gaussian model fit of the normalised fluorescence emission spectra of **12** recorded at 310 nm excitation against β.

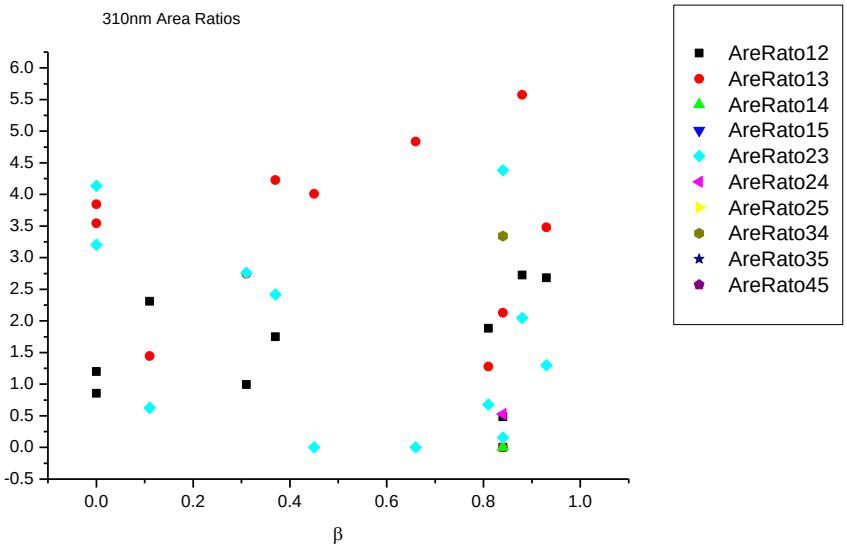

Figure 2.2.11. Area ratios from Gaussian model fit of the normalised fluorescence emission spectra of **12** recorded at 310 nm excitation against β.

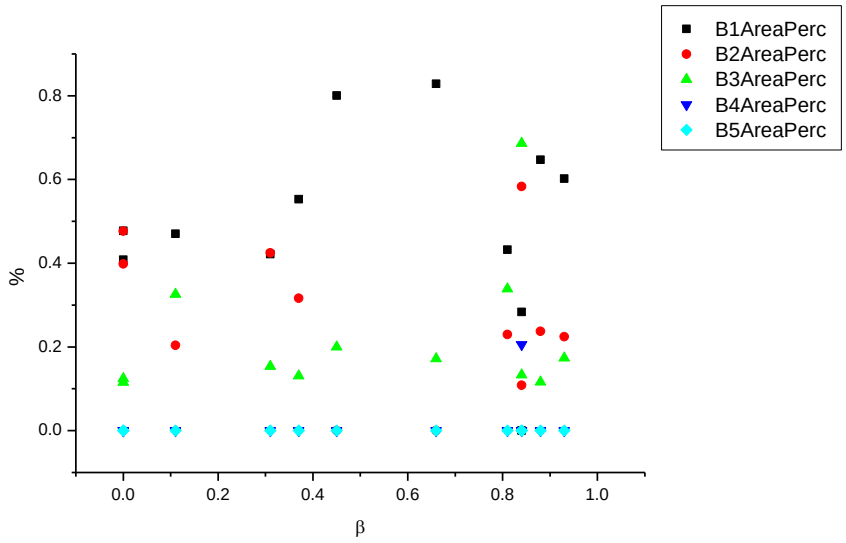

Figure 2.2.12. Area percentages from Gaussian model fit of the normalised fluorescence emission spectra of **12** recorded at 310 nm excitation against β.

2.2.4.3 π.*

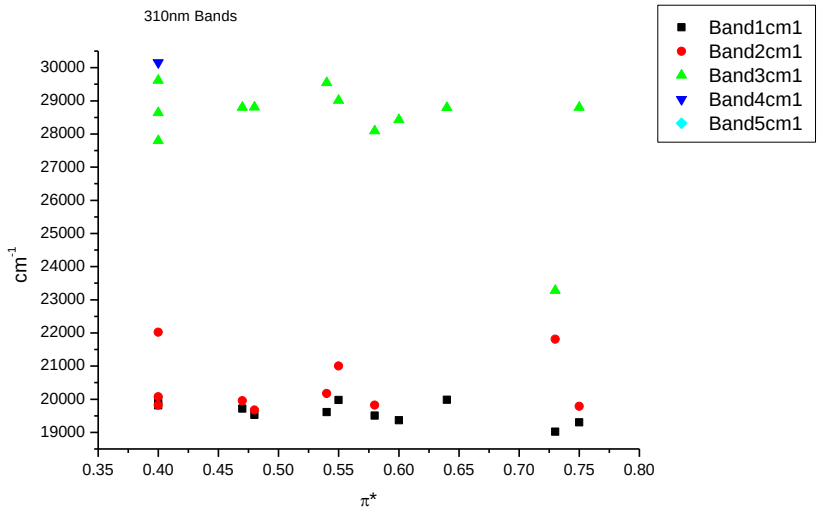

Figure 2.2.13. Band maxima from Gaussian model fit of the normalised fluorescence emission spectra of **12** recorded at 310 nm excitation against π*.

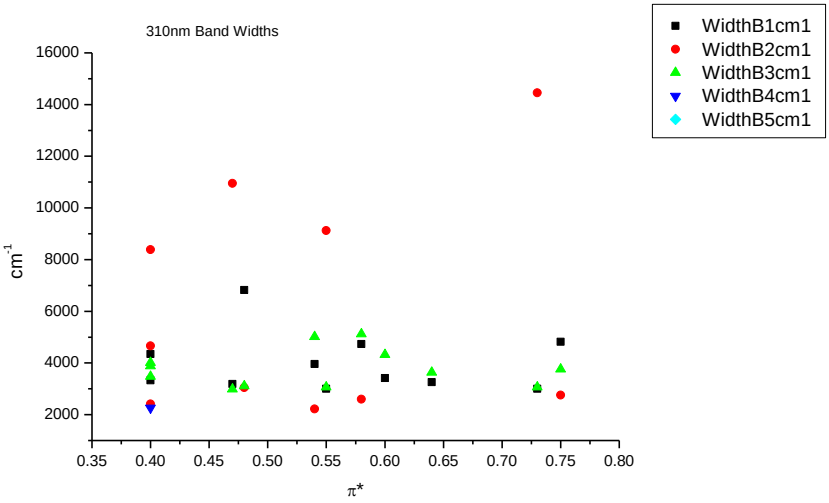

Figure 2.2.14. Band widths from Gaussian model fit of the normalised fluorescence emission spectra of **12** recorded at 310 nm excitation against π*.

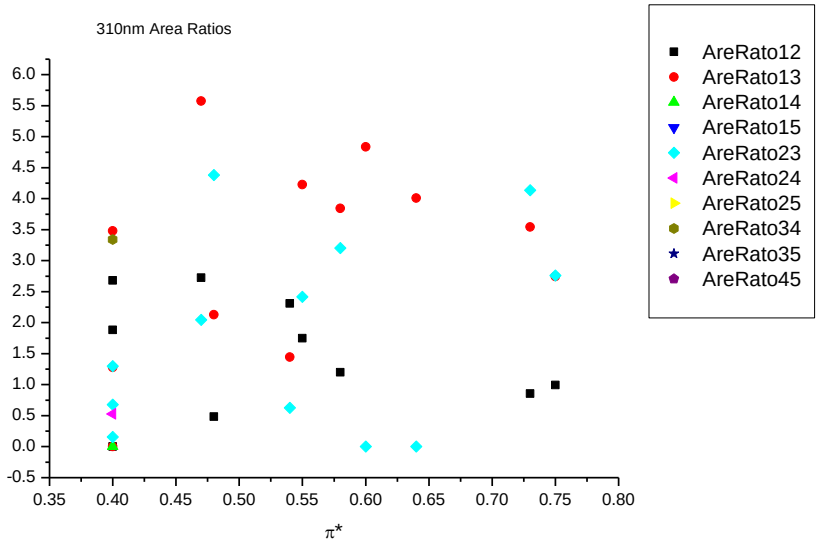

Figure 2.2.15. Area ratios from Gaussian model fit of the normalised fluorescence emission spectra of **12** recorded at 310 nm excitation against π*.

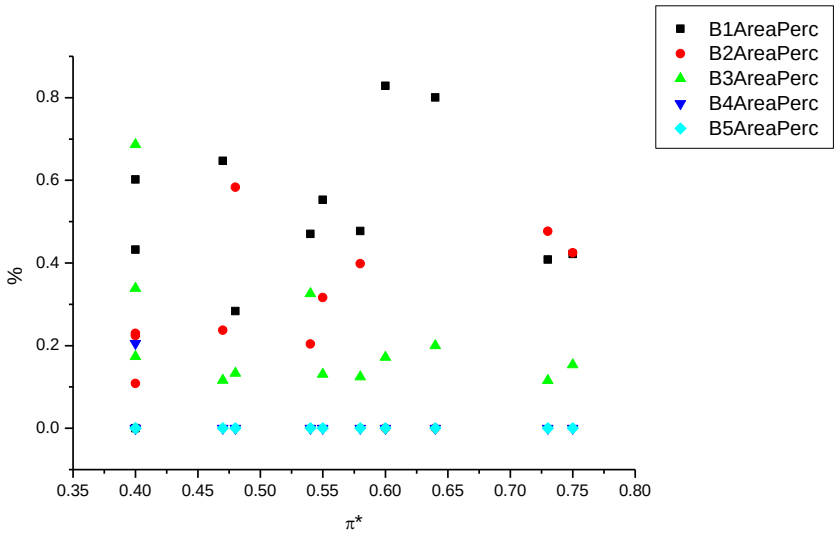

Figure 2.2.16. Area percentages from Gaussian model fit of the normalised fluorescence emission spectra of **12** recorded at 310 nm excitation against π*.

2.2.4.5 μ(D).

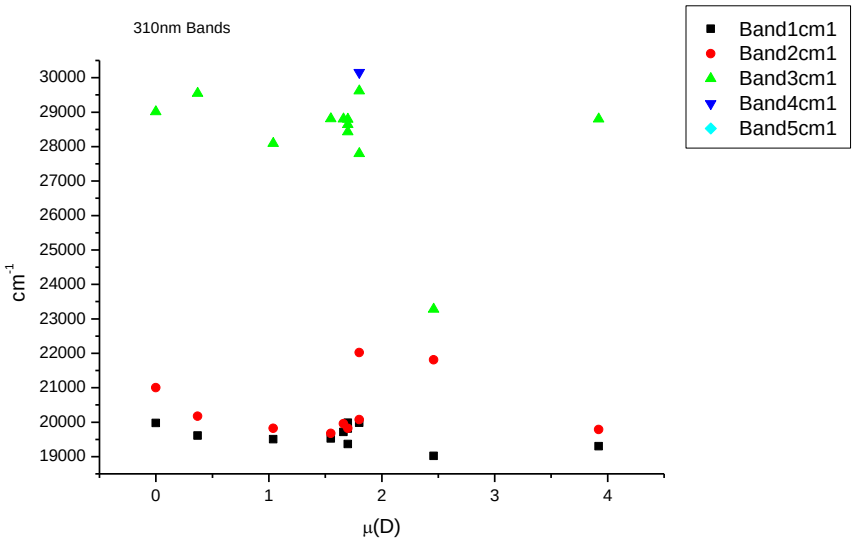

Figure 2.2.17. Band maxima from Gaussian model fit of the normalised fluorescence emission spectra of **12** recorded at 310 nm excitation against μ(D).

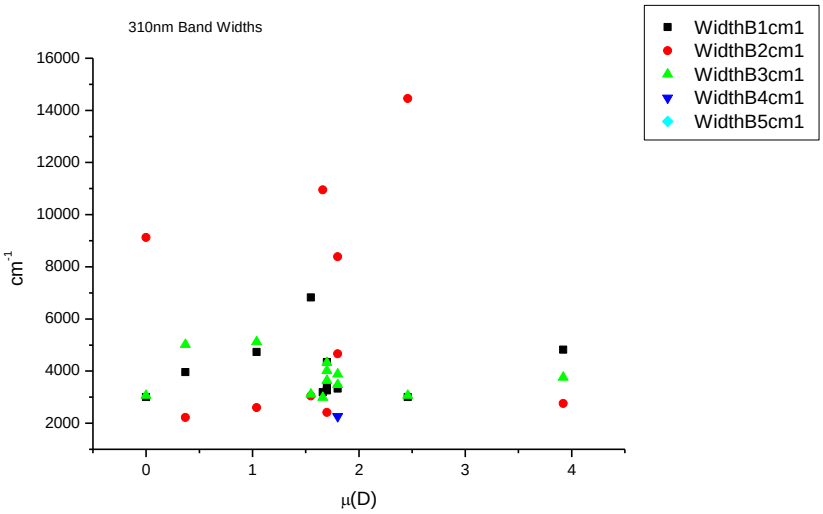

Figure 2.2.18. Band widths from Gaussian model fit of the normalised fluorescence emission spectra of **12** recorded at 310 nm excitation against μ(D).

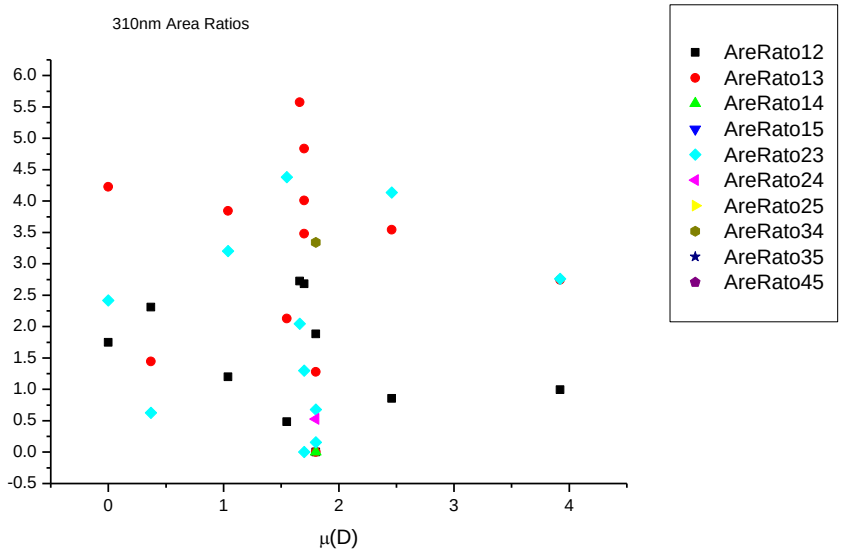

Figure 2.2.19. Area ratios from Gaussian model fit of the normalised fluorescence emission spectra of **12** recorded at 310 nm excitation against μ(D).

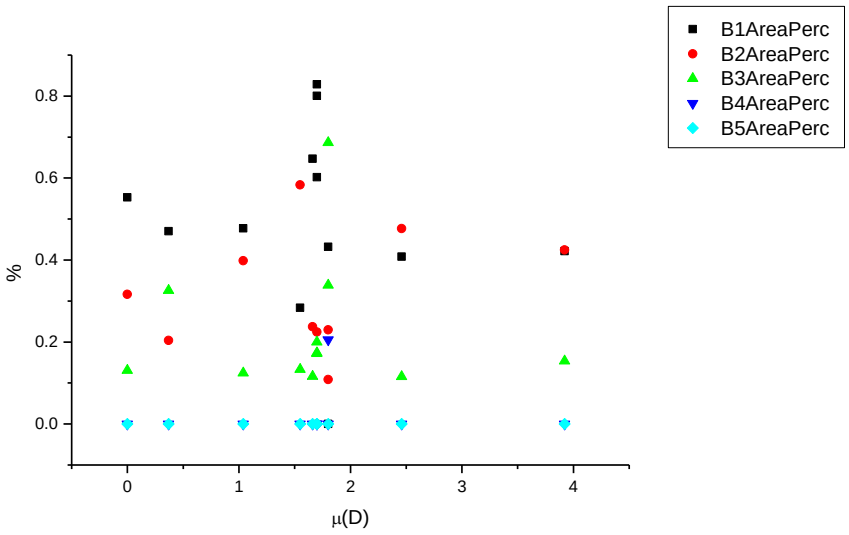

Figure 2.2.20. Area percentages from Gaussian model fit of the normalised fluorescence emission spectra of **12** recorded at 310 nm excitation against μ(D).

2.2.4.6 η(Cp).

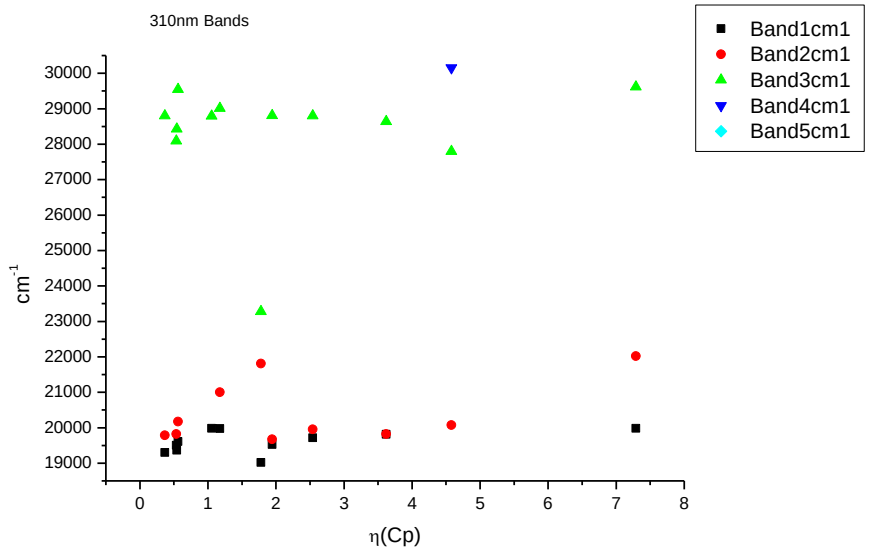

Figure 2.2.21. Band maxima from Gaussian model fit of the normalised fluorescence emission spectra of **12** recorded at 310 nm excitation against η(Cp).

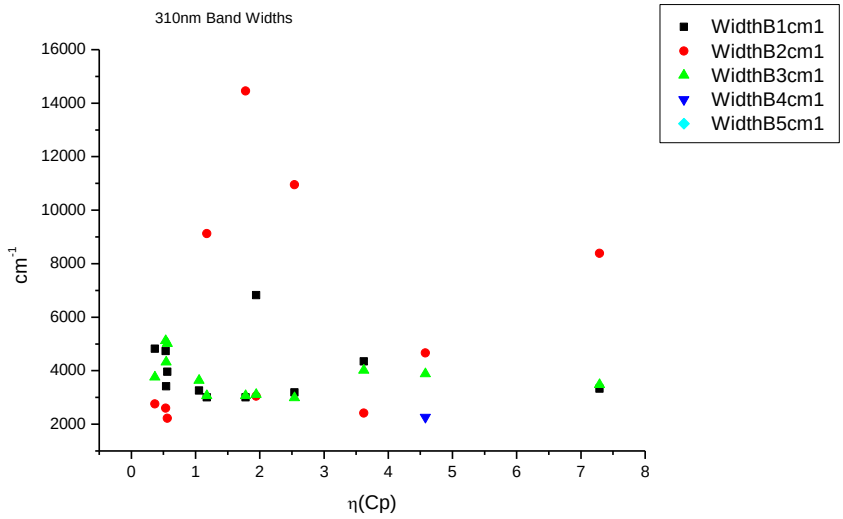

Figure 2.2.22. Band widths from Gaussian model fit of the normalised fluorescence emission spectra of **12** recorded at 310 nm excitation against η(Cp).

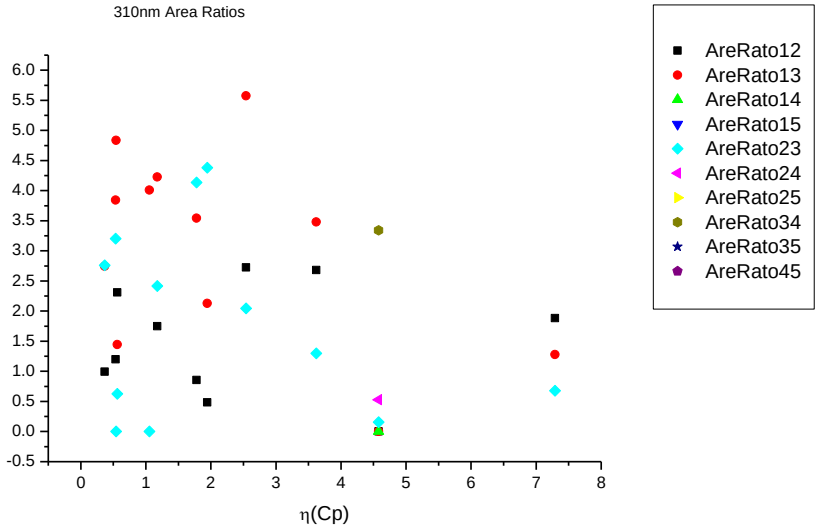

Figure 2.2.23. Area ratios from Gaussian model fit of the normalised fluorescence emission spectra of **12** recorded at 310 nm excitation against η(Cp).

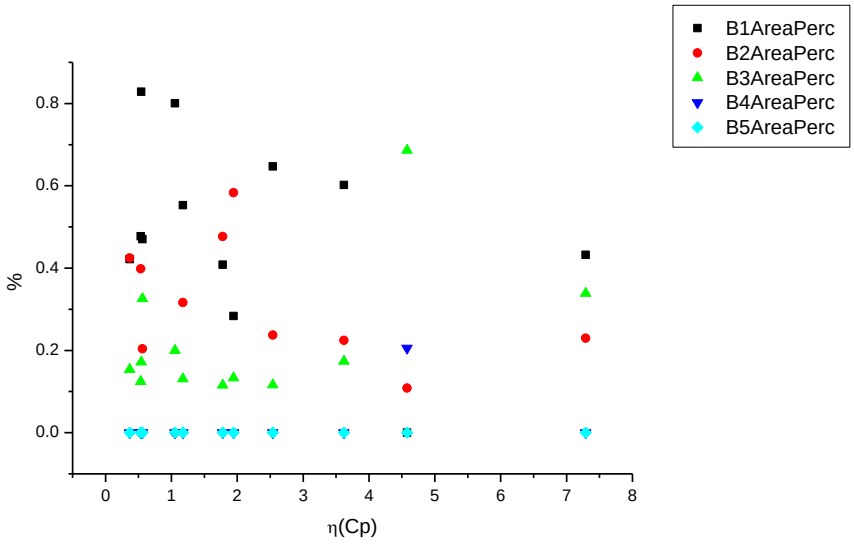

Figure 2.2.24. Area percentages from Gaussian model fit of the normalised fluorescence emission spectra of **12** recorded at 310 nm excitation against η(Cp).

2.2.5 400 nm Gaussian band fit - Solvatochromic analysis.

2.2.5.1 E_T^N.

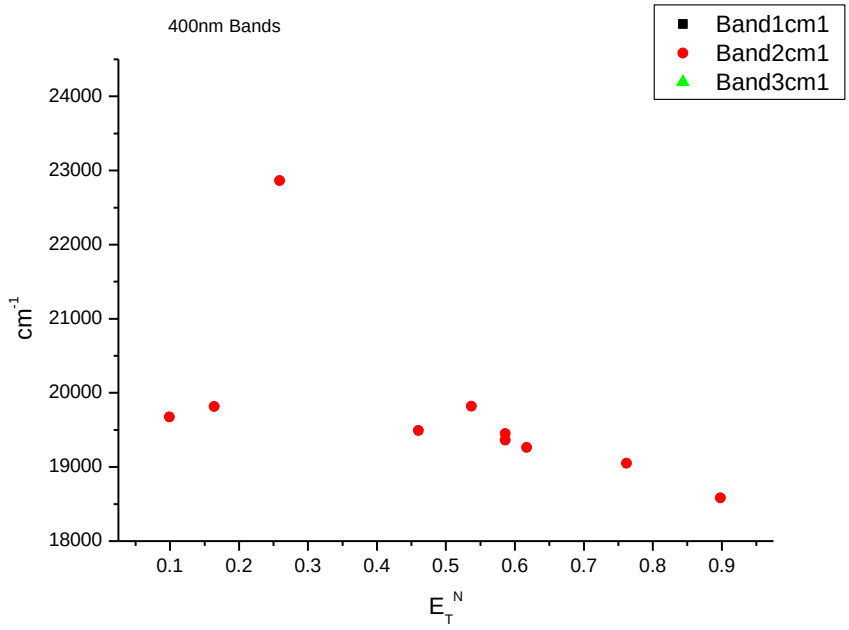

Figure 2.2.25. Band maxima from Gaussian model fit of the normalised fluorescence emission spectra of **12** recorded at 400 nm excitation against E_T^N.

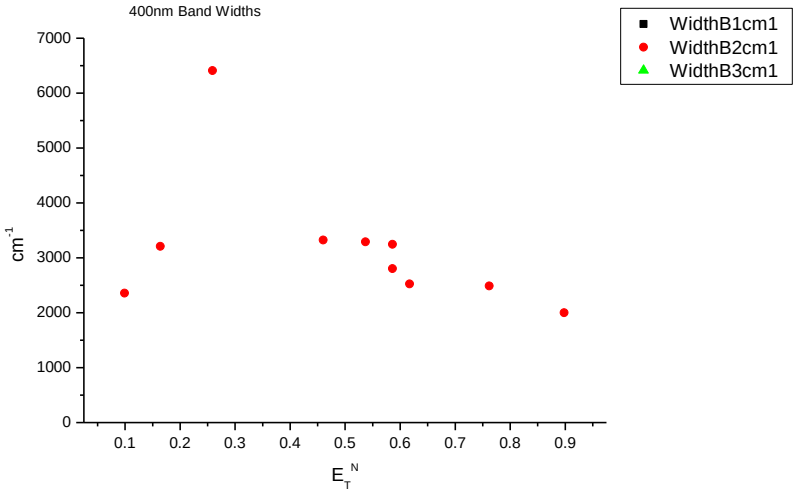

Figure 2.2.26. Band widths from Gaussian model fit of the normalised fluorescence emission spectra of **12** recorded at 400 nm excitation against E_T^N.

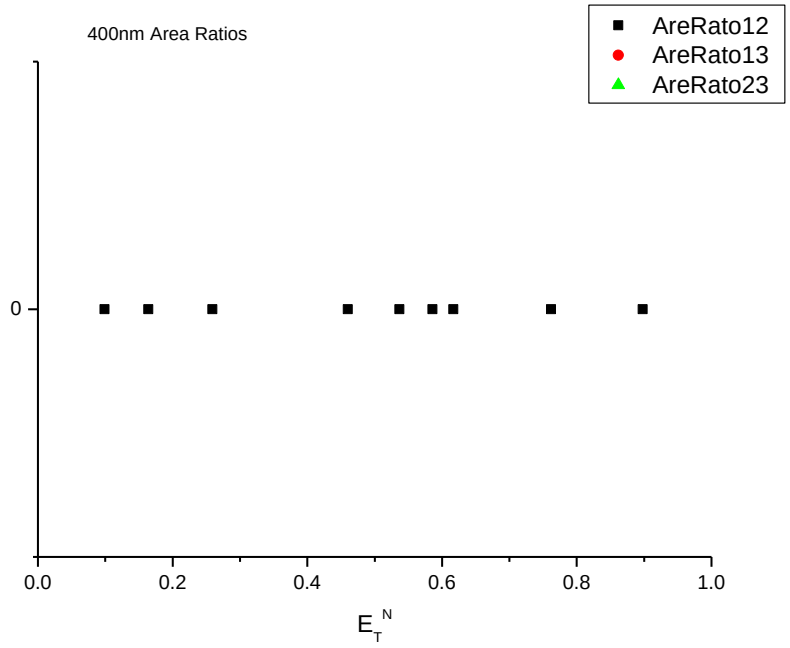

Figure 2.2.27. Area ratios from Gaussian model fit of the normalised fluorescence emission spectra of **12** recorded at 400 nm excitation against E_T^N.

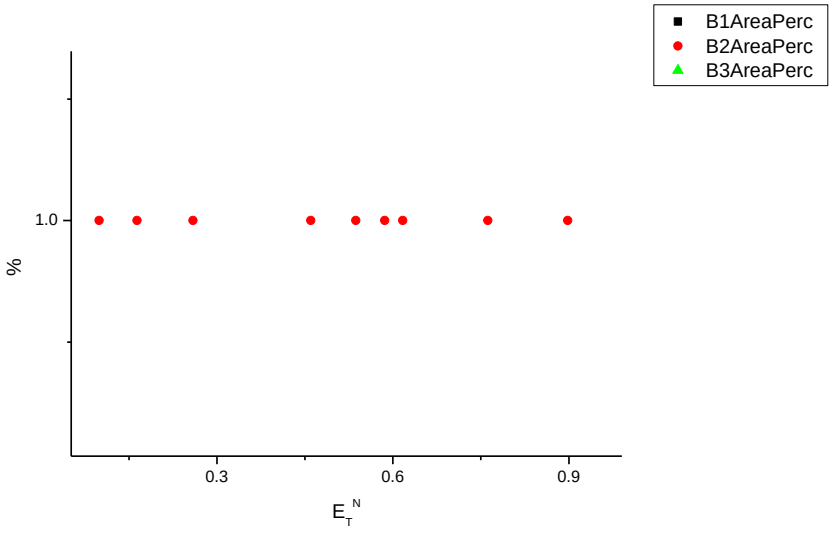

Figure 2.2.28. Area percentages from Gaussian model fit of the normalised fluorescence emission spectra of **12** recorded at 400 nm excitation against E_T^N.

2.2.5.2 α

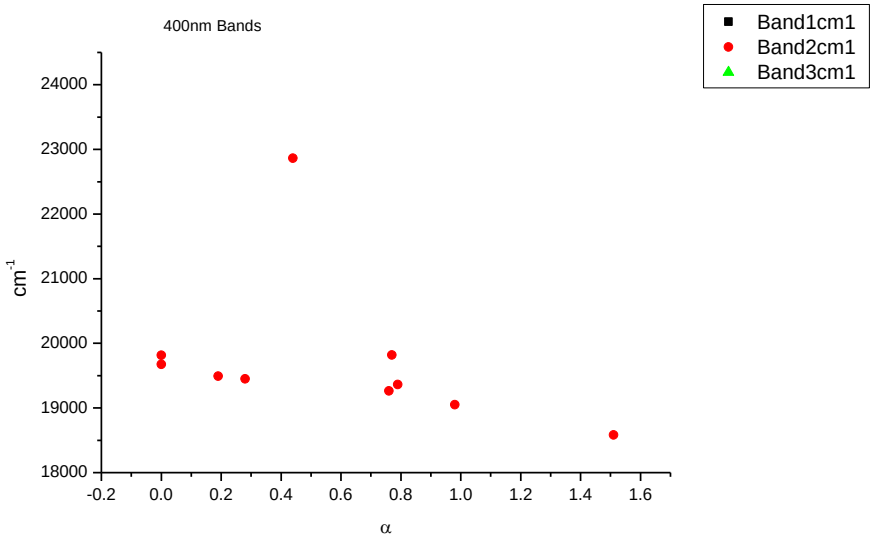

Figure 2.2.29. Band maxima from Gaussian model fit of the normalised fluorescence emission spectra of **12** recorded at 400 nm excitation against α.

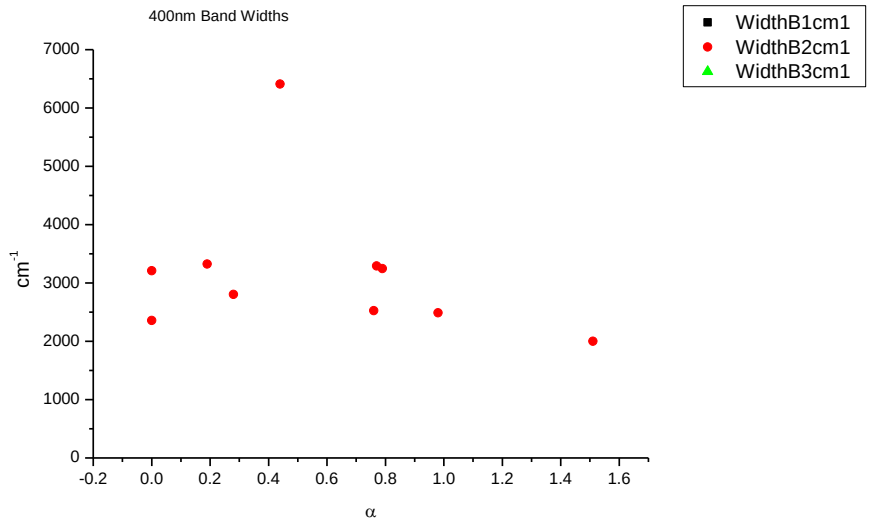

Figure 2.2.30. Band widths from Gaussian model fit of the normalised fluorescence emission spectra of **12** recorded at 400 nm excitation against α.

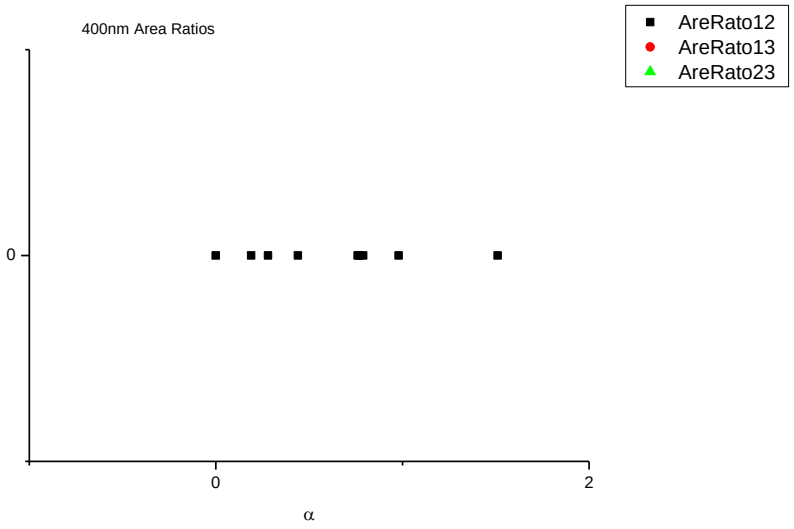

Figure 2.2.31. Area ratios from Gaussian model fit of the normalised fluorescence emission spectra of **12** recorded at 400 nm excitation against α.

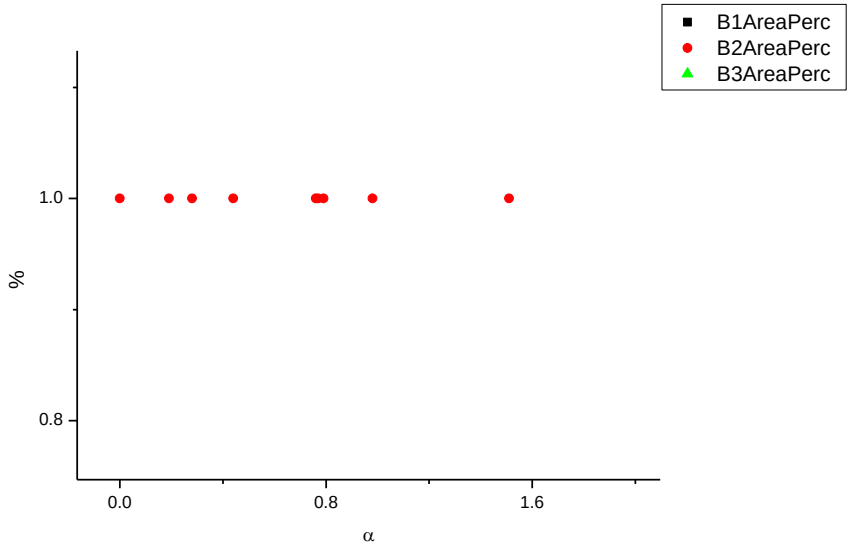

Figure 2.2.32. Area percentages from Gaussian model fit of the normalised fluorescence emission spectra of **12** recorded at 400 nm excitation against α.

2.2.5.3 β.

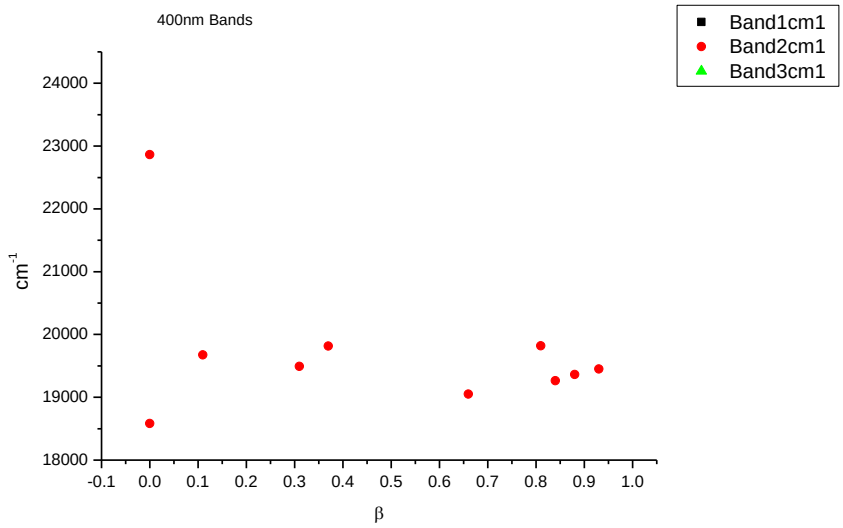

Figure 2.2.33. Band maxima from Gaussian model fit of the normalised fluorescence emission spectra of **12** recorded at 400 nm excitation against β.

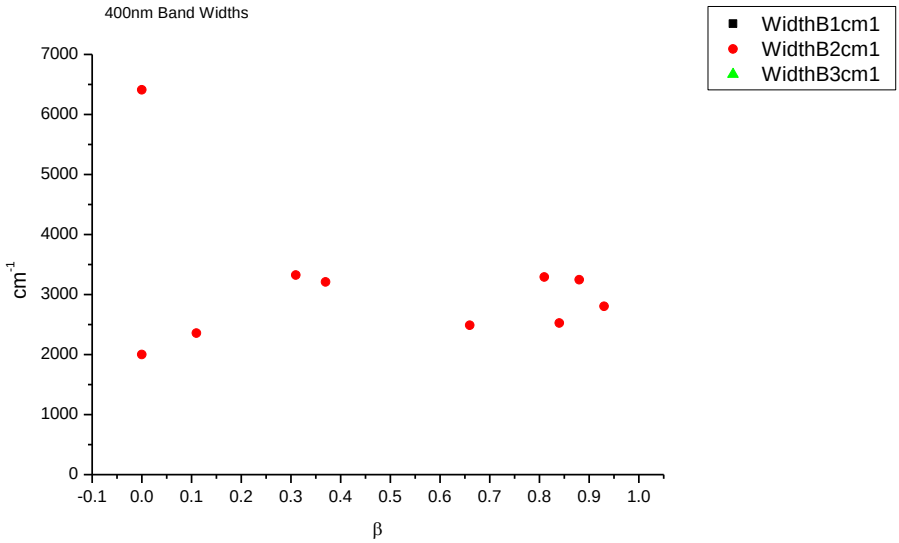

Figure 2.2.34. Band widths from Gaussian model fit of the normalised fluorescence emission spectra of **12** recorded at 400 nm excitation against β.

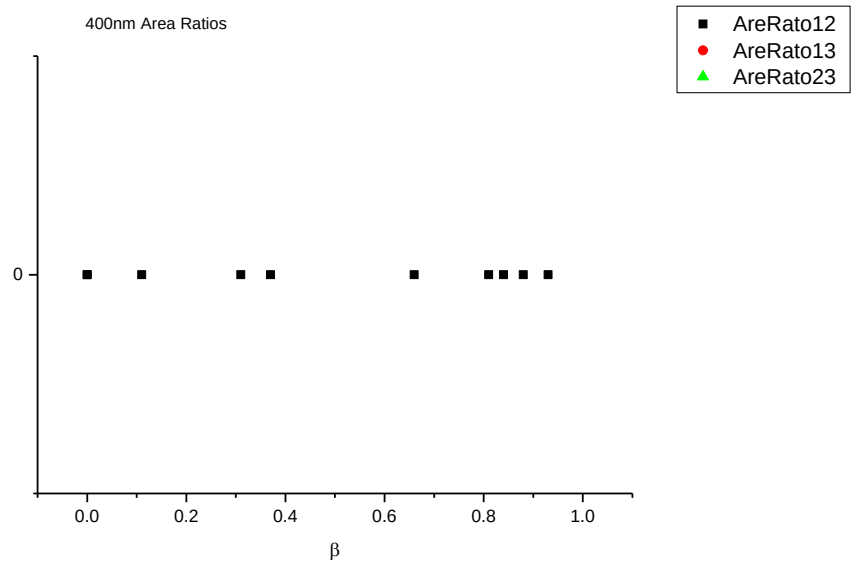

Figure 2.2.35. Area ratios from Gaussian model fit of the normalised fluorescence emission spectra of **12** recorded at 400 nm excitation against β.

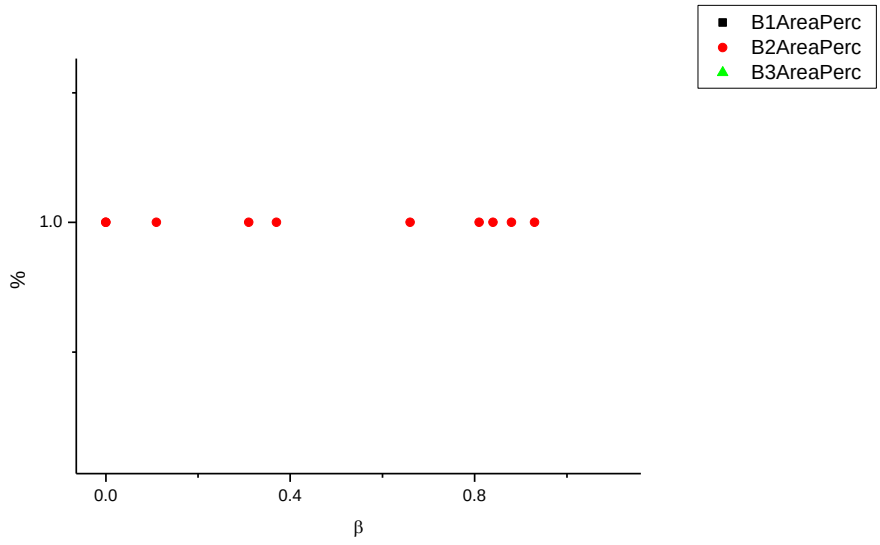

Figure 2.2.36. Area percentages from Gaussian model fit of the normalised fluorescence emission spectra of **12** recorded at 400 nm excitation against β.

2.2.5.4 π.*

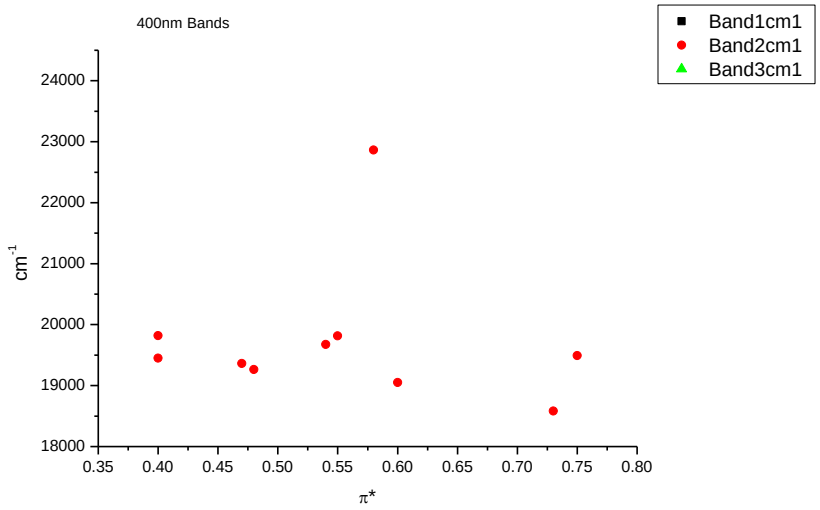

Figure 2.2.37. Band maxima from Gaussian model fit of the normalised fluorescence emission spectra of **12** recorded at 400 nm excitation against π*.

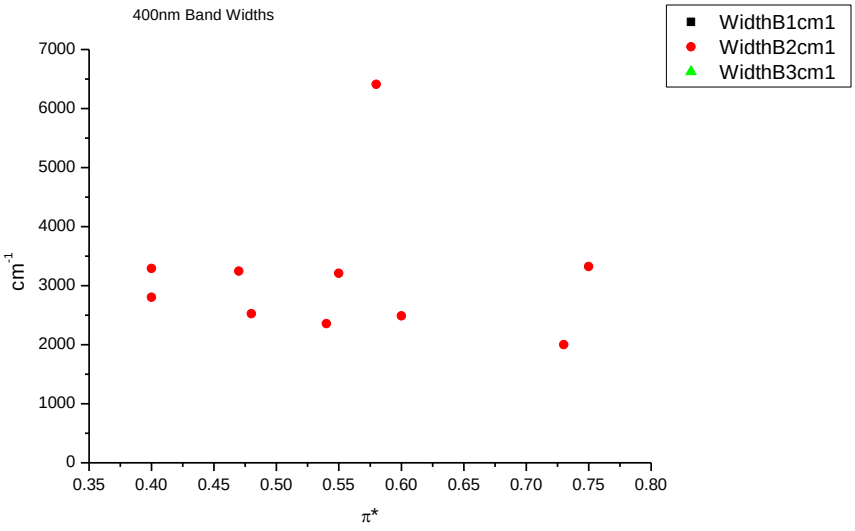

Figure 2.2.38. Band widths from Gaussian model fit of the normalised fluorescence emission spectra of **12** recorded at 400 nm excitation against π*.

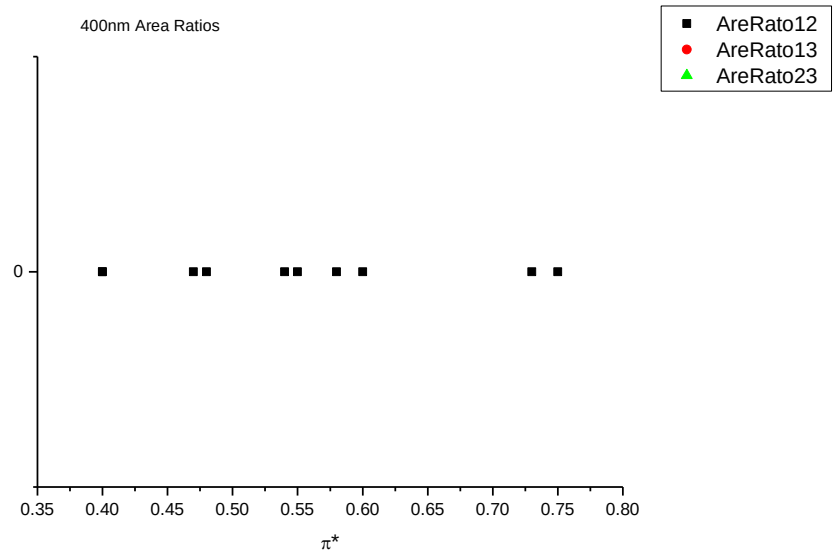

Figure 2.2.39. Area ratios from Gaussian model fit of the normalised fluorescence emission spectra of **12** recorded at 400 nm excitation against π*.

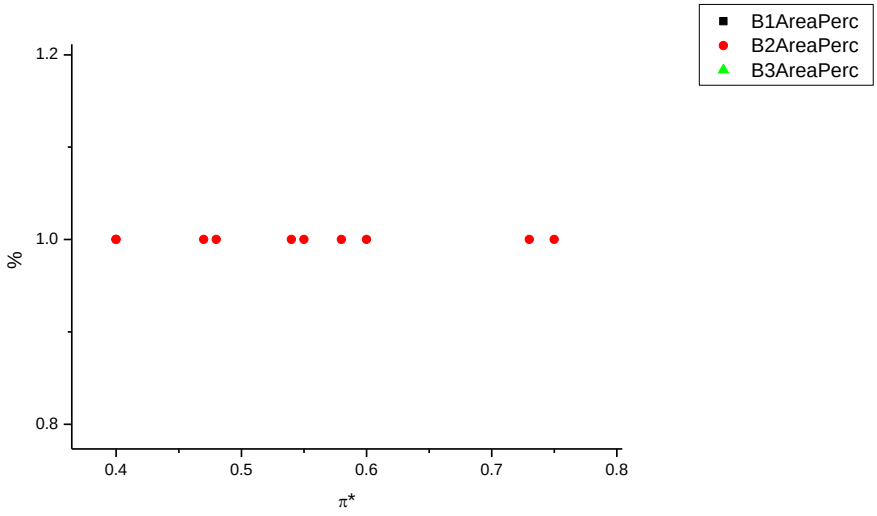

Figure 2.2.40. Area percentages from Gaussian model fit of the normalised fluorescence emission spectra of **12** recorded at 400 nm excitation against π*.

2.2.5.5 μ(D).

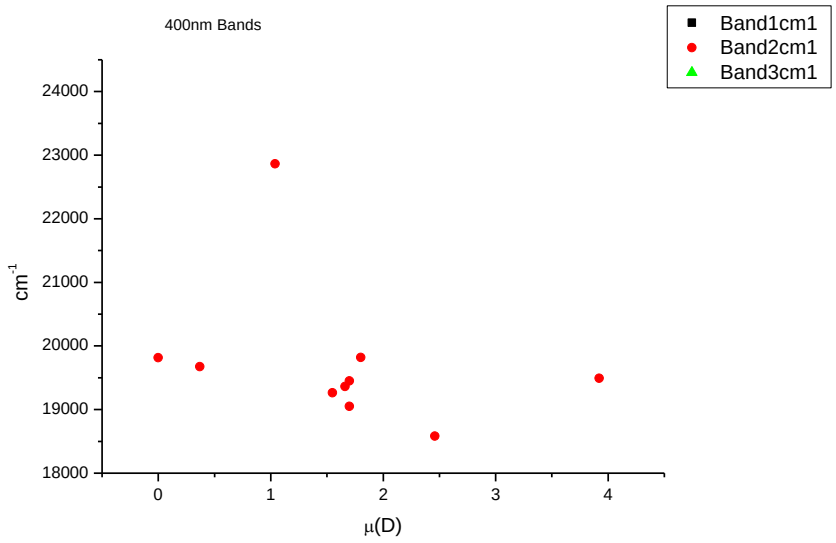

Figure 2.2.41. Band maxima from Gaussian model fit of the normalised fluorescence emission spectra of **12** recorded at 400 nm excitation against μ(D).

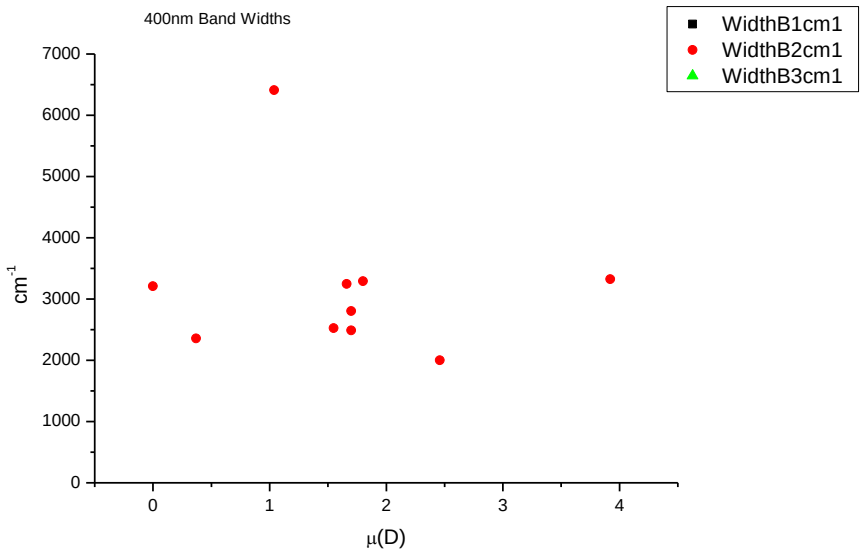

Figure 2.2.42. Band widths from Gaussian model fit of the normalised fluorescence emission spectra of **12** recorded at 400 nm excitation against μ(D).

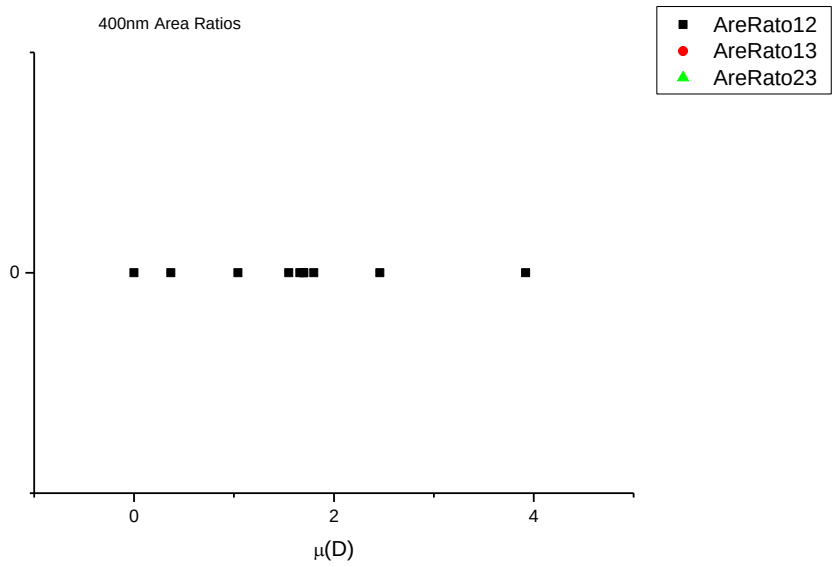

Figure 2.2.43. Area ratios from Gaussian model fit of the normalised fluorescence emission spectra of **12** recorded at 400 nm excitation against μ(D).

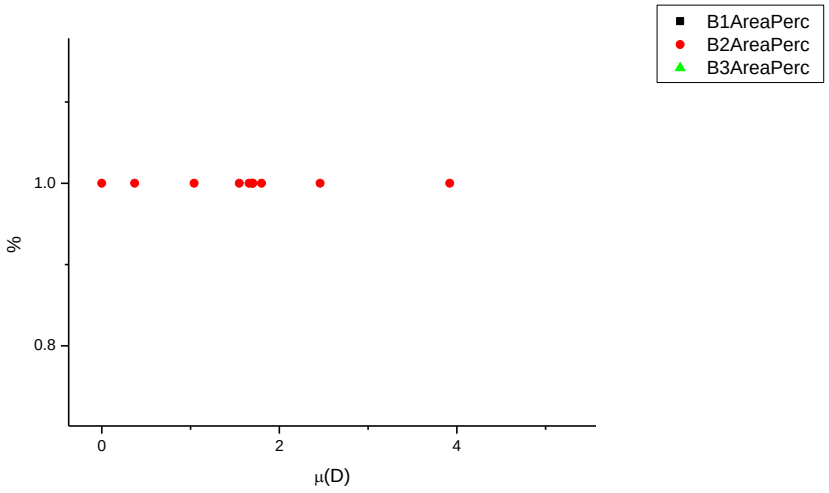

Figure 2.2.44. Area percentages from Gaussian model fit of the normalised fluorescence emission spectra of **12** recorded at 400 nm excitation against μ(D).

2.2.5.6 η(Cp).

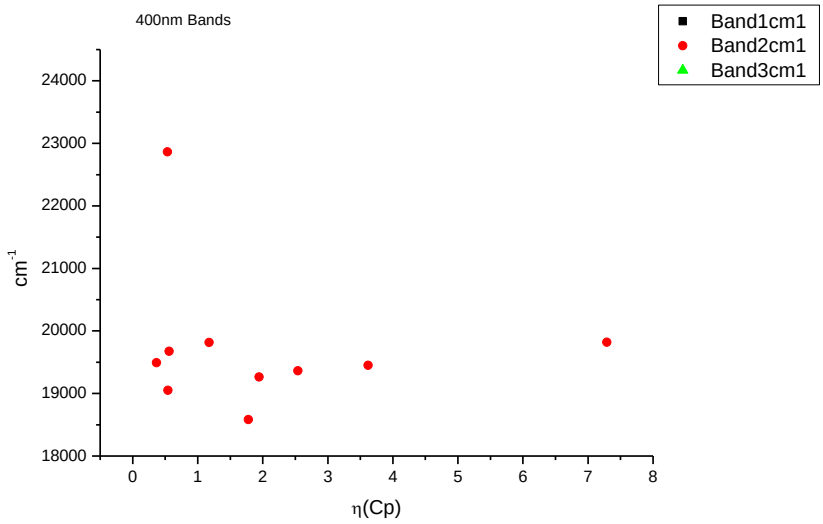

Figure 2.2.45. Band maxima from Gaussian model fit of the normalised fluorescence emission spectra of **12** recorded at 400 nm excitation against η(Cp).

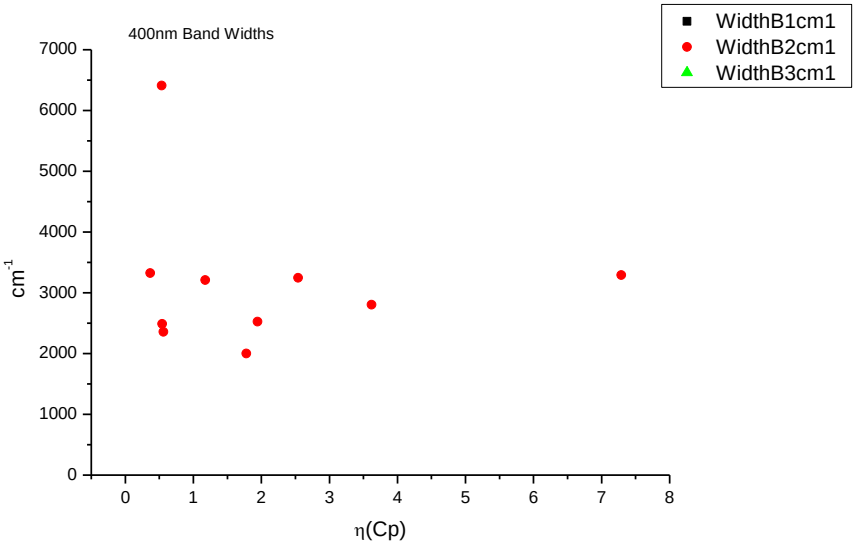

Figure 2.2.46. Band widths from Gaussian model fit of the normalised fluorescence emission spectra of **12** recorded at 400 nm excitation against η(Cp).

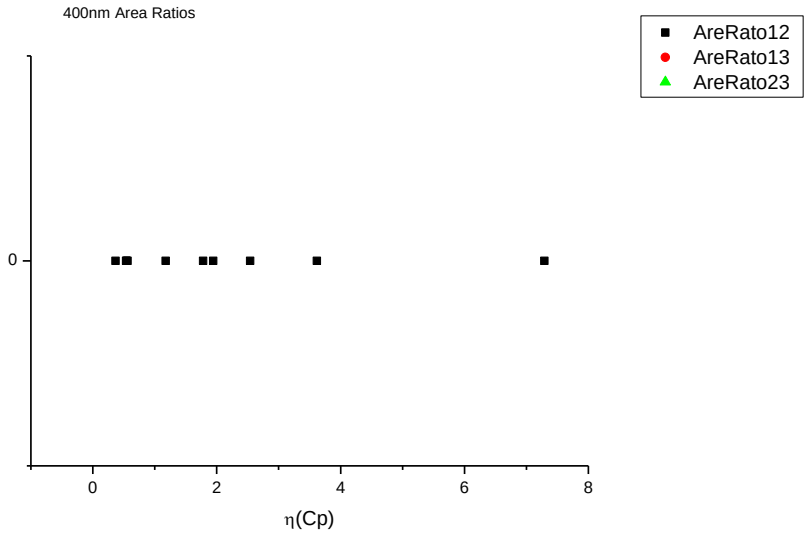

Figure 2.2.47. Area ratios from Gaussian model fit of the normalised fluorescence emission spectra of **12** recorded at 400 nm excitation against η(Cp).

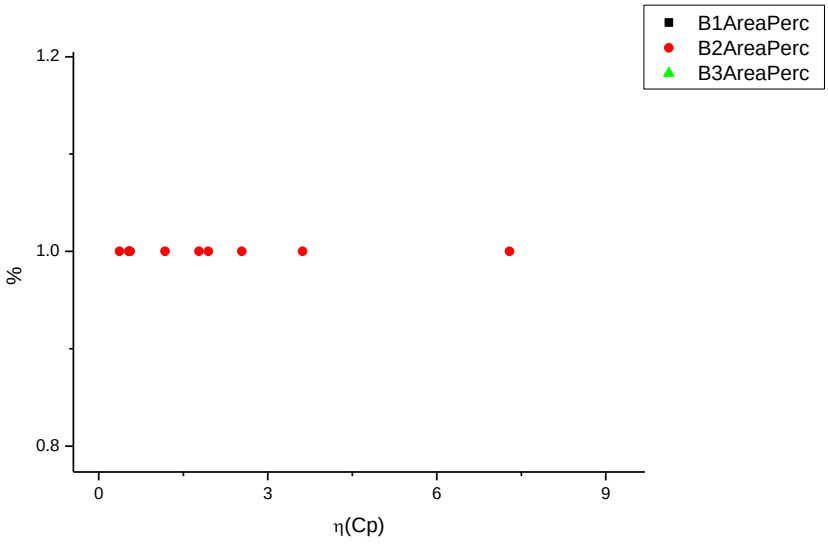

Figure 2.2.48. Area percentages from Gaussian model fit of the normalised fluorescence emission spectra of **12** recorded at 400 nm excitation against η(Cp).

2.2.6 295 nm (LED) fluorescent lifetime results.

2.2.6.1 Intensity weighted.

Wavelength (nm)	Solvent	τ_1 (ns)	A_1 (%)	τ_2 (ns)	A_2 (%)	τ_3 (ns)	A_3 (%)	τ_f (ns) (Intensity Weighted)	$1/\tau_f$	χ^2
350	Toluene	-	-	-	-	-	-	-	-	-
350	1,4-Dioxane	0.77	38.64	3.04	43.22	11.39	18.15	3.77	0.27	1.23
350	Chloroform	1.03	46.05	3.81	28.44	12.39	25.51	4.72	0.21	1.15
350	Acetonitrile	-	-	-	-	-	-	-	-	-
350	1-Octanol	1.90	46.27	8.67	53.73	-	-	5.54	0.18	1.27
350	1-Hexanol	1.07	28.66	4.04	42.49	15.36	28.85	6.46	0.15	1.16
350	1-Butanol	-	-	-	-	-	-	-	-	-
350	1-Pentanol	-	-	-	-	-	-	-	-	-
350	1-Propanol	-	-	-	-	-	-	-	-	-
350	Acetic acid	-	-	-	-	-	-	-	-	-
350	Methanol	-	-	-	-	-	-	-	-	-
350	2,2,2-Trifluoroethanol	-	-	-	-	-	-	-	-	-

Wavelength (nm)	Solvent	τ_1 (ns)	A_1 (%)	τ_2 (ns)	A_2 (%)	τ_3 (ns)	A_3 (%)	τ_f (ns) (Intensity Weighted)	$1/\tau_f$	χ^2
500	Toluene	-	-	-	-	-	-	-	-	-
500	1,4-Dioxane	0.22	30.81	1.42	32.95	6.50	36.24	2.89	0.35	1.06
500	Chloroform	0.18	77.87	1.49	15.53	7.83	6.60	0.89	1.13	1.21
500	Acetonitrile	-	-	-	-	-	-	-	-	-
500	1-Octanol	-	-	-	-	-	-	-	-	-
500	1-Hexanol	-	-	-	-	-	-	-	-	-
500	1-Butanol	-	-	-	-	-	-	-	-	-
500	1-Pentanol	-	-	-	-	-	-	-	-	-
500	1-Propanol	-	-	-	-	-	-	-	-	-
500	Acetic acid	-	-	-	-	-	-	-	-	-
500	Methanol	-	-	-	-	-	-	-	-	-
500	2,2,2-Trifluoroethanol	-	-	-	-	-	-	-	-	-

Table 2.2.8. Summary of Time Correlated Single Photon Counting (TCSPC) fluorescent lifetimes (intensity weighted) of **12** at (a.) 350 nm and (b.) 500 nm, recorded using a 295 nm Light Emitting Diode (LED) light source.

2.2.6.2 Amplitude weighted.

Wavelength (nm)	Solvent	τ_1 (ns)	A_1 (%)	τ_2 (ns)	A_2 (%)	τ_3 (ns)	A_3 (%)	τ_f (ns) (Amplitude Weighted)	$1/\tau_f$	χ^2
350	Toluene	-	-	-	-	-	-	-	-	-
350	1,4-Dioxane	0.77	76.12	3.04	21.56	11.39	2.32	1.52	0.66	1.23
350	Chloroform	1.03	82.44	3.81	13.77	12.39	3.79	1.84	0.54	1.15
350	Acetonitrile	-	-	-	-	-	-	-	-	-
350	1-Octanol	1.90	79.70	8.67	20.30	-	-	3.27	0.31	1.27
350	1-Hexanol	1.07	68.46	4.04	26.75	15.36	4.78	2.55	0.39	1.16
350	1-Butanol	-	-	-	-	-	-	-	-	-
350	1-Pentanol	-	-	-	-	-	-	-	-	-
350	1-Propanol	-	-	-	-	-	-	-	-	-
350	Acetic acid	-	-	-	-	-	-	-	-	-
350	Methanol	-	-	-	-	-	-	-	-	-
350	2,2,2-Trifluoroethanol	-	-	-	-	-	-	-	-	-

Wavelength (nm)	Solvent	τ_1 (ns)	A_1 (%)	τ_2 (ns)	A_2 (%)	τ_3 (ns)	A_3 (%)	τ_f (ns) (Amplitude Weighted)	$1/\tau_f$	χ^2
500	Toluene	-	-	-	-	-	-	-	-	-
500	1,4-Dioxane	0.22	82.69	1.42	13.95	6.50	3.35	0.60	1.66	1.06
500	Chloroform	0.18	97.36	1.49	2.45	7.83	0.19	0.23	4.33	1.21
500	Acetonitrile	-	-	-	-	-	-	-	-	-
500	1-Octanol	-	-	-	-	-	-	-	-	-
500	1-Hexanol	-	-	-	-	-	-	-	-	-
500	1-Butanol	-	-	-	-	-	-	-	-	-
500	1-Pentanol	-	-	-	-	-	-	-	-	-
500	1-Propanol	-	-	-	-	-	-	-	-	-
500	Acetic acid	-	-	-	-	-	-	-	-	-
500	Methanol	-	-	-	-	-	-	-	-	-
500	2,2,2-Trifluoroethanol	-	-	-	-	-	-	-	-	-

Table 2.2.9. Summary of Time Correlated Single Photon Counting (TCSPC) fluorescent lifetimes (amplitude weighted) of **12** at (a.) 350 nm and (b.) 500 nm, recorded using a 295 nm Light Emitting Diode (LED) light source.

2.2.7 400 nm fluorescent lifetime results.

2.2.7.1 Intensity weighted.

Wavelength (nm)	Solvent	τ_1 (ns)	A_1 (%)	τ_2 (ns)	A_2 (%)	τ_3 (ns)	A_3 (%)	τ_f (ns) (Intensity Weighted)	$1/\tau_f$	χ^2
450	Toluene	-	-	-	-	-	-	-	-	-
450	1,4-Dioxane	-	-	-	-	-	-	-	-	-
450	Chloroform	0.64	12.35	1.41	87.65	-	-	1.31	0.76	2.10
450	Acetonitrile	-	-	-	-	-	-	-	-	-
450	1-Octanol	-	-	-	-	-	-	-	-	-
450	1-Hexanol	-	-	-	-	-	-	-	-	-
450	1-Butanol	-	-	-	-	-	-	-	-	-
450	1-Pentanol	-	-	-	-	-	-	-	-	-
450	1-Propanol	-	-	-	-	-	-	-	-	-
450	Acetic acid	-	-	-	-	-	-	-	-	-
450	Methanol	-	-	-	-	-	-	-	-	-
450	2,2,2-Trifluoroethanol	-	-	-	-	-	-	-	-	-

Table 2.2.10. Summary of Time Correlated Single Photon Counting (TCSPC) fluorescent lifetimes (intensity weighted) of **12** at 450 nm, recorded using a 405 nm Laser Diode excitation source source.

Wavelength (nm)	Solvent	τ_1 (ns)	A_1 (%)	τ_2 (ns)	A_2 (%)	τ_3 (ns)	A_3 (%)	τ_f (ns) (Amplitude Weighted)	$1/\tau_f$	χ^2
500	Toluene	-	-	-	-	-	-	-	-	-
500	1,4-Dioxane	-	-	-	-	-	-	-	-	-
500	Chloroform	0.23	20.18	1.39	76.65	7.04	3.17	1.34	0.75	1.07
500	Acetonitrile	-	-	-	-	-	-	-	-	-
500	1-Octanol	-	-	-	-	-	-	-	-	-
500	1-Hexanol	-	-	-	-	-	-	-	-	-
500	1-Butanol	-	-	-	-	-	-	-	-	-
500	1-Pentanol	-	-	-	-	-	-	-	-	-
500	1-Propanol	0.29	69.33	1.20	14.31	5.22	16.37	1.23	0.81	1.20
500	Acetic acid	-	-	-	-	-	-	-	-	-
500	Methanol	-	-	-	-	-	-	-	-	-
500	2,2,2-Trifluoroethanol	-	-	-	-	-	-	-	-	-

Table 2.2.11. Summary of Time Correlated Single Photon Counting (TCSPC) fluorescent lifetimes (intensity weighted) of **12** at 500 nm, recorded using a 405 nm Laser Diode excitation source source.

2.2.7.2 Amplitude weighted.

Wavelength (nm)	Solvent	τ_1 (ns)	A_1 (%)	τ_2 (ns)	A_2 (%)	τ_3 (ns)	A_3 (%)	τ_f (ns) (Intensity Weighted)	$1/\tau_f$	χ^2
450	Toluene	-	-	-	-	-	-	-	-	-
450	1,4-Dioxane	-	-	-	-	-	-	-	-	-
450	Chloroform	0.64	23.76	1.41	76.24	-	-	1.22	0.82	2.10
450	Acetonitrile	-	-	-	-	-	-	-	-	-
450	1-Octanol	-	-	-	-	-	-	-	-	-
450	1-Hexanol	-	-	-	-	-	-	-	-	-
450	1-Butanol	-	-	-	-	-	-	-	-	-
450	1-Pentanol	-	-	-	-	-	-	-	-	-
450	1-Propanol	-	-	-	-	-	-	-	-	-
450	Acetic acid	-	-	-	-	-	-	-	-	-
450	Methanol	-	-	-	-	-	-	-	-	-
450	2,2,2-Trifluoroethanol	-	-	-	-	-	-	-	-	-

Table 2.2.12. Summary of Time Correlated Single Photon Counting (TCSPC) fluorescent lifetimes (amplitude weighted) of **12** at 450 nm, recorded using a 405 nm Laser Diode excitation source source.

Wavelength (nm)	Solvent	τ_1 (ns)	A_1 (%)	τ_2 (ns)	A_2 (%)	τ_3 (ns)	A_3 (%)	τ_f (ns) (Amplitude Weighted)	$1/\tau_f$	χ^2
500	Toluene	-	-	-	-	-	-	-	-	-
500	1,4-Dioxane	-	-	-	-	-	-	-	-	-
500	Chloroform	0.62	20.02	1.51	71.92	6.53	7.06	1.68	0.59	1.14
500	Acetonitrile	-	-	-	-	-	-	-	-	-
500	1-Octanol	-	-	-	-	-	-	-	-	-
500	1-Hexanol	-	-	-	-	-	-	-	-	-
500	1-Butanol	-	-	-	-	-	-	-	-	-
500	1-Pentanol	-	-	-	-	-	-	-	-	-
500	1-Propanol	-	-	-	-	-	-	-	-	-
500	Acetic acid	-	-	-	-	-	-	-	-	-
500	Methanol	-	-	-	-	-	-	-	-	-
500	2,2,2-Trifluoroethanol	-	-	-	-	-	-	-	-	-

Table 2.2.13. Summary of Time Correlated Single Photon Counting (TCSPC) fluorescent lifetimes (amplitude weighted) of **11a** at 500 nm, recorded using a 405 nm Laser Diode excitation source source.

2.2.8 400 nm average fluorescent lifetimes - Solvatochromic analysis.

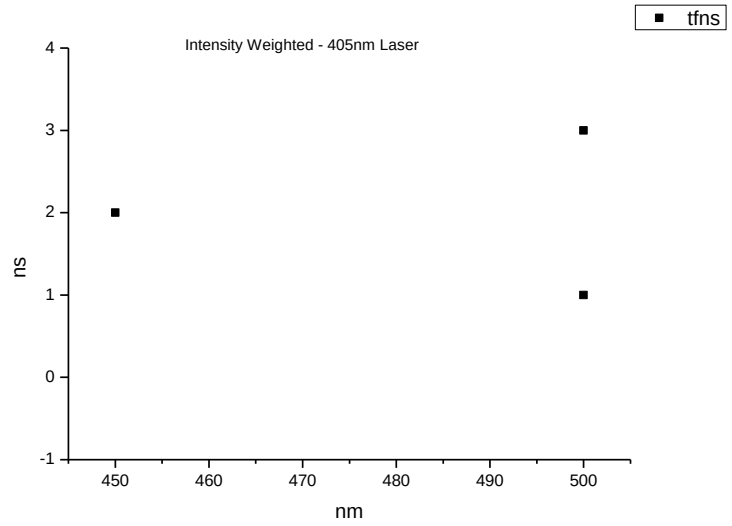

Figure 2.2.49. Intensity weighted average lifetime (τ_f) of **12** versus wavelength (nm).

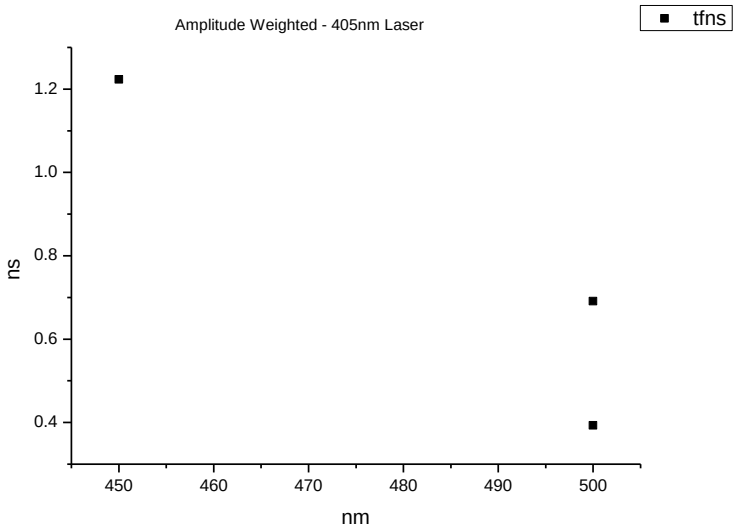

Figure 2.2.50. Amplitude weighted average lifetime (τ_f) of **12** versus wavelength (nm).

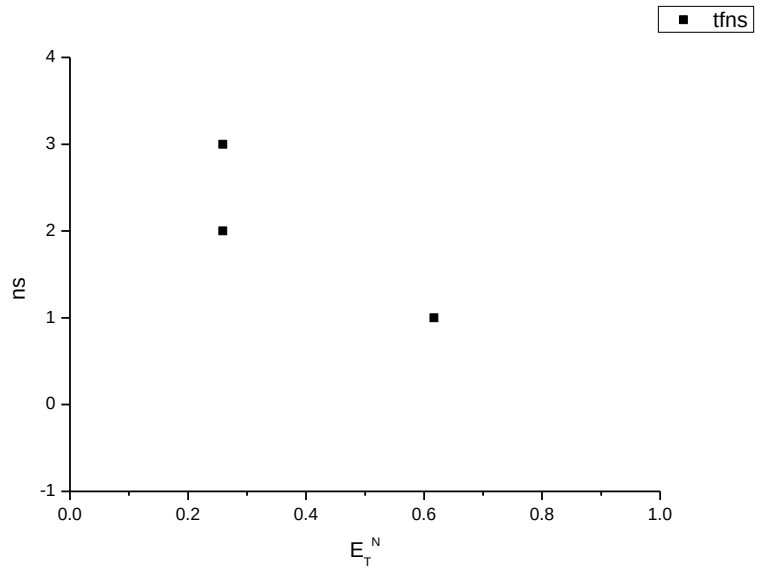

Figure 2.2.51. Intensity weighted average lifetime (τ_f) of N=C-Ph**3a** versus E_T^N.

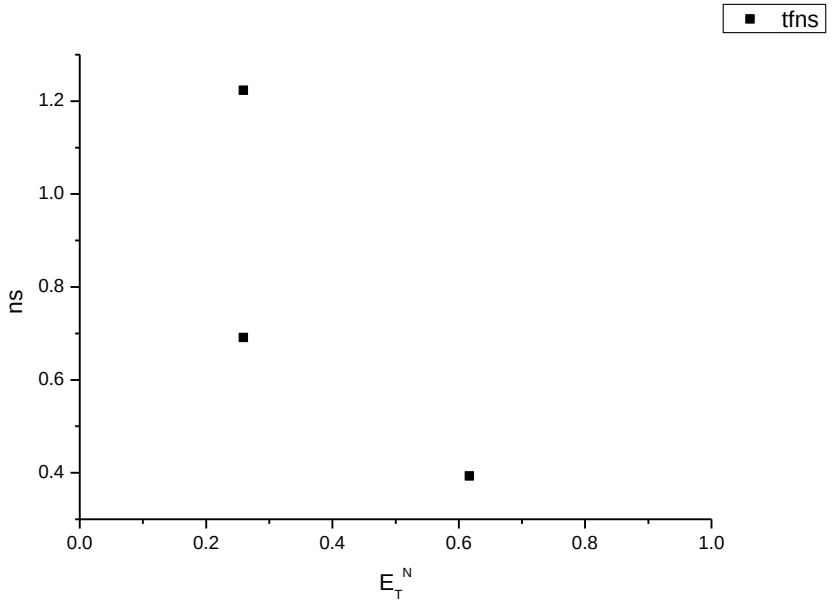

Figure 2.2.52. Amplitude weighted average lifetime (τ_f) of **12** versus E_T^N.

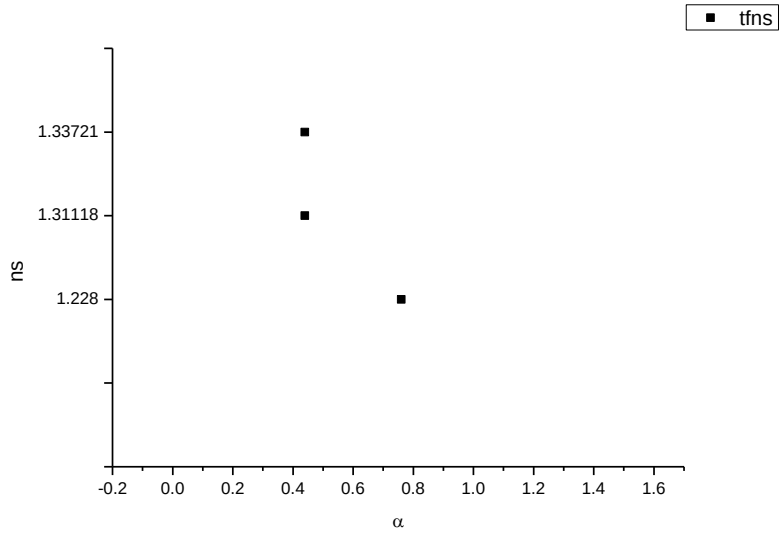

Figure 2.2.53. Intensity weighted average lifetime (τ_f) of **12** versus α.

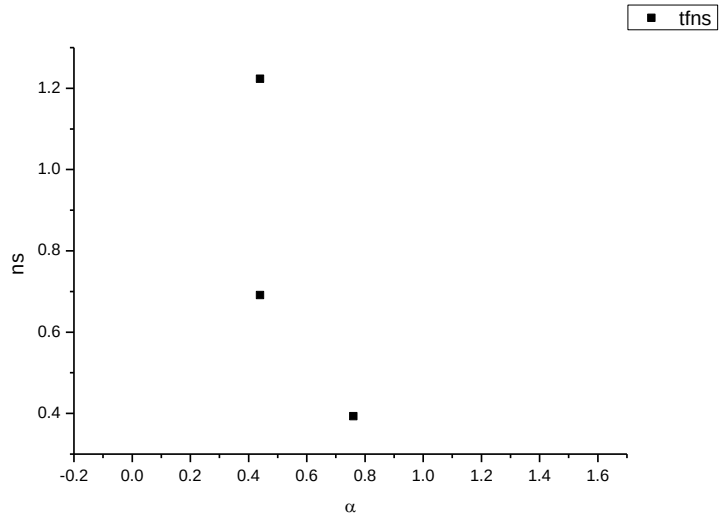

Figure 2.2.54. Amplitude weighted average lifetime (τ_f) of **12** versus α.

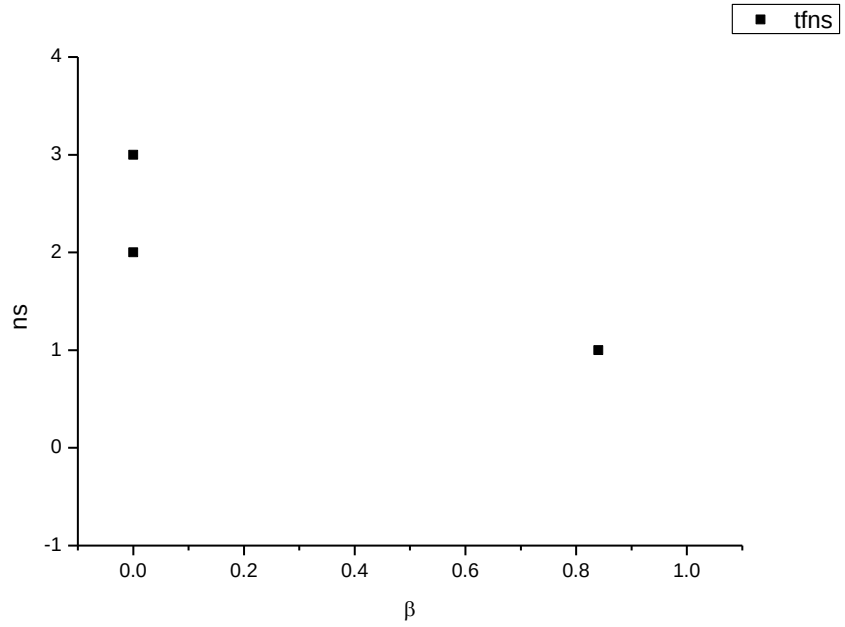

Figure 2.2.55. Intensity weighted average lifetime (τ_f) of **12** versus β.

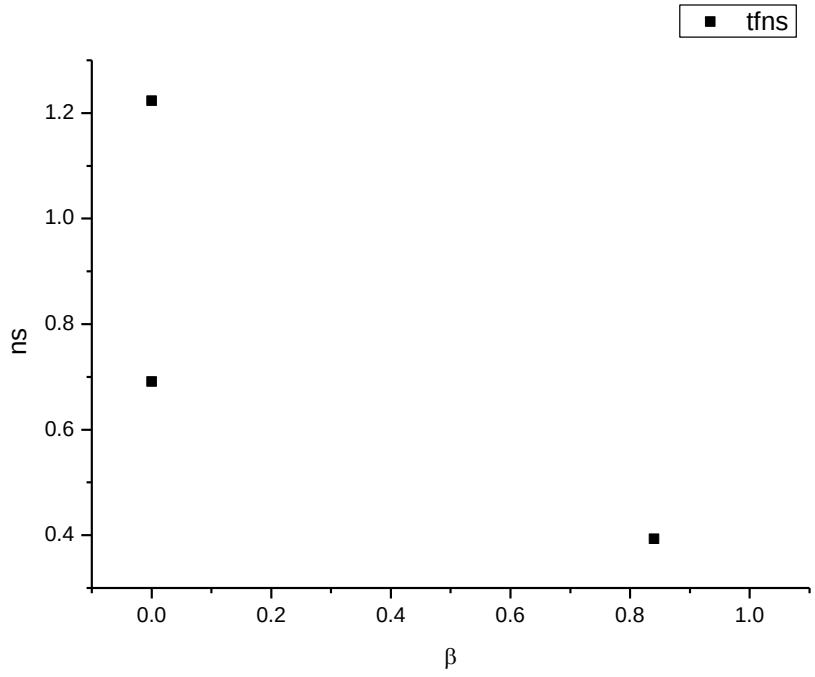

Figure 2.2.56. Amplitude weighted average lifetime (τ_f) of **12** versus β.

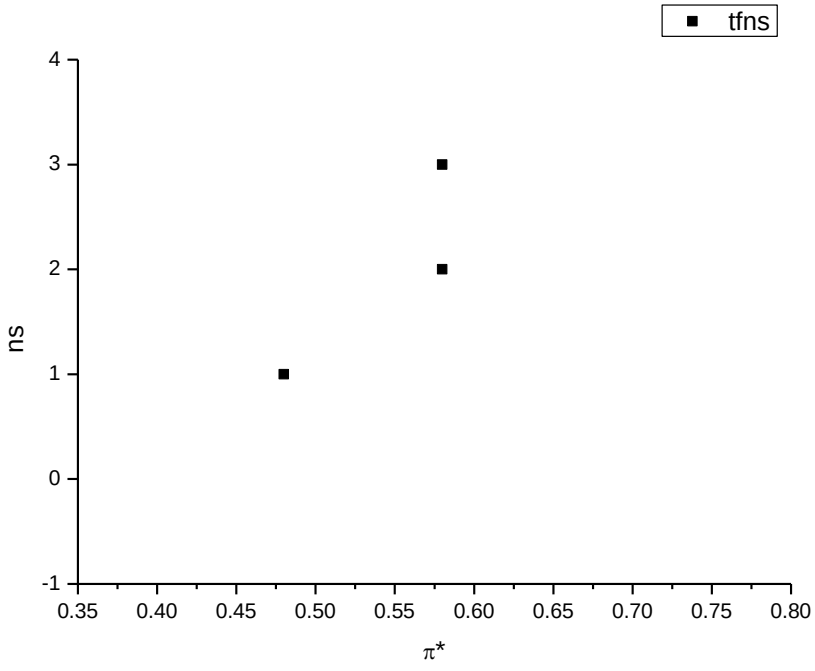

Figure 2.2.57. Intensity weighted average lifetime (τ_f) of **12** versus π*.

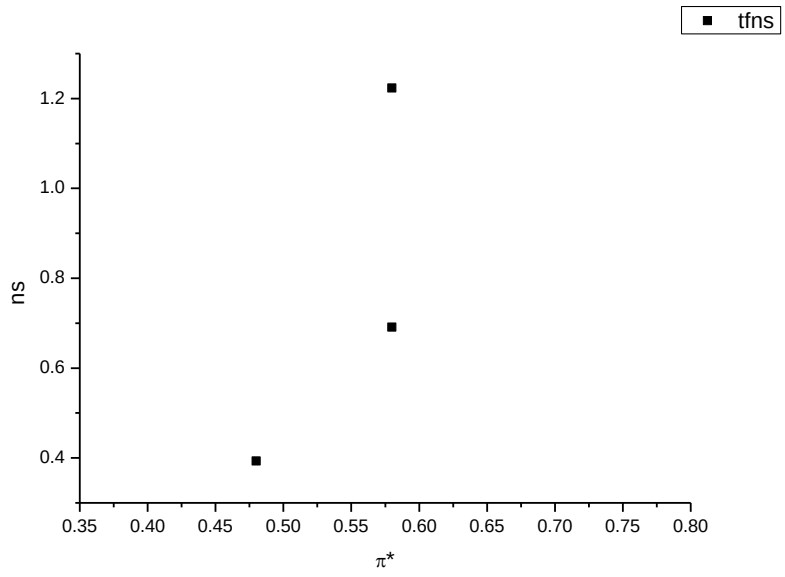

Figure 2.2.58. Amplitude weighted average lifetime (τ_f) of **12** versus π*.

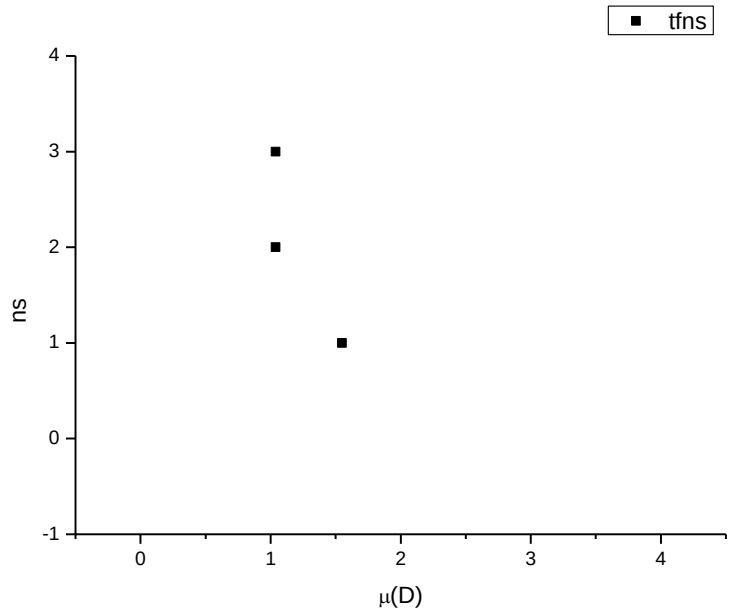

Figure 2.2.59. Intensity weighted average lifetime (τ_f) of **12** versus μ(D).

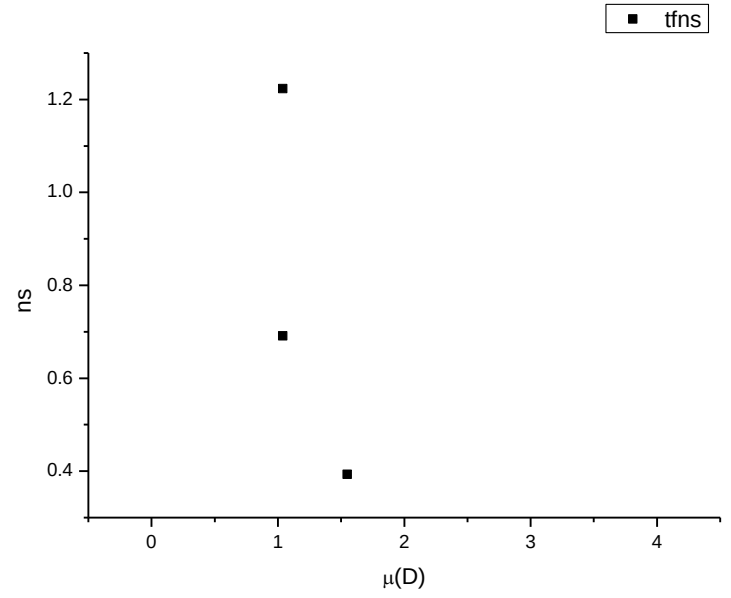

Figure 2.2.60. Amplitude weighted average lifetime (τ_f) of **12** versus μ(D).

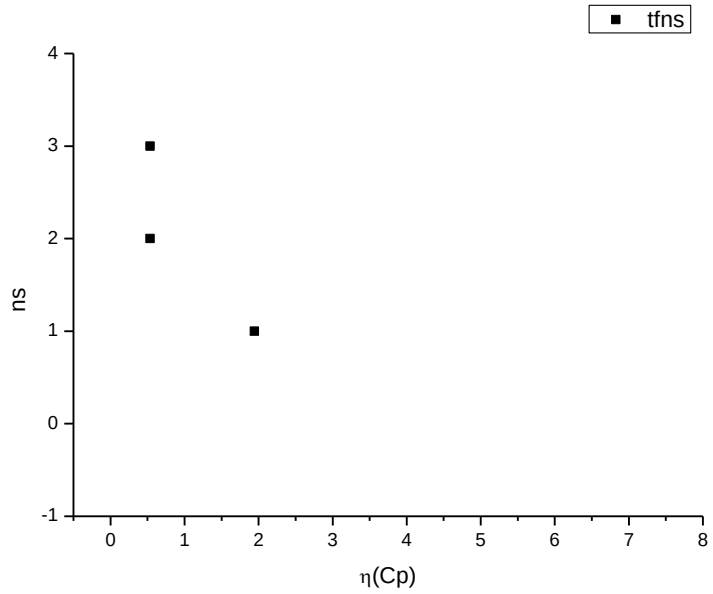

Figure 2.2.61. Intensity weighted average lifetime (τ_f) of **12** versus η(Cp).

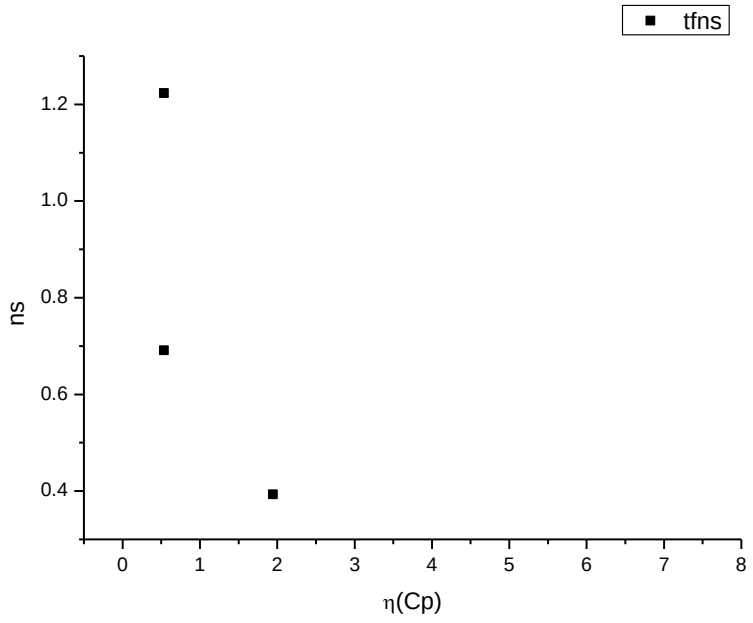

Figure 2.2.62. Amplitude weighted average lifetime (τ_f) of **12** versus η(Cp).

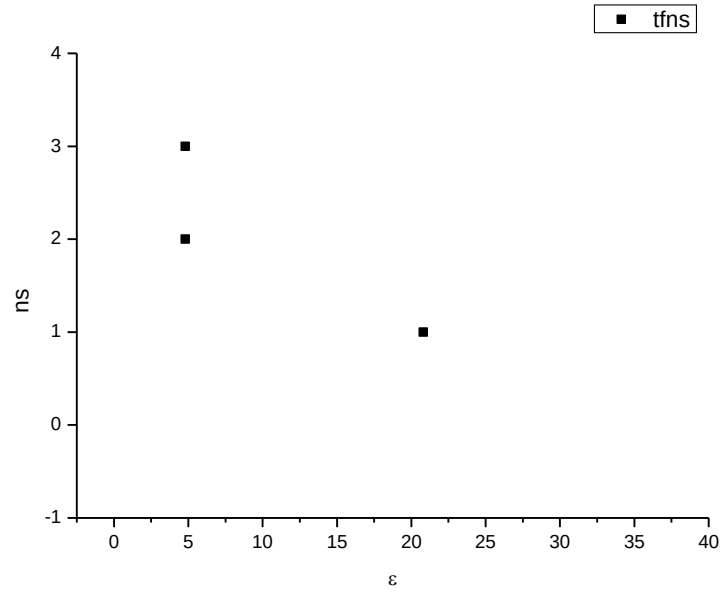

Figure 2.2.63. Intensity weighted average lifetime (τ_f) of **12** versus ε.

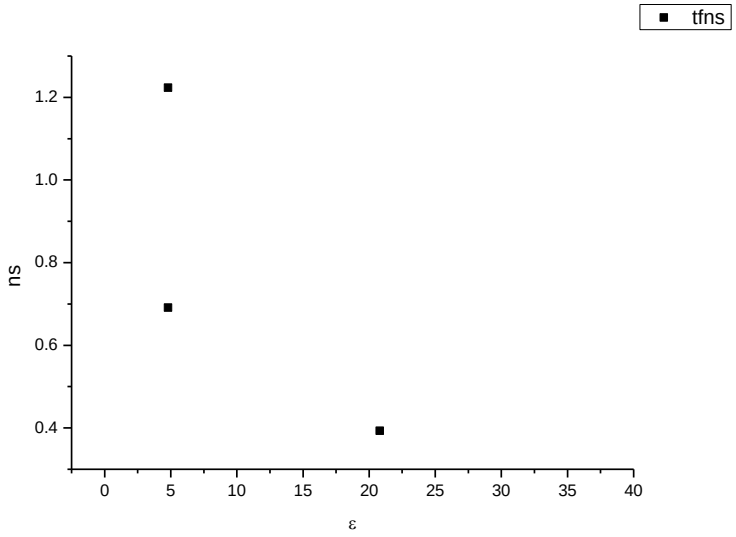

Figure 2.2.64. Amplitude weighted average lifetime (τ_f) of **12** versus ε.

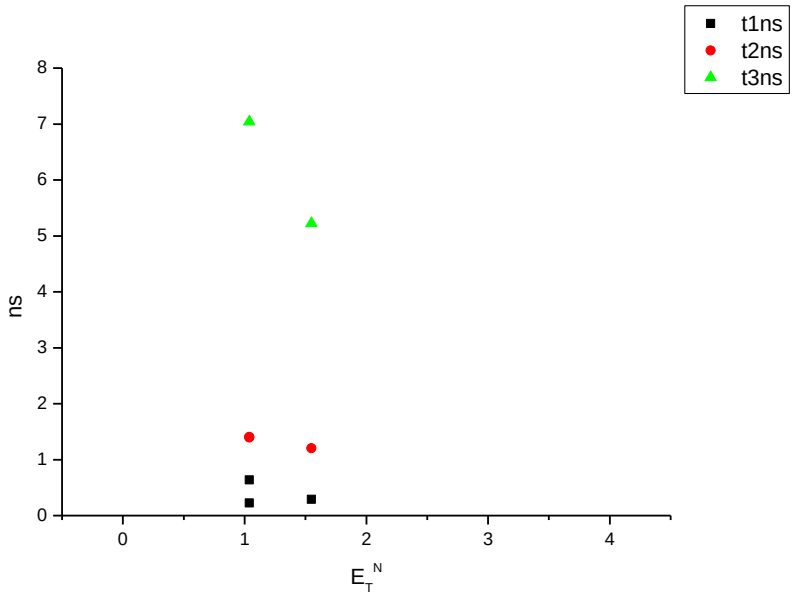

Figure 2.2.65. Intensity weighted components of TCSPC lifetime decay of **12** (450 to 500 nm) versus E_T^N.

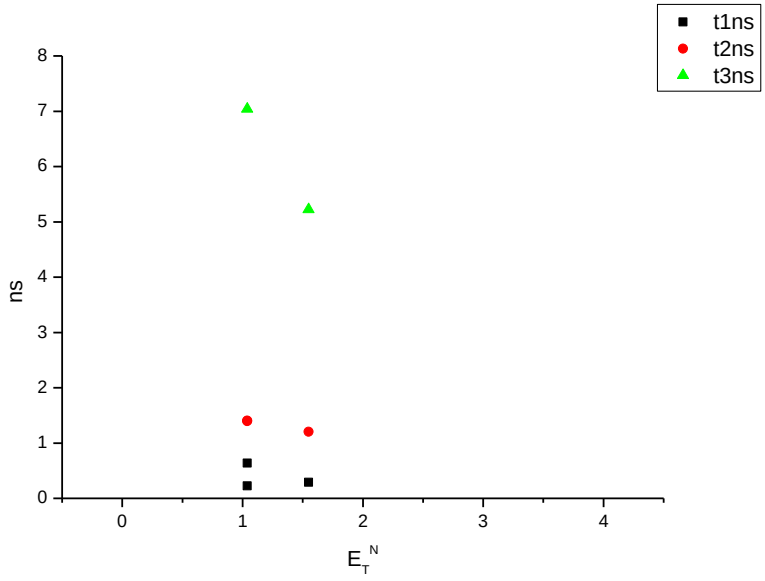

Figure 2.2.66. Amplitude weighted components of TCSPC lifetime decay of **12** (450 to 500 nm) versus E_T^N.

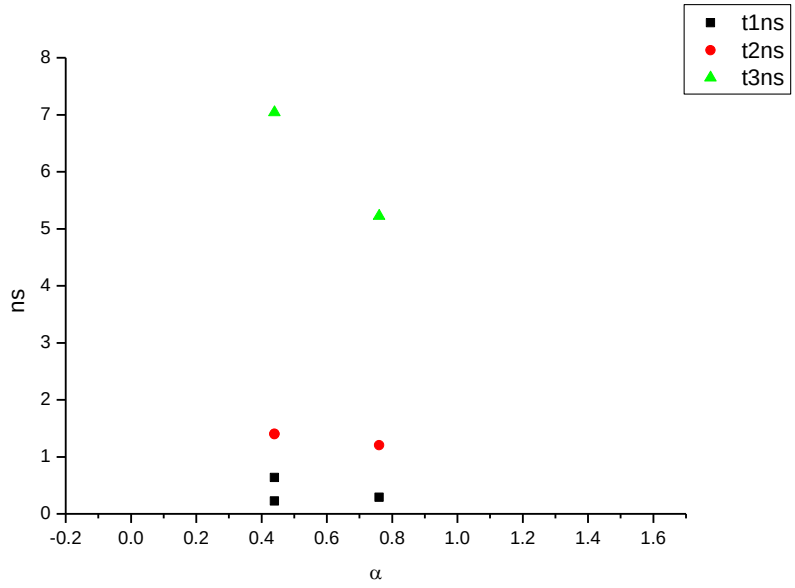

Figure 2.2.67. Intensity weighted components of TCSPC lifetime decay of **12** (450 to 500 nm) versus α.

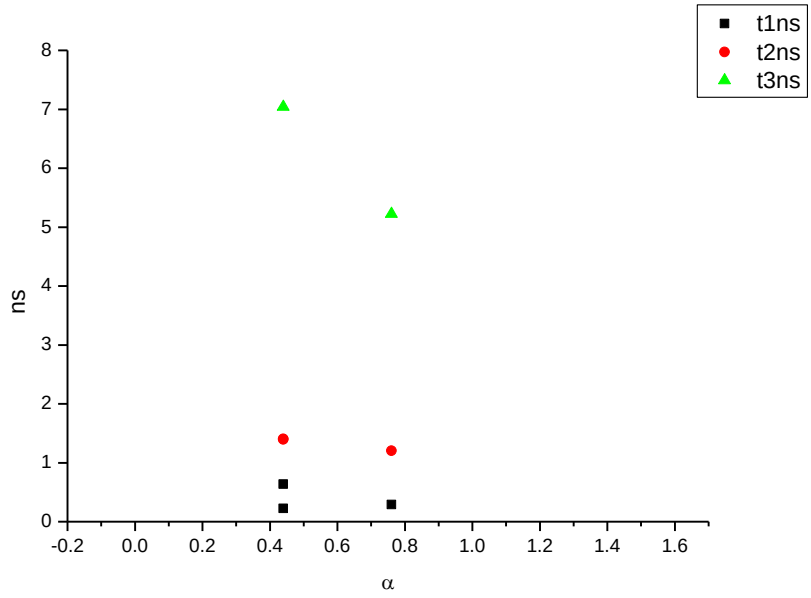

Figure 2.2.68. Amplitude weighted components of TCSPC lifetime decay of **12** (450 to 500 nm) versus α.

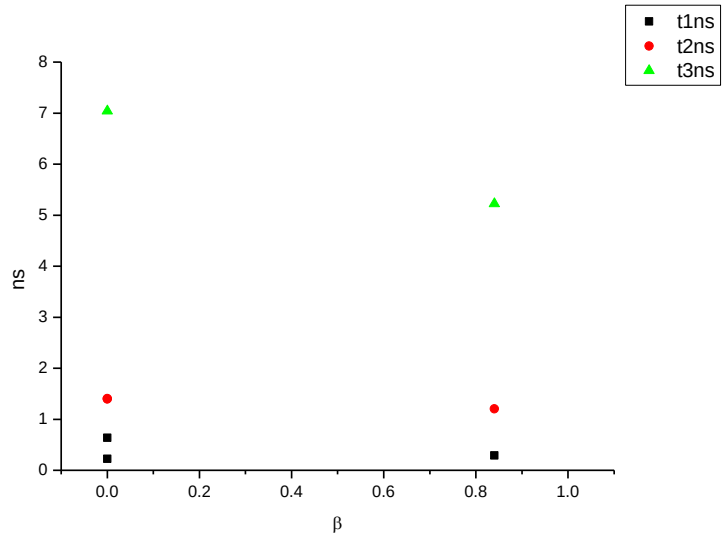

Figure 2.2.69. Intensity weighted components of TCSPC lifetime decay of **12** (450 to 500 nm) versus β.

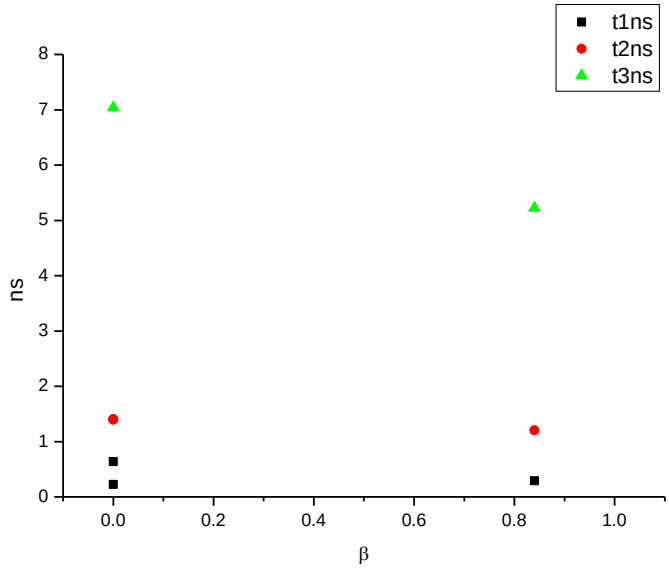

Figure 2.2.70. Amplitude weighted components of TCSPC lifetime decay of **15** (450 to 500 nm) versus β.

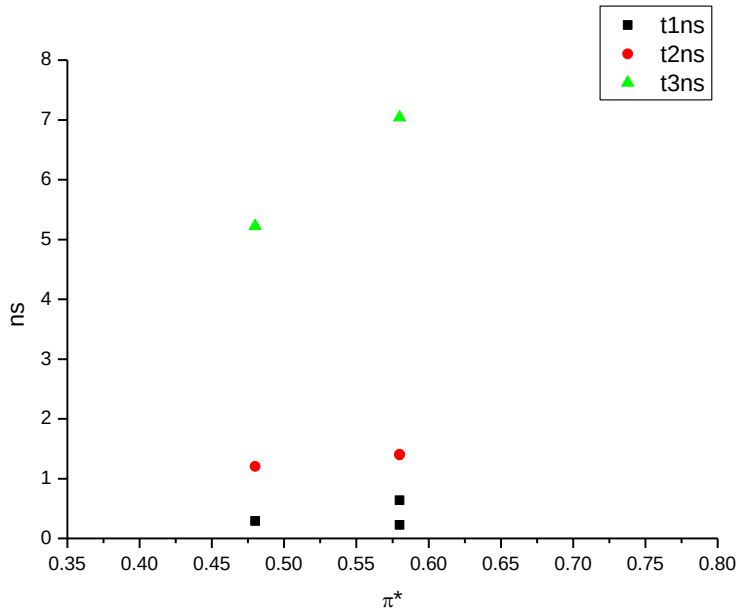

Figure 2.2.71. Intensity weighted components of TCSPC lifetime decay of **12** (450 to 500 nm) versus π*.

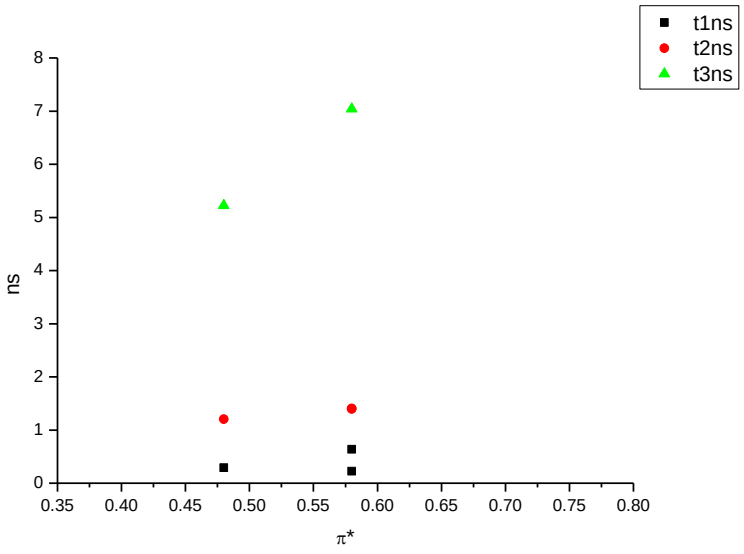

Figure 2.2.72. Amplitude weighted components of TCSPC lifetime decay of **12** (450 to 500 nm) versus π*.

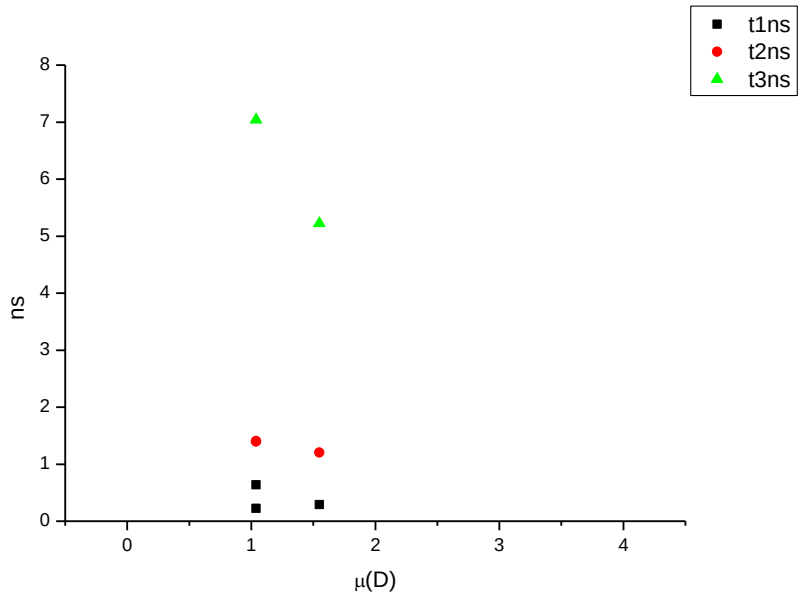

Figure 2.2.73. Intensity weighted components of TCSPC lifetime decay of **12** (450 to 500 nm) versus μ(D).

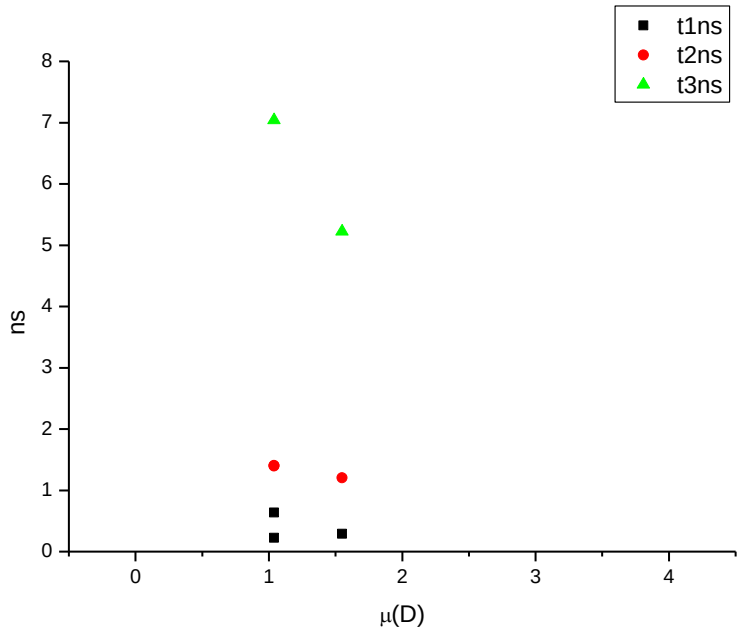

Figure 2.2.74. Amplitude weighted components of TCSPC lifetime decay of **12** (450 to 500 nm) versus μ(D).

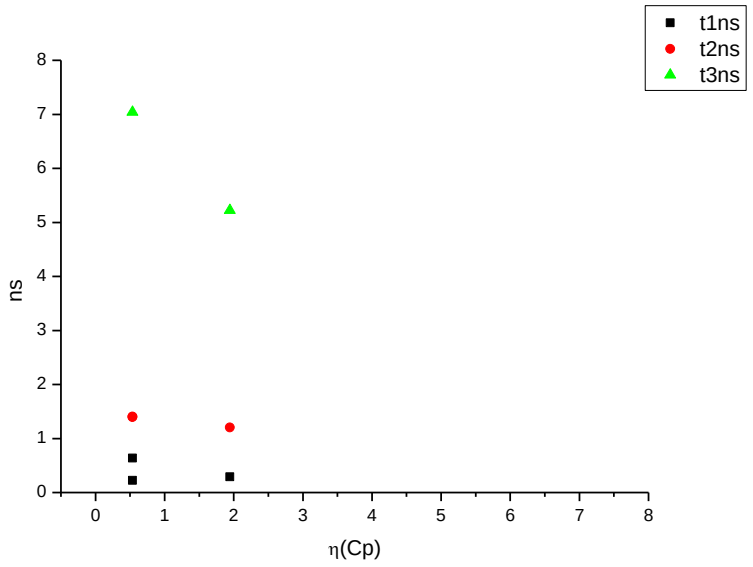

Figure 2.2.75. Intensity weighted components of TCSPC lifetime decay of **12** (450 to 500 nm) versus η(Cp).

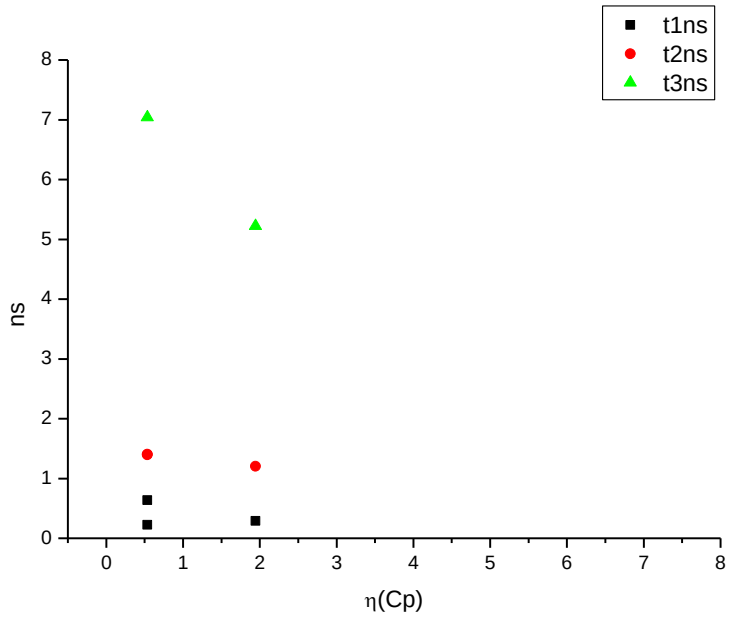

Figure 2.2.76. Amplitude weighted components of TCSPC lifetime decay of **12** (450 to 500 nm) versus η(Cp).

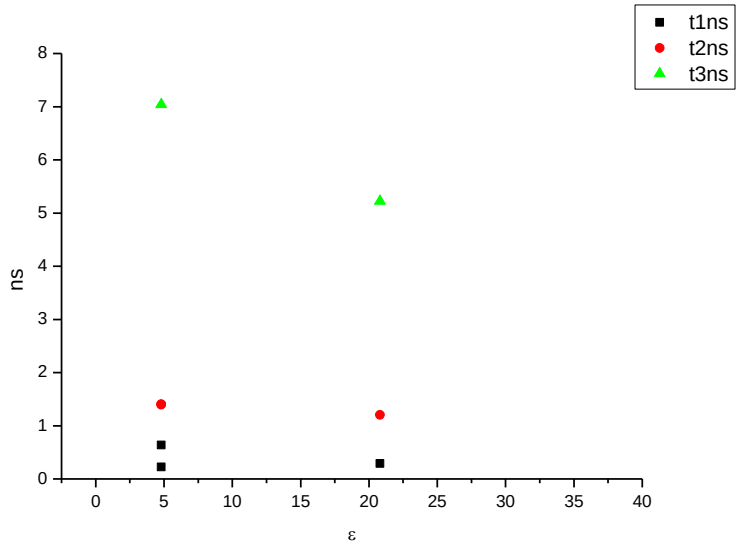

Figure 2.2.77. Intensity weighted components of TCSPC lifetime decay of **12** (450 to 500 nm) versus ε.

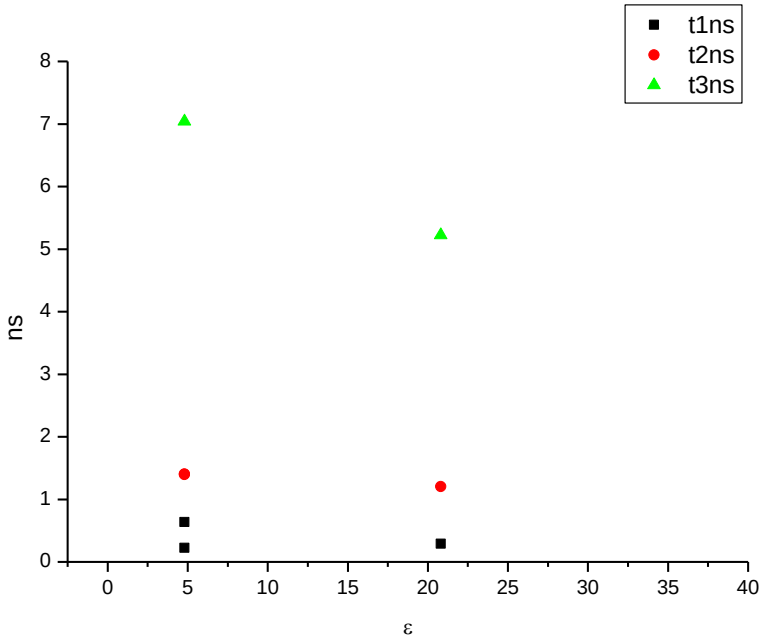

Figure 2.2.78. Amplitude weighted components of TCSPC lifetime decay of **12** (450 to 500 nm) versus ε.

2.2.8.1 500 nm Lifetime – Solvatochromic analysis.

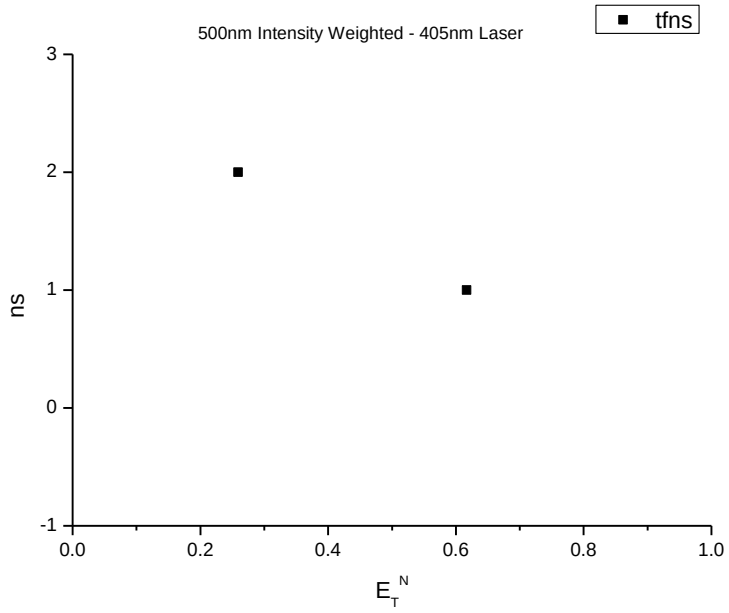

Figure 2.2.79. Intensity weighted average lifetime (τ_f) of **12** at 500 nm versus E_T^N.

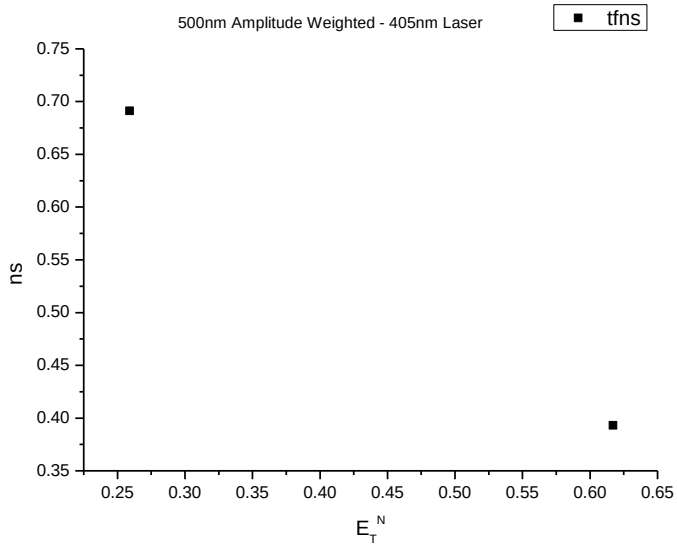

Figure 2.2.80. Amplitude weighted average lifetime (τ_f) of **12** at 500 nm versus E_T^N.

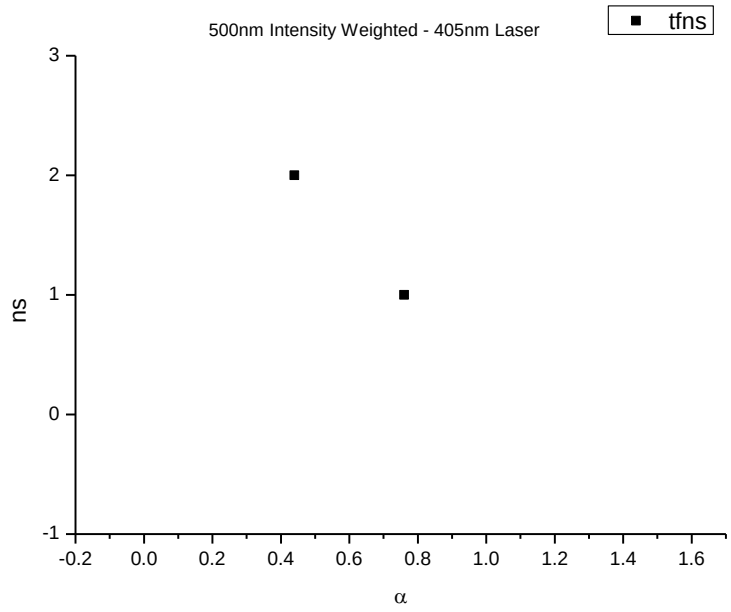

Figure 2.2.81. Intensity weighted average lifetime (τ_f) of **12** at 500 nm versus α.

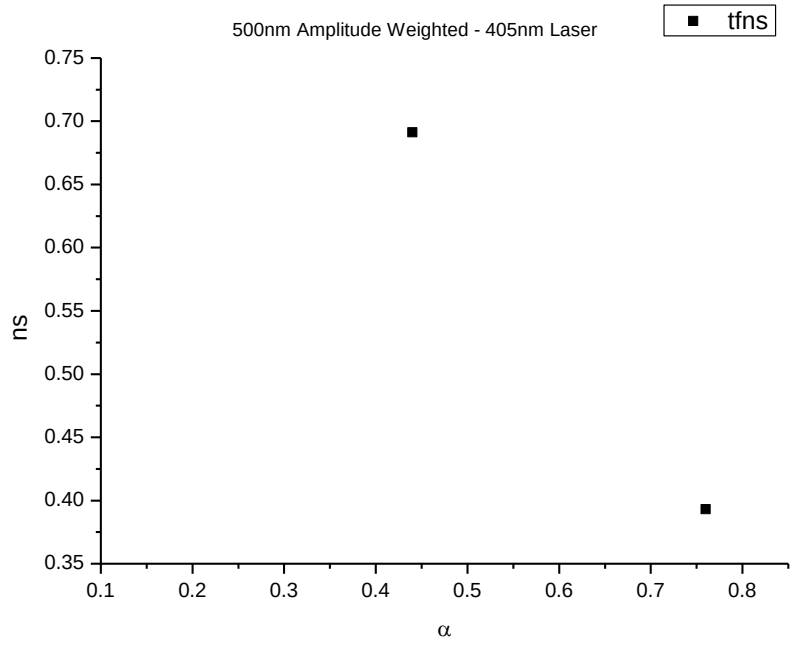

Figure 2.2.82. Amplitude weighted average lifetime (τ_f) of **12** at 500 nm versus α.

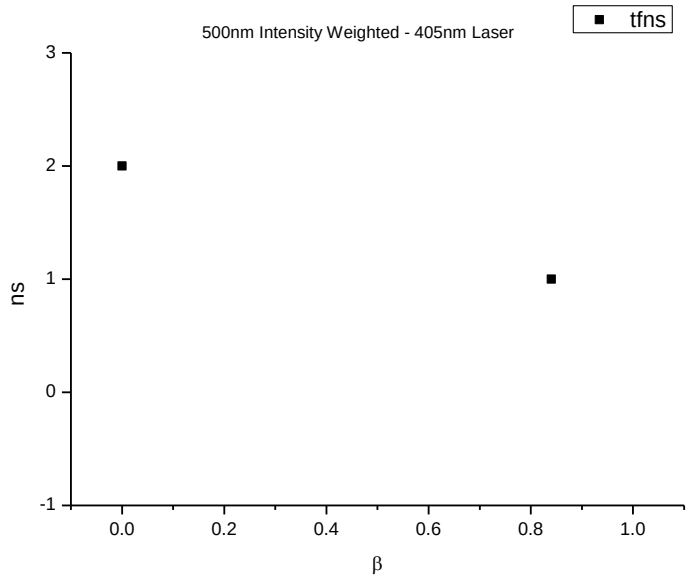

Figure 2.2.83. Intensity weighted average lifetime (τ_f) of **12** at 500 nm versus β.

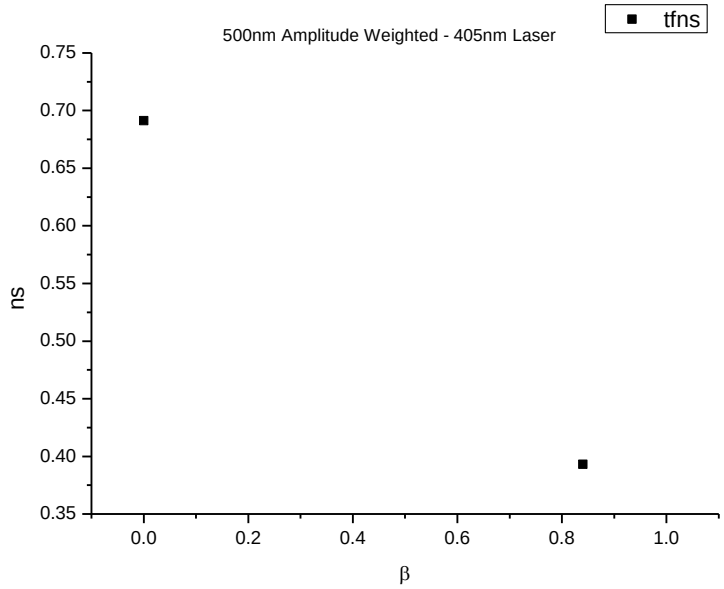

Figure 2.2.84. Amplitude weighted average lifetime (τ_f) of **12** at 500 nm versus β.

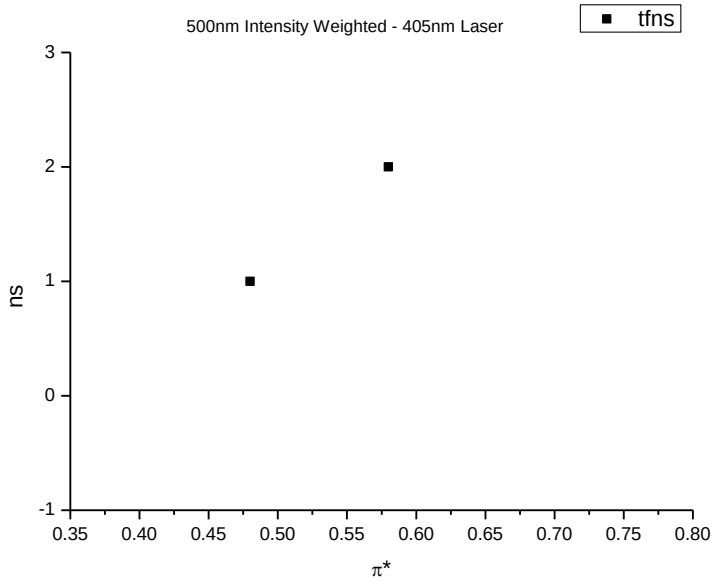

Figure 2.2.85. Intensity weighted average lifetime (τ_f) of **12** at 500 nm versus π*.

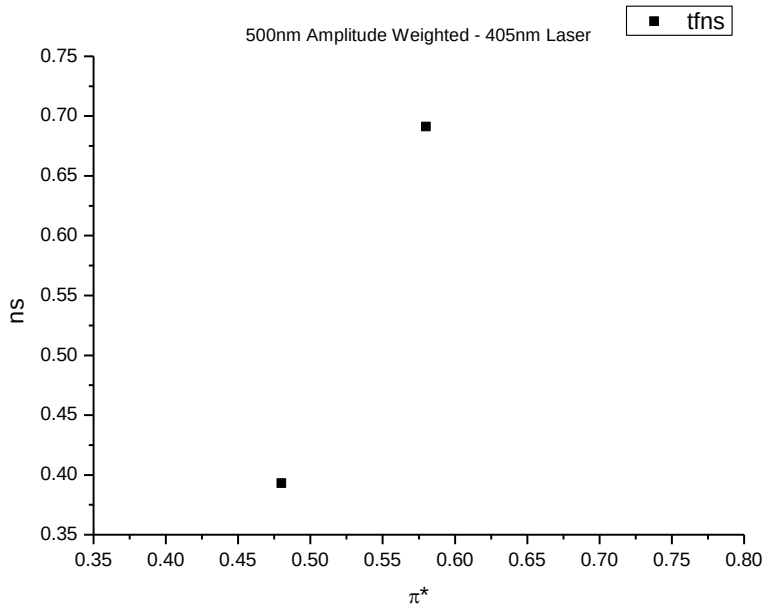

Figure 2.2.86. Amplitude weighted average lifetime (τ_f) of **12** at 500 nm versus π*.

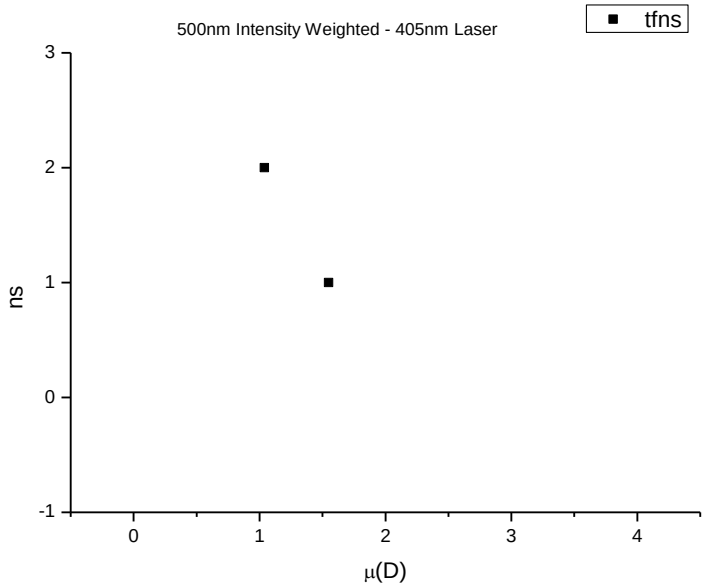

Figure 2.2.87. Intensity weighted average lifetime (τ_f) of **12** at 500 nm versus μ(D).

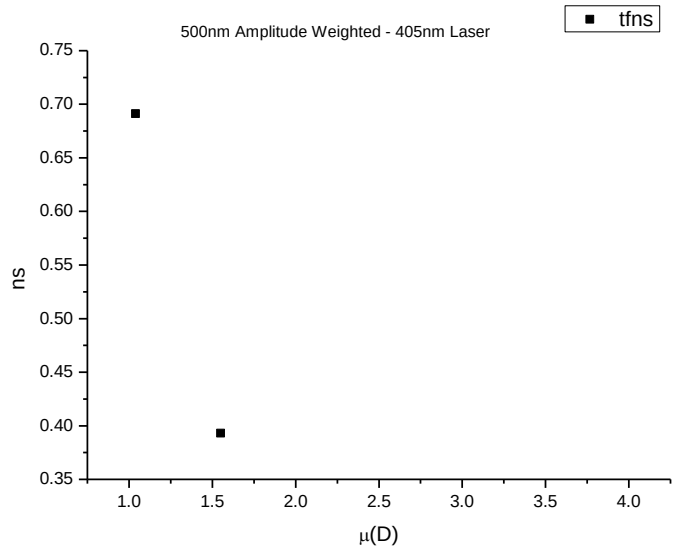

Figure 2.2.88. Amplitude weighted average lifetime (τ_f) of **12** at 500 nm versus μ(D).

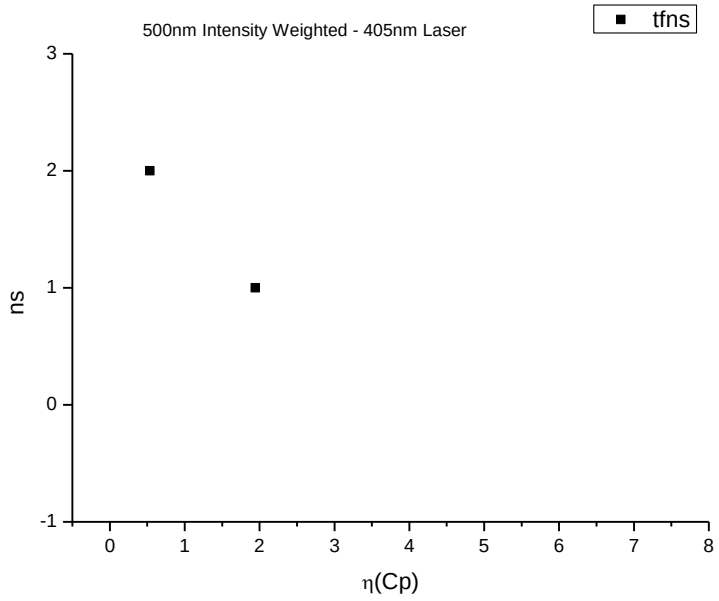

Figure 2.2.89. Intensity weighted average lifetime (τ_f) of **12** at 500 nm versus η(Cp).

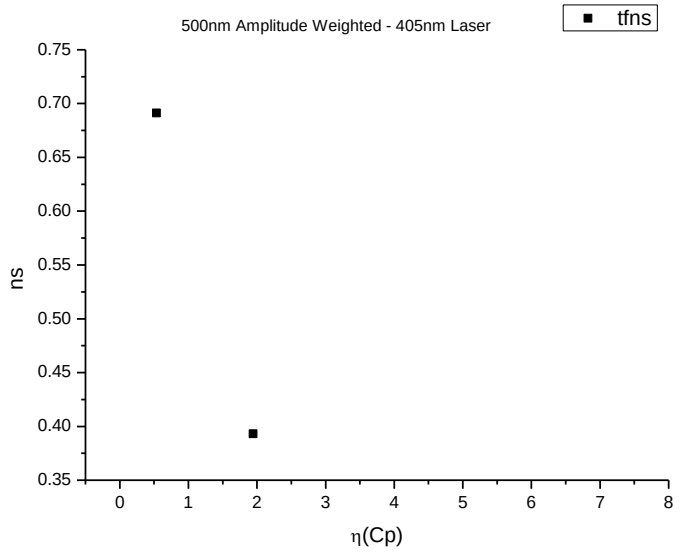

Figure 2.2.90. Amplitude weighted average lifetime (τ_f) of **12** at 500 nm versus η(Cp).

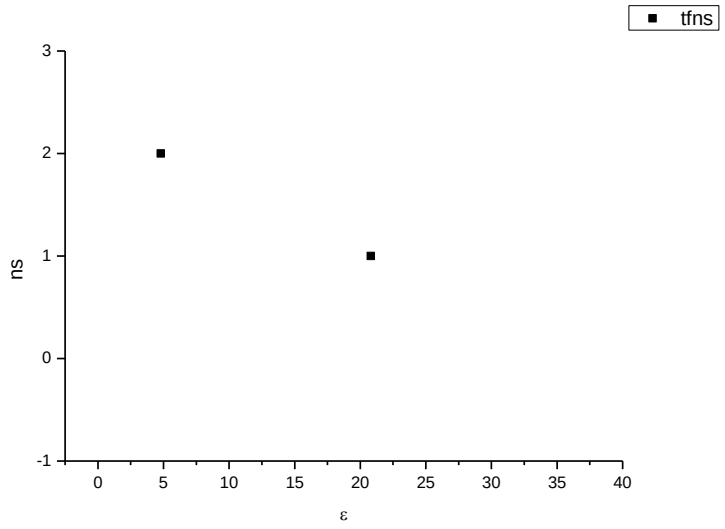

Figure 2.2.91. Intensity weighted average lifetime (τ_f) of **12** at 500 nm versus ε.

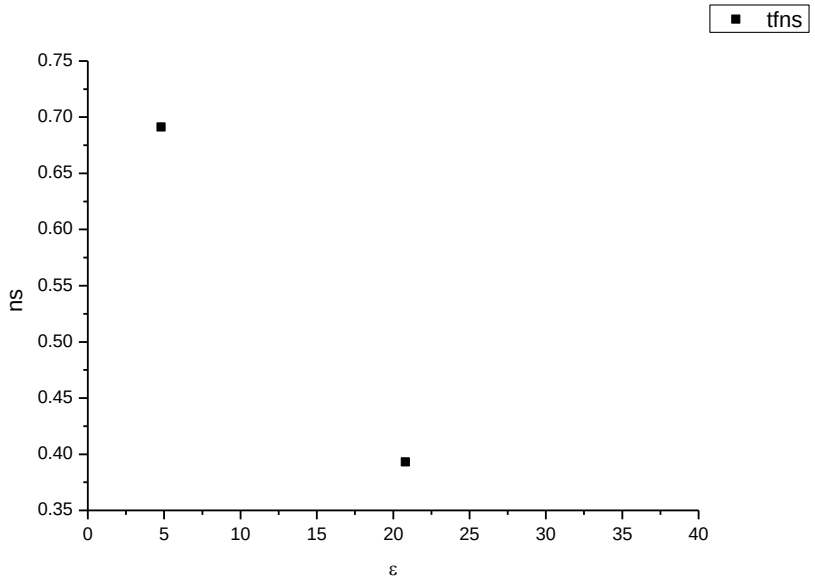

Figure 2.2.92. Amplitude weighted average lifetime (τ_f) of **12** at 500 nm versus ε.

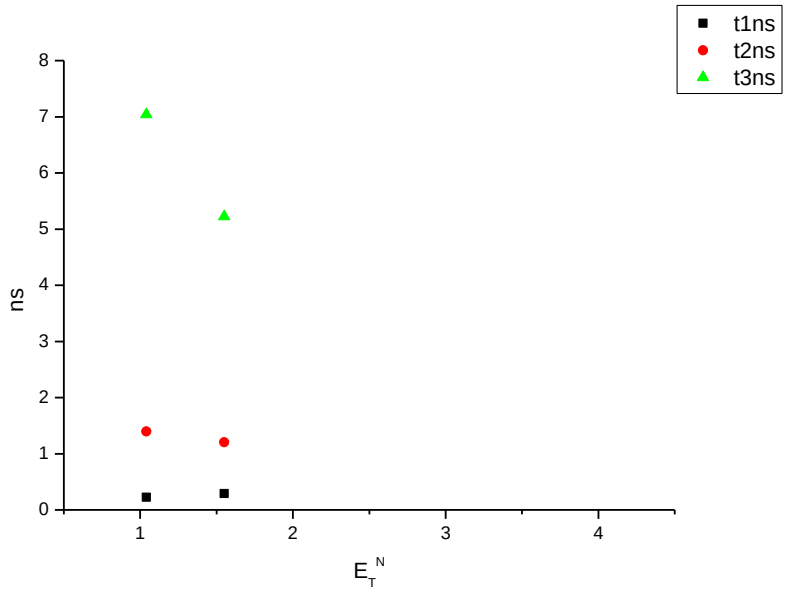

Figure 2.2.93. Intensity weighted components of TCSPC lifetime decay of **12** (500 nm) versus E_T^N.

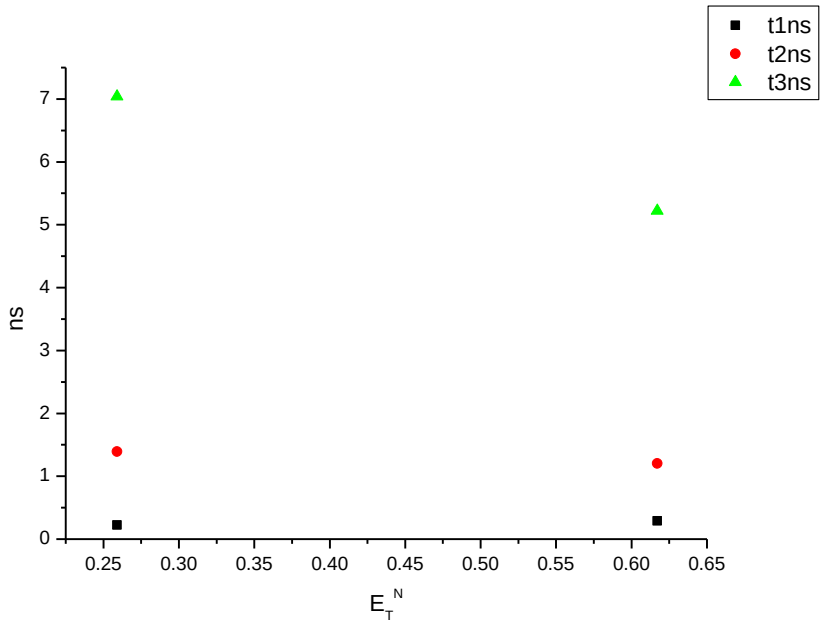

Figure 2.2.94. Amplitude weighted components of TCSPC lifetime decay of **12** (500 nm) versus E_T^N.

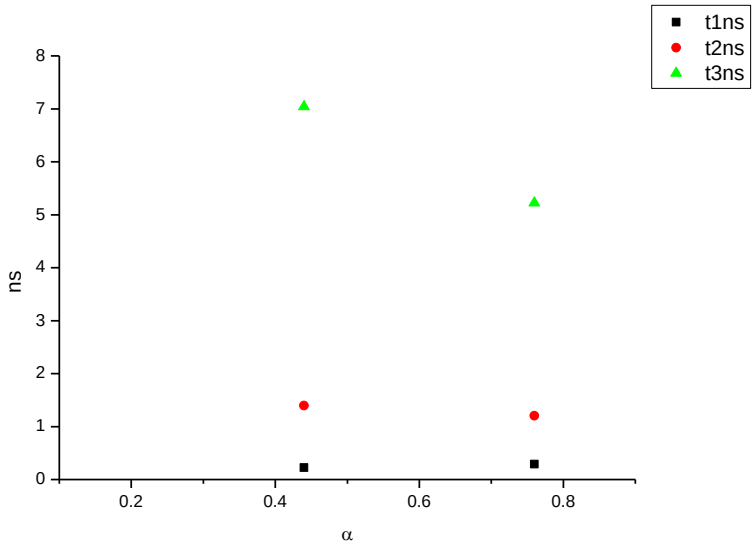

Figure 2.2.95. Intensity weighted components of TCSPC lifetime decay of **12** (500 nm) versus α.

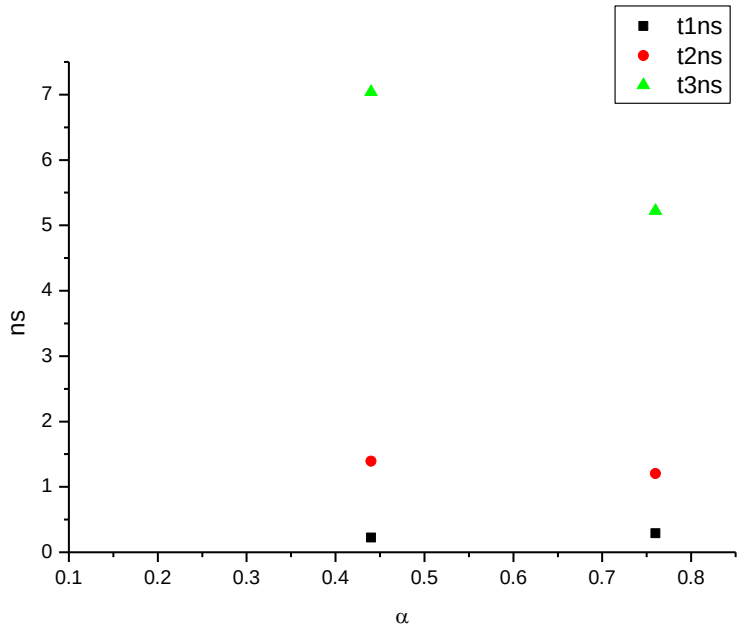

Figure 2.2.96. Amplitude weighted components of TCSPC lifetime decay of **12** (500 nm) versus α.

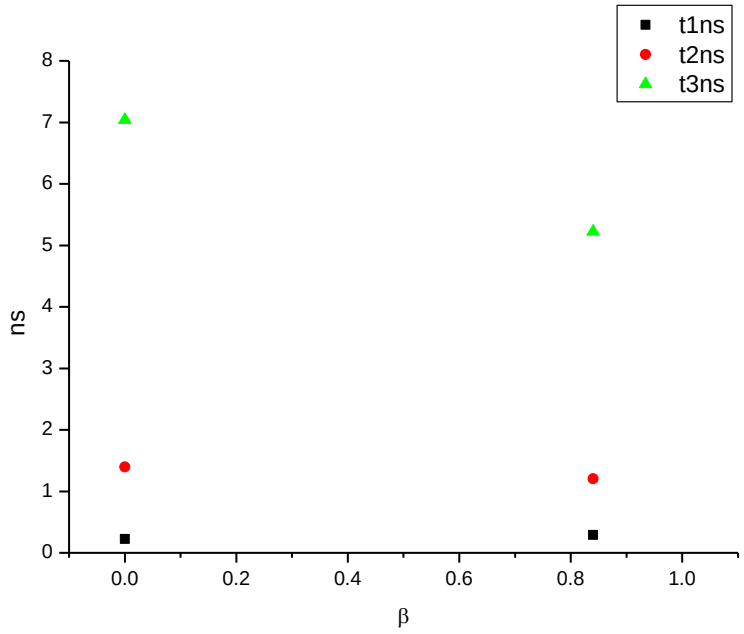

Figure 2.2.97. Intensity weighted components of TCSPC lifetime decay of **12** (500 nm) versus β.

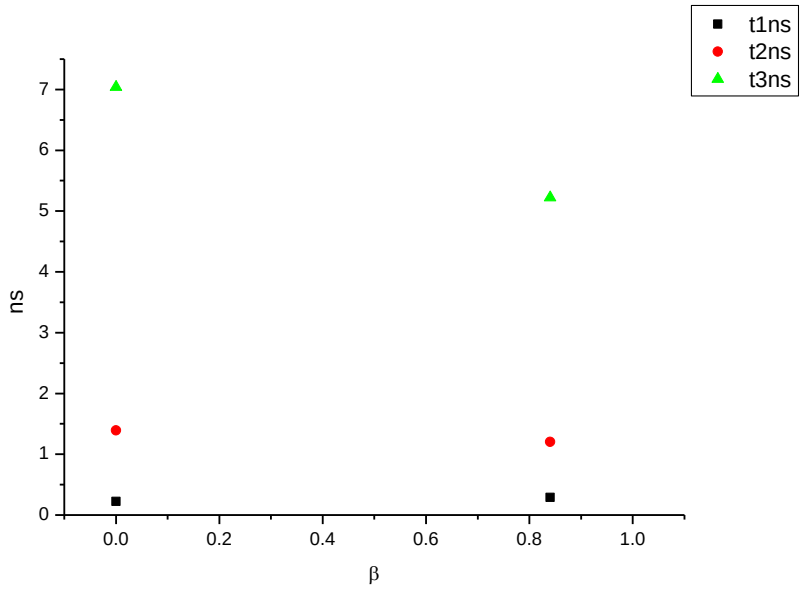

Figure 2.2.98. Amplitude weighted components of TCSPC lifetime decay of **12** (500 nm) versus β.

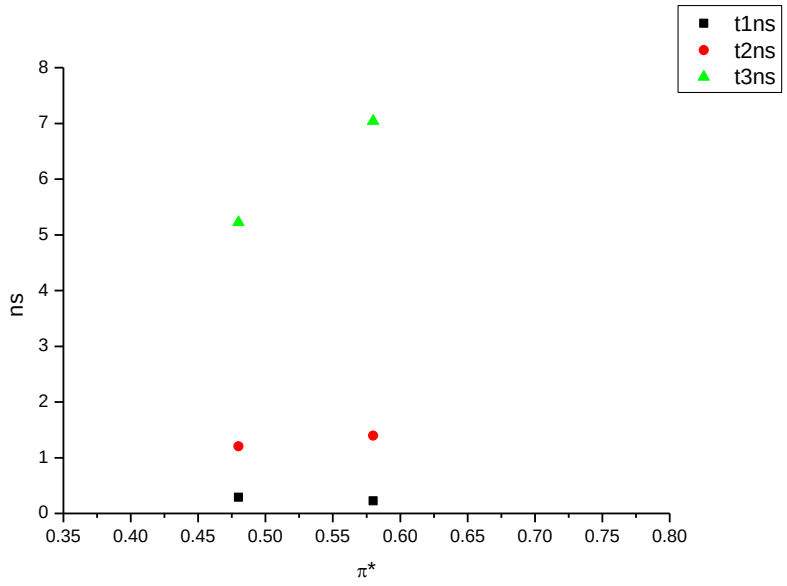

Figure 2.2.99. Intensity weighted components of TCSPC lifetime decay of **12** (500 nm) versus π*.

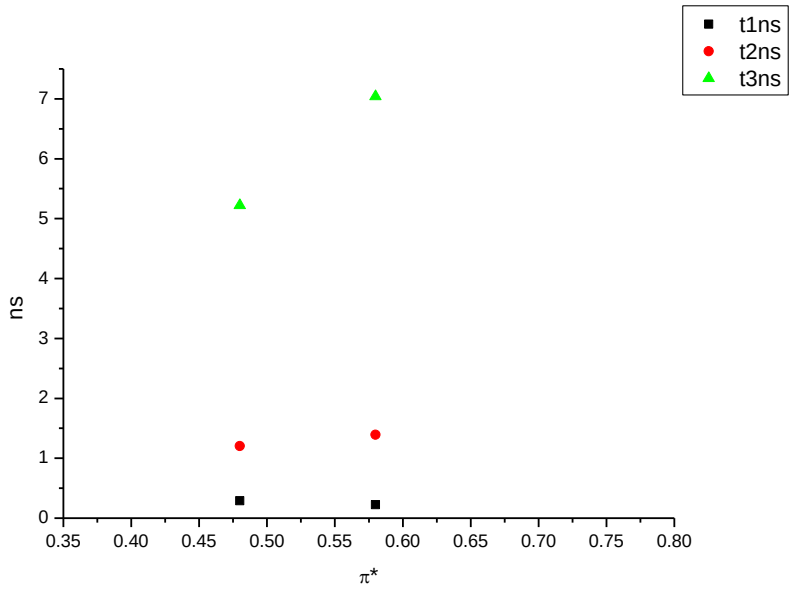

Figure 2.2.100. Amplitude weighted components of TCSPC lifetime decay of **12** (500 nm) versus π*.

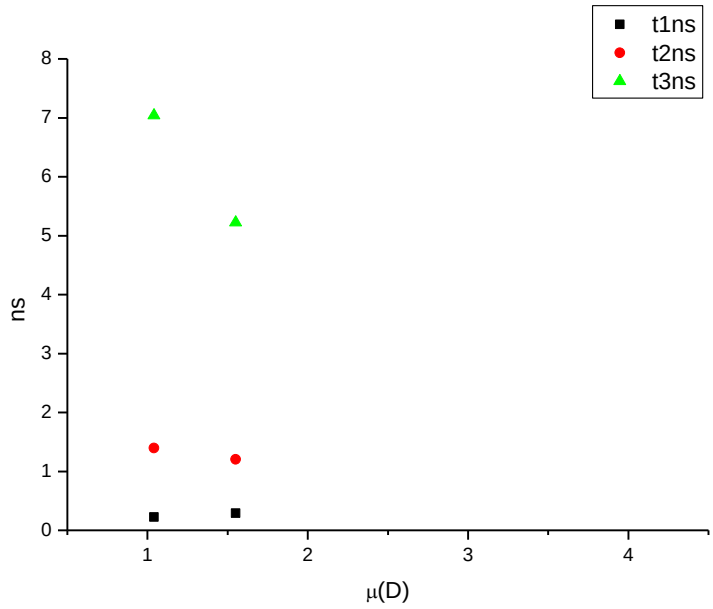

Figure 2.2.101. Intensity weighted components of TCSPC lifetime decay of **12** (500 nm) versus μ(D).

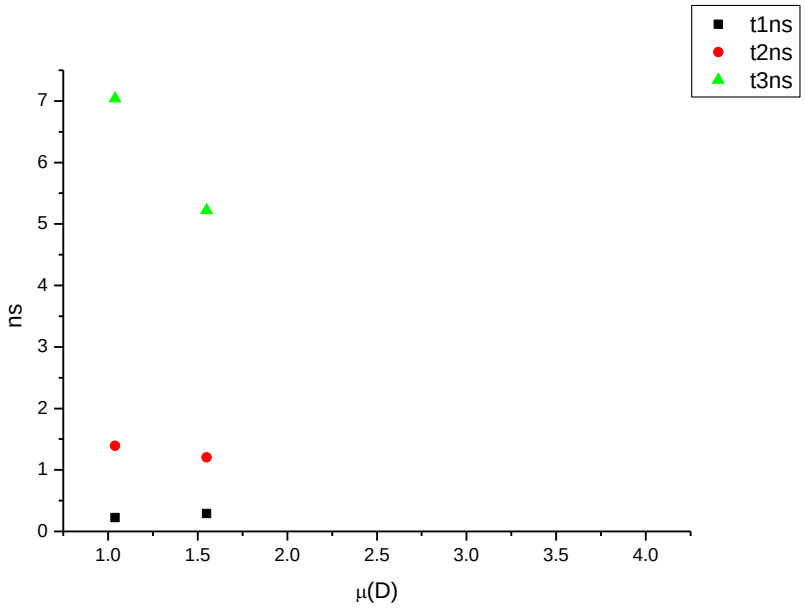

Figure 2.2.102. Amplitude weighted components of TCSPC lifetime decay of **12** (500 nm) versus μ(D).

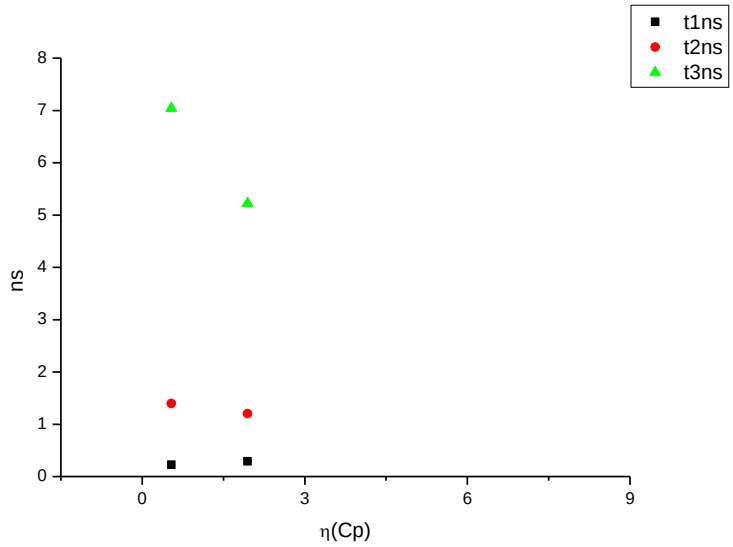

Figure 2.2.103. Intensity weighted components of TCSPC lifetime decay of **12** (500 nm) versus η(Cp).

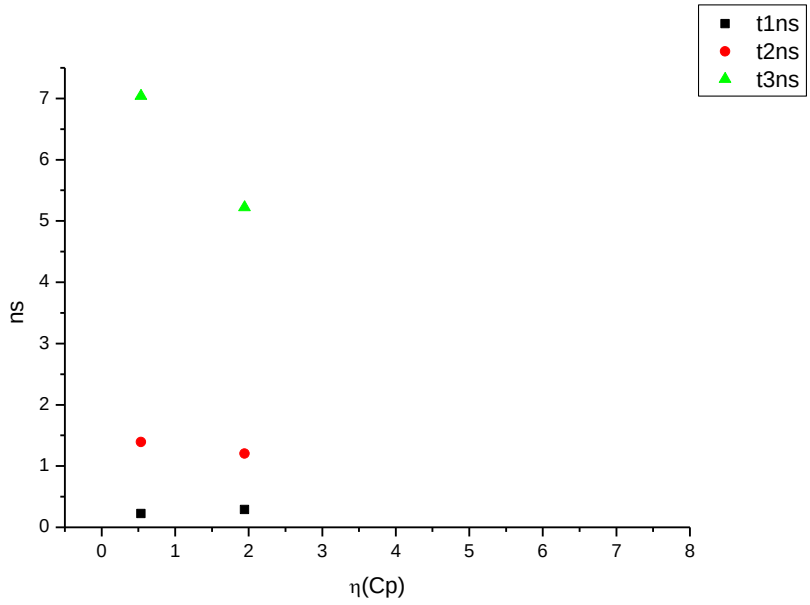

Figure 2.2.104. Amplitude weighted components of TCSPC lifetime decay of **12** (500 nm) versus η(Cp).

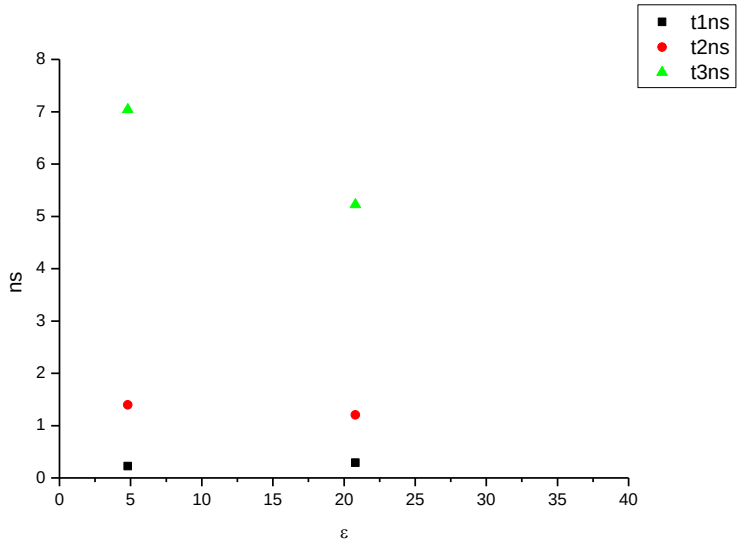

Figure 2.2.105. Intensity weighted components of TCSPC lifetime decay of **12** (500 nm) versus ε.

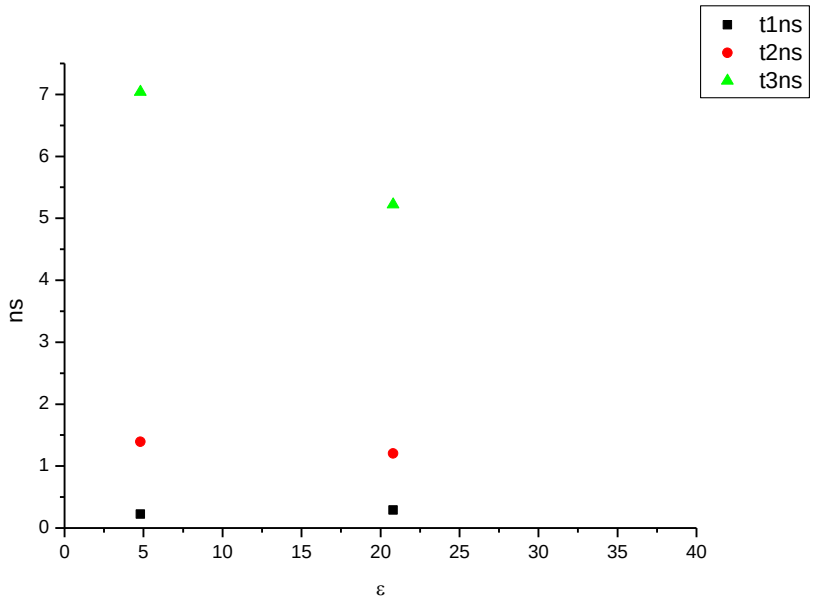

Figure 2.2.106. Amplitude weighted components of TCSPC lifetime decay of **12** (500 nm) versus ε.

2.2.9 295 nm (LED) average fluorescent lifetimes - Solvatochromic analysis.

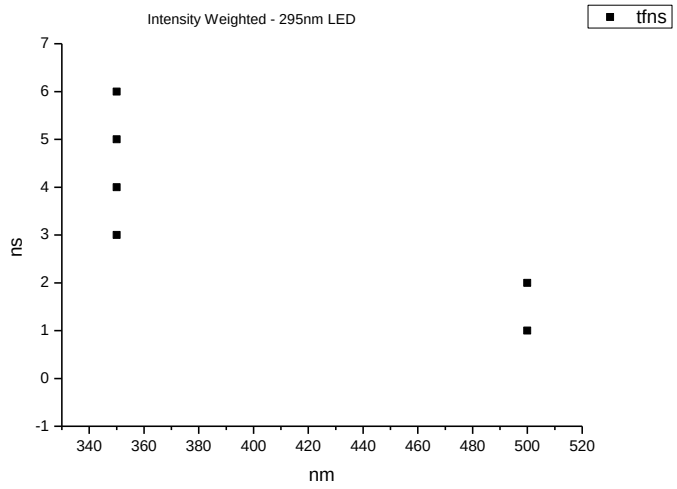

Figure 2.2.107. Intensity weighted average lifetime (τ_f) of **12** versus wavelength (nm).

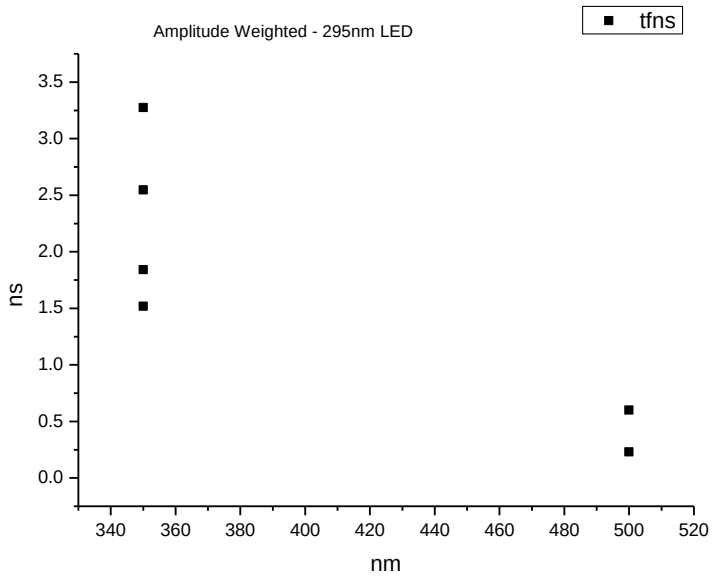

Figure 2.2.108. Amplitude weighted average lifetime (τ_f) of **12** versus wavelength (nm).

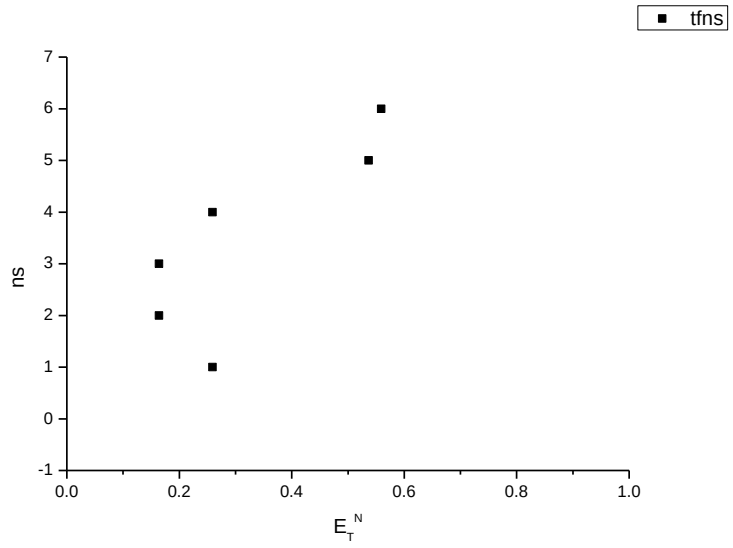

Figure 2.2.109. Intensity weighted average lifetime (τ_f) of **12** versus E_T^N.

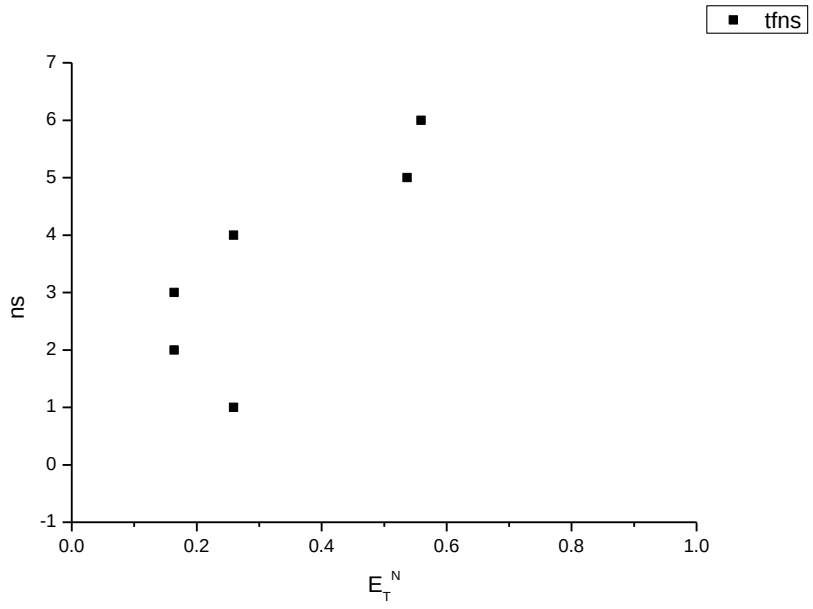

Figure 2.2.110. Amplitude weighted average lifetime (τ_f) of **12** versus E_T^N.

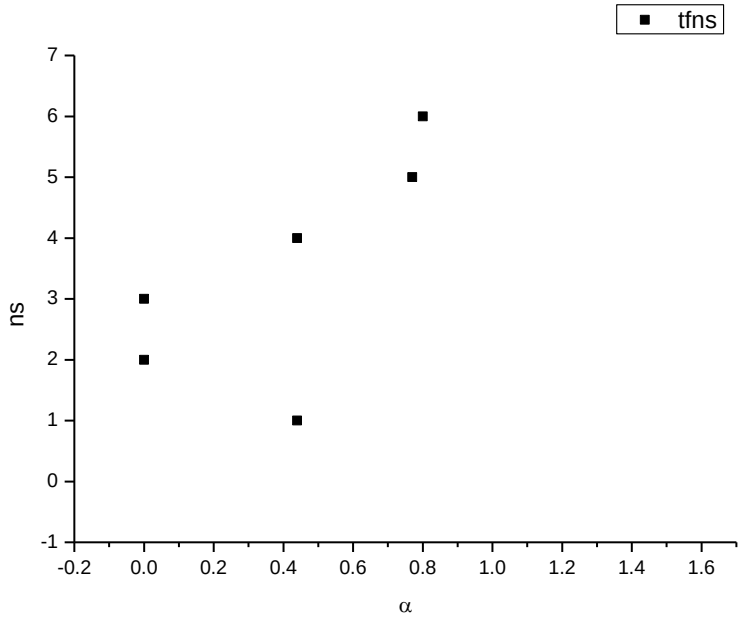

Figure 2.2.111. Intensity weighted average lifetime (τ_f) of **12** versus α.

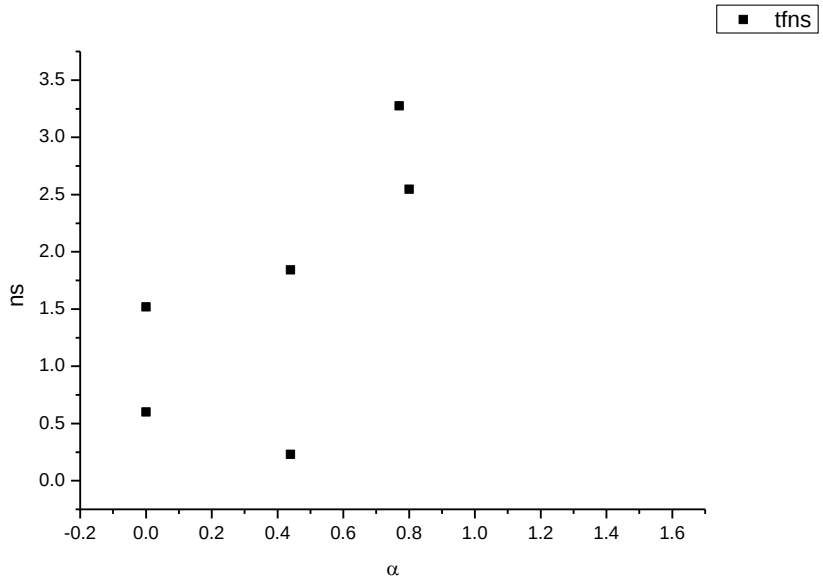

Figure 2.2.112. Amplitude weighted average lifetime (τ_f) of **12** versus α.

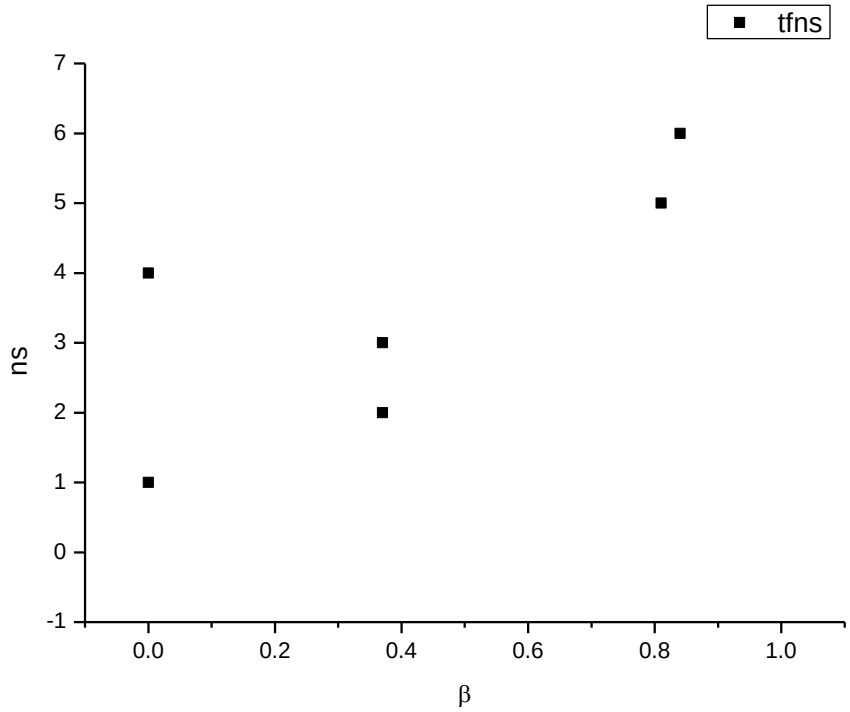

Figure 2.2.113. Intensity weighted average lifetime (τ_f) of **12** versus β.

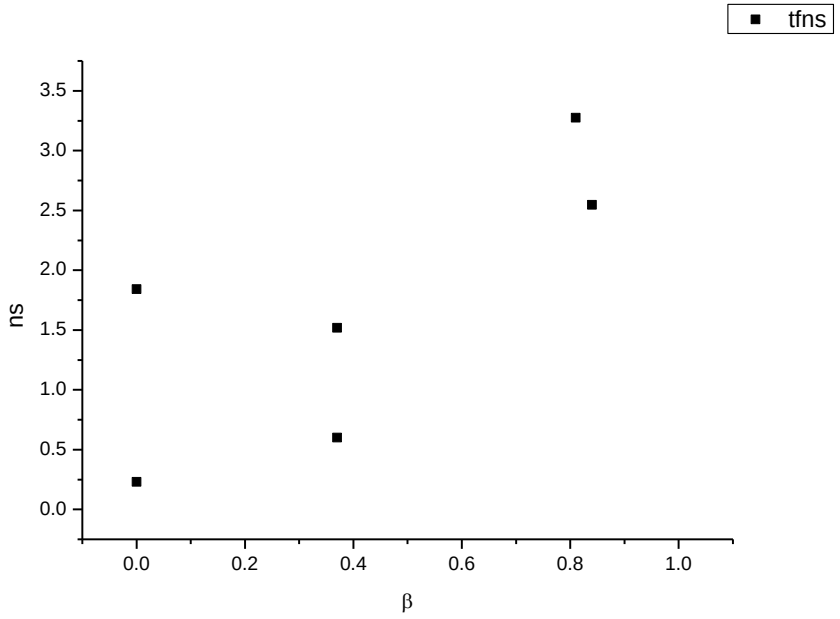

Figure 2.2.114. Amplitude weighted average lifetime (τ_f) of **12** versus β.

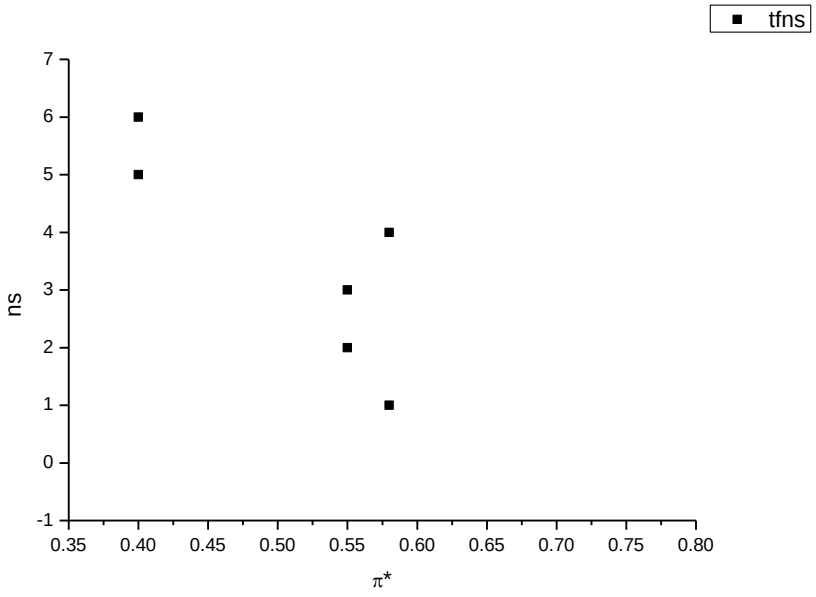

Figure 2.2.115. Intensity weighted average lifetime (τ_f) of **12** versus π*.

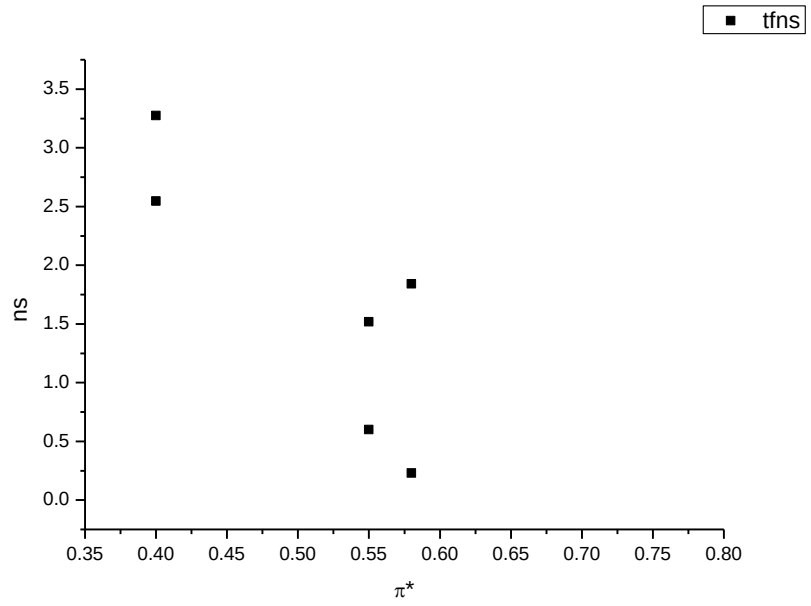

Figure 2.2.116. Amplitude weighted average lifetime (τ_f) of **12** versus π*.

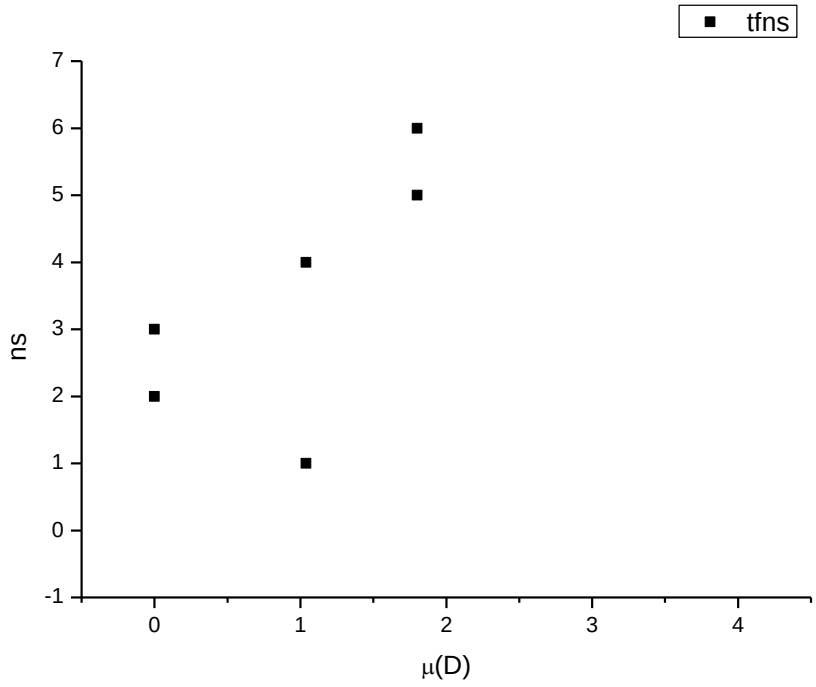

Figure 2.2.117. Intensity weighted average lifetime (τ_f) of **12** versus μ(D).

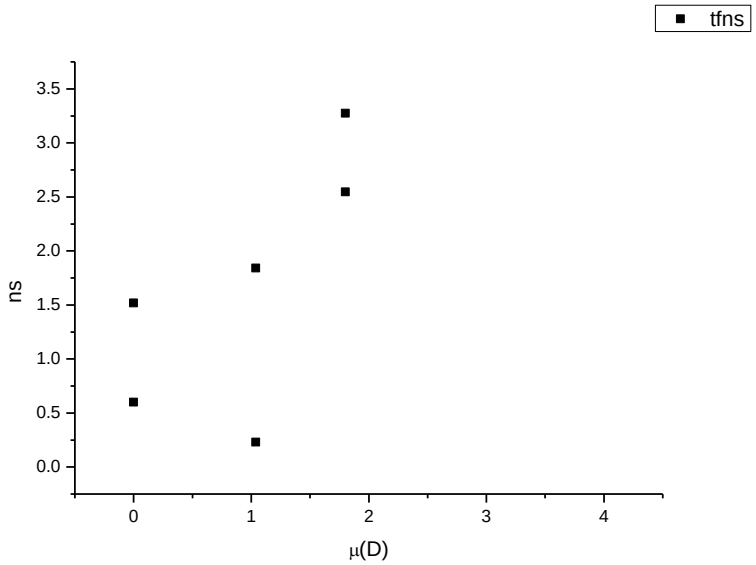

Figure 2.2.118. Amplitude weighted average lifetime (τ_f) of **12** versus μ(D).

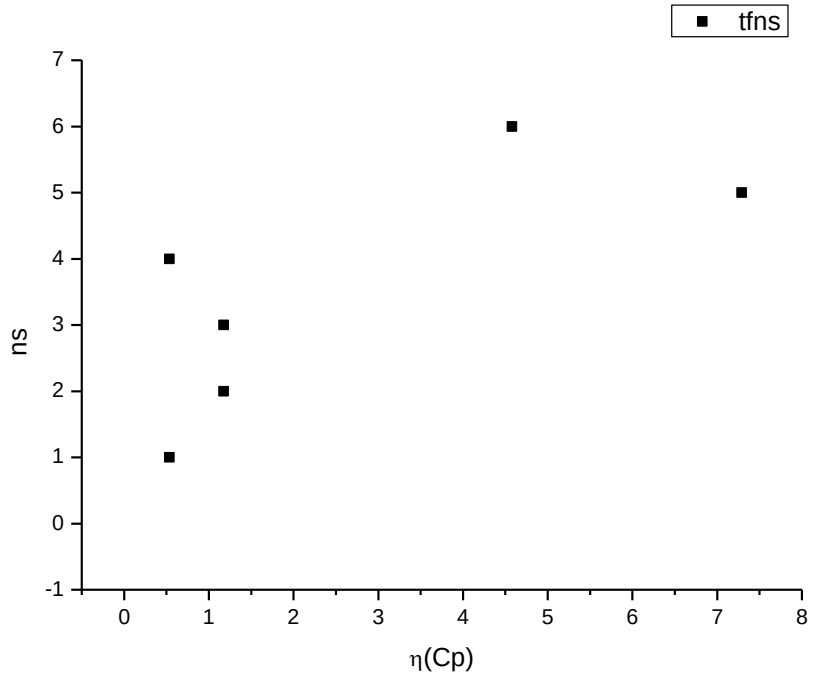

Figure 2.2.119. Intensity weighted average lifetime (τ_f) of **12** versus η(Cp).

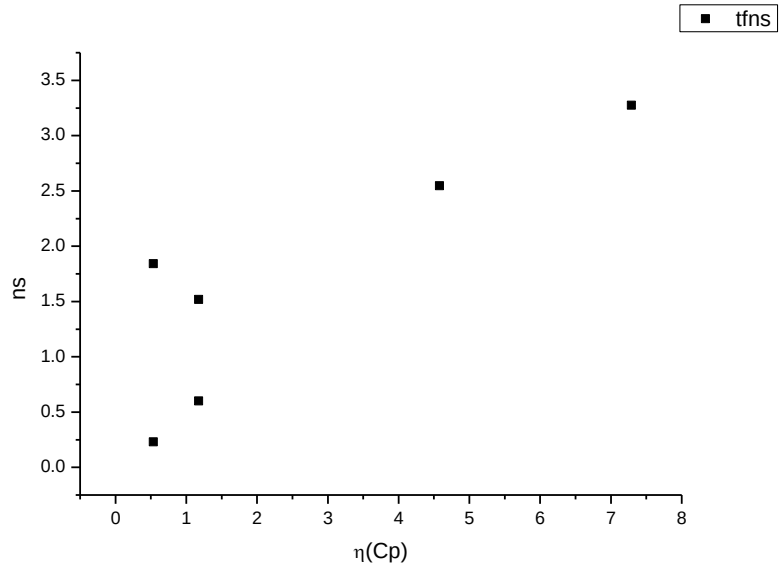

Figure 2.2.120. Amplitude weighted average lifetime (τ_f) of **12** versus η(Cp).

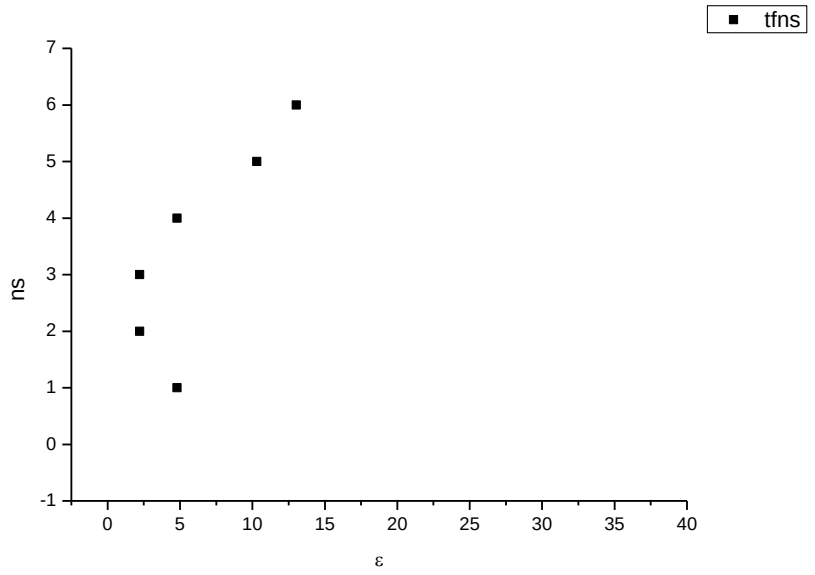

Figure 2.2.121. Intensity weighted average lifetime (τ_f) of **12** versus ε.

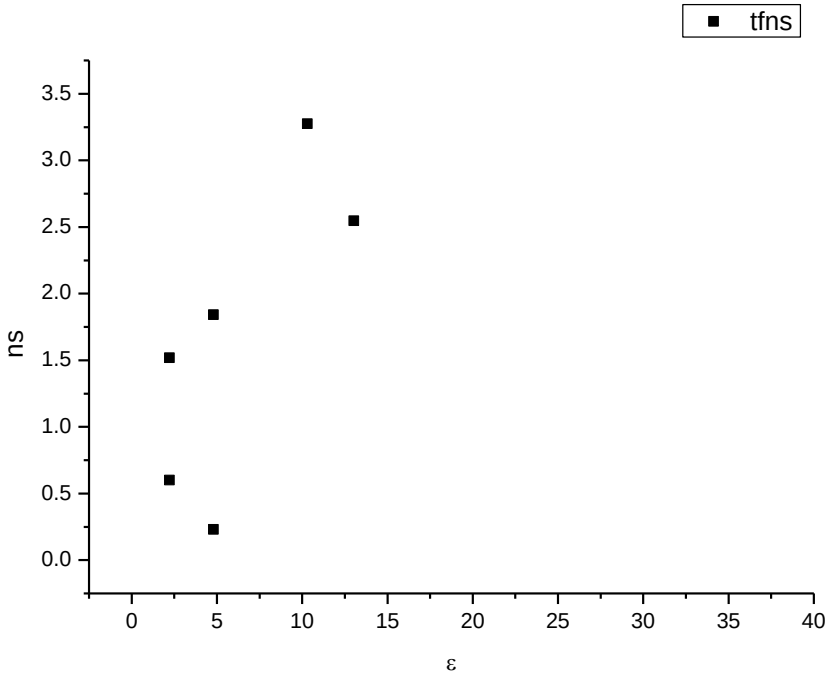

Figure 2.2.122. Amplitude weighted average lifetime (τ_f) of **12** versus ε.

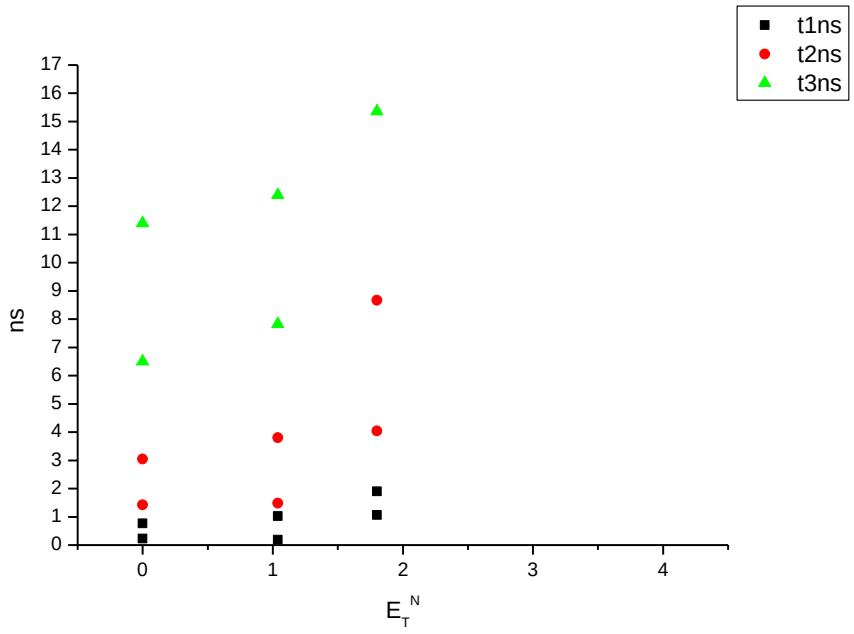

Figure 2.2.123. Intensity weighted components of TCSPC lifetime decay of **12** (350 to 500 nm) versus E_T^N.

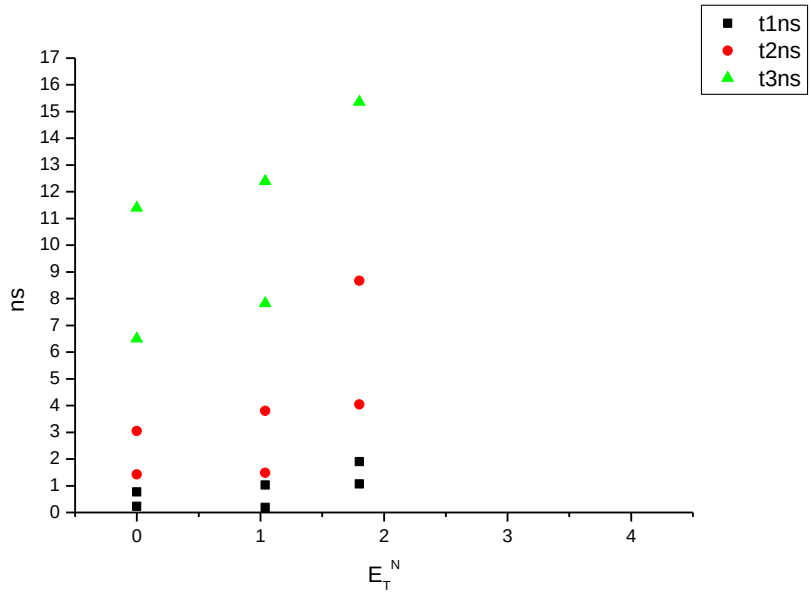

Figure 2.2.124. Amplitude weighted components of TCSPC lifetime decay of **12** (350 to 500 nm) versus E_T^N.

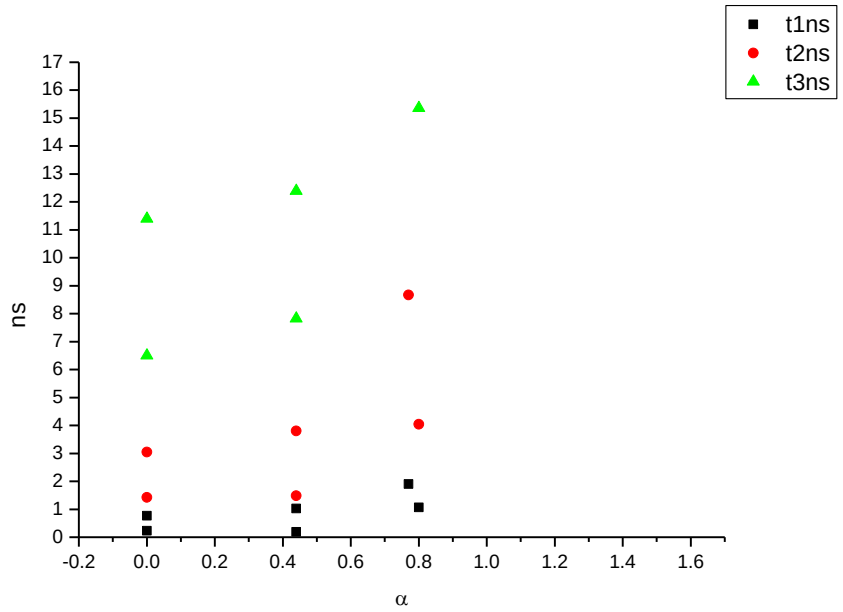

Figure 2.2.125. Intensity weighted components of TCSPC lifetime decay of **12** (350 to 500 nm) versus α.

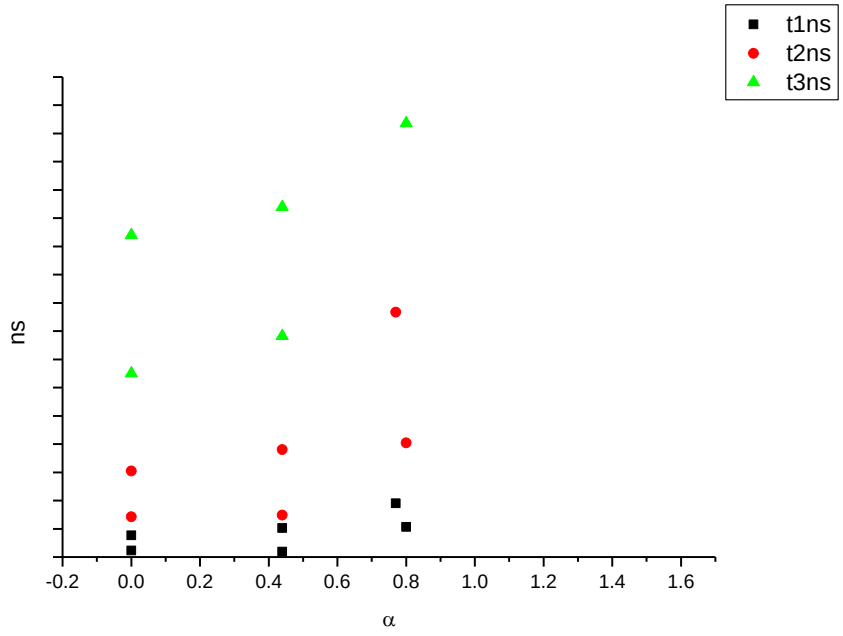

Figure 2.2.126. Amplitude weighted components of TCSPC lifetime decay of **12** (350 to 500 nm) versus α.

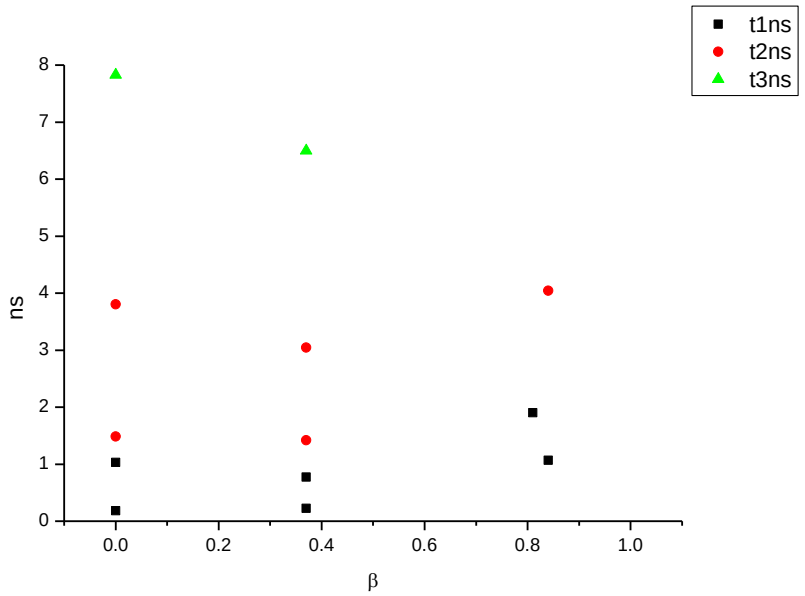

Figure 2.2.127. Intensity weighted components of TCSPC lifetime decay of **12** (350 to 500 nm) versus β.

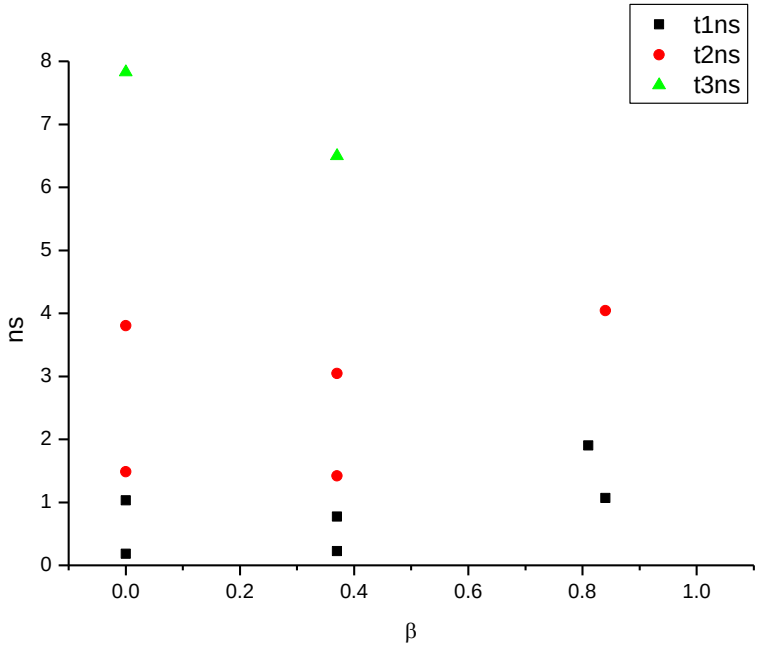

Figure 2.2.128. Amplitude weighted components of TCSPC lifetime decay of **12** (350 to 500 nm) versus β.

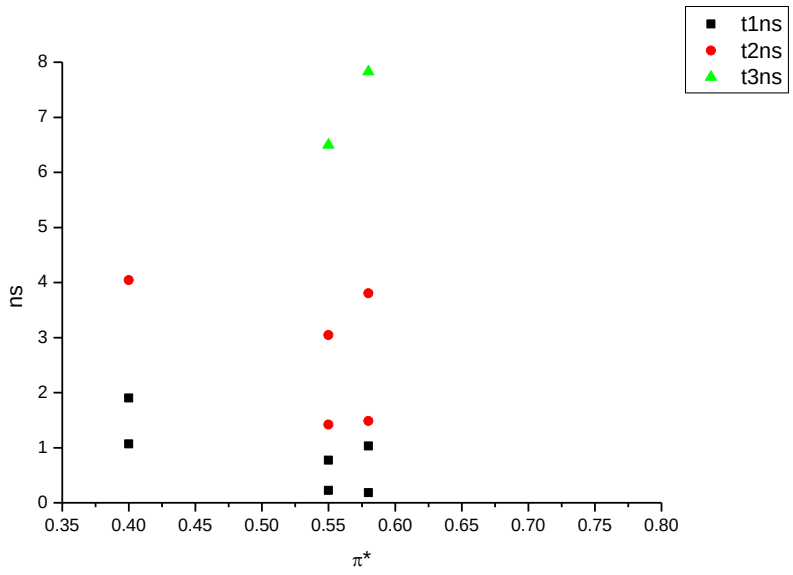

Figure 2.2.129. Intensity weighted components of TCSPC lifetime decay of **12** (350 to 500 nm) versus π*.

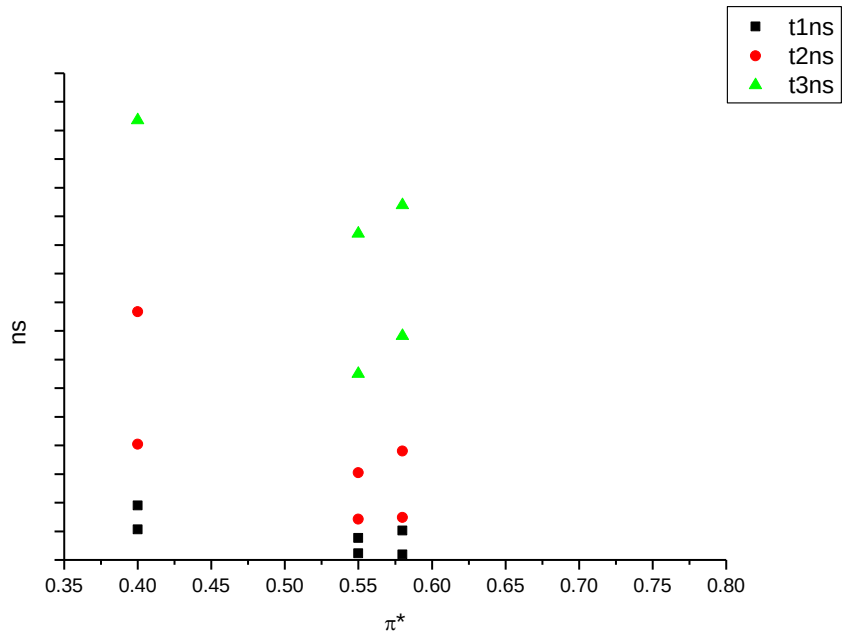

Figure 2.2.130. Amplitude weighted components of TCSPC lifetime decay of **12** (350 to 500 nm) versus π*.

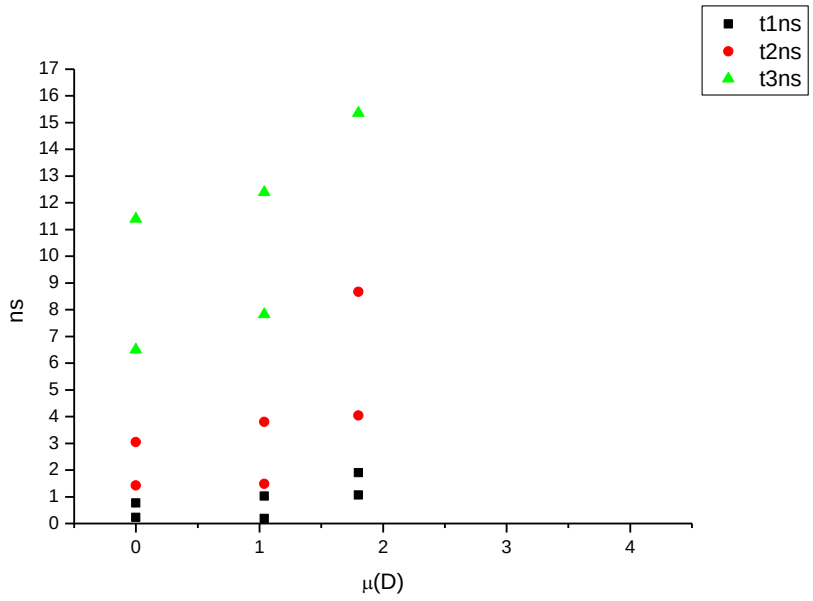

Figure 2.2.131. Intensity weighted components of TCSPC lifetime decay of **12** (350 to 500 nm) versus μ(D).

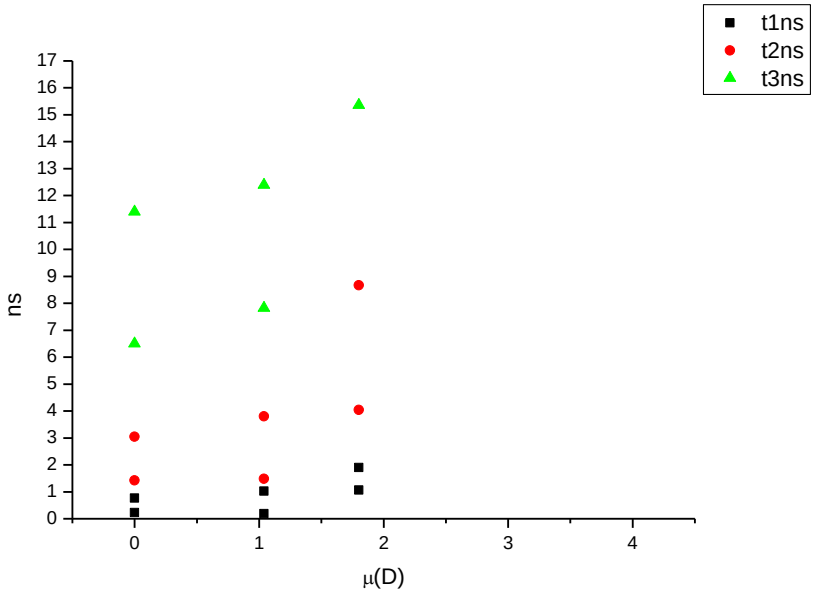

Figure 2.2.132. Amplitude weighted components of TCSPC lifetime decay of **12** (350 to 500 nm) versus μ(D).

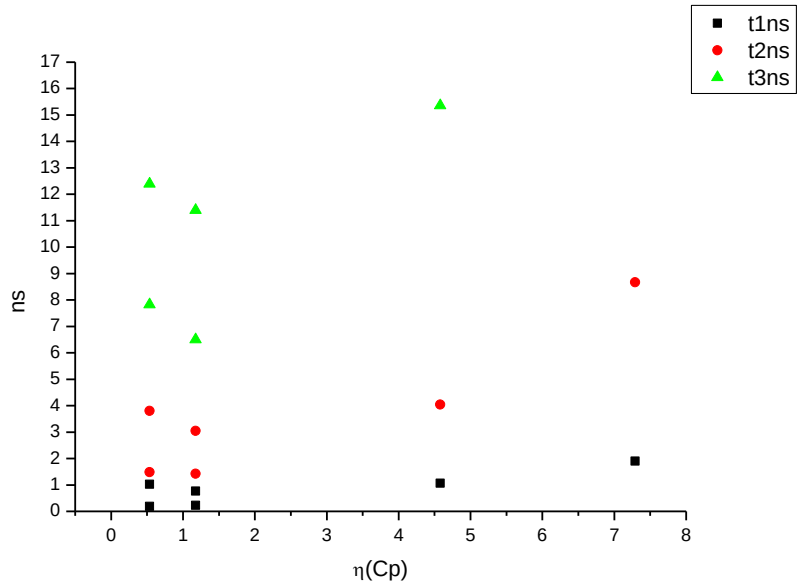

Figure 2.2.133. Intensity weighted components of TCSPC lifetime decay of **12** (350 to 500 nm) versus η(Cp).

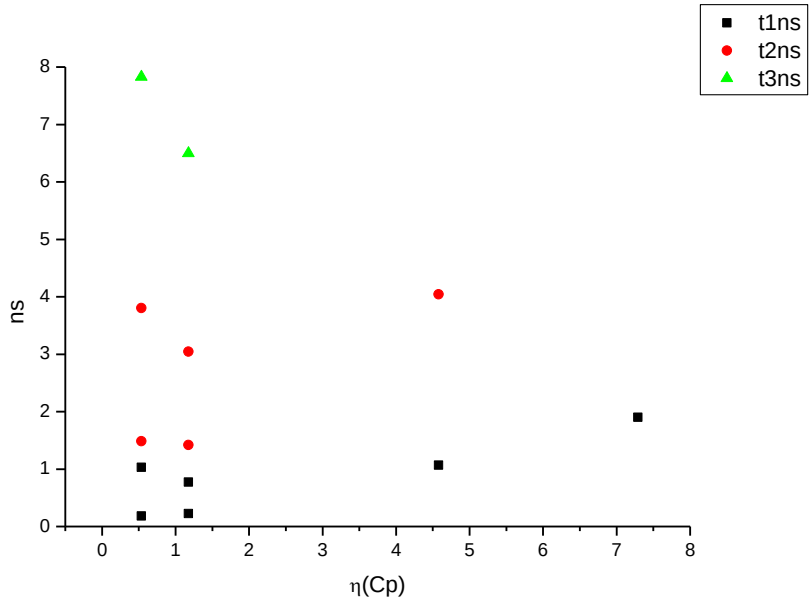

Figure 2.2.134. Amplitude weighted components of TCSPC lifetime decay of **12** (350 to 500 nm) versus η(Cp).

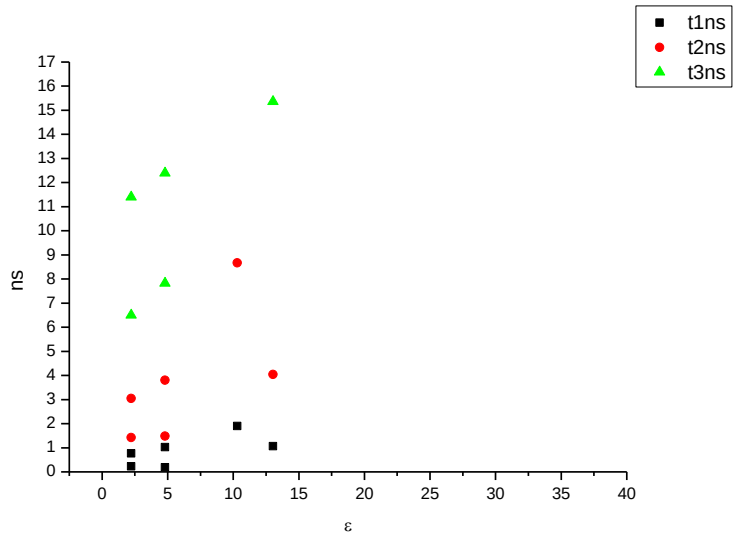

Figure 2.2.135. Intensity weighted components of TCSPC lifetime decay of **12** (350 to 500 nm) versus ε.

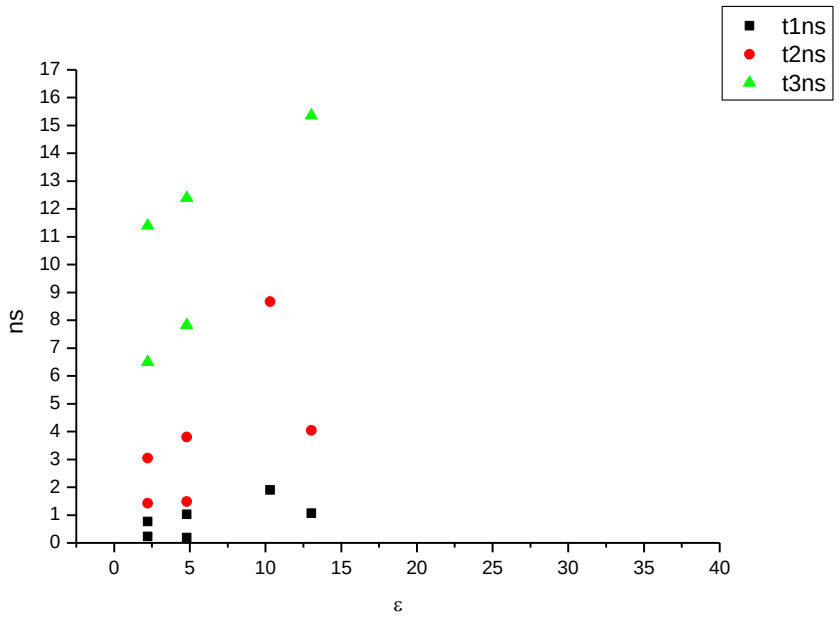

Figure 2.2.136. Amplitude weighted components of TCSPC lifetime decay of **12** (350 to 500 nm) versus ε.

2.2.9.1 350 nm (LED) Lifetime – Solvatochromic analysis.

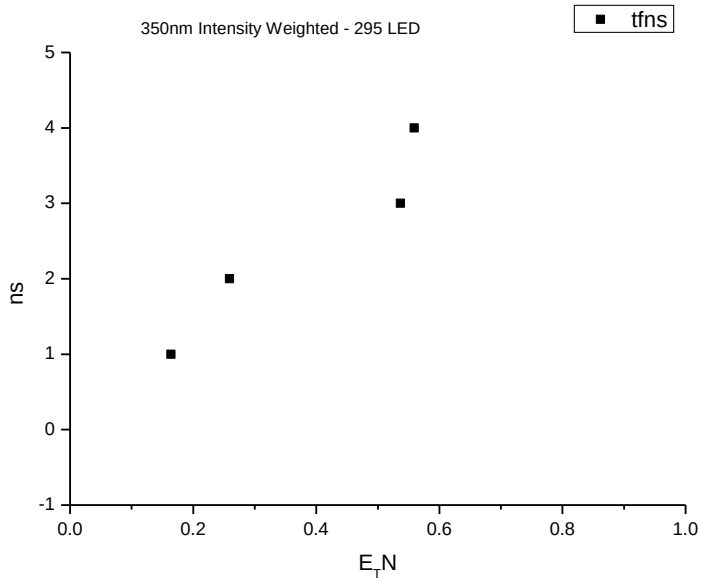

Figure 2.2.137. Intensity weighted average lifetime (τ_f) of **12** at 350 nm versus E_T^N.

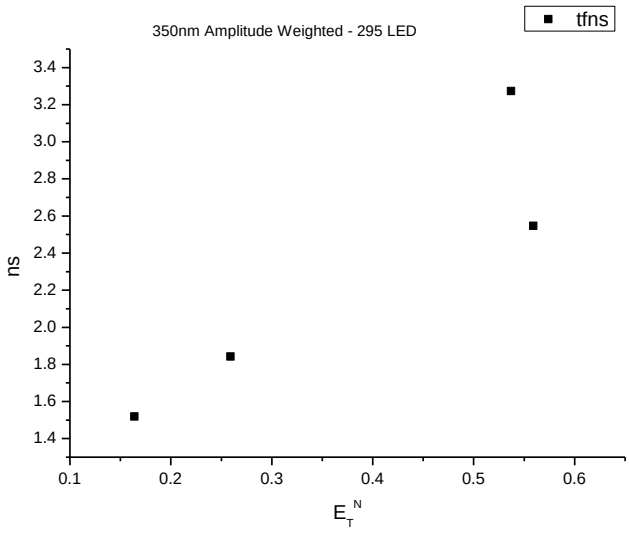

Figure 2.2.138. Amplitude weighted average lifetime (τ_f) of **12** at 350 nm versus E_T^N.

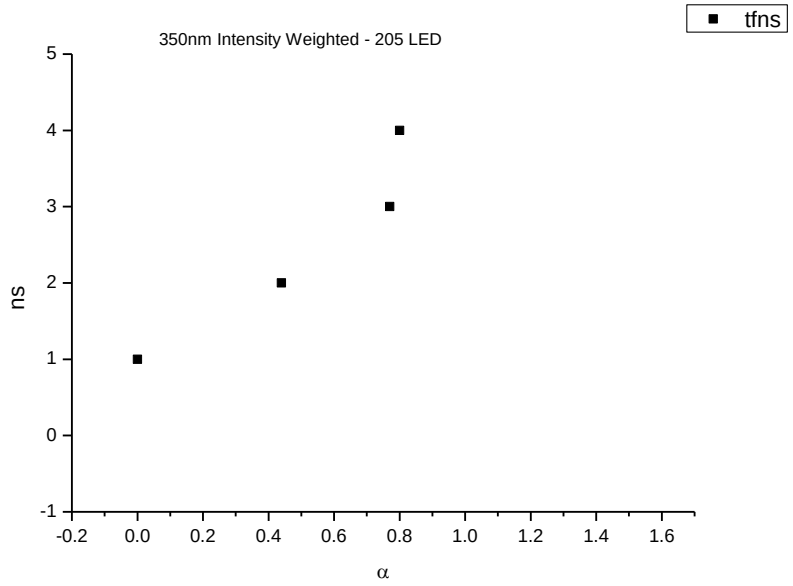

Figure 2.2.139. Intensity weighted average lifetime (τ_f) of **12** at 350 nm versus α.

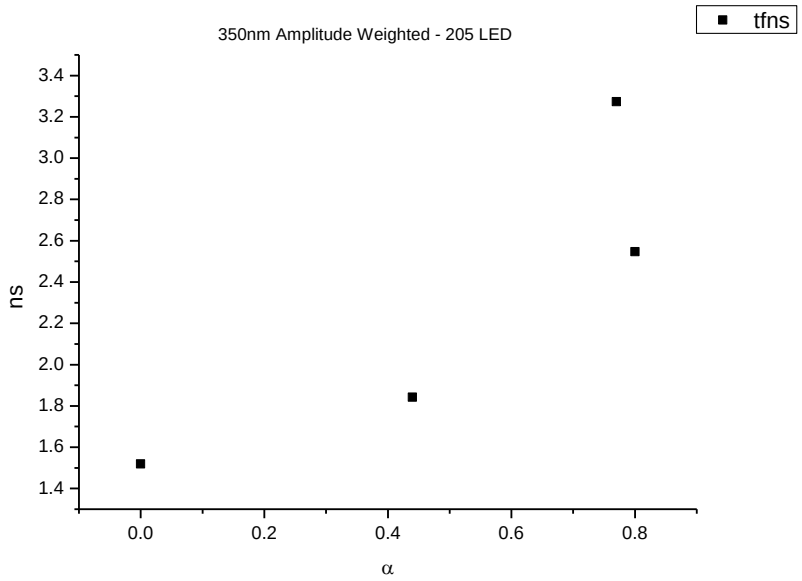

Figure 2.2.140. Amplitude weighted average lifetime (τ_f) of **12** at 350 nm versus α.

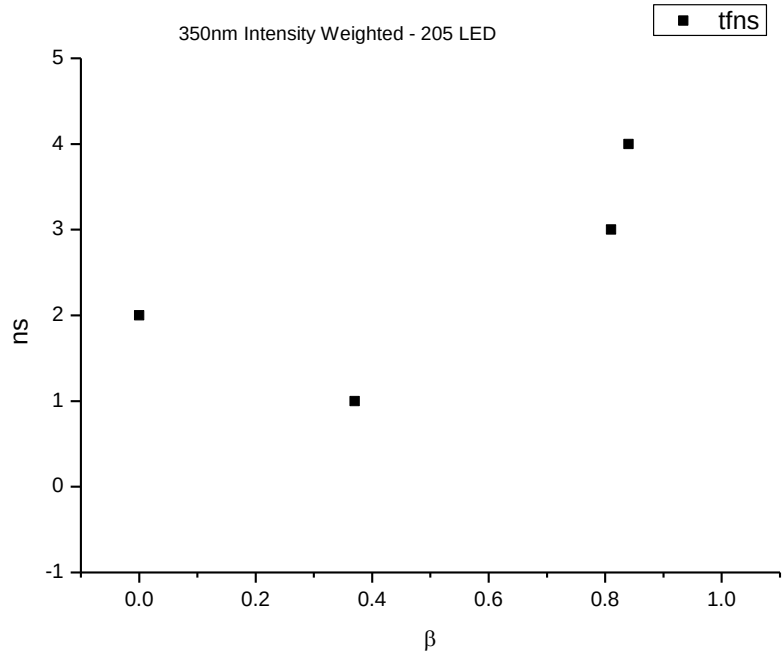

Figure 2.2.141. Intensity weighted average lifetime (τ_f) of **12** at 350 nm versus β.

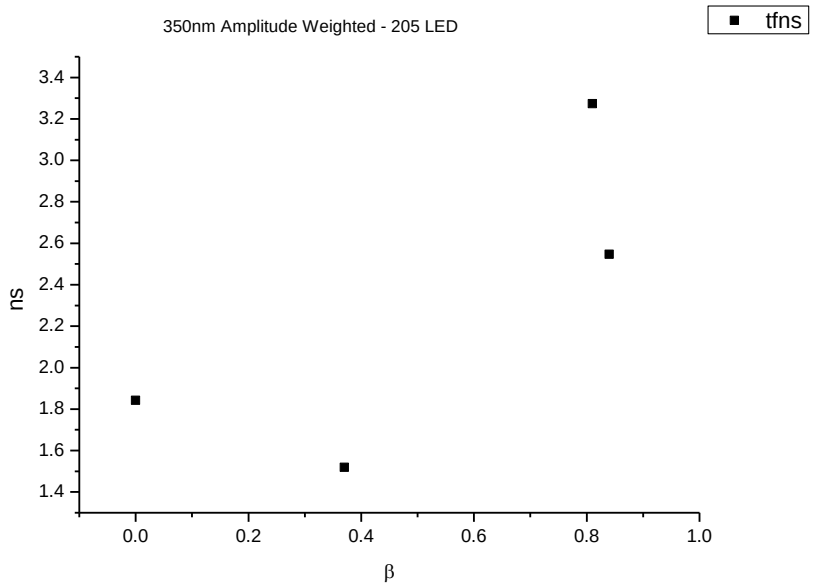

Figure 2.2.142. Amplitude weighted average lifetime (τ_f) of **12** at 350 nm versus β.

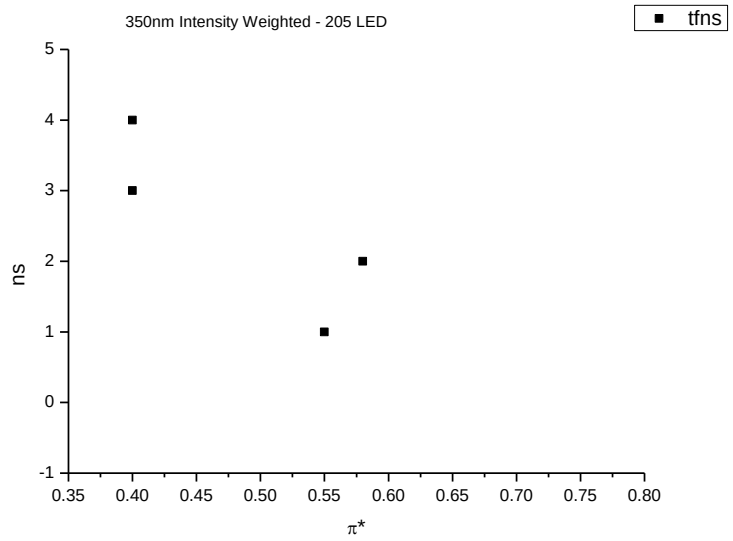

Figure 2.2.143. Intensity weighted average lifetime (τ_f) of **12** at 350 nm versus π*.

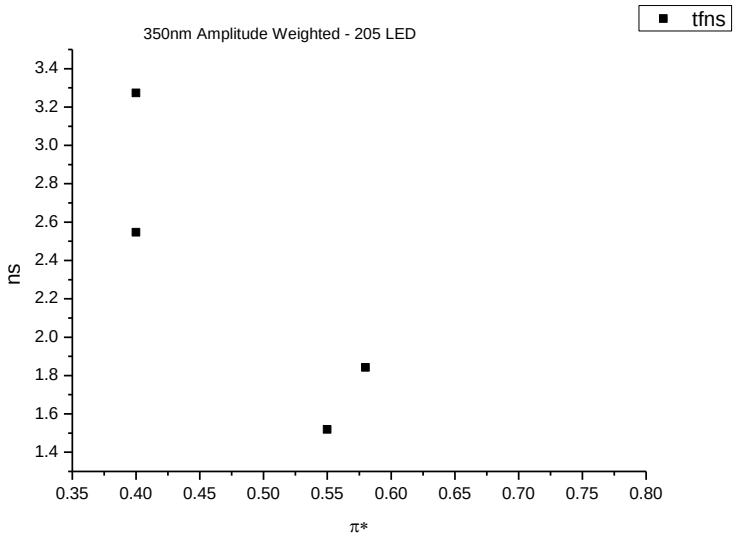

Figure 2.2.144. Amplitude weighted average lifetime (τ_f) of **12** at 350 nm versus π*.

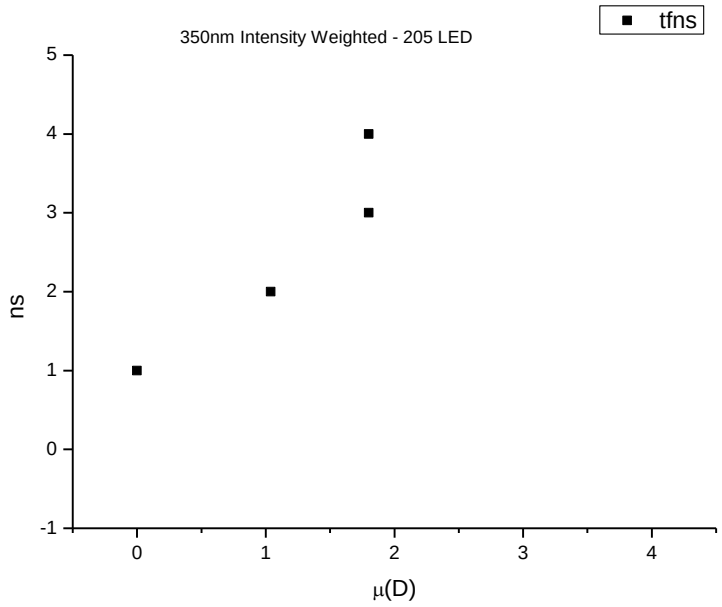

Figure 2.2.145. Intensity weighted average lifetime (τ_f) of **12** at 350 nm versus μ(D).

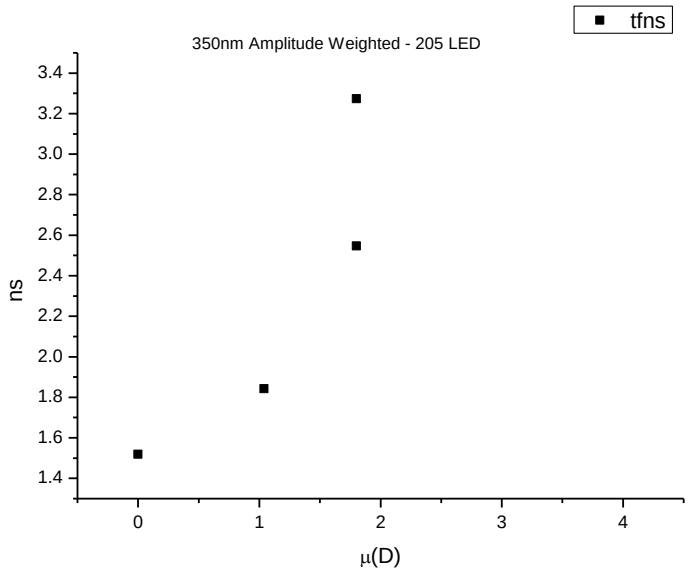

Figure 2.2.146. Amplitude weighted average lifetime (τ_f) of **12** at 350 nm versus μ(D).

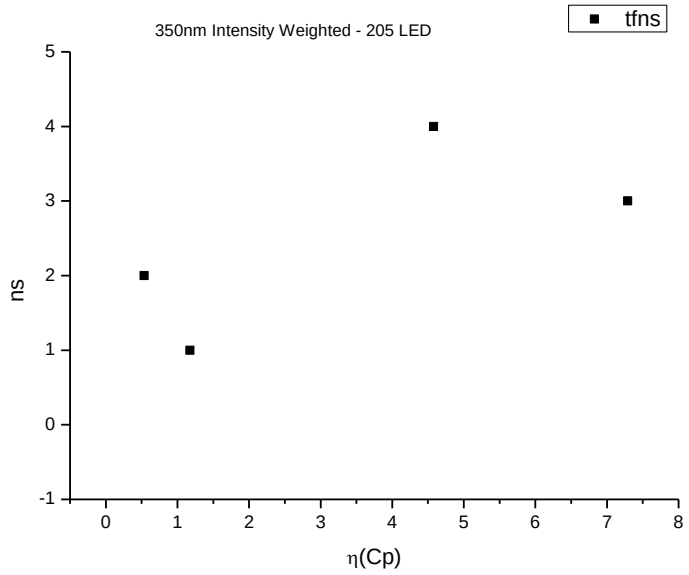

Figure 2.2.147. Intensity weighted average lifetime (τ_f) of **12** at 350 nm versus η(Cp).

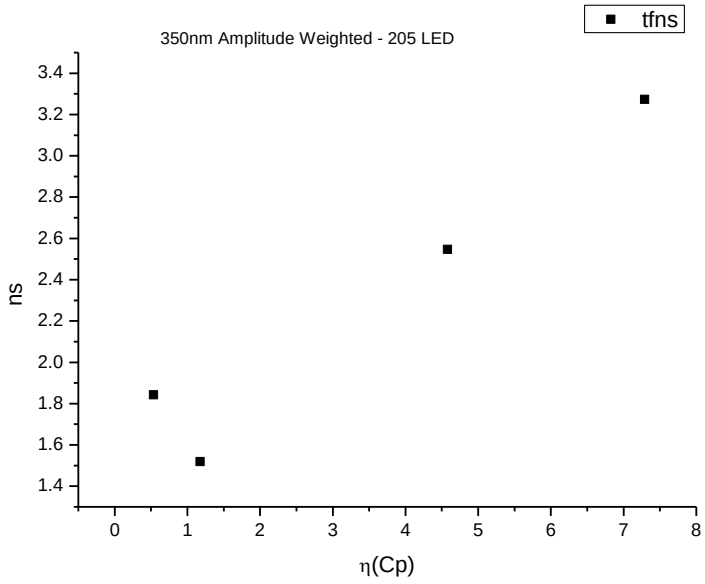

Figure 2.2.148. Amplitude weighted average lifetime (τ_f) of **12** at 350 nm versus η(Cp).

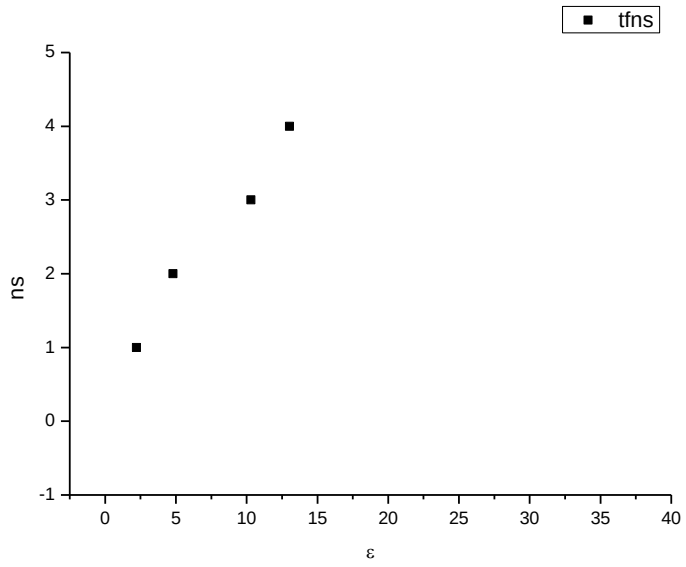

Figure 2.2.149. Intensity weighted average lifetime (τ_f) of **12** at 350 nm versus ε.

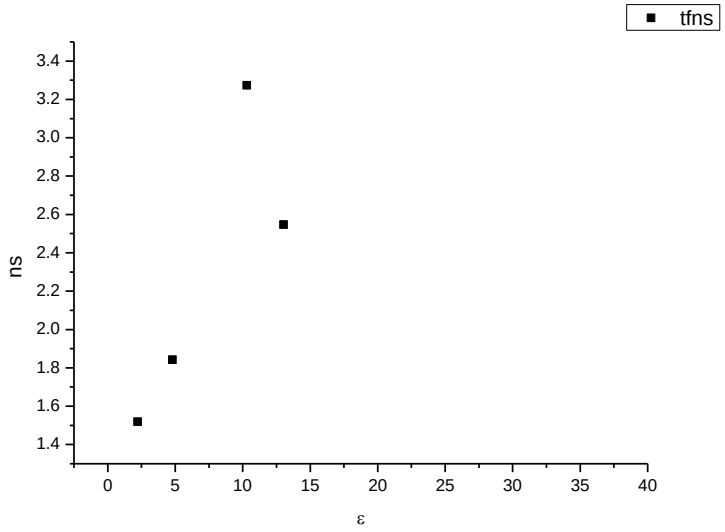

Figure 2.2.150. Amplitude weighted average lifetime (τ_f) of **12** at 350 nm versus ε.

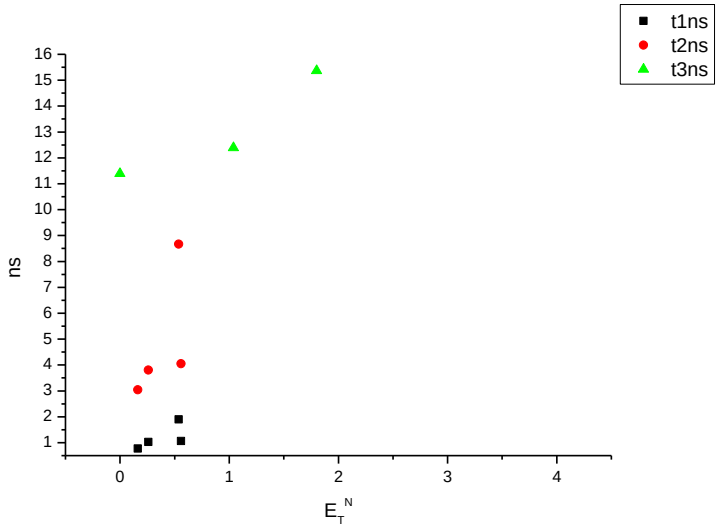

Figure 2.2.151. Intensity weighted components of TCSPC lifetime decay of **12** (350 nm) versus E_T^N.

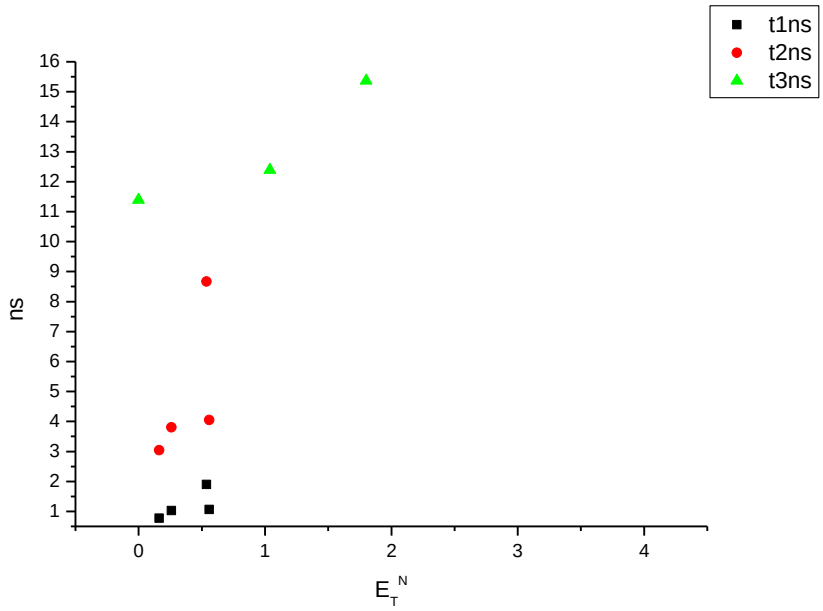

Figure 2.2.152. Amplitude weighted components of TCSPC lifetime decay of **12** (350 nm) versus E_T^N.

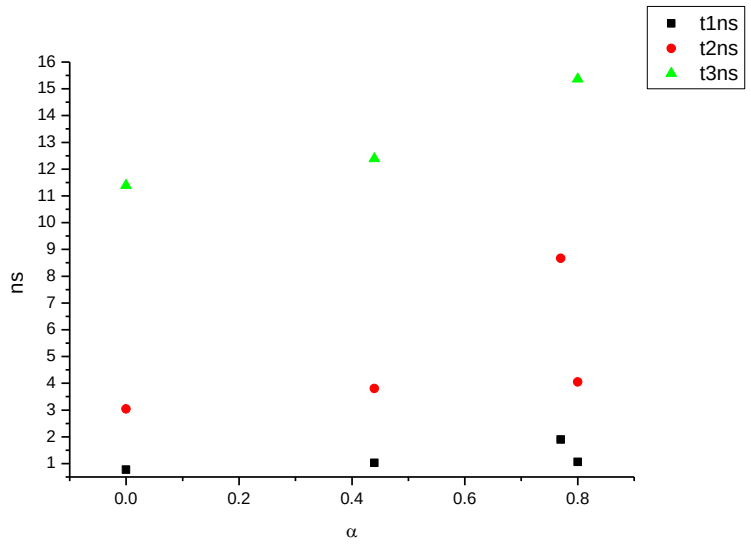

Figure 2.2.153. Intensity weighted components of TCSPC lifetime decay of **12** (350 nm) versus α.

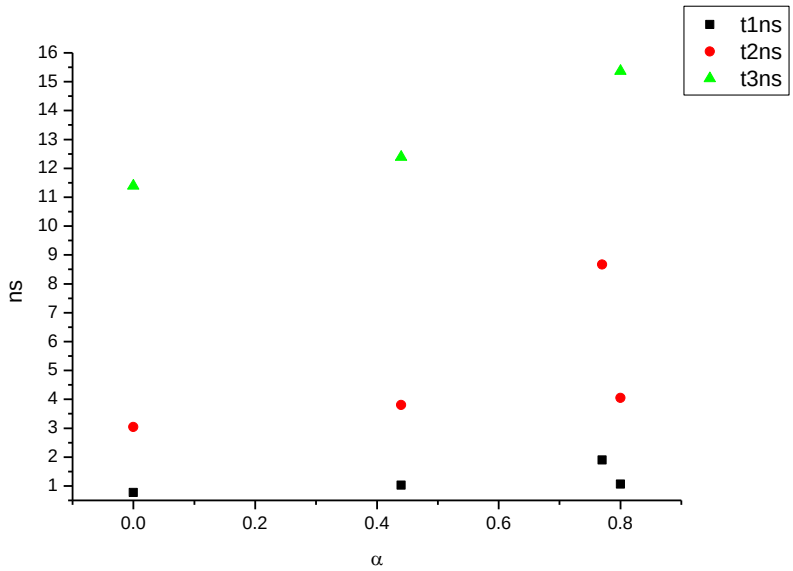

Figure 2.2.154. Amplitude weighted components of TCSPC lifetime decay of **12** (350 nm) versus α.

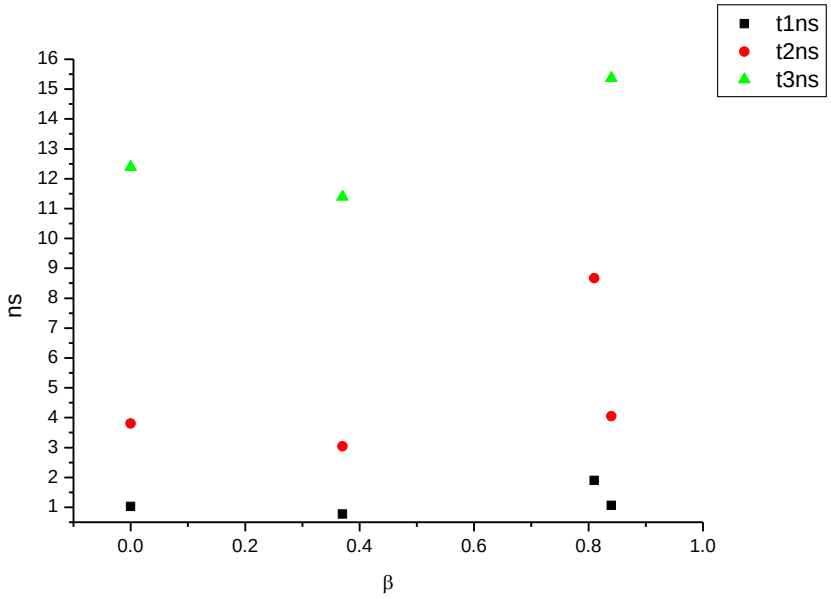

Figure 2.2.155. Intensity weighted components of TCSPC lifetime decay of **12** (350 nm) versus β.

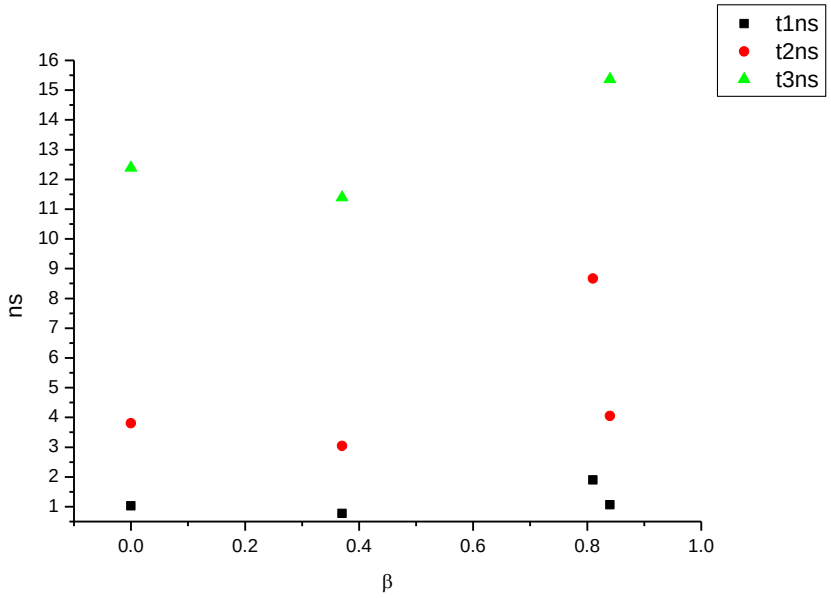

Figure 2.2.156. Amplitude weighted components of TCSPC lifetime decay of **12** (350 nm) versus β.

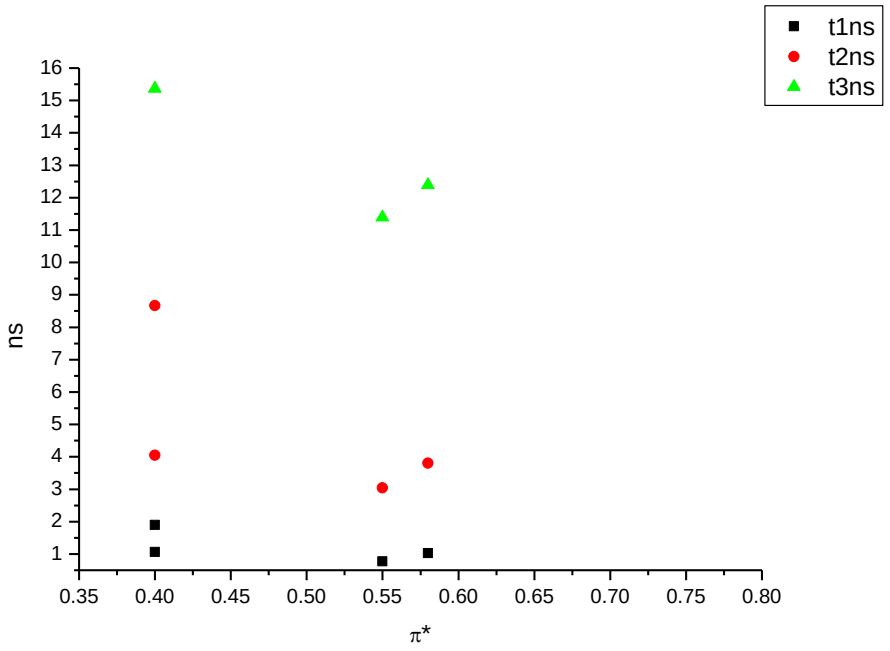

Figure 2.2.157. Intensity weighted components of TCSPC lifetime decay of **12** (350 nm) versus π*.

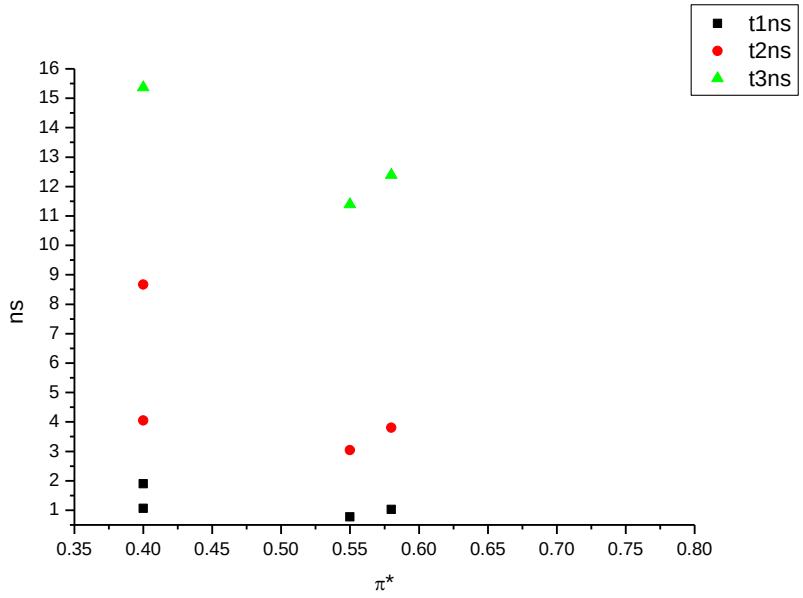

Figure 2.2.158. Amplitude weighted components of TCSPC lifetime decay of **12** (350 nm) versus π*.

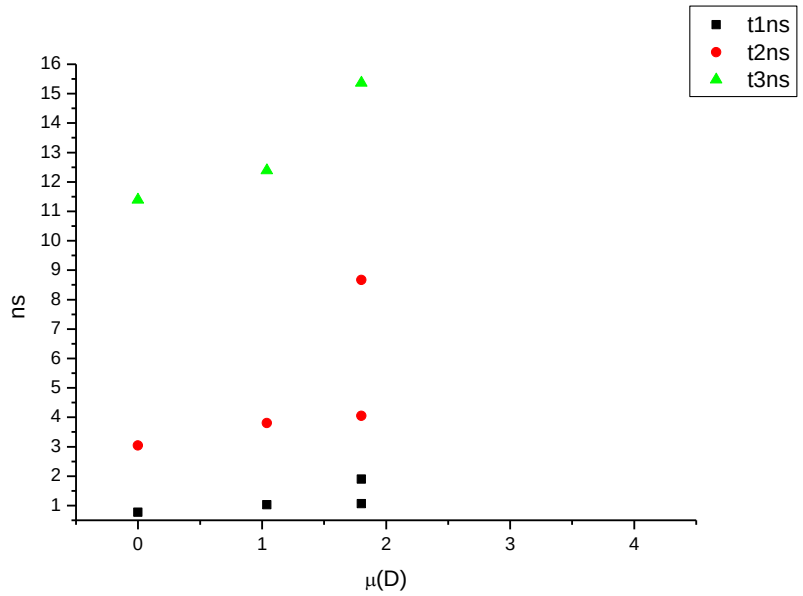

Figure 2.2.159. Intensity weighted components of TCSPC lifetime decay of **12** (350 nm) versus μ(D).

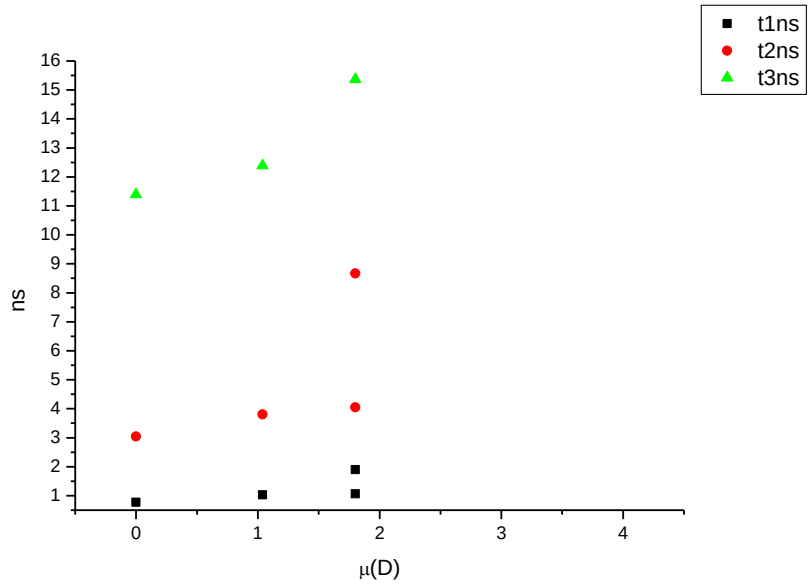

Figure 2.2.160. Amplitude weighted components of TCSPC lifetime decay of **12** (350 nm) versus μ(D).

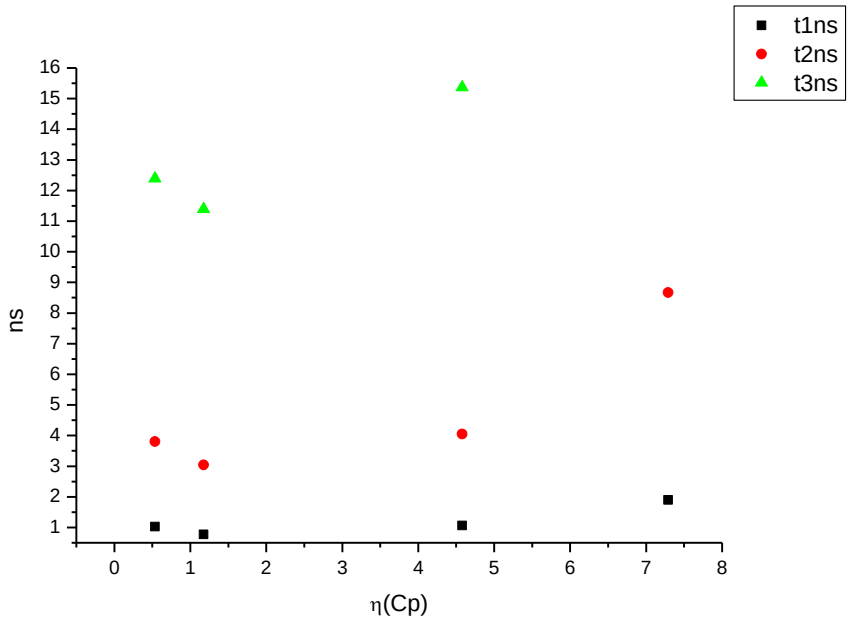

Figure 2.2.161. Intensity weighted components of TCSPC lifetime decay of **12** (350 nm) versus η(Cp).

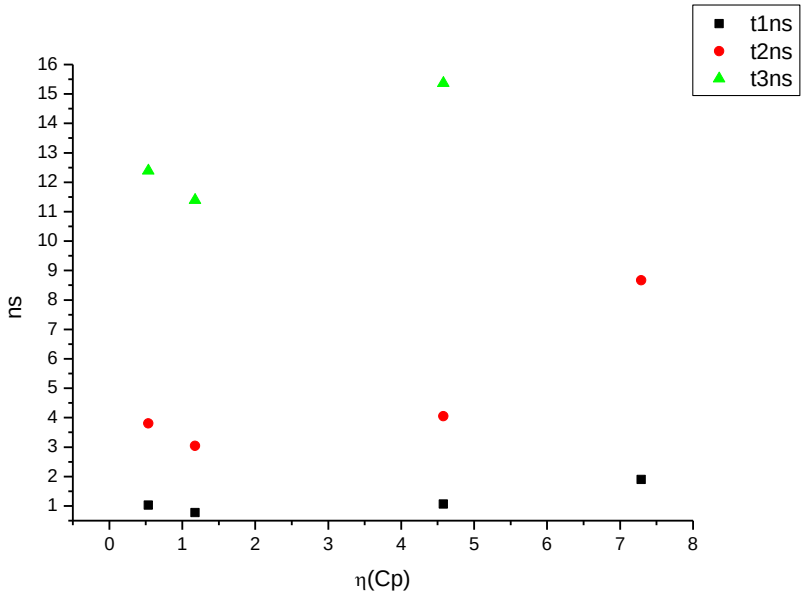

Figure 2.2.162. Amplitude weighted components of TCSPC lifetime decay of **12** (350 nm) versus η(Cp).

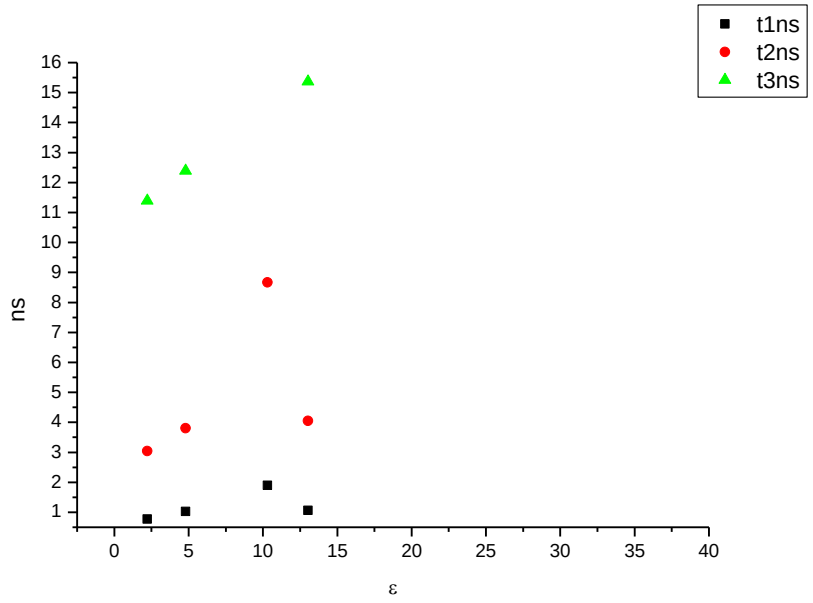

Figure 2.2.163. Intensity weighted components of TCSPC lifetime decay of **12** (350 nm) versus ε.

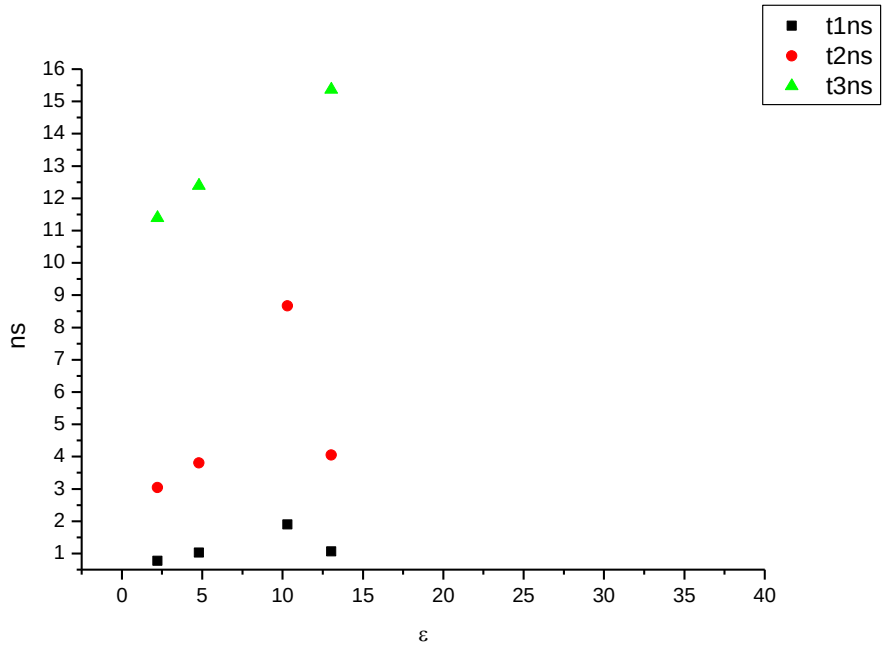

Figure 2.2.164. Amplitude weighted components of TCSPC lifetime decay of **12** (350 nm) versus ε.

2.2.9.2 500 nm (LED) Lifetime – Solvatochromic analysis.

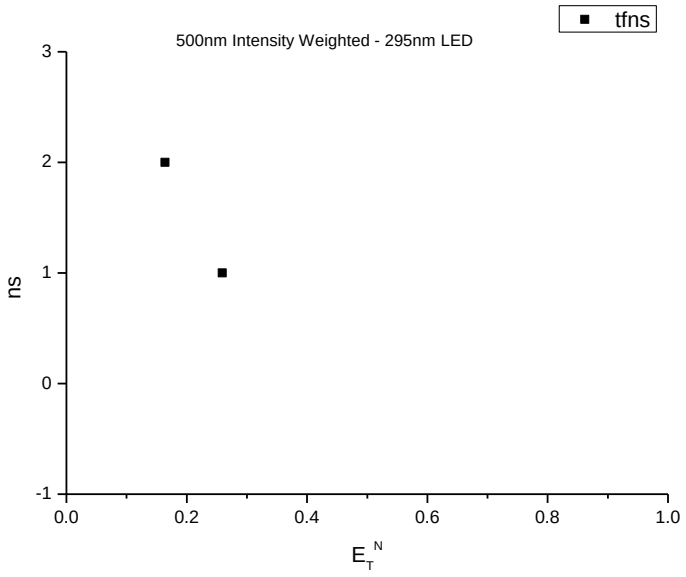

Figure 2.2.165. Intensity weighted average lifetime (τ_f) of **12** at 500 nm versus E_T^N.

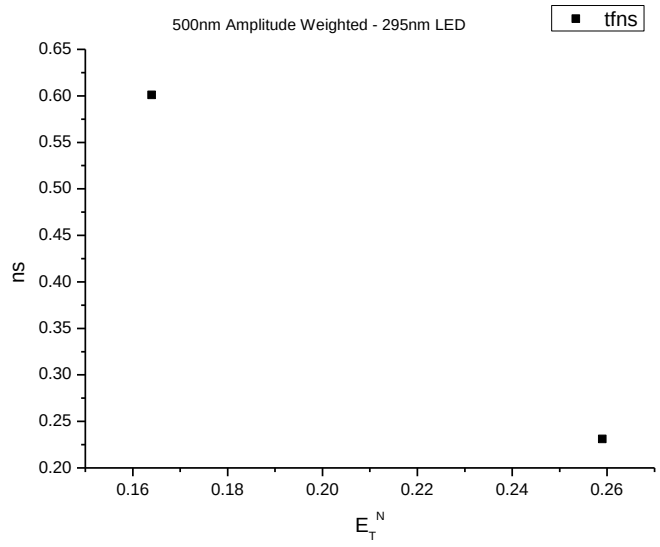

Figure 2.2.166. Amplitude weighted average lifetime (τ_f) of **12** at 500 nm versus E_T^N.

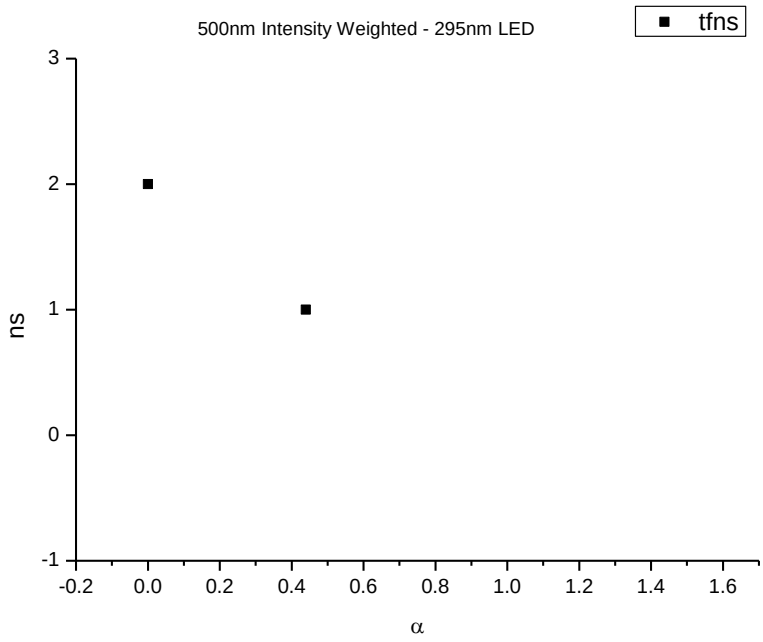

Figure 2.2.167. Intensity weighted average lifetime (τ_f) of **12** at 500 nm versus α.

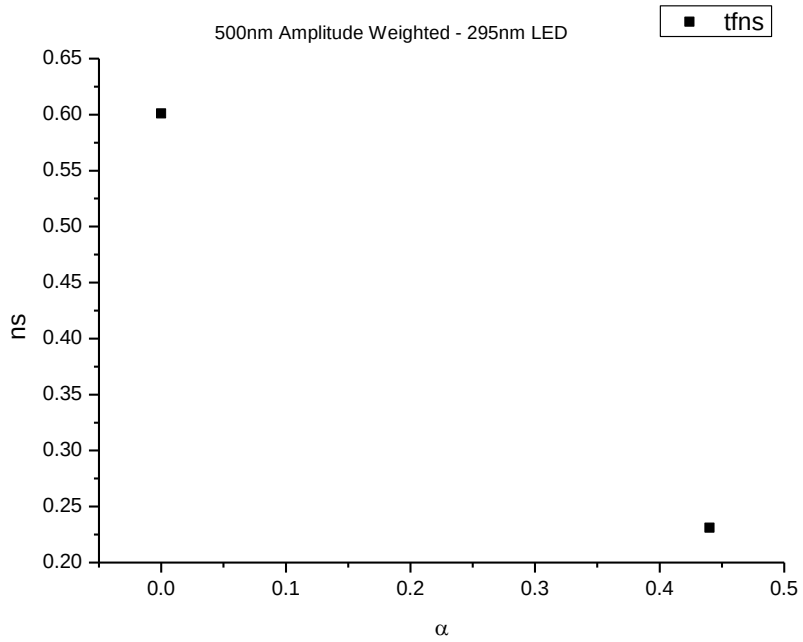

Figure 2.2.168. Amplitude weighted average lifetime (τ_f) of **12** at 500 nm versus α.

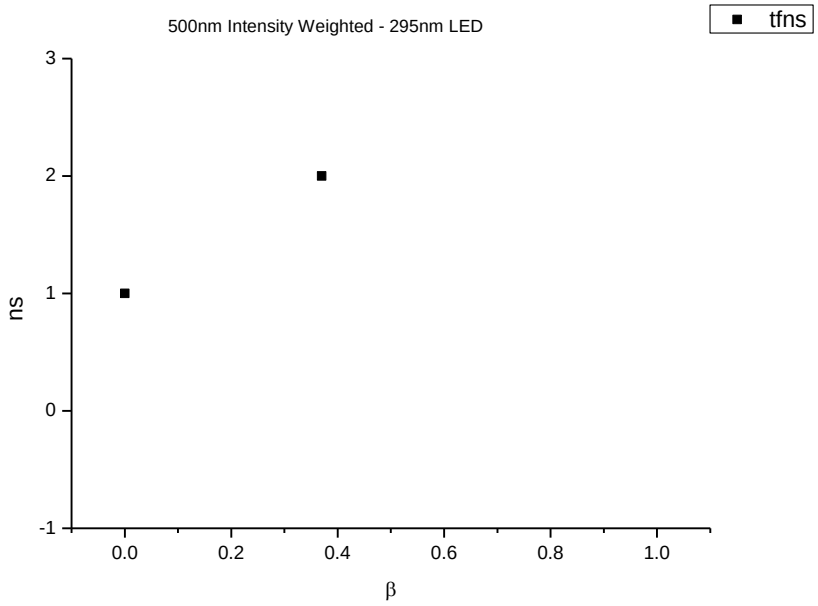

Figure 2.2.169. Intensity weighted average lifetime (τ_f) of **12** at 500 nm versus β.

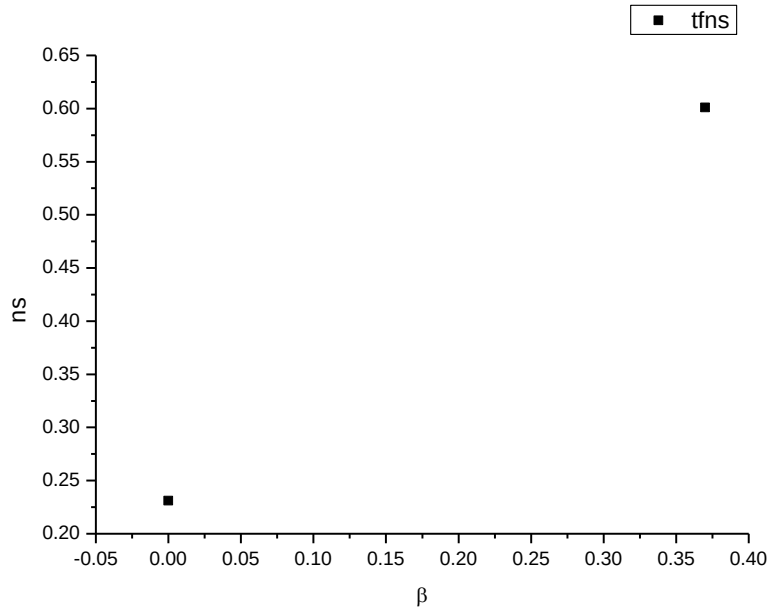

Figure 2.2.170. Amplitude weighted average lifetime (τ_f) of **12** at 500 nm versus β.

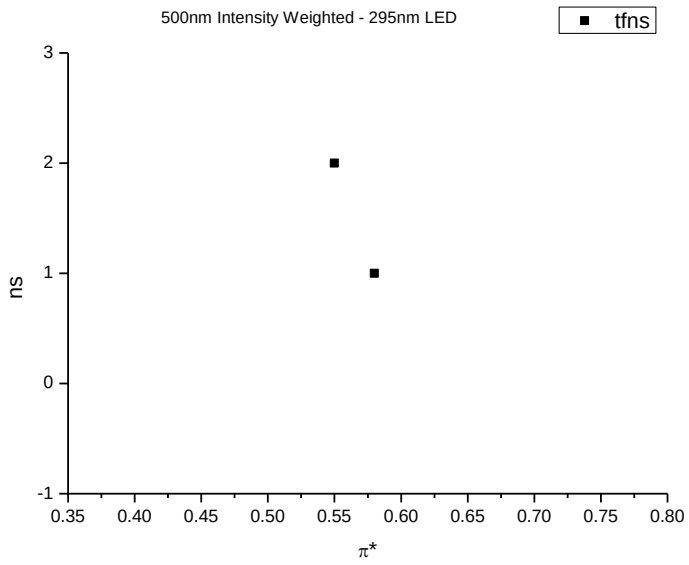

Figure 2.2.171. Intensity weighted average lifetime (τ_f) of **12** at 500 nm versus π*.

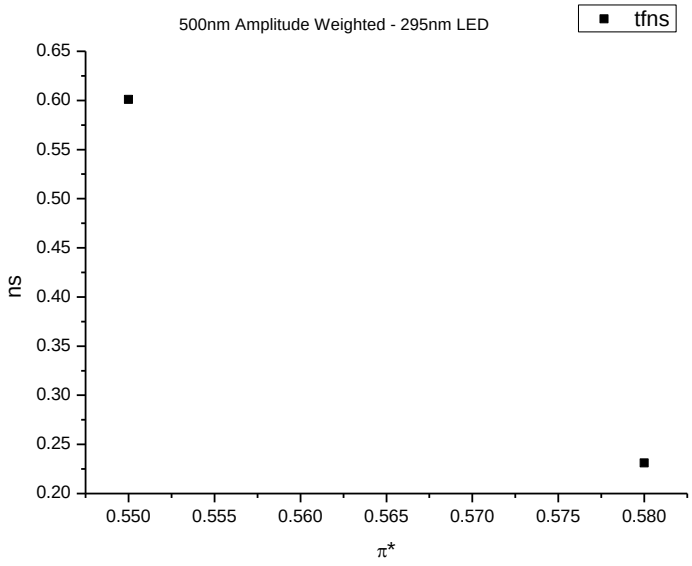

Figure 2.2.172. Amplitude weighted average lifetime (τ_f) of **12** at 500 nm versus π*.

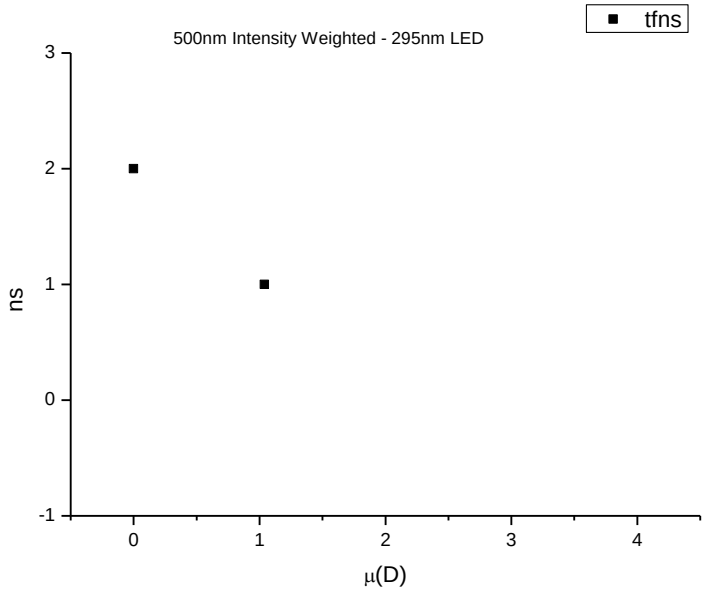

Figure 2.2.173. Intensity weighted average lifetime (τ_f) of **12** at 500 nm versus μ(D).

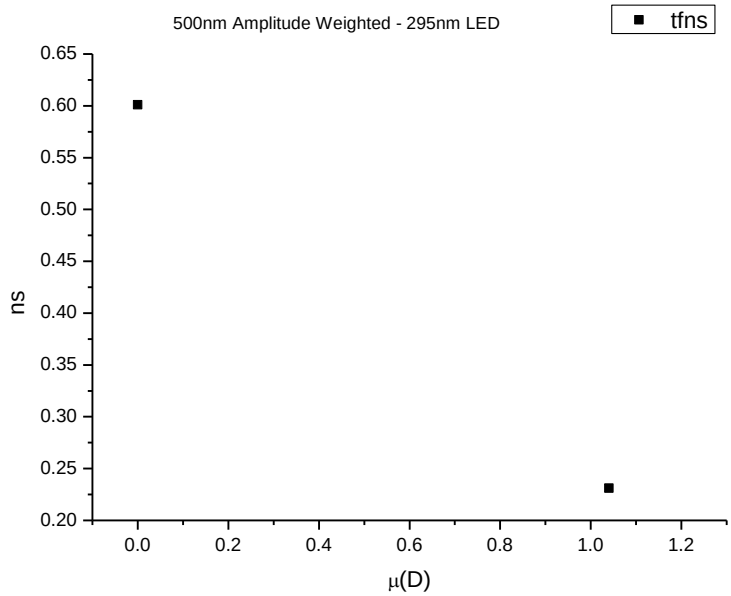

Figure 2.2.174. Amplitude weighted average lifetime (τ_f) of **12** at 500 nm versus μ(D).

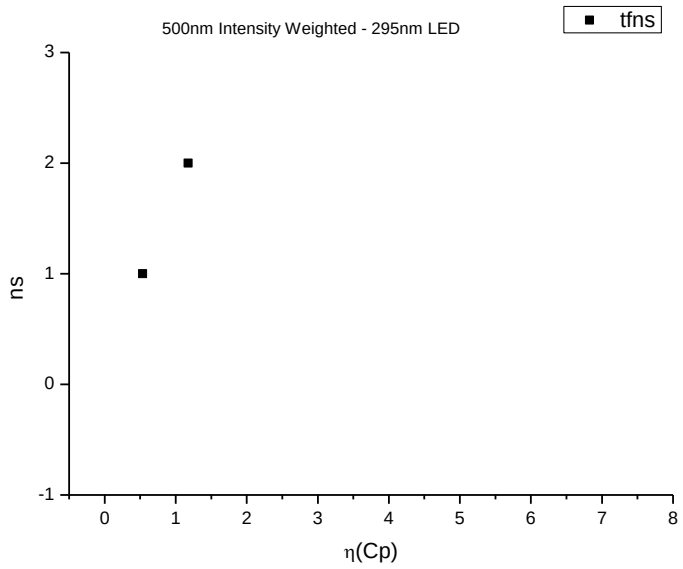

Figure 2.2.175. Intensity weighted average lifetime (τ_f) of **12** at 500 nm versus η(Cp).

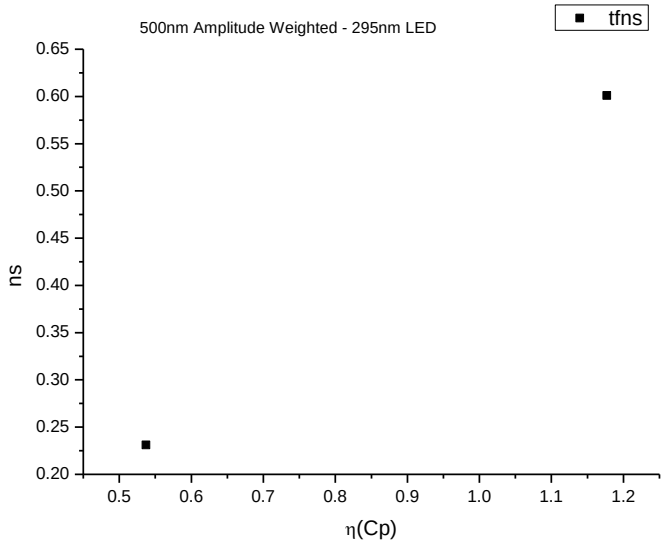

Figure 2.2.176. Amplitude weighted average lifetime (τ_f) of **12** at 500 nm versus η(Cp).

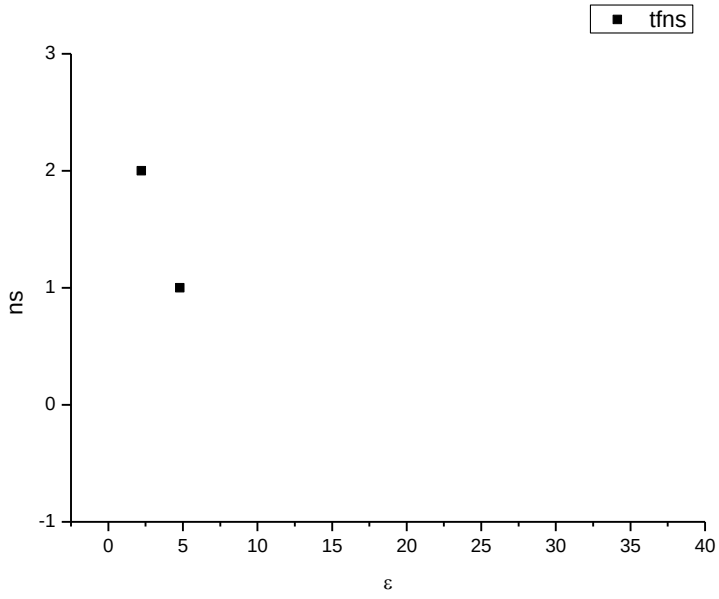

Figure 2.2.177. Intensity weighted average lifetime (τ_f) of **12** at 500 nm versus ε.

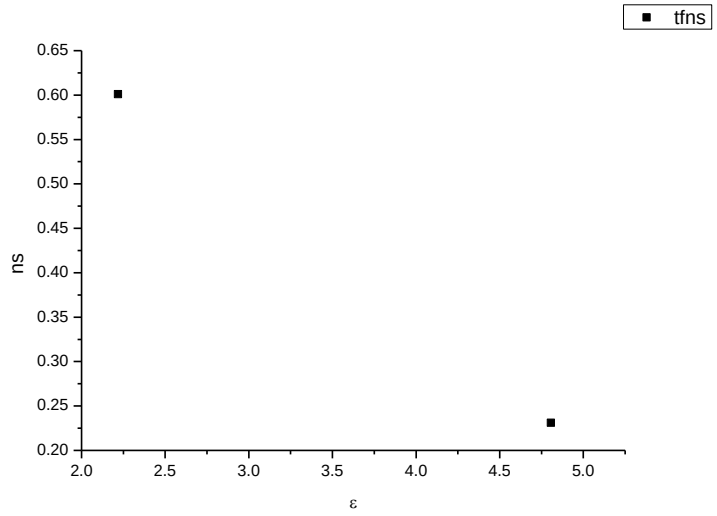

Figure 2.2.178. Amplitude weighted average lifetime (τ_f) of **12** at 500 nm versus ε.

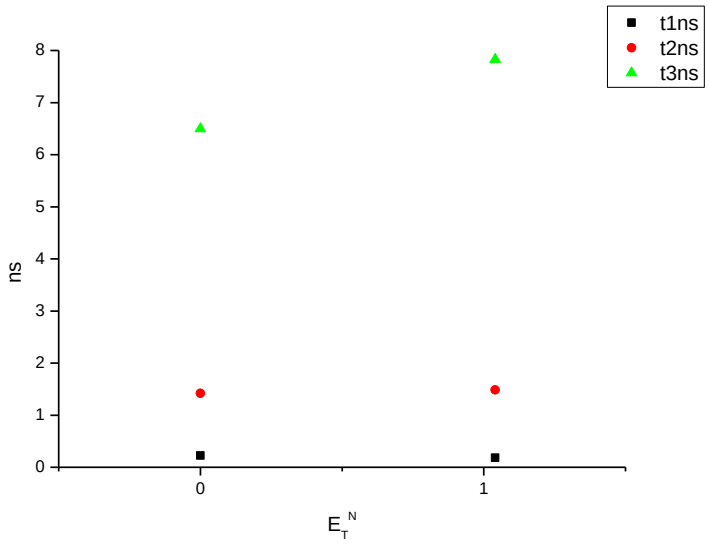

Figure 2.2.179. Intensity weighted components of TCSPC lifetime decay of **12** (500 nm) versus E_T^N.

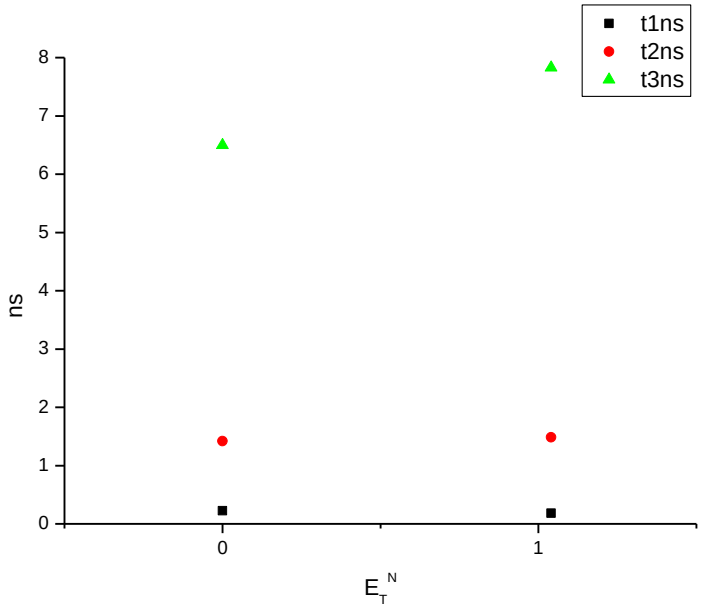

Figure 2.2.180. Amplitude weighted components of TCSPC lifetime decay of **12** (500 nm) versus E_T^N.

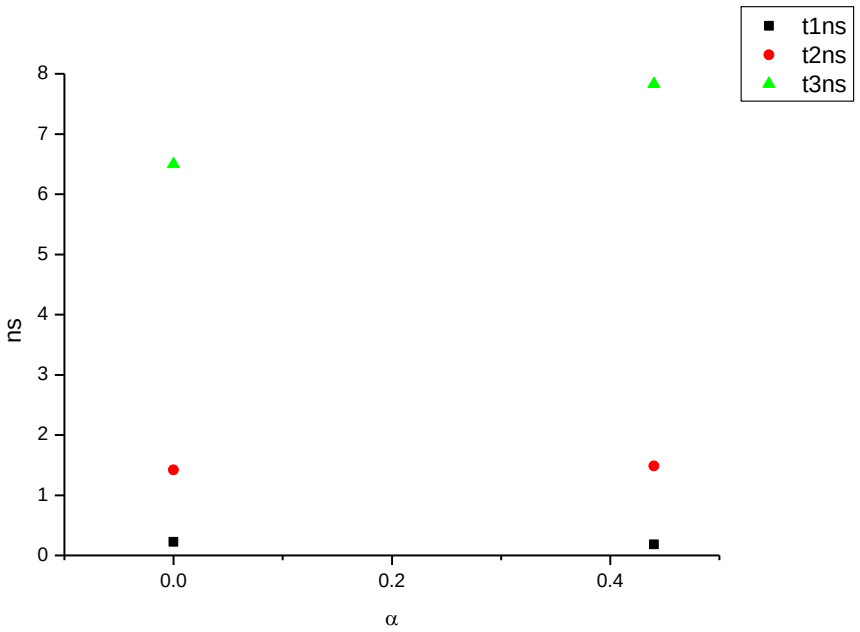

Figure 2.2.181. Intensity weighted components of TCSPC lifetime decay of **12** (500 nm) versus α.

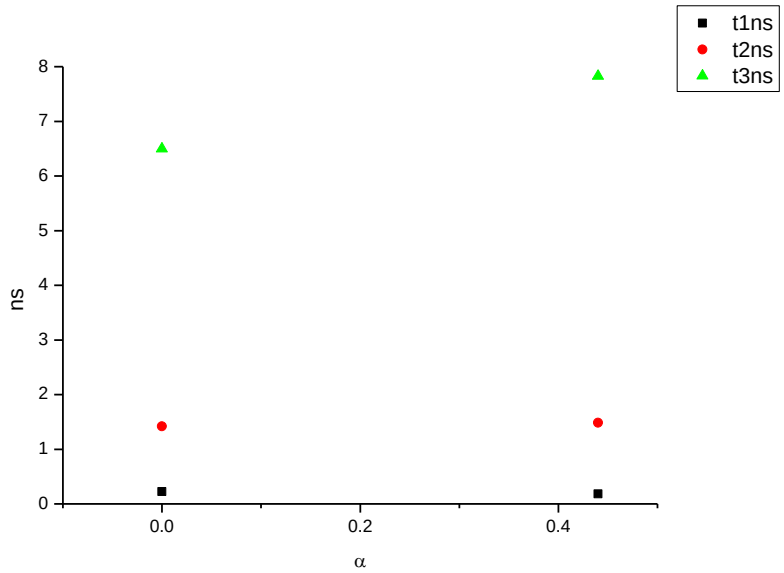

Figure 2.2.182. Amplitude weighted components of TCSPC lifetime decay of **12** (500 nm) versus α.

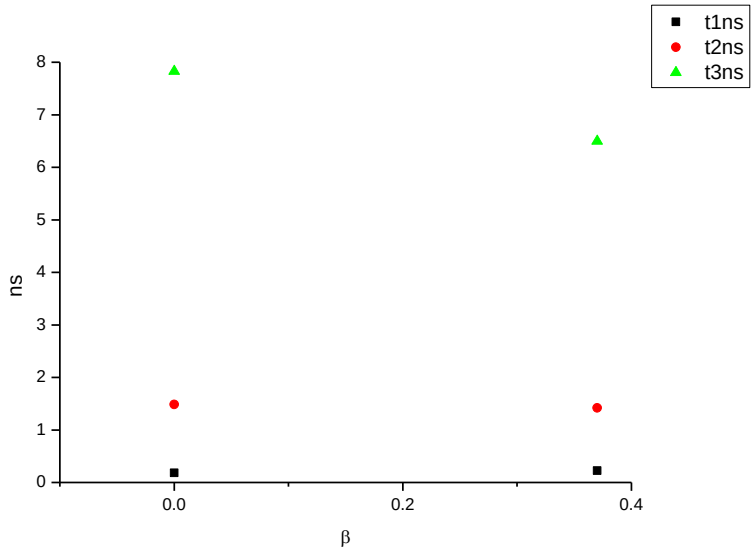

Figure 2.2.183. Intensity weighted components of TCSPC lifetime decay of **12** (500 nm) versus β.

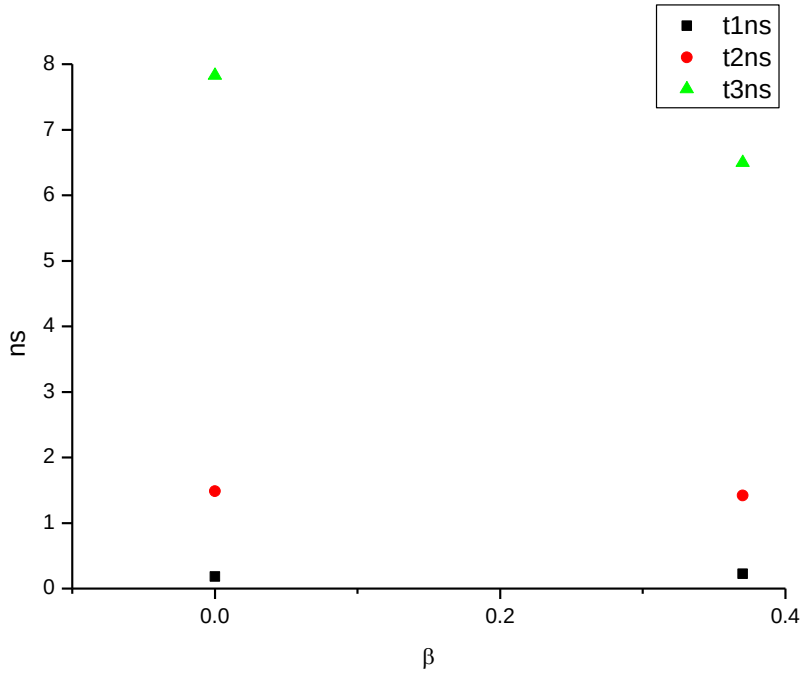

Figure 2.2.184. Amplitude weighted components of TCSPC lifetime decay of **12** (500 nm) versus β.

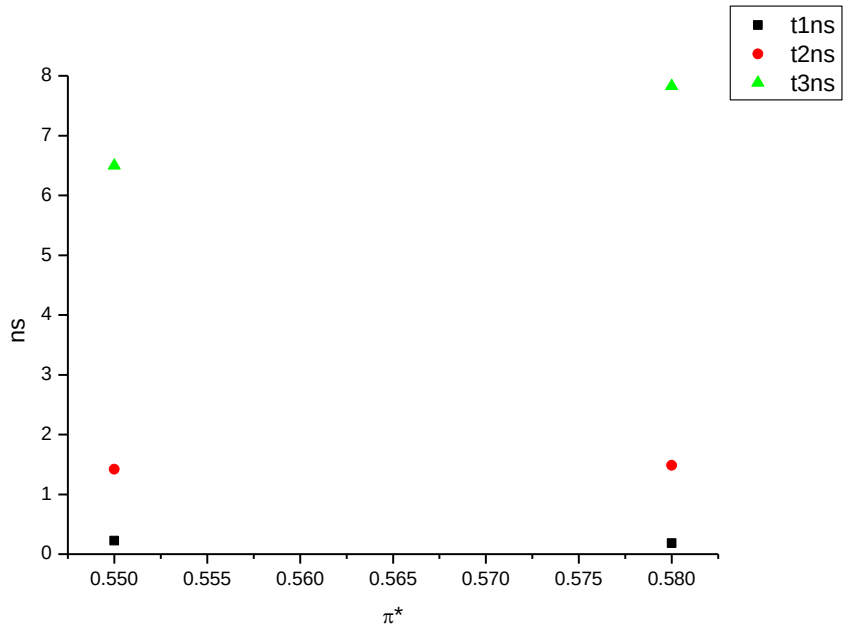

Figure 2.2.185. Intensity weighted components of TCSPC lifetime decay of **12** (500 nm) versus π*.

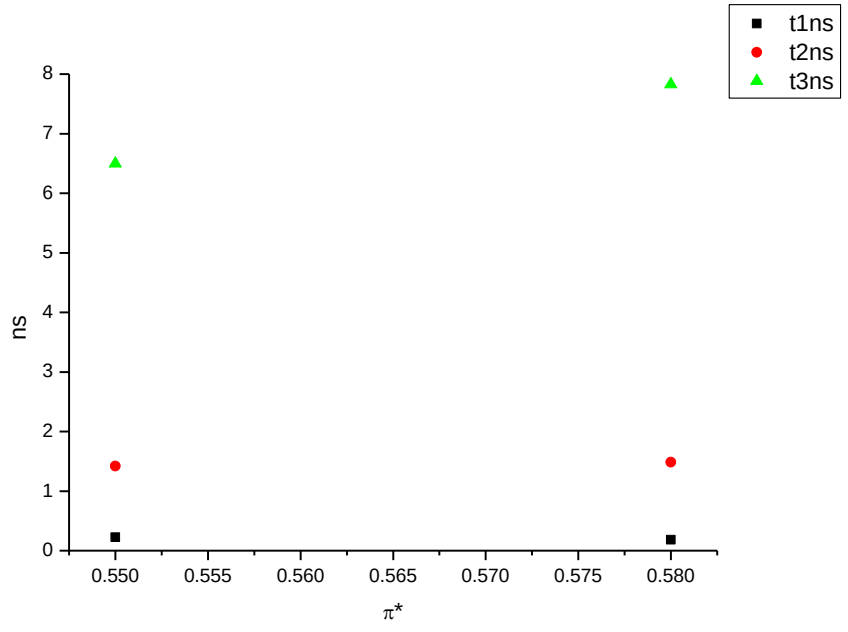

Figure 2.2.186. Amplitude weighted components of TCSPC lifetime decay of **12** (500 nm) versus π*.

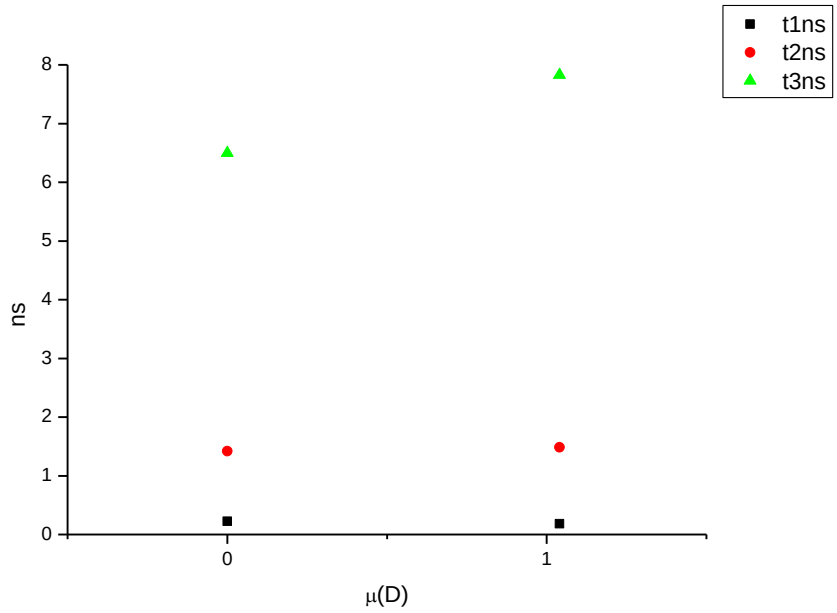

Figure 2.2.187. Intensity weighted components of TCSPC lifetime decay of **12** (500 nm) versus μ(D).

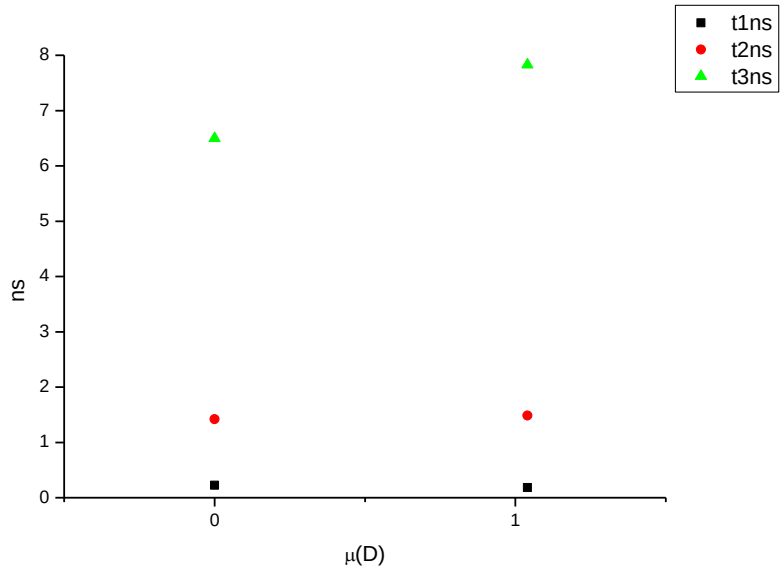

Figure 2.2.188. Amplitude weighted components of TCSPC lifetime decay of **12** (500 nm) versus μ(D).

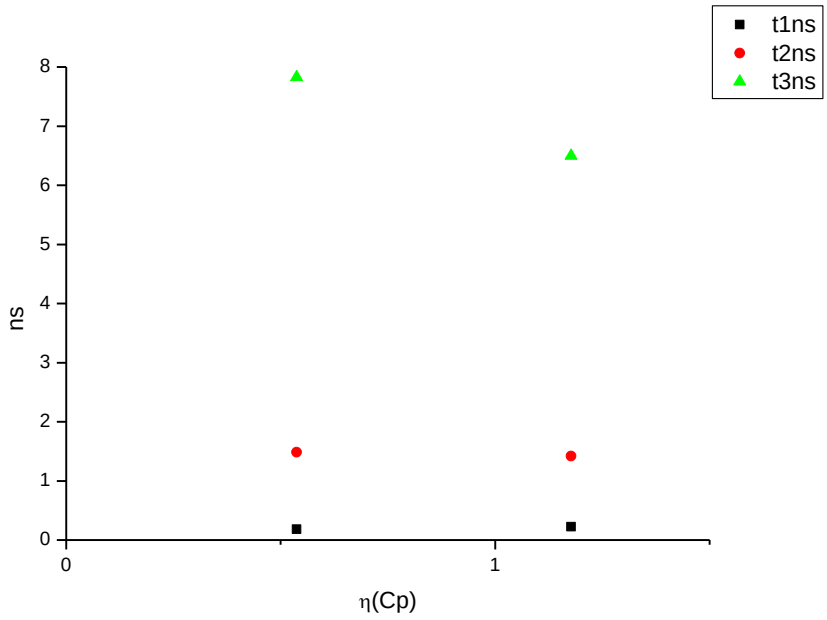

Figure 2.2.189. Intensity weighted components of TCSPC lifetime decay of **12** (500 nm) versus η(Cp).

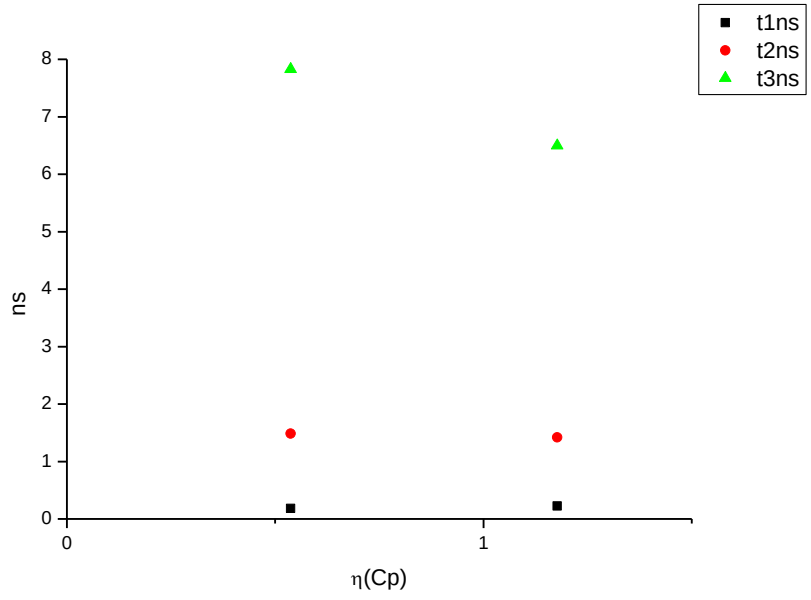

Figure 2.2.190. Amplitude weighted components of TCSPC lifetime decay of **12** (500 nm) versus η(Cp).

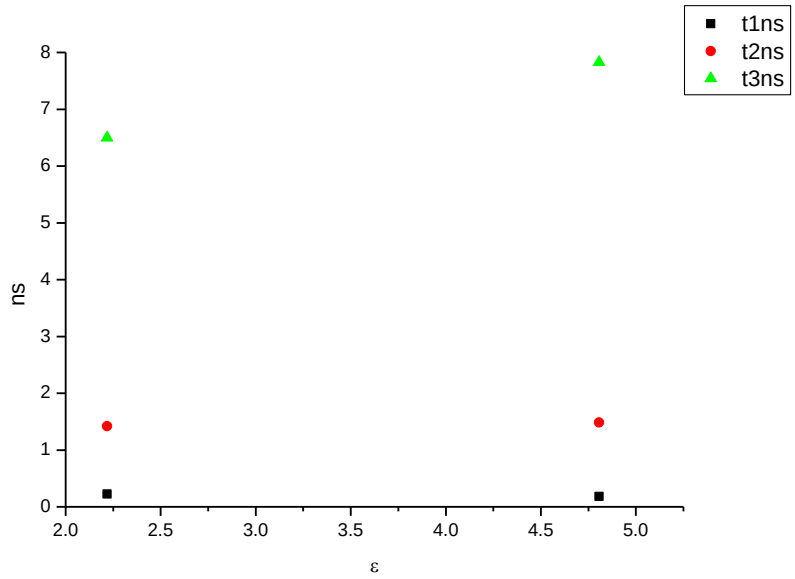

Figure 2.2.191. Intensity weighted components of TCSPC lifetime decay of **12** (500 nm) versus ε.

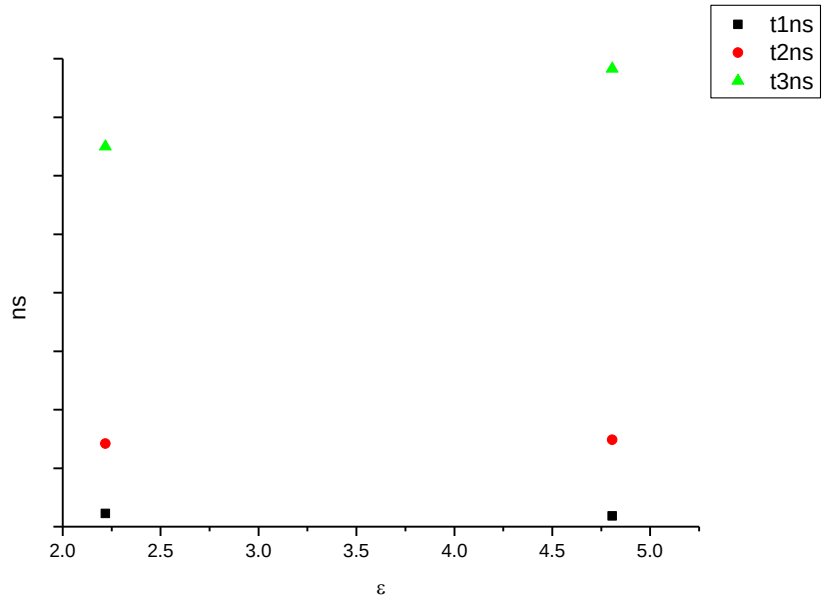

Figure 2.2.192. Amplitude weighted components of TCSPC lifetime decay of **12** (500 nm) versus ε.

2.2.10 Ultraviolet-visible absorption spectra.

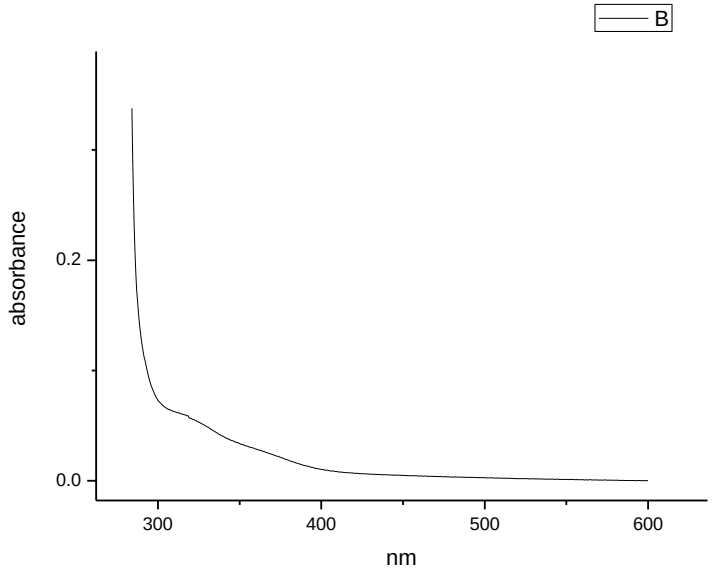

Figure 2.2.193. Ultraviolet-Visible absorption spectrum of **12** recorded in Toluene.

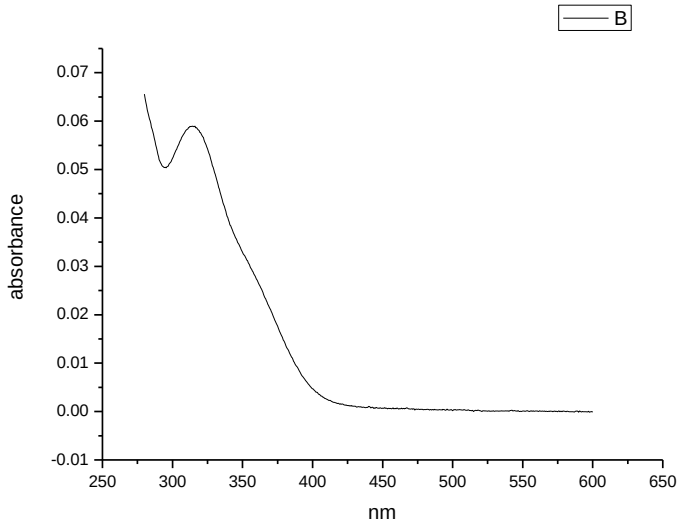

Figure 2.2.194. Ultraviolet-Visible absorption spectrum of **12** recorded in 1,4-dioxane.

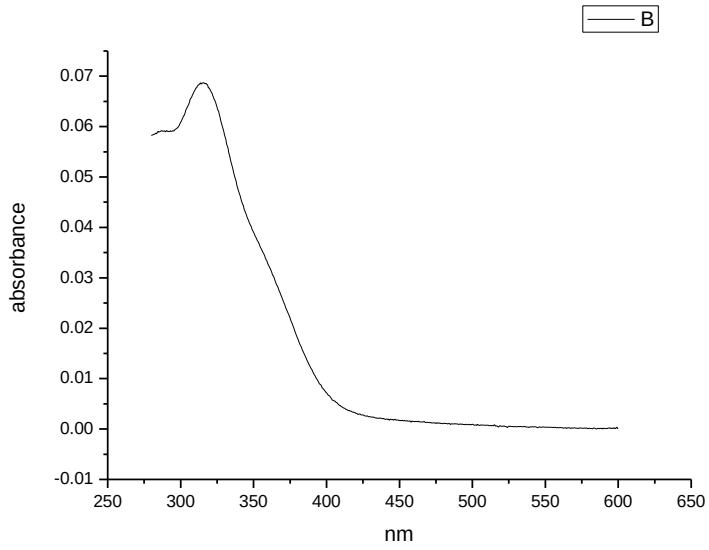

Figure 2.2.195. Ultraviolet-Visible absorption spectrum of **12** recorded in Chloroform.

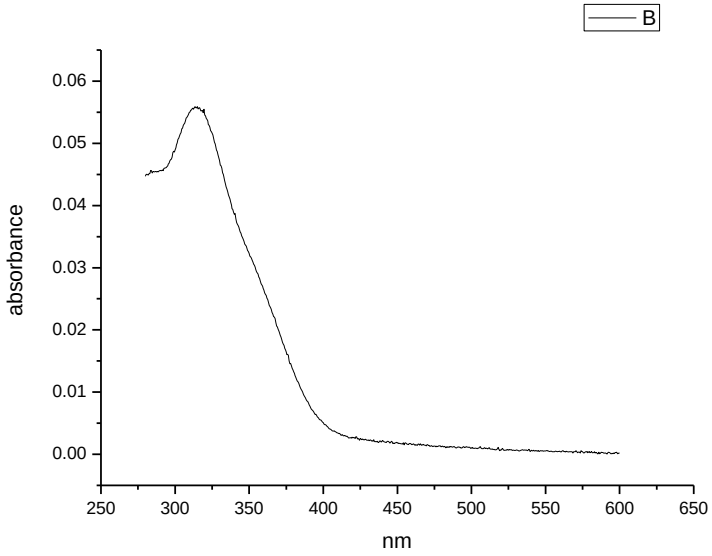

Figure 2.2.196. Ultraviolet-Visible absorption spectrum of **12** recorded in Acetonitrile.

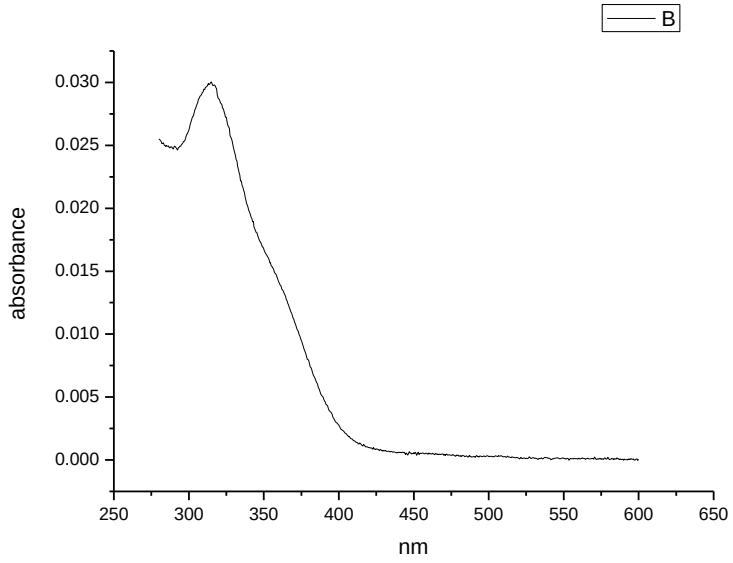

Figure 2.2.197. Ultraviolet-Visible absorption spectrum of **12** recorded in 1-octanol.

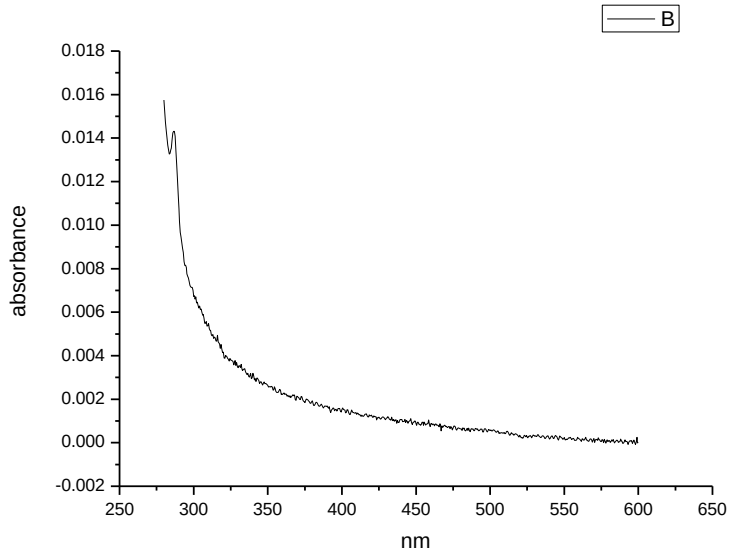

Figure 2.2.198. Ultraviolet-Visible absorption spectrum of **12** recorded in 1-hexanol.

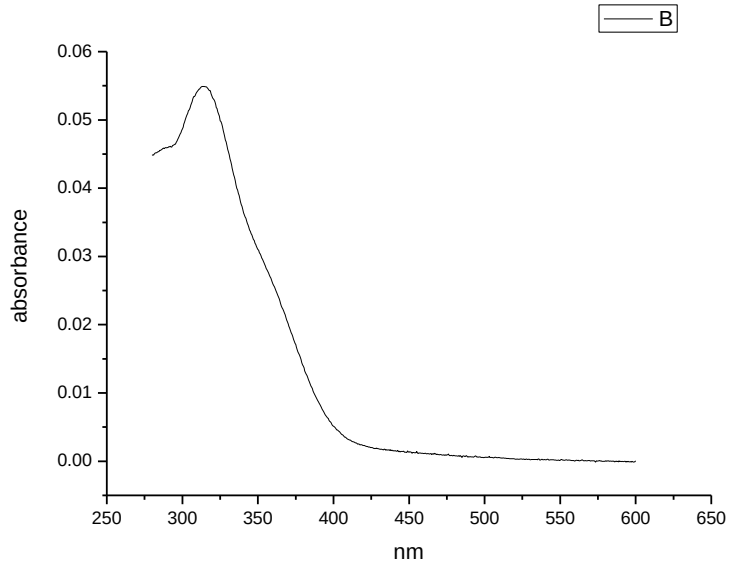

Figure 2.2.199. Ultraviolet-Visible absorption spectrum of **12** recorded in 1-butanol.

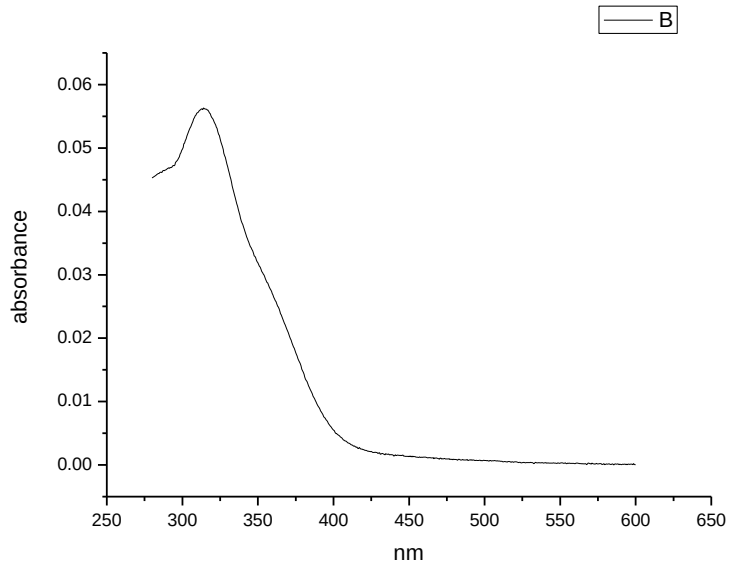

Figure 2.2.200. Ultraviolet-Visible absorption spectrum of **12** recorded in 1-pentanol.

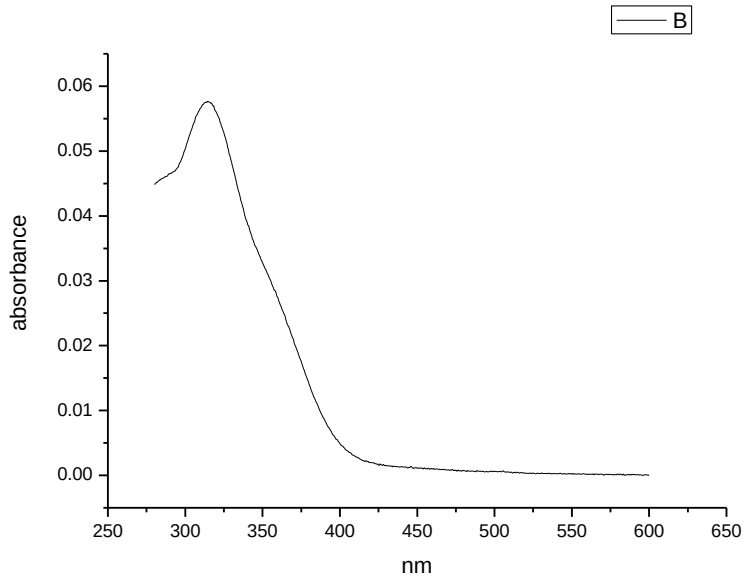

Figure 2.2.201. Ultraviolet-Visible absorption spectrum of **12** recorded in 1-propanol.

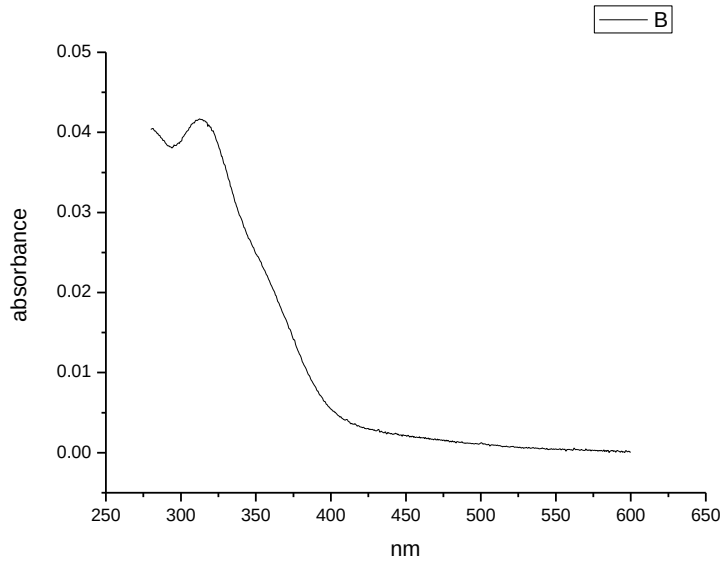

Figure 2.2.202. Ultraviolet-Visible absorption spectrum of **12** recorded in Acetic Acid.

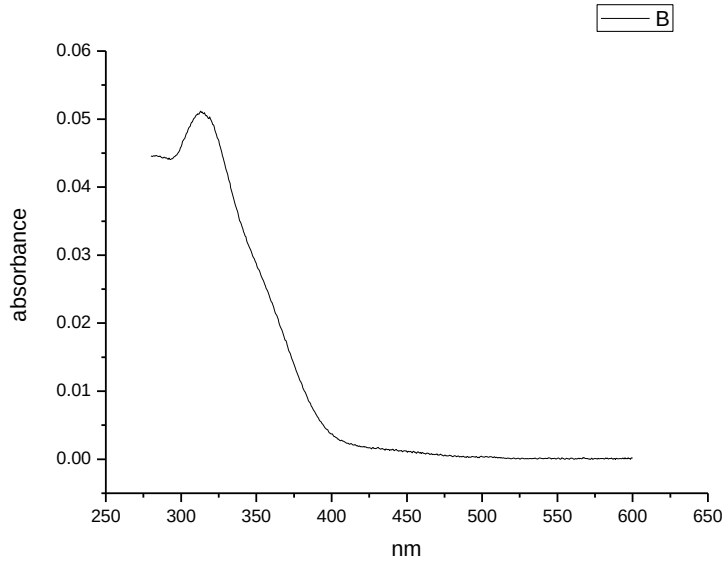

Figure 2.2.203. Ultraviolet-Visible absorption spectrum of **12** recorded in Methanol.

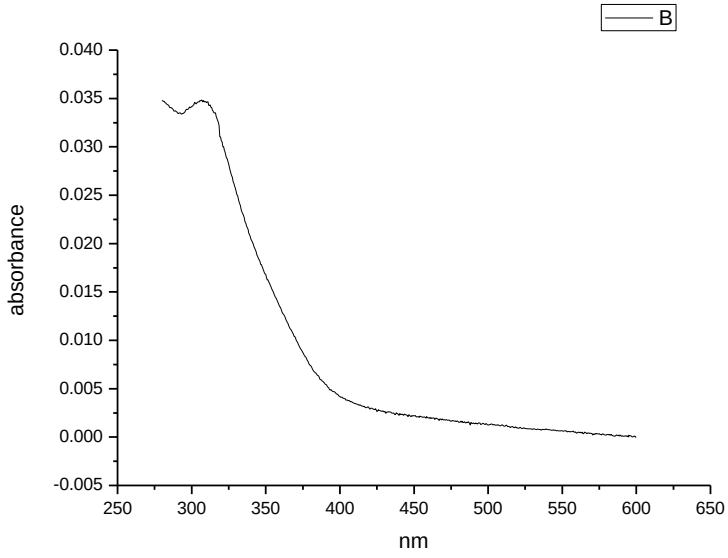

Figure 2.2.204. Ultraviolet-Visible absorption spectrum of **12** recorded in 2,2,2-trifluoroethanol.

2.2.11 Fluorescence Emission spectra.

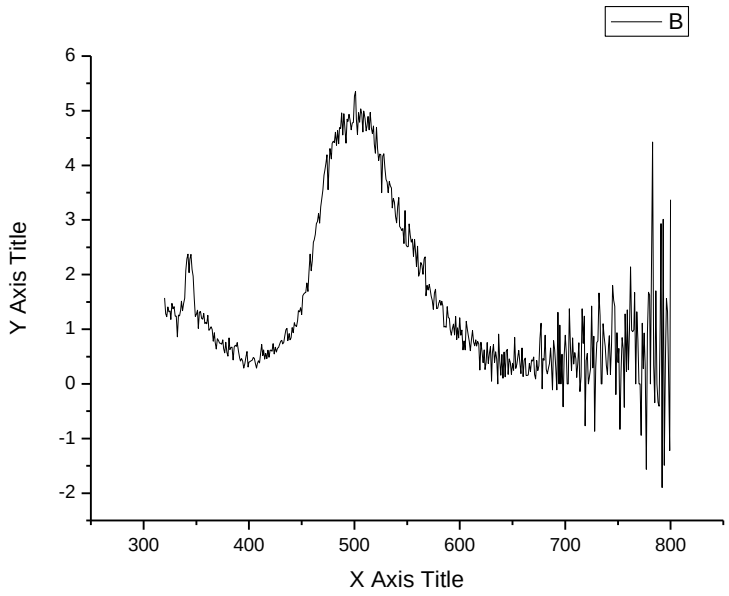

Figure 2.2.205. Fluorescence emission spectrum of **12** recorded in Toluene at 310 nm excitation.

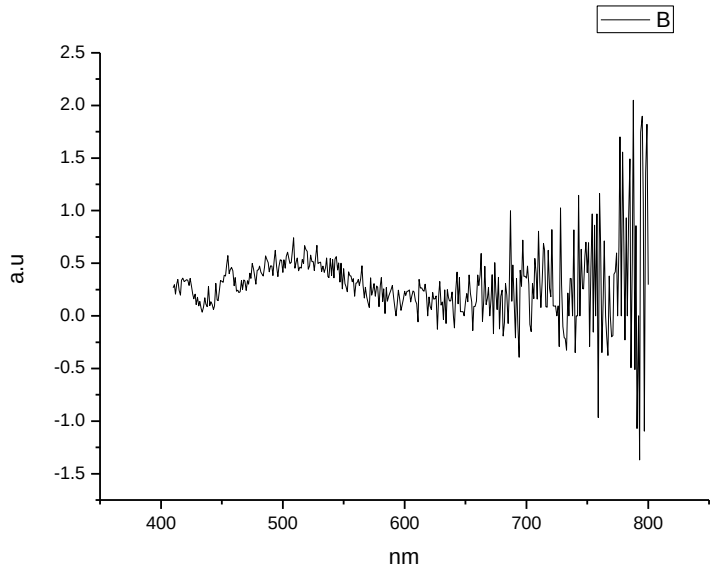

Figure 2.2.206. Fluorescence emission spectrum of **12** recorded in Toluene at 400 nm excitation.

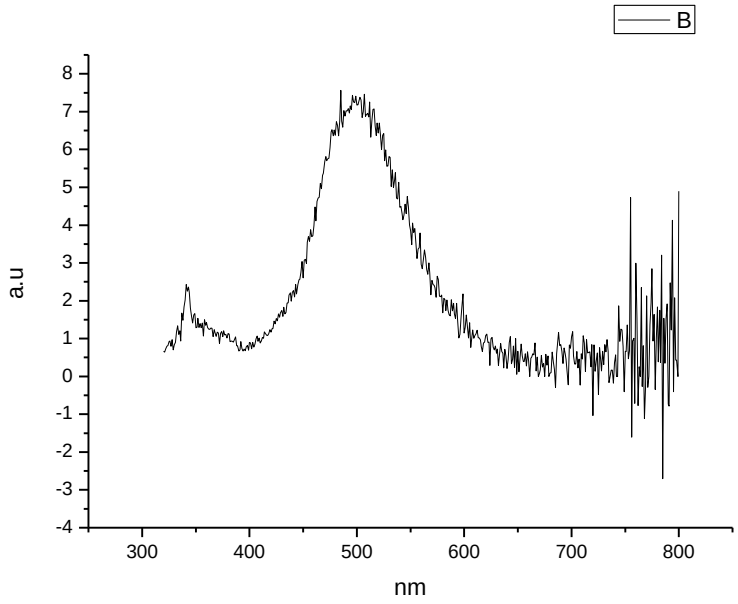

Figure 2.2.207. Fluorescence emission spectrum of **12** recorded in 1,4-dioxane at 310 nm excitation.

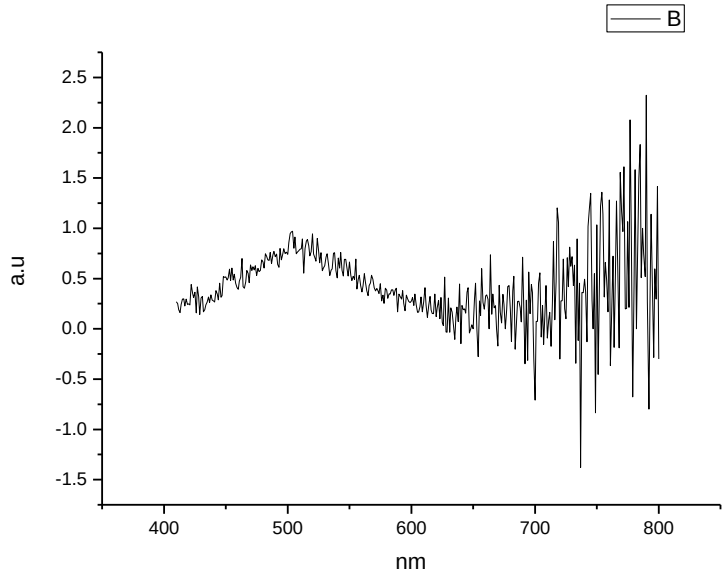

Figure 2.2.208. Fluorescence emission spectrum of **12** recorded in 1,4-dioxane at 400 nm excitation.

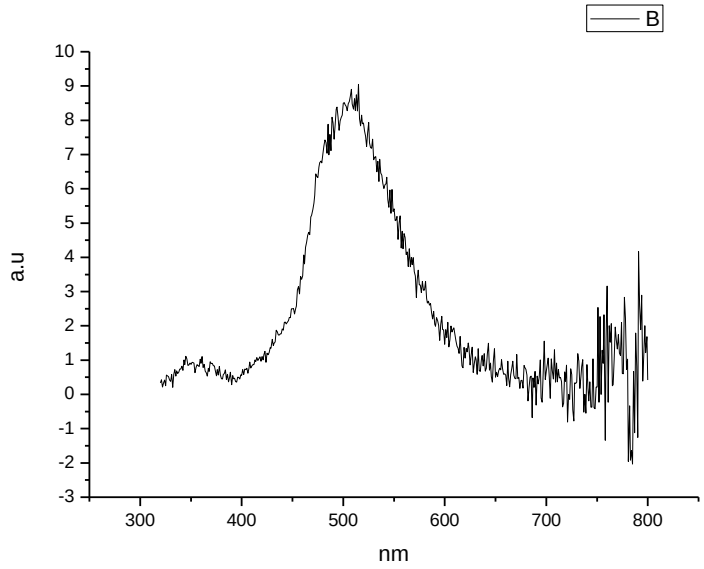

Figure 2.2.209. Fluorescence emission spectrum of **12** recorded in Chloroform at 310 nm excitation.

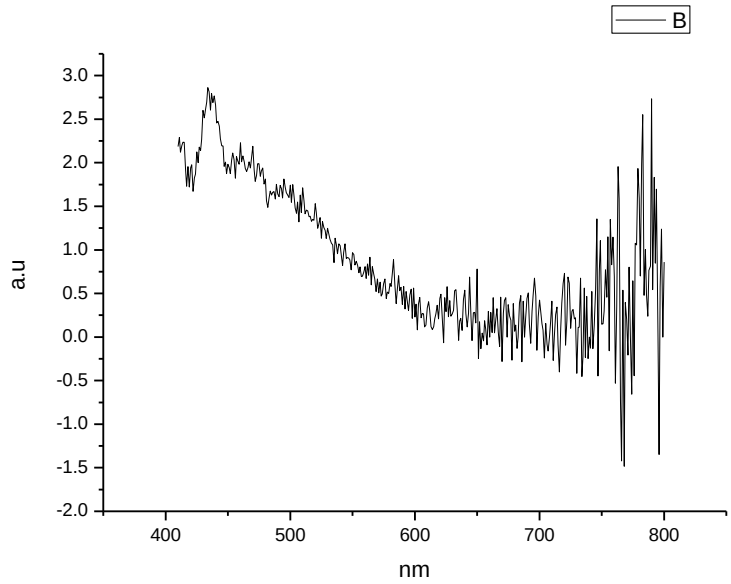

Figure 2.2.210. Fluorescence emission spectrum of **12** recorded in Chloroform at 400 nm excitation.

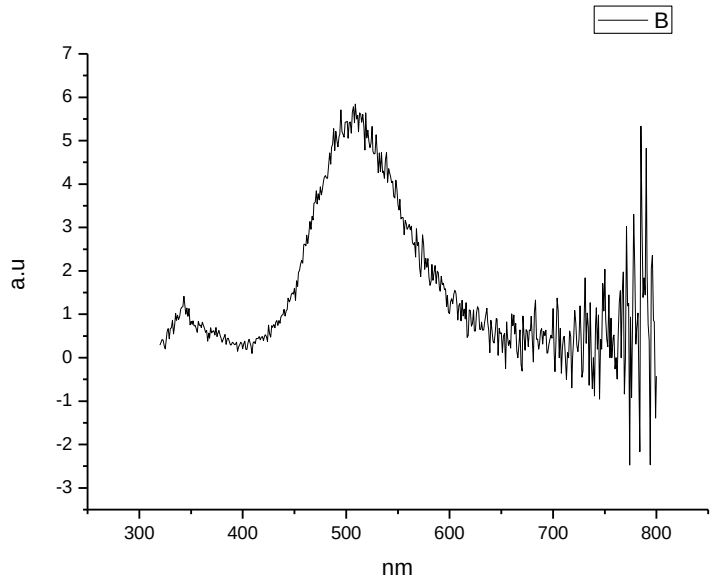

Figure 2.2.211. Fluorescence emission spectrum of **12** recorded in Acetonitrile at 310 nm excitation.

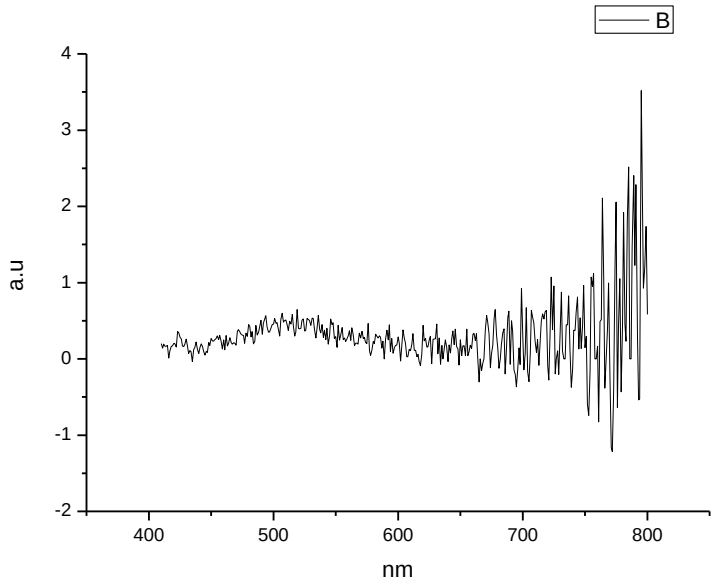

Figure 2.2.212. Fluorescence emission spectrum of **12** recorded in Acetonitrile at 400 nm excitation.

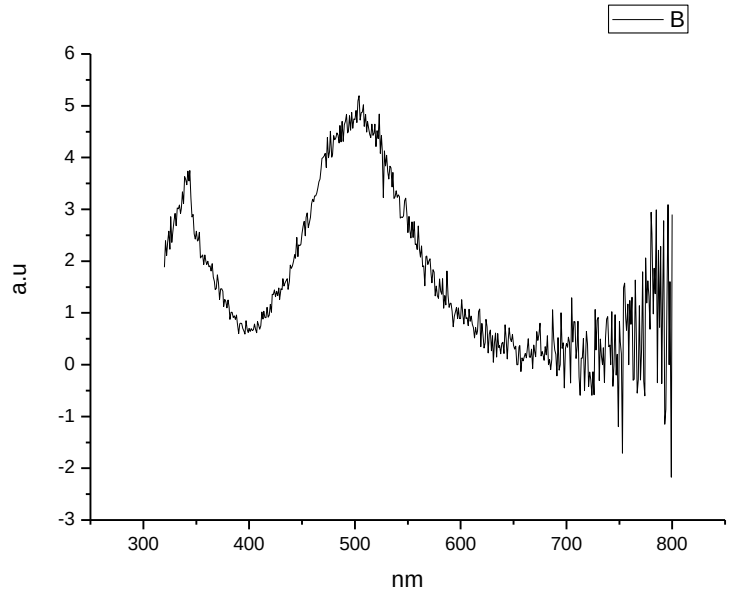

Figure 2.2.213. Fluorescence emission spectrum of **12** recorded in 1-octanol at 310 nm excitation.

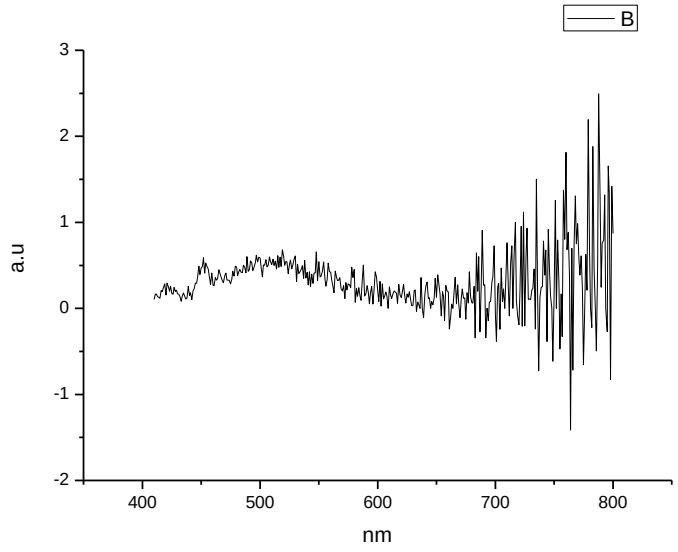

Figure 2.2.214. Fluorescence emission spectrum of **12** recorded in 1-octanol at 400 nm excitation.

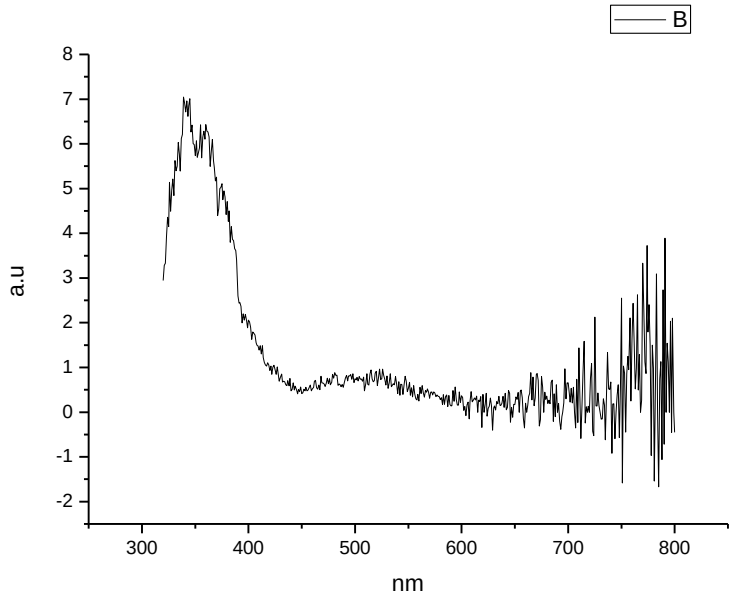

Figure 2.2.215. Fluorescence emission spectrum of **12** recorded in 1-hexanol at 310 nm excitation.

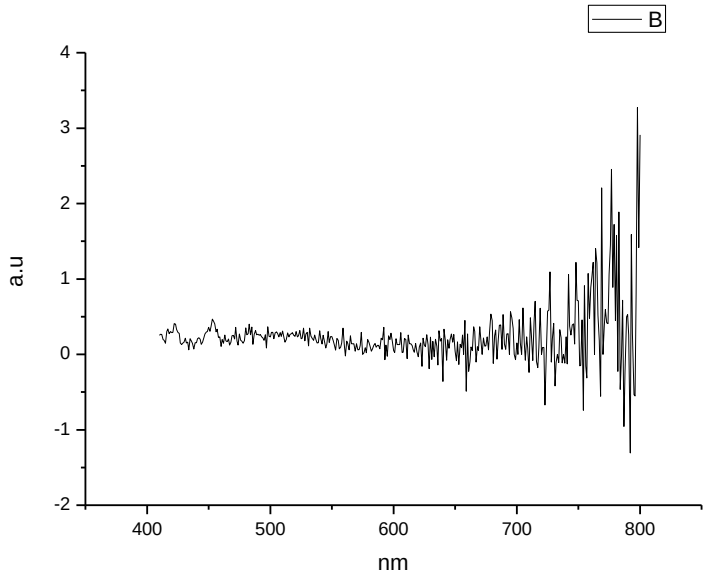

Figure 2.2.216. Fluorescence emission spectrum of **12** recorded in 1-hexanol at 400 nm excitation.

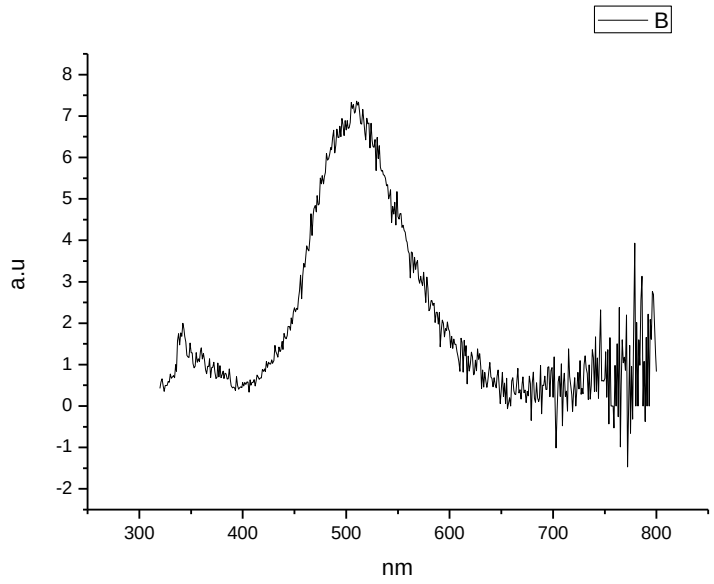

Figure 2.2.217. Fluorescence emission spectrum of **12** recorded in 1-butanol at 310 nm excitation.

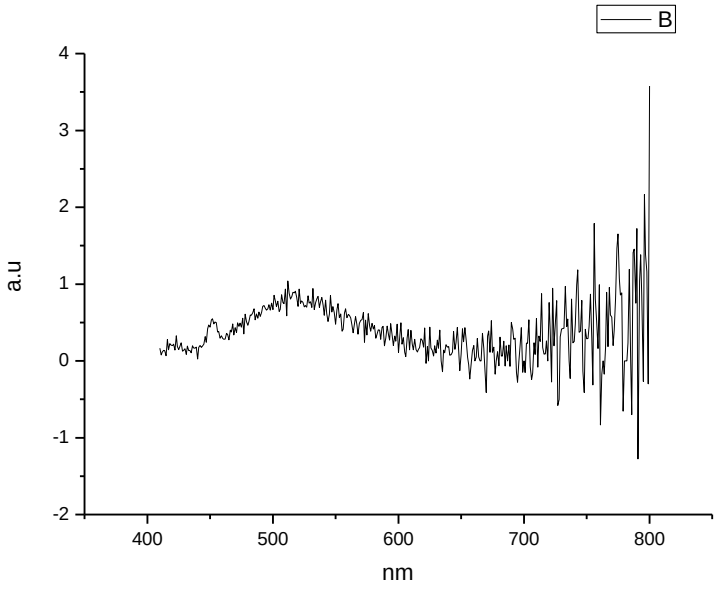

Figure 2.2.218. Fluorescence emission spectrum of **12** recorded in 1-butanol at 400 nm excitation.

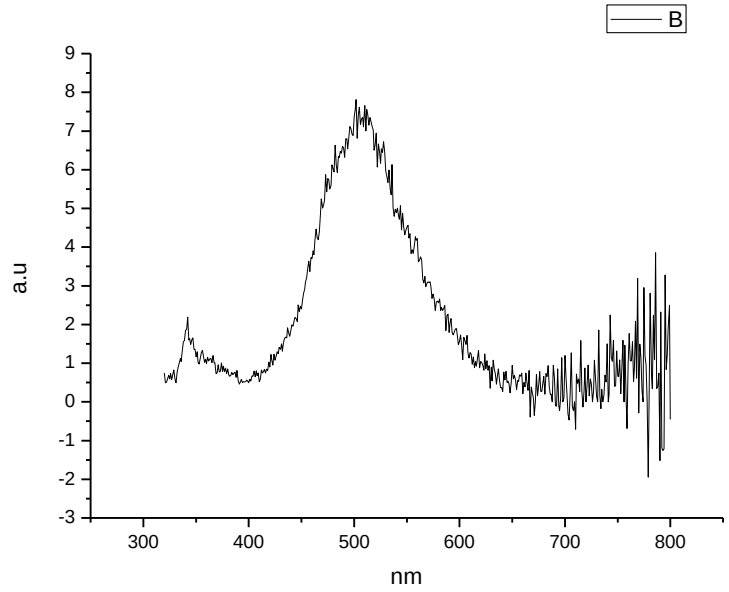

Figure 2.2.219. Fluorescence emission spectrum of **12** recorded in 1-pentanol at 310 nm excitation.

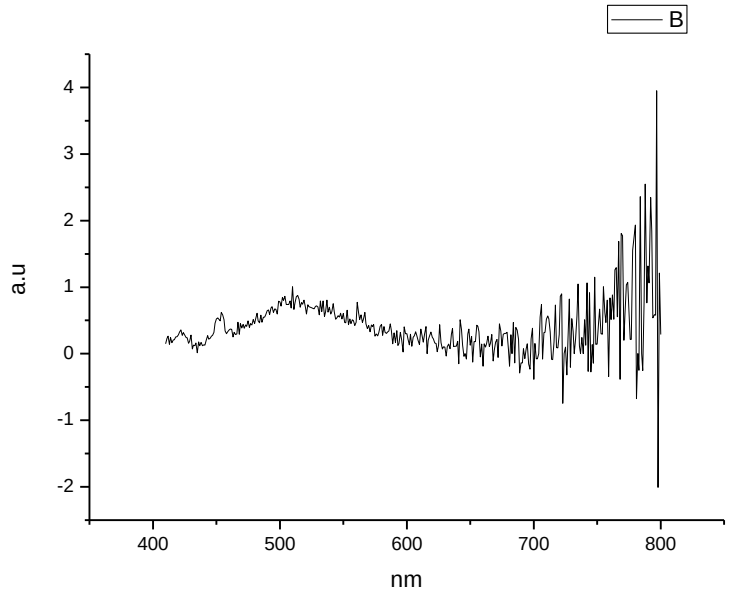

Figure 2.2.220. Fluorescence emission spectrum of **12** recorded in 1-pentanol at 400 nm excitation.

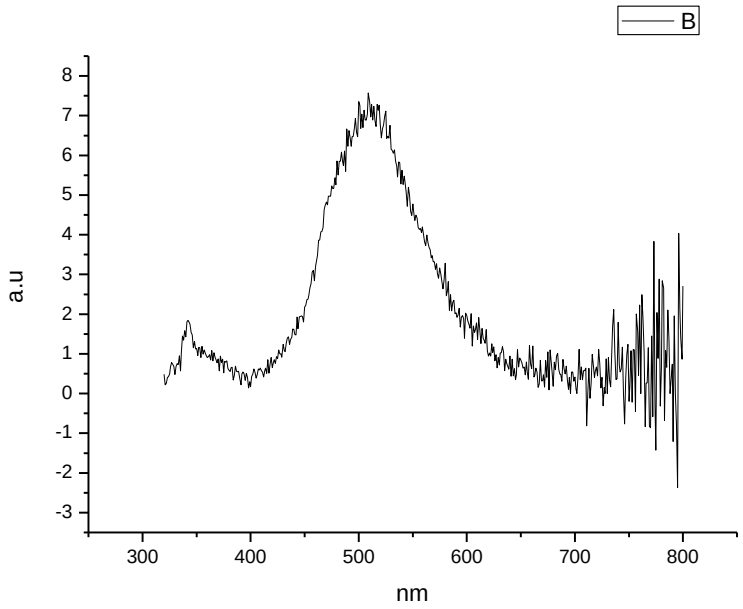

Figure 2.2.221. Fluorescence emission spectrum of **12** recorded in 1-propanol at 310 nm excitation.

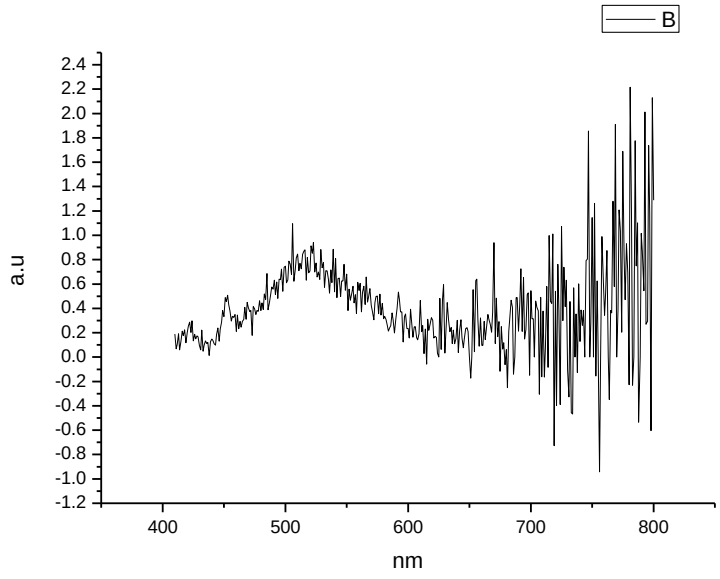

Figure 2.2.222. Fluorescence emission spectrum of **12** recorded in 1-propanol at 400 nm excitation.

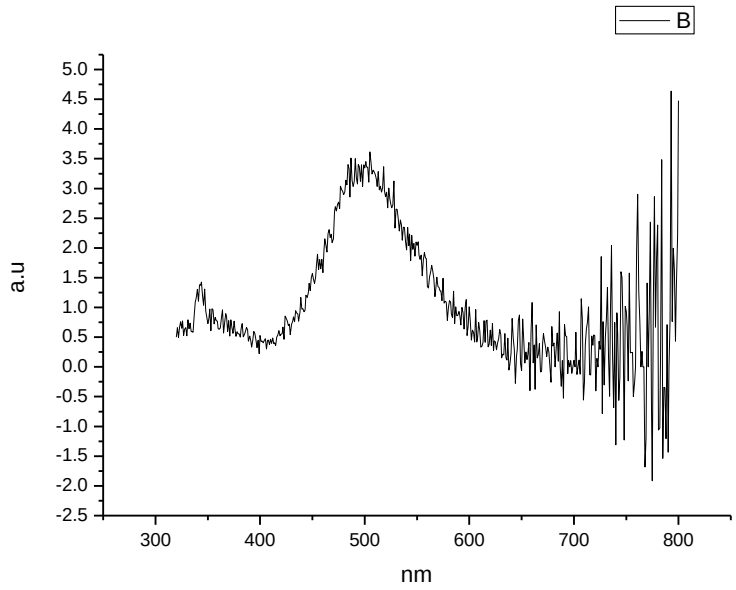

Figure 2.2.223. Fluorescence emission spectrum of **12** recorded in Acetic Acid at 310 nm excitation.

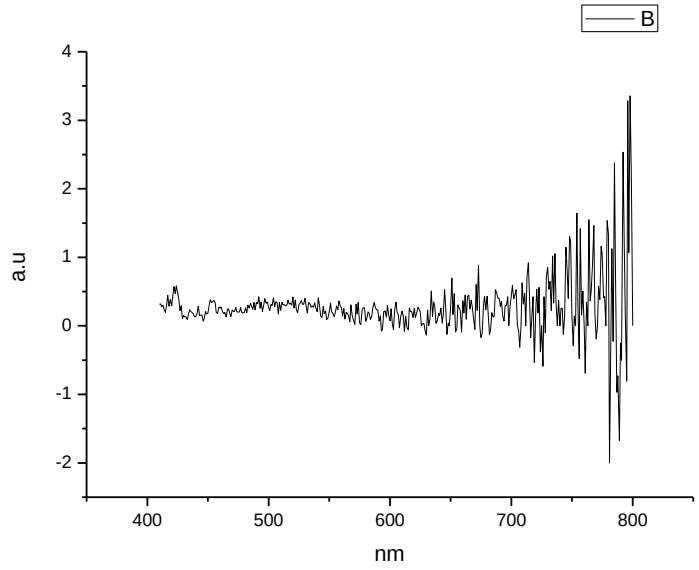

Figure 2.2.224. Fluorescence emission spectrum of **12** recorded in Acetic Acid at 400 nm excitation.

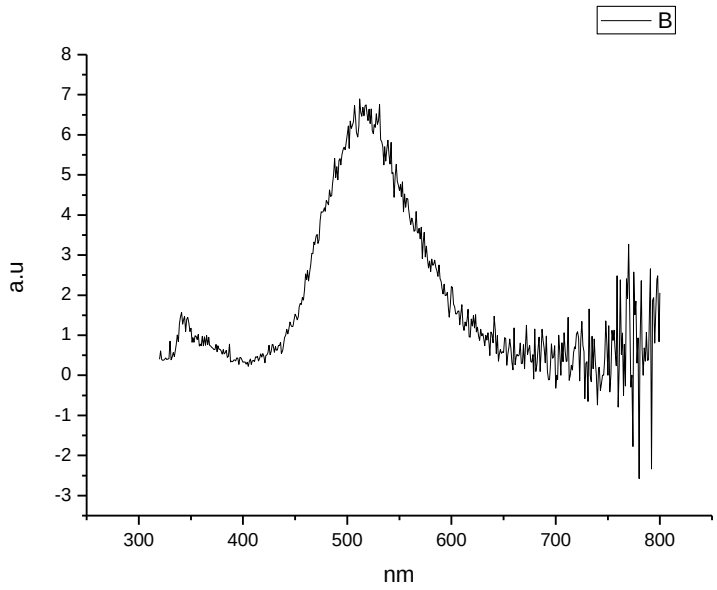

Figure 2.2.225. Fluorescence emission spectrum of **12** recorded in Methanol at 310 nm excitation.

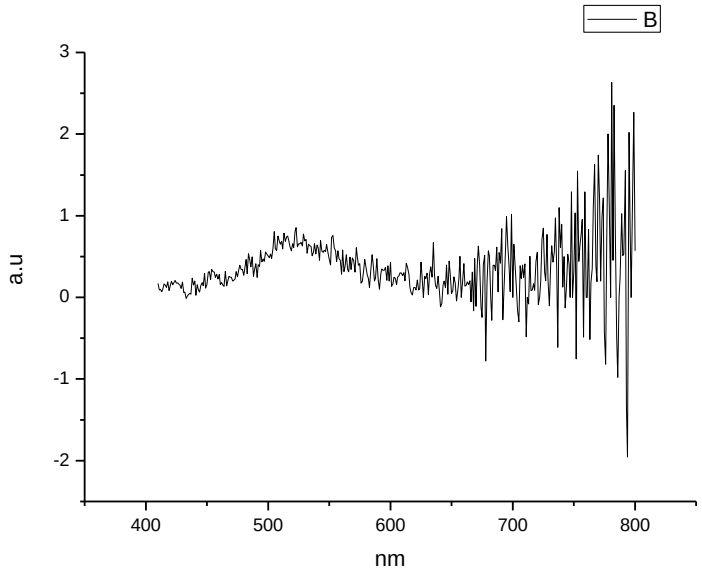

Figure 2.2.226. Fluorescence emission spectrum of **12** recorded in Methanol at 400 nm excitation.

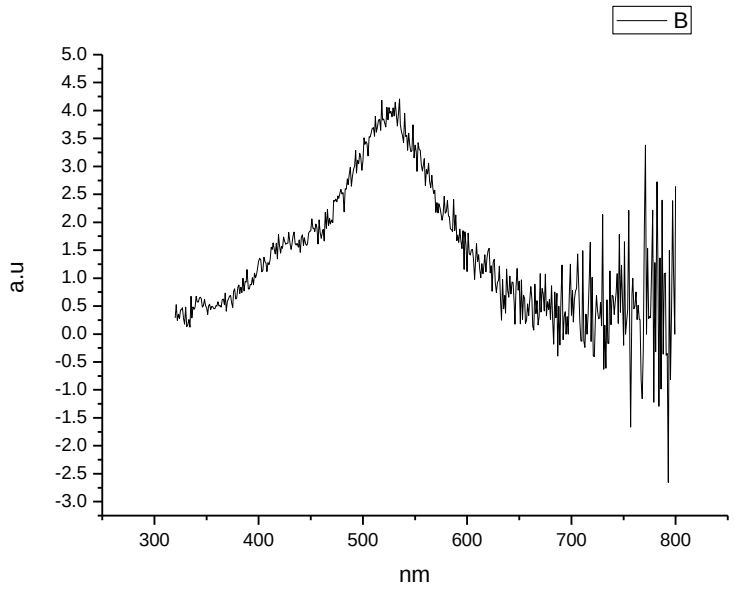

Figure 2.2.227. Fluorescence emission spectrum of **12** recorded in 2,2,2-trifluoroethanol at 310 nm excitation.

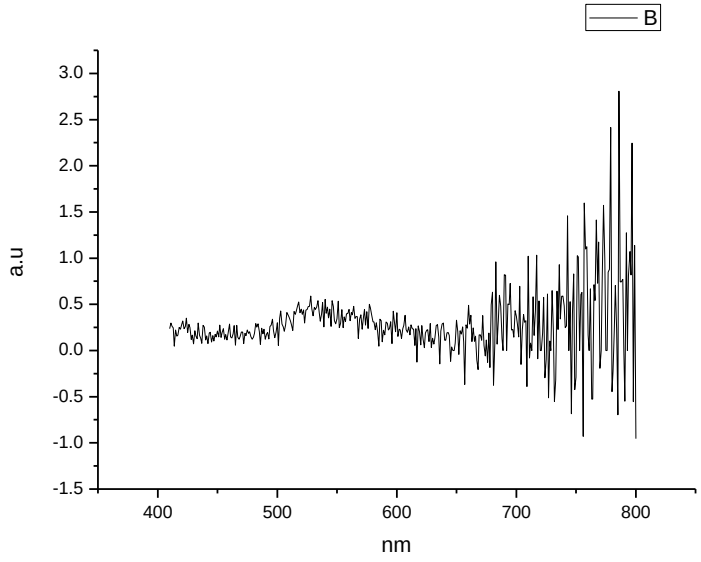

Figure 2.2.228. Fluorescence emission spectrum of **12** recorded in 2,2,2-trifluoroethanol at 400 nm excitation.

2.2.12 Normalised Fluorescence Emission spectra (Gaussian fitted).

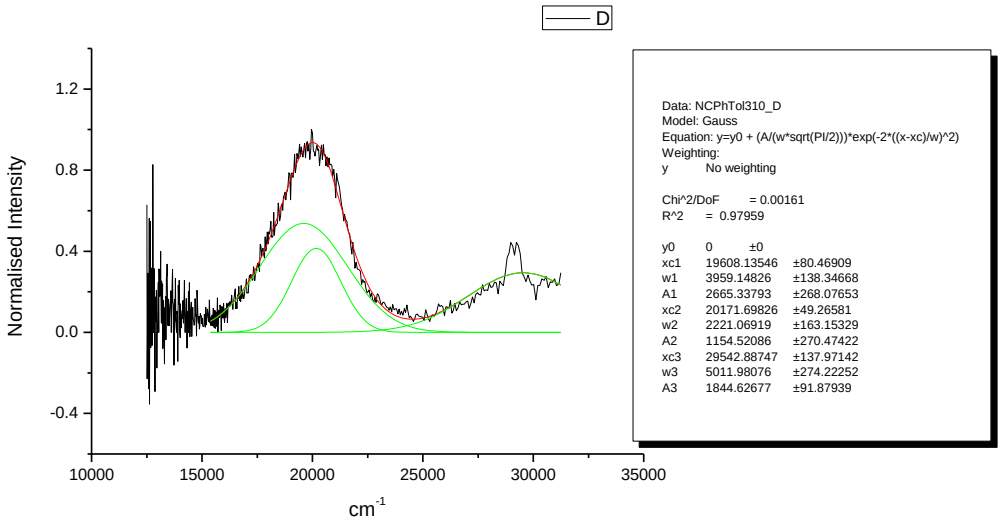

Figure 2.2.229. Gaussian model fit of the normalised fluorescence emission spectrum of **12** recorded in Toluene at 310 nm excitation.

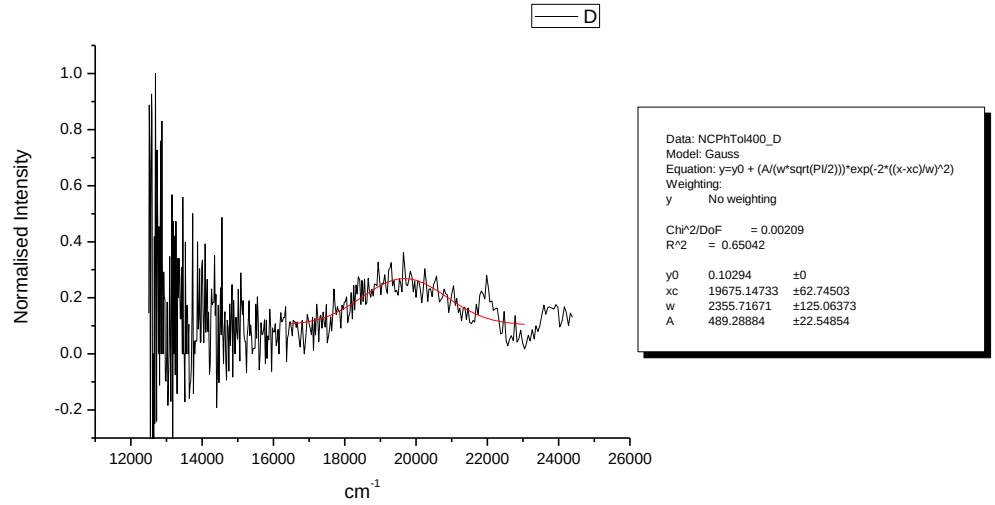

Figure 2.2.230. Gaussian model fit of the normalised fluorescence emission spectrum of **12** recorded in Toluene at 400 nm excitation.

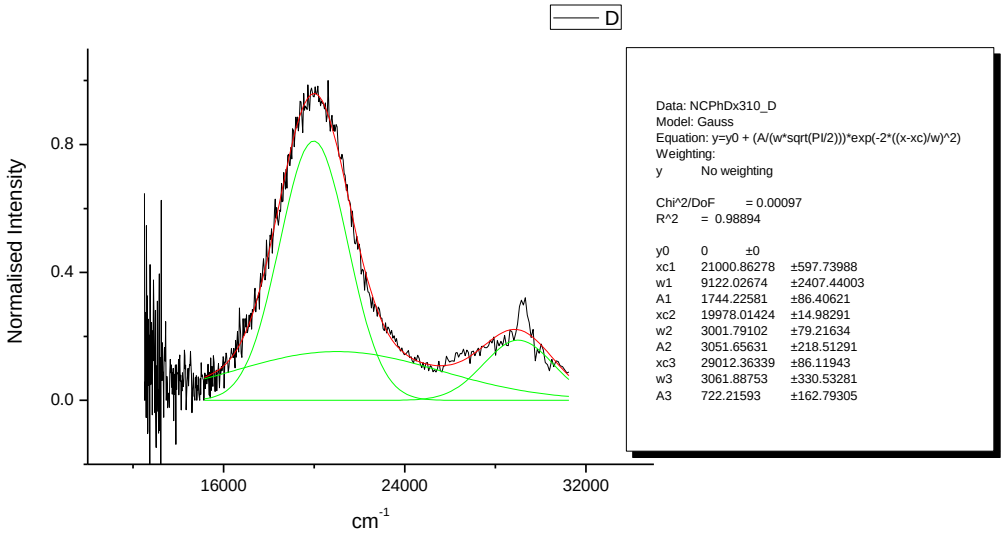

Figure 2.2.231. Gaussian model fit of the normalised fluorescence emission spectrum of **12** recorded in 1,4-dioxane at 310 nm excitation.

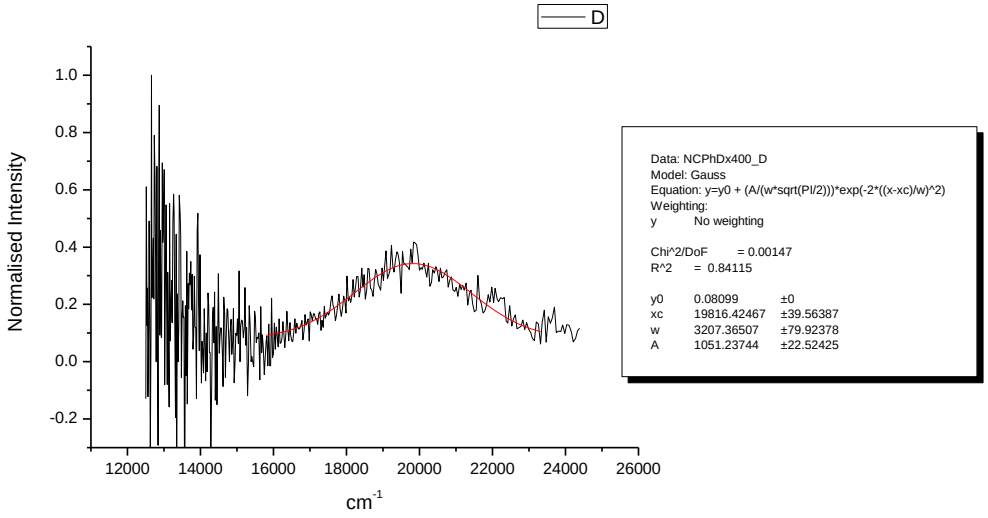

Figure 2.2.232. Gaussian model fit of the normalised fluorescence emission spectrum of **12** recorded in 1,4-dioxane at 400 nm excitation.

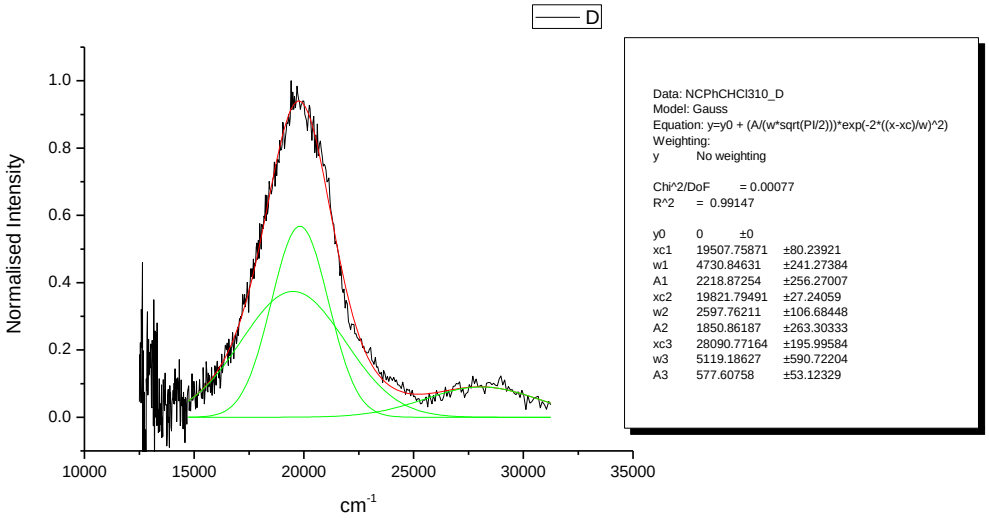

Figure 2.2.233. Gaussian model fit of the normalised fluorescence emission spectrum of **12** recorded in Chloroform at 310 nm excitation.

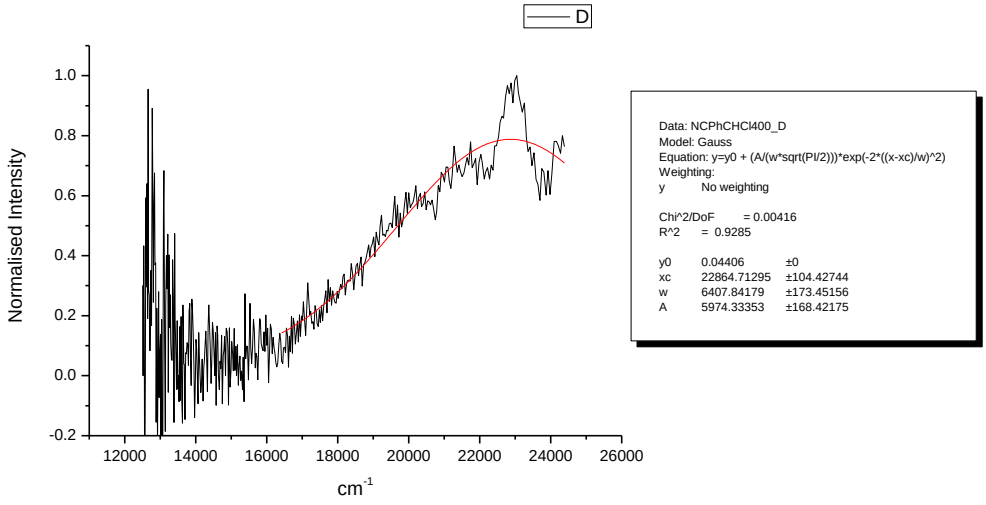

Figure 2.2.234. Gaussian model fit of the normalised fluorescence emission spectrum of **12** recorded in Chloroform at 400 nm excitation.

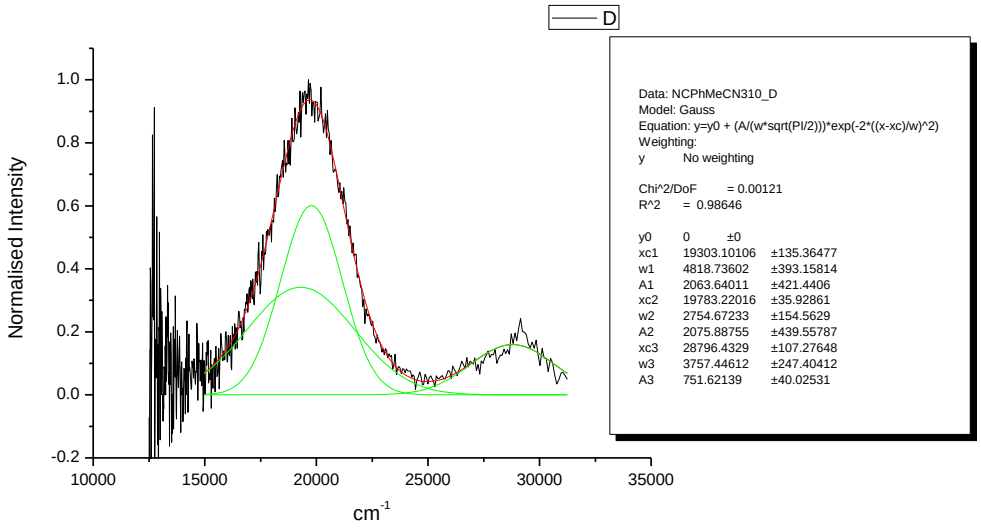

Figure 2.2.235. Gaussian model fit of the normalised fluorescence emission spectrum of **12** recorded in Acetonitrile at 310 nm excitation.

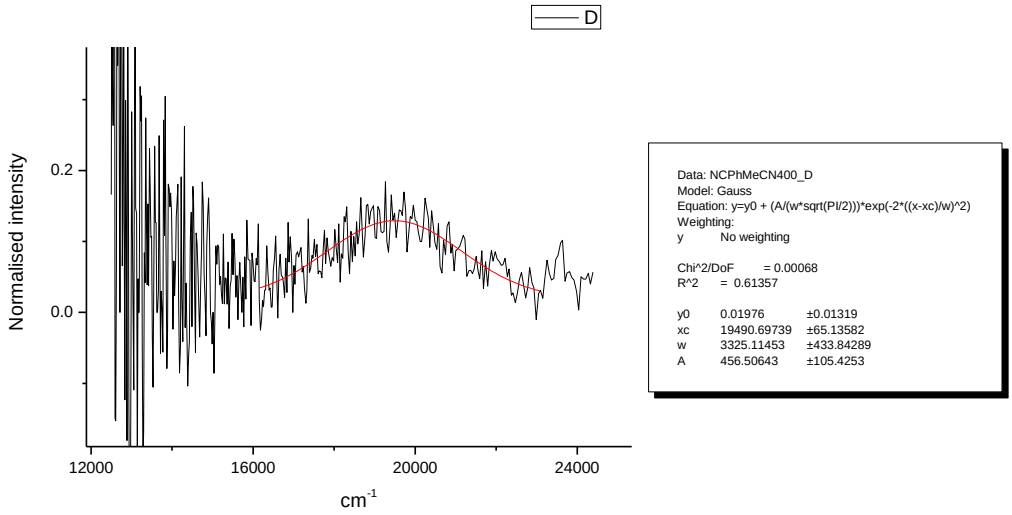

Figure 2.2.236. Gaussian model fit of the normalised fluorescence emission spectrum of **12** recorded in Acetonitrile at 400 nm excitation.

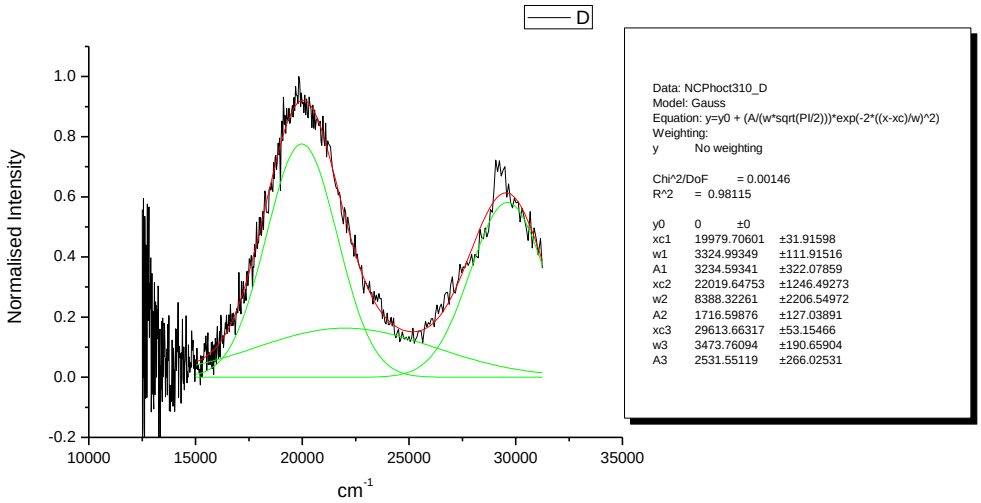

Figure 2.2.237. Gaussian model fit of the normalised fluorescence emission spectrum of **12** recorded in 1-octanol at 310 nm excitation.

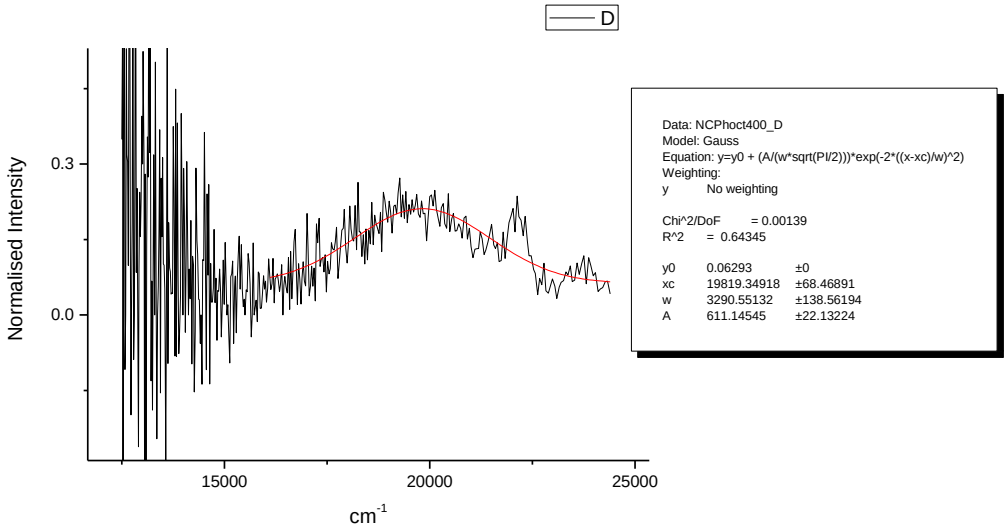

Figure 2.2.238. Gaussian model fit of the normalised fluorescence emission spectrum of **12** recorded in 1-octanol at 400 nm excitation.

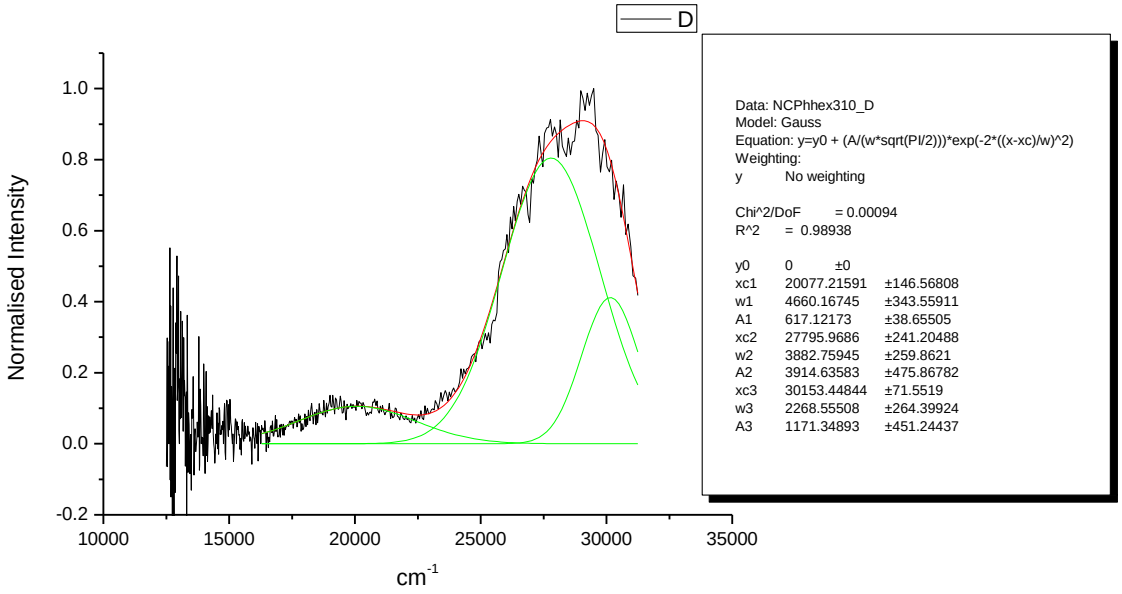

Figure 2.2.239. Gaussian model fit of the normalised fluorescence emission spectrum of **12** recorded in 1-hexanol at 310 nm excitation.

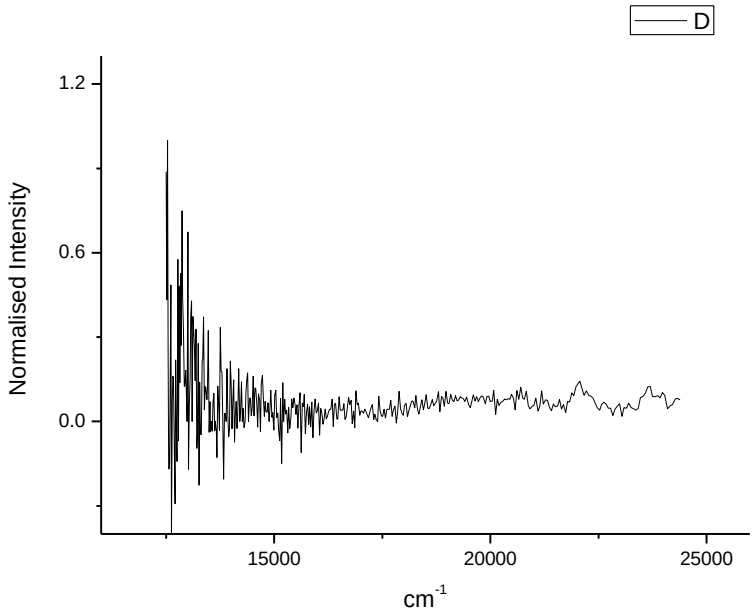

Figure 2.2.240. Attempted gaussian model fit of the normalised fluorescence emission spectrum of **12** recorded in 1-hexanol at 400 nm excitation.

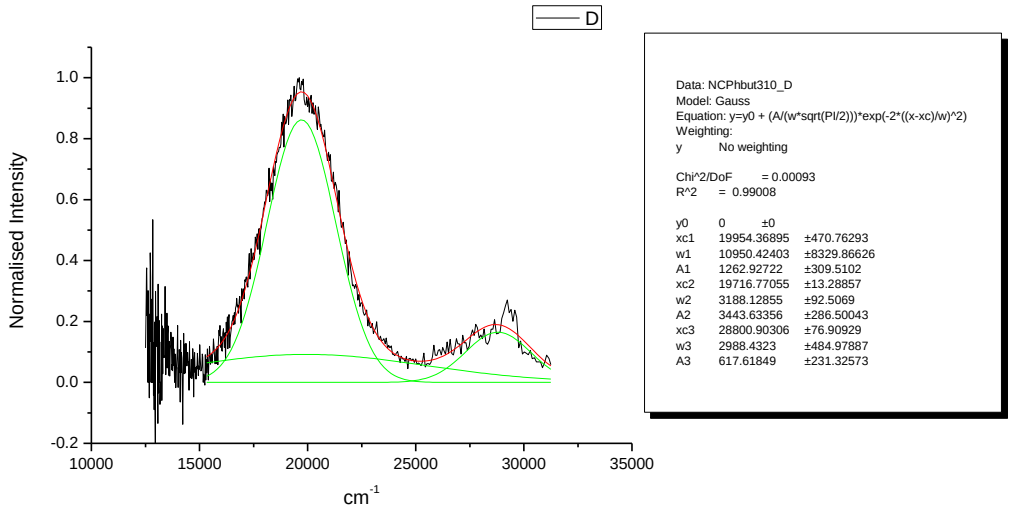

Figure 2.2.241. Gaussian model fit of the normalised fluorescence emission spectrum of **12** recorded in 1-butanol at 310 nm excitation.

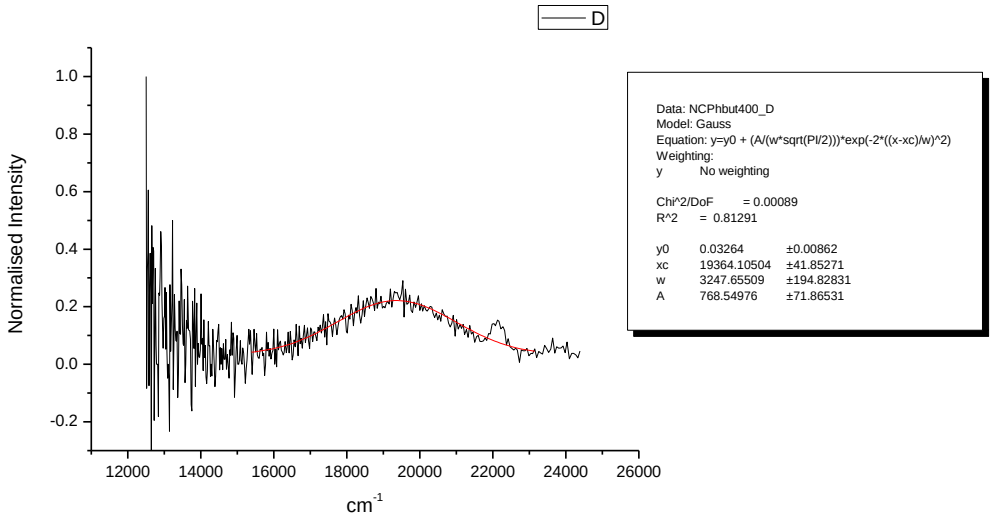

Figure 2.2.242. Gaussian model fit of the normalised fluorescence emission spectrum of **12** recorded in 1-butanol at 400 nm excitation.

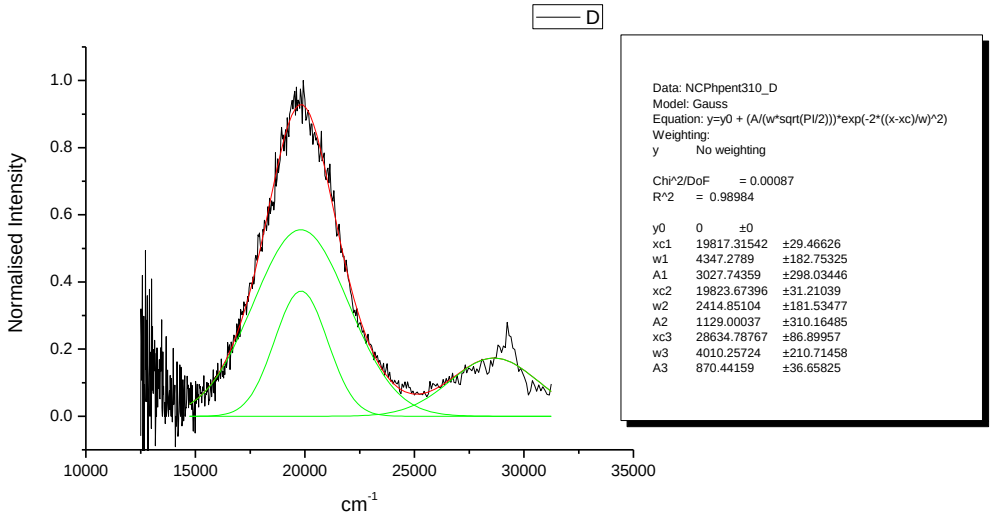

Figure 2.2.243. Gaussian model fit of the normalised fluorescence emission spectrum of **12** recorded in 1-pentanol at 310 nm excitation.

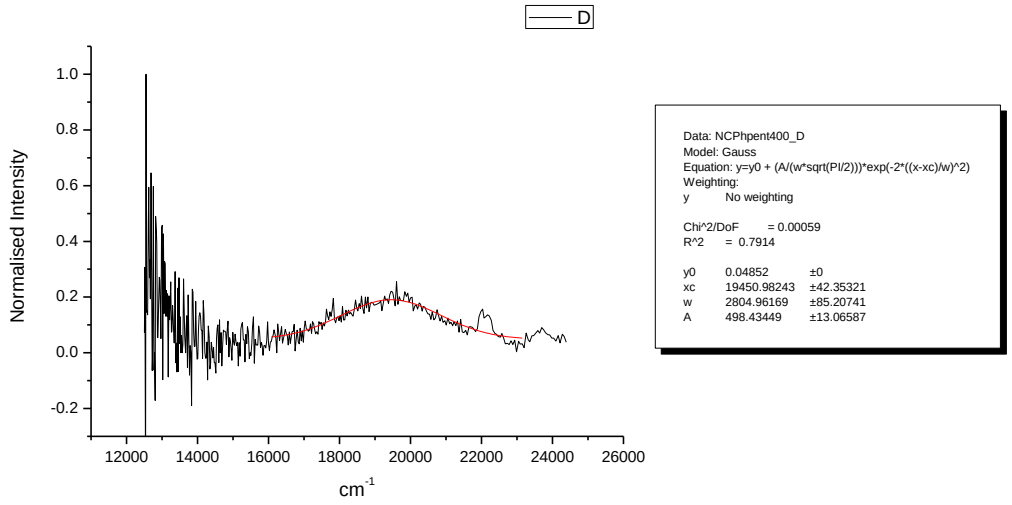

Figure 2.2.244. Gaussian model fit of the normalised fluorescence emission spectrum of **12** recorded in 1-pentanol at 400 nm excitation.

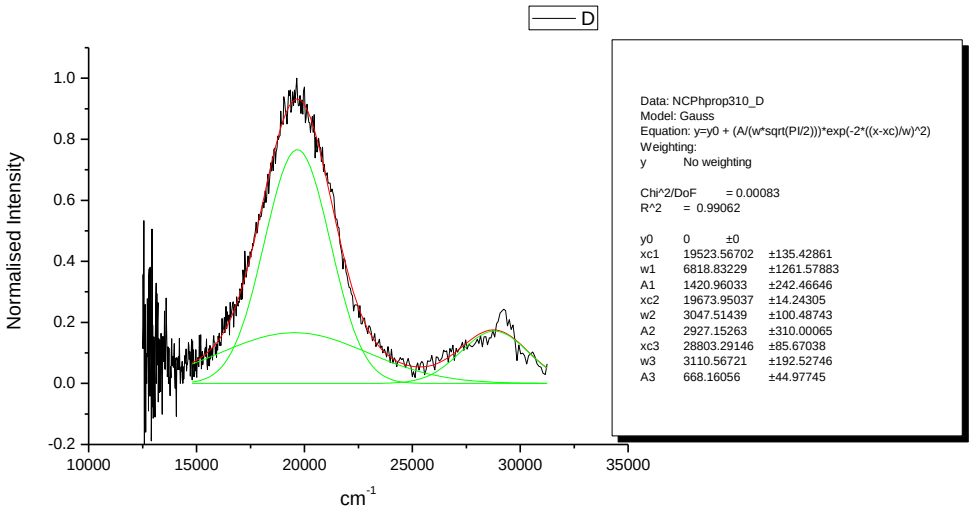

Figure 2.2.245. Gaussian model fit of the normalised fluorescence emission spectrum of **12** recorded in 1-propanol at 310 nm excitation.

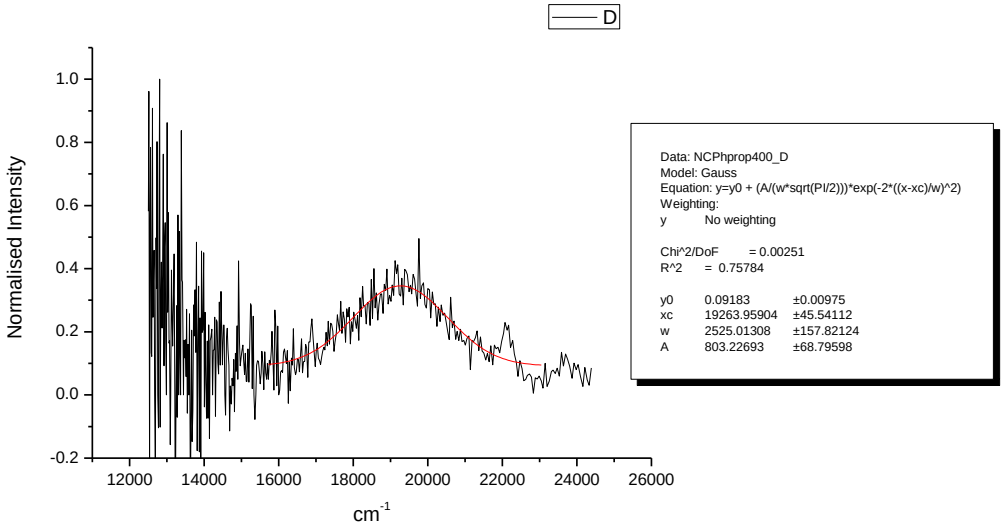

Figure 2.2.246. Gaussian model fit of the normalised fluorescence emission spectrum of **12** recorded in 1-propanol at 400 nm excitation.

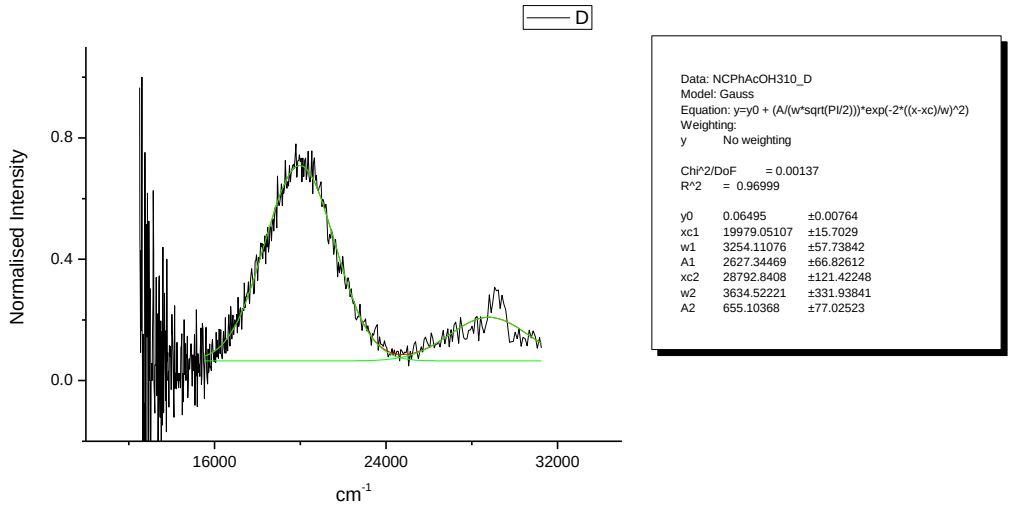

Figure 2.2.247. Gaussian model fit of the normalised fluorescence emission spectrum of **12** recorded in Acetic Acid at 310 nm excitation.

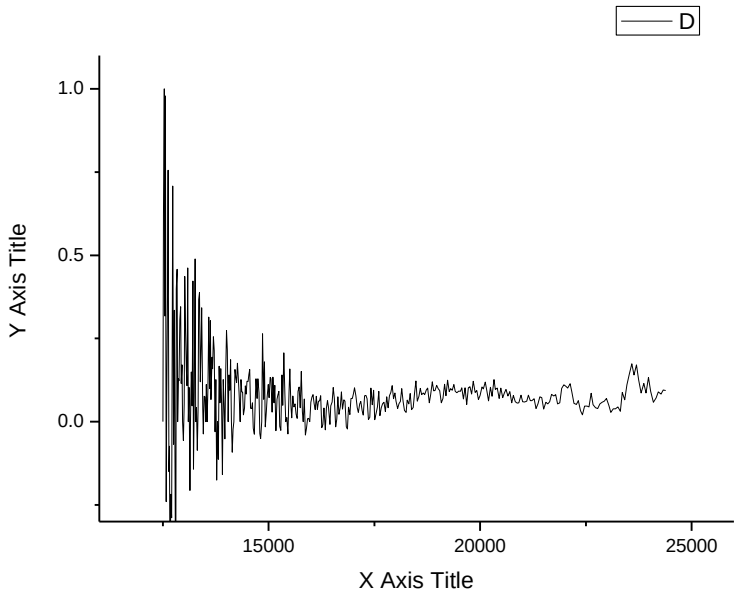

Figure 2.2.248. Attempted gaussian model fit of the normalised fluorescence emission spectrum of **12** recorded in Acetic Acid at 400 nm excitation.

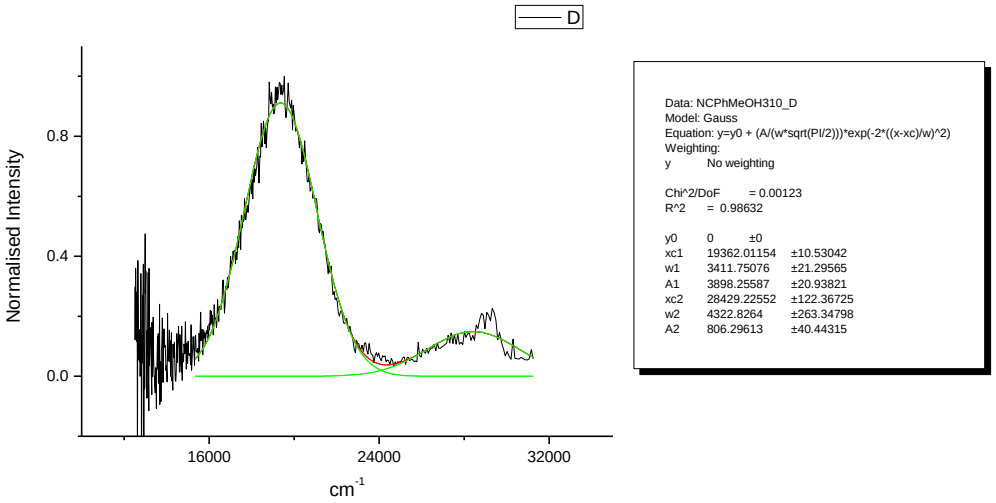

Figure 2.2.249. Gaussian model fit of the normalised fluorescence emission spectrum of **12** recorded in Methanol at 310 nm excitation.

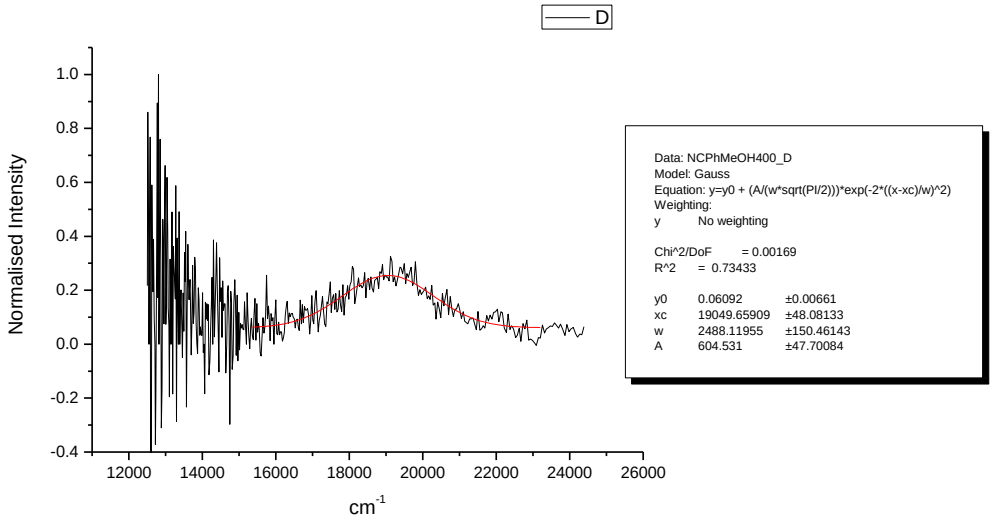

Figure 2.2.250. Gaussian model fit of the normalised fluorescence emission spectrum of **12** recorded in Methanol at 400 nm excitation.

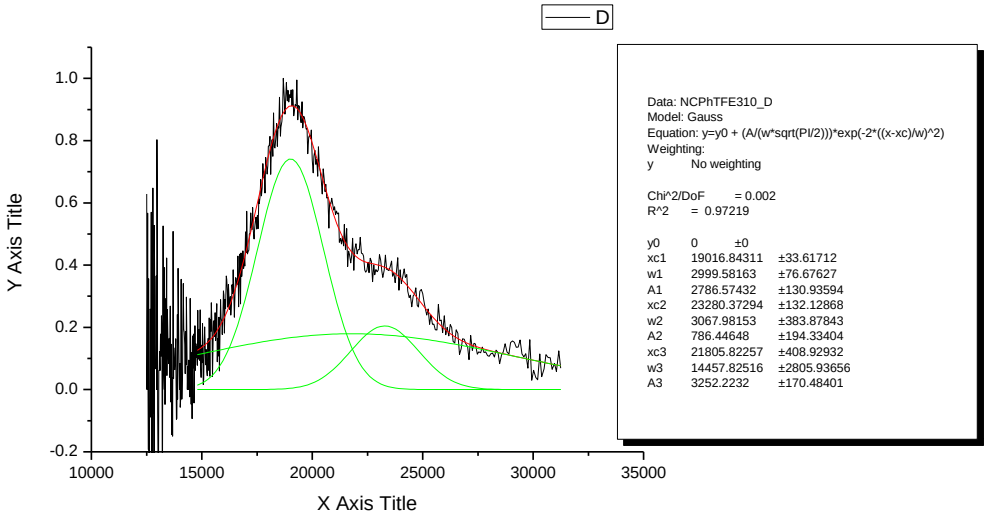

Figure 2.2.251. Gaussian model fit of the normalised fluorescence emission spectrum of **12** recorded in 2,2,2-trifluoroethanol at 310 nm excitation.

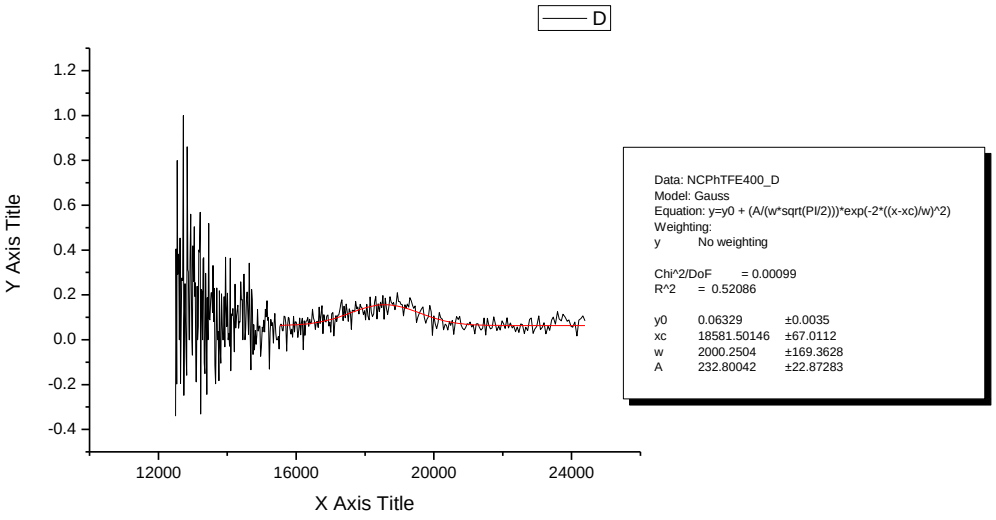

Figure 2.2.252. Gaussian model fit of the normalised fluorescence emission spectrum of **12** recorded in 2,2,2-trifluoroethanol at 400 nm excitation.

2.2.13 Fluorescence Excitation spectra.

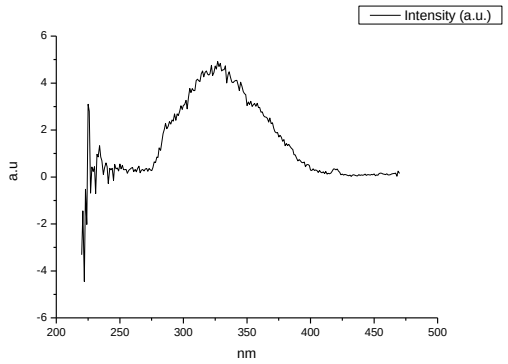

Figure 2.2.253. Fluorescence excitation spectrum of **12** recorded in Toluene with emission fixed at 480 nm.

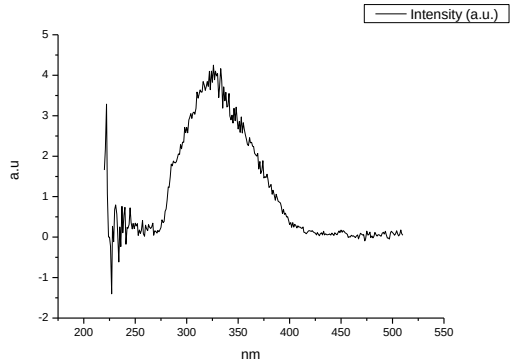

Figure 2.2.254. Fluorescence excitation spectrum of **12** recorded in Toluene with emission fixed at 520 nm.

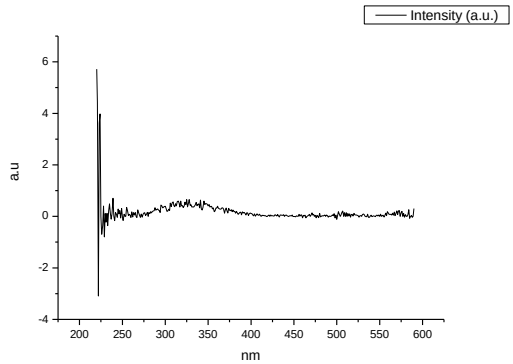

Figure 2.2.255. Fluorescence excitation spectrum of **12** recorded in Toluene with emission fixed at 600 nm.

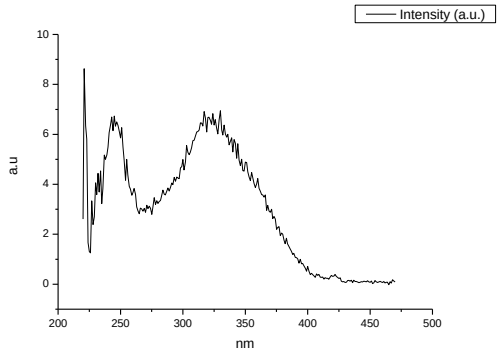

Figure 2.2.256. Fluorescence excitation spectrum of **12** recorded in 1,4-dioxane with emission fixed at 480 nm.

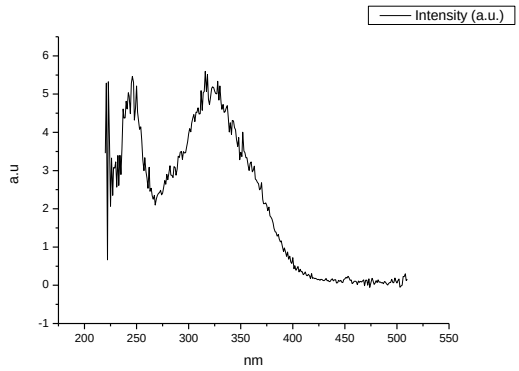

Figure 2.2.257. Fluorescence excitation spectrum of **12** recorded in 1,4-dioxane with emission fixed at 520 nm.

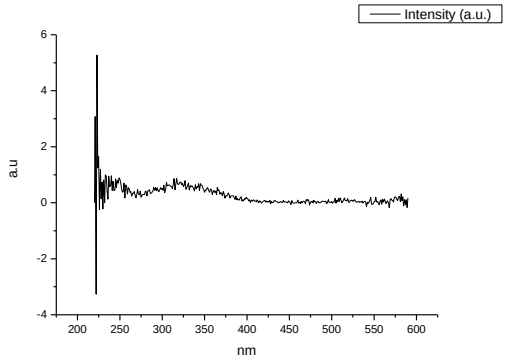

Figure 2.2.258. Fluorescence excitation spectrum of **12** recorded in 1,4-dioxane with emission fixed at 600 nm.

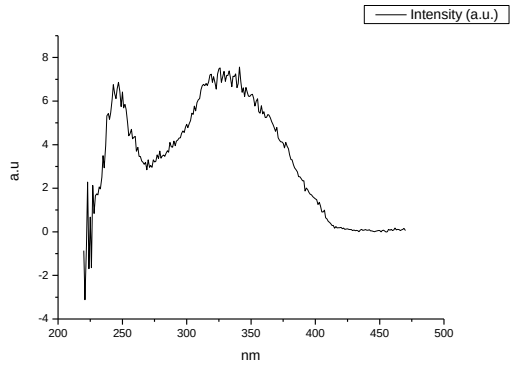

Figure 2.2.259. Fluorescence excitation spectrum of **12** recorded in Chloroform with emission fixed at 480 nm.

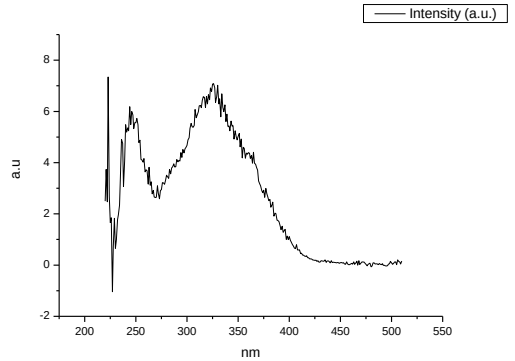

Figure 2.2.260. Fluorescence excitation spectrum of **12** recorded in Chloroform with emission fixed at 520 nm.

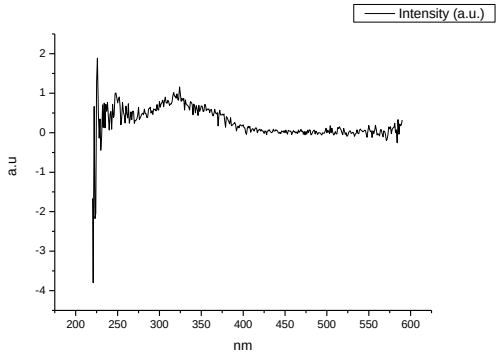

Figure 2.2.261. Fluorescence excitation spectrum of **12** recorded in Chloroform with emission fixed at 600 nm.

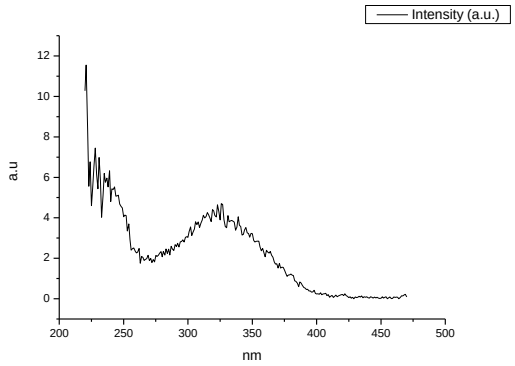

Figure 2.2.262. Fluorescence excitation spectrum of **12** recorded in Acetonitrile with emission fixed at 480 nm.

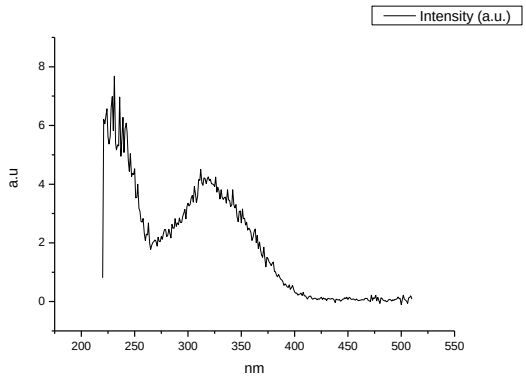

Figure 2.2.263. Fluorescence excitation spectrum of **12** recorded in Acetonitrile with emission fixed at 520 nm.

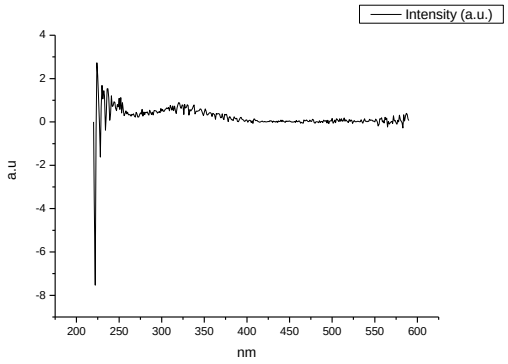

Figure 2.2.264. Fluorescence excitation spectrum of **12** recorded in Acetonitrile with emission fixed at 600 nm.

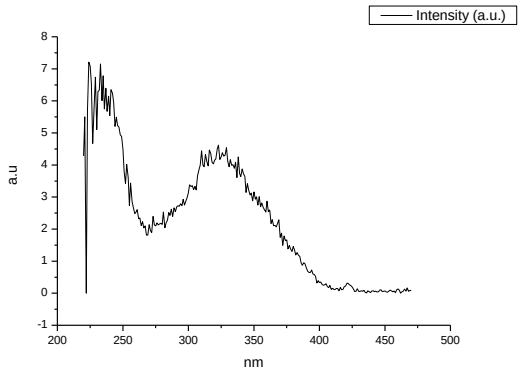

Figure 2.2.265. Fluorescence excitation spectrum of **12** recorded in 1-octanol with emission fixed at 480 nm.

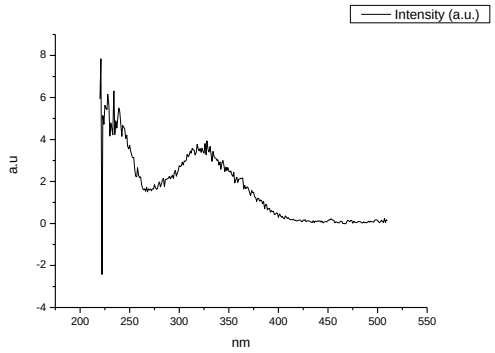

Figure 2.2.266. Fluorescence excitation spectrum of **12** recorded in 1-octanol with emission fixed at 520 nm.

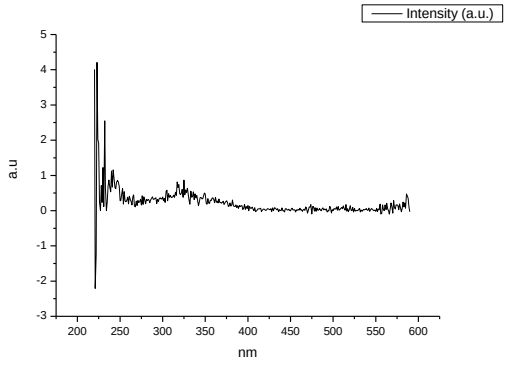

Figure 2.2.267. Fluorescence excitation spectrum of **12** recorded in 1-octanol with emission fixed at 600 nm.

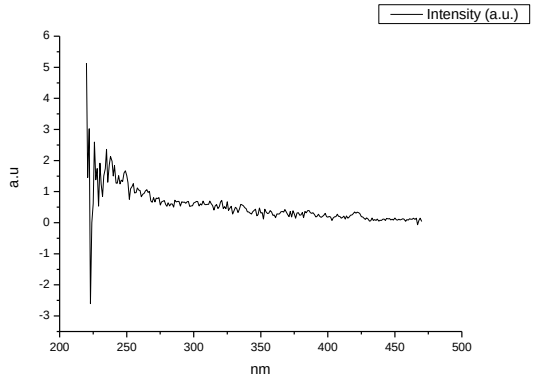

Figure 2.2.268. Fluorescence excitation spectrum of **12** recorded in 1-hexanol with emission fixed at 480 nm.

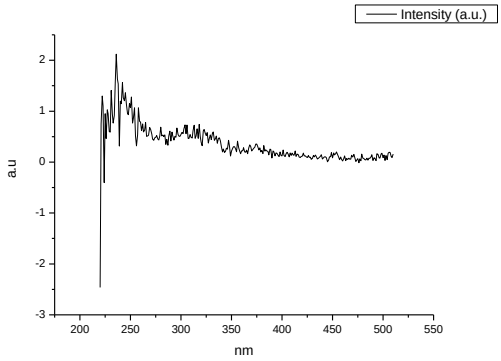

Figure 2.2.269. Fluorescence excitation spectrum of **12** recorded in 1-hexanol with emission fixed at 520 nm.

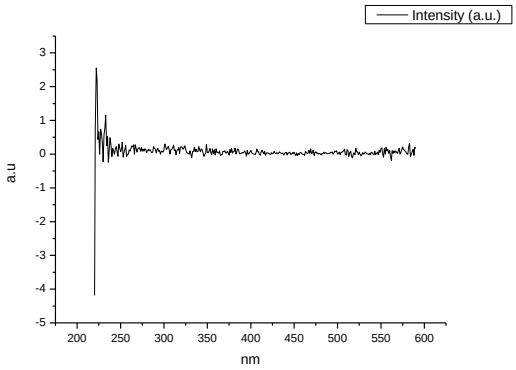

Figure 2.2.270. Fluorescence excitation spectrum of **12** recorded in 1-hexanol with emission fixed at 600 nm.

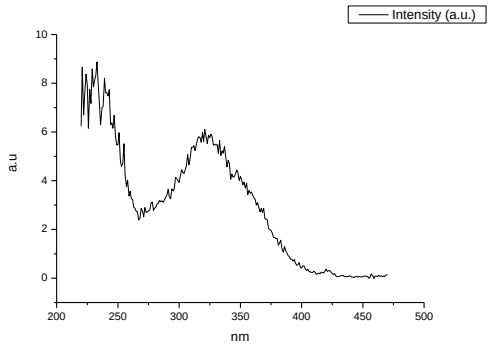

Figure 2.2.271. Fluorescence excitation spectrum of **12** recorded in 1-butanol with emission fixed at 480 nm.

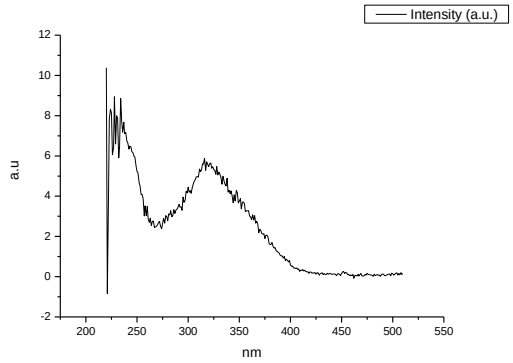

Figure 2.2.272. Fluorescence excitation spectrum of **12** recorded in 1-butanol with emission fixed at 520 nm.

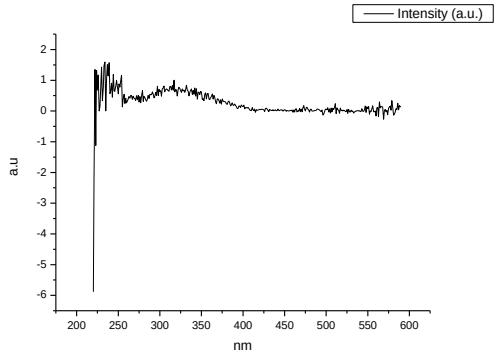

Figure 2.2.273. Fluorescence excitation spectrum of **12** recorded in 1-butanol with emission fixed at 600 nm.

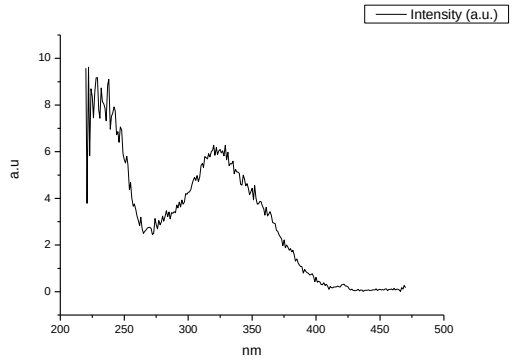

Figure 2.2.274. Fluorescence excitation spectrum of **12** recorded in 1-pentanol with emission fixed at 480 nm.

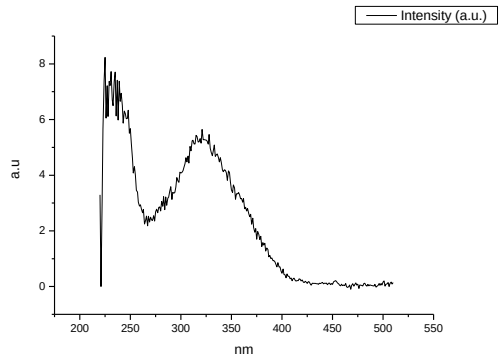

Figure 2.2.275. Fluorescence excitation spectrum of **12** recorded in 1-pentanol with emission fixed at 520 nm.

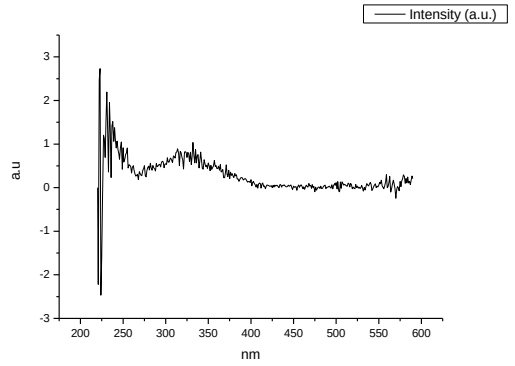

Figure 2.2.276. Fluorescence excitation spectrum of **12** recorded in 1-pentanol with emission fixed at 600 nm.

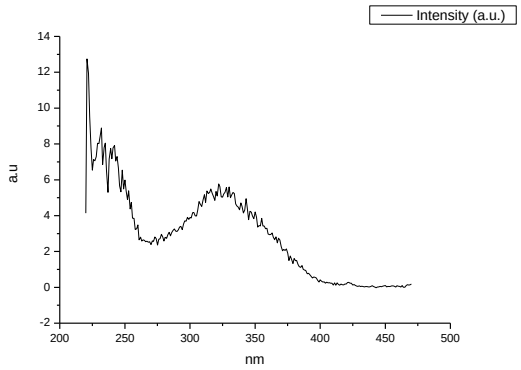

Figure 2.2.277. Fluorescence excitation spectrum of **12** recorded in 1-propanol with emission fixed at 480 nm.

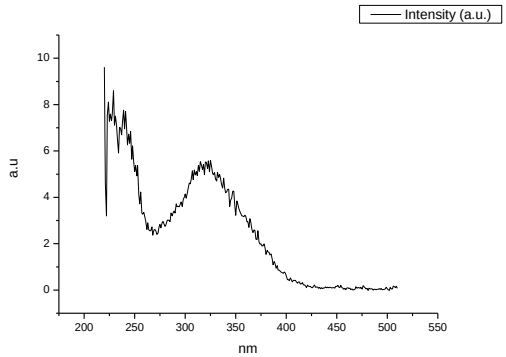

Figure 2.2.278. Fluorescence excitation spectrum of **12** recorded in 1-propanol with emission fixed at 520 nm.

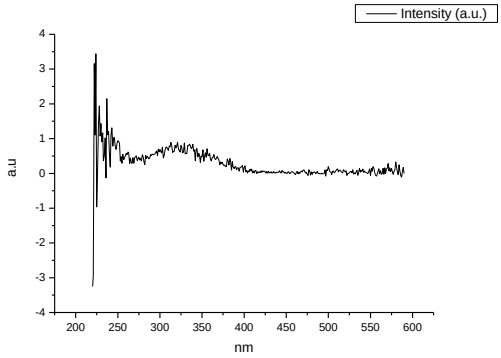

Figure 2.2.279. Fluorescence excitation spectrum of **12** recorded in 1-propanol with emission fixed at 600 nm.

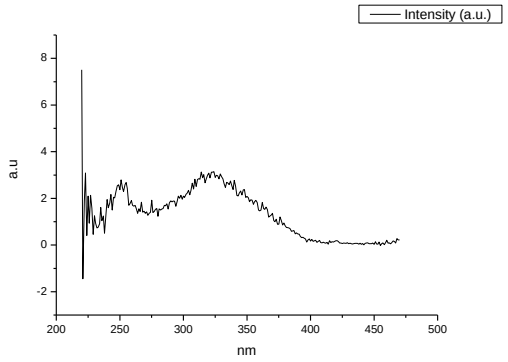

Figure 2.2.280. Fluorescence excitation spectrum of **12** recorded in Acetic Acid with emission fixed at 480 nm.

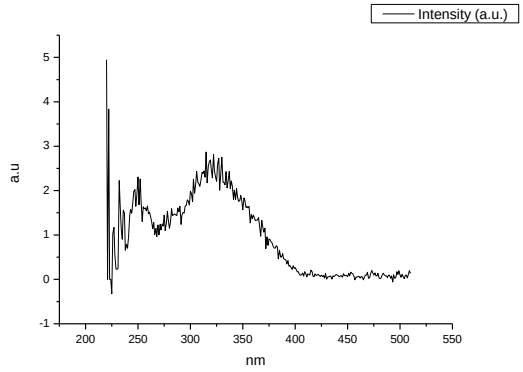

Figure 2.2.281. Fluorescence excitation spectrum of **12** recorded in Acetic Acid with emission fixed at 520 nm.

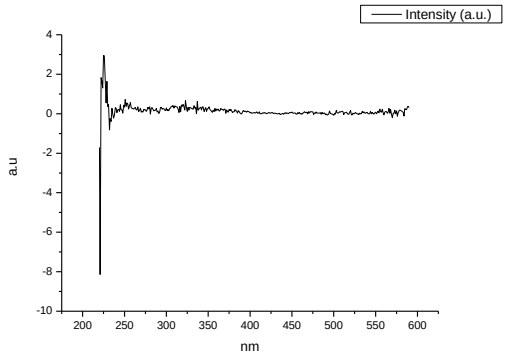

Figure 2.2.282. Fluorescence excitation spectrum of **12** recorded in Acetic Acid with emission fixed at 600 nm.

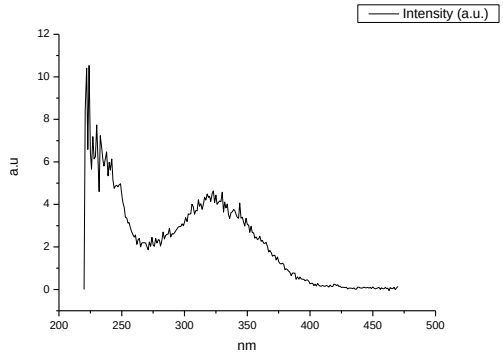

Figure 2.2.283. Fluorescence excitation spectrum of **12** recorded in Methanol with emission fixed at 480 nm.

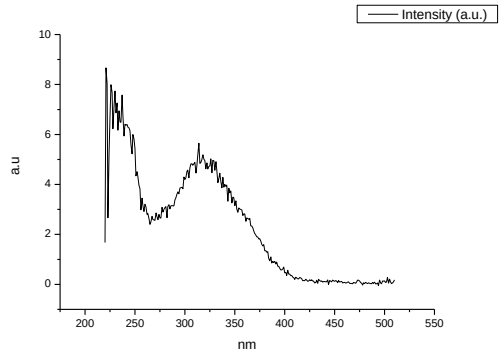

Figure 2.2.284. Fluorescence excitation spectrum of **12** recorded in Methanol with emission fixed at 520 nm.

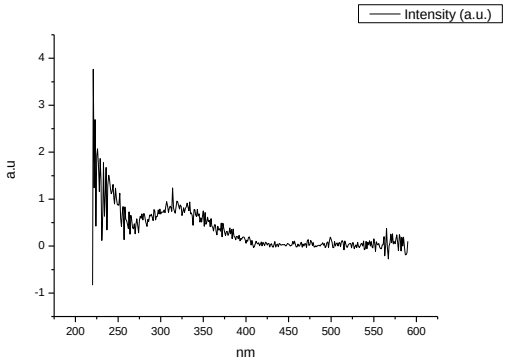

Figure 2.2.285. Fluorescence excitation spectrum of **12** recorded in Methanol with emission fixed at 600 nm.

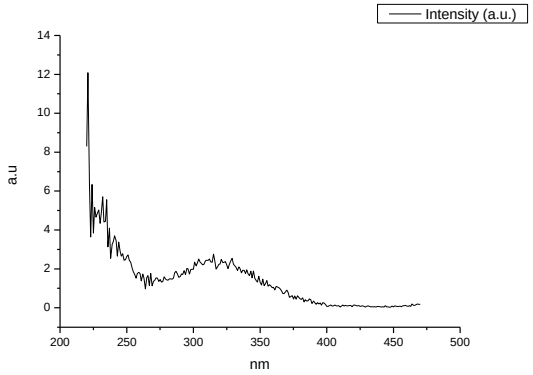

Figure 2.2.286. Fluorescence excitation spectrum of **12** recorded in 2,2,2-trifluoroethanol with emission fixed at 480 nm.

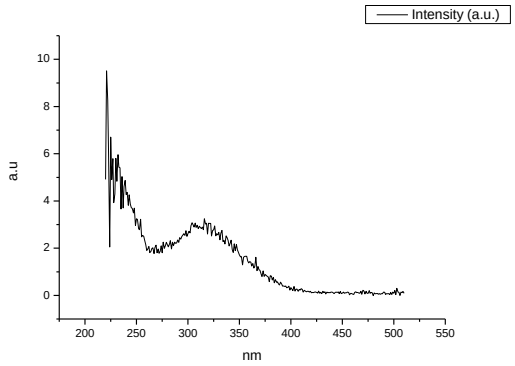

Figure 2.2.287. Fluorescence excitation spectrum of **12** recorded in 2,2,2-trifluoroethanol with emission fixed at 520 nm.

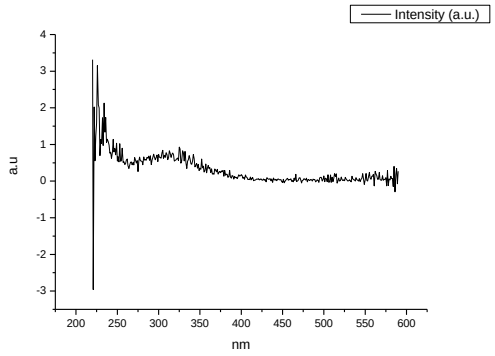

Figure 2.2.288. Fluorescence excitation spectrum of **12** recorded in 2,2,2-trifluoroethanol with emission fixed at 600 nm.

2.3 COMPOUND 13

2.3.1 Quantum Yield Summary.

Solvent	abs (310 nm)	$\lambda_{ems\ (max)}$	$\Phi_{310\ nm}$	abs (400 nm)	$\Phi_{400\ nm}$
Toluene	0.10	786.98	0.00	0.04	0.00
1,4-Dioxane	0.06	779.02	0.00	0.00	0.00
Chloroform	0.07	790.00	0.00	0.01	0.00
Acetonitrile	0.06	783.97	0.00	0.01	0.00
1-Octanol	0.03	341.07	0.00	0.00	0.00
1-Hexanol	0.01	343.07	0.01	0.00	0.00
1-Butanol	0.05	797.94	0.00	0.01	0.00
1-Pentanol	0.06	793.01	0.00	0.01	0.00
1-Propanol	0.06	793.01	0.00	0.00	0.00
Acetic acid	0.04	799.04	0.00	0.01	0.00
Methanol	0.05	786.02	0.00	0.00	0.00
2,2,2-Trifluoroethanol	0.03	796.02	0.00	0.00	0.00

Table 2.3.1. Summary of ultraviolet-visible absorbance values at 310 nm and 400 nm, emission maxima and quantum yield (Φ) of **13** at 310 nm and 400 nm excitation.

2.3.2 310 nm excitation Gaussian band fit summaries.

Solvent	λ max$_{em}$ Band 1 (cm^{-1})	λ max$_{em}$ Band 1 (nm)	λ max$_{em}$ Band 2 (cm^{-1})	λ max$_{em}$ Band 2 (nm)	λ max$_{em}$ Band 3 (cm^{-1})	λ max$_{em}$ Band 3 (nm)
Toluene	-	-	-	-	29512.96	338.83
1,4-Dioxane	-	-	-	-	27131.26	368.58
Chloroform	-	-	-	-	27984.95	357.33
Acetonitrile	-	-	20193.27	495.21	28558.37	350.16
1-Octanol	-	-	21567.50	463.66	29575.15	338.12
1-Hexanol	-	-	20112.50	497.20	28500.02	350.88
1-Butanol	-	-	-	-	28451.33	351.48
1-Pentanol	-	-	-	-	28166.87	355.03
1-Propanol	-	-	-	-	28638.58	349.18
Acetic acid	-	-	-	-	28620.78	349.40
Methanol	-	-	-	-	28592.91	349.74
2,2,2-Trifluoroethanol	-	-	-	-	23978.86	417.03

Solvent	λ max$_{em}$ Band 4 (cm^{-1})	λ max$_{em}$ Band 4 (nm)	λ max$_{em}$ Band 5 (cm^{-1})	λ max$_{em}$ Band 5 (nm)
Toluene	-	-	-	-
1,4-Dioxane	29091.97	343.74	-	-
Chloroform	-	-	-	-
Acetonitrile	-	-	-	-
1-Octanol	-	-	-	-
1-Hexanol	-	-	-	-
1-Butanol	-	-	-	-
1-Pentanol	29236.31	342.04	-	-
1-Propanol	-	-	-	-
Acetic acid	-	-	-	-
Methanol	-	-	-	-
2,2,2-Trifluoroethanol	-	-	-	-

Table 2.3.1. Summary of band maxima of 5 band fit using Gaussian model for normalised **13** emission spectra recorded at 310 nm excitation.

(a)

Solvent	Width Band 1 (cm^{-1})	Width Band 2 (cm^{-1})	Width Band 3 (cm^{-1})	Width Band 4 (cm^{-1})	Width Band 5 (cm^{-1})
Toluene	-	-	3728.24	-	-
1,4-Dioxane	-	-	4278.11	1159.32	-
Chloroform	-	-	3092.81	-	-
Acetonitrile	-	2491.01	-	3499.17	-
1-Octanol	-	10950.16	3984.18	-	-
1-Hexanol	-	5060.30	4708.25	-	-
1-Butanol	-	-	3356.34	-	-
1-Pentanol	-	-	4621.00	618.16	-
1-Propanol	-	-	3188.60	-	-
Acetic acid	-	-	3346.71	-	-
Methanol	-	-	2859.78	-	-
2,2,2-Trifluoroethanol	-	-	4479.42	-	-

(b)

Solvent	Area Band 1 (cm^{-1})	Area Band 2 (cm^{-1})	Area Band 3 (cm^{-1})	Area Band 4 (cm^{-1})	Area Band 5 (cm^{-1})
Toluene	-	-	1641.49	-	-
1,4-Dioxane	-	-	705.83	324.48	-
Chloroform	-	-	589.98	-	-
Acetonitrile	-	151.73	-	679.18	-
1-Octanol	-	1338.29	3843.52	-	-
1-Hexanol	-	528.98	5421.54	-	-
1-Butanol	-	-	640.86	-	-
1-Pentanol	-	-	2211.74	263.42	-
1-Propanol	-	-	900.80	-	-
Acetic acid	-	-	380.83	-	-
Methanol	-	-	566.69	-	-
2,2,2-Trifluoroethanol	-	-	1213.01	-	-

Tables 2.3.2 (a) and (b). Summary band width and band area of 5 band fit using Gaussian model for normalised **13** emission spectra recorded at 310 nm excitation.

Solvent	Band 1 Area Percentage (%)	Band 2 Area Percentage (%)	Band 3 Area Percentage (%)	Band 4 Area Percentage (%)	Band 5 Area Percentage (%)
Toluene	-	-	100.00	-	-
1,4-Dioxane	-	-	68.51	31.49	-
Chloroform	-	-	100.00	-	-
Acetonitrile	-	18.26	-	81.74	-
1-Octanol	-	25.83	74.17	-	-
1-Hexanol	-	8.89	91.11	-	-
1-Butanol	-	-	100.00	-	-
1-Pentanol	-	-	89.36	10.64	-
1-Propanol	-	-	100.00	-	-
Acetic acid	-	-	100.00	-	-
Methanol	-	-	100.00	-	-
2,2,2-Trifluoroethanol	-	-	100.00	-	-

Table 2.3.4. Total Area Percentages of 5 band fit using Gaussian model for normalised **13** emission spectra recorded at 310 nm excitation.

Solvent	Area Ratio Band 1/2 (310 nm ex)	Area Ratio Band 1/3 (310 nm ex)	Area Ratio Band 1/4 (310 nm ex)	Area Ratio Band 1/5 (310 nm ex)
Toluene	-	-	-	-
1,4-Dioxane	-	-	-	-
Chloroform	-	-	-	-
Acetonitrile	-	-	-	-
1-Octanol	-	-	-	-
1-Hexanol	-	-	-	-
1-Butanol	-	-	-	-
1-Pentanol	-	-	-	-
1-Propanol	-	-	-	-
Acetic acid	-	-	-	-
Methanol	-	-	-	-
2,2,2-Trifluoroethanol	-	-	-	-

Solvent	Area Ratio Band 2/3 (310 nm ex)	Area Ratio Band 2/4 (310 nm ex)	Area Ratio Band 2/5 (310 nm ex)	Area Ratio Band 3/4 (310 nm ex)	Area Ratio Band 3/5 (310 nm ex)	Area Ratio Band 4/5 (310 nm ex)
Toluene	-	-	-	-	-	-
1,4-Dioxane	-	-	-	2.18	-	-
Chloroform	-	-	-	-	-	-
Acetonitrile	-	0.22	-	-	-	-
1-Octanol	0.35	-	-	-	-	-
1-Hexanol	0.10	-	-	-	-	-
1-Butanol	-	-	-	-	-	-
1-Pentanol	-	-	-	8.40	-	-
1-Propanol	-	-	-	-	-	-
Acetic acid	-	-	-	-	-	-
Methanol	-	-	-	-	-	-
2,2,2-Trifluoroethanol	-	-	-	-	-	-

Table 2.3.5. Area Ratios of 5 band fit using Gaussian model for normalised **13** emission spectra recorded at 310 nm excitation.

2.3.3 310 nm Gaussian band fit - Solvatochromic analysis.

2.3.3.1 E_T^N.

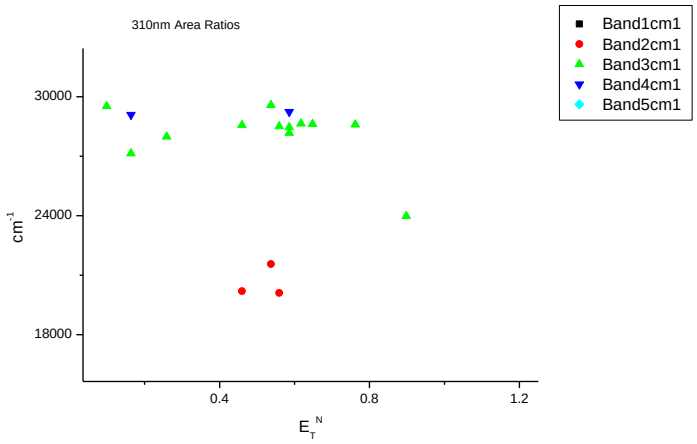

Figure 2.3.1. Band maxima from Gaussian model fit of the normalised fluorescence emission spectra of **13** recorded at 310 nm excitation against E_T^N.

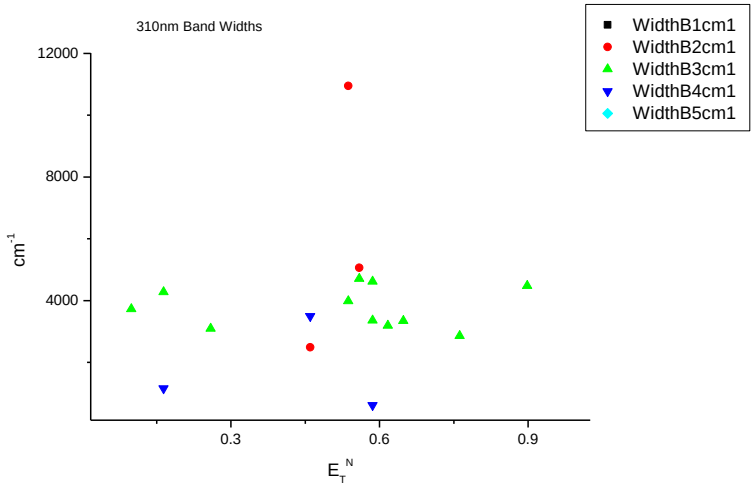

Figure 2.3.2. Band widths from Gaussian model fit of the normalised fluorescence emission spectra of **13** recorded at 310 nm excitation against E_T^N.

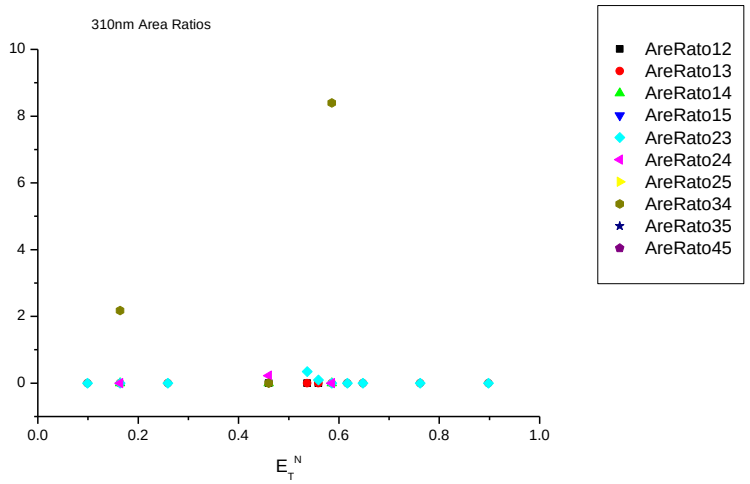

Figure 2.3.3. Area ratios from Gaussian model fit of the normalised fluorescence emission spectra of **13** recorded at 310 nm excitation against E_T^N.

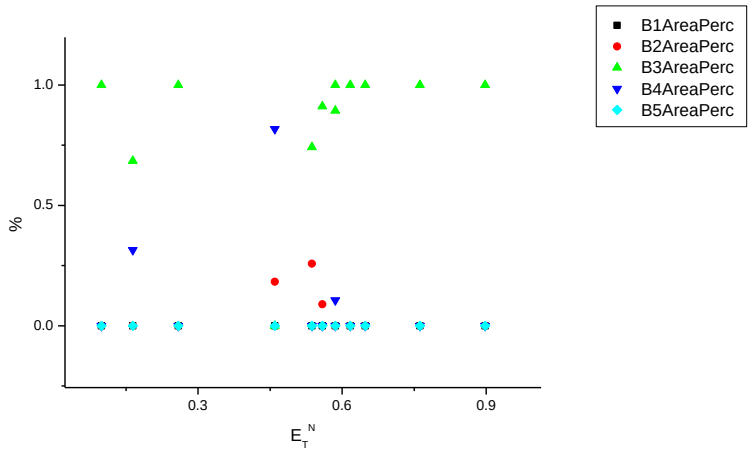

Figure 2.3.4. Area percentages from Gaussian model fit of the normalised fluorescence emission spectra of **13** recorded at 310 nm excitation against E_T^N.

2.3.3.2 *α*

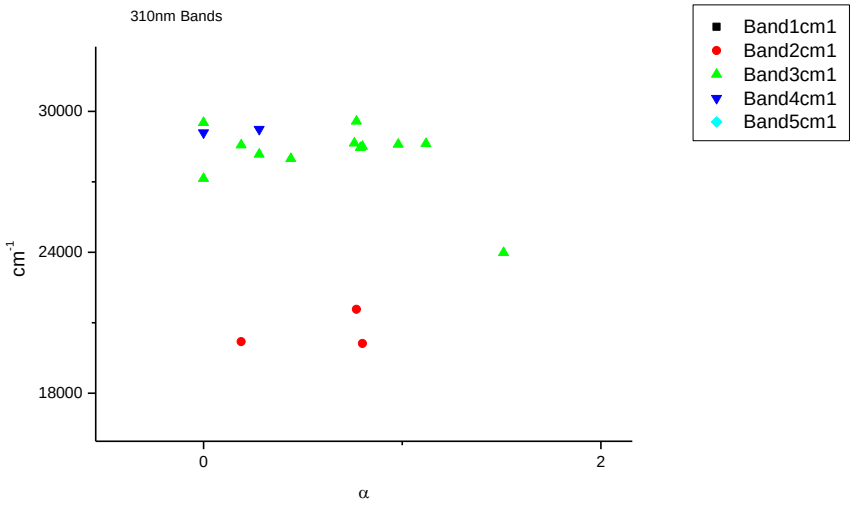

Figure 2.3.5. Band maxima from Gaussian model fit of the normalised fluorescence emission spectra of **13** recorded at 310 nm excitation against α.

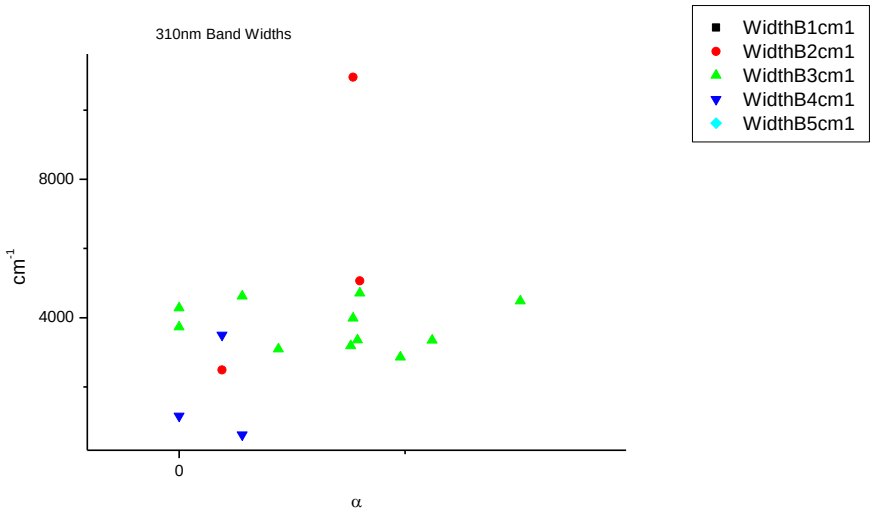

Figure 2.3.6. Band widths from Gaussian model fit of the normalised fluorescence emission spectra of **13** recorded at 310 nm excitation against α.

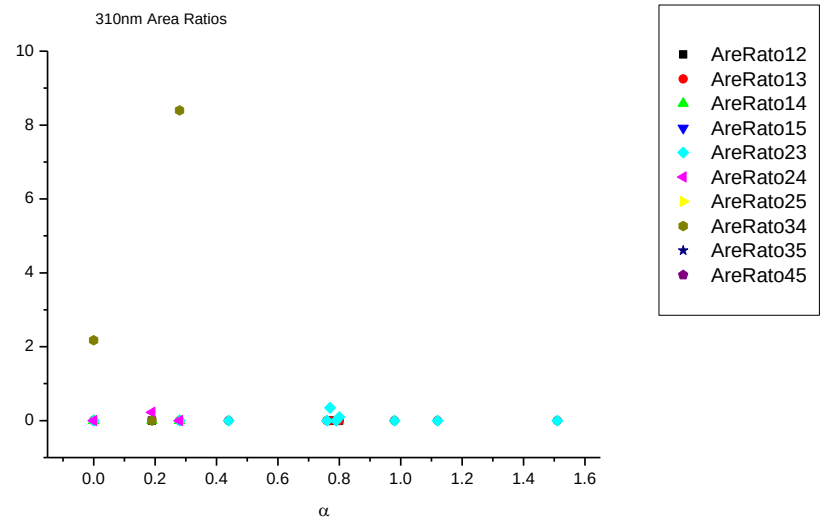

Figure 2.3.7. Area Ratios from Gaussian model fit of the normalised fluorescence emission spectra of **13** recorded at 310 nm excitation against α.

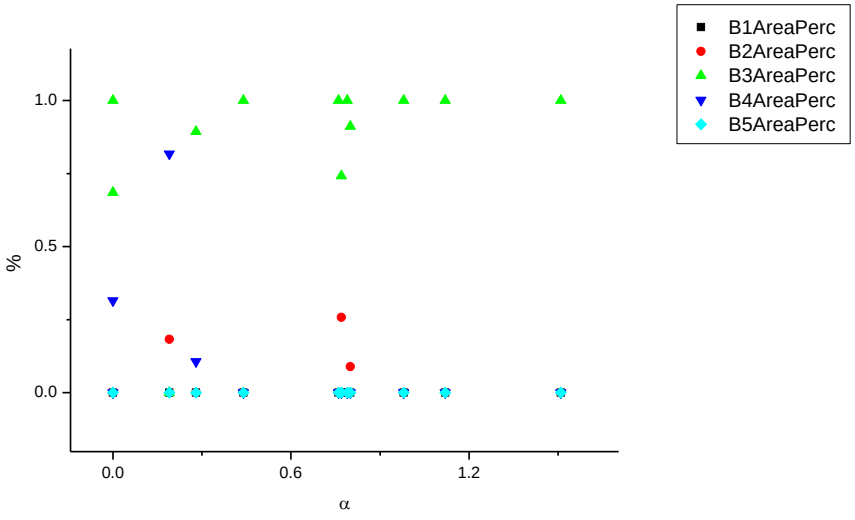

Figure 2.3.8. Area percentages from Gaussian model fit of the normalised fluorescence emission spectra of **13** recorded at 310 nm excitation against α.

2.3.3.3 β.

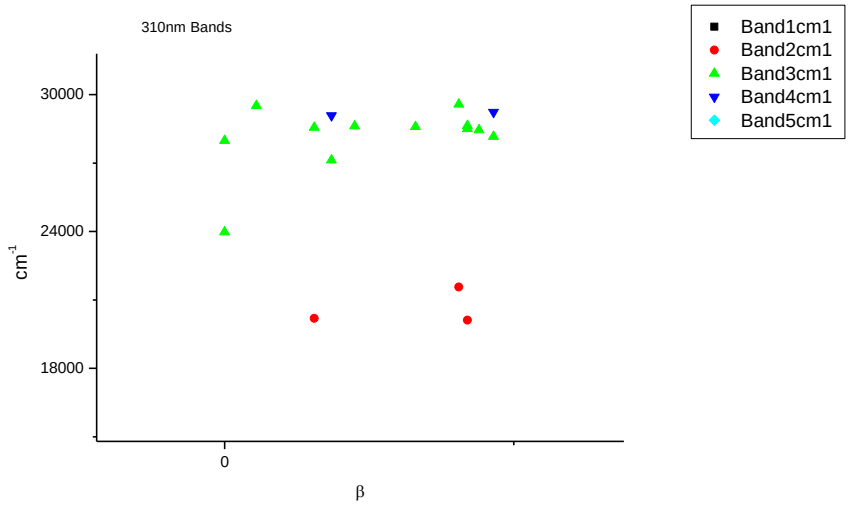

Figure 2.3.9. Band maxima from Gaussian model fit of the normalised fluorescence emission spectra of **13** recorded at 310 nm excitation against β.

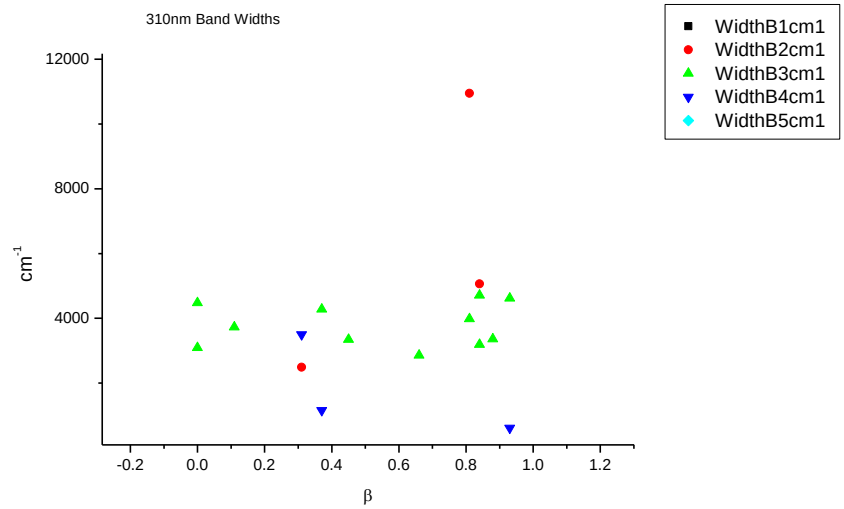

Figure 2.3.10. Band widths from Gaussian model fit of the normalised fluorescence emission spectra of **13** recorded at 310 nm excitation against β.

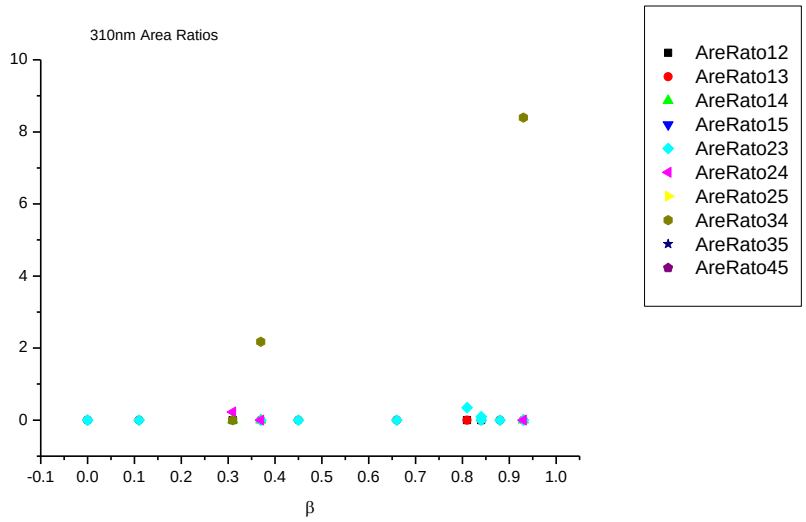

Figure 2.3.11. Area ratios from Gaussian model fit of the normalised fluorescence emission spectra of **13** recorded at 310 nm excitation against β.

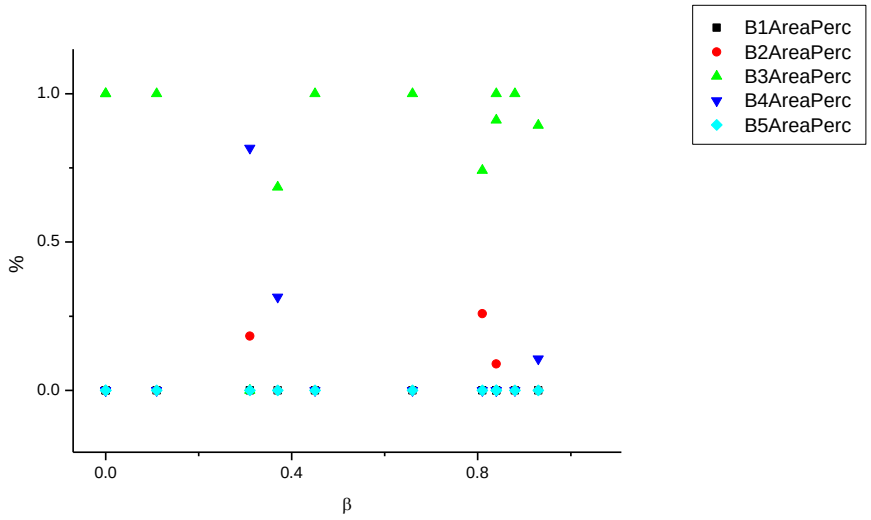

Figure 2.3.12. Area percentages from Gaussian model fit of the normalised fluorescence emission spectra of **13** recorded at 310 nm excitation against β.

2.3.3.4 π.*

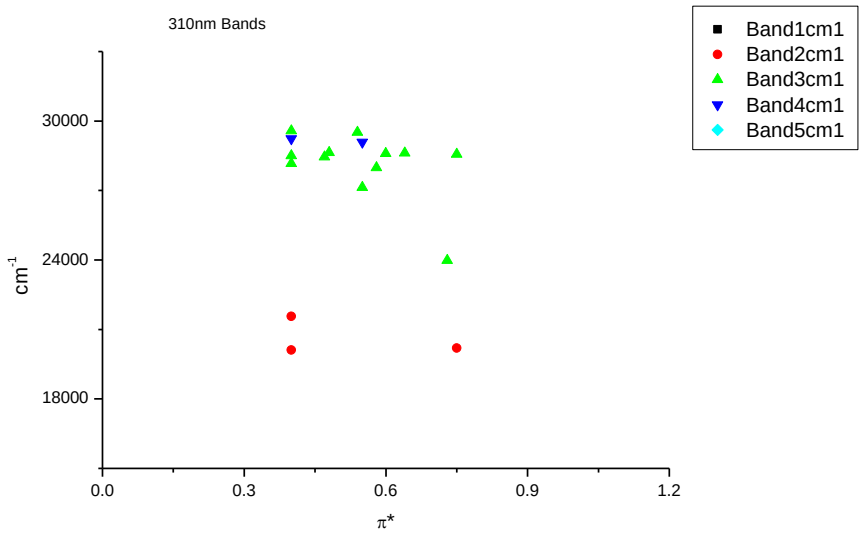

Figure 2.3.13. Band maxima from Gaussian model fit of the normalised fluorescence emission spectra of **13** recorded at 310 nm excitation against π*.

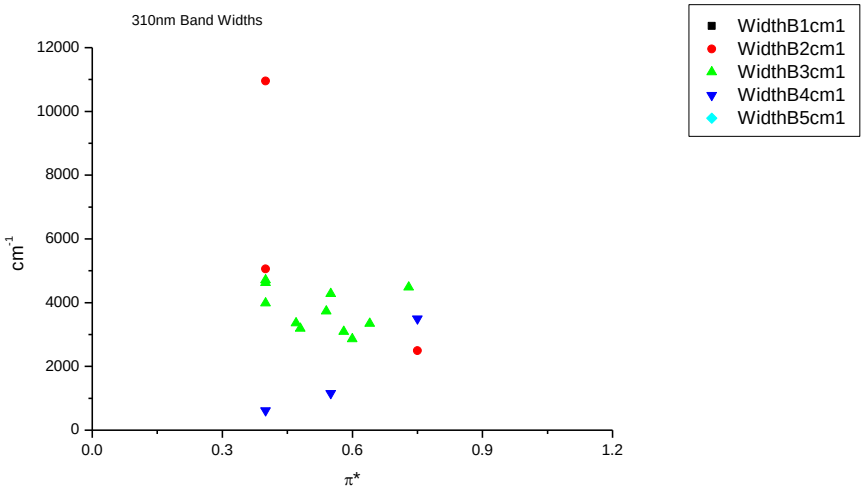

Figure 2.3.14. Band widths from Gaussian model fit of the normalised fluorescence emission spectra of **13** recorded at 310 nm excitation against π*.

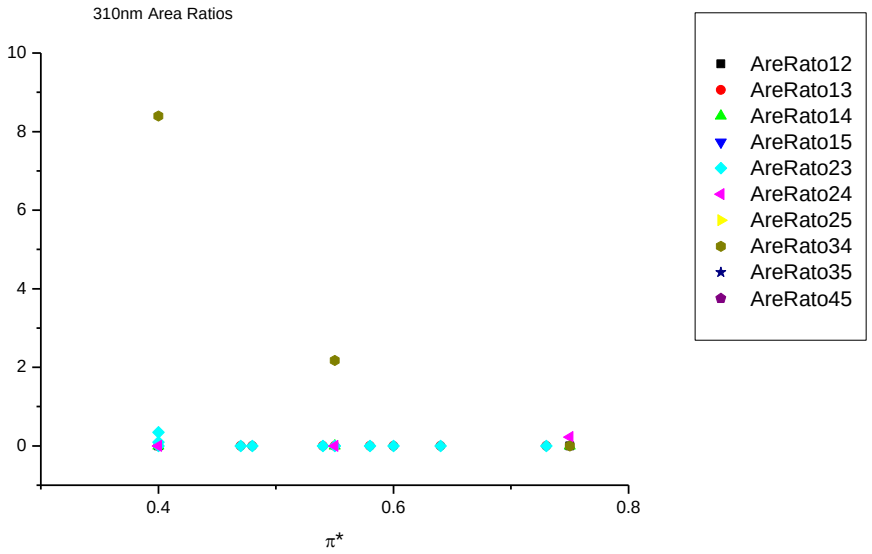

Figure 2.3.15. Area ratios from Gaussian model fit of the normalised fluorescence emission spectra of **13** recorded at 310 nm excitation against π*.

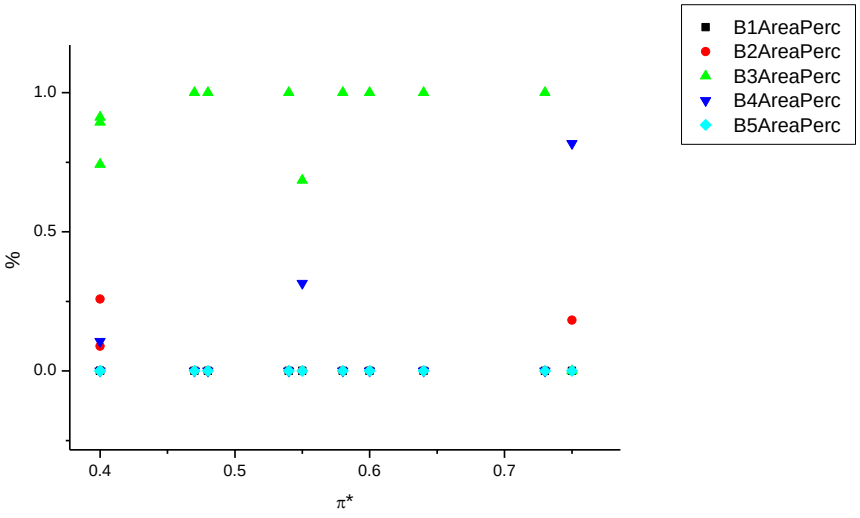

Figure 2.3.16. Area percentages from Gaussian model fit of the normalised fluorescence emission spectra of **13** recorded at 310 nm excitation against π*.

2.3.3.5 μ(D).

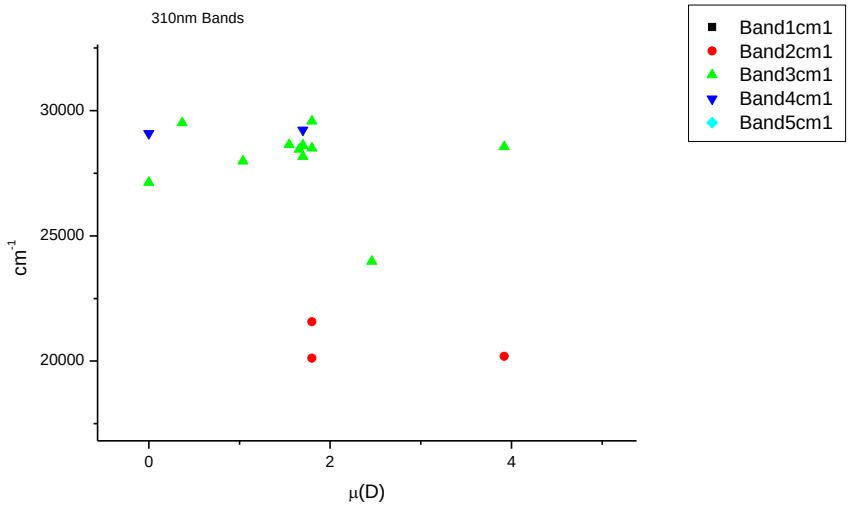

Figure 2.3.17. Band maxima from Gaussian model fit of the normalised fluorescence emission spectra of **13** recorded at 310 nm excitation against μ(D).

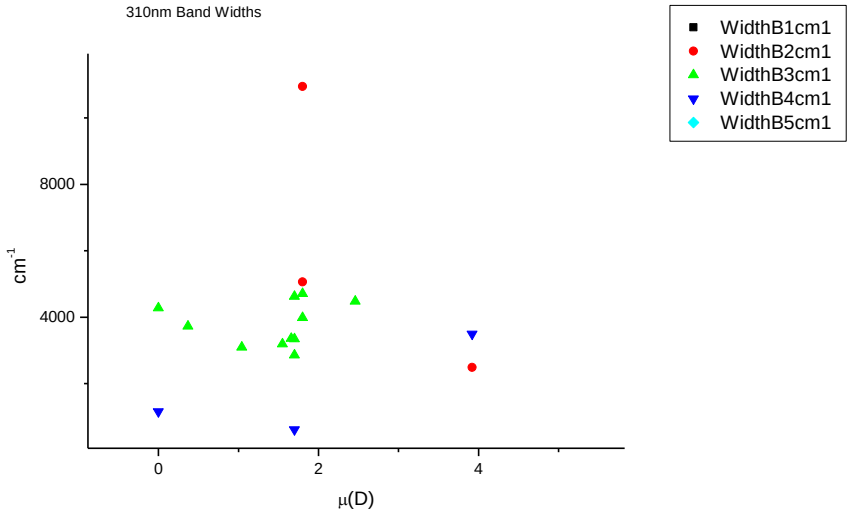

Figure 2.3.18. Band widths from Gaussian model fit of the normalised fluorescence emission spectra of **13** recorded at 310 nm excitation against μ(D).

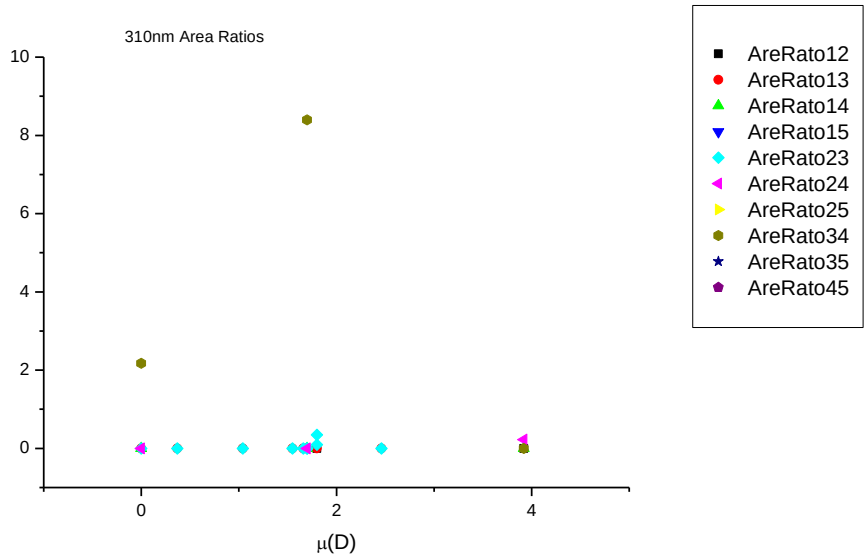

Figure 2.3.19. Area ratios from Gaussian model fit of the normalised fluorescence emission spectra of **13** recorded at 310 nm excitation against μ(D).

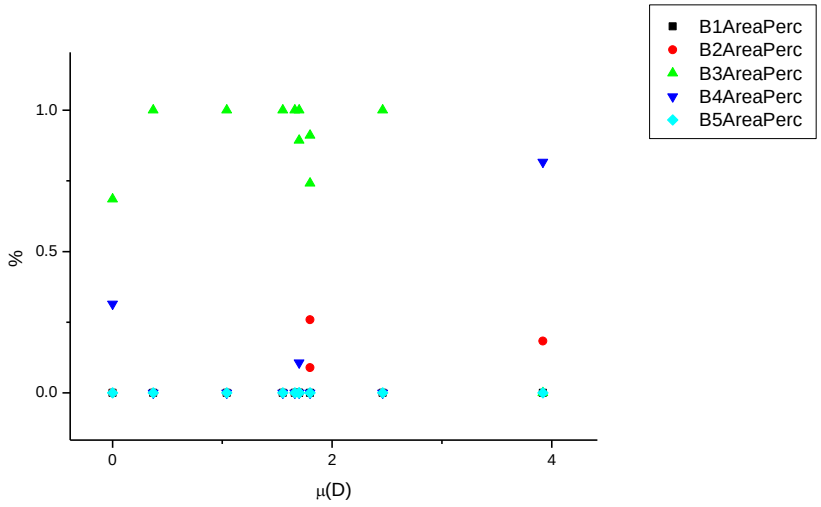

Figure 2.3.20. Area percentages from Gaussian model fit of the normalised fluorescence emission spectra of **13** recorded at 310 nm excitation against μ(D).

2.3.3.6 η(Cp).

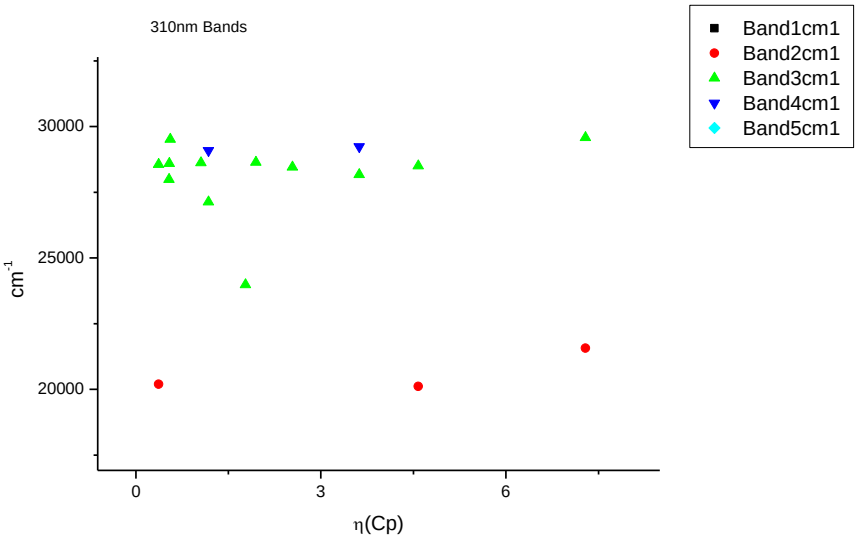

Figure 2.3.21. Band maxima from Gaussian model fit of the normalised fluorescence emission spectra of **13** recorded at 310 nm excitation against η(Cp).

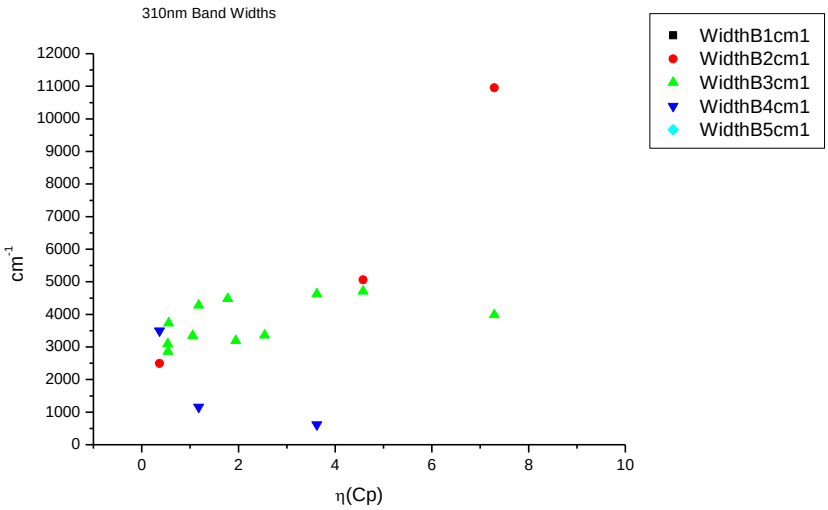

Figure 2.3.22. Band widths from Gaussian model fit of the normalised fluorescence emission spectra of **13** recorded at 310 nm excitation against η(Cp).

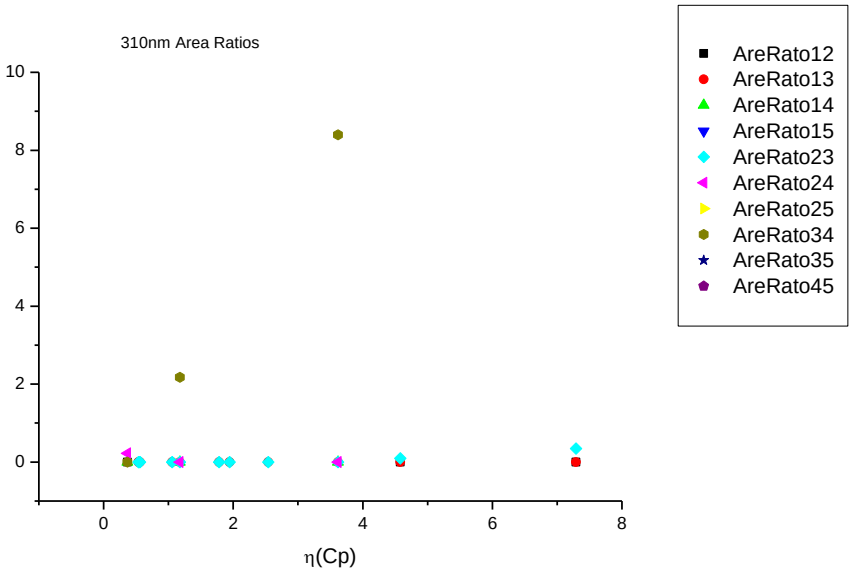

Figure 2.3.23. Area ratios from Gaussian model fit of the normalised fluorescence emission spectra of **13** recorded at 310 nm excitation against η(Cp).

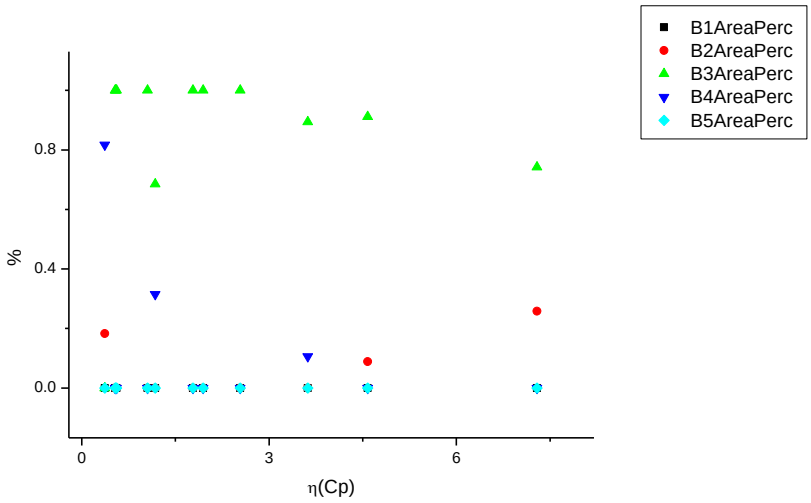

Figure 2.3.24. Area percentages from Gaussian model fit of the normalised fluorescence emission spectra of **13** recorded at 310 nm excitation against η(Cp).

2.3.4 295 nm (LED) fluorescent lifetime results.

2.3.4.1 Intensity weighted.

Wavelength (nm)	Solvent	τ_1 (ns)	A_1 (%)	τ_2 (ns)	A_2 (%)	τ_3 (ns)	A_3 (%)	τ_f (ns) (Intensity Weighted)	$1/\tau_f$	χ^2
370	Toluene	-	-	-	-	-	-	-	-	-
370	1,4-Dioxane	-	-	-	-	-	-	-	-	-
370	Chloroform	-	-	-	-	-	-	-	-	-
370	Acetonitrile	-	-	-	-	-	-	-	-	-
370	1-Octanol	0.74	40.83	3.21	38.70	13.13	20.47	4.29	0.23	1.07
370	1-Hexanol	0.74	30.54	3.06	40.01	13.38	29.45	5.39	0.19	1.34
370	1-Butanol	-	-	-	-	-	-	-	-	-
370	1-Pentanol	-	-	-	-	-	-	-	-	-
370	1-Propanol	-	-	-	-	-	-	-	-	-
370	Acetic acid	-	-	-	-	-	-	-	-	-
370	Methanol	-	-	-	-	-	-	-	-	-
370	2,2,2-Trifluoroethanol	-	-	-	-	-	-	-	-	-

Table 2.3.6. Summary of Time Correlated Single Photon Counting (TCSPC) fluorescent lifetimes (intensity weighted) of **13** at 370 nm, recorded using a 295 nm Light Emitting Diode (LED) light source.

2.3.4.2 Amplitude weighted.

Wavelength (nm)	Solvent	τ_1 (ns)	A_1 (%)	τ_2 (ns)	A_2 (%)	τ_3 (ns)	A_3 (%)	τ_f (ns) (Amplitude Weighted)	$1/\tau_f$	χ^2
370	Toluene	-	-	-	-	-	-	-	-	-
370	1,4-Dioxane	-	-	-	-	-	-	-	-	-
370	Chloroform	-	-	-	-	-	-	-	-	-
370	Acetonitrile	-	-	-	-	-	-	-	-	-
370	1-Octanol	0.74	80.27	3.21	17.47	13.13	2.26	1.45	0.69	1.07
370	1-Hexanol	0.74	73.01	3.06	23.10	13.38	3.88	1.77	0.57	1.34
370	1-Butanol	-	-	-	-	-	-	-	-	-
370	1-Pentanol	-	-	-	-	-	-	-	-	-
370	1-Propanol	-	-	-	-	-	-	-	-	-
370	Acetic acid	-	-	-	-	-	-	-	-	-
370	Methanol	-	-	-	-	-	-	-	-	-
370	2,2,2-Trifluoroethanol	-	-	-	-	-	-	-	-	-

Table 2.3.7. Summary of Time Correlated Single Photon Counting (TCSPC) fluorescent lifetimes (amplitude weighted) of **13** at 370 nm, recorded using a 295 nm Light Emitting Diode (LED) light source.

2.3.4 295 nm (LED) average fluorescent lifetimes - Solvatochromic analysis.

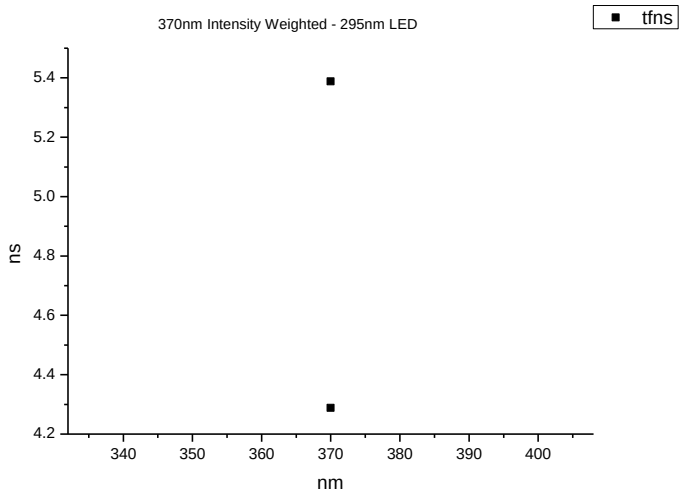

Figure 2.3.25. Intensity weighted average lifetime (τ_f) of **13** versus wavelength (nm).

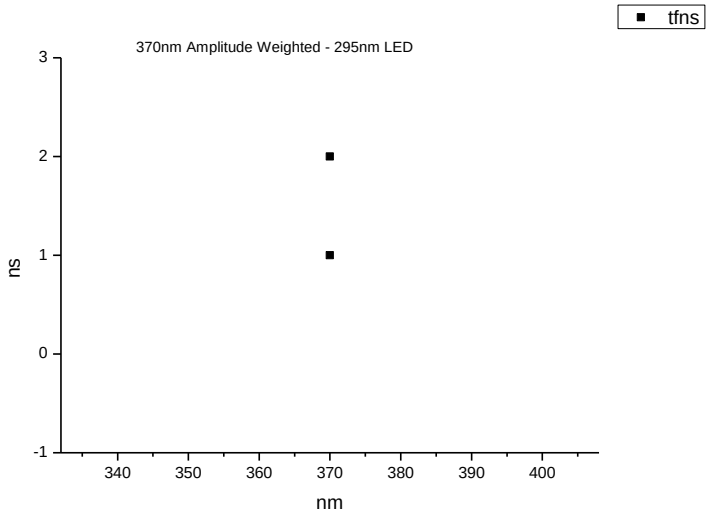

Figure 2.3.26. Amplitude weighted average lifetime (τ_f) of **13** versus wavelength (nm).

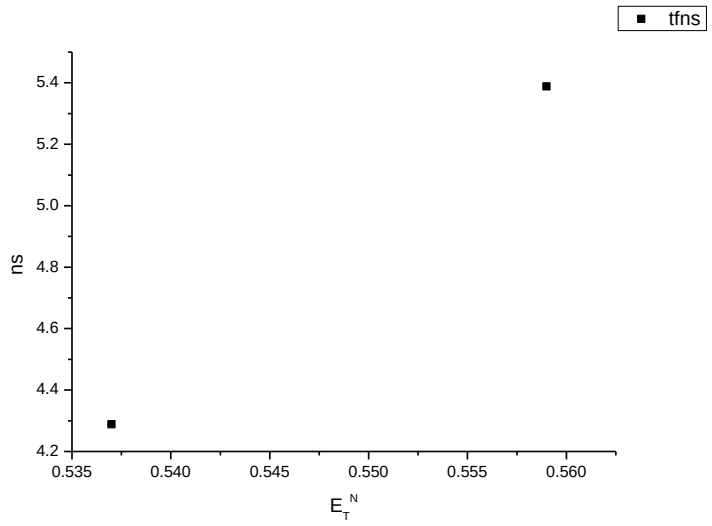

Figure 2.3.27. Intensity weighted average lifetime (τ_f) of **13** versus E_T^N.

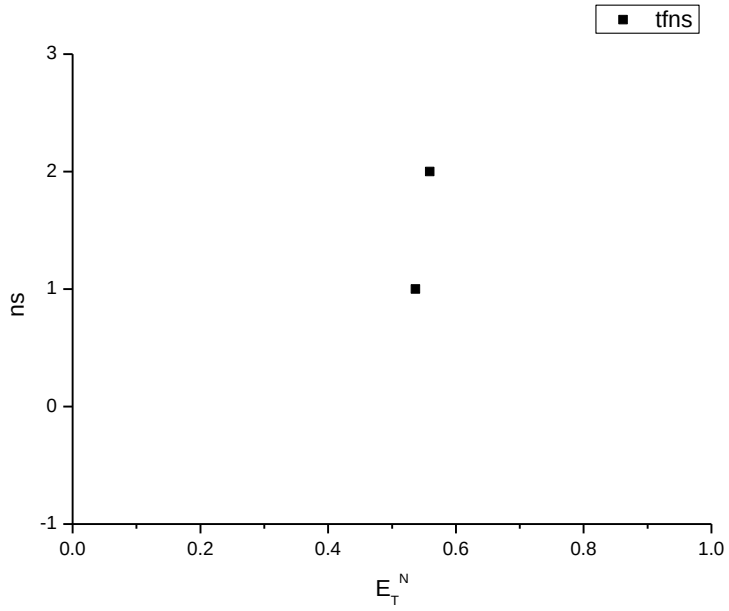

Figure 2.3.28. Amplitude weighted average lifetime (τ_f) of **13** versus E_T^N.

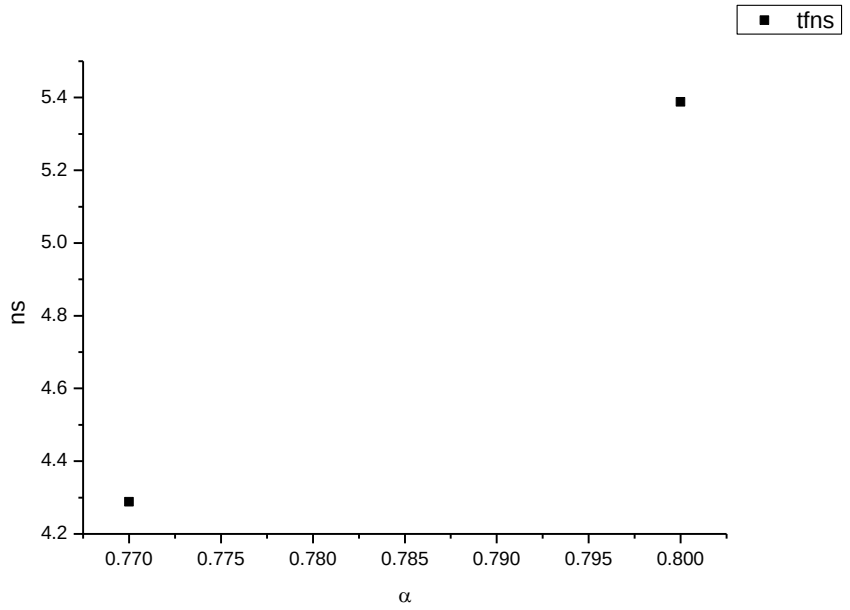

Figure 2.3.29. Intensity weighted average lifetime (τ_f) of **13** versus α.

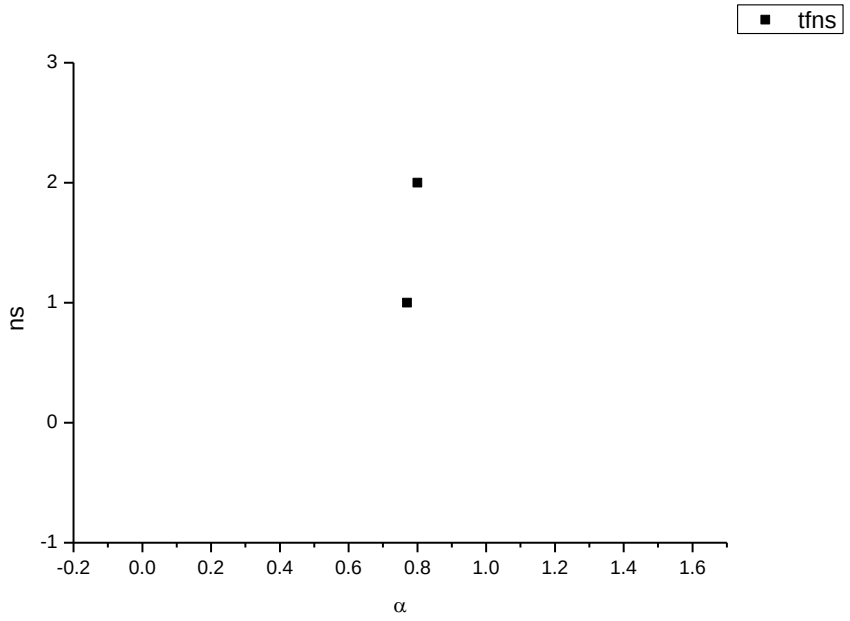

Figure 2.3.30. Amplitude weighted average lifetime (τ_f) of **13** versus α.

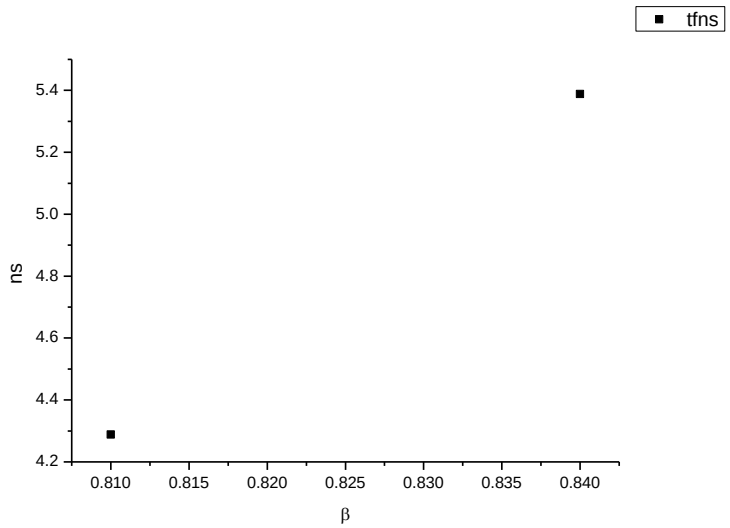

Figure 2.3.31. Intensity weighted average lifetime (τ_f) of **13** versus β.

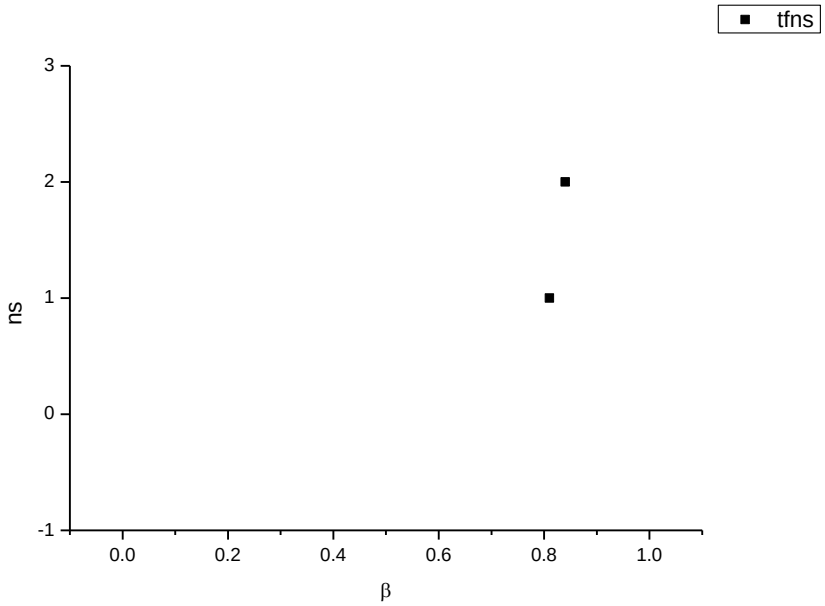

Figure 2.3.32. Amplitude weighted average lifetime (τ_f) of **13** versus β.

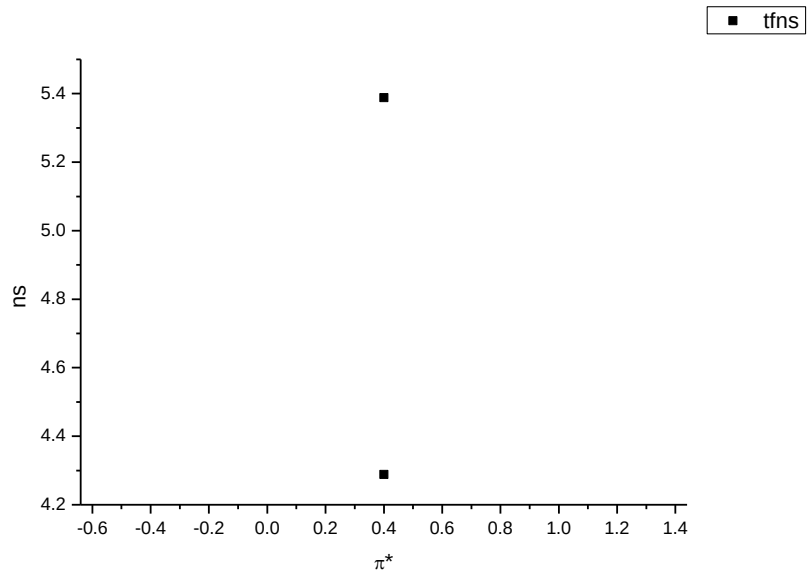

Figure 2.3.33. Intensity weighted average lifetime (τ_f) of **13** versus π*.

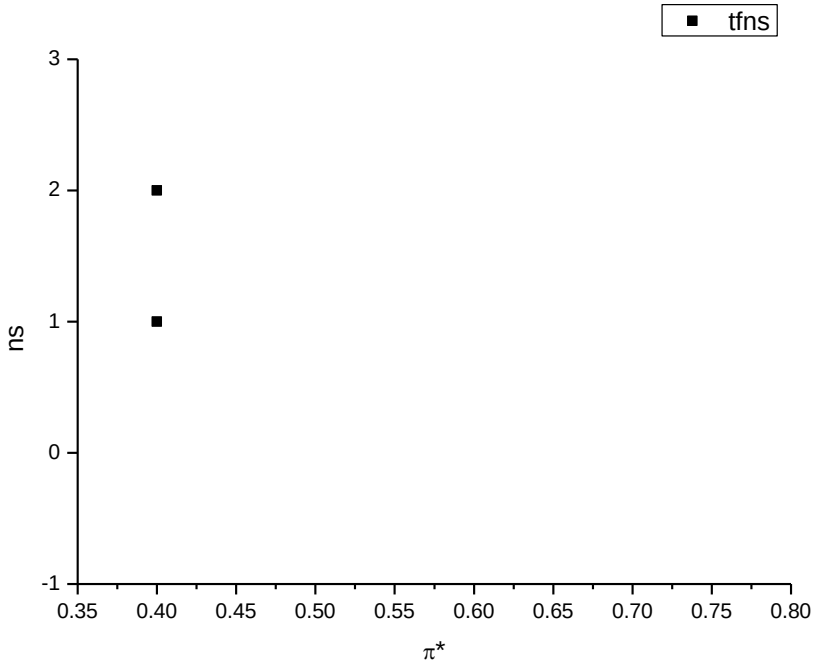

Figure 2.3.34. Amplitude weighted average lifetime (τ_f) of **13** versus π*.

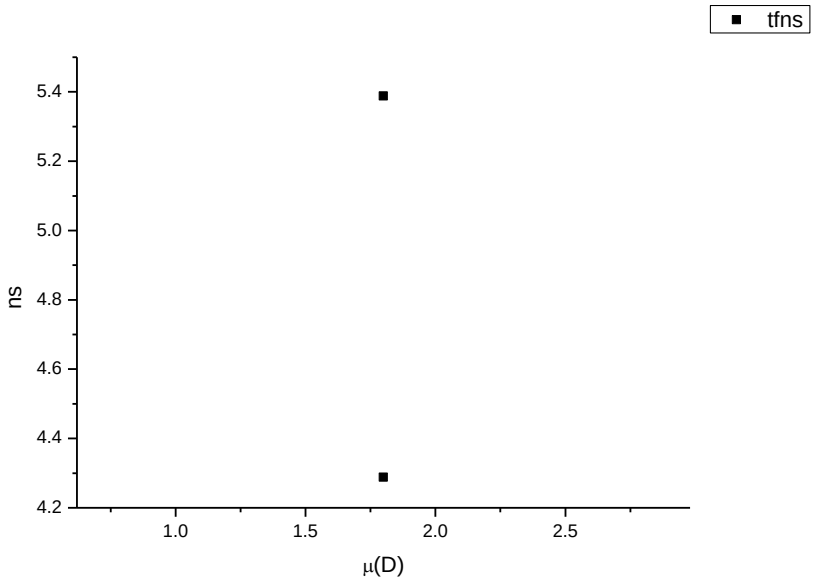

Figure 2.3.35. Intensity weighted average lifetime (τ_f) of **13** versus μ(D).

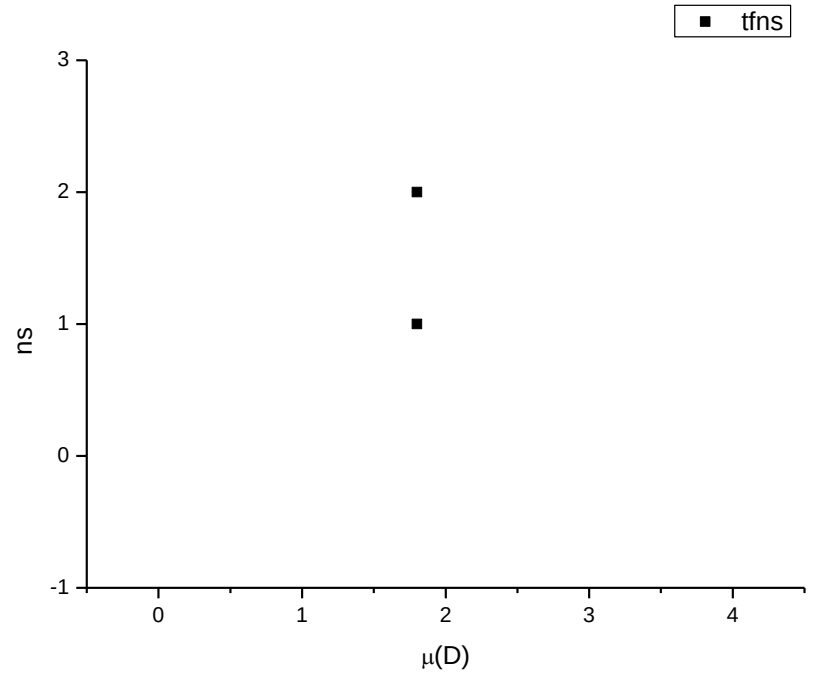

Figure 2.3.36. Amplitude weighted average lifetime (τ_f) of **13** versus μ(D).

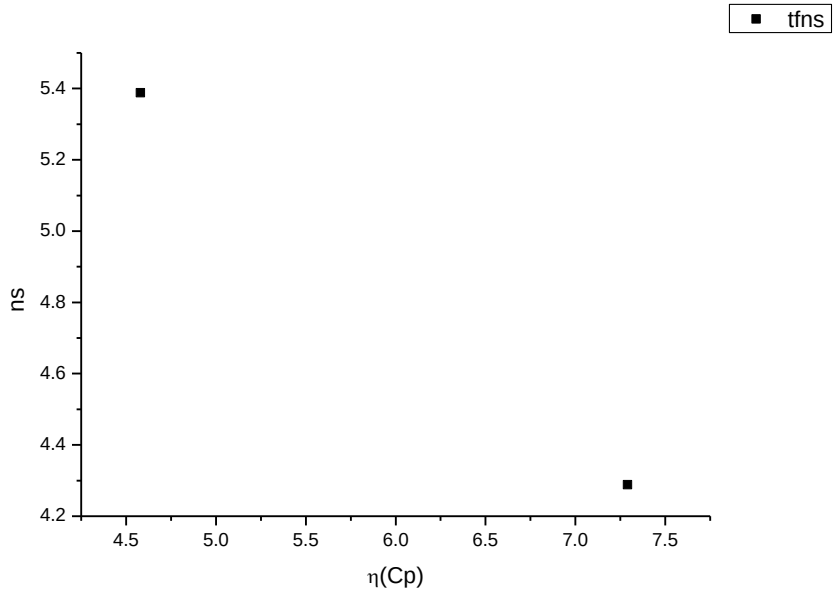

Figure 2.3.37. Intensity weighted average lifetime (τ_f) of **13** versus η(Cp).

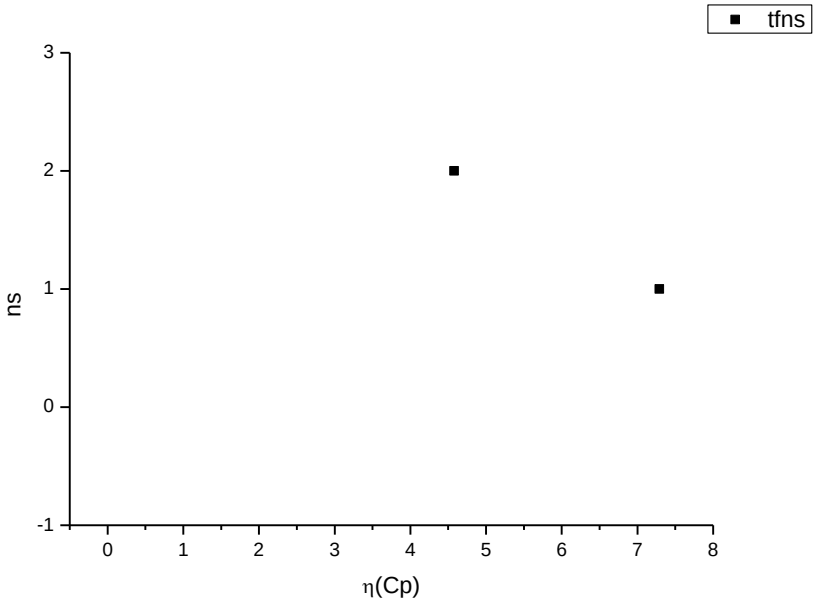

Figure 2.3.38. Amplitude weighted average lifetime (τ_f) of **13** versus η(Cp).

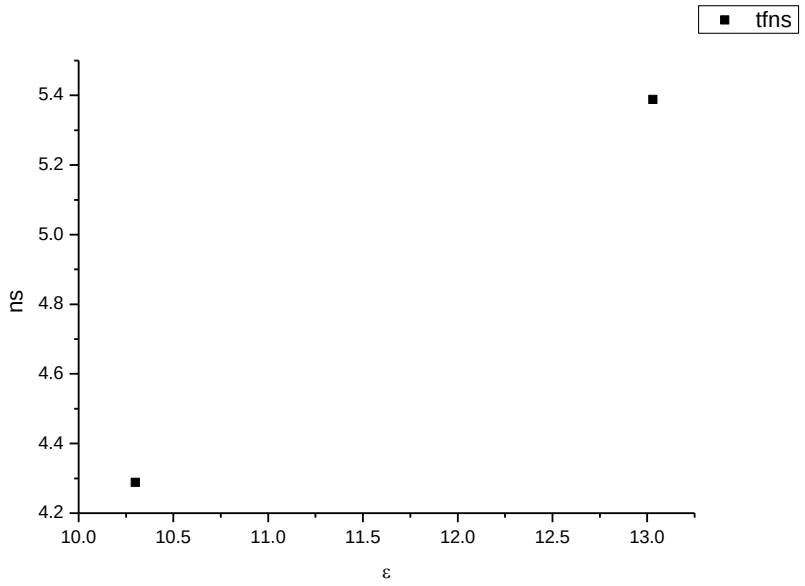

Figure 2.3.39. Intensity weighted average lifetime (τ_f) of **13** versus ε.

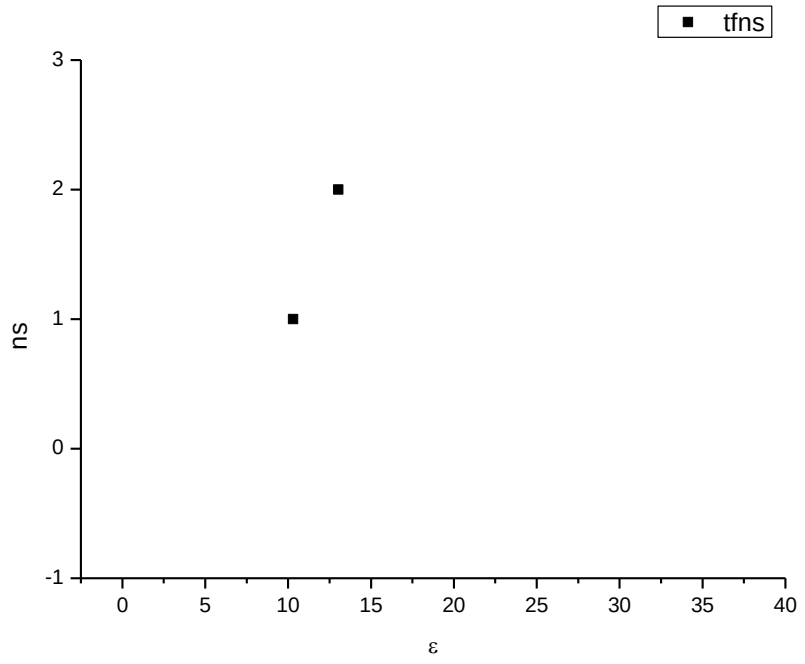

Figure 2.3.40. Amplitude weighted average lifetime (τ_f) of **13** versus ε.

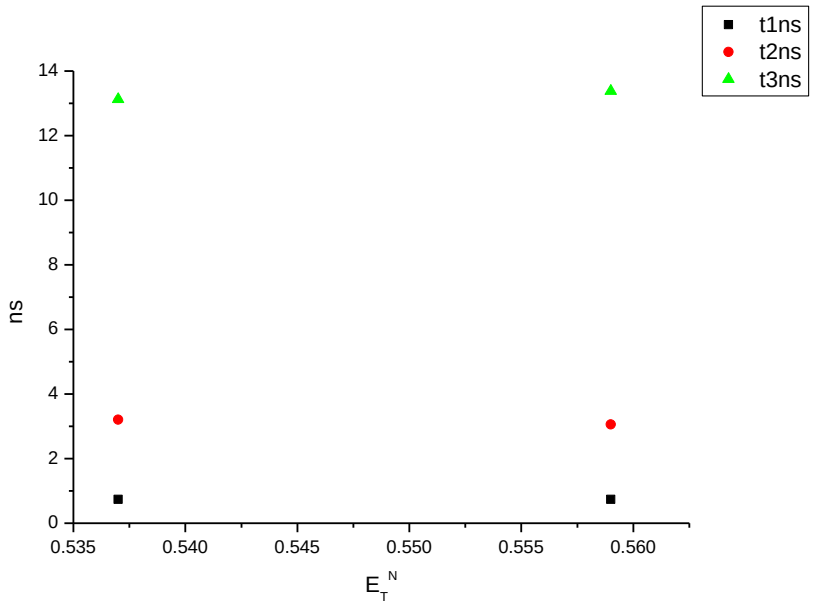

Figure 2.3.41. Intensity weighted components of TCSPC lifetime decay of **13** (370 nm) versus E_T^N.

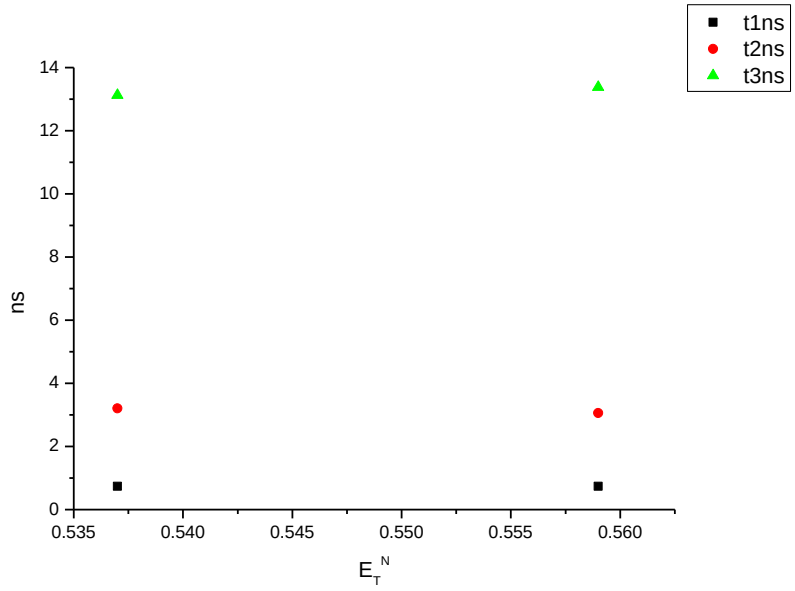

Figure 2.3.42. Amplitude weighted components of TCSPC lifetime decay of **13** (370 nm) versus E_T^N.

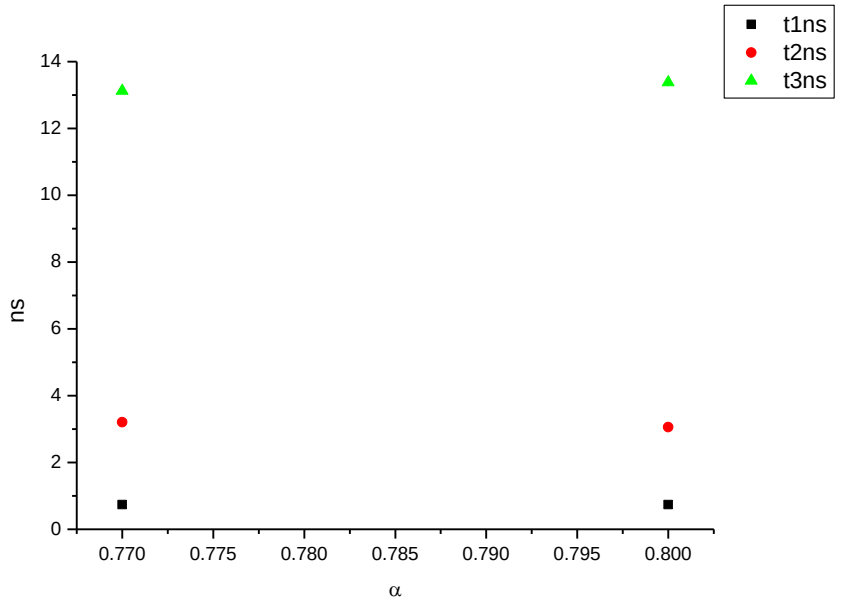

Figure 2.3.43. Intensity weighted components of TCSPC lifetime decay of **13** (370 nm) versus α.

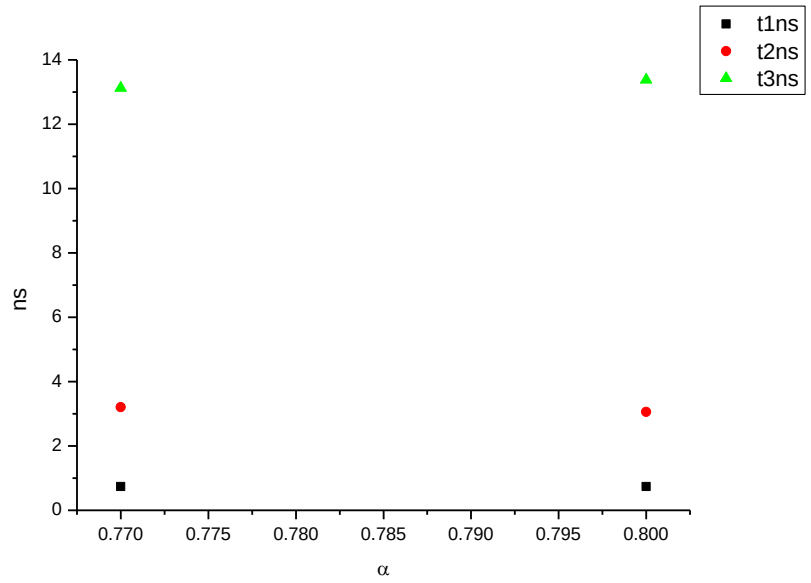

Figure 2.3.44. Amplitude weighted components of TCSPC lifetime decay of **13** (370 nm) versus α.

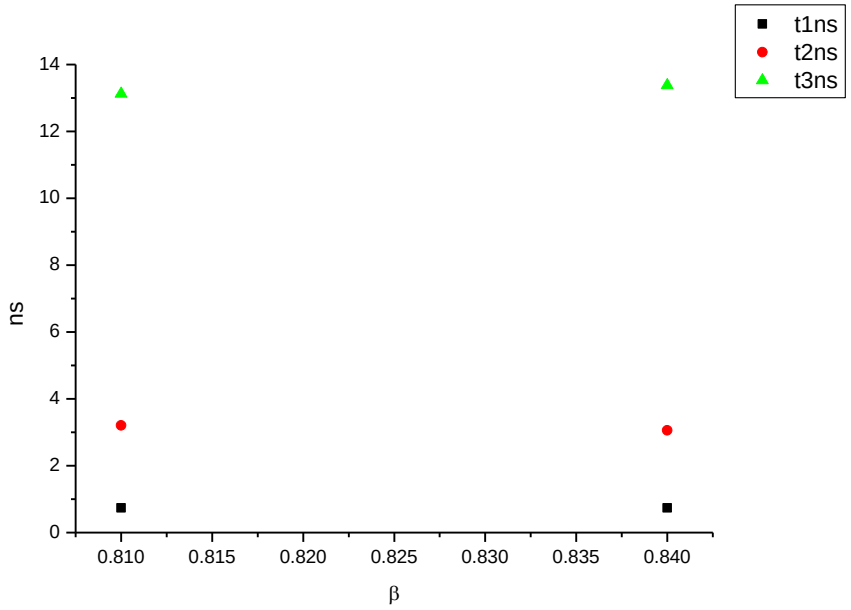

Figure 2.3.45. Intensity weighted components of TCSPC lifetime decay of **13** (370 nm) versus β.

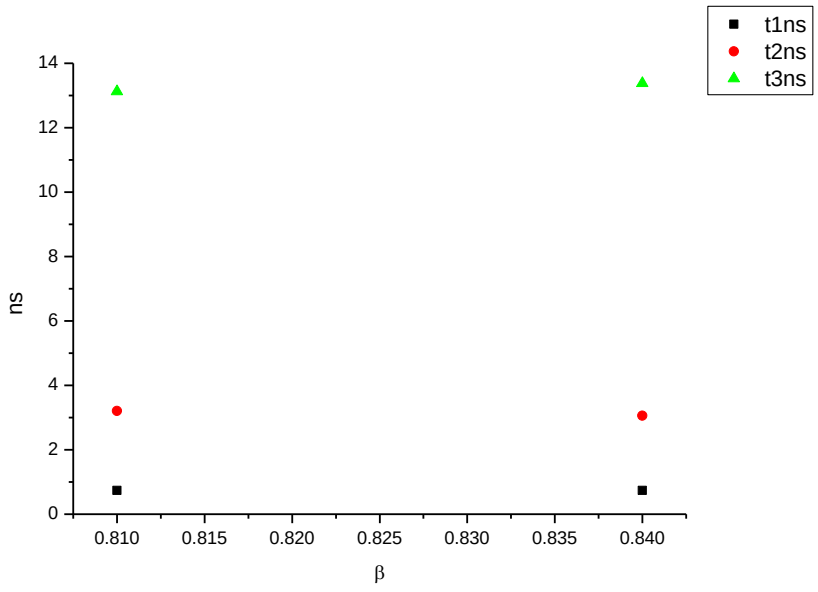

Figure 2.3.46. Amplitude weighted components of TCSPC lifetime decay of **13** (500 nm) versus β.

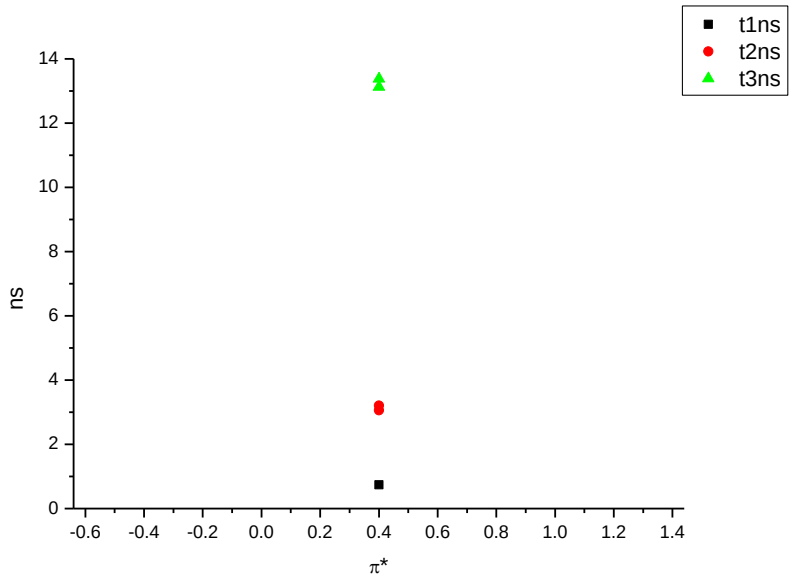

Figure 2.3.47. Intensity weighted components of TCSPC lifetime decay of **13** (370 nm) versus π*.

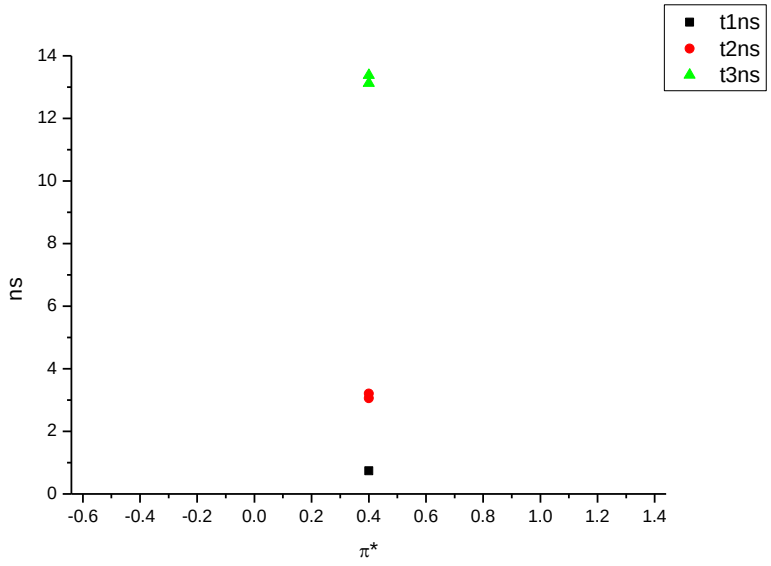

Figure 2.3.48. Amplitude weighted components of TCSPC lifetime decay of **13** (370 nm) versus π*.

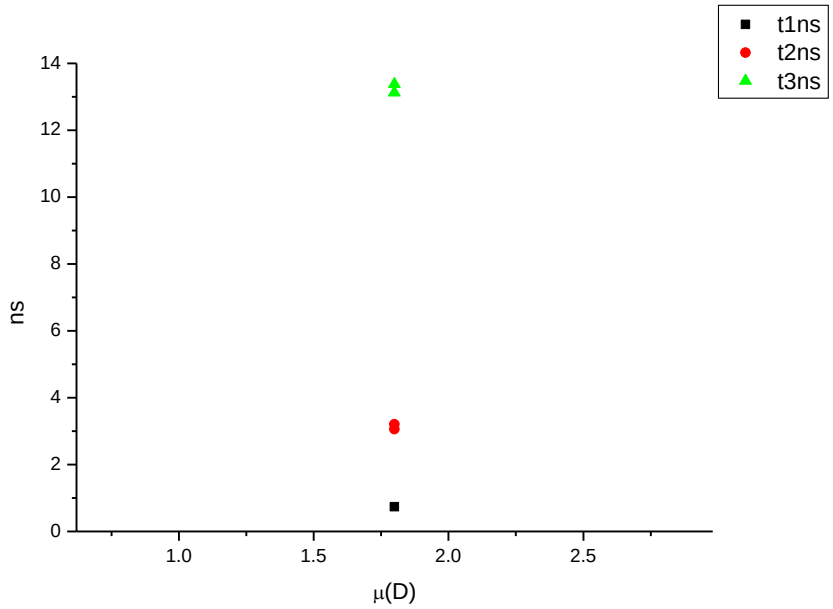

Figure 2.3.49. Intensity weighted components of TCSPC lifetime decay of **13** (370 nm) versus μ(D).

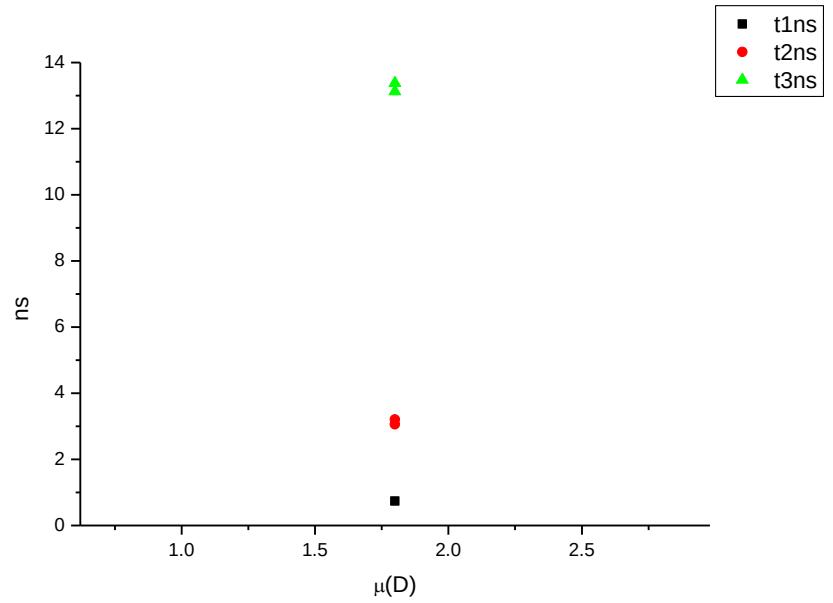

Figure 2.3.50. Amplitude weighted components of TCSPC lifetime decay of **13** (370 nm) versus μ(D).

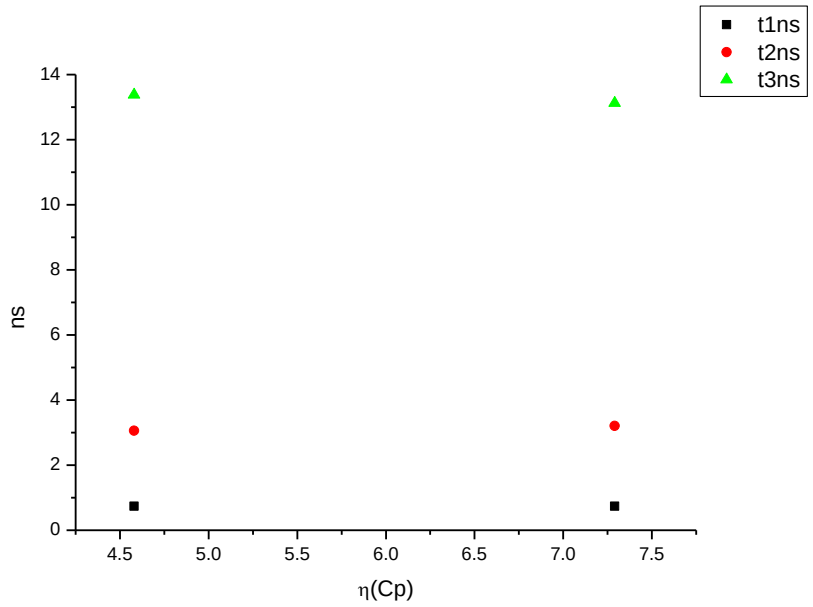

Figure 2.3.51. Intensity weighted components of TCSPC lifetime decay of **13** (370 nm) versus η(Cp).

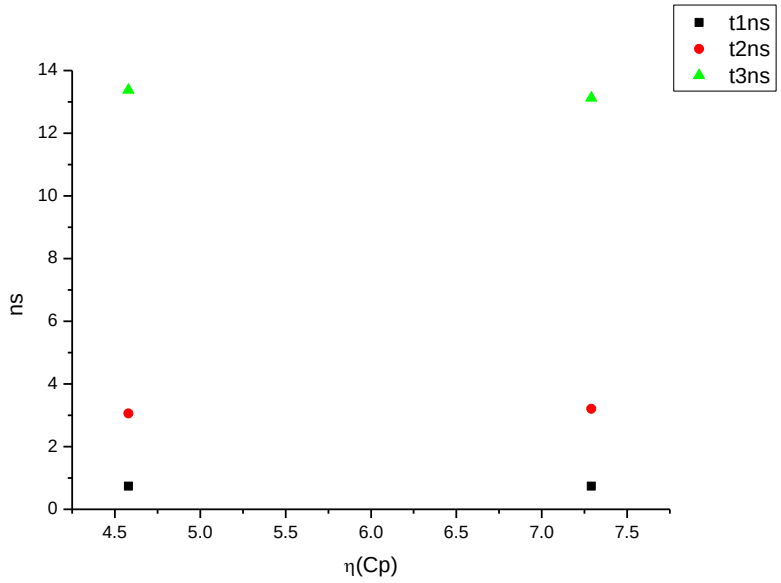

Figure 2.3.52. Amplitude weighted components of TCSPC lifetime decay of **13** (500 nm) versus η(Cp).

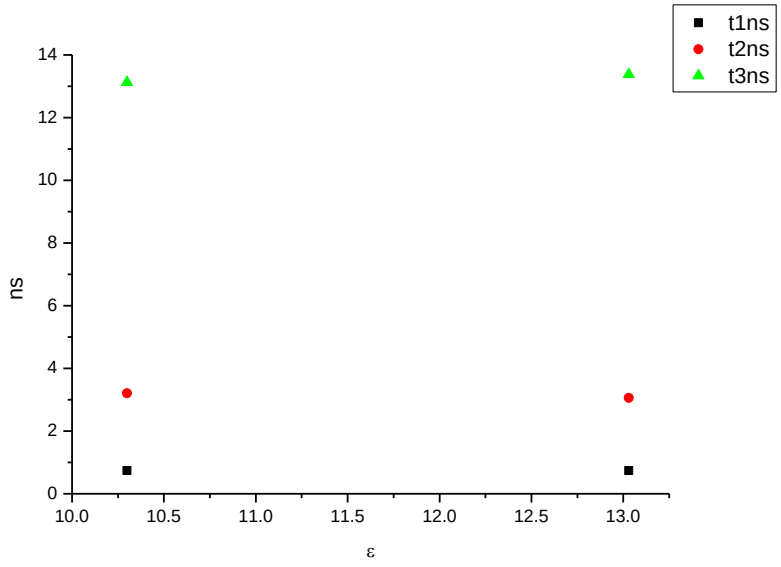

Figure 2.3.53. Intensity weighted components of TCSPC lifetime decay of **13** (370 nm) versus ε.

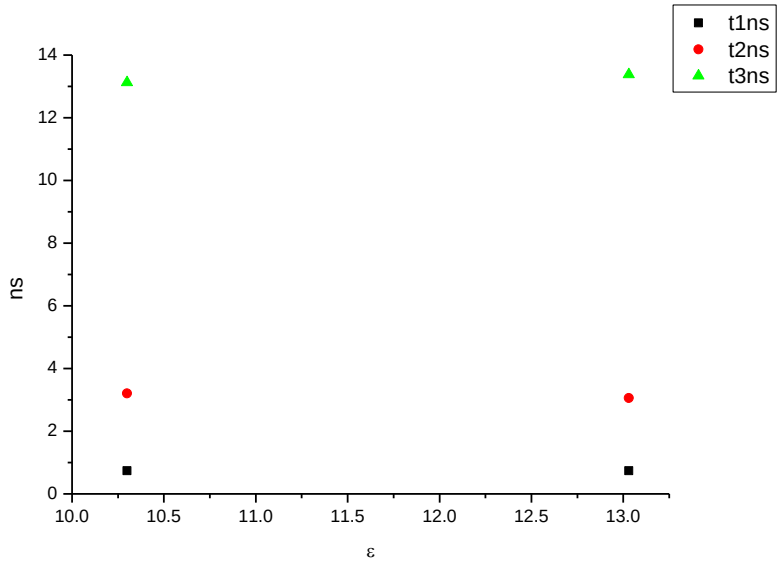

Figure 2.3.54. Amplitude weighted components of TCSPC lifetime decay of **13** (370 nm) versus ε.

2.3.5 Ultraviolet-visible absorption spectra.

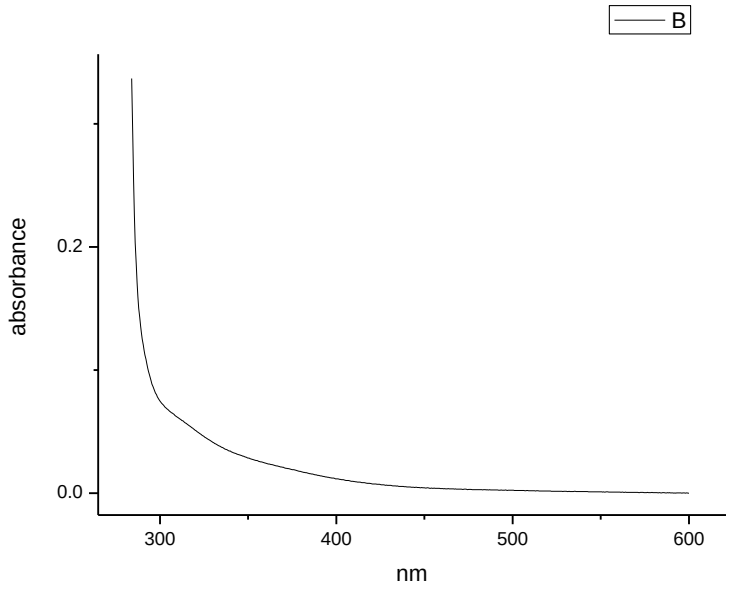

Figure 2.3.55. Ultraviolet-Visible absorption spectrum of **13** recorded in Toluene.

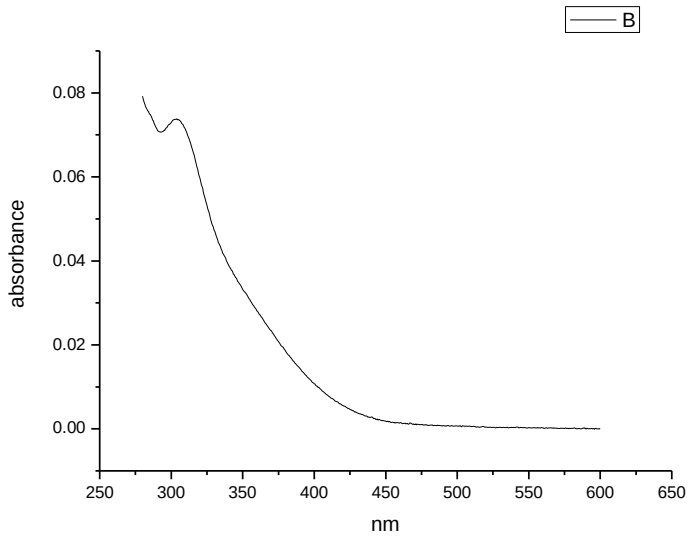

Figure 2.3.56. Ultraviolet-Visible absorption spectrum of **13** recorded in 1,4-dioxane.

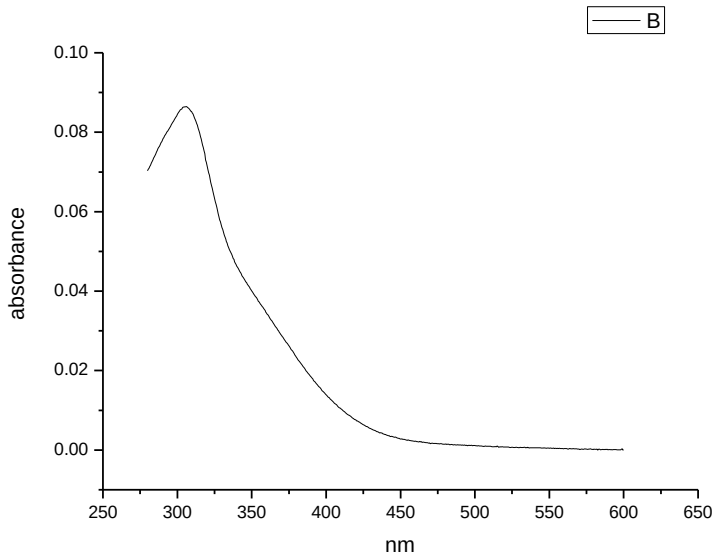

Figure 2.3.57. Ultraviolet-Visible absorption spectrum of **13** recorded in Chloroform.

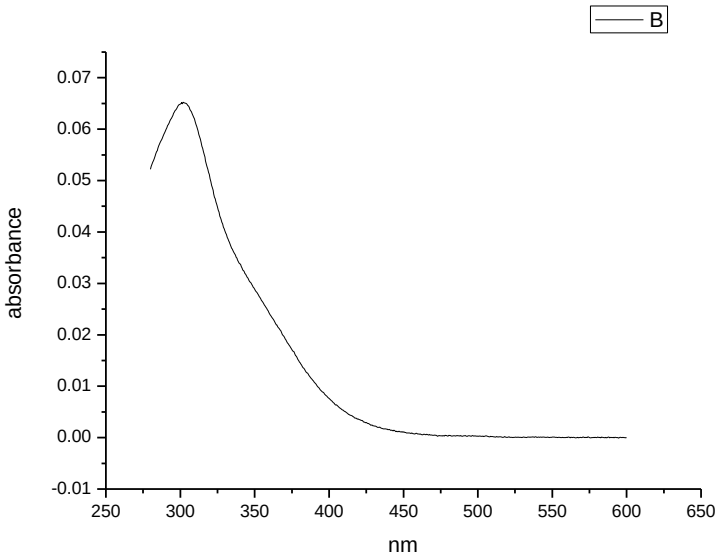

Figure 2.3.58. Ultraviolet-Visible absorption spectrum of **13** recorded in Acetonitrile.

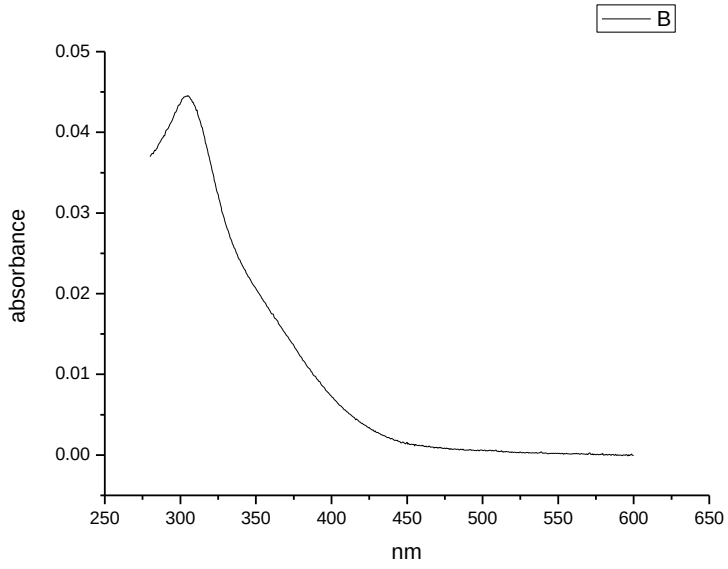

Figure 2.3.59. Ultraviolet-Visible absorption spectrum of **13** recorded in 1-octanol.

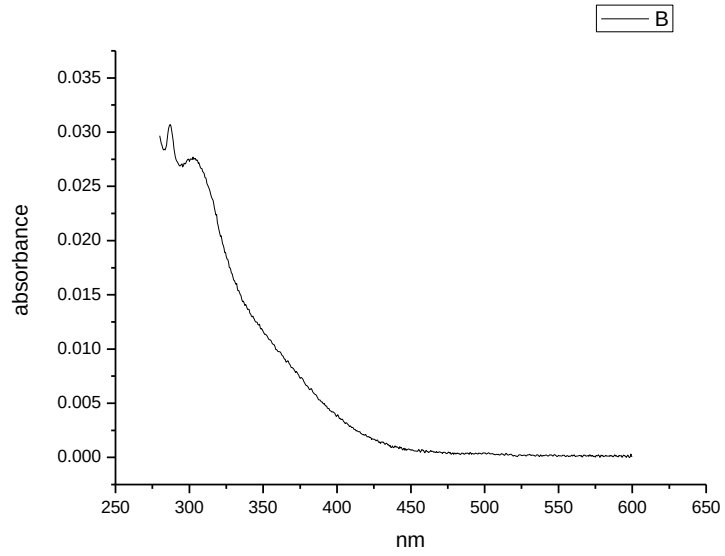

Figure 2.3.60. Ultraviolet-Visible absorption spectrum of **13** recorded in 1-hexanol.

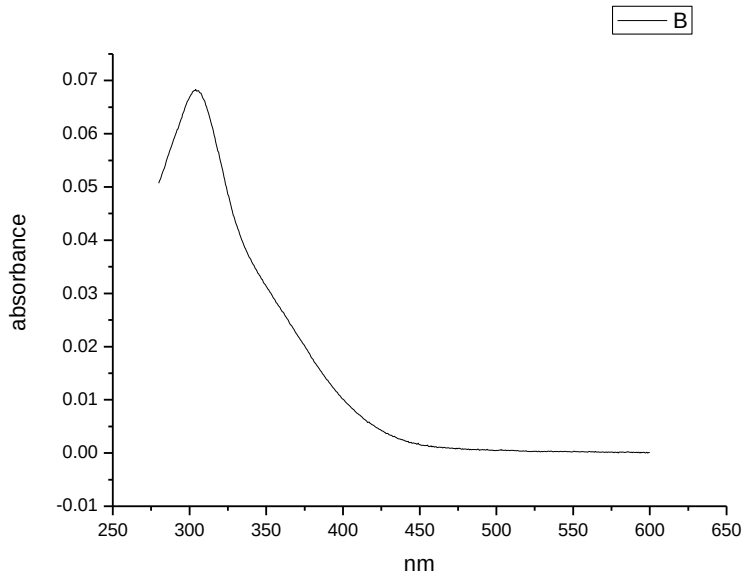

Figure 2.3.61. Ultraviolet-Visible absorption spectrum of **13** recorded in 1-butanol.

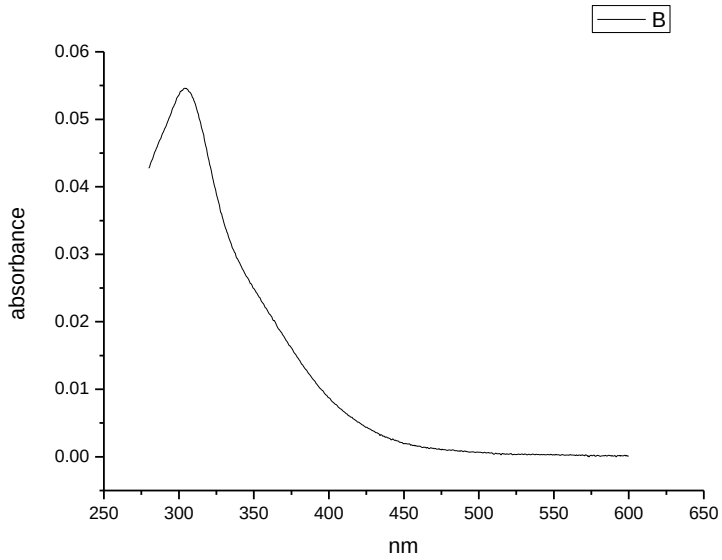

Figure 2.3.62. Ultraviolet-Visible absorption spectrum of **13** recorded in 1-pentanol.

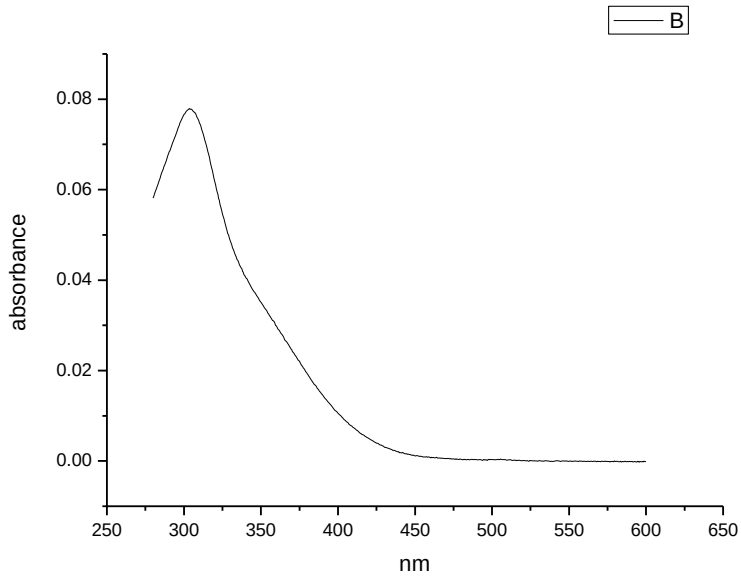

Figure 2.3.63. Ultraviolet-Visible absorption spectrum of **13** recorded in 1-propanol.

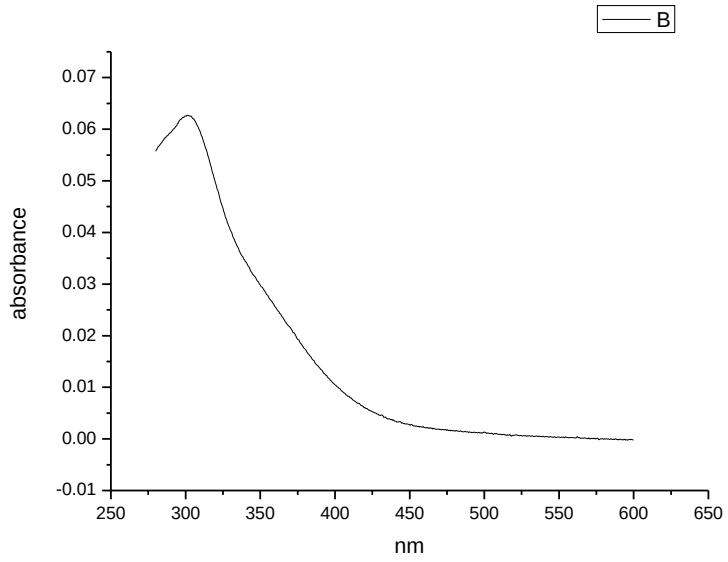

Figure 2.3.64. Ultraviolet-Visible absorption spectrum of **13** recorded in Acetic Acid.

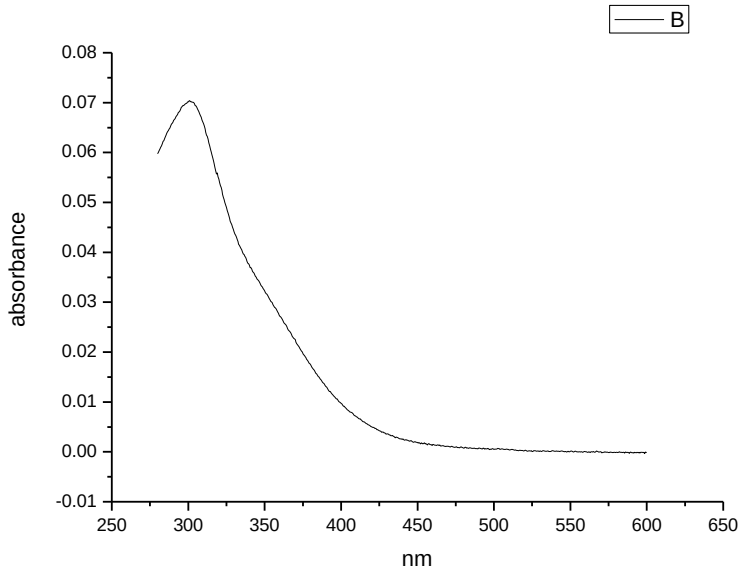

Figure 2.3.65. Ultraviolet-Visible absorption spectrum of **13** recorded in Methanol.

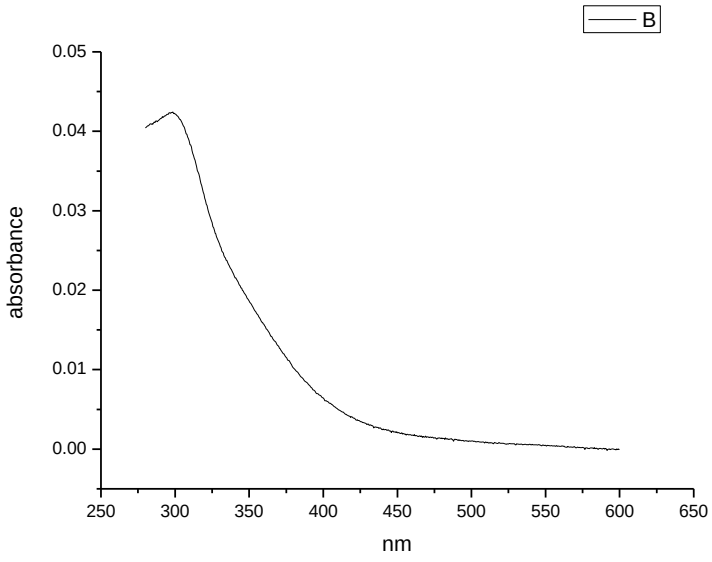

Figure 2.3.66. Ultraviolet-Visible absorption spectrum of **13** recorded in 2,2,2-trifluoroethanol.

2.3.6 Fluorescence Emission spectra.

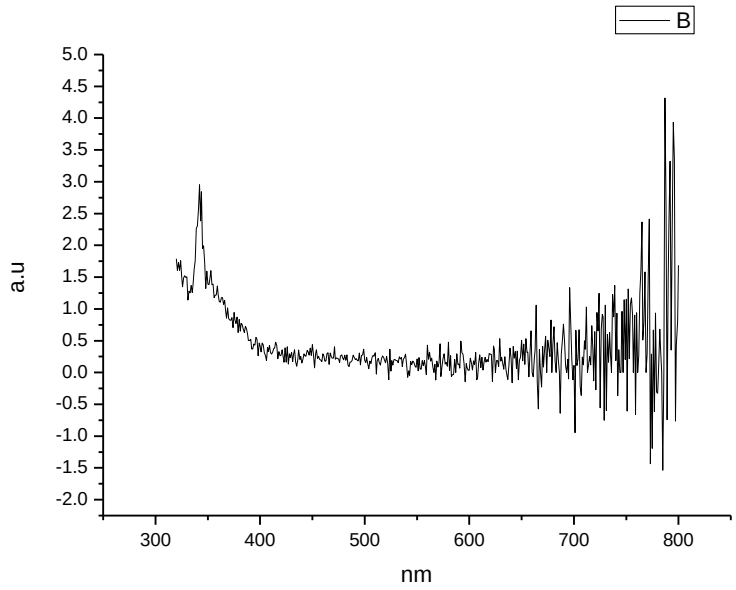

Figure 2.3.67. Fluorescence emission spectrum of **13** recorded in Toluene at 310 nm excitation.

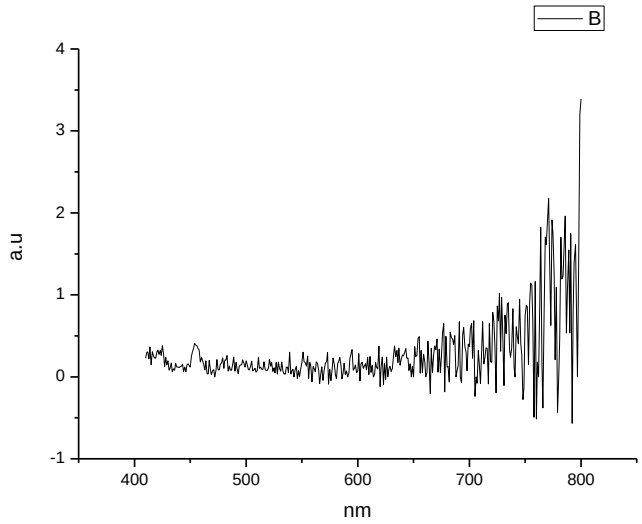

Figure 2.3.68. Fluorescence emission spectrum of **13** recorded in Toluene at 400 nm excitation.

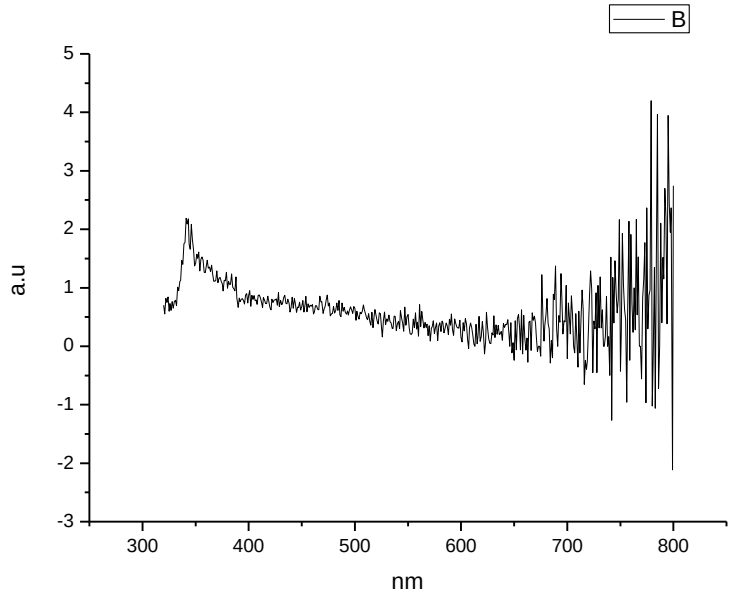

Figure 2.3.69. Fluorescence emission spectrum of **13** recorded in 1,4-dioxane at 310 nm excitation.

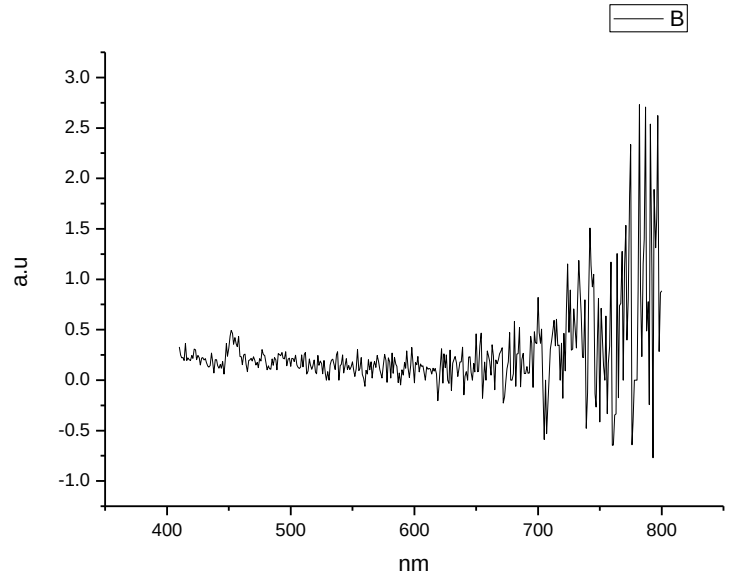

Figure 2.3.70. Fluorescence emission spectrum of **13** recorded in 1,4-dioxane at 400 nm excitation.

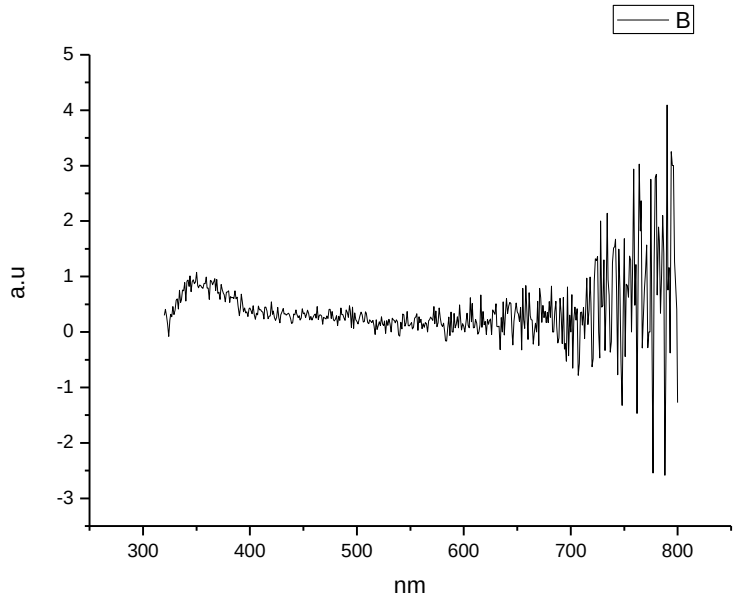

Figure 2.3.71. Fluorescence emission spectrum of **13** recorded in Chloroform at 310 nm excitation.

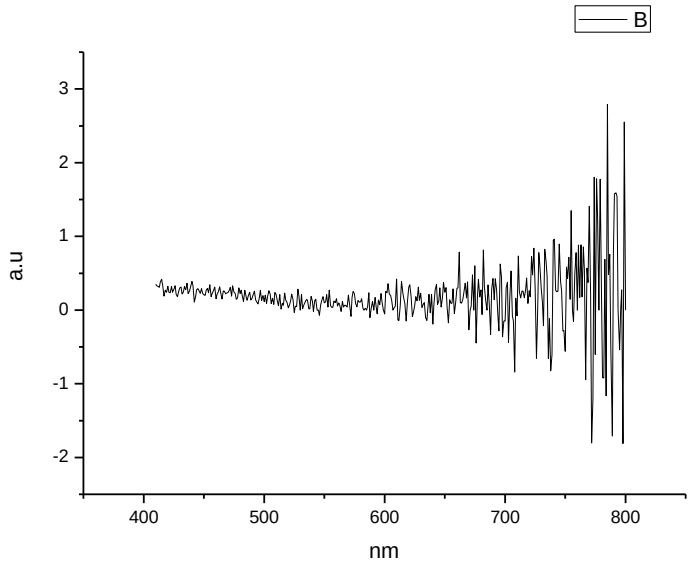

Figure 2.3.72. Fluorescence emission spectrum of **13** recorded in Chloroform at 400 nm excitation.

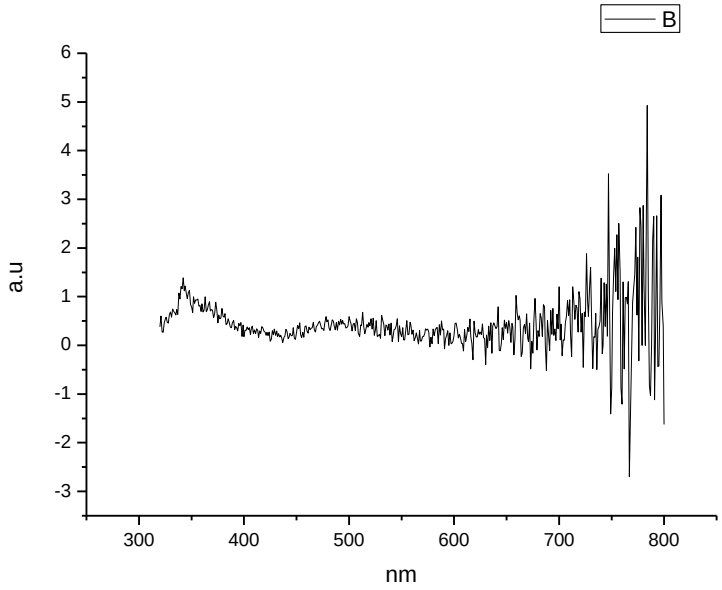

Figure 2.3.73. Fluorescence emission spectrum of **13** recorded in Acetonitrile at 310 nm excitation.

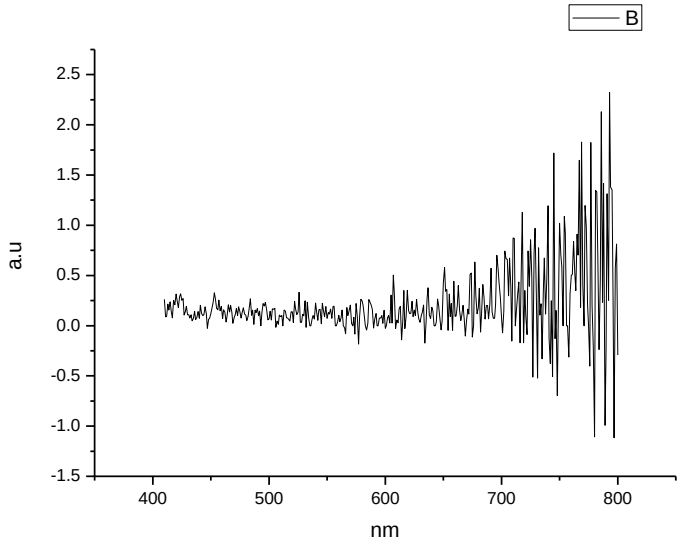

Figure 2.3.74. Fluorescence emission spectrum of **13** recorded in Acetonitrile at 400 nm excitation.

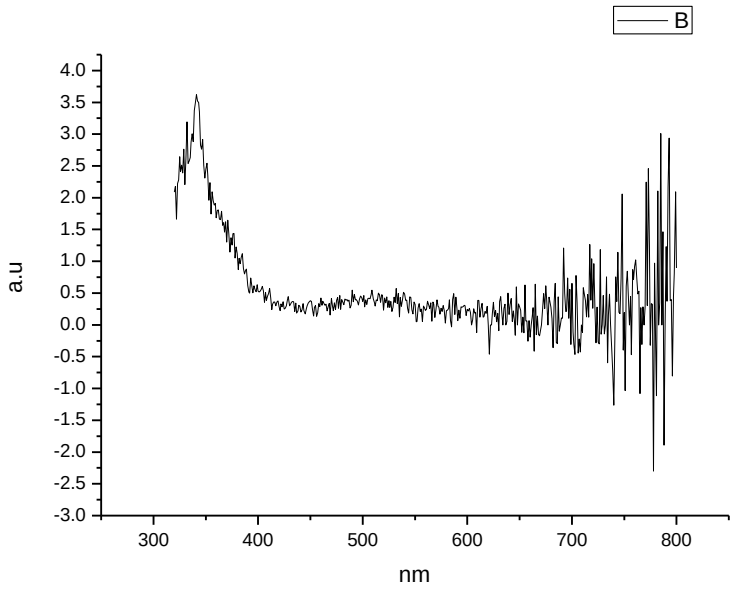

Figure 2.3.75. Fluorescence emission spectrum of **13** recorded in 1-octanol at 310 nm excitation.

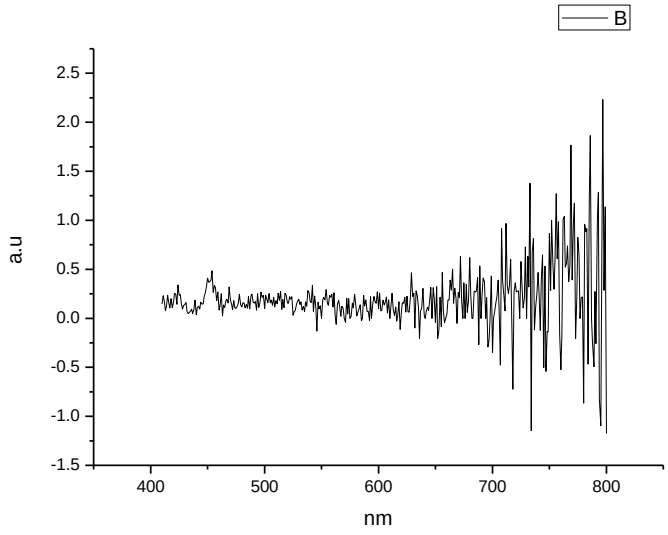

Figure 2.3.76. Fluorescence emission spectrum of **13** recorded in 1-octanol at 400 nm excitation.

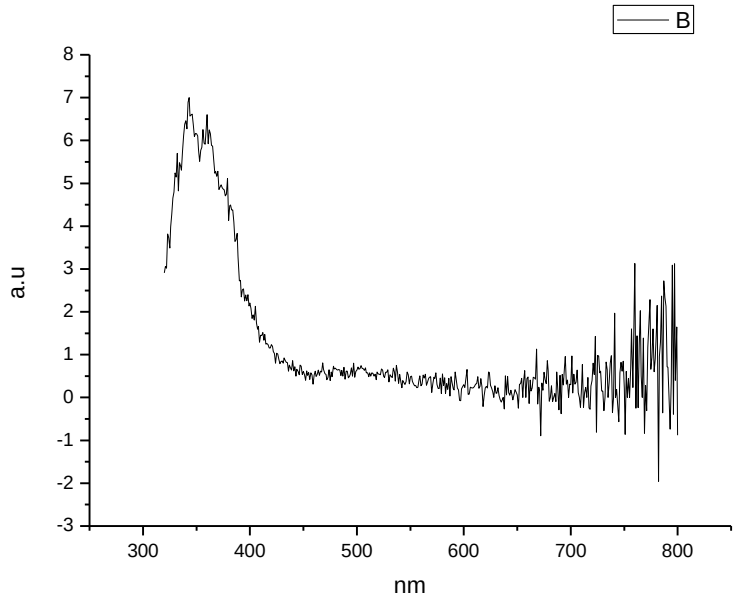

Figure 2.3.77. Fluorescence emission spectrum of **13** recorded in 1-hexanol at 310 nm excitation.

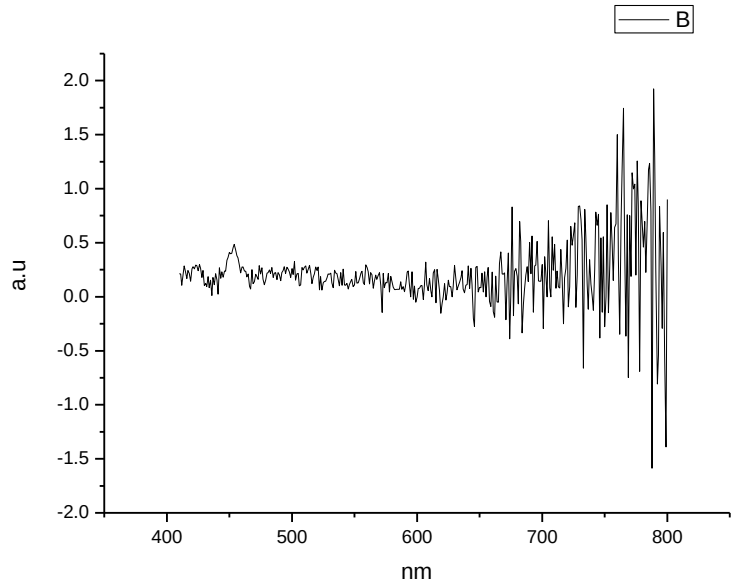

Figure 2.3.78. Fluorescence emission spectrum of **13** recorded in 1-hexanol at 400 nm excitation.

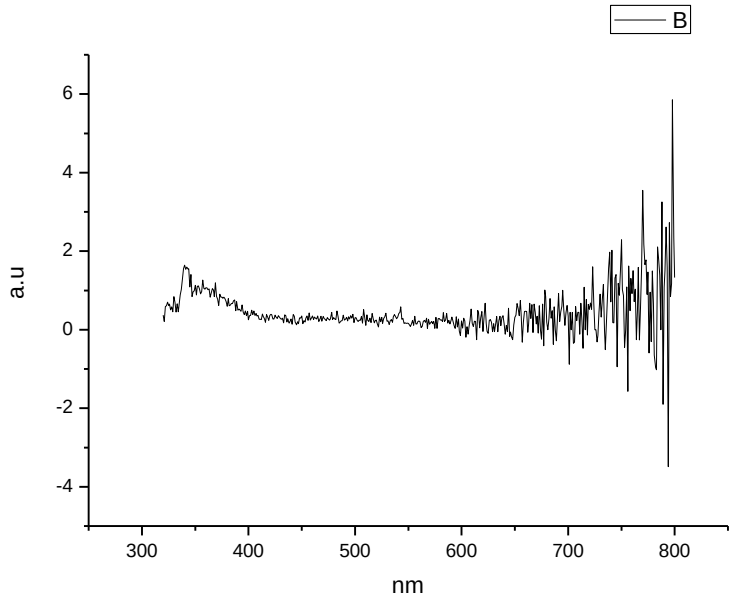

Figure 2.3.79. Fluorescence emission spectrum of **13** recorded in 1-butanol at 310 nm excitation.

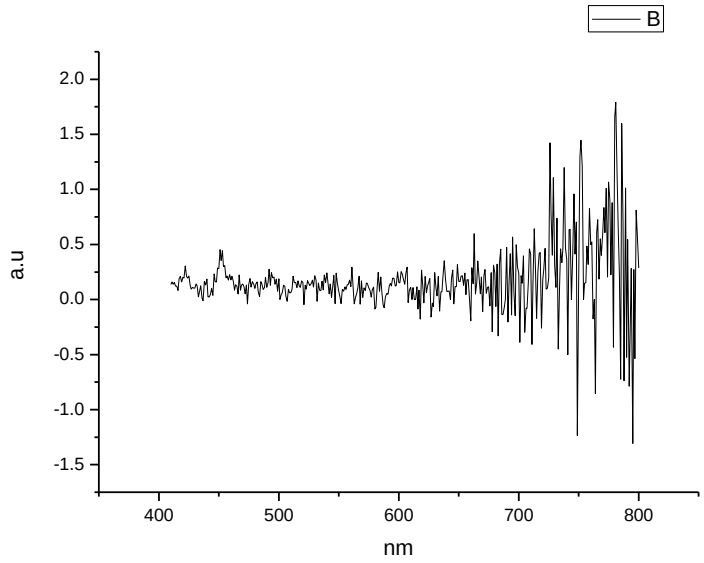

Figure 2.3.80. Fluorescence emission spectrum of **13** recorded in 1-butanol at 400 nm excitation.

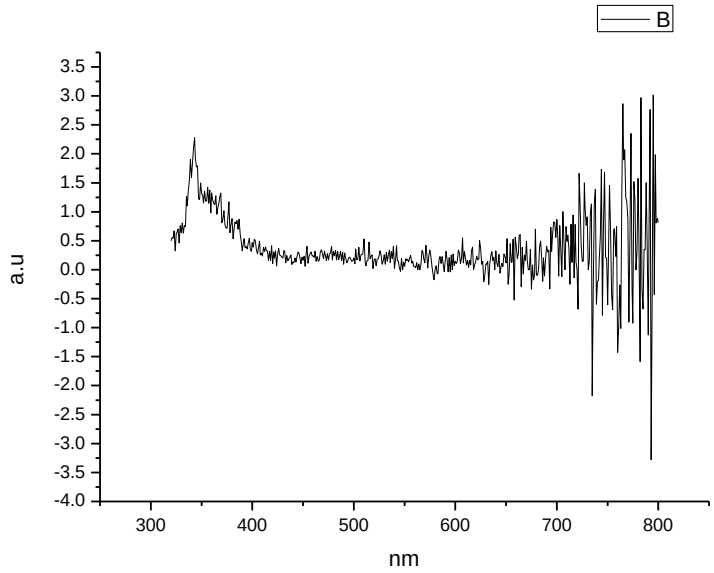

Figure 2.3.81. Fluorescence emission spectrum of **13** recorded in 1-pentanol at 310 nm excitation.

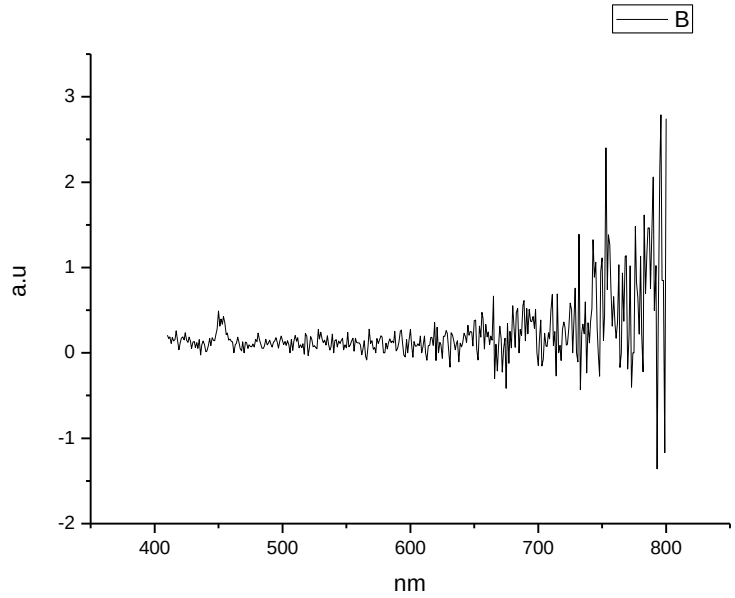

Figure 2.3.82. Fluorescence emission spectrum of **13** recorded in 1-pentanol at 400 nm excitation.

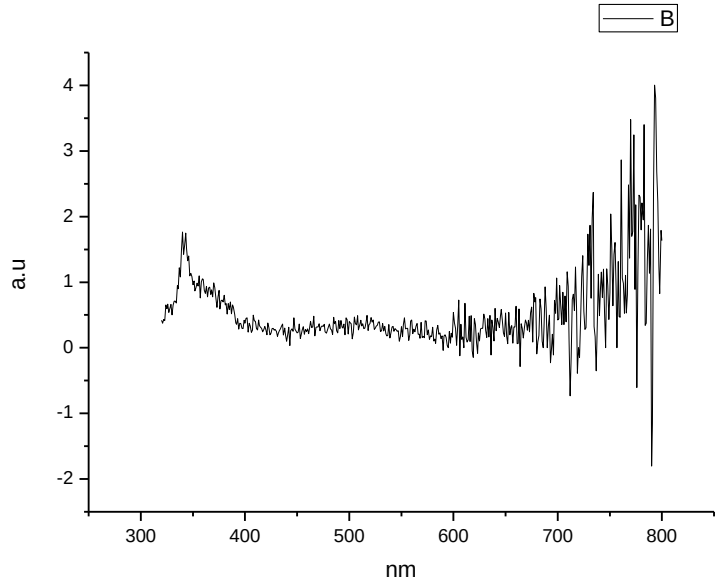

Figure 2.3.83. Fluorescence emission spectrum of **13** recorded in 1-propanol at 310 nm excitation.

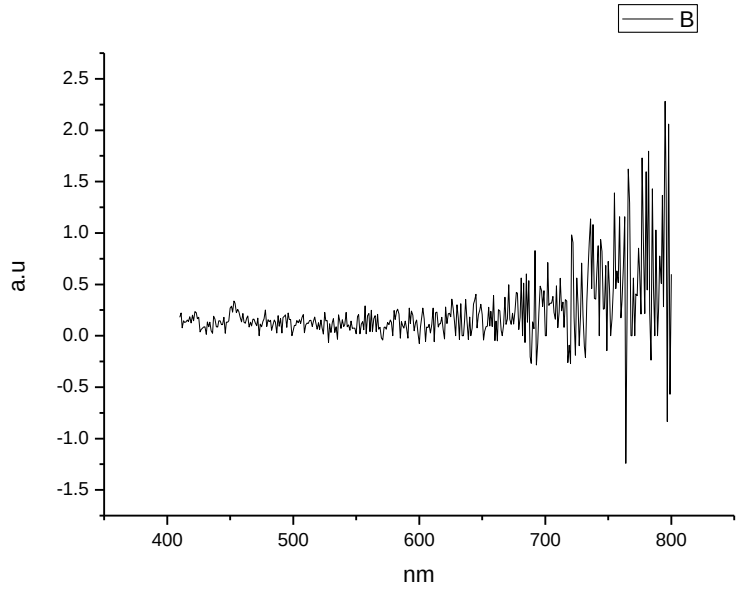

Figure 2.3.84. Fluorescence emission spectrum of **13** recorded in 1-propanol at 400 nm excitation.

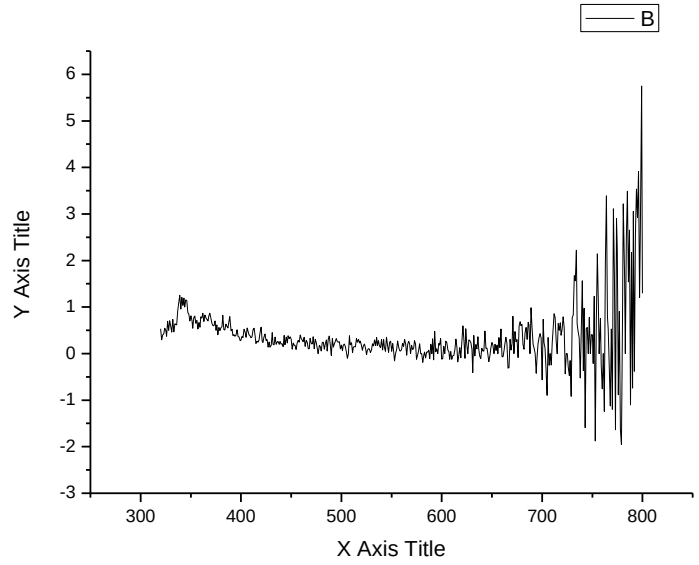

Figure 2.3.85. Fluorescence emission spectrum of **13** recorded in Acetic Acid at 310 nm excitation.

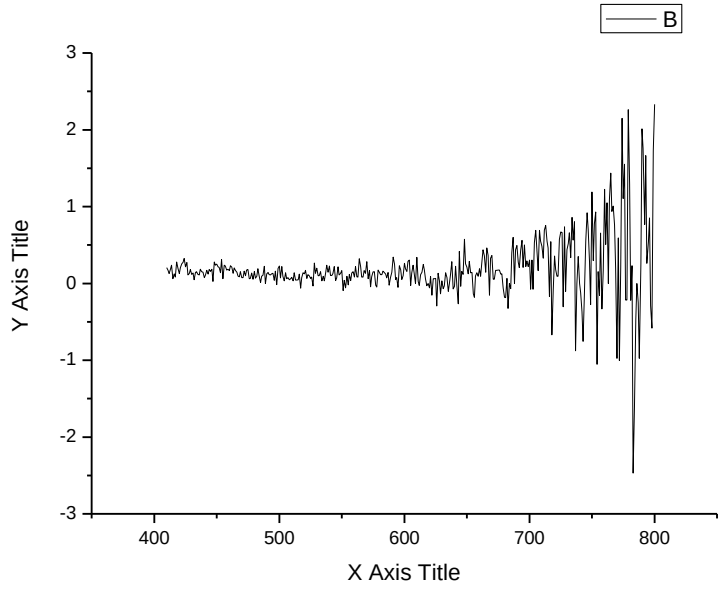

Figure 2.3.86. Fluorescence emission spectrum of **13** recorded in Acetic Acid at 400 nm excitation.

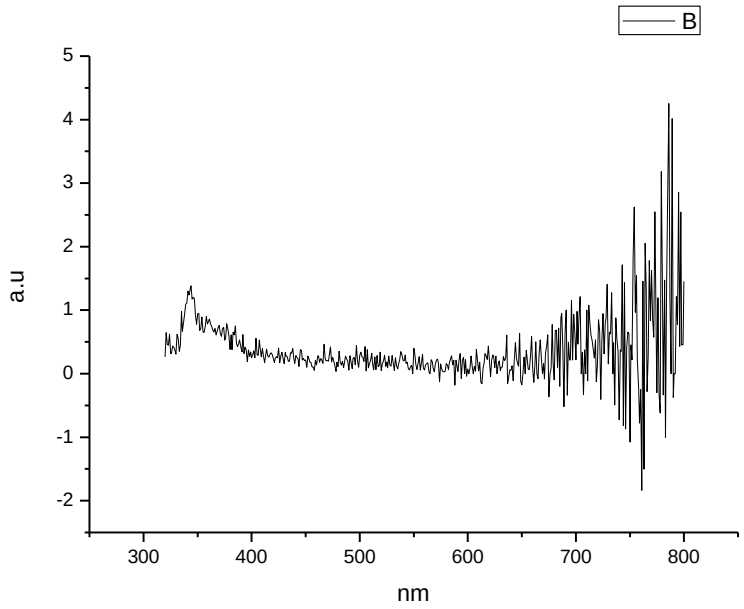

Figure 2.3.87. Fluorescence emission spectrum of **13** recorded in Methanol at 310 nm excitation.

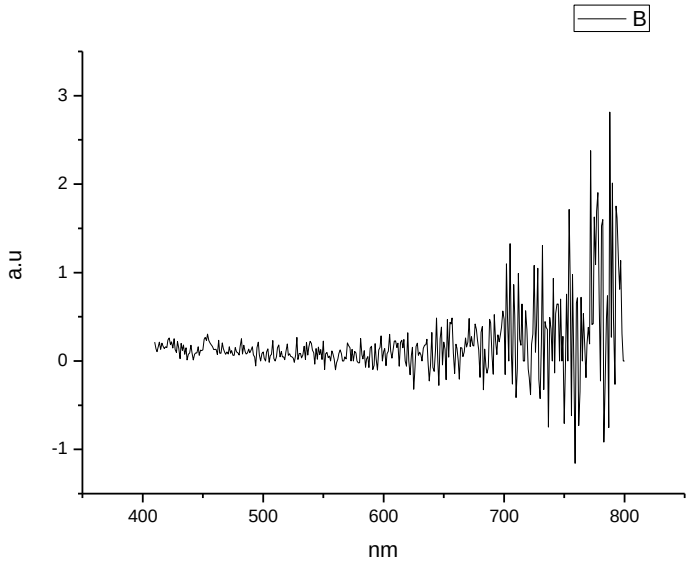

Figure 2.3.88. Fluorescence emission spectrum of **13** recorded in Methanol at 400 nm excitation.

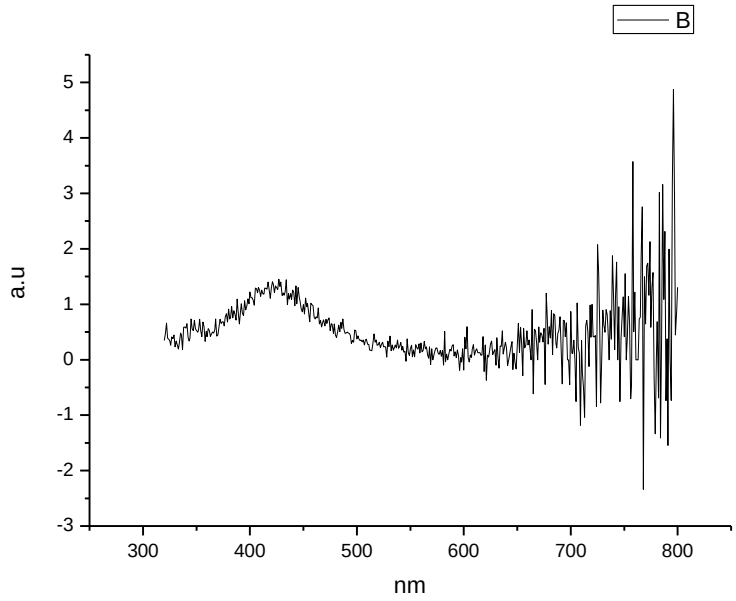

Figure 2.3.89. Fluorescence emission spectrum of **13** recorded in 2,2,2-trifluoroethanol at 310 nm excitation.

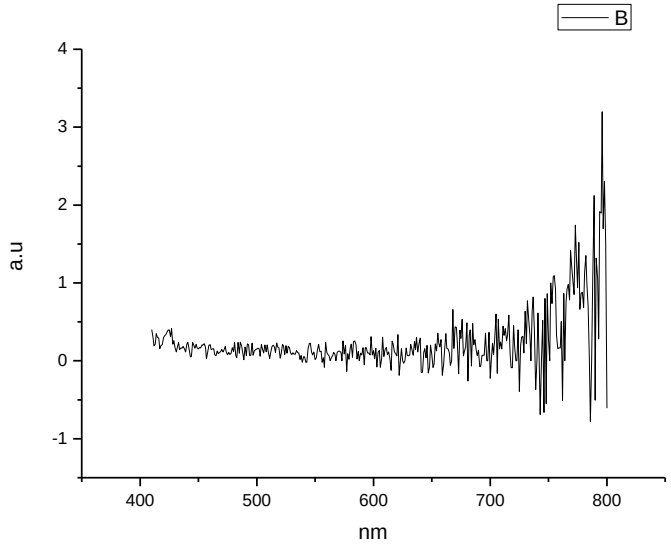

Figure 2.3.90. Fluorescence emission spectrum of **13** recorded in 2,2,2-trifluoroethanol at 400 nm excitation.

2.3.7 Normalised Fluorescence Emission spectra (Gaussian fitted).

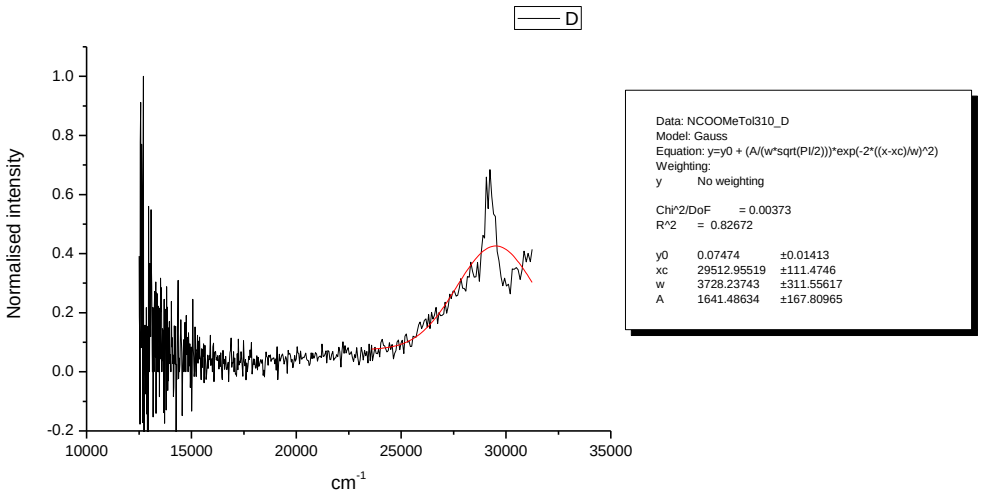

Figure 2.3.91. Gaussian model fit of the normalised fluorescence emission spectrum of **13** recorded in Toluene at 310 nm excitation.

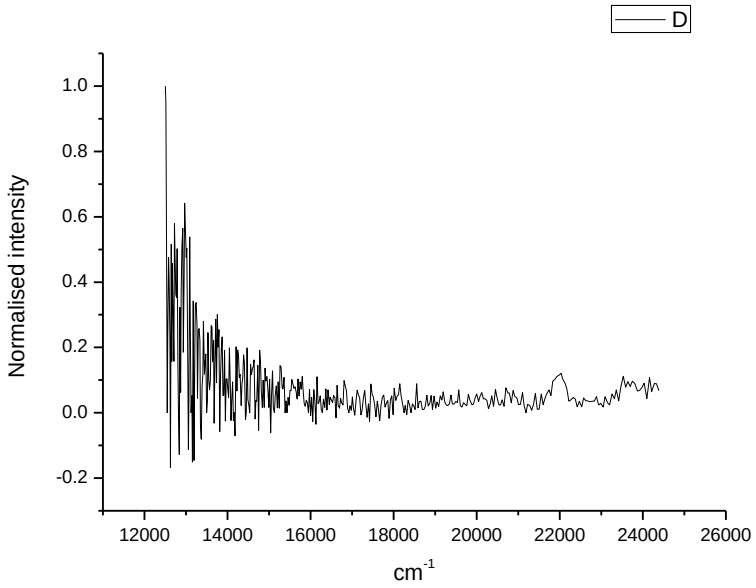

Figure 2.3.92. Attempted gaussian model fit of the normalised fluorescence emission spectrum of **13** recorded in Toluene at 400 nm excitation.

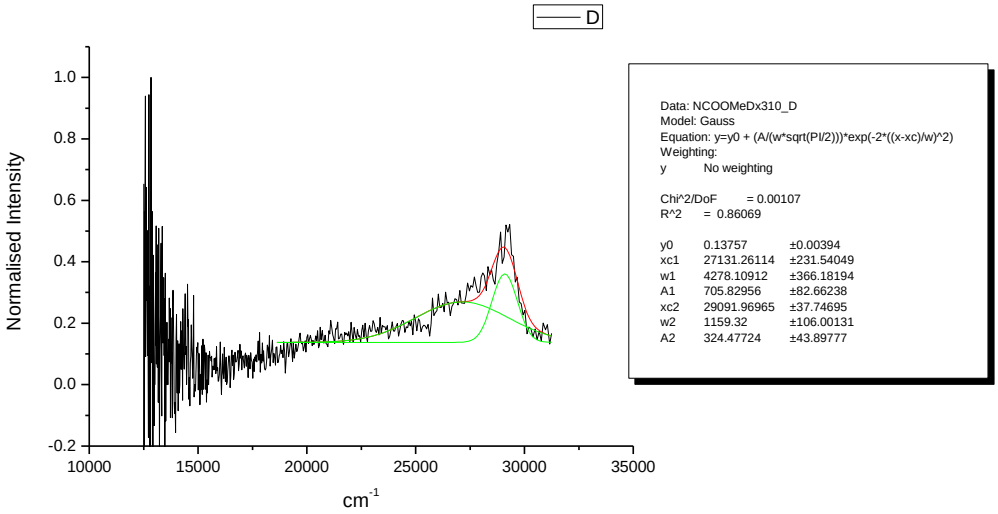

Figure 2.3.93. Gaussian model fit of the normalised fluorescence emission spectrum of **13** recorded in 1,4-dioxane at 310 nm excitation.

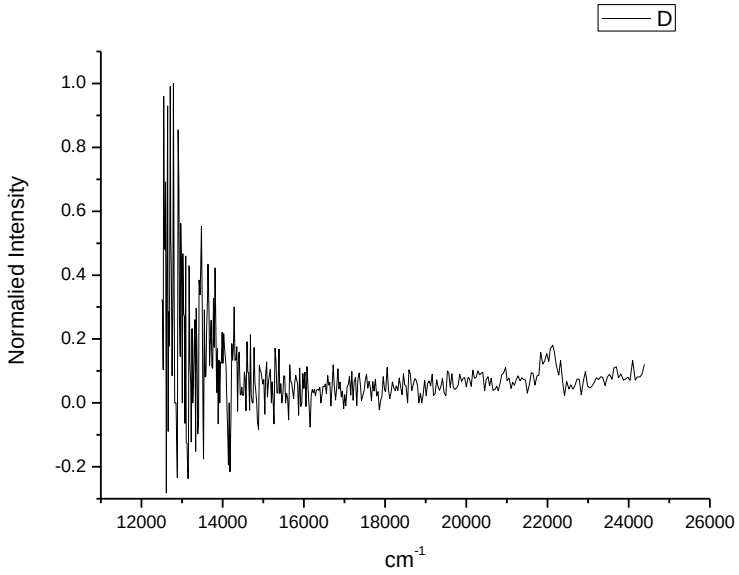

Figure 2.3.94. Attempted gaussian model fit of the normalised fluorescence emission spectrum of **13** recorded in 1,4-dioxane at 400 nm excitation.

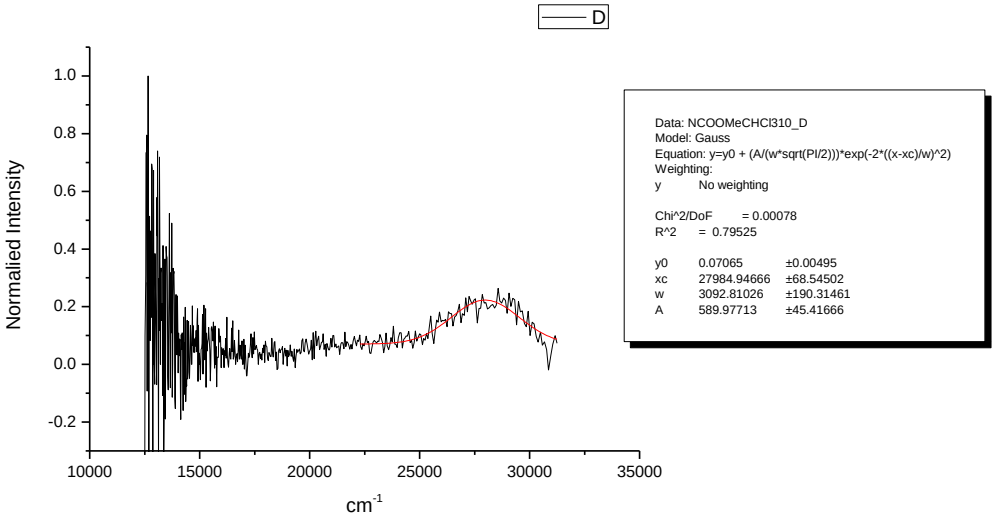

Figure 2.3.95. Gaussian model fit of the normalised fluorescence emission spectrum of **13** recorded in Chloroform at 310 nm excitation.

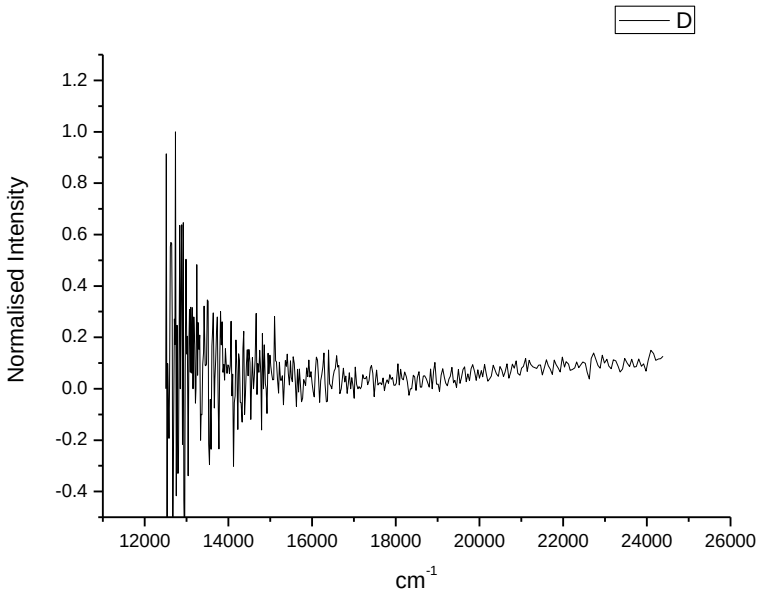

Figure 2.3.96. Attempted gaussian model fit of the normalised fluorescence emission spectrum of **13** recorded in Chloroform at 400 nm excitation.

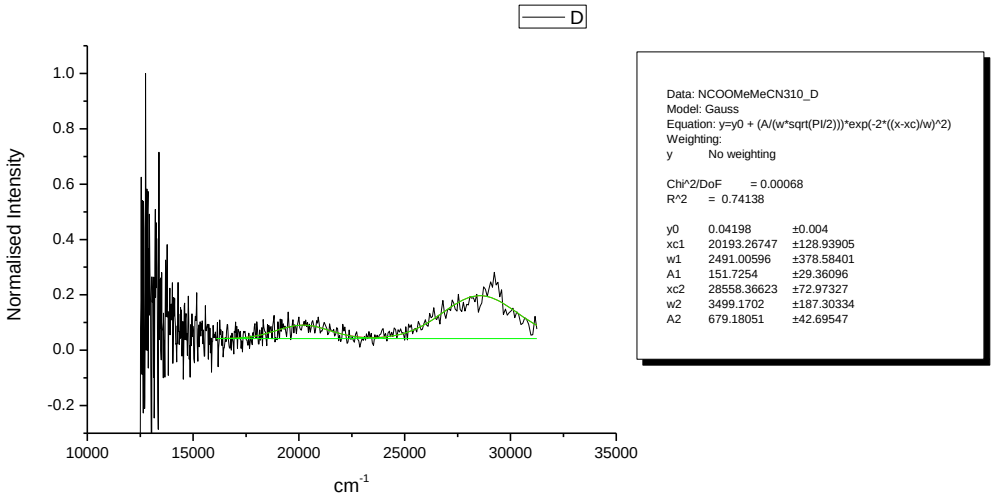

Figure 2.3.97. Gaussian model fit of the normalised fluorescence emission spectrum of **13** recorded in Acetonitrile at 310 nm excitation.

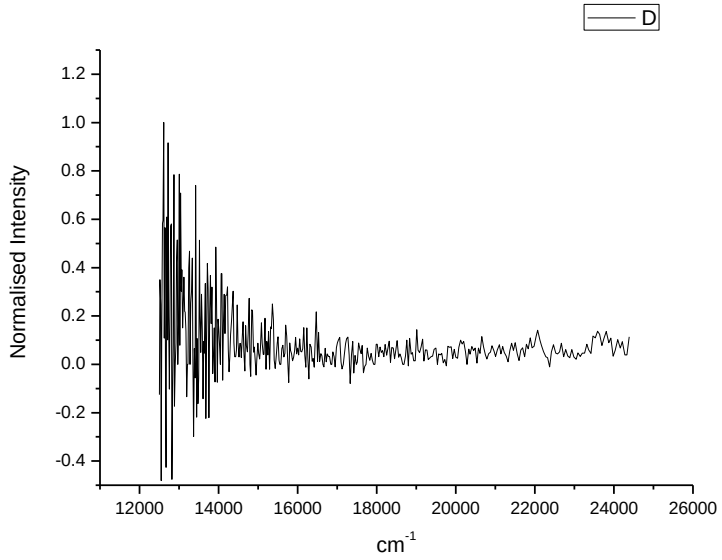

Figure 2.3.98. Attempted gaussian model fit of the normalised fluorescence emission spectrum of **13** recorded in Acetonitrile at 400 nm excitation.

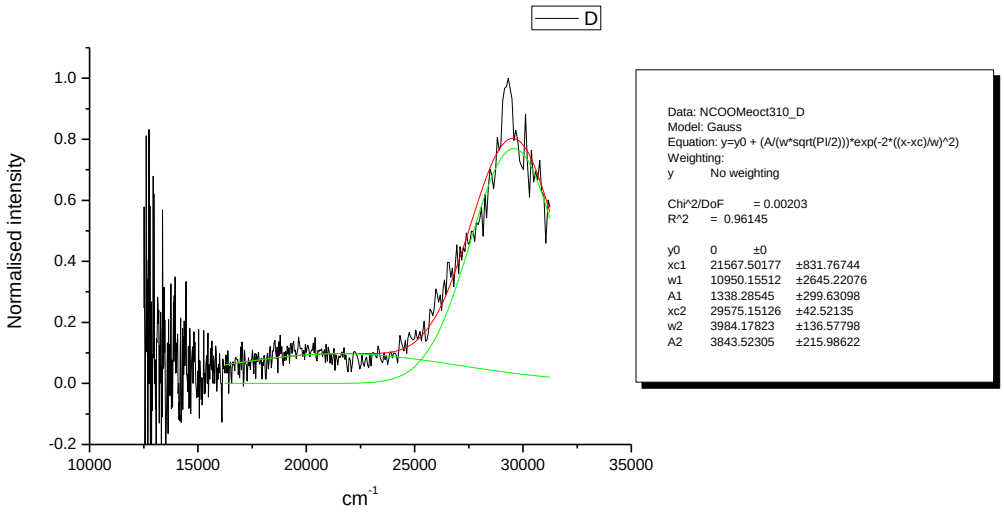

Figure 2.3.99. Gaussian model fit of the normalised fluorescence emission spectrum of **13** recorded in 1-octanol at 310 nm excitation.

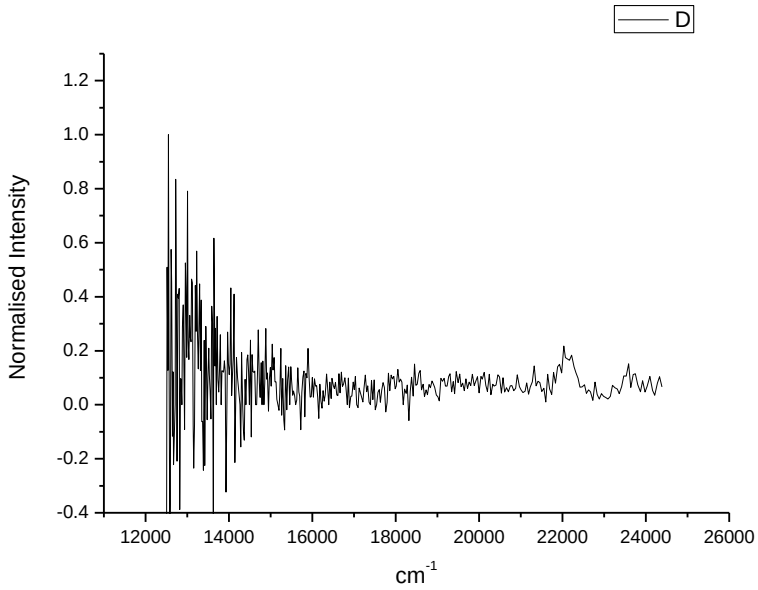

Figure 2.3.100. Attempted gaussian model fit of the normalised fluorescence emission spectrum of **13** recorded in 1-octanol at 400 nm excitation.

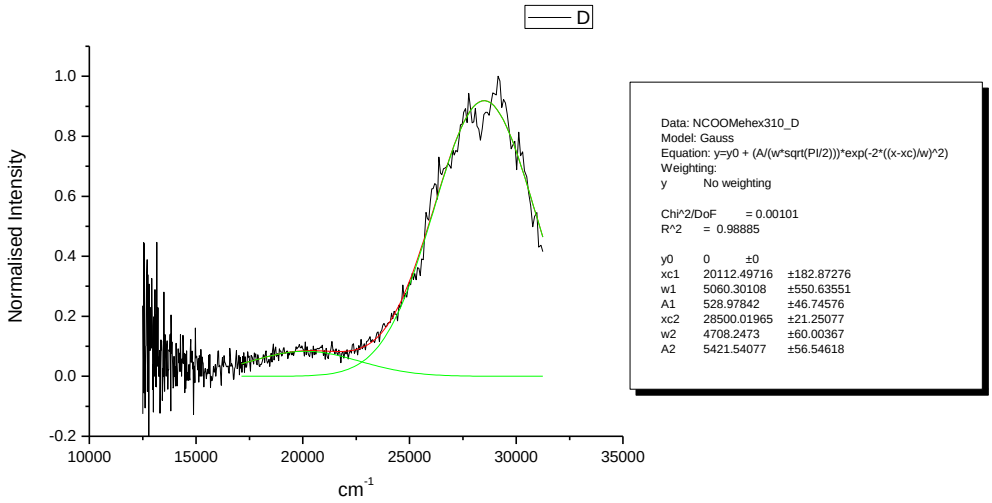

Figure 2.3.101. Gaussian model fit of the normalised fluorescence emission spectrum of **13** recorded in 1-hexanol at 310 nm excitation.

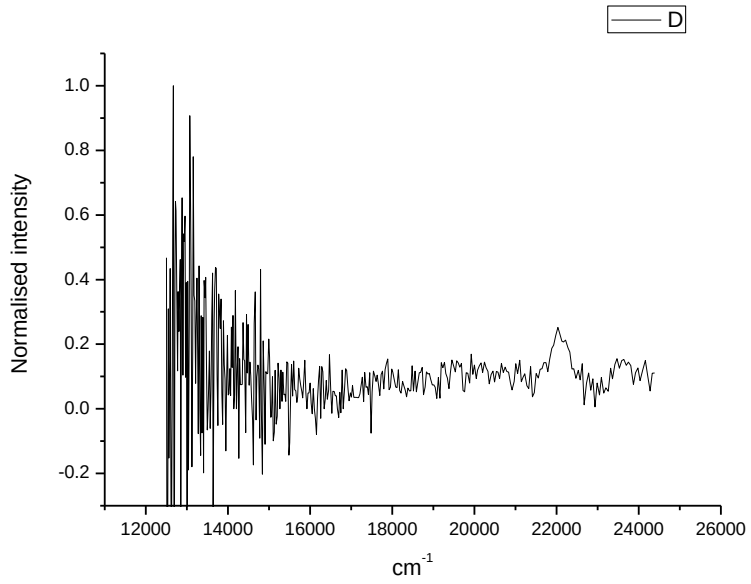

Figure 2.3.102. Attempted gaussian model fit of the normalised fluorescence emission spectrum of **13** recorded in 1-hexanol at 400 nm excitation.

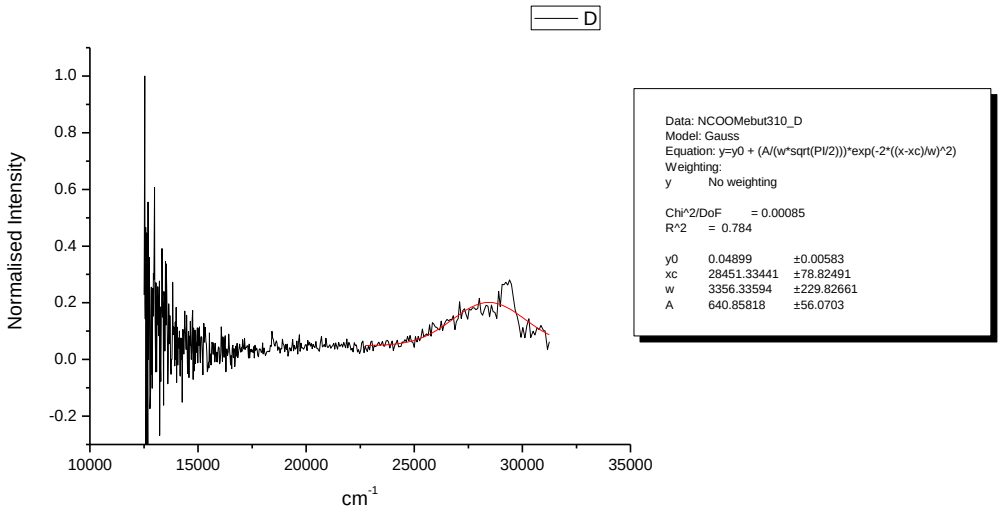

Figure 2.3.103. Gaussian model fit of the normalised fluorescence emission spectrum of **13** recorded in 1-butanol at 310 nm excitation.

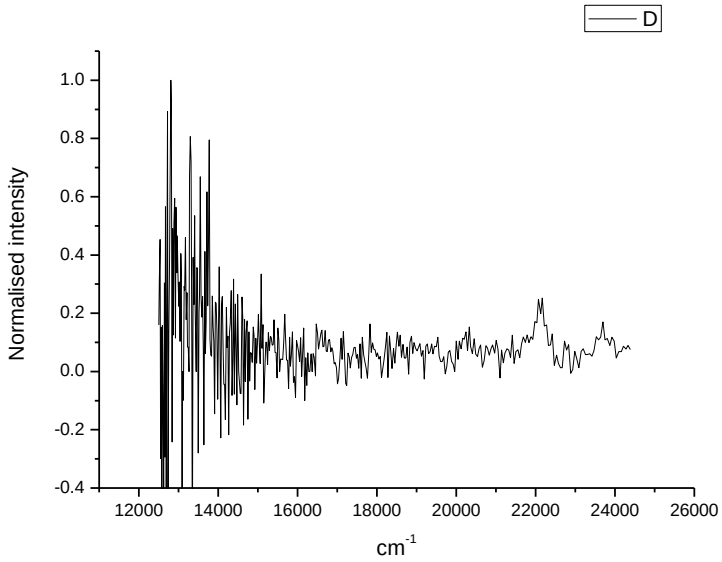

Figure 2.3.104. Attempted gaussian model fit of the normalised fluorescence emission spectrum of **13** recorded in 1-butanol at 400 nm excitation.

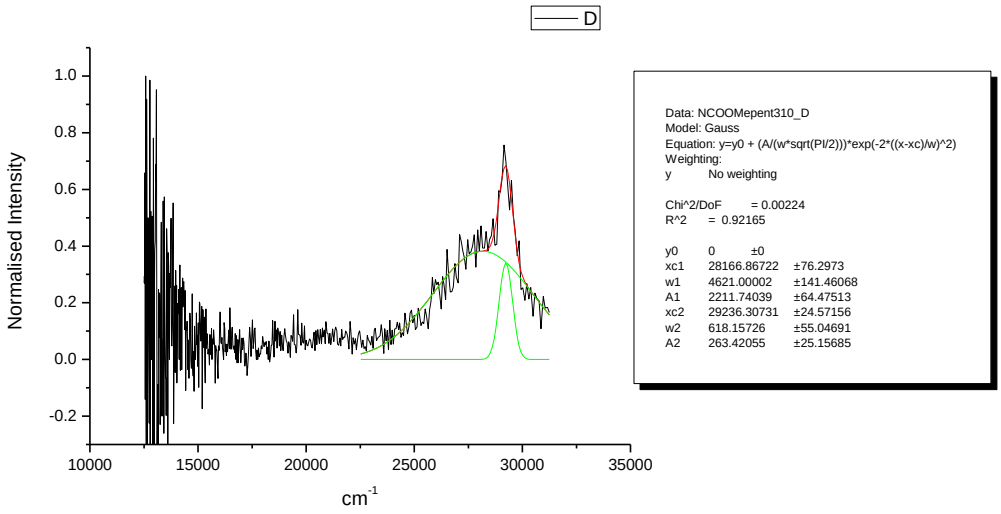

Figure 2.3.105. Gaussian model fit of the normalised fluorescence emission spectrum of **13** recorded in 1-pentanol at 310 nm excitation.

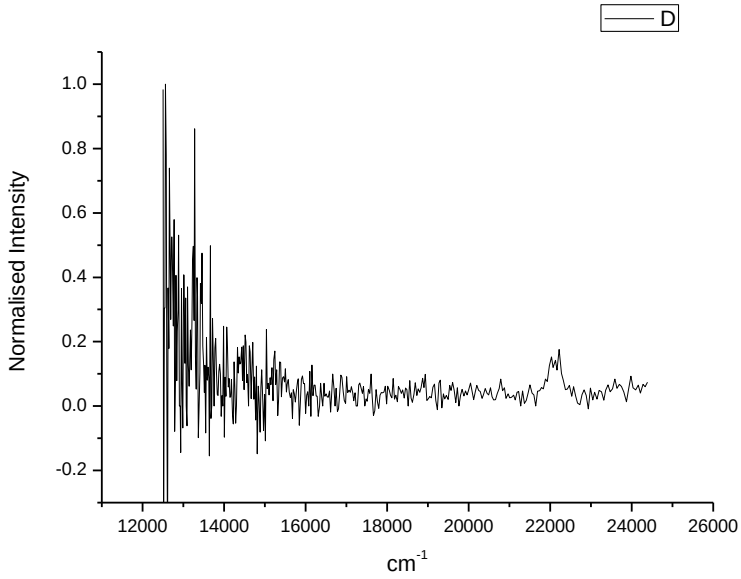

Figure 2.3.106. Attempted gaussian model fit of the normalised fluorescence emission spectrum of **13** recorded in 1-pentanol at 400 nm excitation.

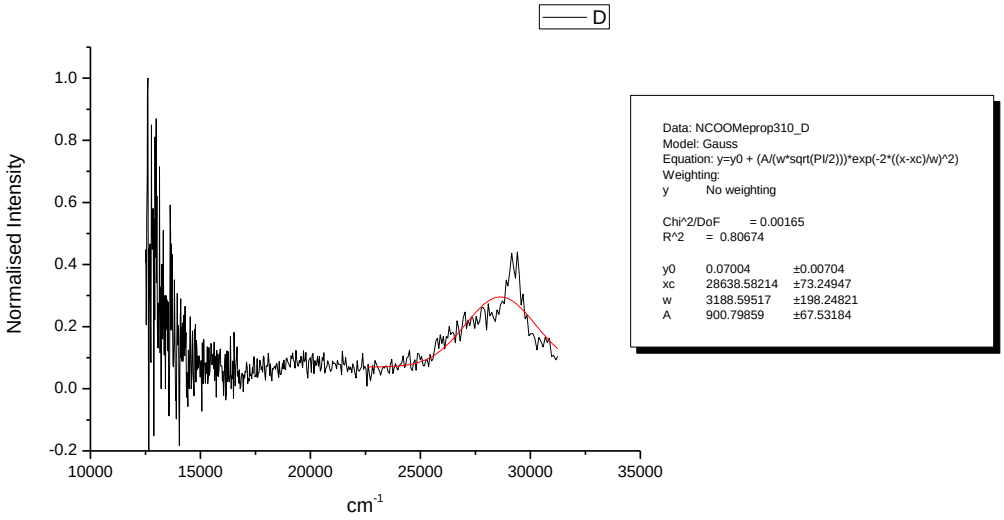

Figure 2.3.107. Gaussian model fit of the normalised fluorescence emission spectrum of **13** recorded in 1-propanol at 310 nm excitation.

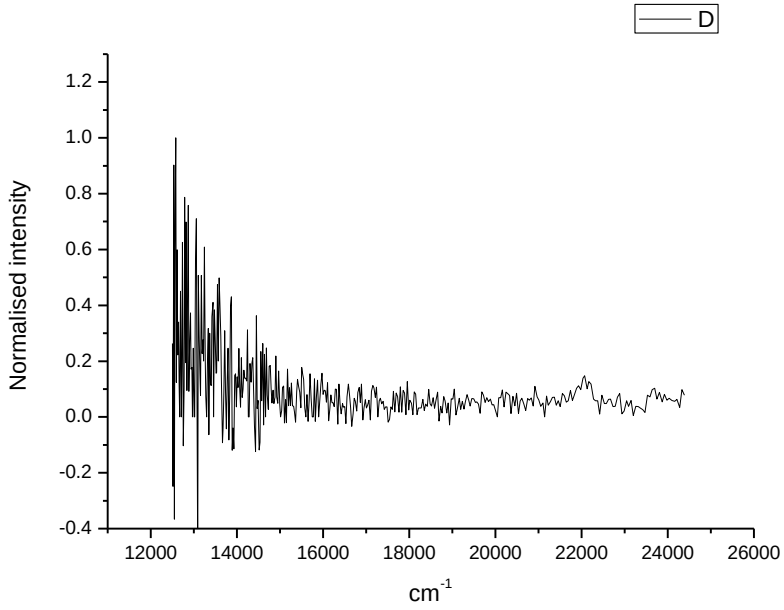

Figure 2.3.108. Attempted gaussian model fit of the normalised fluorescence emission spectrum of **13** recorded in 1-propanol at 400 nm excitation.

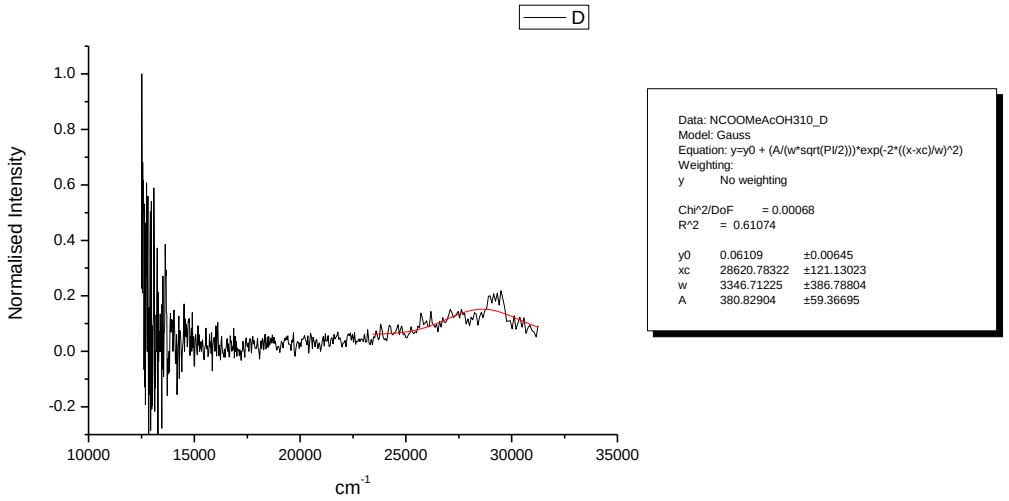

Figure 2.3.109. Gaussian model fit of the normalised fluorescence emission spectrum of **13** recorded in Acetic Acid at 310 nm excitation.

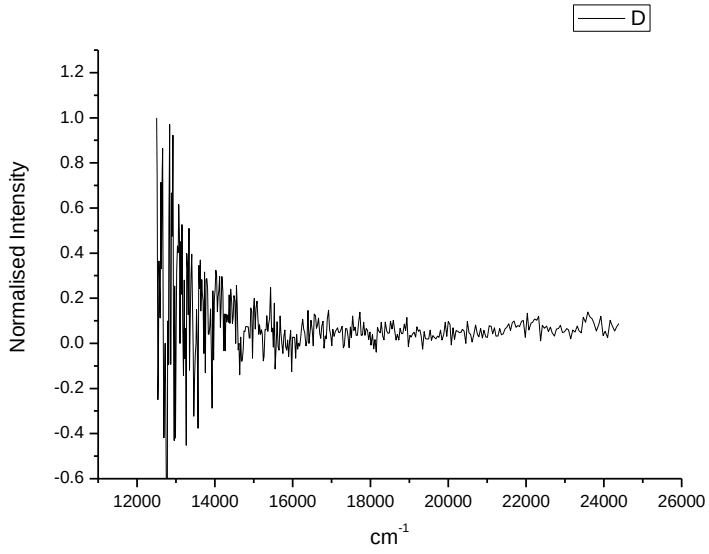

Figure 2.3.110. Attempted Gaussian model fit of the normalised fluorescence emission spectrum of **13** recorded in Acetic Acid at 400 nm excitation.

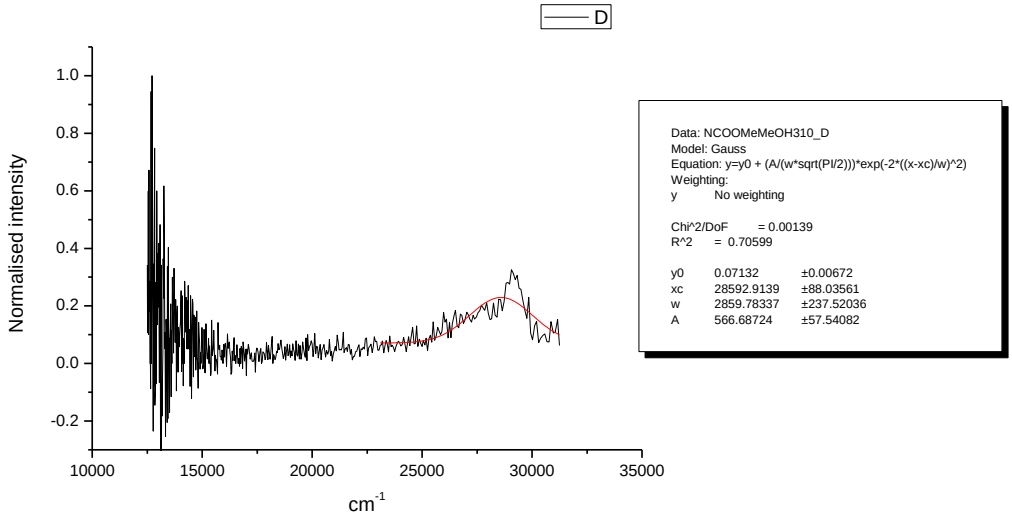

Figure 2.3.111. Gaussian model fit of the normalised fluorescence emission spectrum of **13** recorded in Methanol at 310 nm excitation.

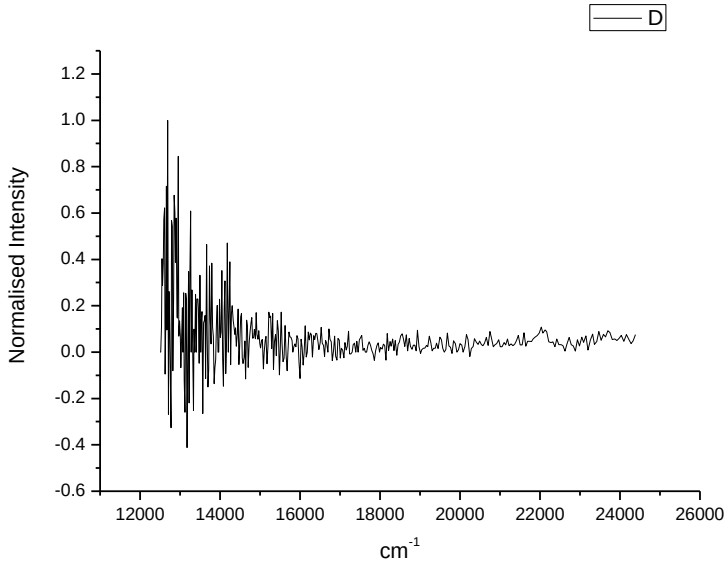

Figure 2.3.112. Attempted gaussian model fit of the normalised fluorescence emission spectrum of **13** recorded in Methanol at 400 nm excitation.

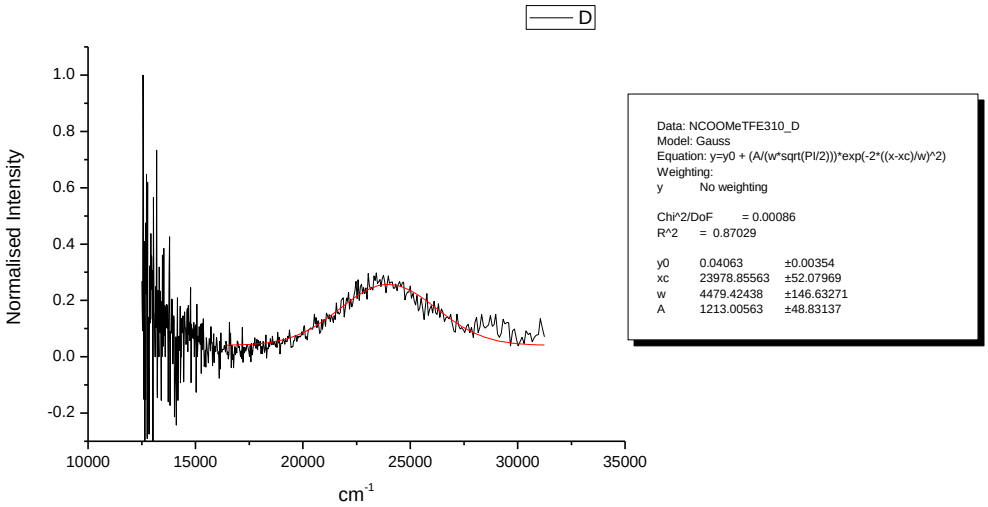

Figure 2.3.113. Gaussian model fit of the normalised fluorescence emission spectrum of **13** recorded in 2,2,2-trifluoroethanol at 310 nm excitation.

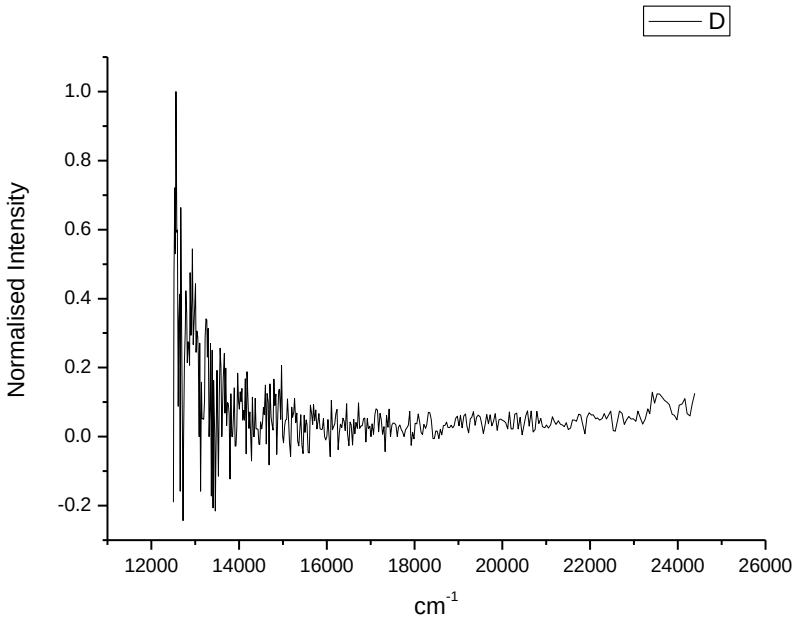

Figure 2.3.114. Gaussian model fit of the normalised fluorescence emission spectrum of **13** recorded in 2,2,2-trifluoroethanol at 400 nm excitation.

2.3.8 Fluorescence Excitation spectra.

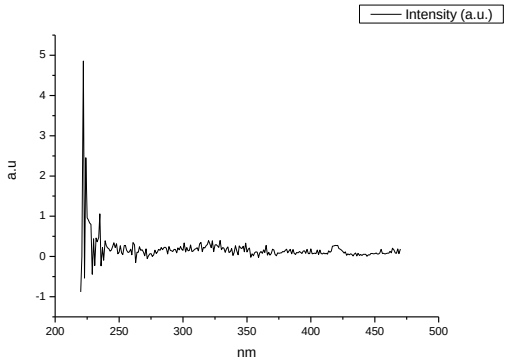

Figure 2.3.115. Fluorescence excitation spectrum of **13** recorded in Toluene with emission fixed at 480 nm.

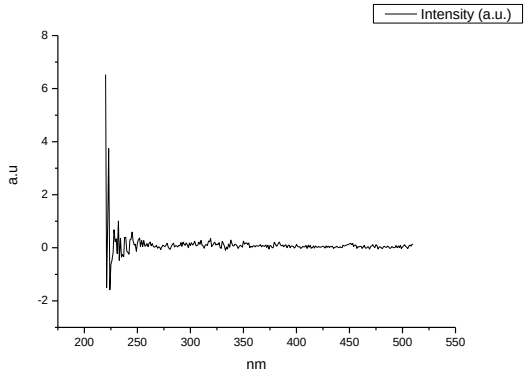

Figure 2.3.116. Fluorescence excitation spectrum of **13** recorded in Toluene with emission fixed at 520 nm.

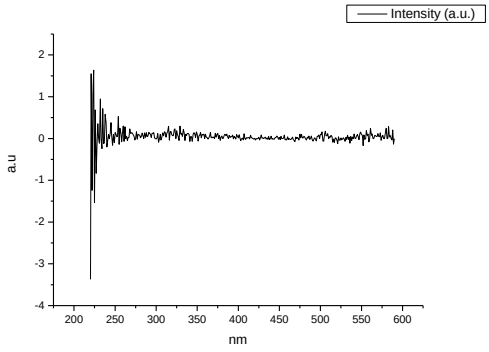

Figure 2.3.117. Fluorescence excitation spectrum of **13** recorded in Toluene with emission fixed at 600 nm.

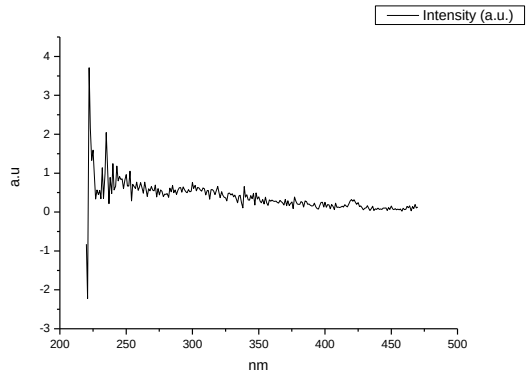

Figure 2.3.118. Fluorescence excitation spectrum of **13** recorded in 1,4-dioxane with emission fixed at 480 nm.

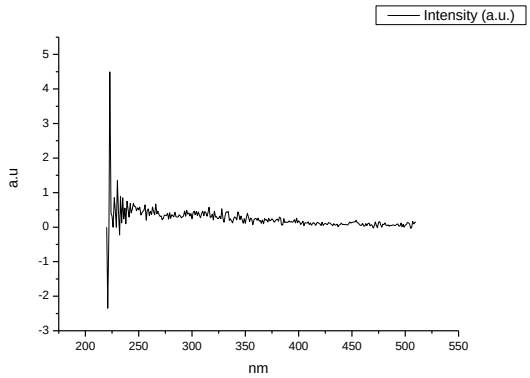

Figure 2.3.119. Fluorescence excitation spectrum of **13** recorded in 1,4-dioxane with emission fixed at 520 nm.

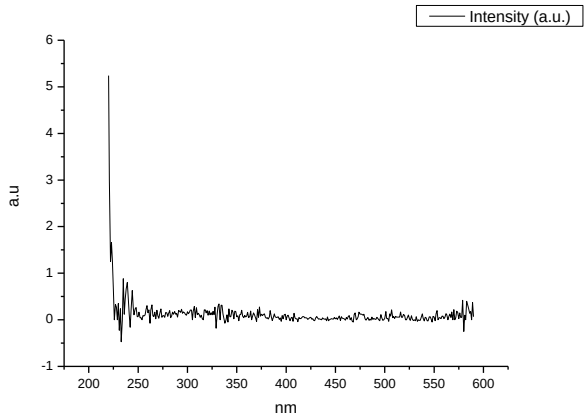

Figure 2.3.120. Fluorescence excitation spectrum of **13** recorded in 1,4-dioxane with emission fixed at 600 nm.

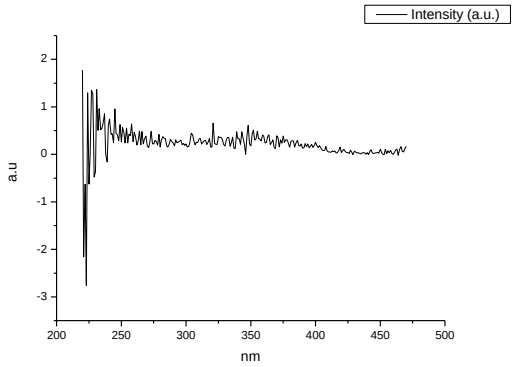

Figure 2.3.121. Fluorescence excitation spectrum of **13** recorded in Chloroform with emission fixed at 480 nm.

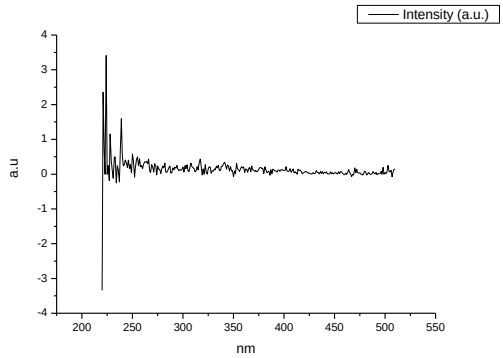

Figure 2.3.122. Fluorescence excitation spectrum of **13** recorded in Chloroform with emission fixed at 520 nm.

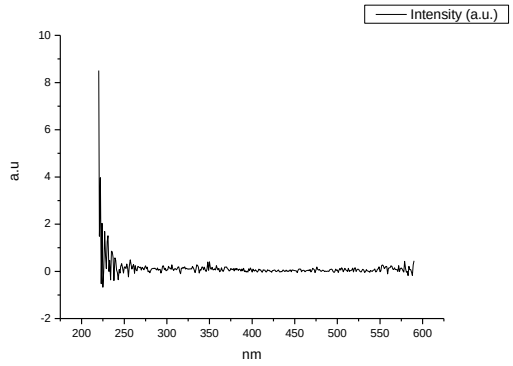

Figure 2.3.123. Fluorescence excitation spectrum of **13** recorded in Chloroform with emission fixed at 600 nm.

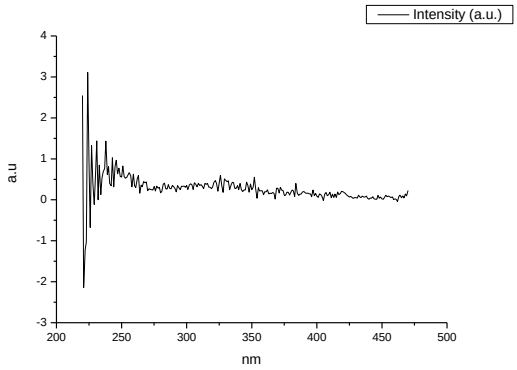

Figure 2.3.124. Fluorescence excitation spectrum of **13** recorded in Acetonitrile with emission fixed at 480 nm.

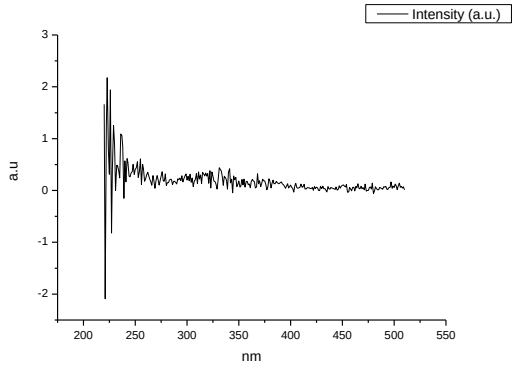

Figure 2.3.125. Fluorescence excitation spectrum of **13** recorded in Acetonitrile with emission fixed at 520 nm.

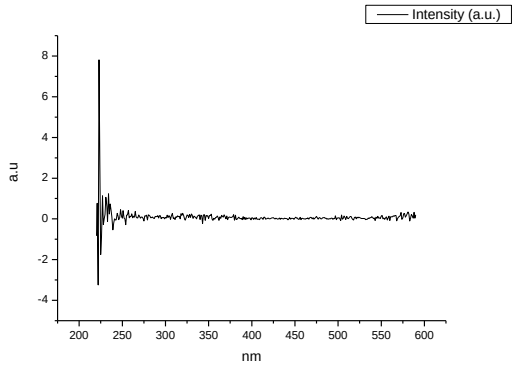

Figure 2.3.126. Fluorescence excitation spectrum of **13** recorded in Acetonitrile with emission fixed at 600 nm.

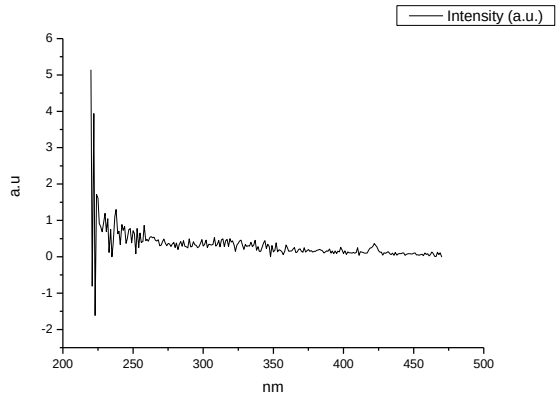

Figure 2.3.127. Fluorescence excitation spectrum of **13** recorded in 1-octanol with emission fixed at 480 nm.

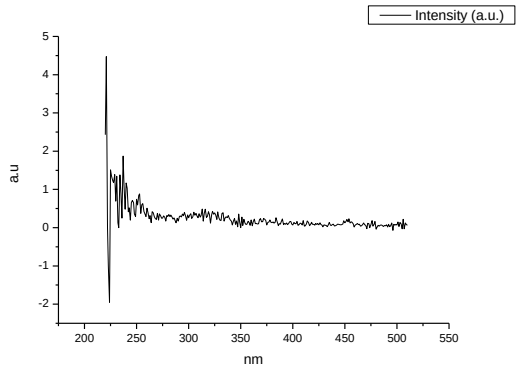

Figure 2.3.128. Fluorescence excitation spectrum of **13** recorded in 1-octanol with emission fixed at 520 nm.

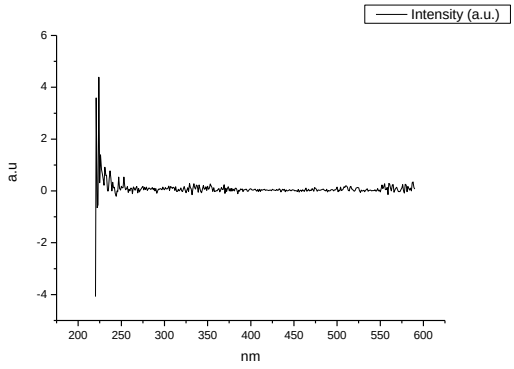

Figure 2.3.129. Fluorescence excitation spectrum of **13** recorded in 1-octanol with emission fixed at 600 nm.

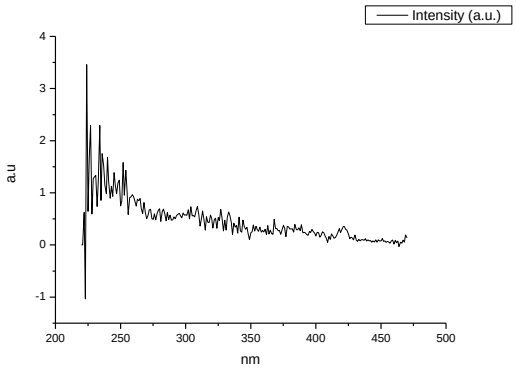

Figure 2.3.130. Fluorescence excitation spectrum of **13** recorded in 1-hexanol with emission fixed at 480 nm.

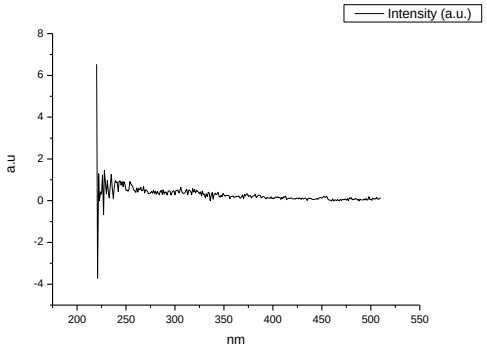

Figure 2.3.131. Fluorescence excitation spectrum of **13** recorded in 1-hexanol with emission fixed at 520 nm.

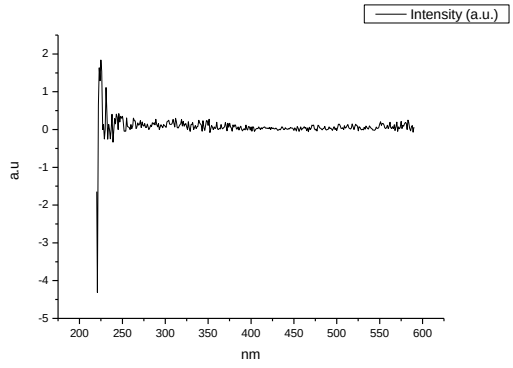

Figure 2.3.132. Fluorescence excitation spectrum of **13** recorded in 1-hexanol with emission fixed at 600 nm.

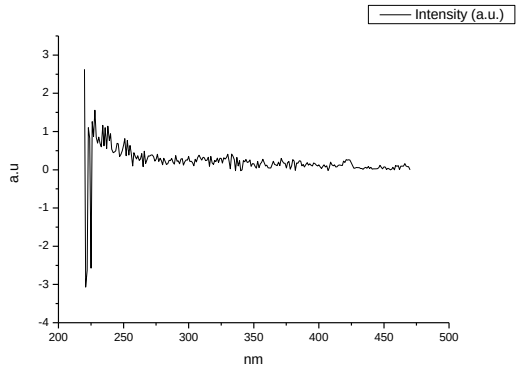

Figure 2.3.133. Fluorescence excitation spectrum of **13** recorded in 1-butanol with emission fixed at 480 nm.

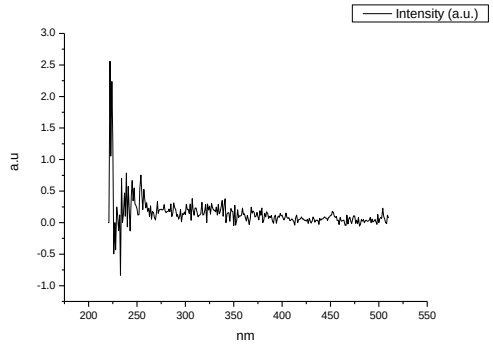

Figure 2.3.134. Fluorescence excitation spectrum of **13** recorded in 1-butanol with emission fixed at 520 nm.

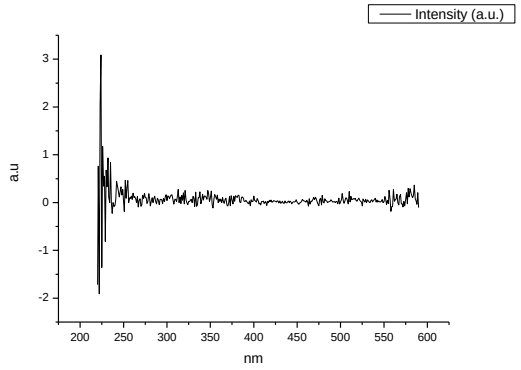

Figure 2.3.135. Fluorescence excitation spectrum of **13** recorded in 1-butanol with emission fixed at 600 nm.

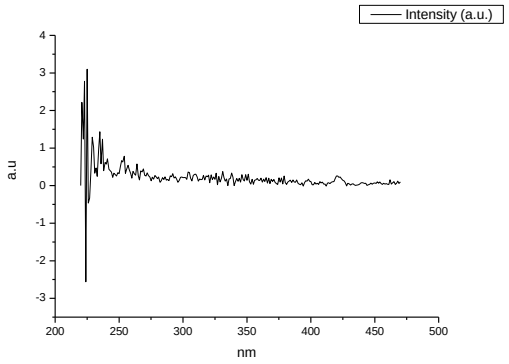

Figure 2.3.136. Fluorescence excitation spectrum of **13** recorded in 1-pentanol with emission fixed at 480 nm.

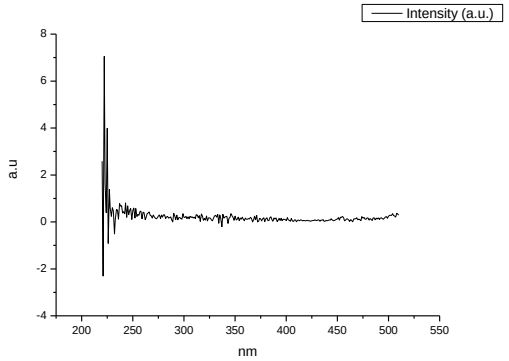

Figure 2.3.137. Fluorescence excitation spectrum of **13** recorded in 1-pentanol with emission fixed at 520 nm.

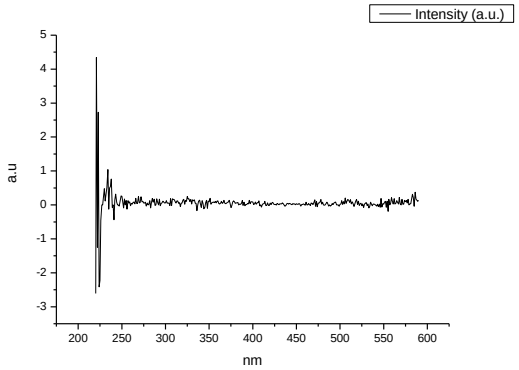

Figure 2.3.138. Fluorescence excitation spectrum of **13** recorded in 1-pentanol with emission fixed at 600 nm.

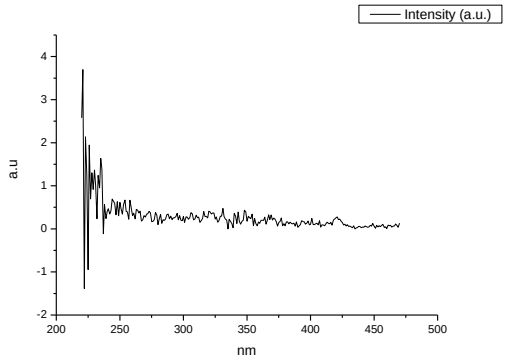

Figure 2.3.139. Fluorescence excitation spectrum of **13** recorded in 1-propanol with emission fixed at 480 nm.

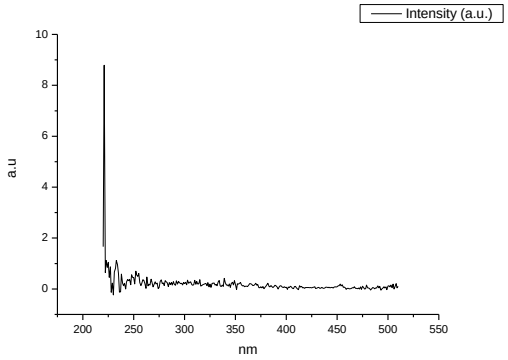

Figure 2.3.140. Fluorescence excitation spectrum of **13** recorded in 1-propanol with emission fixed at 520 nm.

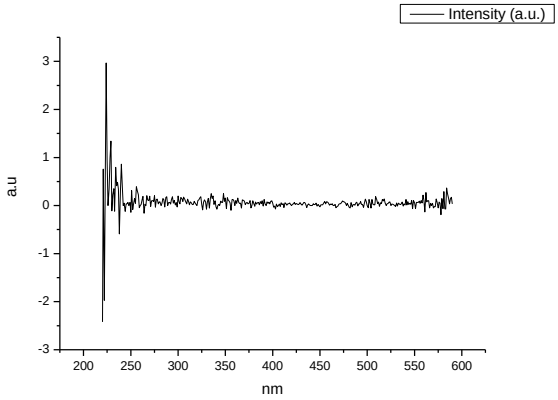

Figure 2.3.141. Fluorescence excitation spectrum of **13** recorded in 1-propanol with emission fixed at 600 nm.

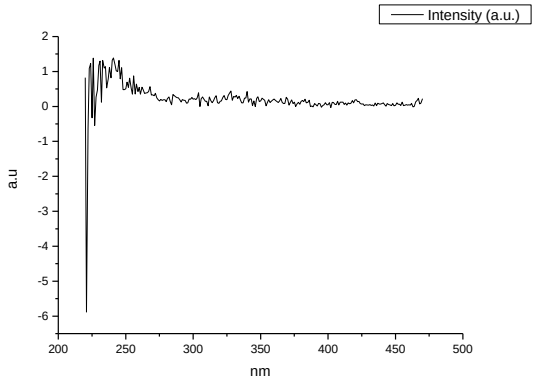

Figure 2.3.142. Fluorescence excitation spectrum of **13** recorded in Acetic Acid with emission fixed at 480 nm.

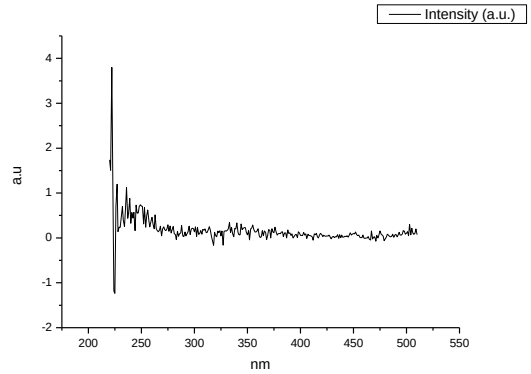

Figure 2.3.143. Fluorescence excitation spectrum of **13** recorded in Acetic Acid with emission fixed at 520 nm.

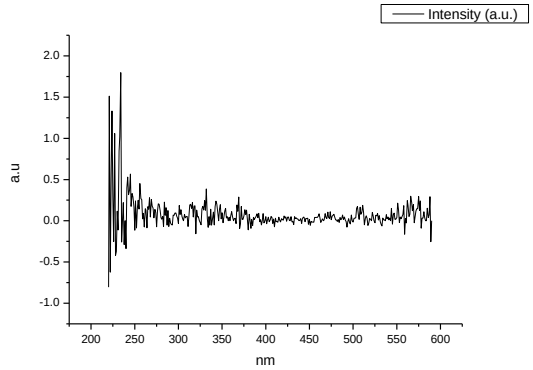

Figure 2.3.144. Fluorescence excitation spectrum of **13** recorded in Acetic Acid with emission fixed at 600 nm.

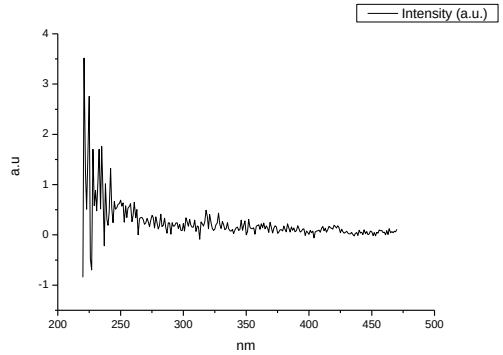

Figure 2.3.145. Fluorescence excitation spectrum of **13** recorded in Methanol with emission fixed at 480 nm.

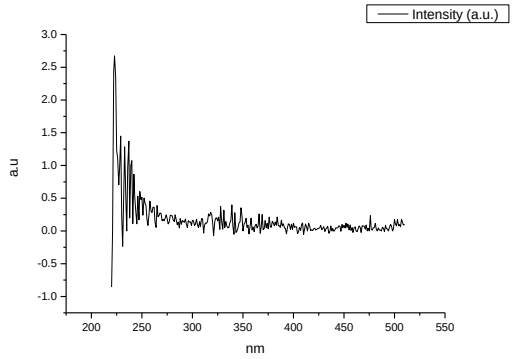

Figure 2.3.146. Fluorescence excitation spectrum of **13** recorded in Methanol with emission fixed at 520 nm.

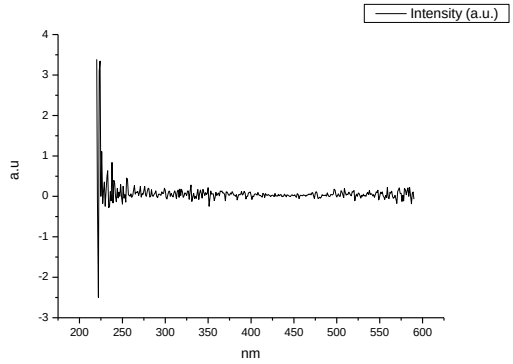

Figure 2.3.147. Fluorescence excitation spectrum of **13** recorded in Methanol with emission fixed at 600 nm.

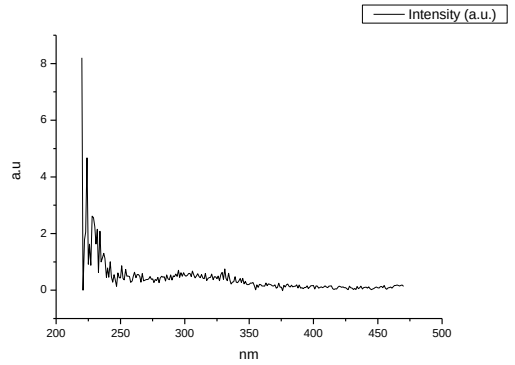

Figure 2.3.148. Fluorescence excitation spectrum of **13** recorded in 2,2,2-trifluoroethanol with emission fixed at 480 nm.

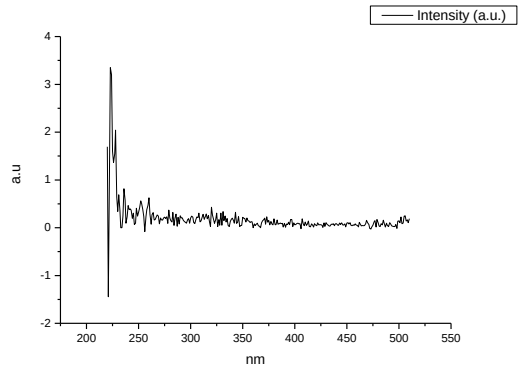

Figure 2.3.149. Fluorescence excitation spectrum of **13** recorded in 2,2,2-trifluoroethanol with emission fixed at 520 nm.

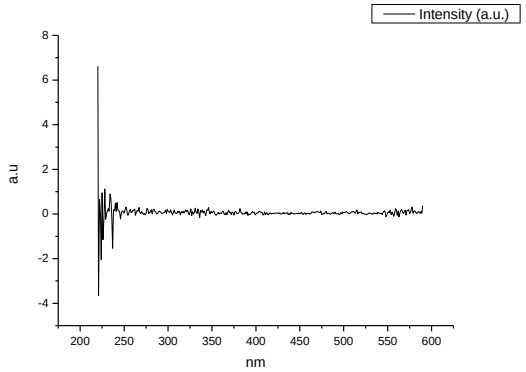

Figure 2.3.150. Fluorescence excitation spectrum of **13** recorded in 2,2,2-trifluoroethanol with emission fixed at 600 nm.

2.4 COMPOUND 15

2.4.1 Quantum Yield Summary.

Solvent	abs (310 nm)	$\lambda_{ems\ (max)}$	$\Phi_{310\ nm}$	abs (400 nm)	$\lambda_{ems\ (max)}$	$\Phi_{400\ nm}$
Toluene	0.12	511.94	0.34	0.07	508.05	0.30
1,4-Dioxane	0.08	511.94	0.60	0.02	508.95	0.64
Chloroform	0.07	518.95	0.63	0.02	511.04	0.64
Acetonitrile	0.06	512.98	0.51	0.02	508.95	0.49
1-Octanol	0.04	512.98	0.59	0.01	511.94	0.57
1-Hexanol	0.02	511.94	0.53	0.01	508.05	0.54
1-Butanol	0.07	515.97	0.50	0.02	507.01	0.46
1-Pentanol	0.05	512.98	0.49	0.01	508.05	0.45
1-Propanol	0.08	515.97	0.44	0.02	508.05	0.41
Acetic acid	0.06	504.02	0.01	0.02	502.98	0.01
Methanol	0.08	518.95	0.34	0.02	501.94	0.29
2,2,2-Trifluoroethanol	0.04	548.97	0.02	0.01	513.98	0.01

Table 2.4.1. Summary of ultraviolet-visible absorbance values at 310 nm and 400 nm, emission maxima and quantum yield (Φ) of **15** at 310 nm and 400 nm excitation.

2.4.2 310 nm excitation Gaussian band fit summaries.

Solvent	λ max$_{em}$ Band 1 (cm^{-1})	λ max$_{em}$ Band 1 (nm)	λ max$_{em}$ Band 2 (cm^{-1})	λ max$_{em}$ Band 2 (nm)	λ max$_{em}$ Band 3 (cm^{-1})	λ max$_{em}$ Band 3 (nm)
Toluene	18789.67	532.21	19826.90	504.37	21224.92	471.14
1,4-Dioxane	18702.66	534.68	19824.09	504.44	21262.29	470.32
Chloroform	18554.75	538.95	19645.82	509.01	21081.40	474.35
Acetonitrile	18314.86	546.00	19660.98	508.62	21117.48	473.54
1-Octanol	18526.82	539.76	19777.96	505.61	21248.19	470.63
1-Hexanol	18497.76	540.61	19743.06	506.51	21222.58	471.20
1-Butanol	18438.10	542.36	19736.34	506.68	21193.25	471.85
1-Pentanol	18463.80	541.60	19731.54	506.80	21201.83	471.66
1-Propanol	18423.89	542.77	19733.32	506.76	21184.89	472.03
Acetic acid	18423.49	542.79	20226.02	494.41	-	-
Methanol	18232.66	548.47	19605.44	510.06	21122.81	473.42
2,2,2-Trifluoroethanol	18240.38	548.23	18659.32	535.93	-	-

Solvent	λ max$_{em}$ Band 4 (cm^{-1})	λ max$_{em}$ Band 4 (nm)	λ max$_{em}$ Band 5 (cm^{-1})	λ max$_{em}$ Band 5 (nm)
Toluene	28556.87	350.18	-	-
1,4-Dioxane	28413.61	351.94	-	-
Chloroform	28192.71	354.70	-	-
Acetonitrile	28496.09	350.93	-	-
1-Octanol	28676.87	348.71	-	-
1-Hexanol	28450.12	351.49	-	-
1-Butanol	28386.63	352.28	-	-
1-Pentanol	28405.86	352.04	-	-
1-Propanol	28393.57	352.19	-	-
Acetic acid	27285.17	366.50	29096.97	343.68
Methanol	28368.55	352.50	-	-
2,2,2-Trifluoroethanol	27298.52	366.32	-	-

Table 2.4.1. Summary of band maxima of 5 band fit using Gaussian model for normalised **15** emission spectra recorded at 310 nm excitation.

(a)

Solvent	Width Band 1 (cm^{-1})	Width Band 2 (cm^{-1})	Width Band 3 (cm^{-1})	Width Band 4 (cm^{-1})	Width Band 5 (cm^{-1})
Toluene	3090.41	1726.50	963.88	3441.45	-
1,4-Dioxane	3144.56	1908.18	975.30	3491.91	-
Chloroform	3160.48	1922.96	1006.27	3363.18	-
Acetonitrile	3235.53	2289.35	1136.82	3407.22	-
1-Octanol	3179.39	2092.97	1003.75	3628.90	-
1-Hexanol	3215.50	2132.32	1015.54	4109.25	-
1-Butanol	3188.95	2151.39	1028.19	3385.13	-
1-Pentanol	3206.93	2135.74	1016.43	3454.40	-
1-Propanol	3189.21	2159.92	1043.69	3375.56	-
Acetic acid	3816.06	2517.98	-	3269.97	2223.42
Methanol	3261.13	2315.35	1089.26	3391.95	-
2,2,2-Trifluoroethanol	3634.56	1726.58	-	5365.92	-

(b)

Solvent	Area Band 1 (cm^{-1})	Area Band 2 (cm^{-1})	Area Band 3 (cm^{-1})	Area Band 4 (cm^{-1})	Area Band 5 (cm^{-1})
Toluene	2163.74	1101.47	343.27	56.81	-
1,4-Dioxane	2101.36	1306.12	300.17	52.16	-
Chloroform	2086.30	1315.23	323.57	43.81	-
Acetonitrile	1914.68	1815.62	300.78	51.80	-
1-Octanol	2003.49	1545.69	303.07	78.88	-
1-Hexanol	1996.48	1572.96	295.70	190.32	-
1-Butanol	1946.83	1643.40	300.69	58.01	-
1-Pentanol	1954.81	1607.71	300.29	63.29	-
1-Propanol	1953.20	1659.48	303.58	58.58	-
Acetic acid	2726.54	1815.87	-	1431.93	1034.09
Methanol	1931.12	1835.17	286.48	72.87	-
2,2,2-Trifluoroethanol	3359.44	502.99	-	1106.01	-

Tables 2.4.2 (a) and (b). Summary band width and band area of 5 band fit using Gaussian model for normalised **15** emission spectra recorded at 310 nm excitation.

Solvent	Band 1 Area Percentage (%)	Band 2 Area Percentage (%)	Band 3 Area Percentage (%)	Band 4 Area Percentage (%)	Band 5 Area Percentage (%)
Toluene	59.03	30.05	9.37	1.55	-
1,4-Dioxane	55.89	34.74	7.98	1.39	-
Chloroform	55.36	34.90	8.59	1.16	-
Acetonitrile	46.90	44.47	7.37	1.27	-
1-Octanol	50.96	39.32	7.71	2.01	-
1-Hexanol	49.23	38.79	7.29	4.69	-
1-Butanol	49.30	41.62	7.61	1.47	-
1-Pentanol	49.79	40.95	7.65	1.61	-
1-Propanol	49.14	41.75	7.64	1.47	-
Acetic acid	38.90	25.91	-	20.43	14.75
Methanol	46.81	44.48	6.94	1.77	-
2,2,2-Trifluoroethanol	67.62	10.12	-	22.26	-

Table 2.4.3. Total Area Percentages of 5 band fit using Gaussian model for normalised **15** emission spectra recorded at 310 nm excitation.

Solvent	Area Ratio Band 1/2 (310 nm ex)	Area Ratio Band 1/3 (310 nm ex)	Area Ratio Band 1/4 (310 nm ex)	Area Ratio Band 1/5 (310 nm ex)
Toluene	1.96	6.30	38.09	-
1,4-Dioxane	1.61	7.00	40.29	-
Chloroform	1.59	6.45	47.62	-
Acetonitrile	1.05	6.37	36.97	-
1-Octanol	1.30	6.61	25.40	-
1-Hexanol	1.27	6.75	10.49	-
1-Butanol	1.18	6.47	33.56	-
1-Pentanol	1.22	6.51	30.89	-
1-Propanol	1.18	6.43	33.34	-
Acetic acid	1.50	-	1.90	2.64
Methanol	1.05	6.74	26.50	-
2,2,2-Trifluoroethanol	6.68	-	3.04	-

Solvent	Area Ratio Band 2/3 (310 nm ex)	Area Ratio Band 2/4 (310 nm ex)	Area Ratio Band 2/5 (310 nm ex)	Area Ratio Band 3/4 (310 nm ex)	Area Ratio Band 3/5 (310 nm ex)	Area Ratio Band 4/5 (310 nm ex)
Toluene	3.21	19.39	-	6.04	-	-
1,4-Dioxane	4.35	25.04	-	5.75	-	-
Chloroform	4.06	30.02	-	7.39	-	-
Acetonitrile	6.04	35.05	-	5.81	-	-
1-Octanol	5.10	19.59	-	3.84	-	-
1-Hexanol	5.32	8.27	-	1.55	-	-
1-Butanol	5.47	28.33	-	5.18	-	-
1-Pentanol	5.35	25.40	-	4.74	-	-
1-Propanol	5.47	28.33	-	5.18	-	-
Acetic acid	-	1.27	1.76	-	-	1.38
Methanol	6.41	25.18	-	3.93	-	-
2,2,2-Trifluoroethanol	-	0.45	-	-	-	-

Table 2.4.4. Area Ratios of 5 band fit using Gaussian model for normalised **15** emission spectra recorded at 310 nm excitation.

2.4.3 400 nm excitation Gaussian band fit summaries.

Solvent	λ max$_{em}$ Band 1 (cm^{-1})	λ max$_{em}$ Band 1 (nm)	λ max$_{em}$ Band 2 (cm^{-1})	λ max$_{em}$ Band 2 (nm)	λmax$_{em}$ Band 3 (cm^{-1})	λmax$_{em}$ Band 3 (nm)
Toluene	18800.74	531.89	19919.29	502.03	21213.49	471.40
1,4-Dioxane	18689.22	535.07	19939.94	501.51	21237.23	470.87
Chloroform	18648.14	536.25	19782.47	505.50	21045.61	475.16
Acetonitrile	18451.77	541.95	19794.12	505.20	21059.20	474.85
1-Octanol	18595.40	537.77	19910.09	502.26	21202.37	471.65
1-Hexanol	18561.83	538.74	19877.27	503.09	21164.58	472.49
1-Butanol	18574.65	538.37	19900.49	502.50	21137.87	473.08
1-Pentanol	18579.73	538.22	19901.17	502.48	21160.41	472.58
1-Propanol	18569.12	538.53	19900.22	502.51	21134.07	473.17
Acetic acid	18237.56	548.32	19855.26	503.64	21112.19	473.66
Methanol	18505.27	540.39	19850.28	503.77	21062.44	474.78
2,2,2-Trifluoroethanol	17788.17	562.17	19780.44	505.55	-	-

Table 2.4.5. Summary of band maxima of 3 band fit using Gaussian model for normalised **15** emission spectra recorded at 400 nm excitation.

Solvent	Width Band 1 (cm^{-1})	Width Band 2 (cm^{-1})	Width Band 3 (cm^{-1})
Toluene	3086.27	1849.59	984.14
1,4-Dioxane	3092.96	2009.51	995.63
Chloroform	3183.50	2028.38	1031.68
Acetonitrile	3172.31	2173.08	1242.09
1-Octanol	3120.89	2074.38	1067.35
1-Hexanol	3164.13	2103.00	1123.72
1-Butanol	3100.99	2076.27	1112.85
1-Pentanol	3132.10	2083.16	1096.89
1-Propanol	3103.04	2083.65	1126.22
Acetic acid	3781.19	2459.42	1322.01
Methanol	3140.88	2112.02	1218.49
2,2,2-Trifluoroethanol	3747.17	2720.34	-

Table 2.4.6. Summary of band width of 3 band fit using Gaussian model for normalised **15** emission spectra recorded at 400 nm excitation.

Solvent	Area Band 1 (cm^{-1})	Area Band 2 (cm^{-1})	Area Band 3 (cm^{-1})	Area Ratio Band 1/2 (400 nm ex)	Area Ratio Band 1/3 (400 nm ex)	Area Ratio Band 2/3 (400 nm ex)
Toluene	1893.06	1361.28	418.24	1.39	4.53	3.25
1,4-Dioxane	1796.76	1583.56	364.26	1.13	4.93	4.35
Chloroform	1865.73	1539.90	391.09	1.21	4.77	3.94
Acetonitrile	1632.21	1807.81	479.18	0.90	3.41	3.77
1-Octanol	1722.57	1706.49	422.25	1.01	4.08	4.04
1-Hexanol	1644.28	1751.56	454.43	0.94	3.62	3.85
1-Butanol	1637.99	1740.15	470.43	0.94	3.48	3.70
1-Pentanol	1669.83	1735.68	447.62	0.96	3.73	3.88
1-Propanol	1618.48	1750.71	473.20	0.92	3.42	3.70
Acetic acid	1561.17	2069.70	412.73	0.75	3.78	5.01
Methanol	1555.80	1758.23	525.20	0.88	2.96	3.35
2,2,2-Trifluoroethanol	1002.13	1728.63	-	0.58	-	-

Solvent	Band 1 Area Percentage (%)	Band 2 Area Percentage (%)	Band 3 Area Percentage (%)
Toluene	51.55	37.07	11.39
1,4-Dioxane	47.98	42.29	9.73
Chloroform	49.14	40.56	10.30
Acetonitrile	41.65	46.13	12.23
1-Octanol	44.73	44.31	10.96
1-Hexanol	42.71	45.49	11.80
1-Butanol	42.56	45.22	12.22
1-Pentanol	43.34	45.05	11.62
1-Propanol	42.12	45.56	12.32
Acetic acid	38.61	51.18	10.21
Methanol	40.52	45.80	13.68
2,2,2-Trifluoroethanol	36.70	63.30	-

Table 2.4.7. Band area, area ratios and total area percentage of 3 band fit using Gaussian model for normalised **15** emission spectra recorded at 400 nm excitation.

2.4.4 310 nm Gaussian band fit - Solvatochromic analysis.

2.4.4.1 E_T^N.

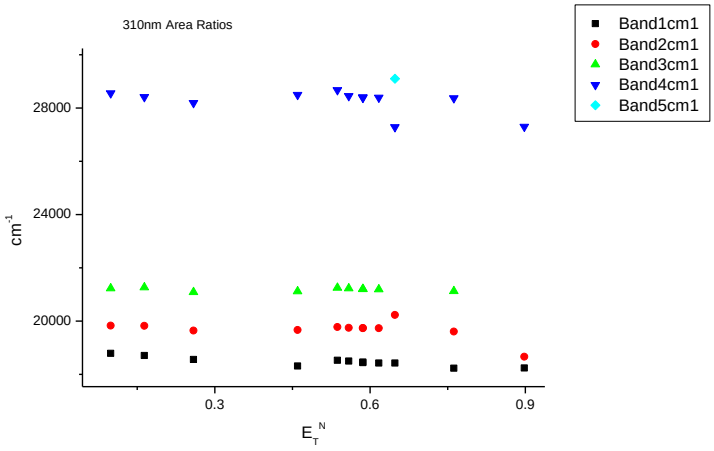

Figure 2.4.1. Band maxima from Gaussian model fit of the normalised fluorescence emission spectra of **15** recorded at 310 nm excitation against E_T^N.

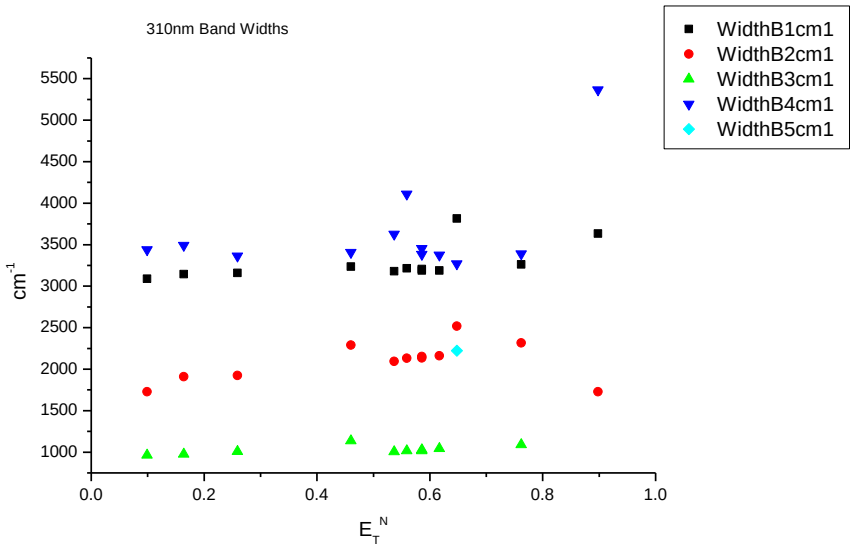

Figure 2.4.2. Band widths from Gaussian model fit of the normalised fluorescence emission spectra of **15** recorded at 310 nm excitation against E_T^N.

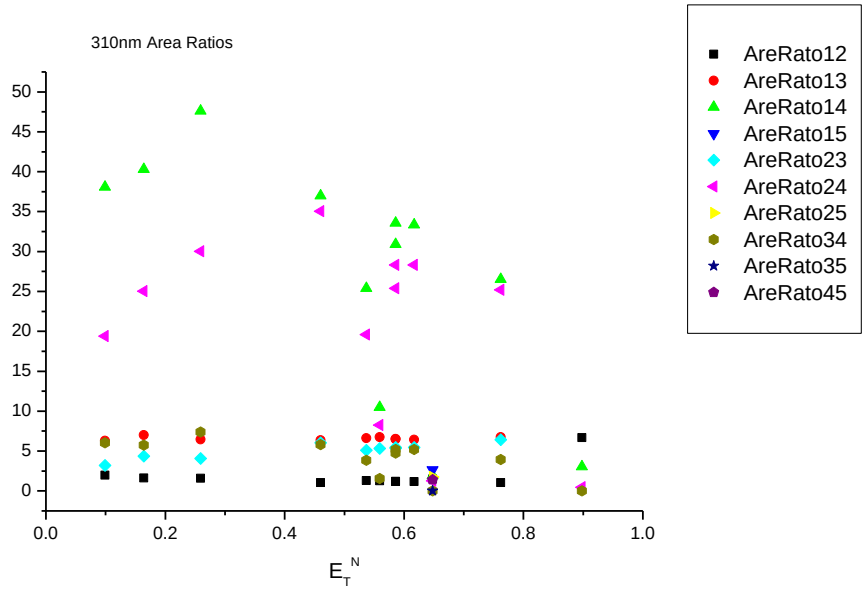

Figure 2.4.3. Area ratios from Gaussian model fit of the normalised fluorescence emission spectra of **15** recorded at 310 nm excitation against E_T^N.

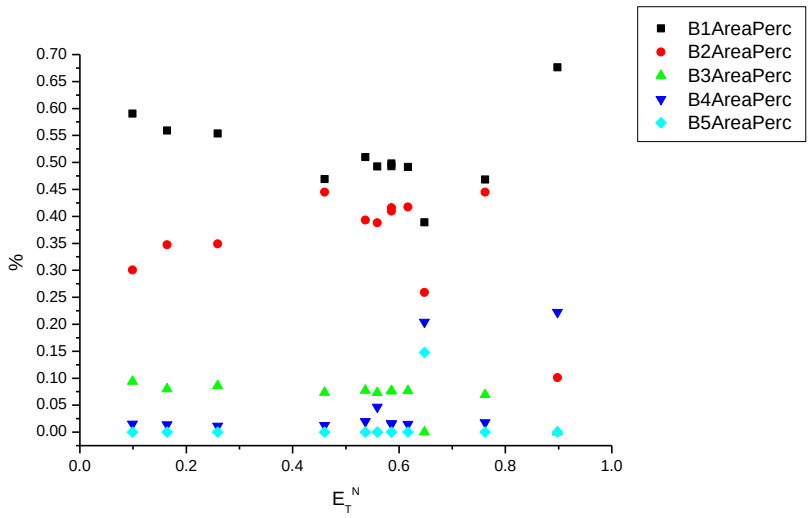

Figure 2.4.4. Area percentages from Gaussian model fit of the normalised fluorescence emission spectra of **15** recorded at 310 nm excitation against E_T^N.

2.4.4.2 α.

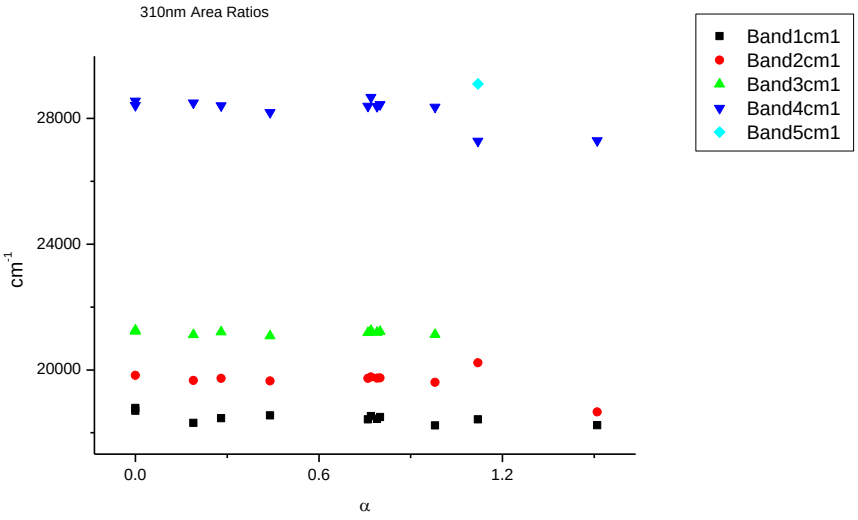

Figure 2.4.5. Band maxima from Gaussian model fit of the normalised fluorescence emission spectra of **15** recorded at 310 nm excitation against α.

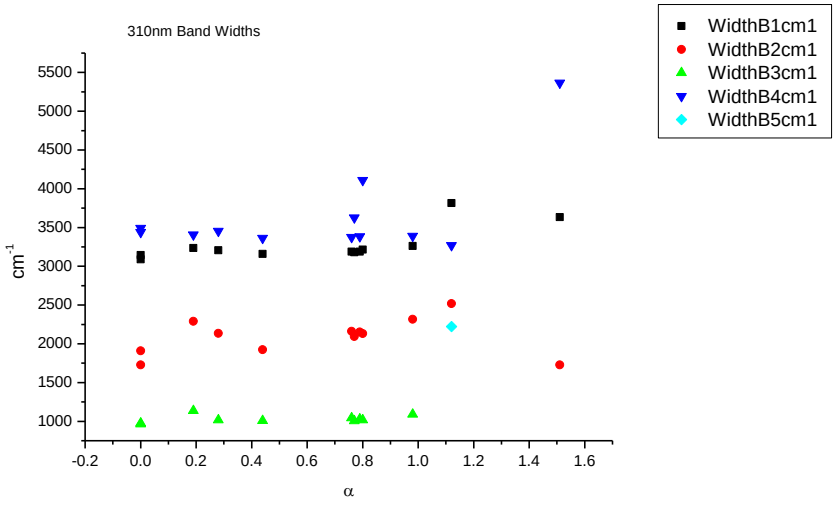

Figure 2.4.6. Band widths from Gaussian model fit of the normalised fluorescence emission spectra of **15** recorded at 310 nm excitation against α.

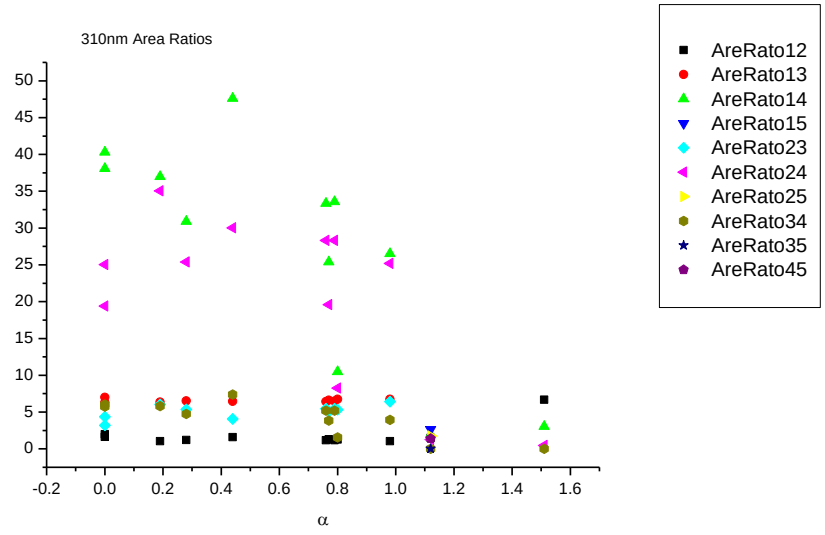

Figure 2.4.7. Area Ratios from Gaussian model fit of the normalised fluorescence emission spectra of **15** recorded at 310 nm excitation against α.

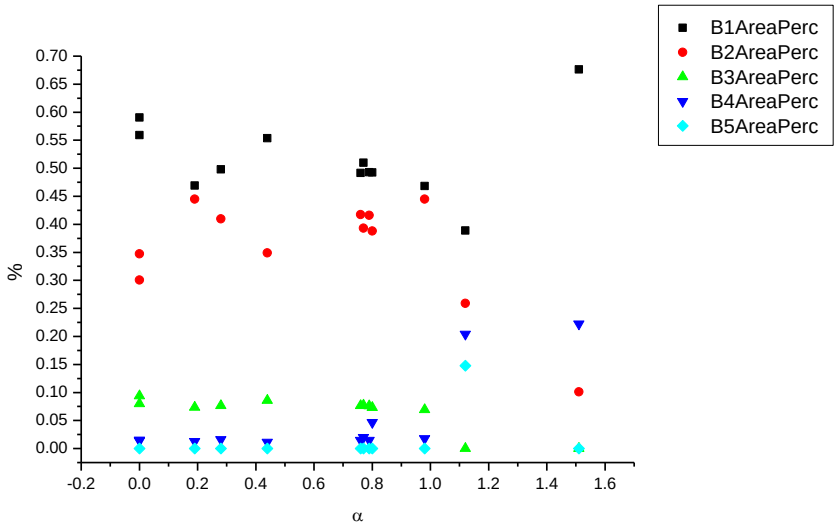

Figure 2.4.8. Area percentages from Gaussian model fit of the normalised fluorescence emission spectra of **15** recorded at 310 nm excitation against α.

2.4.4.3 β.

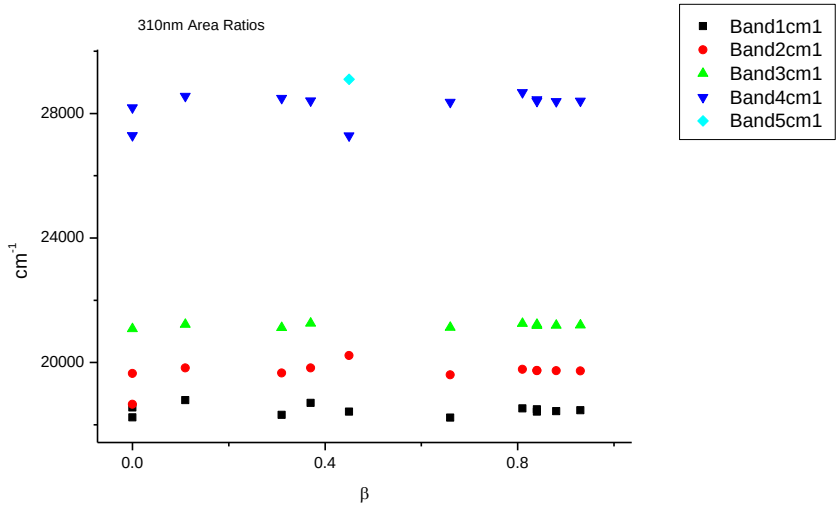

Figure 2.4.9. Band maxima from Gaussian model fit of the normalised fluorescence emission spectra of **15** recorded at 310 nm excitation against β.

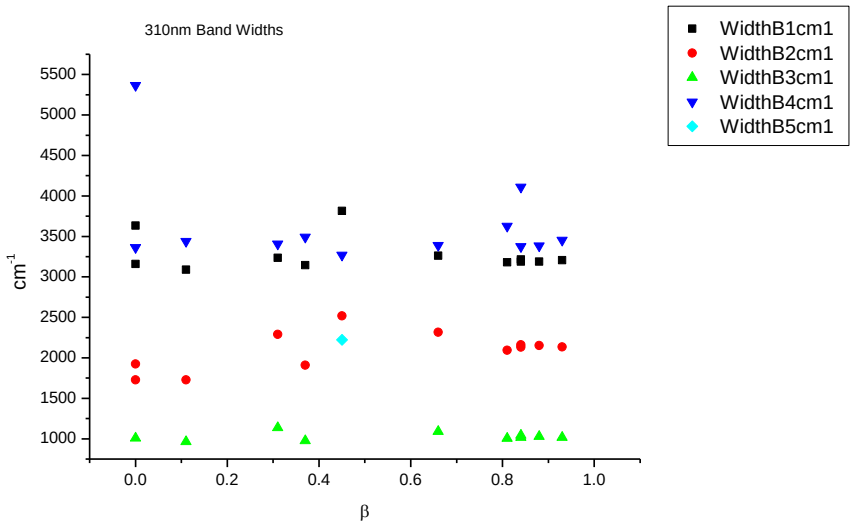

Figure 2.4.10. Band widths from Gaussian model fit of the normalised fluorescence emission spectra of **15** recorded at 310 nm excitation against β.

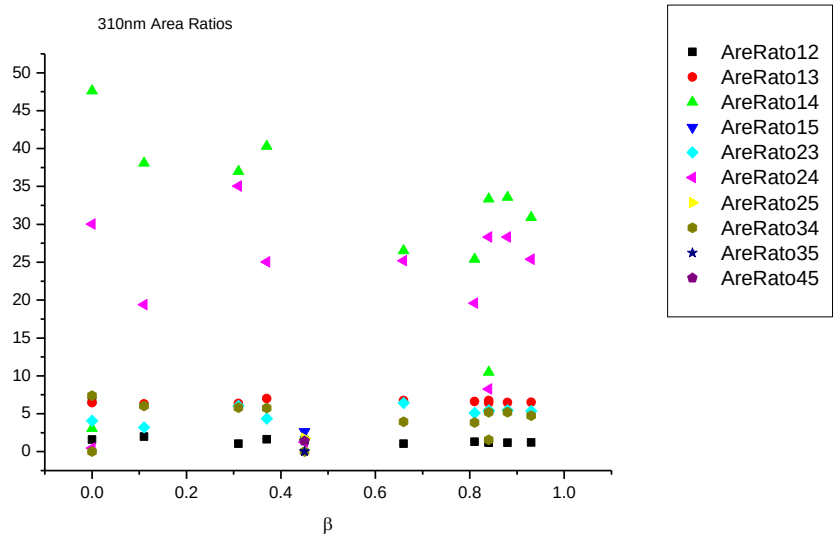

Figure 2.4.11. Area ratios from Gaussian model fit of the normalised fluorescence emission spectra of **15** recorded at 310 nm excitation against β.

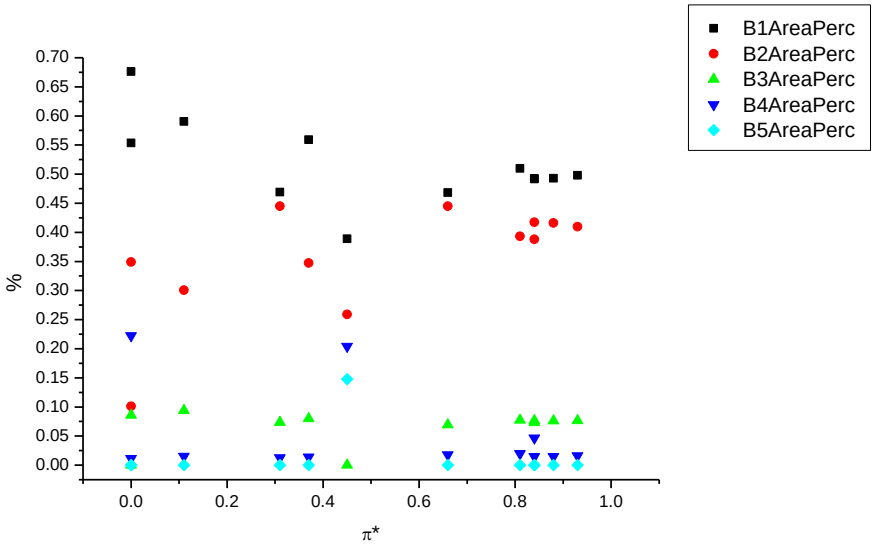

Figure 2.4.12. Area percentages from Gaussian model fit of the normalised fluorescence emission spectra of **15** recorded at 310 nm excitation against β.

2.4.4.4 π.*

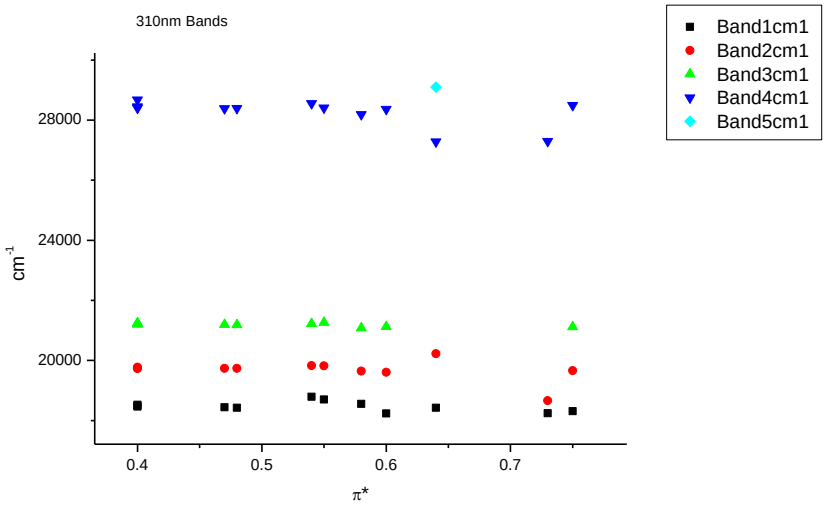

Figure 2.4.13. Band maxima from Gaussian model fit of the normalised fluorescence emission spectra of **15** recorded at 310 nm excitation against π*.

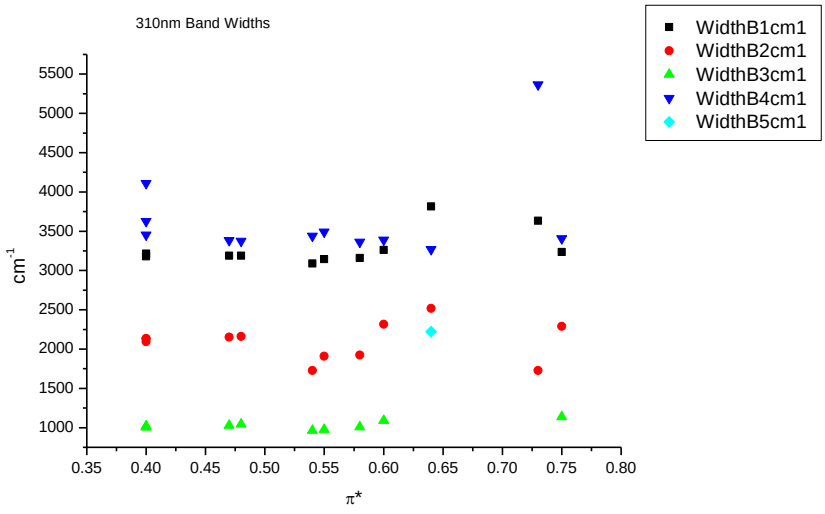

Figure 2.4.14. Band widths from Gaussian model fit of the normalised fluorescence emission spectra of **15** recorded at 310 nm excitation against π*.

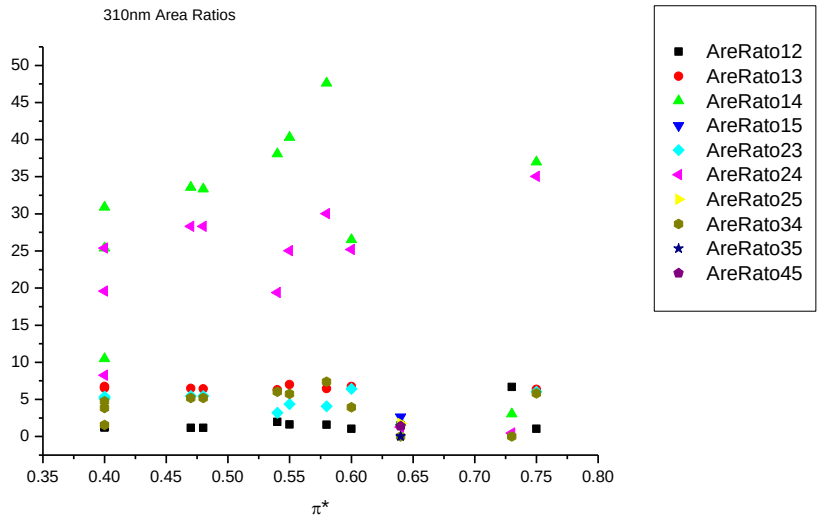

Figure 2.4.15. Area ratios from Gaussian model fit of the normalised fluorescence emission spectra of **15** recorded at 310 nm excitation against π*.

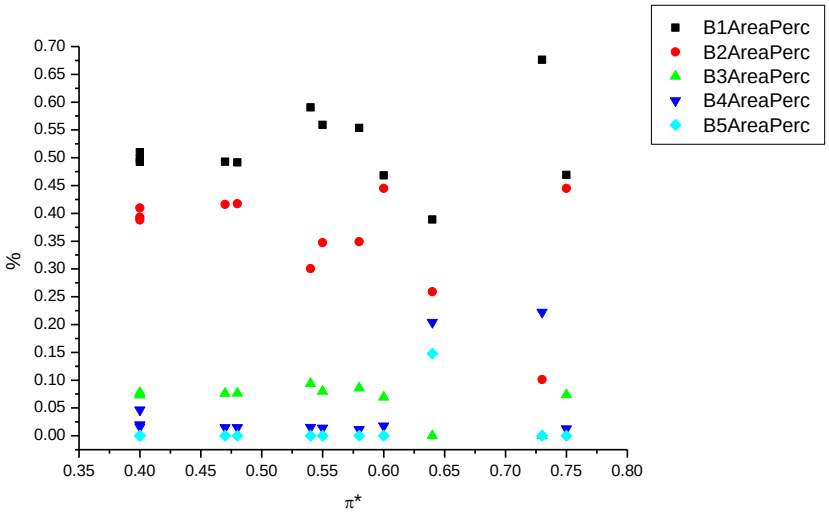

Figure 2.4.16. Area percentages from Gaussian model fit of the normalised fluorescence emission spectra of **15** recorded at 310 nm excitation against π*.

2.4.4.5 μ(D).

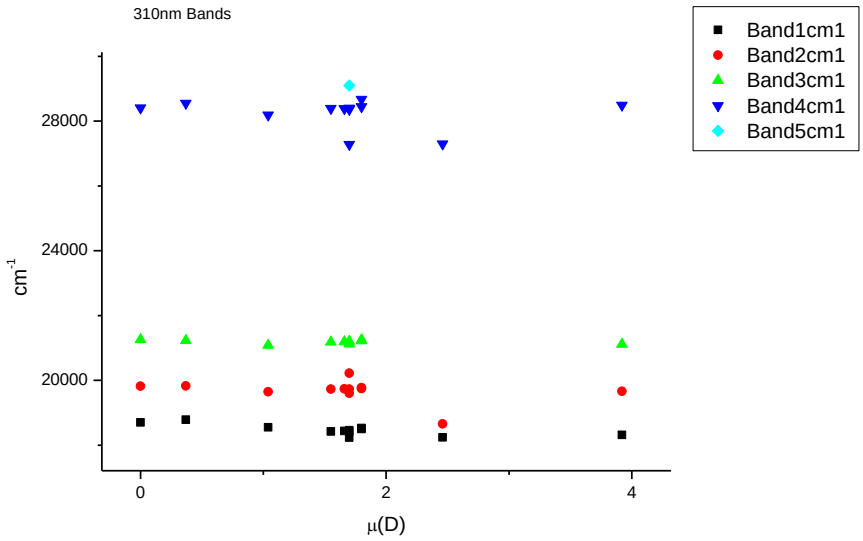

Figure 2.4.17. Band maxima from Gaussian model fit of the normalised fluorescence emission spectra of **15** recorded at 310 nm excitation against μ(D).

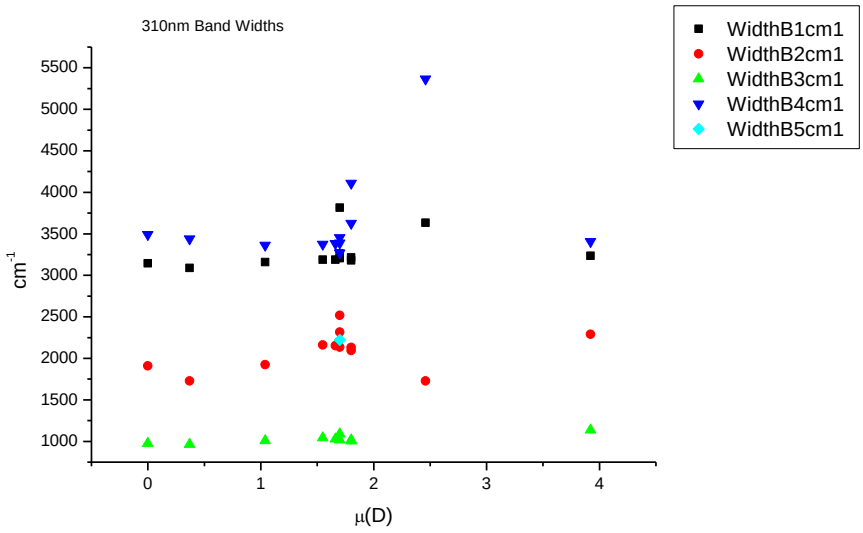

Figure 2.4.18. Band widths from Gaussian model fit of the normalised fluorescence emission spectra of **15** recorded at 310 nm excitation against μ(D).

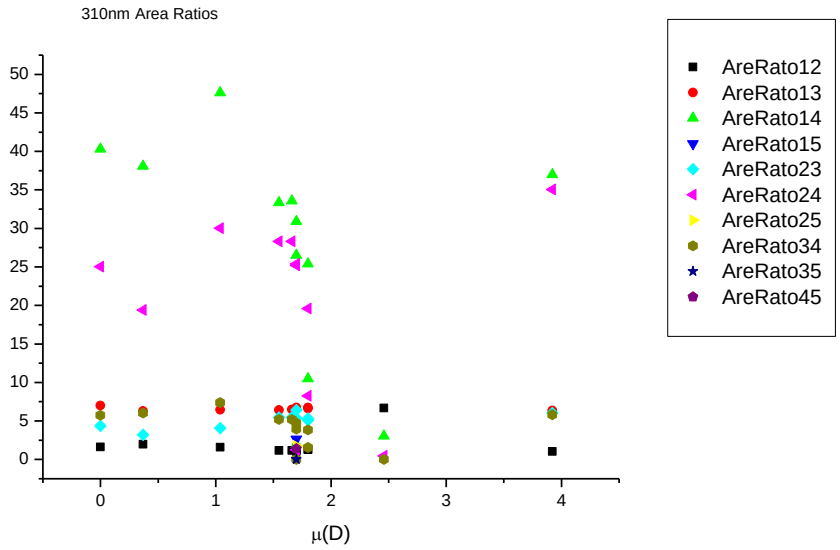

Figure 2.4.19. Area ratios from Gaussian model fit of the normalised fluorescence emission spectra of **15** recorded at 310 nm excitation against μ(D).

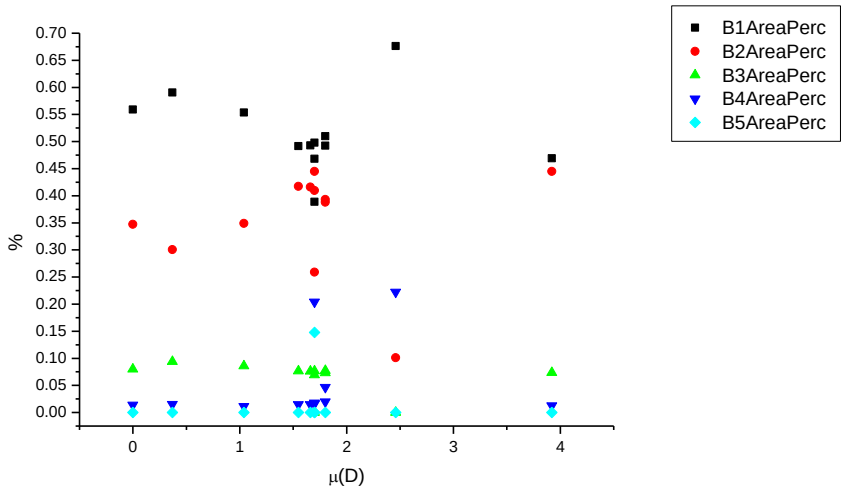

Figure 2.4.20. Area percentages from Gaussian model fit of the normalised fluorescence emission spectra of **15** recorded at 310 nm excitation against μ(D).

2.4.4.6 η(Cp).

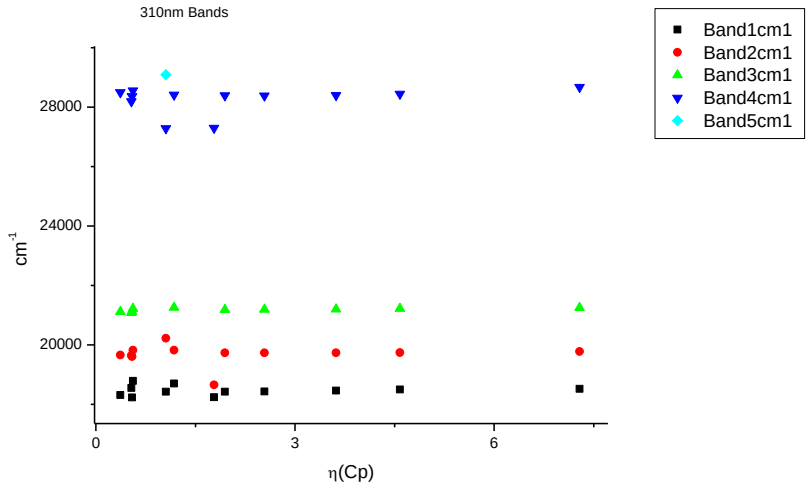

Figure 2.4.21. Band maxima from Gaussian model fit of the normalised fluorescence emission spectra of **15** recorded at 310 nm excitation against η(Cp).

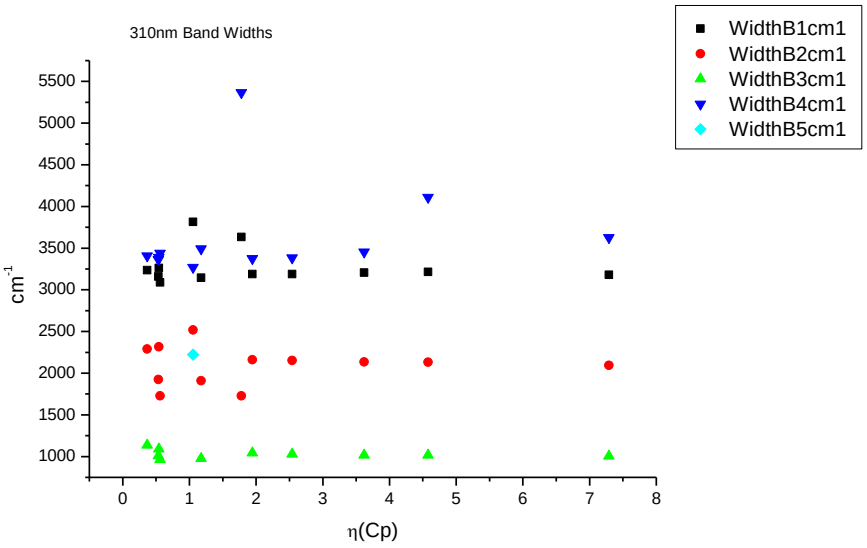

Figure 2.4.22. Band widths from Gaussian model fit of the normalised fluorescence emission spectra of **15** recorded at 310 nm excitation against η(Cp).

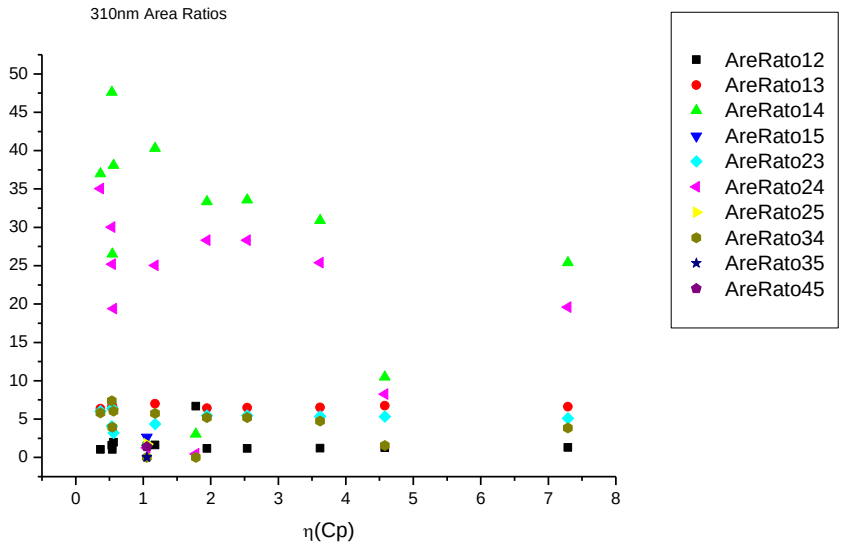

Figure 2.4.23. Area ratios from Gaussian model fit of the normalised fluorescence emission spectra of **15** recorded at 310 nm excitation against η(Cp).

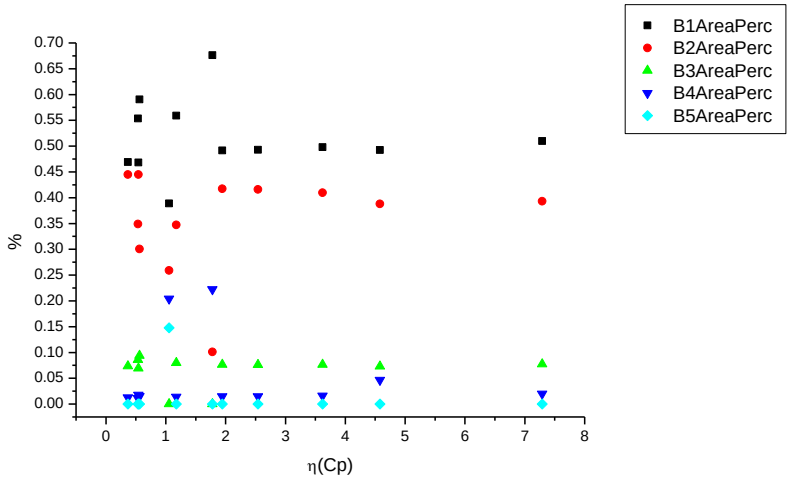

Figure 2.4.24. Area percentages from Gaussian model fit of the normalised fluorescence emission spectra of **15** recorded at 310 nm excitation against η(Cp).

2.4.5 400 nm Gaussian band fit - Solvatochromic analysis.

2.4.5.1 E_T^N.

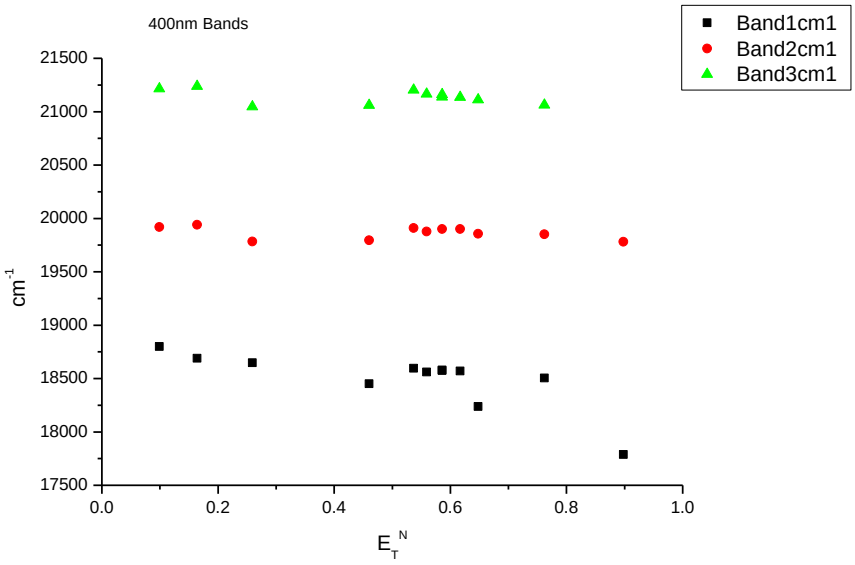

Figure 2.4.25. Band maxima from Gaussian model fit of the normalised fluorescence emission spectra of **15** recorded at 400 nm excitation against E_T^N.

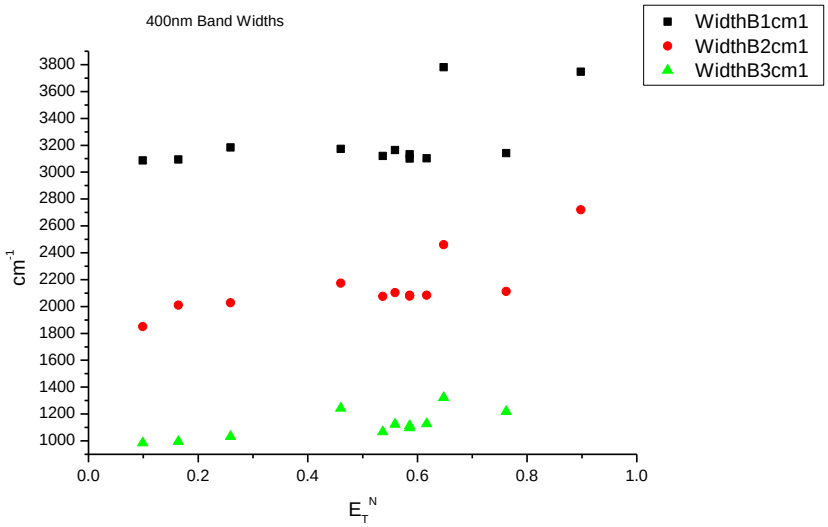

Figure 2.4.26. Band widths from Gaussian model fit of the normalised fluorescence emission spectra of **15** recorded at 400 nm excitation against E_T^N.

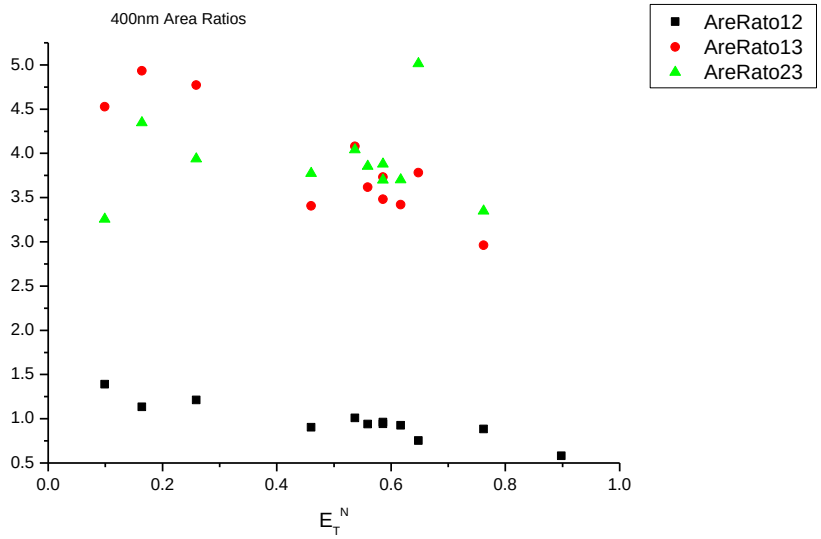

Figure 2.4.27. Area ratios from Gaussian model fit of the normalised fluorescence emission spectra of **15** recorded at 400 nm excitation against E_T^N.

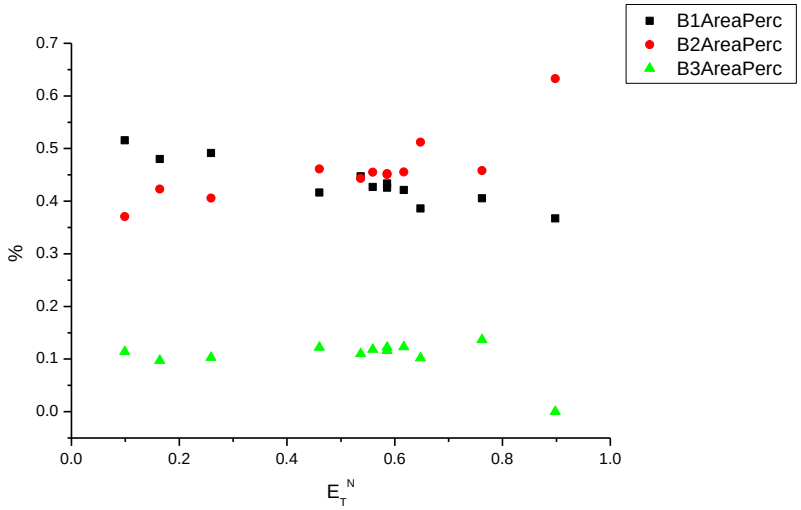

Figure 2.4.28. Area percentages from Gaussian model fit of the normalised fluorescence emission spectra of **15** recorded at 400 nm excitation against E_T^N.

2.4.5.2 α

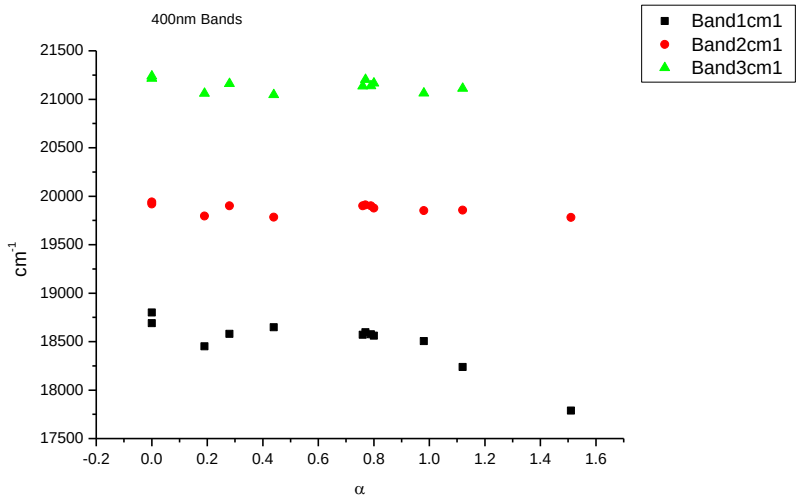

Figure 2.4.29. Band maxima from Gaussian model fit of the normalised fluorescence emission spectra of **15** recorded at 400 nm excitation against α.

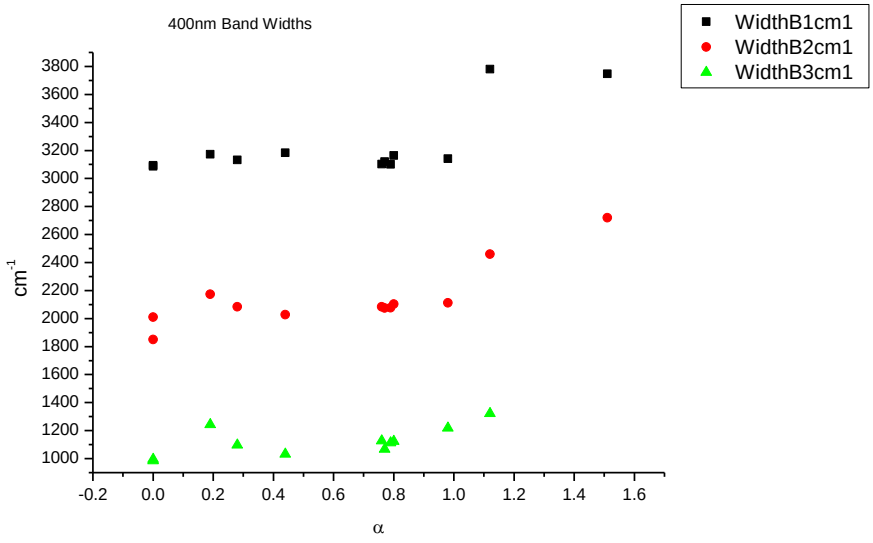

Figure 2.4.30. Band widths from Gaussian model fit of the normalised fluorescence emission spectra of **15** recorded at 400 nm excitation against α.

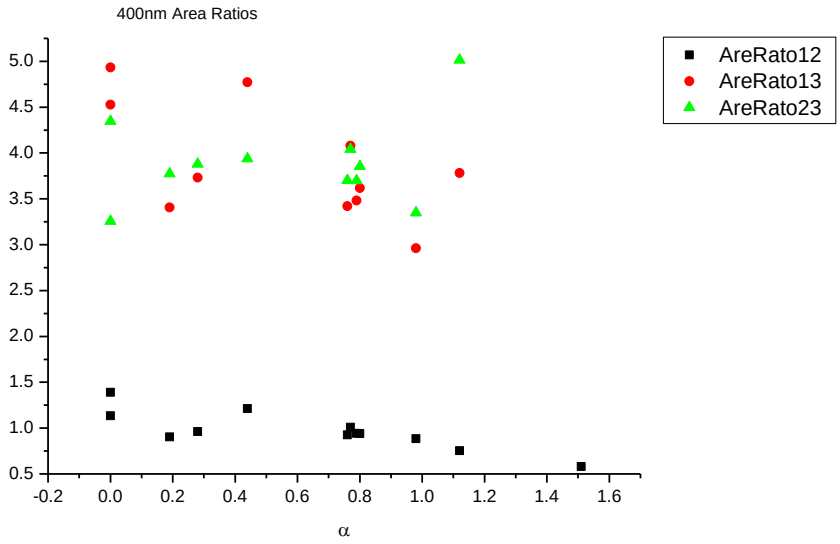

Figure 2.4.31. Area ratios from Gaussian model fit of the normalised fluorescence emission spectra of **15** recorded at 400 nm excitation against α.

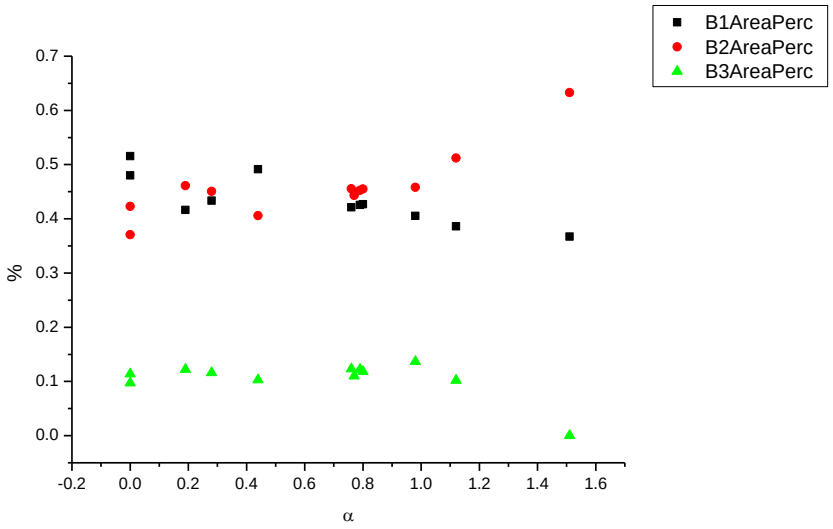

Figure 2.4.32. Area percentages from Gaussian model fit of the normalised fluorescence emission spectra of **15** recorded at 400 nm excitation against α.

2.4.5.3 β.

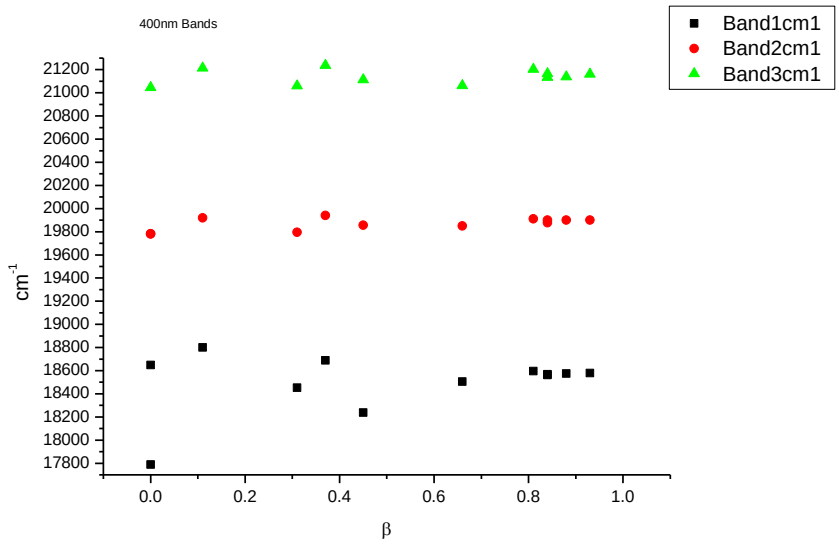

Figure 2.4.33. Band maxima from Gaussian model fit of the normalised fluorescence emission spectra of **15** recorded at 400 nm excitation against β.

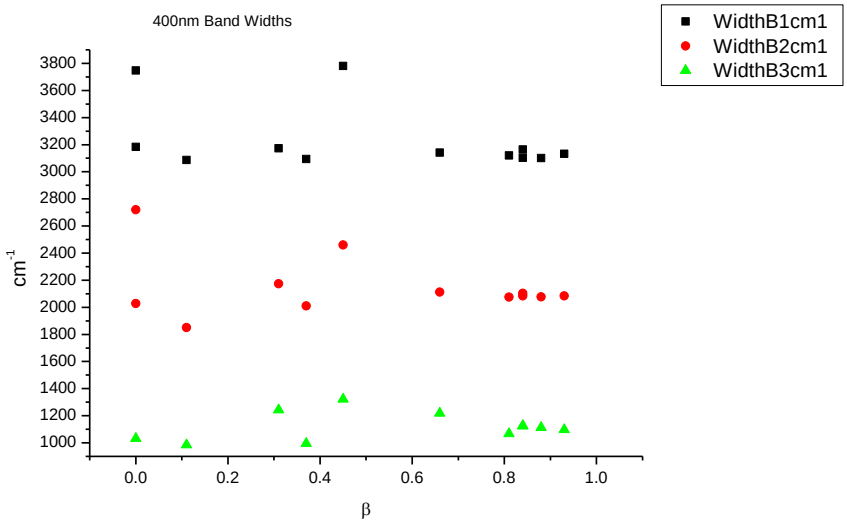

Figure 2.4.34. Band widths from Gaussian model fit of the normalised fluorescence emission spectra of **15** recorded at 400 nm excitation against β.

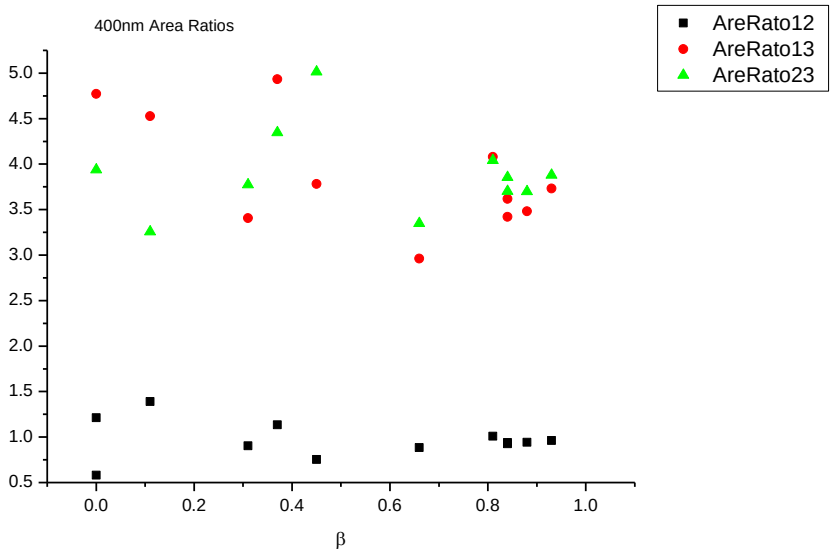

Figure 2.4.35. Area ratios from Gaussian model fit of the normalised fluorescence emission spectra of **15** recorded at 400 nm excitation against β.

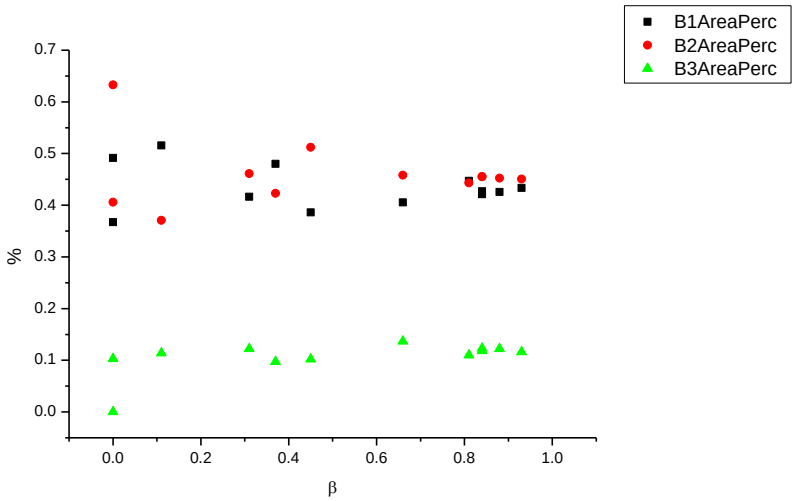

Figure 2.4.36. Area percentages from Gaussian model fit of the normalised fluorescence emission spectra of **15** recorded at 400 nm excitation against β.

2.4.5.4 π.*

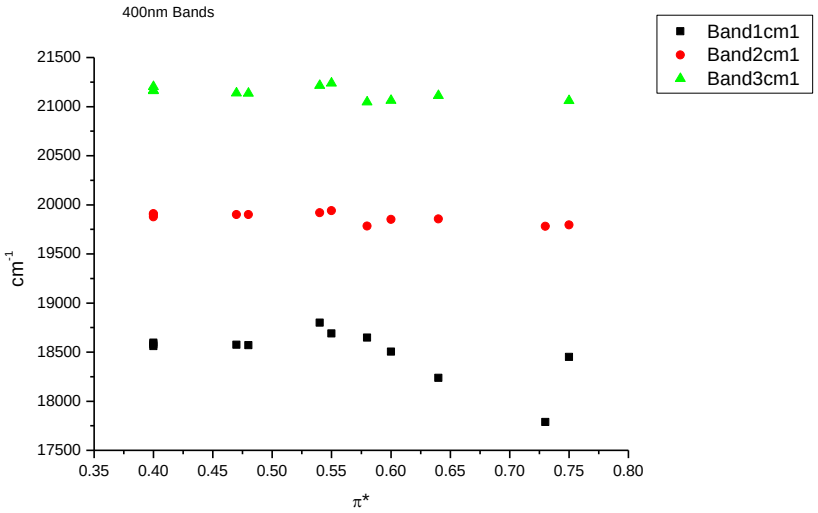

Figure 2.4.37. Band maxima from Gaussian model fit of the normalised fluorescence emission spectra of **15** recorded at 400 nm excitation against π*.

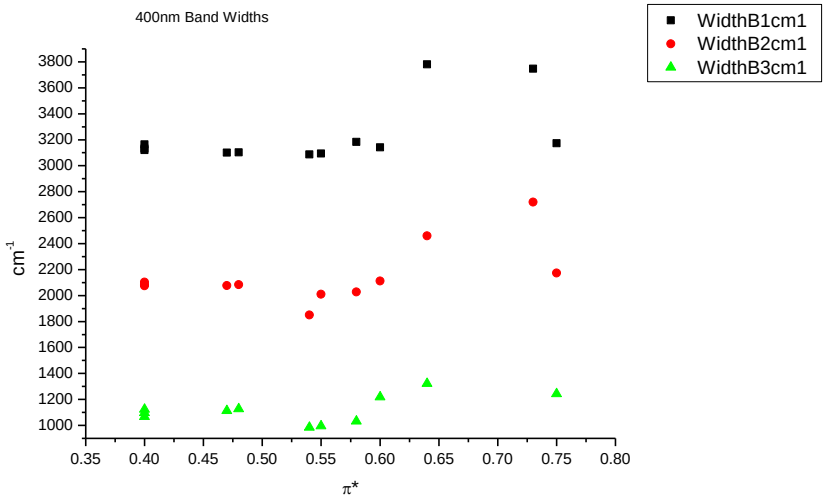

Figure 2.4.38. Band widths from Gaussian model fit of the normalised fluorescence emission spectra of **15** recorded at 400 nm excitation against π*.

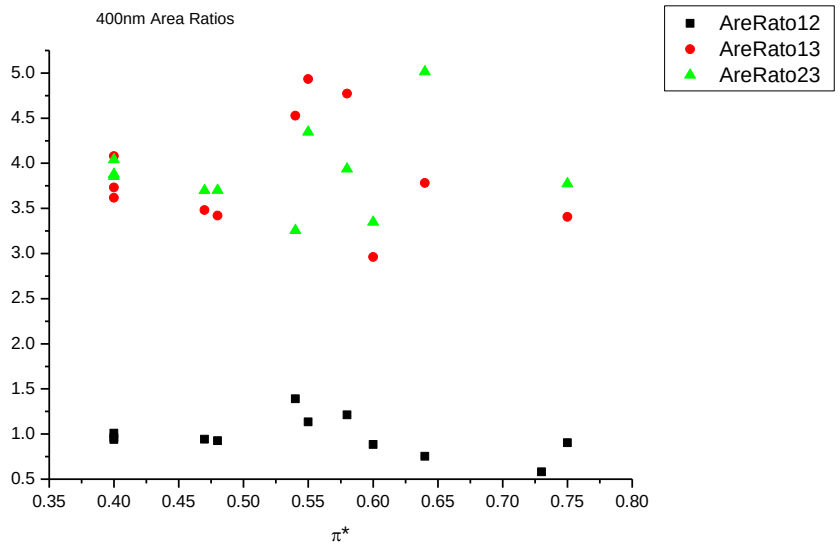

Figure 2.4.39. Area ratios from Gaussian model fit of the normalised fluorescence emission spectra of **15** recorded at 400 nm excitation against π*.

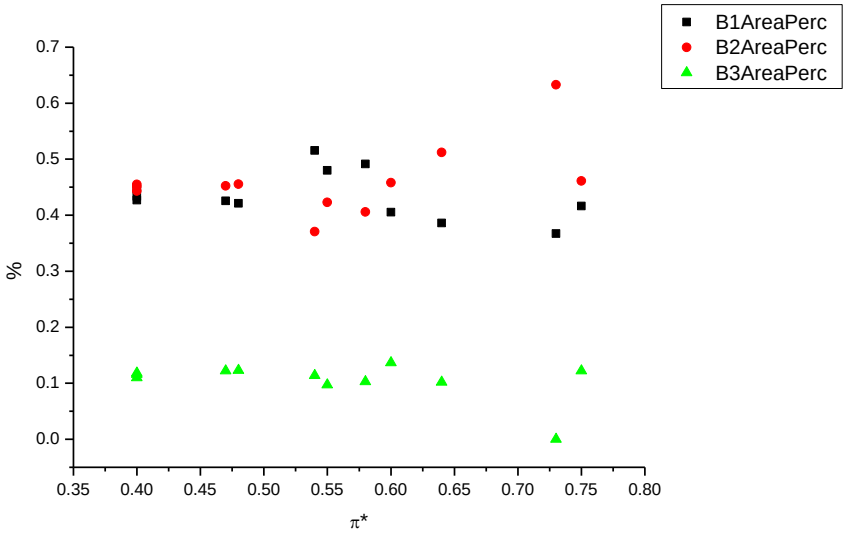

Figure 2.4.40. Area percentages from Gaussian model fit of the normalised fluorescence emission spectra of **15** recorded at 400 nm excitation against π*.

2.4.5.5 μ(D).

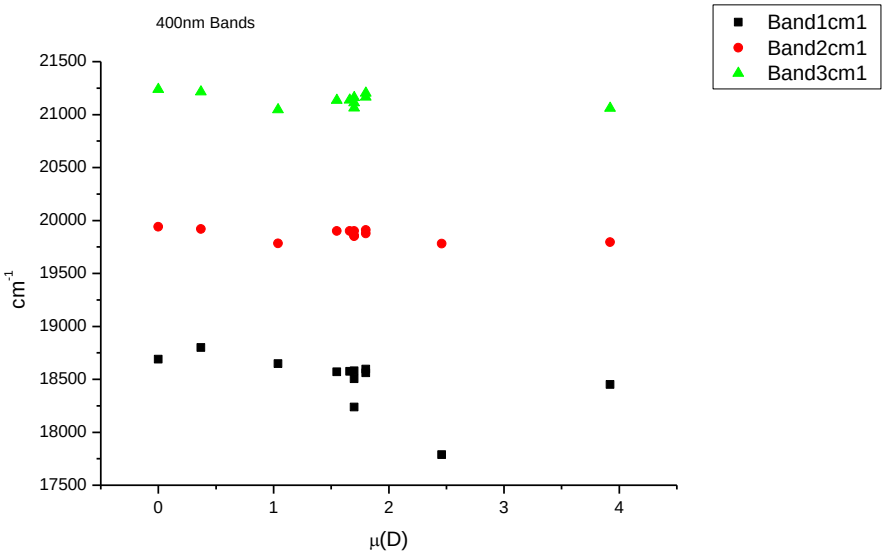

Figure 2.4.41. Band maxima from Gaussian model fit of the normalised fluorescence emission spectra of **15** recorded at 400 nm excitation against μ(D).

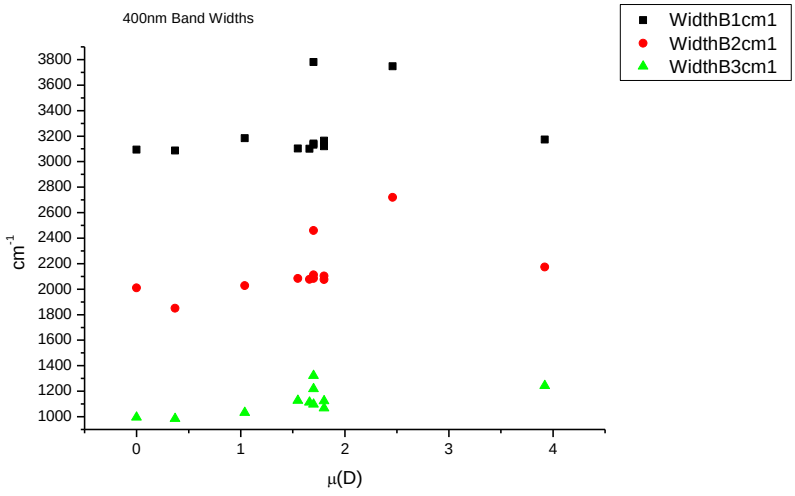

Figure 2.4.42. Band widths from Gaussian model fit of the normalised fluorescence emission spectra of **15** recorded at 400 nm excitation against μ(D).

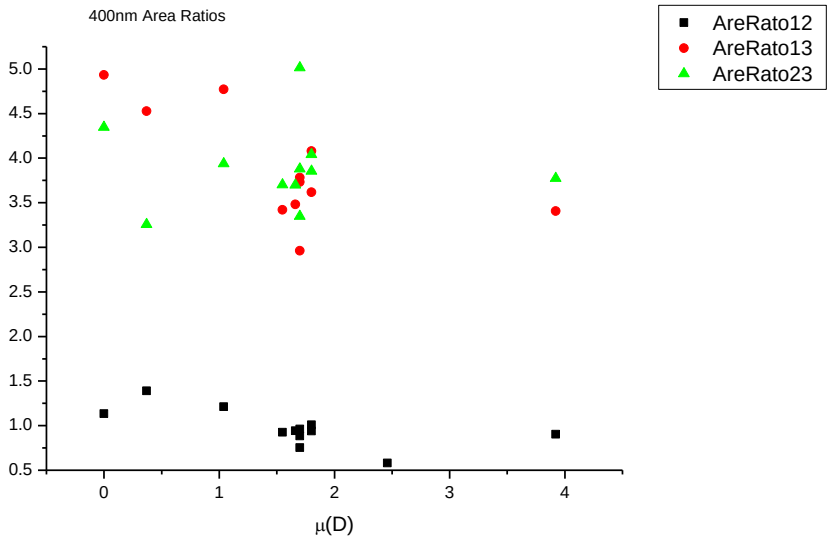

Figure 2.4.43. Area ratios from Gaussian model fit of the normalised fluorescence emission spectra of **11a** recorded at 400 nm excitation against μ(D).

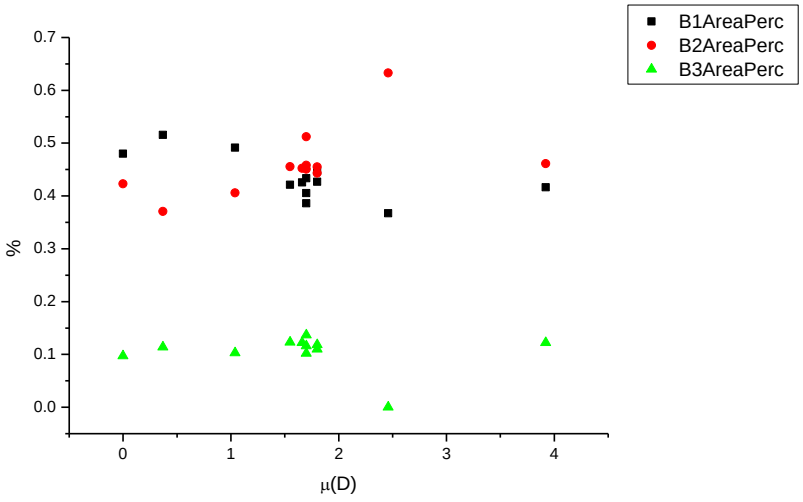

Figure 2.4.44. Area percentages from Gaussian model fit of the normalised fluorescence emission spectra of **15** recorded at 400 nm excitation against μ(D).

2.4.5.6 η(Cp).

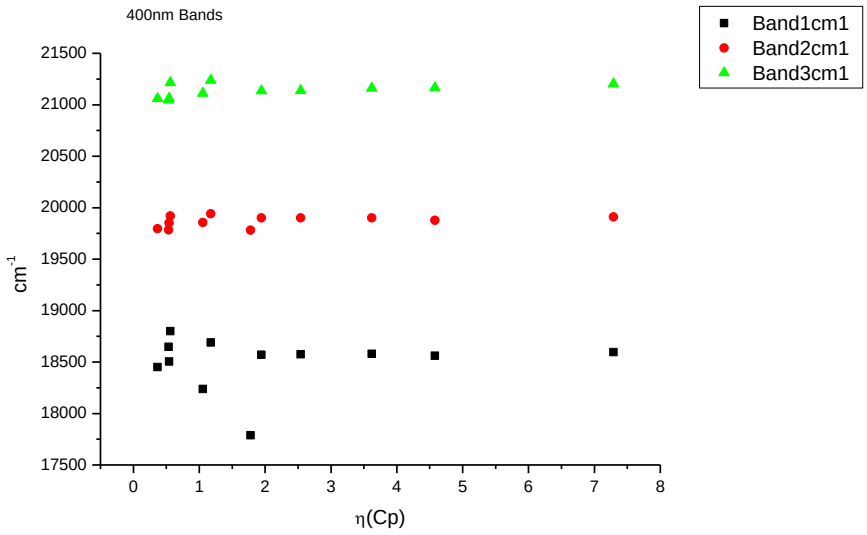

Figure 2.4.45. Band maxima from Gaussian model fit of the normalised fluorescence emission spectra of **15** recorded at 400 nm excitation against η(Cp).

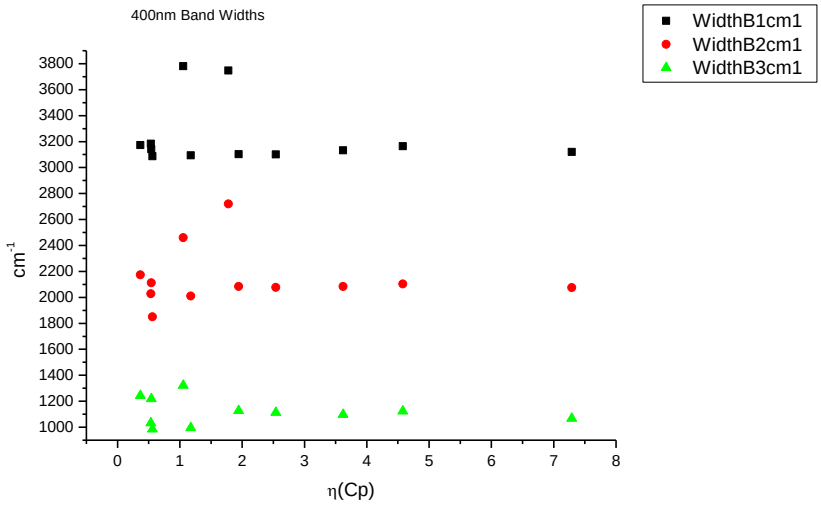

Figure 2.4.46. Band widths from Gaussian model fit of the normalised fluorescence emission spectra of **15** recorded at 400 nm excitation against η(Cp).

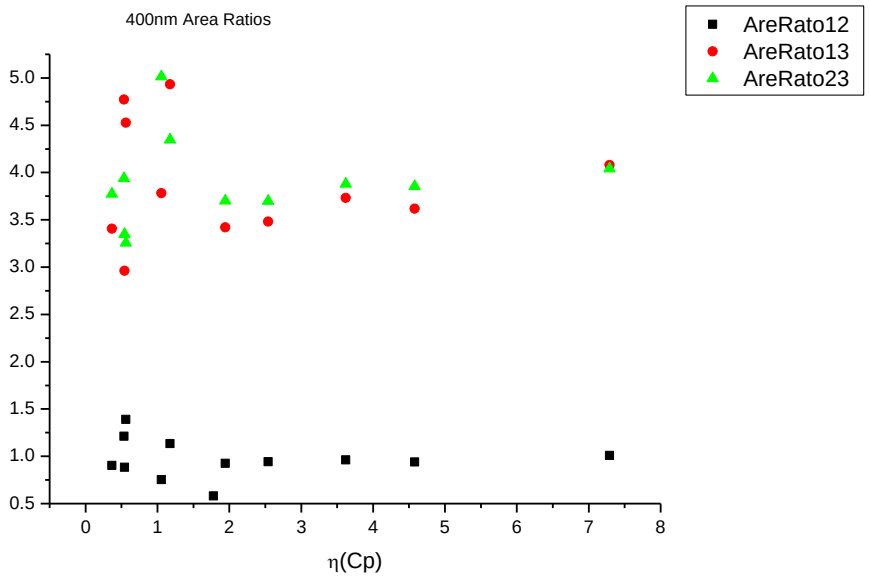

Figure 2.4.47. Area ratios from Gaussian model fit of the normalised fluorescence emission spectra of **15** recorded at 400 nm excitation against η(Cp).

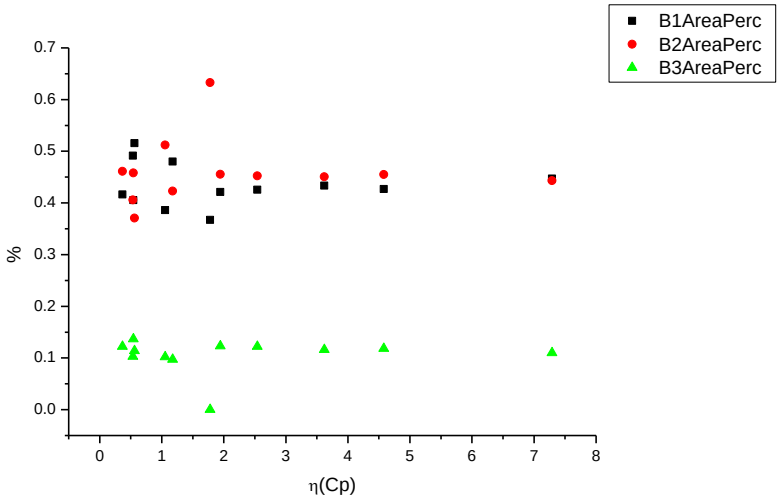

Figure 2.4.48. Area percentages from Gaussian model fit of the normalised fluorescence emission spectra of **15** recorded at 400 nm excitation against η(Cp).

2.4.6 295 nm (LED) fluorescent lifetime results.

2.4.6.1 Intensity weighted.

Wavelength (nm)	Solvent	τ_1 (ns)	A_1 (%)	τ_2 (ns)	A_2 (%)	τ_3 (ns)	A_3 (%)	τ_f (ns) (Intensity Weighted)	$1/\tau_f$	χ^2
470	Toluene	-	-	4.56	58.84	9.92	41.16	6.76	0.15	1.47
470	1,4-Dioxane	0.26	0.84	4.72	55.99	11.24	43.17	7.50	0.13	1.45
470	Chloroform	1.09	1.14	5.73	70.24	12.23	28.62	7.54	0.13	1.52
470	Acetonitrile	1.02	2.25	5.59	70.23	12.30	27.51	7.33	0.14	1.42
470	1-Octanol	1.00	6.35	5.58	73.12	12.00	20.53	6.61	0.15	1.49
470	1-Hexanol	0.78	2.92	5.52	81.07	12.71	16.01	6.54	0.15	1.42
470	1-Butanol	1.52	7.35	4.65	69.86	9.22	22.79	5.46	0.18	1.42
470	1-Pentanol	0.81	2.97	5.37	74.02	10.09	23.01	6.32	0.16	1.41
470	1-Propanol	1.55	2.90	5.03	80.00	10.28	17.11	5.83	0.17	1.52
470	Acetic acid	0.81	56.55	2.28	21.50	8.86	21.94	2.89	0.35	1.05
470	Methanol	1.40	27.62	2.73	72.38	-	-	2.36	0.42	1.27
470	2,2,2-Trifluoroethanol	0.45	51.53	1.82	26.21	8.45	22.26	2.59	0.39	1.08

Table 2.4.8. Summary of Time Correlated Single Photon Counting (TCSPC) fluorescent lifetimes (intensity weighted) of **15** recorded at 470 nm using a 295 nm Light Emitting Diode (LED) light source.

Wavelength (nm)	Solvent	τ_1 (ns)	A_1 (%)	τ_2 (ns)	A_2 (%)	τ_3 (ns)	A_3 (%)	τ_f (ns) (Intensity Weighted)	$1/\tau_f$	χ^2
490	Toluene	-	-	4.34	43.03	9.88	56.97	7.52	0.13	1.59
490	1,4-Dioxane	-	-	4.77	44.80	11.28	55.20	8.36	0.12	1.48
490	Chloroform	-	-	5.57	57.96	11.80	42.04	8.19	0.12	1.45
490	Acetonitrile	1.13	1.32	5.74	64.77	12.76	33.91	8.06	0.12	1.48
490	1-Octanol	1.03	3.58	5.68	66.15	12.61	30.27	7.62	0.13	1.45
490	1-Hexanol	1.13	1.99	5.65	73.75	13.00	24.26	7.34	0.14	1.45
490	1-Butanol	1.62	5.78	5.01	71.01	11.60	23.21	6.34	0.16	1.44
490	1-Pentanol	1.02	1.74	5.69	75.47	12.86	22.79	7.24	0.14	1.43
490	1-Propanol	1.66	2.30	5.23	75.70	12.26	22.01	6.70	0.15	1.46
490	Acetic acid	-	-	-	-	-	-	-	-	-
490	Methanol	1.34	24.63	2.74	75.37	-	-	2.39	0.42	1.27
490	2,2,2-Trifluoroethanol	-	-	-	-	-	-	-	-	-

Table 2.4.9. Summary of Time Correlated Single Photon Counting (TCSPC) fluorescent lifetimes (intensity weighted) of **15** recorded at 490 nm using a 295 nm Light Emitting Diode (LED) light source.

Wavelength (nm)	Solvent	τ_1 (ns)	A_1 (%)	τ_2 (ns)	A_2 (%)	τ_3 (ns)	A_3 (%)	τ_f (ns) (Intensity Weighted)	$1/\tau_f$	χ^2
520	Toluene	-	-	4.50	20.15	10.06	79.85	8.94	0.11	1.59
520	1,4-Dioxane	-	-	4.74	19.61	11.46	80.39	10.14	0.10	1.58
520	Chloroform	-	-	5.70	30.45	12.15	69.55	10.18	0.10	1.58
520	Acetonitrile	1.33	0.75	5.83	40.73	13.14	58.52	10.07	0.10	1.54
520	1-Octanol	1.26	1.87	5.84	40.56	13.21	57.58	10.00	0.10	1.62
520	1-Hexanol	0.93	1.05	5.77	46.36	13.33	52.59	9.69	0.10	1.52
520	1-Butanol	1.72	4.07	5.28	49.76	13.19	46.17	8.79	0.11	1.57
520	1-Pentanol	0.88	0.78	5.71	47.05	13.17	52.16	9.56	0.10	1.64
520	1-Propanol	1.25	0.93	5.23	50.61	12.99	48.46	8.96	0.11	1.45
520	Acetic acid	0.37	18.53	1.13	55.98	6.69	25.49	2.40	0.42	1.15
520	Methanol	1.57	32.87	2.87	67.13	-	-	2.44	0.41	1.27
520	2,2,2-Trifluoroethanol	0.36	48.24	2.35	41.50	8.33	10.27	2.01	0.50	1.08

Table 2.4.10. Summary of Time Correlated Single Photon Counting (TCSPC) fluorescent lifetimes (intensity weighted) of **15** recorded at 520 nm using a 295 nm Light Emitting Diode (LED) light source.

Wavelength (nm)	Solvent	τ_1 (ns)	A_1 (%)	τ_2 (ns)	A_2 (%)	τ_3 (ns)	A_3 (%)	τ_f (ns) (Intensity Weighted)	$1/\tau_f$	χ^2
540	Toluene	-	-	4.17	11.70	9.95	88.30	9.27	0.11	1.66
540	1,4-Dioxane	-	-	4.97	13.65	11.56	86.35	10.66	0.09	1.59
540	Chloroform	-	-	5.64	20.81	12.10	79.19	10.75	0.09	1.69
540	Acetonitrile	1.22	0.77	5.82	29.78	13.18	69.45	10.90	0.09	1.64
540	1-Octanol	1.08	1.21	5.68	29.91	13.09	68.88	10.73	0.09	1.68
540	1-Hexanol	1.04	0.69	5.69	35.56	13.26	63.75	10.48	0.10	1.62
540	1-Butanol	1.60	2.96	5.19	28.85	13.07	58.19	9.67	0.10	1.64
540	1-Pentanol	1.34	0.78	5.74	37.12	13.16	62.10	10.31	0.10	1.68
540	1-Propanol	1.03	0.91	5.28	40.65	13.03	58.44	9.77	0.10	1.59
540	Acetic acid	-	-	-	-	-	-	-	-	-
540	Methanol	0.19	2.58	1.82	47.59	3.11	49.83	2.42	0.41	1.30
540	2,2,2-Trifluoroethanol	-	-	-	-	-	-	-	-	-

Table 2.4.11. Summary of Time Correlated Single Photon Counting (TCSPC) fluorescent lifetimes (intensity weighted) of **15** recorded at 540 nm using a 295 nm Light Emitting Diode (LED) light source.

Wavelength (nm)	Solvent	τ_1 (ns)	A_1 (%)	τ_2 (ns)	A_2 (%)	τ_3 (ns)	A_3 (%)	τ_f (ns) (Intensity Weighted)	$1/\tau_f$	χ^2
570	Toluene	-		5.77	6.76	10.11	93.24	9.82	0.10	1.32
570	1,4-Dioxane	-	-	6.64	7.29	11.68	92.71	11.32	0.09	1.47
570	Chloroform	-	-	6.53	13.66	12.33	86.34	11.54	0.09	1.30
570	Acetonitrile	-	-	5.80	17.71	12.97	82.29	11.70	0.09	1.25
570	1-Octanol	13.91	50.37	5.11	14.08	11.50	35.55	11.81	0.08	1.41
570	1-Hexanol	-	-	5.25	19.55	12.98	80.45	11.47	0.09	1.32
570	1-Butanol	-	-	4.61	20.59	12.62	79.41	10.97	0.09	1.33
570	1-Pentanol	-	-	5.87	24.83	13.26	75.17	11.42	0.09	1.49
570	1-Propanol	-	-	5.19	29.22	13.05	70.78	10.76	0.09	1.34
570	Acetic acid	-	-	-	-	-	-	-	-	-
570	Methanol	1.92	58.98	3.37	41.02	-	-	2.51	0.40	1.41
570	2,2,2-Trifluoroethanol	-	-	-	-	-	-	-	-	-

Table 2.4.12. Summary of Time Correlated Single Photon Counting (TCSPC) fluorescent lifetimes (intensity weighted) of **15** recorded at 570 nm using a 295 nm Light Emitting Diode (LED) light source.

2.4.6.2 Amplitude weighted.

Wavelength (nm)	Solvent	τ_1 (ns)	A_1 (%)	τ_2 (ns)	A_2 (%)	τ_3 (ns)	A_3 (%)	τ_f (ns) (Amplitude Weighted)	$1/\tau_f$	χ^2
470	Toluene	-	-	4.56	75.68	9.92	24.32	5.86	0.17	1.47
470	1,4-Dioxane	0.26	16.99	4.72	62.70	11.24	20.31	5.29	0.19	1.45
470	Chloroform	1.09	1.14	5.73	78.32	12.23	14.96	6.39	0.16	1.52
470	Acetonitrile	1.02	13.02	5.59	73.83	12.30	13.15	5.88	0.17	1.42
470	1-Octanol	1.00	29.98	5.58	61.93	12.00	8.09	6.73	0.15	1.49
470	1-Hexanol	0.78	19.08	5.52	74.53	12.71	6.40	5.08	0.20	1.42
470	1-Butanol	1.52	21.65	4.65	67.27	9.22	11.08	4.48	0.22	1.42
470	1-Pentanol	0.81	18.67	5.37	69.78	10.09	11.55	5.07	0.20	1.41
470	1-Propanol	1.55	9.60	5.03	81.84	10.28	8.56	5.15	0.19	1.52
470	Acetic acid	0.81	85.40	2.28	11.56	8.86	3.04	1.23	0.82	1.05
470	Methanol	1.40	42.69	2.73	57.31	-	-	2.16	0.46	1.27
470	2,2,2-Trifluoroethanol	0.45	87.01	1.82	10.98	8.45	2.01	0.76	1.31	1.08

Table 2.4.13. Summary of Time Correlated Single Photon Counting (TCSPC) fluorescent lifetimes (amplitude weighted) of **15** recorded at 470 nm using a 295 nm Light Emitting Diode (LED) light source.

Wavelength (nm)	Solvent	τ_1 (ns)	A_1 (%)	τ_2 (ns)	A_2 (%)	τ_3 (ns)	A_3 (%)	τ_f (ns) (Amplitude Weighted)	$1/\tau_f$	χ^2
490	Toluene	-	-	4.34	62.98	9.88	37.02	6.42	0.16	1.59
490	1,4-Dioxane	-	-	4.77	65.75	11.28	34.25	7.00	0.14	1.48
490	Chloroform	-	-	5.57	74.49	11.80	25.51	7.16	0.14	1.45
490	Acetonitrile	1.13	7.73	5.74	74.68	12.76	17.59	6.62	0.15	1.48
490	1-Octanol	1.03	19.89	5.68	66.41	12.61	13.70	5.71	0.18	1.45
490	1-Hexanol	1.13	10.54	5.65	78.27	13.00	11.19	6.00	0.17	1.45
490	1-Butanol	1.62	18.09	5.01	71.77	11.60	10.13	5.06	0.20	1.44
490	1-Pentanol	1.02	10.20	5.69	79.22	12.86	10.58	5.97	0.17	1.43
490	1-Propanol	1.66	7.82	5.23	82.00	12.26	10.17	5.67	0.18	1.46
490	Acetic acid	-	-	-	-	-	-	-	-	-
490	Methanol	1.34	40.07	2.74	59.93	-	-	2.17	0.46	1.27
490	2,2,2-Trifluoroethanol	-	-	-	-	-	-	-	-	-

Table 2.4.14. Summary of Time Correlated Single Photon Counting (TCSPC) fluorescent lifetimes (amplitude weighted) of **15** recorded at 490 nm using a 295 nm Light Emitting Diode (LED) light source.

Wavelength (nm)	Solvent	τ_1 (ns)	A_1 (%)	τ_2 (ns)	A_2 (%)	τ_3 (ns)	A_3 (%)	τ_f (ns) (Amplitude Weighted)	$1/\tau_f$	χ^2
520	Toluene	-	-	4.50	36.06	10.06	63.94	8.05	0.12	1.59
520	1,4-Dioxane	-	-	4.74	37.10	11.46	62.90	8.96	0.11	1.58
520	Chloroform	-	-	5.70	48.27	12.15	51.73	9.03	0.11	1.58
520	Acetonitrile	1.33	4.73	5.83	58.17	13.14	37.10	8.33	0.12	1.54
520	1-Octanol	1.26	11.60	5.84	54.33	13.21	34.07	7.82	0.13	1.62
520	1-Hexanol	0.93	8.59	5.77	61.31	13.33	30.11	7.63	0.13	1.52
520	1-Butanol	1.72	15.49	5.28	61.62	13.19	22.90	6.54	0.15	1.57
520	1-Pentanol	0.88	6.81	5.71	62.93	13.17	30.25	7.64	0.13	1.64
520	1-Propanol	1.25	5.24	5.23	68.39	12.99	26.36	7.07	0.14	1.45
520	Acetic acid	0.37	48.28	1.13	48.04	6.69	3.68	0.97	1.04	1.15
520	Methanol	1.57	47.21	2.87	52.79	-	-	2.26	0.44	1.27
520	2,2,2-Trifluoroethanol	0.36	87.52	2.35	11.67	8.33	0.82	0.66	1.51	1.08

Table 2.4.15. Summary of Time Correlated Single Photon Counting (TCSPC) fluorescent lifetimes (amplitude weighted) of **15** recorded at 520 nm using a 295 nm Light Emitting Diode (LED) light source.

Wavelength (nm)	Solvent	τ_1 (ns)	A_1 (%)	τ_2 (ns)	A_2 (%)	τ_3 (ns)	A_3 (%)	τ_f (ns) (Amplitude Weighted)	$1/\tau_f$	χ^2
540	Toluene	-	-	4.17	24.02	9.95	75.98	8.56	0.12	1.66
540	1,4-Dioxane	-	-	4.97	26.89	11.56	73.11	9.79	0.10	1.59
540	Chloroform	-	-	5.64	36.06	12.10	63.94	9.77	0.10	1.69
540	Acetonitrile	1.22	5.70	5.82	46.44	13.18	47.86	9.08	0.11	1.64
540	1-Octanol	1.08	9.60	5.68	45.22	13.10	45.18	8.59	0.12	1.68
540	1-Hexanol	1.04	5.69	5.69	53.31	13.26	41.00	8.53	0.12	1.62
540	1-Butanol	1.60	13.40	5.19	54.31	13.07	32.29	7.25	0.14	1.64
540	1-Pentanol	1.34	0.78	5.74	54.95	13.16	40.12	8.50	0.12	1.68
540	1-Propanol	1.03	6.72	5.28	58.96	13.04	34.31	7.65	0.13	1.59
540	Acetic acid	-	-	-	-	-	-	-	-	-
540	Methanol	0.19	24.86	1.82	46.59	3.11	28.55	1.78	0.56	1.30
540	2,2,2-Trifluoroethanol	-	-	-	-	-	-	-	-	-

Table 2.4.16. Summary of Time Correlated Single Photon Counting (TCSPC) fluorescent lifetimes (amplitude weighted) of **15** recorded at 540 nm using a 295 nm Light Emitting Diode (LED) light source.

Wavelength (nm)	Solvent	τ_1 (ns)	A_1 (%)	τ_2 (ns)	A_2 (%)	τ_3 (ns)	A_3 (%)	τ_f (ns) (Amplitude Weighted)	$1/\tau_f$	χ^2
570	Toluene	-	-	5.77	11.27	10.11	88.73	9.62	0.10	1.32
570	1,4-Dioxane	-	-	6.64	12.15	11.69	87.85	11.07	0.09	1.47
570	Chloroform	-	-	6.53	23.01	12.33	76.99	11.00	0.09	1.30
570	Acetonitrile	-	-	5.80	32.51	12.97	67.49	10.64	0.09	1.25
570	1-Octanol	13.91	38.23	5.11	29.11	11.50	32.66	10.56	0.09	1.41
570	1-Hexanol	-	-	5.25	37.55	12.98	62.45	10.08	0.10	1.32
570	1-Butanol	-	-	4.61	41.52	12.62	58.48	9.30	0.11	1.33
570	1-Pentanol	-	-	5.87	42.73	13.26	57.27	10.10	0.10	1.49
570	1-Propanol	-	-	5.19	50.94	13.06	49.06	9.05	0.11	1.34
570	Acetic acid	-	-	-	-	-	-	-	-	-
570	Methanol	1.92	71.69	3.37	28.31	-	-	2.33	0.43	1.41
570	2,2,2-Trifluoroethanol	-	-	-	-	-	-	-	-	-

Table 2.4.17. Summary of Time Correlated Single Photon Counting (TCSPC) fluorescent lifetimes (amplitude weighted) of **15** recorded at 570 nm using a 295 nm Light Emitting Diode (LED) light source.

2.4.7 400 nm fluorescent lifetime results.

2.4.7.1 Intensity weighted.

Wavelength (nm)	Solvent	τ_1 (ns)	A_1 (%)	τ_2 (ns)	A_2 (%)	τ_3 (ns)	A_3 (%)	τ_f (ns) (Intensity Weighted)	$1/\tau_f$	χ^2
500	Toluene	-	-	4.35	44.63	9.78	55.37	7.35	0.14	1.20
500	1,4-Dioxane	-	-	4.64	44.27	11.09	55.73	8.24	0.12	1.20
500	Chloroform	-	-	5.50	57.28	11.39	42.72	8.02	0.12	1.21
500	Acetonitrile	-	-	5.47	63.10	11.56	36.90	7.72	0.13	1.23
500	1-Octanol	0.62	2.52	5.33	61.82	11.69	35.66	7.48	0.13	1.16
500	1-Hexanol	0.45	2.95	5.07	64.01	11.23	33.04	1.18	0.85	1.18
500	1-Butanol	0.75	2.27	4.57	67.81	10.35	29.92	6.21	0.16	1.18
500	1-Pentanol	0.34	2.02	5.48	70.43	11.84	27.55	7.13	0.14	1.19
500	1-Propanol	0.39	1.40	4.93	72.71	10.74	25.89	6.37	0.16	1.10
500	Acetic acid	0.28	18.70	5.34	3.51	1.12	77.79	1.10	0.91	1.08
500	Methanol	1.28	17.86	2.62	82.14	-	-	2.38	0.42	1.20
500	2,2,2-Trifluoroethanol	0.26	65.32	4.52	2.74	0.57	31.95	0.48	2.11	1.07

Table 2.4.18. Summary of Time Correlated Single Photon Counting (TCSPC) fluorescent lifetimes (intensity weighted) of **15** recorded at 500 nm using a 405 nm Laser Diode excitation source source.

2.4.7.2 Amplitude weighted.

Wavelength (nm)	Solvent	τ_1 (ns)	A_1 (%)	τ_2 (ns)	A_2 (%)	τ_3 (ns)	A_3 (%)	τ_f (ns) (Amplitude Weighted)	$1/\tau_f$	χ^2
500	Toluene	-	-	4.35	64.45	9.78	35.55	6.28	0.16	1.20
500	1,4-Dioxane	-	-	4.64	65.50	11.09	34.50	6.87	0.15	1.20
500	Chloroform	-	-	5.50	73.53	11.39	26.47	7.06	0.14	1.21
500	Acetonitrile	-	-	5.47	78.34	11.56	21.66	6.79	0.15	1.23
500	1-Octanol	0.62	21.79	5.33	61.92	11.69	16.29	5.34	0.19	1.16
500	1-Hexanol	0.45	29.70	5.07	57.01	11.23	13.29	4.52	0.22	1.18
500	1-Butanol	0.75	14.58	4.57	71.50	10.35	13.92	4.81	0.21	1.18
500	1-Pentanol	0.34	28.16	5.48	60.83	11.84	11.01	4.73	0.21	1.19
500	1-Propanol	0.39	17.24	4.93	71.12	10.74	11.64	4.83	0.21	1.10
500	Acetic acid	0.28	48.53	5.34	0.48	1.12	52.00	0.73	1.37	1.08
500	Methanol	1.28	30.81	2.62	69.19	-	-	2.21	0.45	1.20
500	2,2,2-Trifluoroethanol	0.26	81.73	4.52	0.20	0.57	18.07	0.32	3.09	1.07

Table 2.4.19. Summary of Time Correlated Single Photon Counting (TCSPC) fluorescent lifetimes (amplitude weighted) of **15** recorded at 500 nm using a 405 nm Light source.

2.4.8 400 nm average fluorescent lifetimes - Solvatochromic analysis.

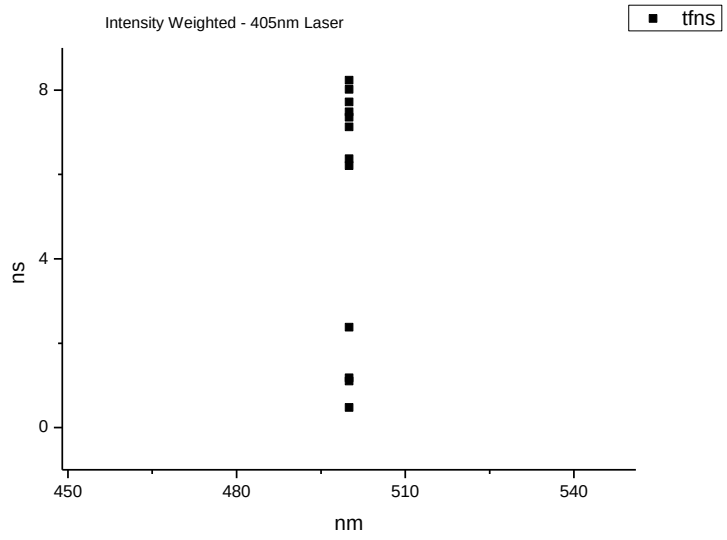

Figure 2.4.49. Intensity weighted average lifetime (τ_f) of **15** versus wavelength (nm).

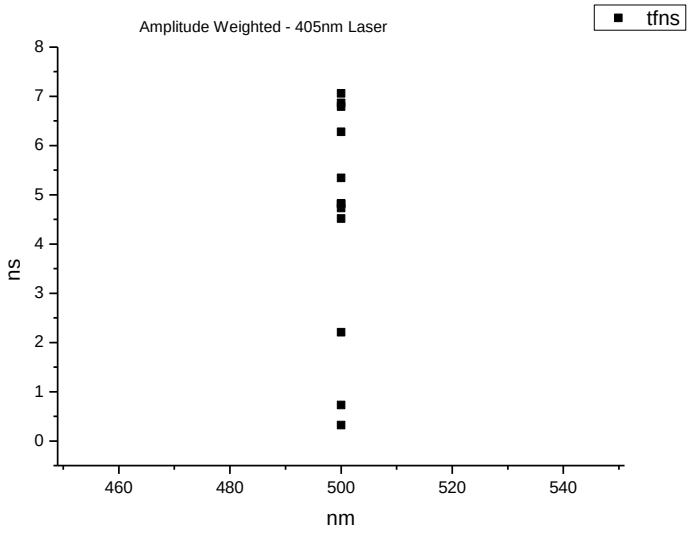

Figure 2.4.50. Amplitude weighted average lifetime (τ_f) of **15** versus wavelength (nm).

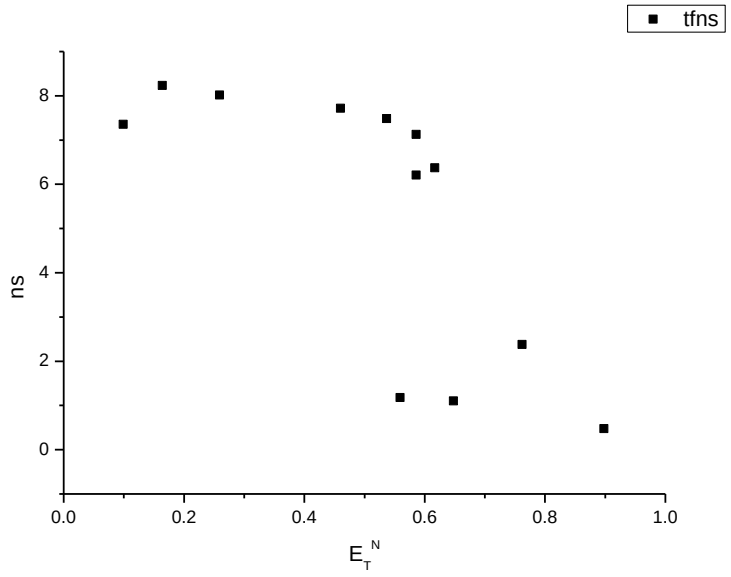

Figure 2.4.51. Intensity weighted average lifetime (τ_f) of **15** versus E_T^N.

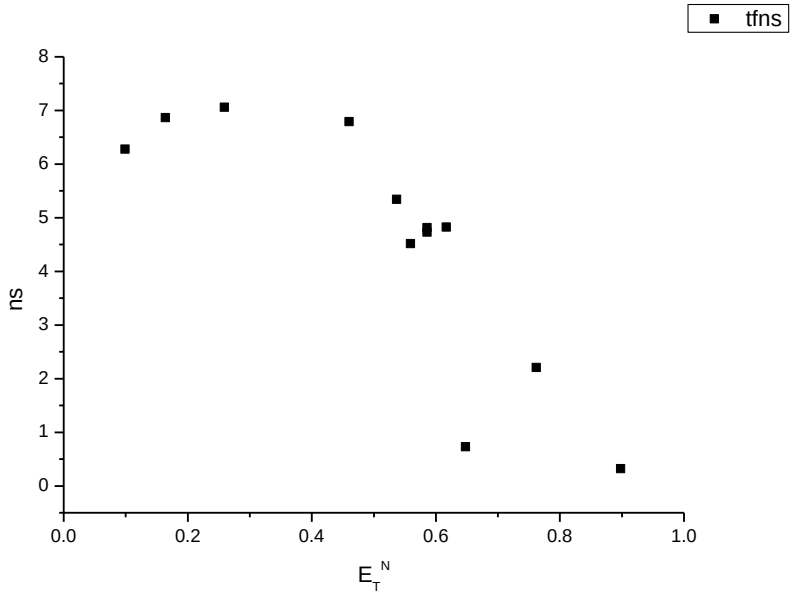

Figure 2.4.52. Amplitude weighted average lifetime (τ_f) of **15** versus E_T^N.

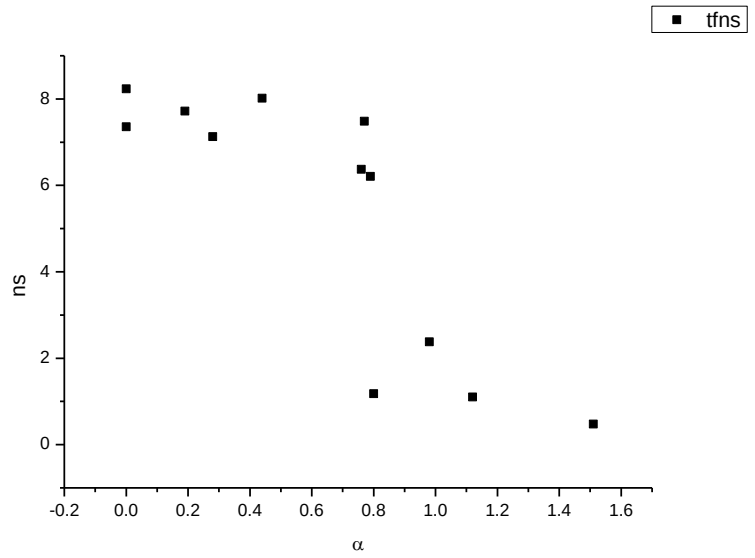

Figure 2.4.53. Intensity weighted average lifetime (τ_f) of **15** versus α.

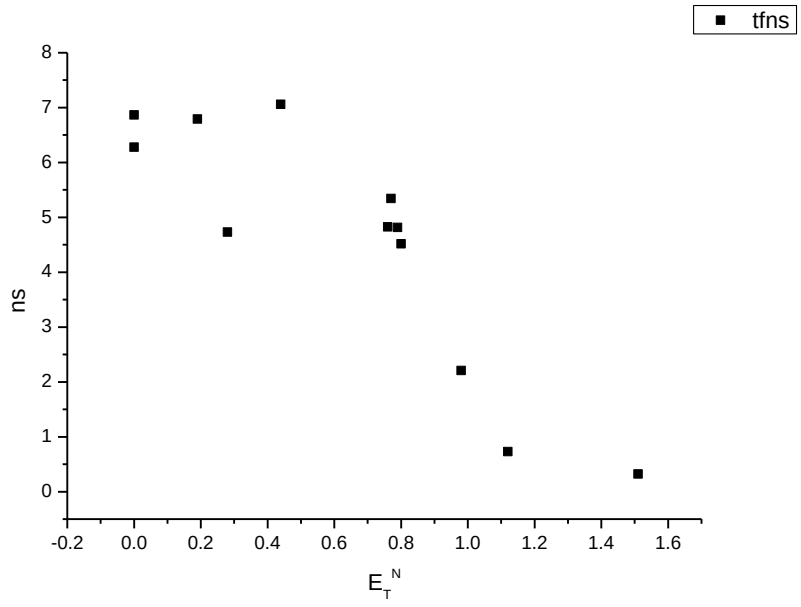

Figure 2.4.54. Amplitude weighted average lifetime (τ_f) of **15** versus α.

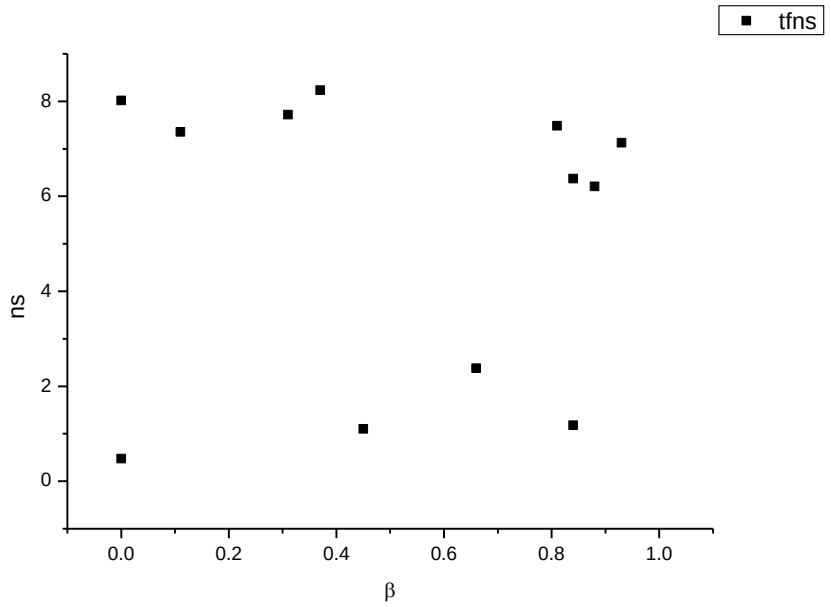

Figure 2.4.55. Intensity weighted average lifetime (τ_f) of **15** versus β.

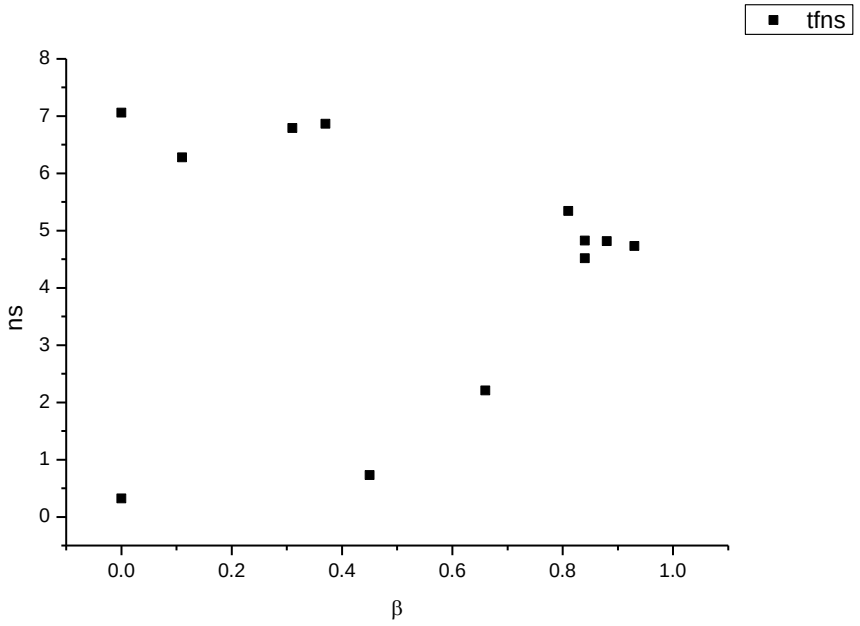

Figure 2.4.56. Amplitude weighted average lifetime (τ_f) of **15** versus β.

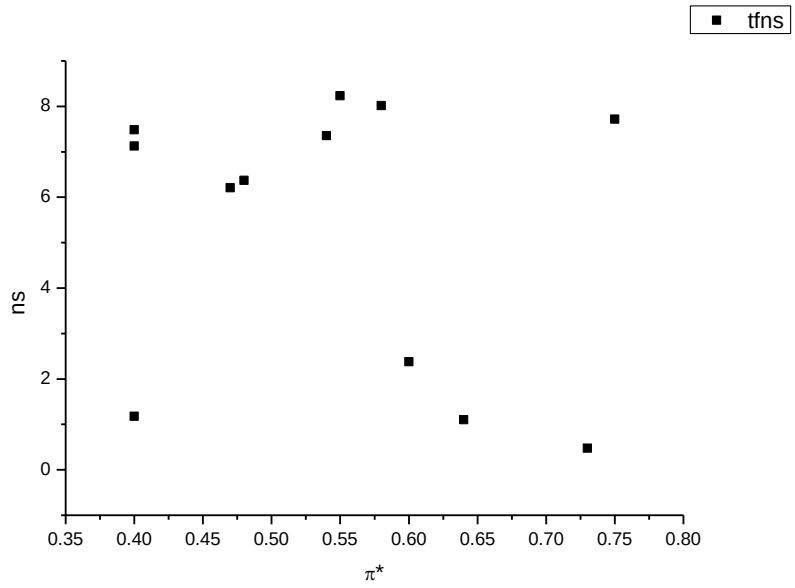

Figure 2.4.57. Intensity weighted average lifetime (τ_f) of **15** versus π^*.

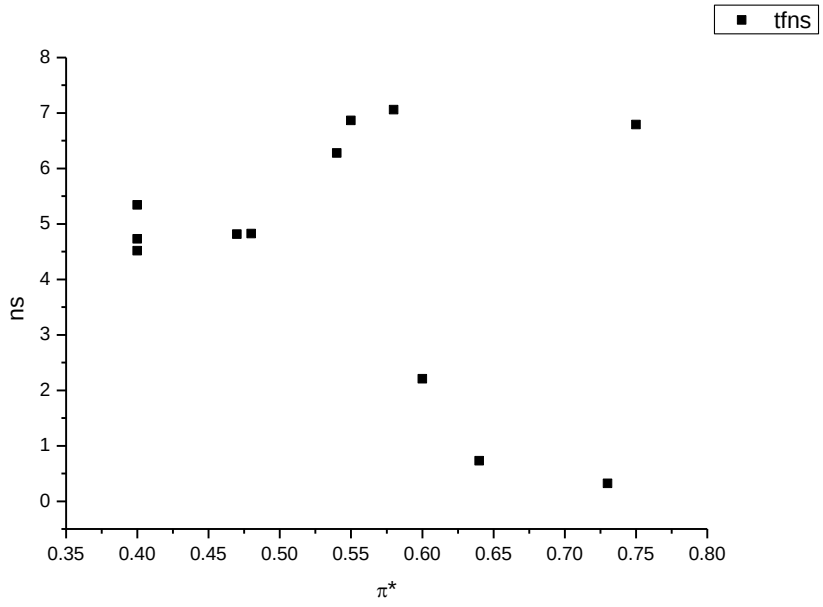

Figure 2.4.58. Amplitude weighted average lifetime (τ_f) of **15** versus π^*.

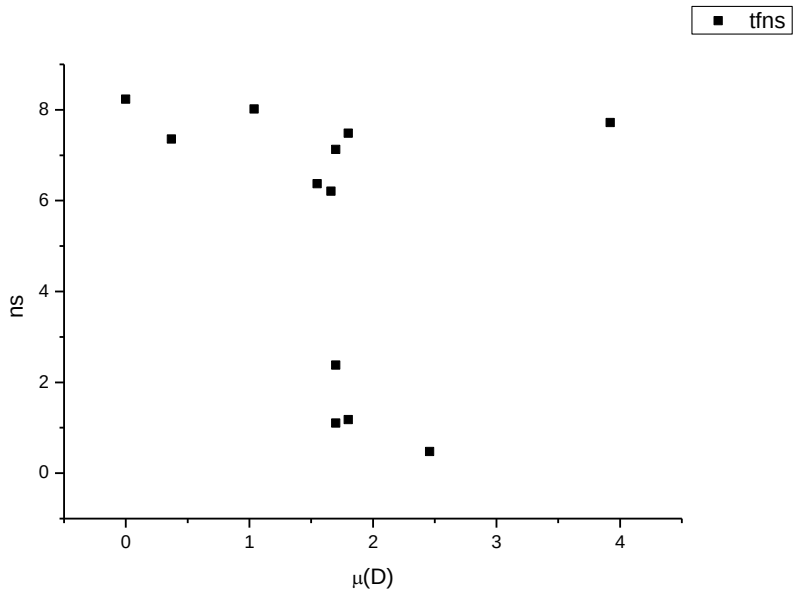

Figure 2.4.59. Intensity weighted average lifetime (τ_f) of **15** versus μ(D).

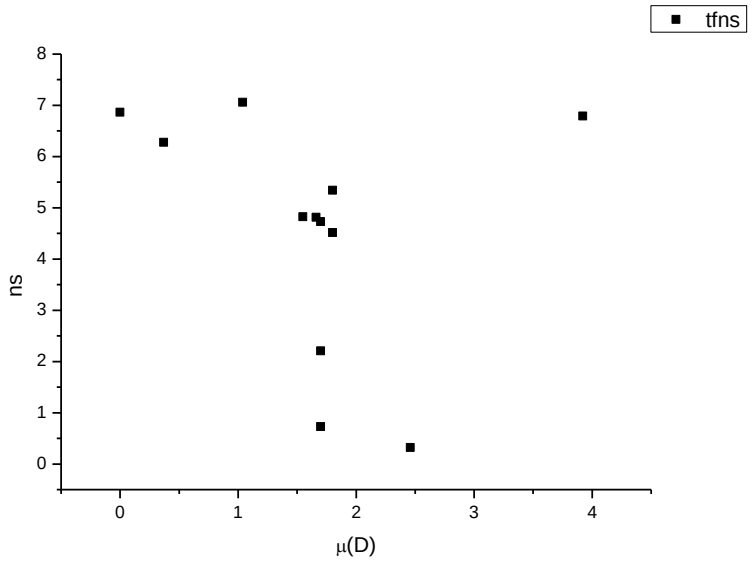

Figure 2.4.60. Amplitude weighted average lifetime (τ_f) of **15** versus μ(D).

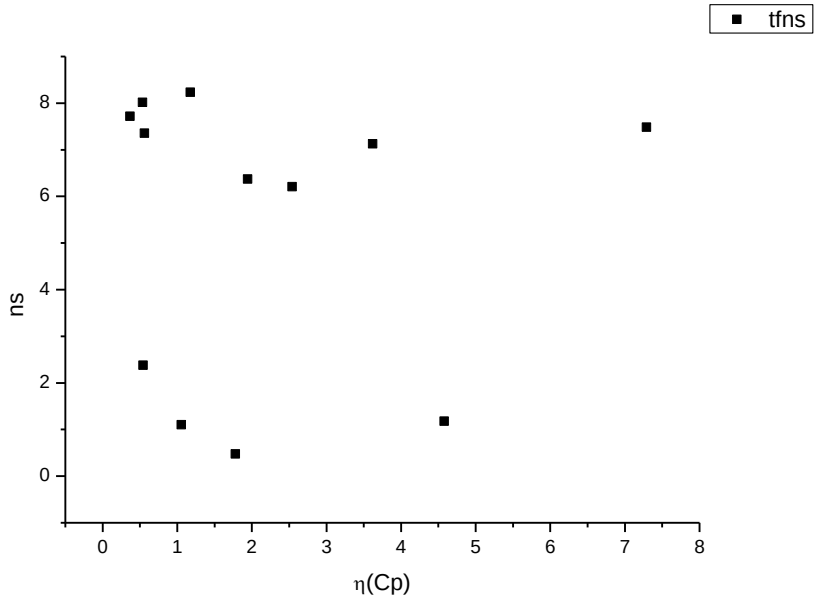

Figure 2.4.61. Intensity weighted average lifetime (τ_f) of **15** versus η(Cp).

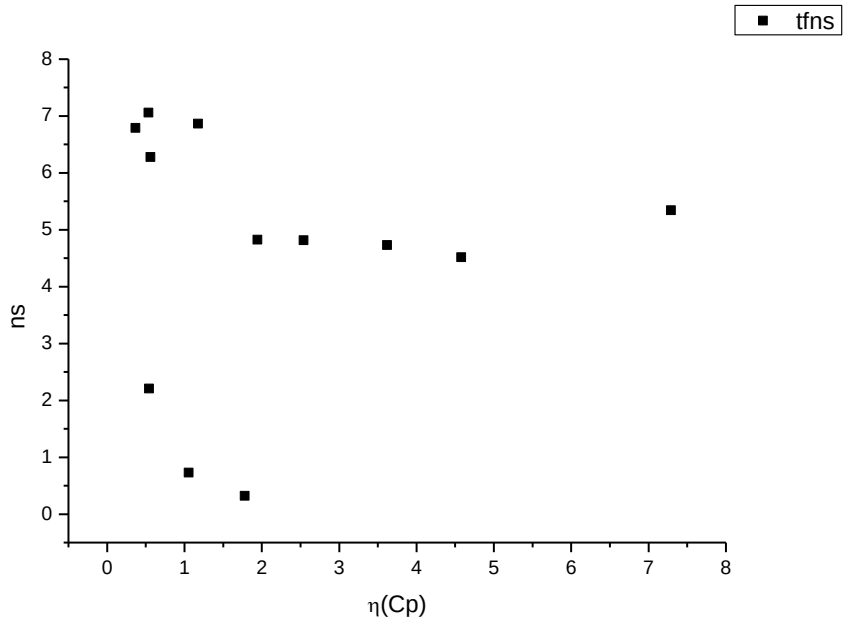

Figure 2.4.62. Amplitude weighted average lifetime (τ_f) of **15** versus η(Cp).

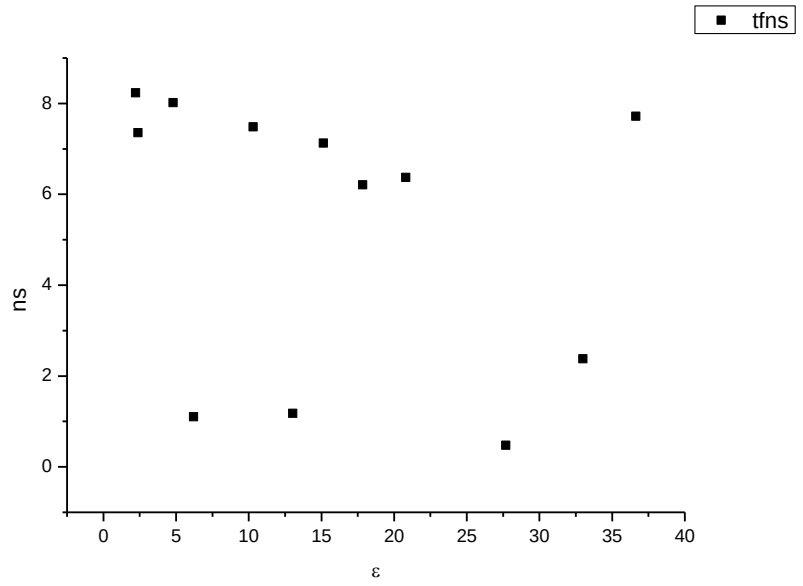

Figure 2.4.63. Intensity weighted average lifetime (τ_f) of **15** versus ε.

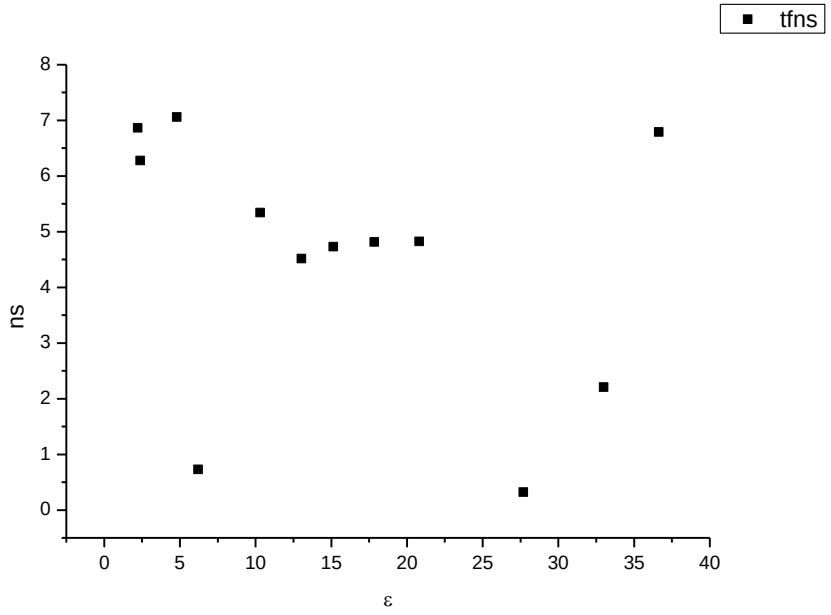

Figure 2.4.64. Amplitude weighted average lifetime (τ_f) of **15** versus ε.

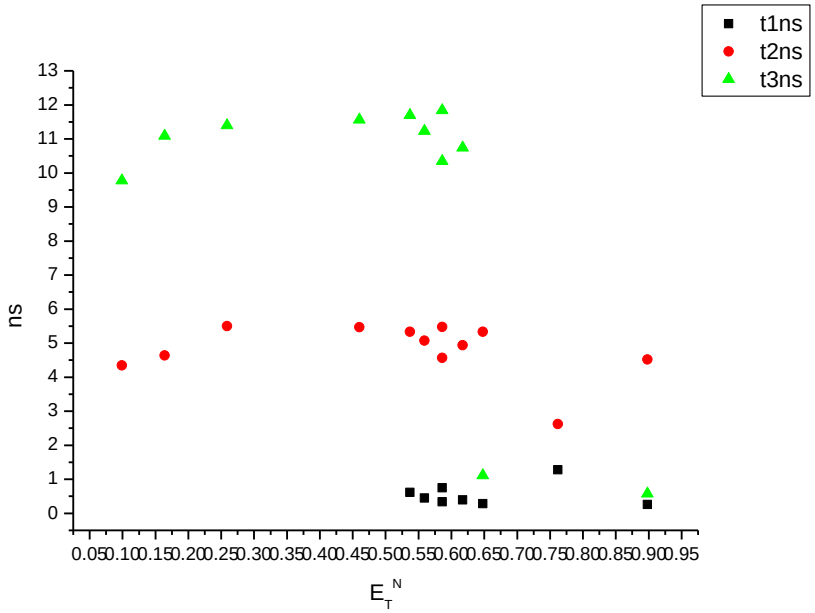

Figure 2.4.65. Intensity weighted components of TCSPC lifetime decay of **15** (500 nm) versus E_T^N.

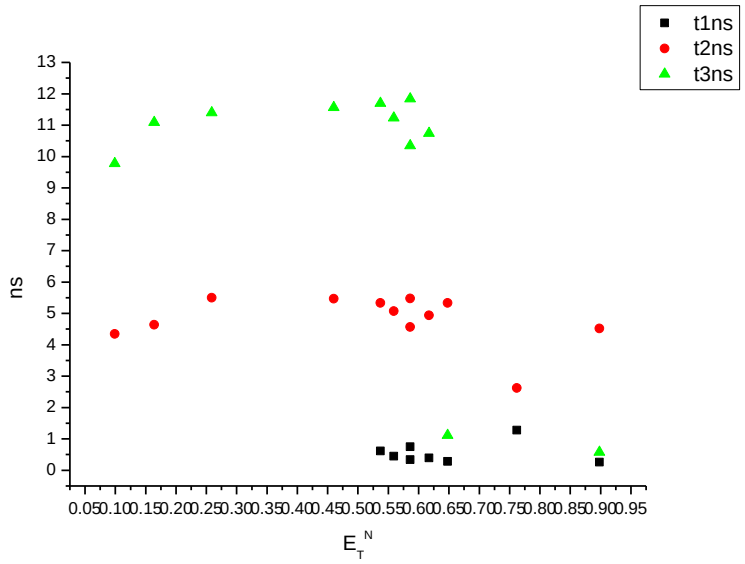

Figure 2.4.66. Amplitude weighted components of TCSPC lifetime decay of **15** (500 nm) versus E_T^N.

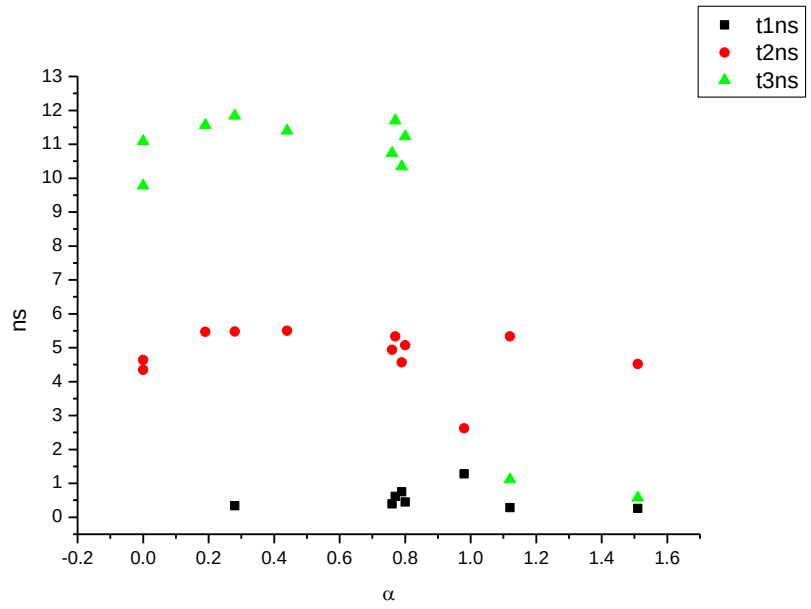

Figure 2.4.67. Intensity weighted components of TCSPC lifetime decay of **15** (500 nm) versus α.

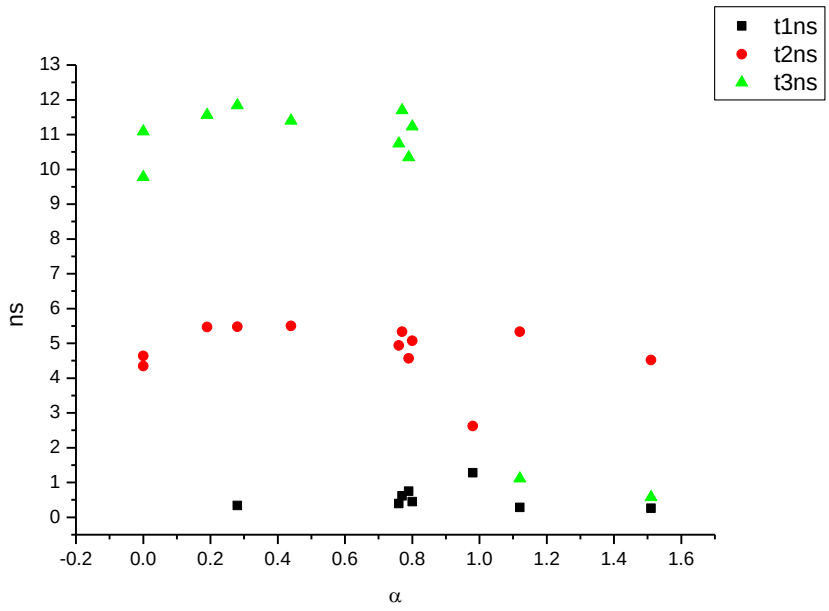

Figure 2.4.68. Amplitude weighted components of TCSPC lifetime decay of **15** (500 nm) versus α.

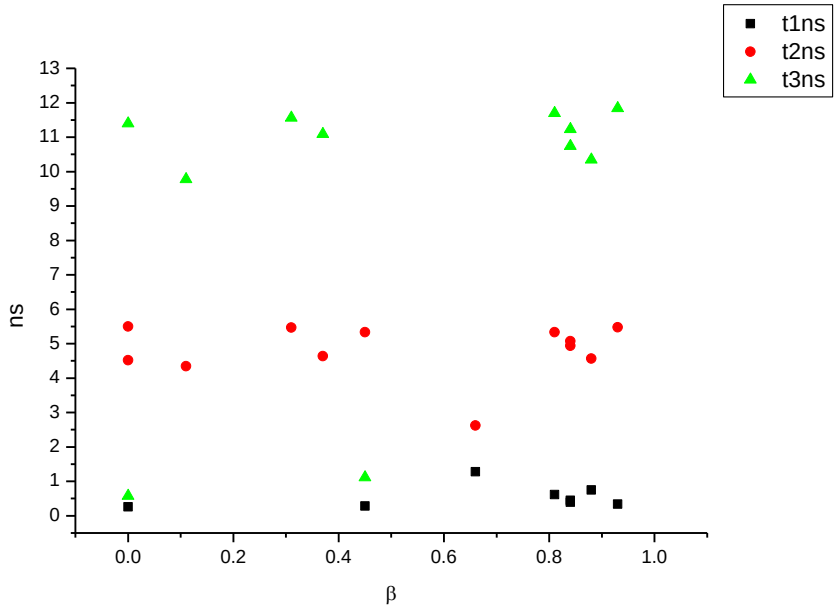

Figure 2.4.69. Intensity weighted components of TCSPC lifetime decay of **15** (500 nm) versus β.

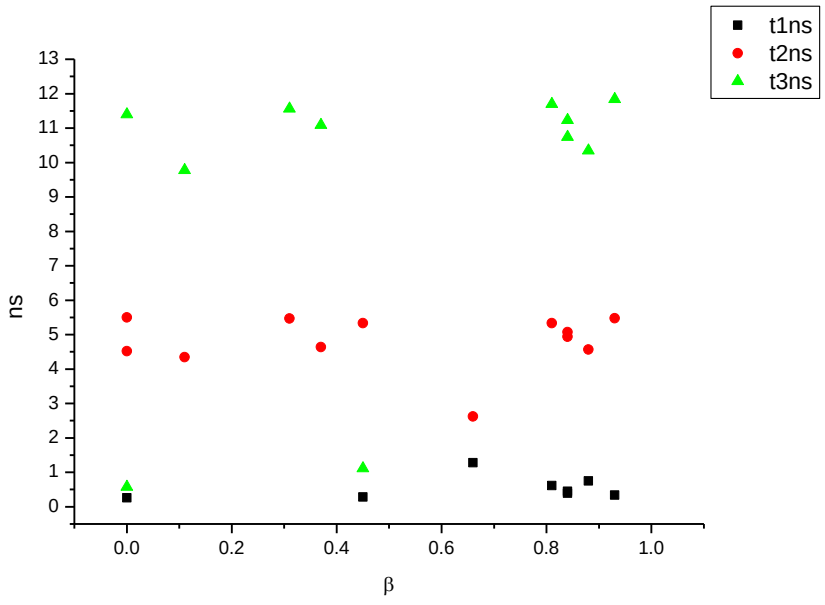

Figure 2.4.70. Amplitude weighted components of TCSPC lifetime decay of **15** (500 nm) versus β.

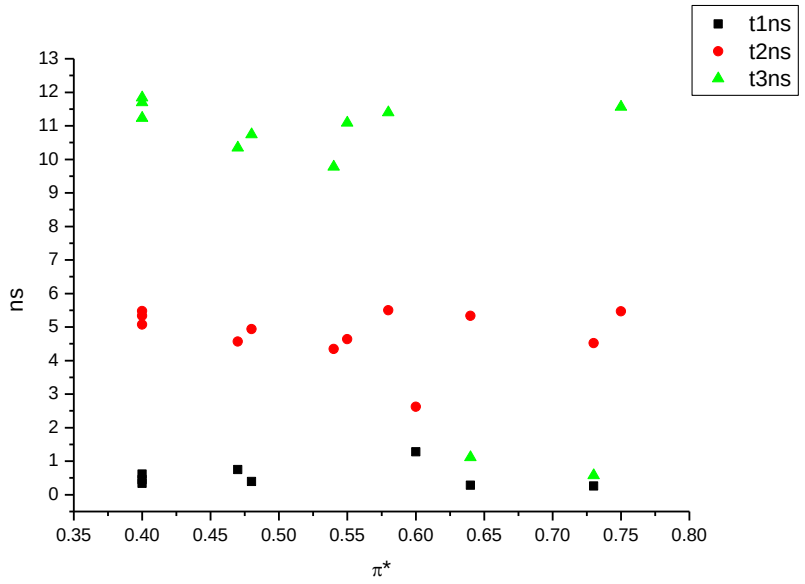

Figure 2.4.71. Intensity weighted components of TCSPC lifetime decay of **15** (500 nm) versus π*.

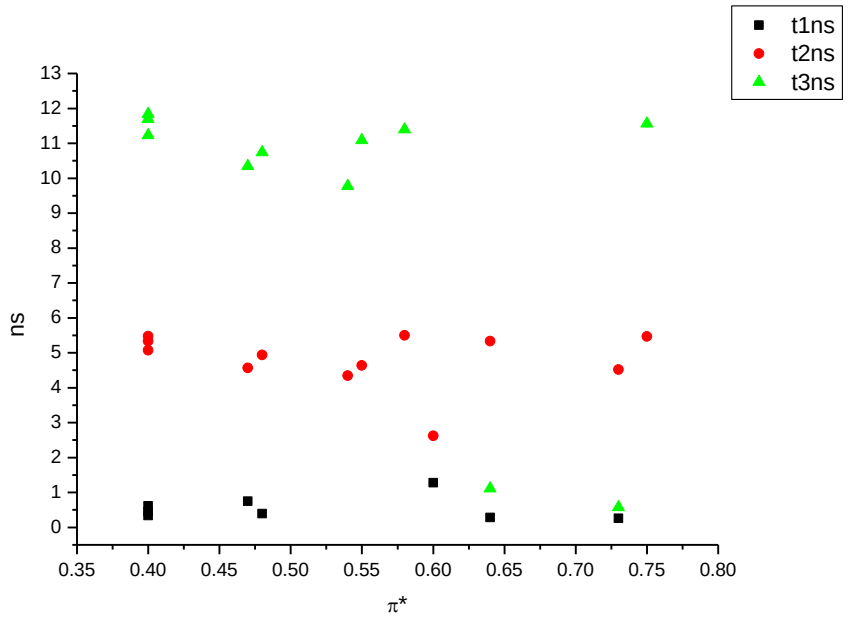

Figure 2.4.72. Amplitude weighted components of TCSPC lifetime decay of **15** (500 nm) versus π*.

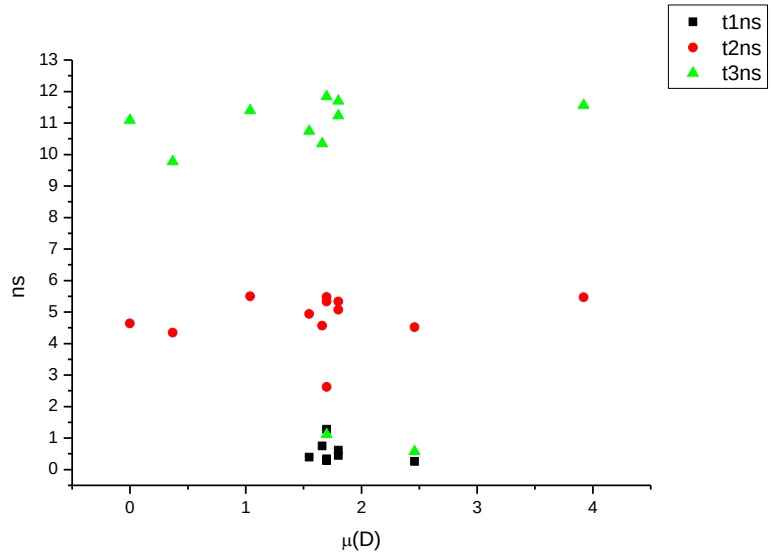

Figure 2.4.73. Intensity weighted components of TCSPC lifetime decay of **15** (500 nm) versus μ(D).

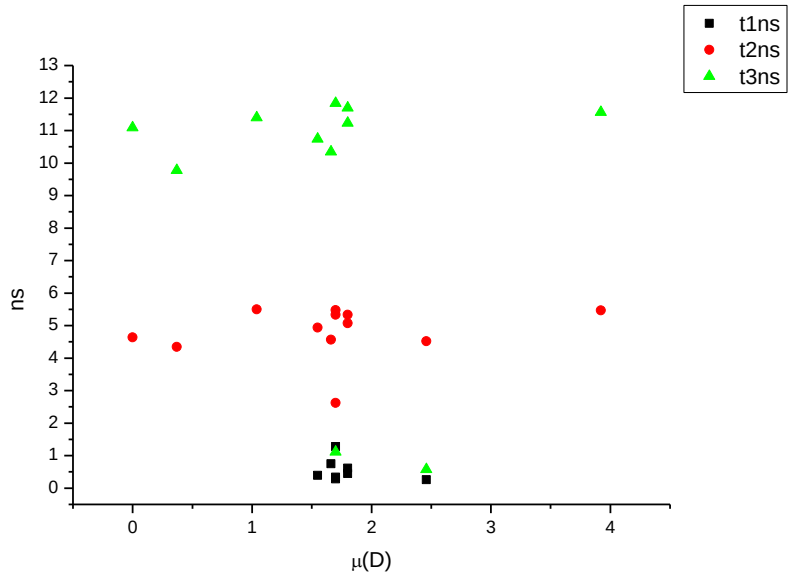

Figure 2.4.74. Amplitude weighted components of TCSPC lifetime decay of **15** (500 nm) versus μ(D).

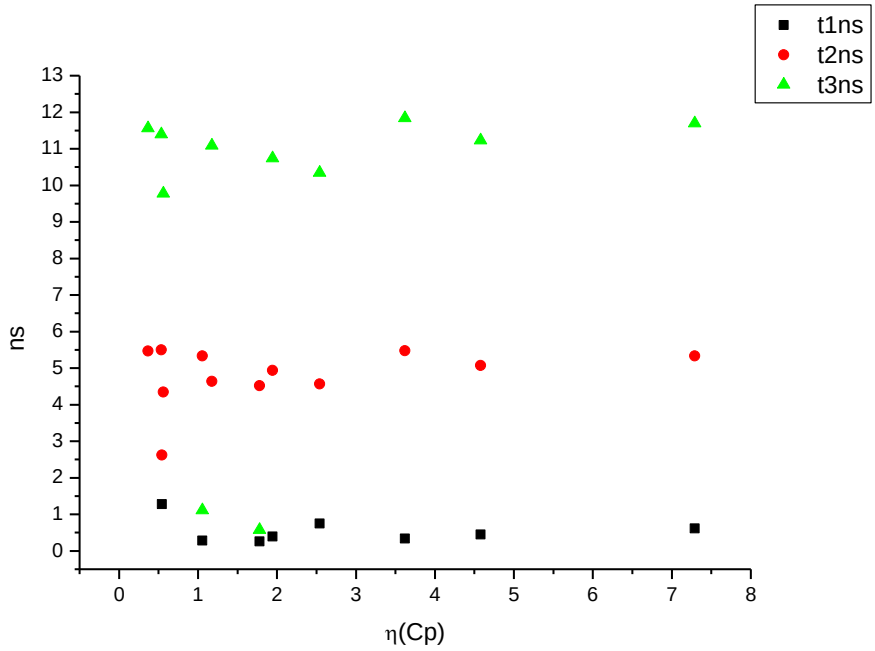

Figure 2.4.75. Intensity weighted components of TCSPC lifetime decay of **15** (500 nm) versus η(Cp).

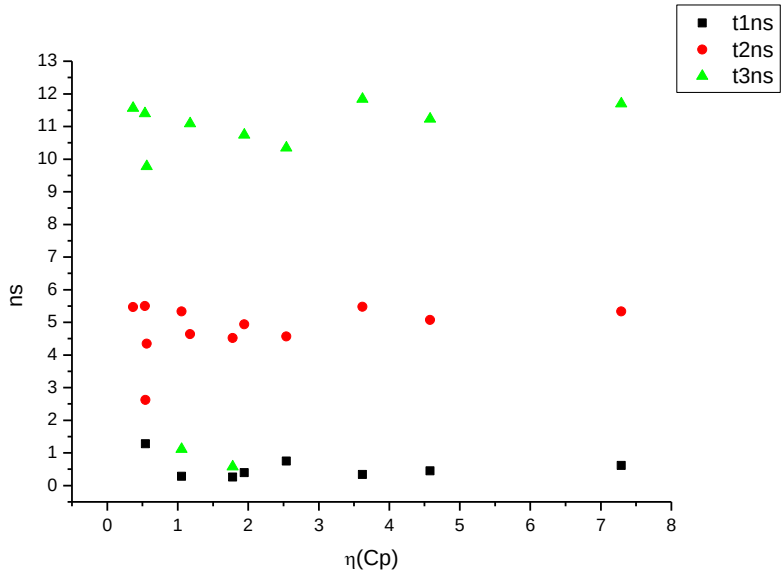

Figure 2.4.76. Amplitude weighted components of TCSPC lifetime decay of **15** (500 nm) versus η(Cp).

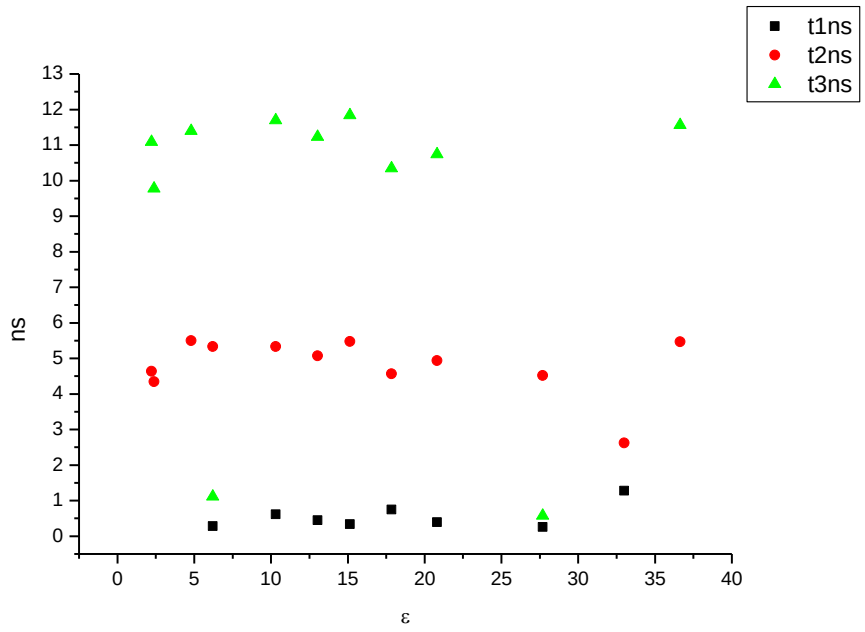

Figure 2.4.77. Intensity weighted components of TCSPC lifetime decay of **15** (500 nm) versus ε.

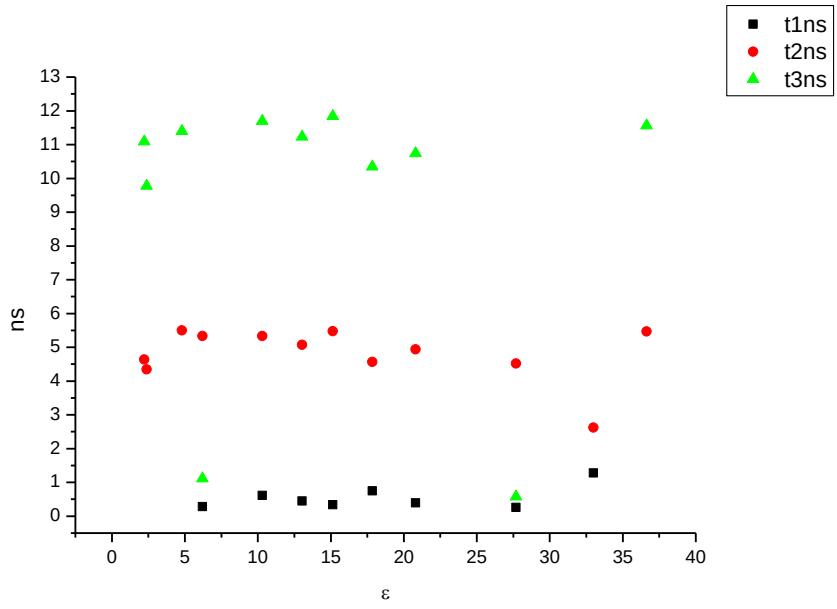

Figure 2.4.78. Amplitude weighted components of TCSPC lifetime decay of **15** (500 nm) versus ε.

2.4.9 295 nm (LED) average fluorescent lifetimes - Solvatochromic analysis.

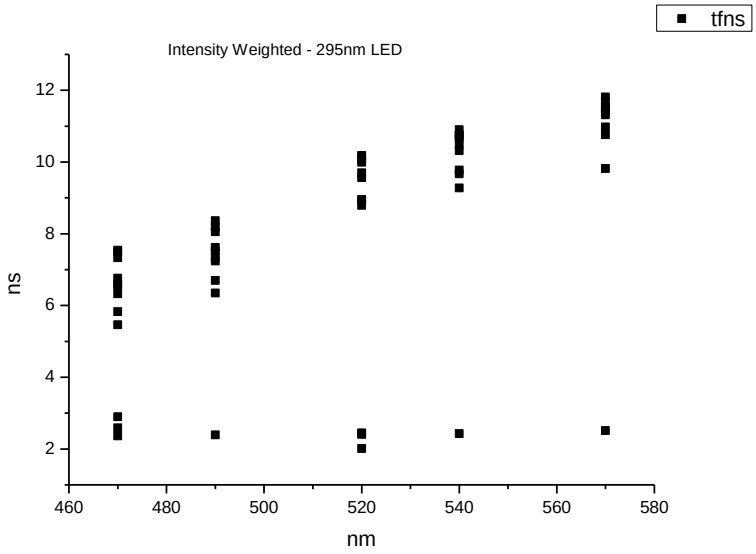

Figure 2.4.79. Intensity weighted average lifetime (τ_f) of **15** versus wavelength (nm).

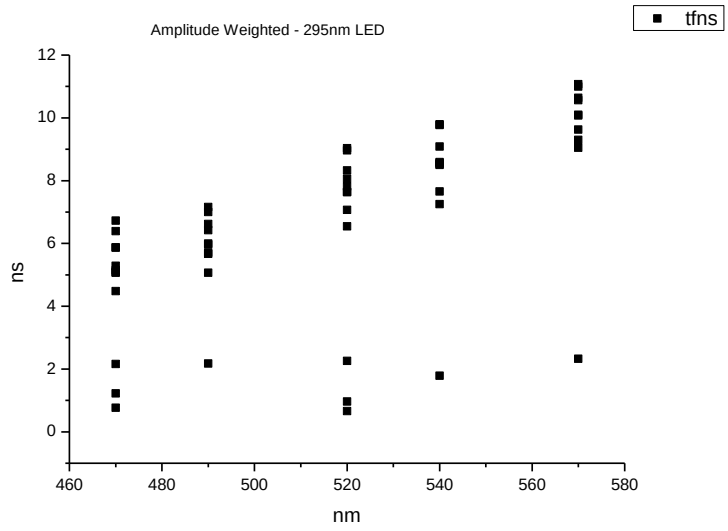

Figure 2.4.80. Amplitude weighted average lifetime (τ_f) of **15** versus wavelength (nm).

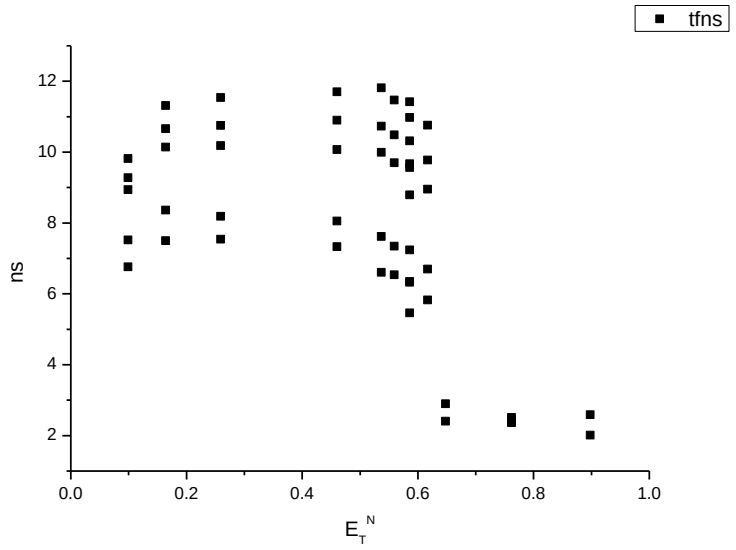

Figure 2.4.81. Intensity weighted average lifetime (τ_f) of **15** versus E_T^N.

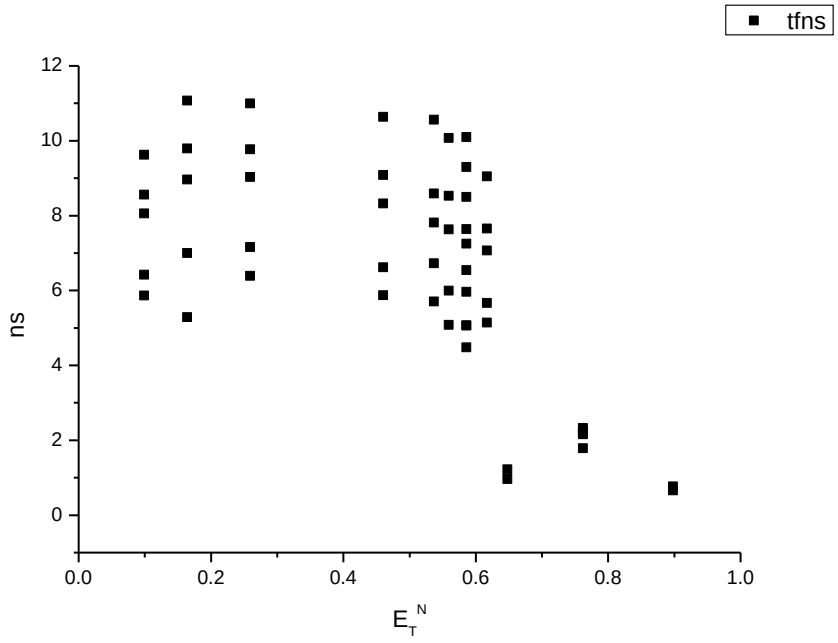

Figure 2.4.82. Amplitude weighted average lifetime (τ_f) of **15** versus E_T^N.

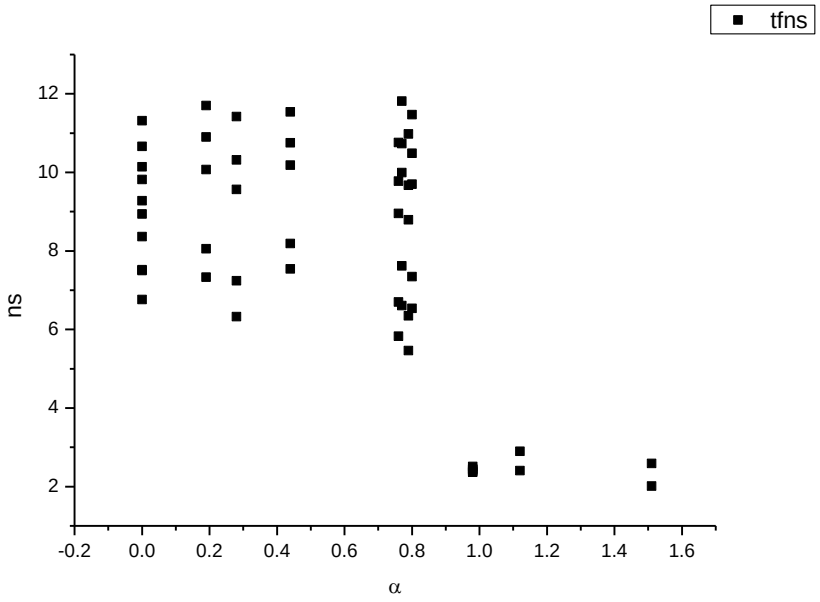

Figure 2.4.83. Intensity weighted average lifetime (τ_f) of **15** versus α.

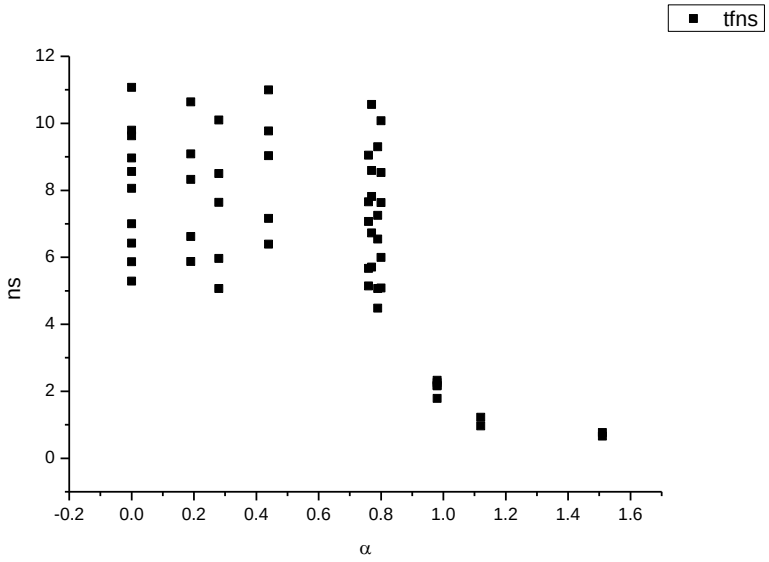

Figure 2.4.84. Amplitude weighted average lifetime (τ_f) of **15** versus α.

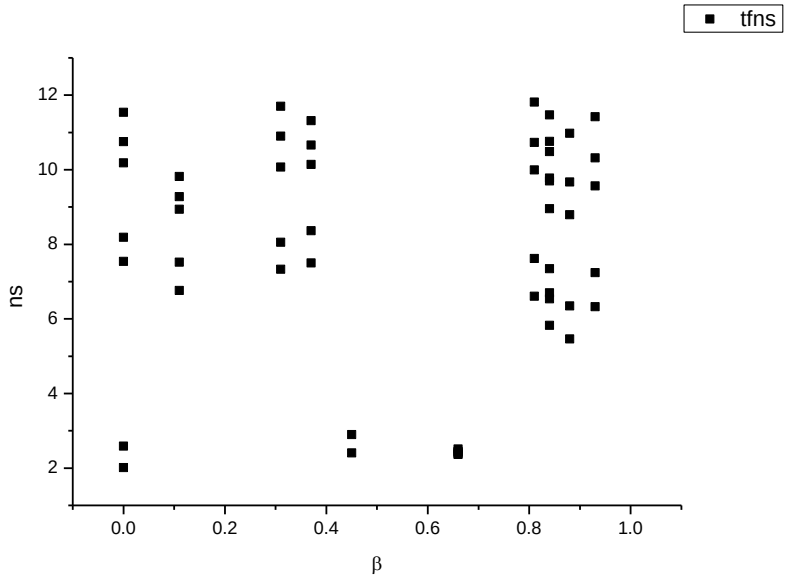

Figure 2.4.85. Intensity weighted average lifetime (τ_f) of **15** versus β.

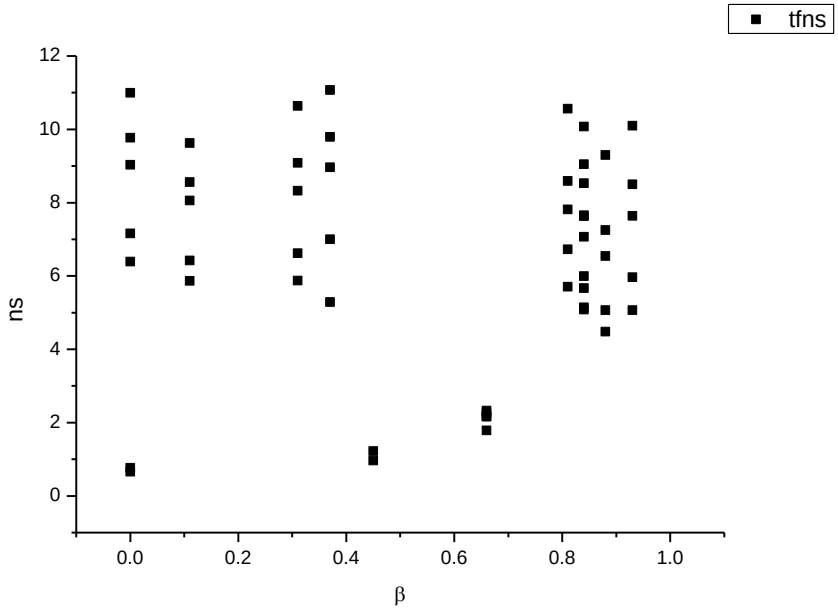

Figure 2.4.86. Amplitude weighted average lifetime (τ_f) of **15** versus β.

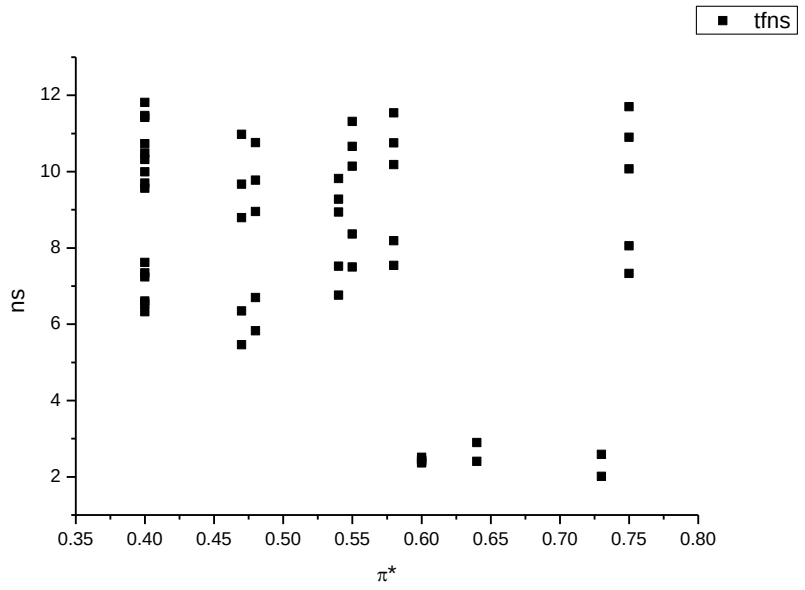

Figure 2.4.87. Intensity weighted average lifetime (τ_f) of **15** versus π*.

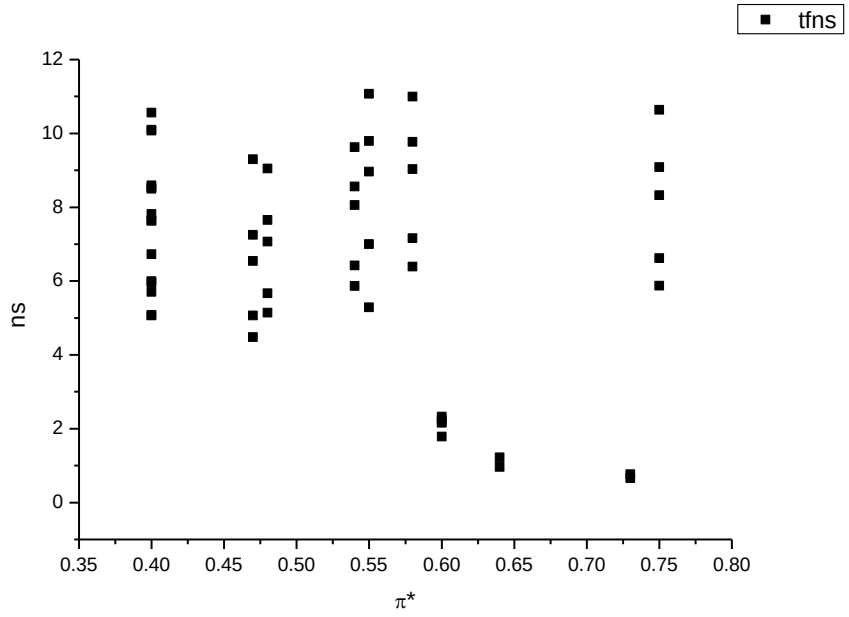

Figure 2.4.88. Amplitude weighted average lifetime (τ_f) of **15** versus π*.

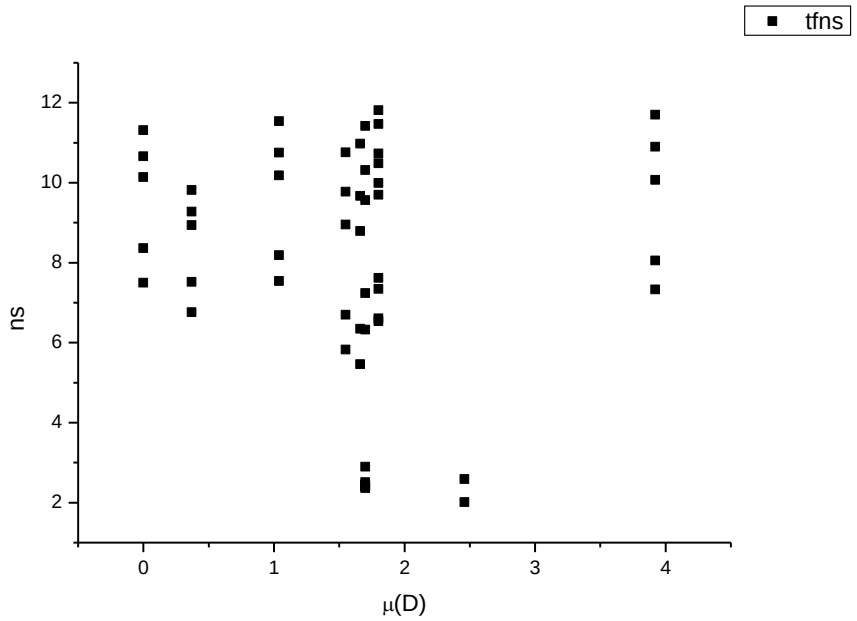

Figure 2.4.89. Intensity weighted average lifetime (τ_f) of **15** versus μ(D).

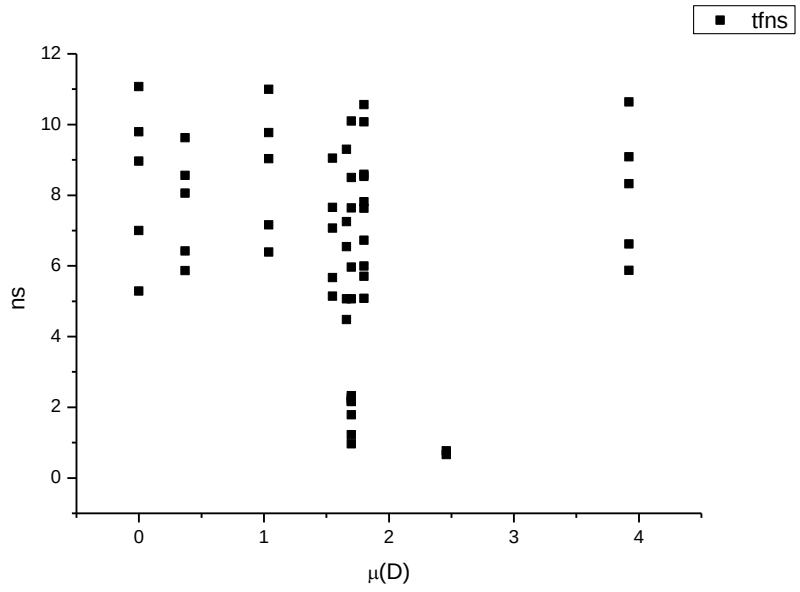

Figure 2.4.90. Amplitude weighted average lifetime (τ_f) of **15** versus μ(D).

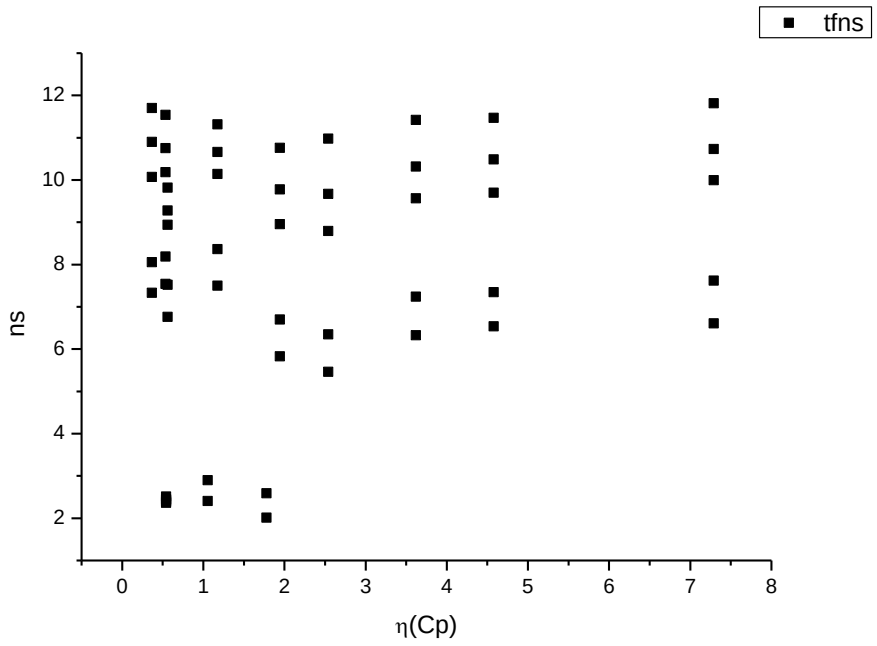

Figure 2.4.91. Intensity weighted average lifetime (τ_f) of **15** versus η(Cp).

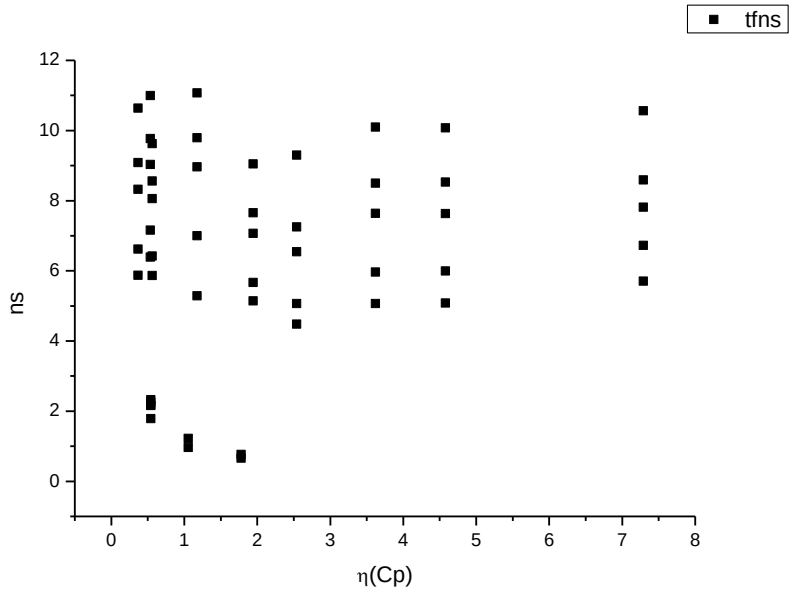

Figure 2.4.92. Amplitude weighted average lifetime (τ_f) of **15** versus η(Cp).

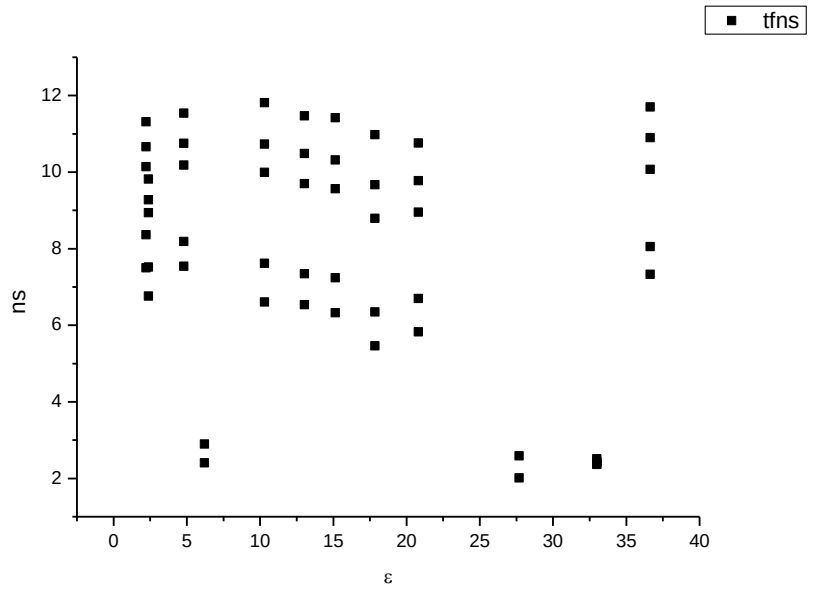

Figure 2.4.93. Intensity weighted average lifetime (τ_f) of **15** versus ε.

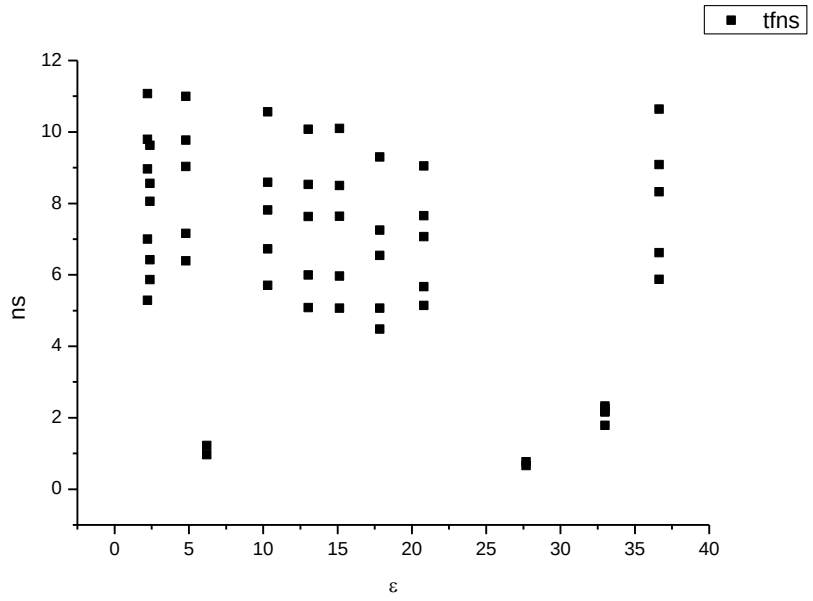

Figure 2.4.94. Amplitude weighted average lifetime (τ_f) of **15** versus ε.

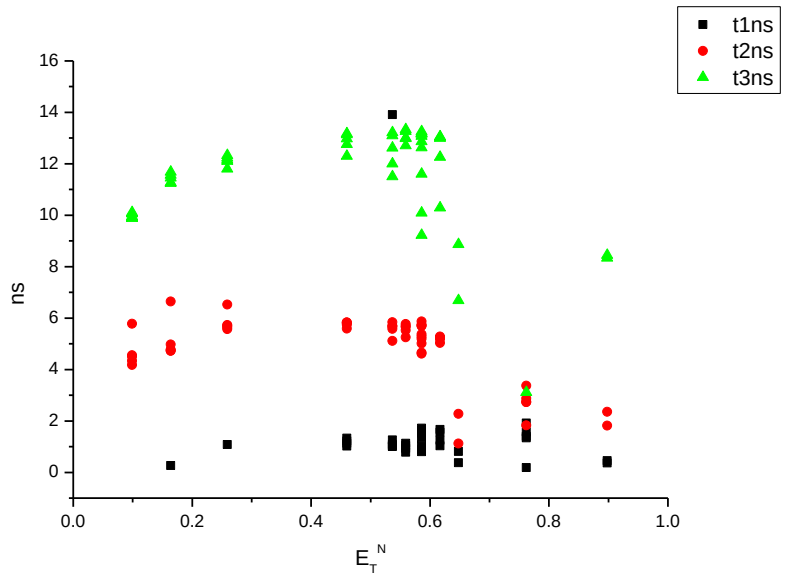

Figure 2.4.95. Intensity weighted components of TCSPC lifetime decay of **15** (470 to 570 nm) versus E_T^N.

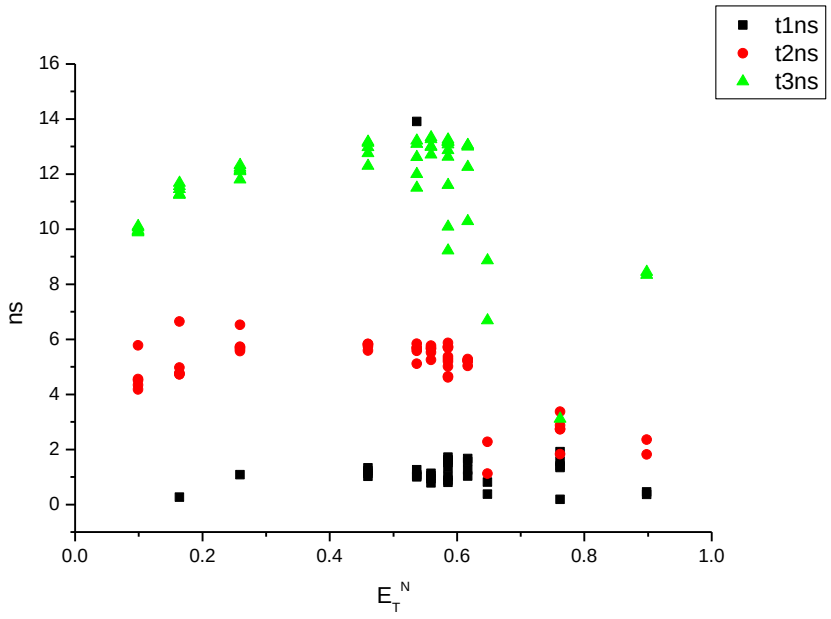

Figure 2.4.96. Amplitude weighted components of TCSPC lifetime decay of **15** (470 to 570 nm) versus E_T^N.

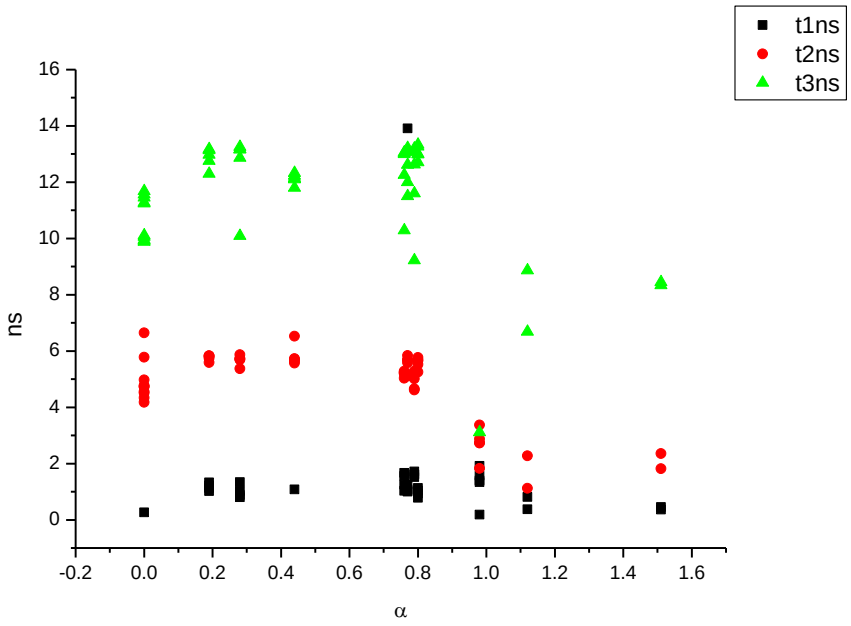

Figure 2.4.97. Intensity weighted components of TCSPC lifetime decay of **15** (470 to 570 nm) versus α.

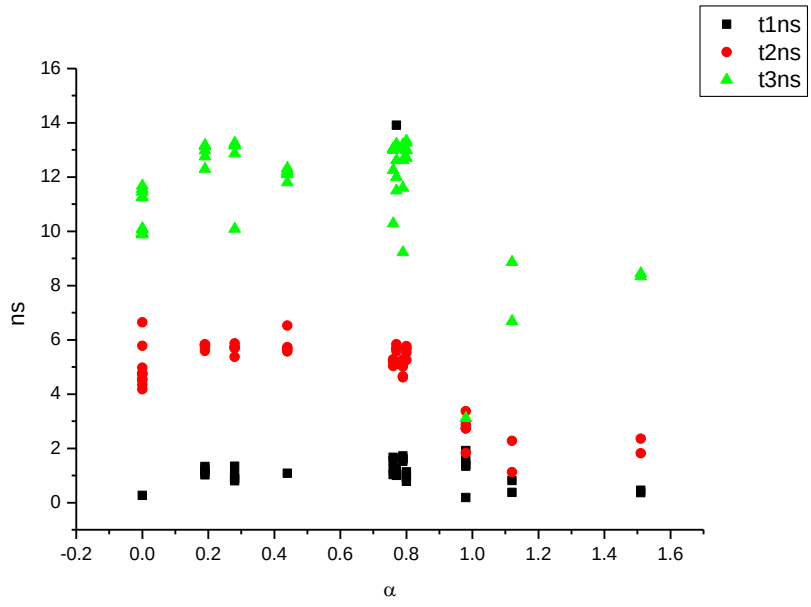

Figure 2.4.98. Amplitude weighted components of TCSPC lifetime decay of **15** (470 to 570 nm) versus α.

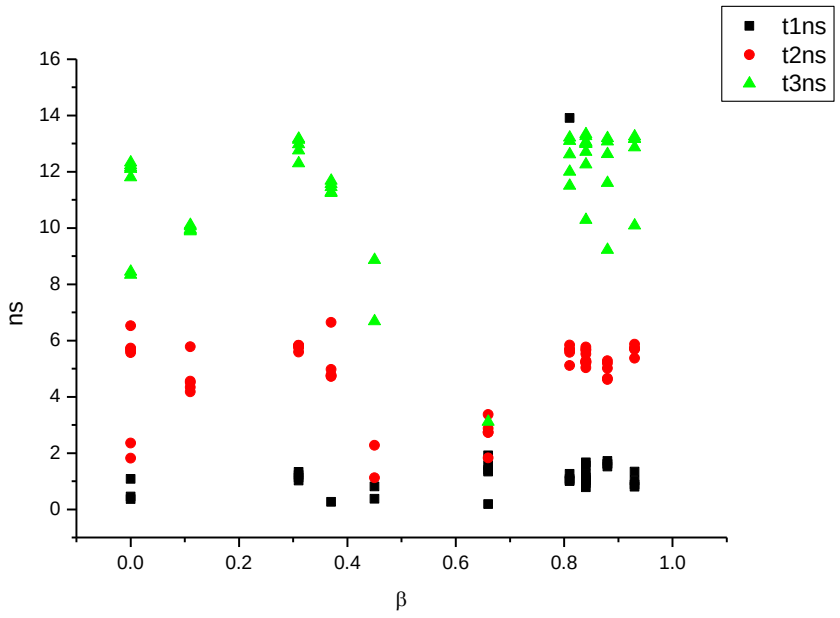

Figure 2.4.99. Intensity weighted components of TCSPC lifetime decay of **15** (470 to 570 nm) versus β.

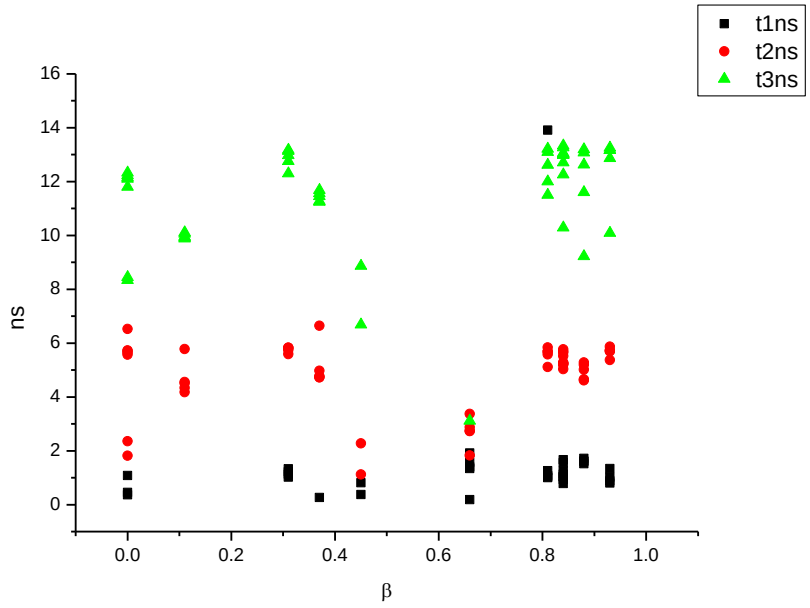

Figure 2.4.100. Amplitude weighted components of TCSPC lifetime decay of **15** (470 to 570 nm) versus β.

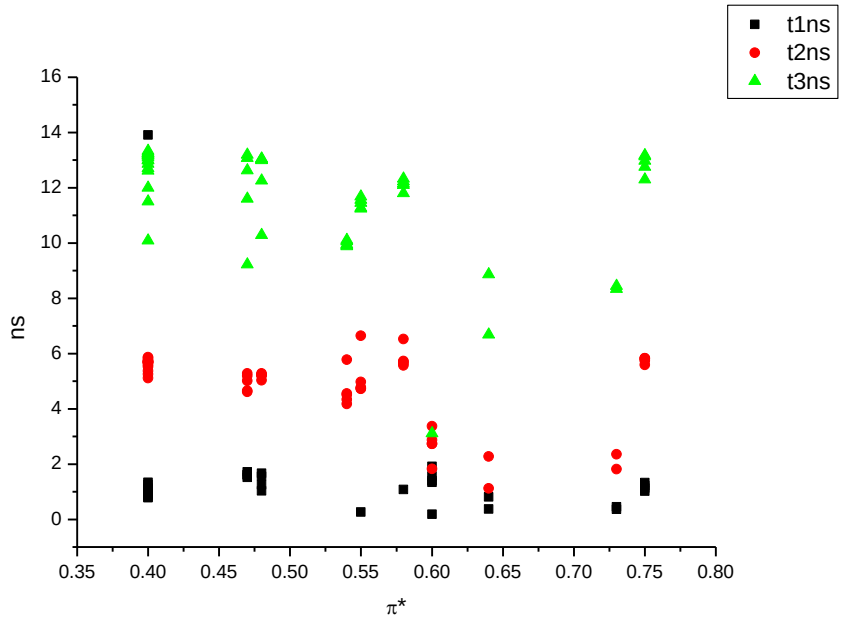

Figure 2.4.101. Intensity weighted components of TCSPC lifetime decay of **15** (470 to 570 nm) versus π*.

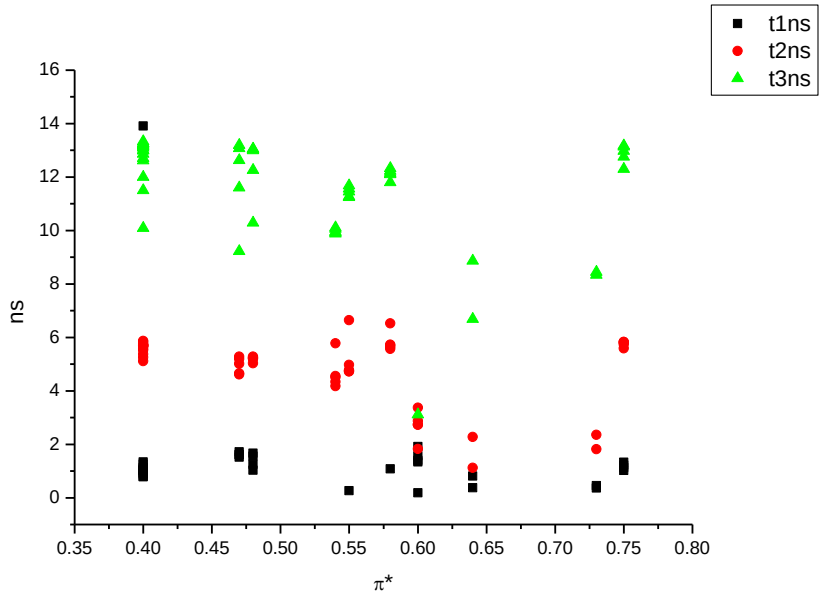

Figure 2.4.102. Amplitude weighted components of TCSPC lifetime decay of **15** (470 to 570 nm) versus π*.

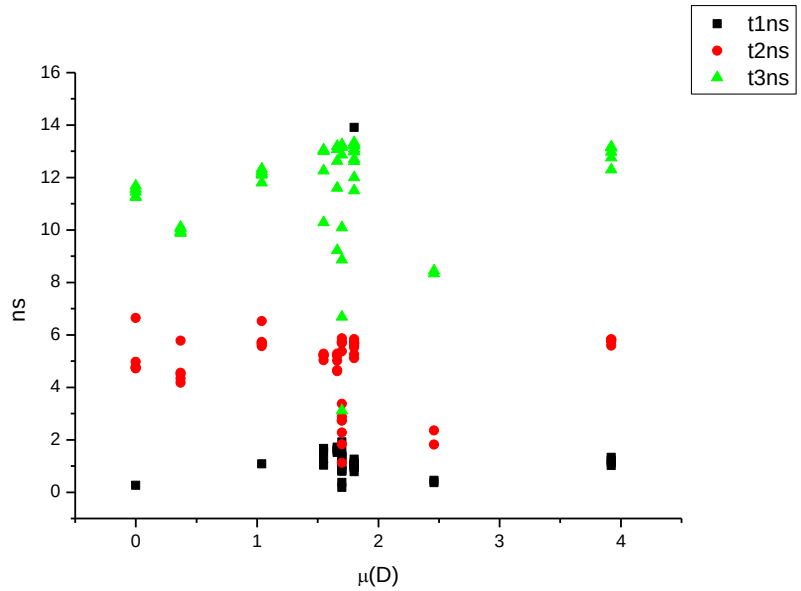

Figure 2.4.103. Intensity weighted components of TCSPC lifetime decay of **15** (470 to 570 nm) versus μ(D).

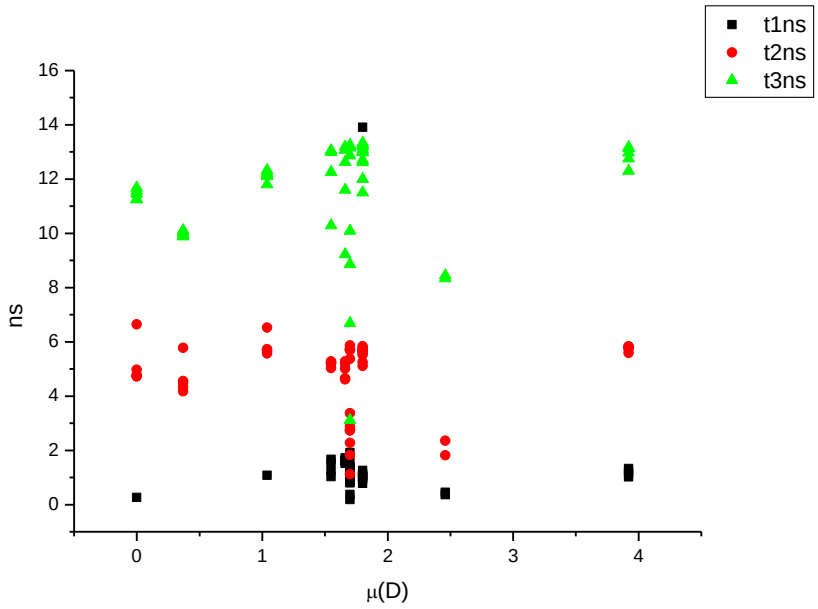

Figure 2.4.104. Amplitude weighted components of TCSPC lifetime decay of **15** (470 to 570 nm) versus μ(D).

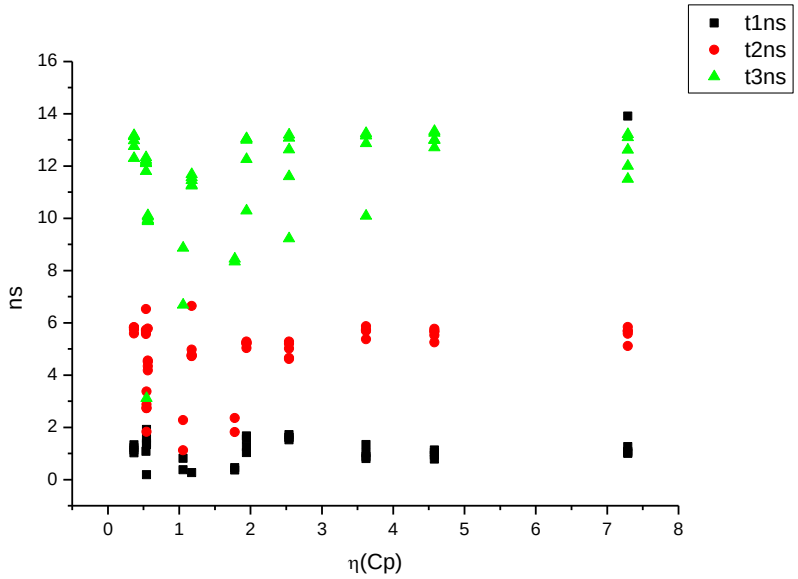

Figure 2.4.105. Intensity weighted components of TCSPC lifetime decay of **15** (470 to 570 nm) versus η(Cp).

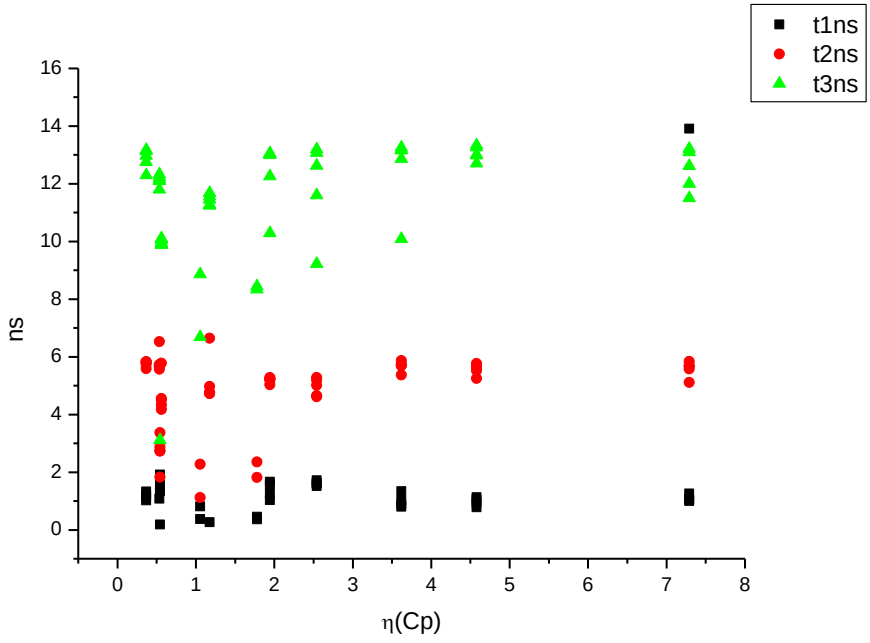

Figure 2.4.106. Amplitude weighted components of TCSPC lifetime decay of **15** (470 to 570 nm) versus η(Cp).

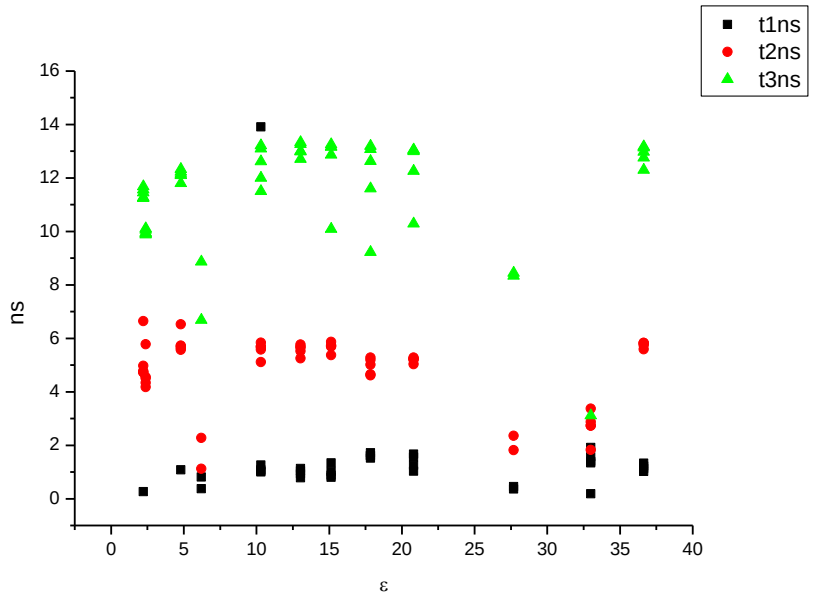

Figure 2.4.107. Intensity weighted components of TCSPC lifetime decay of **15** (470 to 570 nm) versus ε.

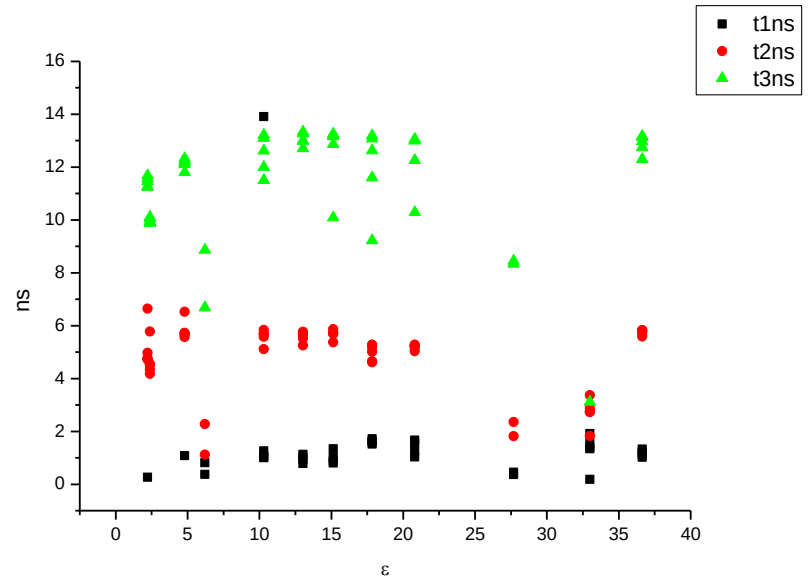

Figure 2.4.108. Amplitude weighted components of TCSPC lifetime decay of **15** (470 to 570 nm) versus ε.

2.4.9.1 470 nm (LED) Lifetime – Solvatochromic analysis.

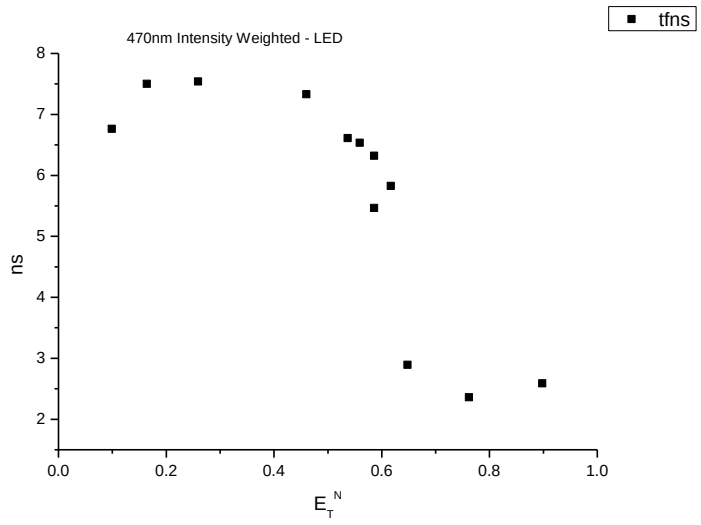

Figure 2.4.109. Intensity weighted average lifetime (τ_f) of **15** at 470 nm versus E_T^N.

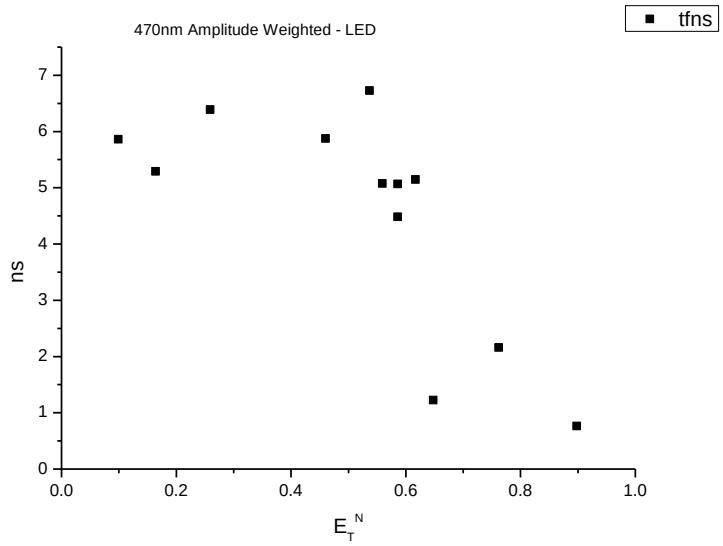

Figure 2.4.110. Amplitude weighted average lifetime (τ_f) of **15** at 470 nm versus E_T^N.

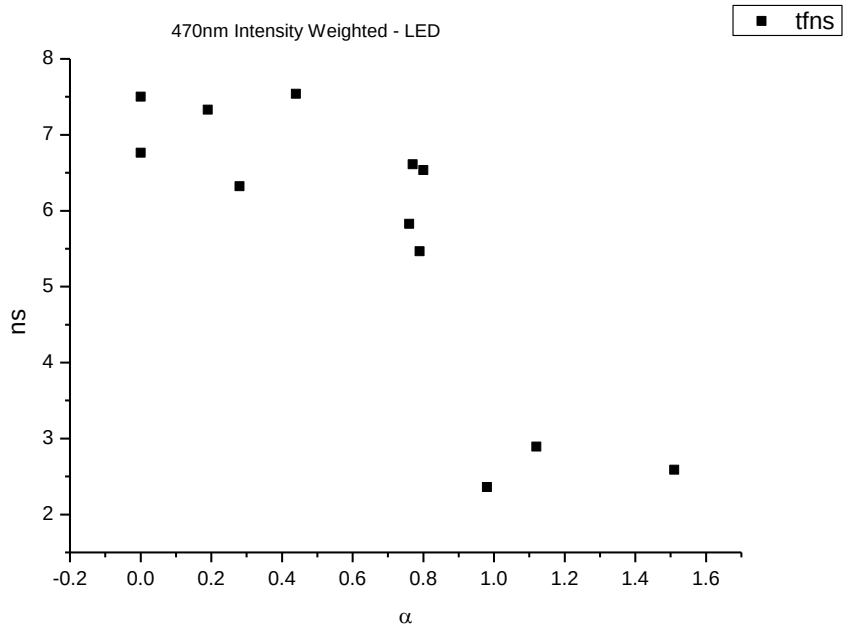

Figure 2.4.111. Intensity weighted average lifetime (τ_f) of **15** at 470 nm versus α.

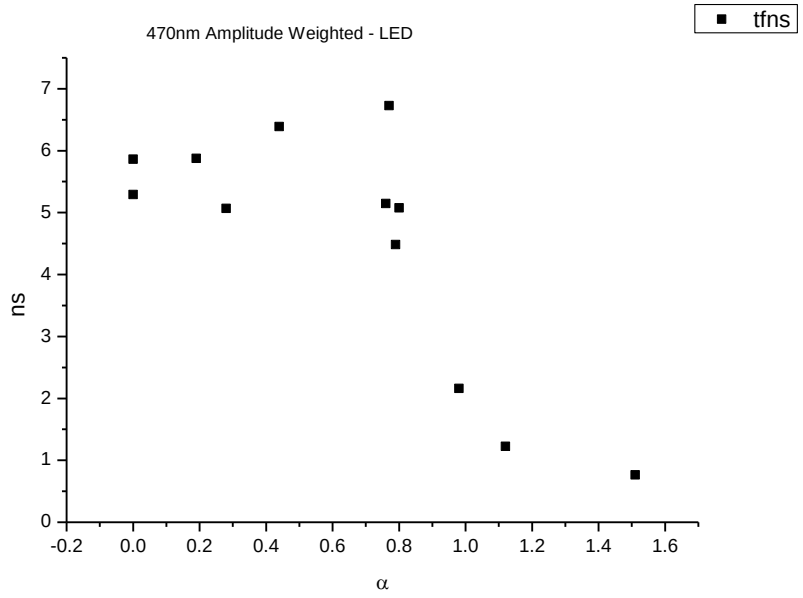

Figure 2.4.112. Amplitude weighted average lifetime (τ_f) of **15** at 470 nm versus α.

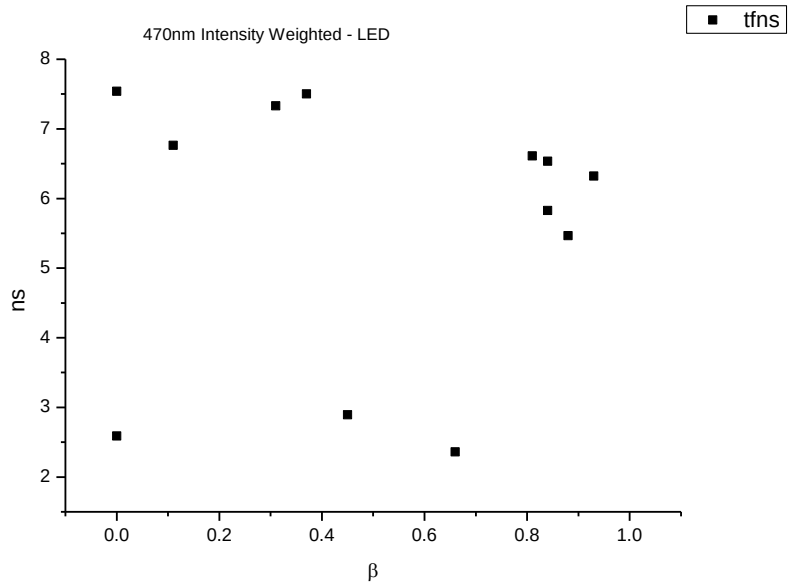

Figure 2.4.113. Intensity weighted average lifetime (τ_f) of **15** at 470 nm versus β.

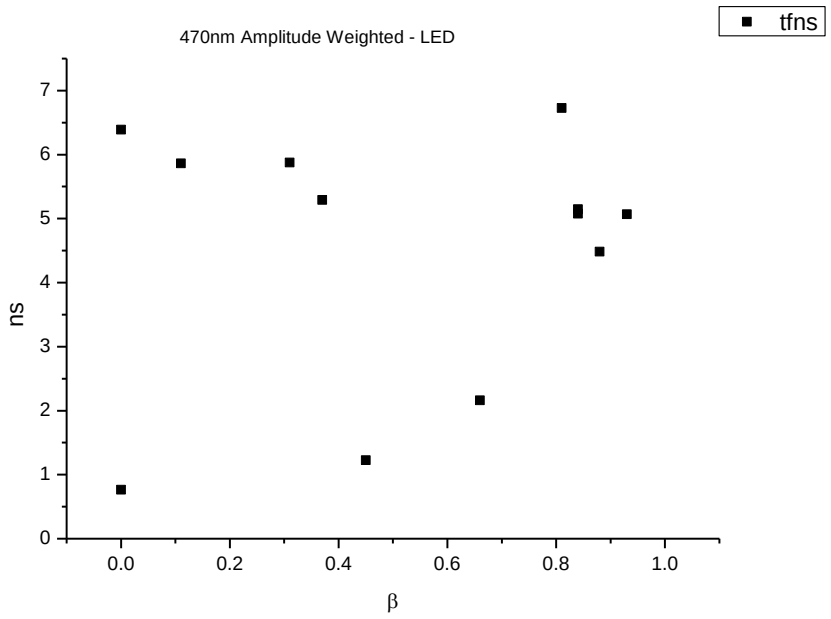

Figure 2.4.114. Amplitude weighted average lifetime (τ_f) of **15** at 470 nm versus β.

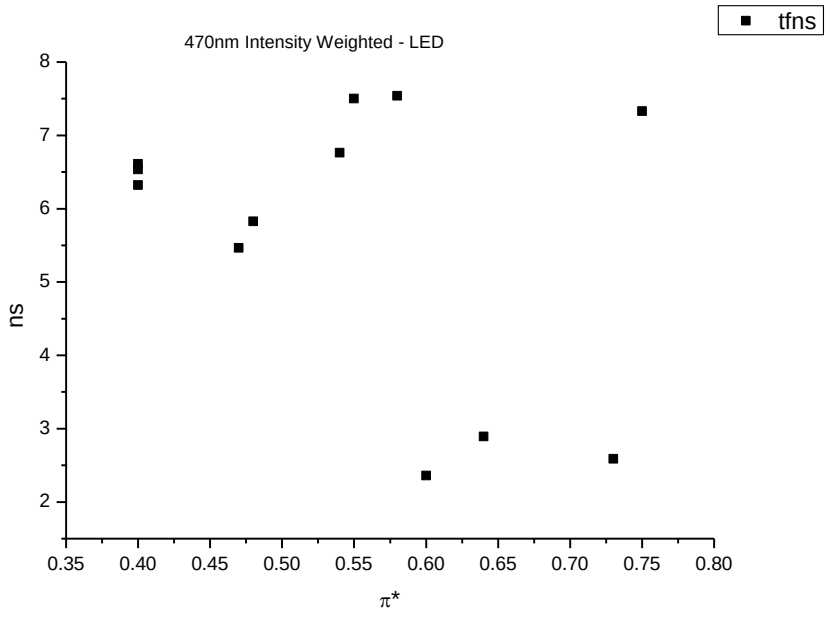

Figure 2.4.115. Intensity weighted average lifetime (τ_f) of **15** at 470 nm versus π*.

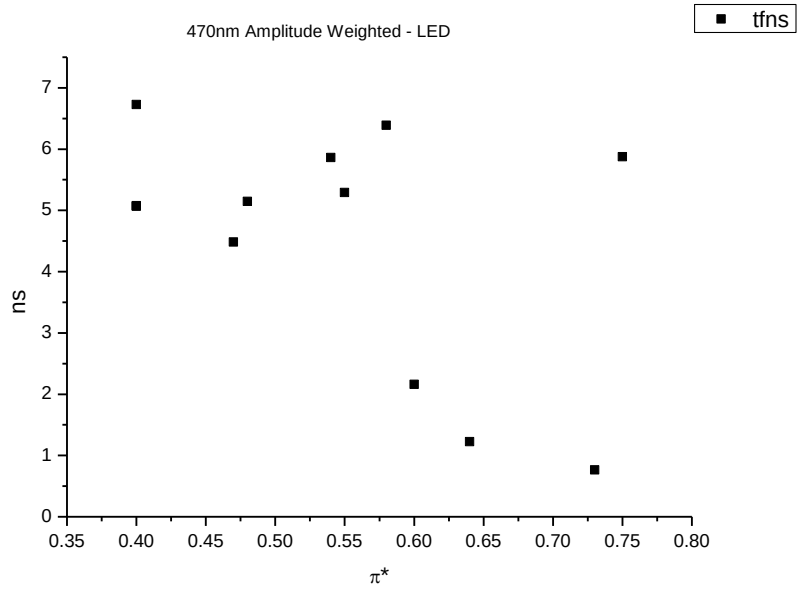

Figure 2.4.116. Amplitude weighted average lifetime (τ_f) of **15** at 470 nm versus π*.

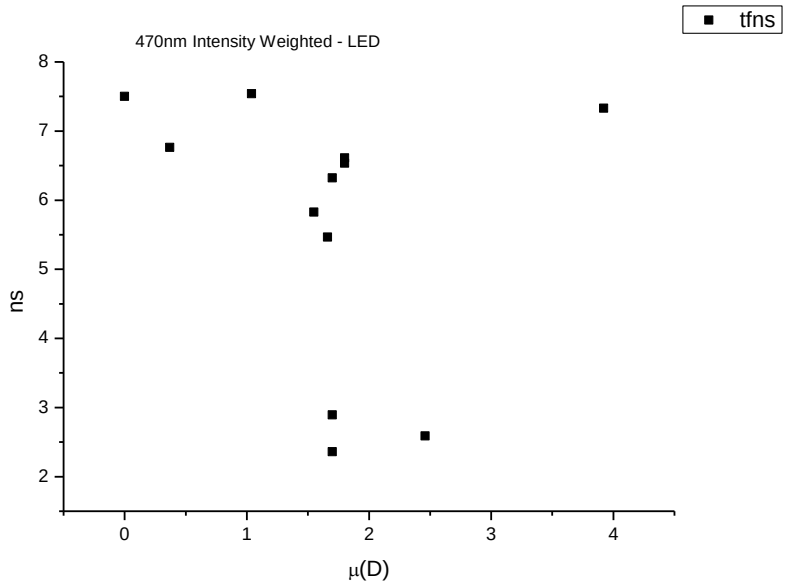

Figure 2.4.117. Intensity weighted average lifetime (τ_f) of **15** at 470 nm versus μ(D).

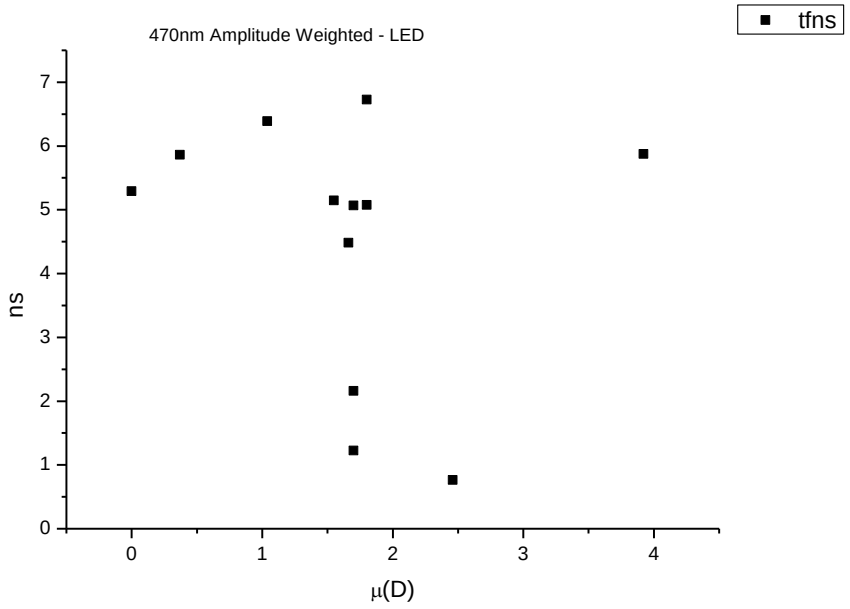

Figure 2.4.118. Amplitude weighted average lifetime (τ_f) of **15** at 470 nm versus μ(D).

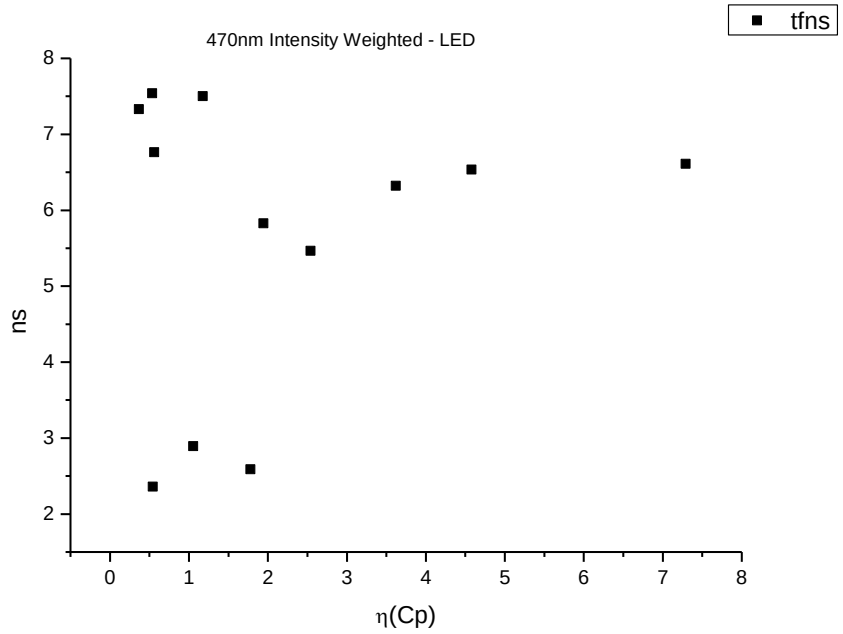

Figure 2.4.119. Intensity weighted average lifetime (τ_f) of **15** at 470 nm versus η(Cp).

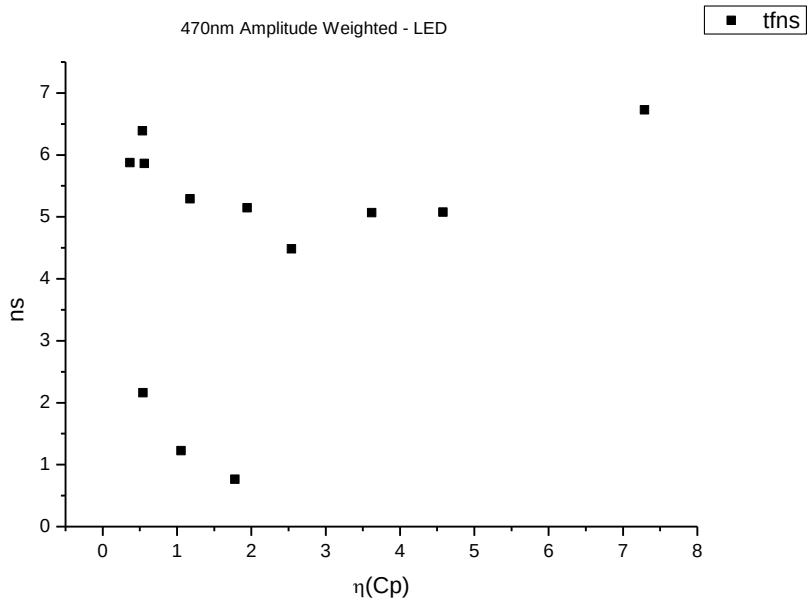

Figure 2.4.120. Amplitude weighted average lifetime (τ_f) of **15** at 470 nm versus η(Cp).

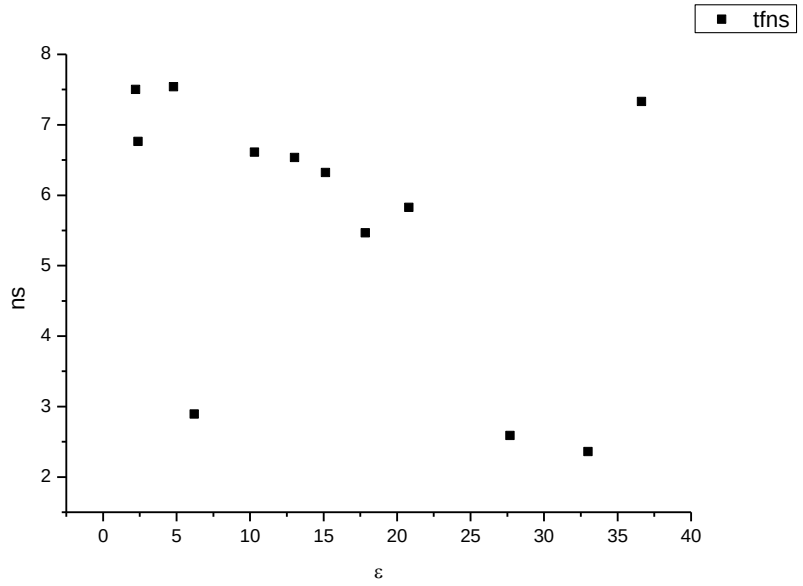

Figure 2.4.121. Intensity weighted average lifetime (τ_f) of **15** at 470 nm versus ε.

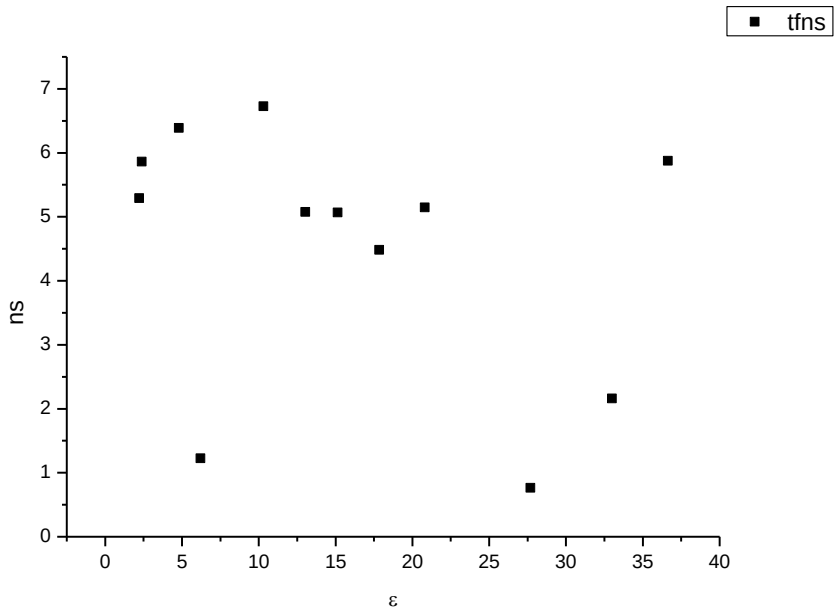

Figure 2.4.122. Amplitude weighted average lifetime (τ_f) of **15** at 470 nm versus ε.

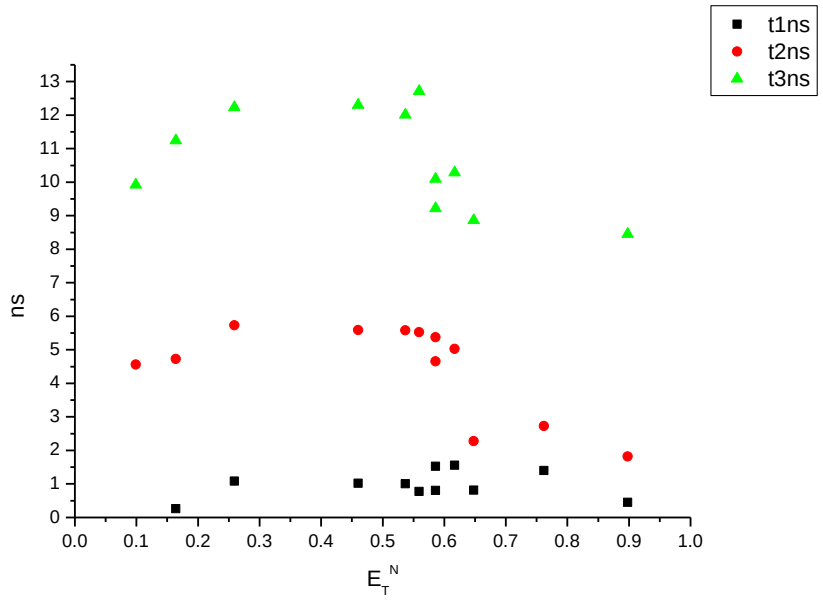

Figure 2.4.123. Intensity weighted components of TCSPC lifetime decay of **15** (470 nm) versus E_T^N.

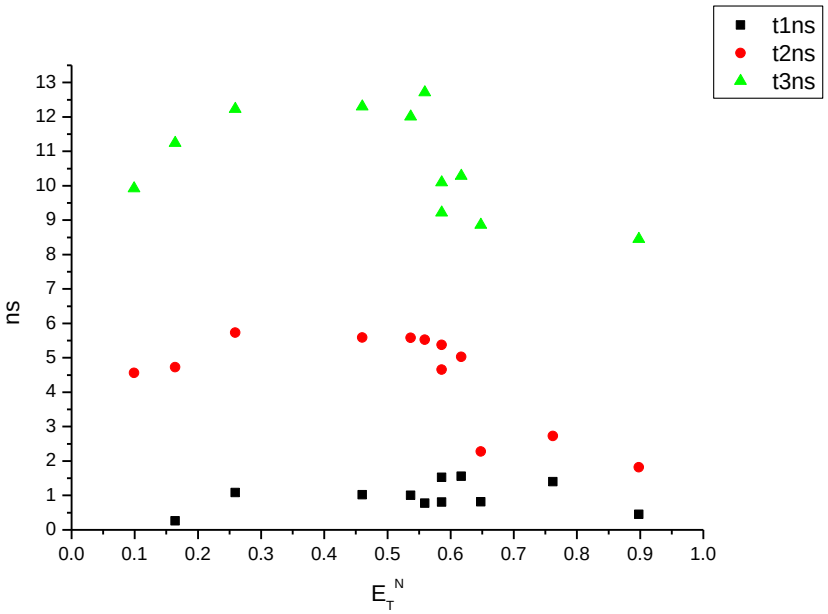

Figure 2.4.124. Amplitude weighted components of TCSPC lifetime decay of **15** (470 nm) versus E_T^N.

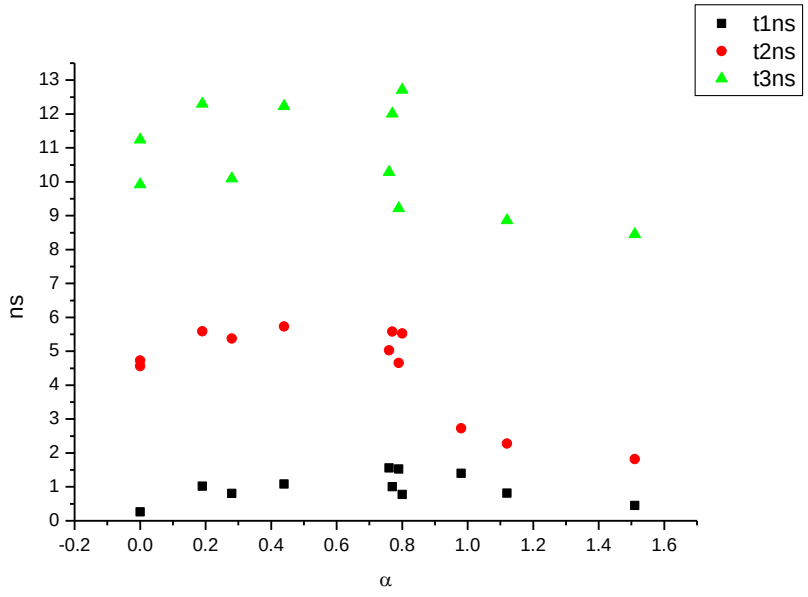

Figure 2.4.125. Intensity weighted components of TCSPC lifetime decay of **15** (470 nm) versus α.

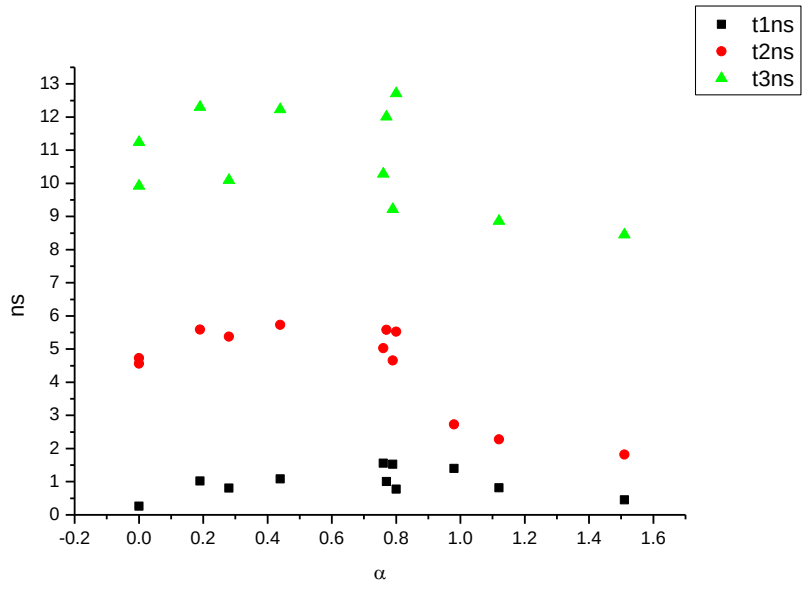

Figure 2.4.126. Amplitude weighted components of TCSPC lifetime decay of **15** (470 nm) versus α.

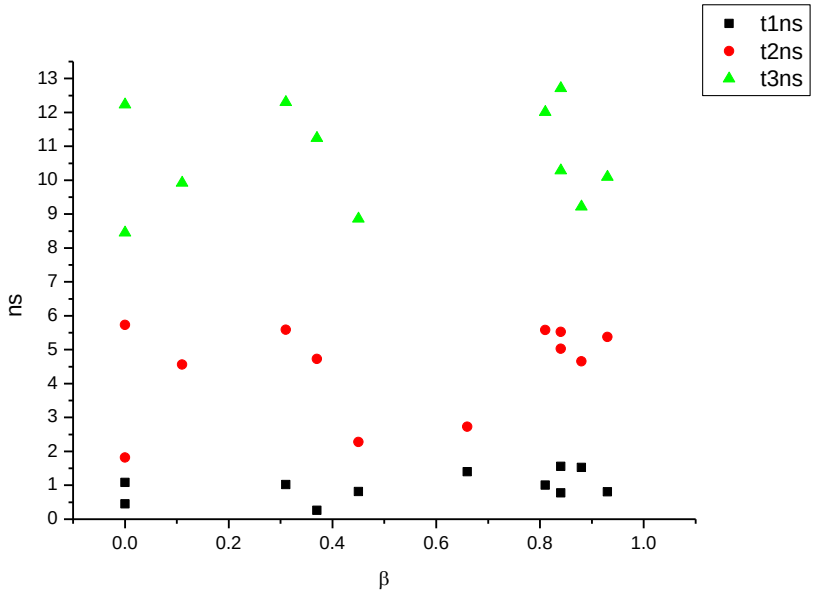

Figure 2.4.127. Intensity weighted components of TCSPC lifetime decay of **15** (470 nm) versus β.

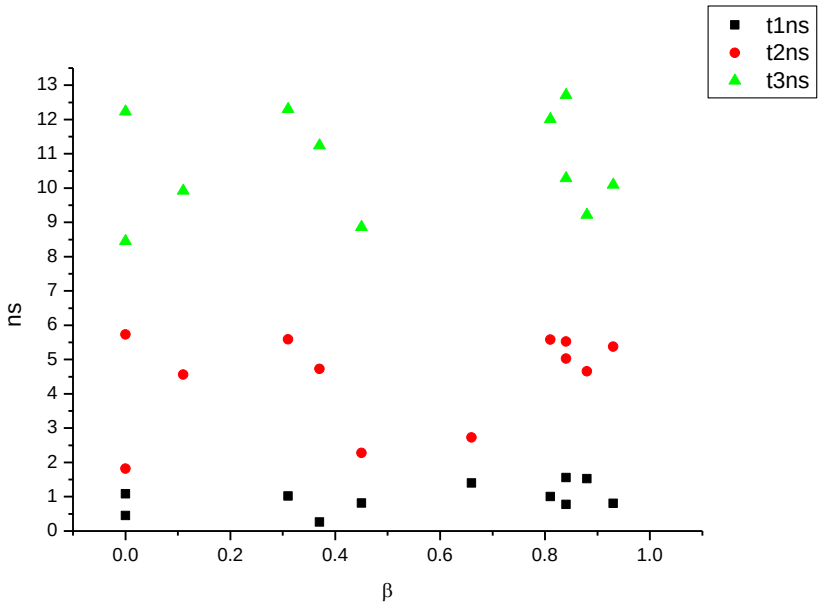

Figure 2.4.128. Amplitude weighted components of TCSPC lifetime decay of **15** (470 nm) versus β.

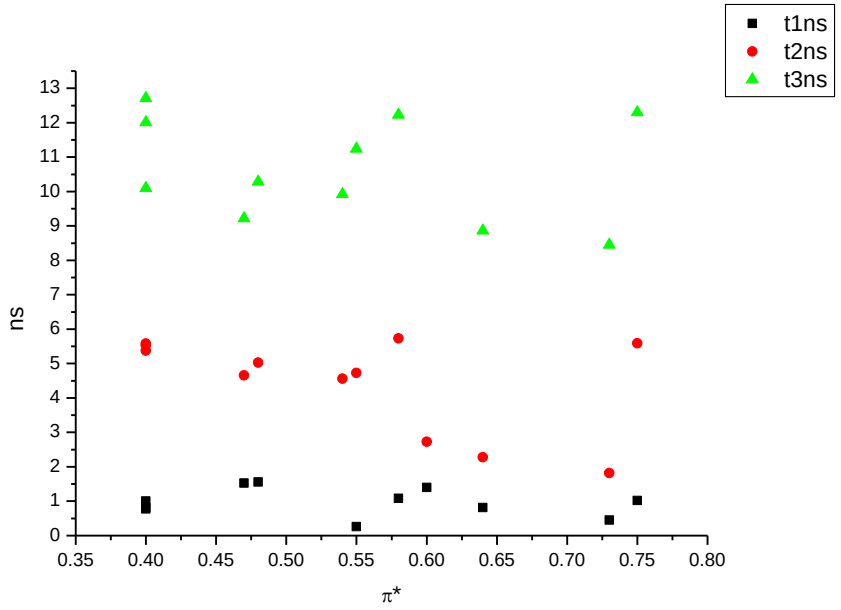

Figure 2.4.129. Intensity weighted components of TCSPC lifetime decay of **15** (470 nm) versus π*.

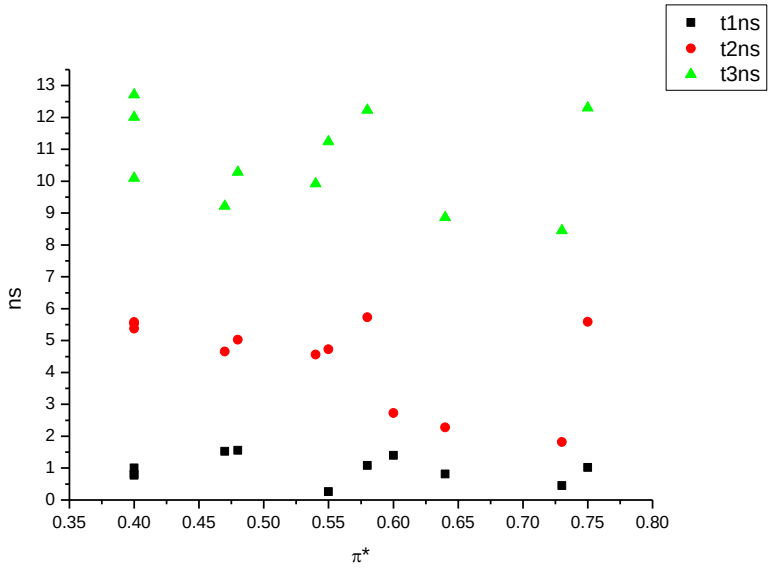

Figure 2.4.130. Amplitude weighted components of TCSPC lifetime decay of **15** (470 nm) versus π*.

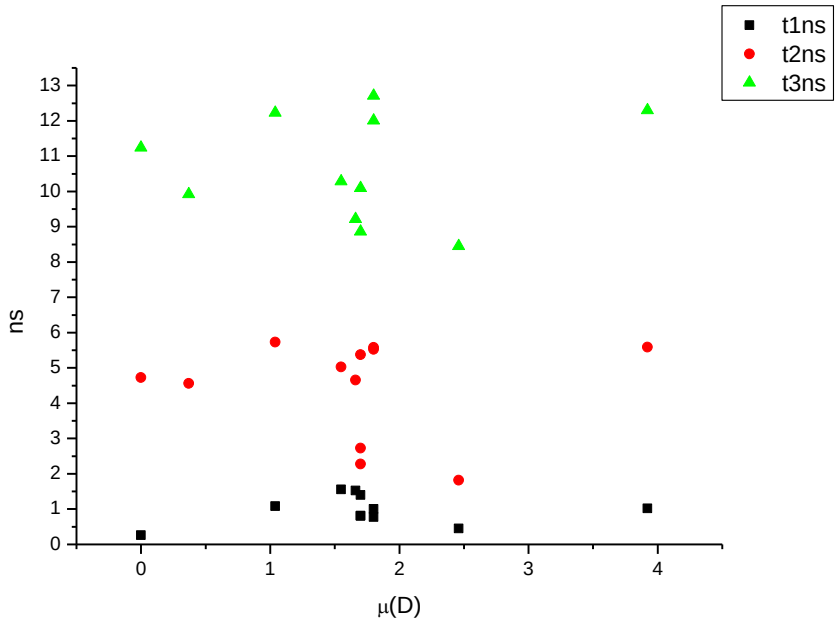

Figure 2.4.131. Intensity weighted components of TCSPC lifetime decay of **15** (470 nm) versus μ(D).

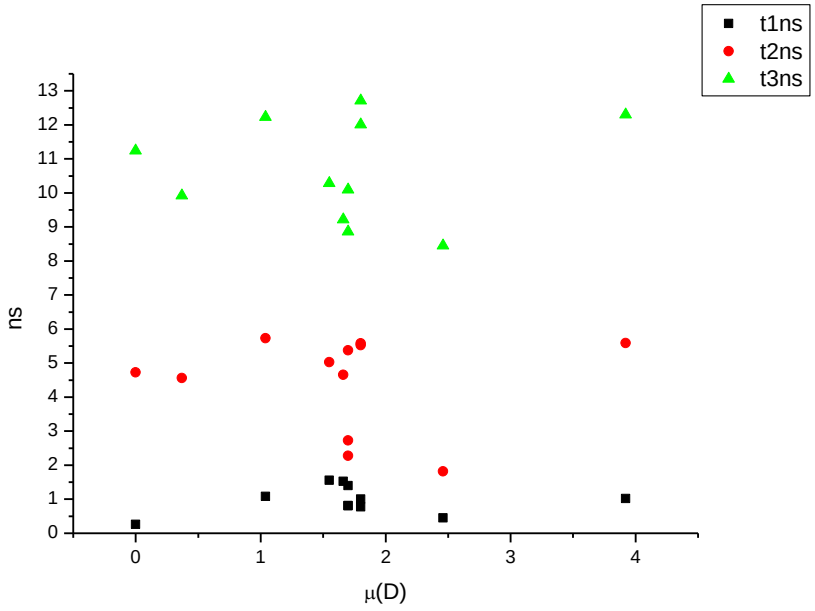

Figure 2.4.132. Amplitude weighted components of TCSPC lifetime decay of **15** (470 nm) versus μ(D).

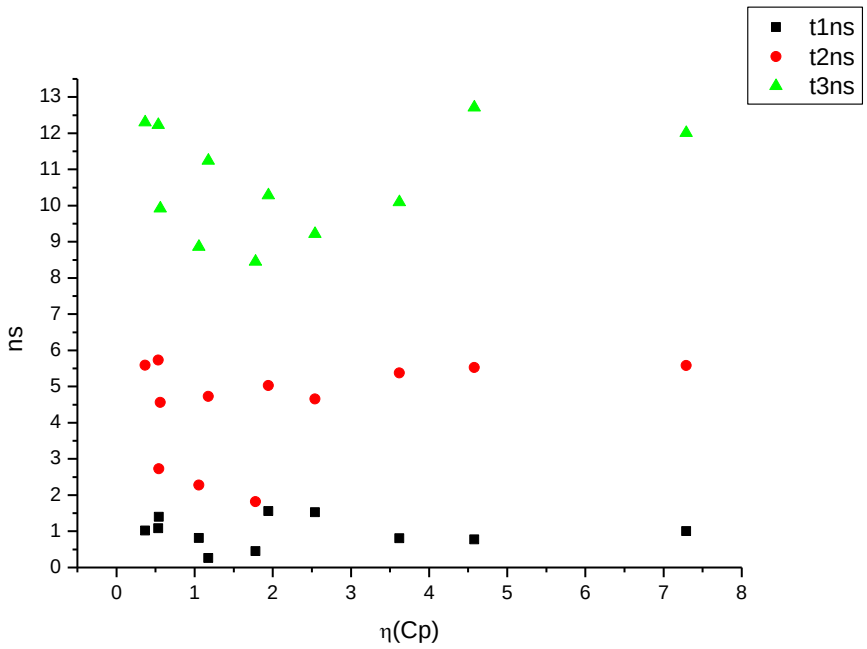

Figure 2.4.133. Intensity weighted components of TCSPC lifetime decay of **15** (470 nm) versus η(Cp).

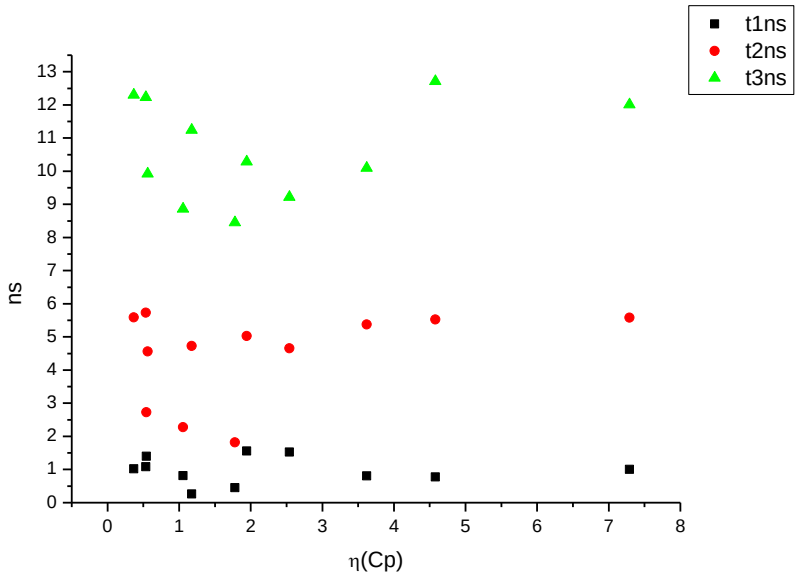

Figure 2.4.134. Amplitude weighted components of TCSPC lifetime decay of **15** (470 nm) versus η(Cp).

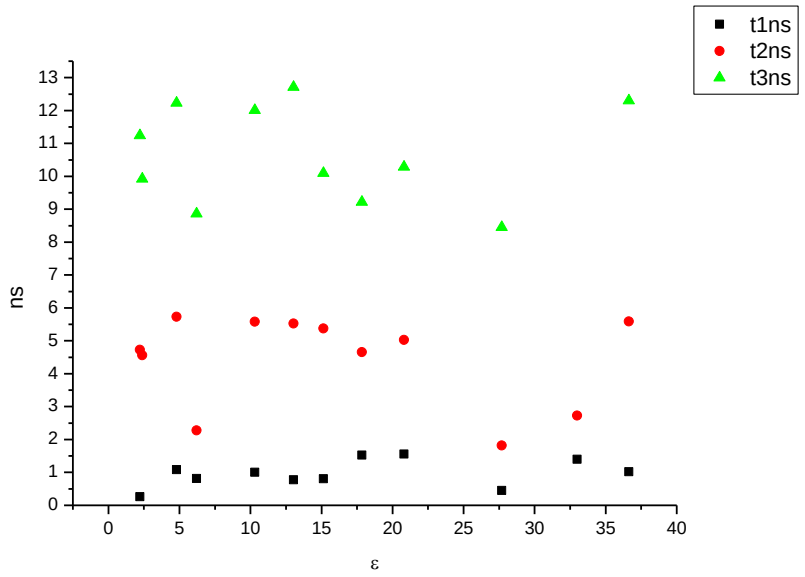

Figure 2.4.135. Intensity weighted components of TCSPC lifetime decay of **15** (470 nm) versus ε.

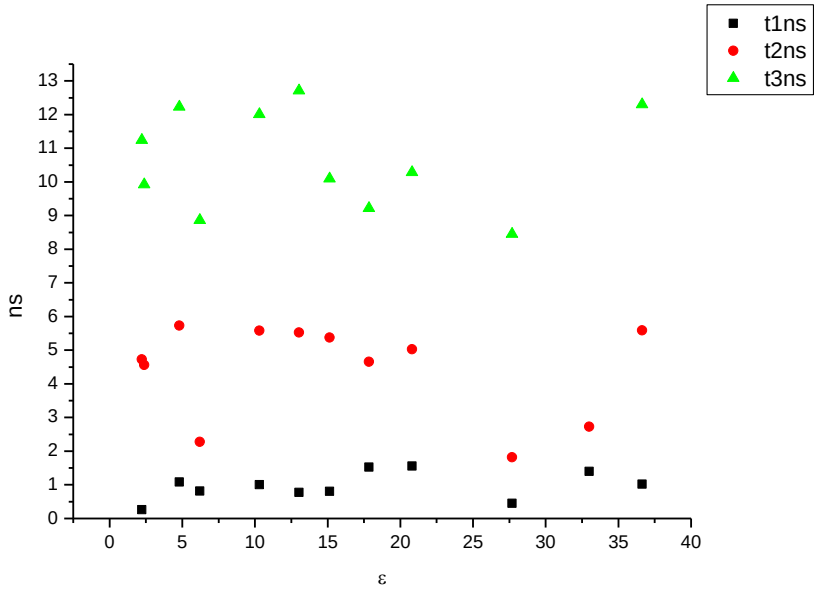

Figure 2.4.136. Amplitude weighted components of TCSPC lifetime decay of **15** (470 nm) versus ε.

2.4.9.2 570 nm (LED) Lifetime – Solvatochromic analysis.

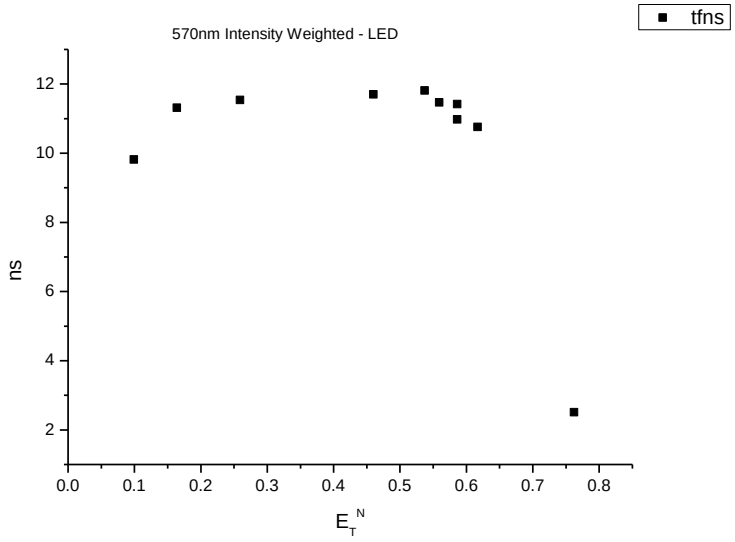

Figure 2.4.137. Intensity weighted average lifetime (τ_f) of **15** at 570 nm versus E_T^N.

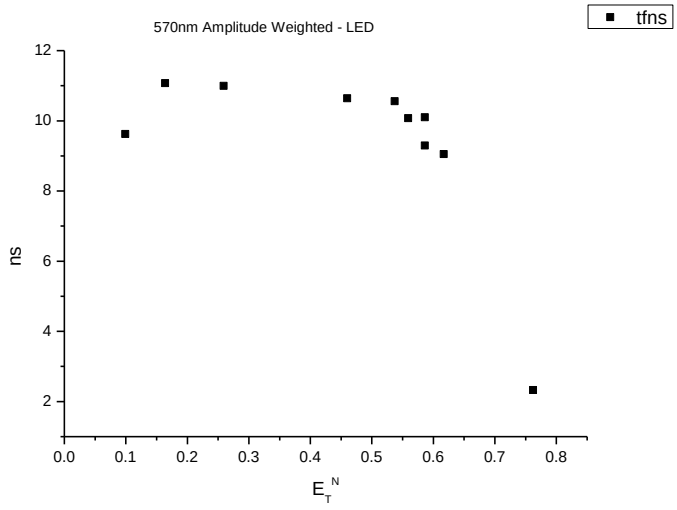

Figure 2.4.138. Amplitude weighted average lifetime (τ_f) of **15** at 570 nm versus E_T^N.

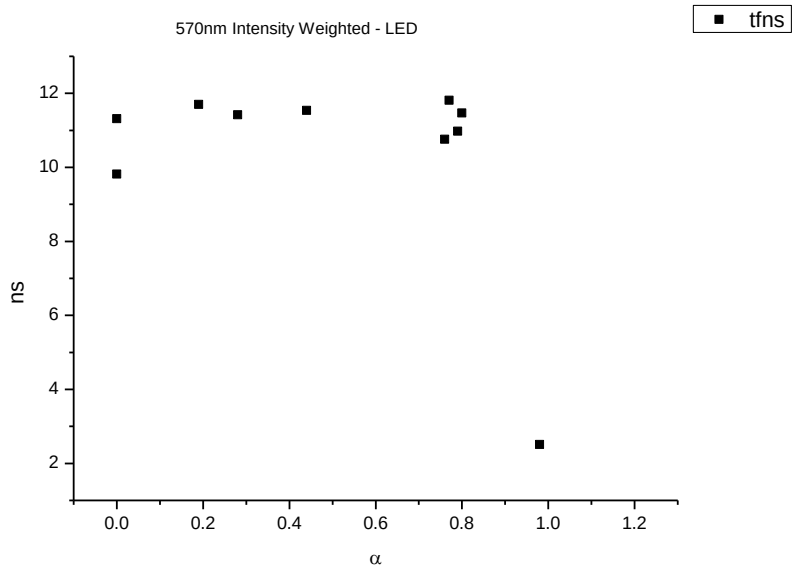

Figure 2.4.139. Intensity weighted average lifetime (τ_f) of **15** at 570 nm versus α.

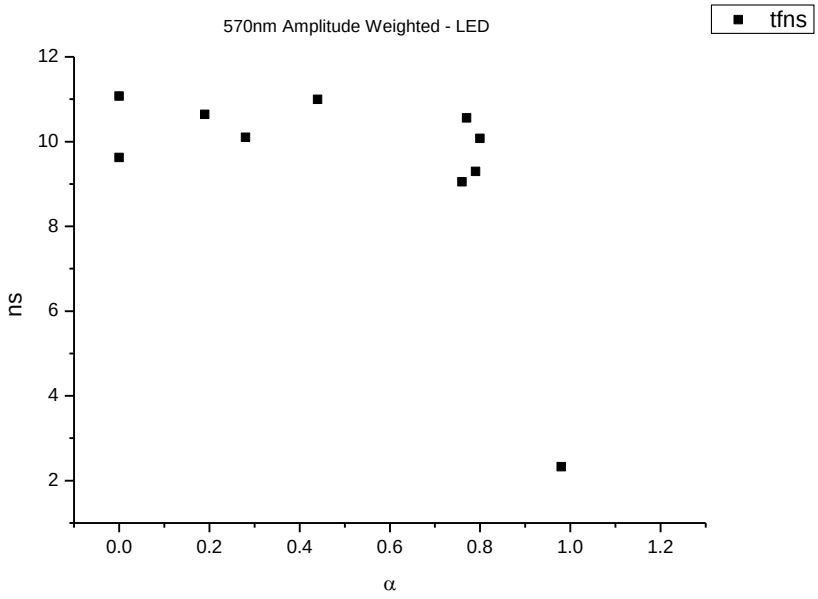

Figure 2.4.140. Amplitude weighted average lifetime (τ_f) of **11a** at 570 nm versus α.

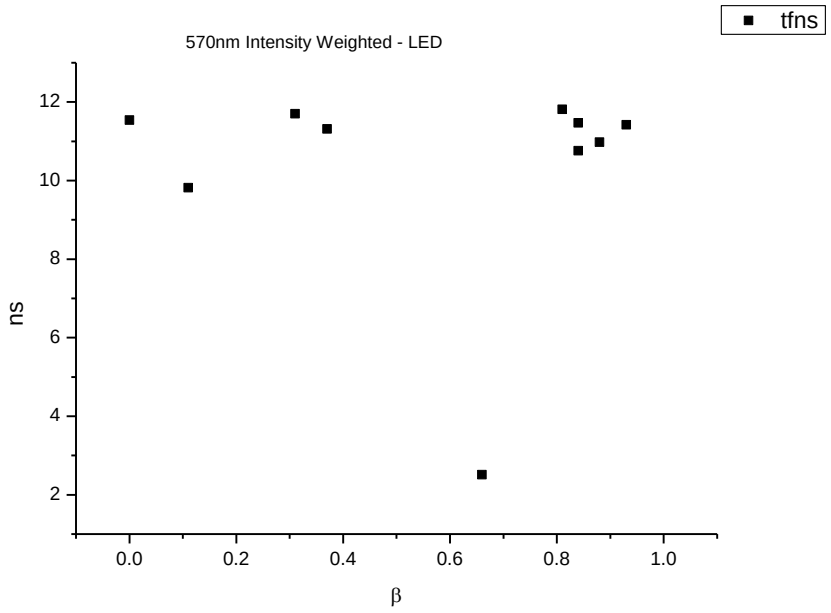

Figure 2.4.141. Intensity weighted average lifetime (τ_f) of **15** at 570 nm versus β.

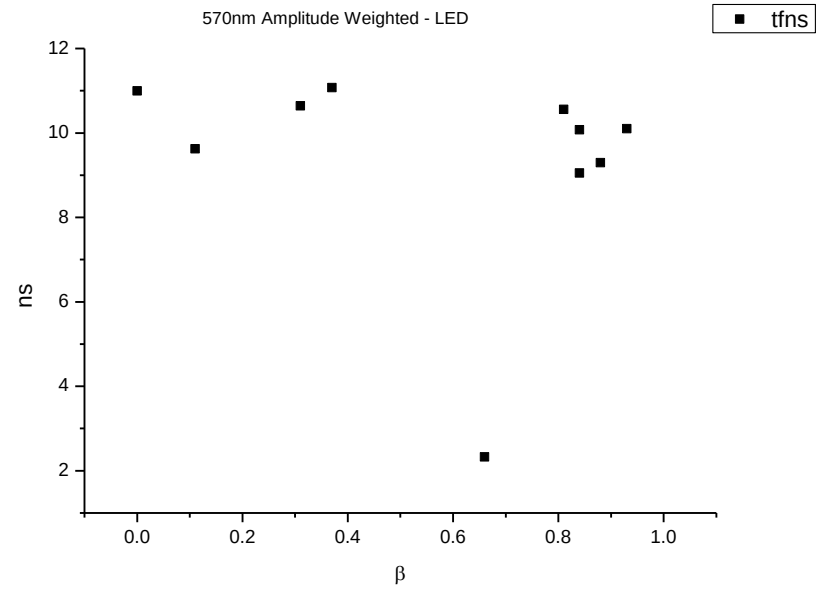

Figure 2.4.142. Amplitude weighted average lifetime (τ_f) of **15** at 570 nm versus β.

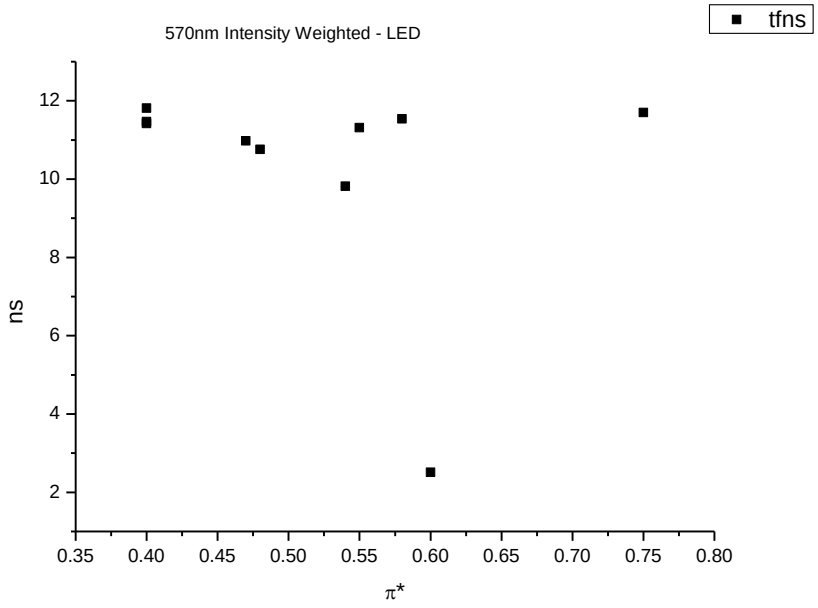

Figure 2.4.143. Intensity weighted average lifetime (τ_f) of **15** at 570 nm versus π*.

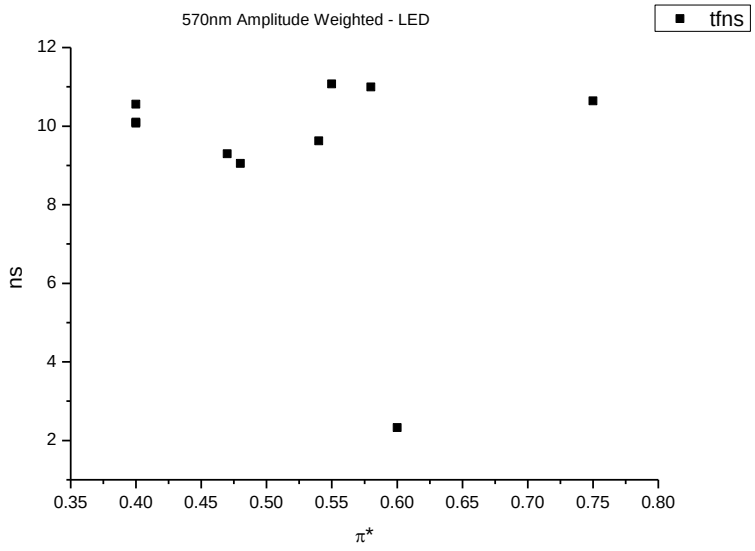

Figure 2.4.144. Amplitude weighted average lifetime (τ_f) of **15** at 570 nm versus π*.

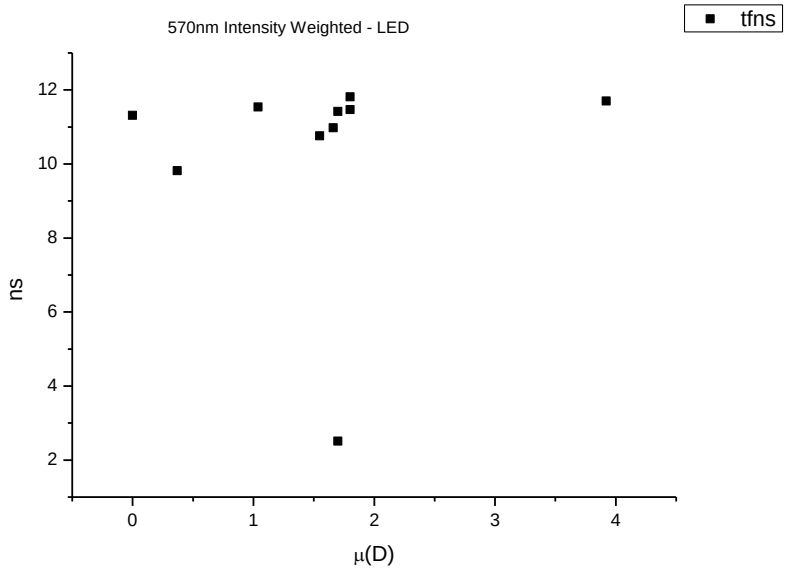

Figure 2.4.145. Intensity weighted average lifetime (τ_f) of **15** at 570 nm versus μ(D).

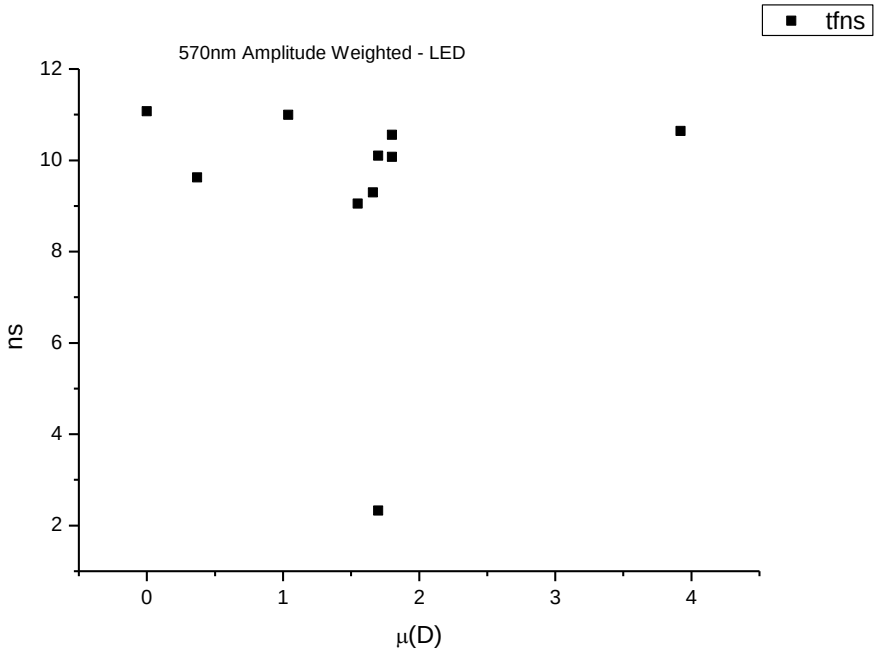

Figure 2.4.146. Amplitude weighted average lifetime (τ_f) of **15** at 570 nm versus μ(D).

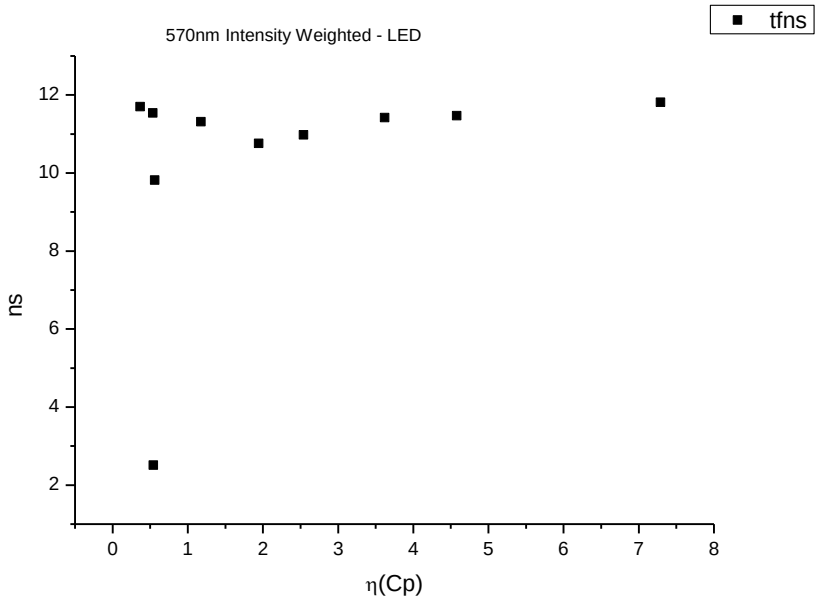

Figure 2.4.147. Intensity weighted average lifetime (τ_f) of **15** at 570 nm versus η(Cp).

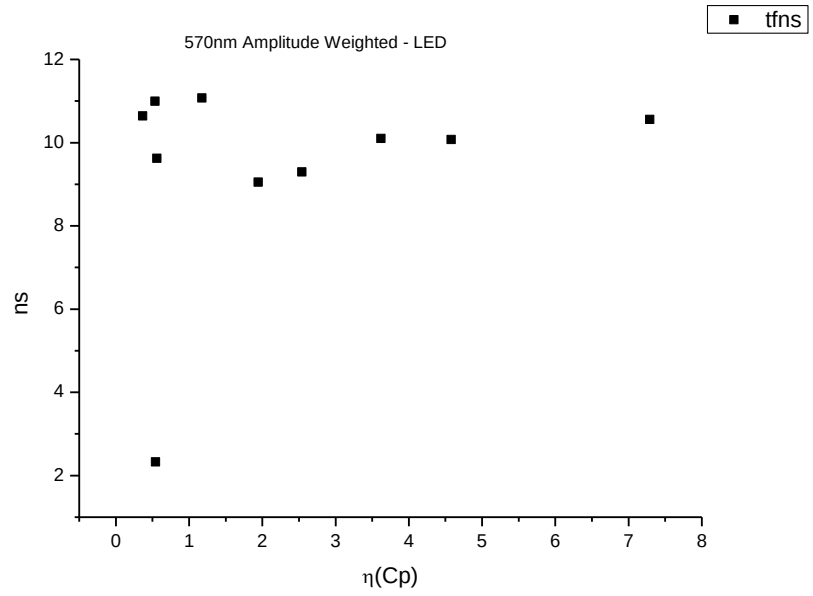

Figure 2.4.148. Amplitude weighted average lifetime (τ_f) of **15** at 570 nm versus η(Cp).

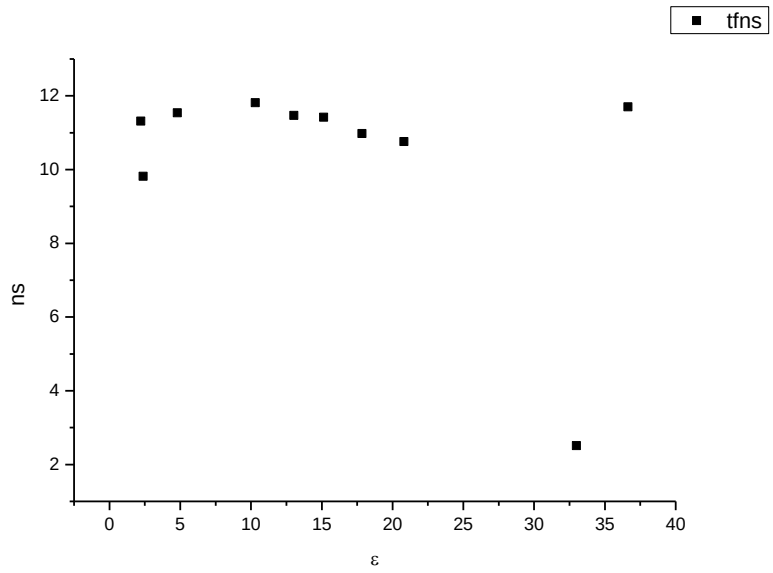

Figure 2.4.149. Intensity weighted average lifetime (τ_f) of **15** at 570 nm versus ε.

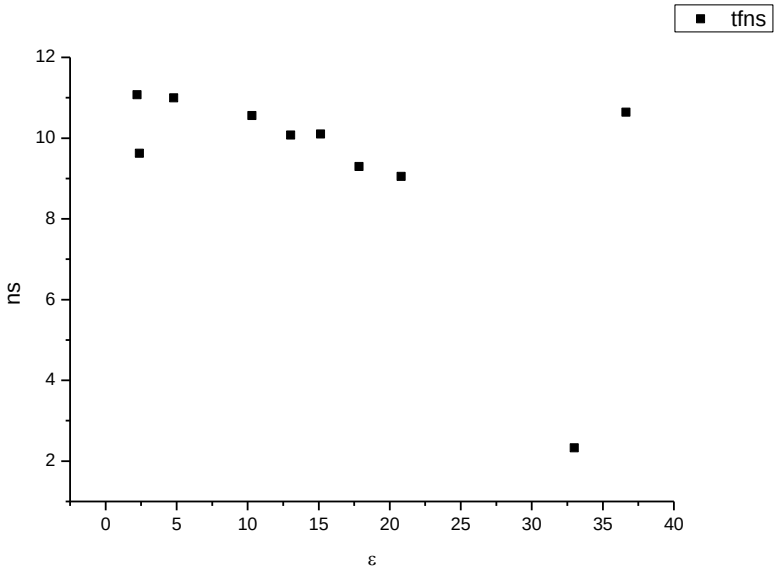

Figure 2.4.150. Amplitude weighted average lifetime (τ_f) of **15** at 570 nm versus ε.

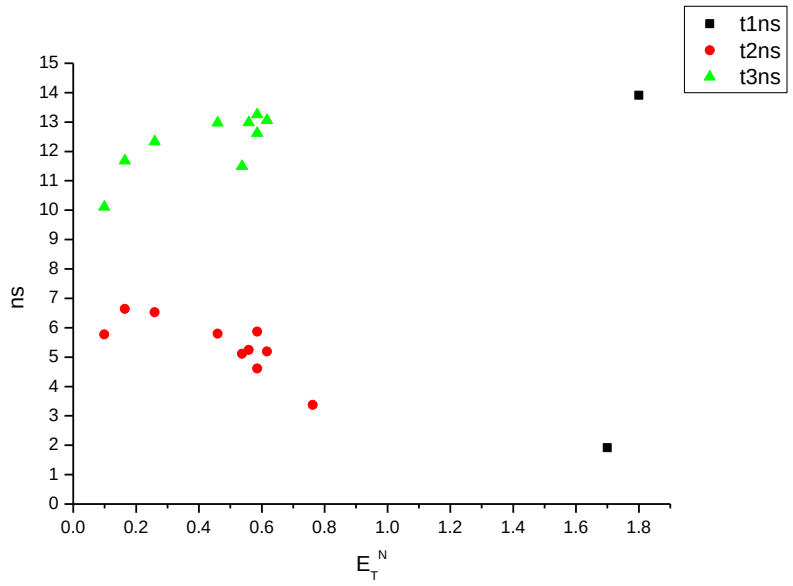

Figure 2.4.151. Intensity weighted components of TCSPC lifetime decay of **15** (570 nm) versus E_T^N.

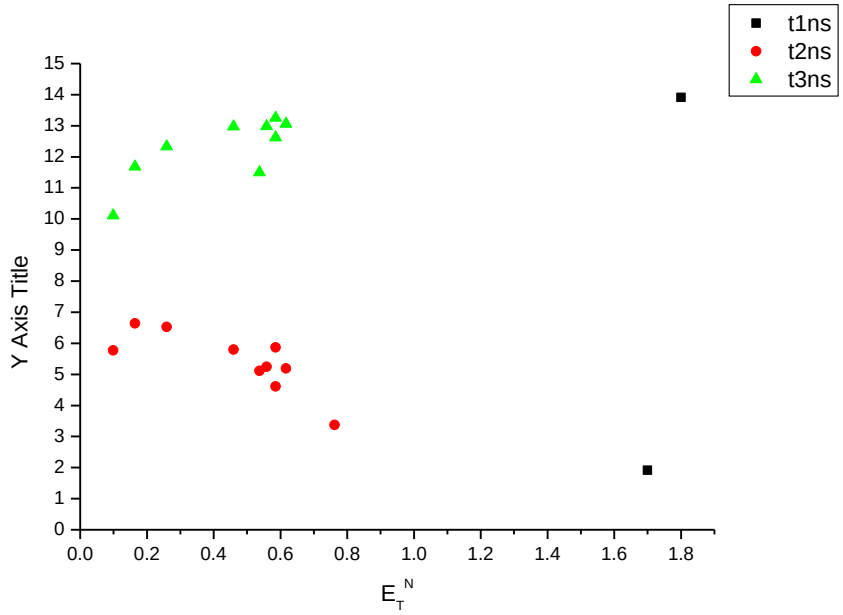

Figure 2.4.152. Amplitude weighted components of TCSPC lifetime decay of **15** (570 nm) versus E_T^N.

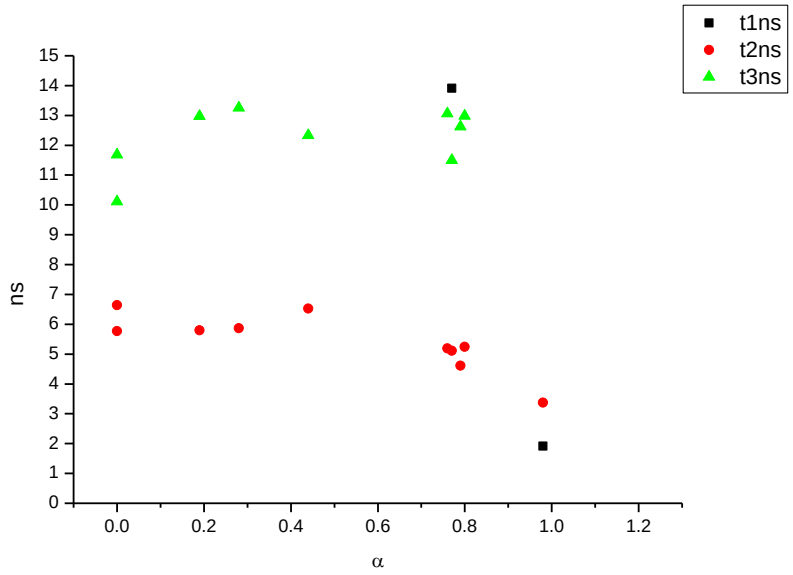

Figure 2.4.153. Intensity weighted components of TCSPC lifetime decay of **15** (570 nm) versus α.

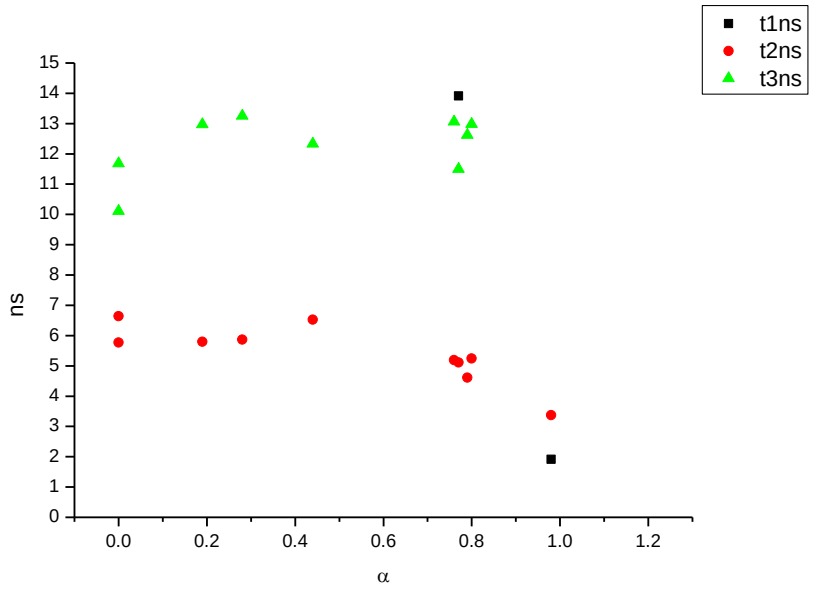

Figure 2.4.154. Amplitude weighted components of TCSPC lifetime decay of **15** (570 nm) versus α.

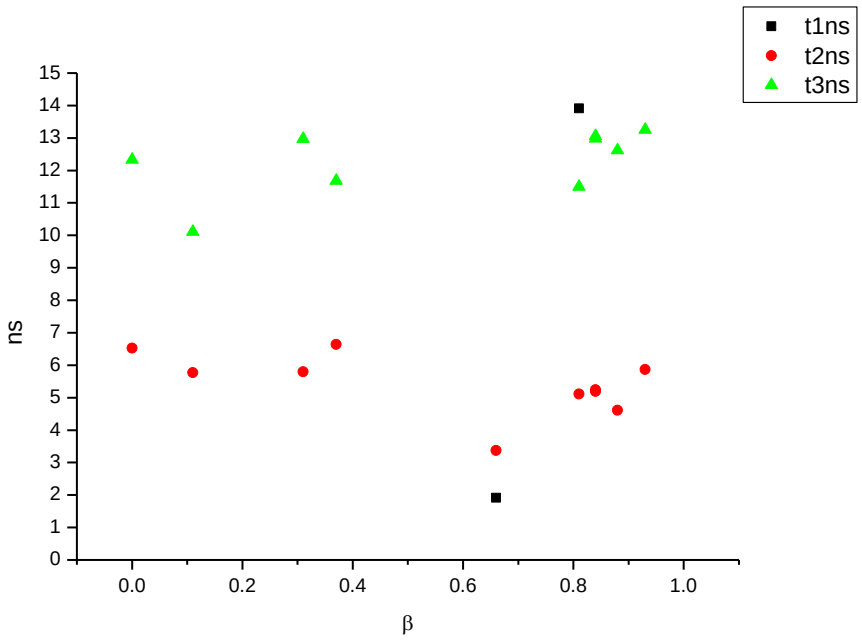

Figure 2.4.155. Intensity weighted components of TCSPC lifetime decay of **15** (570 nm) versus β.

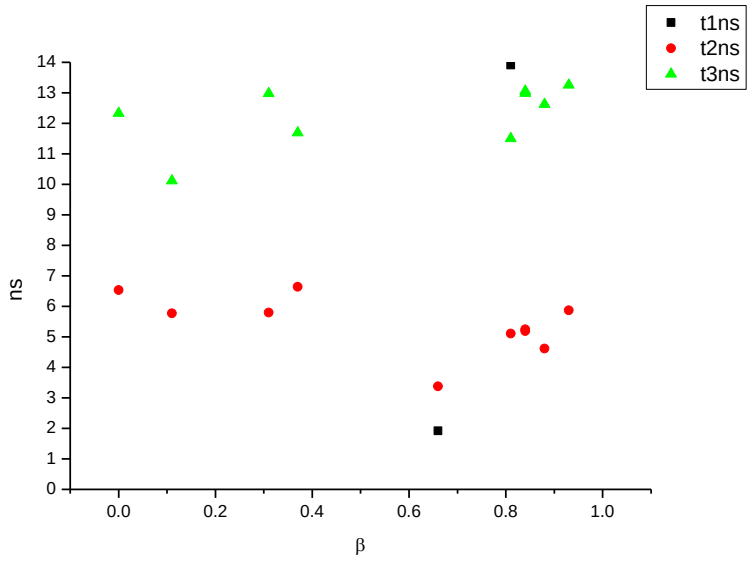

Figure 2.4.156. Amplitude weighted components of TCSPC lifetime decay of **15** (570 nm) versus β.

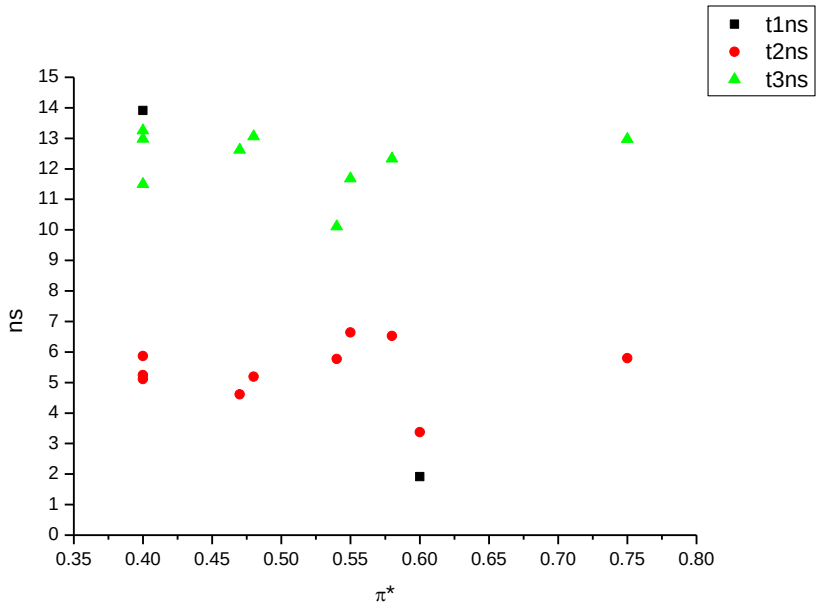

Figure 2.4.157. Intensity weighted components of TCSPC lifetime decay of **15** (570 nm) versus π*.

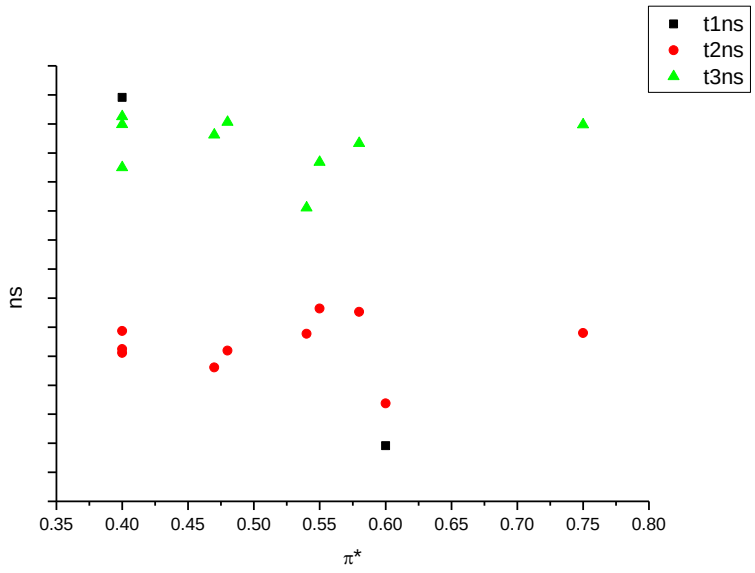

Figure 2.4.158. Amplitude weighted components of TCSPC lifetime decay of **15** (570 nm) versus π*.

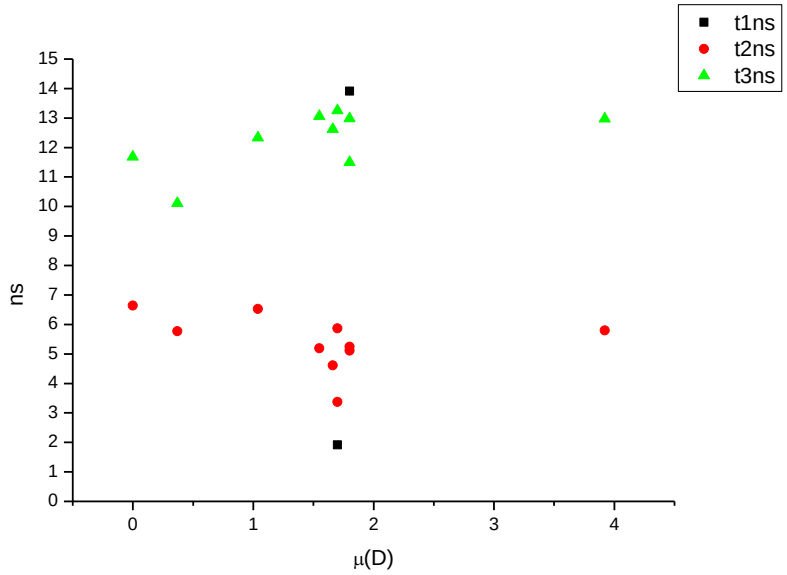

Figure 2.4.159. Intensity weighted components of TCSPC lifetime decay of **15** (570 nm) versus μ(D).

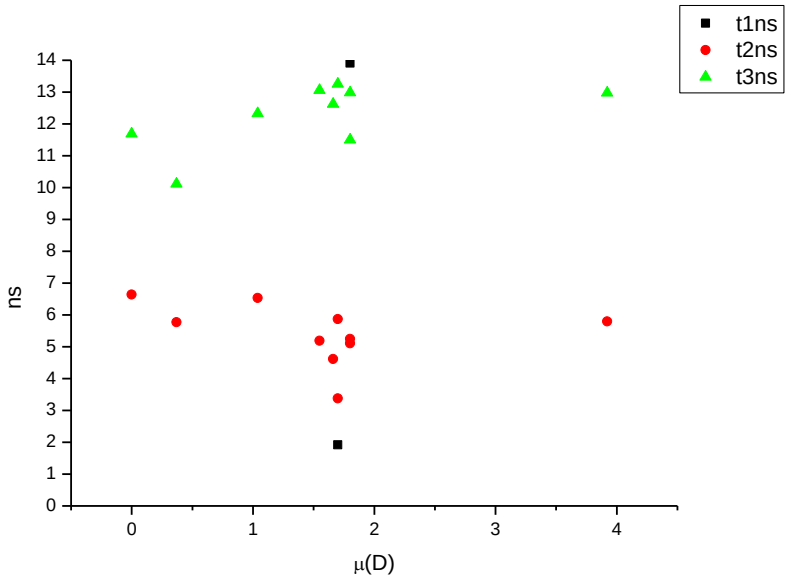

Figure 2.4.160. Amplitude weighted components of TCSPC lifetime decay of **15** (570 nm) versus μ(D).

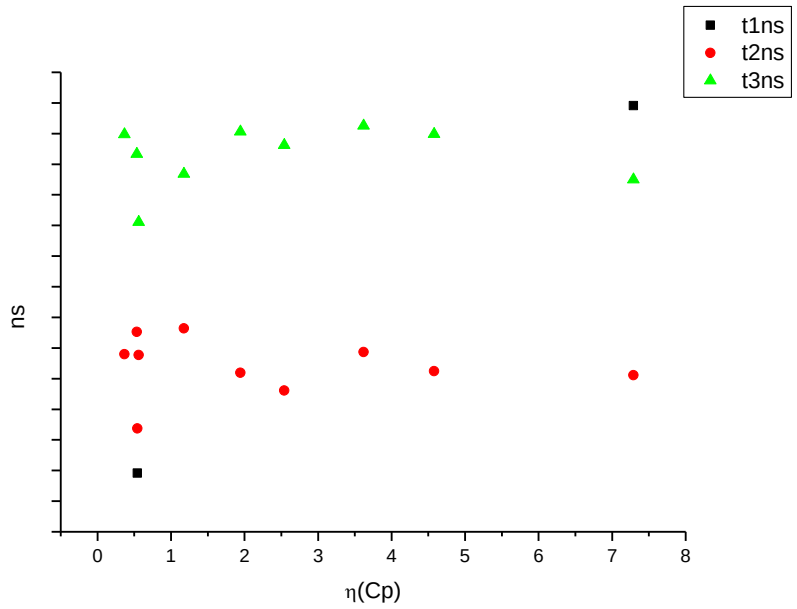

Figure 2.4.161. Intensity weighted components of TCSPC lifetime decay of **15** (570 nm) versus η(Cp).

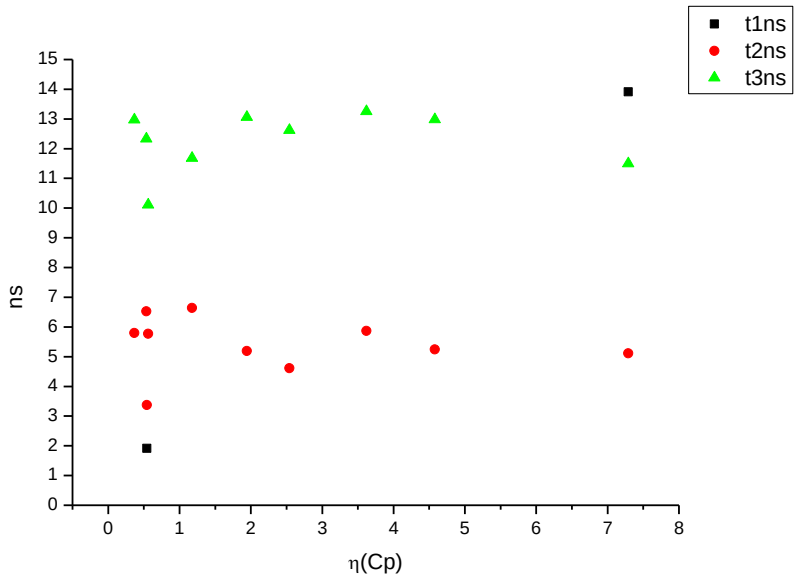

Figure 2.4.162. Amplitude weighted components of TCSPC lifetime decay of **15** (570 nm) versus η(Cp).

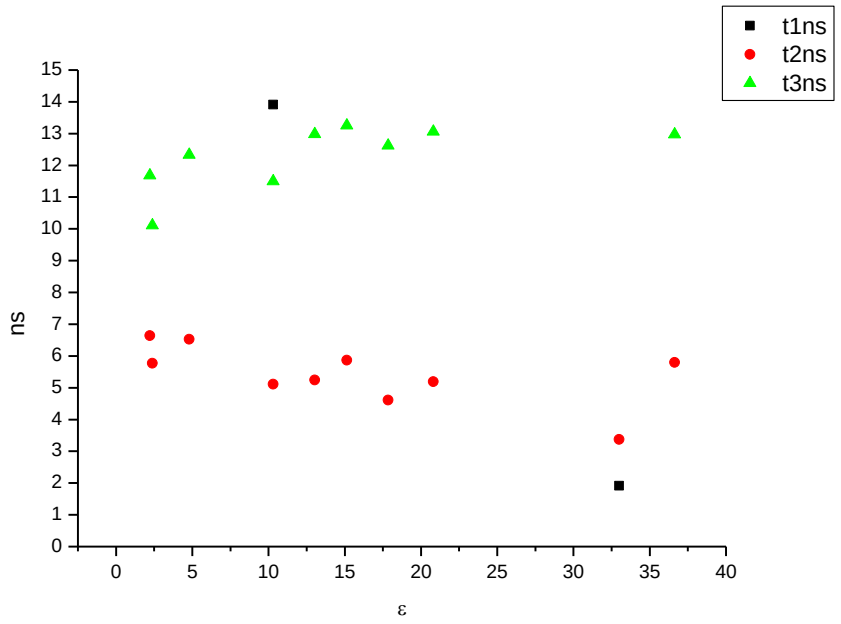

Figure 2.4.163. Intensity weighted components of TCSPC lifetime decay of **15** (570 nm) versus ε.

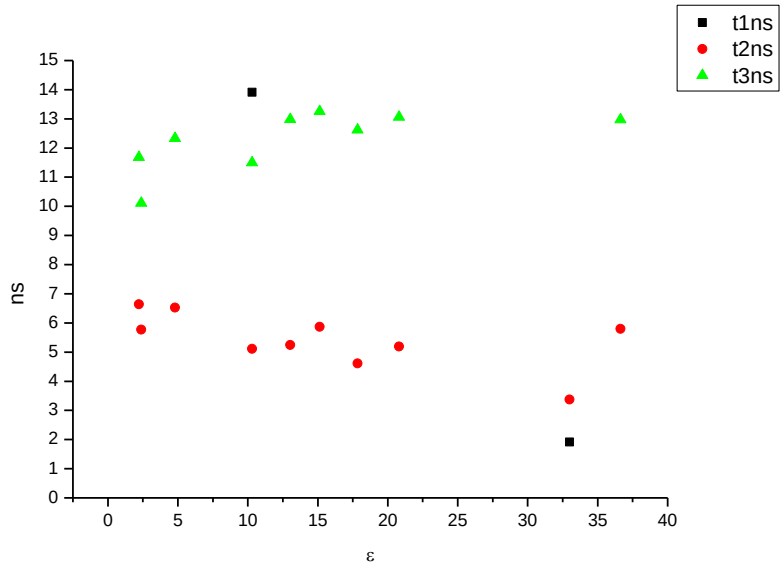

Figure 2.4.164. Amplitude weighted components of TCSPC lifetime decay of **15** (570 nm) versus ε.

2.4.10 Ultraviolet-visible absorption spectra.

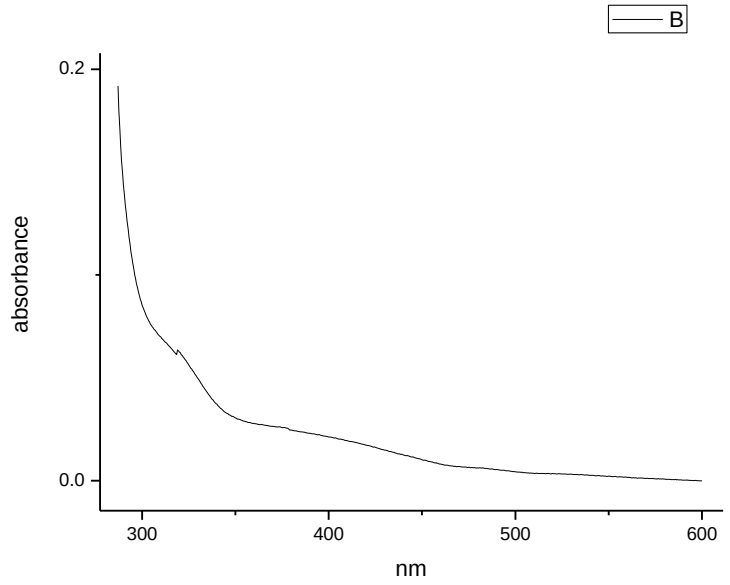

Figure 2.4.165. Ultraviolet-Visible absorption spectrum of **15** recorded in Toluene.

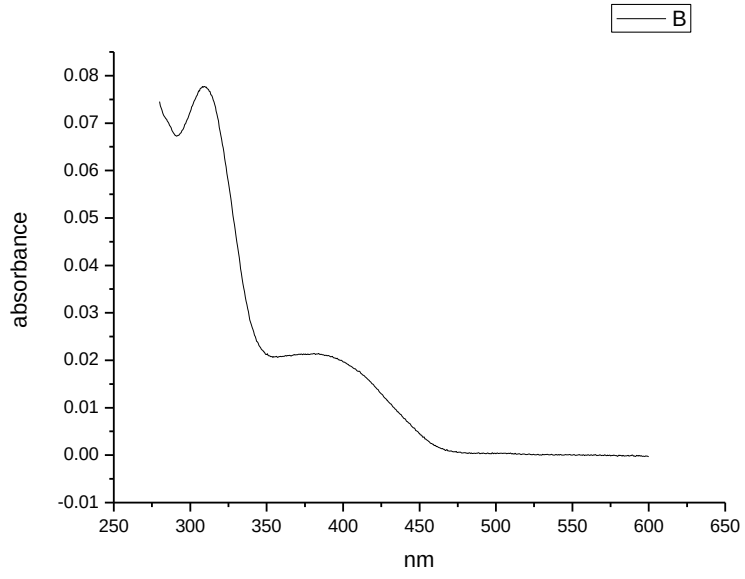

Figure 2.4.166. Ultraviolet-Visible absorption spectrum of **15** recorded in 1,4-dioxane.

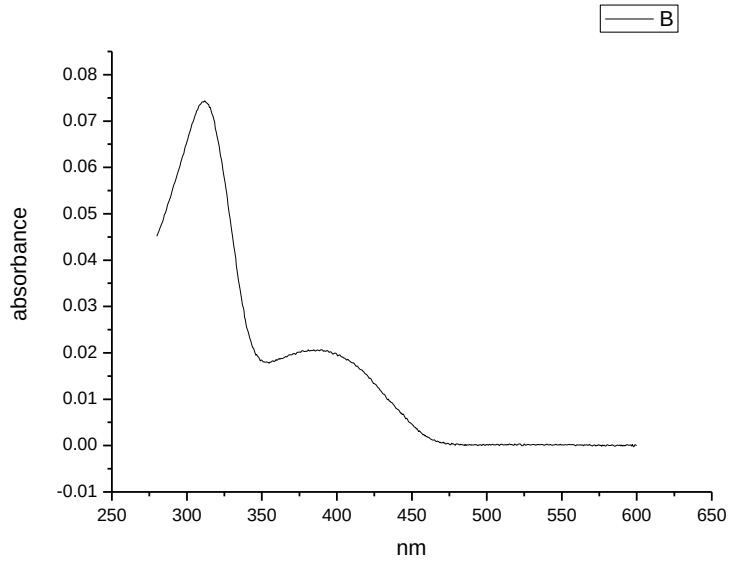

Figure 2.4.167. Ultraviolet-Visible absorption spectrum of **15** recorded in Chloroform.

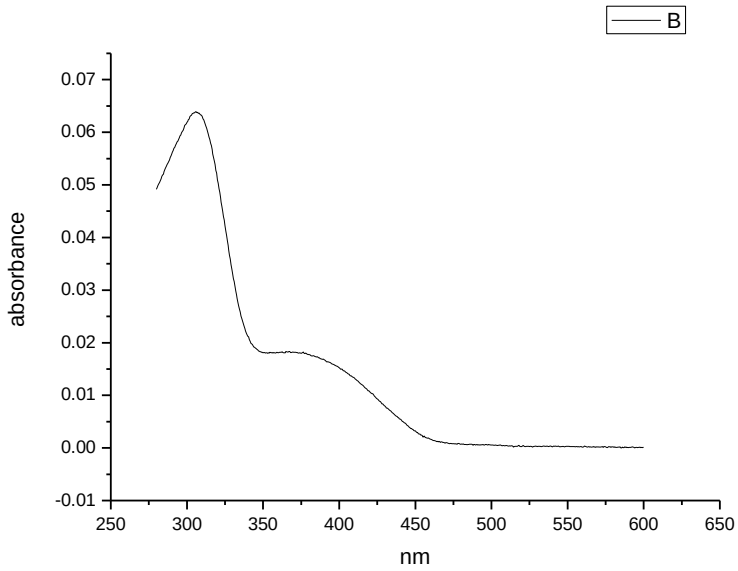

Figure 2.4.168. Ultraviolet-Visible absorption spectrum of **15** recorded in Acetonitrile.

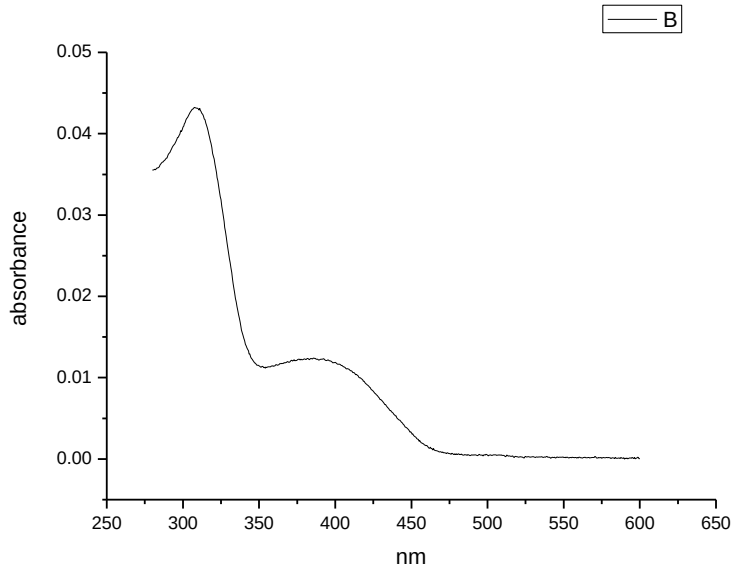

Figure 2.4.169. Ultraviolet-Visible absorption spectrum of **15** recorded in 1-octanol.

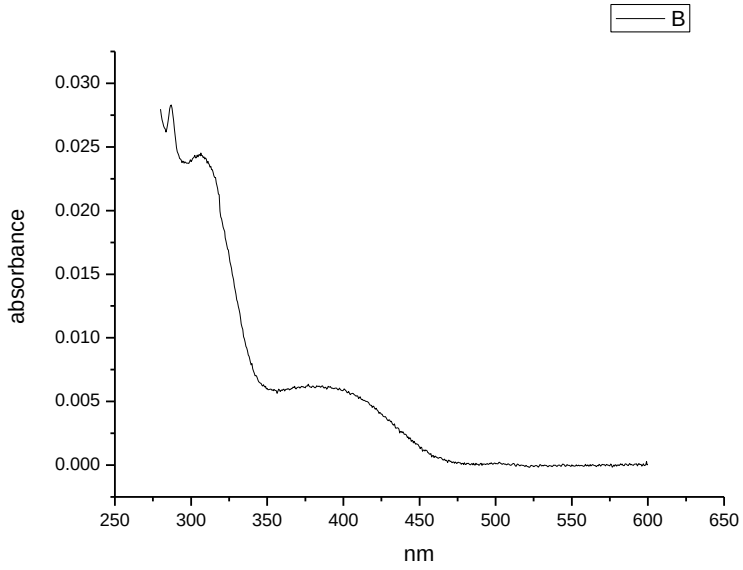

Figure 2.4.170. Ultraviolet-Visible absorption spectrum of **15** recorded in 1-hexanol.

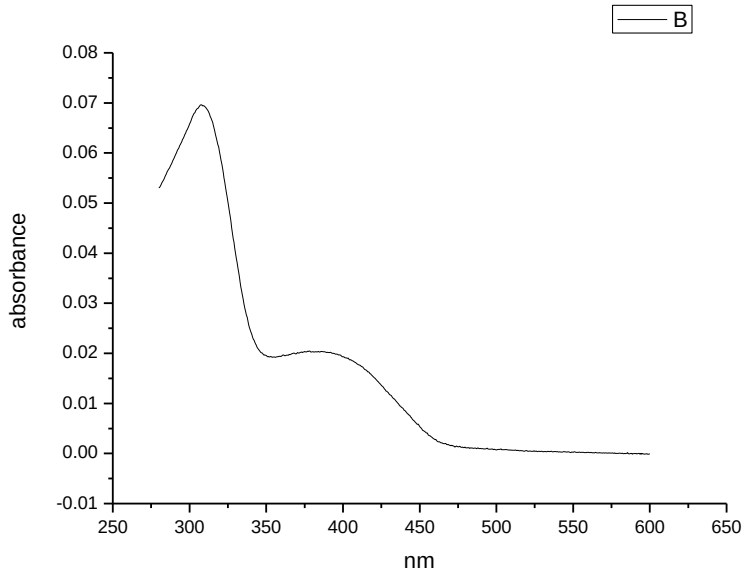

Figure 2.4.171. Ultraviolet-Visible absorption spectrum of **15** recorded in 1-butanol.

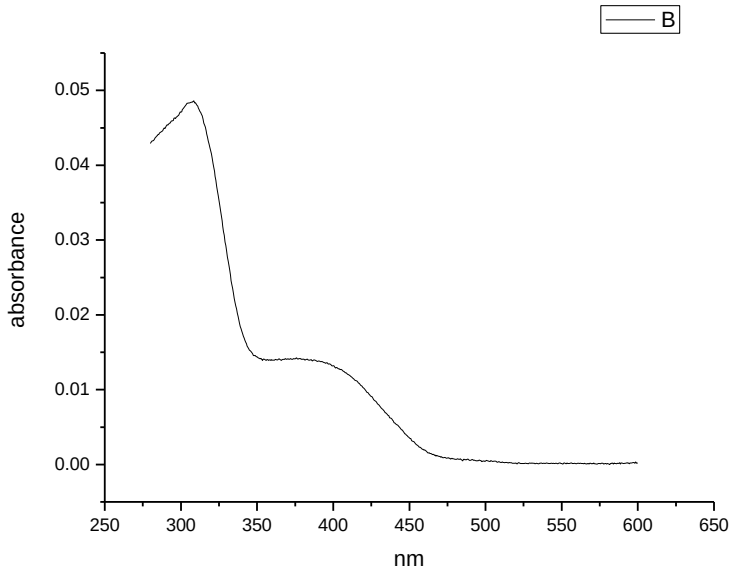

Figure 2.4.172. Ultraviolet-Visible absorption spectrum of **15** recorded in 1-pentanol.

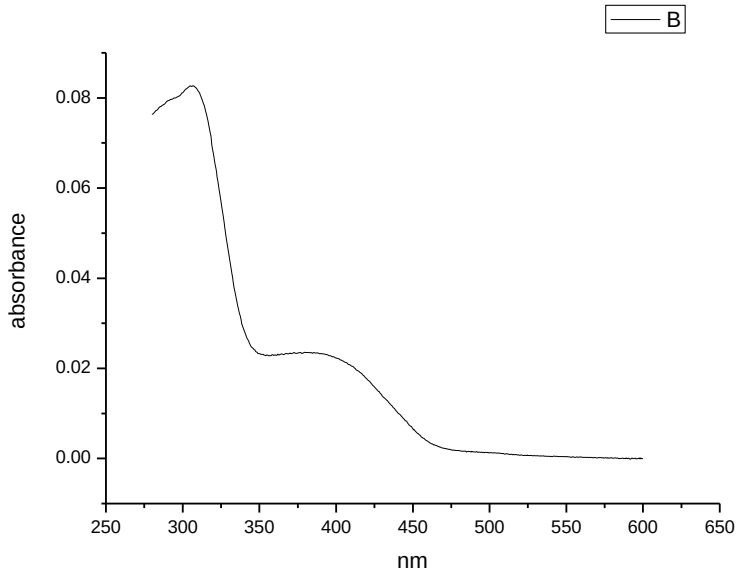

Figure 2.4.173. Ultraviolet-Visible absorption spectrum of **15** recorded in 1-propanol.

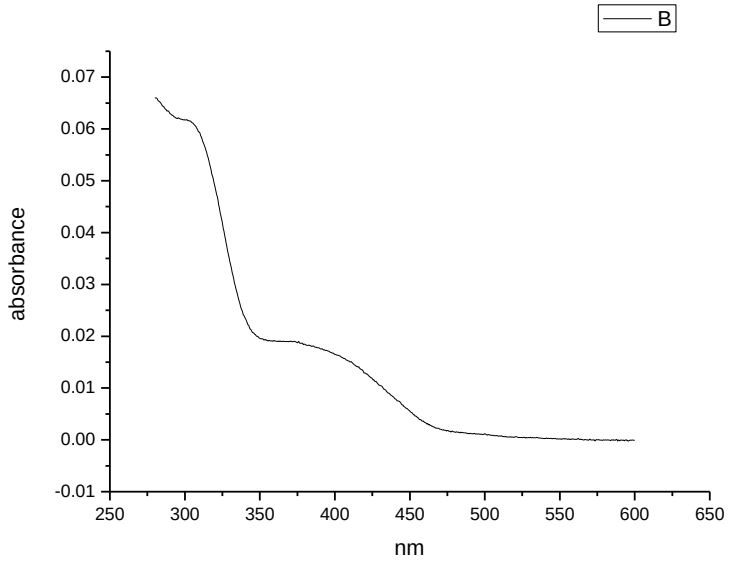

Figure 2.4.174. Ultraviolet-Visible absorption spectrum of **15** recorded in Acetic Acid.

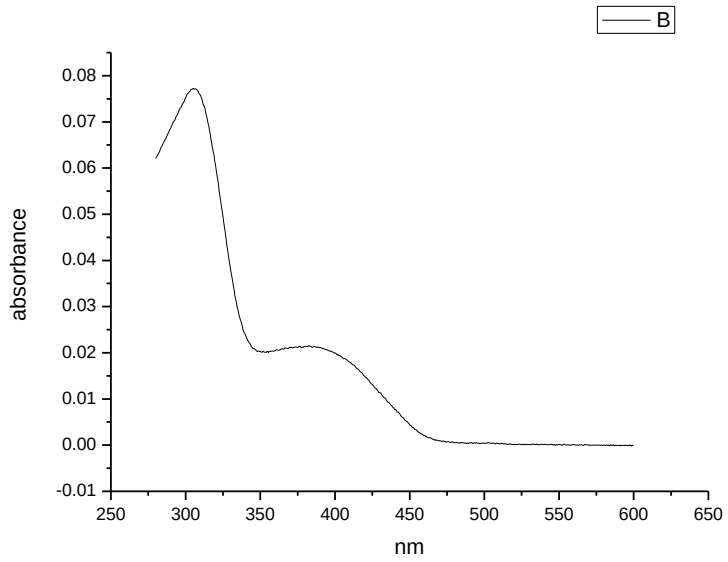

Figure 2.4.175. Ultraviolet-Visible absorption spectrum of **15** recorded in Methanol.

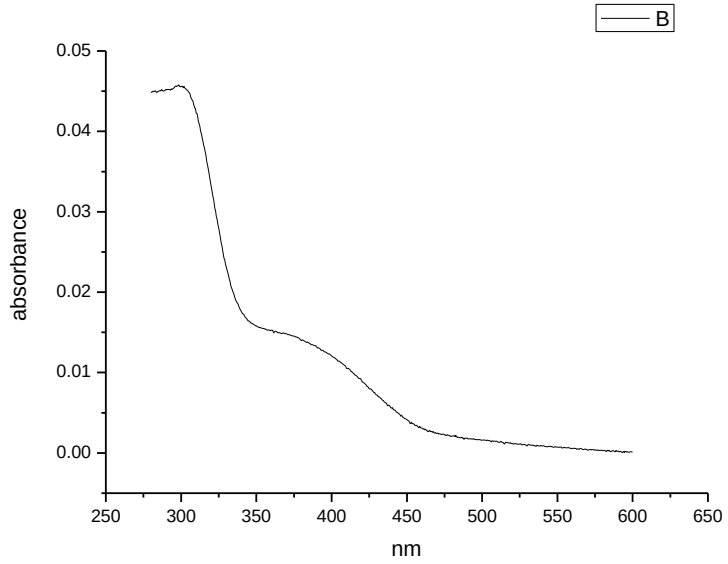

Figure 2.4.176. Ultraviolet-Visible absorption spectrum of **15** recorded in 2,2,2-trifluoroethanol.

2.4.11 Fluorescence Emission spectra.

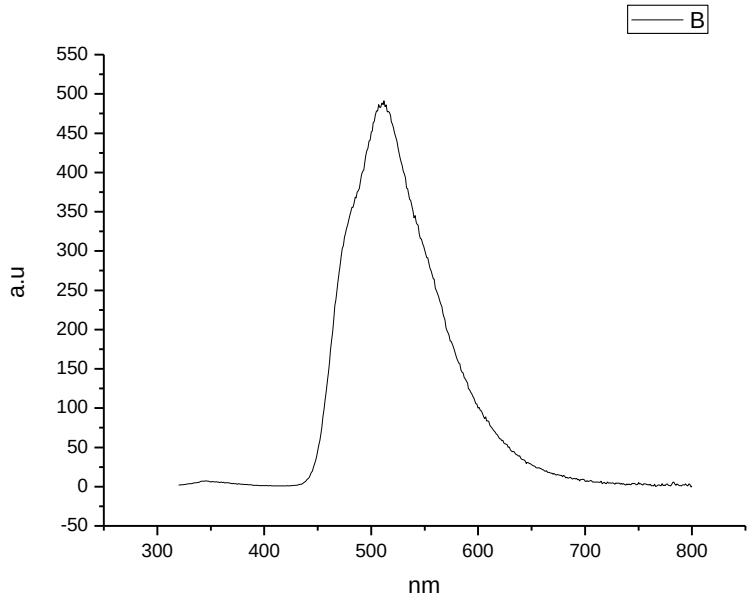

Figure 2.4.177. Fluorescence emission spectrum of **15** recorded in Toluene at 310 nm excitation.

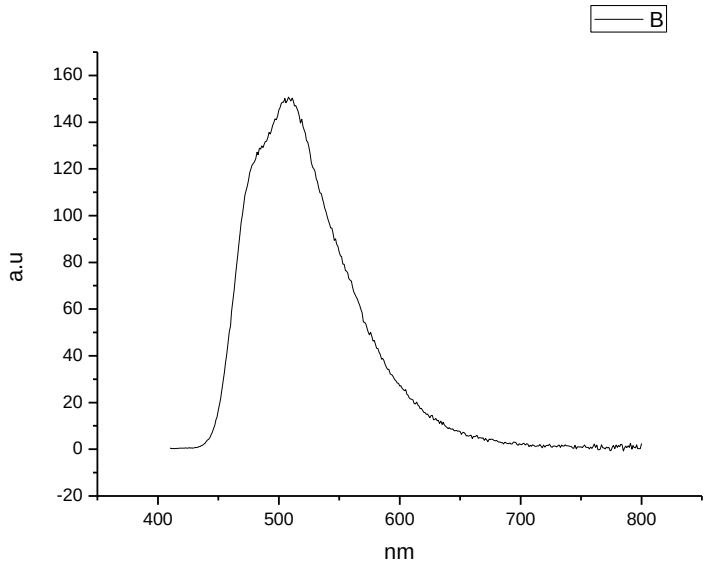

Figure 2.4.178. Fluorescence emission spectrum of **15** recorded in Toluene at 400 nm excitation.

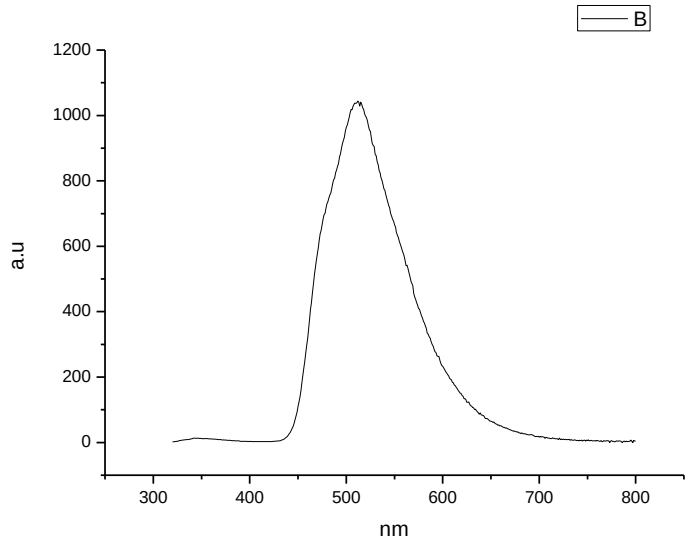

Figure 2.4.179. Fluorescence emission spectrum of **15** recorded in 1,4-dioxane at 310 nm excitation.

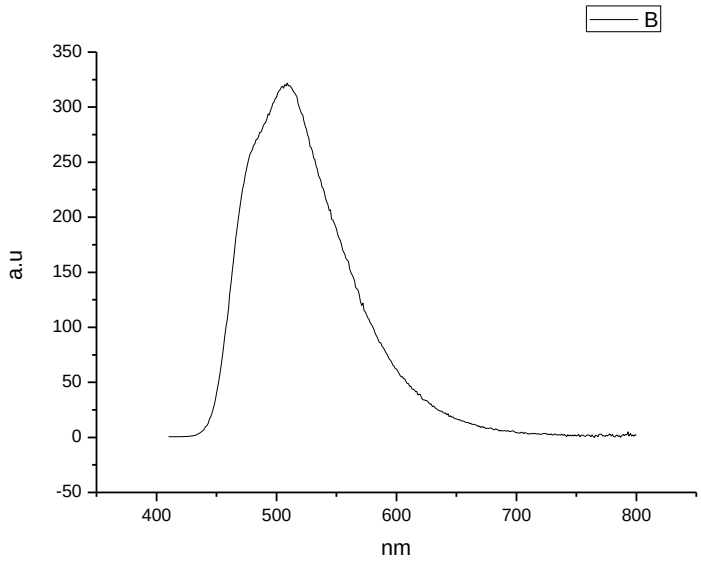

Figure 2.4.180. Fluorescence emission spectrum of **15** recorded in 1,4-dioxane at 400 nm excitation.

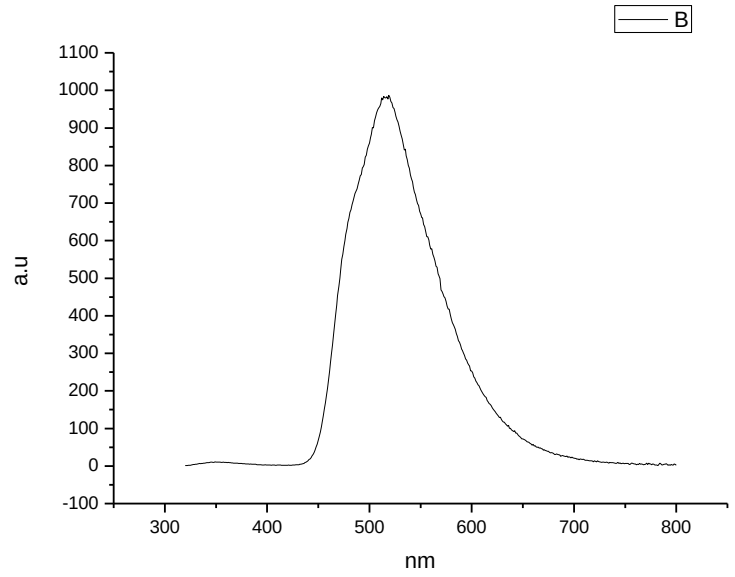

Figure 2.4.181. Fluorescence emission spectrum of **15** recorded in Chloroform at 310 nm excitation.

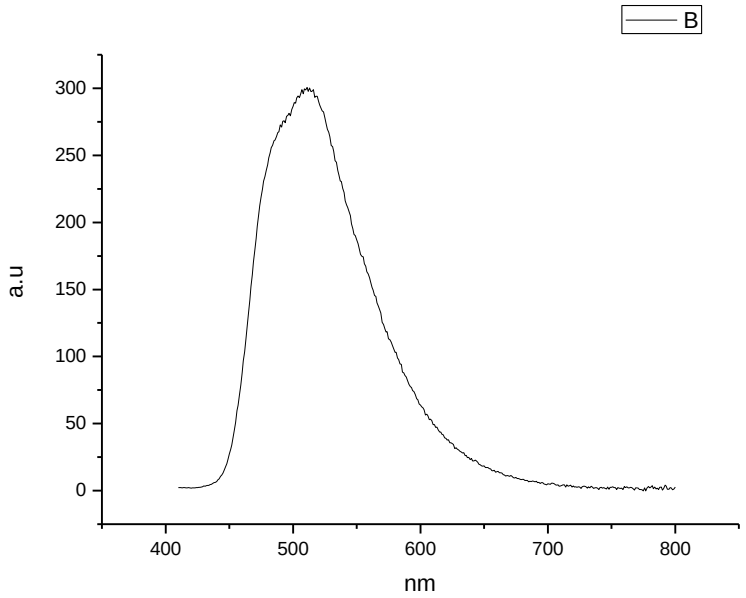

Figure 2.4.182. Fluorescence emission spectrum of **15** recorded in Chloroform at 400 nm excitation.

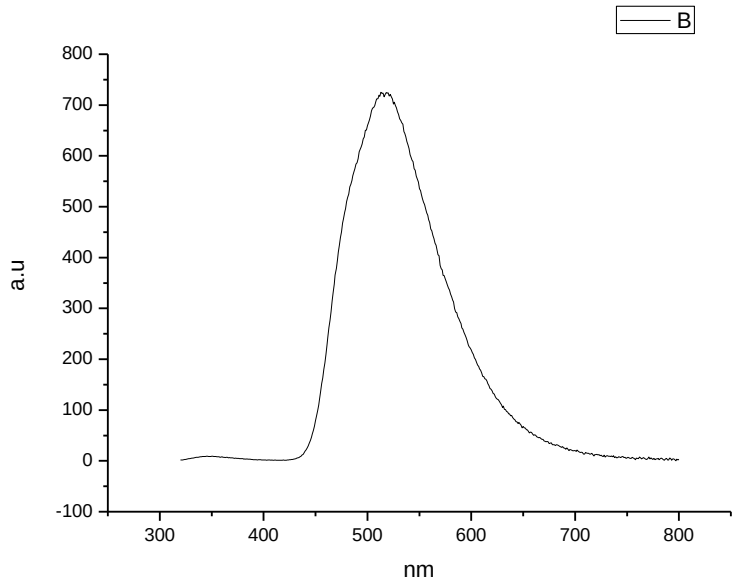

Figure 2.4.183. Fluorescence emission spectrum of **15** recorded in Acetonitrile at 310 nm excitation.

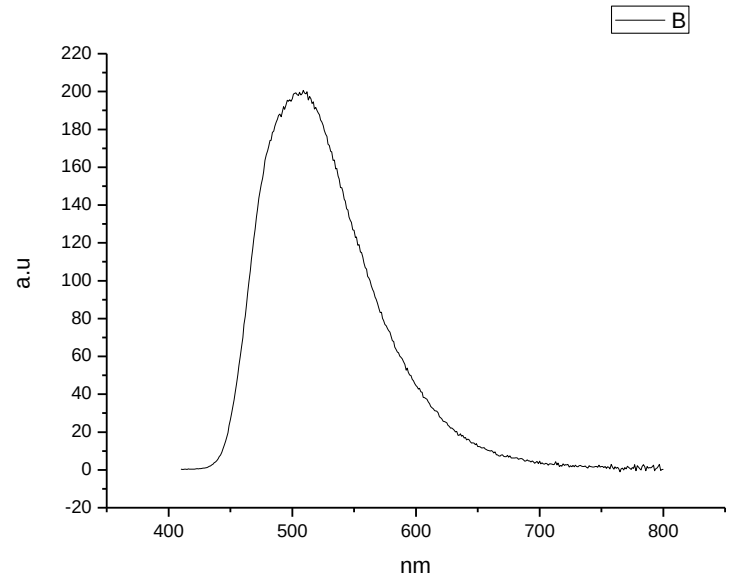

Figure 2.4.184. Fluorescence emission spectrum of **15** recorded in Acetonitrile at 400 nm excitation.

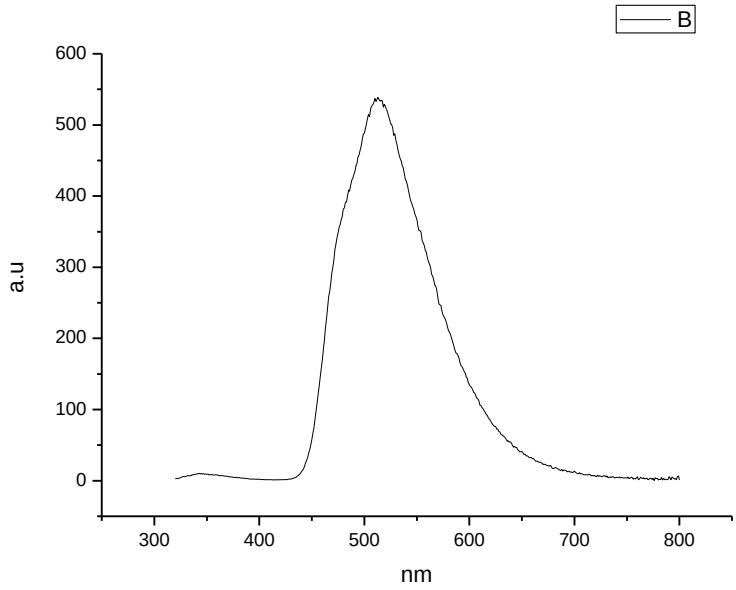

Figure 2.4.185. Fluorescence emission spectrum of **15** recorded in 1-octanol at 310 nm excitation.

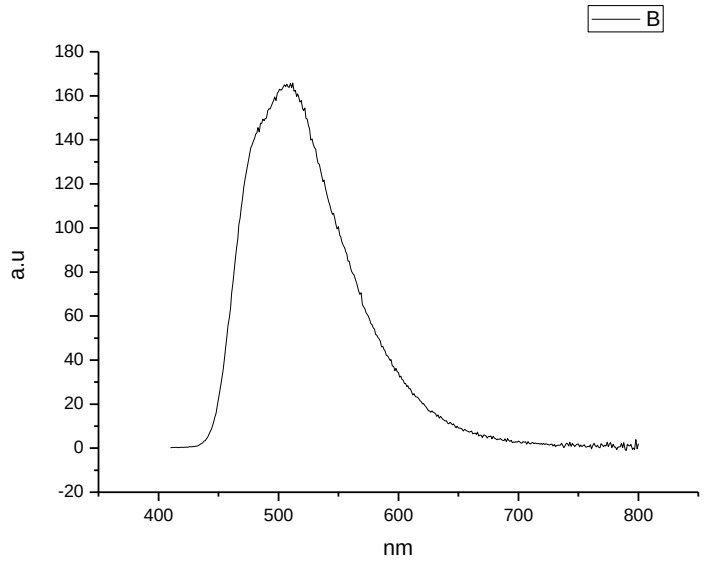

Figure 2.4.186. Fluorescence emission spectrum of **15** recorded in 1-octanol at 400 nm excitation.

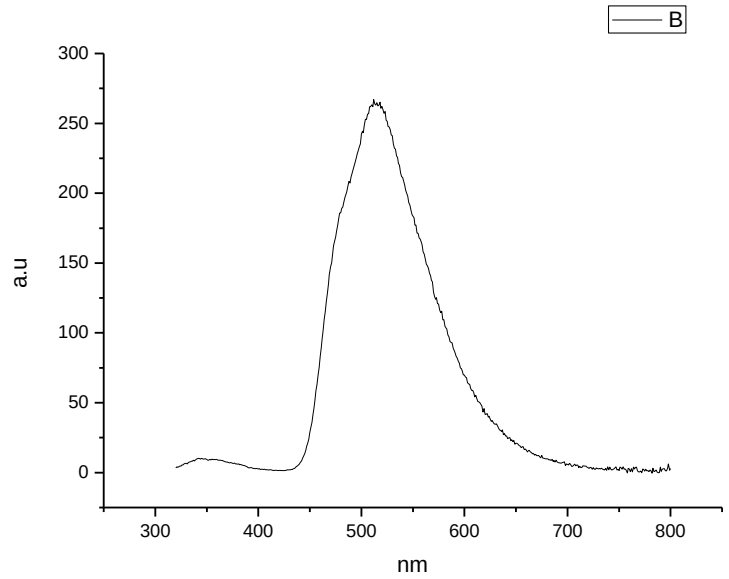

Figure 2.4.187. Fluorescence emission spectrum of **15** recorded in 1-hexanol at 310 nm excitation.

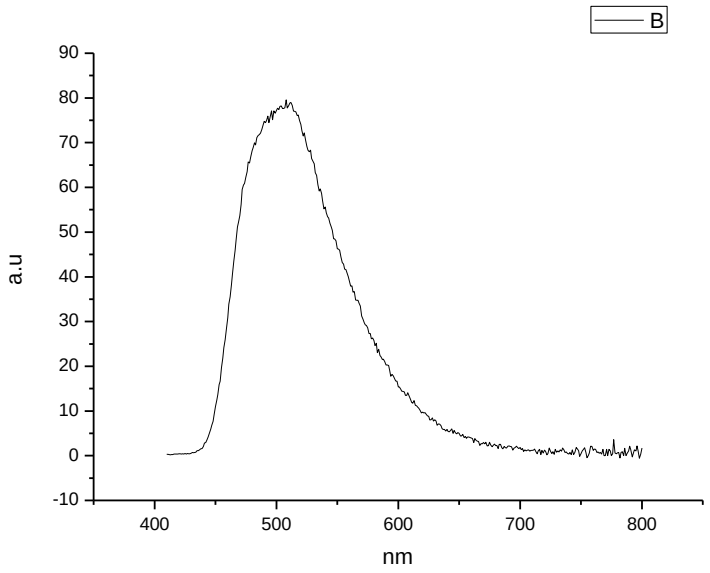

Figure 2.4.188. Fluorescence emission spectrum of **15** recorded in 1-hexanol at 400 nm excitation.

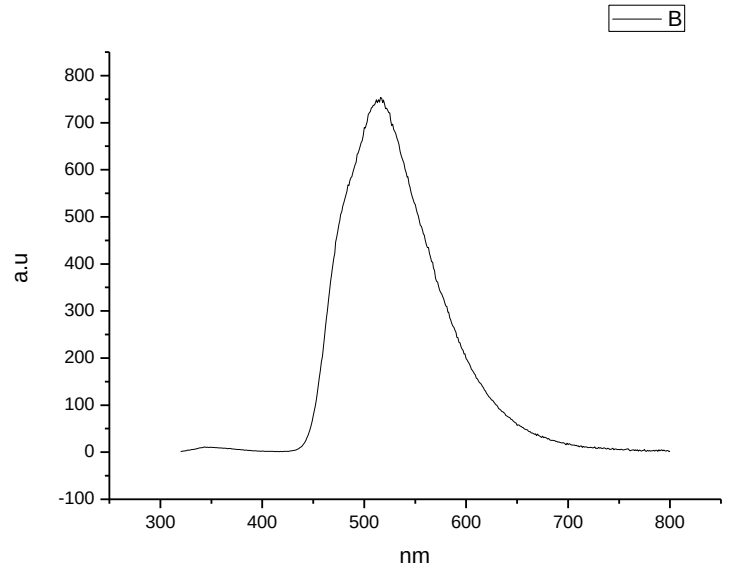

Figure 2.4.189. Fluorescence emission spectrum of **15** recorded in 1-butanol at 310 nm excitation.

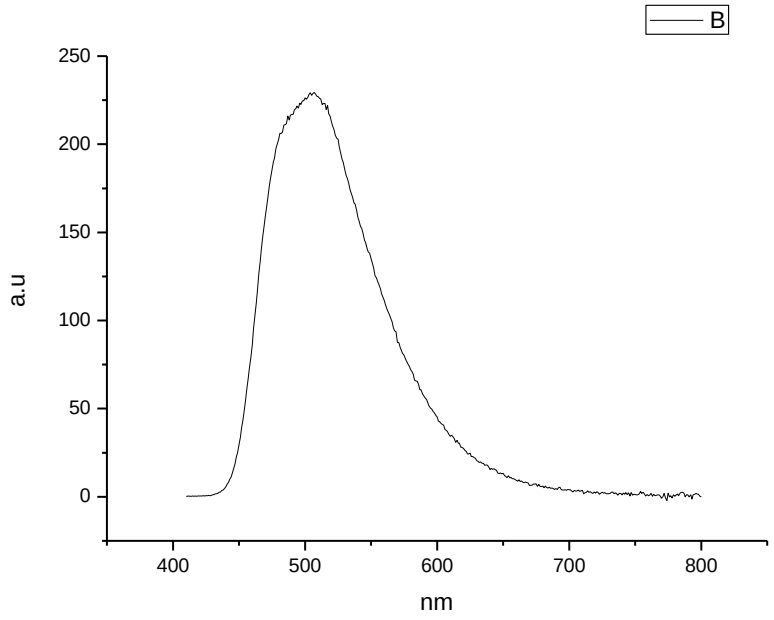

Figure 2.4.190. Fluorescence emission spectrum of **15** recorded in 1-butanol at 400 nm excitation.

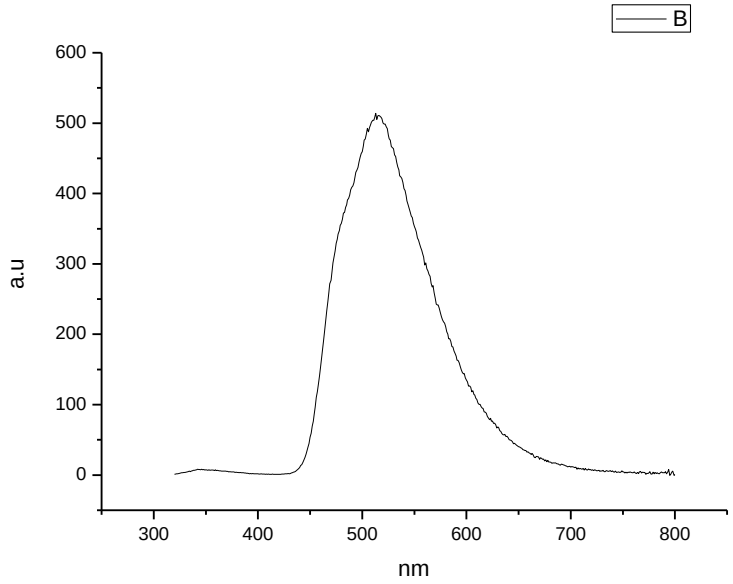

Figure 2.4.191. Fluorescence emission spectrum of **15** recorded in 1-pentanol at 310 nm excitation.

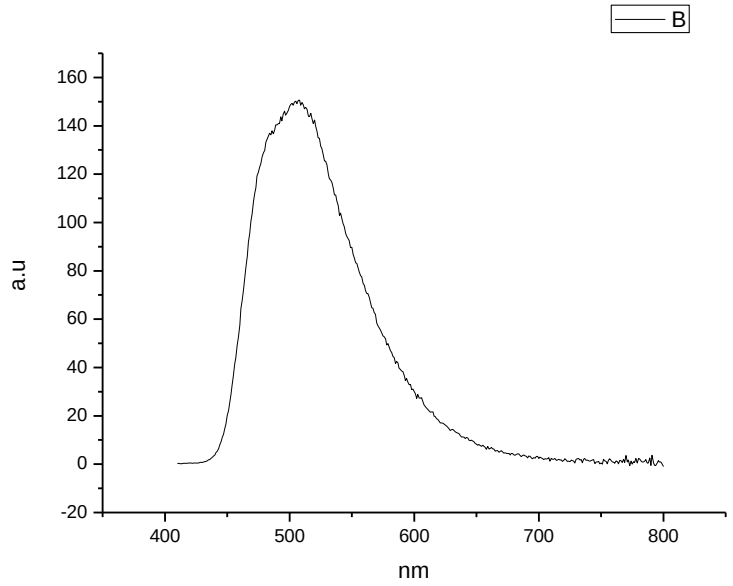

Figure 2.4.192. Fluorescence emission spectrum of **15** recorded in 1-pentanol at 400 nm excitation.

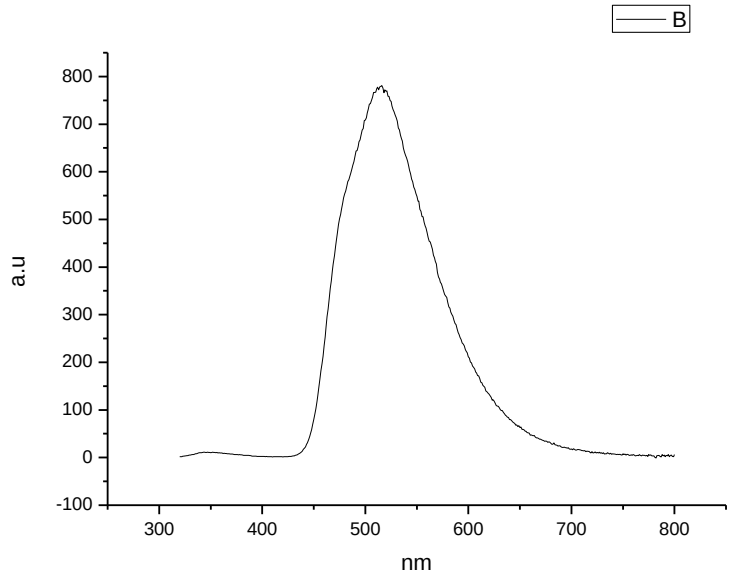

Figure 2.4.193. Fluorescence emission spectrum of **15** recorded in 1-propanol at 310 nm excitation.

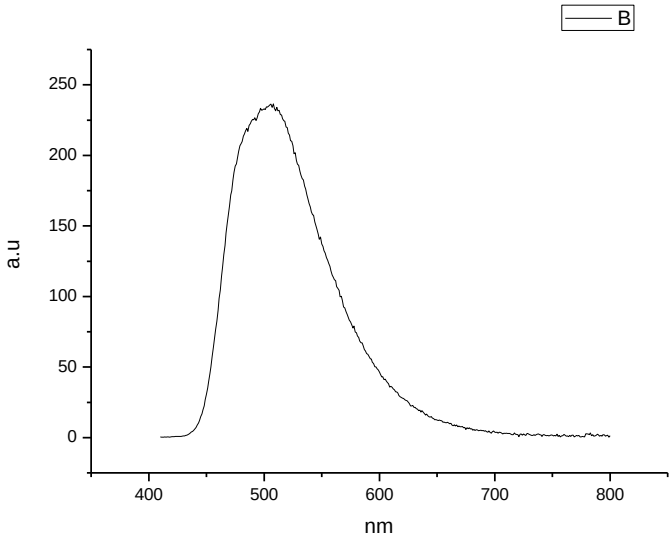

Figure 2.4.194. Fluorescence emission spectrum of **15** recorded in 1-propanol at 400 nm excitation.

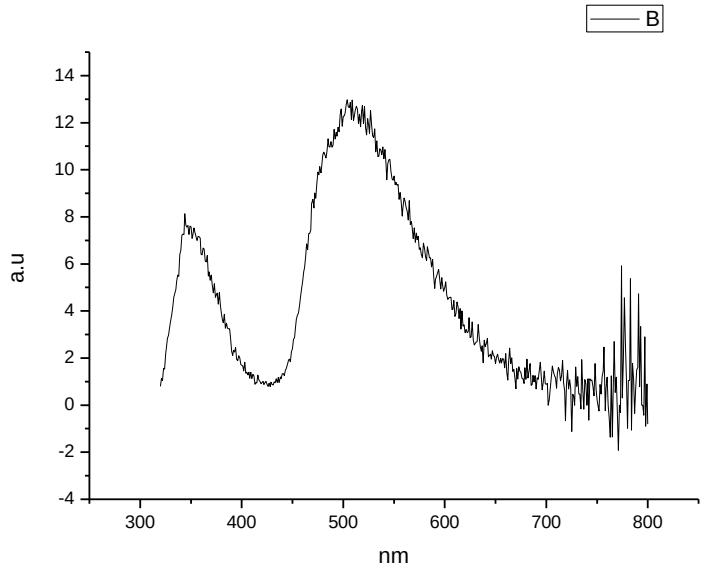

Figure 2.4.195. Fluorescence emission spectrum of **15** recorded in Acetic Acid at 310 nm excitation.

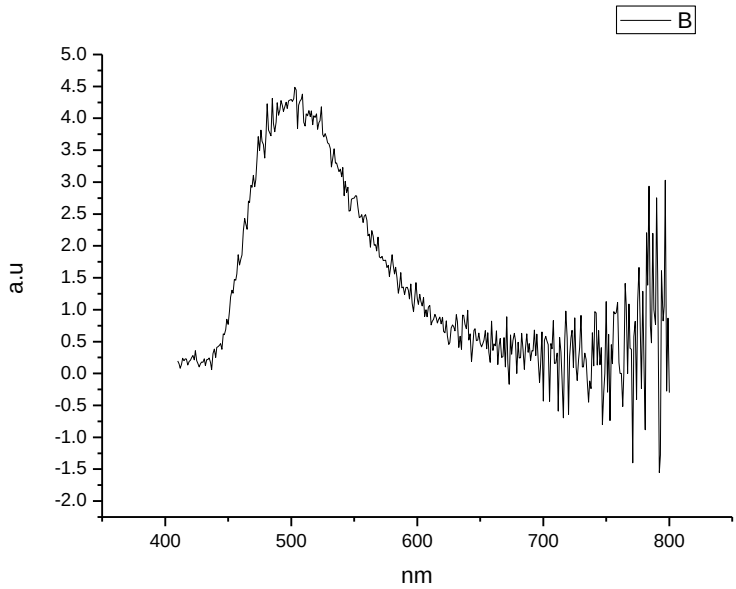

Figure 2.4.196. Fluorescence emission spectrum of **15** recorded in Acetic Acid at 400 nm excitation.

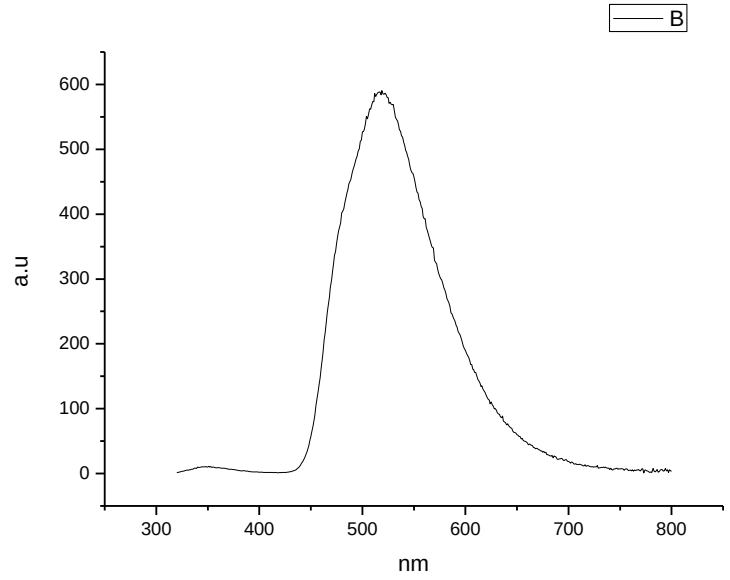

Figure 2.4.197. Fluorescence emission spectrum of **15** recorded in Methanol at 310 nm excitation.

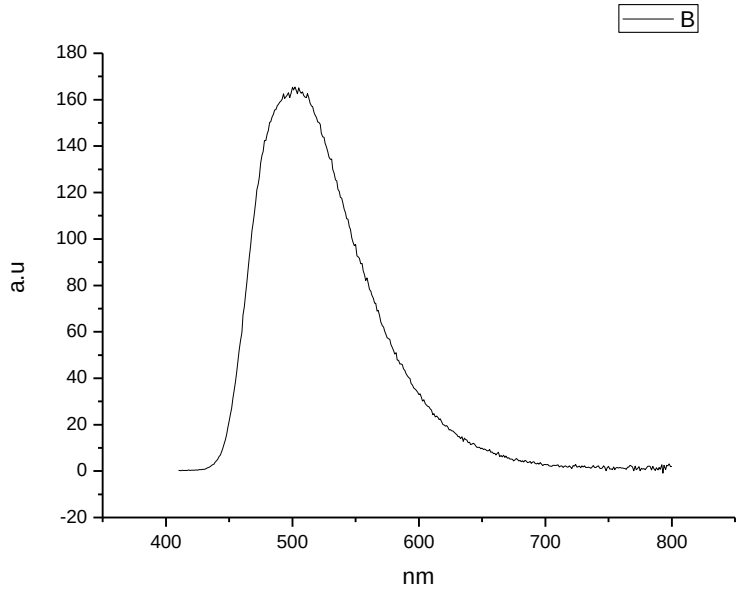

Figure 2.4.198. Fluorescence emission spectrum of **15** recorded in Methanol at 400 nm excitation.

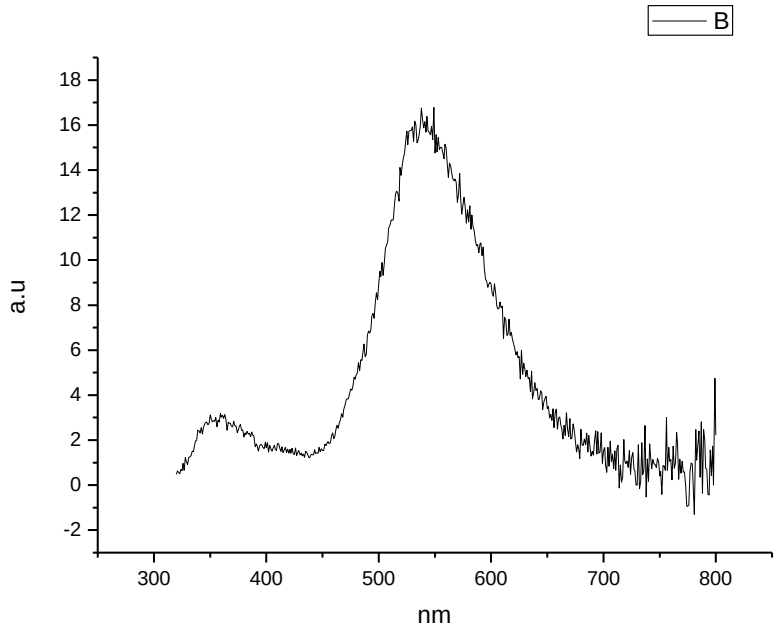

Figure 2.4.199. Fluorescence emission spectrum of **15** recorded in 2,2,2-trifluoroethanol at 310 nm excitation.

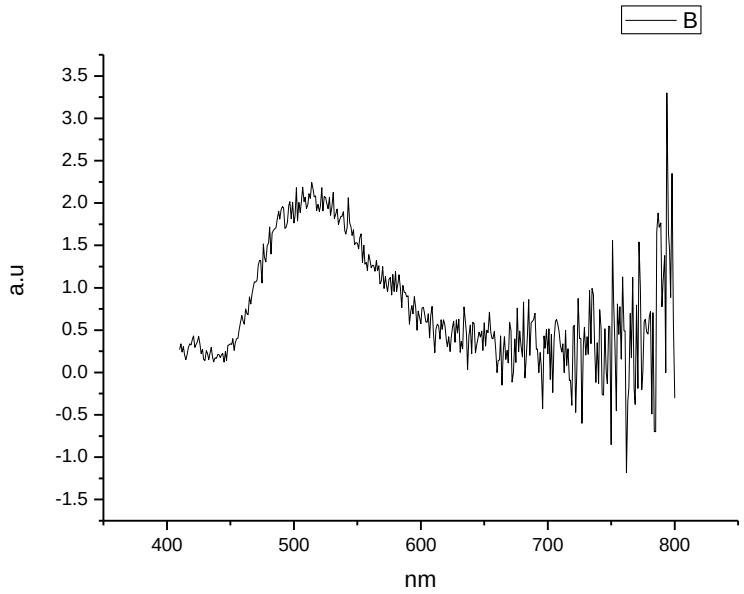

Figure 2.4.200. Fluorescence emission spectrum of **15** recorded in 2,2,2-trifluoroethanol at 400 nm excitation.

2.4.12 Normalised Fluorescence Emission spectra (Gaussian fitted).

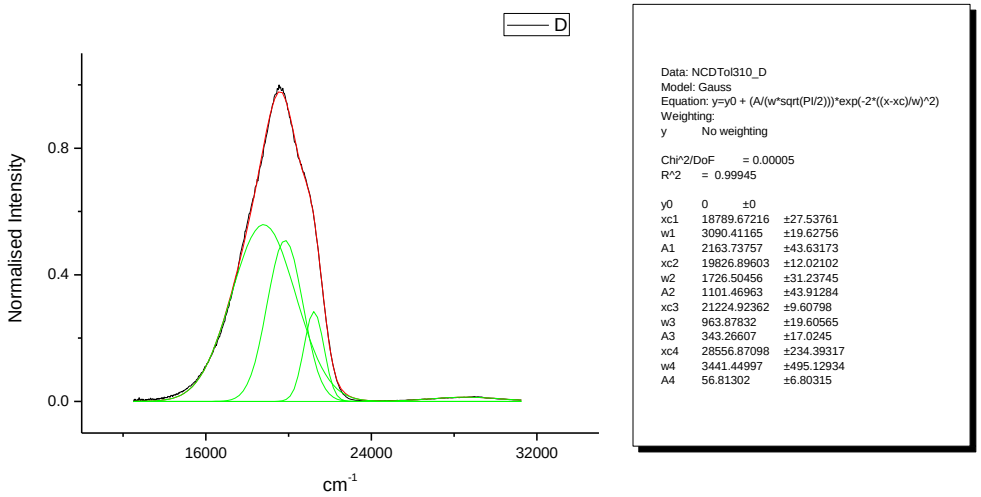

Figure 2.4.201. Gaussian model fit of the normalised fluorescence emission spectrum of **15** recorded in Toluene at 310 nm excitation.

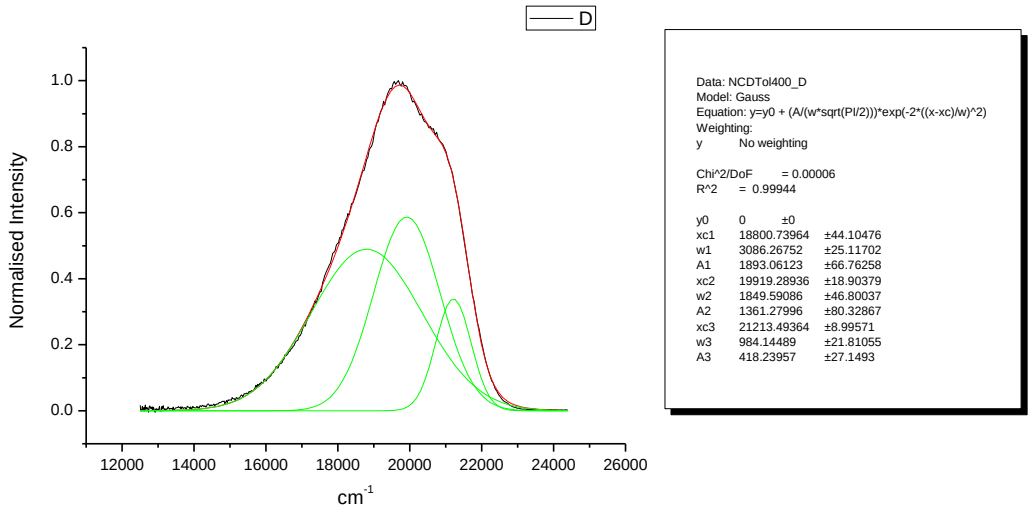

Figure 2.4.202. Gaussian model fit of the normalised fluorescence emission spectrum of **15** recorded in Toluene at 400 nm excitation.

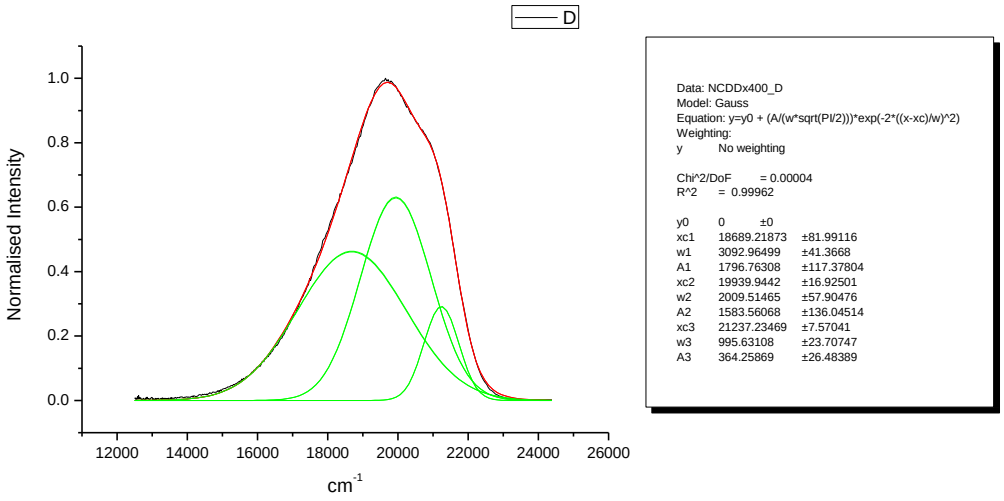

Figure 2.4.203. Gaussian model fit of the normalised fluorescence emission spectrum of **15** recorded in 1,4-dioxane at 310 nm excitation.

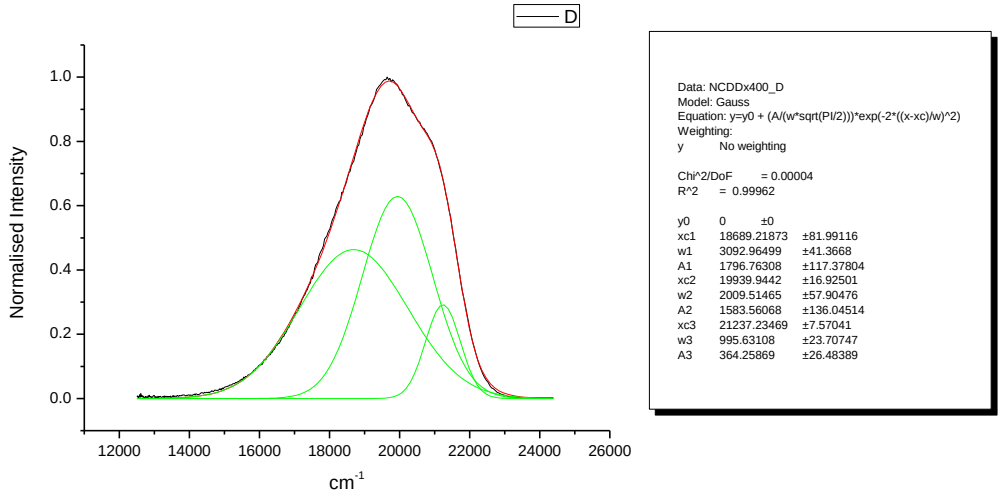

Figure 2.4.204. Gaussian model fit of the normalised fluorescence emission spectrum of **15** recorded in 1,4-dioxane at 400 nm excitation.

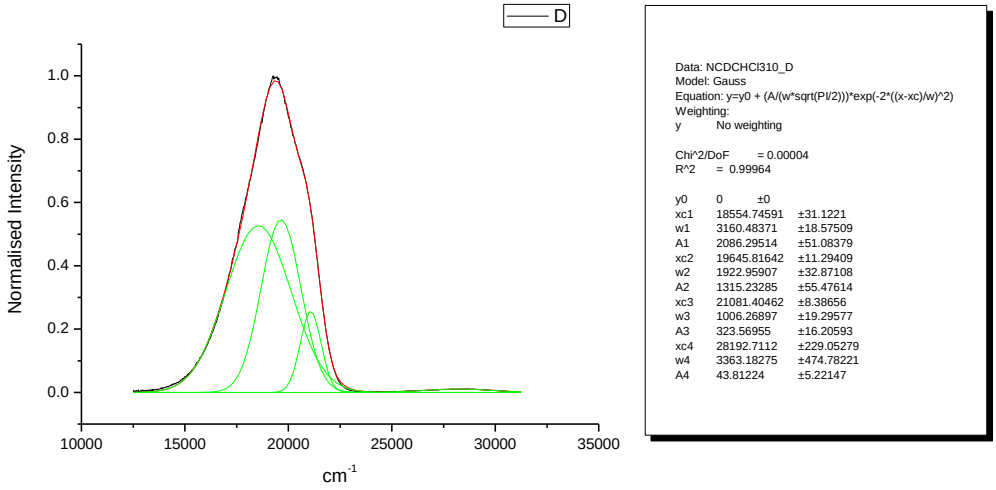

Figure 2.4.205. Gaussian model fit of the normalised fluorescence emission spectrum of **15** recorded in Chloroform at 310 nm excitation.

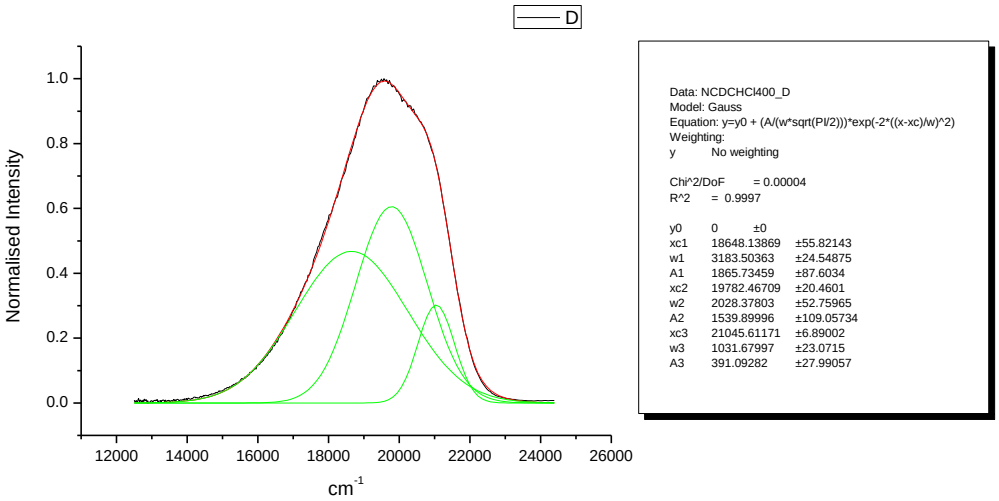

Figure 2.4.206. Gaussian model fit of the normalised fluorescence emission spectrum of **15** recorded in Chloroform at 400 nm excitation.

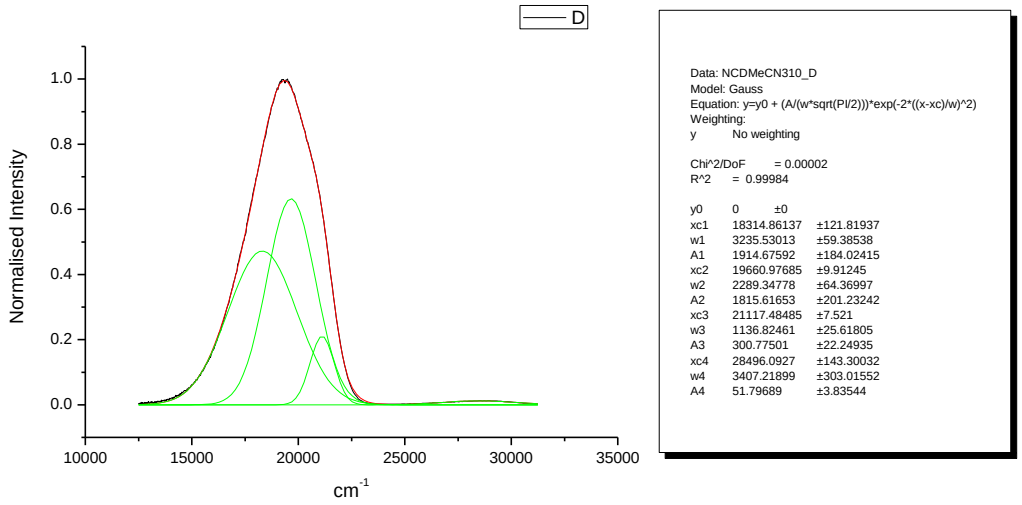

Figure 2.4.207. Gaussian model fit of the normalised fluorescence emission spectrum of **15** recorded in Acetonitrile at 310 nm excitation.

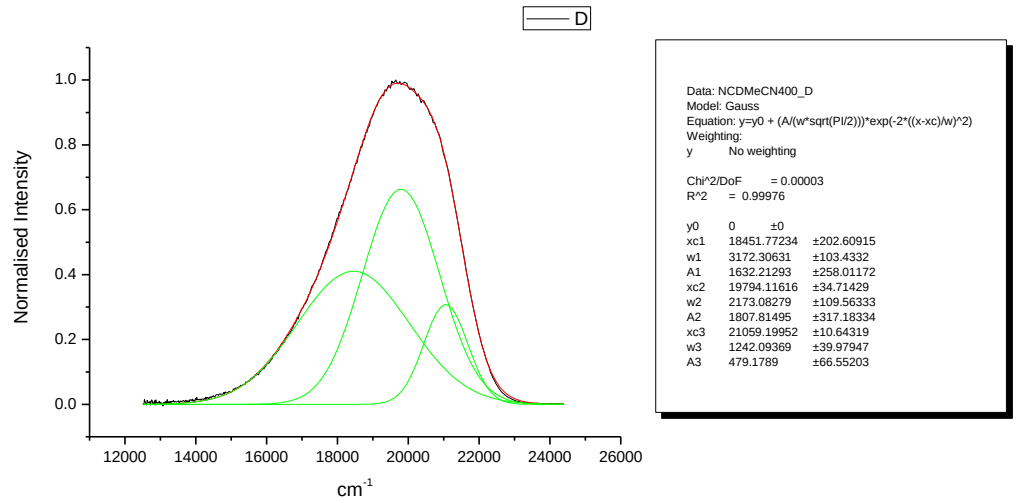

Figure 2.4.208. Gaussian model fit of the normalised fluorescence emission spectrum of **15** recorded in Acetonitrile at 400 nm excitation.

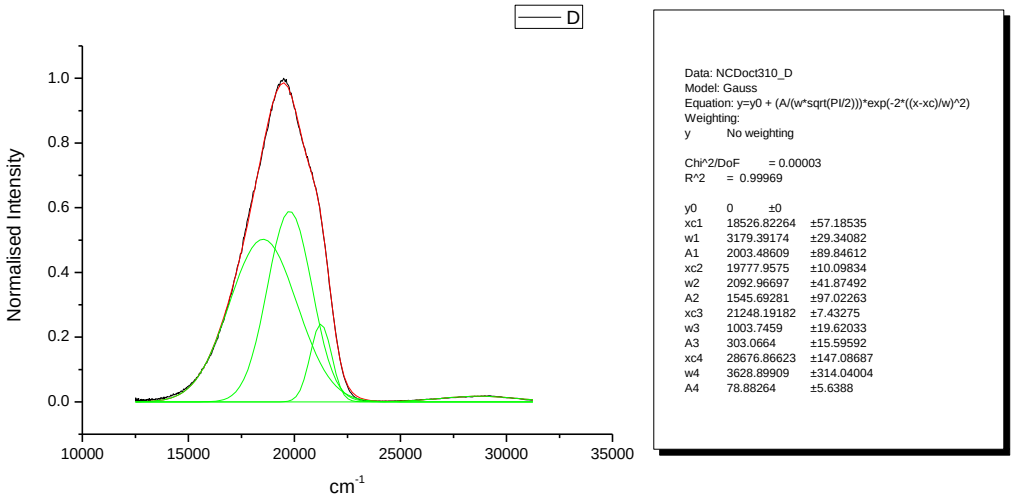

Figure 2.4.209. Gaussian model fit of the normalised fluorescence emission spectrum of **15** recorded in 1-octanol at 310 nm excitation.

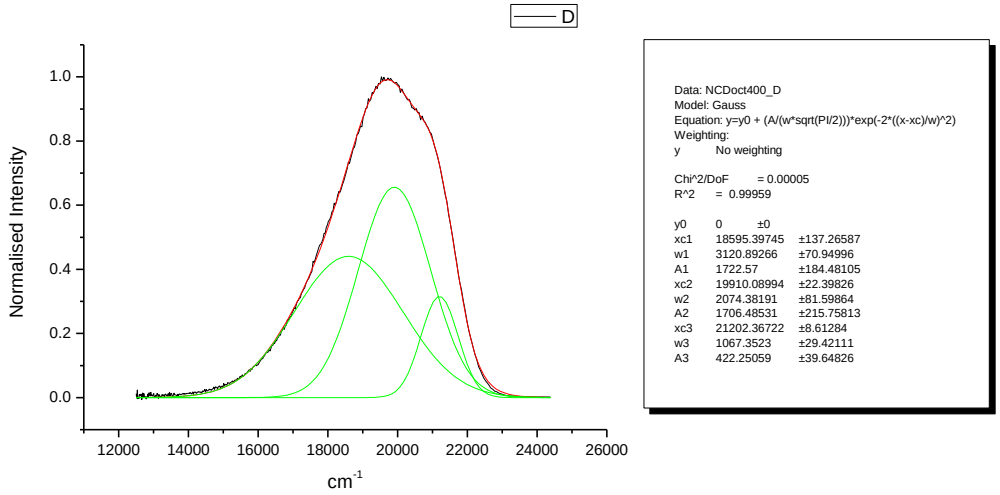

Figure 2.4.210. Gaussian model fit of the normalised fluorescence emission spectrum of **15** recorded in 1-octanol at 400 nm excitation.

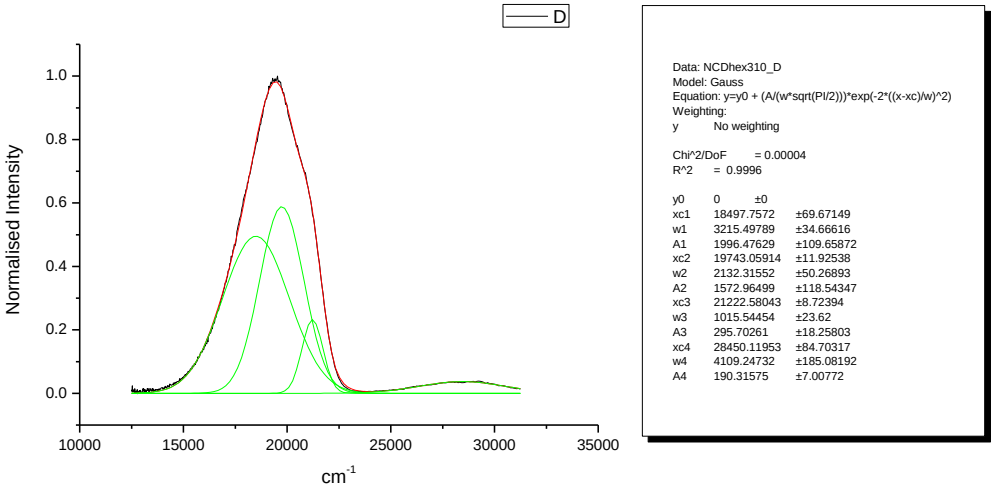

Figure 2.4.211. Gaussian model fit of the normalised fluorescence emission spectrum of **15** recorded in 1-hexanol at 310 nm excitation.

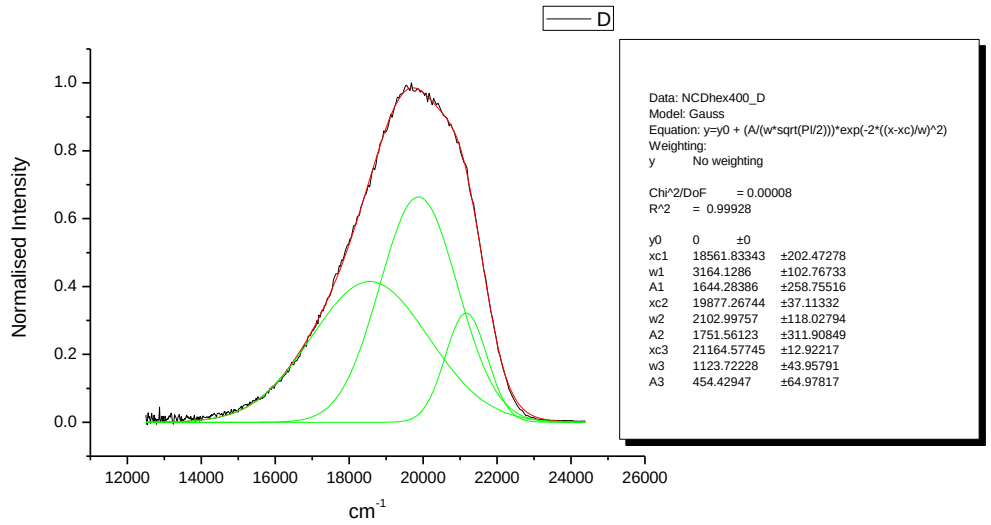

Figure 2.4.212. Gaussian model fit of the normalised fluorescence emission spectrum of **15** recorded in 1-hexanol at 400 nm excitation.

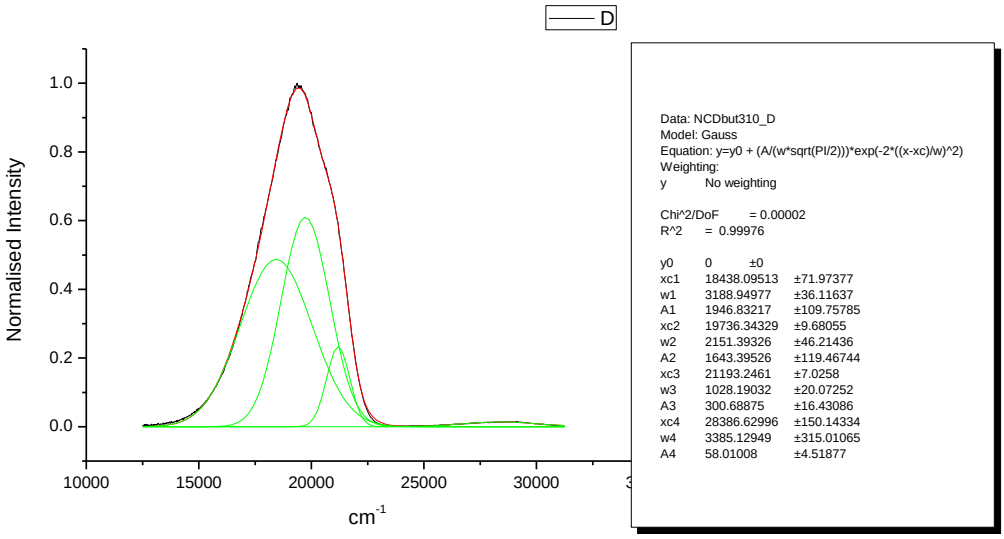

Figure 2.4.213. Gaussian model fit of the normalised fluorescence emission spectrum of **15** recorded in 1-butanol at 310 nm excitation.

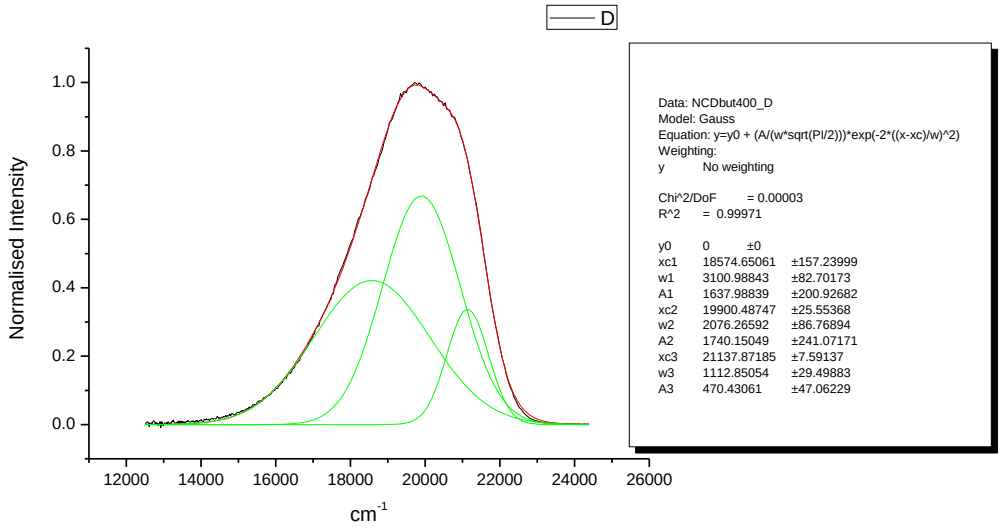

Figure 2.4.214. Gaussian model fit of the normalised fluorescence emission spectrum of **15** recorded in 1-butanol at 400 nm excitation.

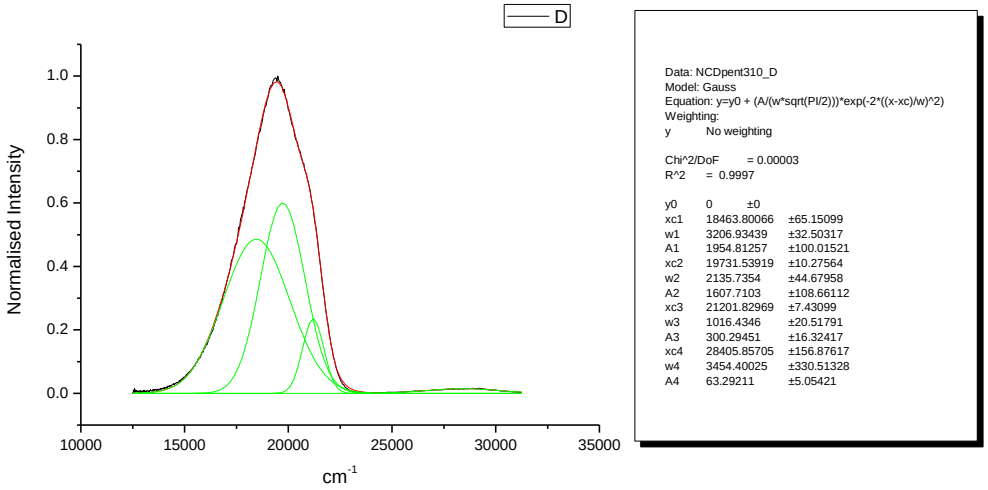

Figure 2.4.215. Gaussian model fit of the normalised fluorescence emission spectrum of **15** recorded in 1-pentanol at 310 nm excitation.

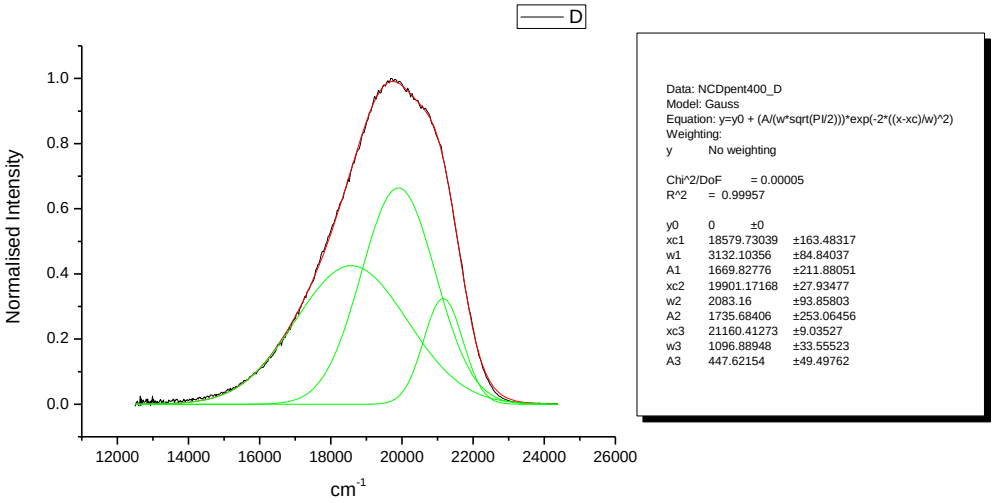

Figure 2.4.216. Gaussian model fit of the normalised fluorescence emission spectrum of **15** recorded in 1-pentanol at 400 nm excitation.

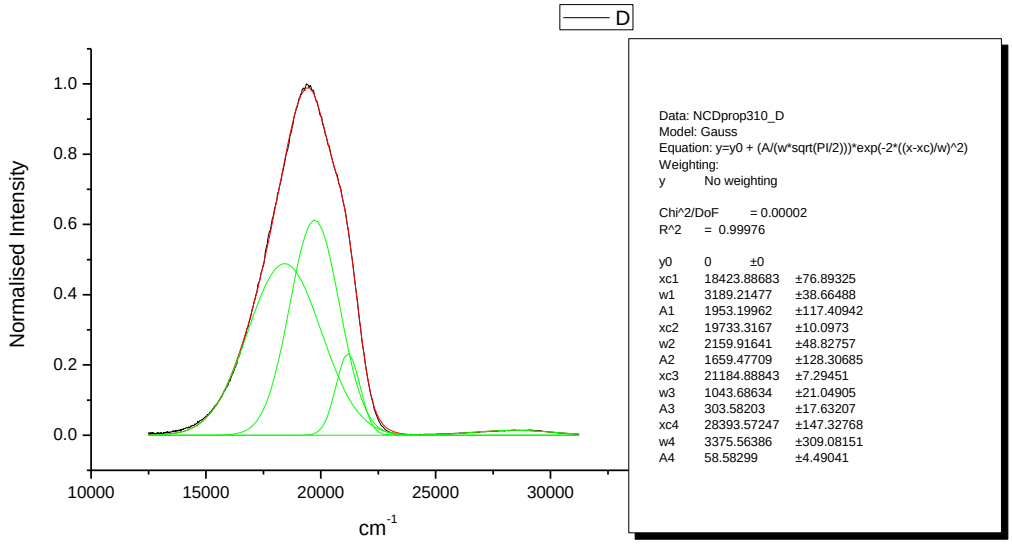

Figure 2.4.217. Gaussian model fit of the normalised fluorescence emission spectrum of **15** recorded in 1-propanol at 310 nm excitation.

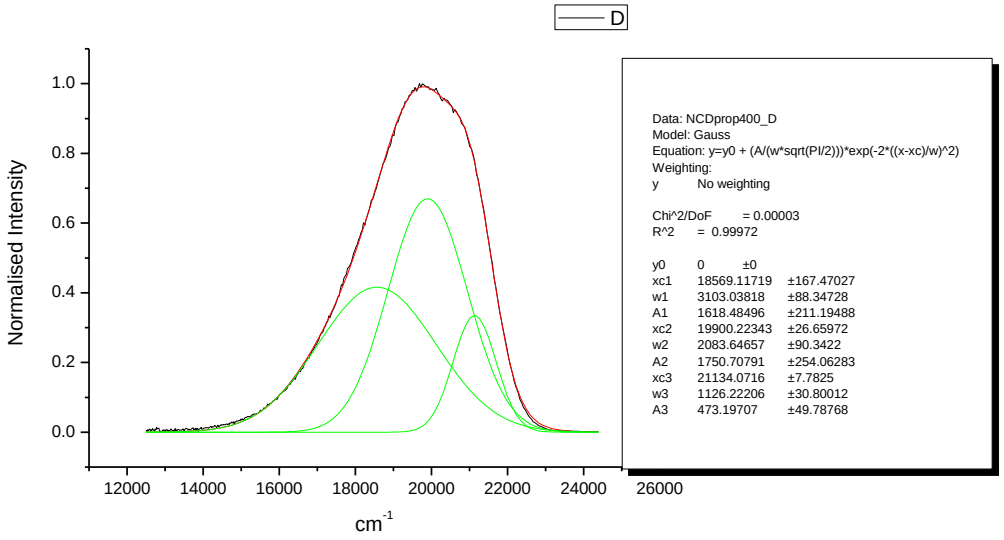

Figure 2.4.218. Gaussian model fit of the normalised fluorescence emission spectrum of **15** recorded in 1-propanol at 400 nm excitation.

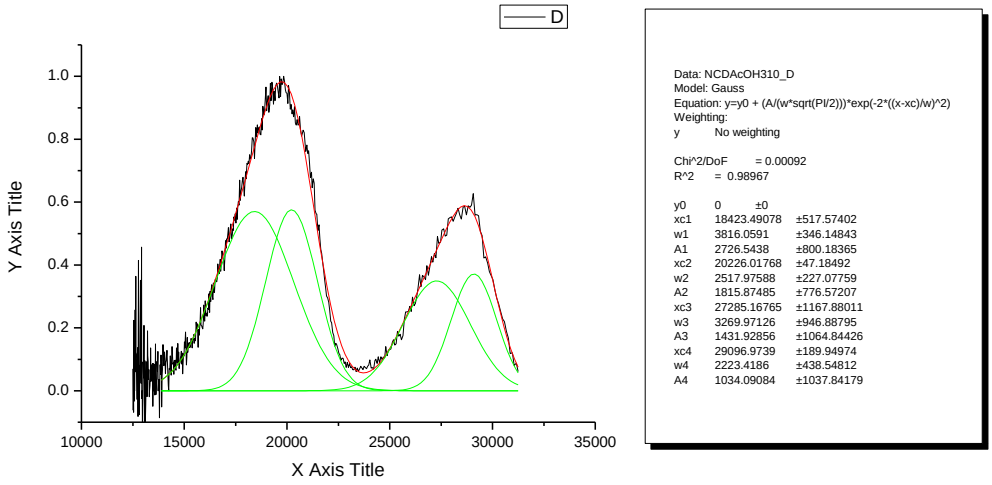

Figure 2.4.219. Gaussian model fit of the normalised fluorescence emission spectrum of **15** recorded in Acetic Acid at 310 nm excitation.

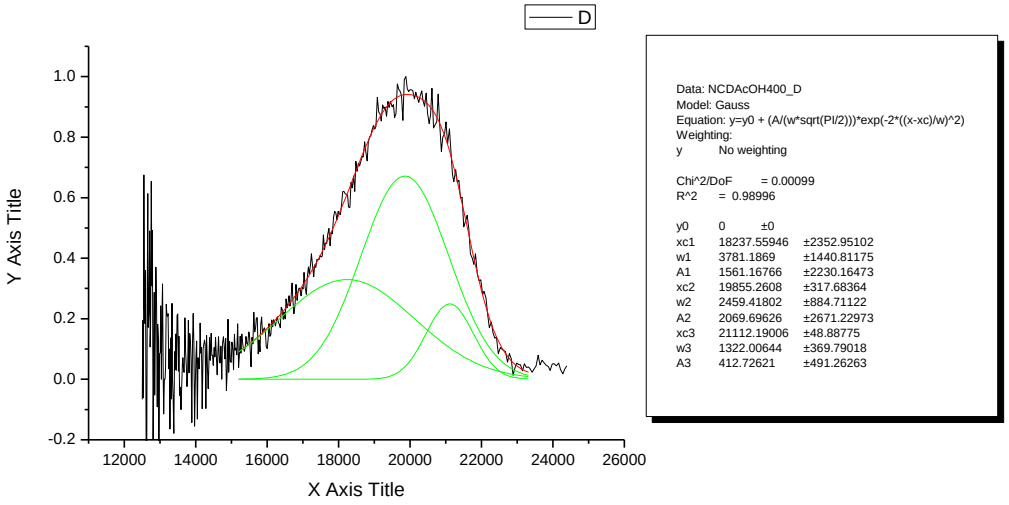

Figure 2.4.220. Gaussian model fit of the normalised fluorescence emission spectrum of **15** recorded in Acetic Acid at 400 nm excitation.

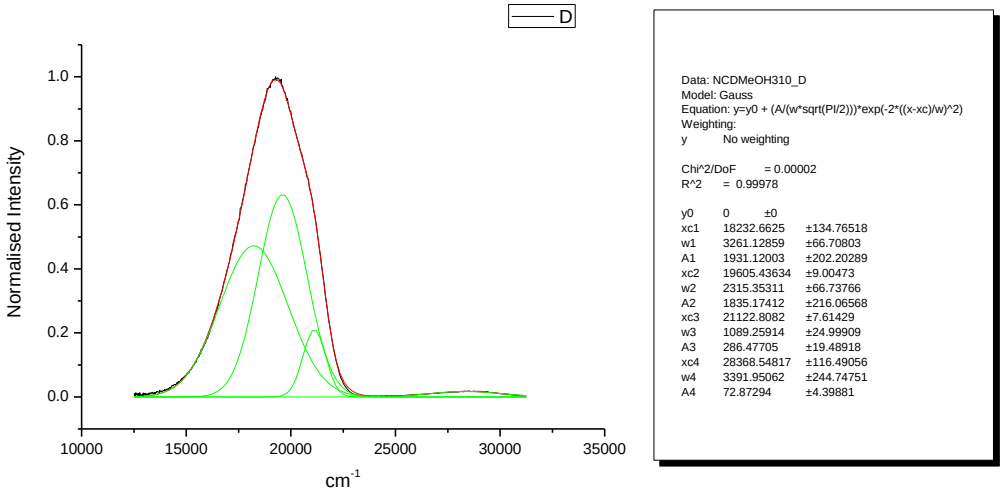

Figure 2.4.221. Gaussian model fit of the normalised fluorescence emission spectrum of **15** recorded in Methanol at 310 nm excitation.

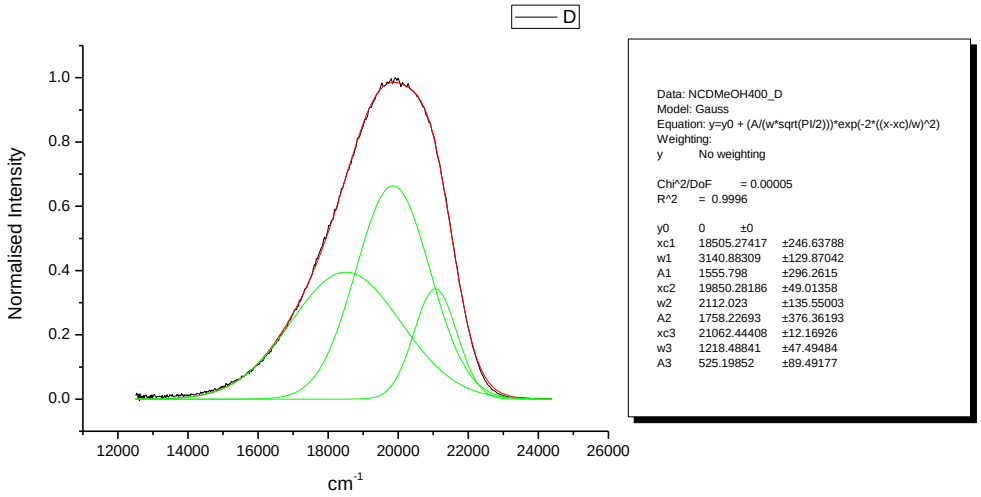

Figure 2.4.222. Gaussian model fit of the normalised fluorescence emission spectrum of **15** recorded in Methanol at 400 nm excitation.

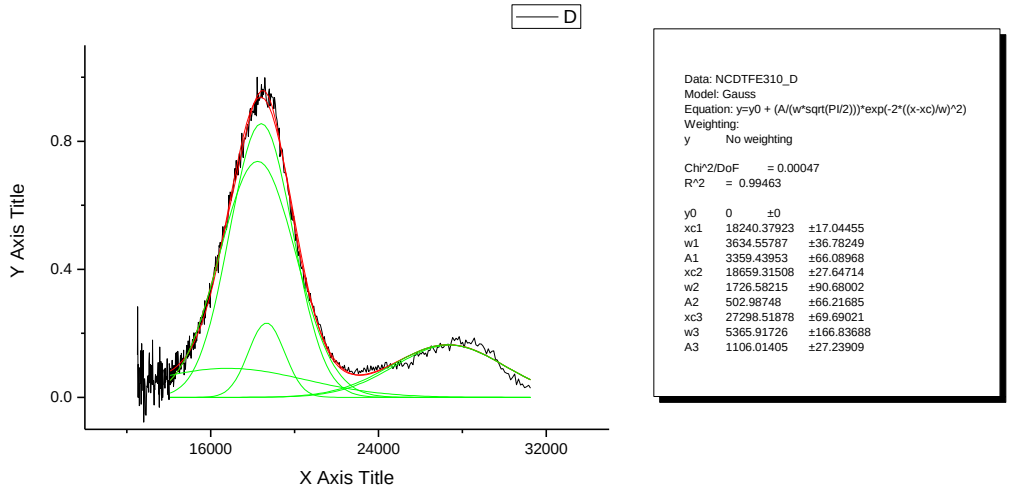

Figure 2.4.223. Gaussian model fit of the normalised fluorescence emission spectrum of **15** recorded in 2,2,2-trifluoroethanol at 310 nm excitation.

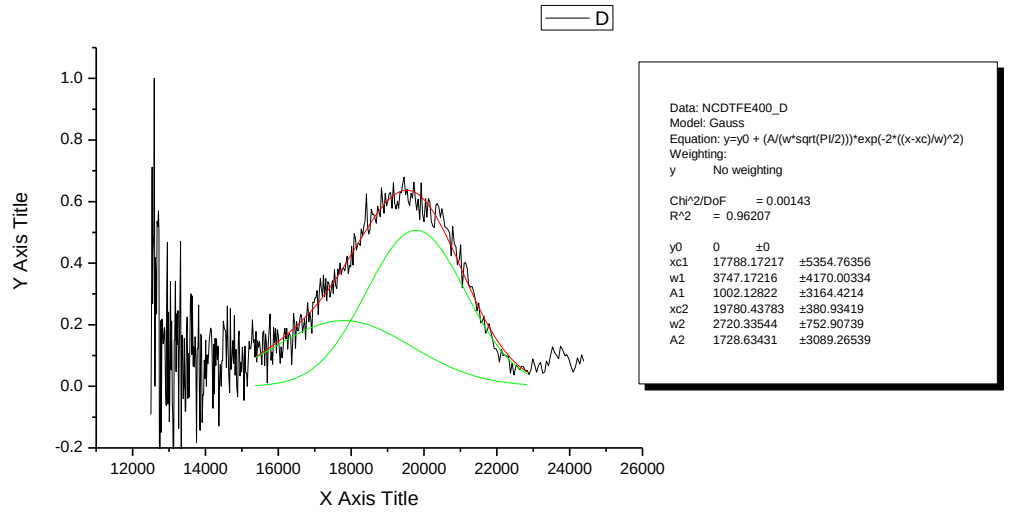

Figure 2.4.224. Gaussian model fit of the normalised fluorescence emission spectrum of **15** recorded in 2,2,2-trifluoroethanol at 400 nm excitation.

2.4.13 Fluorescence Excitation spectra.

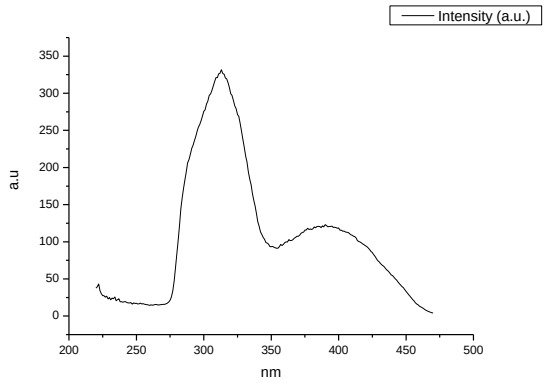

Figure 2.4.225. Fluorescence excitation spectrum of **15** recorded in Toluene with emission fixed at 480 nm.

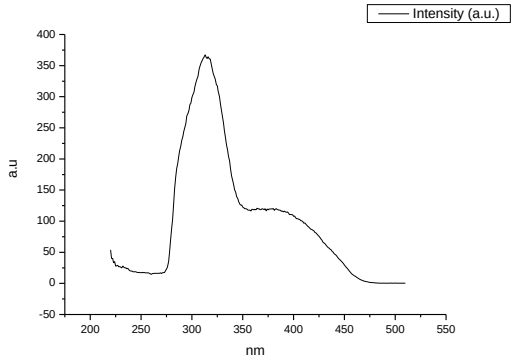

Figure 2.4.226. Fluorescence excitation spectrum of **15** recorded in Toluene with emission fixed at 520 nm.

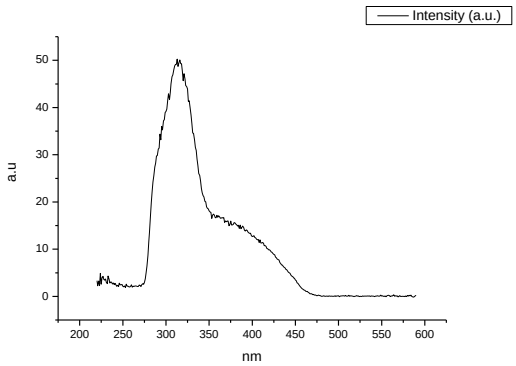

Figure 2.4.227. Fluorescence excitation spectrum of **15** recorded in Toluene with emission fixed at 600 nm.

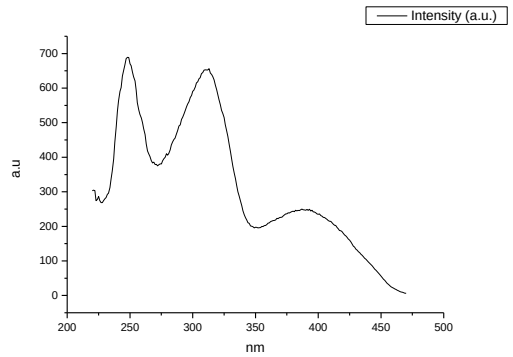

Figure 2.4.228. Fluorescence excitation spectrum of **15** recorded in 1,4-dioxane with emission fixed at 480 nm.

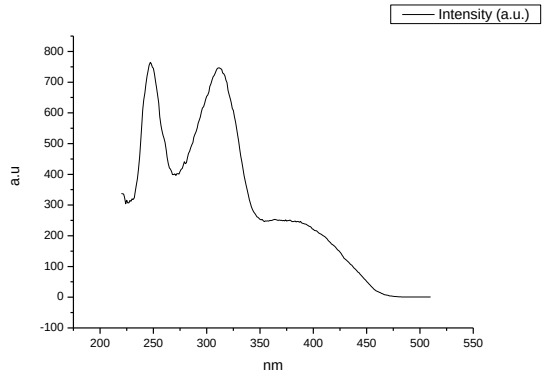

Figure 2.4.229. Fluorescence excitation spectrum of **15** recorded in 1,4-dioxane with emission fixed at 520 nm.

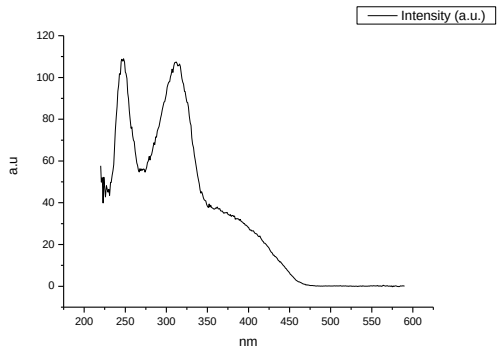

Figure 2.4.230. Fluorescence excitation spectrum of **15** recorded in 1,4-dioxane with emission fixed at 600 nm.

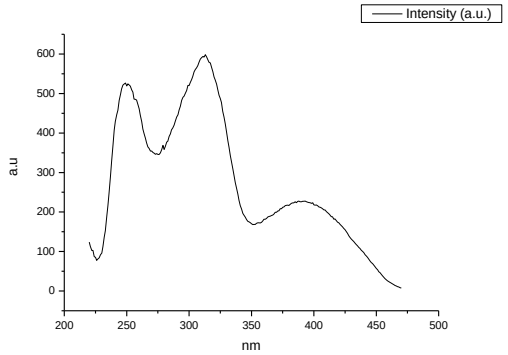

Figure 2.4.231. Fluorescence excitation spectrum of **15** recorded in Chloroform with emission fixed at 480 nm.

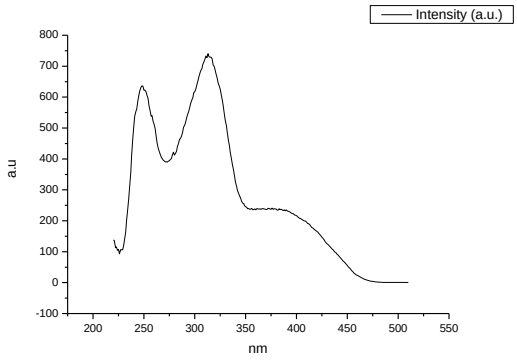

Figure 2.4.232. Fluorescence excitation spectrum of **15** recorded in Chloroform with emission fixed at 520 nm.

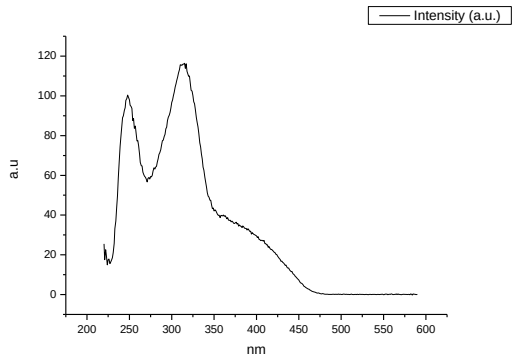

Figure 2.4.233. Fluorescence excitation spectrum of **15** recorded in Chloroform with emission fixed at 600 nm.

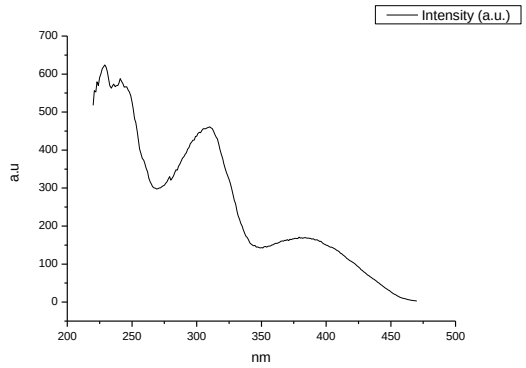

Figure 2.4.234. Fluorescence excitation spectrum of **15** recorded in Acetonitrile with emission fixed at 480 nm.

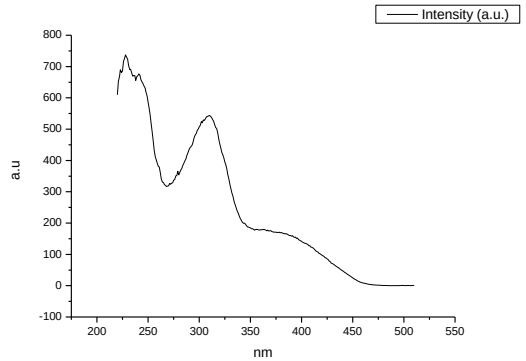

Figure 2.4.235. Fluorescence excitation spectrum of **15** recorded in Acetonitrile with emission fixed at 520 nm.

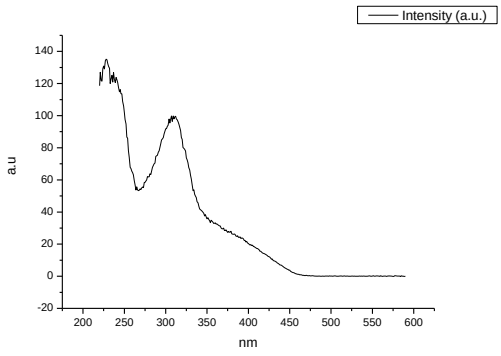

Figure 2.4.236. Fluorescence excitation spectrum of **15** recorded in Acetonitrile with emission fixed at 600 nm.

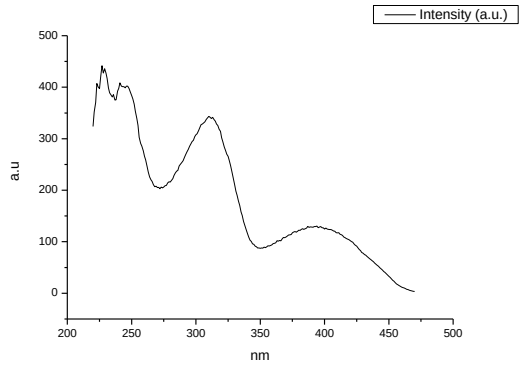

Figure 2.4.237. Fluorescence excitation spectrum of **15** recorded in 1-octanol with emission fixed at 480 nm.

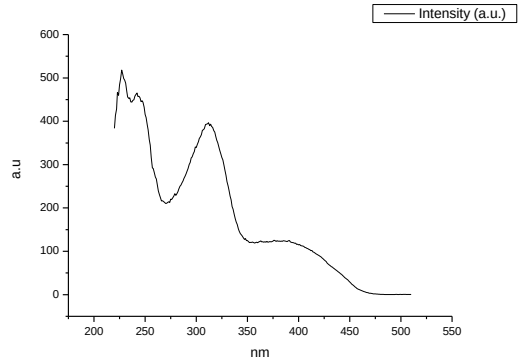

Figure 2.4.238. Fluorescence excitation spectrum of **15** recorded in 1-octanol with emission fixed at 520 nm.

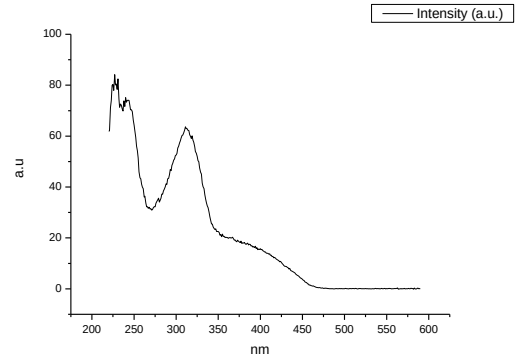

Figure 2.4.239. Fluorescence excitation spectrum of **15** recorded in 1-octanol with emission fixed at 600 nm.

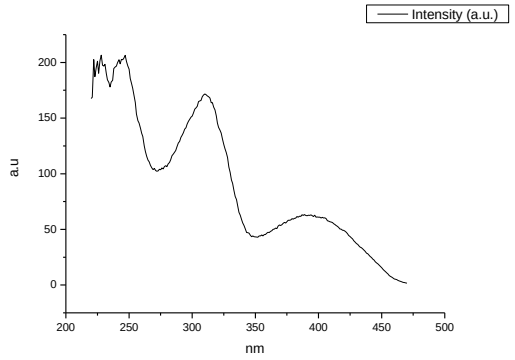

Figure 2.4.240. Fluorescence excitation spectrum of **15** recorded in 1-hexanol with emission fixed at 480 nm.

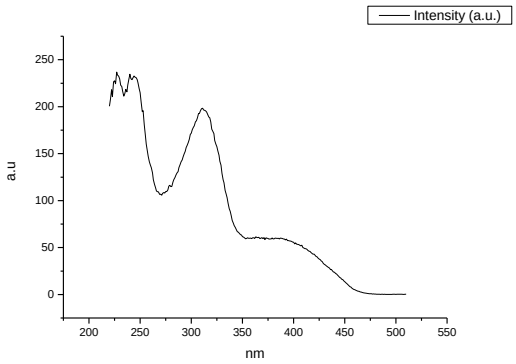

Figure 2.4.241. Fluorescence excitation spectrum of **15** recorded in 1-hexanol with emission fixed at 520 nm.

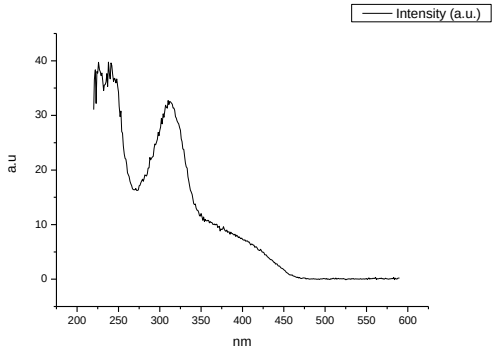

Figure 2.4.242. Fluorescence excitation spectrum of **15** recorded in 1-hexanol with emission fixed at 600 nm.

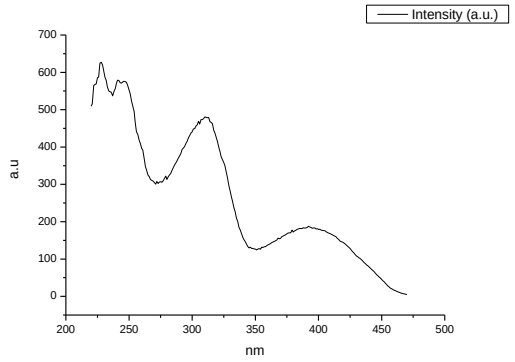

Figure 2.4.243. Fluorescence excitation spectrum of **15** recorded in 1-butanol with emission fixed at 480 nm.

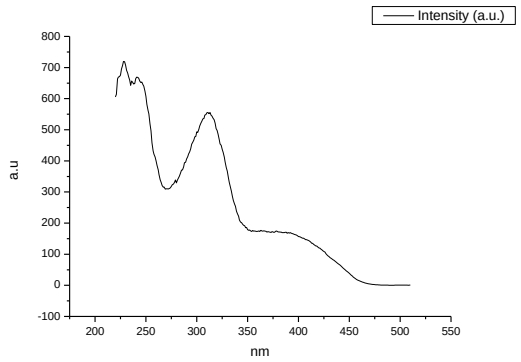

Figure 2.4.244. Fluorescence excitation spectrum of **15** recorded in 1-butanol with emission fixed at 520 nm.

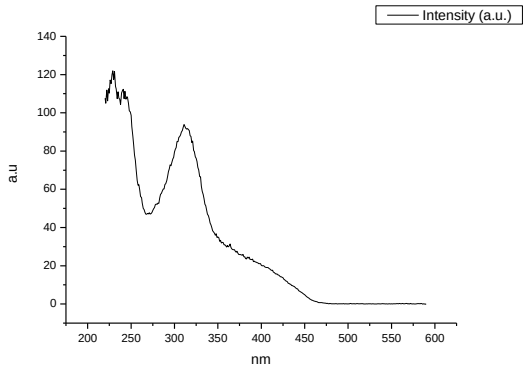

Figure 2.4.245. Fluorescence excitation spectrum of **15** recorded in 1-butanol with emission fixed at 600 nm.

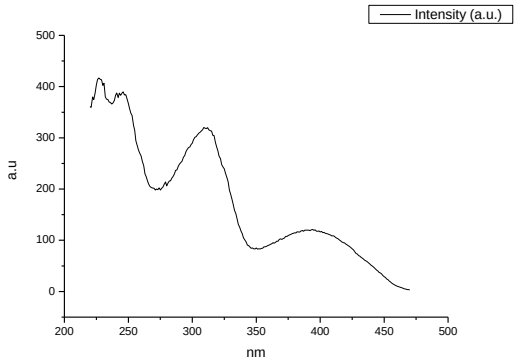

Figure 2.4.246. Fluorescence excitation spectrum of **15** recorded in 1-pentanol with emission fixed at 480 nm.

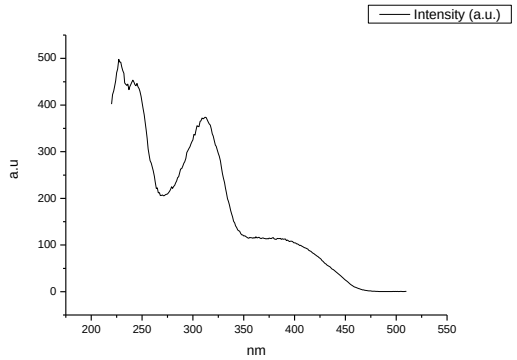

Figure 2.4.247. Fluorescence excitation spectrum of **15** recorded in 1-pentanol with emission fixed at 520 nm.

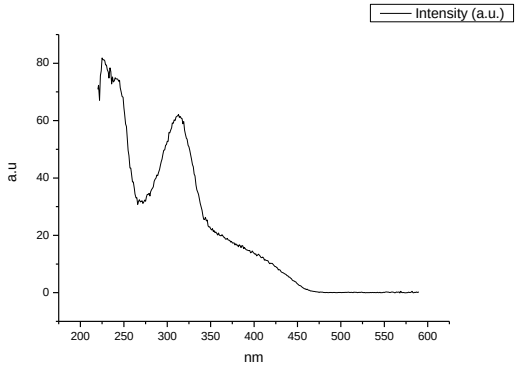

Figure 2.4.248. Fluorescence excitation spectrum of **15** recorded in 1-pentanol with emission fixed at 600 nm.

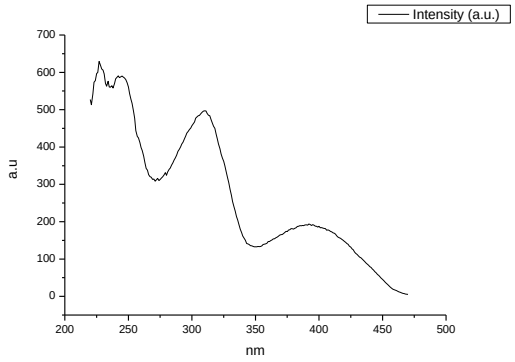

Figure 2.4.249. Fluorescence excitation spectrum of **15** recorded in 1-propanol with emission fixed at 480 nm.

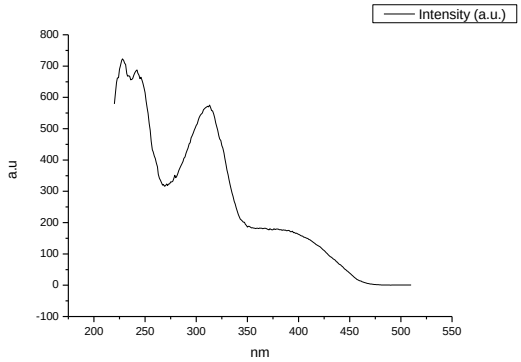

Figure 2.4.250. Fluorescence excitation spectrum of **15** recorded in 1-propanol with emission fixed at 520 nm.

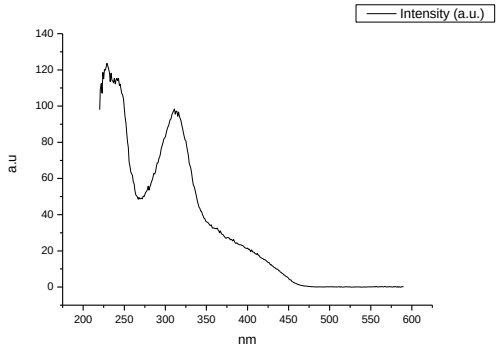

Figure 2.4.251. Fluorescence excitation spectrum of **15** recorded in 1-propanol with emission fixed at 600 nm.

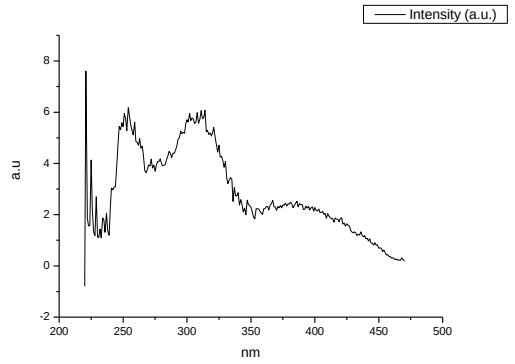

Figure 2.4.252. Fluorescence excitation spectrum of **15** recorded in Acetic Acid with emission fixed at 480 nm.

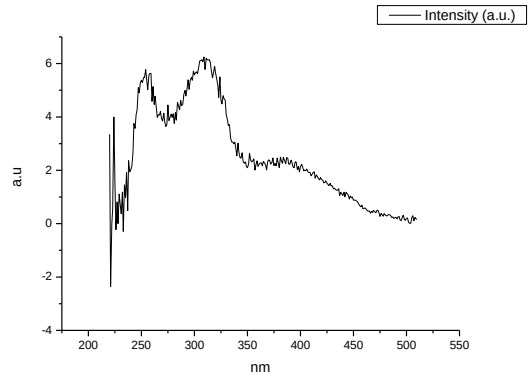

Figure 2.4.253. Fluorescence excitation spectrum of **15** recorded in Acetic Acid with emission fixed at 520 nm.

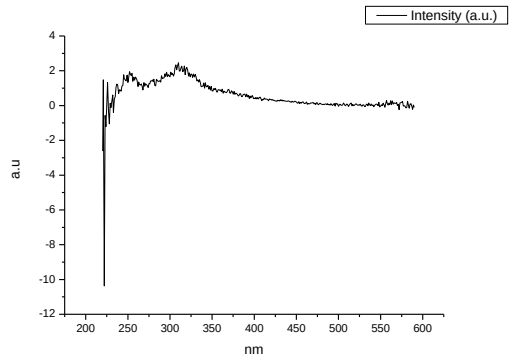

Figure 2.4.254. Fluorescence excitation spectrum of **15** recorded in Acetic Acid with emission fixed at 600 nm.

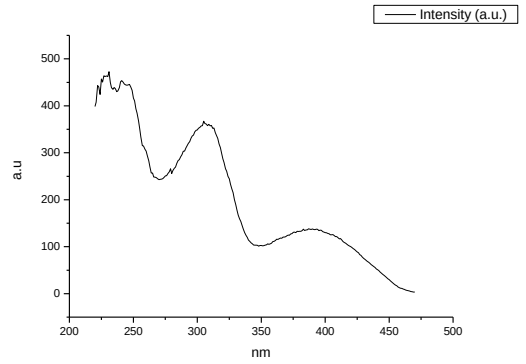

Figure 2.4.255. Fluorescence excitation spectrum of **15** recorded in Methanol with emission fixed at 480 nm.

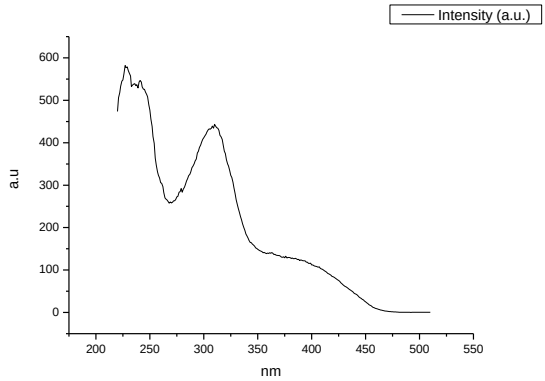

Figure 2.4.256. Fluorescence excitation spectrum of **15** recorded in Methanol with emission fixed at 520 nm.

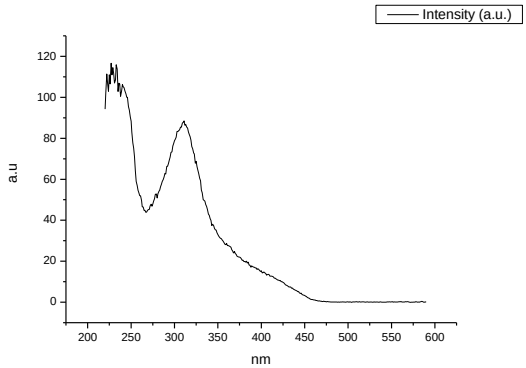

Figure 2.4.257. Fluorescence excitation spectrum of **15** recorded in Methanol with emission fixed at 600 nm.

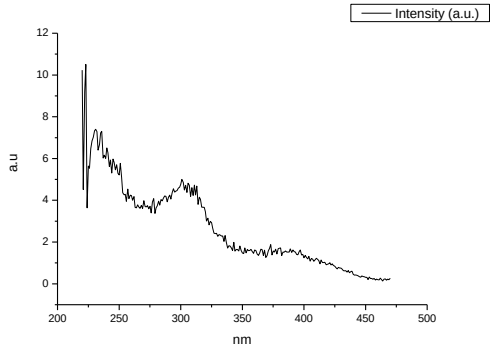

Figure 2.4.258. Fluorescence excitation spectrum of **15** recorded in 2,2,2-trifluoroethanol with emission fixed at 480 nm.

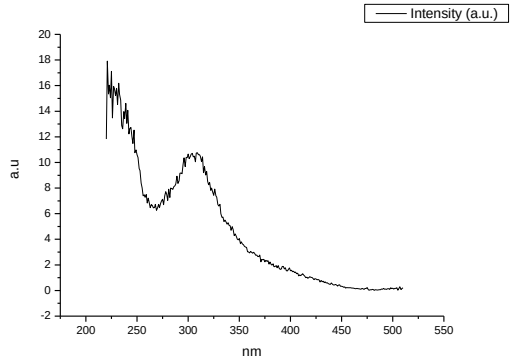

Figure 2.4.259. Fluorescence excitation spectrum of **15** recorded in 2,2,2-trifluoroethanol with emission fixed at 520 nm.

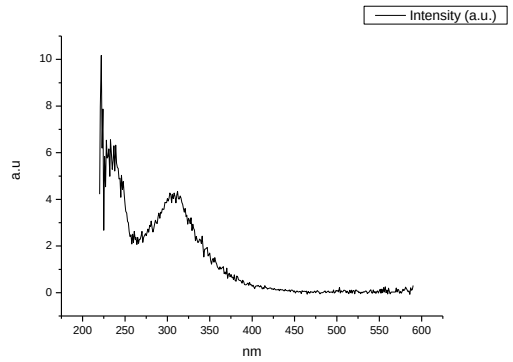

Figure 2.4.260. Fluorescence excitation spectrum of **15** recorded in 2,2,2-trifluoroethanol with emission fixed at 600 nm.

Appendix 3: Imine hydrolysis of the 2,5-dihydro-1,2,3-triazines with substituted aryl groups.

3.1 COMPOUND 16

3.1.1 Quantum Yield Summary.

Solvent	abs (310 nm)	$\lambda_{ems\ (max)}$	$\Phi_{310\ nm}$	abs (400 nm)	$\lambda_{ems\ (max)}$	$\Phi_{400\ nm}$
Toluene	0.06	480.00	0.21	0.03	478.93	0.27
1,4-Dioxane	0.06	481.04	0.27	0.03	480.00	0.28
Chloroform	0.05	482.98	0.27	0.03	485.97	0.25
Acetonitrile	0.06	488.05	0.29	0.02	487.01	0.26
1-Octanol	0.04	481.94	0.23	0.03	480.00	0.21
1-Hexanol	0.03	480.00	0.24	0.01	481.04	0.23
1-Butanol	0.04	482.98	0.25	0.02	481.94	0.22
1-Pentanol	0.04	481.94	0.24	0.02	481.94	0.22
1-Propanol	0.05	481.94	0.24	0.02	481.04	0.22
Acetic acid	0.06	482.98	0.07	0.03	485.07	0.07
Methanol	0.06	488.95	0.18	0.03	484.02	0.17
2,2,2-Trifluoroethanol	0.05	496.96	0.03	0.02	498.93	0.03

Table 3.1.1. Summary of ultraviolet-visible absorbance values at 310 nm and 400 nm, emission maxima and quantum yield (Φ) of **16** at 310 nm and 400 nm excitation.

3.1.2 310 nm excitation Gaussian band fit summaries.

Solvent	λ max$_{em}$ Band 1 (cm^{-1})	λ max$_{em}$ Band 1 (nm)	λ max$_{em}$ Band 2 (cm^{-1})	λ max$_{em}$ Band 2 (nm)	λ max$_{em}$ Band 3 (cm^{-1})	λ max$_{em}$ Band 3 (nm)
Toluene	19166.04	521.76	19922.88	501.94	21142.64	472.98
1,4-Dioxane	19089.20	523.86	20092.20	497.71	21197.52	471.75
Chloroform	18858.87	530.25	19960.73	500.98	21032.25	475.46
Acetonitrile	18855.12	530.36	20022.70	499.43	21109.05	473.73
1-Octanol	19095.79	523.68	20171.82	495.74	21278.26	469.96
1-Hexanol	19061.39	524.62	20157.19	496.10	21261.95	470.32
1-Butanol	19002.57	526.24	20161.11	496.00	21253.03	470.52
1-Pentanol	19032.03	525.43	20149.81	496.28	21254.48	470.49
1-Propanol	19007.33	526.11	20167.28	495.85	21255.10	470.48
Acetic acid	18974.71	527.02	20153.32	496.20	21232.70	470.97
Methanol	18930.94	528.24	20105.39	497.38	21209.10	471.50
2,2,2-Trifluoroethanol	19027.55	525.55	20435.02	489.36		

Solvent	λ max$_{em}$ Band 4 (cm^{-1})	λ max$_{em}$ Band 4 (nm)	λ max$_{em}$ Band 5 (cm^{-1})	λ max$_{em}$ Band 5 (nm)
Toluene	-	-	-	-
1,4-Dioxane	-	-	-	-
Chloroform	-	-	-	-
Acetonitrile	-	-	-	-
1-Octanol	-	-	-	-
1-Hexanol	28445.15	351.55	-	-
1-Butanol	-	-	-	-
1-Pentanol	-	-	-	-
1-Propanol	-	-	-	-
Acetic acid	28428.51	351.76	-	-
Methanol	-	-	-	-
2,2,2-Trifluoroethanol	-	-	-	-

Table 3.1.2. Summary of band maxima of 5 band fit using Gaussian model for normalised **16** emission spectra recorded at 310 nm excitation.

(a)

Solvent	Width Band 1 (cm^{-1})	Width Band 2 (cm^{-1})	Width Band 3 (cm^{-1})	Width Band 4 (cm^{-1})	Width Band 5 (cm^{-1})
Toluene	2936.89	1570.99	1083.43	-	-
1,4-Dioxane	3012.55	1879.73	1086.05	-	-
Chloroform	3030.37	1996.52	1121.45	-	-
Acetonitrile	3014.09	2041.79	1250.53	-	-
1-Octanol	2979.23	1893.22	1081.88	-	-
1-Hexanol	2990.79	1925.30	1118.83	4525.86	-
1-Butanol	2970.53	1964.31	1127.56	-	-
1-Pentanol	2985.51	1937.93	1126.95	-	-
1-Propanol	2971.33	1958.82	1143.06	-	-
Acetic acid	3095.85	2075.10	1169.89	4294.52	-
Methanol	3023.67	2005.05	1187.28	-	-
2,2,2-Trifluoroethanol	3176.03	2038.84	-	-	-

(b)

Solvent	Area Band 1 (cm^{-1})	Area Band 2 (cm^{-1})	Area Band 3 (cm^{-1})	Area Band 4 (cm^{-1})	Area Band 5 (cm^{-1})
Toluene	1405.63	993.79	858.10	-	-
1,4-Dioxane	1295.27	1402.32	653.21	-	-
Chloroform	1149.61	1577.92	620.30	-	-
Acetonitrile	1177.31	1627.36	635.60	-	-
1-Octanol	1256.36	1471.17	636.98	-	-
1-Hexanol	1242.94	1504.89	646.64	220.48	-
1-Butanol	1205.66	1584.93	626.54	-	-
1-Pentanol	1216.40	1530.51	641.89	-	-
1-Propanol	1223.49	1568.42	622.59	-	-
Acetic acid	1158.10	1712.42	565.09	61.00	-
Methanol	1237.02	1621.74	614.23	-	-
2,2,2-Trifluoroethanol	2144.28	1559.91	-	-	-

Tables 3.1.3 (a) and (b). Summary band width and band area of 5 band fit using Gaussian model for normalised **16** emission spectra recorded at 310 nm excitation.

Solvent	Band 1 Area Percentage (%)	Band 2 Area Percentage(%)	Band 3 Area Percentage (%)	Band 4 Area Percentag e (%)	Band 5 Area Percentage (%)
Toluene	43.15	30.51	26.34	-	-
1,4-Dioxane	38.66	41.85	19.49	-	-
Chloroform	34.34	47.13	18.53	-	-
Acetonitrile	34.22	47.30	18.48	-	-
1-Octanol	37.34	43.73	18.93	-	-
1-Hexanol	34.38	41.63	17.89	6.10	-
1-Butanol	35.28	46.38	18.34	-	-
1-Pentanol	35.89	45.16	18.94	-	-
1-Propanol	35.83	45.93	18.23	-	-
Acetic acid	33.12	48.97	16.16	1.74	-
Methanol	35.62	46.70	17.69	-	-
2,2,2-Trifluoroethanol	57.89	42.11	-	-	-

Table 3.1.4. Total Area Percentages of 5 band fit using Gaussian model for normalised **16** emission spectra recorded at 310 nm excitation.

Solvent	Area Ratio Band 1/2 (310 nm ex)	Area Ratio Band 1/3 (310 nm ex)	Area Ratio Band 1/4 (310 nm ex)	Area Ratio Band 1/5 (310 nm ex)
Toluene	1.41	1.64	-	-
1,4-Dioxane	0.92	1.98	-	-
Chloroform	0.73	1.85	-	-
Acetonitrile	0.72	1.85	-	-
1-Octanol	0.85	1.97	-	-
1-Hexanol	0.83	1.92	5.64	-
1-Butanol	0.76	1.92	-	-
1-Pentanol	0.79	1.90	-	-
1-Propanol	0.78	1.97	-	-
Acetic acid	0.68	2.05	18.98	-
Methanol	0.76	2.01	-	-
2,2,2-Trifluoroethanol	1.37	-	-	-

Solvent	Area Ratio Band 2/3 (310 nm ex)	Area Ratio Band 2/4 (310 nm ex)	Area Ratio Band 2/5 (310 nm ex)	Area Ratio Band 3/4 (310 nm ex)	Area Ratio Band 3/5 (310 nm ex)	Area Ratio Band 4/5 (310 nm ex)
Toluene	1.16	-	-	-	-	-
1,4-Dioxane	2.15	-	-	-	-	-
Chloroform	2.54	-	-	-	-	-
Acetonitrile	2.56	-	-	-	-	-
1-Octanol	2.31	-	-	-	-	-
1-Hexanol	2.33	6.83	-	2.93	-	-
1-Butanol	2.53	-	-	-	-	-
1-Pentanol	2.38	-	-	-	-	-
1-Propanol	2.52	-	-	-	-	-
Acetic acid	3.03	28.07	-	9.26	-	-
Methanol	2.64	-	-	-	-	-
2,2,2-Trifluoroethanol	-	-	-	-	-	-

Table 3.1.5. Area Ratios of 5 band fit using Gaussian model for normalised **16** emission spectra recorded at 310 nm excitation.

3.1.3 400 nm excitation Gaussian band fit summaries.

Solvent	λ max$_{em}$ Band 1 (cm^{-1})	λ max$_{em}$ Band 1 (nm)	λ max$_{em}$ Band 2 (cm^{-1})	λ max$_{em}$ Band 2 (nm)	λmax$_{em}$ Band 3 (cm^{-1})	λmax$_{em}$ Band 3 (nm)
Toluene	19137.04	522.55	19927.70	501.81	21135.58	473.14
1,4-Dioxane	19028.50	525.53	20085.68	497.87	21188.91	471.94
Chloroform	18843.01	530.70	19949.47	501.27	21029.01	475.53
Acetonitrile	18844.18	530.67	20024.31	499.39	21109.15	473.73
1-Octanol	19123.91	522.91	20158.15	496.08	21265.29	470.25
1-Hexanol	19012.09	525.98	20155.12	496.15	21246.23	470.67
1-Butanol	18995.89	526.43	20138.53	496.56	21242.60	470.75
1-Pentanol	18990.92	526.57	20147.88	496.33	21254.86	470.48
1-Propanol	18953.07	527.62	20136.21	496.62	21241.14	470.78
Acetic acid	18968.55	527.19	20103.54	497.42	21205.74	471.57
Methanol	18872.22	529.88	20067.04	498.33	21182.88	472.08
2,2,2-Trifluoroethanol	18400.65	543.46	19808.79	504.83	20935.44	477.66

Table 3.1.6. Summary of band maxima of 3 band fit using Gaussian model for normalised **16** emission spectra recorded at 400 nm excitation.

Solvent	Width Band 1 (cm^{-1})	Width Band 2 (cm^{-1})	Width Band 3 (cm^{-1})
Toluene	2938.32	1619.02	1078.30
1,4-Dioxane	2959.86	1889.63	1079.99
Chloroform	2982.03	1965.12	1120.33
Acetonitrile	2985.04	2024.50	1235.41
1-Octanol	2980.62	1864.50	1074.21
1-Hexanol	2963.12	1930.14	1114.52
1-Butanol	2964.92	1947.61	1122.17
1-Pentanol	2950.29	1937.07	1112.32
1-Propanol	2950.03	1965.59	1147.20
Acetic acid	3031.75	2010.85	1194.02
Methanol	2995.71	2008.97	1213.65
2,2,2-Trifluoroethanol	3305.76	2263.30	1395.21

Table 3.1.7. Summary of band width of 3 band fit using Gaussian model for normalised **16** emission spectra recorded at 400 nm excitation.

Solvent	Area Band 1 (cm^{-1})	Area Band 2 (cm^{-1})	Area Band 3 (cm^{-1})	Area Ratio Band 1/2 (400 nm ex)	Area Ratio Band 1/3 (400 nm ex)	Area Ratio Band 2/3 (400 nm ex)
Toluene	1341.84	1042.21	837.90	1.29	1.60	1.24
1,4-Dioxane	1220.61	1435.19	654.44	0.85	1.87	2.19
Chloroform	1134.62	1540.08	632.78	0.74	1.79	2.43
Acetonitrile	1180.13	2024.50	625.68	0.58	1.89	3.24
1-Octanol	1288.75	1411.22	647.39	0.91	1.99	2.18
1-Hexanol	1177.97	1528.12	634.10	0.77	1.86	2.41
1-Butanol	1179.98	1563.47	640.29	0.75	1.84	2.44
1-Pentanol	1174.28	1570.79	639.58	0.75	1.84	2.46
1-Propanol	1155.55	1606.08	641.09	0.72	1.80	2.51
Acetic acid	1195.66	1605.98	630.98	0.74	1.89	2.55
Methanol	1163.60	1638.98	659.91	0.71	1.76	2.48
2,2,2-Trifluoroethanol	1178.58	1893.30	559.71	0.62	2.11	3.38

Solvent	Band 1 Area Percentage (%)	Band 2 Area Percentage (%)	Band 3 Area Percentage (%)
Toluene	41.65	32.35	26.01
1,4-Dioxane	36.87	43.36	19.77
Chloroform	34.30	46.56	19.13
Acetonitrile	30.81	52.85	16.33
1-Octanol	38.50	42.16	19.34
1-Hexanol	35.27	45.75	18.98
1-Butanol	34.87	46.21	18.92
1-Pentanol	34.69	46.41	18.90
1-Propanol	33.96	47.20	18.84
Acetic acid	34.83	46.79	18.38
Methanol	33.61	47.34	19.06
2,2,2-Trifluoroethanol	32.45	52.13	15.41

Table 3.1.8. Band areas, area ratios and total area percentage of 3 band fit using Gaussian model for normalised **16** emission spectra recorded at 400 nm excitation.

3.1.4 310 nm Gaussian band fit - Solvatochromic analysis.

3.1.4.1 E_T^N.

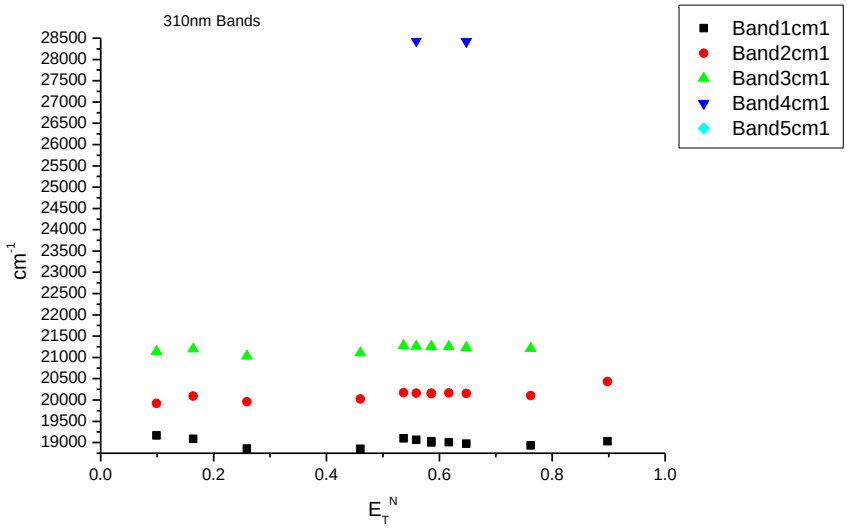

Figure 3.1.1. Band maxima from Gaussian model fit of the normalised fluorescence emission spectra of **16** recorded at 310 nm excitation against E_T^N.

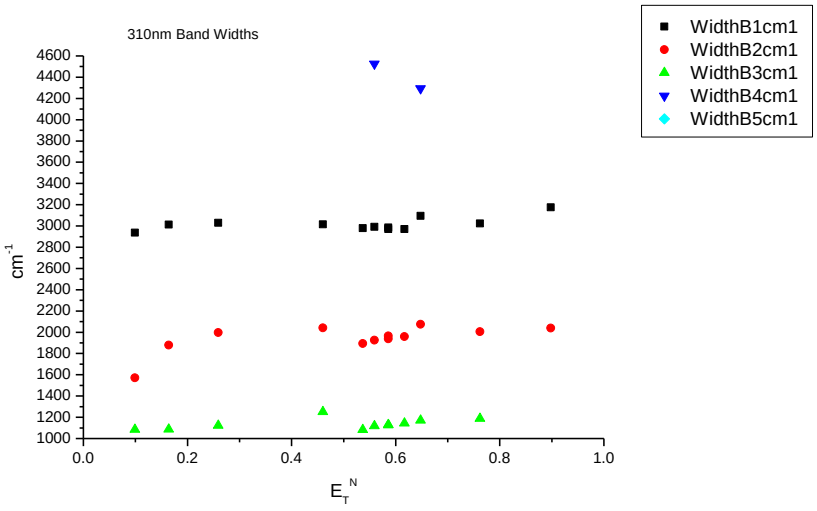

Figure 3.1.2. Band widths from Gaussian model fit of the normalised fluorescence emission spectra of **16** recorded at 310 nm excitation against E_T^N.

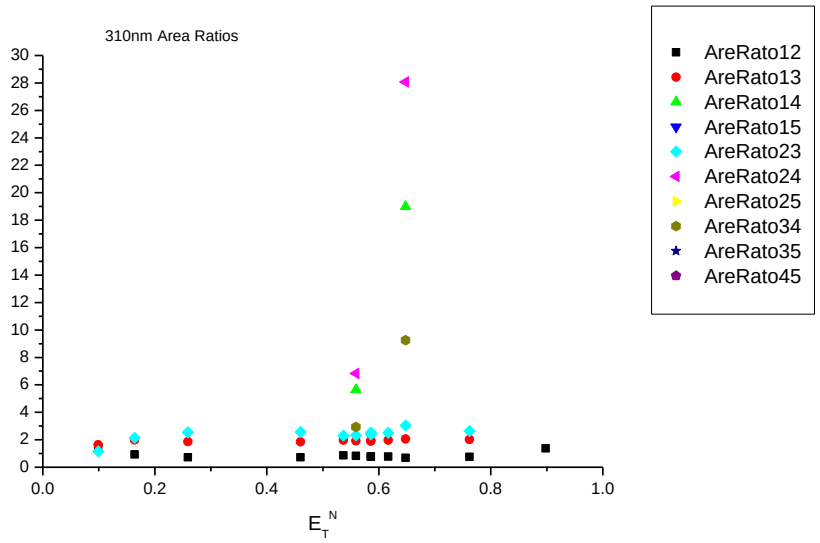

Figure 3.1.3. Area ratios from Gaussian model fit of the normalised fluorescence emission spectra of **16** recorded at 310 nm excitation against E_T^N.

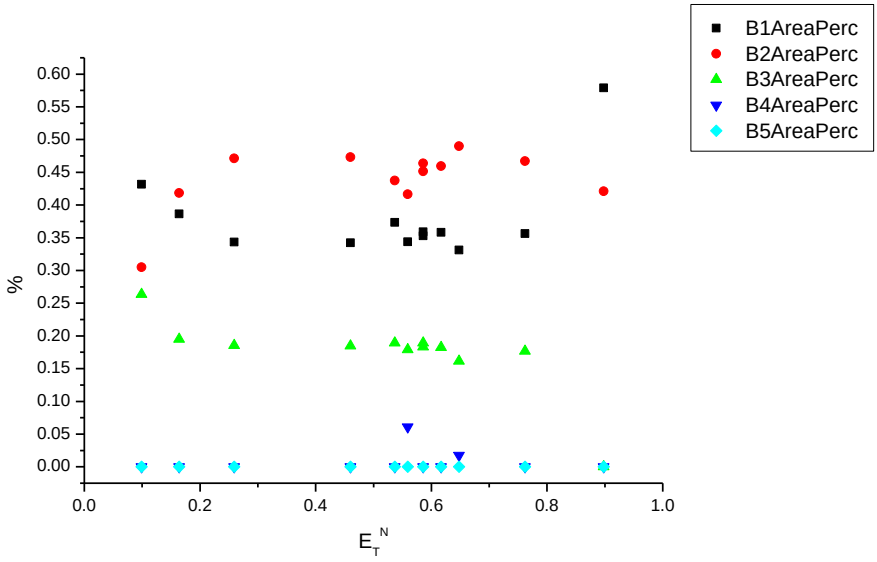

Figure 3.1.4. Area percentages from Gaussian model fit of the normalised fluorescence emission spectra of **16** recorded at 310 nm excitation against E_T^N.

3.1.4.2 α

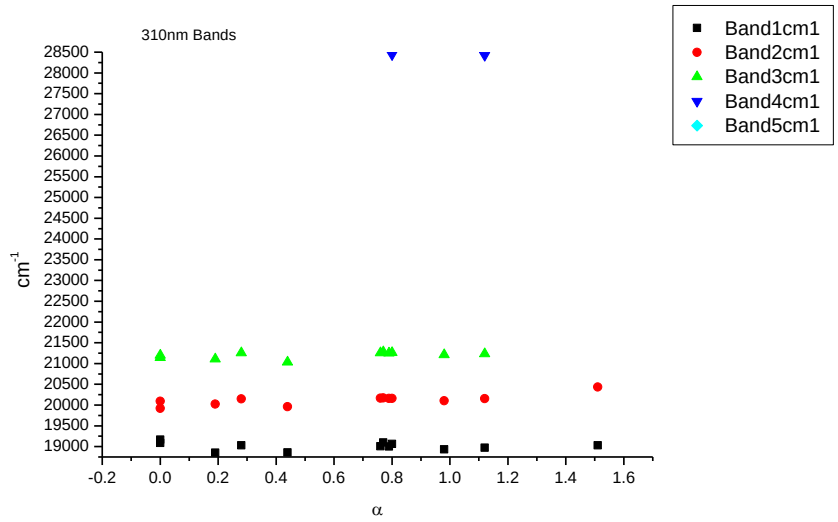

Figure 3.1.5. Band maxima from Gaussian model fit of the normalised fluorescence emission spectra of **16** recorded at 310 nm excitation against α.

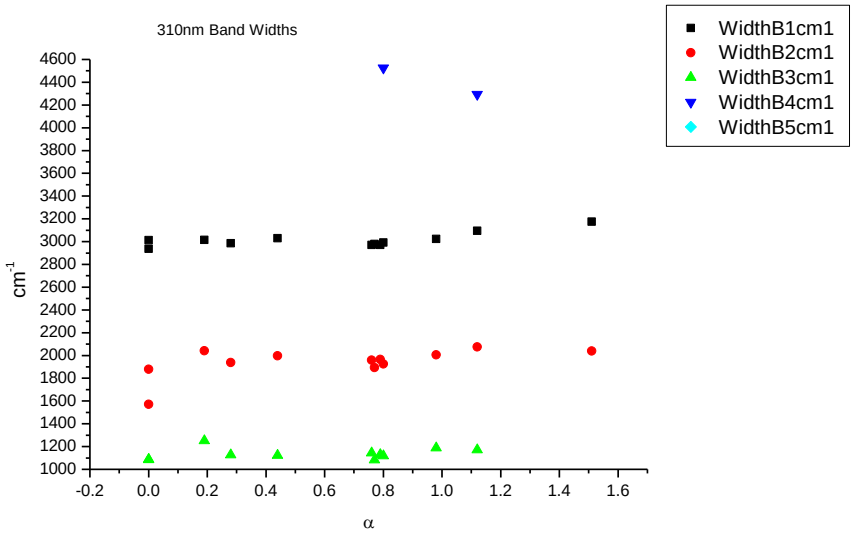

Figure 3.1.6. Band widths from Gaussian model fit of the normalised fluorescence emission spectra of **16** recorded at 310 nm excitation against α.

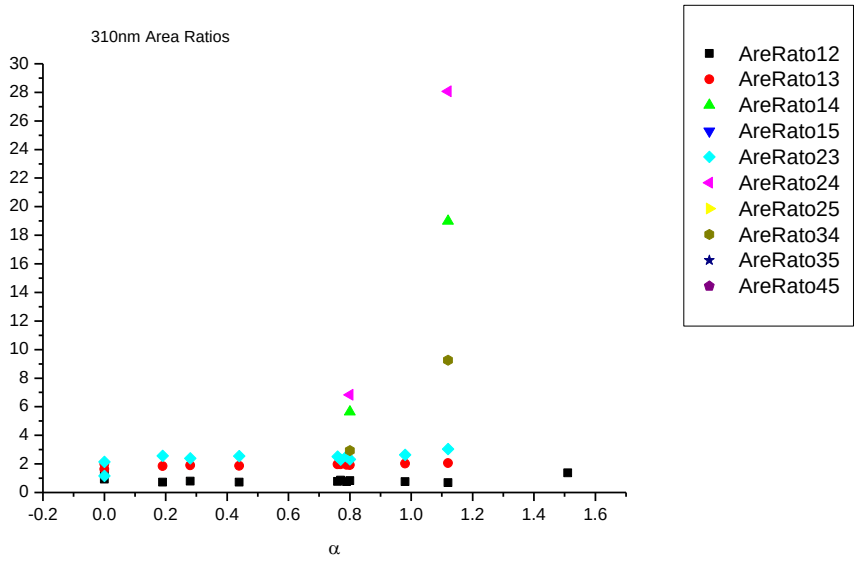

Figure 3.1.7. Area Ratios from Gaussian model fit of the normalised fluorescence emission spectra of **16** recorded at 310 nm excitation against α.

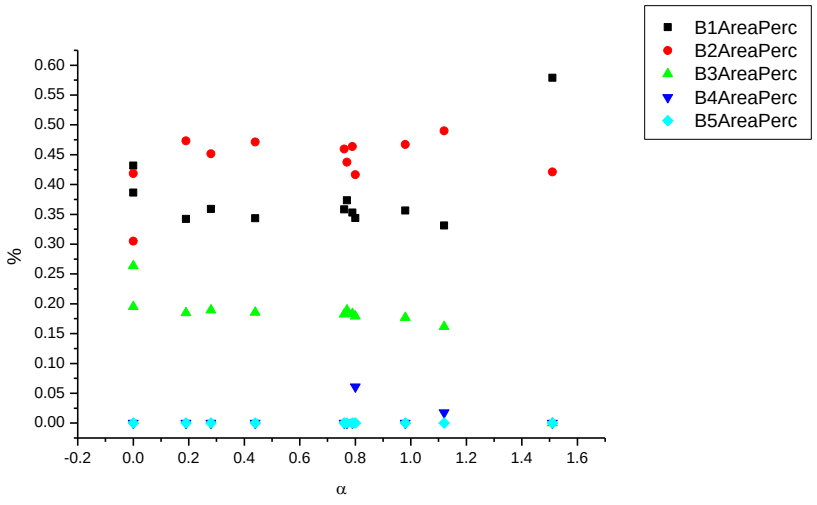

Figure 3.1.8. Area percentages from Gaussian model fit of the normalised fluorescence emission spectra of **16** recorded at 310 nm excitation against α.

3.1.4.3 β.

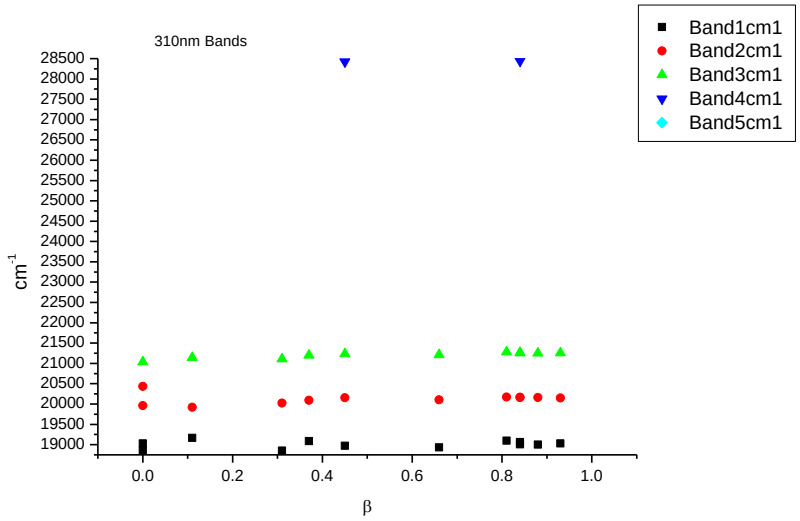

Figure 3.1.9. Band maxima from Gaussian model fit of the normalised fluorescence emission spectra of **16** recorded at 310 nm excitation against β.

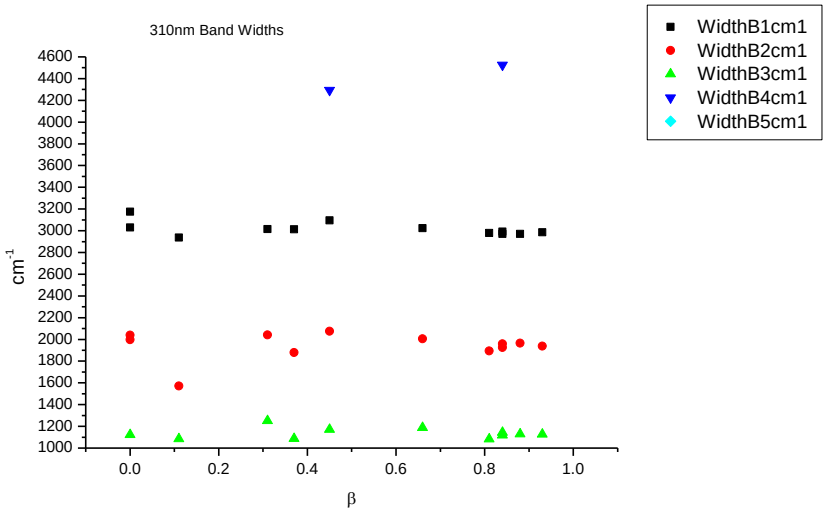

Figure 3.1.10. Band widths from Gaussian model fit of the normalised fluorescence emission spectra of **16** recorded at 310 nm excitation against β.

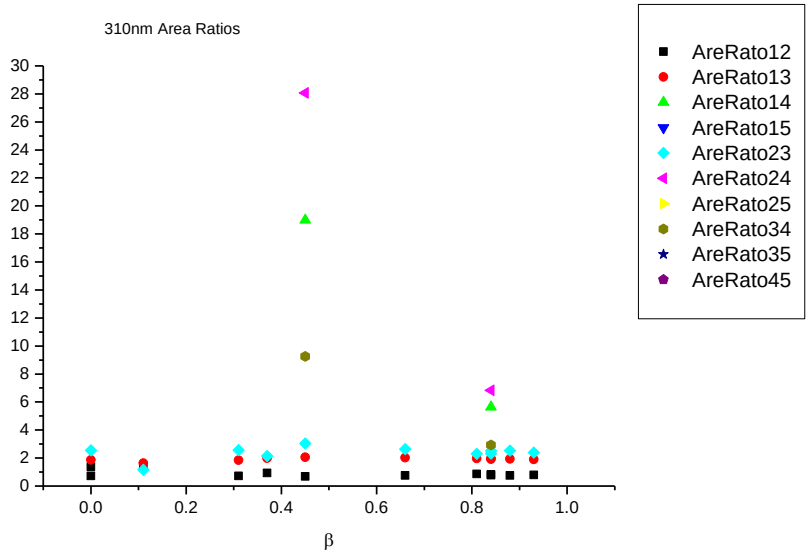

Figure 3.1.11. Area ratios from Gaussian model fit of the normalised fluorescence emission spectra of **16** recorded at 310 nm excitation against β.

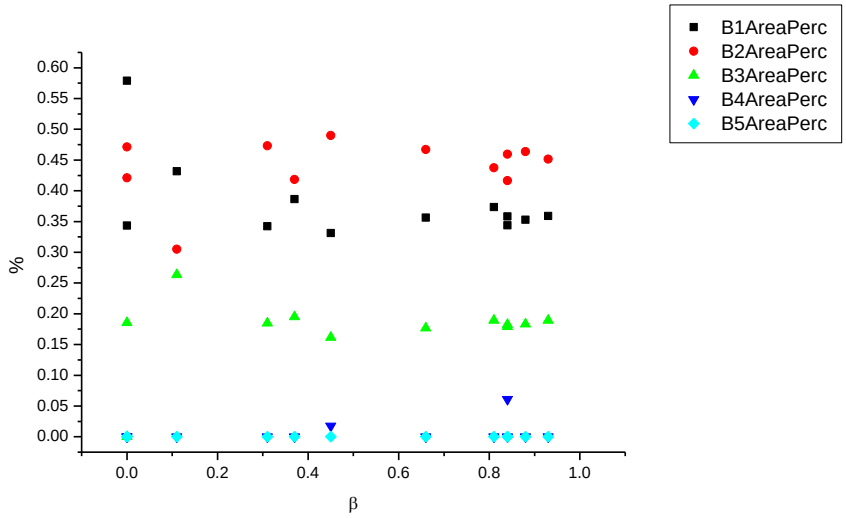

Figure 3.1.12. Area percentages from Gaussian model fit of the normalised fluorescence emission spectra of **16** recorded at 310 nm excitation against β.

3.1.4.4 π.*

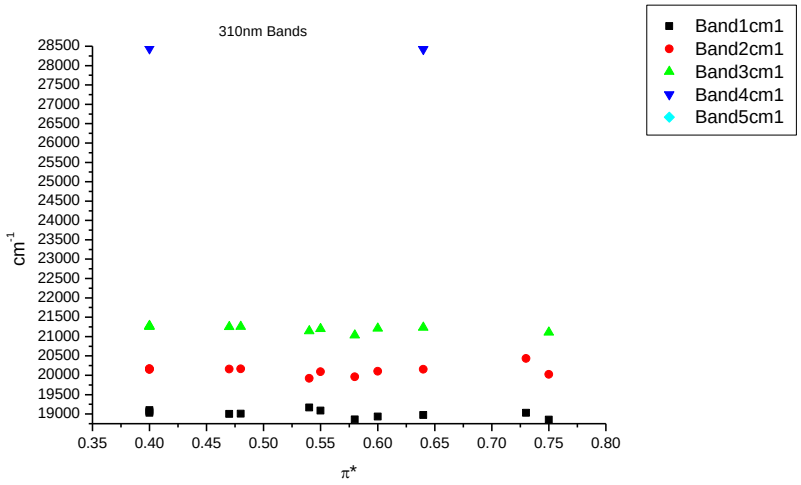

Figure 3.1.13. Band maxima from Gaussian model fit of the normalised fluorescence emission spectra of **16** recorded at 310 nm excitation against π*.

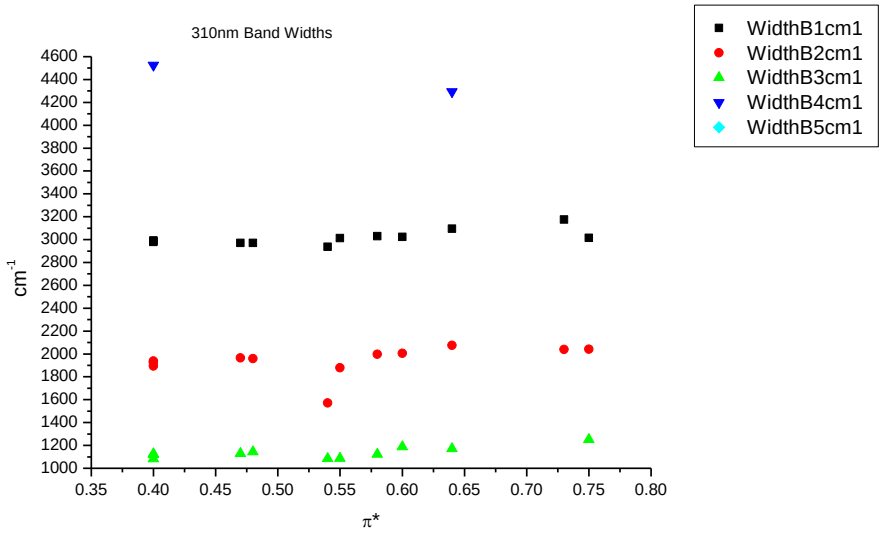

Figure 3.1.14. Band widths from Gaussian model fit of the normalised fluorescence emission spectra of **16** recorded at 310 nm excitation against π*.

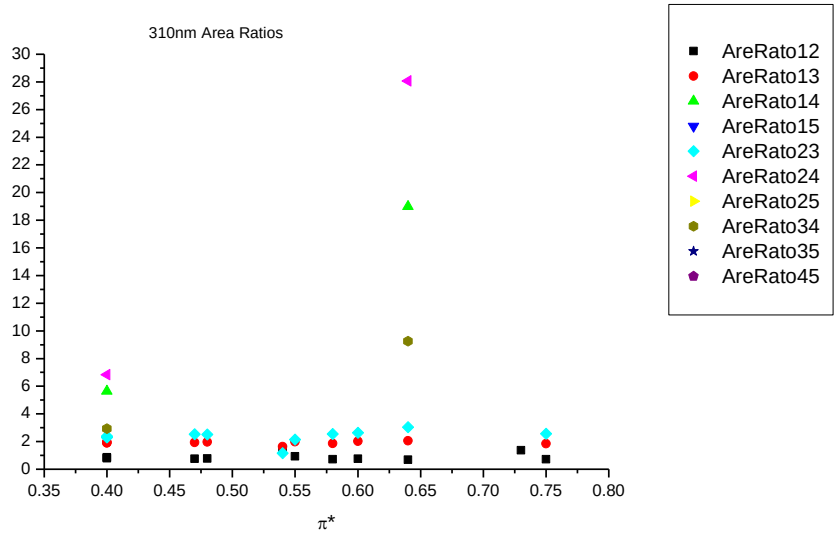

Figure 3.1.15. Area ratios from Gaussian model fit of the normalised fluorescence emission spectra of **16** recorded at 310 nm excitation against π*.

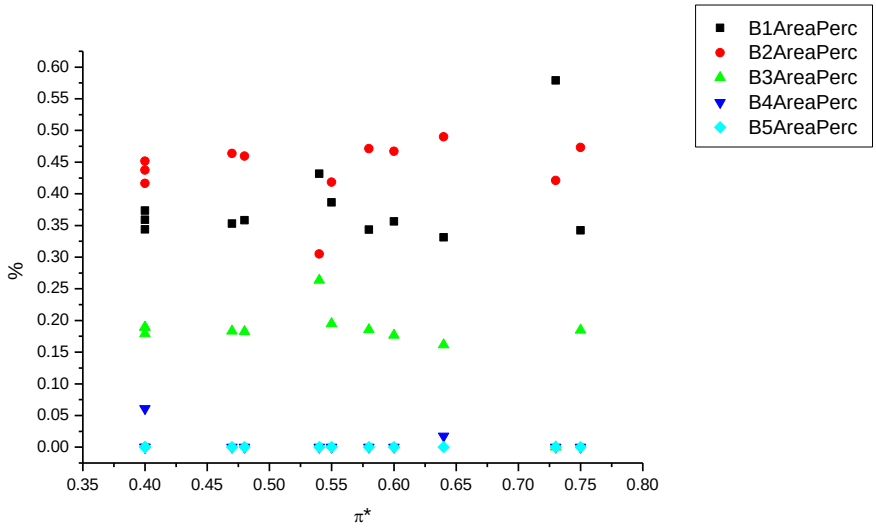

Figure 3.1.16. Area percentages from Gaussian model fit of the normalised fluorescence emission spectra of **16** recorded at 310 nm excitation against π*.

3.1.4.5 μ(D).

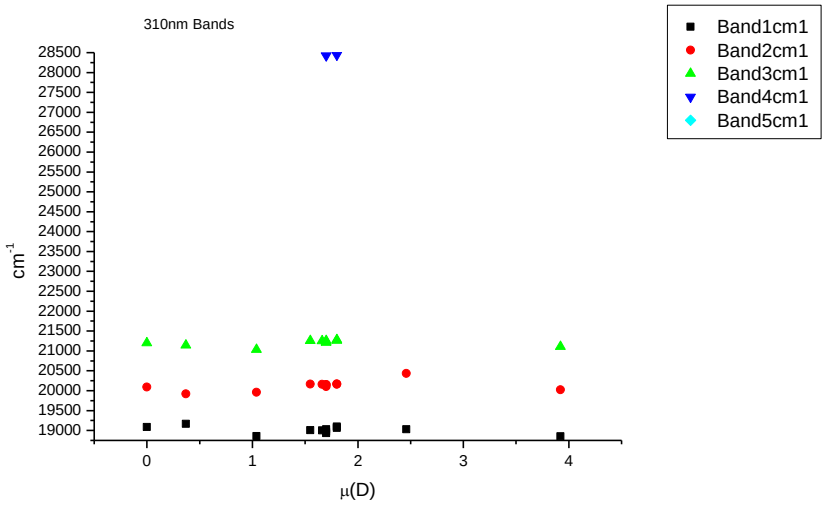

Figure 3.1.17. Band maxima from Gaussian model fit of the normalised fluorescence emission spectra of **16** recorded at 310 nm excitation against μ(D).

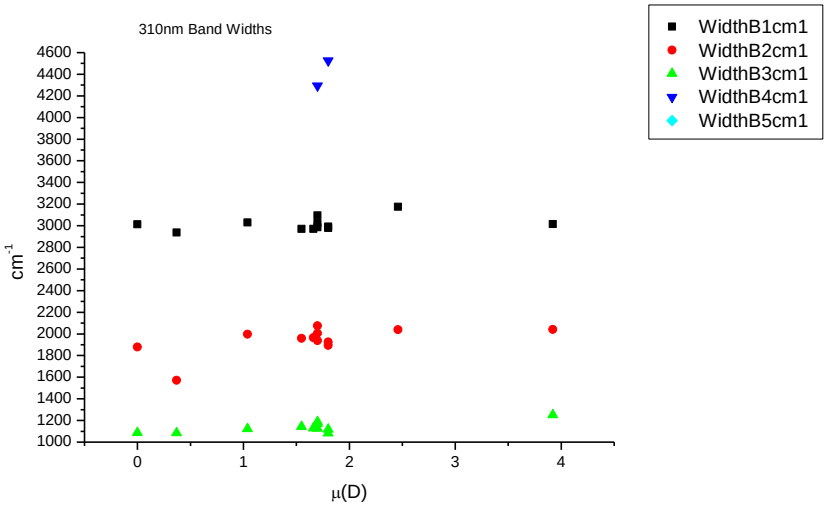

Figure 3.1.18. Band widths from Gaussian model fit of the normalised fluorescence emission spectra of **16** recorded at 310 nm excitation against μ(D).

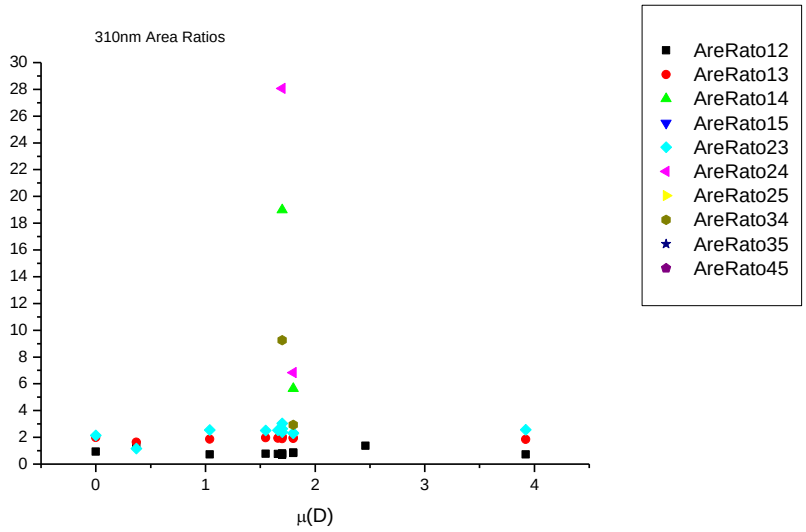

Figure 3.1.19. Area ratios from Gaussian model fit of the normalised fluorescence emission spectra of **16** recorded at 310 nm excitation against μ(D).

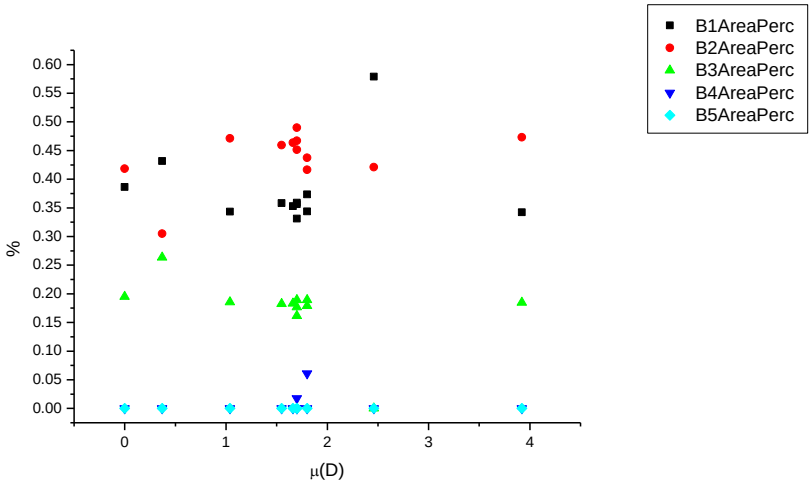

Figure 3.1.20. Area percentages from Gaussian model fit of the normalised fluorescence emission spectra of **16** recorded at 310 nm excitation against μ(D).

3.1.4.6 η(Cp).

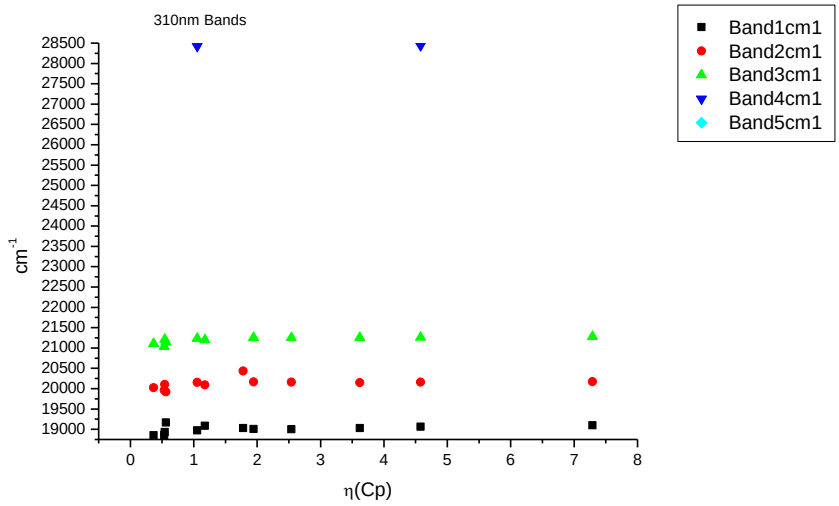

Figure 3.1.21. Band maxima from Gaussian model fit of the normalised fluorescence emission spectra of **16** recorded at 310 nm excitation against η(Cp).

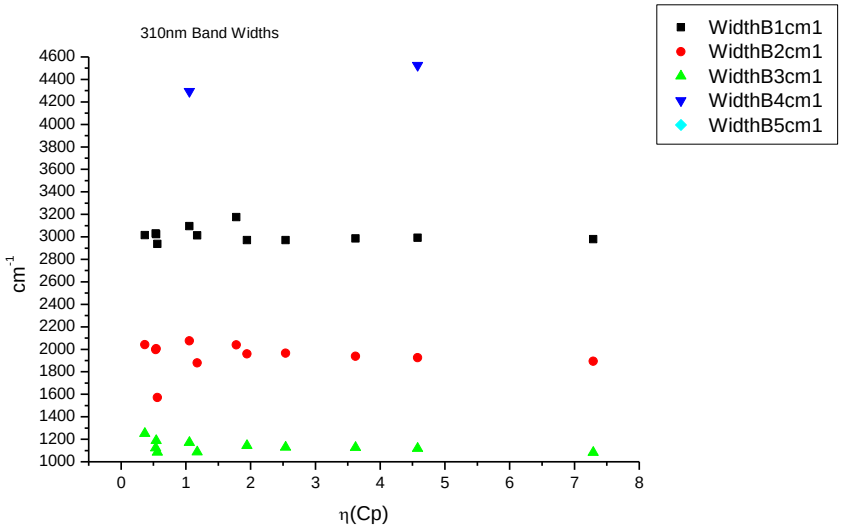

Figure 3.1.22. Band widths from Gaussian model fit of the normalised fluorescence emission spectra of **16** recorded at 310 nm excitation against η(Cp).

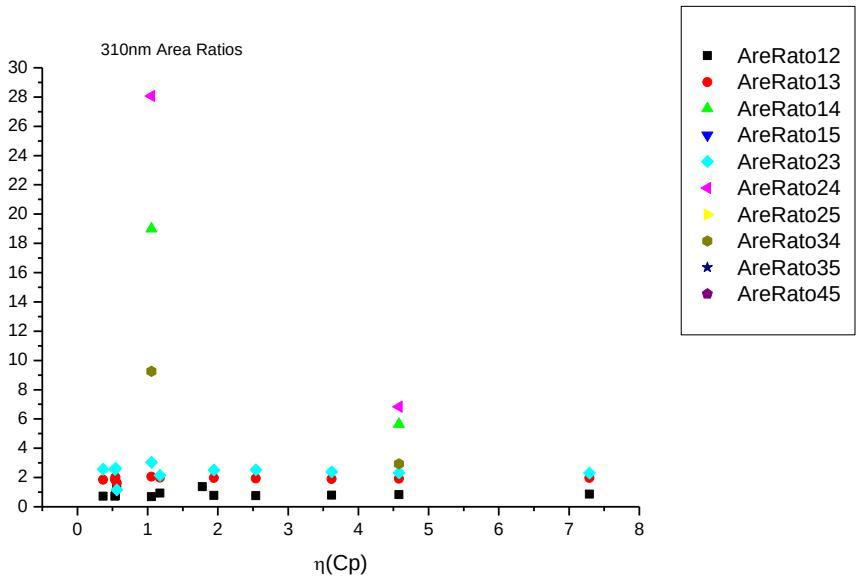

Figure 3.1.23. Area ratios from Gaussian model fit of the normalised fluorescence emission spectra of **16** recorded at 310 nm excitation against η(Cp).

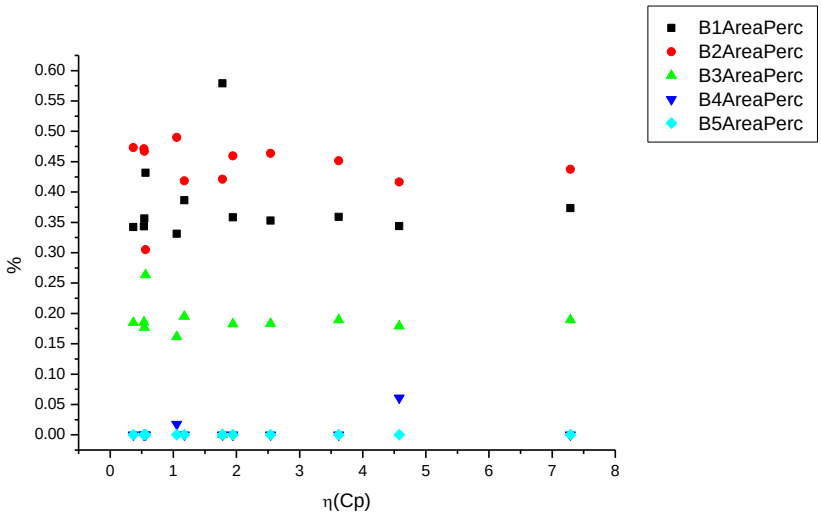

Figure 3.1.24. Area percentages from Gaussian model fit of the normalised fluorescence emission spectra of **16** recorded at 310 nm excitation against η(Cp).

3.1.5 400 nm Gaussian band fit - Solvatochromic analysis.

3.1.5.1 E_T^N.

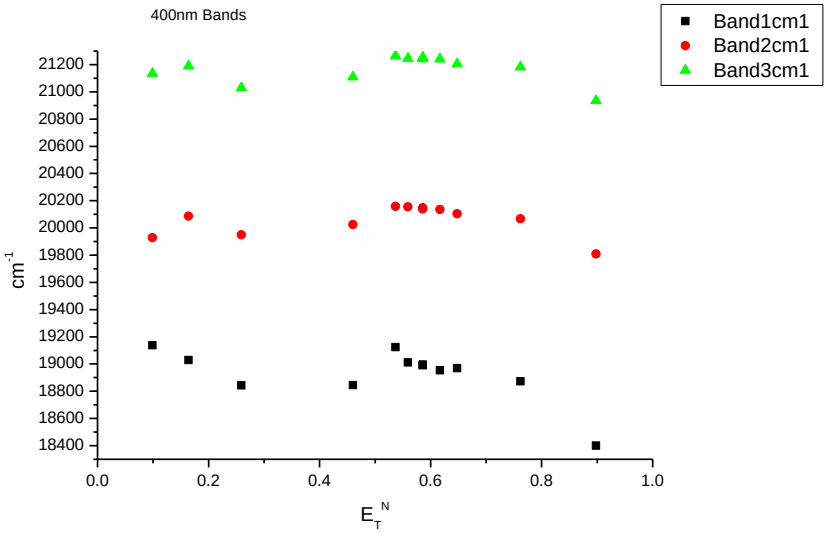

Figure 3.1.25. Band maxima from Gaussian model fit of the normalised fluorescence emission spectra of **16** recorded at 400 nm excitation against E_T^N.

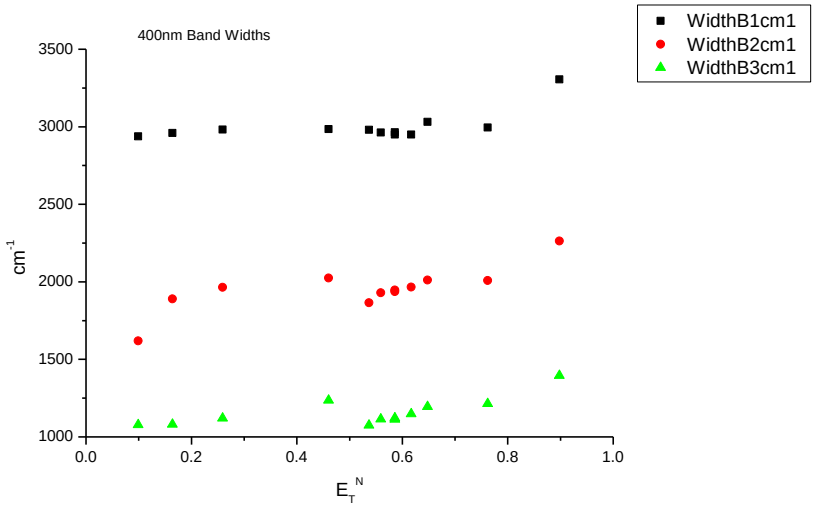

Figure 3.1.26. Band widths from Gaussian model fit of the normalised fluorescence emission spectra of **16** recorded at 400 nm excitation against E_T^N.

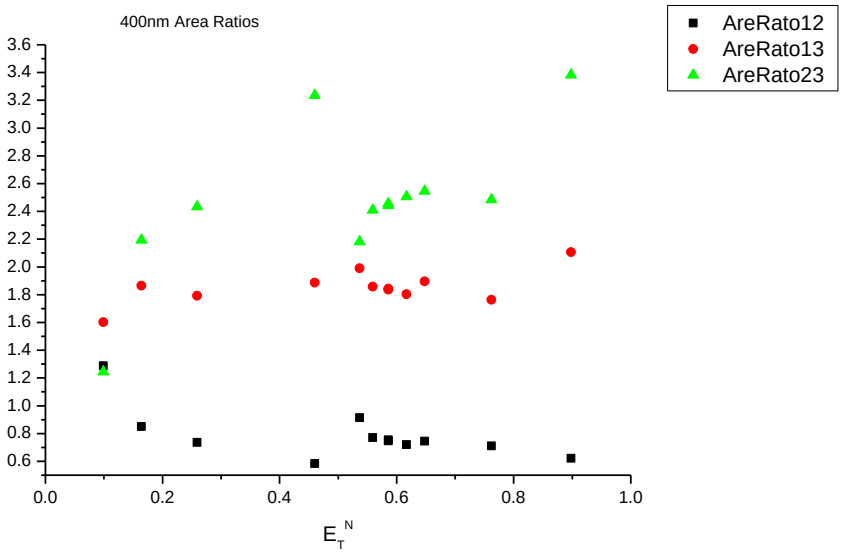

Figure 3.1.27. Area ratios from Gaussian model fit of the normalised fluorescence emission spectra of **16** recorded at 400 nm excitation against E_T^N.

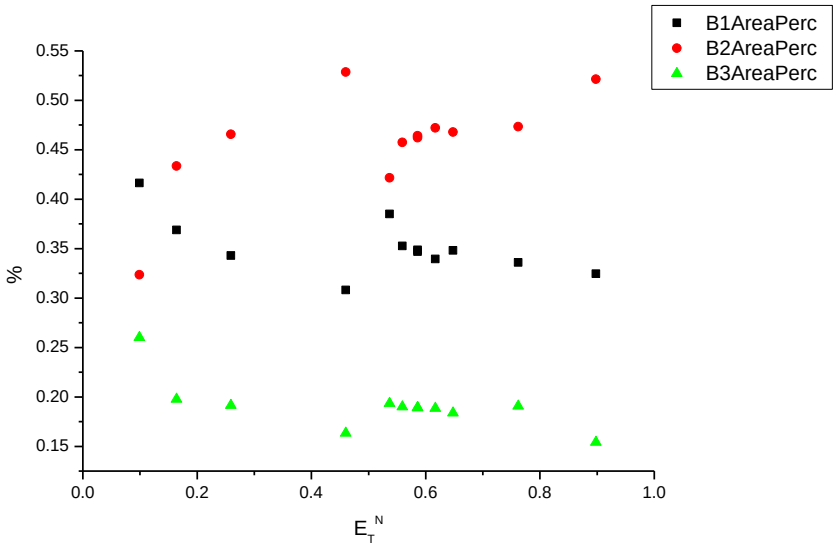

Figure 3.1.28. Area percentages from Gaussian model fit of the normalised fluorescence emission spectra of **16** recorded at 400 nm excitation against E_T^N.

3.1.5.2 *α*

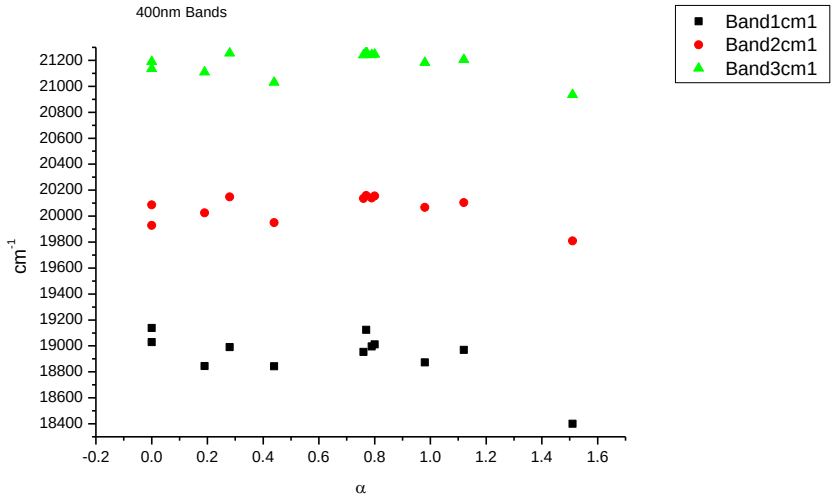

Figure 3.1.29. Band maxima from Gaussian model fit of the normalised fluorescence emission spectra of **16** recorded at 400 nm excitation against α.

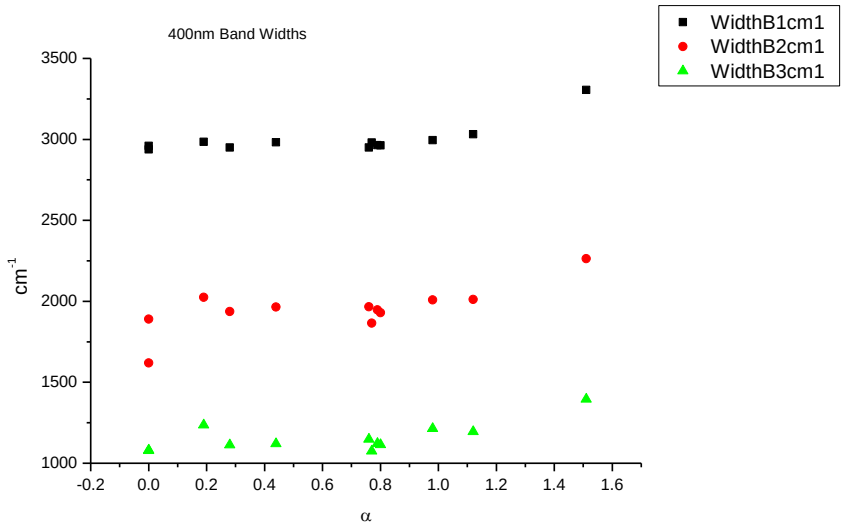

Figure 3.1.30. Band widths from Gaussian model fit of the normalised fluorescence emission spectra of **16** recorded at 400 nm excitation against α.

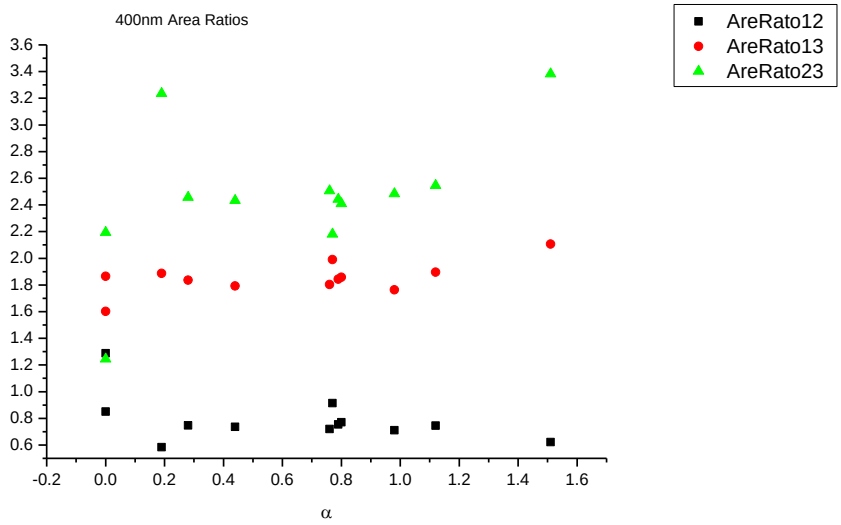

Figure 3.1.31. Area ratios from Gaussian model fit of the normalised fluorescence emission spectra of **16** recorded at 400 nm excitation against α.

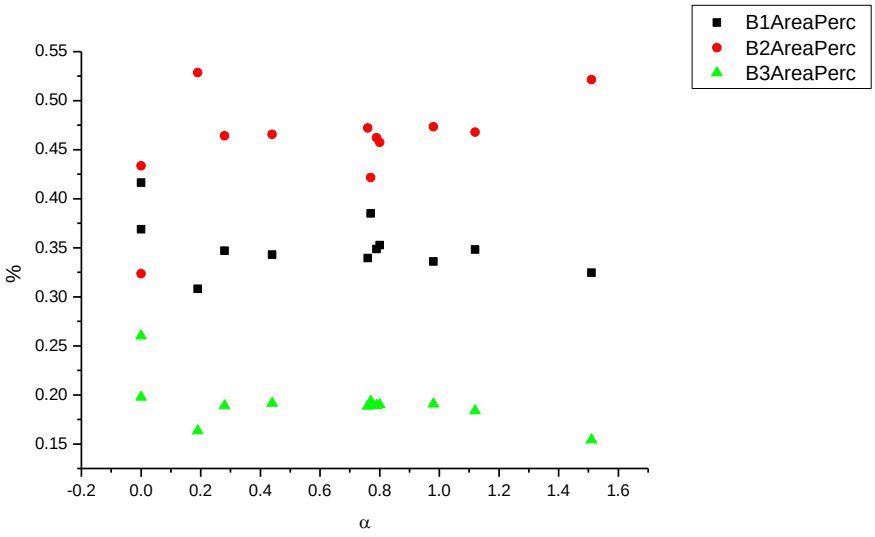

Figure 3.1.32. Area percentages from Gaussian model fit of the normalised fluorescence emission spectra of **16** recorded at 400 nm excitation against α.

3.1.5.3 β.

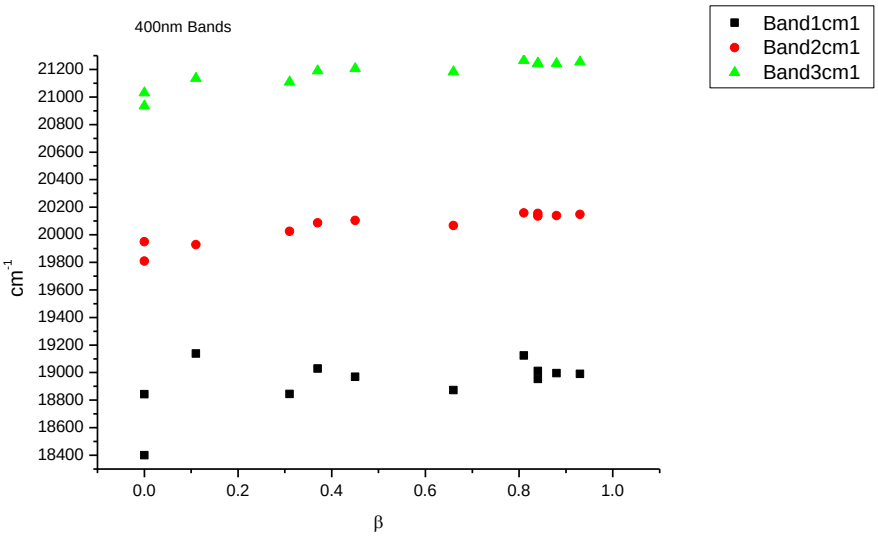

Figure 3.1.33. Band maxima from Gaussian model fit of the normalised fluorescence emission spectra of **16** recorded at 400 nm excitation against β.

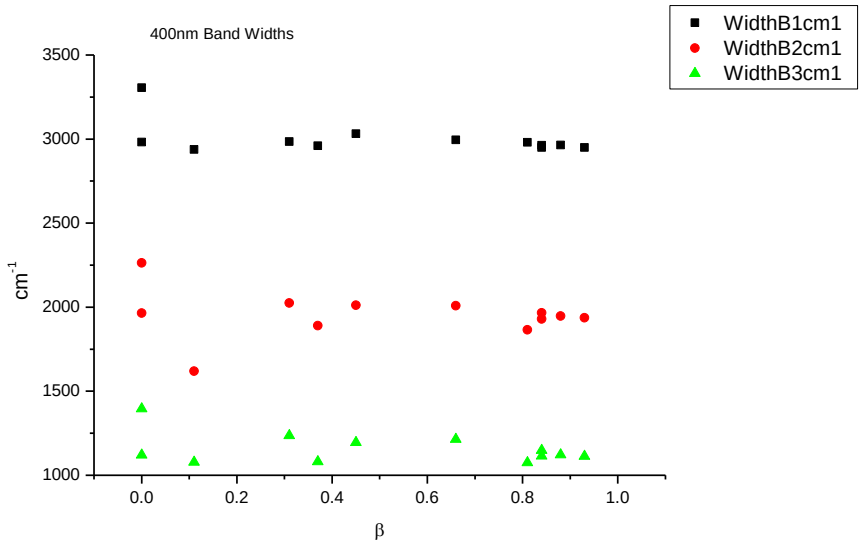

Figure 3.1.34. Band widths from Gaussian model fit of the normalised fluorescence emission spectra of **16** recorded at 400 nm excitation against β.

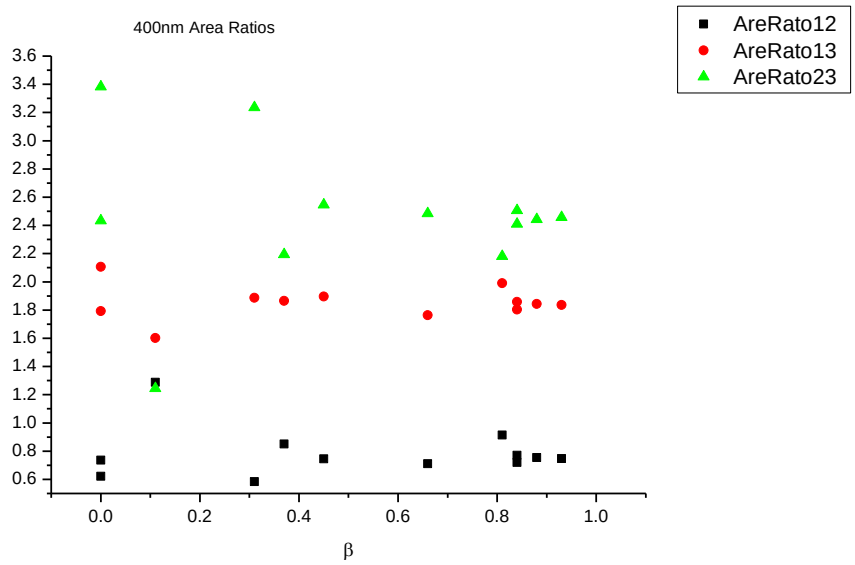

Figure 3.1.35. Area ratios from Gaussian model fit of the normalised fluorescence emission spectra of **16** recorded at 400 nm excitation against β.

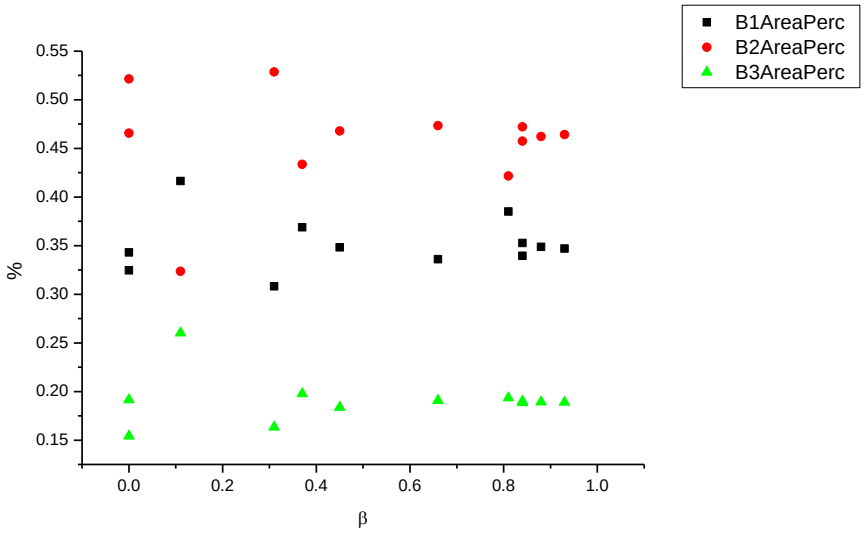

Figure 3.1.36. Area percentages from Gaussian model fit of the normalised fluorescence emission spectra of **16** recorded at 400 nm excitation against β.

3.1.5.4 π.*

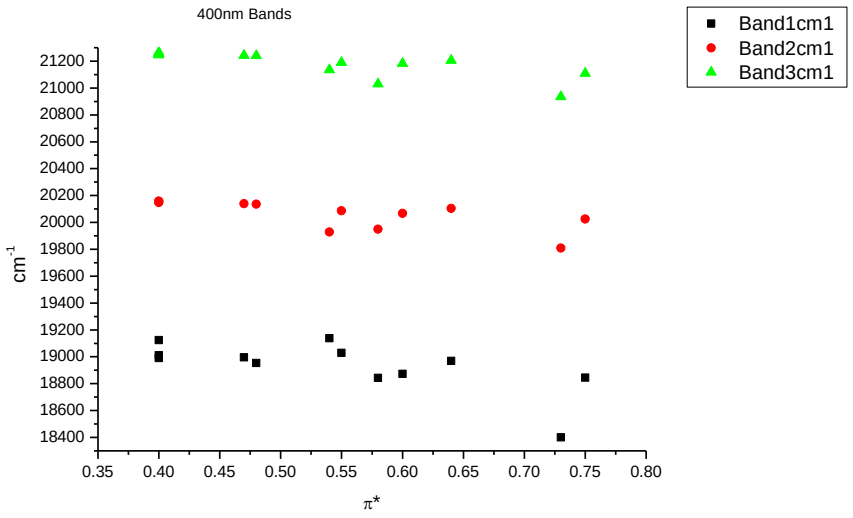

Figure 3.1.37. Band maxima from Gaussian model fit of the normalised fluorescence emission spectra of **16** recorded at 400 nm excitation against π*.

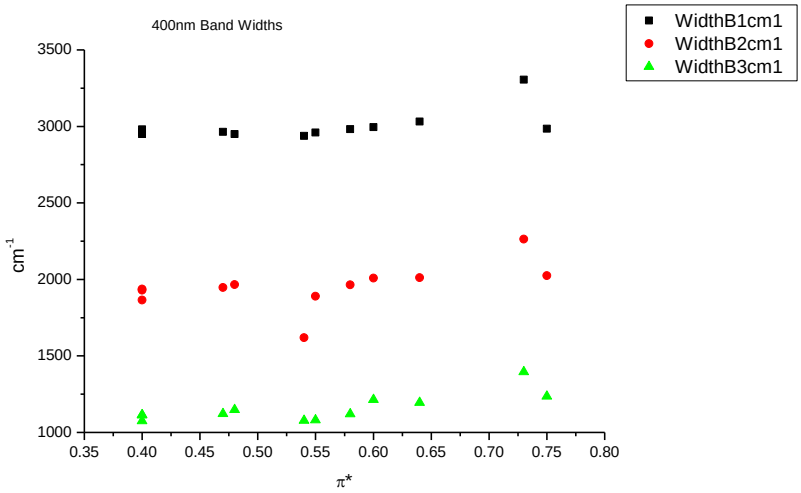

Figure 3.1.38. Band widths from Gaussian model fit of the normalised fluorescence emission spectra of **16** recorded at 400 nm excitation against π*.

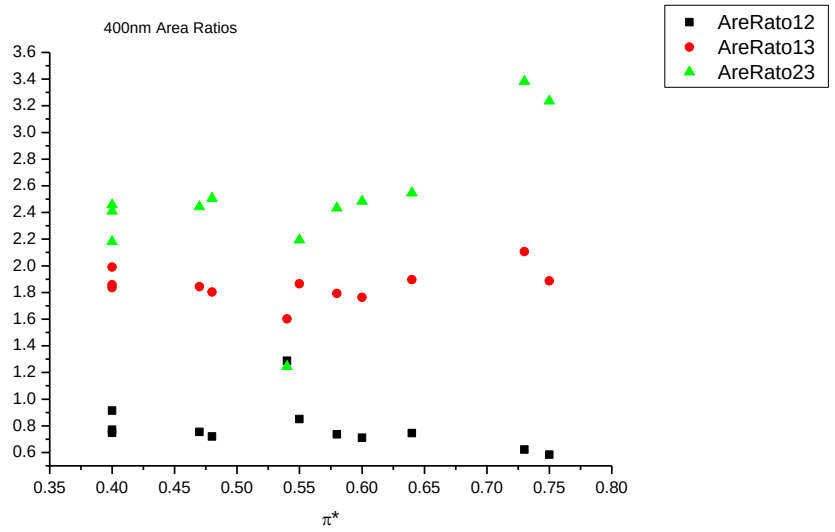

Figure 3.1.39. Area ratios from Gaussian model fit of the normalised fluorescence emission spectra of **16** recorded at 400 nm excitation against π*.

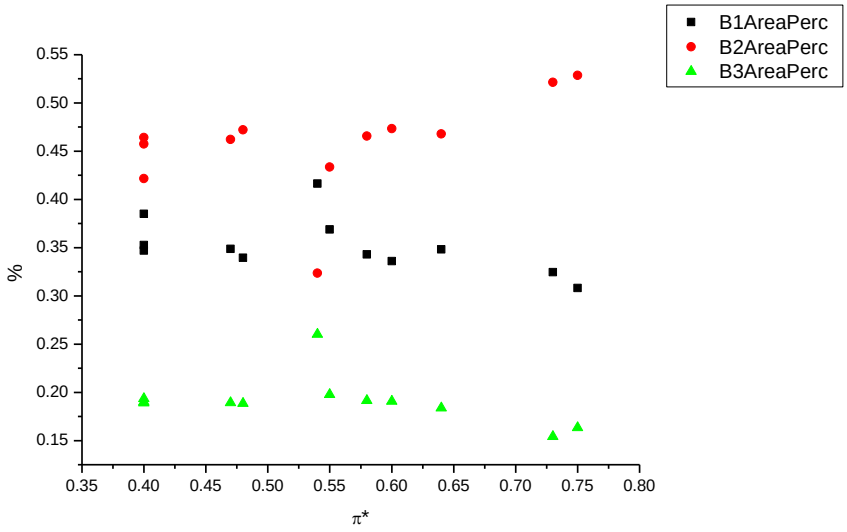

Figure 3.1.40. Area percentages from Gaussian model fit of the normalised fluorescence emission spectra of **16** recorded at 400 nm excitation against π*.

3.1.5.5 μ(D).

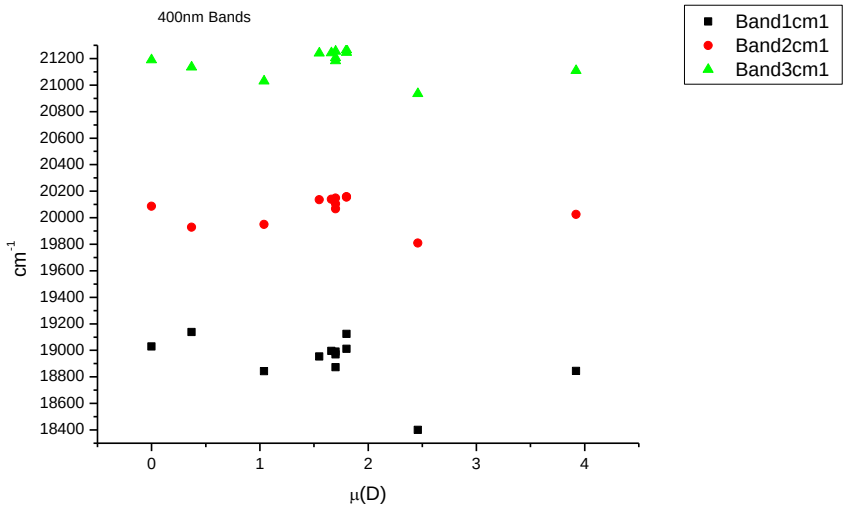

Figure 3.1.41. Band maxima from Gaussian model fit of the normalised fluorescence emission spectra of **16** recorded at 400 nm excitation against μ(D).

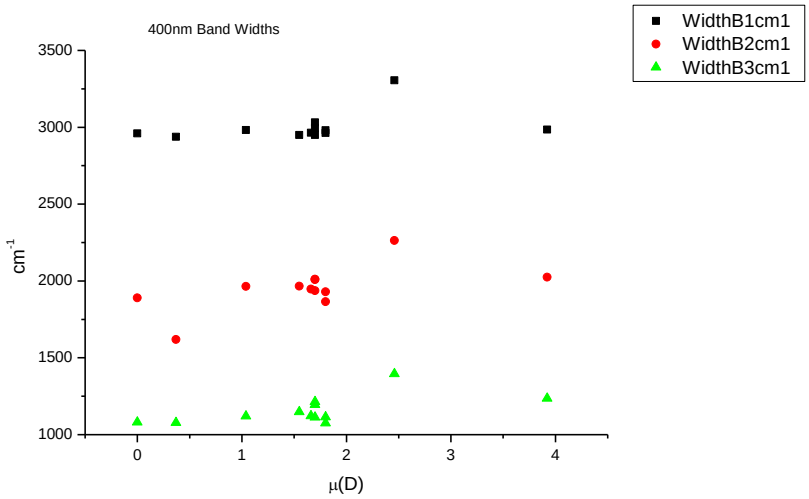

Figure 3.1.42. Band widths from Gaussian model fit of the normalised fluorescence emission spectra of **16** recorded at 400 nm excitation against μ(D).

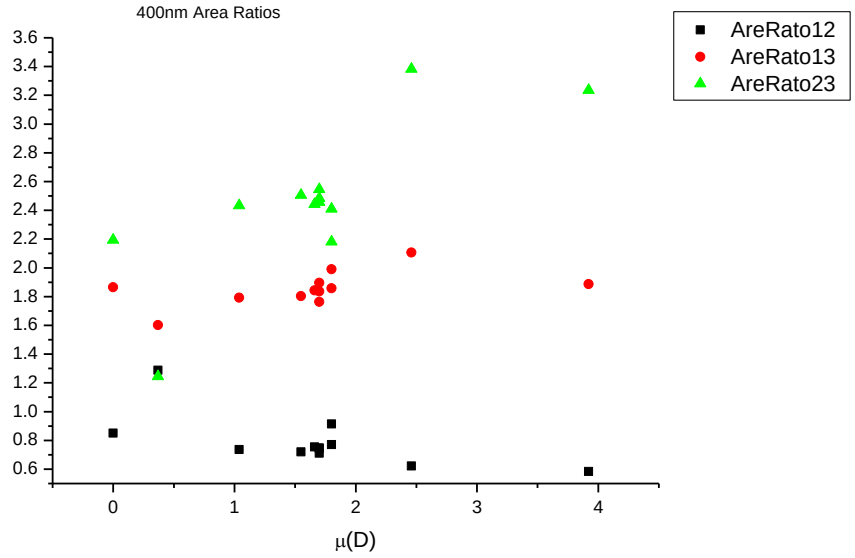

Figure 3.1.43. Area ratios from Gaussian model fit of the normalised fluorescence emission spectra of **16** recorded at 400 nm excitation against μ(D).

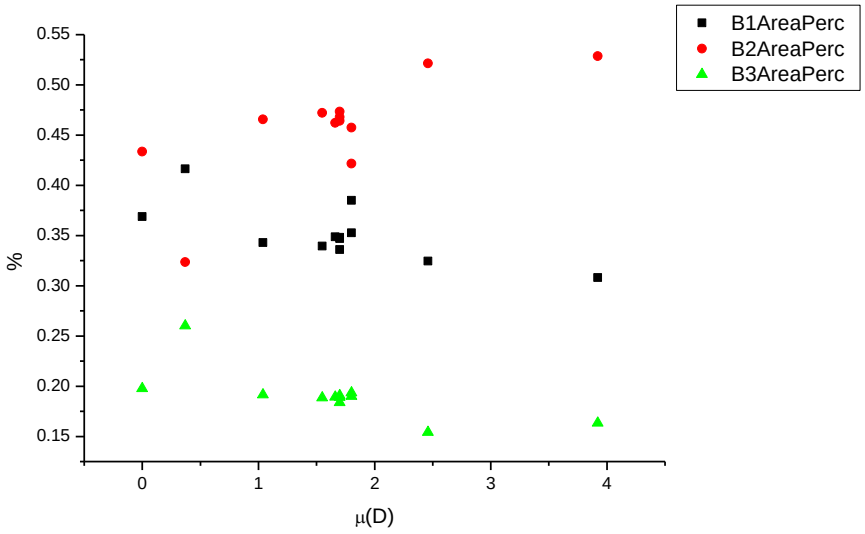

Figure 3.1.44. Area percentages from Gaussian model fit of the normalised fluorescence emission spectra of **16** recorded at 400 nm excitation against μ(D).

3.1.5.6 η(Cp).

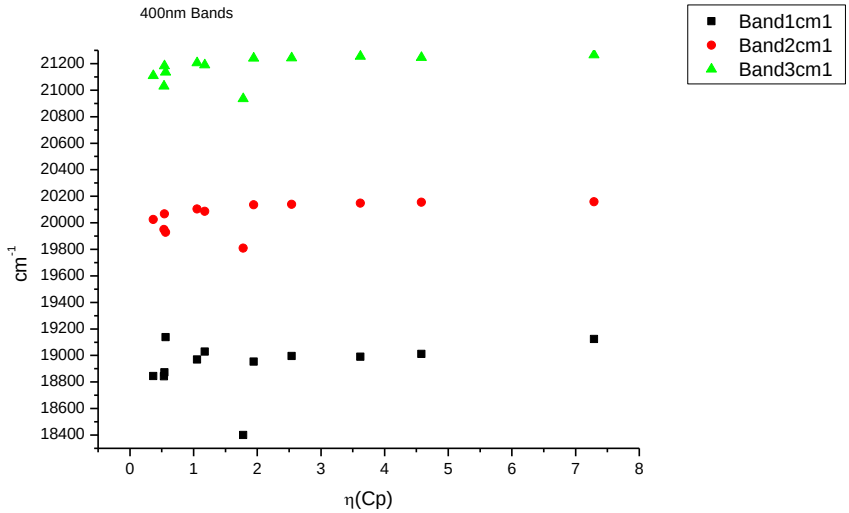

Figure 3.1.45. Band maxima from Gaussian model fit of the normalised fluorescence emission spectra of **16** recorded at 400 nm excitation against η(Cp).

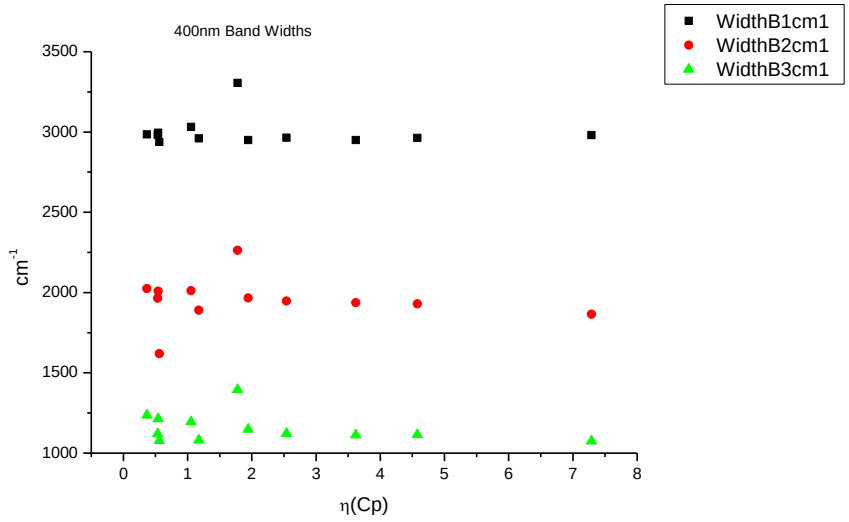

Figure 3.1.46. Band widths from Gaussian model fit of the normalised fluorescence emission spectra of **16** recorded at 400 nm excitation against η(Cp).

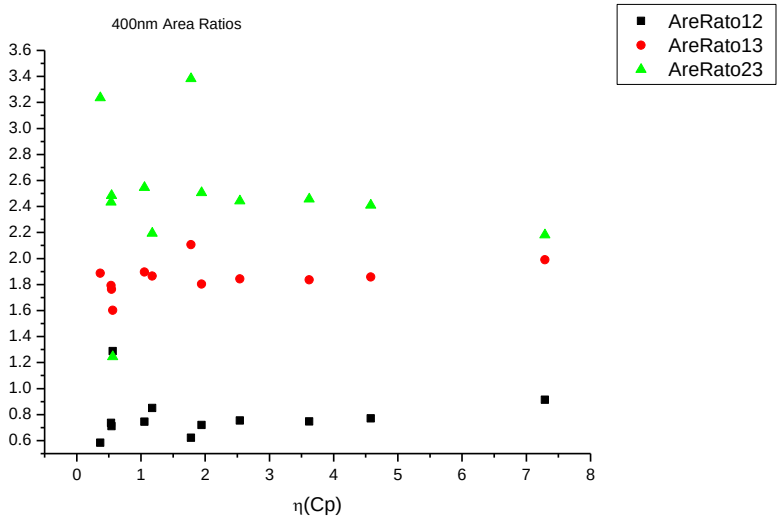

Figure 3.1.47. Area ratios from Gaussian model fit of the normalised fluorescence emission spectra of **16** recorded at 400 nm excitation against η(Cp).

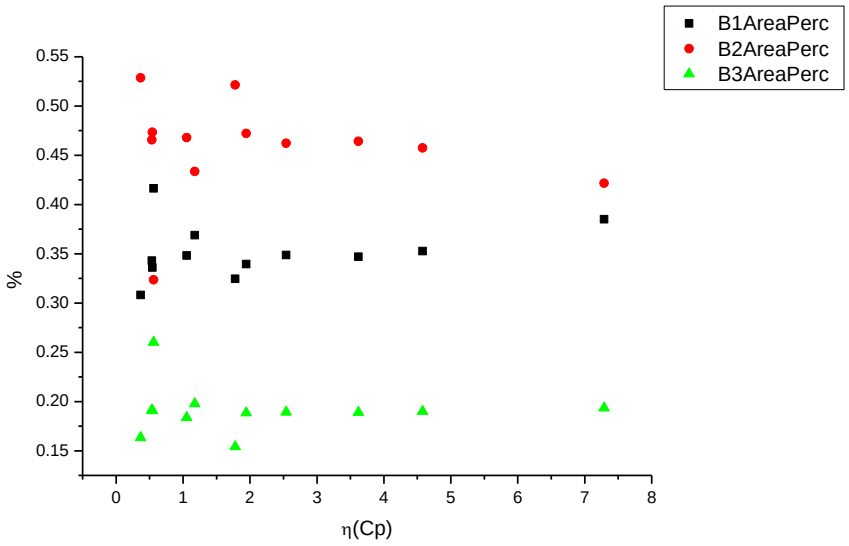

Figure 3.1.48. Area percentages from Gaussian model fit of the normalised fluorescence emission spectra of **16** recorded at 400 nm excitation against η(Cp).

3.1.6 400 nm fluorescent lifetime results.

3.1.6.1 Intensity weighted.

Wavelength (nm)	Solvent	τ_1 (ns)	A_1 (%)	τ_2 (ns)	A_2 (%)	τ_3 (ns)	A_3 (%)	τ_f (ns) (Intensity Weighted)	$1/\tau_f$	χ^2
470	Toluene	-	-	1.89	19.25	3.61	80.75	3.28	0.31	1.21
470	1,4-Dioxane	-	-	2.09	22.73	3.86	77.27	3.46	0.29	1.04
470	Chloroform	-	-	1.96	26.44	3.64	73.56	3.19	0.31	1.11
470	Acetonitrile	-	-	2.25	34.38	4.14	65.62	3.49	0.29	1.16
470	1-Octanol	0.19	11.73	2.45	58.99	3.63	29.28	2.53	0.40	1.21
470	1-Hexanol	0.70	3.73	2.53	76.21	3.97	20.06	2.75	0.36	1.29
470	1-Butanol	0.35	2.43	2.30	60.85	3.48	36.72	2.68	0.37	1.03
470	1-Pentanol	0.39	2.83	2.23	55.29	3.34	41.88	2.64	0.38	1.07
470	1-Propanol	1.40	7.04	2.39	59.19	3.50	33.77	2.70	0.37	1.11
470	Acetic acid	0.57	36.49	1.01	62.69	4.53	0.81	0.88	1.14	1.07
470	Methanol	-	-	1.52	23.36	2.95	76.64	2.62	0.38	1.10
470	2,2,2-Trifluoroethanol	0.60	98.19	3.12	1.81	-	-	0.65	1.55	1.06

Table 3.1.9. Summary of Time Correlated Single Photon Counting (TCSPC) fluorescent lifetimes (intensity weighted) of **16** recorded at 470 nm.

Wavelength (nm)	Solvent	τ_1 (ns)	A_1 (%)	τ_2 (ns)	A_2 (%)	τ_3 (ns)	A_3 (%)	τ_f (ns) (Intensity Weighted)	$1/\tau_f$	χ^2
490	Toluene	-	-	1.79	17.96	3.62	82.04	3.29	0.30	1.16
490	1,4-Dioxane	-	-	2.09	22.16	3.88	77.84	3.48	0.29	1.01
490	Chloroform	-	-	2.05	26.56	3.64	73.44	3.22	0.31	1.02
490	Acetonitrile	-	-	2.23	30.26	4.14	69.74	3.56	0.28	1.20
490	1-Octanol	0.20	10.17	2.48	60.37	3.73	29.46	2.62	0.38	1.24
490	1-Hexanol	0.34	3.09	2.24	47.69	3.38	49.21	2.74	0.36	1.19
490	1-Butanol	0.28	1.82	2.15	49.35	3.32	48.83	2.68	0.37	1.05
490	1-Pentanol	0.25	2.21	1.95	35.76	3.14	62.03	2.65	0.38	1.07
490	1-Propanol	0.36	2.18	2.24	56.59	3.40	41.23	2.67	0.37	1.11
490	Acetic acid	0.41	21.43	0.96	77.63	5.30	0.94	0.88	1.13	0.95
490	Methanol	-	-	1.62	25.32	2.99	74.68	2.65	0.38	1.11
490	2,2,2-Trifluoroethanol	0.37	21.96	0.67	77.22	6.05	0.83	0.65	1.54	1.10

Table 3.1.10. Summary of Time Correlated Single Photon Counting (TCSPC) fluorescent lifetimes (intensity weighted) of **16** recorded at 490 nm.

Wavelength (nm)	Solvent	τ_1 (ns)	A_1 (%)	τ_2 (ns)	A_2 (%)	τ_3 (ns)	A_3 (%)	τ_f (ns) (Intensity Weighted)	$1/\tau_f$	χ^2
520	Toluene	-	-	1.94	20.54	3.67	79.42	3.31	0.30	1.21
520	1,4-Dioxane	-	-	1.89	16.67	3.81	83.33	3.49	0.29	1.05
520	Chloroform	-	-	2.37	42.59	3.93	57.41	3.26	0.31	1.13
520	Acetonitrile	-	-	2.21	29.39	4.16	70.61	3.58	0.28	1.22
520	1-Octanol	0.18	9.56	2.66	77.51	4.56	12.93	2.67	0.37	1.46
520	1-Hexanol	0.22	1.67	2.14	46.09	3.40	52.24	2.76	0.36	1.22
520	1-Butanol	0.17	2.31	2.12	45.82	3.29	51.87	2.68	0.37	1.08
520	1-Pentanol	0.38	1.77	2.25	58.46	3.46	39.77	2.70	0.37	1.08
520	1-Propanol	0.28	1.96	2.23	55.84	3.43	42.20	2.70	0.37	1.06
520	Acetic acid	0.43	19.39	0.97	79.23	3.91	1.38	0.91	1.10	0.91
520	Methanol	-	-	1.56	22.50	2.98	77.50	2.66	0.38	0.96
520	2,2,2-Trifluoroethanol	0.48	45.49	0.73	53.75	6.08	0.75	0.66	1.52	0.99

Table 3.1.11. Summary of Time Correlated Single Photon Counting (TCSPC) fluorescent lifetimes (intensity weighted) of **16** recorded at 520 nm.

Wavelength (nm)	Solvent	τ_1 (ns)	A_1 (%)	τ_2 (ns)	A_2 (%)	τ_3 (ns)	A_3 (%)	τ_f (ns) (Intensity Weighted)	$1/\tau_f$	χ^2
540	Toluene	0.57	2.61	3.12	83.92	5.25	13.48	3.34	0.30	1.21
540	1,4-Dioxane	-	-	2.29	28.21	3.99	71.79	3.51	0.29	1.10
540	Chloroform	-	-	2.36	41.21	3.91	58.79	3.27	0.31	1.07
540	Acetonitrile	-	-	2.32	31.49	4.19	68.51	3.60	0.28	1.10
540	1-Octanol	0.19	9.05	2.61	73.68	4.37	17.27	2.69	0.37	1.27
540	1-Hexanol	0.41	1.52	2.18	45.89	3.39	52.60	2.79	0.36	1.18
540	1-Butanol	0.30	1.85	2.33	64.17	3.57	33.98	2.71	0.37	1.11
540	1-Pentanol	-	-	2.04	45.74	3.29	54.26	2.72	0.37	1.20
540	1-Propanol	0.38	1.70	2.33	67.62	3.67	30.68	2.71	0.37	1.07
540	Acetic acid	0.51	26.49	1.01	72.47	5.26	1.04	0.92	1.08	1.03
540	Methanol	-	-	1.54	20.85	2.95	79.15	2.66	0.38	1.15
540	2,2,2-Trifluoroethanol	0.40	18.47	0.68	80.70	4.98	0.83	0.66	1.52	1.13

Table 3.1.12. Summary of Time Correlated Single Photon Counting (TCSPC) fluorescent lifetimes (intensity weighted) of **16** recorded at 540 nm.

Wavelength (nm)	Solvent	τ_1 (ns)	A_1 (%)	τ_2 (ns)	A_2 (%)	τ_3 (ns)	A_3 (%)	τ_f (ns) (Intensity Weighted)	$1/\tau_f$	χ^2
570	Toluene	0.55	2.11	3.09	82.23	5.27	15.66	3.36	0.30	1.23
570	1,4-Dioxane	-	-	2.30	29.11	4.03	70.89	3.53	0.28	1.01
570	Chloroform	-	-	2.34	40.66	3.91	59.34	3.27	0.31	1.12
570	Acetonitrile	-	-	2.39	34.13	4.28	65.87	3.63	0.28	1.12
570	1-Octanol	0.23	7.70	2.72	83.64	5.44	8.67	2.76	0.36	1.28
570	1-Hexanol	0.77	4.12	2.57	78.31	4.38	17.57	2.81	0.36	1.25
570	1-Butanol	0.35	1.55	2.32	64.13	3.66	34.32	2.75	0.36	1.10
570	1-Pentanol	-	-	2.37	71.75	3.77	28.54	2.76	0.36	1.19
570	1-Propanol	0.39	1.68	2.36	70.45	3.84	27.87	2.74	0.36	1.09
570	Acetic acid	0.42	22.64	0.99	76.03	5.01	1.33	0.92	1.09	1.06
570	Methanol	-	-	1.57	21.91	2.98	78.09	2.67	0.37	1.14
570	2,2,2-Trifluoroethanol	0.60	82.47	0.89	16.88	5.08	0.65	0.67	1.48	1.18

Table 3.1.13. Summary of Time Correlated Single Photon Counting (TCSPC) fluorescent lifetimes (intensity weighted) of **16** recorded at 570 nm.

3.1.6.2 Amplitude weighted.

Wavelength (nm)	Solvent	τ_1 (ns)	A_1 (%)	τ_2 (ns)	A_2 (%)	τ_3 (ns)	A_3 (%)	τ_f (ns) (Amplitude Weighted)	$1/\tau_f$	χ^2
470	Toluene	-	-	1.89	31.27	3.61	68.73	3.07	0.33	1.21
470	1,4-Dioxane	-	-	2.09	35.18	3.86	64.82	3.24	0.31	1.04
470	Chloroform	-	-	1.96	40.05	3.64	59.95	2.97	0.34	1.11
470	Acetonitrile	-	-	2.25	49.13	4.14	50.87	3.21	0.31	1.16
470	1-Octanol	0.19	65.84	2.45	25.58	3.63	8.57	1.06	0.94	1.21
470	1-Hexanol	0.70	13.10	2.53	74.43	3.97	12.46	2.47	0.41	1.29
470	1-Butanol	0.35	15.90	2.30	60.10	3.48	23.99	2.27	0.44	1.03
470	1-Pentanol	0.39	16.16	2.23	55.63	3.34	28.21	2.25	0.45	1.07
470	1-Propanol	1.40	12.74	2.39	62.83	3.50	24.43	2.53	0.39	1.11
470	Acetic acid	0.57	50.50	1.01	49.36	4.53	0.14	0.80	1.26	1.07
470	Methanol	-	-	1.52	37.09	2.95	62.91	2.42	0.41	1.10
470	2,2,2-Trifluoroethanol	0.60	99.65	3.12	0.35	-	-	0.61	1.64	1.06

Table 3.1.14. Summary of Time Correlated Single Photon Counting (TCSPC) fluorescent lifetimes (amplitude weighted) of **16** recorded at 470 nm.

Wavelength (nm)	Solvent	τ_1 (ns)	A_1 (%)	τ_2 (ns)	A_2 (%)	τ_3 (ns)	A_3 (%)	τ_f (ns) (Amplitude Weighted)	$1/\tau_f$	χ^2
490	Toluene	-	-	1.79	30.63	3.62	69.37	3.06	0.33	1.16
490	1,4-Dioxane	-	-	2.09	34.61	3.88	65.39	3.26	0.31	1.01
490	Chloroform	-	-	2.05	39.09	3.64	60.91	3.02	0.33	1.02
490	Acetonitrile	-	-	2.23	44.58	4.14	55.42	3.29	0.30	1.20
490	1-Octanol	0.20	61.56	2.48	29.02	3.73	9.43	1.19	0.84	1.24
490	1-Hexanol	0.34	20.03	2.24	47.48	3.38	32.49	2.23	0.45	1.19
490	1-Butanol	0.28	14.62	2.15	52.03	3.32	33.36	2.26	0.44	1.05
490	1-Pentanol	0.25	18.83	1.95	39.03	3.14	42.15	2.13	0.47	1.07
490	1-Propanol	0.36	13.92	2.24	58.18	3.40	27.90	2.30	0.43	1.11
490	Acetic acid	0.41	39.17	0.96	60.70	5.30	0.13	0.75	1.33	0.95
490	Methanol	-	-	1.62	38.68	2.99	61.52	2.47	0.41	1.11
490	2,2,2-Trifluoroethanol	0.37	34.22	0.67	65.70	6.05	0.08	0.57	1.75	1.10

Table 3.1.15. Summary of Time Correlated Single Photon Counting (TCSPC) fluorescent lifetimes (amplitude weighted) of **16** recorded at 490 nm.

Wavelength (nm)	Solvent	τ_1 (ns)	A_1 (%)	τ_2 (ns)	A_2 (%)	τ_3 (ns)	A_3 (%)	τ_f (ns) (Amplitude Weighted)	$1/\tau_f$	χ^2
520	Toluene	-	-	1.94	32.88	3.67	67.12	3.10	0.32	1.21
520	1,4-Dioxane	-	-	1.89	28.76	3.81	71.24	3.25	0.31	1.05
520	Chloroform	-	-	2.37	55.14	3.93	44.86	3.07	0.33	1.13
520	Acetonitrile	-	-	2.21	43.96	4.16	56.04	3.30	0.30	1.22
520	1-Octanol	0.18	62.24	2.66	34.41	4.56	3.35	1.18	0.85	1.46
520	1-Hexanol	0.22	17.06	2.14	48.38	3.40	34.56	2.25	0.45	1.22
520	1-Butanol	0.17	26.37	2.12	42.54	3.29	31.09	1.97	0.51	1.08
520	1-Pentanol	0.38	11.14	2.25	61.62	3.46	27.24	2.37	0.42	1.08
520	1-Propanol	0.28	15.71	2.23	56.52	3.43	27.77	2.26	0.44	1.06
520	Acetic acid	0.43	35.79	0.97	63.93	3.91	0.28	0.79	1.27	0.91
520	Methanol	-	-	1.56	35.59	2.98	64.41	2.47	0.40	0.96
520	2,2,2-Trifluoroethanol	0.48	56.23	0.73	43.70	6.08	0.07	0.60	1.68	0.99

Table 3.1.16. Summary of Time Correlated Single Photon Counting (TCSPC) fluorescent lifetimes (amplitude weighted) of **16** recorded at 520 nm.

Wavelength (nm)	Solvent	τ_1 (ns)	A_1 (%)	τ_2 (ns)	A_2 (%)	τ_3 (ns)	A_3 (%)	τ_f (ns) (Amplitude Weighted)	$1/\tau_f$	χ^2
540	Toluene	0.57	13.44	3.12	79.03	5.25	7.54	2.93	0.34	1.21
540	1,4-Dioxane	-	-	2.29	40.67	3.99	59.33	3.30	0.30	1.10
540	Chloroform	-	-	2.36	53.73	3.91	46.27	3.08	0.33	1.07
540	Acetonitrile	-	-	2.32	45.36	4.19	54.64	3.34	0.30	1.10
540	1-Octanol	0.19	59.89	2.61	35.19	4.37	4.92	1.24	0.80	1.27
540	1-Hexanol	0.41	9.12	2.18	52.38	3.39	38.51	2.48	0.40	1.18
540	1-Butanol	0.30	14.45	2.33	63.59	3.57	21.96	2.31	0.43	1.11
540	1-Pentanol	-	-	2.04	57.65	3.29	42.35	2.57	0.39	1.20
540	1-Propanol	0.38	10.71	2.33	69.32	3.67	19.97	2.39	0.42	1.07
540	Acetic acid	0.51	42.07	1.01	57.77	5.26	0.16	0.81	1.24	1.03
540	Methanol	-	-	1.54	33.53	2.95	66.47	2.48	0.40	1.15
540	2,2,2-Trifluoroethanol	0.40	28.10	0.68	71.80	4.98	0.10	0.60	1.66	1.13

Table 3.1.17. Summary of Time Correlated Single Photon Counting (TCSPC) fluorescent lifetimes (amplitude weighted) of **16** recorded at 540 nm.

Wavelength (nm)	Solvent	τ_1 (ns)	A_1 (%)	τ_2 (ns)	A_2 (%)	τ_3 (ns)	A_3 (%)	τ_f (ns) (Amplitude Weighted)	$1/\tau_f$	χ^2
570	Toluene	0.55	11.51	3.09	79.67	5.27	8.82	2.97	0.34	1.23
570	1,4-Dioxane	-	-	2.30	41.82	4.03	58.18	3.31	0.30	1.01
570	Chloroform	-	-	2.34	53.40	3.91	46.60	3.07	0.33	1.12
570	Acetonitrile	-	-	2.39	48.13	4.28	51.87	3.37	0.30	1.12
570	1-Octanol	0.23	51.41	2.72	46.19	5.44	2.39	1.50	0.67	1.28
570	1-Hexanol	0.77	13.39	2.57	76.53	4.38	10.07	2.51	0.40	1.25
570	1-Butanol	0.35	10.79	2.32	66.60	3.66	22.61	2.41	0.42	1.10
570	1-Pentanol	-	-	2.37	80.16	3.77	19.84	2.65	0.38	1.19
570	1-Propanol	0.39	10.52	2.36	71.96	3.84	17.52	1.09	0.92	1.09
570	Acetic acid	0.42	41.00	0.99	58.79	5.01	0.20	0.77	1.30	1.06
570	Methanol	-	-	1.57	34.70	2.98	65.30	2.49	0.40	1.14
570	2,2,2-Trifluoroethanol	0.60	87.93	0.89	11.99	5.08	0.08	0.63	1.58	1.18

Table 3.1.18. Summary of Time Correlated Single Photon Counting (TCSPC) fluorescent lifetimes (amplitude weighted) of **16** recorded at 570 nm.

3.1.7 400 nm average fluorescent lifetimes - Solvatochromic analysis.

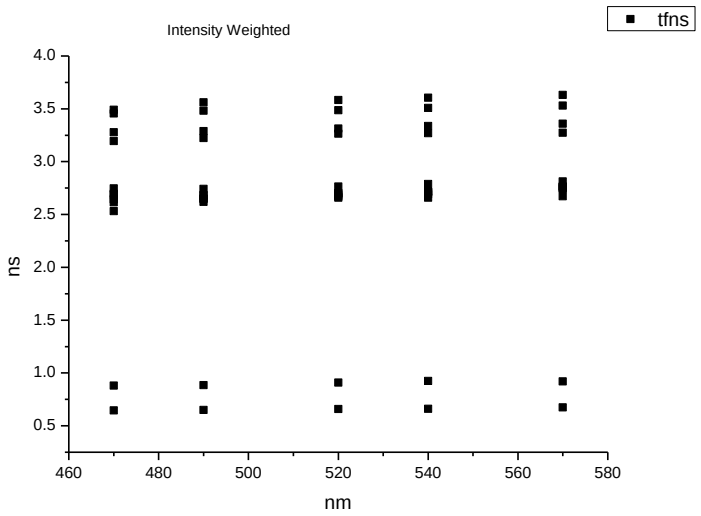

Figure 3.1.49. Intensity weighted average lifetime (τ_f) of **16** versus wavelength (nm).

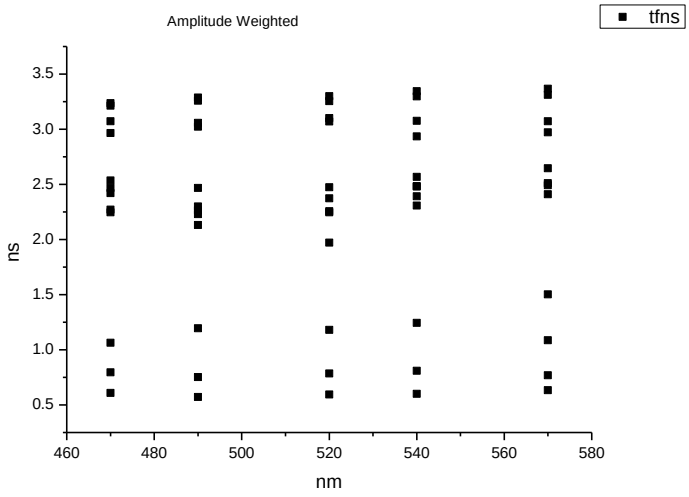

Figure 3.1.50. Amplitude weighted average lifetime (τ_f) of **16** versus wavelength (nm).

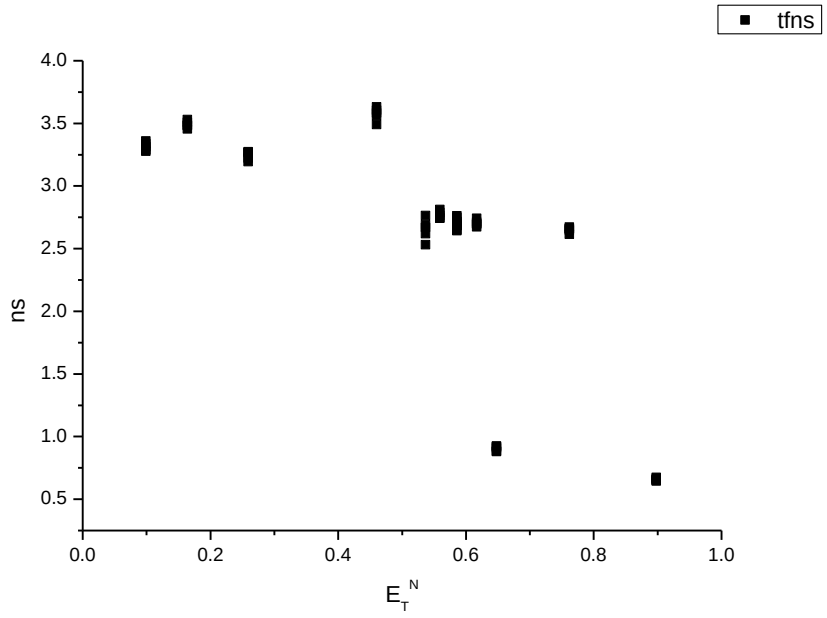

Figure 3.1.51. Intensity weighted average lifetime (τ_f) of **16** versus E_T^N.

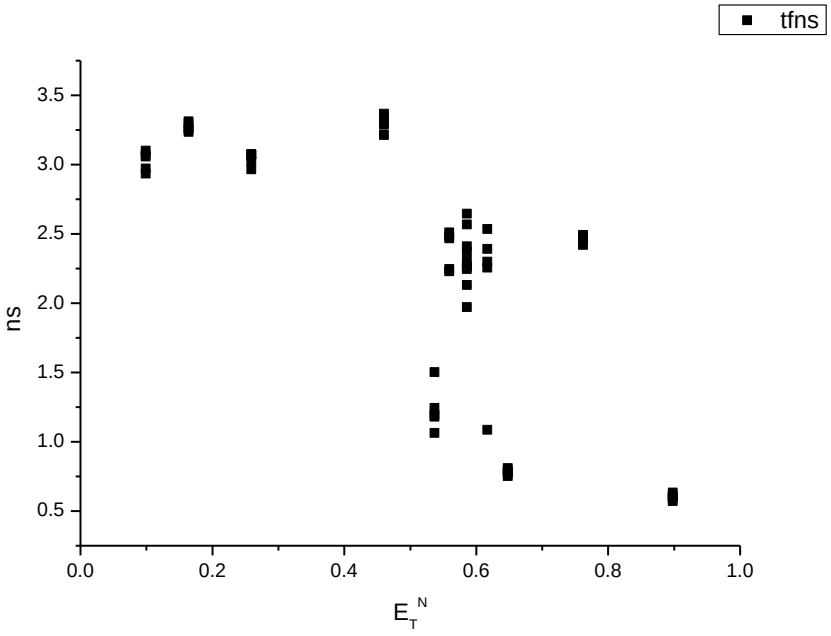

Figure 3.1.52. Amplitude weighted average lifetime (τ_f) of **16** versus E_T^N.

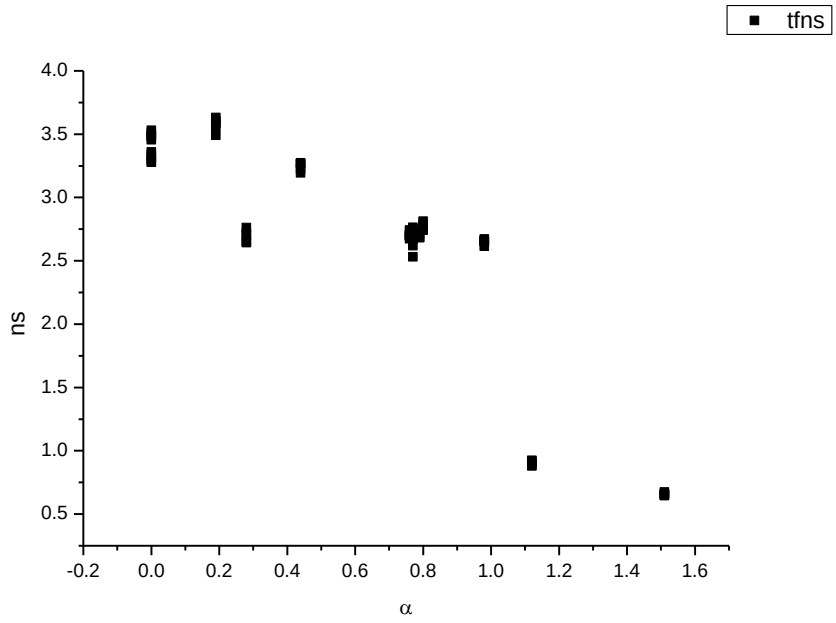

Figure 3.1.53. Intensity weighted average lifetime (τ_f) of **16** versus α.

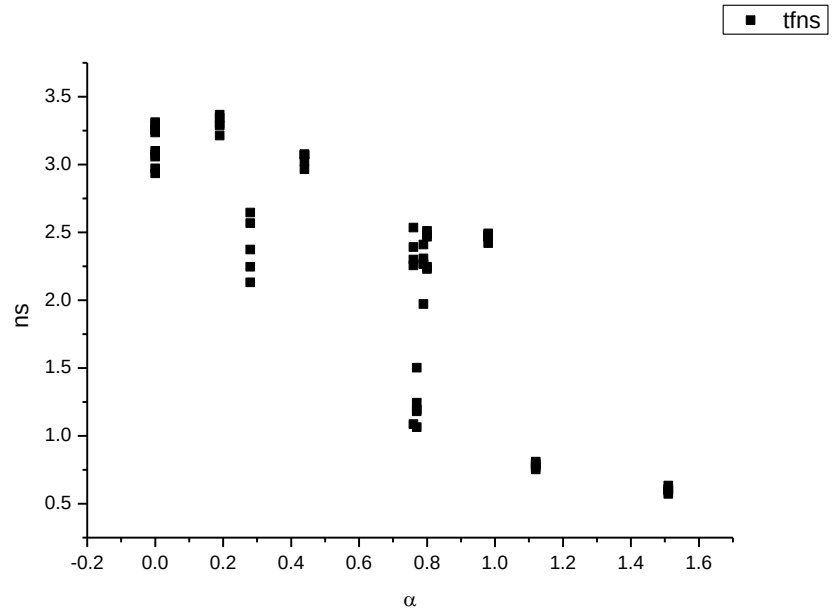

Figure 3.1.54. Amplitude weighted average lifetime (τ_f) of **16** versus α.

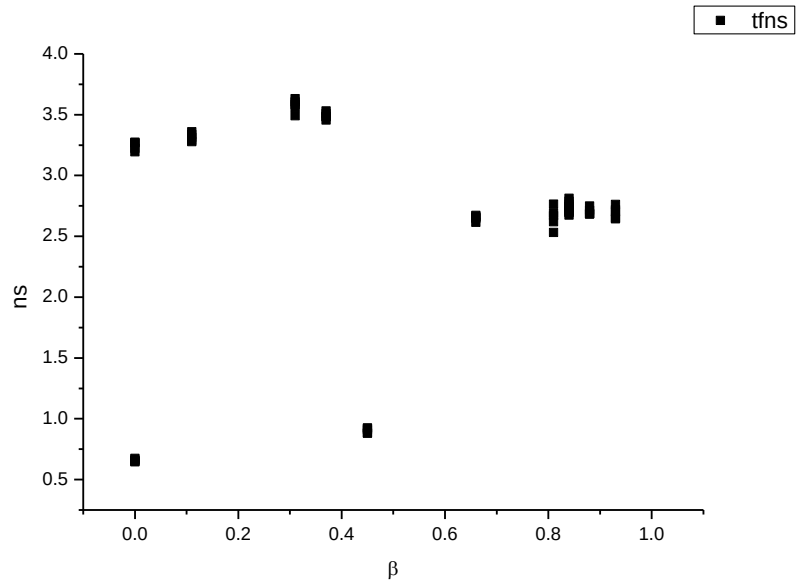

Figure 3.1.55. Intensity weighted average lifetime (τ_f) of **16** versus β.

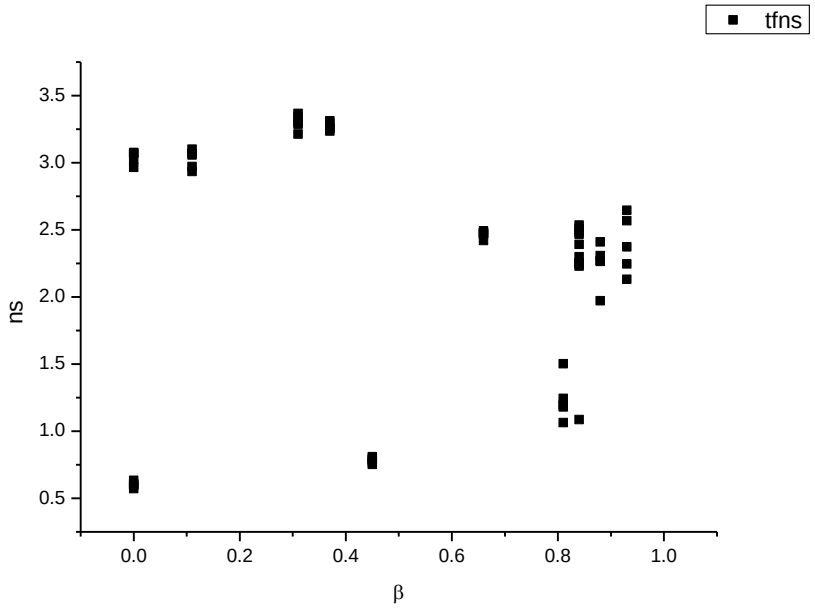

Figure 3.1.56. Amplitude weighted average lifetime (τ_f) of **16** versus β.

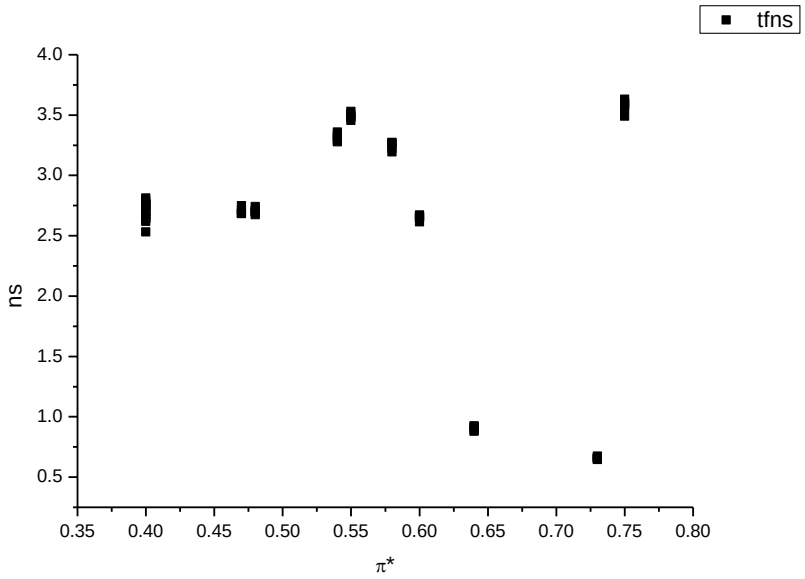

Figure 3.1.57. Intensity weighted average lifetime (τ_f) of **16** versus π*.

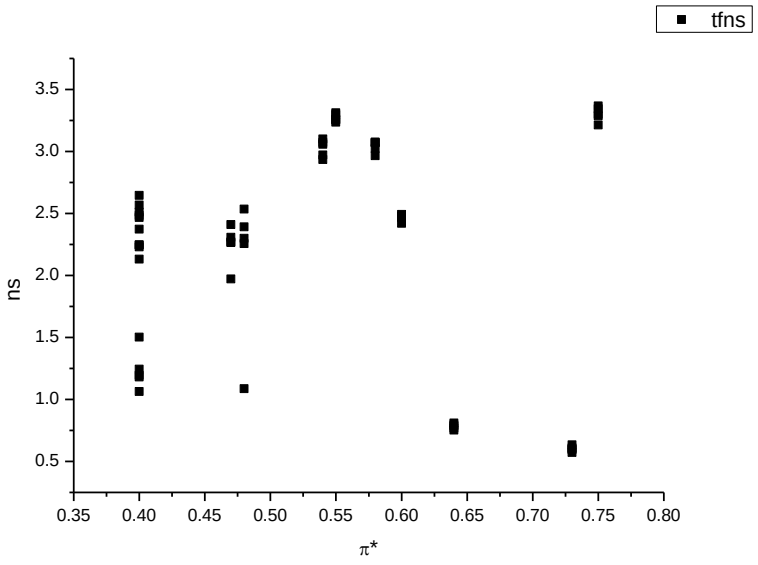

Figure 3.1.58. Amplitude weighted average lifetime (τ_f) of **16** versus π*.

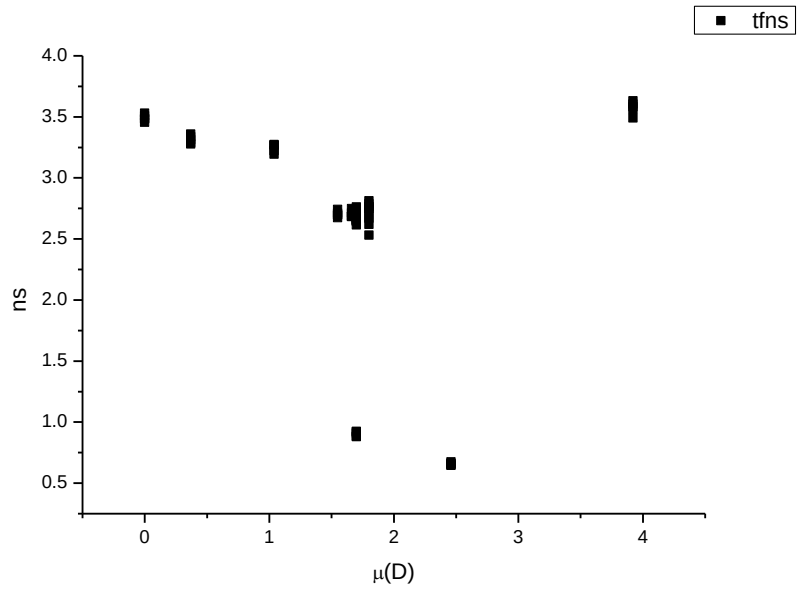

Figure 3.1.59. Intensity weighted average lifetime (τ_f) of **16** versus μ(D).

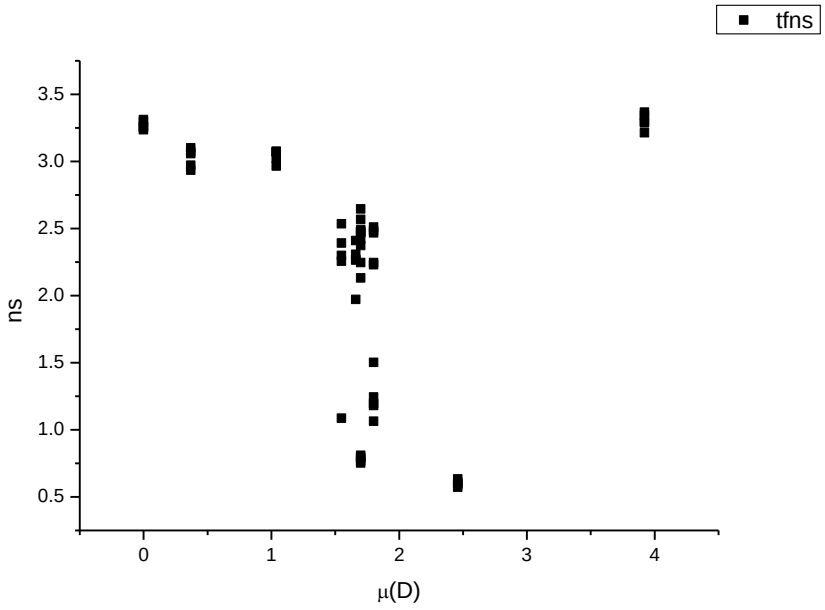

Figure 3.1.60. Amplitude weighted average lifetime (τ_f) of **16** versus μ(D).

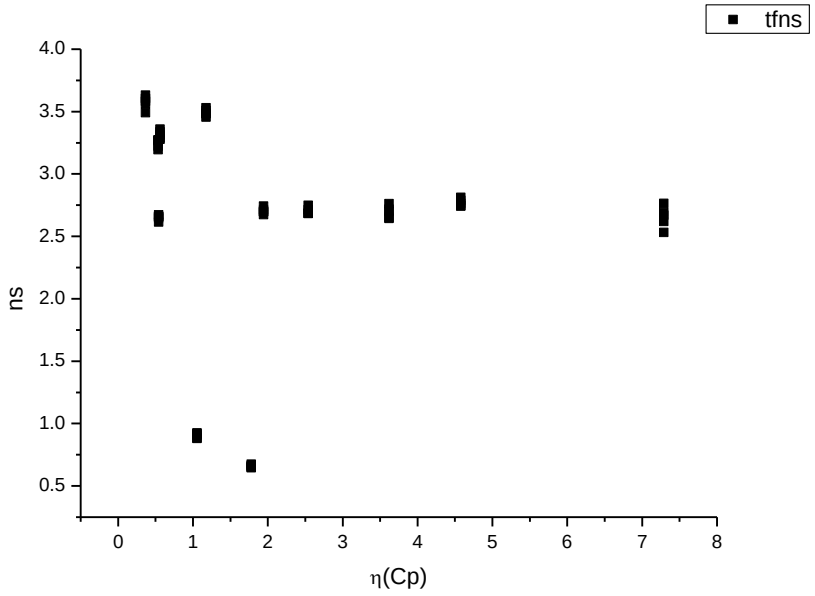

Figure 3.1.61. Intensity weighted average lifetime (τ_f) of **16** versus η(Cp).

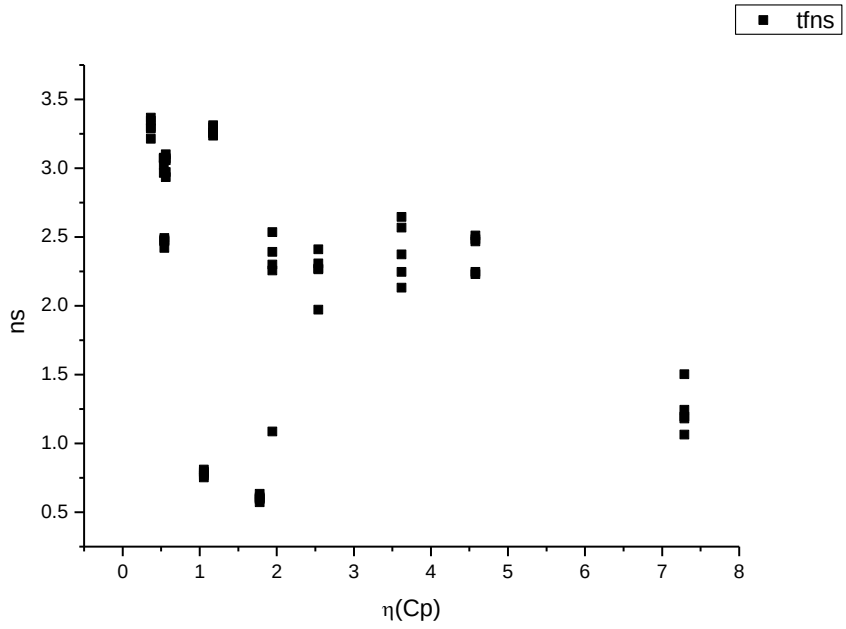

Figure 3.1.62. Amplitude weighted average lifetime (τ_f) of **16** versus η(Cp).

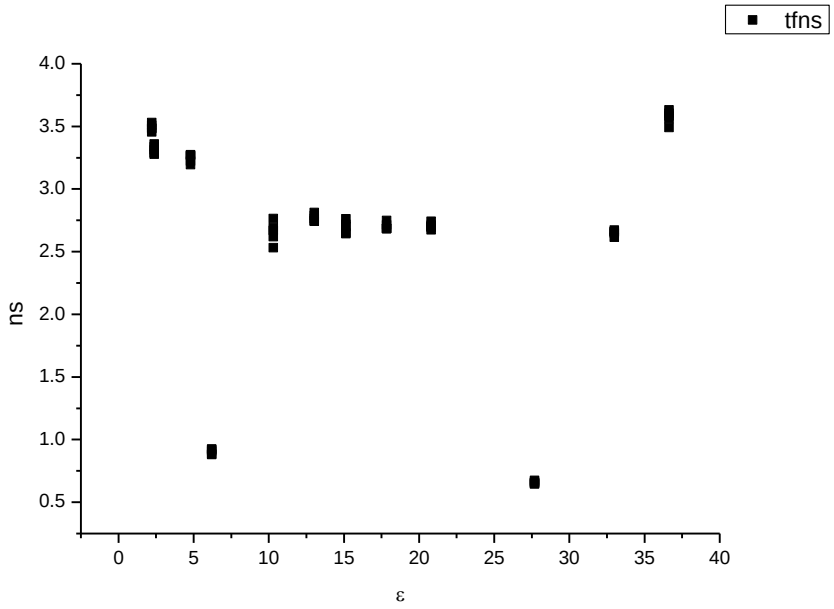

Figure 3.1.63. Intensity weighted average lifetime (τ_f) of **16** versus ε.

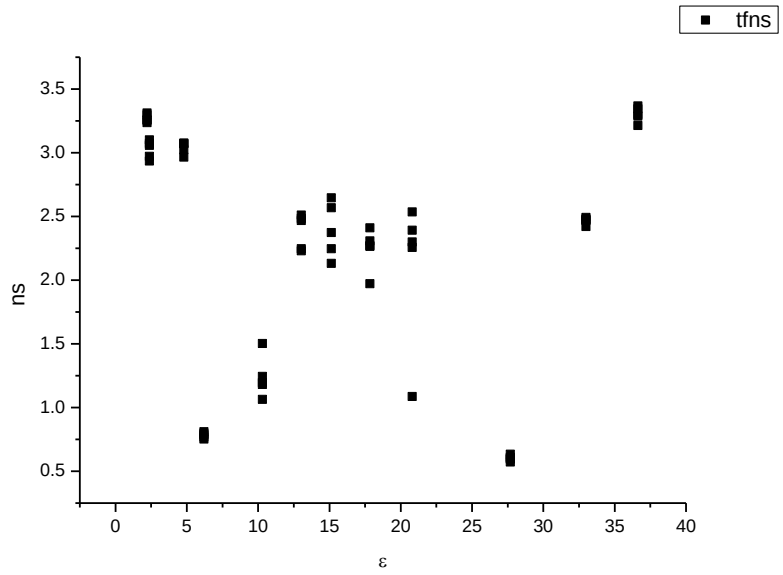

Figure 3.1.64. Amplitude weighted average lifetime (τ_f) of **16** versus ε.

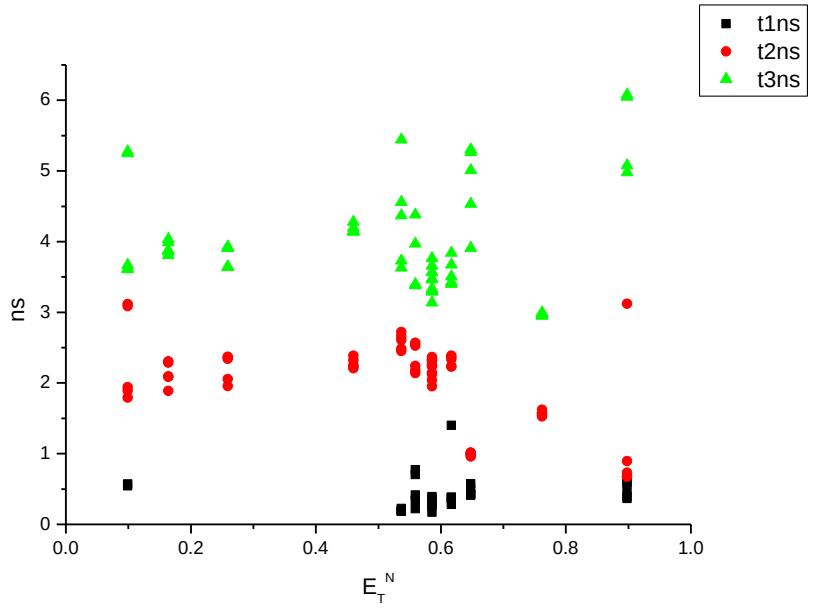

Figure 3.1.65. Intensity weighted components of TCSPC lifetime decay of **16** (470 nm to 570 nm) versus E_T^N.

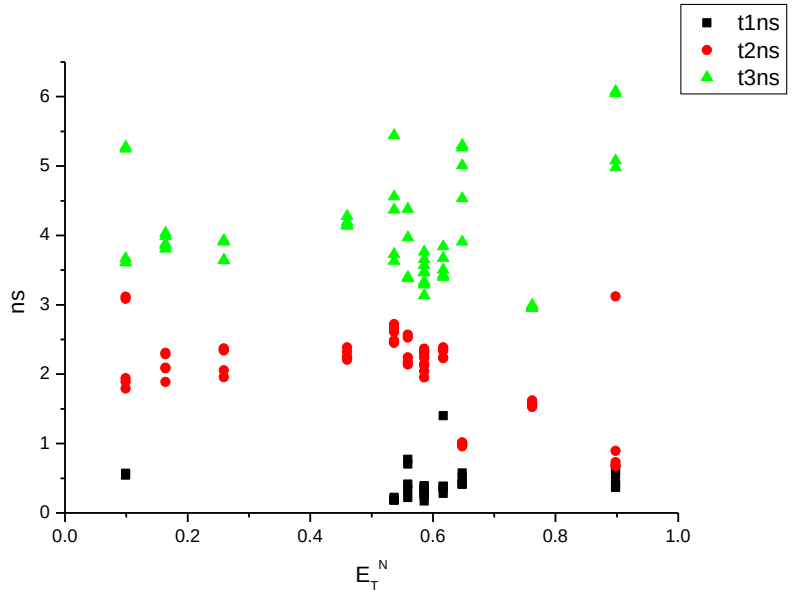

Figure 3.1.66. Amplitude weighted components of TCSPC lifetime decay of **16** (470 nm to 570 nm) versus E_T^N.

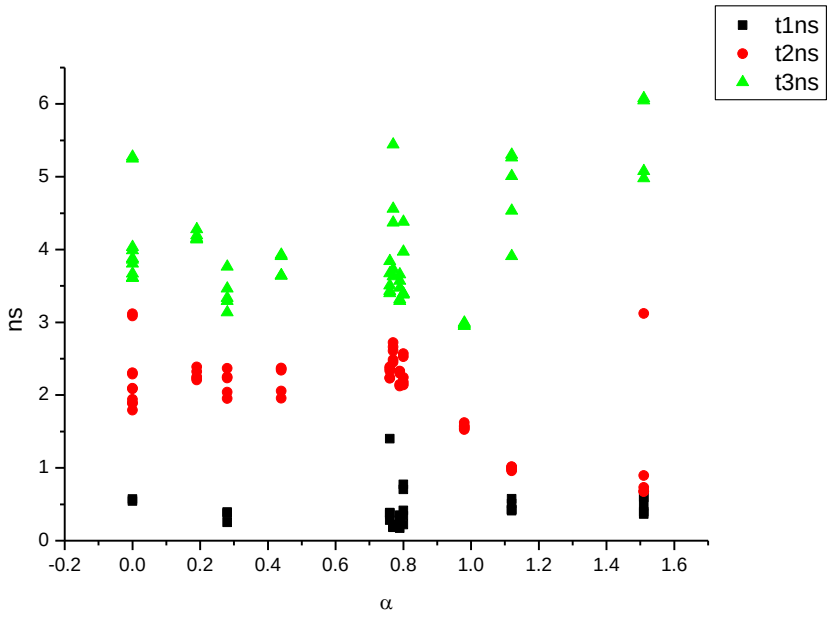

Figure 3.1.67. Intensity weighted components of TCSPC lifetime decay of **16** (470 nm to 570 nm) versus α.

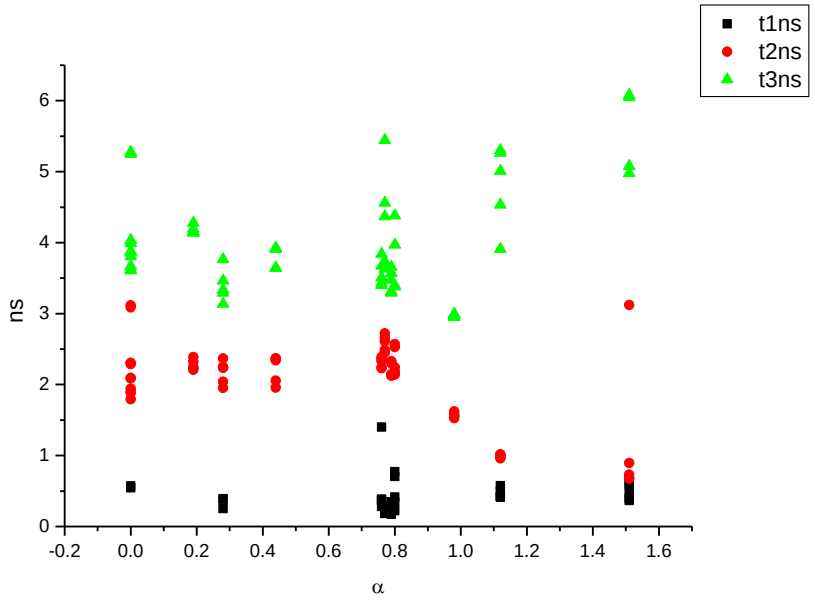

Figure 3.1.68. Amplitude weighted components of TCSPC lifetime decay of **16** (470 nm to 570 nm) versus α.

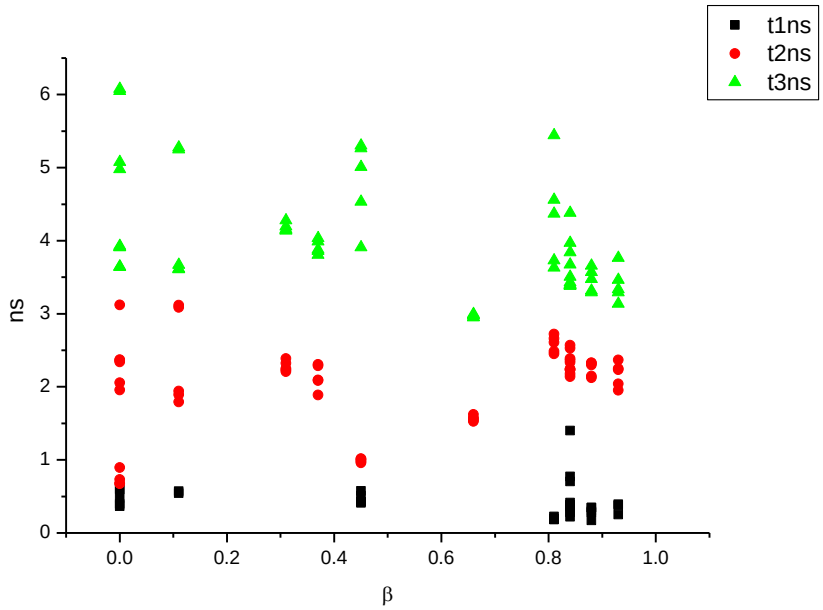

Figure 3.1.69. Intensity weighted components of TCSPC lifetime decay of **16** (470 nm to 570 nm) versus β.

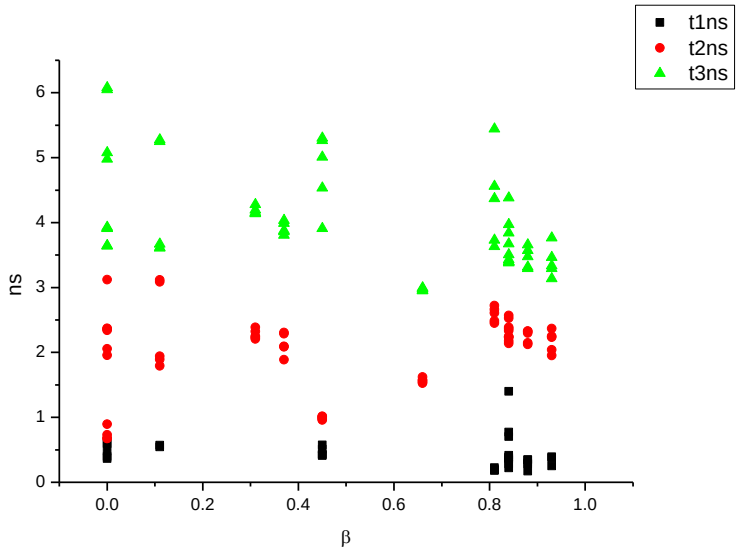

Figure 3.1.70. Amplitude weighted components of TCSPC lifetime decay of **16** (470 nm to 570 nm) versus β.

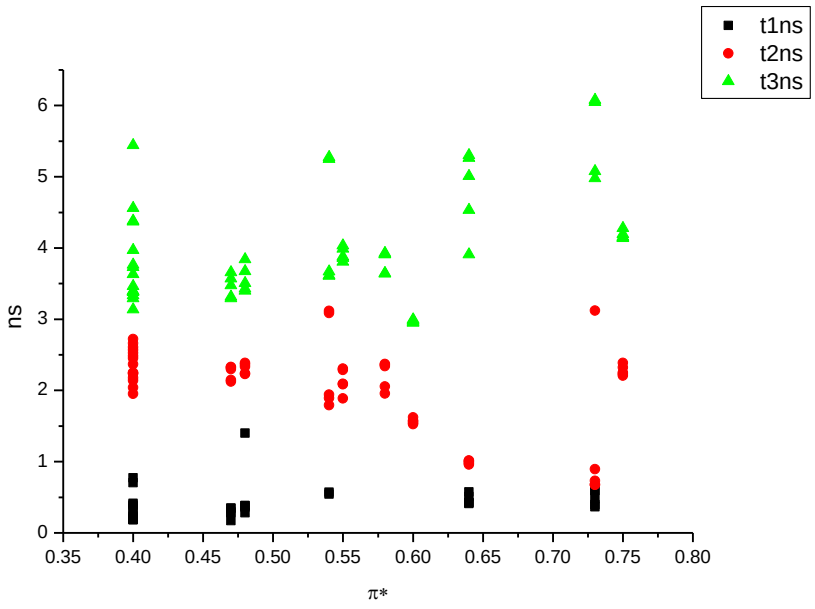

Figure 3.1.71. Intensity weighted components of TCSPC lifetime decay of **16** (470 nm to 570 nm) versus π*.

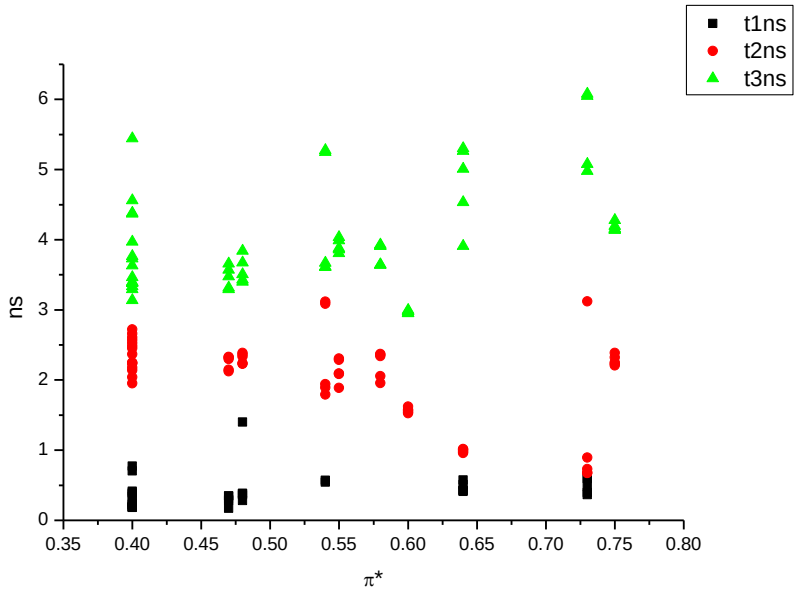

Figure 3.1.72. Amplitude weighted components of TCSPC lifetime decay of **16** (470 nm to 570 nm) versus π*.

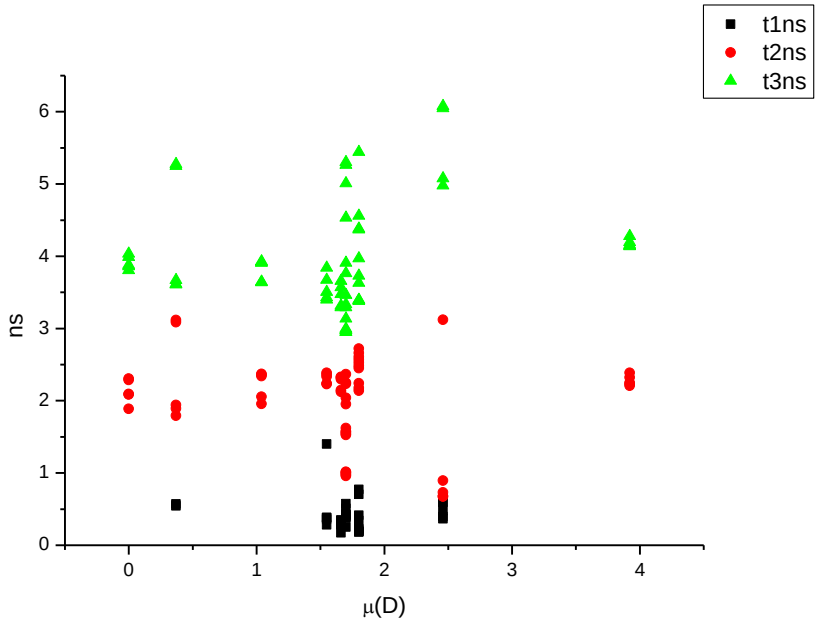

Figure 3.1.73. Intensity weighted components of TCSPC lifetime decay of **16** (470 nm to 570 nm) versus μ(D).

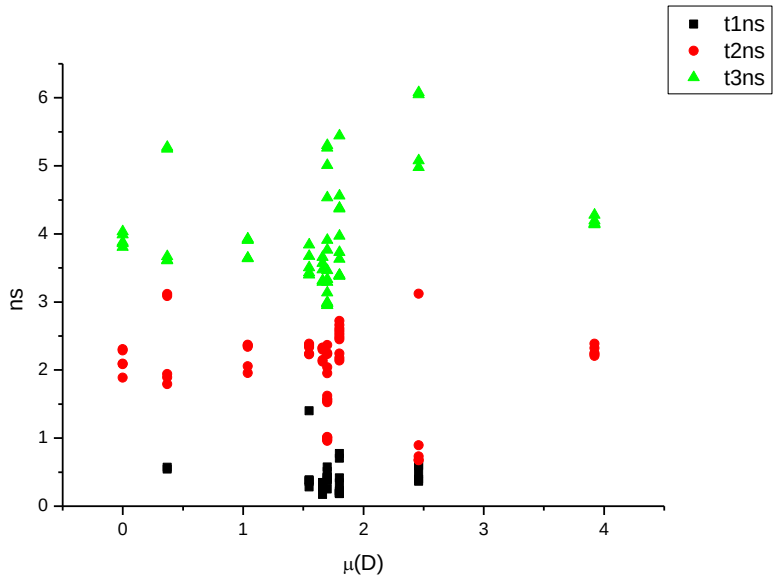

Figure 3.1.74. Amplitude weighted components of TCSPC lifetime decay of **16** (470 nm to 570 nm) versus μ(D).

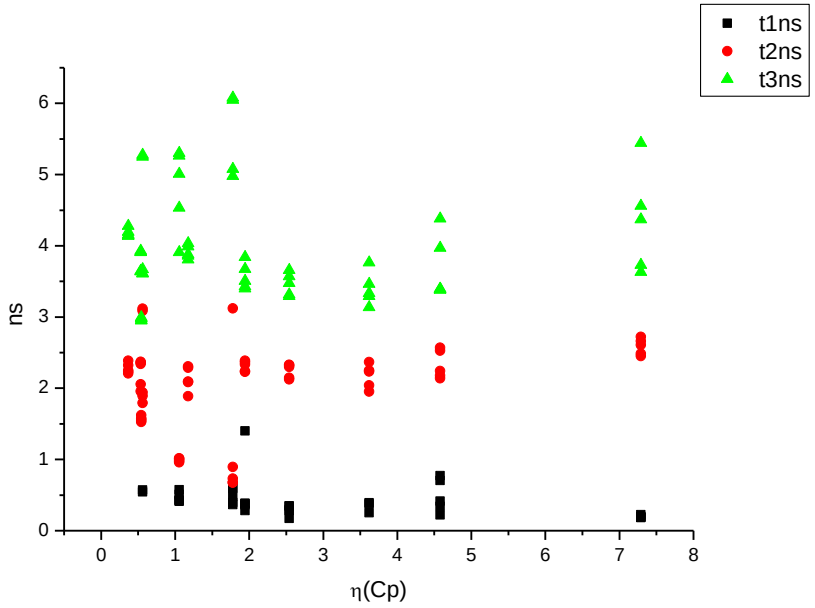

Figure 3.1.75. Intensity weighted components of TCSPC lifetime decay of **16** (470 nm to 570 nm) versus η(Cp).

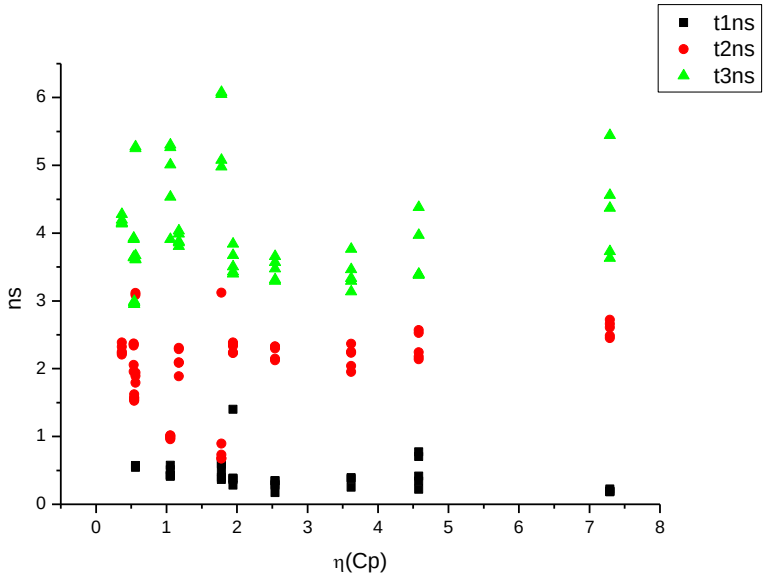

Figure 3.1.76. Amplitude weighted components of TCSPC lifetime decay of **16** (470 nm to 570 nm) versus η(Cp).

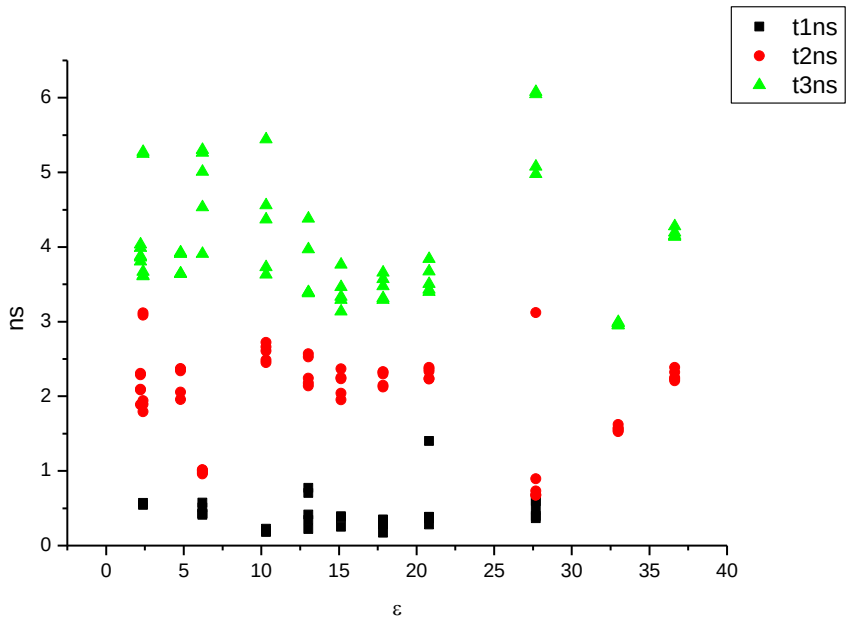

Figure 3.1.77. Intensity weighted components of TCSPC lifetime decay of **16** (470 nm to 570 nm) versus ε.

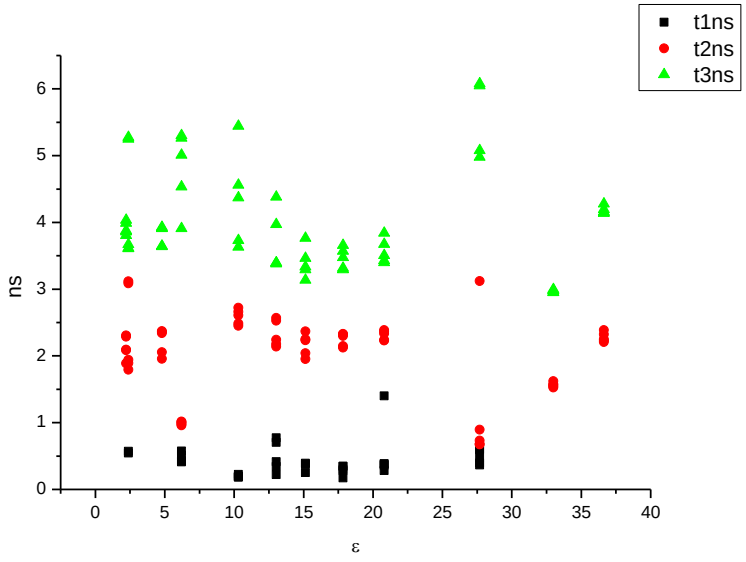

Figure 3.1.78. Amplitude weighted components of TCSPC lifetime decay of **16** (470 nm to 570 nm) versus ε.

3.1.7.1 470 nm Lifetime – Solvatochromic analysis.

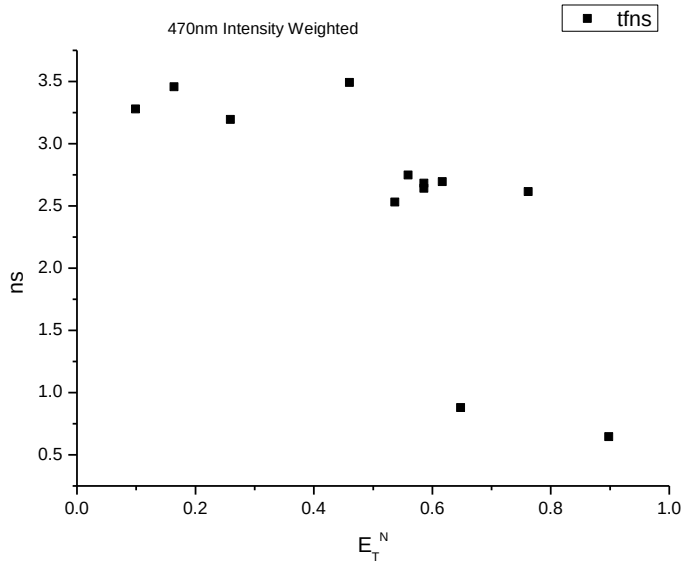

Figure 3.1.79. Intensity weighted average lifetime (τ_f) of **16** at 470 nm versus E_T^N.

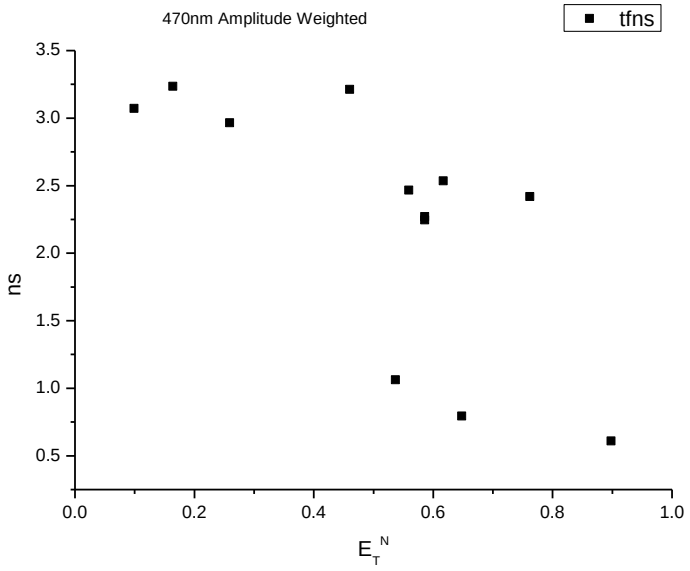

Figure 3.1.80. Amplitude weighted average lifetime (τ_f) of **16** at 470 nm versus E_T^N.

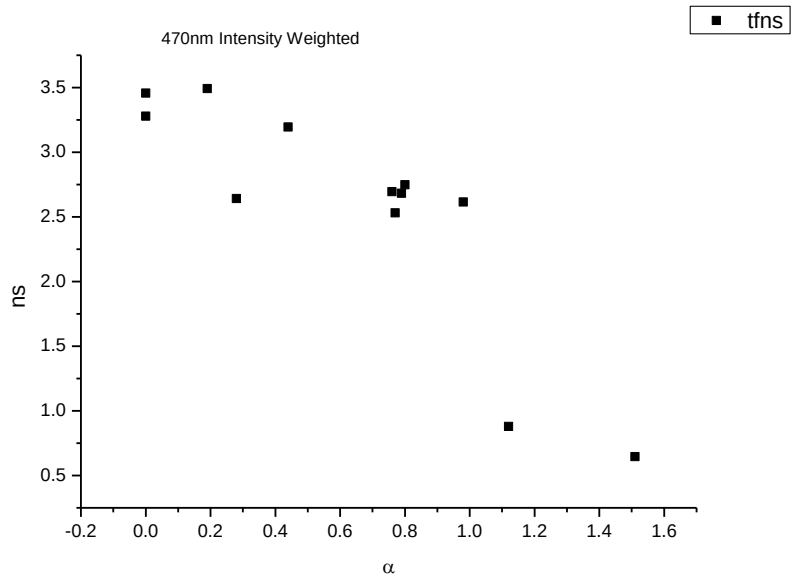

Figure 3.1.81. Intensity weighted average lifetime (τ_f) of **16** at 470 nm versus α.

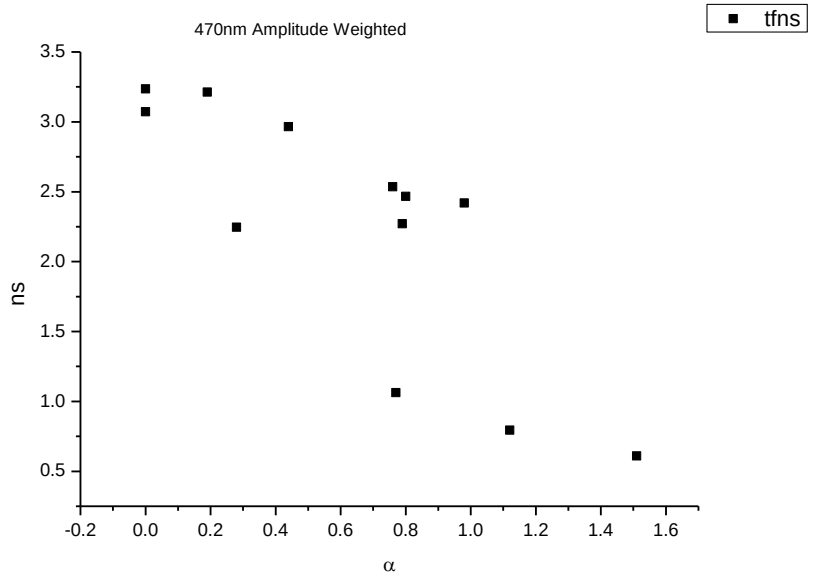

Figure 3.1.82. Amplitude weighted average lifetime (τ_f) of **16** at 470 nm versus α.

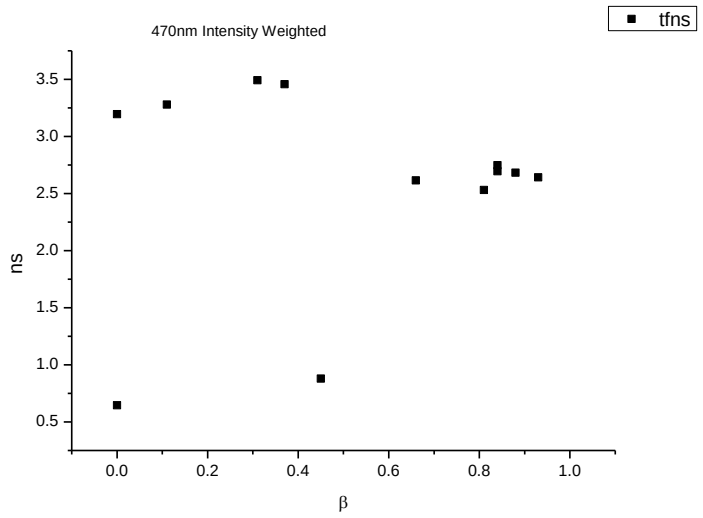

Figure 3.1.83. Intensity weighted average lifetime (τ_f) of **16** at 470 nm versus β.

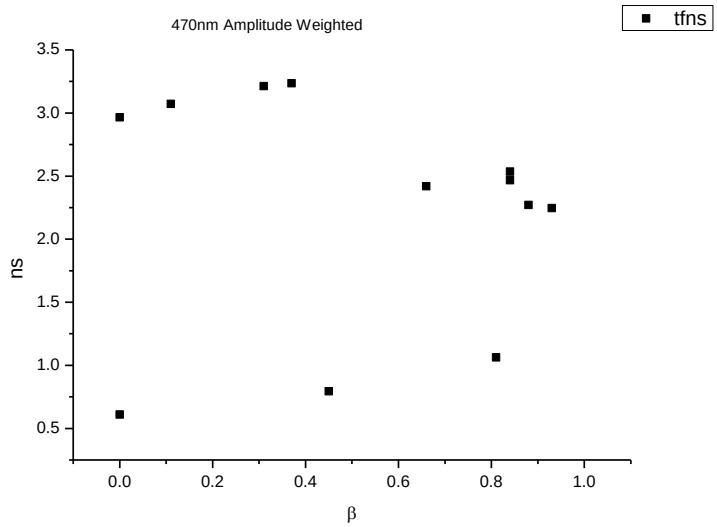

Figure 3.1.84. Amplitude weighted average lifetime (τ_f) of **16** at 470 nm versus β.

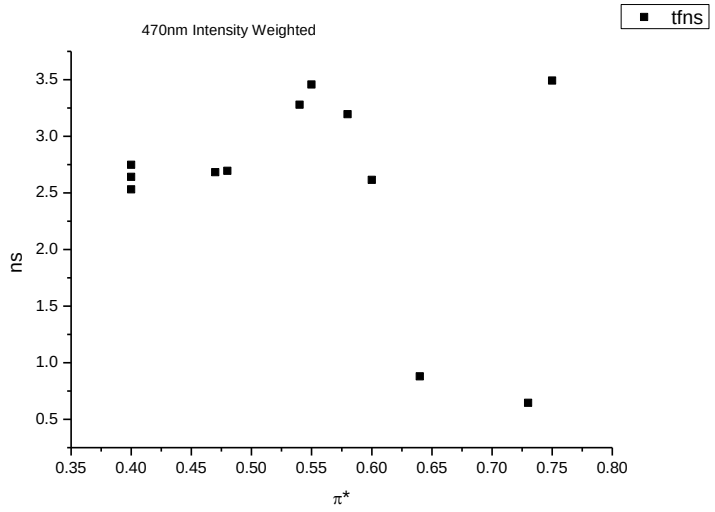

Figure 3.1.85. Intensity weighted average lifetime (τ_f) of **16** at 470 nm versus π*.

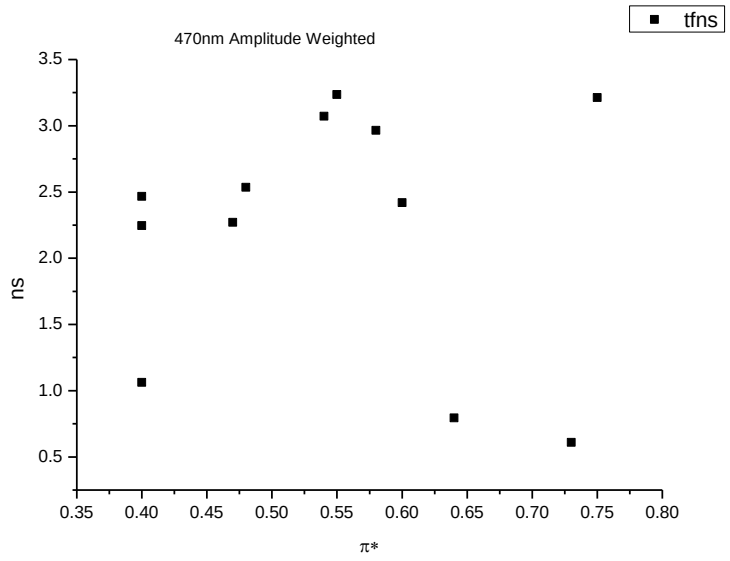

Figure 3.1.86. Amplitude weighted average lifetime (τ_f) of **16** at 470 nm versus π*.

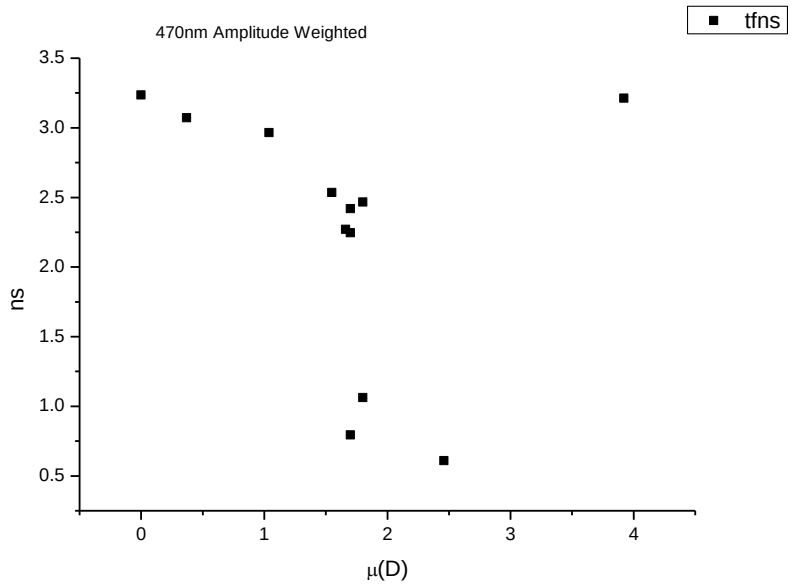

Figure 3.1.87. Intensity weighted average lifetime (τ_f) of **16** at 470 nm versus μ(D).

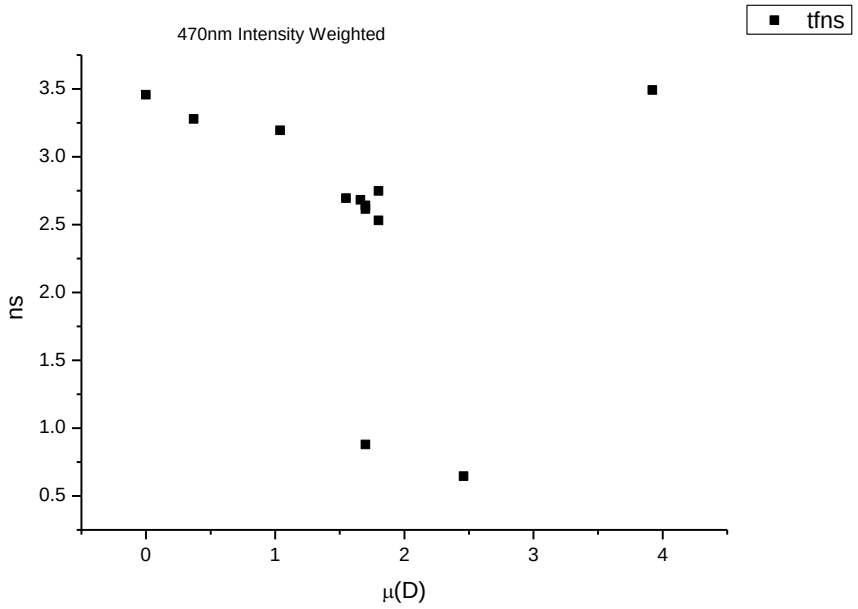

Figure 3.1.88. Amplitude weighted average lifetime (τ_f) of **16** at 470 nm versus μ(D).

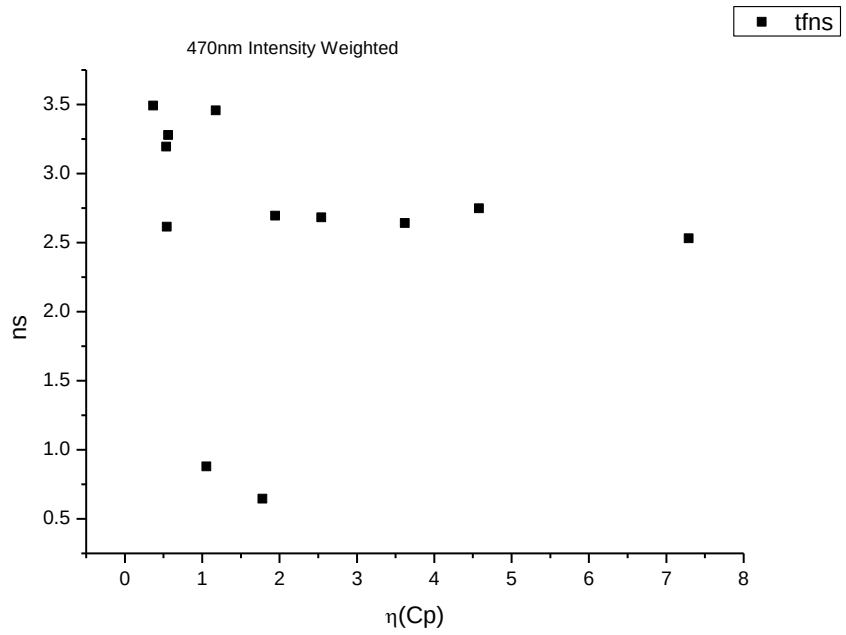

Figure 3.1.89. Intensity weighted average lifetime (τ_f) of **16** at 470 nm versus η(Cp).

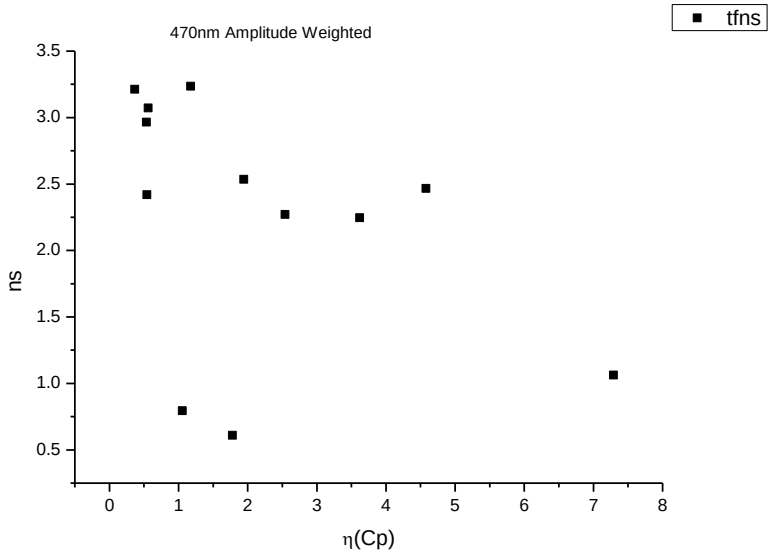

Figure 3.1.90. Amplitude weighted average lifetime (τ_f) of **16** at 470 nm versus η(Cp).

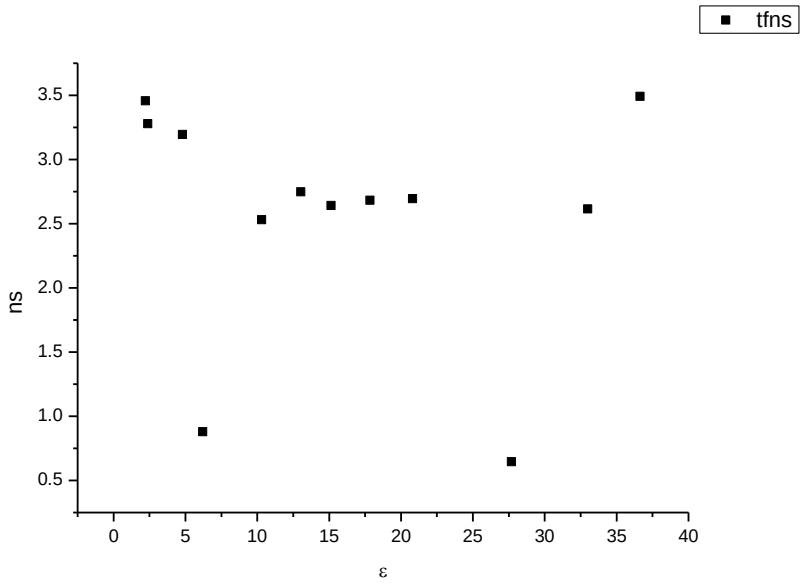

Figure 3.1.91. Intensity weighted average lifetime (τ_f) of **16** at 470 nm versus ε.

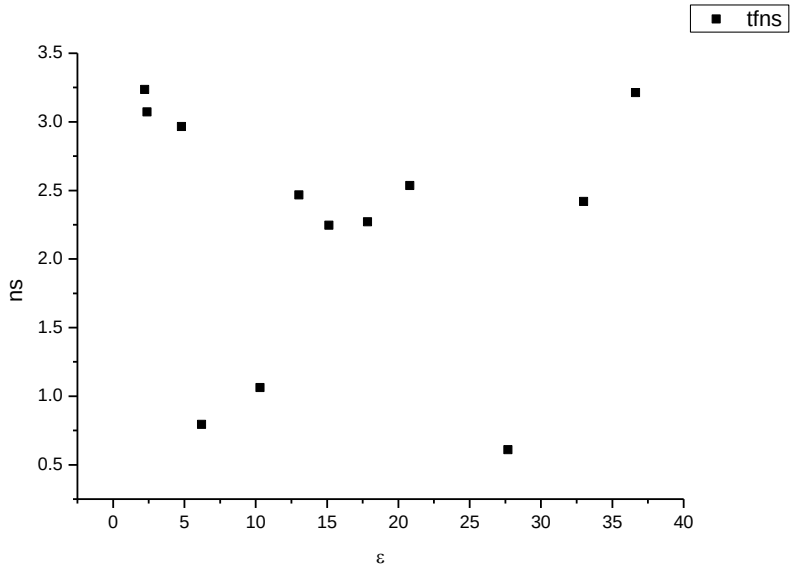

Figure 3.1.92. Amplitude weighted average lifetime (τ_f) of **16** at 470 nm versus ε.

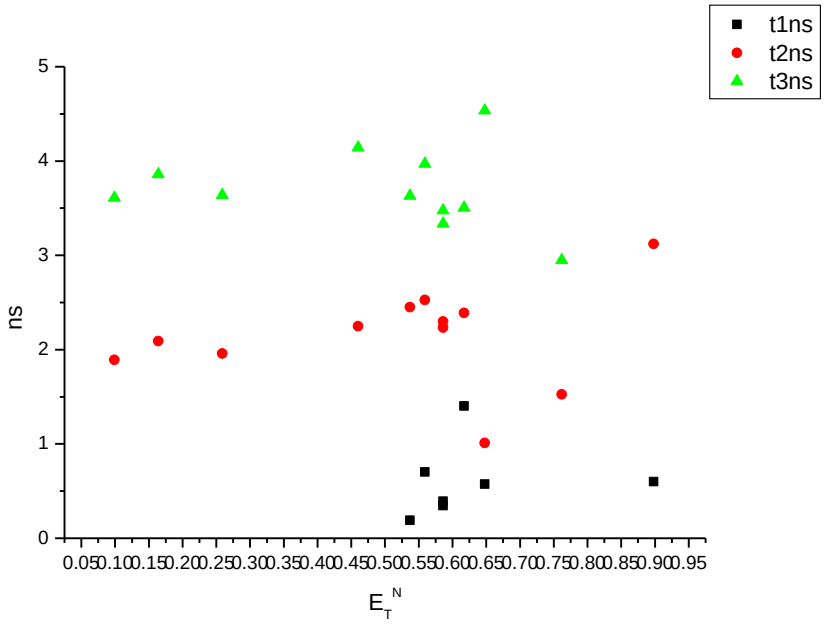

Figure 3.1.93. Intensity weighted components of TCSPC lifetime decay of **16** (470 nm) versus E_T^N.

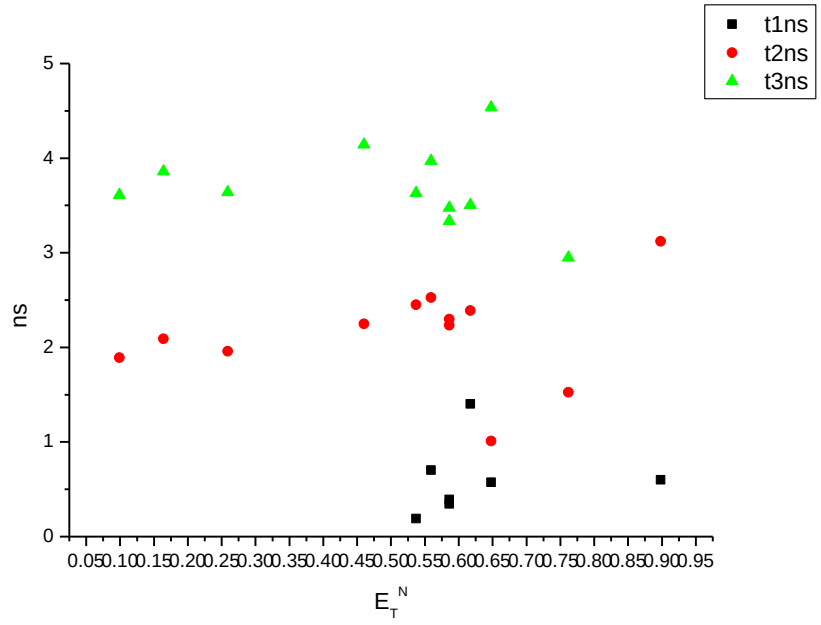

Figure 3.1.94. Amplitude weighted components of TCSPC lifetime decay of **16** (470 nm) versus E_T^N.

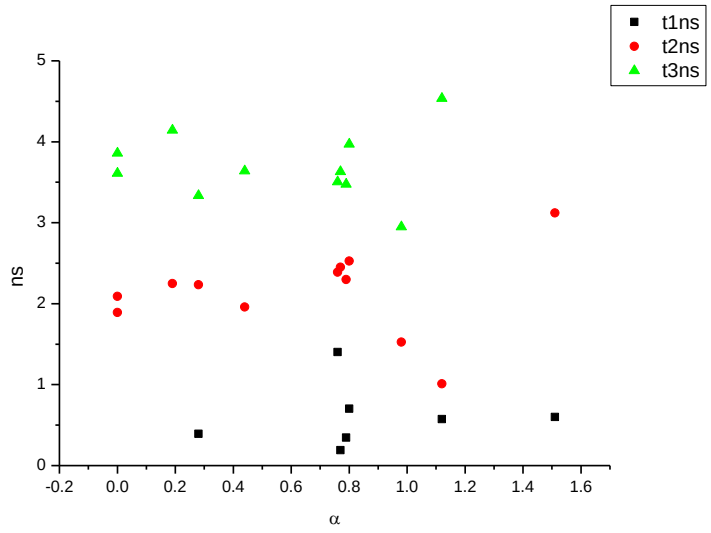

Figure 3.1.95. Intensity weighted components of TCSPC lifetime decay of **16** (470 nm) versus α.

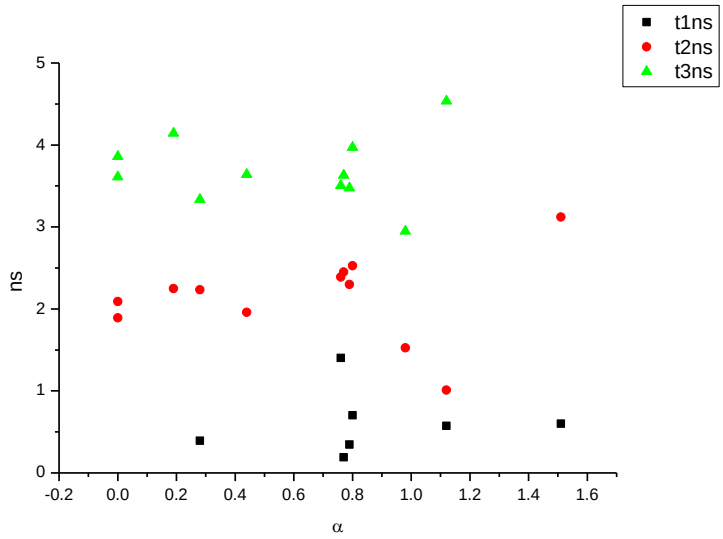

Figure 3.1.96. Amplitude weighted components of TCSPC lifetime decay of **16** (470 nm) versus α.

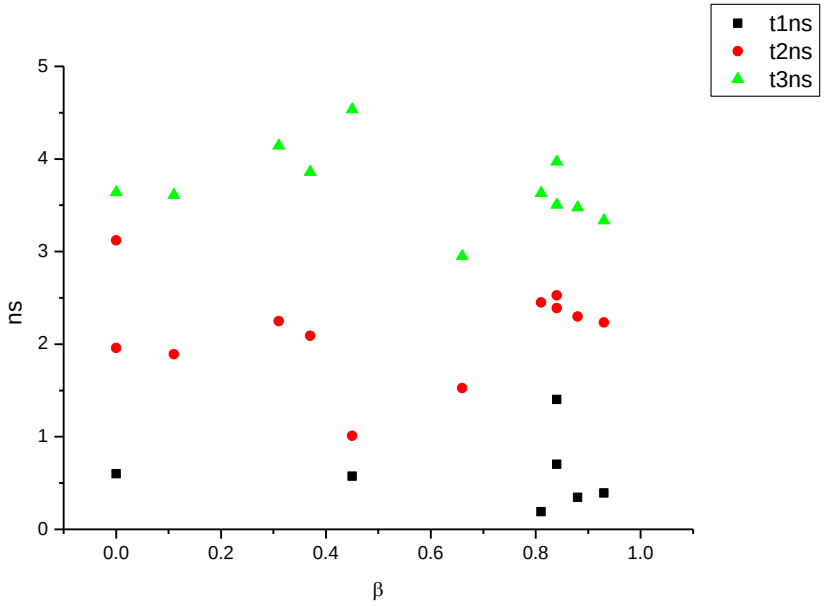

Figure 3.1.97. Intensity weighted components of TCSPC lifetime decay of **16** (470 nm) versus β.

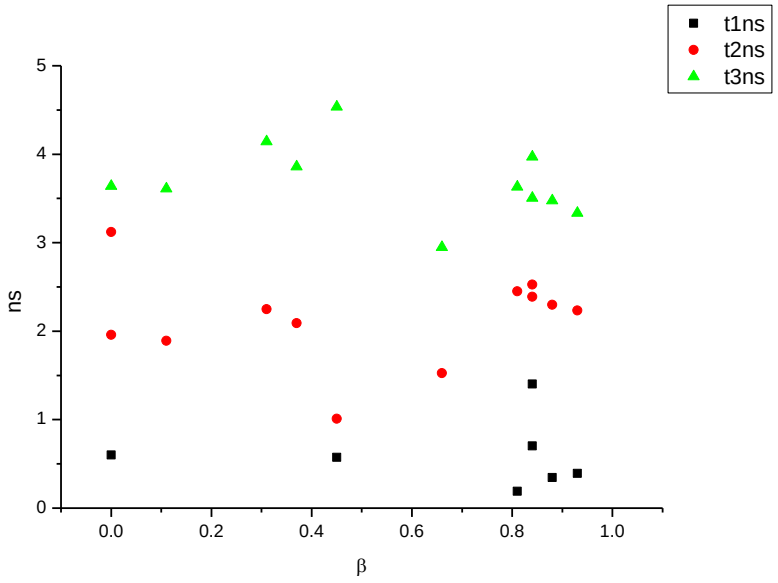

Figure 3.1.98. Amplitude weighted components of TCSPC lifetime decay of **16** (470 nm) versus β.

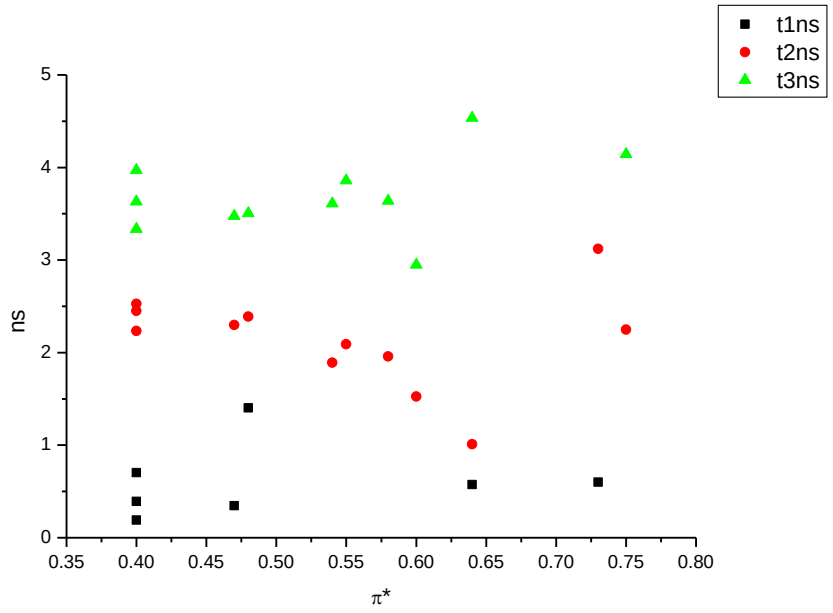

Figure 3.1.99. Intensity weighted components of TCSPC lifetime decay of **16** (470 nm) versus π*.

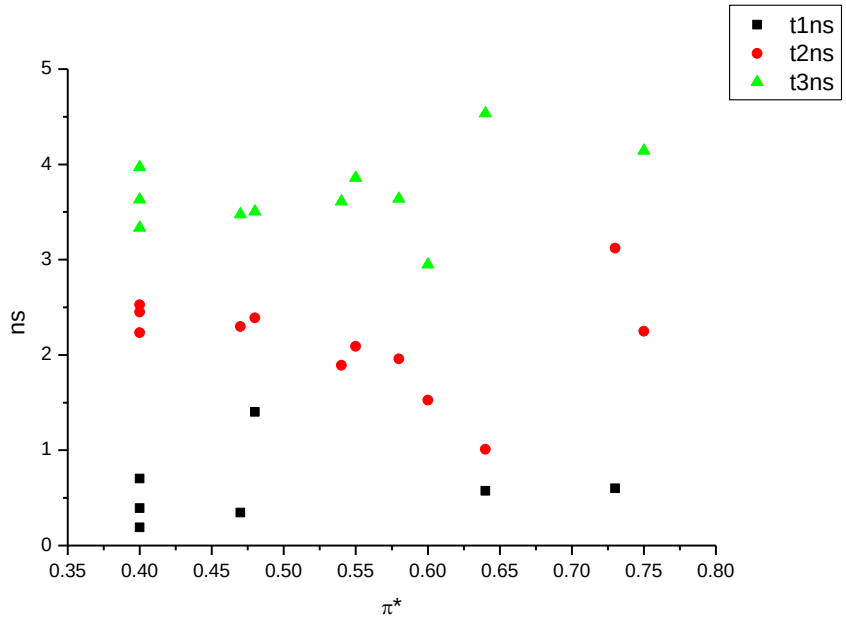

Figure 3.1.100. Amplitude weighted components of TCSPC lifetime decay of **16** (470 nm) versus π*.

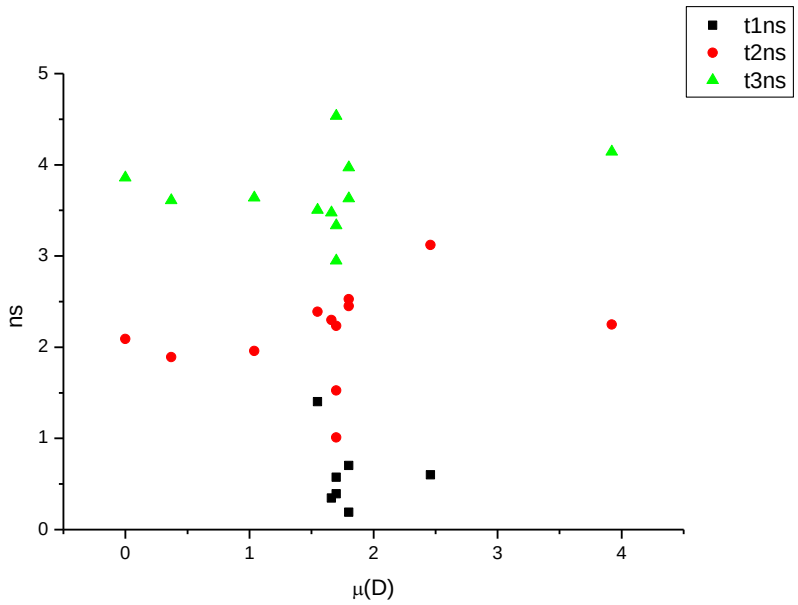

Figure 3.1.101. Intensity weighted components of TCSPC lifetime decay of **16** (470 nm) versus μ(D).

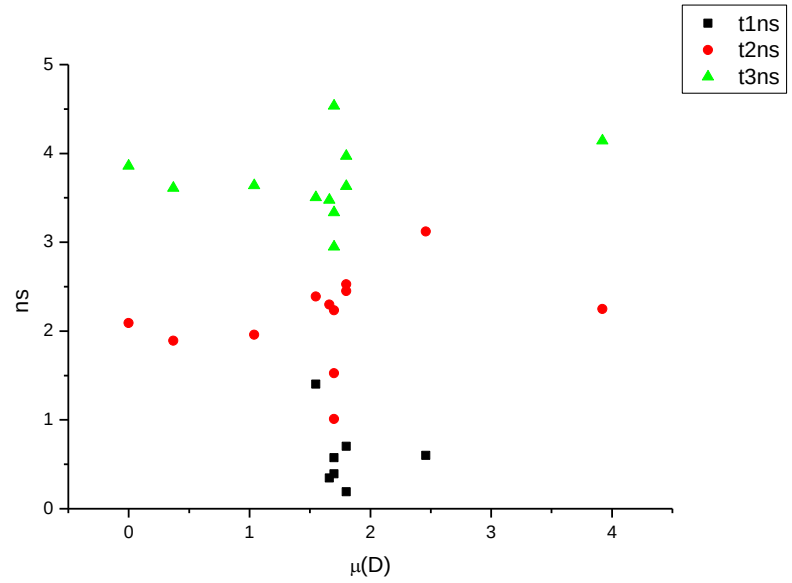

Figure 3.1.102. Amplitude weighted components of TCSPC lifetime decay of **16** (470 nm) versus μ(D).

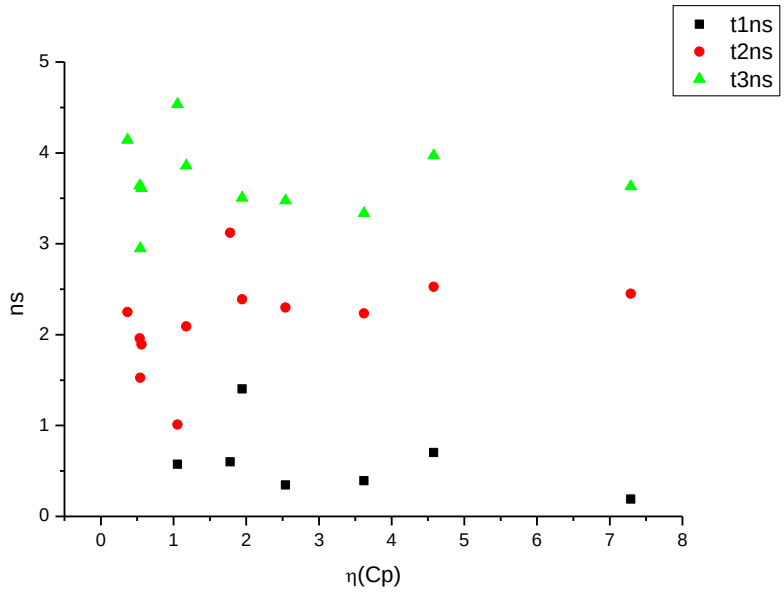

Figure 3.1.103. Intensity weighted components of TCSPC lifetime decay of **16** (470 nm) versus η(Cp).

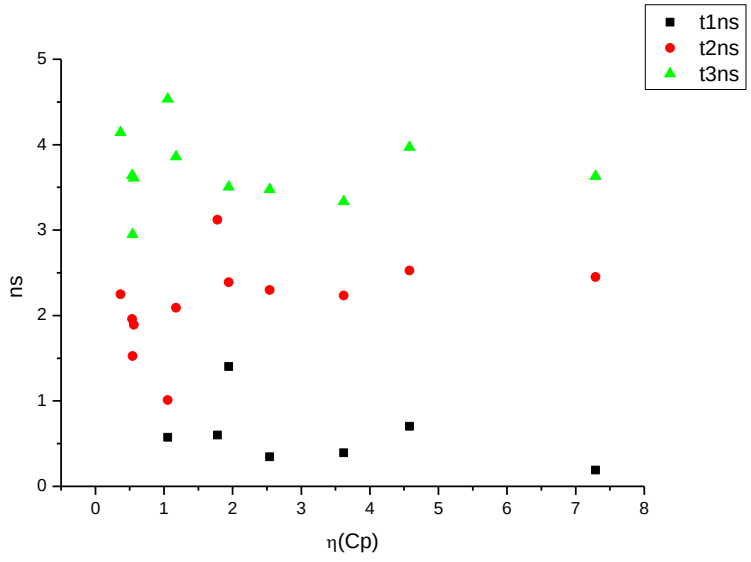

Figure 3.1.104. Amplitude weighted components of TCSPC lifetime decay of **16** (470 nm) versus η(Cp).

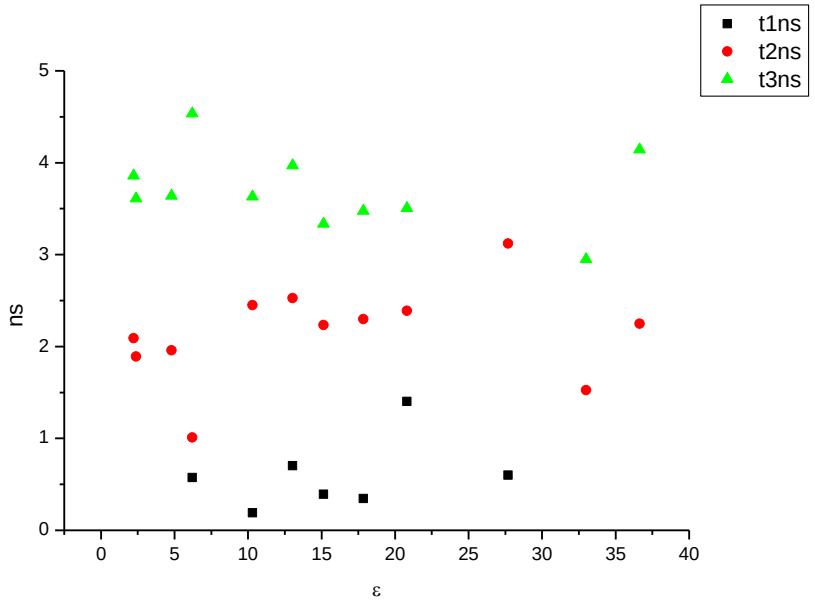

Figure 3.1.105. Intensity weighted components of TCSPC lifetime decay of **16** (470 nm) versus ε.

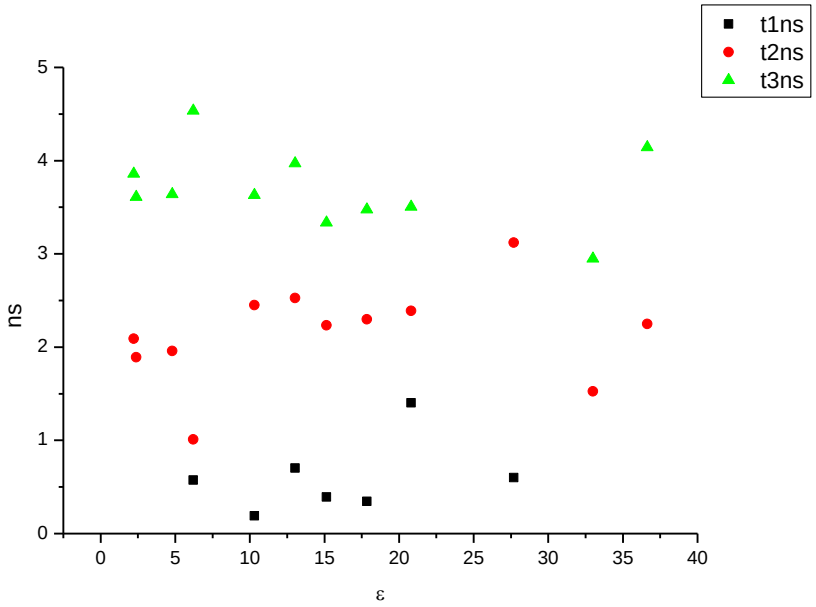

Figure 3.1.106. Amplitude weighted components of TCSPC lifetime decay of **16** (470 nm) versus ε.

3.1.7.2 570 nm Lifetime – Solvatochromic analysis.

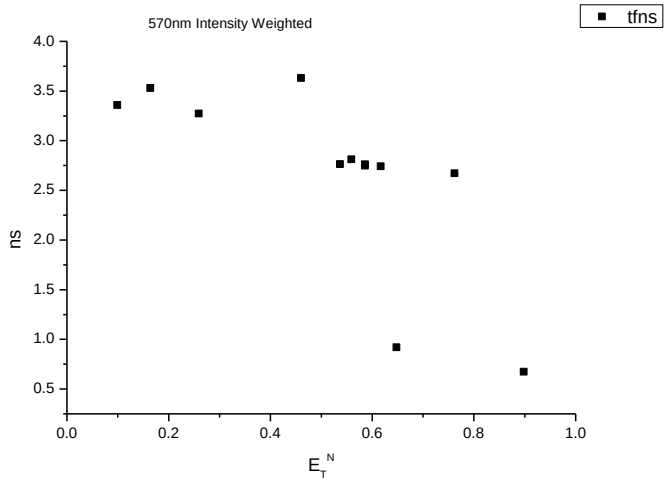

Figure 3.1.107. Intensity weighted average lifetime (τ_f) of **16** at 570 nm versus E_T^N.

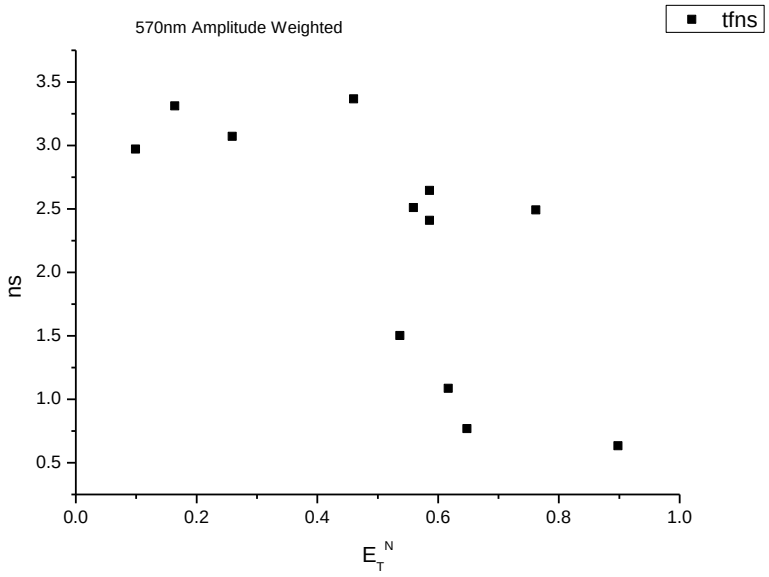

Figure 3.1.108. Amplitude weighted average lifetime (τ_f) of **16** at 570 nm versus E_T^N.

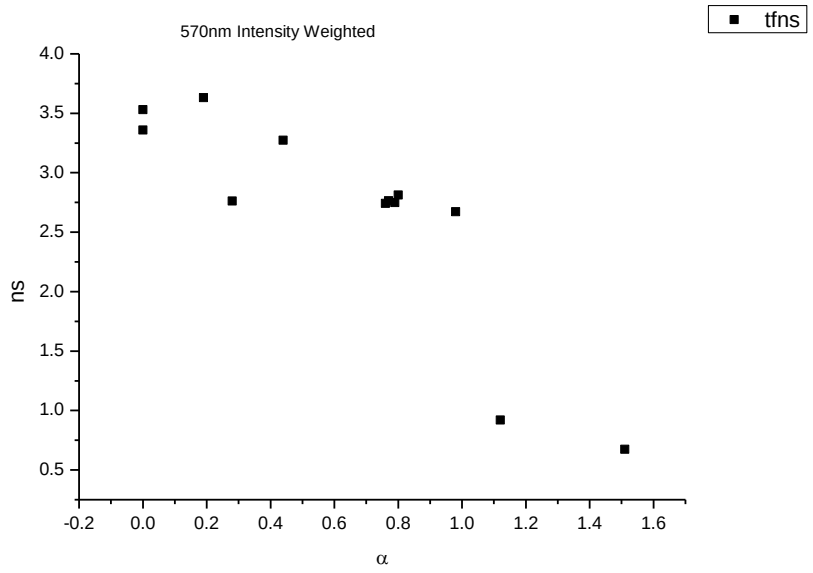

Figure 3.1.109. Intensity weighted average lifetime (τ_f) of **16** at 570 nm versus α.

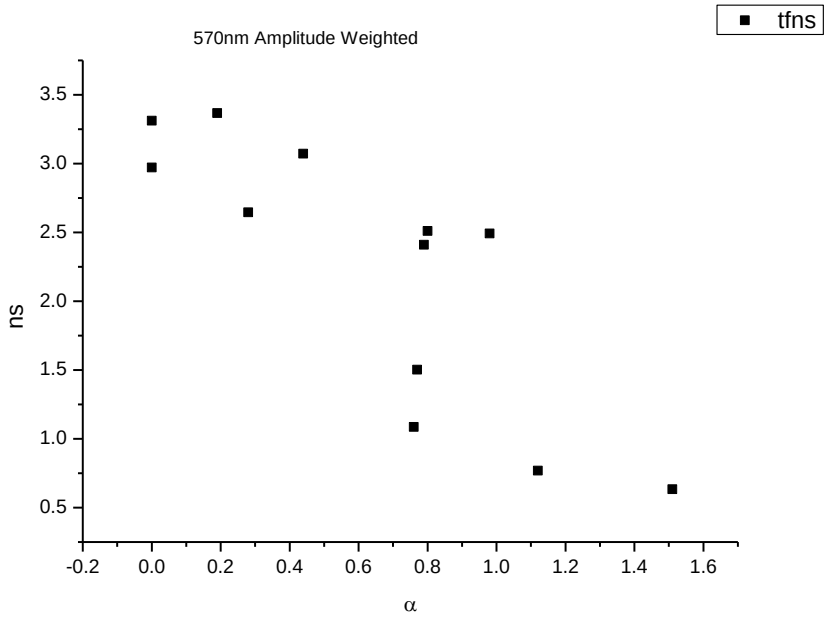

Figure 3.1.110. Amplitude weighted average lifetime (τ_f) of **16** at 570 nm versus α.

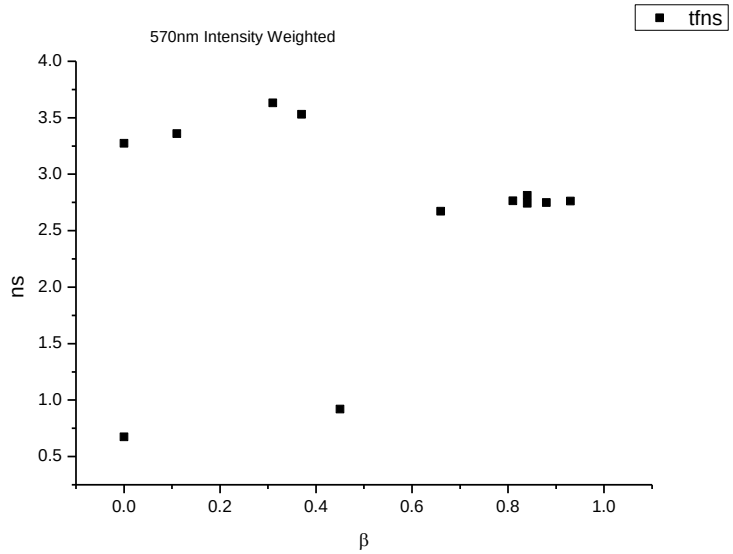

Figure 3.1.111. Intensity weighted average lifetime (τ_f) of **16** at 570 nm versus β.

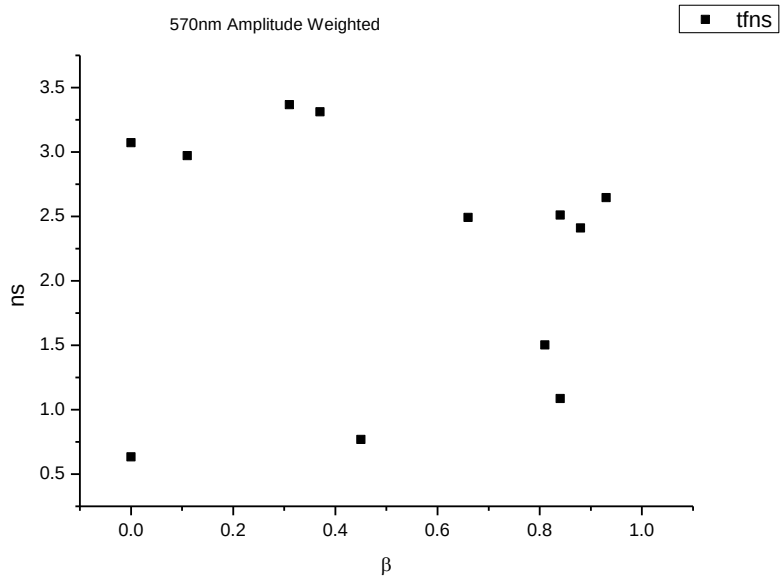

Figure 3.1.112. Amplitude weighted average lifetime (τ_f) of **16** at 570 nm versus β.

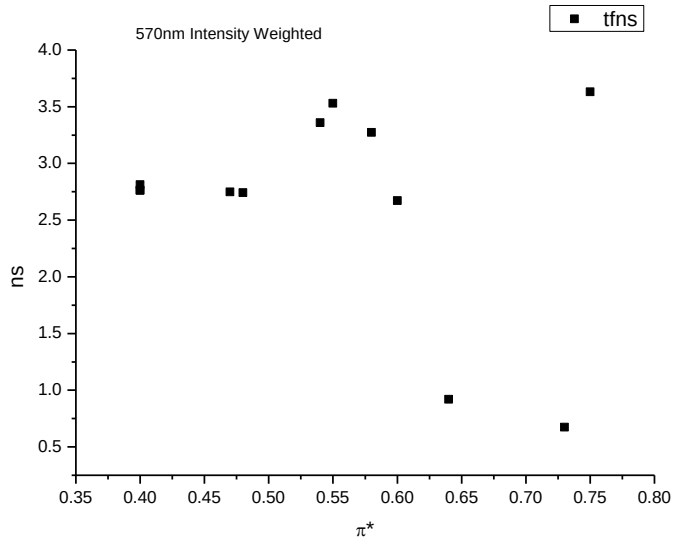

Figure 3.1.113. Intensity weighted average lifetime (τ_f) of **16** at 570 nm versus π*.

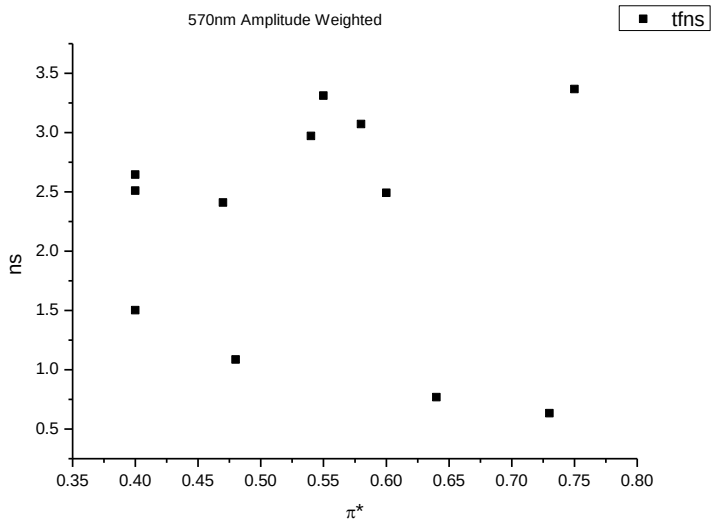

Figure 3.1.114. Amplitude weighted average lifetime (τ_f) of **16** at 570 nm versus π*.

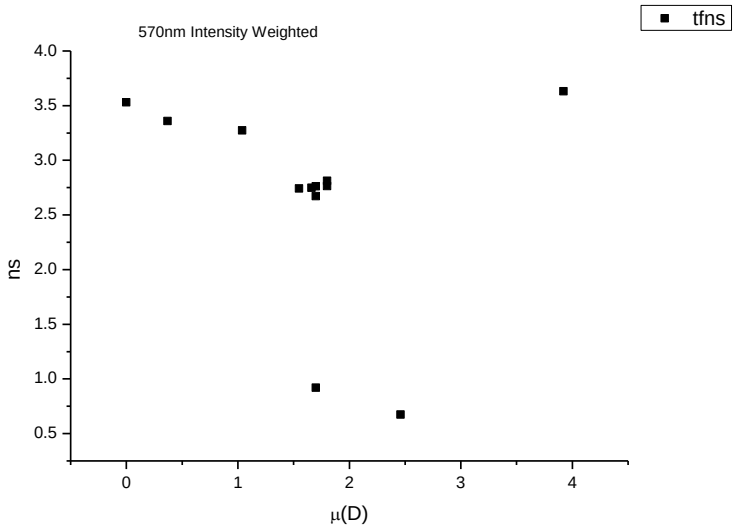

Figure 3.1.115. Intensity weighted average lifetime (τ_f) of **16** at 570 nm versus μ(D).

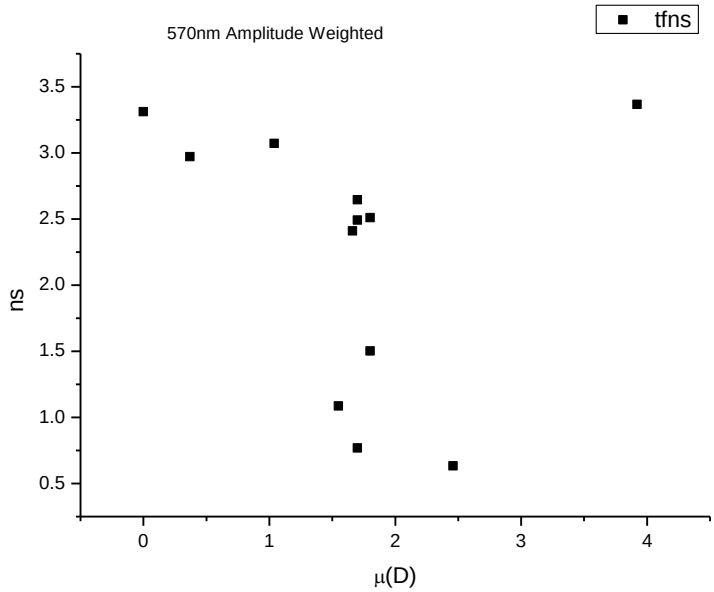

Figure 3.1.116. Amplitude weighted average lifetime (τ_f) of **16** at 570 nm versus μ(D).

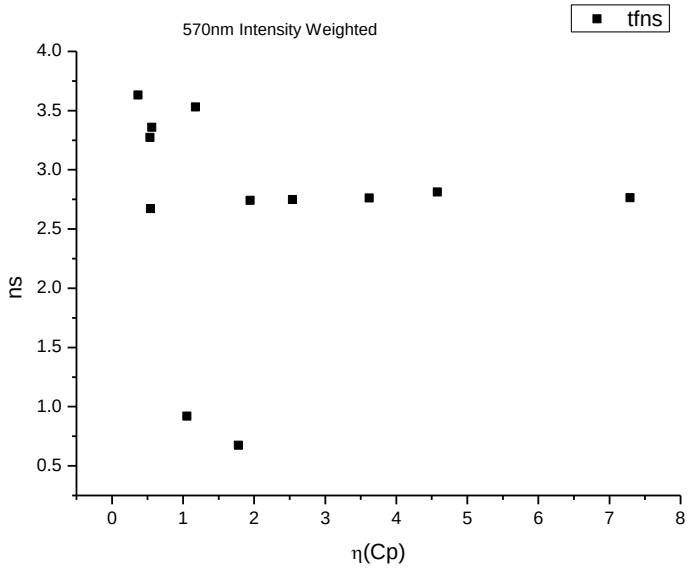

Figure 3.1.117. Intensity weighted average lifetime (τ_f) of **16** at 570 nm versus η(Cp).

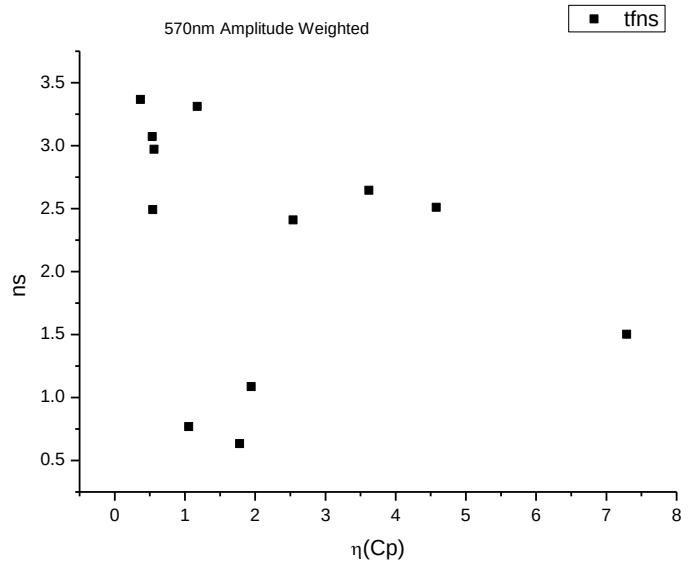

Figure 3.1.118. Amplitude weighted average lifetime (τ_f) of **16** at 570 nm versus η(Cp).

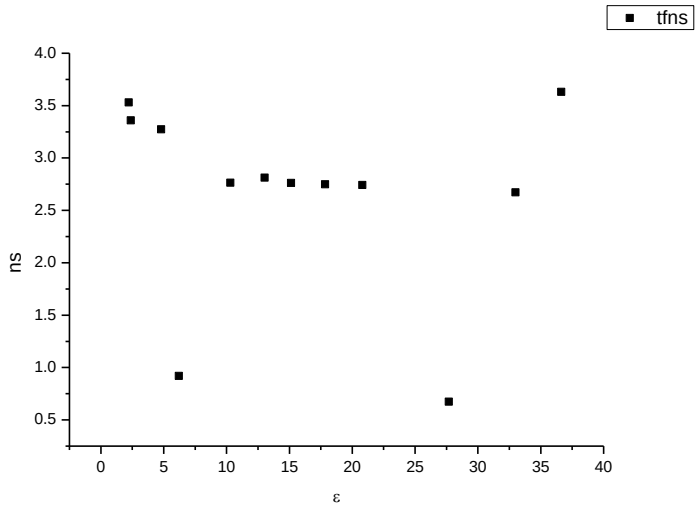

Figure 3.1.119. Intensity weighted average lifetime (τ_f) of **16** at 570 nm versus ε.

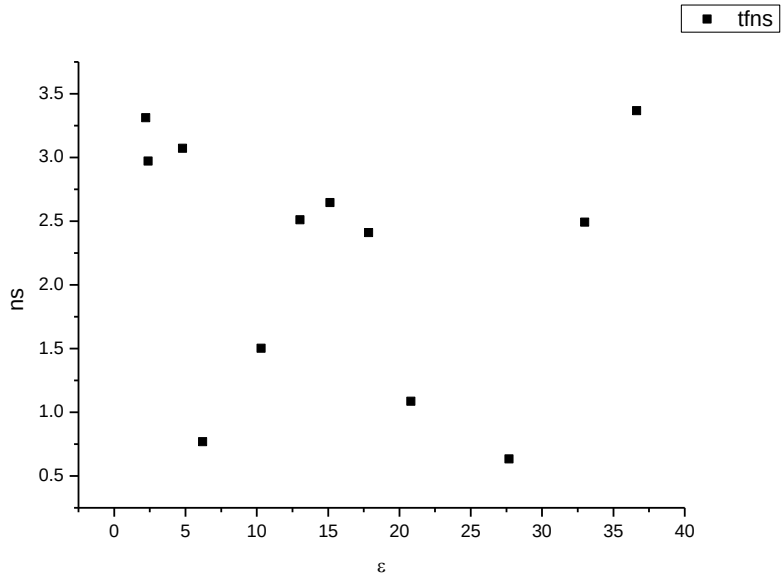

Figure 3.1.120. Amplitude weighted average lifetime (τ_f) of **16** at 570 nm versus ε.

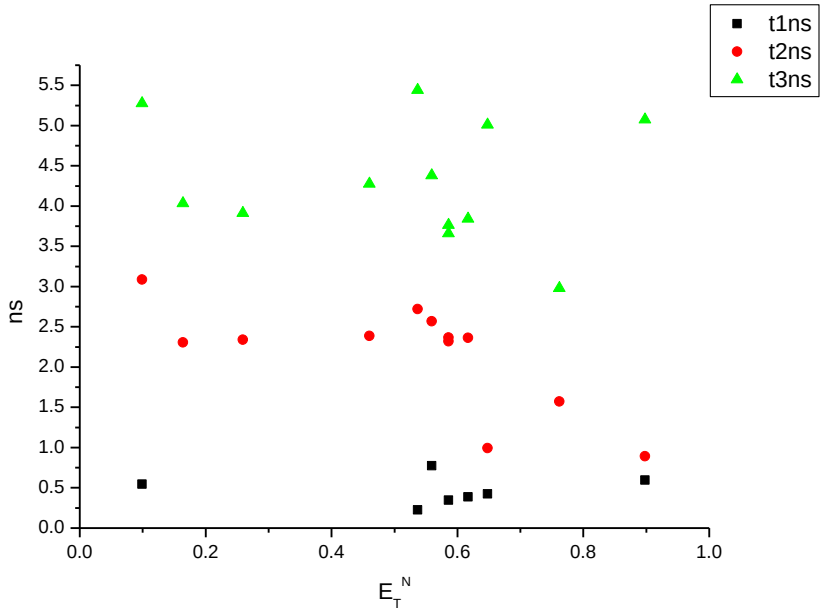

Figure 3.1.121. Intensity weighted components of TCSPC lifetime decay of **16** (570 nm) versus E_T^N.

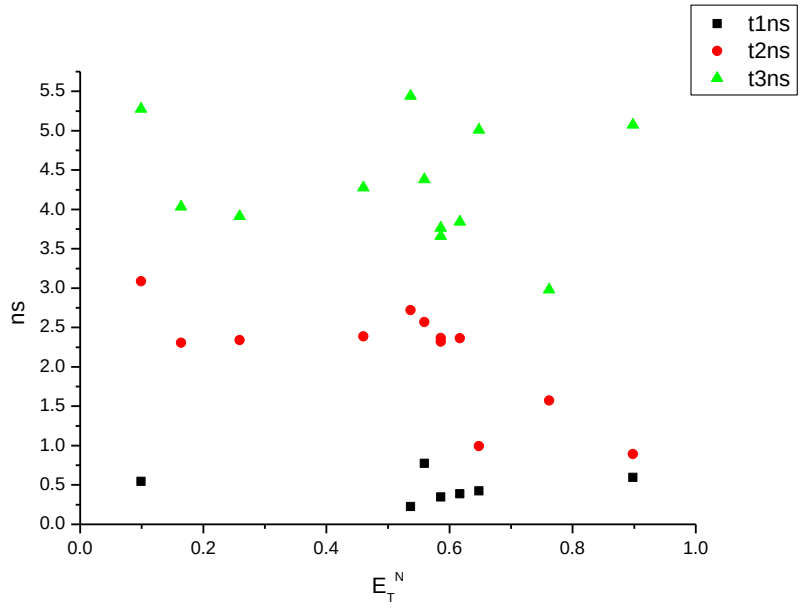

Figure 3.1.122. Amplitude weighted components of TCSPC lifetime decay of **16** (570 nm) versus E_T^N.

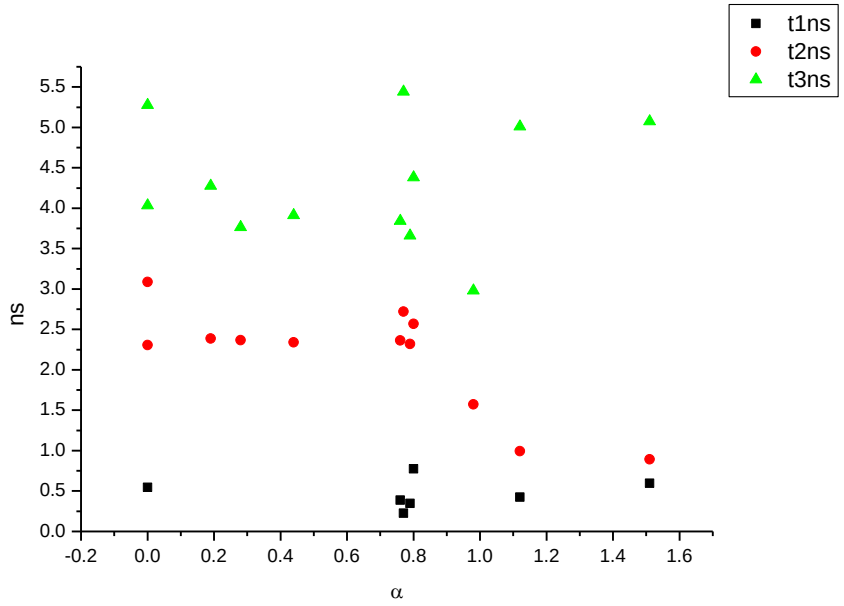

Figure 3.1.123. Intensity weighted components of TCSPC lifetime decay of **16** (570 nm) versus α.

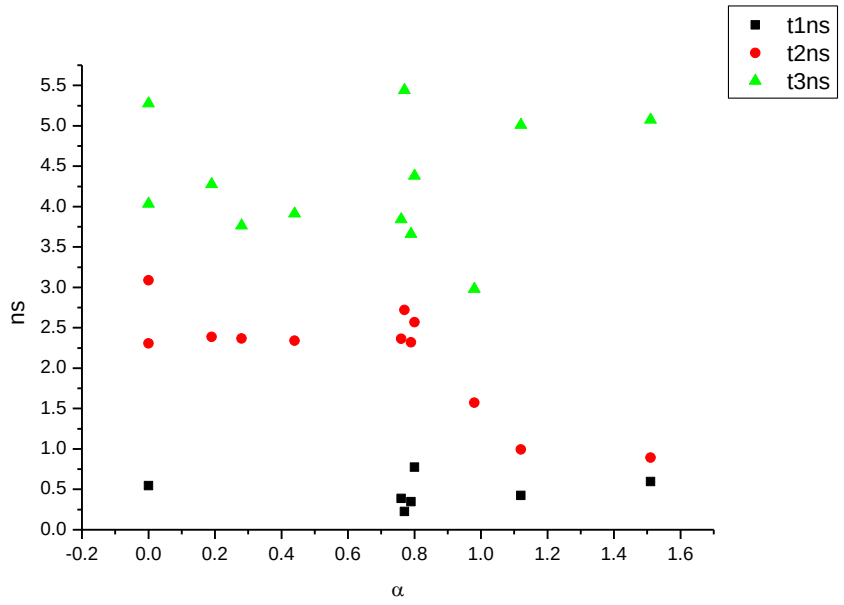

Figure 3.1.124. Amplitude weighted components of TCSPC lifetime decay of **16** (570 nm) versus α.

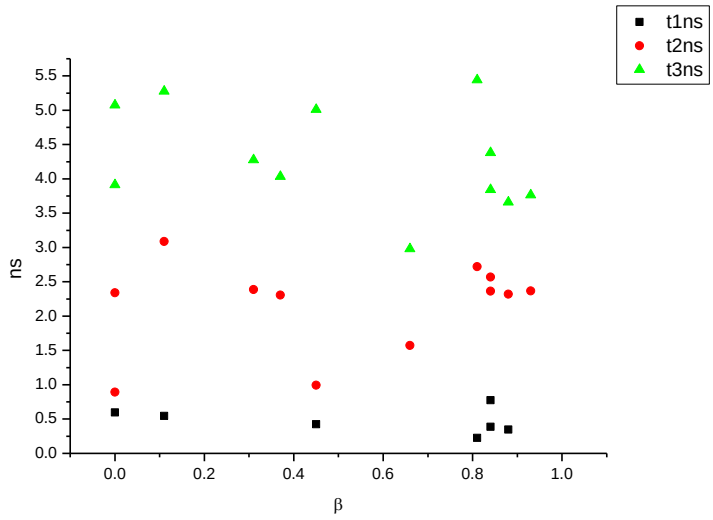

Figure 3.1.125. Intensity weighted components of TCSPC lifetime decay of **16** (570 nm) versus β.

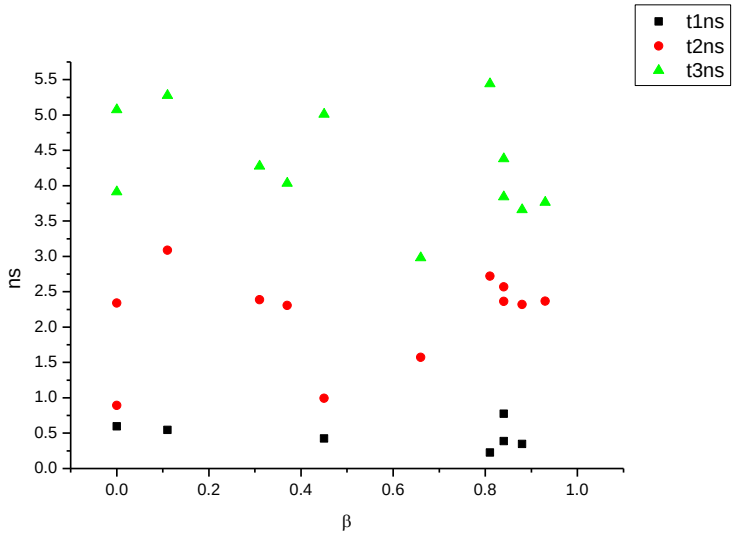

Figure 3.1.126. Amplitude weighted components of TCSPC lifetime decay of **16** (570 nm) versus β.

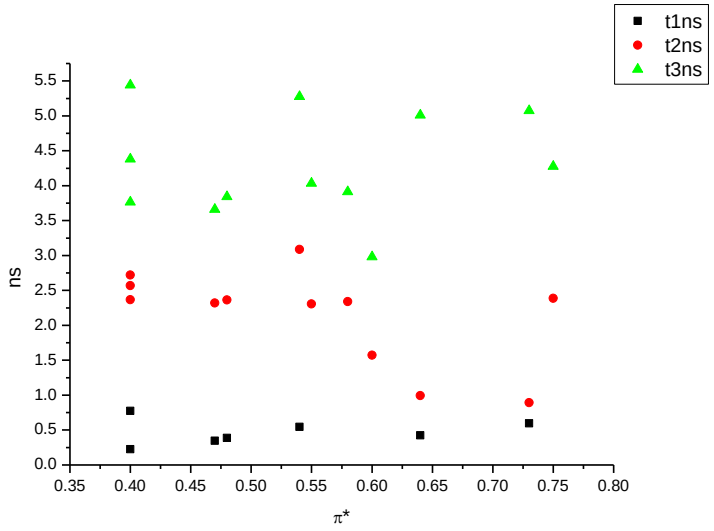

Figure 3.1.127. Intensity weighted components of TCSPC lifetime decay of **16** (570 nm) versus π*.

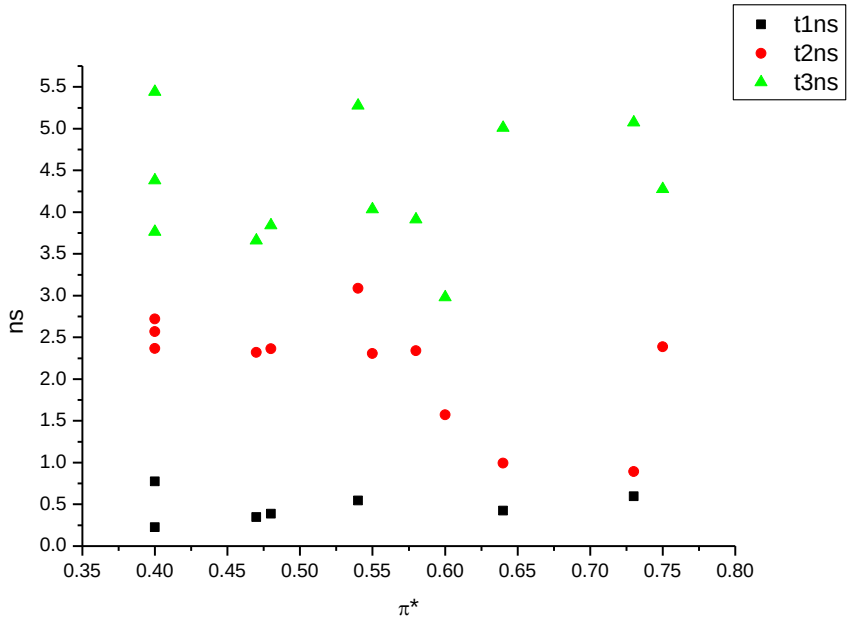

Figure 3.1.128. Amplitude weighted components of TCSPC lifetime decay of **16** (570 nm) versus π*.

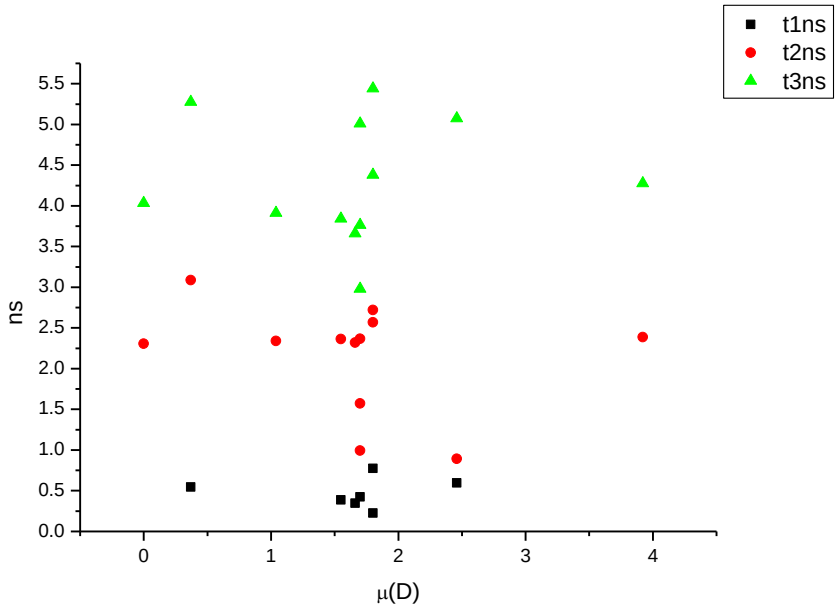

Figure 3.1.129. Intensity weighted components of TCSPC lifetime decay of **16** (570 nm) versus μ(D).

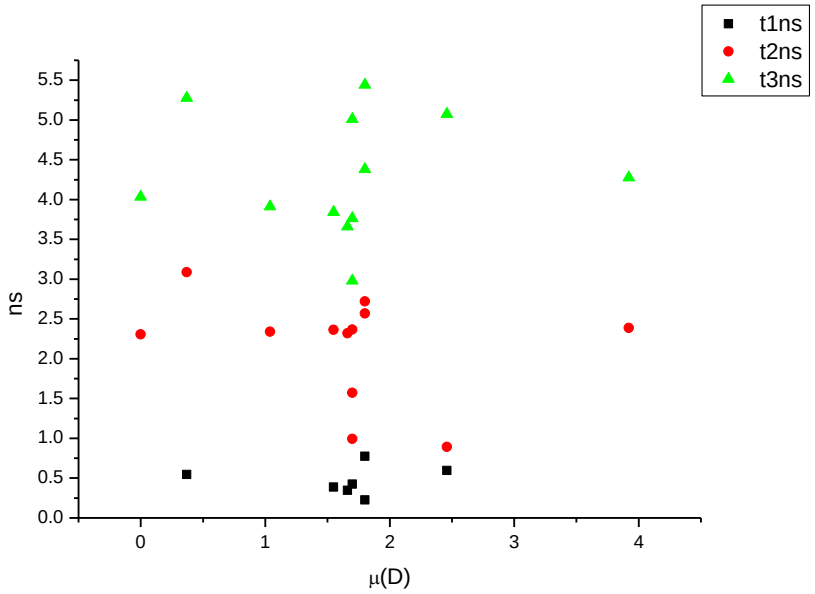

Figure 3.1.130. Amplitude weighted components of TCSPC lifetime decay of **16** (570 nm) versus μ(D).

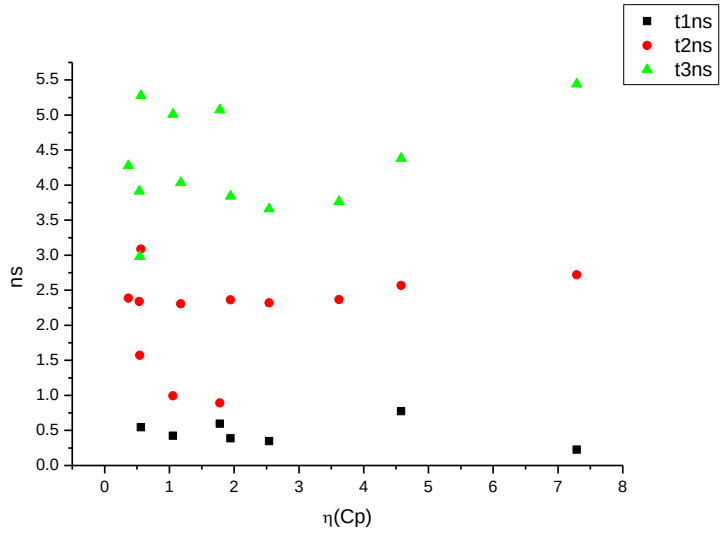

Figure 3.1.131. Intensity weighted components of TCSPC lifetime decay of **16** (570 nm) versus η(Cp).

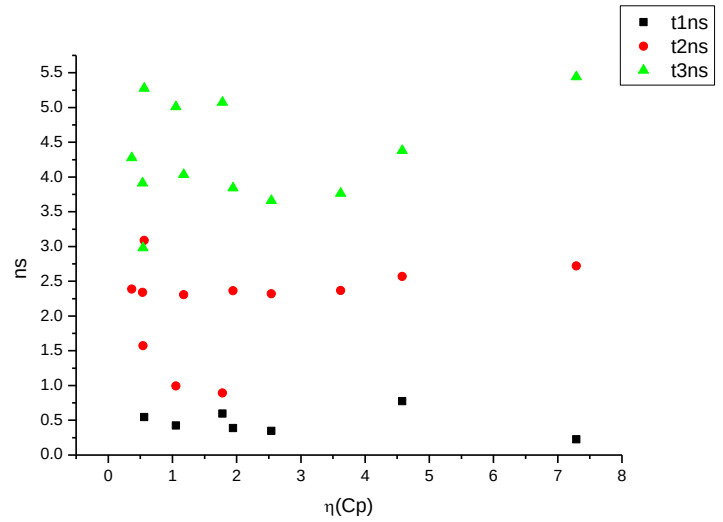

Figure 3.1.132. Amplitude weighted components of TCSPC lifetime decay of **16** (570 nm) versus η(Cp).

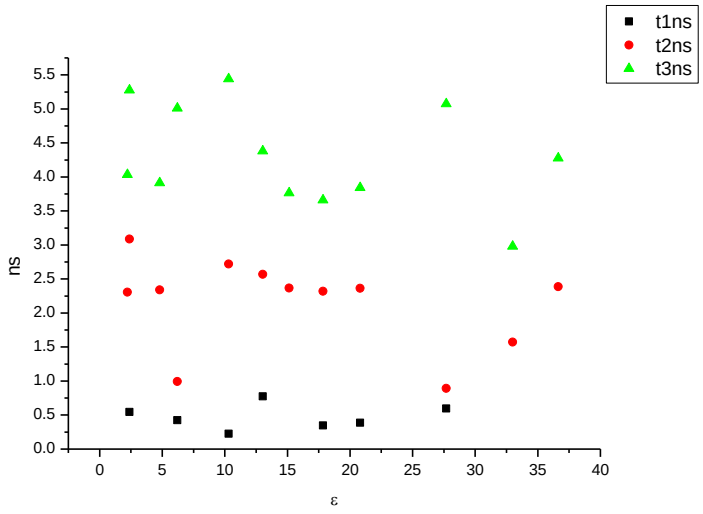

Figure 3.1.133. Intensity weighted components of TCSPC lifetime decay of **16** (570 nm) versus ε.

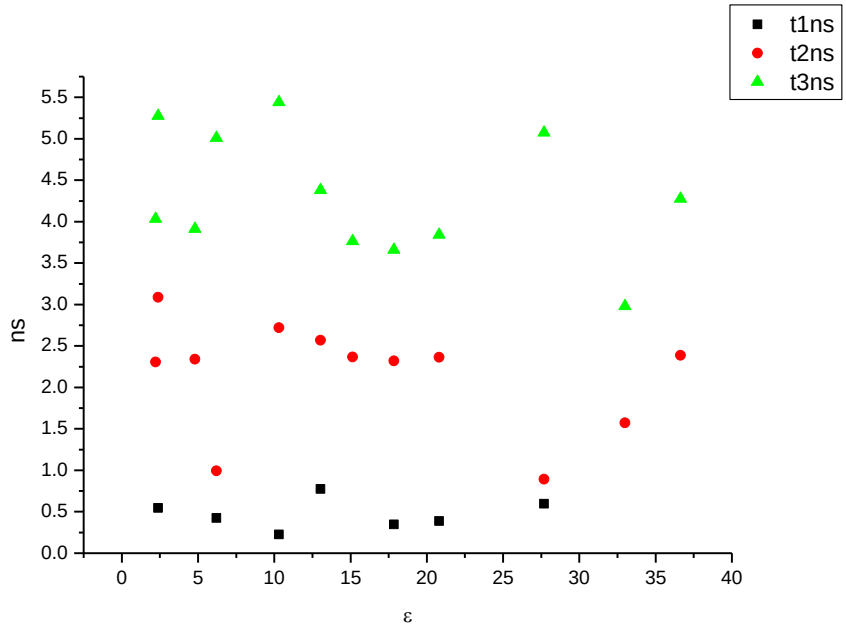

Figure 3.1.134. Amplitude weighted components of TCSPC lifetime decay of **16** (570 nm) versus ε.

3.1.8 Ultraviolet-visible absorption spectra.

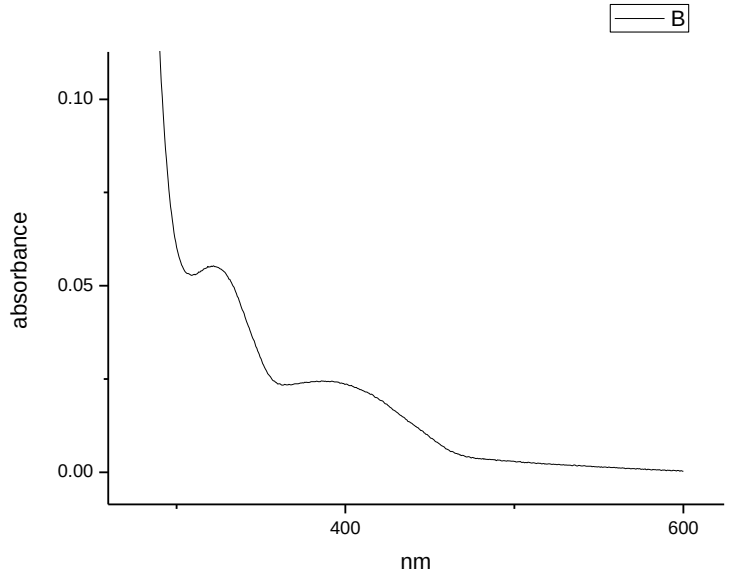

Figure 3.1.135. Ultraviolet-Visible absorption spectrum of **16** recorded in Toluene.

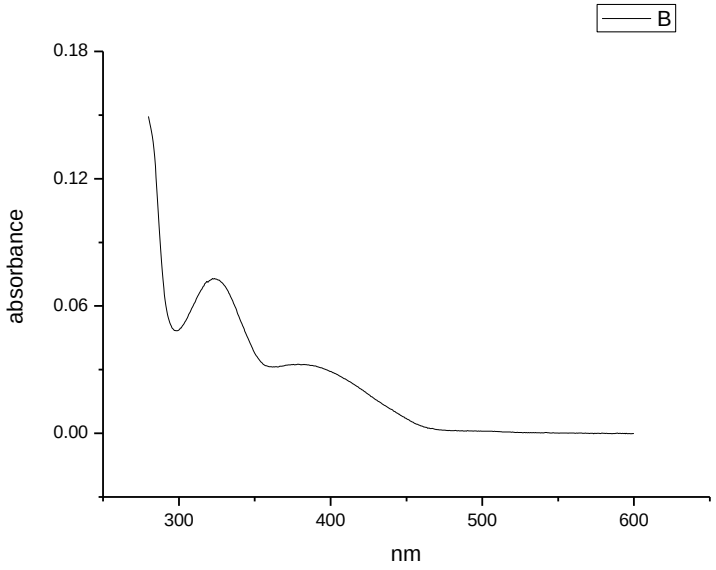

Figure 3.1.136. Ultraviolet-Visible absorption spectrum of **16** recorded in 1,4-dioxane.

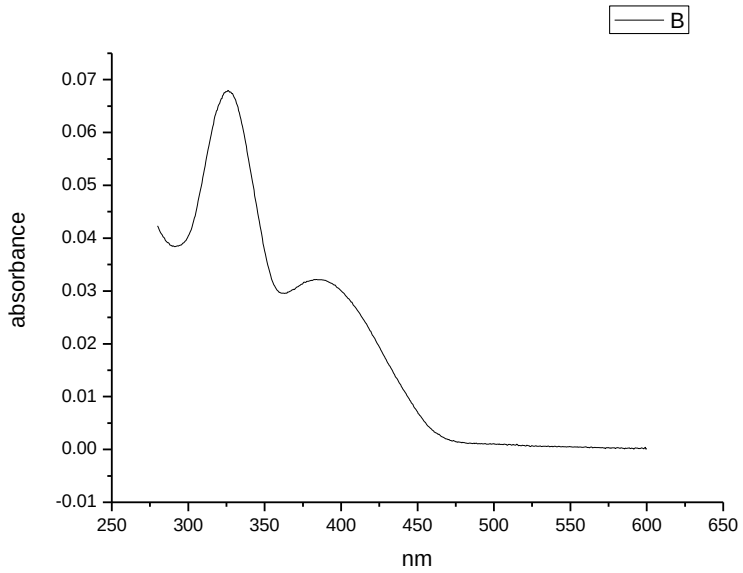

Figure 3.1.137. Ultraviolet-Visible absorption spectrum of **16** recorded in Chloroform.

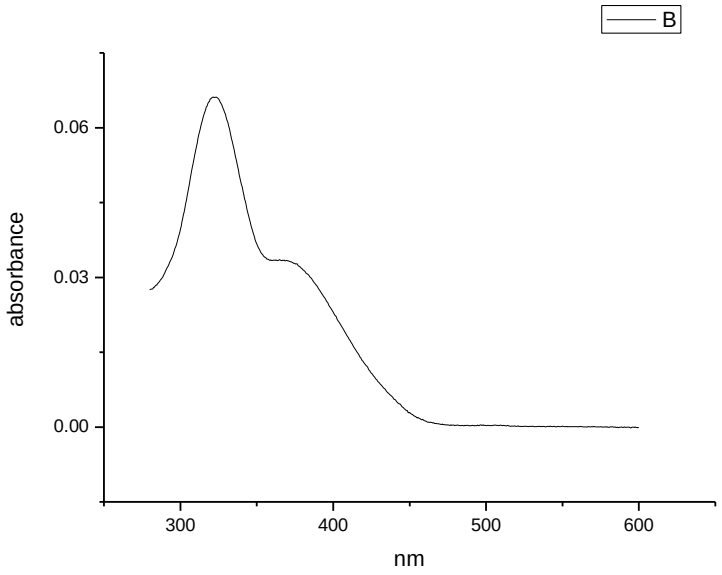

Figure 3.1.138. Ultraviolet-Visible absorption spectrum of **16** recorded in Acetonitrile.

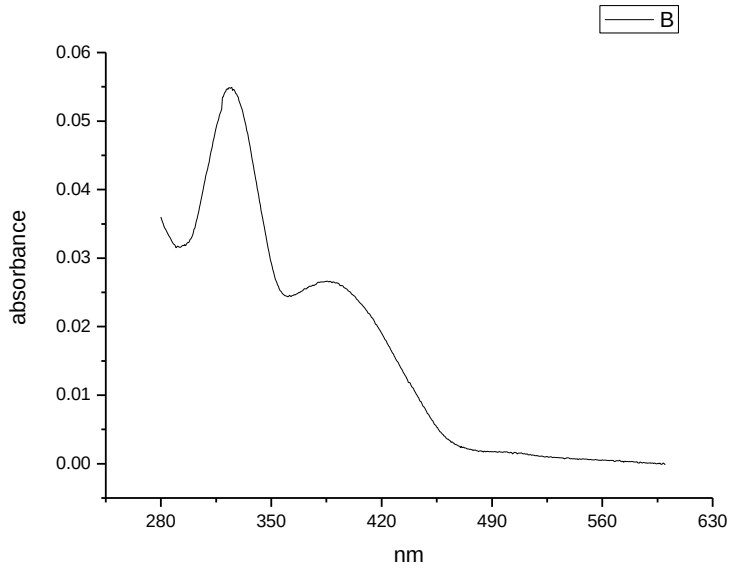

Figure 3.1.139. Ultraviolet-Visible absorption spectrum of **16** recorded in 1-octanol.

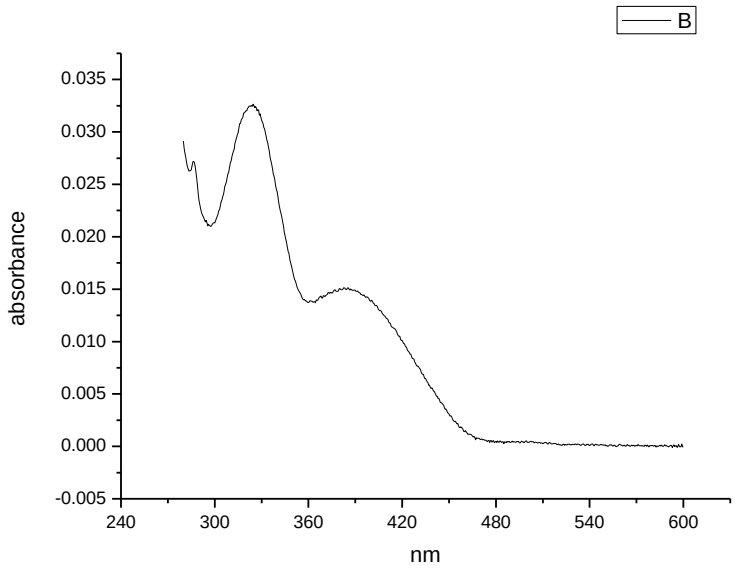

Figure 3.1.140. Ultraviolet-Visible absorption spectrum of **16** recorded in 1-hexanol.

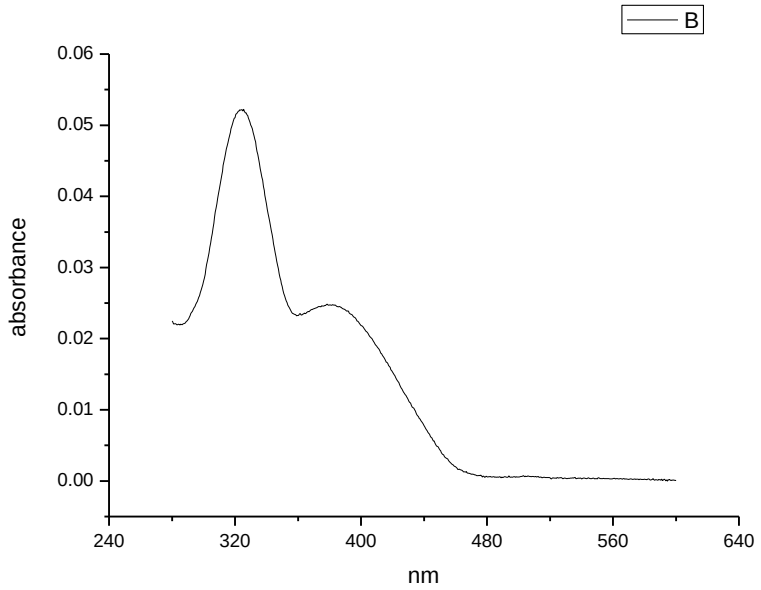

Figure 3.1.141. Ultraviolet-Visible absorption spectrum of **16** recorded in 1-butanol.

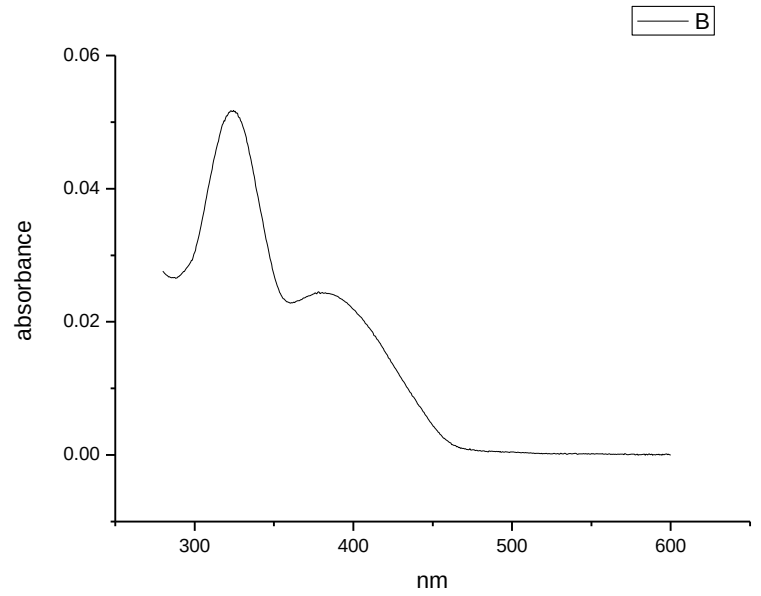

Figure 3.1.142. Ultraviolet-Visible absorption spectrum of **16** recorded in 1-pentanol.

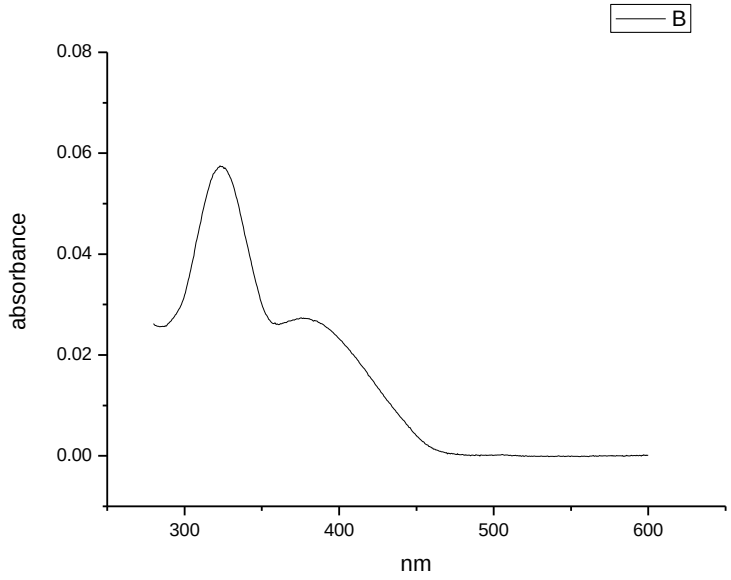

Figure 3.1.143. Ultraviolet-Visible absorption spectrum of **16** recorded in 1-propanol.

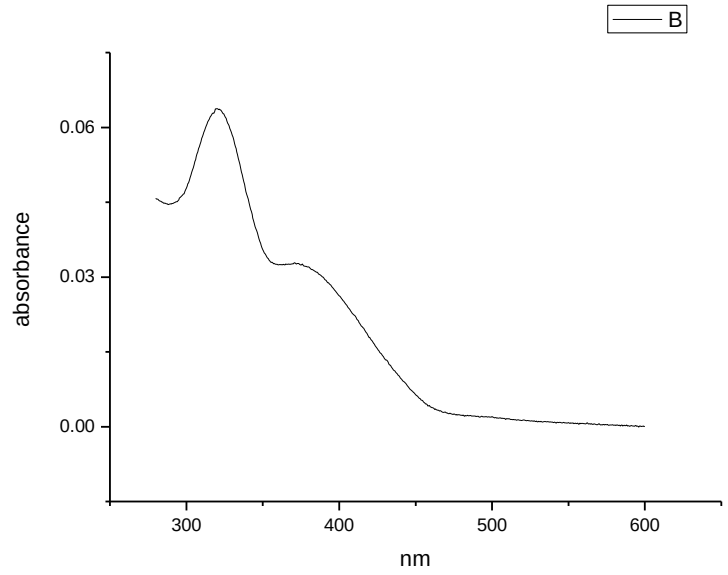

Figure 3.1.144. Ultraviolet-Visible absorption spectrum of **16** recorded in Acetic Acid.

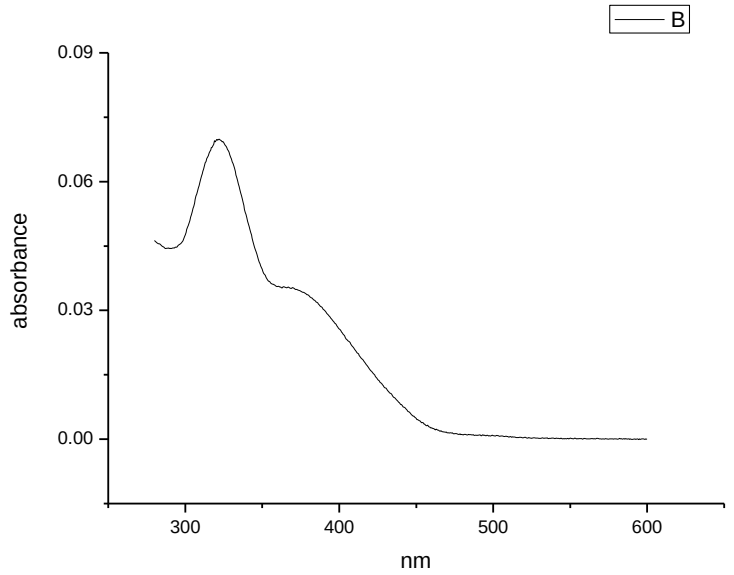

Figure 3.1.145. Ultraviolet-Visible absorption spectrum of **16** recorded in Methanol.

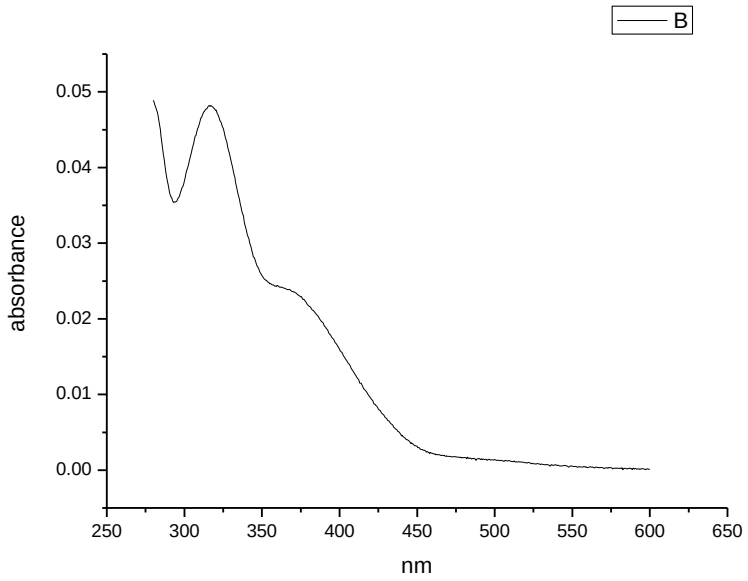

Figure 3.1.146. Ultraviolet-Visible absorption spectrum of **16** recorded in 2,2,2-trifluoroethanol.

3.1.9 Fluorescence Emission spectra.

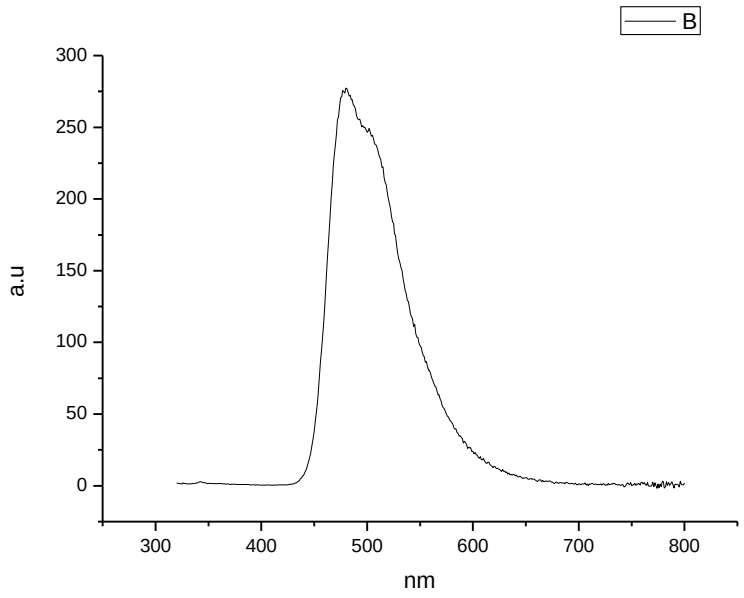

Figure 3.1.147. Fluorescence emission spectrum of **16** recorded in Toluene at 310 nm excitation.

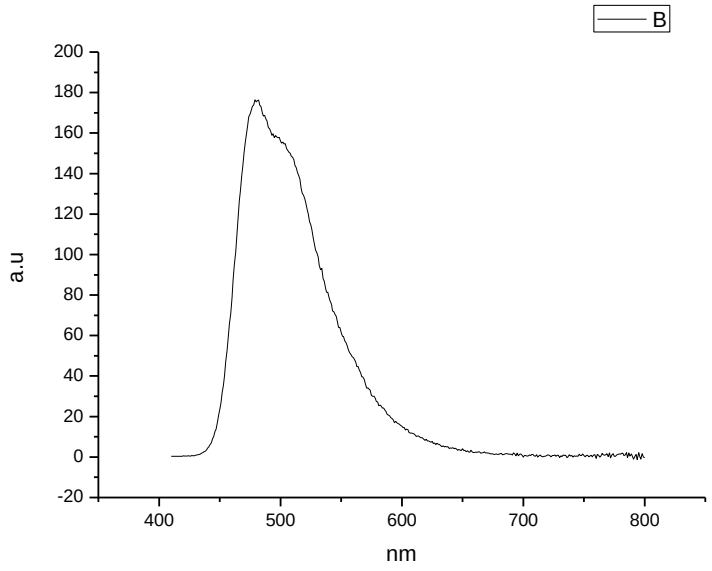

Figure 3.1.148. Fluorescence emission spectrum of **16** recorded in Toluene at 400 nm excitation.

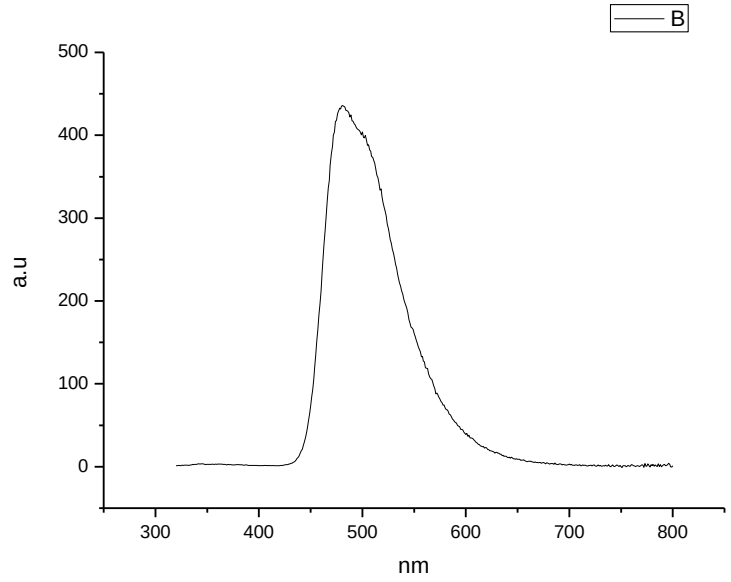

Figure 3.1.149. Fluorescence emission spectrum of **16** recorded in 1,4-dioxane at 310 nm excitation.

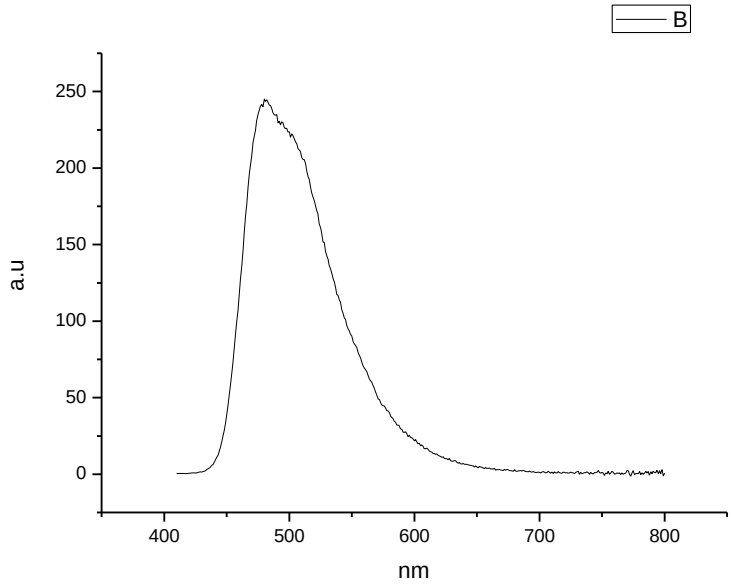

Figure 3.1.150. Fluorescence emission spectrum of **16** recorded in 1,4-dioxane at 400 nm excitation.

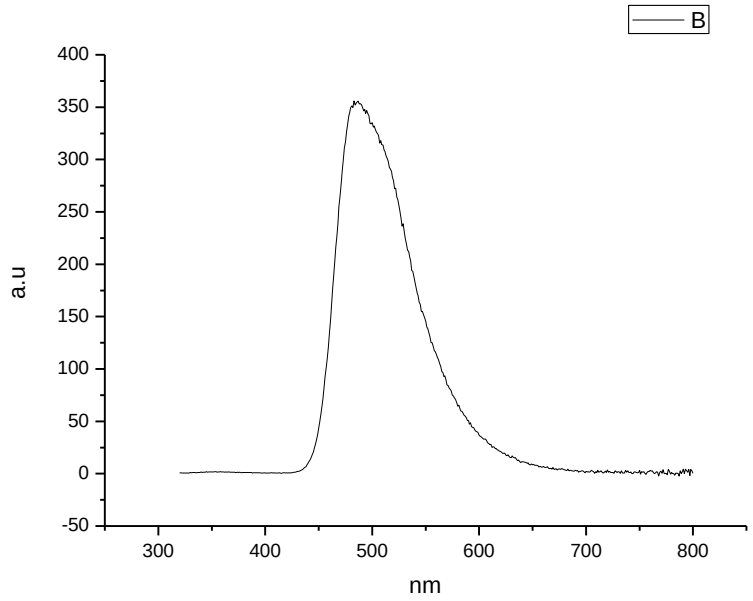

Figure 3.1.151. Fluorescence emission spectrum of **16** recorded in Chloroform at 310 nm excitation.

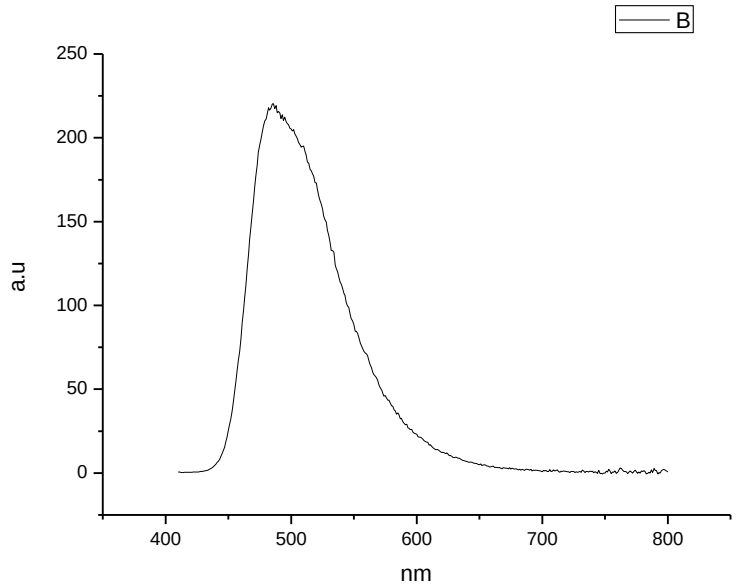

Figure 3.1.152. Fluorescence emission spectrum of **16** recorded in Chloroform at 400 nm excitation.

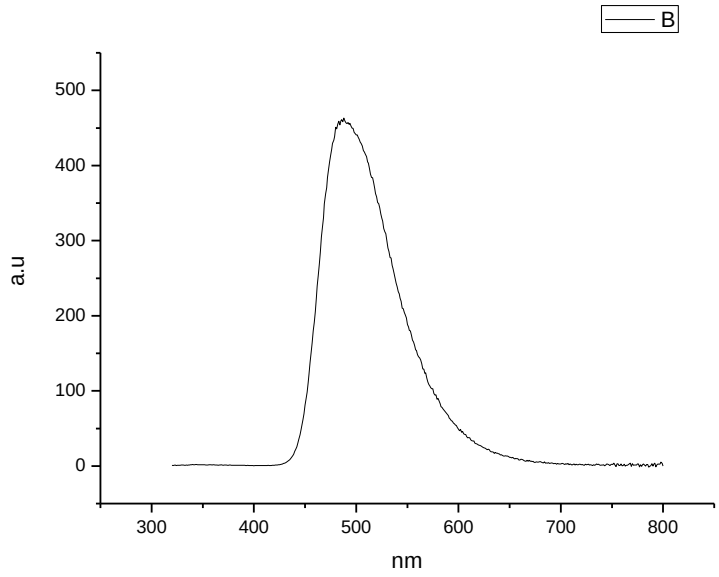

Figure 3.1.153. Fluorescence emission spectrum of **16** recorded in Acetonitrile at 310 nm excitation.

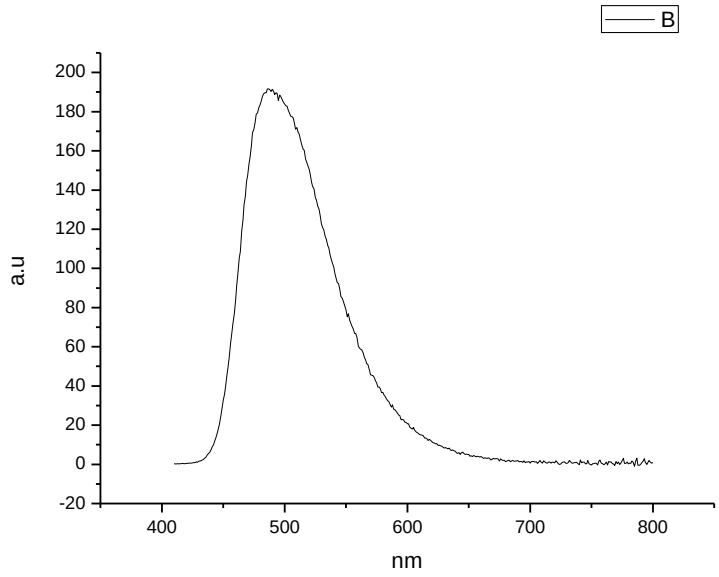

Figure 3.1.154. Fluorescence emission spectrum of **16** recorded in Acetonitrile at 400 nm excitation.

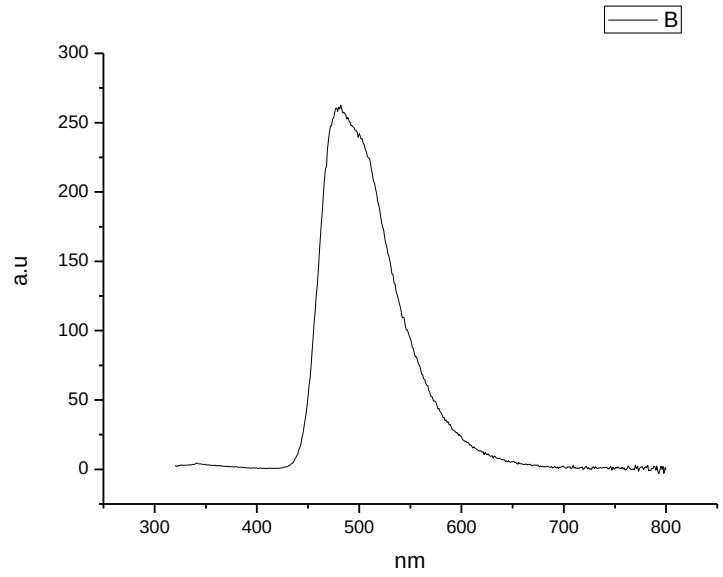

Figure 3.1.155. Fluorescence emission spectrum of **16** recorded in 1-octanol at 310 nm excitation.

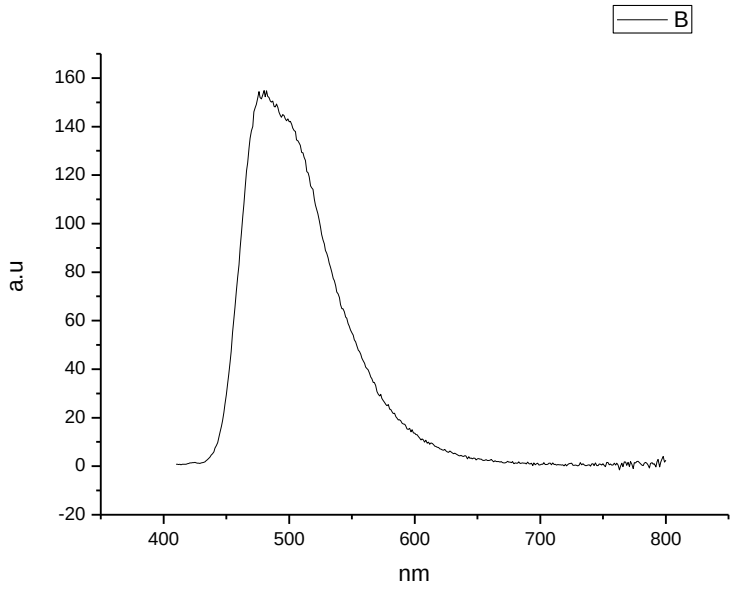

Figure 3.1.156. Fluorescence emission spectrum of **16** recorded in 1-octanol at 400 nm excitation.

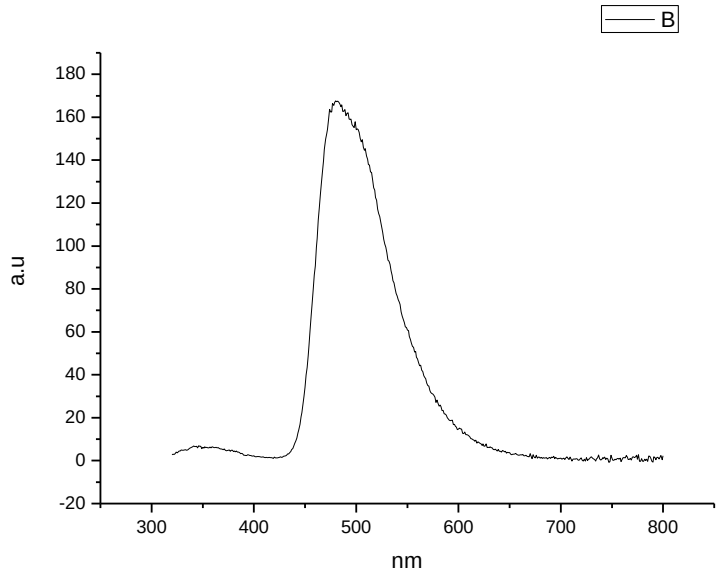

Figure 3.1.157. Fluorescence emission spectrum of **16** recorded in 1-hexanol at 310 nm excitation.

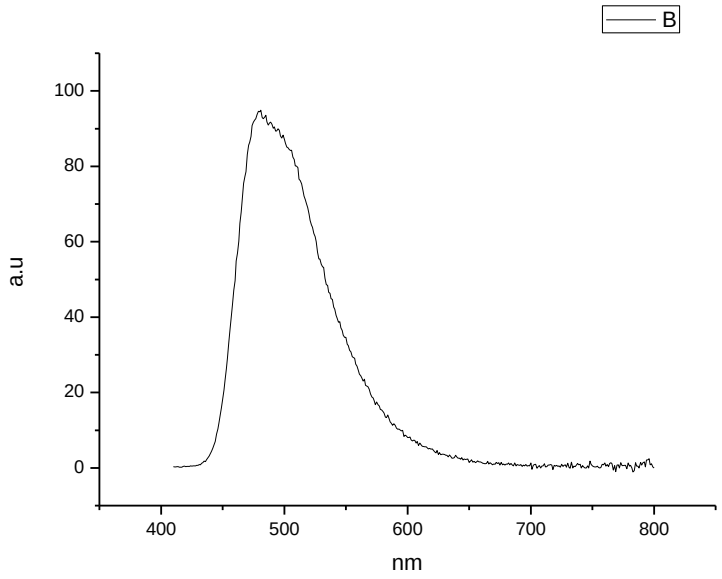

Figure 3.1.158. Fluorescence emission spectrum of **16** recorded in 1-hexanol at 400 nm excitation.

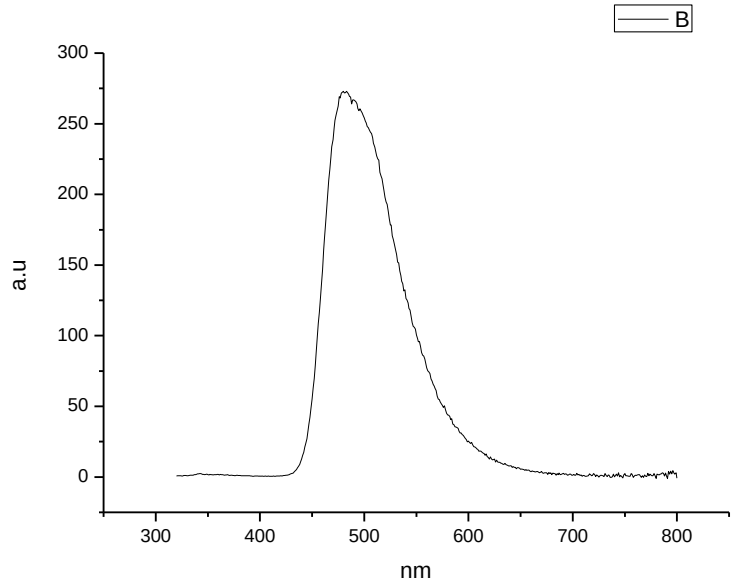

Figure 3.1.159. Fluorescence emission spectrum of **16** recorded in 1-butanol at 310 nm excitation.

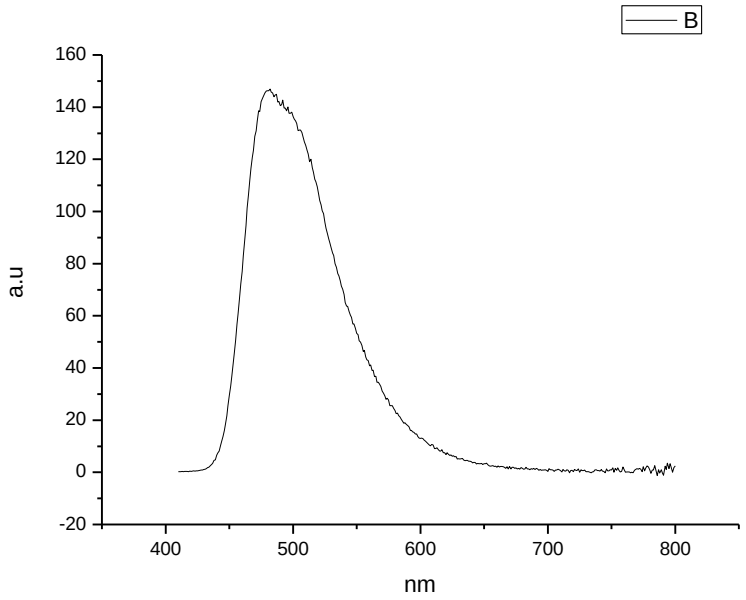

Figure 3.1.160. Fluorescence emission spectrum of **16** recorded in 1-butanol at 400 nm excitation.

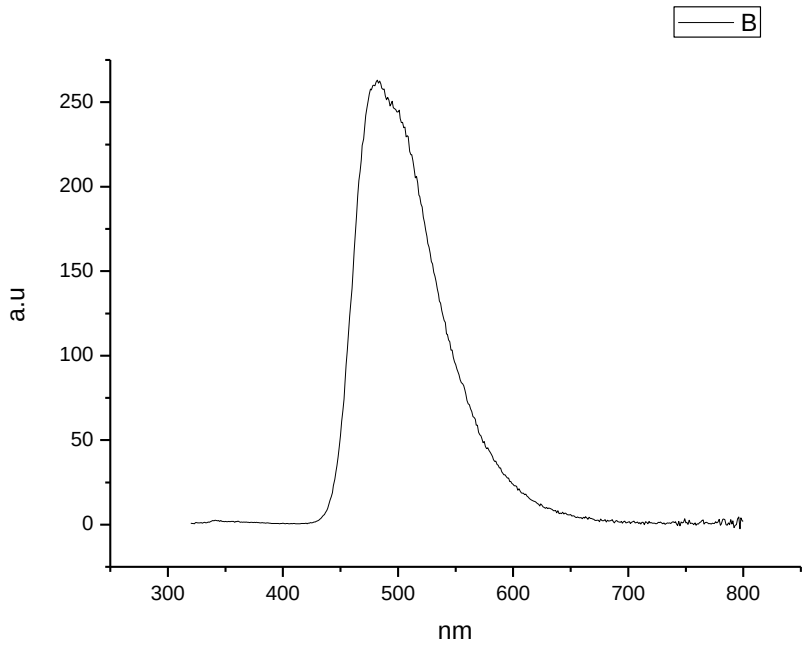

Figure 3.1.161. Fluorescence emission spectrum of **16** recorded in 1-pentanol at 310 nm excitation.

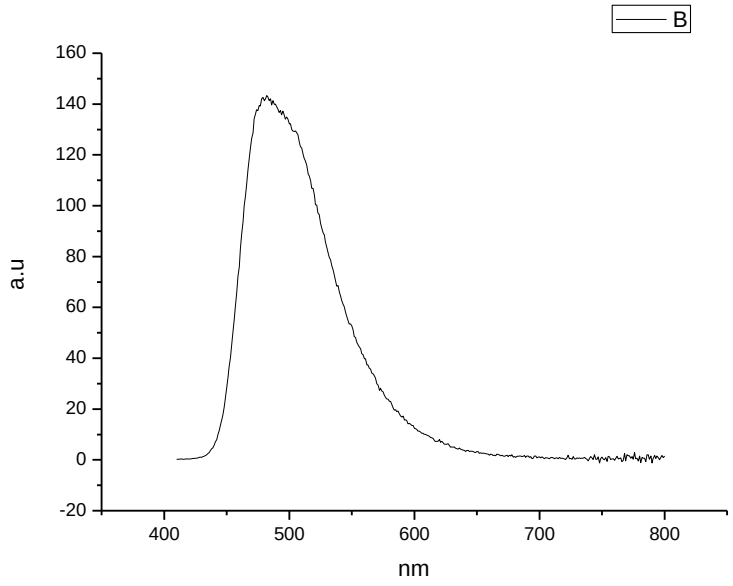

Figure 3.1.162. Fluorescence emission spectrum of **16** recorded in 1-pentanol at 400 nm excitation.

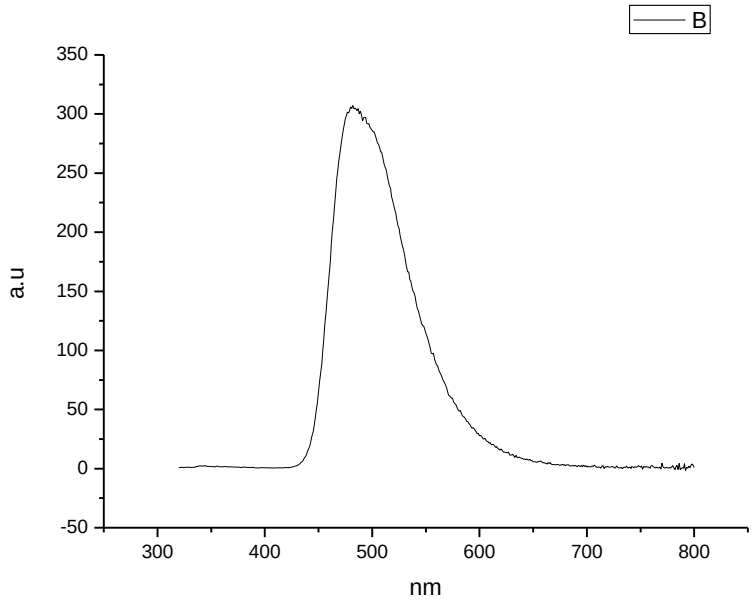

Figure 3.1.163. Fluorescence emission spectrum of **16** recorded in 1-propanol at 310 nm excitation.

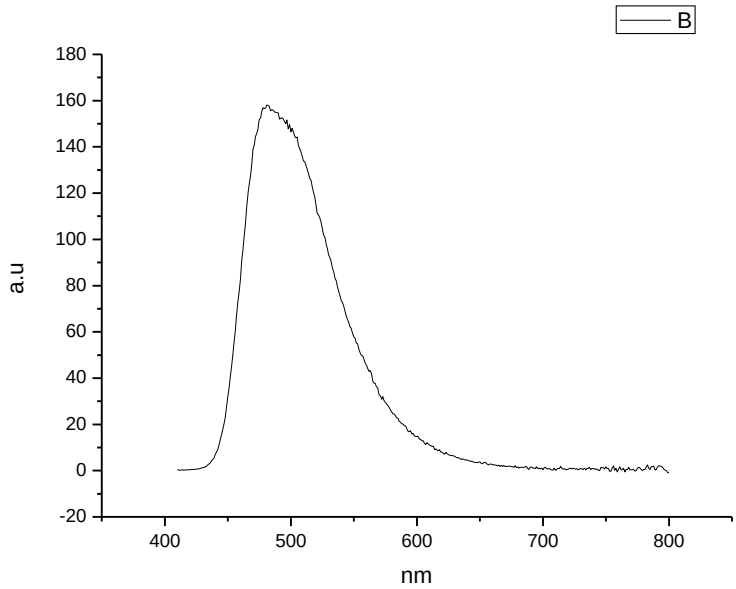

Figure 3.1.164. Fluorescence emission spectrum of **16** recorded in 1-propanol at 400 nm excitation.

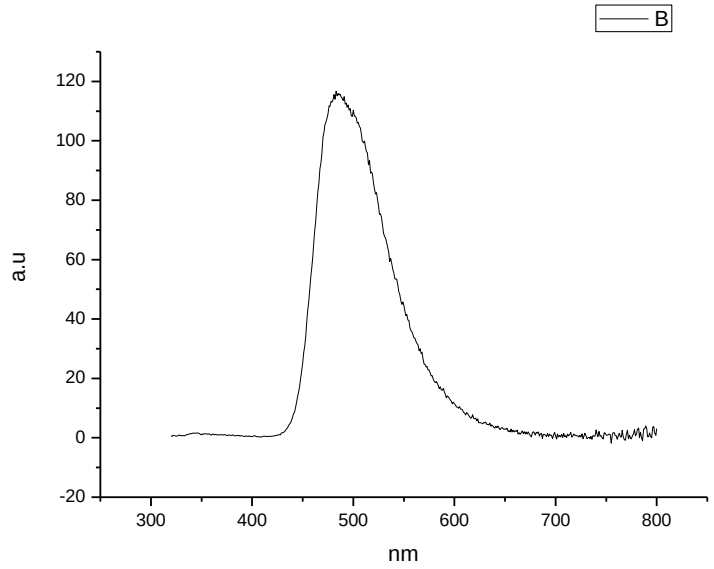

Figure 3.1.165. Fluorescence emission spectrum of **16** recorded in Acetic Acid at 310 nm excitation.

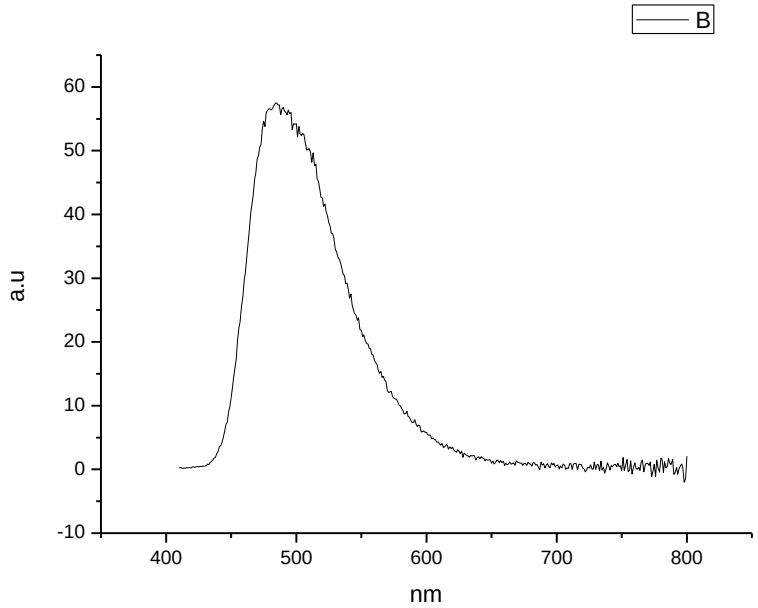

Figure 3.1.166. Fluorescence emission spectrum of **16** recorded in Acetic Acid at 400 nm excitation.

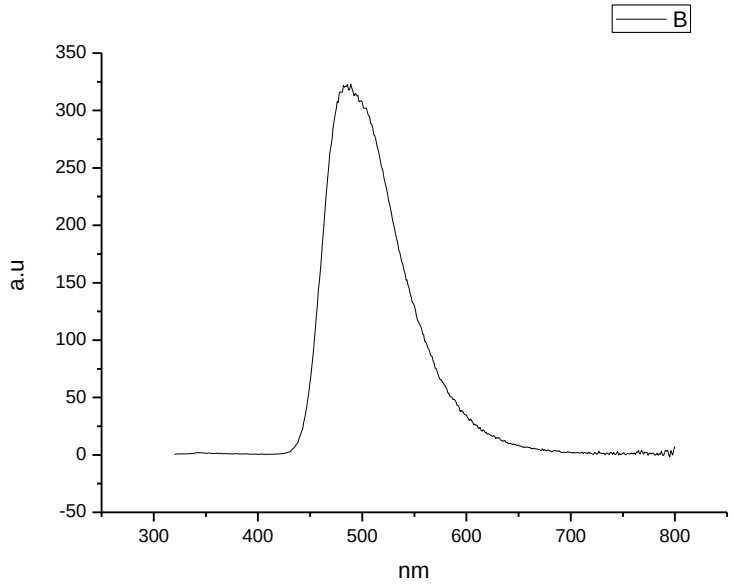

Figure 3.1.167. Fluorescence emission spectrum of **16** recorded in Methanol at 310 nm excitation.

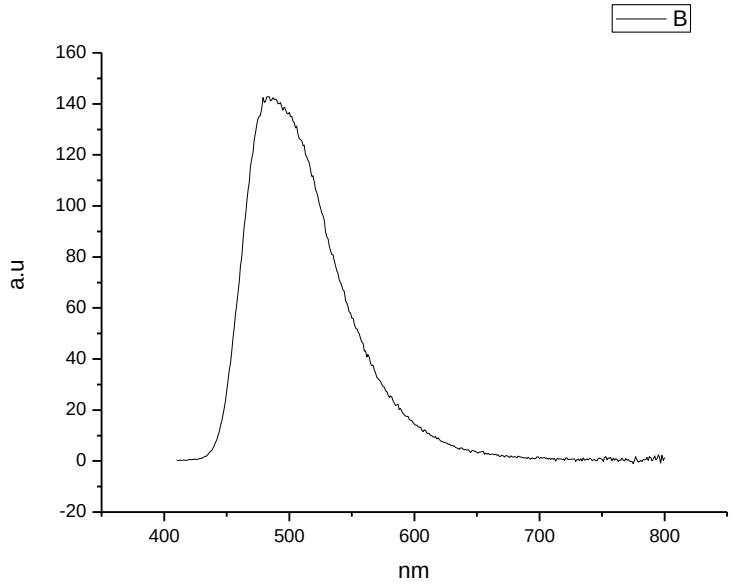

Figure 3.1.168. Fluorescence emission spectrum of **16** recorded in Methanol at 400 nm excitation.

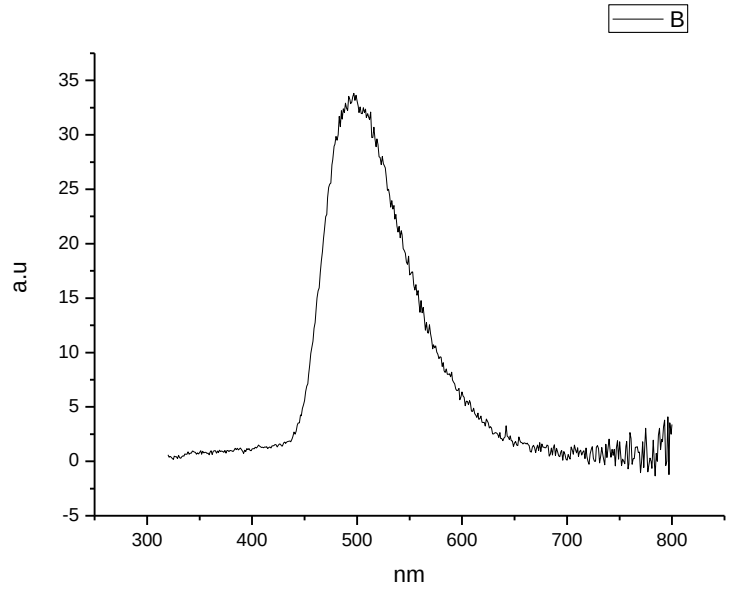

Figure 3.1.169. Fluorescence emission spectrum of **16** recorded in 2,2,2-trifluoroethanol at 310 nm excitation.

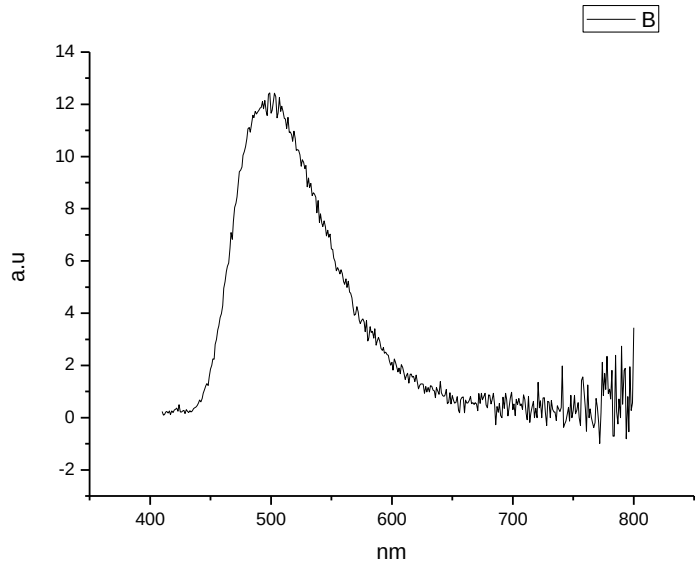

Figure 3.1.170. Fluorescence emission spectrum of **16** recorded in 2,2,2-trifluoroethanol at 400 nm excitation.

3.1.10 Normalised Fluorescence Emission spectra (Gaussian fitted).

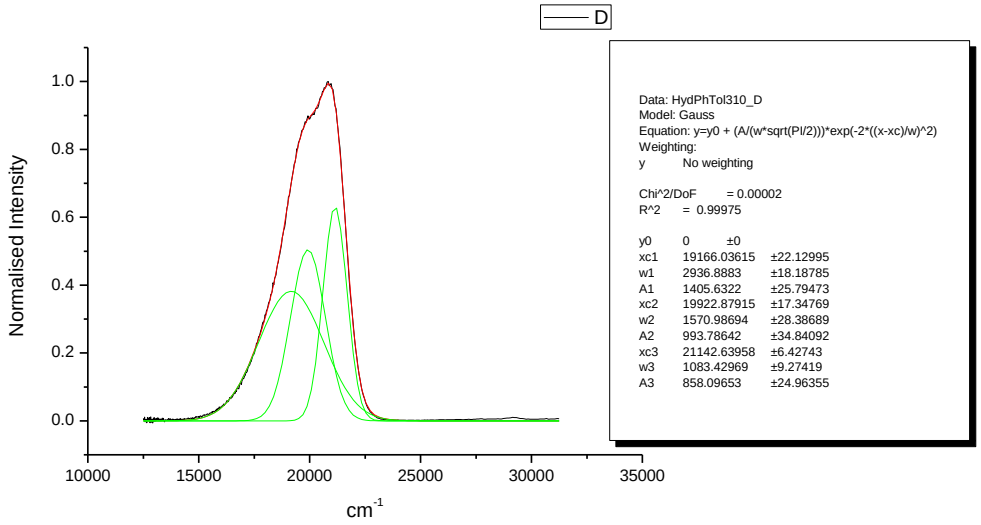

Figure 3.1.171. Gaussian model fit of the normalised fluorescence emission spectrum of **16** recorded in Toluene at 310 nm excitation.

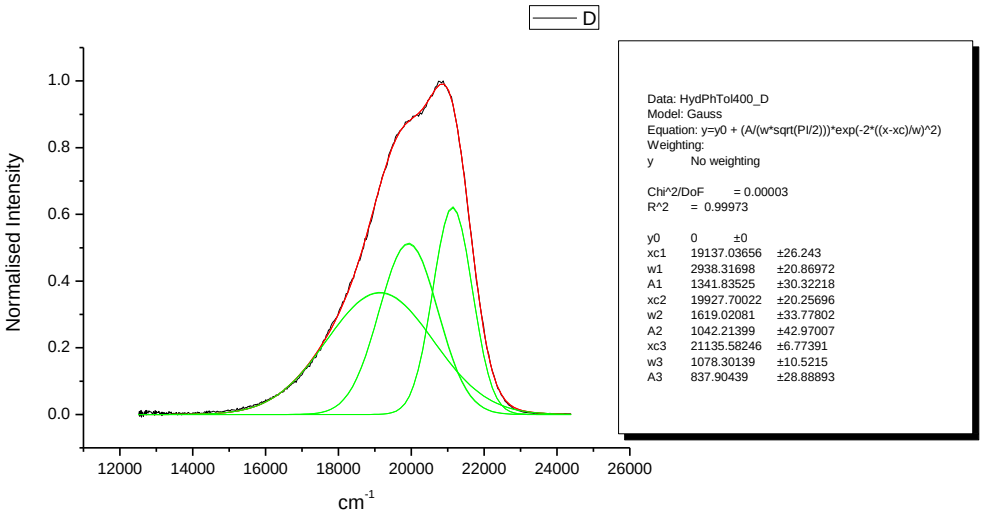

Figure 3.1.172. Gaussian model fit of the normalised fluorescence emission spectrum of **16** recorded in Toluene at 400 nm excitation.

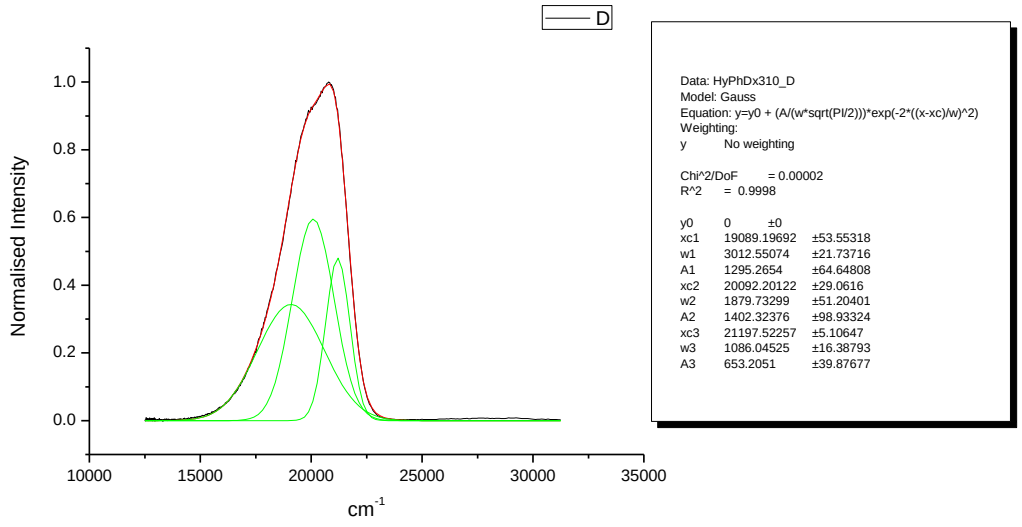

Figure 3.1.173. Gaussian model fit of the normalised fluorescence emission spectrum of **16** recorded in 1,4-dioxane at 310 nm excitation.

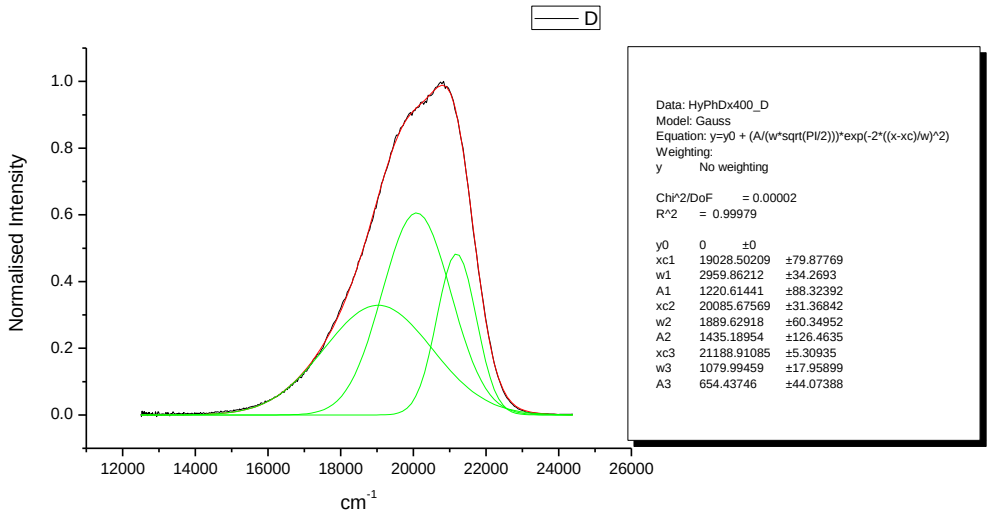

Figure 3.1.174. Gaussian model fit of the normalised fluorescence emission spectrum of **16** recorded in 1,4-dioxane at 400 nm excitation.

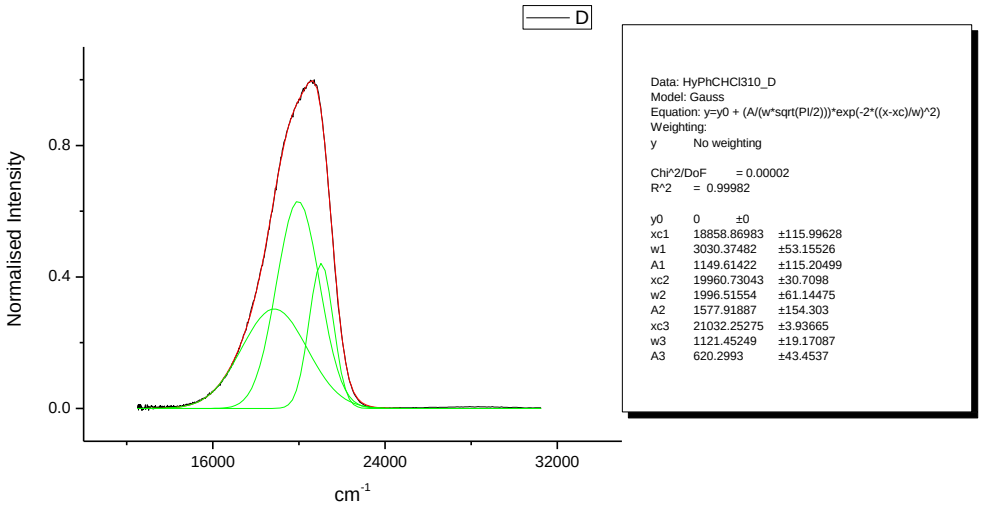

Figure 3.1.175. Gaussian model fit of the normalised fluorescence emission spectrum of **16** recorded in Chloroform at 310 nm excitation.

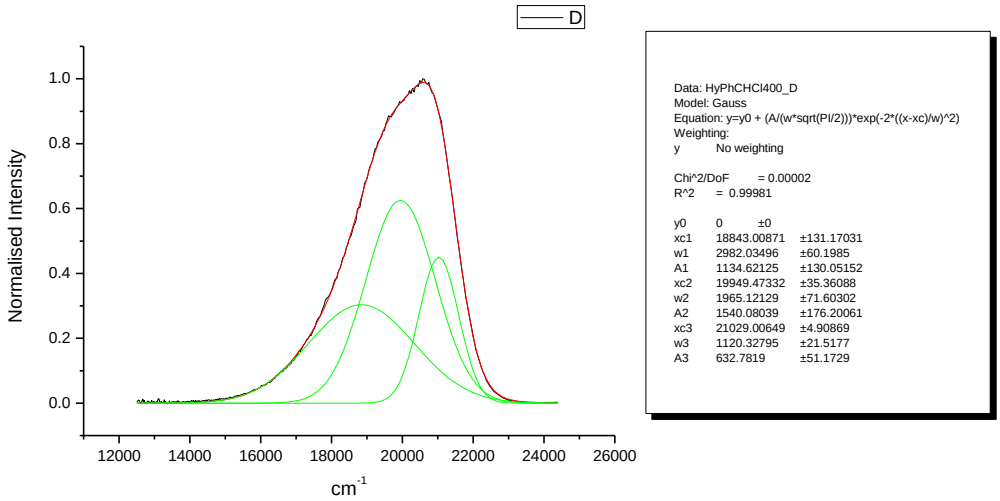

Figure 3.1.176. Gaussian model fit of the normalised fluorescence emission spectrum of **16** recorded in Chloroform at 400 nm excitation.

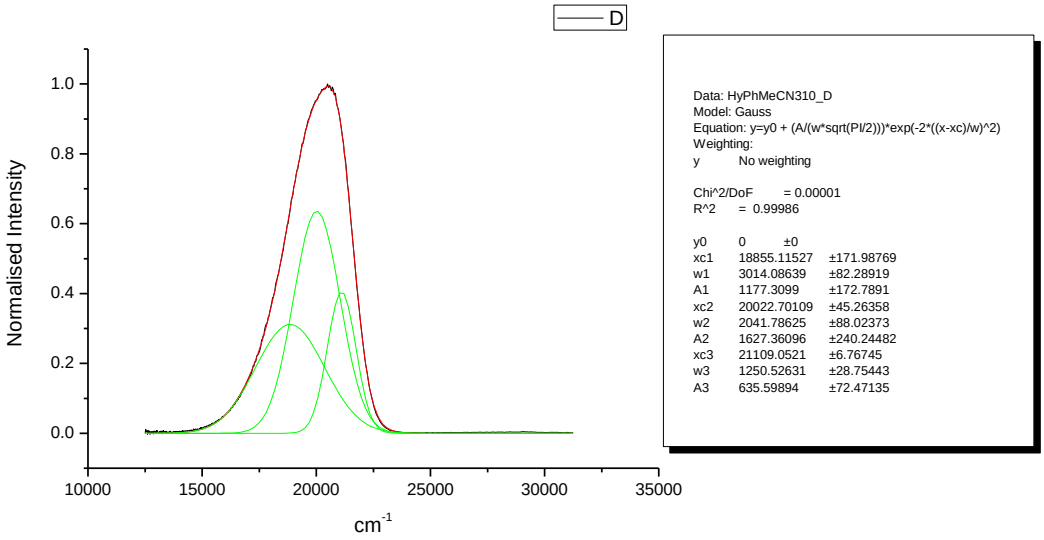

Figure 3.1.177. Gaussian model fit of the normalised fluorescence emission spectrum of **16** recorded in Acetonitrile at 310 nm excitation.

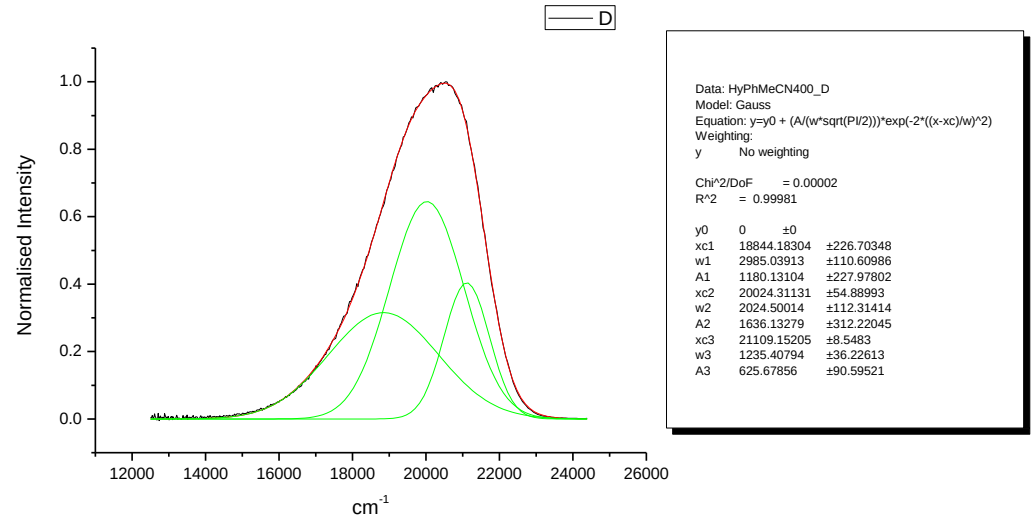

Figure 3.1.178. Gaussian model fit of the normalised fluorescence emission spectrum of **16** recorded in Acetonitrile at 400 nm excitation.

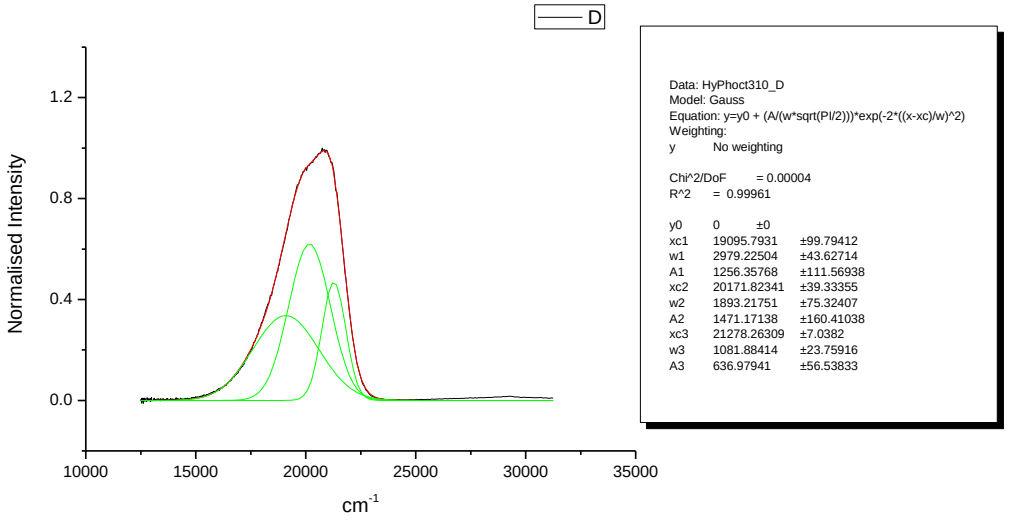

Figure 3.1.179. Gaussian model fit of the normalised fluorescence emission spectrum of **16** recorded in 1-octanol at 310 nm excitation.

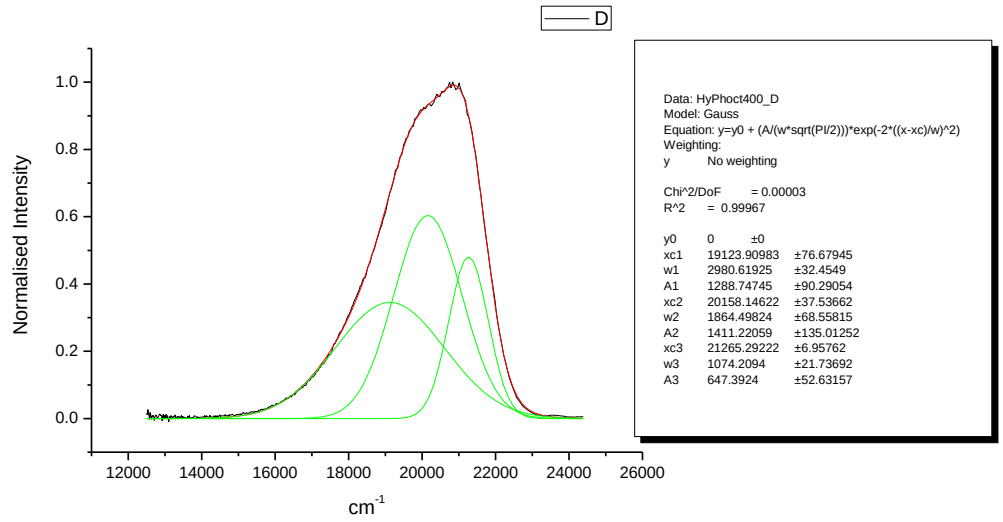

Figure 3.1.180. Gaussian model fit of the normalised fluorescence emission spectrum of **16** recorded in 1-octanol at 400 nm excitation.

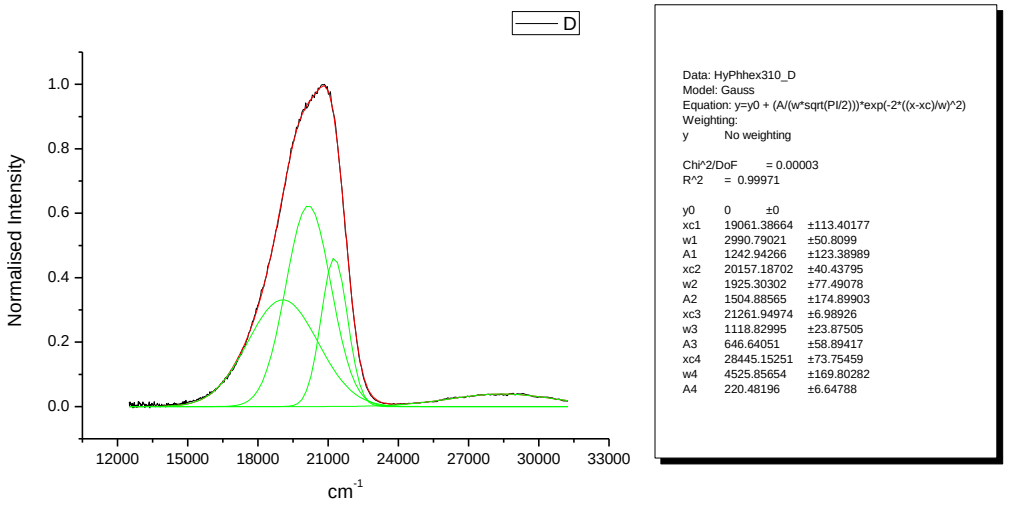

Figure 3.1.181. Gaussian model fit of the normalised fluorescence emission spectrum of **16** recorded in 1-hexanol at 310 nm excitation.

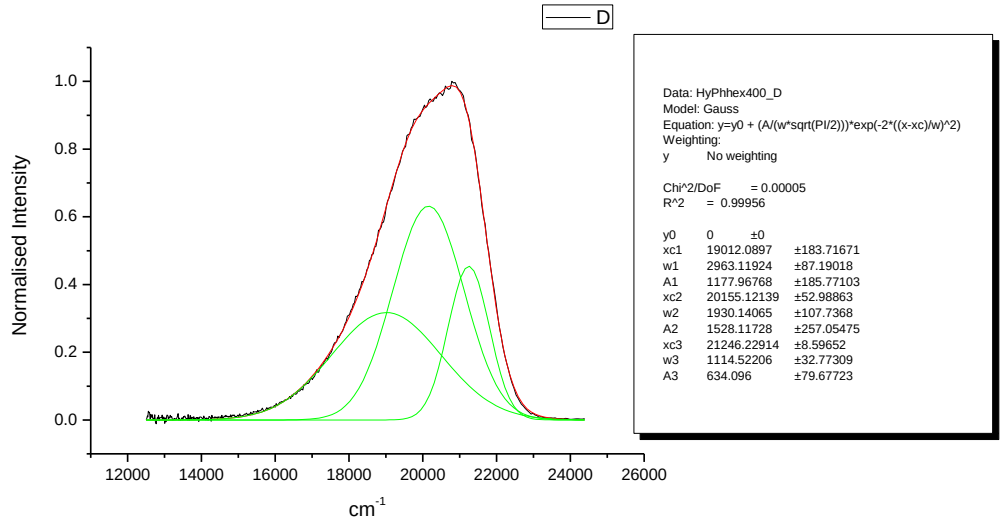

Figure 3.1.182. Gaussian model fit of the normalised fluorescence emission spectrum of **16** recorded in 1-hexanol at 400 nm excitation.

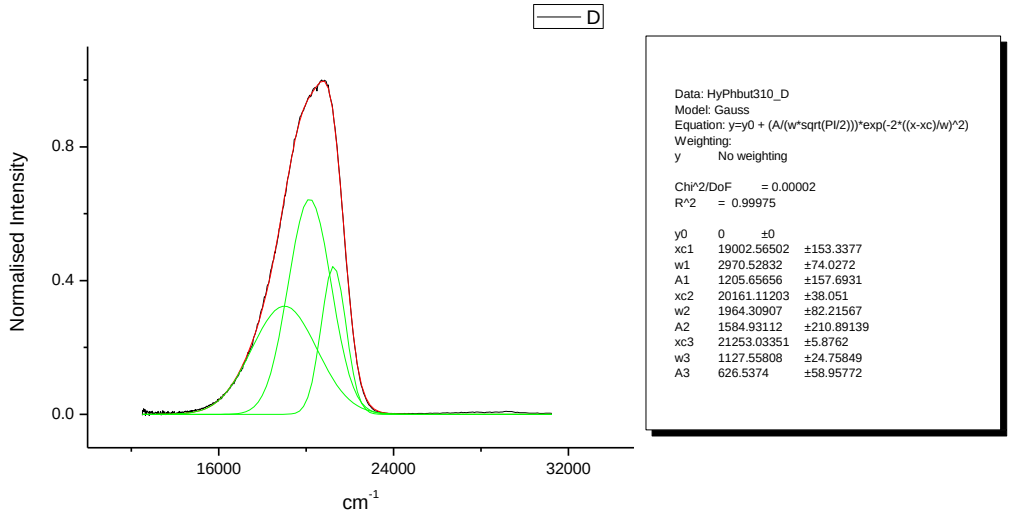

Figure 3.1.183. Gaussian model fit of the normalised fluorescence emission spectrum of **16** recorded in 1-butanol at 310 nm excitation.

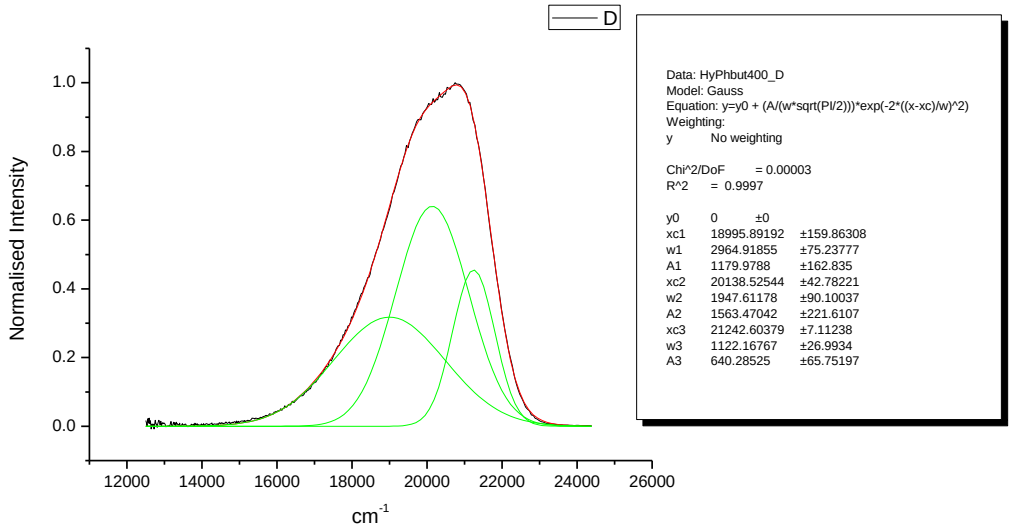

Figure 3.1.184. Gaussian model fit of the normalised fluorescence emission spectrum of **16** recorded in 1-butanol at 400 nm excitation.

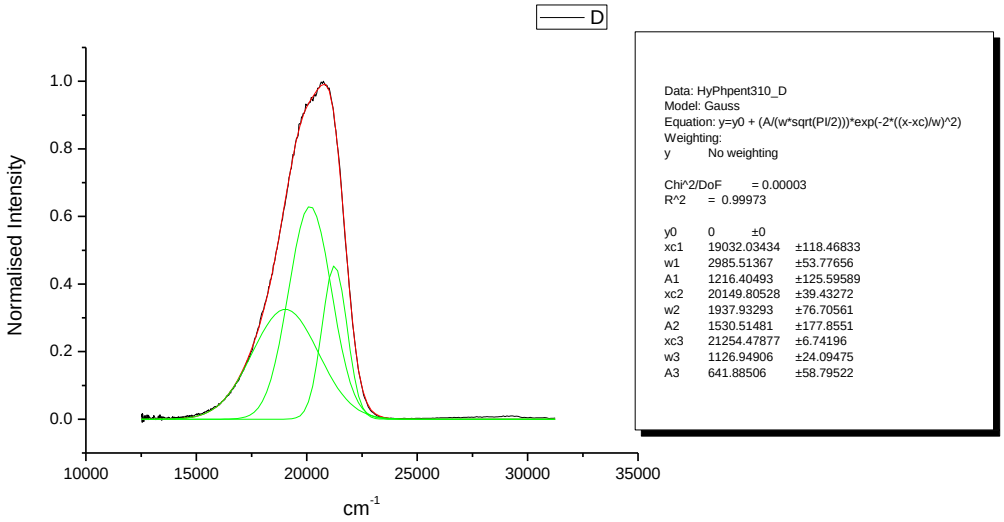

Figure 3.1.185. Gaussian model fit of the normalised fluorescence emission spectrum of **16** recorded in 1-pentanol at 310 nm excitation.

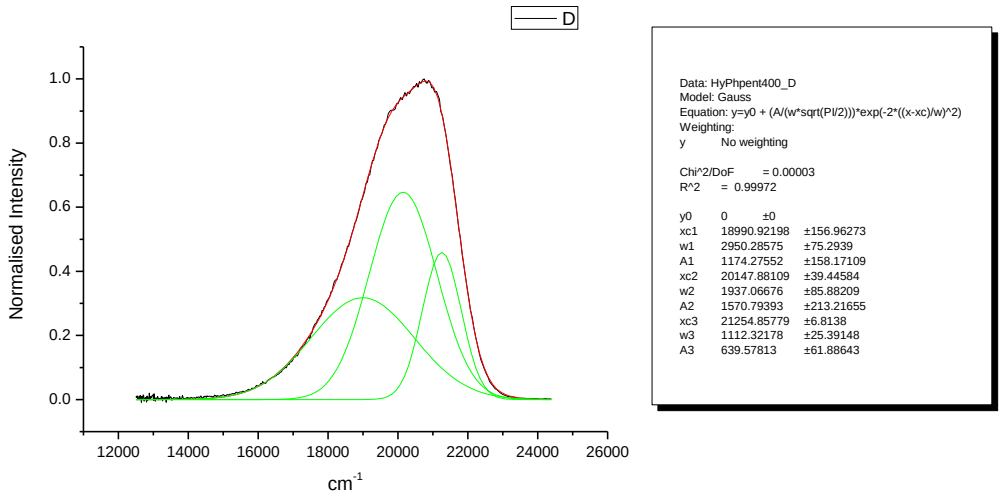

Figure 3.1.186. Gaussian model fit of the normalised fluorescence emission spectrum of **16** recorded in 1-pentanol at 400 nm excitation.

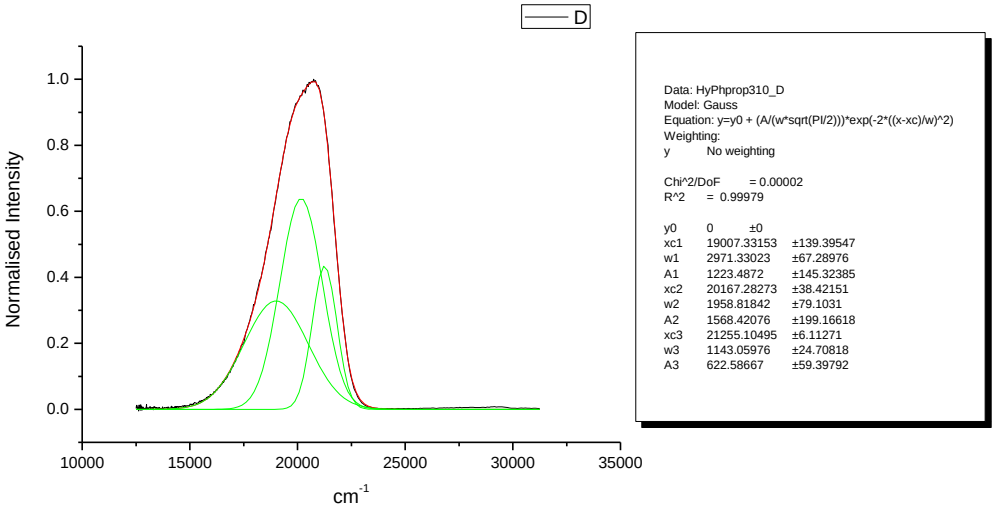

Figure 3.1.187. Gaussian model fit of the normalised fluorescence emission spectrum of **16** recorded in 1-propanol at 310 nm excitation.

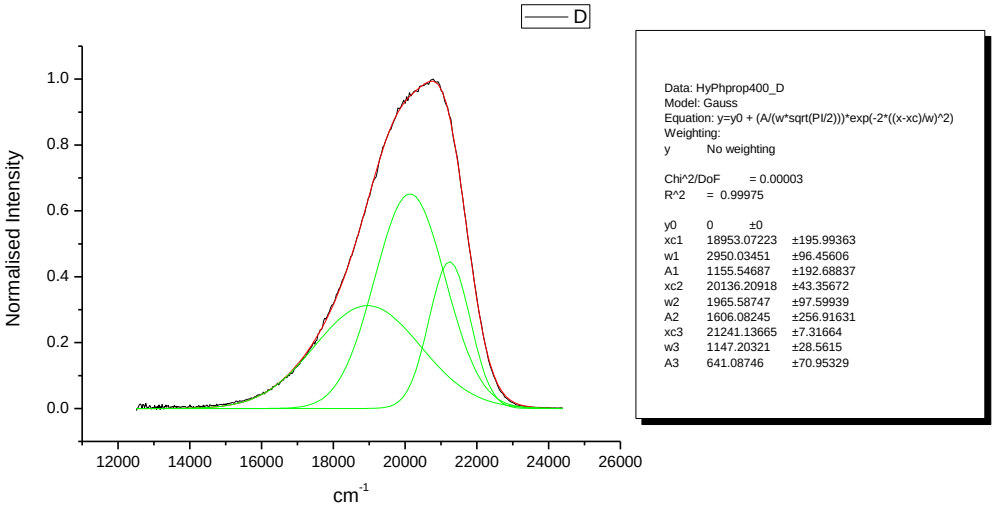

Figure 3.1.188. Gaussian model fit of the normalised fluorescence emission spectrum of **16** recorded in 1-propanol at 400 nm excitation.

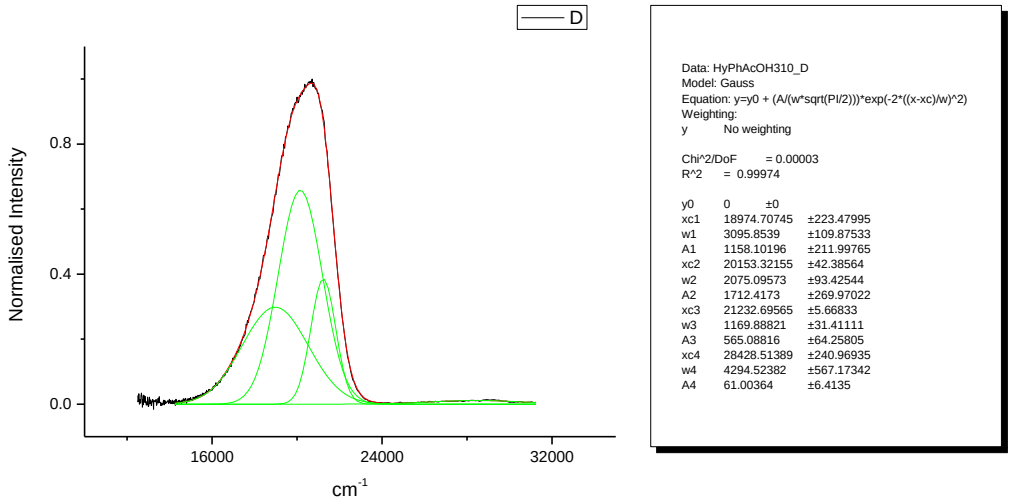

Figure 3.1.189. Gaussian model fit of the normalised fluorescence emission spectrum of **16** recorded in Acetic Acid at 310 nm excitation.

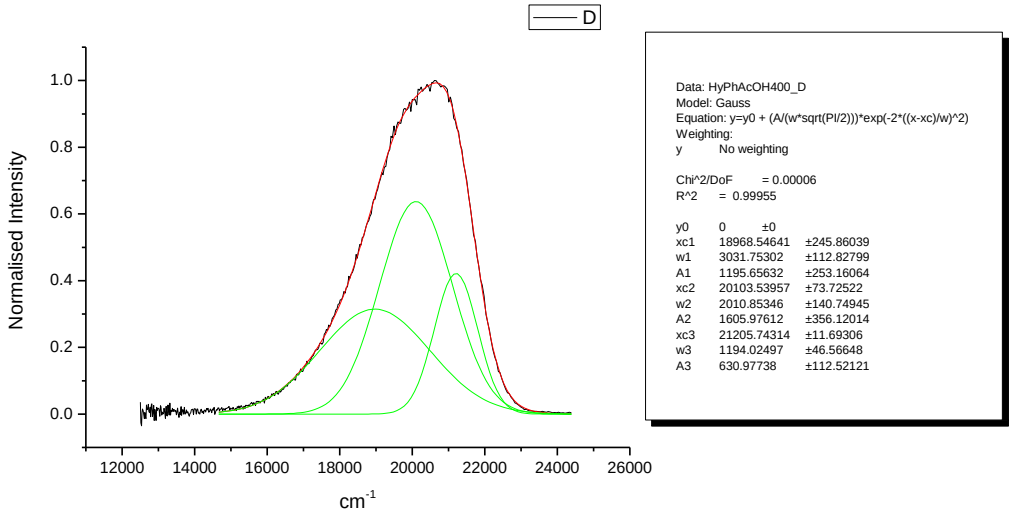

Figure 3.1.190. Gaussian model fit of the normalised fluorescence emission spectrum of **16** recorded in Acetic Acid at 400 nm excitation.

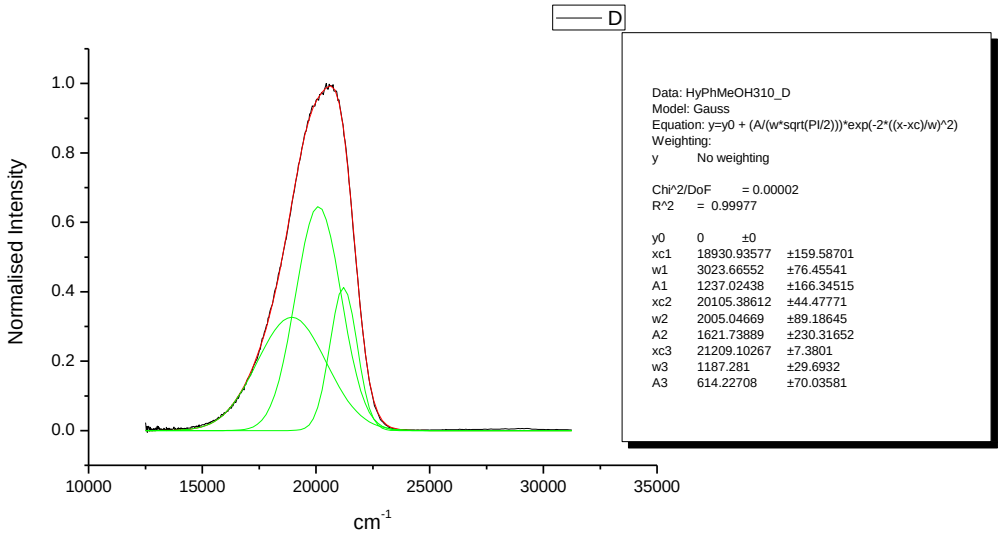

Figure 3.1.191. Gaussian model fit of the normalised fluorescence emission spectrum of **16** recorded in Methanol at 310 nm excitation.

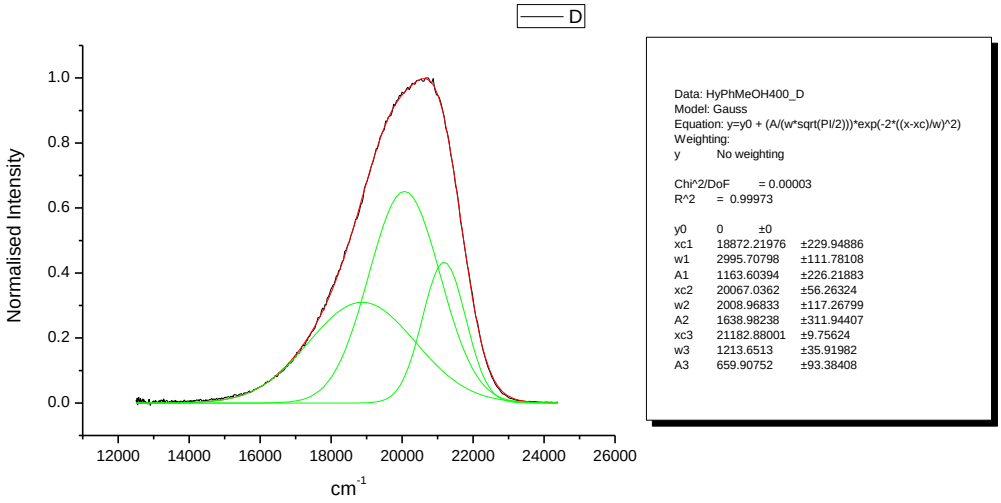

Figure 3.1.192. Gaussian model fit of the normalised fluorescence emission spectrum of **16** recorded in Methanol at 400 nm excitation.

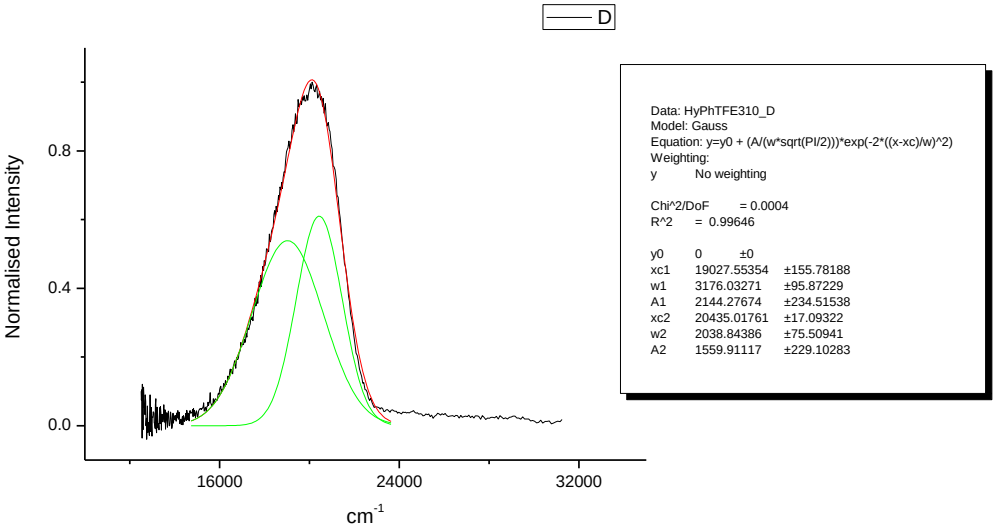

Figure 3.1.193. Gaussian model fit of the normalised fluorescence emission spectrum of **16** recorded in 2,2,2-trifluoroethanol at 310 nm excitation.

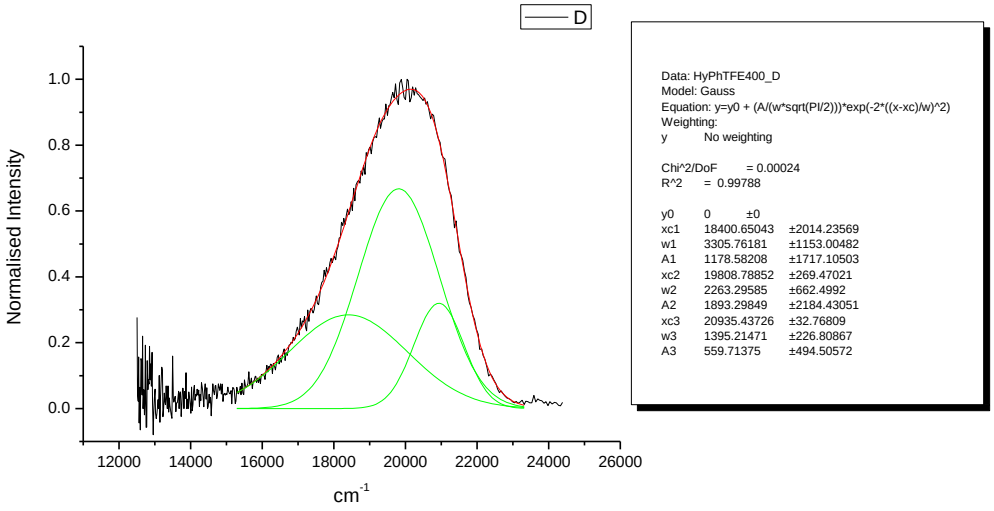

Figure 3.1.194. Gaussian model fit of the normalised fluorescence emission spectrum of **16** recorded in 2,2,2-trifluoroethanol at 400 nm excitation.

3.1.11 Fluorescence Excitation spectra.

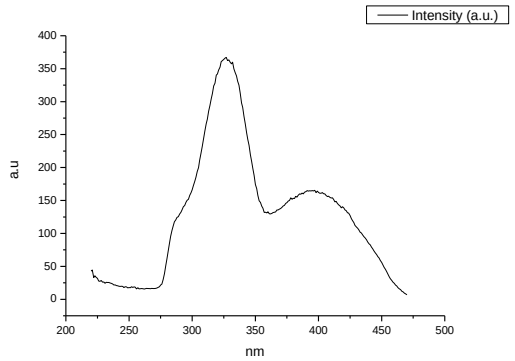

Figure 3.1.195. Fluorescence excitation spectrum of **16** recorded in Toluene with emission fixed at 480 nm.

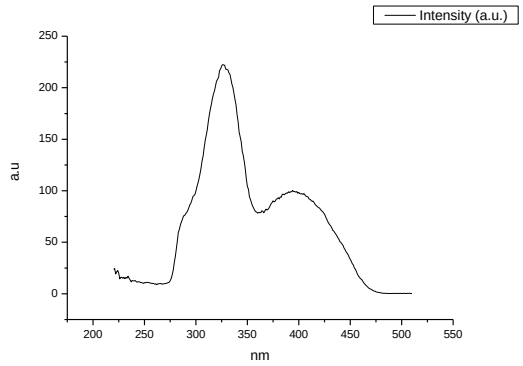

Figure 3.1.196. Fluorescence excitation spectrum of **16** recorded in Toluene with emission fixed at 520 nm.

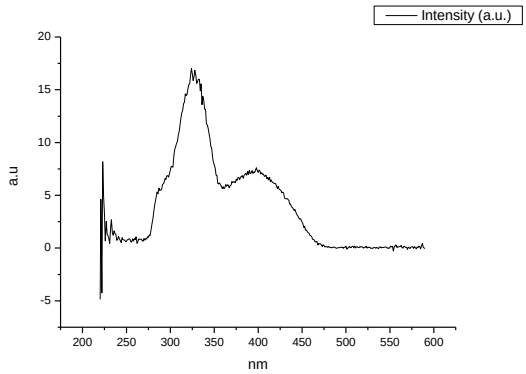

Figure 3.1.197. Fluorescence excitation spectrum of **16** recorded in Toluene with emission fixed at 600 nm.

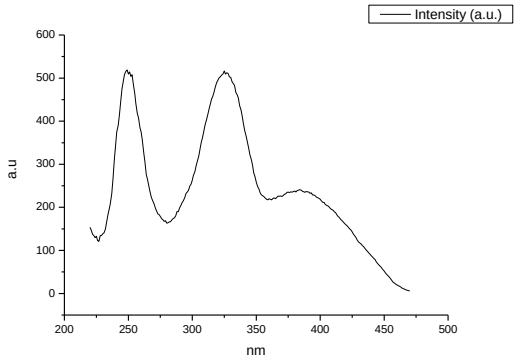

Figure 3.1.198. Fluorescence excitation spectrum of **16** recorded in 1,4-dioxane with emission fixed at 480 nm.

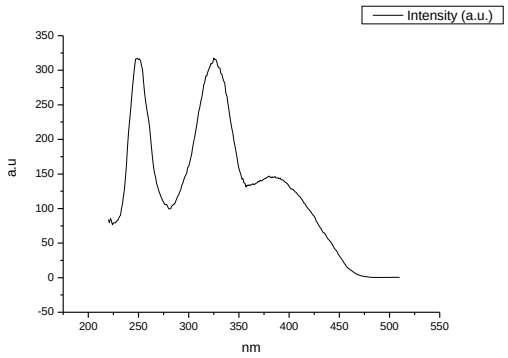

Figure 3.1.199. Fluorescence excitation spectrum of **16** recorded in 1,4-dioxane with emission fixed at 520 nm.

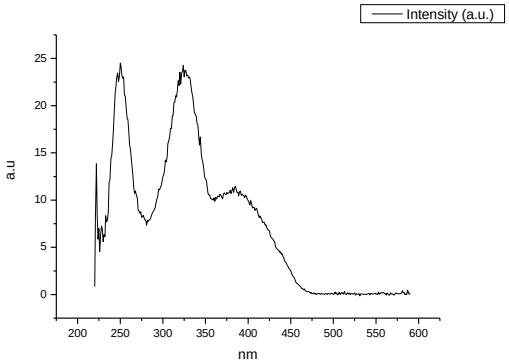

Figure 3.1.200. Fluorescence excitation spectrum of **16** recorded in 1,4-dioxane with emission fixed at 600 nm.

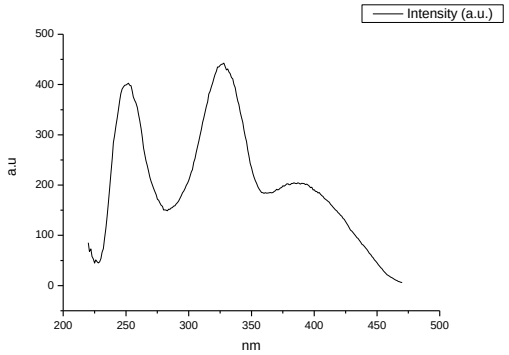

Figure 3.1.201. Fluorescence excitation spectrum of **16** recorded in Chloroform with emission fixed at 480 nm.

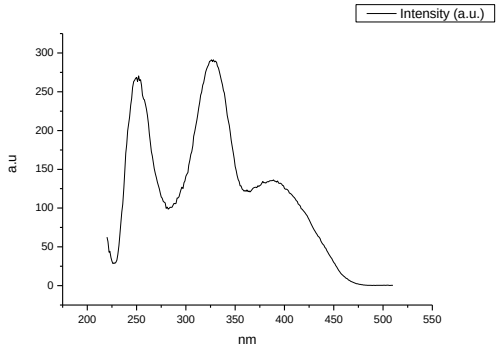

Figure 3.1.202. Fluorescence excitation spectrum of **16** recorded in Chloroform with emission fixed at 520 nm.

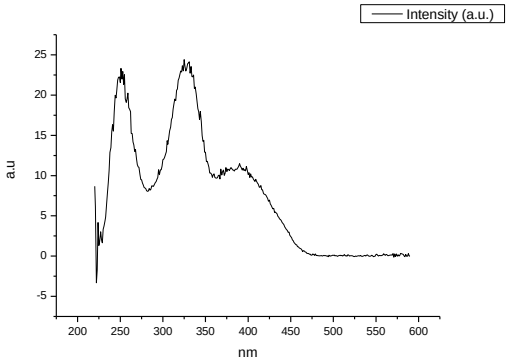

Figure 3.1.203. Fluorescence excitation spectrum of **16** recorded in Chloroform with emission fixed at 600 nm.

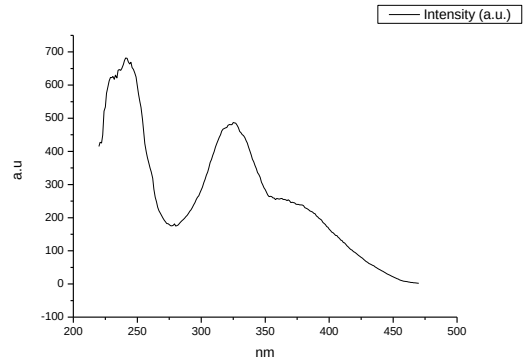

Figure 3.1.204. Fluorescence excitation spectrum of **16** recorded in Acetonitrile with emission fixed at 480 nm.

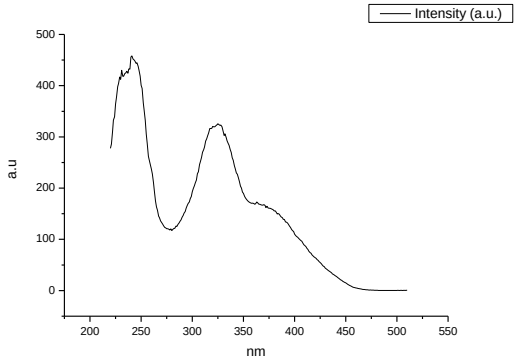

Figure 3.1.205. Fluorescence excitation spectrum of **16** recorded in Acetonitrile with emission fixed at 520 nm.

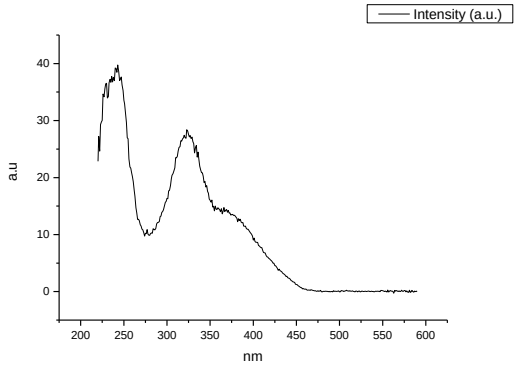

Figure 3.1.206. Fluorescence excitation spectrum of **16** recorded in Acetonitrile with emission fixed at 600 nm.

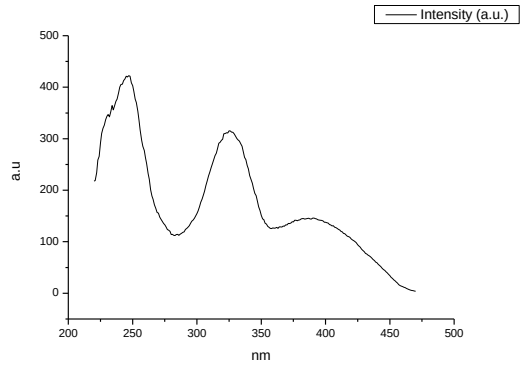

Figure 3.1.207. Fluorescence excitation spectrum of **16** recorded in 1-octanol with emission fixed at 480 nm.

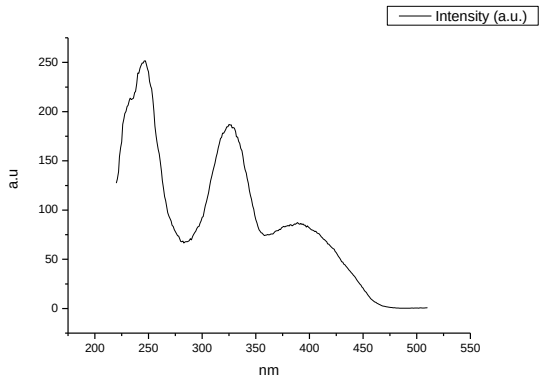

Figure 3.1.208. Fluorescence excitation spectrum of **16** recorded in 1-octanol with emission fixed at 520 nm.

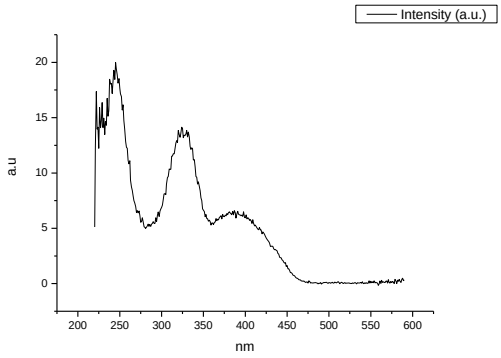

Figure 3.1.209. Fluorescence excitation spectrum of **16** recorded in 1-octanol with emission fixed at 600 nm.

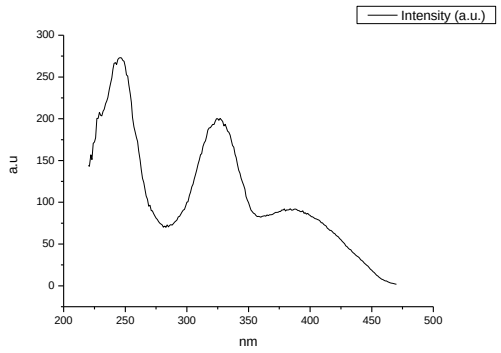

Figure 3.1.210. Fluorescence excitation spectrum of **16** recorded in 1-hexanol with emission fixed at 480 nm.

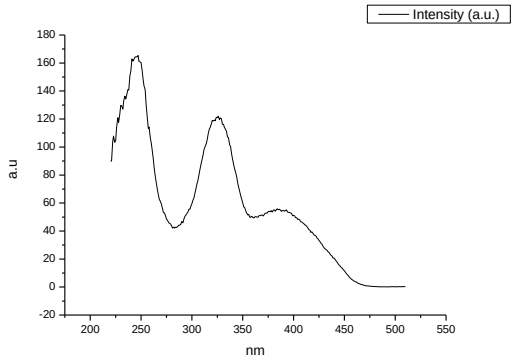

Figure 3.1.211. Fluorescence excitation spectrum of **16** recorded in 1-hexanol with emission fixed at 520 nm.

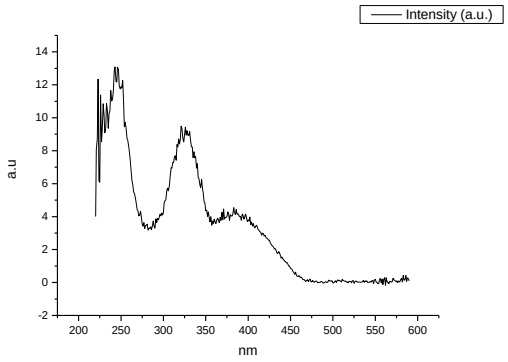

Figure 3.1.212. Fluorescence excitation spectrum of **16** recorded in 1-hexanol with emission fixed at 600 nm.

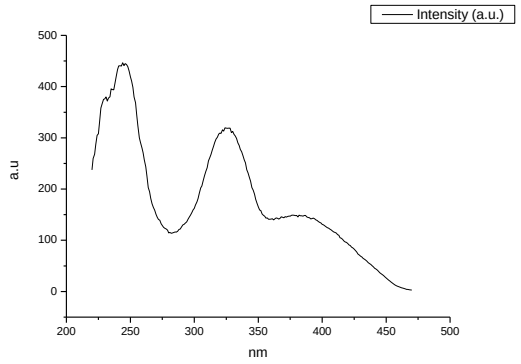

Figure 3.1.213. Fluorescence excitation spectrum of **16** recorded in 1-butanol with emission fixed at 480 nm.

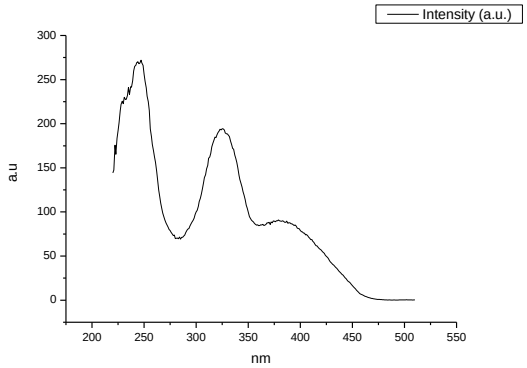

Figure 3.1.214. Fluorescence excitation spectrum of **16** recorded in 1-butanol with emission fixed at 520 nm.

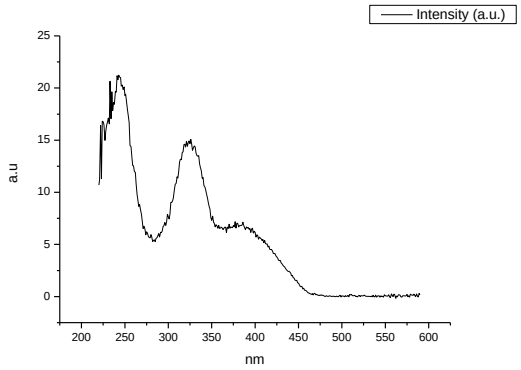

Figure 3.1.215. Fluorescence excitation spectrum of **16** recorded in 1-butanol with emission fixed at 600 nm.

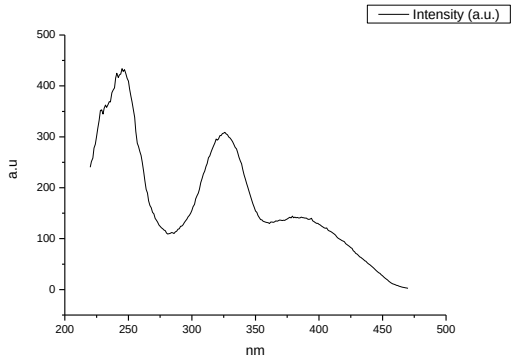

Figure 3.1.216. Fluorescence excitation spectrum of **16** recorded in 1-pentanol with emission fixed at 480 nm.

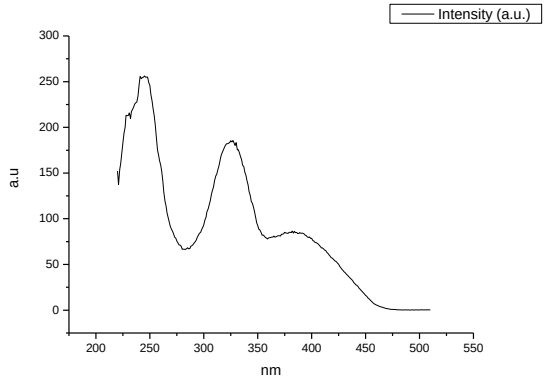

Figure 3.1.217. Fluorescence excitation spectrum of **16** recorded in 1-pentanol with emission fixed at 520 nm.

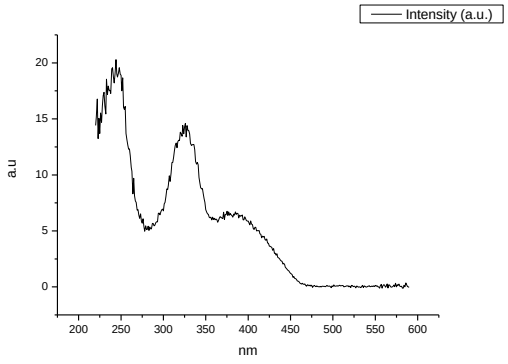

Figure 3.1.218. Fluorescence excitation spectrum of **16** recorded in 1-pentanol with emission fixed at 600 nm.

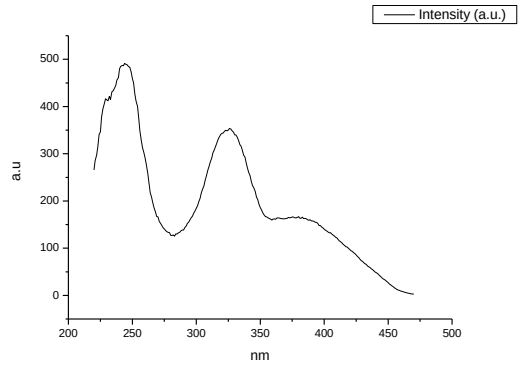

Figure 3.1.219. Fluorescence excitation spectrum of **16** recorded in 1-propanol with emission fixed at 480 nm.

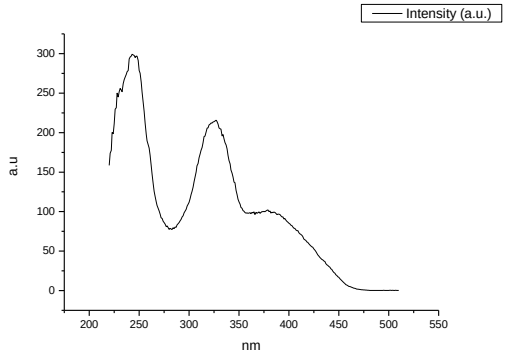

Figure 3.1.220. Fluorescence excitation spectrum of **16** recorded in 1-propanol with emission fixed at 520 nm.

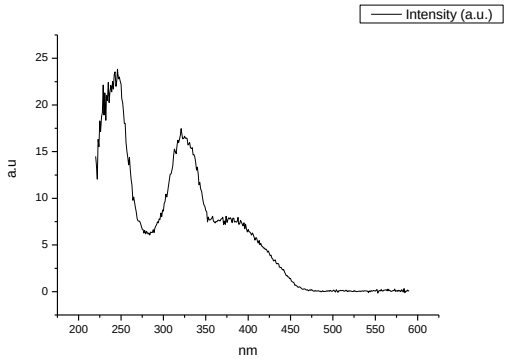

Figure 3.1.221. Fluorescence excitation spectrum of **16** recorded in 1-propanol with emission fixed at 600 nm.

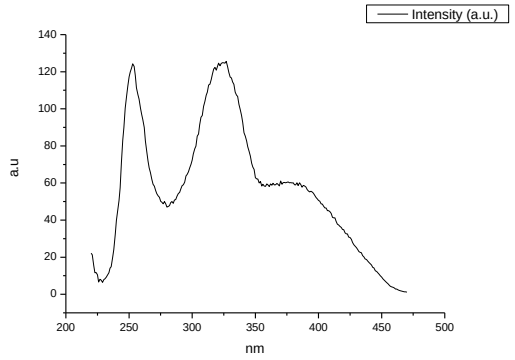

Figure 3.1.222. Fluorescence excitation spectrum of **16** recorded in Acetic Acid with emission fixed at 480 nm.

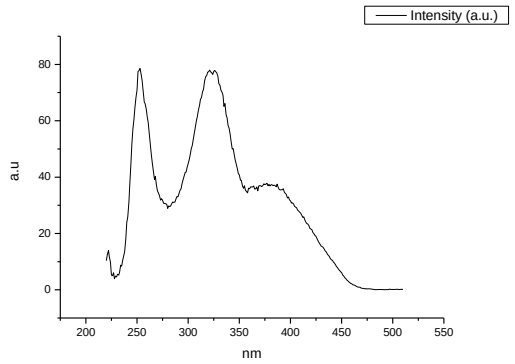

Figure 3.1.223. Fluorescence excitation spectrum of **16** recorded in Acetic Acid with emission fixed at 520 nm.

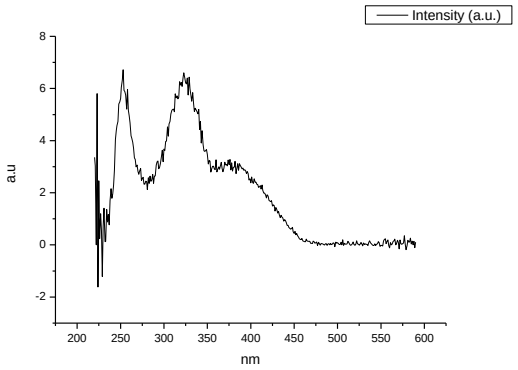

Figure 3.1.224. Fluorescence excitation spectrum of **16** recorded in Acetic Acid with emission fixed at 600 nm.

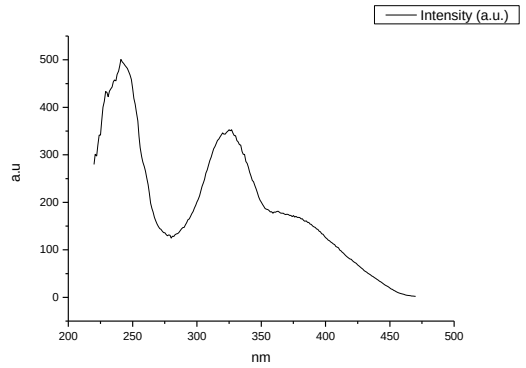

Figure 3.1.225. Fluorescence excitation spectrum of **16** recorded in Methanol with emission fixed at 480 nm.

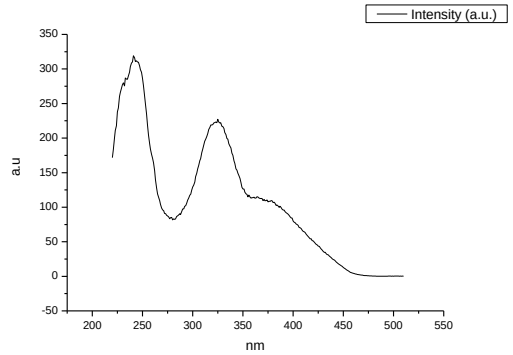

Figure 3.1.226. Fluorescence excitation spectrum of **16** recorded in Methanol with emission fixed at 520 nm.

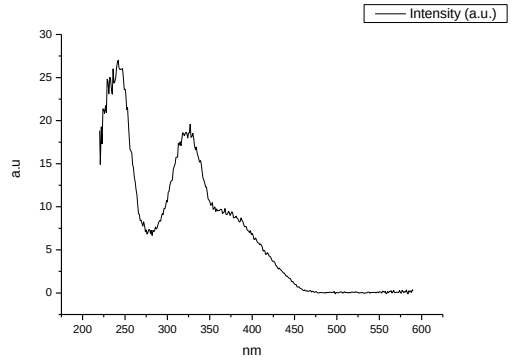

Figure 3.1.227. Fluorescence excitation spectrum of **16** recorded in Methanol with emission fixed at 600 nm.

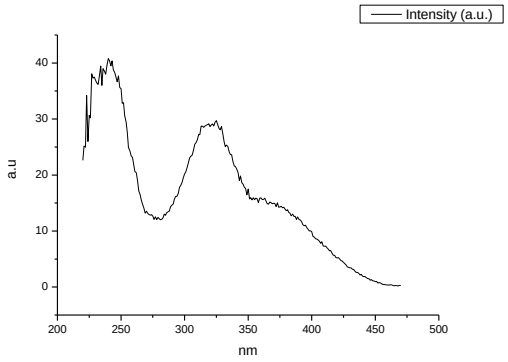

Figure 3.1.228. Fluorescence excitation spectrum of **16** recorded in 2,2,2-trifluoroethanol with emission fixed at 480 nm.

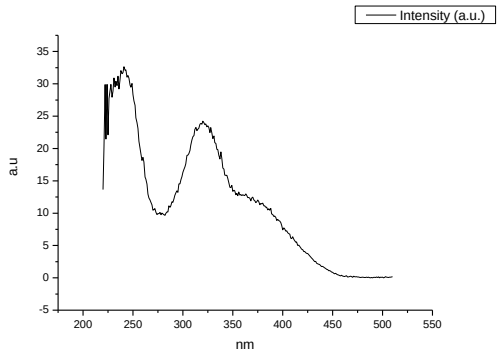

Figure 3.1.229. Fluorescence excitation spectrum of **16** recorded in 2,2,2-trifluoroethanol with emission fixed at 520 nm.

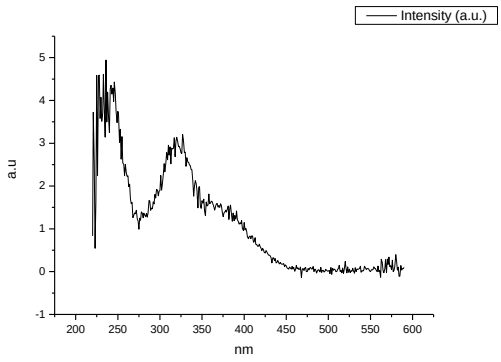

Figure 3.1.230. Fluorescence excitation spectrum of **16** recorded in 2,2,2-trifluoroethanol with emission fixed at 600 nm.

3.2 COMPOUND 17.

3.2.1 Quantum Yield Summary.

Solvent	$\lambda_{abs\ (310\ nm)}$	$\lambda_{ems\ (max)}$	$\Phi_{310\ nm}$	$\lambda_{abs\ (400\ nm)}$	$\lambda_{ems\ (max)}$	$\Phi_{400\ nm}$
Toluene	0.07	478.03	0.15	0.05	478.03	0.17
1,4-Dioxane	0.05	476.96	0.22	0.02	476.06	0.21
Chloroform	0.05	482.98	0.19	0.02	488.05	0.18
Acetonitrile	0.05	487.01	0.19	0.02	485.97	0.17
1-Octanol	0.03	476.06	0.18	0.02	476.06	0.16
1-Hexanol	0.02	481.94	0.16	0.01	478.93	0.14
1-Butanol	0.04	481.94	0.14	0.02	478.03	0.12
1-Pentanol	0.04	481.04	0.15	0.02	481.94	0.13
1-Propanol	0.05	476.96	0.16	0.02	481.04	0.14
Acetic acid	0.07	482.98	0.06	0.03	478.93	0.06
Methanol	0.04	485.97	0.16	0.01	485.97	0.13
2,2,2-Trifluoroethanol	0.06	496.06	0.03	0.02	491.96	0.03

Table 3.2.1. Summary of ultraviolet-visible absorbance values at 310 nm and 400 nm, emission maxima and quantum yield (Φ) of **17** at 310 nm and 400 nm excitation.

3.2.2 310 nm excitation Gaussian band fit summaries.

Solvent	λ max$_{em}$ Band 1 (cm^{-1})	λ max$_{em}$ Band 1 (nm)	λ max$_{em}$ Band 2 (cm^{-1})	λ max$_{em}$ Band 2 (nm)	λ max$_{em}$ Band 3 (cm^{-1})	λ max$_{em}$ Band 3 (nm)
Toluene	19213.04	520.48	19966.38	500.84	21183.70	472.06
1,4-Dioxane	19201.20	520.80	20112.11	497.21	21247.35	470.65
Chloroform	19128.85	522.77	19980.11	500.50	21091.72	474.12
Acetonitrile	18950.75	527.68	20092.71	497.69	21198.21	471.74
1-Octanol	19257.53	519.28	20235.30	494.19	21356.12	468.25
1-Hexanol	19331.43	517.29	20250.73	493.81	21351.87	468.34
1-Butanol	19196.29	520.93	20220.02	494.56	21335.67	468.70
1-Pentanol	19186.68	521.20	20224.80	494.44	21340.32	468.60
1-Propanol	19181.16	521.35	20254.91	493.71	21349.51	468.39
Acetic acid	19302.56	518.07	20224.60	494.45	21297.91	469.53
Methanol	19094.11	523.72	20226.77	494.39	21317.01	469.11
2,2,2-Trifluoroethanol	18508.27	540.30	19735.44	506.70	20914.09	478.15

Solvent	λ max$_{em}$ Band 4 (cm^{-1})	λ max$_{em}$ Band 4 (nm)	λ max$_{em}$ Band 5 (cm^{-1})	λ max$_{em}$ Band 5 (nm)
Toluene	28128.38	355.51	-	-
1,4-Dioxane	28050.60	356.50	-	-
Chloroform	27827.97	359.35	-	-
Acetonitrile	28156.35	355.16	-	-
1-Octanol	28183.65	354.82	-	-
1-Hexanol	28147.72	355.27	-	-
1-Butanol	28081.26	356.11	-	-
1-Pentanol	28059.90	356.38	-	-
1-Propanol	28064.88	356.32	-	-
Acetic acid	28018.27	356.91	-	-
Methanol	28106.14	355.79	-	-
2,2,2-Trifluoroethanol	25244.76	396.12	27897.71	358.45

Table 3.2.2. Summary of band maxima of 5 band fit using Gaussian model for normalised **17** emission spectra recorded at 310 nm excitation.

(a)

Solvent	Width Band 1 (cm^{-1})	Width Band 2 (cm^{-1})	Width Band 3 (cm^{-1})	Width Band 4 (cm^{-1})	Width Band 5 (cm^{-1})
Toluene	2982.60	1635.08	1093.28	3283.45	-
1,4-Dioxane	3063.06	1843.74	1088.14	3204.67	-
Chloroform	3136.52	1894.98	1124.10	3172.68	-
Acetonitrile	3076.26	2066.15	1252.56	3221.85	-
1-Octanol	3064.27	1877.03	1093.87	3325.16	-
1-Hexanol	3119.33	1896.55	1090.15	3631.34	-
1-Butanol	3092.49	1952.08	1141.53	3211.80	-
1-Pentanol	3054.35	1933.57	1139.43	3197.51	-
1-Propanol	3056.22	1959.71	1130.60	3193.60	-
Acetic acid	3195.85	2000.28	1191.49	3244.83	-
Methanol	3080.62	2013.69	1193.61	3258.40	-
2,2,2-Trifluoroethanol	3753.80	2424.88	1522.05	2865.55	2748.48968

(b)

Solvent	Area Band 1 (cm^{-1})	Area Band 2 (cm^{-1})	Area Band 3 (cm^{-1})	Area Band 4 (cm^{-1})	Area Band 5 (cm^{-1})
Toluene	1419.16	1026.81	822.49	325.95	-
1,4-Dioxane	1413.66	1323.68	665.46	303.56	-
Chloroform	1415.10	1300.45	641.40	308.40	-
Acetonitrile	1219.91	1648.49	624.05	266.77	-
1-Octanol	1389.24	1374.66	640.91	476.15	-
1-Hexanol	1508.67	1358.94	597.32	832.29	-
1-Butanol	1327.60	1471.77	627.87	443.03	-
1-Pentanol	1334.23	1455.37	637.17	430.37	-
1-Propanol	1351.37	1510.77	594.25	404.22	-
Acetic acid	1488.01	1417.06	572.33	639.80	-
Methanol	1370.76	1589.33	576.37	434.11	-
2,2,2-Trifluoroethanol	1060.73	1973.65	681.53	271.85	791.30662

Tables 3.2.3 (a) and (b). Summary band width and band area of 5 band fit using Gaussian model for normalised **17** emission spectra recorded at 310 nm excitation.

Solvent	Band 1 Area Percentage (%)	Band 2 Area Percentage (%)	Band 3 Area Percentage (%)	Band 4 Area Percentage (%)	Band 5 Area Percentage (%)
Toluene	39.48	28.57	22.88	9.07	-
1,4-Dioxane	38.14	35.71	17.95	8.19	-
Chloroform	38.61	35.48	17.50	8.41	-
Acetonitrile	32.45	43.85	16.60	7.10	-
1-Octanol	35.80	35.42	16.51	12.27	-
1-Hexanol	35.11	31.62	13.90	19.37	-
1-Butanol	34.30	38.03	16.22	11.45	-
1-Pentanol	34.59	37.73	16.52	11.16	-
1-Propanol	35.00	39.13	15.39	10.47	-
Acetic acid	36.14	34.42	13.90	15.54	-
Methanol	34.52	40.03	14.52	10.93	-
2,2,2-Trifluoroethanol	22.20	41.30	14.26	5.69	16.56

Table 3.2.4. Total Area Percentages of 5 band fit using Gaussian model for normalised **17** emission spectra recorded at 310 nm excitation.

Solvent	Area Ratio Band 1/2 (310 nm ex)	Area Ratio Band 1/3 (310 nm ex)	Area Ratio Band 1/4 (310 nm ex)	Area Ratio Band 1/5 (310 nm ex)
Toluene	1.38	1.73	4.35	-
1,4-Dioxane	1.07	2.12	4.66	-
Chloroform	1.09	2.21	4.59	-
Acetonitrile	0.74	1.95	4.57	-
1-Octanol	1.01	2.17	2.92	-
1-Hexanol	1.11	2.53	1.81	-
1-Butanol	0.90	2.11	3.00	-
1-Pentanol	0.92	2.09	3.10	-
1-Propanol	0.89	2.27	3.34	-
Acetic acid	1.05	2.60	2.33	-
Methanol	0.86	2.38	3.16	-
2,2,2-Trifluoroethanol	0.54	1.56	3.90	1.34

Solvent	Area Ratio Band 2/3 (310 nm ex)	Area Ratio Band 2/4 (310 nm ex)	Area Ratio Band 2/5 (310 nm ex)	Area Ratio Band 3/4 (310 nm ex)	Area Ratio Band 3/5 (310 nm ex)	Area Ratio Band 4/5 (310 nm ex)
Toluene	1.25	3.15	-	2.52	-	-
1,4-Dioxane	1.99	4.36	-	2.19	-	-
Chloroform	2.03	4.22	-	2.08	-	-
Acetonitrile	2.64	6.18	-	2.34	-	-
1-Octanol	2.14	2.89	-	1.35	-	-
1-Hexanol	2.28	1.63	-	0.72	-	-
1-Butanol	2.34	3.32	-	1.42	-	-
1-Pentanol	2.28	3.38	-	1.48	-	-
1-Propanol	2.54	3.74	-	1.47	-	-
Acetic acid	2.48	2.21	-	0.89	-	-
Methanol	2.76	3.66	-	1.33	-	-
2,2,2-Trifluoroethanol	2.90	7.26	2.49	2.51	0.86	0.34

Table 3.2.5. Area Ratios of 5 band fit using Gaussian model for normalised **17** emission spectra recorded at 310 nm excitation.

3.2.3 400 nm excitation Gaussian band fit summaries.

Solvent	λ max$_{em}$ Band 1 (cm^{-1})	λ max$_{em}$ Band 1 (nm)	λ max$_{em}$ Band 2 (cm^{-1})	λ max$_{em}$ Band 2 (nm)	λmax$_{em}$ Band 3 (cm^{-1})	λmax$_{em}$ Band 3 (nm)
Toluene	19138.16	522.52	19999.86	500.00	21195.67	471.79
1,4-Dioxane	19004.78	526.18	20132.54	496.71	21243.61	470.73
Chloroform	19441.79	514.36	19960.60	500.99	21066.92	474.68
Acetonitrile	18955.50	527.55	20114.69	497.15	21205.58	471.57
1-Octanol	19137.86	522.52	20238.87	494.10	21349.63	468.39
1-Hexanol	19142.91	522.39	20197.68	495.11	21339.95	468.60
1-Butanol	19113.26	523.20	20192.97	495.22	21336.18	468.69
1-Pentanol	19020.03	525.76	20202.24	494.99	21329.75	468.83
1-Propanol	19085.19	523.97	20236.91	494.15	21344.38	468.51
Acetic acid	19066.61	524.48	20180.02	495.54	21261.87	470.33
Methanol	19007.85	526.10	20197.84	495.10	21306.15	469.35
2,2,2-Trifluoroethanol	18384.73	543.93	19820.59	504.53	21010.96	475.94

Table 3.2.6. Summary of band maxima of 3 band fit using Gaussian model for normalised **17** emission spectra recorded at 400 nm excitation.

Solvent	Width Band 1 (cm^{-1})	Width Band 2 (cm^{-1})	Width Band 3 (cm^{-1})
Toluene	2970.25	1688.79	1079.34
1,4-Dioxane	2954.94	1920.47	1090.13
Chloroform	3311.74	1818.46	1069.22
Acetonitrile	3030.93	2025.12	1232.33
1-Octanol	2961.58	1893.33	1092.46
1-Hexanol	3053.45	1938.74	1128.53
1-Butanol	3019.70	1902.46	1150.08
1-Pentanol	2998.88	1977.07	1136.51
1-Propanol	2984.77	1953.98	1133.62
Acetic acid	3113.36	2064.38	1181.68
Methanol	3052.82	2024.77	1185.65
2,2,2-Trifluoroethanol	2659.40	1968.97	1434.81

Table 3.2.7. Summary of band width of 3 band fit using Gaussian model for normalised **17** emission spectra recorded at 400 nm excitation.

Solvent	Area Band 1 (cm^{-1})	Area Band 2 (cm^{-1})	Area Band 3 (cm^{-1})	Area Ratio Band 1/2 (400 nm ex)	Area Ratio Band 1/3 (400 nm ex)	Area Ratio Band 2/3 (400 nm ex)
Toluene	1322.61	1135.62	788.14	1.16	1.68	1.44
1,4-Dioxane	1201.03	1536.00	650.52	0.78	1.85	2.36
Chloroform	1755.86	1054.43	578.71	1.67	3.03	1.82
Acetonitrile	1237.71	1613.63	602.79	0.77	2.05	2.68
1-Octanol	1268.03	1458.30	652.22	0.87	1.94	2.24
1-Hexanol	1252.52	1508.99	654.24	0.83	1.91	2.31
1-Butanol	1271.80	1480.01	677.96	0.86	1.88	2.18
1-Pentanol	1148.75	1613.79	650.80	0.71	1.77	2.48
1-Propanol	1247.82	1552.88	618.25	0.80	2.02	2.51
Acetic acid	1249.04	1602.54	599.34	0.78	2.08	2.67
Methanol	1261.10	1661.62	594.59	0.76	2.12	2.79
2,2,2-Trifluoroethanol	1054.53	1576.92	772.27	0.67	1.37	2.04

Solvent	Band 1 Area Percentage(%)	Band 2 Area Percentage (%)	Band 3 Area Percentage (%)
Toluene	40.74	34.98	24.28
1,4-Dioxane	35.45	45.34	19.20
Chloroform	51.81	31.11	17.08
Acetonitrile	35.83	46.72	17.45
1-Octanol	37.53	43.16	19.30
1-Hexanol	36.67	44.18	19.15
1-Butanol	37.08	43.15	19.77
1-Pentanol	33.65	47.28	19.07
1-Propanol	36.50	45.42	18.08
Acetic acid	36.19	46.44	17.37
Methanol	35.85	47.24	16.90
2,2,2-Trifluoroethanol	30.98	46.33	22.69

Table 3.2.8. Band areas, area ratios and total area percentage of 3 band fit using Gaussian model for normalised **17** emission spectra recorded at 400 nm excitation.

3.2.4 310 nm Gaussian band fit - Solvatochromic analysis.

3.2.4.1 E_T^N.

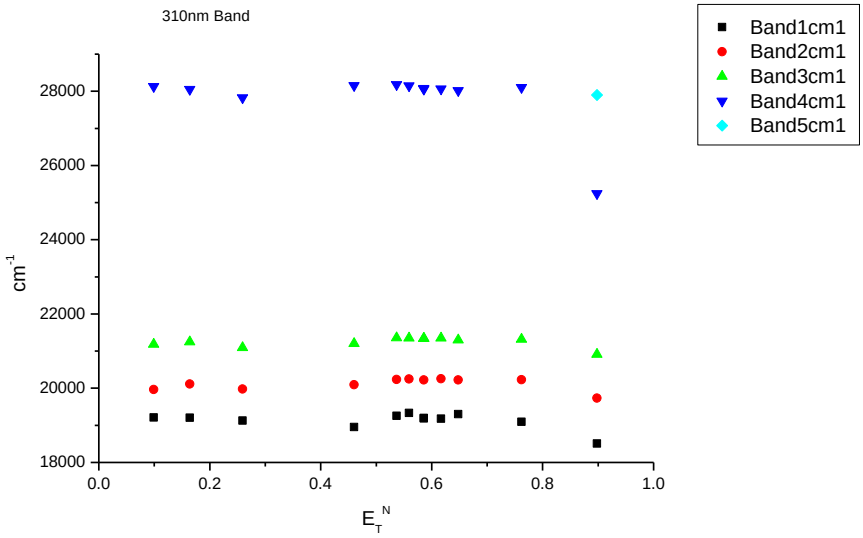

Figure 3.2.1. Band maxima from Gaussian model fit of the normalised fluorescence emission spectra of **17** recorded at 310 nm excitation against E_T^N.

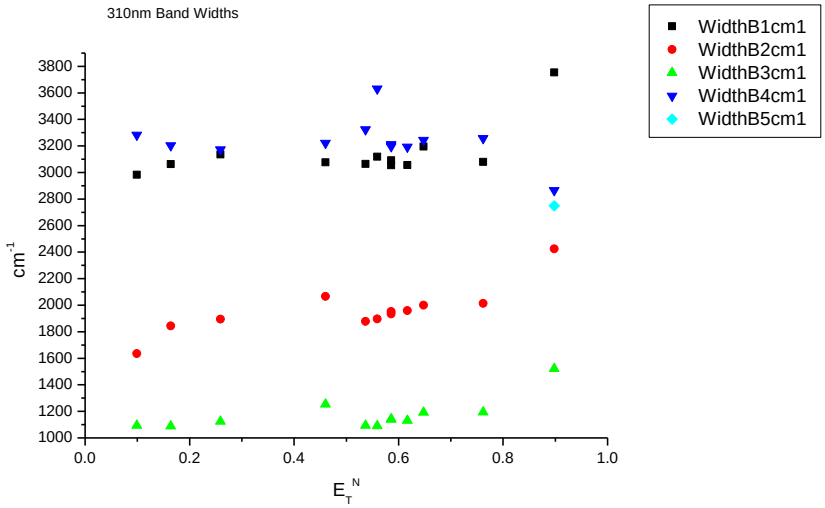

Figure 3.2.2. Band widths from Gaussian model fit of the normalised fluorescence emission spectra of **17** recorded at 310 nm excitation against E_T^N.

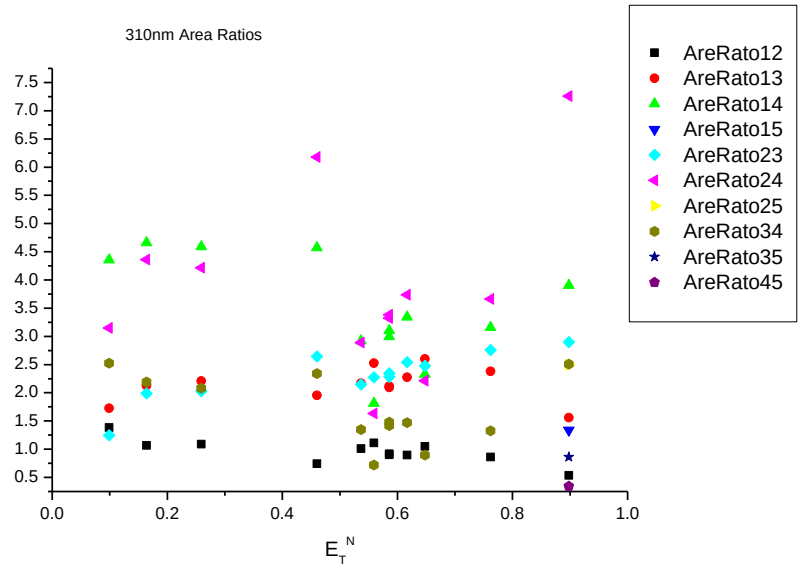

Figure 3.2.3. Area ratios from Gaussian model fit of the normalised fluorescence emission spectra of **17** recorded at 310 nm excitation against E_T^N.

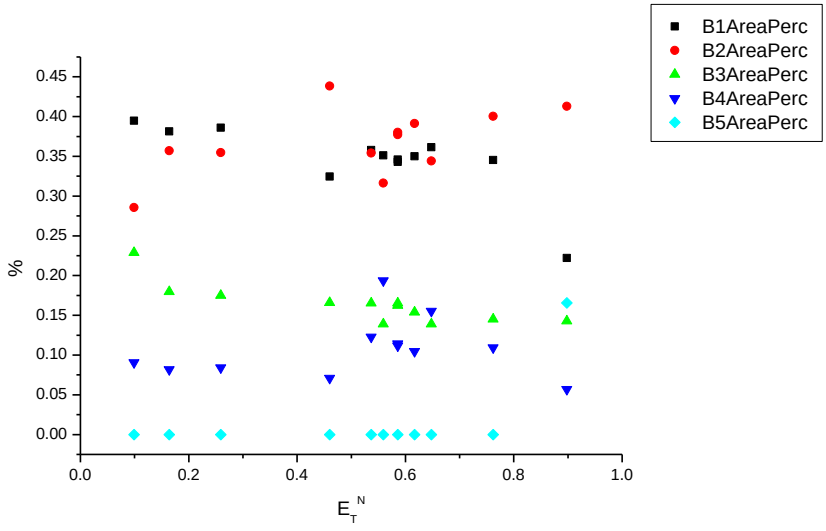

Figure 3.2.4. Area percentages from Gaussian model fit of the normalised fluorescence emission spectra of **17** recorded at 310 nm excitation against E_T^N.

3.2.4.2 *α*

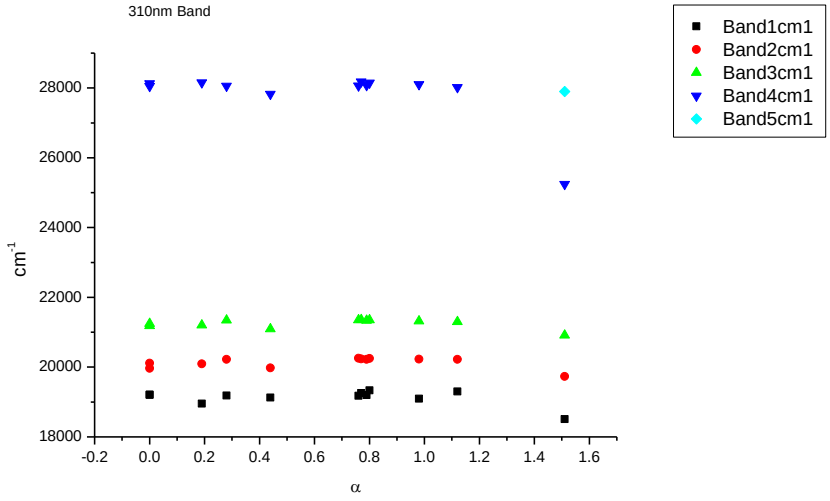

Figure 3.2.5. Band maxima from Gaussian model fit of the normalised fluorescence emission spectra of **17** recorded at 310 nm excitation against α.

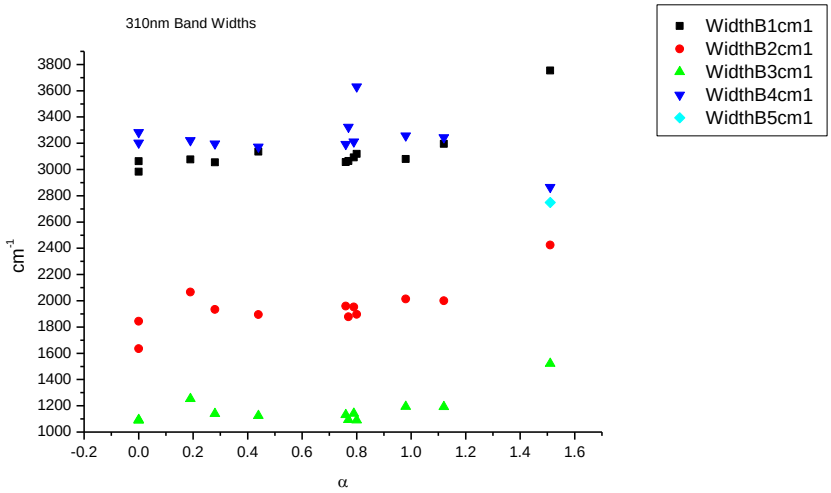

Figure 3.2.6. Band widths from Gaussian model fit of the normalised fluorescence emission spectra of **17** recorded at 310 nm excitation against α.

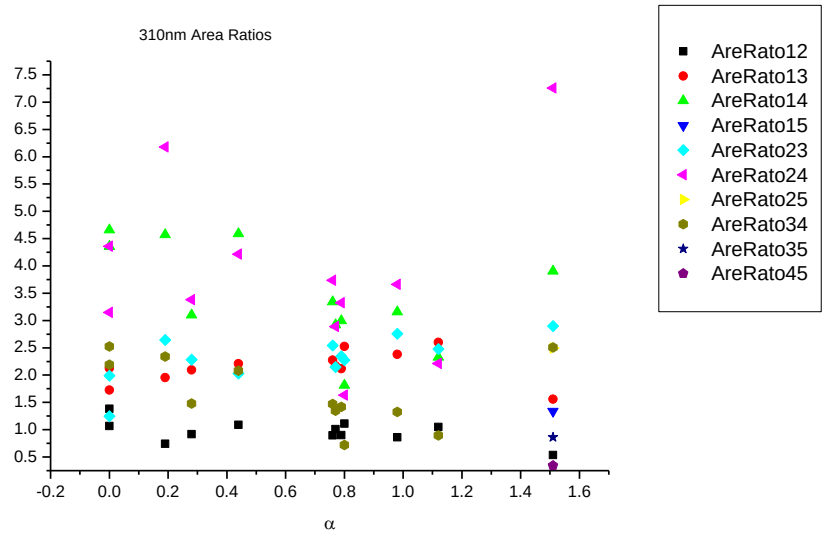

Figure 3.2.7. Area Ratios from Gaussian model fit of the normalised fluorescence emission spectra of **17** recorded at 310 nm excitation against α.

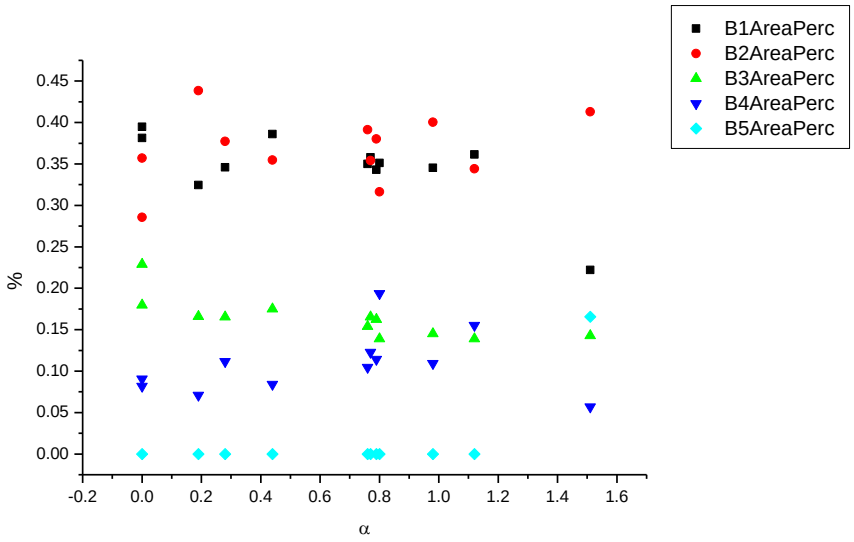

Figure 3.2.8. Area percentages from Gaussian model fit of the normalised fluorescence emission spectra of **17** recorded at 310 nm excitation against α.

3.2.4.3 β.

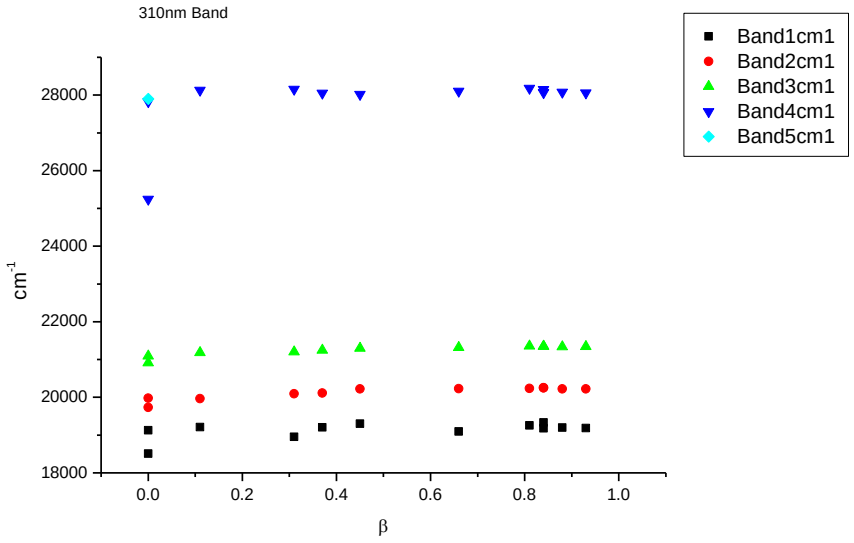

Figure 3.2.9. Band maxima from Gaussian model fit of the normalised fluorescence emission spectra of **17** recorded at 310 nm excitation against β.

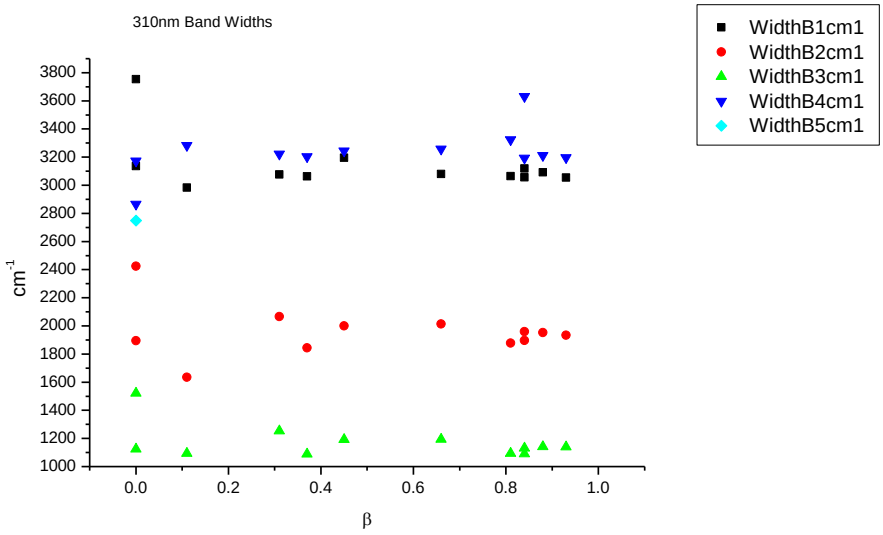

Figure 3.2.10. Band widths from Gaussian model fit of the normalised fluorescence emission spectra of **17** recorded at 310 nm excitation against β.

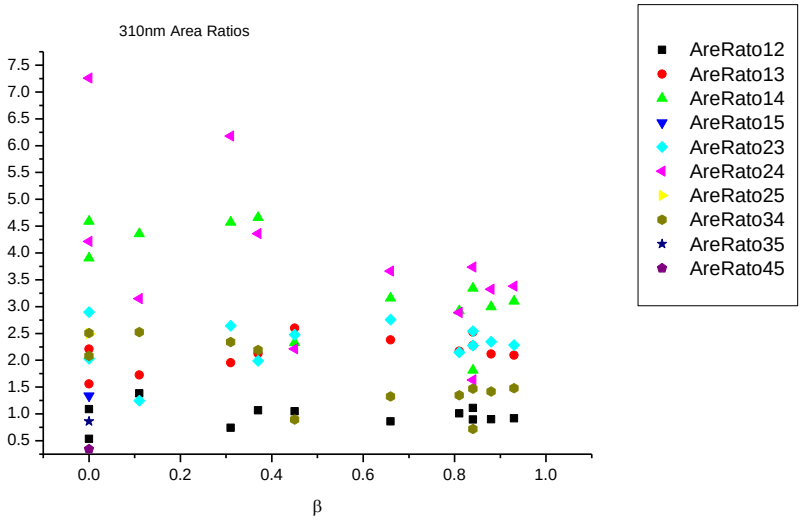

Figure 3.2.11. Area ratios from Gaussian model fit of the normalised fluorescence emission spectra of **17** recorded at 310 nm excitation against β.

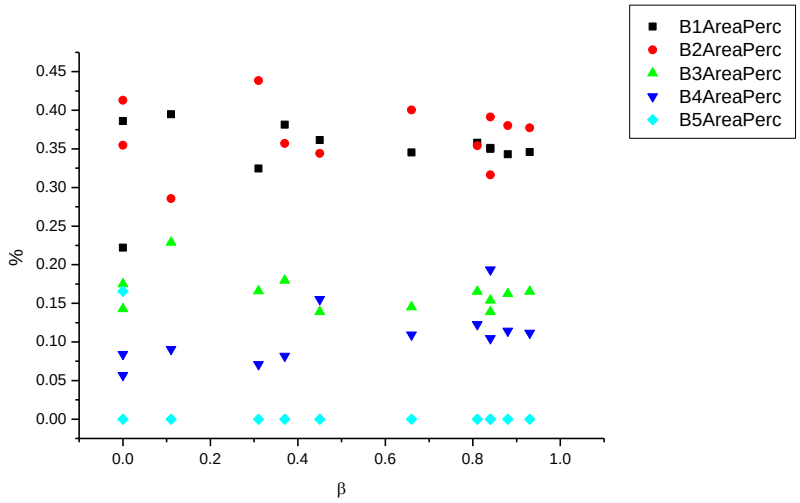

Figure 3.2.12. Area percentages from Gaussian model fit of the normalised fluorescence emission spectra of **17** recorded at 310 nm excitation against β.

3.2.4.4 π.*

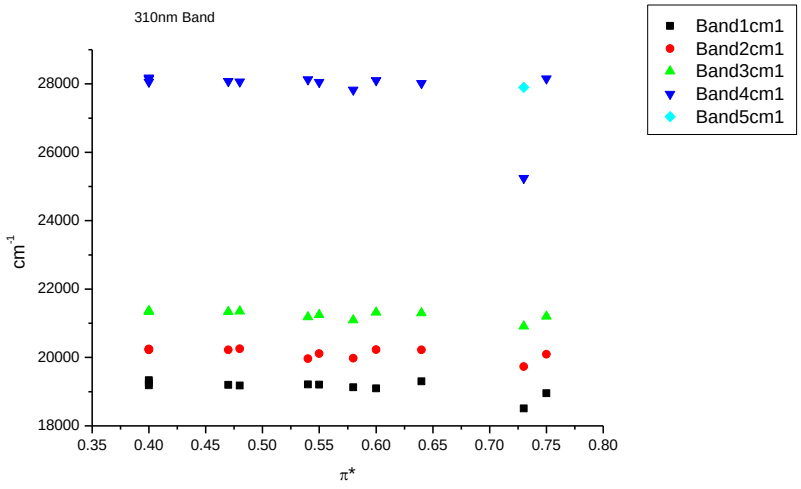

Figure 3.2.13. Band maxima from Gaussian model fit of the normalised fluorescence emission spectra of **17** recorded at 310 nm excitation against π*.

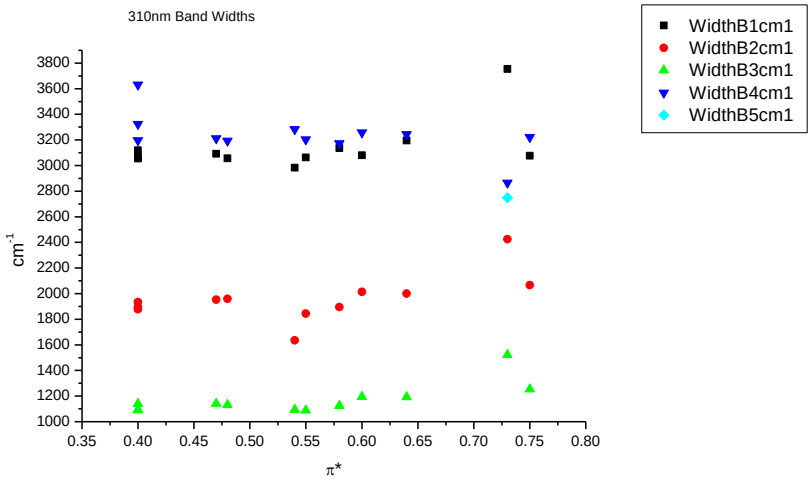

Figure 3.2.14. Band widths from Gaussian model fit of the normalised fluorescence emission spectra of **17** recorded at 310 nm excitation against π*.

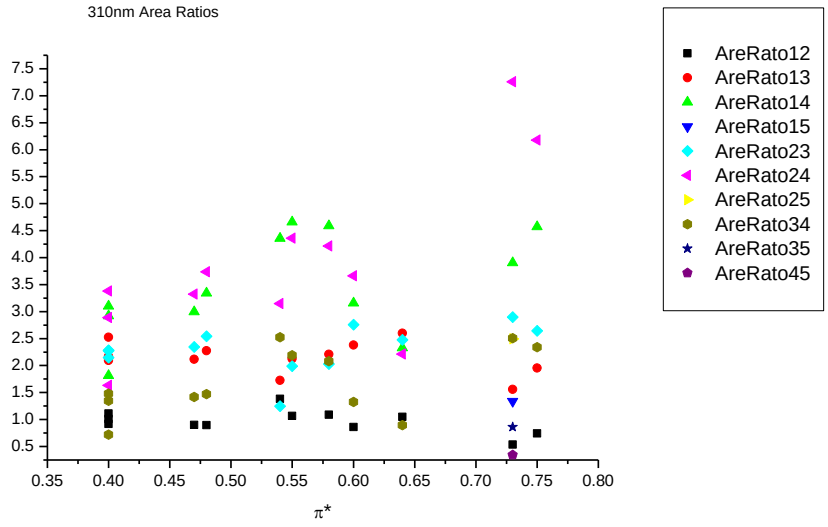

Figure 3.2.15. Area ratios from Gaussian model fit of the normalised fluorescence emission spectra of **17** recorded at 310 nm excitation against π*.

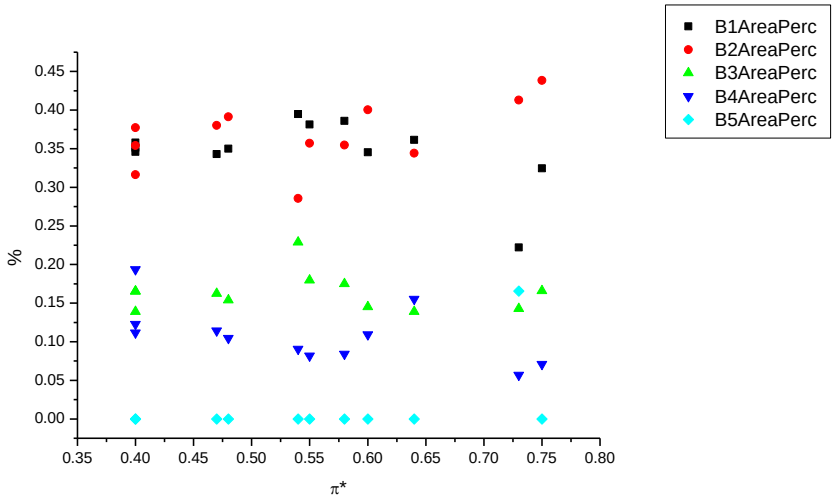

Figure 3.2.16. Area percentages from Gaussian model fit of the normalised fluorescence emission spectra of **17** recorded at 310 nm excitation against π*.

3.2.4.5 μ(D).

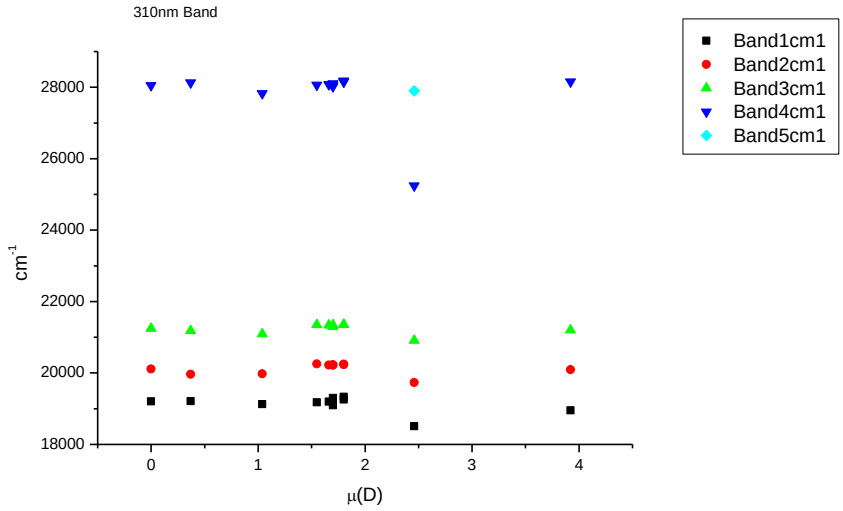

Figure 3.2.17. Band maxima from Gaussian model fit of the normalised fluorescence emission spectra of **17** recorded at 310 nm excitation against μ(D).

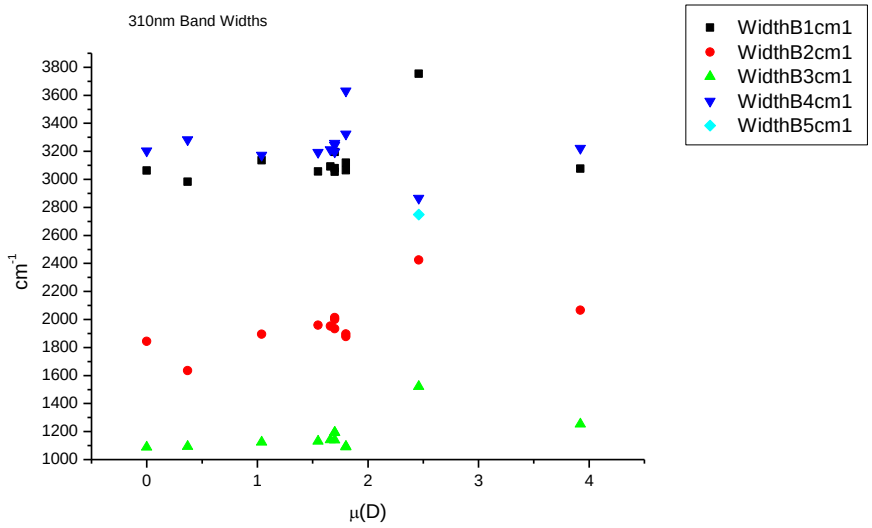

Figure 3.2.18. Band widths from Gaussian model fit of the normalised fluorescence emission spectra of **17** recorded at 310 nm excitation against μ(D).

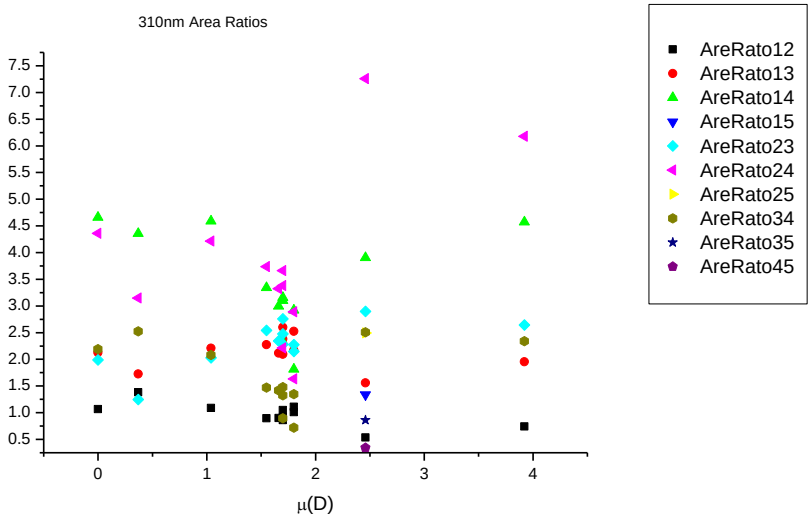

Figure 3.2.19. Area ratios from Gaussian model fit of the normalised fluorescence emission spectra of **17** recorded at 310 nm excitation against μ(D).

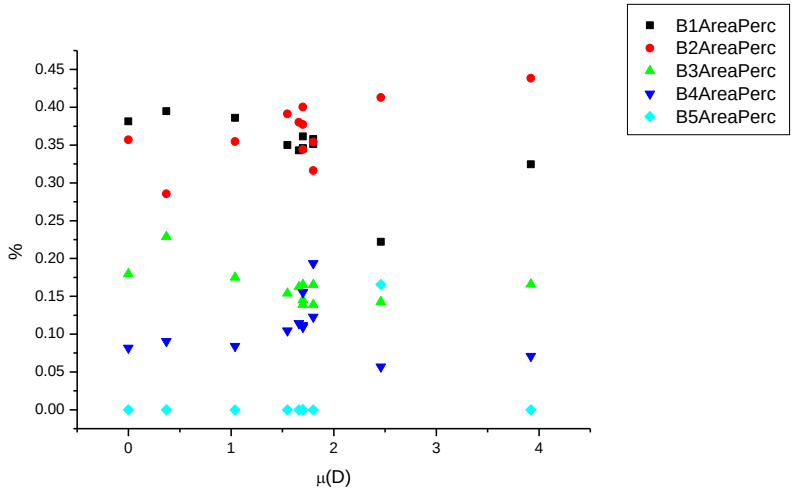

Figure 3.2.20. Area percentages from Gaussian model fit of the normalised fluorescence emission spectra of **17** recorded at 310 nm excitation against μ(D).

3.2.4.6 η(Cp).

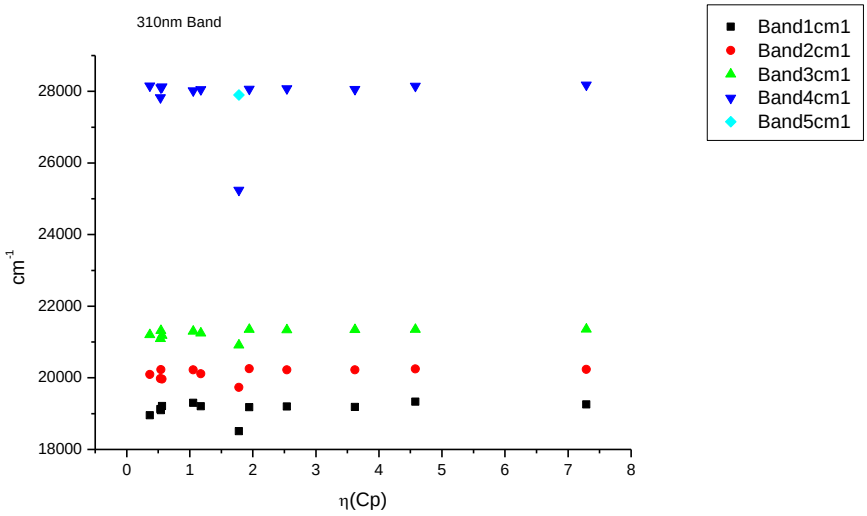

Figure 3.2.21. Band maxima from Gaussian model fit of the normalised fluorescence emission spectra of **17** recorded at 310 nm excitation against η(Cp).

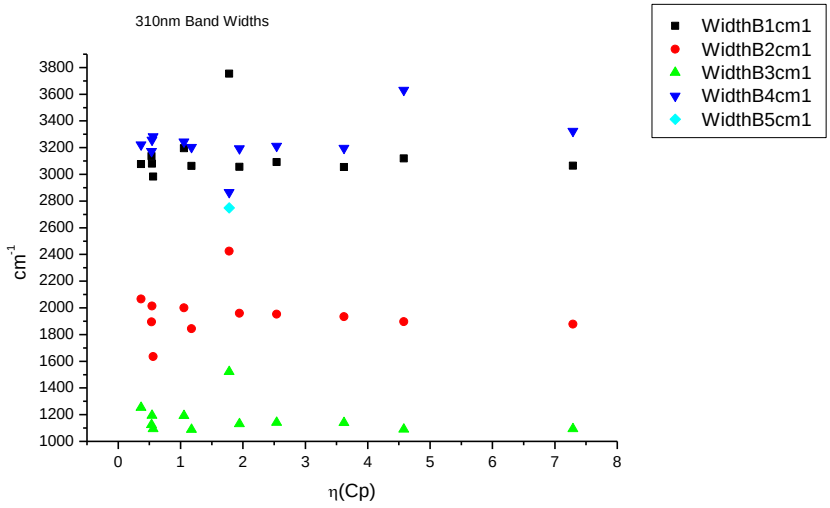

Figure 3.2.22. Band widths from Gaussian model fit of the normalised fluorescence emission spectra of **17** recorded at 310 nm excitation against η(Cp).

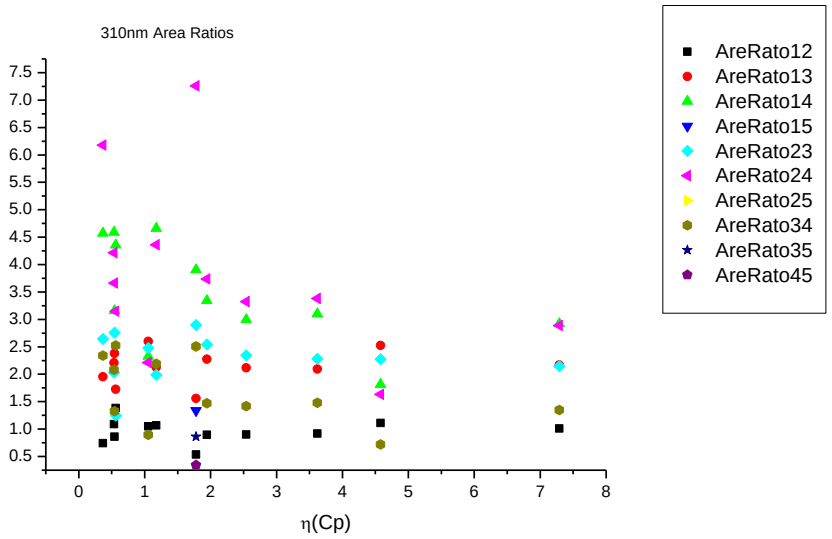

Figure 3.2.23. Area ratios from Gaussian model fit of the normalised fluorescence emission spectra of **17** recorded at 310 nm excitation against η(Cp).

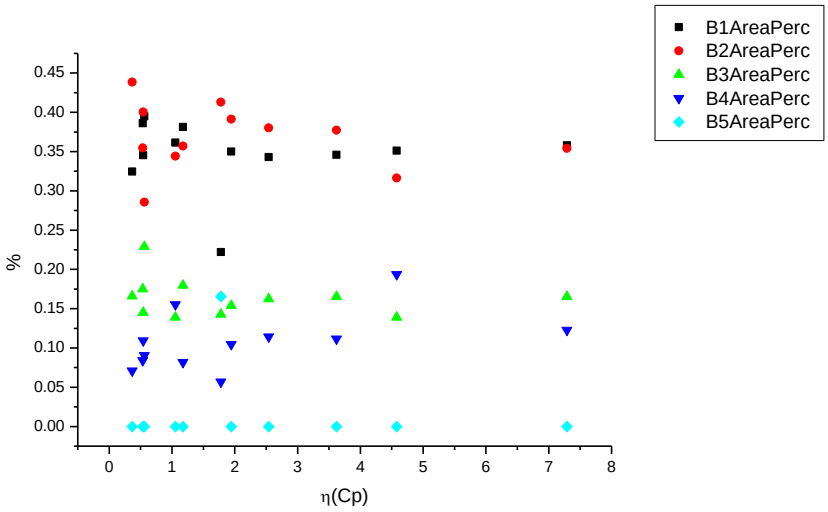

Figure 3.2.24. Area percentages from Gaussian model fit of the normalised fluorescence emission spectra of **17** recorded at 310 nm excitation against η(Cp).

3.2.5 400 nm Gaussian band fit - Solvatochromic analysis.

3.2.5.1 E_T^N.

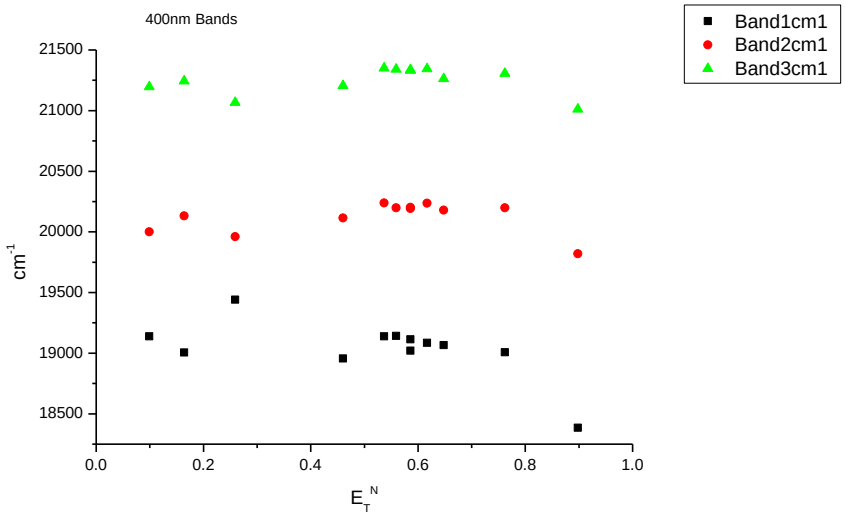

Figure 3.2.25. Band maxima from Gaussian model fit of the normalised fluorescence emission spectra of **17** recorded at 400 nm excitation against E_T^N.

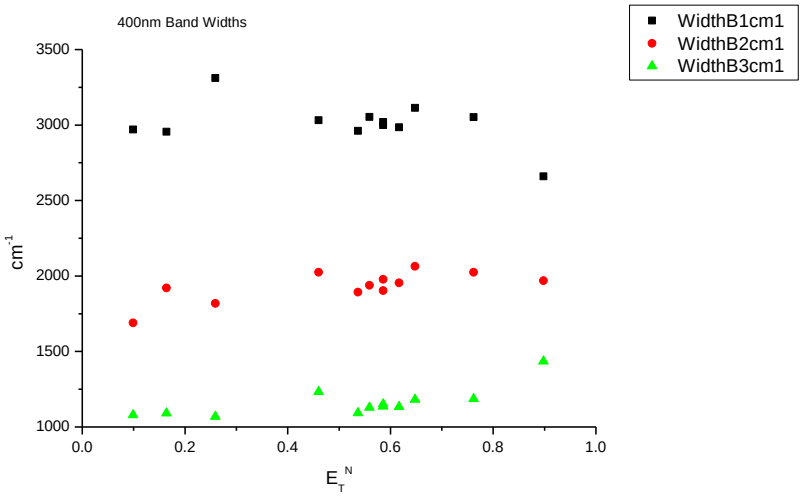

Figure 3.2.26. Band widths from Gaussian model fit of the normalised fluorescence emission spectra of **17** recorded at 400 nm excitation against E_T^N.

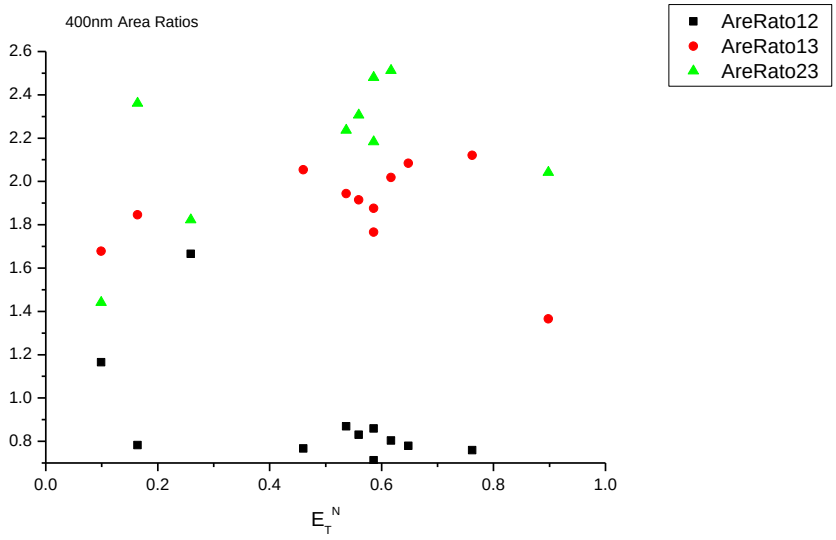

Figure 3.2.27. Area ratios from Gaussian model fit of the normalised fluorescence emission spectra of **17** recorded at 400 nm excitation against E_T^N.

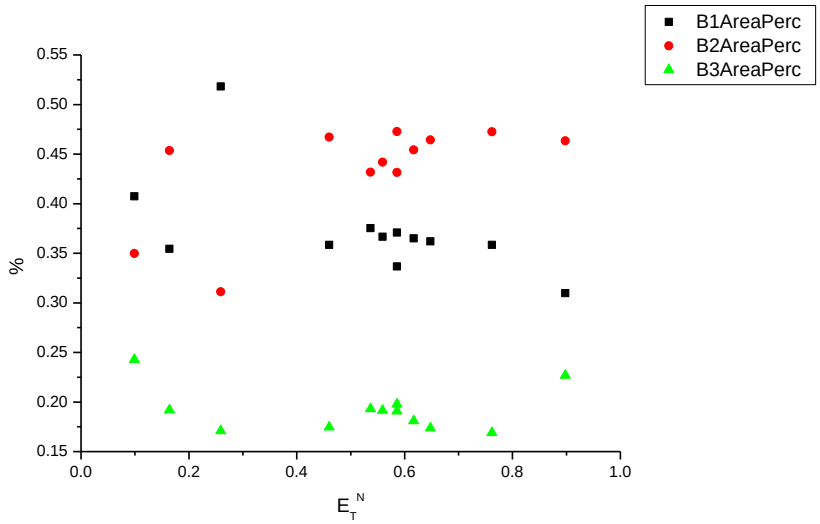

Figure 3.2.28. Area percentages from Gaussian model fit of the normalised fluorescence emission spectra of **17** recorded at 400 nm excitation against E_T^N.

3.2.5.2 *α*

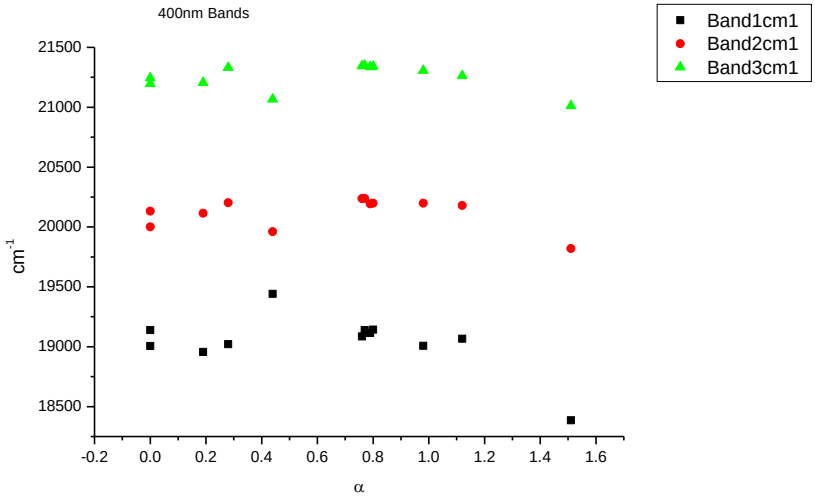

Figure 3.2.29. Band maxima from Gaussian model fit of the normalised fluorescence emission spectra of **17** recorded at 400 nm excitation against α.

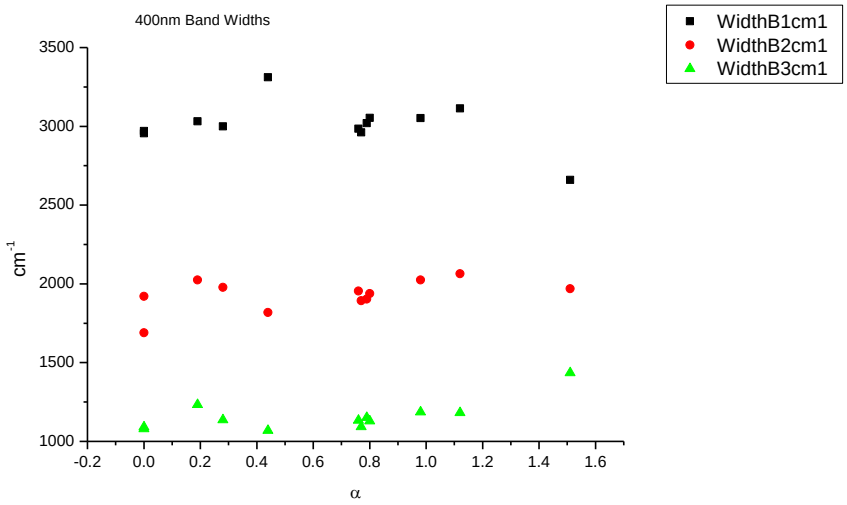

Figure 3.2.30. Band widths from Gaussian model fit of the normalised fluorescence emission spectra of **17** recorded at 400 nm excitation against α.

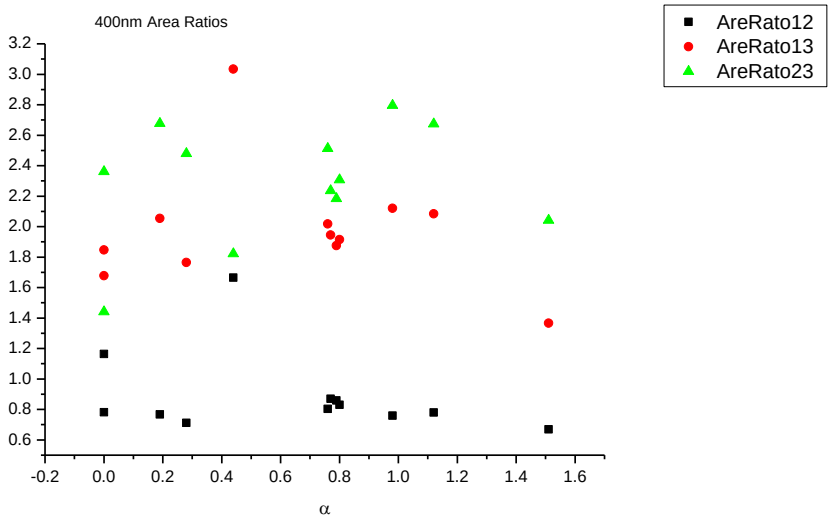

Figure 3.2.31. Area ratios from Gaussian model fit of the normalised fluorescence emission spectra of **17** recorded at 400 nm excitation against α.

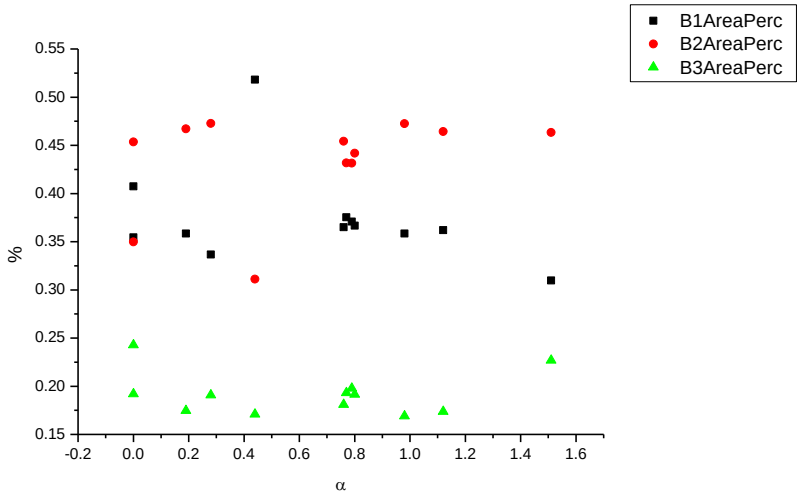

Figure 3.2.32. Area percentages from Gaussian model fit of the normalised fluorescence emission spectra of **17** recorded at 400 nm excitation against α.

3.2.5.3 β.

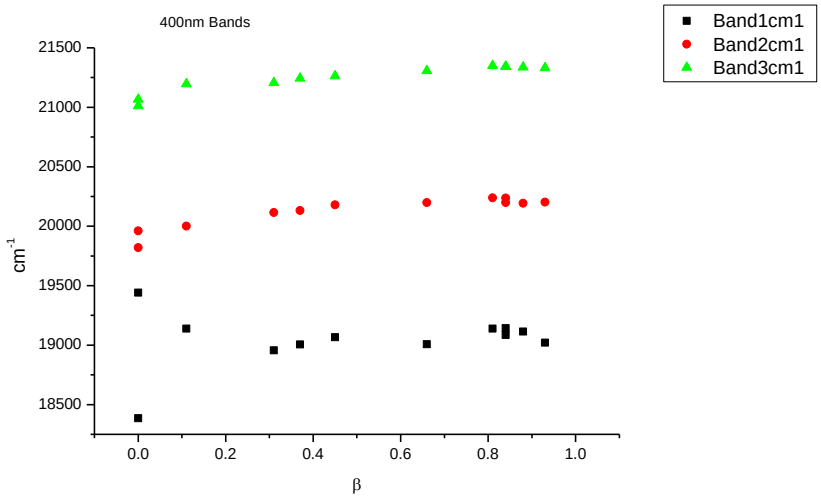

Figure 3.2.33. Band maxima from Gaussian model fit of the normalised fluorescence emission spectra of **17** recorded at 400 nm excitation against β.

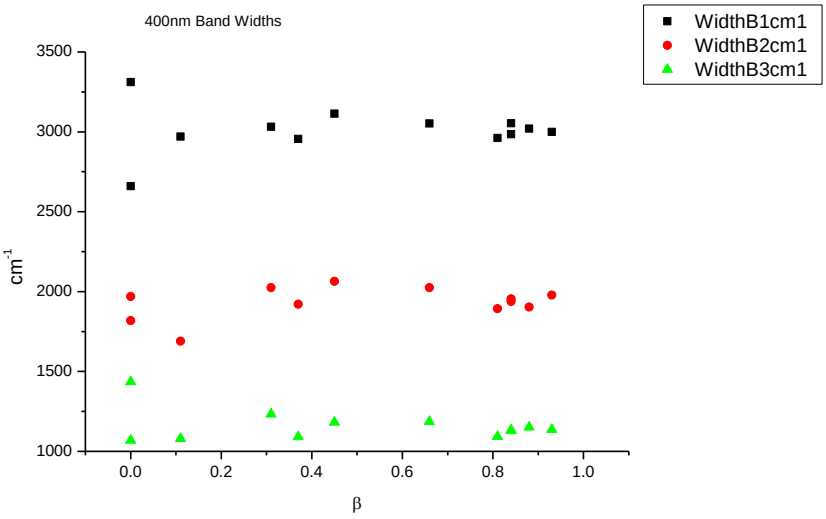

Figure 3.2.34. Band widths from Gaussian model fit of the normalised fluorescence emission spectra of **17** recorded at 400 nm excitation against β.

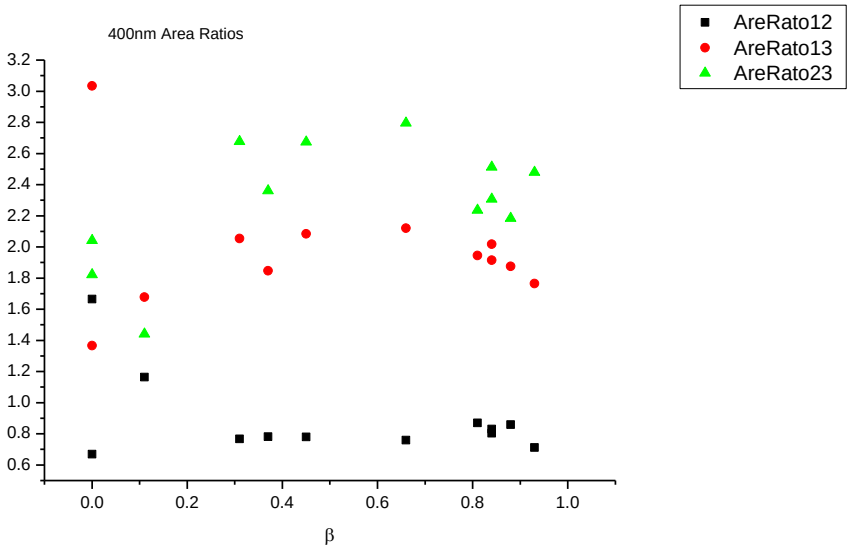

Figure 3.2.35. Area ratios from Gaussian model fit of the normalised fluorescence emission spectra of **17** recorded at 400 nm excitation against β.

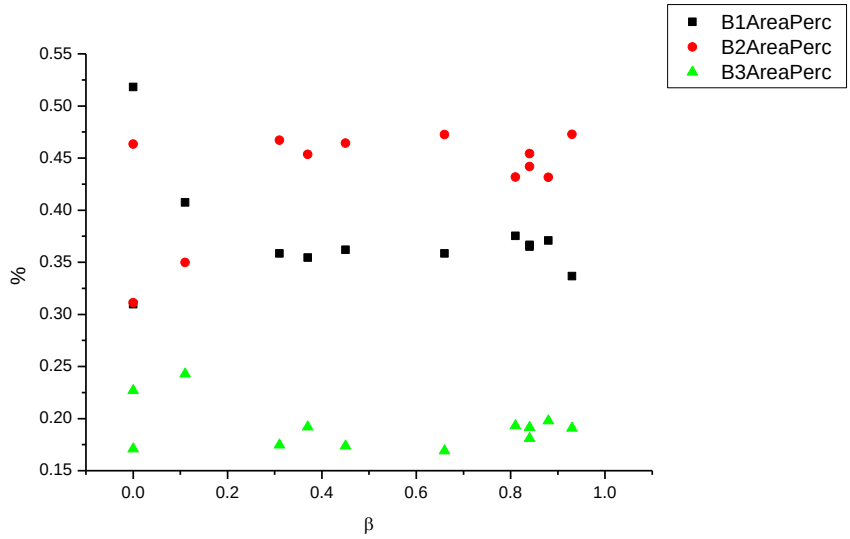

Figure 3.2.36. Area percentages from Gaussian model fit of the normalised fluorescence emission spectra of **17** recorded at 400 nm excitation against β.

3.2.5.4 π.*

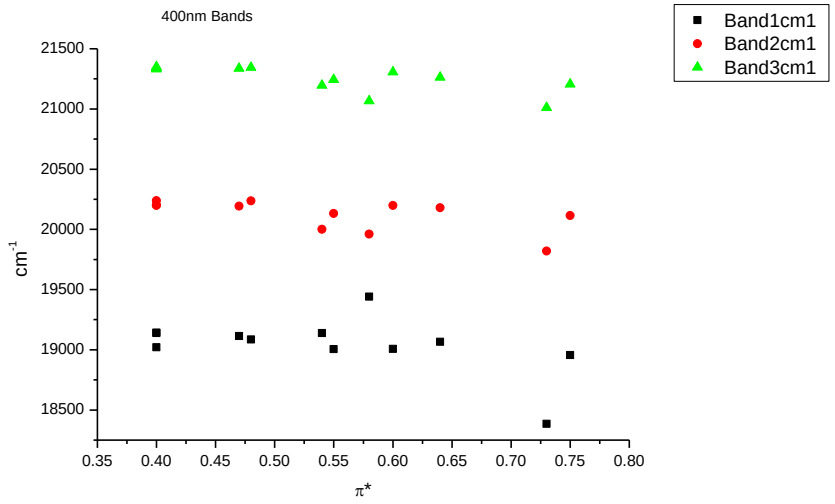

Figure 3.2.37. Band maxima from Gaussian model fit of the normalised fluorescence emission spectra of **17** recorded at 400 nm excitation against π*.

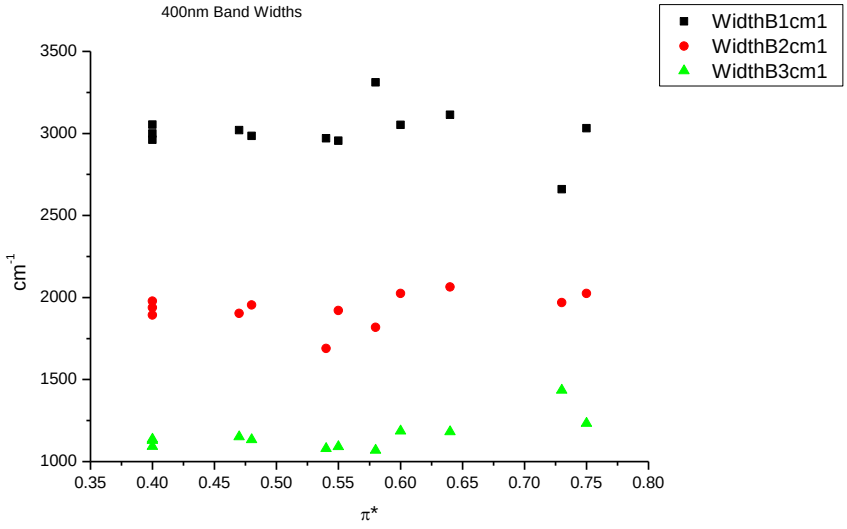

Figure 3.2.38. Band widths from Gaussian model fit of the normalised fluorescence emission spectra of **17** recorded at 400 nm excitation against π*.

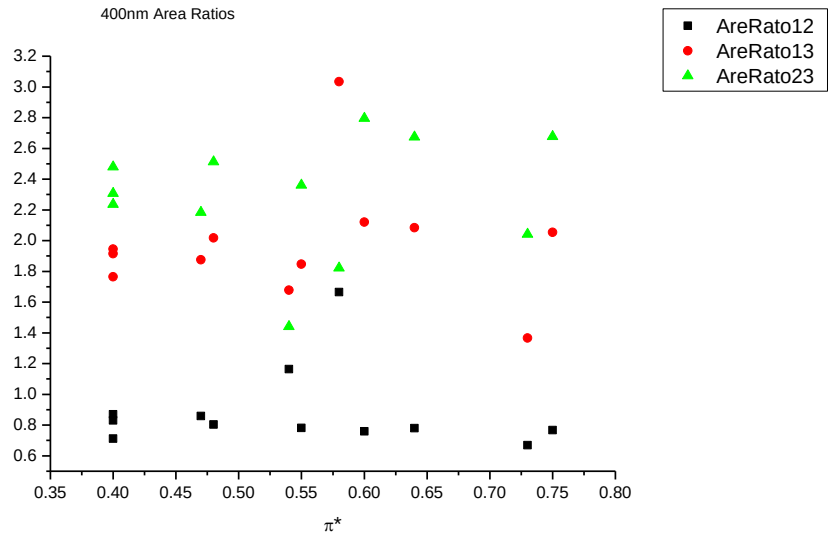

Figure 3.2.39. Area ratios from Gaussian model fit of the normalised fluorescence emission spectra of **17** recorded at 400 nm excitation against π*.

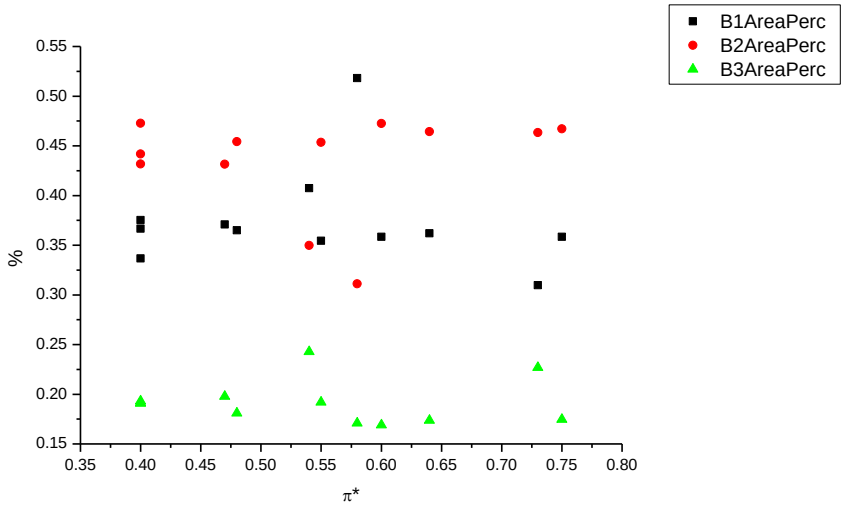

Figure 3.2.40. Area percentages from Gaussian model fit of the normalised fluorescence emission spectra of **17** recorded at 400 nm excitation against π*.

3.2.5.5 μ(D).

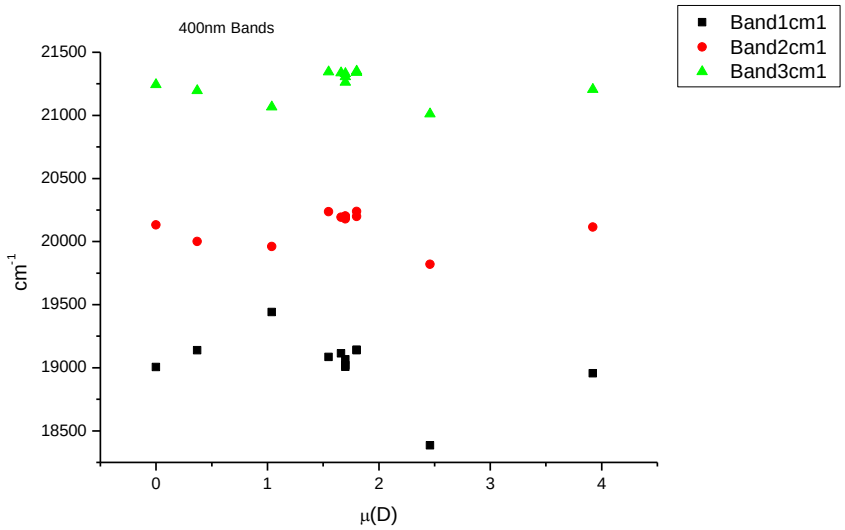

Figure 3.2.41. Band maxima from Gaussian model fit of the normalised fluorescence emission spectra of **17** recorded at 400 nm excitation against μ(D).

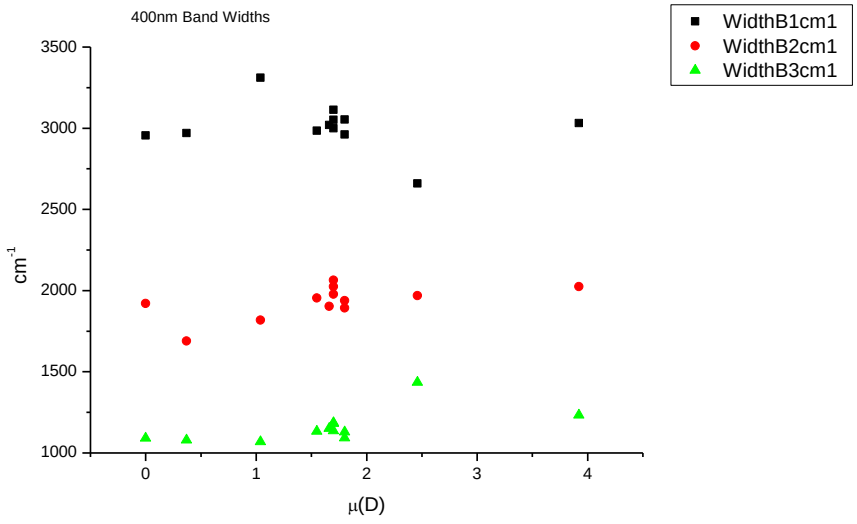

Figure 3.2.42. Band widths from Gaussian model fit of the normalised fluorescence emission spectra of **17** recorded at 400 nm excitation against μ(D).

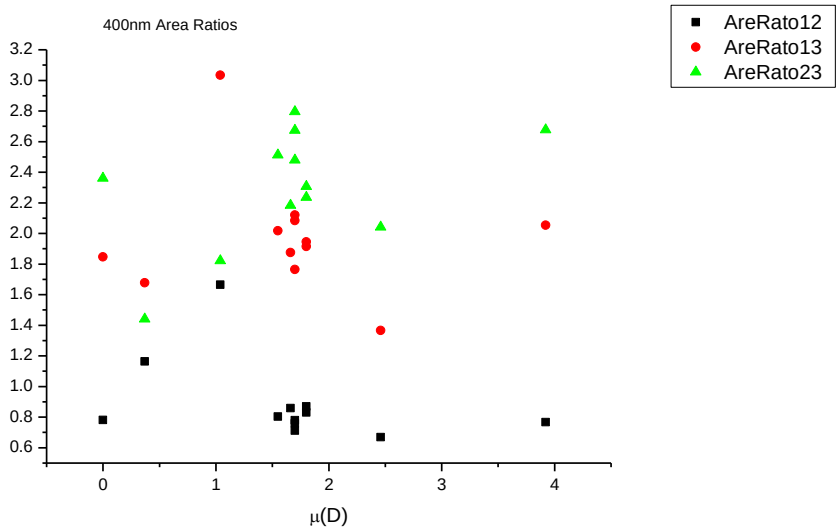

Figure 3.2.43. Area ratios from Gaussian model fit of the normalised fluorescence emission spectra of **17** recorded at 400 nm excitation against μ(D).

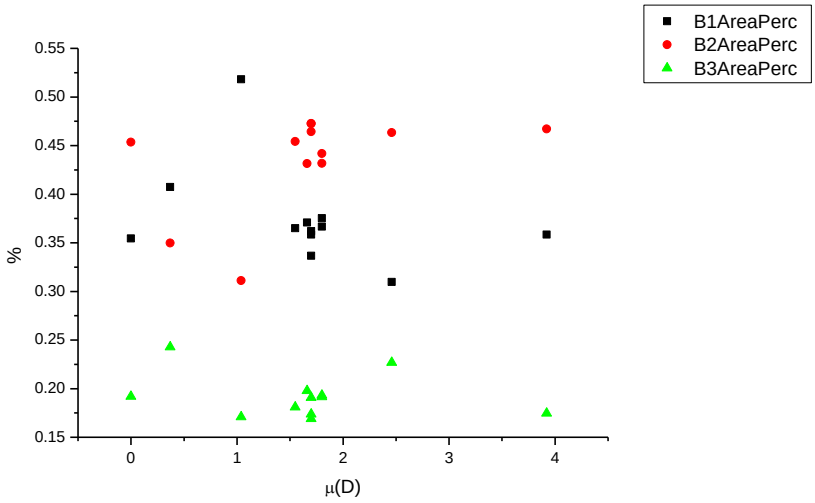

Figure 3.2.44. Area percentages from Gaussian model fit of the normalised fluorescence emission spectra of **17** recorded at 400 nm excitation against μ(D).

3.2.5.6 η(Cp).

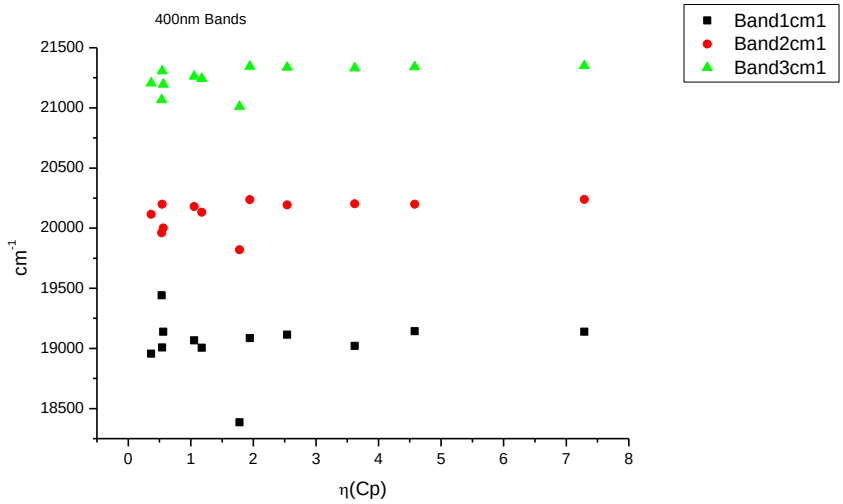

Figure 3.2.45. Band maxima from Gaussian model fit of the normalised fluorescence emission spectra of **17** recorded at 400 nm excitation against η(Cp).

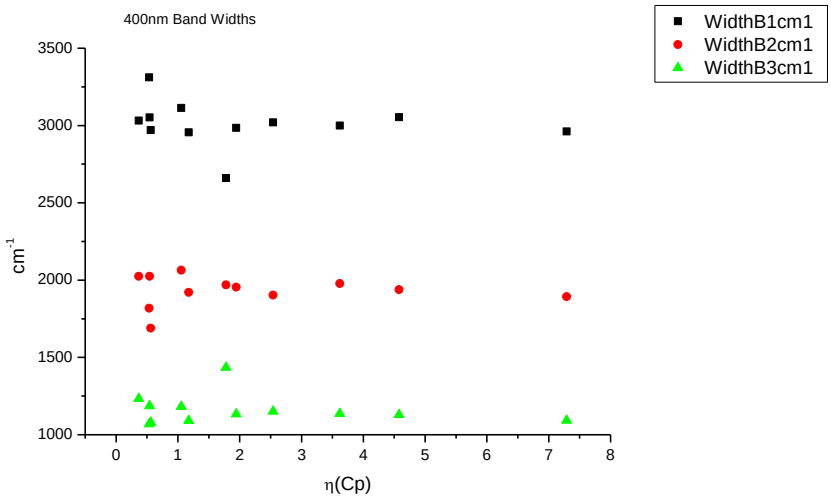

Figure 3.2.46. Band widths from Gaussian model fit of the normalised fluorescence emission spectra of **17** recorded at 400 nm excitation against η(Cp).

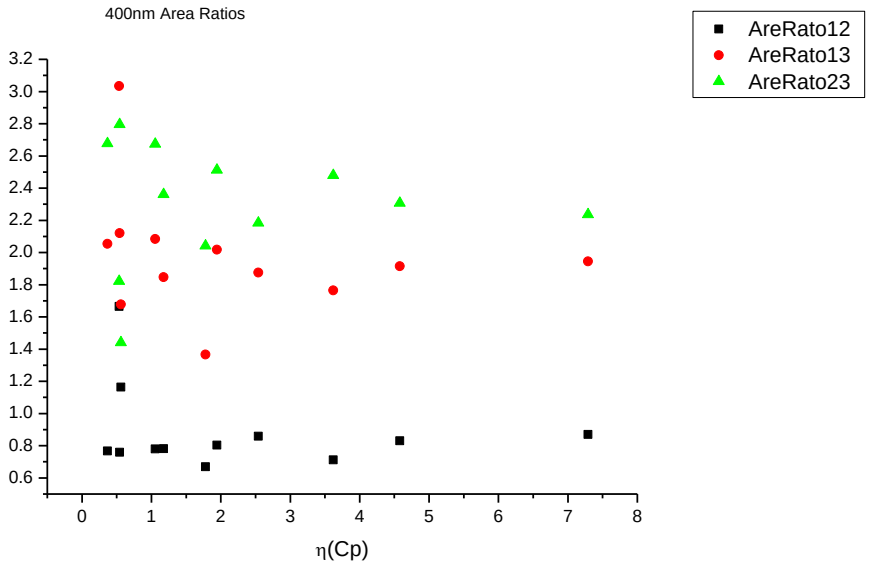

Figure 3.2.47. Area ratios from Gaussian model fit of the normalised fluorescence emission spectra of **17** recorded at 400 nm excitation against η(Cp).

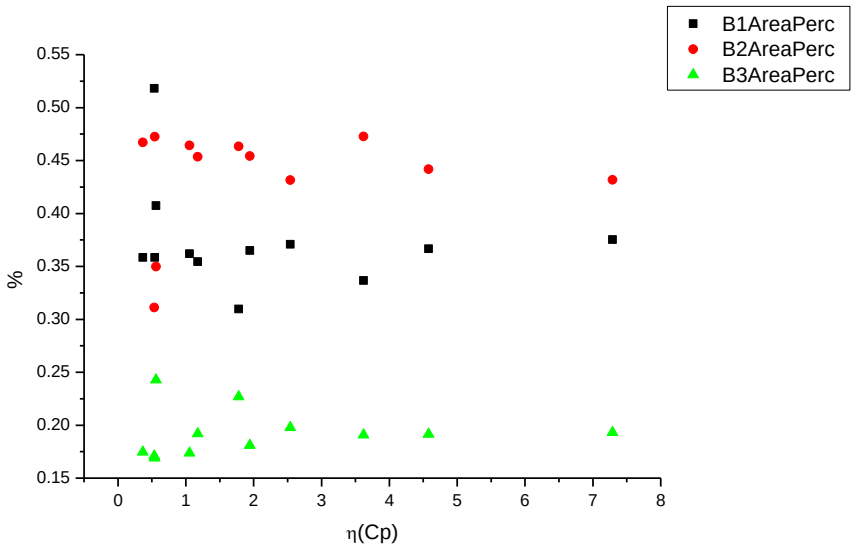

Figure 3.2.48. Area percentages from Gaussian model fit of the normalised fluorescence emission spectra of **17** recorded at 400 nm excitation against η(Cp).

3.2.6 400 nm fluorescent lifetime results.

3.2.6.1 Intensity weighted.

Wavelength (nm)	Solvent	τ_1 (ns)	A_1 (%)	τ_2 (ns)	A_2 (%)	τ_3 (ns)	A_3 (%)	τ_f (ns) (Intensity Weighted)	$1/\tau_f$	χ^2
470	Toluene	-	-	1.17	16.81	2.70	83.19	2.44	0.41	1.19
470	1,4-Dioxane	0.30	1.45	1.70	28.77	2.78	69.79	2.43	0.41	1.13
470	Chloroform	-	-	1.41	34.93	2.65	65.07	2.21	0.45	1.19
470	Acetonitrile	-	-	1.64	37.50	3.11	62.50	2.56	0.39	1.14
470	1-Octanol	0.19	19.94	1.74	54.48	2.40	25.57	1.60	0.62	1.41
470	1-Hexanol	0.53	4.74	1.54	57.08	2.36	38.18	1.81	0.55	1.15
470	1-Butanol	0.52	5.18	1.60	61.05	2.41	33.77	1.82	0.55	1.19
470	1-Pentanol	0.59	10.32	1.80	81.25	3.00	8.43	1.78	0.56	1.28
470	1-Propanol	-	-	1.25	39.92	2.16	60.08	1.80	0.56	1.08
470	Acetic acid	0.49	22.83	0.99	74.22	2.41	2.96	0.92	1.09	1.03
470	Methanol	0.34	4.82	1.52	41.38	2.38	53.80	1.92	0.52	1.21
470	2,2,2-Trifluoroethanol	0.42	68.59	0.68	30.34	5.01	1.08	0.54	1.84	1.08

Table 3.2.9. Summary of Time Correlated Single Photon Counting (TCSPC) fluorescent lifetimes (intensity weighted) of **17** recorded at 470 nm.

Wavelength (nm)	Solvent	τ_1 (ns)	A_1 (%)	τ_2 (ns)	A_2 (%)	τ_3 (ns)	A_3 (%)	τ_f (ns) (Intensity Weighted)	$1/\tau_f$	χ^2
490	Toluene	-	-	1.06	13.77	2.67	86.23	2.45	0.41	1.12
490	1,4-Dioxane	0.37	1.59	1.78	31.25	2.82	67.17	2.45	0.41	1.10
490	Chloroform	-	-	1.53	37.83	2.74	62.17	2.28	0.44	1.07
490	Acetonitrile	-	-	1.54	29.62	3.03	70.38	2.59	0.39	1.22
490	1-Octanol	0.19	18.15	1.72	59.61	2.59	22.04	1.63	0.61	1.28
490	1-Hexanol	0.30	4.82	1.67	76.95	2.81	18.23	1.81	0.55	1.16
490	1-Butanol	0.34	5.47	1.67	75.41	2.74	19.12	1.80	0.55	1.05
490	1-Pentanol	0.56	6.14	1.79	86.47	3.49	7.39	1.84	0.54	1.19
490	1-Propanol	-	-	1.29	44.37	2.22	55.63	1.81	0.55	1.17
490	Acetic acid	0.44	18.41	1.03	78.47	2.39	3.12	0.96	1.04	0.93
490	Methanol	0.33	4.50	1.53	42.82	2.40	1.94	1.94	0.52	1.04
490	2,2,2-Trifluoroethanol	0.43	65.22	0.66	33.88	5.45	0.91	0.55	1.81	1.18

Table 3.2.10. Summary of Time Correlated Single Photon Counting (TCSPC) fluorescent lifetimes (intensity weighted) of **17** recorded at 490 nm.

Wavelength (nm)	Solvent	τ_1 (ns)	A_1 (%)	τ_2 (ns)	A_2 (%)	τ_3 (ns)	A_3 (%)	τ_f (ns) (Intensity Weighted)	$1/\tau_f$	χ^2
520	Toluene	-	-	1.29	19.25	2.76	80.75	2.48	0.40	1.17
520	1,4-Dioxane	0.28	1.64	1.91	42.69	2.97	55.68	2.47	0.40	1.10
520	Chloroform	0.36	2.75	1.96	66.07	3.21	31.17	2.31	0.43	1.15
520	Acetonitrile	-	-	1.71	37.15	3.16	62.85	2.63	0.38	1.13
520	1-Octanol	0.17	16.55	1.79	68.69	2.81	14.75	1.67	0.60	1.37
520	1-Hexanol	0.44	4.54	1.71	77.88	2.84	17.58	1.85	0.54	1.16
520	1-Butanol	0.49	6.21	1.81	88.07	3.75	5.72	1.84	0.54	1.20
520	1-Pentanol	0.47	6.06	1.80	88.02	3.85	5.91	1.84	0.54	1.21
520	1-Propanol	0.36	4.66	1.73	88.07	3.72	7.27	1.81	0.55	0.99
520	Acetic acid	0.56	23.03	1.09	73.89	2.46	3.08	1.01	0.99	1.10
520	Methanol	0.30	2.90	1.47	39.99	2.41	57.11	1.98	0.51	1.08
520	2,2,2-Trifluoroethanol	0.42	66.47	0.69	32.71	4.48	0.82	0.54	1.85	1.02

Table 3.2.11. Summary of Time Correlated Single Photon Counting (TCSPC) fluorescent lifetimes (intensity weighted) of **17** recorded at 520 nm.

Wavelength (nm)	Solvent	τ_1 (ns)	A_1 (%)	τ_2 (ns)	A_2 (%)	τ_3 (ns)	A_3 (%)	τ_f (ns) (Intensity Weighted)	$1/\tau_f$	χ^2
540	Toluene	-	-	1.31	19.94	2.77	80.06	2.48	0.40	1.23
540	1,4-Dioxane	0.40	1.33	1.93	44.91	3.00	53.76	2.49	0.40	1.14
540	Chloroform	0.32	2.42	1.88	57.83	3.07	39.75	2.31	0.43	1.10
540	Acetonitrile	-	-	1.72	37.53	3.17	62.47	2.63	0.38	1.02
540	1-Octanol	0.18	16.52	1.89	79.47	4.10	4.01	1.69	0.59	1.36
540	1-Hexanol	0.76	10.91	1.92	86.74	6.36	2.35	1.90	0.53	1.17
540	1-Butanol	0.78	9.03	1.88	87.31	4.51	3.66	1.87	0.53	1.06
540	1-Pentanol	0.48	6.15	1.80	88.30	3.95	5.56	1.84	0.54	1.20
540	1-Propanol	0.41	5.16	1.75	88.03	3.81	6.82	1.82	0.55	0.99
540	Acetic acid	0.39	14.21	1.06	82.59	2.50	3.20	1.01	0.99	0.91
540	Methanol	0.28	2.16	1.46	41.67	2.45	56.17	1.99	0.50	1.03
540	2,2,2-Trifluoroethanol	0.44	74.55	0.73	24.50	6.63	0.95	0.58	1.74	1.18

Table 3.2.12. Summary of Time Correlated Single Photon Counting (TCSPC) fluorescent lifetimes (intensity weighted) of **17** recorded at 540 nm.

Wavelength (nm)	Solvent	τ_1 (ns)	A_1 (%)	τ_2 (ns)	A_2 (%)	τ_3 (ns)	A_3 (%)	τ_f (ns) (Intensity Weighted)	$1/\tau_f$	χ^2
570	Toluene	-	-	1.44	24.59	2.84	75.41	2.49	0.40	1.22
570	1,4-Dioxane	0.34	3.49	2.05	55.88	3.22	40.63	2.46	0.41	0.93
570	Chloroform	0.34	2.25	1.98	69.27	3.36	28.48	2.34	0.43	1.19
570	Acetonitrile	-	-	1.70	36.23	3.22	63.77	2.67	0.37	1.16
570	1-Octanol	0.20	15.28	1.89	80.78	4.73	3.94	1.75	0.57	1.27
570	1-Hexanol	0.47	9.54	1.86	86.62	5.51	3.84	1.87	0.54	1.14
570	1-Butanol	0.43	9.21	1.85	86.84	4.88	3.95	1.84	0.54	1.18
570	1-Pentanol	0.55	9.05	1.85	87.52	5.58	3.43	1.86	0.54	1.22
570	1-Propanol	0.85	10.54	1.86	86.27	5.50	3.19	1.87	0.53	1.09
570	Acetic acid	0.37	24.59	1.11	73.78	3.41	1.64	0.97	1.04	0.95
570	Methanol	0.32	6.40	1.69	56.53	2.63	37.07	1.95	0.51	1.05
570	2,2,2-Trifluoroethanol	0.47	80.63	0.77	18.33	5.14	1.04	0.57	1.75	1.13

Table 3.2.13. Summary of Time Correlated Single Photon Counting (TCSPC) fluorescent lifetimes (intensity weighted) of **17** recorded at 570 nm.

3.2.6.2 Amplitude weighted.

Wavelength (nm)	Solvent	τ_1 (ns)	A_1 (%)	τ_2 (ns)	A_2 (%)	τ_3 (ns)	A_3 (%)	τ_f (ns) (Amplitude Weighted)	$1/\tau_f$	χ^2
470	Toluene	-	-	1.17	31.86	2.70	68.14	2.21	0.45	1.19
470	1,4-Dioxane	0.30	10.43	1.70	36.08	2.78	53.49	2.13	0.47	1.13
470	Chloroform	-	-	1.41	50.16	2.65	49.84	2.03	0.49	1.19
470	Acetonitrile	-	-	1.64	53.26	3.11	46.74	2.33	0.43	1.14
470	1-Octanol	0.19	70.95	1.74	21.67	2.40	7.38	0.69	1.45	1.41
470	1-Hexanol	0.53	14.32	1.54	59.58	2.36	26.10	1.61	0.62	1.15
470	1-Butanol	0.52	16.00	1.60	61.51	2.41	22.49	1.61	0.62	1.19
470	1-Pentanol	0.59	26.79	1.80	68.91	3.00	4.30	1.53	0.65	1.28
470	1-Propanol	-	-	1.25	53.39	2.16	46.61	1.68	0.60	1.08
470	Acetic acid	0.49	38.22	0.99	60.78	2.41	1.00	0.81	1.23	1.03
470	Methanol	0.34	22.30	1.52	42.47	2.38	35.23	1.56	0.64	1.21
470	2,2,2-Trifluoroethanol	0.42	78.60	0.68	21.30	5.01	0.10	0.48	2.10	1.08

Table 3.2.14. Summary of Time Correlated Single Photon Counting (TCSPC) fluorescent lifetimes (amplitude weighted) of **17** recorded at 470 nm.

Wavelength (nm)	Solvent	τ_1 (ns)	A_1 (%)	τ_2 (ns)	A_2 (%)	τ_3 (ns)	A_3 (%)	τ_f (ns) (Amplitude Weighted)	$1/\tau_f$	χ^2
490	Toluene	-	-	1.06	28.64	2.67	71.36	2.21	0.45	1.12
490	1,4-Dioxane	0.37	9.28	1.78	38.51	2.82	52.21	2.19	0.46	1.10
490	Chloroform	-	-	1.53	52.07	2.74	47.93	2.11	0.47	1.07
490	Acetonitrile	-	-	1.54	45.26	3.03	54.74	2.36	0.42	1.22
490	1-Octanol	0.19	68.86	1.72	25.01	2.59	6.13	0.72	1.39	1.28
490	1-Hexanol	0.30	23.45	1.67	67.11	2.81	9.44	1.46	0.69	1.16
490	1-Butanol	0.34	23.50	1.67	66.26	2.74	10.24	1.47	0.68	1.05
490	1-Pentanol	0.56	17.85	1.79	78.71	3.49	3.44	1.63	0.61	1.19
490	1-Propanol	-	-	1.29	57.78	2.22	42.22	1.68	0.59	1.17
490	Acetic acid	0.44	35.17	1.03	63.74	2.39	1.10	0.84	1.19	0.93
490	Methanol	0.33	21.59	1.53	43.93	2.40	34.48	1.57	0.64	1.04
490	2,2,2-Trifluoroethanol	0.43	74.60	0.66	25.31	5.45	0.08	0.49	2.04	1.18

Table 3.2.15. Summary of Time Correlated Single Photon Counting (TCSPC) fluorescent lifetimes (amplitude weighted) of **17** recorded at 490 nm.

Wavelength (nm)	Solvent	τ_1 (ns)	A_1 (%)	τ_2 (ns)	A_2 (%)	τ_3 (ns)	A_3 (%)	τ_f (ns) (Amplitude Weighted)	$1/\tau_f$	χ^2
520	Toluene	-	-	1.29	33.81	2.76	66.19	2.26	0.44	1.17
520	1,4-Dioxane	0.28	12.34	1.91	47.65	2.97	40.02	2.13	0.47	1.10
520	Chloroform	0.36	15.14	1.96	65.85	3.21	19.01	1.96	0.51	1.15
520	Acetonitrile	-	-	1.71	52.17	3.16	47.83	2.41	0.42	1.13
520	1-Octanol	0.17	68.51	1.79	27.61	2.81	3.78	0.72	1.39	1.37
520	1-Hexanol	0.44	16.72	1.71	73.30	2.84	9.98	1.61	0.62	1.16
520	1-Butanol	0.49	20.33	1.81	77.25	3.75	2.42	1.59	0.63	1.20
520	1-Pentanol	0.47	20.18	1.80	77.39	3.85	2.42	1.58	0.63	1.21
520	1-Propanol	0.36	19.71	1.73	77.32	3.72	2.97	1.52	0.66	0.99
520	Acetic acid	0.56	37.52	1.09	61.35	2.46	1.13	0.91	1.10	1.10
520	Methanol	0.30	15.86	1.47	44.94	2.41	39.20	1.66	0.60	1.08
520	2,2,2-Trifluoroethanol	0.42	76.83	0.69	23.08	4.48	0.09	0.49	2.05	1.02

Table 3.2.16. Summary of Time Correlated Single Photon Counting (TCSPC) fluorescent lifetimes (amplitude weighted) of **17** recorded at 520 nm.

Wavelength (nm)	Solvent	τ_1 (ns)	A_1 (%)	τ_2 (ns)	A_2 (%)	τ_3 (ns)	A_3 (%)	τ_f (ns) (Amplitude Weighted)	$1/\tau_f$	χ^2
540	Toluene	-	-	1.31	34.52	2.77	65.48	2.27	0.44	1.23
540	1,4-Dioxane	0.40	7.40	1.93	52.37	3.00	40.23	2.25	0.44	1.14
540	Chloroform	0.32	14.81	1.88	60.00	3.07	25.18	1.95	0.51	1.10
540	Acetonitrile	-	-	1.72	52.58	3.17	47.42	2.41	0.41	1.02
540	1-Octanol	0.18	67.74	1.89	31.53	4.10	0.73	0.75	1.34	1.36
540	1-Hexanol	0.76	23.90	1.92	75.49	6.36	0.62	1.67	0.60	1.17
540	1-Butanol	0.78	19.59	1.88	79.03	4.51	1.38	1.70	0.59	1.06
540	1-Pentanol	0.48	20.39	1.80	77.39	3.95	2.22	1.58	0.63	1.20
540	1-Propanol	0.41	19.30	1.75	77.93	3.81	2.78	1.55	0.65	0.99
540	Acetic acid	0.39	31.48	1.06	67.41	2.50	1.11	0.86	1.16	0.91
540	Methanol	0.28	13.23	1.46	48.11	2.45	38.66	1.69	0.59	1.03
540	2,2,2-Trifluoroethanol	0.44	83.33	0.73	16.60	6.63	0.07	0.50	2.01	1.18

Table 3.2.17. Summary of Time Correlated Single Photon Counting (TCSPC) fluorescent lifetimes (amplitude weighted) of **17** recorded at 540 nm.

Wavelength (nm)	Solvent	τ_1 (ns)	A_1 (%)	τ_2 (ns)	A_2 (%)	τ_3 (ns)	A_3 (%)	τ_f (ns) (Amplitude Weighted)	$1/\tau_f$	χ^2
570	Toluene	-	-	1.44	39.19	2.84	60.81	2.29	0.44	1.22
570	1,4-Dioxane	0.34	20.64	2.05	54.24	3.22	25.12	1.99	0.50	0.93
570	Chloroform	0.34	13.05	1.98	69.97	3.36	16.98	2.00	0.50	1.19
570	Acetonitrile	-	-	1.70	51.92	3.22	48.08	2.43	0.41	1.16
570	1-Octanol	0.20	63.33	1.89	35.97	4.73	35.97	0.84	1.19	1.27
570	1-Hexanol	0.47	30.16	1.86	68.81	5.51	1.03	1.48	0.68	1.14
570	1-Butanol	0.43	30.74	1.85	68.09	4.88	1.17	1.45	0.69	1.18
570	1-Pentanol	0.55	25.69	1.85	73.35	5.58	0.96	1.55	0.64	1.22
570	1-Propanol	0.85	20.87	1.86	78.15	5.50	0.98	1.69	0.59	1.09
570	Acetic acid	0.37	49.72	1.11	49.92	3.41	0.36	0.75	1.33	0.95
570	Methanol	0.32	29.90	1.69	49.32	2.63	20.78	1.48	0.68	1.05
570	2,2,2-Trifluoroethanol	0.47	87.85	0.77	12.05	5.14	0.10	0.51	1.97	1.13

Table 3.2.18. Summary of Time Correlated Single Photon Counting (TCSPC) fluorescent lifetimes (amplitude weighted) of **17** recorded at 570 nm.

3.2.7 400 nm average fluorescent lifetimes - Solvatochromic analysis.

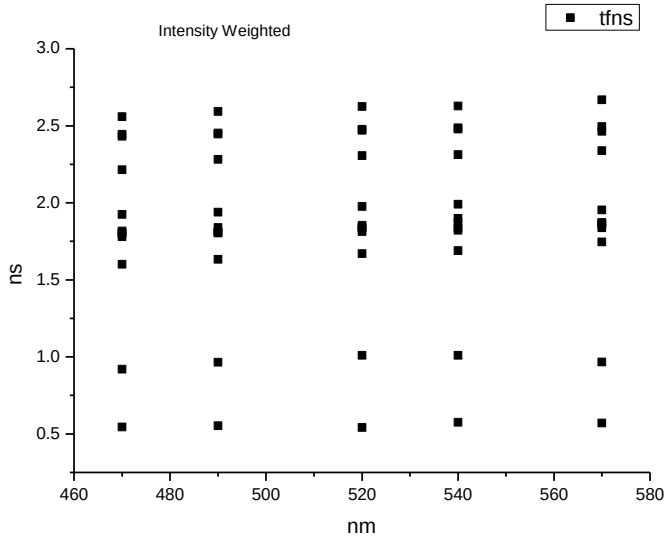

Figure 3.2.49. Intensity weighted average lifetime (τ_f) of **17** versus wavelength (nm).

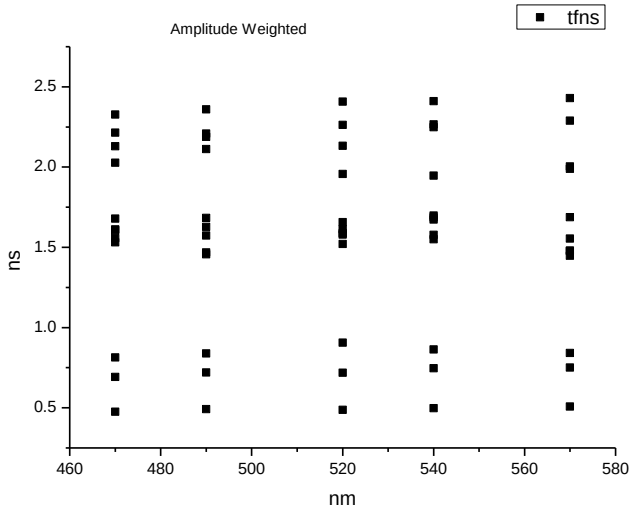

Figure 3.2.50. Amplitude weighted average lifetime (τ_f) of **17** versus wavelength (nm).

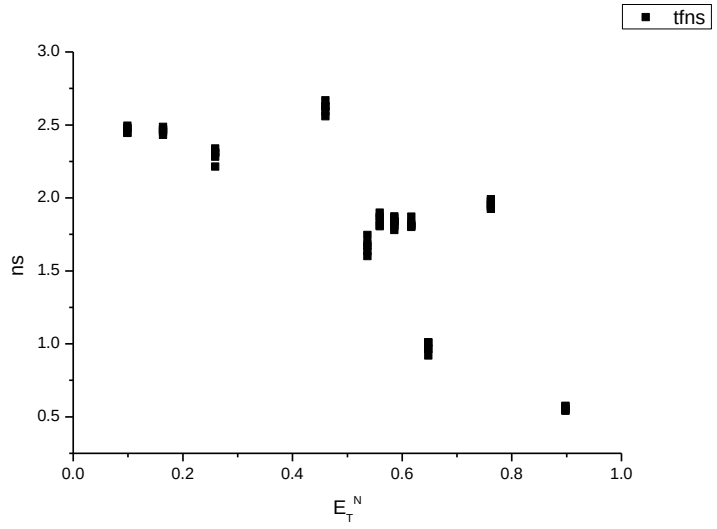

Figure 3.2.51. Intensity weighted average lifetime (τ_f) of **17** versus E_T^N.

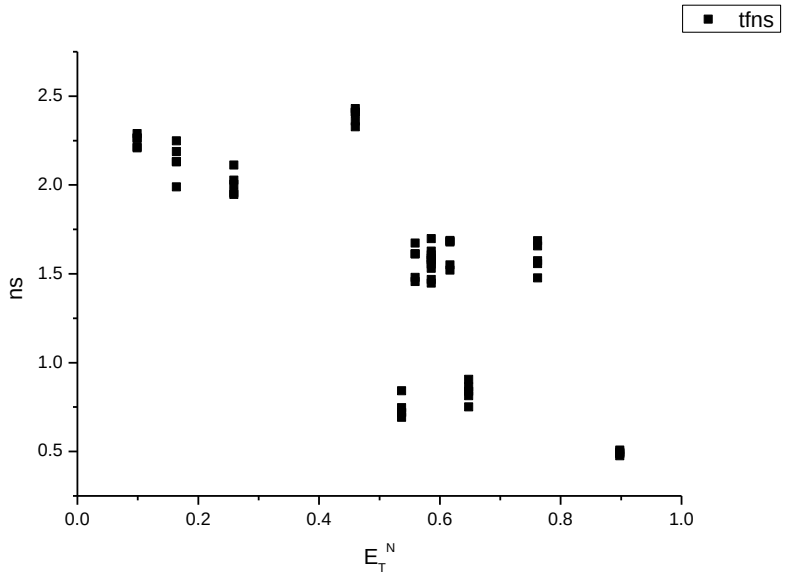

Figure 3.2.52. Amplitude weighted average lifetime (τ_f) of **17** versus E_T^N.

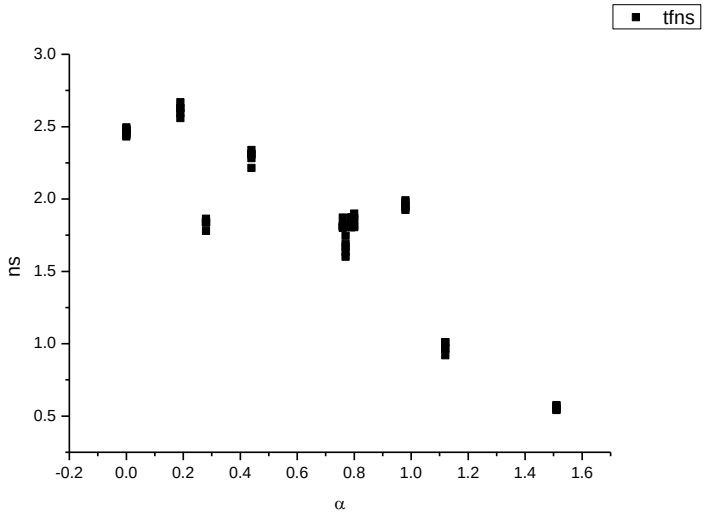

Figure 3.2.53. Intensity weighted average lifetime (τ_f) of **17** versus α.

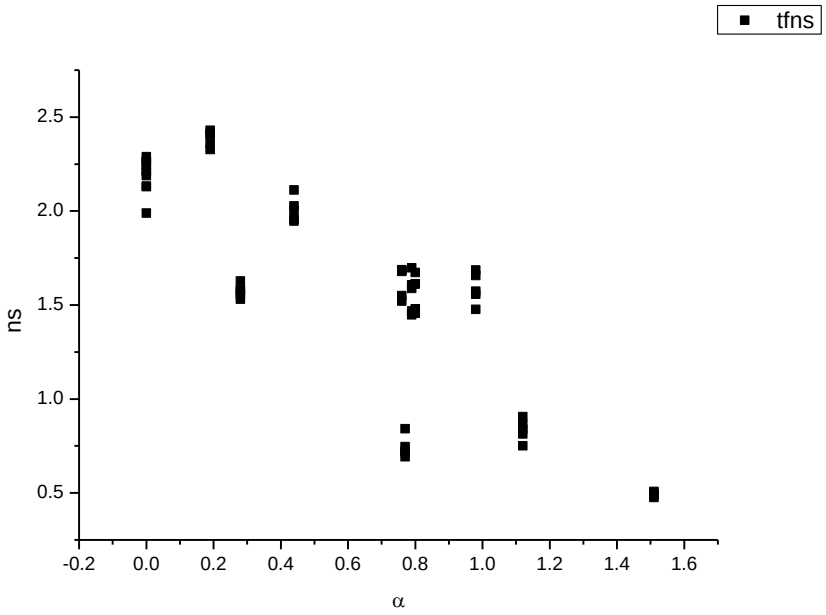

Figure 3.2.54. Amplitude weighted average lifetime (τ_f) of **17** versus α.

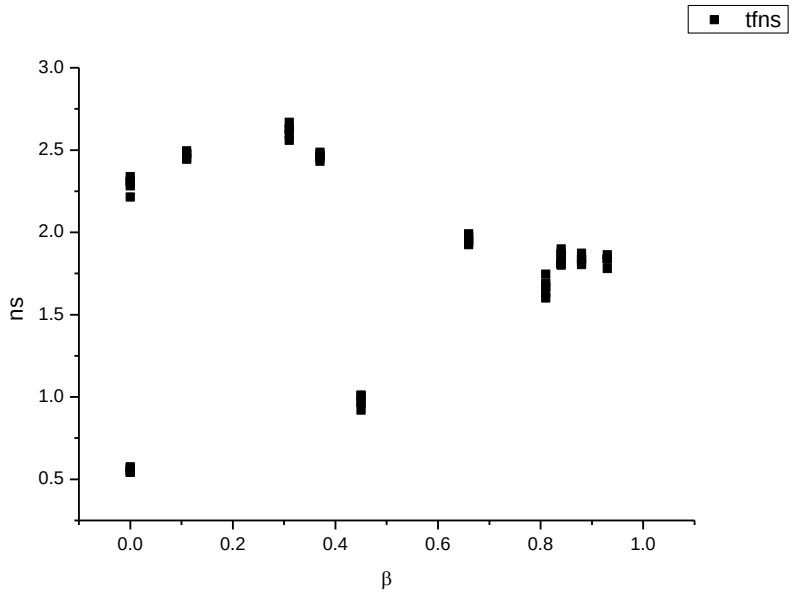

Figure 3.2.55. Intensity weighted average lifetime (τ_f) of **17** versus β.

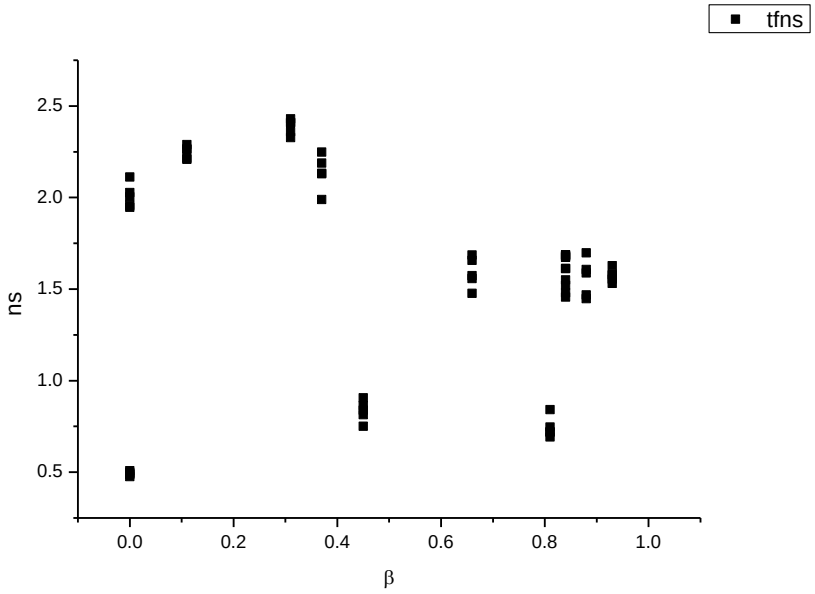

Figure 3.2.56. Amplitude weighted average lifetime (τ_f) of **17** versus β.

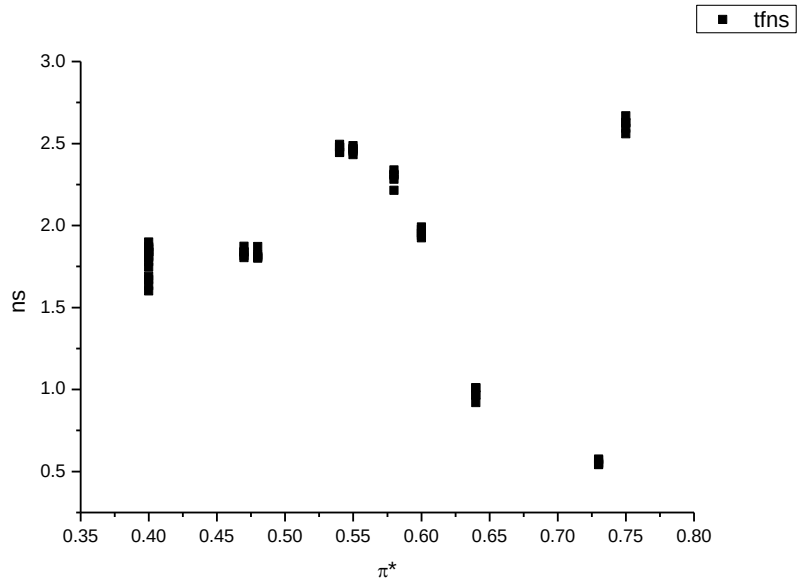

Figure 3.2.57. Intensity weighted average lifetime (τ_f) of **17** versus π*.

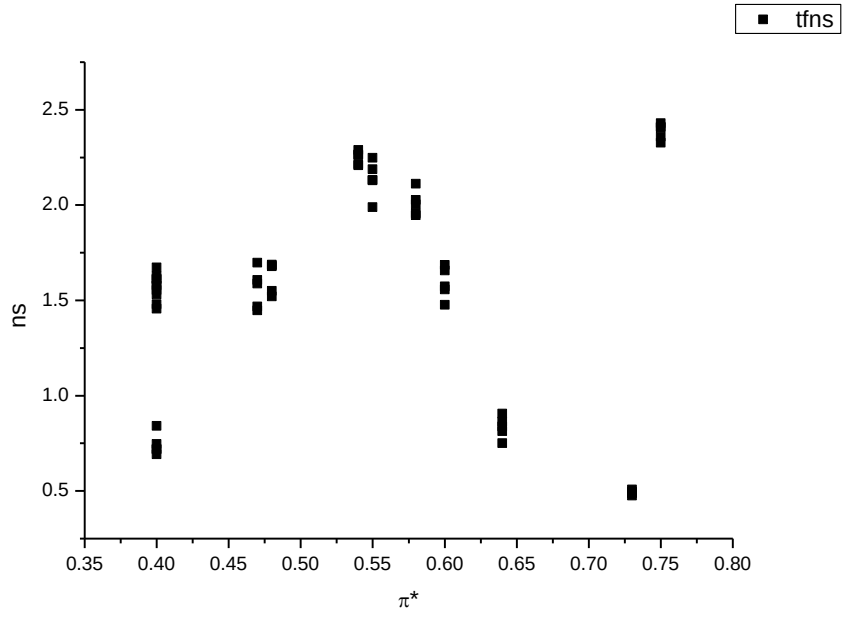

Figure 3.2.58. Amplitude weighted average lifetime (τ_f) of **17** versus π*.

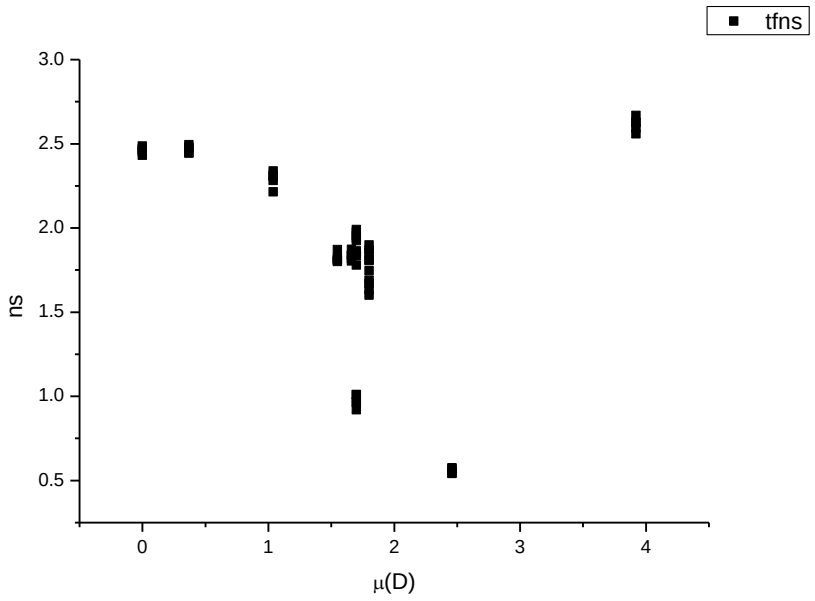

Figure 3.2.59. Intensity weighted average lifetime (τ_f) of **17** versus μ(D).

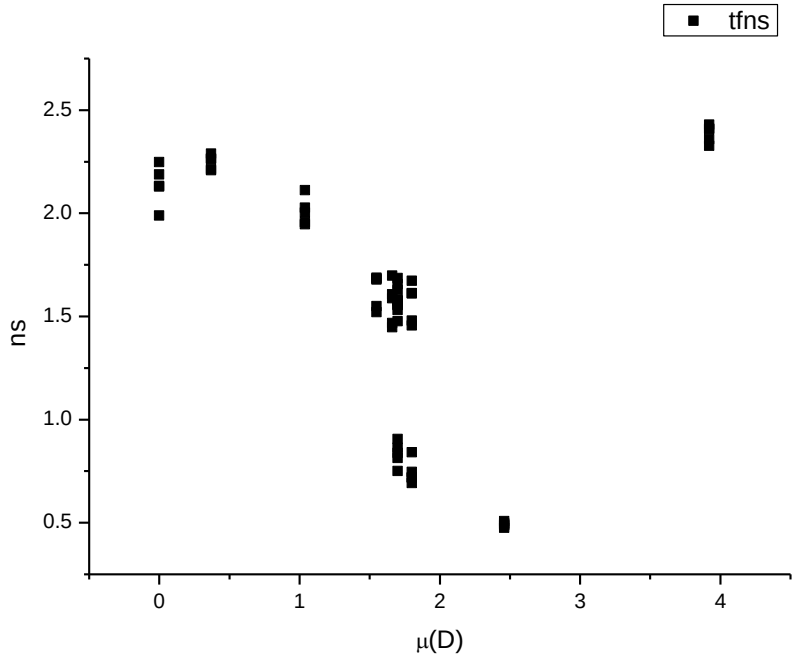

Figure 3.2.60. Amplitude weighted average lifetime (τ_f) of **17** versus μ(D).

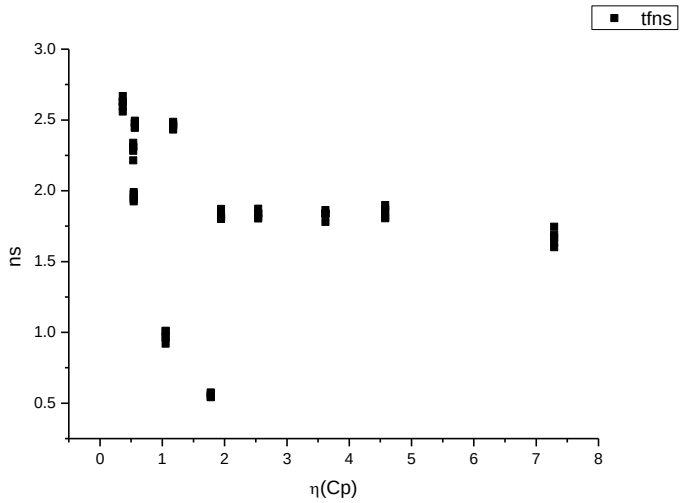

Figure 3.2.61. Intensity weighted average lifetime (τ_f) of **17** versus η(Cp).

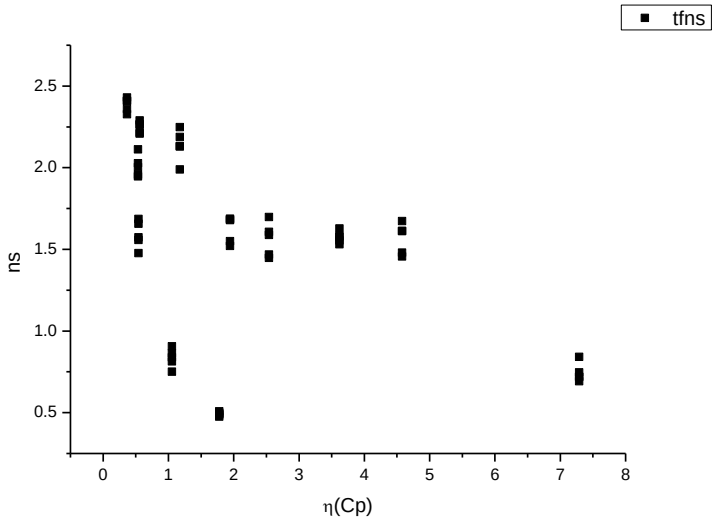

Figure 3.2.62. Amplitude weighted average lifetime (τ_f) of **17** versus η(Cp).

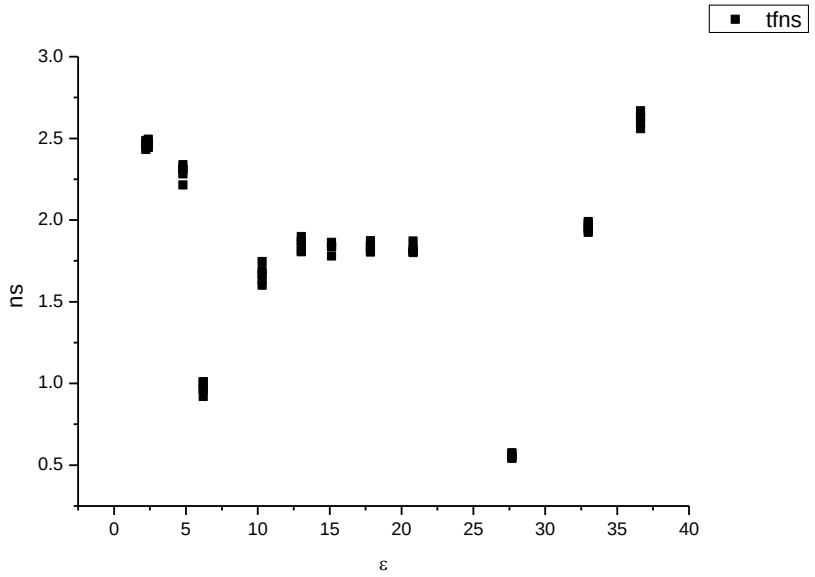

Figure 3.2.63. Intensity weighted average lifetime (τ_f) of **17** versus ε.

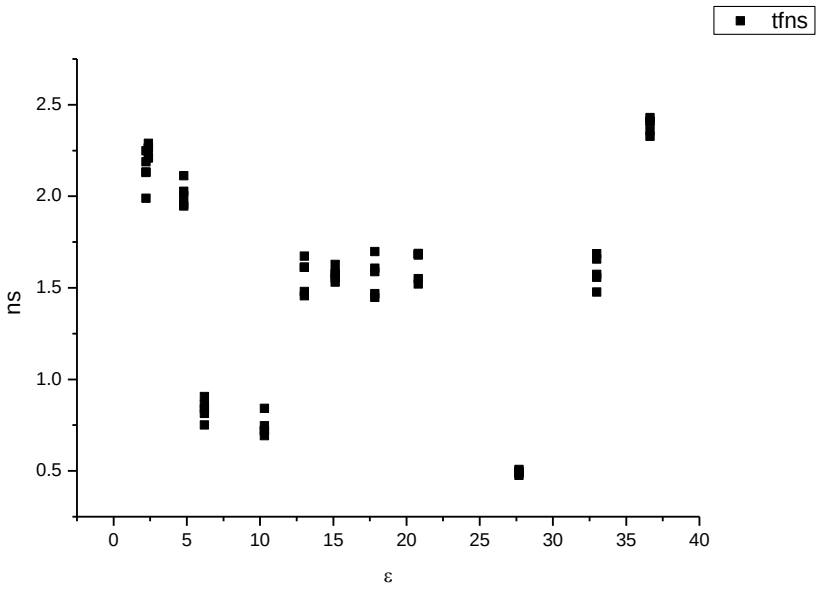

Figure 3.2.64. Amplitude weighted average lifetime (τ_f) of **17** versus ε.

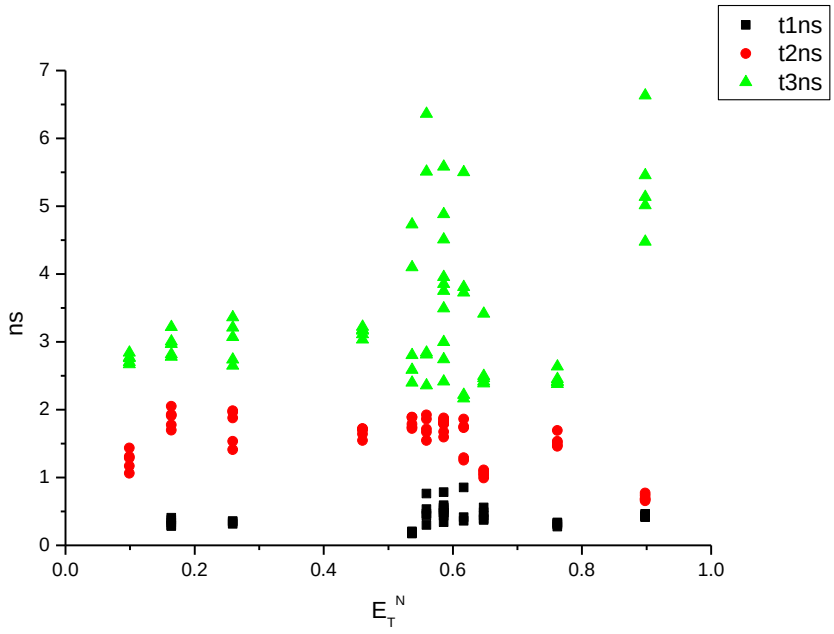

Figure 3.2.65. Intensity weighted components of TCSPC lifetime decay of **17** (470 nm to 570 nm) versus E_T^N.

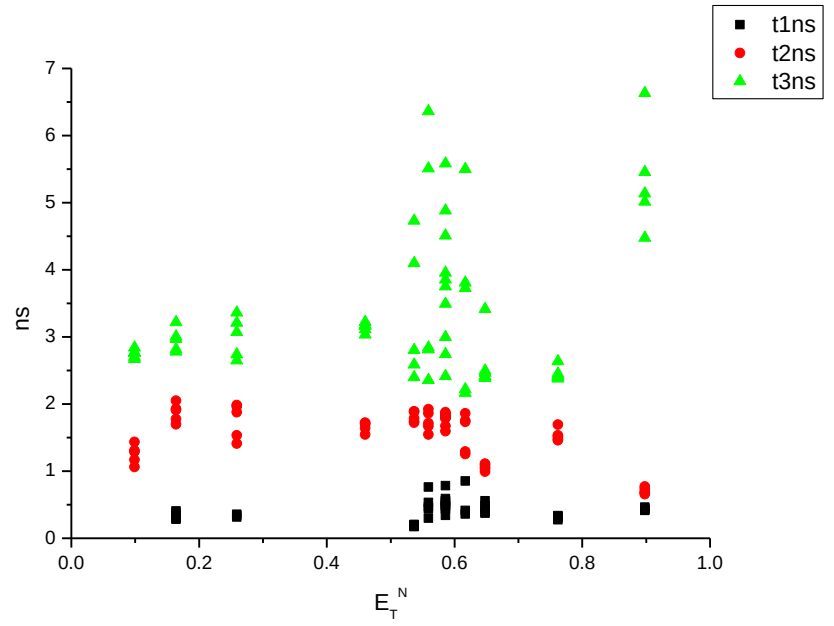

Figure 3.2.66. Amplitude weighted components of TCSPC lifetime decay of **17** (470 nm to 570 nm) versus E_T^N.

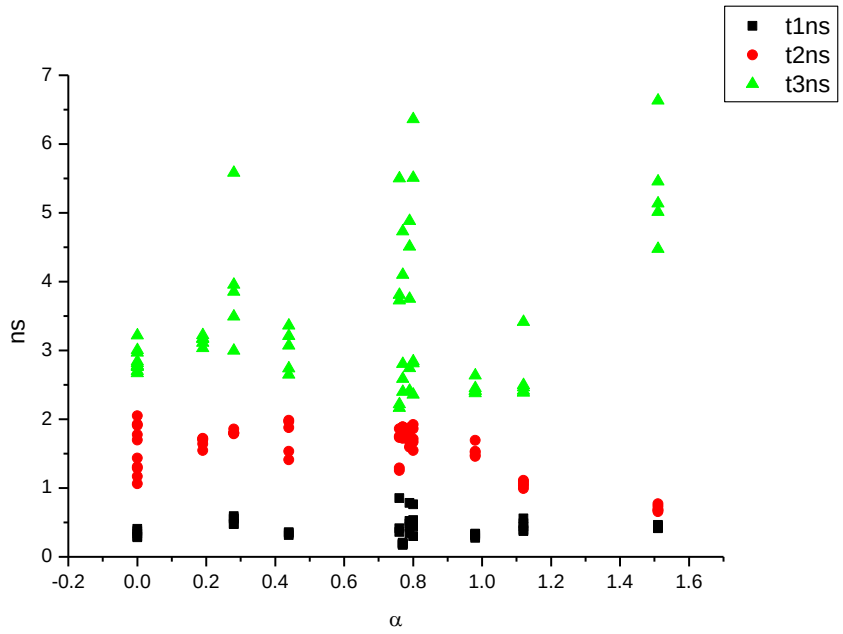

Figure 3.2.67. Intensity weighted components of TCSPC lifetime decay of **17** (470 nm to 570 nm) versus α.

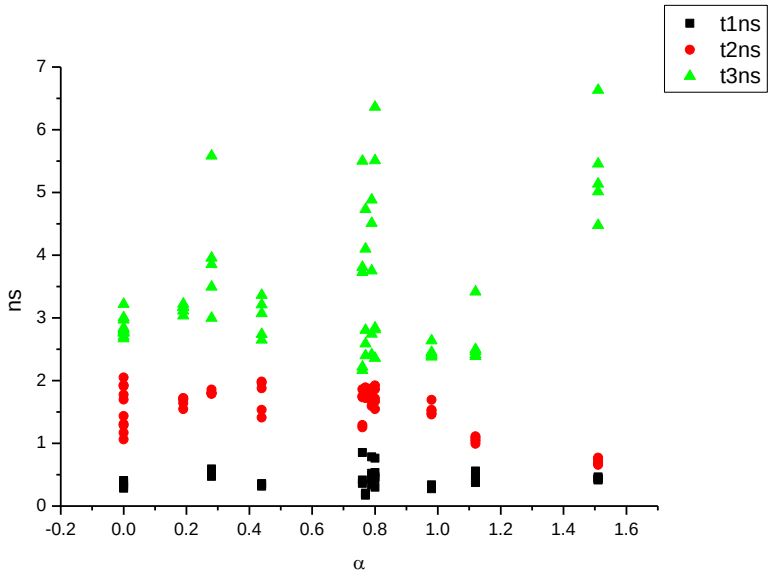

Figure 3.2.68. Amplitude weighted components of TCSPC lifetime decay of **17** (470 nm to 570 nm) versus α.

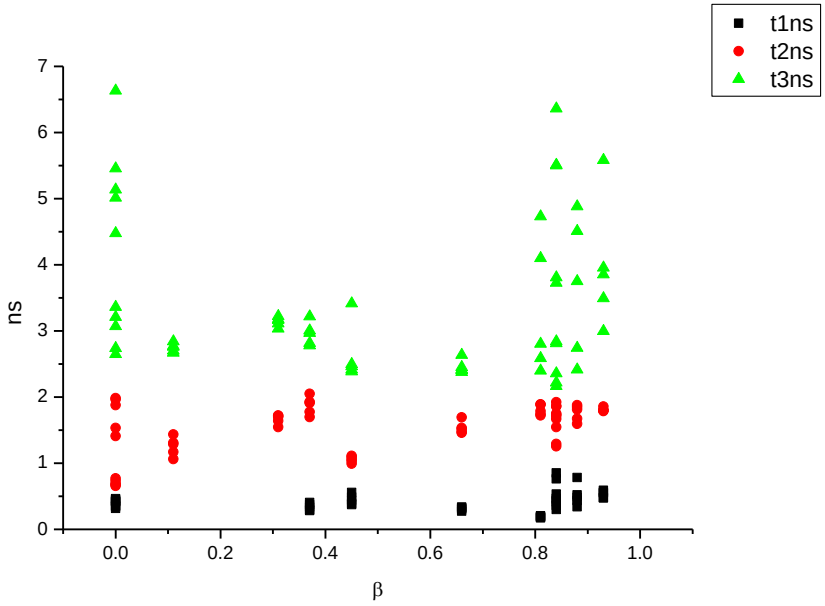

Figure 3.2.69. Intensity weighted components of TCSPC lifetime decay of **17** (470 nm to 570 nm) versus β.

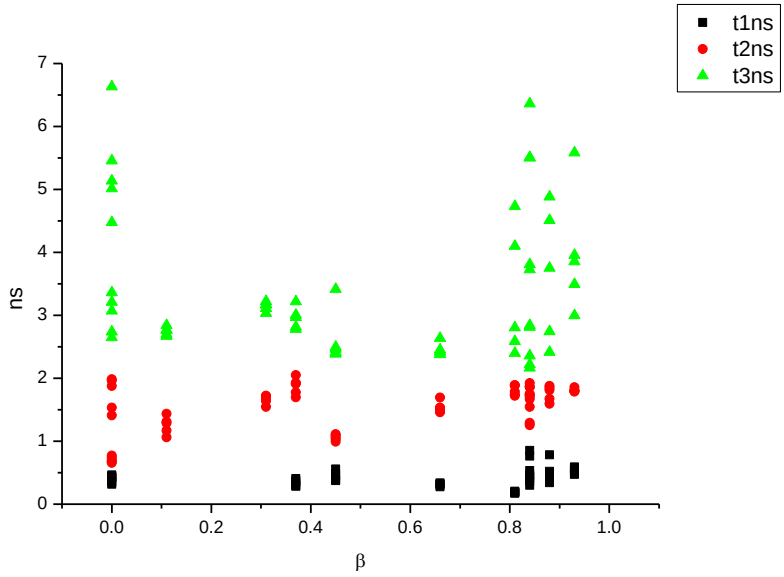

Figure 3.2.70. Amplitude weighted components of TCSPC lifetime decay of **17** (470 nm to 570 nm) versus β.

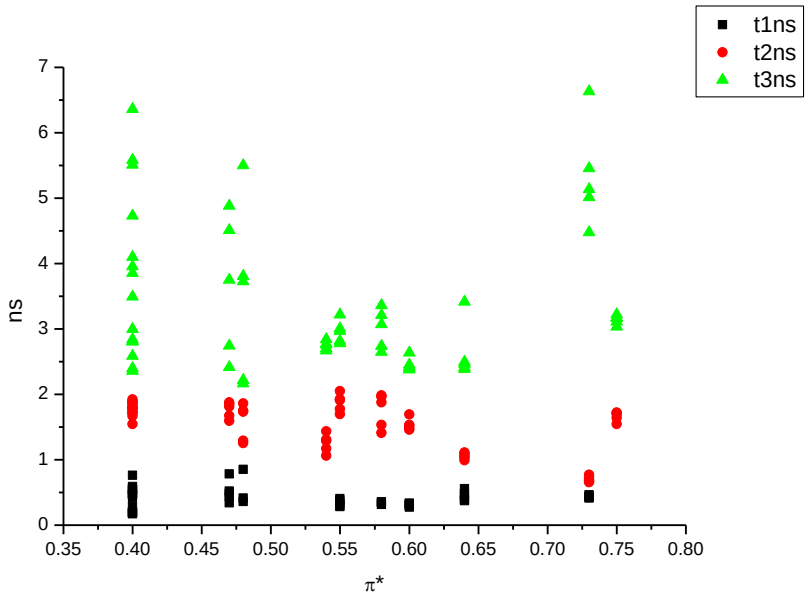

Figure 3.2.71. Intensity weighted components of TCSPC lifetime decay of **17** (470 nm to 570 nm) versus π*.

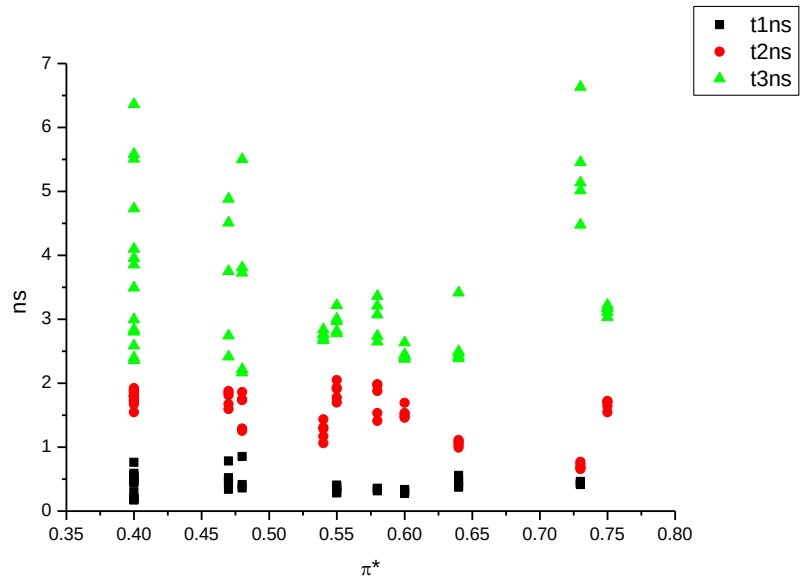

Figure 3.2.72. Amplitude weighted components of TCSPC lifetime decay of **17** (470 nm to 570 nm) versus π*.

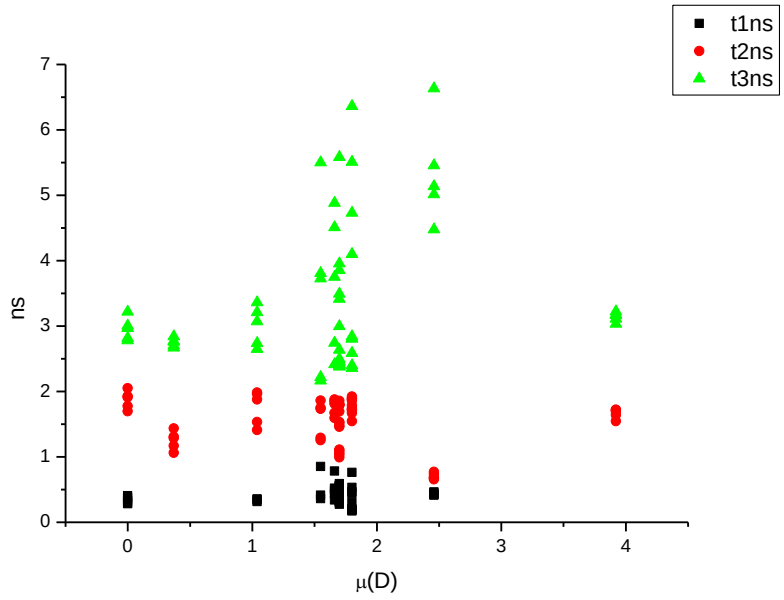

Figure 3.2.73. Intensity weighted components of TCSPC lifetime decay of **17** (470 nm to 570 nm) versus μ(D).

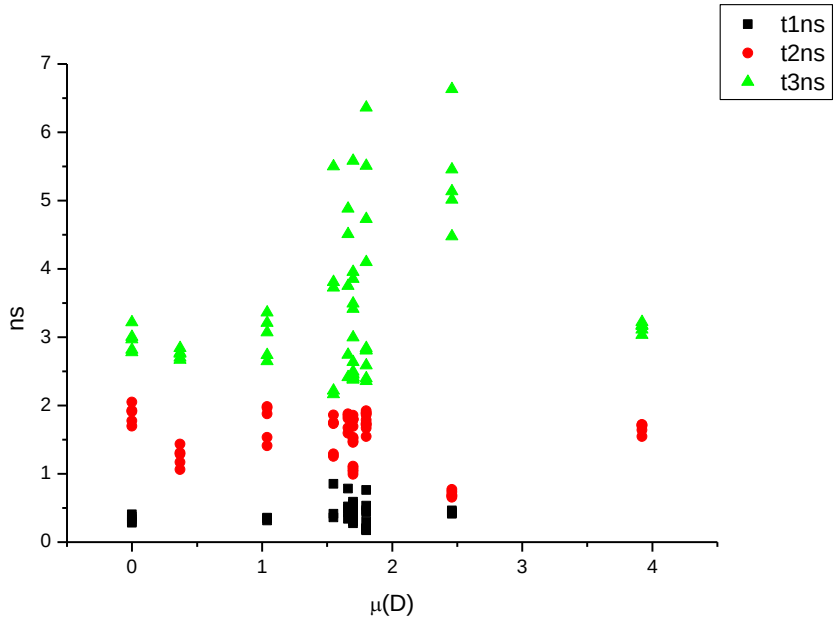

Figure 3.2.74. Amplitude weighted components of TCSPC lifetime decay of **17** (470 nm to 570 nm) versus μ(D).

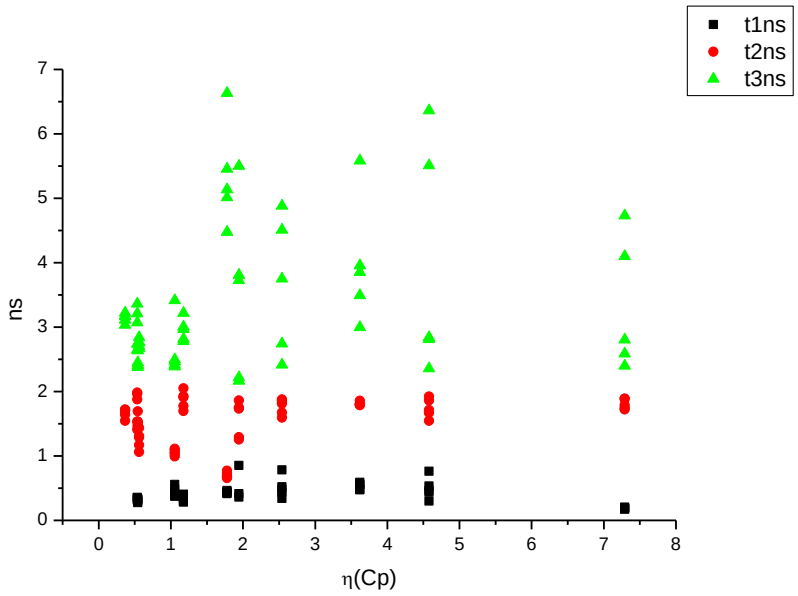

Figure 3.2.75. Intensity weighted components of TCSPC lifetime decay of **17** (470 nm to 570 nm) versus η(Cp).

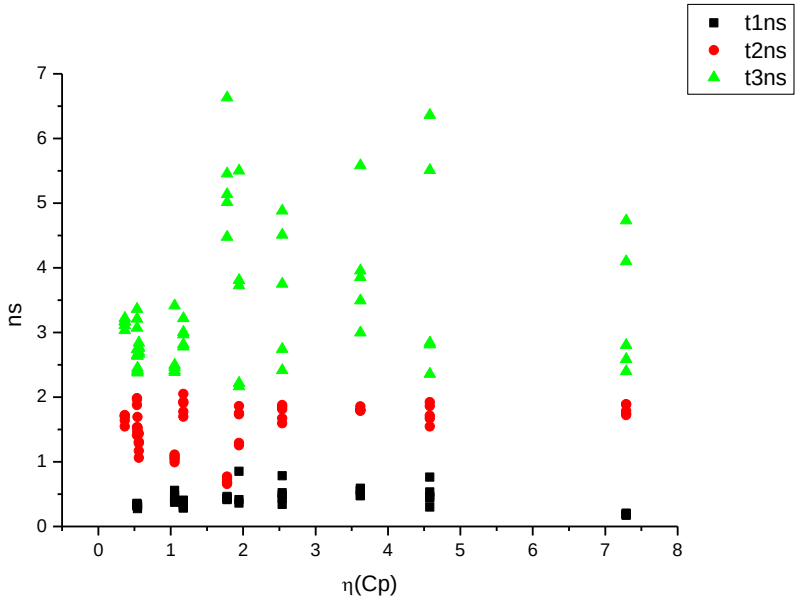

Figure 3.2.76. Amplitude weighted components of TCSPC lifetime decay of **17** (470 nm to 570 nm) versus η(Cp).

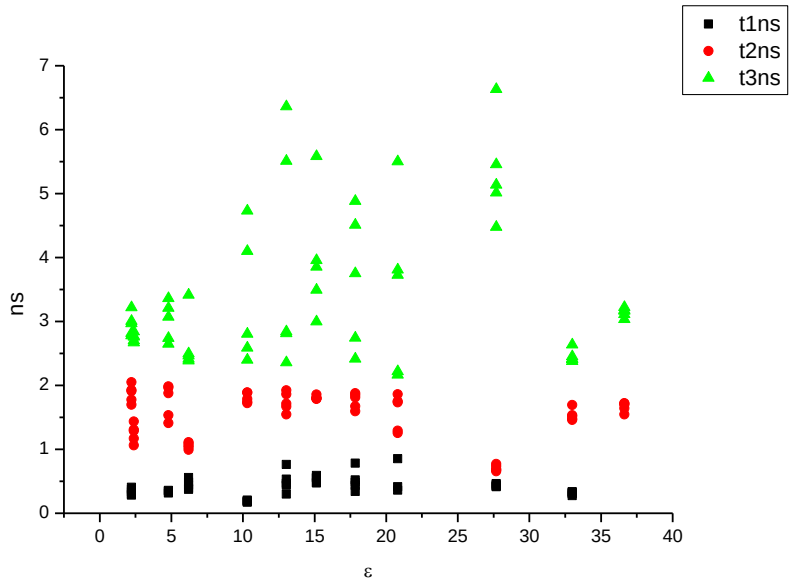

Figure 3.2.77. Intensity weighted components of TCSPC lifetime decay of **17** (470 nm to 570 nm) versus ε.

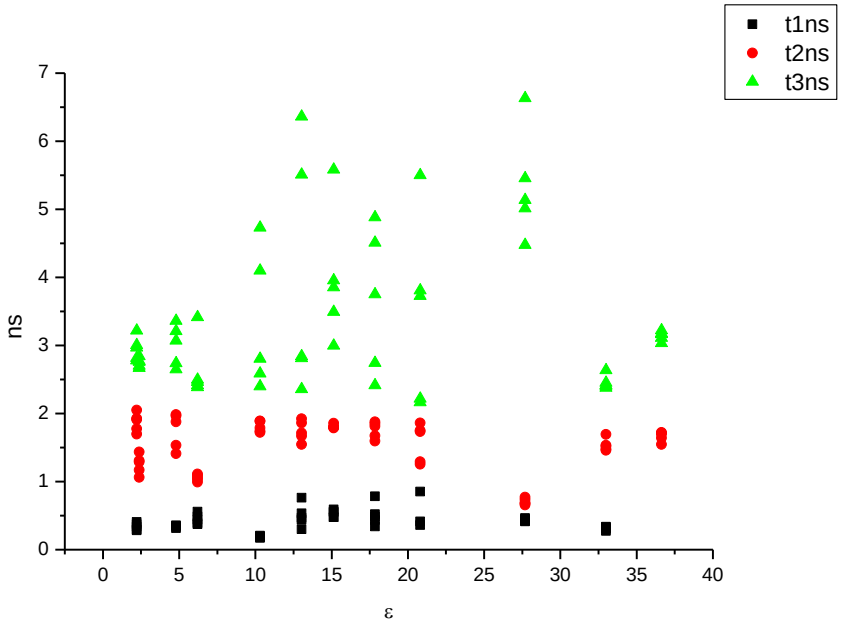

Figure 3.2.78. Amplitude weighted components of TCSPC lifetime decay of **17** (470 nm to 570 nm) versus ε.

3.2.7.1 470 nm Lifetime – Solvatochromic analysis.

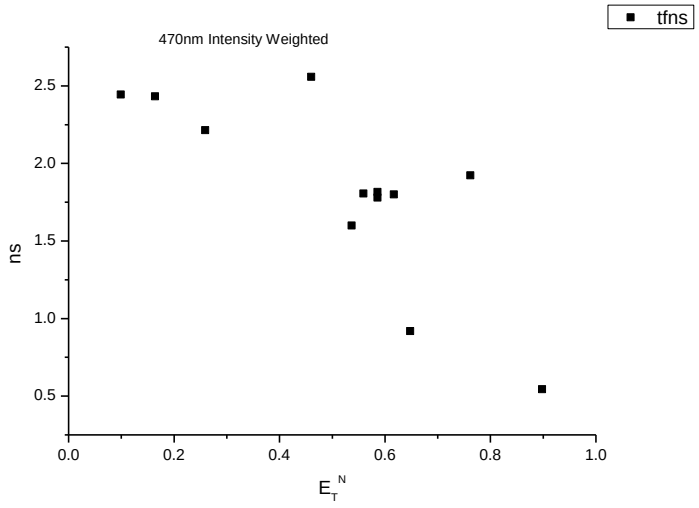

Figure 3.2.79. Intensity weighted average lifetime (τ_f) of **17** at 470 nm versus E_T^N.

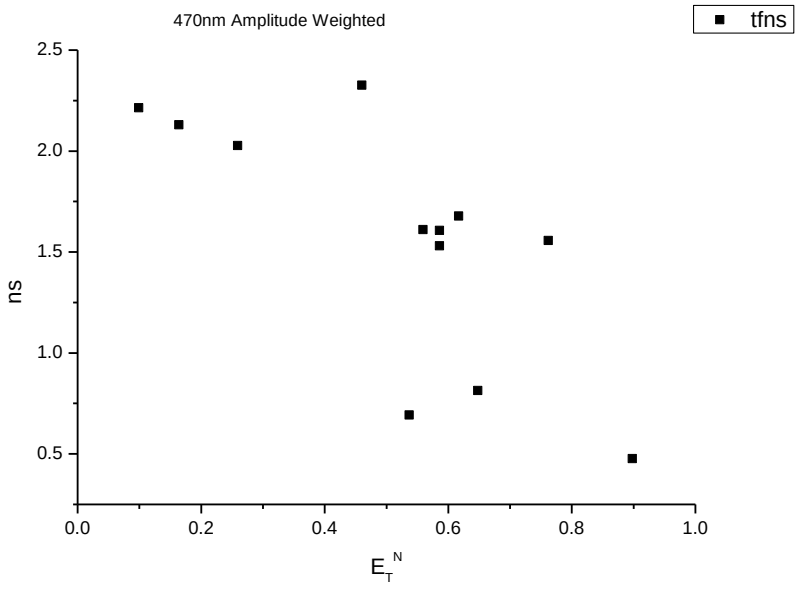

Figure 3.2.80. Amplitude weighted average lifetime (τ_f) of **17** at 470 nm versus E_T^N.

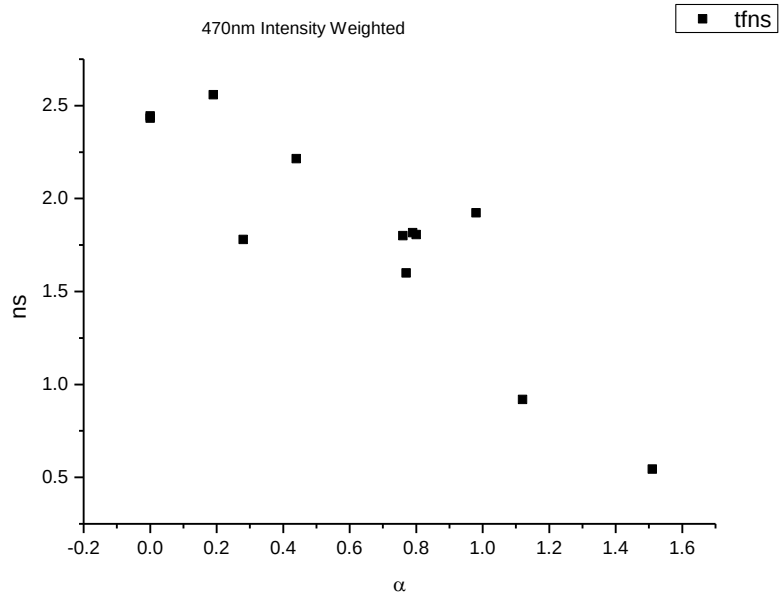

Figure 3.2.81. Intensity weighted average lifetime (τ_f) of **17** at 470 nm versus α.

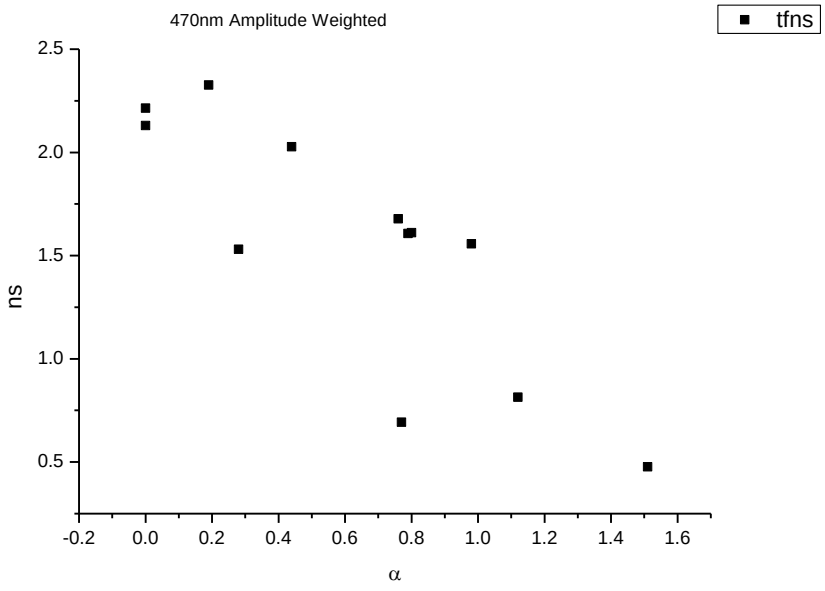

Figure 3.2.82. Amplitude weighted average lifetime (τ_f) of **17** at 470 nm versus α.

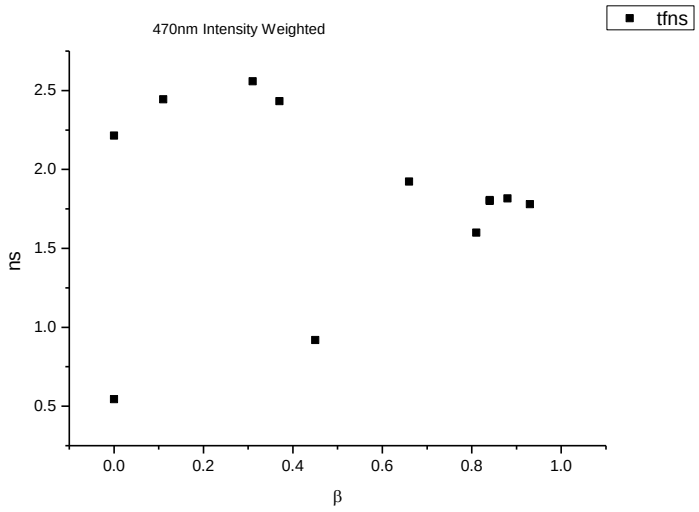

Figure 3.2.83. Intensity weighted average lifetime (τ_f) of **17** at 470 nm versus β.

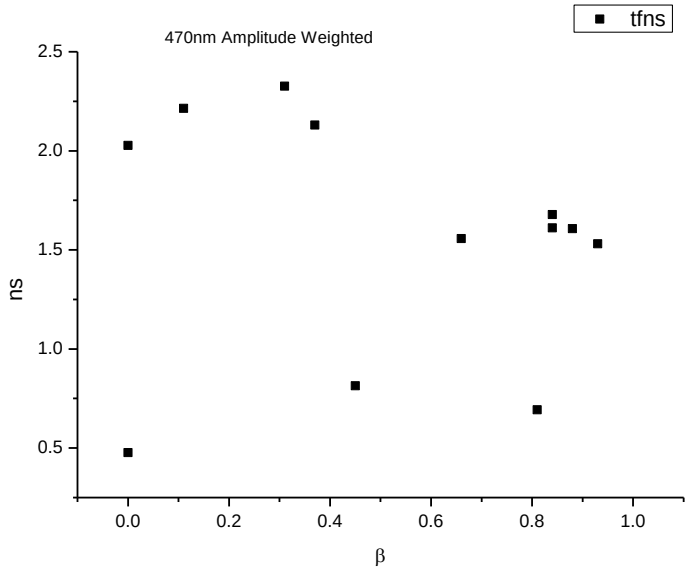

Figure 3.2.84. Amplitude weighted average lifetime (τ_f) of **17** at 470 nm versus β.

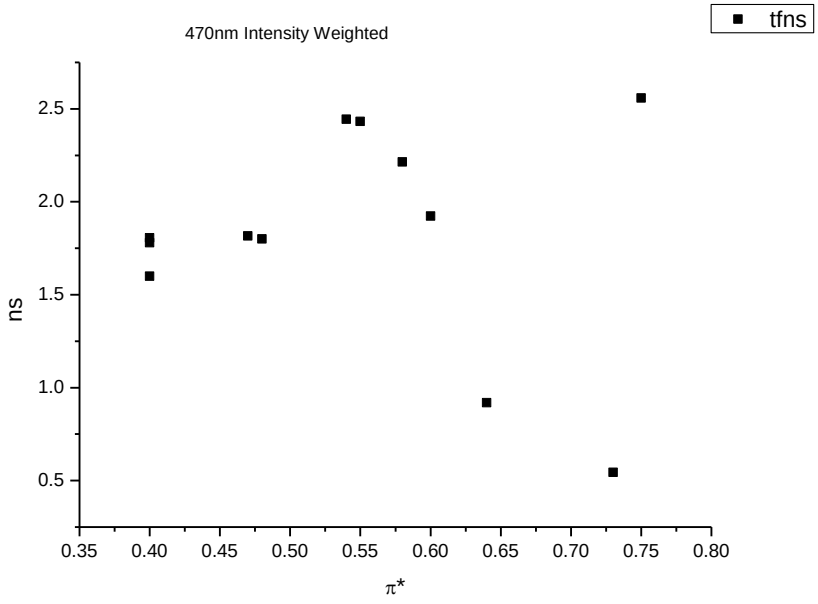

Figure 3.2.85. Intensity weighted average lifetime (τ_f) of **17** at 470 nm versus π*.

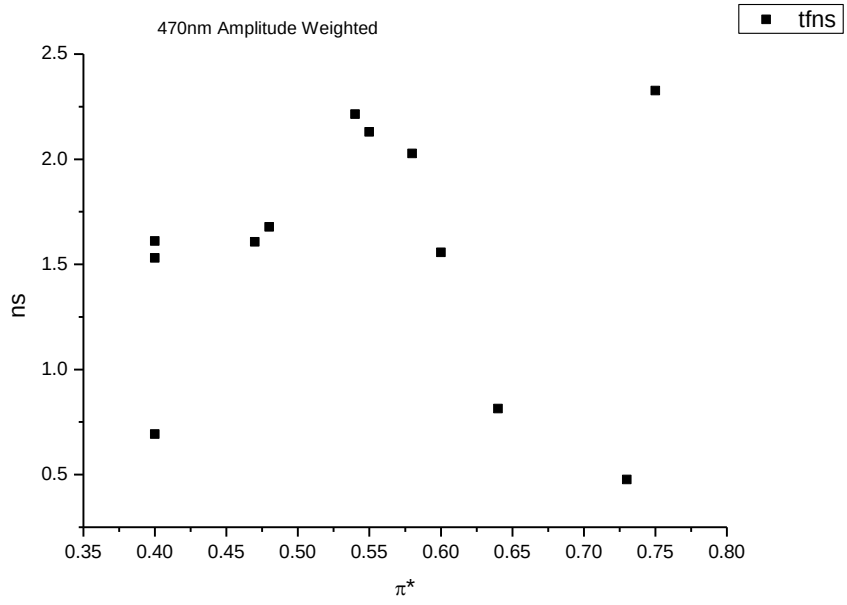

Figure 3.2.86. Amplitude weighted average lifetime (τ_f) of **17** at 470 nm versus π*.

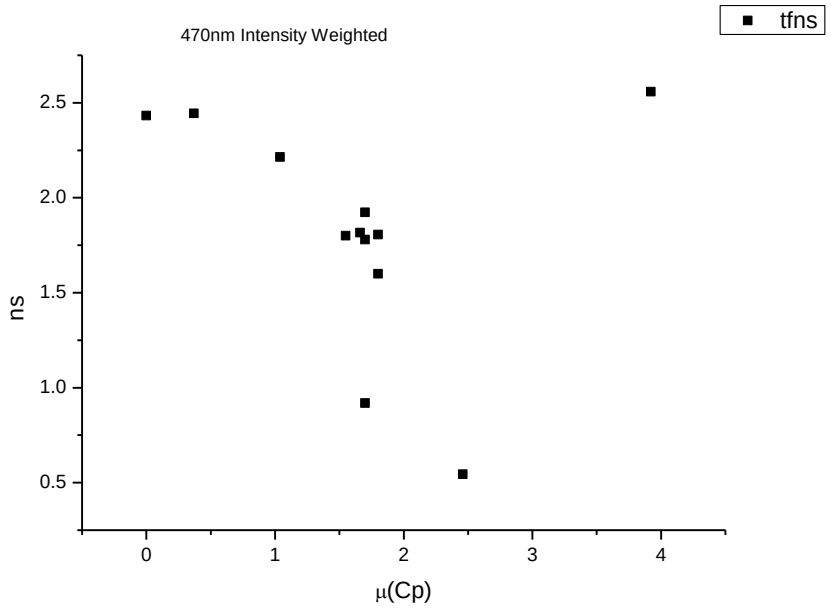

Figure 3.2.87. Intensity weighted average lifetime (τ_f) of **17** at 470 nm versus μ(D).

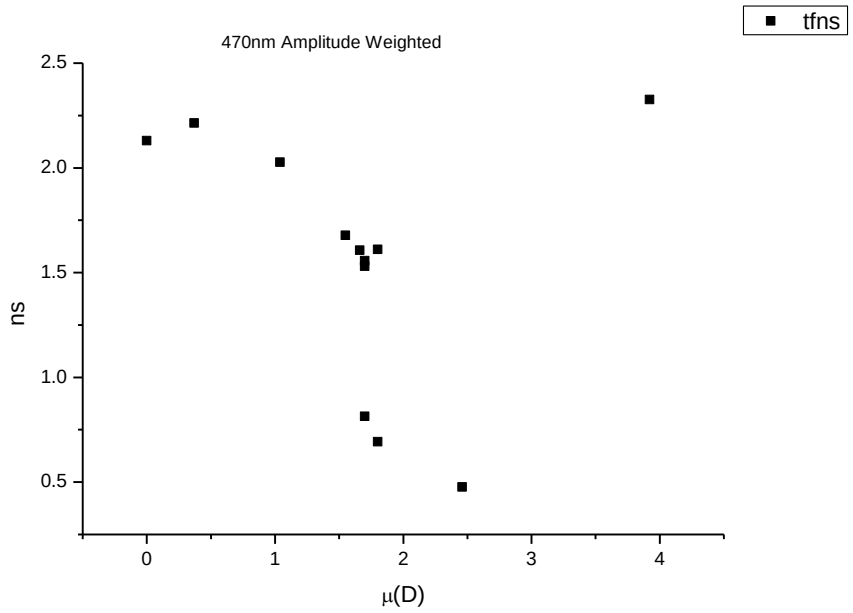

Figure 3.2.88. Amplitude weighted average lifetime (τ_f) of **17** at 470 nm versus μ(D).

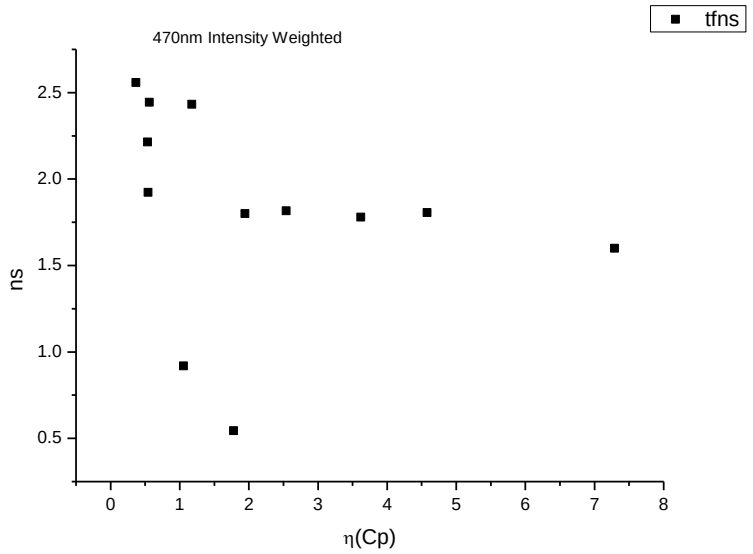

Figure 3.2.89. Intensity weighted average lifetime (τ_f) of **17** at 470 nm versus η(Cp).

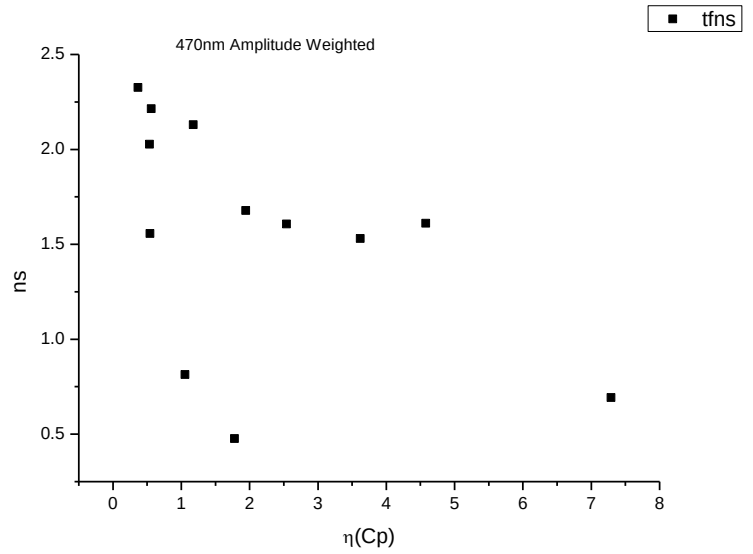

Figure 3.2.90. Amplitude weighted average lifetime (τ_f) of **17** at 470 nm versus η(Cp).

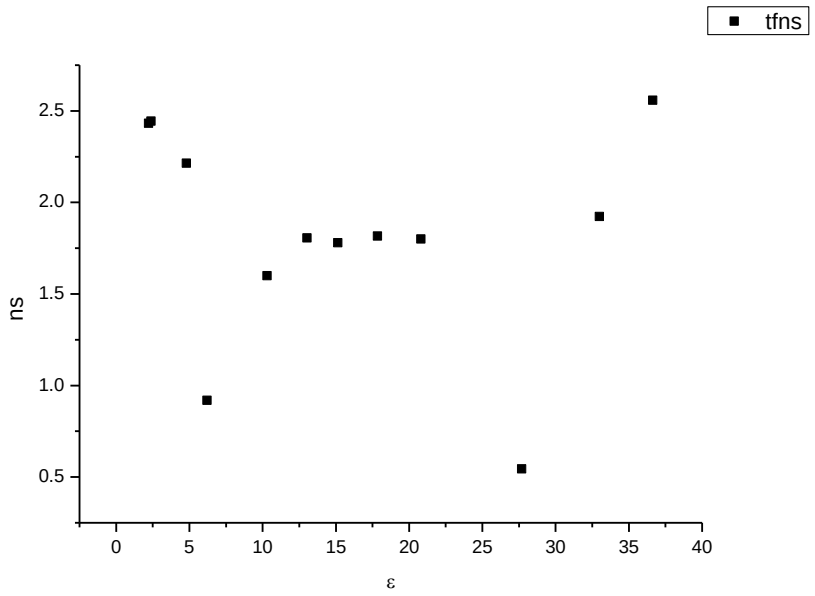

Figure 3.2.91. Intensity weighted average lifetime (τ_f) of **17** at 470 nm versus ε.

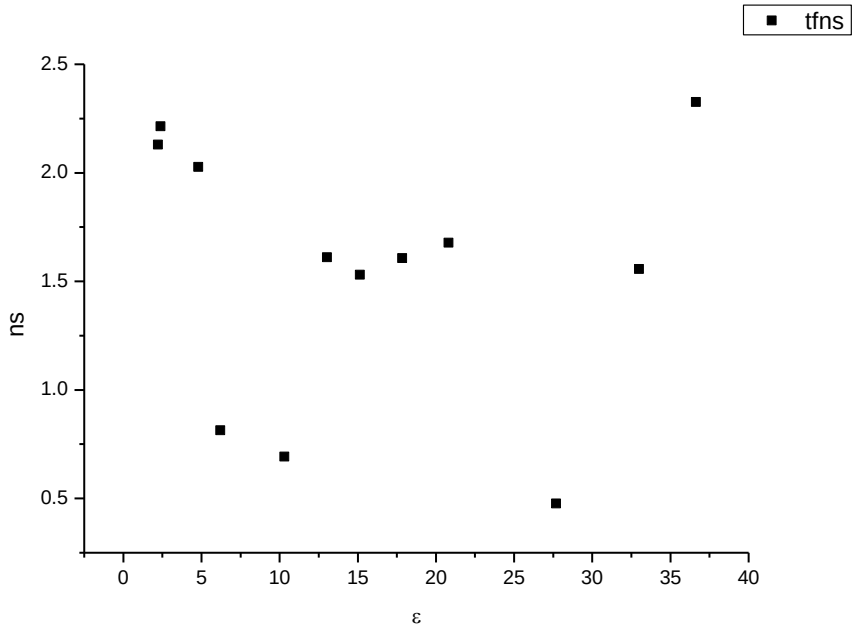

Figure 3.2.92. Amplitude weighted average lifetime (τ_f) of **17** at 470 nm versus ε.

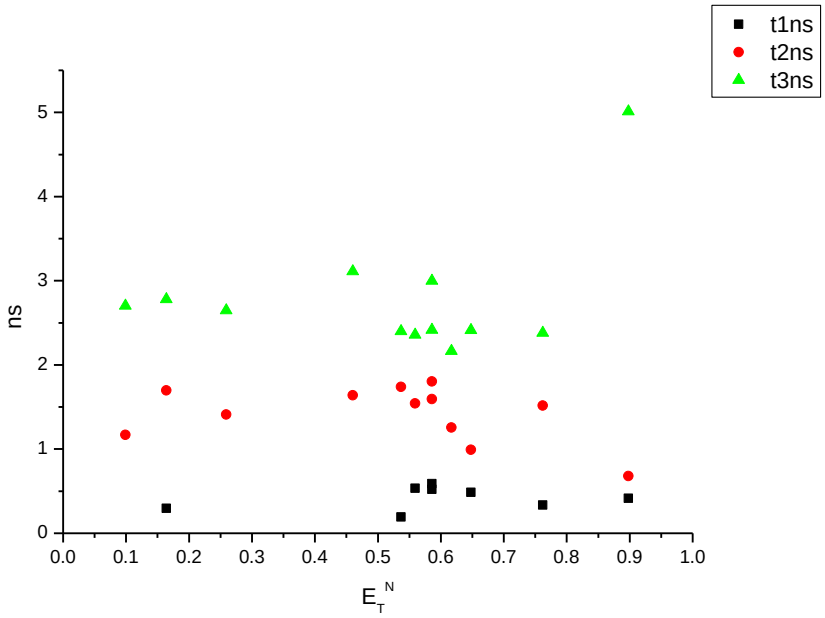

Figure 3.2.93. Intensity weighted components of TCSPC lifetime decay of **17** (470 nm) versus E_T^N.

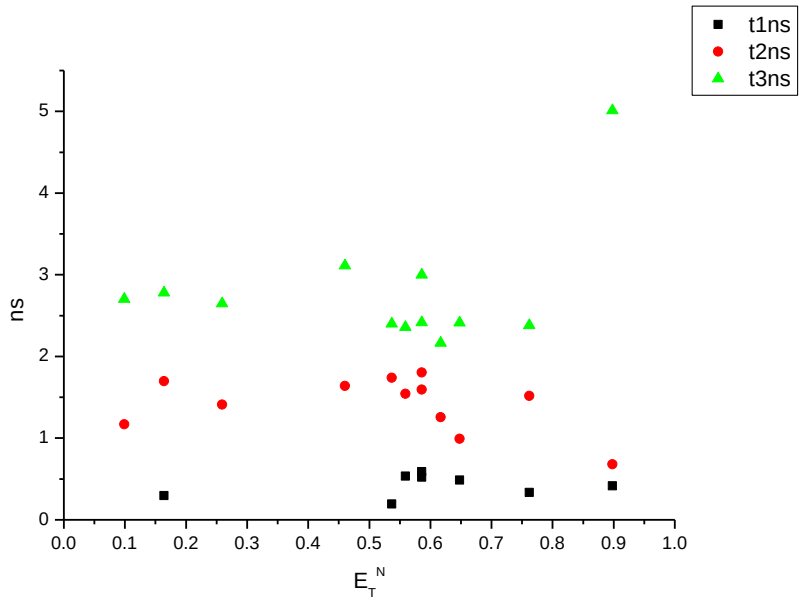

Figure 3.2.94. Amplitude weighted components of TCSPC lifetime decay of **17** (470 nm) versus E_T^N.

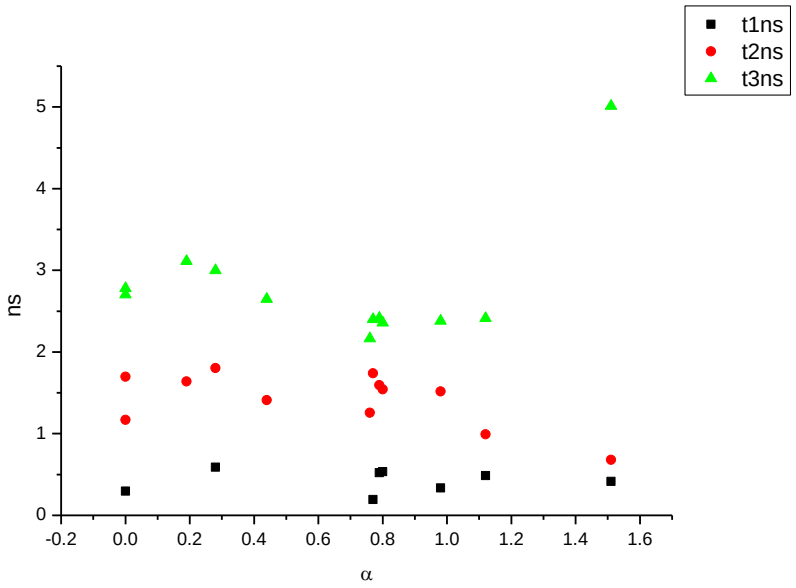

Figure 3.2.95. Intensity weighted components of TCSPC lifetime decay of **17** (470 nm) versus α.

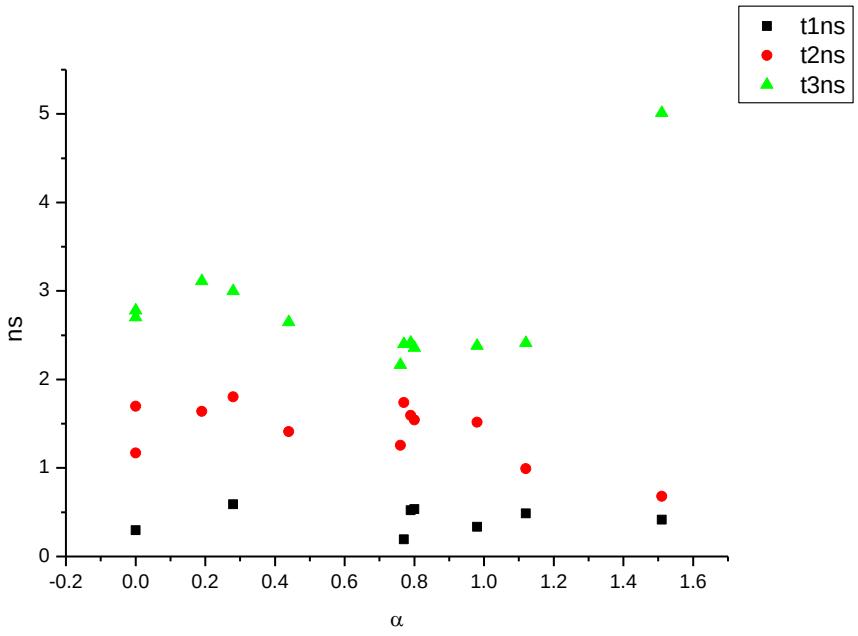

Figure 3.2.96. Amplitude weighted components of TCSPC lifetime decay of **17** (470 nm) versus α.

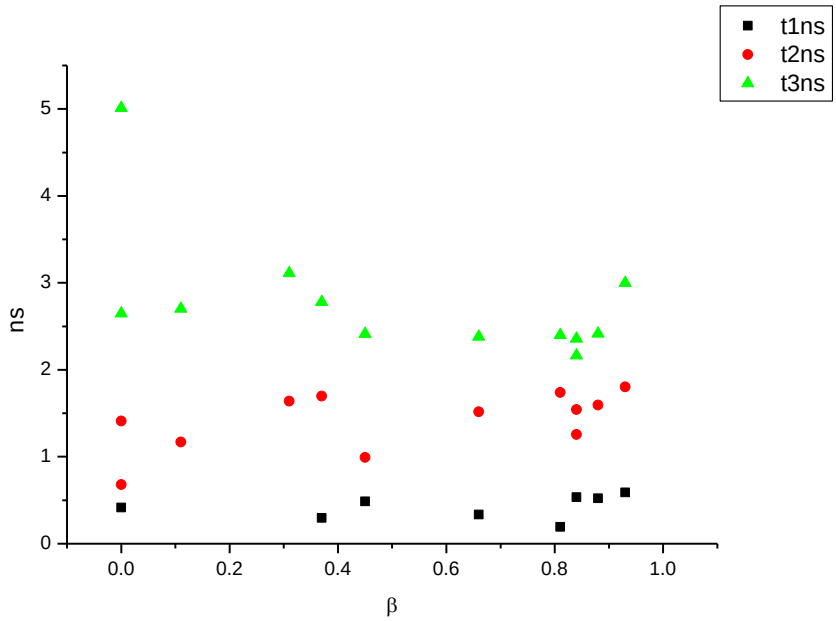

Figure 3.2.97. Intensity weighted components of TCSPC lifetime decay of **17** (470 nm) versus β.

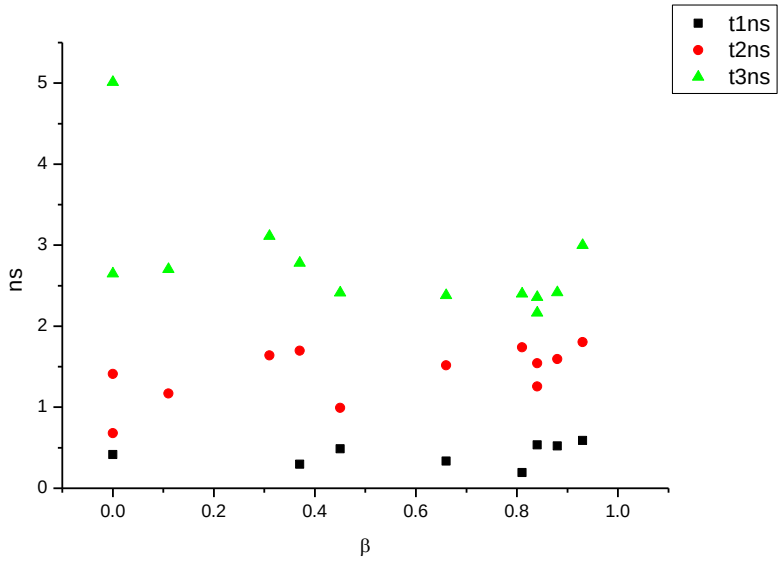

Figure 3.2.98. Amplitude weighted components of TCSPC lifetime decay of **17** (470 nm) versus β.

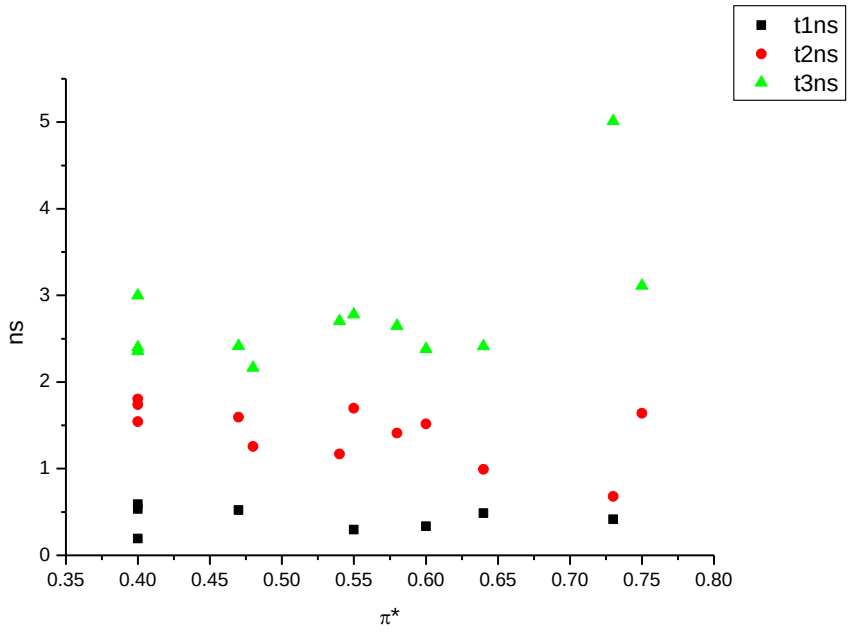

Figure 3.2.99. Intensity weighted components of TCSPC lifetime decay of **17** (470 nm) versus π*.

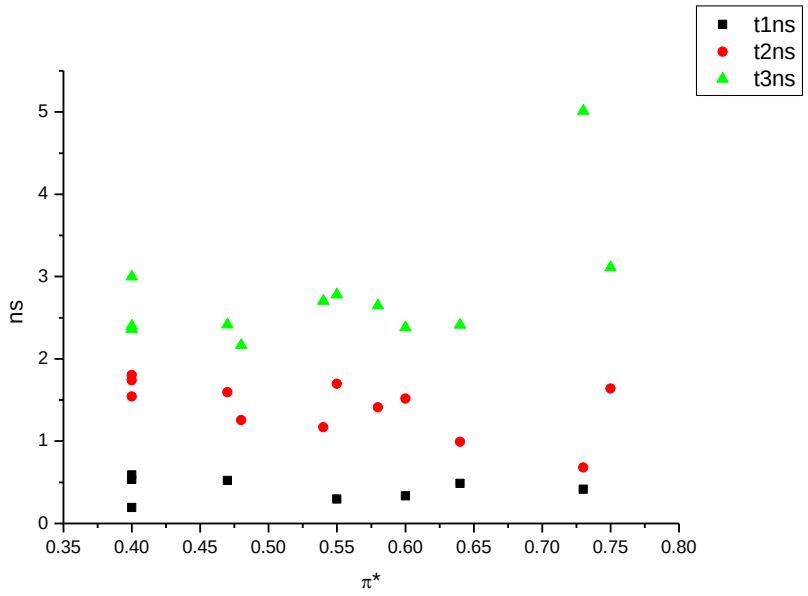

Figure 3.2.100. Amplitude weighted components of TCSPC lifetime decay of **17** (470 nm) versus π*.

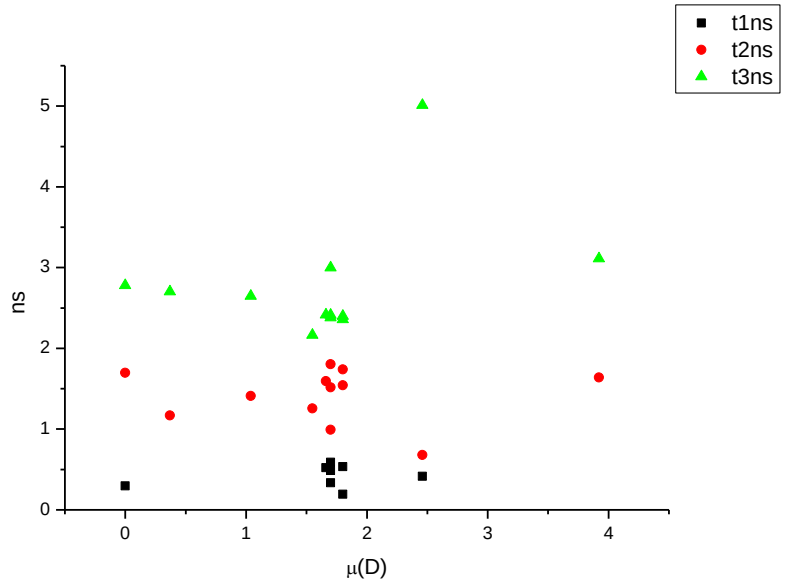

Figure 3.2.101. Intensity weighted components of TCSPC lifetime decay of **17** (470 nm) versus μ(D).

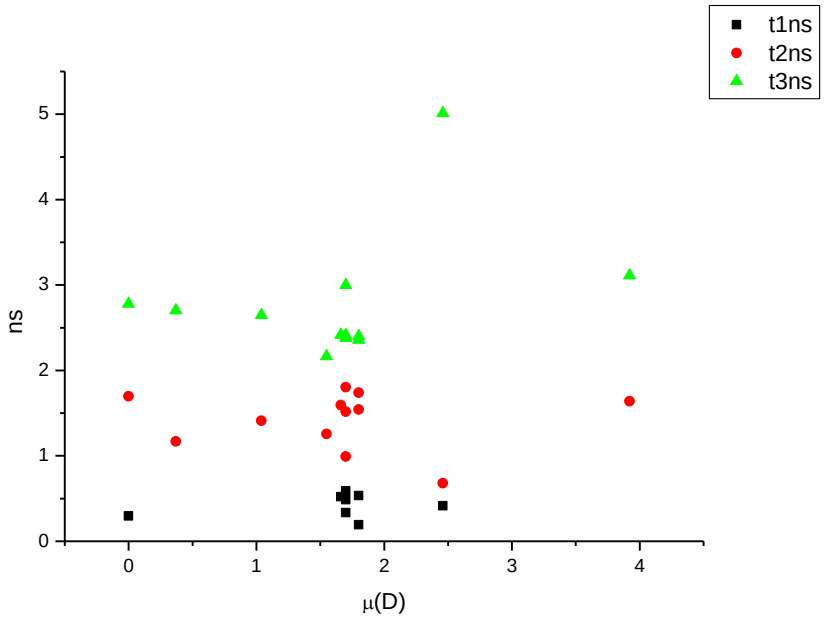

Figure 3.2.102. Amplitude weighted components of TCSPC lifetime decay of **17** (470 nm) versus μ(D).

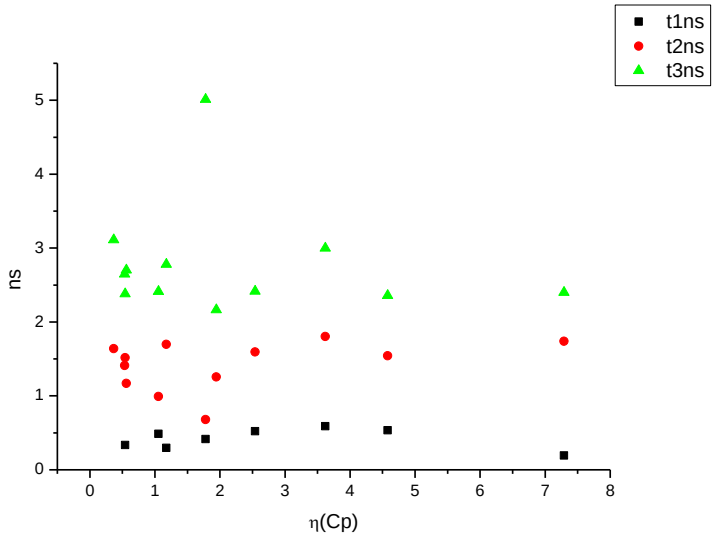

Figure 3.2.103. Intensity weighted components of TCSPC lifetime decay of **17** (470 nm) versus η(Cp).

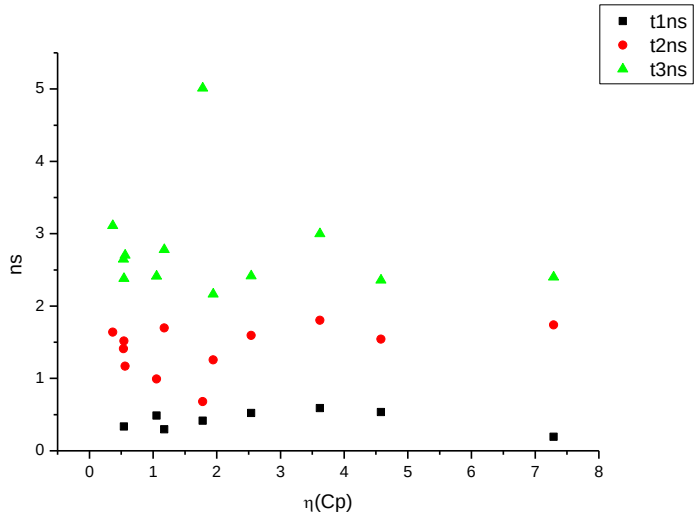

Figure 3.2.104. Amplitude weighted components of TCSPC lifetime decay of **17** (470 nm) versus η(Cp).

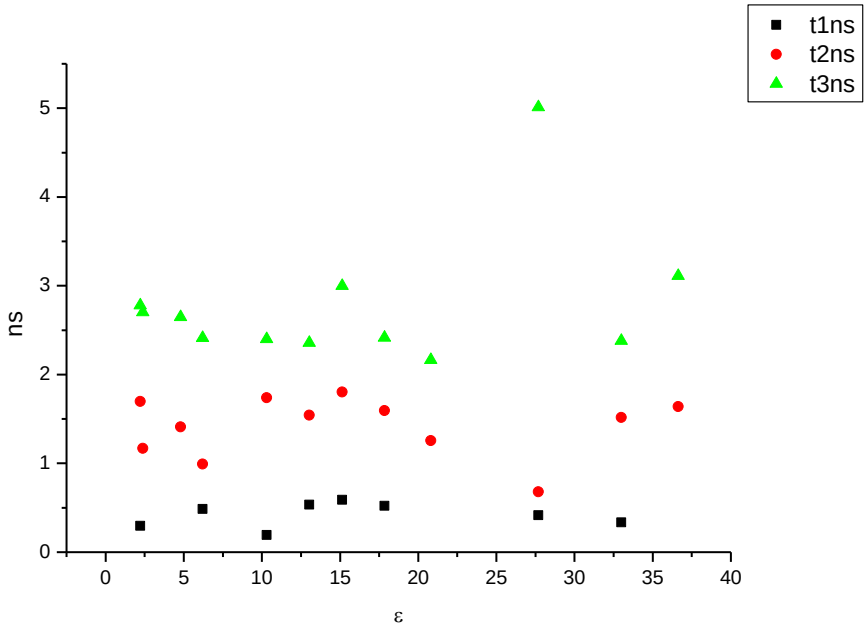

Figure 3.2.105. Intensity weighted components of TCSPC lifetime decay of **17** (470 nm) versus ε.

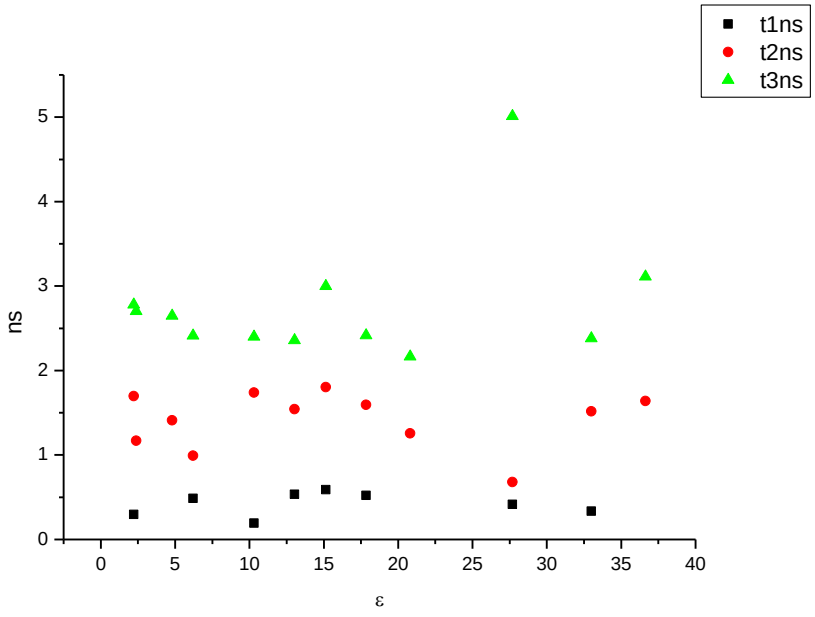

Figure 3.2.106. Amplitude weighted components of TCSPC lifetime decay of **17** (470 nm) versus ε.

3.2.7.2 570 nm Lifetime – Solvatochromic analysis.

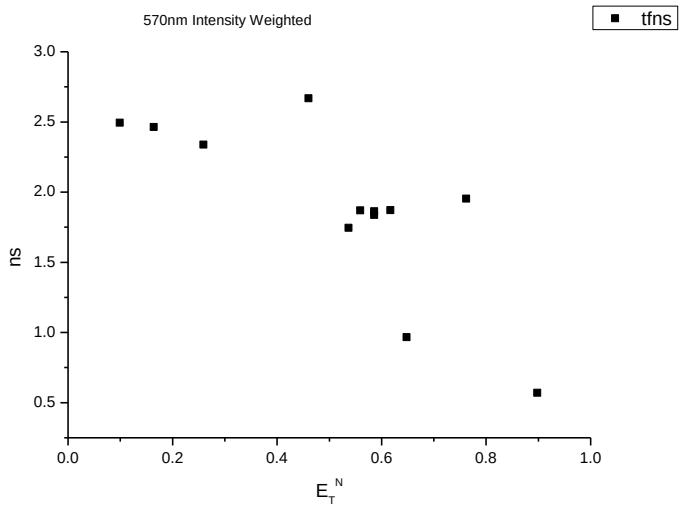

Figure 3.2.107. Intensity weighted average lifetime (τ_f) of **17** at 570 nm versus E_T^N.

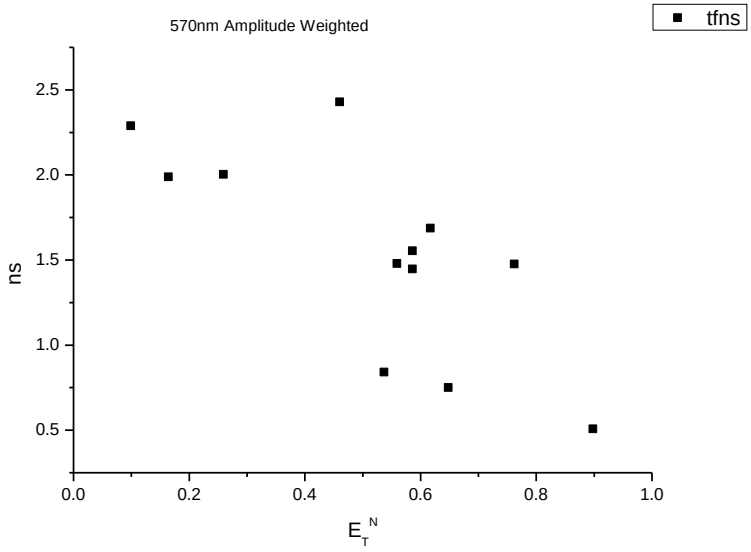

Figure 3.2.108. Amplitude weighted average lifetime (τ_f) of **17** at 570 nm versus E_T^N.

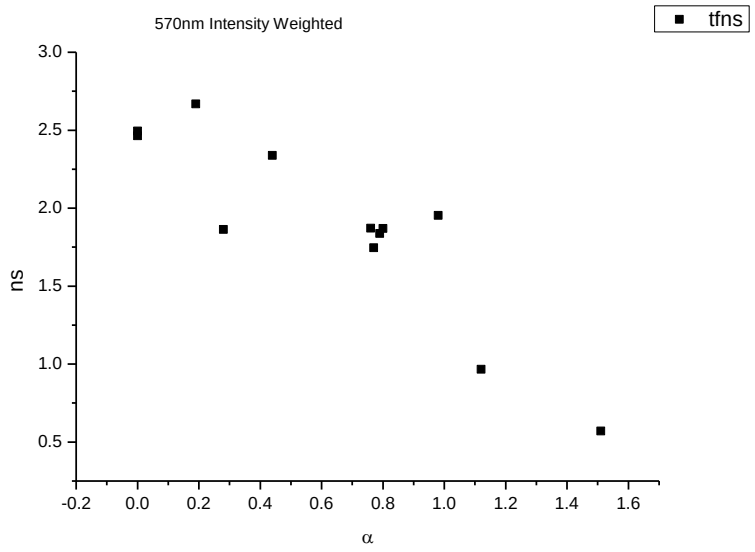

Figure 3.2.109. Intensity weighted average lifetime (τ_f) of **17** at 570 nm versus α.

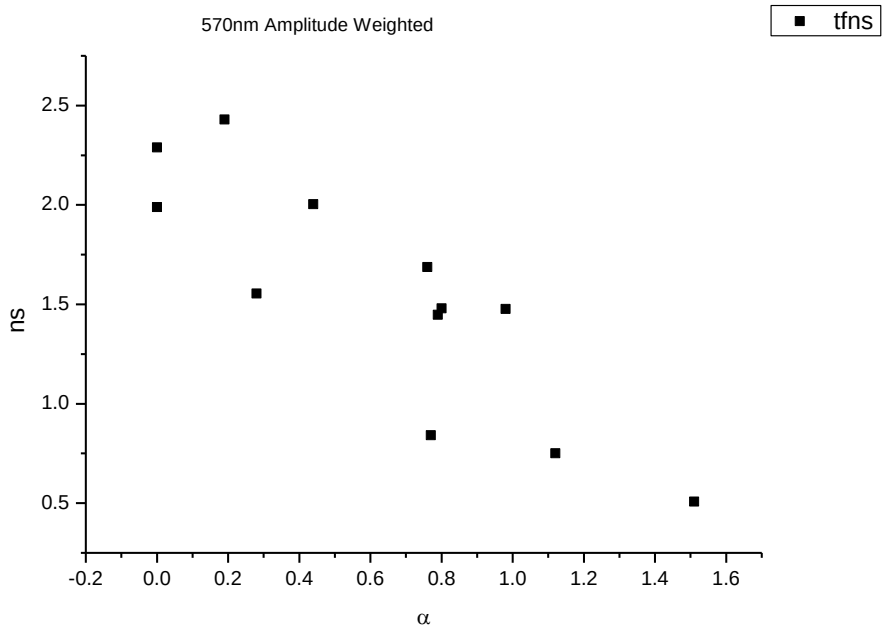

Figure 3.2.110. Amplitude weighted average lifetime (τ_f) of **17** at 570 nm versus α.

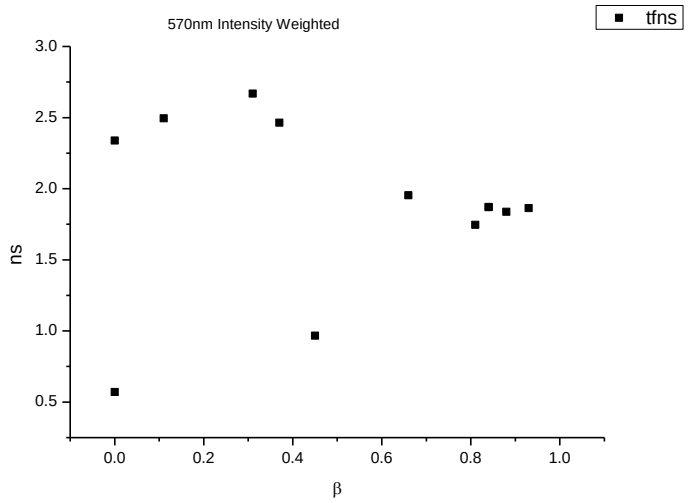

Figure 3.2.111. Intensity weighted average lifetime (τ_f) of **17** at 570 nm versus β.

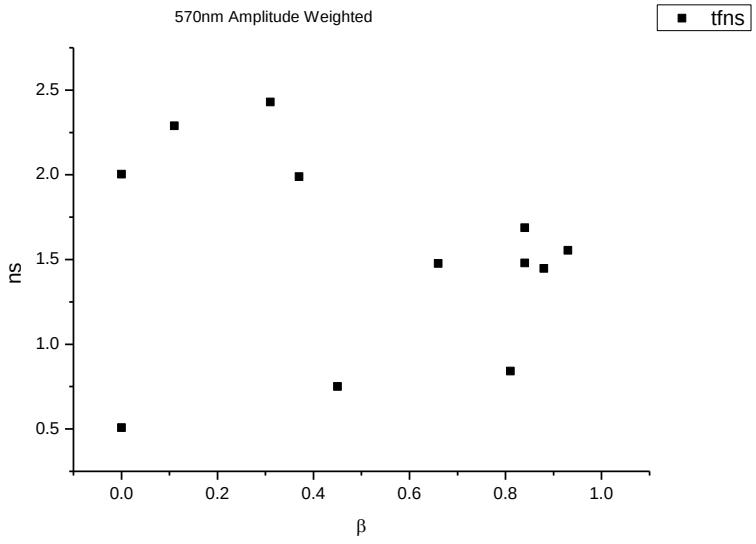

Figure 3.2.112. Amplitude weighted average lifetime (τ_f) of **17** at 570 nm versus β.

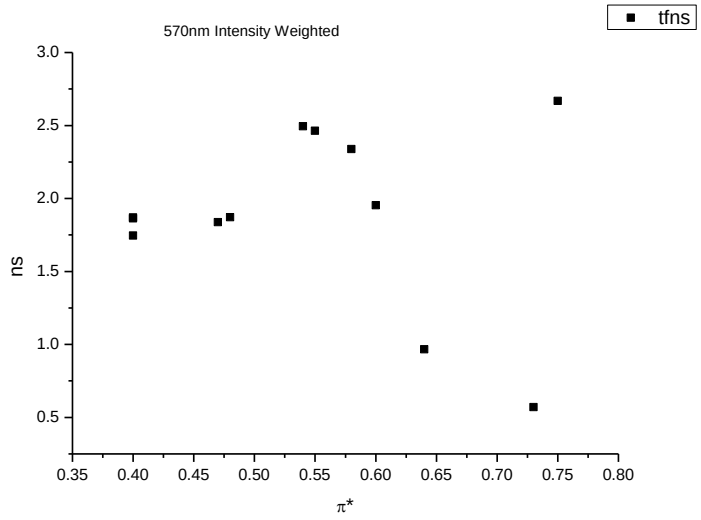

Figure 3.2.113. Intensity weighted average lifetime (τ_f) of **17** at 570 nm versus π*.

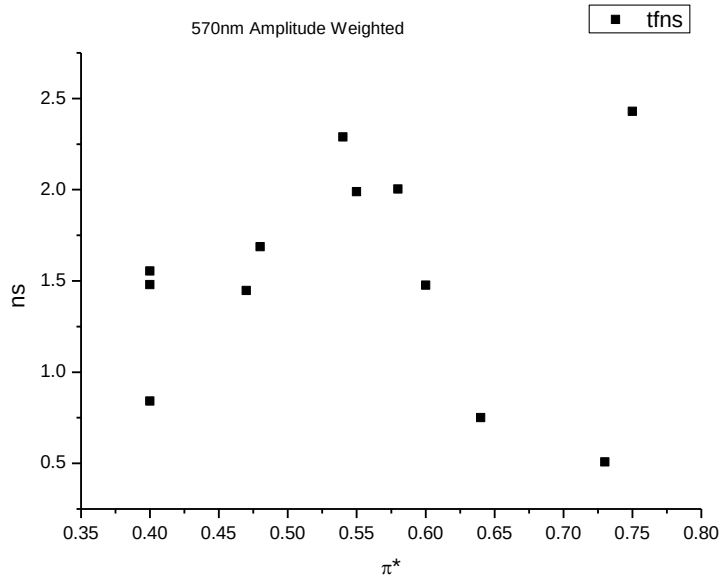

Figure 3.2.114. Amplitude weighted average lifetime (τ_f) of **17** at 570 nm versus π*.

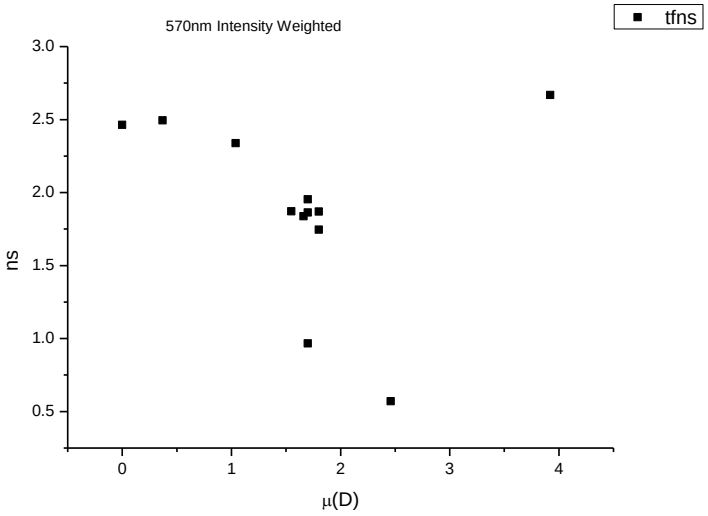

Figure 3.2.115. Intensity weighted average lifetime (τ_f) of **17** at 570 nm versus μ(D).

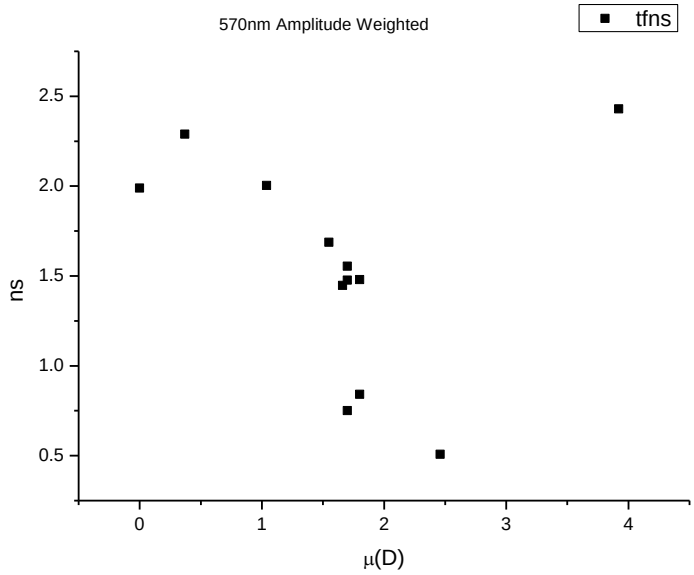

Figure 3.2.116. Amplitude weighted average lifetime (τ_f) of **17** at 570 nm versus μ(D).

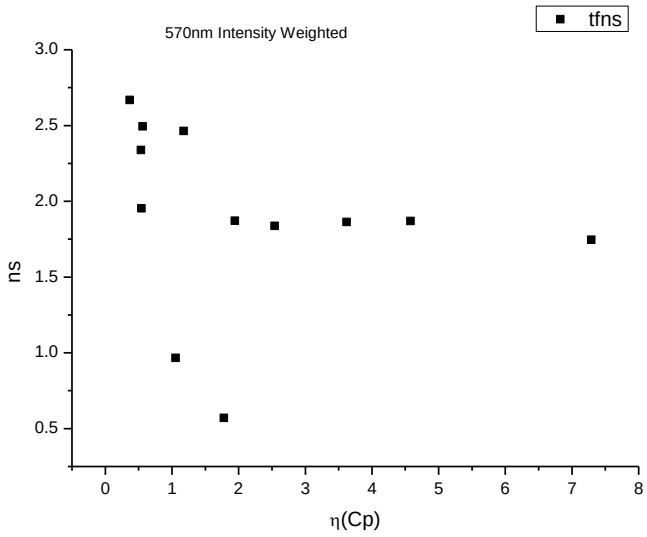

Figure 3.2.117. Intensity weighted average lifetime (τ_f) of **17** at 570 nm versus η(Cp).

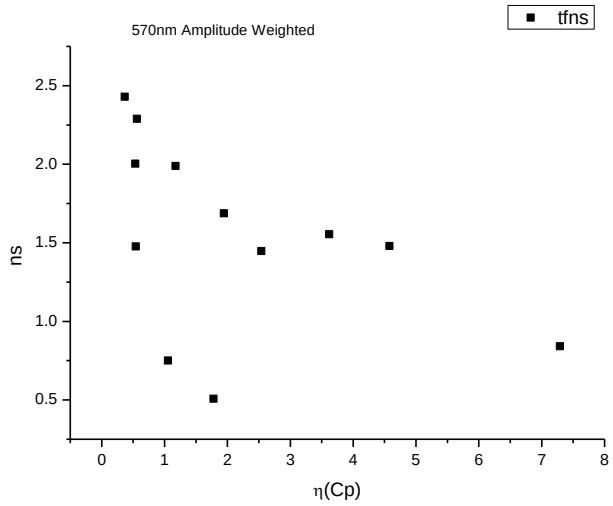

Figure 3.2.118. Amplitude weighted average lifetime (τ_f) of **17** at 570 nm versus η(Cp).

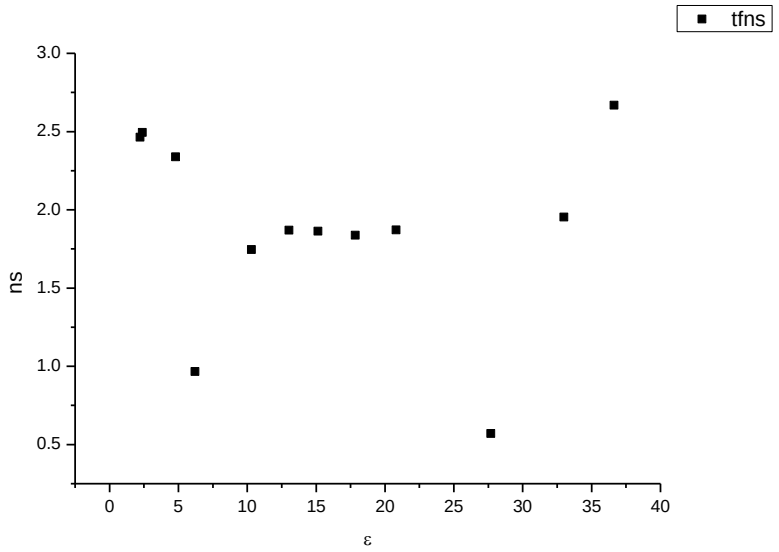

Figure 3.2.119. Intensity weighted average lifetime (τ_f) of **17** at 570 nm versus ε.

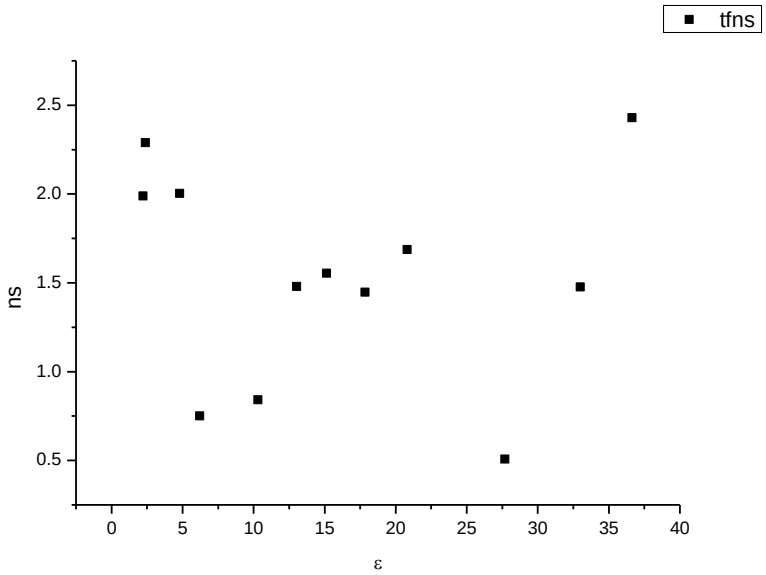

Figure 3.2.120. Amplitude weighted average lifetime (τ_f) of **17** at 570 nm versus ε.

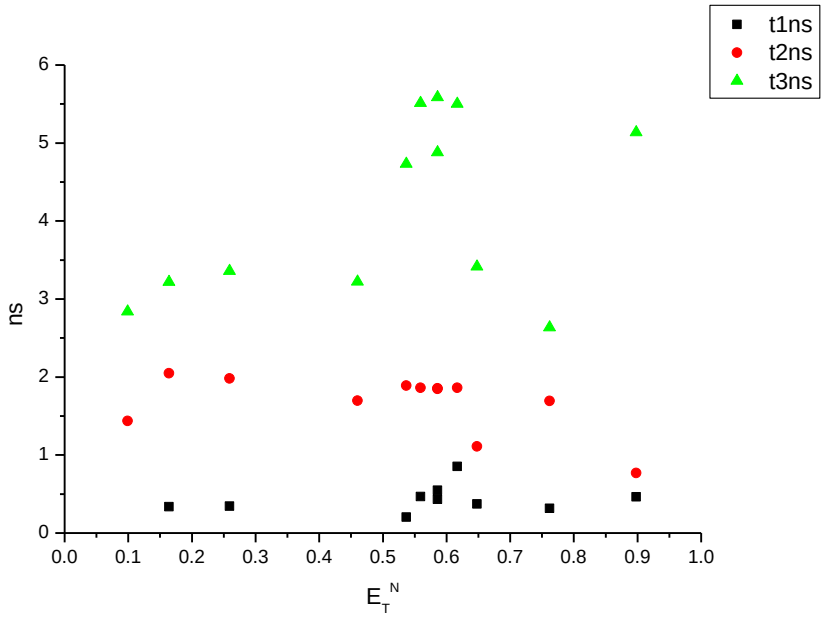

Figure 3.2.121. Intensity weighted components of TCSPC lifetime decay of **17** (570 nm) versus E_T^N.

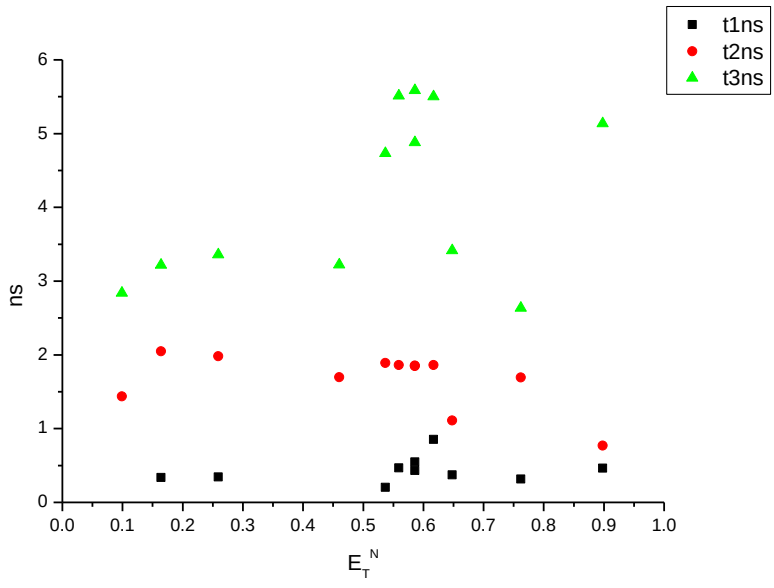

Figure 3.2.122. Amplitude weighted components of TCSPC lifetime decay of **17** (570 nm) versus E_T^N.

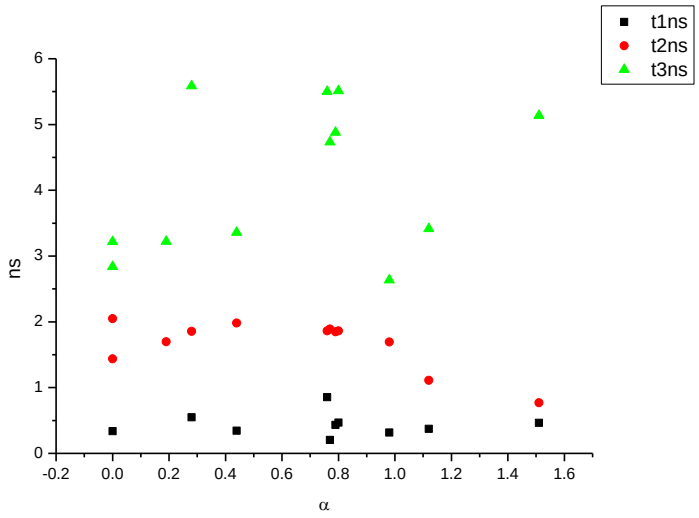

Figure 3.2.123. Intensity weighted components of TCSPC lifetime decay of **17** (570 nm) versus α.

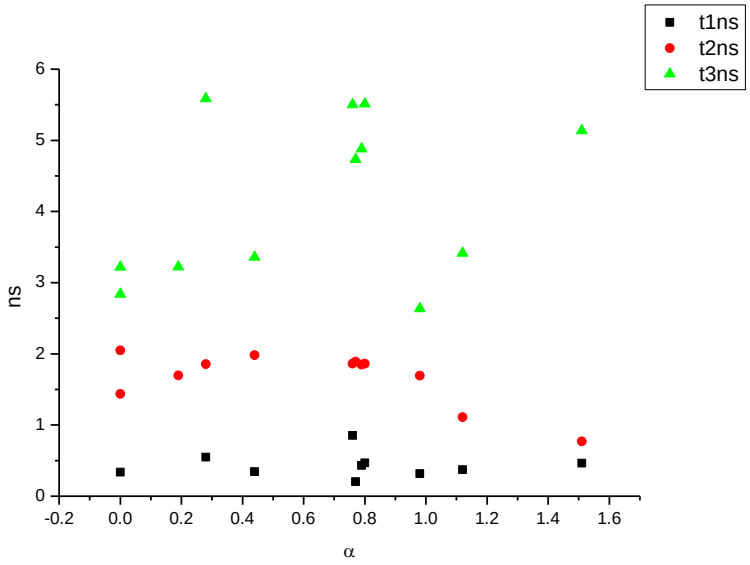

Figure 3.2.124. Amplitude weighted components of TCSPC lifetime decay of **17** (570 nm) versus α.

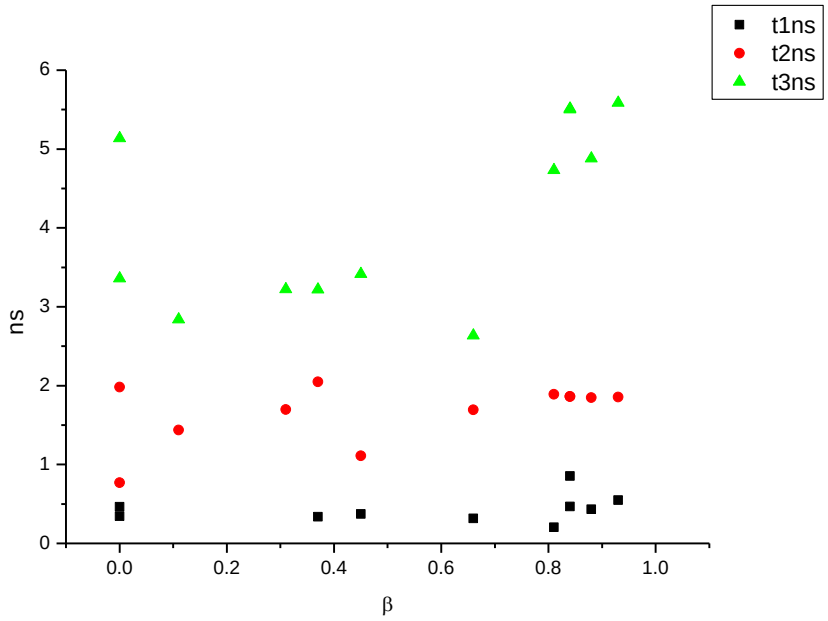

Figure 3.2.125. Intensity weighted components of TCSPC lifetime decay of **17** (570 nm) versus β.

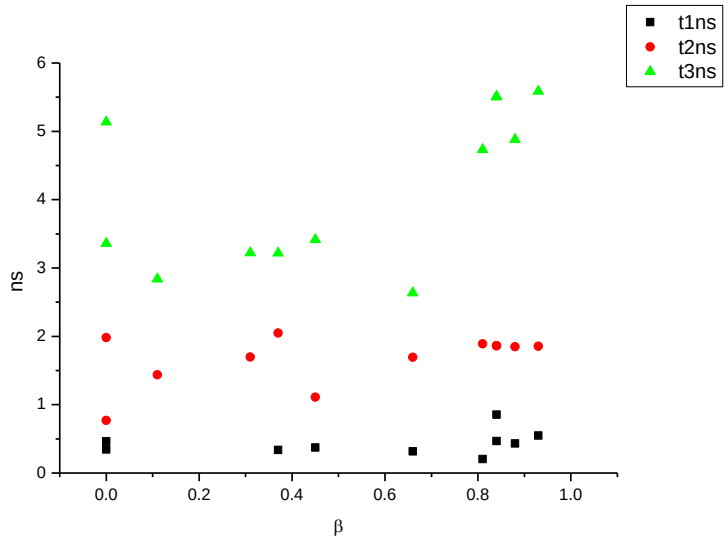

Figure 3.2.126. Amplitude weighted components of TCSPC lifetime decay of **17** (570 nm) versus β.

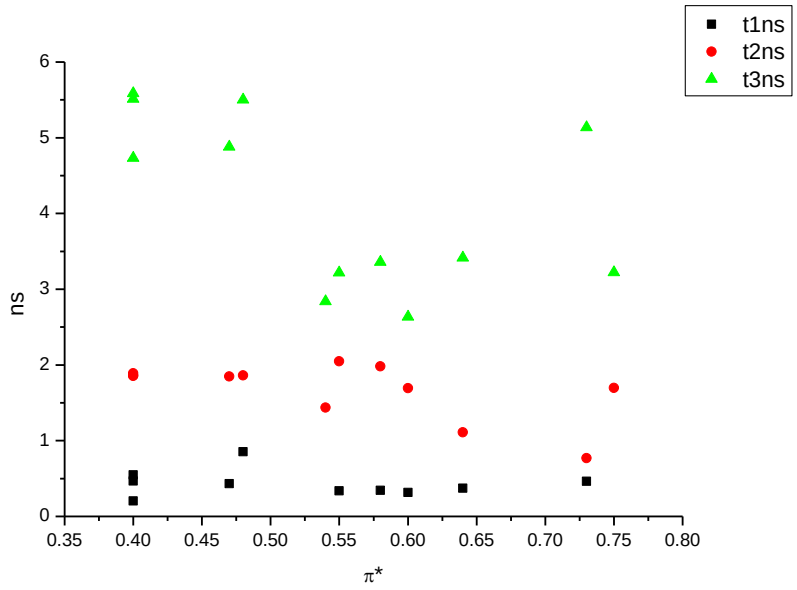

Figure 3.2.127. Intensity weighted components of TCSPC lifetime decay of **17** (570 nm) versus π*.

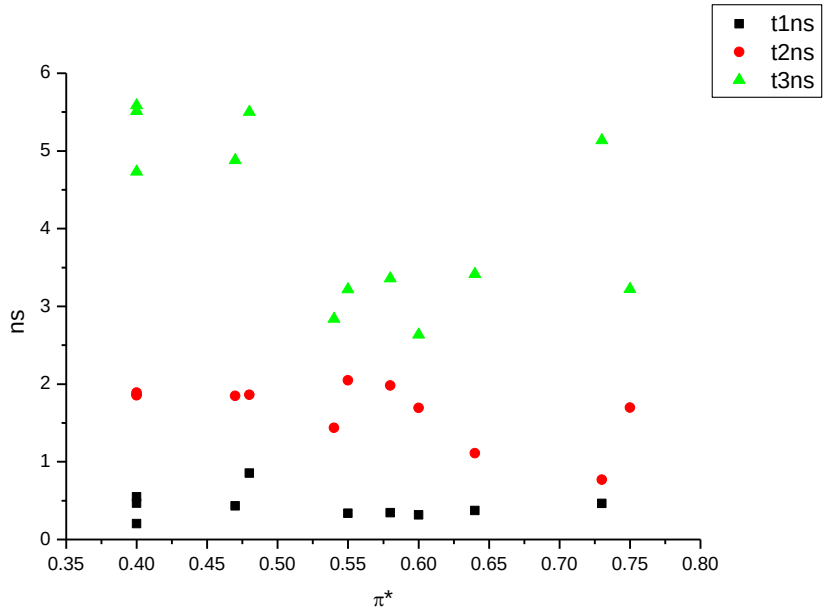

Figure 3.2.128. Amplitude weighted components of TCSPC lifetime decay of **17** (570 nm) versus π*.

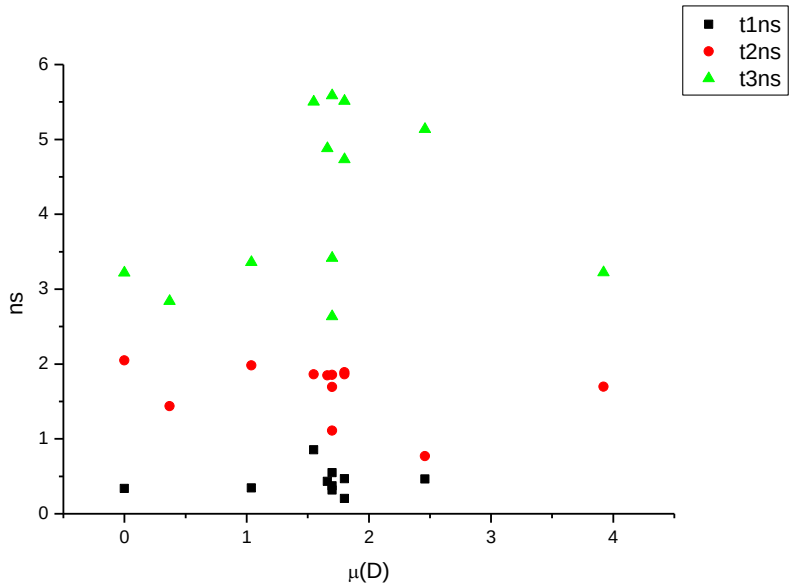

Figure 3.2.129. Intensity weighted components of TCSPC lifetime decay of **17** (570 nm) versus μ(D).

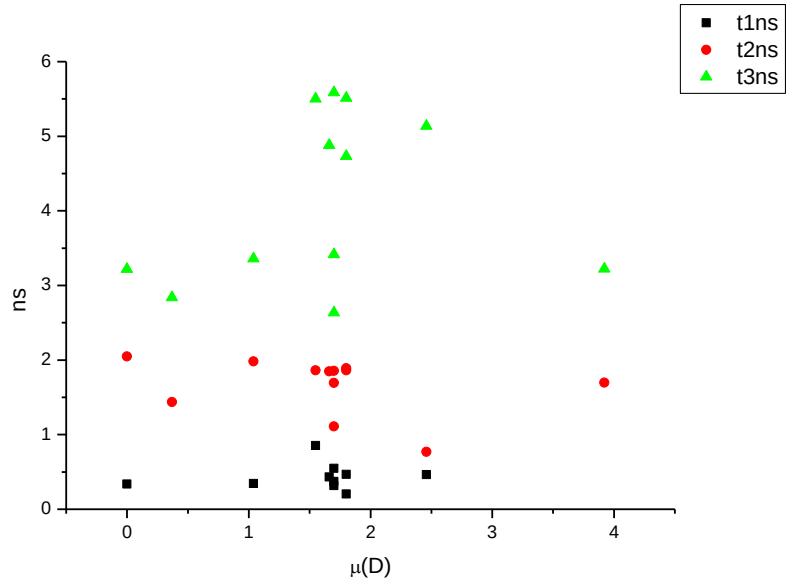

Figure 3.2.130. Amplitude weighted components of TCSPC lifetime decay of **17** (570 nm) versus μ(D).

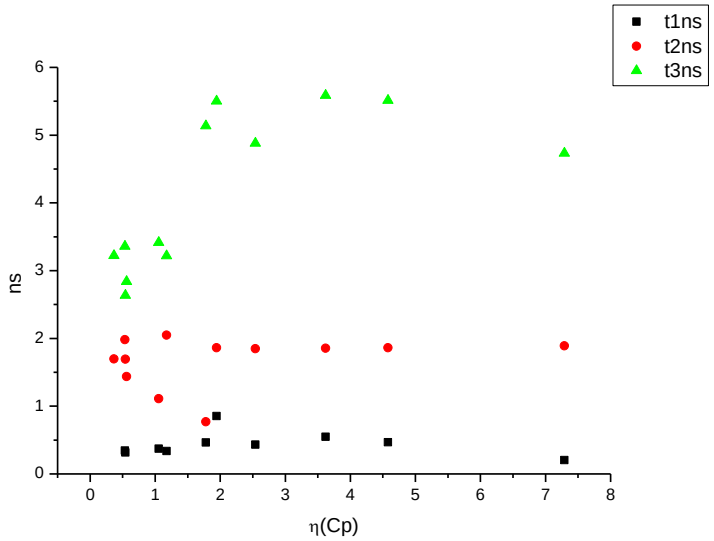

Figure 3.2.131. Intensity weighted components of TCSPC lifetime decay of **17** (570 nm) versus η(Cp).

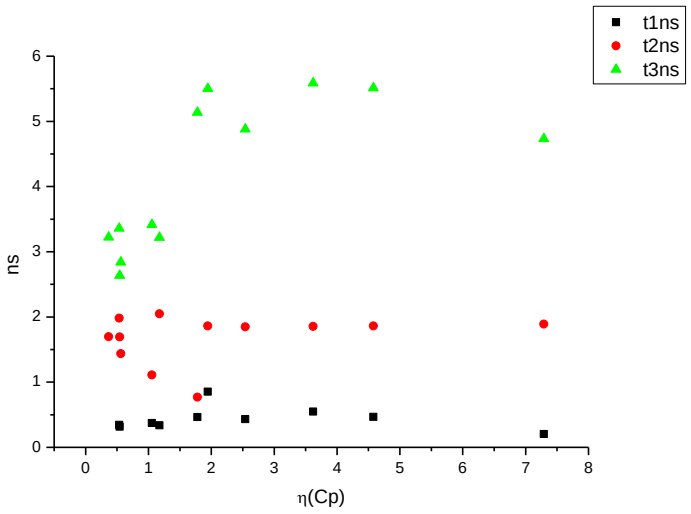

Figure 3.2.132. Amplitude weighted components of TCSPC lifetime decay of **17** (570 nm) versus η(Cp).

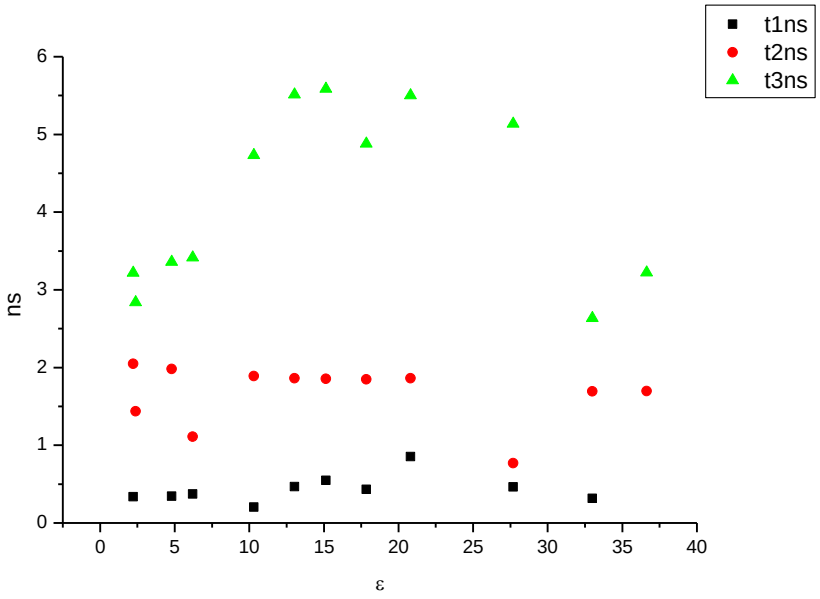

Figure 3.2.133. Intensity weighted components of TCSPC lifetime decay of **17** (570 nm) versus ε.

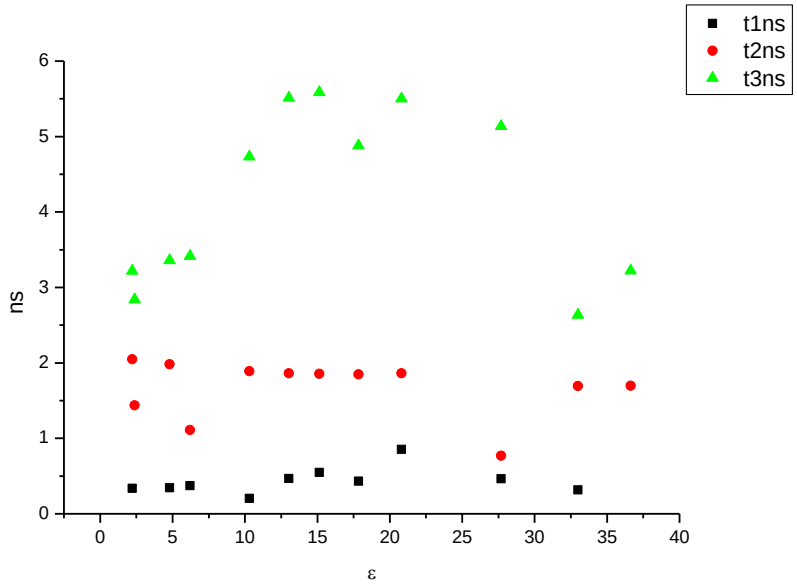

Figure 3.2.134. Amplitude weighted components of TCSPC lifetime decay of **17** (570 nm) versus ε.

3.2.8 Ultraviolet-visible absorption spectra.

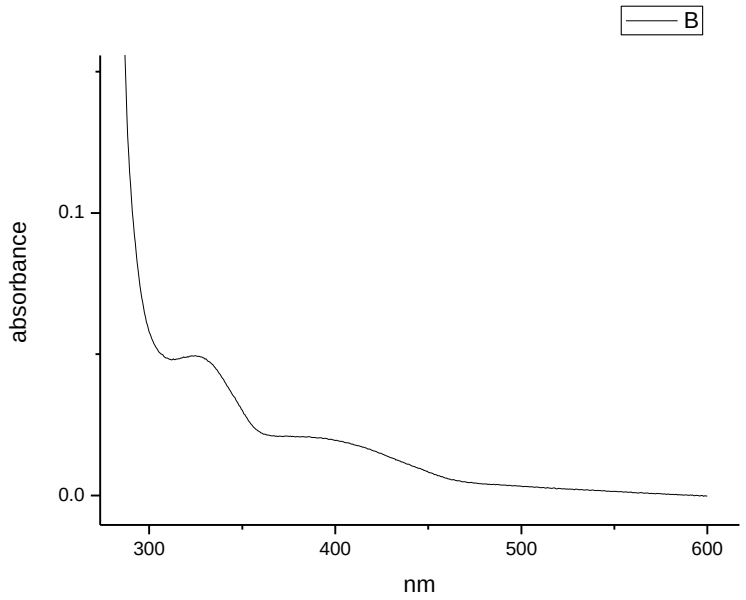

Figure 3.2.135. Ultraviolet-Visible absorption spectrum of **17** recorded in Toluene.

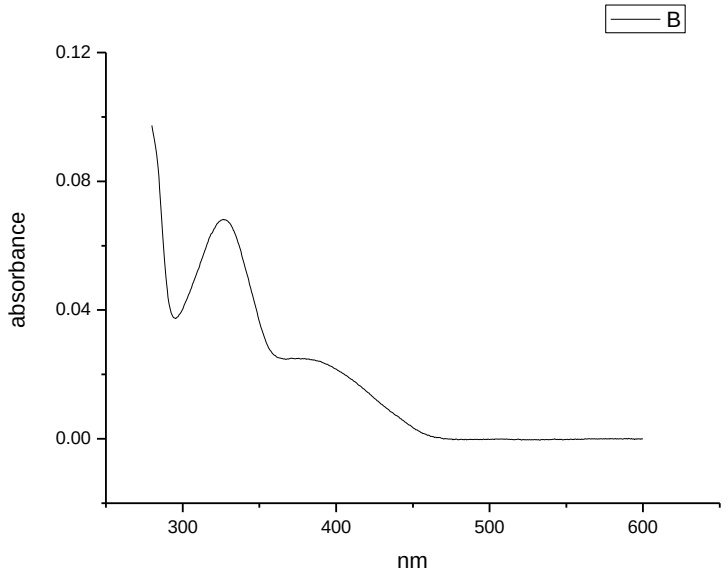

Figure 3.2.136. Ultraviolet-Visible absorption spectrum of **17** recorded in 1,4-dioxane.

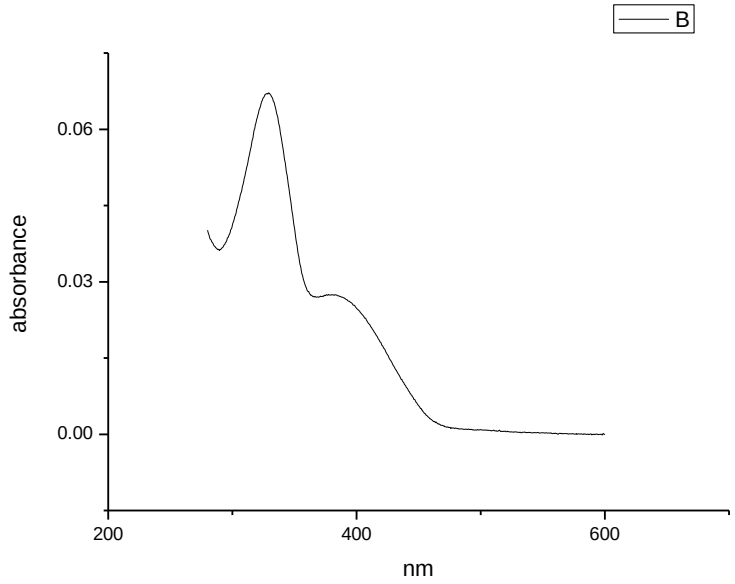

Figure 3.2.137. Ultraviolet-Visible absorption spectrum of **17** recorded in Chloroform.

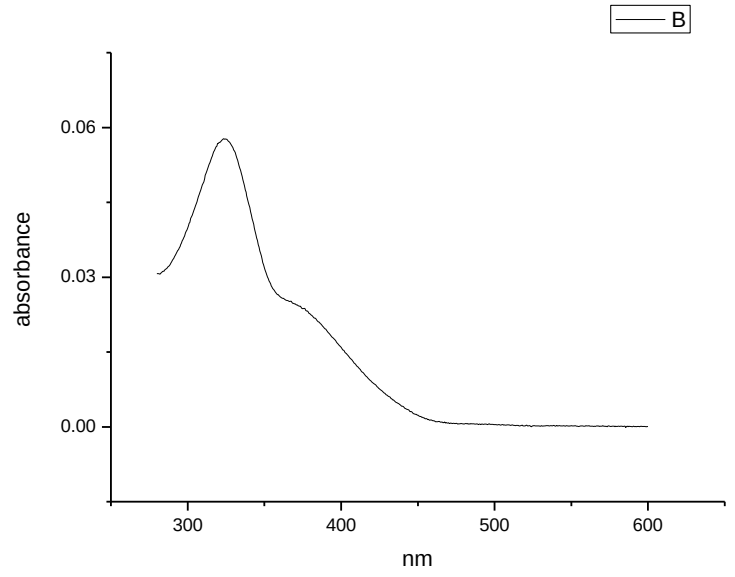

Figure 3.2.138. Ultraviolet-Visible absorption spectrum of **17** recorded in Acetonitrile.

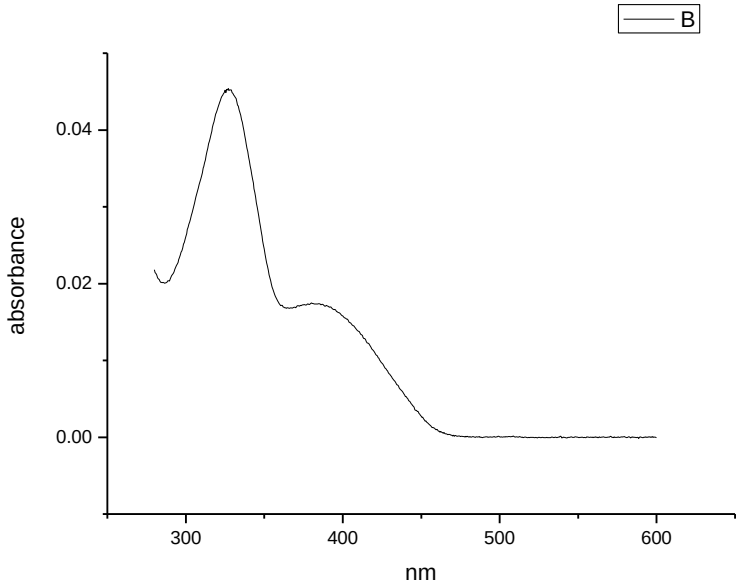

Figure 3.2.139. Ultraviolet-Visible absorption spectrum of **17** recorded in 1-octanol.

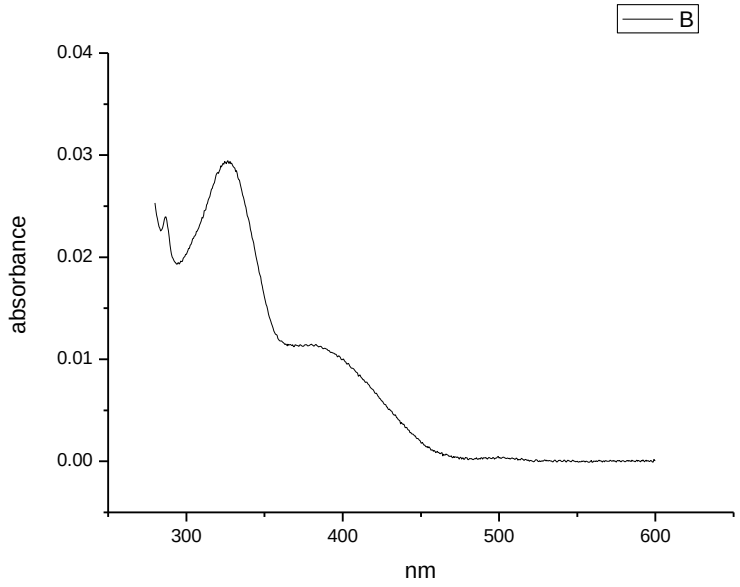

Figure 3.2.140. Ultraviolet-Visible absorption spectrum of **17** recorded in 1-hexanol.

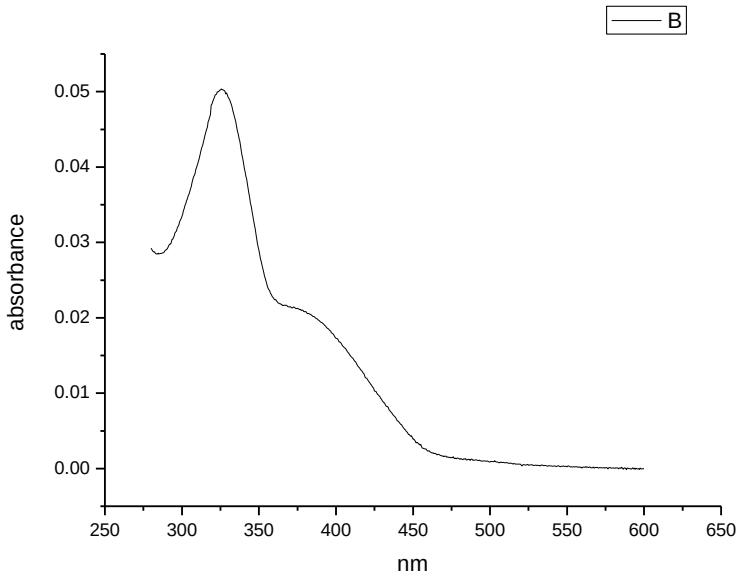

Figure 3.2.141. Ultraviolet-Visible absorption spectrum of **17** recorded in 1-butanol.

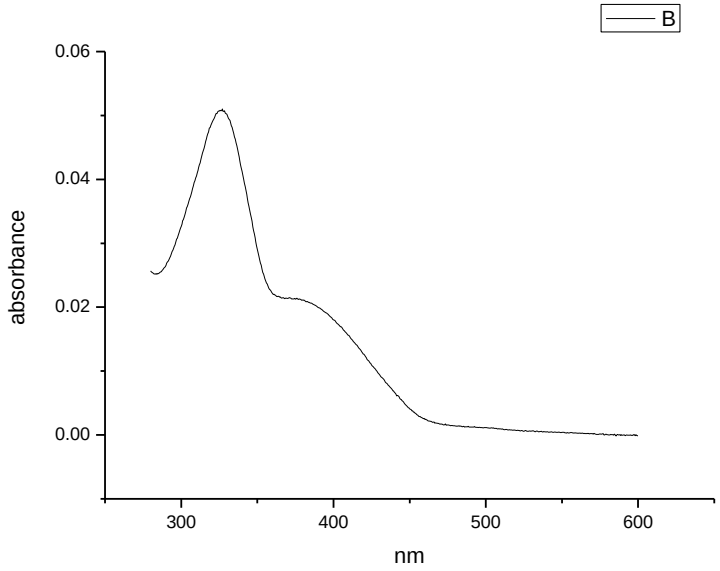

Figure 3.2.142. Ultraviolet-Visible absorption spectrum of **17** recorded in 1-pentanol.

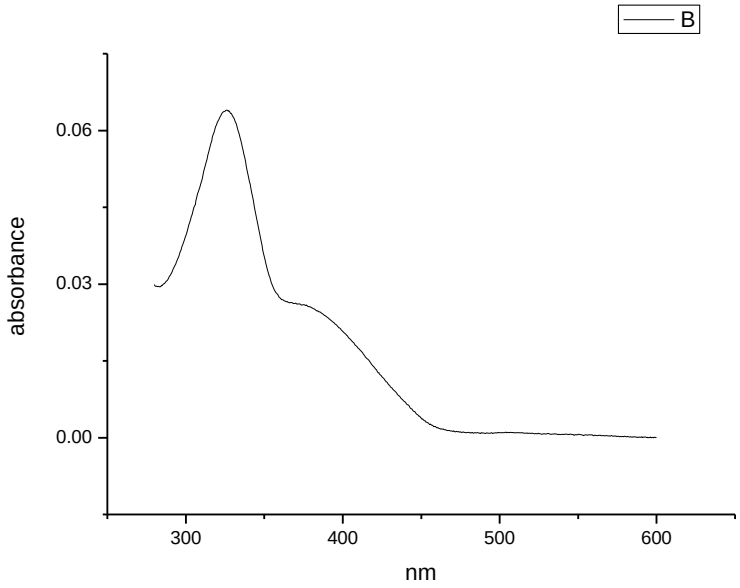

Figure 3.2.143. Ultraviolet-Visible absorption spectrum of **17** recorded in 1-propanol.

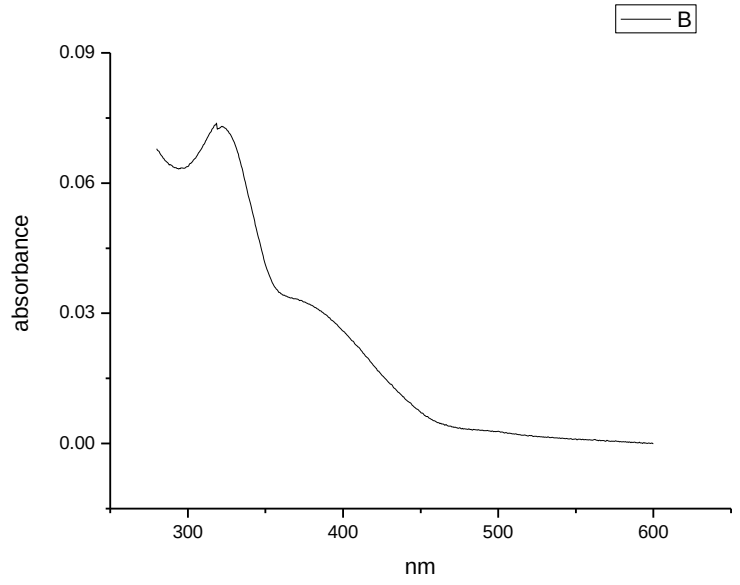

Figure 3.2.144. Ultraviolet-Visible absorption spectrum of **17** recorded in Acetic Acid.

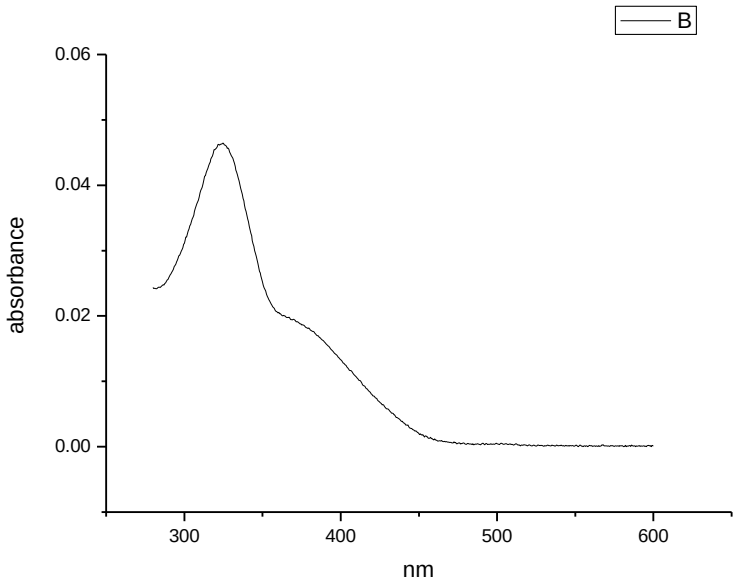

Figure 3.2.145. Ultraviolet-Visible absorption spectrum of **17** recorded in Methanol.

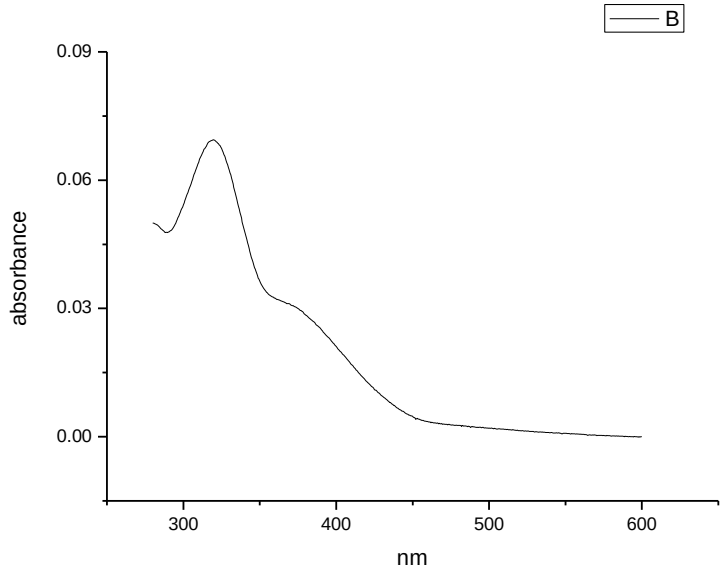

Figure 3.2.146. Ultraviolet-Visible absorption spectrum of **17** recorded in 2,2,2-trifluoroethanol.

3.2.9 Fluorescence Emission spectra.

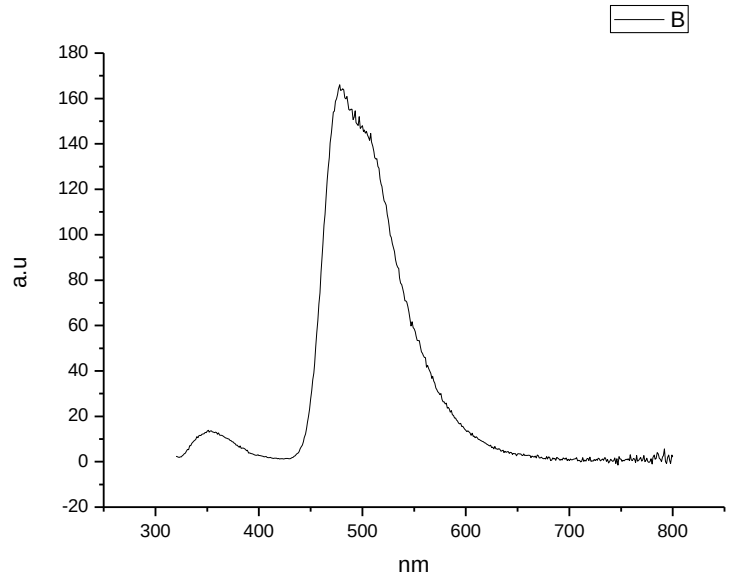

Figure 3.2.147. Fluorescence emission spectrum of **17** recorded in Toluene at 310 nm excitation.

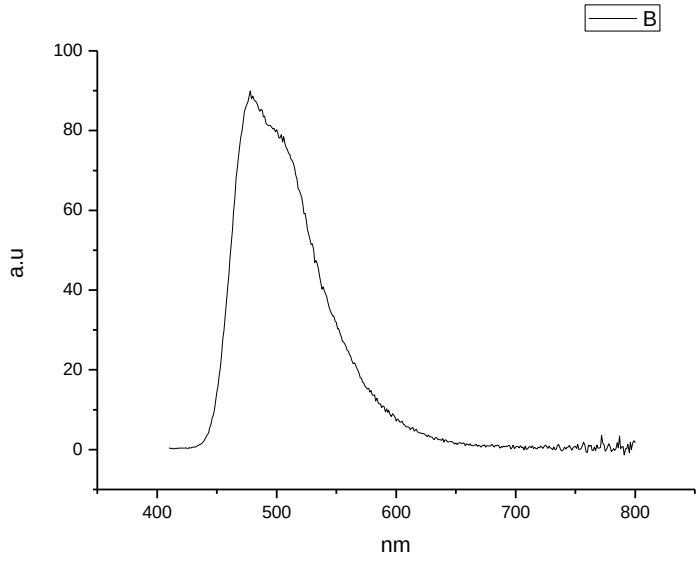

Figure 3.2.148. Fluorescence emission spectrum of **17** recorded in Toluene at 400 nm excitation.

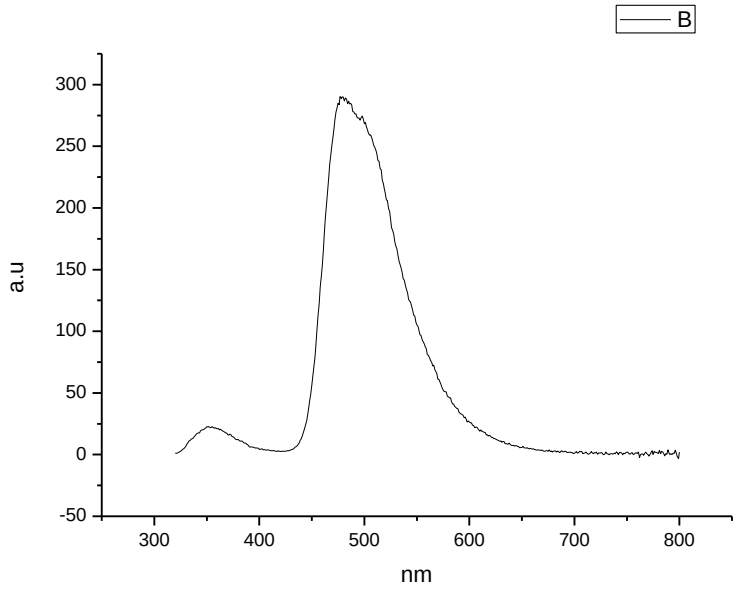

Figure 3.2.149. Fluorescence emission spectrum of **17** recorded in 1,4-dioxane at 310 nm excitation.

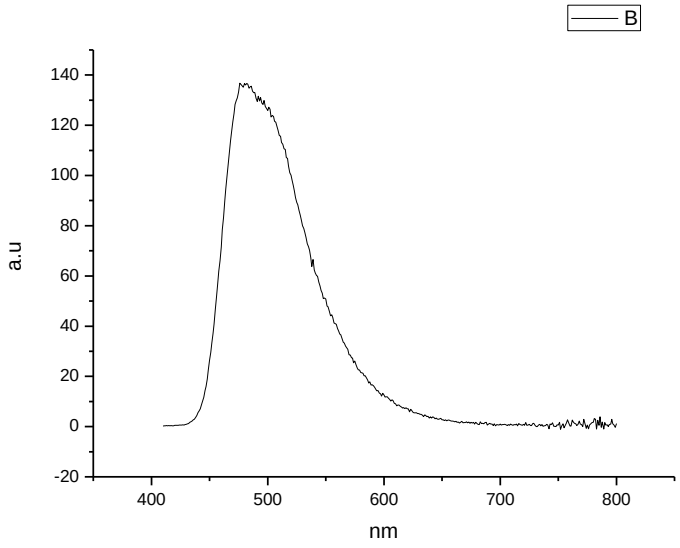

Figure 3.2.150. Fluorescence emission spectrum of **17** recorded in 1,4-dioxane at 400 nm excitation.

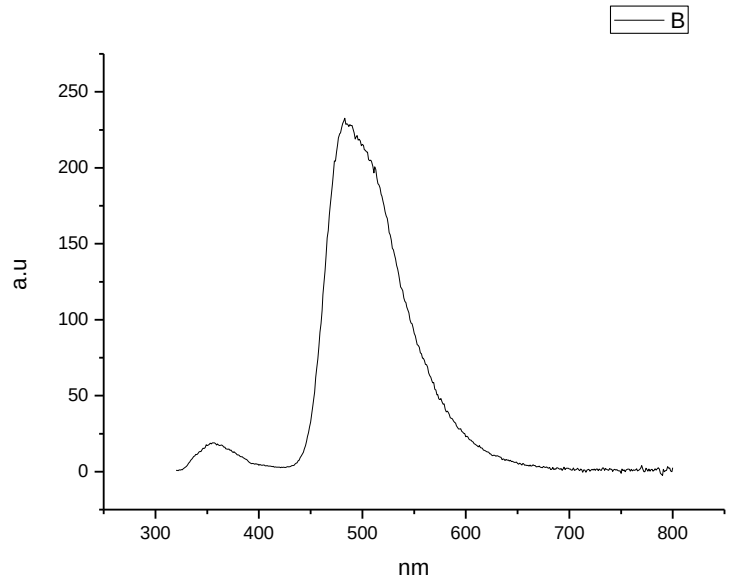

Figure 3.2.151. Fluorescence emission spectrum of **17** recorded in Chloroform at 310 nm excitation.

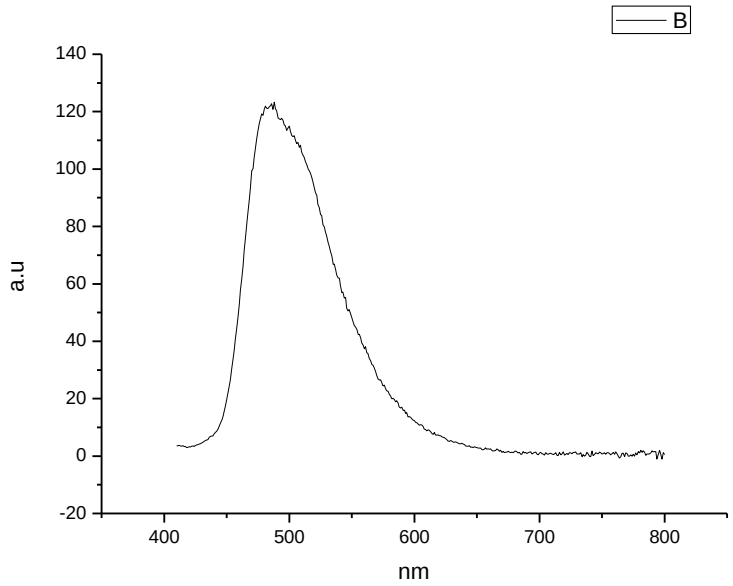

Figure 3.2.152. Fluorescence emission spectrum of **17** recorded in Chloroform at 400 nm excitation.

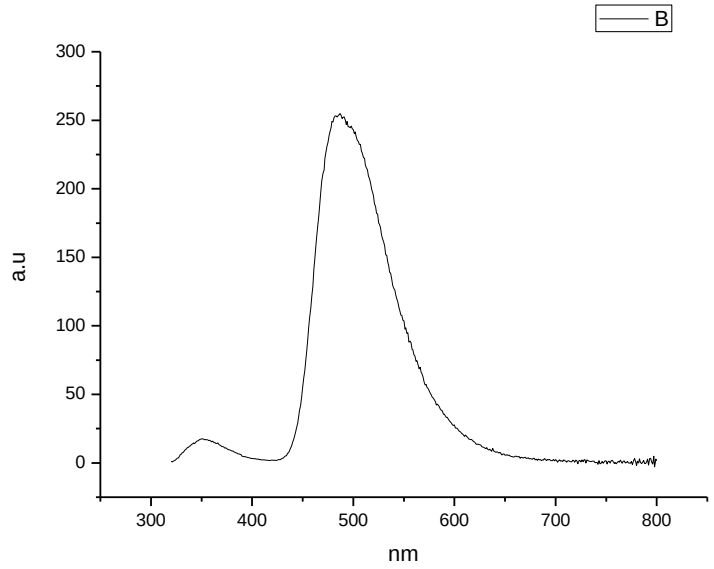

Figure 3.2.153. Fluorescence emission spectrum of **17** recorded in Acetonitrile at 310 nm excitation.

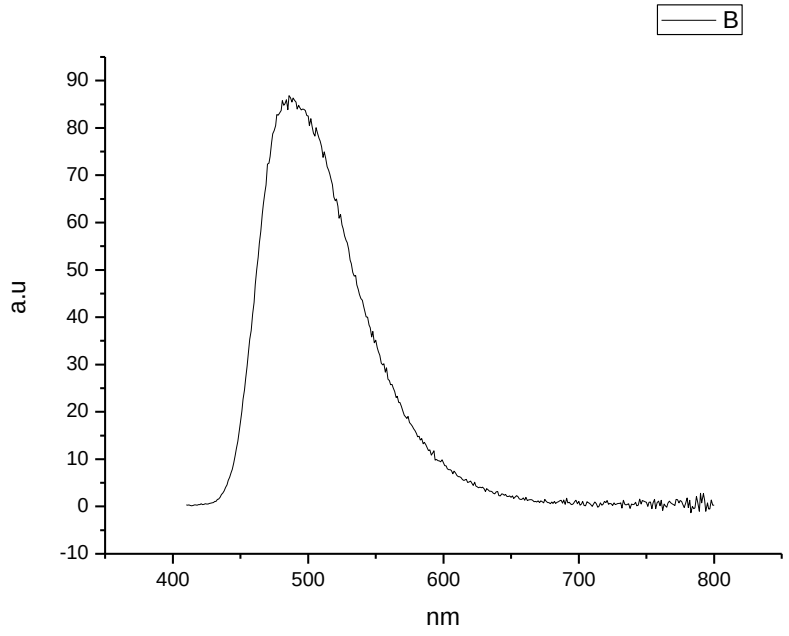

Figure 3.2.154. Fluorescence emission spectrum of **17** recorded in Acetonitrile at 400 nm excitation.

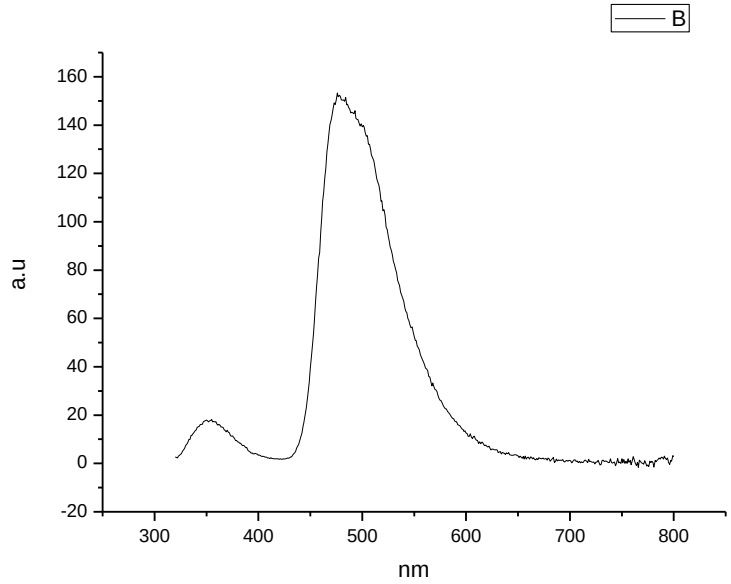

Figure 3.2.155. Fluorescence emission spectrum of **17** recorded in 1-octanol at 310 nm excitation.

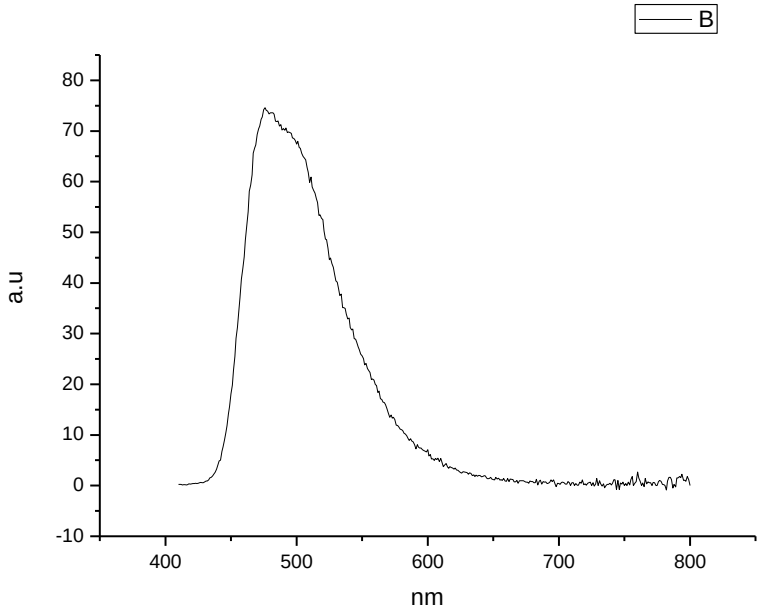

Figure 3.2.156. Fluorescence emission spectrum of **17** recorded in 1-octanol at 400 nm excitation.

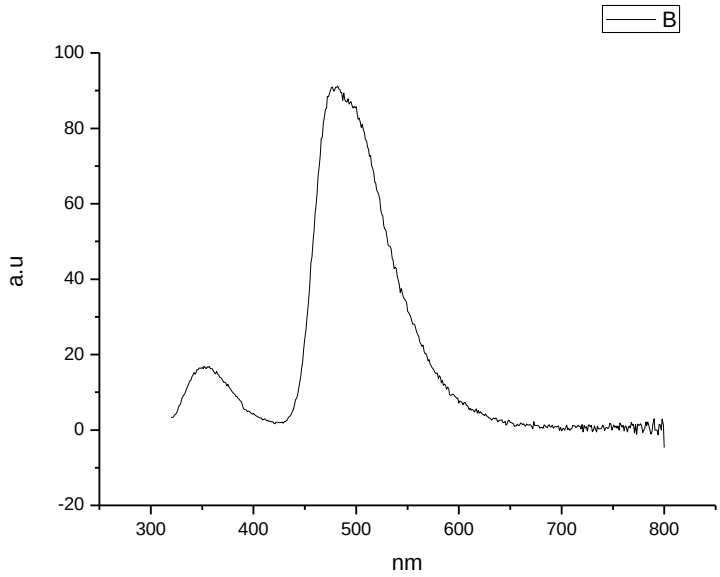

Figure 3.2.157. Fluorescence emission spectrum of **17** recorded in 1-hexanol at 310 nm excitation.

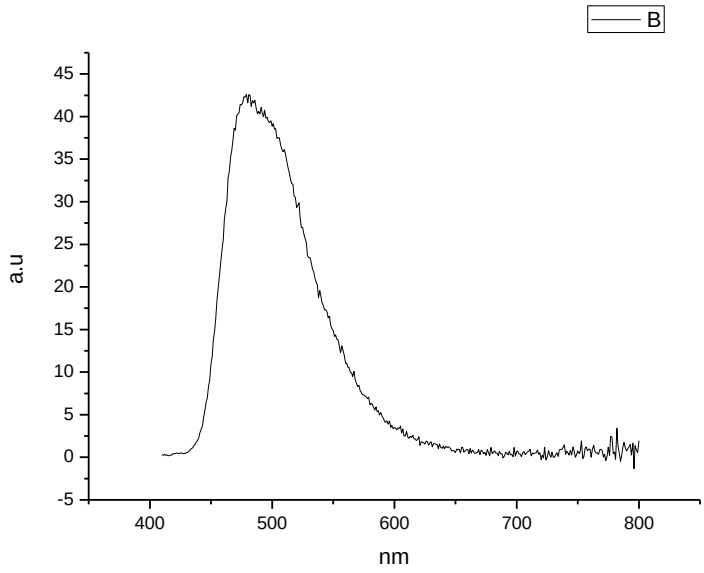

Figure 3.2.158. Fluorescence emission spectrum of **17** recorded in 1-hexanol at 400 nm excitation.

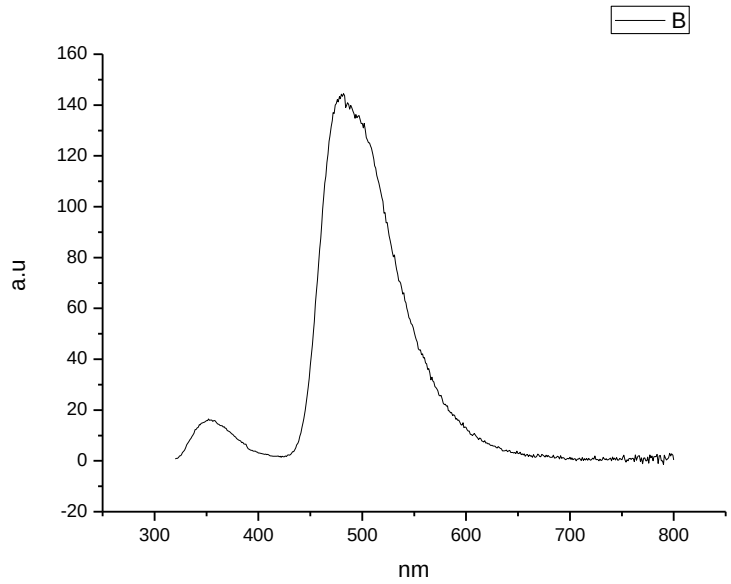

Figure 3.2.159. Fluorescence emission spectrum of **17** recorded in 1-butanol at 310 nm excitation.

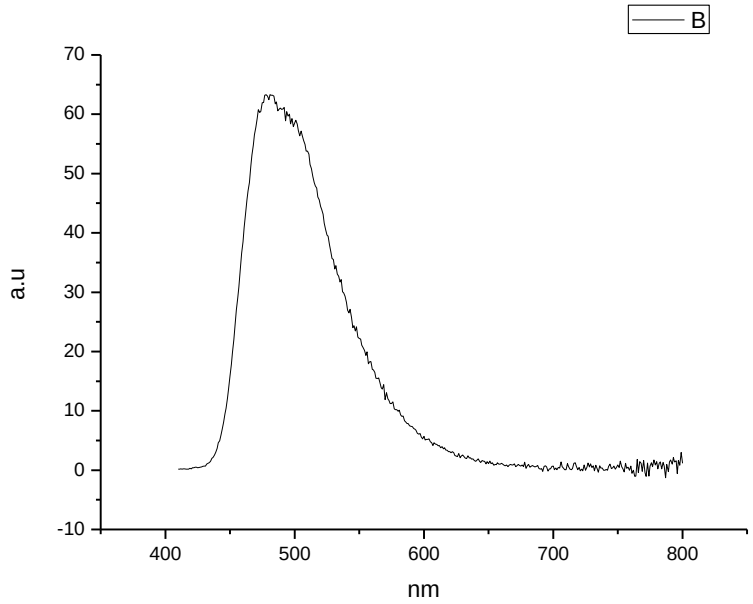

Figure 3.2.160. Fluorescence emission spectrum of **17** recorded in 1-butanol at 400 nm excitation.

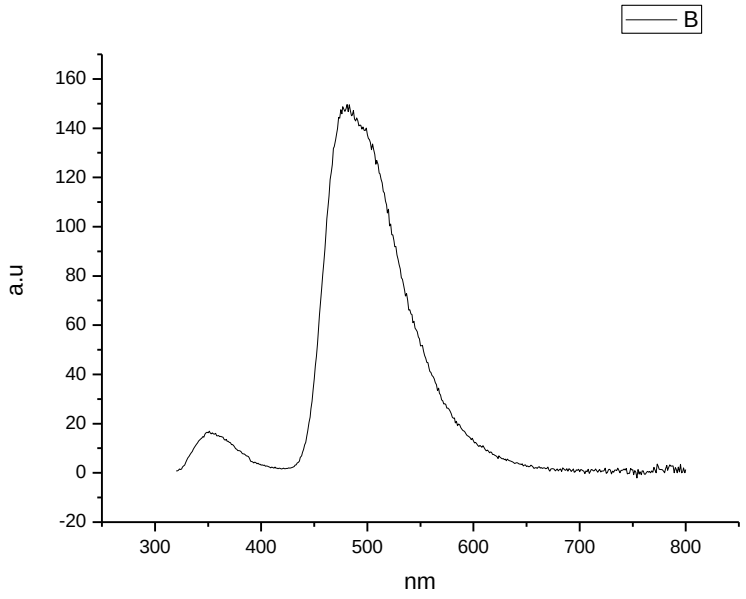

Figure 3.2.161. Fluorescence emission spectrum of **17** recorded in 1-pentanol at 310 nm excitation.

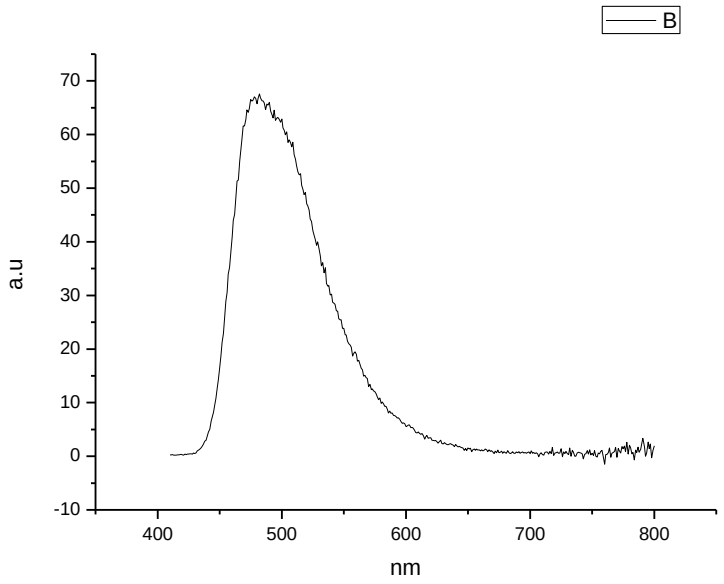

Figure 3.2.162. Fluorescence emission spectrum of **17** recorded in 1-pentanol at 400 nm excitation.

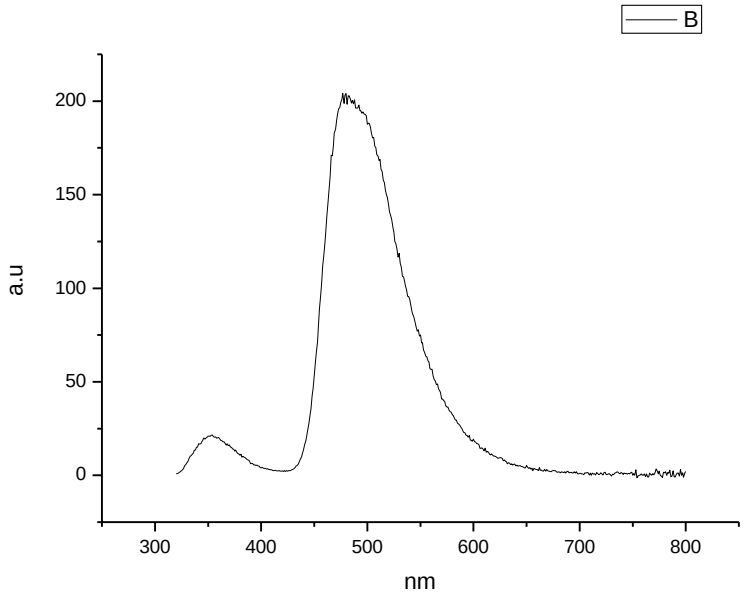

Figure 3.2.163. Fluorescence emission spectrum of **17** recorded in 1-propanol at 310 nm excitation.

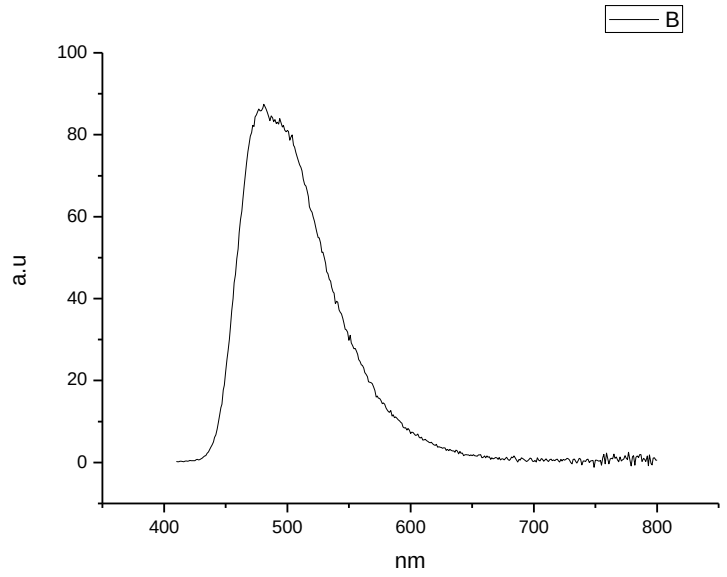

Figure 3.2.164. Fluorescence emission spectrum of **17** recorded in 1-propanol at 400 nm excitation.

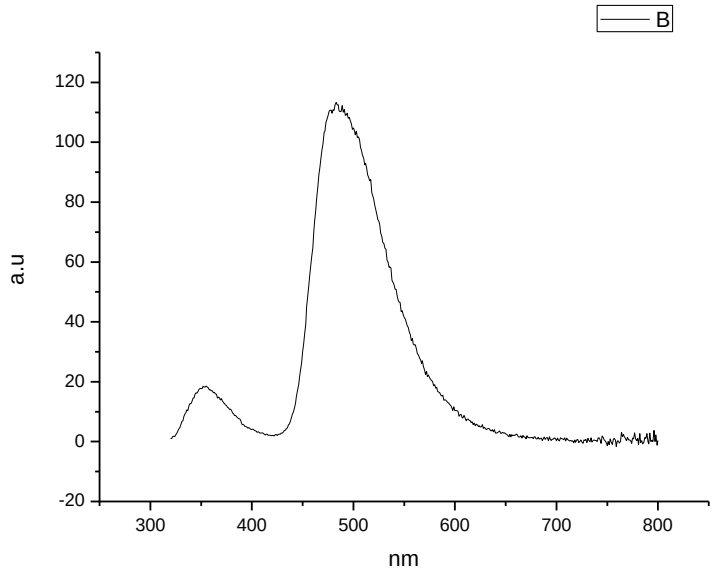

Figure 3.2.165. Fluorescence emission spectrum of **17** recorded in Acetic Acid at 310 nm excitation.

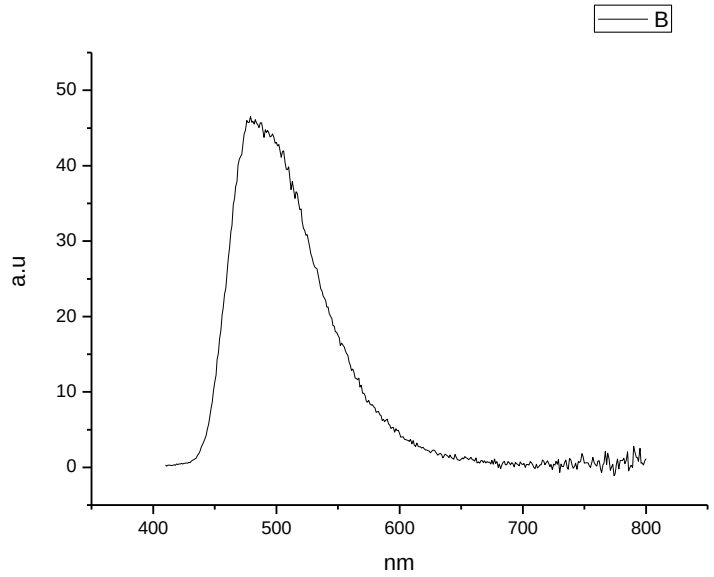

Figure 3.2.166. Fluorescence emission spectrum of **17** recorded in Acetic Acid at 400 nm excitation.

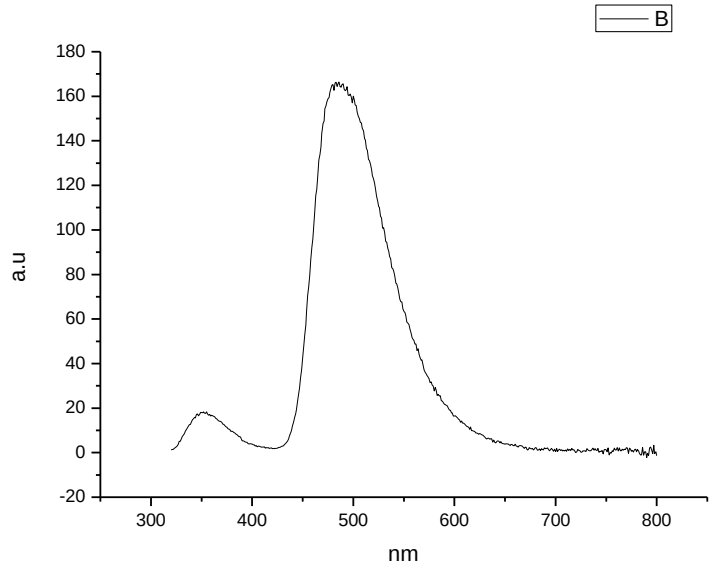

Figure 3.2.167. Fluorescence emission spectrum of **17** recorded in Methanol at 310 nm excitation.

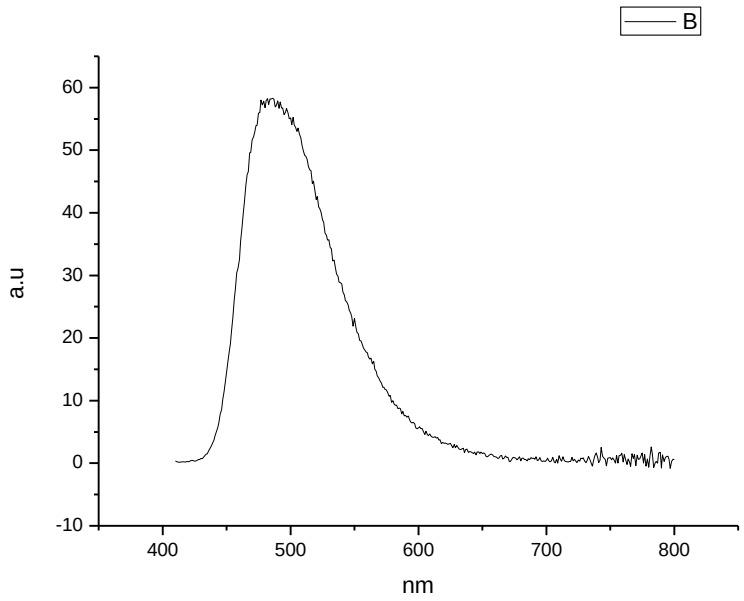

Figure 3.2.168. Fluorescence emission spectrum of **17** recorded in Methanol at 400 nm excitation.

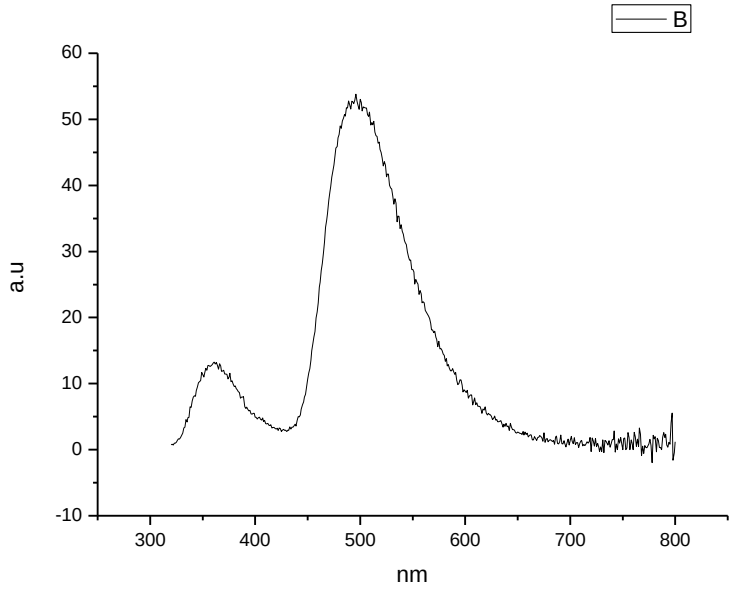

Figure 3.2.169. Fluorescence emission spectrum of **17** recorded in 2,2,2-trifluoroethanol at 310 nm excitation.

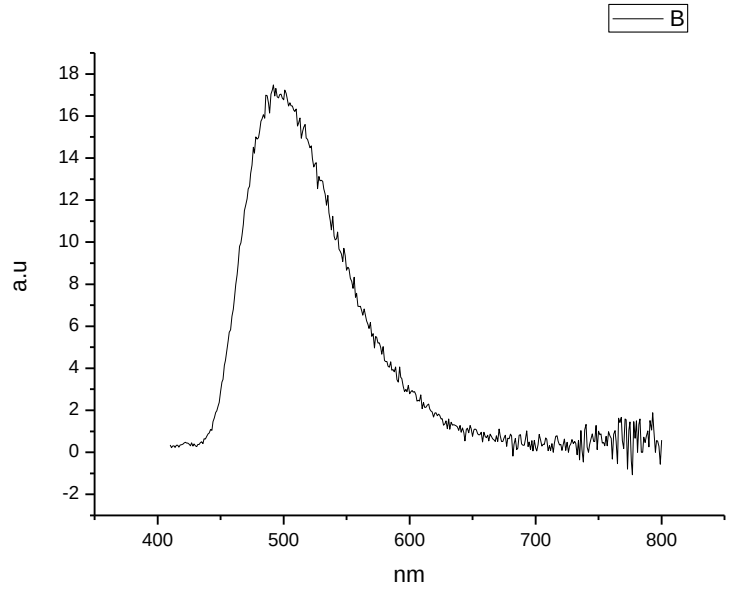

Figure 3.2.170. Fluorescence emission spectrum of **17** recorded in 2,2,2-trifluoroethanol at 400 nm excitation.

3.2.10 Normalised Fluorescence Emission spectra (Gaussian fitted).

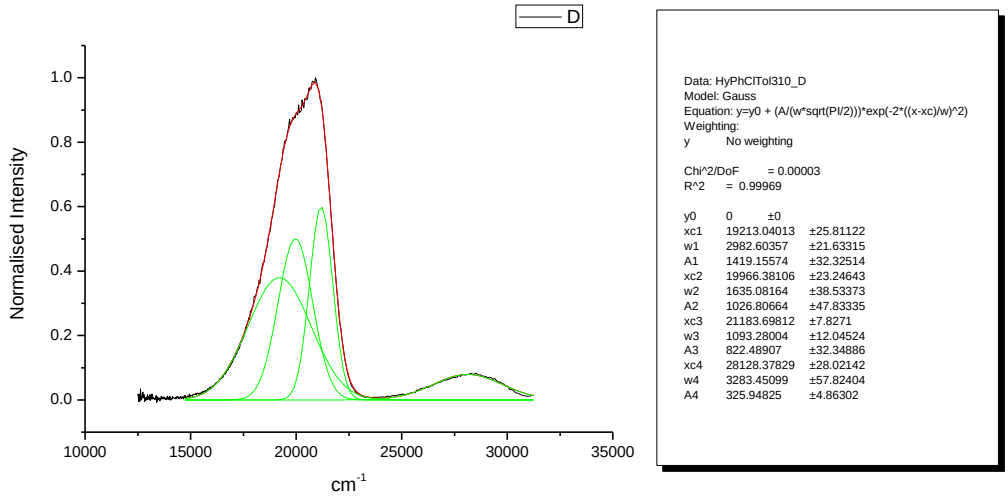

Figure 3.2.171. Gaussian model fit of the normalised fluorescence emission spectrum of **17** recorded in Toluene at 310 nm excitation.

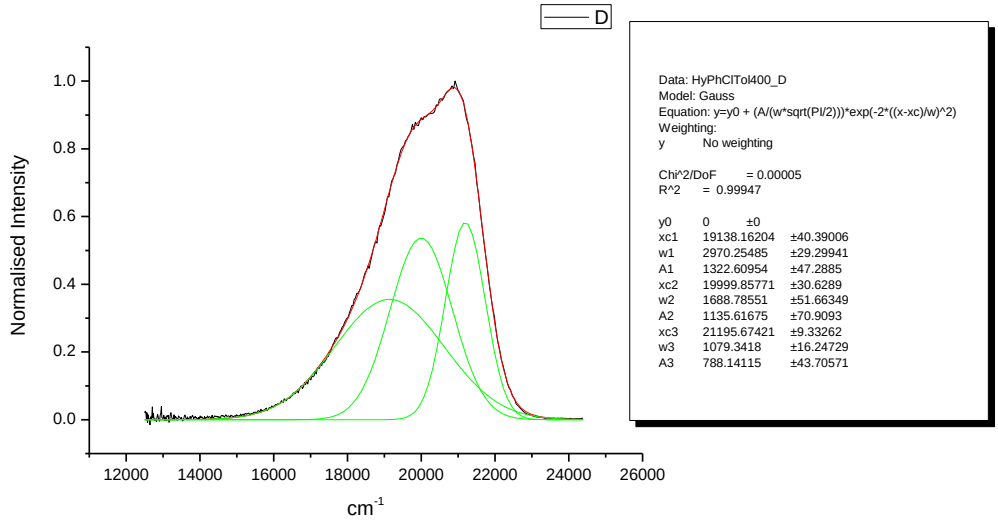

Figure 3.2.172. Gaussian model fit of the normalised fluorescence emission spectrum of **17** recorded in Toluene at 400 nm excitation.

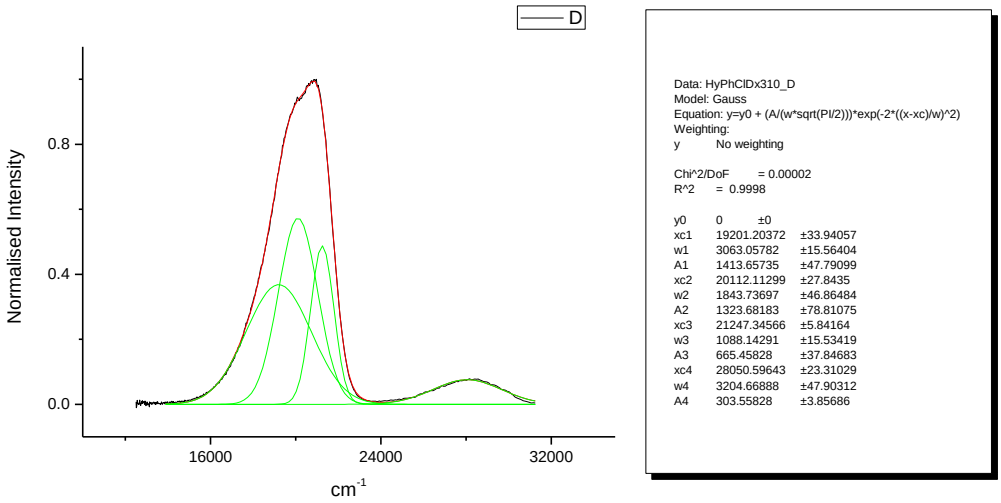

Figure 3.2.173. Gaussian model fit of the normalised fluorescence emission spectrum of **17** recorded in 1,4-dioxane at 310 nm excitation.

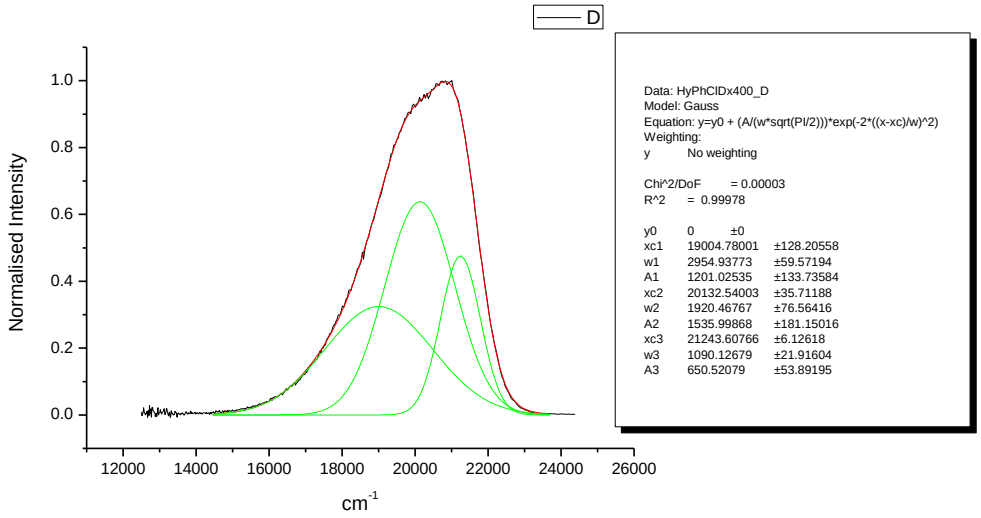

Figure 3.2.174. Gaussian model fit of the normalised fluorescence emission spectrum of **17** recorded in 1,4-dioxane at 400 nm excitation.

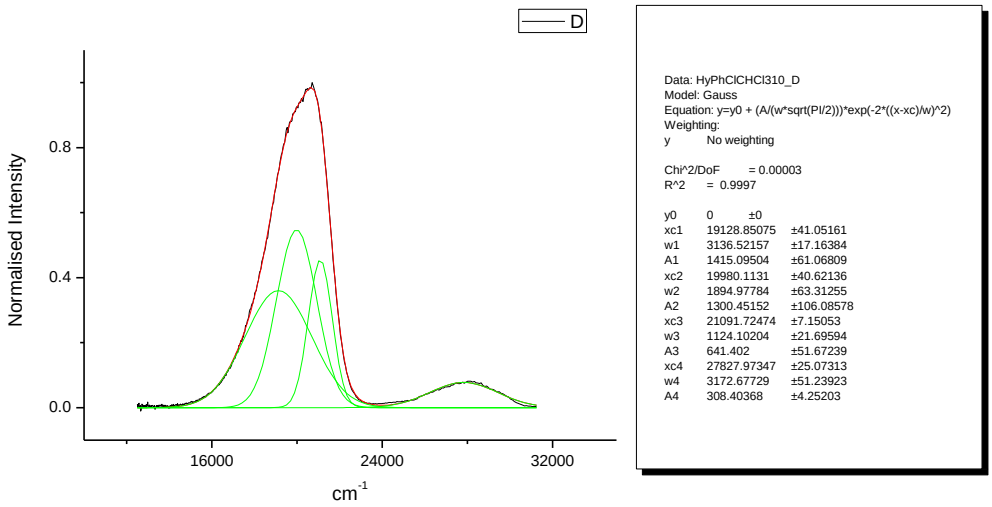

Figure 3.2.175. Gaussian model fit of the normalised fluorescence emission spectrum of **17** recorded in Chloroform at 310 nm excitation.

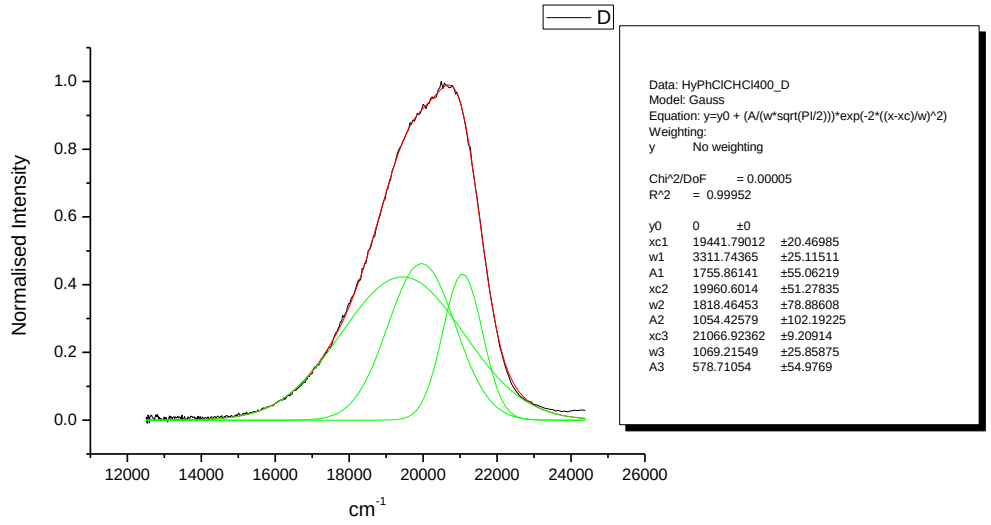

Figure 3.2.176. Gaussian model fit of the normalised fluorescence emission spectrum of **17** recorded in Chloroform at 400 nm excitation.

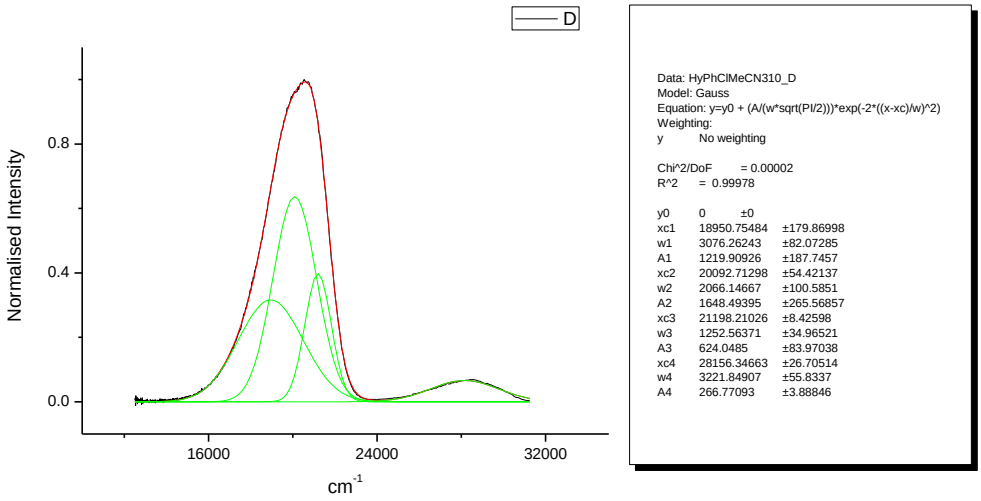

Figure 3.2.177. Gaussian model fit of the normalised fluorescence emission spectrum of **17** recorded in Acetonitrile at 310 nm excitation.

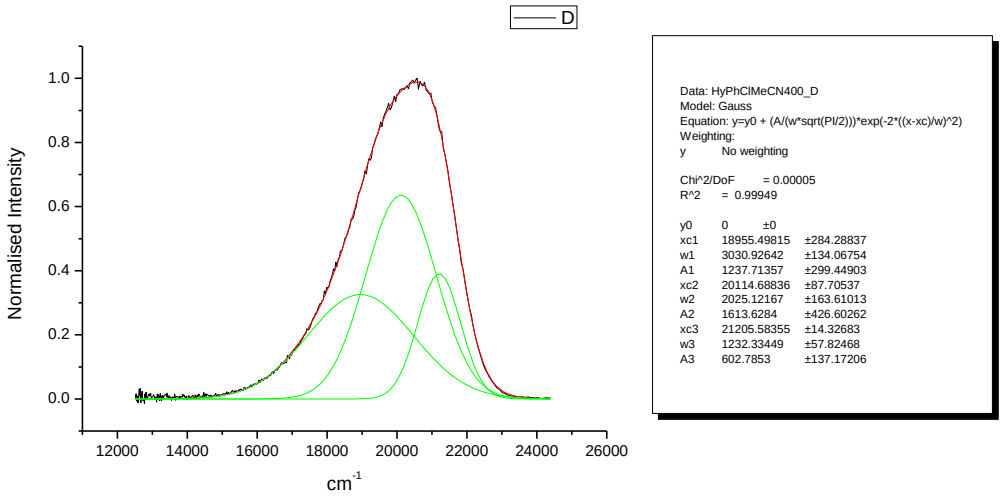

Figure 3.2.178. Gaussian model fit of the normalised fluorescence emission spectrum of **17** recorded in Acetonitrile at 400 nm excitation.

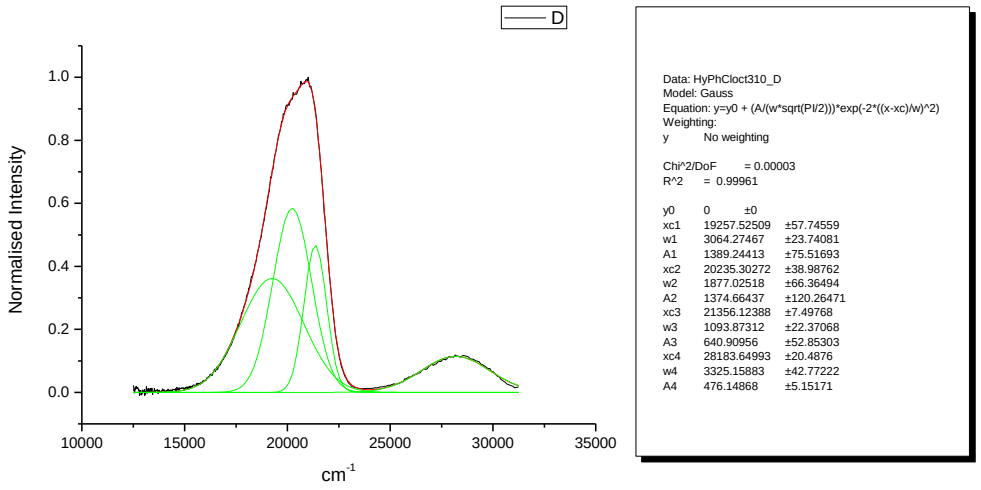

Figure 3.2.179. Gaussian model fit of the normalised fluorescence emission spectrum of **17** recorded in 1-octanol at 310 nm excitation.

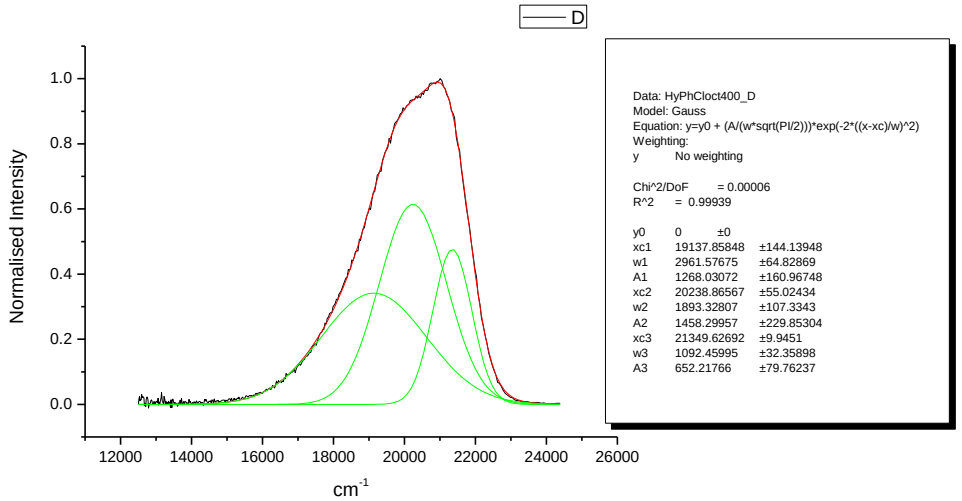

Figure 3.2.180. Gaussian model fit of the normalised fluorescence emission spectrum of **17** recorded in 1-octanol at 400 nm excitation.

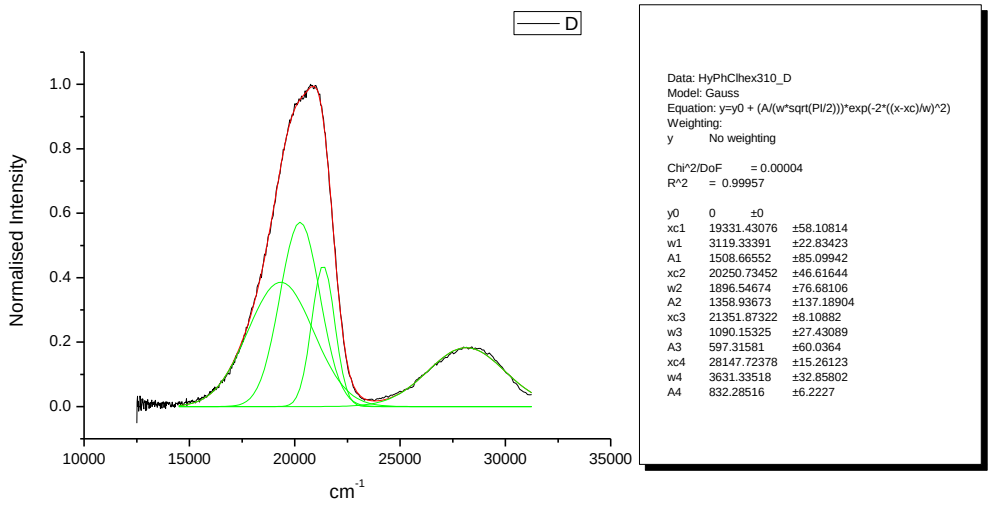

Figure 3.2.181. Gaussian model fit of the normalised fluorescence emission spectrum of **17** recorded in 1-hexanol at 310 nm excitation.

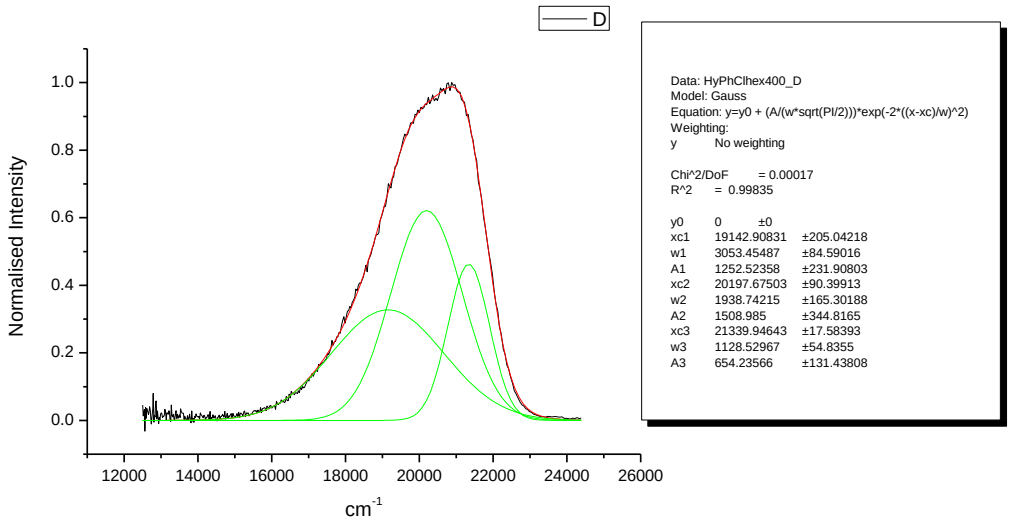

Figure 3.2.182. Gaussian model fit of the normalised fluorescence emission spectrum of **17** recorded in 1-hexanol at 400 nm excitation.

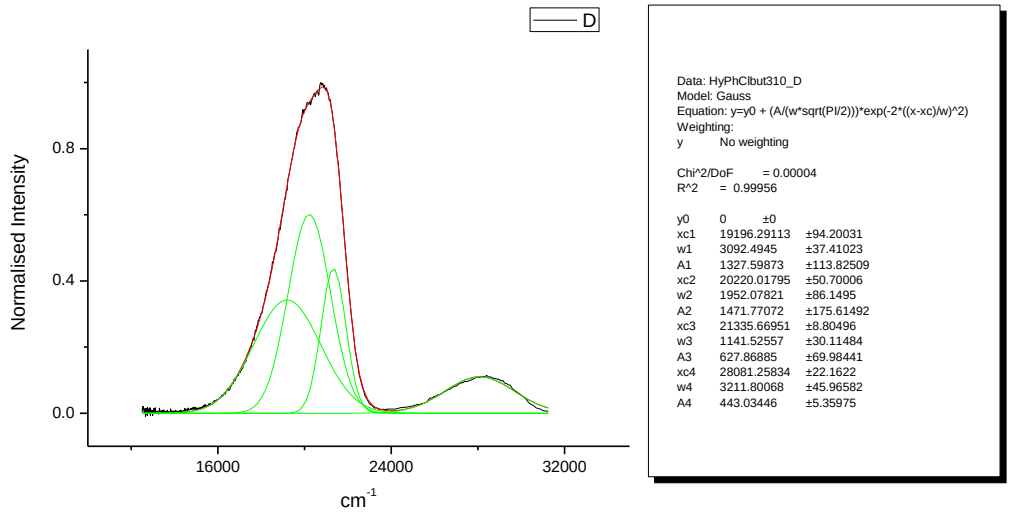

Figure 3.2.183. Gaussian model fit of the normalised fluorescence emission spectrum of **17** recorded in 1-butanol at 310 nm excitation.

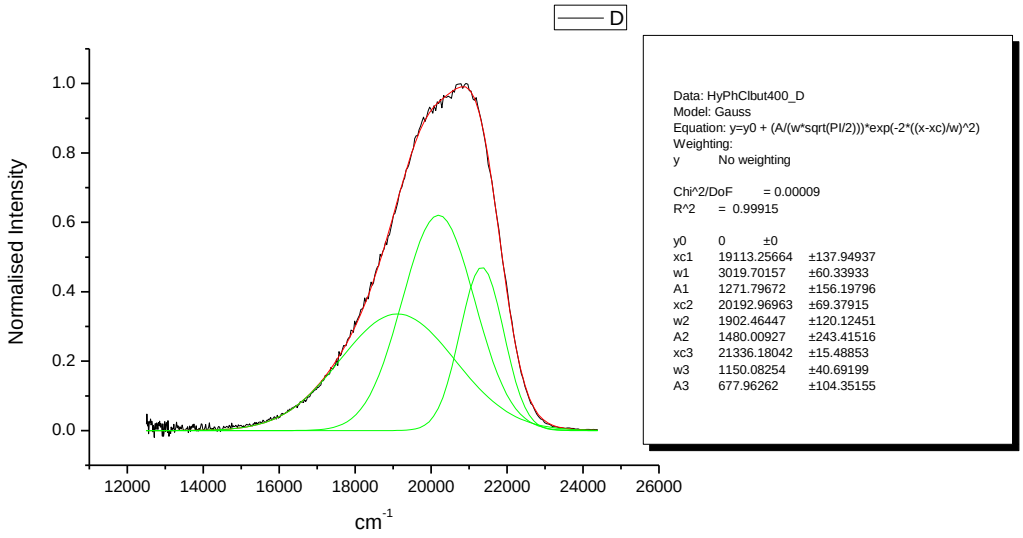

Figure 3.2.184. Gaussian model fit of the normalised fluorescence emission spectrum of **17** recorded in 1-butanol at 400 nm excitation.

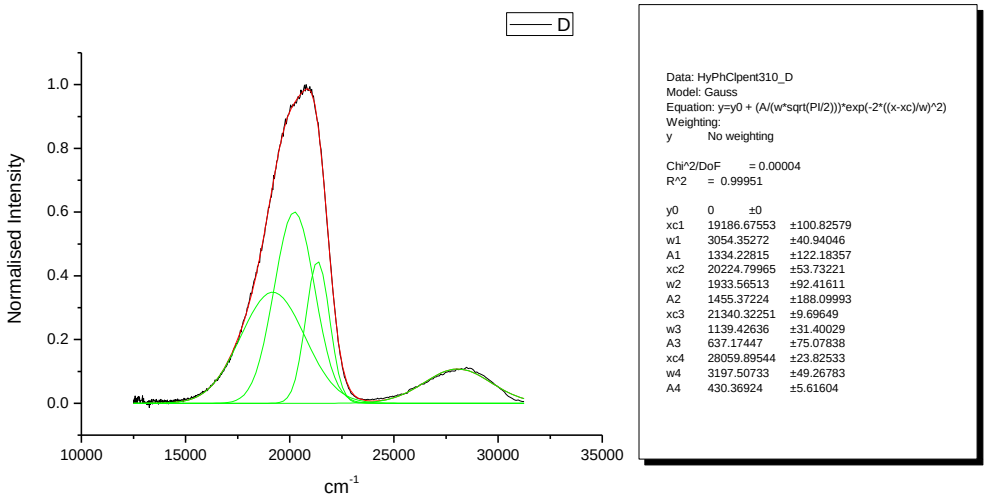

Figure 3.2.185. Gaussian model fit of the normalised fluorescence emission spectrum of **17** recorded in 1-pentanol at 310 nm excitation.

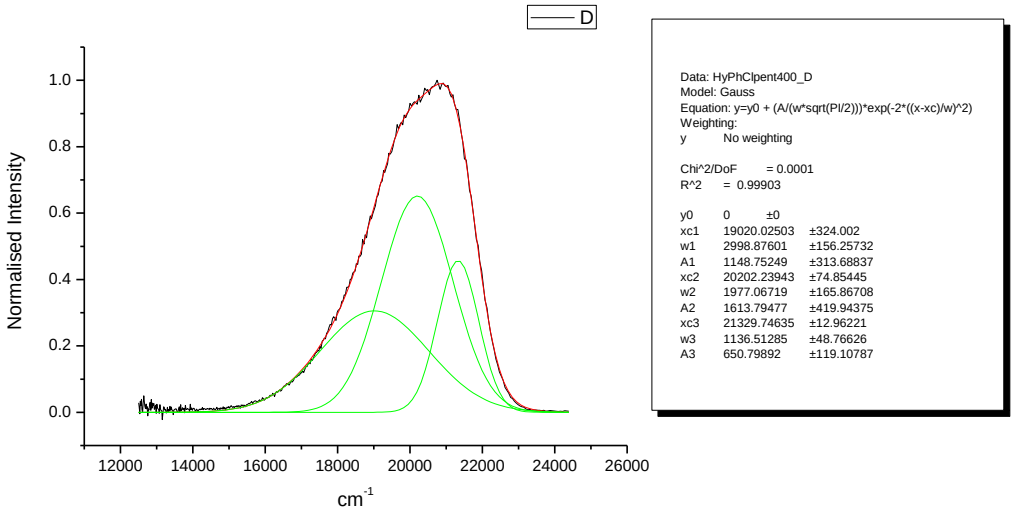

Figure 3.2.186. Gaussian model fit of the normalised fluorescence emission spectrum of **17** recorded in 1-pentanol at 400 nm excitation.

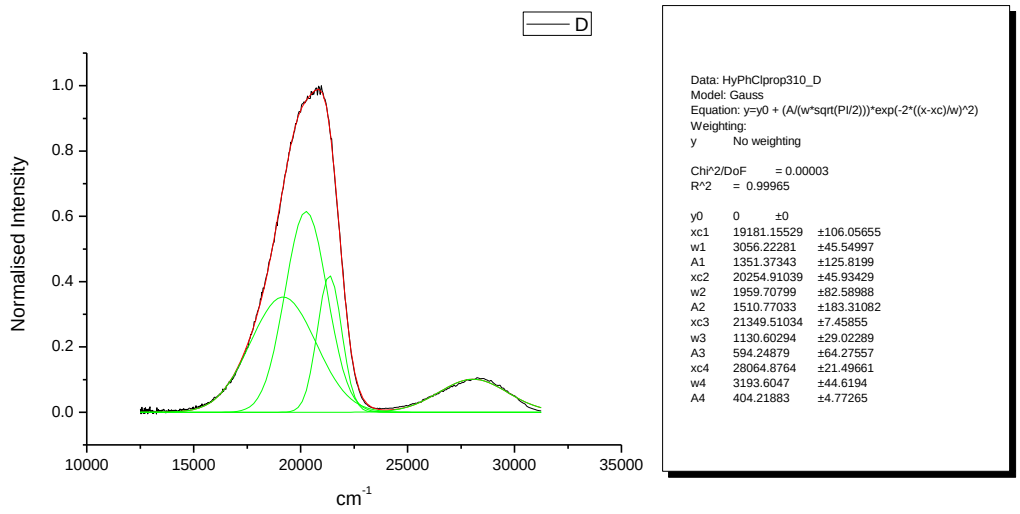

Figure 3.2.187. Gaussian model fit of the normalised fluorescence emission spectrum of **17** recorded in 1-propanol at 310 nm excitation.

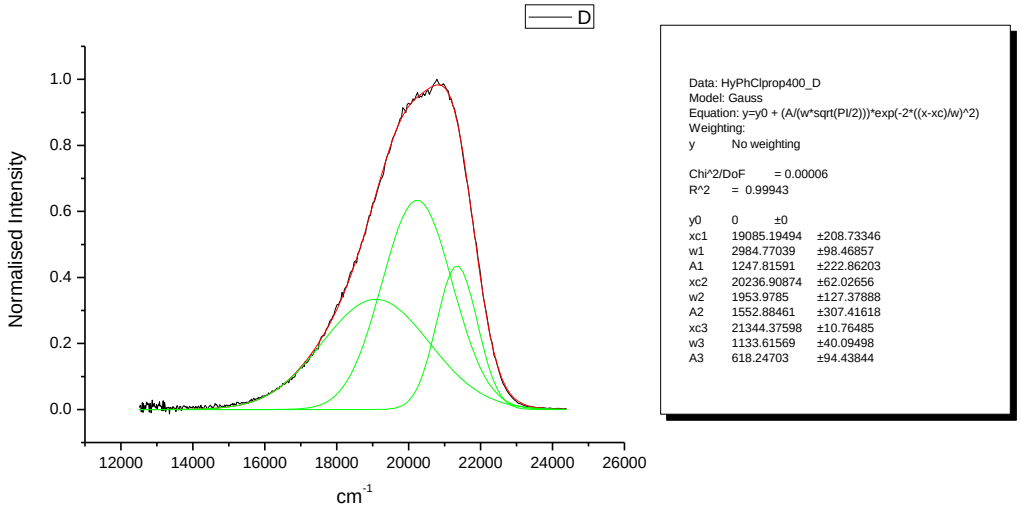

Figure 3.2.188. Gaussian model fit of the normalised fluorescence emission spectrum of **17** recorded in 1-propanol at 400 nm excitation.

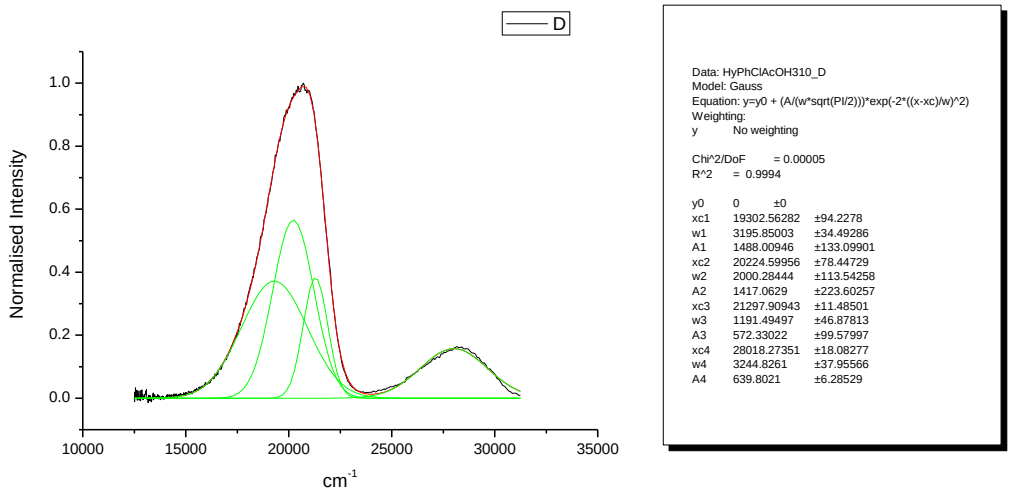

Figure 3.2.189. Gaussian model fit of the normalised fluorescence emission spectrum of **17** recorded in Acetic Acid at 310 nm excitation.

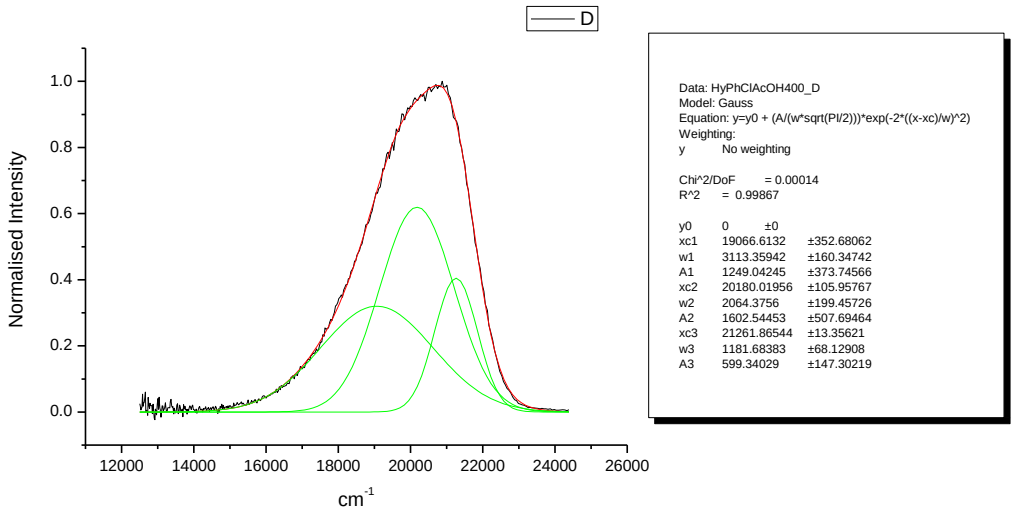

Figure 3.2.190. Gaussian model fit of the normalised fluorescence emission spectrum of **17** recorded in Acetic Acid at 400 nm excitation.

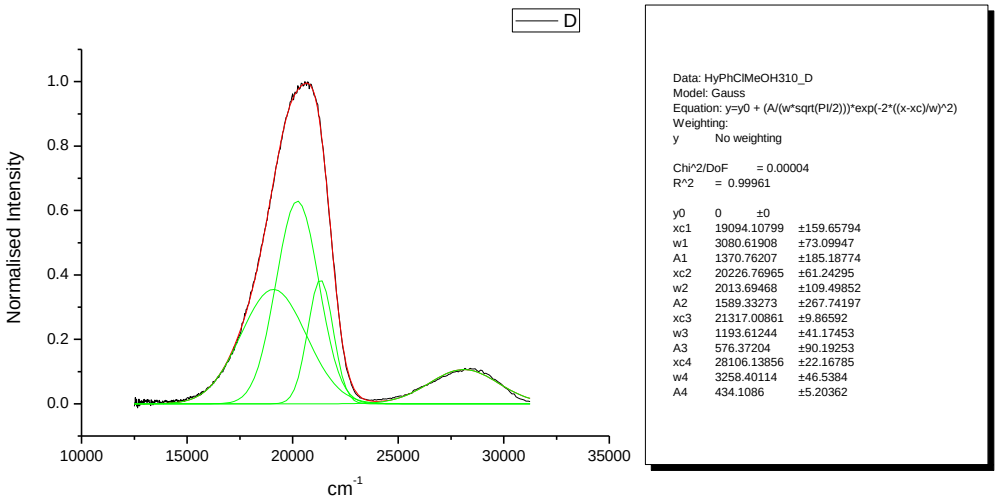

Figure 3.2.191. Gaussian model fit of the normalised fluorescence emission spectrum of **17** recorded in Methanol at 310 nm excitation.

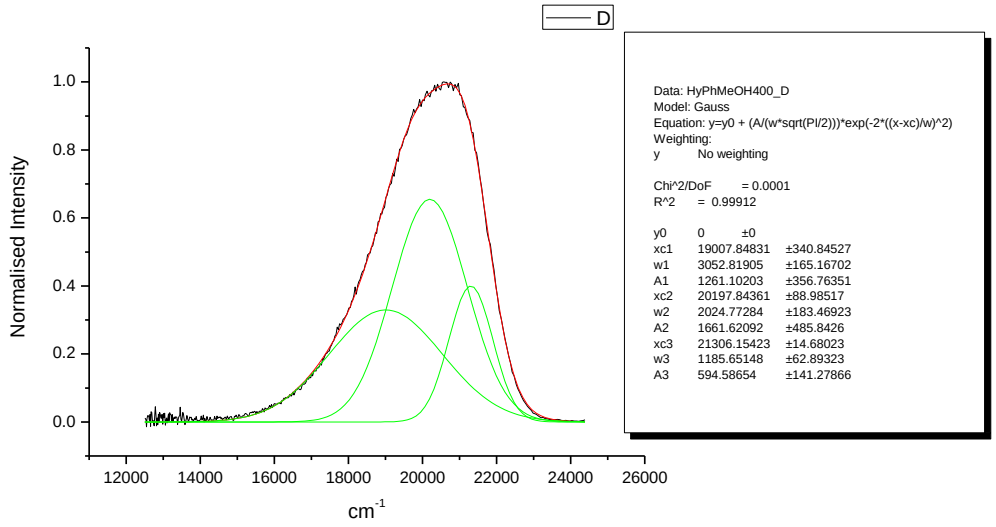

Figure 3.2.192. Gaussian model fit of the normalised fluorescence emission spectrum of **17** recorded in Methanol at 400 nm excitation.

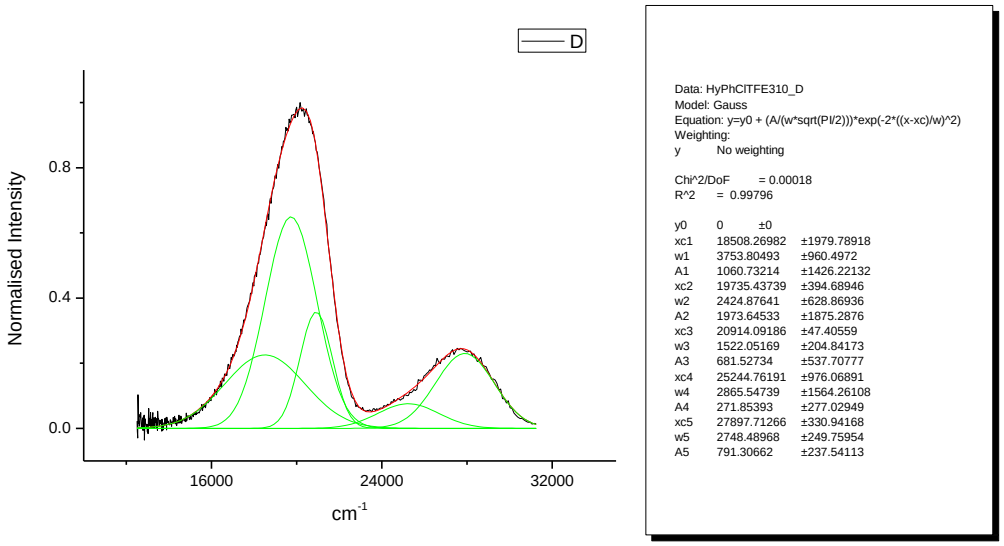

Figure 3.2.193. Gaussian model fit of the normalised fluorescence emission spectrum of **17** recorded in 2,2,2-trifluoroethanol at 310 nm excitation.

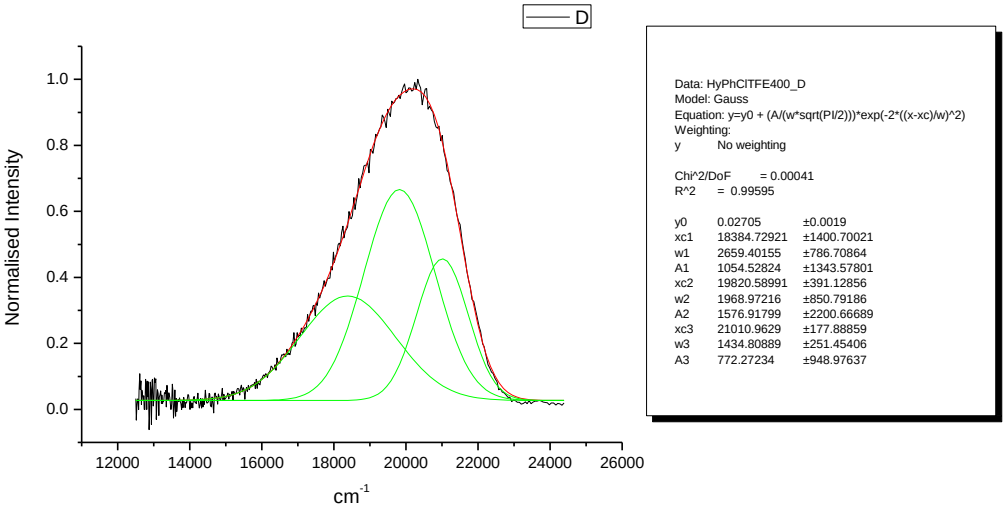

Figure 3.2.194. Gaussian model fit of the normalised fluorescence emission spectrum of **17** recorded in 2,2,2-trifluoroethanol at 400 nm excitation.

3.2.11 Fluorescence Excitation spectra.

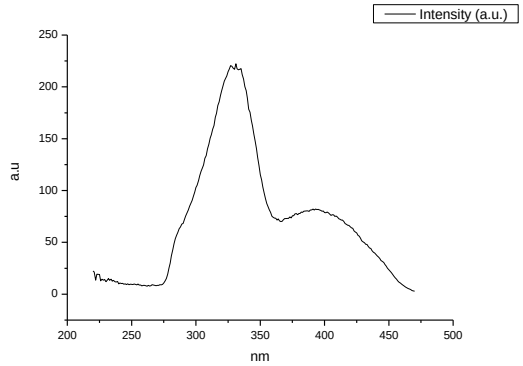

Figure 3.2.195. Fluorescence excitation spectrum of **17** recorded in Toluene with emission fixed at 480 nm.

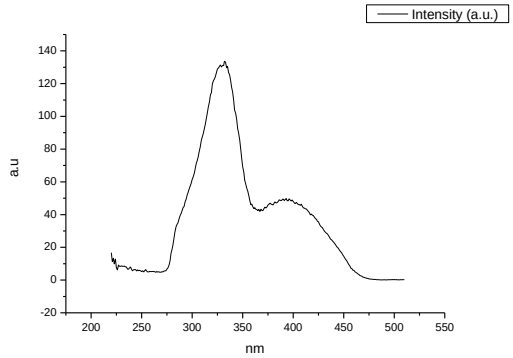

Figure 3.2.196. Fluorescence excitation spectrum of **17** recorded in Toluene with emission fixed at 520 nm.

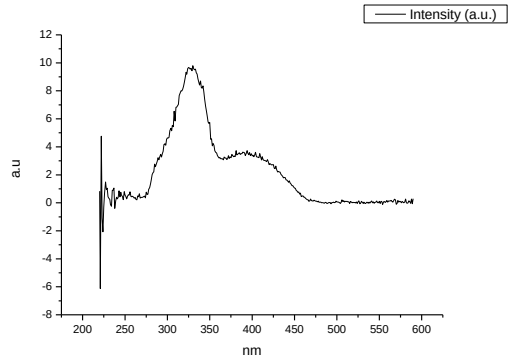

Figure 3.2.197. Fluorescence excitation spectrum of **17** recorded in Toluene with emission fixed at 600 nm.

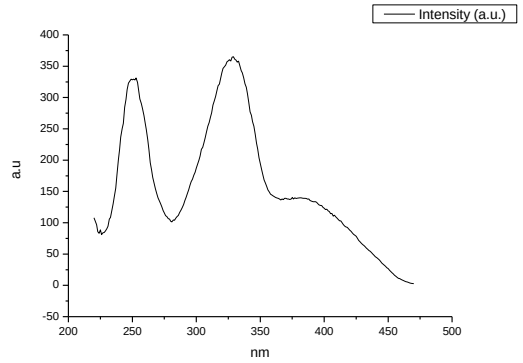

Figure 3.2.198. Fluorescence excitation spectrum of **17** recorded in 1,4-dioxane with emission fixed at 480 nm.

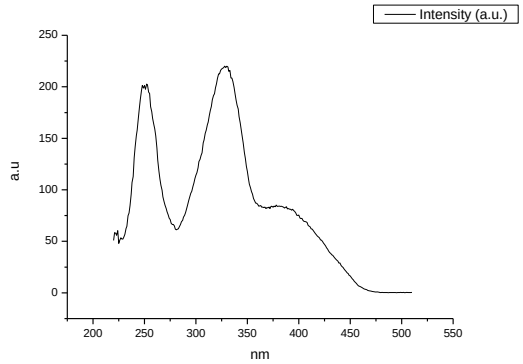

Figure 3.2.199. Fluorescence excitation spectrum of **17** recorded in 1,4-dioxane with emission fixed at 520 nm.

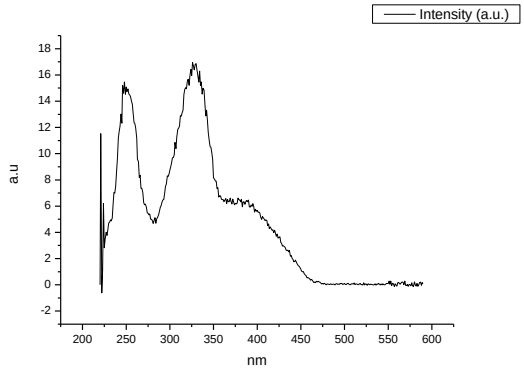

Figure 3.2.200. Fluorescence excitation spectrum of **17** recorded in 1,4-dioxane with emission fixed at 600 nm.

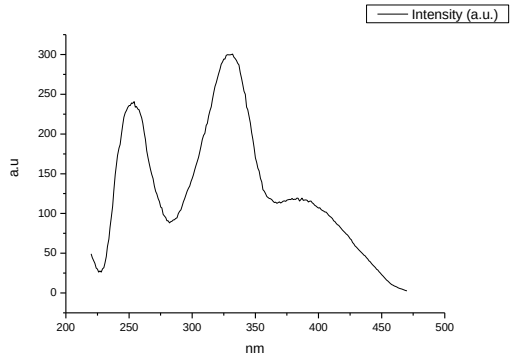

Figure 3.2.201. Fluorescence excitation spectrum of **17** recorded in Chloroform with emission fixed at 480 nm.

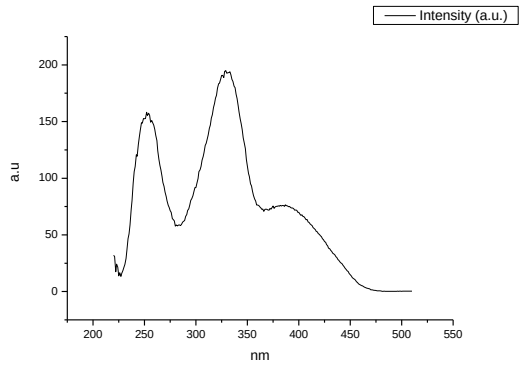

Figure 3.2.202. Fluorescence excitation spectrum of **17** recorded in Chloroform with emission fixed at 520 nm.

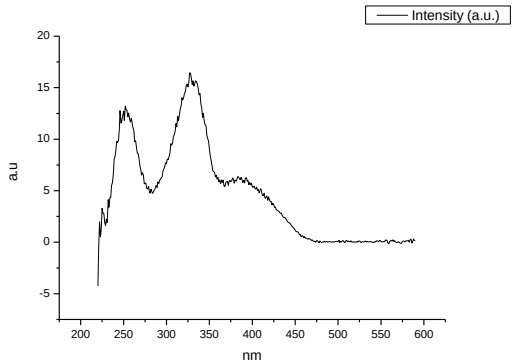

Figure 3.2.203. Fluorescence excitation spectrum of **17** recorded in Chloroform with emission fixed at 600 nm.

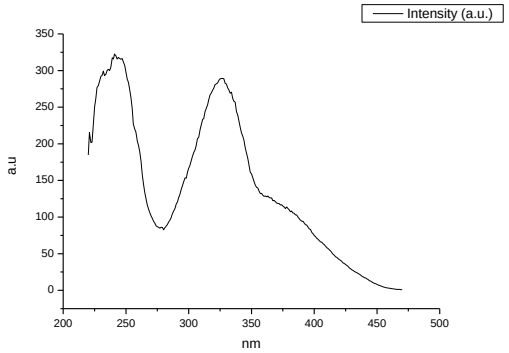

Figure 3.2.204. Fluorescence excitation spectrum of **17** recorded in Acetonitrile with emission fixed at 480 nm.

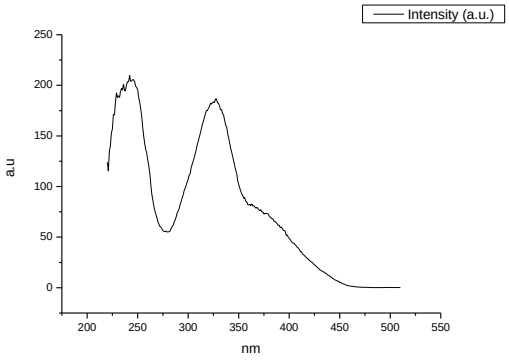

Figure 3.2.205. Fluorescence excitation spectrum of **17** recorded in Acetonitrile with emission fixed at 520 nm.

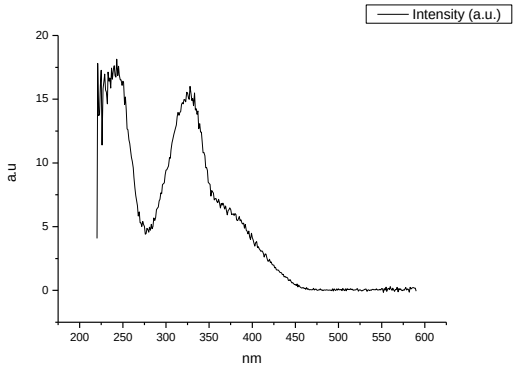

Figure 3.2.206. Fluorescence excitation spectrum of **17** recorded in Acetonitrile with emission fixed at 600 nm.

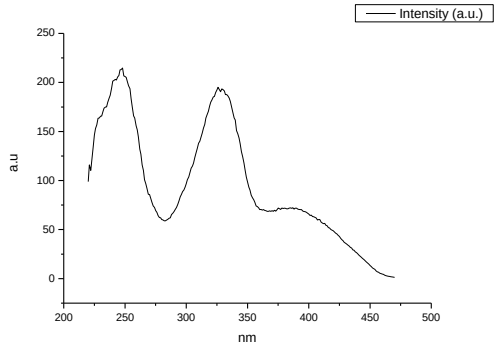

Figure 3.2.207. Fluorescence excitation spectrum of **17** recorded in 1-octanol with emission fixed at 480 nm.

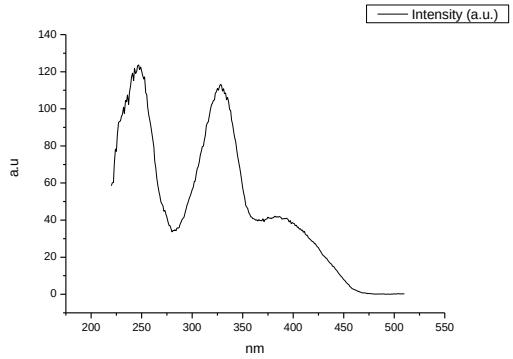

Figure 3.2.208. Fluorescence excitation spectrum of **17** recorded in 1-octanol with emission fixed at 520 nm.

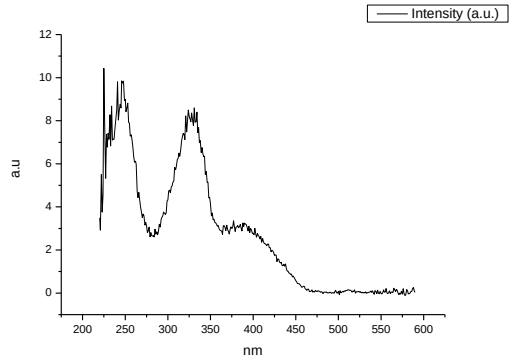

Figure 3.2.209. Fluorescence excitation spectrum of **17** recorded in 1-octanol with emission fixed at 600 nm.

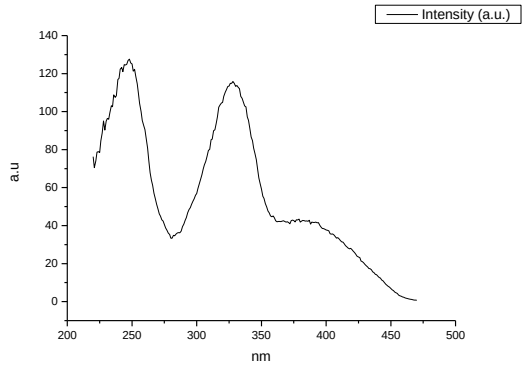

Figure 3.2.210. Fluorescence excitation spectrum of **17** recorded in 1-hexanol with emission fixed at 480 nm.

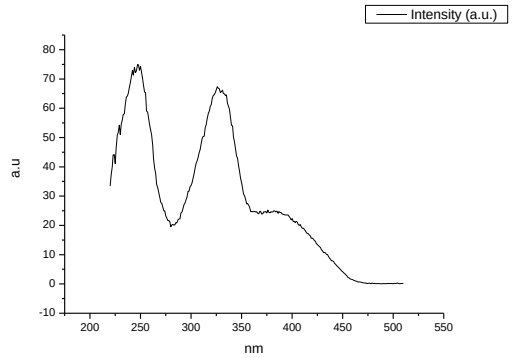

Figure 3.2.211. Fluorescence excitation spectrum of **17** recorded in 1-hexanol with emission fixed at 520 nm.

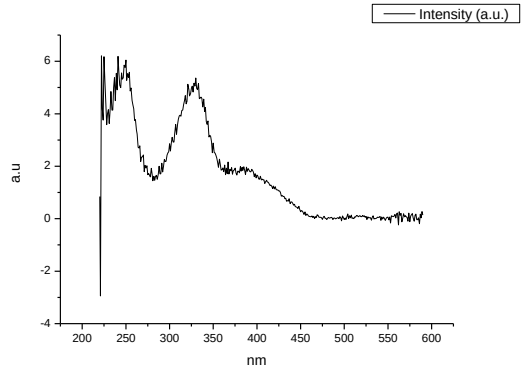

Figure 3.2.212. Fluorescence excitation spectrum of **17** recorded in 1-hexanol with emission fixed at 600 nm.

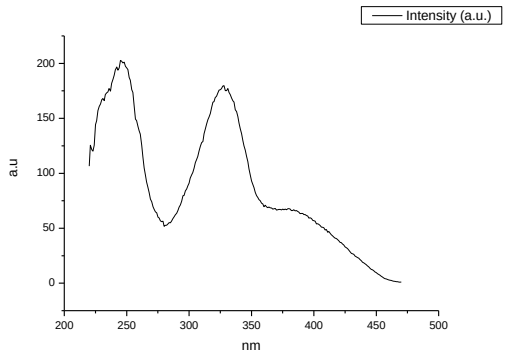

Figure 3.2.213. Fluorescence excitation spectrum of **17** recorded in 1-butanol with emission fixed at 480 nm.

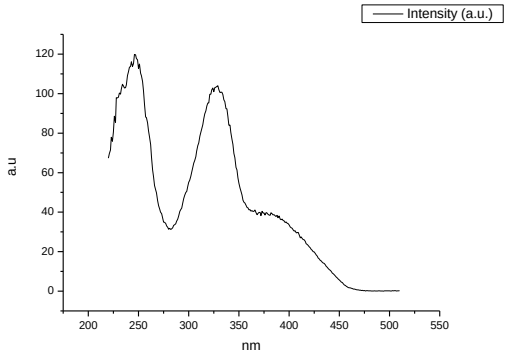

Figure 3.2.214. Fluorescence excitation spectrum of **17** recorded in 1-butanol with emission fixed at 520 nm.

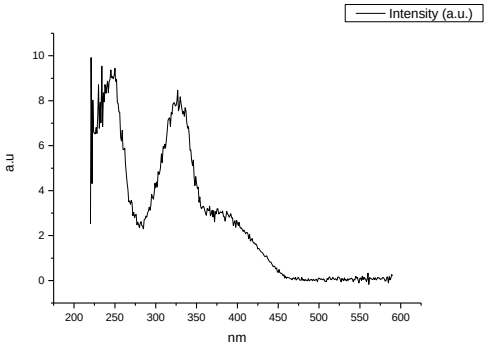

Figure 3.2.215. Fluorescence excitation spectrum of **17** recorded in 1-butanol with emission fixed at 600 nm.

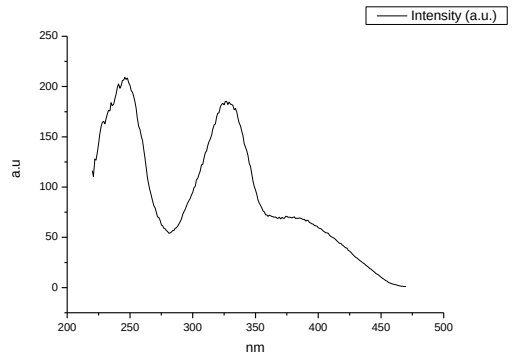

Figure 3.2.216. Fluorescence excitation spectrum of **17** recorded in 1-pentanol with emission fixed at 480 nm.

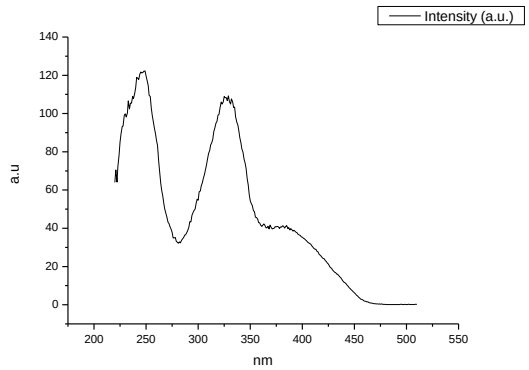

Figure 3.2.217. Fluorescence excitation spectrum of **17** recorded in 1-pentanol with emission fixed at 520 nm.

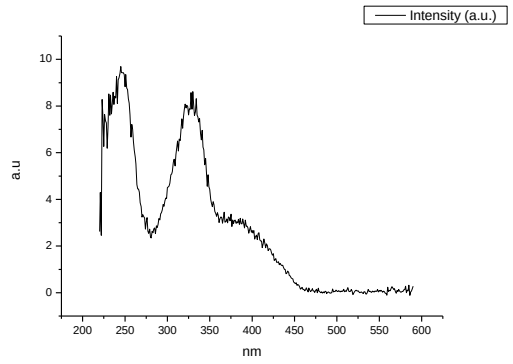

Figure 3.2.218. Fluorescence excitation spectrum of **17** recorded in 1-pentanol with emission fixed at 600 nm.

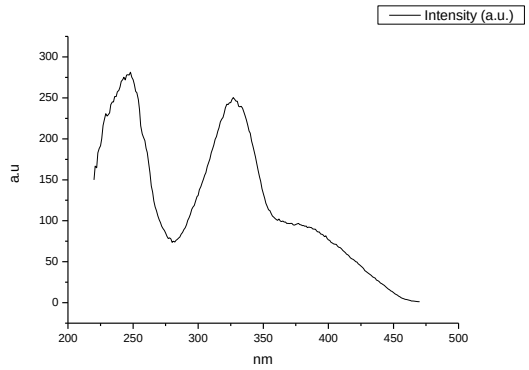

Figure 3.2.219. Fluorescence excitation spectrum of **17** recorded in 1-propanol with emission fixed at 480 nm.

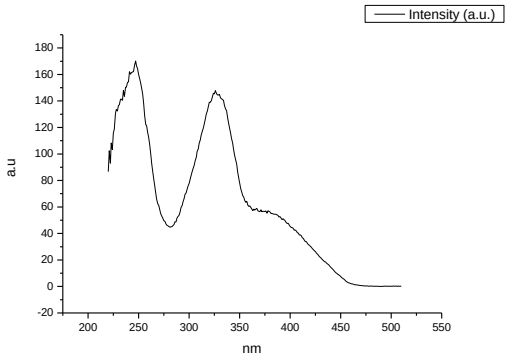

Figure 3.2.220. Fluorescence excitation spectrum of **17** recorded in 1-propanol with emission fixed at 520 nm.

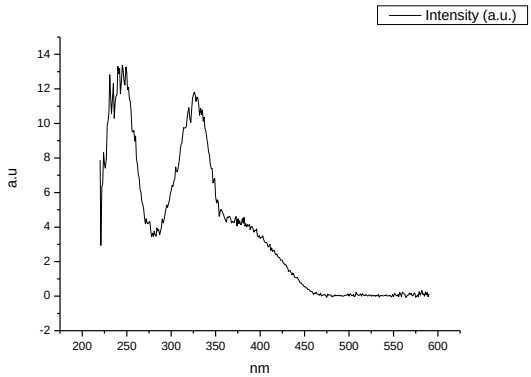

Figure 3.2.221. Fluorescence excitation spectrum of **17** recorded in 1-propanol with emission fixed at 600 nm.

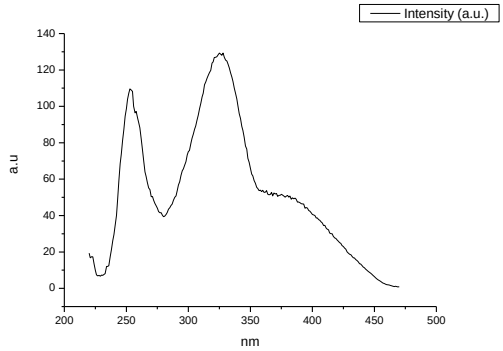

Figure 3.2.222. Fluorescence excitation spectrum of **17** recorded in Acetic Acid with emission fixed at 480 nm.

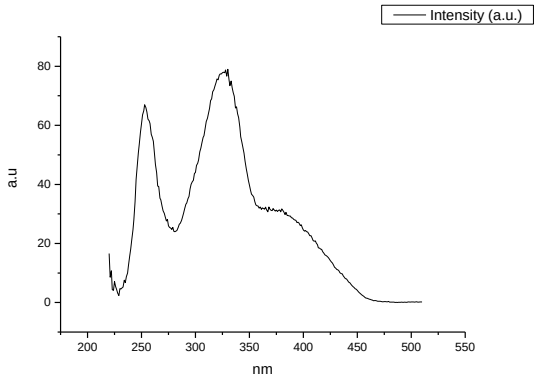

Figure 3.2.223. Fluorescence excitation spectrum of **17** recorded in Acetic Acid with emission fixed at 520 nm.

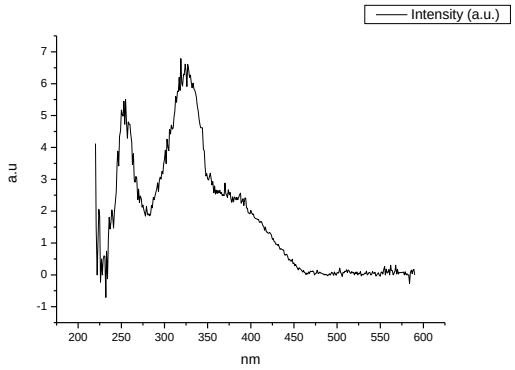

Figure 3.2.224. Fluorescence excitation spectrum of **17** recorded in Acetic Acid with emission fixed at 600 nm.

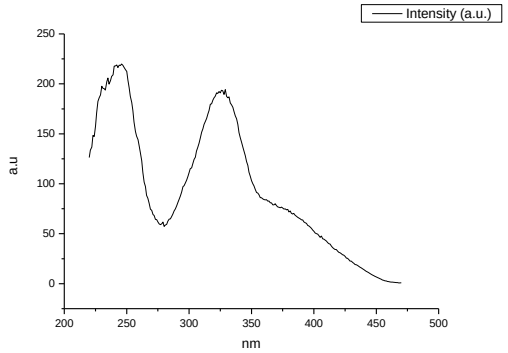

Figure 3.2.225. Fluorescence excitation spectrum of **17** recorded in Methanol with emission fixed at 480 nm.

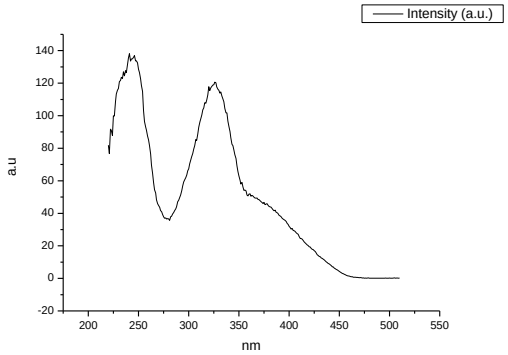

Figure 3.2.226. Fluorescence excitation spectrum of **17** recorded in Methanol with emission fixed at 520 nm.

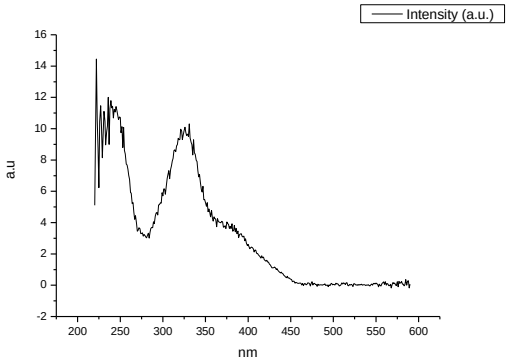

Figure 3.2.227. Fluorescence excitation spectrum of **17** recorded in Methanol with emission fixed at 600 nm.

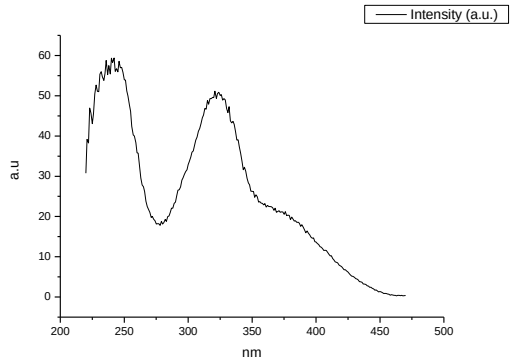

Figure 3.2.228. Fluorescence excitation spectrum of **17** recorded in 2,2,2-trifluoroethanol with emission fixed at 480 nm.

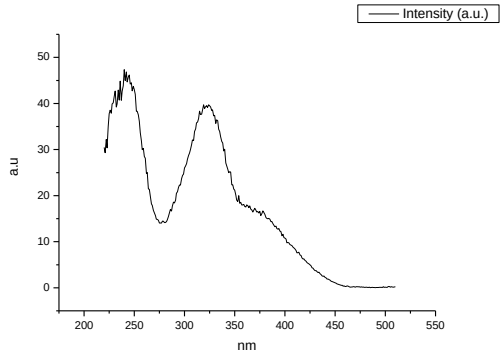

Figure 3.2.229. Fluorescence excitation spectrum of **17** recorded in 2,2,2-trifluoroethanol with emission fixed at 520 nm.

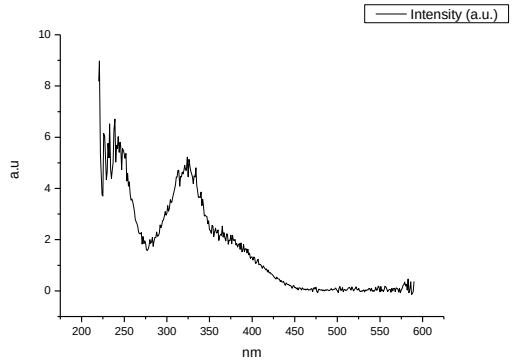

Figure 3.2.230. Fluorescence excitation spectrum of **17** recorded in 2,2,2-trifluoroethanol with emission fixed at 600 nm.

3.3 COMPOUND 18.

3.3.1 Quantum Yield Summary.

Solvent	abs (310 nm)	$\lambda_{ems\ (max)}$	$\Phi_{310\ nm}$	abs (400 nm)	$\lambda_{ems\ (max)}$	$\Phi_{400\ nm}$
Toluene	0.07	481.04	0.15	0.05	476.06	0.20
1,4-Dioxane	0.08	476.96	0.19	0.03	481.04	0.18
Chloroform	0.04	485.97	0.18	0.02	481.94	0.17
Acetonitrile	0.04	481.94	0.20	0.01	482.98	0.18
1-Octanol	0.04	473.93	0.16	0.02	475.00	0.15
1-Hexanol	0.03	478.03	0.14	0.01	476.96	0.13
1-Butanol	0.04	480.00	0.16	0.02	481.04	0.14
1-Pentanol	0.03	476.96	0.14	0.01	480.00	0.12
1-Propanol	0.04	480.00	0.16	0.02	480.00	0.14
Acetic acid	0.06	481.04	0.08	0.02	480.00	0.07
Methanol	0.05	481.94	0.13	0.02	480.00	0.11
2,2,2-Trifluoroethanol	0.04	495.00	0.03	0.01	500.00	0.03

Table 3.3.1. Summary of ultraviolet-visible absorbance values at 310 nm and 400 nm, emission maxima and quantum yield (Φ) of **18** at 310 nm and 400 nm excitation.

3.3.2 310 nm excitation Gaussian band fit summaries.

Solvent	λ max$_{em}$ Band 1 (cm^{-1})	λ max$_{em}$ Band 1 (nm)	λ max$_{em}$ Band 2 (cm^{-1})	λ max$_{em}$ Band 2 (nm)	λ max$_{em}$ Band 3 (cm^{-1})	λ max$_{em}$ Band 3 (nm)
Toluene	19263.65	519.11	20042.57	498.94	21238.74	470.84
1,4-Dioxane	19182.31	521.31	20172.91	495.71	21289.05	469.72
Chloroform	19149.13	522.22	20096.18	497.61	21158.06	472.63
Acetonitrile	19017.38	525.83	20182.01	495.49	21256.56	470.44
1-Octanol	19284.02	518.56	20268.63	493.37	21412.41	467.02
1-Hexanol	19253.92	519.37	20293.59	492.77	21403.26	467.22
1-Butanol	19220.19	520.29	20310.88	492.35	21412.47	467.02
1-Pentanol	19210.45	520.55	20298.58	492.65	21405.44	467.17
1-Propanol	19183.66	521.28	20294.35	492.75	21403.95	467.20
Acetic acid	19201.21	520.80	20217.38	494.62	21339.83	468.61
Methanol	19055.30	524.79	20233.59	494.23	21348.97	468.41
2,2,2-Trifluoroethanol	17088.82	585.18	19429.19	514.69	20760.68	481.68

Solvent	λ max$_{em}$ Band 4 (cm^{-1})	λ max$_{em}$ Band 4 (nm)	λ max$_{em}$ Band 5 (cm^{-1})	λ max$_{em}$ Band 5 (nm)
Toluene	28313.16	353.19	-	-
1,4-Dioxane	27962.27	357.62	-	-
Chloroform	27770.60	360.09	-	-
Acetonitrile	28149.31	355.25	-	-
1-Octanol	28401.94	352.09	-	-
1-Hexanol	28264.55	353.80	-	-
1-Butanol	28074.79	356.19	-	-
1-Pentanol	28088.63	356.02	-	-
1-Propanol	28061.79	356.36	-	-
Acetic acid	27992.28	357.24	-	-
Methanol	28066.34	356.30	-	-
2,2,2-Trifluoroethanol	27209.10	367.52	-	-

Table 3.3.2. Summary of band maxima of 5 band fit using Gaussian model for normalised **18** emission spectra recorded at 310 nm excitation.

(a)

Solvent	Width Band 1 (cm^{-1})	Width Band 2 (cm^{-1})	Width Band 3 (cm^{-1})	Width Band 4 (cm^{-1})	Width Band 5 (cm^{-1})
Toluene	3016.32	1682.03	1088.91	3579.79	-
1,4-Dioxane	3035.73	1898.35	1098.82	3399.35	-
Chloroform	3136.04	2001.35	1118.06	3462.52	-
Acetonitrile	3039.62	2062.78	1243.29	3337.01	-
1-Octanol	3031.70	1867.82	1117.40	3741.52	-
1-Hexanol	3090.52	1956.47	1117.80	4132.47	-
1-Butanol	3037.50	1966.48	1123.26	3351.43	-
1-Pentanol	3046.98	1969.05	1123.52	3391.69	-
1-Propanol	3032.98	1973.08	1144.65	3306.04	-
Acetic acid	3154.88	2015.50	1220.85	3422.93	-
Methanol	3041.84	2025.06	1225.41	3435.65	-
2,2,2-Trifluoroethanol	6878.57	2801.38	1786.91	4349.25	-

(b)

Solvent	Area Band 1 (cm^{-1})	Area Band 2 (cm^{-1})	Area Band 3 (cm^{-1})	Area Band 4 (cm^{-1})	Area Band 5 (cm^{-1})
Toluene	1383.90	1084.43	786.06	127.77	-
1,4-Dioxane	1310.95	1411.84	650.50	95.61	-
Chloroform	1305.98	1469.29	586.55	117.04	-
Acetonitrile	1233.19	1655.78	597.76	90.15	-
1-Octanol	1321.88	1384.64	684.26	206.20	-
1-Hexanol	1282.75	1482.50	616.43	482.69	-
1-Butanol	1292.30	1541.34	596.19	146.82	-
1-Pentanol	1250.40	1527.27	609.77	158.62	-
1-Propanol	1264.17	1573.58	617.47	132.11	-
Acetic acid	1326.81	1505.83	644.89	197.35	-
Methanol	1227.01	1622.46	622.82	115.48	-
2,2,2-Trifluoroethanol	428.06	2342.76	1057.01	480.83	-

Tables 3.3.3 (a) and (b). Summary band width and band area of 5 band fit using Gaussian model for normalised **18** emission spectra recorded at 310 nm excitation.

Solvent	Band 1 Area Percentage (%)	Band 2 Area Percentage (%)	Band 3 Area Percentage (%)	Band 4 Area Percentage (%)	Band 5 Area Percentage (%)
Toluene	40.92	32.06	23.24	3.78	-
1,4-Dioxane	37.79	40.70	18.75	2.76	-
Chloroform	37.54	42.23	16.86	3.36	-
Acetonitrile	34.48	46.29	16.71	2.52	-
1-Octanol	36.75	38.49	19.02	5.73	-
1-Hexanol	33.19	38.36	15.95	12.49	-
1-Butanol	36.13	43.09	16.67	4.11	-
1-Pentanol	35.26	43.07	17.20	4.47	-
1-Propanol	35.24	43.86	17.21	3.68	-
Acetic acid	36.10	40.98	17.55	5.37	-
Methanol	34.20	45.22	17.36	3.22	-
2,2,2-Trifluoroethanol	9.93	54.37	24.53	11.16	-

Table 3.3.4. Total Area Percentages of 5 band fit using Gaussian model for normalised **18** emission spectra recorded at 310 nm excitation.

Solvent	Area Ratio Band 1/2 (310 nm ex)	Area Ratio Band 1/3 (310 nm ex)	Area Ratio Band 1/4 (310 nm ex)	Area Ratio Band 1/5 (310 nm ex)
Toluene	1.28	1.76	10.83	-
1,4-Dioxane	0.93	2.02	13.71	-
Chloroform	0.89	2.23	11.16	-
Acetonitrile	0.74	2.06	13.68	-
1-Octanol	0.95	1.93	6.41	-
1-Hexanol	0.87	2.08	2.66	-
1-Butanol	0.84	2.17	8.80	-
1-Pentanol	0.82	2.05	7.88	-
1-Propanol	0.80	2.05	9.57	-
Acetic acid	0.88	2.06	6.72	-
Methanol	0.76	1.97	10.63	-
2,2,2-Trifluoroethanol	0.18	0.40	0.89	-

Solvent	Area Ratio Band 2/3 (310 nm ex)	Area Ratio Band 2/4 (310 nm ex)	Area Ratio Band 2/5 (310 nm ex)	Area Ratio Band 3/4 (310 nm ex)	Area Ratio Band 3/5 (310 nm ex)	Area Ratio Band 4/5 (310 nm ex)
Toluene	1.38	8.49	-	6.15	-	-
1,4-Dioxane	2.17	14.77	-	6.80	-	-
Chloroform	2.50	12.55	-	5.01	-	-
Acetonitrile	2.77	18.37	-	6.63	-	-
1-Octanol	2.02	6.71	-	3.32	-	-
1-Hexanol	2.40	3.07	-	1.28	-	-
1-Butanol	2.59	10.50	-	4.06	-	-
1-Pentanol	2.50	9.63	-	3.84	-	-
1-Propanol	2.55	11.91	-	4.67	-	-
Acetic acid	2.34	7.63	-	3.27	-	-
Methanol	2.61	14.05	-	5.39	-	-
2,2,2-Trifluoroethanol	2.22	4.87	-	2.20	-	-

Table 3.3.5. Area Ratios of 5 band fit using Gaussian model for normalised **18** emission spectra recorded at 310 nm excitation.

3.3.3 400 nm excitation Gaussian band fit summaries.

Solvent	λ max$_{em}$ Band 1 (cm^{-1})	λ max$_{em}$ Band 1 (nm)	λ max$_{em}$ Band 2 (cm^{-1})	λ max$_{em}$ Band 2 (nm)	λmax$_{em}$ Band 3 (cm^{-1})	λmax$_{em}$ Band 3 (nm)
Toluene	19230.77	520.00	20009.21	499.77	21225.62	471.13
1,4-Dioxane	19154.39	522.07	20112.52	497.20	21273.05	470.08
Chloroform	19502.65	512.75	20018.76	499.53	21127.36	473.32
Acetonitrile	18970.67	527.13	20134.70	496.65	21242.40	470.76
1-Octanol	19293.69	518.30	20277.01	493.17	21411.65	467.04
1-Hexanol	19260.88	519.19	20272.34	493.28	21409.61	467.08
1-Butanol	19145.53	522.32	20282.36	493.04	21399.38	467.30
1-Pentanol	19201.27	520.80	20291.01	492.83	21403.03	467.22
1-Propanol	19119.02	523.04	20261.83	493.54	21397.99	467.33
Acetic acid	19127.46	522.81	20216.28	494.65	21329.25	468.84
Methanol	18980.74	526.85	20198.02	495.10	21329.92	468.82
2,2,2-Trifluoroethanol	18186.69	549.85	19714.54	507.24	20956.85	477.17

Table 3.3.6. Summary of band maxima of 3 band fit using Gaussian model for normalised **18** emission spectra recorded at 400 nm excitation.

Solvent	Width Band 1 (cm^{-1})	Width Band 2 (cm^{-1})	Width Band 3 (cm^{-1})
Toluene	2945.03	1586.95	1091.22
1,4-Dioxane	2997.55	1814.46	1111.48
Chloroform	3338.33	1857.35	1065.22
Acetonitrile	3055.05	2053.08	1244.61
1-Octanol	2988.13	1815.18	1079.75
1-Hexanol	3069.22	1879.41	1092.19
1-Butanol	2982.10	1939.68	1130.07
1-Pentanol	3006.60	1913.48	1105.90
1-Propanol	2980.79	1922.25	1158.02
Acetic acid	3126.71	1998.49	1164.70
Methanol	3065.52	2056.23	1214.33
2,2,2-Trifluoroethanol	3530.70	2352.29	1558.60

Table 3.3.7. Summary of band width of 3 band fit using Gaussian model for normalised **18** emission spectra recorded at 400 nm excitation

Solvent	Area Band 1 (cm^{-1})	Area Band 2 (cm^{-1})	Area Band 3 (cm^{-1})	Area Ratio Band 1/2 (400 nm ex)	Area Ratio Band 1/3 (400 nm ex)	Area Ratio Band 2/3 (400 nm ex)
Toluene	1409.37	1000.02	842.98	1.41	1.67	1.19
1,4-Dioxane	1311.71	1315.89	724.74	1.00	1.81	1.82
Chloroform	1704.33	1109.67	562.98	1.54	3.03	1.97
Acetonitrile	1181.44	1651.56	623.36	0.72	1.90	2.65
1-Octanol	1389.79	1323.08	668.14	1.05	2.08	1.98
1-Hexanol	1358.92	1417.24	633.55	0.96	2.14	2.24
1-Butanol	1257.35	1551.14	634.54	0.81	1.98	2.44
1-Pentanol	1295.14	1486.10	623.36	0.87	2.08	2.38
1-Propanol	1237.93	1539.74	662.29	0.80	1.87	2.32
Acetic acid	1286.99	1561.93	596.98	0.82	2.16	2.62
Methanol	1161.14	1716.81	635.63	0.68	1.83	2.70
2,2,2-Trifluoroethanol	925.46	1954.73	793.69	0.47	1.17	2.46

Solvent	Band 1 Area Percentage (%)	Band 2 Area Percentage (%)	Band 3 Area Percentage (%)
Toluene	43.33	30.75	25.92
1,4-Dioxane	39.13	39.25	21.62
Chloroform	50.47	32.86	16.67
Acetonitrile	34.18	47.78	18.04
1-Octanol	41.11	39.13	19.76
1-Hexanol	39.85	41.56	18.58
1-Butanol	36.52	45.05	18.43
1-Pentanol	38.04	43.65	18.31
1-Propanol	35.99	44.76	19.25
Acetic acid	37.35	45.33	17.32
Methanol	33.05	48.86	18.09
2,2,2-Trifluoroethanol	25.19	53.21	21.60

Table 3.3.8. Band areas, area ratios and total area percentage of 3 band fit using Gaussian model for normalised **18** emission spectra recorded at 400 nm excitation.

3.3.4 310 nm Gaussian band fit - Solvatochromic analysis.

3.3.4.1 E_T^N.

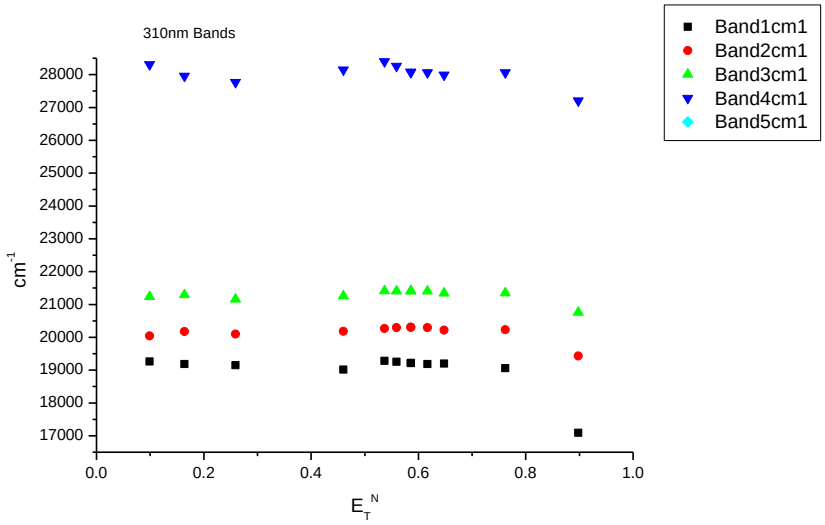

Figure 3.3.1. Band maxima from Gaussian model fit of the normalised fluorescence emission spectra of **18** recorded at 310 nm excitation against E_T^N.

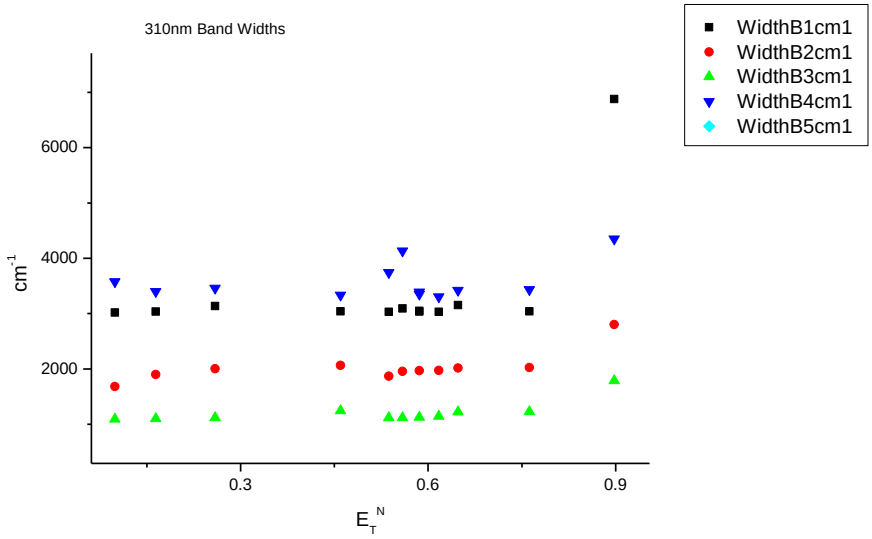

Figure 3.3.2. Band widths from Gaussian model fit of the normalised fluorescence emission spectra of **18** recorded at 310 nm excitation against E_T^N.

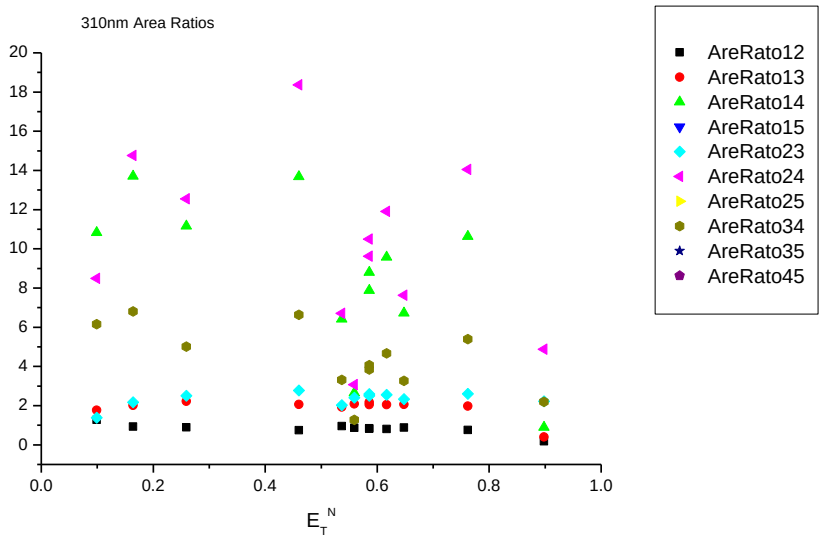

Figure 3.3.3. Area ratios from Gaussian model fit of the normalised fluorescence emission spectra of **18** recorded at 310 nm excitation against E_T^N.

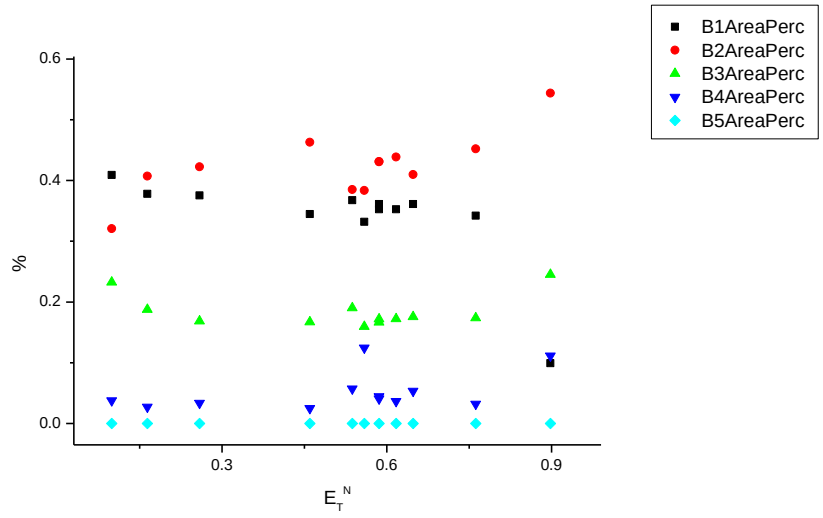

Figure 3.3.4. Area percentages from Gaussian model fit of the normalised fluorescence emission spectra of **18** recorded at 310 nm excitation against E_T^N.

3.3.4.2 *α*

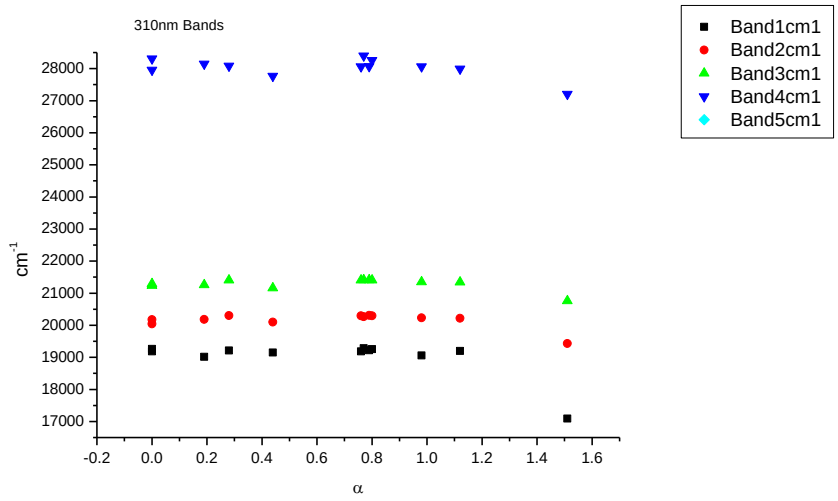

Figure 3.3.5. Band maxima from Gaussian model fit of the normalised fluorescence emission spectra of **18** recorded at 310 nm excitation against α.

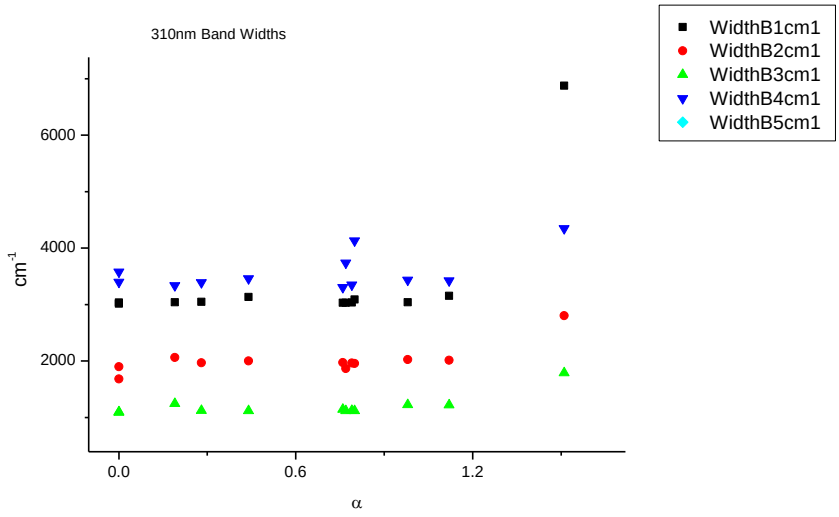

Figure 3.3.6. Band widths from Gaussian model fit of the normalised fluorescence emission spectra of **18** recorded at 310 nm excitation against α.

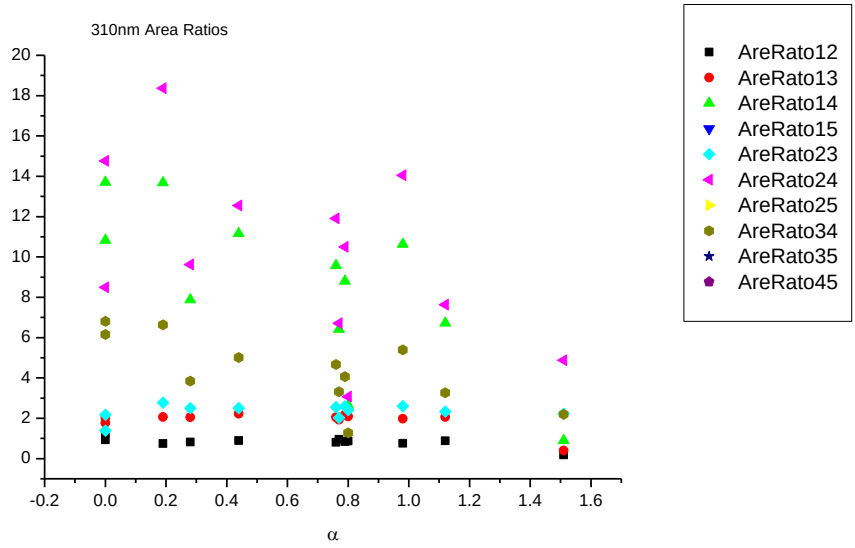

Figure 3.3.7. Area Ratios from Gaussian model fit of the normalised fluorescence emission spectra of **18** recorded at 310 nm excitation against α.

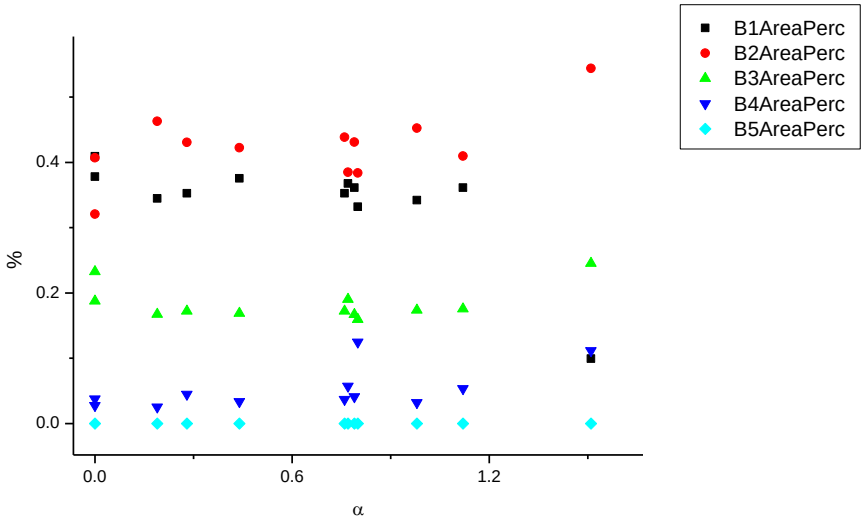

Figure 3.3.8. Area percentages from Gaussian model fit of the normalised fluorescence emission spectra of **18** recorded at 310 nm excitation against α.

3.3.4.3 β.

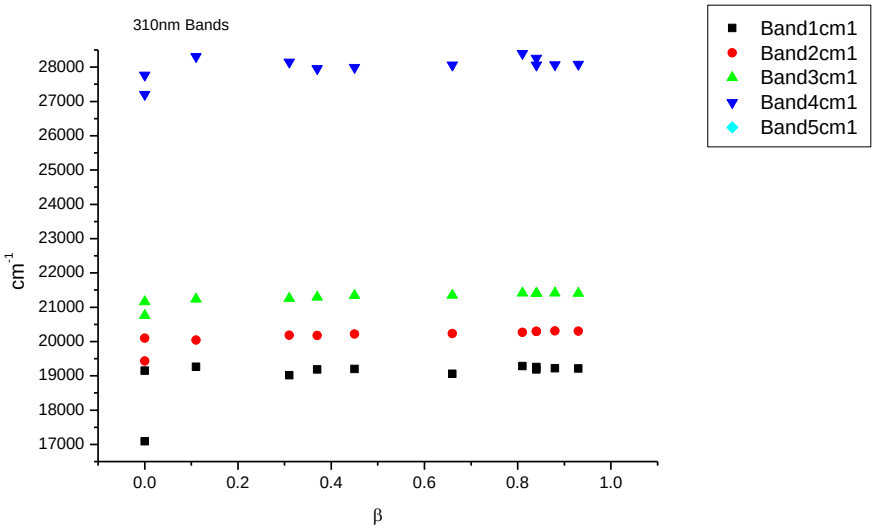

Figure 3.3.9. Band maxima from Gaussian model fit of the normalised fluorescence emission spectra of **18** recorded at 310 nm excitation against β.

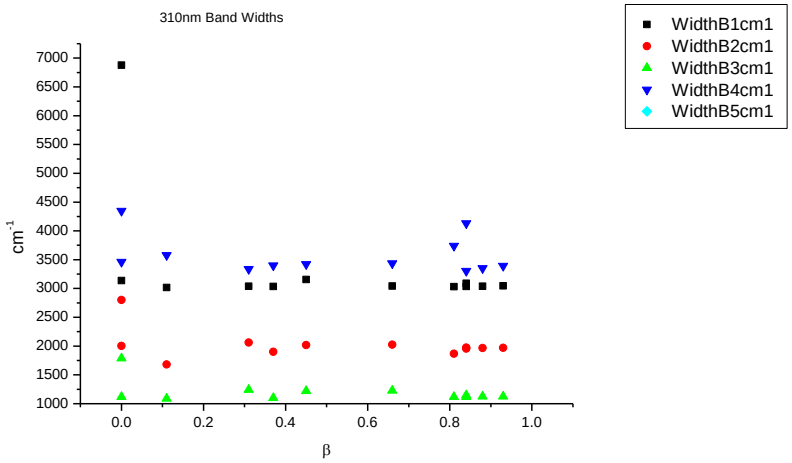

Figure 3.3.10. Band widths from Gaussian model fit of the normalised fluorescence emission spectra of **18** recorded at 310 nm excitation against β.

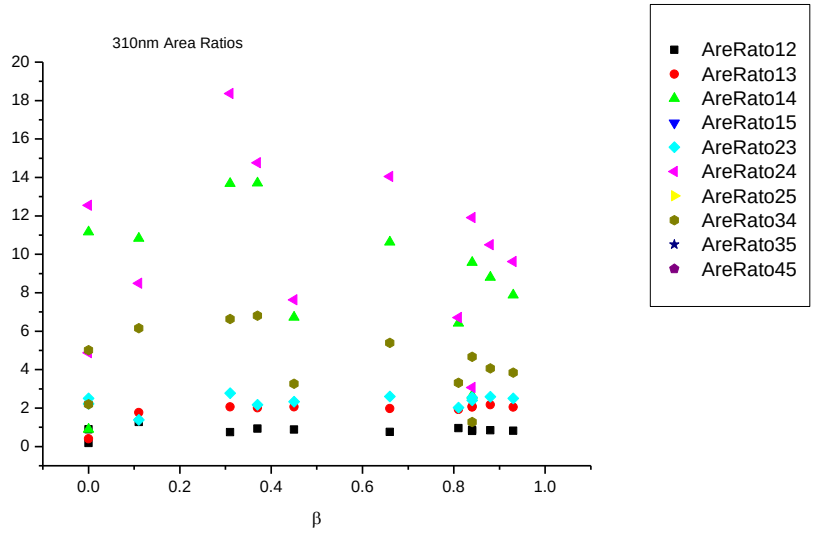

Figure 3.3.11. Area ratios from Gaussian model fit of the normalised fluorescence emission spectra of **18** recorded at 310 nm excitation against β.

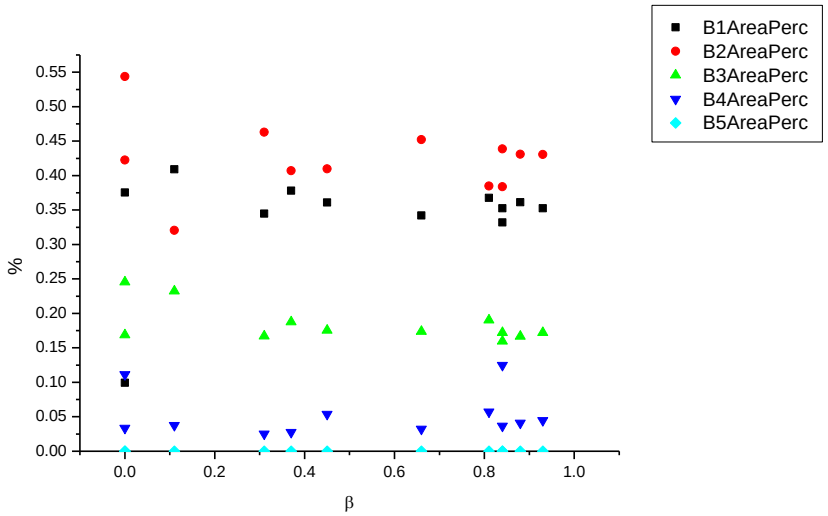

Figure 3.3.12. Area percentages from Gaussian model fit of the normalised fluorescence emission spectra of **18** recorded at 310 nm excitation against β.

3.3.4.4 π.*

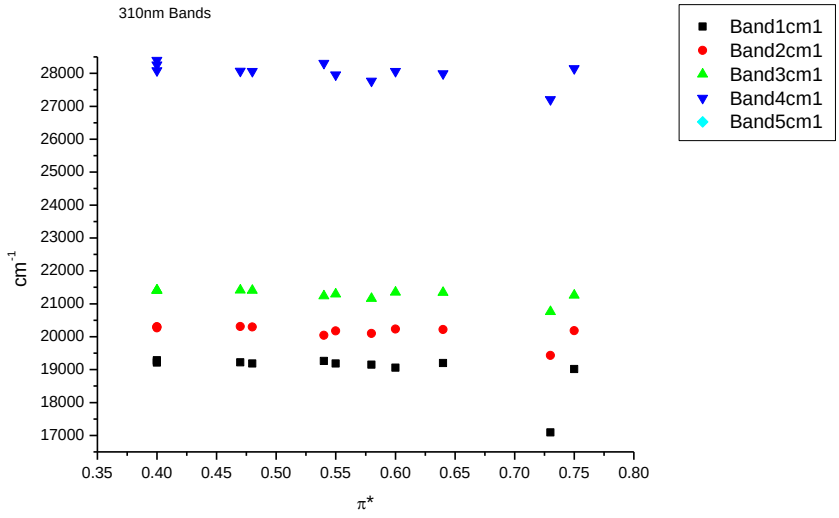

Figure 3.3.13. Band maxima from Gaussian model fit of the normalised fluorescence emission spectra of **18** recorded at 310 nm excitation against π*.

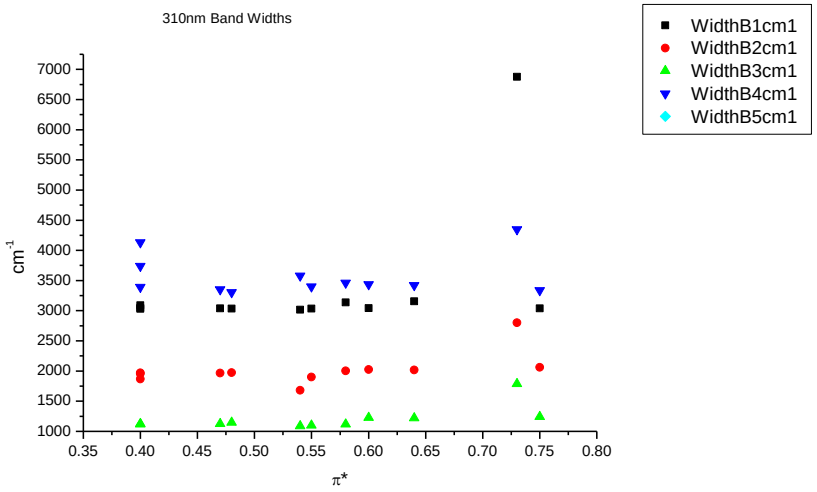

Figure 3.3.14. Band widths from Gaussian model fit of the normalised fluorescence emission spectra of **18** recorded at 310 nm excitation against π*.

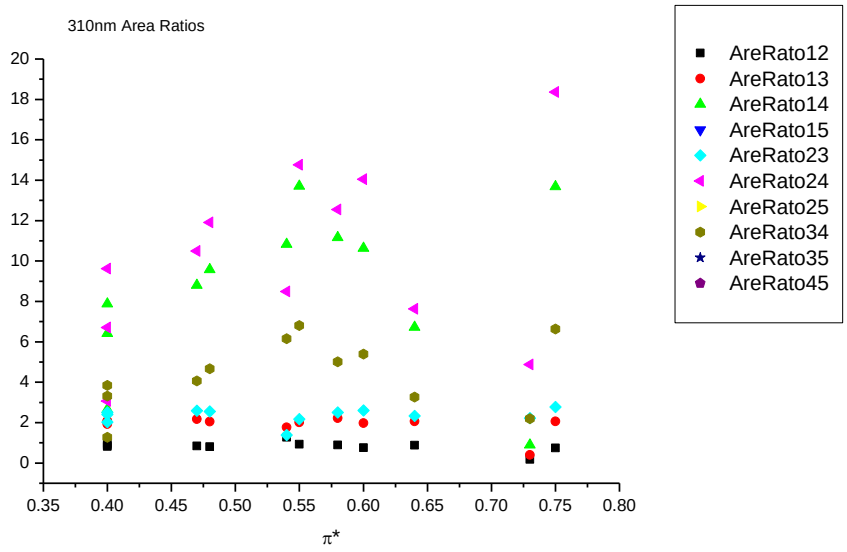

Figure 3.3.15. Area ratios from Gaussian model fit of the normalised fluorescence emission spectra of **18** recorded at 310 nm excitation against π*.

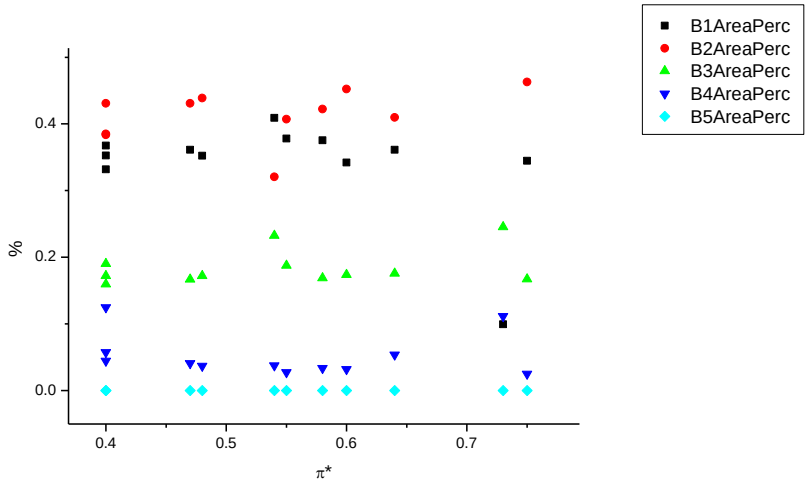

Figure 3.3.16. Area percentages from Gaussian model fit of the normalised fluorescence emission spectra of **18** recorded at 310 nm excitation against π*.

3.3.4.5 μ(D).

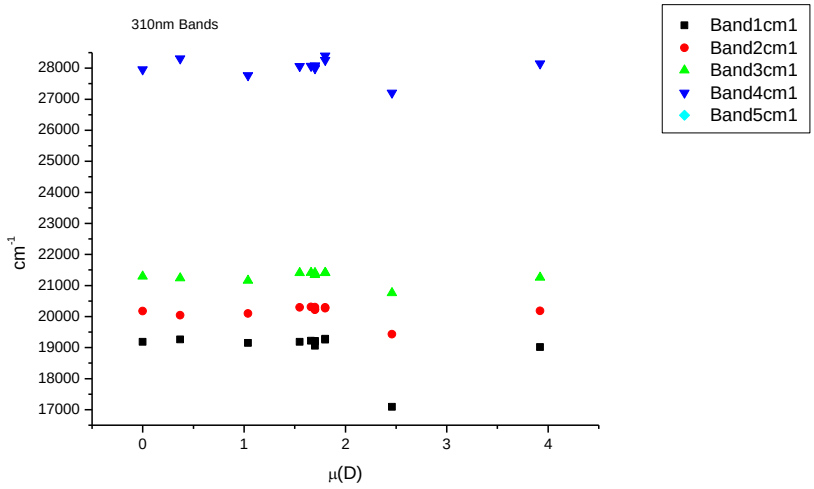

Figure 3.3.17. Band maxima from Gaussian model fit of the normalised fluorescence emission spectra of **18** recorded at 310 nm excitation against μ(D).

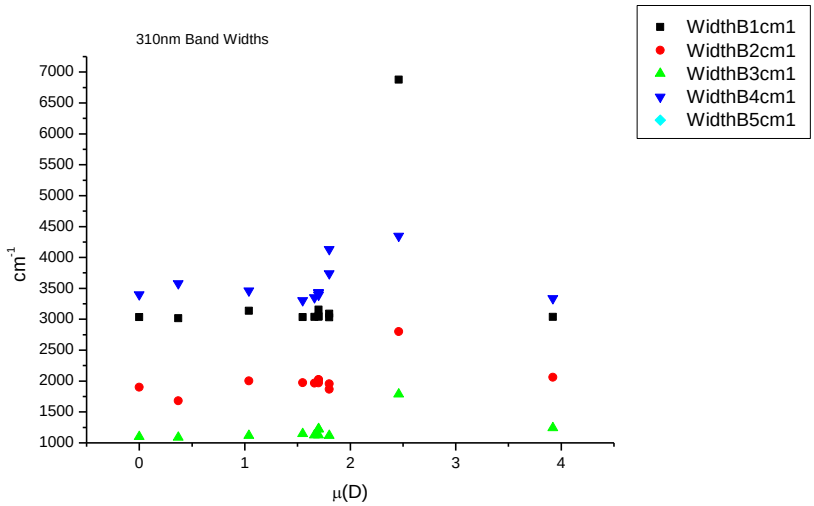

Figure 3.3.18. Band widths from Gaussian model fit of the normalised fluorescence emission spectra of **18** recorded at 310 nm excitation against μ(D).

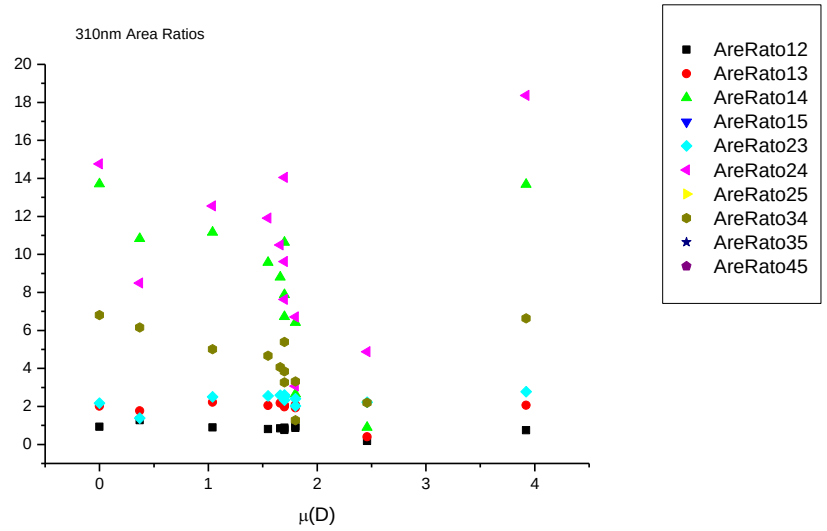

Figure 3.3.19. Area ratios from Gaussian model fit of the normalised fluorescence emission spectra of **18** recorded at 310 nm excitation against μ(D).

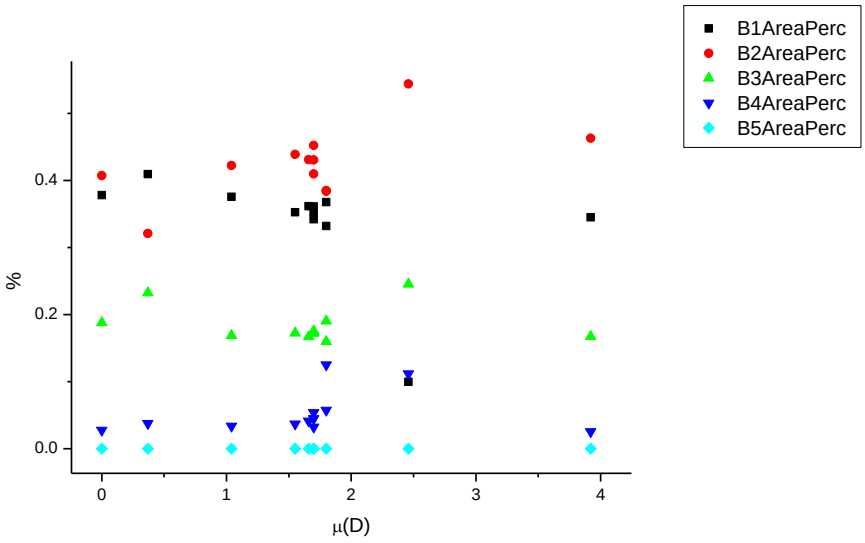

Figure 3.3.20. Area percentages from Gaussian model fit of the normalised fluorescence emission spectra of **18** recorded at 310 nm excitation against μ(D).

3.3.4.6 η(Cp).

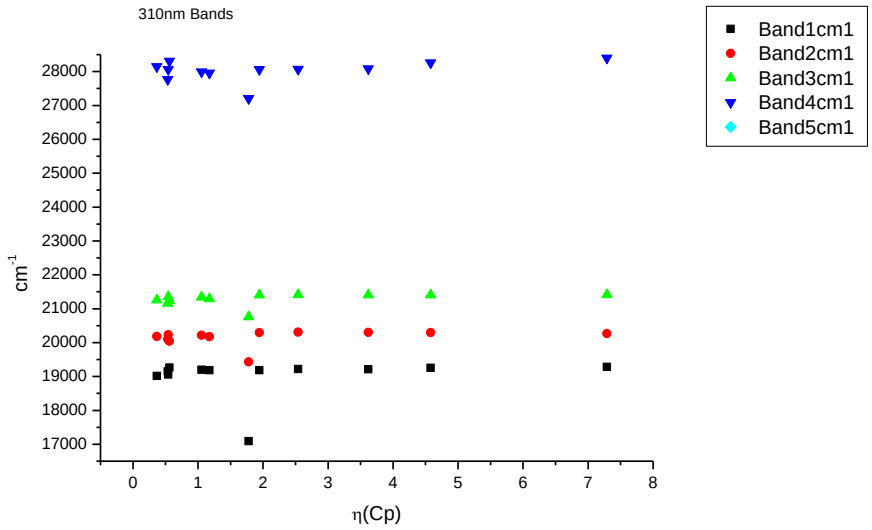

Figure 3.3.21. Band maxima from Gaussian model fit of the normalised fluorescence emission spectra of **18** recorded at 310 nm excitation against η(Cp).

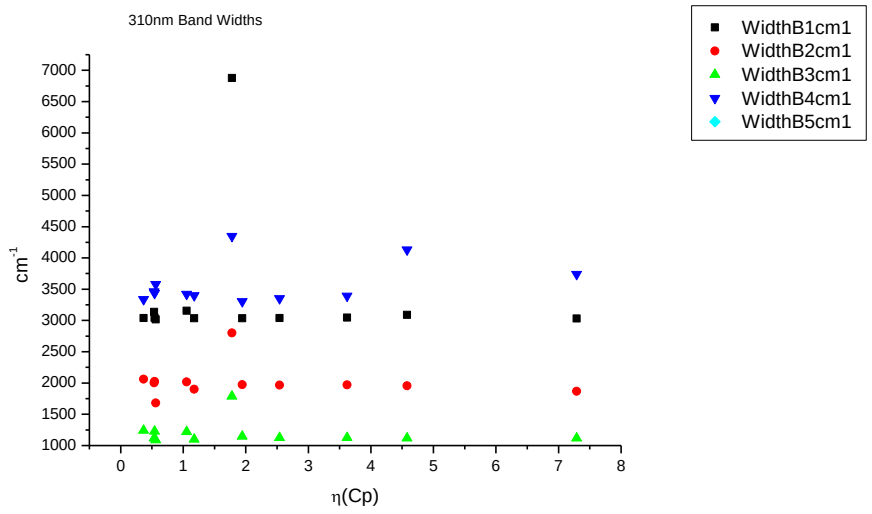

Figure 3.3.22. Band widths from Gaussian model fit of the normalised fluorescence emission spectra of **18** recorded at 310 nm excitation against η(Cp).

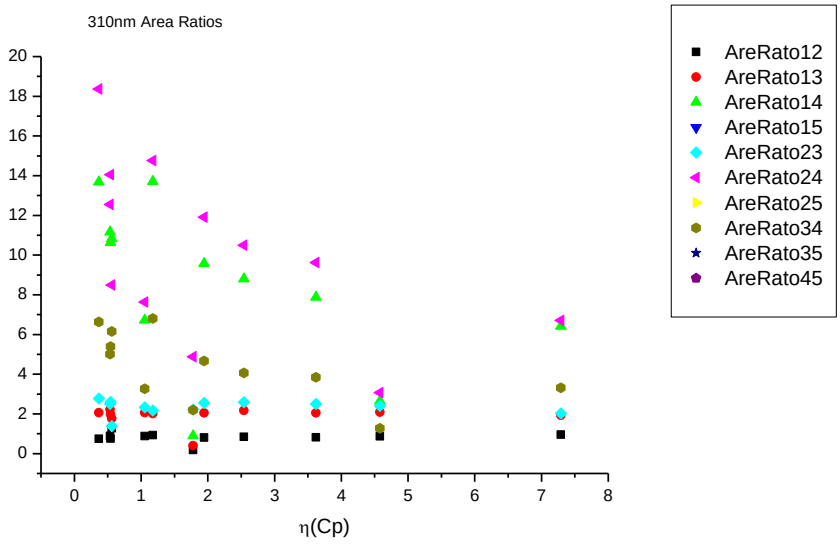

Figure 3.3.23. Area ratios from Gaussian model fit of the normalised fluorescence emission spectra of **18** recorded at 310 nm excitation against η(Cp).

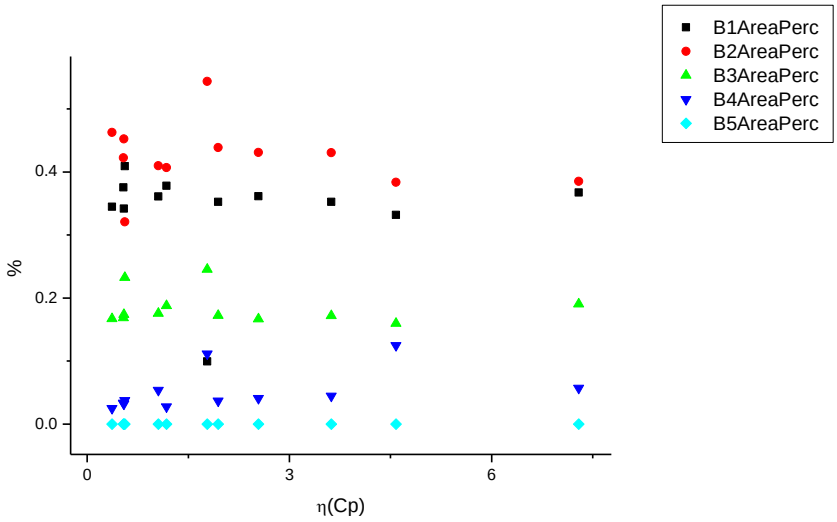

Figure 3.3.24. Area percentages from Gaussian model fit of the normalised fluorescence emission spectra of **18** recorded at 310 nm excitation against η(Cp).

3.3.5 400 nm Gaussian band fit - Solvatochromic analysis.

3.3.5.1 E_T^N.

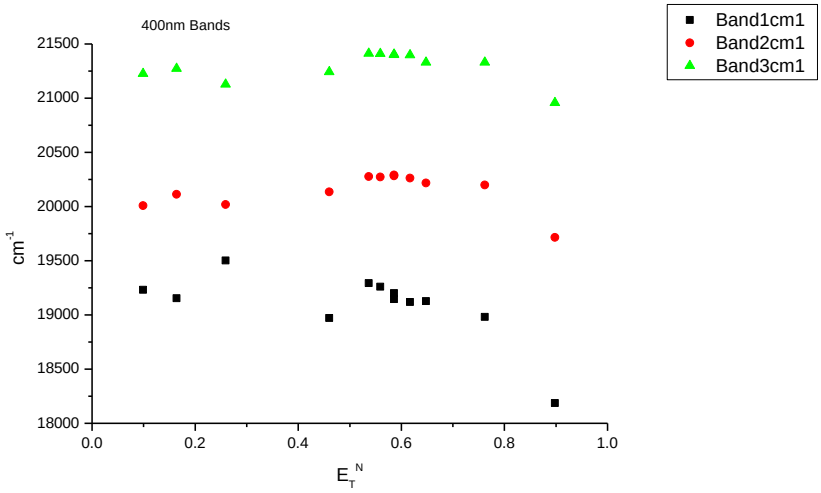

Figure 3.3.25. Band maxima from Gaussian model fit of the normalised fluorescence emission spectra of **18** recorded at 400 nm excitation against E_T^N.

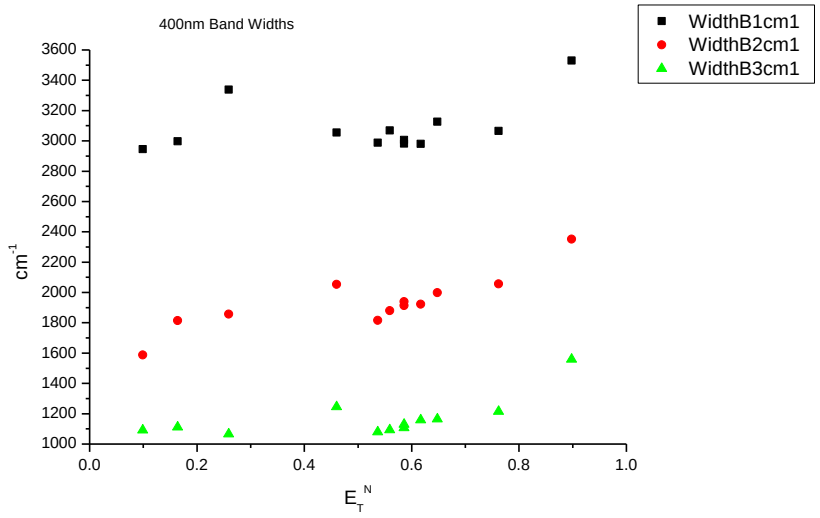

Figure 3.3.26. Band widths from Gaussian model fit of the normalised fluorescence emission spectra of **18** recorded at 400 nm excitation against E_T^N.

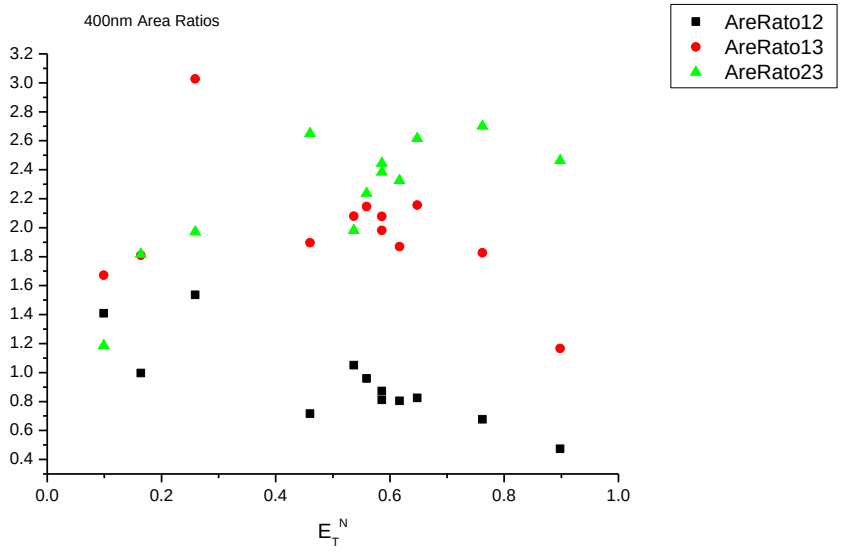

Figure 3.3.27. Area ratios from Gaussian model fit of the normalised fluorescence emission spectra of **18** recorded at 400 nm excitation against E_T^N.

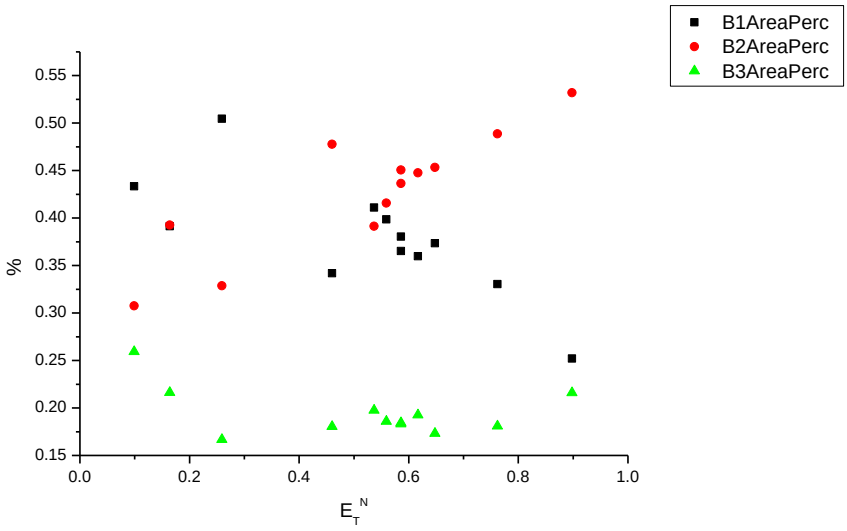

Figure 3.3.28. Area percentages from Gaussian model fit of the normalised fluorescence emission spectra of **18** recorded at 400 nm excitation against E_T^N.

3.3.5.2 *α*

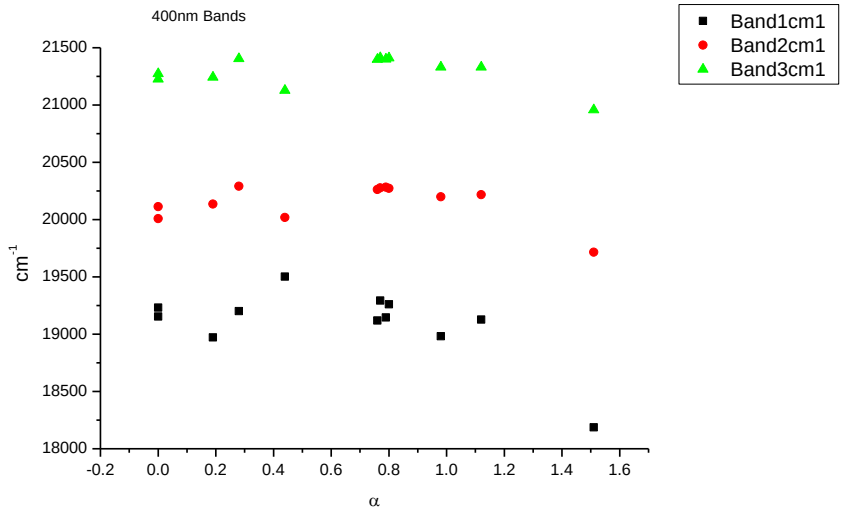

Figure 3.3.29. Band maxima from Gaussian model fit of the normalised fluorescence emission spectra of **18** recorded at 400 nm excitation against α.

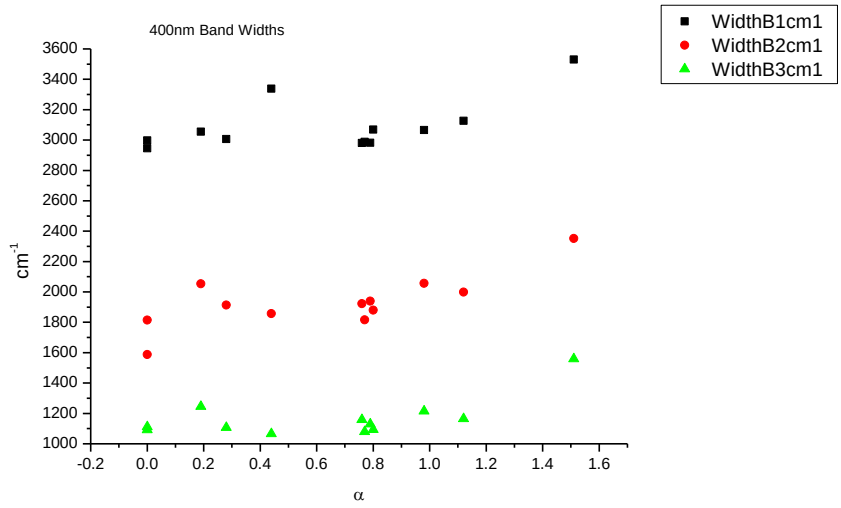

Figure 3.3.30. Band widths from Gaussian model fit of the normalised fluorescence emission spectra of **17** recorded at 400 nm excitation against α.

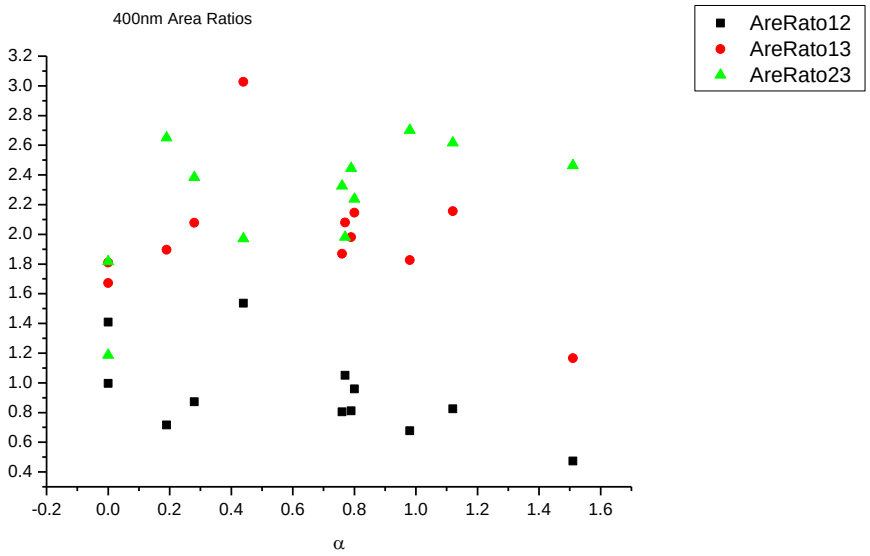

Figure 3.3.31. Area ratios from Gaussian model fit of the normalised fluorescence emission spectra of **18** recorded at 400 nm excitation against α.

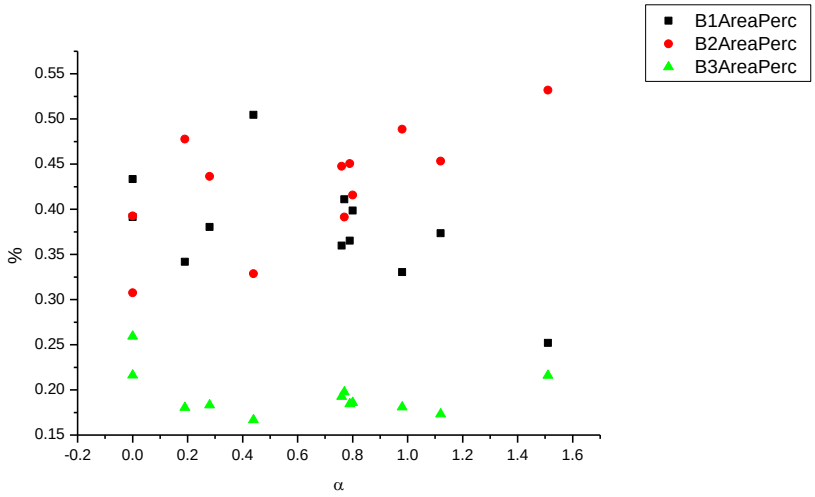

Figure 3.3.32. Area percentages from Gaussian model fit of the normalised fluorescence emission spectra of **18** recorded at 400 nm excitation against α.

3.3.5.3 β.

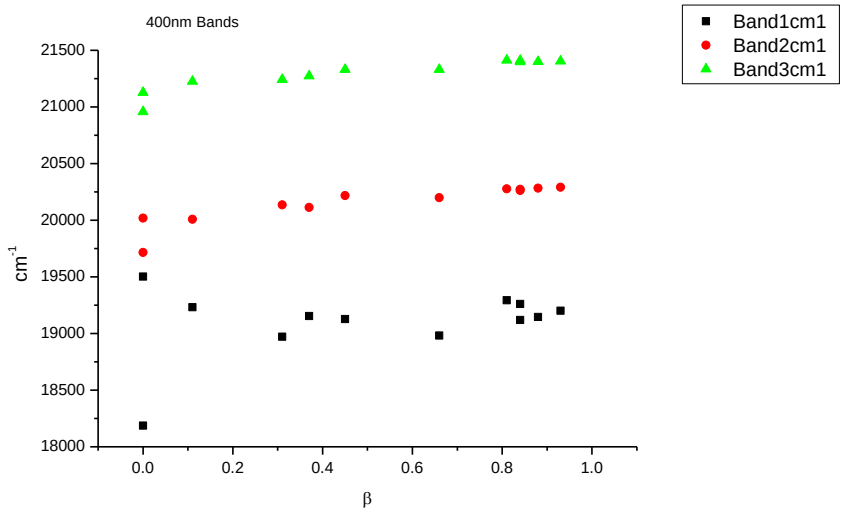

Figure 3.3.33. Band maxima from Gaussian model fit of the normalised fluorescence emission spectra of **18** recorded at 400 nm excitation against β.

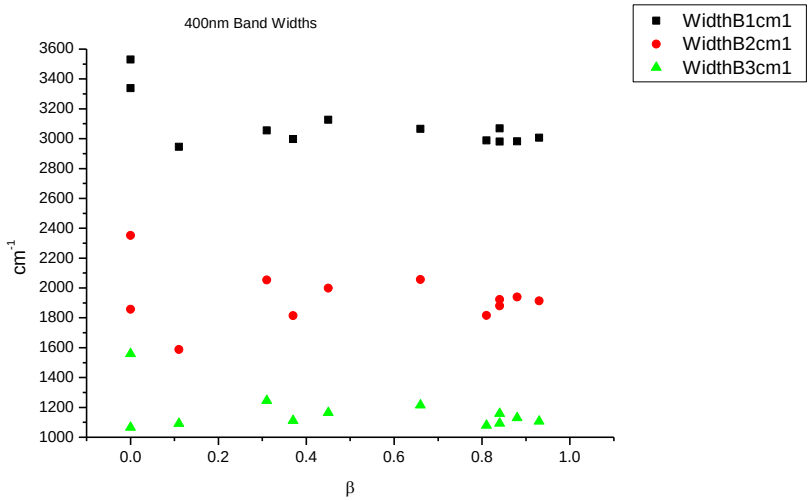

Figure 3.3.34. Band widths from Gaussian model fit of the normalised fluorescence emission spectra of **18** recorded at 400 nm excitation against β.

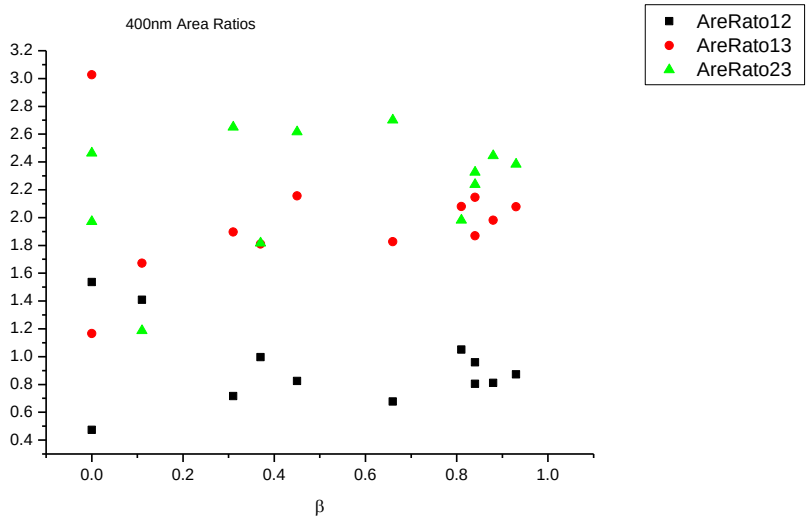

Figure 3.3.35. Area ratios from Gaussian model fit of the normalised fluorescence emission spectra of **18** recorded at 400 nm excitation against β.

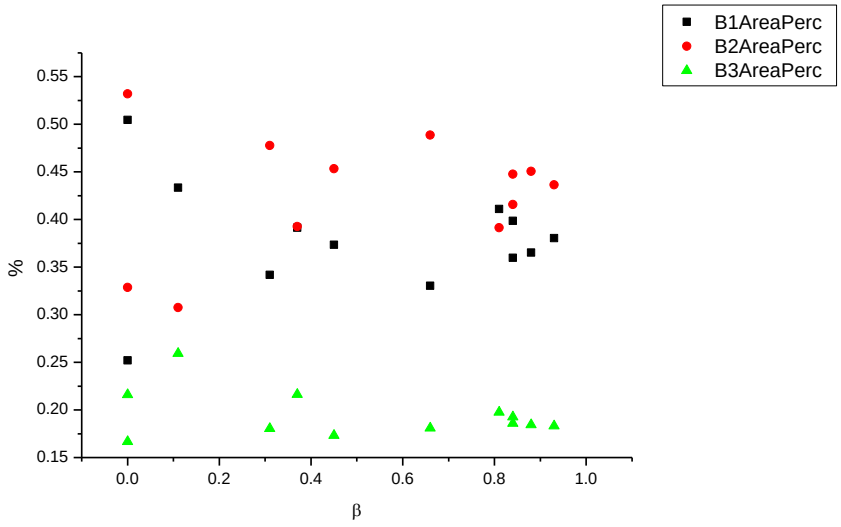

Figure 3.3.36. Area percentages from Gaussian model fit of the normalised fluorescence emission spectra of **18** recorded at 400 nm excitation against β.

3.3.5.4 π.*

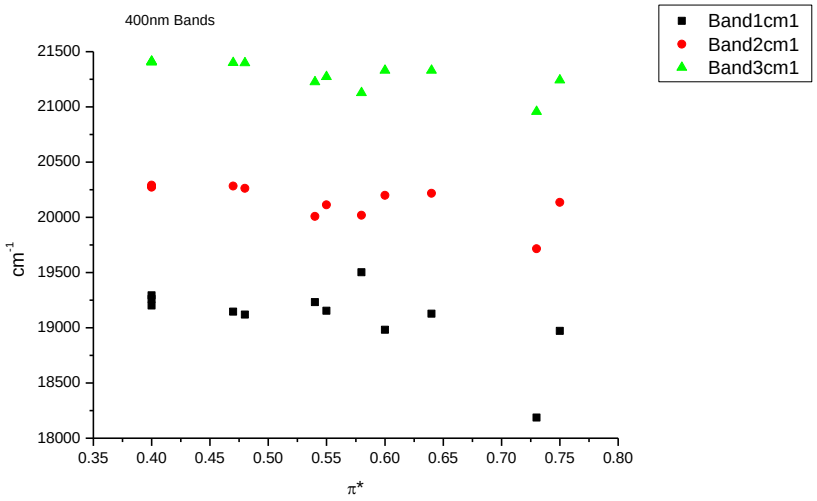

Figure 3.3.37. Band maxima from Gaussian model fit of the normalised fluorescence emission spectra of **18** recorded at 400 nm excitation against π*.

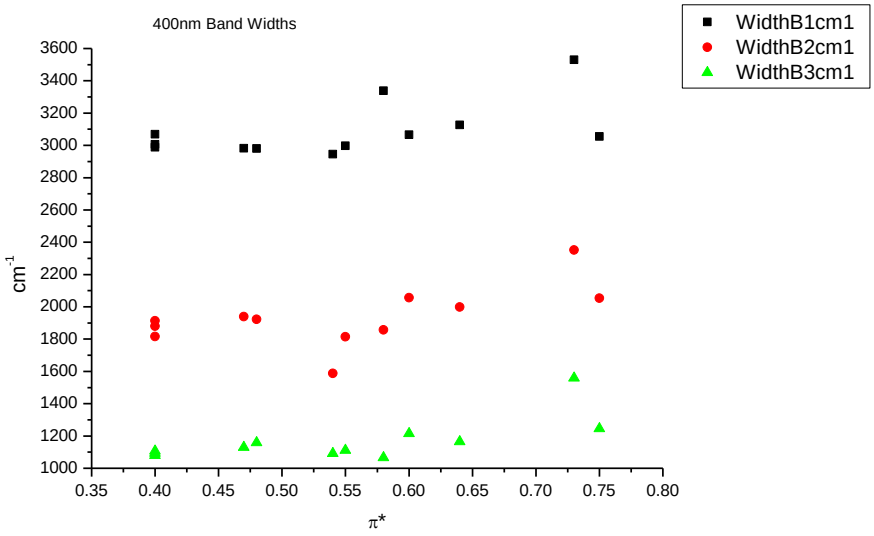

Figure 3.3.38. Band widths from Gaussian model fit of the normalised fluorescence emission spectra of **18** recorded at 400 nm excitation against π*.

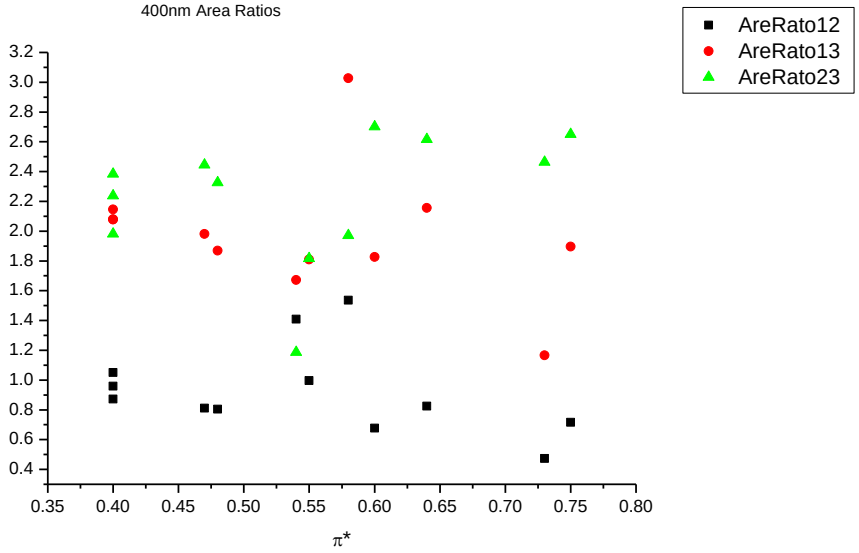

Figure 3.3.39. Area ratios from Gaussian model fit of the normalised fluorescence emission spectra of **18** recorded at 400 nm excitation against π*.

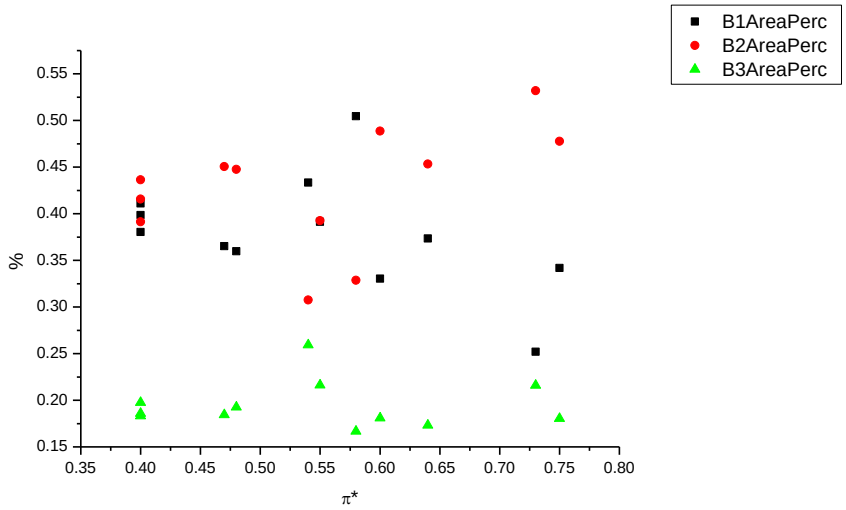

Figure 3.3.40. Area percentages from Gaussian model fit of the normalised fluorescence emission spectra of **18** recorded at 400 nm excitation against π*.

3.3.5.5 μ(D).

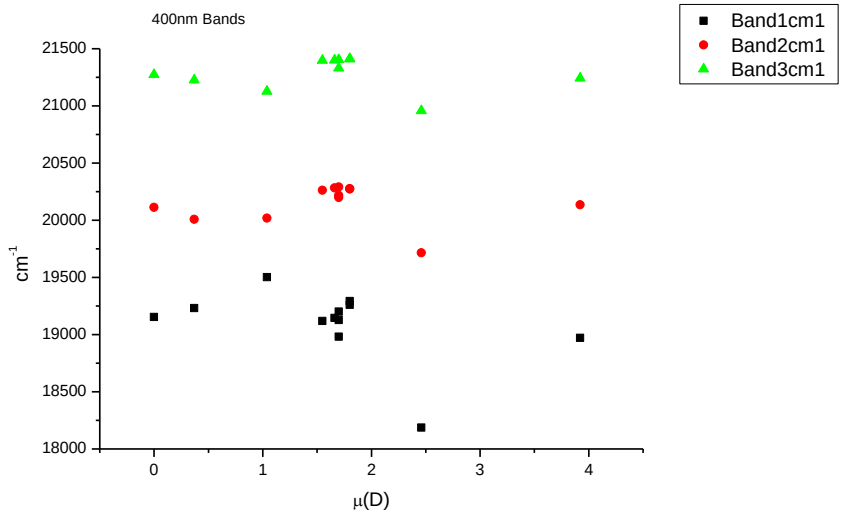

Figure 3.3.41. Band maxima from Gaussian model fit of the normalised fluorescence emission spectra of **18** recorded at 400 nm excitation against μ(D).

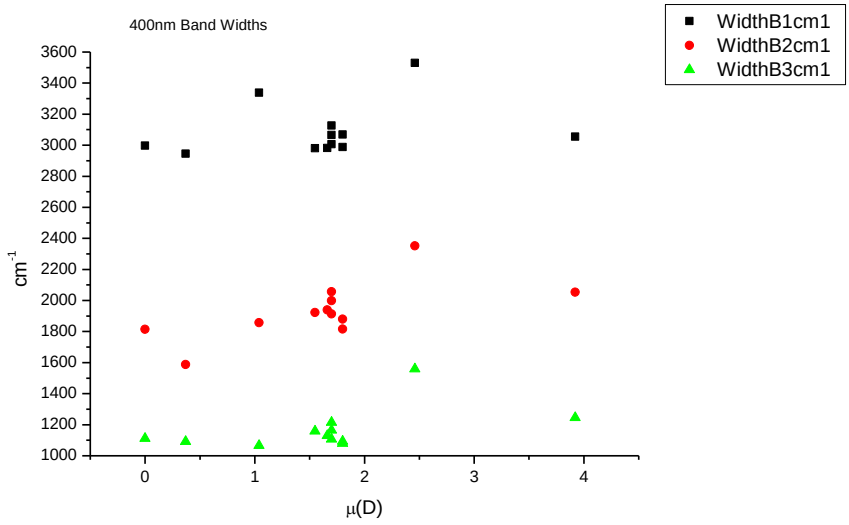

Figure 3.3.42. Band widths from Gaussian model fit of the normalised fluorescence emission spectra of **18** recorded at 400 nm excitation against μ(D).

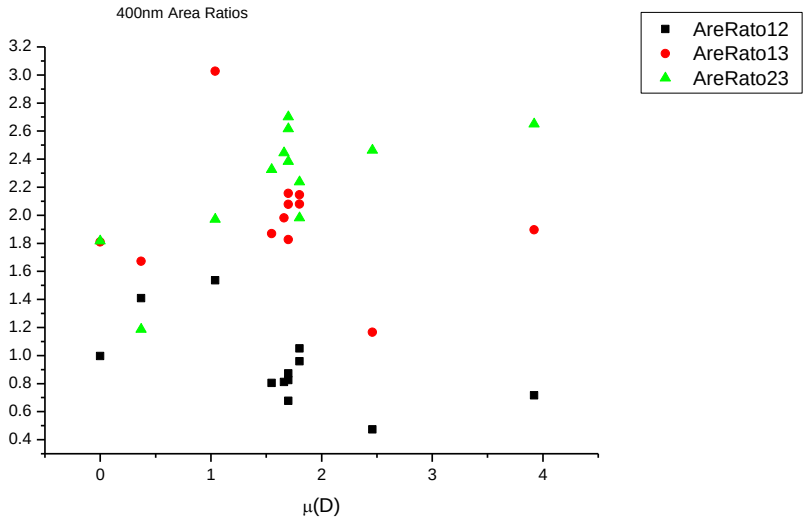

Figure 3.3.43. Area ratios from Gaussian model fit of the normalised fluorescence emission spectra of **18** recorded at 400 nm excitation against μ(D).

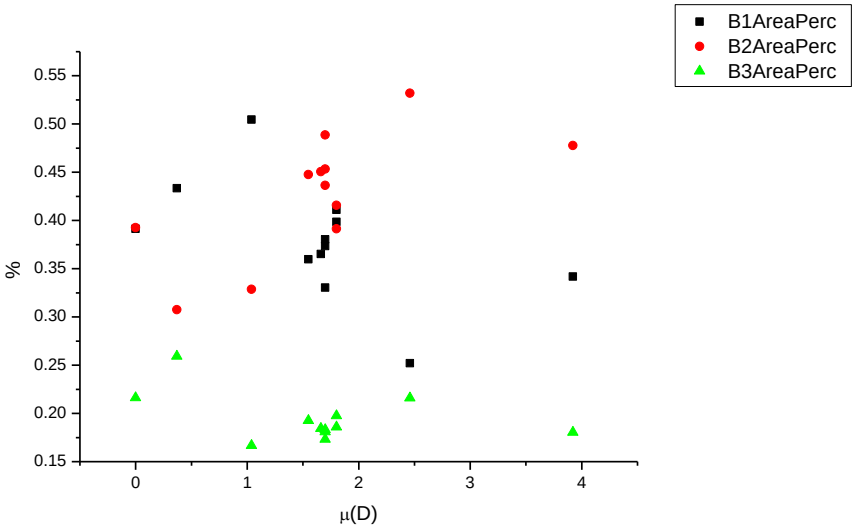

Figure 3.3.44. Area percentages from Gaussian model fit of the normalised fluorescence emission spectra of **18** recorded at 400 nm excitation against μ(D).

3.3.5.6 η(Cp).

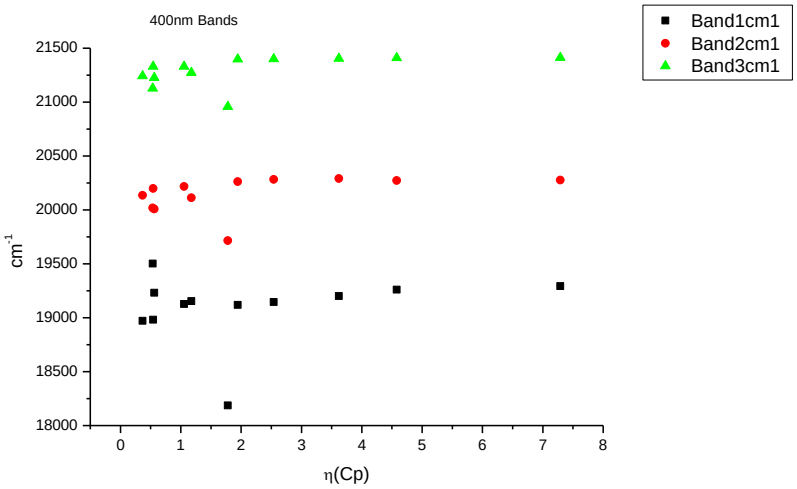

Figure 3.3.45. Band maxima from Gaussian model fit of the normalised fluorescence emission spectra of **18** recorded at 400 nm excitation against η(Cp).

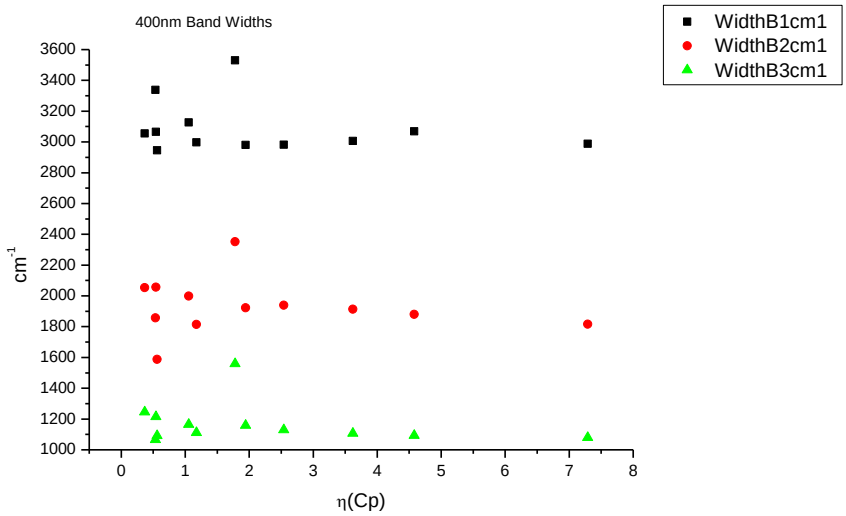

Figure 3.3.46. Band widths from Gaussian model fit of the normalised fluorescence emission spectra of **18** recorded at 400 nm excitation against η(Cp).

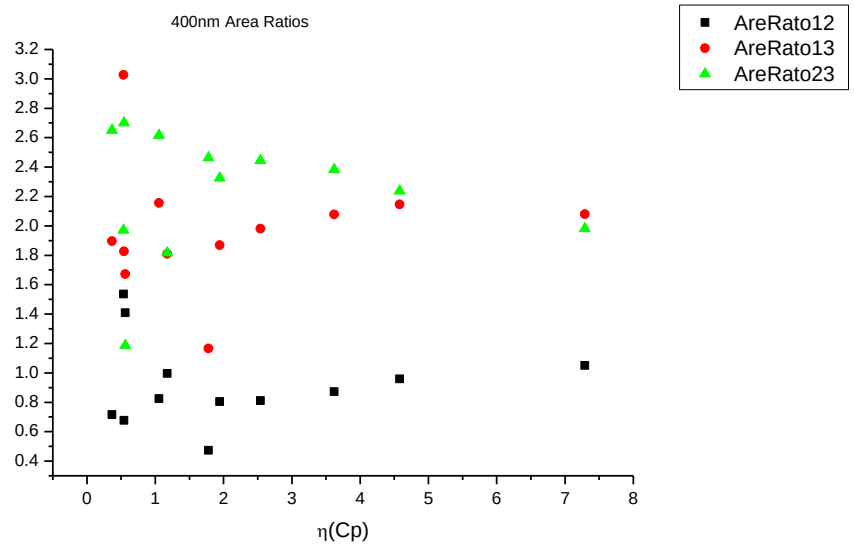

Figure 3.3.47. Area ratios from Gaussian model fit of the normalised fluorescence emission spectra of **18** recorded at 400 nm excitation against η(Cp).

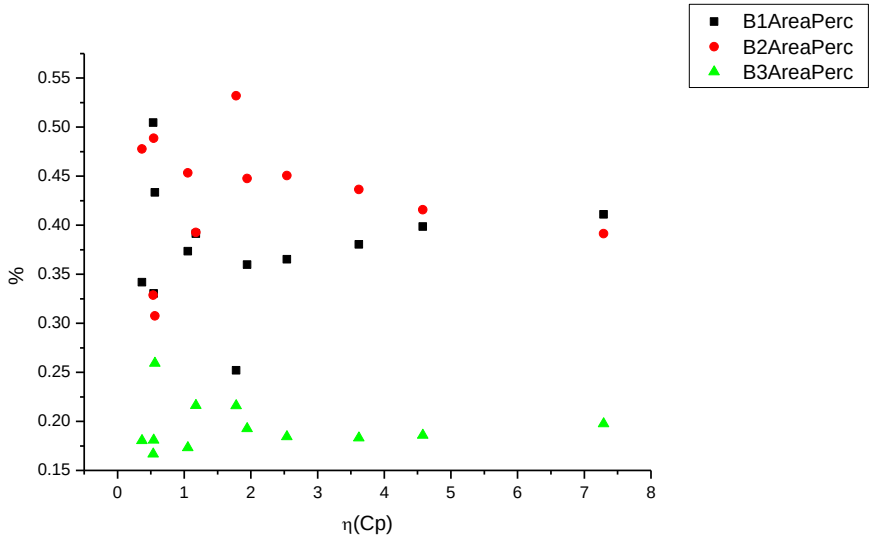

Figure 3.3.48. Area percentages from Gaussian model fit of the normalised fluorescence emission spectra of **18** recorded at 400 nm excitation against η(Cp).

3.3.6 400 nm fluorescent lifetime results.

3.3.6.1 Intensity weighted.

Wavelength (nm)	Solvent	τ_1 (ns)	A_1 (%)	τ_2 (ns)	A_2 (%)	τ_3 (ns)	A_3 (%)	τ_f (ns) (Intensity Weighted)	$1/\tau_f$	χ^2
470	Toluene	0.39	3.98	1.87	36.19	2.78	59.83	2.36	0.42	1.17
470	1,4-Dioxane	0.54	2.14	1.72	32.71	2.73	65.16	2.35	0.42	1.18
470	Chloroform	0.49	4.44	1.94	70.14	3.13	25.41	2.18	0.46	1.02
470	Acetonitrile	0.35	2.50	1.95	57.88	3.38	39.63	2.48	0.40	1.12
470	1-Octanol	0.79	20.72	-	-	2.00	79.28	1.75	0.57	1.19
470	1-Hexanol	0.57	10.17	1.76	84.92	3.55	4.92	1.73	0.58	1.10
470	1-Butanol	0.39	5.02	1.54	63.72	2.31	31.26	1.72	0.58	1.04
470	1-Pentanol	-	-	1.18	35.50	2.06	64.50	1.75	0.57	1.20
470	1-Propanol	0.51	2.78	1.44	49.72	2.21	47.50	1.78	0.56	1.16
470	Acetic acid	0.43	18.28	1.02	79.79	2.68	1.93	0.95	1.06	1.06
470	Methanol	0.26	4.12	1.29	25.87	2.27	70.01	1.93	0.52	0.90
470	2,2,2-Trifluoroethanol	0.41	59.07	0.73	39.42	6.72	1.51	0.63	1.58	1.08

Table 3.3.9. Summary of Time Correlated Single Photon Counting (TCSPC) fluorescent lifetimes (intensity weighted) of **18** recorded at 470 nm.

Wavelength (nm)	Solvent	τ_1 (ns)	A_1 (%)	τ_2 (ns)	A_2 (%)	τ_3 (ns)	A_3 (%)	τ_f (ns) (Intensity Weighted)	$1/\tau_f$	χ^2
490	Toluene	0.31	4.80	1.93	41.33	2.82	53.87	2.33	0.43	1.12
490	1,4-Dioxane	0.31	2.05	1.74	37.93	2.80	60.01	2.34	0.43	1.16
490	Chloroform	0.48	4.38	1.93	68.49	3.08	27.14	2.18	0.46	1.02
490	Acetonitrile	0.28	2.39	1.85	46.17	3.17	51.44	2.49	0.40	1.02
490	1-Octanol	0.31	8.01	1.43	38.92	2.19	53.07	1.74	0.57	1.05
490	1-Hexanol	0.42	7.99	1.70	82.17	2.95	9.84	1.72	0.58	1.06
490	1-Butanol	0.28	4.40	1.51	64.18	2.31	31.42	1.71	0.59	1.03
490	1-Pentanol	0.52	7.00	1.68	79.09	2.73	13.92	1.74	0.57	1.12
490	1-Propanol	0.66	6.78	1.71	79.15	2.73	14.06	1.78	0.56	1.00
490	Acetic acid	0.39	16.67	1.07	81.86	3.01	1.47	0.98	1.02	0.97
490	Methanol	0.31	4.40	1.49	35.28	2.34	60.31	1.95	0.51	1.02
490	2,2,2-Trifluoroethanol	0.50	84.01	0.85	15.17	8.60	0.82	0.62	1.62	1.43

Table 3.3.10. Summary of Time Correlated Single Photon Counting (TCSPC) fluorescent lifetimes (intensity weighted) of **18** recorded at 490 nm.

Wavelength (nm)	Solvent	τ_1 (ns)	A_1 (%)	τ_2 (ns)	A_2 (%)	τ_3 (ns)	A_3 (%)	τ_f (ns) (Intensity Weighted)	$1/\tau_f$	χ^2
520	Toluene	0.32	4.15	1.85	35.19	2.78	60.65	2.35	0.43	1.06
520	1,4-Dioxane	0.32	2.40	1.92	51.94	2.97	45.66	2.36	0.42	0.99
520	Chloroform	0.57	5.03	1.97	67.92	2.99	27.06	2.18	0.46	1.05
520	Acetonitrile	0.30	2.50	1.85	41.72	3.12	55.78	2.52	0.40	1.08
520	1-Octanol	0.80	17.01	2.01	82.99	-	-	1.80	0.55	1.13
520	1-Hexanol	0.59	5.45	1.73	86.00	3.02	8.55	1.78	0.56	1.15
520	1-Butanol	0.33	3.64	1.54	70.96	2.42	25.40	1.72	0.58	1.28
520	1-Pentanol	0.69	7.87	1.74	83.82	3.00	8.31	1.77	0.57	0.99
520	1-Propanol	0.60	4.82	1.68	78.21	2.67	16.97	1.80	0.56	0.96
520	Acetic acid	0.47	18.51	1.12	80.61	4.04	0.88	1.02	0.98	1.00
520	Methanol	0.29	3.77	1.41	30.70	2.33	65.53	1.97	0.51	0.94
520	2,2,2-Trifluoroethanol	0.46	68.57	0.74	30.66	8.06	0.77	0.60	1.66	1.24

Table 3.3.11. Summary of Time Correlated Single Photon Counting (TCSPC) fluorescent lifetimes (intensity weighted) of **18** recorded at 520 nm.

Wavelength (nm)	Solvent	τ_1 (ns)	A_1 (%)	τ_2 (ns)	A_2 (%)	τ_3 (ns)	A_3 (%)	τ_f (ns) (Intensity Weighted)	$1/\tau_f$	χ^2
540	Toluene	0.38	3.72	1.87	34.81	2.77	61.47	2.37	0.42	1.14
540	1,4-Dioxane	0.36	2.33	1.93	51.56	2.97	46.11	2.37	0.42	0.97
540	Chloroform	0.60	4.50	2.04	77.79	3.33	17.71	2.21	0.45	1.11
540	Acetonitrile	0.30	2.23	1.95	50.77	3.28	47.01	2.54	0.39	1.09
540	1-Octanol	0.37	7.24	1.72	76.88	2.75	15.88	1.78	0.56	1.04
540	1-Hexanol	0.48	7.45	1.73	85.20	3.25	7.36	1.75	0.57	1.16
540	1-Butanol	0.37	4.33	1.61	78.53	2.60	17.14	1.72	0.58	0.96
540	1-Pentanol	0.64	7.66	1.74	83.55	2.98	8.80	1.77	0.57	1.09
540	1-Propanol	0.75	5.37	1.68	78.01	2.73	16.61	1.80	0.55	1.03
540	Acetic acid	0.50	18.80	1.13	80.28	4.61	0.92	1.04	0.96	0.95
540	Methanol	0.34	5.02	1.52	35.35	2.37	59.63	1.97	0.51	1.10
540	2,2,2-Trifluoroethanol	0.45	58.47	0.70	40.68	7.84	0.86	0.61	1.64	0.93

Table 3.3.12. Summary of Time Correlated Single Photon Counting (TCSPC) fluorescent lifetimes (intensity weighted) of **18** recorded at 540 nm.

Wavelength (nm)	Solvent	τ_1 (ns)	A_1 (%)	τ_2 (ns)	A_2 (%)	τ_3 (ns)	A_3 (%)	τ_f (ns) (Intensity Weighted)	$1/\tau_f$	χ^2
570	Toluene	0.73	4.22	2.00	35.77	2.77	60.01	2.41	0.42	1.16
570	1,4-Dioxane	-	-	1.72	38.70	2.83	61.30	2.40	0.42	1.23
570	Chloroform	0.29	3.52	1.89	61.54	2.88	34.94	2.18	0.46	1.24
570	Acetonitrile	0.70	2.19	1.99	49.96	3.27	47.85	2.57	0.39	1.13
570	1-Octanol	0.40	8.63	1.66	65.78	2.51	25.59	1.77	0.57	0.98
570	1-Hexanol	0.32	14.04	1.75	80.82	3.73	5.15	1.65	0.61	1.16
570	1-Butanol	0.65	6.93	1.74	88.71	3.83	4.36	1.76	0.57	1.12
570	1-Pentanol	0.62	7.30	1.77	88.73	4.05	3.97	1.77	0.56	1.14
570	1-Propanol	1.09	9.61	1.71	72.27	2.68	18.12	1.82	0.55	1.06
570	Acetic acid	0.43	14.05	1.11	84.36	3.52	1.60	1.05	0.95	0.94
570	Methanol	0.37	4.37	1.49	34.19	2.38	61.44	1.99	0.50	1.14
570	2,2,2-Trifluoroethanol	0.39	45.93	0.67	53.22	5.81	0.85	0.58	1.71	1.15

Table 3.3.13. Summary of Time Correlated Single Photon Counting (TCSPC) fluorescent lifetimes (intensity weighted) of **18** recorded at 570 nm.

3.3.6.2 Amplitude weighted.

Wavelength (nm)	Solvent	τ_1 (ns)	A_1 (%)	τ_2 (ns)	A_2 (%)	τ_3 (ns)	A_3 (%)	τ_f (ns) (Amplitude Weighted)	$1/\tau_f$	χ^2
470	Toluene	0.39	20.14	1.87	37.83	2.78	42.03	1.95	0.51	1.17
470	1,4-Dioxane	0.54	8.39	1.72	40.71	2.73	50.90	2.14	0.47	1.18
470	Chloroform	0.49	17.07	1.94	67.72	3.13	15.20	1.87	0.53	1.02
470	Acetonitrile	0.35	14.86	1.95	61.06	3.38	24.08	2.05	0.49	1.12
470	1-Octanol	0.79	39.87	-	-	2.00	60.13	1.52	0.66	1.19
470	1-Hexanol	0.57	26.41	1.76	71.53	3.55	2.06	1.49	0.67	1.10
470	1-Butanol	0.39	18.79	1.54	61.17	2.31	20.04	1.48	0.68	1.04
470	1-Pentanol	-	-	1.18	48.99	2.06	51.01	1.63	0.61	1.20
470	1-Propanol	0.51	2.78	1.44	56.20	2.21	34.97	1.63	0.61	1.16
470	Acetic acid	0.43	35.13	1.02	64.28	2.68	0.60	0.83	1.21	1.06
470	Methanol	0.26	24.04	1.29	29.87	2.27	46.10	1.49	0.67	0.90
470	2,2,2-Trifluoroethanol	0.41	72.61	0.73	27.27	6.72	0.11	0.51	1.98	1.08

Table 3.3.14. Summary of Time Correlated Single Photon Counting (TCSPC) fluorescent lifetimes (amplitude weighted) of **18** recorded at 470 nm.

Wavelength (nm)	Solvent	τ_1 (ns)	A_1 (%)	τ_2 (ns)	A_2 (%)	τ_3 (ns)	A_3 (%)	τ_f (ns) (Amplitude Weighted)	$1/\tau_f$	χ^2
490	Toluene	0.31	27.58	1.93	38.31	2.82	34.12	1.79	0.56	1.12
490	1,4-Dioxane	0.31	13.34	1.74	43.75	2.80	42.91	2.00	0.50	1.16
490	Chloroform	0.48	17.07	1.93	66.53	3.08	16.46	1.87	0.53	1.02
490	Acetonitrile	0.28	17.39	1.85	50.01	3.17	32.61	2.01	0.50	1.02
490	1-Octanol	0.31	33.34	1.43	35.25	2.19	31.42	1.29	0.77	1.05
490	1-Hexanol	0.42	26.91	1.70	68.37	2.95	4.72	1.42	0.71	1.06
490	1-Butanol	0.28	22.05	1.51	59.05	2.31	18.90	1.39	0.72	1.03
490	1-Pentanol	0.52	20.58	1.68	71.66	2.73	7.76	1.52	0.66	1.12
490	1-Propanol	0.66	16.67	1.71	74.99	2.73	8.35	1.62	0.62	1.00
490	Acetic acid	0.39	35.90	1.07	63.70	3.01	0.40	0.83	1.20	0.97
490	Methanol	0.31	22.13	1.49	37.33	2.34	40.55	1.58	0.63	1.02
490	2,2,2-Trifluoroethanol	0.50	90.39	0.85	9.56	8.60	0.05	0.53	1.87	1.43

Table 3.3.15. Summary of Time Correlated Single Photon Counting (TCSPC) fluorescent lifetimes (amplitude weighted) of **18** recorded at 490 nm.

Wavelength (nm)	Solvent	τ_1 (ns)	A_1 (%)	τ_2 (ns)	A_2 (%)	τ_3 (ns)	A_3 (%)	τ_f (ns) (Amplitude Weighted)	$1/\tau_f$	χ^2
520	Toluene	0.32	23.98	1.85	35.43	2.78	40.59	1.86	0.54	1.06
520	1,4-Dioxane	0.32	15.21	1.92	54.06	2.97	30.73	2.00	0.50	0.99
520	Chloroform	0.57	16.83	1.97	65.85	2.99	17.32	1.91	0.52	1.05
520	Acetonitrile	0.30	17.33	1.85	46.11	3.12	36.55	2.04	0.49	1.08
520	1-Octanol	0.80	34.03	2.01	65.97	-	-	1.60	0.63	1.13
520	1-Hexanol	0.59	14.91	1.73	80.50	3.02	4.59	1.62	0.62	1.15
520	1-Butanol	0.33	16.42	1.54	68.06	2.42	15.52	1.48	0.68	1.28
520	1-Pentanol	0.69	18.40	1.74	77.15	3.00	4.45	1.61	0.62	0.99
520	1-Propanol	0.60	13.18	1.68	76.38	2.67	10.43	1.64	0.61	0.96
520	Acetic acid	0.47	35.15	1.12	64.65	4.04	0.20	0.90	1.12	1.00
520	Methanol	0.29	20.82	1.41	34.57	2.33	44.61	1.59	0.63	0.94
520	2,2,2-Trifluoroethanol	0.46	78.46	0.74	21.49	8.06	0.05	0.52	1.92	1.24

Table 3.3.16. Summary of Time Correlated Single Photon Counting (TCSPC) fluorescent lifetimes (amplitude weighted) of **18** recorded at 520 nm.

Wavelength (nm)	Solvent	τ_1 (ns)	A_1 (%)	τ_2 (ns)	A_2 (%)	τ_3 (ns)	A_3 (%)	τ_f (ns) (Amplitude Weighted)	$1/\tau_f$	χ^2
540	Toluene	0.38	19.45	1.87	36.75	2.77	43.80	1.98	0.51	1.14
540	1,4-Dioxane	0.36	13.30	1.93	54.78	2.97	31.92	2.05	0.49	0.97
540	Chloroform	0.60	14.66	2.04	74.88	3.33	10.45	1.97	0.51	1.11
540	Acetonitrile	0.30	15.71	1.95	54.38	3.28	29.91	2.09	0.48	1.09
540	1-Octanol	0.37	27.88	1.72	63.86	2.75	8.26	1.43	0.70	1.04
540	1-Hexanol	0.48	23.07	1.73	73.54	3.25	3.38	1.50	0.67	1.16
540	1-Butanol	0.37	17.28	1.61	72.89	2.60	9.83	1.49	0.67	0.96
540	1-Pentanol	0.64	19.07	1.74	76.23	2.98	4.70	1.59	0.63	1.09
540	1-Propanol	0.75	12.04	1.68	77.78	2.73	10.19	1.67	0.60	1.03
540	Acetic acid	0.50	34.47	1.13	65.35	4.61	0.18	0.92	1.09	0.95
540	Methanol	0.34	23.32	1.52	36.79	2.37	39.89	1.59	0.63	1.10
540	2,2,2-Trifluoroethanol	0.45	69.21	0.70	30.73	7.84	0.06	0.53	1.90	0.93

Table 3.3.17. Summary of Time Correlated Single Photon Counting (TCSPC) fluorescent lifetimes (amplitude weighted) of **18** recorded at 540 nm.

Wavelength (nm)	Solvent	τ_1 (ns)	A_1 (%)	τ_2 (ns)	A_2 (%)	τ_3 (ns)	A_3 (%)	τ_f (ns) (Amplitude Weighted)	$1/\tau_f$	χ^2
570	Toluene	0.73	12.73	2.00	39.43	2.77	47.84	2.21	0.45	1.16
570	1,4-Dioxane	-	-	1.72	50.96	2.83	49.04	2.26	0.44	1.23
570	Chloroform	0.29	21.43	1.89	57.43	2.88	21.14	1.77	0.57	1.24
570	Acetonitrile	0.70	7.36	1.99	58.55	3.27	34.10	2.33	0.43	1.13
570	1-Octanol	0.40	30.21	1.66	55.54	2.51	14.25	1.40	0.72	0.98
570	1-Hexanol	0.32	47.68	1.75	50.81	3.73	1.51	1.10	0.91	1.16
570	1-Butanol	0.65	16.99	1.74	81.20	3.83	1.82	1.60	0.63	1.12
570	1-Pentanol	0.62	18.82	1.77	79.63	4.05	1.55	1.59	0.63	1.14
570	1-Propanol	1.09	15.22	1.71	73.10	2.68	11.69	1.73	0.58	1.06
570	Acetic acid	0.43	29.72	1.11	69.86	3.52	0.42	0.92	1.09	0.94
570	Methanol	0.37	19.41	1.49	37.95	2.38	42.64	1.65	0.61	1.14
570	2,2,2-Trifluoroethanol	0.39	59.55	0.67	40.38	5.81	0.07	0.51	1.97	1.15

Table 3.3.18. Summary of Time Correlated Single Photon Counting (TCSPC) fluorescent lifetimes (amplitude weighted) of **18** recorded at 570 nm.

3.3.7 400 nm average fluorescent lifetimes - Solvatochromic analysis.

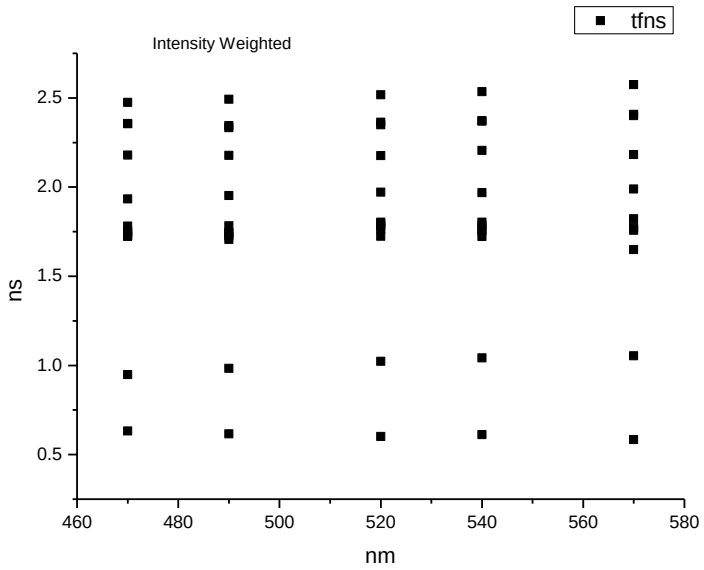

Figure 3.3.49. Intensity weighted average lifetime (τ_f) of **18** versus wavelength (nm).

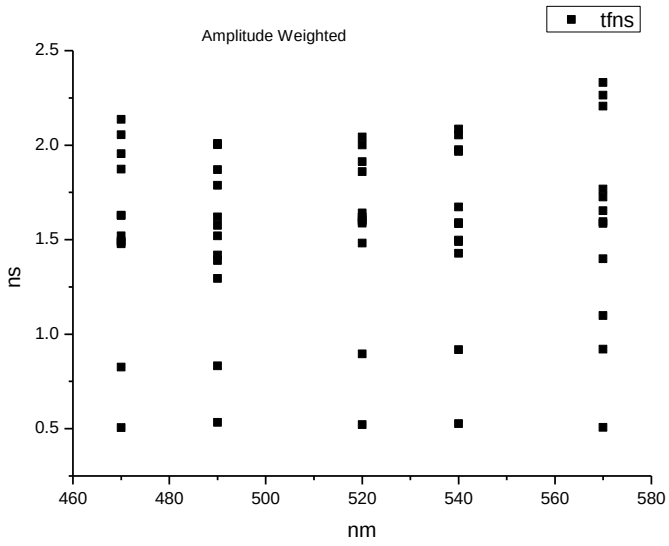

Figure 3.3.50. Amplitude weighted average lifetime (τ_f) of **18** versus wavelength (nm).

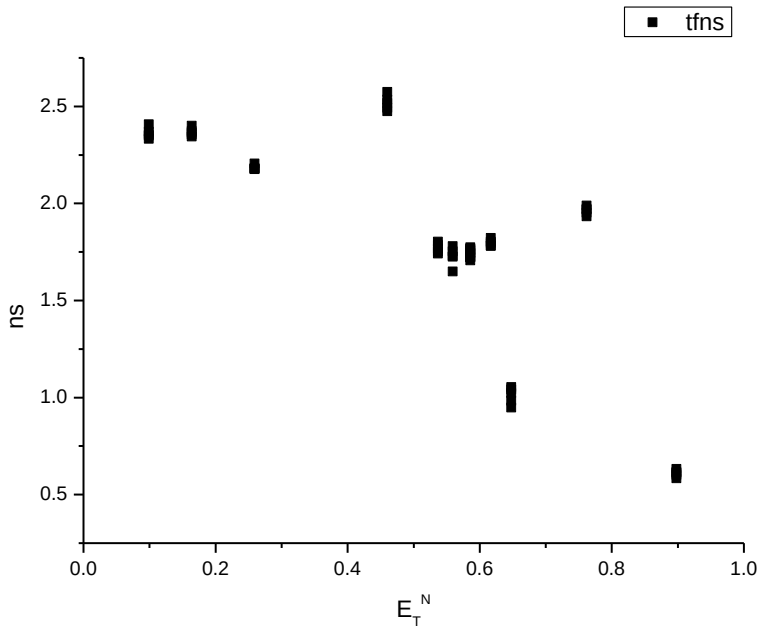

Figure 3.3.51. Intensity weighted average lifetime (τ_f) of **18** versus E_T^N.

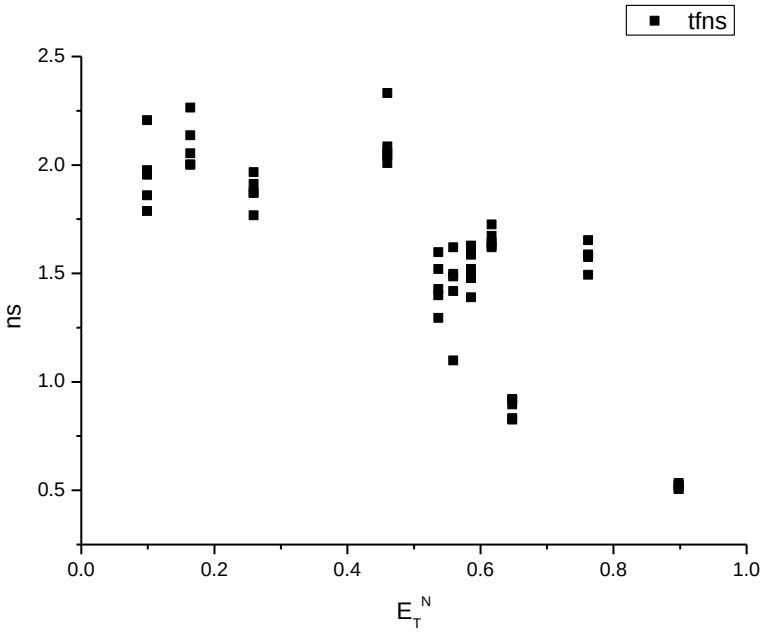

Figure 3.3.52. Amplitude weighted average lifetime (τ_f) of **18** versus E_T^N.

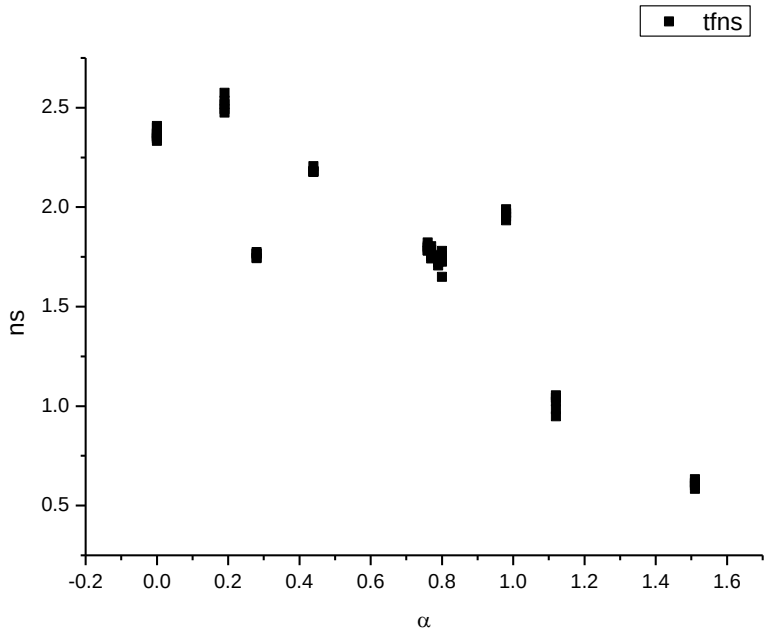

Figure 3.3.53. Intensity weighted average lifetime (τ_f) of **18** versus α.

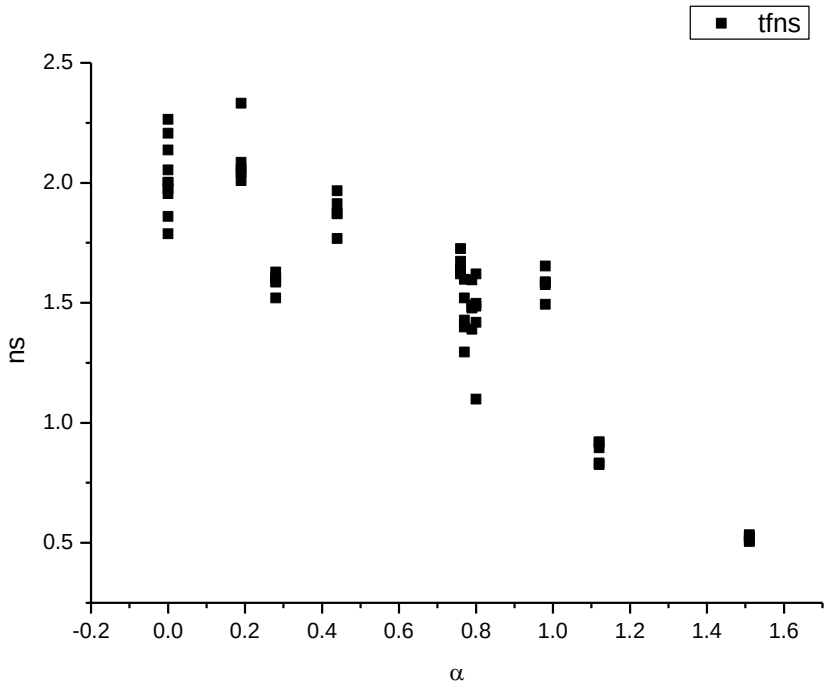

Figure 3.3.54. Amplitude weighted average lifetime (τ_f) of **18** versus α.

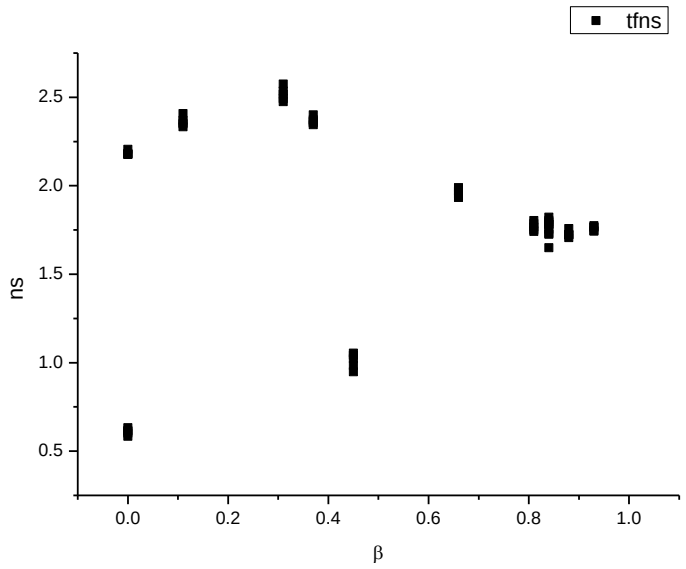

Figure 3.3.55. Intensity weighted average lifetime (τ_f) of **18** versus β.

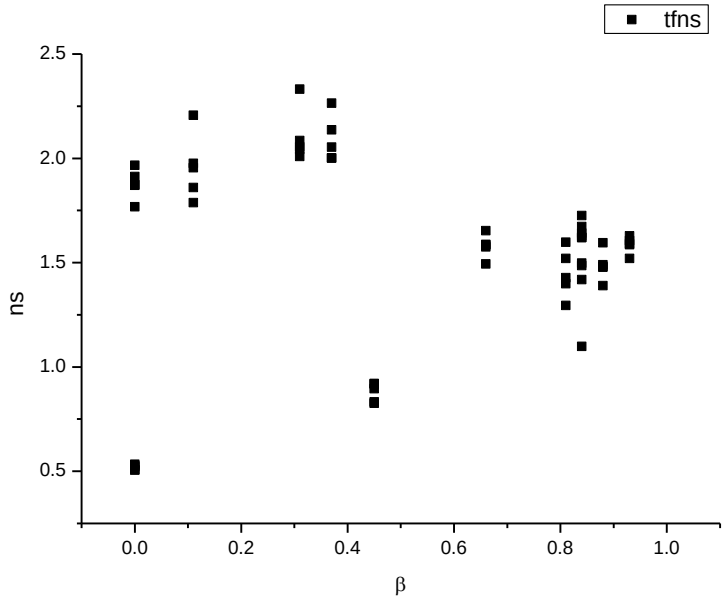

Figure 3.3.56. Amplitude weighted average lifetime (τ_f) of **18** versus β.

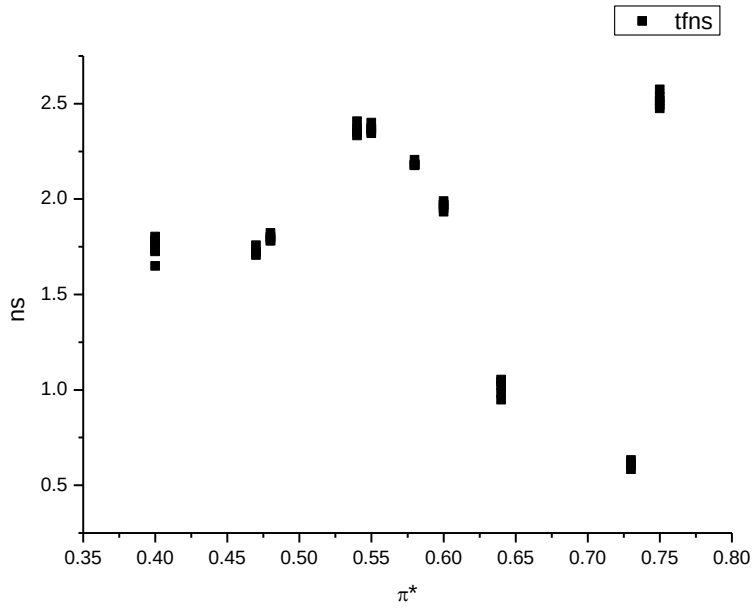

Figure 3.3.57. Intensity weighted average lifetime (τ_f) of **18** versus π*.

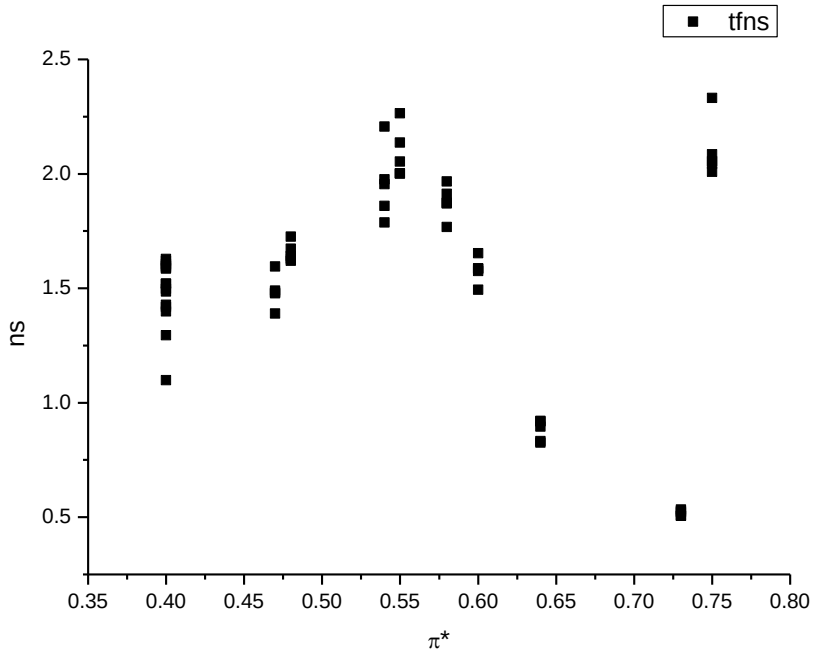

Figure 3.3.58. Amplitude weighted average lifetime (τ_f) of **18** versus π*.

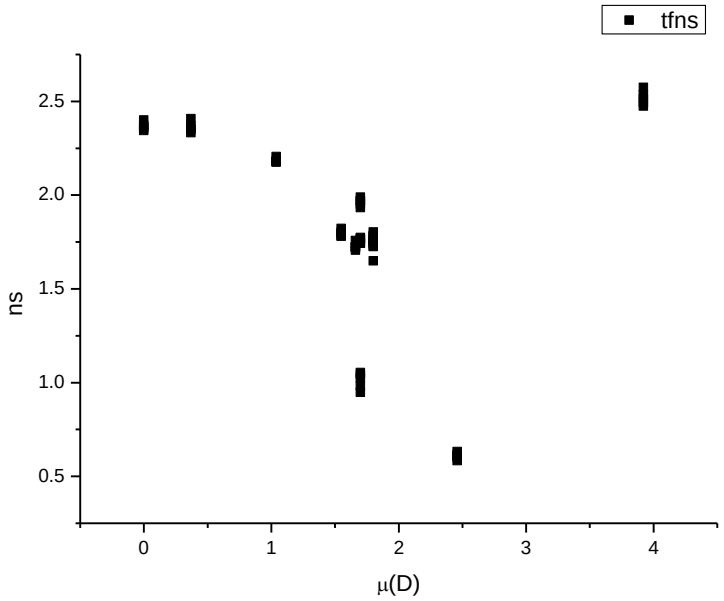

Figure 3.3.59. Intensity weighted average lifetime (τ_f) of **18** versus μ(D).

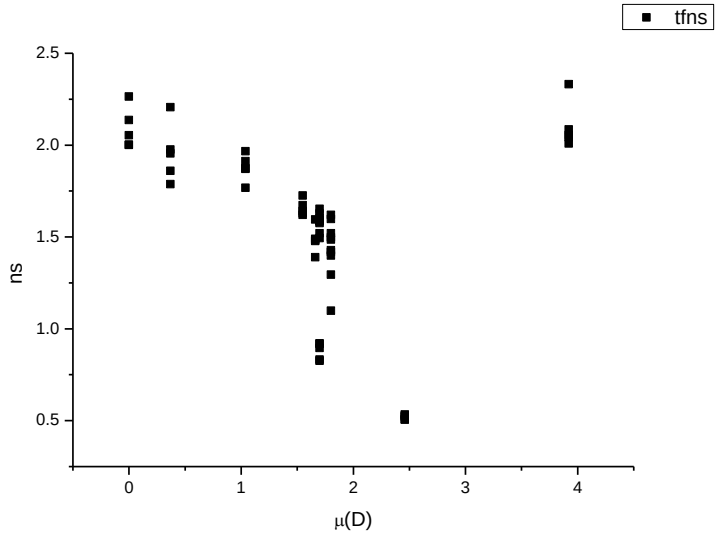

Figure 3.3.60. Amplitude weighted average lifetime (τ_f) of **18** versus μ(D).

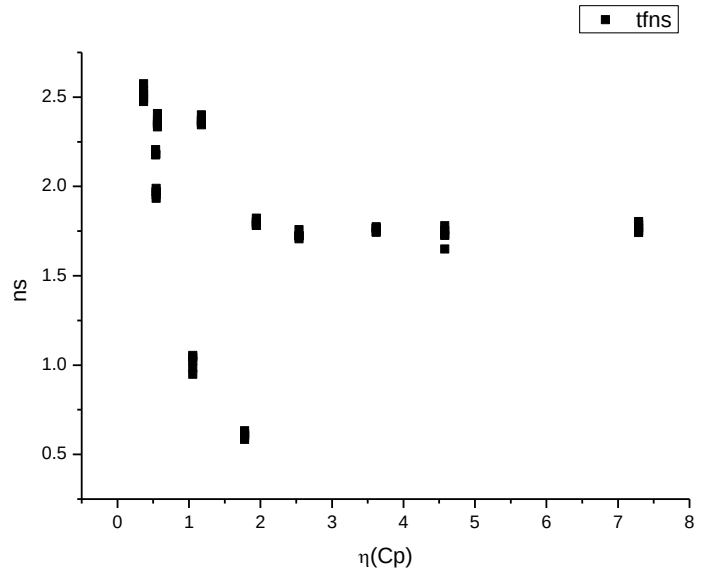

Figure 3.3.61. Intensity weighted average lifetime (τ_f) of **18** versus η(Cp).

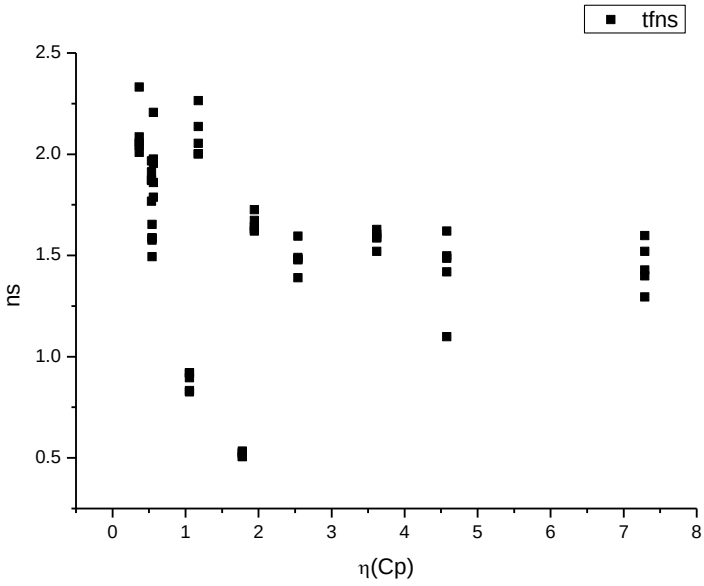

Figure 3.3.62. Amplitude weighted average lifetime (τ_f) of **18** versus η(Cp).

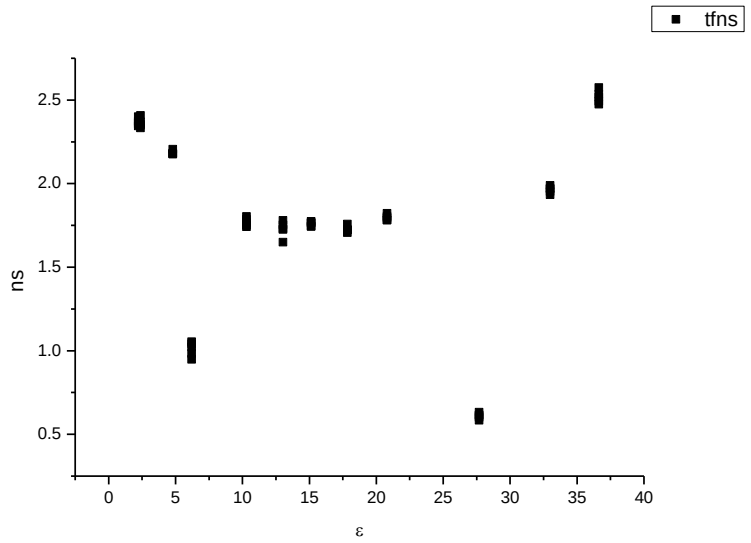

Figure 3.3.63. Intensity weighted average lifetime (τ_f) of **18** versus ε.

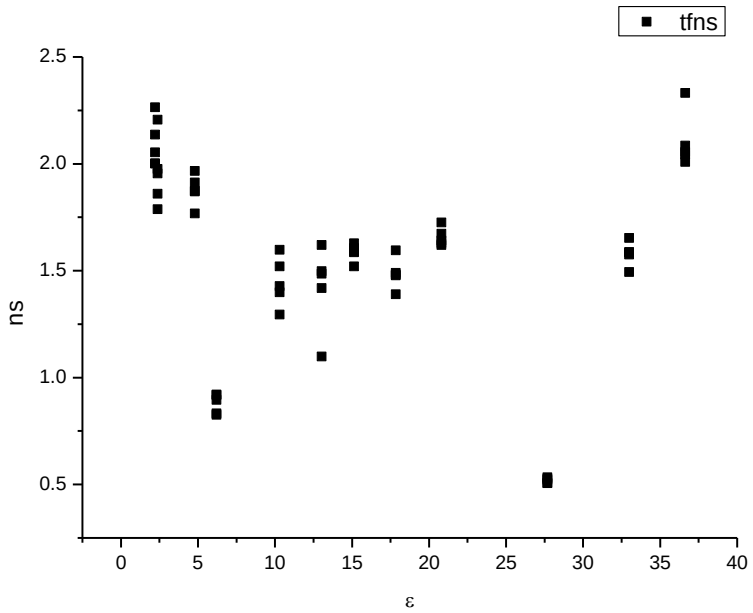

Figure 3.3.64. Amplitude weighted average lifetime (τ_f) of **18** versus ε.

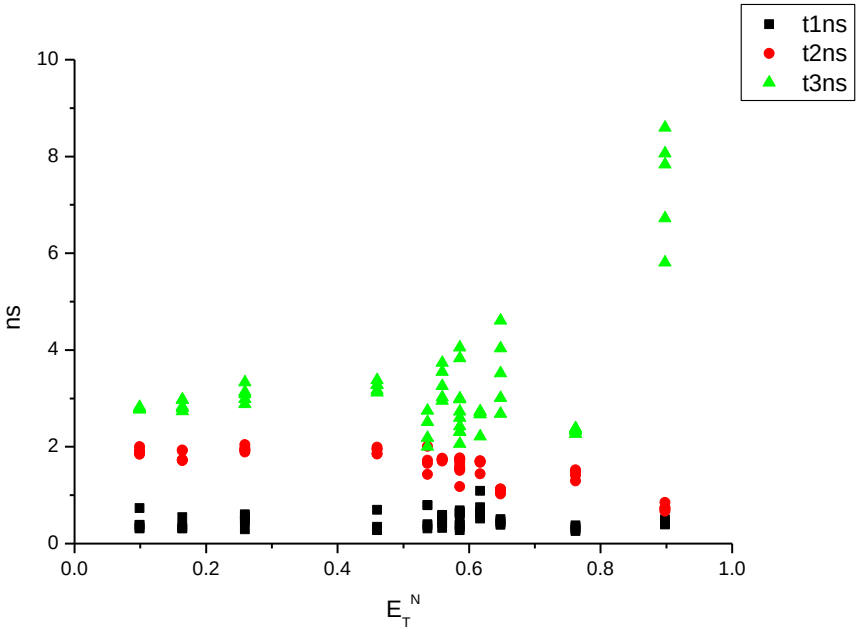

Figure 3.3.65. Intensity weighted components of TCSPC lifetime decay of **18** (470 nm to 570 nm) versus E_T^N.

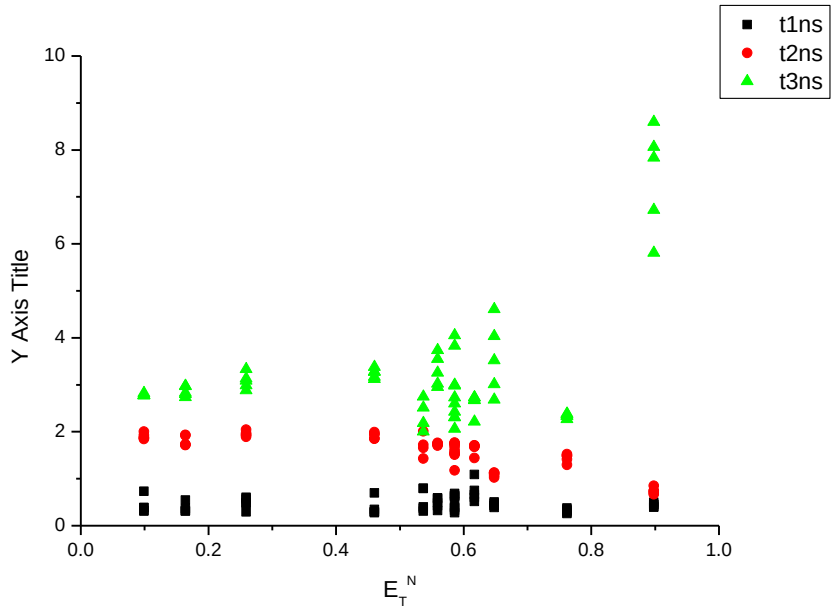

Figure 3.3.66. Amplitude weighted components of TCSPC lifetime decay of **18** (470 nm to 570 nm) versus E_T^N.

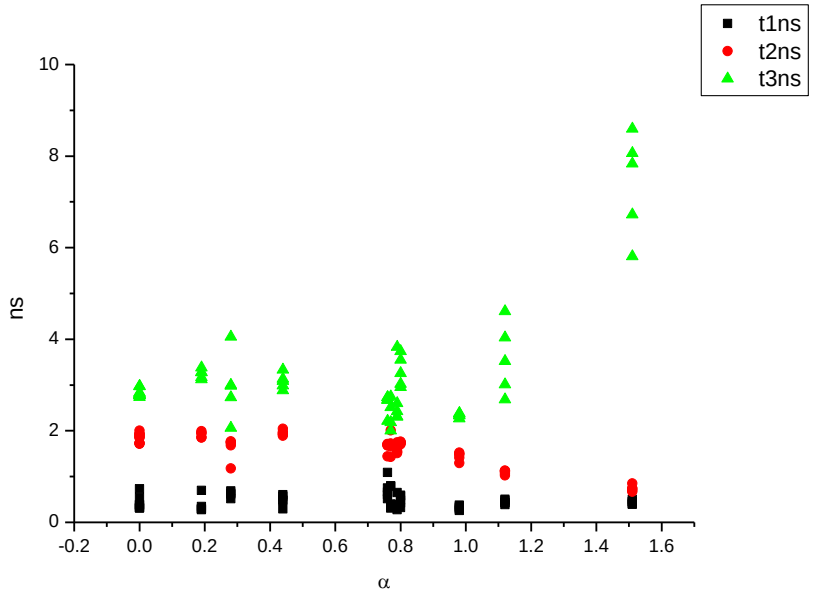

Figure 3.3.67. Intensity weighted components of TCSPC lifetime decay of **18** (470 nm to 570 nm) versus α.

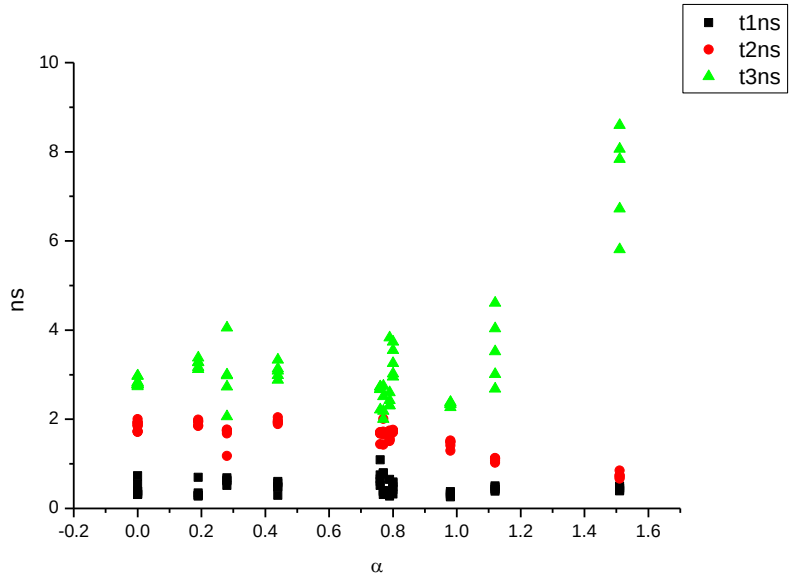

Figure 3.3.68. Amplitude weighted components of TCSPC lifetime decay of **18** (470 nm to 570 nm) versus α.

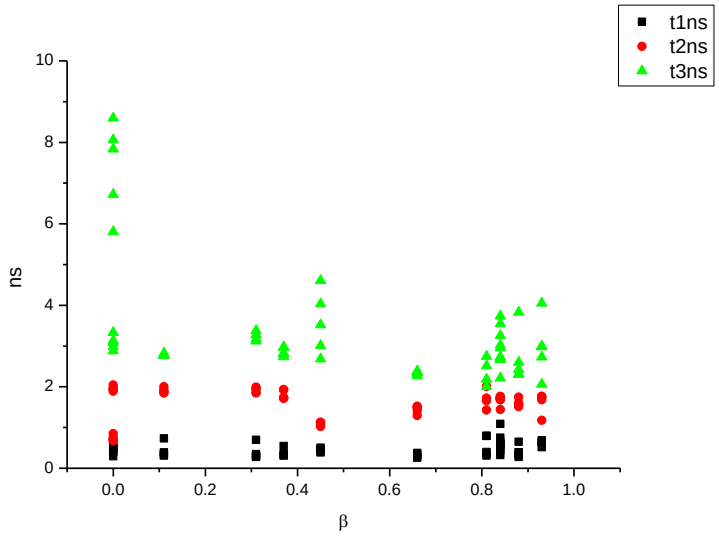

Figure 3.3.69. Intensity weighted components of TCSPC lifetime decay of **18** (470 nm to 570 nm) versus β.

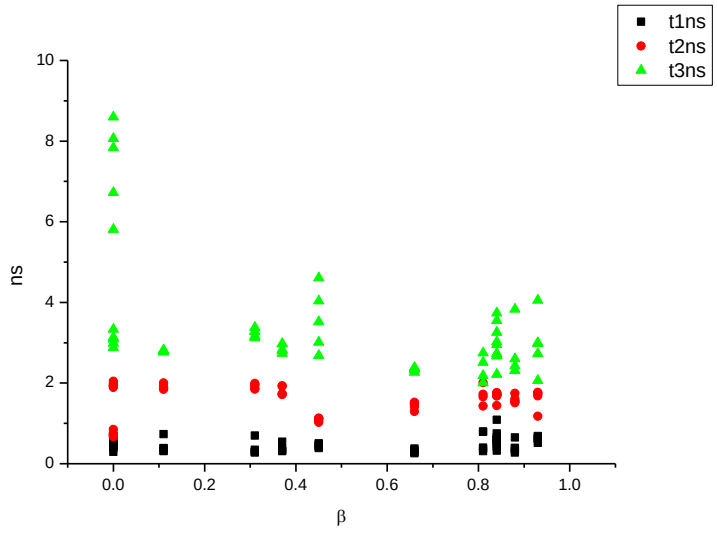

Figure 3.3.70. Amplitude weighted components of TCSPC lifetime decay of **18** (470 nm to 570 nm) versus β.

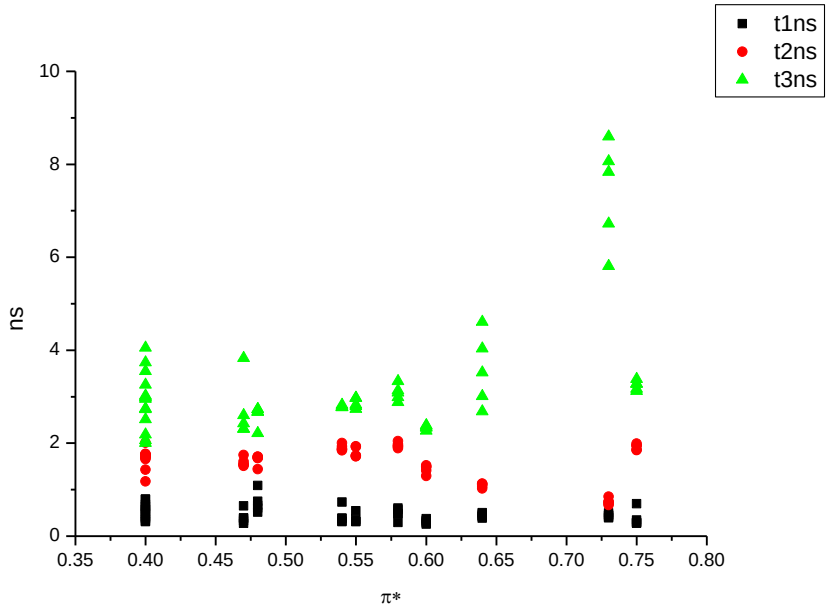

Figure 3.3.71. Intensity weighted components of TCSPC lifetime decay of **18** (470 nm to 570 nm) versus π*.

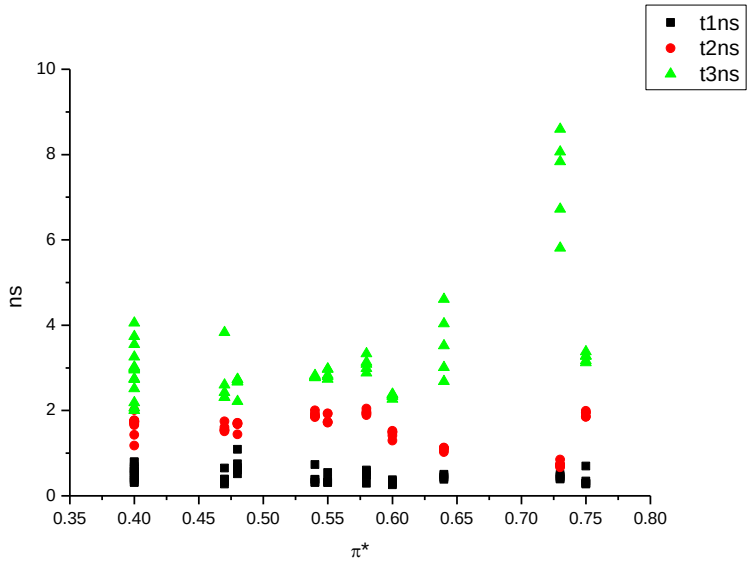

Figure 3.3.72. Amplitude weighted components of TCSPC lifetime decay of **18** (470 nm to 570 nm) versus π*.

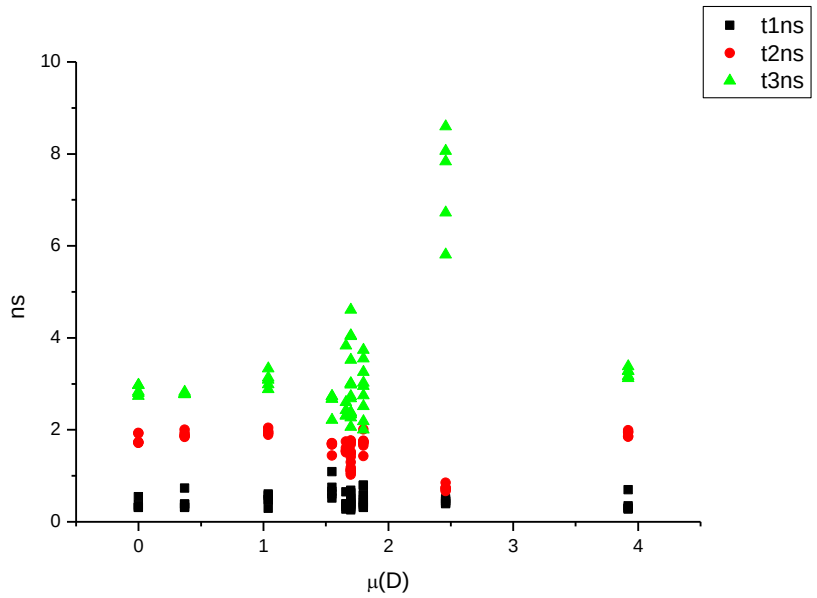

Figure 3.3.73. Intensity weighted components of TCSPC lifetime decay of **18** (470 nm to 570 nm) versus μ(D).

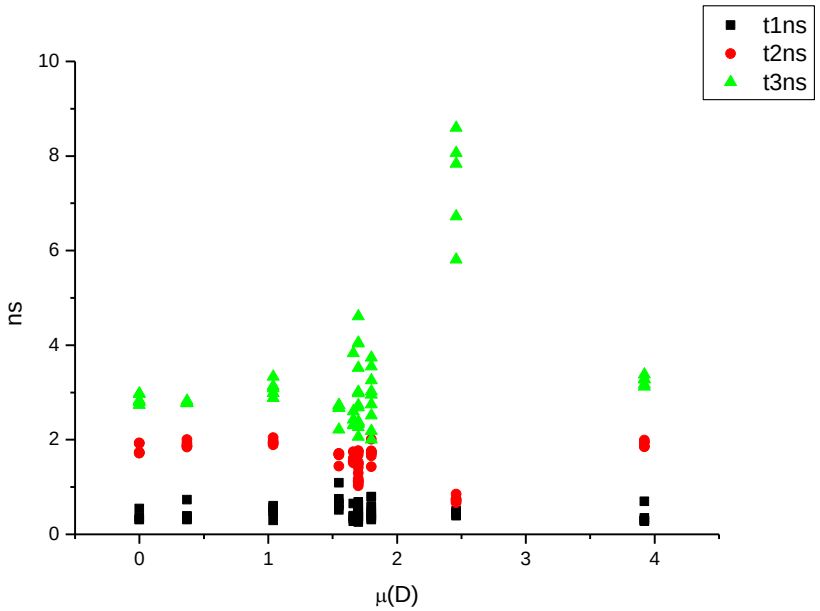

Figure 3.3.74. Amplitude weighted components of TCSPC lifetime decay of **18** (470 nm to 570 nm) versus μ(D).

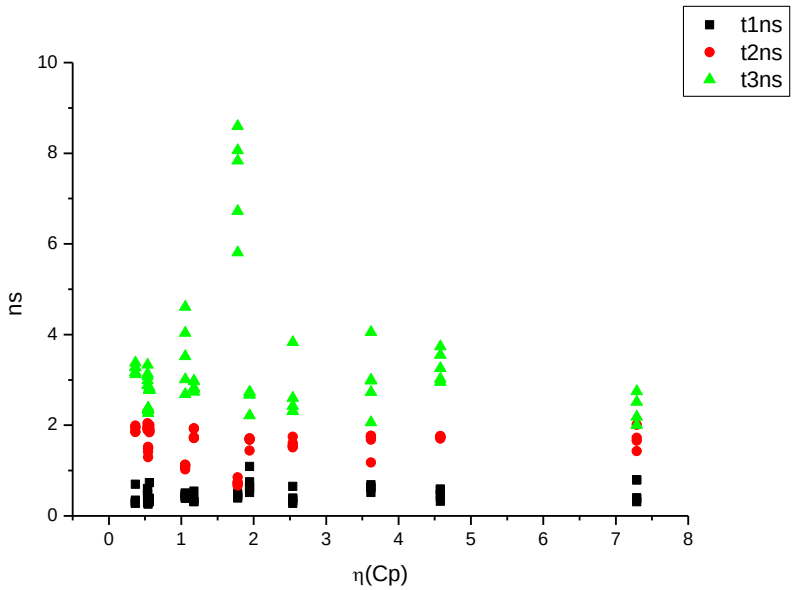

Figure 3.3.75. Intensity weighted components of TCSPC lifetime decay of **18** (470 nm to 570 nm) versus η(Cp).

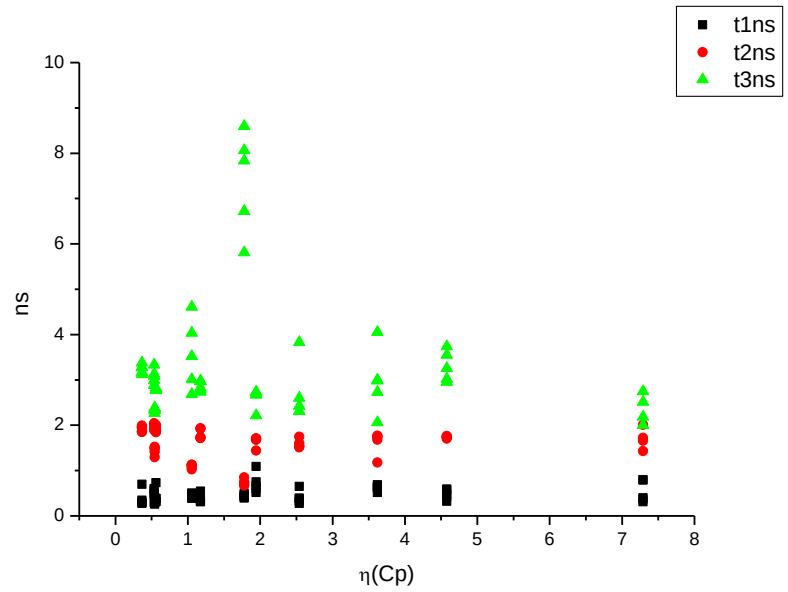

Figure 3.3.76. Amplitude weighted components of TCSPC lifetime decay of **18** (470 nm to 570 nm) versus η(Cp).

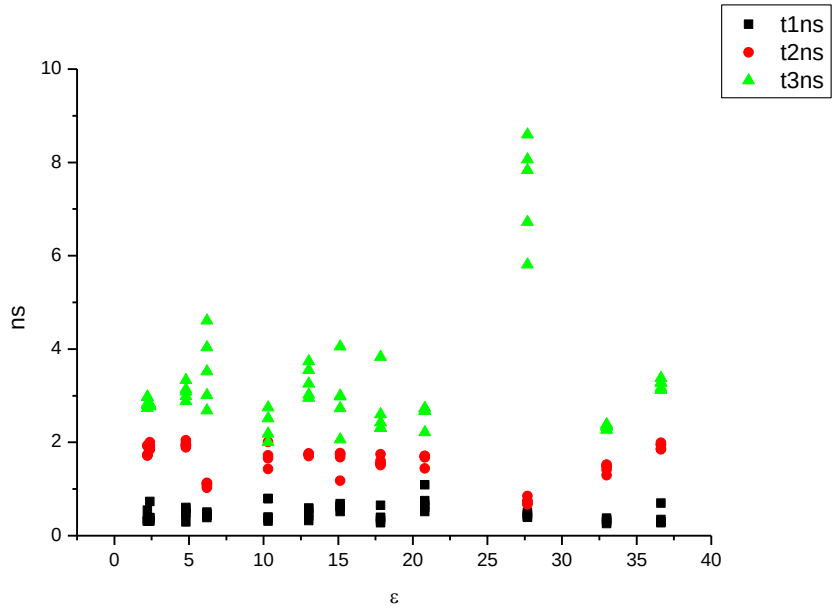

Figure 3.3.77. Intensity weighted components of TCSPC lifetime decay of **18** (470 nm to 570 nm) versus ε.

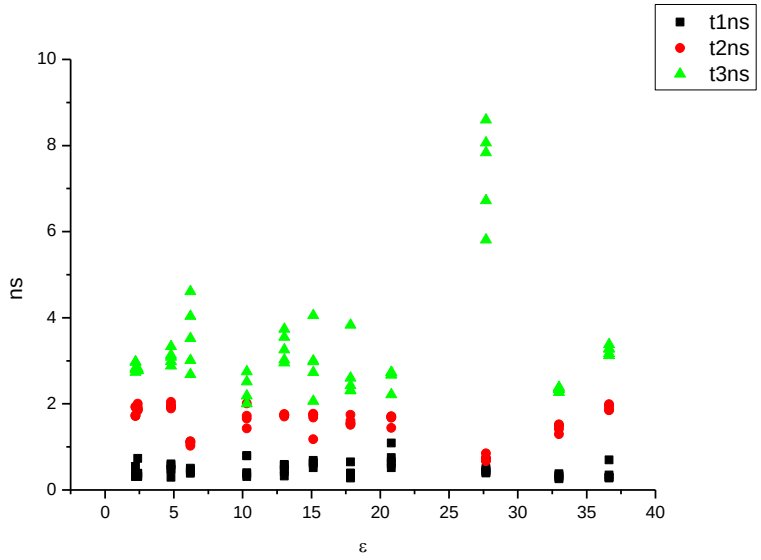

Figure 3.3.78. Amplitude weighted components of TCSPC lifetime decay of **18** (470 nm to 570 nm) versus ε.

3.3.7.1 470 nm Lifetime – Solvatochromic analysis.

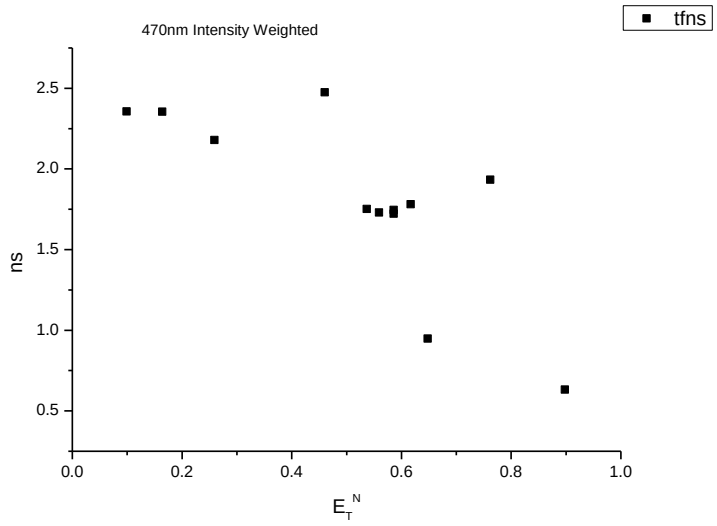

Figure 3.3.79. Intensity weighted average lifetime (τ_f) of **18** at 470 nm versus E_T^N.

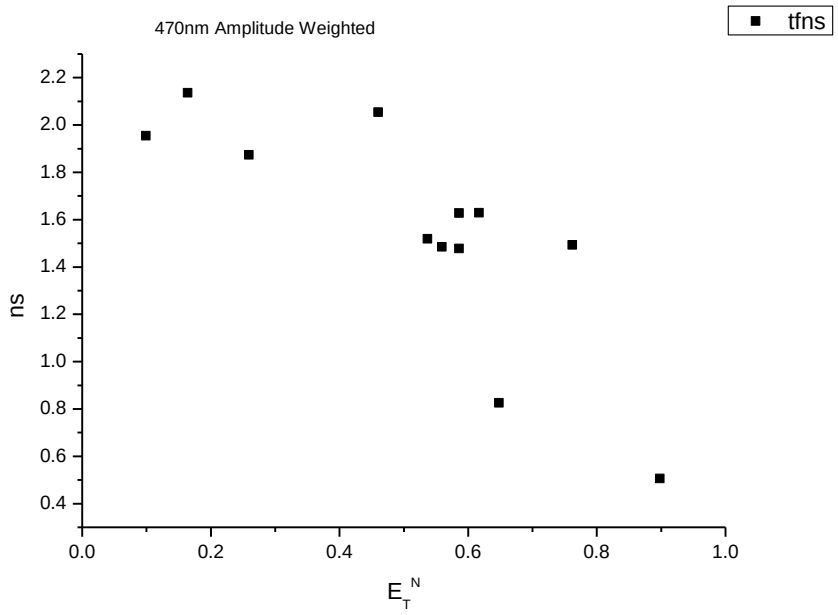

Figure 3.3.80. Amplitude weighted average lifetime (τ_f) of **18** at 470 nm versus E_T^N.

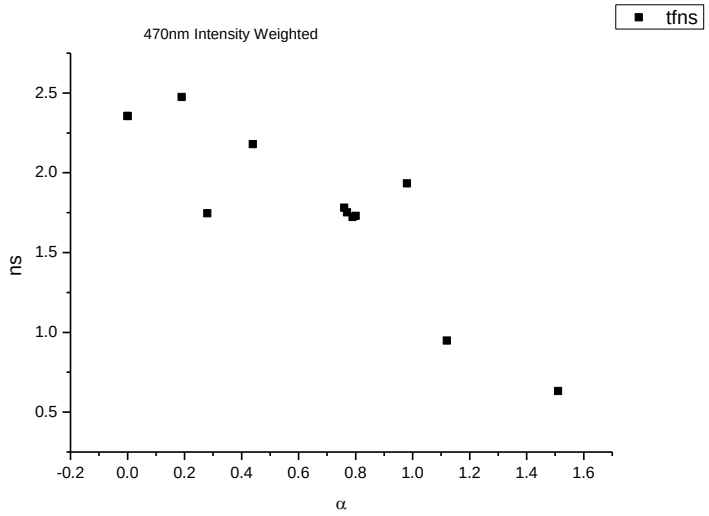

Figure 3.3.81. Intensity weighted average lifetime (τ_f) of **18** at 470 nm versus α.

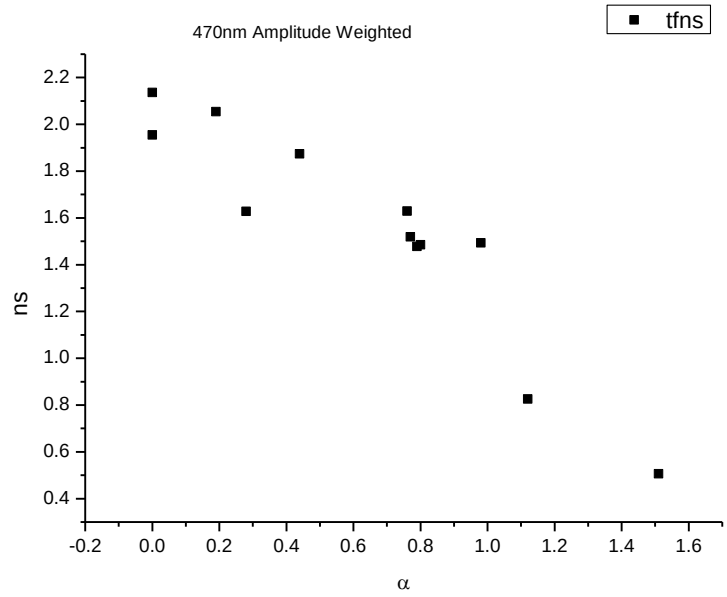

Figure 3.3.82. Amplitude weighted average lifetime (τ_f) of **18** at 470 nm versus α.

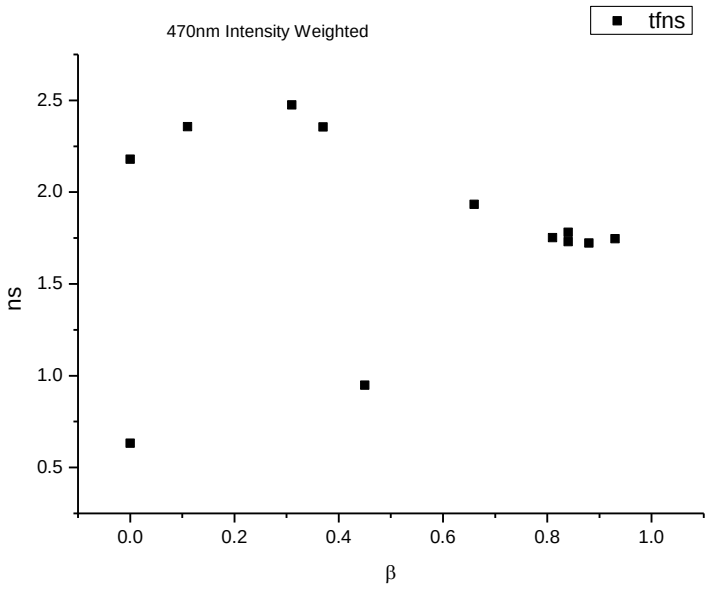

Figure 3.3.83. Intensity weighted average lifetime (τ_f) of **18** at 470 nm versus β.

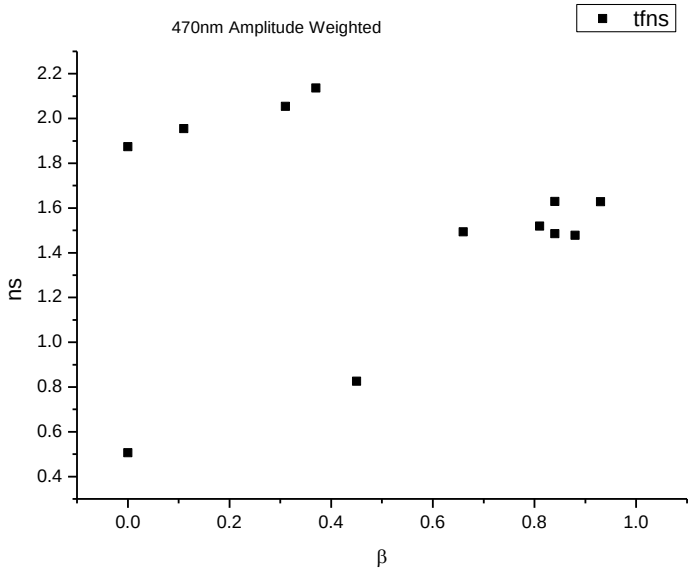

Figure 3.3.84. Amplitude weighted average lifetime (τ_f) of **18** at 470 nm versus β.

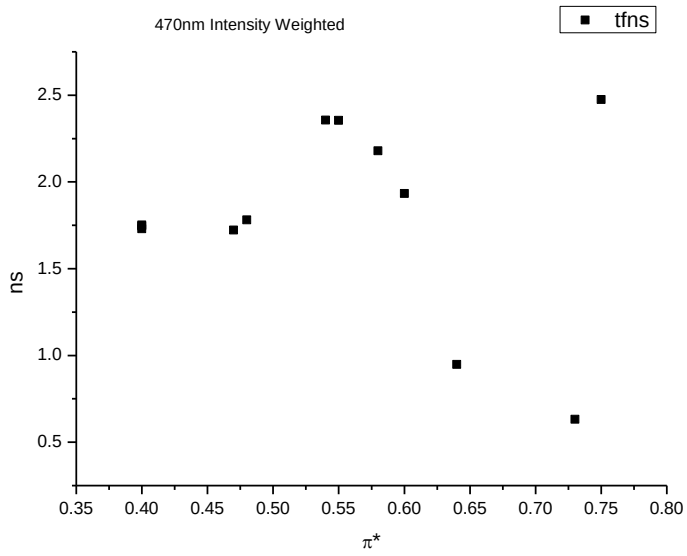

Figure 3.3.85. Intensity weighted average lifetime (τ_f) of **18** at 470 nm versus π*.

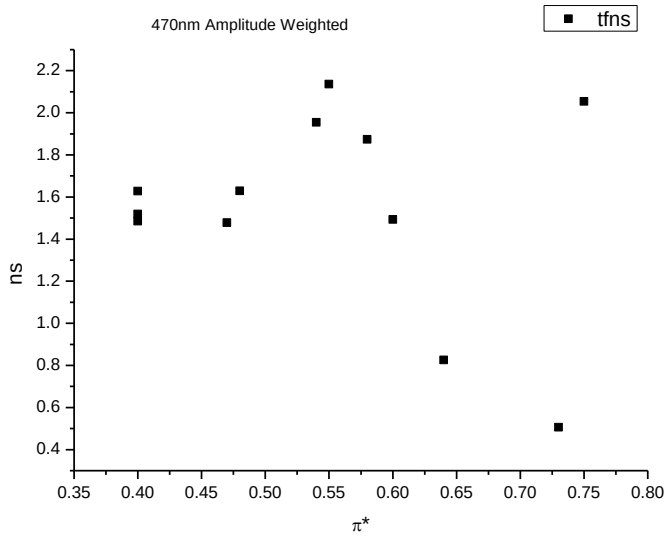

Figure 3.3.86. Amplitude weighted average lifetime (τ_f) of **18** at 470 nm versus π*.

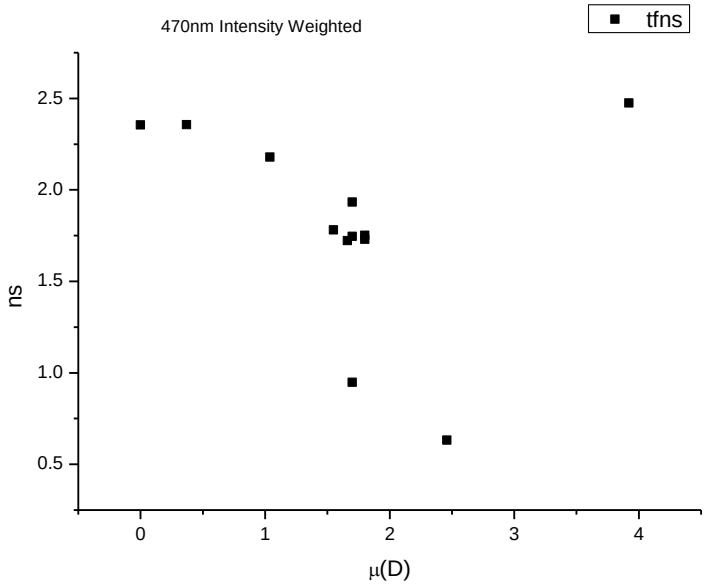

Figure 3.3.87. Intensity weighted average lifetime (τ_f) of **18** at 470 nm versus μ(D).

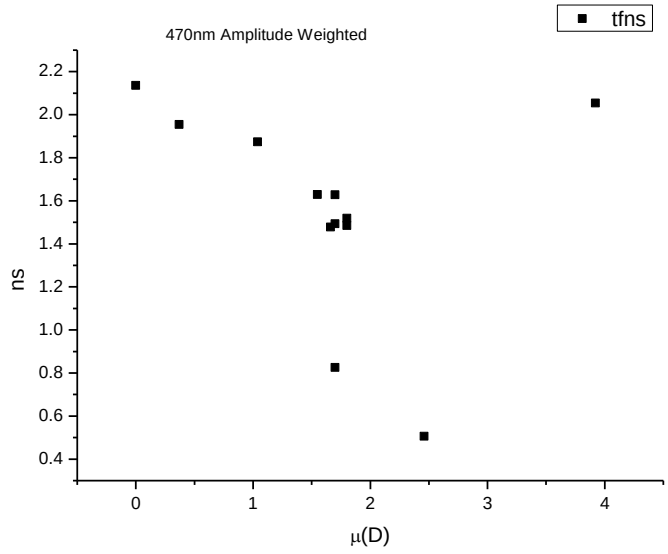

Figure 3.3.88. Amplitude weighted average lifetime (τ_f) of **18** at 470 nm versus μ(D).

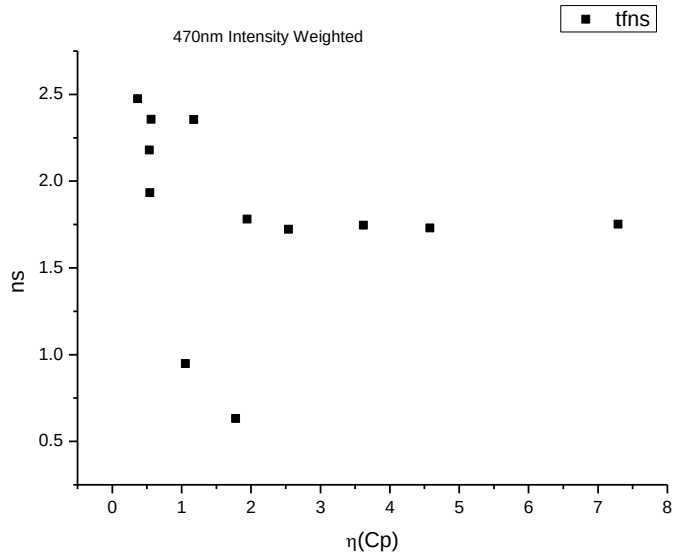

Figure 3.3.89. Intensity weighted average lifetime (τ_f) of **18** at 470 nm versus η(Cp).

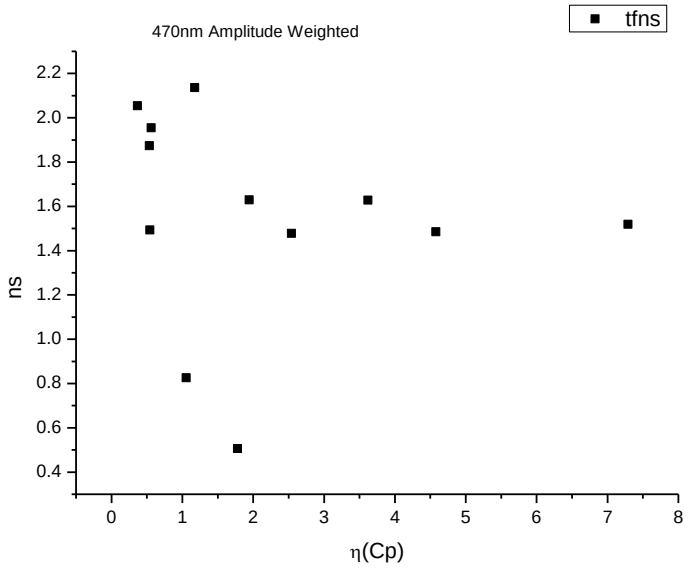

Figure 3.3.90. Amplitude weighted average lifetime (τ_f) of **18** at 470 nm versus η(Cp).

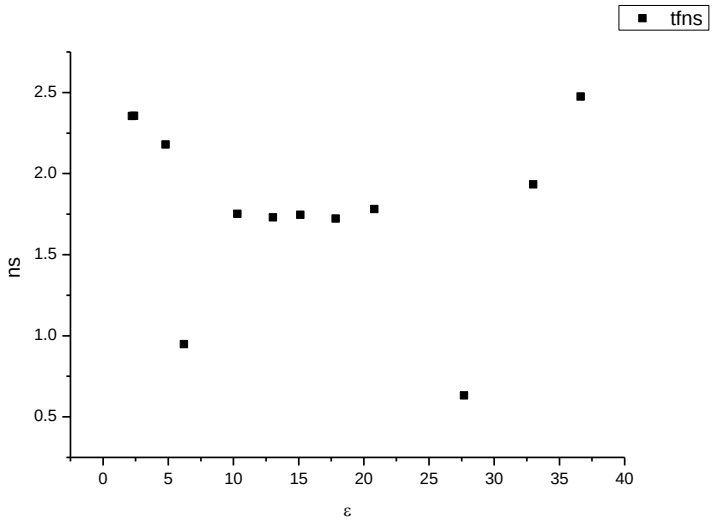

Figure 3.3.91. Intensity weighted average lifetime (τ_f) of **18** at 470 nm versus ε.

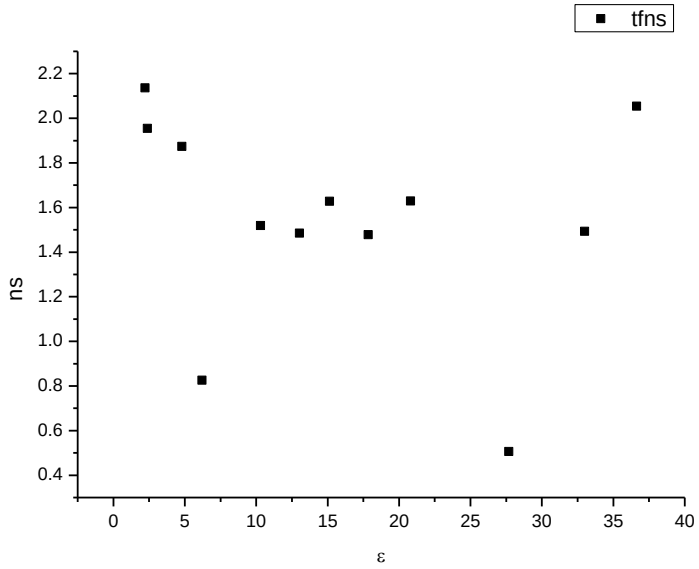

Figure 3.3.92. Amplitude weighted average lifetime (τ_f) of **18** at 470 nm versus ε.

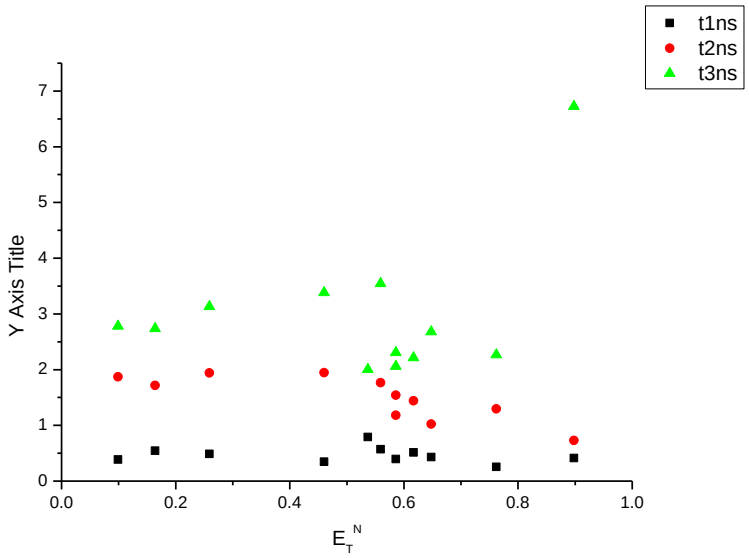

Figure 3.3.91. Intensity weighted components of TCSPC lifetime decay of **18** (470 nm) versus E_T^N.

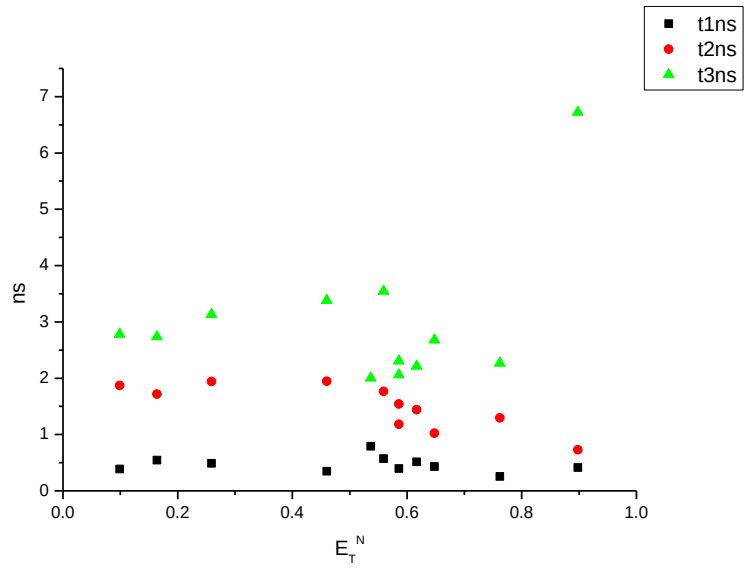

Figure 3.3.92. Amplitude weighted components of TCSPC lifetime decay of **18** (470 nm) versus E_T^N.

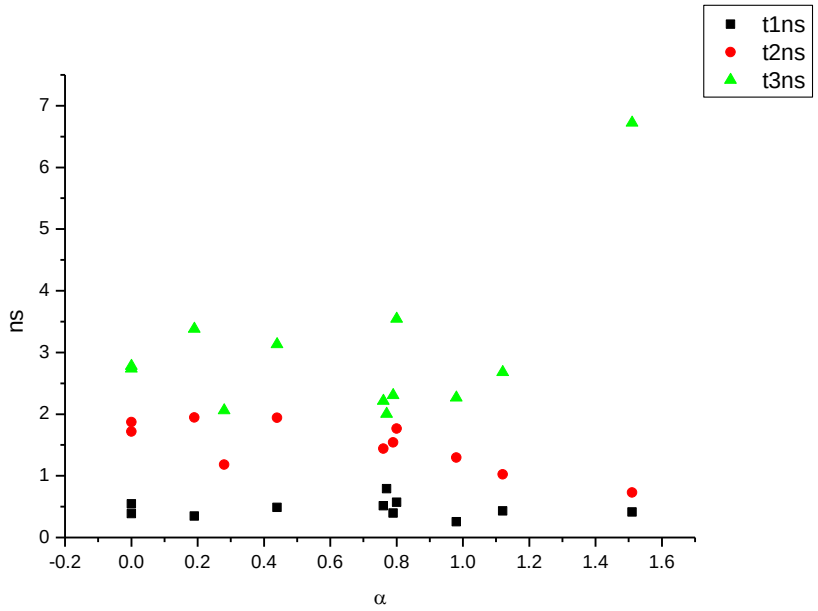

Figure 3.3.93. Intensity weighted components of TCSPC lifetime decay of **18** (470 nm) versus α.

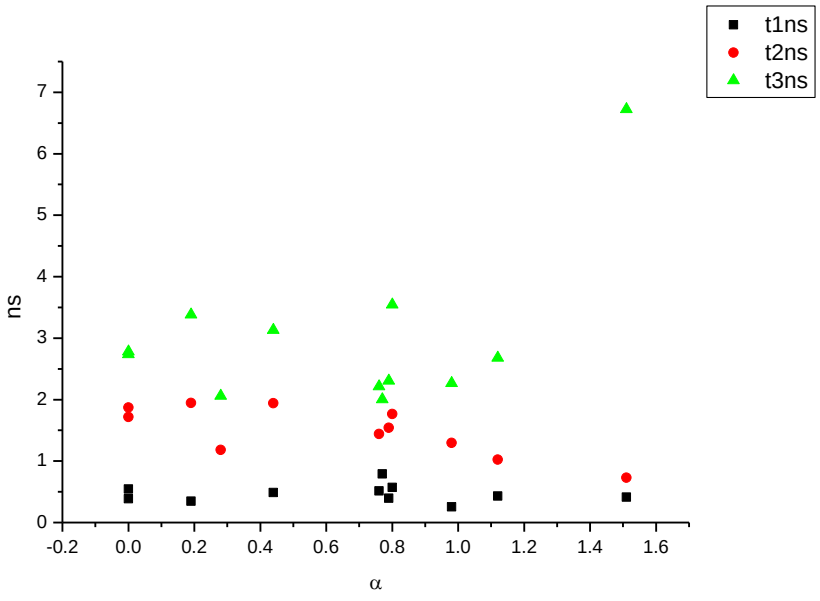

Figure 3.3.94. Amplitude weighted components of TCSPC lifetime decay of **18** (470 nm) versus α.

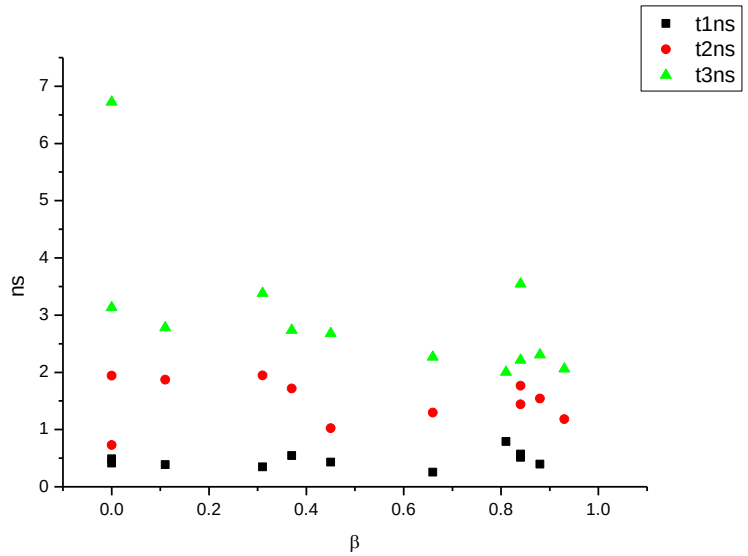

Figure 3.3.95. Intensity weighted components of TCSPC lifetime decay of **18** (470 nm) versus β.

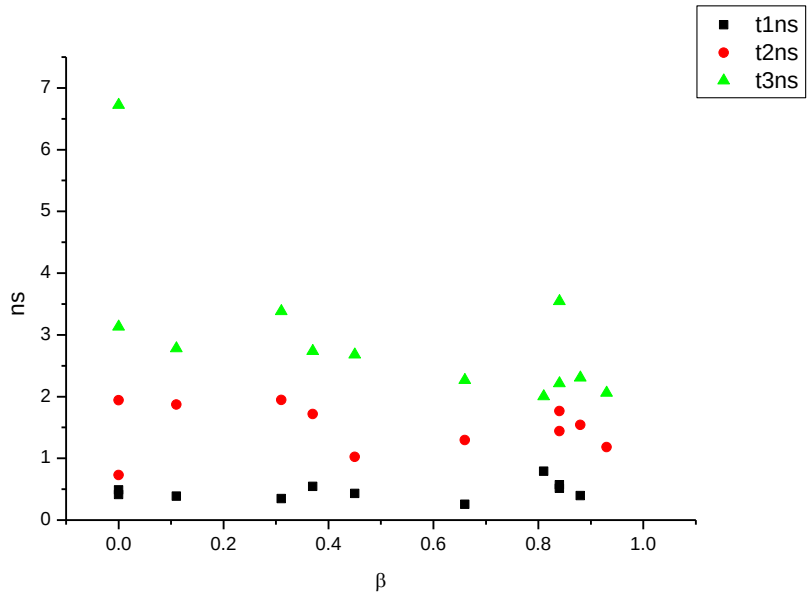

Figure 3.3.96. Amplitude weighted components of TCSPC lifetime decay of **18** (470 nm) versus β.

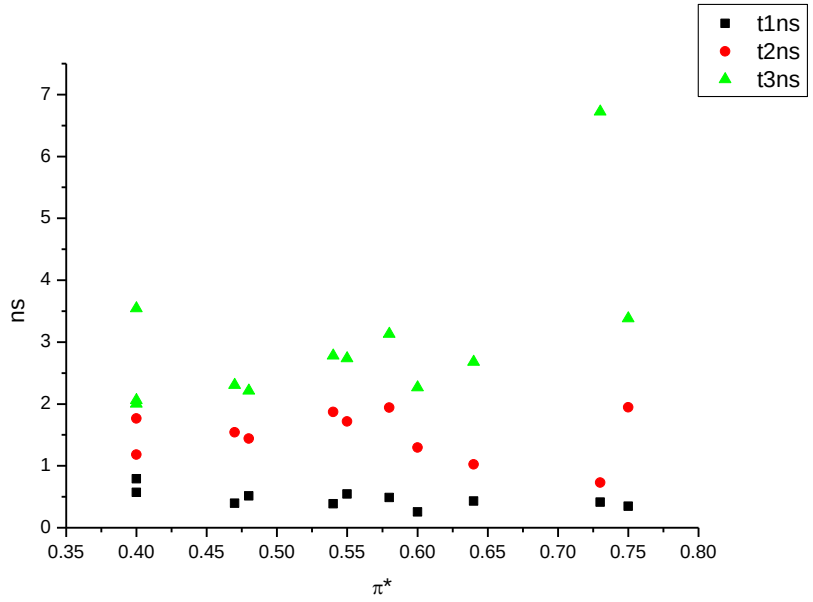

Figure 3.3.97. Intensity weighted components of TCSPC lifetime decay of **18** (470 nm) versus π*.

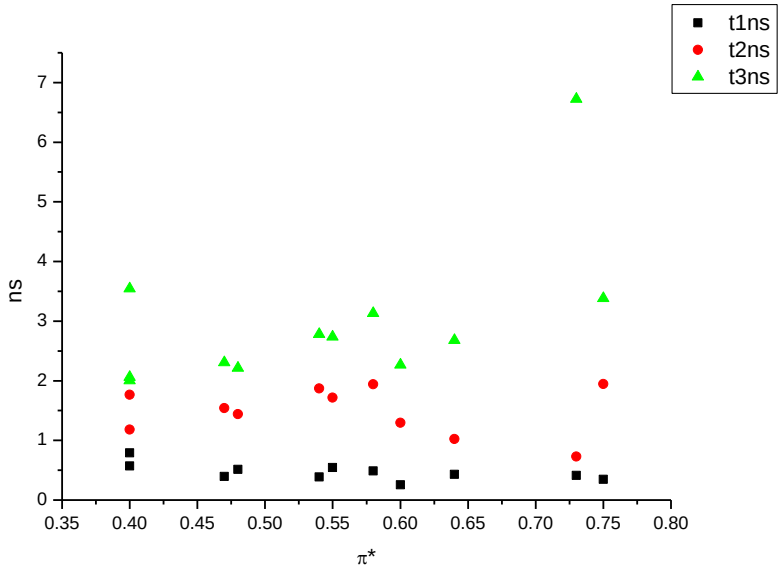

Figure 3.3.98. Amplitude weighted components of TCSPC lifetime decay of **18** (470 nm) versus π*.

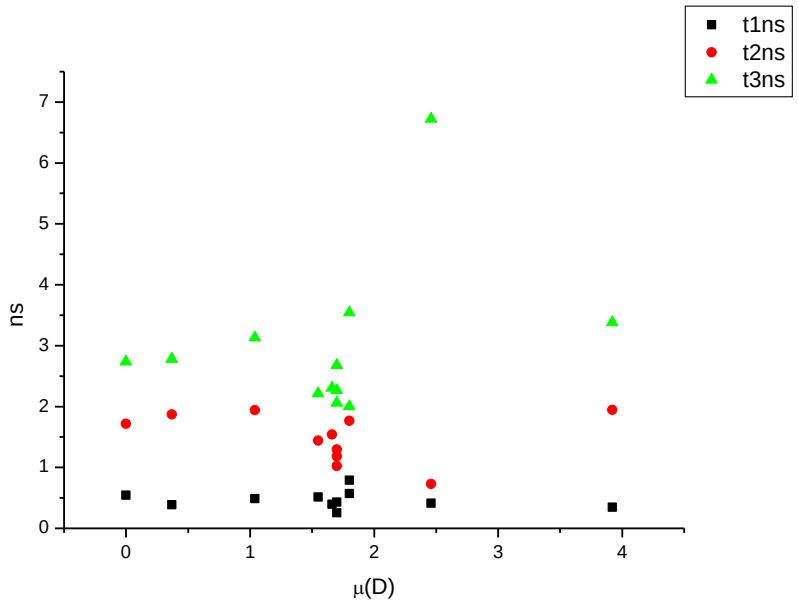

Figure 3.3.99. Intensity weighted components of TCSPC lifetime decay of **18** (470 nm) versus μ(D).

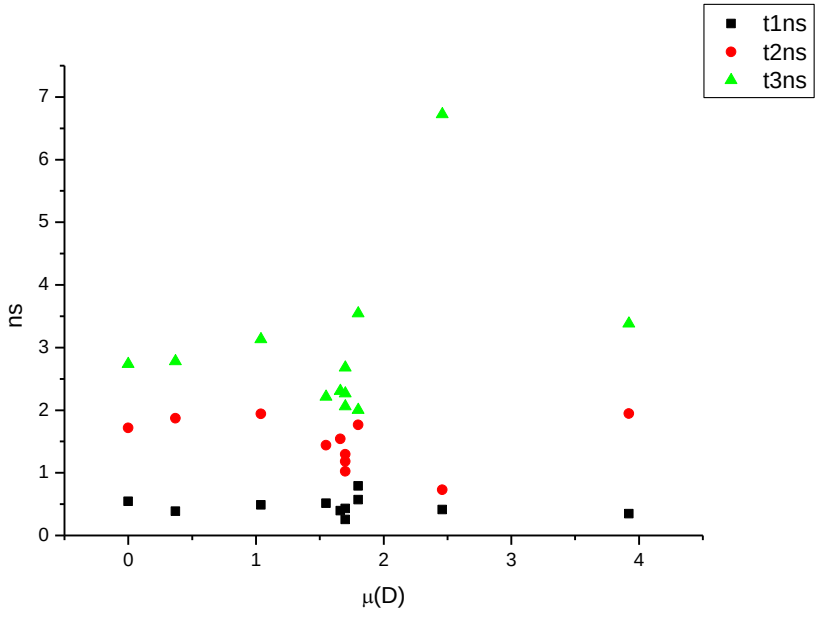

Figure 3.3.100. Amplitude weighted components of TCSPC lifetime decay of **18** (470 nm) versus μ(D).

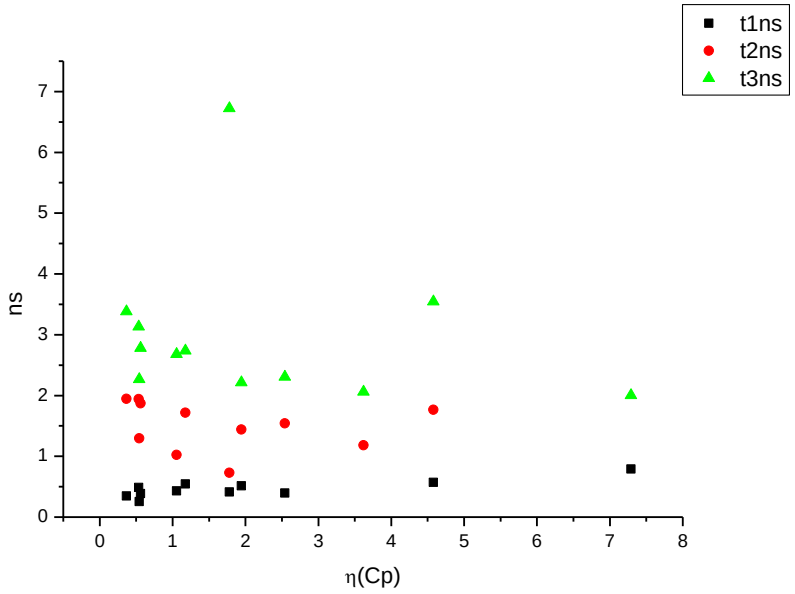

Figure 3.3.101. Intensity weighted components of TCSPC lifetime decay of **18** (470 nm) versus η(Cp).

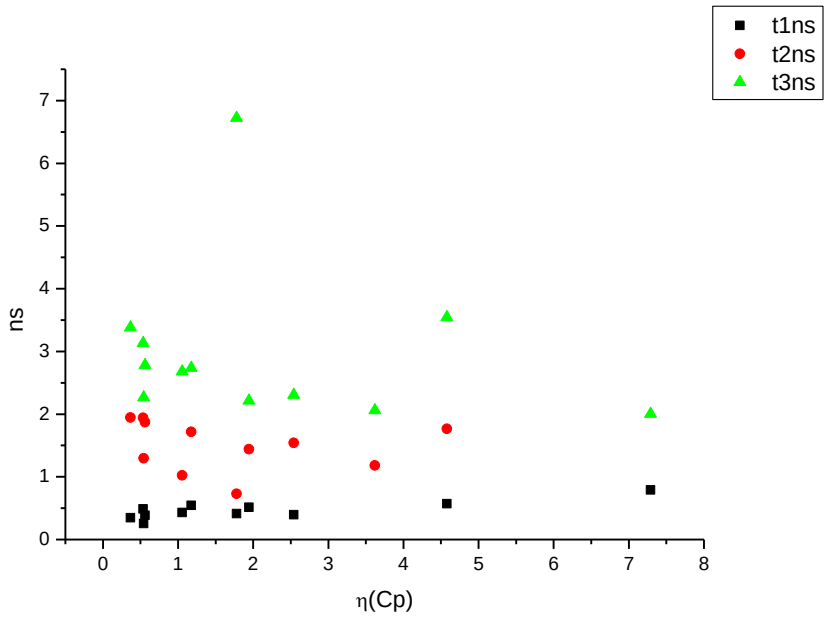

Figure 3.3.102. Amplitude weighted components of TCSPC lifetime decay of **18** (470 nm) versus η(Cp).

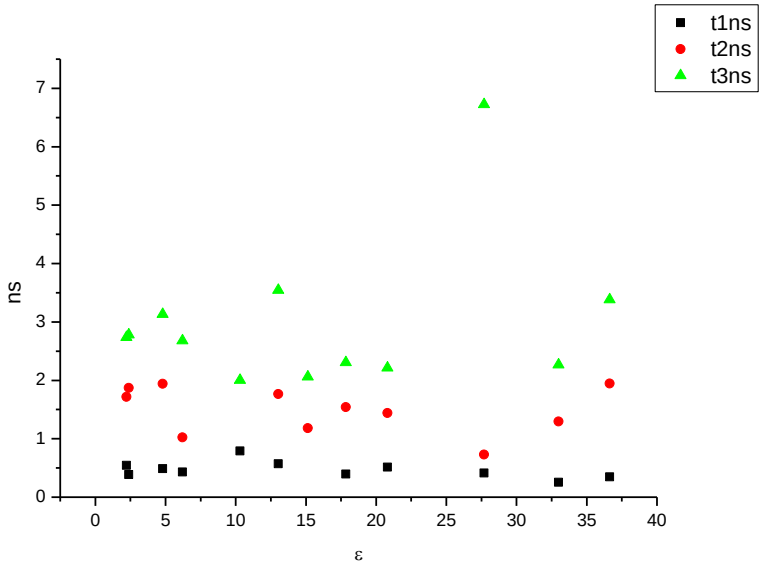

Figure 3.3.103. Intensity weighted components of TCSPC lifetime decay of **18** (470 nm) versus ε.

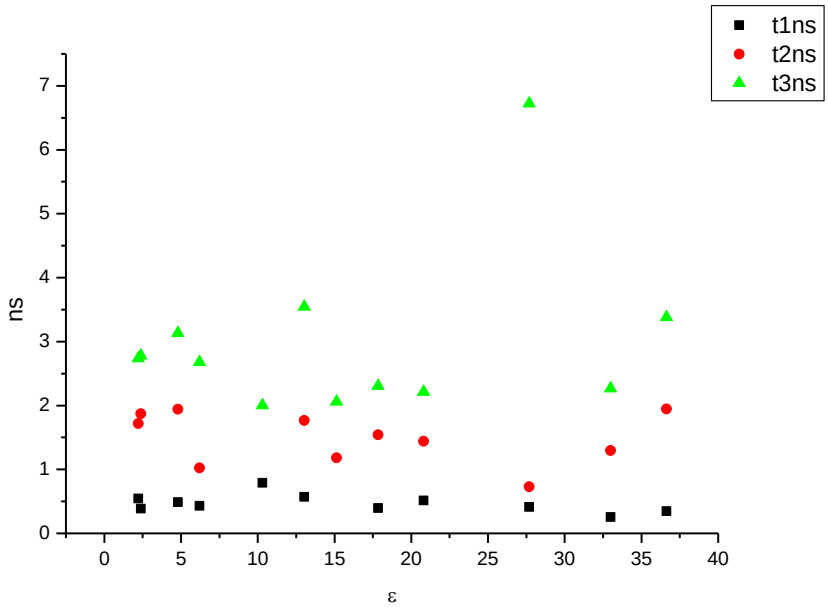

Figure 3.3.104. Amplitude weighted components of TCSPC lifetime decay of **18** (470 nm) versus ε.

3.3.7.2 570 nm Lifetime – Solvatochromic analysis.

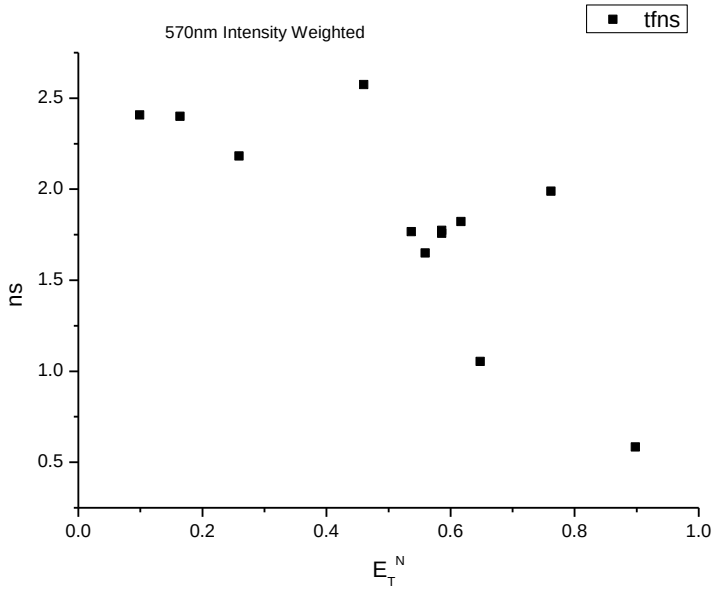

Figure 3.3.105. Intensity weighted average lifetime (τ_f) of **18** at 570 nm versus E_T^N.

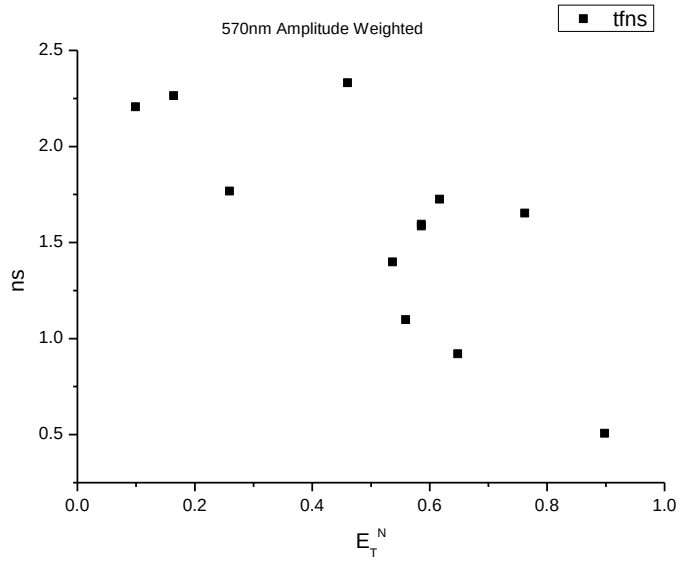

Figure 3.3.106. Amplitude weighted average lifetime (τ_f) of **18** at 570 nm versus E_T^N.

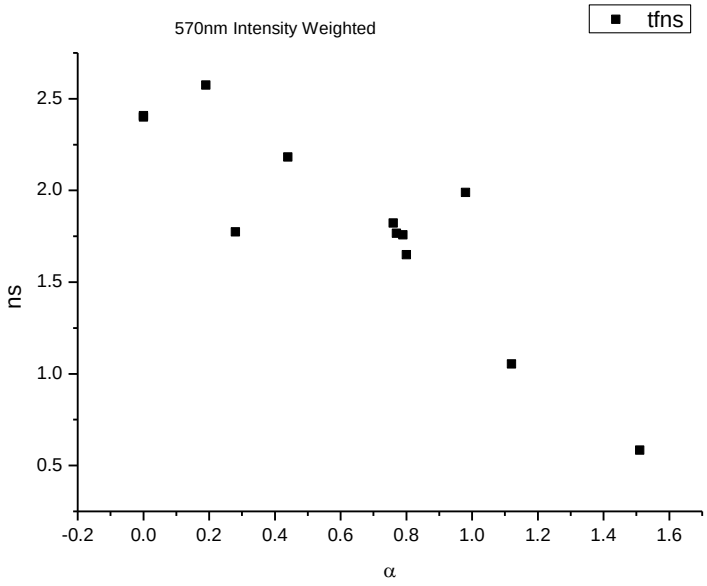

Figure 3.3.107. Intensity weighted average lifetime (τ_f) of **18** at 570 nm versus α.

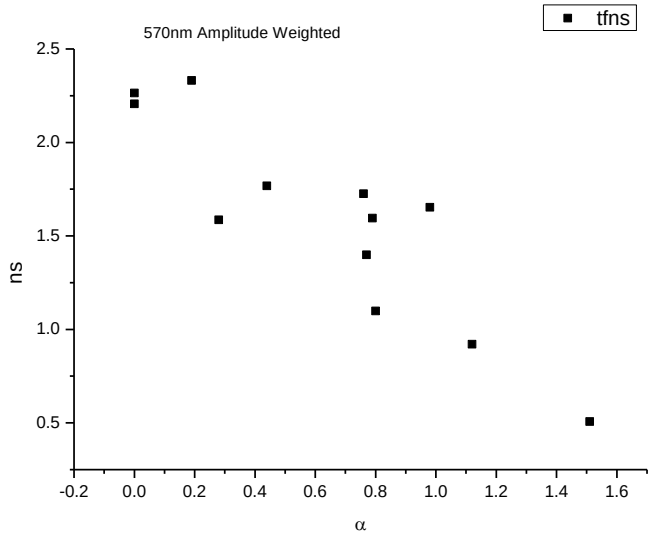

Figure 3.3.108. Amplitude weighted average lifetime (τ_f) of **18** at 570 nm versus α.

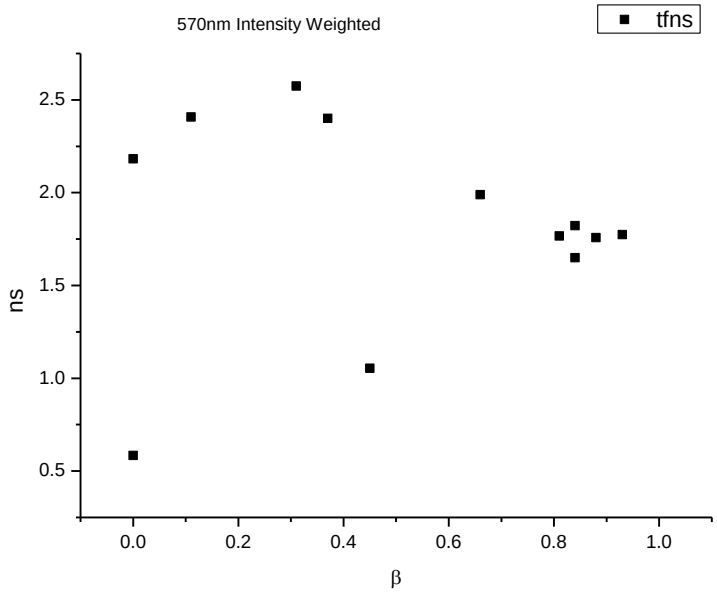

Figure 3.3.109. Intensity weighted average lifetime (τ_f) of **18** at 570 nm versus β.

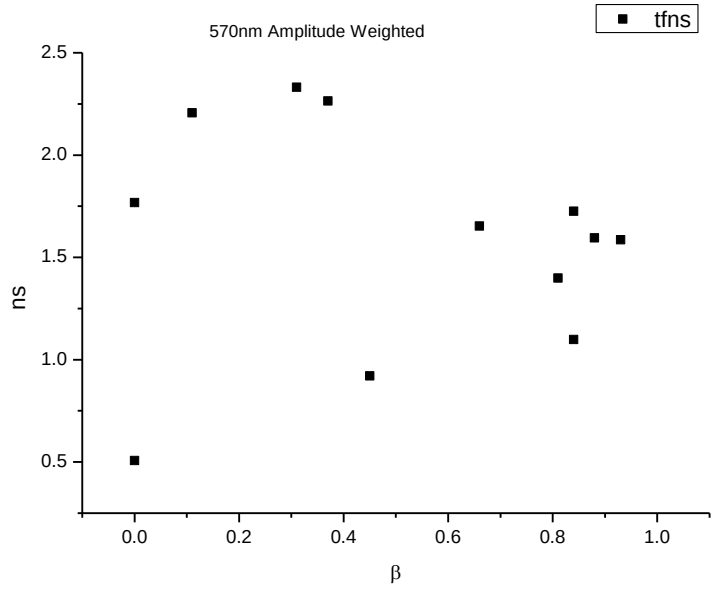

Figure 3.3.110. Amplitude weighted average lifetime (τ_f) of **18** at 570 nm versus β.

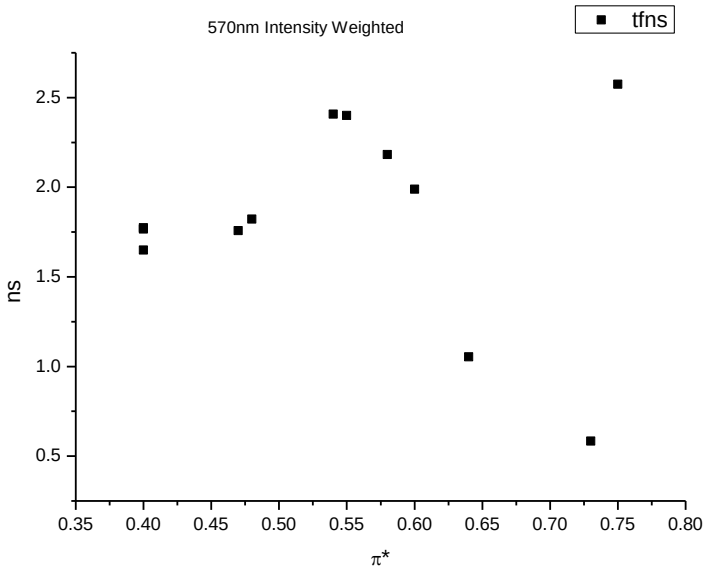

Figure 3.3.111. Intensity weighted average lifetime (τ_f) of **18** at 570 nm versus π*.

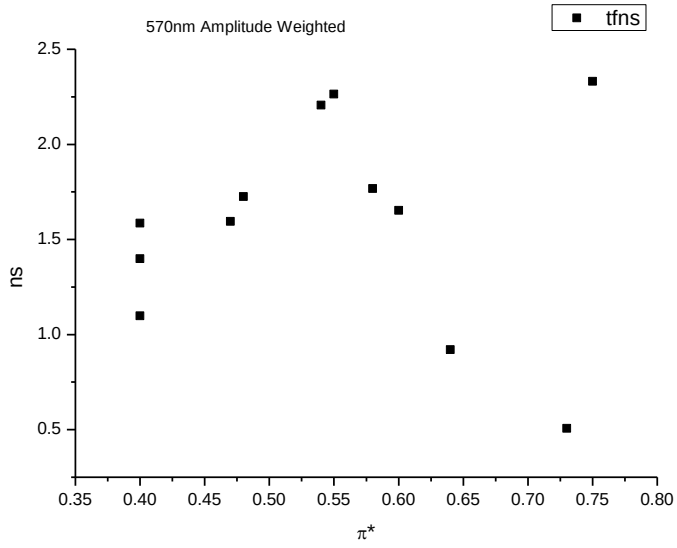

Figure 3.3.112. Amplitude weighted average lifetime (τ_f) of **18** at 570 nm versus π*.

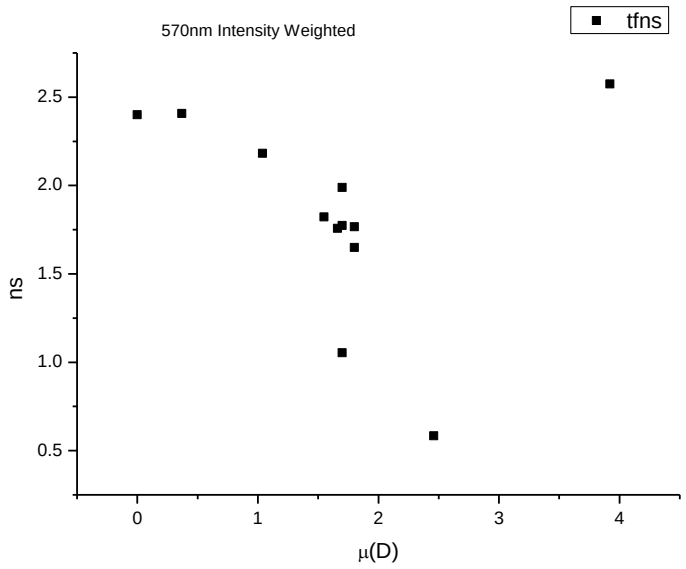

Figure 3.3.113. Intensity weighted average lifetime (τ_f) of **18** at 570 nm versus μ(D).

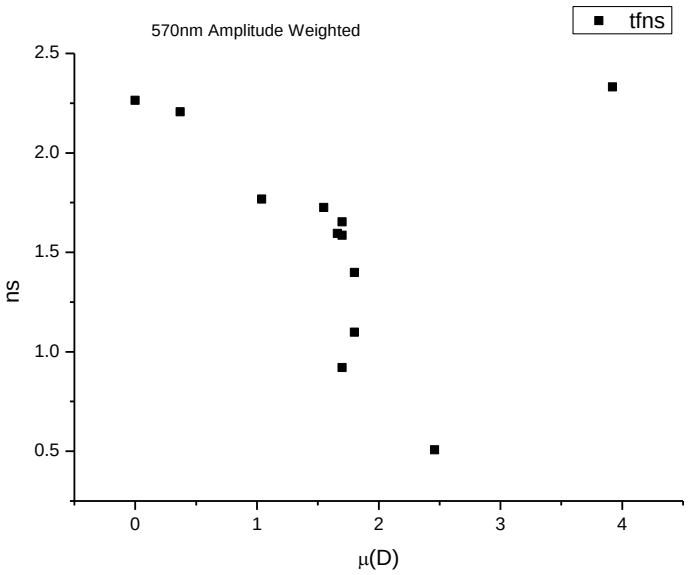

Figure 3.3.114. Amplitude weighted average lifetime (τ_f) of **18** at 570 nm versus μ(D).

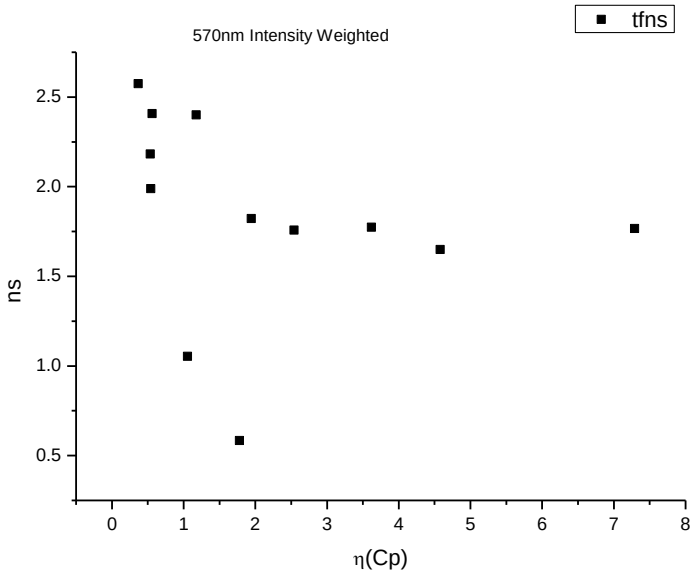

Figure 3.3.115. Intensity weighted average lifetime (τ_f) of **18** at 570 nm versus η(Cp).

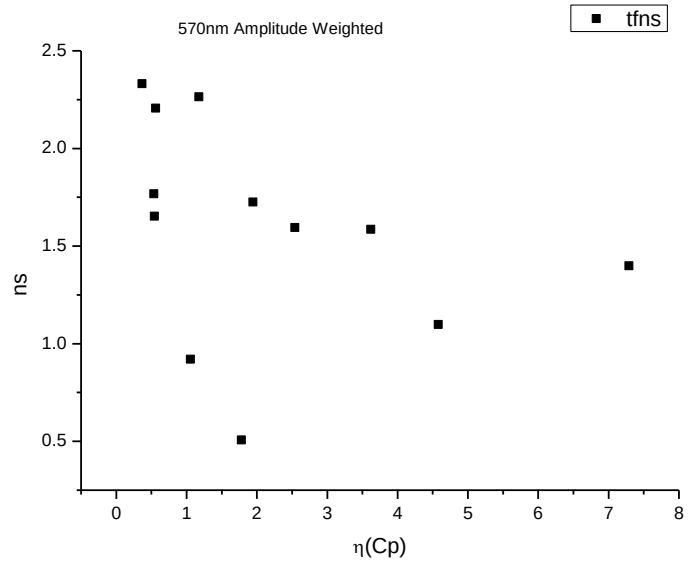

Figure 3.3.116. Amplitude weighted average lifetime (τ_f) of **18** at 570 nm versus η(Cp).

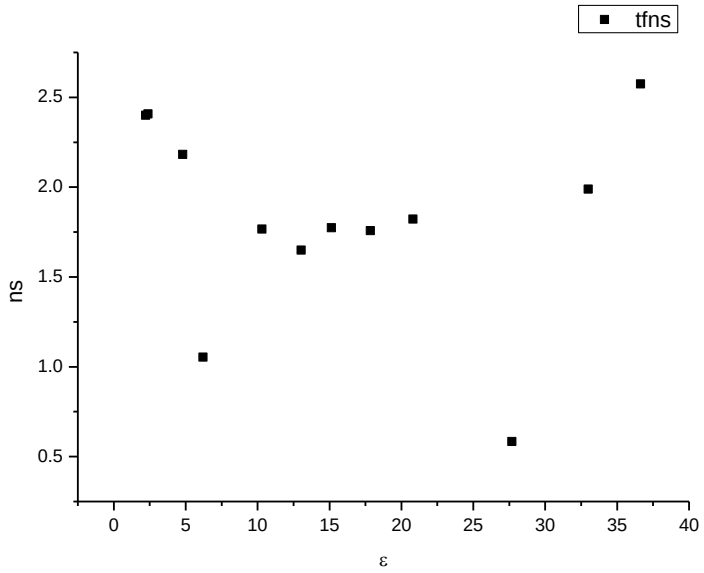

Figure 3.3.117. Intensity weighted average lifetime (τ_f) of **18** at 570 nm versus ε.

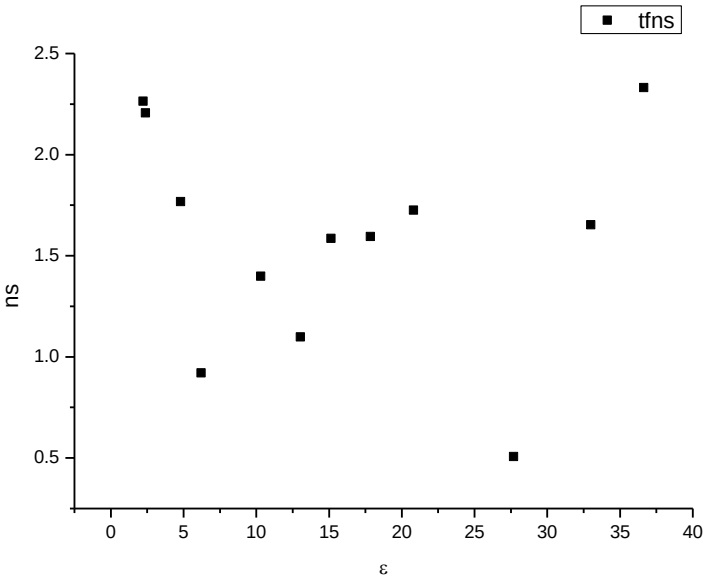

Figure 3.3.118. Amplitude weighted average lifetime (τ_f) of **18** at 570 nm versus ε.

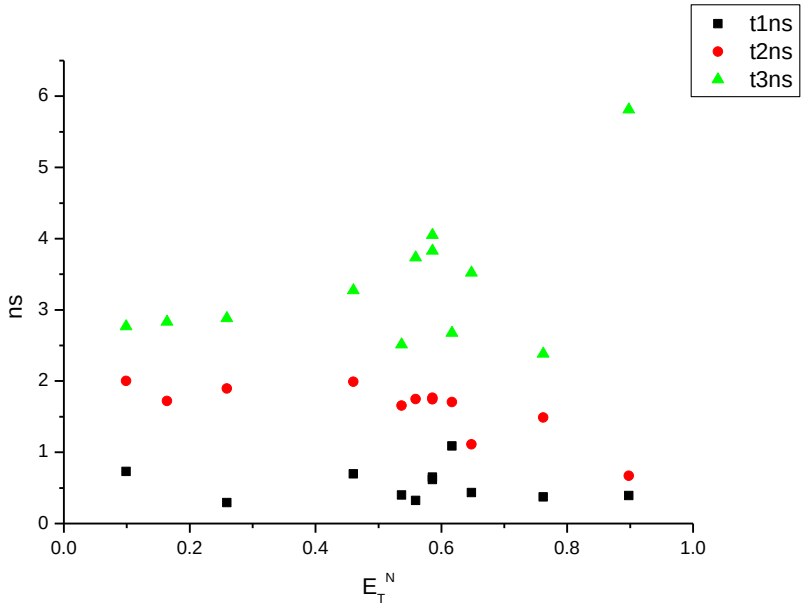

Figure 3.3.119. Intensity weighted components of TCSPC lifetime decay of **18** (570 nm) versus E_T^N.

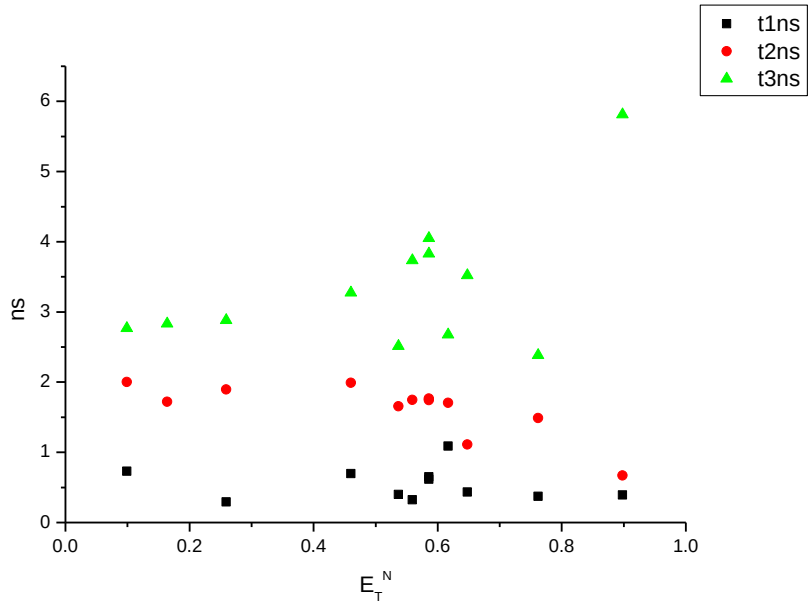

Figure 3.3.120. Amplitude weighted components of TCSPC lifetime decay of **18** (570 nm) versus E_T^N.

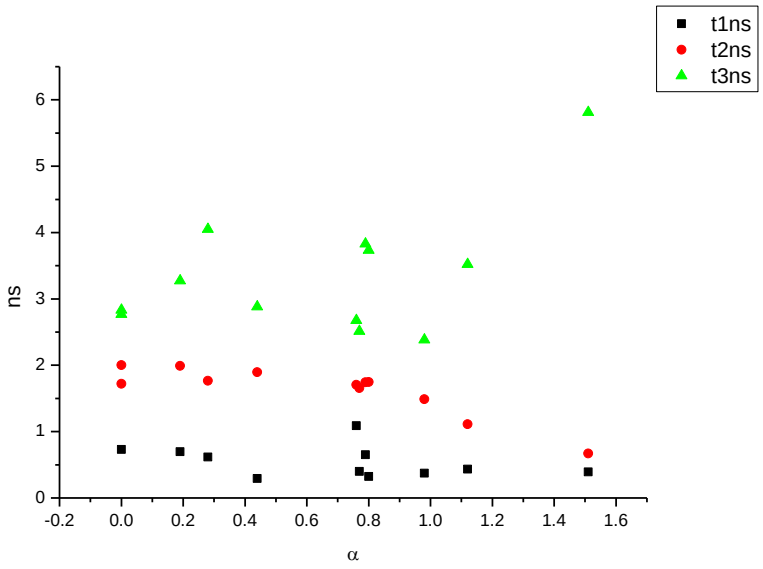

Figure 3.3.121. Intensity weighted components of TCSPC lifetime decay of **18** (570 nm) versus α.

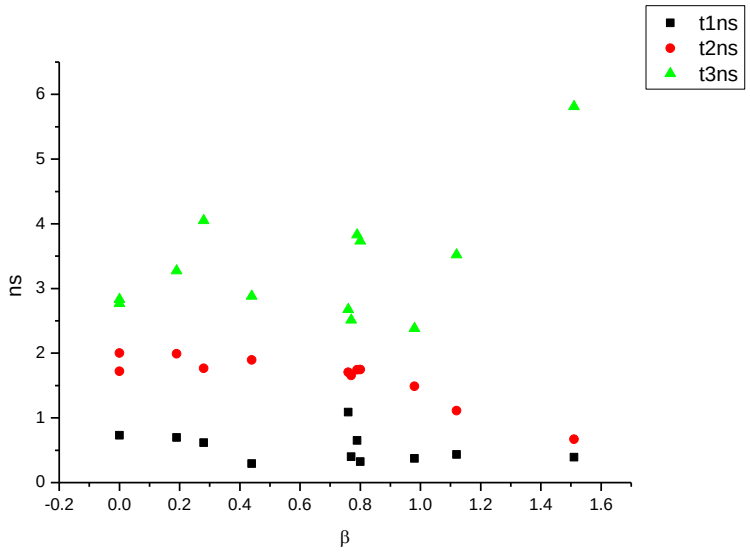

Figure 3.3.122. Amplitude weighted components of TCSPC lifetime decay of **18** (570 nm) versus α.

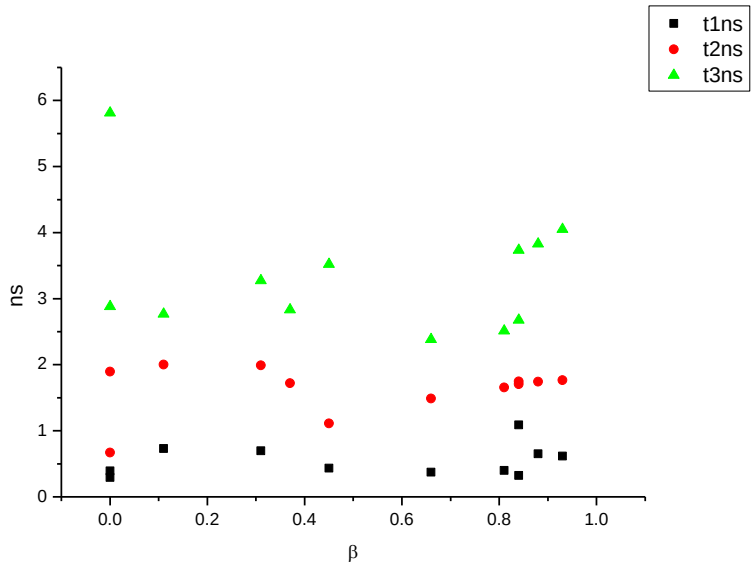

Figure 3.3.123. Intensity weighted components of TCSPC lifetime decay of **18** (570 nm) versus β.

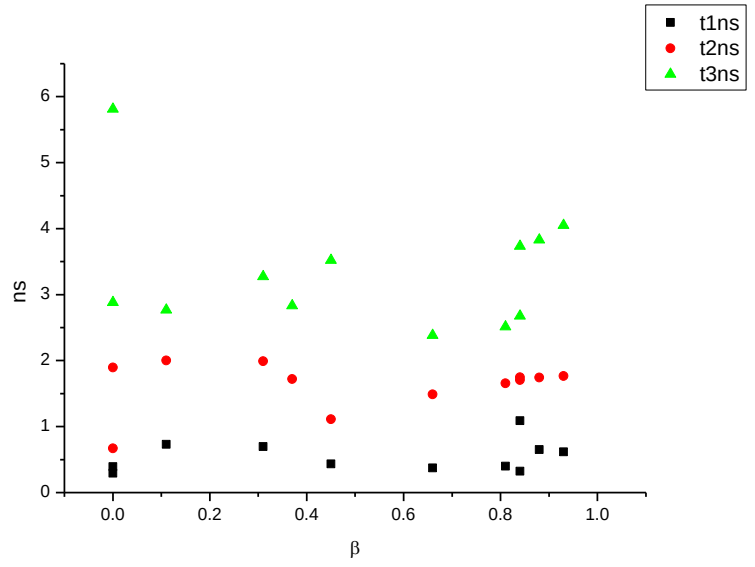

Figure 3.3.124. Amplitude weighted components of TCSPC lifetime decay of **18** (570 nm) versus β.

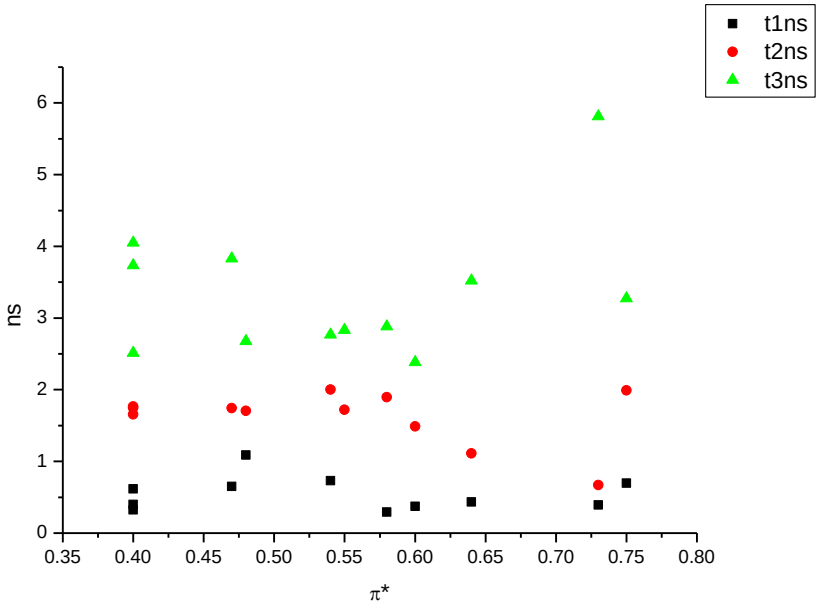

Figure 3.3.125. Intensity weighted components of TCSPC lifetime decay of **18** (570 nm) versus π*.

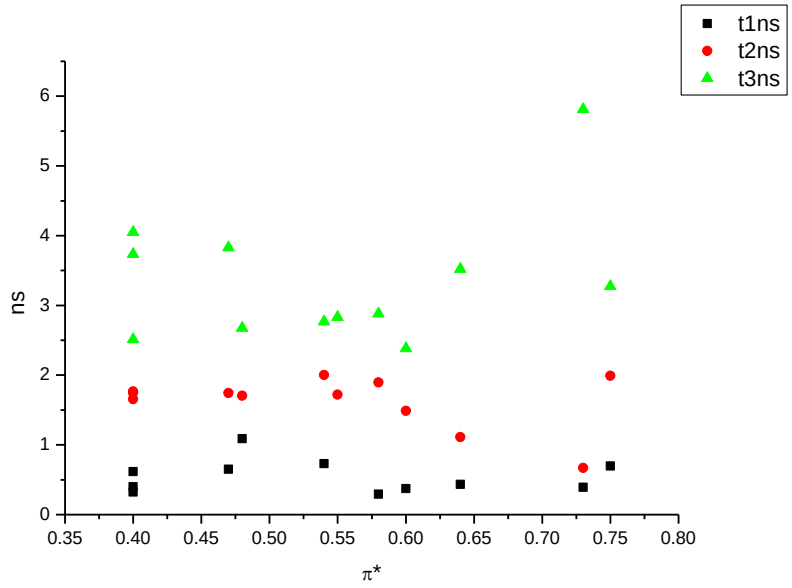

Figure 3.3.126. Amplitude weighted components of TCSPC lifetime decay of **18** (570 nm) versus π*.

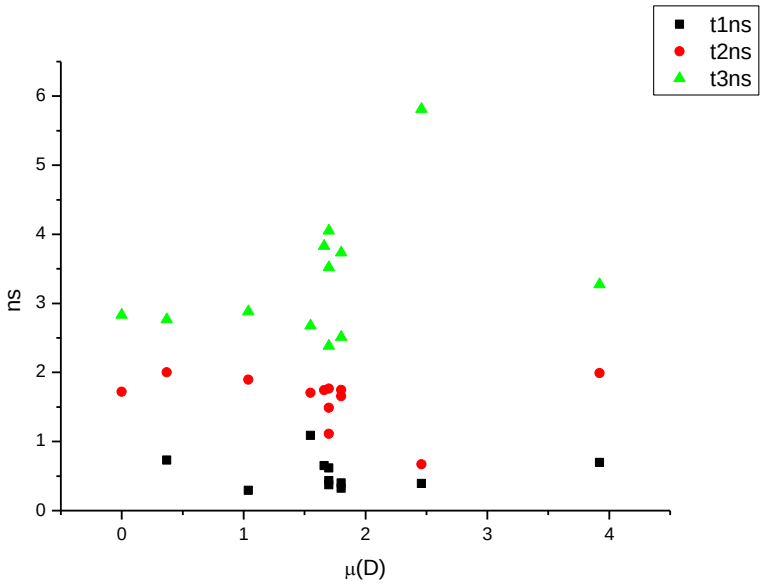

Figure 3.3.127. Intensity weighted components of TCSPC lifetime decay of **18** (570 nm) versus μ(D).

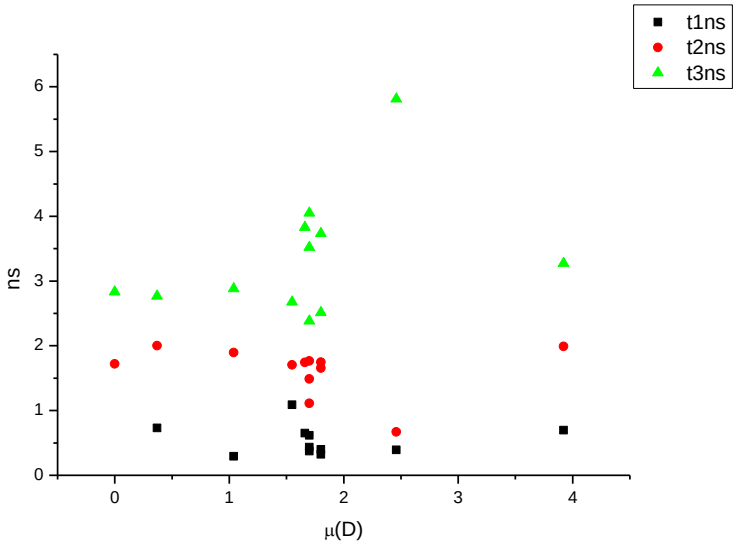

Figure 3.3.128. Amplitude weighted components of TCSPC lifetime decay of **18** (570 nm) versus μ(D).

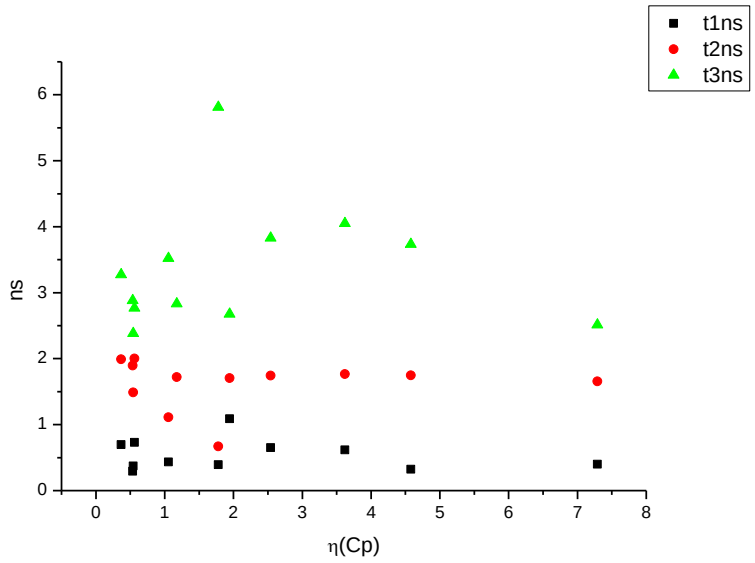

Figure 3.3.129. Intensity weighted components of TCSPC lifetime decay of **18** (570 nm) versus η(Cp).

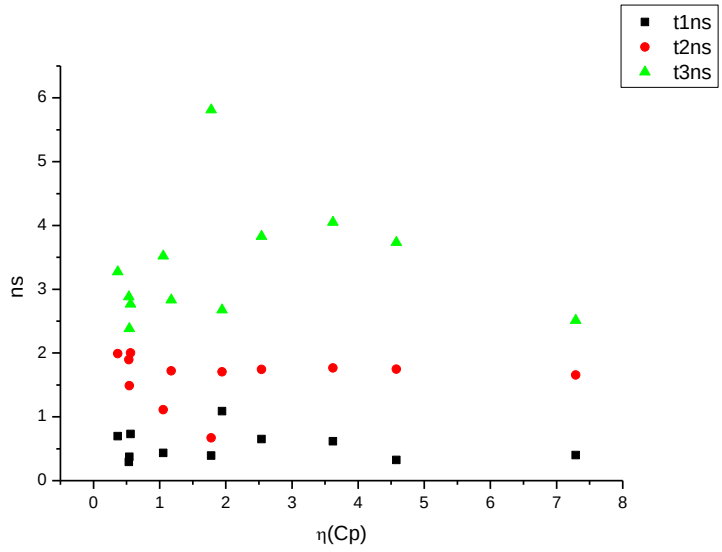

Figure 3.3.130. Amplitude weighted components of TCSPC lifetime decay of **18** (570 nm) versus η(Cp).

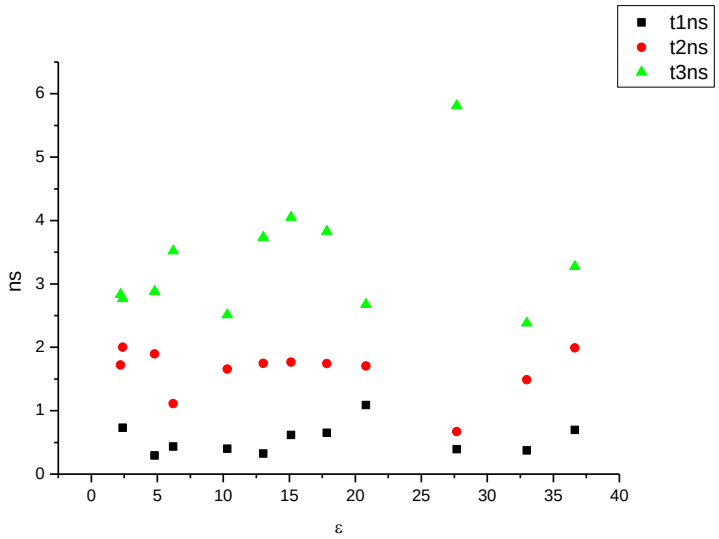

Figure 3.3.131. Intensity weighted components of TCSPC lifetime decay of **18** (570 nm) versus ε.

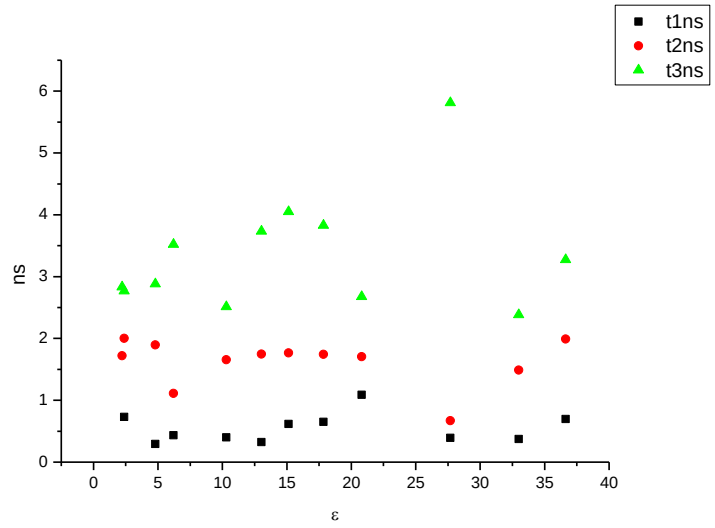

Figure 3.3.132. Amplitude weighted components of TCSPC lifetime decay of **18** (570 nm) versus ε.

3.3.8 Ultraviolet-visible absorption spectra.

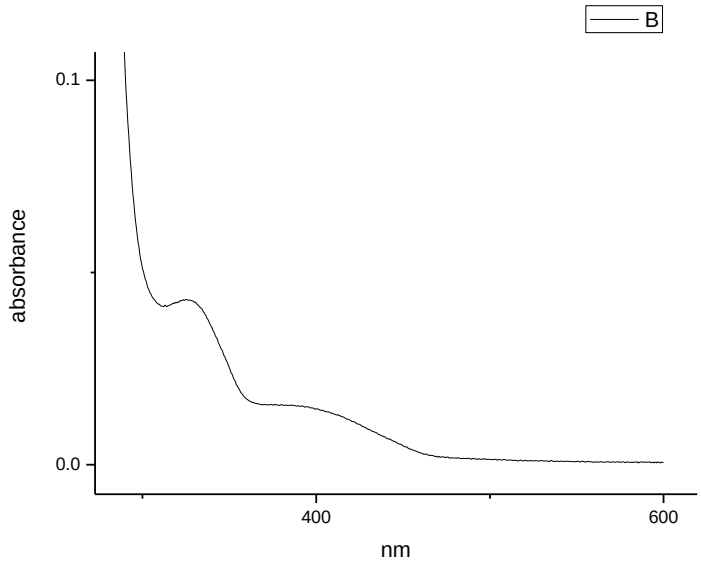

Figure 3.3.133. Ultraviolet-Visible absorption spectrum of **18** recorded in Toluene.

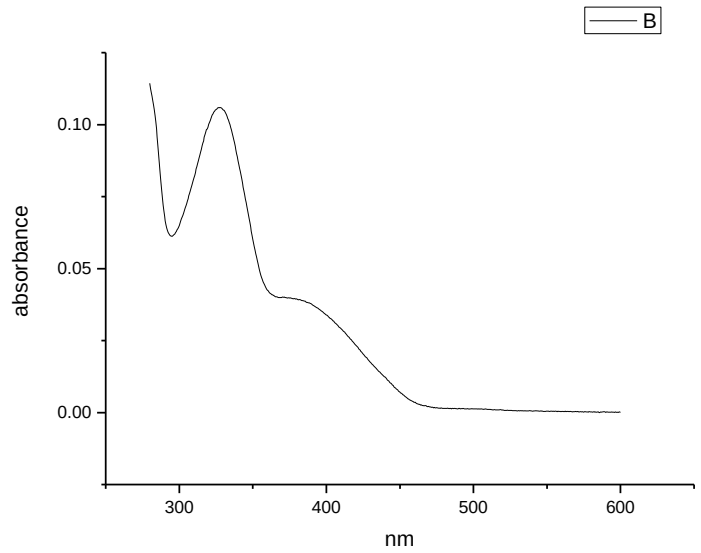

Figure 3.3.134. Ultraviolet-Visible absorption spectrum of **18** recorded in 1,4-dioxane.

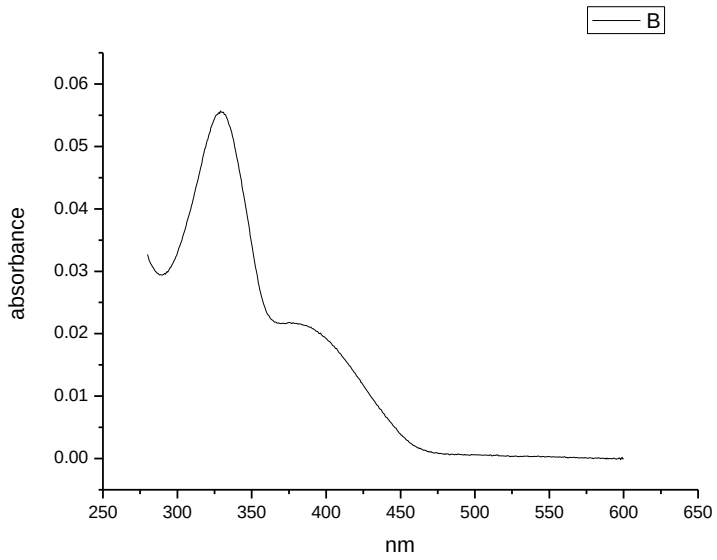

Figure 3.3.135. Ultraviolet-Visible absorption spectrum of **18** recorded in Chloroform.

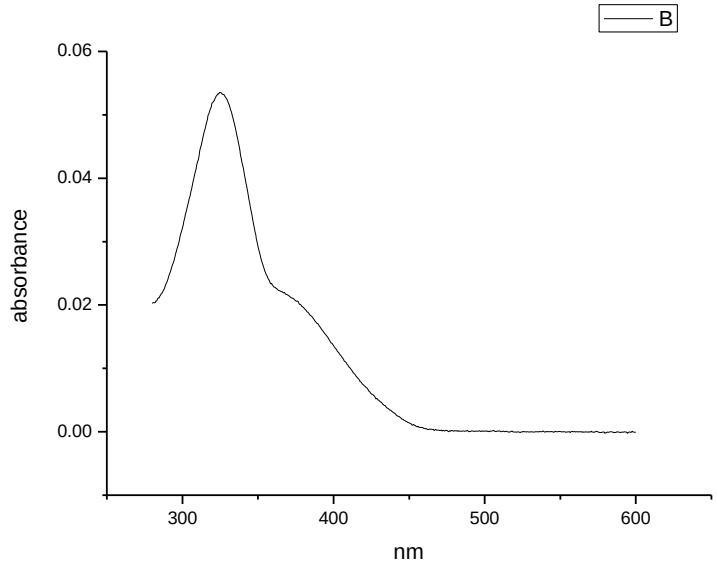

Figure 3.3.136. Ultraviolet-Visible absorption spectrum of **18** recorded in Acetonitirile.

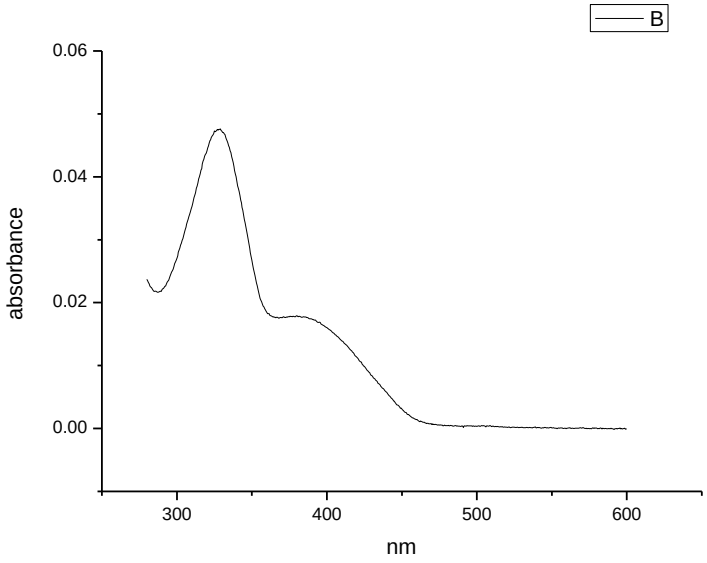

Figure 3.3.137. Ultraviolet-Visible absorption spectrum of **18** recorded in 1-octanol.

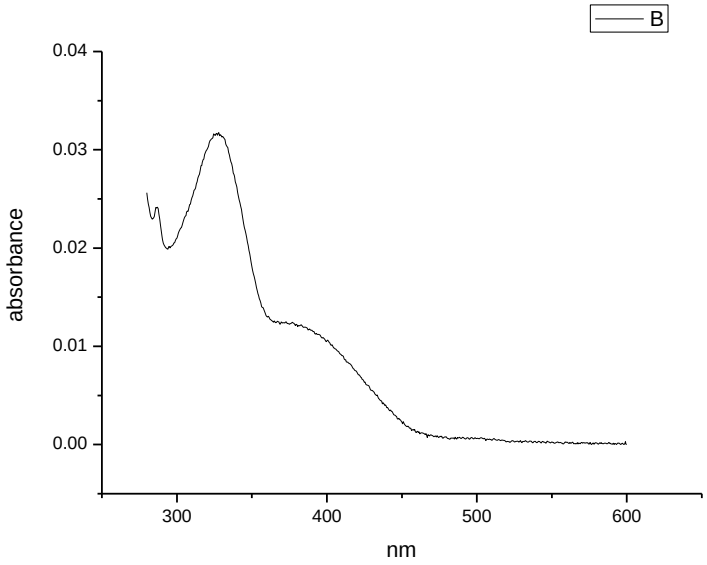

Figure 3.3.138. Ultraviolet-Visible absorption spectrum of **18** recorded in 1-hexanol.

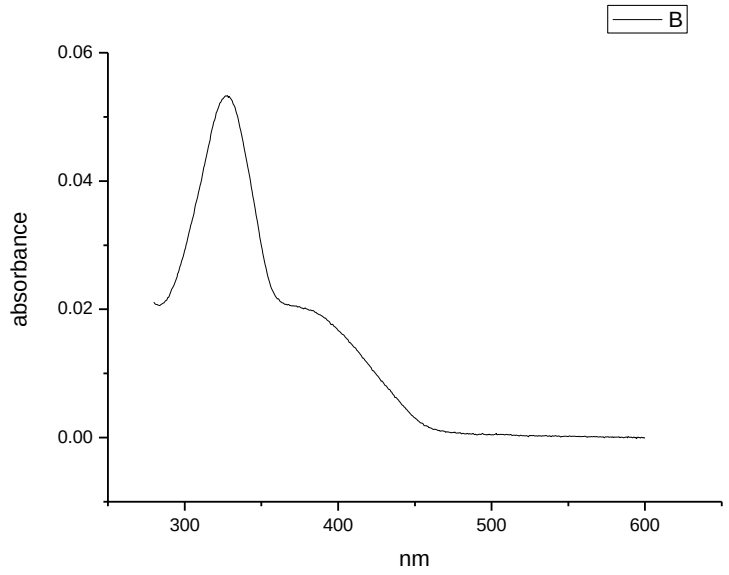

Figure 3.3.139. Ultraviolet-Visible absorption spectrum of **18** recorded in 1-butanol.

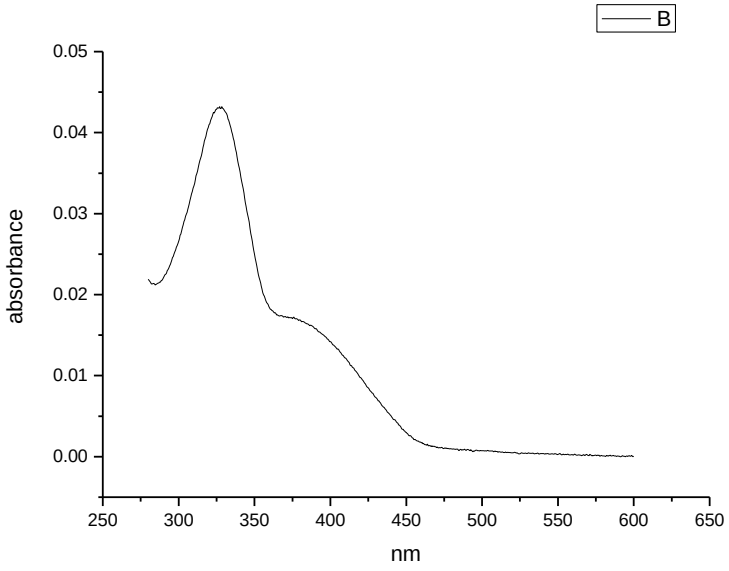

Figure 3.3.140. Ultraviolet-Visible absorption spectrum of **18** recorded in 1-pentanol.

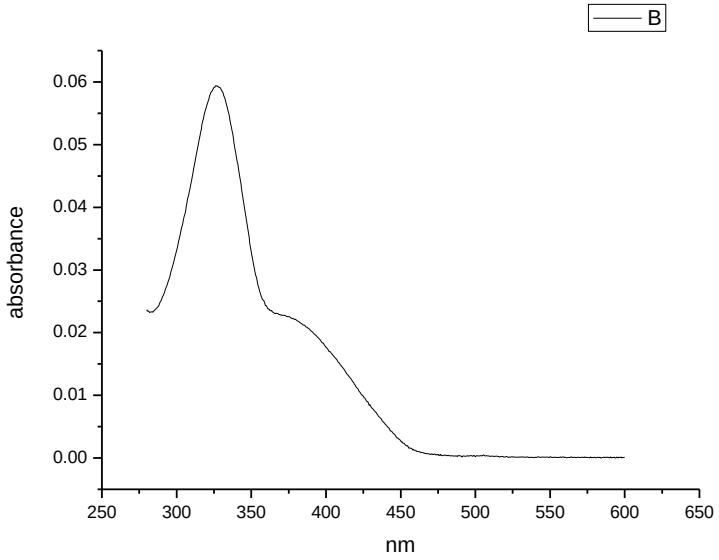

Figure 3.3.141. Ultraviolet-Visible absorption spectrum of **18** recorded in 1-propanol.

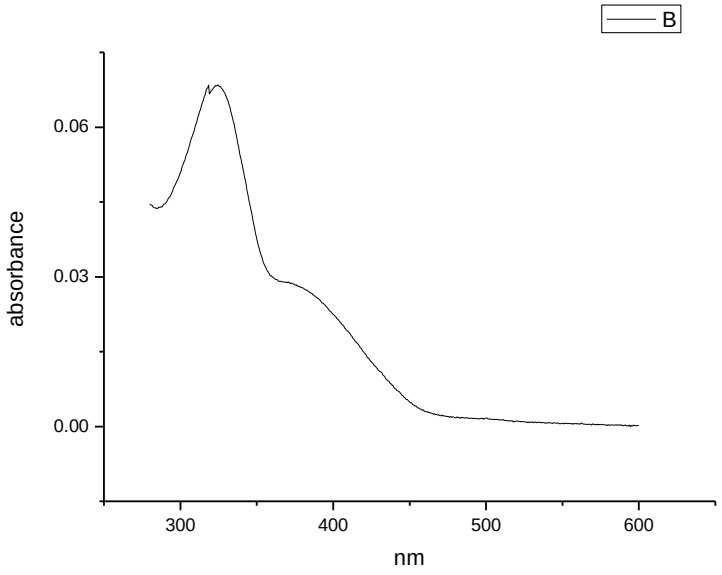

Figure 3.3.142. Ultraviolet-Visible absorption spectrum of **18** recorded in Acetic Acid.

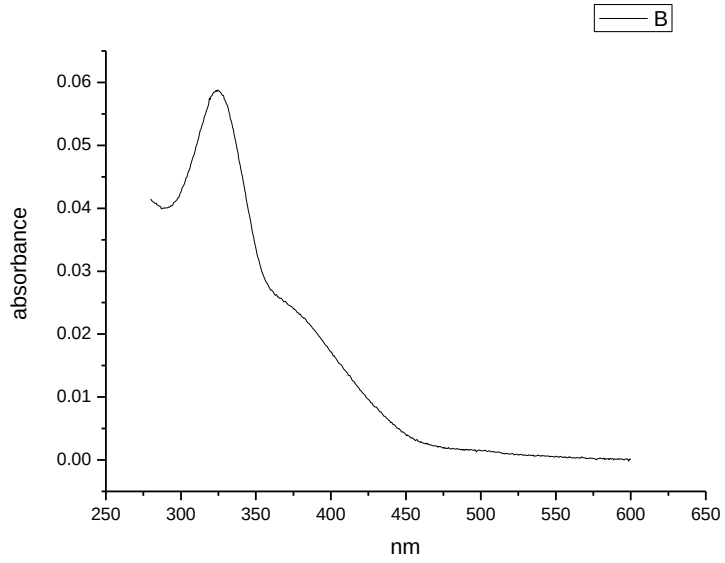

Figure 3.3.143. Ultraviolet-Visible absorption spectrum of **18** recorded in Methanol.

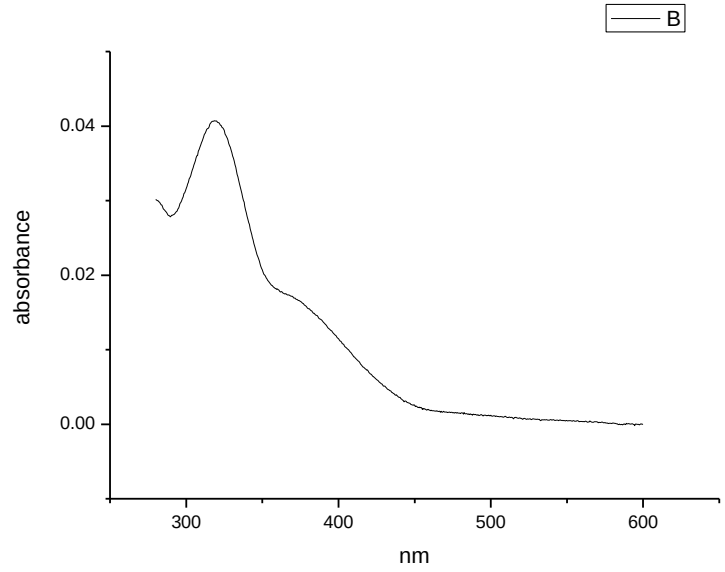

Figure 3.3.144. Ultraviolet-Visible absorption spectrum of **18** recorded in 2,2,2-trifluoroethanol.

3.3.9 Fluorescence Emission spectra.

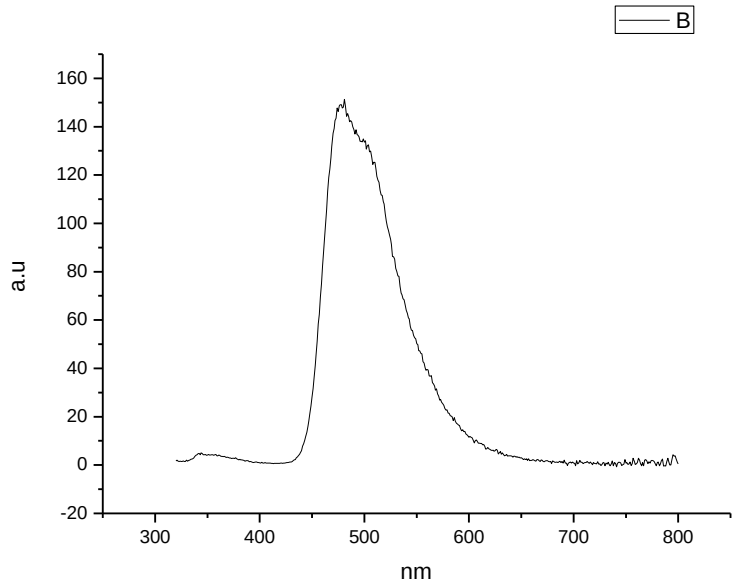

Figure 3.3.145. Fluorescence emission spectrum of **18** recorded in Toluene at 310 nm excitation.

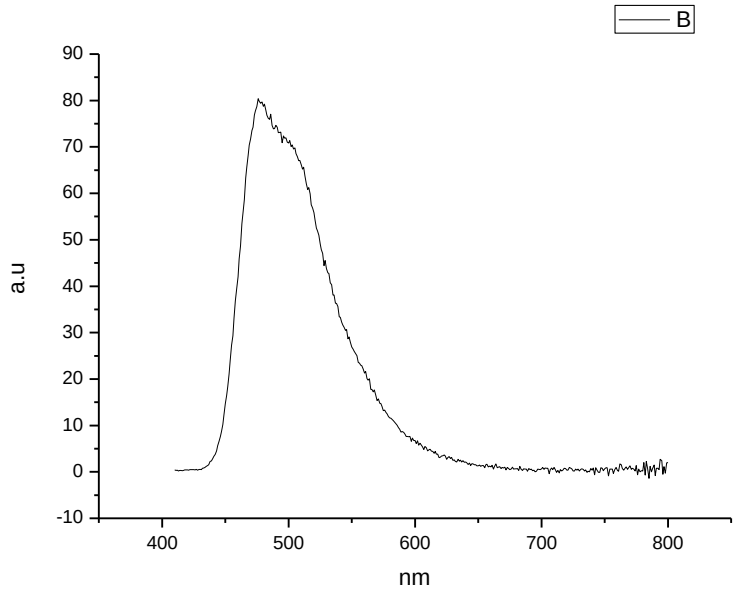

Figure 3.3.146. Fluorescence emission spectrum of **18** recorded in Toluene at 400 nm excitation.

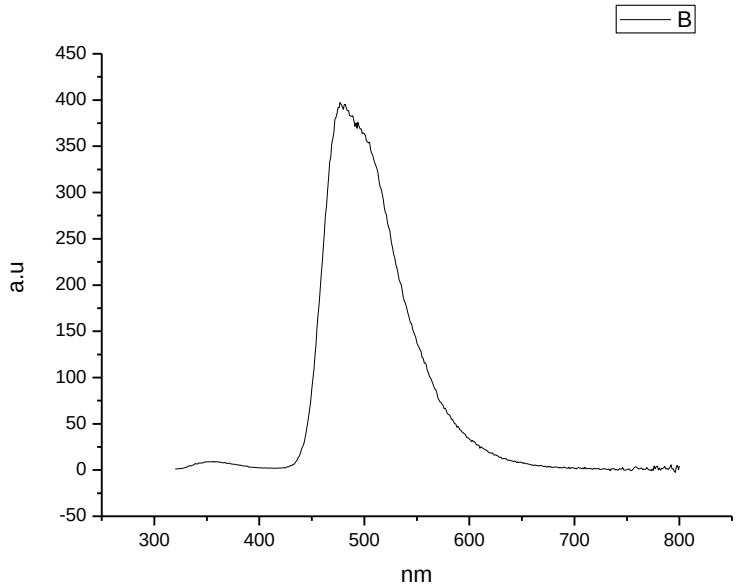

Figure 3.3.147. Fluorescence emission spectrum of **18** recorded in 1,4-dioxane at 310 nm excitation.

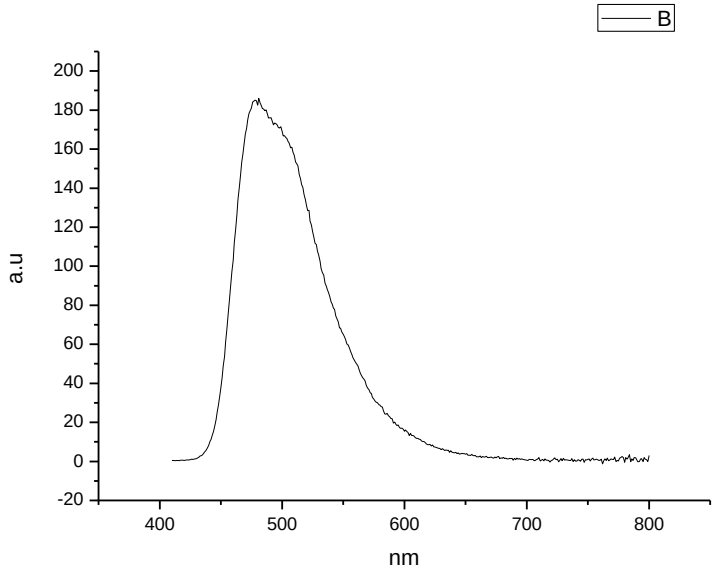

Figure 3.3.148. Fluorescence emission spectrum of **18** recorded in 1,4-dioxane at 400 nm excitation.

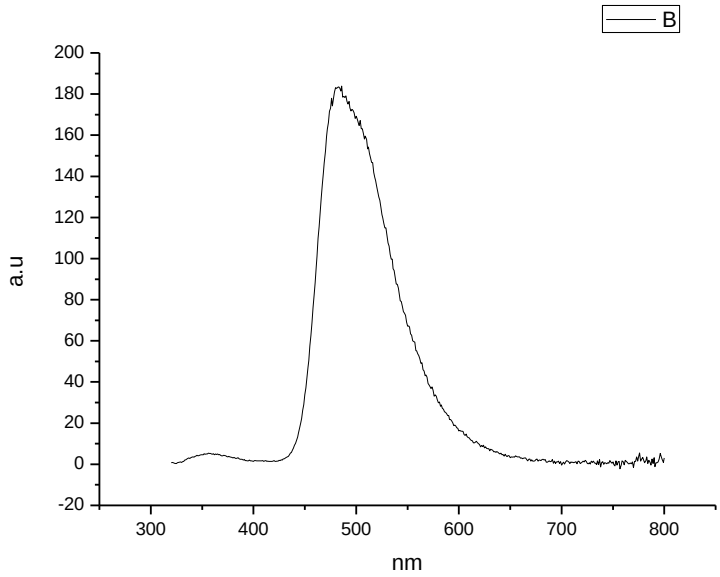

Figure 3.3.149. Fluorescence emission spectrum of **18** recorded in Chloroform at 310 nm excitation.

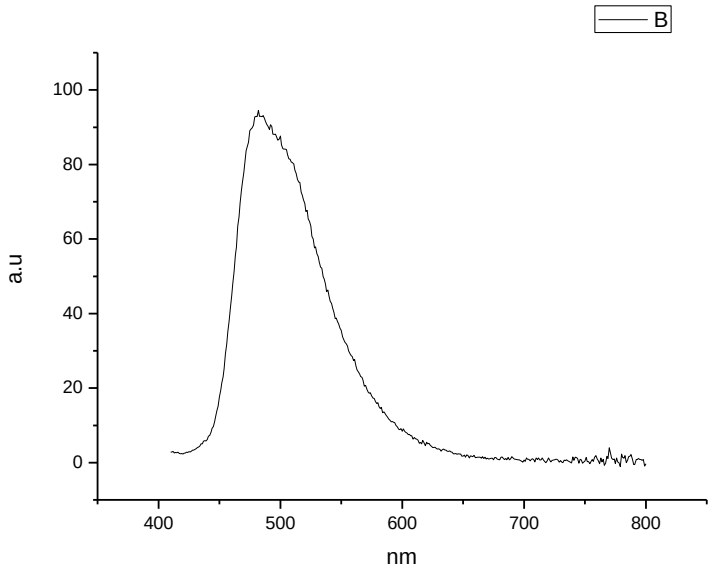

Figure 3.3.150. Fluorescence emission spectrum of **18** recorded in Chloroform at 400 nm excitation.

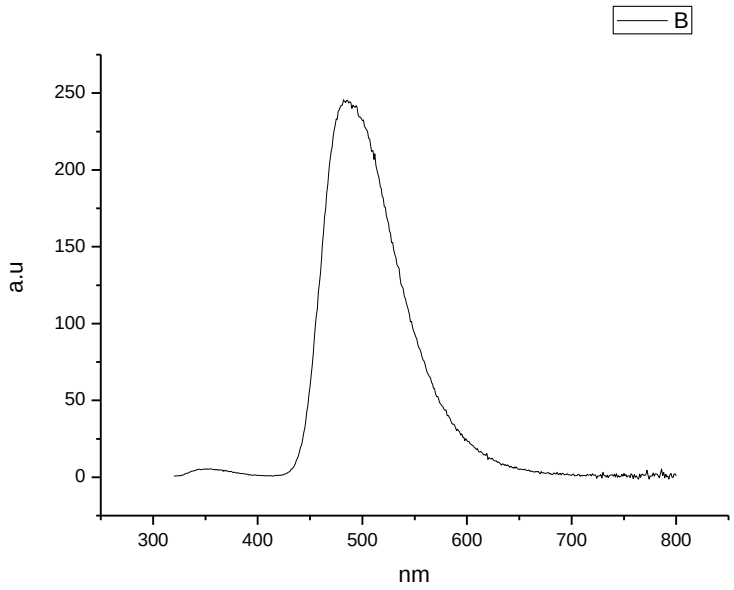

Figure 3.3.151. Fluorescence emission spectrum of **18** recorded in Acetonitrile at 310 nm excitation.

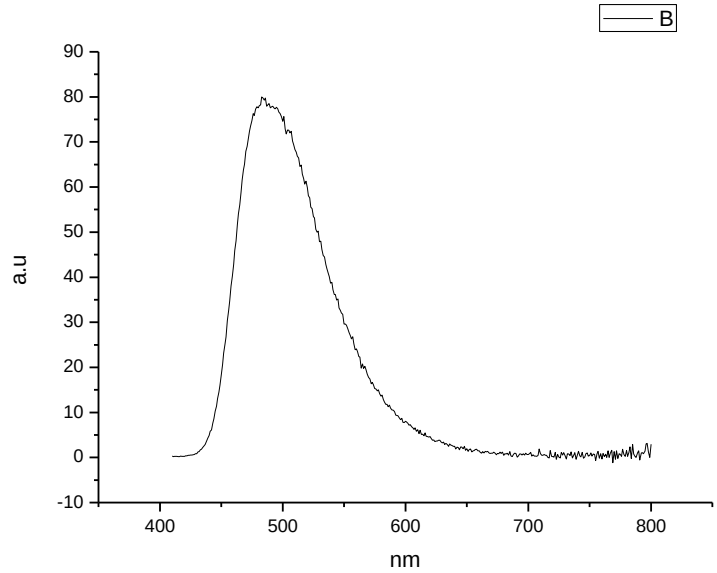

Figure 3.3.152. Fluorescence emission spectrum of **18** recorded in Acetonitrile at 400 nm excitation.

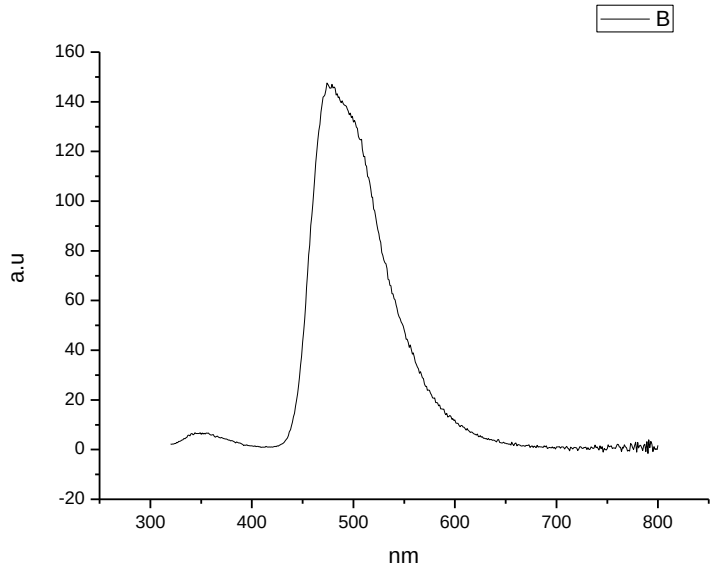

Figure 3.3.153. Fluorescence emission spectrum of **18** recorded in 1-octanol at 310 nm excitation.

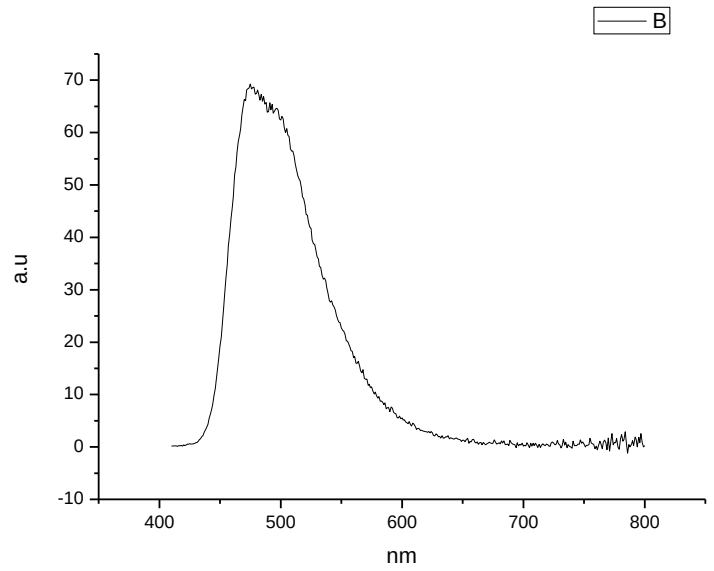

Figure 3.3.154. Fluorescence emission spectrum of **18** recorded in 1-octanol at 400 nm excitation.

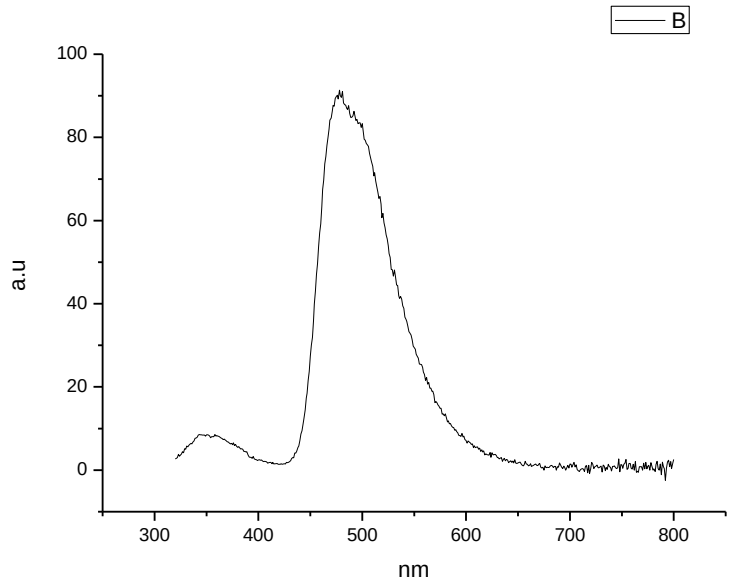

Figure 3.3.155. Fluorescence emission spectrum of **18** recorded in 1-hexanol at 310 nm excitation.

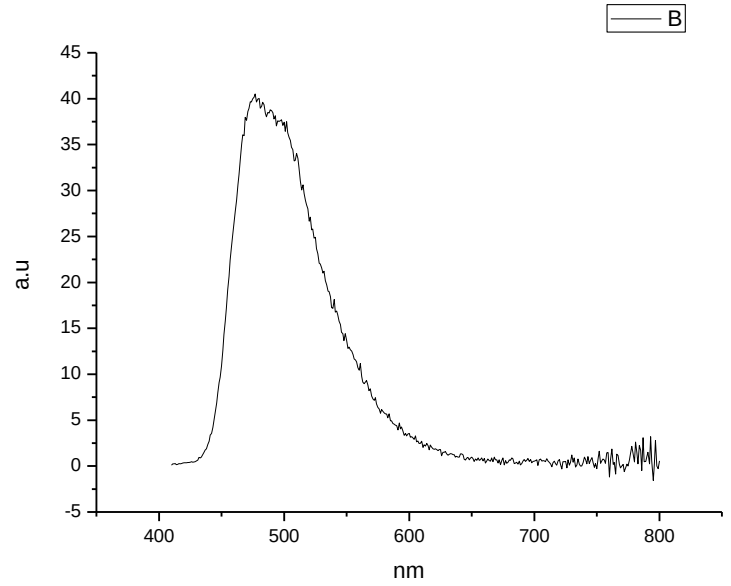

Figure 3.3.156. Fluorescence emission spectrum of **18** recorded in 1-hexanol at 400 nm excitation.

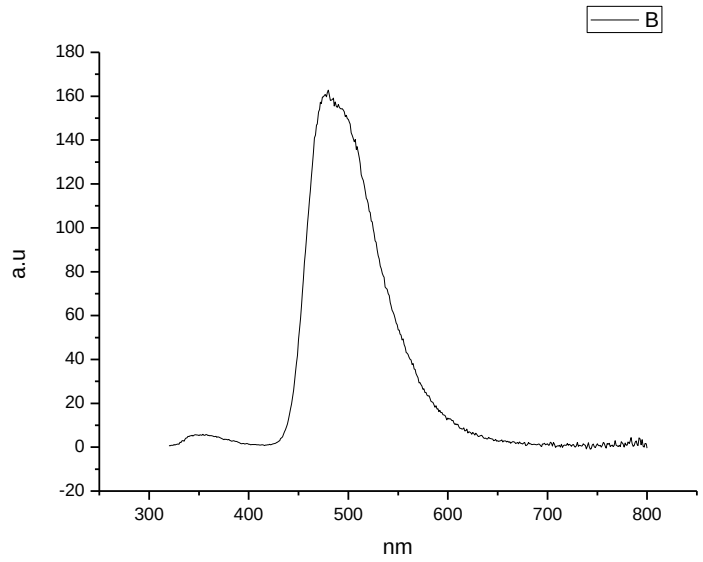

Figure 3.3.157. Fluorescence emission spectrum of **18** recorded in 1-butanol at 310 nm excitation.

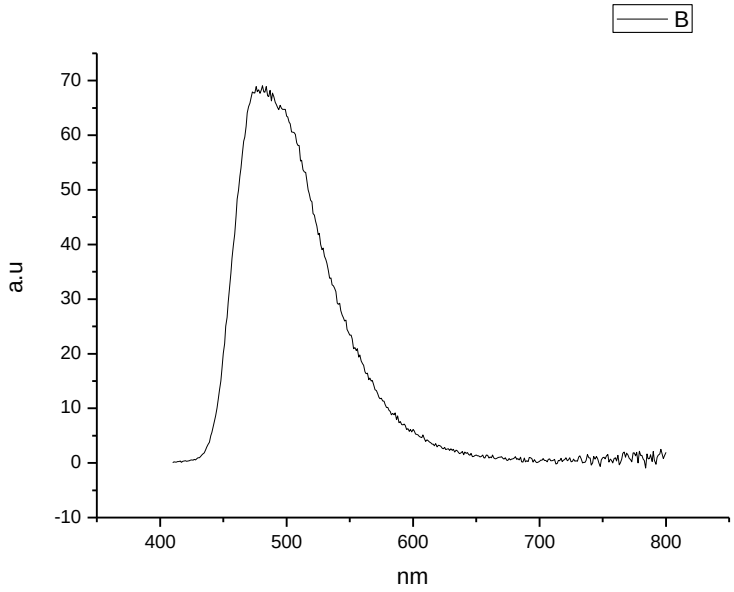

Figure 3.3.158. Fluorescence emission spectrum of **18** recorded in 1-butanol at 400 nm excitation.

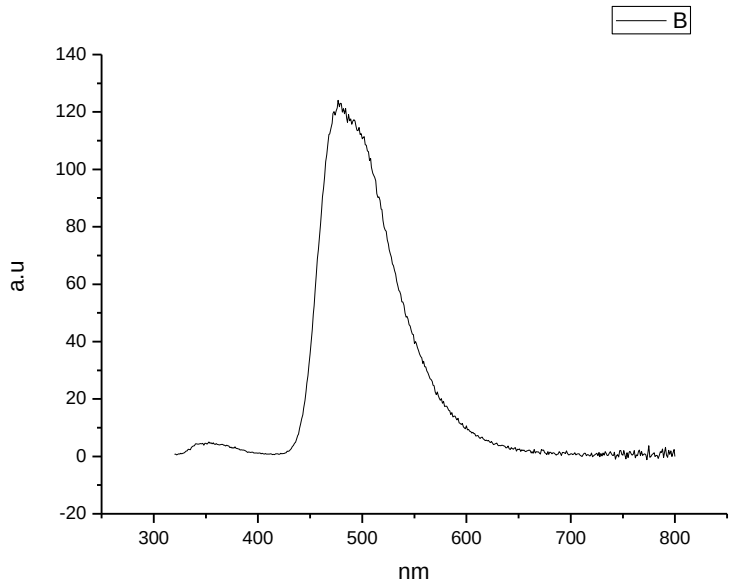

Figure 3.3.159. Fluorescence emission spectrum of **18** recorded in 1-pentanol at 310 nm excitation.

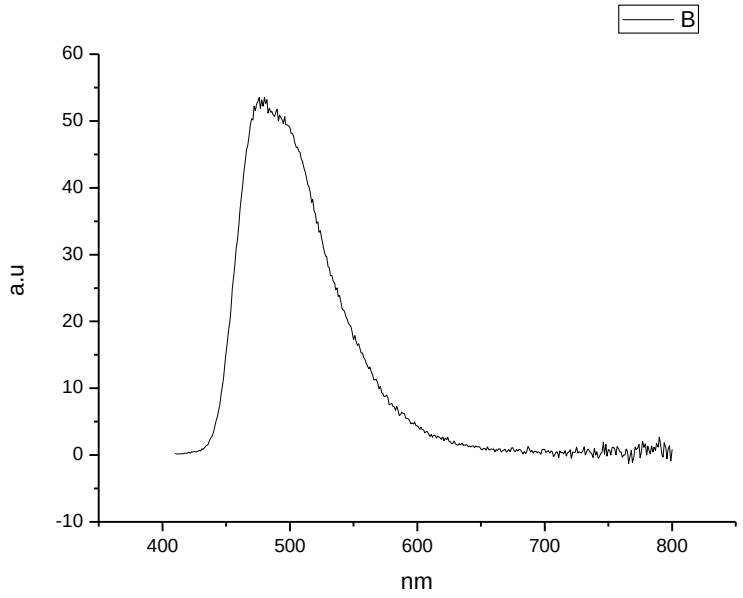

Figure 3.3.160. Fluorescence emission spectrum of **18** recorded in 1-pentanol at 400 nm excitation.

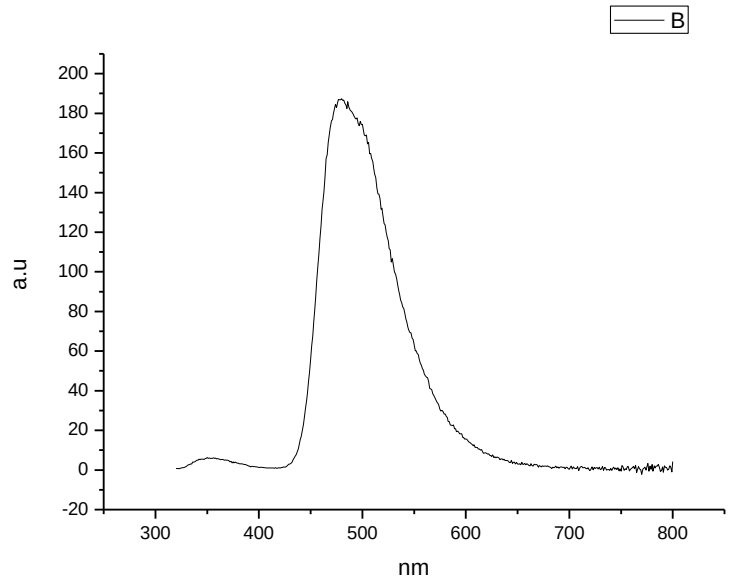

Figure 3.3.161. Fluorescence emission spectrum of **18** recorded in 1-propanol at 310 nm excitation.

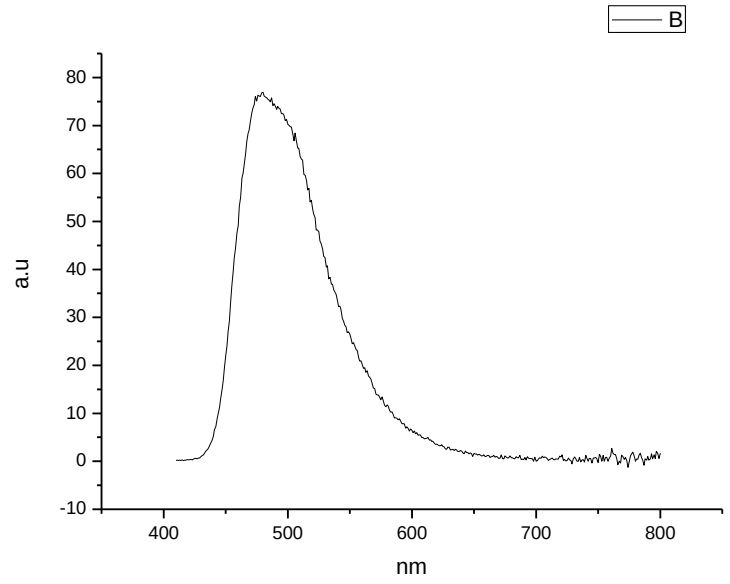

Figure 3.3.162. Fluorescence emission spectrum of **18** recorded in 1-propanol at 400 nm excitation.

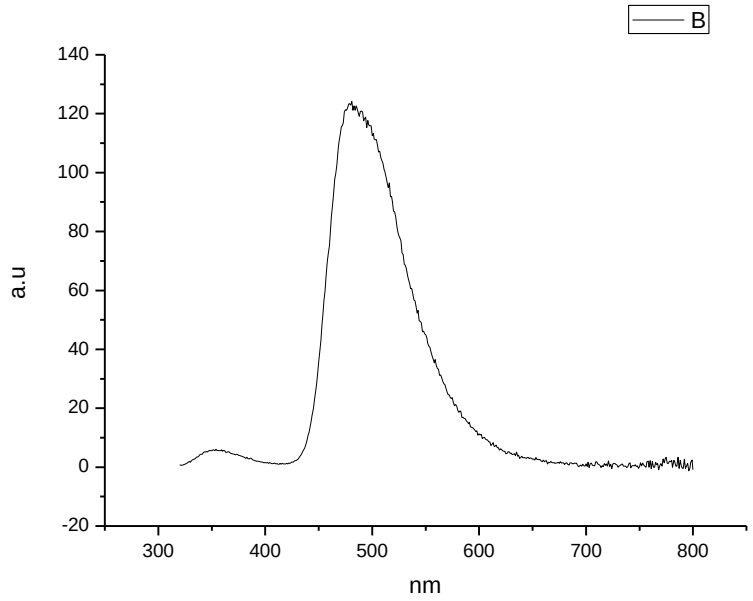

Figure 3.3.163. Fluorescence emission spectrum of **18** recorded in Acetic Acid at 310 nm excitation.

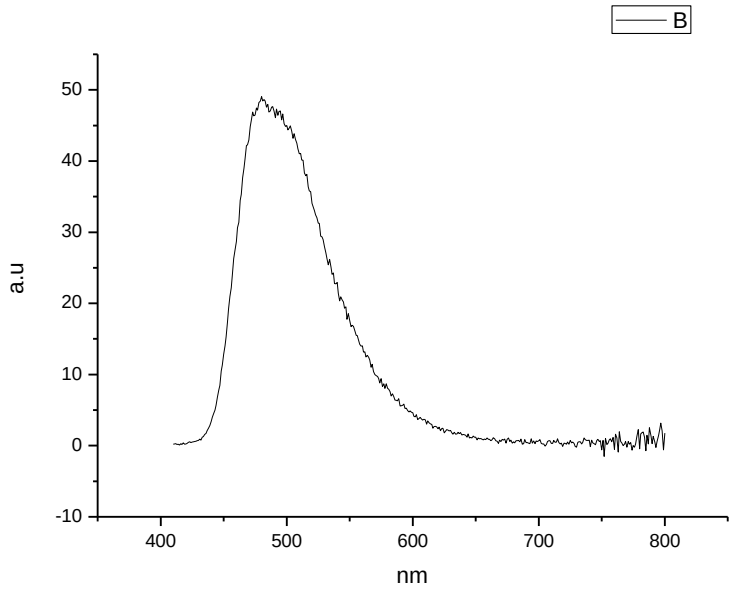

Figure 3.3.164. Fluorescence emission spectrum of **18** recorded in Acetic Acid at 400 nm excitation.

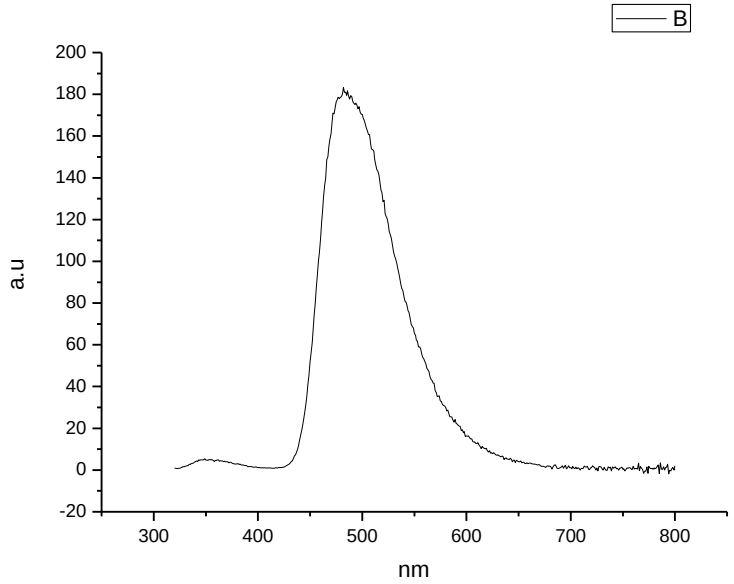

Figure 3.3.165. Fluorescence emission spectrum of **18** recorded in Methanol at 310 nm excitation.

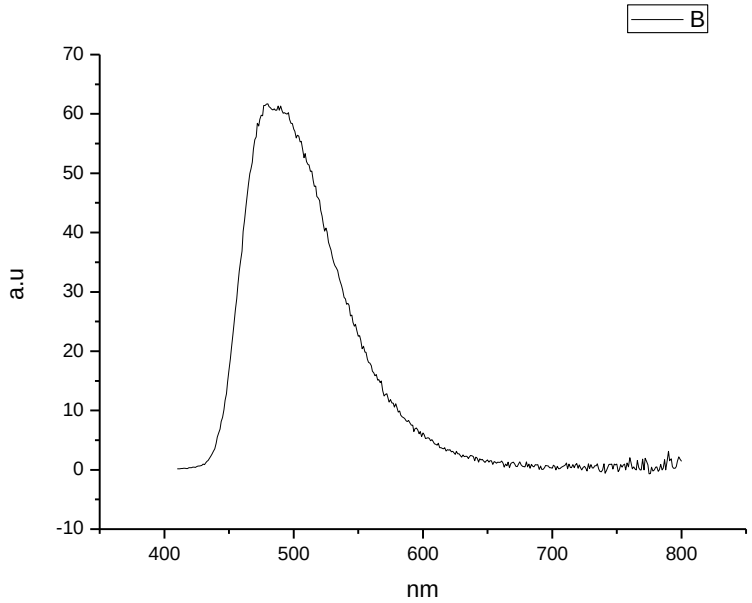

Figure 3.3.166. Fluorescence emission spectrum of **18** recorded in Methanol at 400 nm excitation.

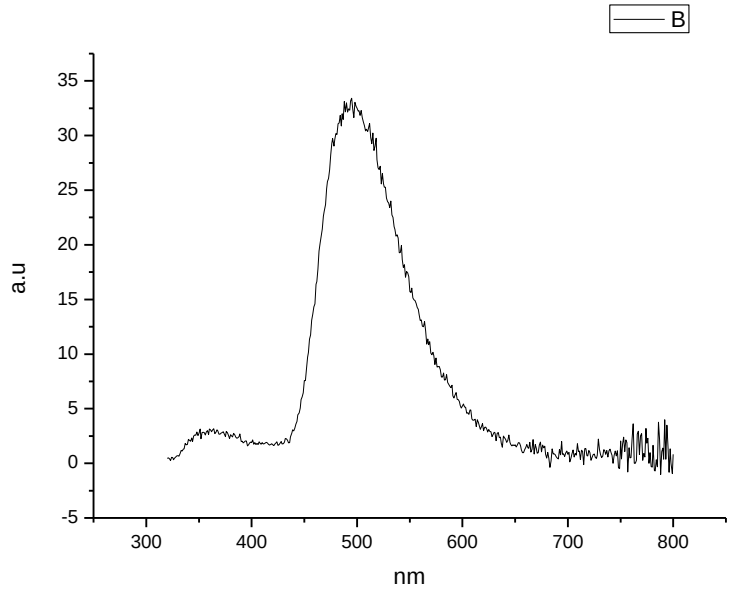

Figure 3.3.167. Fluorescence emission spectrum of **18** recorded in 2,2,2-trifluoroethanol at 310 nm excitation.

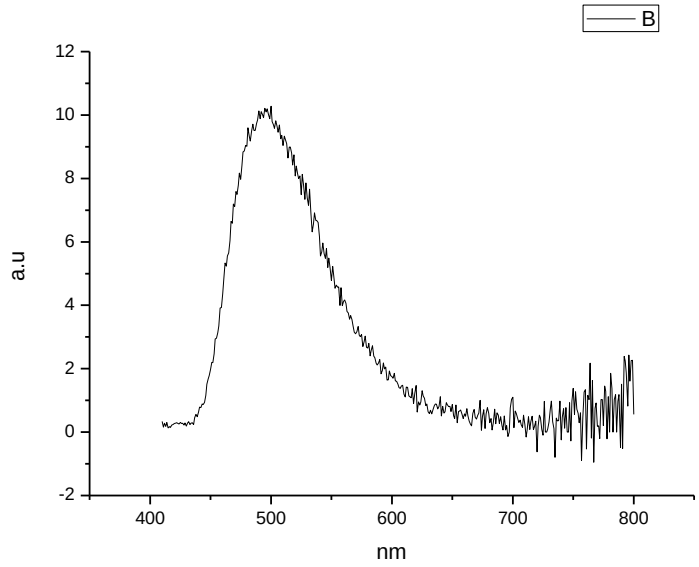

Figure 3.3.168. Fluorescence emission spectrum of **18** recorded in 2,2,2-trifluoroethanol at 400 nm excitation.

3.3.10 Normalised Fluorescence Emission spectra (Gaussian fitted).

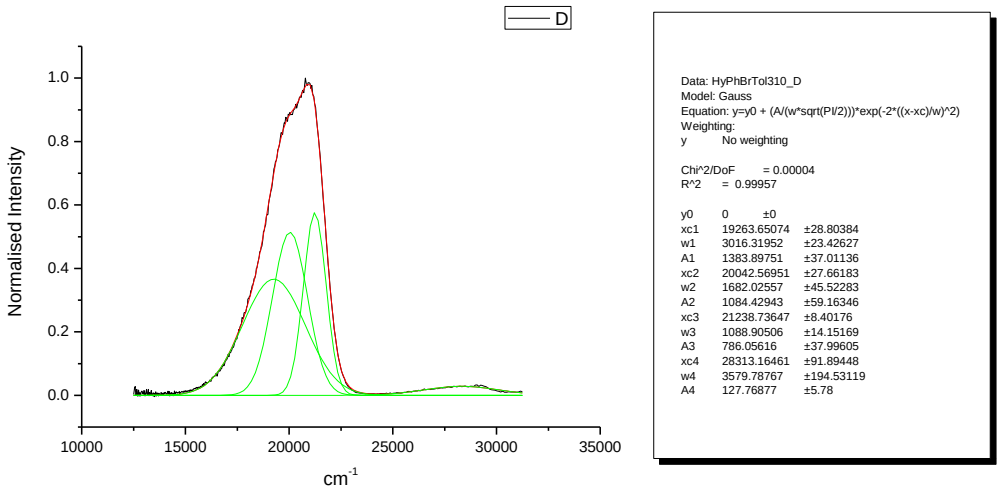

Figure 3.3.169. Gaussian model fit of the normalised fluorescence emission spectrum of **18** recorded in Toluene at 310 nm excitation.

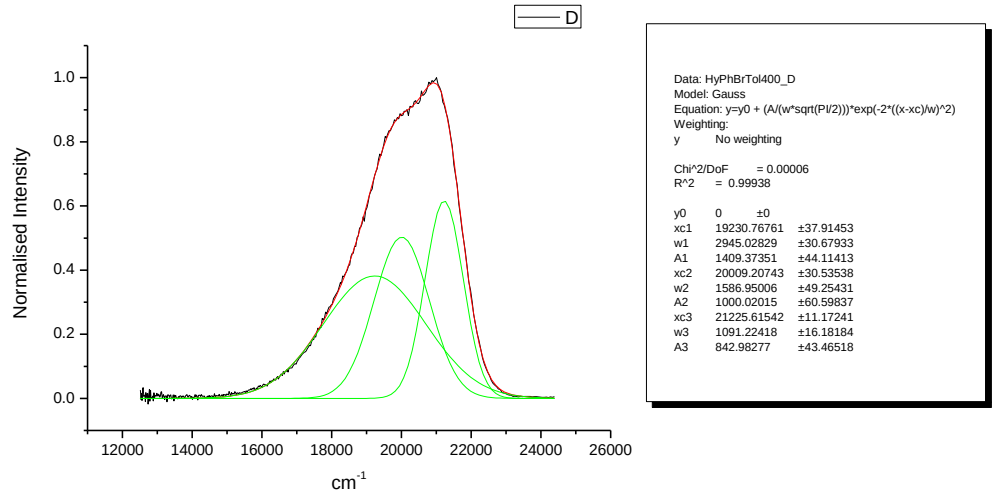

Figure 3.3.170. Gaussian model fit of the normalised fluorescence emission spectrum of **18** recorded in Toluene at 400 nm excitation.

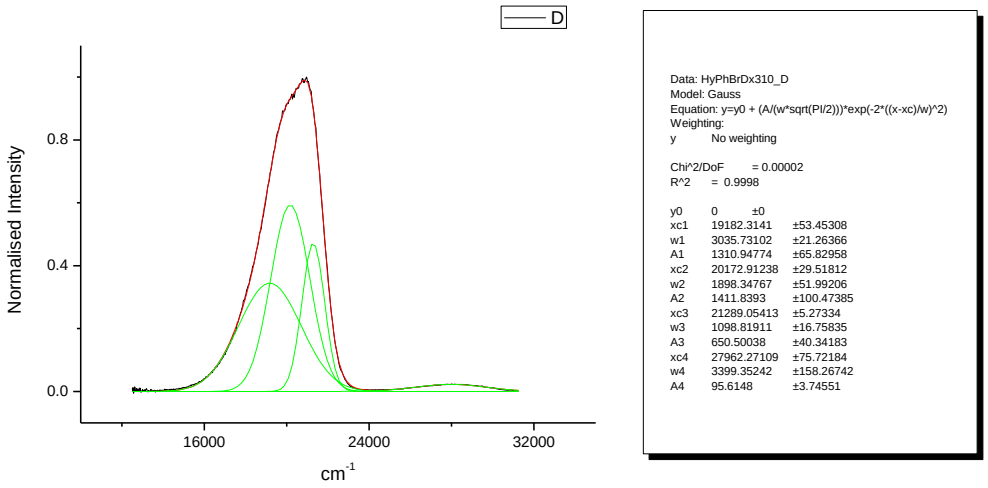

Figure 3.3.171. Gaussian model fit of the normalised fluorescence emission spectrum of **18** recorded in 1,4-dioxane at 310 nm excitation.

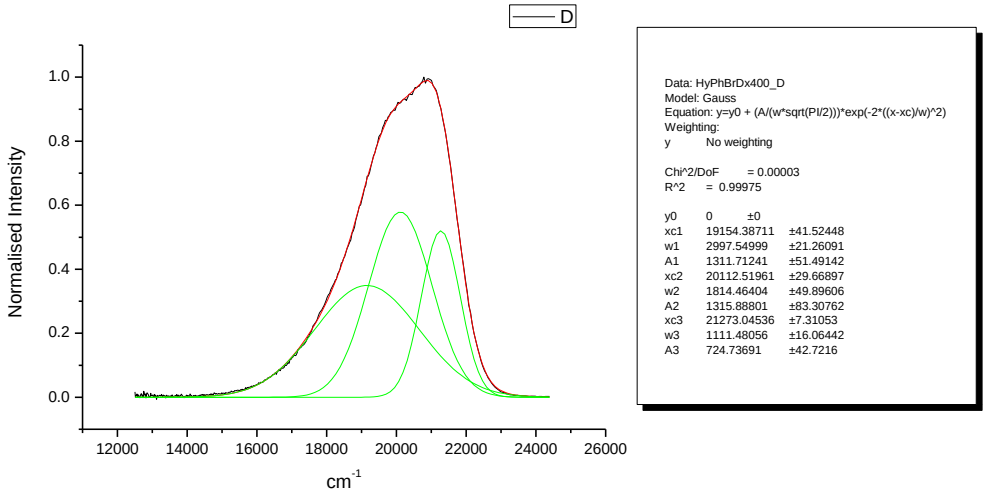

Figure 3.3.172. Gaussian model fit of the normalised fluorescence emission spectrum of **18** recorded in 1,4-dioxane at 400 nm excitation.

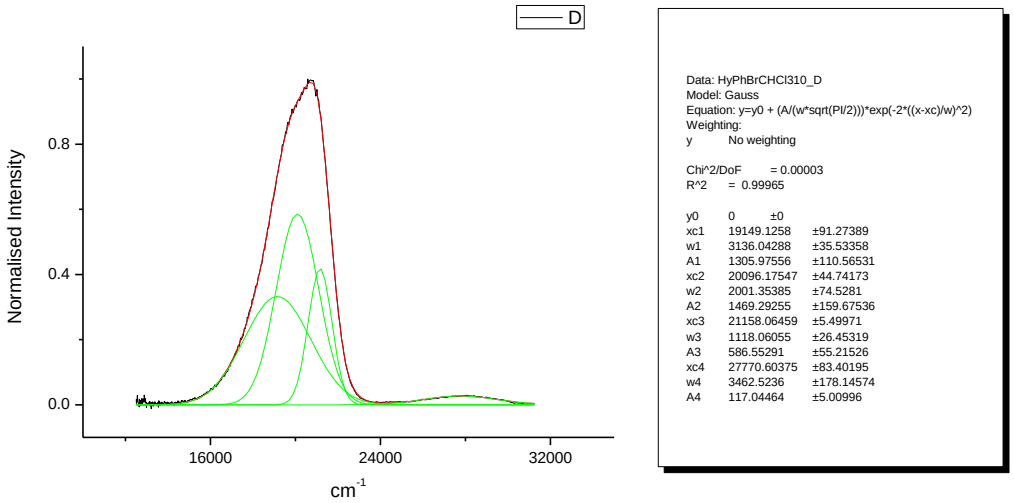

Figure 3.3.173. Gaussian model fit of the normalised fluorescence emission spectrum of **18** recorded in Chloroform at 310 nm excitation.

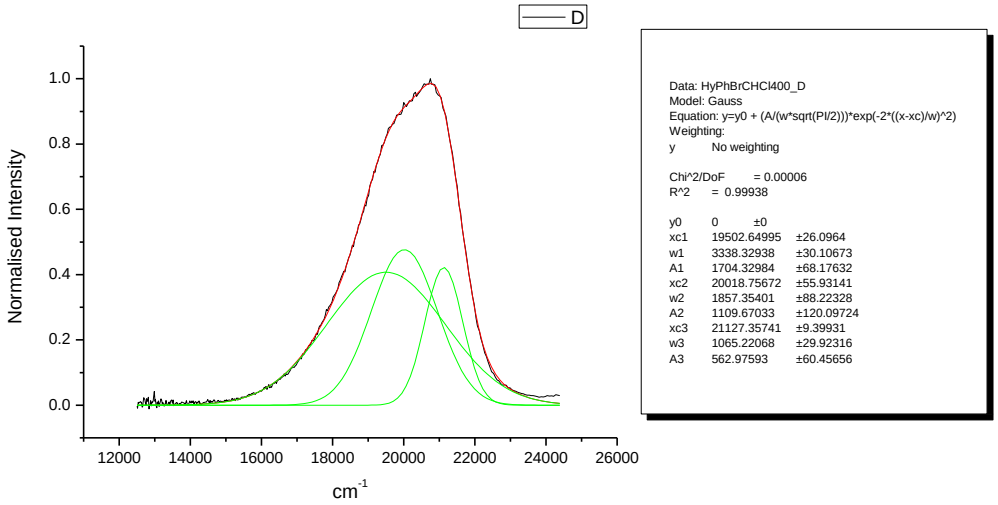

Figure 3.3.174. Gaussian model fit of the normalised fluorescence emission spectrum of **18** recorded in Chloroform at 400 nm excitation.

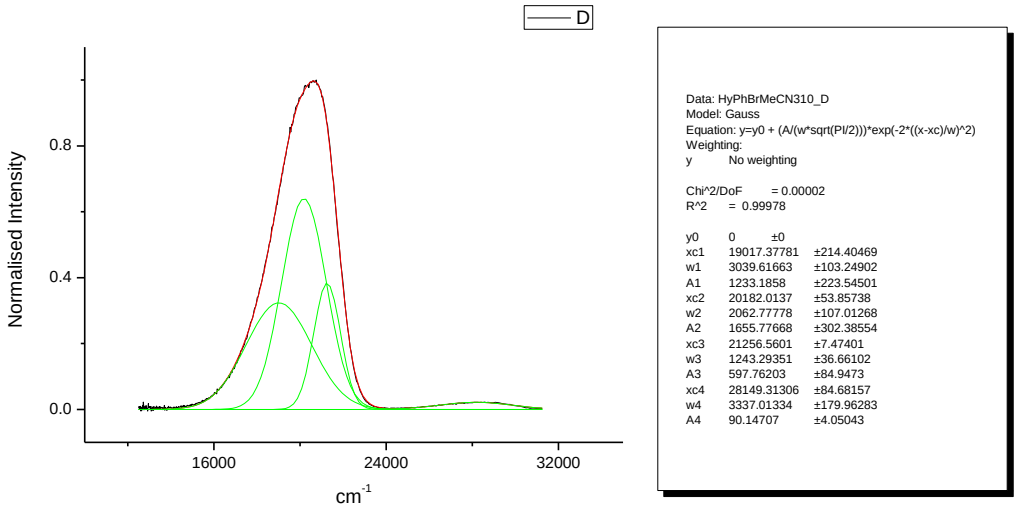

Figure 3.3.175. Gaussian model fit of the normalised fluorescence emission spectrum of **18** recorded in Acetonitrile at 310 nm excitation.

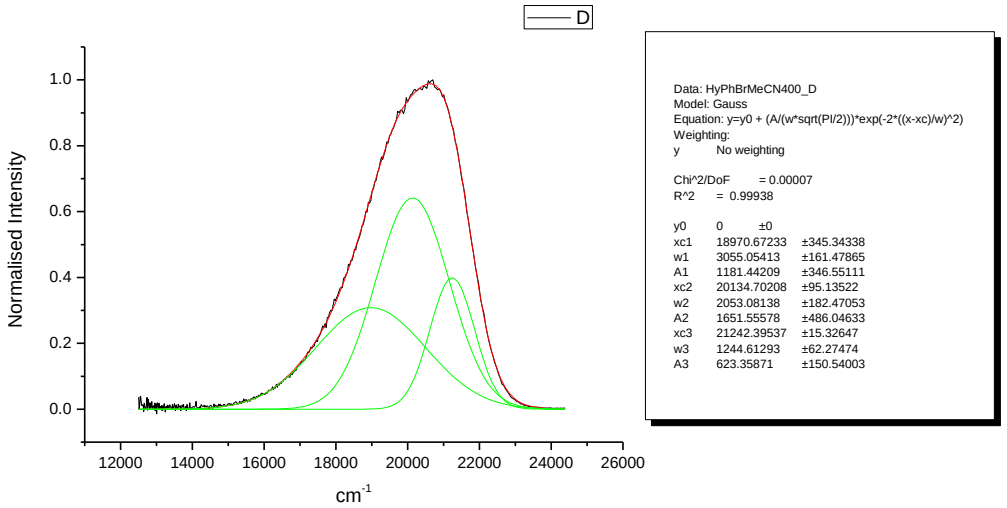

Figure 3.3.176. Gaussian model fit of the normalised fluorescence emission spectrum of **18** recorded in Acetonitrile at 400 nm excitation.

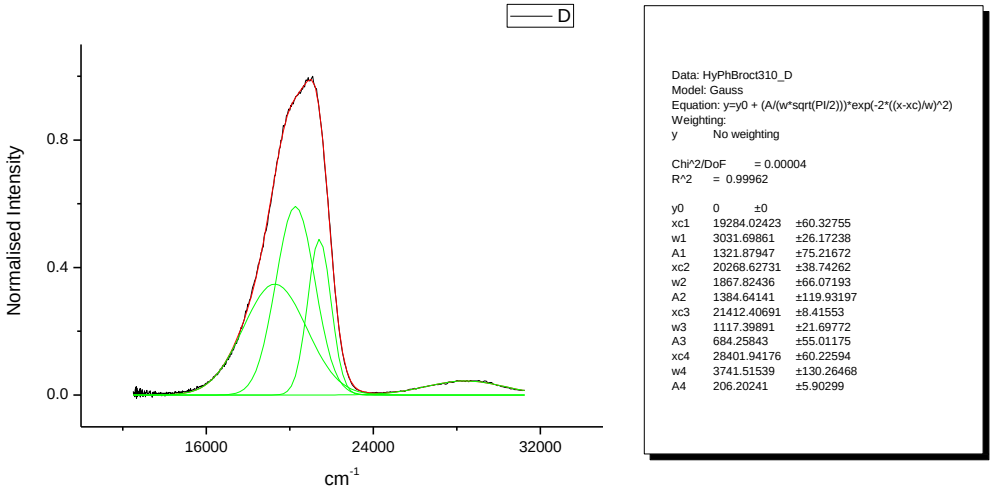

Figure 3.3.177. Gaussian model fit of the normalised fluorescence emission spectrum of **18** recorded in 1-octanol at 310 nm excitation.

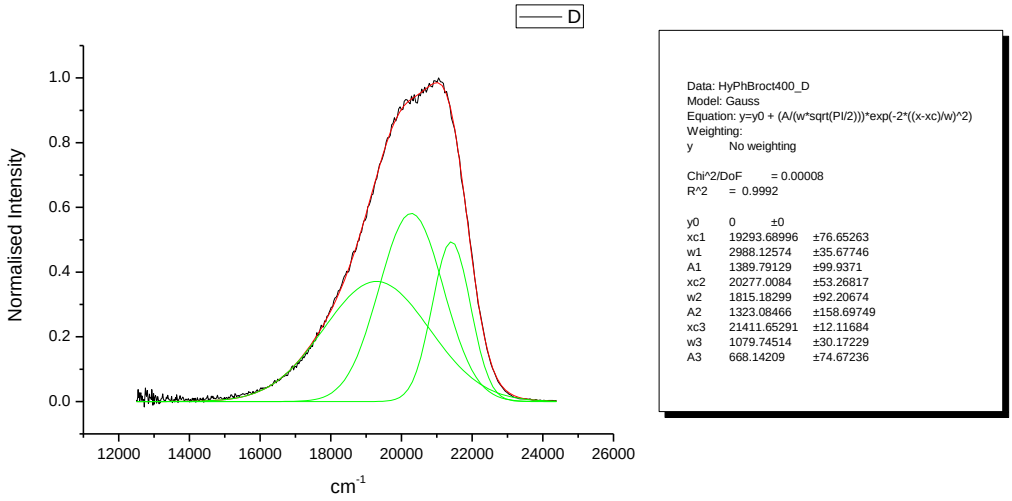

Figure 3.3.178. Gaussian model fit of the normalised fluorescence emission spectrum of **18** recorded in 1-octanol at 400 nm excitation.

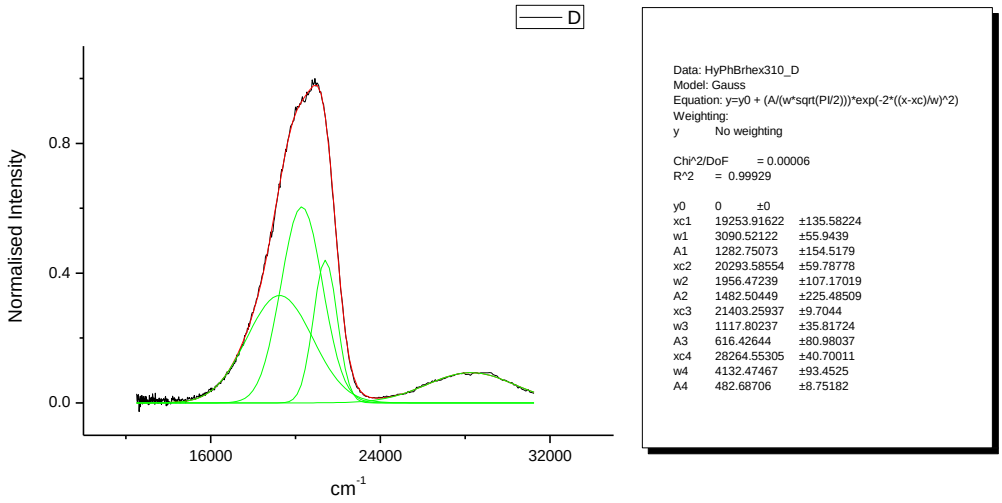

Figure 3.3.179. Gaussian model fit of the normalised fluorescence emission spectrum of **18** recorded in 1-hexanol at 310 nm excitation.

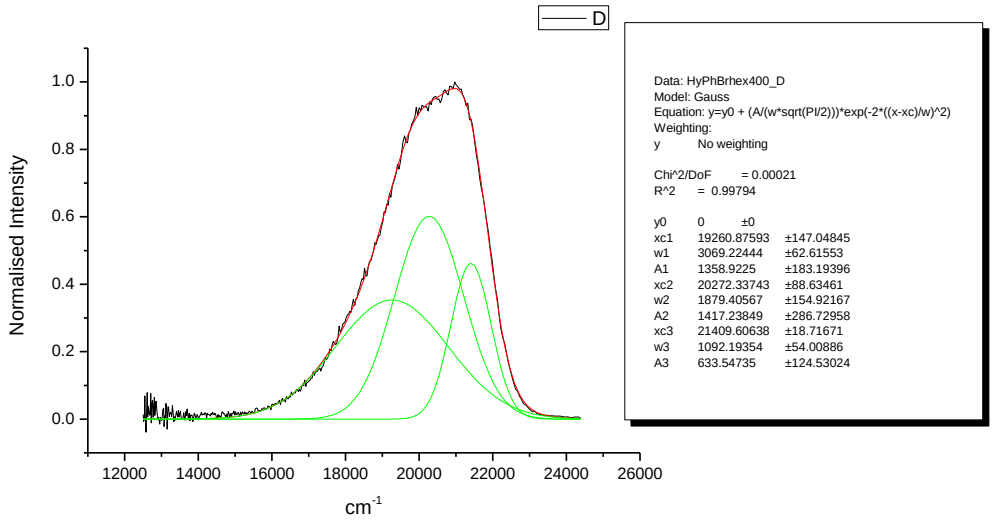

Figure 3.3.180. Gaussian model fit of the normalised fluorescence emission spectrum of **18** recorded in 1-hexanol at 400 nm excitation.

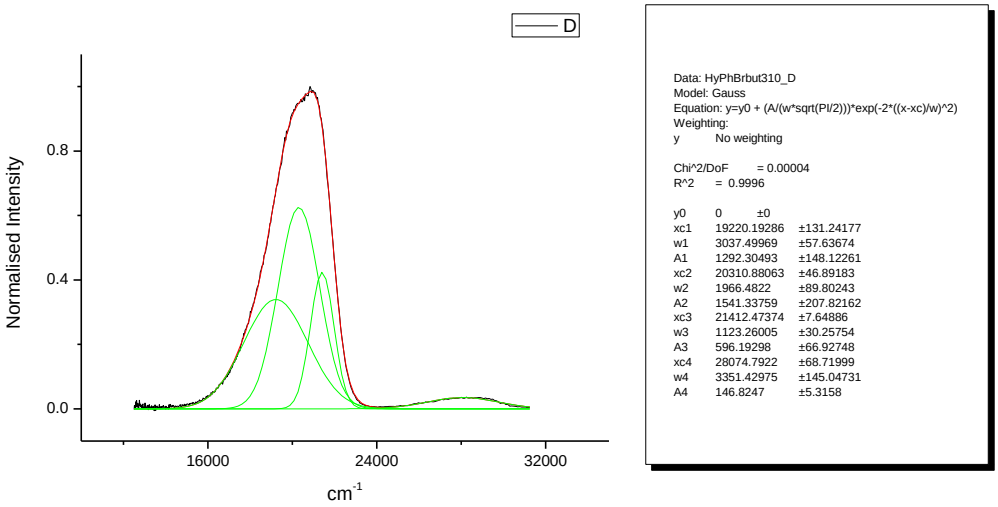

Figure 3.3.181. Gaussian model fit of the normalised fluorescence emission spectrum of **18** recorded in 1-butanol at 310 nm excitation.

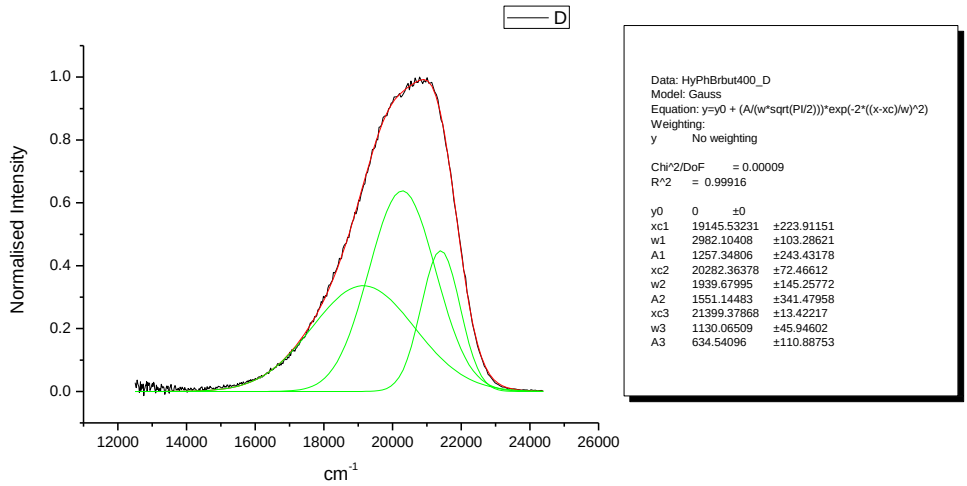

Figure 3.3.182. Gaussian model fit of the normalised fluorescence emission spectrum of **18** recorded in 1-butanol at 400 nm excitation.

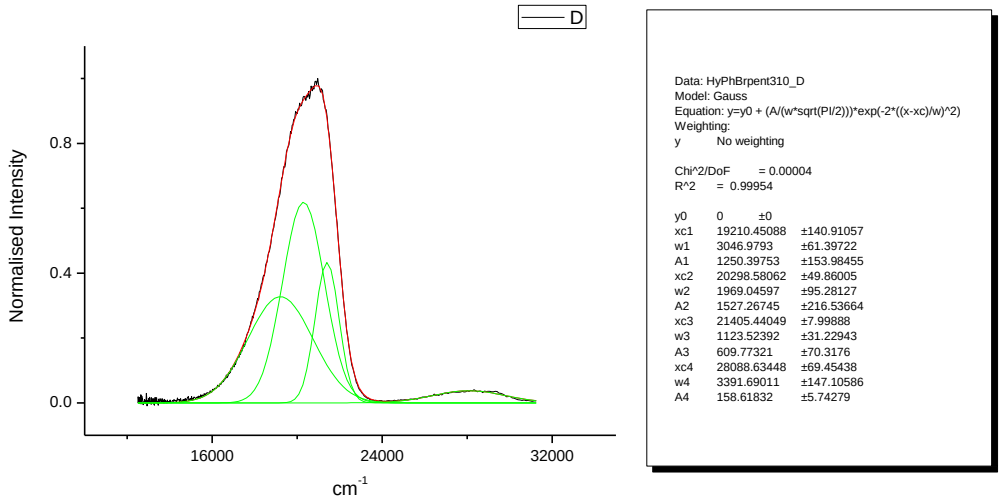

Figure 3.3.183. Gaussian model fit of the normalised fluorescence emission spectrum of **18** recorded in 1-pentanol at 310 nm excitation.

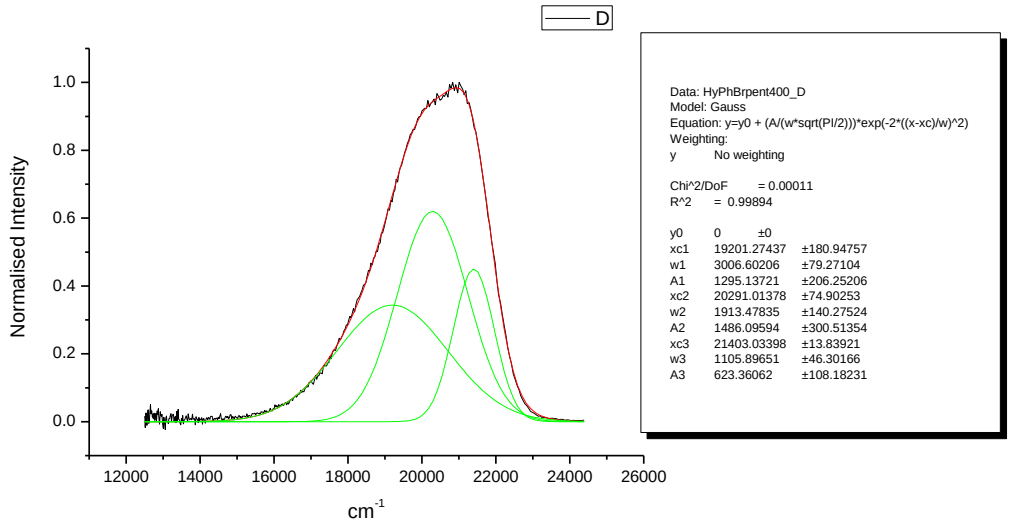

Figure 3.3.184. Gaussian model fit of the normalised fluorescence emission spectrum of **18** recorded in 1-pentanol at 400 nm excitation.

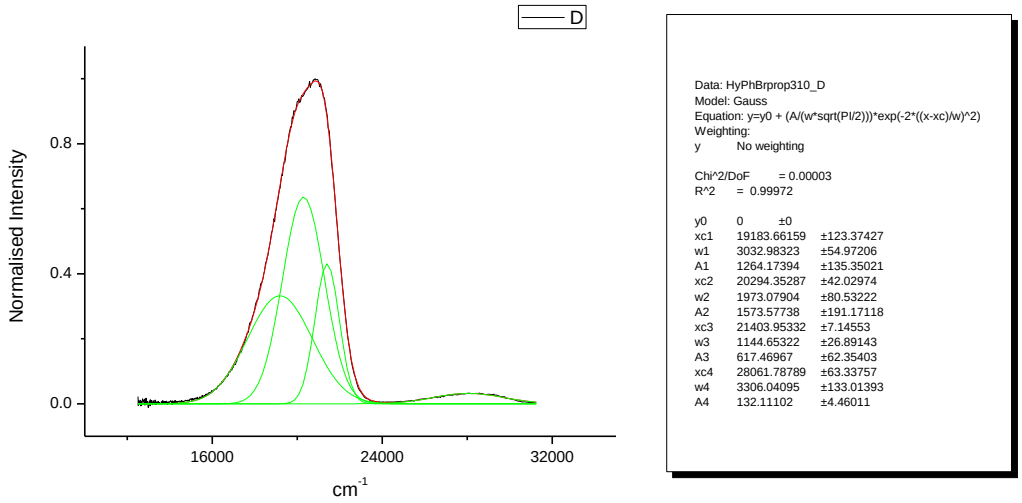

Figure 3.3.185. Gaussian model fit of the normalised fluorescence emission spectrum of **18** recorded in 1-propanol at 310 nm excitation.

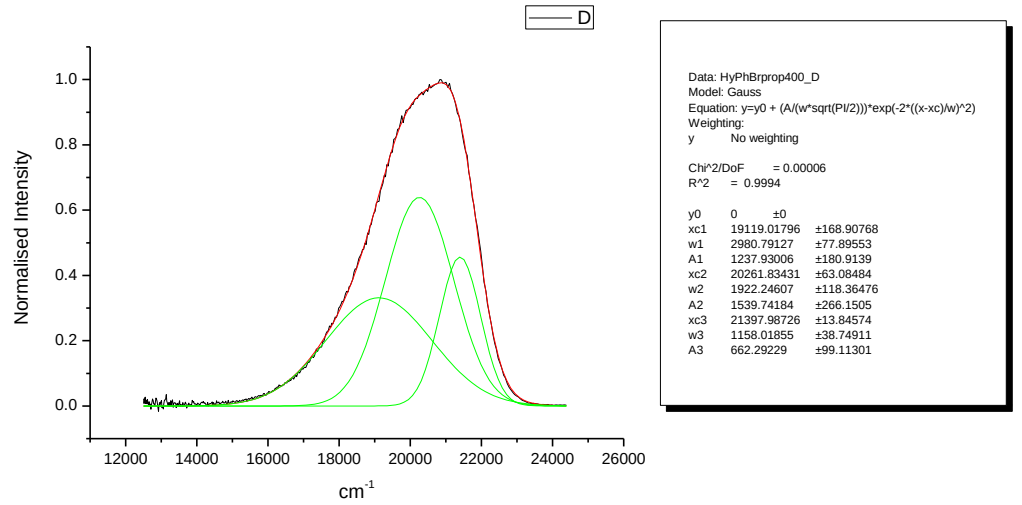

Figure 3.3.186. Gaussian model fit of the normalised fluorescence emission spectrum of **18** recorded in 1-propanol at 400 nm excitation.

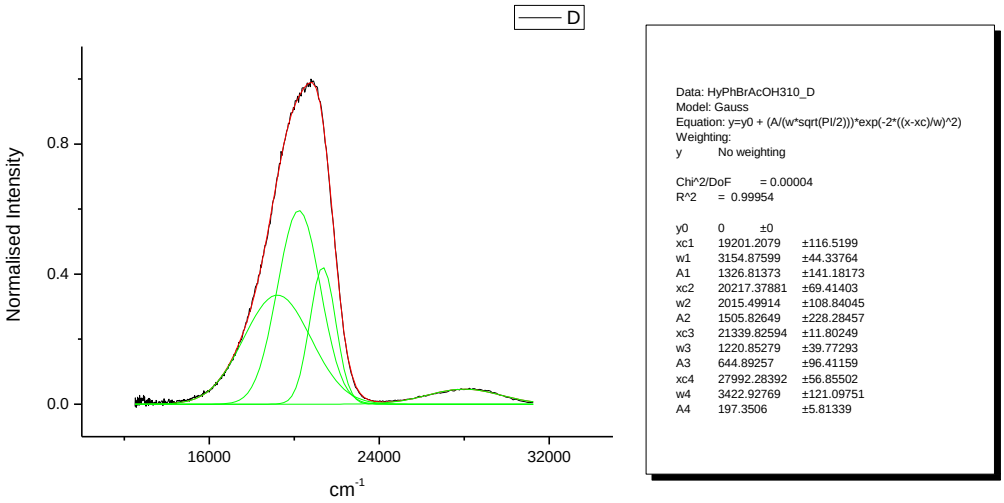

Figure 3.3.187. Gaussian model fit of the normalised fluorescence emission spectrum of **18** recorded in Acetic Acid at 310 nm excitation.

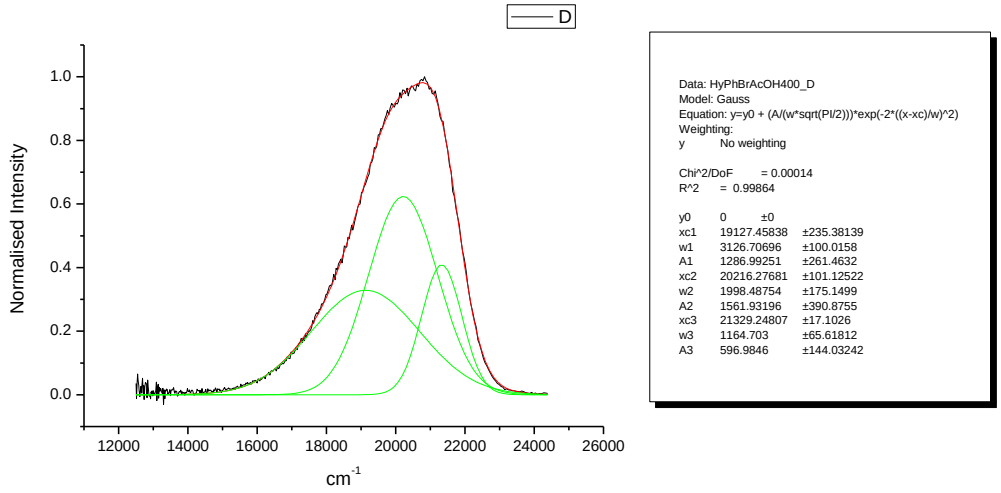

Figure 3.3.188. Gaussian model fit of the normalised fluorescence emission spectrum of **18** recorded in Acetic Acid at 400 nm excitation.

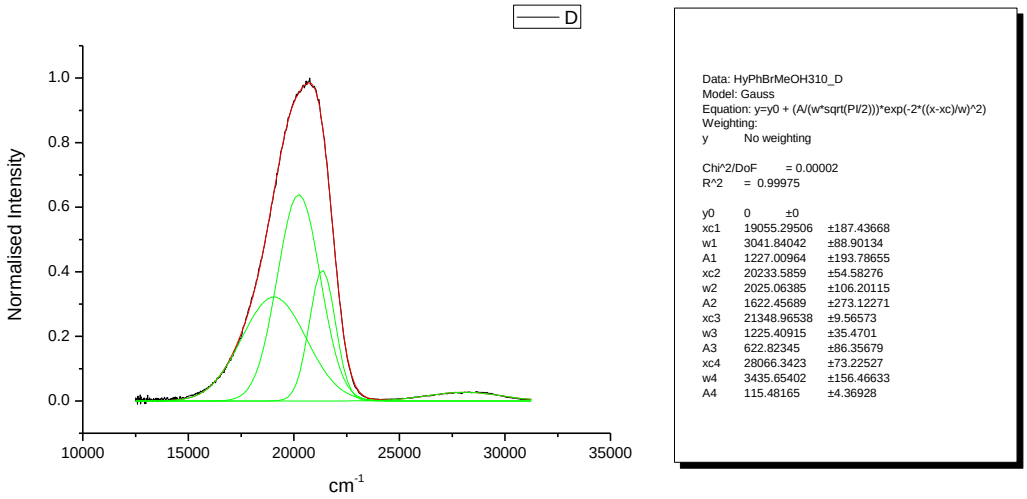

Figure 3.3.189. Gaussian model fit of the normalised fluorescence emission spectrum of **18** recorded in Methanol at 310 nm excitation.

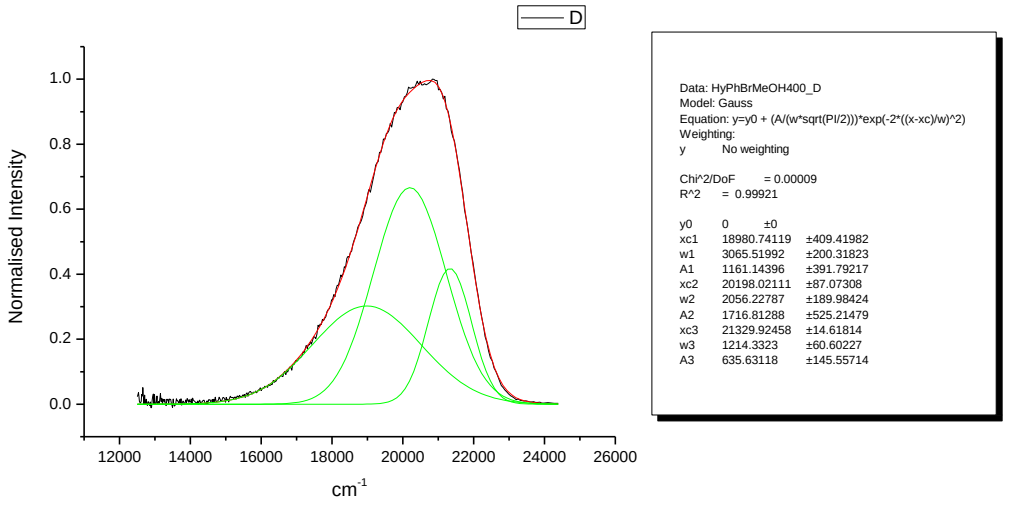

Figure 3.3.190. Gaussian model fit of the normalised fluorescence emission spectrum of **18** recorded in Methanol at 400 nm excitation.

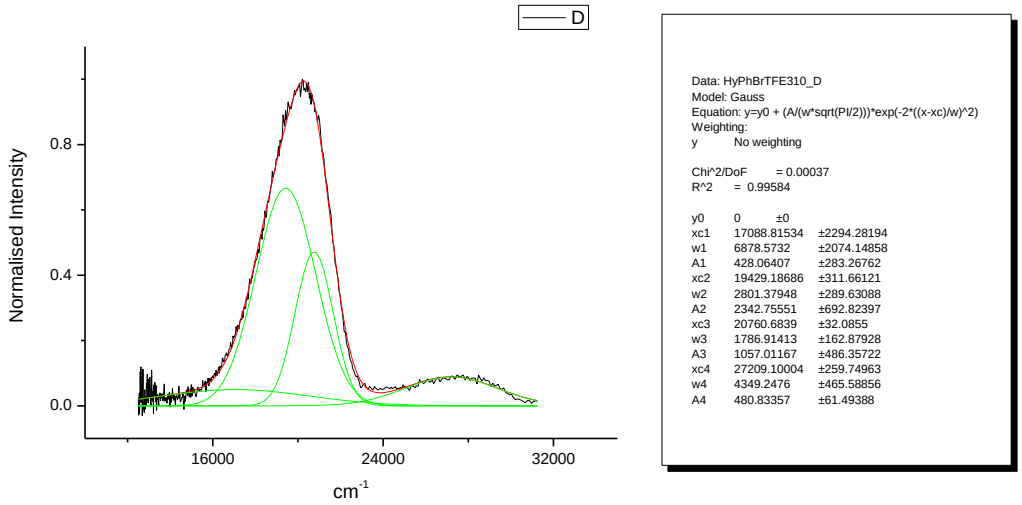

Figure 3.3.191. Gaussian model fit of the normalised fluorescence emission spectrum of **18** recorded in 2,2,2-trifluoroethanol at 310 nm excitation.

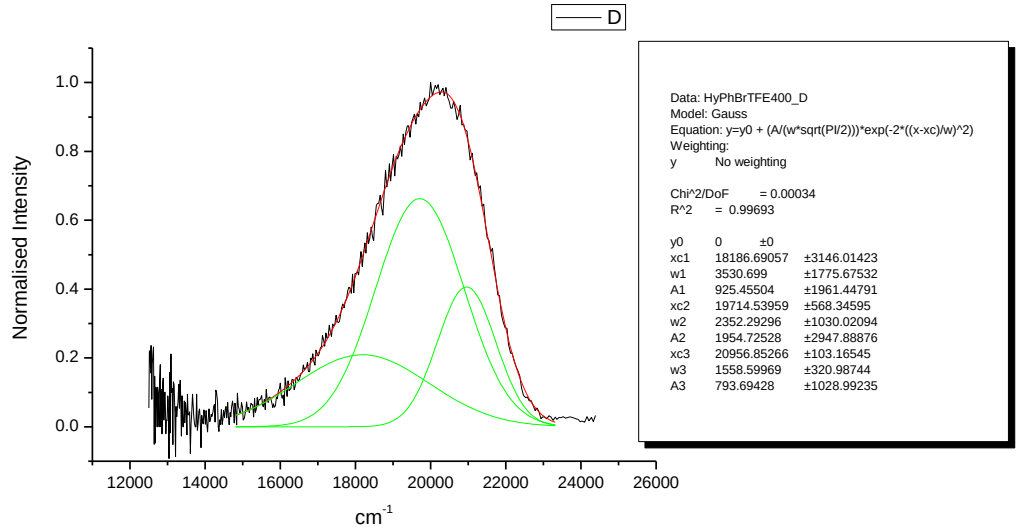

Figure 3.3.192. Gaussian model fit of the normalised fluorescence emission spectrum of **18** recorded in 2,2,2-trifluoroethanol at 400 nm excitation.

3.3.11 Fluorescence Excitation spectra.

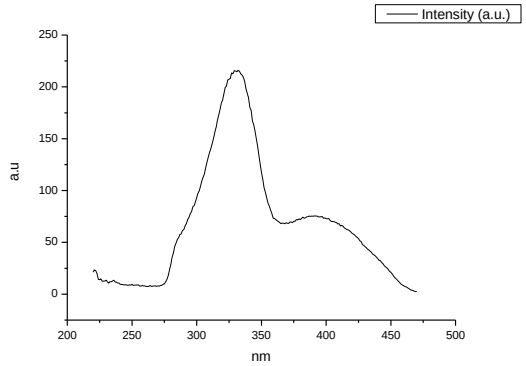

Figure 3.3.193. Fluorescence excitation spectrum of **18** recorded in Toluene with emission fixed at 480 nm.

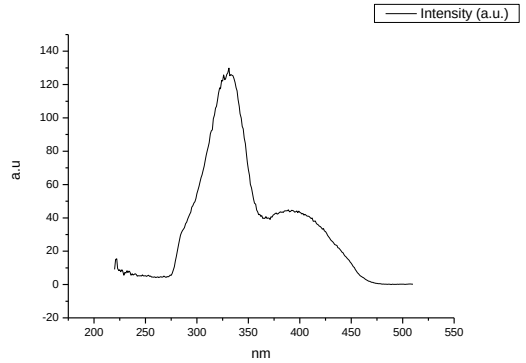

Figure 3.3.194. Fluorescence excitation spectrum of **18** recorded in Toluene with emission fixed at 520 nm.

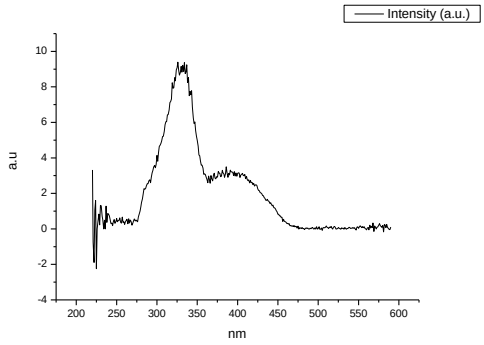

Figure 3.3.195. Fluorescence excitation spectrum of **18** recorded in Toluene with emission fixed at 600 nm.

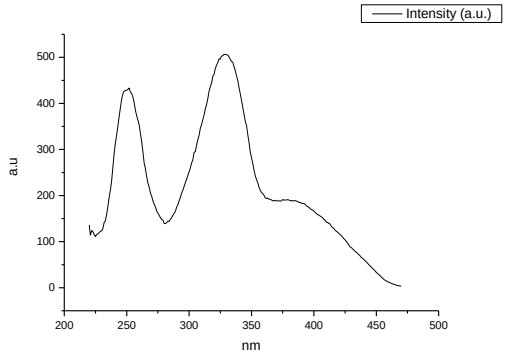

Figure 3.3.196. Fluorescence excitation spectrum of **18** recorded in 1,4-dioxane with emission fixed at 480 nm.

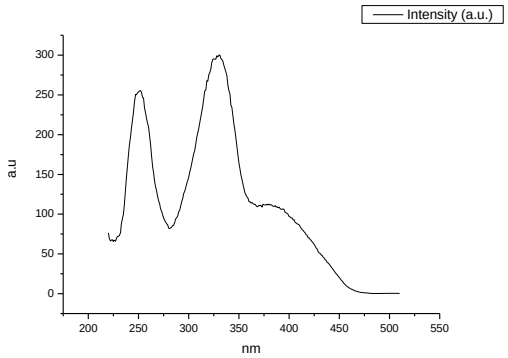

Figure 3.3.197. Fluorescence excitation spectrum of **18** recorded in 1,4-dioxane with emission fixed at 520 nm.

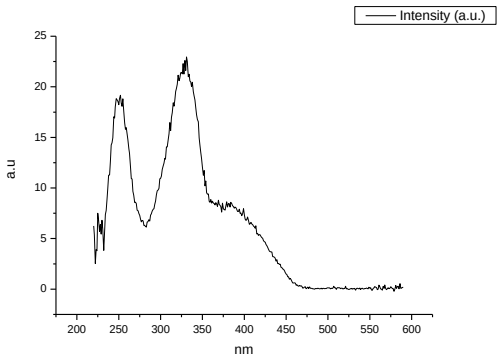

Figure 3.3.198. Fluorescence excitation spectrum of **18** recorded in 1,4-dioxane with emission fixed at 600 nm.

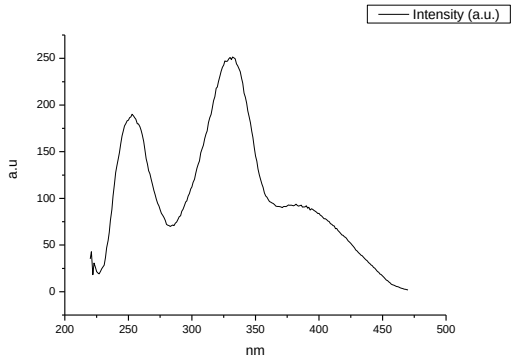

Figure 3.3.199. Fluorescence excitation spectrum of **18** recorded in Chloroform with emission fixed at 480 nm.

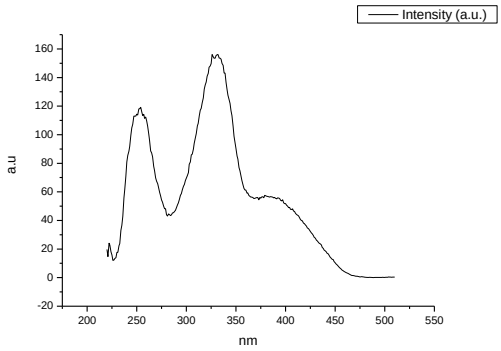

Figure 3.3.200. Fluorescence excitation spectrum of **18** recorded in Chloroform with emission fixed at 520 nm.

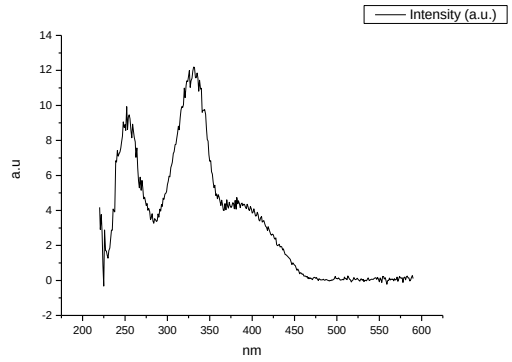

Figure 3.3.201. Fluorescence excitation spectrum of **18** recorded in Chloroform with emission fixed at 600 nm.

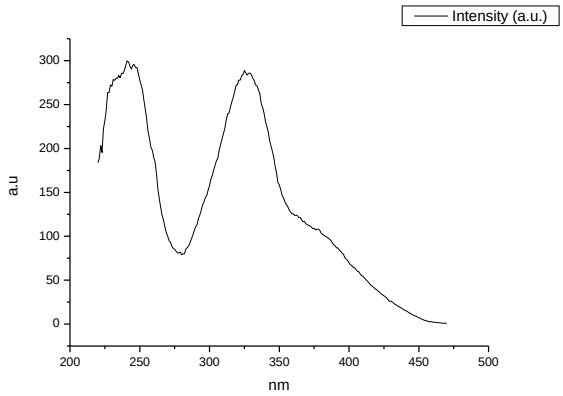

Figure 3.3.202. Fluorescence excitation spectrum of **18** recorded in Acetonitrile with emission fixed at 480 nm.

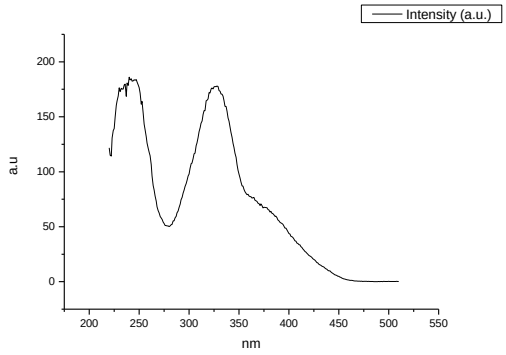

Figure 3.3.203. Fluorescence excitation spectrum of **18** recorded in Acetonitrile with emission fixed at 520 nm.

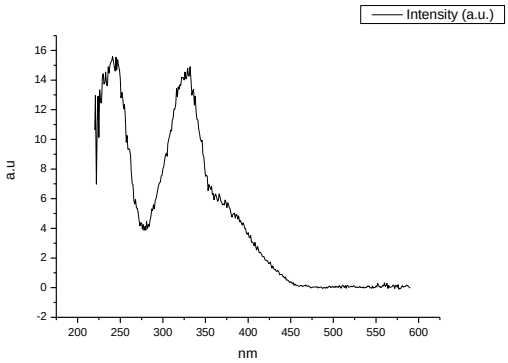

Figure 3.3.204. Fluorescence excitation spectrum of **18** recorded in Acetonitrile with emission fixed at 600 nm.

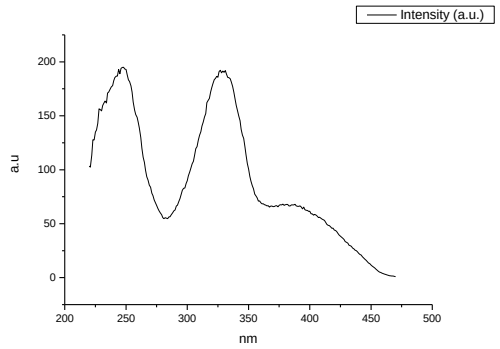

Figure 3.3.205. Fluorescence excitation spectrum of **18** recorded in 1-octanol with emission fixed at 480 nm.

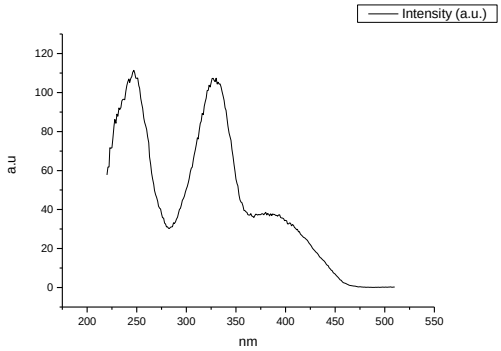

Figure 3.3.206. Fluorescence excitation spectrum of **18** recorded in 1-octanol with emission fixed at 520 nm.

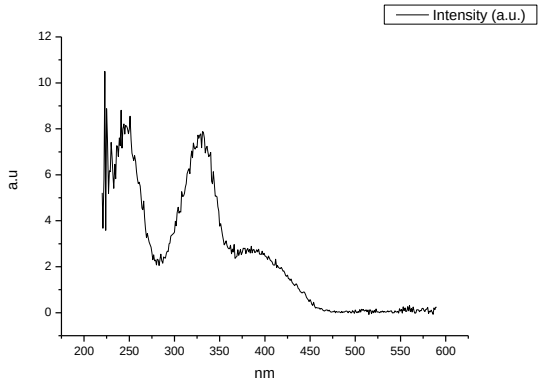

Figure 3.3.207. Fluorescence excitation spectrum of **18** recorded in 1-octanol with emission fixed at 600 nm.

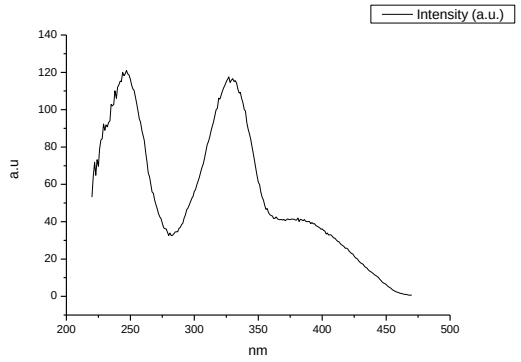

Figure 3.3.208. Fluorescence excitation spectrum of **18** recorded in 1-hexanol with emission fixed at 480 nm.

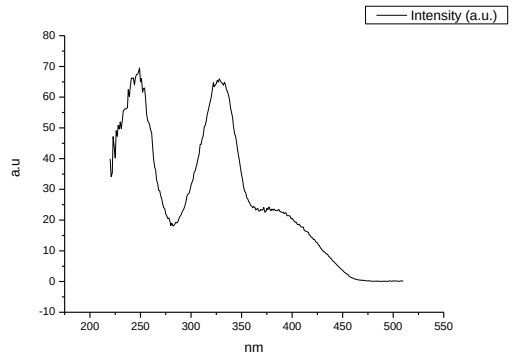

Figure 3.3.209. Fluorescence excitation spectrum of **18** recorded in 1-hexanol with emission fixed at 520 nm.

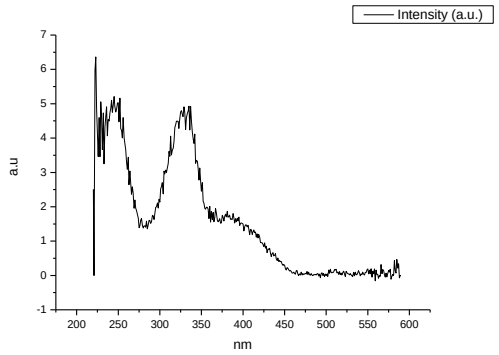

Figure 3.3.210. Fluorescence excitation spectrum of **18** recorded in 1-hexanol with emission fixed at 600 nm.

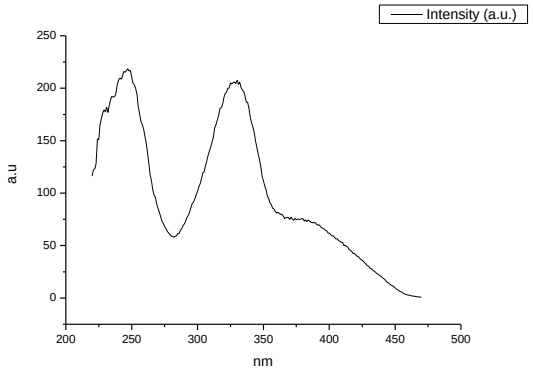

Figure 3.3.211. Fluorescence excitation spectrum of **18** recorded in 1-butanol with emission fixed at 480 nm.

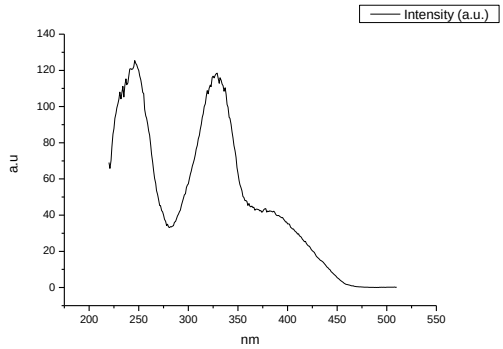

Figure 3.3.212. Fluorescence excitation spectrum of **18** recorded in 1-butanol with emission fixed at 520 nm.

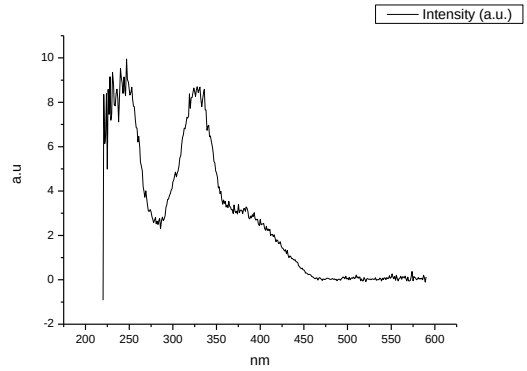

Figure 3.3.213. Fluorescence excitation spectrum of **18** recorded in 1-butanol with emission fixed at 600 nm.

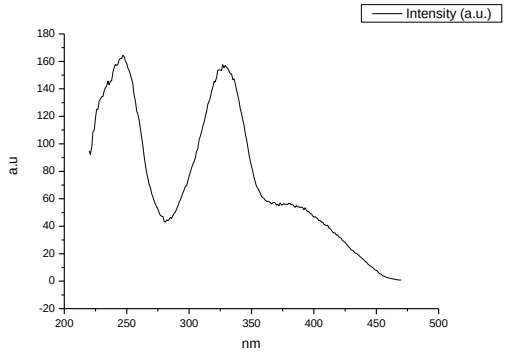

Figure 3.3.214. Fluorescence excitation spectrum of **18** recorded in 1-pentanol with emission fixed at 480 nm.

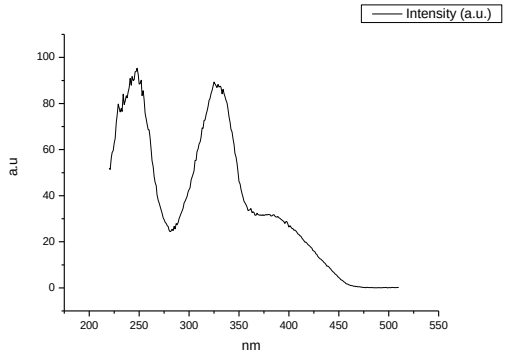

Figure 3.3.215. Fluorescence excitation spectrum of **18** recorded in 1-pentanol with emission fixed at 520 nm.

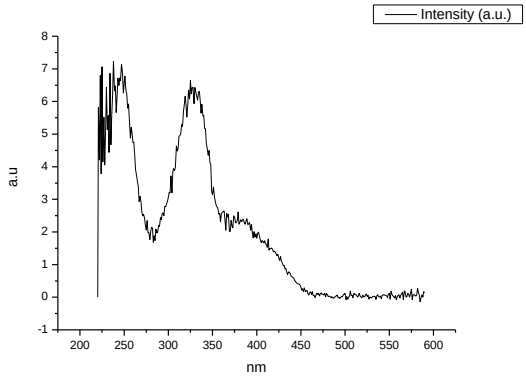

Figure 3.3.216. Fluorescence excitation spectrum of **18** recorded in 1-pentanol with emission fixed at 600 nm.

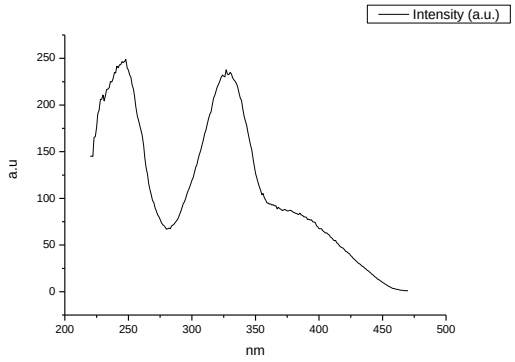

Figure 3.3.217. Fluorescence excitation spectrum of **18** recorded in 1-propanol with emission fixed at 480 nm.

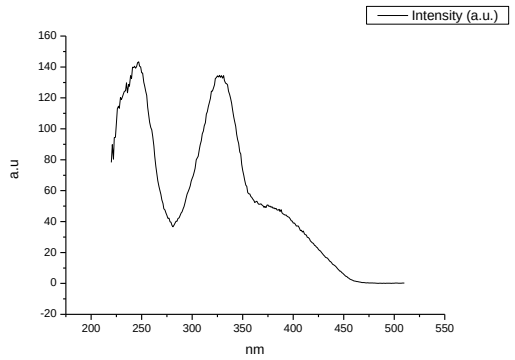

Figure 3.3.218. Fluorescence excitation spectrum of **18** recorded in 1-propanol with emission fixed at 520 nm.

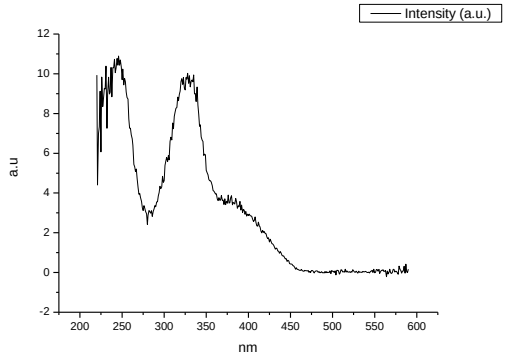

Figure 3.3.219. Fluorescence excitation spectrum of **18** recorded in 1-propanol with emission fixed at 600 nm.

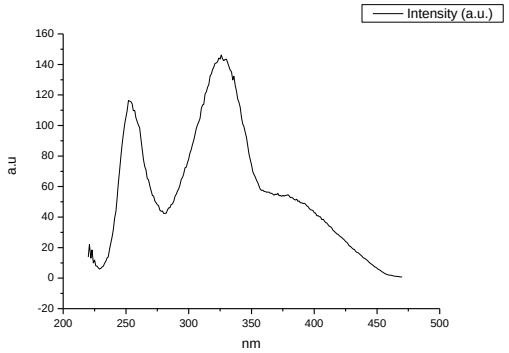

Figure 3.3.220. Fluorescence excitation spectrum of **18** recorded in Acetic Acid with emission fixed at 480 nm.

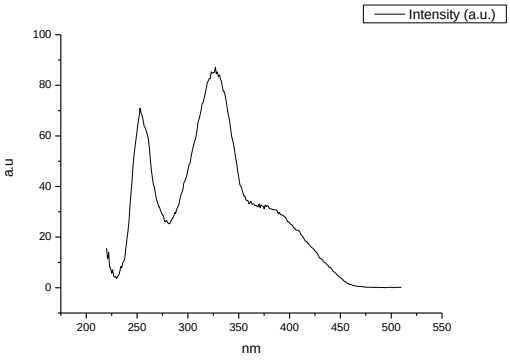

Figure 3.3.221. Fluorescence excitation spectrum of **18** recorded in Acetic Acid with emission fixed at 520 nm.

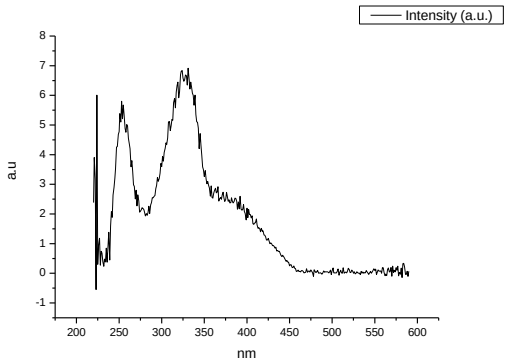

Figure 3.3.222. Fluorescence excitation spectrum of **18** recorded in Acetic Acid with emission fixed at 600 nm.

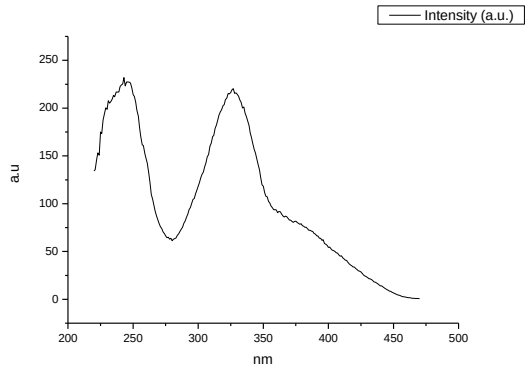

Figure 3.3.223. Fluorescence excitation spectrum of **18** recorded in Methanol with emission fixed at 480 nm.

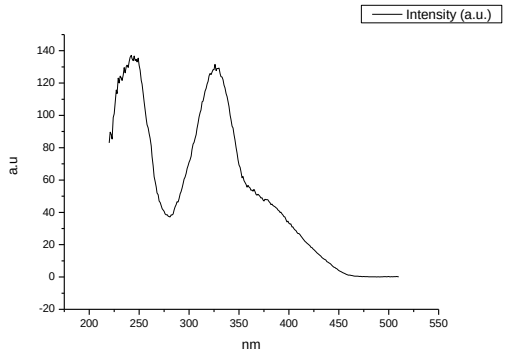

Figure 3.3.224. Fluorescence excitation spectrum of **18** recorded in Methanol with emission fixed at 520 nm.

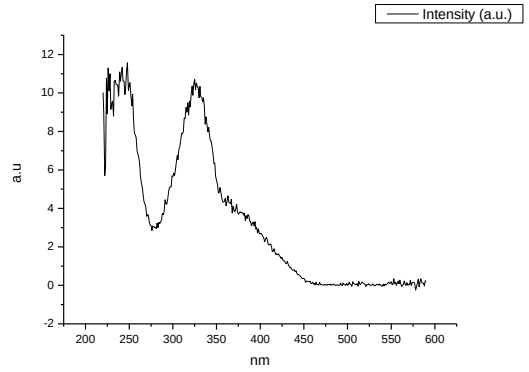

Figure 3.3.225. Fluorescence excitation spectrum of **18** recorded in Methanol with emission fixed at 600 nm.

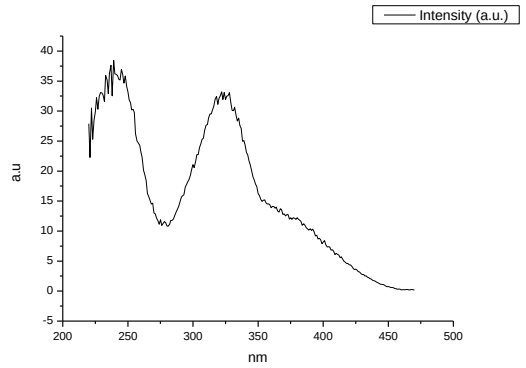

Figure 3.3.226. Fluorescence excitation spectrum of **18** recorded in 2,2,2-trifluoroethanol with emission fixed at 480 nm.

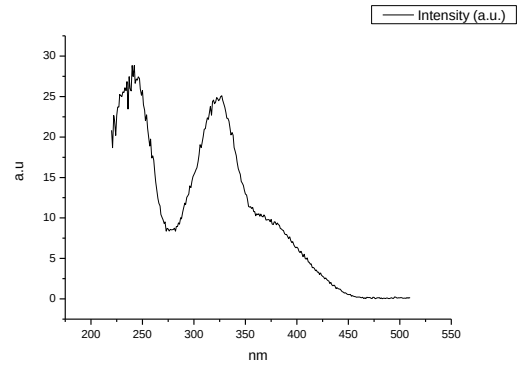

Figure 3.3.227. Fluorescence excitation spectrum of **18** recorded in 2,2,2-trifluoroethanol with emission fixed at 520 nm.

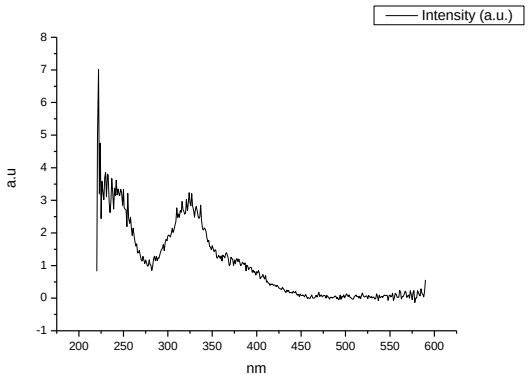

Figure 3.3.228. Fluorescence excitation spectrum of **18** recorded in 2,2,2-trifluoroethanol with emission fixed at 600 nm.

3.4 COMPOUND 19.

3.4.1 Quantum Yield Summary.

Solvent	abs (310 nm)	$\lambda_{ems\ (max)}$	$\Phi_{310\ nm}$	abs (400 nm)	$\lambda_{ems\ (max)}$	$\Phi_{400\ nm}$
Toluene	0.07	522.98	0.33	0.04	525.97	0.39
1,4-Dioxane	0.04	525.97	0.44	0.01	528.05	0.44
Chloroform	0.03	530.00	0.46	0.01	534.02	0.45
Acetonitrile	0.03	534.02	0.39	0.01	532.98	0.35
1-Octanol	0.03	531.04	0.46	0.01	531.04	0.40
1-Hexanol	0.02	534.02	0.46	0.01	532.98	0.43
1-Butanol	0.04	537.01	0.35	0.01	538.95	0.32
1-Pentanol	0.03	535.07	0.45	0.01	534.02	0.40
1-Propanol	0.03	534.02	0.41	0.01	538.95	0.36
Acetic acid	0.02	546.02	0.03	0.01	542.05	0.03
Methanol	0.04	534.02	0.25	0.01	534.02	0.23
2,2,2-Trifluoroethanol	0.03	538.05	0.02	0.01	538.95	0.02

Table 3.4.1. Summary of ultraviolet-visible absorbance values at 310 nm and 400 nm, emission maxima and quantum yield (Φ) of **19** at 310 nm and 400 nm excitation.

3.4.2 310 nm excitation Gaussian band fit summaries.

Solvent	λ max$_{em}$ Band 1 (cm^{-1})	λ max$_{em}$ Band 1 (nm)	λ max$_{em}$ Band 2 (cm^{-1})	λ max$_{em}$ Band 2 (nm)	λ max$_{em}$ Band 3 (cm^{-1})	λ max$_{em}$ Band 3 (nm)
Toluene	17523.22	570.67	18515.50	540.09	19546.16	511.61
1,4-Dioxane	17639.20	566.92	18476.46	541.23	19505.80	512.67
Chloroform	17377.06	575.47	18293.59	546.64	19319.35	517.62
Acetonitrile	17555.70	569.62	18215.75	548.98	19324.12	517.49
1-Octanol	17444.32	573.25	18356.15	544.78	19391.45	515.69
1-Hexanol	17366.97	575.81	18273.24	547.25	19339.34	517.08
1-Butanol	17375.19	575.53	18219.57	548.86	19304.64	518.01
1-Pentanol	17379.02	575.41	18239.05	548.27	19317.55	517.66
1-Propanol	17367.68	575.78	18185.85	549.88	19276.53	518.77
Acetic acid	17144.38	583.28	18082.49	553.02	19262.14	519.15
Methanol	17320.73	577.34	18075.72	553.23	19195.66	520.95
2,2,2-Trifluoroethanol	14106.65	708.89	18045.74	554.15	18566.85	538.59

Solvent	λ max$_{em}$ Band 4 (cm^{-1})	λ max$_{em}$ Band 4 (nm)	λ max$_{em}$ Band 5 (cm^{-1})	λ max$_{em}$ Band 5 (nm)
Toluene	28390.17	352.23	-	-
1,4-Dioxane	28173.48	354.94	-	-
Chloroform	28160.43	355.11	-	-
Acetonitrile	28326.01	353.03	-	-
1-Octanol	28543.57	350.34	-	-
1-Hexanol	28333.47	352.94	-	-
1-Butanol	28250.67	353.97	-	-
1-Pentanol	28256.08	353.91	-	-
1-Propanol	28202.51	354.58	-	-
Acetic acid	26007.67	384.50	28670.56	348.79
Methanol	28112.43	355.71	-	-
2,2,2-Trifluoroethanol	24436.15	409.23	27685.79	361.20

Table 3.4.2. Summary of band maxima of 5 band fit using Gaussian model for normalised **19** emission spectra recorded at 310 nm excitation.

(a)

Solvent	Width Band 1 (cm^{-1})	Width Band 2 (cm^{-1})	Width Band 3 (cm^{-1})	Width Band 4 (cm^{-1})	Width Band 5 (cm^{-1})
Toluene	3176.46	2053.58	1122.11	4638.89	-
1,4-Dioxane	3231.89	2029.62	1212.74	4374.99	-
Chloroform	3228.85	2133.01	1268.38	3784.79	-
Acetonitrile	3513.11	2293.29	1544.53	4305.57	-
1-Octanol	3251.68	2122.41	1291.16	4493.15	-
1-Hexanol	3302.03	2183.99	1370.80	4617.91	-
1-Butanol	3341.59	2185.50	1416.64	4592.96	-
1-Pentanol	3336.56	2209.41	1383.70	4297.30	-
1-Propanol	3350.49	2219.34	1448.49	4400.18	-
Acetic acid	3731.97	2290.77	1512.77	5275.66	3102.23
Methanol	3480.50	2299.64	1560.34	4471.59	-
2,2,2-Trifluoroethanol	48.08	1877.46	4588.27	2036.84	4026.34

(b)

Solvent	Area Band 1 (cm^{-1})	Area Band 2 (cm^{-1})	Area Band 3 (cm^{-1})	Area Band 4 (cm^{-1})	Area Band 5 (cm^{-1})
Toluene	1339.69	1510.04	548.48	117.75	-
1,4-Dioxane	1556.35	1331.59	574.83	196.48	-
Chloroform	1315.39	1503.98	606.45	154.23	-
Acetonitrile	1295.56	1482.04	738.38	126.68	-
1-Octanol	1408.32	1497.36	573.58	152.79	-
1-Hexanol	1288.80	1546.91	634.95	266.30	-
1-Butanol	1322.28	1505.54	671.68	139.51	-
1-Pentanol	1289.85	1574.10	653.44	138.36	-
1-Propanol	1310.97	1501.85	703.35	129.42	-
Acetic acid	1272.18	1662.32	704.87	389.80	745.46
Methanol	1292.38	1518.61	749.48	145.63	-
2,2,2-Trifluoroethanol	5.55	380.05	4560.20	337.25	1353.91

Tables 3.4.3 (a.) and (b.). Summary band width and band area of 5 band fit using Gaussian model for normalised **19** emission spectra recorded at 310 nm excitation.

Solvent	Band 1 Area Percentage (%)	Band 2 Area Percentage (%)	Band 3 Area Percentage (%)	Band 4 Area Percentage (%)	Band 5 Area Percentage (%)
Toluene	38.10	42.95	15.60	3.35	-
1,4-Dioxane	42.53	36.39	15.71	5.37	-
Chloroform	36.74	42.01	16.94	4.31	-
Acetonitrile	35.57	40.69	20.27	3.48	-
1-Octanol	38.77	41.23	15.79	4.21	-
1-Hexanol	34.49	41.39	16.99	7.13	-
1-Butanol	36.34	41.37	18.46	3.83	-
1-Pentanol	35.28	43.06	17.87	3.78	-
1-Propanol	35.96	41.20	19.29	3.55	-
Acetic acid	26.64	34.82	14.76	8.16	15.61
Methanol	34.87	40.98	20.22	3.93	-
2,2,2-Trifluoroethanol	0.08	5.73	68.71	5.08	20.40

Table 3.4.4. Total Area Percentages of 5 band fit using Gaussian model for normalised **19** emission spectra recorded at 310 nm excitation.

Solvent	Area Ratio Band 1/2 (310 nm ex)	Area Ratio Band 1/3 (310 nm ex)	Area Ratio Band 1/4 (310 nm ex)	Area Ratio Band 1/5 (310 nm ex)
Toluene	0.89	2.44	11.38	-
1,4-Dioxane	1.17	2.71	7.92	-
Chloroform	0.87	2.17	8.53	-
Acetonitrile	0.87	1.75	10.23	-
1-Octanol	0.94	2.46	9.22	-
1-Hexanol	0.83	2.03	4.84	-
1-Butanol	0.88	1.97	9.48	-
1-Pentanol	0.82	1.97	9.32	-
1-Propanol	0.87	1.86	10.13	-
Acetic acid	0.77	1.80	3.26	1.71
Methanol	0.85	1.72	8.87	-
2,2,2-Trifluoroethanol	0.01	0.00	0.02	0.00

Solvent	Area Ratio Band 2/3 (310 nm ex)	Area Ratio Band 2/4 (310 nm ex)	Area Ratio Band 2/5 (310 nm ex)	Area Ratio Band 3/4 (310 nm ex)	Area Ratio Band 3/5 (310 nm ex)	Area Ratio Band 4/5 (310 nm ex)
Toluene	2.75	12.82	-	4.66	-	-
1,4-Dioxane	2.32	6.78	-	2.93	-	-
Chloroform	2.48	9.75	-	3.93	-	-
Acetonitrile	2.01	11.70	-	5.83	-	-
1-Octanol	2.61	9.80	-	3.75	-	-
1-Hexanol	2.44	5.81	-	2.38	-	-
1-Butanol	2.24	10.79	-	4.81	-	-
1-Pentanol	2.41	11.38	-	4.72	-	-
1-Propanol	2.14	11.60	-	5.43	-	-
Acetic acid	2.36	4.26	2.23	1.81	0.95	0.52
Methanol	2.03	10.43	-	5.15	-	-
2,2,2-Trifluoroethanol	0.08	1.13	0.28	13.52	3.37	0.25

Table 3.4.5. Area Ratios of 5 band fit using Gaussian model for normalised **19** emission spectra recorded at 310 nm excitation.

3.4.3 400 nm excitation Gaussian band fit summaries.

Solvent	λ max$_{em}$ Band 1 (cm^{-1})	λ max$_{em}$ Band 1 (nm)	λ max$_{em}$ Band 2 (cm^{-1})	λ max$_{em}$ Band 2 (nm)	λmax$_{em}$ Band 3 (cm^{-1})	λmax$_{em}$ Band 3 (nm)
Toluene	17456.71	572.85	18493.74	540.72	19535.15	511.90
1,4-Dioxane	17584.47	568.68	18491.63	540.79	19511.76	512.51
Chloroform	17415.03	574.22	18249.30	547.97	19305.48	517.99
Acetonitrile	17214.93	580.89	18164.13	550.54	19297.78	518.19
1-Octanol	17269.37	579.06	18282.56	546.97	19361.34	516.49
1-Hexanol	17200.00	581.40	18238.24	548.30	19328.10	517.38
1-Butanol	17202.43	581.31	18191.62	549.70	19298.17	518.18
1-Pentanol	17163.48	582.63	18218.40	548.90	19317.34	517.67
1-Propanol	17207.42	581.14	18204.12	549.33	19293.25	518.32
Acetic acid	16234.74	615.96	17754.32	563.24	19167.26	521.72
Methanol	17146.97	583.19	18076.07	553.22	19218.46	520.33
2,2,2-Trifluoroethanol	18484.38	541.00	-	-	21039.80	475.29

Table 3.4.6. Summary of band maxima of 3 band fit using Gaussian model for normalised **19** emission spectra recorded at 400 nm excitation.

Solvent	Width Band 1 (cm^{-1})	Width Band 2 (cm^{-1})	Width Band 3 (cm^{-1})
Toluene	3174.69	2068.75	1148.79
1,4-Dioxane	3168.38	2027.03	1222.77
Chloroform	3306.94	2091.43	1303.18
Acetonitrile	3531.67	2403.21	1621.55
1-Octanol	3240.59	2182.59	1390.15
1-Hexanol	3321.88	2241.03	1415.71
1-Butanol	3351.51	2254.96	1446.65
1-Pentanol	3322.47	2247.14	1429.31
1-Propanol	3315.94	2243.40	1468.18
Acetic acid	6105.11	2354.28	1623.69
Methanol	3500.37	2347.43	1556.24
2,2,2-Trifluoroethanol	4086.80	-	982.24

Table 3.4.7. Summary of band width of 3 band fit using Gaussian model for normalised **19** emission spectra recorded at 400 nm excitation

Solvent	Area Band 1 (cm^{-1})	Area Band 2 (cm^{-1})	Area Band 3 (cm^{-1})	Area Ratio Band 1/2 (400 nm ex)	Area Ratio Band 1/3 (400 nm ex)	Area Ratio Band 2/3 (400 nm ex)
Toluene	1277.51	1552.04	570.63	0.82	2.24	2.72
1,4-Dioxane	1506.34	1350.55	577.76	1.12	2.61	2.34
Chloroform	1351.76	1425.78	641.39	0.95	2.11	2.22
Acetonitrile	921.55	1771.60	841.66	0.52	1.09	2.10
1-Octanol	1174.56	1614.89	678.67	0.73	1.73	2.38
1-Hexanol	1094.13	1709.92	673.06	0.64	1.63	2.54
1-Butanol	1098.79	1694.67	695.28	0.65	1.58	2.44
1-Pentanol	1084.45	1719.51	692.58	0.63	1.57	2.48
1-Propanol	1164.46	1655.42	687.51	0.70	1.69	2.41
Acetic acid	913.14	1807.01	967.07	0.51	0.94	1.87
Methanol	1122.79	1754.21	737.96	0.64	1.52	2.38
2,2,2-Trifluoroethanol	4579.88	-	120.10	-	38.13	-

Solvent	Band 1 Area Percentage (%)	Band 2 Area Percentage (%)	Band 3 Area Percentage (%)
Toluene	37.57	45.65	16.78
1,4-Dioxane	43.86	39.32	16.82
Chloroform	39.54	41.70	18.76
Acetonitrile	26.07	50.12	23.81
1-Octanol	33.87	46.56	19.57
1-Hexanol	31.47	49.18	19.36
1-Butanol	31.50	48.58	19.93
1-Pentanol	31.01	49.18	19.81
1-Propanol	33.20	47.20	19.60
Acetic acid	24.76	49.01	26.23
Methanol	31.06	48.53	20.41
2,2,2-Trifluoroethanol	97.44	-	2.56

Table 3.4.8. Band areas, area ratios and total area percentage of 3 band fit using Gaussian model for normalised **19** emission spectra recorded at 400 nm excitation.

3.4.4 310 nm Gaussian band fit - Solvatochromic analysis.

3.4.4.1 E_T^N.

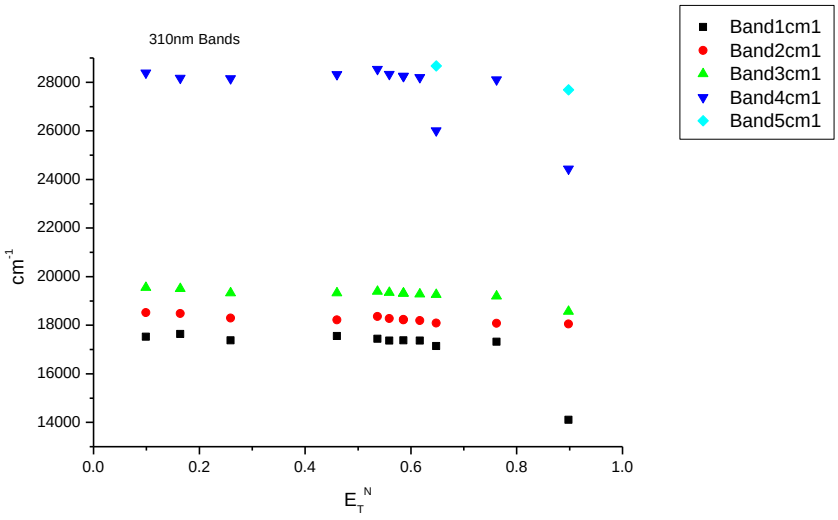

Figure 3.4.1. Band maxima from Gaussian model fit of the normalised fluorescence emission spectra of **19** recorded at 310 nm excitation against E_T^N.

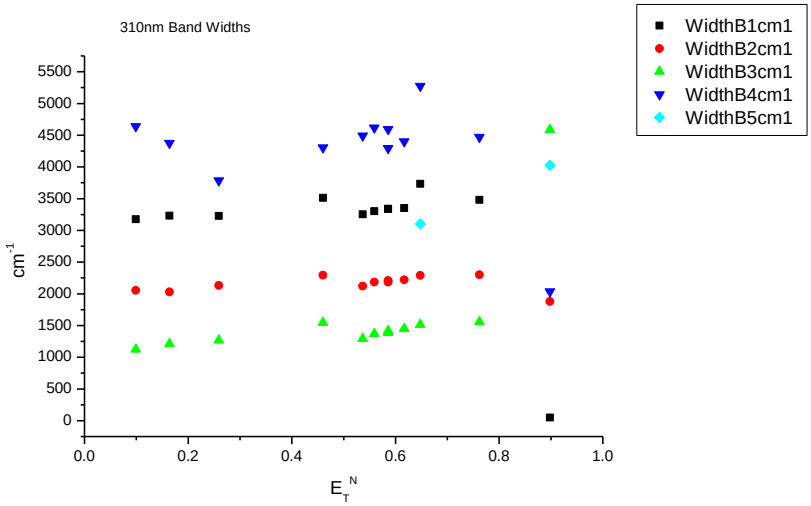

Figure 3.4.2. Band widths from Gaussian model fit of the normalised fluorescence emission spectra of **19** recorded at 310 nm excitation against E_T^N.

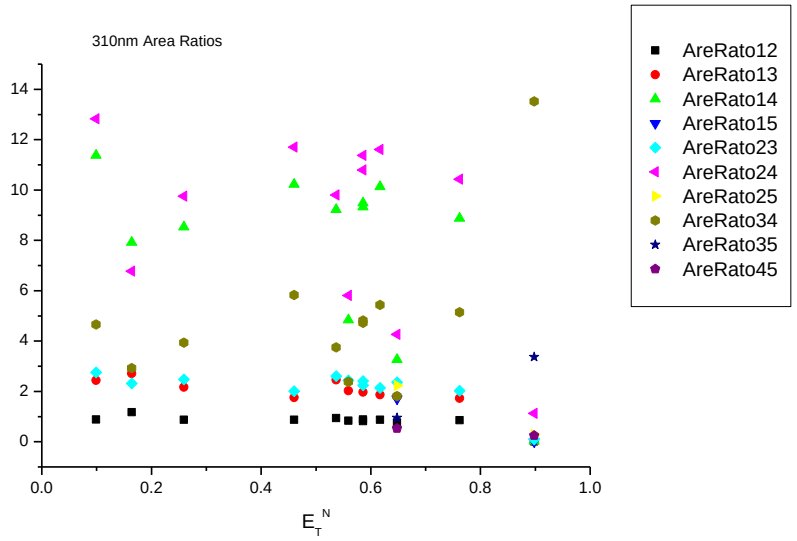

Figure 3.4.3. Area ratios from Gaussian model fit of the normalised fluorescence emission spectra of **19** recorded at 310 nm excitation against E_T^N.

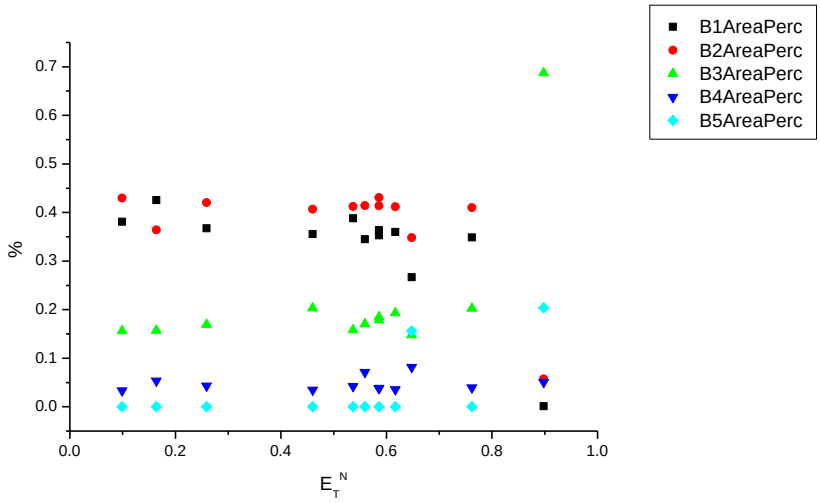

Figure 3.4.4. Area percentages from Gaussian model fit of the normalised fluorescence emission spectra of **19** recorded at 310 nm excitation against E_T^N.

3.4.4.2 *α*

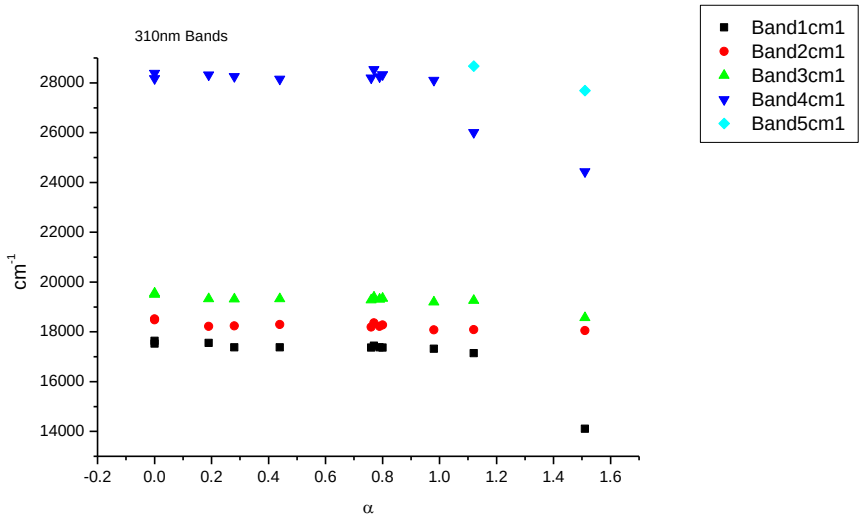

Figure 3.4.5. Band maxima from Gaussian model fit of the normalised fluorescence emission spectra of **19** recorded at 310 nm excitation against α.

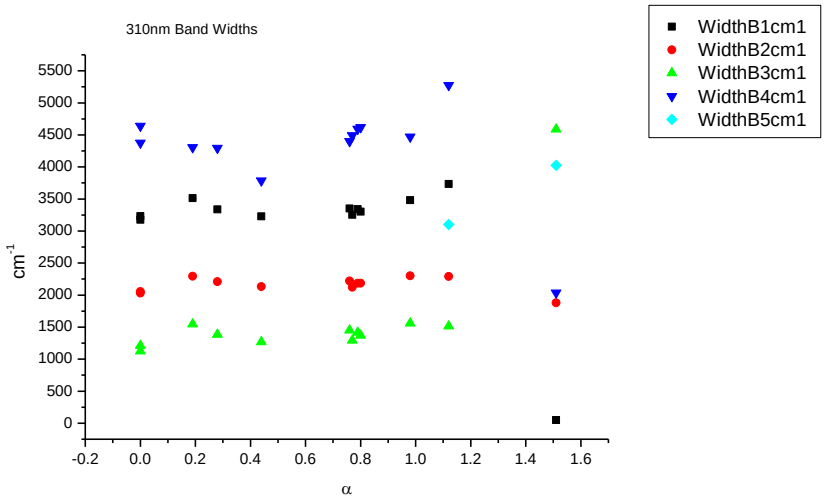

Figure 3.4.6. Band widths from Gaussian model fit of the normalised fluorescence emission spectra of **19** recorded at 310 nm excitation against α.

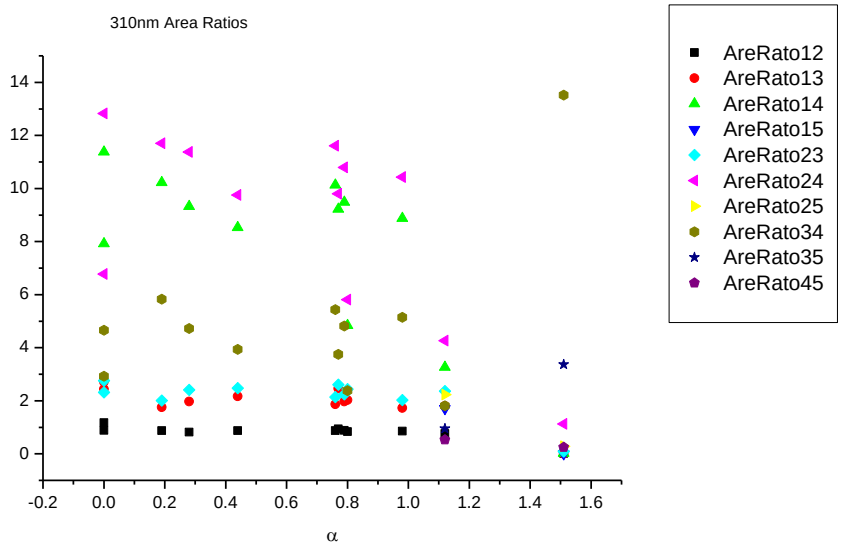

Figure 3.4.7. Area Ratios from Gaussian model fit of the normalised fluorescence emission spectra of **19** recorded at 310 nm excitation against α.

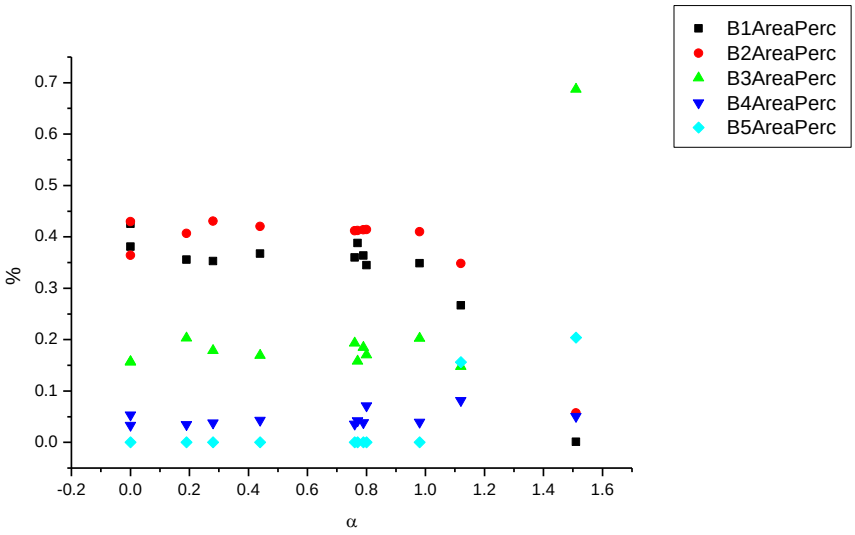

Figure 3.4.8. Area percentages from Gaussian model fit of the normalised fluorescence emission spectra of **19** recorded at 310 nm excitation against α.

3.4.4.3 β.

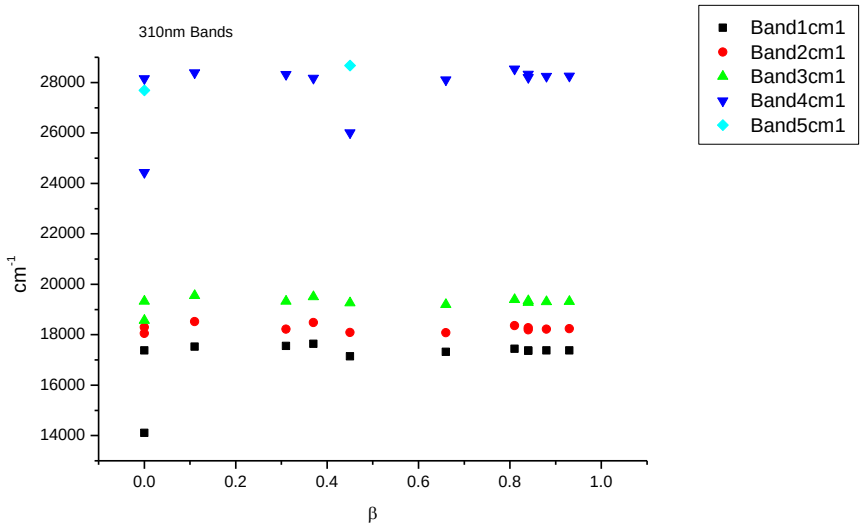

Figure 3.4.9. Band maxima from Gaussian model fit of the normalised fluorescence emission spectra of **19** recorded at 310 nm excitation against β.

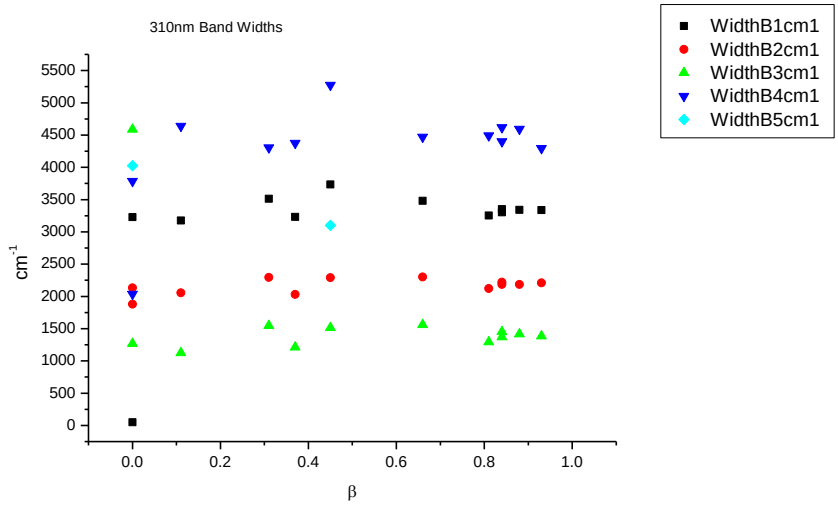

Figure 3.4.10. Band widths from Gaussian model fit of the normalised fluorescence emission spectra of **19** recorded at 310 nm excitation against β.

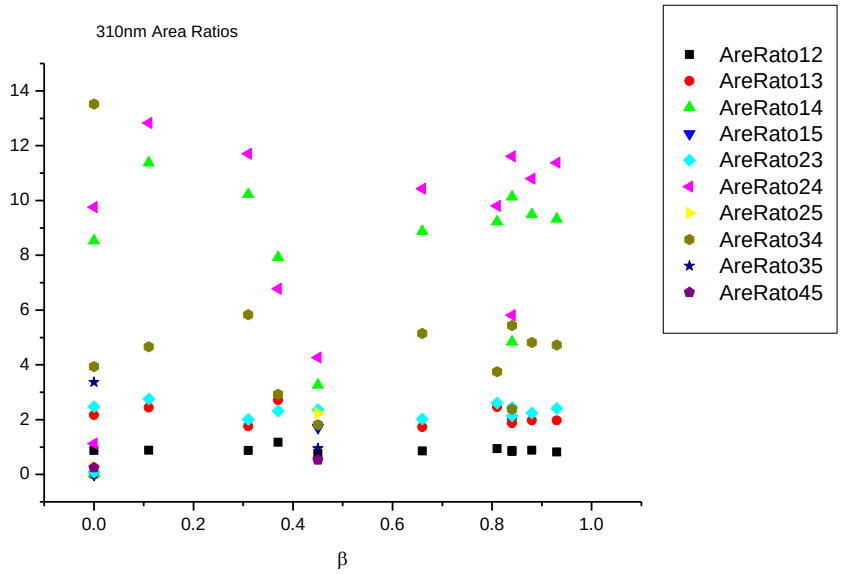

Figure 3.4.11. Area ratios from Gaussian model fit of the normalised fluorescence emission spectra of **19** recorded at 310 nm excitation against β.

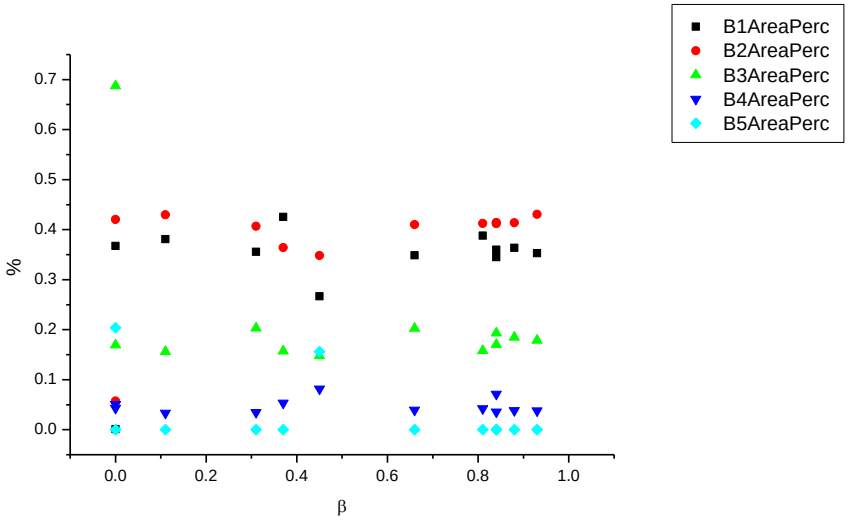

Figure 3.4.12. Area percentages from Gaussian model fit of the normalised fluorescence emission spectra of **19** recorded at 310 nm excitation against β.

3.4.4.4 π.*

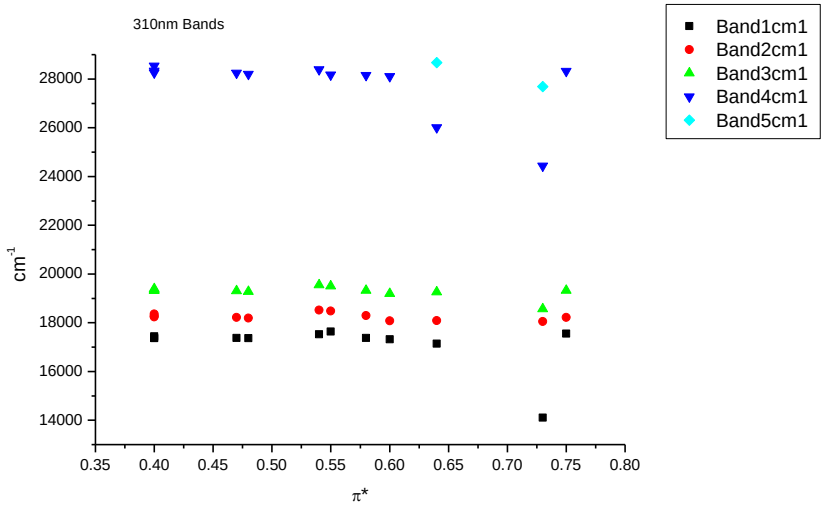

Figure 3.4.13. Band maxima from Gaussian model fit of the normalised fluorescence emission spectra of **19** recorded at 310 nm excitation against π*.

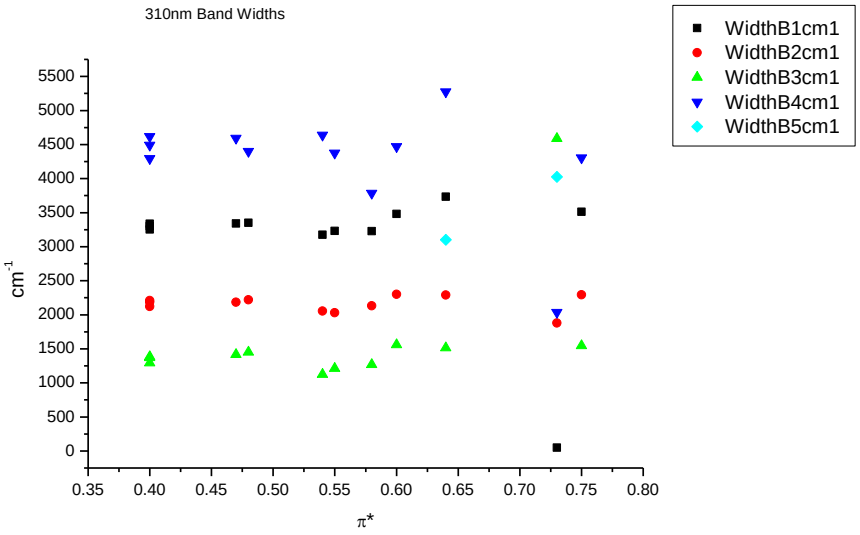

Figure 3.4.14. Band widths from Gaussian model fit of the normalised fluorescence emission spectra of **19** recorded at 310 nm excitation against π*.

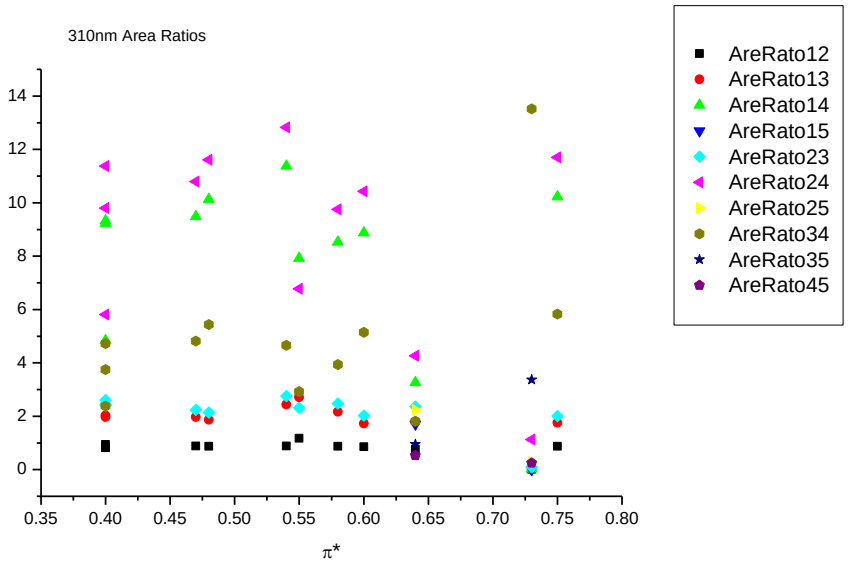

Figure 3.4.15. Area ratios from Gaussian model fit of the normalised fluorescence emission spectra of **19** recorded at 310 nm excitation against π*.

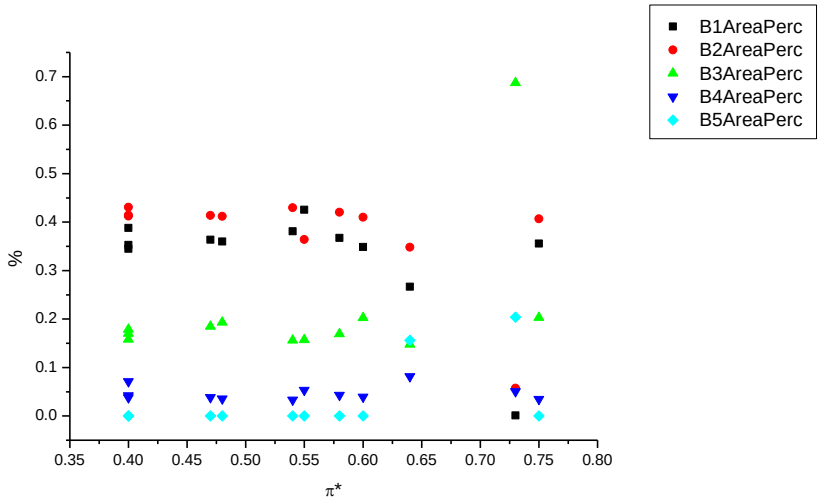

Figure 3.4.16. Area percentages from Gaussian model fit of the normalised fluorescence emission spectra of **19** recorded at 310 nm excitation against π*.

3.4.4.5 μ(D).

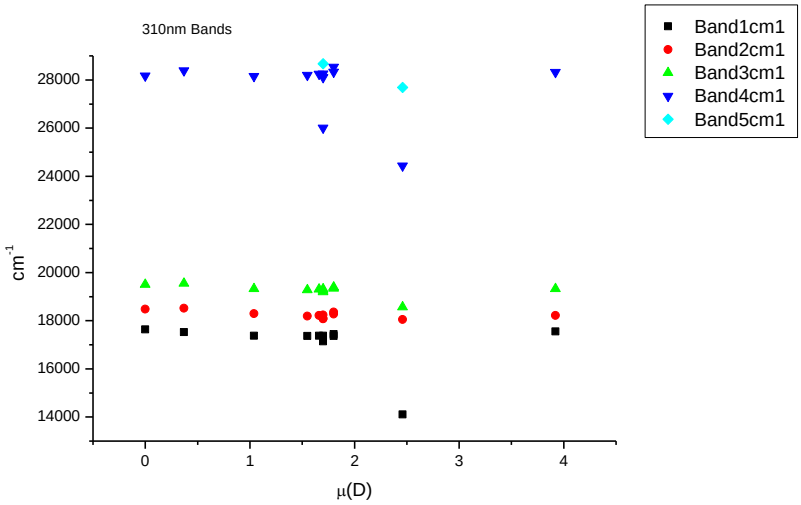

Figure 3.4.17. Band maxima from Gaussian model fit of the normalised fluorescence emission spectra of **19** recorded at 310 nm excitation against μ(D).

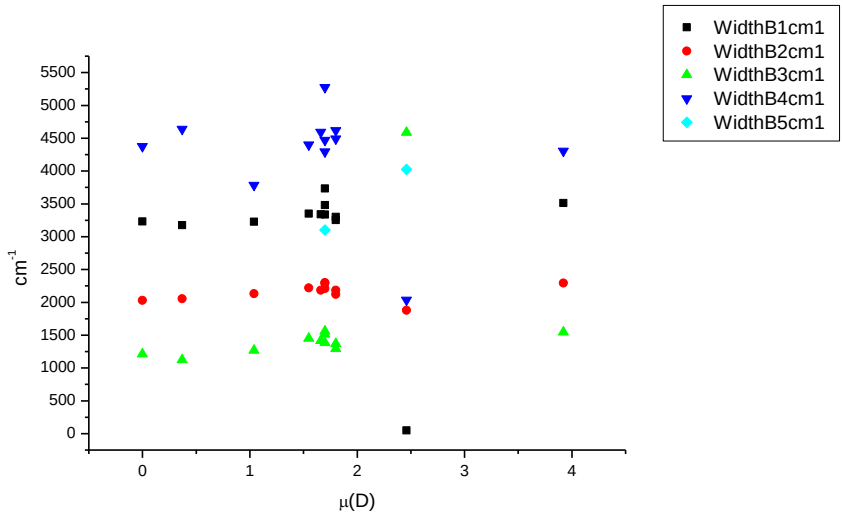

Figure 3.4.18. Band widths from Gaussian model fit of the normalised fluorescence emission spectra of **19** recorded at 310 nm excitation against μ(D).

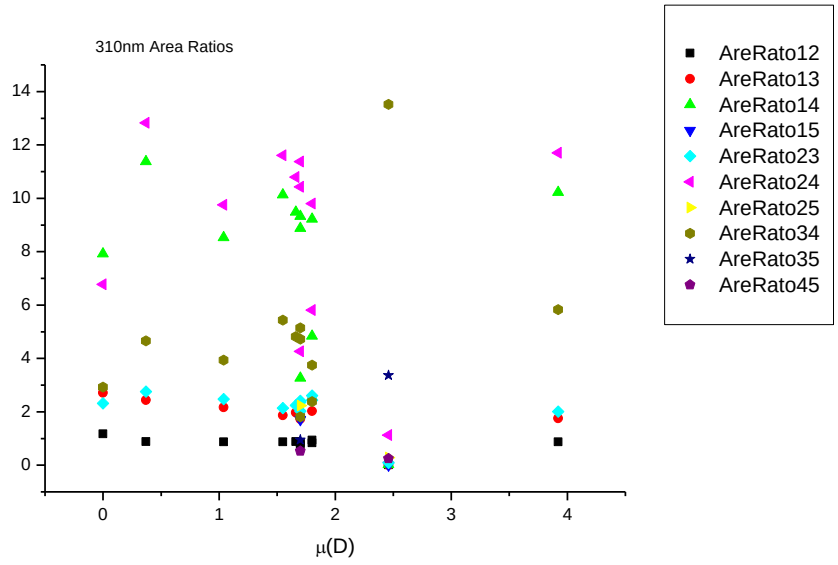

Figure 3.4.19. Area ratios from Gaussian model fit of the normalised fluorescence emission spectra of **19** recorded at 310 nm excitation against μ(D).

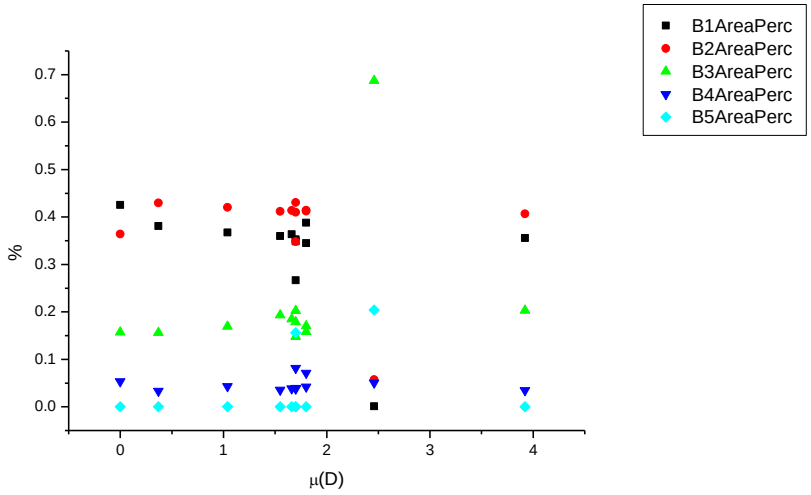

Figure 3.4.20. Area percentages from Gaussian model fit of the normalised fluorescence emission spectra of **19** recorded at 310 nm excitation against μ(D).

3.4.4.6 η(Cp).

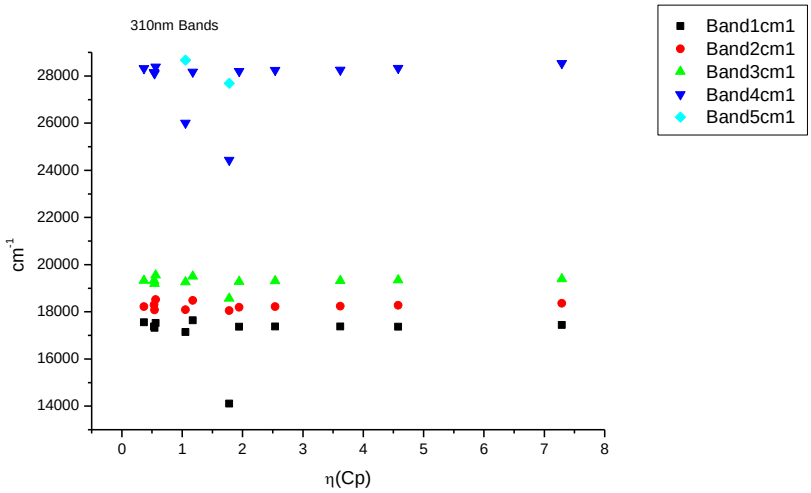

Figure 3.4.21. Band maxima from Gaussian model fit of the normalised fluorescence emission spectra of **19** recorded at 310 nm excitation against η(Cp).

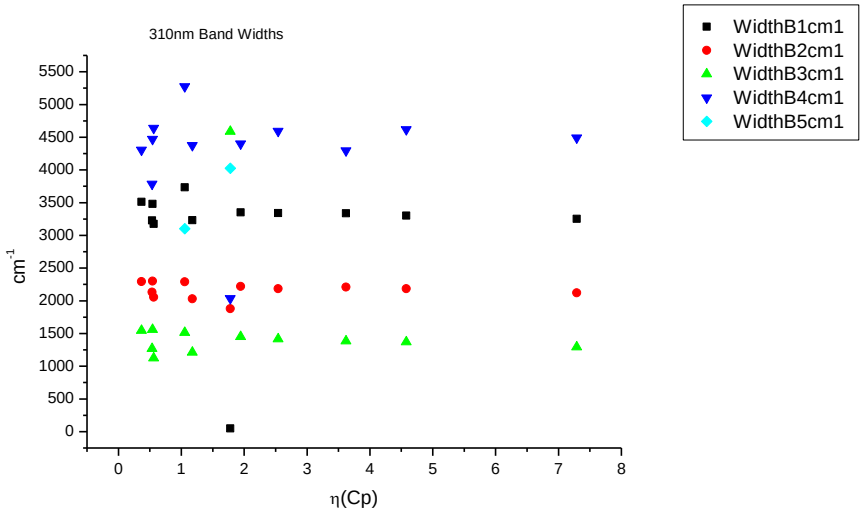

Figure 3.4.22. Band widths from Gaussian model fit of the normalised fluorescence emission spectra of **19** recorded at 310 nm excitation against η(Cp).

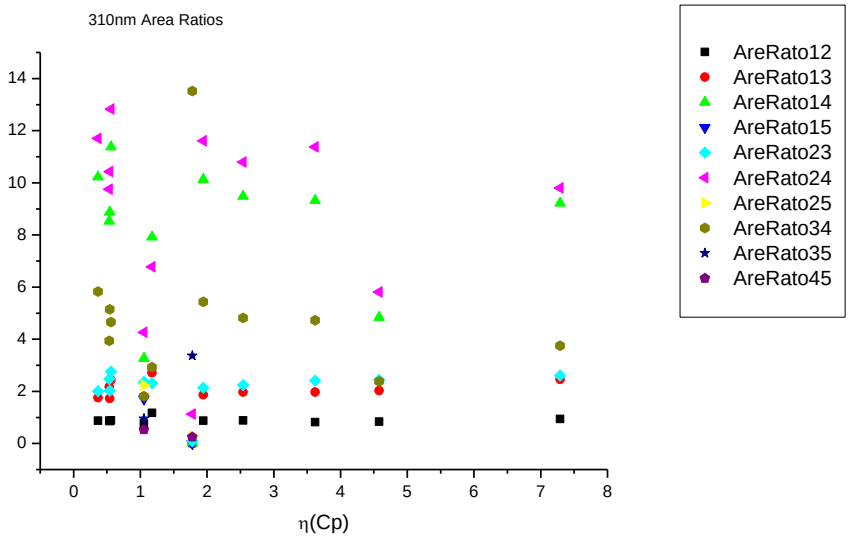

Figure 3.4.23. Area ratios from Gaussian model fit of the normalised fluorescence emission spectra of **19** recorded at 310 nm excitation against η(Cp).

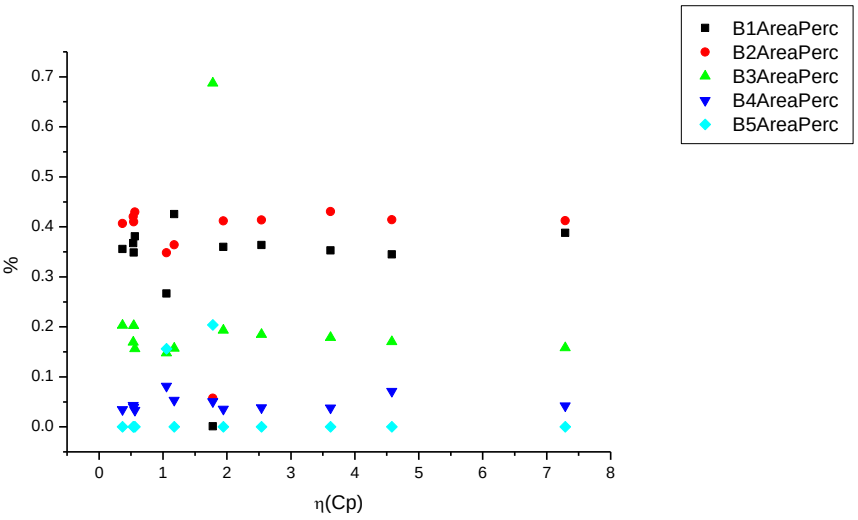

Figure 3.4.24. Area percentages from Gaussian model fit of the normalised fluorescence emission spectra of **19** recorded at 310 nm excitation against η(Cp).

3.4.5 400 nm Gaussian band fit - Solvatochromic analysis.

3.4.5.1 E_T^N.

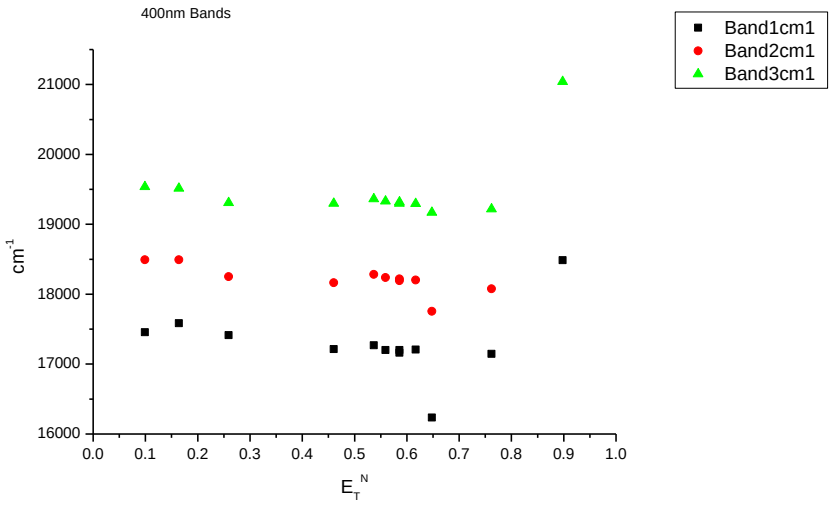

Figure 3.4.25. Band maxima from Gaussian model fit of the normalised fluorescence emission spectra of **19** recorded at 400 nm excitation against E_T^N.

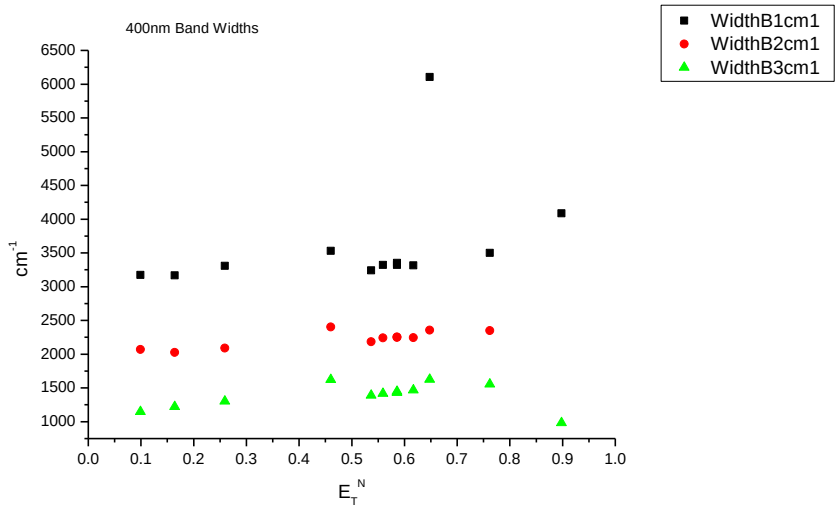

Figure 3.4.26. Band widths from Gaussian model fit of the normalised fluorescence emission spectra of **19** recorded at 400 nm excitation against E_T^N.

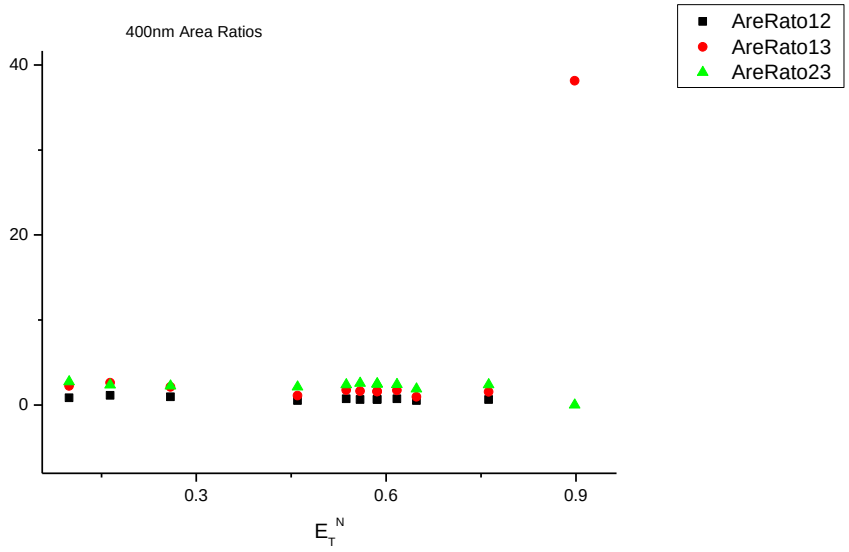

Figure 3.4.27. Area ratios from Gaussian model fit of the normalised fluorescence emission spectra of **19** recorded at 400 nm excitation against E_T^N.

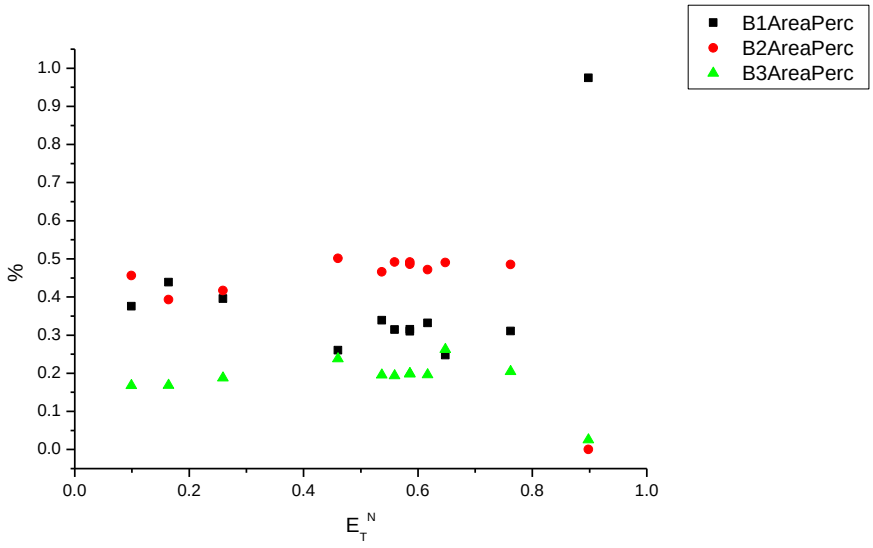

Figure 3.4.28. Area percentages from Gaussian model fit of the normalised fluorescence emission spectra of **19** recorded at 400 nm excitation against E_T^N.

3.4.5.2 *α*

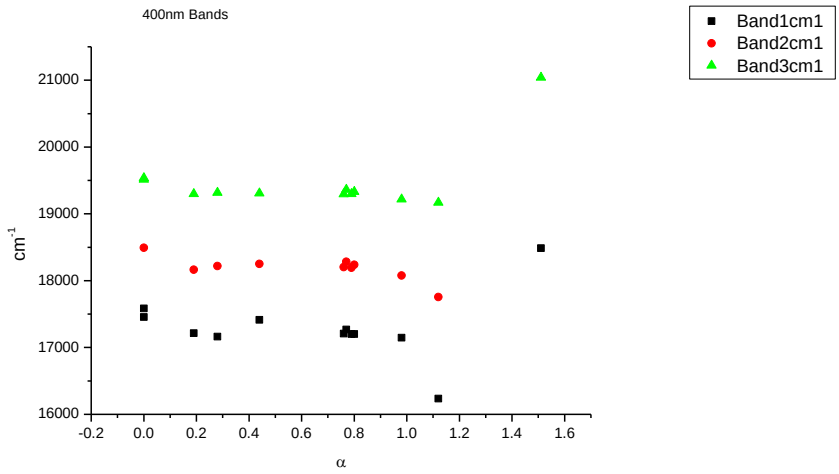

Figure 3.4.29. Band maxima from Gaussian model fit of the normalised fluorescence emission spectra of **19** recorded at 400 nm excitation against α.

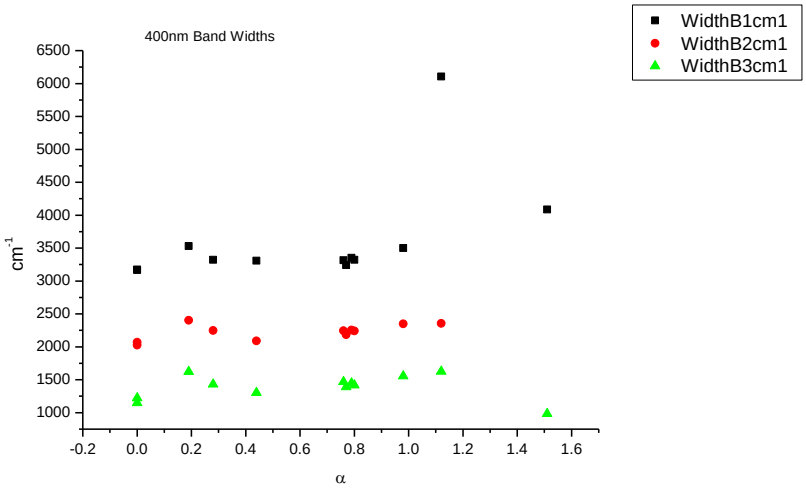

Figure 3.4.30. Band widths from Gaussian model fit of the normalised fluorescence emission spectra of **19** recorded at 400 nm excitation against α.

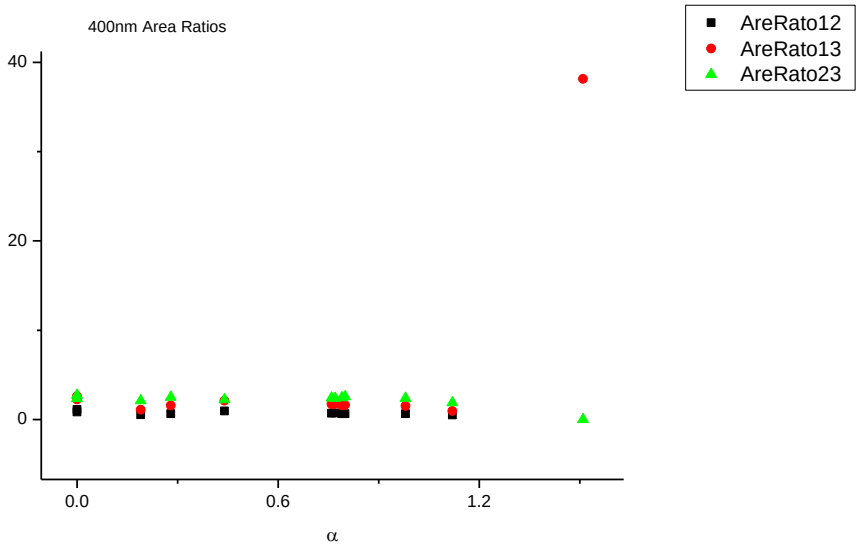

Figure 3.4.31. Area ratios from Gaussian model fit of the normalised fluorescence emission spectra of **19** recorded at 400 nm excitation against α.

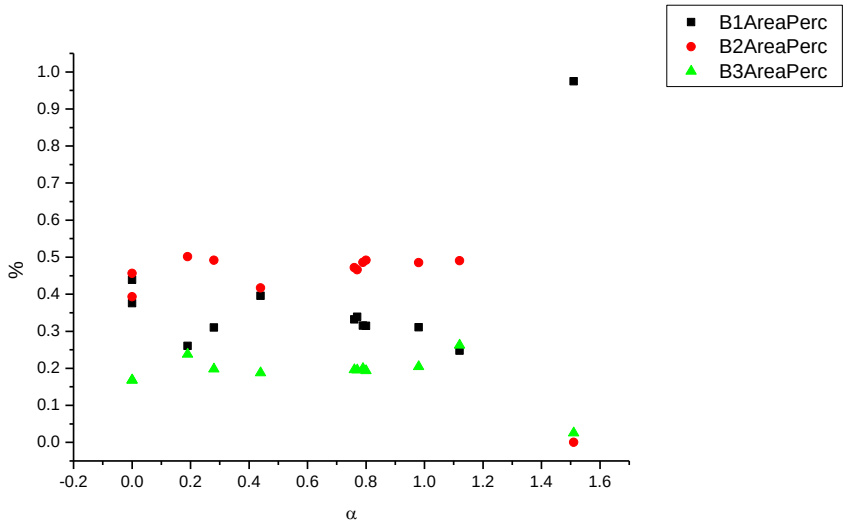

Figure 3.4.32. Area percentages from Gaussian model fit of the normalised fluorescence emission spectra of **19** recorded at 400 nm excitation against α.

3.4.5.3 β.

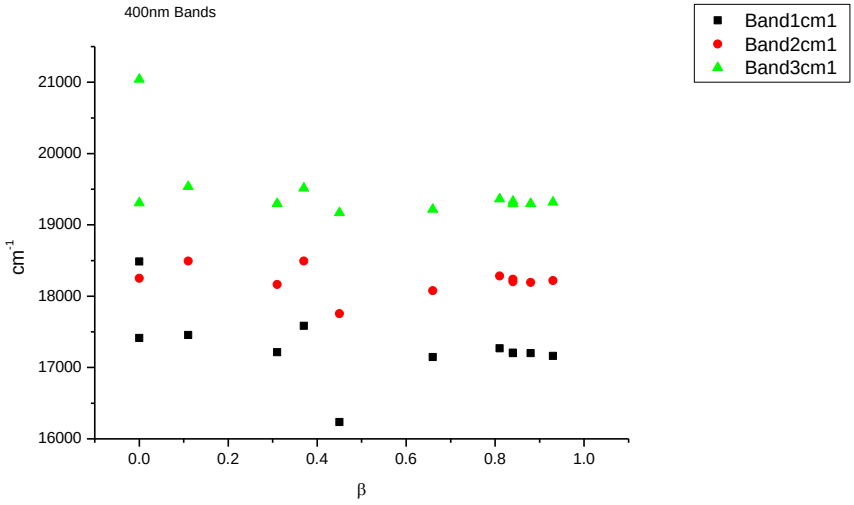

Figure 3.4.33. Band maxima from Gaussian model fit of the normalised fluorescence emission spectra of **19** recorded at 400 nm excitation against β.

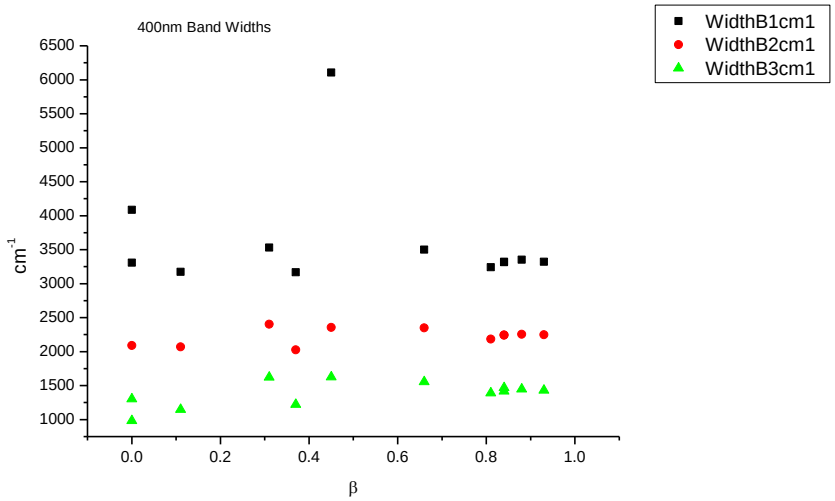

Figure 3.4.34. Band widths from Gaussian model fit of the normalised fluorescence emission spectra of **19** recorded at 400 nm excitation against β.

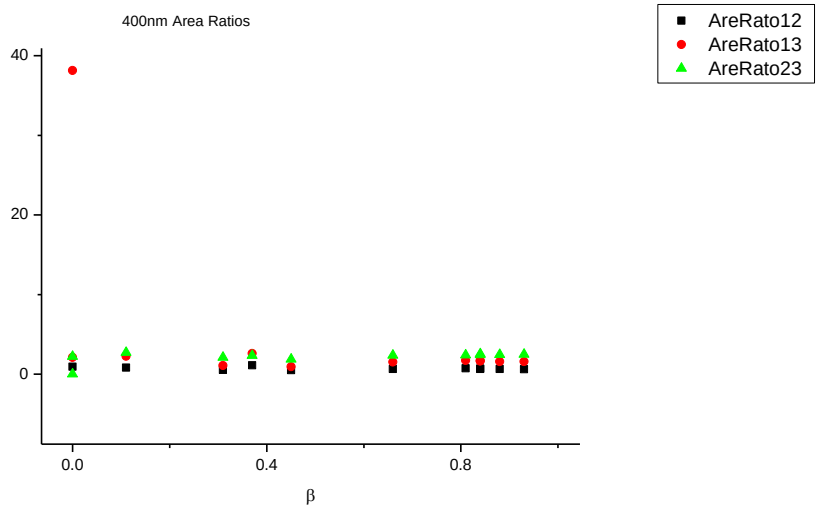

Figure 3.4.35. Area ratios from Gaussian model fit of the normalised fluorescence emission spectra of **19** recorded at 400 nm excitation against β.

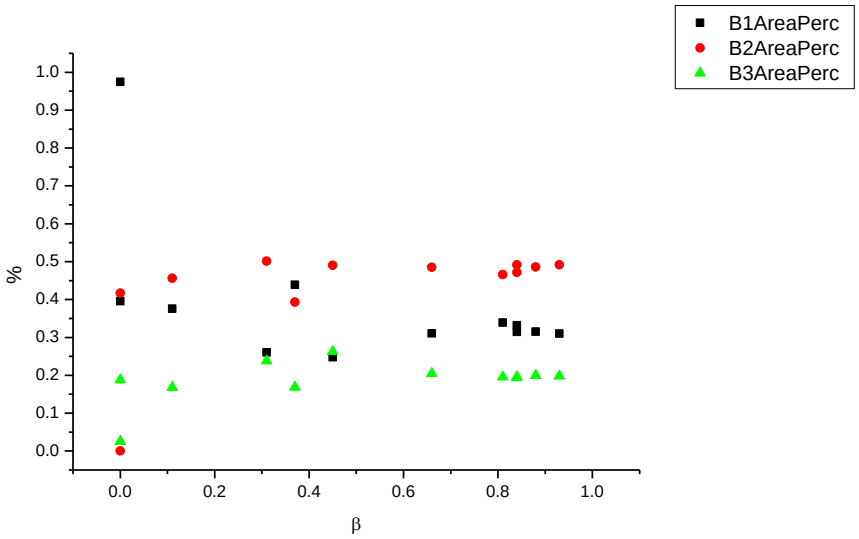

Figure 3.4.36. Area percentages from Gaussian model fit of the normalised fluorescence emission spectra of **19** recorded at 400 nm excitation against β.

3.4.5.4 π.*

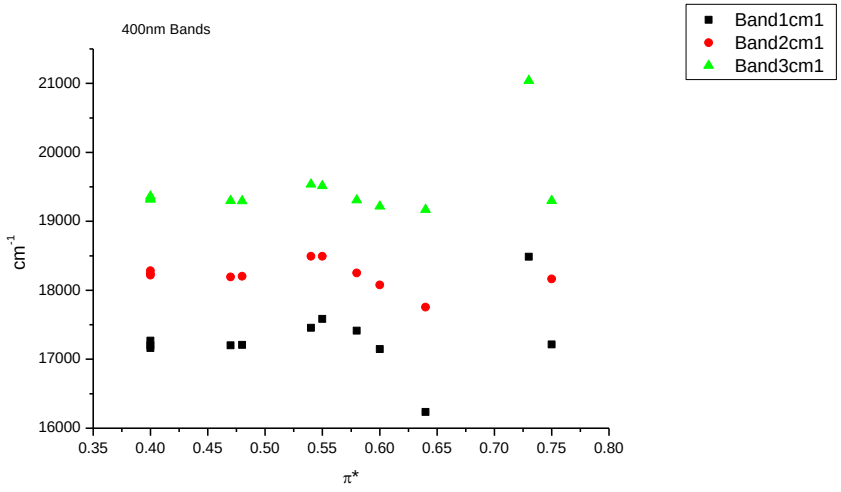

Figure 3.4.37. Band maxima from Gaussian model fit of the normalised fluorescence emission spectra of **19** recorded at 400 nm excitation against π*.

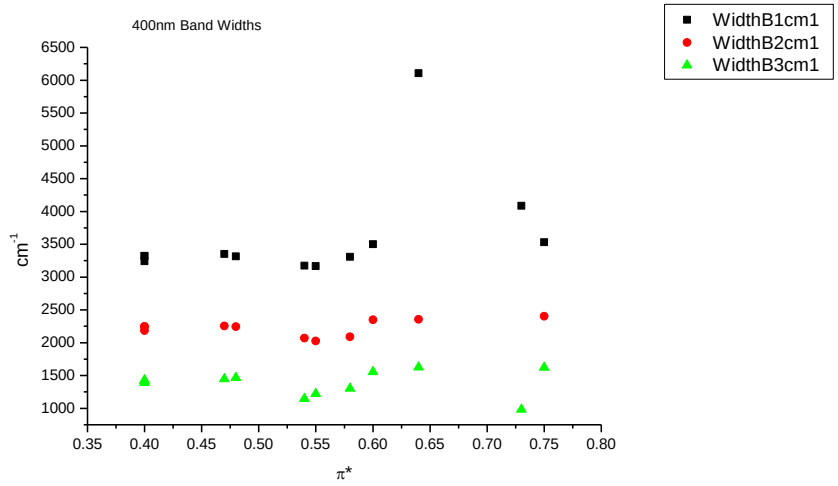

Figure 3.4.38. Band widths from Gaussian model fit of the normalised fluorescence emission spectra of **19** recorded at 400 nm excitation against π*.

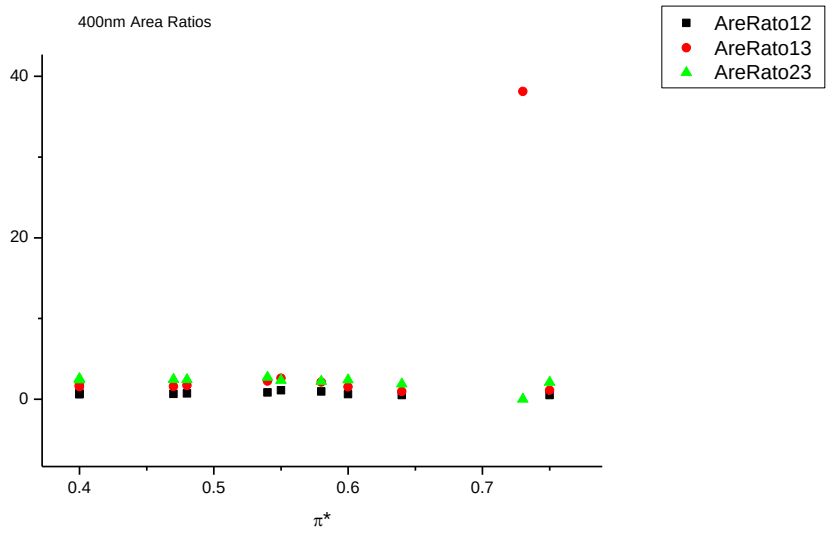

Figure 3.4.39. Area ratios from Gaussian model fit of the normalised fluorescence emission spectra of **19** recorded at 400 nm excitation against π*.

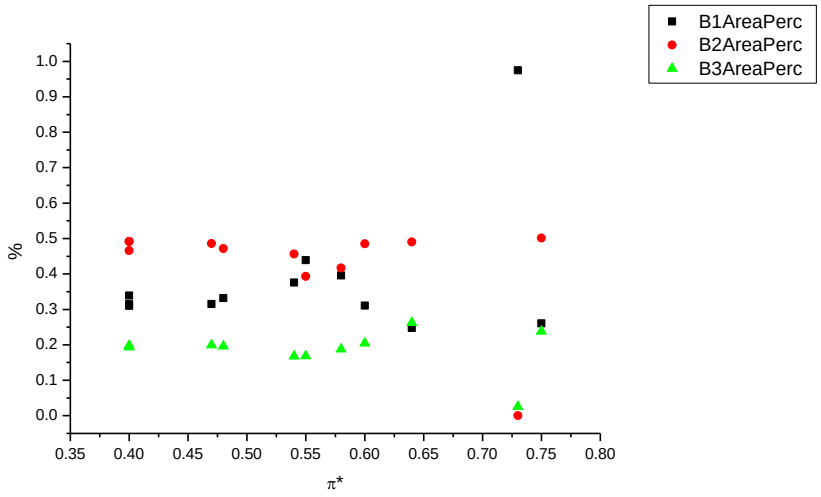

Figure 3.4.40. Area percentages from Gaussian model fit of the normalised fluorescence emission spectra of **19** recorded at 400 nm excitation against π*.

3.4.5.5 μ(D).

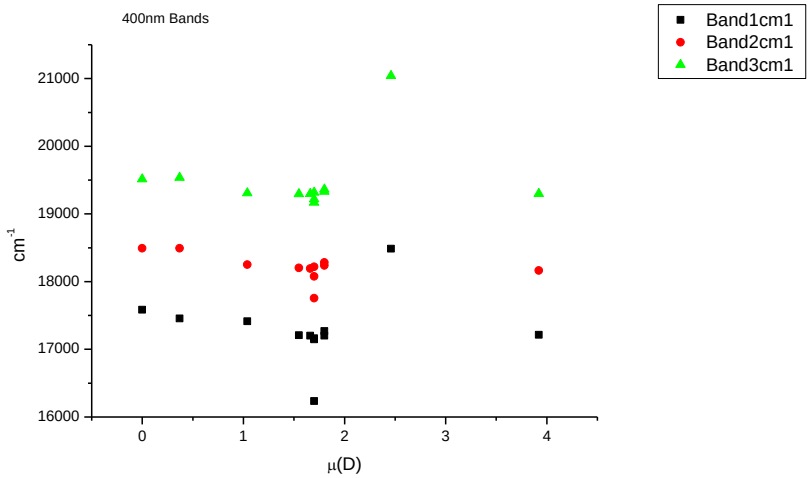

Figure 3.4.41. Band maxima from Gaussian model fit of the normalised fluorescence emission spectra of **19** recorded at 400 nm excitation against μ(D).

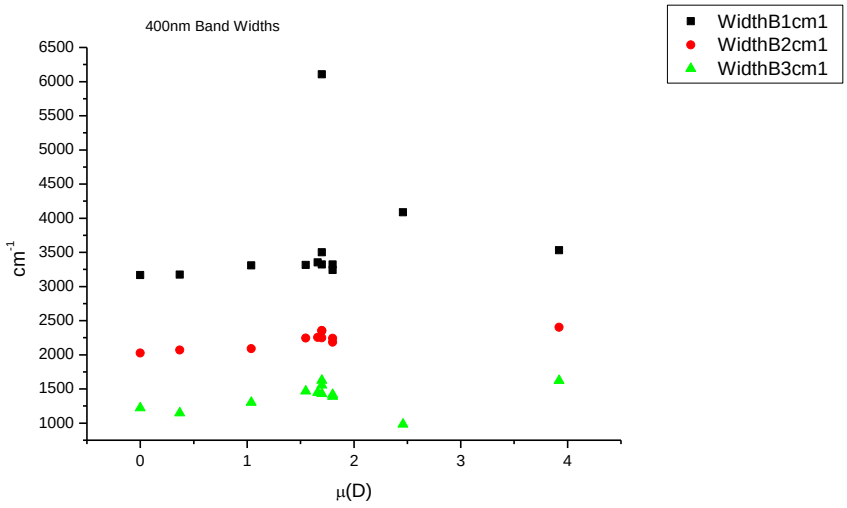

Figure 3.4.42. Band widths from Gaussian model fit of the normalised fluorescence emission spectra of **19** recorded at 400 nm excitation against μ(D).

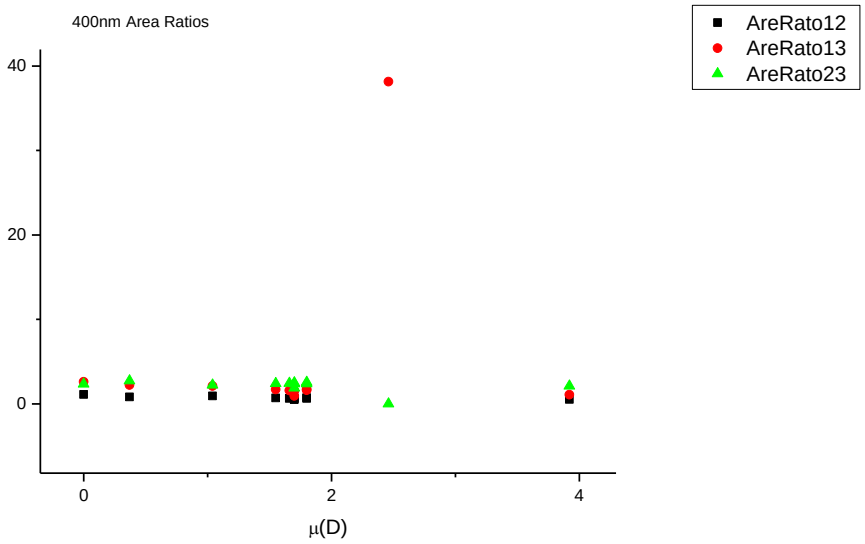

Figure 3.4.43. Area ratios from Gaussian model fit of the normalised fluorescence emission spectra of **19** recorded at 400 nm excitation against μ(D).

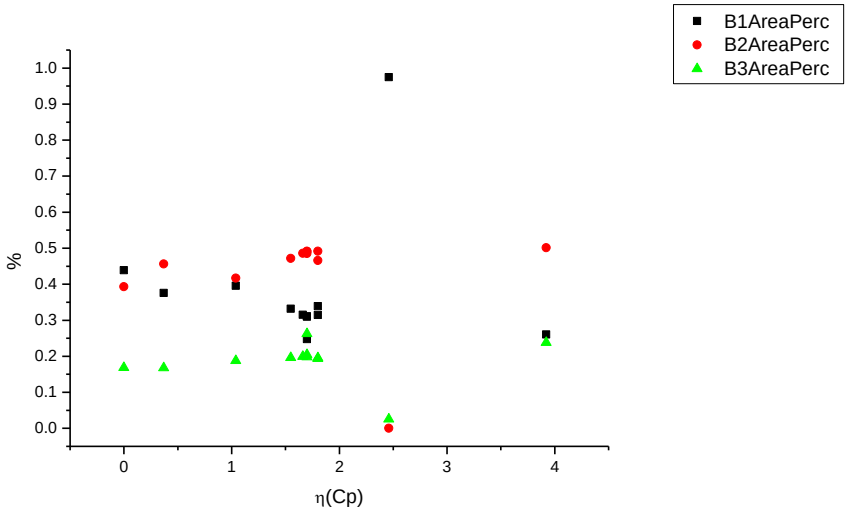

Figure 3.4.44. Area percentages from Gaussian model fit of the normalised fluorescence emission spectra of **19** recorded at 400 nm excitation against μ(D).

3.4.5.6 η(Cp).

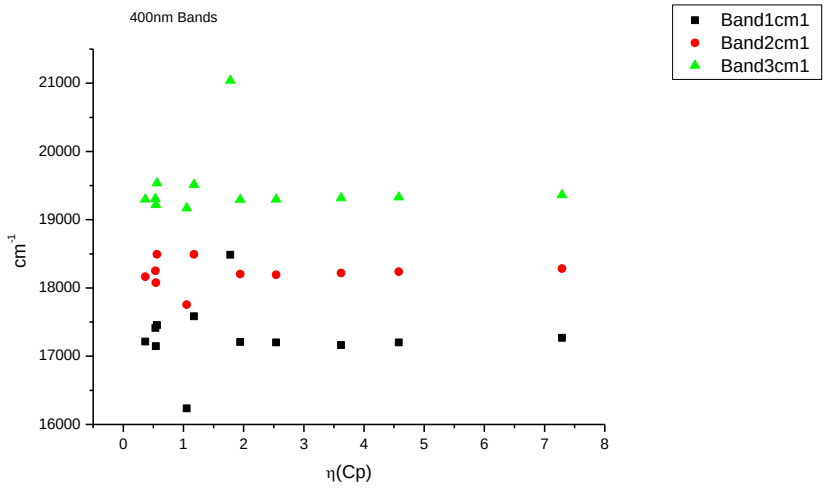

Figure 3.4.45. Band maxima from Gaussian model fit of the normalised fluorescence emission spectra of **19** recorded at 400 nm excitation against η(Cp).

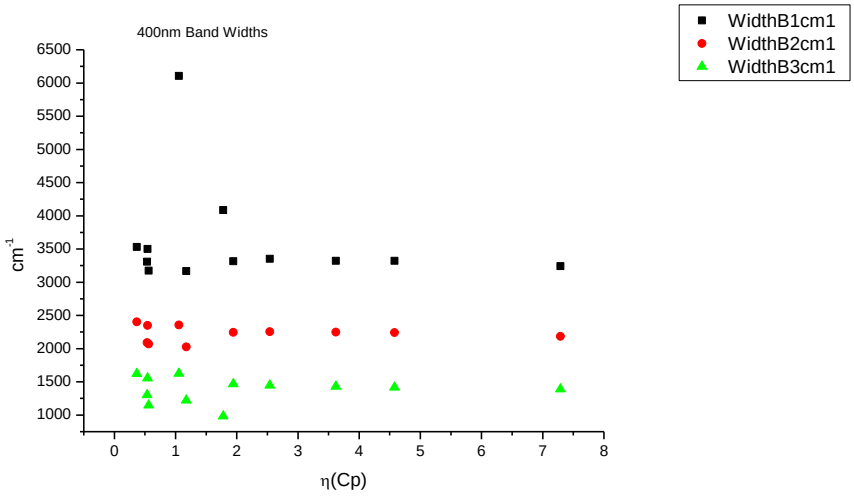

Figure 3.4.46. Band widths from Gaussian model fit of the normalised fluorescence emission spectra of **19** recorded at 400 nm excitation against η(Cp).

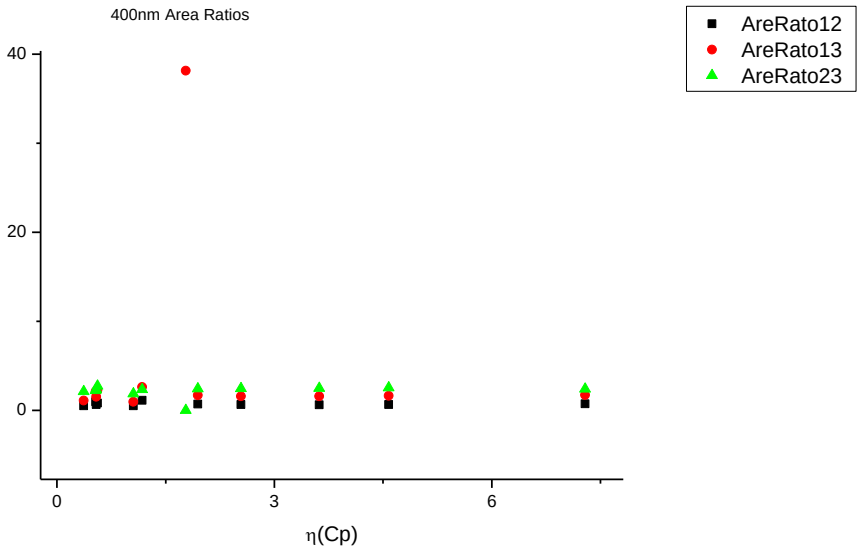

Figure 3.4.47. Area ratios from Gaussian model fit of the normalised fluorescence emission spectra of **19** recorded at 400 nm excitation against η(Cp).

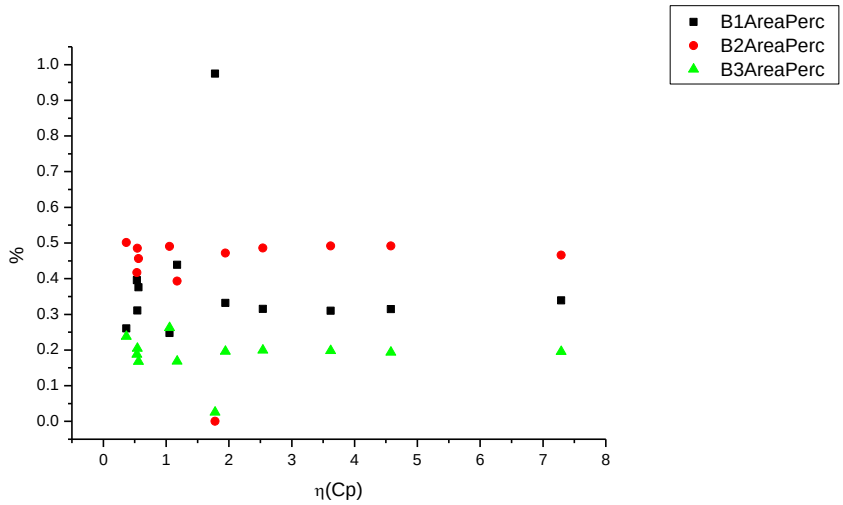

Figure 3.4.48. Area percentages from Gaussian model fit of the normalised fluorescence emission spectra of **19** recorded at 400 nm excitation against η(Cp).

3.4.6 400 nm fluorescent lifetime results.

3.4.6.1 Intensity weighted.

Wavelength (nm)	Solvent	τ_1 (ns)	A_1 (%)	τ_2 (ns)	A_2 (%)	τ_3 (ns)	A_3 (%)	τ_f (ns) (Intensity Weighted)	$1/\tau_f$	χ^2
470	Toluene	0.34	30.10	2.15	13.88	9.03	56.02	5.46	0.18	1.17
470	1,4-Dioxane	0.37	24.19	1.92	14.54	8.59	61.27	5.63	0.18	1.14
470	Chloroform	0.38	19.17	1.64	26.64	8.72	54.19	5.24	0.19	1.15
470	Acetonitrile	0.63	26.77	1.80	29.11	6.95	44.12	3.76	0.27	1.08
470	1-Octanol	0.30	36.37	2.11	11.06	8.85	52.56	4.99	0.20	1.11
470	1-Hexanol	0.35	46.18	2.26	13.83	8.90	40.00	4.03	0.25	1.11
470	1-Butanol	0.35	52.96	2.39	12.21	9.10	34.82	3.64	0.27	1.05
470	1-Pentanol	0.31	56.04	1.98	9.38	8.47	34.57	3.29	0.30	1.12
470	1-Propanol	0.27	68.72	2.23	7.17	8.35	24.11	2.36	0.42	1.47
470	Acetic acid	0.30	45.18	1.39	45.24	6.77	9.57	1.41	0.71	1.26
470	Methanol	0.27	21.10	2.56	24.70	7.43	54.20	4.72	0.21	1.03
470	2,2,2-Trifluoroethanol	0.40	30.99	1.00	64.18	6.18	4.83	1.07	0.94	1.06

Table 3.4.9. Summary of Time Correlated Single Photon Counting (TCSPC) fluorescent lifetimes (intensity weighted) of **19** recorded at 470 nm.

Wavelength (nm)	Solvent	τ_1 (ns)	A_1 (%)	τ_2 (ns)	A_2 (%)	τ_3 (ns)	A_3 (%)	τ_f (ns) (Intensity Weighted)	$1/\tau_f$	χ^2
490	Toluene	0.40	5.56	4.96	11.00	10.06	83.45	8.96	0.11	1.12
490	1,4-Dioxane	0.44	4.06	4.10	9.64	10.34	86.30	9.33	0.11	1.23
490	Chloroform	0.46	2.91	2.78	7.02	10.15	90.07	9.35	0.11	1.18
490	Acetonitrile	0.65	8.66	2.38	14.72	8.23	76.62	6.71	0.15	1.11
490	1-Octanol	0.34	10.39	3.46	6.83	10.13	82.78	8.65	0.12	1.14
490	1-Hexanol	0.37	11.64	4.17	11.81	10.22	76.55	8.36	0.12	1.11
490	1-Butanol	0.32	18.35	4.26	11.68	10.07	69.97	7.60	0.13	1.49
490	1-Pentanol	0.33	15.74	4.46	12.69	10.31	71.56	8.00	0.13	1.10
490	1-Propanol	0.35	10.31	3.66	9.98	9.54	79.71	8.01	0.12	1.26
490	Acetic acid	0.30	24.21	1.31	69.85	5.75	5.94	1.33	0.75	1.09
490	Methanol	0.35	3.80	3.93	37.17	9.53	59.02	7.10	0.14	1.01
490	2,2,2-Trifluoroethanol	0.45	26.19	1.04	67.79	5.64	6.01	1.16	0.86	1.00

Table 3.4.10. Summary of Time Correlated Single Photon Counting (TCSPC) fluorescent lifetimes (intensity weighted) of **19** recorded at 490 nm.

Wavelength (nm)	Solvent	τ_1 (ns)	A_1 (%)	τ_2 (ns)	A_2 (%)	τ_3 (ns)	A_3 (%)	τ_f (ns) (Intensity Weighted)	$1/\tau_f$	χ^2
520	Toluene	-	-	3.48	4.42	9.98	95.58	9.69	0.10	1.30
520	1,4-Dioxane	0.39	0.59	5.05	9.75	10.71	89.66	10.10	0.10	1.16
520	Chloroform	-	-	4.17	5.56	10.55	94.44	10.20	0.10	1.15
520	Acetonitrile	0.42	1.48	3.04	8.25	8.88	90.27	8.28	0.12	1.15
520	1-Octanol	0.40	2.83	4.66	6.71	10.53	90.47	9.85	0.10	1.11
520	1-Hexanol	0.37	2.34	5.92	15.75	10.86	81.92	9.83	0.10	1.06
520	1-Butanol	0.29	2.45	5.17	11.10	10.37	86.45	9.55	0.10	1.12
520	1-Pentanol	0.36	1.71	5.82	15.53	10.78	82.76	9.83	0.10	1.10
520	1-Propanol	0.34	1.42	5.60	16.73	10.48	81.86	9.52	0.11	1.14
520	Acetic acid	0.31	18.57	1.28	77.46	5.22	3.97	1.26	0.79	1.07
520	Methanol	0.30	1.37	4.17	31.49	9.70	67.15	7.81	0.13	1.11
520	2,2,2-Trifluoroethanol	0.31	21.16	1.22	69.98	5.10	9.17	1.38	0.72	1.06

Table 3.4.11. Summary of Time Correlated Single Photon Counting (TCSPC) fluorescent lifetimes (intensity weighted) of **19** recorded at 520 nm.

Wavelength (nm)	Solvent	τ_1 (ns)	A_1 (%)	τ_2 (ns)	A_2 (%)	τ_3 (ns)	A_3 (%)	τ_f (ns) (Intensity Weighted)	$1/\tau_f$	χ^2
540	Toluene	-	-	3.43	3.84	9.92	96.16	9.67	0.10	1.28
540	1,4-Dioxane	0.29	0.44	5.60	12.15	10.78	87.41	10.11	0.10	1.11
540	Chloroform	-	-	5.36	8.54	10.70	91.46	10.24	0.10	1.22
540	Acetonitrile	0.54	1.14	5.33	22.98	9.89	75.89	8.74	0.11	1.15
540	1-Octanol	0.42	1.76	6.06	14.75	11.03	83.49	10.11	0.10	0.98
540	1-Hexanol	0.39	1.23	6.22	18.19	10.97	80.59	9.98	0.10	1.09
540	1-Butanol	0.32	1.47	6.14	18.84	10.76	79.69	9.73	0.10	1.02
540	1-Pentanol	0.35	0.93	5.84	15.30	10.76	83.77	9.91	0.10	1.17
540	1-Propanol	0.32	0.76	5.43	14.42	10.38	84.82	9.59	0.10	1.11
540	Acetic acid	0.30	15.21	1.28	81.22	5.40	3.57	1.28	0.78	0.98
540	Methanol	-	-	3.93	28.89	9.57	71.11	7.94	0.13	1.20
540	2,2,2-Trifluoroethanol	0.31	19.15	1.33	71.98	5.20	8.87	1.48	0.68	0.98

Table 3.4.12. Summary of Time Correlated Single Photon Counting (TCSPC) fluorescent lifetimes (intensity weighted) of **19** recorded at 540 nm.

Wavelength (nm)	Solvent	τ_1 (ns)	A_1 (%)	τ_2 (ns)	A_2 (%)	τ_3 (ns)	A_3 (%)	τ_f (ns) (Intensity Weighted)	$1/\tau_f$	χ^2
570	Toluene	-	-	4.16	5.16	10.02	94.84	9.72	0.10	1.26
570	1,4-Dioxane	-	-	4.83	8.41	10.67	91.59	10.18	0.10	1.17
570	Chloroform	-	-	6.19	9.01	10.69	90.99	10.29	0.10	1.21
570	Acetonitrile	-	-	4.50	13.82	9.53	86.18	8.84	0.11	1.19
570	1-Octanol	0.47	1.20	6.39	16.41	11.10	82.38	10.20	0.10	1.09
570	1-Hexanol	0.42	0.74	6.15	16.50	10.92	82.76	10.06	0.10	1.17
570	1-Butanol	0.32	1.02	5.82	15.16	10.62	83.82	9.79	0.10	1.15
570	1-Pentanol	0.52	0.81	8.36	59.70	12.98	39.49	10.12	0.10	1.19
570	1-Propanol	-	-	5.63	16.42	10.50	83.58	9.70	0.10	1.19
570	Acetic acid	0.28	15.81	1.26	80.78	5.15	3.41	1.24	0.81	1.05
570	Methanol	-	-	3.94	28.47	9.59	71.53	7.98	0.13	1.08
570	2,2,2-Trifluoroethanol	0.29	18.52	1.40	73.72	5.56	7.75	1.52	0.66	1.04

Table 3.4.13. Summary of Time Correlated Single Photon Counting (TCSPC) fluorescent lifetimes (intensity weighted) of **19** recorded at 570 nm.

Wavelength (nm)	Solvent	τ_1 (ns)	A_1 (%)	τ_2 (ns)	A_2 (%)	τ_3 (ns)	A_3 (%)	τ_f (ns) (Intensity Weighted)	$1/\tau_f$	χ^2
600	Toluene	-	-	3.60	3.61	9.93	96.39	9.70	0.10	1.23
600	1,4-Dioxane	-	-	6.35	16.53	11.05	83.47	10.27	0.10	1.20
600	Chloroform	-	-	9.13	64.62	12.82	35.38	10.44	0.10	1.24
600	Acetonitrile	-	-	4.71	13.46	9.55	86.54	8.90	0.11	1.32
600	1-Octanol	0.40	0.86	6.00	12.82	10.97	86.33	10.24	0.10	1.06
600	1-Hexanol	0.44	0.79	6.73	20.63	11.07	78.58	10.09	0.10	1.12
600	1-Butanol	0.33	1.22	6.04	17.13	10.72	81.65	9.79	0.10	1.14
600	1-Pentanol	0.40	0.75	6.84	24.06	11.14	75.20	10.02	0.10	1.13
600	1-Propanol	-	-	6.31	23.32	10.79	76.68	9.75	0.10	1.28
600	Acetic acid	0.17	29.45	1.23	67.05	4.49	3.50	1.03	0.97	1.28
600	Methanol	-	-	3.94	28.07	9.53	71.93	7.96	0.13	1.15
600	2,2,2-Trifluoroethanol	0.31	19.27	1.46	74.31	6.09	6.42	1.53	0.65	1.09

Table 3.4.14. Summary of Time Correlated Single Photon Counting (TCSPC) fluorescent lifetimes (intensity weighted) of **19** recorded at 600 nm.

3.4.6.2 Amplitude weighted.

Wavelength (nm)	Solvent	τ_1 (ns)	A_1 (%)	τ_2 (ns)	A_2 (%)	τ_3 (ns)	A_3 (%)	τ_f (ns) (Amplitude Weighted)	$1/\tau_f$	χ^2
470	Toluene	0.34	87.44	2.15	6.41	9.03	6.15	0.99	1.01	1.17
470	1,4-Dioxane	0.37	81.58	1.92	9.48	8.59	8.94	1.25	0.80	1.14
470	Chloroform	0.38	69.04	1.64	22.39	8.72	8.57	1.38	0.73	1.15
470	Acetonitrile	0.63	65.28	1.80	24.94	6.95	9.79	1.54	0.65	1.08
470	1-Octanol	0.30	91.62	2.11	3.93	8.85	4.46	0.75	1.33	1.11
470	1-Hexanol	0.35	92.49	2.26	4.33	8.90	3.18	0.71	1.41	1.11
470	1-Butanol	0.35	94.50	2.39	3.15	9.10	2.36	0.62	1.62	1.05
470	1-Pentanol	0.31	95.31	1.98	2.52	8.47	2.17	0.53	1.88	1.12
470	1-Propanol	0.27	97.69	2.23	1.22	8.35	1.09	0.38	2.65	1.47
470	Acetic acid	0.30	81.86	1.39	17.38	6.77	0.76	0.54	1.87	1.26
470	Methanol	0.27	81.90	2.56	10.32	7.43	7.79	1.07	0.94	1.03
470	2,2,2-Trifluoroethanol	0.40	54.52	1.00	44.93	6.18	0.55	0.70	1.42	1.06

Table 3.4.15. Summary of Time Correlated Single Photon Counting (TCSPC) fluorescent lifetimes (amplitude weighted) of **19** recorded at 470 nm.

Wavelength (nm)	Solvent	τ_1 (ns)	A_1 (%)	τ_2 (ns)	A_2 (%)	τ_3 (ns)	A_3 (%)	τ_f (ns) (Amplitude Weighted)	$1/\tau_f$	χ^2
490	Toluene	0.40	57.19	4.96	9.04	10.06	33.78	4.07	0.25	1.12
490	1,4-Dioxane	0.44	46.10	4.10	11.84	10.34	42.06	5.04	0.20	1.23
490	Chloroform	0.46	35.77	2.78	14.21	10.15	50.02	5.64	0.18	1.18
490	Acetonitrile	0.65	46.23	2.38	21.45	8.23	32.32	3.47	0.29	1.11
490	1-Octanol	0.34	75.01	3.46	4.86	10.13	20.13	2.46	0.41	1.14
490	1-Hexanol	0.37	75.38	4.17	6.75	10.22	17.87	2.38	0.42	1.11
490	1-Butanol	0.32	85.60	4.26	4.07	10.07	10.32	1.49	0.67	1.49
490	1-Pentanol	0.33	83.09	4.46	4.92	10.31	11.99	1.73	0.58	1.10
490	1-Propanol	0.35	72.84	3.66	6.69	9.54	20.48	2.45	0.41	1.26
490	Acetic acid	0.30	59.80	1.31	39.44	5.75	0.76	0.74	1.36	1.09
490	Methanol	0.35	41.09	3.93	35.61	9.53	23.30	3.76	0.27	1.01
490	2,2,2-Trifluoroethanol	0.45	46.65	1.04	52.50	5.64	0.85	0.80	1.25	1.00

Table 3.4.16. Summary of Time Correlated Single Photon Counting (TCSPC) fluorescent lifetimes (amplitude weighted) of **19** recorded at 490 nm.

Wavelength (nm)	Solvent	τ_1 (ns)	A_1 (%)	τ_2 (ns)	A_2 (%)	τ_3 (ns)	A_3 (%)	τ_f (ns) (Amplitude Weighted)	$1/\tau_f$	χ^2
520	Toluene	-	-	3.48	11.73	9.98	88.27	9.21	0.11	1.30
520	1,4-Dioxane	0.39	12.73	5.05	16.36	10.71	70.91	8.47	0.12	1.16
520	Chloroform	-	-	4.17	12.98	10.55	87.02	9.72	0.10	1.15
520	Acetonitrile	0.42	21.28	3.04	16.60	8.88	62.11	6.11	0.16	1.15
520	1-Octanol	0.40	41.36	4.66	8.42	10.53	50.21	5.84	0.17	1.11
520	1-Hexanol	0.37	37.93	5.92	16.17	10.86	45.90	6.08	0.16	1.06
520	1-Butanol	0.29	45.02	5.17	11.27	10.37	43.72	5.24	0.19	1.12
520	1-Pentanol	0.36	31.32	5.82	17.70	10.78	50.98	6.64	0.15	1.10
520	1-Propanol	0.34	28.10	5.60	19.89	10.48	52.00	6.66	0.15	1.14
520	Acetic acid	0.31	48.83	1.28	49.55	5.22	0.62	0.82	1.22	1.07
520	Methanol	0.30	24.17	4.17	39.83	9.70	35.99	5.20	0.19	1.11
520	2,2,2-Trifluoroethanol	0.31	53.37	1.22	45.21	5.10	1.43	0.79	1.26	1.06

Table 3.4.17. Summary of Time Correlated Single Photon Counting (TCSPC) fluorescent lifetimes (amplitude weighted) of **19** recorded at 520 nm.

Wavelength (nm)	Solvent	τ_1 (ns)	A_1 (%)	τ_2 (ns)	A_2 (%)	τ_3 (ns)	A_3 (%)	τ_f (ns) (Amplitude Weighted)	$1/\tau_f$	χ^2
540	Toluene	-	-	3.43	10.35	9.92	89.65	9.25	0.11	1.28
540	1,4-Dioxane	0.29	12.80	5.60	18.41	10.78	68.79	8.49	0.12	1.11
540	Chloroform	-	-	5.36	15.71	10.70	84.29	9.86	0.10	1.22
540	Acetonitrile	0.54	15.00	5.33	30.59	9.89	54.41	7.09	0.14	1.15
540	1-Octanol	0.42	29.73	6.06	17.09	11.03	53.18	7.03	0.14	0.98
540	1-Hexanol	0.39	23.53	6.22	21.77	10.97	54.69	7.45	0.13	1.09
540	1-Butanol	0.32	30.32	6.14	20.40	10.76	49.28	6.65	0.15	1.02
540	1-Pentanol	0.35	20.25	5.84	20.09	10.76	59.67	7.66	0.13	1.17
540	1-Propanol	0.32	18.07	5.43	20.11	10.38	61.82	7.57	0.13	1.11
540	Acetic acid	0.30	43.94	1.28	55.48	5.40	0.58	0.87	1.14	0.98
540	Methanol	-	-	3.93	49.73	9.57	50.27	6.77	0.15	1.20
540	2,2,2-Trifluoroethanol	0.31	52.90	1.33	45.66	5.20	1.44	0.84	1.18	0.98

Table 3.4.18. Summary of Time Correlated Single Photon Counting (TCSPC) fluorescent lifetimes (amplitude weighted) of **19** recorded at 540 nm.

Wavelength (nm)	Solvent	τ_1 (ns)	A_1 (%)	τ_2 (ns)	A_2 (%)	τ_3 (ns)	A_3 (%)	τ_f (ns) (Amplitude Weighted)	$1/\tau_f$	χ^2
570	Toluene	-	-	4.16	11.60	10.02	88.40	9.34	0.11	1.26
570	1,4-Dioxane	-	-	4.83	16.87	10.67	83.13	9.68	0.10	1.17
570	Chloroform	-	-	6.19	14.59	10.69	85.41	10.04	0.10	1.21
570	Acetonitrile	-	-	4.50	25.33	9.53	74.67	8.26	0.12	1.19
570	1-Octanol	0.47	20.44	6.39	20.46	11.10	59.10	7.96	0.13	1.09
570	1-Hexanol	0.42	14.57	6.15	22.35	10.92	63.08	8.33	0.12	1.17
570	1-Butanol	0.32	23.38	5.82	19.02	10.62	57.60	7.30	0.14	1.15
570	1-Pentanol	0.52	13.36	8.36	60.76	12.98	25.88	8.51	0.12	1.19
570	1-Propanol	-	-	5.63	26.80	10.50	73.20	9.19	0.11	1.19
570	Acetic acid	0.28	46.29	1.26	53.16	5.15	0.55	0.83	1.21	1.05
570	Methanol	-	-	3.94	49.21	9.59	50.79	6.81	0.15	1.08
570	2,2,2-Trifluoroethanol	0.29	54.33	1.40	44.49	5.56	1.18	0.85	1.18	1.04

Table 3.4.19. Summary of Time Correlated Single Photon Counting (TCSPC) fluorescent lifetimes (amplitude weighted) of **19** recorded at 570 nm.

Wavelength (nm)	Solvent	τ_1 (ns)	A_1 (%)	τ_2 (ns)	A_2 (%)	τ_3 (ns)	A_3 (%)	τ_f (ns) (Amplitude Weighted)	$1/\tau_f$	χ^2
600	Toluene	-	-	3.60	9.37	9.93	90.63	9.33	0.11	1.23
600	1,4-Dioxane	-	-	6.35	25.65	11.05	74.35	9.84	0.10	1.20
600	Chloroform	-	-	9.13	71.94	12.82	28.06	10.17	0.10	1.24
600	Acetonitrile	-	-	4.71	23.95	9.55	76.05	8.39	0.12	1.32
600	1-Octanol	0.40	17.64	6.00	17.59	10.97	64.77	8.23	0.12	1.06
600	1-Hexanol	0.44	15.03	6.73	25.62	11.07	59.35	8.36	0.12	1.12
600	1-Butanol	0.33	26.12	6.04	20.05	10.72	53.83	7.06	0.14	1.14
600	1-Pentanol	0.40	15.34	6.84	29.00	11.14	55.66	8.24	0.12	1.13
600	1-Propanol	-	-	6.31	34.20	10.79	65.80	9.26	0.11	1.28
600	Acetic acid	0.17	75.72	1.23	23.94	4.49	0.34	0.44	2.28	1.28
600	Methanol	-	-	3.94	48.57	9.53	51.43	6.82	0.15	1.15
600	2,2,2-Trifluoroethanol	0.31	54.71	1.46	44.37	6.09	0.92	0.87	1.15	1.09

Table 3.4.20. Summary of Time Correlated Single Photon Counting (TCSPC) fluorescent lifetimes (amplitude weighted) of **19** recorded at 600 nm.

3.4.7 400 nm average fluorescent lifetimes - Solvatochromic analysis.

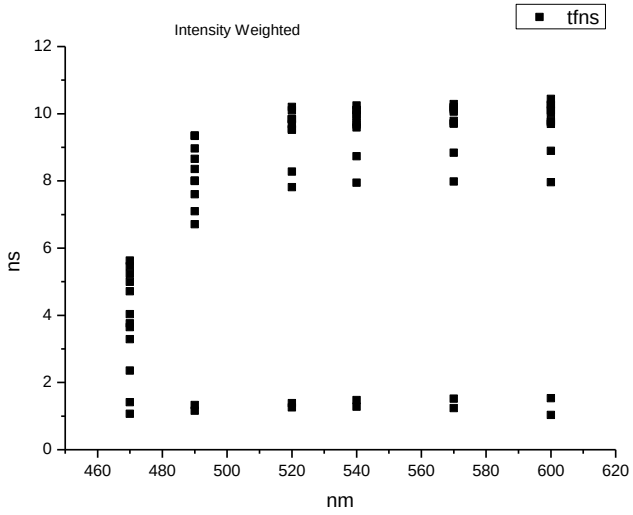

Figure 3.4.49. Intensity weighted average lifetime (τ_f) of **19** versus wavelength (nm).

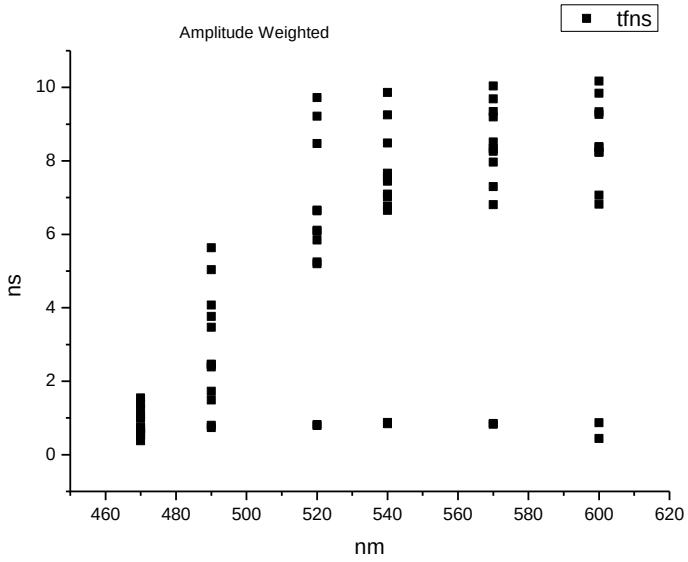

Figure 3.4.50. Amplitude weighted average lifetime (τ_f) of **19** versus wavelength (nm).

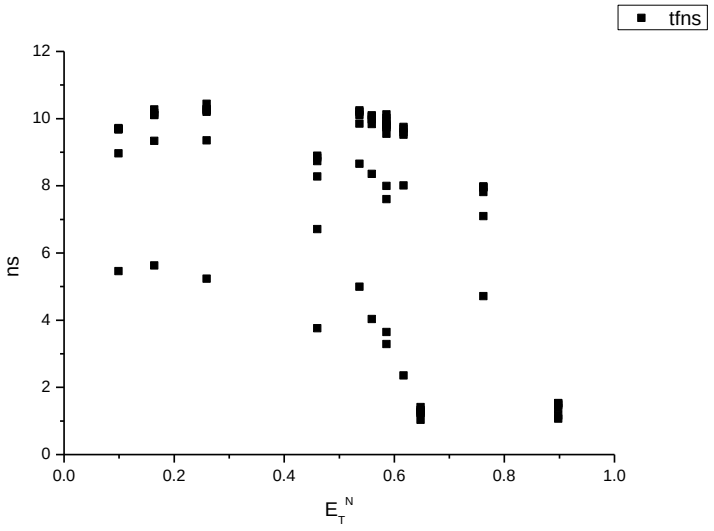

Figure 3.4.51. Intensity weighted average lifetime (τ_f) of **19** versus E_T^N.

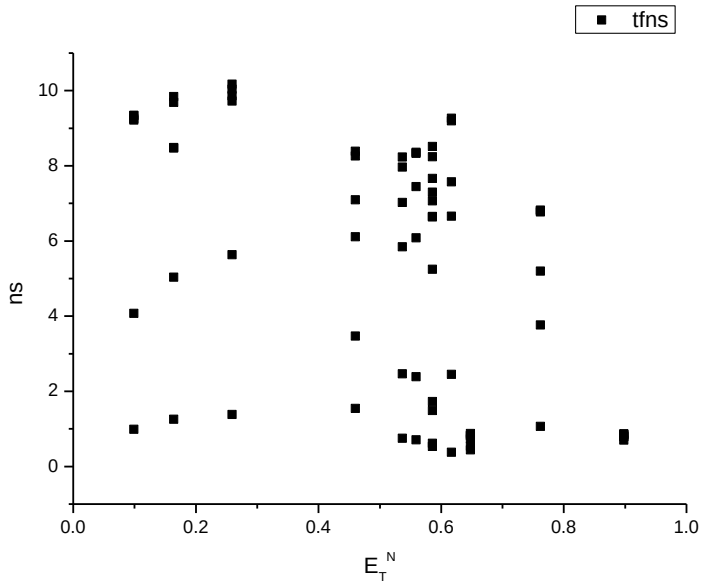

Figure 3.4.52. Amplitude weighted average lifetime (τ_f) of **19** versus E_T^N.

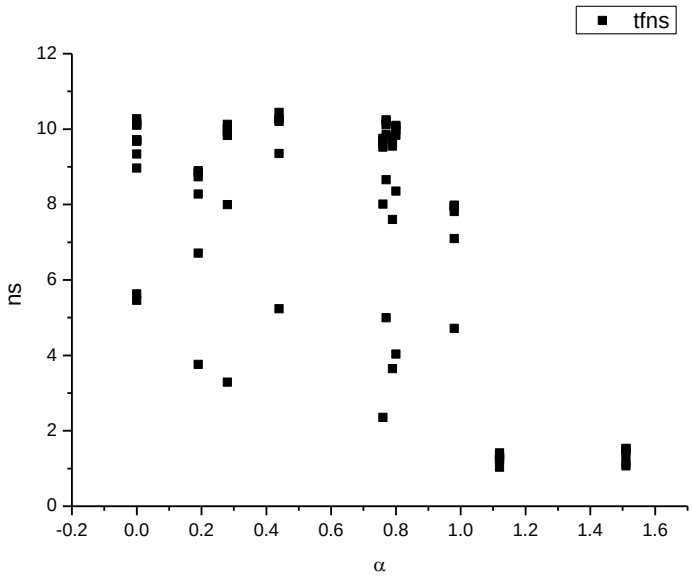

Figure 3.4.53. Intensity weighted average lifetime (τ_f) of **19** versus α.

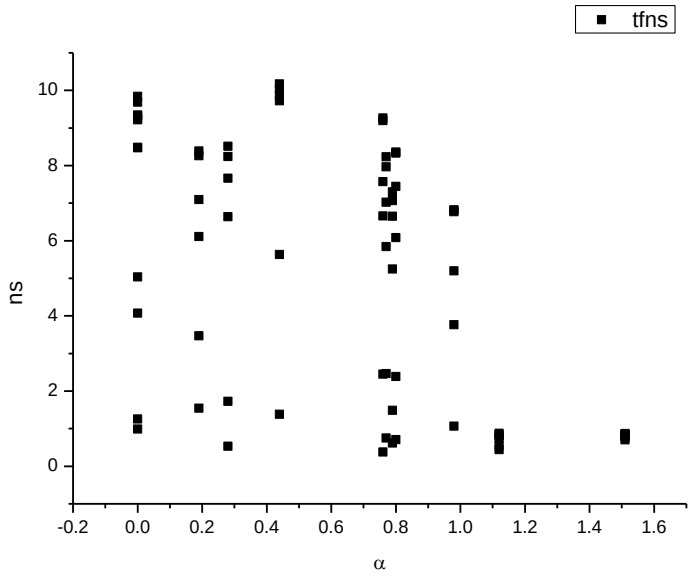

Figure 3.4.54. Amplitude weighted average lifetime (τ_f) of **19** versus α.

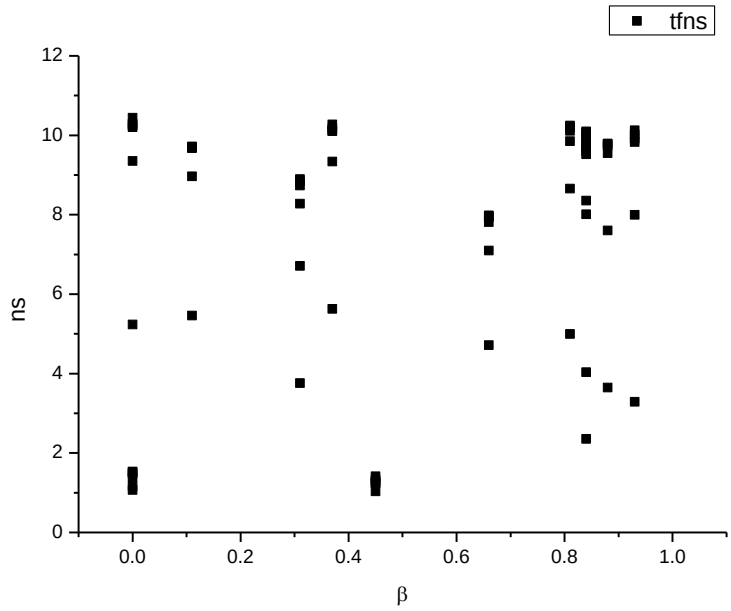

Figure 3.4.55. Intensity weighted average lifetime (τ_f) of **19** versus β.

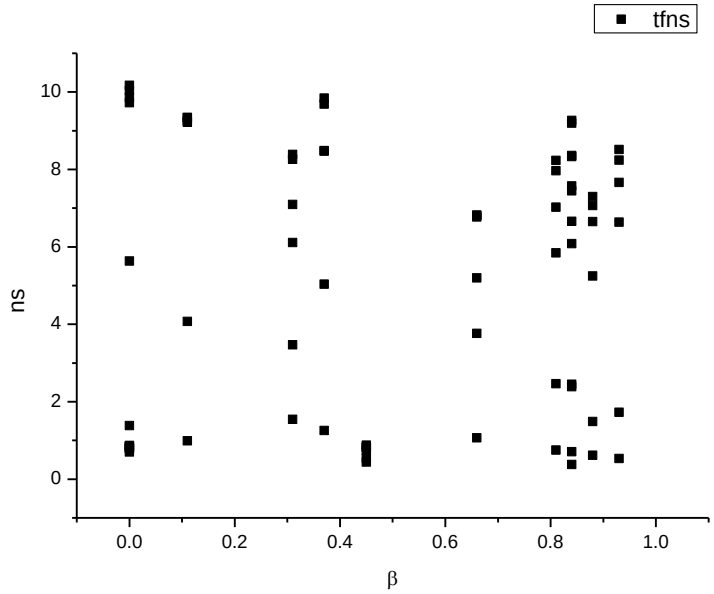

Figure 3.4.56. Amplitude weighted average lifetime (τ_f) of **19** versus β.

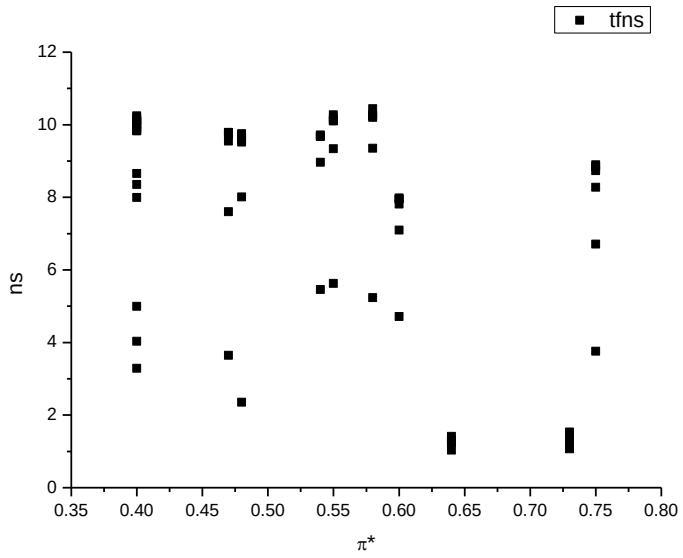

Figure 3.4.57. Intensity weighted average lifetime (τ_f) of **19** versus π*.

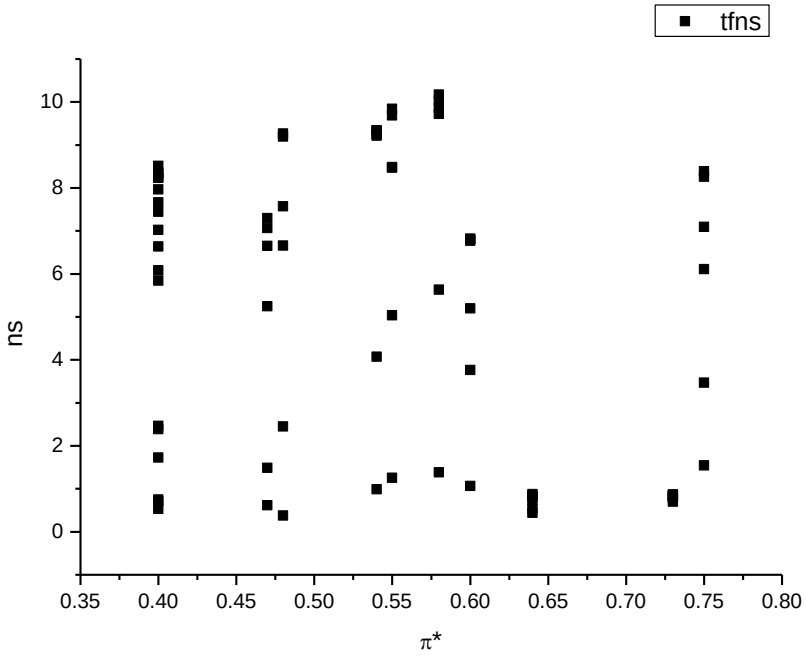

Figure 3.4.58. Amplitude weighted average lifetime (τ_f) of **19** versus π*.

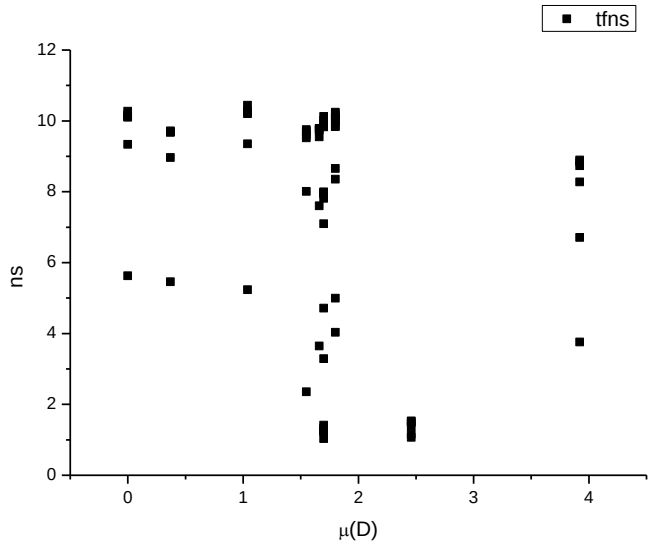

Figure 3.4.59. Intensity weighted average lifetime (τ_f) of **19** versus μ(D).

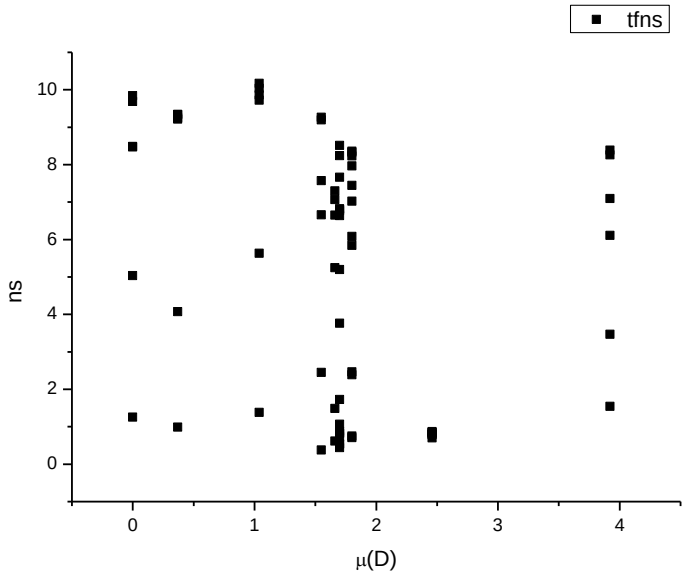

Figure 3.4.60. Amplitude weighted average lifetime (τ_f) of **19** versus μ(D).

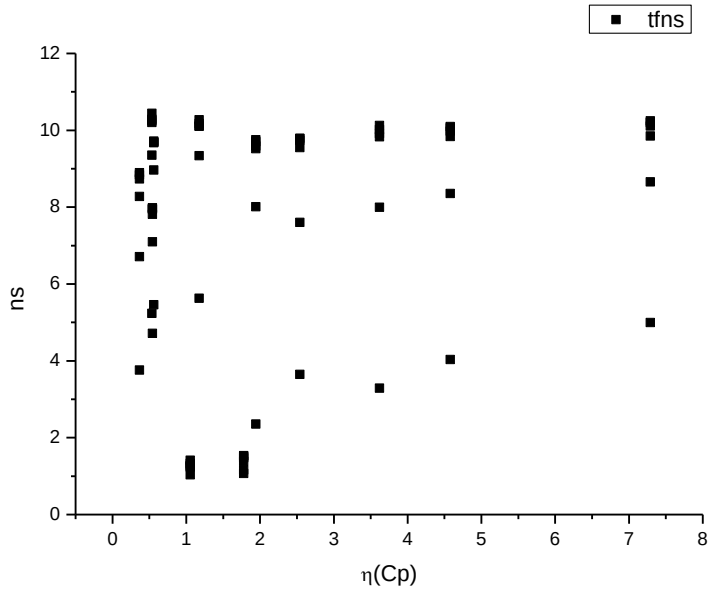

Figure 3.4.61. Intensity weighted average lifetime (τ_f) of **19** versus η(Cp).

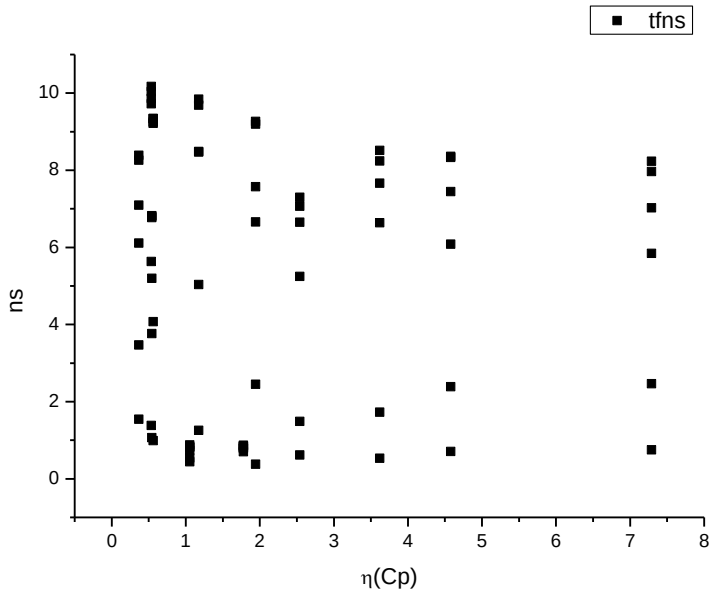

Figure 3.4.62. Amplitude weighted average lifetime (τ_f) of **19** versus η(Cp).

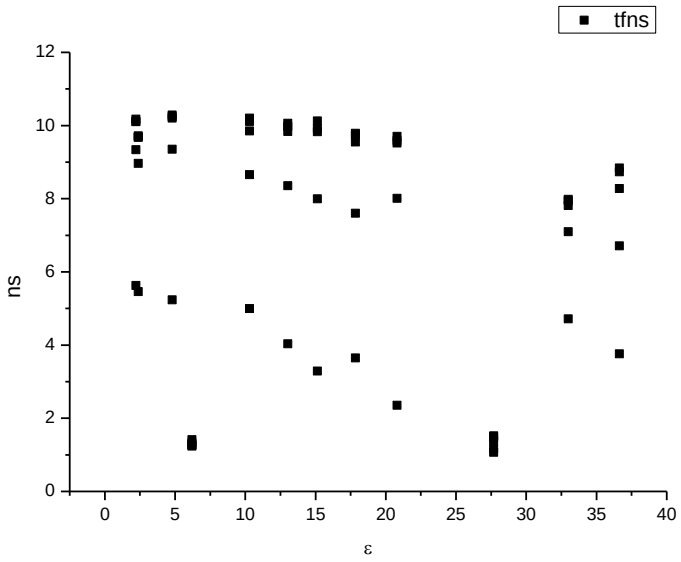

Figure 3.4.63. Intensity weighted average lifetime (τ_f) of **19** versus ε.

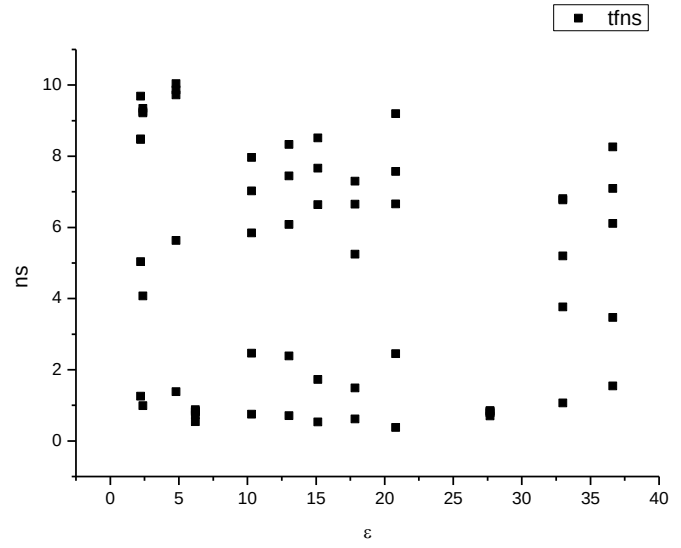

Figure 3.4.64. Amplitude weighted average lifetime (τ_f) of **19** versus ε.

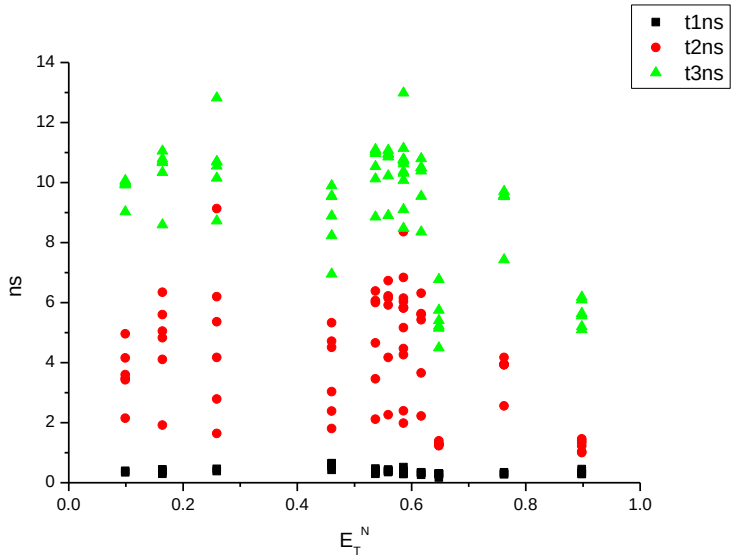

Figure 3.4.65. Intensity weighted components of TCSPC lifetime decay of **19** (470 nm to 600 nm) versus E_T^N.

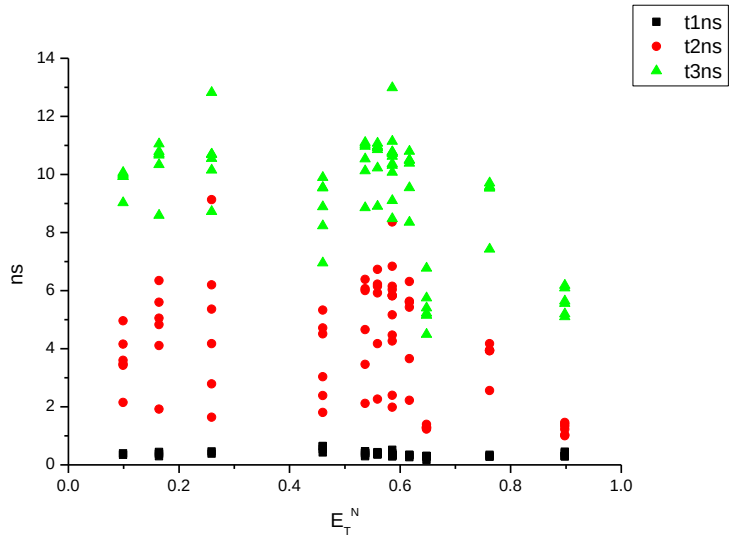

Figure 3.4.66. Amplitude weighted components of TCSPC lifetime decay of **19** (470 nm to 600 nm) versus E_T^N.

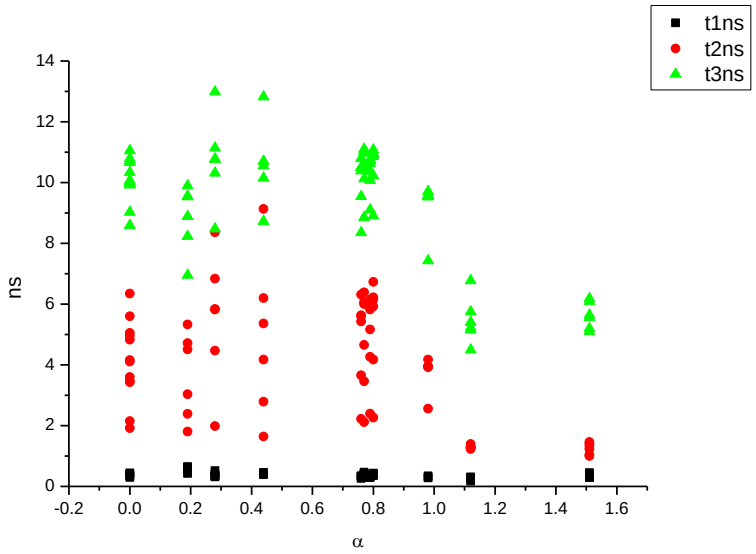

Figure 3.4.67. Intensity weighted components of TCSPC lifetime decay of **19** (470 nm to 600 nm) versus α.

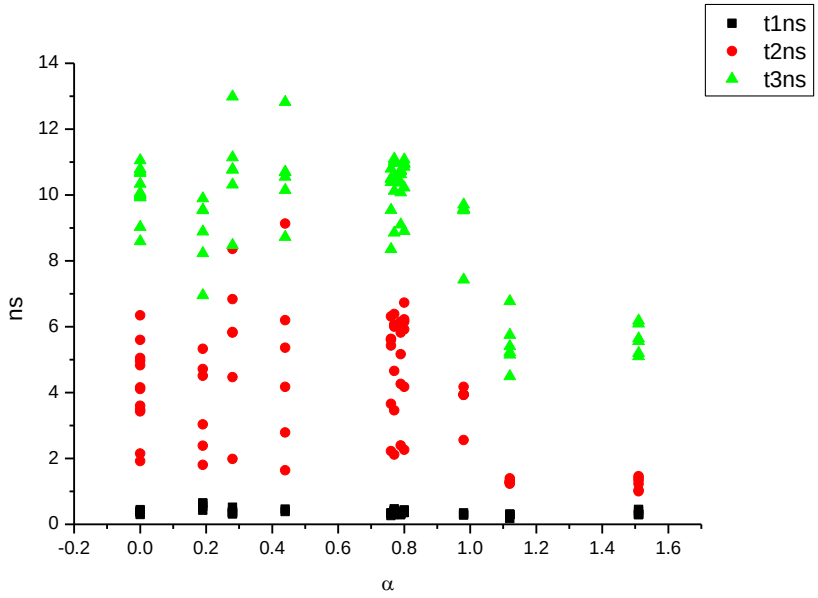

Figure 3.4.68. Amplitude weighted components of TCSPC lifetime decay of **19** (470 nm to 600 nm) versus α.

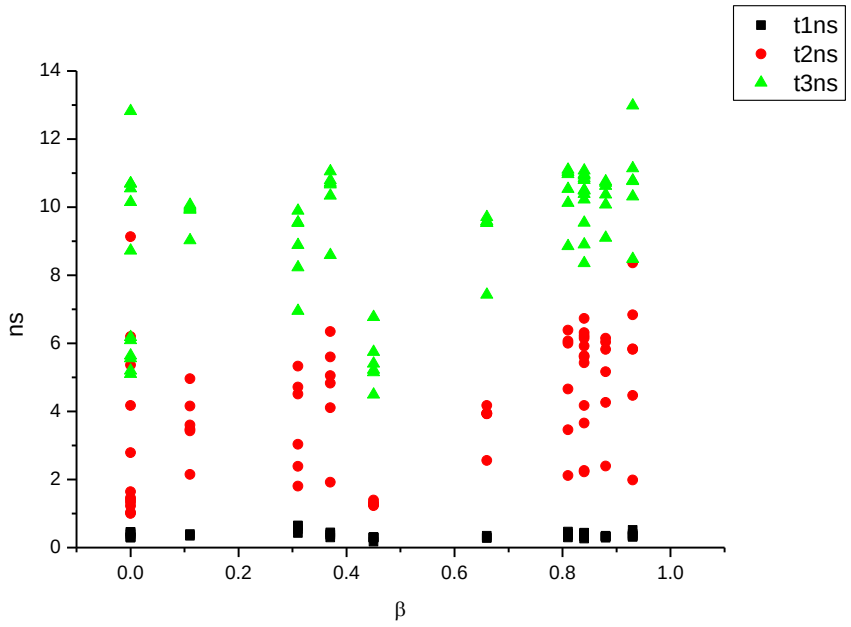

Figure 3.4.69. Intensity weighted components of TCSPC lifetime decay of **19** (470 nm to 600 nm) versus β.

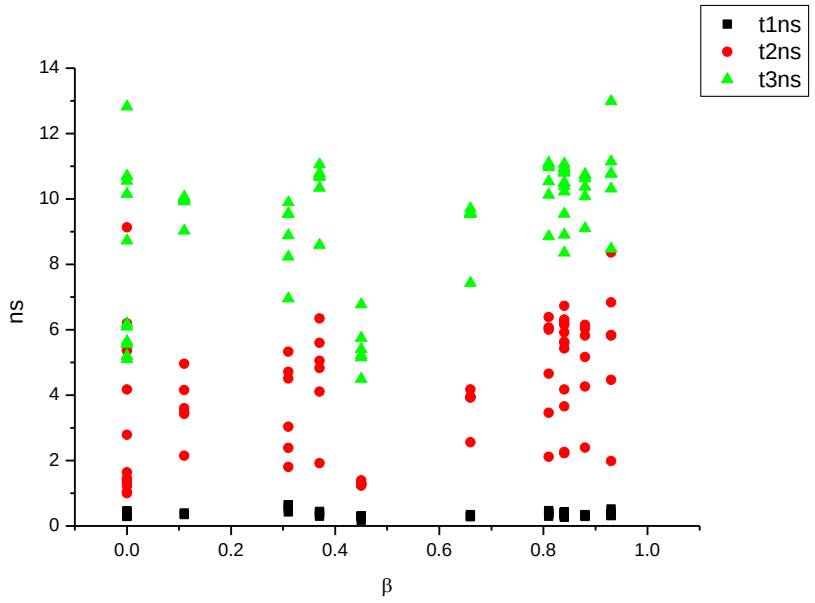

Figure 3.4.70. Amplitude weighted components of TCSPC lifetime decay of **19** (470 nm to 600 nm) versus β.

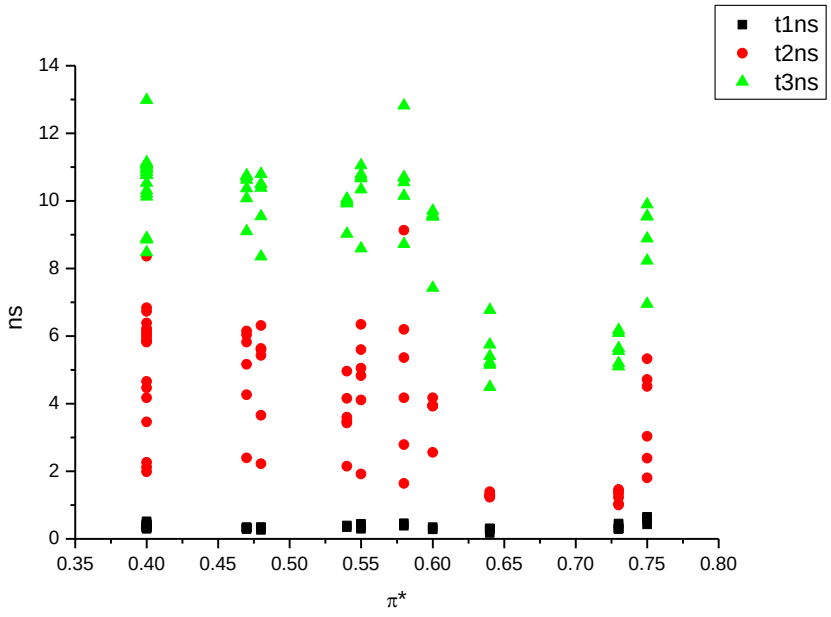

Figure 3.4.71. Intensity weighted components of TCSPC lifetime decay of **19** (470 nm to 600 nm) versus π*.

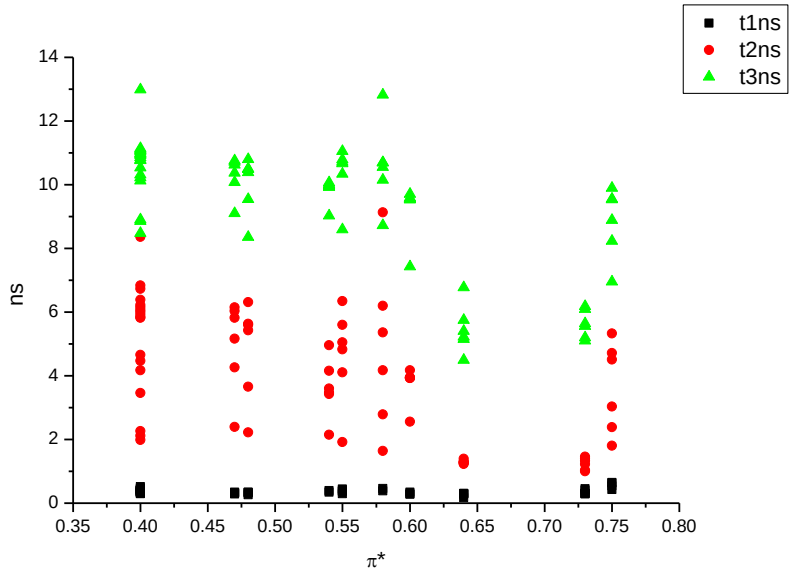

Figure 3.4.72. Amplitude weighted components of TCSPC lifetime decay of **19** (470 nm to 600 nm) versus π*.

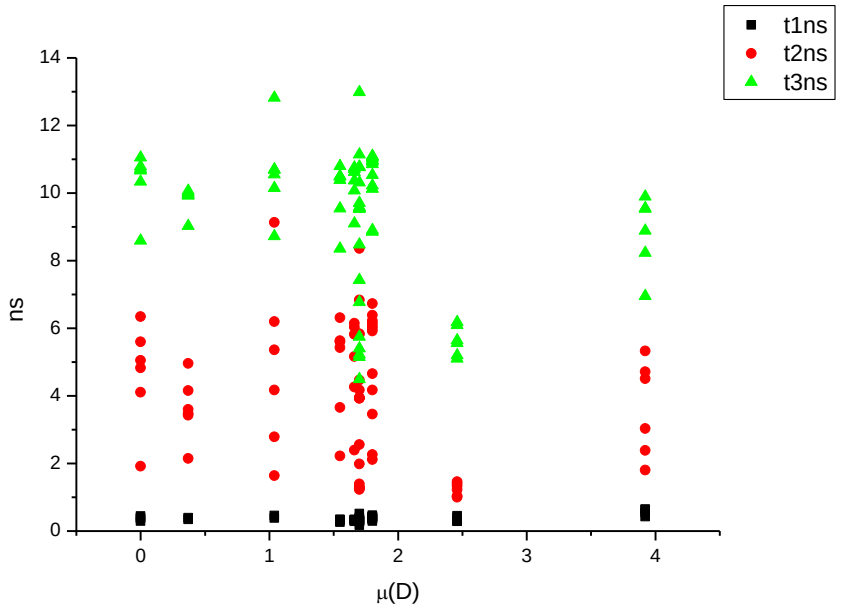

Figure 3.4.73. Intensity weighted components of TCSPC lifetime decay of **19** (470 nm to 600 nm) versus μ(D).

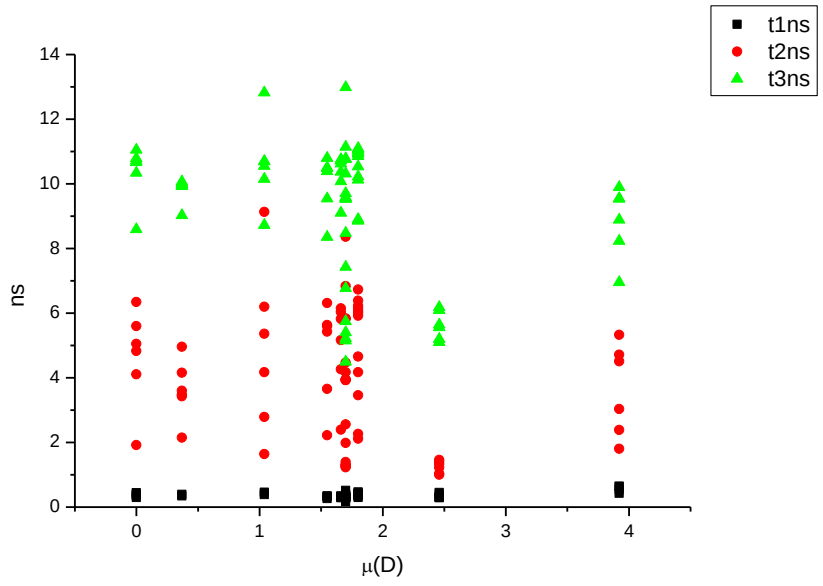

Figure 3.4.74. Amplitude weighted components of TCSPC lifetime decay of **19** (470 nm to 600 nm) versus μ(D).

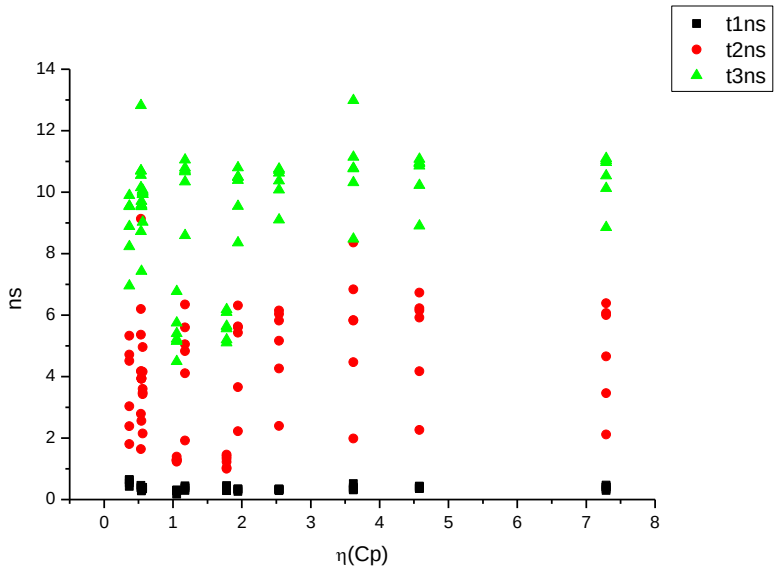

Figure 3.4.75. Intensity weighted components of TCSPC lifetime decay of **19** (470 nm to 600 nm) versus η(Cp).

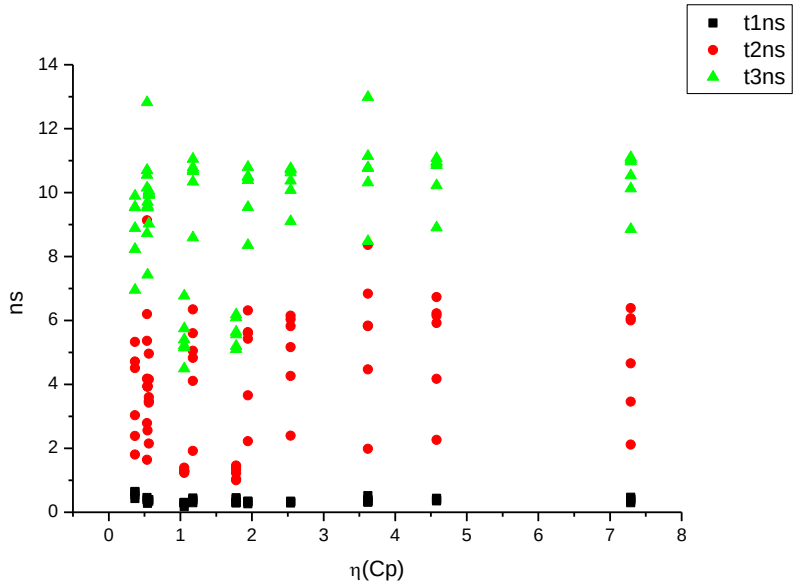

Figure 3.4.76. Amplitude weighted components of TCSPC lifetime decay of **19** (470 nm to 600 nm) versus η(Cp).

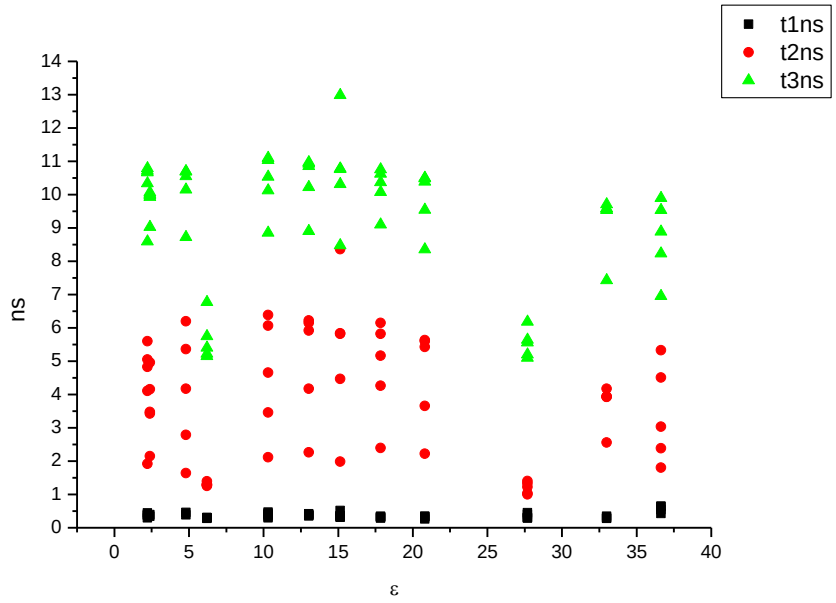

Figure 3.4.77. Intensity weighted components of TCSPC lifetime decay of **19** (470 nm to 600 nm) versus ε.

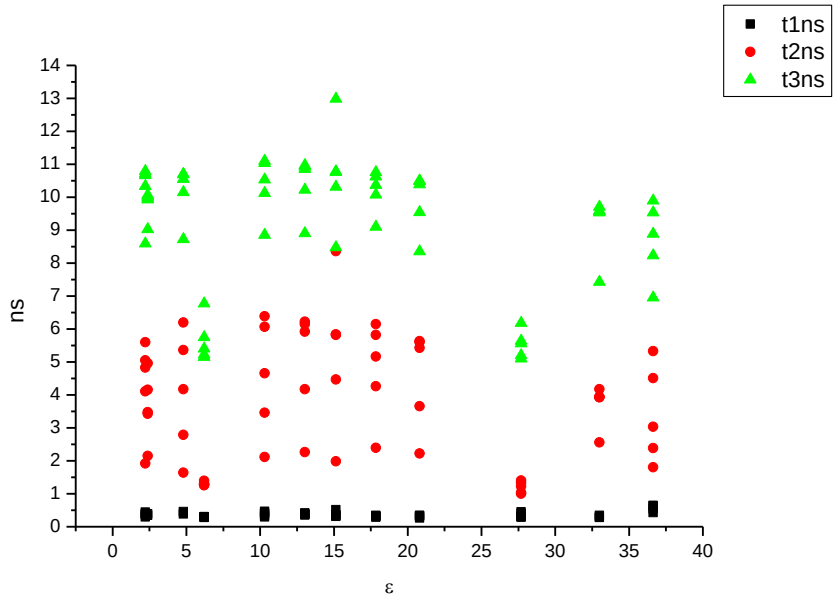

Figure 3.4.78. Amplitude weighted components of TCSPC lifetime decay of **19** (470 nm to 600 nm) versus ε.

3.4.7.1 470 nm Lifetime – Solvatochromic analysis.

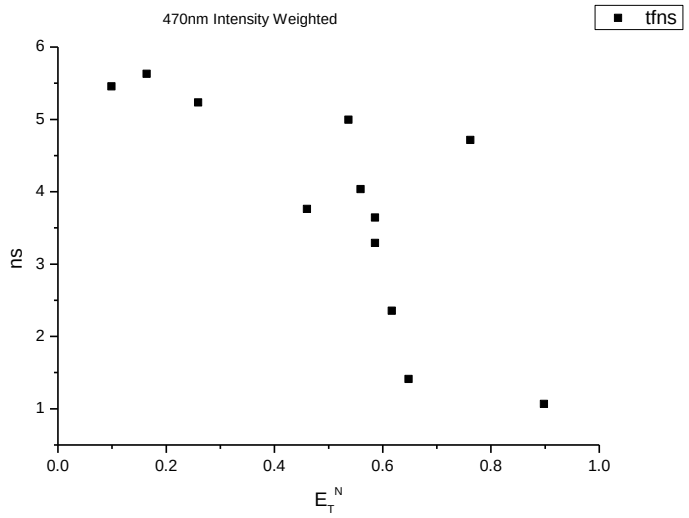

Figure 3.4.79. Intensity weighted average lifetime (τ_f) of **19** at 470 nm versus E_T^N.

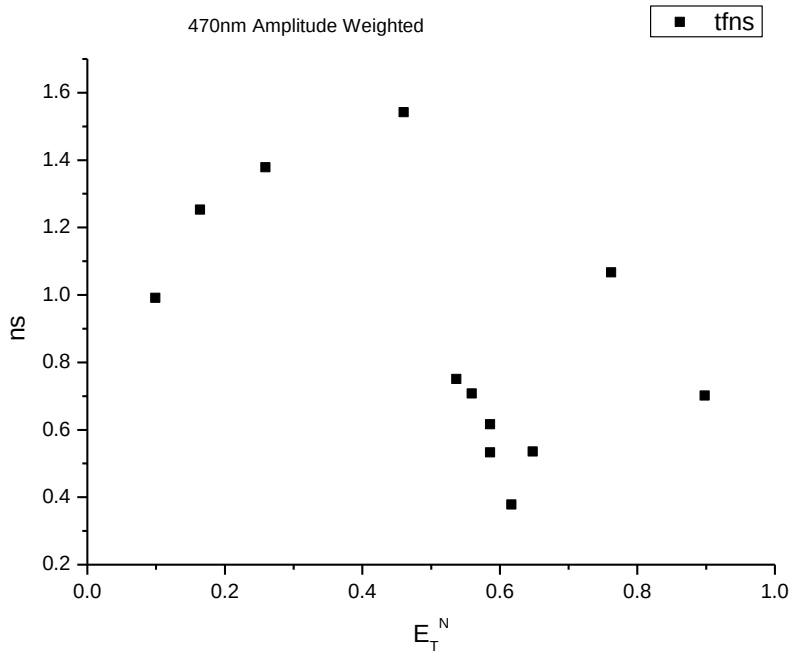

Figure 3.4.78. Amplitude weighted average lifetime (τ_f) of **19** at 470 nm versus E_T^N.

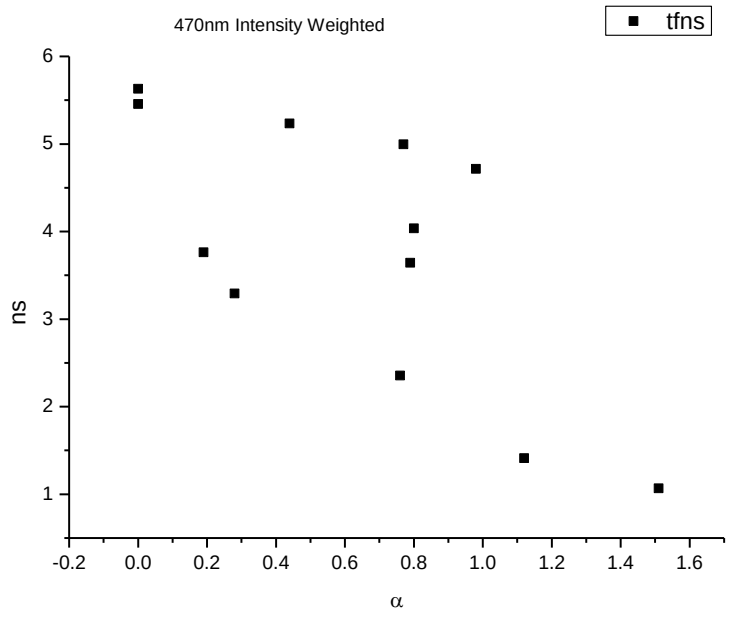

Figure 3.4.79. Intensity weighted average lifetime (τ_f) of **19** at 470 nm versus α.

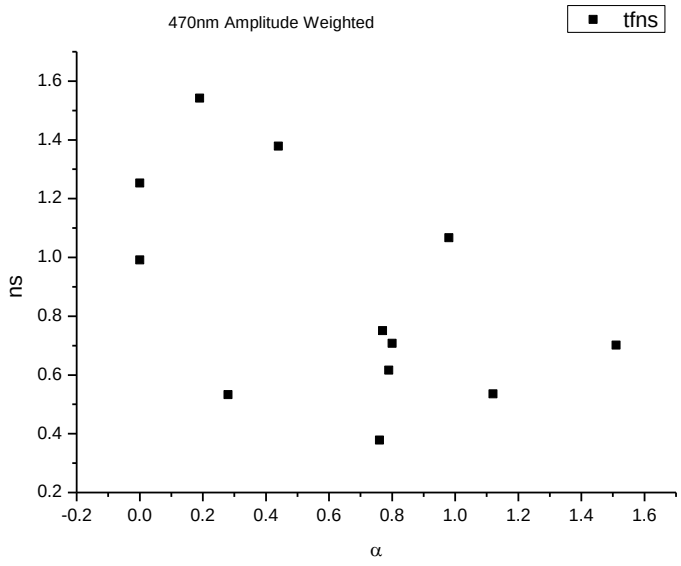

Figure 3.4.80. Amplitude weighted average lifetime (τ_f) of **19** at 470 nm versus α.

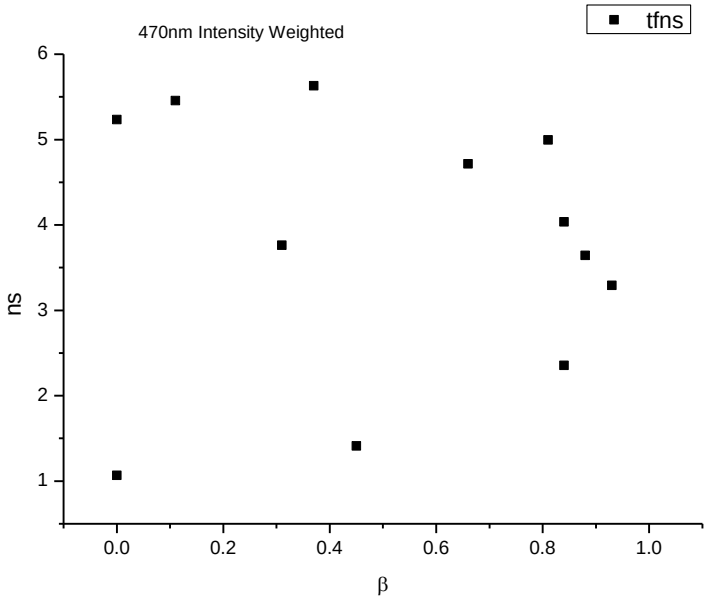

Figure 3.4.81. Intensity weighted average lifetime (τ_f) of **19** at 470 nm versus β.

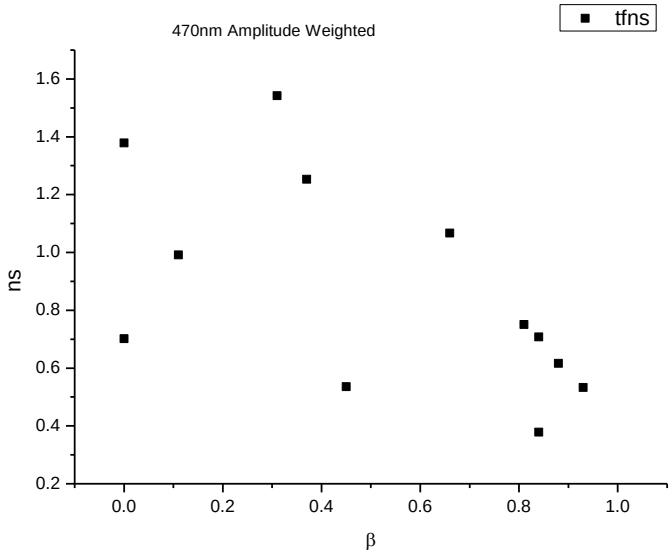

Figure 3.4.82. Amplitude weighted average lifetime (τ_f) of **19** at 470 nm versus β.

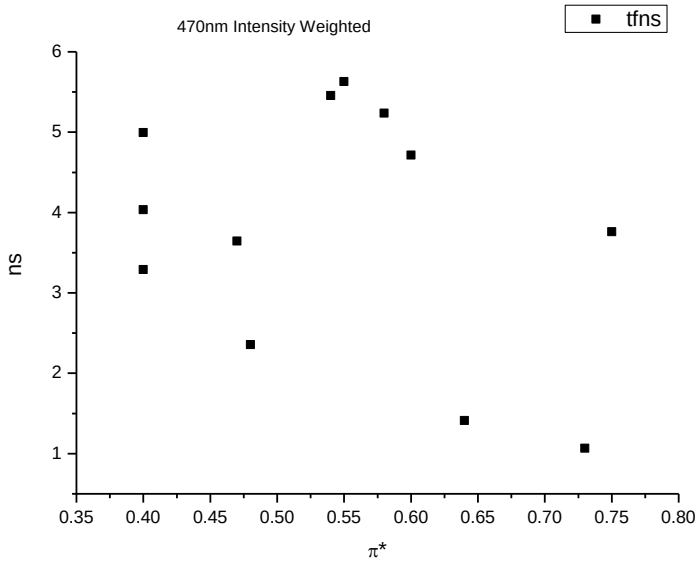

Figure 3.4.83. Intensity weighted average lifetime (τ_f) of **19** at 470 nm versus π*.

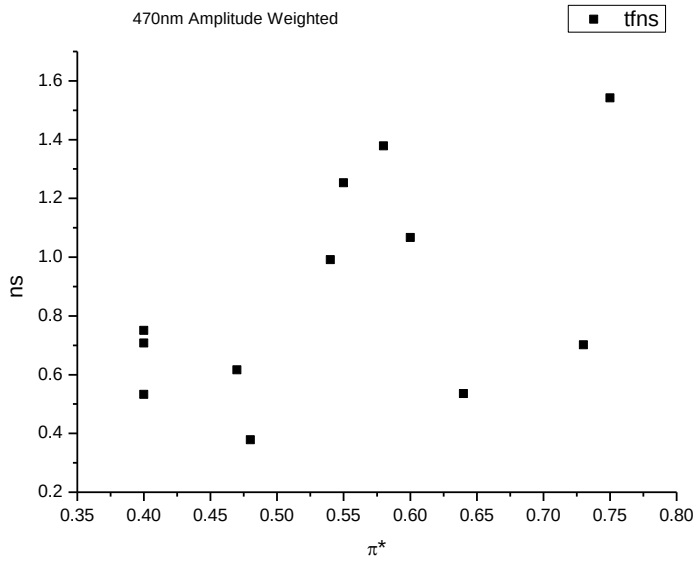

Figure 3.4.84. Amplitude weighted average lifetime (τ_f) of **19** at 470 nm versus π*.

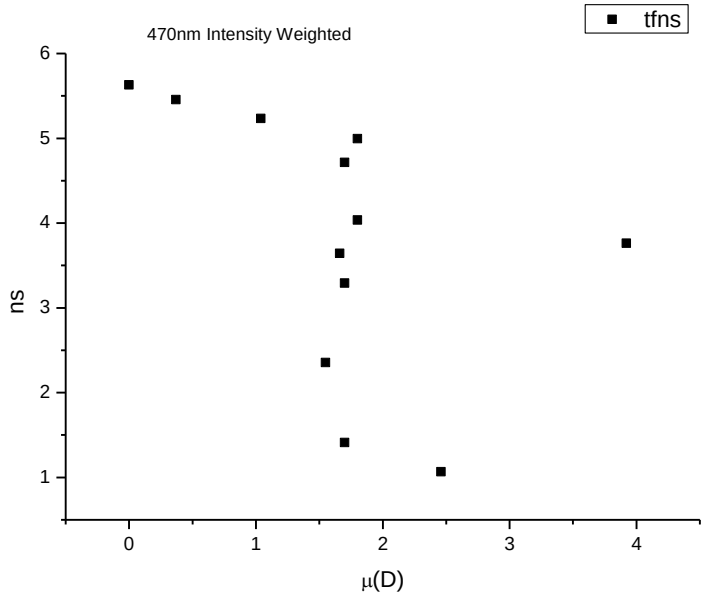

Figure 3.4.85. Intensity weighted average lifetime (τ_f) of **19** at 470 nm versus μ(D).

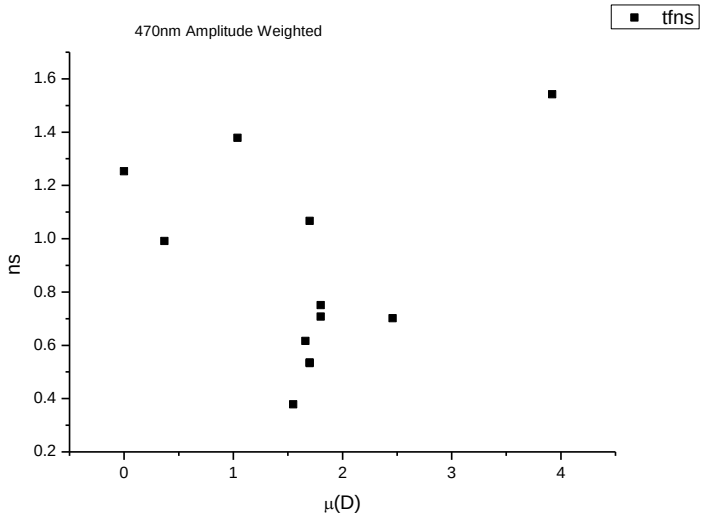

Figure 3.4.86. Amplitude weighted average lifetime (τ_f) of **19** at 470 nm versus μ(D).

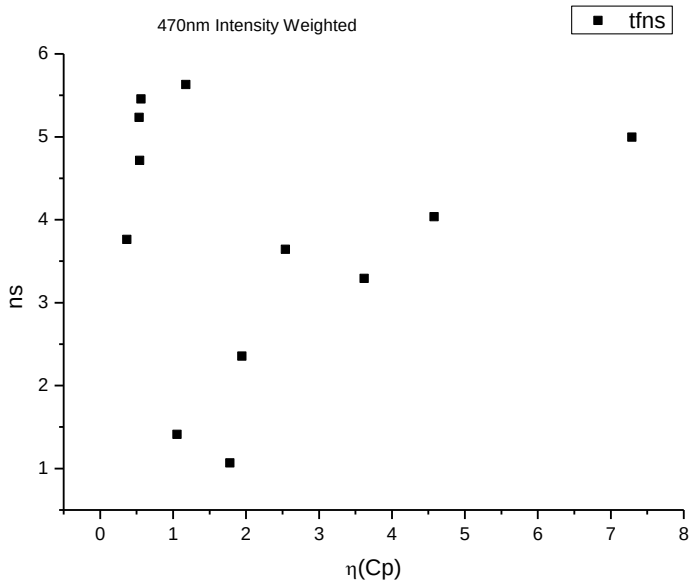

Figure 3.4.87. Intensity weighted average lifetime (τ_f) of **19** at 470 nm versus η(Cp).

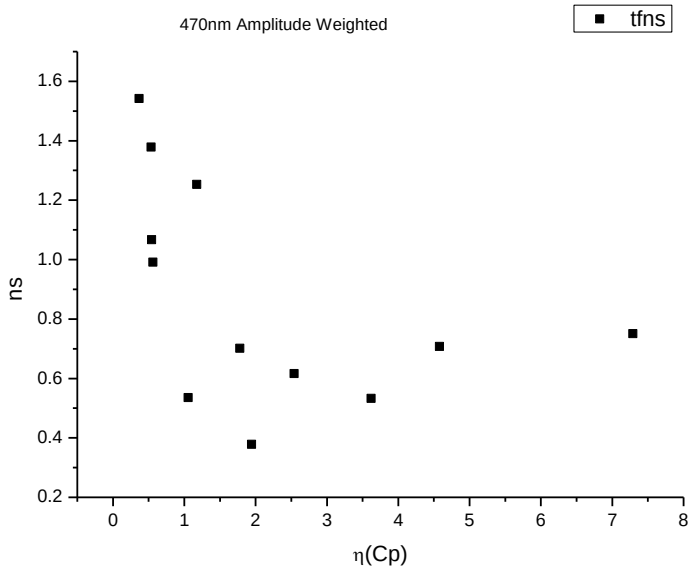

Figure 3.4.88. Amplitude weighted average lifetime (τ_f) of **19** at 470 nm versus η(Cp).

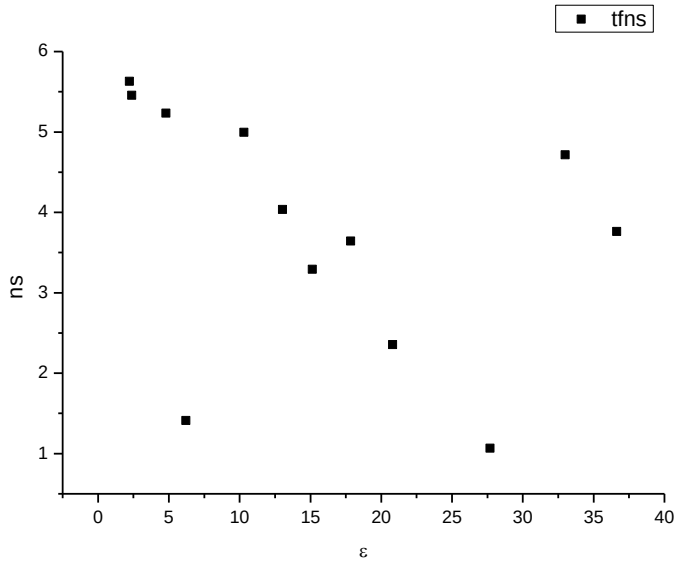

Figure 3.4.89. Intensity weighted average lifetime (τ_f) of **19** at 470 nm versus ε.

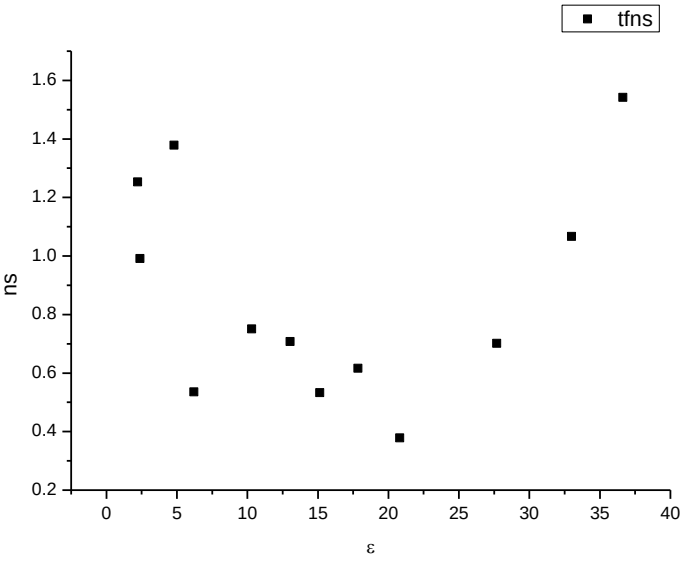

Figure 3.4.90. Amplitude weighted average lifetime (τ_f) of **19** at 470 nm versus ε.

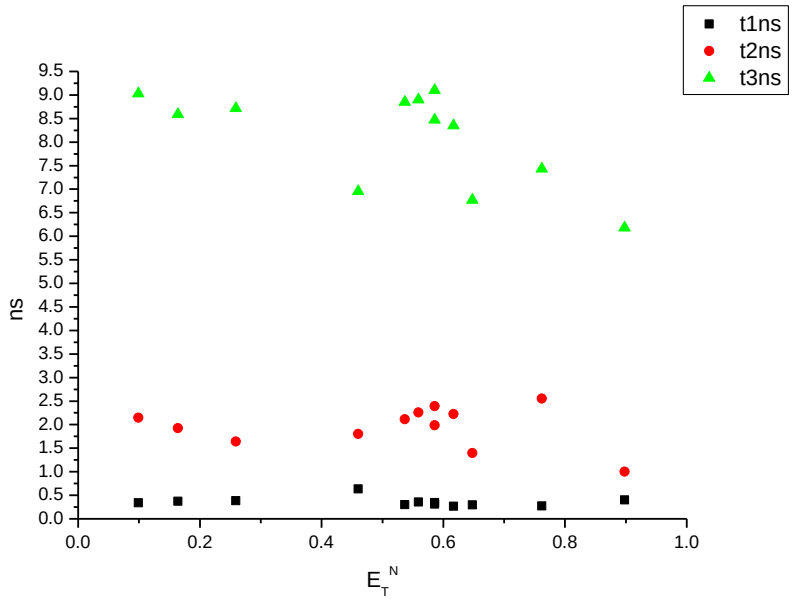

Figure 3.4.91. Intensity weighted components of TCSPC lifetime decay of **19** (470 nm) versus E_T^N.

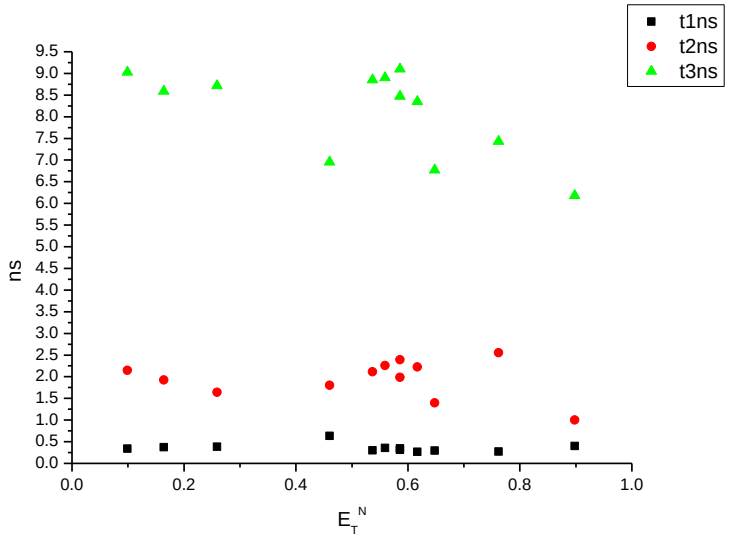

Figure 3.4.92. Amplitude weighted components of TCSPC lifetime decay of **19** (470 nm) versus E_T^N.

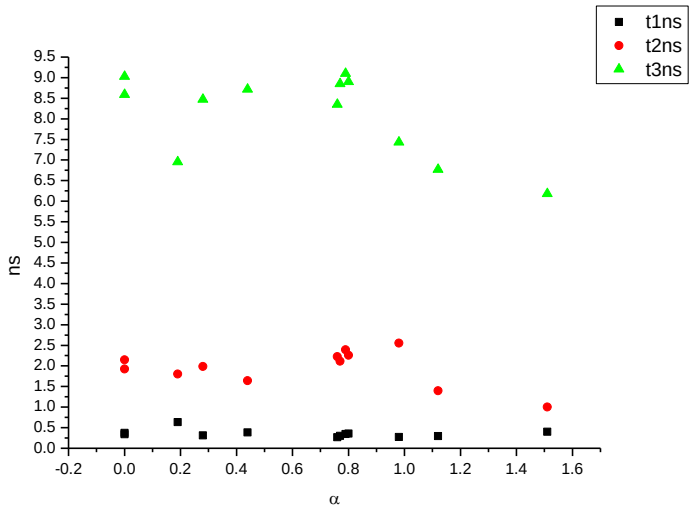

Figure 3.4.93. Intensity weighted components of TCSPC lifetime decay of **19** (470 nm) versus α.

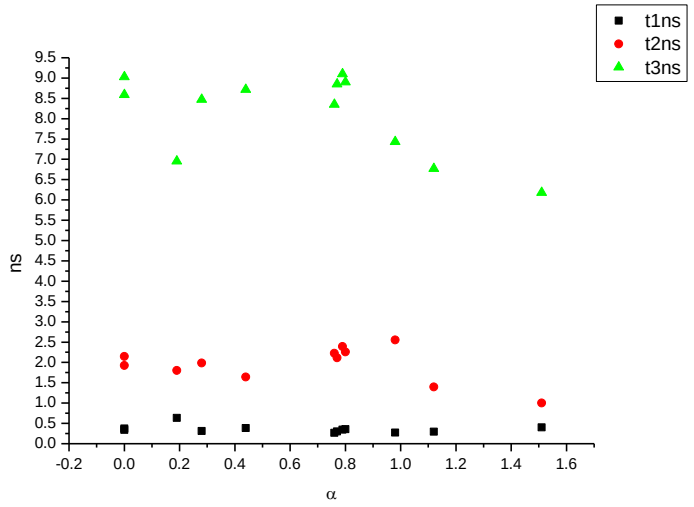

Figure 3.4.94. Amplitude weighted components of TCSPC lifetime decay of **19** (470 nm) versus α.

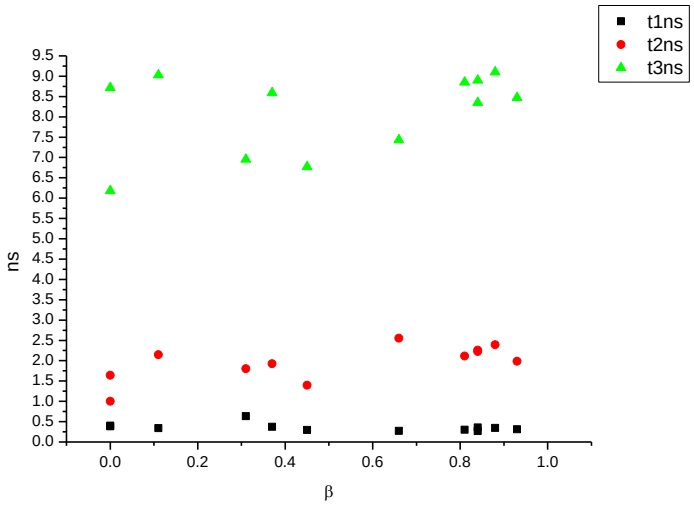

Figure 3.4.95. Intensity weighted components of TCSPC lifetime decay of **19** (470 nm) versus β.

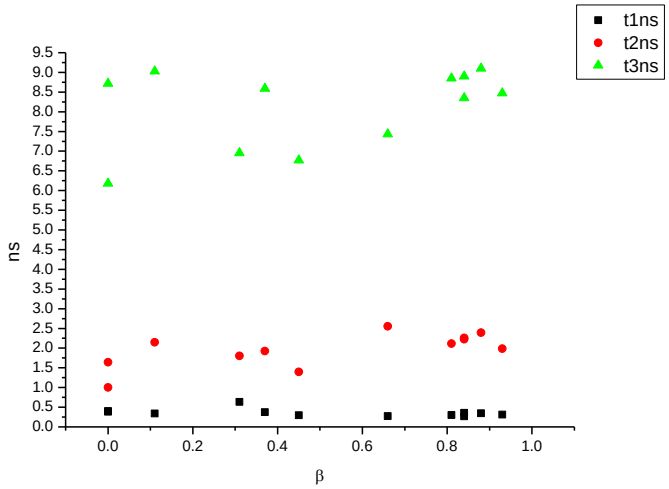

Figure 3.4.96. Amplitude weighted components of TCSPC lifetime decay of **19** (470 nm) versus β.

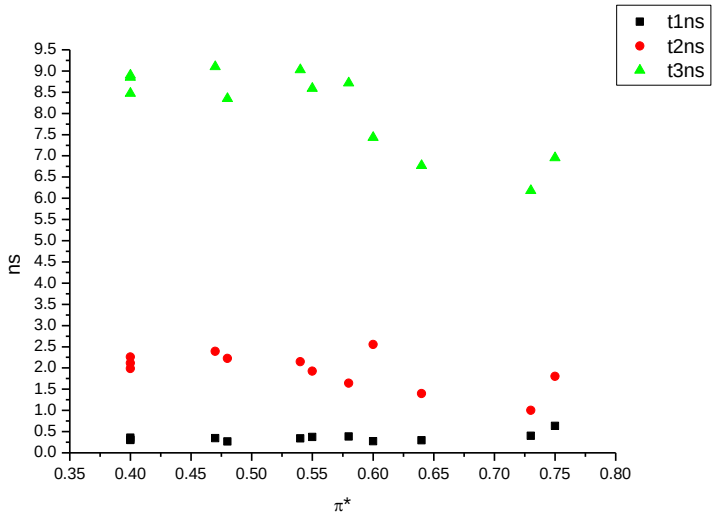

Figure 3.4.97. Intensity weighted components of TCSPC lifetime decay of **19** (470 nm) versus π*.

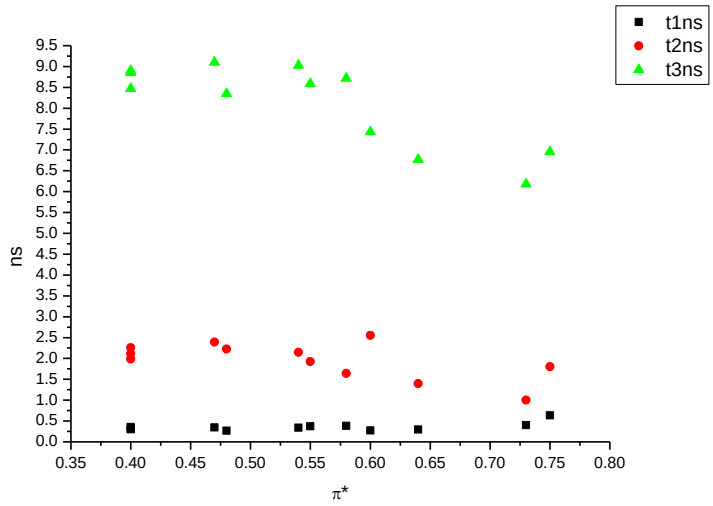

Figure 3.4.98. Amplitude weighted components of TCSPC lifetime decay of **19** (470 nm) versus π*.

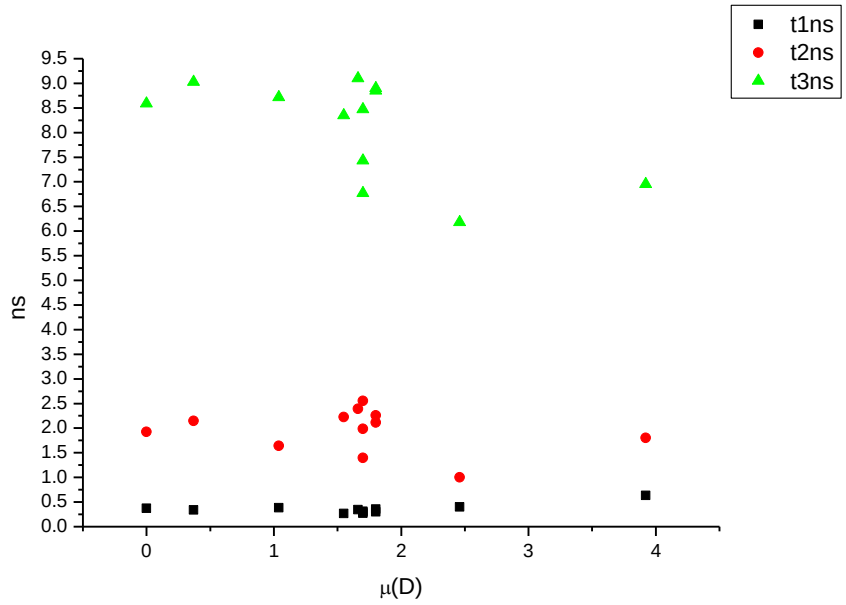

Figure 3.4.99. Intensity weighted components of TCSPC lifetime decay of **19** (470 nm) versus μ(D).

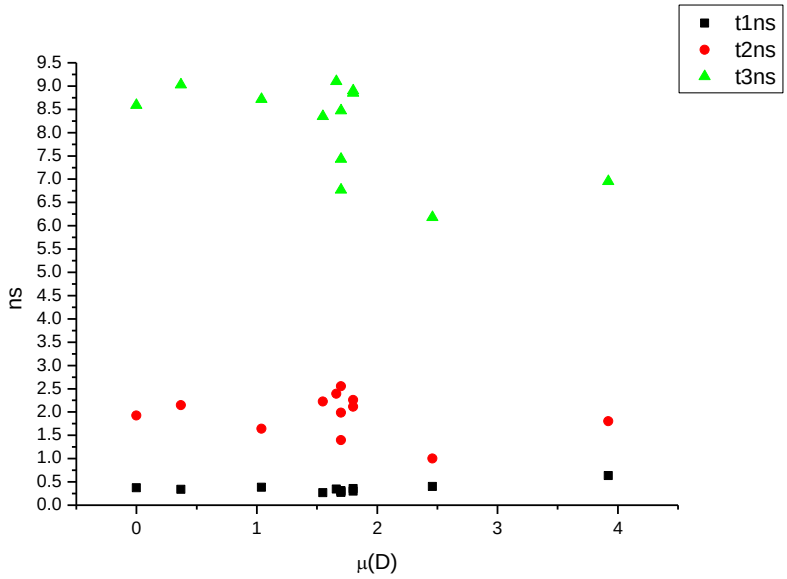

Figure 3.4.100. Amplitude weighted components of TCSPC lifetime decay of **19** (470 nm) versus μ(D).

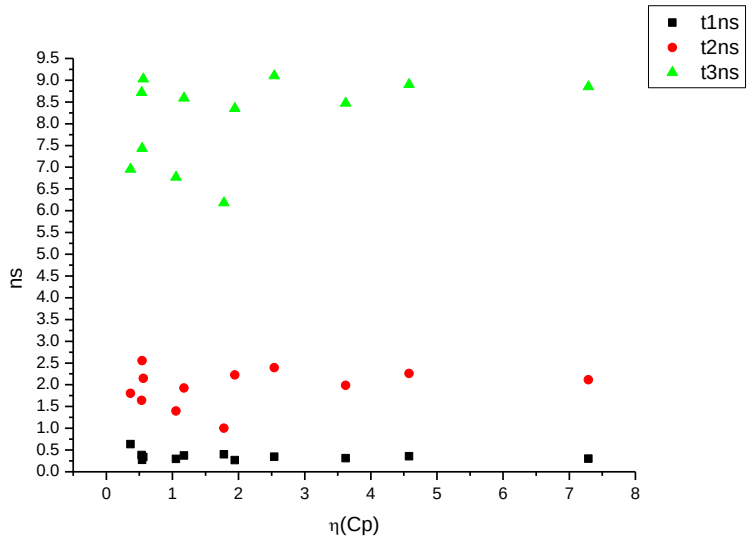

Figure 3.4.101. Intensity weighted components of TCSPC lifetime decay of **19** (470 nm) versus η(Cp).

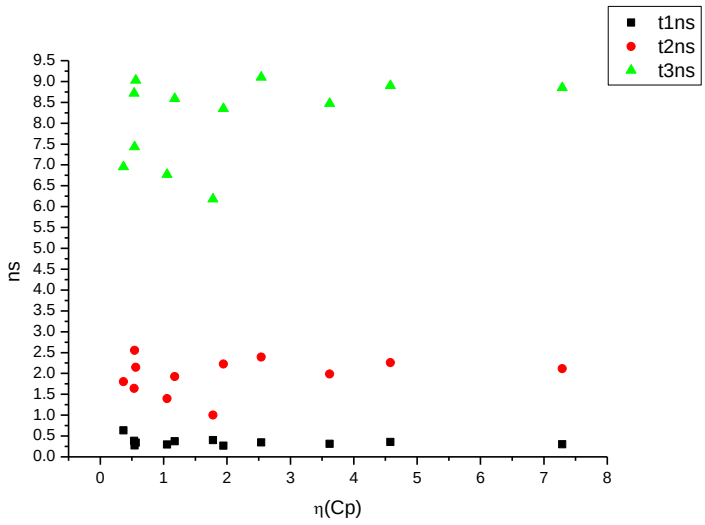

Figure 3.4.102. Amplitude weighted components of TCSPC lifetime decay of **19** (470 nm) versus η(Cp).

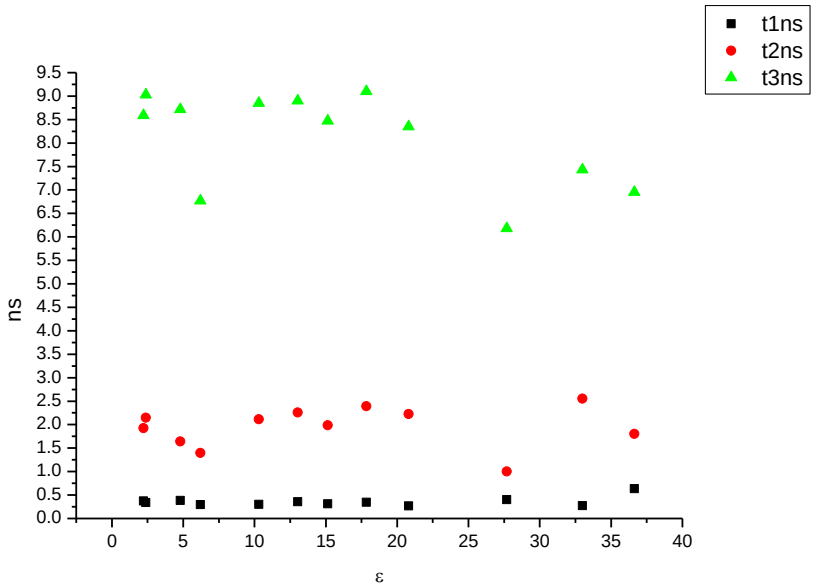

Figure 3.4.103. Intensity weighted components of TCSPC lifetime decay of **19** (470 nm) versus ε.

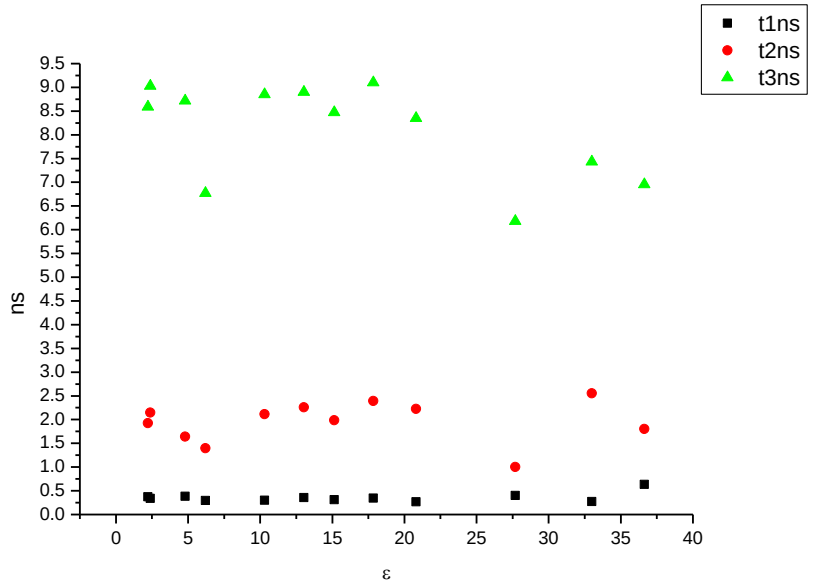

Figure 3.4.104. Amplitude weighted components of TCSPC lifetime decay of **19** (470 nm) versus ε.

3.4.7.2 600 nm Lifetime – Solvatochromic analysis.

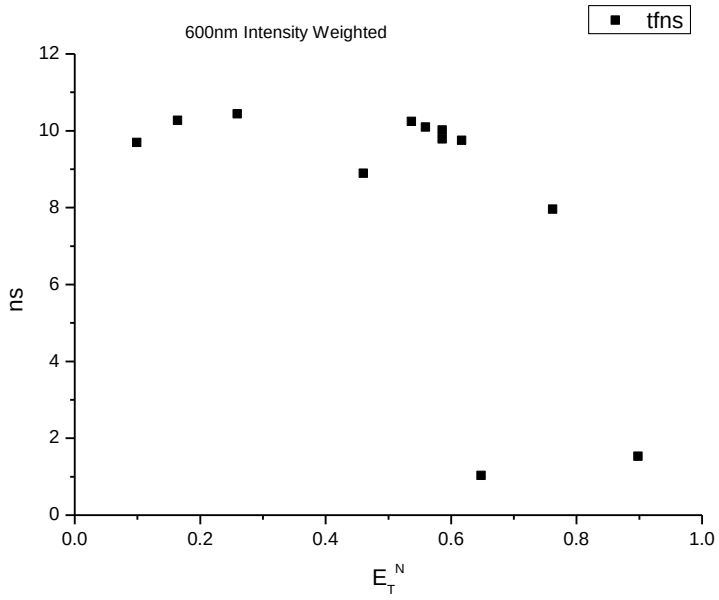

Figure 3.4.105. Intensity weighted average lifetime (τ_f) of **19** at 600 nm versus E_T^N.

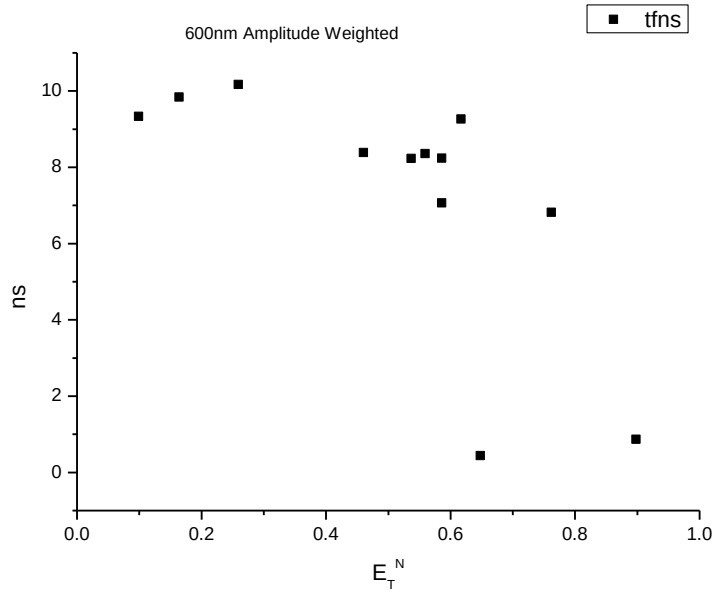

Figure 3.4.106. Amplitude weighted average lifetime (τ_f) of **19** at 600 nm versus E_T^N.

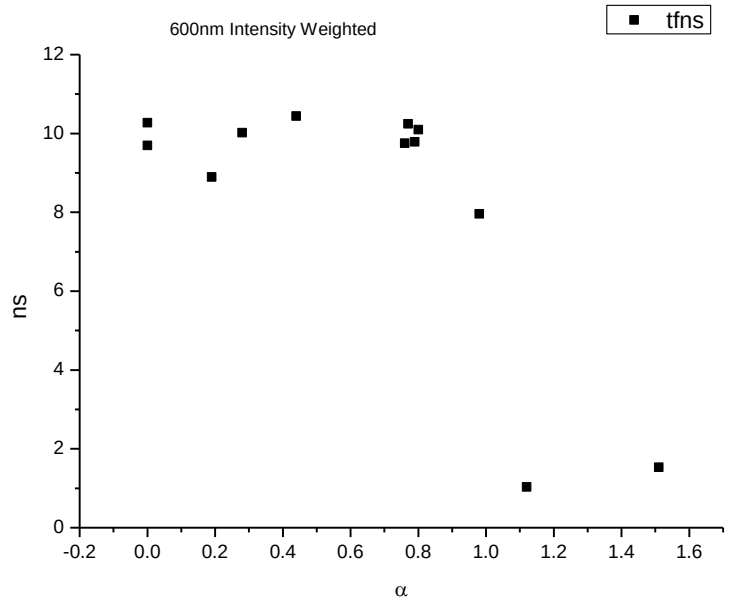

Figure 3.4.107. Intensity weighted average lifetime (τ_f) of **19** at 600 nm versus α.

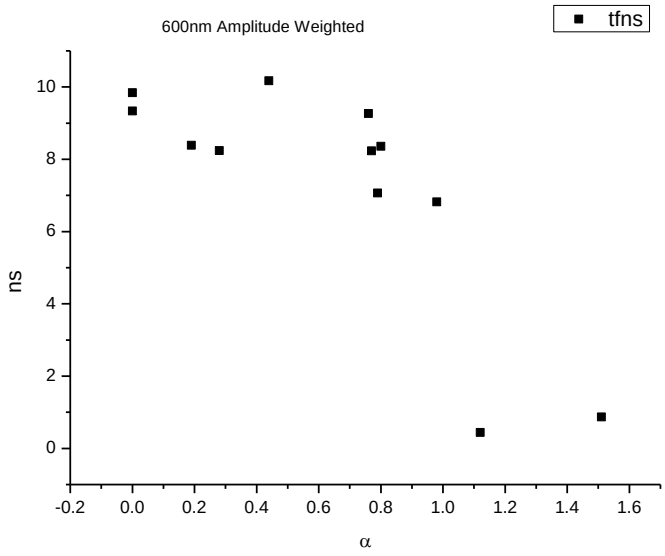

Figure 3.4.108. Amplitude weighted average lifetime (τ_f) of **19** at 600 nm versus α.

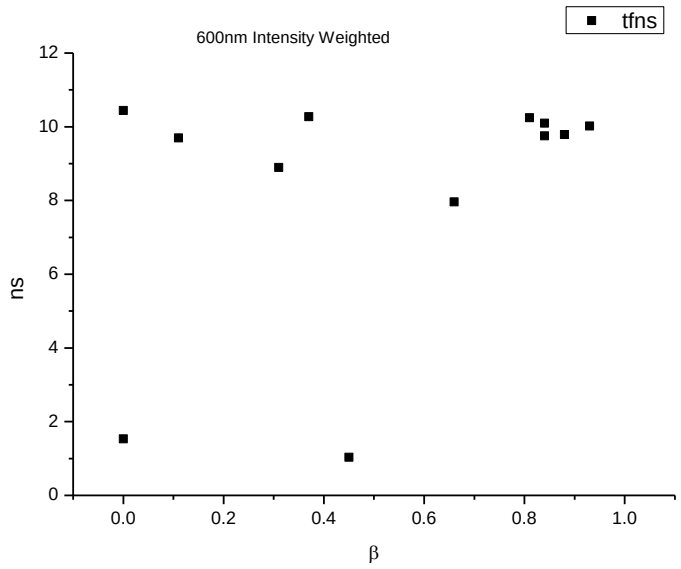

Figure 3.4.109. Intensity weighted average lifetime (τ_f) of **19** at 600 nm versus β.

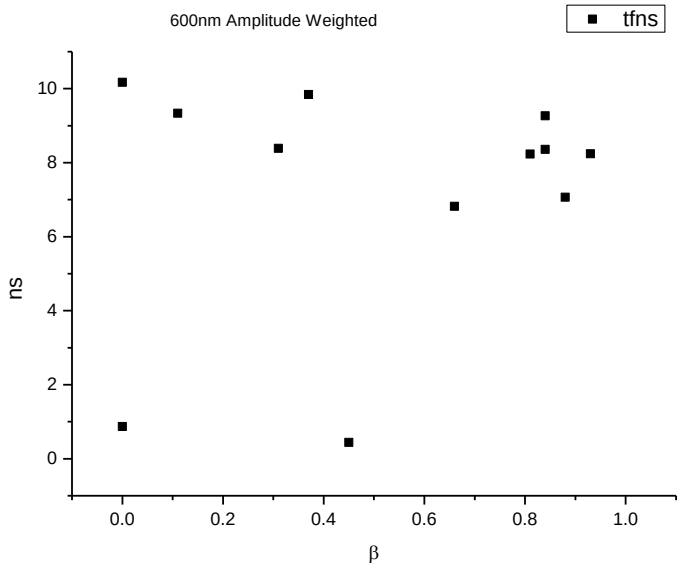

Figure 3.4.110. Amplitude weighted average lifetime (τ_f) of **19** at 600 nm versus β.

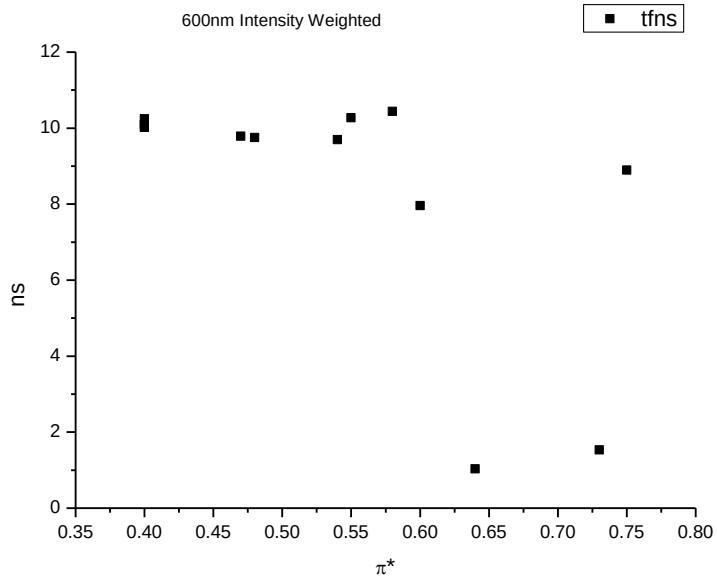

Figure 3.4.111. Intensity weighted average lifetime (τ_f) of **19** at 600 nm versus π*.

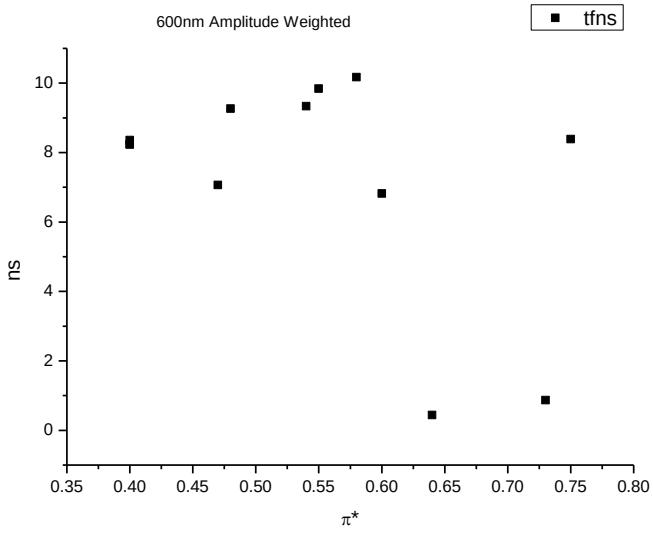

Figure 3.4.112. Amplitude weighted average lifetime (τ_f) of **19** at 600 nm versus π*.

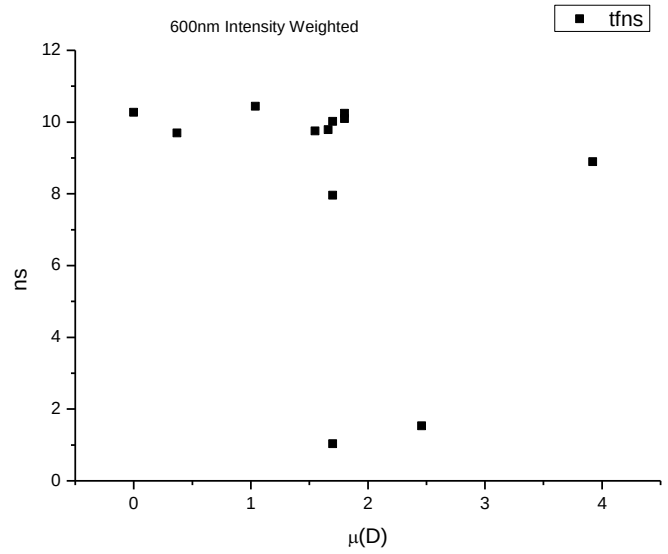

Figure 3.4.113. Intensity weighted average lifetime (τ_f) of **19** at 600 nm versus μ(D).

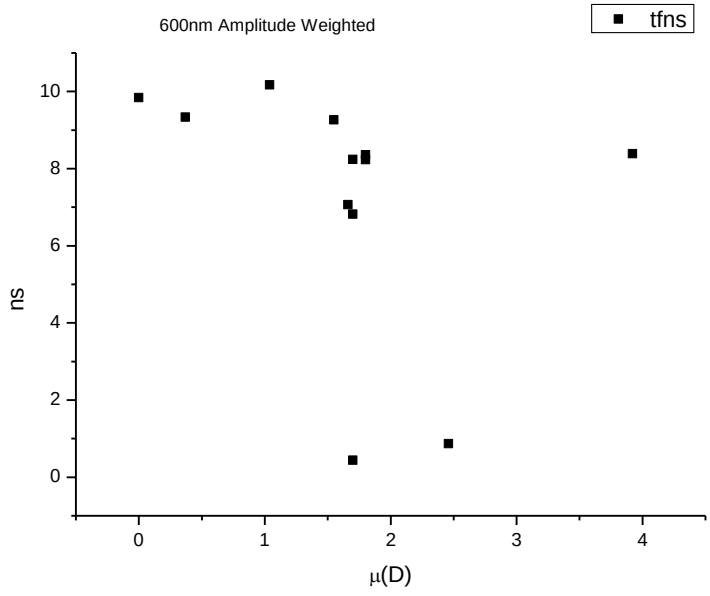

Figure 3.4.114. Amplitude weighted average lifetime (τ_f) of **19** at 600 nm versus μ(D).

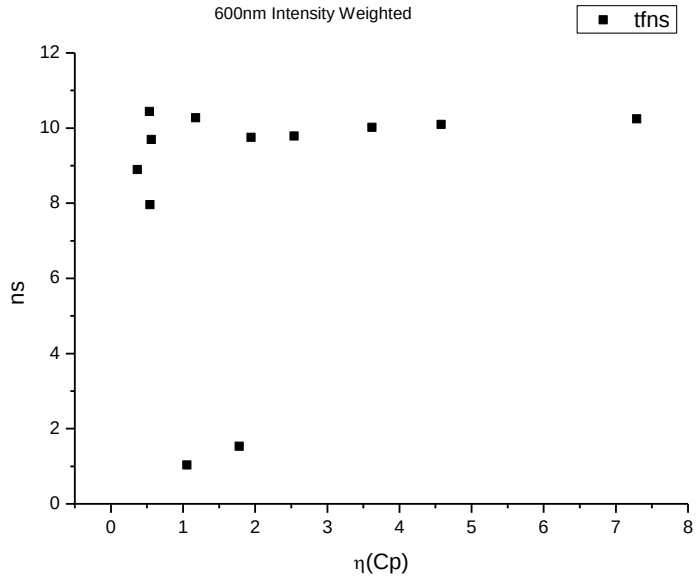

Figure 3.4.115. Intensity weighted average lifetime (τ_f) of **19** at 600 nm versus η(Cp).

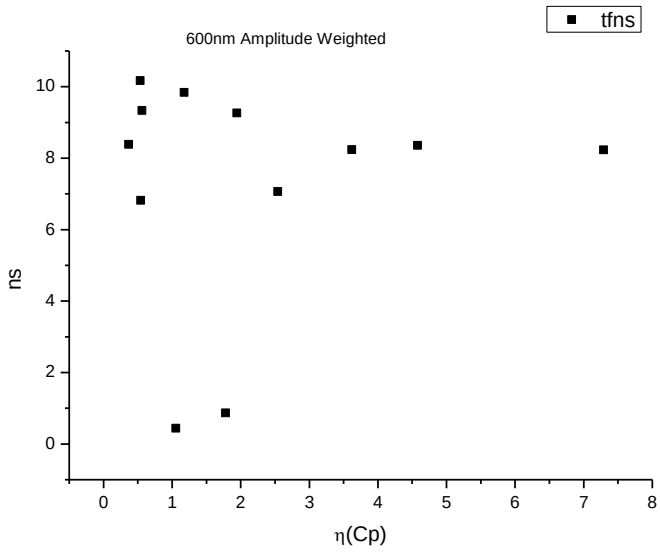

Figure 3.4.116. Amplitude weighted average lifetime (τ_f) of **19** at 600 nm versus η(Cp).

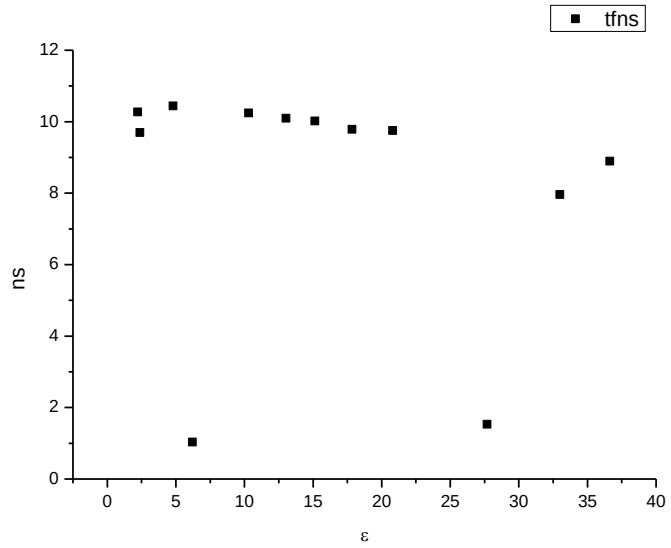

Figure 3.4.117. Intensity weighted average lifetime (τ_f) of **19** at 600 nm versus ε.

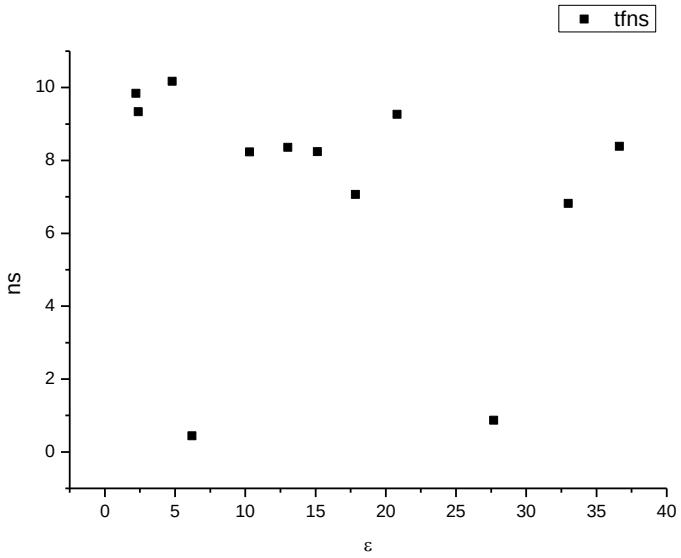

Figure 3.4.118. Amplitude weighted average lifetime (τ_f) of **19** at 600 nm versus ε.

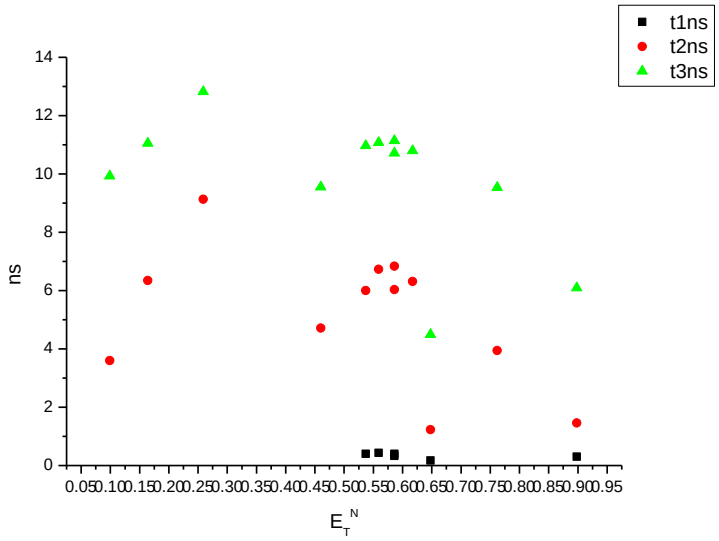

Figure 3.4.119. Intensity weighted components of TCSPC lifetime decay of **19** (600 nm) versus E_T^N.

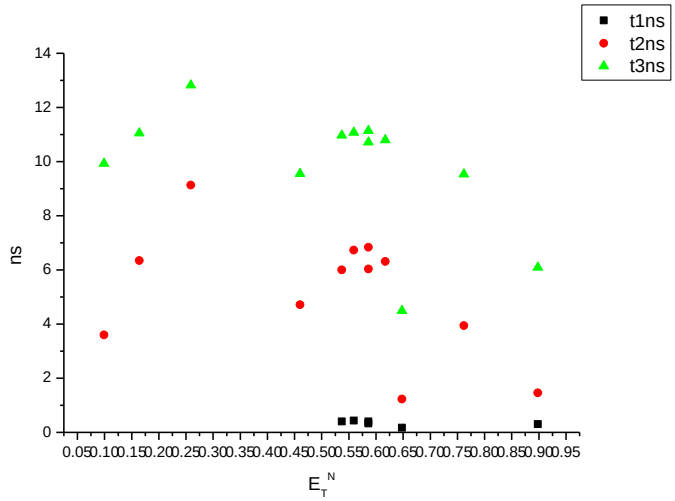

Figure 3.4.120. Amplitude weighted components of TCSPC lifetime decay of **19** (600 nm) versus E_T^N.

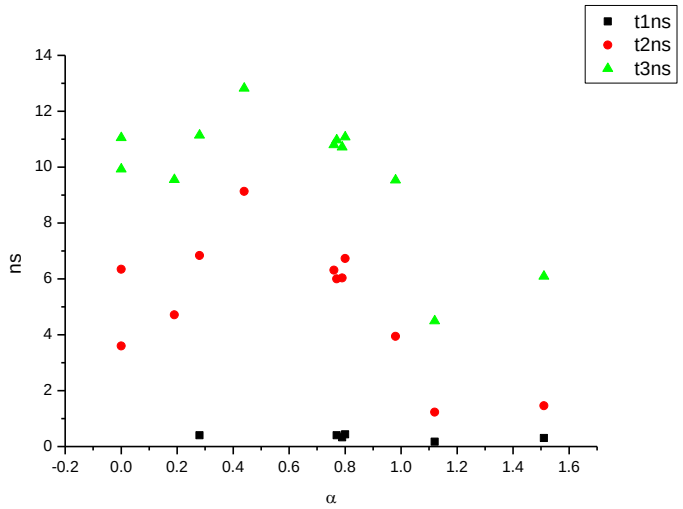

Figure 3.4.121. Intensity weighted components of TCSPC lifetime decay of **19** (600 nm) versus α.

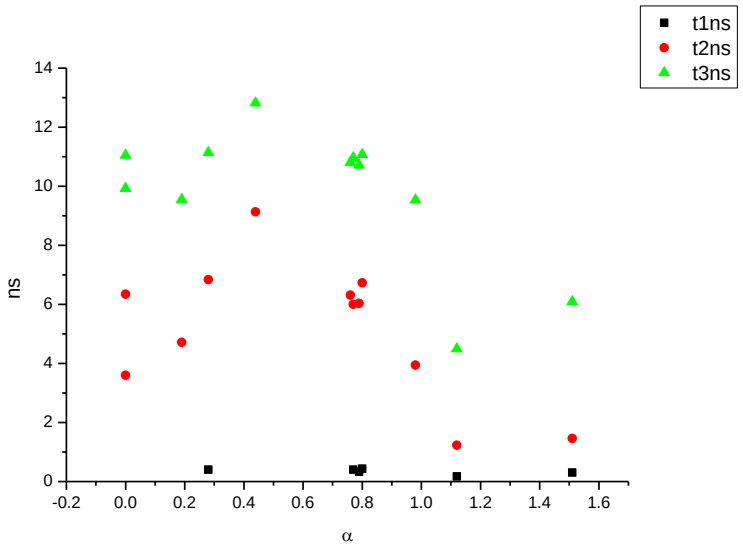

Figure 3.4.122. Amplitude weighted components of TCSPC lifetime decay of **19** (600 nm) versus α.

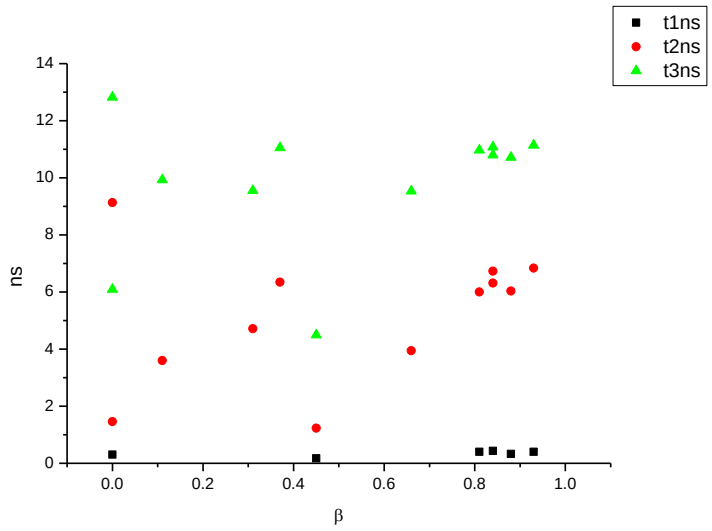

Figure 3.4.123. Intensity weighted components of TCSPC lifetime decay of **19** (600 nm) versus β.

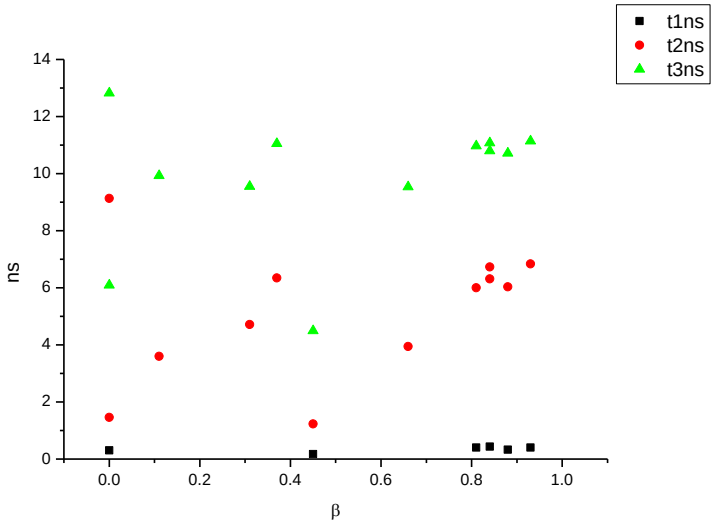

Figure 3.4.124. Amplitude weighted components of TCSPC lifetime decay of **19** (600 nm) versus β.

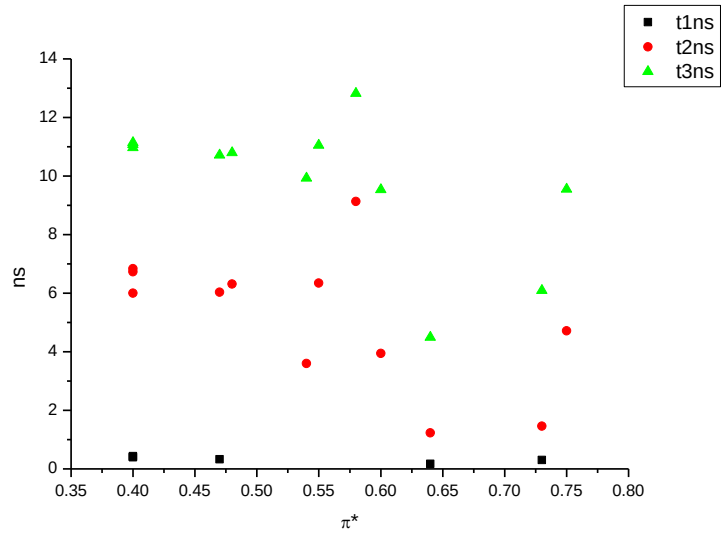

Figure 3.4.125. Intensity weighted components of TCSPC lifetime decay of **19** (600 nm) versus π*.

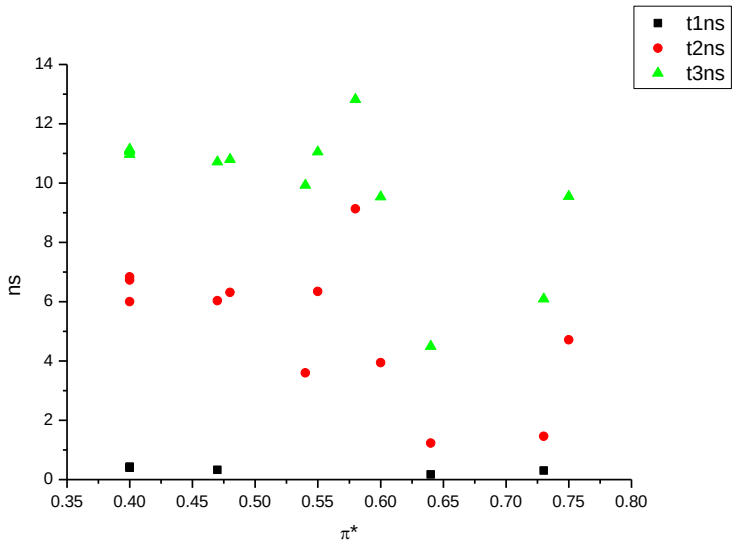

Figure 3.4.126. Amplitude weighted components of TCSPC lifetime decay of **19** (600 nm) versus π*.

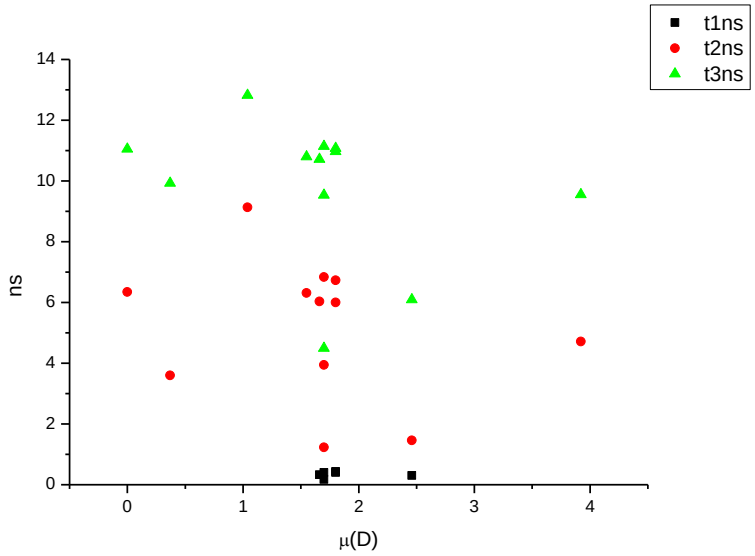

Figure 3.4.127. Intensity weighted components of TCSPC lifetime decay of **19** (600 nm) versus μ(D).

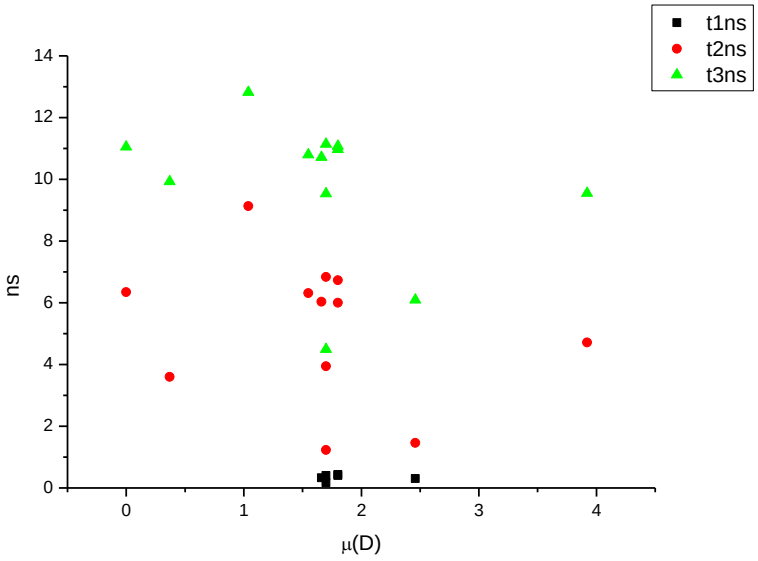

Figure 3.4.128. Amplitude weighted components of TCSPC lifetime decay of **19** (600 nm) versus μ(D).

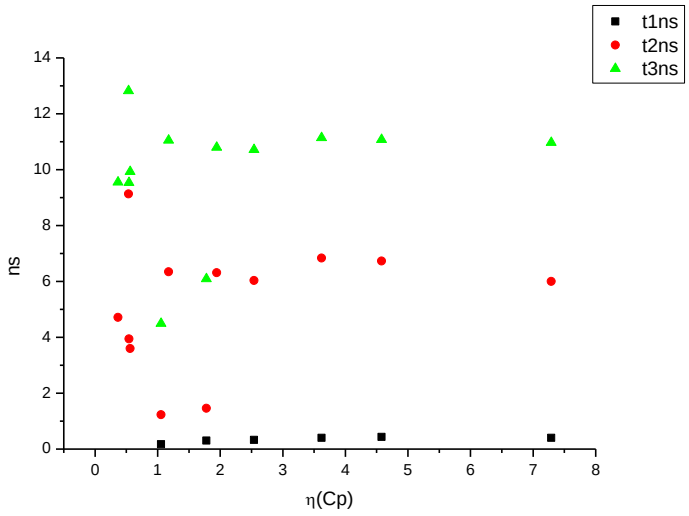

Figure 3.4.129. Intensity weighted components of TCSPC lifetime decay of **19** (600 nm) versus η(Cp).

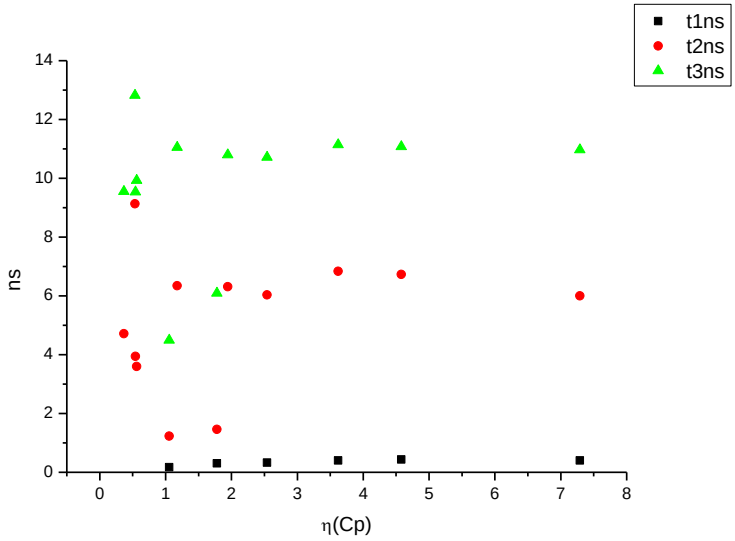

Figure 3.4.130. Amplitude weighted components of TCSPC lifetime decay of **19** (600 nm) versus η(Cp).

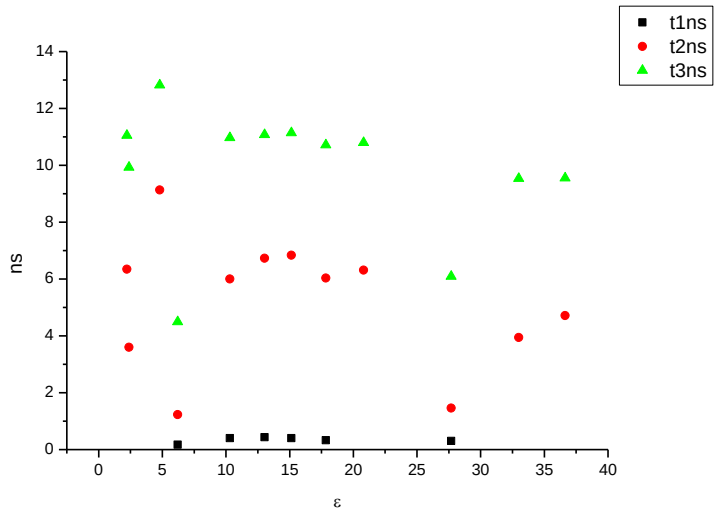

Figure 3.4.131. Intensity weighted components of TCSPC lifetime decay of **19** (600 nm) versus ε.

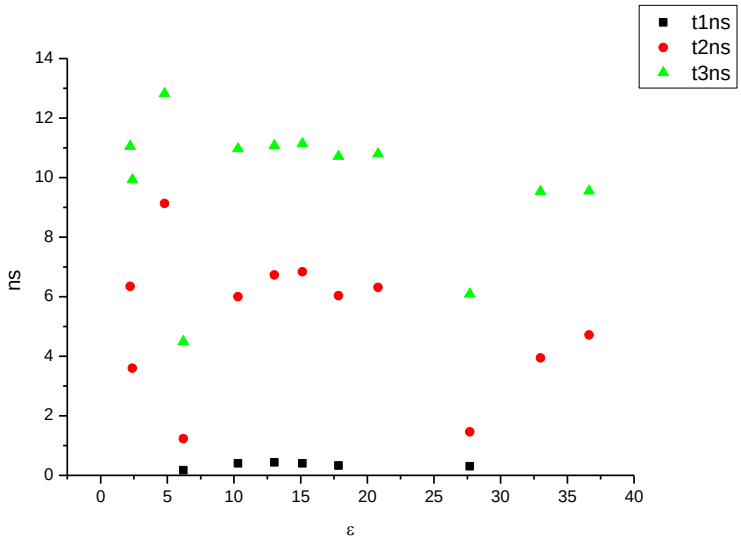

Figure 3.4.132. Amplitude weighted components of TCSPC lifetime decay of **19** (600 nm) versus ε.

3.4.8 Ultraviolet-visible absorption spectra.

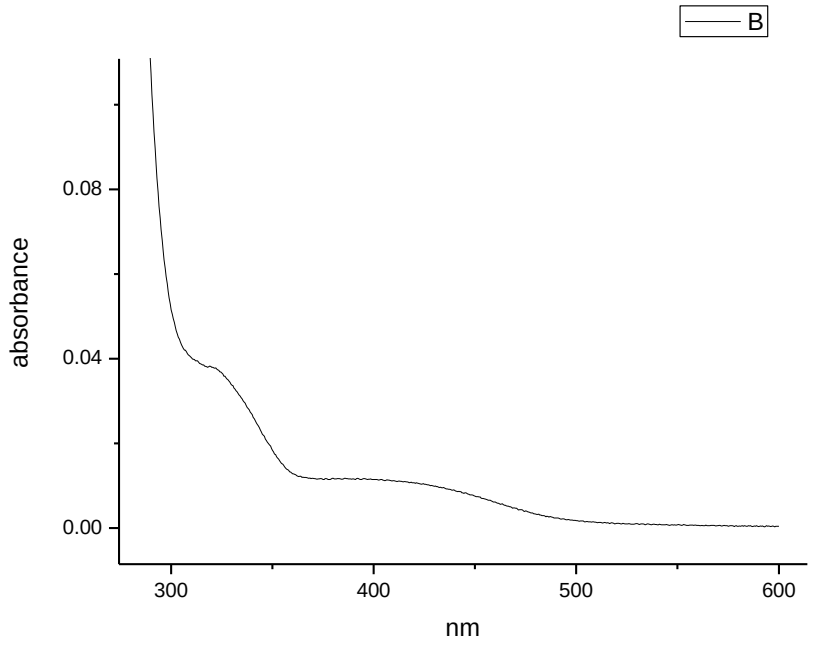

Figure 181. Ultraviolet-Visible absorption spectrum of **19** recorded in Toluene.

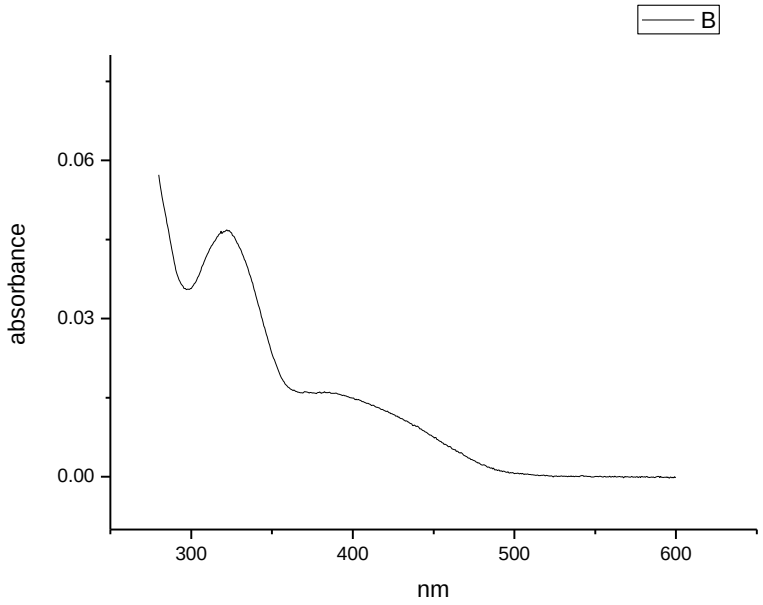

Figure 182. Ultraviolet-Visible absorption spectrum of **19** recorded in 1,4-dioxane.

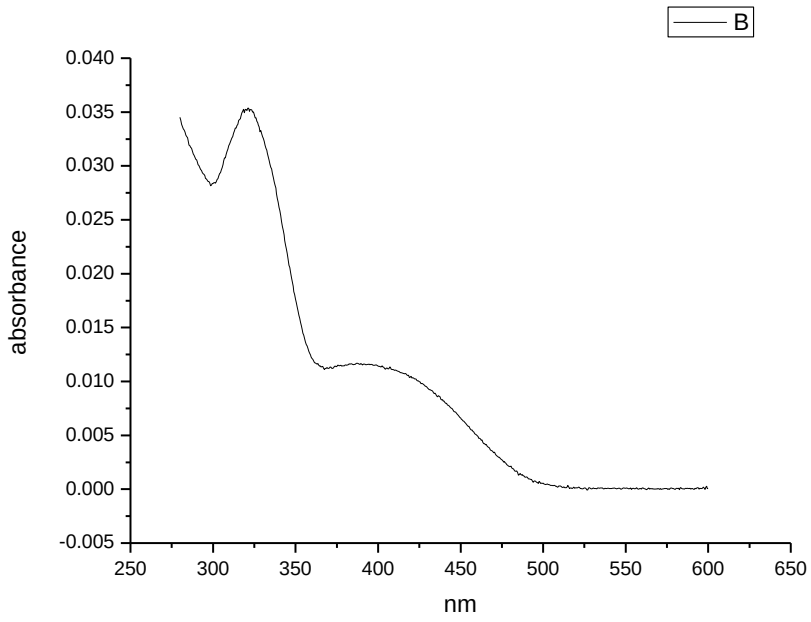

Figure 183. Ultraviolet-Visible absorption spectrum of **19** recorded in Chloroform.

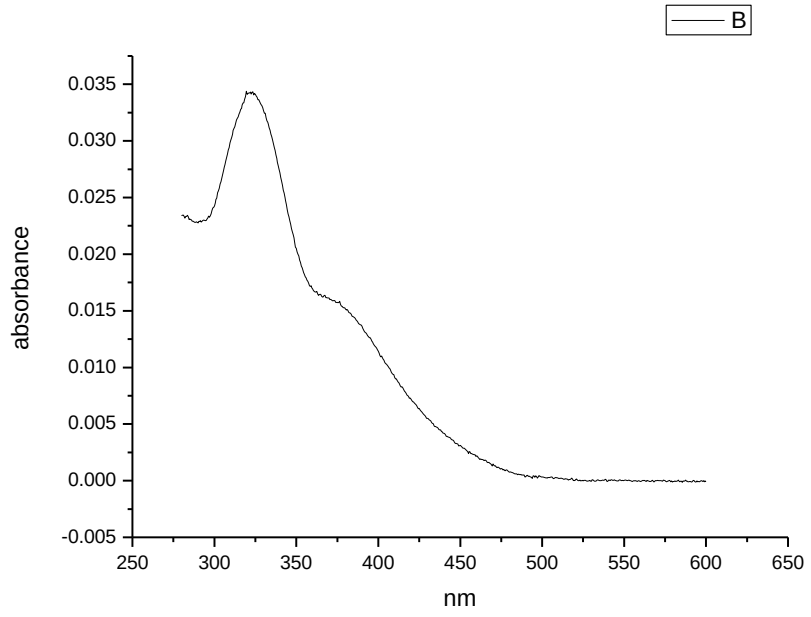

Figure 184. Ultraviolet-Visible absorption spectrum of **19** recorded in Acetonitrile.

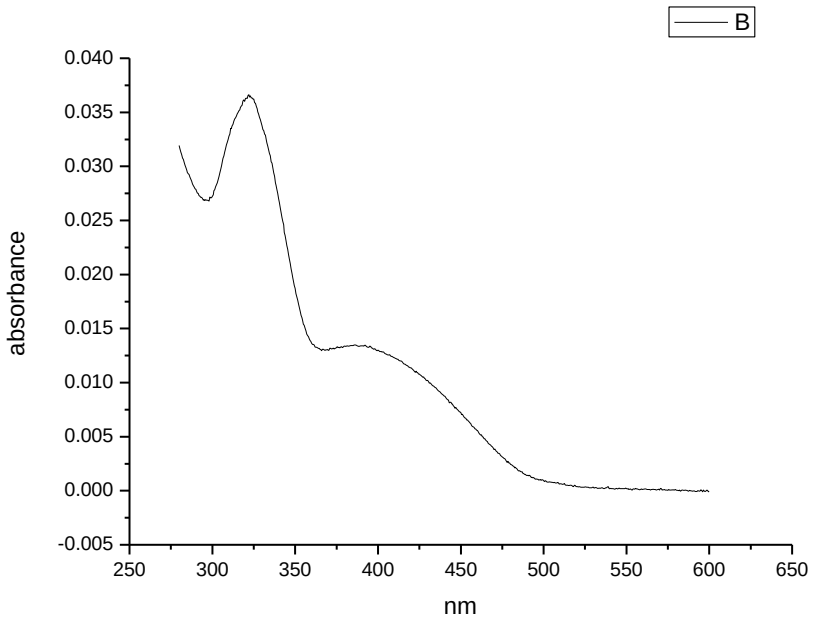

Figure 185. Ultraviolet-Visible absorption spectrum of **19** recorded in 1-octanol.

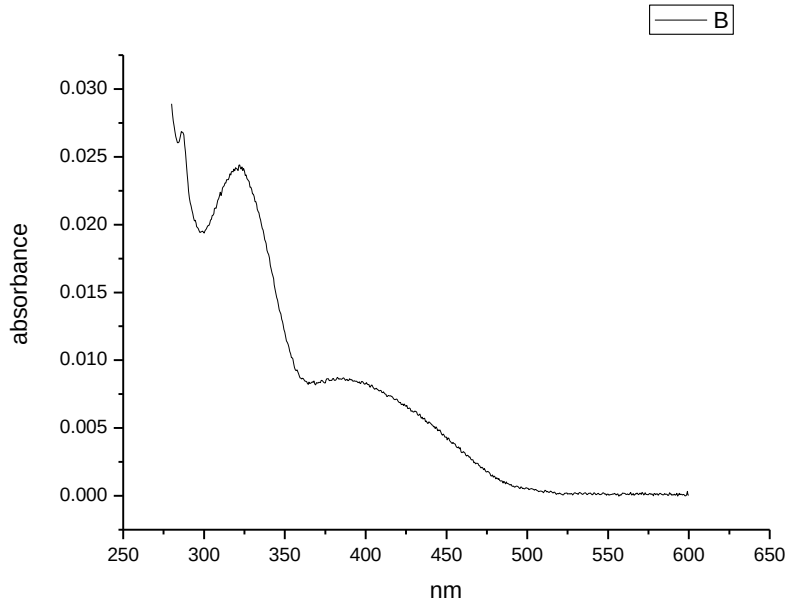

Figure 186. Ultraviolet-Visible absorption spectrum of **19** recorded in 1-hexanol.

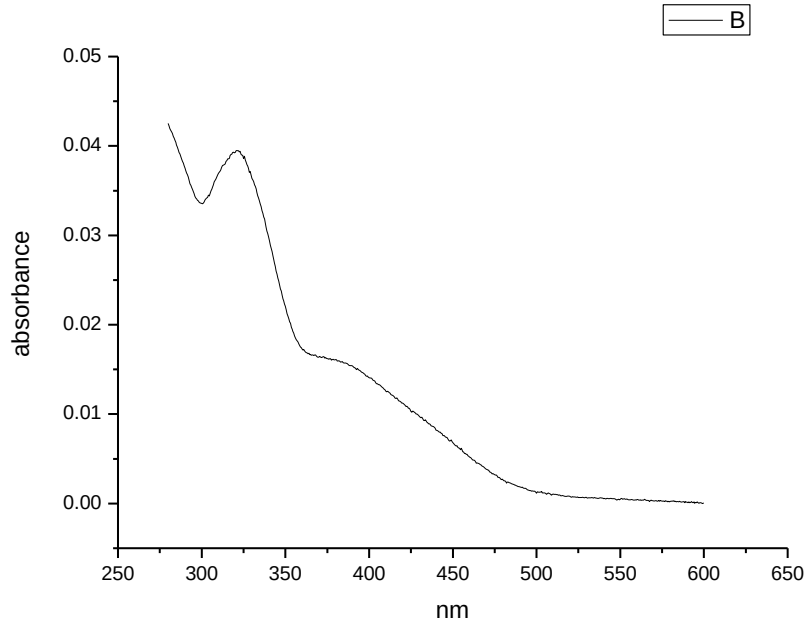

Figure 187. Ultraviolet-Visible absorption spectrum of **19** recorded in 1-butanol.

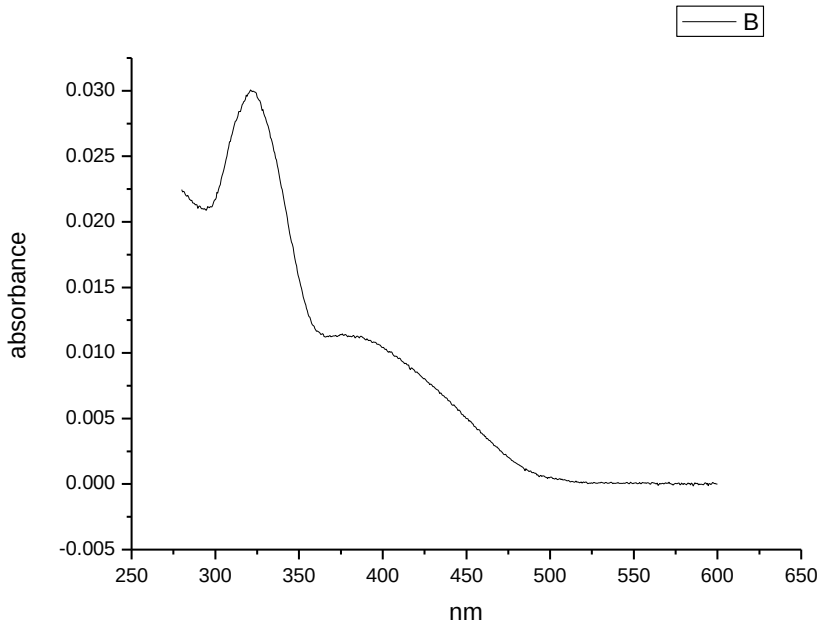

Figure 188. Ultraviolet-Visible absorption spectrum of **19** recorded in 1-pentanol.

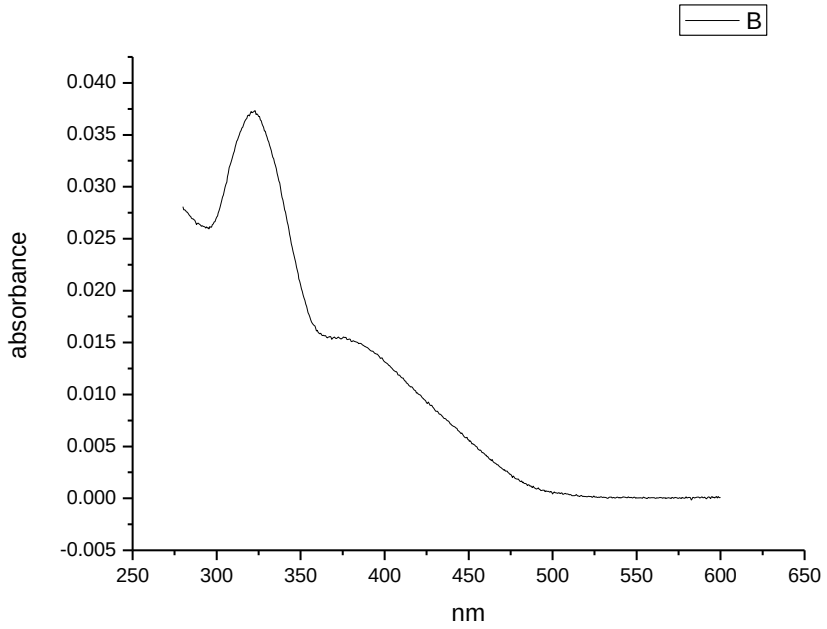

Figure 189. Ultraviolet-Visible absorption spectrum of **19** recorded in 1-propanol.

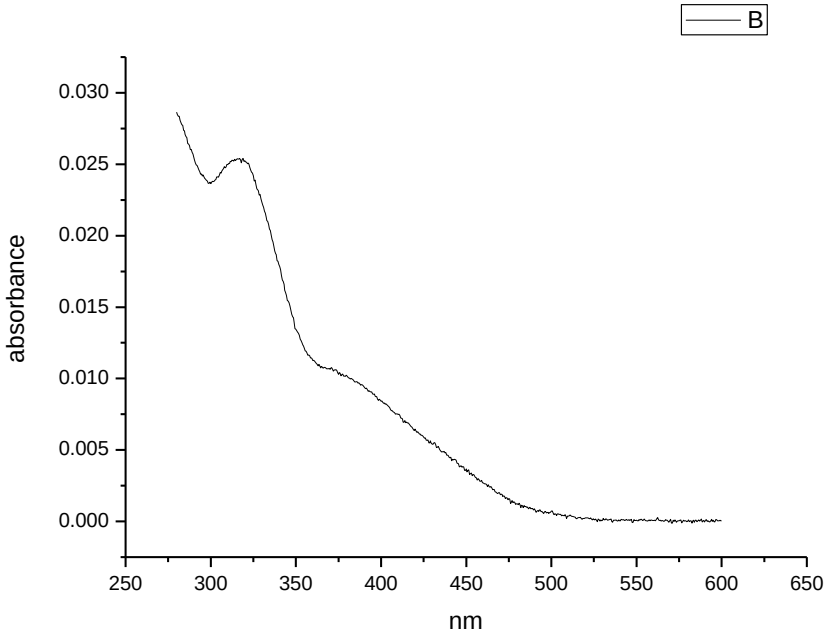

Figure 190. Ultraviolet-Visible absorption spectrum of **19** recorded in Acetic Acid.

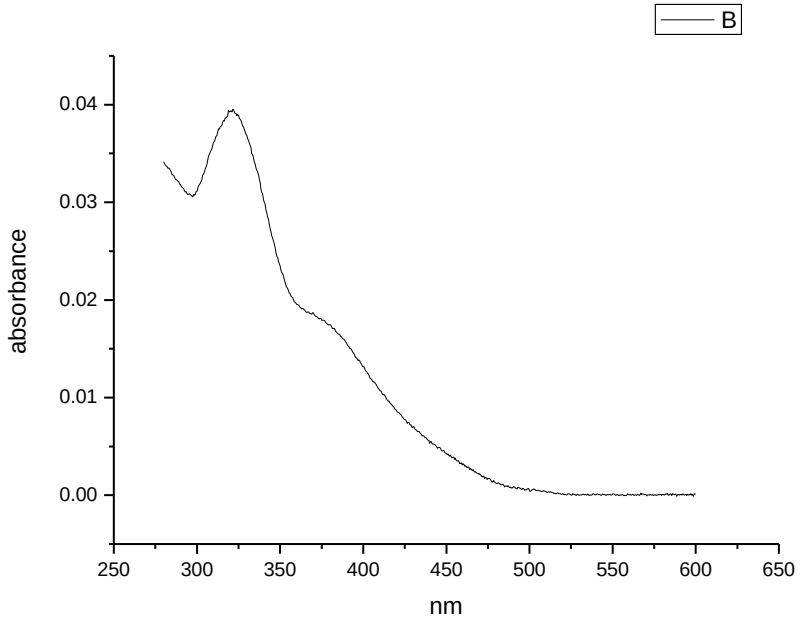

Figure 191. Ultraviolet-Visible absorption spectrum of **19** recorded in Methanol.

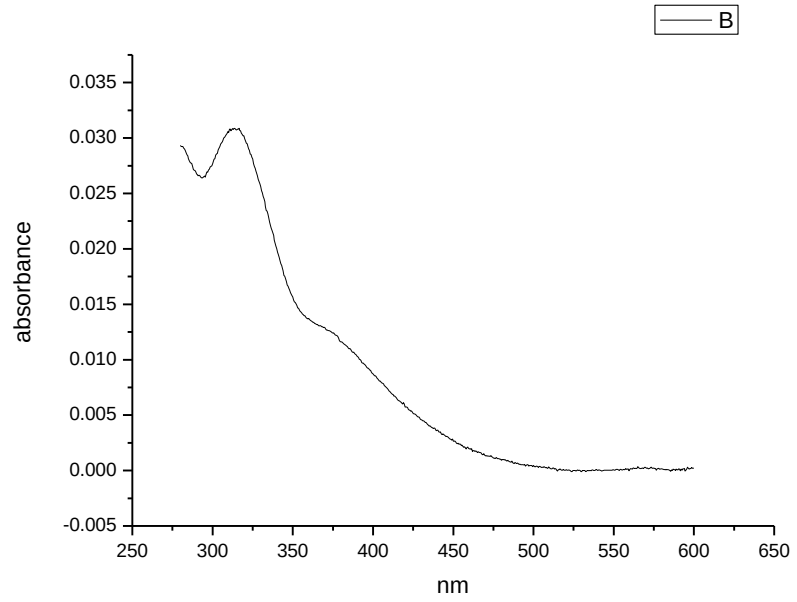

Figure 192. Ultraviolet-Visible absorption spectrum of **19** recorded in 2,2,2-trifluoroethanol.

3.4.9 Fluorescence Emission spectra.

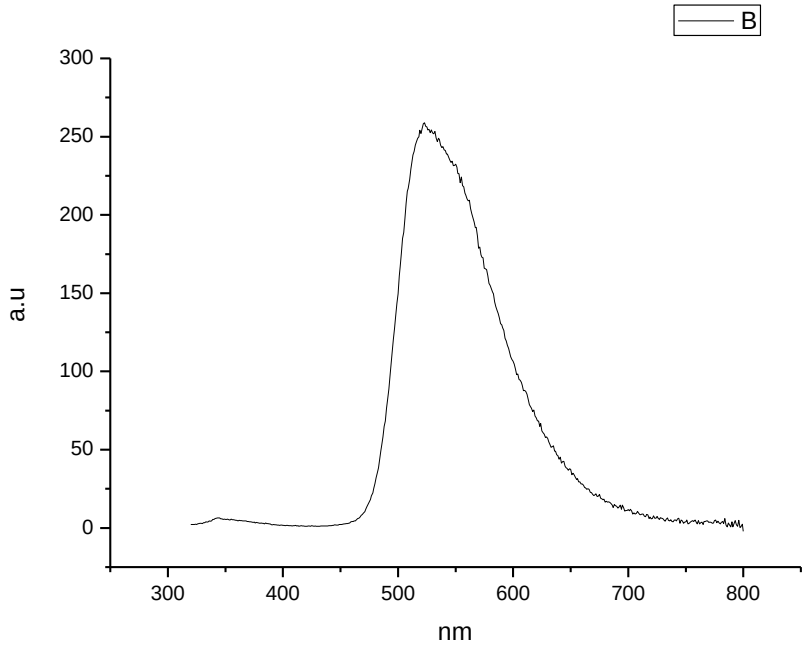

Figure 359. Fluorescence emission spectrum of **19** recorded in Toluene at 310 nm excitation.

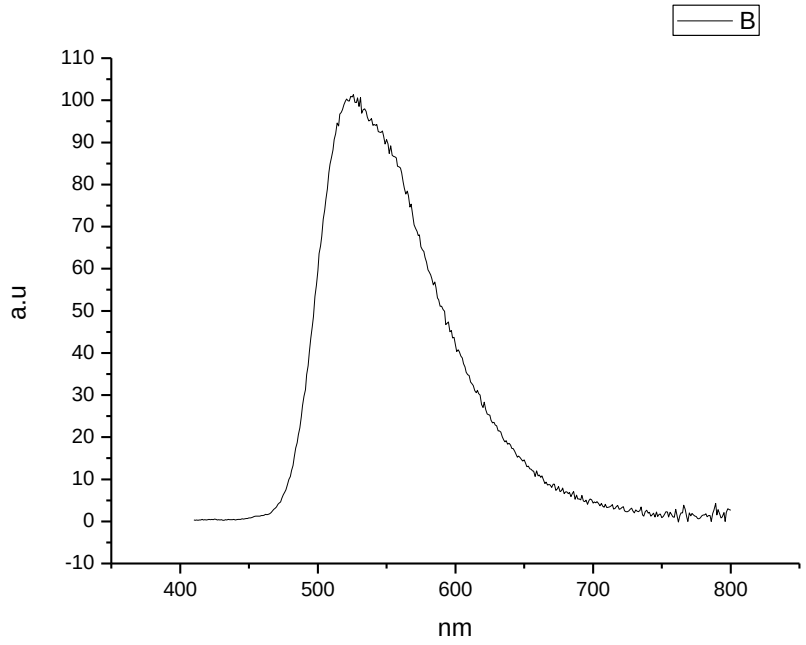

Figure 360. Fluorescence emission spectrum of **19** recorded in Toluene at 400 nm excitation.

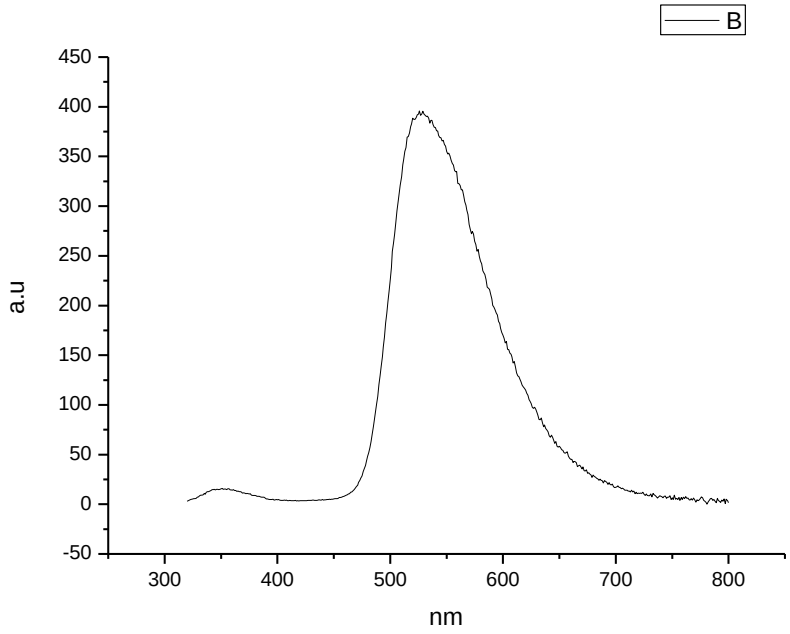

Figure 361. Fluorescence emission spectrum of **19** recorded in 1,4-dioxane at 310 nm excitation.

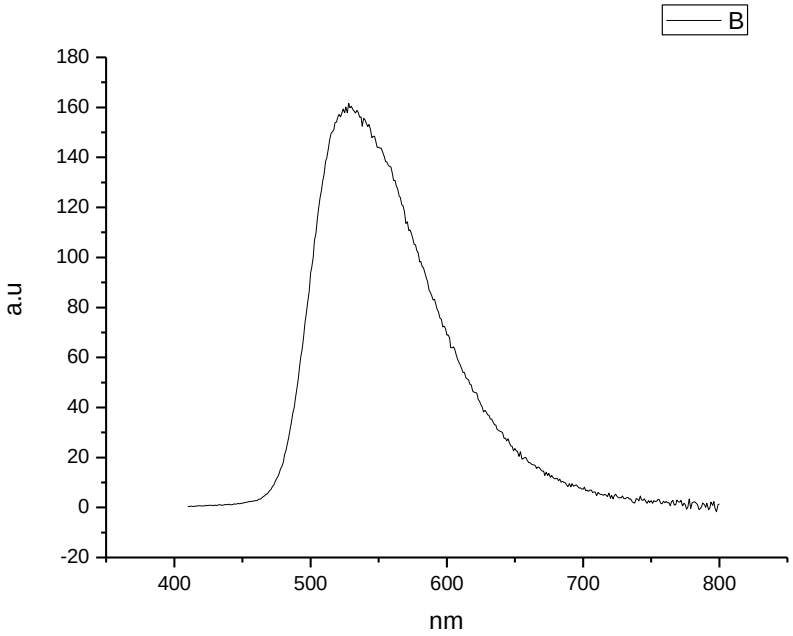

Figure 362. Fluorescence emission spectrum of **19** recorded in 1,4-dioxane at 400 nm excitation.

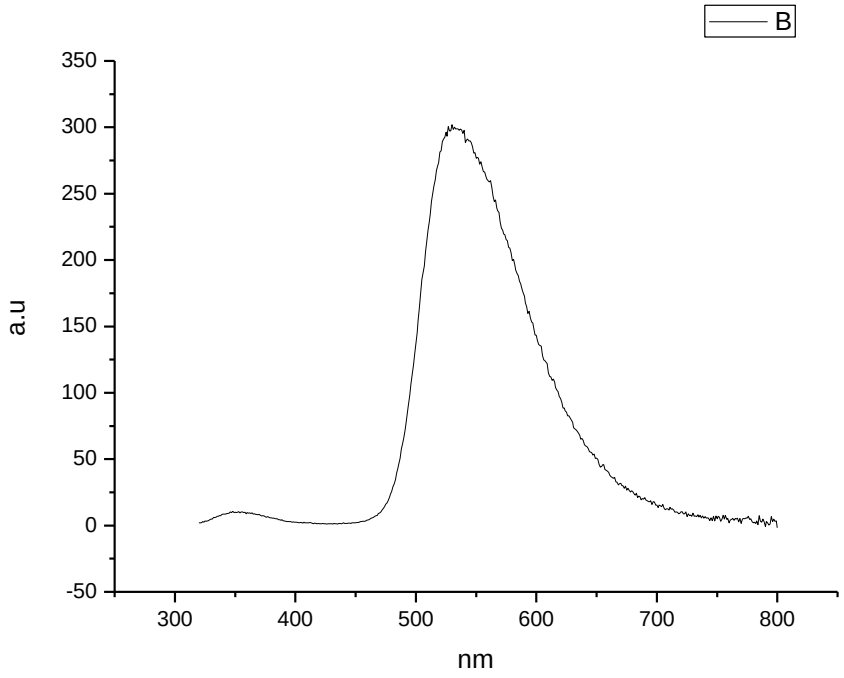

Figure 363. Fluorescence emission spectrum of **19** recorded in Chloroform at 310 nm excitation.

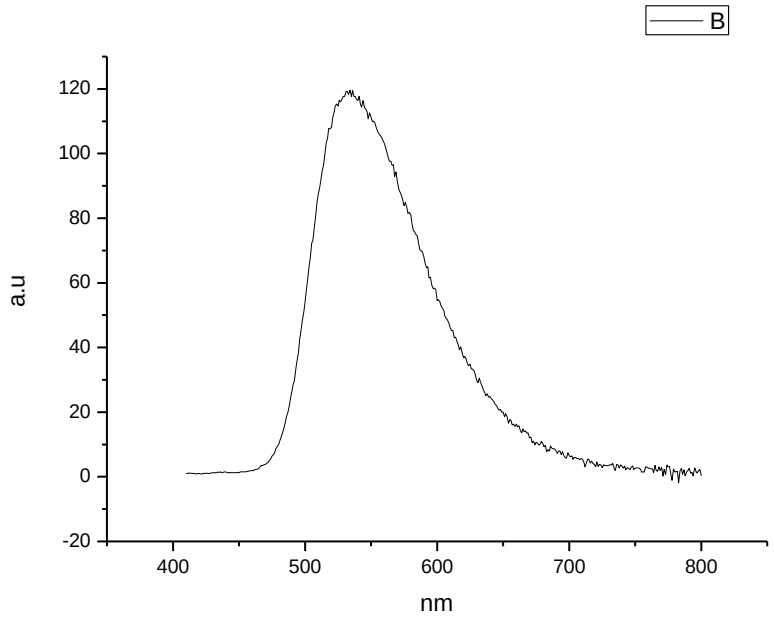

Figure 364. Fluorescence emission spectrum of **19** recorded in Chloroform at 400 nm excitation.

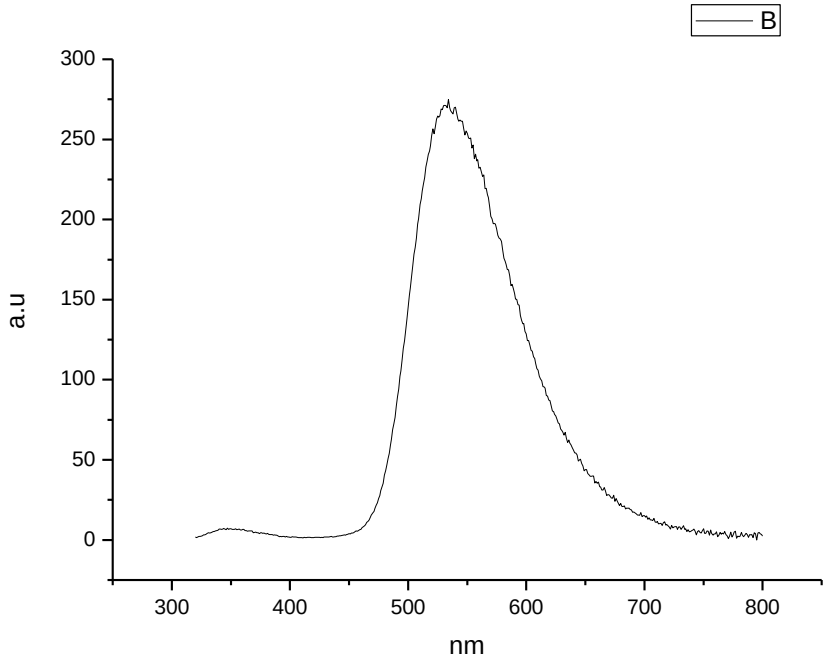

Figure 365. Fluorescence emission spectrum of **19** recorded in Acetonitrile at 310 nm excitation.

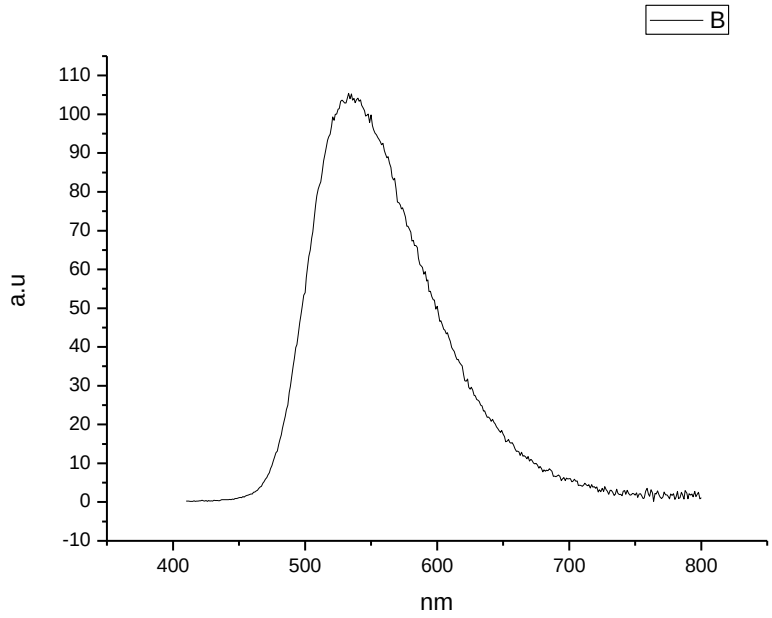

Figure 366. Fluorescence emission spectrum of **19** recorded in Acetonitrile at 400 nm excitation.

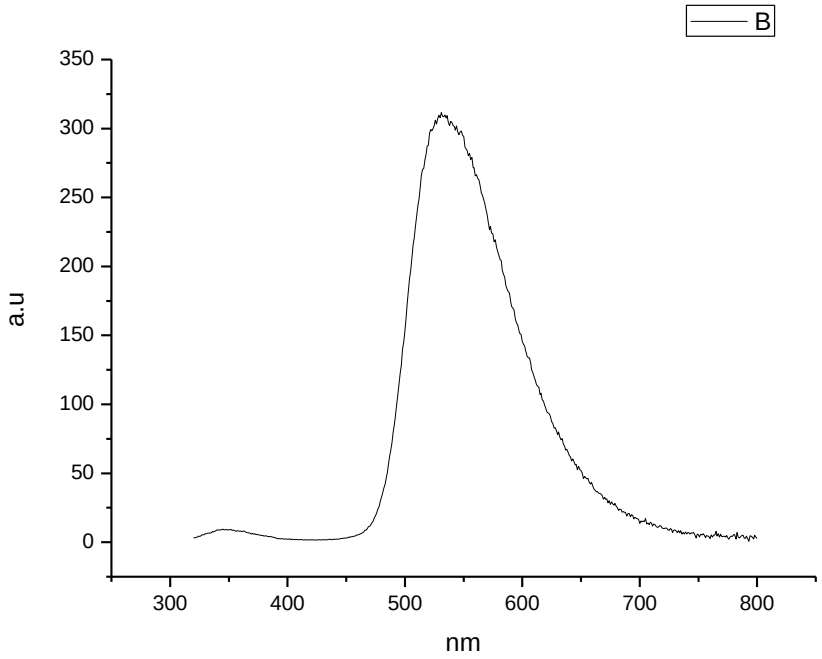

Figure 367. Fluorescence emission spectrum of **19** recorded in 1-octanol at 310 nm excitation.

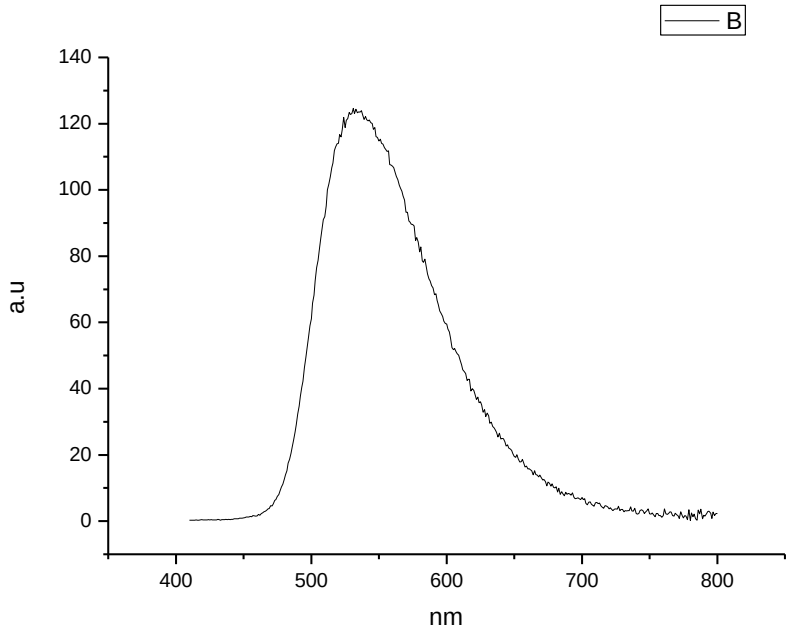

Figure 368. Fluorescence emission spectrum of **19** recorded in 1-octanol at 400 nm excitation.

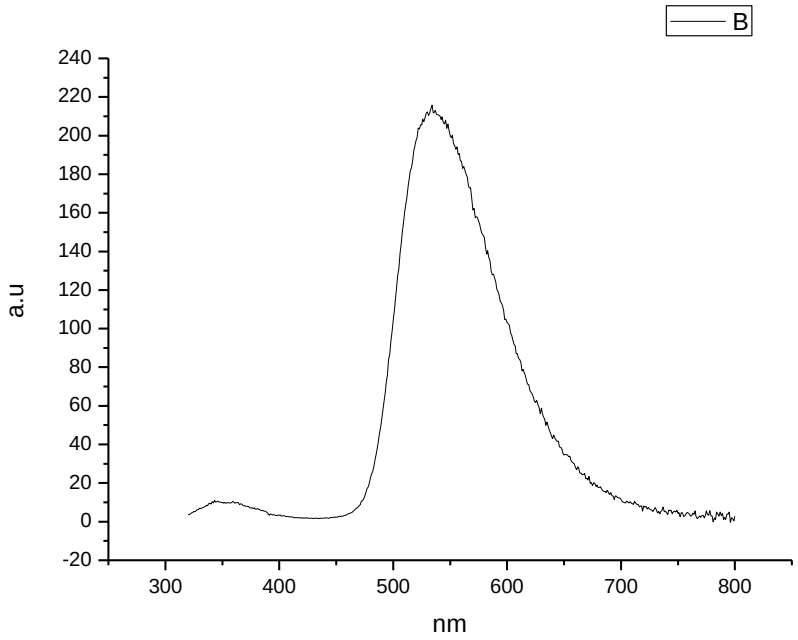

Figure 369. Fluorescence emission spectrum of **19** recorded in 1-hexanol at 310 nm excitation.

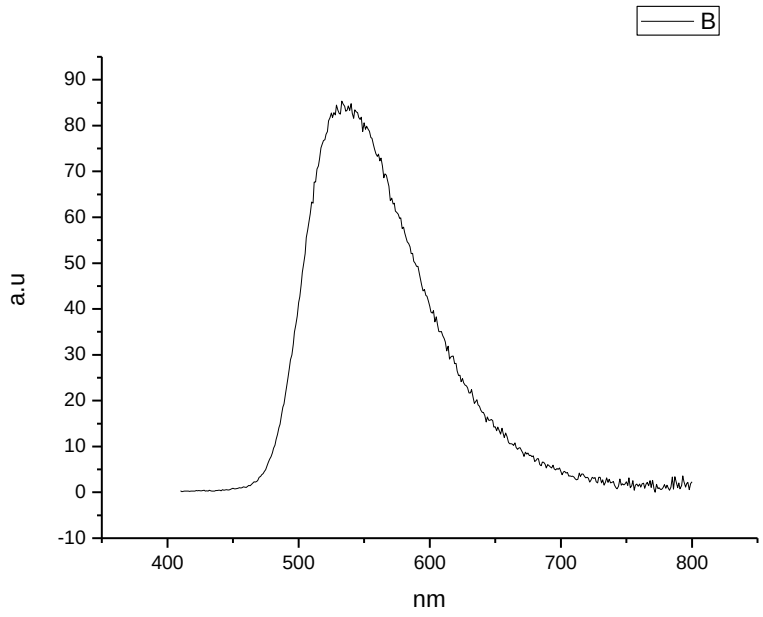

Figure 370. Fluorescence emission spectrum of **19** recorded in 1-hexanol at 400 nm excitation.

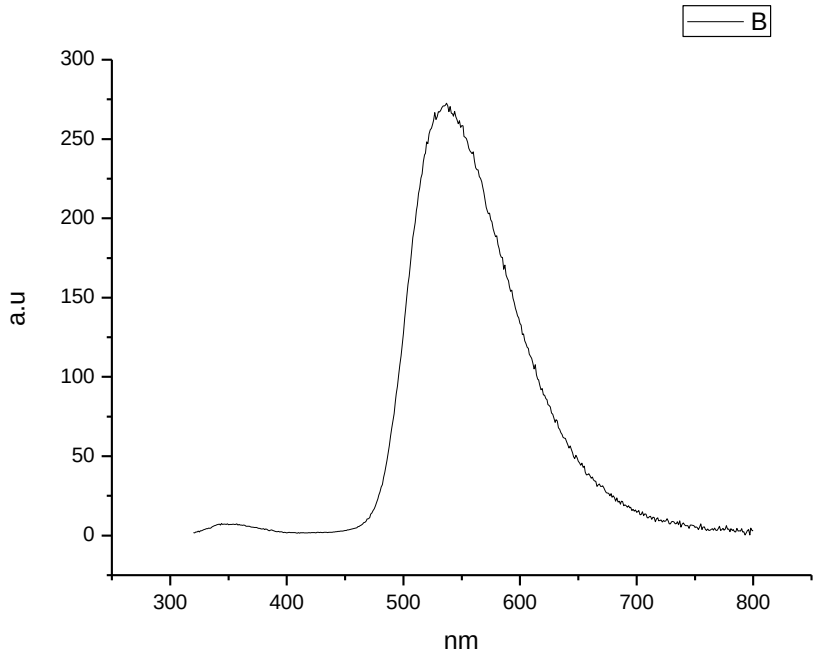

Figure 371. Fluorescence emission spectrum of **19** recorded in 1-butanol at 310 nm excitation.

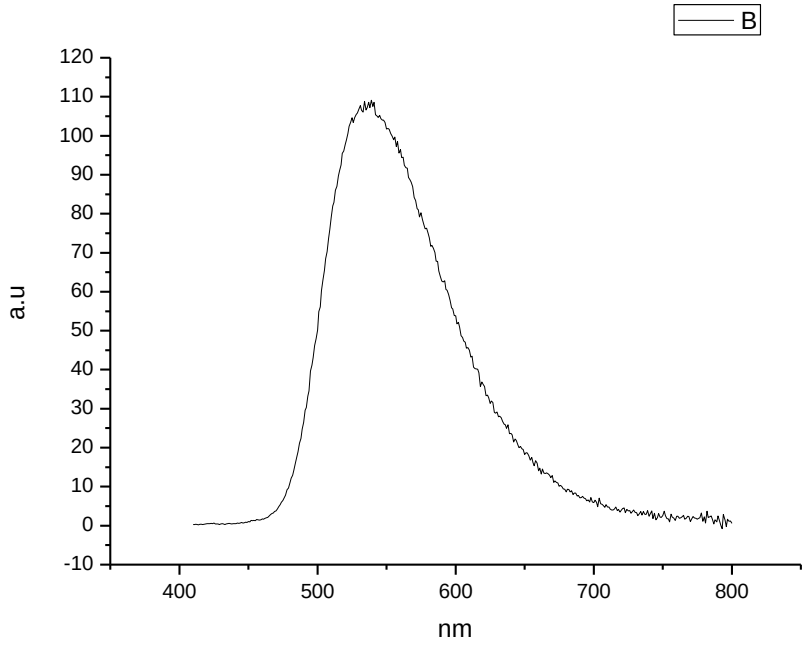

Figure 372. Fluorescence emission spectrum of **19** recorded in 1-butanol at 400 nm excitation.

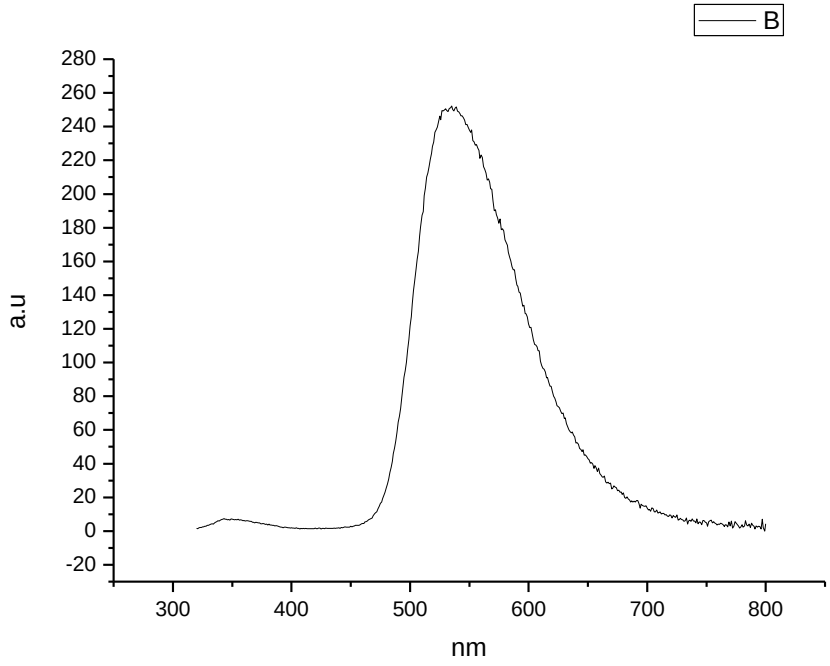

Figure 373. Fluorescence emission spectrum of **19** recorded in 1-pentanol at 310 nm excitation.

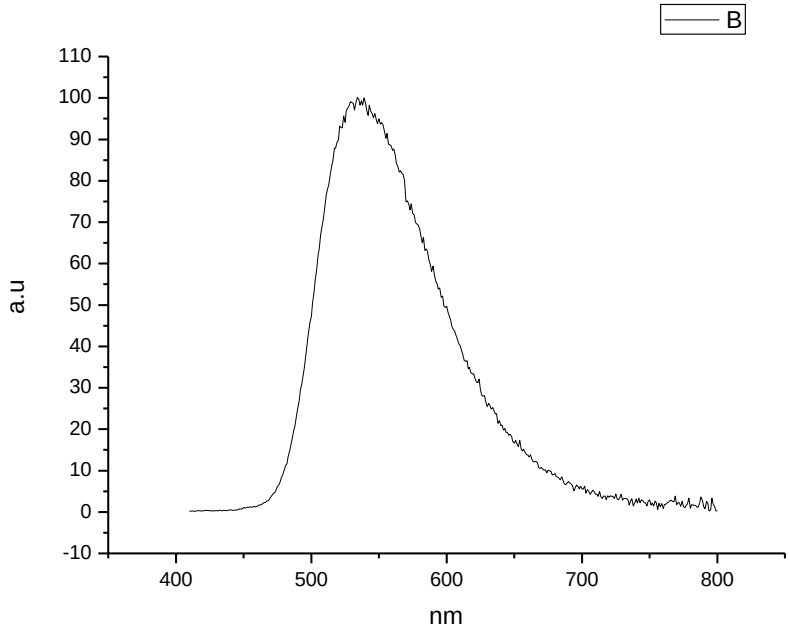

Figure 374. Fluorescence emission spectrum of **19** recorded in 1-pentanol at 400 nm excitation.

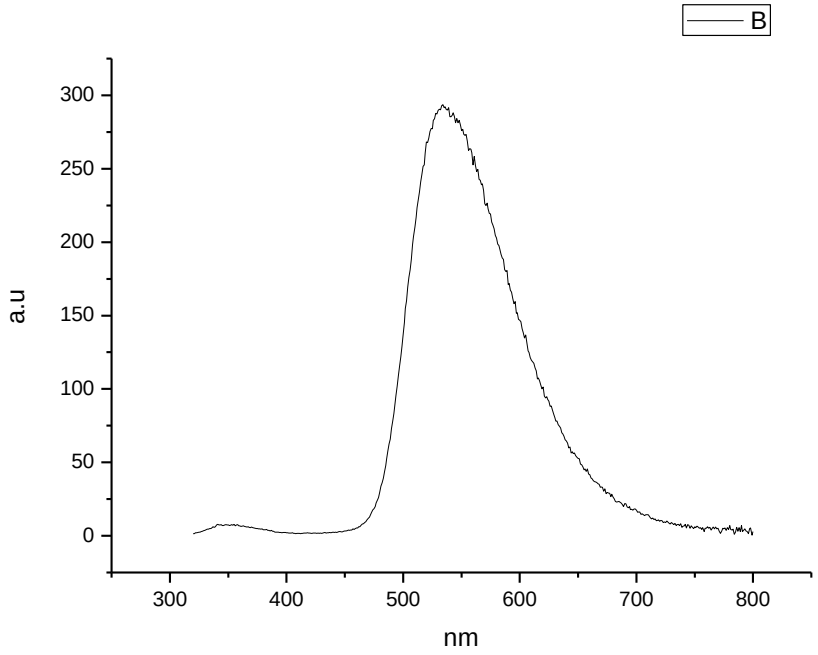

Figure 375. Fluorescence emission spectrum of **19** recorded in 1-propanol at 310 nm excitation.

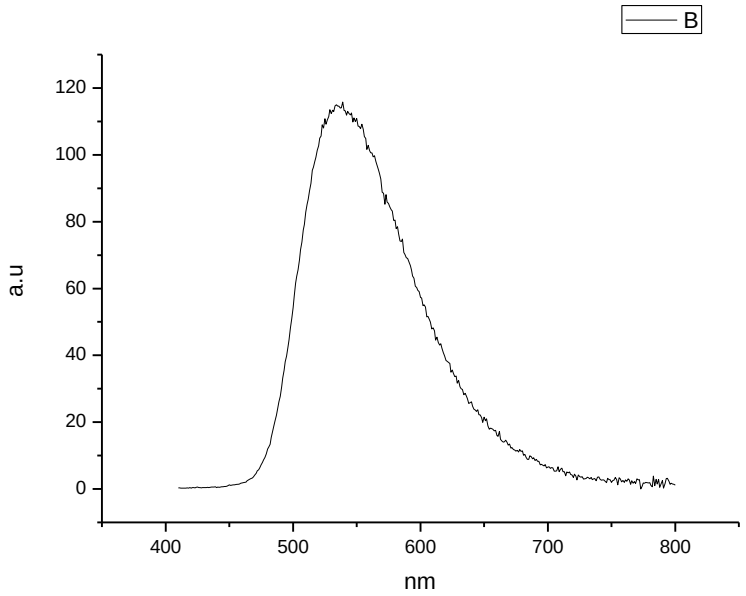

Figure 376. Fluorescence emission spectrum of **19** recorded in 1-propanol at 400 nm excitation.

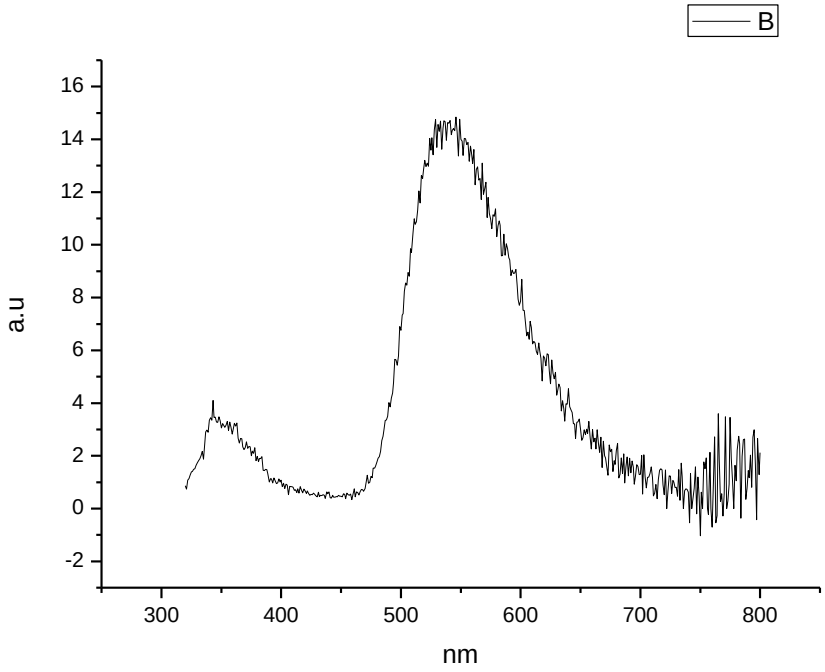

Figure 377. Fluorescence emission spectrum of **19** recorded in Acetic Acid at 310 nm excitation.

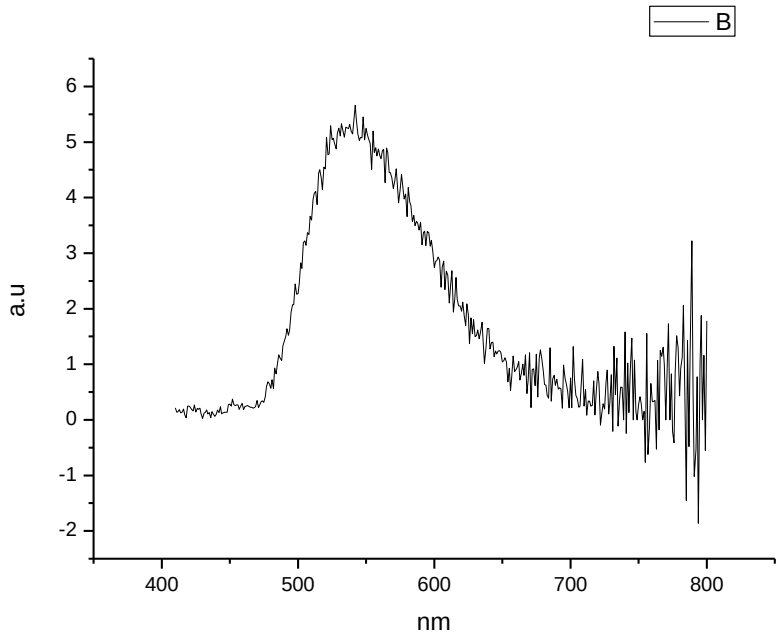

Figure 378. Fluorescence emission spectrum of **19** recorded in Acetic Acid at 400 nm excitation.

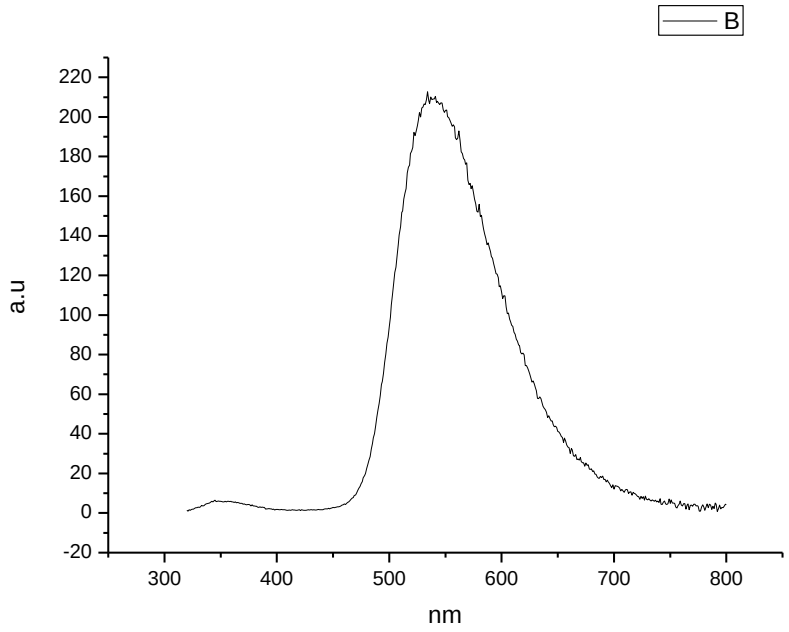

Figure 379. Fluorescence emission spectrum of **19** recorded in Methanol at 310 nm excitation.

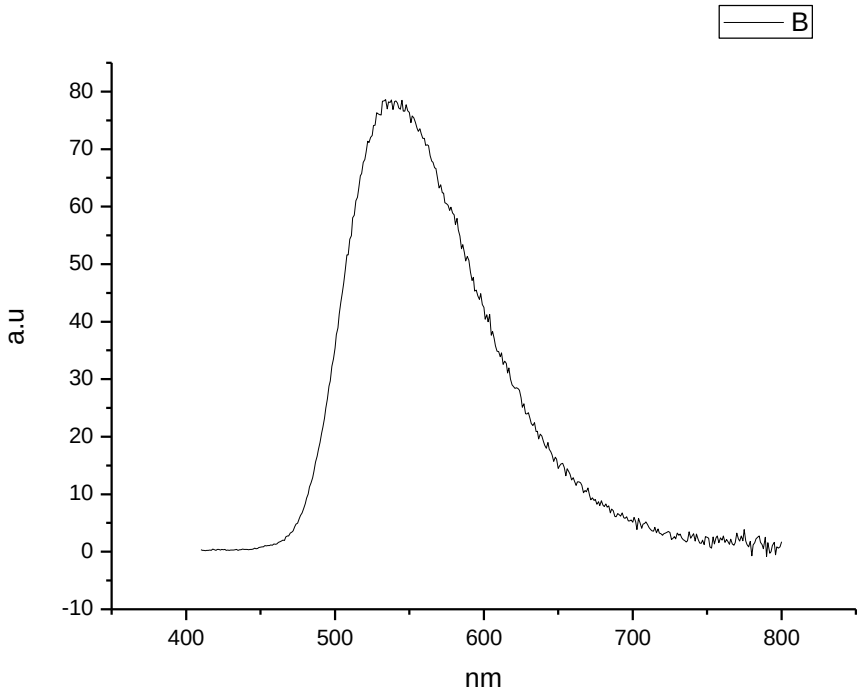

Figure 380. Fluorescence emission spectrum of **19** recorded in Methanol at 400 nm excitation.

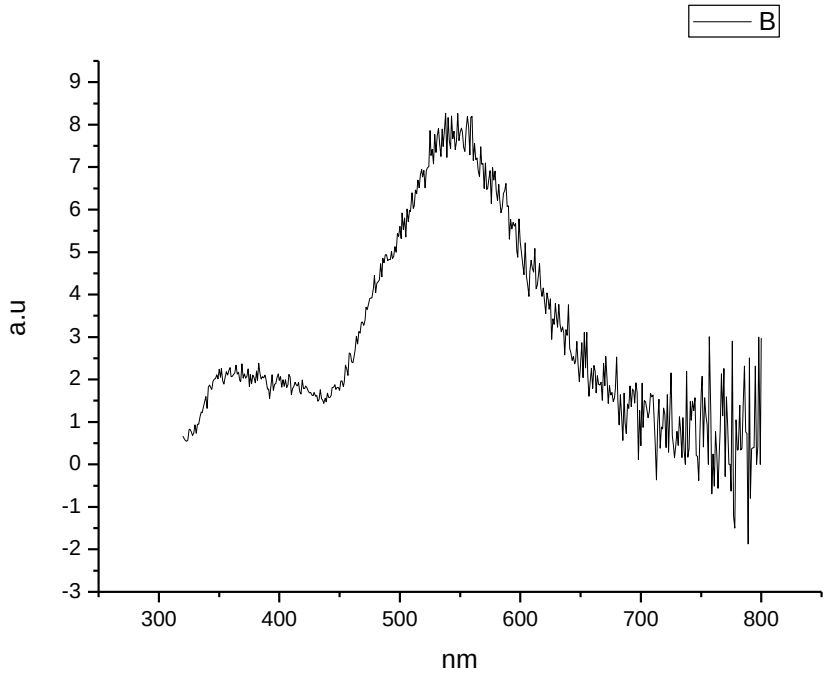

Figure 381. Fluorescence emission spectrum of **19** recorded in 2,2,2-trifluoroethanol at 310 nm excitation.

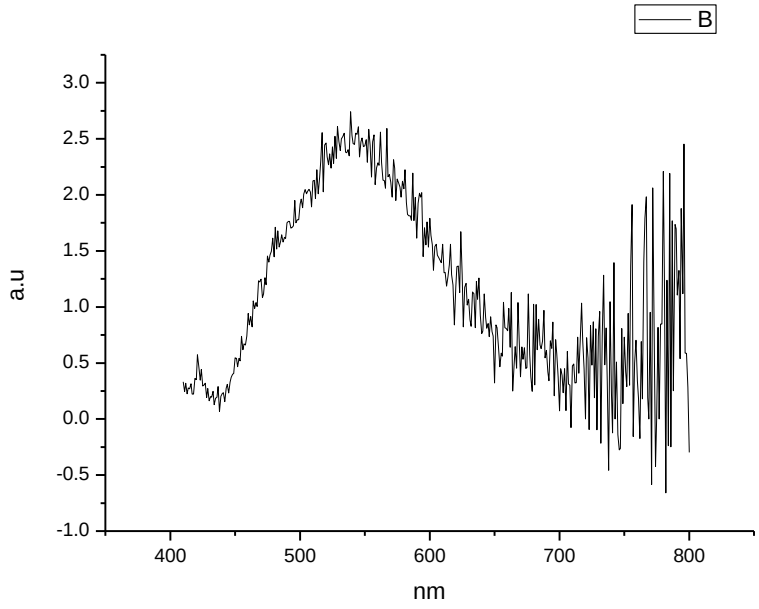

Figure 382. Fluorescence emission spectrum of **19** recorded in 2,2,2-trifluoroethanol at 400 nm excitation.

3.4.10 Normalised Fluorescence Emission spectra (Gaussian fitted).

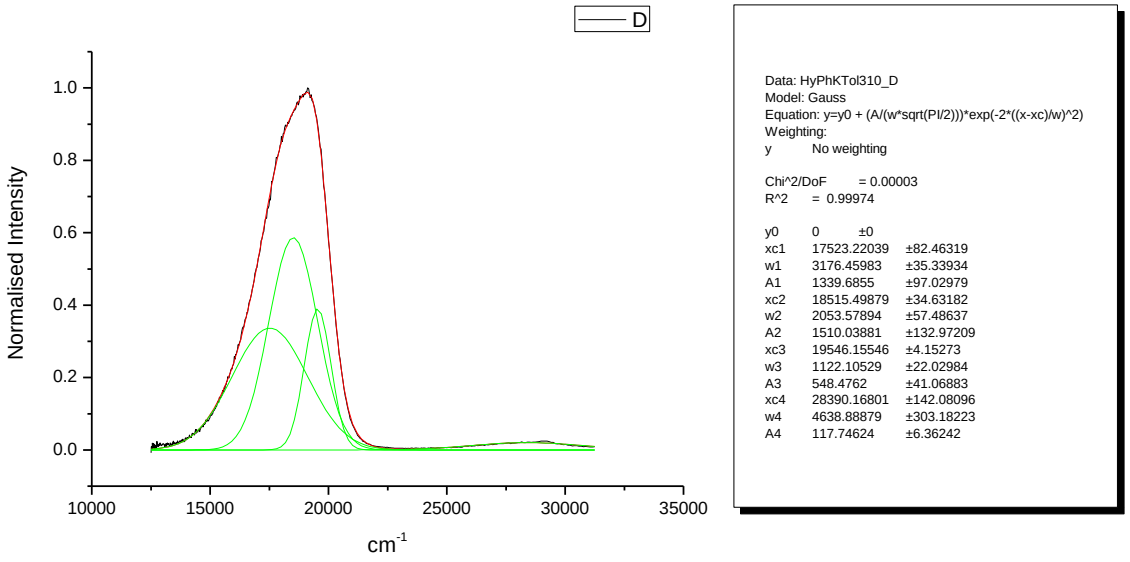

Figure 359. Gaussian model fit of the normalised fluorescence emission spectrum of **19** recorded in Toluene at 310 nm excitation.

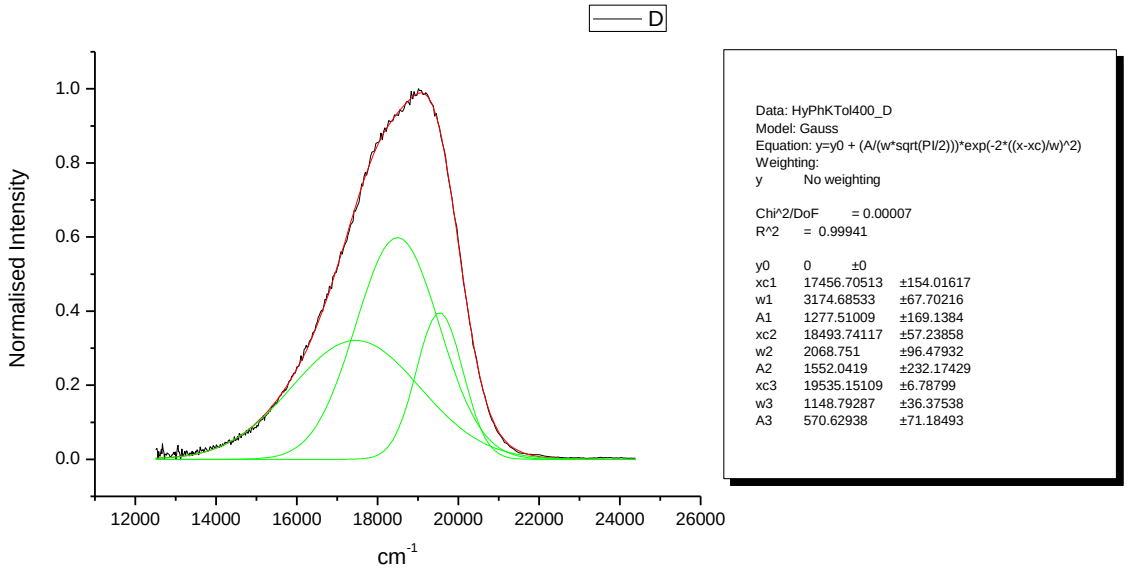

Figure 360. Gaussian model fit of the normalised fluorescence emission spectrum of **19** recorded in Toluene at 400 nm excitation.

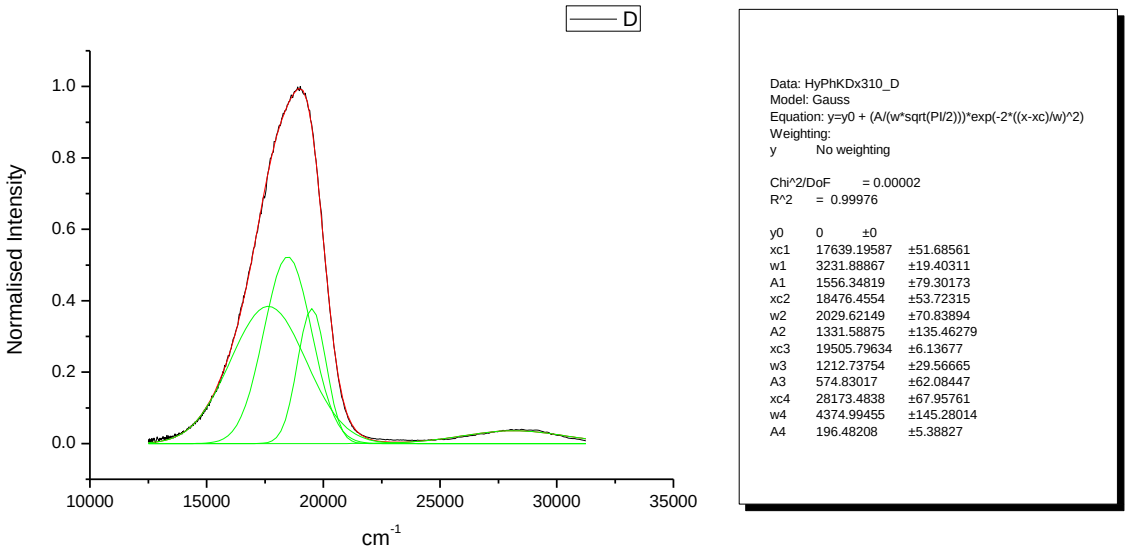

Figure 361. Gaussian model fit of the normalised fluorescence emission spectrum of **19** recorded in 1,4-dioxane at 310 nm excitation.

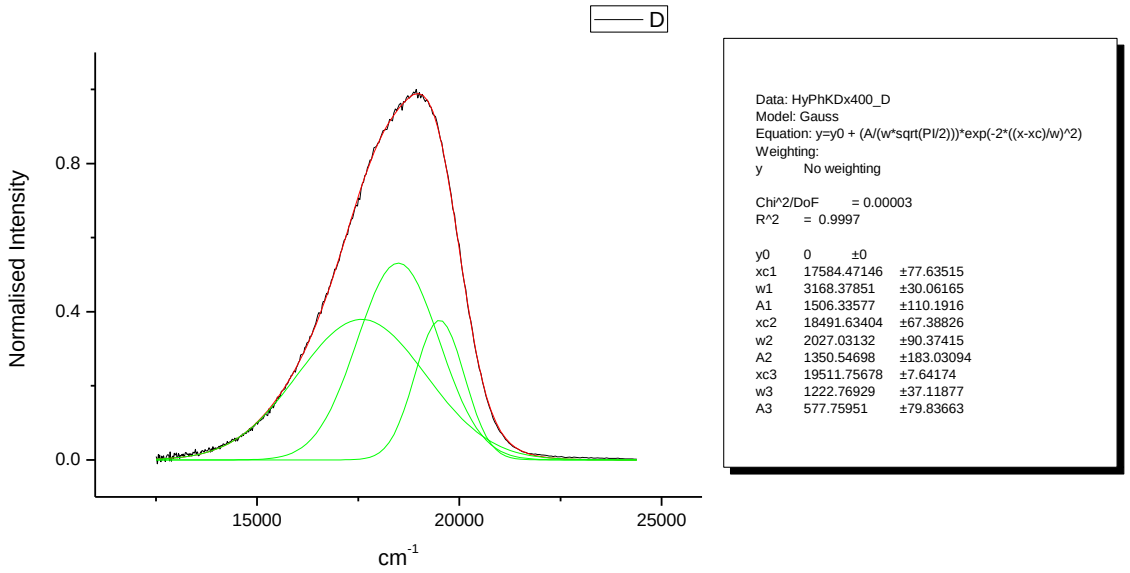

Figure 362. Gaussian model fit of the normalised fluorescence emission spectrum of **19** recorded in 1,4-dioxane at 400 nm excitation.

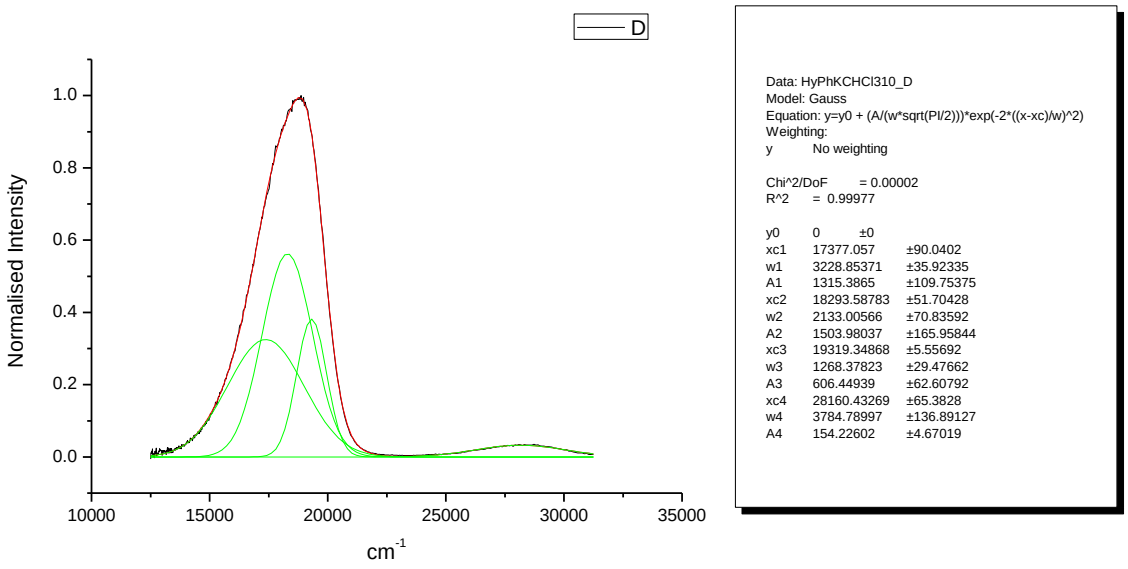

Figure 363. Gaussian model fit of the normalised fluorescence emission spectrum of **19** recorded in Chloroform at 310 nm excitation.

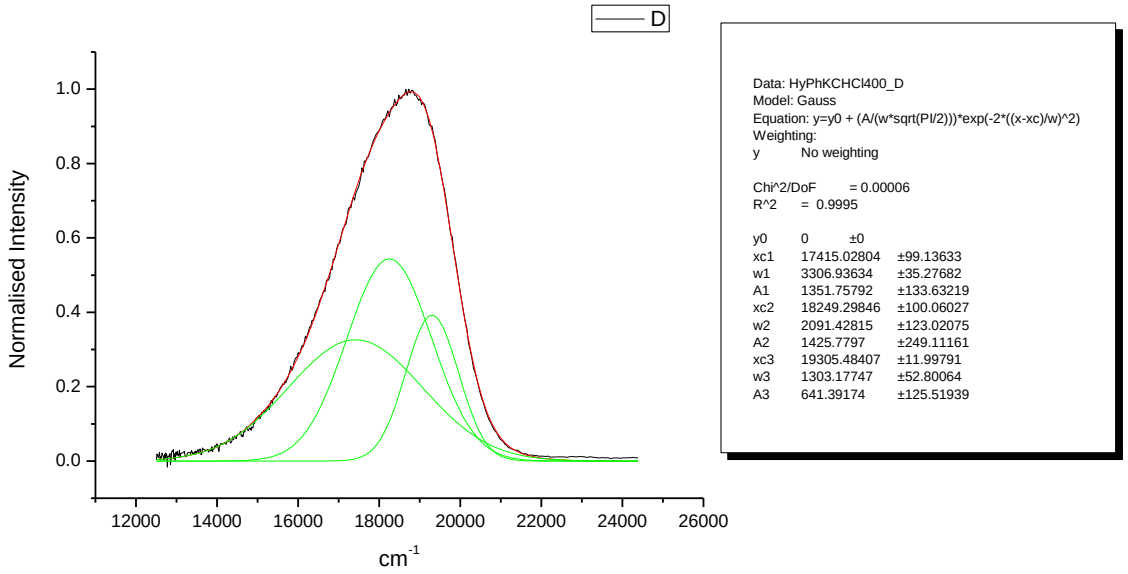

Figure 364. Gaussian model fit of the normalised fluorescence emission spectrum of **19** recorded in Chloroform at 400 nm excitation.

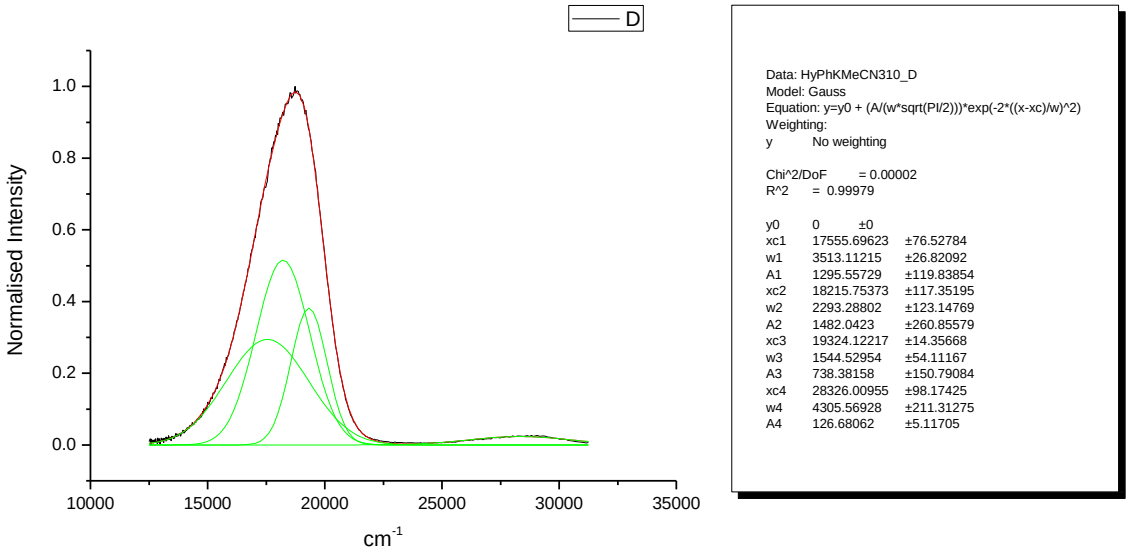

Figure 365. Gaussian model fit of the normalised fluorescence emission spectrum of **19** recorded in Acetonitrile at 310 nm excitation.

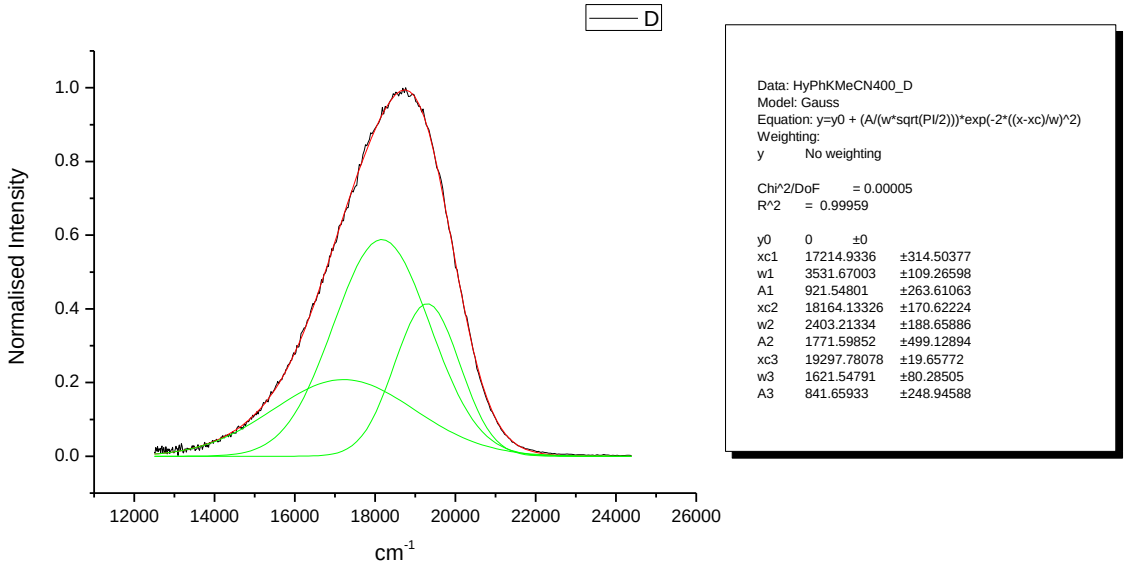

Figure 366. Gaussian model fit of the normalised fluorescence emission spectrum of **19** recorded in Acetonitrile at 400 nm excitation.

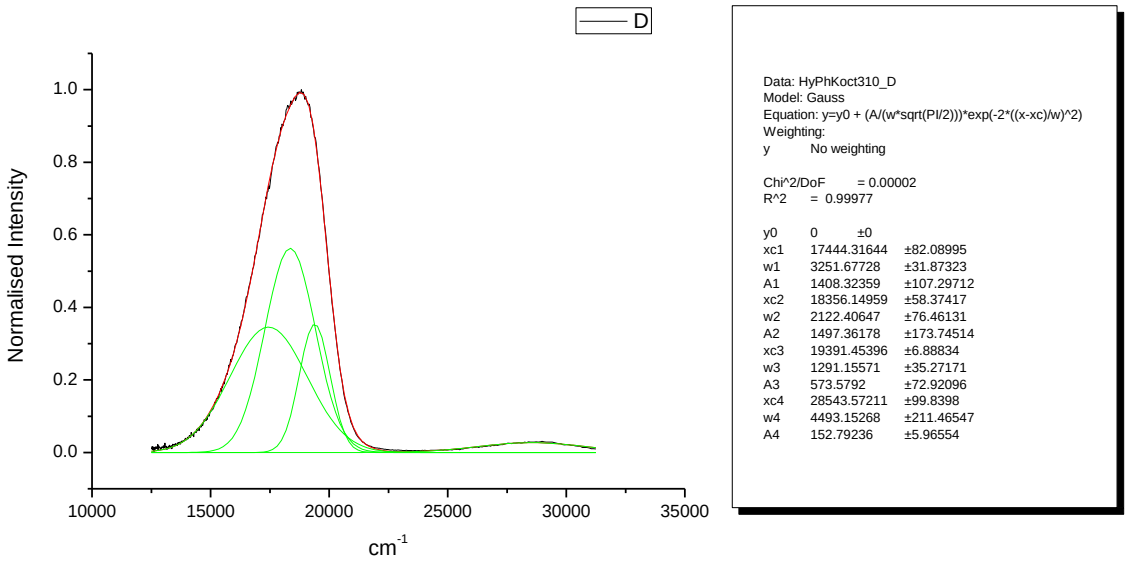

Figure 367. Gaussian model fit of the normalised fluorescence emission spectrum of **19** recorded in 1-octanol at 310 nm excitation.

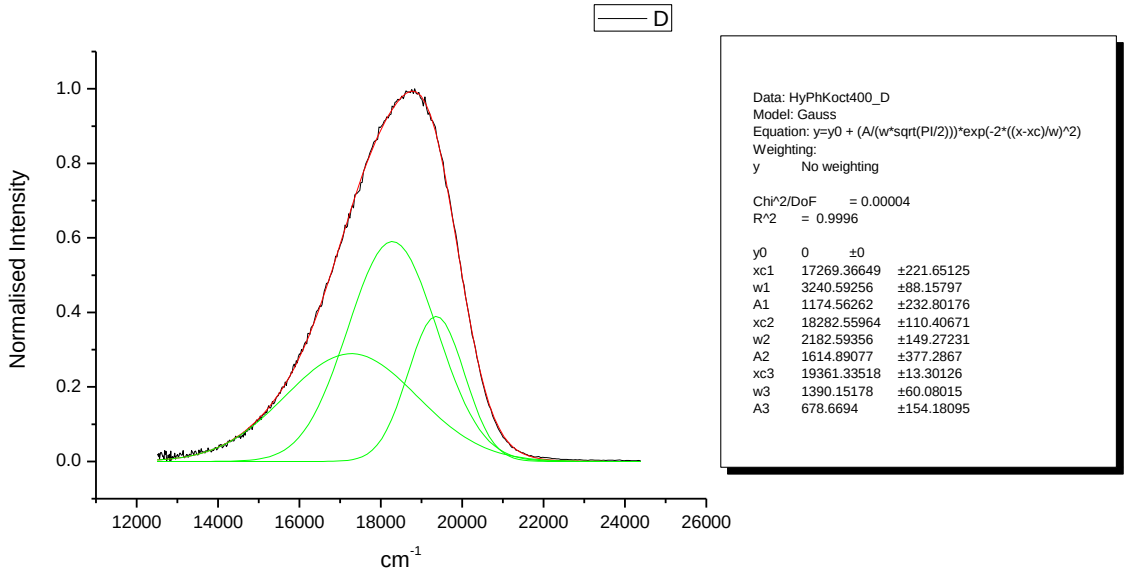

Figure 368. Gaussian model fit of the normalised fluorescence emission spectrum of **19** recorded in 1-octanol at 400 nm excitation.

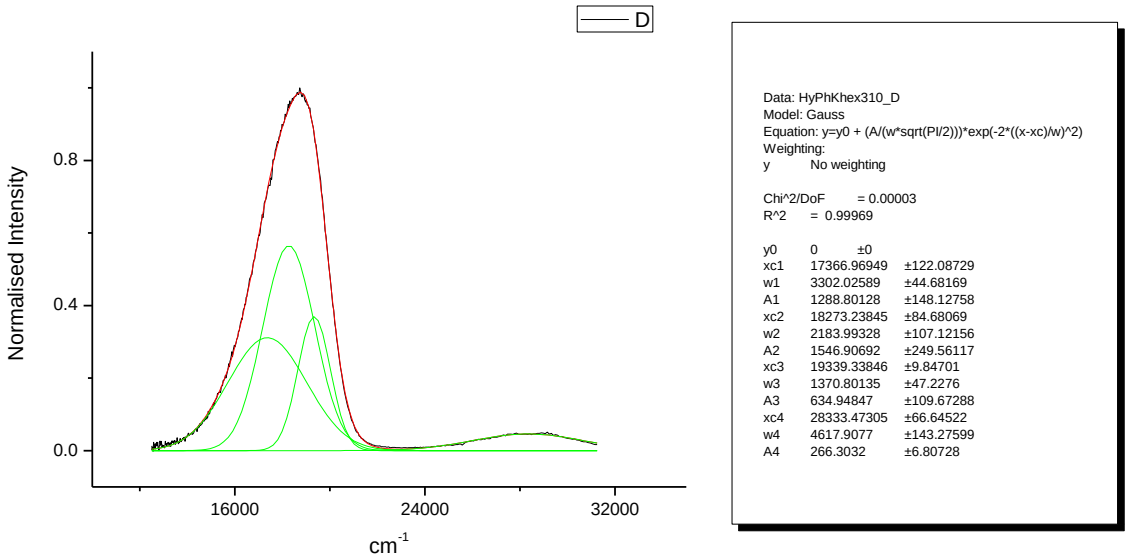

Figure 369. Gaussian model fit of the normalised fluorescence emission spectrum of **19** recorded in 1-hexanol at 310 nm excitation.

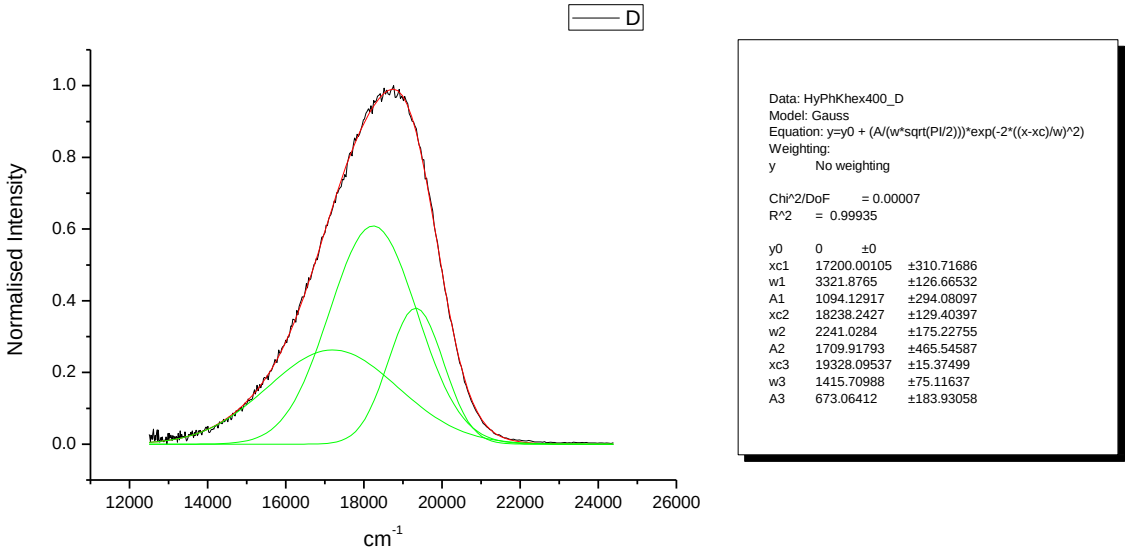

Figure 370. Gaussian model fit of the normalised fluorescence emission spectrum of **19** recorded in 1-hexanol at 400 nm excitation.

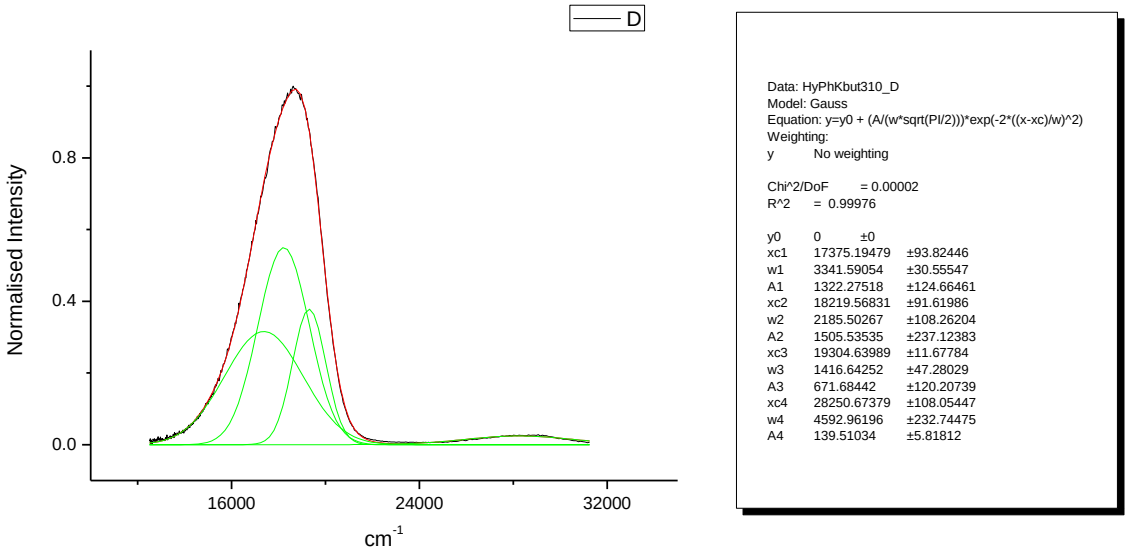

Figure 371. Gaussian model fit of the normalised fluorescence emission spectrum of **19** recorded in 1-butanol at 310 nm excitation.

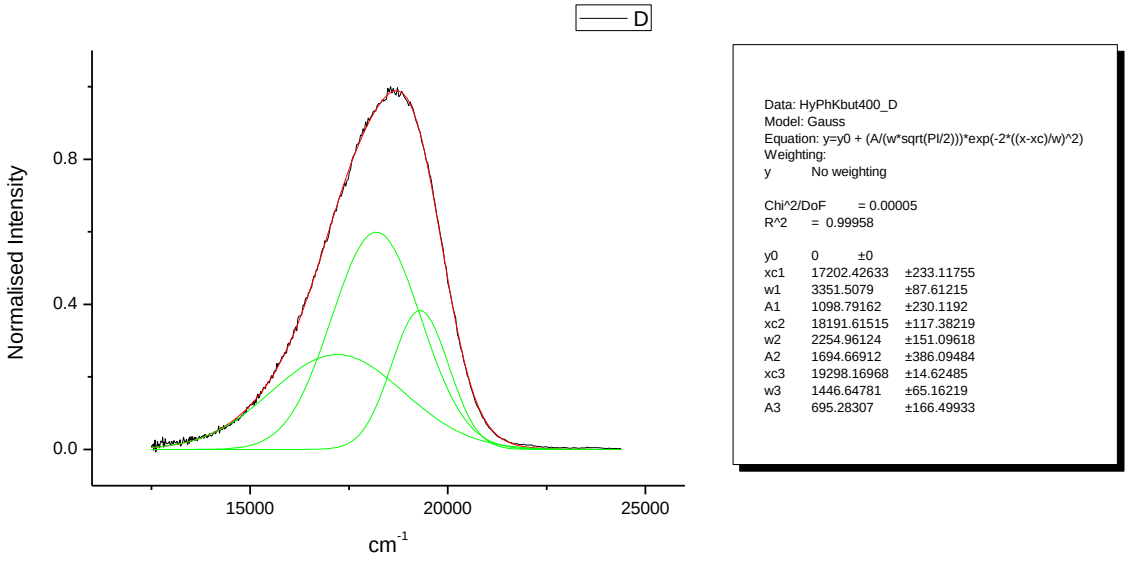

Figure 372. Gaussian model fit of the normalised fluorescence emission spectrum of **19** recorded in 1-butanol at 400 nm excitation.

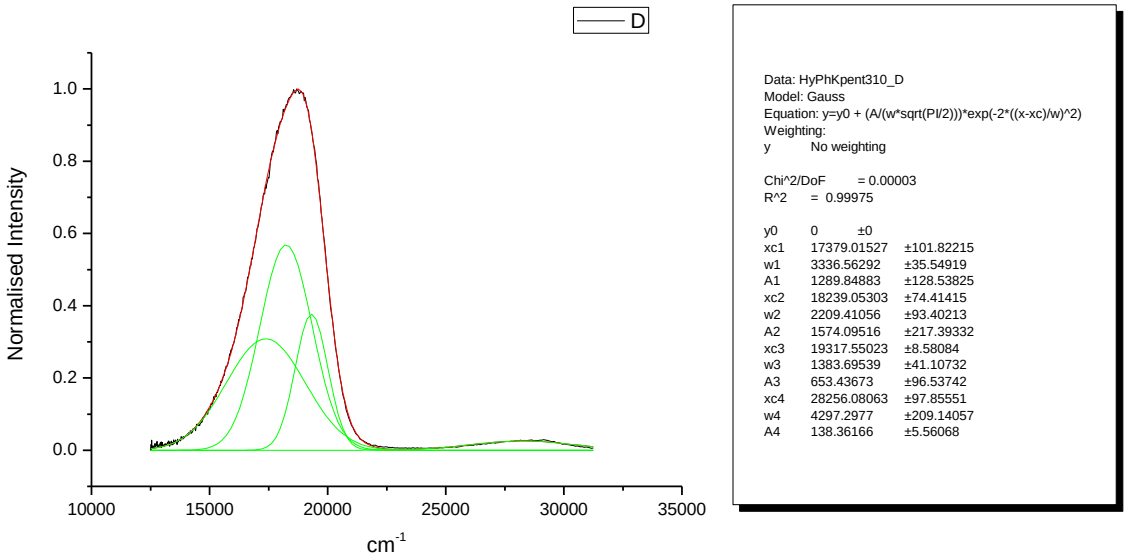

Figure 373. Gaussian model fit of the normalised fluorescence emission spectrum of **19** recorded in 1-pentanol at 310 nm excitation.

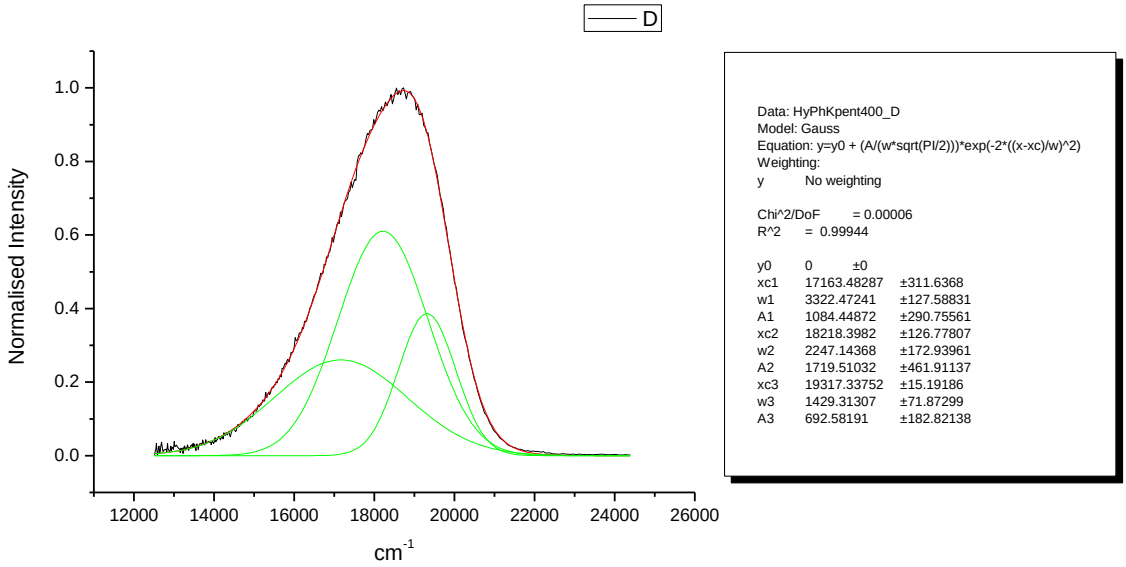

Figure 374. Gaussian model fit of the normalised fluorescence emission spectrum of **19** recorded in 1-pentanol at 400 nm excitation.

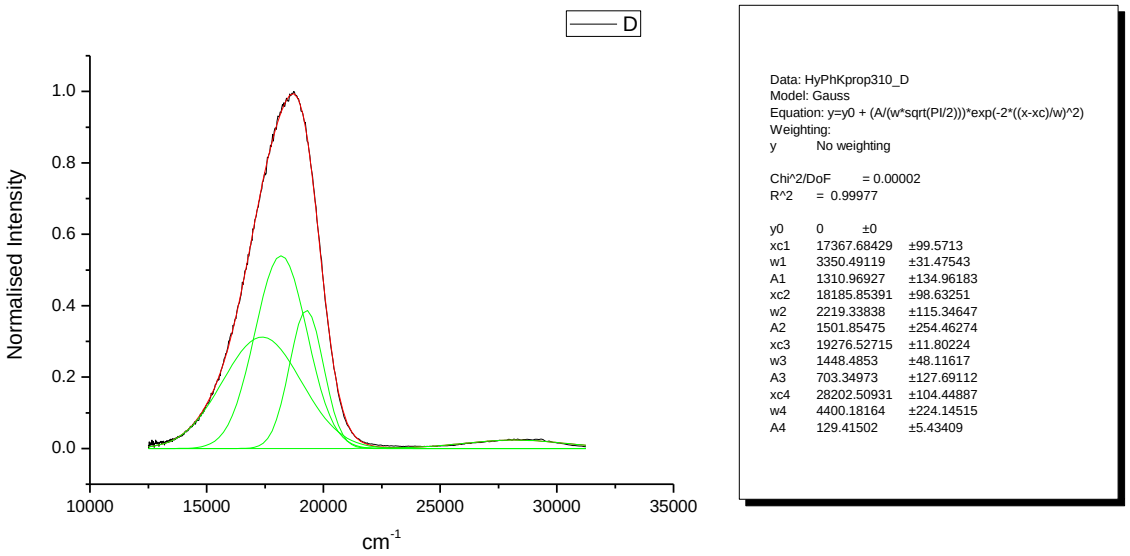

Figure 375. Gaussian model fit of the normalised fluorescence emission spectrum of **19** recorded in 1-propanol at 310 nm excitation.

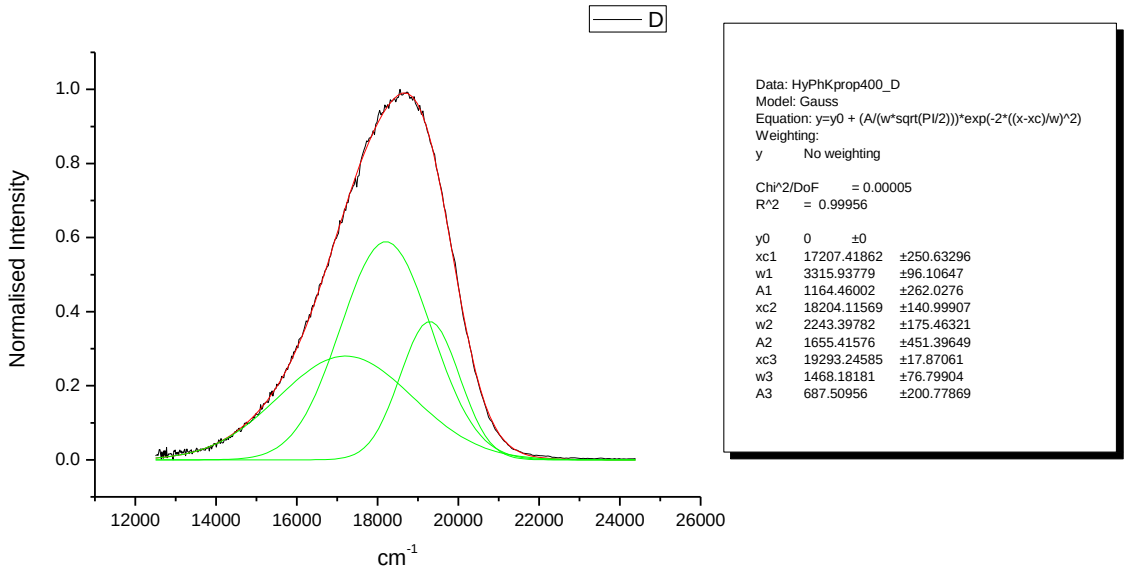

Figure 376. Gaussian model fit of the normalised fluorescence emission spectrum of **19** recorded in 1-propanol at 400 nm excitation.

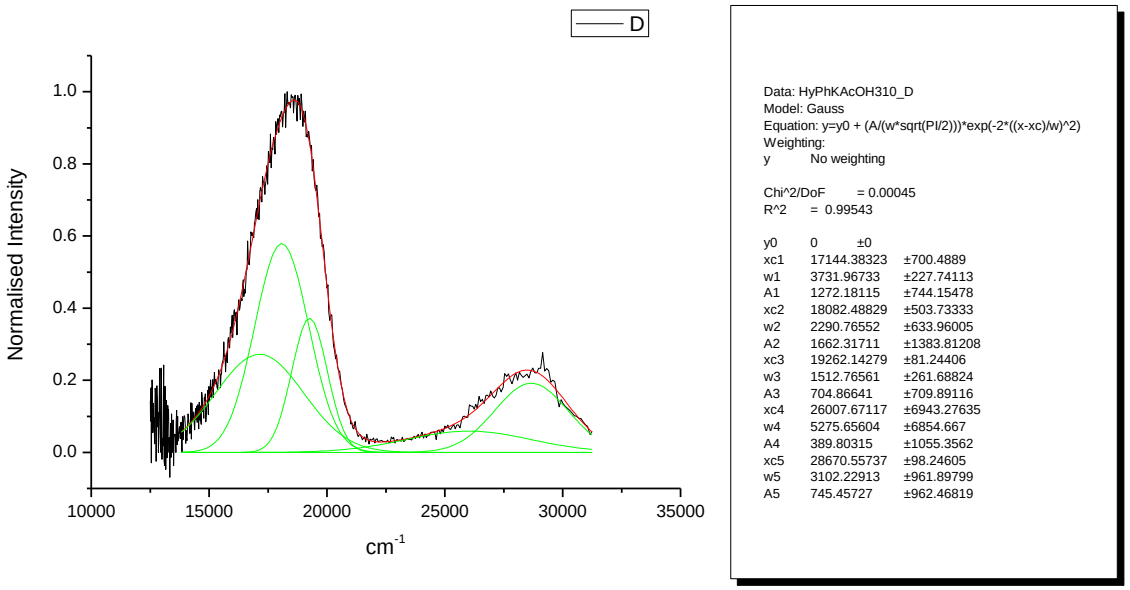

Figure 377. Gaussian model fit of the normalised fluorescence emission spectrum of **19** recorded in Acetic Acid at 310 nm excitation.

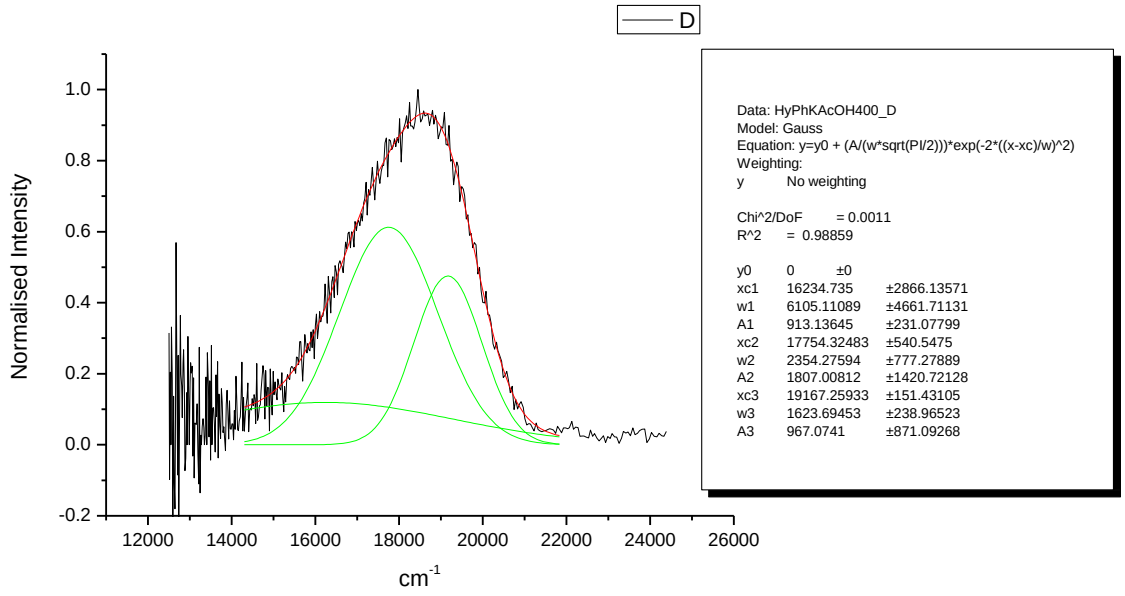

Figure 378. Gaussian model fit of the normalised fluorescence emission spectrum of **19** recorded in Acetic Acid at 400 nm excitation.

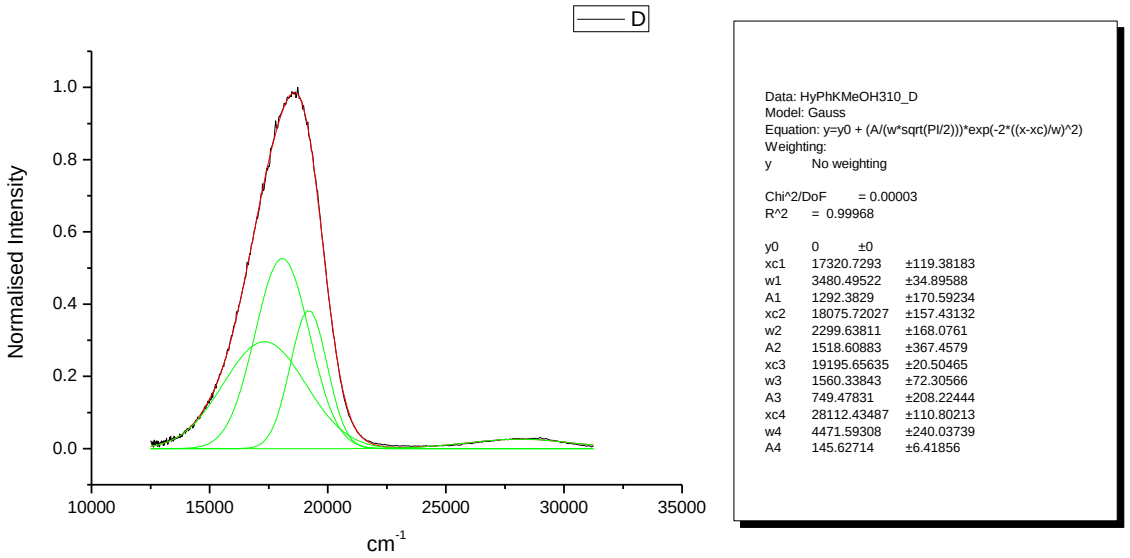

Figure 379. Gaussian model fit of the normalised fluorescence emission spectrum of **19** recorded in Methanol at 310 nm excitation.

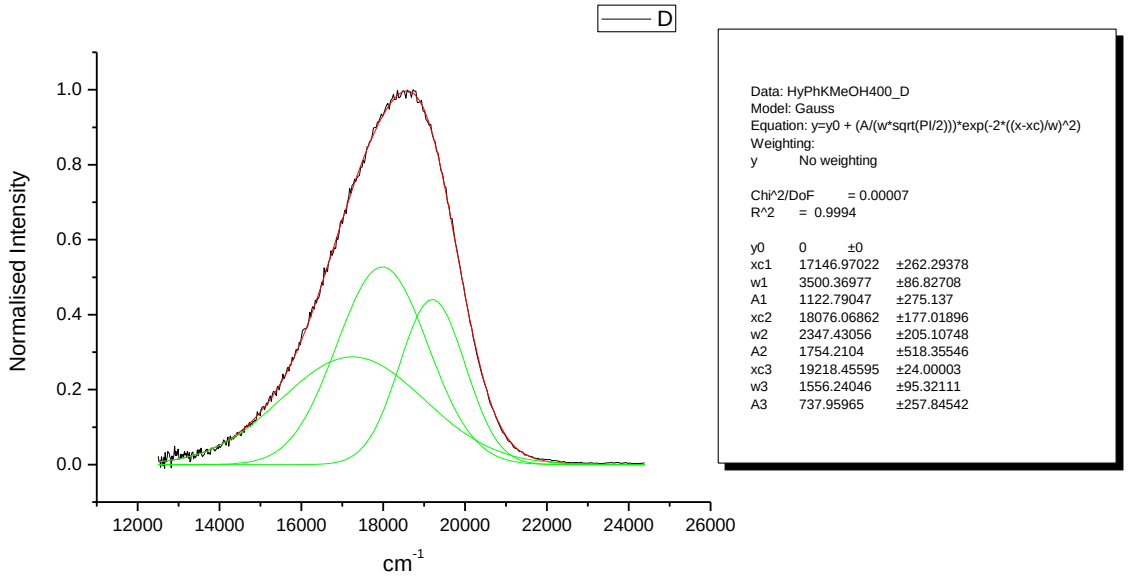

Figure 380. Gaussian model fit of the normalised fluorescence emission spectrum of **19** recorded in Methanol at 400 nm excitation.

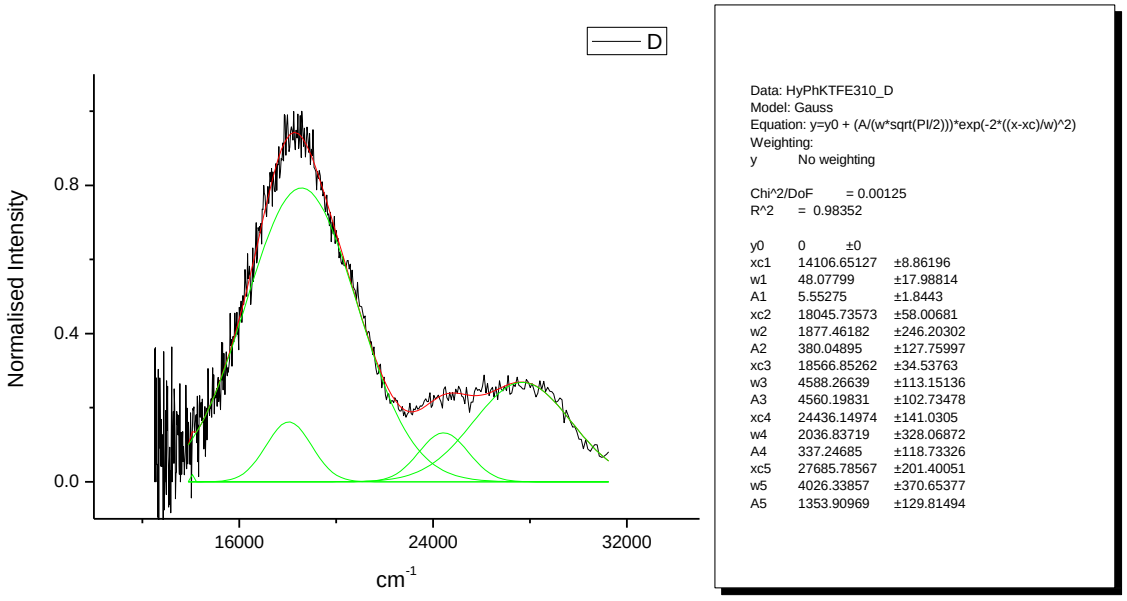

Figure 381. Gaussian model fit of the normalised fluorescence emission spectrum of **19** recorded in 2,2,2-trifluoroethanol at 310 nm excitation.

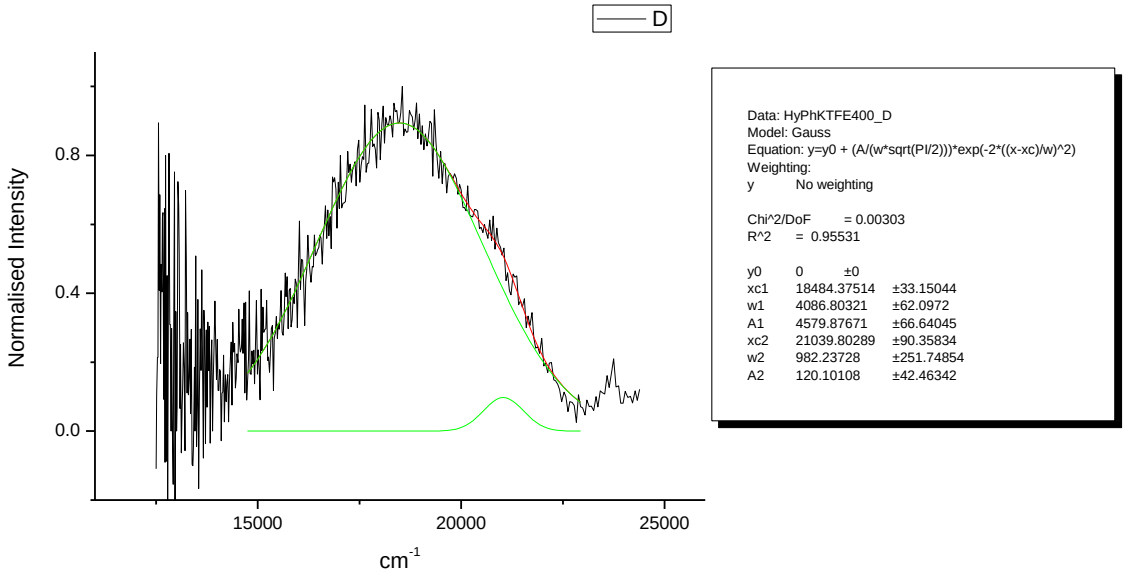

Figure 382. Gaussian model fit of the normalised fluorescence emission spectrum of **19** recorded in 2,2,2-trifluoroethanol at 400 nm excitation.

3.4.11 Fluorescence Excitation spectra.

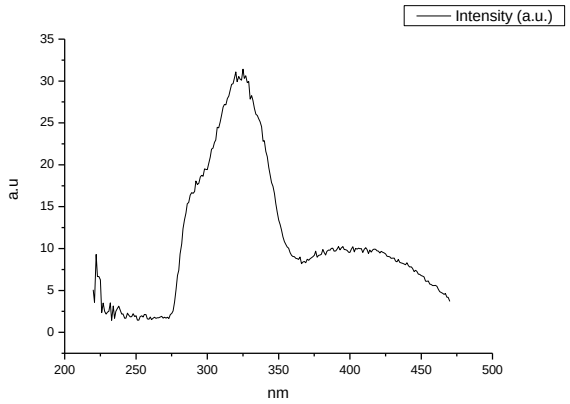

Figure 538. Fluorescence excitation spectrum of **19** recorded in Toluene with emission fixed at 480 nm.

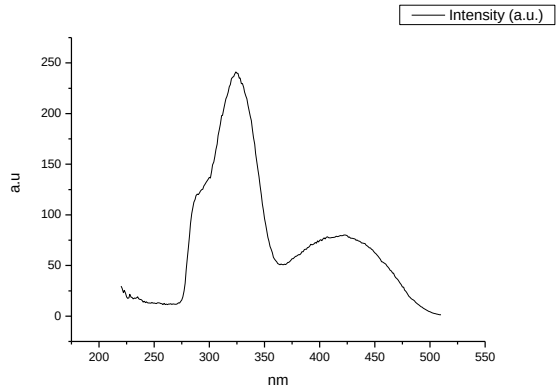

Figure 539. Fluorescence excitation spectrum of **19** recorded in Toluene with emission fixed at 520 nm.

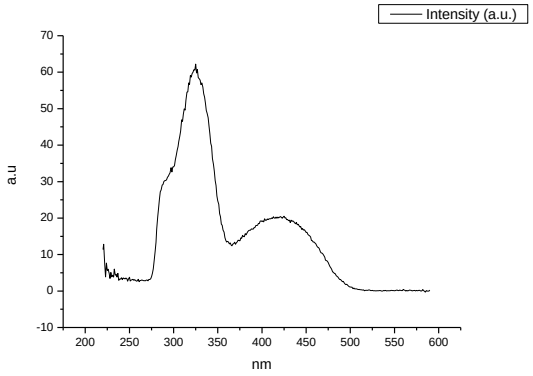

Figure 540. Fluorescence excitation spectrum of **19** recorded in Toluene with emission fixed at 600 nm.

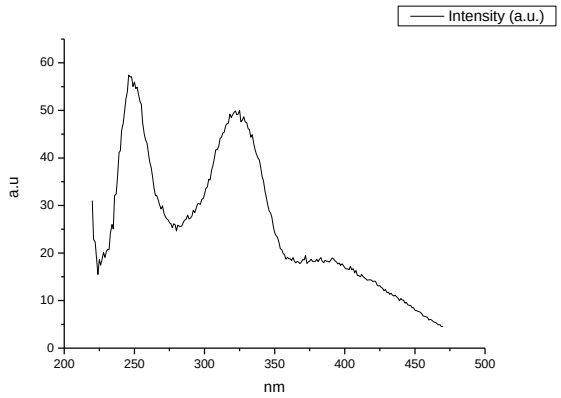

Figure 541. Fluorescence excitation spectrum of **19** recorded in 1,4-dioxane with emission fixed at 480 nm.

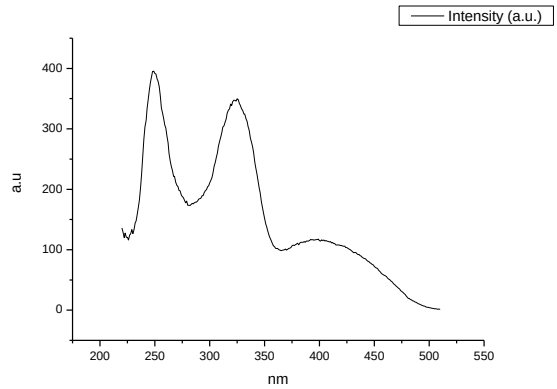

Figure 542. Fluorescence excitation spectrum of **19** recorded in 1,4-dioxane with emission fixed at 520 nm.

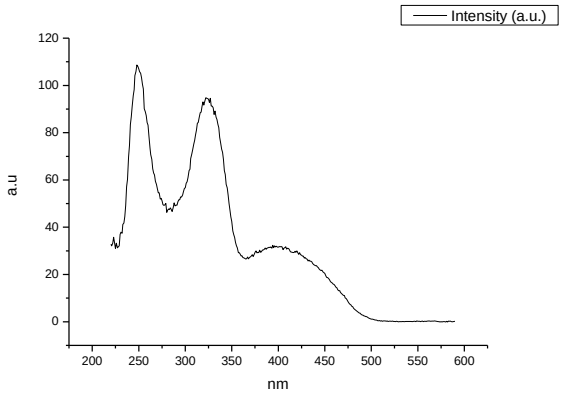

Figure 543. Fluorescence excitation spectrum of **19** recorded in 1,4-dioxane with emission fixed at 600 nm.

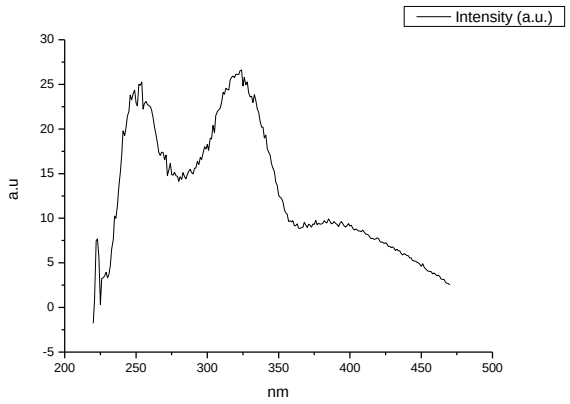

Figure 544. Fluorescence excitation spectrum of **19** recorded in Chloroform with emission fixed at 480 nm.

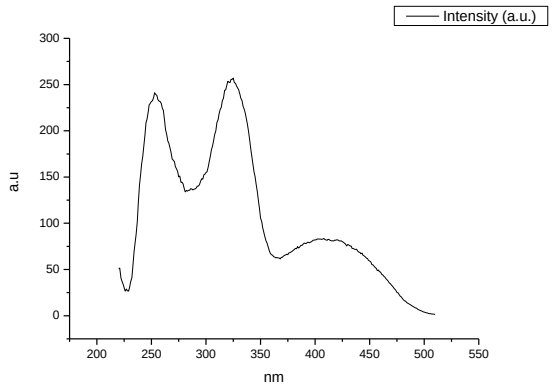

Figure 545. Fluorescence excitation spectrum of **19** recorded in Chloroform with emission fixed at 520 nm.

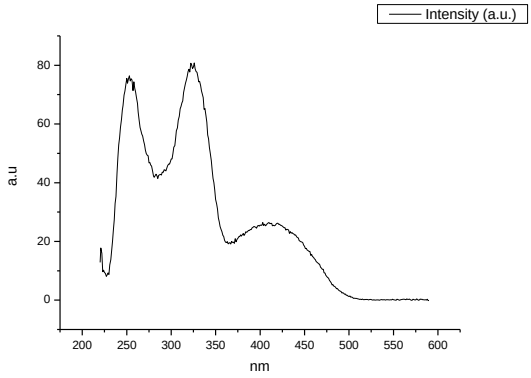

Figure 546. Fluorescence excitation spectrum of **19** recorded in Chloroform with emission fixed at 600 nm.

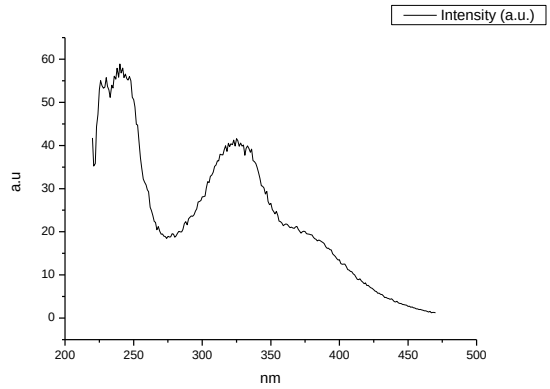

Figure 547. Fluorescence excitation spectrum of **19** recorded in Acetonitrile with emission fixed at 480 nm.

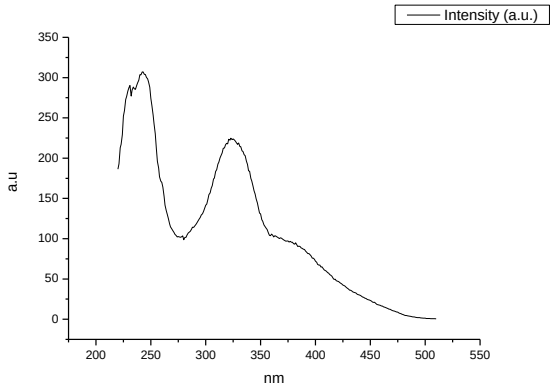

Figure 548. Fluorescence excitation spectrum of **19** recorded in Acetonitrile with emission fixed at 520 nm.

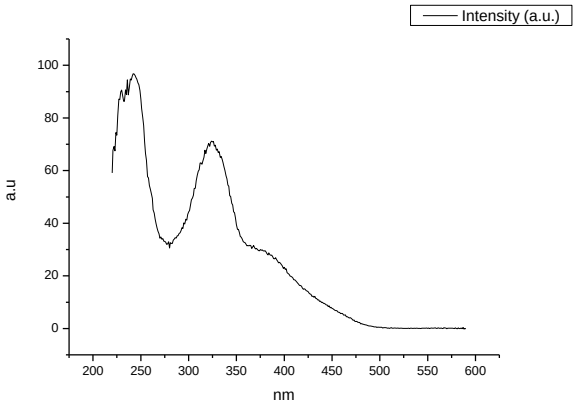

Figure 549. Fluorescence excitation spectrum of **19** recorded in Acetonitrile with emission fixed at 600 nm.

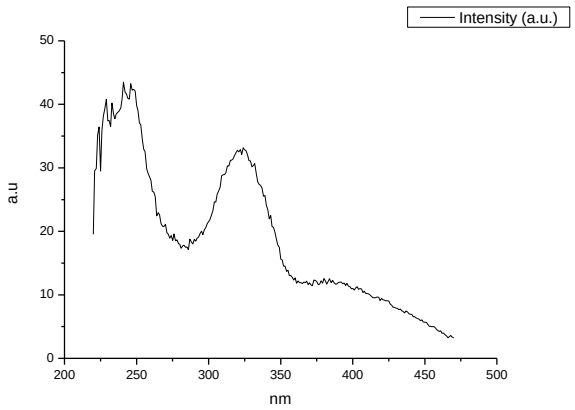

Figure 550. Fluorescence excitation spectrum of **19** recorded in 1-octanol with emission fixed at 480 nm.

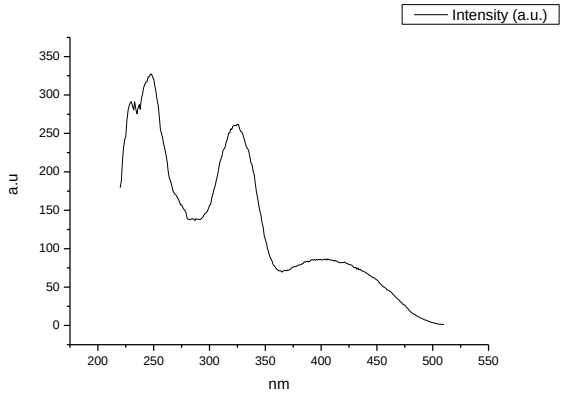

Figure 551. Fluorescence excitation spectrum of **19** recorded in 1-octanol with emission fixed at 520 nm.

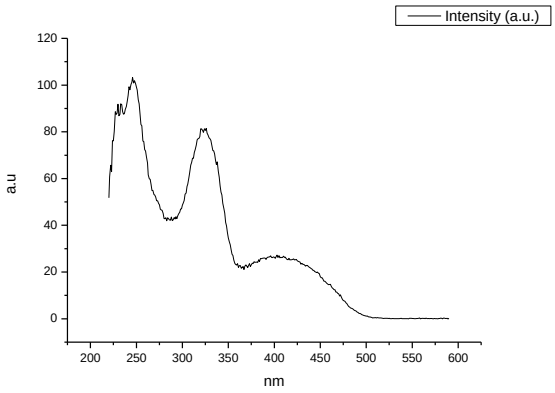

Figure 552. Fluorescence excitation spectrum of **19** recorded in 1-octanol with emission fixed at 600 nm.

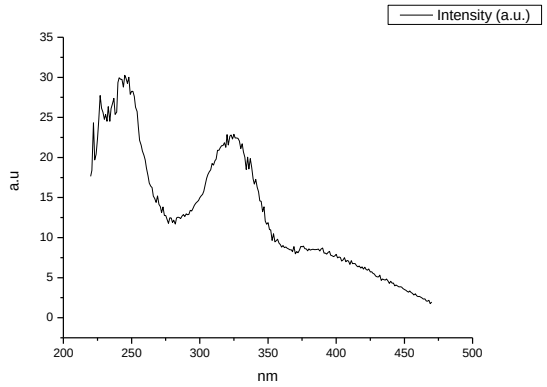

Figure 553. Fluorescence excitation spectrum of **19** recorded in 1-hexanol with emission fixed at 480 nm.

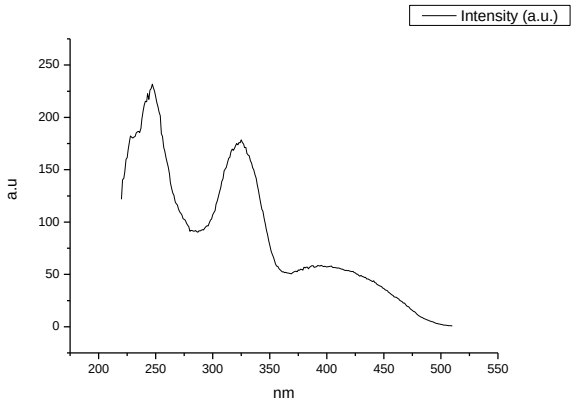

Figure 554. Fluorescence excitation spectrum of **19** recorded in 1-hexanol with emission fixed at 520 nm.

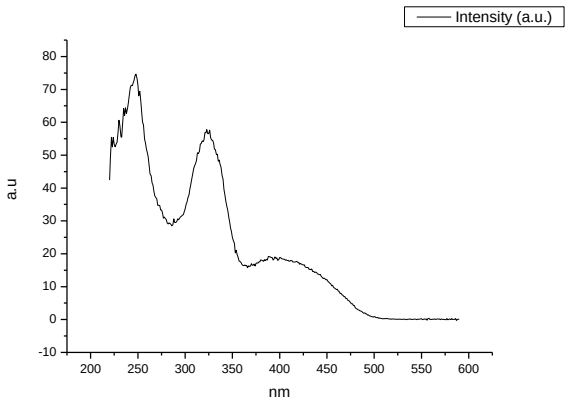

Figure 555. Fluorescence excitation spectrum of **19** recorded in 1-hexanol with emission fixed at 600 nm.

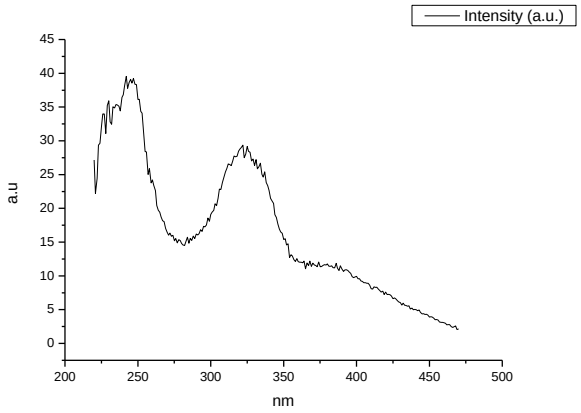

Figure 556. Fluorescence excitation spectrum of **19** recorded in 1-butanol with emission fixed at 480 nm.

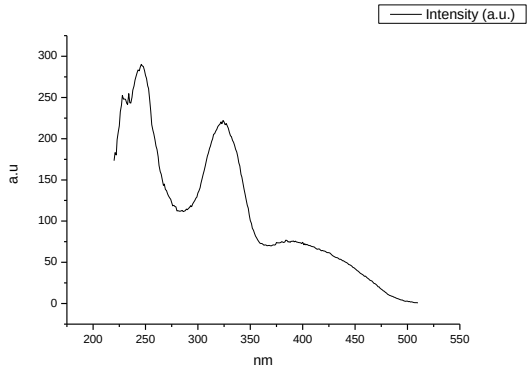

Figure 557. Fluorescence excitation spectrum of **19** recorded in 1-butanol with emission fixed at 520 nm.

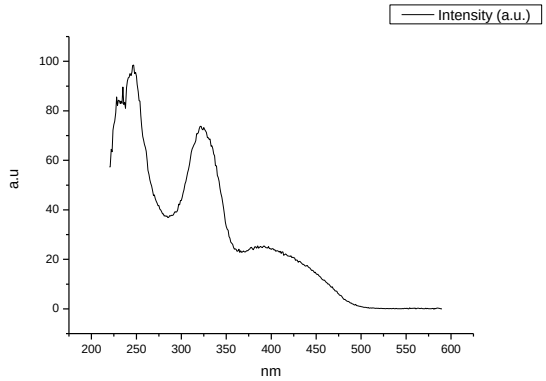

Figure 558. Fluorescence excitation spectrum of **19** recorded in 1-butanol with emission fixed at 600 nm.

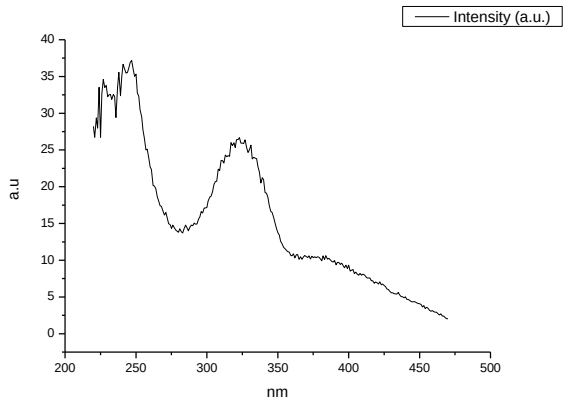

Figure 559. Fluorescence excitation spectrum of **19** recorded in 1-pentanol with emission fixed at 480 nm.

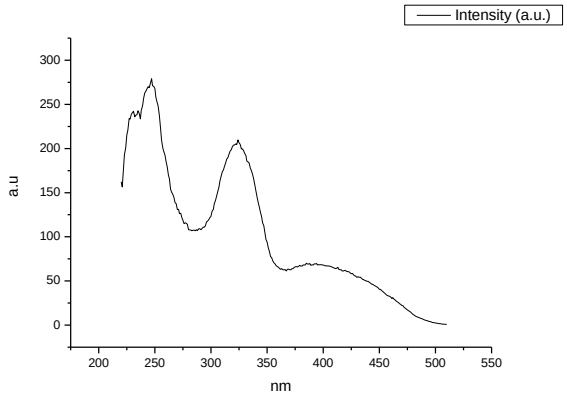

Figure 560. Fluorescence excitation spectrum of **19** recorded in 1-pentanol with emission fixed at 520 nm.

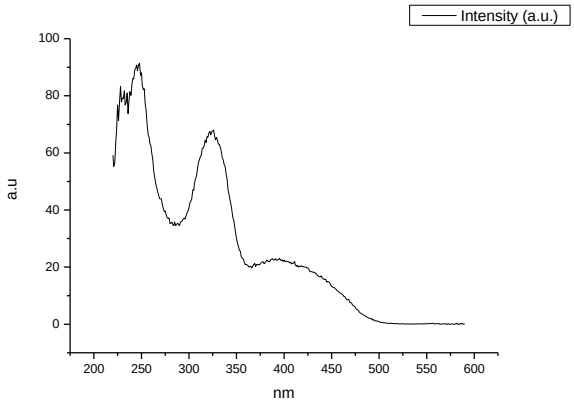

Figure 561. Fluorescence excitation spectrum of **19** recorded in 1-pentanol with emission fixed at 600 nm.

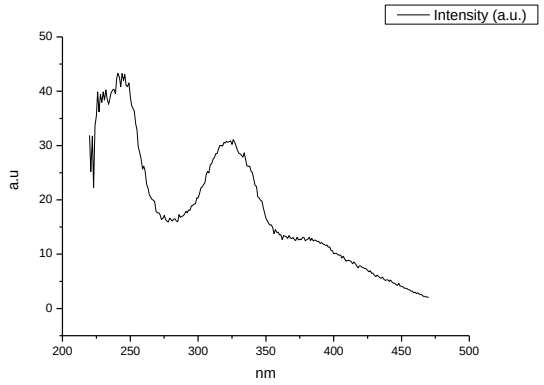

Figure 562. Fluorescence excitation spectrum of **19** recorded in 1-propanol with emission fixed at 480 nm.

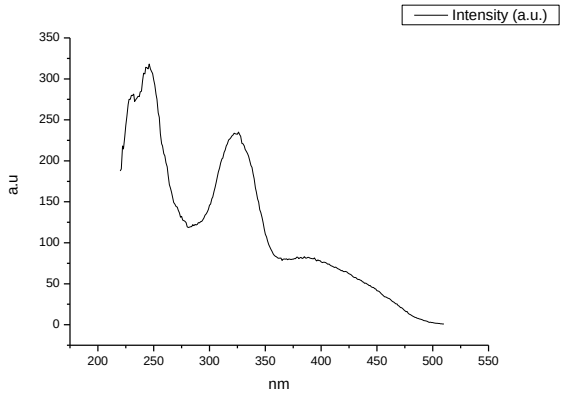

Figure 563. Fluorescence excitation spectrum of **19** recorded in 1-propanol with emission fixed at 520 nm.

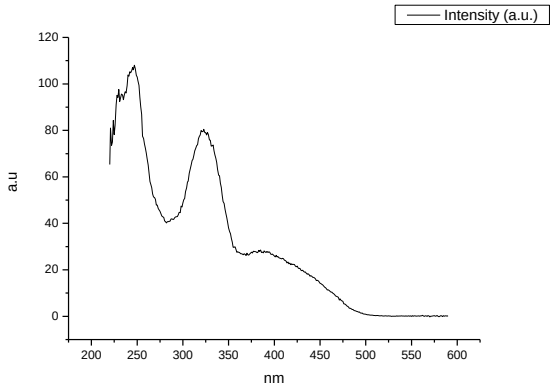

Figure 564. Fluorescence excitation spectrum of **19** recorded in 1-propanol with emission fixed at 600 nm.

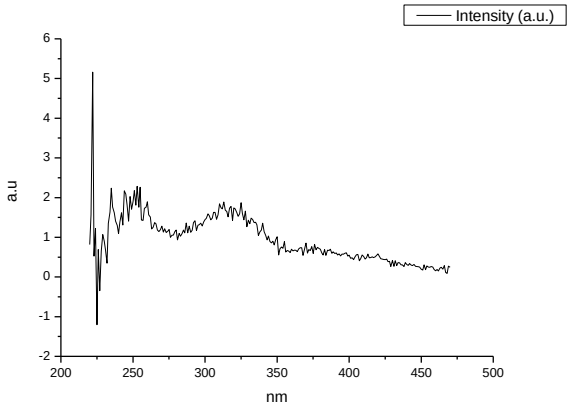

Figure 565. Fluorescence excitation spectrum of **19** recorded in Acetic Acid with emission fixed at 480 nm.

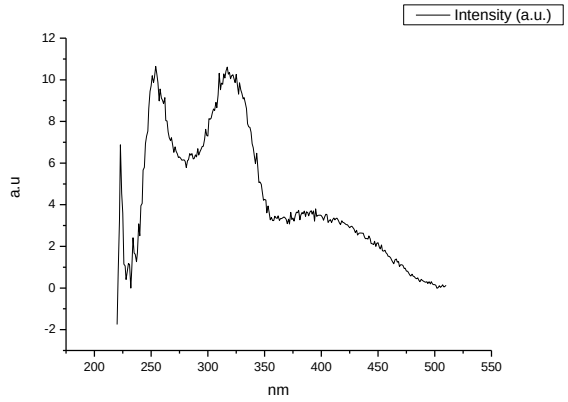

Figure 566. Fluorescence excitation spectrum of **19** recorded in Acetic Acid with emission fixed at 520 nm.

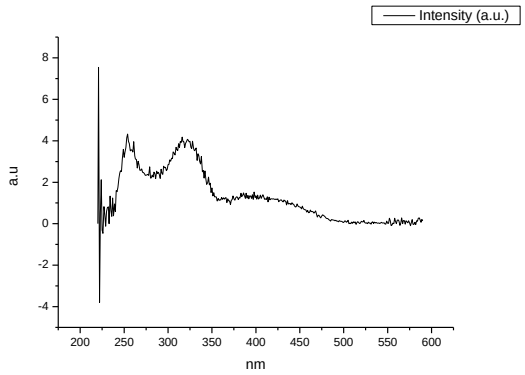

Figure 567. Fluorescence excitation spectrum of **19** recorded in Acetic Acid with emission fixed at 600 nm.

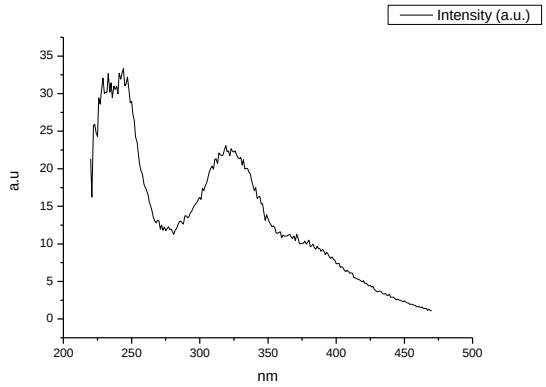

Figure 568. Fluorescence excitation spectrum of **19** recorded in Methanol with emission fixed at 480 nm.

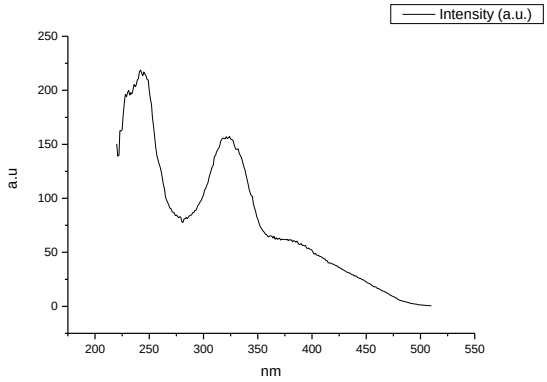

Figure 569. Fluorescence excitation spectrum of **19** recorded in Methanol with emission fixed at 520 nm.

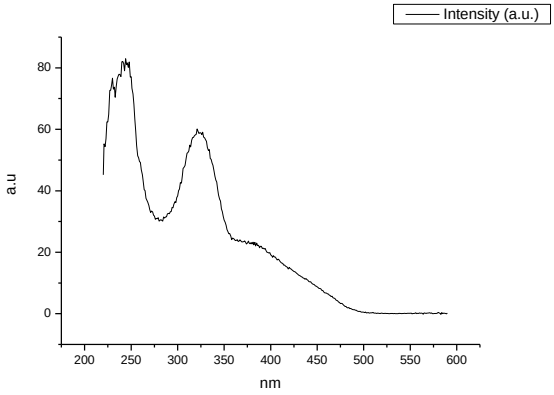

Figure 570. Fluorescence excitation spectrum of **19** recorded in Methanol with emission fixed at 600 nm.

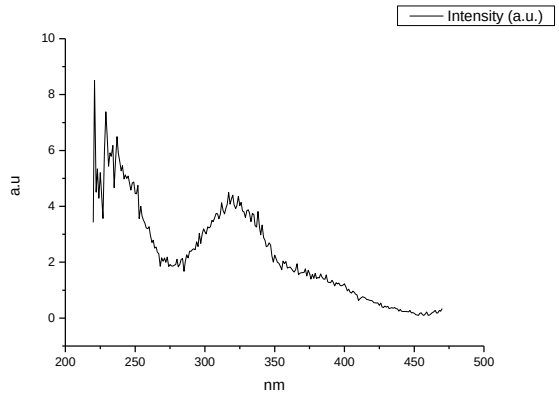

Figure 571. Fluorescence excitation spectrum of **19** recorded in 2,2,2-trifluoroethanol with emission fixed at 480 nm.

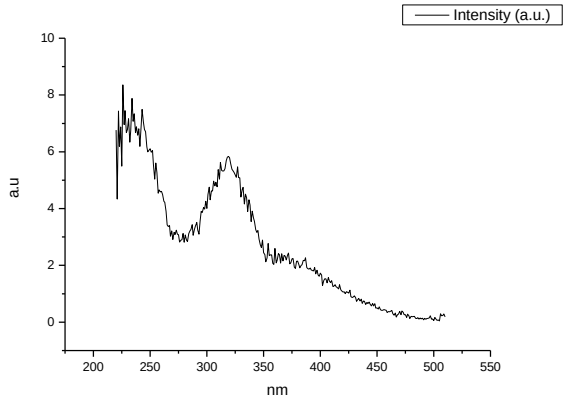

Figure 572. Fluorescence excitation spectrum of **19** recorded in 2,2,2-trifluoroethanol with emission fixed at 520 nm.

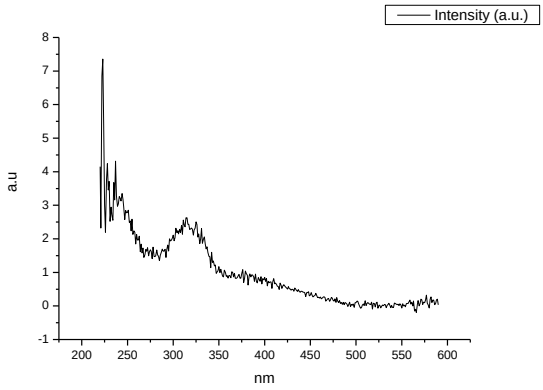

Figure 573. Fluorescence excitation spectrum of **19** recorded in 2,2,2-trifluoroethanol with emission fixed at 600 nm.

Appendix 4: Substituted phenyl ester 2,5-dihydro-1,2,3-triazines.

4.1 COMPOUND 21.

4.1.1 Quantum Yield Summary.

Solvent	abs (310 nm)	$\lambda_{ems\ (max)}$	$\Phi_{310\ nm}$	abs (400 nm)	$\lambda_{ems\ (max)}$	$\Phi_{400\ nm}$
Toluene	0.08	511.94	0.27	0.03	512.98	0.20
1,4-Dioxane	0.06	515.07	0.47	0.01	510.00	0.54
Chloroform	0.06	515.97	0.48	0.02	514.02	0.49
Acetonitrile	0.05	520.00	0.44	0.01	512.98	0.44
1-Octanol	0.04	515.97	0.50	0.01	512.98	0.50
1-Hexanol	0.02	512.98	0.46	0.01	511.04	0.45
1-Butanol	0.05	514.02	0.47	0.01	508.05	0.46
1-Pentanol	0.04	515.97	0.44	0.01	511.04	0.46
1-Propanol	0.07	517.01	0.41	0.02	508.05	0.40
Acetic acid	0.06	508.95	0.02	0.02	501.94	0.01
Methanol	0.06	515.97	0.34	0.01	514.02	0.34
2,2,2-Trifluoroethanol	0.03	535.97	0.02	0.01	517.20	0.01

Table 4.1.1. Summary of ultraviolet-visible absorbance values at 310 nm and 400 nm, emission maxima and quantum yield (Φ) of **21** at 310 nm and 400 nm excitation.

4.1.2 310 nm excitation Gaussian band fit summaries.

Solvent	λ max$_{em}$ Band 1 (cm^{-1})	λ max$_{em}$ Band 1 (nm)	λ max$_{em}$ Band 2 (cm^{-1})	λ max$_{em}$ Band 2 (nm)	λ max$_{em}$ Band 3 (cm^{-1})	λ max$_{em}$ Band 3 (nm)
Toluene	18730.26	533.90	19733.66	506.75	21058.83	474.86
1,4-Dioxane	18694.70	534.91	19742.90	506.51	21069.70	474.62
Chloroform	18483.06	541.04	19604.91	510.08	20904.09	478.38
Acetonitrile	18338.23	545.31	19541.31	511.74	20897.77	478.52
1-Octanol	18606.01	537.46	19709.07	507.38	21054.59	474.96
1-Hexanol	18589.50	537.94	19699.94	507.62	21015.24	475.85
1-Butanol	18516.11	540.07	19670.34	508.38	20962.49	477.04
1-Pentanol	19033.02	525.40	19729.28	506.86	20987.47	476.47
1-Propanol	18490.23	540.83	19667.35	508.46	20954.66	477.22
Acetic acid	18707.68	534.54	20250.71	493.81	-	-
Methanol	18374.05	544.25	19595.77	510.31	20876.40	479.01
2,2,2-Trifluoroethanol	18214.79	549.00	18705.84	534.59	-	-

Solvent	λ max$_{em}$ Band 4 (cm^{-1})	λ max$_{em}$ Band 4 (nm)	λ max$_{em}$ Band 5 (cm^{-1})	λ max$_{em}$ Band 5 (nm)
Toluene	27977.44	357.43	-	-
1,4-Dioxane	27832.99	359.29	-	-
Chloroform	28039.58	356.64	-	-
Acetonitrile	28235.78	354.16	-	-
1-Octanol	28349.32	352.74	-	-
1-Hexanol	28324.43	353.05	-	-
1-Butanol	28130.84	355.48	-	-
1-Pentanol	27704.63	360.95	-	-
1-Propanol	28136.11	355.42	-	-
Acetic acid	26945.91	371.11	28839.76	346.74
Methanol	28179.85	354.86	-	-
2,2,2-Trifluoroethanol	25238.83	396.21	28348.26	352.76

Table 4.1.2. Summary of band maxima of 5 band fit using Gaussian model for normalised **21** emission spectra recorded at 310 nm excitation.

(a)

Solvent	Width Band 1 (cm^{-1})	Width Band 2 (cm^{-1})	Width Band 3 (cm^{-1})	Width Band 4 (cm^{-1})	Width Band 5 (cm^{-1})
Toluene	3163.67	1857.71	976.51	4644.21	-
1,4-Dioxane	3222.49	1981.68	1010.47	5260.52	-
Chloroform	3173.72	2025.83	1036.49	3778.67	-
Acetonitrile	3321.65	2296.37	1137.12	4505.62	-
1-Octanol	3284.35	2110.16	1031.01	4592.46	-
1-Hexanol	3294.47	2133.47	1007.16	4550.67	-
1-Butanol	3266.78	2137.64	1073.30	4313.33	-
1-Pentanol	3002.34	1802.23	1150.25	4854.11	-
1-Propanol	3264.36	2159.49	1086.54	4290.15	-
Acetic acid	3693.08	2377.93	-	3694.66	2495.87
Methanol	3298.06	2211.67	1155.00	4124.47	-
2,2,2-Trifluoroethanol	4131.47	2782.82	-	4517.96	2897.17

(b)

Solvent	Area Band 1 (cm^{-1})	Area Band 2 (cm^{-1})	Area Band 3 (cm^{-1})	Area Band 4 (cm^{-1})	Area Band 5 (cm^{-1})
Toluene	2146.48	1215.59	298.14	169.05	-
1,4-Dioxane	2127.17	1329.81	281.00	171.91	-
Chloroform	1943.94	1485.10	314.26	107.39	-
Acetonitrile	2053.88	1689.47	259.68	138.35	-
1-Octanol	2067.61	1499.64	296.56	182.57	-
1-Hexanol	2070.74	1486.40	274.04	315.95	-
1-Butanol	1998.57	1561.74	311.39	148.34	-
1-Pentanol	2037.28	1075.78	519.29	170.88	-
1-Propanol	1985.22	1607.64	307.12	142.95	-
Acetic acid	2231.14	1848.32	-	1828.91	1976.85
Methanol	1979.57	1671.64	340.09	158.91	-
2,2,2-Trifluoroethanol	2475.87	1674.71	-	1337.61	1203.68

Tables 4.1.3 (a) and (b). Summary band width and band area of 5 band fit using Gaussian model for normalised **21** emission spectra recorded at 310 nm excitation.

Solvent	Band 1 Area Percentage (%)	Band 2 Area Percentage (%)	Band 3 Area Percentage (%)	Band 4 Area Percentage (%)	Band 5 Area Percentage (%)
Toluene	56.05	31.74	7.79	4.41	-
1,4-Dioxane	54.40	34.01	7.19	4.40	-
Chloroform	50.48	38.57	8.16	2.79	-
Acetonitrile	49.59	40.79	6.27	3.34	-
1-Octanol	51.10	37.06	7.33	4.51	-
1-Hexanol	49.93	35.84	6.61	7.62	-
1-Butanol	49.72	38.85	7.75	3.69	-
1-Pentanol	53.57	28.29	13.65	4.49	-
1-Propanol	49.10	39.76	7.60	3.54	-
Acetic acid	28.30	23.44	-	23.19	25.07
Methanol	47.70	40.28	8.19	3.83	-
2,2,2-Trifluoroethanol	37.00	25.03	-	19.99	17.99

Table 4.1.4. Total Area Percentages of 5 band fit using Gaussian model for normalised **21** emission spectra recorded at 310 nm excitation.

Solvent	Area Ratio Band 1/2 (310 nm ex)	Area Ratio Band 1/3 (310 nm ex)	Area Ratio Band 1/4 (310 nm ex)	Area Ratio Band 1/5 (310 nm ex)
Toluene	1.77	7.20	12.70	-
1,4-Dioxane	1.60	7.57	12.37	-
Chloroform	1.31	6.19	18.10	-
Acetonitrile	1.22	7.91	14.85	-
1-Octanol	1.38	6.97	11.32	-
1-Hexanol	1.39	7.56	6.55	-
1-Butanol	1.28	6.42	13.47	-
1-Pentanol	1.89	3.92	11.92	-
1-Propanol	1.23	6.46	13.89	-
Acetic acid	1.21	-	1.22	1.13
Methanol	1.18	5.82	12.46	-
2,2,2-Trifluoroethanol	1.48	-	1.85	2.06

Solvent	Area Ratio Band 2/3 (310 nm ex)	Area Ratio Band 2/4 (310 nm ex)	Area Ratio Band 2/5 (310 nm ex)	Area Ratio Band 3/4 (310 nm ex)	Area Ratio Band 3/5 (310 nm ex)	Area Ratio Band 4/5 (310 nm ex)
Toluene	4.08	7.19	-	1.76	-	-
1,4-Dioxane	4.73	7.74	-	1.63	-	-
Chloroform	4.73	13.83	-	2.93	-	-
Acetonitrile	6.51	12.21	-	1.88	-	-
1-Octanol	5.06	8.21	-	1.62	-	-
1-Hexanol	5.42	4.70	-	0.87	-	-
1-Butanol	5.02	10.53	-	2.10	-	-
1-Pentanol	2.07	6.30	-	3.04	-	-
1-Propanol	5.23	11.25	-	2.15	-	-
Acetic acid	-	1.01	0.93	-	-	0.93
Methanol	4.92	10.52	-	2.14	-	-
2,2,2-Trifluoroethanol	-	1.25	1.39	-	-	1.11

Table 4.1.5. Area Ratios of 5 band fit using Gaussian model for normalised **21** emission spectra recorded at 310 nm excitation.

4.1.3 400 nm excitation Gaussian band fit summaries.

Solvent	λ max_{em} Band 1 (cm^{-1})	λ max_{em} Band 1 (nm)	λ max_{em} Band 2 (cm^{-1})	λ max_{em} Band 2 (nm)	λmax_{em} Band 3 (cm^{-1})	λmax_{em} Band 3 (nm)
Toluene	18601.76	537.58	19787.89	505.36	21045.39	475.16
1,4-Dioxane	18555.28	538.93	19778.63	505.60	21045.40	475.16
Chloroform	18688.18	535.10	19640.40	509.15	20863.55	479.30
Acetonitrile	18279.32	547.07	19589.10	510.49	20852.13	479.57
1-Octanol	18481.52	541.08	19763.59	505.98	21019.77	475.74
1-Hexanol	18465.50	541.55	19720.37	507.09	20969.98	476.87
1-Butanol	18416.36	543.00	19704.43	507.50	20925.33	477.89
1-Pentanol	18507.13	540.33	19727.35	506.91	20954.32	477.23
1-Propanol	18410.72	543.16	19703.98	507.51	20920.50	478.00
Acetic acid	18730.40	533.89	20326.82	491.96	-	-
Methanol	18351.76	544.91	19640.28	509.16	20827.80	480.13
2,2,2-Trifluoroethanol	18473.67	541.31	19653.40	508.82	-	-

Table 4.1.6. Summary of band maxima of 3 band fit using Gaussian model for normalised **21** emission spectra recorded at 400 nm excitation.

Solvent	Width Band 1 (cm^{-1})	Width Band 2 (cm^{-1})	Width Band 3 (cm^{-1})
Toluene	3098.09	1992.45	1006.27
1,4-Dioxane	3127.52	2071.55	1058.17
Chloroform	3285.42	2004.99	1056.76
Acetonitrile	3223.81	2239.36	1235.61
1-Octanol	3144.57	2108.47	1092.32
1-Hexanol	3250.16	2160.76	1116.15
1-Butanol	3136.49	2114.22	1162.77
1-Pentanol	3201.38	2117.10	1123.57
1-Propanol	3141.81	2113.99	1171.26
Acetic acid	3285.90	2145.14	-
Methanol	3174.62	2133.97	1262.70
2,2,2-Trifluoroethanol	4128.01	2421.13	-

Table 4.1.7. Summary of band width and band area of 3 band fit using Gaussian model for normalised **21** emission spectra recorded at 400 nm excitation.

Solvent	Area Band 1 (cm^{-1})	Area Band 2 (cm^{-1})	Area Band 3 (cm^{-1})	Area Ratio Band 1/2 (400 nm ex)	Area Ratio Band 1/3 (400 nm ex)	Area Ratio Band 2/3 (400 nm ex)
Toluene	1783.35	1544.35	345.77	1.15	5.16	4.47
1,4-Dioxane	1754.99	1642.93	349.11	1.07	5.03	4.71
Chloroform	2032.58	1399.54	374.53	1.45	5.43	3.74
Acetonitrile	1684.06	1826.37	407.17	0.92	4.14	4.49
1-Octanol	1720.50	1715.01	396.58	1.00	4.34	4.32
1-Hexanol	1665.22	1753.69	390.93	0.95	4.26	4.49
1-Butanol	1611.02	1758.70	456.17	0.92	3.53	3.86
1-Pentanol	1745.82	1688.38	410.64	1.03	4.25	4.11
1-Propanol	1599.03	1768.95	453.67	0.90	3.52	3.90
Acetic acid	2002.75	1748.01	-	1.15	-	-
Methanol	1554.32	1730.85	517.17	0.90	3.01	3.35
2,2,2-Trifluoroethanol	2135.88	1481.13	-	1.44	-	-

Solvent	Band 1 Area Percentage(%)	Band 2 Area Percentage (%)	Band 3 Area Percentage (%)
Toluene	48.55	42.04	9.41
1,4-Dioxane	46.84	43.85	9.32
Chloroform	53.40	36.77	9.84
Acetonitrile	42.99	46.62	10.39
1-Octanol	44.90	44.75	10.35
1-Hexanol	43.71	46.03	10.26
1-Butanol	42.11	45.97	11.92
1-Pentanol	45.41	43.91	10.68
1-Propanol	41.84	46.29	11.87
Acetic acid	53.40	46.60	-
Methanol	40.88	45.52	13.60
2,2,2-Trifluoroethanol	59.05	40.95	-

Table 4.1.8. Band areas, area ratios and total area percentage of 3 band fit using Gaussian model for normalised **21** emission spectra recorded at 400 nm excitation.

4.1.4 310 nm Gaussian band fit - Solvatochromic analysis.

4.1.4.1 E_T^N.

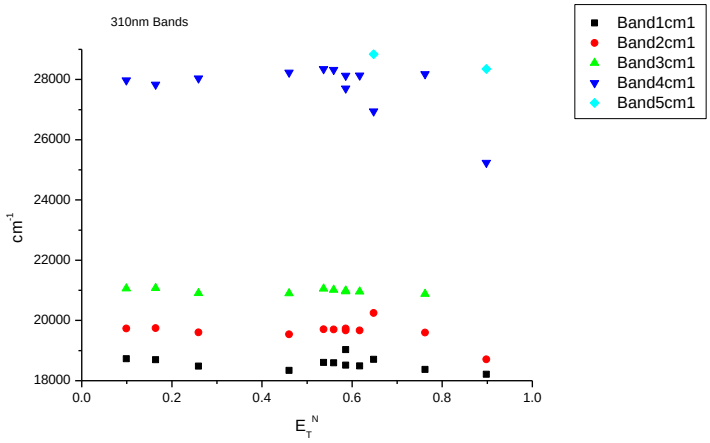

Figure 4.1.1. Band maxima from Gaussian model fit of the normalised fluorescence emission spectra of **21** recorded at 310 nm excitation against E_T^N.

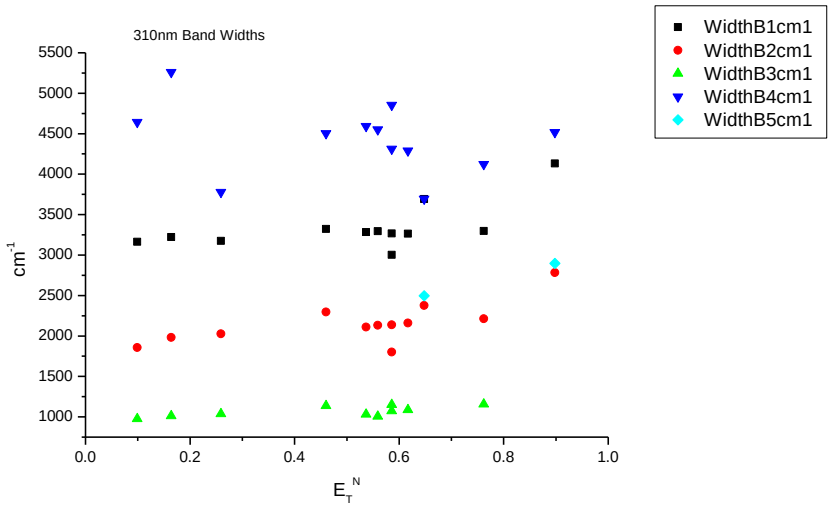

Figure 4.1.2. Band widths from Gaussian model fit of the normalised fluorescence emission spectra of **21** recorded at 310 nm excitation against E_T^N.

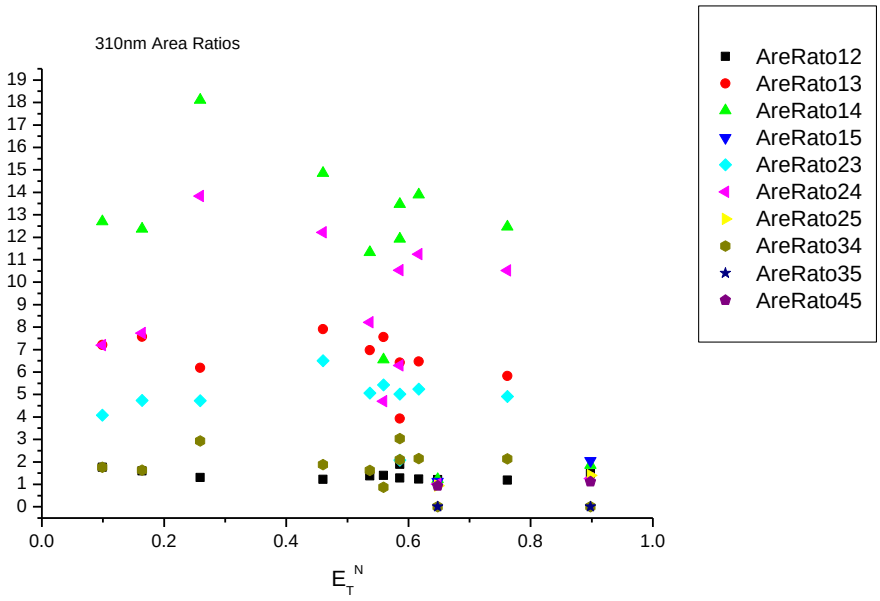

Figure 4.1.3. Area ratios from Gaussian model fit of the normalised fluorescence emission spectra of **21** recorded at 310 nm excitation against E_T^N.

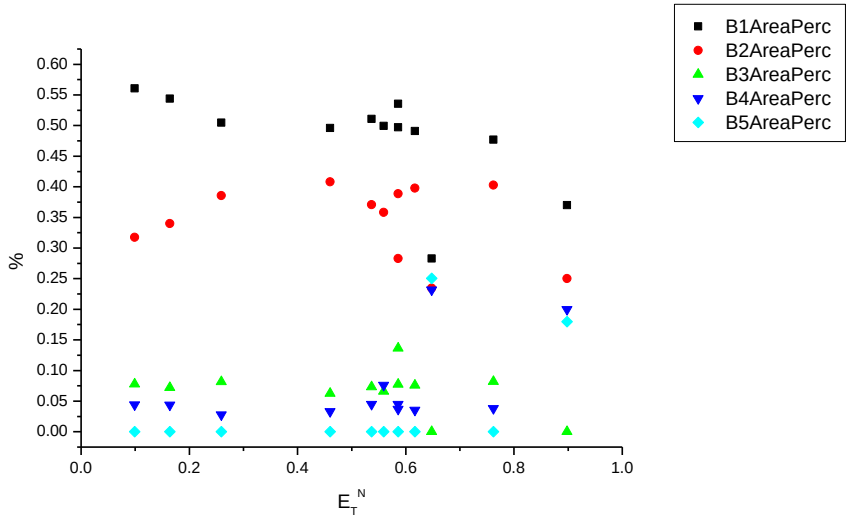

Figure 4.1.4. Area percentages from Gaussian model fit of the normalised fluorescence emission spectra of **21** recorded at 310 nm excitation against E_T^N.

4.1.4.2 α

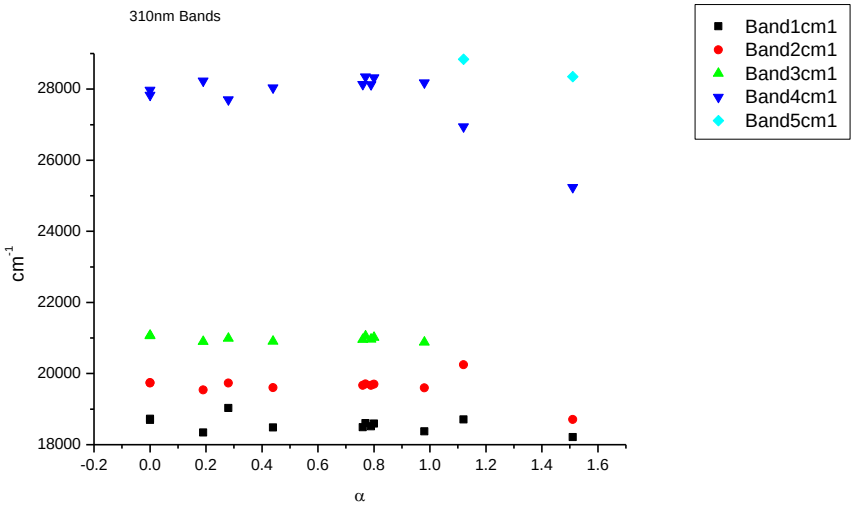

Figure 4.1.5. Band maxima from Gaussian model fit of the normalised fluorescence emission spectra of **21** recorded at 310 nm excitation against α.

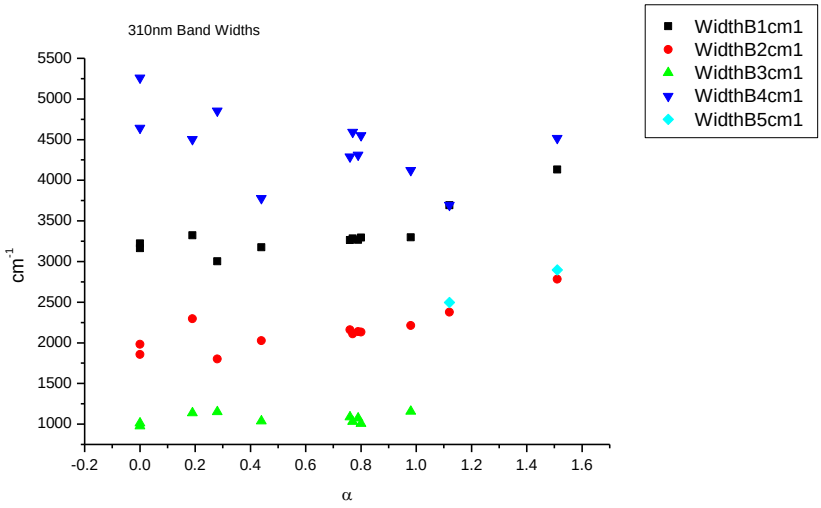

Figure 4.1.6. Band widths from Gaussian model fit of the normalised fluorescence emission spectra of **21** recorded at 310 nm excitation against α.

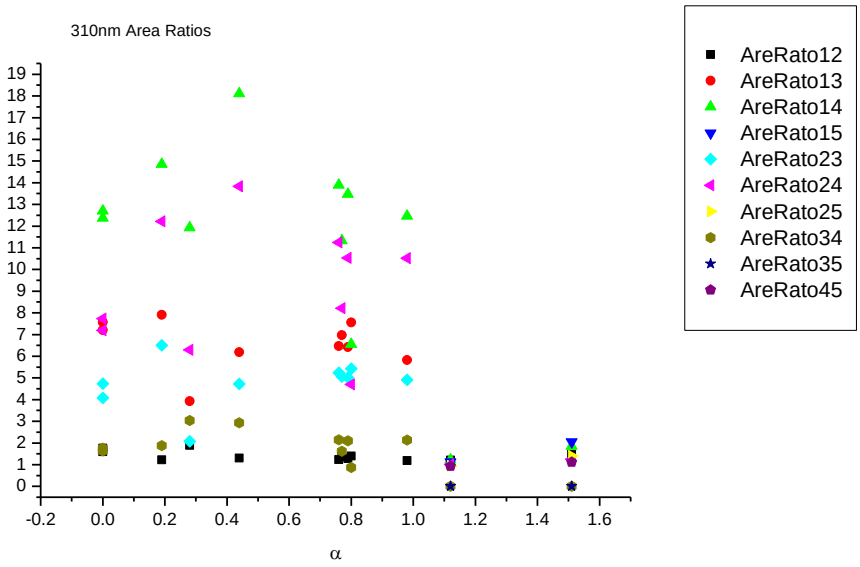

Figure 4.1.7. Area Ratios from Gaussian model fit of the normalised fluorescence emission spectra of **21** recorded at 310 nm excitation against α.

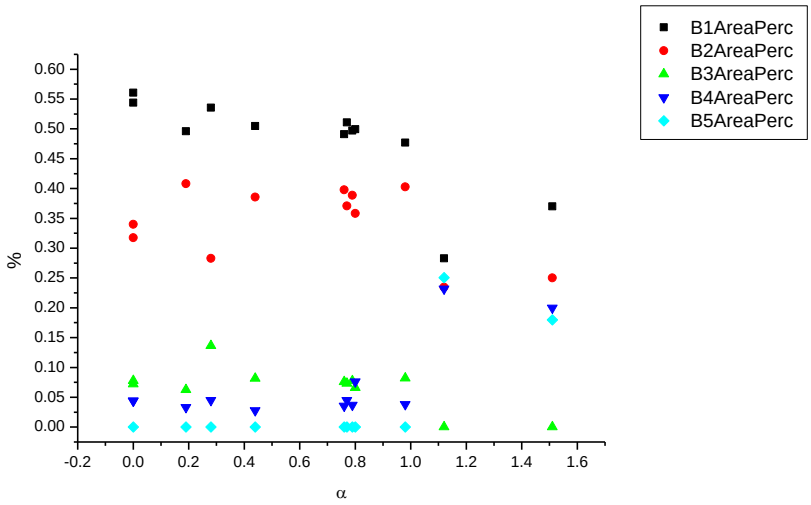

Figure 4.1.8. Area percentages from Gaussian model fit of the normalised fluorescence emission spectra of **21** recorded at 310 nm excitation against α.

4.1.4.3 β.

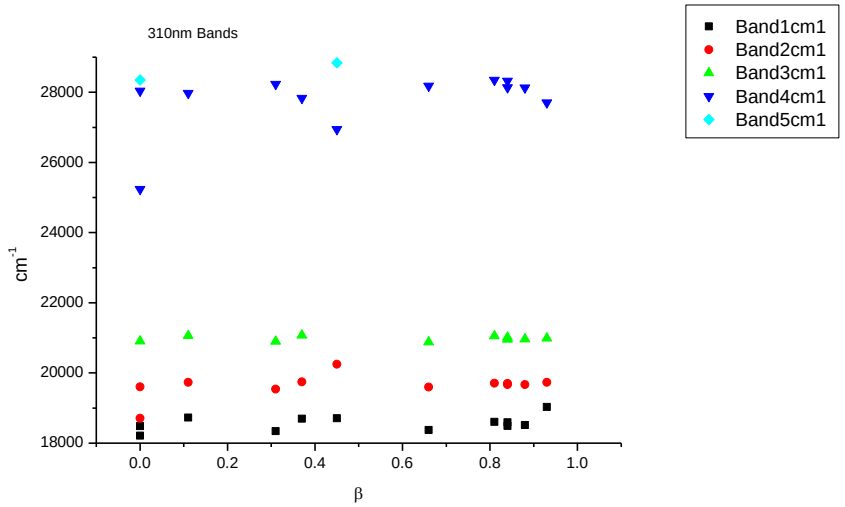

Figure 4.1.9. Band maxima from Gaussian model fit of the normalised fluorescence emission spectra of **21** recorded at 310 nm excitation against β.

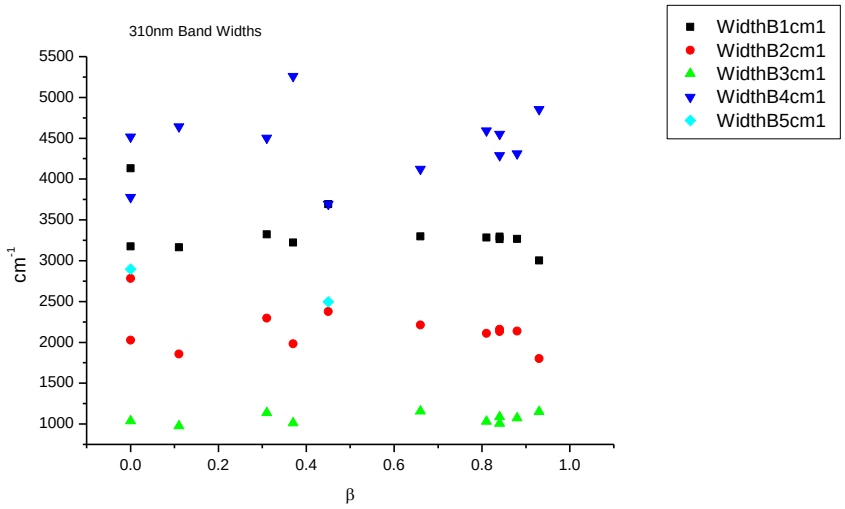

Figure 4.1.10. Band widths from Gaussian model fit of the normalised fluorescence emission spectra of **21** recorded at 310 nm excitation against β.

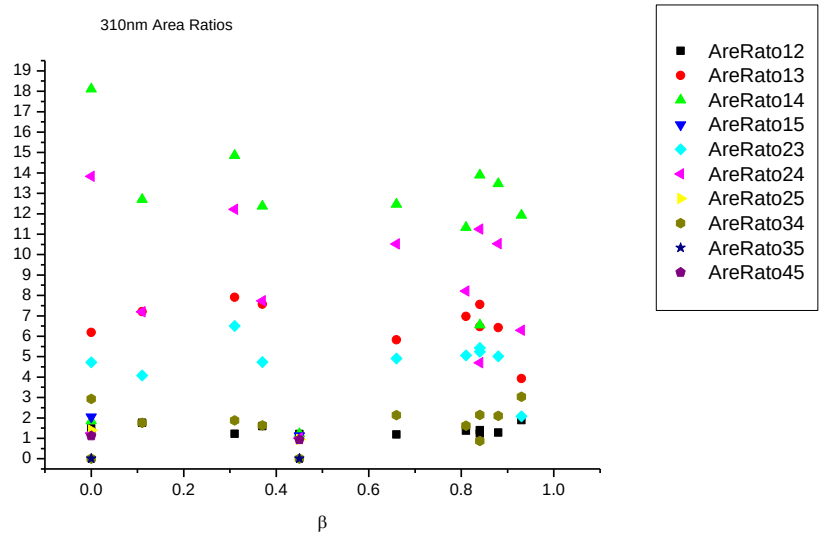

Figure 4.1.11. Area ratios from Gaussian model fit of the normalised fluorescence emission spectra of **21** recorded at 310 nm excitation against β.

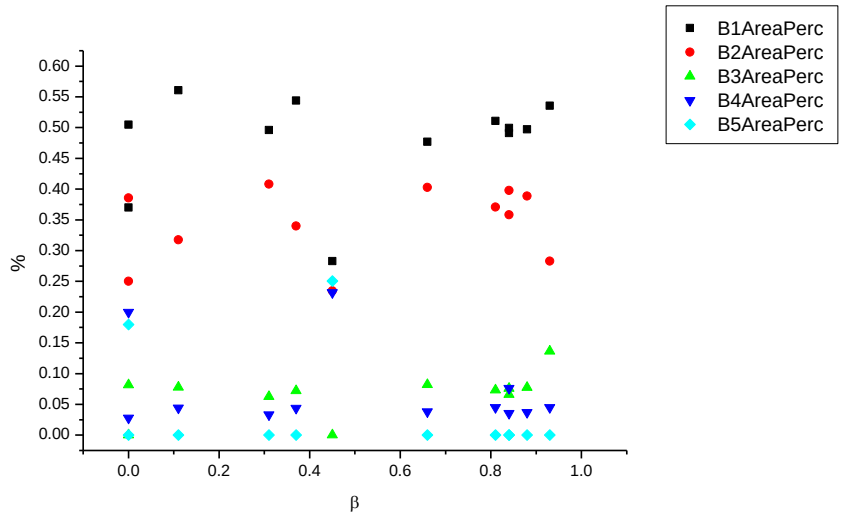

Figure 4.1.12. Area percentages from Gaussian model fit of the normalised fluorescence emission spectra of **21** recorded at 310 nm excitation against β.

4.1.4.4 π.*

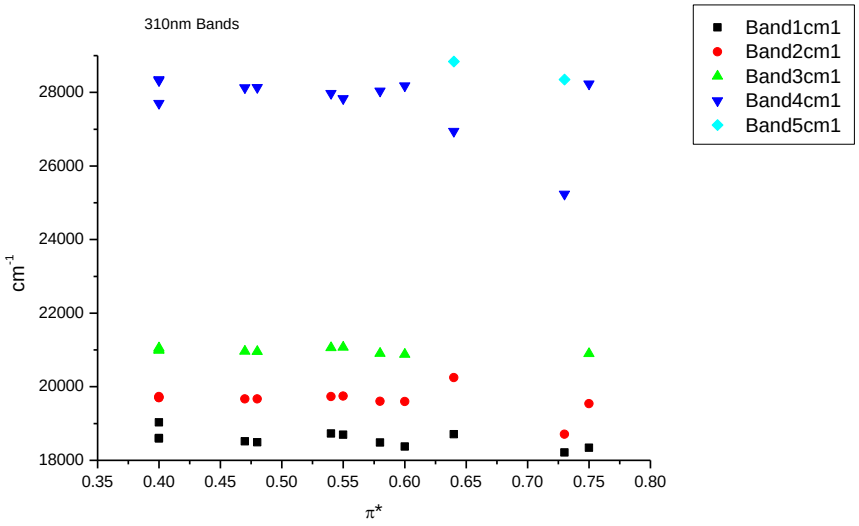

Figure 4.1.13. Band maxima from Gaussian model fit of the normalised fluorescence emission spectra of **21** recorded at 310 nm excitation against π*.

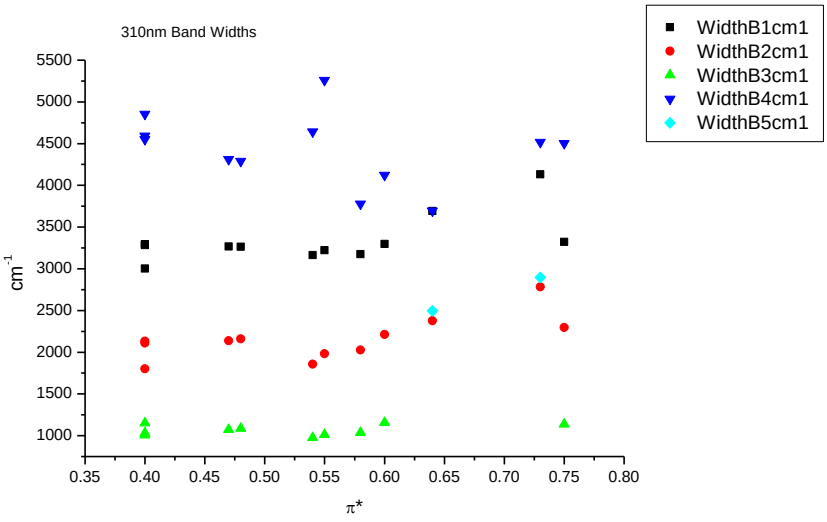

Figure 4.1.14. Band widths from Gaussian model fit of the normalised fluorescence emission spectra of **21** recorded at 310 nm excitation against π*.

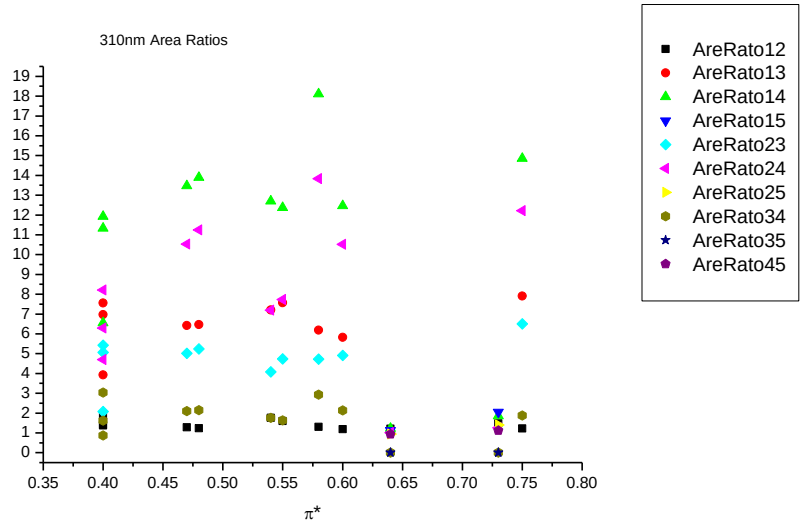

Figure 4.1.15. Area ratios from Gaussian model fit of the normalised fluorescence emission spectra of **21** recorded at 310 nm excitation against π*.

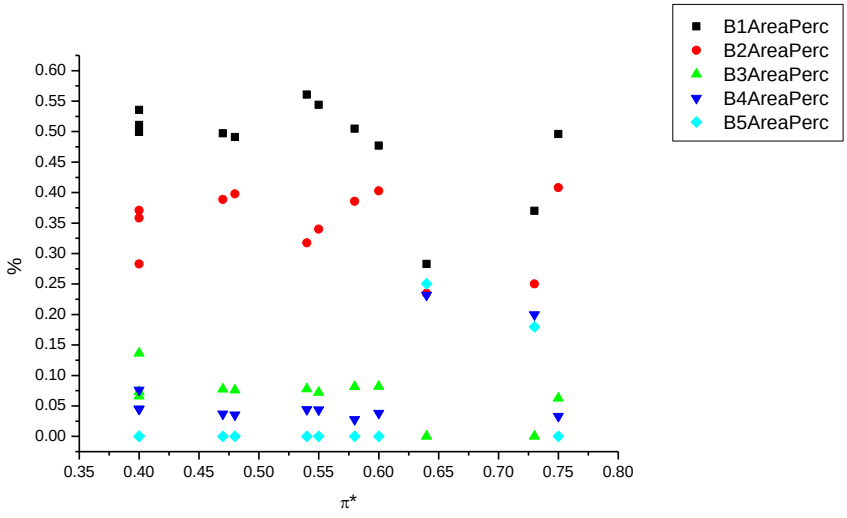

Figure 4.1.16. Area percentages from Gaussian model fit of the normalised fluorescence emission spectra of **21** recorded at 310 nm excitation against π*.

4.1.4.5 μ(D).

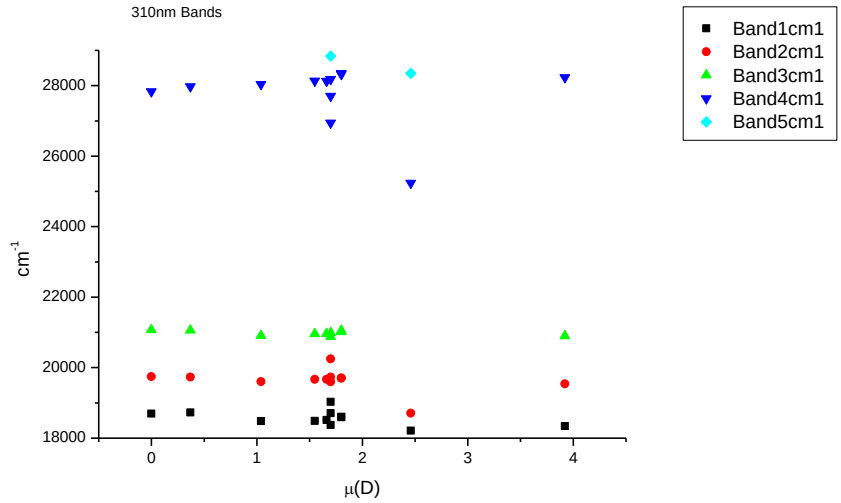

Figure 4.1.17. Band maxima from Gaussian model fit of the normalised fluorescence emission spectra of **21** recorded at 310 nm excitation against μ(D).

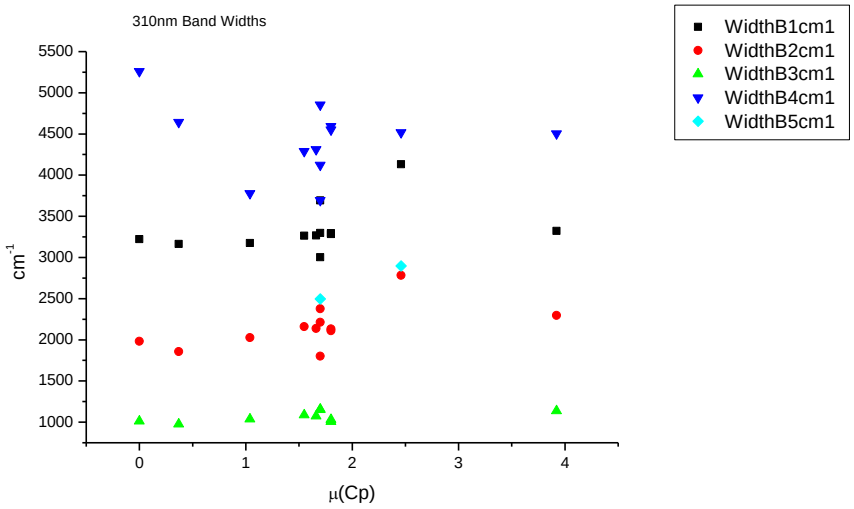

Figure 4.1.18. Band widths from Gaussian model fit of the normalised fluorescence emission spectra of **21** recorded at 310 nm excitation against μ(D).

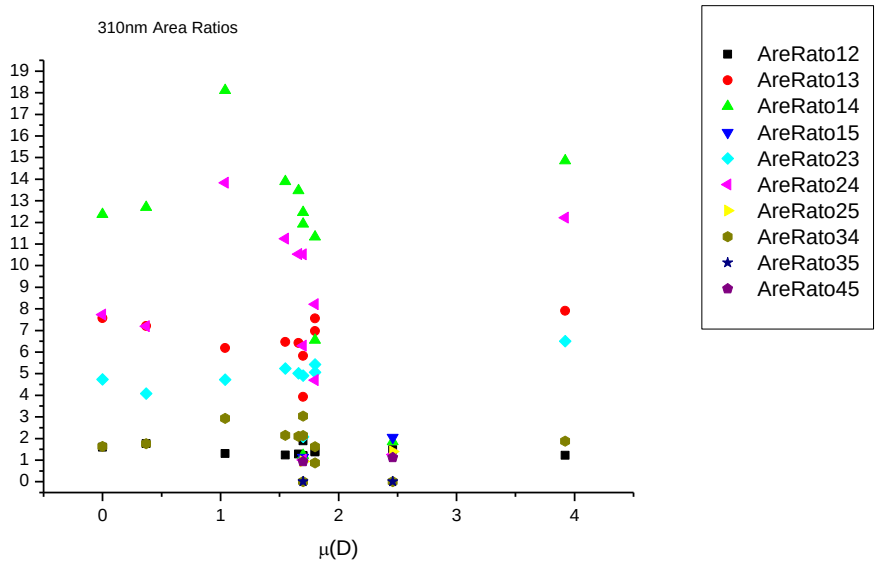

Figure 4.1.19. Area ratios from Gaussian model fit of the normalised fluorescence emission spectra of **21** recorded at 310 nm excitation against μ(D).

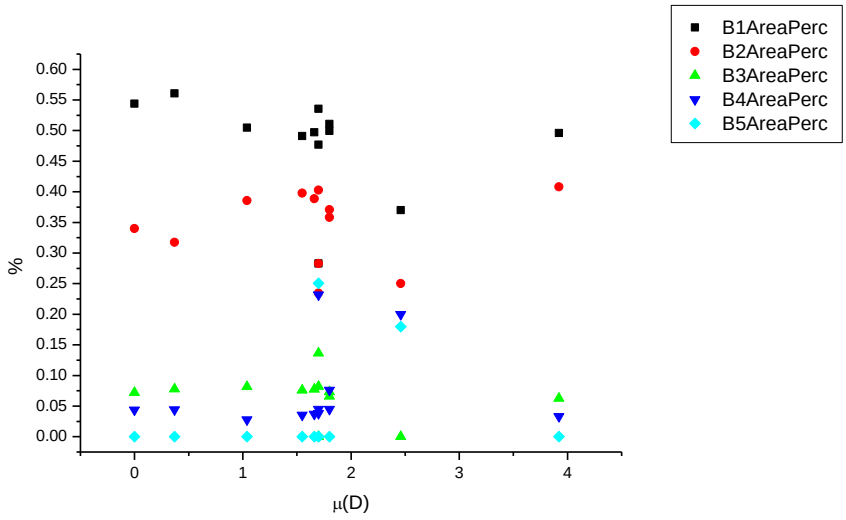

Figure 4.1.20. Area percentages from Gaussian model fit of the normalised fluorescence emission spectra of **21** recorded at 310 nm excitation against μ(D).

4.1.4.6 η(Cp).

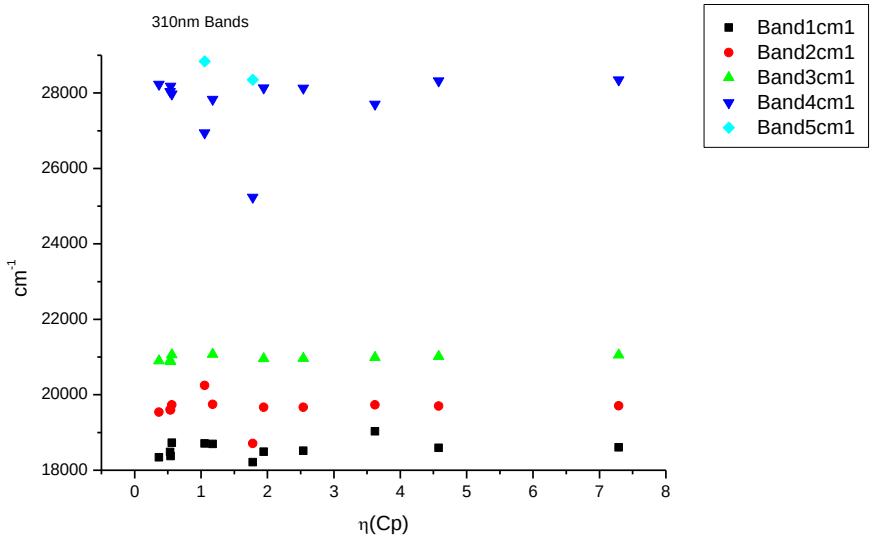

Figure 4.1.21. Band maxima from Gaussian model fit of the normalised fluorescence emission spectra of **21** recorded at 310 nm excitation against η(Cp).

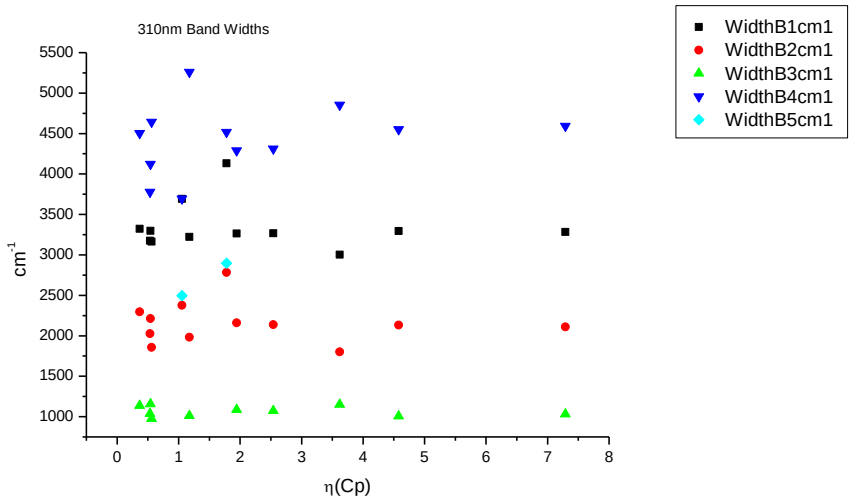

Figure 4.1.22. Band widths from Gaussian model fit of the normalised fluorescence emission spectra of **21** recorded at 310 nm excitation against η(Cp).

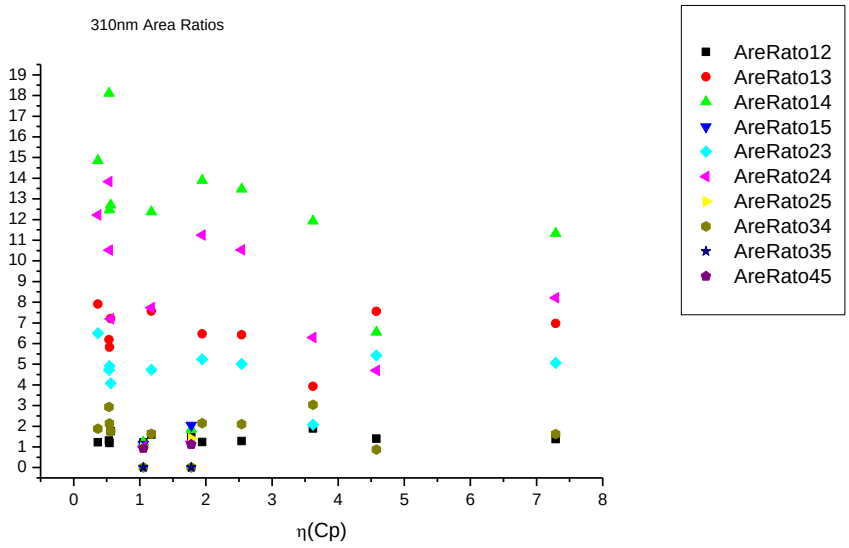

Figure 4.1.23. Area ratios from Gaussian model fit of the normalised fluorescence emission spectra of **21** recorded at 310 nm excitation against η(Cp).

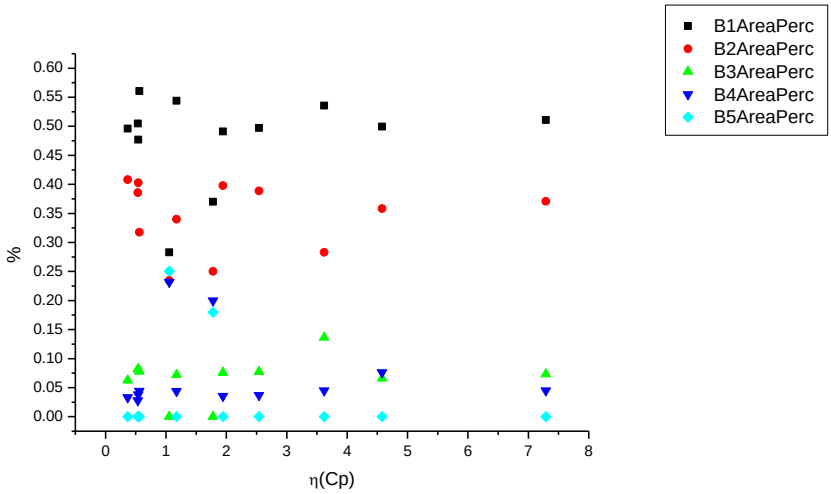

Figure 4.1.24. Area percentages from Gaussian model fit of the normalised fluorescence emission spectra of **21** recorded at 310 nm excitation against η(Cp).

4.1.5 400 nm Gaussian band fit - Solvatochromic analysis.

4.1.5.1 E_T^N.

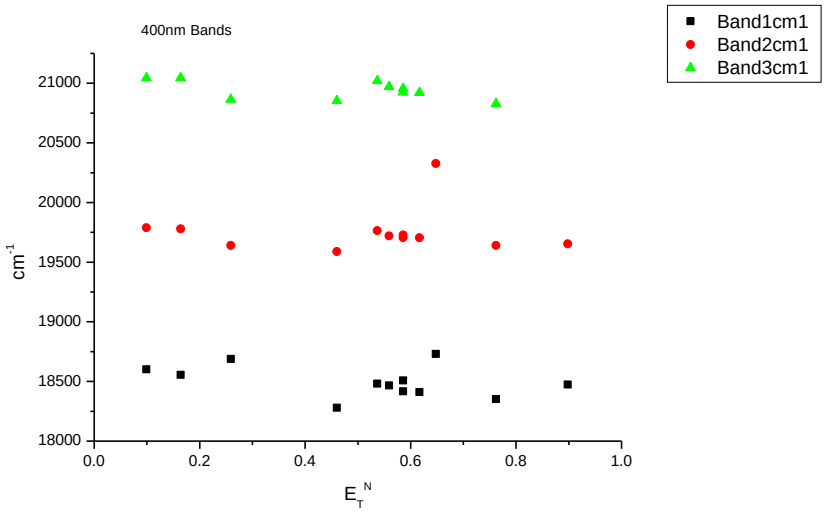

Figure 4.1.25. Band maxima from Gaussian model fit of the normalised fluorescence emission spectra of **21** recorded at 400 nm excitation against E_T^N.

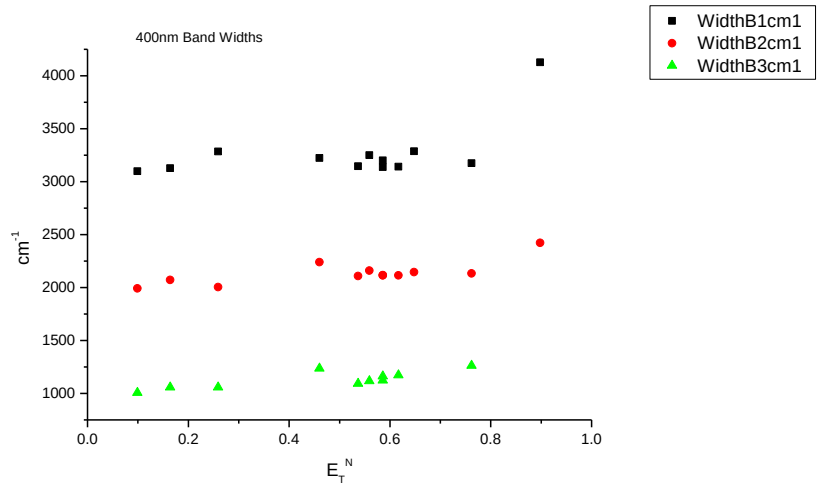

Figure 4.1.26. Band widths from Gaussian model fit of the normalised fluorescence emission spectra of **21** recorded at 400 nm excitation against E_T^N.

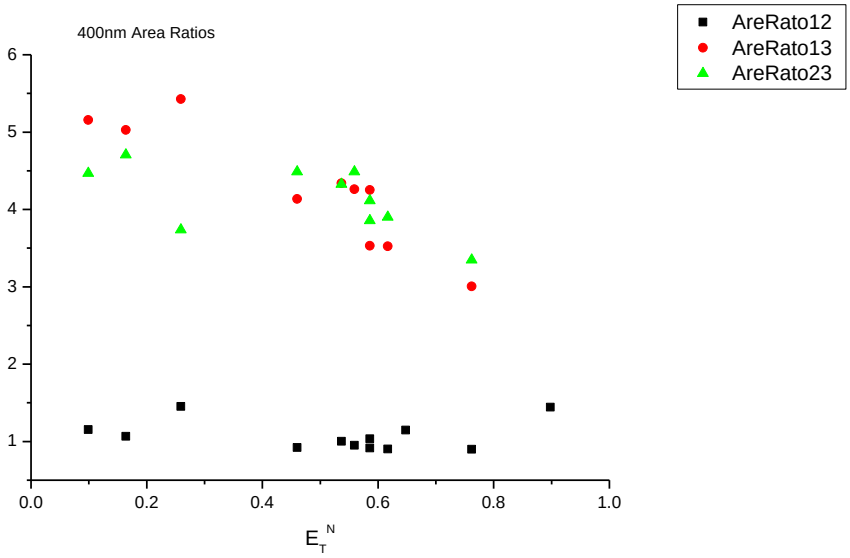

Figure 4.1.27. Area ratios from Gaussian model fit of the normalised fluorescence emission spectra of **21** recorded at 400 nm excitation against E_T^N.

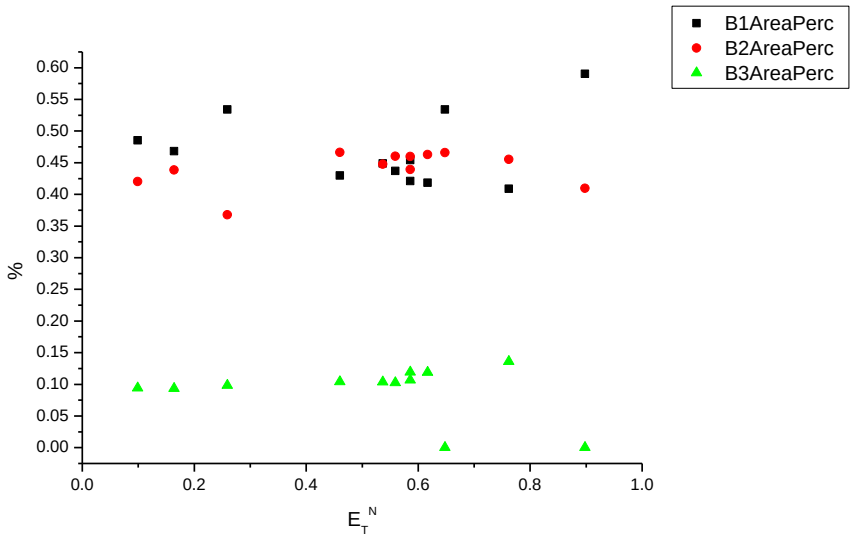

Figure 4.1.28. Area percentages from Gaussian model fit of the normalised fluorescence emission spectra of **21** recorded at 400 nm excitation against E_T^N.

4.1.5.2 α

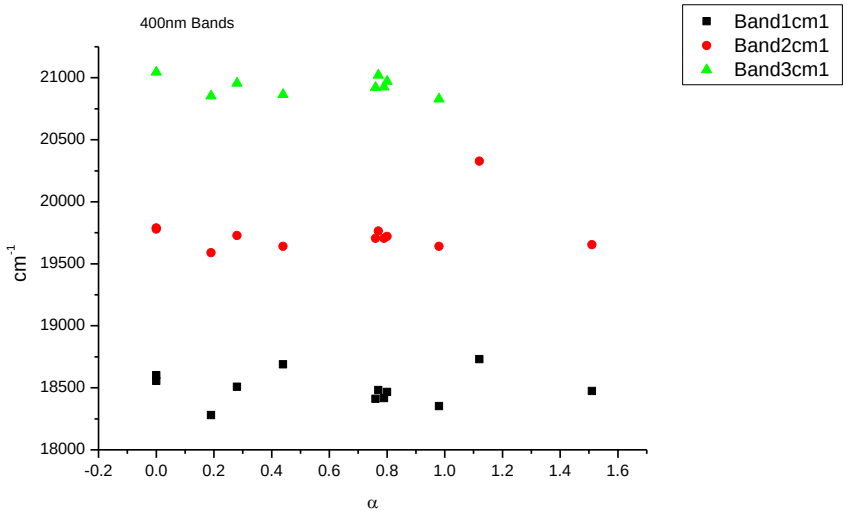

Figure 4.1.29. Band maxima from Gaussian model fit of the normalised fluorescence emission spectra of **21** recorded at 400 nm excitation against α.

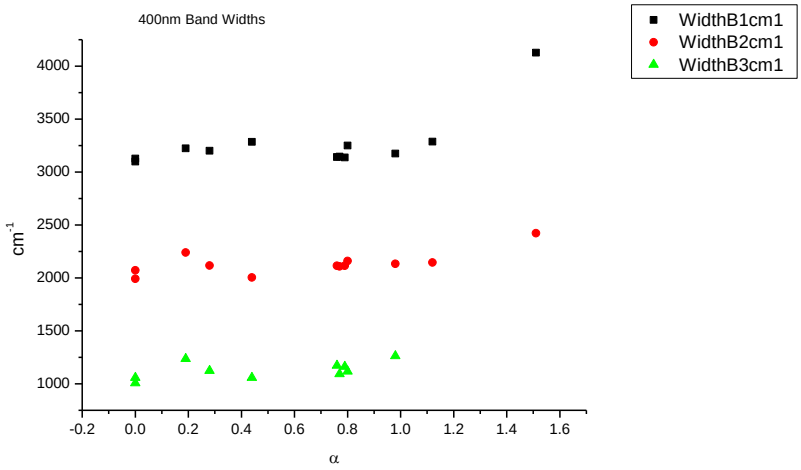

Figure 4.1.30. Band widths from Gaussian model fit of the normalised fluorescence emission spectra of **21** recorded at 400 nm excitation against α.

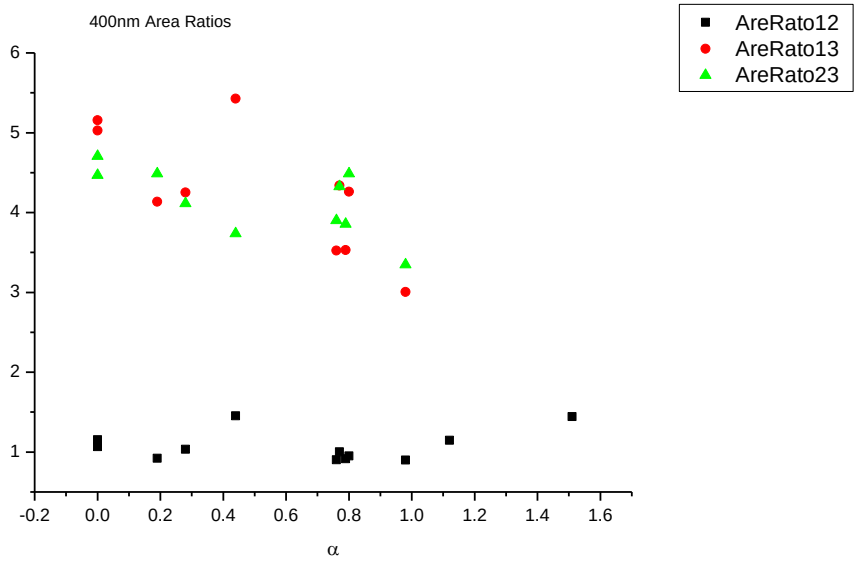

Figure 4.1.31. Area ratios from Gaussian model fit of the normalised fluorescence emission spectra of **21** recorded at 400 nm excitation against α.

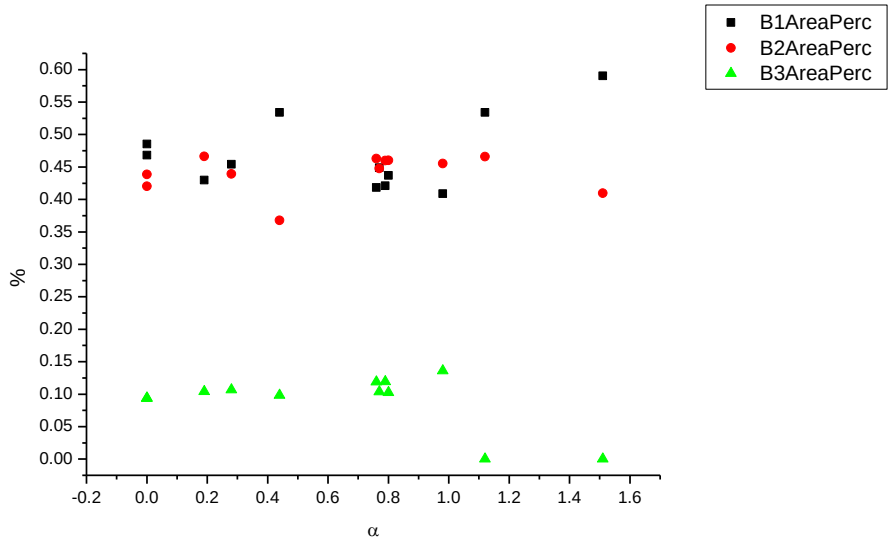

Figure 4.1.32. Area percentages from Gaussian model fit of the normalised fluorescence emission spectra of **21** recorded at 400 nm excitation against α.

4.1.5.3 β.

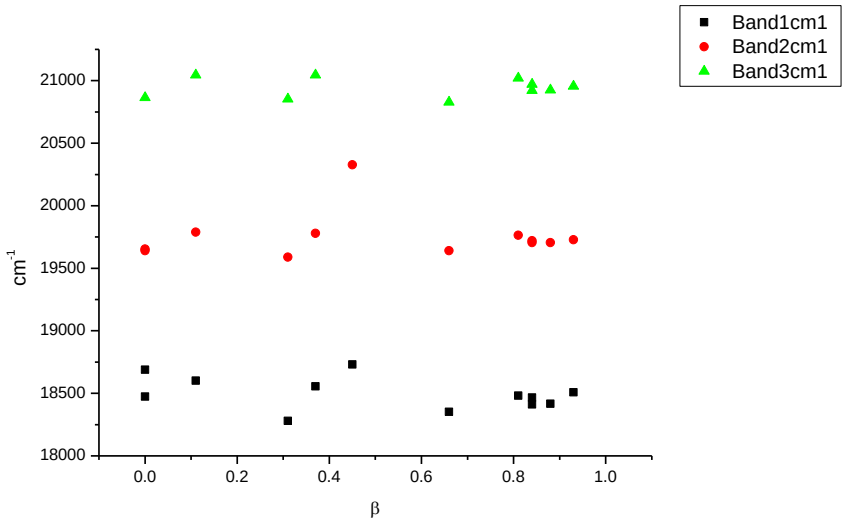

Figure 4.1.33. Band maxima from Gaussian model fit of the normalised fluorescence emission spectra of **21** recorded at 400 nm excitation against β.

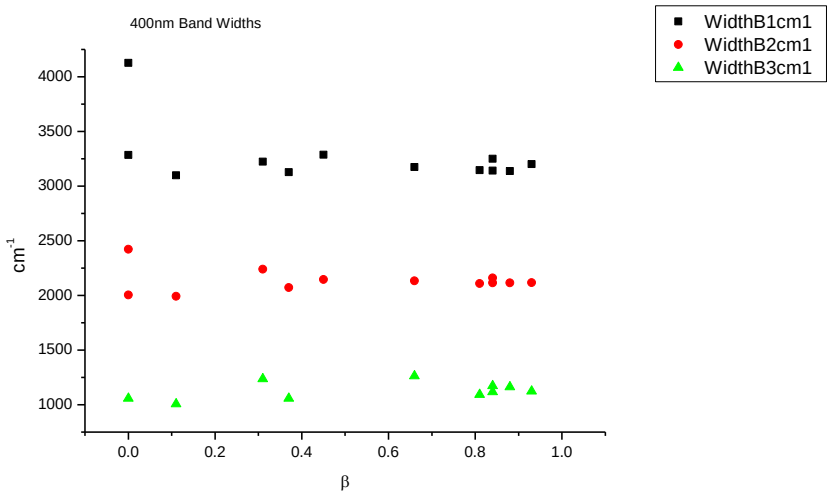

Figure 4.1.34. Band widths from Gaussian model fit of the normalised fluorescence emission spectra of **21** recorded at 400 nm excitation against β.

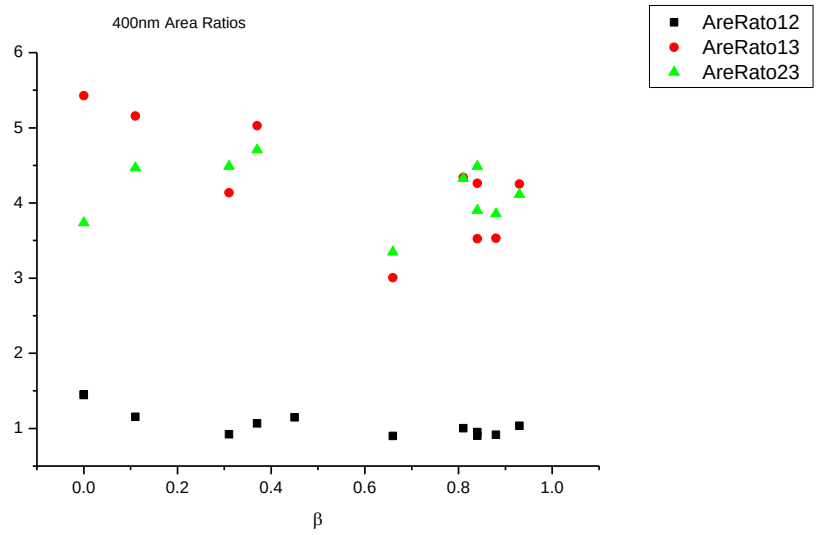

Figure 4.1.35. Area ratios from Gaussian model fit of the normalised fluorescence emission spectra of **21** recorded at 400 nm excitation against β.

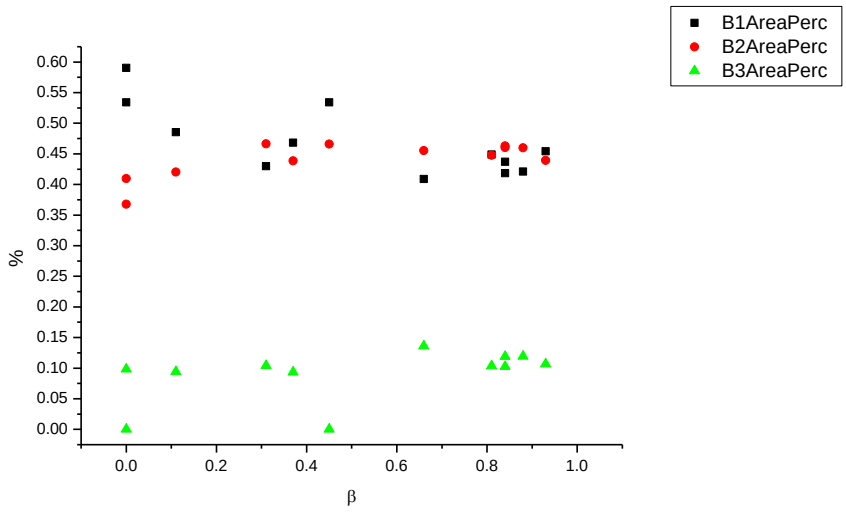

Figure 4.1.36. Area percentages from Gaussian model fit of the normalised fluorescence emission spectra of **21** recorded at 400 nm excitation against β.

4.1.5.4 π.*

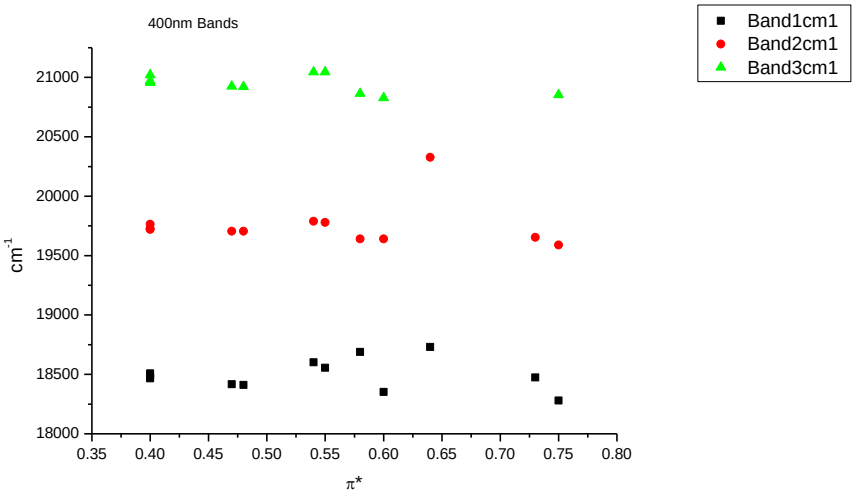

Figure 4.1.37. Band maxima from Gaussian model fit of the normalised fluorescence emission spectra of **21** recorded at 400 nm excitation against π*.

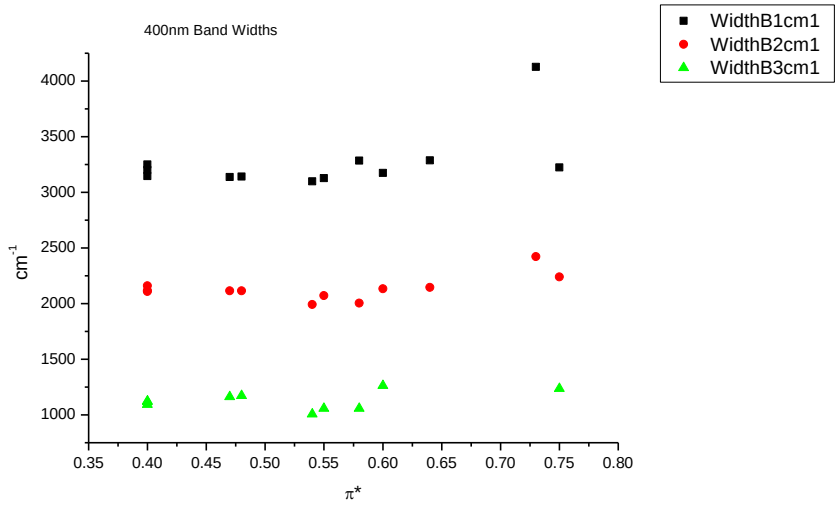

Figure 4.1.38. Band widths from Gaussian model fit of the normalised fluorescence emission spectra of **21** recorded at 400 nm excitation against π*.

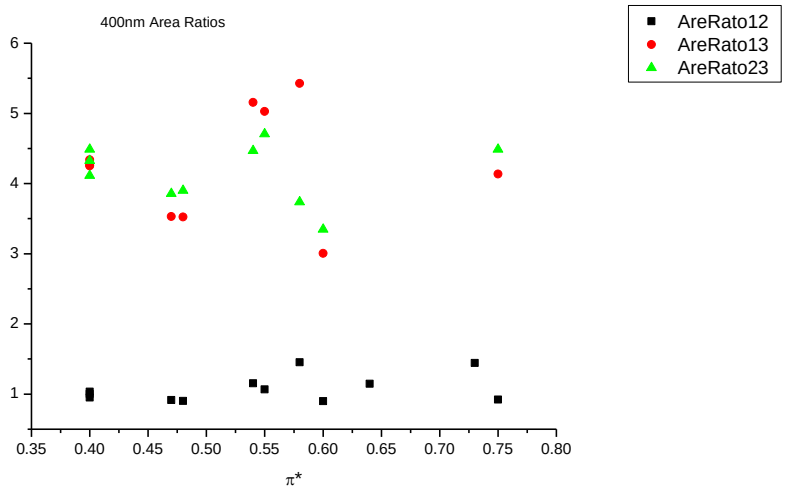

Figure 4.1.39. Area ratios from Gaussian model fit of the normalised fluorescence emission spectra of **21** recorded at 400 nm excitation against π*.

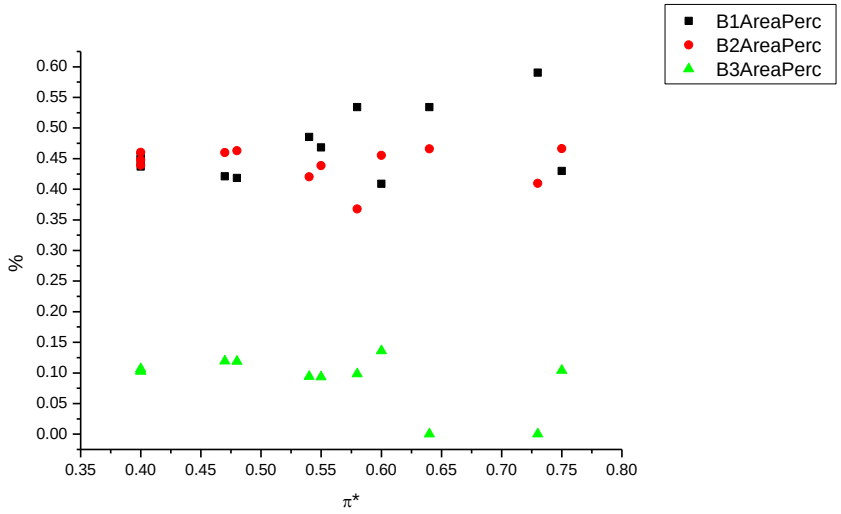

Figure 4.1.40. Area percentages from Gaussian model fit of the normalised fluorescence emission spectra of **21** recorded at 400 nm excitation against π*.

4.1.5.5 μ(D).

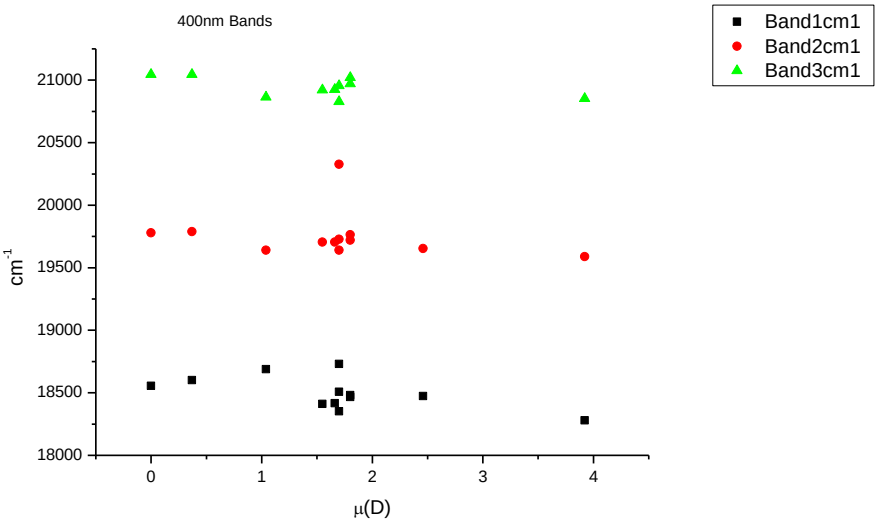

Figure 4.1.41. Band maxima from Gaussian model fit of the normalised fluorescence emission spectra of **21** recorded at 400 nm excitation against μ(D).

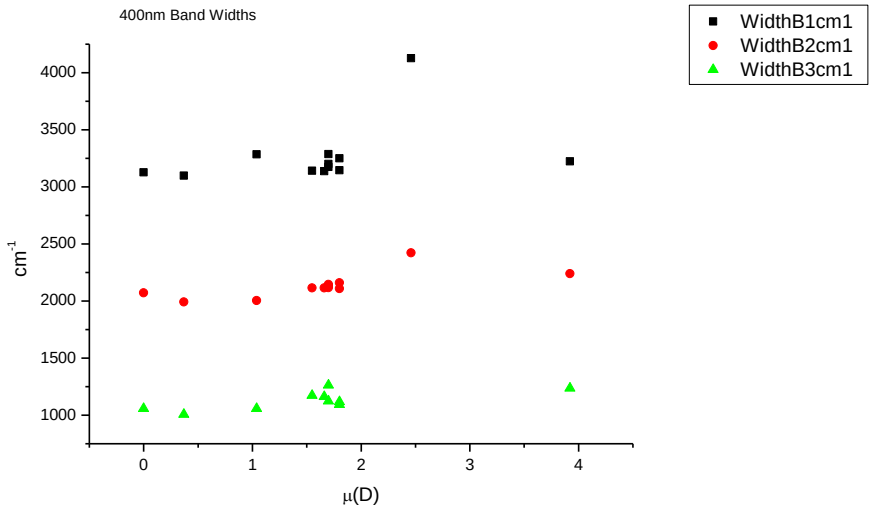

Figure 4.1.42. Band widths from Gaussian model fit of the normalised fluorescence emission spectra of **21** recorded at 400 nm excitation against μ(D).

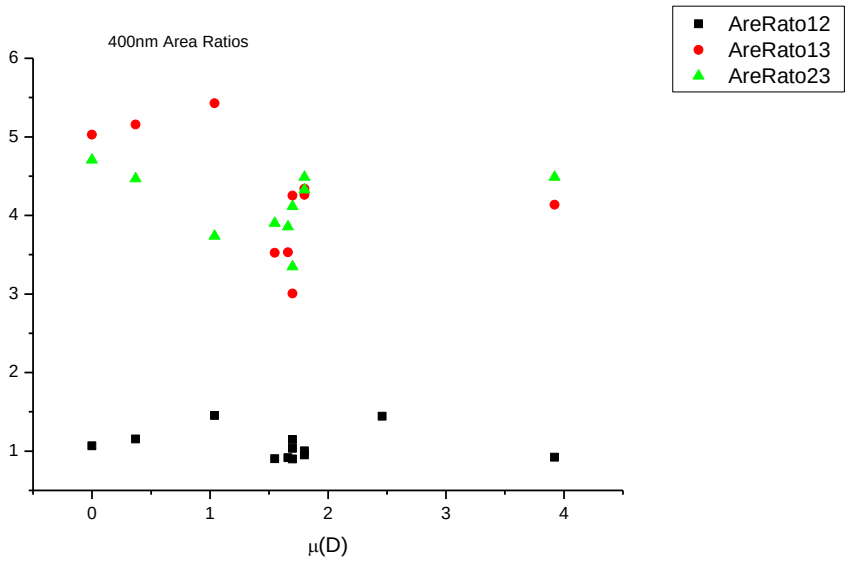

Figure 4.1.43. Area ratios from Gaussian model fit of the normalised fluorescence emission spectra of **21** recorded at 400 nm excitation against μ(D).

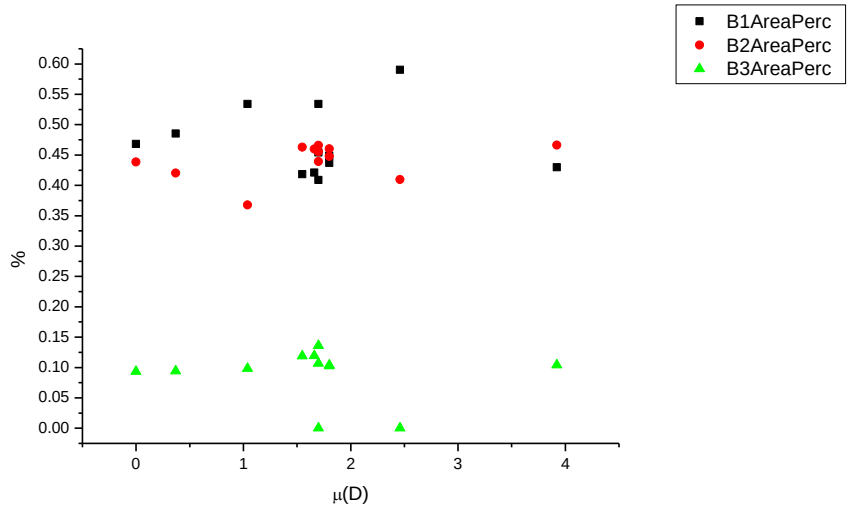

Figure 4.1.44. Area percentages from Gaussian model fit of the normalised fluorescence emission spectra of **21** recorded at 400 nm excitation against μ(D).

4.1.5.6 η(Cp).

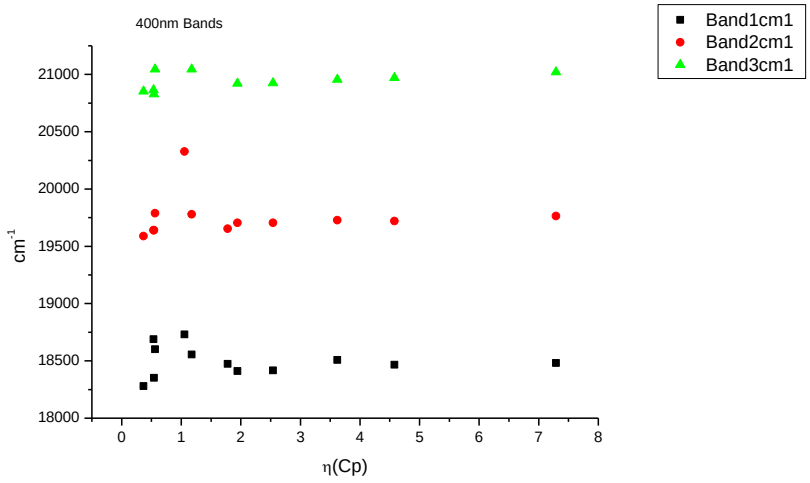

Figure 4.1.45. Band maxima from Gaussian model fit of the normalised fluorescence emission spectra of **21** recorded at 400 nm excitation against η(Cp).

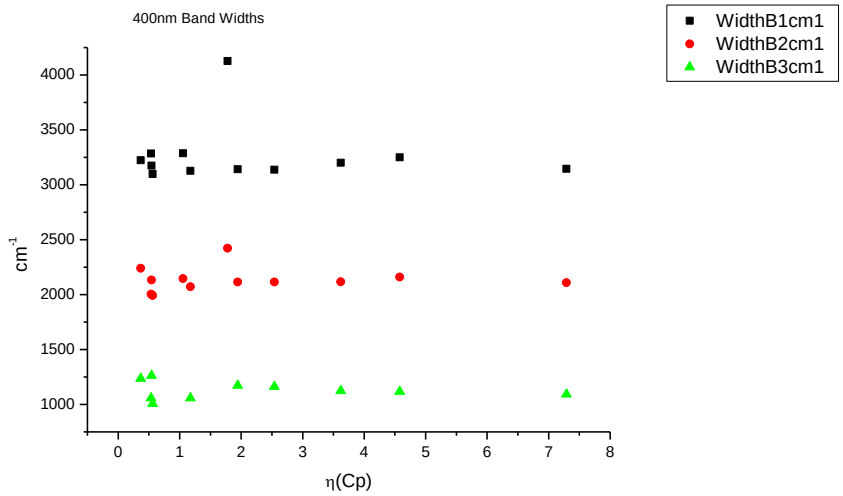

Figure 4.1.46. Band widths from Gaussian model fit of the normalised fluorescence emission spectra of **21** recorded at 400 nm excitation against η(Cp).

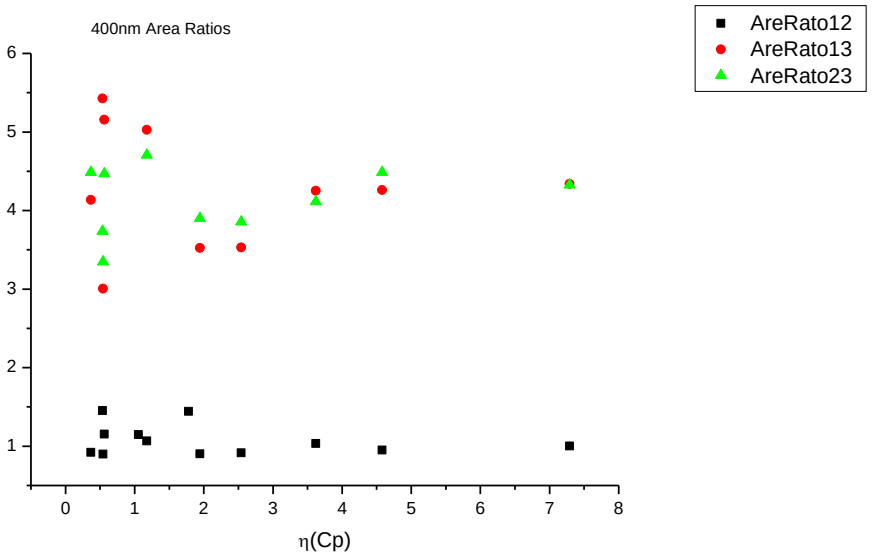

Figure 4.1.47. Area ratios from Gaussian model fit of the normalised fluorescence emission spectra of **21** recorded at 400 nm excitation against η(Cp).

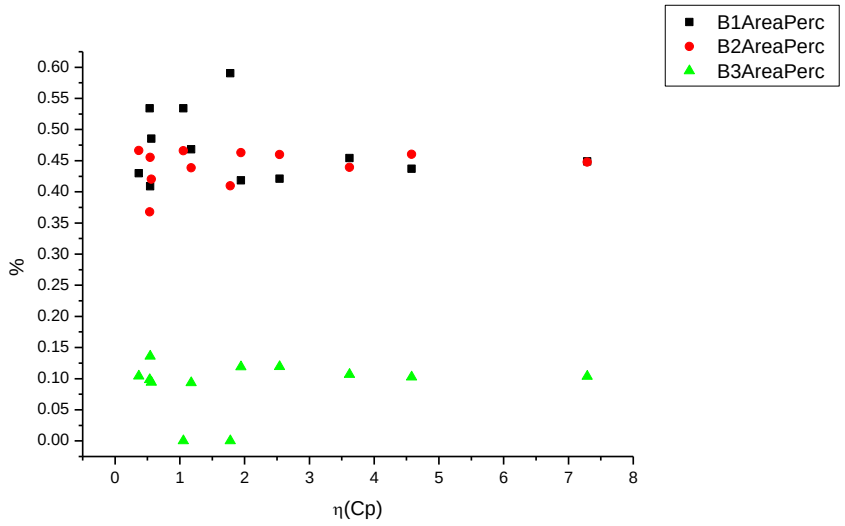

Figure 4.1.48. Area percentages from Gaussian model fit of the normalised fluorescence emission spectra of **21** recorded at 400 nm excitation against η(Cp).

4.1.6 400 nm fluorescent lifetime results.

4.1.6.1 Intensity weighted.

Wavelength (nm)	Solvent	τ_1 (ns)	A_1 (%)	τ_2 (ns)	A_2 (%)	τ_3 (ns)	A_3 (%)	τ_f (ns) (Intensity Weighted)	$1/\tau_f$	χ^2
470	Toluene	-	-	3.87	71.01	9.83	28.93	5.59	0.18	1.23
470	1,4-Dioxane	0.49	0.39	4.36	67.11	9.52	32.51	6.02	0.17	1.12
470	Chloroform	1.49	10.01	5.42	74.59	13.54	15.40	6.28	0.16	1.09
470	Acetonitrile	-	-	4.79	66.39	8.67	33.61	6.09	0.16	1.21
470	1-Octanol	0.25	8.41	5.06	58.00	9.40	33.58	6.11	0.16	1.23
470	1-Hexanol	0.41	5.79	5.54	80.78	12.35	13.43	6.16	0.16	1.12
470	1-Butanol	0.33	2.35	5.57	79.59	9.92	18.06	6.23	0.16	1.10
470	1-Pentanol	0.33	2.56	4.78	40.44	7.34	57.00	6.13	0.16	1.08
470	1-Propanol	0.33	2.19	5.35	71.05	8.33	26.76	6.04	0.17	1.10
470	Acetic acid	0.31	20.39	1.63	76.51	4.98	3.10	1.47	0.68	1.07
470	Methanol	0.17	5.05	4.68	71.91	7.12	23.04	5.01	0.20	1.23
470	2,2,2-Trifluoroethanol	0.24	82.80	1.07	13.46	7.15	3.74	0.61	1.64	1.29

Table 4.1.9. Summary of Time Correlated Single Photon Counting (TCSPC) fluorescent lifetimes (intensity weighted) of **21** recorded at 470 nm.

Wavelength (nm)	Solvent	τ_1 (ns)	A_1 (%)	τ_2 (ns)	A_2 (%)	τ_3 (ns)	A_3 (%)	τ_f (ns) (Intensity Weighted)	$1/\tau_f$	χ^2
490	Toluene	-	-	3.79	58.68	9.54	41.32	6.17	0.16	1.21
490	1,4-Dioxane	0.24	0.70	4.47	62.24	10.53	37.06	6.68	0.15	1.14
490	Chloroform	0.57	1.54	4.72	57.21	9.72	41.25	6.72	0.15	1.18
490	Acetonitrile	-	-	5.03	69.83	10.10	30.17	5.93	0.17	1.18
490	1-Octanol	0.24	5.46	5.35	60.49	10.82	34.04	6.93	0.14	1.25
490	1-Hexanol	0.38	5.34	5.55	73.63	11.82	21.03	6.59	0.15	1.18
490	1-Butanol	0.29	1.10	5.54	73.84	10.17	25.06	6.64	0.15	1.22
490	1-Pentanol	0.26	1.35	5.58	75.90	11.25	22.74	6.80	0.15	1.08
490	1-Propanol	0.37	1.30	5.69	85.39	13.14	13.30	6.61	0.15	1.12
490	Acetic acid	0.29	16.60	1.70	81.40	5.87	2.00	1.55	0.64	1.17
490	Methanol	0.18	4.90	4.95	81.56	9.52	13.55	5.34	0.19	1.15
490	2,2,2-Trifluoroethanol	0.26	66.69	0.84	30.79	5.63	2.52	0.58	1.74	1.11

Table 4.1.10. Summary of Time Correlated Single Photon Counting (TCSPC) fluorescent lifetimes (intensity weighted) of **21** recorded at 490 nm.

Wavelength (nm)	Solvent	τ_1 (ns)	A_1 (%)	τ_2 (ns)	A_2 (%)	τ_3 (ns)	A_3 (%)	τ_f (ns) (Intensity Weighted)	$1/\tau_f$	χ^2
520	Toluene	-	-	3.70	29.99	9.70	70.01	7.90	0.13	1.15
520	1,4-Dioxane	-	-	4.44	35.61	11.21	64.39	8.80	0.11	1.13
520	Chloroform	0.29	0.66	4.88	39.29	11.46	60.05	8.80	0.11	1.04
520	Acetonitrile	-	-	5.39	58.31	13.65	41.69	8.83	0.11	1.19
520	1-Octanol	0.22	3.11	5.60	43.68	12.49	53.21	9.10	0.11	1.16
520	1-Hexanol	0.33	2.11	5.46	50.36	12.65	47.53	8.77	0.11	1.12
520	1-Butanol	-	-	5.53	57.03	12.08	42.97	8.35	0.12	1.13
520	1-Pentanol	-	-	5.57	55.20	12.68	44.80	8.75	0.11	1.15
520	1-Propanol	4.93	39.49	8.50	46.59	19.77	13.92	1.13	0.89	1.13
520	Acetic acid	0.19	23.77	1.69	73.49	4.72	2.75	1.41	0.71	1.02
520	Methanol	0.15	4.48	5.05	73.08	12.60	22.45	6.53	0.15	1.26
520	2,2,2-Trifluoroethanol	0.24	65.53	0.86	30.78	5.07	3.69	0.61	1.63	1.10

Table 4.1.11. Summary of Time Correlated Single Photon Counting (TCSPC) fluorescent lifetimes (intensity weighted) of **21** recorded at 520 nm.

Wavelength (nm)	Solvent	τ_1 (ns)	A_1 (%)	τ_2 (ns)	A_2 (%)	τ_3 (ns)	A_3 (%)	τ_f (ns) (Intensity Weighted)	$1/\tau_f$	χ^2
540	Toluene	-	-	3.71	22.13	9.73	77.87	8.40	0.12	1.17
540	1,4-Dioxane	-	-	4.51	27.20	11.38	72.80	9.51	0.11	1.14
540	Chloroform	0.25	0.48	4.95	30.70	11.67	68.82	9.55	0.10	1.05
540	Acetonitrile	-	-	5.38	44.60	13.62	55.40	9.95	0.10	1.15
540	1-Octanol	0.20	2.64	5.61	33.54	12.64	63.82	9.95	0.10	1.18
540	1-Hexanol	0.31	1.90	5.57	42.30	13.26	55.80	9.76	0.10	1.15
540	1-Butanol	-	-	5.58	48.80	12.77	51.20	9.26	0.11	1.23
540	1-Pentanol	-	-	5.66	46.44	13.17	53.56	9.68	0.10	1.08
540	1-Propanol	-	-	5.53	52.71	12.80	47.29	8.97	0.11	1.22
540	Acetic acid	0.16	29.96	1.61	63.10	3.23	6.94	1.29	0.78	1.08
540	Methanol	0.15	4.44	5.05	65.35	13.07	30.21	7.26	0.14	1.23
540	2,2,2-Trifluoroethanol	0.24	65.03	0.85	30.02	4.34	4.95	0.63	1.60	1.16

Table 4.1.12. Summary of Time Correlated Single Photon Counting (TCSPC) fluorescent lifetimes (intensity weighted) of **21** recorded at 540 nm.

Wavelength (nm)	Solvent	τ_1 (ns)	A_1 (%)	τ_2 (ns)	A_2 (%)	τ_3 (ns)	A_3 (%)	τ_f (ns) (Intensity Weighted)	$1/\tau_f$	χ^2
570	Toluene	-	-	3.74	10.86	9.81	89.14	9.15	0.11	1.24
570	1,4-Dioxane	-	-	4.56	15.59	11.61	84.41	9.36	0.11	1.14
570	Chloroform	0.34	0.23	5.07	19.52	11.95	80.24	10.58	0.09	1.22
570	Acetonitrile	-	-	5.38	30.00	13.69	70.00	11.20	0.09	1.18
570	1-Octanol	0.22	2.07	5.89	24.41	13.02	73.52	11.02	0.09	1.16
570	1-Hexanol	0.31	1.78	5.33	25.83	12.91	72.39	10.73	0.09	1.15
570	1-Butanol	-	-	5.67	38.60	13.37	61.40	10.40	0.10	1.14
570	1-Pentanol	-	-	5.90	35.05	13.48	64.95	10.82	0.09	1.27
570	1-Propanol	-	-	5.36	38.07	12.74	61.93	9.93	0.10	1.13
570	Acetic acid	0.19	39.10	1.63	55.95	3.83	4.96	1.18	0.85	0.89
570	Methanol	0.17	2.77	4.97	55.66	13.24	41.47	8.27	0.12	1.14
570	2,2,2-Trifluoroethanol	0.23	66.68	0.85	26.50	4.34	6.83	0.68	1.48	1.13

Table 4.1.13. Summary of Time Correlated Single Photon Counting (TCSPC) fluorescent lifetimes (intensity weighted) of **21** recorded at 570 nm.

4.1.6.2 Amplitude weighted.

Wavelength (nm)	Solvent	τ_1 (ns)	A_1 (%)	τ_2 (ns)	A_2 (%)	τ_3 (ns)	A_3 (%)	τ_f (ns) (Amplitude Weighted)	$1/\tau_f$	χ^2
470	Toluene	-	-	3.87	86.18	9.83	13.82	4.69	0.21	1.23
470	1,4-Dioxane	0.49	4.02	4.36	78.55	9.52	27.43	5.10	0.20	1.12
470	Chloroform	1.49	31.11	5.42	63.63	13.54	5.26	4.62	0.22	1.09
470	Acetonitrile	-	-	4.79	78.15	8.67	21.85	5.63	0.18	1.21
470	1-Octanol	0.25	68.98	5.06	23.66	9.40	7.37	2.06	0.48	1.23
470	1-Hexanol	0.41	47.68	5.54	48.69	12.35	3.63	3.34	0.30	1.12
470	1-Butanol	0.33	30.87	5.57	61.32	9.92	7.81	4.29	0.23	1.10
470	1-Pentanol	0.33	33.03	4.78	34.91	7.34	32.07	4.13	0.24	1.08
470	1-Propanol	0.33	28.77	5.35	57.34	8.33	13.89	4.32	0.23	1.10
470	Acetic acid	0.31	57.99	1.63	41.46	4.98	0.55	0.89	1.13	1.07
470	Methanol	0.17	61.98	4.68	31.41	7.12	6.61	2.04	0.49	1.23
470	2,2,2-Trifluoroethanol	0.24	96.35	1.07	3.51	7.15	0.15	0.28	3.58	1.29

Table 4.1.14. Summary of Time Correlated Single Photon Counting (TCSPC) fluorescent lifetimes (amplitude weighted) of **21** recorded at 470 nm.

Wavelength (nm)	Solvent	τ_1 (ns)	A_1 (%)	τ_2 (ns)	A_2 (%)	τ_3 (ns)	A_3 (%)	τ_f (ns) (Amplitude Weighted)	$1/\tau_f$	χ^2
490	Toluene	-	-	3.79	78.16	9.54	21.84	5.05	0.20	1.21
490	1,4-Dioxane	0.24	14.30	4.47	68.43	10.53	17.28	4.91	0.20	1.14
490	Chloroform	0.57	14.21	4.72	63.54	9.72	22.25	5.24	0.19	1.18
490	Acetonitrile	-	-	5.03	82.29	10.10	17.71	5.93	0.17	1.18
490	1-Octanol	0.24	61.20	5.35	30.35	10.82	8.45	2.69	0.37	1.25
490	1-Hexanol	0.38	48.36	5.55	45.54	11.82	6.10	3.43	0.29	1.18
490	1-Butanol	0.29	19.20	5.54	68.20	10.17	12.60	5.12	0.20	1.22
490	1-Pentanol	0.26	25.22	5.58	65.11	11.25	9.67	4.78	0.21	1.08
490	1-Propanol	0.37	17.84	5.69	76.97	13.14	5.19	5.13	0.20	1.12
490	Acetic acid	0.29	53.95	1.70	45.73	5.87	0.33	0.96	1.05	1.17
490	Methanol	0.18	60.95	4.95	35.95	9.52	3.10	2.18	0.46	1.15
490	2,2,2-Trifluoroethanol	0.26	87.41	0.84	12.44	5.63	0.15	0.34	2.93	1.11

Table 4.1.15. Summary of Time Correlated Single Photon Counting (TCSPC) fluorescent lifetimes (amplitude weighted) of **21** recorded at 490 nm.

Wavelength (nm)	Solvent	τ_1 (ns)	A_1 (%)	τ_2 (ns)	A_2 (%)	τ_3 (ns)	A_3 (%)	τ_f (ns) (Amplitude Weighted)	$1/\tau_f$	χ^2
520	Toluene	-	-	3.70	52.90	9.70	47.10	6.53	0.15	1.15
520	1,4-Dioxane	-	-	4.44	58.28	11.21	41.72	7.26	0.14	1.13
520	Chloroform	0.29	14.78	4.88	51.61	11.46	33.61	6.41	0.16	1.04
520	Acetonitrile	-	-	5.39	78.00	13.65	22.00	7.20	0.14	1.19
520	1-Octanol	0.22	54.38	5.60	29.52	12.49	16.11	3.78	0.26	1.16
520	1-Hexanol	0.33	32.69	5.46	47.84	12.65	19.48	5.18	0.19	1.12
520	1-Butanol	-	-	5.53	74.37	12.08	25.63	7.21	0.14	1.13
520	1-Pentanol	-	-	5.57	73.73	12.68	26.27	7.44	0.13	1.15
520	1-Propanol	4.93	56.44	8.50	38.61	19.77	4.96	7.04	0.14	1.13
520	Acetic acid	0.19	73.46	1.69	26.19	4.72	0.35	0.60	1.67	1.02
520	Methanol	0.15	64.26	5.05	31.82	12.60	3.92	2.20	0.45	1.26
520	2,2,2-Trifluoroethanol	0.24	88.03	0.86	11.73	5.07	0.24	0.33	3.04	1.10

Table 4.1.16. Summary of Time Correlated Single Photon Counting (TCSPC) fluorescent lifetimes (amplitude weighted) of **21** recorded at 520 nm.

Wavelength (nm)	Solvent	τ_1 (ns)	A_1 (%)	τ_2 (ns)	A_2 (%)	τ_3 (ns)	A_3 (%)	τ_f (ns) (Amplitude Weighted)	$1/\tau_f$	χ^2
540	Toluene	-	-	3.71	42.67	9.73	57.33	7.16	0.14	1.17
540	1,4-Dioxane	-	-	4.51	48.52	11.38	51.48	8.04	0.12	1.14
540	Chloroform	0.25	13.79	4.95	44.20	11.67	42.01	7.12	0.14	1.05
540	Acetonitrile	-	-	5.38	67.07	13.62	32.93	8.10	0.12	1.15
540	1-Octanol	0.20	34.32	5.61	24.76	12.64	20.92	4.14	0.24	1.18
540	1-Hexanol	0.31	33.87	5.57	42.54	13.26	23.59	5.61	0.18	1.15
540	1-Butanol	-	-	5.58	68.56	12.77	31.44	7.84	0.13	1.23
540	1-Pentanol	-	-	5.66	66.85	13.17	33.15	8.15	0.12	1.08
540	1-Propanol	-	-	5.53	72.07	12.80	27.93	7.56	0.13	1.22
540	Acetic acid	0.16	82.04	1.61	17.03	3.23	0.93	0.43	2.31	1.08
540	Methanol	0.15	65.93	5.05	28.91	13.07	5.16	2.23	0.45	1.23
540	2,2,2-Trifluoroethanol	0.24	88.23	0.85	11.40	4.34	0.37	0.32	3.09	1.16

Table 4.1.17. Summary of Time Correlated Single Photon Counting (TCSPC) fluorescent lifetimes (amplitude weighted) of **21** recorded at 540 nm.

Wavelength (nm)	Solvent	τ_1 (ns)	A_1 (%)	τ_2 (ns)	A_2 (%)	τ_3 (ns)	A_3 (%)	τ_f (ns) (Amplitude Weighted)	$1/\tau_f$	χ^2
570	Toluene	-	-	3.74	24.22	9.81	75.78	8.34	0.12	1.24
570	1,4-Dioxane	-	-	4.56	31.97	11.61	68.03	9.36	0.11	1.14
570	Chloroform	0.34	6.03	5.07	34.26	11.95	59.71	8.89	0.11	1.22
570	Acetonitrile	-	-	5.38	52.14	13.69	47.86	9.36	0.11	1.18
570	1-Octanol	0.22	49.48	5.89	21.38	13.02	29.14	5.16	0.19	1.16
570	1-Hexanol	0.31	35.47	5.33	29.93	12.91	34.60	6.17	0.16	1.15
570	1-Butanol	-	-	5.67	59.71	13.37	40.29	8.77	0.11	1.14
570	1-Pentanol	-	-	5.90	55.21	13.48	44.79	9.30	0.11	1.27
570	1-Propanol	-	-	5.36	59.39	12.74	40.61	8.36	0.12	1.13
570	Acetic acid	0.19	85.20	1.63	14.26	3.83	0.54	0.42	2.40	0.89
570	Methanol	0.17	52.65	4.97	36.99	13.24	10.36	3.30	0.30	1.14
570	2,2,2-Trifluoroethanol	0.23	89.75	0.85	9.76	4.34	0.49	0.31	3.20	1.13

Table 4.1.18. Summary of Time Correlated Single Photon Counting (TCSPC) fluorescent lifetimes (amplitude weighted) of **21** recorded at 570 nm.

4.1.7 400 nm average fluorescent lifetimes - Solvatochromic analysis.

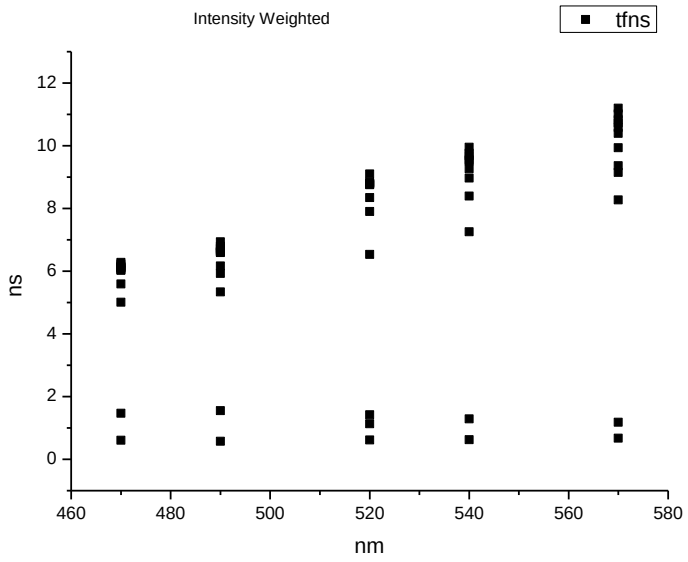

Figure 4.1.49. Intensity weighted average lifetime (τ_f) of **21** versus wavelength (nm).

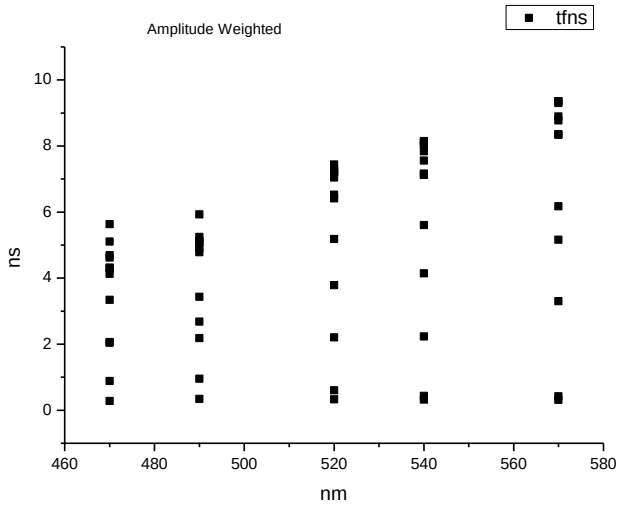

Figure 4.1.50. Amplitude weighted average lifetime (τ_f) of **21** versus wavelength (nm).

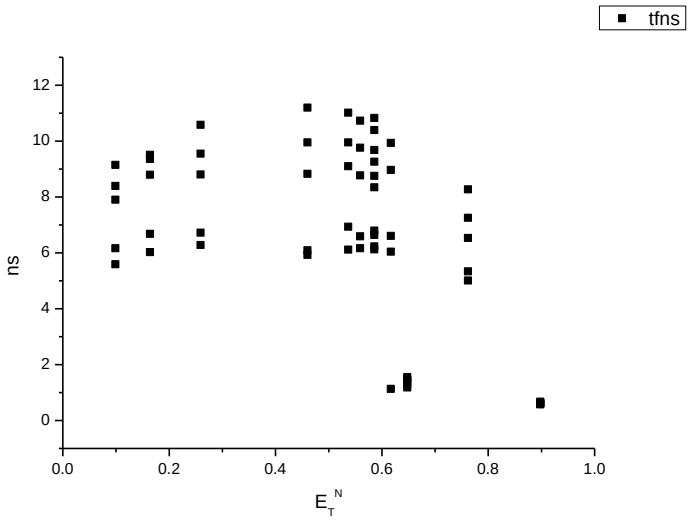

Figure 4.1.51. Intensity weighted average lifetime (τ_f) of **21** versus E_T^N.

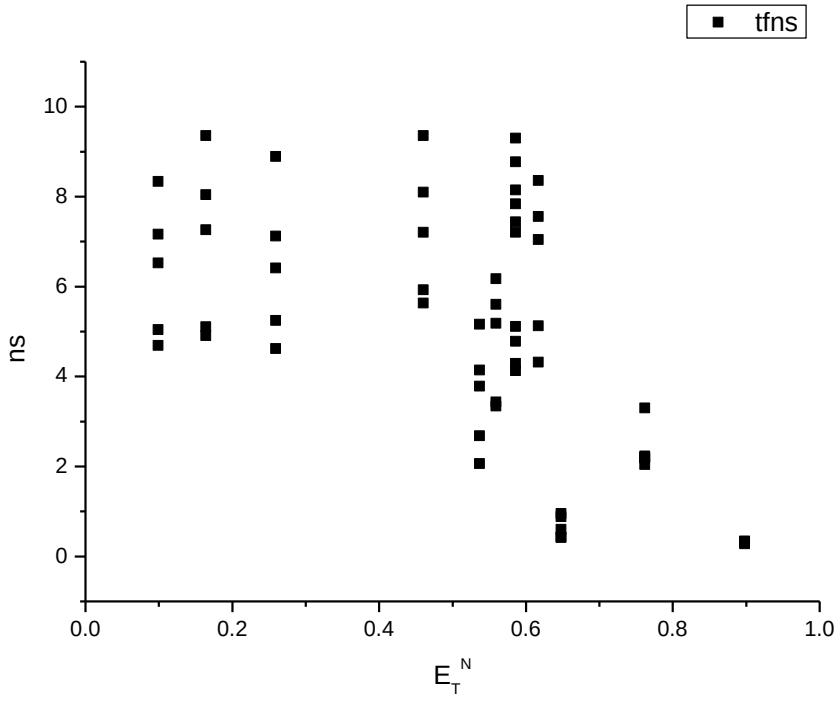

Figure 4.1.52. Amplitude weighted average lifetime (τ_f) of **21** versus E_T^N.

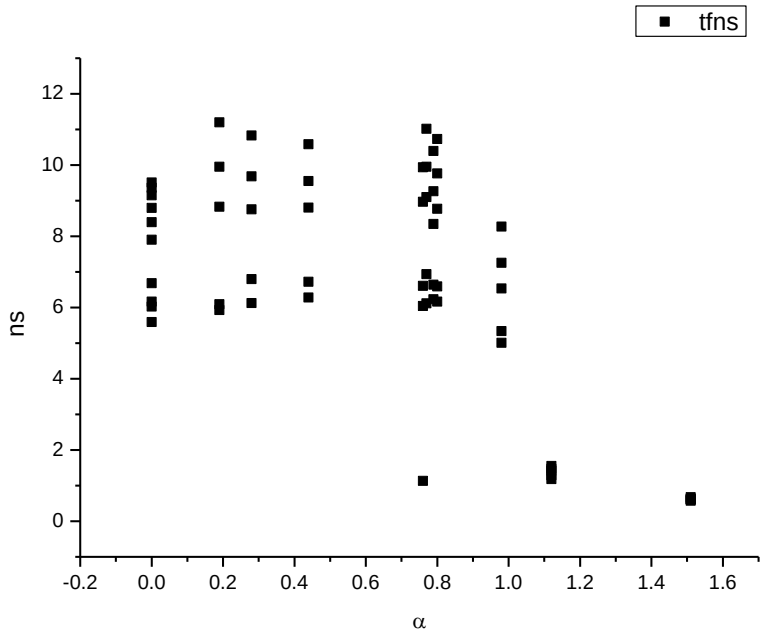

Figure 4.1.53. Intensity weighted average lifetime (τ_f) of **21** versus α.

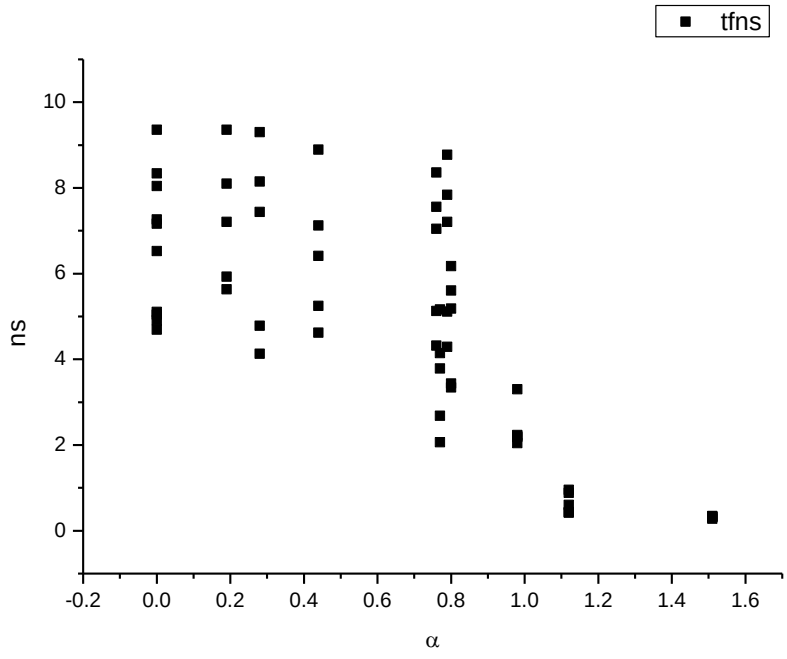

Figure 4.1.54. Amplitude weighted average lifetime (τ_f) of **21** versus α.

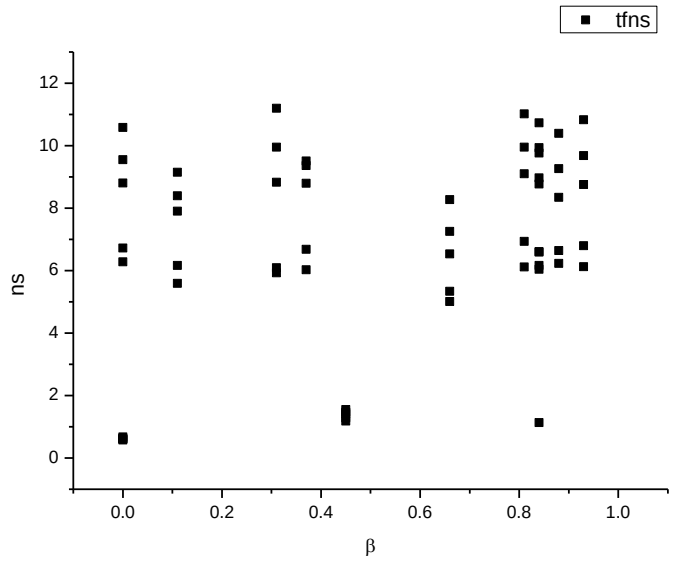

Figure 4.1.55. Intensity weighted average lifetime (τ_f) of **21** versus β.

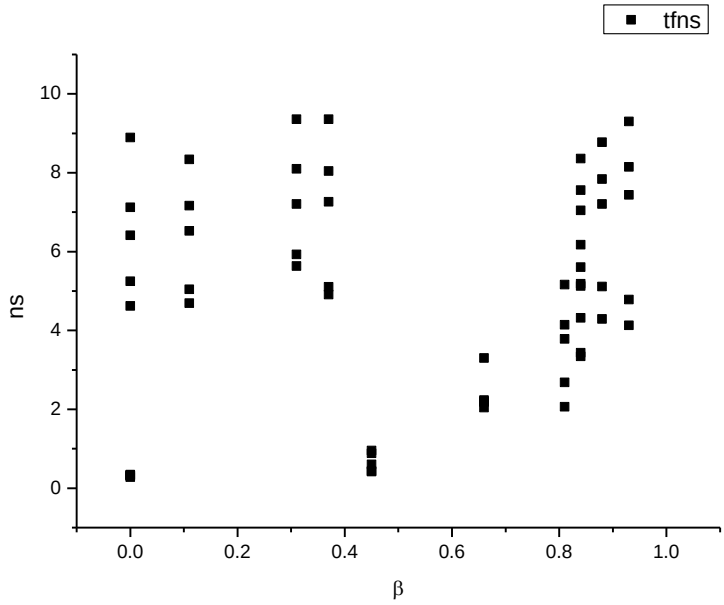

Figure 4.1.56. Amplitude weighted average lifetime (τ_f) of **21** versus β.

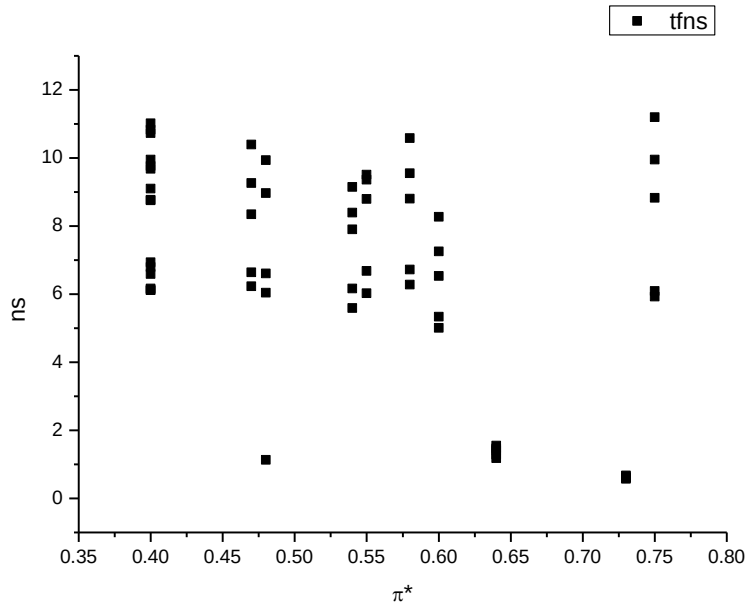

Figure 4.1.57. Intensity weighted average lifetime (τ_f) of **21** versus π*.

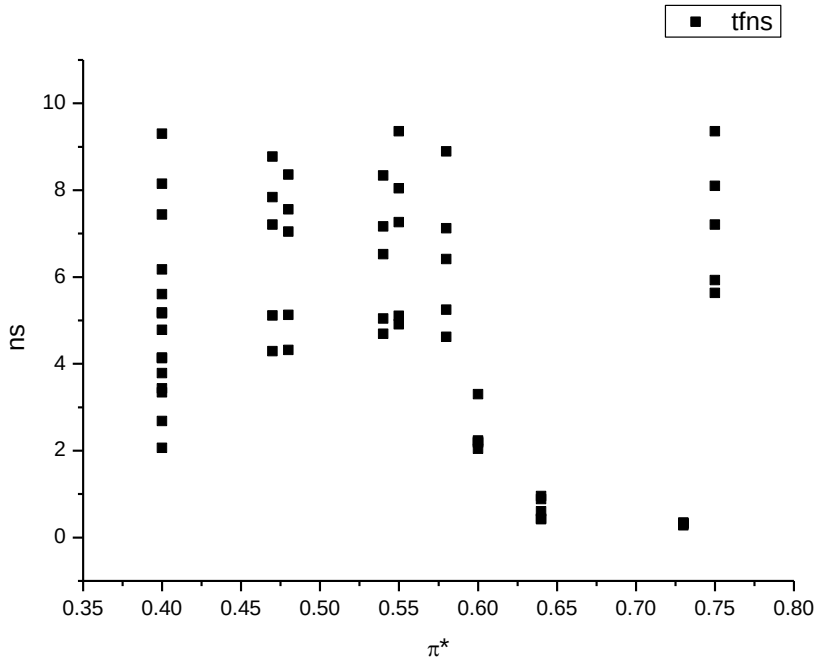

Figure 4.1.58. Amplitude weighted average lifetime (τ_f) of **21** versus π*.

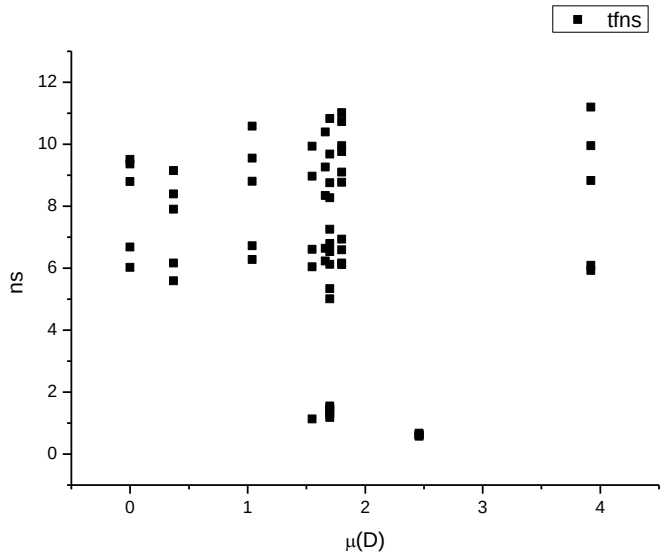

Figure 4.1.59. Intensity weighted average lifetime (τ_f) of **21** versus μ(D).

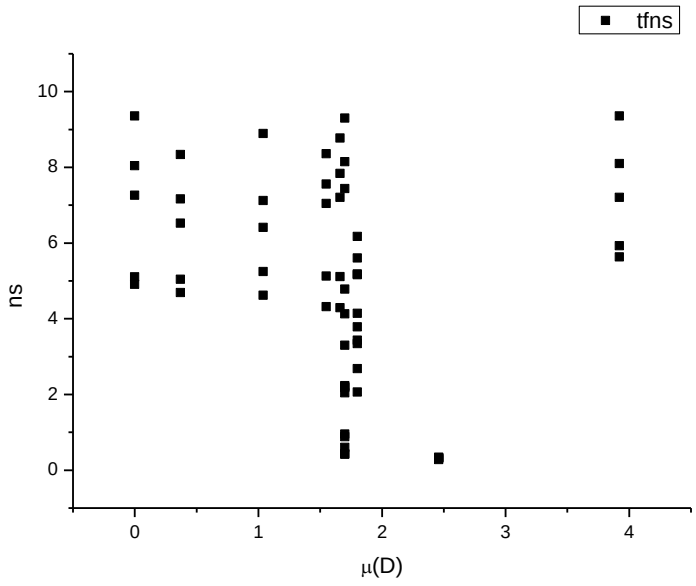

Figure 4.1.60. Amplitude weighted average lifetime (τ_f) of **21** versus μ(D).

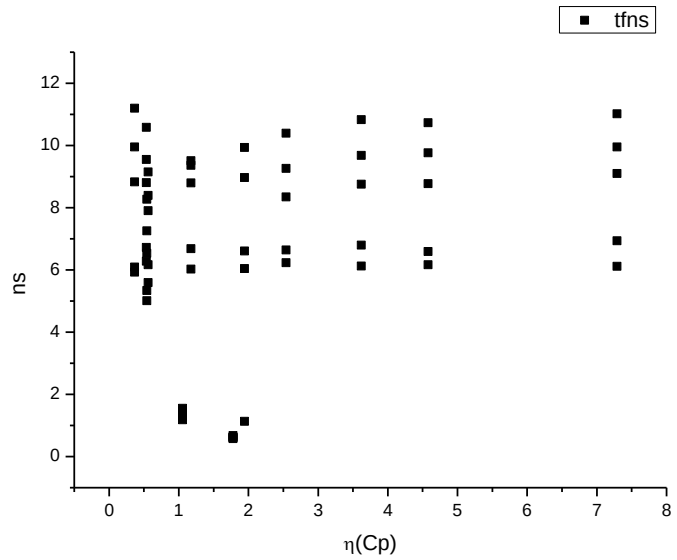

Figure 4.1.61. Intensity weighted average lifetime (τ_f) of **21** versus η(Cp).

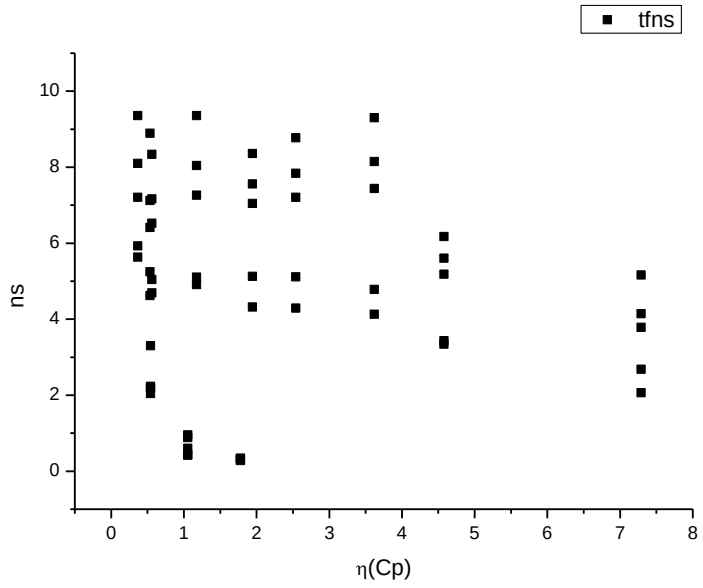

Figure 4.1.62. Amplitude weighted average lifetime (τ_f) of **21** versus η(Cp).

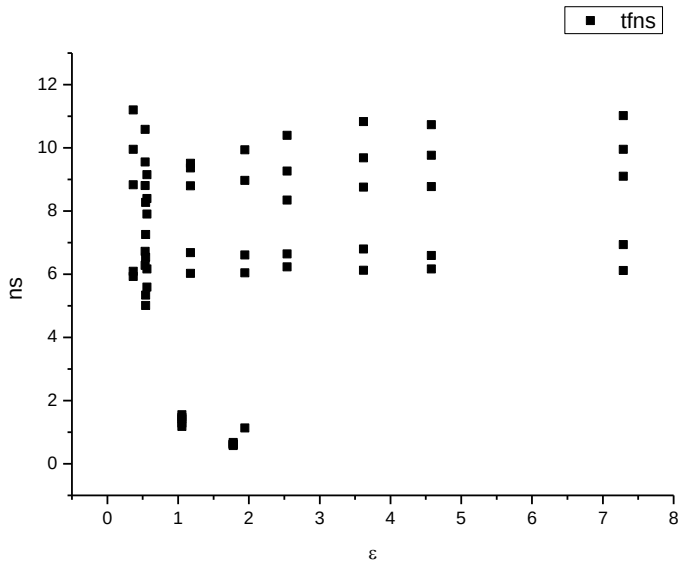

Figure 4.1.63. Intensity weighted average lifetime (τ_f) of **21** versus ε.

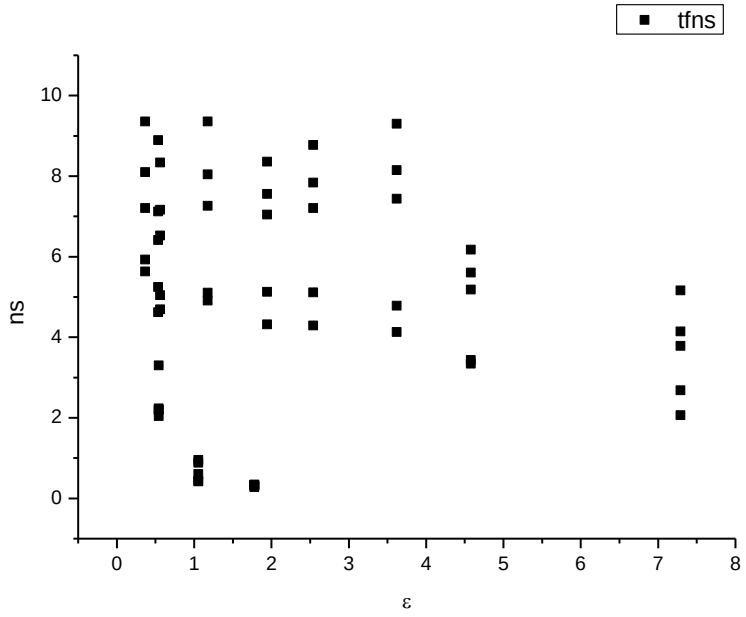

Figure 4.1.64. Amplitude weighted average lifetime (τ_f) of **21** versus ε.

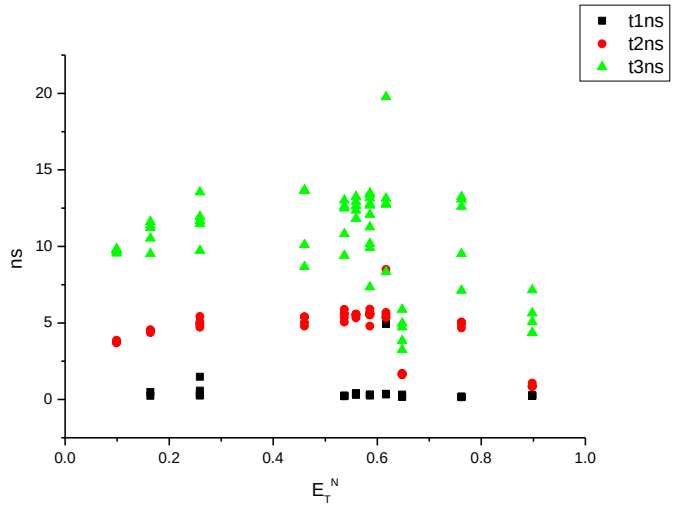

Figure 4.1.65. Intensity weighted components of TCSPC lifetime decay of **21** (470 nm to 570 nm) versus E_T^N.

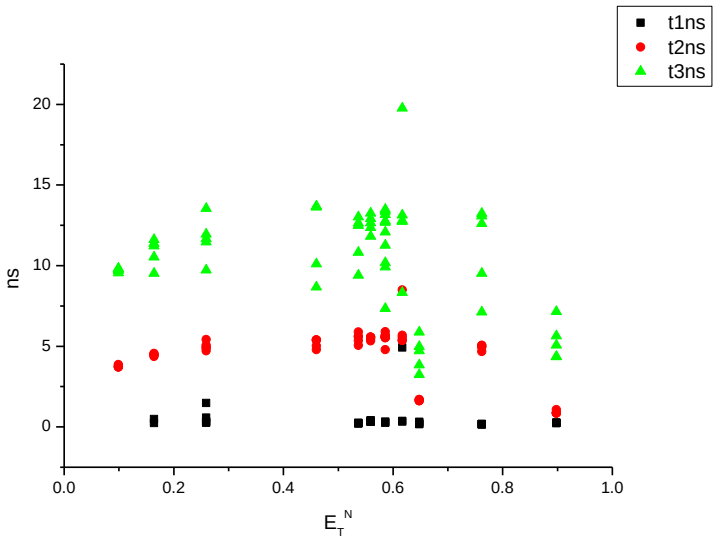

Figure 4.1.66. Amplitude weighted components of TCSPC lifetime decay of **21** (470 nm to 570 nm) versus E_T^N.

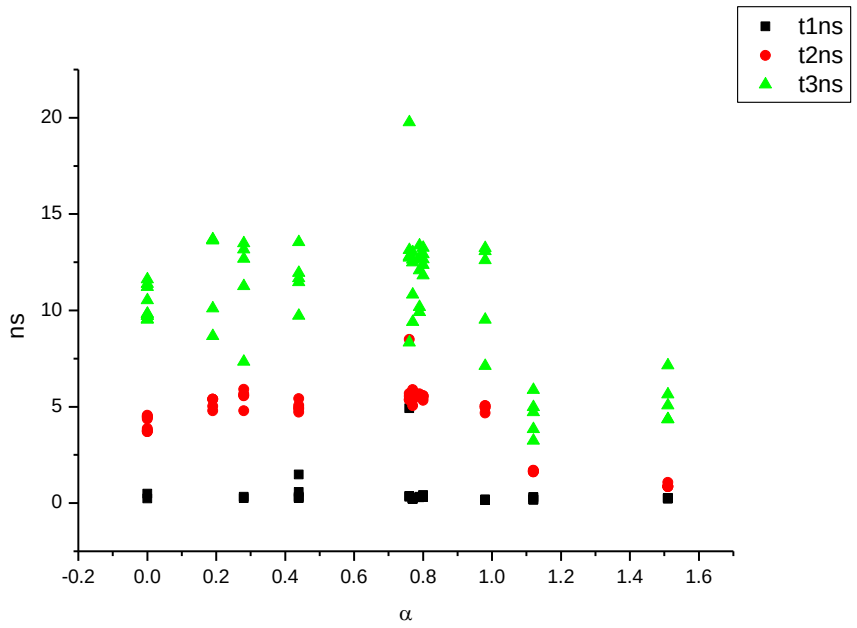

Figure 4.1.67. Intensity weighted components of TCSPC lifetime decay of **21** (470 nm to 570 nm) versus α.

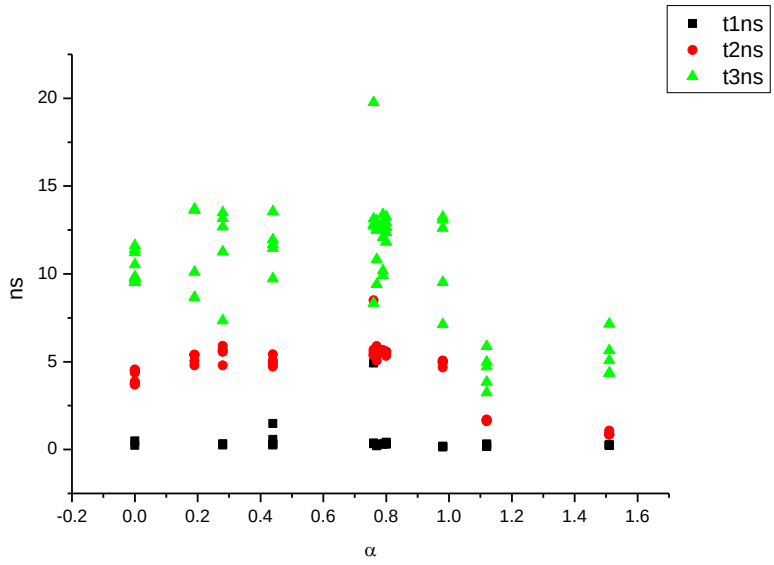

Figure 4.1.68. Amplitude weighted components of TCSPC lifetime decay of **21** (470 nm to 570 nm) versus α.

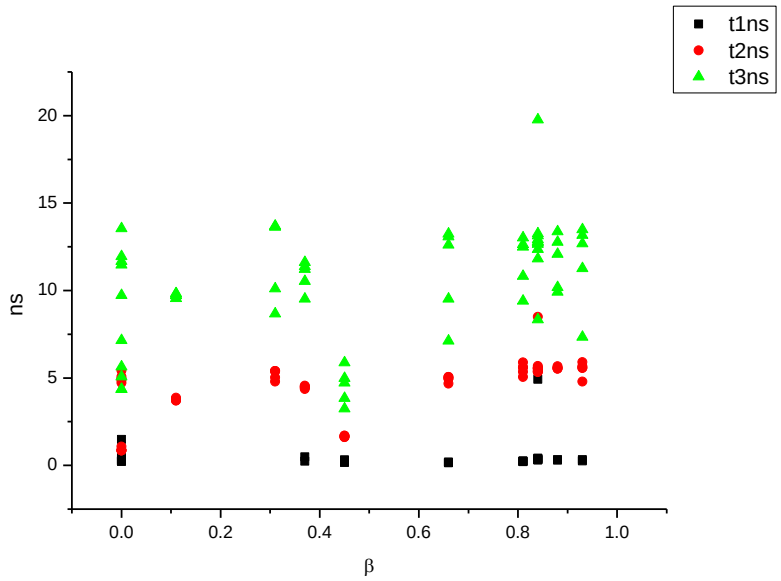

Figure 4.1.69. Intensity weighted components of TCSPC lifetime decay of **21** (470 nm to 570 nm) versus β.

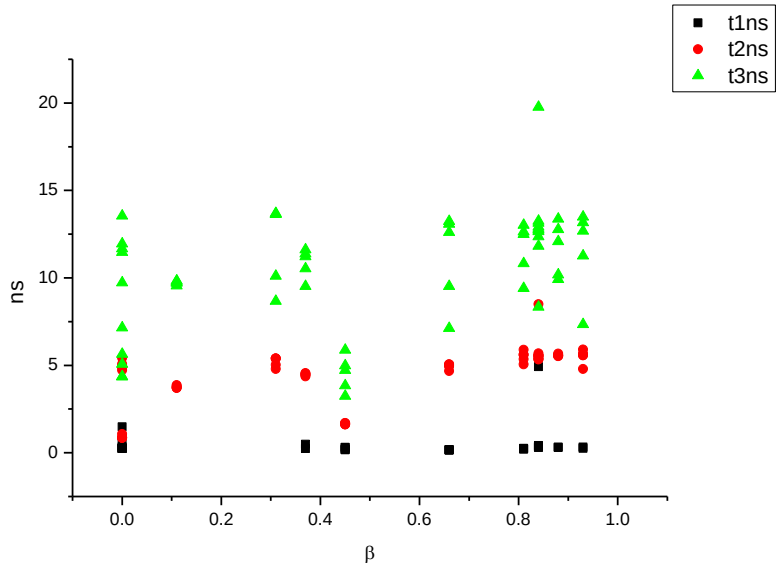

Figure 4.1.70. Amplitude weighted components of TCSPC lifetime decay of **21** (470 nm to 570 nm) versus β.

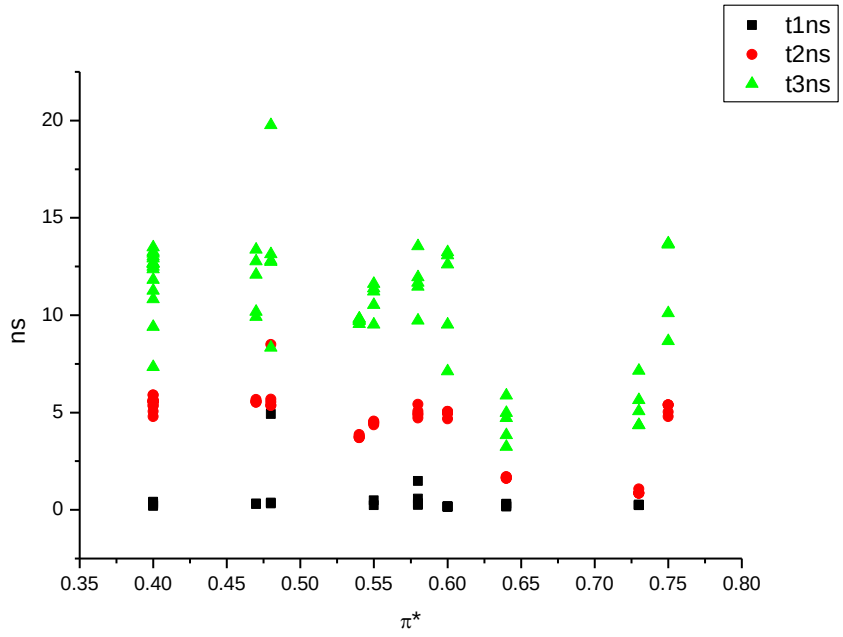

Figure 4.1.71. Intensity weighted components of TCSPC lifetime decay of **21** (470 nm to 570 nm) versus π*.

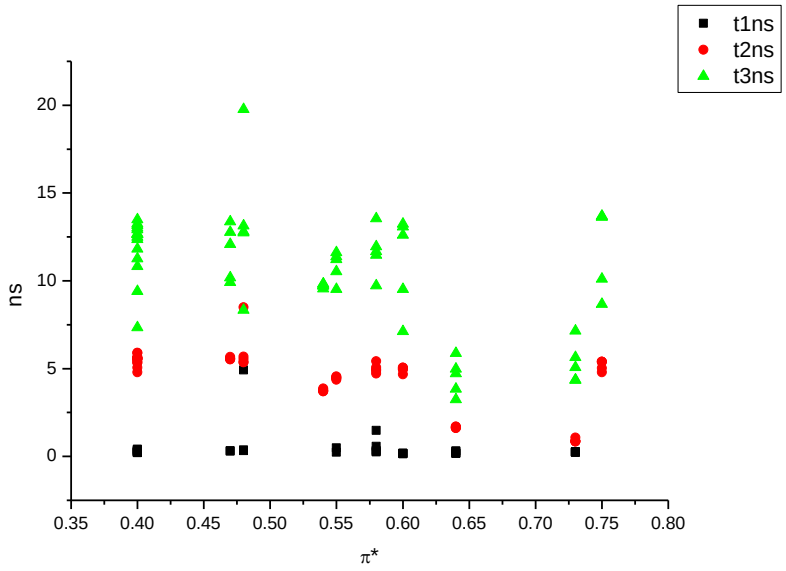

Figure 4.1.72. Amplitude weighted components of TCSPC lifetime decay of **21** (470 nm to 570 nm) versus π*.

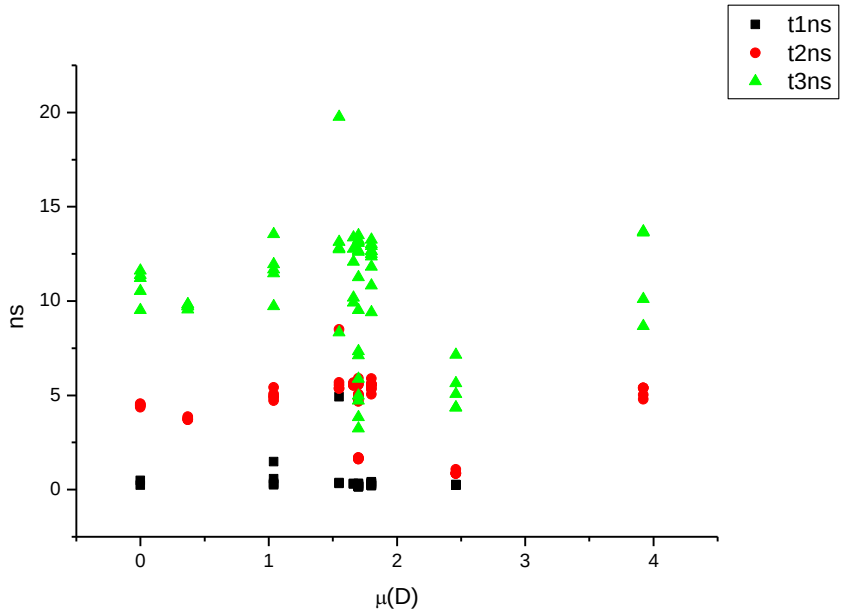

Figure 4.1.73. Intensity weighted components of TCSPC lifetime decay of **21** (470 nm to 570 nm) versus μ(D).

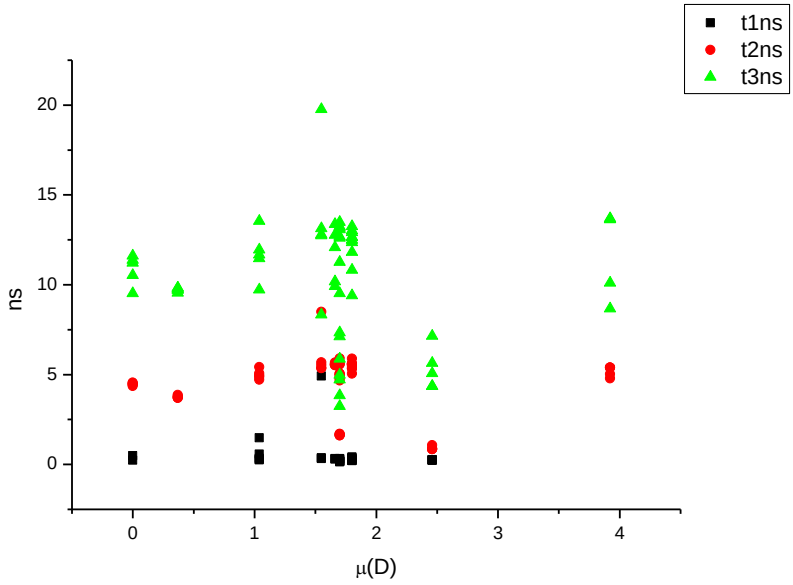

Figure 4.1.74. Amplitude weighted components of TCSPC lifetime decay of **21** (470 nm to 570 nm) versus μ(D).

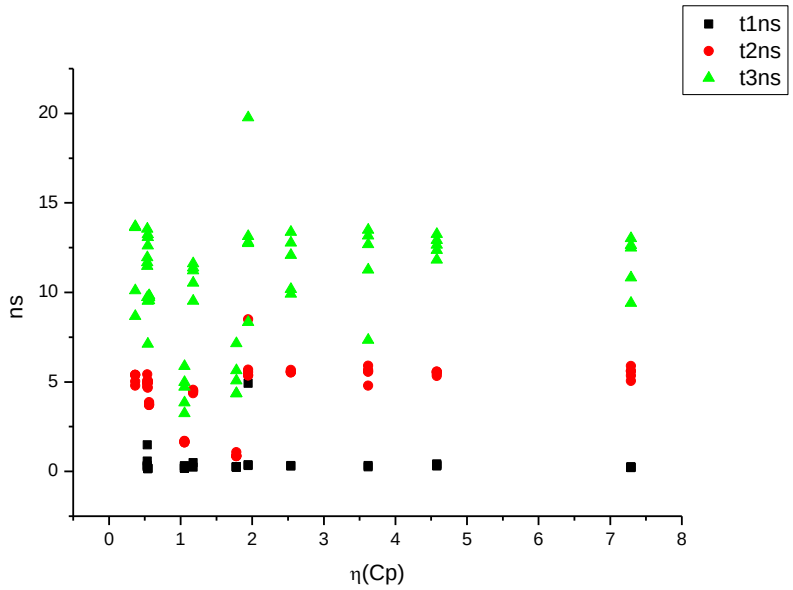

Figure 4.1.75. Intensity weighted components of TCSPC lifetime decay of **21** (470 nm to 570 nm) versus η(Cp).

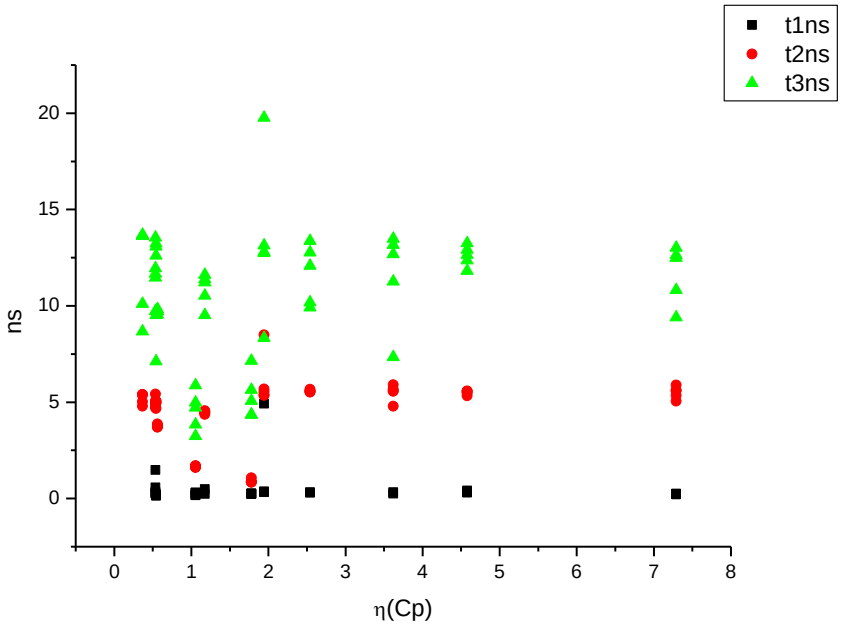

Figure 4.1.76. Amplitude weighted components of TCSPC lifetime decay of **21** (470 nm to 570 nm) versus η(Cp).

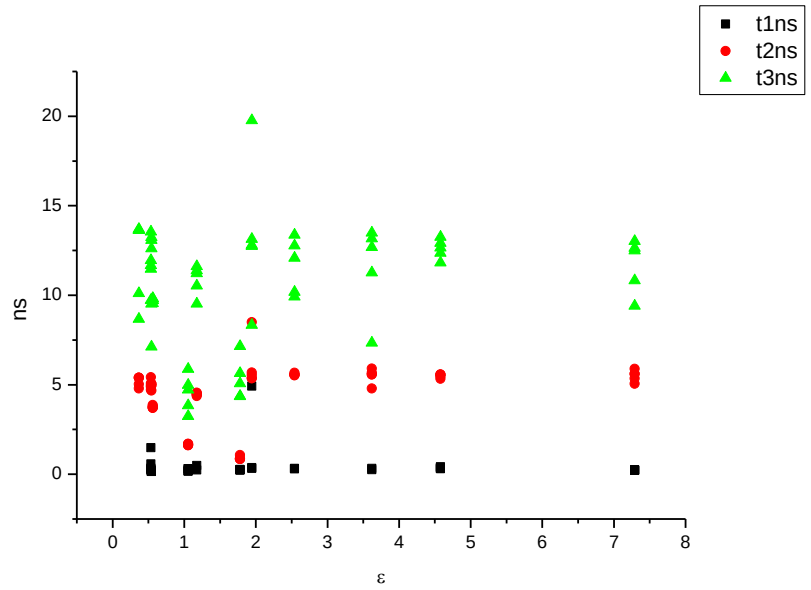

Figure 4.1.77. Intensity weighted components of TCSPC lifetime decay of **21** (470 nm to 570 nm) versus ε.

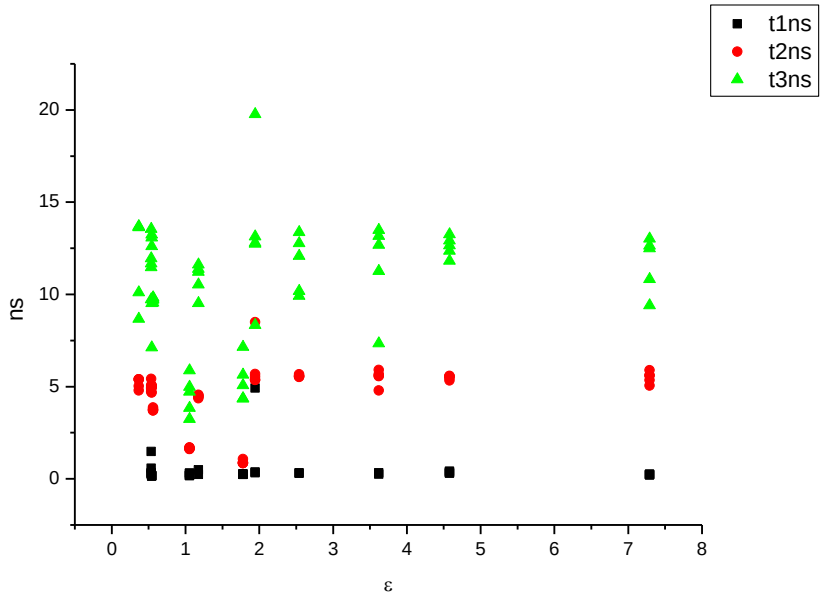

Figure 4.1.78. Amplitude weighted components of TCSPC lifetime decay of **21** (470 nm to 570 nm) versus ε.

4.1.7.1 470 nm Lifetime – Solvatochromic analysis.

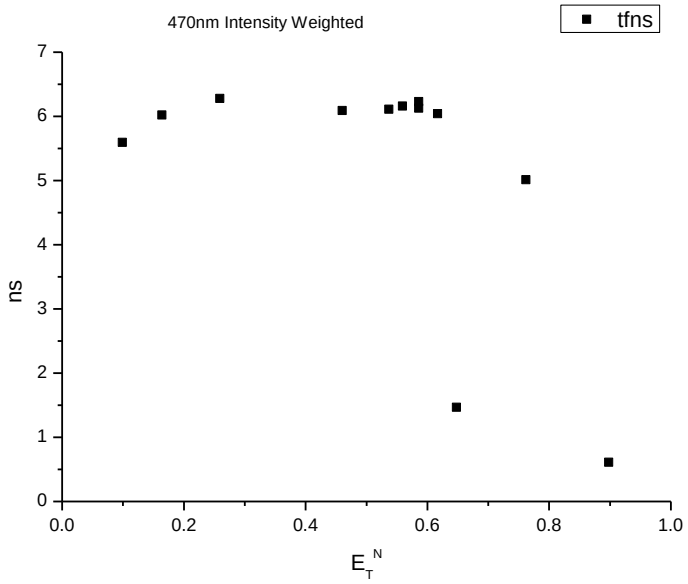

Figure 4.1.79. Intensity weighted average lifetime (τ_f) of **21** at 470 nm versus E_T^N.

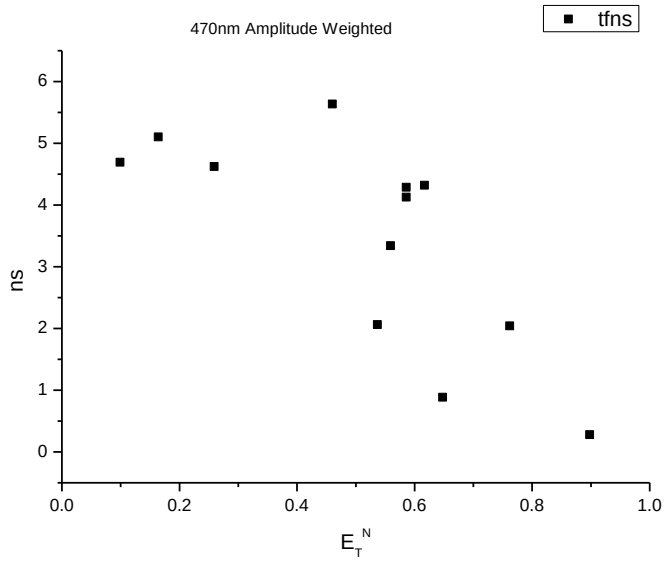

Figure 4.1.80. Amplitude weighted average lifetime (τ_f) of **21** at 470 nm versus E_T^N.

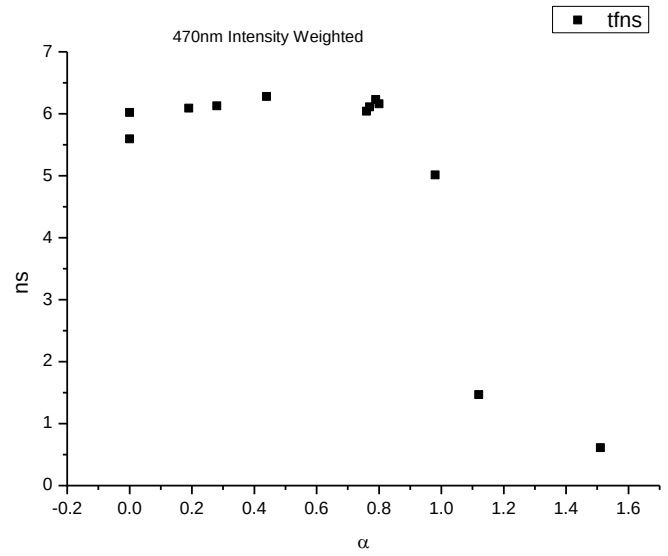

Figure 4.1.81. Intensity weighted average lifetime (τ_f) of **21** at 470 nm versus α.

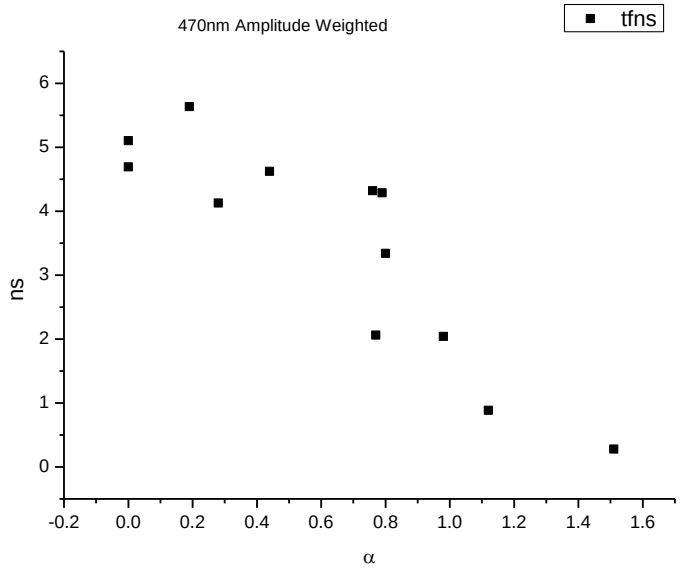

Figure 4.1.82. Amplitude weighted average lifetime (τ_f) of **21** at 470 nm versus α.

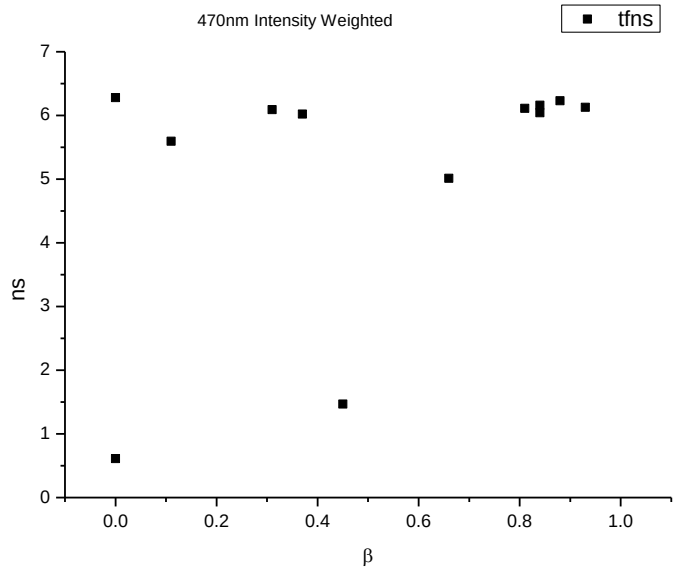

Figure 4.1.83. Intensity weighted average lifetime (τ_f) of **21** at 470 nm versus β.

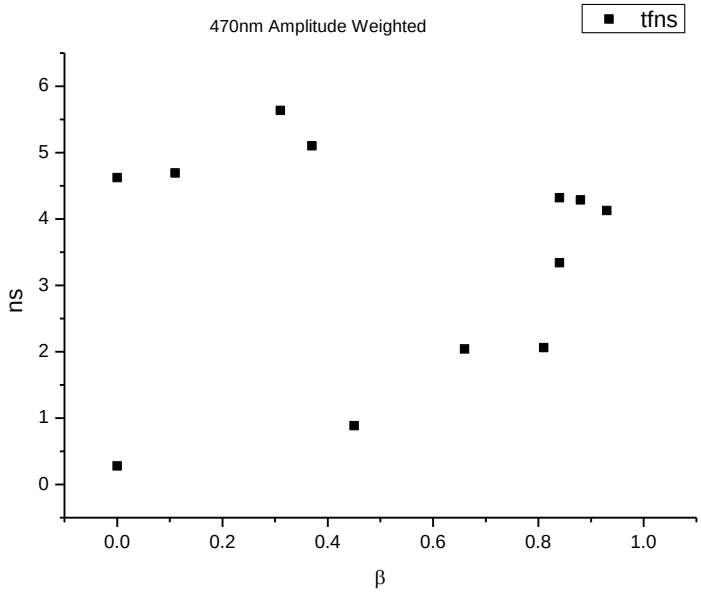

Figure 4.1.84. Amplitude weighted average lifetime (τ_f) of **21** at 470 nm versus β.

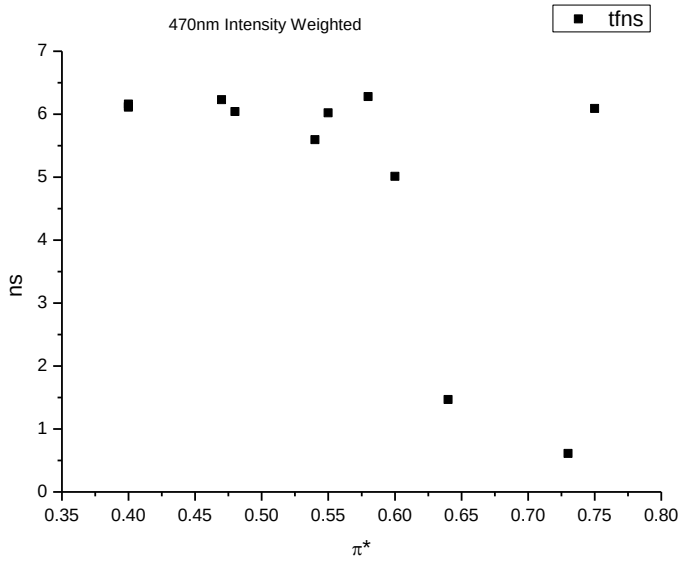

Figure 4.1.85. Intensity weighted average lifetime (τ_f) of **21** at 470 nm versus π*.

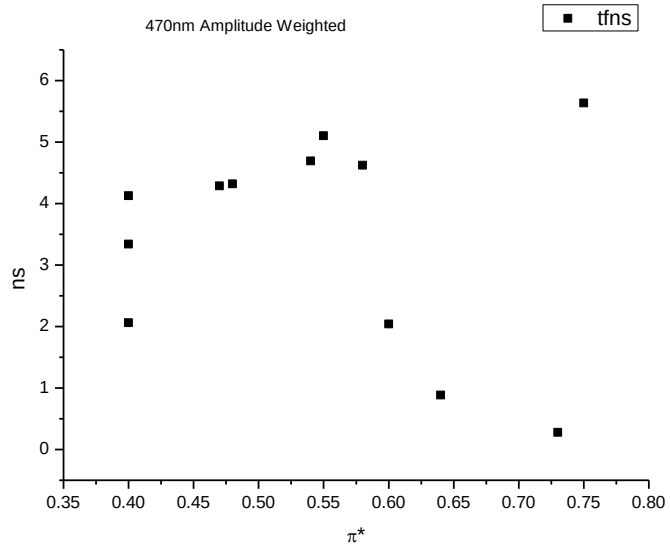

Figure 4.1.86. Amplitude weighted average lifetime (τ_f) of **21** at 470 nm versus π*.

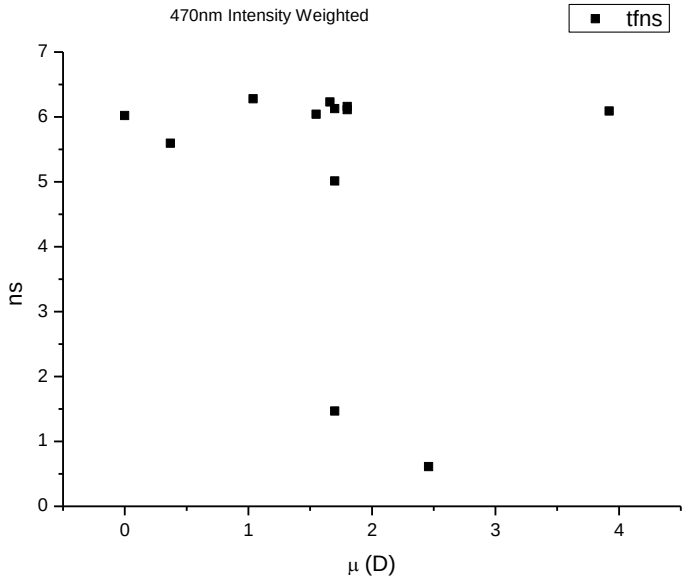

Figure 4.1.87. Intensity weighted average lifetime (τ_f) of **21** at 470 nm versus μ(D).

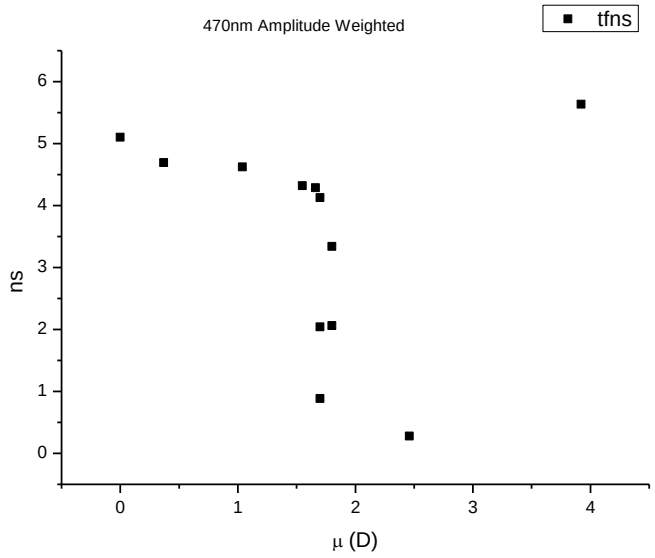

Figure 4.1.88. Amplitude weighted average lifetime (τ_f) of **21** at 470 nm versus μ(D).

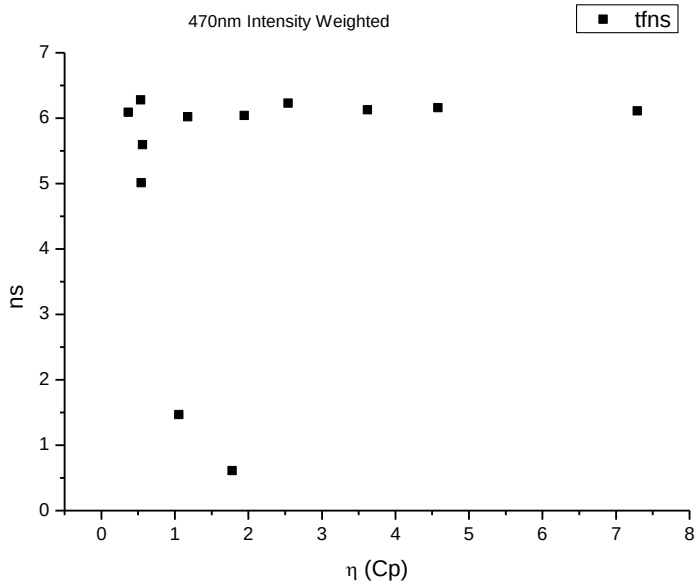

Figure 4.1.89. Intensity weighted average lifetime (τ_f) of **21** at 470 nm versus η(Cp).

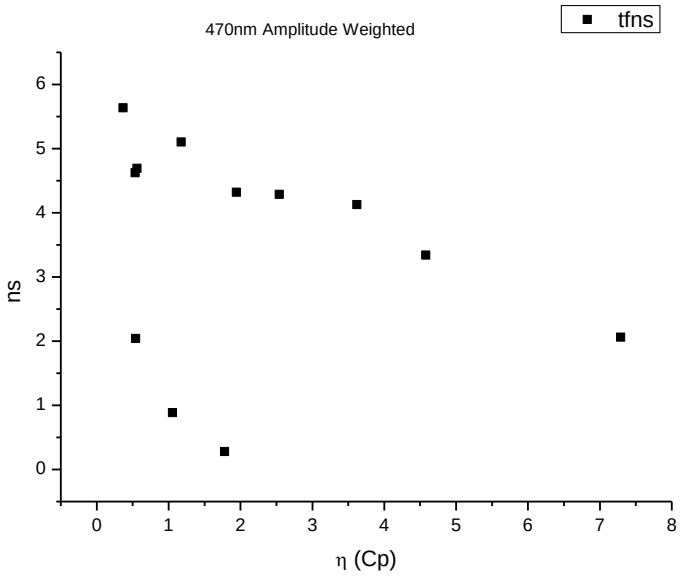

Figure 4.1.90. Amplitude weighted average lifetime (τ_f) of **21** at 470 nm versus η(Cp).

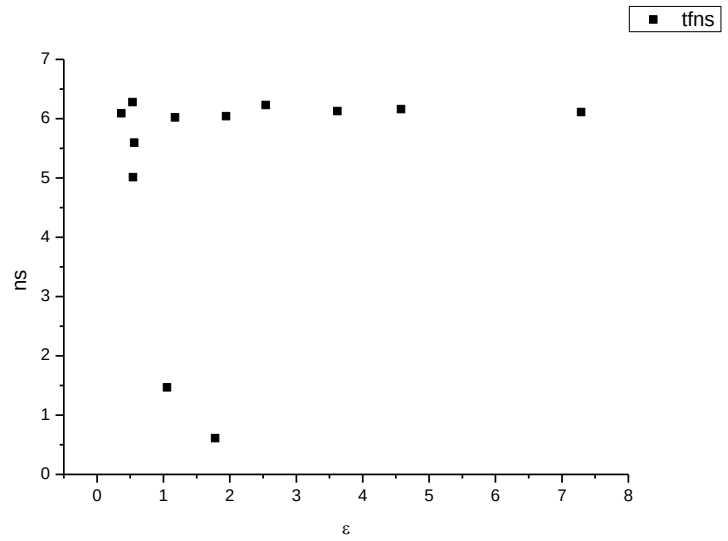

Figure 4.1.91. Intensity weighted average lifetime (τ_f) of **21** at 470 nm versus ε.

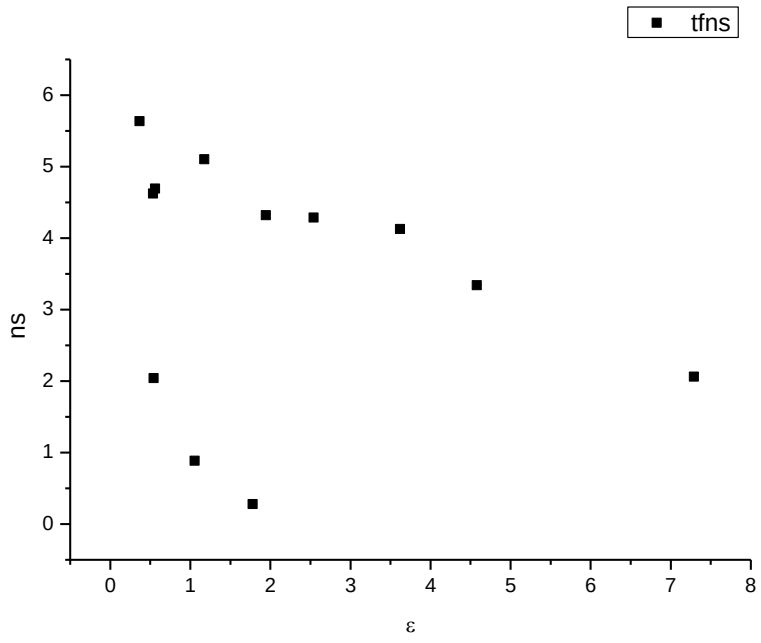

Figure 4.1.92. Amplitude weighted average lifetime (τ_f) of **21** at 470 nm versus ε.

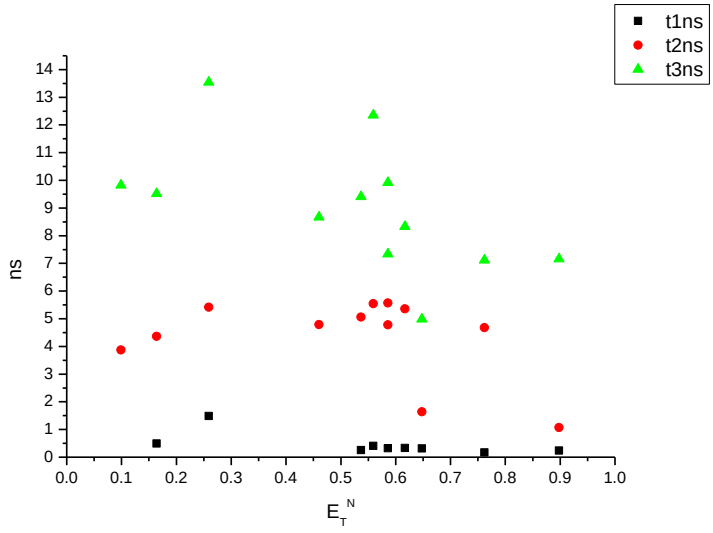

Figure 4.1.93. Intensity weighted components of TCSPC lifetime decay of **21** (470 nm) versus E_T^N.

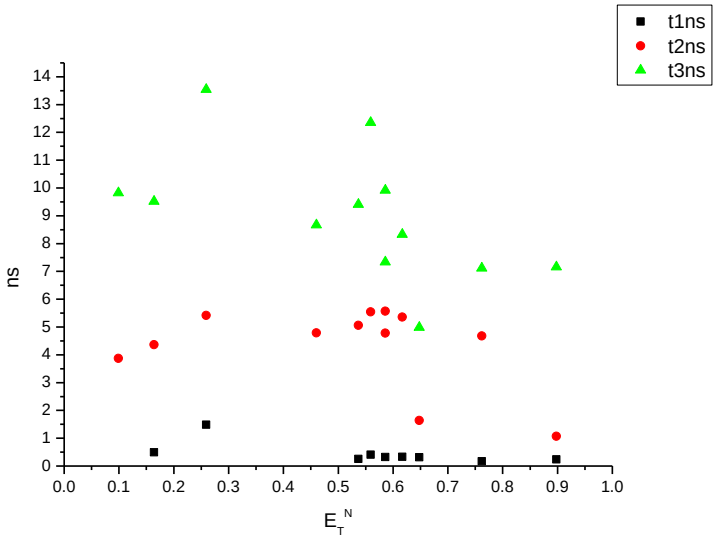

Figure 4.1.94. Amplitude weighted components of TCSPC lifetime decay of **21** (470 nm) versus E_T^N.

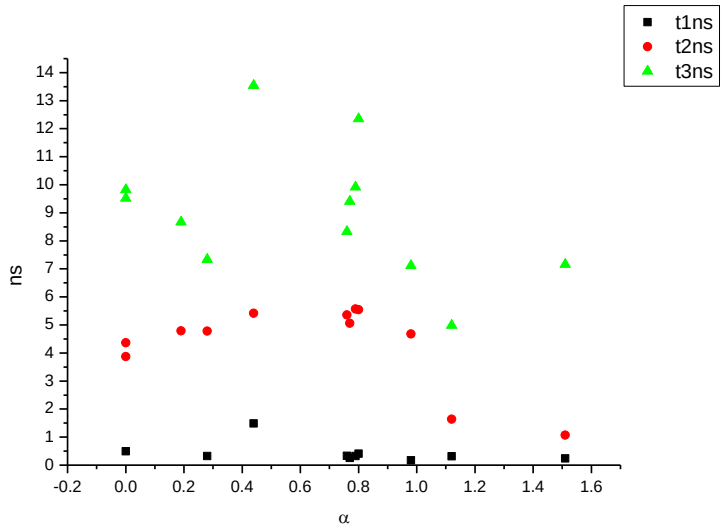

Figure 4.1.95. Intensity weighted components of TCSPC lifetime decay of **21** (470 nm) versus α.

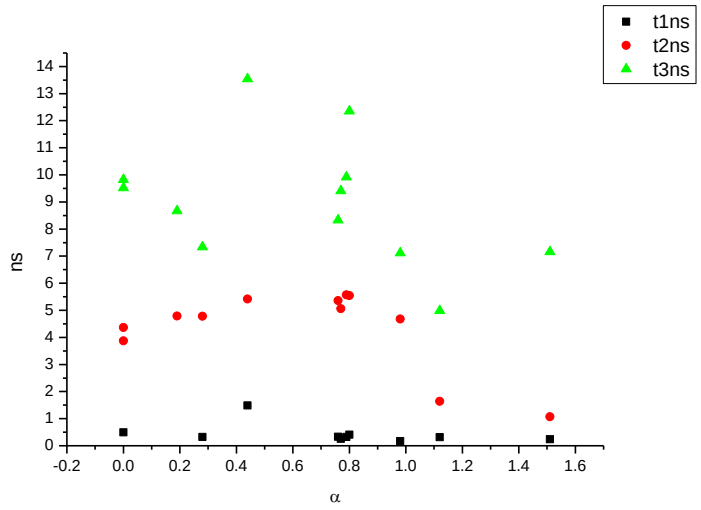

Figure 4.1.96. Amplitude weighted components of TCSPC lifetime decay of **21** (470 nm) versus α.

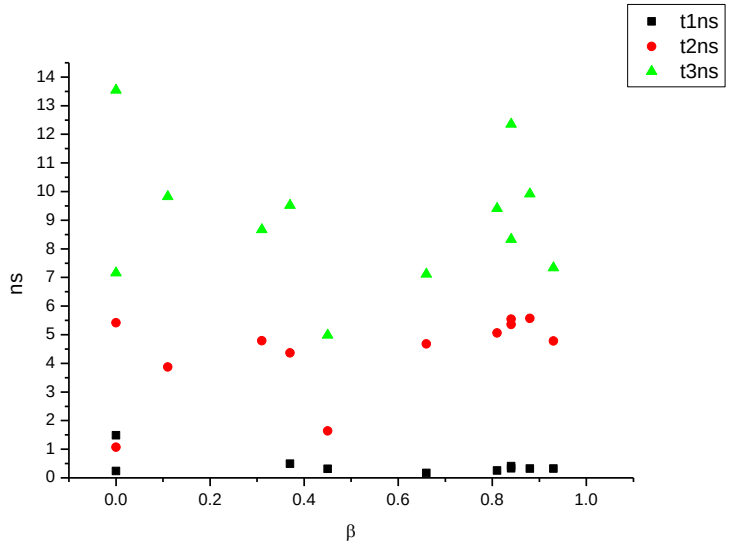

Figure 4.1.97. Intensity weighted components of TCSPC lifetime decay of **21** (470 nm) versus β.

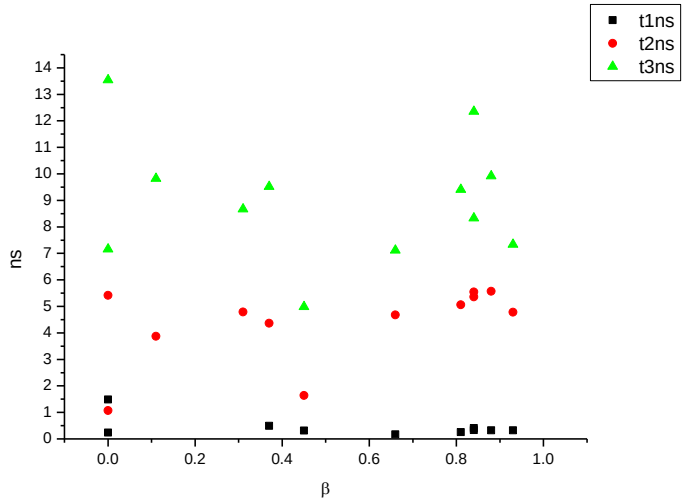

Figure 4.1.98. Amplitude weighted components of TCSPC lifetime decay of **21** (470 nm) versus β.

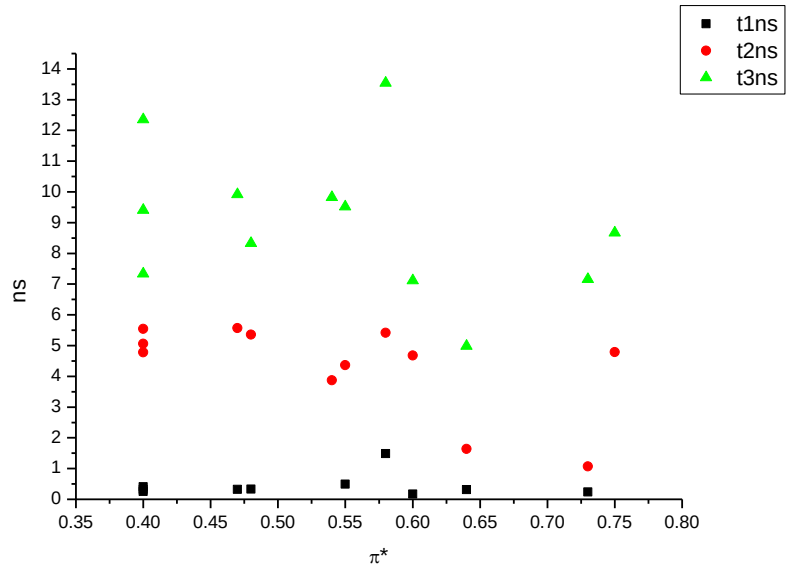

Figure 4.1.99. Intensity weighted components of TCSPC lifetime decay of **21** (470 nm) versus π*.

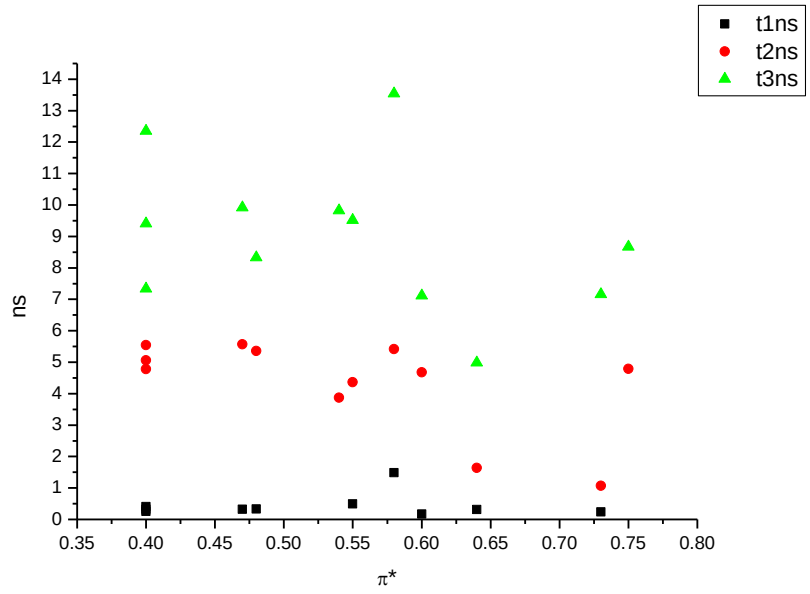

Figure 4.1.100. Amplitude weighted components of TCSPC lifetime decay of **21** (470 nm) versus π*.

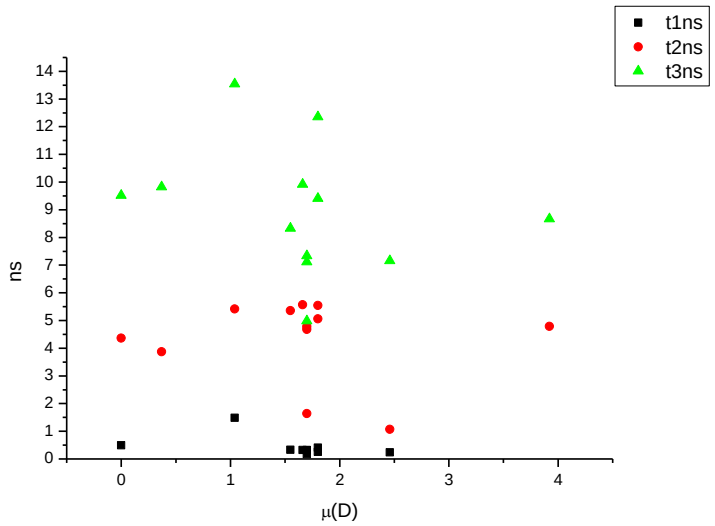

Figure 4.1.101. Intensity weighted components of TCSPC lifetime decay of **21** (470 nm) versus μ(D).

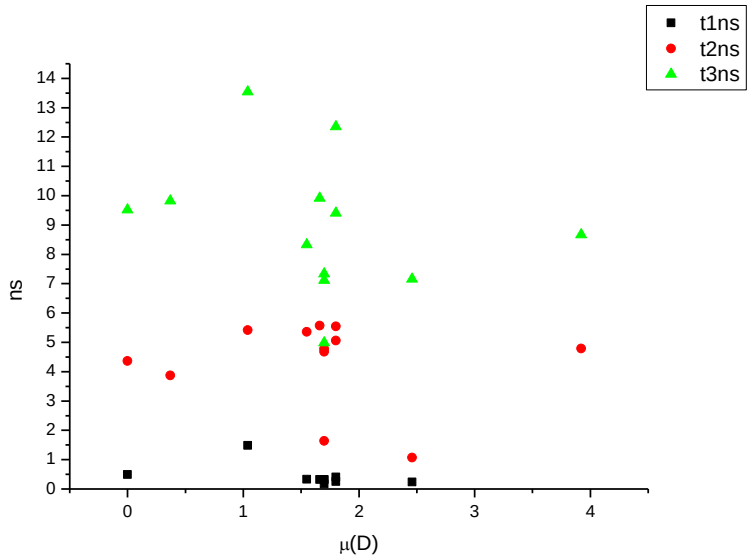

Figure 4.1.102. Amplitude weighted components of TCSPC lifetime decay of **21** (470 nm) versus μ(D).

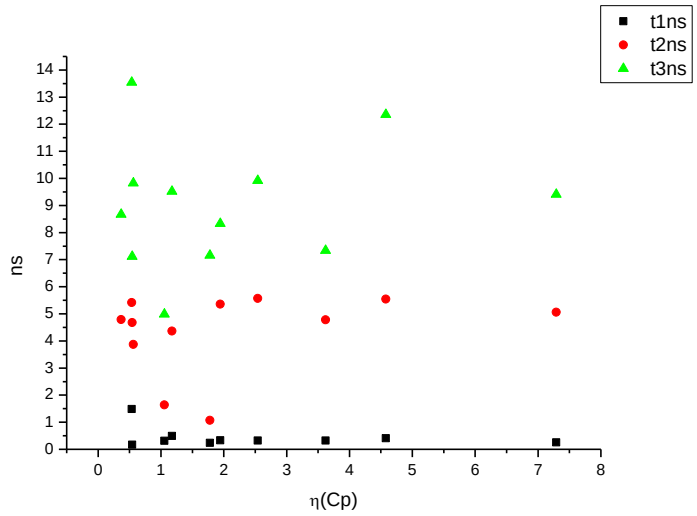

Figure 4.1.103. Intensity weighted components of TCSPC lifetime decay of **21** (470 nm) versus η(Cp).

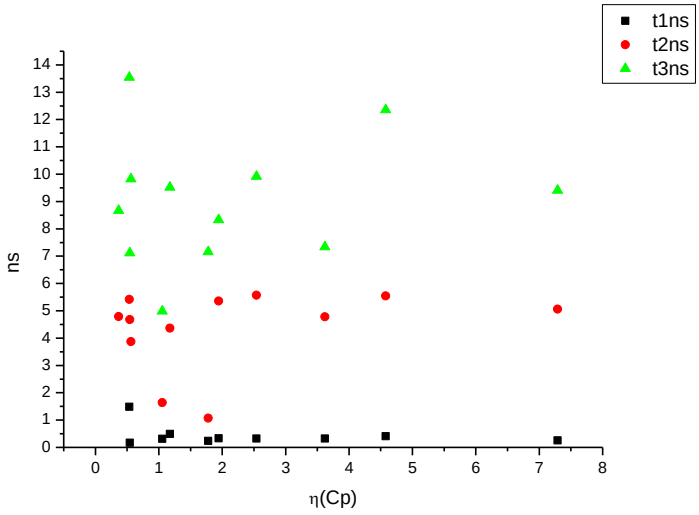

Figure 4.1.104. Amplitude weighted components of TCSPC lifetime decay of **21** (470 nm) versus η(Cp).

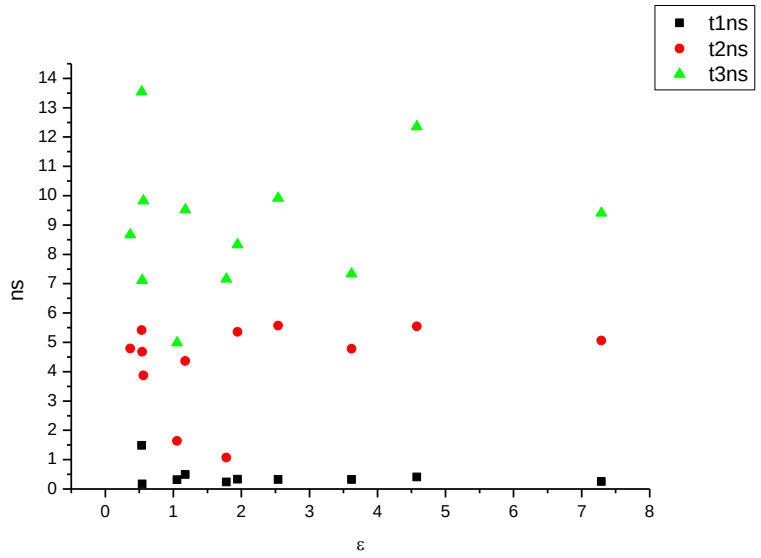

Figure 4.1.105. Intensity weighted components of TCSPC lifetime decay of **21** (470 nm) versus ε.

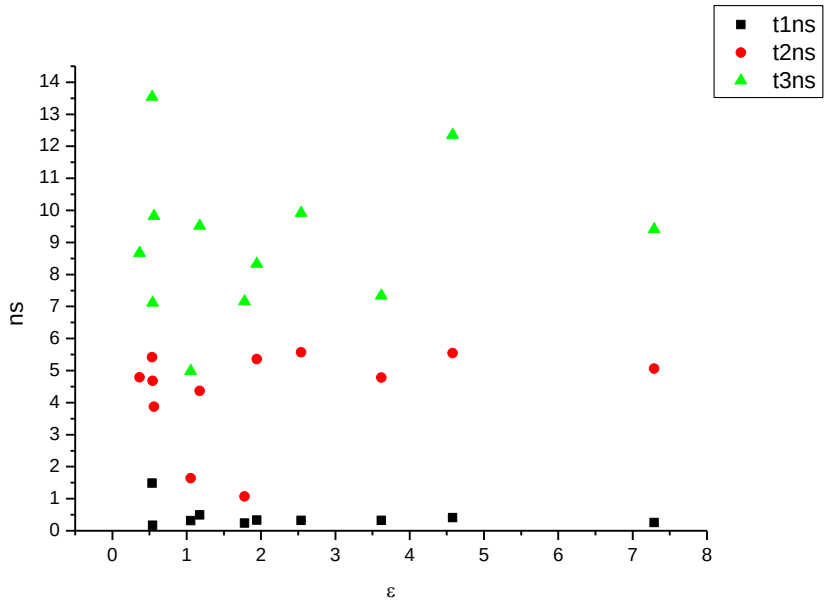

Figure 4.1.106. Amplitude weighted components of TCSPC lifetime decay of **21** (470 nm) versus ε.

4.1.7.2 570 nm Lifetime – Solvatochromic analysis.

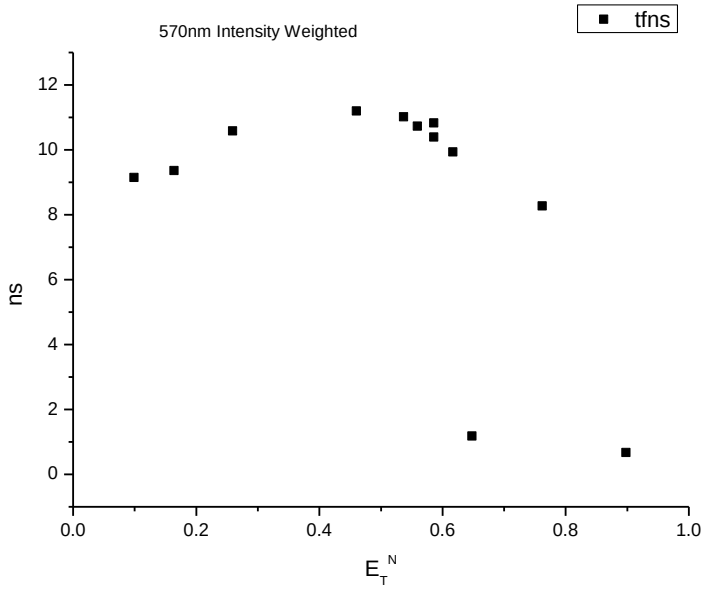

Figure 4.1.107. Intensity weighted average lifetime (τ_f) of **21** at 570 nm versus E_T^N.

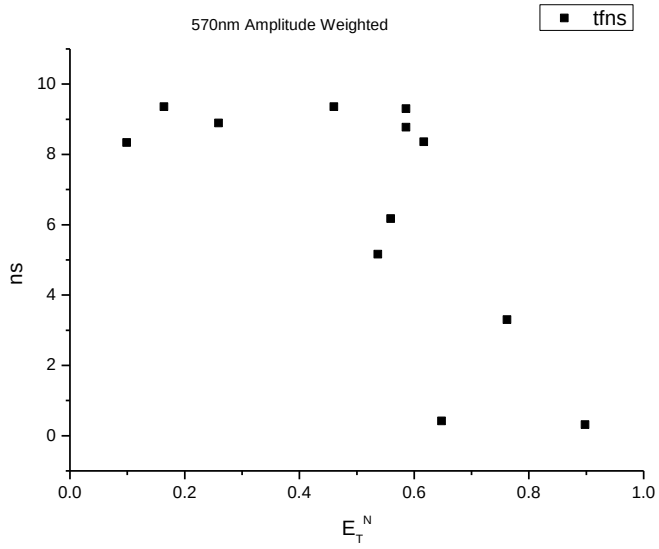

Figure 4.1.108. Amplitude weighted average lifetime (τ_f) of **21** at 570 nm versus E_T^N.

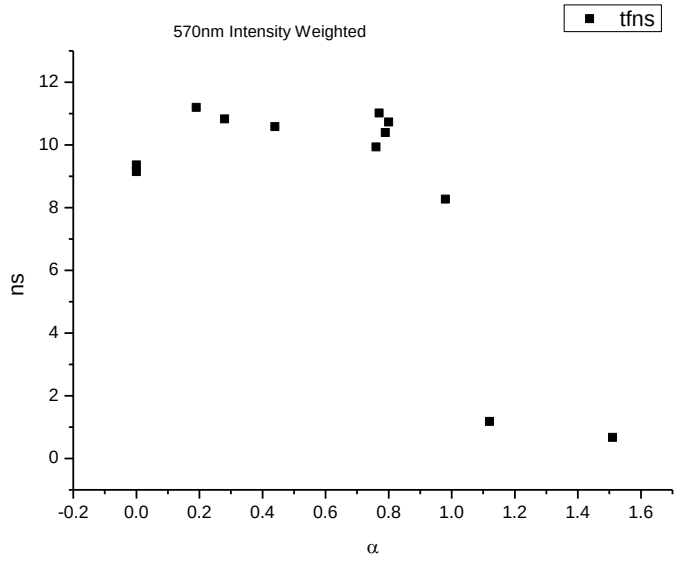

Figure 4.1.109. Intensity weighted average lifetime (τ_f) of **21** at 570 nm versus α.

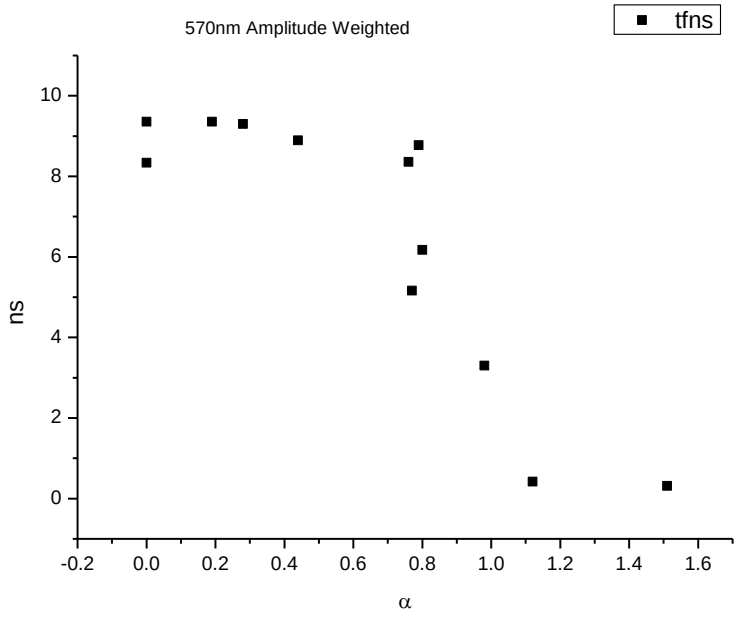

Figure 4.1.110. Amplitude weighted average lifetime (τ_f) of **21** at 570 nm versus α.

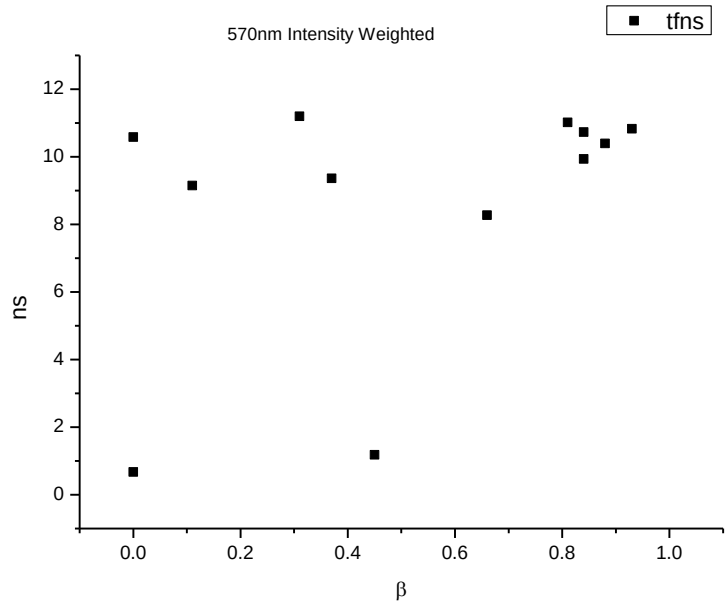

Figure 4.1.111. Intensity weighted average lifetime (τ_f) of **21** at 570 nm versus β.

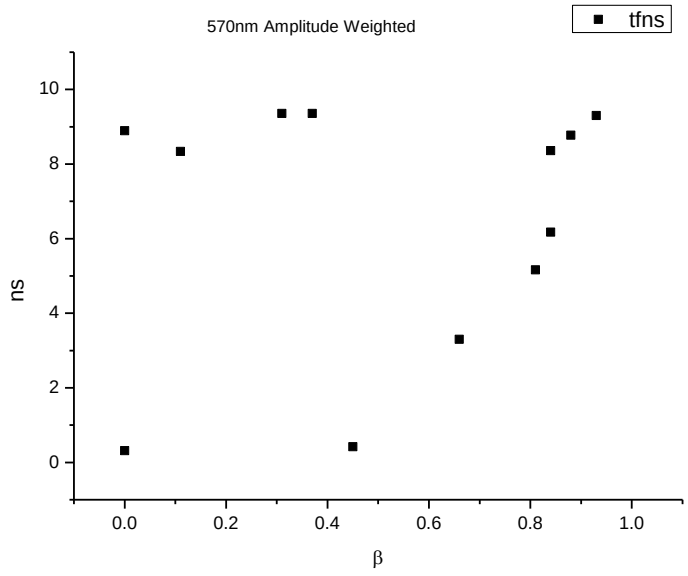

Figure 4.1.112. Amplitude weighted average lifetime (τ_f) of **21** at 570 nm versus β.

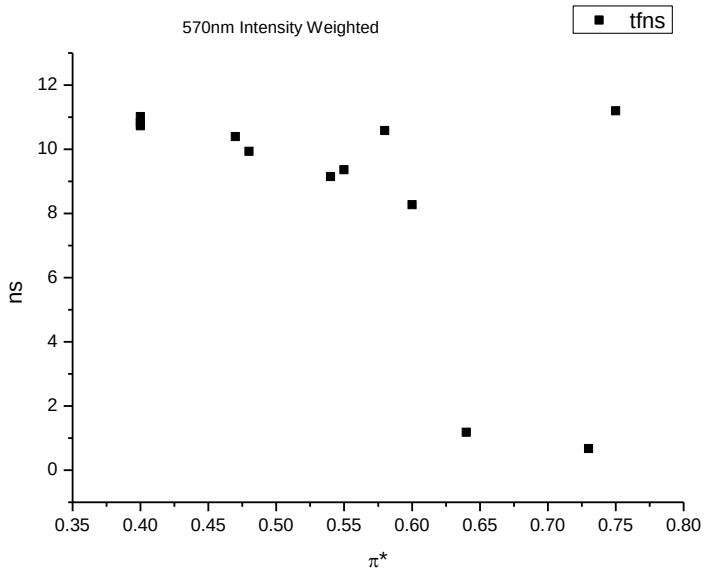

Figure 4.1.113. Intensity weighted average lifetime (τ_f) of **21** at 570 nm versus π*.

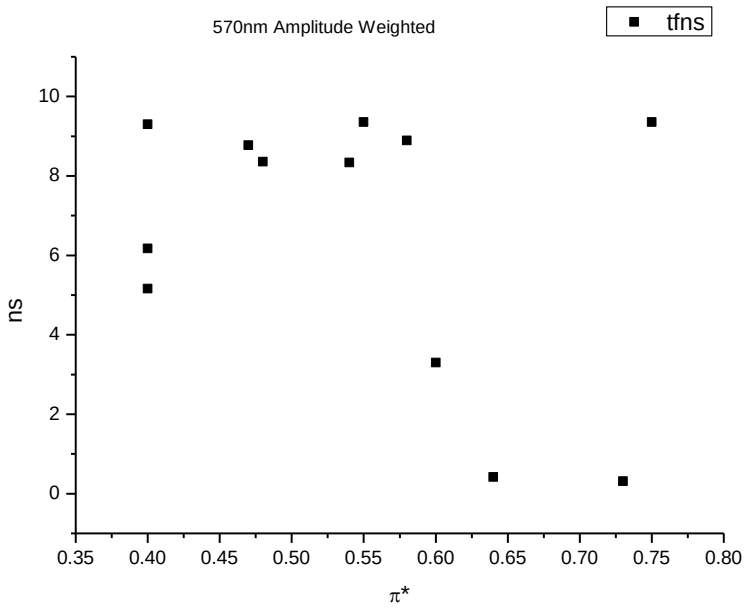

Figure 4.1.114. Amplitude weighted average lifetime (τ_f) of **21** at 570 nm versus π*.

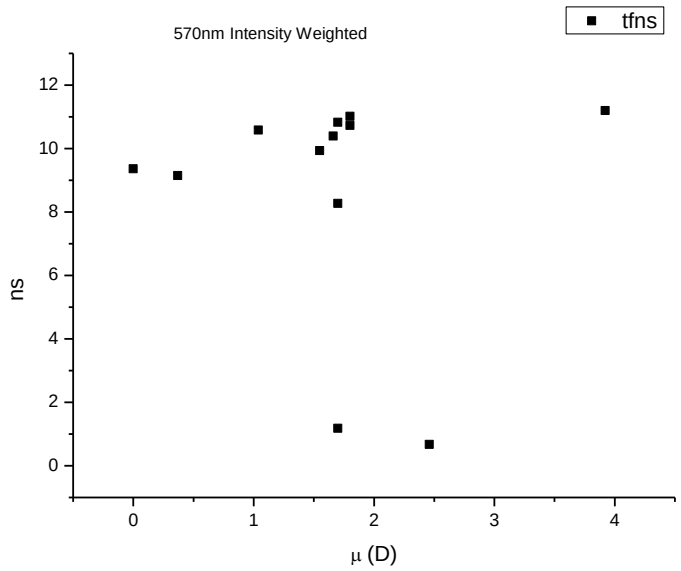

Figure 4.1.115. Intensity weighted average lifetime (τ_f) of **21** at 570 nm versus μ(D).

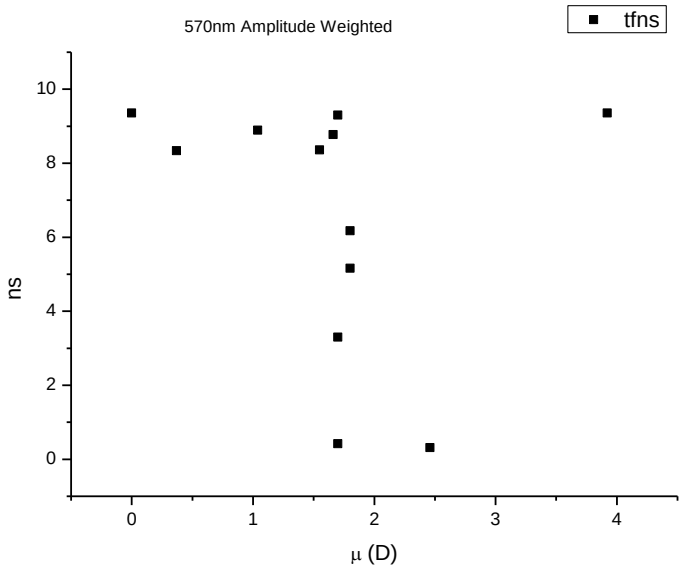

Figure 4.1.116. Amplitude weighted average lifetime (τ_f) of **21** at 570 nm versus μ(D).

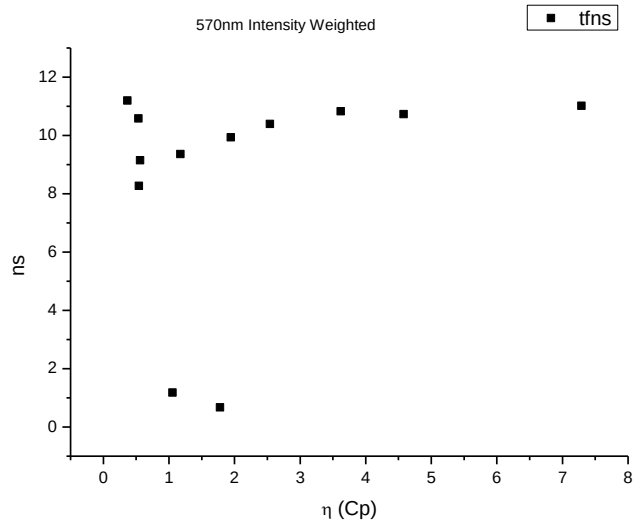

Figure 4.1.117. Intensity weighted average lifetime (τ_f) of **21** at 570 nm versus η(Cp).

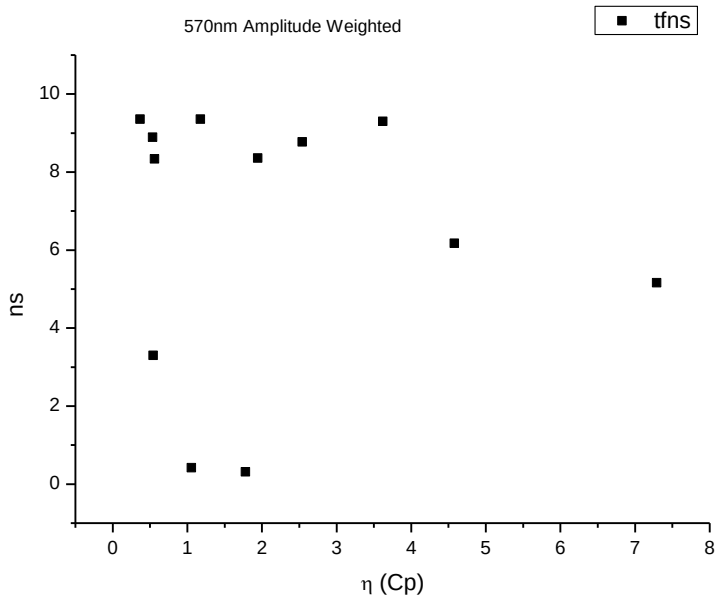

Figure 4.1.118. Amplitude weighted average lifetime (τ_f) of **21** at 570 nm versus η(Cp).

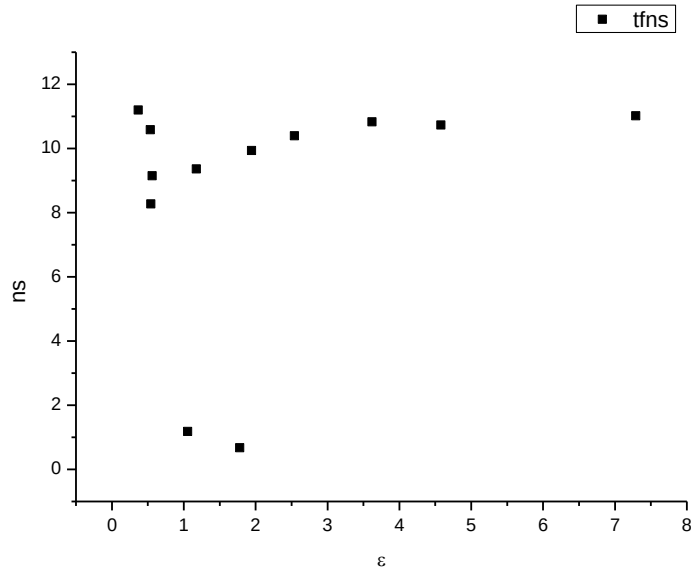

Figure 4.1.119. Intensity weighted average lifetime (τ_f) of **21** at 570 nm versus ε.

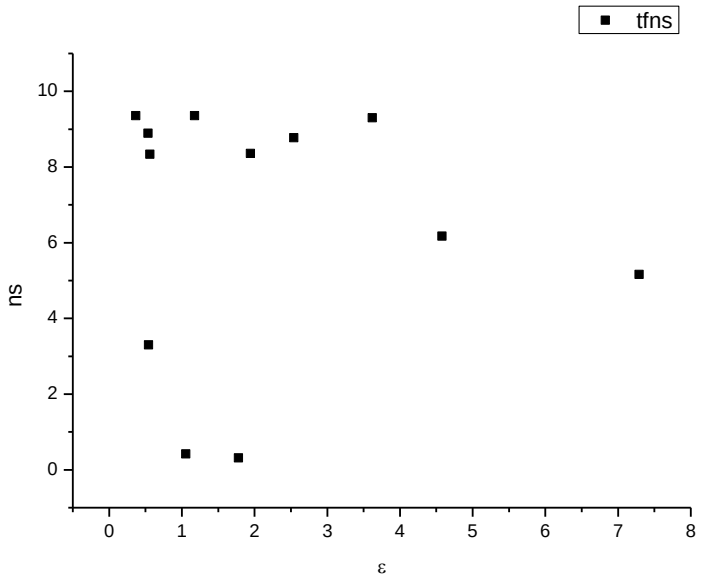

Figure 4.1.120. Amplitude weighted average lifetime (τ_f) of **21** at 570 nm versus ε.

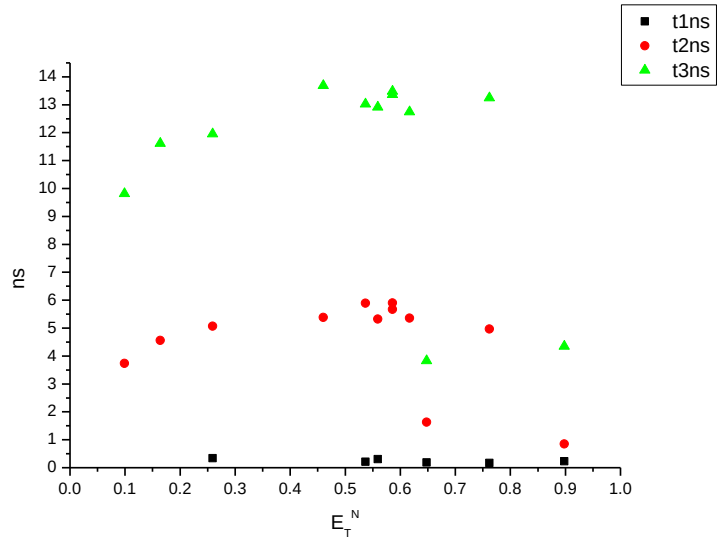

Figure 4.1.121. Intensity weighted components of TCSPC lifetime decay of **21** (570 nm) versus E_T^N.

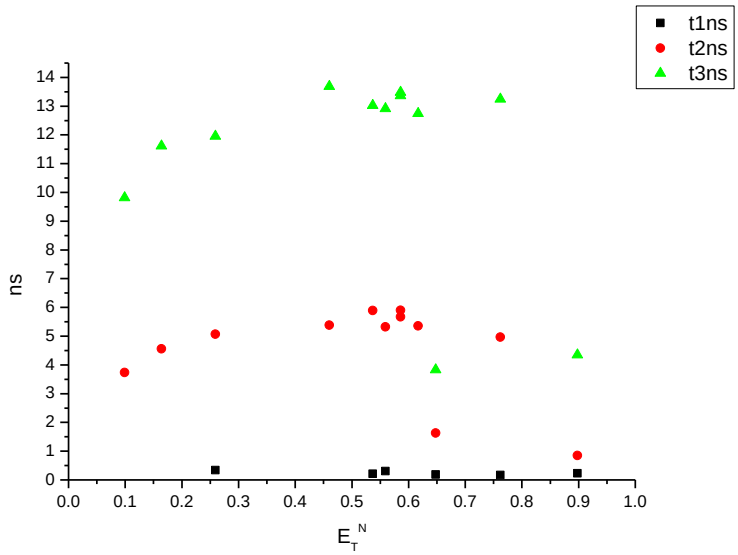

Figure 4.1.122. Amplitude weighted components of TCSPC lifetime decay of **21** (570 nm) versus E_T^N.

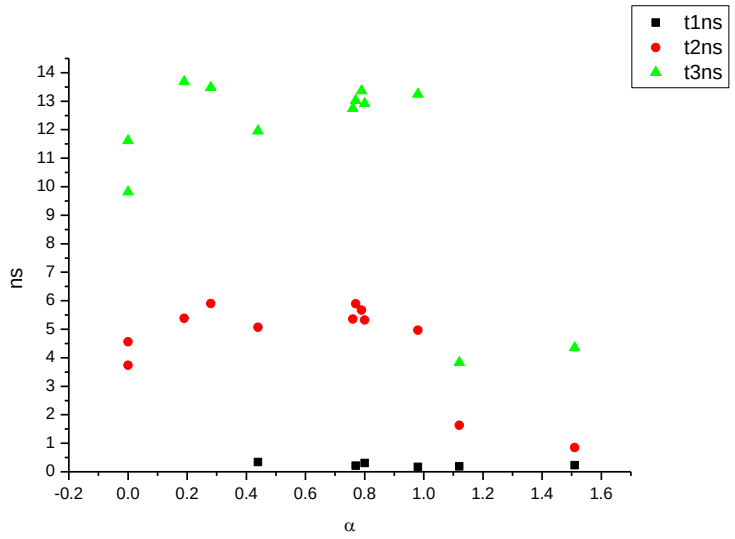

Figure 4.1.123. Intensity weighted components of TCSPC lifetime decay of **21** (570 nm) versus α.

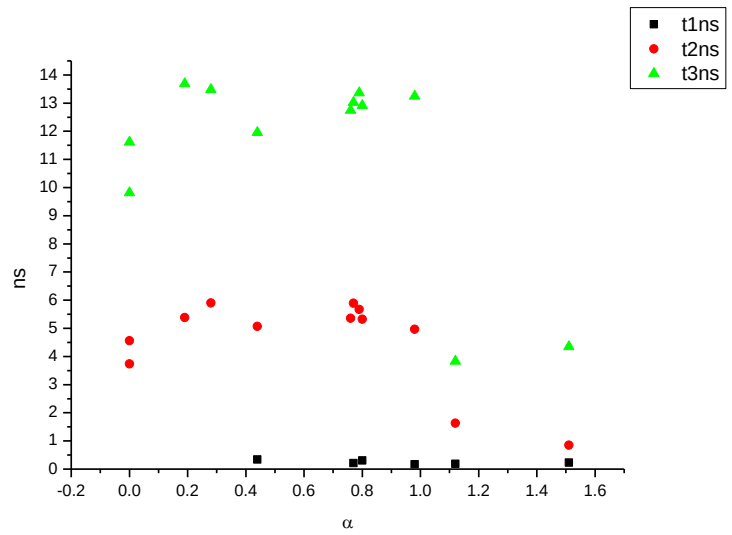

Figure 4.1.124. Amplitude weighted components of TCSPC lifetime decay of **21** (570 nm) versus α.

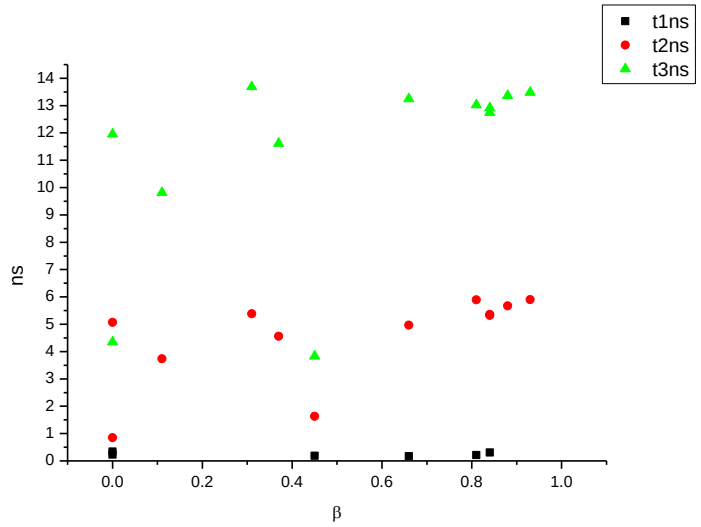

Figure 4.1.125. Intensity weighted components of TCSPC lifetime decay of **21** (570 nm) versus β.

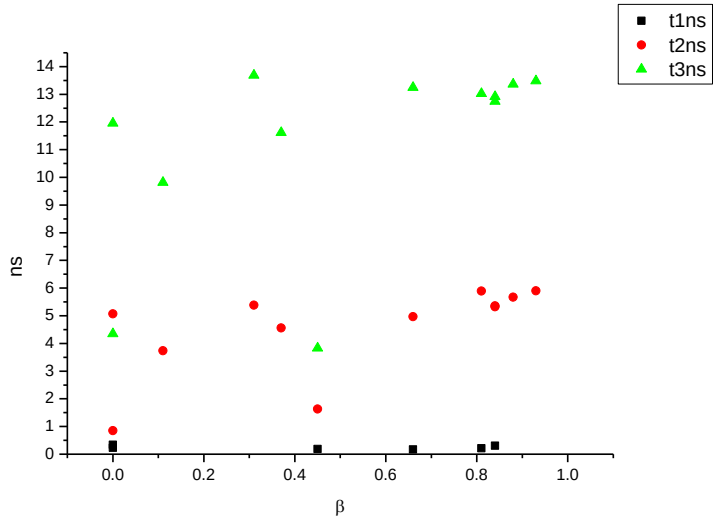

Figure 4.1.126. Amplitude weighted components of TCSPC lifetime decay of **21** (570 nm) versus β.

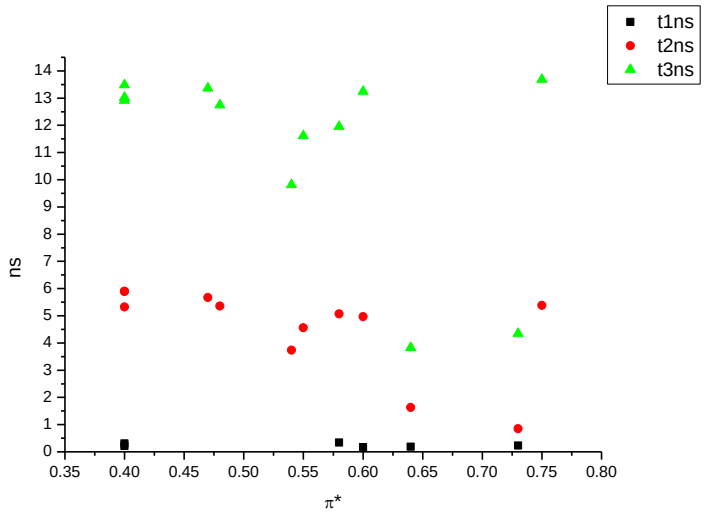

Figure 4.1.127. Intensity weighted components of TCSPC lifetime decay of **21** (570 nm) versus π*.

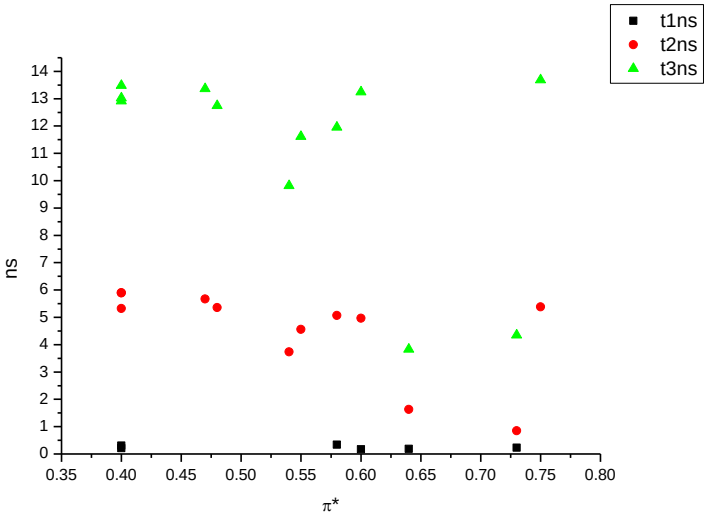

Figure 4.1.128. Amplitude weighted components of TCSPC lifetime decay of **21** (570 nm) versus π*.

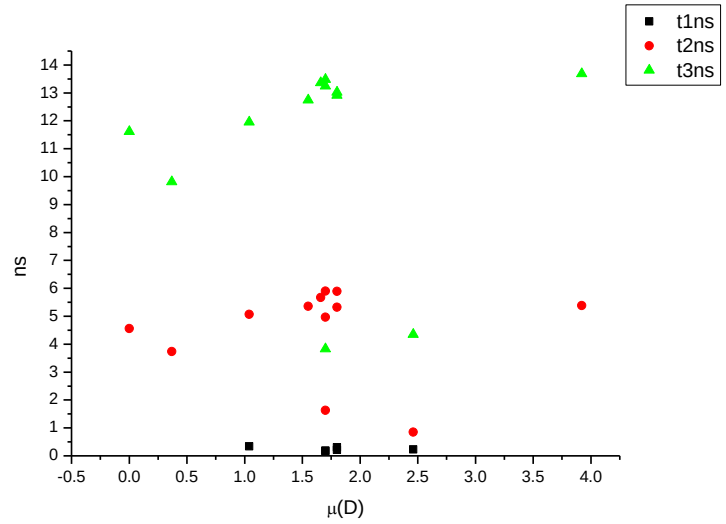

Figure 4.1.129. Intensity weighted components of TCSPC lifetime decay of **21** (570 nm) versus μ(D).

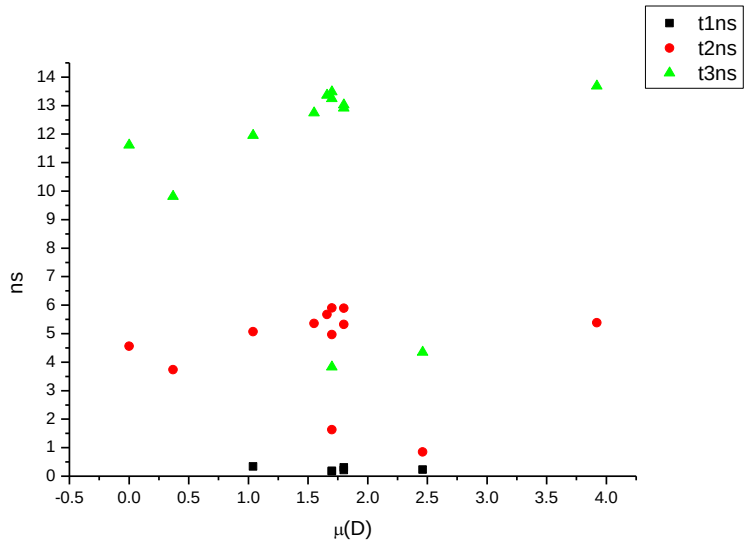

Figure 4.1.130. Amplitude weighted components of TCSPC lifetime decay of **21** (570 nm) versus μ(D).

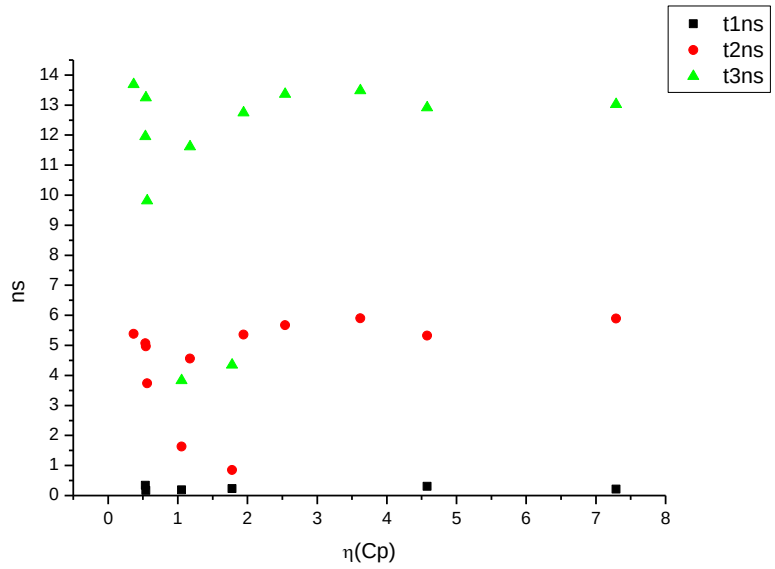

Figure 4.1.131. Intensity weighted components of TCSPC lifetime decay of **21** (570 nm) versus η(Cp).

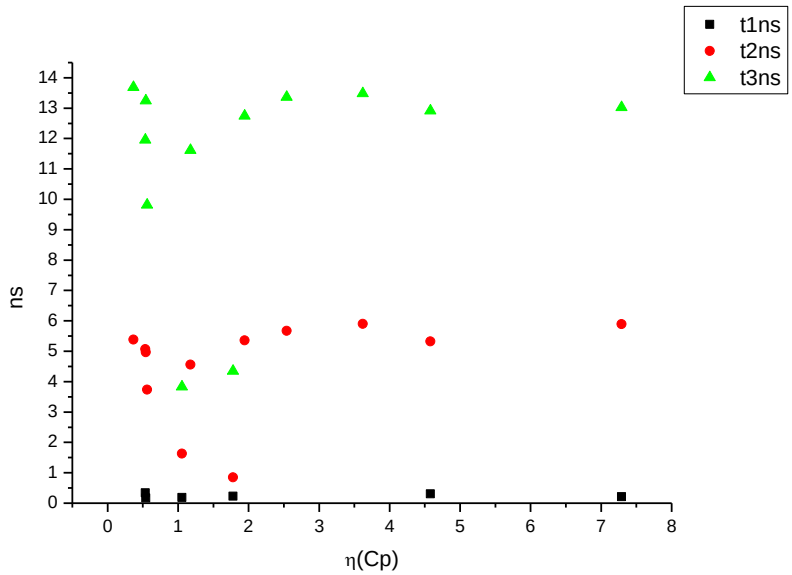

Figure 4.1.132. Amplitude weighted components of TCSPC lifetime decay of **21** (570 nm) versus η(Cp).

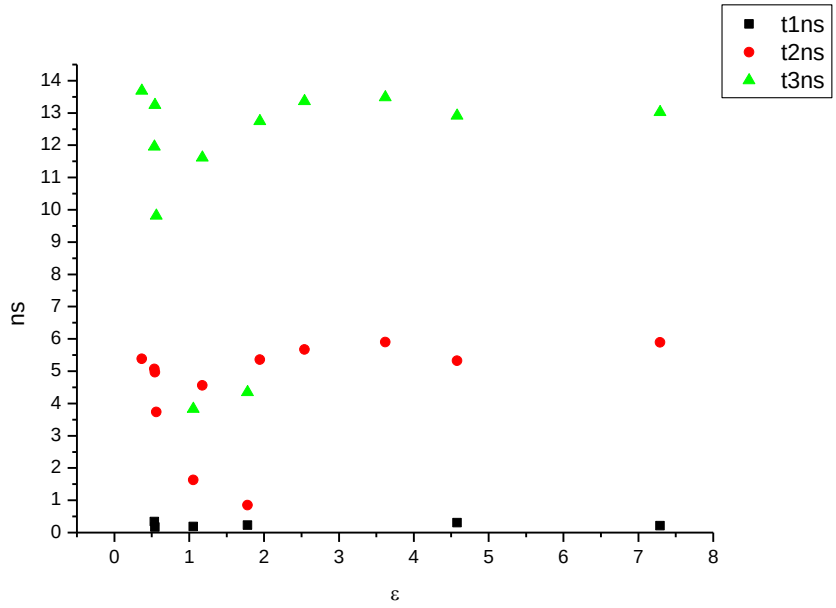

Figure 4.1.133. Intensity weighted components of TCSPC lifetime decay of **21** (570 nm) versus ε.

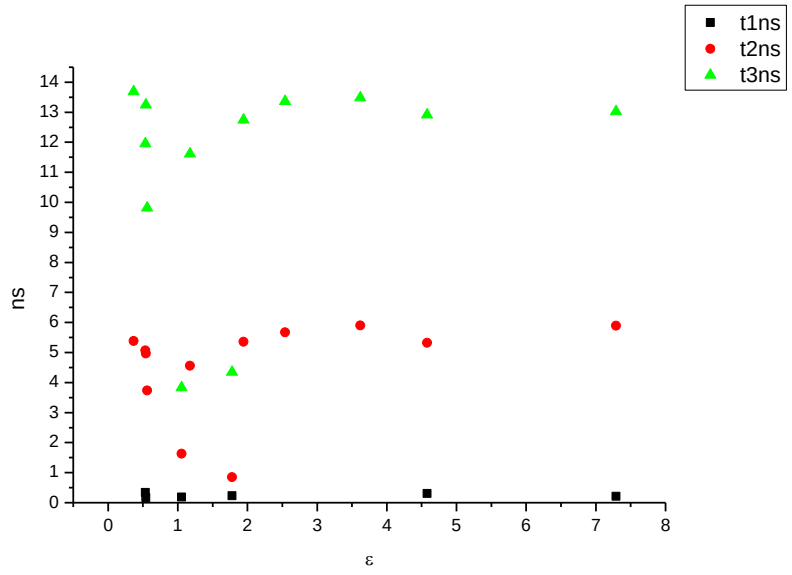

Figure 4.1.134. Amplitude weighted components of TCSPC lifetime decay of **21** (570 nm) versus ε.

4.1.8 Ultraviolet-visible absorption spectra.

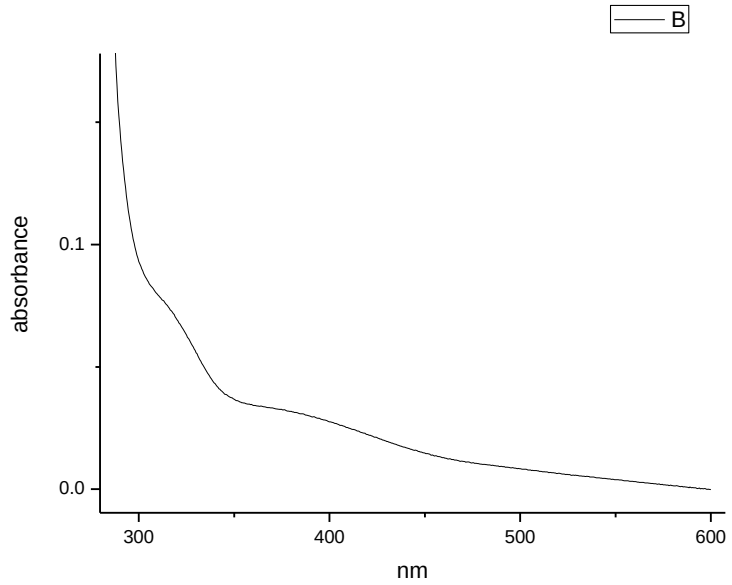

Figure 4.1.135. Ultraviolet-Visible absorption spectrum of **21** recorded in Toluene.

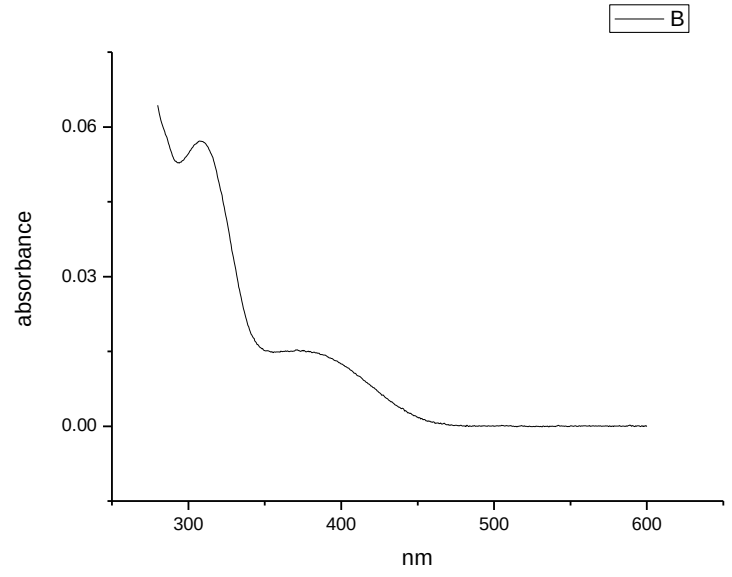

Figure 4.1.136. Ultraviolet-Visible absorption spectrum of **21** recorded in 1,4-dioxane.

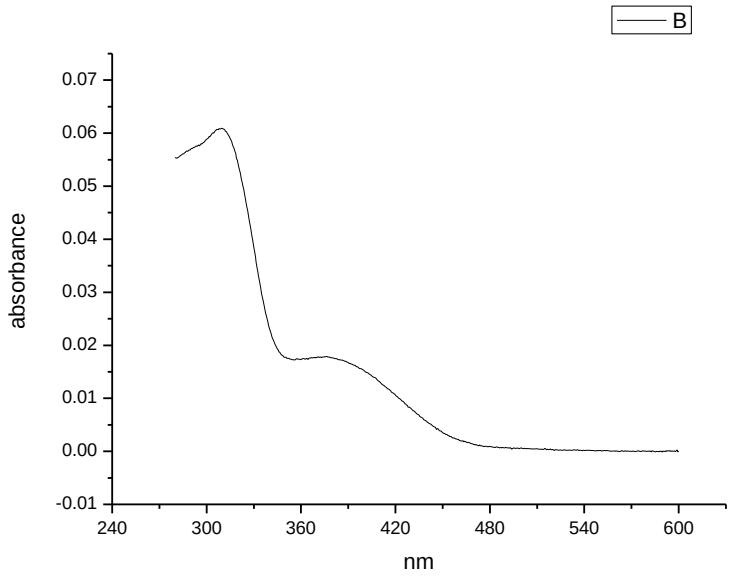

Figure 4.1.137. Ultraviolet-Visible absorption spectrum of **21** recorded in Chloroform.

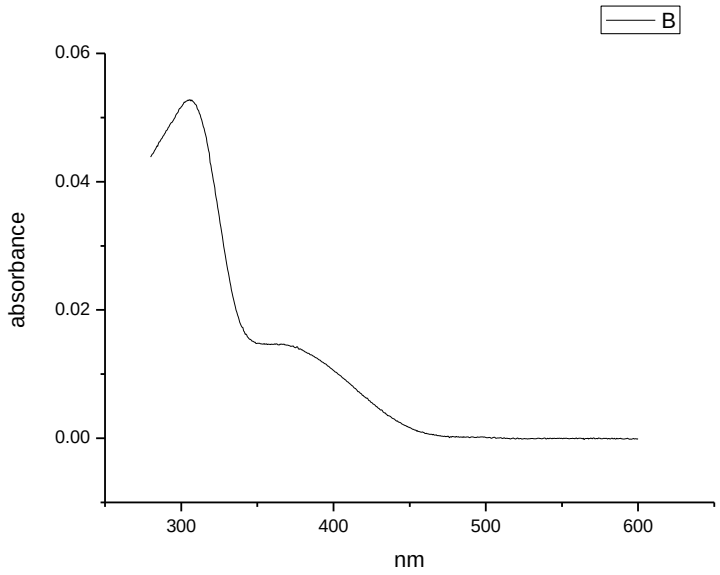

Figure 4.1.138. Ultraviolet-Visible absorption spectrum of **21** recorded in Acetonitrile.

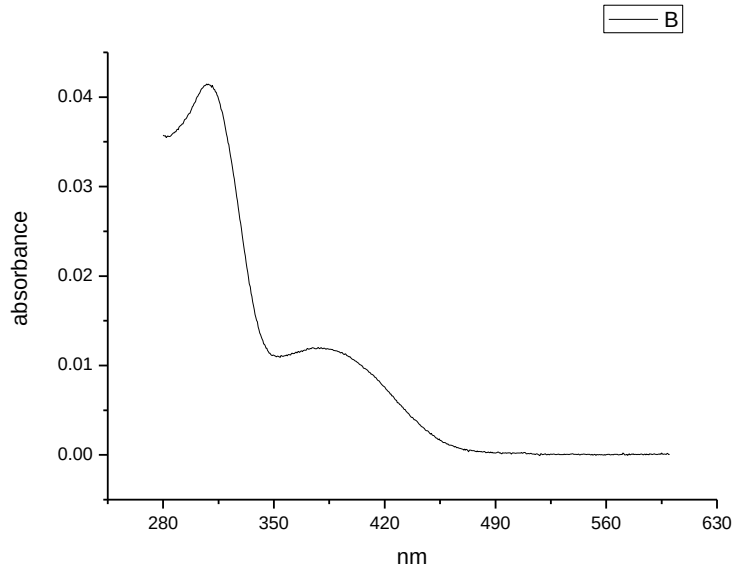

Figure 4.1.139. Ultraviolet-Visible absorption spectrum of **21** recorded in 1-octanol.

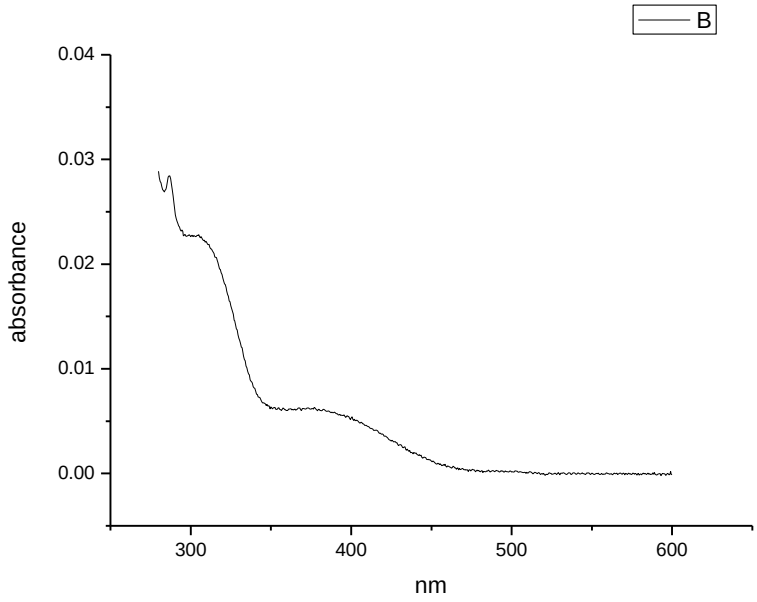

Figure 4.1.140. Ultraviolet-Visible absorption spectrum of **21** recorded in 1-hexanol.

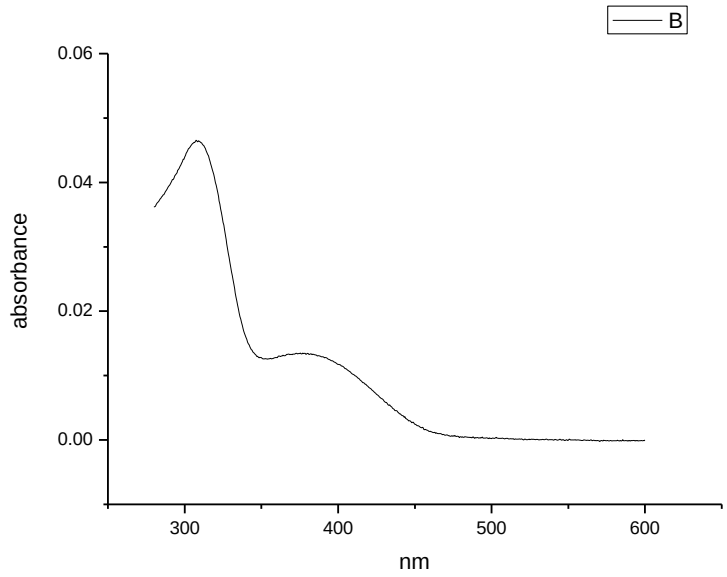

Figure 4.1.141. Ultraviolet-Visible absorption spectrum of **21** recorded in 1-butanol.

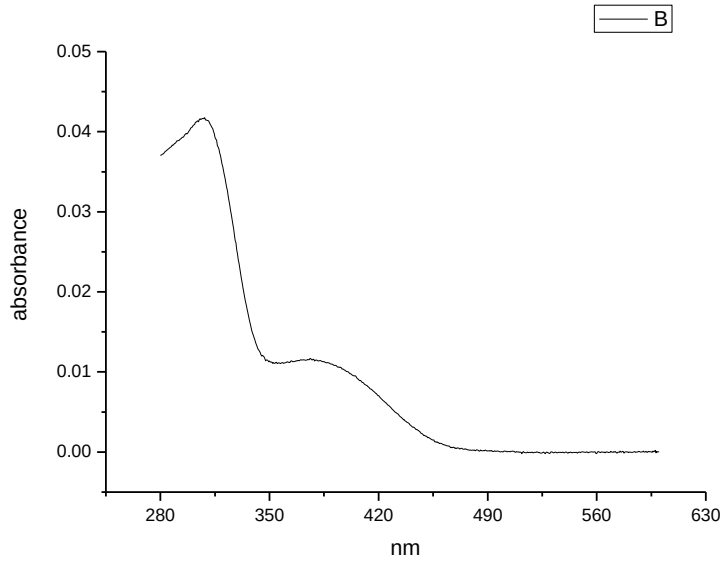

Figure 4.1.142. Ultraviolet-Visible absorption spectrum of **21** recorded in 1-pentanol.

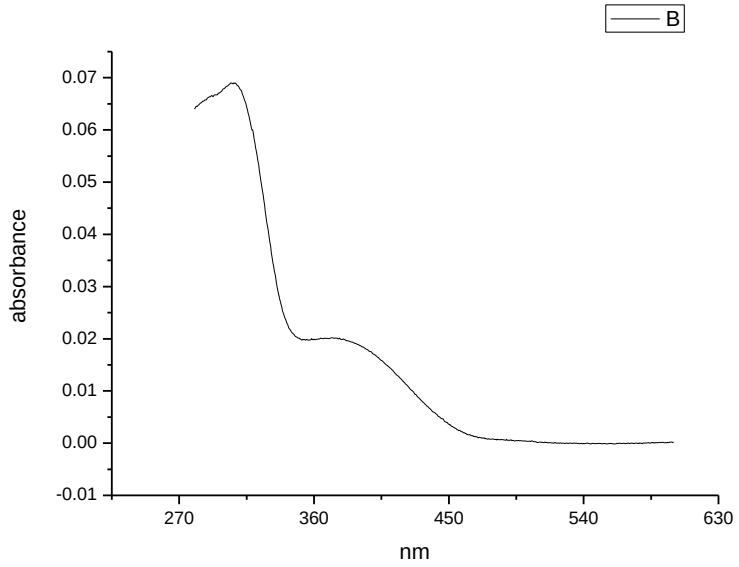

Figure 4.1.143. Ultraviolet-Visible absorption spectrum of **21** recorded in 1-propanol.

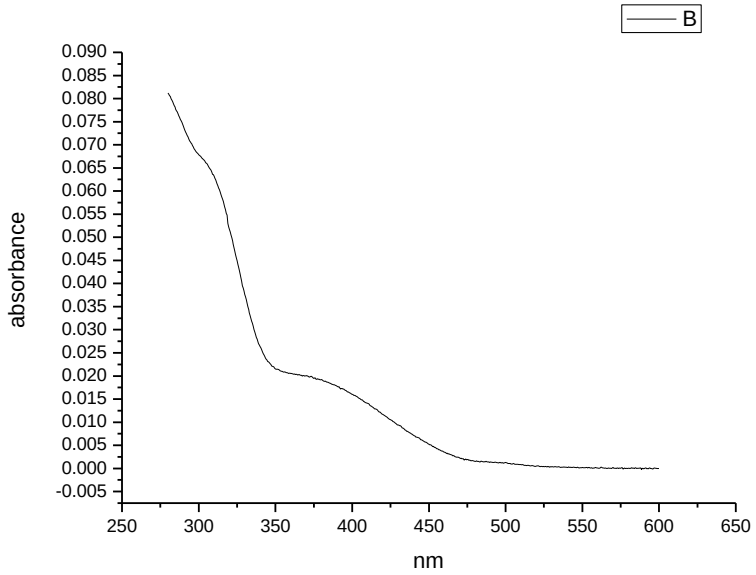

Figure 4.1.144. Ultraviolet-Visible absorption spectrum of **21** recorded in Acetic Acid.

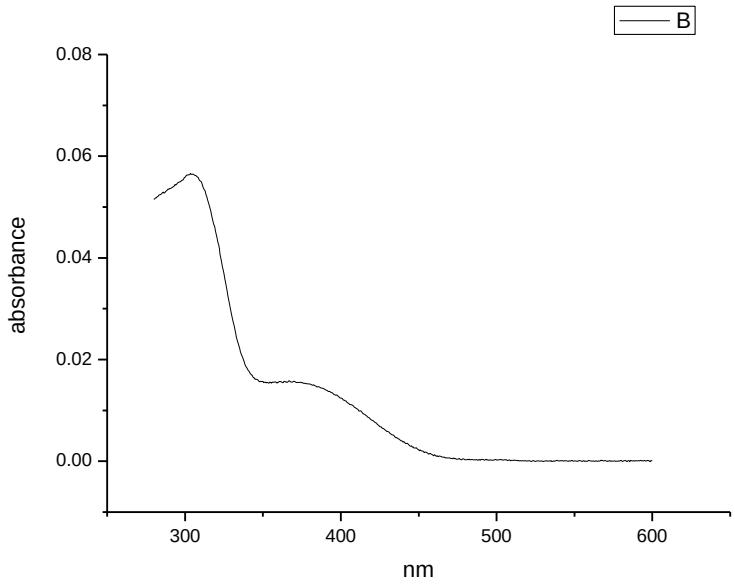

Figure 4.1.145. Ultraviolet-Visible absorption spectrum of **21** recorded in Methanol.

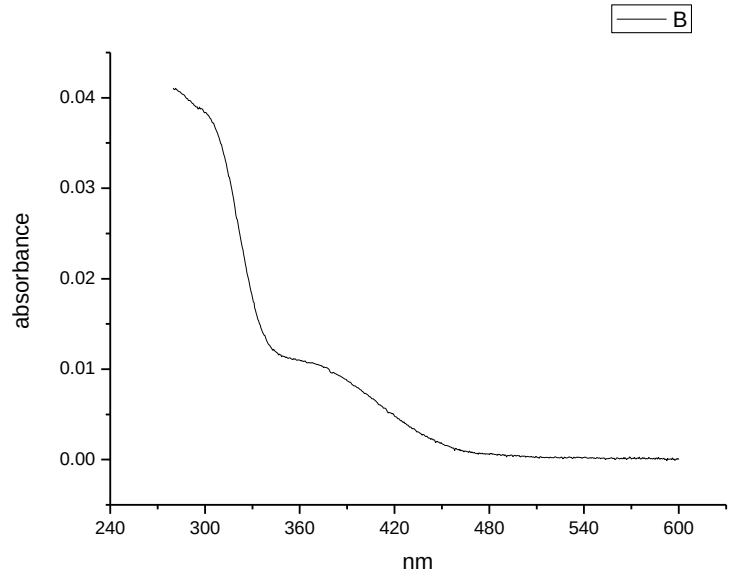

Figure 4.1.146. Ultraviolet-Visible absorption spectrum of **21** recorded in 2,2,2-trifluoroethanol.

4.1.9 Fluorescence Emission spectra.

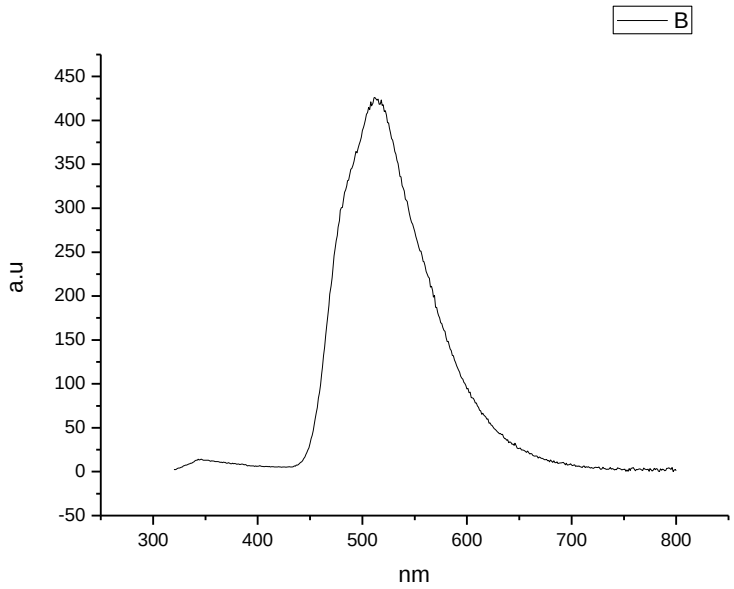

Figure 4.1.147. Fluorescence emission spectrum of **21** recorded in Toluene at 310 nm excitation.

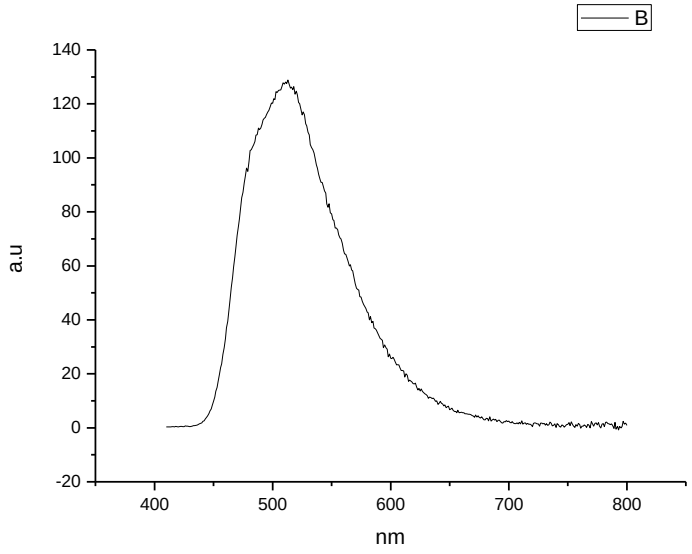

Figure 4.1.148. Fluorescence emission spectrum of **21** recorded in Toluene at 400 nm excitation.

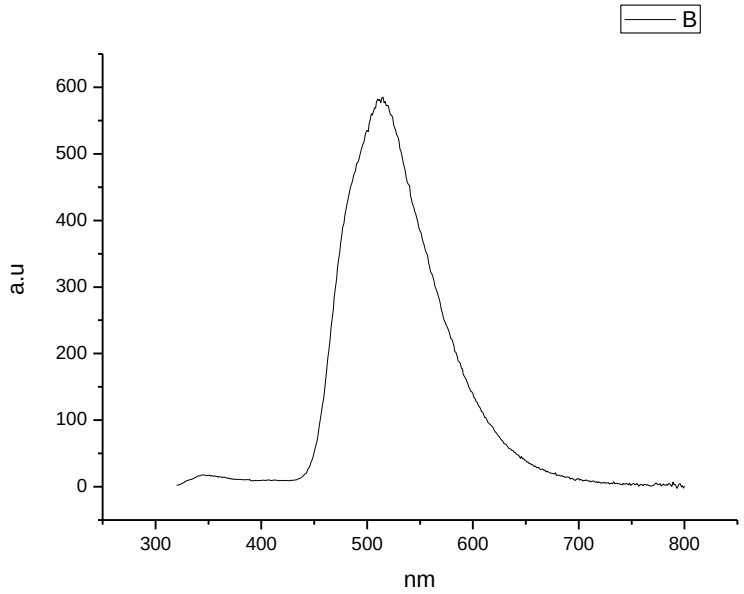

Figure 4.1.149. Fluorescence emission spectrum of **21** recorded in 1,4-dioxane at 310 nm excitation.

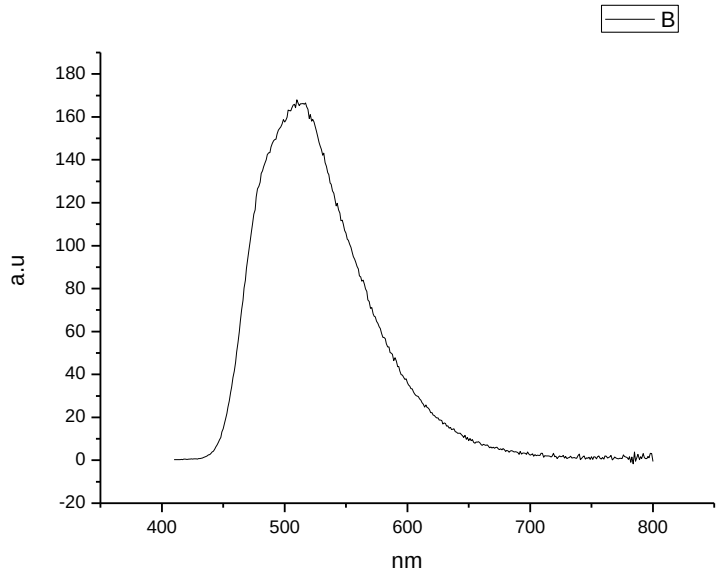

Figure 4.1.150. Fluorescence emission spectrum of **21** recorded in 1,4-dioxane at 400 nm excitation.

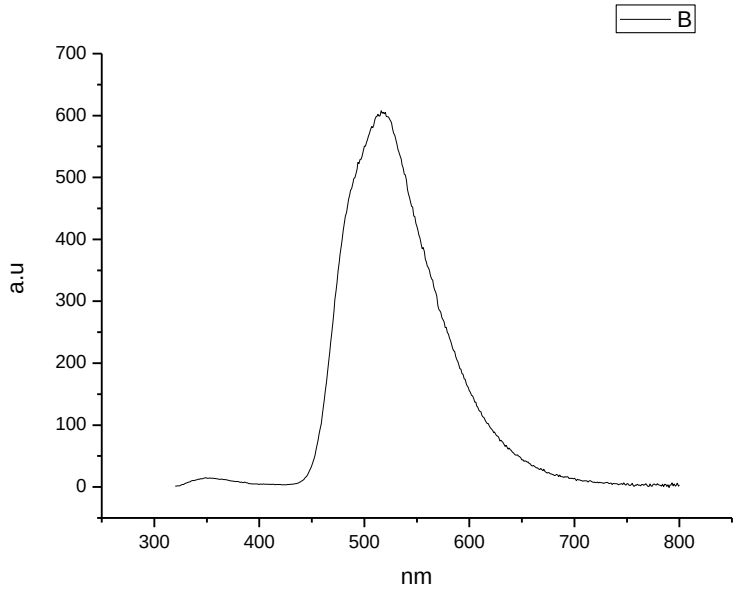

Figure 4.1.151. Fluorescence emission spectrum of **21** recorded in Chloroform at 310 nm excitation.

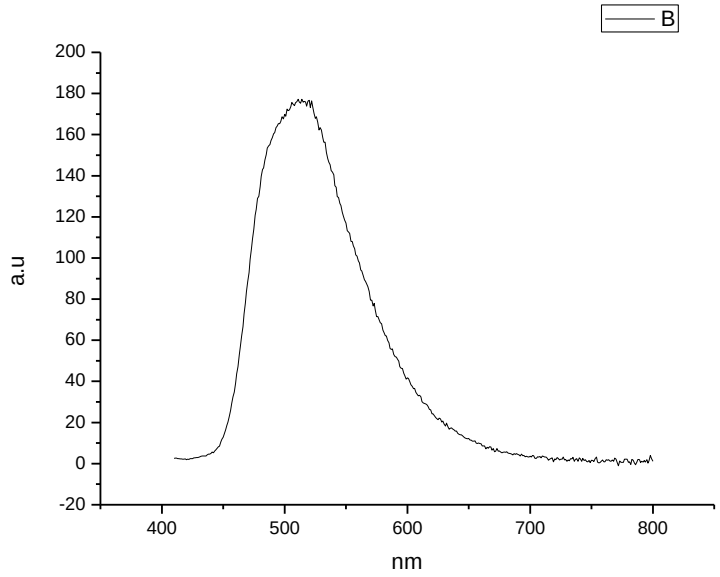

Figure 4.1.152. Fluorescence emission spectrum of **21** recorded in Chloroform at 400 nm excitation.

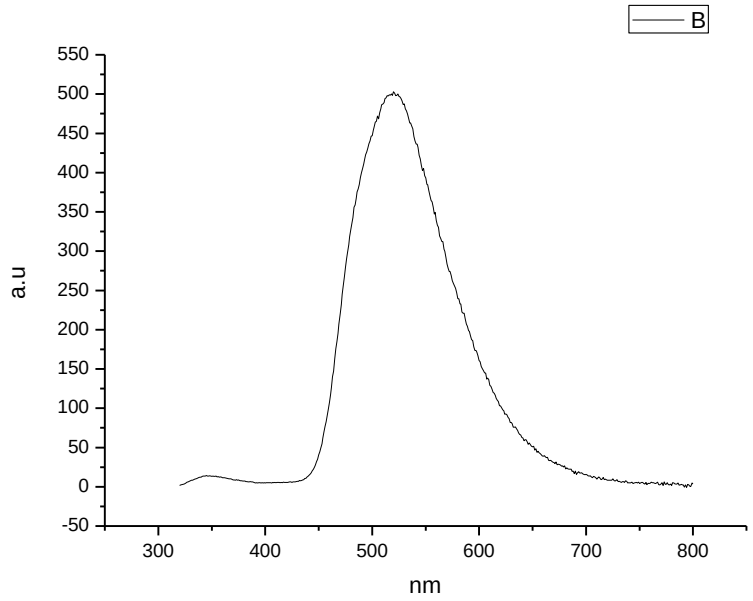

Figure 4.1.153. Fluorescence emission spectrum of **21** recorded in Acetonitrile at 310 nm excitation.

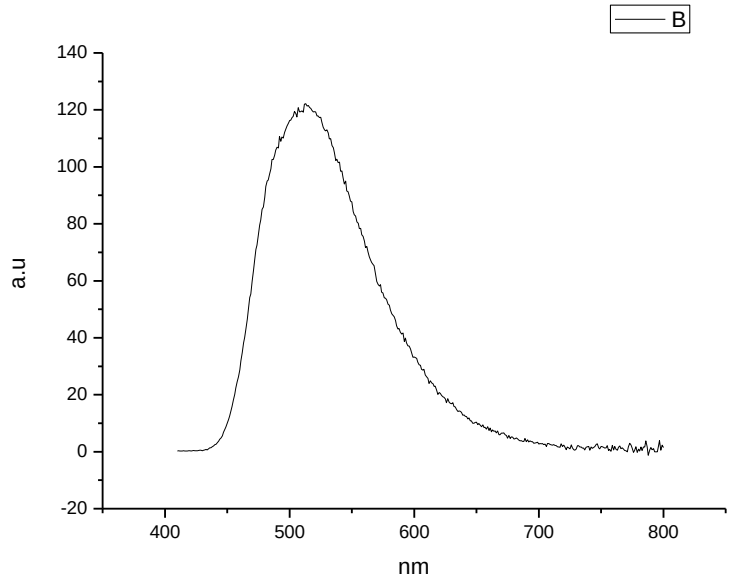

Figure 4.1.154. Fluorescence emission spectrum of **21** recorded in Acetonitrile at 400 nm excitation.

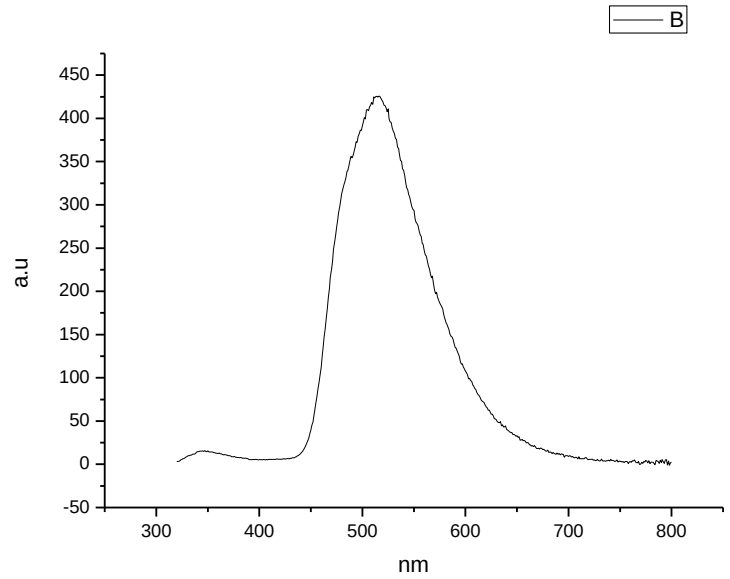

Figure 4.1.155. Fluorescence emission spectrum of **21** recorded in 1-octanol at 310 nm excitation.

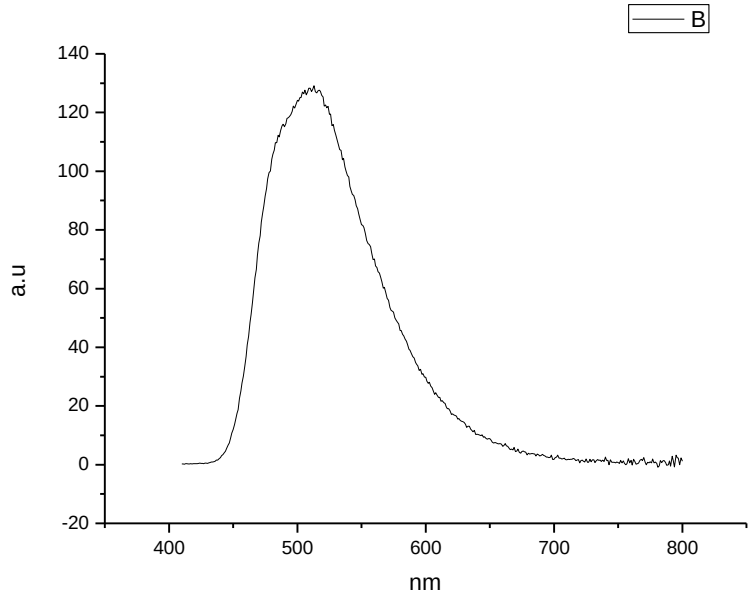

Figure 4.1.156. Fluorescence emission spectrum of **21** recorded in 1-octanol at 400 nm excitation.

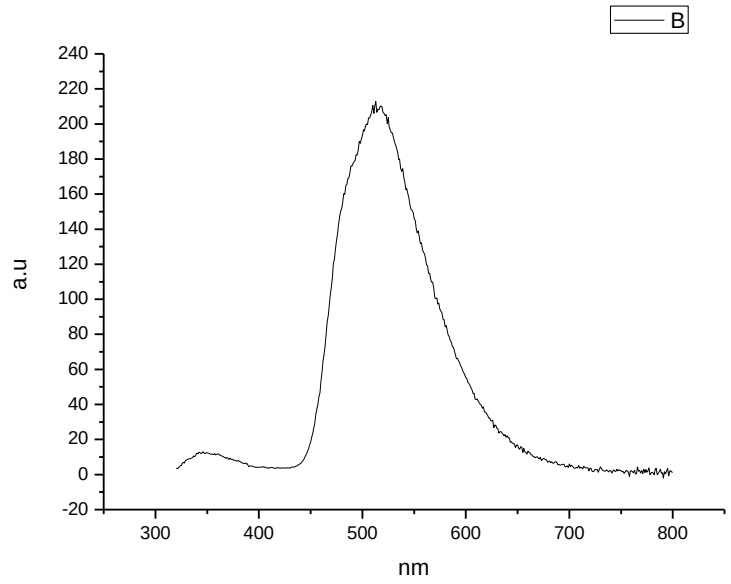

Figure 4.1.157. Fluorescence emission spectrum of **21** recorded in 1-hexanol at 310 nm excitation.

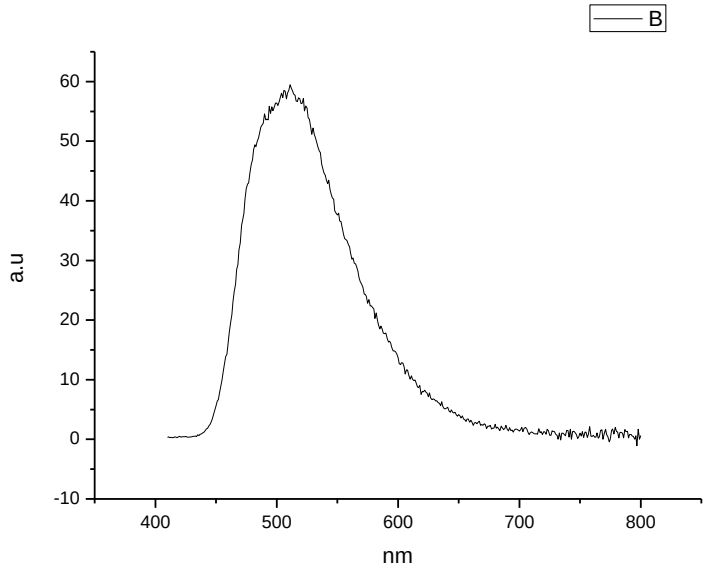

Figure 4.1.158. Fluorescence emission spectrum of **21** recorded in 1-hexanol at 400 nm excitation.

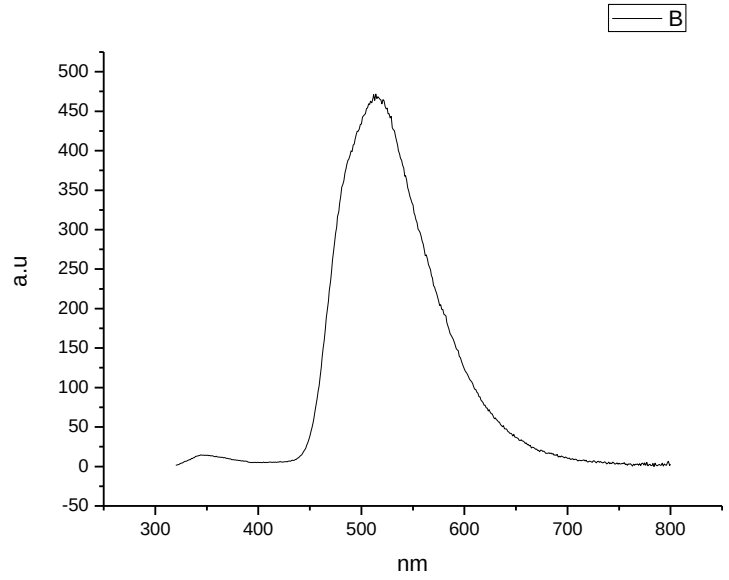

Figure 4.1.159. Fluorescence emission spectrum of **21** recorded in 1-butanol at 310 nm excitation.

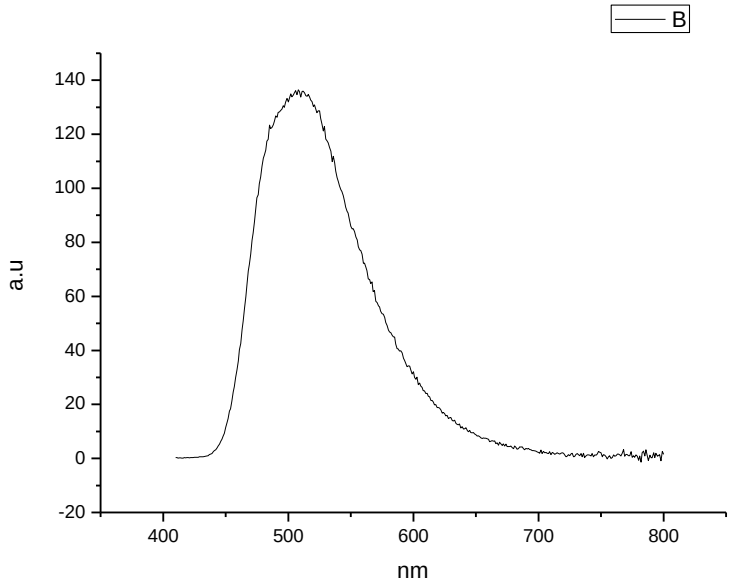

Figure 4.1.160. Fluorescence emission spectrum of **21** recorded in 1-butanol at 400 nm excitation.

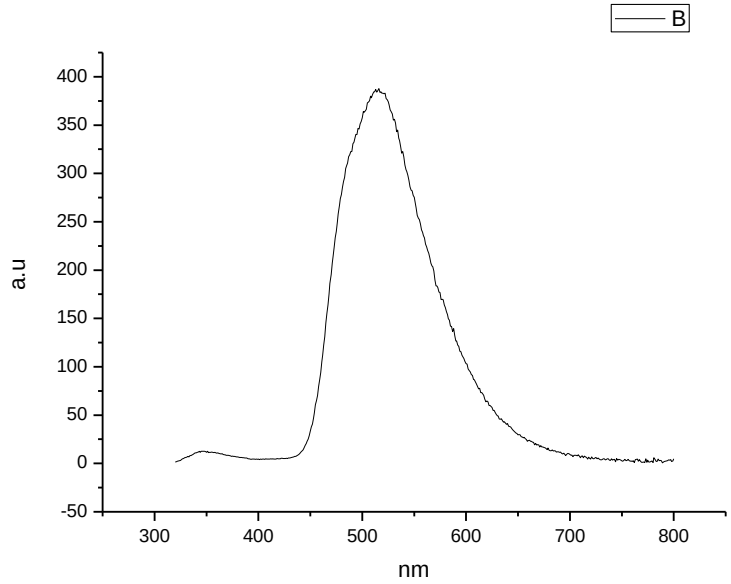

Figure 4.1.161. Fluorescence emission spectrum of **21** recorded in 1-pentanol at 310 nm excitation.

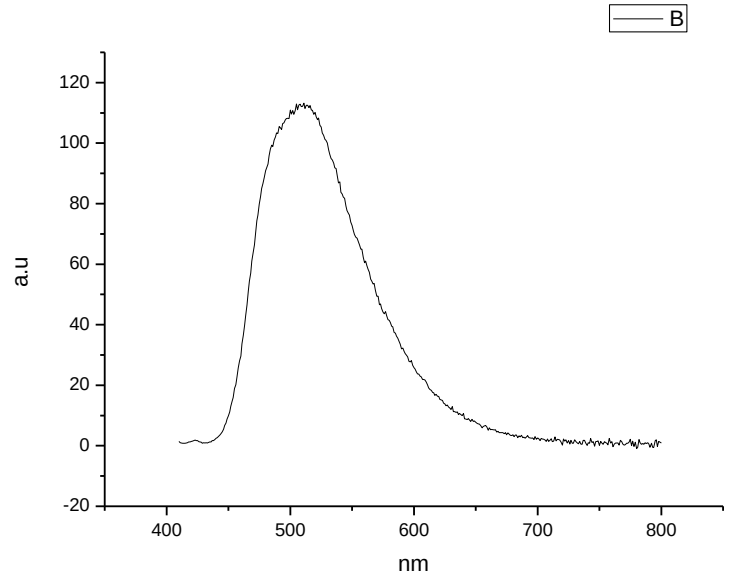

Figure 4.1.162. Fluorescence emission spectrum of **21** recorded in 1-pentanol at 400 nm excitation.

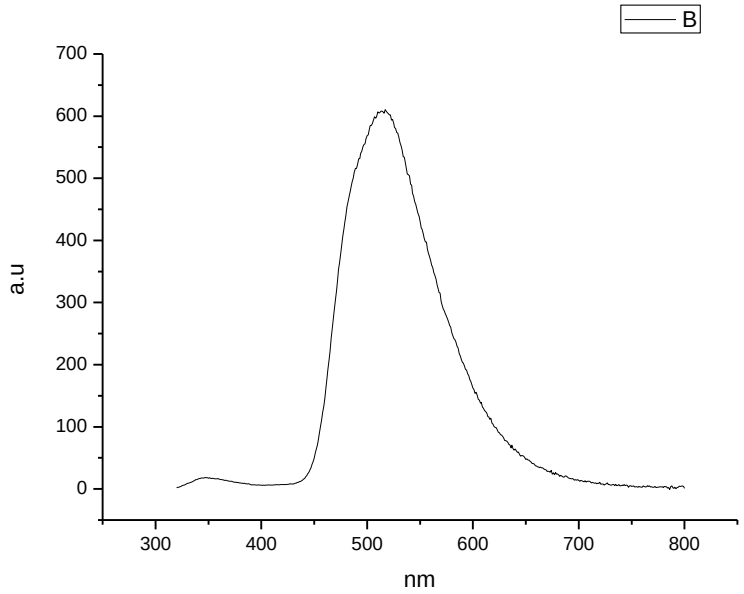

Figure 4.1.163. Fluorescence emission spectrum of **21** recorded in 1-propanol at 310 nm excitation.

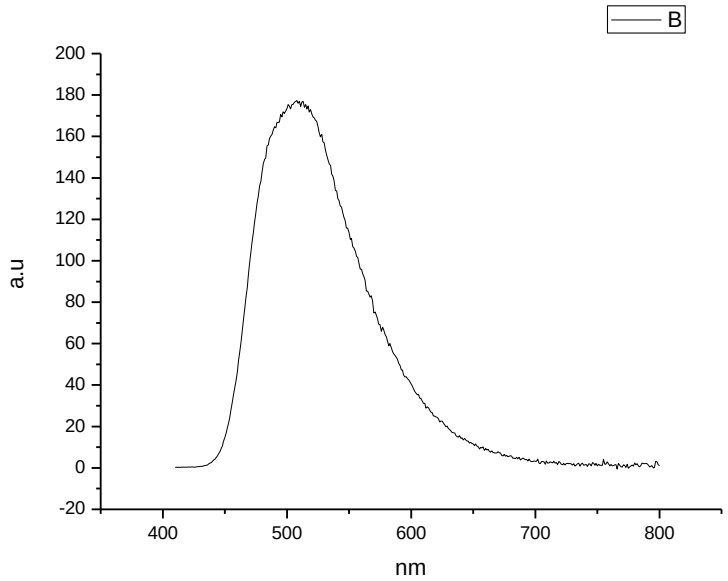

Figure 4.1.164. Fluorescence emission spectrum of **21** recorded in 1-propanol at 400 nm excitation.

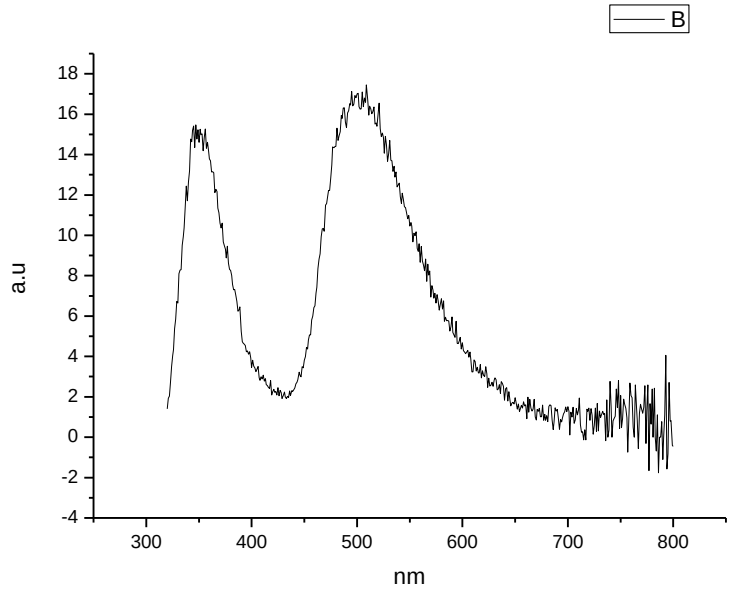

Figure 4.1.165. Fluorescence emission spectrum of **21** recorded in Acetic Acid at 310 nm excitation.

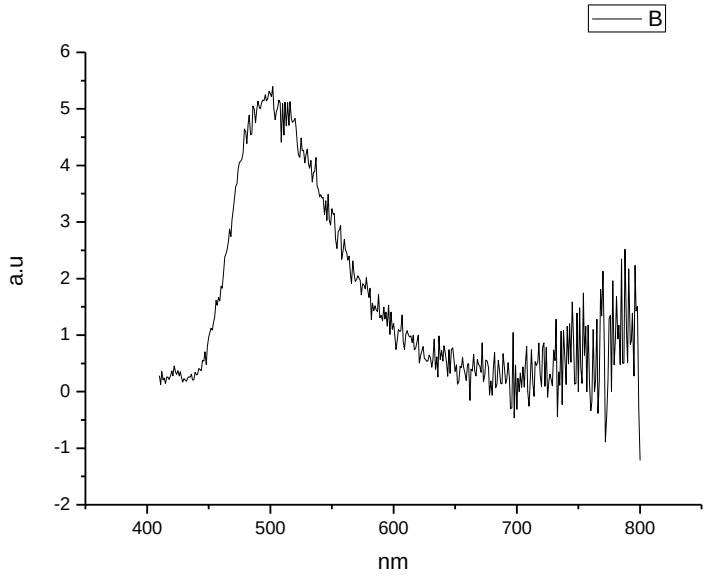

Figure 4.1.166. Fluorescence emission spectrum of **21** recorded in Acetic Acid at 400 nm excitation.

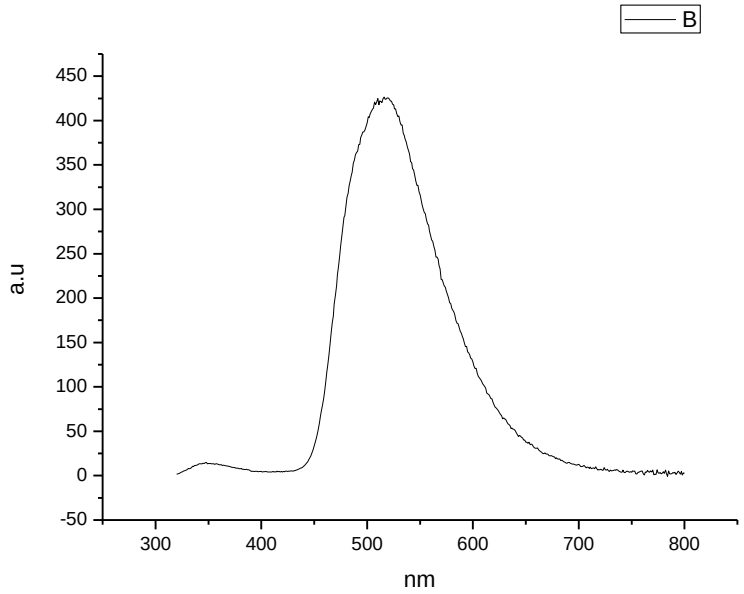

Figure 4.1.167. Fluorescence emission spectrum of **21** recorded in Methanol at 310 nm excitation.

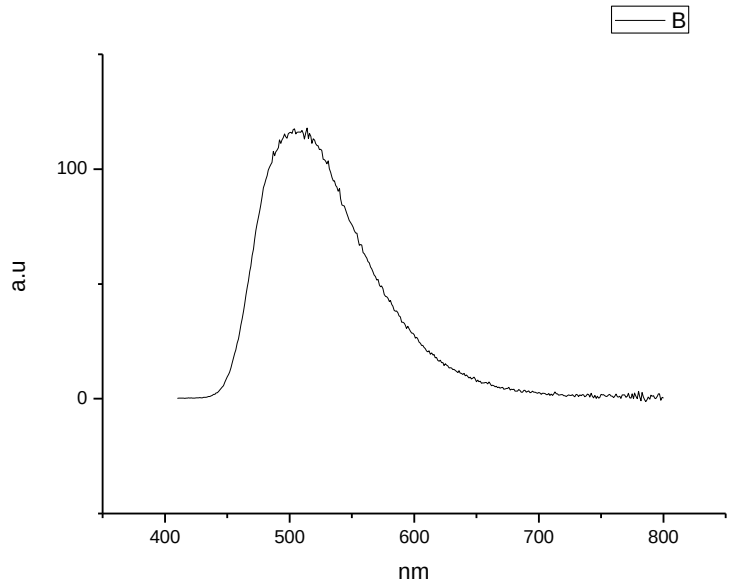

Figure 4.1.168. Fluorescence emission spectrum of **21** recorded in Methanol at 400 nm excitation.

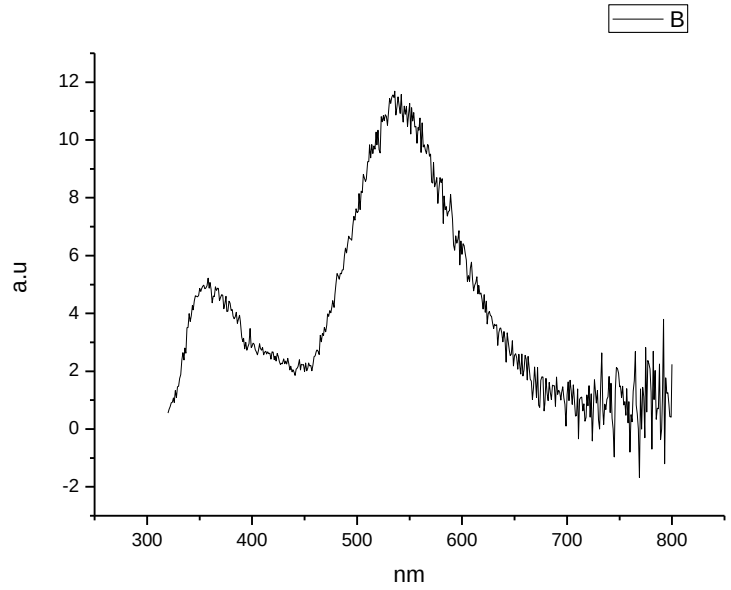

Figure 4.1.169. Fluorescence emission spectrum of **21** recorded in 2,2,2-trifluoroethanol at 310 nm excitation.

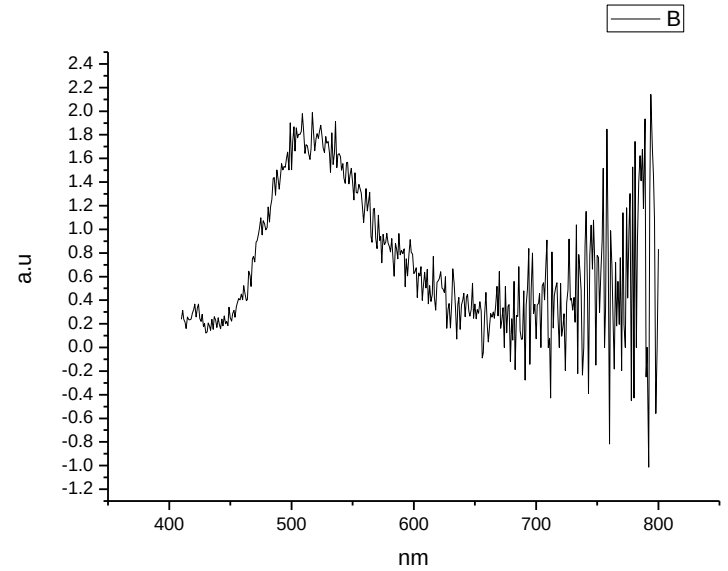

Figure 4.1.170. Fluorescence emission spectrum of **21** recorded in 2,2,2-trifluoroethanol at 400 nm excitation.

4.1.10 Normalised Fluorescence Emission spectra (Gaussian fitted).

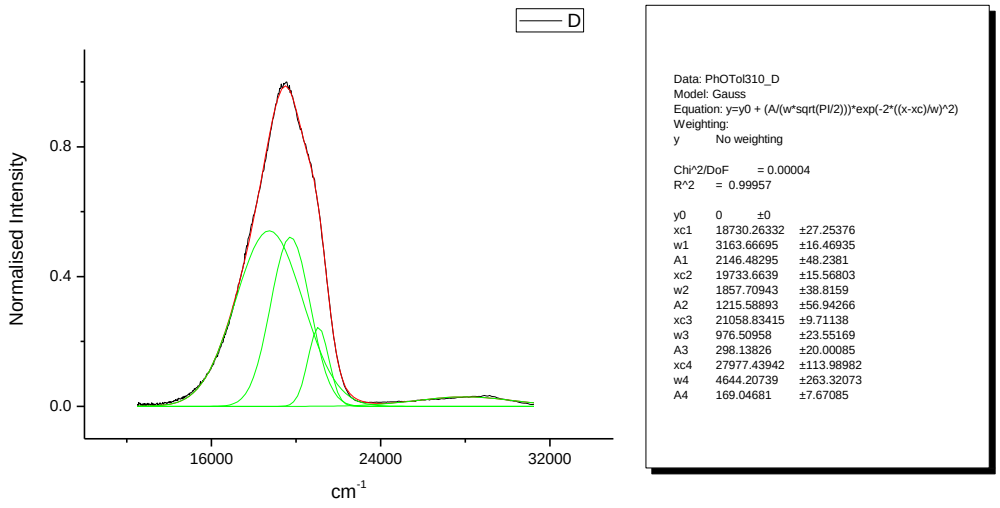

Figure 4.1.171. Gaussian model fit of the normalised fluorescence emission spectrum of **21** recorded in Toluene at 310 nm excitation.

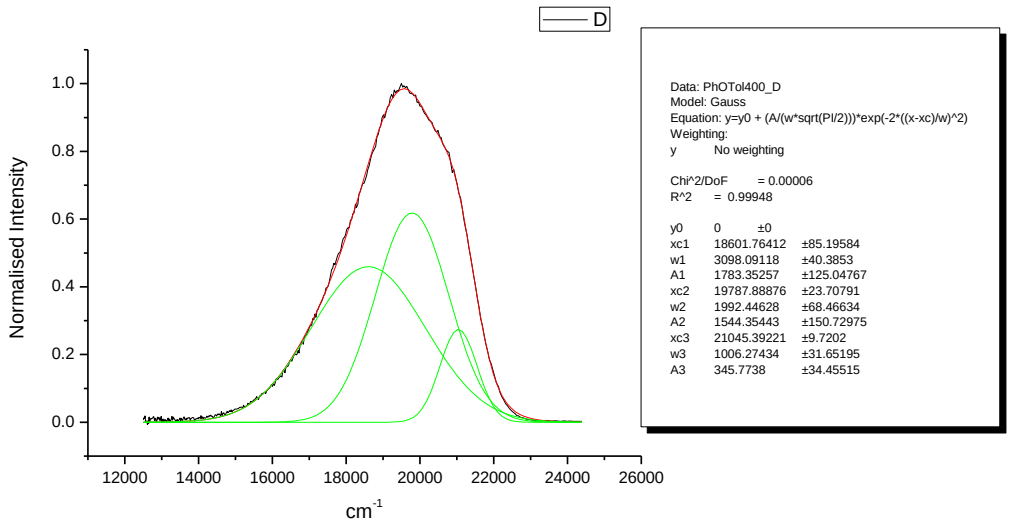

Figure 4.1.172. Gaussian model fit of the normalised fluorescence emission spectrum of **21** recorded in Toluene at 400 nm excitation.

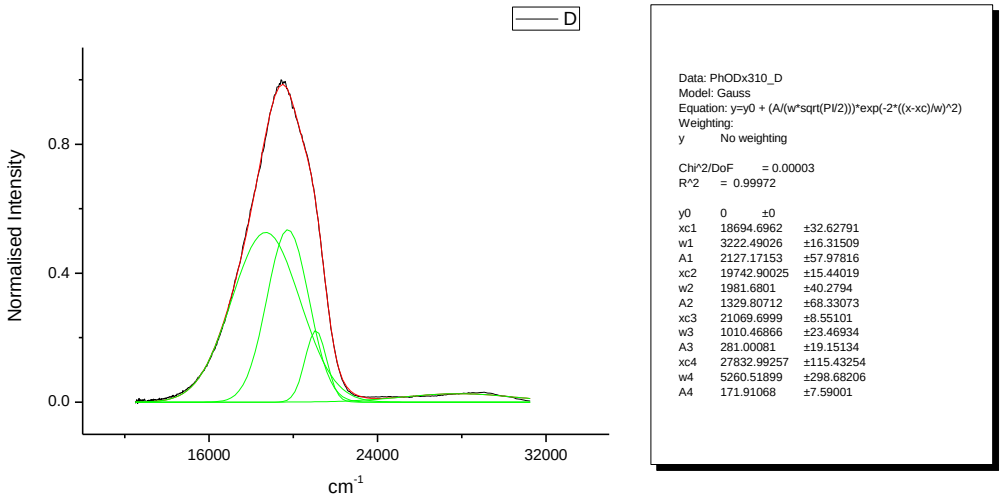

Figure 4.1.173. Gaussian model fit of the normalised fluorescence emission spectrum of **21** recorded in 1,4-dioxane at 310 nm excitation.

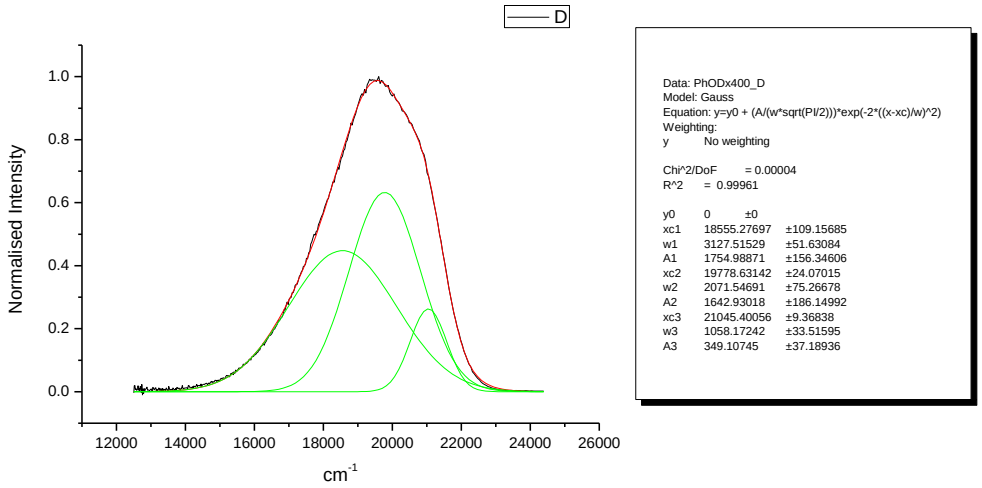

Figure 4.1.174. Gaussian model fit of the normalised fluorescence emission spectrum of **21** recorded in 1,4-dioxane at 400 nm excitation.

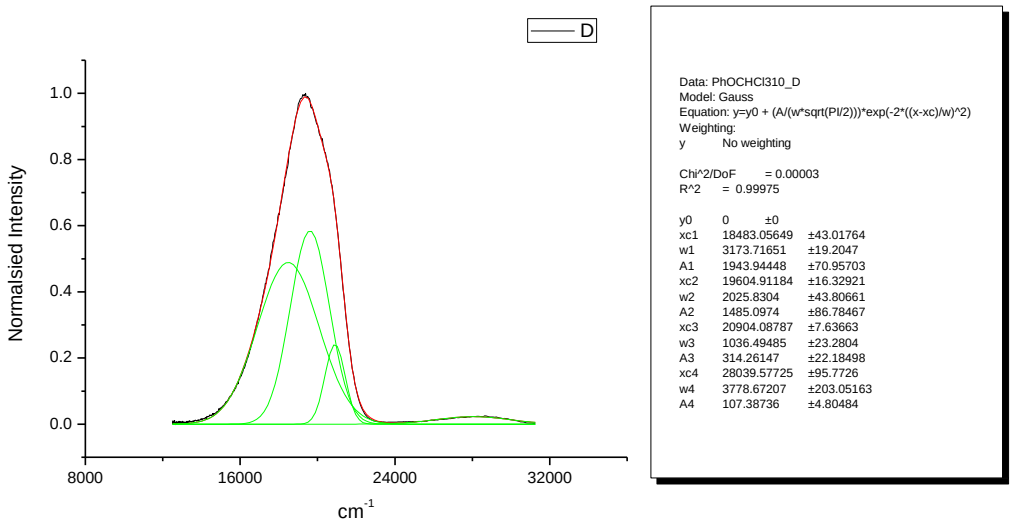

Figure 4.1.175. Gaussian model fit of the normalised fluorescence emission spectrum of **21** recorded in Chloroform at 310 nm excitation.

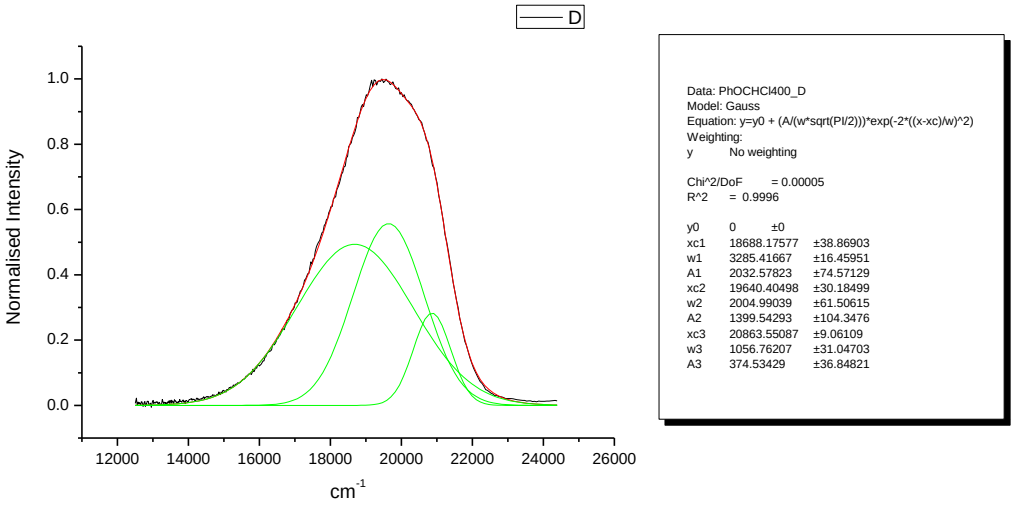

Figure 4.1.176. Gaussian model fit of the normalised fluorescence emission spectrum of **21** recorded in Chloroform at 400 nm excitation.

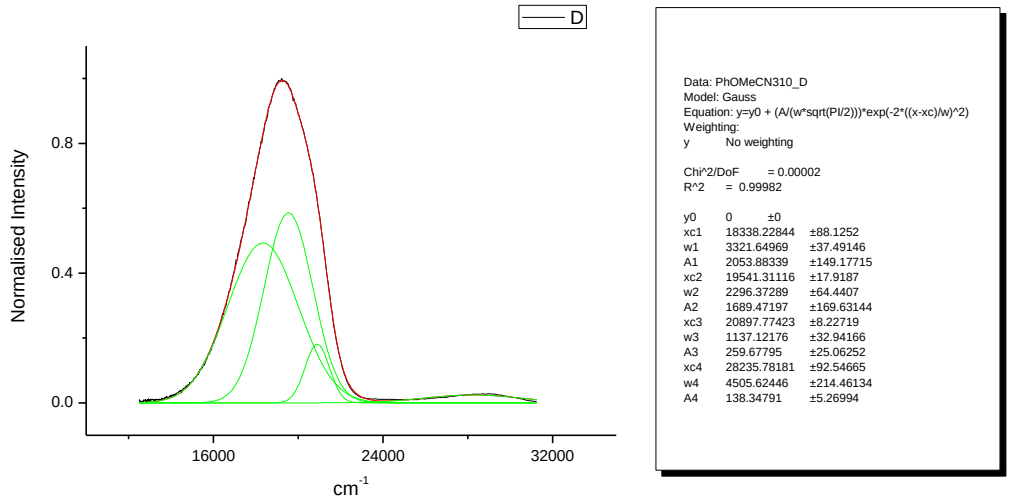

Figure 4.1.177. Gaussian model fit of the normalised fluorescence emission spectrum of **21** recorded in Acetonitrile at 310 nm excitation.

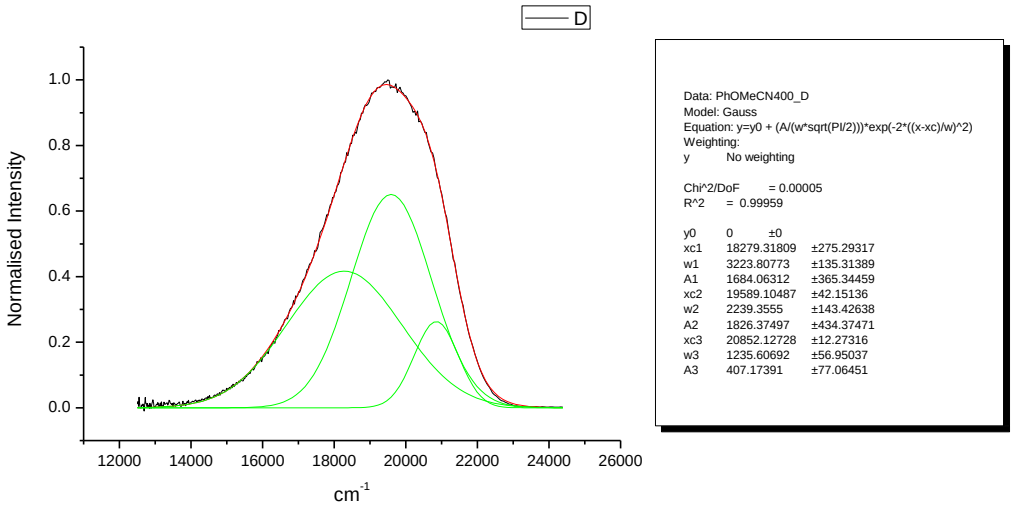

Figure 4.1.178. Gaussian model fit of the normalised fluorescence emission spectrum of **21** recorded in Acetonitrile at 400 nm excitation.

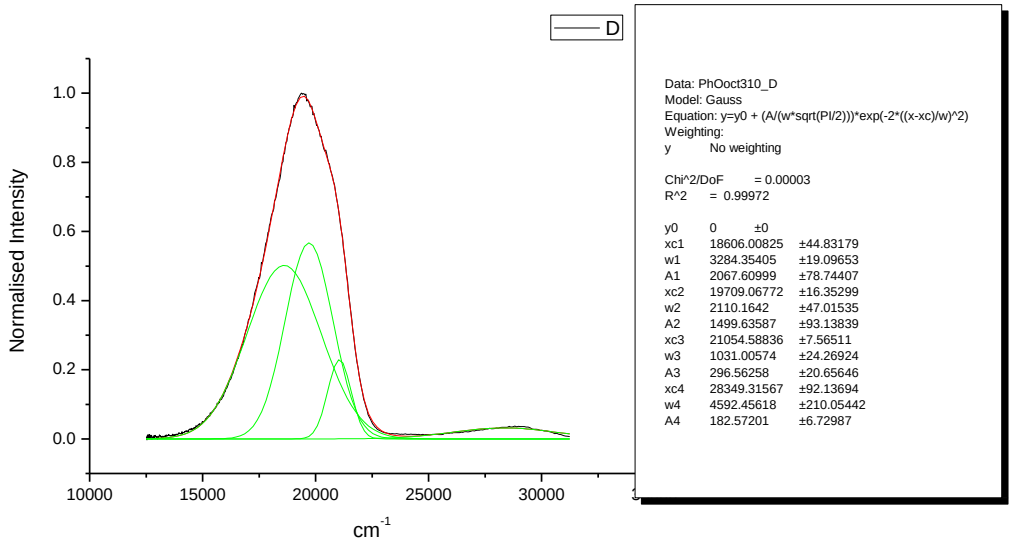

Figure 4.1.179. Gaussian model fit of the normalised fluorescence emission spectrum of **21** recorded in 1-octanol at 310 nm excitation.

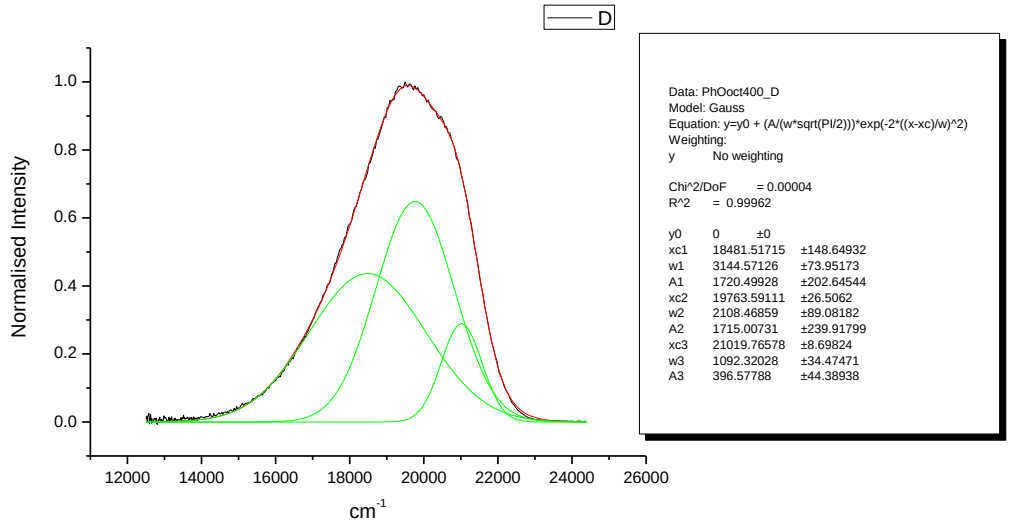

Figure 4.1.180. Gaussian model fit of the normalised fluorescence emission spectrum of **21** recorded in 1-octanol at 400 nm excitation.

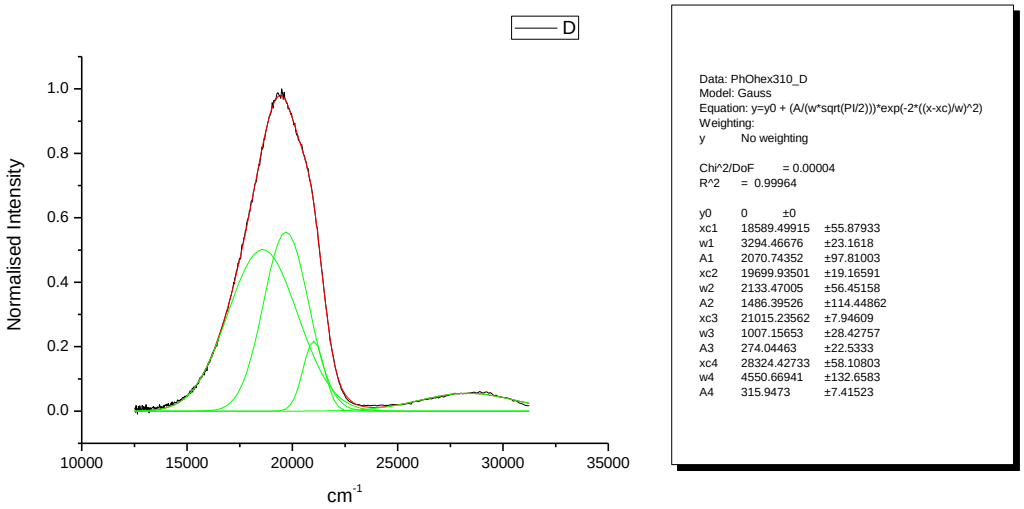

Figure 4.1.181. Gaussian model fit of the normalised fluorescence emission spectrum of **21** recorded in 1-hexanol at 310 nm excitation.

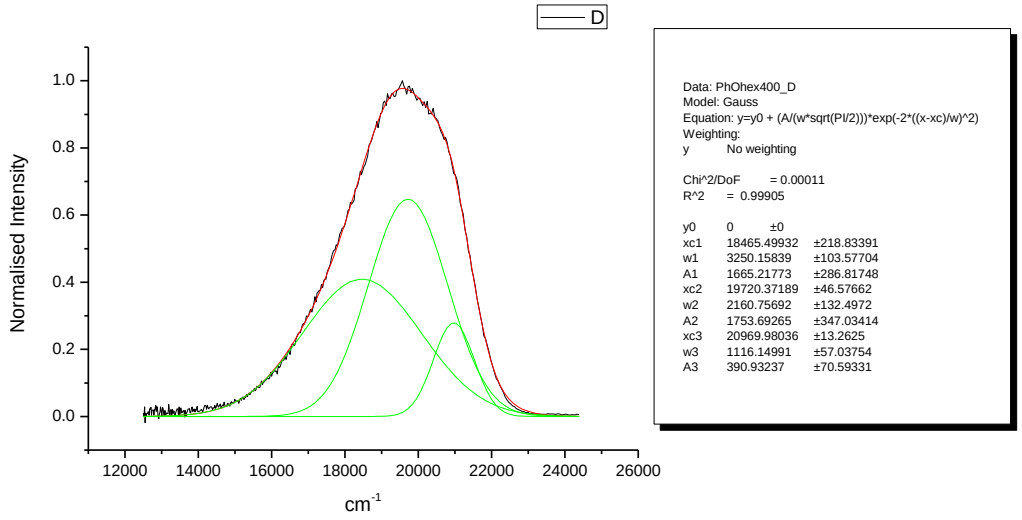

Figure 4.1.182. Gaussian model fit of the normalised fluorescence emission spectrum of **21** recorded in 1-hexanol at 400 nm excitation.

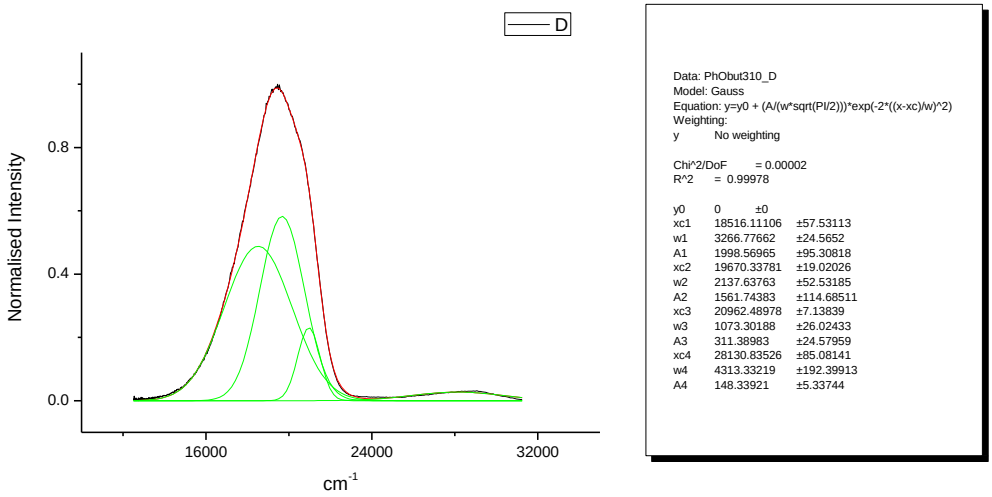

Figure 4.1.183. Gaussian model fit of the normalised fluorescence emission spectrum of **21** recorded in 1-butanol at 310 nm excitation.

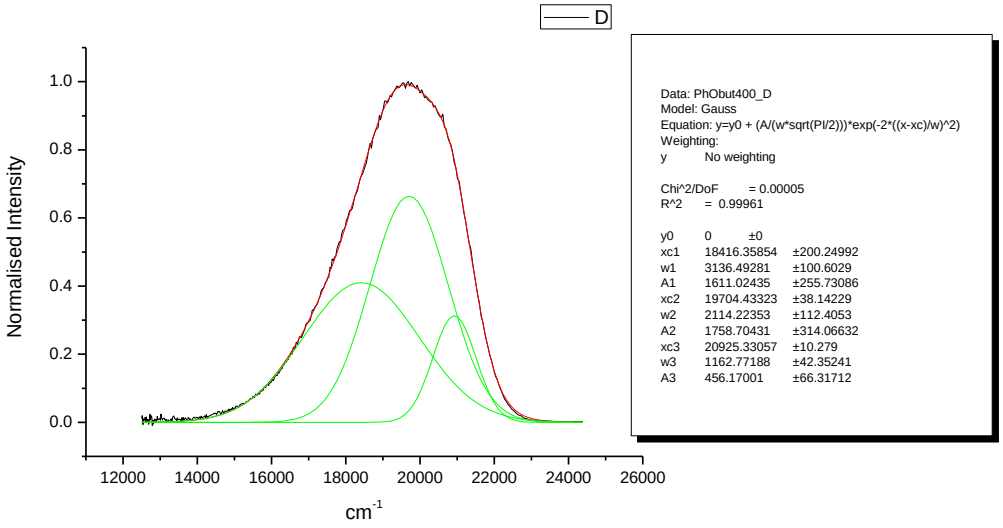

Figure 4.1.184. Gaussian model fit of the normalised fluorescence emission spectrum of **21** recorded in 1-butanol at 400 nm excitation.

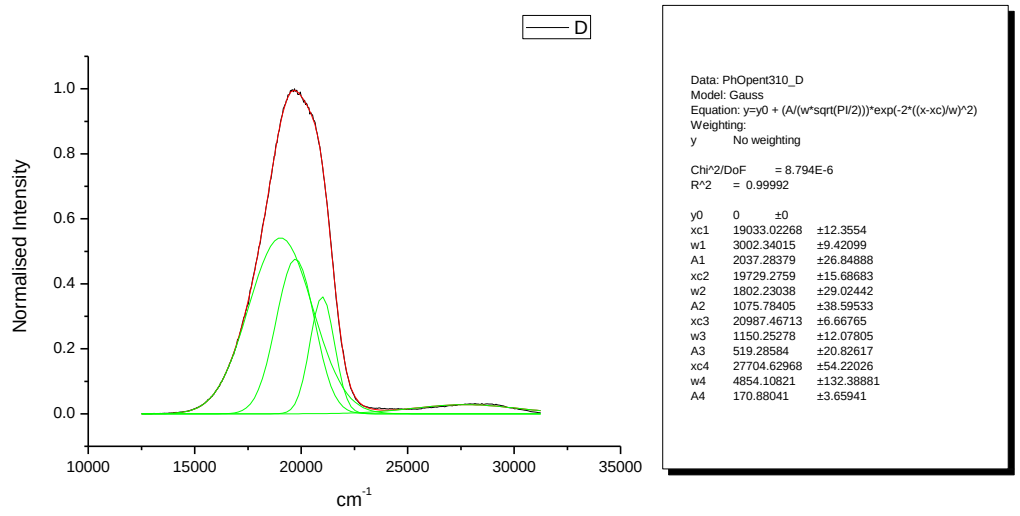

Figure 4.1.185. Gaussian model fit of the normalised fluorescence emission spectrum of **21** recorded in 1-pentanol at 310 nm excitation.

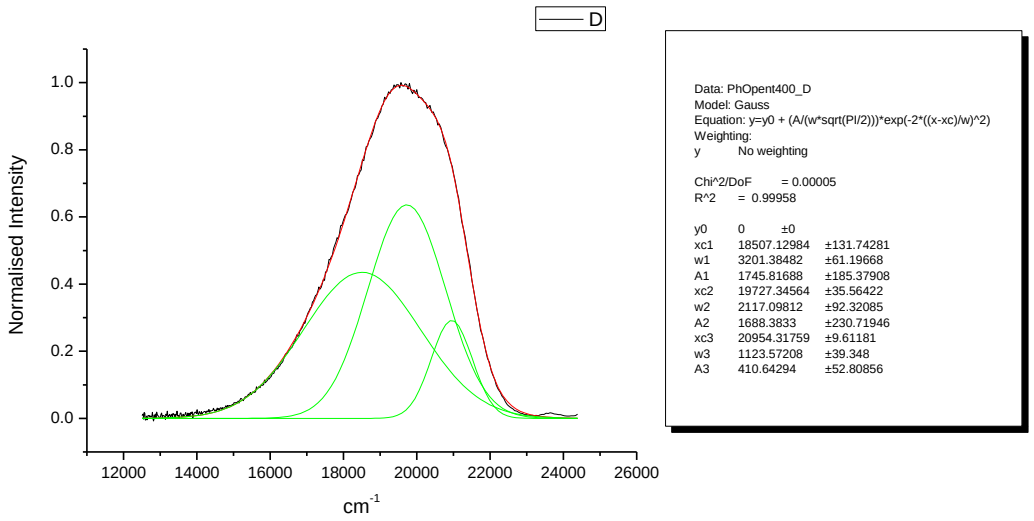

Figure 4.1.186. Gaussian model fit of the normalised fluorescence emission spectrum of **21** recorded in 1-pentanol at 400 nm excitation.

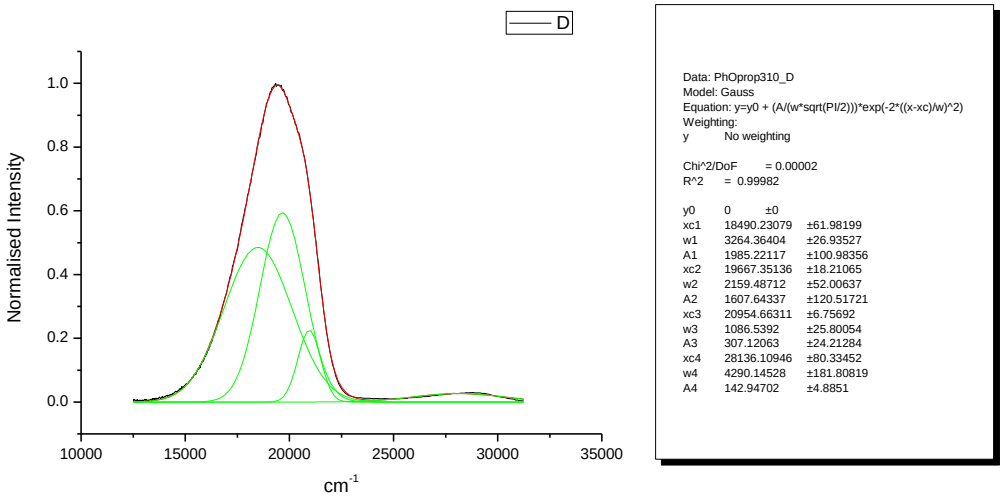

Figure 4.1.187. Gaussian model fit of the normalised fluorescence emission spectrum of **21** recorded in 1-propanol at 310 nm excitation.

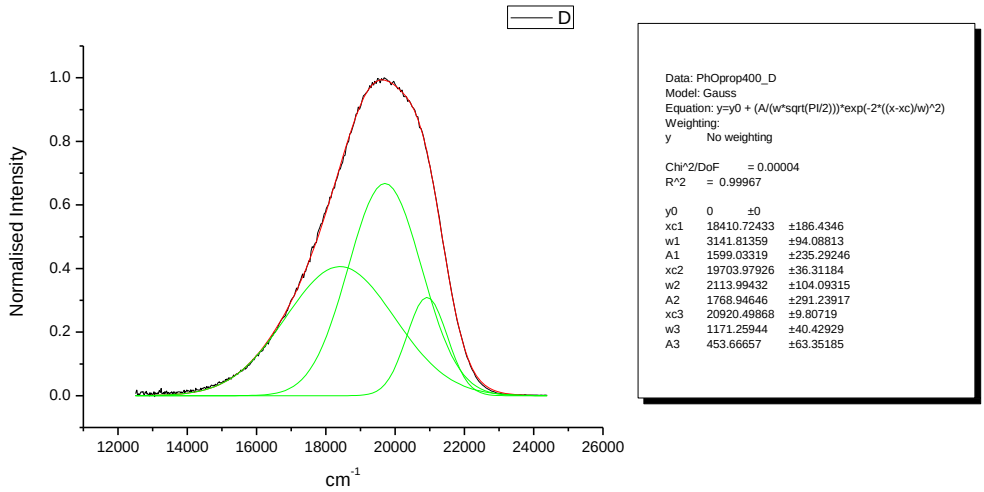

Figure 4.1.188. Gaussian model fit of the normalised fluorescence emission spectrum of **21** recorded in 1-propanol at 400 nm excitation.

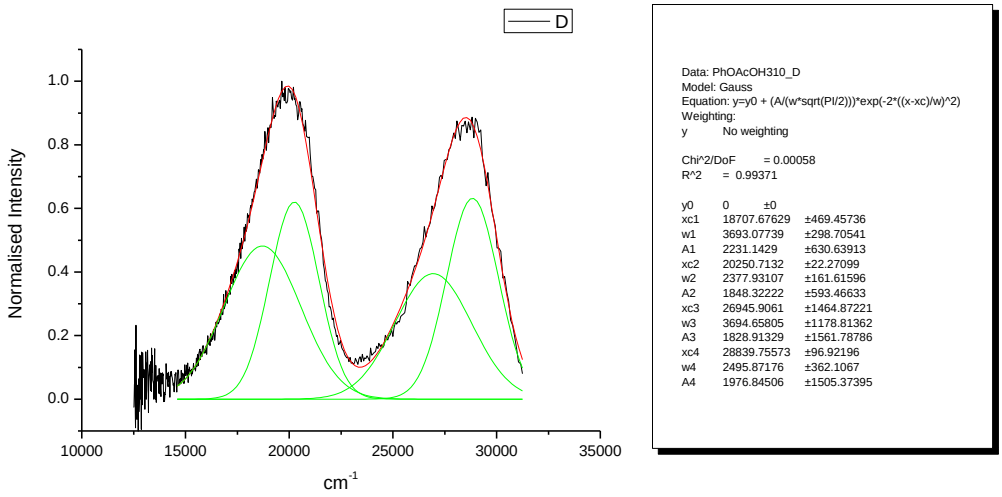

Figure 4.1.189. Gaussian model fit of the normalised fluorescence emission spectrum of **21** recorded in Acetic Acid at 310 nm excitation.

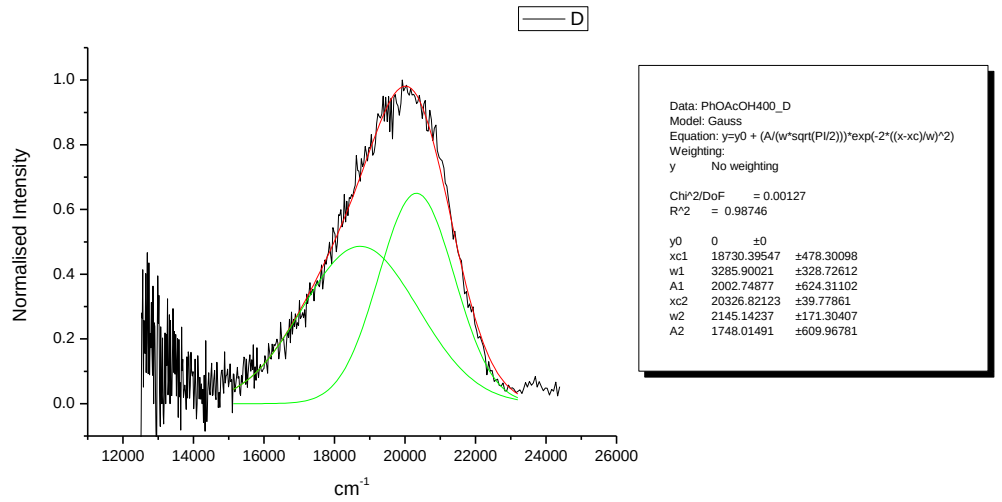

Figure 4.1.190. Gaussian model fit of the normalised fluorescence emission spectrum of **21** recorded in Acetic Acid at 400 nm excitation.

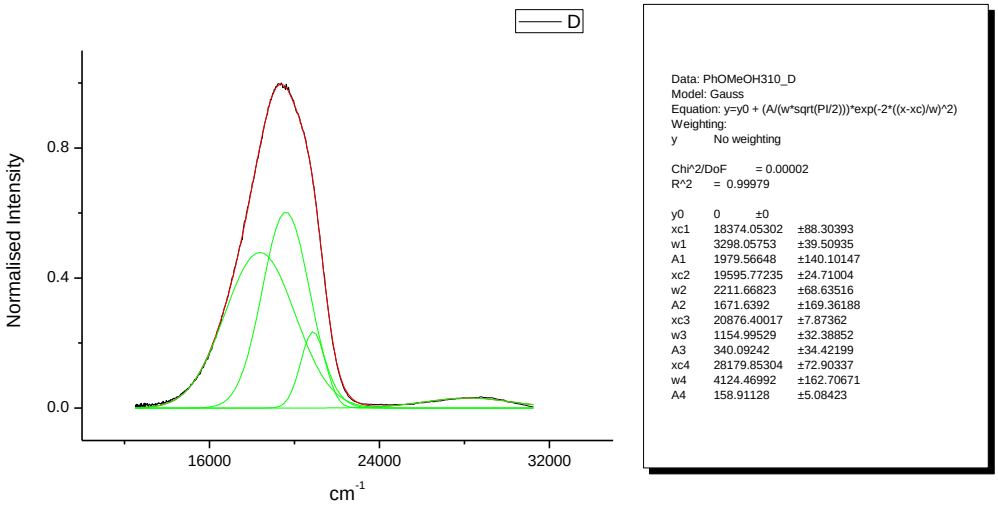

Figure 4.1.191. Gaussian model fit of the normalised fluorescence emission spectrum of **21** recorded in Methanol at 310 nm excitation.

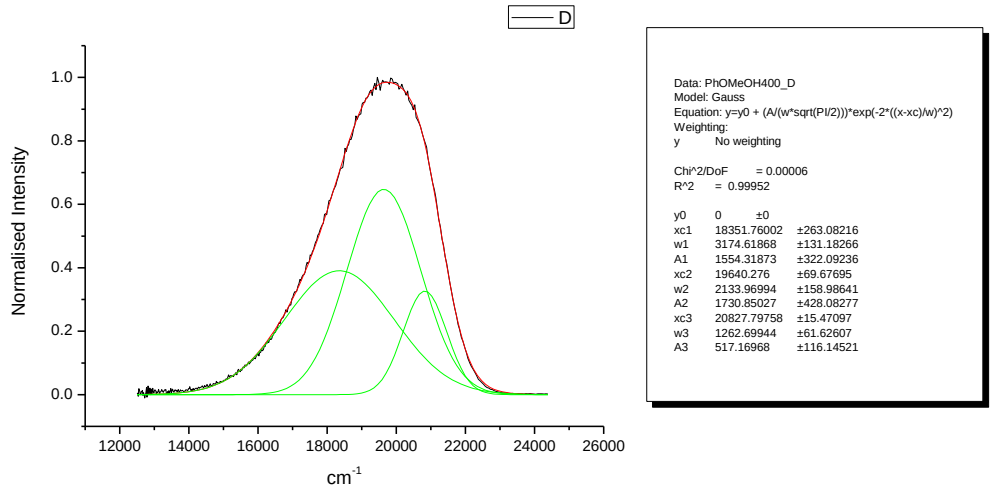

Figure 4.1.192. Gaussian model fit of the normalised fluorescence emission spectrum of **21** recorded in Methanol at 400 nm excitation.

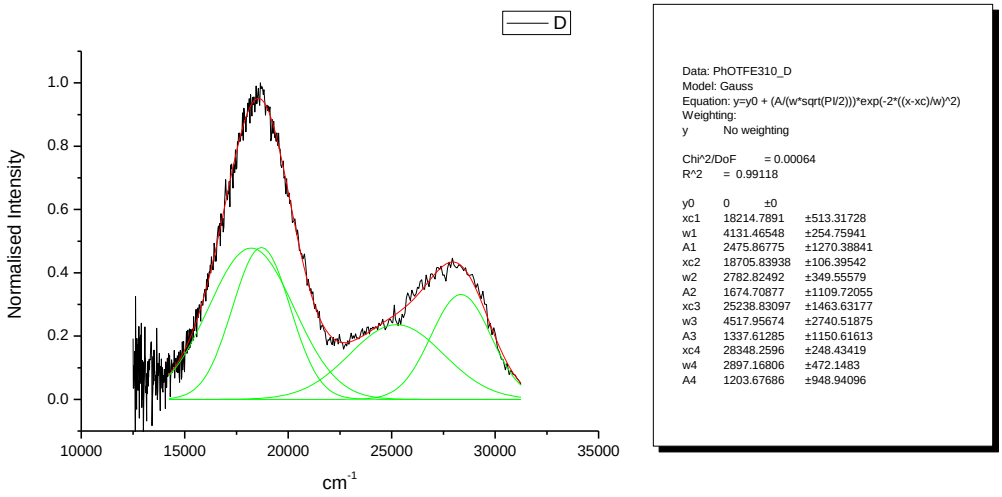

Figure 4.1.193. Gaussian model fit of the normalised fluorescence emission spectrum of **21** recorded in 2,2,2-trifluoroethanol at 310 nm excitation.

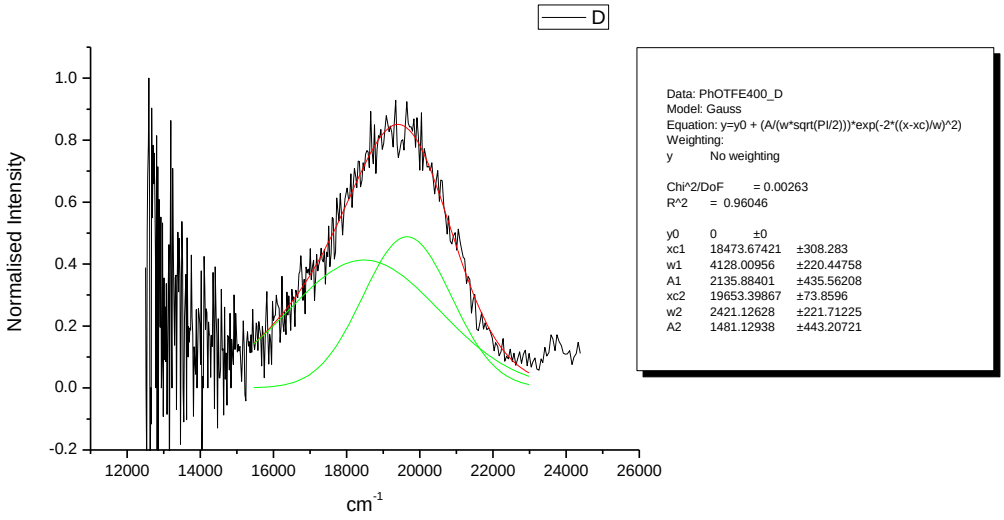

Figure 4.1.194. Gaussian model fit of the normalised fluorescence emission spectrum of **21** recorded in 2,2,2-trifluoroethanol at 400 nm excitation.

4.1.11 Fluorescence Excitation spectra.

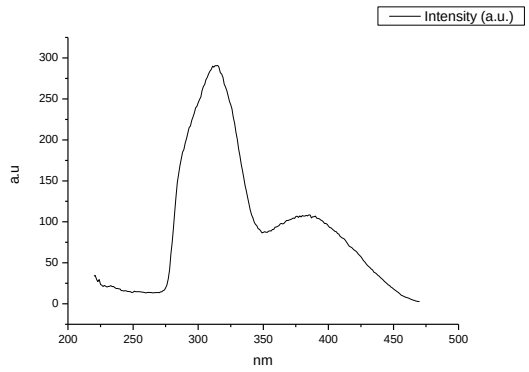

Figure 4.1.195. Fluorescence excitation spectrum of **21** recorded in Toluene with emission fixed at 480 nm.

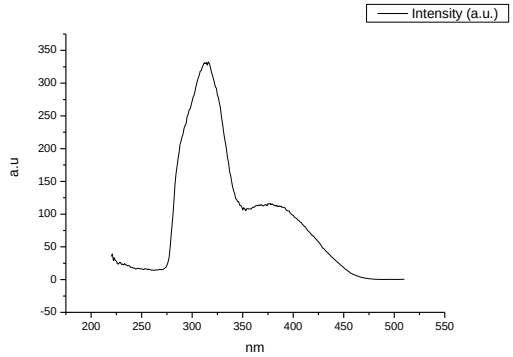

Figure 4.1.196. Fluorescence excitation spectrum of **21** recorded in Toluene with emission fixed at 520 nm.

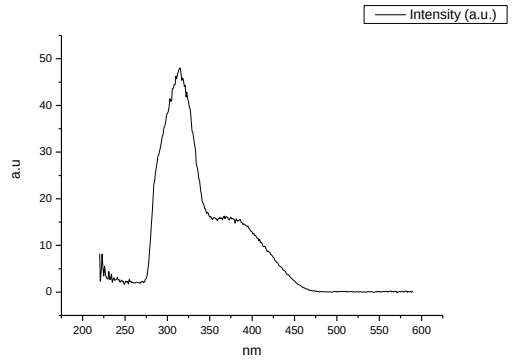

Figure 4.1.197. Fluorescence excitation spectrum of **21** recorded in Toluene with emission fixed at 600 nm.

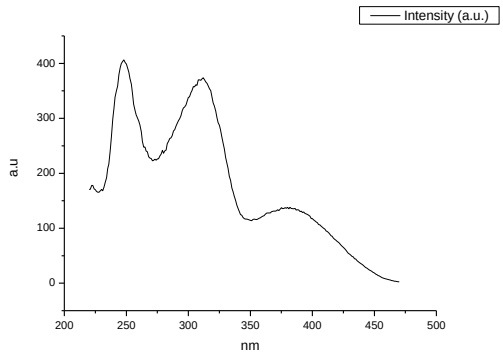

Figure 4.1.198. Fluorescence excitation spectrum of **21** recorded in 1,4-dioxane with emission fixed at 480 nm.

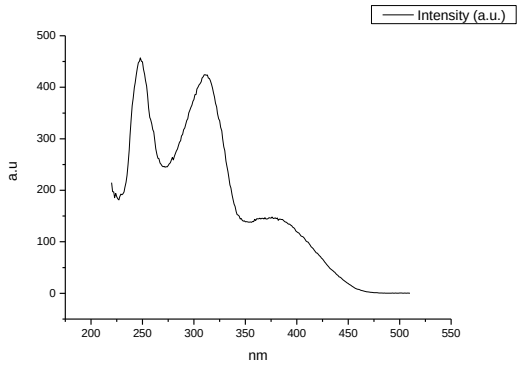

Figure 4.1.199. Fluorescence excitation spectrum of **21** recorded in 1,4-dioxane with emission fixed at 520 nm.

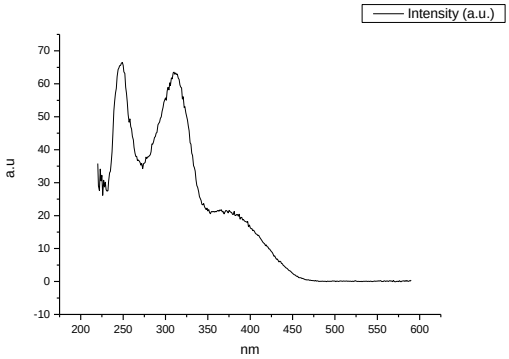

Figure 4.1.200. Fluorescence excitation spectrum of **21** recorded in 1,4-dioxane with emission fixed at 600 nm.

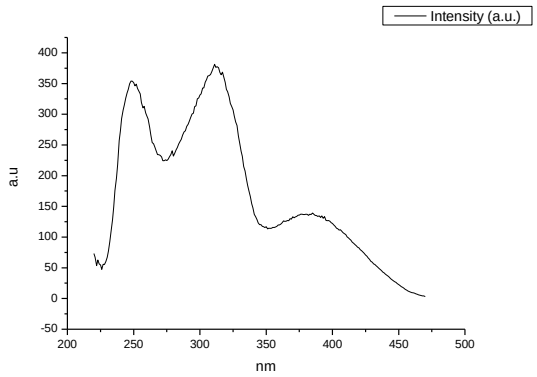

Figure 4.1.201. Fluorescence excitation spectrum of **21** recorded in Chloroform with emission fixed at 480 nm.

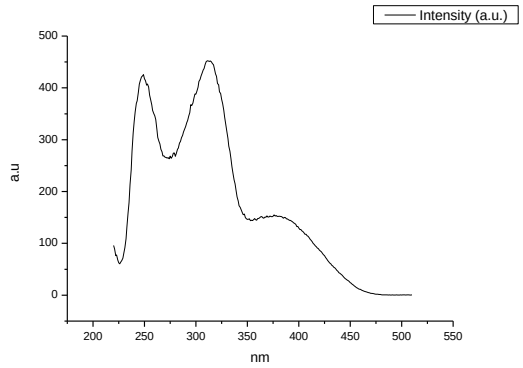

Figure 4.1.202. Fluorescence excitation spectrum of **21** recorded in Chloroform with emission fixed at 520 nm.

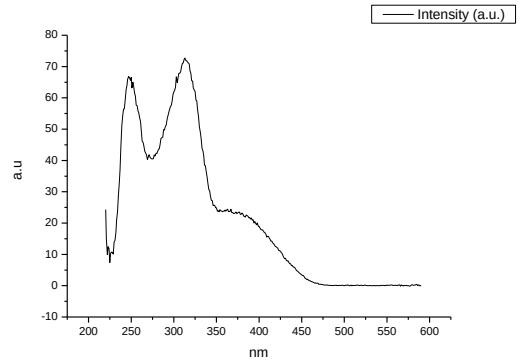

Figure 4.1.203. Fluorescence excitation spectrum of **21** recorded in Chloroform with emission fixed at 600 nm.

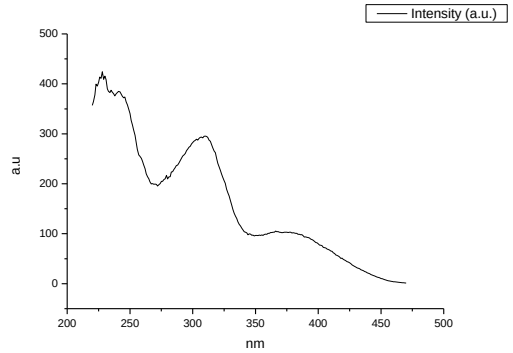

Figure 4.1.204. Fluorescence excitation spectrum of **21** recorded in Acetonitrile with emission fixed at 480 nm.

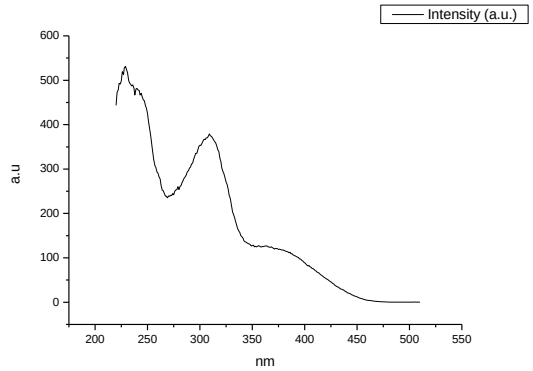

Figure 4.1.205. Fluorescence excitation spectrum of **21** recorded in Acetonitrile with emission fixed at 520 nm.

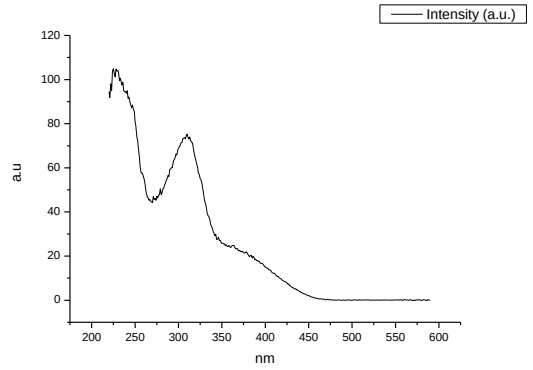

Figure 4.1.206. Fluorescence excitation spectrum of **21** recorded in Acetonitrile with emission fixed at 600 nm.

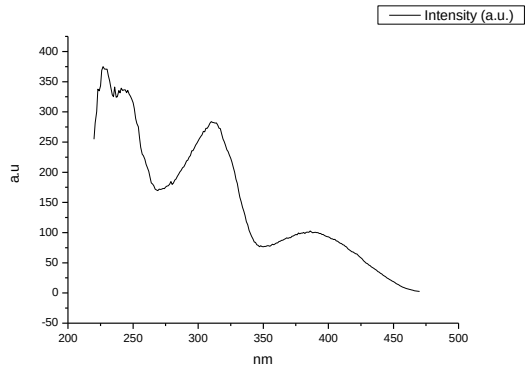

Figure 4.1.207. Fluorescence excitation spectrum of **21** recorded in 1-octanol with emission fixed at 480 nm.

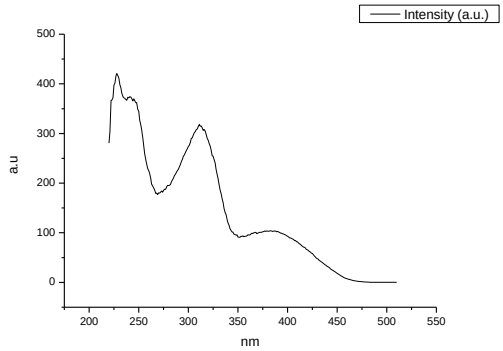

Figure 4.1.208. Fluorescence excitation spectrum of **21** recorded in 1-octanol with emission fixed at 520 nm.

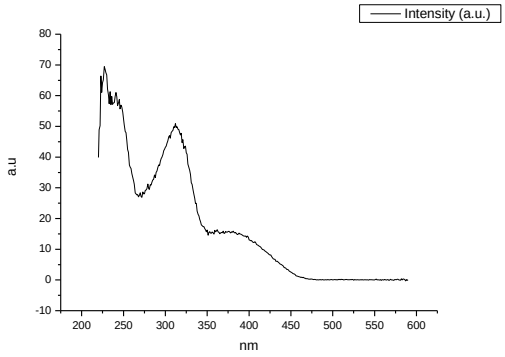

Figure 4.1.209. Fluorescence excitation spectrum of **21** recorded in 1-octanol with emission fixed at 600 nm.

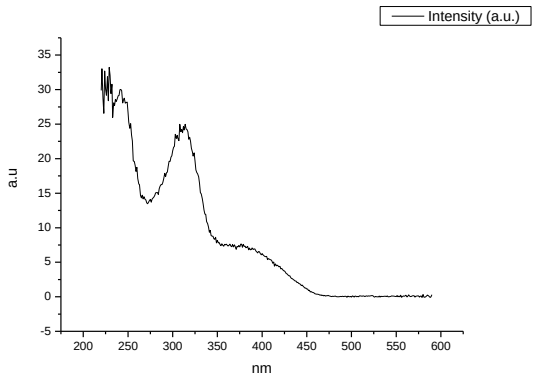

Figure 4.1.210. Fluorescence excitation spectrum of **21** recorded in 1-hexanol with emission fixed at 480 nm.

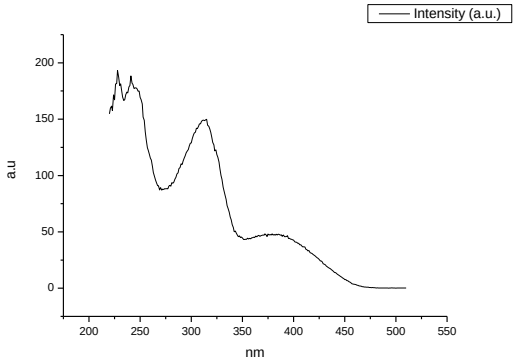

Figure 4.1.211. Fluorescence excitation spectrum of **21** recorded in 1-hexanol with emission fixed at 520 nm.

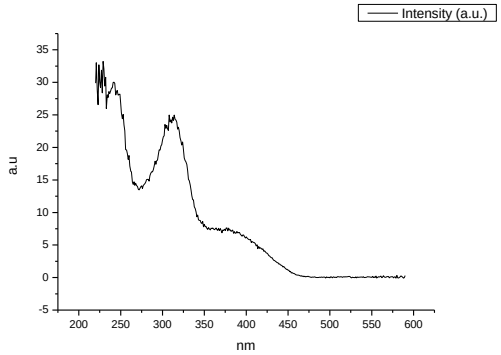

Figure 4.1.212. Fluorescence excitation spectrum of **21** recorded in 1-hexanol with emission fixed at 600 nm.

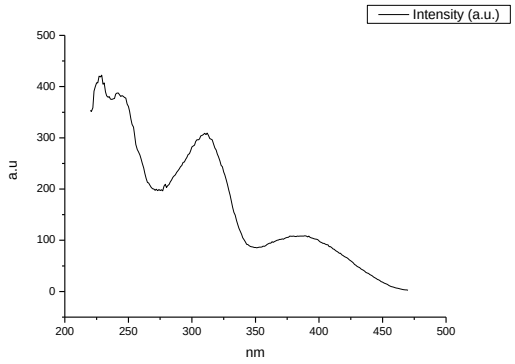

Figure 4.1.213. Fluorescence excitation spectrum of **21** recorded in 1-butanol with emission fixed at 480 nm.

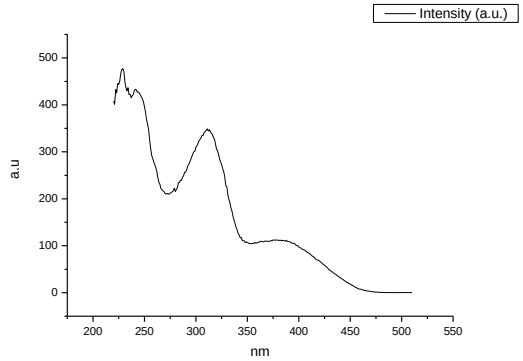

Figure 4.1.214. Fluorescence excitation spectrum of **21** recorded in 1-butanol with emission fixed at 520 nm.

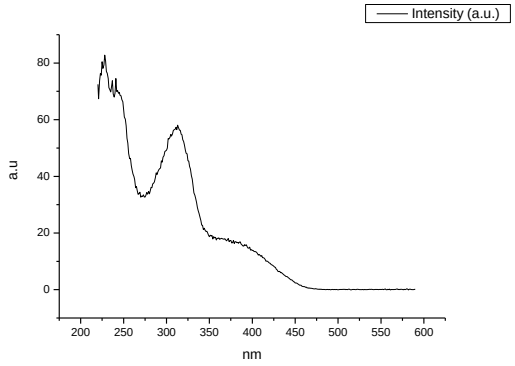

Figure 4.1.215. Fluorescence excitation spectrum of **21** recorded in 1-butanol with emission fixed at 600 nm.

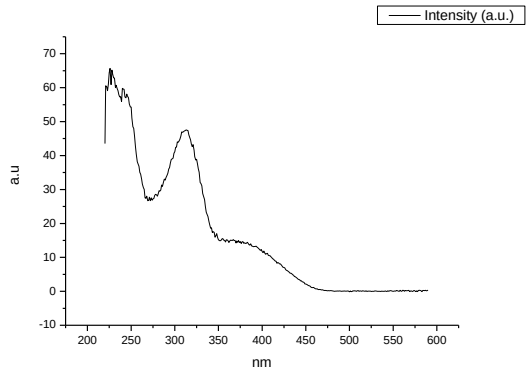

Figure 4.1.216. Fluorescence excitation spectrum of **21** recorded in 1-pentanol with emission fixed at 480 nm.

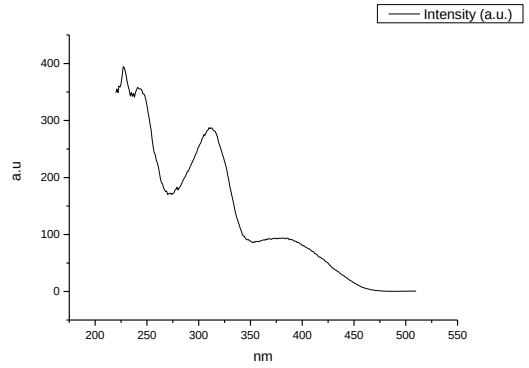

Figure 4.1.217. Fluorescence excitation spectrum of **21** recorded in 1-pentanol with emission fixed at 520 nm.

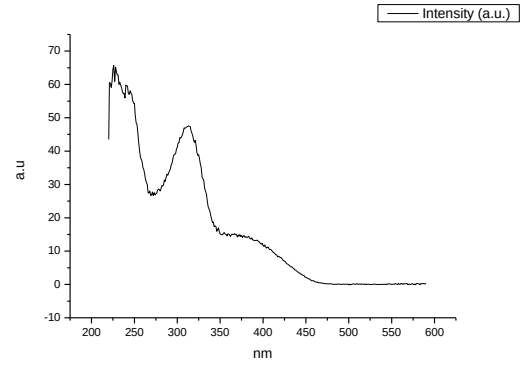

Figure 4.1.218. Fluorescence excitation spectrum of **21** recorded in 1-pentanol with emission fixed at 600 nm.

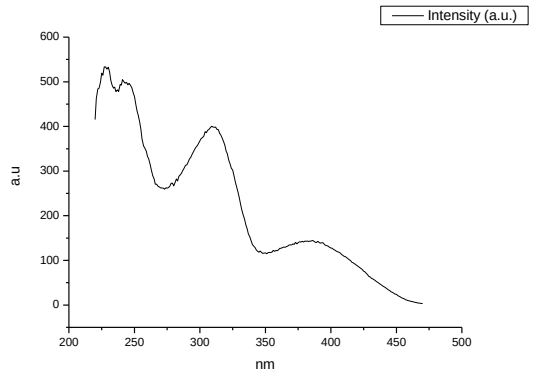

Figure 4.1.219. Fluorescence excitation spectrum of **21** recorded in 1-propanol with emission fixed at 480 nm.

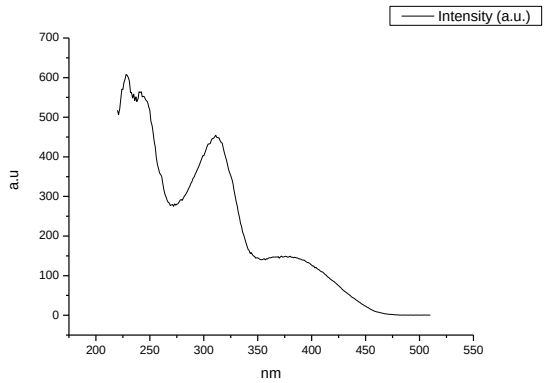

Figure 4.1.220. Fluorescence excitation spectrum of **21** recorded in 1-propanol with emission fixed at 520 nm.

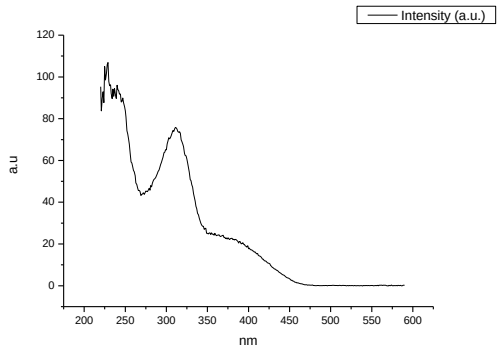

Figure 4.1.221. Fluorescence excitation spectrum of **21** recorded in 1-propanol with emission fixed at 600 nm.

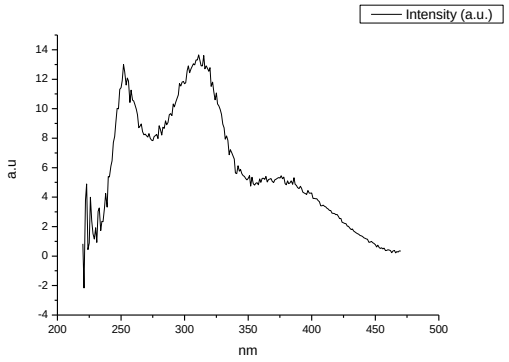

Figure 4.1.222. Fluorescence excitation spectrum of **21** recorded in Acetic Acid with emission fixed at 480 nm.

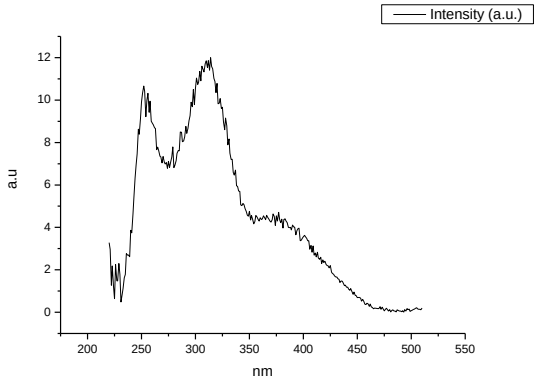

Figure 4.1.223. Fluorescence excitation spectrum of **21** recorded in Acetic Acid with emission fixed at 520 nm.

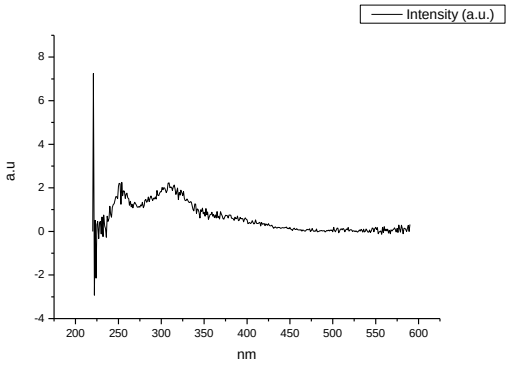

Figure 4.1.224. Fluorescence excitation spectrum of **21** recorded in Acetic Acid with emission fixed at 600 nm.

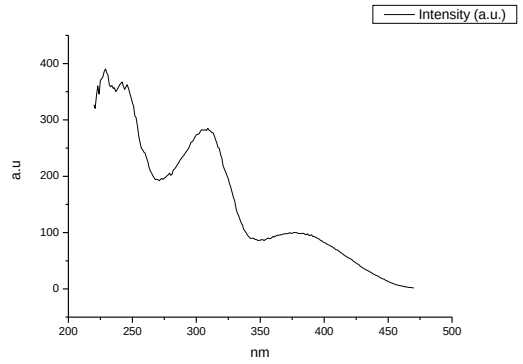

Figure 4.1.225. Fluorescence excitation spectrum of **21** recorded in Methanol with emission fixed at 480 nm.

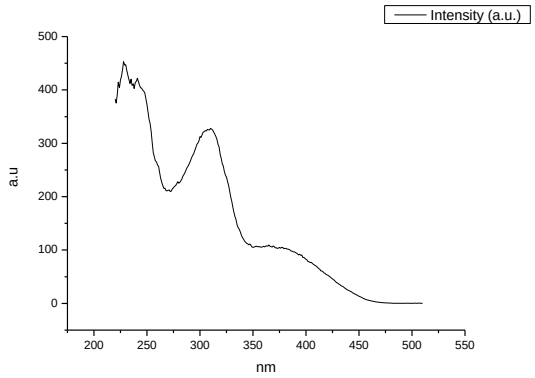

Figure 4.1.226. Fluorescence excitation spectrum of **21** recorded in Methanol with emission fixed at 520 nm.

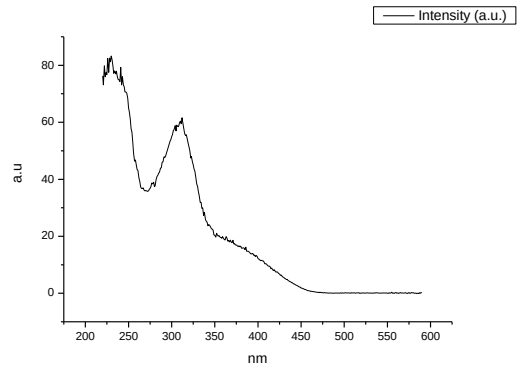

Figure 4.1.227. Fluorescence excitation spectrum of **21** recorded in Methanol with emission fixed at 600 nm.

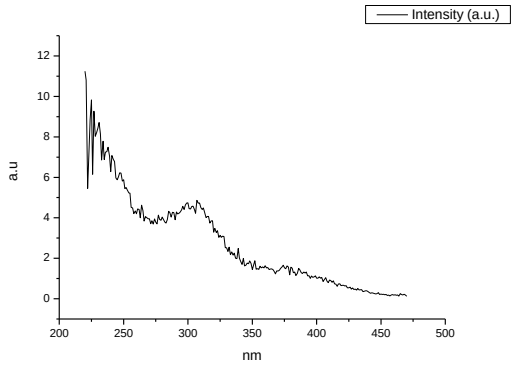

Figure 4.1.228. Fluorescence excitation spectrum of **21** recorded in 2,2,2-trifluoroethanol with emission fixed at 480 nm.

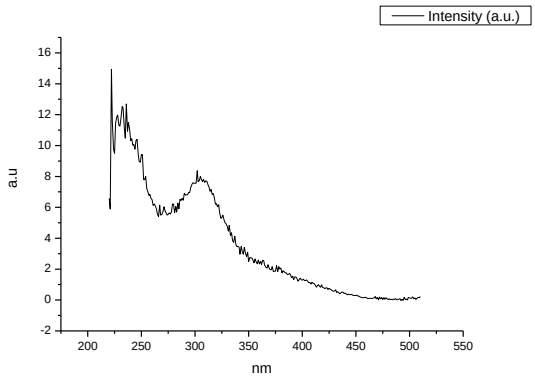

Figure 4.1.229. Fluorescence excitation spectrum of **21** recorded in 2,2,2-trifluoroethanol with emission fixed at 520 nm.

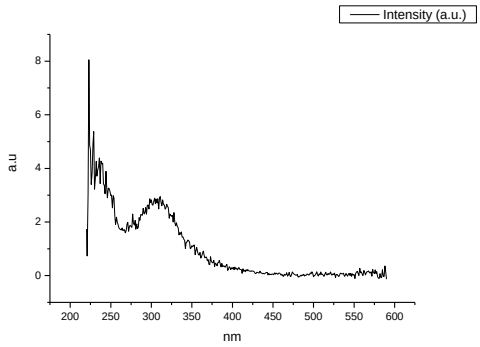

Figure 4.1.230. Fluorescence excitation spectrum of **21** recorded in 2,2,2-trifluoroethanol with emission fixed at 600 nm.

4.2 COMPOUND 23.

4.2.1 Quantum Yield Summary.

Solvent	abs (310 nm)	$\lambda_{ems\ (max)}$	$\Phi_{310\ nm}$	abs (400 nm)	$\lambda_{ems\ (max)}$	$\Phi_{400\ nm}$
Toluene	0.06	511.94	0.31	0.02	515.07	0.31
1,4-Dioxane	0.06	515.97	0.47	0.01	508.05	0.53
Chloroform	0.07	515.97	0.47	0.02	511.94	0.50
Acetonitrile	0.06	520.00	0.44	0.01	511.04	0.44
1-Octanol	0.04	514.02	0.49	0.01	508.05	0.49
1-Hexanol	0.02	518.05	0.43	0.01	508.05	0.45
1-Butanol	0.05	512.98	0.48	0.01	508.95	0.48
1-Pentanol	0.05	514.02	0.45	0.01	511.94	0.44
1-Propanol	0.06	515.07	0.44	0.01	511.94	0.43
Acetic acid	0.05	350.00	0.03	0.01	497.85	0.01
Methanol	0.06	511.94	0.33	0.01	505.97	0.31
2,2,2-Trifluoroethanol	0.03	356.00	0.02	0.01	520.33	0.01

Table 4.2.1. Summary of ultraviolet-visible absorbance values at 310 nm and 400 nm, emission maxima and quantum yield (Φ) of **23** at 310 nm and 400 nm excitation.

4.2.2 310 nm excitation Gaussian band fit summaries.

Solvent	λ max$_{em}$ Band 1 (cm^{-1})	λ max$_{em}$ Band 1 (nm)	λ max$_{em}$ Band 2 (cm^{-1})	λ max$_{em}$ Band 2 (nm)	λ max$_{em}$ Band 3 (cm^{-1})	λ max$_{em}$ Band 3 (nm)
Toluene	18745.41	533.46	19732.75	506.77	21067.55	474.66
1,4-Dioxane	18686.47	535.15	19765.91	505.92	21098.14	473.98
Chloroform	18553.06	538.99	19615.34	509.81	20929.58	477.79
Acetonitrile	18315.00	546.00	19548.46	511.55	20918.81	478.04
1-Octanol	18582.79	538.13	19729.32	506.86	21075.27	474.49
1-Hexanol	18580.77	538.19	19685.31	507.99	21031.86	475.47
1-Butanol	18454.84	541.86	19679.12	508.15	20977.84	476.69
1-Pentanol	18478.81	541.16	19680.66	508.11	21007.20	476.03
1-Propanol	18443.92	542.18	19680.56	508.12	20979.37	476.66
Acetic acid	19066.46	524.48	20095.52	497.62	-	-
Methanol	18323.12	545.76	19592.77	510.39	20895.74	478.57
2,2,2-Trifluoroethanol	15256.86	655.44	18534.54	539.53	-	-

Solvent	λ max$_{em}$ Band 4 (cm^{-1})	λ max$_{em}$ Band 4 (nm)	λ max$_{em}$ Band 5 (cm^{-1})	λ max$_{em}$ Band 5 (nm)
Toluene	28362.68	352.58	-	-
1,4-Dioxane	28358.32	352.63	-	-
Chloroform	28152.23	355.21	-	-
Acetonitrile	28430.00	351.74	-	-
1-Octanol	28437.35	351.65	-	-
1-Hexanol	28374.50	352.43	-	-
1-Butanol	28322.25	353.08	-	-
1-Pentanol	28324.01	353.06	-	-
1-Propanol	28341.29	352.84	-	-
Acetic acid	27560.00	362.84	29121.32	343.39
Methanol	28324.08	353.06	-	-
2,2,2-Trifluoroethanol	25441.60	393.06	28236.42	354.15

Table 4.2.2. Summary of band maxima of 5 band fit using Gaussian model for normalised **23** emission spectra recorded at 310 nm excitation.

(a)

Solvent	Width Band 1 (cm^{-1})	Width Band 2 (cm^{-1})	Width Band 3 (cm^{-1})	Width Band 4 (cm^{-1})	Width Band 5 (cm^{-1})
Toluene	3159.70	1814.76	1000.58	3452.45	-
1,4-Dioxane	3227.17	2025.62	996.92	3531.62	-
Chloroform	3190.92	1960.19	1052.69	3297.92	-
Acetonitrile	3301.45	2287.62	1162.36	3458.91	-
1-Octanol	3263.67	2113.56	1044.40	3503.88	-
1-Hexanol	3298.09	2111.87	1059.04	3780.65	-
1-Butanol	3240.10	2168.87	1086.57	3433.15	-
1-Pentanol	3249.56	2160.97	1076.30	3421.17	-
1-Propanol	3235.37	2164.62	1084.04	3437.18	-
Acetic acid	4239.50	2083.63	-	3286.15	2158.31
Methanol	3274.60	2227.18	1155.63	3468.32	-
2,2,2-Trifluoroethanol	1936.18	3289.87	-	4694.13	2900.68

(b)

Solvent	Area Band 1 (cm^{-1})	Area Band 2 (cm^{-1})	Area Band 3 (cm^{-1})	Area Band 4 (cm^{-1})	Area Band 5 (cm^{-1})
Toluene	2140.85	1172.25	334.42	283.46	-
1,4-Dioxane	2079.05	1404.55	268.61	265.25	-
Chloroform	2026.19	1376.58	348.71	215.24	-
Acetonitrile	2000.13	1711.09	282.47	251.81	-
1-Octanol	2010.94	1527.67	305.75	308.73	-
1-Hexanol	2055.81	1490.44	310.11	448.53	-
1-Butanol	1899.52	1664.46	318.30	276.84	-
1-Pentanol	1920.52	1649.48	314.40	281.72	-
1-Propanol	1894.22	1676.25	311.81	271.86	-
Acetic acid	1138.26	242.73	-	2622.58	1399.43
Methanol	1900.02	1732.56	343.04	307.86	-
2,2,2-Trifluoroethanol	166.31	3612.93	-	2175.17	2863.59

Tables 4.2.3 (a) and (b). Summary band width and band area of 5 band fit using Gaussian model for normalised **23** emission spectra recorded at 310 nm excitation.

Solvent	Band 1 Area Percentage(%)	Band 2 Area Percentage(%)	Band 3 Area Percentage (%)	Band 4 Area Percentage (%)	Band 5 Area Percentage (%)
Toluene	54.46	29.82	8.51	7.21	-
1,4-Dioxane	51.75	34.96	6.69	6.60	-
Chloroform	51.08	34.70	8.79	5.43	-
Acetonitrile	47.11	40.30	6.65	5.93	-
1-Octanol	48.42	36.78	7.36	7.43	-
1-Hexanol	47.76	34.62	7.20	10.42	-
1-Butanol	45.67	40.02	7.65	6.66	-
1-Pentanol	46.10	39.59	7.55	6.76	-
1-Propanol	45.60	40.35	7.51	6.54	-
Acetic acid	21.07	4.49	-	48.54	25.90
Methanol	44.36	40.45	8.01	7.19	-
2,2,2-Trifluoroethanol	1.89	40.97	-	24.67	32.47

Table 4.2.4. Total Area Percentages of 5 band fit using Gaussian model for normalised **23** emission spectra recorded at 310 nm excitation.

Solvent	Area Ratio Band 1/2 (310 nm ex)	Area Ratio Band 1/3 (310 nm ex)	Area Ratio Band 1/4 (310 nm ex)	Area Ratio Band 1/5 (310 nm ex)
Toluene	1.83	6.40	7.55	-
1,4-Dioxane	1.48	7.74	7.84	-
Chloroform	1.47	5.81	9.41	-
Acetonitrile	1.17	7.08	7.94	-
1-Octanol	1.32	6.58	6.51	-
1-Hexanol	1.38	6.63	4.58	-
1-Butanol	1.14	5.97	6.86	-
1-Pentanol	1.16	6.11	6.82	-
1-Propanol	1.13	6.07	6.97	-
Acetic acid	4.69	-	0.43	0.81
Methanol	1.10	5.54	6.17	-
2,2,2-Trifluoroethanol	0.05	-	0.08	0.06

Solvent	Area Ratio Band 2/3 (310 nm ex)	Area Ratio Band 2/4 (310 nm ex)	Area Ratio Band 2/5 (310 nm ex)	Area Ratio Band 3/4 (310 nm ex)	Area Ratio Band 3/5 (310 nm ex)	Area Ratio Band 4/5 (310 nm ex)
Toluene	3.51	4.14	-	1.18	-	-
1,4-Dioxane	5.23	5.30	-	1.01	-	-
Chloroform	3.95	6.40	-	1.62	-	-
Acetonitrile	6.06	6.80	-	1.12	-	-
1-Octanol	5.00	4.95	-	0.99	-	-
1-Hexanol	4.81	3.32	-	0.69	-	-
1-Butanol	5.23	6.01	-	1.15	-	-
1-Pentanol	5.25	5.85	-	1.12	-	-
1-Propanol	5.38	6.17	-	1.15	-	-
Acetic acid	-	0.09	0.17	-	-	1.87
Methanol	5.05	5.63	-	1.11	-	-
2,2,2-Trifluoroethanol	-	1.66	1.26	-	-	0.76

Table 4.2.5. Area Ratios of 5 band fit using Gaussian model for normalised **23** emission spectra recorded at 310 nm excitation.

4.2.3 400 nm excitation Gaussian band fit summaries.

Solvent	λ max$_{em}$ Band 1 (cm^{-1})	λ max$_{em}$ Band 1 (nm)	λ max$_{em}$ Band 2 (cm^{-1})	λ max$_{em}$ Band 2 (nm)	λmax$_{em}$ Band 3 (cm^{-1})	λmax$_{em}$ Band 3 (nm)
Toluene	18655.02	536.05	19802.53	504.99	21051.80	475.02
1,4-Dioxane	18578.49	538.26	19798.67	505.08	21069.33	474.62
Chloroform	18785.76	532.32	19632.80	509.35	20879.17	478.95
Acetonitrile	18301.03	546.42	19604.94	510.08	20868.52	479.19
1-Octanol	18508.58	540.29	19775.71	505.67	21040.49	475.27
1-Hexanol	18460.49	541.70	19730.65	506.83	20993.59	476.34
1-Butanol	18422.65	542.81	19718.26	507.14	20946.16	477.41
1-Pentanol	18452.18	541.94	19727.06	506.92	20969.03	476.89
1-Propanol	18461.62	541.66	19745.40	506.45	20943.76	477.47
Acetic acid	17944.21	557.28	19996.16	500.10	-	-
Methanol	18371.97	544.31	19659.99	508.65	20854.45	479.51
2,2,2-Trifluoroethanol	18413.61	543.08	19696.66	507.70	-	-

Table 4.2.6. Summary of band maxima of 3 band fit using Gaussian model for normalised **23** emission spectra recorded at 400 nm excitation.

Solvent	Width Band 1 (cm^{-1})	Width Band 2 (cm^{-1})	Width Band 3 (cm^{-1})
Toluene	3130.34	1980.70	987.66
1,4-Dioxane	3148.94	2076.97	1050.18
Chloroform	3332.55	1957.28	1056.82
Acetonitrile	3229.88	2254.70	1247.70
1-Octanol	3175.29	2122.62	1093.92
1-Hexanol	3221.96	2171.51	1111.91
1-Butanol	3154.43	2128.89	1159.31
1-Pentanol	3171.02	2136.47	1141.03
1-Propanol	3145.77	2126.51	1148.47
Acetic acid	3822.76	2614.30	-
Methanol	3188.04	2142.94	1237.13
2,2,2-Trifluoroethanol	4773.55	2592.03	-

Table 4.2.7. Summary of band width of 3 band fit using Gaussian model for normalised **23** emission spectra recorded at 400 nm excitation.

Solvent	Area Band 1 (cm^{-1})	Area Band 2 (cm^{-1})	Area Band 3 (cm^{-1})	Area Ratio Band 1/2 (400 nm ex)	Area Ratio Band 1/3 (400 nm ex)	Area Ratio Band 2/3 (400 nm ex)
Toluene	1797.23	1500.04	344.92	1.20	5.21	4.35
1,4-Dioxane	1765.15	1633.96	337.73	1.08	5.23	4.84
Chloroform	2136.53	1288.20	394.03	1.66	5.42	3.27
Acetonitrile	1691.46	1833.56	403.41	0.92	4.19	4.55
1-Octanol	1721.26	1705.41	391.37	1.01	4.40	4.36
1-Hexanol	1662.53	1799.34	401.55	0.92	4.14	4.48
1-Butanol	1583.43	1769.30	443.12	0.89	3.57	3.99
1-Pentanol	1647.83	1758.38	430.16	0.94	3.83	4.09
1-Propanol	1650.05	1752.04	427.80	0.94	3.86	4.10
Acetic acid	1406.69	2284.74	-	0.62	-	-
Methanol	1579.77	1762.03	499.90	0.90	3.16	3.52
2,2,2-Trifluoroethanol	1043.43	646.27	-	1.61	-	-

Solvent	Band 1 Area Percentage (%)	Band 2 Area Percentage (%)	Band 3 Area Percentage (%)
Toluene	49.34	41.19	9.47
1,4-Dioxane	47.24	43.73	9.04
Chloroform	55.95	33.73	10.32
Acetonitrile	43.06	46.67	10.27
1-Octanol	45.08	44.67	10.25
1-Hexanol	43.03	46.57	10.39
1-Butanol	41.71	46.61	11.67
1-Pentanol	42.95	45.83	11.21
1-Propanol	43.08	45.75	11.17
Acetic acid	38.11	61.89	-
Methanol	41.12	45.87	13.01
2,2,2-Trifluoroethanol	61.75	38.25	-

Table 4.2.8. Band areas, area ratios and total area percentage of 3 band fit using Gaussian model for normalised **23** emission spectra recorded at 400 nm excitation.

4.2.4 310 nm Gaussian band fit - Solvatochromic analysis.

4.2.4.1 E_T^N.

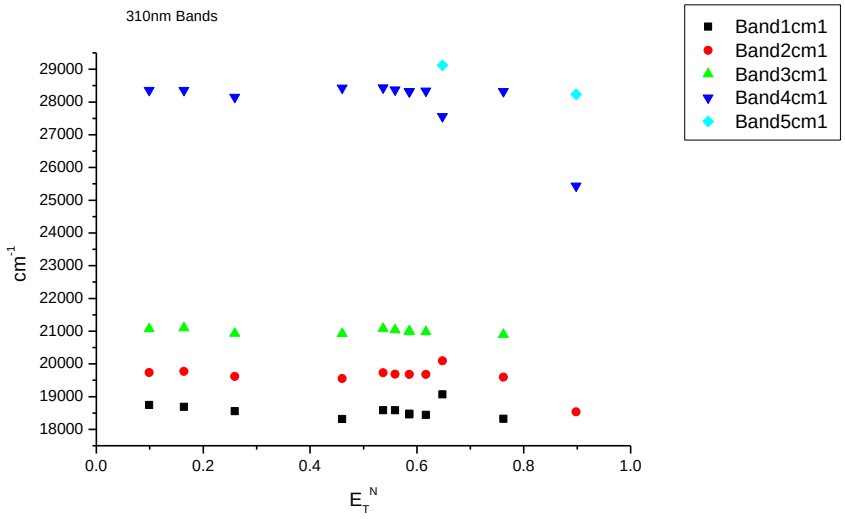

Figure 4.2.1. Band maxima from Gaussian model fit of the normalised fluorescence emission spectra of **23** recorded at 310 nm excitation against E_T^N.

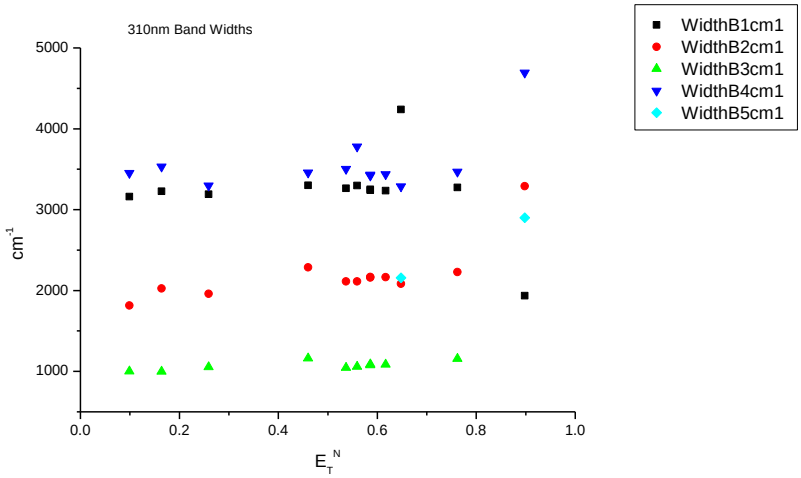

Figure 4.2.2. Band widths from Gaussian model fit of the normalised fluorescence emission spectra of **23** recorded at 310 nm excitation against E_T^N.

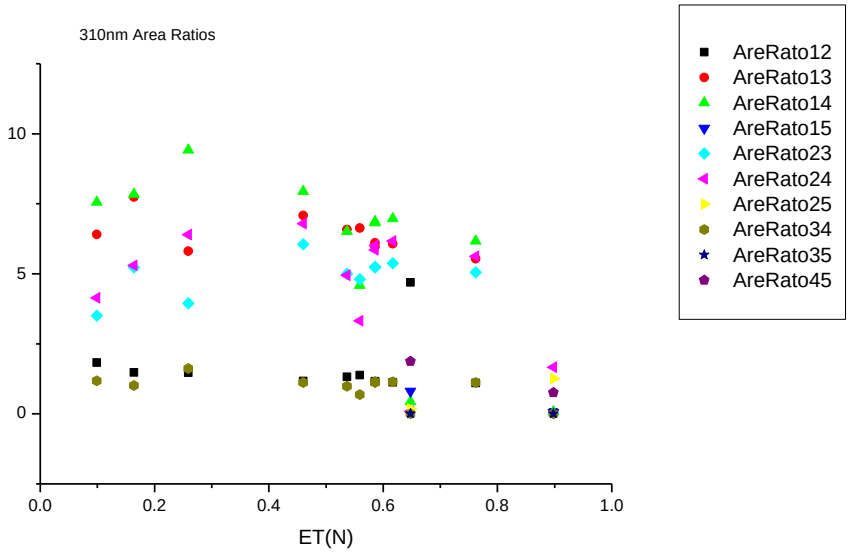

Figure 4.2.3. Area ratios from Gaussian model fit of the normalised fluorescence emission spectra of **23** recorded at 310 nm excitation against E_T^N.

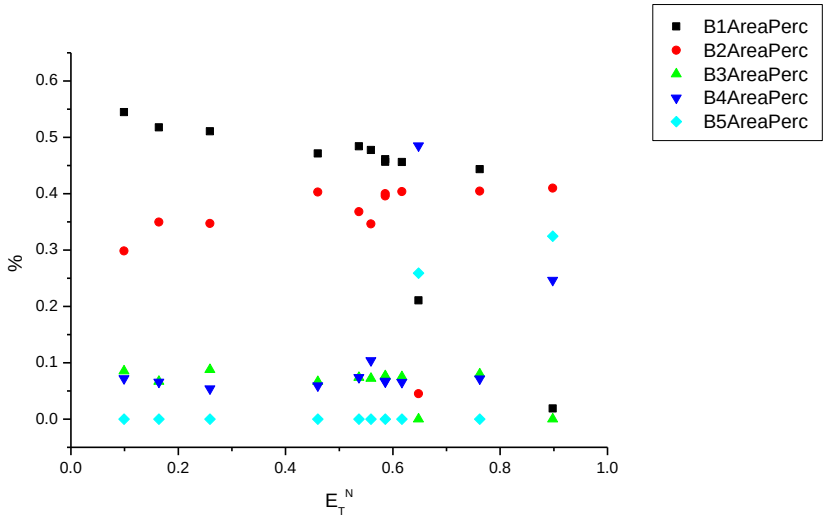

Figure 4.2.4. Area percentages from Gaussian model fit of the normalised fluorescence emission spectra of **23** recorded at 310 nm excitation against E_T^N.

4.2.4.2 α

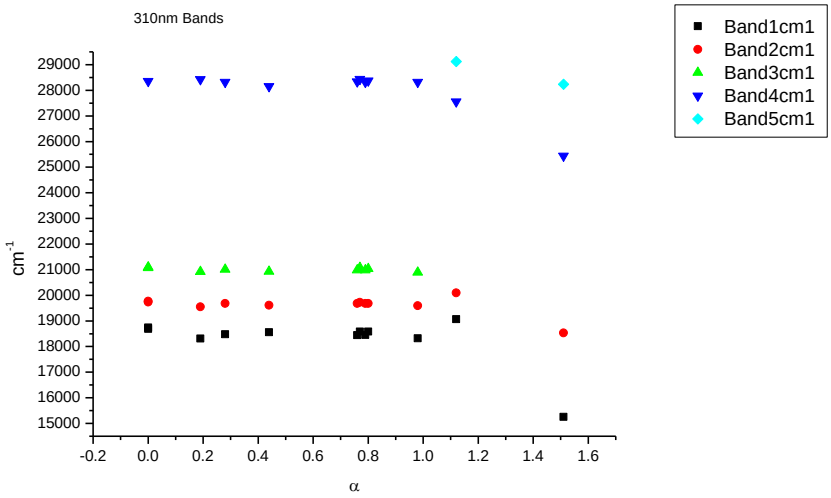

Figure 4.2.5. Band maxima from Gaussian model fit of the normalised fluorescence emission spectra of **23** recorded at 310 nm excitation against α.

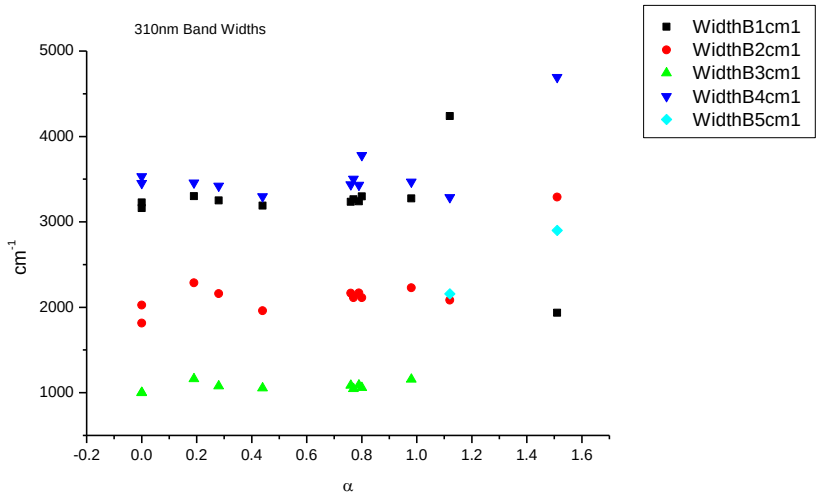

Figure 4.2.6. Band widths from Gaussian model fit of the normalised fluorescence emission spectra of **23** recorded at 310 nm excitation against α.

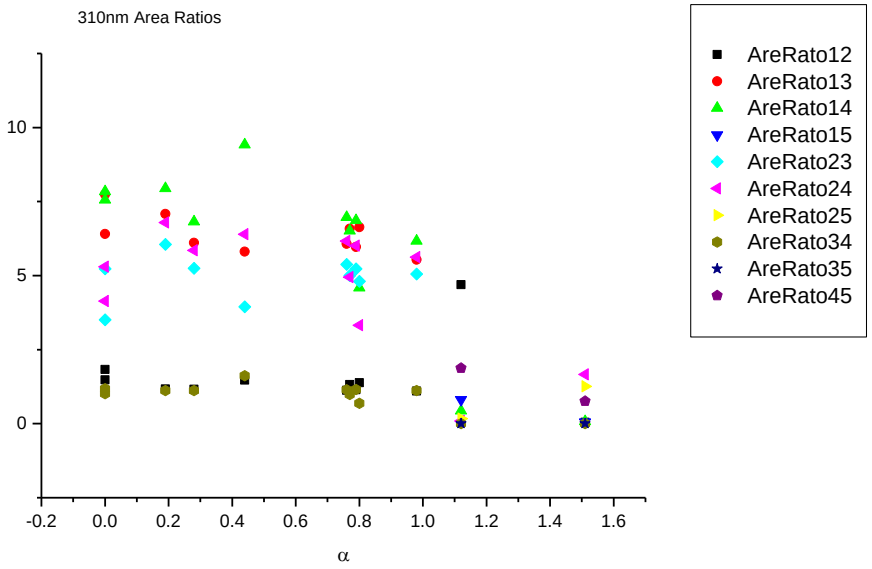

Figure 4.2.7. Area Ratios from Gaussian model fit of the normalised fluorescence emission spectra of **23** recorded at 310 nm excitation against α.

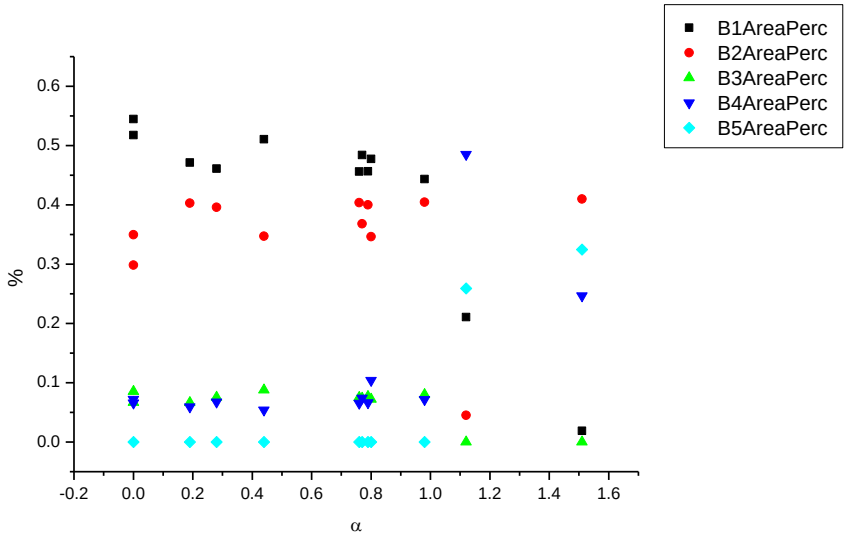

Figure 4.2.8. Area percentages from Gaussian model fit of the normalised fluorescence emission spectra of **23** recorded at 310 nm excitation against α.

4.2.4.3 β.

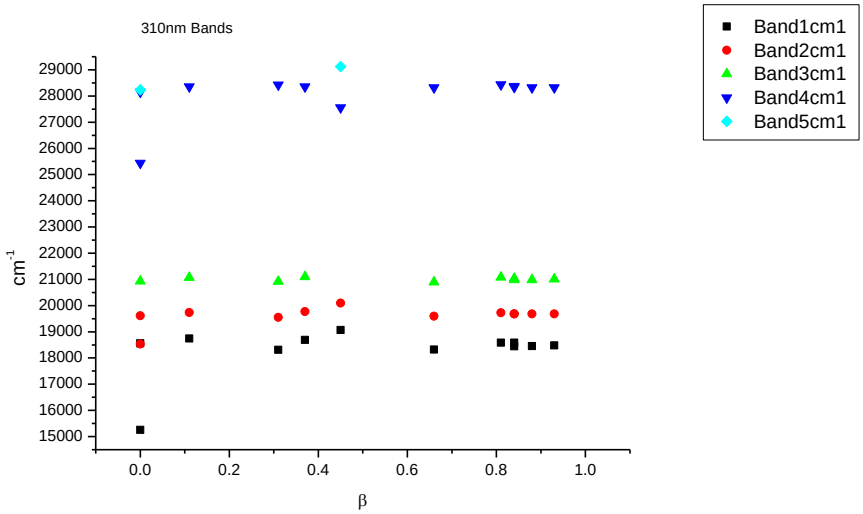

Figure 4.2.9. Band maxima from Gaussian model fit of the normalised fluorescence emission spectra of **23** recorded at 310 nm excitation against β.

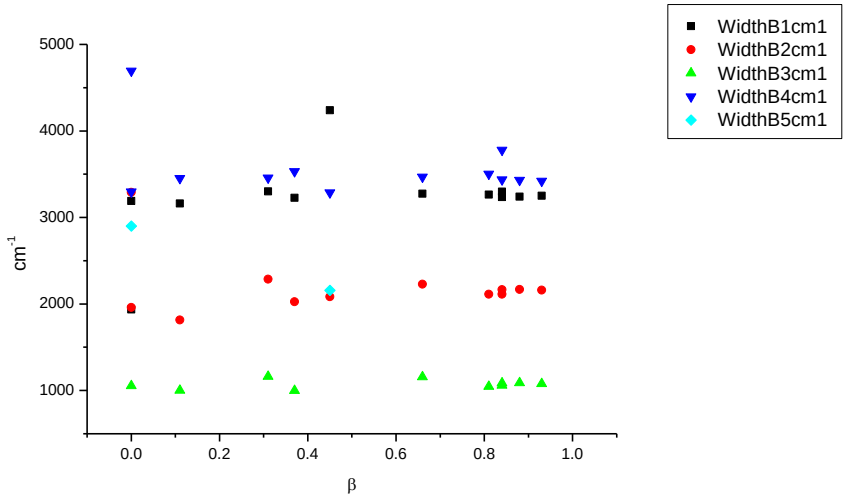

Figure 4.2.10. Band widths from Gaussian model fit of the normalised fluorescence emission spectra of **23** recorded at 310 nm excitation against β.

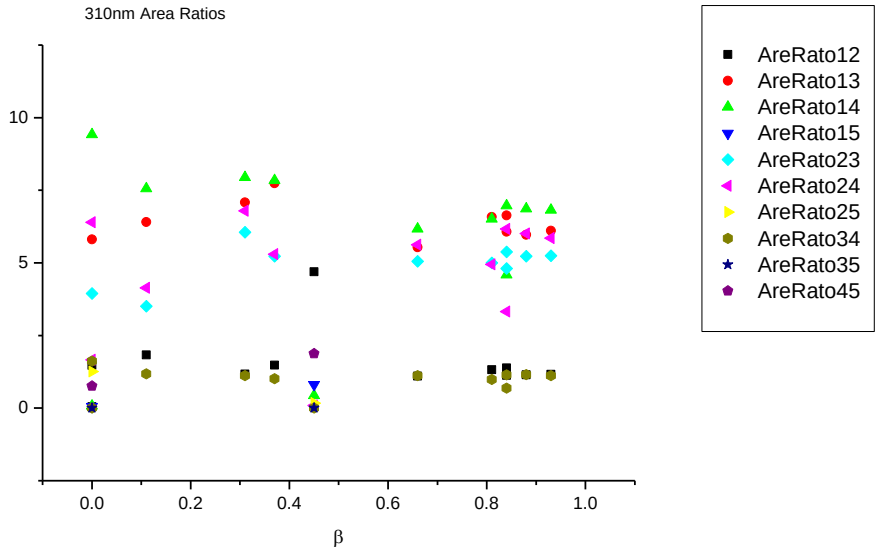

Figure 4.2.11. Area ratios from Gaussian model fit of the normalised fluorescence emission spectra of **23** recorded at 310 nm excitation against β.

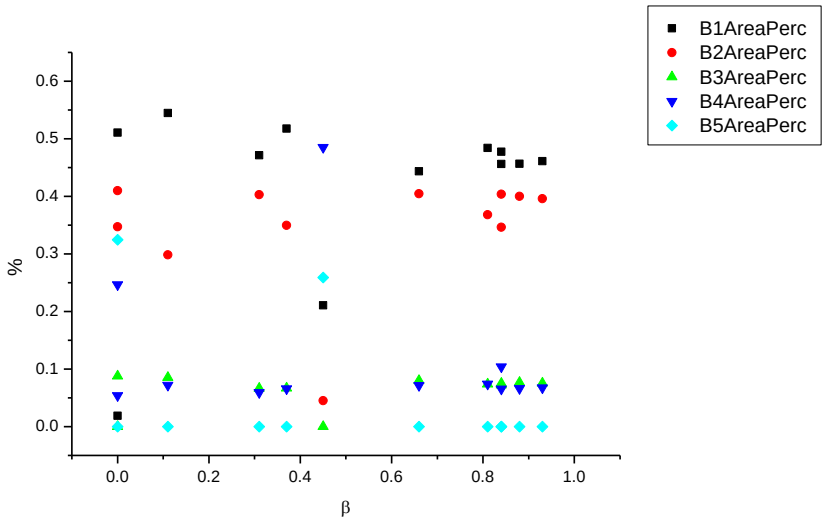

Figure 4.2.12. Area percentages from Gaussian model fit of the normalised fluorescence emission spectra of **23** recorded at 310 nm excitation against β.

4.2.4.4 π.*

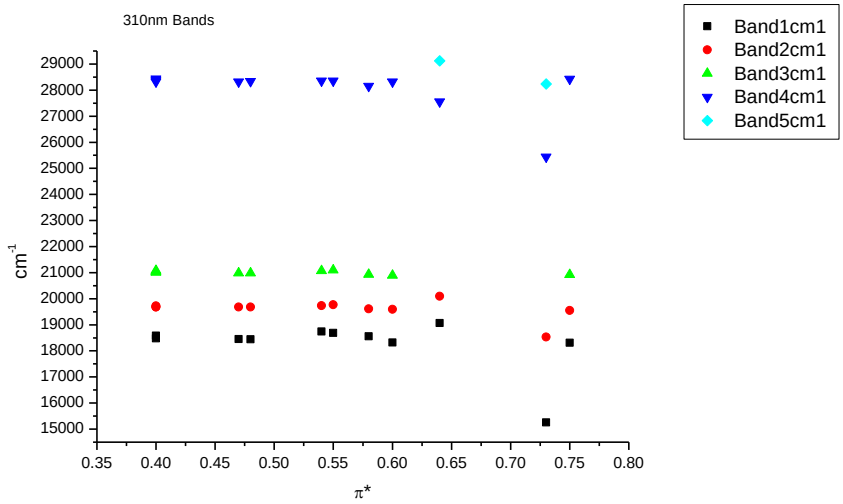

Figure 4.2.13. Band maxima from Gaussian model fit of the normalised fluorescence emission spectra of **23** recorded at 310 nm excitation against π*.

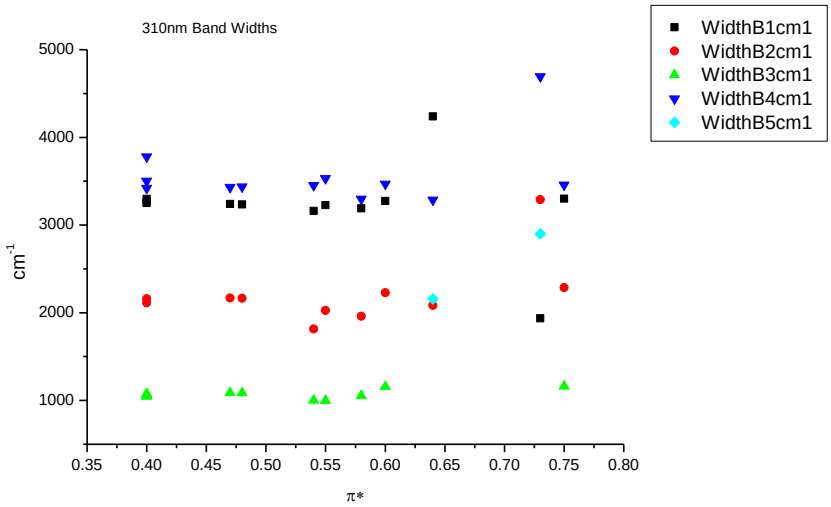

Figure 4.2.14. Band widths from Gaussian model fit of the normalised fluorescence emission spectra of **23** recorded at 310 nm excitation against π*.

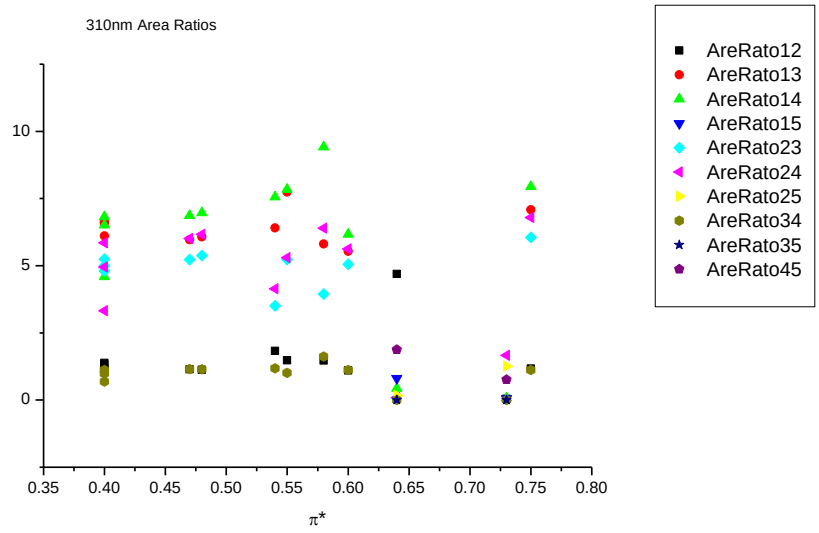

Figure 4.2.15. Area ratios from Gaussian model fit of the normalised fluorescence emission spectra of **23** recorded at 310 nm excitation against π*.

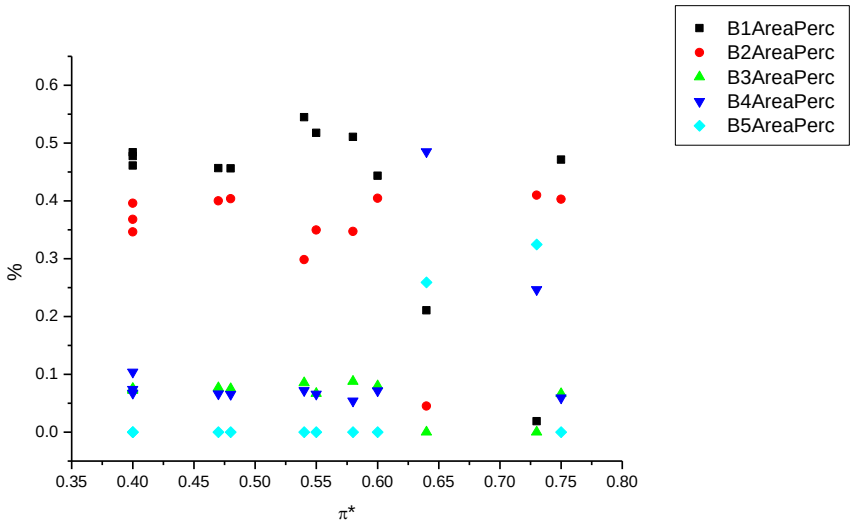

Figure 4.2.16. Area percentages from Gaussian model fit of the normalised fluorescence emission spectra of **23** recorded at 310 nm excitation against π*.

4.2.4.5 μ(D).

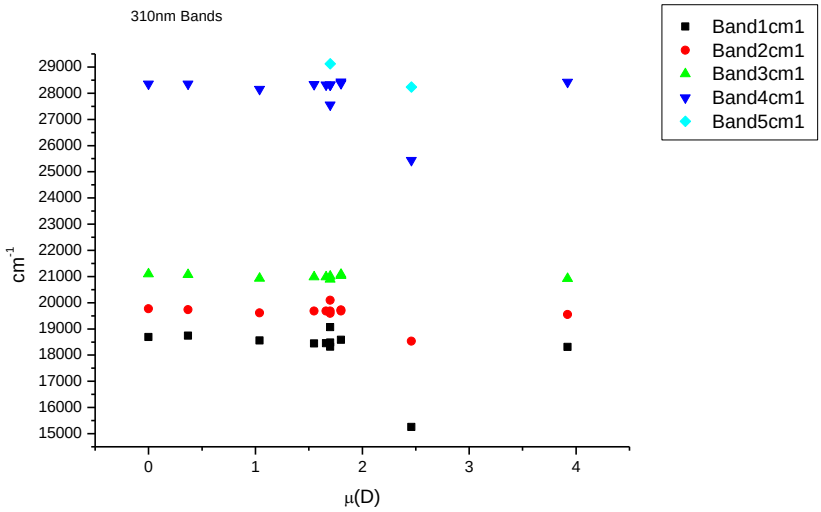

Figure 4.2.17. Band maxima from Gaussian model fit of the normalised fluorescence emission spectra of **23** recorded at 310 nm excitation against μ(D).

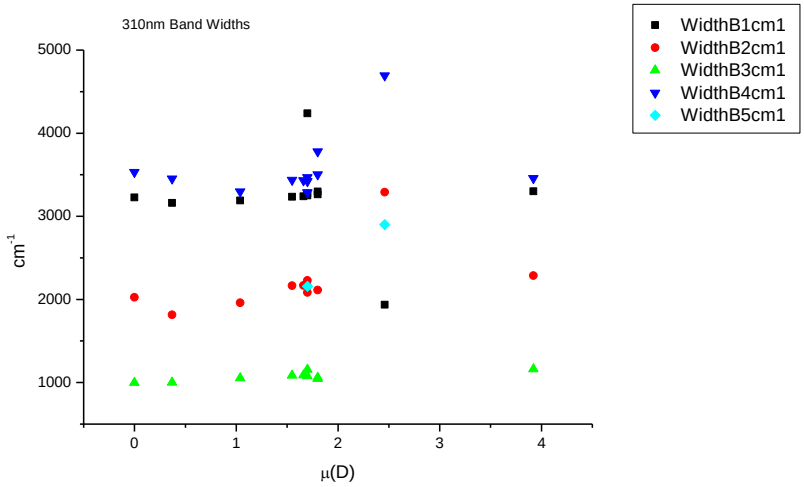

Figure 4.2.18. Band widths from Gaussian model fit of the normalised fluorescence emission spectra of **23** recorded at 310 nm excitation against μ(D).

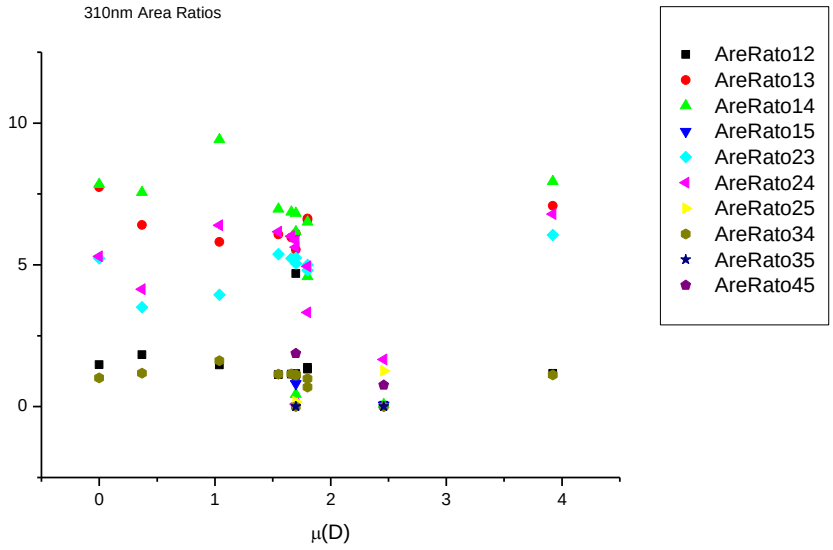

Figure 4.2.19. Area ratios from Gaussian model fit of the normalised fluorescence emission spectra of **23** recorded at 310 nm excitation against μ(D).

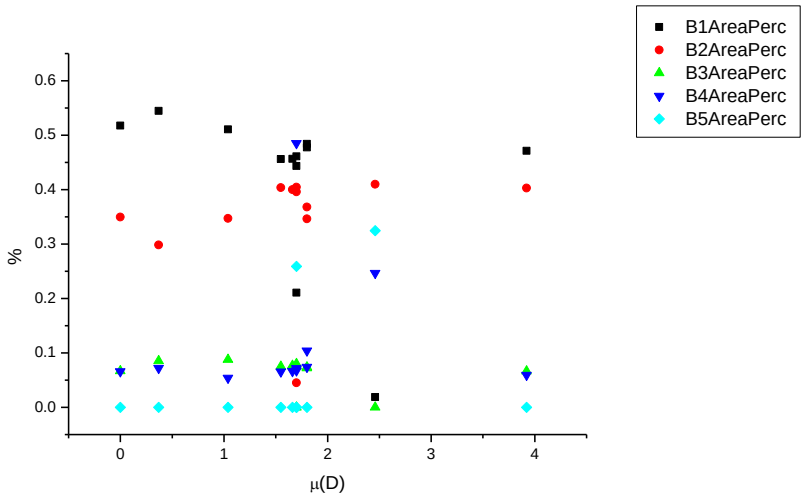

Figure 4.2.20. Area percentages from Gaussian model fit of the normalised fluorescence emission spectra of **23** recorded at 310 nm excitation against μ(D).

4.2.4.6 η(Cp).

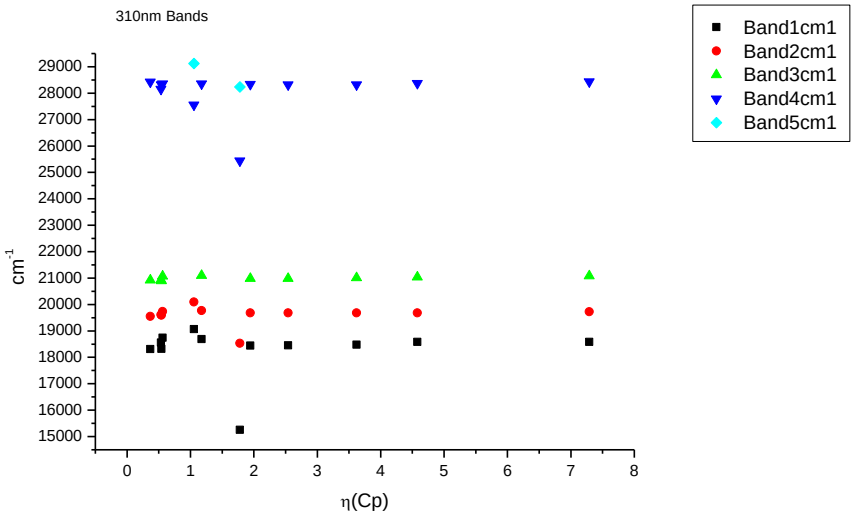

Figure 4.2.21. Band maxima from Gaussian model fit of the normalised fluorescence emission spectra of **23** recorded at 310 nm excitation against η(Cp).

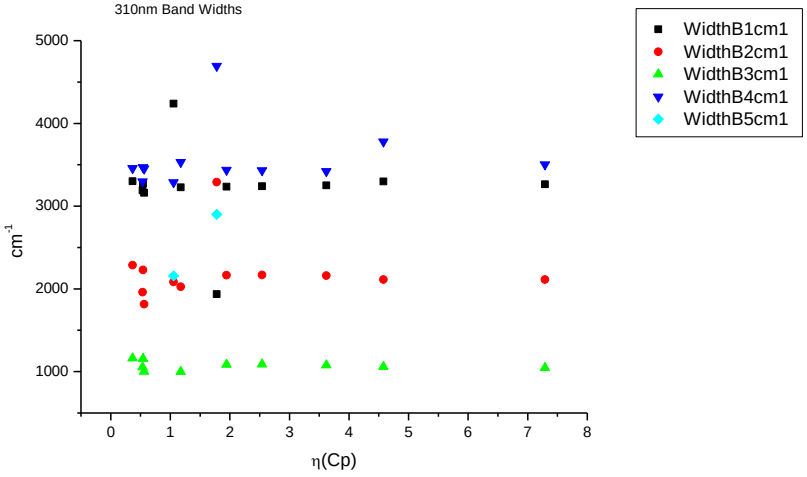

Figure 4.2.22. Band widths from Gaussian model fit of the normalised fluorescence emission spectra of **23** recorded at 310 nm excitation against η(Cp).

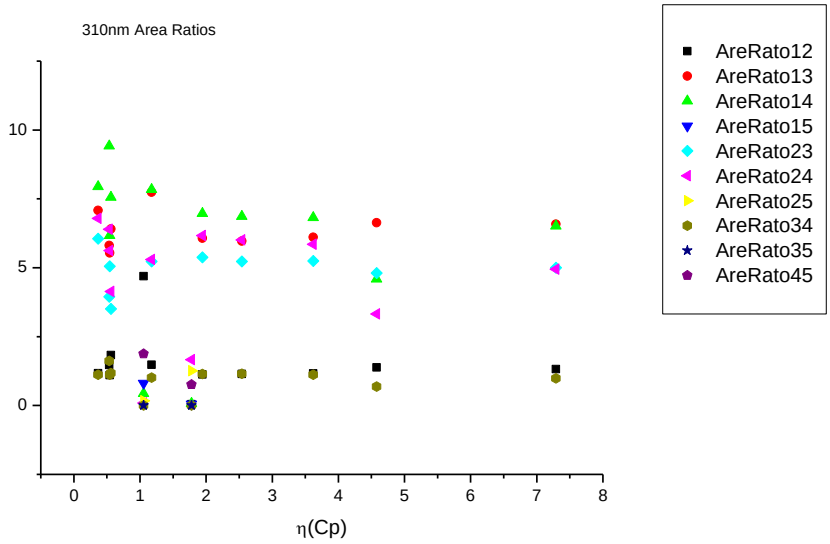

Figure 4.2.23. Area ratios from Gaussian model fit of the normalised fluorescence emission spectra of **23** recorded at 310 nm excitation against η(Cp).

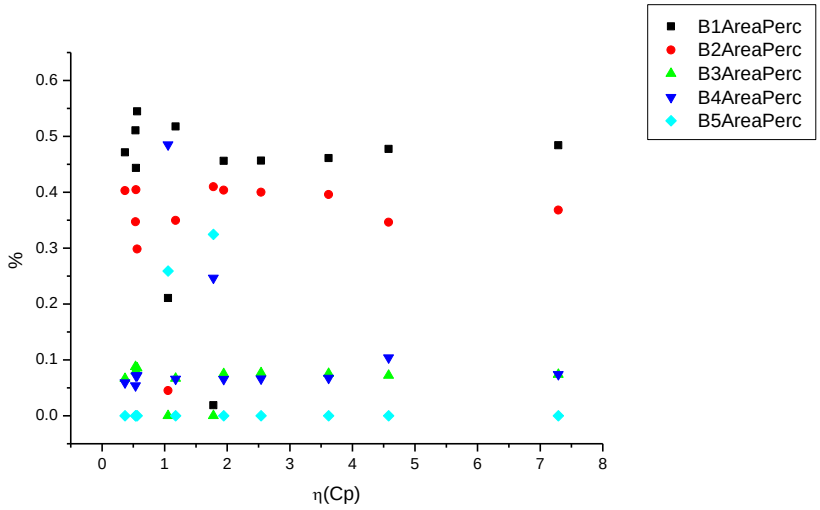

Figure 4.2.24. Area percentages from Gaussian model fit of the normalised fluorescence emission spectra of **23** recorded at 310 nm excitation against η(Cp).

4.2.5 400 nm Gaussian band fit - Solvatochromic analysis.

4.2.5.1 E_T^N.

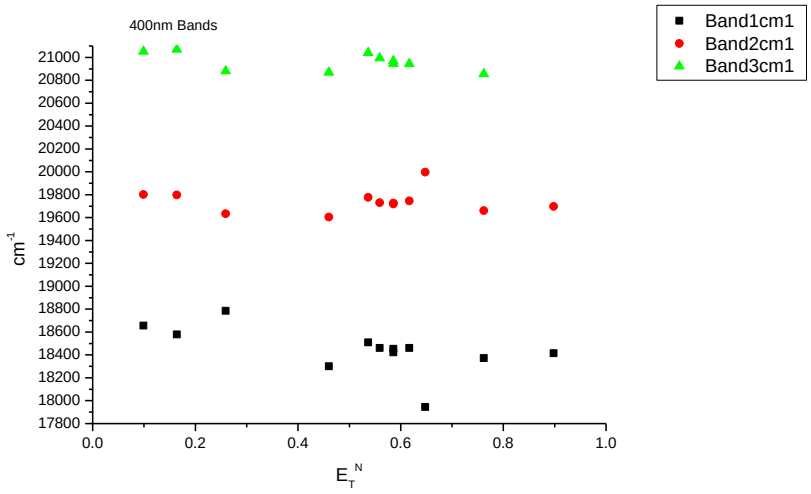

Figure 4.2.25. Band maxima from Gaussian model fit of the normalised fluorescence emission spectra of **23** recorded at 400 nm excitation against E_T^N.

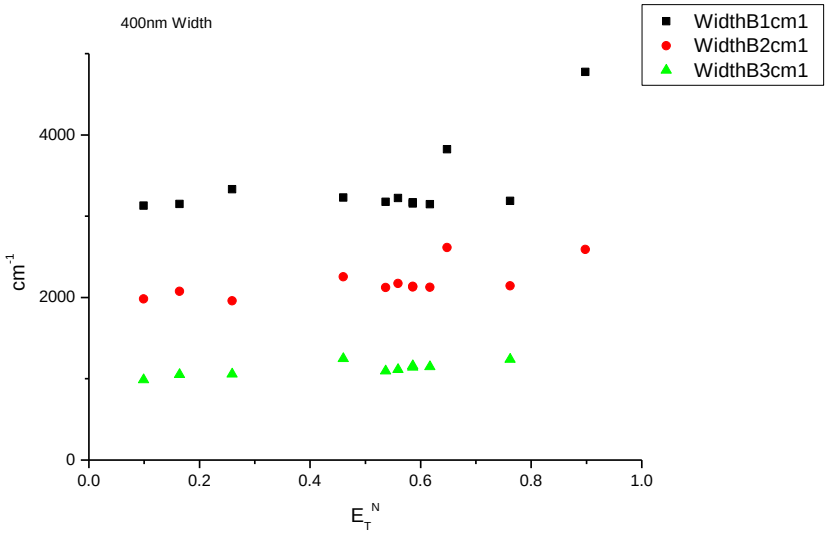

Figure 4.2.26. Band widths from Gaussian model fit of the normalised fluorescence emission spectra of **23** recorded at 400 nm excitation against E_T^N.

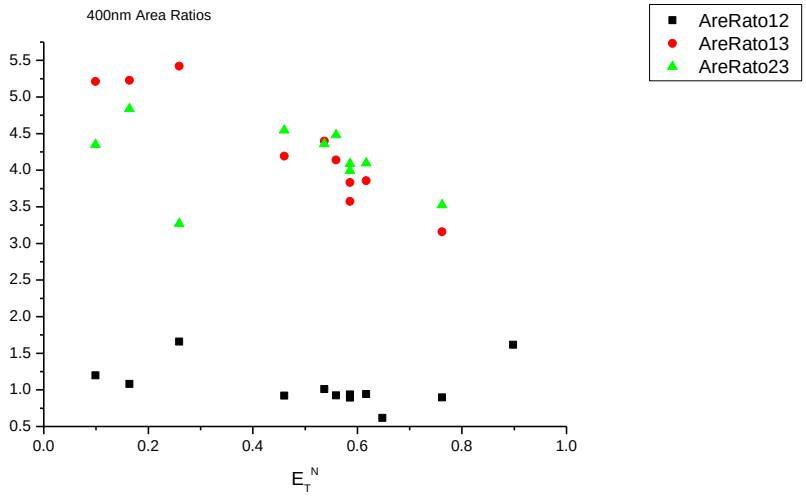

Figure 4.2.27. Area ratios from Gaussian model fit of the normalised fluorescence emission spectra of **23** recorded at 400 nm excitation against E_T^N.

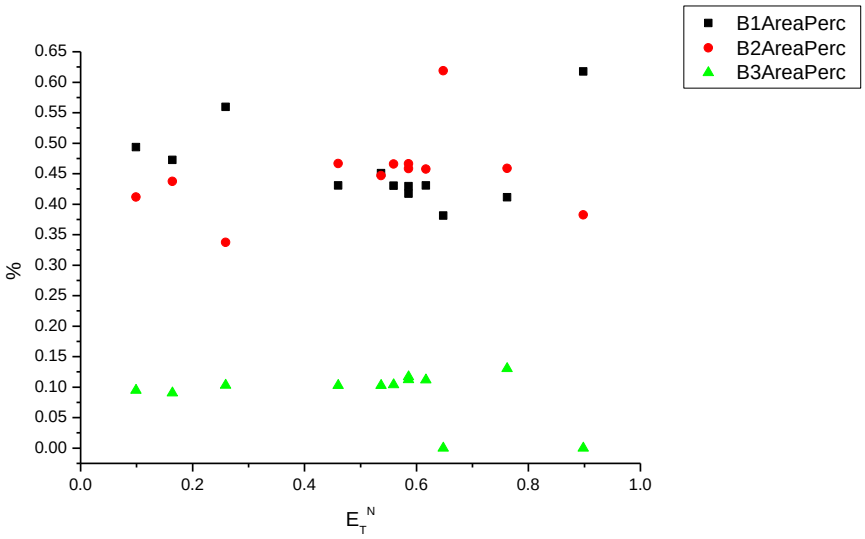

Figure 4.2.28. Area percentages from Gaussian model fit of the normalised fluorescence emission spectra of **23** recorded at 400 nm excitation against E_T^N.

4.2.5.2 *α*

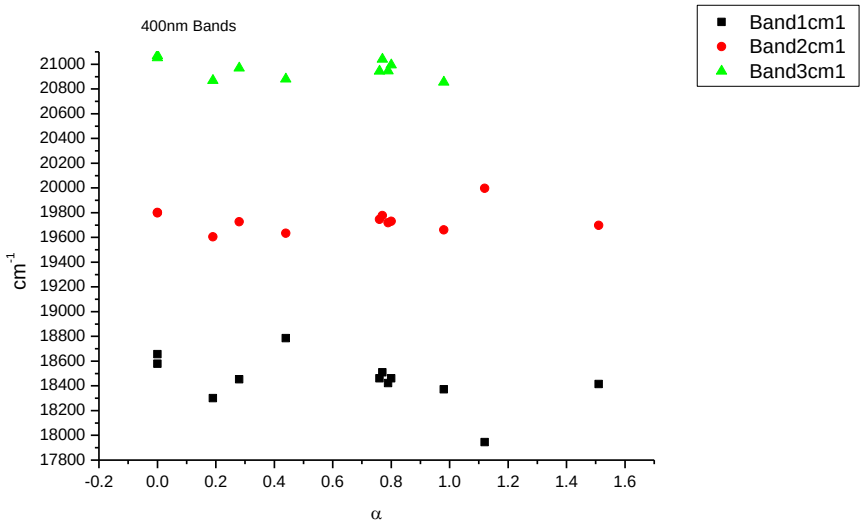

Figure 4.2.29. Band maxima from Gaussian model fit of the normalised fluorescence emission spectra of **23** recorded at 400 nm excitation against α.

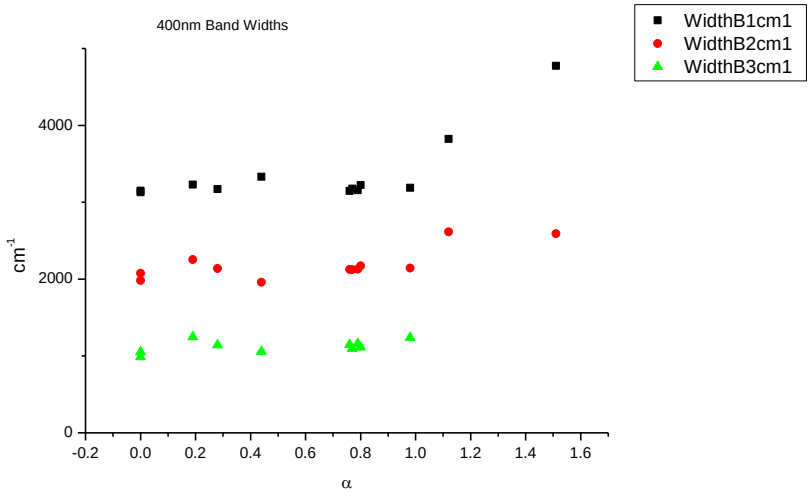

Figure 4.2.30. Band widths from Gaussian model fit of the normalised fluorescence emission spectra of **23** recorded at 400 nm excitation against α.

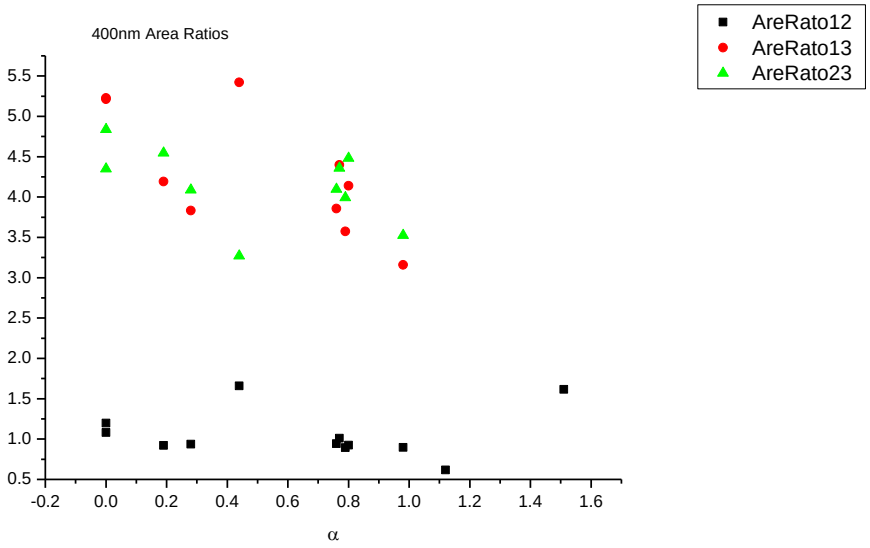

Figure 4.2.31. Area ratios from Gaussian model fit of the normalised fluorescence emission spectra of **23** recorded at 400 nm excitation against α.

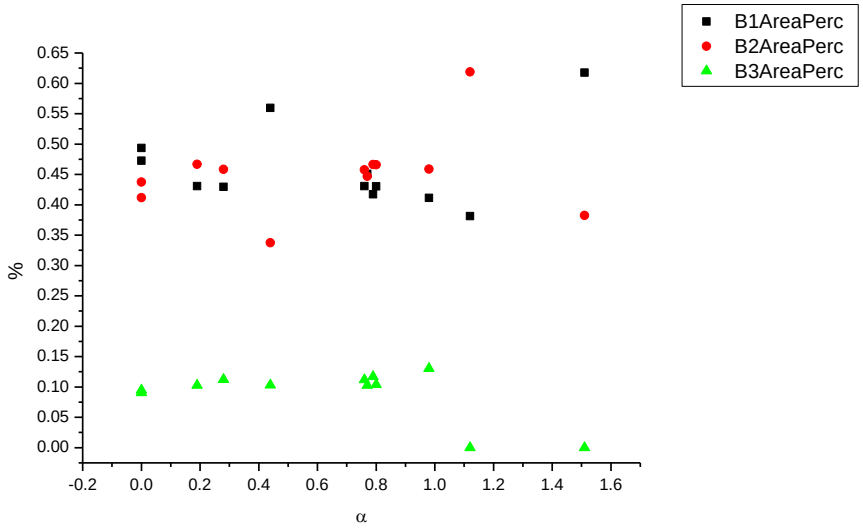

Figure 4.2.32. Area percentages from Gaussian model fit of the normalised fluorescence emission spectra of **23** recorded at 400 nm excitation against α.

4.2.5.3 β.

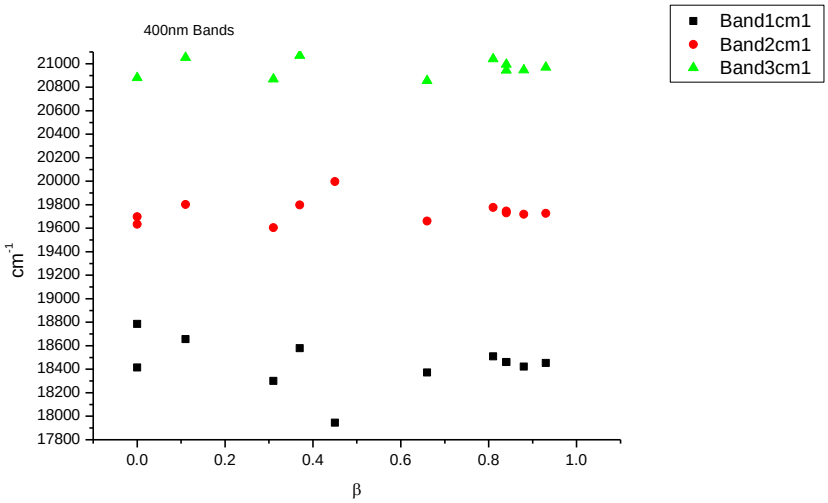

Figure 4.2.33. Band maxima from Gaussian model fit of the normalised fluorescence emission spectra of **23** recorded at 400 nm excitation against β.

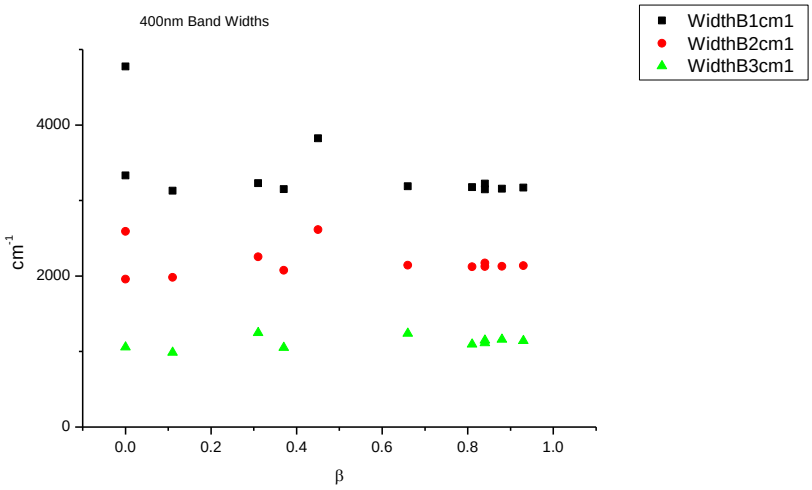

Figure 4.2.34. Band widths from Gaussian model fit of the normalised fluorescence emission spectra of **23** recorded at 400 nm excitation against β.

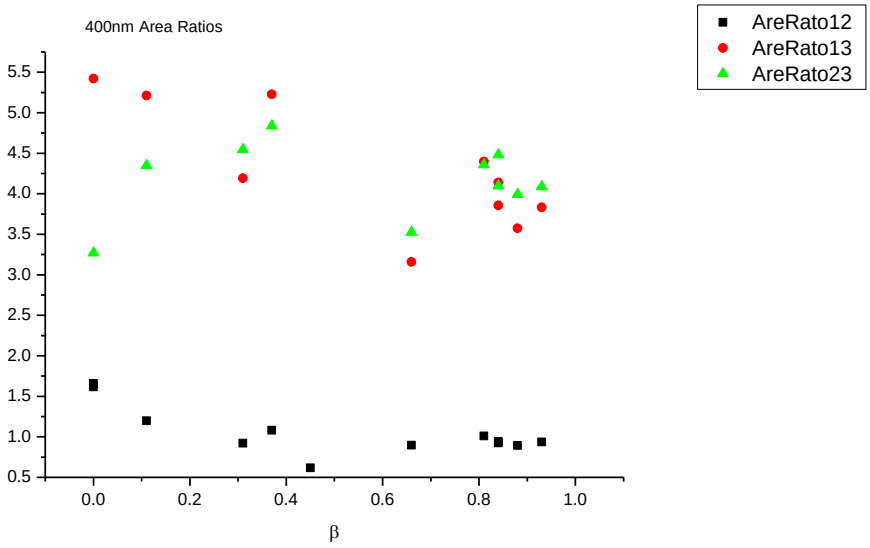

Figure 4.2.35. Area ratios from Gaussian model fit of the normalised fluorescence emission spectra of **23** recorded at 400 nm excitation against β.

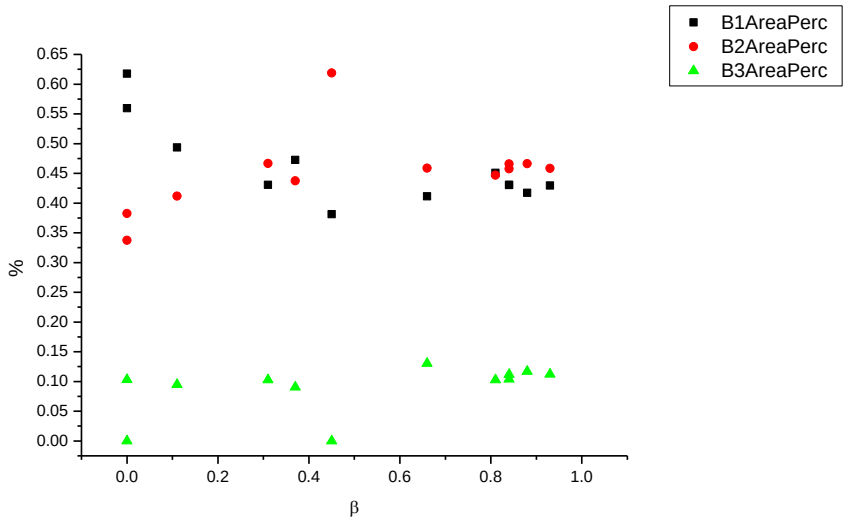

Figure 4.2.36. Area percentages from Gaussian model fit of the normalised fluorescence emission spectra of **23** recorded at 400 nm excitation against β.

4.2.5.4 π.*

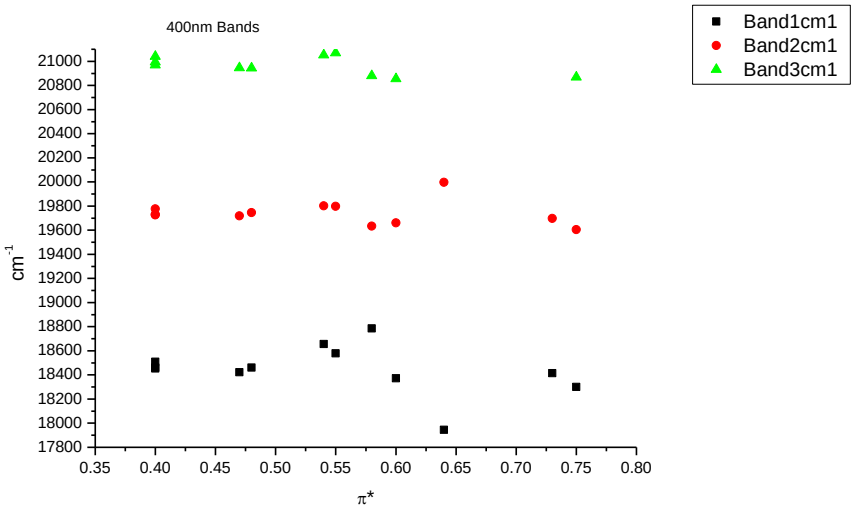

Figure 4.2.37. Band maxima from Gaussian model fit of the normalised fluorescence emission spectra of **23** recorded at 400 nm excitation against π*.

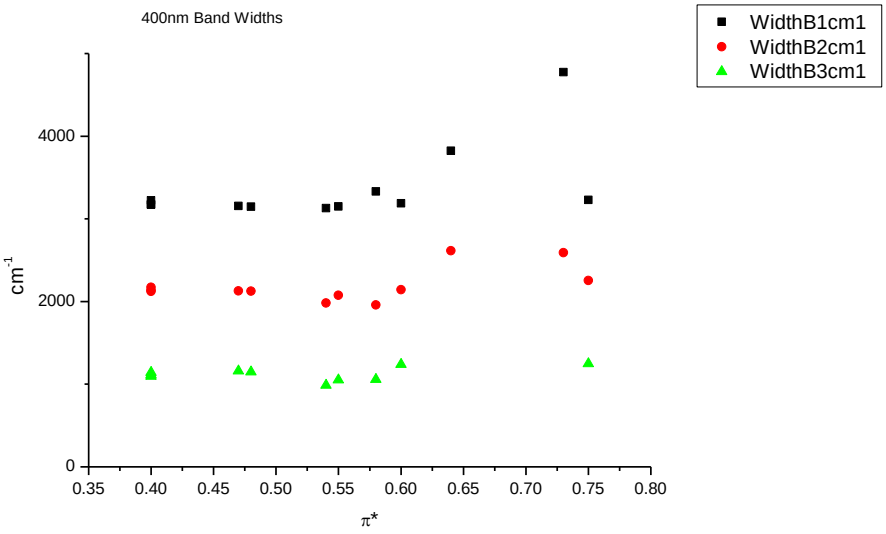

Figure 4.2.38. Band widths from Gaussian model fit of the normalised fluorescence emission spectra of **23** recorded at 400 nm excitation against π*.

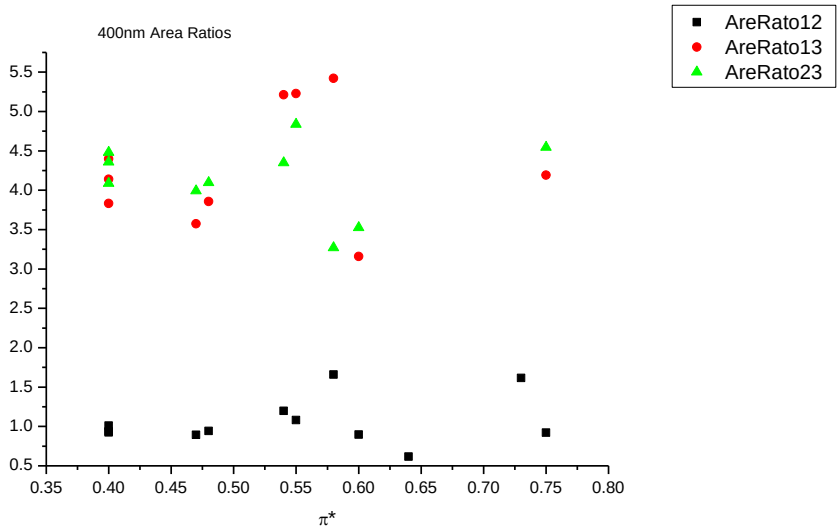

Figure 4.2.39. Area ratios from Gaussian model fit of the normalised fluorescence emission spectra of **23** recorded at 400 nm excitation against π*.

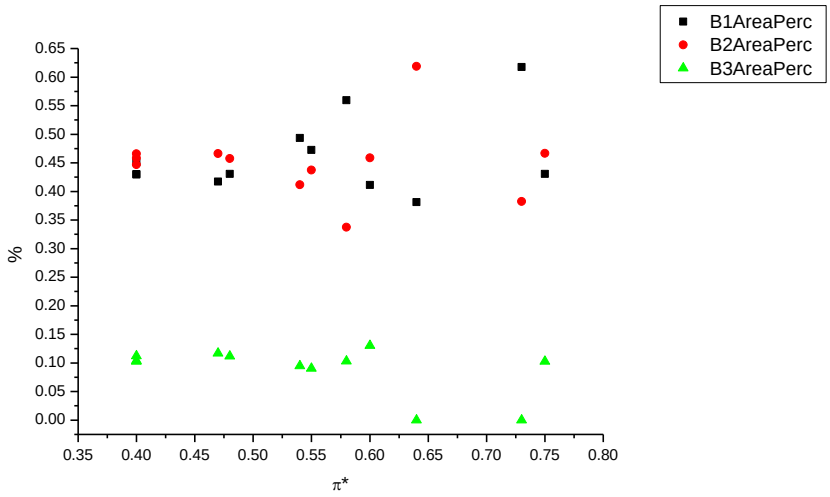

Figure 4.2.40. Area percentages from Gaussian model fit of the normalised fluorescence emission spectra of **23** recorded at 400 nm excitation against π*.

4.2.5.5 μ(D).

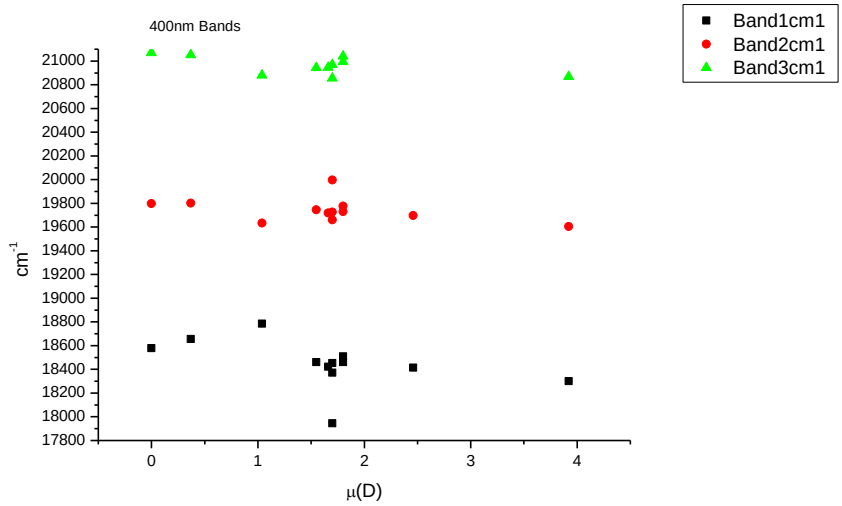

Figure 4.2.41. Band maxima from Gaussian model fit of the normalised fluorescence emission spectra of **23** recorded at 400 nm excitation against μ(D).

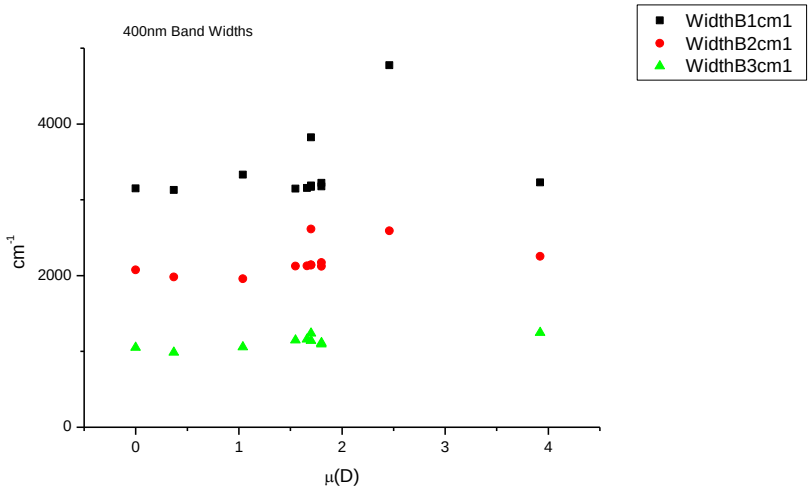

Figure 4.2.42. Band widths from Gaussian model fit of the normalised fluorescence emission spectra of **23** recorded at 400 nm excitation against μ(D).

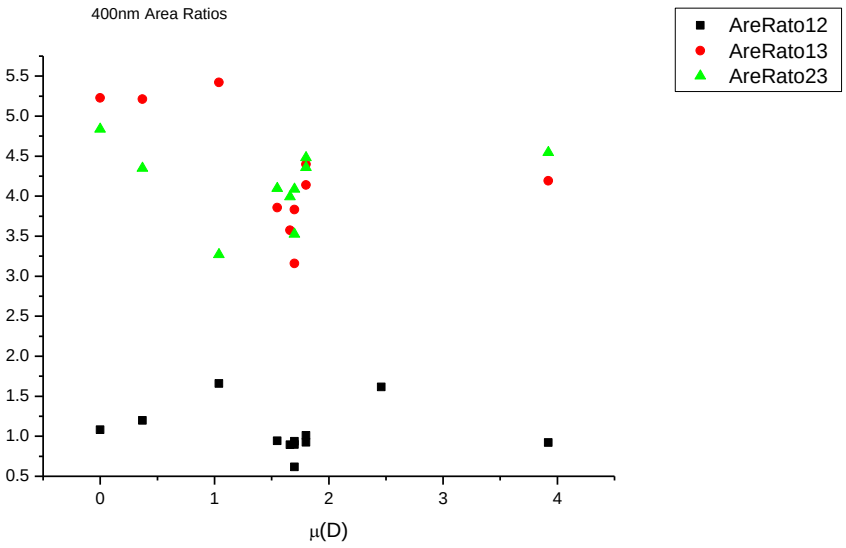

Figure 4.2.43. Area ratios from Gaussian model fit of the normalised fluorescence emission spectra of **23** recorded at 400 nm excitation against μ(D).

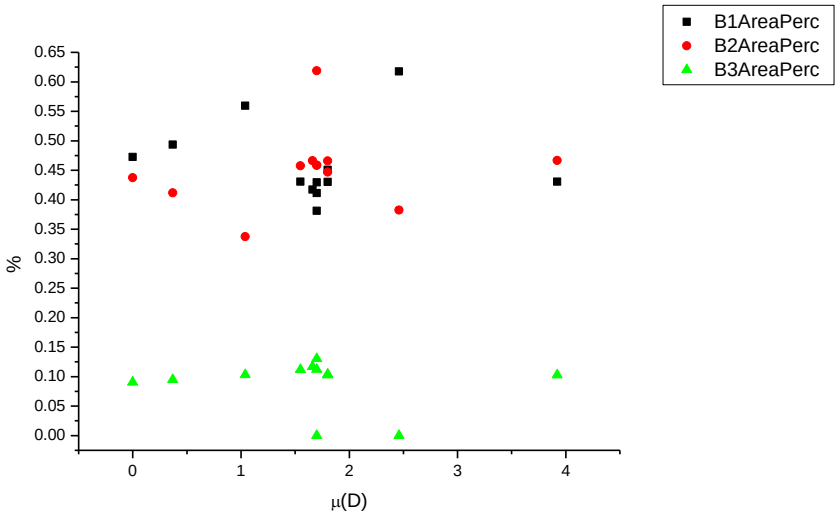

Figure 4.2.44. Area percentages from Gaussian model fit of the normalised fluorescence emission spectra of **23** recorded at 400 nm excitation against μ(D).

4.2.5.6 η(Cp).

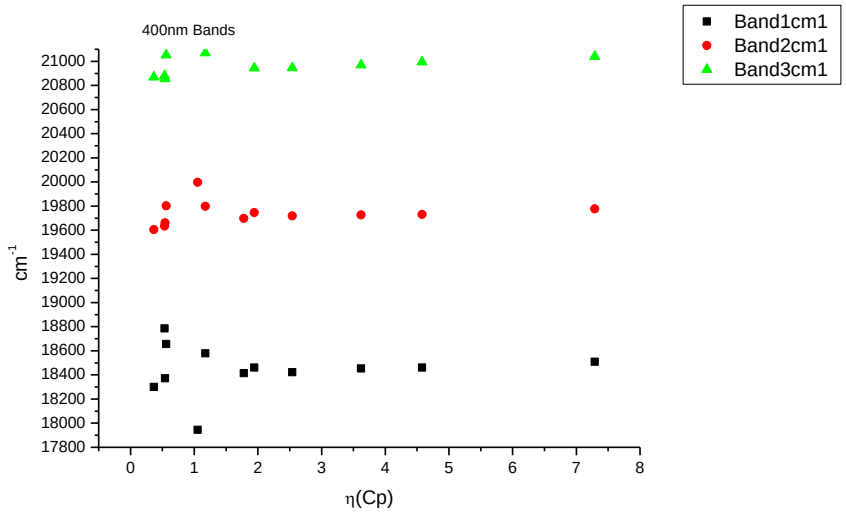

Figure 4.2.45. Band maxima from Gaussian model fit of the normalised fluorescence emission spectra of **23** recorded at 400 nm excitation against η(Cp).

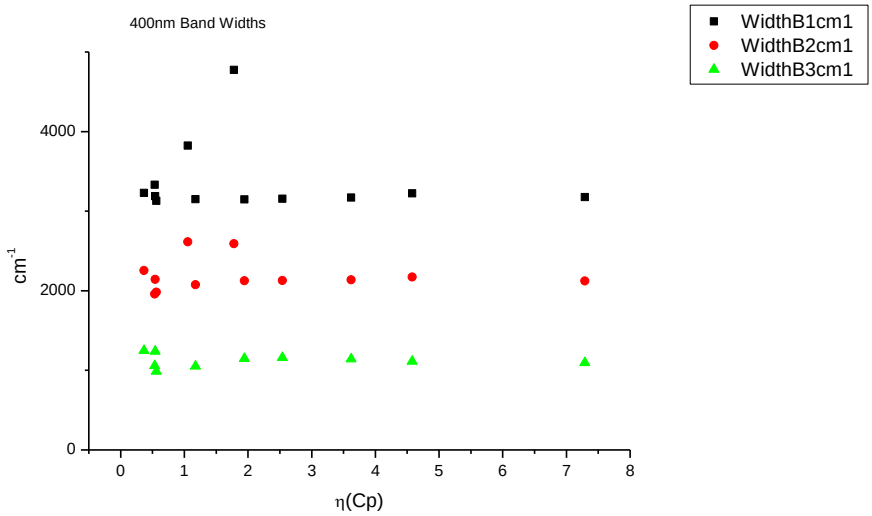

Figure 4.2.46. Band widths from Gaussian model fit of the normalised fluorescence emission spectra of **23** recorded at 400 nm excitation against η(Cp).

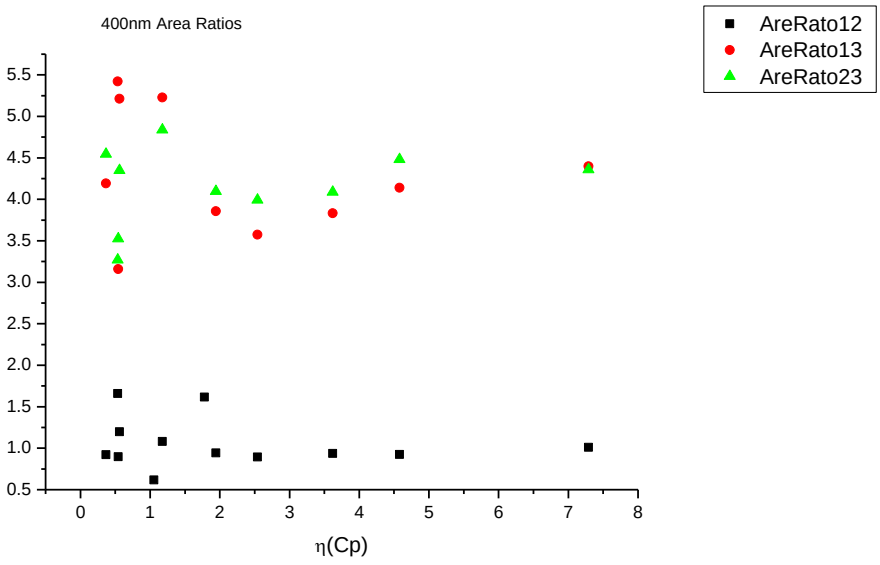

Figure 4.2.47. Area ratios from Gaussian model fit of the normalised fluorescence emission spectra of **23** recorded at 400 nm excitation against η(Cp).

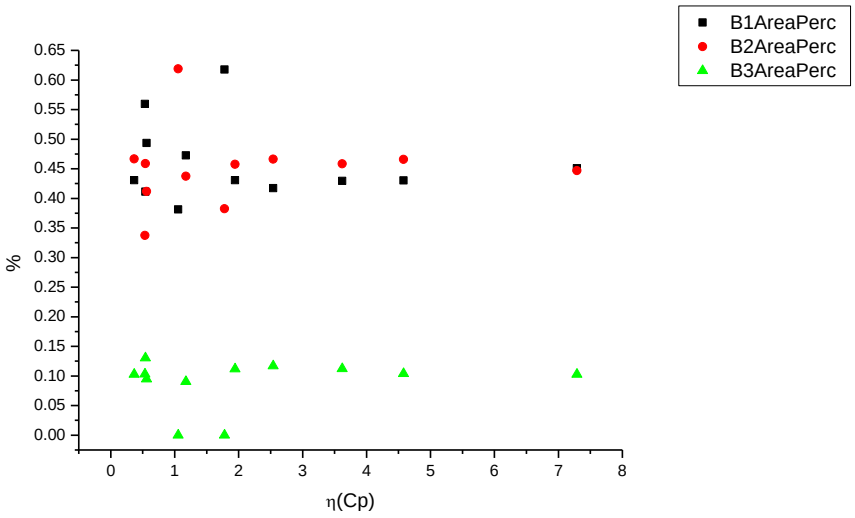

Figure 4.2.48. Area percentages from Gaussian model fit of the normalised fluorescence emission spectra of **23** recorded at 400 nm excitation against η(Cp).

4.2.6 400 nm fluorescent lifetime results.

4.2.6.1 Intensity weighted.

Wavelength (nm)	Solvent	τ_1 (ns)	A_1 (%)	τ_2 (ns)	A_2 (%)	τ_3 (ns)	A_3 (%)	τ_f (ns) (Intensity Weighted)	$1/\tau_f$	χ^2
470	Toluene	-	-	3.45	67.87	9.26	32.13	5.32	0.19	1.24
470	1,4-Dioxane	0.45	0.42	4.40	70.99	10.47	28.59	6.11	0.16	1.22
470	Chloroform	1.19	6.42	4.65	62.58	9.47	31.00	5.92	0.17	1.16
470	Acetonitrile	0.39	0.64	5.10	80.04	10.63	19.32	6.13	0.16	1.21
470	1-Octanol	0.24	7.15	5.27	65.42	10.05	27.43	6.22	0.16	1.17
470	1-Hexanol	0.40	6.19	5.34	68.35	9.04	25.45	5.97	0.17	1.20
470	1-Butanol	0.38	3.36	5.51	79.14	9.67	17.51	6.07	0.16	1.21
470	1-Pentanol	0.40	3.34	5.54	82.32	11.00	14.34	6.15	0.16	1.11
470	1-Propanol	0.32	1.19	5.37	79.45	9.37	19.36	6.08	0.16	1.13
470	Acetic acid	0.25	31.99	1.57	63.07	5.55	4.94	1.34	0.74	1.19
470	Methanol	0.47	2.31	3.97	63.13	6.31	34.56	4.70	0.21	1.04
470	2,2,2-Trifluoroethanol	0.22	72.07	0.88	22.02	5.67	5.91	0.68	1.46	1.07

Table 4.2.9. Summary of Time Correlated Single Photon Counting (TCSPC) fluorescent lifetimes (intensity weighted) of **23** recorded at 470 nm.

Wavelength (nm)	Solvent	τ_1 (ns)	A_1 (%)	τ_2 (ns)	A_2 (%)	τ_3 (ns)	A_3 (%)	τ_f (ns) (Intensity Weighted)	$1/\tau_f$	χ^2
490	Toluene	-	-	3.56	58.94	9.40	41.06	5.96	0.17	1.19
490	1,4-Dioxane	0.20	0.84	4.41	60.93	10.55	38.24	6.72	0.15	1.11
490	Chloroform	0.39	1.16	4.43	52.73	9.00	46.11	6.49	0.15	1.18
490	Acetonitrile	-	-	5.08	73.15	10.76	26.85	6.60	0.15	1.19
490	1-Octanol	0.22	4.79	5.50	64.60	11.10	30.61	6.96	0.14	1.20
490	1-Hexanol	0.40	2.33	5.34	63.92	9.56	33.76	6.65	0.15	1.11
490	1-Butanol	0.33	2.48	5.52	73.99	9.91	23.54	6.42	0.16	1.22
490	1-Pentanol	0.34	1.52	5.44	72.05	10.35	26.43	6.66	0.15	1.06
490	1-Propanol	0.25	0.92	5.51	80.13	10.77	18.95	6.46	0.15	1.07
490	Acetic acid	0.23	30.73	1.62	64.59	4.64	4.70	1.33	0.75	1.08
490	Methanol	0.39	1.93	3.97	59.77	6.73	38.30	4.96	0.20	1.19
490	2,2,2-Trifluoroethanol	0.24	70.53	0.89	25.31	6.38	4.16	0.66	1.52	1.14

Table 4.2.10. Summary of Time Correlated Single Photon Counting (TCSPC) fluorescent lifetimes (intensity weighted) of **23** recorded at 490 nm.

Wavelength (nm)	Solvent	τ_1 (ns)	A_1 (%)	τ_2 (ns)	A_2 (%)	τ_3 (ns)	A_3 (%)	τ_f (ns) (Intensity Weighted)	$1/\tau_f$	χ^2
520	Toluene	-	-	3.61	33.32	9.57	66.68	7.58	0.13	1.10
520	1,4-Dioxane	-	-	4.41	34.93	11.18	65.07	8.81	0.11	1.05
520	Chloroform	0.31	0.66	4.81	40.94	11.32	58.40	8.58	0.12	0.99
520	Acetonitrile	-	-	5.25	55.40	13.03	44.60	8.72	0.11	1.14
520	1-Octanol	0.22	2.76	5.74	46.94	12.72	50.30	9.10	0.11	1.16
520	1-Hexanol	0.38	1.15	5.63	52.17	12.61	46.68	8.83	0.11	0.99
520	1-Butanol	-	-	5.50	60.21	12.54	39.79	8.30	0.12	1.18
520	1-Pentanol	-	-	5.36	51.83	12.08	48.17	8.60	0.12	1.15
520	1-Propanol	-	-	5.46	60.41	12.04	39.59	8.07	0.12	1.12
520	Acetic acid	0.20	41.91	1.64	54.07	4.48	4.02	1.15	0.87	1.11
520	Methanol	0.31	1.65	4.41	71.96	11.12	26.39	6.10	0.16	1.12
520	2,2,2-Trifluoroethanol	0.26	68.93	0.89	25.61	5.36	5.46	0.70	1.44	1.31

Table 4.2.11. Summary of Time Correlated Single Photon Counting (TCSPC) fluorescent lifetimes (intensity weighted) of **23** recorded at 520 nm.

Wavelength (nm)	Solvent	τ_1 (ns)	A_1 (%)	τ_2 (ns)	A_2 (%)	τ_3 (ns)	A_3 (%)	τ_f (ns) (Intensity Weighted)	$1/\tau_f$	χ^2
540	Toluene	-	-	3.71	25.93	9.64	74.07	8.10	0.12	1.11
540	1,4-Dioxane	-	-	4.36	25.28	11.22	74.72	9.48	0.11	1.14
540	Chloroform	-	-	4.59	28.85	11.21	71.15	9.30	0.11	1.23
540	Acetonitrile	-	-	5.24	42.01	13.20	57.99	9.85	0.10	1.06
540	1-Octanol	0.24	1.86	5.84	38.30	13.06	59.85	10.06	0.10	1.20
540	1-Hexanol	-	-	5.49	41.54	12.94	58.46	9.85	0.10	1.14
540	1-Butanol	-	-	5.51	51.08	12.95	48.92	9.15	0.11	1.17
540	1-Pentanol	-	-	5.50	44.50	12.71	55.50	9.51	0.11	1.15
540	1-Propanol	-	-	5.57	54.04	13.02	45.96	8.99	0.11	1.12
540	Acetic acid	0.15	44.92	1.56	47.71	3.30	7.38	1.06	0.95	1.06
540	Methanol	0.31	1.47	4.41	71.98	11.12	26.55	6.13	0.16	1.06
540	2,2,2-Trifluoroethanol	0.23	70.30	0.91	23.87	6.21	5.82	0.74	1.36	1.09

Table 4.2.12. Summary of Time Correlated Single Photon Counting (TCSPC) fluorescent lifetimes (intensity weighted) of **23** recorded at 540 nm.

Wavelength (nm)	Solvent	τ_1 (ns)	A_1 (%)	τ_2 (ns)	A_2 (%)	τ_3 (ns)	A_3 (%)	τ_f (ns) (Intensity Weighted)	$1/\tau_f$	χ^2
570	Toluene	-	-	3.64	13.97	9.63	86.03	8.79	0.11	1.25
570	1,4-Dioxane	-	-	4.35	13.25	11.33	86.75	10.40	0.10	1.18
570	Chloroform	-	-	4.72	19.57	11.68	80.43	10.32	0.10	1.13
570	Acetonitrile	-	-	5.19	27.57	13.36	72.43	11.11	0.09	1.09
570	1-Octanol	0.22	1.36	6.04	27.29	13.28	71.35	11.12	0.09	1.19
570	1-Hexanol	-	-	5.68	30.22	13.30	69.78	11.00	0.09	1.21
570	1-Butanol	0.39	1.20	5.74	40.47	13.47	58.34	10.18	0.10	1.19
570	1-Pentanol	-	-	5.64	34.02	13.28	65.98	10.68	0.09	1.11
570	1-Propanol	-	-	5.45	39.89	12.97	60.11	9.97	0.10	1.09
570	Acetic acid	0.17	55.51	1.56	40.37	4.76	4.12	0.92	1.09	1.14
570	Methanol	0.40	1.40	4.53	59.07	12.94	39.53	7.80	0.13	1.08
570	2,2,2-Trifluoroethanol	0.25	63.21	0.76	29.50	4.13	7.29	0.69	1.46	1.19

Table 4.2.13. Summary of Time Correlated Single Photon Counting (TCSPC) fluorescent lifetimes (intensity weighted) of **23** recorded at 570 nm.

4.2.6.2 Amplitude weighted.

Wavelength (nm)	Solvent	τ_1 (ns)	A_1 (%)	τ_2 (ns)	A_2 (%)	τ_3 (ns)	A_3 (%)	τ_f (ns) (Amplitude Weighted)	$1/\tau_f$	χ^2
470	Toluene	-	-	3.45	85.01	9.26	14.99	4.32	0.23	1.24
470	1,4-Dioxane	0.45	4.72	4.40	81.51	10.47	13.78	5.05	0.20	1.22
470	Chloroform	1.19	24.45	4.65	60.76	9.47	14.78	4.51	0.22	1.16
470	Acetonitrile	0.39	8.54	5.10	81.98	10.63	9.48	5.22	0.19	1.21
470	1-Octanol	0.24	66.08	5.27	27.81	10.05	6.12	2.24	0.45	1.17
470	1-Hexanol	0.40	49.92	5.34	41.05	9.04	9.03	3.21	0.31	1.20
470	1-Butanol	0.38	35.20	5.51	57.54	9.67	7.26	4.01	0.25	1.21
470	1-Pentanol	0.40	34.18	5.54	60.51	11.00	5.31	4.07	0.25	1.11
470	1-Propanol	0.32	18.17	5.37	71.80	9.37	10.03	4.85	0.21	1.13
470	Acetic acid	0.25	75.64	1.57	23.84	5.55	0.53	0.59	1.69	1.19
470	Methanol	0.47	18.78	3.97	60.41	6.31	20.81	3.80	0.26	1.04
470	2,2,2-Trifluoroethanol	0.22	92.70	0.88	7.01	5.67	0.29	0.28	3.58	1.07

Table 4.2.14. Summary of Time Correlated Single Photon Counting (TCSPC) fluorescent lifetimes (amplitude weighted) of **23** recorded at 470 nm.

Wavelength (nm)	Solvent	τ_1 (ns)	A_1 (%)	τ_2 (ns)	A_2 (%)	τ_3 (ns)	A_3 (%)	τ_f (ns) (Amplitude Weighted)	$1/\tau_f$	χ^2
490	Toluene	-	-	3.56	79.14	9.40	20.86	4.78	0.21	1.19
490	1,4-Dioxane	0.20	18.97	4.41	64.18	10.55	16.85	4.65	0.22	1.11
490	Chloroform	0.39	14.69	4.43	59.63	9.00	25.68	5.01	0.20	1.18
490	Acetonitrile	-	-	5.08	85.23	10.76	14.77	5.92	0.17	1.19
490	1-Octanol	0.22	60.26	5.50	32.18	11.10	7.55	2.74	0.37	1.20
490	1-Hexanol	0.40	27.53	5.34	55.95	9.56	16.53	4.68	0.21	1.11
490	1-Butanol	0.33	32.52	5.52	57.32	9.91	10.16	4.28	0.23	1.22
490	1-Pentanol	0.34	22.14	5.44	65.26	10.35	12.59	4.93	0.20	1.06
490	1-Propanol	0.25	18.24	5.51	72.93	10.77	8.82	5.02	0.20	1.07
490	Acetic acid	0.23	76.93	1.62	22.50	4.64	0.57	0.56	1.77	1.08
490	Methanol	0.39	19.36	3.97	58.53	6.73	22.11	3.89	0.26	1.19
490	2,2,2-Trifluoroethanol	0.24	91.00	0.89	8.79	6.38	0.20	0.31	3.23	1.14

Table 4.2.15. Summary of Time Correlated Single Photon Counting (TCSPC) fluorescent lifetimes (amplitude weighted) of **23** recorded at 490 nm.

Wavelength (nm)	Solvent	τ_1 (ns)	A_1 (%)	τ_2 (ns)	A_2 (%)	τ_3 (ns)	A_3 (%)	τ_f (ns) (Amplitude Weighted)	$1/\tau_f$	χ^2
520	Toluene	-	-	3.61	56.98	9.57	43.02	6.17	0.16	1.10
520	1,4-Dioxane	-	-	4.41	57.62	11.18	42.38	7.28	0.14	1.05
520	Chloroform	0.31	13.54	4.81	53.83	11.32	32.63	6.33	0.16	0.99
520	Acetonitrile	-	-	5.25	75.52	13.03	24.48	7.15	0.14	1.14
520	1-Octanol	0.22	50.37	5.74	33.45	12.72	16.18	4.09	0.24	1.16
520	1-Hexanol	0.38	19.07	5.63	57.81	12.61	23.12	6.24	0.16	0.99
520	1-Butanol	-	-	5.50	77.52	12.54	22.48	7.08	0.14	1.18
520	1-Pentanol	-	-	5.36	70.81	12.08	29.19	7.32	0.14	1.15
520	1-Propanol	-	-	5.46	77.11	12.04	22.89	6.97	0.14	1.12
520	Acetic acid	0.20	86.27	1.64	13.36	4.48	0.36	0.41	2.46	1.11
520	Methanol	0.31	21.83	4.41	68.25	11.12	9.92	4.18	0.24	1.12
520	2,2,2-Trifluoroethanol	0.26	90.05	0.89	9.61	5.36	0.34	0.33	3.00	1.31

Table 4.2.16. Summary of Time Correlated Single Photon Counting (TCSPC) fluorescent lifetimes (amplitude weighted) of **23** recorded at 520 nm.

Wavelength (nm)	Solvent	τ_1 (ns)	A_1 (%)	τ_2 (ns)	A_2 (%)	τ_3 (ns)	A_3 (%)	τ_f (ns) (Amplitude Weighted)	$1/\tau_f$	χ^2
540	Toluene	-	-	3.71	47.61	9.64	52.39	6.82	0.15	1.11
540	1,4-Dioxane	-	-	4.36	46.55	11.22	53.45	8.02	0.12	1.14
540	Chloroform	-	-	4.59	49.75	11.21	50.25	7.92	0.13	1.23
540	Acetonitrile	-	-	5.24	64.60	13.20	35.40	8.06	0.12	1.06
540	1-Octanol	0.24	40.95	5.84	34.77	13.06	24.28	5.30	0.19	1.20
540	1-Hexanol	-	-	5.49	62.60	12.94	37.40	8.28	0.12	1.14
540	1-Butanol	-	-	5.51	71.03	12.95	28.97	7.67	0.13	1.17
540	1-Pentanol	-	-	5.50	64.95	12.71	35.05	8.03	0.12	1.15
540	1-Propanol	-	-	5.57	73.55	13.02	26.65	7.55	0.13	1.12
540	Acetic acid	0.15	89.86	1.56	9.45	3.30	0.69	0.31	3.24	1.06
540	Methanol	0.31	19.98	4.41	69.81	11.12	10.20	4.27	0.23	1.06
540	2,2,2-Trifluoroethanol	0.23	91.93	0.91	7.80	6.21	0.28	0.30	3.38	1.09

Table 4.2.17. Summary of Time Correlated Single Photon Counting (TCSPC) fluorescent lifetimes (amplitude weighted) of **23** recorded at 540 nm.

Wavelength (nm)	Solvent	τ_1 (ns)	A_1 (%)	τ_2 (ns)	A_2 (%)	τ_3 (ns)	A_3 (%)	τ_f (ns) (Amplitude Weighted)	$1/\tau_f$	χ^2
570	Toluene	-	-	3.64	30.02	9.63	69.98	7.83	0.13	1.25
570	1,4-Dioxane	-	-	4.35	28.45	11.33	71.55	9.34	0.11	1.18
570	Chloroform	-	-	4.72	37.58	11.68	62.42	9.07	0.11	1.13
570	Acetonitrile	-	-	5.19	49.50	13.36	50.50	9.32	0.11	1.09
570	1-Octanol	0.22	38.09	6.04	28.29	13.28	33.62	6.26	0.16	1.19
570	1-Hexanol	-	-	5.68	50.37	13.30	49.63	9.46	0.11	1.21
570	1-Butanol	0.39	21.28	5.74	48.76	13.47	29.96	6.92	0.14	1.19
570	1-Pentanol	-	-	5.64	54.81	13.28	45.19	9.10	0.11	1.11
570	1-Propanol	-	-	5.45	61.23	12.97	38.77	8.36	0.12	1.09
570	Acetic acid	0.17	92.28	1.56	7.47	4.76	0.25	0.29	3.47	1.14
570	Methanol	0.40	17.74	4.53	66.66	12.94	15.60	5.11	0.20	1.08
570	2,2,2-Trifluoroethanol	0.25	86.01	0.76	13.38	4.13	0.61	0.34	2.90	1.19

Table 4.2.18. Summary of Time Correlated Single Photon Counting (TCSPC) fluorescent lifetimes (amplitude weighted) of **23** recorded at 570 nm.

4.2.7 400 nm average fluorescent lifetimes - Solvatochromic analysis.

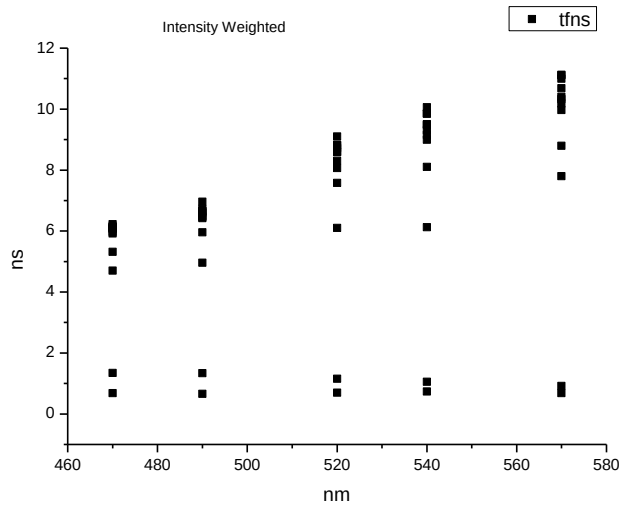

Figure 4.2.49. Intensity weighted average lifetime (τ_f) of **23** versus wavelength (nm).

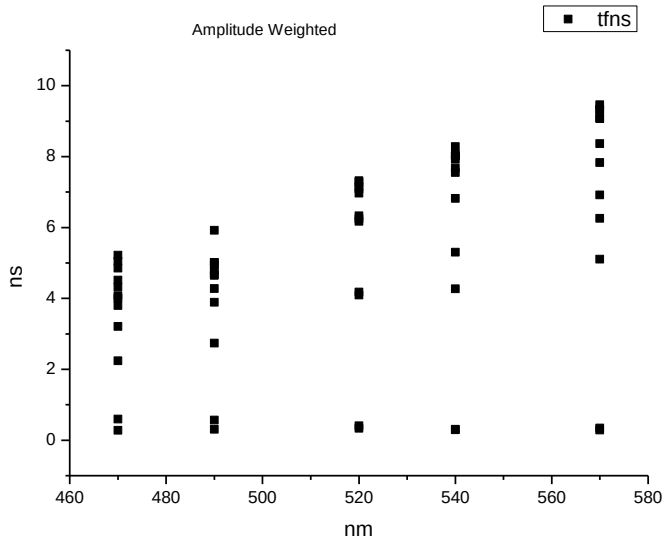

Figure 4.2.50. Amplitude weighted average lifetime (τ_f) of **23** versus wavelength (nm).

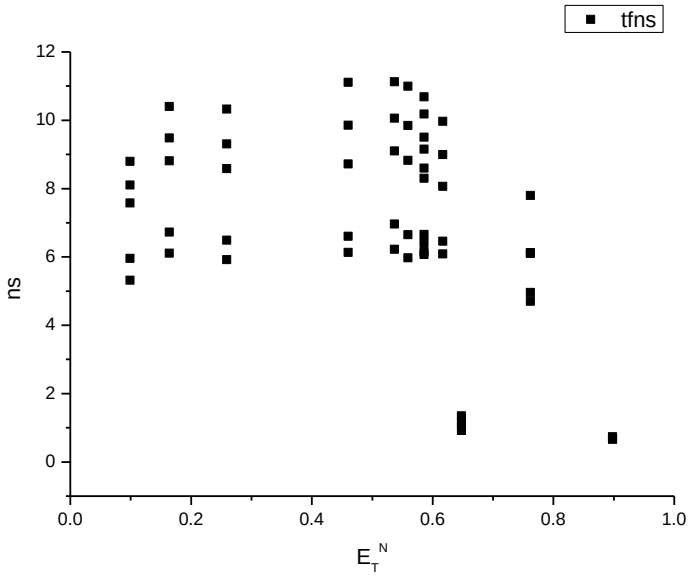

Figure 4.2.51. Intensity weighted average lifetime (τ_f) of **23** versus E_T^N.

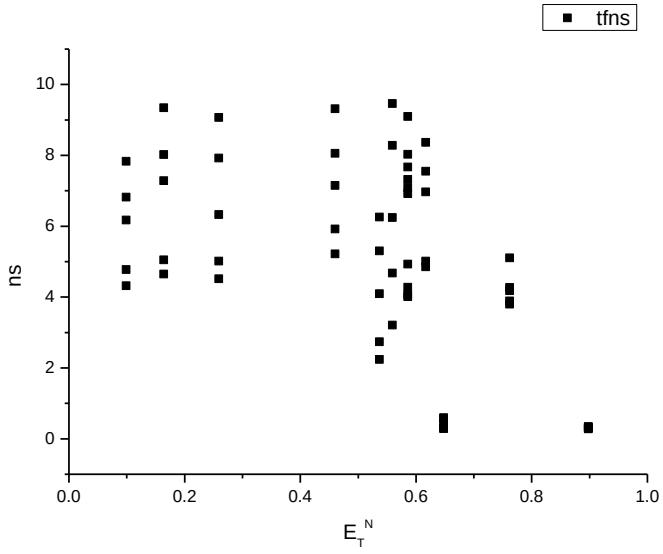

Figure 4.2.52. Amplitude weighted average lifetime (τ_f) of **23** versus E_T^N.

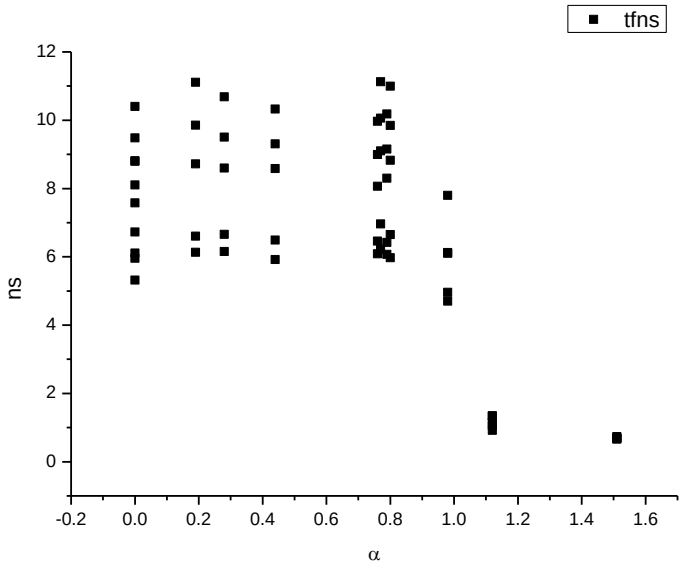

Figure 4.2.53. Intensity weighted average lifetime (τ_f) of **23** versus α.

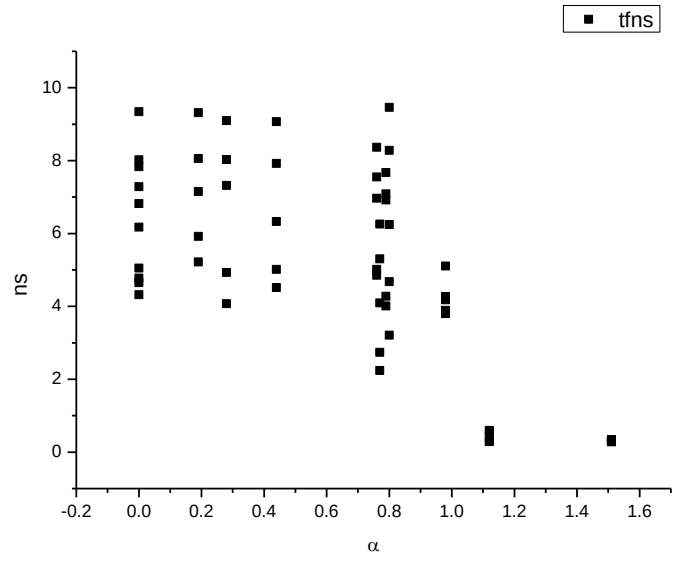

Figure 4.2.54. Amplitude weighted average lifetime (τ_f) of **23** versus α.

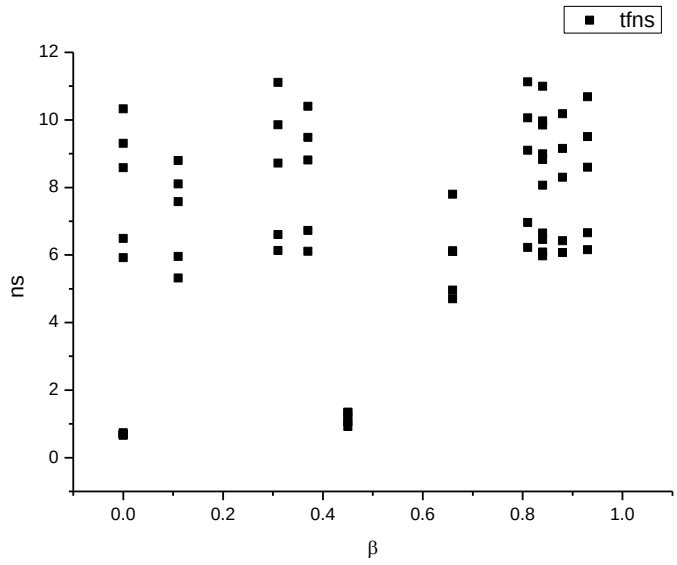

Figure 4.2.55. Intensity weighted average lifetime (τ_f) of **23** versus β.

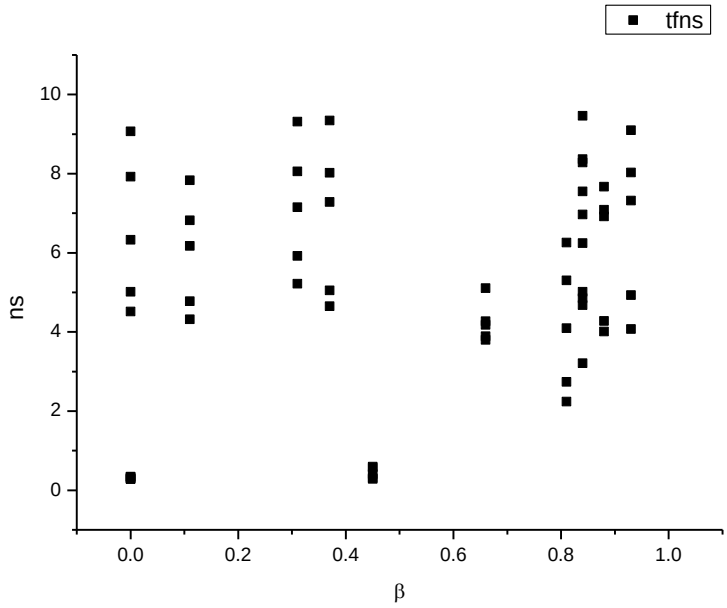

Figure 4.2.56. Amplitude weighted average lifetime (τ_f) of **23** versus β.

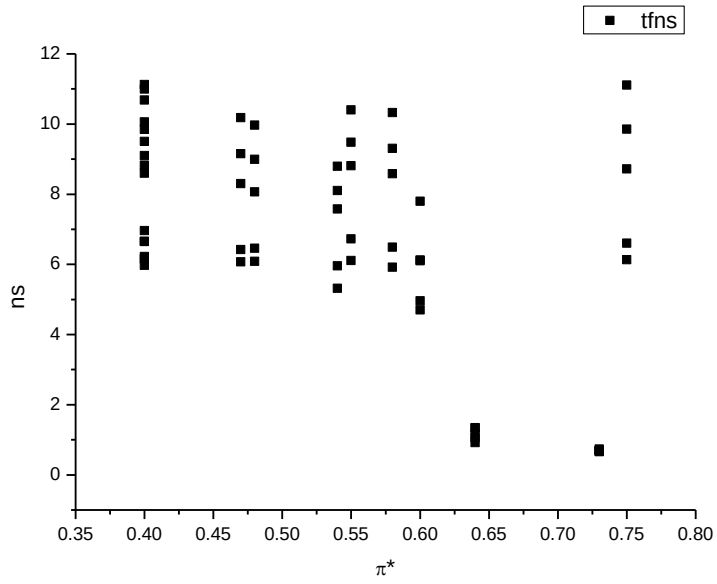

Figure 4.2.57. Intensity weighted average lifetime (τ_f) of **23** versus π*.

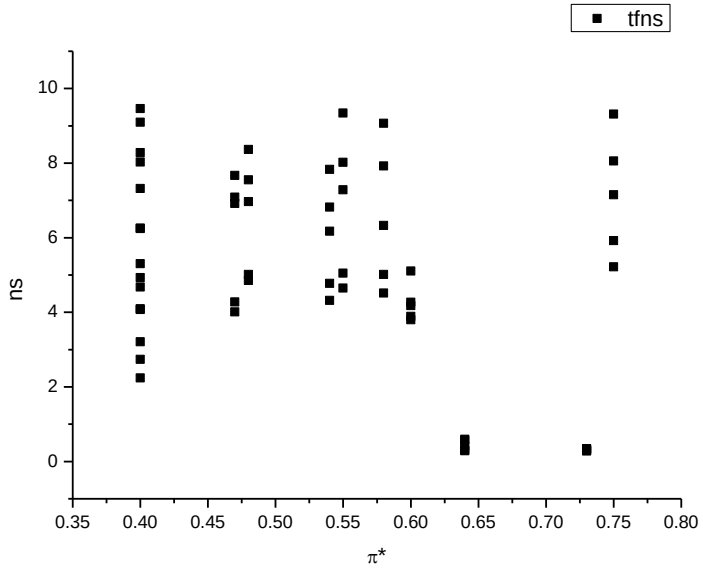

Figure 4.2.58. Amplitude weighted average lifetime (τ_f) of **23** versus π*.

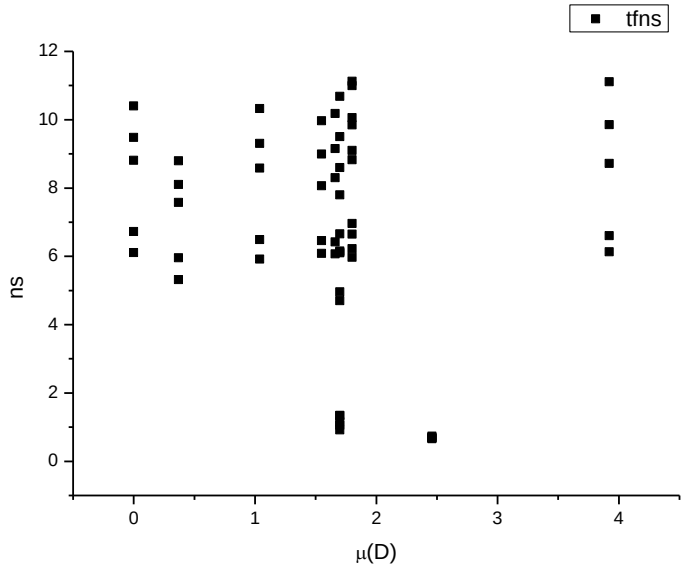

Figure 4.2.59. Intensity weighted average lifetime (τ_f) of **23** versus μ(D).

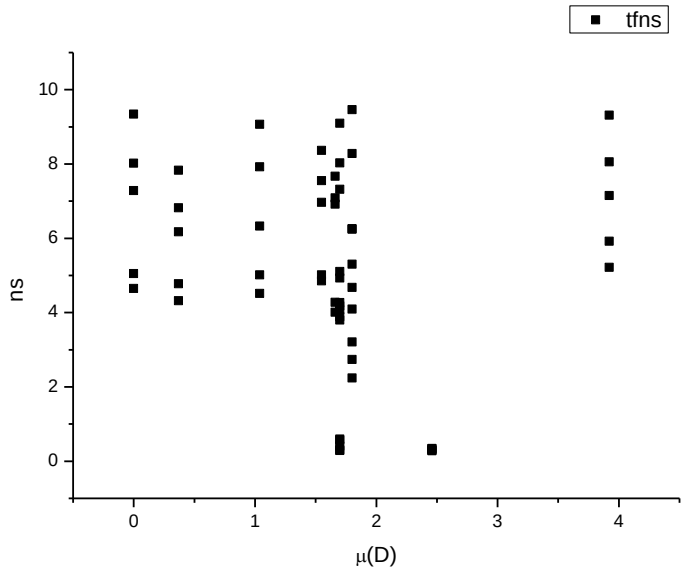

Figure 4.2.60. Amplitude weighted average lifetime (τ_f) of **23** versus μ(D).

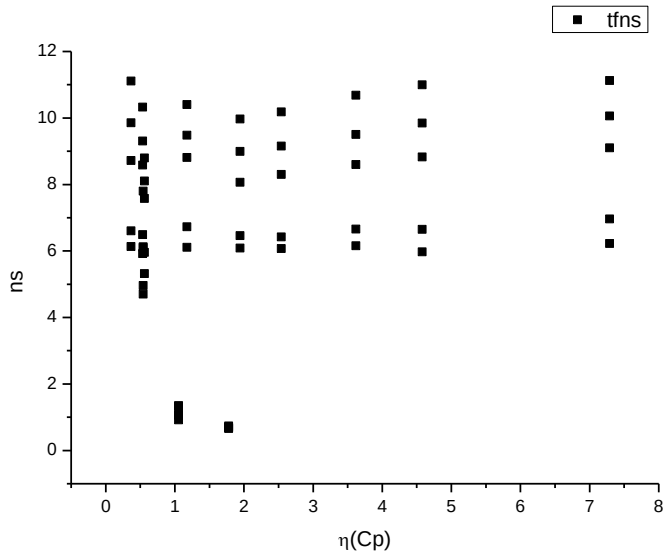

Figure 4.2.61. Intensity weighted average lifetime (τ_f) of **23** versus η(Cp).

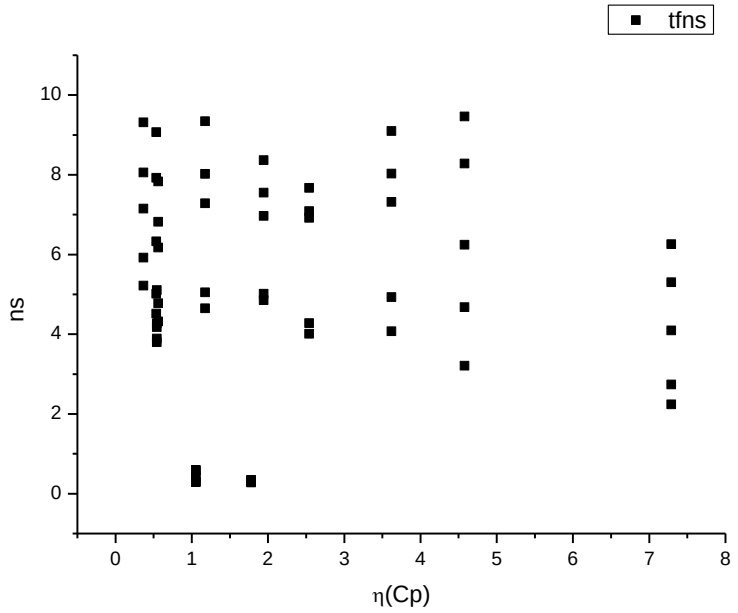

Figure 4.2.62. Amplitude weighted average lifetime (τ_f) of **23** versus η(Cp).

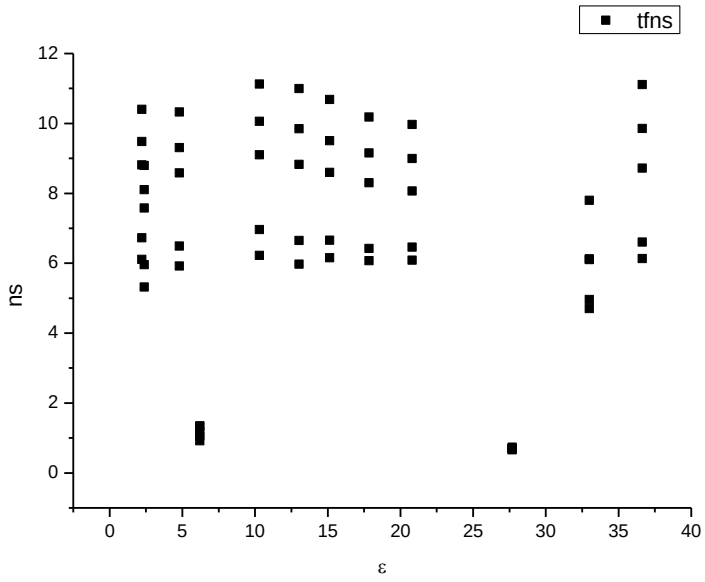

Figure 4.2.63. Intensity weighted average lifetime (τ_f) of **23** versus ε.

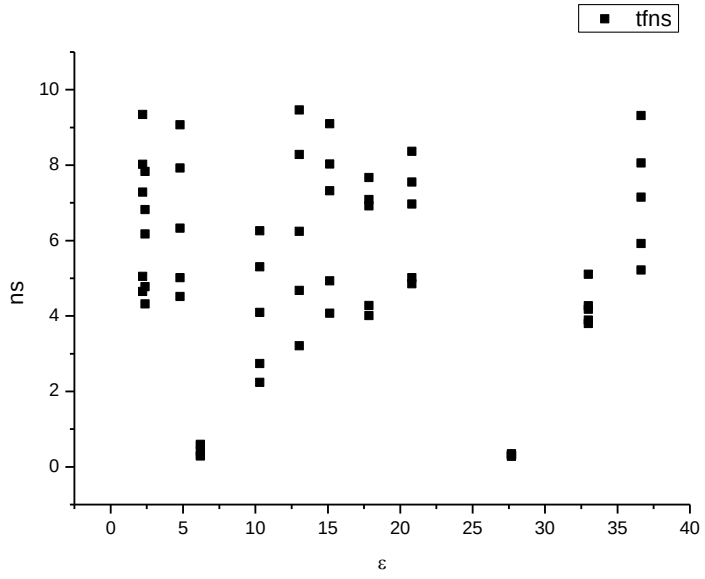

Figure 4.2.64. Amplitude weighted average lifetime (τ_f) of **23** versus ε.

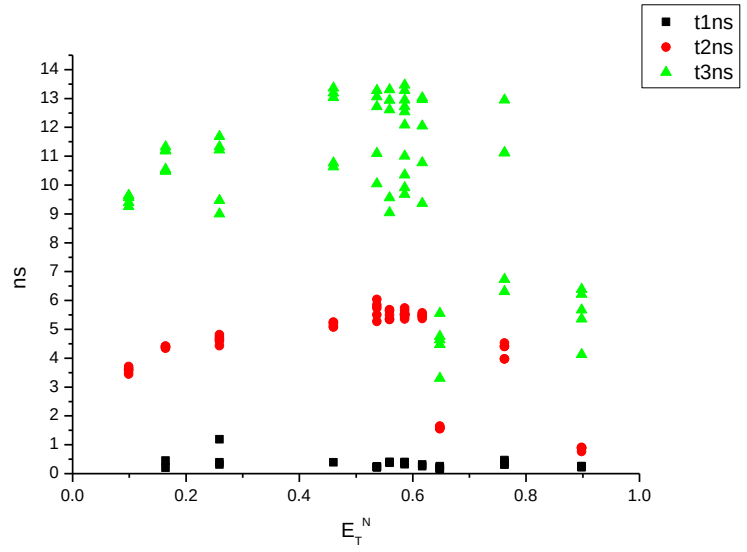

Figure 4.2.65. Intensity weighted components of TCSPC lifetime decay of **23** (470 nm to 570 nm) versus E_T^N.

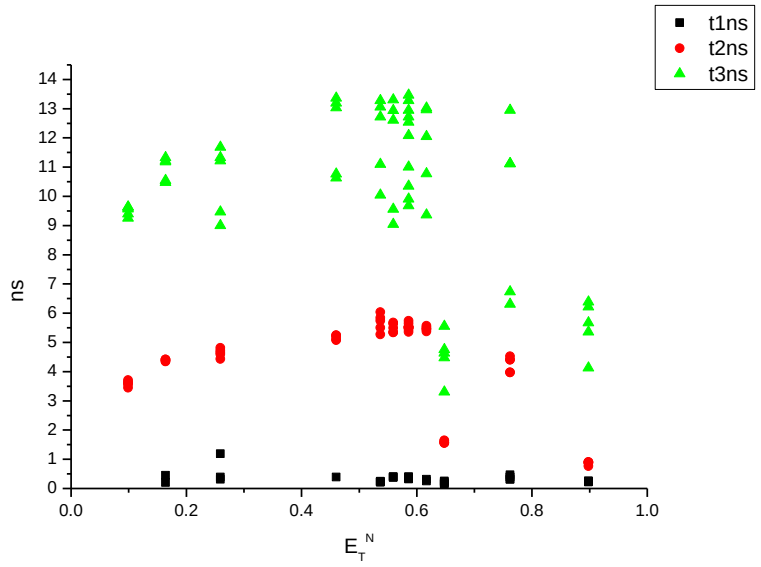

Figure 4.2.66. Amplitude weighted components of TCSPC lifetime decay of **23** (470 nm to 570 nm) versus E_T^N.

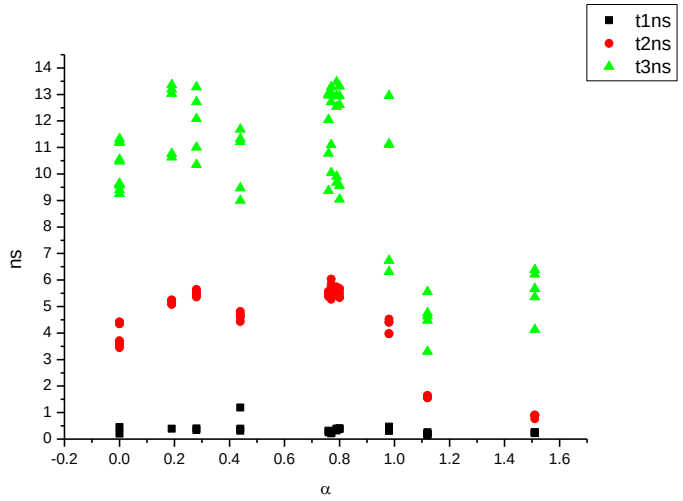

Figure 4.2.67. Intensity weighted components of TCSPC lifetime decay of **23** (470 nm to 570 nm) versus α.

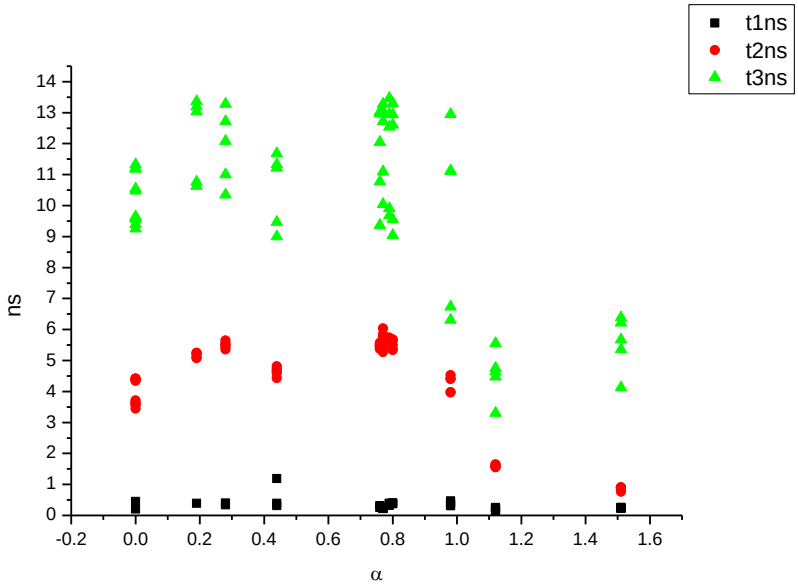

Figure 4.2.68. Amplitude weighted components of TCSPC lifetime decay of **23** (470 nm to 570 nm) versus α.

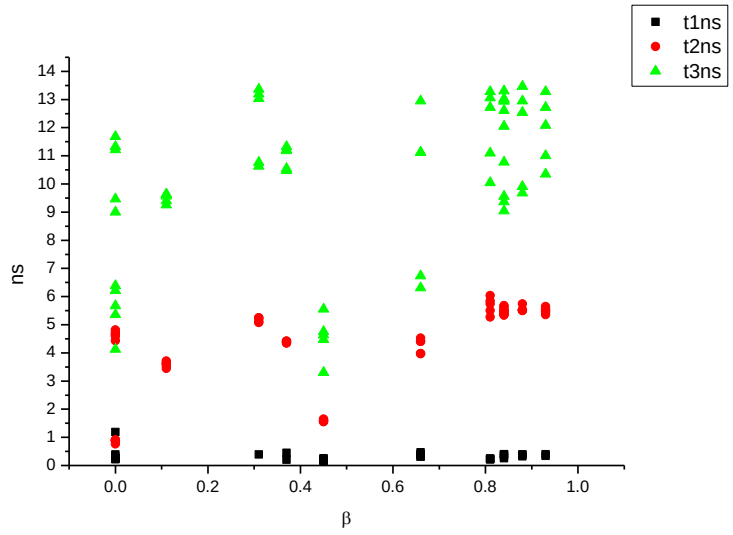

Figure 4.2.69. Intensity weighted components of TCSPC lifetime decay of **23** (470 nm to 570 nm) versus β.

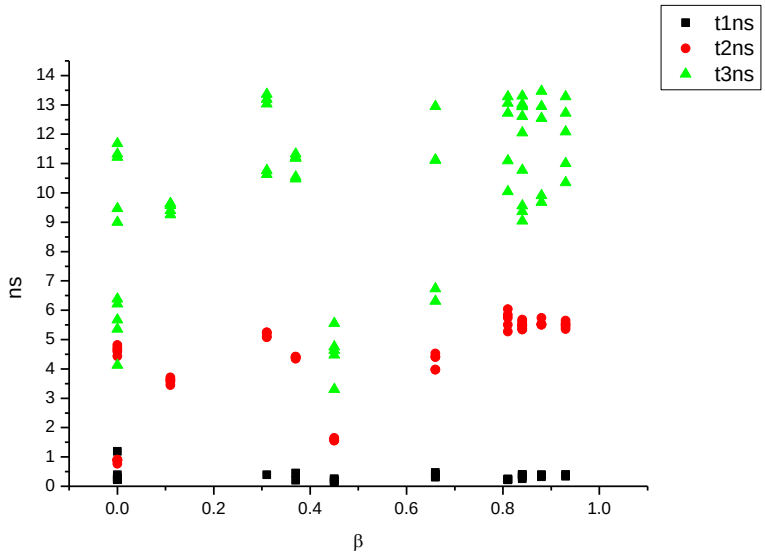

Figure 4.2.70. Amplitude weighted components of TCSPC lifetime decay of **23** (470 nm to 570 nm) versus β.

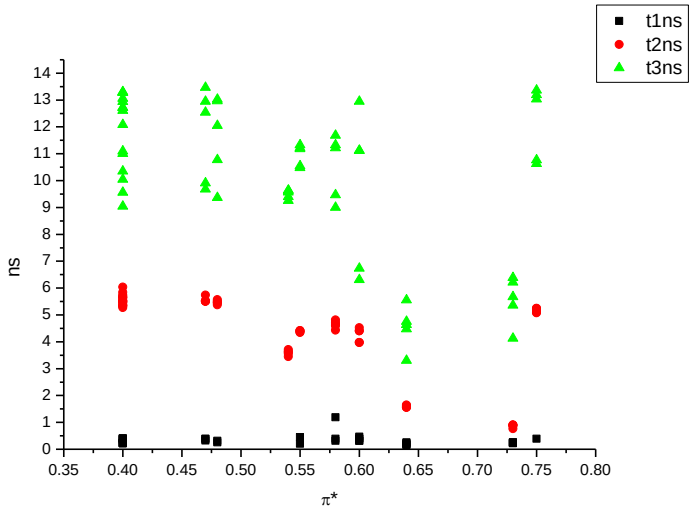

Figure 4.2.71. Intensity weighted components of TCSPC lifetime decay of **23** (470 nm to 570 nm) versus π*.

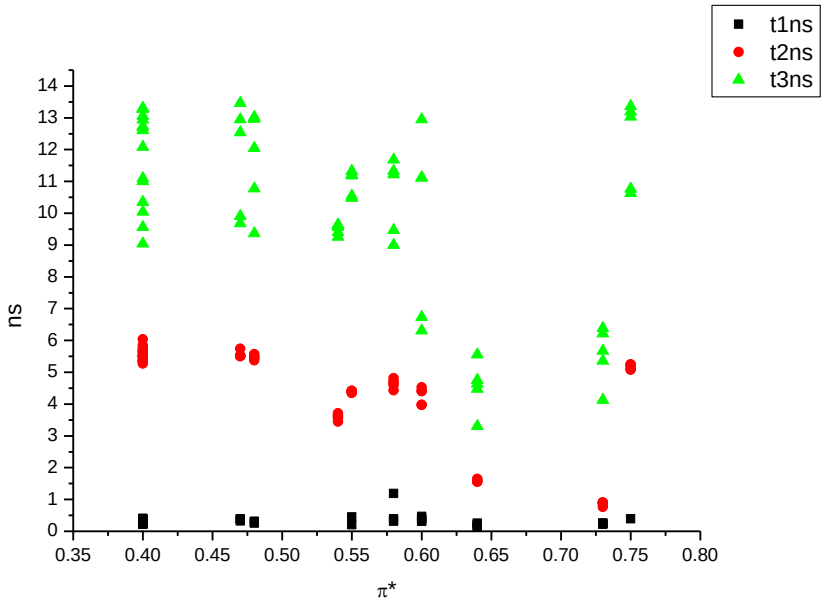

Figure 4.2.72. Amplitude weighted components of TCSPC lifetime decay of **23** (470 nm to 570 nm) versus π*.

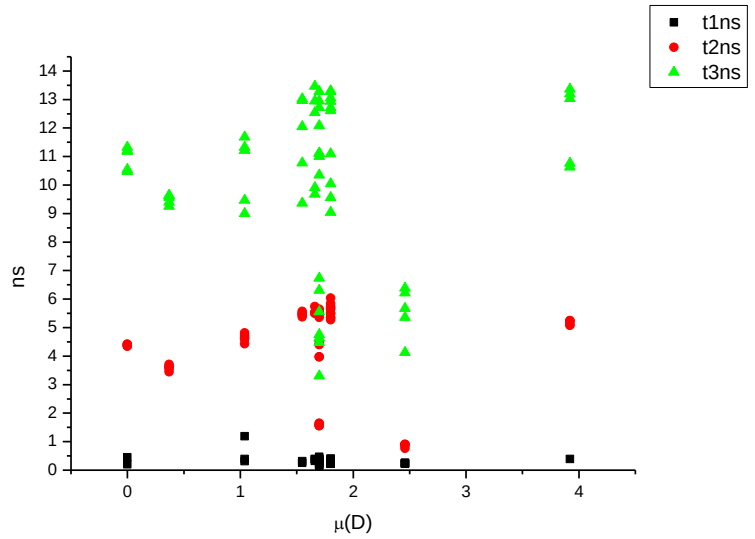

Figure 4.2.73. Intensity weighted components of TCSPC lifetime decay of **23** (470 nm to 570 nm) versus μ(D).

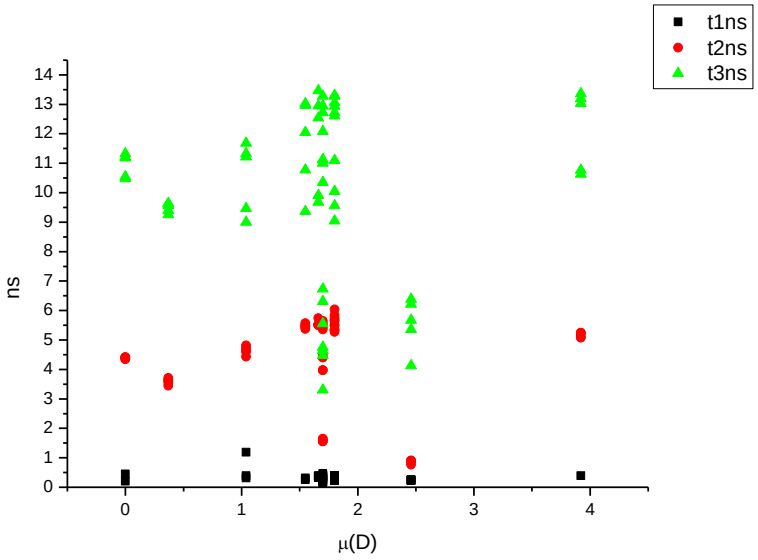

Figure 4.2.74. Amplitude weighted components of TCSPC lifetime decay of **23** (470 nm to 570 nm) versus μ(D).

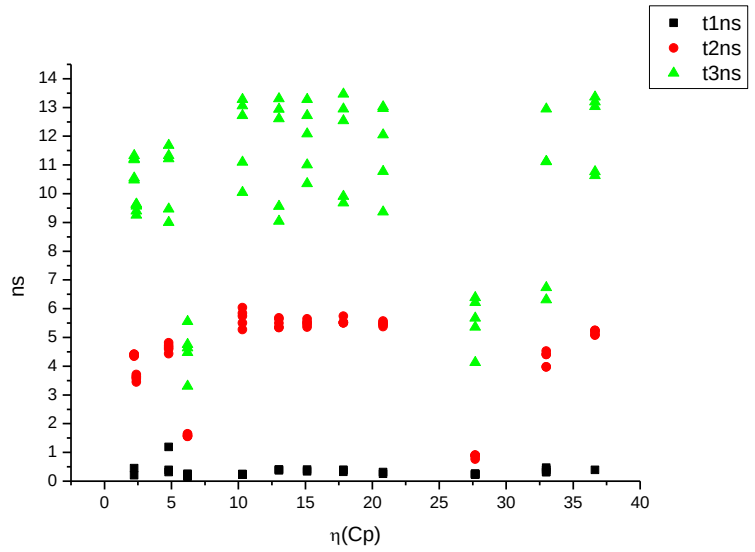

Figure 4.2.75. Intensity weighted components of TCSPC lifetime decay of **23** (470 nm to 570 nm) versus η(Cp).

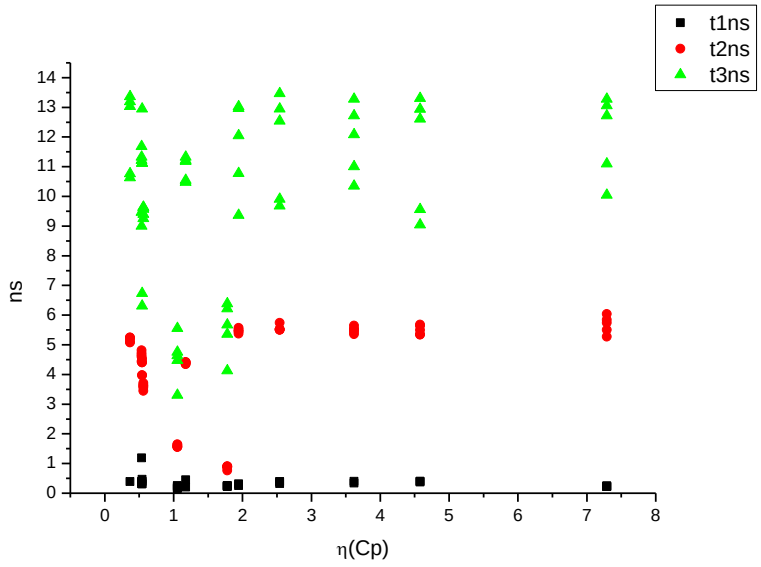

Figure 4.2.76. Amplitude weighted components of TCSPC lifetime decay of **23** (470 nm to 570 nm) versus η(Cp).

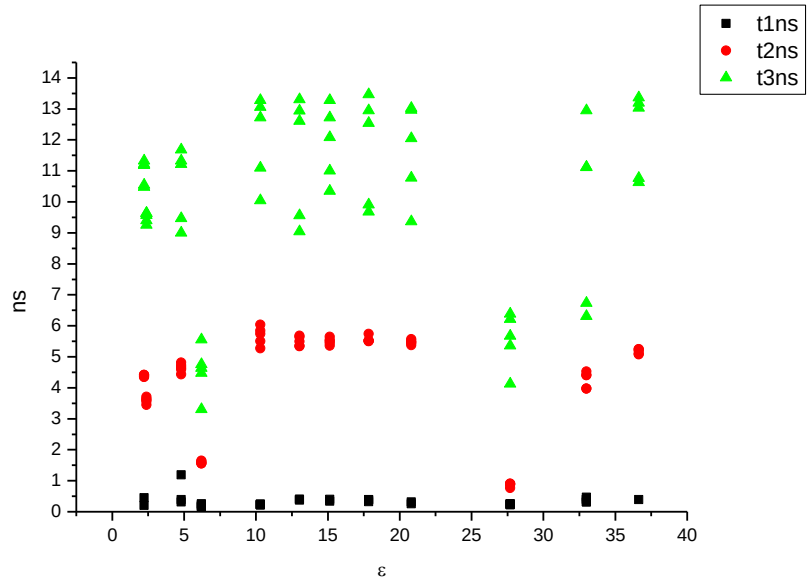

Figure 4.2.77. Intensity weighted components of TCSPC lifetime decay of **23** (470 nm to 570 nm) versus ε.

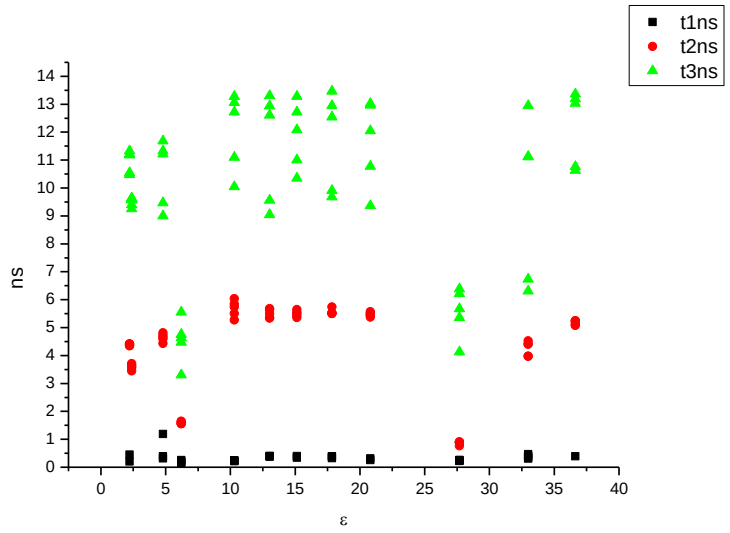

Figure 4.2.78. Amplitude weighted components of TCSPC lifetime decay of **23** (470 nm to 570 nm) versus ε.

4.2.7.1 470 nm Lifetime – Solvatochromic analysis.

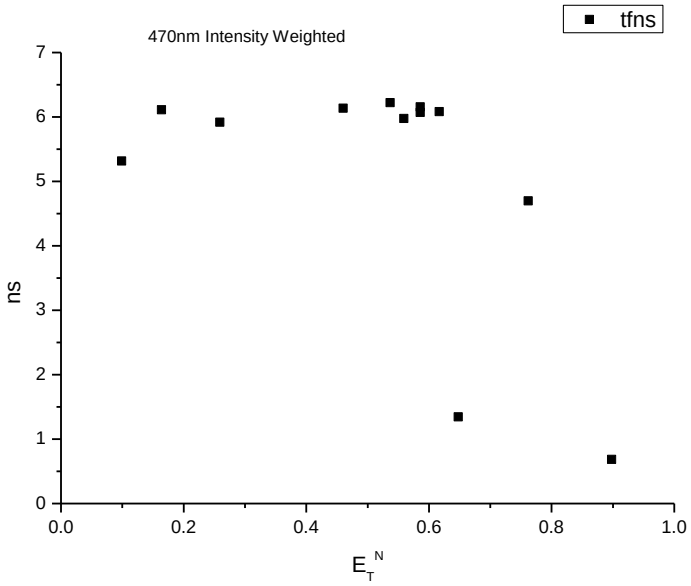

Figure 4.2.79. Intensity weighted average lifetime (τ_f) of **23** at 470 nm versus E_T^N.

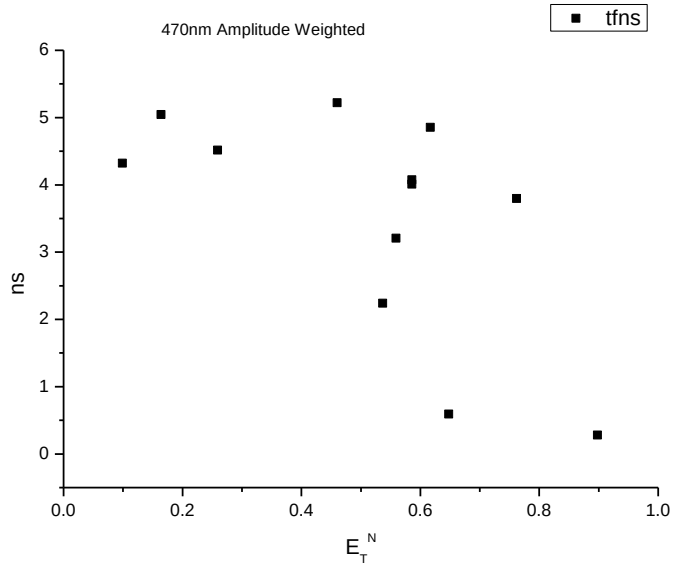

Figure 4.2.80. Amplitude weighted average lifetime (τ_f) of **23** at 470 nm versus E_T^N.

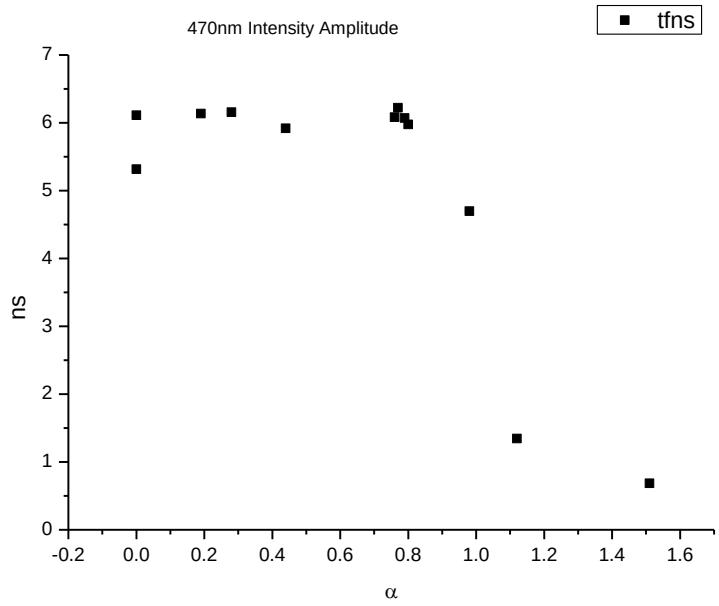

Figure 4.2.81. Intensity weighted average lifetime (τ_f) of **23** at 470 nm versus α.

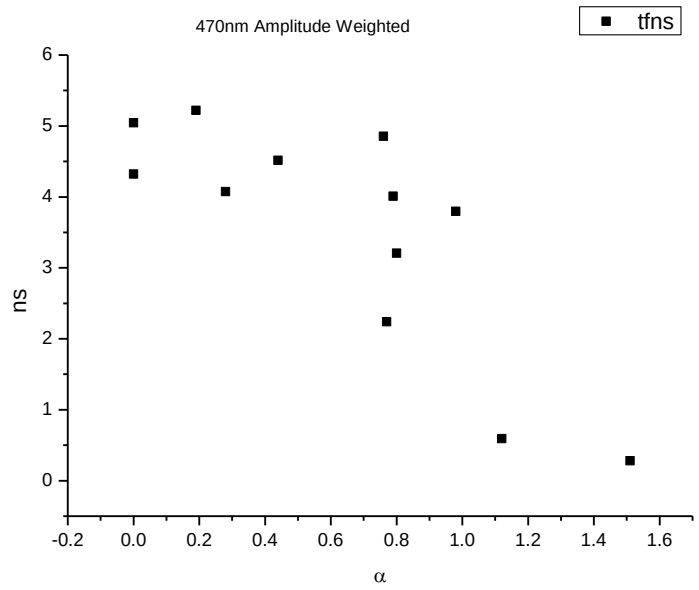

Figure 4.2.82. Amplitude weighted average lifetime (τ_f) of **23** at 470 nm versus α.

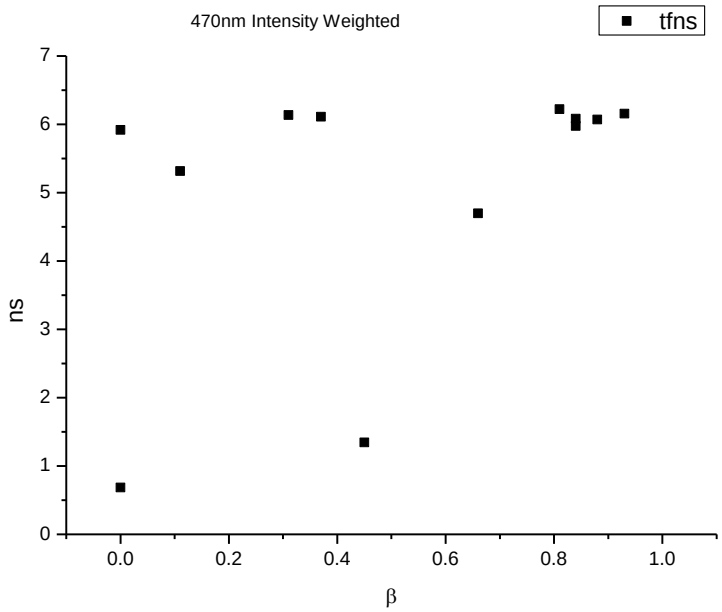

Figure 4.2.83. Intensity weighted average lifetime (τ_f) of **23** at 470 nm versus β.

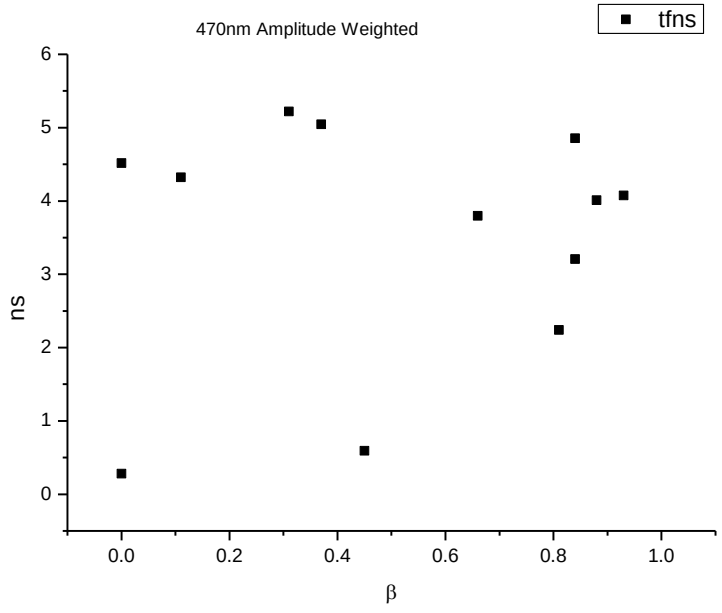

Figure 4.2.84. Amplitude weighted average lifetime (τ_f) of **23** at 470 nm versus β.

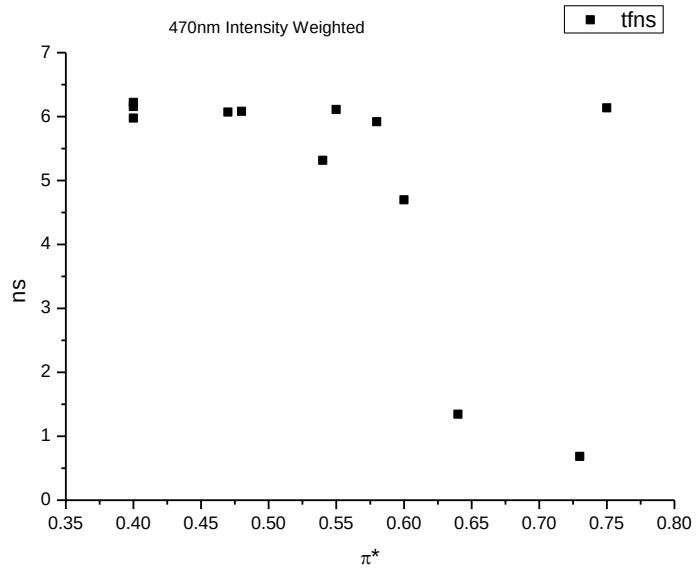

Figure 4.2.85. Intensity weighted average lifetime (τ_f) of **23** at 470 nm versus π*.

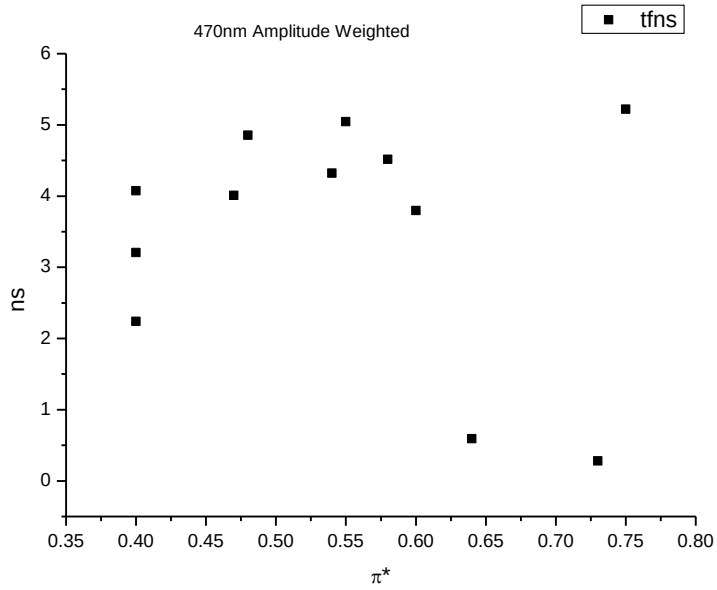

Figure 4.2.86. Amplitude weighted average lifetime (τ_f) of **23** at 470 nm versus π*.

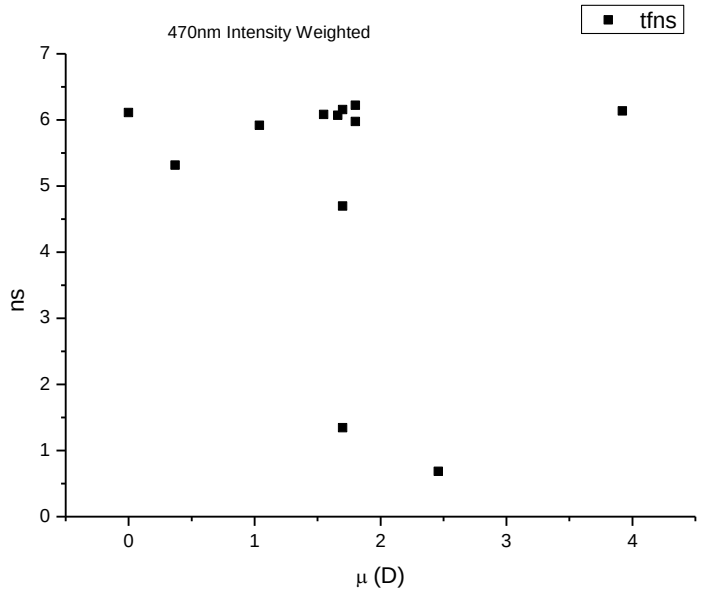

Figure 4.2.87. Intensity weighted average lifetime (τ_f) of **23** at 470 nm versus μ(D).

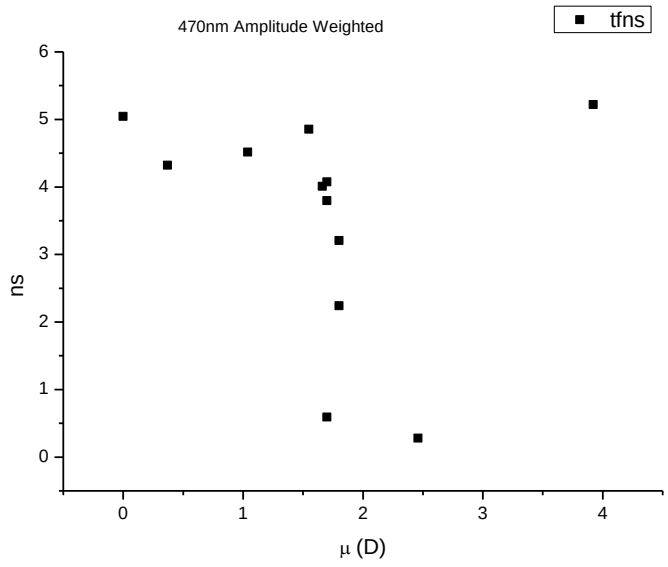

Figure 4.2.88. Amplitude weighted average lifetime (τ_f) of **23** at 470 nm versus μ(D).

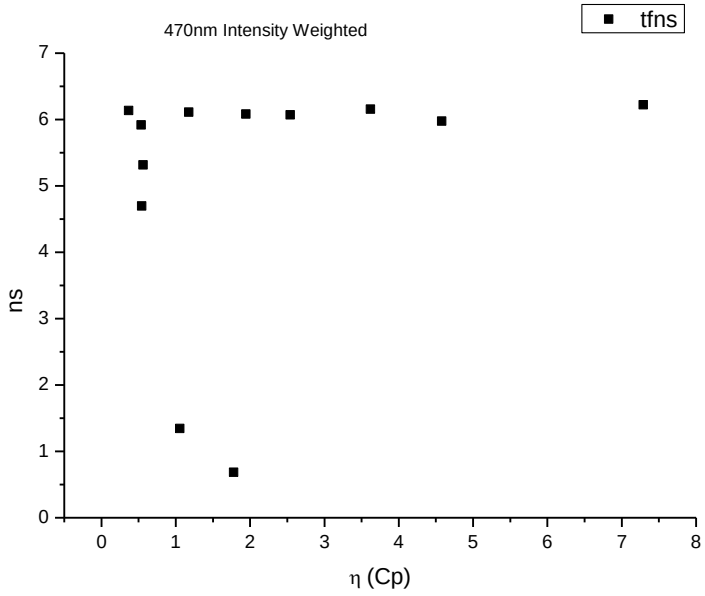

Figure 4.2.89. Intensity weighted average lifetime (τ_f) of **23** at 470 nm versus η(Cp).

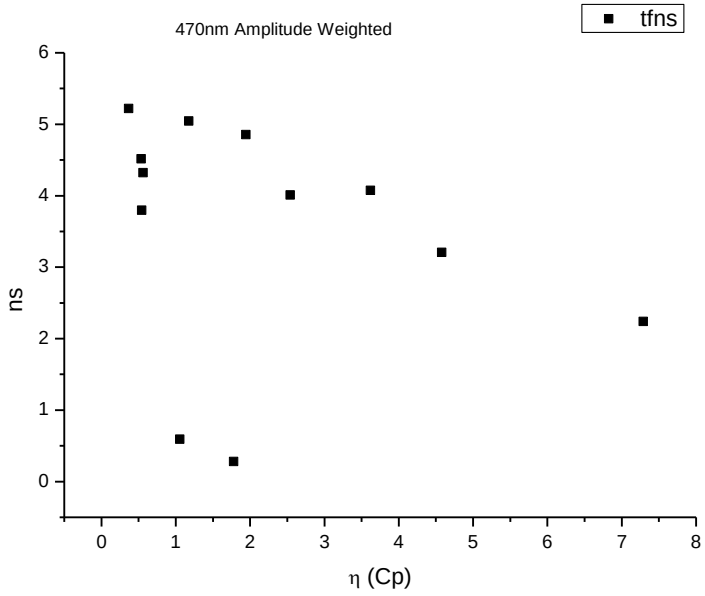

Figure 4.2.90. Amplitude weighted average lifetime (τ_f) of **23** at 470 nm versus η(Cp).

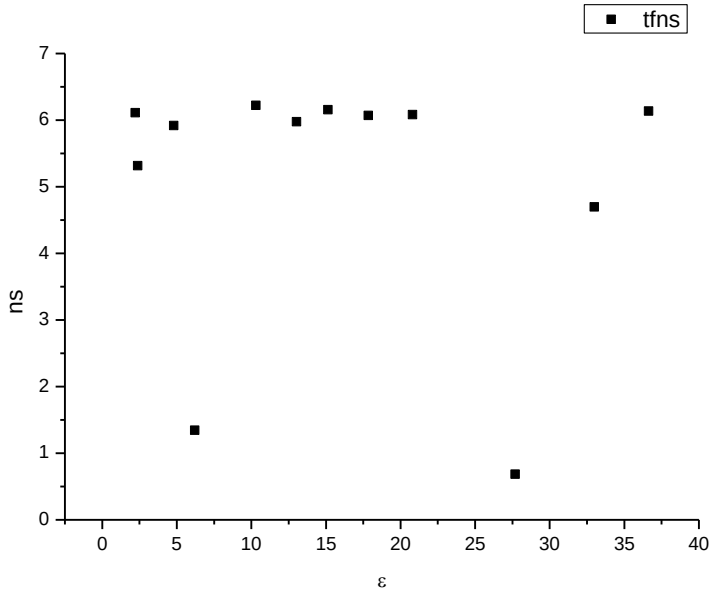

Figure 4.2.91. Intensity weighted average lifetime (τ_f) of **23** at 470 nm versus ε.

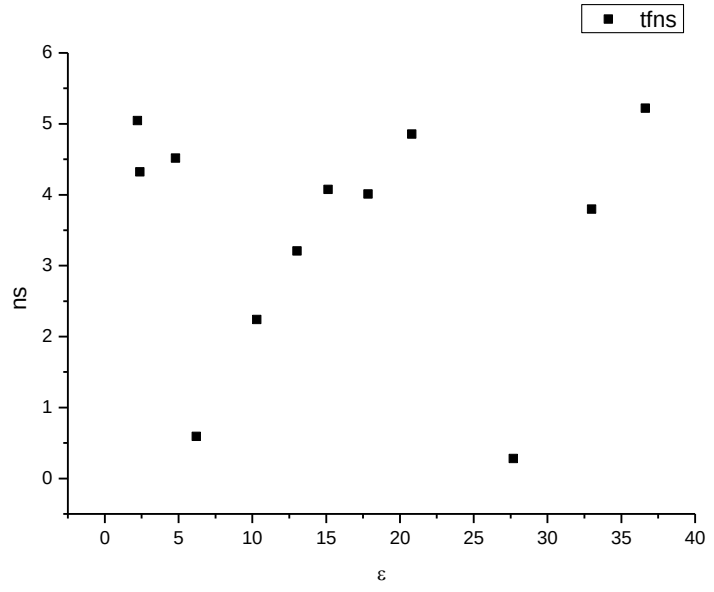

Figure 4.2.92. Amplitude weighted average lifetime (τ_f) of **23** at 470 nm versus ε.

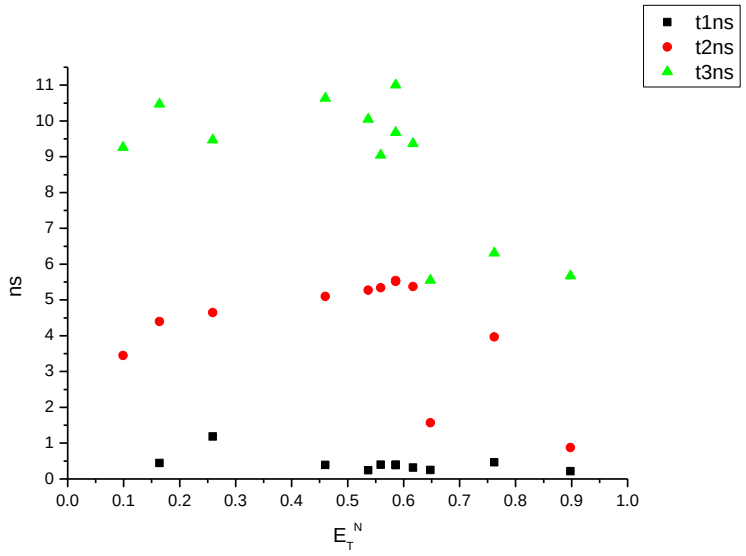

Figure 4.2.93. Intensity weighted components of TCSPC lifetime decay of **23** (470 nm) versus E_T^N.

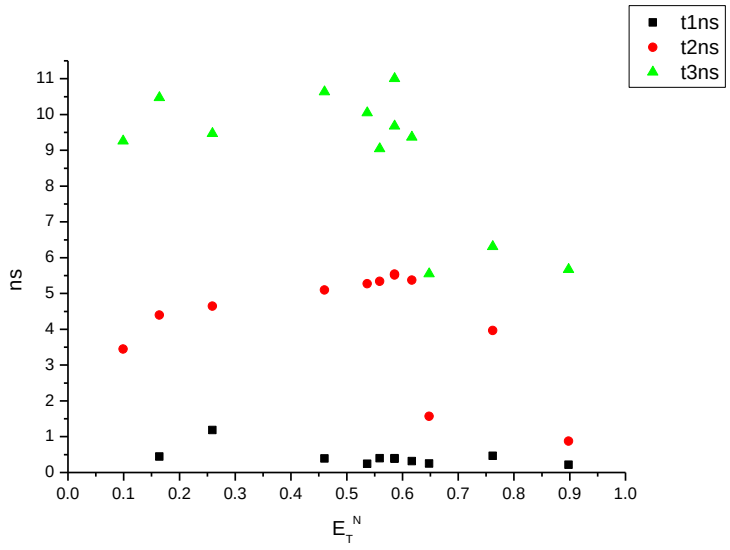

Figure 4.2.94. Amplitude weighted components of TCSPC lifetime decay of **23** (470 nm) versus E_T^N.

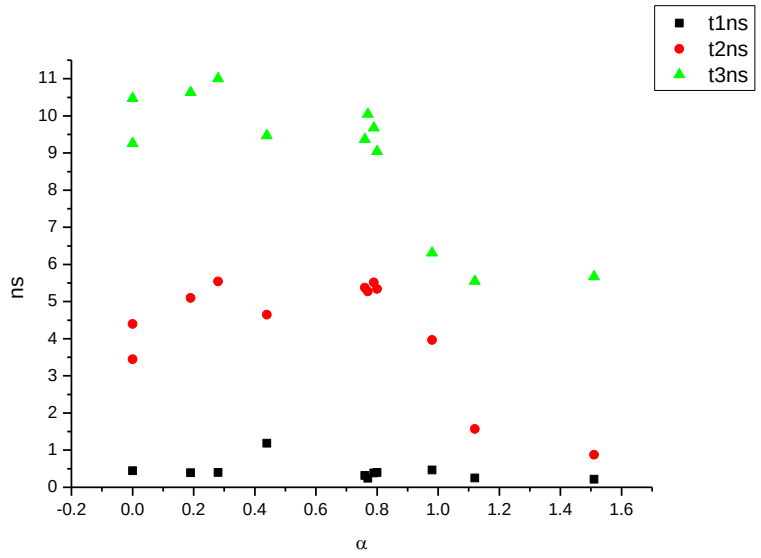

Figure 4.2.95. Intensity weighted components of TCSPC lifetime decay of **23** (470 nm) versus α.

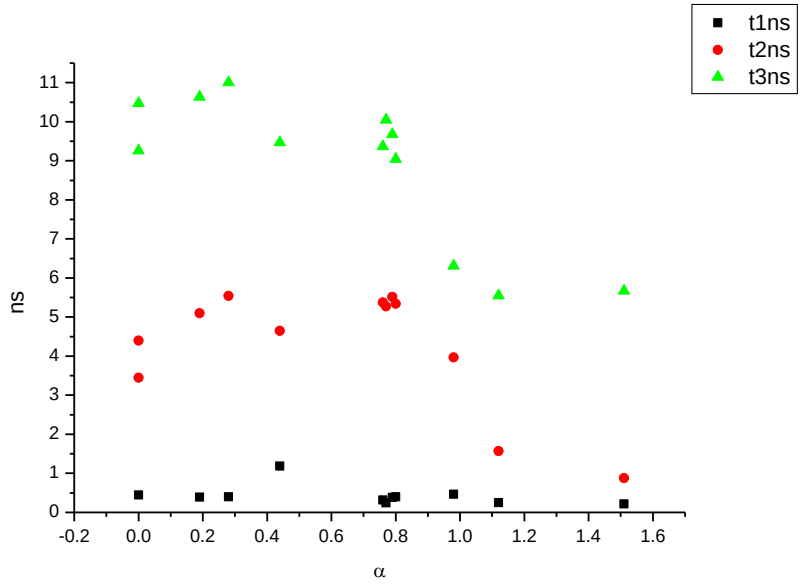

Figure 4.2.96. Amplitude weighted components of TCSPC lifetime decay of **23** (470 nm) versus α.

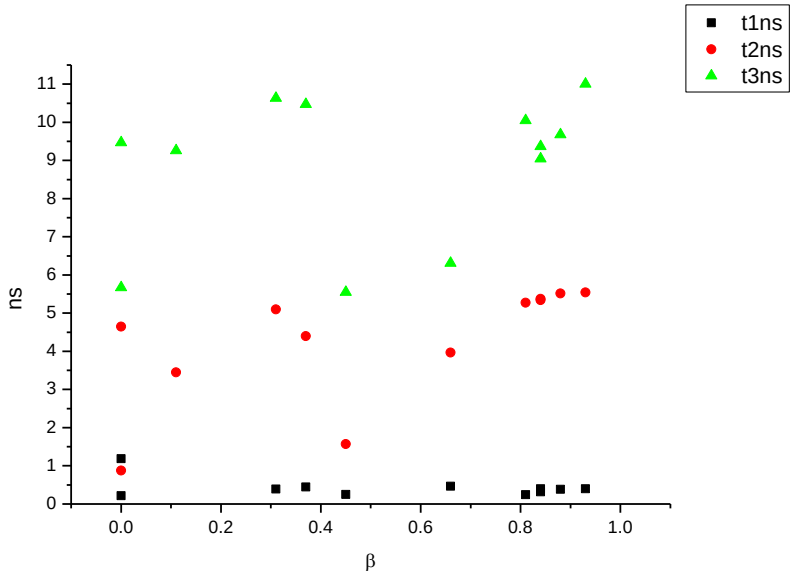

Figure 4.2.97. Intensity weighted components of TCSPC lifetime decay of **23** (470 nm) versus β.

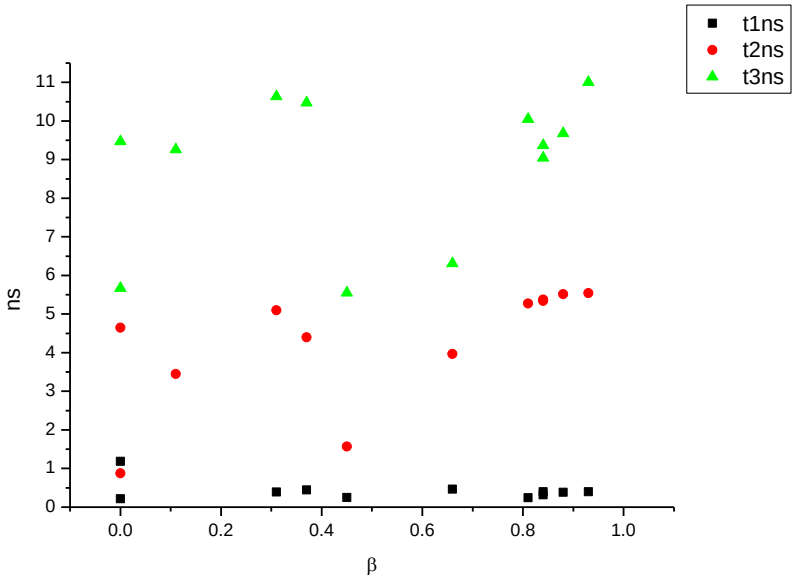

Figure 4.2.98. Amplitude weighted components of TCSPC lifetime decay of **23** (470 nm) versus β.

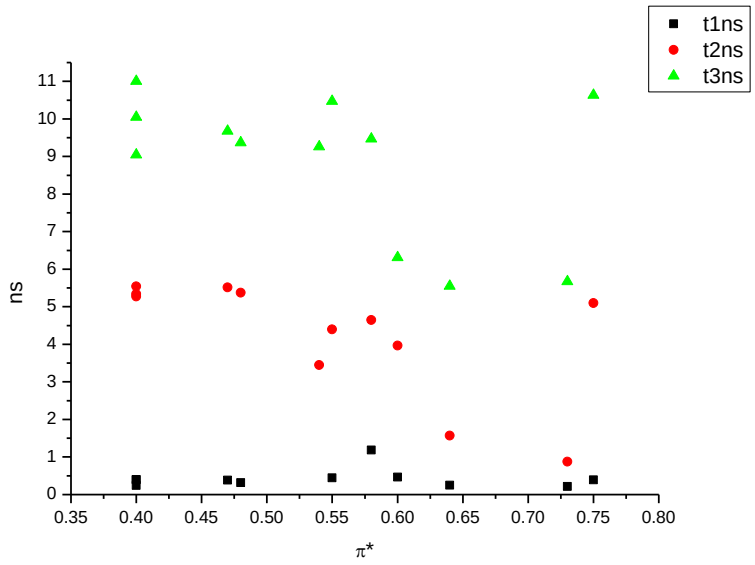

Figure 4.2.99. Intensity weighted components of TCSPC lifetime decay of **23** (470 nm) versus π*.

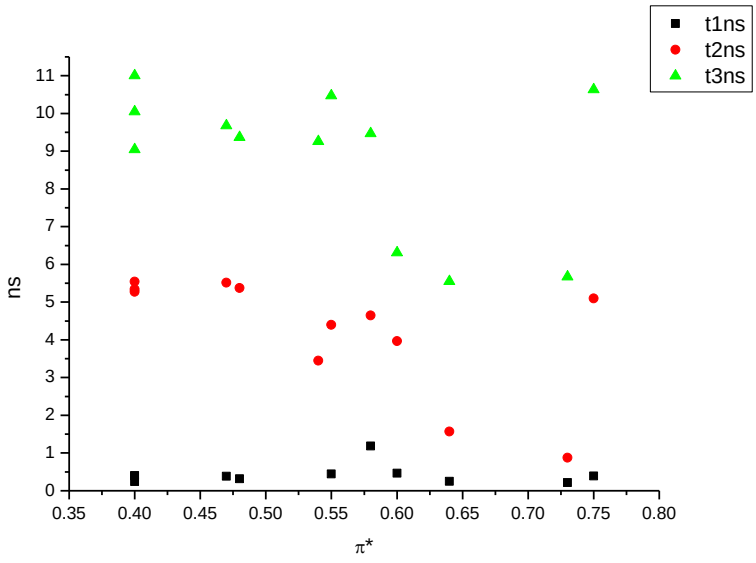

Figure 4.2.100. Amplitude weighted components of TCSPC lifetime decay of **23** (470 nm) versus π*.

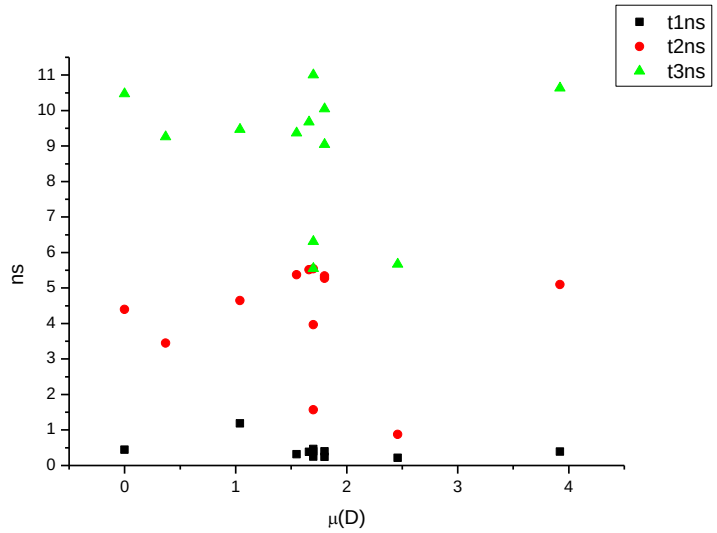

Figure 4.2.101. Intensity weighted components of TCSPC lifetime decay of **23** (470 nm) versus μ(D).

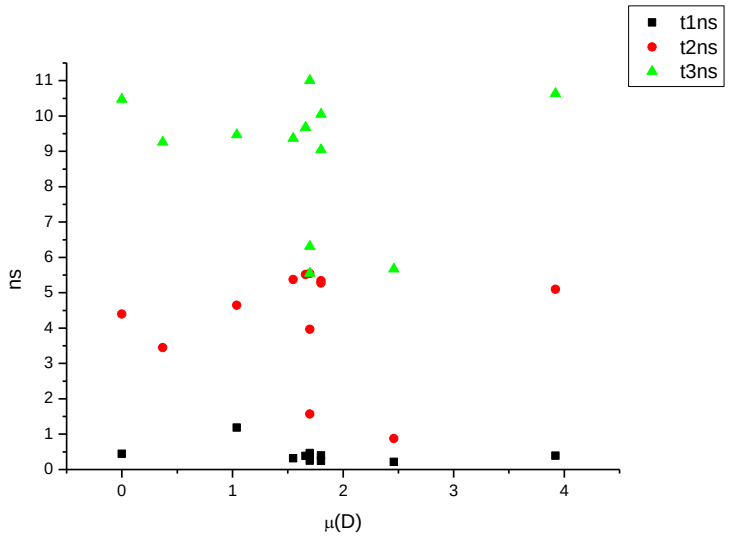

Figure 4.2.102. Amplitude weighted components of TCSPC lifetime decay of **23** (470 nm) versus μ(D).

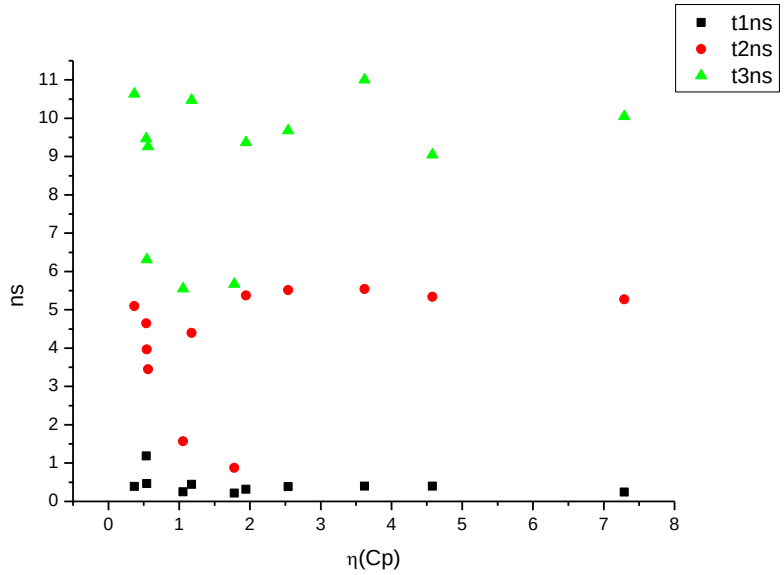

Figure 4.2.103. Intensity weighted components of TCSPC lifetime decay of **23** (470 nm) versus η(Cp).

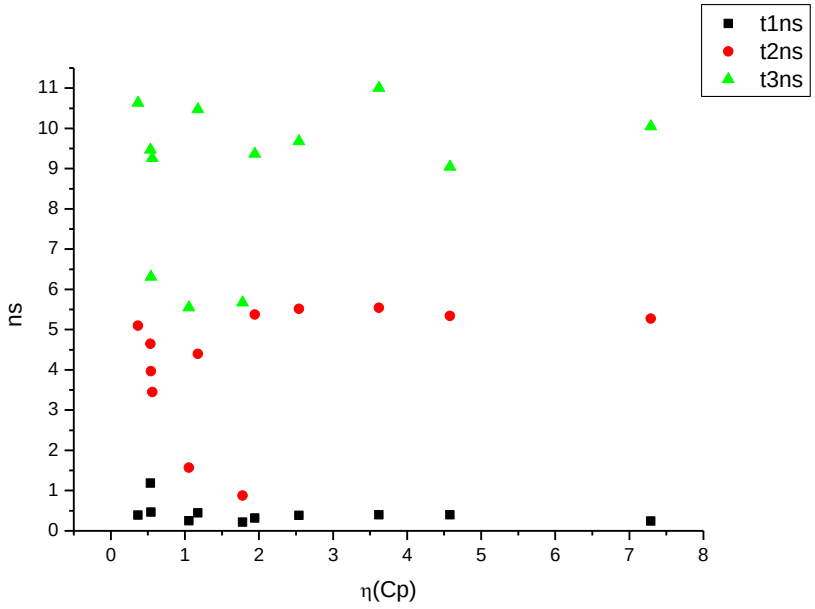

Figure 4.2.104. Amplitude weighted components of TCSPC lifetime decay of **23** (470 nm) versus η(Cp).

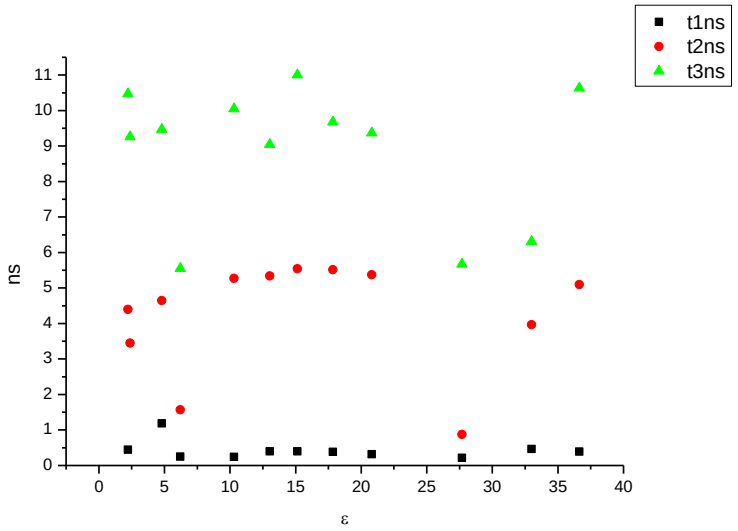

Figure 4.2.105. Intensity weighted components of TCSPC lifetime decay of **23** (470 nm) versus ε.

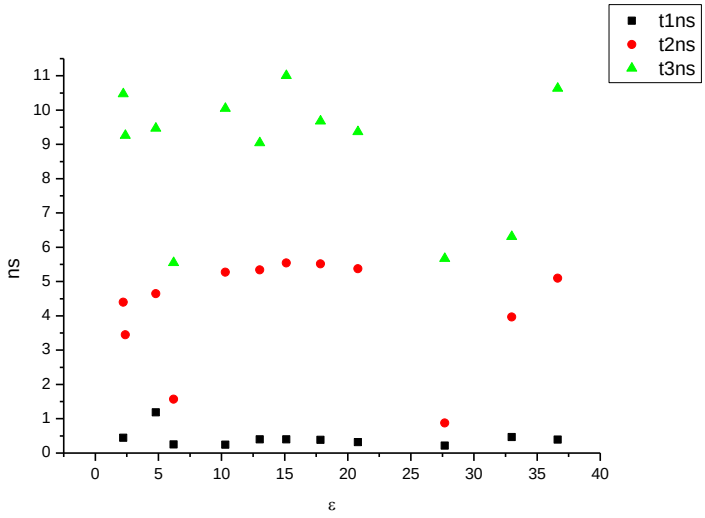

Figure 4.2.106. Amplitude weighted components of TCSPC lifetime decay of **23** (470 nm) versus ε.

4.2.7.2 570 nm Lifetime – Solvatochromic analysis.

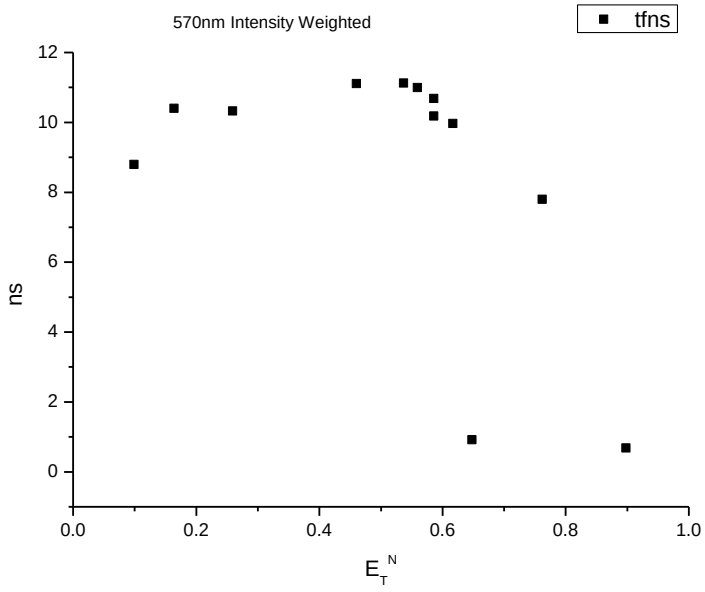

Figure 4.2.107. Intensity weighted average lifetime (τ_f) of **23** at 570 nm versus E_T^N.

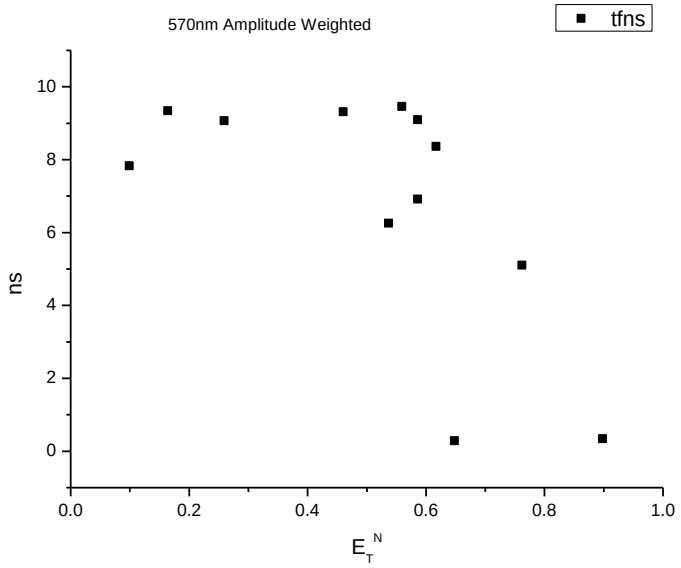

Figure 4.2.108. Amplitude weighted average lifetime (τ_f) of **23** at 570 nm versus E_T^N.

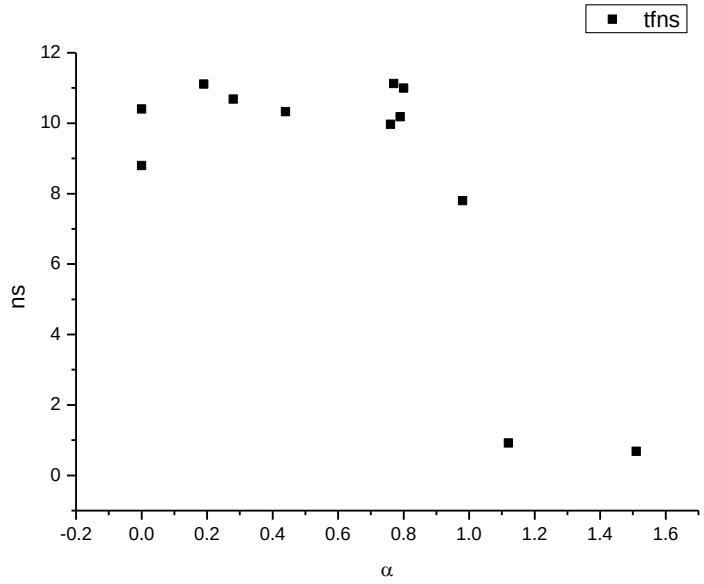

Figure 4.2.109. Intensity weighted average lifetime (τ_f) of **23** at 570 nm versus α.

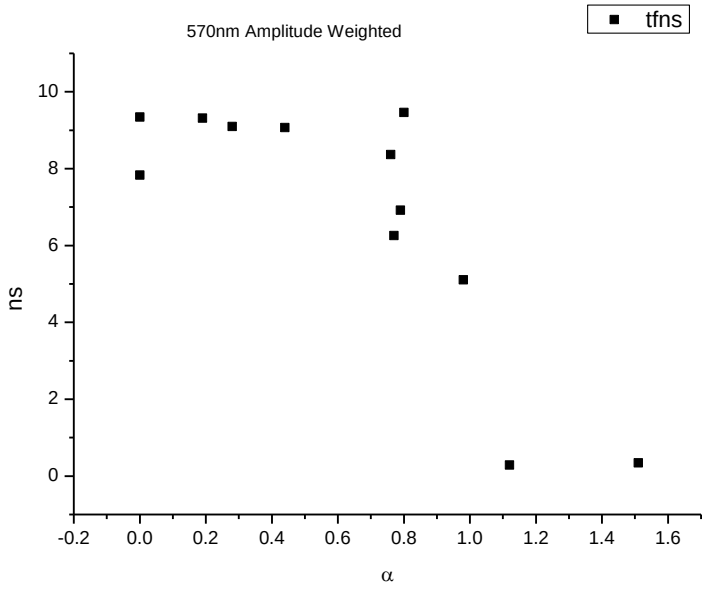

Figure 4.2.110. Amplitude weighted average lifetime (τ_f) of **23** at 570 nm versus α.

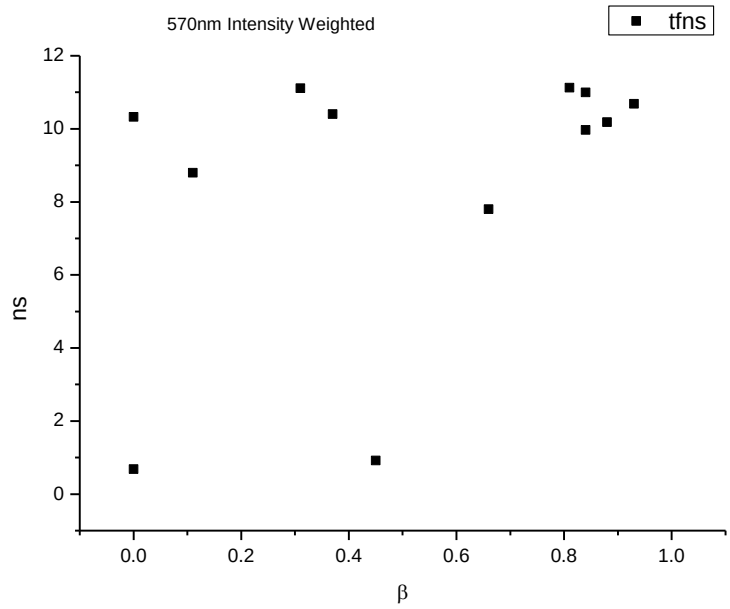

Figure 4.2.111. Intensity weighted average lifetime (τ_f) of **23** at 570 nm versus β.

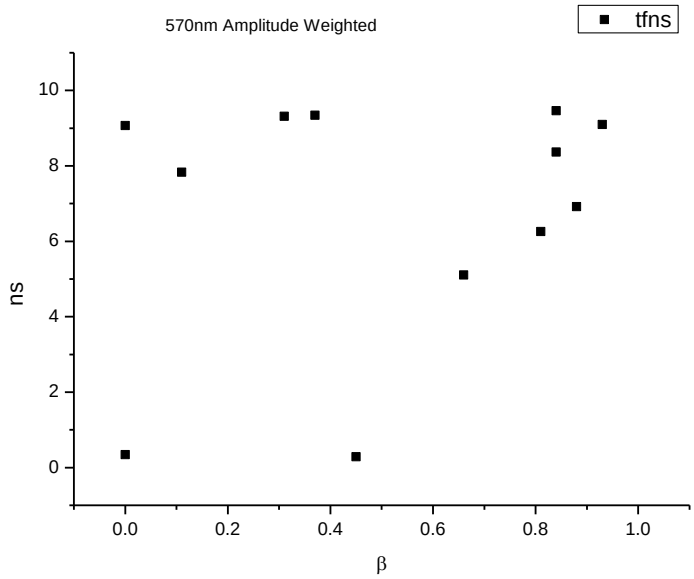

Figure 4.2.112. Amplitude weighted average lifetime (τ_f) of **23** at 570 nm versus β.

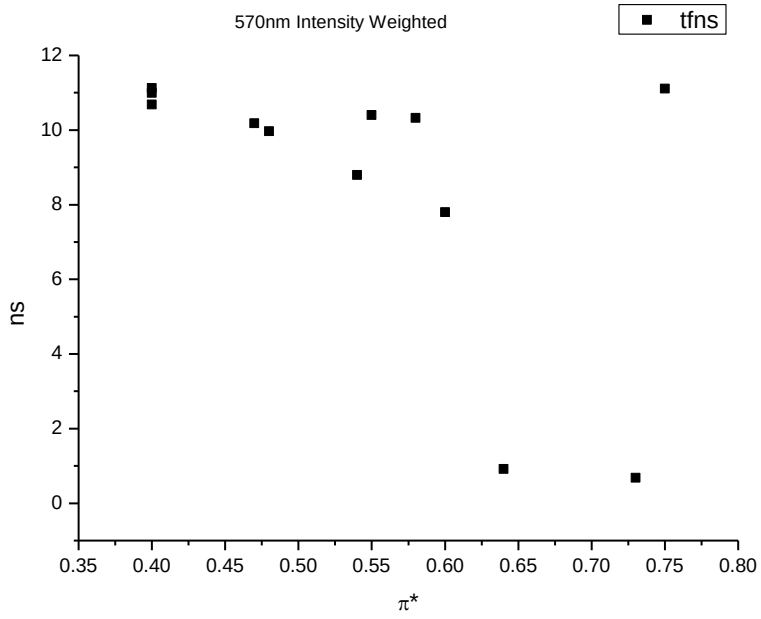

Figure 4.2.113. Intensity weighted average lifetime (τ_f) of **23** at 570 nm versus π*.

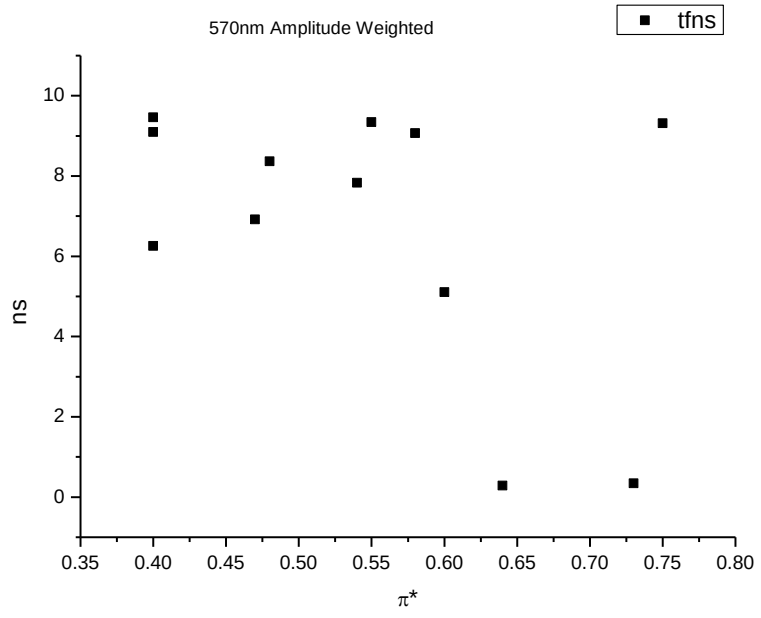

Figure 4.2.114. Amplitude weighted average lifetime (τ_f) of **23** at 570 nm versus π*.

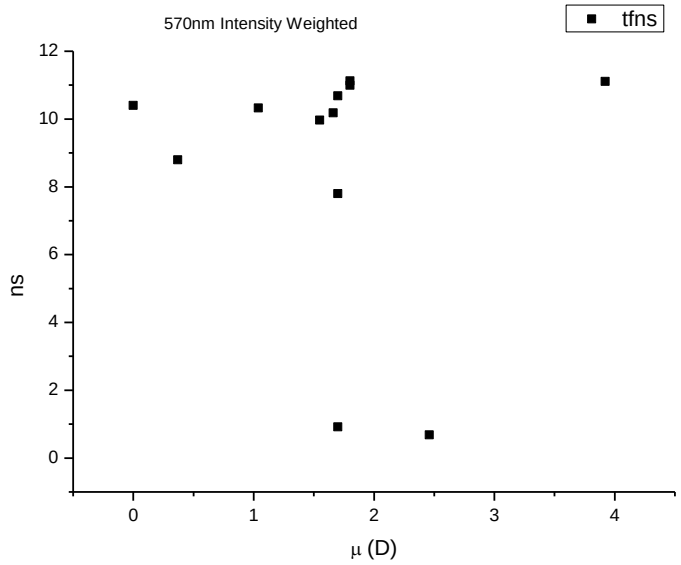

Figure 4.2.115. Intensity weighted average lifetime (τ_f) of **23** at 570 nm versus μ(D).

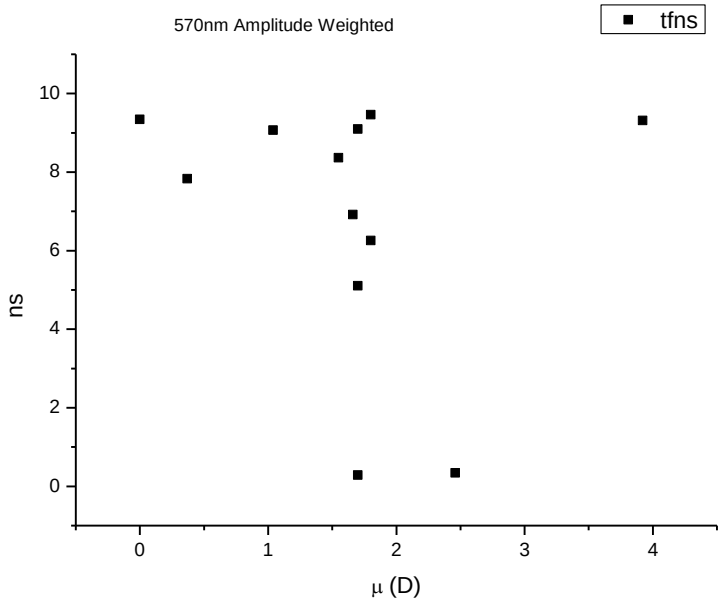

Figure 4.2.116. Amplitude weighted average lifetime (τ_f) of **23** at 570 nm versus μ(D).

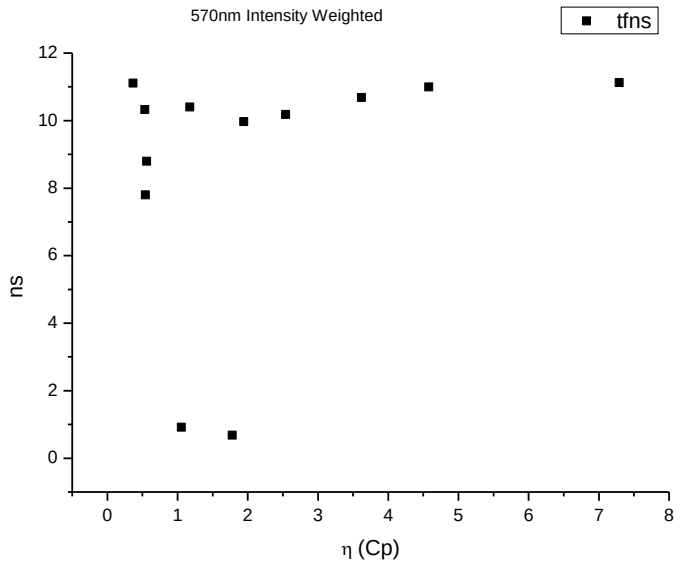

Figure 4.2.117. Intensity weighted average lifetime (τ_f) of **23** at 570 nm versus η(Cp).

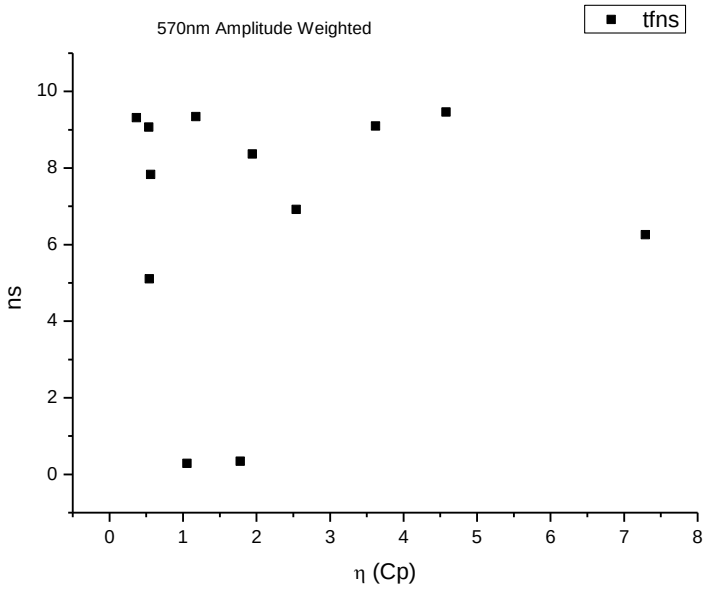

Figure 4.2.118. Amplitude weighted average lifetime (τ_f) of **23** at 570 nm versus η(Cp).

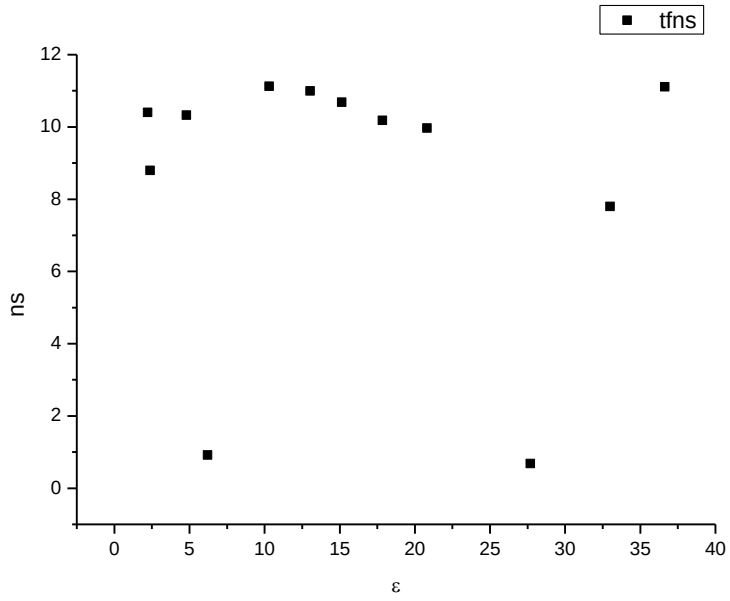

Figure 4.2.119. Intensity weighted average lifetime (τ_f) of **23** at 570 nm versus ε.

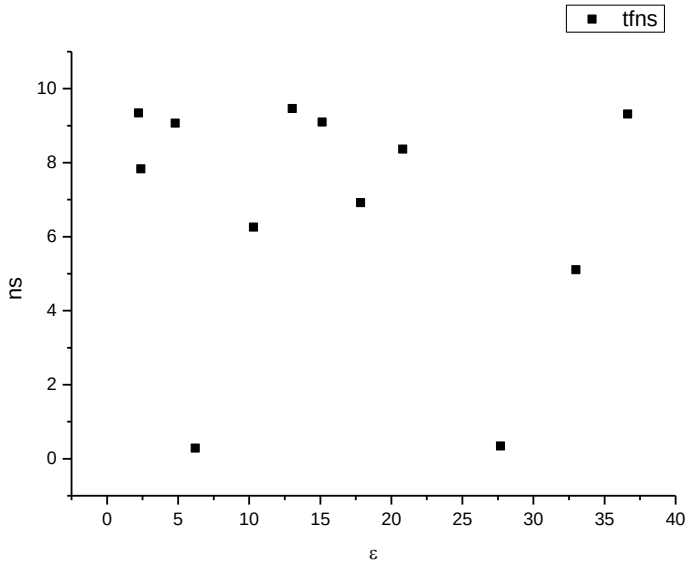

Figure 4.2.120. Amplitude weighted average lifetime (τ_f) of **23** at 570 nm versus ε.

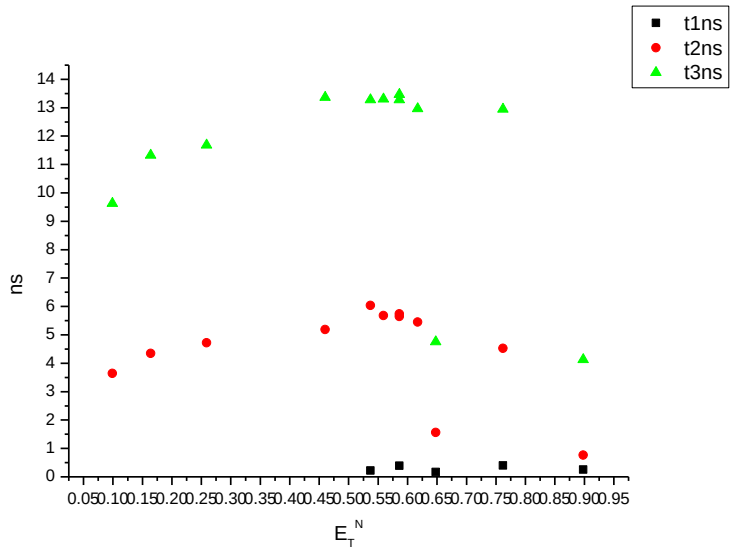

Figure 4.2.121. Intensity weighted components of TCSPC lifetime decay of **23** (570 nm) versus E_T^N.

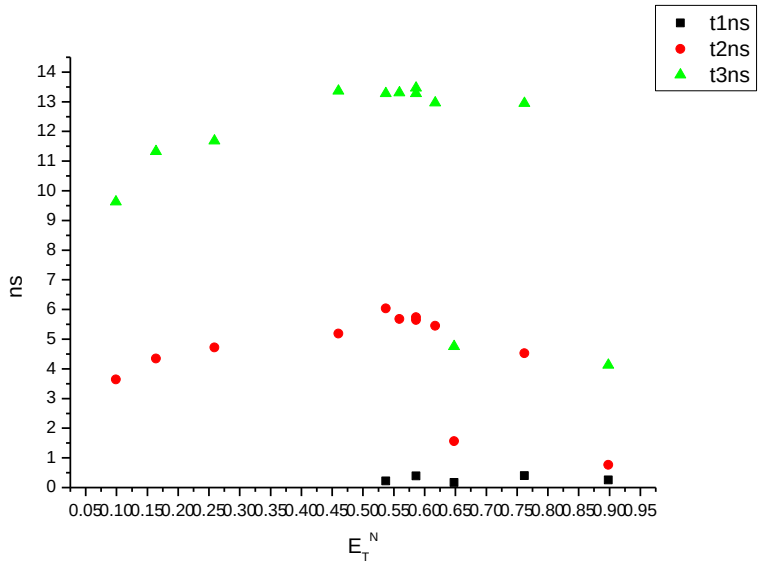

Figure 4.2.122. Amplitude weighted components of TCSPC lifetime decay of **23** (570 nm) versus E_T^N.

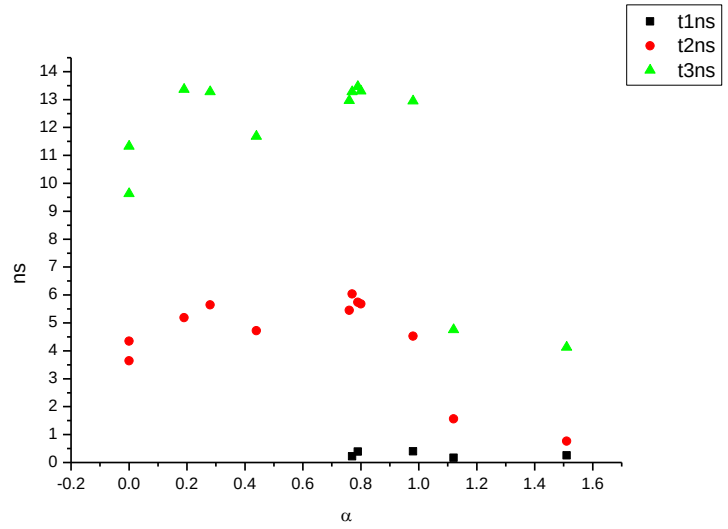

Figure 4.2.123. Intensity weighted components of TCSPC lifetime decay of **23** (570 nm) versus α.

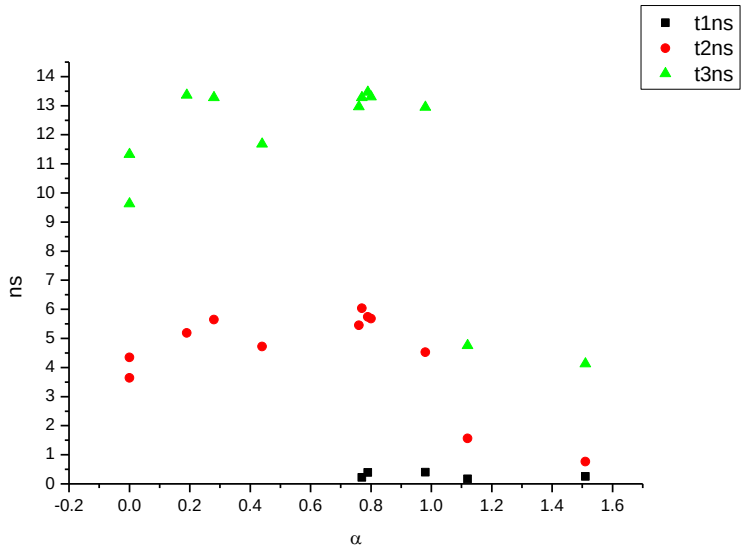

Figure 4.2.124. Amplitude weighted components of TCSPC lifetime decay of **23** (570 nm) versus α.

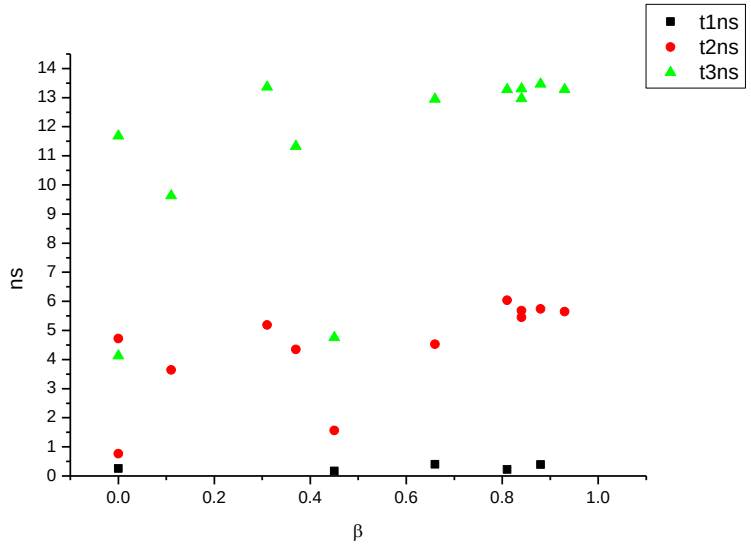

Figure 4.2.125. Intensity weighted components of TCSPC lifetime decay of **23** (570 nm) versus β.

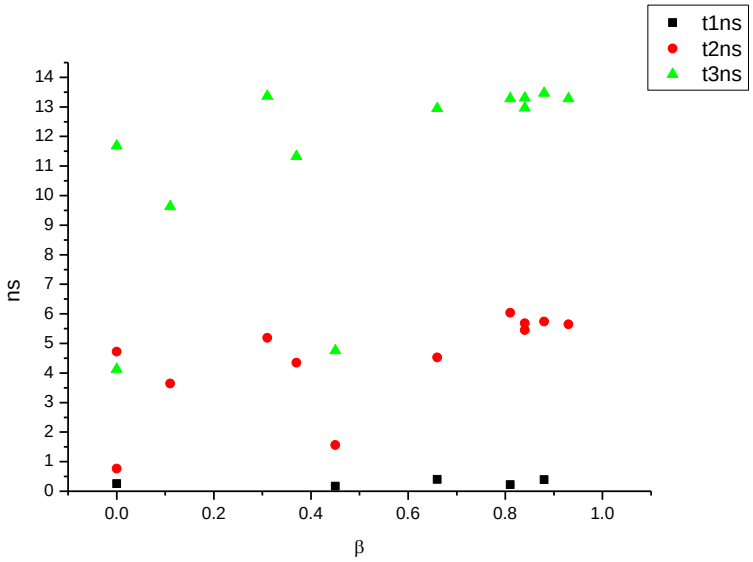

Figure 4.2.126. Amplitude weighted components of TCSPC lifetime decay of **23** (570 nm) versus β.

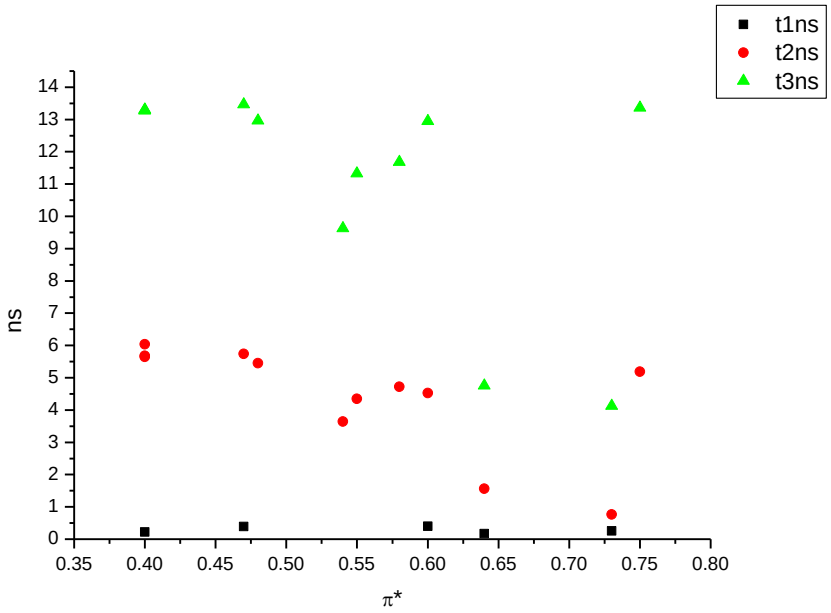

Figure 4.2.127. Intensity weighted components of TCSPC lifetime decay of **23** (570 nm) versus π*.

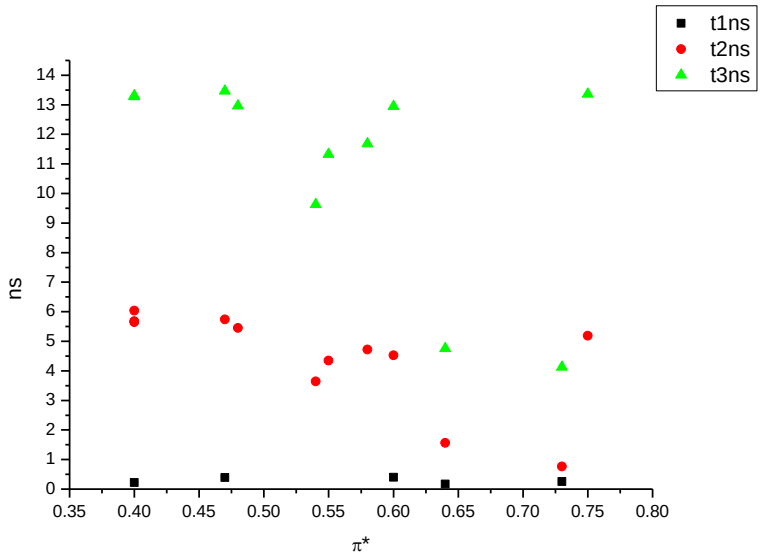

Figure 4.2.128. Amplitude weighted components of TCSPC lifetime decay of **23** (570 nm) versus π*.

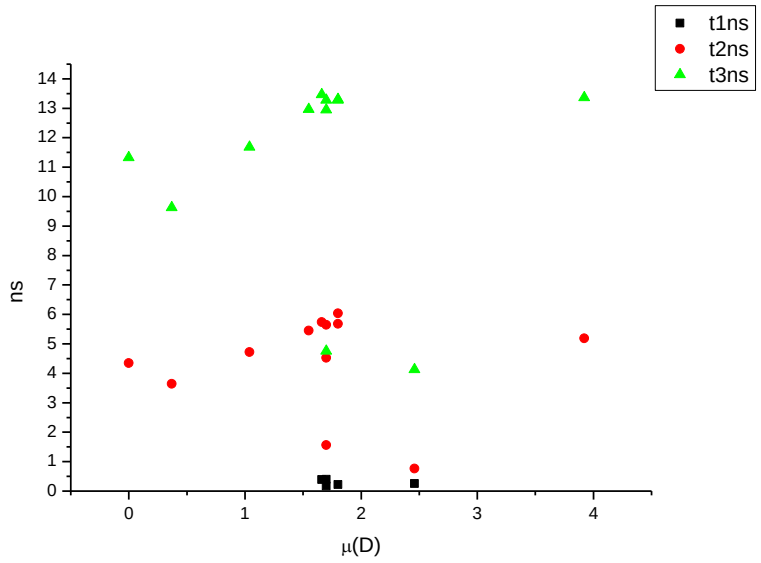

Figure 4.2.129. Intensity weighted components of TCSPC lifetime decay of **23** (570 nm) versus μ(D).

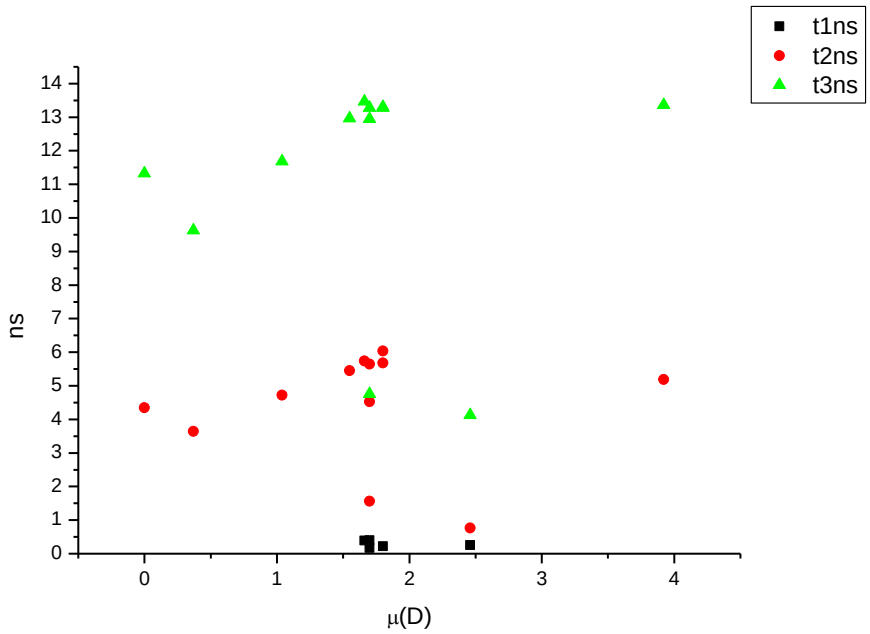

Figure 4.2.130. Amplitude weighted components of TCSPC lifetime decay of **23** (570 nm) versus μ(D).

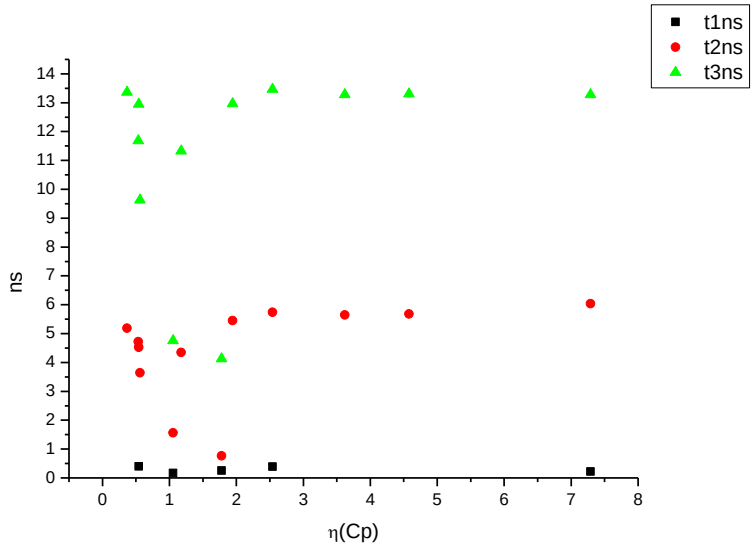

Figure 4.2.131. Intensity weighted components of TCSPC lifetime decay of **23** (570 nm) versus η(Cp).

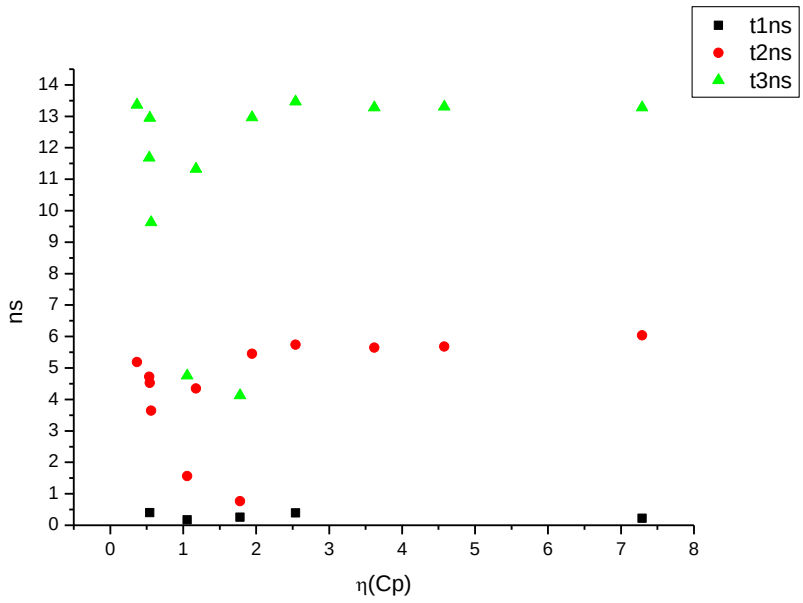

Figure 4.2.132. Amplitude weighted components of TCSPC lifetime decay of **23** (570 nm) versus η(Cp).

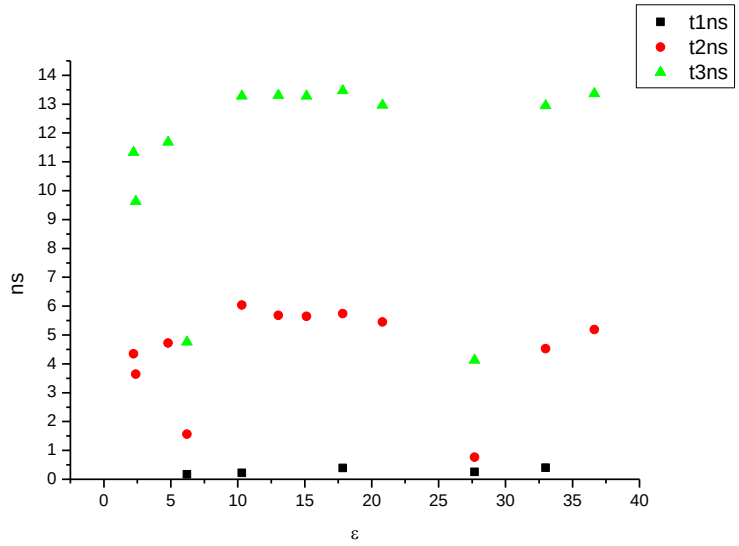

Figure 4.2.133. Intensity weighted components of TCSPC lifetime decay of **23** (570 nm) versus ε.

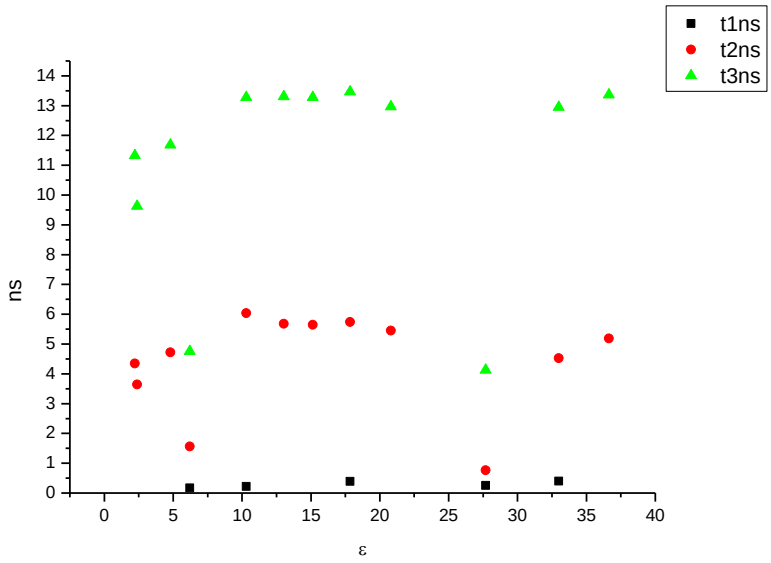

Figure 4.2.134. Amplitude weighted components of TCSPC lifetime decay of **21** (570 nm) versus ε.

4.2.8 Ultraviolet-visible absorption spectra.

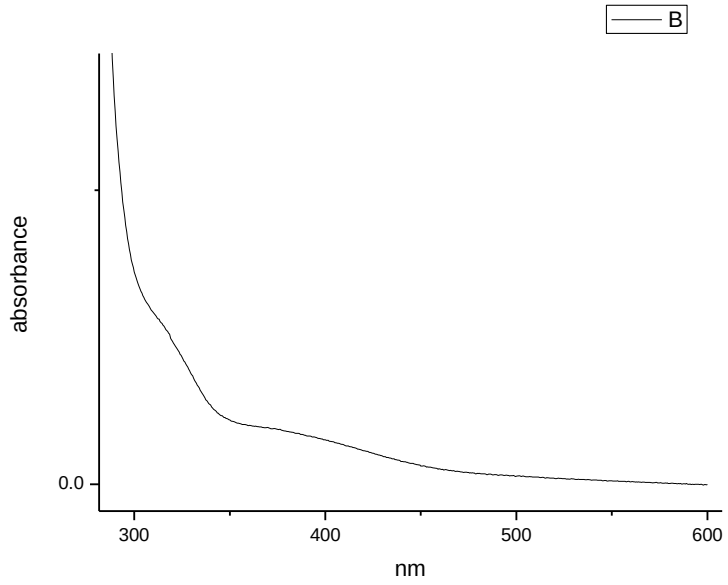

Figure 4.2.135. Ultraviolet-Visible absorption spectrum of **23** recorded in Toluene.

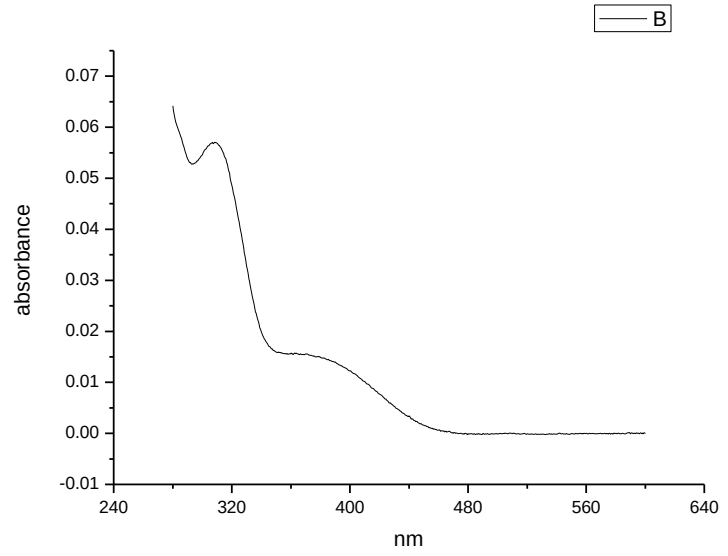

Figure 4.2.136. Ultraviolet-Visible absorption spectrum of **23** recorded in 1,4-dioxane.

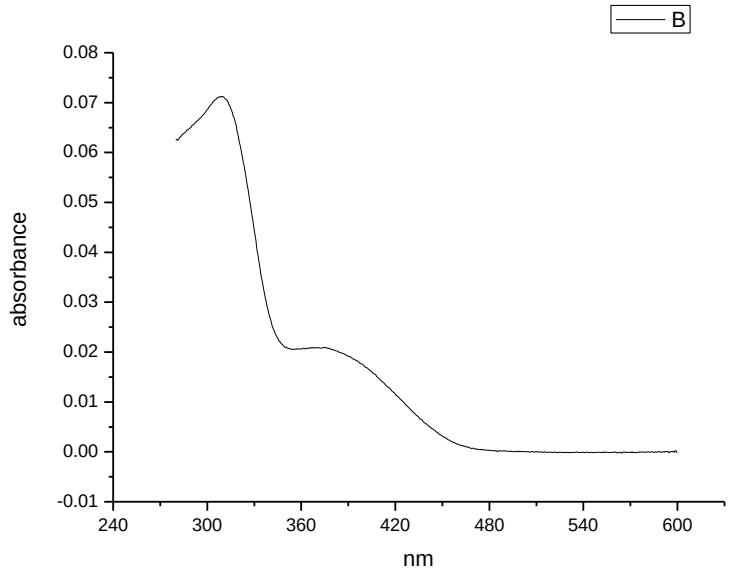

Figure 4.2.137. Ultraviolet-Visible absorption spectrum of **23** recorded in Chloroform.

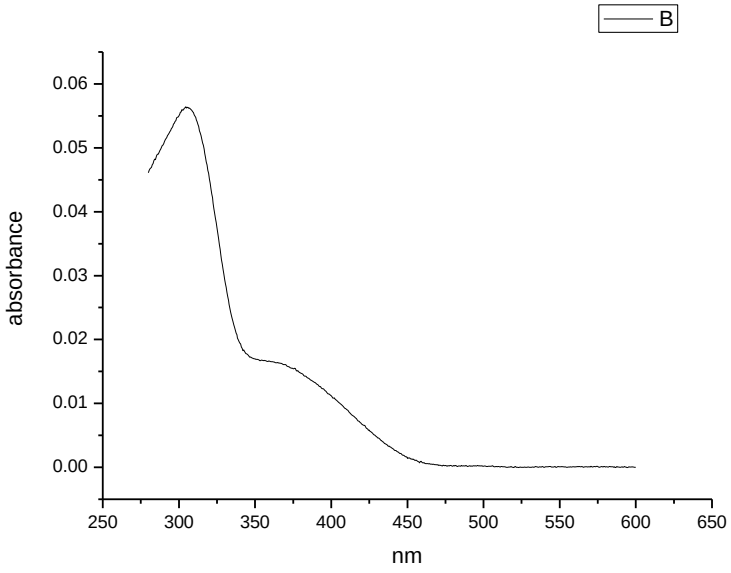

Figure 4.2.138. Ultraviolet-Visible absorption spectrum of **23** recorded in Acetonitrile.

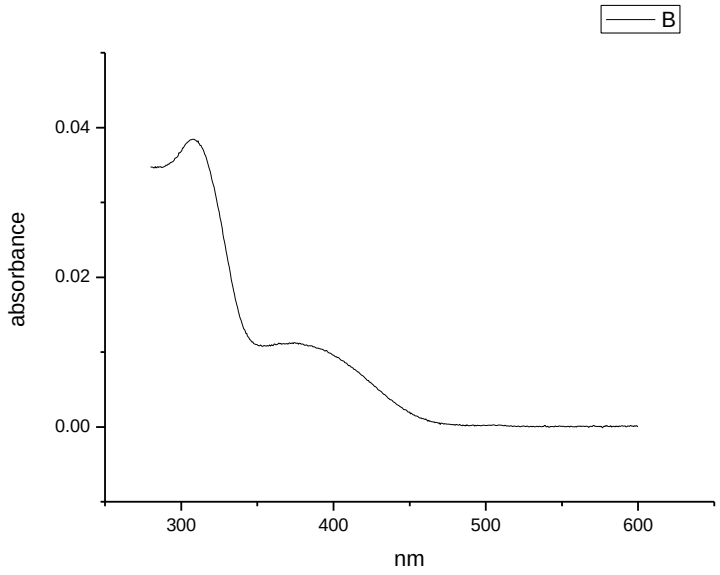

Figure 4.2.139. Ultraviolet-Visible absorption spectrum of **23** recorded in 1-octanol.

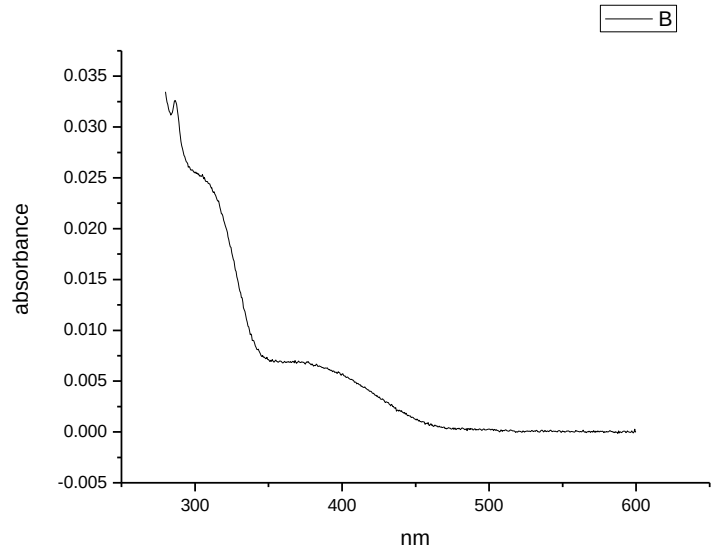

Figure 4.2.140. Ultraviolet-Visible absorption spectrum of **23** recorded in 1-hexanol.

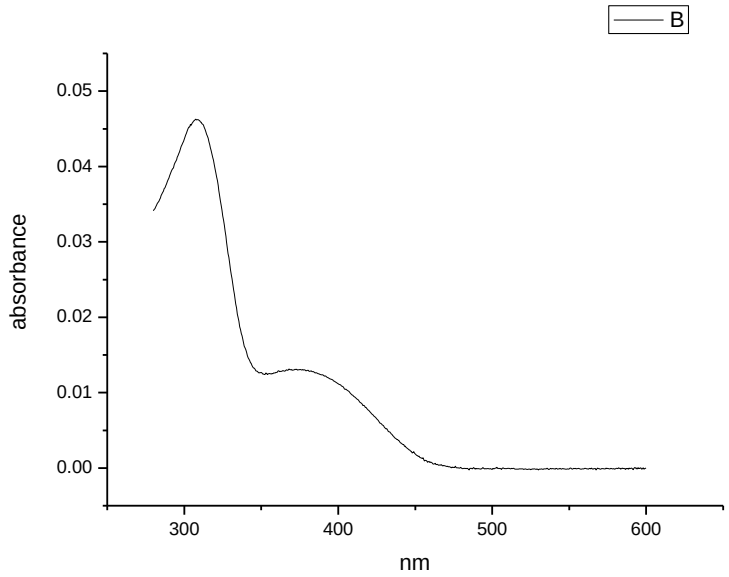

Figure 4.2.141. Ultraviolet-Visible absorption spectrum of **23** recorded in 1-butanol.

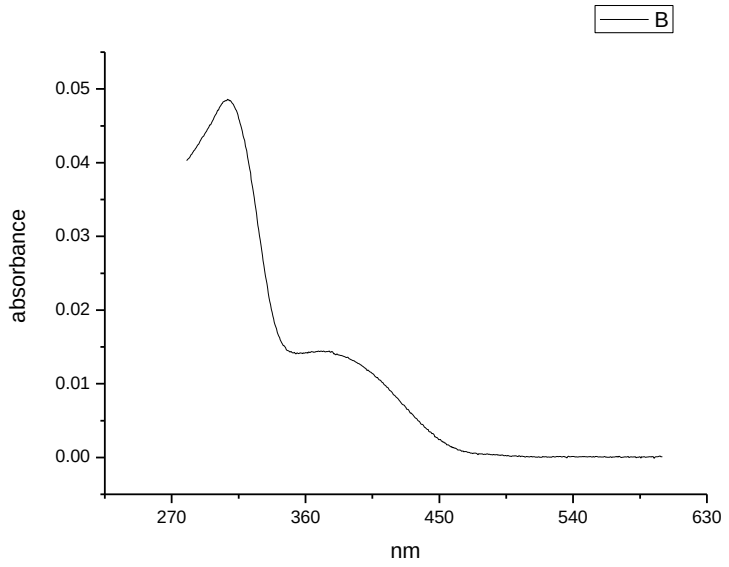

Figure 4.2.142. Ultraviolet-Visible absorption spectrum of **23** recorded in 1-pentanol.

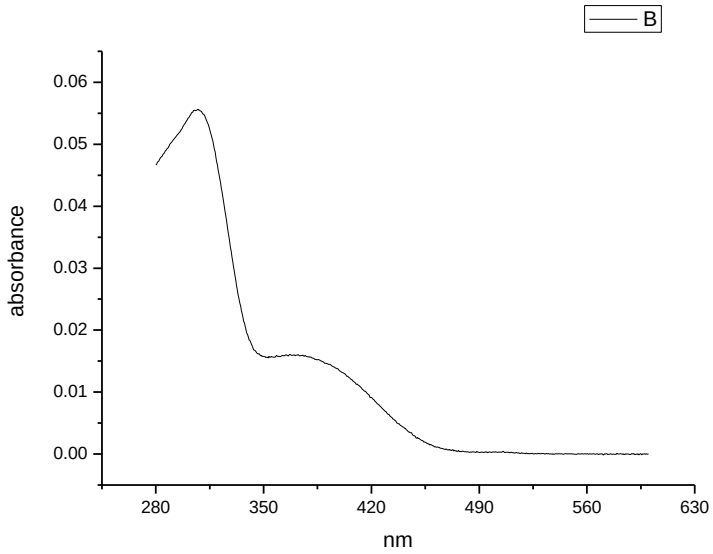

Figure 4.2.143. Ultraviolet-Visible absorption spectrum of **23** recorded in 1-propanol.

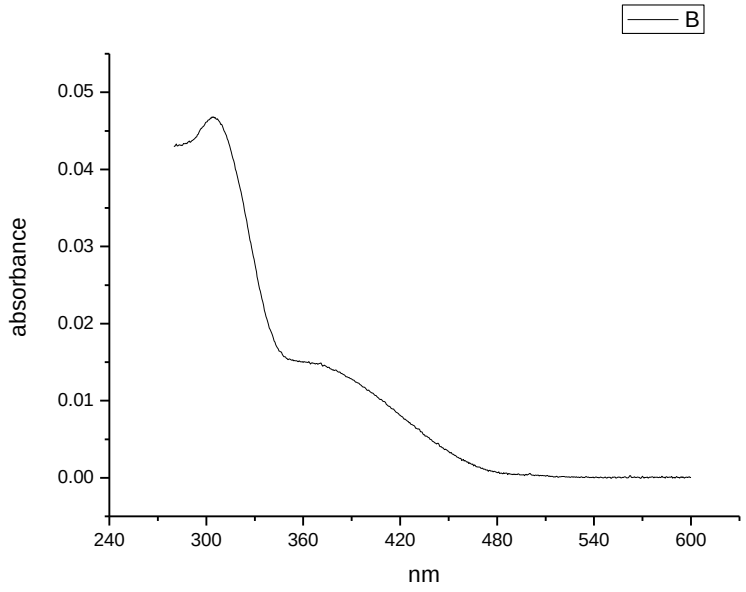

Figure 4.2.144. Ultraviolet-Visible absorption spectrum of **23** recorded in Acetic Acid.

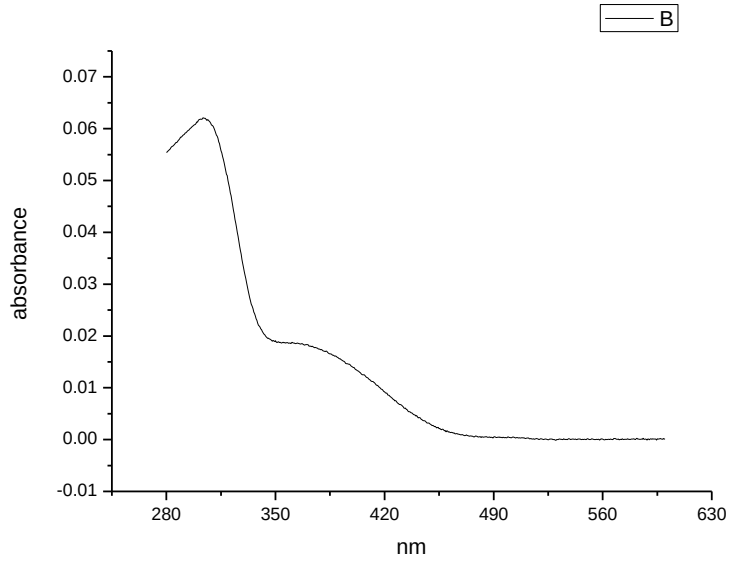

Figure 4.2.145. Ultraviolet-Visible absorption spectrum of **23** recorded in Methanol.

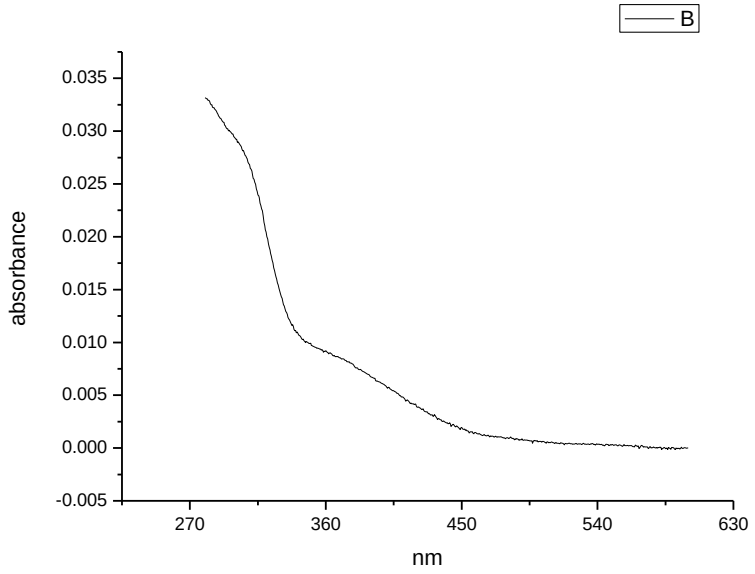

Figure 4.2.146. Ultraviolet-Visible absorption spectrum of **23** recorded in 2,2,2-trifluoroethanol.

4.2.9 Fluorescence Emission spectra.

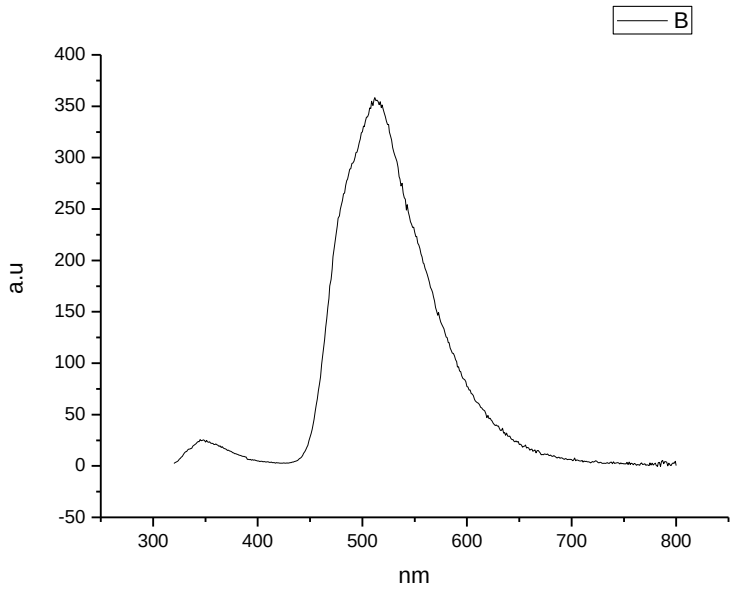

Figure 4.2.147. Fluorescence emission spectrum of **23** recorded in Toluene at 310 nm excitation.

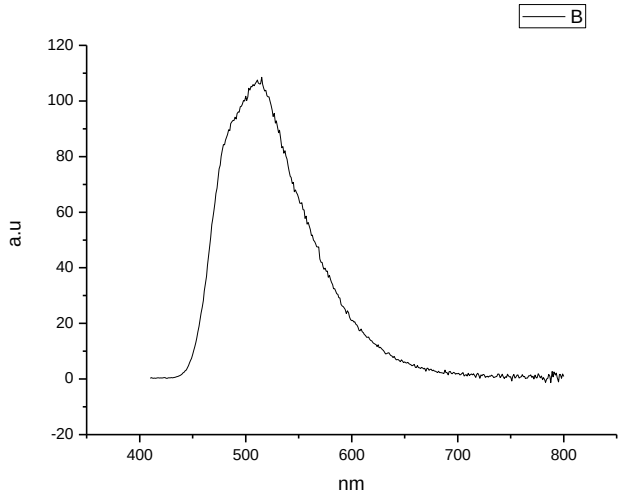

Figure 4.2.148. Fluorescence emission spectrum of **23** recorded in Toluene at 400 nm excitation.

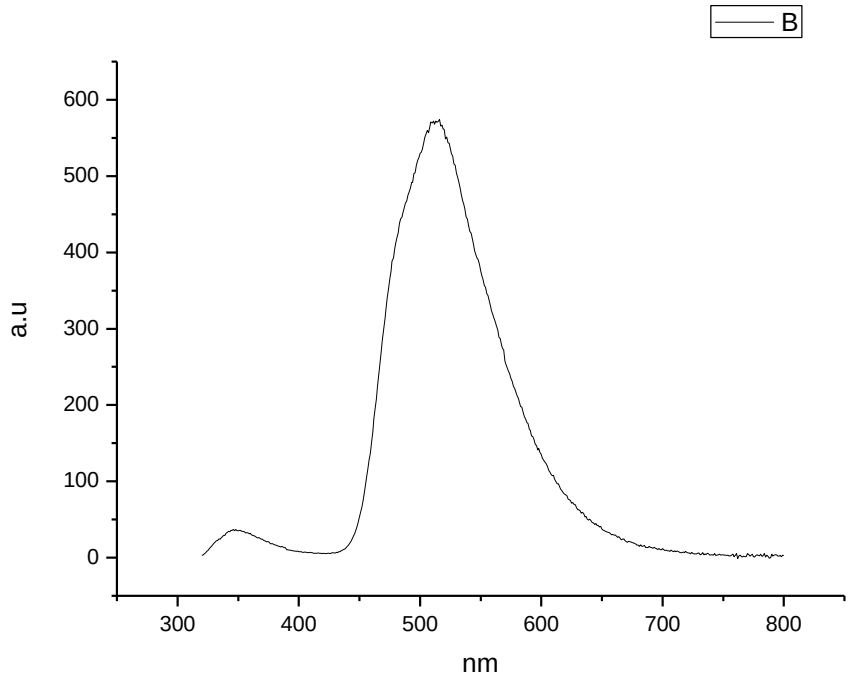

Figure 4.2.149. Fluorescence emission spectrum of **23** recorded in 1,4-dioxane at 310 nm excitation.

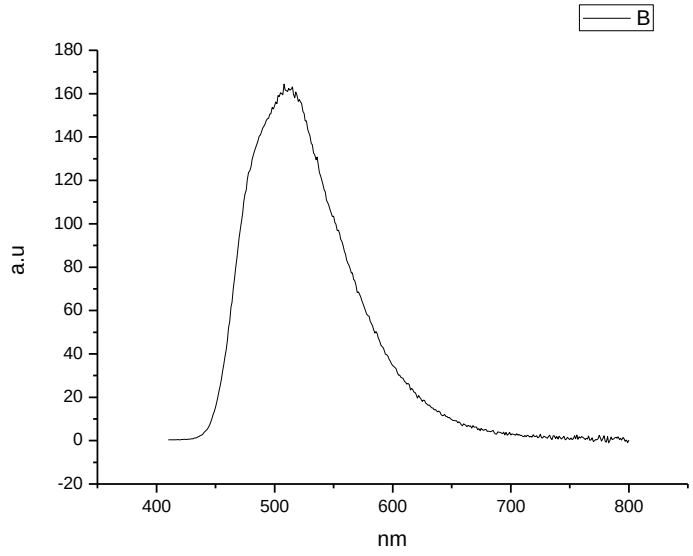

Figure 4.2.150. Fluorescence emission spectrum of **23** recorded in 1,4-dioxane at 400 nm excitation.

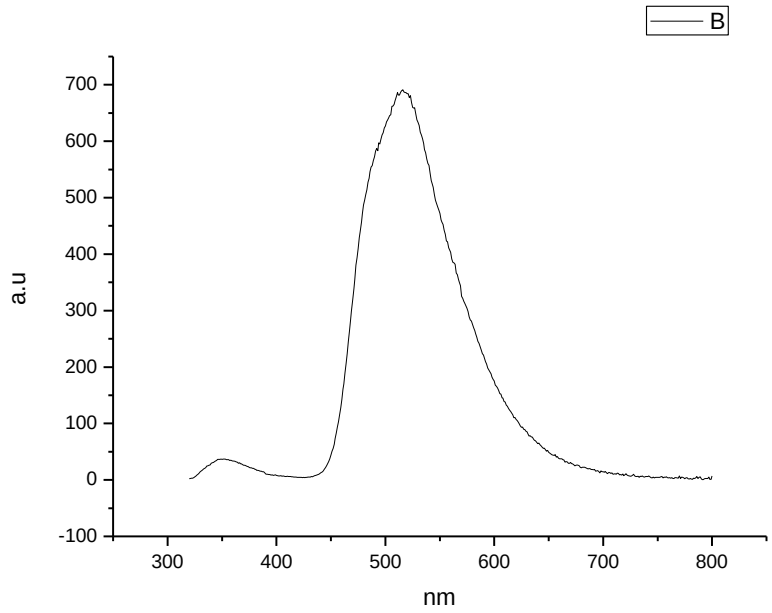

Figure 4.2.151. Fluorescence emission spectrum of **23** recorded in Chloroform at 310 nm excitation.

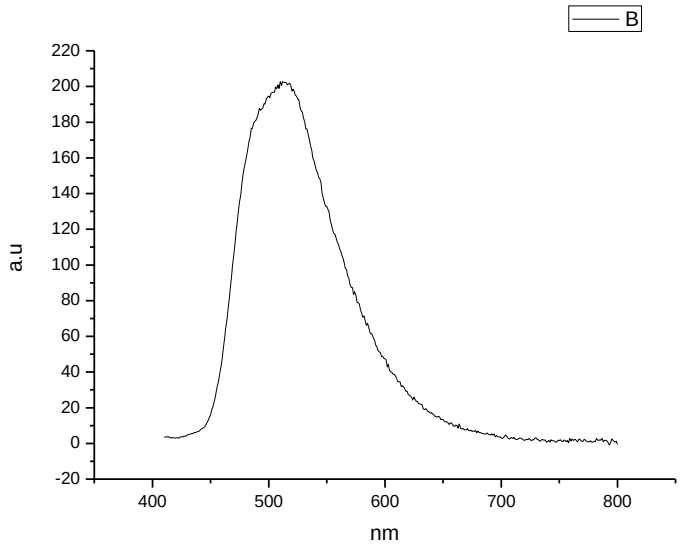

Figure 4.2.152. Fluorescence emission spectrum of **23** recorded in Chloroform at 400 nm excitation.

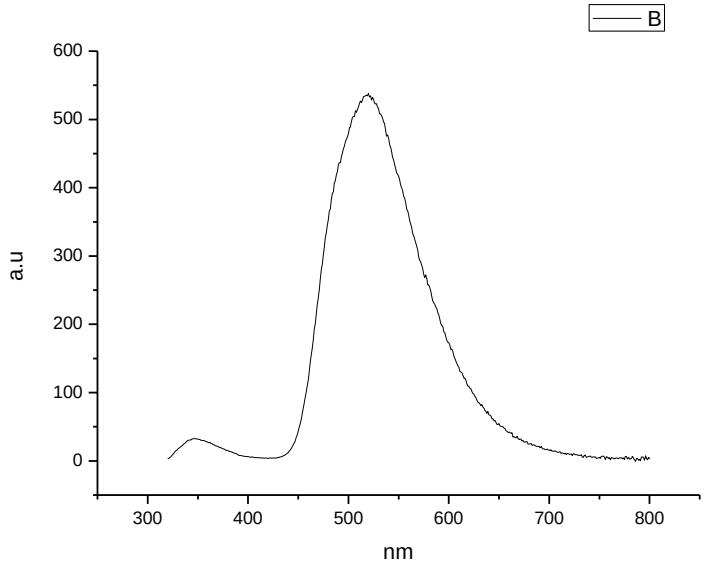

Figure 4.2.153. Fluorescence emission spectrum of **23** recorded in Acetonitrile at 310 nm excitation.

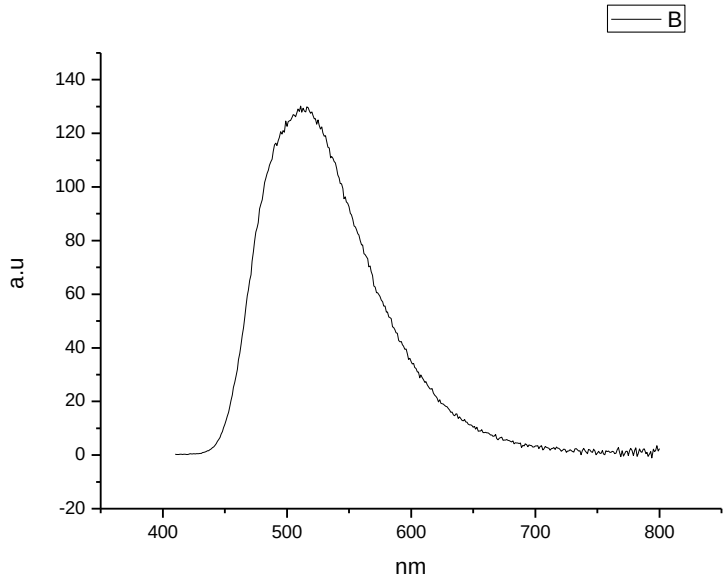

Figure 4.2.154. Fluorescence emission spectrum of **23** recorded in Acetonitrile at 400 nm excitation.

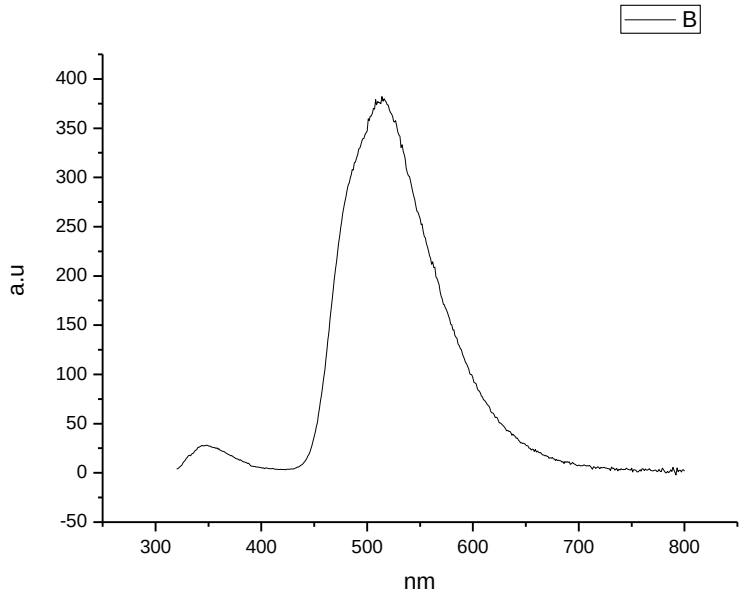

Figure 4.2.155. Fluorescence emission spectrum of **23** recorded in 1-octanol at 310 nm excitation.

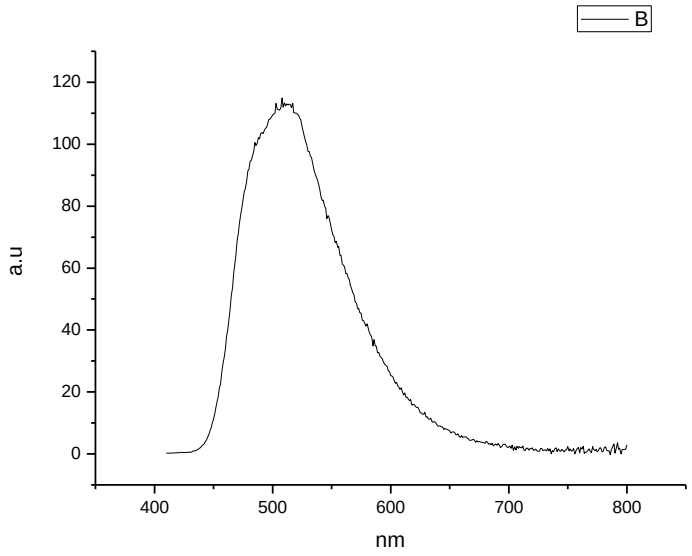

Figure 4.2.156. Fluorescence emission spectrum of **23** recorded in 1-octanol at 400 nm excitation.

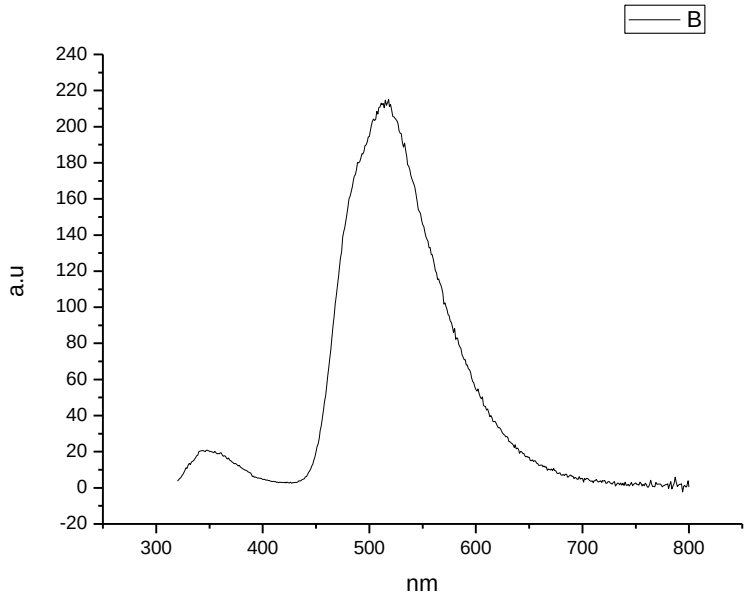

Figure 4.2.157. Fluorescence emission spectrum of **23** recorded in 1-hexanol at 310 nm excitation.

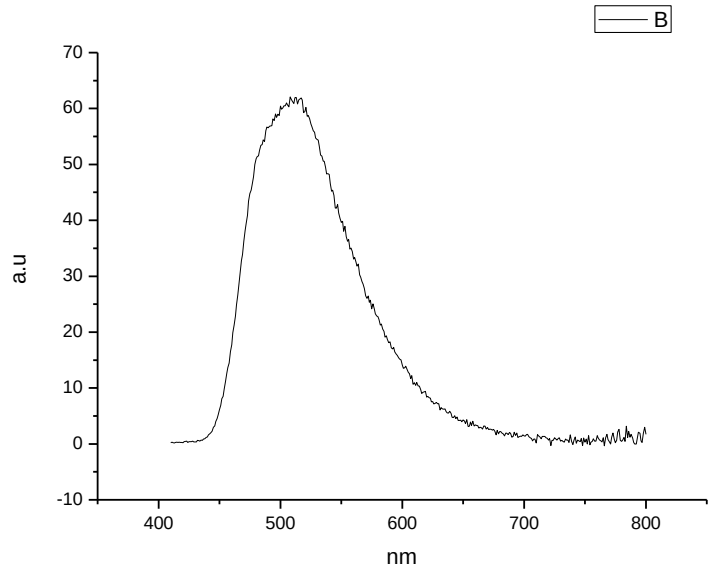

Figure 4.2.158. Fluorescence emission spectrum of **23** recorded in 1-hexanol at 400 nm excitation.

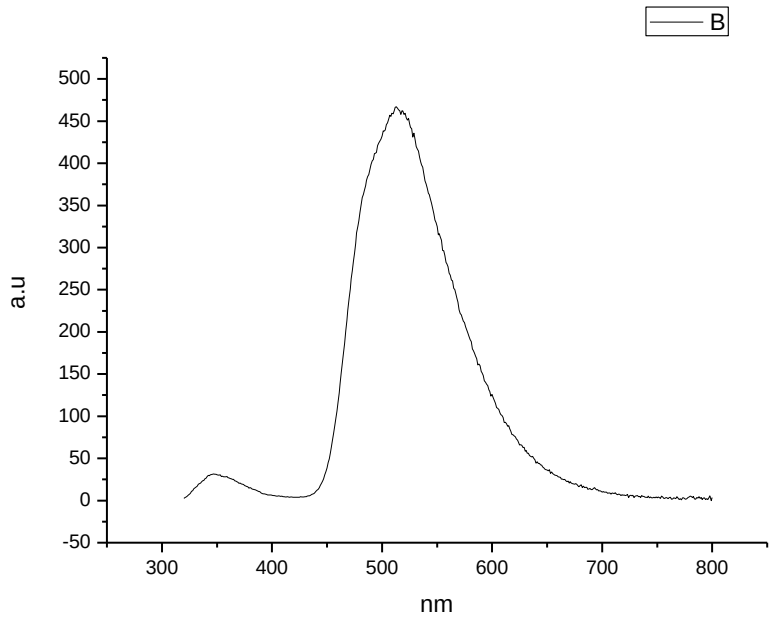

Figure 4.2.159. Fluorescence emission spectrum of **23** recorded in 1-butanol at 310 nm excitation.

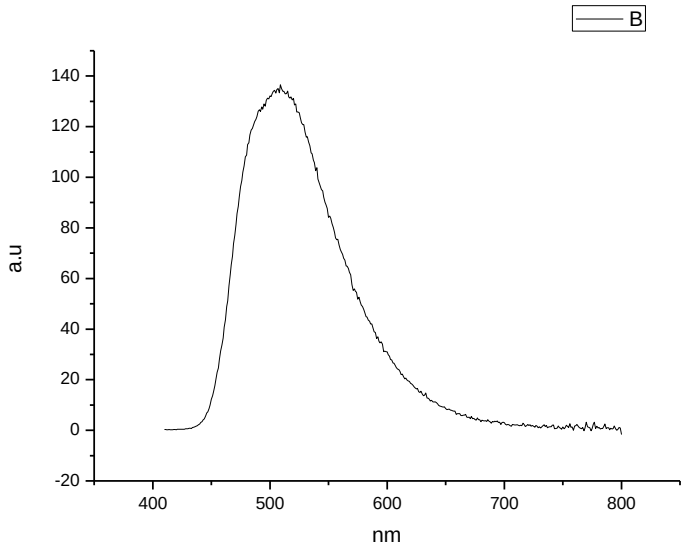

Figure 4.2.160. Fluorescence emission spectrum of **23** recorded in 1-butanol at 400 nm excitation.

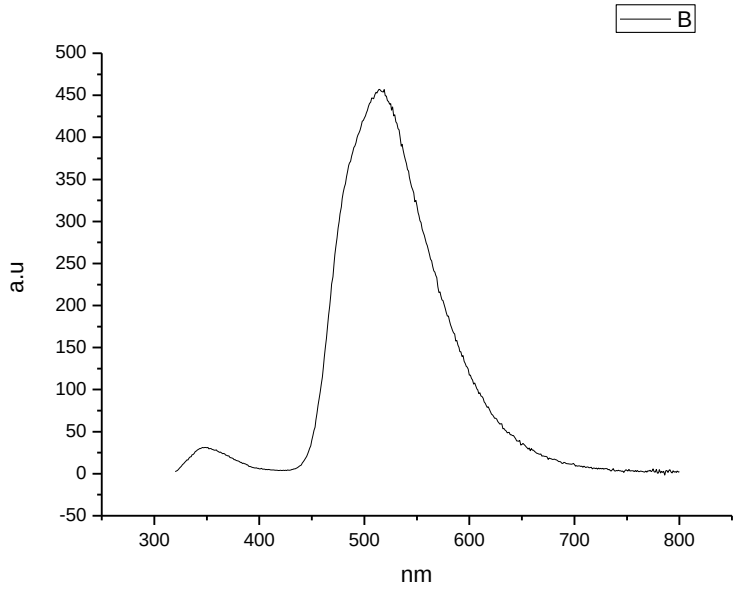

Figure 4.2.161. Fluorescence emission spectrum of **23** recorded in 1-pentanol at 310 nm excitation.

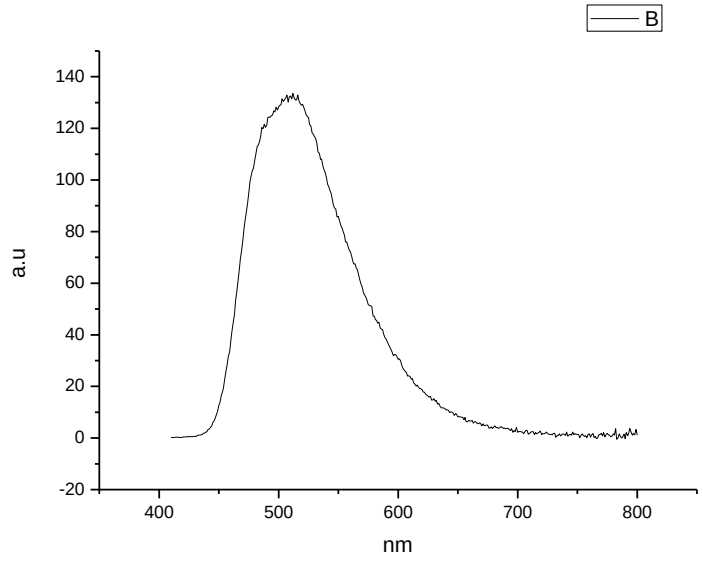

Figure 4.2.162. Fluorescence emission spectrum of **23** recorded in 1-pentanol at 400 nm excitation.

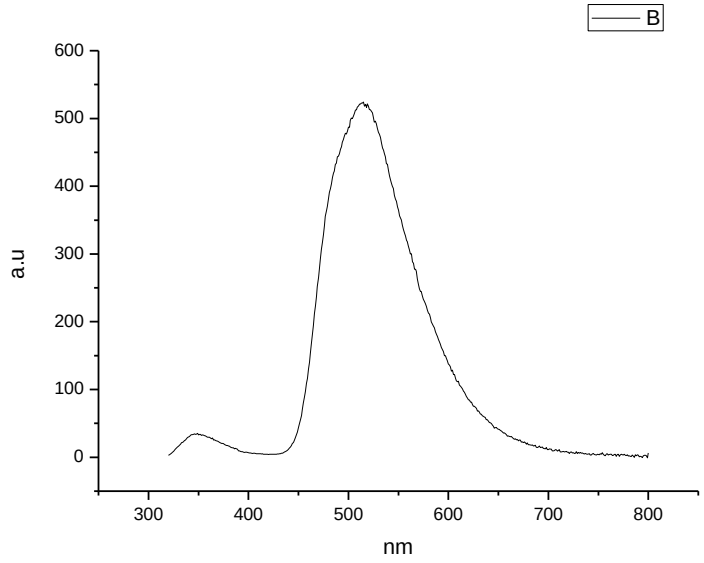

Figure 4.2.163. Fluorescence emission spectrum of **23** recorded in 1-propanol at 310 nm excitation.

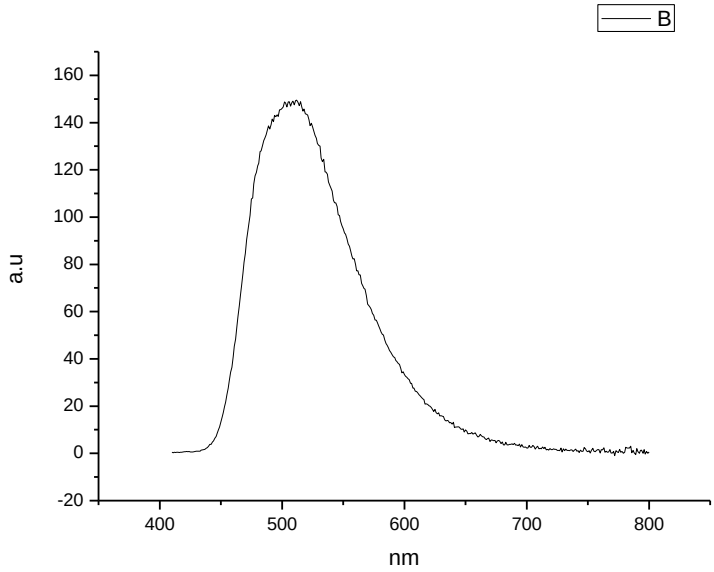

Figure 4.2.164. Fluorescence emission spectrum of **23** recorded in 1-propanol at 400 nm excitation.

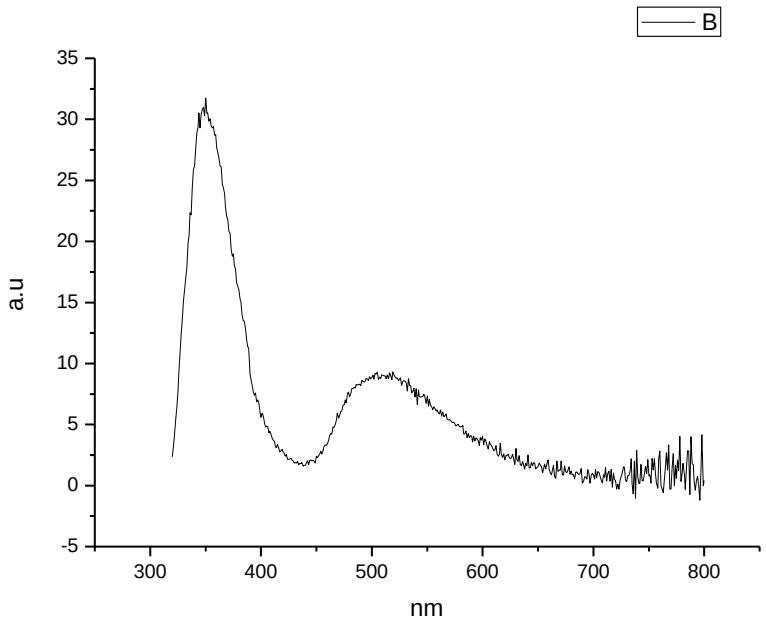

Figure 4.2.165. Fluorescence emission spectrum of **23** recorded in Acetic Acid at 310 nm excitation.

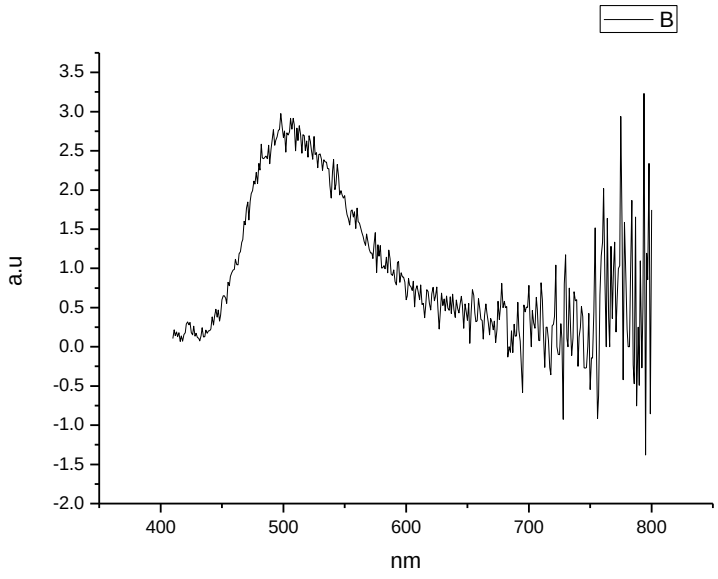

Figure 4.2.166. Fluorescence emission spectrum of **23** recorded in Acetic Acid at 400 nm excitation.

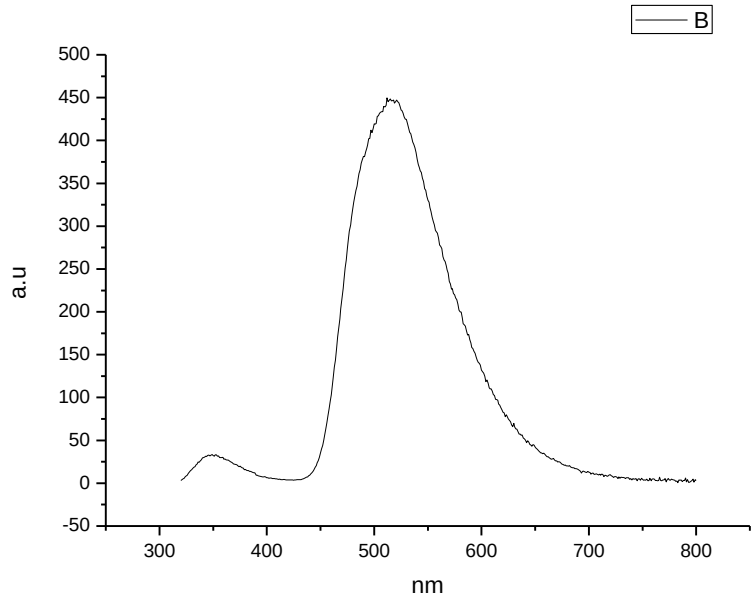

Figure 4.2.167. Fluorescence emission spectrum of **23** recorded in Methanol at 310 nm excitation.

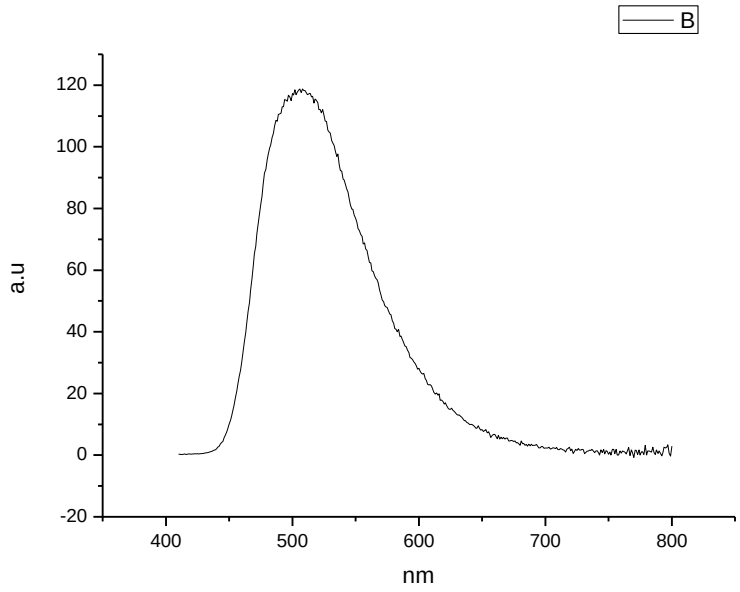

Figure 4.2.168. Fluorescence emission spectrum of **23** recorded in Methanol at 400 nm excitation.

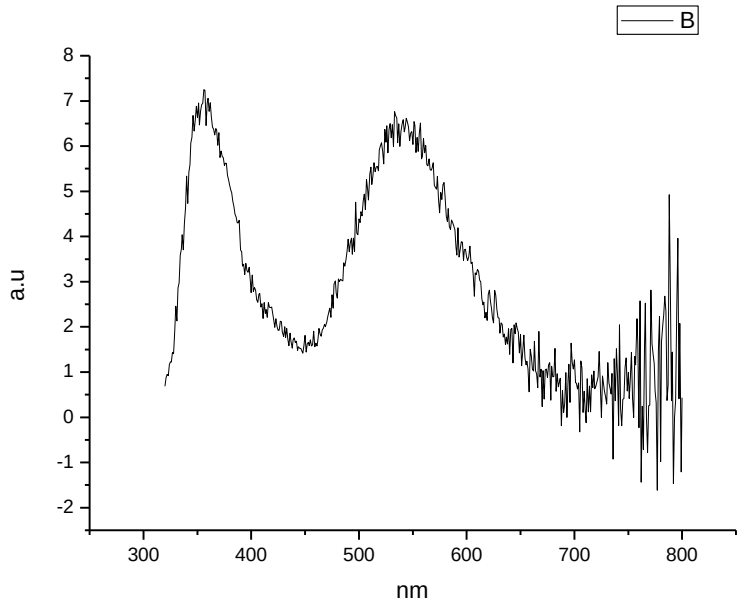

Figure 4.2.169. Fluorescence emission spectrum of **23** recorded in 2,2,2-trifluoroethanol at 310 nm excitation.

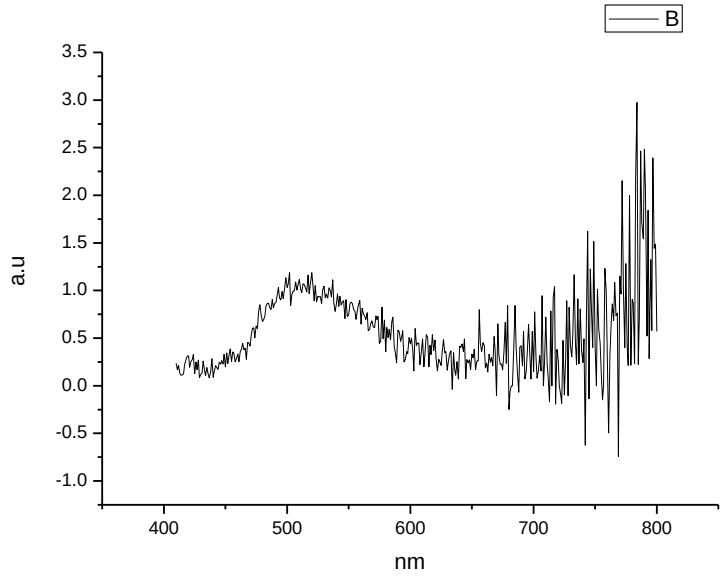

Figure 4.2.170. Fluorescence emission spectrum of **23** recorded in 2,2,2-trifluoroethanol at 400 nm excitation.

4.2.10 Normalised Fluorescence Emission spectra (Gaussian fitted).

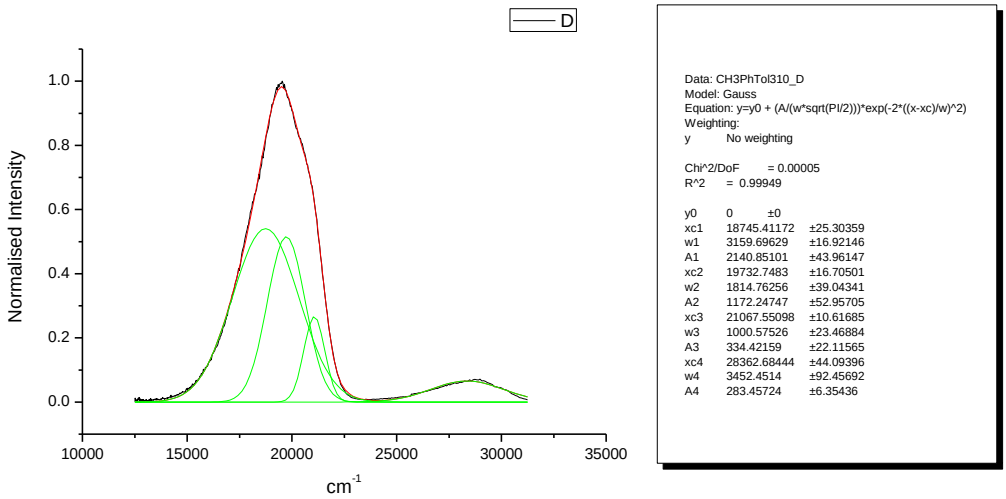

Figure 4.2.171. Gaussian model fit of the normalised fluorescence emission spectrum of **23** recorded in Toluene at 310 nm excitation.

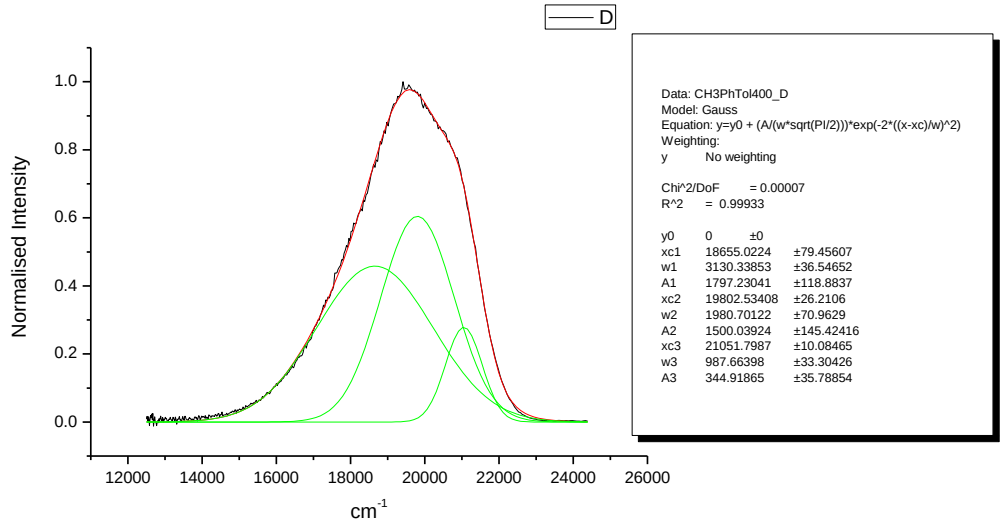

Figure 4.2.172. Gaussian model fit of the normalised fluorescence emission spectrum of **23** recorded in Toluene at 400 nm excitation.

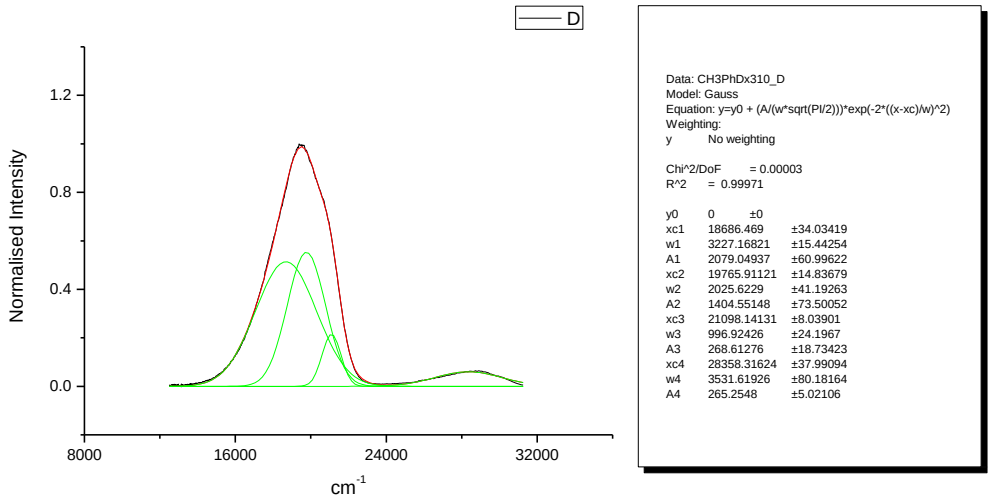

Figure 4.2.173. Gaussian model fit of the normalised fluorescence emission spectrum of **23** recorded in 1,4-dioxane at 310 nm excitation.

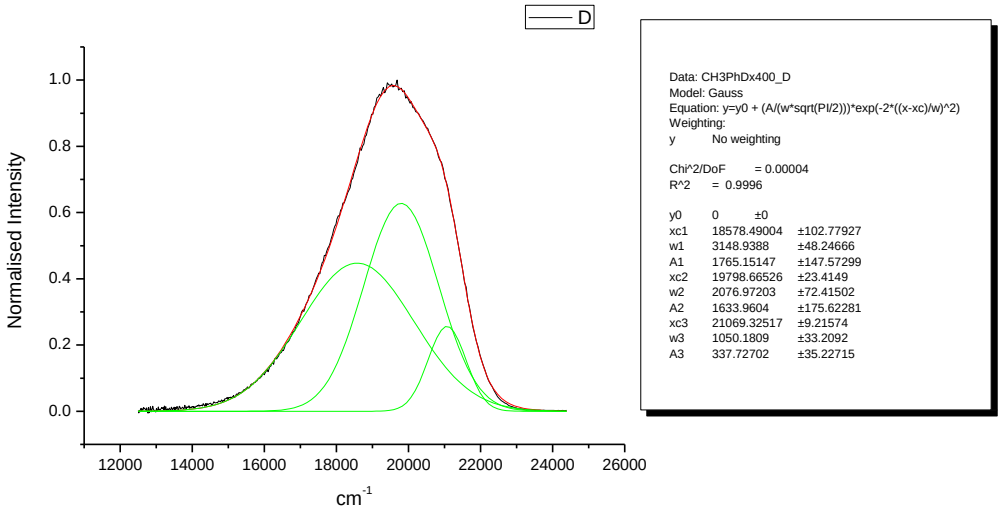

Figure 4.2.174. Gaussian model fit of the normalised fluorescence emission spectrum of **23** recorded in 1,4-dioxane at 400 nm excitation.

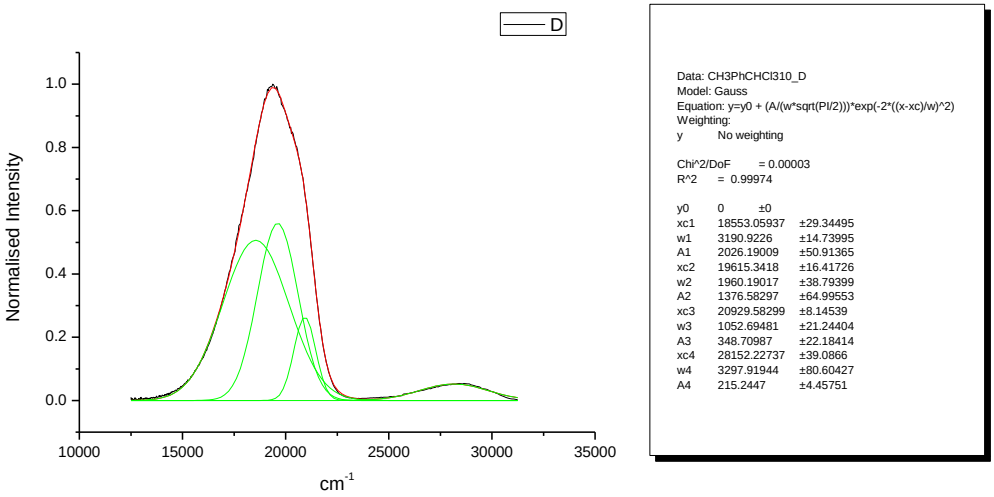

Figure 4.2.175. Gaussian model fit of the normalised fluorescence emission spectrum of **23** recorded in Chloroform at 310 nm excitation.

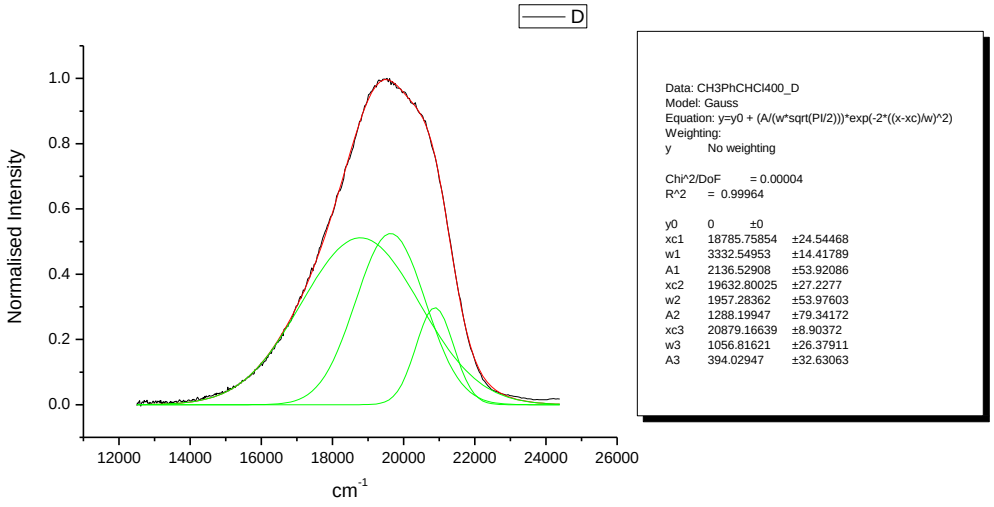

Figure 4.2.176. Gaussian model fit of the normalised fluorescence emission spectrum of **23** recorded in Chloroform at 400 nm excitation.

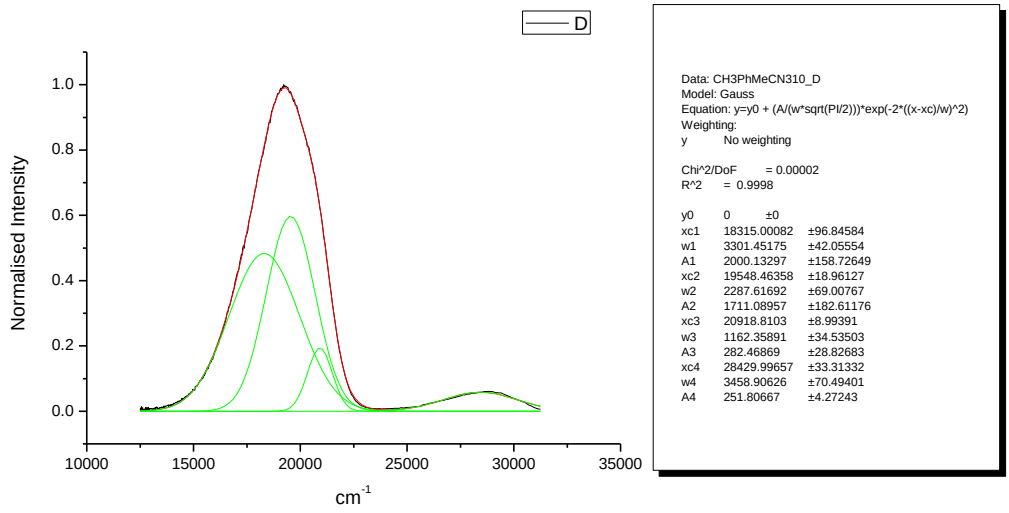

Figure 4.2.177. Gaussian model fit of the normalised fluorescence emission spectrum of **23** recorded in Acetonitrile at 310 nm excitation.

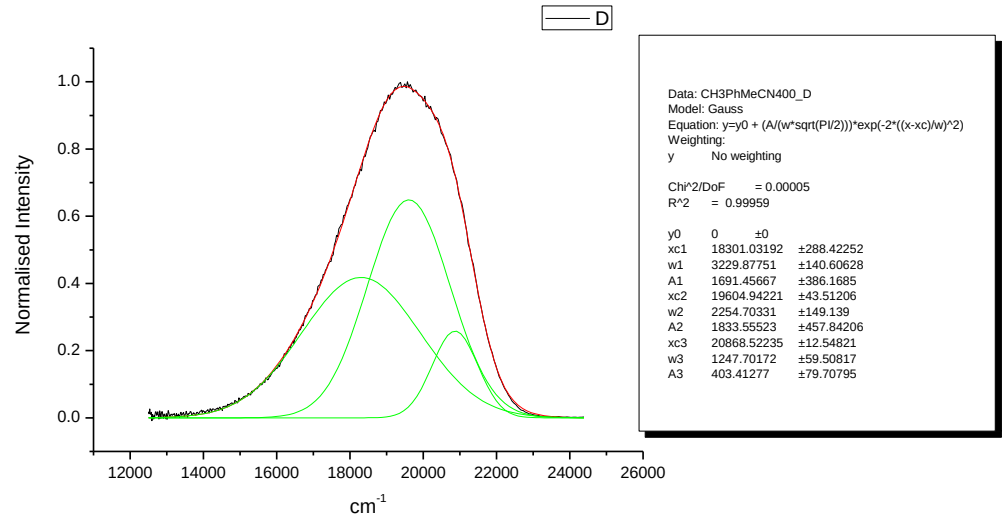

Figure 4.2.178. Gaussian model fit of the normalised fluorescence emission spectrum of **23** recorded in Acetonitrile at 400 nm excitation.

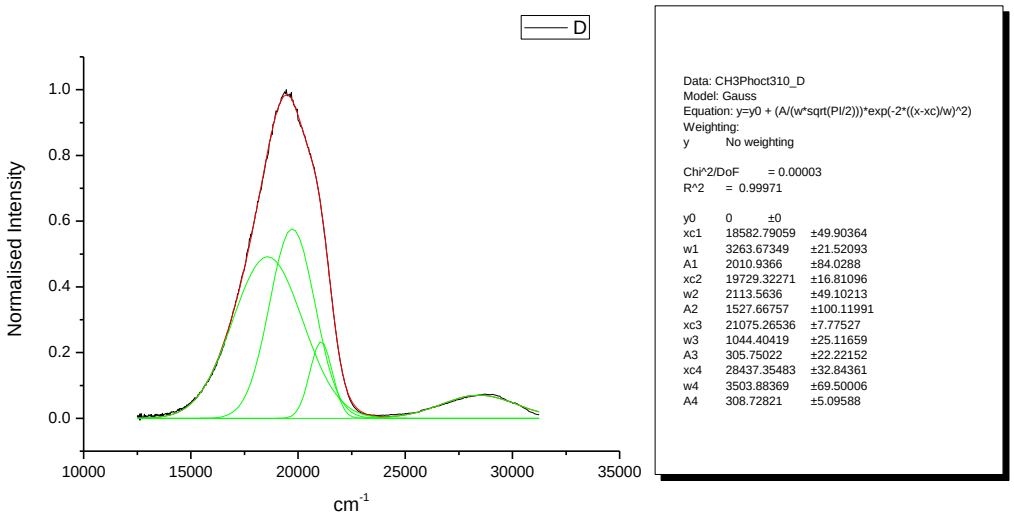

Figure 4.2.179. Gaussian model fit of the normalised fluorescence emission spectrum of **23** recorded in 1-octanol at 310 nm excitation.

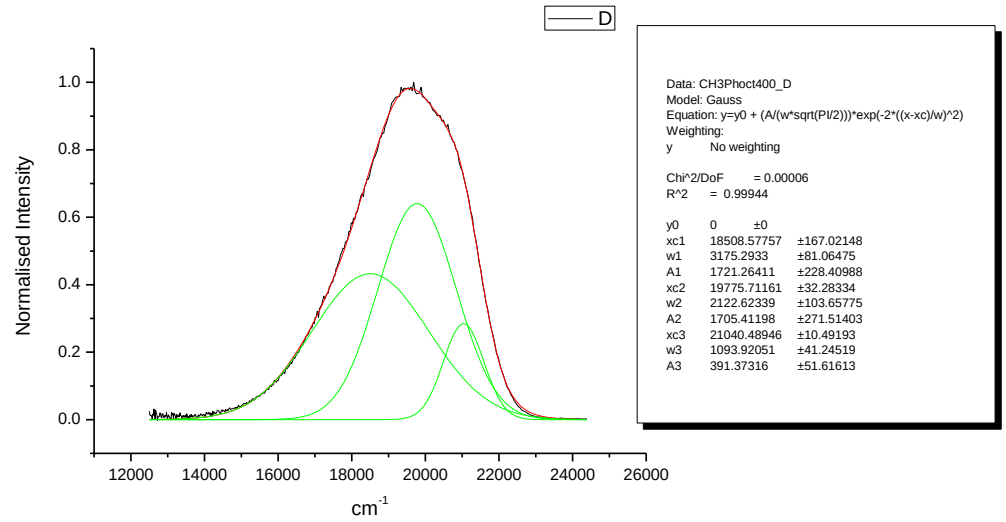

Figure 4.2.180. Gaussian model fit of the normalised fluorescence emission spectrum of **23** recorded in 1-octanol at 400 nm excitation.

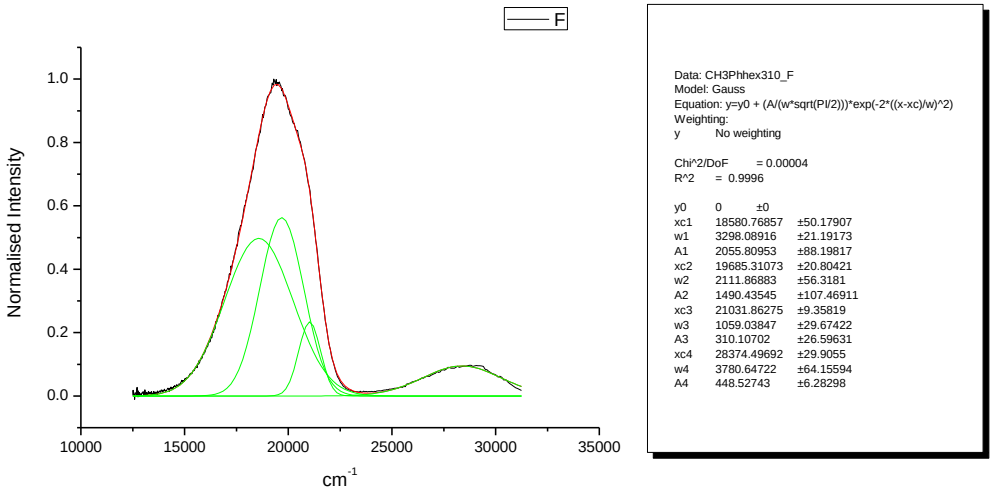

Figure 4.2.181. Gaussian model fit of the normalised fluorescence emission spectrum of **23** recorded in 1-hexanol at 310 nm excitation.

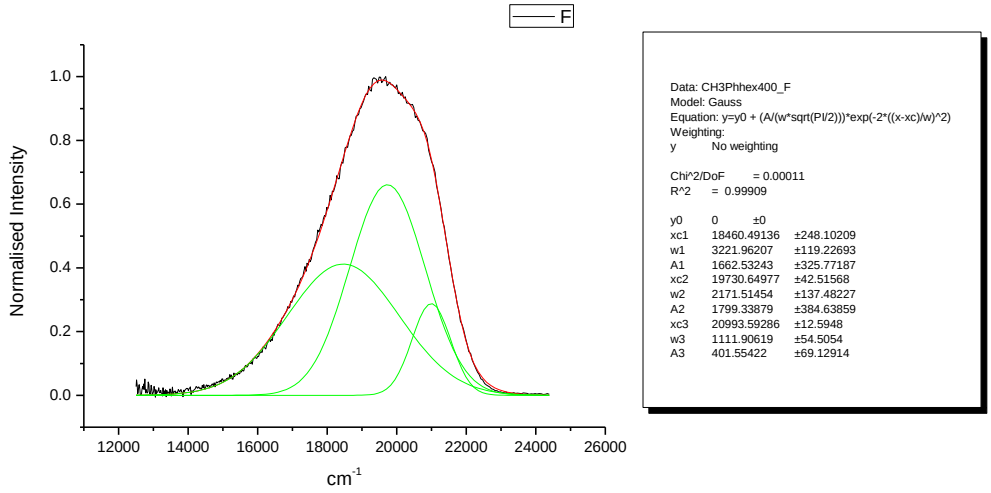

Figure 4.2.182. Gaussian model fit of the normalised fluorescence emission spectrum of **23** recorded in 1-hexanol at 400 nm excitation.

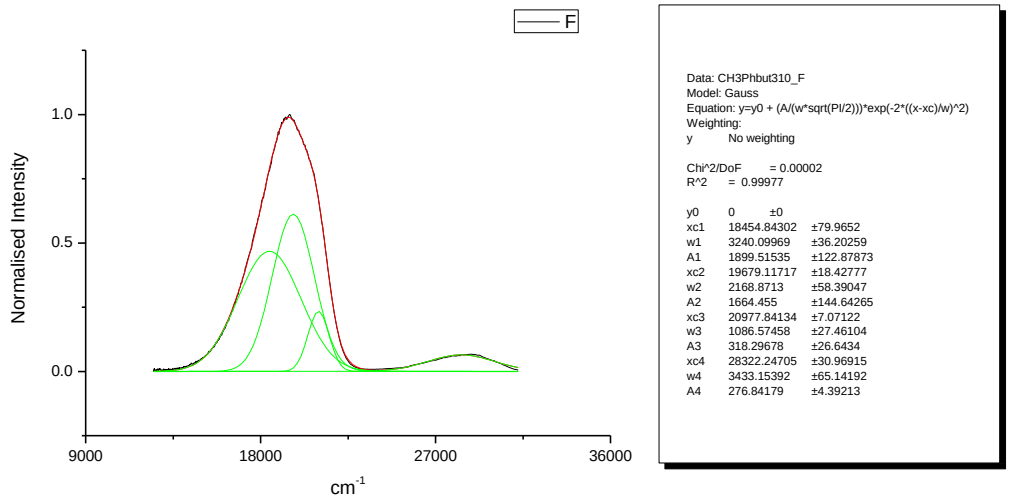

Figure 4.2.183. Gaussian model fit of the normalised fluorescence emission spectrum of **23** recorded in 1-butanol at 310 nm excitation.

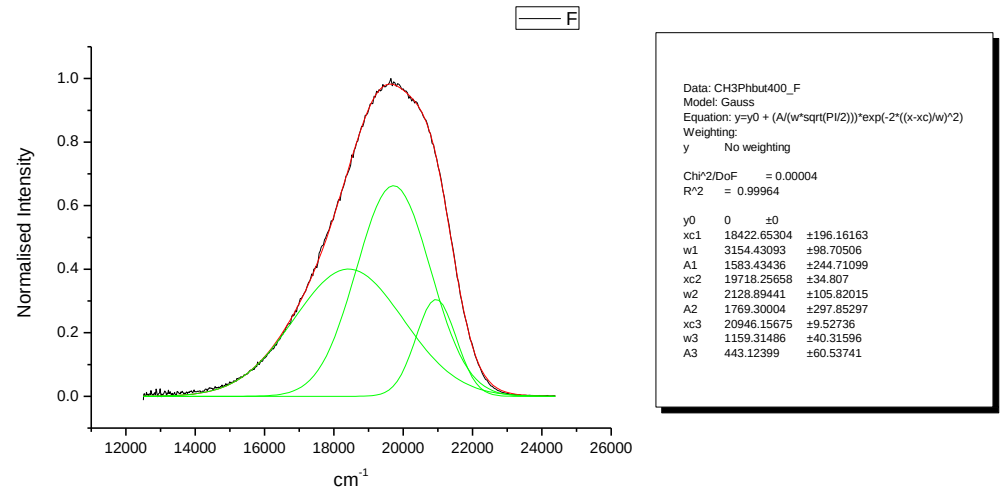

Figure 4.2.184. Gaussian model fit of the normalised fluorescence emission spectrum of **23** recorded in 1-butanol at 400 nm excitation.

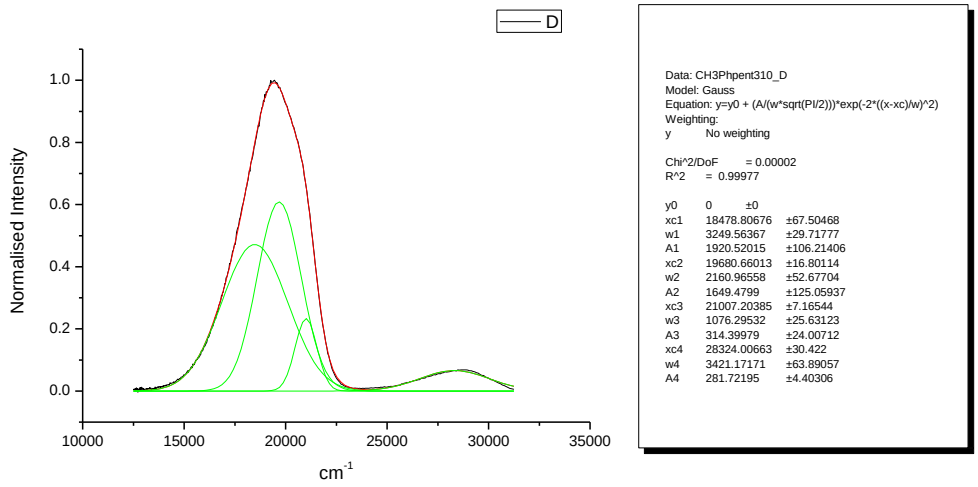

Figure 4.2.185. Gaussian model fit of the normalised fluorescence emission spectrum of **23** recorded in 1-pentanol at 310 nm excitation.

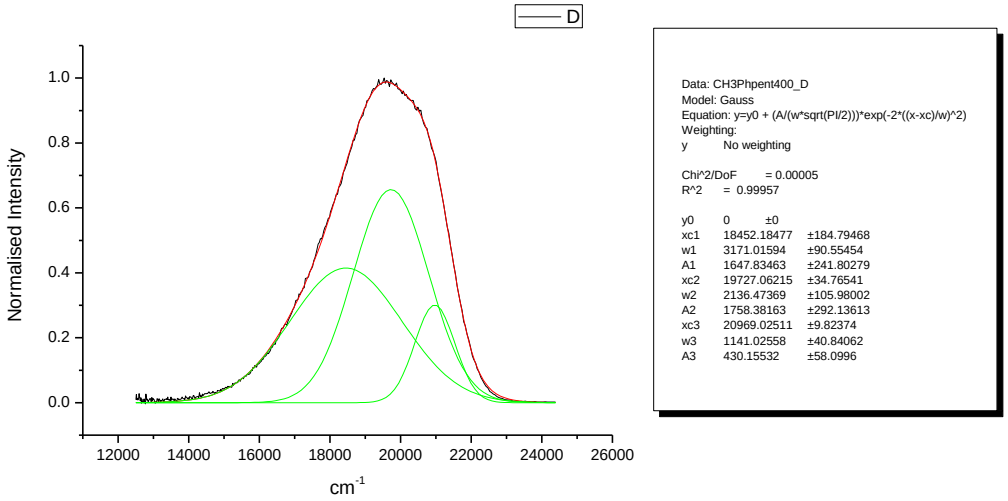

Figure 4.2.186. Gaussian model fit of the normalised fluorescence emission spectrum of **23** recorded in 1-pentanol at 400 nm excitation.

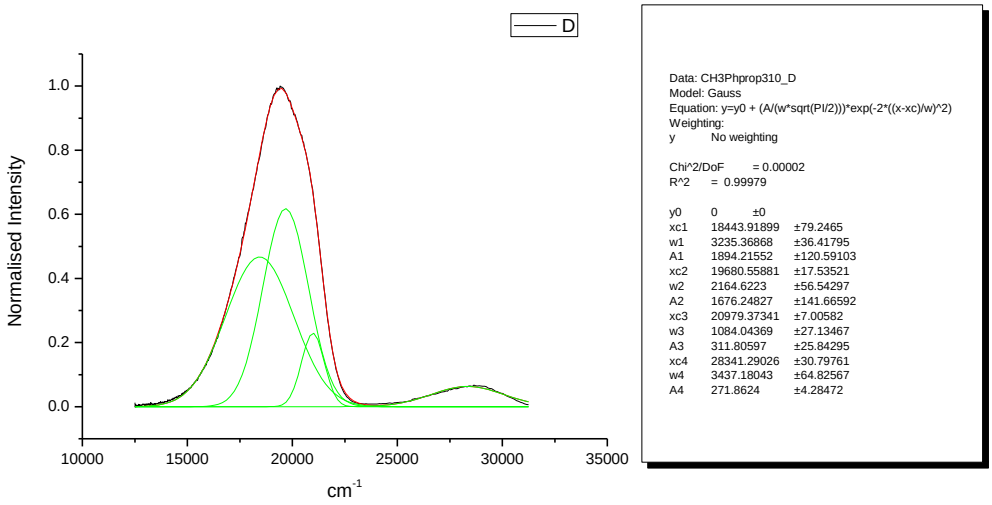

Figure 4.2.187. Gaussian model fit of the normalised fluorescence emission spectrum of **23** recorded in 1-propanol at 310 nm excitation.

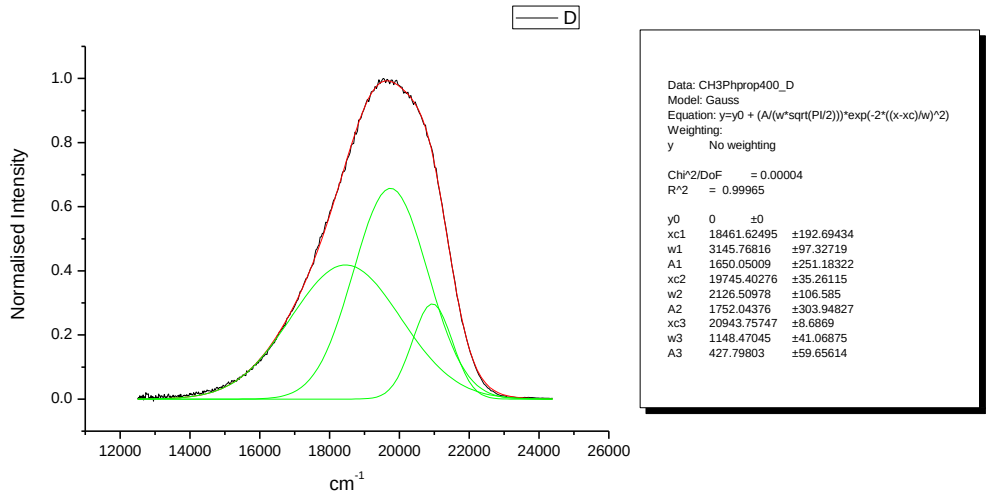

Figure 4.2.188. Gaussian model fit of the normalised fluorescence emission spectrum of **23** recorded in 1-propanol at 400 nm excitation.

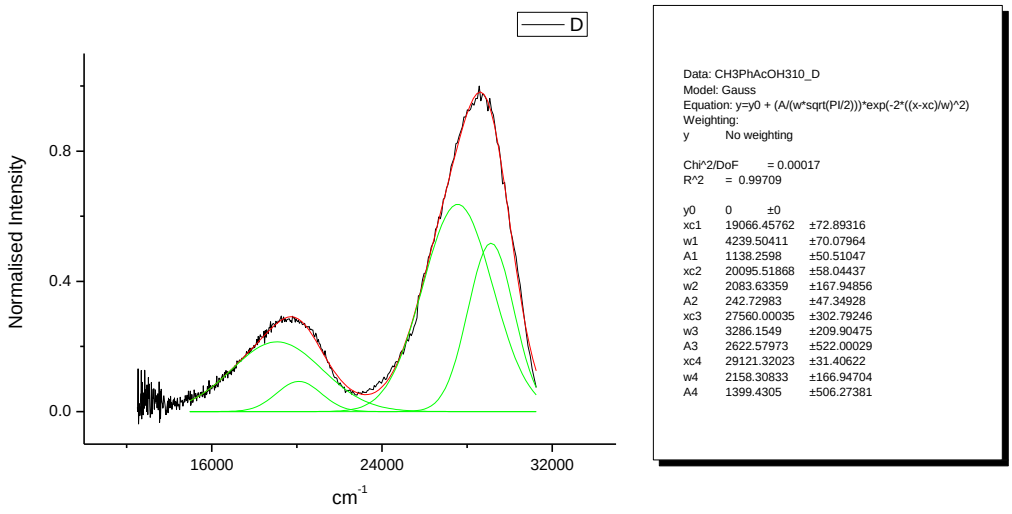

Figure 4.2.189. Gaussian model fit of the normalised fluorescence emission spectrum of **23** recorded in Acetic Acid at 310 nm excitation.

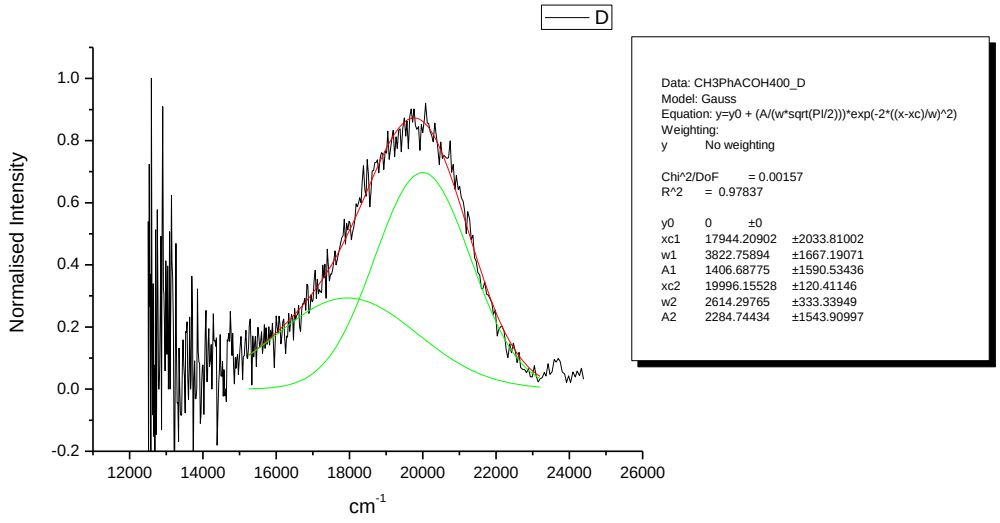

Figure 4.2.190. Gaussian model fit of the normalised fluorescence emission spectrum of **23** recorded in Acetic Acid at 400 nm excitation.

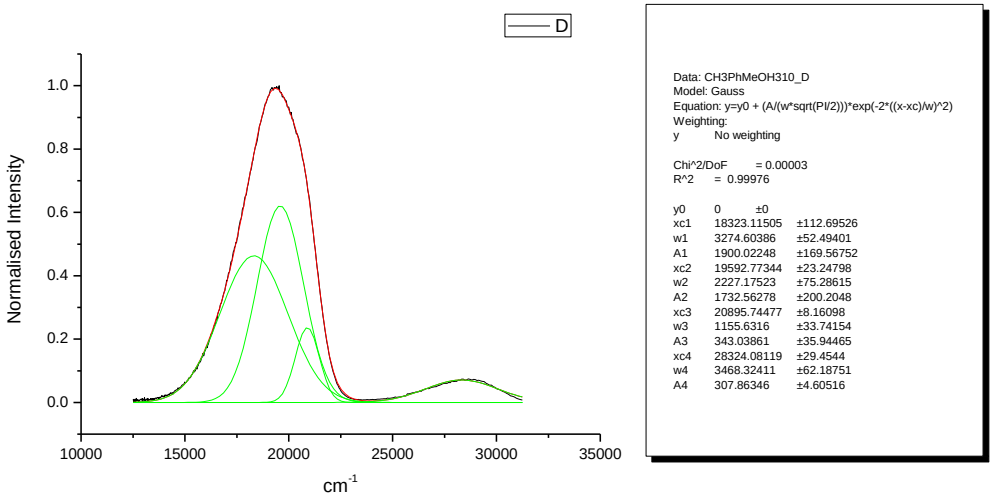

Figure 4.2.191. Gaussian model fit of the normalised fluorescence emission spectrum of **23** recorded in Methanol at 310 nm excitation.

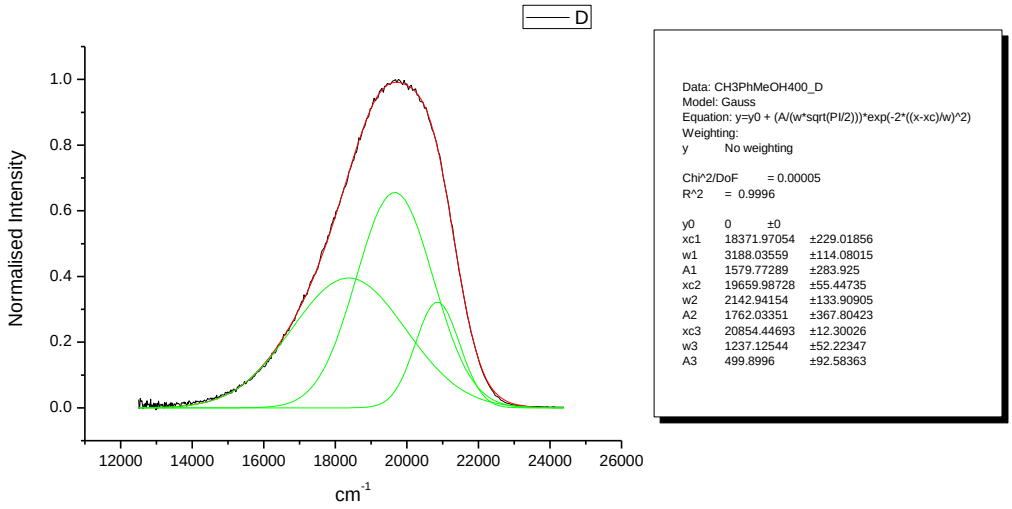

Figure 4.2.192. Gaussian model fit of the normalised fluorescence emission spectrum of **23** recorded in Methanol at 400 nm excitation.

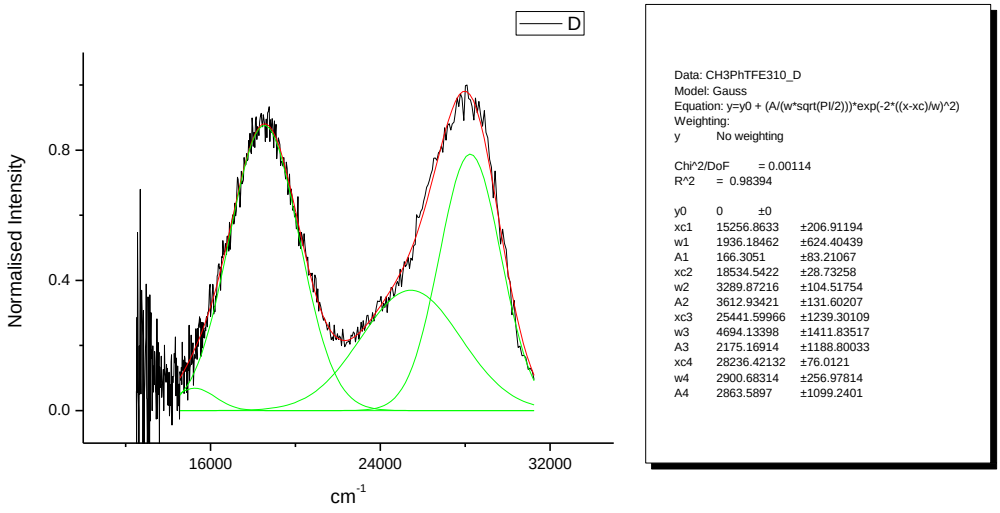

Figure 4.2.193. Gaussian model fit of the normalised fluorescence emission spectrum of **23** recorded in 2,2,2-trifluoroethanol at 310 nm excitation.

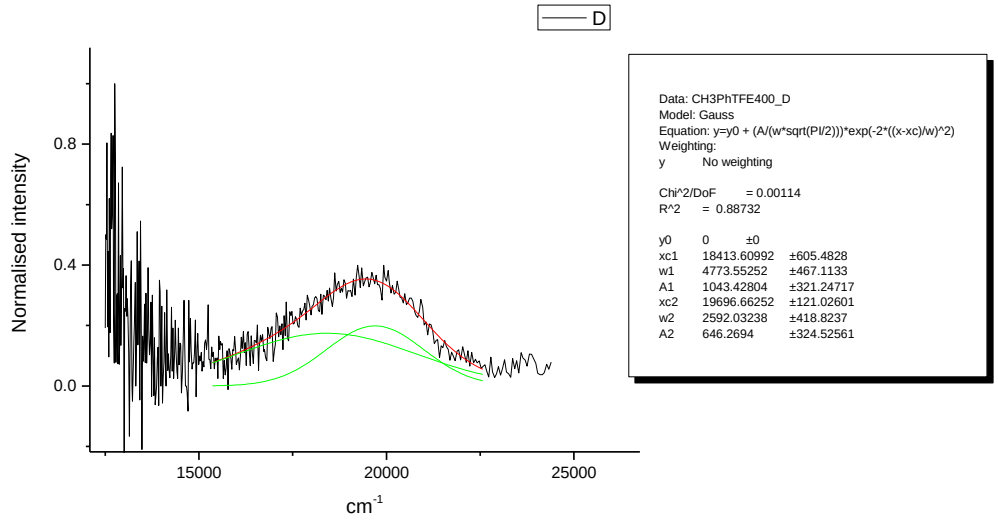

Figure 4.2.194. Gaussian model fit of the normalised fluorescence emission spectrum of **23** recorded in 2,2,2-trifluoroethanol at 400 nm excitation.

4.2.11 Fluorescence Excitation spectra.

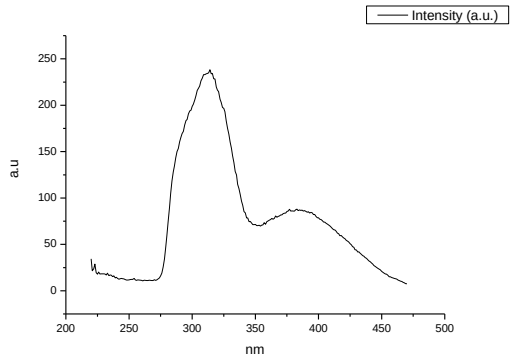

Figure 4.2.195. Fluorescence excitation spectrum of **23** recorded in Toluene with emission fixed at 480 nm.

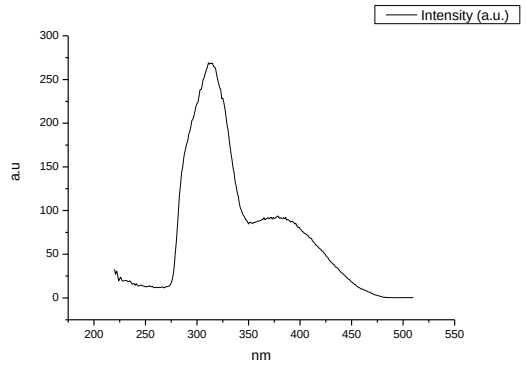

Figure 4.2.196. Fluorescence excitation spectrum of **23** recorded in Toluene with emission fixed at 520 nm.

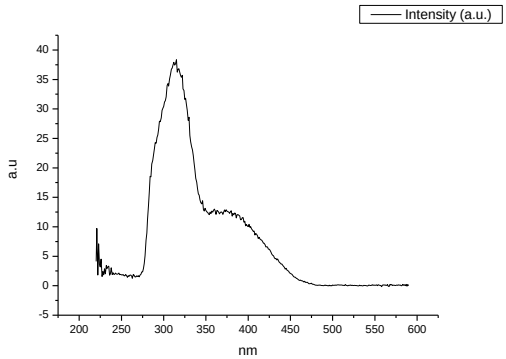

Figure 4.2.197. Fluorescence excitation spectrum of **23** recorded in Toluene with emission fixed at 600 nm.

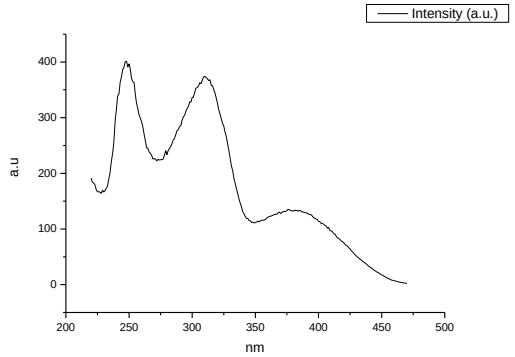

Figure 4.2.198. Fluorescence excitation spectrum of **23** recorded in 1,4-dioxane with emission fixed at 480 nm.

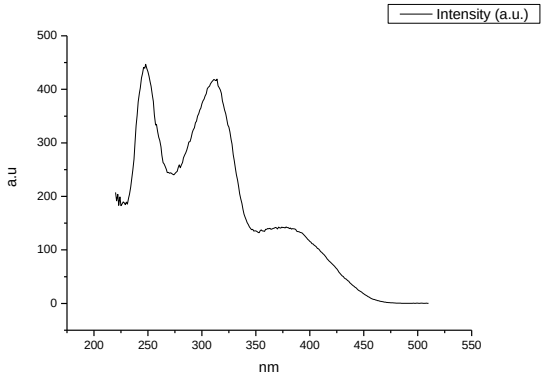

Figure 4.2.199. Fluorescence excitation spectrum of **23** recorded in 1,4-dioxane with emission fixed at 520 nm.

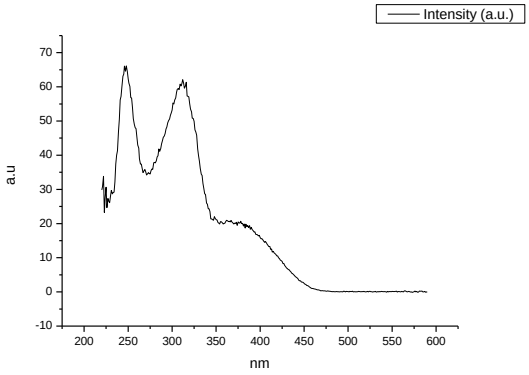

Figure 4.2.200. Fluorescence excitation spectrum of **23** recorded in 1,4-dioxane with emission fixed at 600 nm.

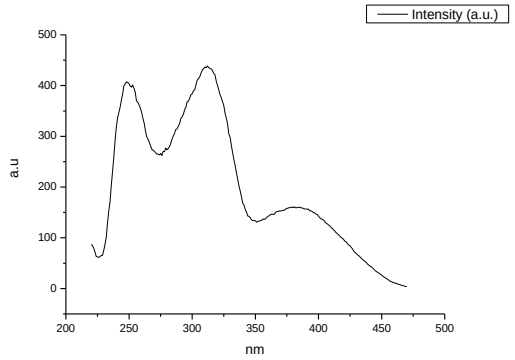

Figure 4.2.201. Fluorescence excitation spectrum of **23** recorded in Chloroform with emission fixed at 480 nm.

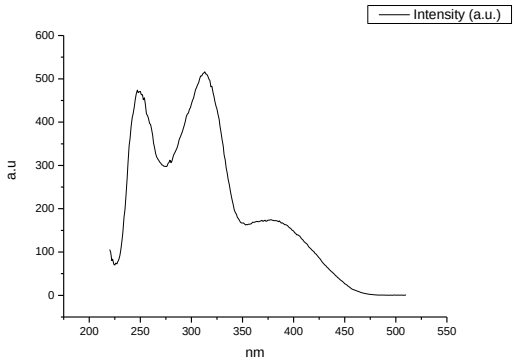

Figure 4.2.202. Fluorescence excitation spectrum of **23** recorded in Chloroform with emission fixed at 520 nm.

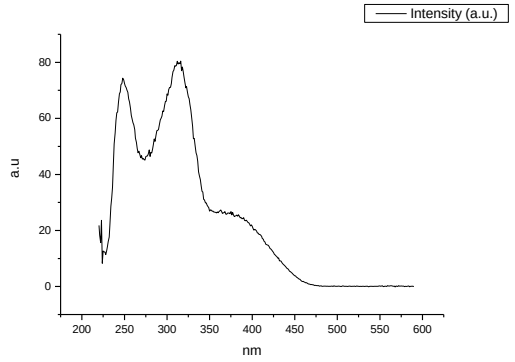

Figure 4.2.203. Fluorescence excitation spectrum of **23** recorded in Chloroform with emission fixed at 600 nm.

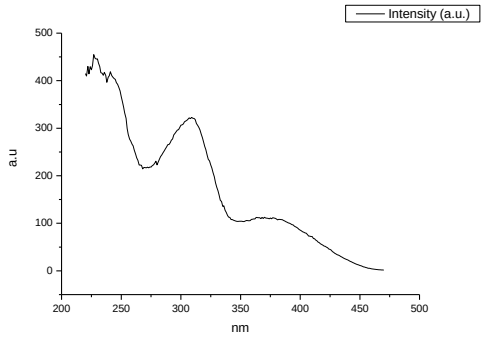

Figure 4.2.204. Fluorescence excitation spectrum of **23** recorded in Acetonitrile with emission fixed at 480 nm.

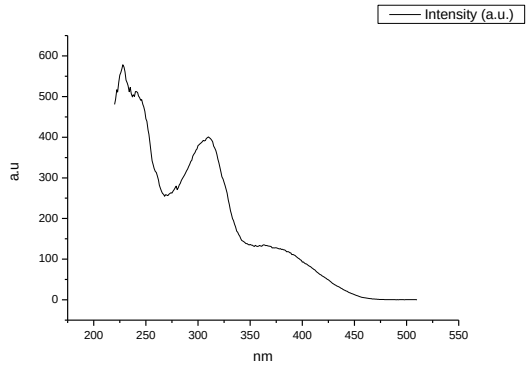

Figure 4.2.205. Fluorescence excitation spectrum of **23** recorded in Acetonitrile with emission fixed at 520 nm.

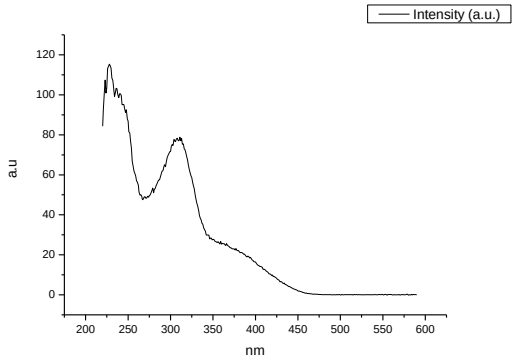

Figure 4.2.206. Fluorescence excitation spectrum of **23** recorded in Acetonitrile with emission fixed at 600 nm.

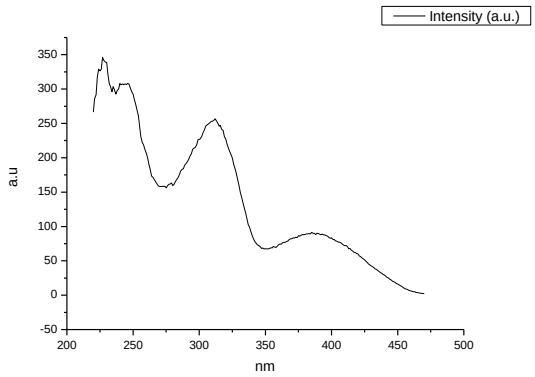

Figure 4.2.207. Fluorescence excitation spectrum of **23** recorded in 1-octanol with emission fixed at 480 nm.

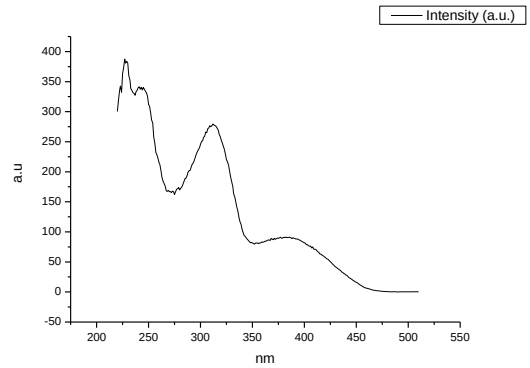

Figure 4.2.208. Fluorescence excitation spectrum of **23** recorded in 1-octanol with emission fixed at 520 nm.

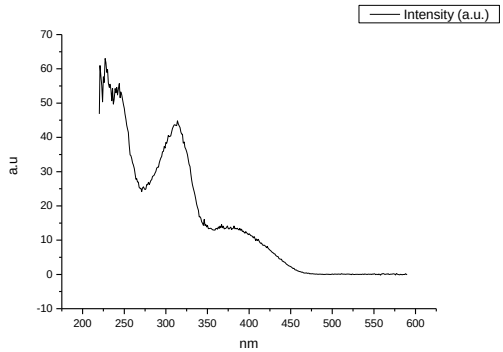

Figure 4.2.209. Fluorescence excitation spectrum of **23** recorded in 1-octanol with emission fixed at 600 nm.

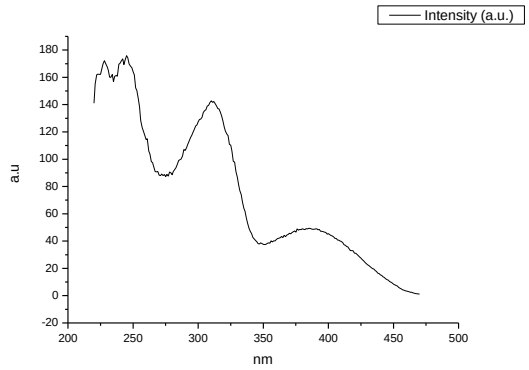

Figure 4.2.210. Fluorescence excitation spectrum of **23** recorded in 1-hexanol with emission fixed at 480 nm.

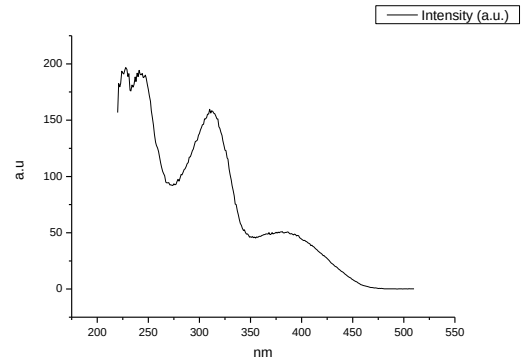

Figure 4.2.211. Fluorescence excitation spectrum of **23** recorded in 1-hexanol with emission fixed at 520 nm.

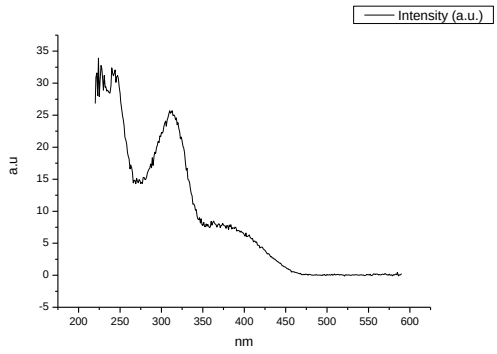

Figure 4.2.212. Fluorescence excitation spectrum of **23** recorded in 1-hexanol with emission fixed at 600 nm.

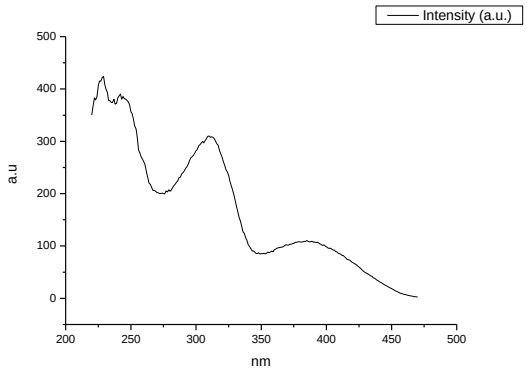

Figure 4.2.213. Fluorescence excitation spectrum of **23** recorded in 1-butanol with emission fixed at 480 nm.

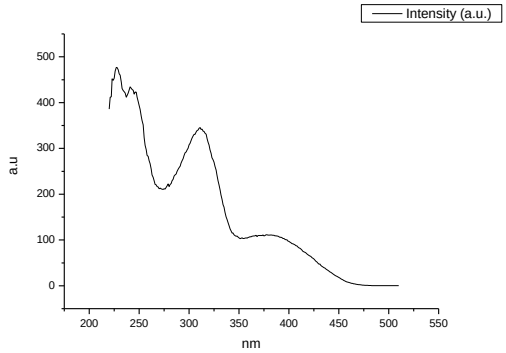

Figure 4.2.214. Fluorescence excitation spectrum of **23** recorded in 1-butanol with emission fixed at 520 nm.

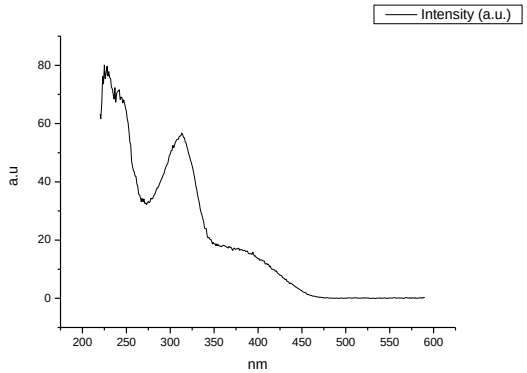

Figure 4.2.215. Fluorescence excitation spectrum of **23** recorded in 1-butanol with emission fixed at 600 nm.

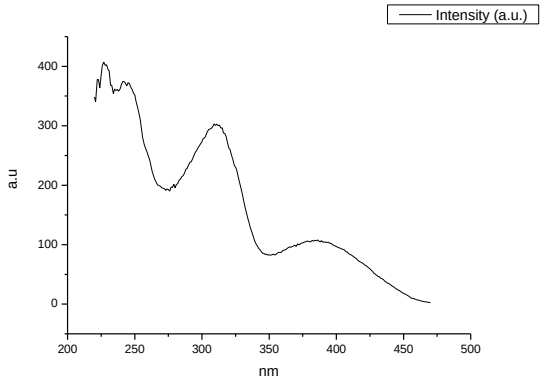

Figure 4.2.216. Fluorescence excitation spectrum of **23** recorded in 1-pentanol with emission fixed at 480 nm.

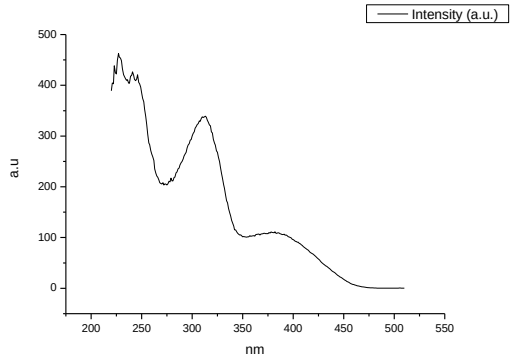

Figure 4.2.217. Fluorescence excitation spectrum of **23** recorded in 1-pentanol with emission fixed at 520 nm.

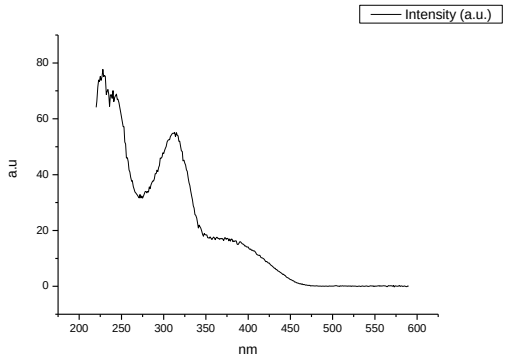

Figure 4.2.218. Fluorescence excitation spectrum of **23** recorded in 1-pentanol with emission fixed at 600 nm.

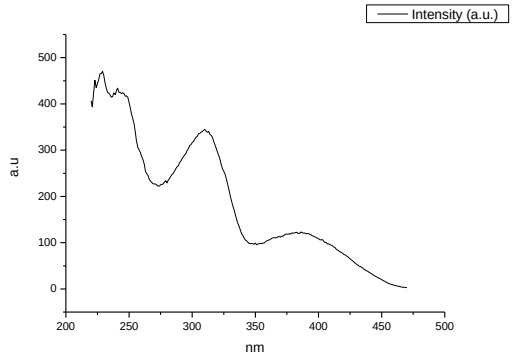

Figure 4.2.219. Fluorescence excitation spectrum of **23** recorded in 1-propanol with emission fixed at 480 nm.

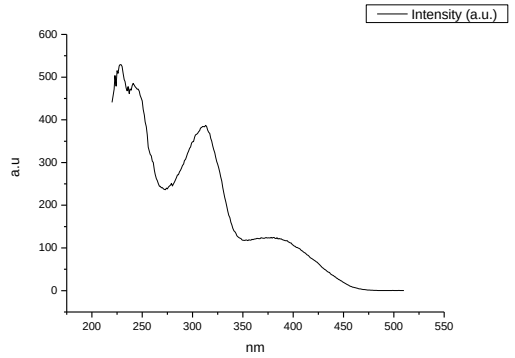

Figure 4.2.220. Fluorescence excitation spectrum of **23** recorded in 1-propanol with emission fixed at 520 nm.

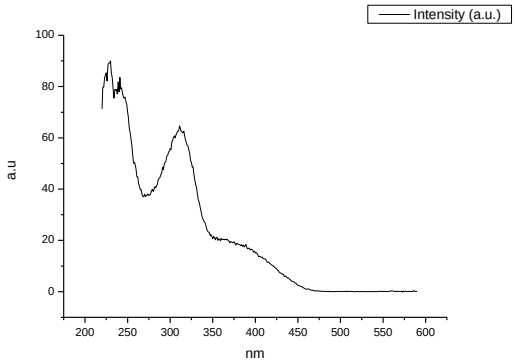

Figure 4.2.221. Fluorescence excitation spectrum of **23** recorded in 1-propanol with emission fixed at 600 nm.

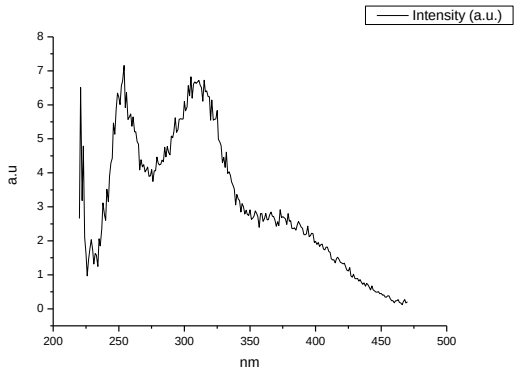

Figure 4.2.222. Fluorescence excitation spectrum of **23** recorded in Acetic Acid with emission fixed at 480 nm.

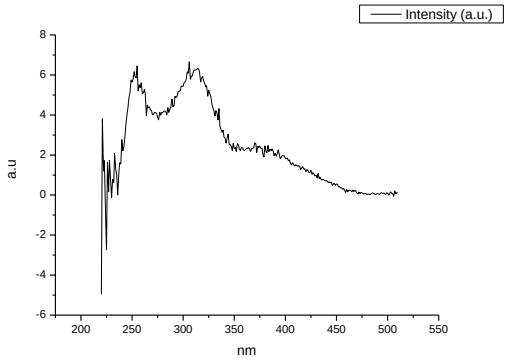

Figure 4.2.223. Fluorescence excitation spectrum of **23** recorded in Acetic Acid with emission fixed at 520 nm.

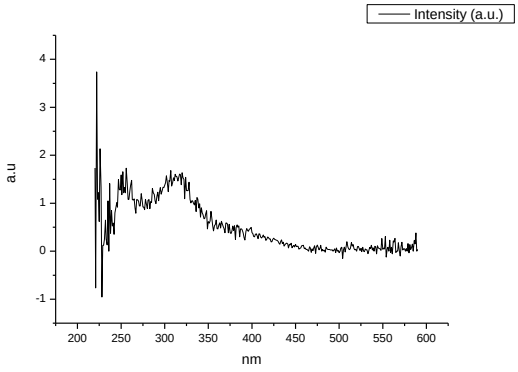

Figure 4.2.224. Fluorescence excitation spectrum of **23** recorded in Acetic Acid with emission fixed at 600 nm.

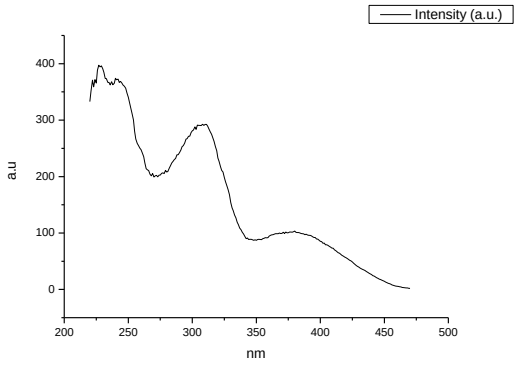

Figure 4.2.225. Fluorescence excitation spectrum of **23** recorded in Methanol with emission fixed at 480 nm.

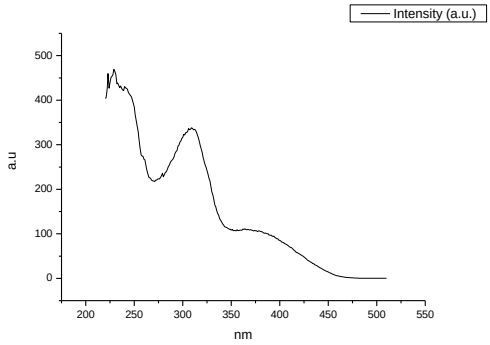

Figure 4.2.226. Fluorescence excitation spectrum of **23** recorded in Methanol with emission fixed at 520 nm.

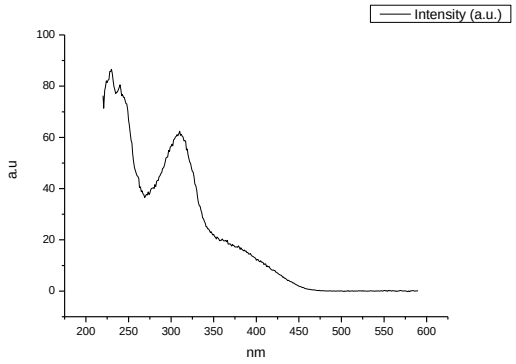

Figure 4.2.227. Fluorescence excitation spectrum of **23** recorded in Methanol with emission fixed at 600 nm.

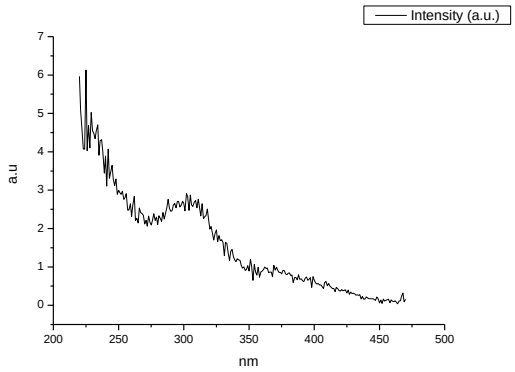

Figure 4.2.228. Fluorescence excitation spectrum of **23** recorded in 2,2,2-trifluoroethanol with emission fixed at 480 nm.

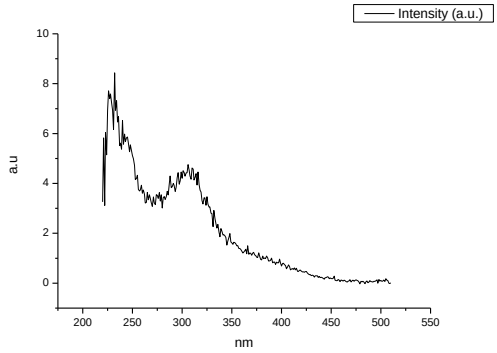

Figure 4.2.229. Fluorescence excitation spectrum of **23** recorded in 2,2,2-trifluoroethanol with emission fixed at 520 nm.

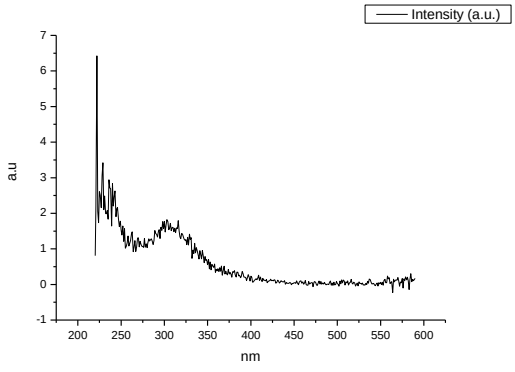

Figure 4.2.230. Fluorescence excitation spectrum of **23** recorded in 2,2,2-trifluoroethanol with emission fixed at 600 nm.

4.3 COMPOUND 25.

4.3.1 Quantum Yield Summary.

Solvent	abs (310 nm)	$\lambda_{ems\ (max)}$	$\Phi_{310\ nm}$	abs (400 nm)	$\lambda_{ems\ (max)}$	$\Phi_{400\ nm}$
Toluene	0.09	514.02	0.40	0.04	508.95	0.41
1,4-Dioxane	0.08	511.94	0.47	0.02	511.94	0.52
Chloroform	0.08	518.05	0.47	0.02	514.02	0.48
Acetonitrile	0.07	518.05	0.45	0.01	515.97	0.44
1-Octanol	0.05	514.02	0.47	0.01	511.04	0.42
1-Hexanol	0.04	515.07	0.46	0.01	507.01	0.44
1-Butanol	0.07	512.98	0.47	0.02	511.94	0.45
1-Pentanol	0.05	517.01	0.44	0.01	511.94	0.41
1-Propanol	0.07	515.97	0.43	0.02	505.97	0.44
Acetic acid	0.07	345.07	0.02	0.02	507.01	0.01
Methanol	0.08	518.95	0.32	0.02	508.95	0.29
2,2,2-Trifluoroethanol	0.05	542.94	0.02	0.01	521.99	0.01

Table 4.3.1. Summary of ultraviolet-visible absorbance values at 310 nm and 400 nm, emission maxima and quantum yield (Φ) of **25** at 310 nm and 400 nm excitation.

4.3.2 310 nm excitation Gaussian band fit summaries.

Solvent	λ max$_{em}$ Band 1 (cm^{-1})	λ max$_{em}$ Band 1 (nm)	λ max$_{em}$ Band 2 (cm^{-1})	λ max$_{em}$ Band 2 (nm)	λ max$_{em}$ Band 3 (cm^{-1})	λ max$_{em}$ Band 3 (nm)
Toluene	18629.38	536.79	19753.44	506.24	21087.34	474.22
1,4-Dioxane	18605.68	537.47	19755.49	506.19	21096.53	474.01
Chloroform	18462.91	541.63	19627.24	509.50	20933.29	477.71
Acetonitrile	18264.76	547.50	19560.23	511.24	20932.29	477.73
1-Octanol	18459.43	541.73	19734.44	506.73	21079.98	474.38
1-Hexanol	18472.07	541.36	19703.61	507.52	21042.26	475.23
1-Butanol	18398.30	543.53	19685.11	508.00	20991.68	476.38
1-Pentanol	18394.21	543.65	19677.09	508.21	21013.61	475.88
1-Propanol	18371.94	544.31	19673.78	508.29	20980.84	476.63
Acetic acid	18686.40	535.15	20266.14	493.43	-	-
Methanol	18264.75	547.50	19595.86	510.31	20897.70	478.52
2,2,2-Trifluoroethanol	15584.01	641.68	18538.82	539.41	-	-

Solvent	λ max$_{em}$ Band 4 (cm^{-1})	λ max$_{em}$ Band 4 (nm)	λ max$_{em}$ Band 5 (cm^{-1})	λ max$_{em}$ Band 5 (nm)
Toluene	28387.72	352.27	-	-
1,4-Dioxane	28289.32	353.49	-	-
Chloroform	28148.46	355.26	-	-
Acetonitrile	28449.60	351.50	-	-
1-Octanol	28507.35	350.79	-	-
1-Hexanol	28385.31	352.29	-	-
1-Butanol	28350.73	352.72	-	-
1-Pentanol	28361.12	352.60	-	-
1-Propanol	28344.35	352.80	-	-
Acetic acid	27517.92	363.40	29032.29	344.44
Methanol	28343.81	352.81	-	-
2,2,2-Trifluoroethanol	25378.63	394.03	28288.60	353.50

Table 4.3.2. Summary of band maxima of 5 band fit using Gaussian model for normalised **25** emission spectra recorded at 310 nm excitation.

(a)

Solvent	Width Band 1 (cm^{-1})	Width Band 2 (cm^{-1})	Width Band 3 (cm^{-1})	Width Band 4 (cm^{-1})	Width Band 5 (cm^{-1})
Toluene	3119.83	1928.17	993.80	3448.80	-
1,4-Dioxane	3170.57	2026.34	1034.07	3635.87	-
Chloroform	3148.25	2021.08	1044.65	3362.45	-
Acetonitrile	3241.88	2255.83	1164.06	3431.71	-
1-Octanol	3177.62	2143.37	1049.57	3578.33	-
1-Hexanol	3196.96	2115.68	1068.01	3885.80	-
1-Butanol	3172.87	2138.13	1098.81	3462.22	-
1-Pentanol	3179.97	2149.66	1095.63	3467.15	-
1-Propanol	3166.77	2148.66	1112.14	3407.32	-
Acetic acid	3545.54	2245.76	-	3406.24	2139.70
Methanol	3213.43	2213.14	1177.42	3446.13	-
2,2,2-Trifluoroethanol	2659.69	3168.82	-	4566.56	2950.63

(b)

Solvent	Area Band 1 (cm^{-1})	Area Band 2 (cm^{-1})	Area Band 3 (cm^{-1})	Area Band 4 (cm^{-1})	Area Band 5 (cm^{-1})
Toluene	1962.25	1393.06	313.18	112.41	-
1,4-Dioxane	1963.04	1488.04	311.16	114.68	-
Chloroform	1909.83	1504.94	329.71	88.92	-
Acetonitrile	1945.19	1741.66	302.02	98.72	-
1-Octanol	1849.20	1672.94	315.64	131.64	-
1-Hexanol	1945.46	1596.90	323.34	213.18	-
1-Butanol	1827.69	1691.09	340.38	108.83	-
1-Pentanol	1821.61	1705.96	338.98	115.11	-
1-Propanol	1824.29	1720.40	342.83	103.87	-
Acetic acid	2405.16	1399.42	-	2625.76	1416.70
Methanol	1842.97	1773.27	362.69	121.57	-
2,2,2-Trifluoroethanol	283.09	3739.31	-	963.48	1196.67

Tables 4.3.3 (a) and (b). Summary band width and band area of 5 band fit using Gaussian model for normalised **25** emission spectra recorded at 310 nm excitation.

Solvent	Band 1 Area Percentage (%)	Band 2 Area Percentage(%)	Band 3 Area Percentage (%)	Band 4 Area Percentage(%)	Band 5 Area Percentage(%)
Toluene	51.90	36.84	8.28	2.97	-
1,4-Dioxane	50.63	38.38	8.03	2.96	-
Chloroform	49.82	39.26	8.60	2.32	-
Acetonitrile	47.59	42.61	7.39	2.42	-
1-Octanol	46.59	42.15	7.95	3.32	-
1-Hexanol	47.70	39.15	7.93	5.23	-
1-Butanol	46.06	42.62	8.58	2.74	-
1-Pentanol	45.75	42.85	8.51	2.89	-
1-Propanol	45.71	43.10	8.59	2.60	-
Acetic acid	30.65	17.83	-	33.46	18.05
Methanol	44.95	43.25	8.85	2.96	-
2,2,2-Trifluoroethanol	4.58	60.48	-	15.58	19.36

Table 4.3.4. Total Area Percentages of 5 band fit using Gaussian model for normalised **25** emission spectra recorded at 310 nm excitation.

Solvent	Area Ratio Band 1/2 (310 nm ex)	Area Ratio Band 1/3 (310 nm ex)	Area Ratio Band 1/4 (310 nm ex)	Area Ratio Band 1/5 (310 nm ex)
Toluene	1.41	6.27	17.46	-
1,4-Dioxane	1.32	6.31	17.12	-
Chloroform	1.27	5.79	21.48	-
Acetonitrile	1.12	6.44	19.70	-
1-Octanol	1.11	5.86	14.05	-
1-Hexanol	1.22	6.02	9.13	-
1-Butanol	1.08	5.37	16.79	-
1-Pentanol	1.07	5.37	15.83	-
1-Propanol	1.06	5.32	17.56	-
Acetic acid	1.72	-	0.92	1.70
Methanol	1.04	5.08	15.16	-
2,2,2-Trifluoroethanol	0.08	-	0.29	0.24

Solvent	Area Ratio Band 2/3 (310 nm ex)	Area Ratio Band 2/4 (310 nm ex)	Area Ratio Band 2/5 (310 nm ex)	Area Ratio Band 3/4 (310 nm ex)	Area Ratio Band 3/5 (310 nm ex)	Area Ratio Band 4/5 (310 nm ex)
Toluene	4.45	12.39	-	2.79	-	-
1,4-Dioxane	4.78	12.98	-	2.71	-	-
Chloroform	4.56	16.92	-	3.71	-	-
Acetonitrile	5.77	17.64	-	3.06	-	-
1-Octanol	5.30	12.71	-	2.40	-	-
1-Hexanol	4.94	7.49	-	1.52	-	-
1-Butanol	4.97	15.54	-	3.13	-	-
1-Pentanol	5.03	14.82	-	2.94	-	-
1-Propanol	5.02	16.56	-	3.30	-	-
Acetic acid	-	0.53	0.99	-	-	1.85
Methanol	4.89	14.59	-	2.98	-	-
2,2,2-Trifluoroethanol	-	3.88	3.12	-	-	0.81

Table 4.3.5. Area Ratios of 5 band fit using Gaussian model for normalised **25** emission spectra recorded at 310 nm excitation.

4.3.3 400 nm excitation Gaussian band fit summaries.

Solvent	λ max$_{em}$ Band 1 (cm^{-1})	λ max$_{em}$ Band 1 (nm)	λ max$_{em}$ Band 2 (cm^{-1})	λ max$_{em}$ Band 2 (nm)	λmax$_{em}$ Band 3 (cm^{-1})	λmax$_{em}$ Band 3 (nm)
Toluene	18609.51	537.36	19798.73	505.08	21067.23	474.67
1,4-Dioxane	18536.93	539.46	19819.32	504.56	21082.91	474.32
Chloroform	18629.42	536.79	19678.65	508.17	20906.53	478.32
Acetonitrile	18308.22	546.20	19606.62	510.03	20875.56	479.03
1-Octanol	18475.45	541.26	19777.73	505.62	21057.82	474.88
1-Hexanol	18423.36	542.79	19729.66	506.85	20992.54	476.36
1-Butanol	18428.67	542.63	19729.59	506.85	20959.90	477.10
1-Pentanol	18437.98	542.36	19751.28	506.30	20992.10	476.37
1-Propanol	18415.59	543.02	19728.16	506.89	20948.61	477.36
Acetic acid	18239.00	548.28	19828.29	504.33	20933.92	477.69
Methanol	18369.33	544.39	19673.93	508.29	20869.17	479.18
2,2,2-Trifluoroethanol	18720.90	534.16	19133.41	522.65	20531.85	487.05

Table 4.3.6. Summary of band maxima of 3 band fit using Gaussian model for normalised **25** emission spectra recorded at 400 nm excitation.

Solvent	Width Band 1 (cm^{-1})	Width Band 2 (cm^{-1})	Width Band 3 (cm^{-1})
Toluene	3102.68	1993.24	1008.90
1,4-Dioxane	3118.47	2106.92	1033.35
Chloroform	3216.02	2013.54	1059.66
Acetonitrile	3203.73	2207.96	1276.91
1-Octanol	3161.45	2123.43	1079.26
1-Hexanol	3177.75	2155.30	1146.58
1-Butanol	3133.07	2112.82	1154.59
1-Pentanol	3144.71	2133.73	1123.06
1-Propanol	3126.08	2118.04	1163.79
Acetic acid	3498.29	2435.73	1246.47
Methanol	3151.50	2120.26	1246.19
2,2,2-Trifluoroethanol	3857.85	1736.25	1093.22

Table 4.3.7. Summary of band width of 3 band fit using Gaussian model for normalised **25** emission spectra recorded at 400 nm excitation.

Solvent	Area Band 1 (cm^{-1})	Area Band 2 (cm^{-1})	Area Band 3 (cm^{-1})	Area Ratio Band 1/2 (400 nm ex)	Area Ratio Band 1/3 (400 nm ex)	Area Ratio Band 2/3 (400 nm ex)
Toluene	1783.27	1566.19	360.81	1.14	4.94	4.34
1,4-Dioxane	1692.53	1731.22	332.28	0.98	5.09	5.21
Chloroform	1934.60	1455.67	373.40	1.33	5.18	3.90
Acetonitrile	1717.30	1775.06	447.94	0.97	3.83	3.96
1-Octanol	1698.09	1759.92	392.96	0.96	4.32	4.48
1-Hexanol	1633.29	1807.12	420.76	0.90	3.88	4.29
1-Butanol	1608.41	1758.04	450.74	0.91	3.57	3.90
1-Pentanol	1637.02	1782.23	406.39	0.92	4.03	4.39
1-Propanol	1588.91	1776.68	448.49	0.89	3.54	3.96
Acetic acid	1408.40	2043.57	362.01	0.69	3.89	5.65
Methanol	1586.62	1739.19	504.69	0.91	3.14	3.45
2,2,2-Trifluoroethanol	2798.26	680.95	324.52	4.11	8.62	2.10

Solvent	Band 1 Area Percentage (%)	Band 2 Area Percentage (%)	Band 3 Area Percentage (%)
Toluene	48.06	42.21	9.72
1,4-Dioxane	45.06	46.09	8.85
Chloroform	51.40	38.68	9.92
Acetonitrile	43.58	45.05	11.37
1-Octanol	44.10	45.70	10.20
1-Hexanol	42.30	46.80	10.90
1-Butanol	42.14	46.06	11.81
1-Pentanol	42.79	46.59	10.62
1-Propanol	41.66	46.58	11.76
Acetic acid	36.93	53.58	9.49
Methanol	41.42	45.40	13.18
2,2,2-Trifluoroethanol	73.57	17.90	8.53

Table 4.3.8. Band areas, area ratios and total area percentage of 3 band fit using Gaussian model for normalised **25** emission spectra recorded at 400 nm excitation.

4.3.4 310 nm Gaussian band fit - Solvatochromic analysis.

4.3.4.1 E_T^N.

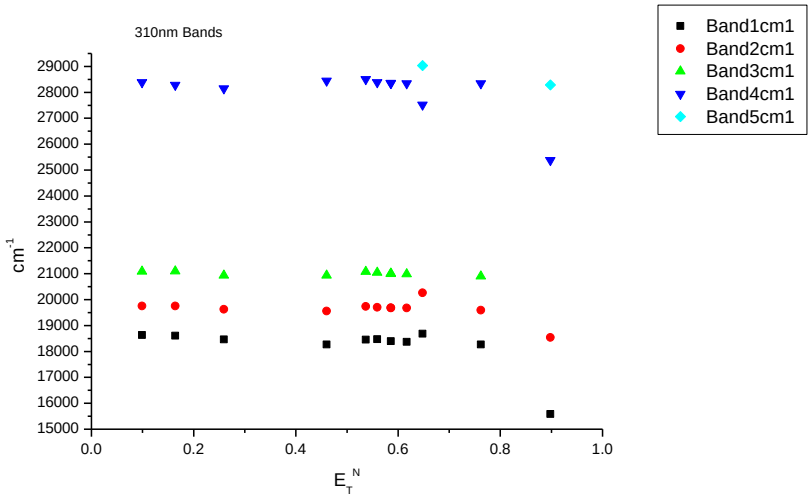

Figure 4.3.1. Band maxima from Gaussian model fit of the normalised fluorescence emission spectra of **25** recorded at 310 nm excitation against E_T^N.

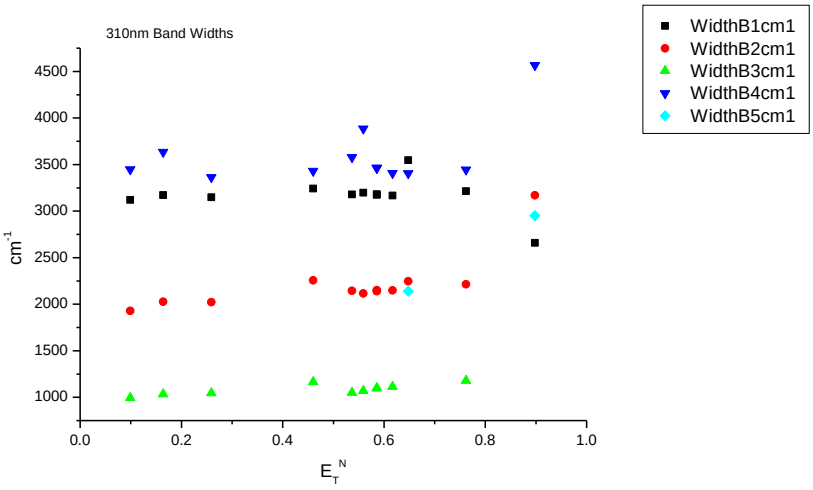

Figure 4.3.2. Band widths from Gaussian model fit of the normalised fluorescence emission spectra of **25** recorded at 310 nm excitation against E_T^N.

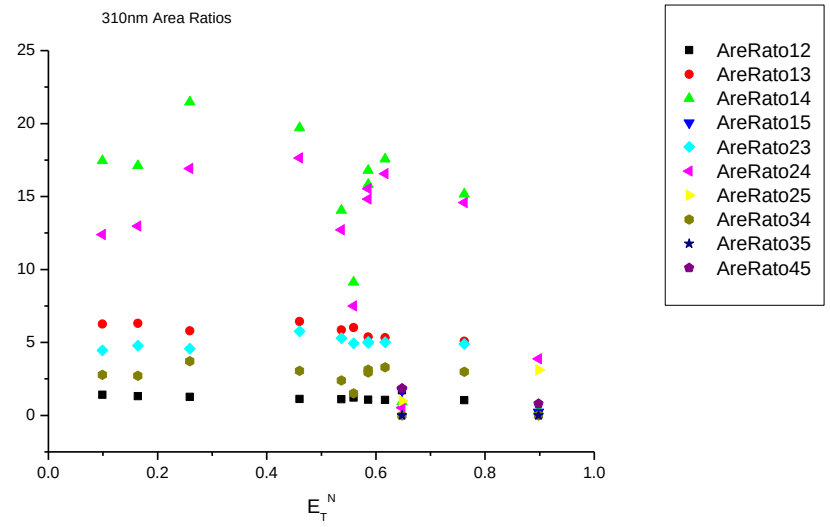

Figure 4.3.3. Area ratios from Gaussian model fit of the normalised fluorescence emission spectra of **25** recorded at 310 nm excitation against E_T^N.

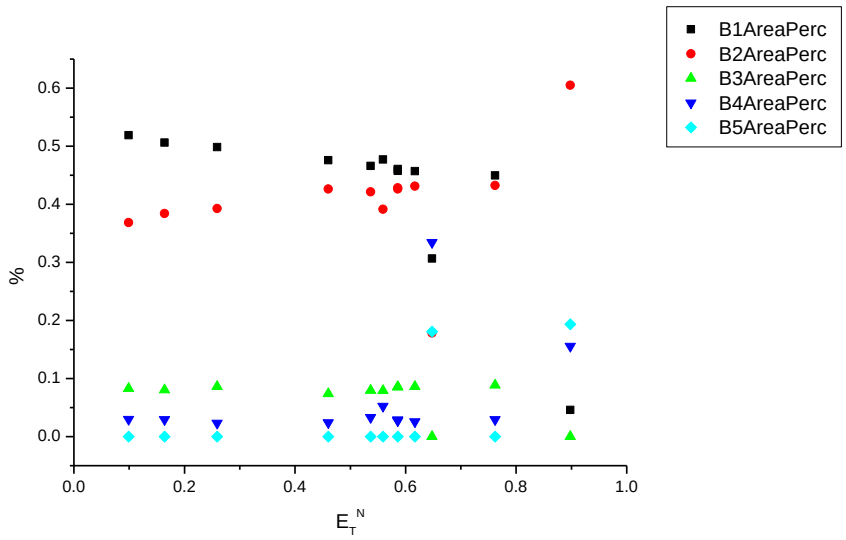

Figure 4.3.4. Area percentages from Gaussian model fit of the normalised fluorescence emission spectra of **25** recorded at 310 nm excitation against E_T^N.

4.3.4.2 α

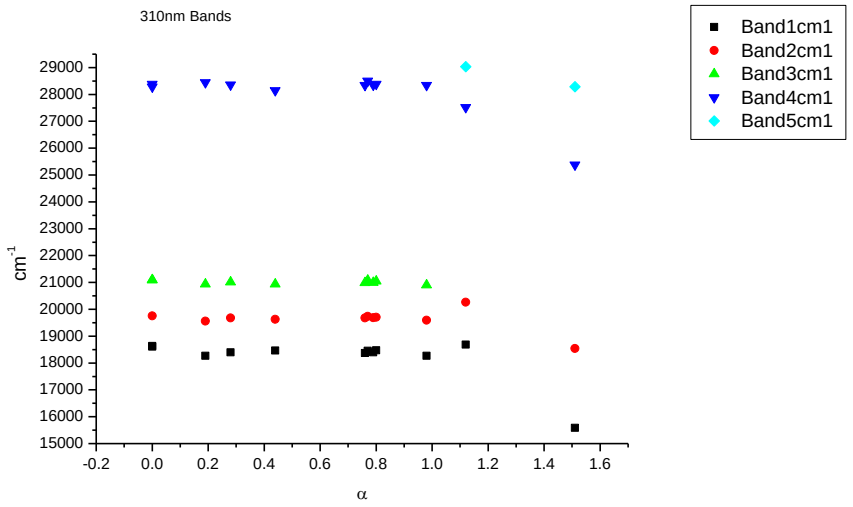

Figure 4.3.5. Band maxima from Gaussian model fit of the normalised fluorescence emission spectra of **25** recorded at 310 nm excitation against α.

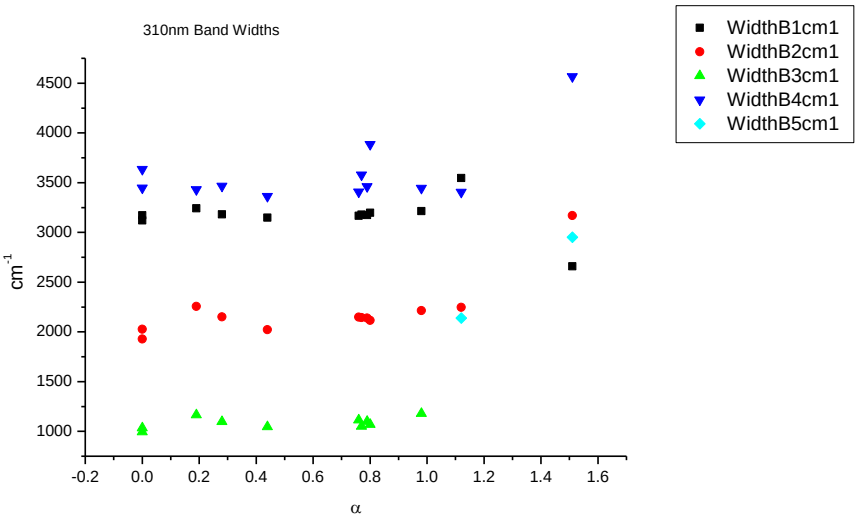

Figure 4.3.6. Band widths from Gaussian model fit of the normalised fluorescence emission spectra of **25** recorded at 310 nm excitation against α.

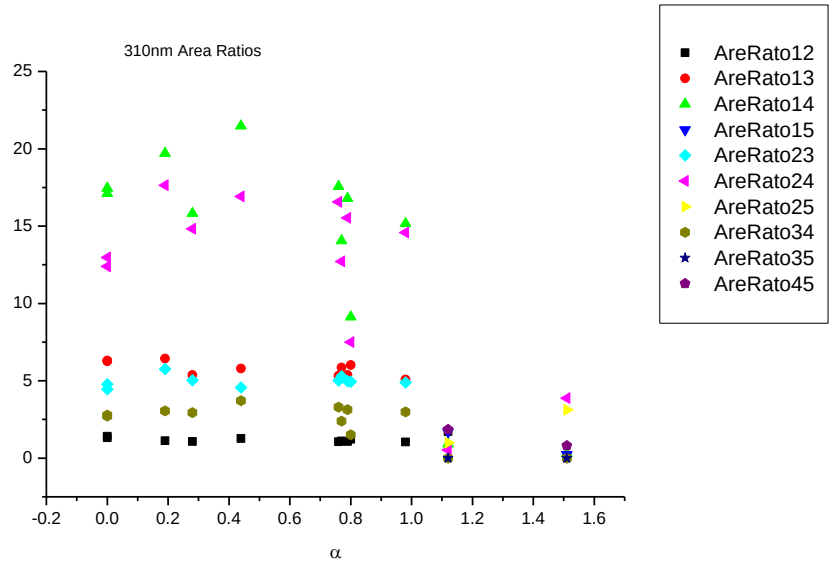

Figure 4.3.7. Area Ratios from Gaussian model fit of the normalised fluorescence emission spectra of **25** recorded at 310 nm excitation against α.

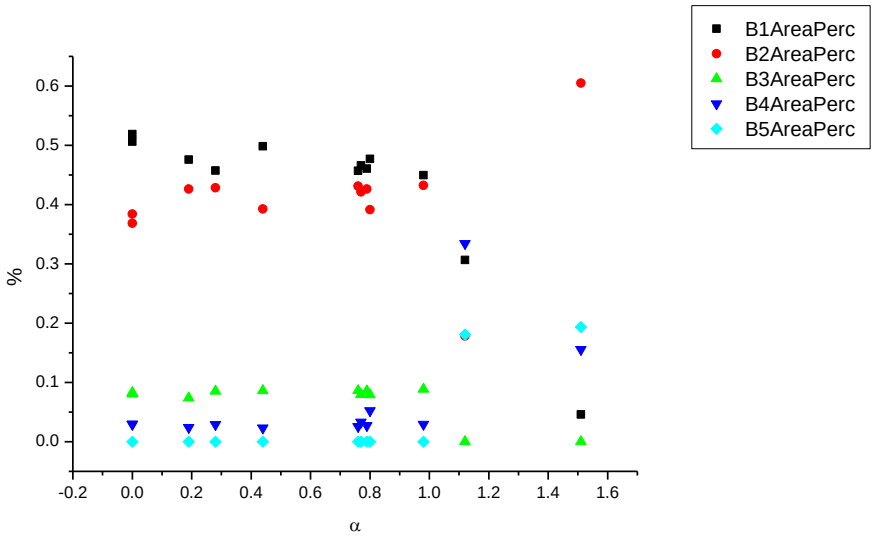

Figure 4.3.8. Area percentages from Gaussian model fit of the normalised fluorescence emission spectra of **25** recorded at 310 nm excitation against α.

4.3.4.3 β.

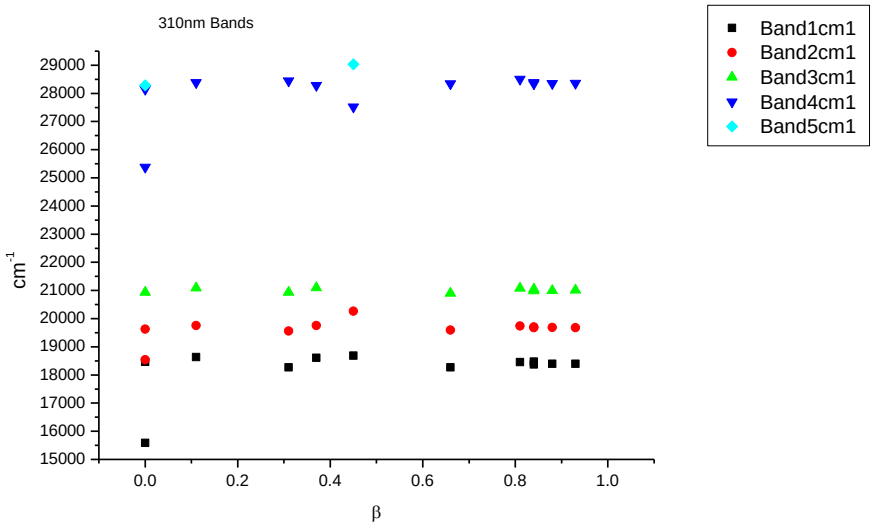

Figure 4.3.9. Band maxima from Gaussian model fit of the normalised fluorescence emission spectra of **25** recorded at 310 nm excitation against β.

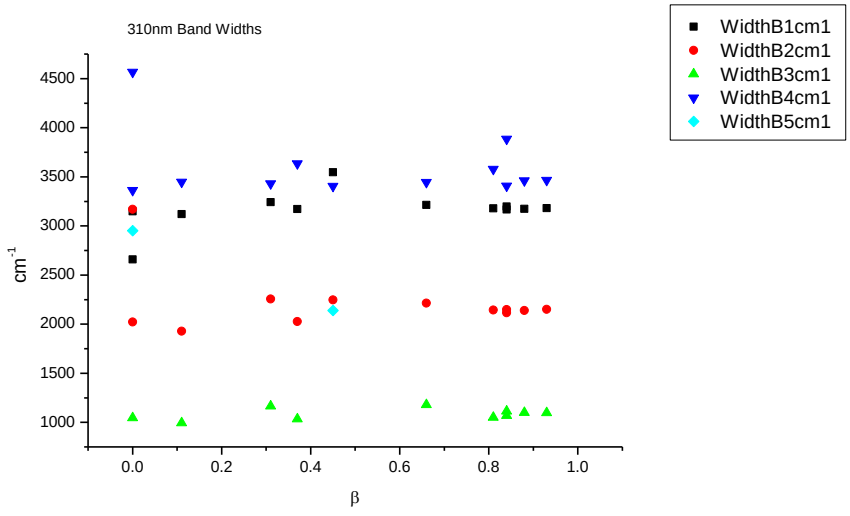

Figure 4.3.10. Band widths from Gaussian model fit of the normalised fluorescence emission spectra of **25** recorded at 310 nm excitation against β.

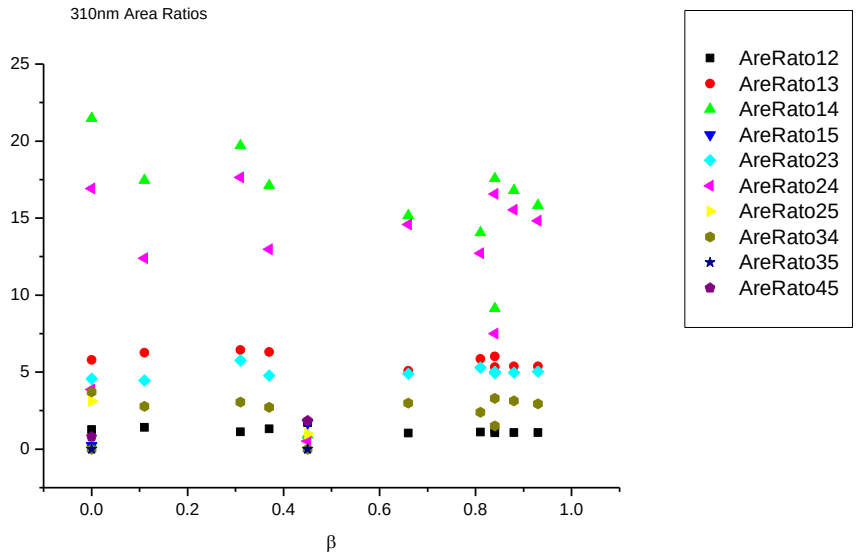

Figure 4.3.11. Area ratios from Gaussian model fit of the normalised fluorescence emission spectra of **25** recorded at 310 nm excitation against β.

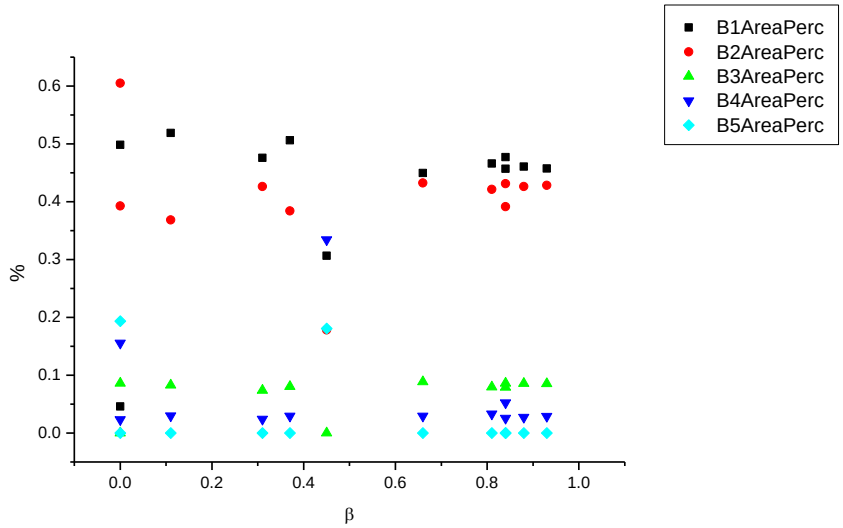

Figure 4.3.12. Area percentages from Gaussian model fit of the normalised fluorescence emission spectra of **25** recorded at 310 nm excitation against β.

4.3.4.4 π.*

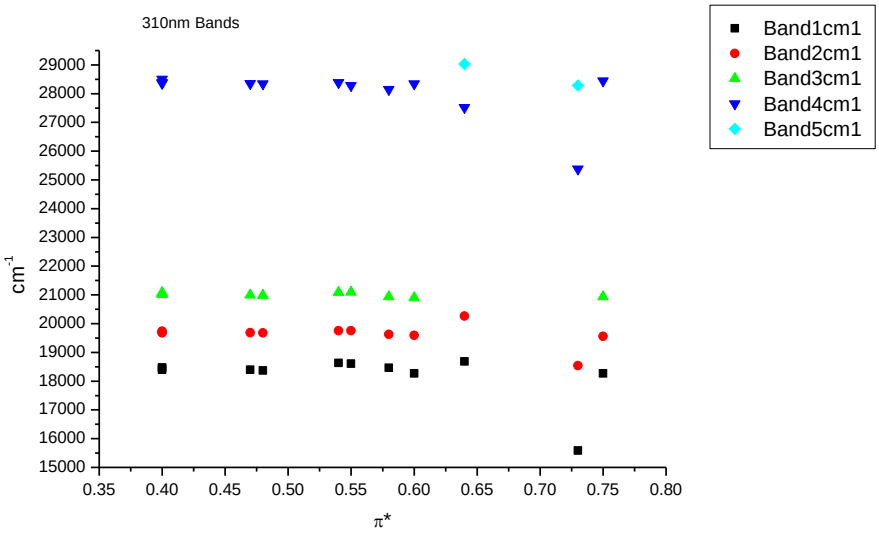

Figure 4.3.13. Band maxima from Gaussian model fit of the normalised fluorescence emission spectra of **25** recorded at 310 nm excitation against π*.

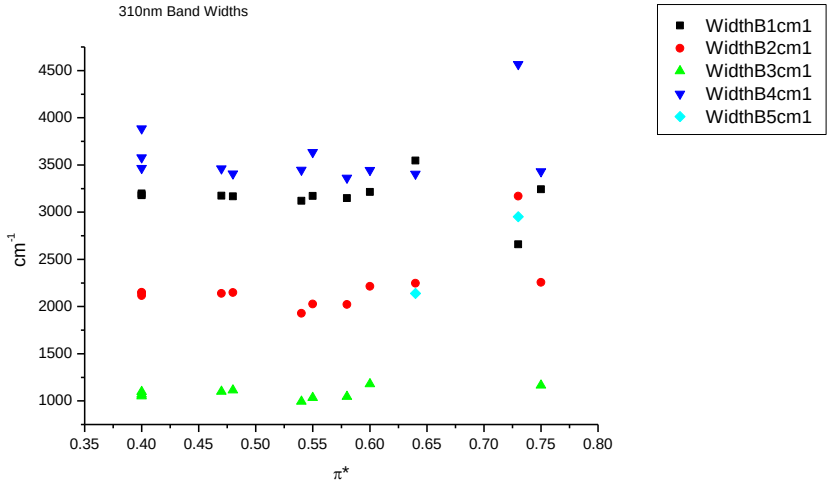

Figure 4.3.14. Band widths from Gaussian model fit of the normalised fluorescence emission spectra of **25** recorded at 310 nm excitation against π*.

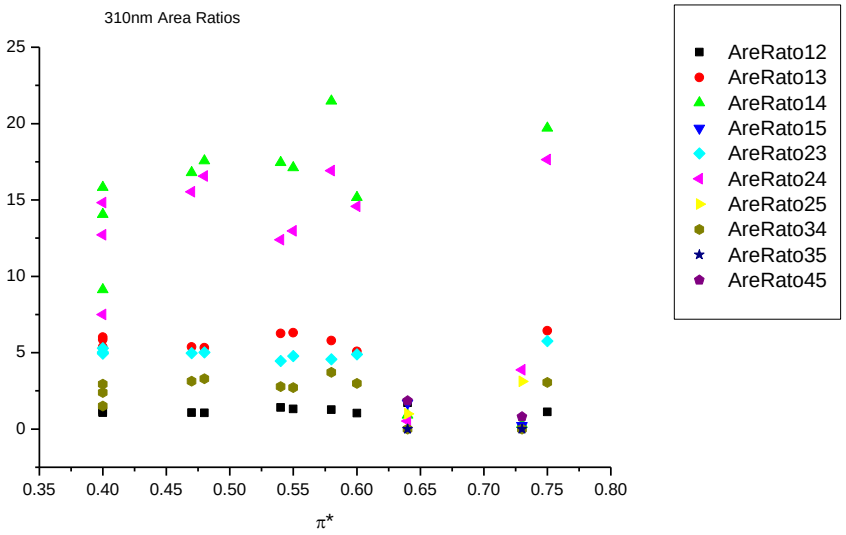

Figure 4.3.15. Area ratios from Gaussian model fit of the normalised fluorescence emission spectra of **25** recorded at 310 nm excitation against π*.

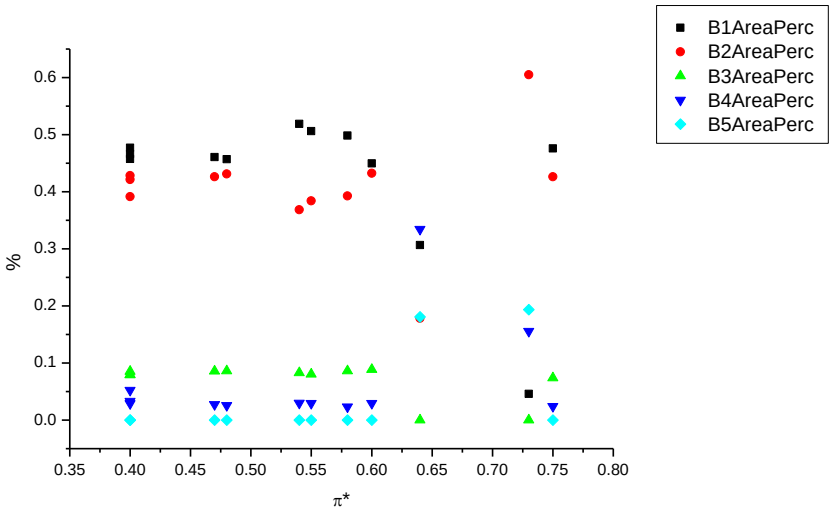

Figure 4.3.16. Area percentages from Gaussian model fit of the normalised fluorescence emission spectra of **25** recorded at 310 nm excitation against π*.

4.3.4.5 μ(D).

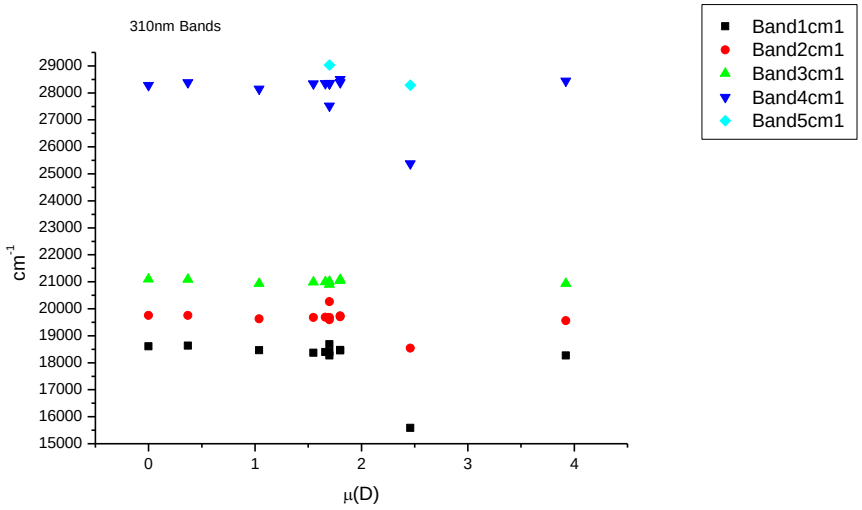

Figure 4.3.17. Band maxima from Gaussian model fit of the normalised fluorescence emission spectra of **25** recorded at 310 nm excitation against μ(D).

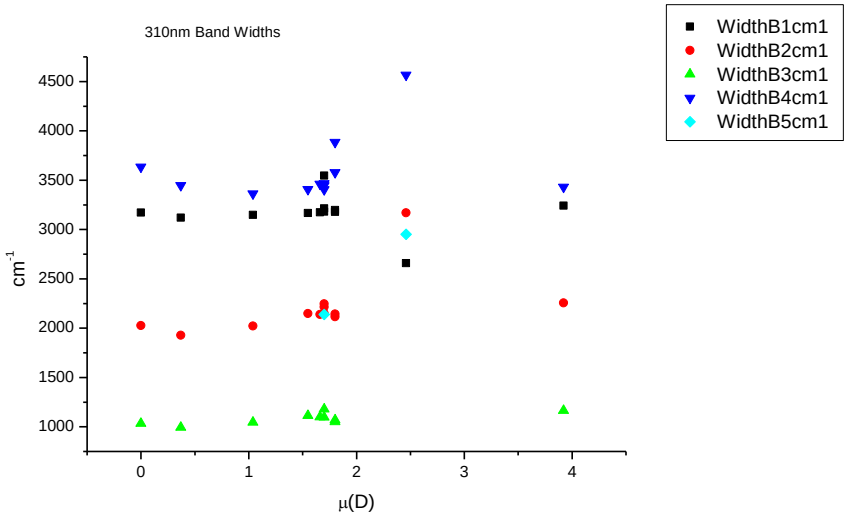

Figure 4.3.18. Band widths from Gaussian model fit of the normalised fluorescence emission spectra of **25** recorded at 310 nm excitation against μ(D).

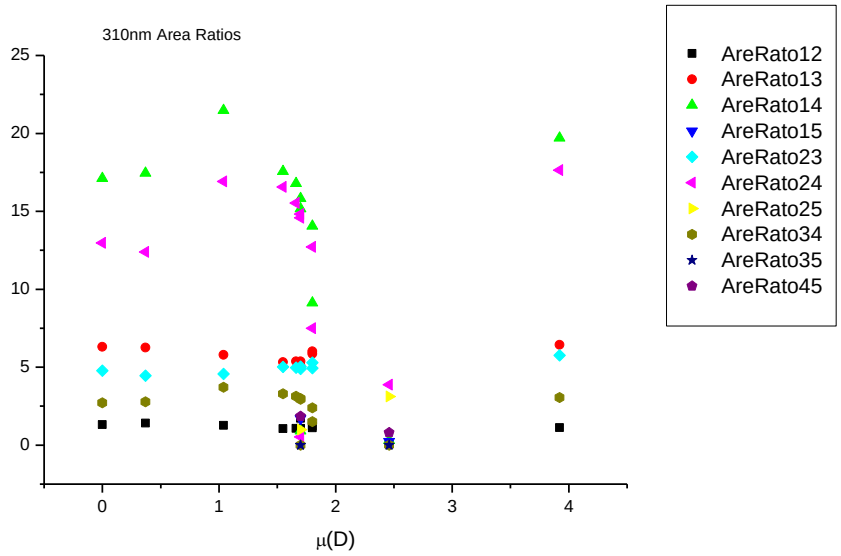

Figure 4.3.19. Area ratios from Gaussian model fit of the normalised fluorescence emission spectra of **25** recorded at 310 nm excitation against μ(D).

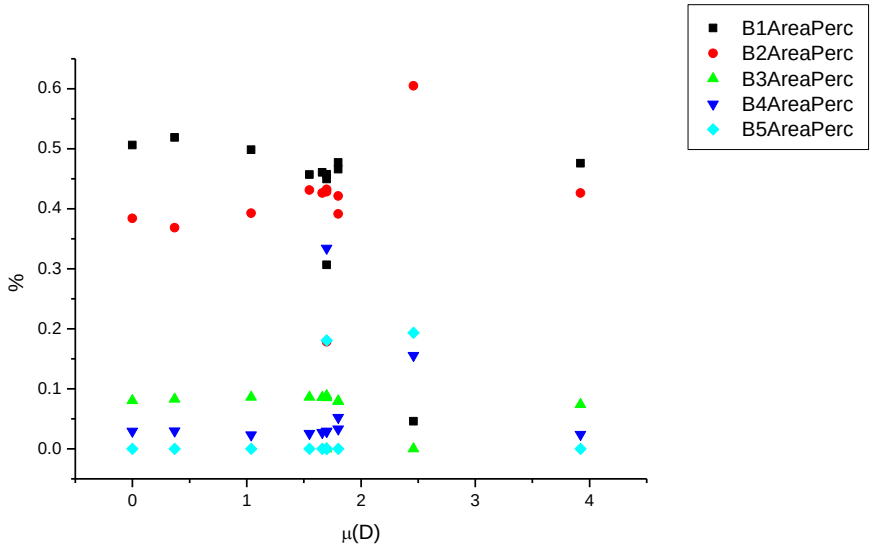

Figure 4.3.20. Area percentages from Gaussian model fit of the normalised fluorescence emission spectra of **25** recorded at 310 nm excitation against μ(D).

4.3.4.6 η(Cp).

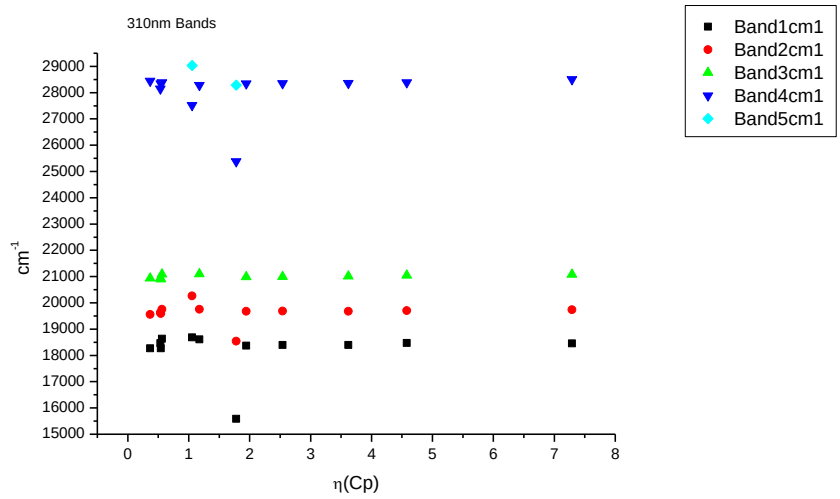

Figure 4.3.21. Band maxima from Gaussian model fit of the normalised fluorescence emission spectra of **25** recorded at 310 nm excitation against η(Cp).

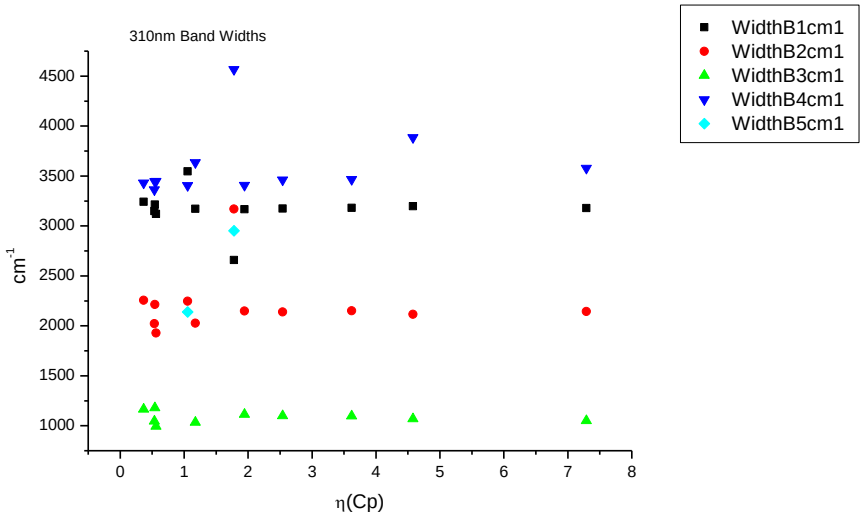

Figure 4.3.22. Band widths from Gaussian model fit of the normalised fluorescence emission spectra of **25** recorded at 310 nm excitation against η(Cp).

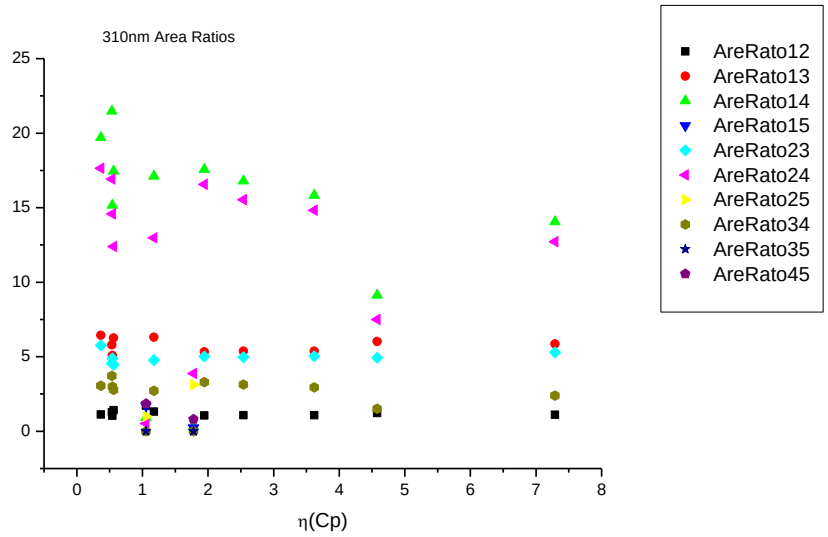

Figure 4.3.23. Area ratios from Gaussian model fit of the normalised fluorescence emission spectra of **25** recorded at 310 nm excitation against η(Cp).

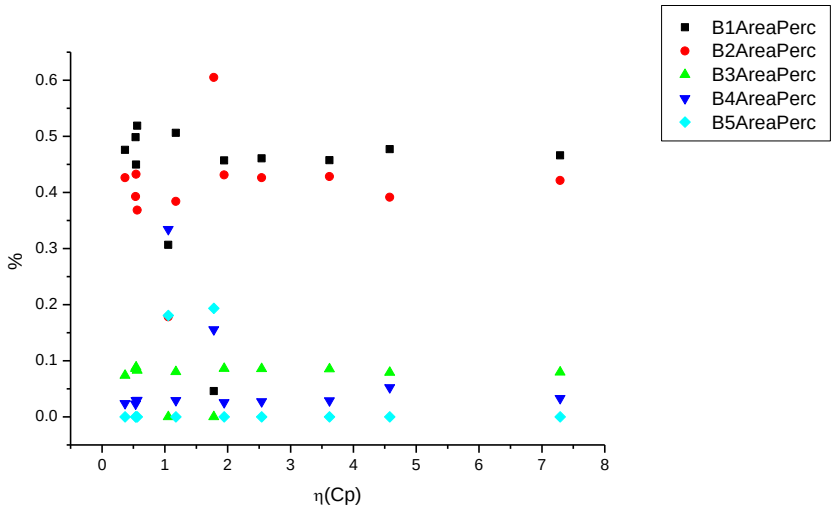

Figure 4.3.24. Area percentages from Gaussian model fit of the normalised fluorescence emission spectra of **25** recorded at 310 nm excitation against η(Cp).

4.3.5 400 nm Gaussian band fit - Solvatochromic analysis.

4.3.5.1 E_T^N.

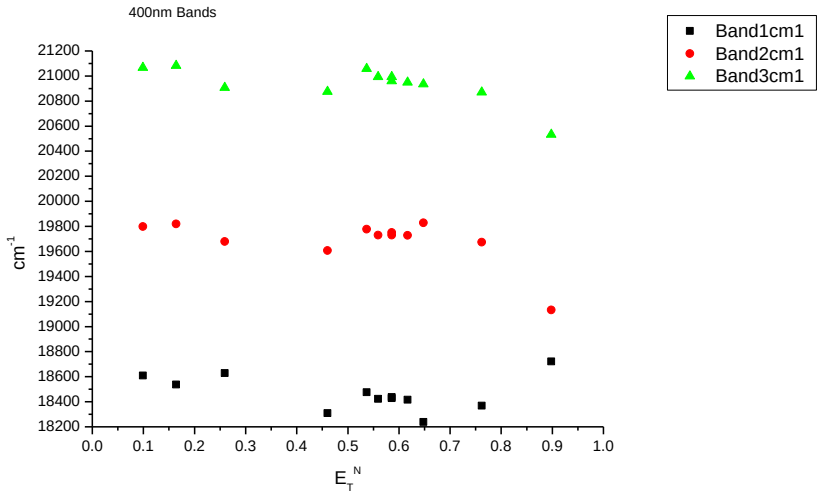

Figure 4.3.25. Band maxima from Gaussian model fit of the normalised fluorescence emission spectra of **25** recorded at 400 nm excitation against E_T^N.

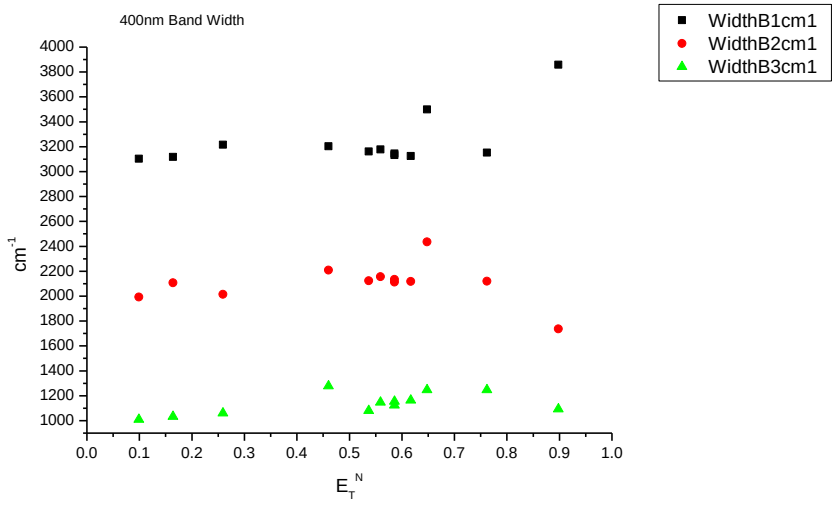

Figure 4.3.26. Band widths from Gaussian model fit of the normalised fluorescence emission spectra of **25** recorded at 400 nm excitation against E_T^N.

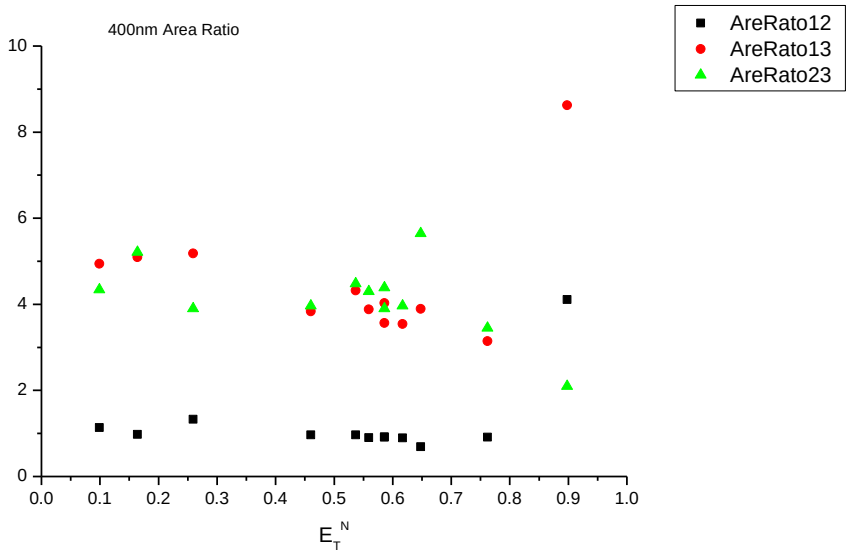

Figure 4.3.27. Area ratios from Gaussian model fit of the normalised fluorescence emission spectra of **25** recorded at 400 nm excitation against E_T^N.

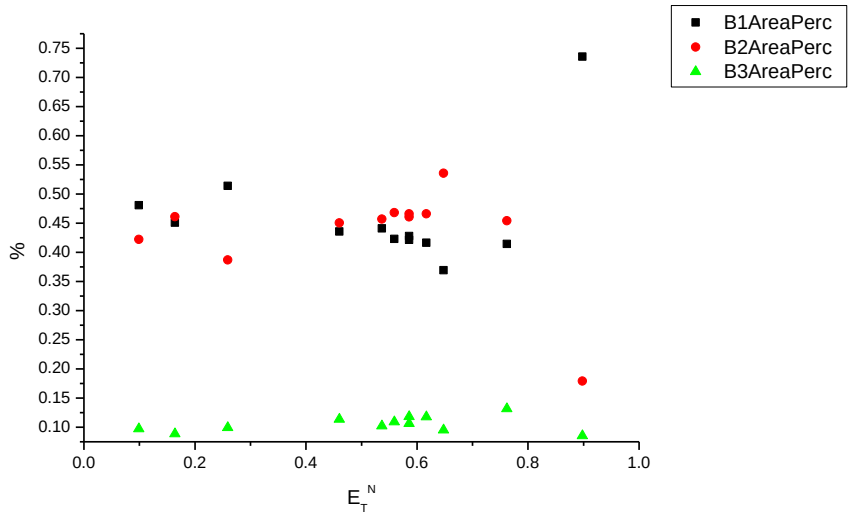

Figure 4.3.28. Area percentages from Gaussian model fit of the normalised fluorescence emission spectra of **25** recorded at 400 nm excitation against E_T^N.

4.3.5.2 α

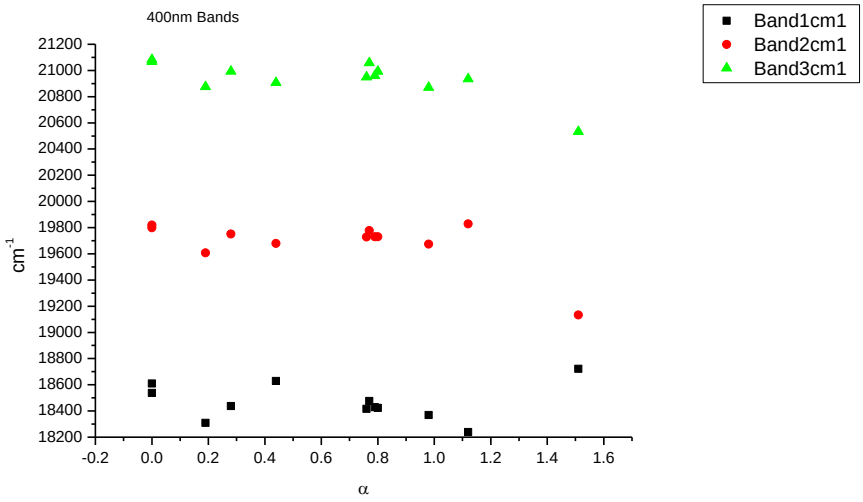

Figure 4.3.29. Band maxima from Gaussian model fit of the normalised fluorescence emission spectra of **25** recorded at 400 nm excitation against α.

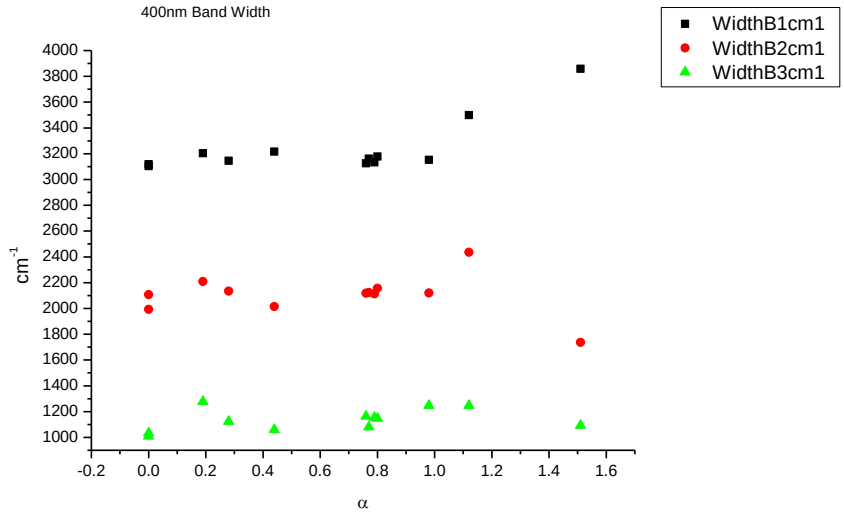

Figure 4.3.30. Band widths from Gaussian model fit of the normalised fluorescence emission spectra of **25** recorded at 400 nm excitation against α.

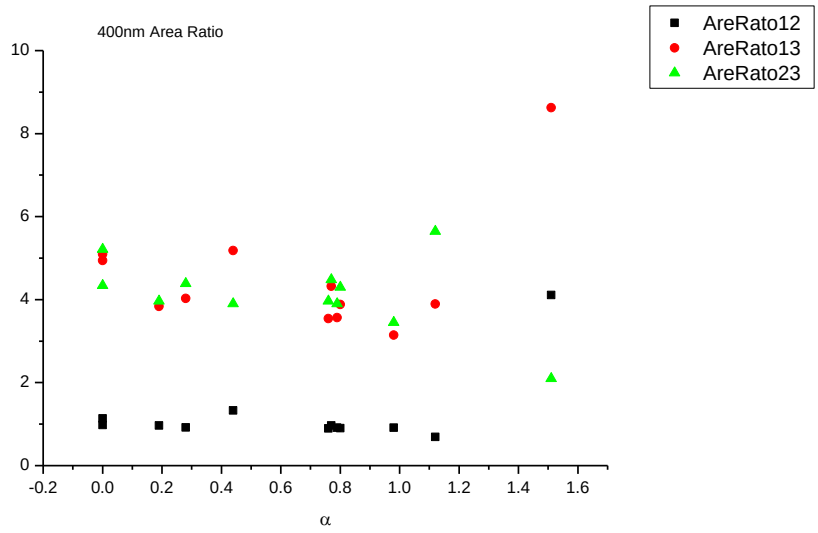

Figure 4.3.31. Area ratios from Gaussian model fit of the normalised fluorescence emission spectra of **25** recorded at 400 nm excitation against α.

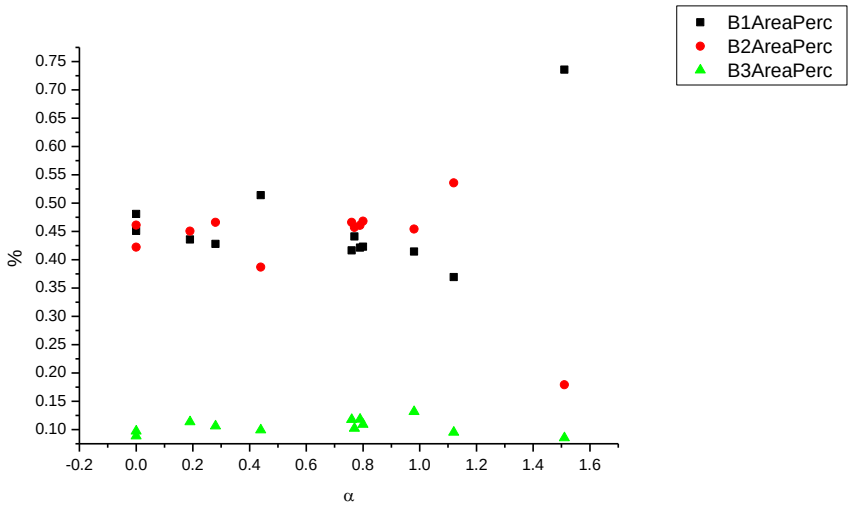

Figure 4.3.32. Area percentages from Gaussian model fit of the normalised fluorescence emission spectra of **25** recorded at 400 nm excitation against α.

4.3.5.3 β.

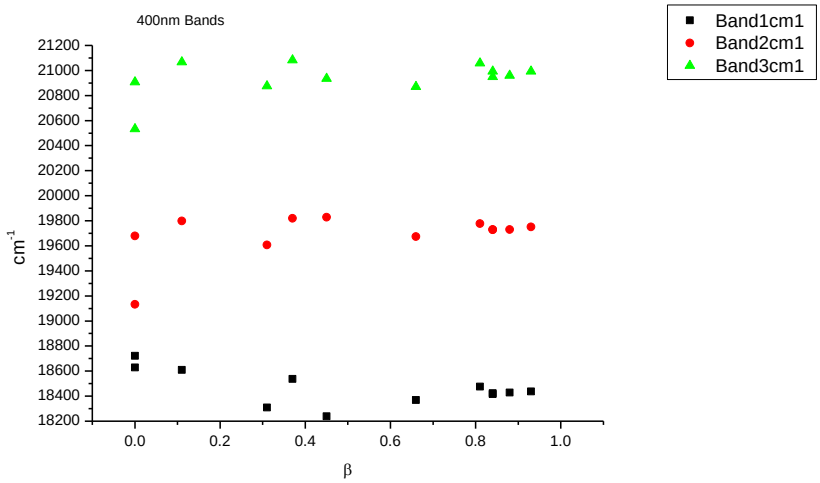

Figure 4.3.33. Band maxima from Gaussian model fit of the normalised fluorescence emission spectra of **25** recorded at 400 nm excitation against β.

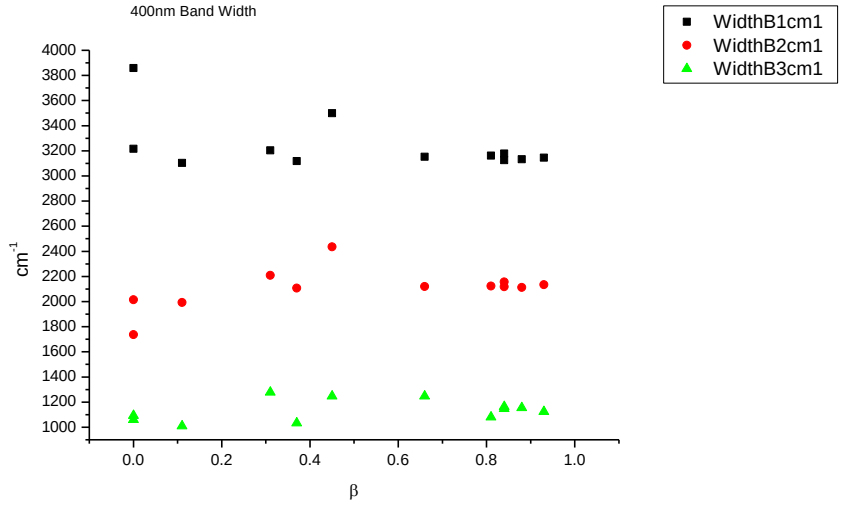

Figure 4.3.34. Band widths from Gaussian model fit of the normalised fluorescence emission spectra of **25** recorded at 400 nm excitation against β.

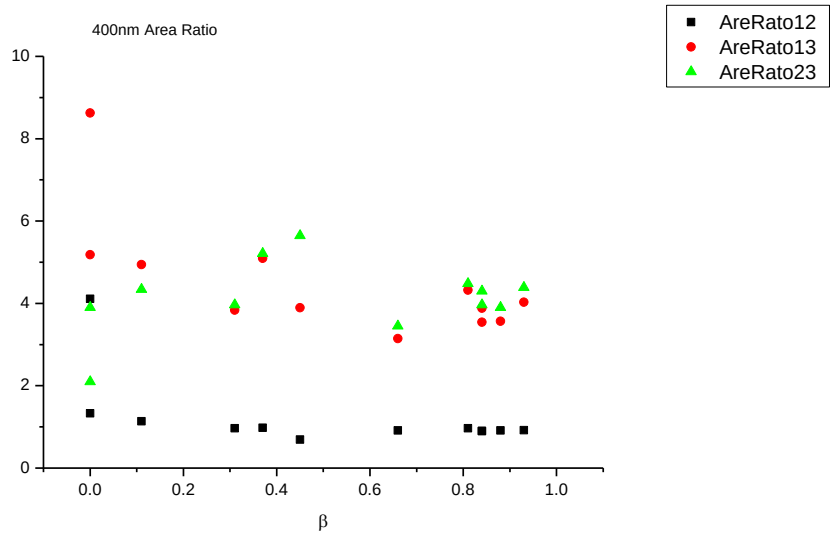

Figure 4.3.35. Area ratios from Gaussian model fit of the normalised fluorescence emission spectra of **25** recorded at 400 nm excitation against β.

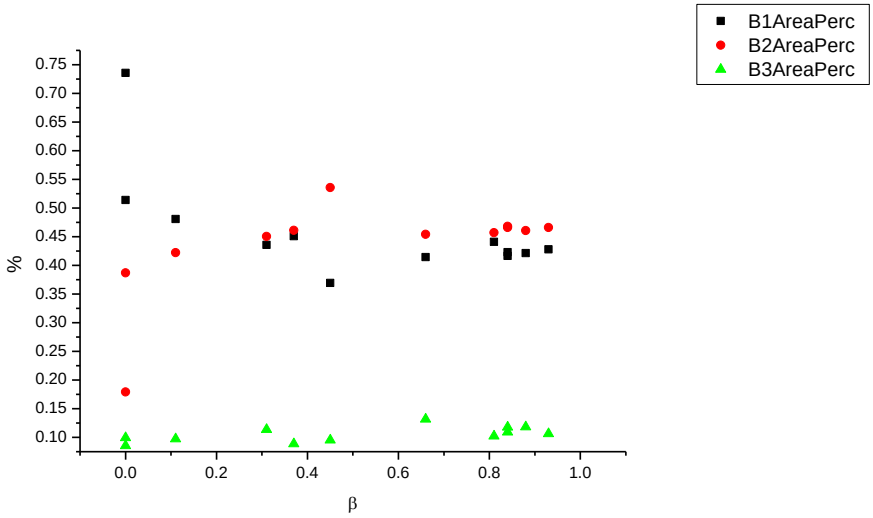

Figure 4.3.36. Area percentages from Gaussian model fit of the normalised fluorescence emission spectra of **25** recorded at 400 nm excitation against β.

4.3.5.4 π.*

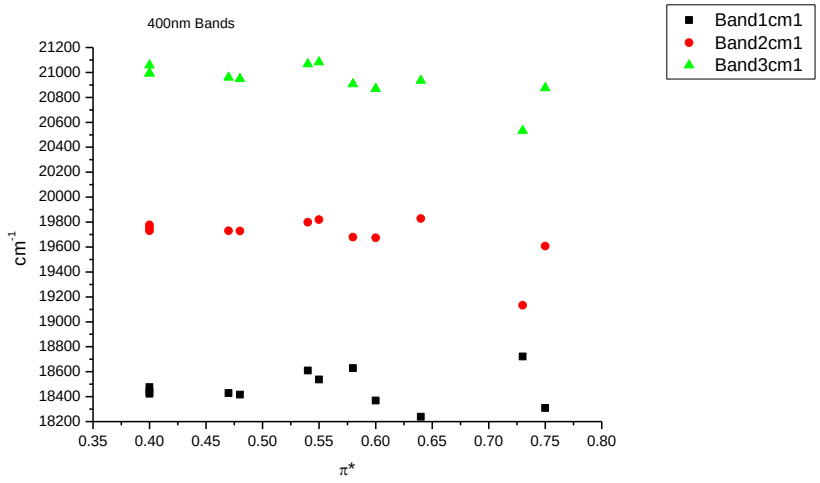

Figure 4.3.37. Band maxima from Gaussian model fit of the normalised fluorescence emission spectra of **25** recorded at 400 nm excitation against π*.

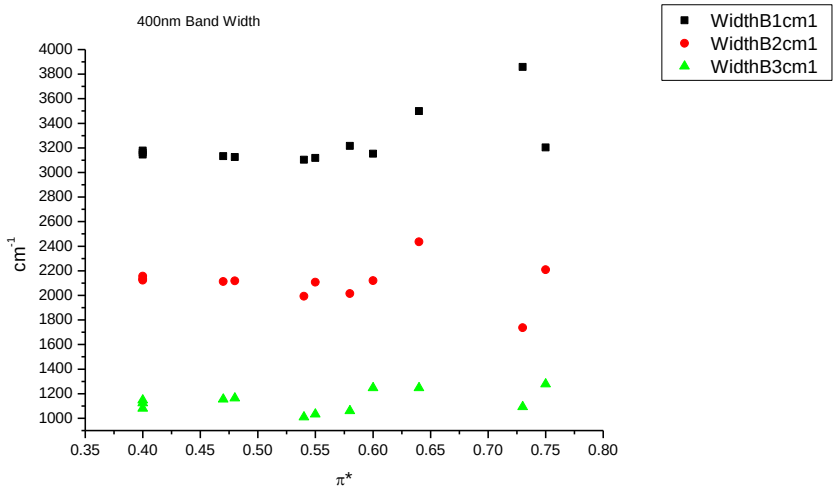

Figure 4.3.38. Band widths from Gaussian model fit of the normalised fluorescence emission spectra of **25** recorded at 400 nm excitation against π*.

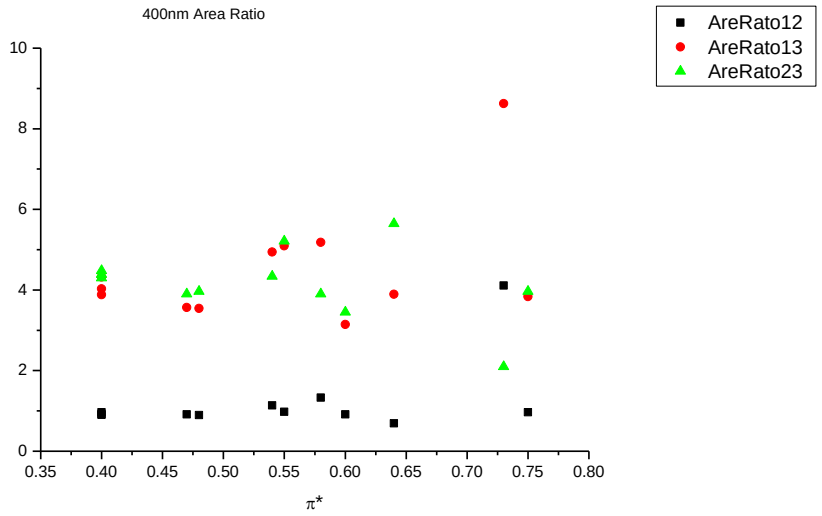

Figure 4.3.39. Area ratios from Gaussian model fit of the normalised fluorescence emission spectra of **25** recorded at 400 nm excitation against π*.

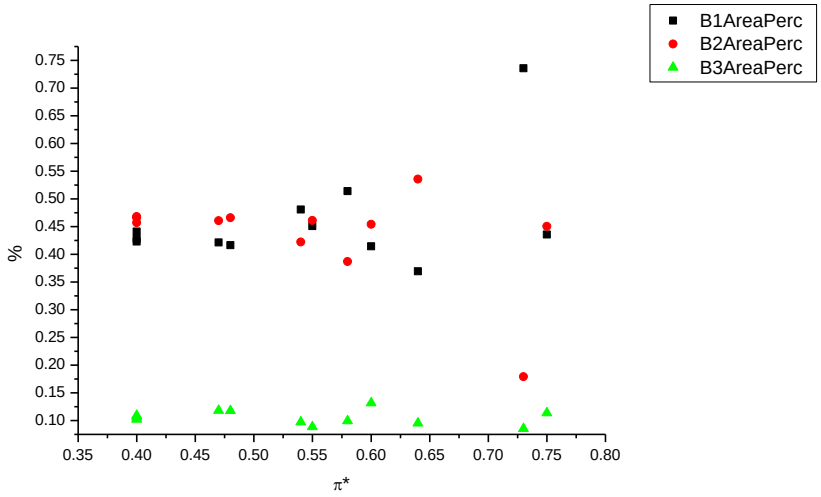

Figure 4.3.40. Area percentages from Gaussian model fit of the normalised fluorescence emission spectra of **25** recorded at 400 nm excitation against π*.

4.3.5.5 μ(D).

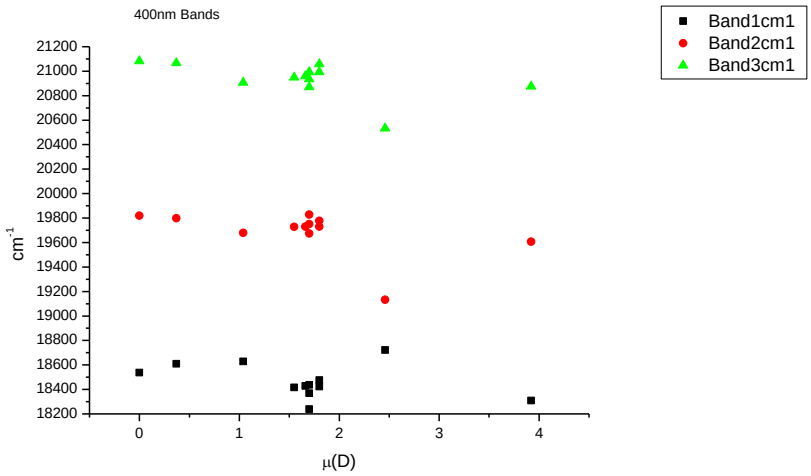

Figure 4.3.41. Band maxima from Gaussian model fit of the normalised fluorescence emission spectra of **25** recorded at 400 nm excitation against μ(D).

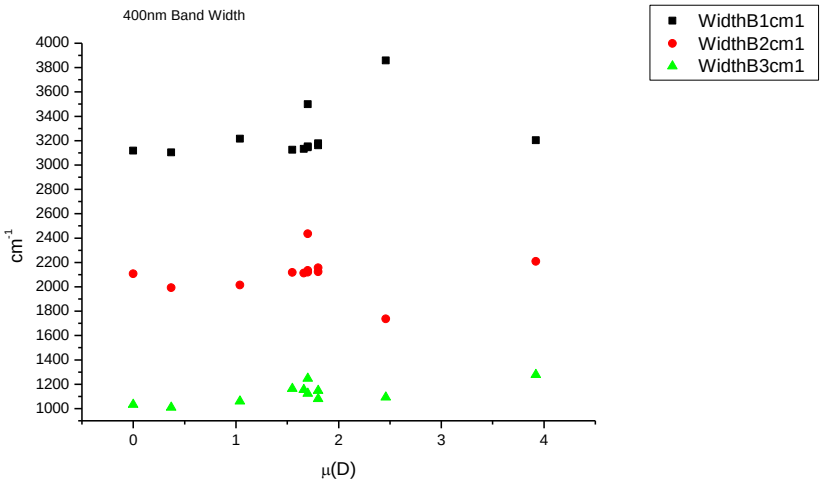

Figure 4.3.42. Band widths from Gaussian model fit of the normalised fluorescence emission spectra of **25** recorded at 400 nm excitation against μ(D).

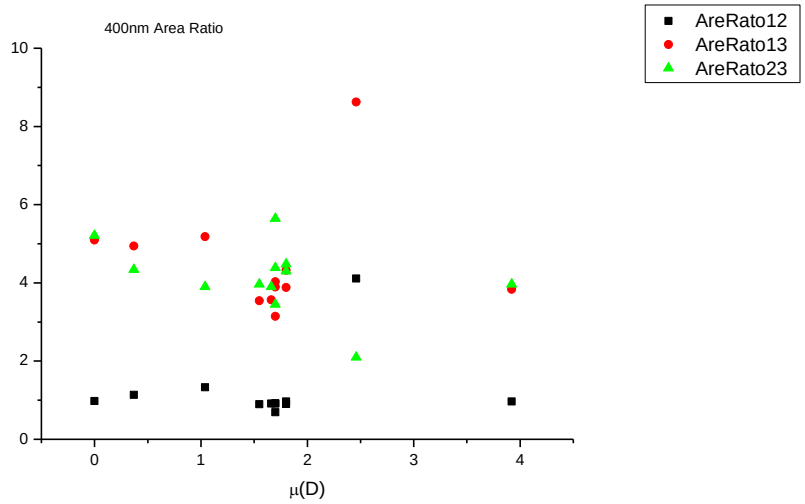

Figure 4.3.43. Area ratios from Gaussian model fit of the normalised fluorescence emission spectra of **25** recorded at 400 nm excitation against μ(D).

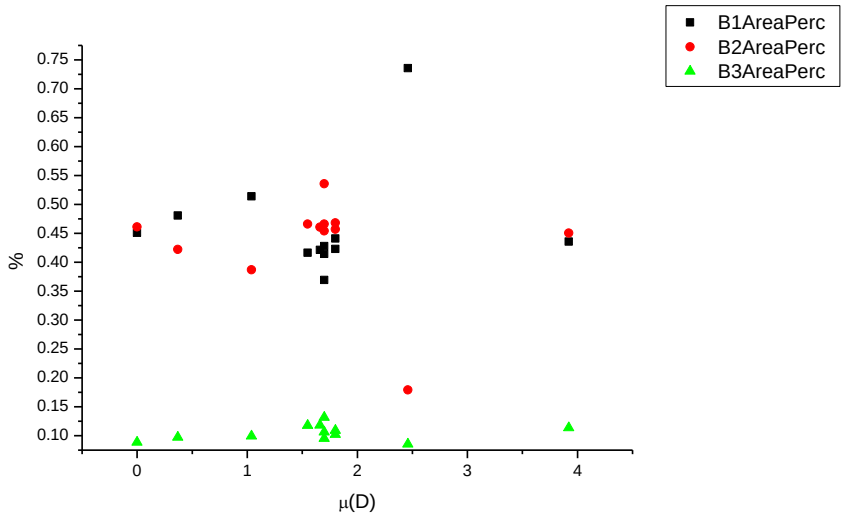

Figure 4.3.44. Area percentages from Gaussian model fit of the normalised fluorescence emission spectra of **25** recorded at 400 nm excitation against μ(D).

4.3.5.6 η(Cp).

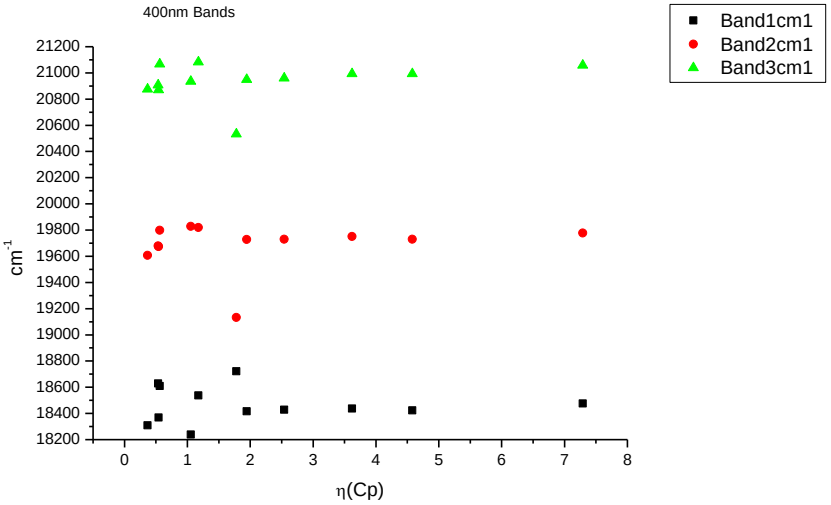

Figure 4.3.45. Band maxima from Gaussian model fit of the normalised fluorescence emission spectra of **25** recorded at 400 nm excitation against η(Cp).

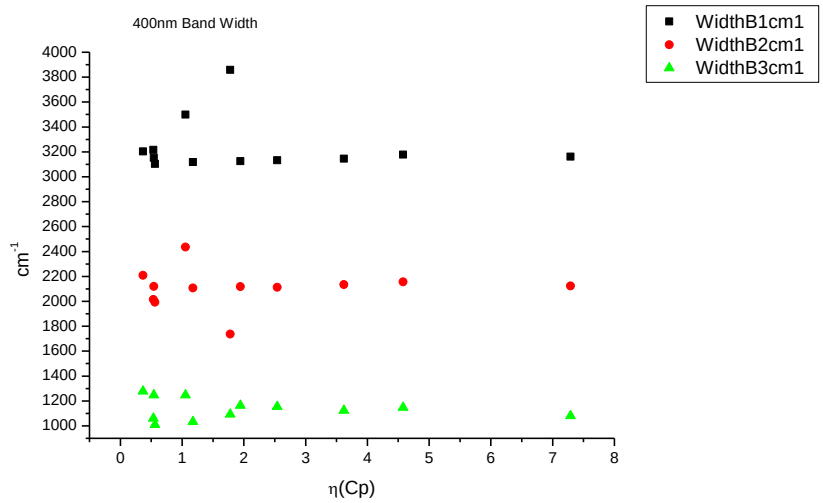

Figure 4.3.46. Band widths from Gaussian model fit of the normalised fluorescence emission spectra of **25** recorded at 400 nm excitation against η(Cp).

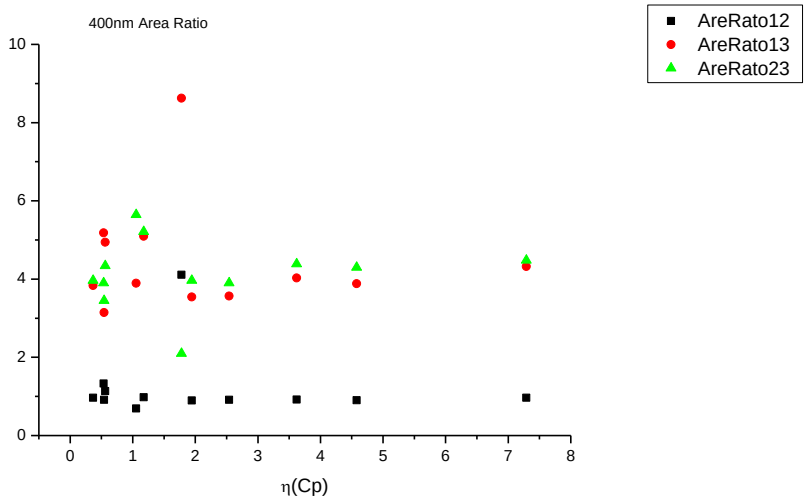

Figure 4.3.47. Area ratios from Gaussian model fit of the normalised fluorescence emission spectra of **25** recorded at 400 nm excitation against η(Cp).

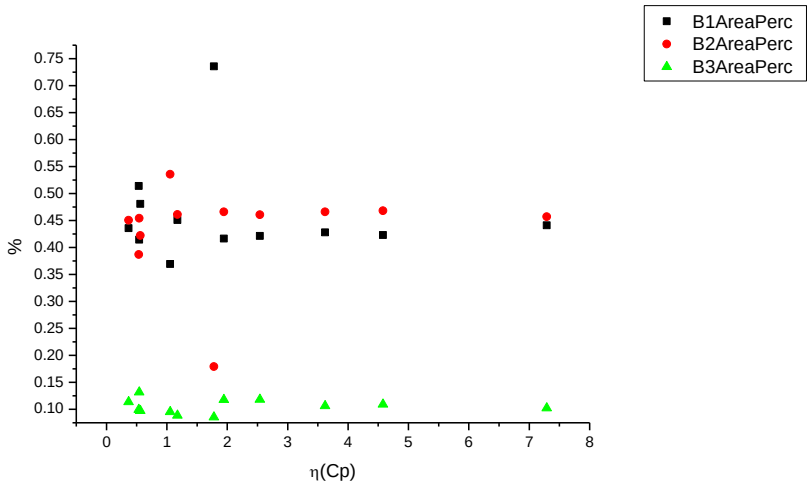

Figure 4.3.48. Area percentages from Gaussian model fit of the normalised fluorescence emission spectra of **25** recorded at 400 nm excitation against η(Cp).

4.3.6 400 nm fluorescent lifetime results.

4.3.6.1 Intensity weighted.

Wavelength (nm)	Solvent	τ_1 (ns)	A_1 (%)	τ_2 (ns)	A_2 (%)	τ_3 (ns)	A_3 (%)	τ_f (ns) (Intensity Weighted)	$1/\tau_f$	χ^2
470	Toluene	-	-	3.59	68.07	9.41	31.13	5.40	0.19	1.19
470	1,4-Dioxane	-	-	4.09	67.89	9.57	32.11	5.85	0.17	1.15
470	Chloroform	1.56	6.22	5.16	74.55	12.07	19.23	6.27	0.16	1.11
470	Acetonitrile	-	-	4.75	70.27	8.61	29.73	5.90	0.17	1.16
470	1-Octanol	0.26	5.70	5.37	71.12	12.40	23.19	6.71	0.15	1.17
470	1-Hexanol	0.47	4.01	5.61	83.43	11.95	12.56	6.20	0.16	1.08
470	1-Butanol	0.25	2.61	5.09	62.14	8.10	35.24	6.03	0.17	1.10
470	1-Pentanol	0.41	2.73	5.30	77.14	9.69	20.13	6.05	0.17	1.12
470	1-Propanol	0.18	1.42	4.62	47.75	7.12	50.82	5.83	0.17	1.17
470	Acetic acid	0.25	36.81	1.56	58.28	5.28	4.91	1.26	0.79	0.98
470	Methanol	0.44	1.98	3.69	44.76	5.76	53.27	4.73	0.21	1.20
470	2,2,2-Trifluoroethanol	0.22	66.70	0.83	29.33	5.66	3.97	0.62	1.62	0.97

Table 4.3.9. Summary of Time Correlated Single Photon Counting (TCSPC) fluorescent lifetimes (intensity weighted) of **25** recorded at 470 nm.

Wavelength (nm)	Solvent	τ_1 (ns)	A_1 (%)	τ_2 (ns)	A_2 (%)	τ_3 (ns)	A_3 (%)	τ_f (ns) (Intensity Weighted)	$1/\tau_f$	χ^2
490	Toluene	-	-	3.67	58.86	9.52	41.14	6.07	0.16	1.12
490	1,4-Dioxane	-	-	4.30	63.04	10.50	36.96	6.59	0.15	1.10
490	Chloroform	0.45	1.00	4.72	61.08	9.90	37.92	6.64	0.15	1.10
490	Acetonitrile	0.21	1.08	5.13	78.92	12.45	20.00	6.54	0.15	1.17
490	1-Octanol	0.26	5.71	5.34	70.49	12.23	23.80	6.69	0.15	1.23
490	1-Hexanol	0.43	1.49	5.60	78.31	12.07	20.21	6.83	0.15	0.97
490	1-Butanol	0.25	1.18	5.13	58.55	8.81	40.27	6.55	0.15	1.15
490	1-Pentanol	0.32	1.31	5.36	75.03	10.69	23.67	6.56	0.15	1.10
490	1-Propanol	0.11	1.30	5.29	77.79	10.58	20.91	6.32	0.16	1.21
490	Acetic acid	0.21	42.23	1.65	54.52	4.76	3.25	1.14	0.88	1.02
490	Methanol	0.31	2.45	4.14	66.73	7.21	30.82	4.99	0.20	1.12
490	2,2,2-Trifluoroethanol	0.24	63.69	0.82	33.80	5.48	2.50	0.57	1.76	1.23

Table 4.3.10. Summary of Time Correlated Single Photon Counting (TCSPC) fluorescent lifetimes (intensity weighted) of **25** recorded at 490 nm.

Wavelength (nm)	Solvent	τ_1 (ns)	A_1 (%)	τ_2 (ns)	A_2 (%)	τ_3 (ns)	A_3 (%)	τ_f (ns) (Intensity Weighted)	$1/\tau_f$	χ^2
520	Toluene	-	-	3.69	30.58	9.58	69.42	7.78	0.13	1.18
520	1,4-Dioxane	-	-	4.27	35.60	10.84	64.40	8.50	0.12	1.23
520	Chloroform	-	-	4.66	37.69	11.08	62.31	8.66	0.12	1.16
520	Acetonitrile	0.12	1.17	5.16	56.24	13.14	42.59	8.50	0.12	1.15
520	1-Octanol	0.26	3.14	5.50	48.52	13.15	48.34	9.03	0.11	1.24
520	1-Hexanol	-	-	5.46	52.38	12.56	47.62	8.84	0.11	1.17
520	1-Butanol	0.21	0.70	5.27	48.78	11.03	50.52	8.14	0.12	1.20
520	1-Pentanol	-	-	5.41	56.11	12.69	43.89	8.60	0.12	1.13
520	1-Propanol	-	-	5.28	61.04	12.18	38.96	7.97	0.13	1.18
520	Acetic acid	0.17	51.92	1.65	45.26	4.99	2.83	0.98	1.02	1.06
520	Methanol	0.40	1.77	4.45	70.85	10.82	27.38	6.12	0.16	1.09
520	2,2,2-Trifluoroethanol	0.24	62.22	0.85	33.13	4.45	4.65	0.64	1.57	1.30

Table 4.3.11. Summary of Time Correlated Single Photon Counting (TCSPC) fluorescent lifetimes (intensity weighted) of **25** recorded at 520 nm.

Wavelength (nm)	Solvent	τ_1 (ns)	A_1 (%)	τ_2 (ns)	A_2 (%)	τ_3 (ns)	A_3 (%)	τ_f (ns) (Intensity Weighted)	$1/\tau_f$	χ^2
540	Toluene	-	-	3.70	23.51	9.68	76.49	8.27	0.12	1.18
540	1,4-Dioxane	-	-	4.37	28.14	11.17	71.86	9.25	0.11	1.12
540	Chloroform	-	-	4.62	28.11	11.24	71.89	9.38	0.11	1.10
540	Acetonitrile	-	-	5.12	43.57	13.24	56.43	9.71	0.10	1.09
540	1-Octanol	0.23	2.23	5.44	36.76	13.06	61.01	9.97	0.10	1.18
540	1-Hexanol	-	-	5.61	44.44	13.19	55.56	9.82	0.10	1.12
540	1-Butanol	-	-	5.61	48.86	12.73	51.14	9.25	0.11	1.14
540	1-Pentanol	-	-	5.49	46.91	13.10	53.09	9.53	0.10	1.22
540	1-Propanol	-	-	5.39	53.56	12.81	46.44	8.84	0.11	1.04
540	Acetic acid	0.16	58.64	1.55	35.93	3.40	5.44	0.84	1.20	0.96
540	Methanol	0.38	1.54	4.46	64.41	11.47	34.05	6.78	0.15	1.12
540	2,2,2-Trifluoroethanol	0.23	58.99	0.85	33.99	4.39	7.01	0.73	1.37	0.95

Table 4.3.12. Summary of Time Correlated Single Photon Counting (TCSPC) fluorescent lifetimes (intensity weighted) of **25** recorded at 540 nm.

Wavelength (nm)	Solvent	τ_1 (ns)	A_1 (%)	τ_2 (ns)	A_2 (%)	τ_3 (ns)	A_3 (%)	τ_f (ns) (Intensity Weighted)	$1/\tau_f$	χ^2
570	Toluene	-	-	3.83	11.83	9.73	88.17	9.03	0.11	1.10
570	1,4-Dioxane	-	-	4.16	14.00	11.11	86.00	10.13	0.10	1.19
570	Chloroform	-	-	4.81	18.36	11.71	81.64	10.44	0.10	1.15
570	Acetonitrile	-	-	5.15	29.42	13.43	70.58	11.00	0.09	1.10
570	1-Octanol	0.14	2.62	5.46	24.16	13.09	73.22	10.90	0.09	1.14
570	1-Hexanol	-	-	5.73	32.27	13.38	67.73	10.91	0.09	1.15
570	1-Butanol	-	-	5.52	35.70	12.73	64.30	10.15	0.10	1.22
570	1-Pentanol	-	-	5.86	37.33	13.50	62.67	10.65	0.09	1.24
570	1-Propanol	-	-	5.48	43.47	13.33	56.53	9.91	0.10	1.06
570	Acetic acid	0.18	59.83	1.51	35.54	3.95	4.62	0.83	1.21	1.00
570	Methanol	0.44	1.74	4.54	57.57	12.60	40.69	7.75	0.13	1.15
570	2,2,2-Trifluoroethanol	0.26	61.79	0.91	28.12	4.10	10.09	0.83	1.21	1.01

Table 4.3.13. Summary of Time Correlated Single Photon Counting (TCSPC) fluorescent lifetimes (intensity weighted) of **25** recorded at 570 nm.

4.3.6.2 Amplitude weighted.

Wavelength (nm)	Solvent	τ_1 (ns)	A_1 (%)	τ_2 (ns)	A_2 (%)	τ_3 (ns)	A_3 (%)	τ_f (ns) (Amplitude Weighted)	$1/\tau_f$	χ^2
470	Toluene	-	-	3.59	85.28	9.41	14.72	4.45	0.22	1.19
470	1,4-Dioxane	-	-	4.09	83.18	9.57	16.82	5.02	0.20	1.15
470	Chloroform	1.56	19.94	5.16	72.11	12.07	7.95	4.99	0.20	1.11
470	Acetonitrile	-	-	4.75	81.08	8.61	18.92	5.48	0.18	1.16
470	1-Octanol	0.26	58.85	5.37	36.06	12.40	5.09	2.72	0.37	1.17
470	1-Hexanol	0.47	35.05	5.61	60.66	11.95	4.29	4.08	0.25	1.08
470	1-Butanol	0.25	39.18	5.09	44.83	8.10	15.99	3.68	0.27	1.10
470	1-Pentanol	0.41	28.58	5.30	62.50	9.69	8.92	4.30	0.23	1.12
470	1-Propanol	0.18	31.23	4.62	40.66	7.12	28.11	3.94	0.25	1.17
470	Acetic acid	0.25	79.04	1.56	20.45	5.28	0.51	0.55	1.83	0.98
470	Methanol	0.44	17.37	3.69	46.89	5.76	35.74	3.87	0.26	1.20
470	2,2,2-Trifluoroethanol	0.22	89.30	0.83	10.49	5.66	0.21	0.30	3.37	0.97

Table 4.3.14. Summary of Time Correlated Single Photon Counting (TCSPC) fluorescent lifetimes (amplitude weighted) of **25** recorded at 470 nm.

Wavelength (nm)	Solvent	τ_1 (ns)	A_1 (%)	τ_2 (ns)	A_2 (%)	τ_3 (ns)	A_3 (%)	τ_f (ns) (Amplitude Weighted)	$1/\tau_f$	χ^2
490	Toluene	-	-	3.67	78.79	9.52	21.21	4.91	0.20	1.12
490	1,4-Dioxane	-	-	4.30	80.63	10.50	19.37	5.50	0.18	1.10
490	Chloroform	0.45	11.59	4.72	68.22	9.90	20.19	5.27	0.19	1.10
490	Acetonitrile	0.21	22.90	5.13	69.81	12.45	7.29	4.54	0.22	1.17
490	1-Octanol	0.26	5.27	5.34	35.72	12.23	5.27	2.71	0.37	1.23
490	1-Hexanol	0.43	18.07	5.60	73.17	12.07	8.76	5.23	0.19	0.97
490	1-Butanol	0.25	22.70	5.13	55.19	8.81	22.12	4.84	0.21	1.15
490	1-Pentanol	0.32	20.21	5.36	68.89	10.69	10.90	4.93	0.20	1.10
490	1-Propanol	0.11	40.46	5.29	52.49	10.58	7.05	3.57	0.28	1.21
490	Acetic acid	0.21	85.43	1.65	14.27	4.76	0.29	0.43	2.32	1.02
490	Methanol	0.31	28.03	4.14	56.87	7.21	15.09	3.53	0.28	1.12
490	2,2,2-Trifluoroethanol	0.24	86.42	0.82	13.43	5.48	0.15	0.33	3.06	1.23

Table 4.3.15. Summary of Time Correlated Single Photon Counting (TCSPC) fluorescent lifetimes (amplitude weighted) of **25** recorded at 490 nm.

Wavelength (nm)	Solvent	τ_1 (ns)	A_1 (%)	τ_2 (ns)	A_2 (%)	τ_3 (ns)	A_3 (%)	τ_f (ns) (Amplitude Weighted)	$1/\tau_f$	χ^2
520	Toluene	-	-	3.69	53.36	9.58	46.64	6.44	0.16	1.18
520	1,4-Dioxane	-	-	4.27	58.41	10.84	41.59	7.00	0.14	1.23
520	Chloroform	-	-	4.66	59.02	11.08	40.98	7.29	0.14	1.16
520	Acetonitrile	0.12	40.97	5.16	45.51	13.14	13.52	4.17	0.24	1.15
520	1-Octanol	0.26	49.49	5.50	35.66	13.15	14.85	4.04	0.25	1.24
520	1-Hexanol	-	-	5.46	71.66	12.56	28.34	7.47	0.13	1.17
520	1-Butanol	0.21	19.19	5.27	54.06	11.03	26.74	5.84	0.17	1.20
520	1-Pentanol	-	-	5.41	74.99	12.69	25.01	7.23	0.14	1.13
520	1-Propanol	-	-	5.28	78.32	12.18	21.68	6.78	0.15	1.18
520	Acetic acid	0.17	91.57	1.65	8.26	4.99	0.17	0.30	3.32	1.06
520	Methanol	0.40	19.37	4.45	69.58	10.82	11.05	4.37	0.23	1.09
520	2,2,2-Trifluoroethanol	0.24	86.77	0.85	12.89	4.45	0.35	0.33	3.02	1.30

Table 4.3.16. Summary of Time Correlated Single Photon Counting (TCSPC) fluorescent lifetimes (amplitude weighted) of **25** recorded at 520 nm.

Wavelength (nm)	Solvent	τ_1 (ns)	A_1 (%)	τ_2 (ns)	A_2 (%)	τ_3 (ns)	A_3 (%)	τ_f (ns) (Amplitude Weighted)	$1/\tau_f$	χ^2
540	Toluene	-	-	3.70	44.60	9.68	55.40	7.01	0.14	1.18
540	1,4-Dioxane	-	-	4.37	50.02	11.17	49.98	7.77	0.13	1.12
540	Chloroform	-	-	4.62	48.75	11.24	51.25	8.02	0.12	1.10
540	Acetonitrile	-	-	5.12	66.63	13.24	33.37	7.83	0.13	1.09
540	1-Octanol	0.23	46.02	5.44	31.91	13.06	22.08	4.72	0.21	1.18
540	1-Hexanol	-	-	5.61	65.31	13.19	34.69	8.24	0.12	1.12
540	1-Butanol	-	-	5.61	68.42	12.73	31.58	7.86	0.13	1.14
540	1-Pentanol	-	-	5.49	67.81	13.10	32.19	7.94	0.13	1.22
540	1-Propanol	-	-	5.39	73.27	12.81	26.73	7.38	0.14	1.04
540	Acetic acid	0.16	93.70	1.55	5.90	3.40	0.41	0.25	3.93	0.96
540	Methanol	0.38	18.96	4.46	67.21	11.47	13.82	4.66	0.21	1.12
540	2,2,2-Trifluoroethanol	0.23	86.20	0.85	13.28	4.39	0.53	0.33	3.02	0.95

Table 4.3.17. Summary of Time Correlated Single Photon Counting (TCSPC) fluorescent lifetimes (amplitude weighted) of **25** recorded at 540 nm.

Wavelength (nm)	Solvent	τ_1 (ns)	A_1 (%)	τ_2 (ns)	A_2 (%)	τ_3 (ns)	A_3 (%)	τ_f (ns) (Amplitude Weighted)	$1/\tau_f$	χ^2
570	Toluene	-	-	3.83	25.44	9.73	74.56	8.23	0.12	1.10
570	1,4-Dioxane	-	-	4.16	30.32	11.11	69.68	9.00	0.11	1.19
570	Chloroform	-	-	4.81	35.38	11.71	64.62	9.27	0.11	1.15
570	Acetonitrile	-	-	5.15	52.08	13.43	47.92	9.12	0.11	1.10
570	1-Octanol	0.14	65.01	5.46	15.44	13.09	19.54	3.49	0.29	1.14
570	1-Hexanol	-	-	5.73	52.66	13.38	47.34	9.35	0.11	1.15
570	1-Butanol	-	-	5.52	56.15	12.73	43.85	8.68	0.12	1.22
570	1-Pentanol	-	-	5.86	57.82	13.50	42.18	9.08	0.11	1.24
570	1-Propanol	-	-	5.48	65.17	13.33	34.83	8.21	0.12	1.06
570	Acetic acid	0.18	92.94	1.51	6.73	3.95	0.33	0.29	3.51	1.00
570	Methanol	0.44	20.00	4.54	63.76	12.60	16.23	5.03	0.20	1.15
570	2,2,2-Trifluoroethanol	0.26	87.84	0.91	11.27	4.10	0.90	0.36	2.75	1.01

Table 4.3.18. Summary of Time Correlated Single Photon Counting (TCSPC) fluorescent lifetimes (amplitude weighted) of **25** recorded at 570 nm.

4.3.7 400 nm average fluorescent lifetimes - Solvatochromic analysis.

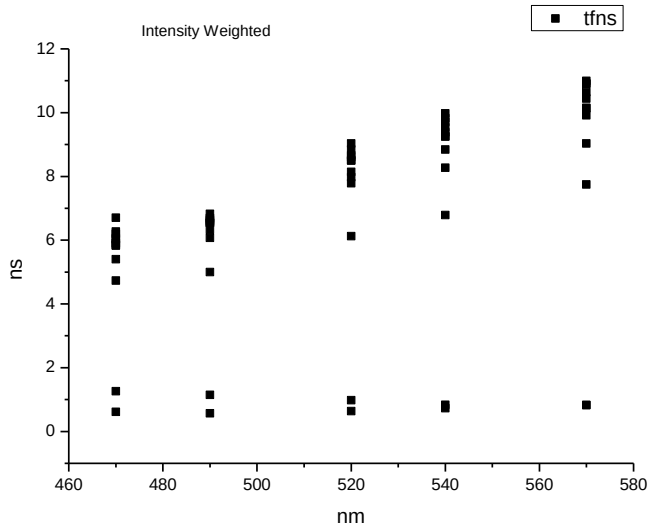

Figure 4.3.49. Intensity weighted average lifetime (τ_f) of **25** versus wavelength (nm).

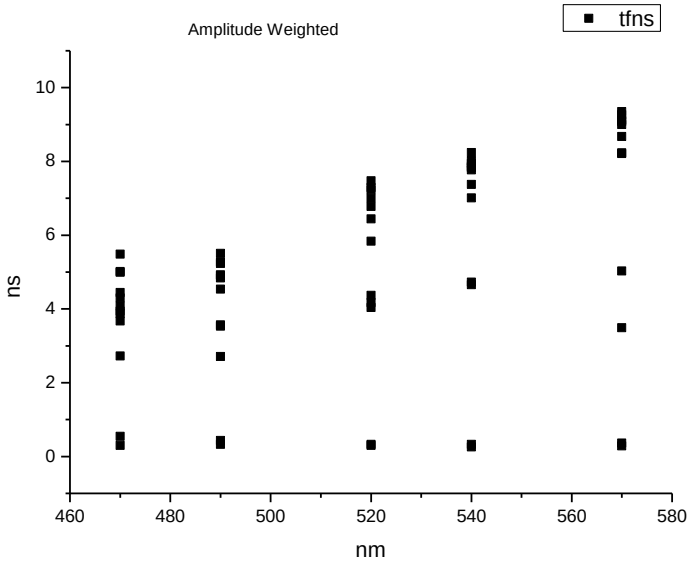

Figure 4.3.50. Amplitude weighted average lifetime (τ_f) of **25** versus wavelength (nm).

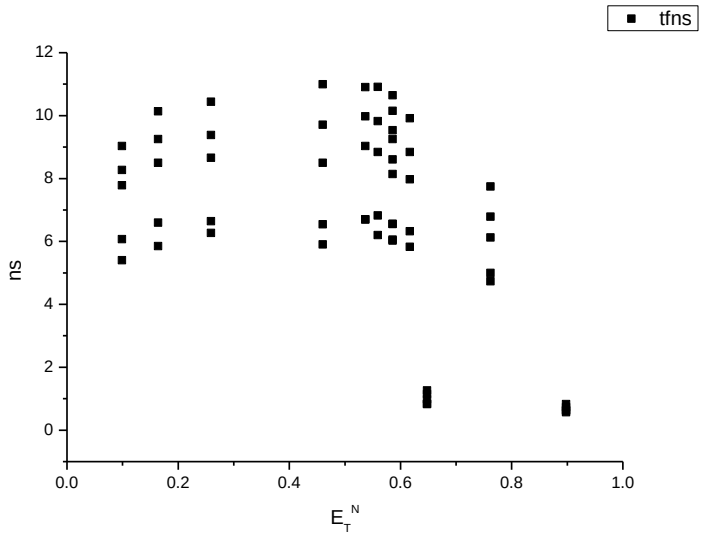

Figure 4.3.51. Intensity weighted average lifetime (τ_f) of **25** versus E_T^N.

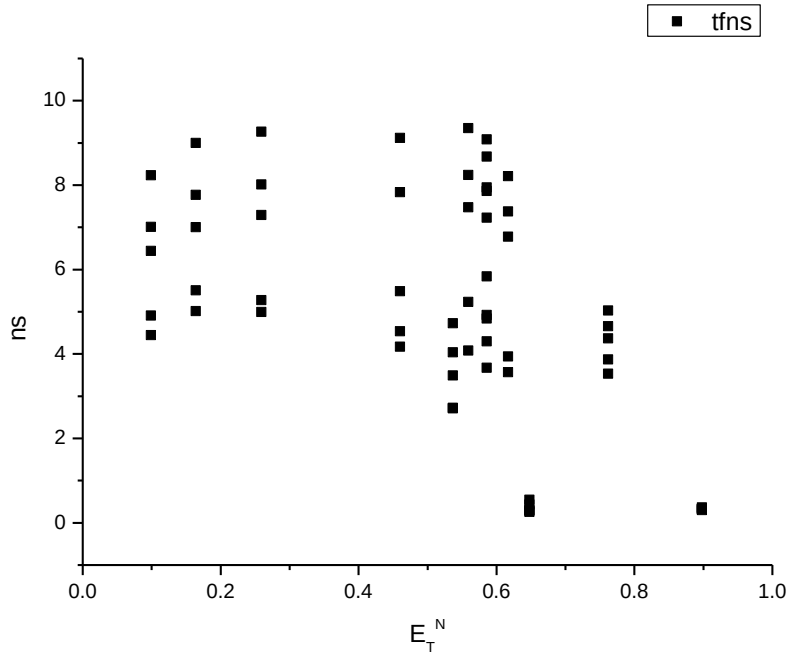

Figure 4.3.52. Amplitude weighted average lifetime (τ_f) of **25** versus E_T^N.

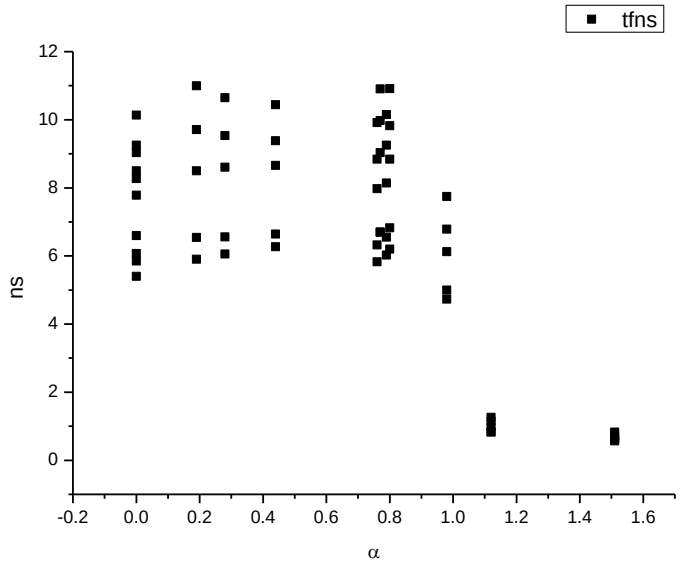

Figure 4.3.53. Intensity weighted average lifetime (τ_f) of **25** versus α.

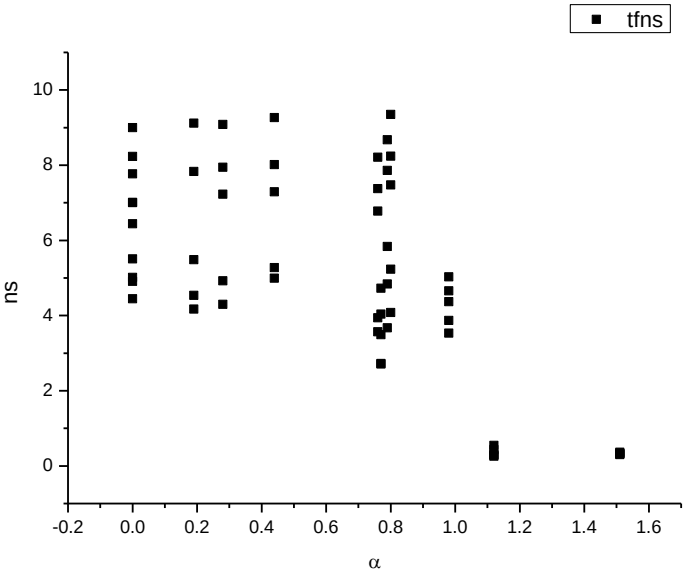

Figure 4.3.54. Amplitude weighted average lifetime (τ_f) of **25** versus α.

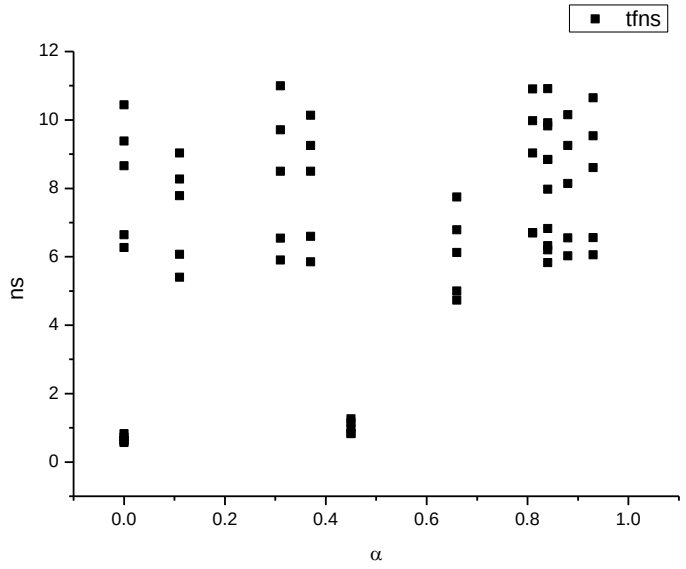

Figure 4.3.55. Intensity weighted average lifetime (τ_f) of **25** versus β.

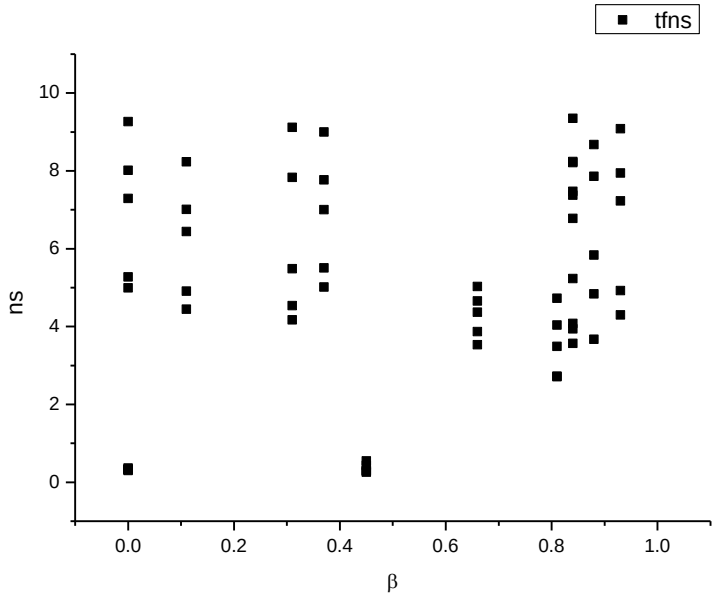

Figure 4.3.56. Amplitude weighted average lifetime (τ_f) of **25** versus β.

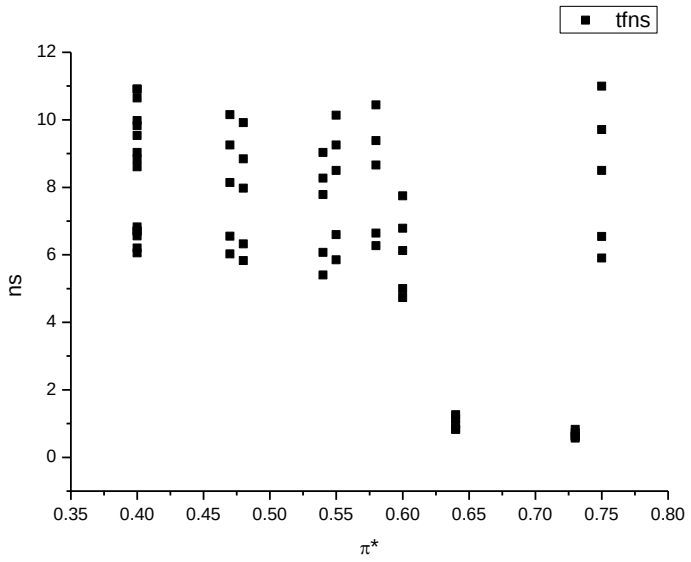

Figure 4.3.57. Intensity weighted average lifetime (τ_f) of **25** versus π*.

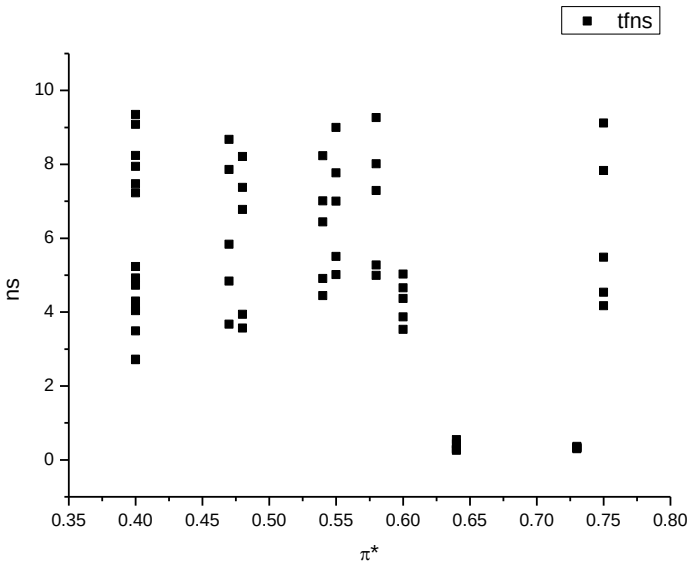

Figure 4.3.58. Amplitude weighted average lifetime (τ_f) of **25** versus π*.

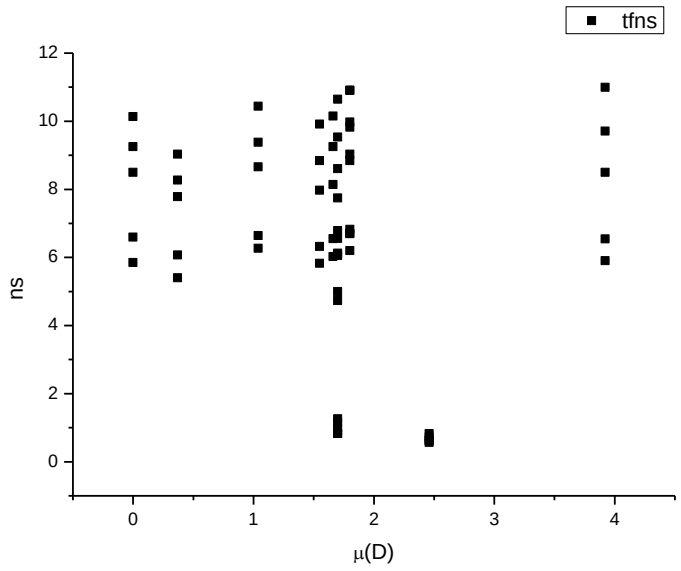

Figure 4.3.59. Intensity weighted average lifetime (τ_f) of **25** versus μ(D).

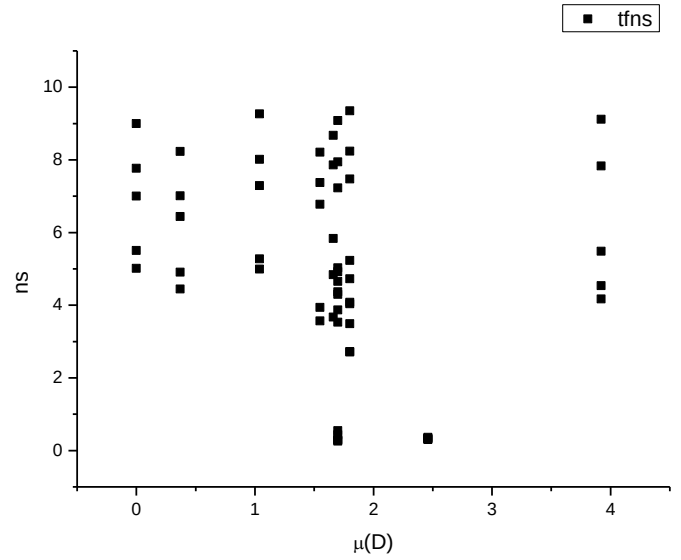

Figure 4.3.60. Amplitude weighted average lifetime (τ_f) of **25** versus μ(D).

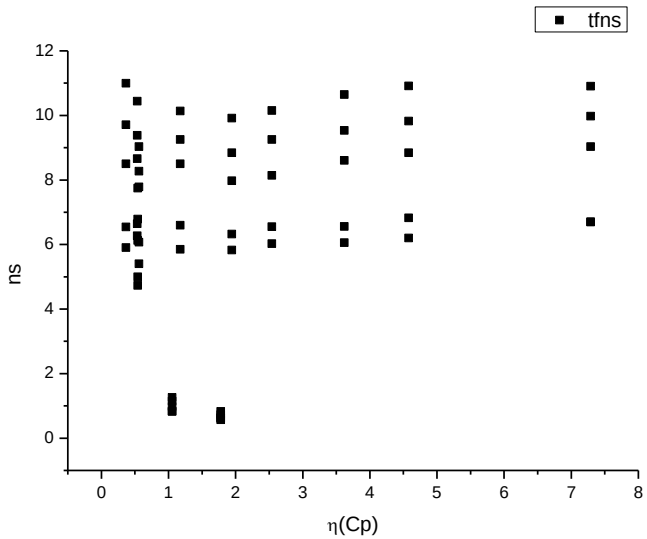

Figure 4.3.61. Intensity weighted average lifetime (τ_f) of **25** versus η(Cp).

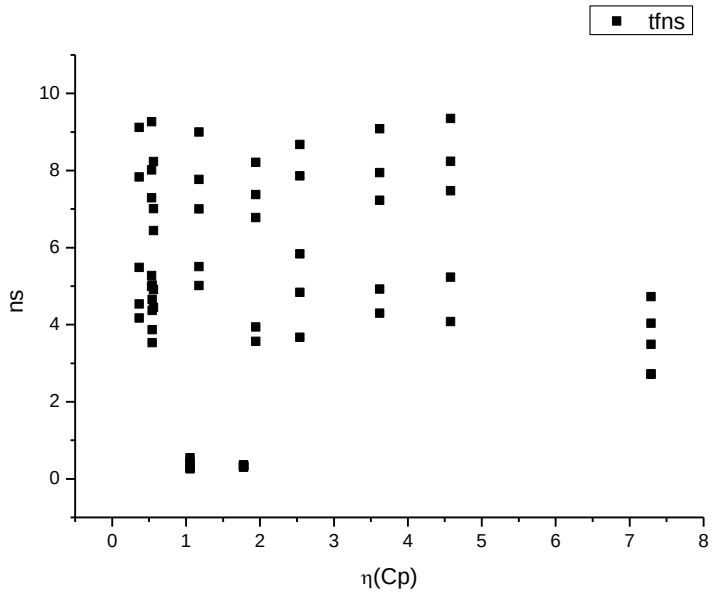

Figure 4.3.62. Amplitude weighted average lifetime (τ_f) of **25** versus η(Cp).

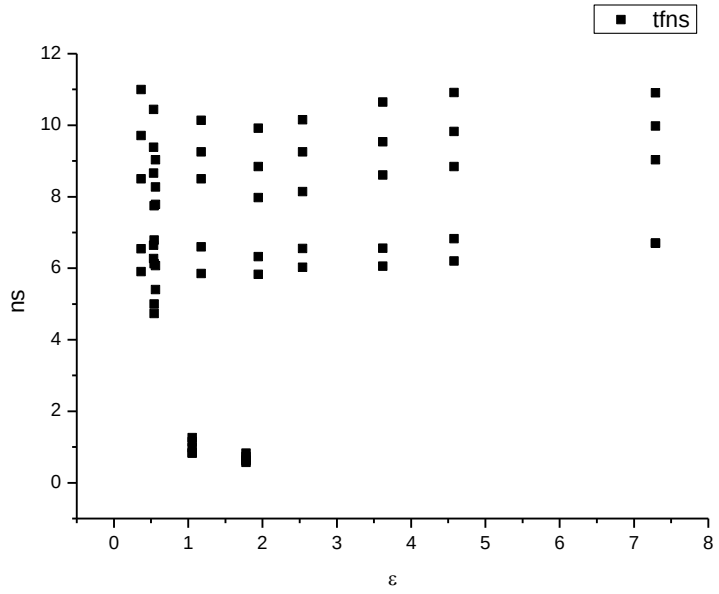

Figure 4.3.63. Intensity weighted average lifetime (τ_f) of **25** versus ε.

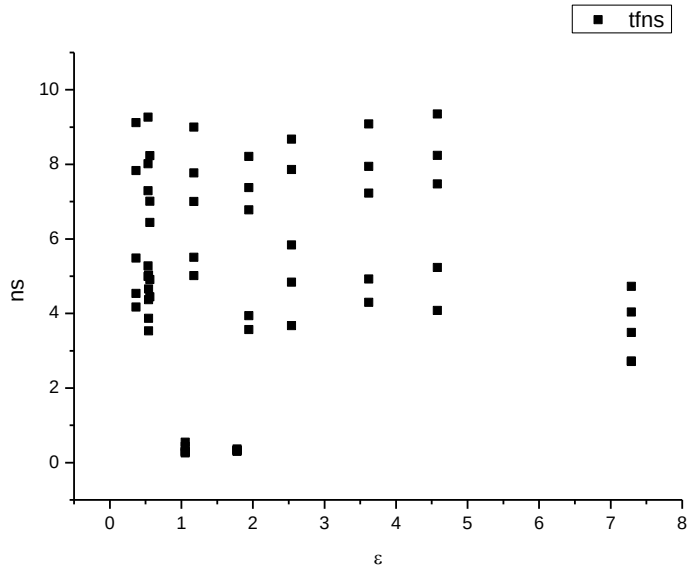

Figure 4.3.64. Amplitude weighted average lifetime (τ_f) of **25** versus ε.

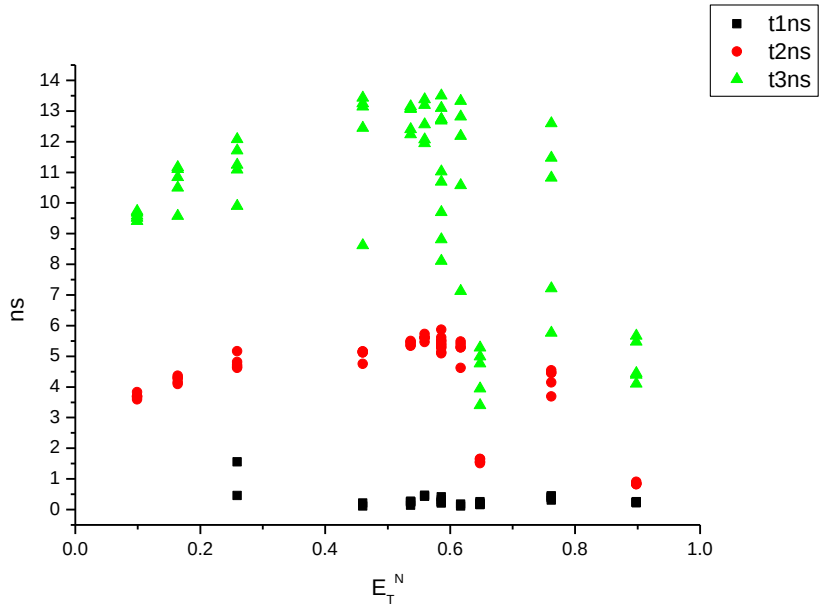

Figure 4.3.65. Intensity weighted components of TCSPC lifetime decay of **25** (470 nm to 570 nm) versus E_T^N.

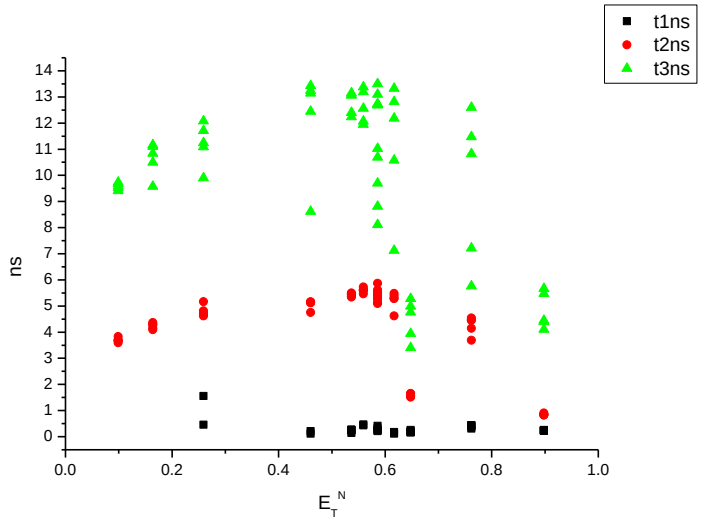

Figure 4.3.66. Amplitude weighted components of TCSPC lifetime decay of **25** (470 nm to 570 nm) versus E_T^N.

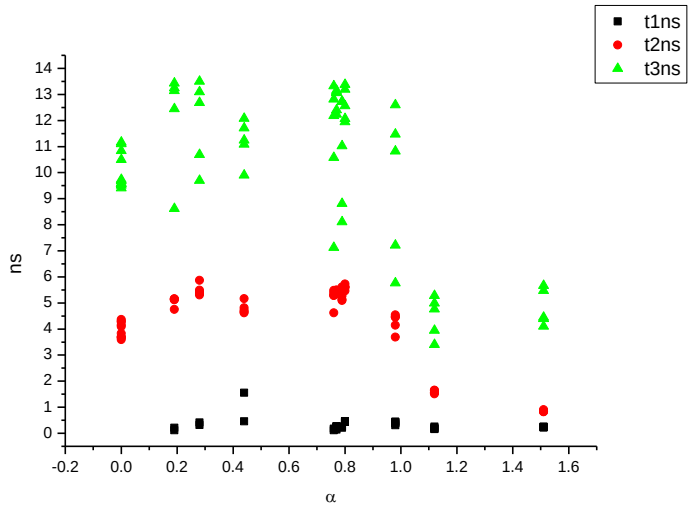

Figure 4.3.67. Intensity weighted components of TCSPC lifetime decay of **25** (470 nm to 570 nm) versus α.

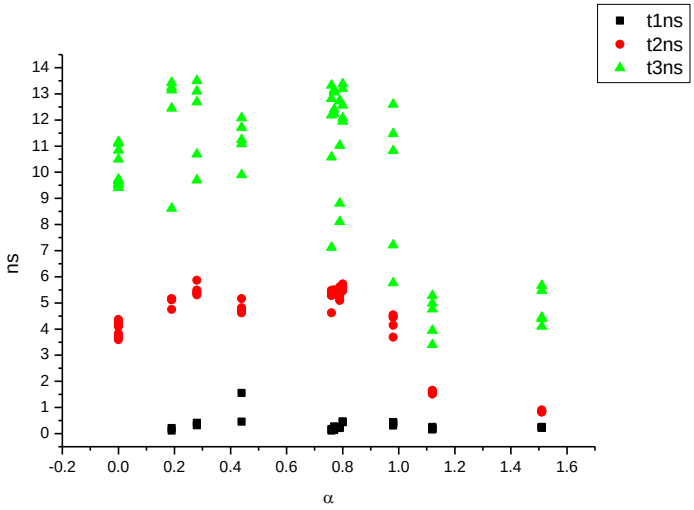

Figure 4.3.68. Amplitude weighted components of TCSPC lifetime decay of **25** (470 nm to 570 nm) versus α.

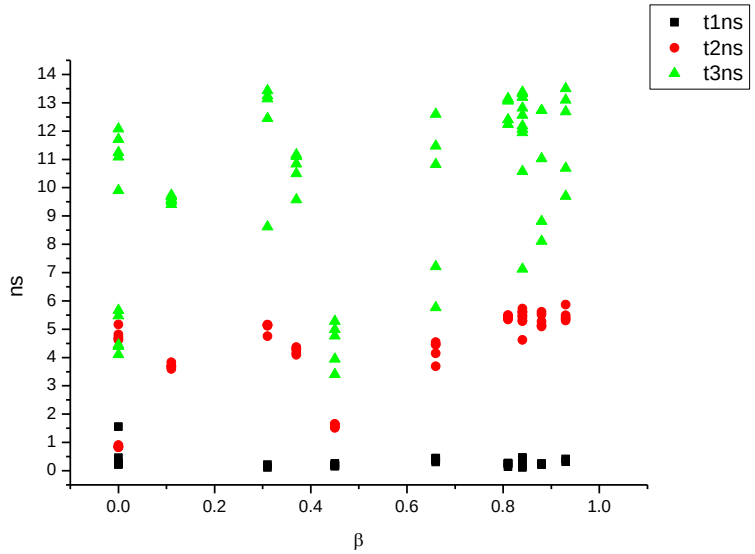

Figure 4.3.67. Intensity weighted components of TCSPC lifetime decay of **25** (470 nm to 570 nm) versus β.

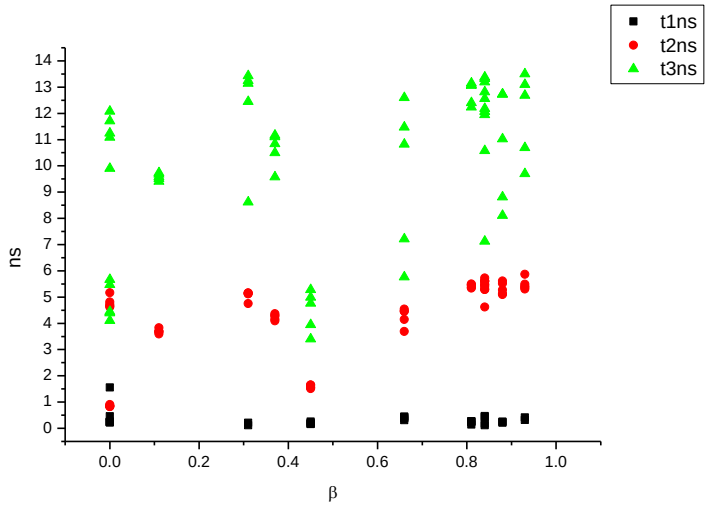

Figure 4.3.68. Amplitude weighted components of TCSPC lifetime decay of **25** (470 nm to 570 nm) versus β.

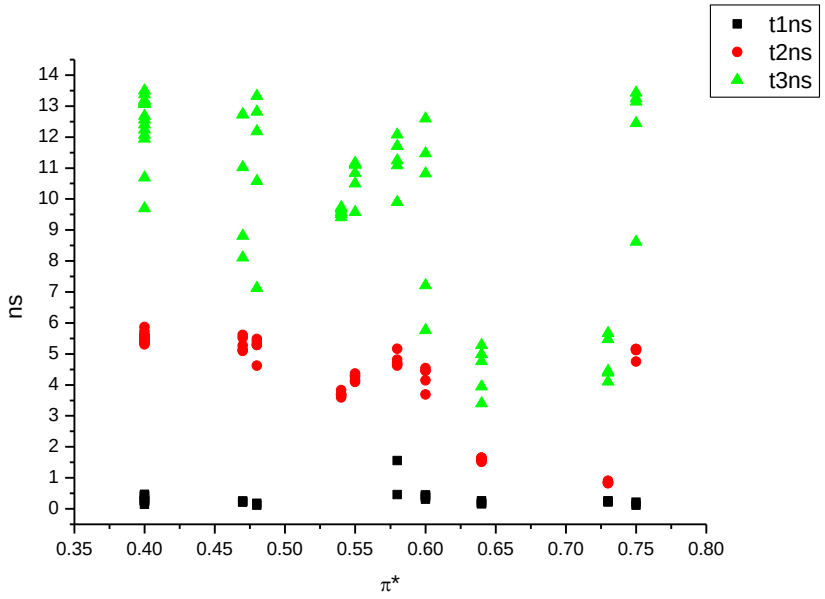

Figure 4.3.69. Intensity weighted components of TCSPC lifetime decay of **25** (470 nm to 570 nm) versus π*.

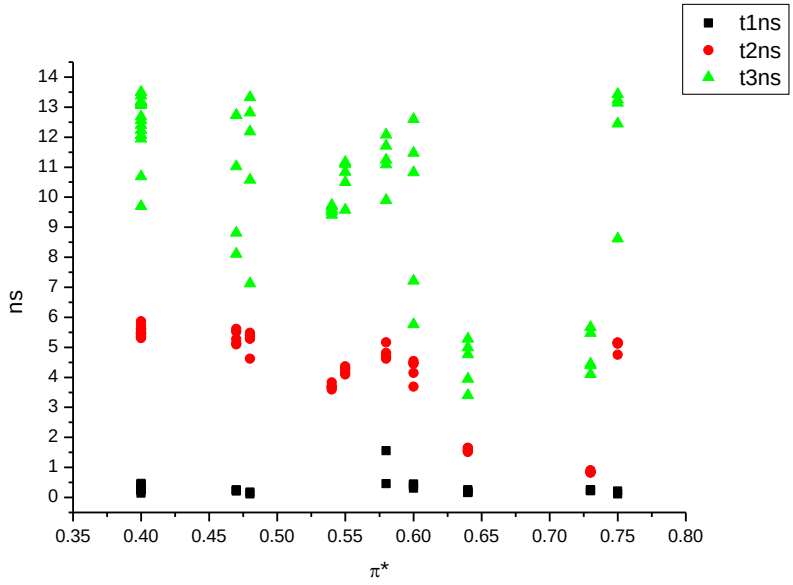

Figure 4.3.70. Amplitude weighted components of TCSPC lifetime decay of **25** (470 nm to 570 nm) versus π*.

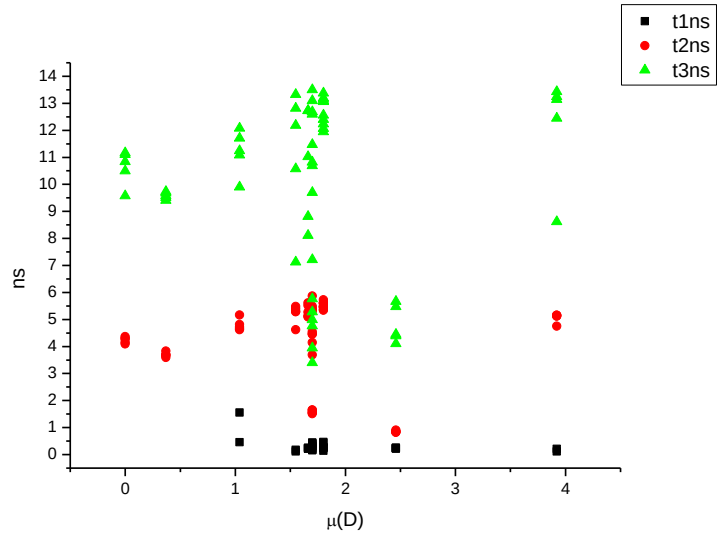

Figure 4.3.71. Intensity weighted components of TCSPC lifetime decay of **25** (470 nm to 570 nm) versus μ(D).

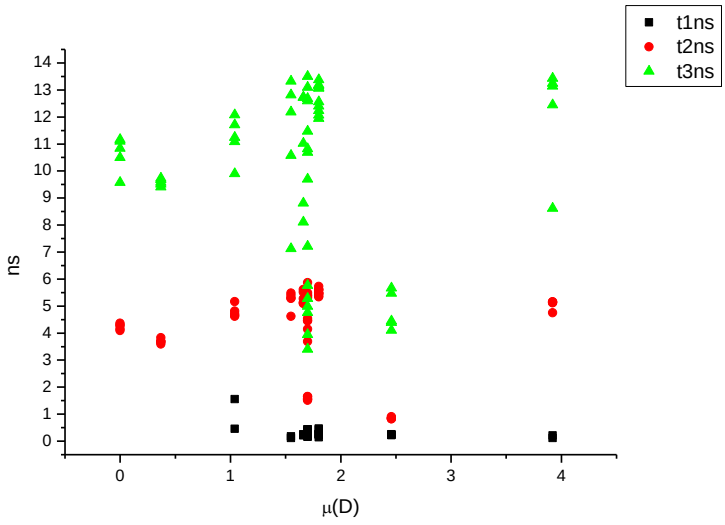

Figure 4.3.72. Amplitude weighted components of TCSPC lifetime decay of **25** (470 nm to 570 nm) versus μ(D).

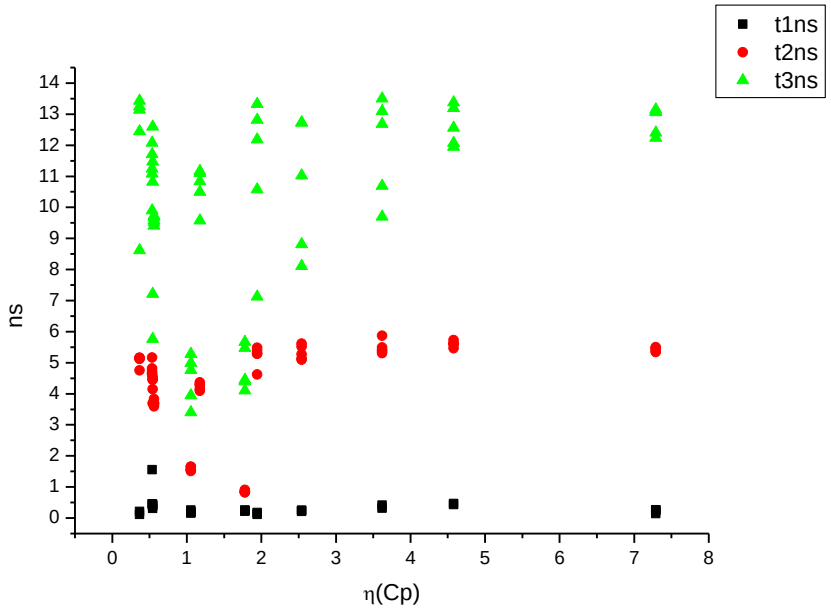

Figure 4.3.73. Intensity weighted components of TCSPC lifetime decay of **25** (470 nm to 570 nm) versus η(Cp).

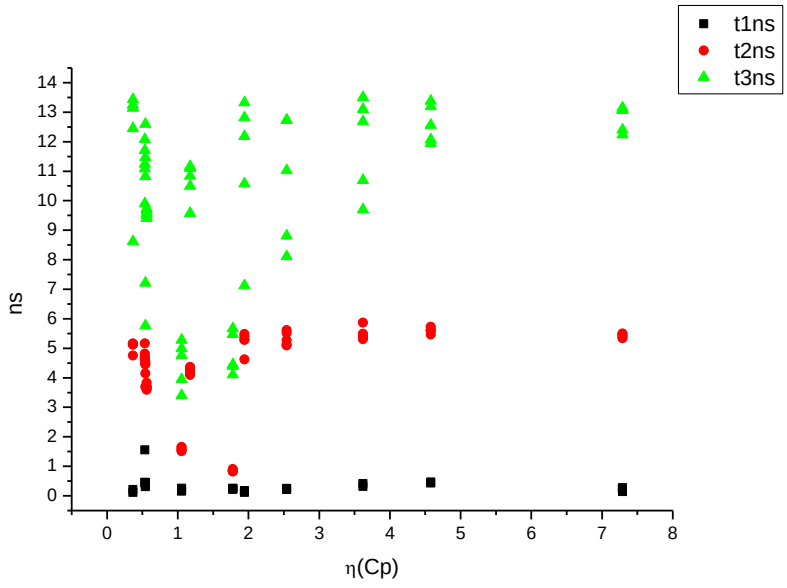

Figure 4.3.74. Amplitude weighted components of TCSPC lifetime decay of **25** (470 nm to 570 nm) versus η(Cp).

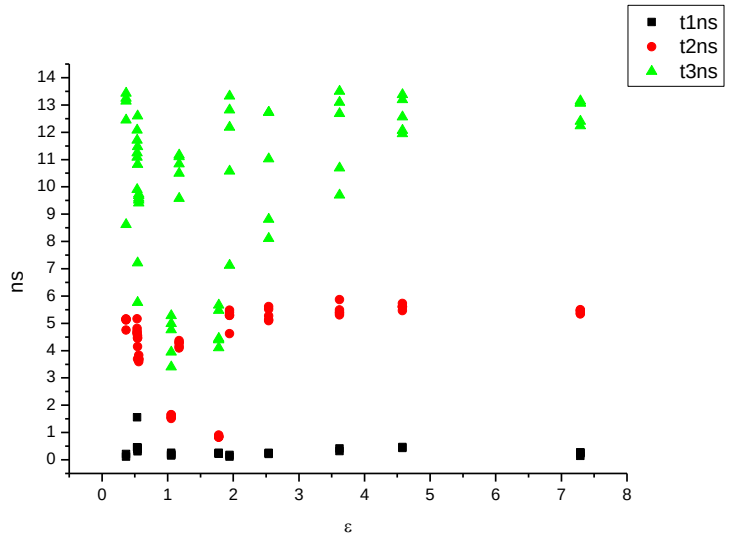

Figure 4.3.75. Intensity weighted components of TCSPC lifetime decay of **25** (470 nm to 570 nm) versus ε.

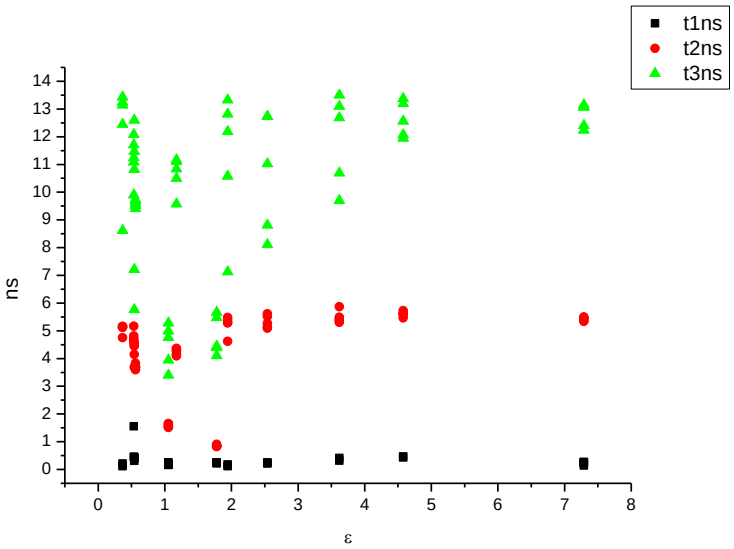

Figure 4.3.76. Amplitude weighted components of TCSPC lifetime decay of **25** (470 nm to 570 nm) versus ε.

4.3.7.1 470 nm Lifetime – Solvatochromic analysis.

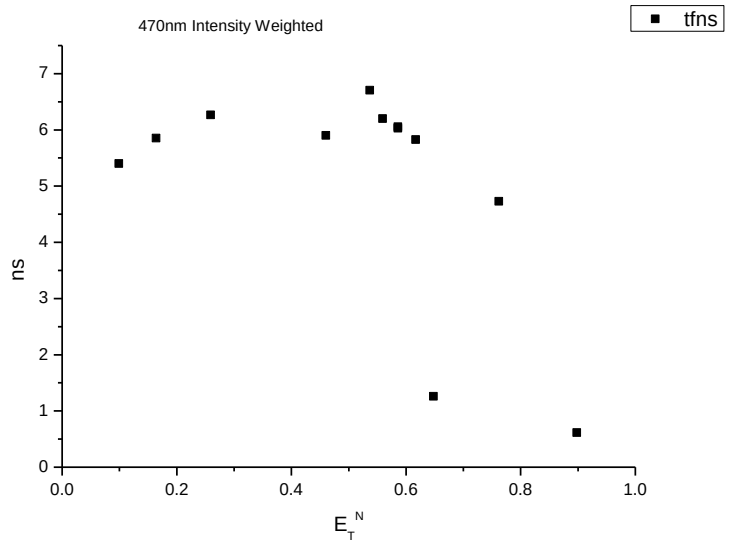

Figure 4.3.77. Intensity weighted average lifetime (τ_f) of **25** at 470 nm versus E_T^N.

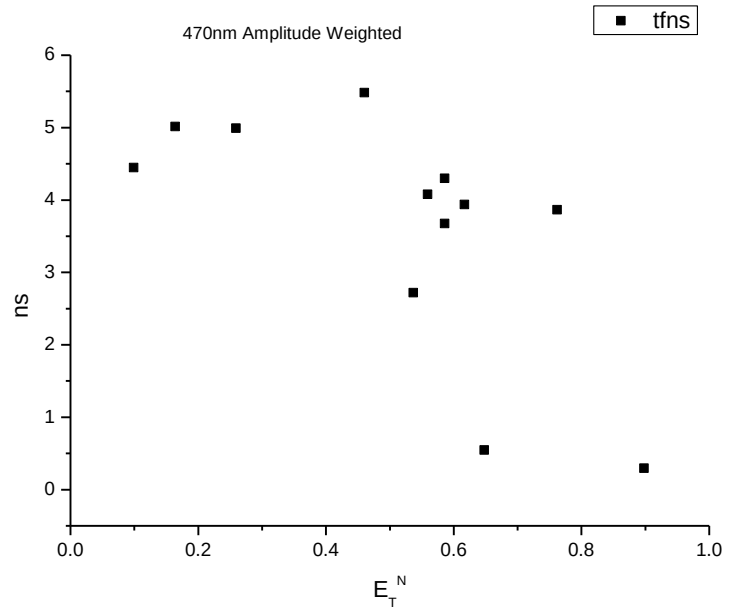

Figure 4.3.78. Amplitude weighted average lifetime (τ_f) of **25** at 470 nm versus E_T^N.

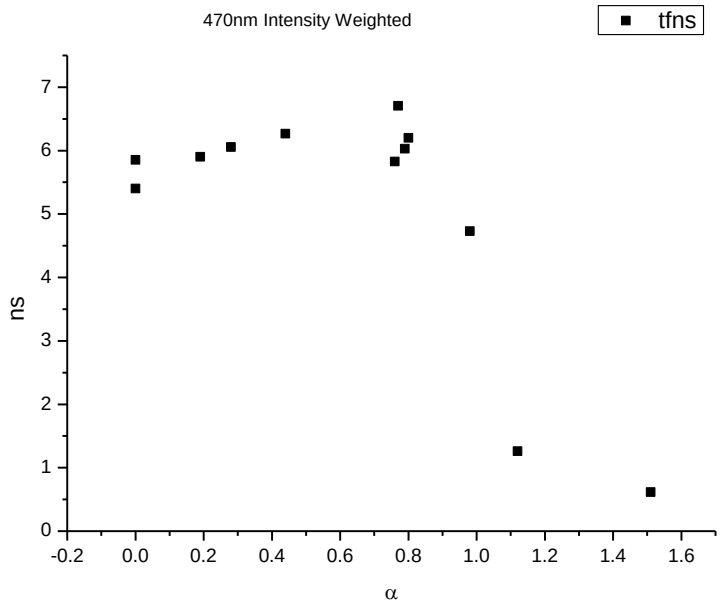

Figure 4.3.79. Intensity weighted average lifetime (τ_f) of **25** at 470 nm versus α.

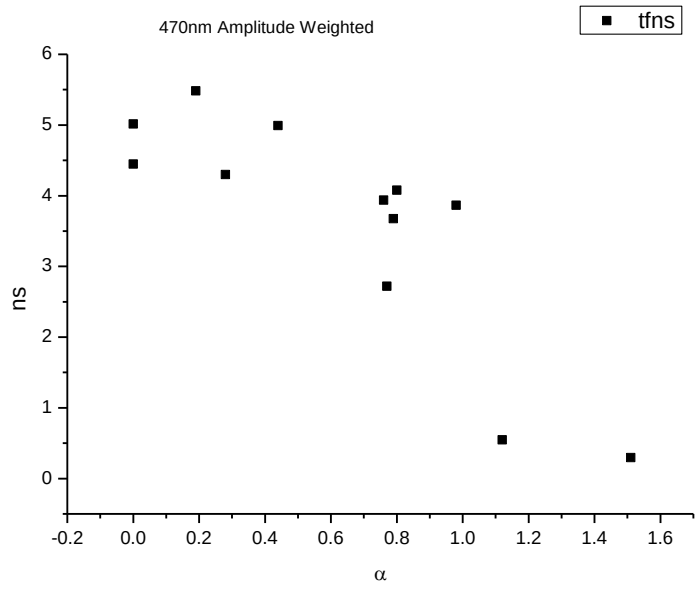

Figure 4.3.80. Amplitude weighted average lifetime (τ_f) of **25** at 470 nm versus α.

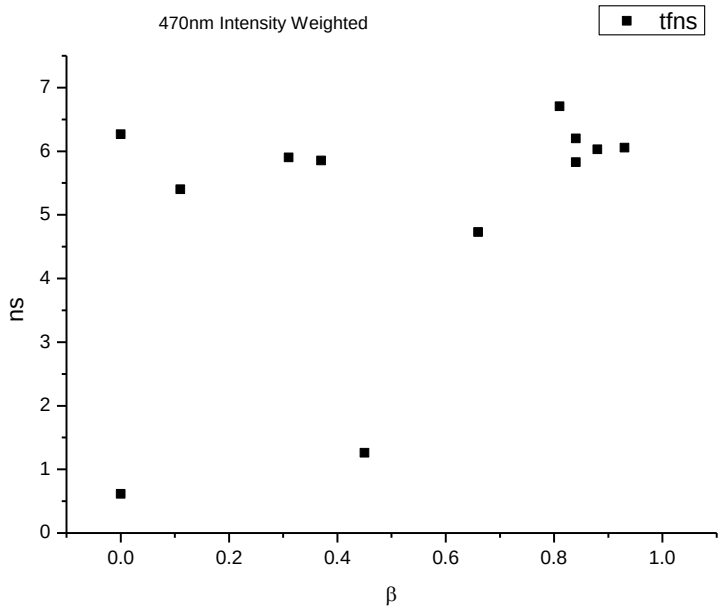

Figure 4.3.81. Intensity weighted average lifetime (τ_f) of **25** at 470 nm versus β.

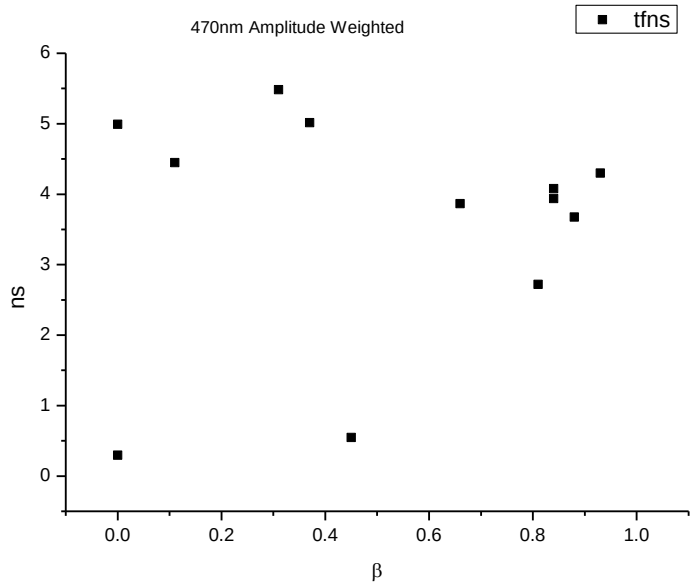

Figure 4.3.82. Amplitude weighted average lifetime (τ_f) of **25** at 470 nm versus β.

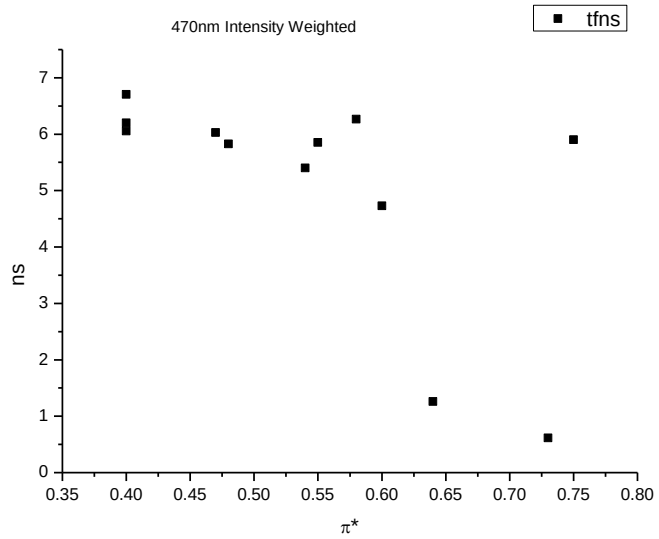

Figure 4.3.83. Intensity weighted average lifetime (τ_f) of **25** at 470 nm versus π*.

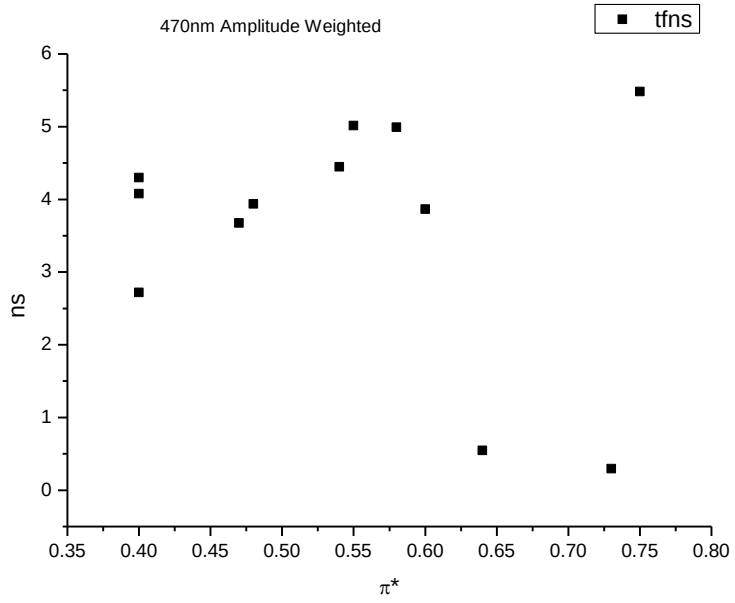

Figure 4.3.84. Amplitude weighted average lifetime (τ_f) of **25** at 470 nm versus π*.

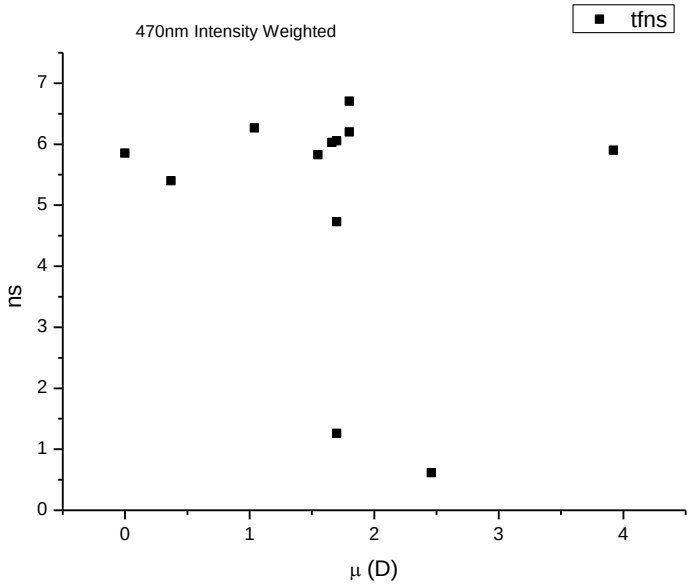

Figure 4.3.85. Intensity weighted average lifetime (τ_f) of **25** at 470 nm versus μ(D).

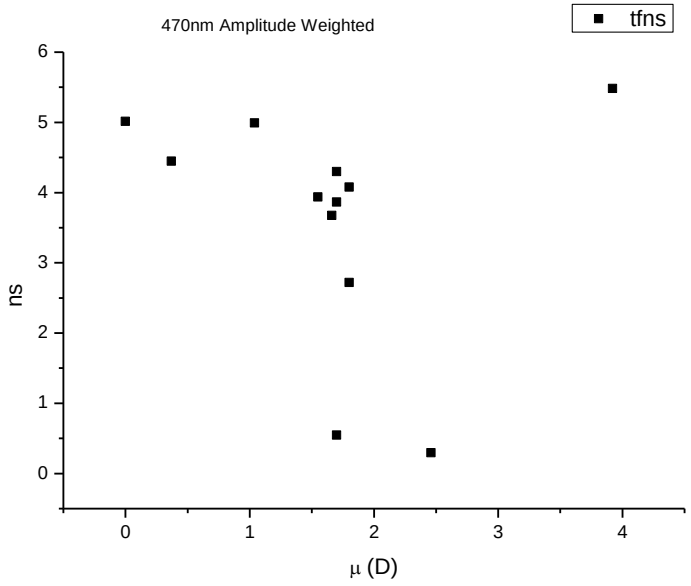

Figure 4.3.86. Amplitude weighted average lifetime (τ_f) of **25** at 470 nm versus μ(D).

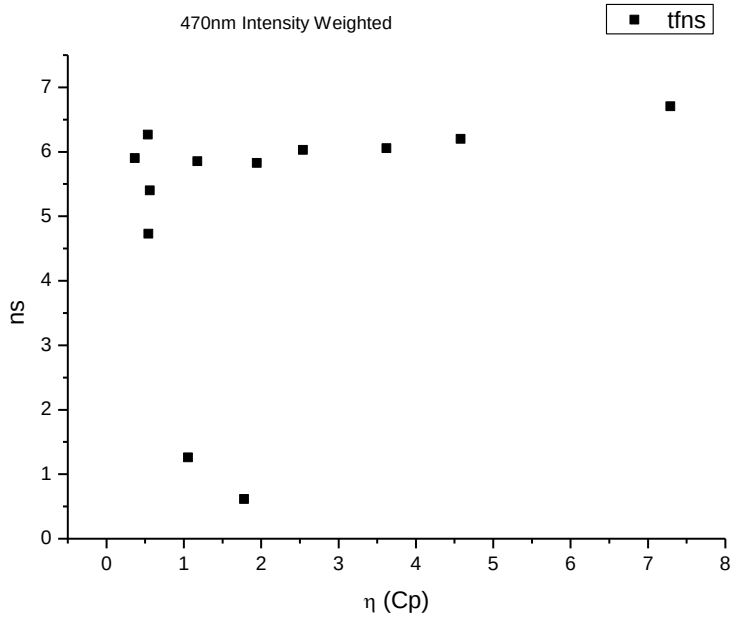

Figure 4.3.87. Intensity weighted average lifetime (τ_f) of **25** at 470 nm versus η(Cp).

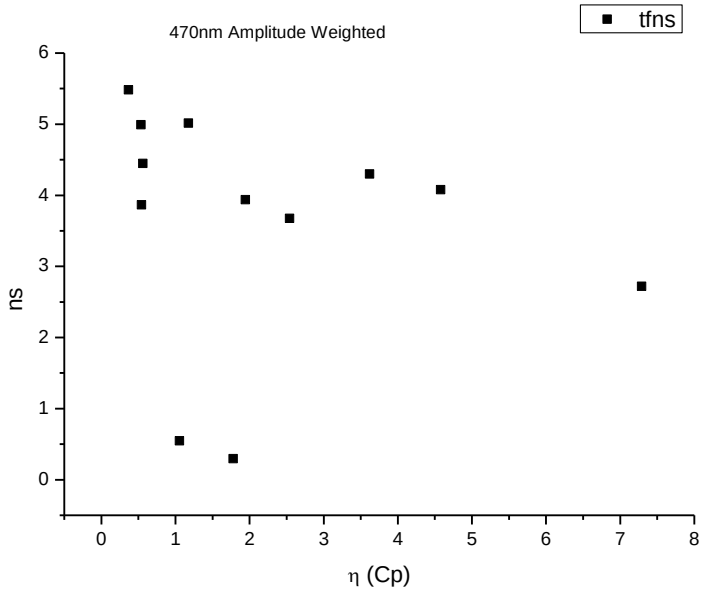

Figure 4.3.88. Amplitude weighted average lifetime (τ_f) of **25** at 470 nm versus η(Cp).

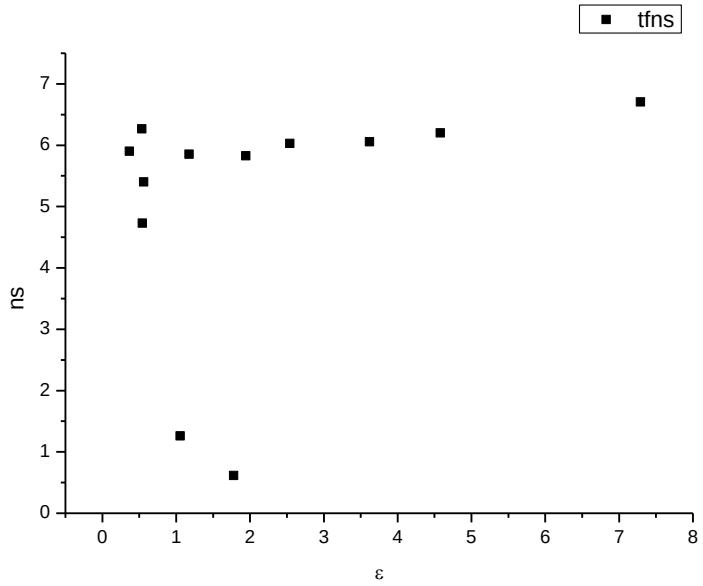

Figure 4.3.89. Intensity weighted average lifetime (τ_f) of **25** at 470 nm versus ε.

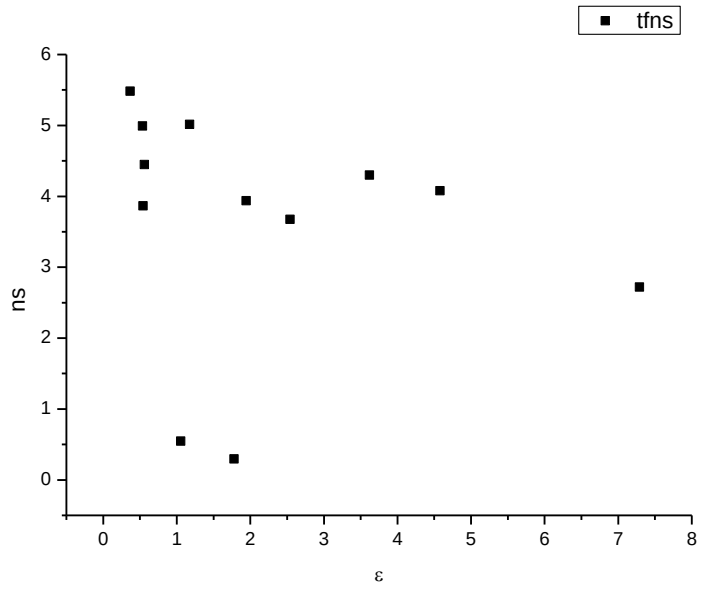

Figure 4.3.90. Amplitude weighted average lifetime (τ_f) of **25** at 470 nm versus ε.

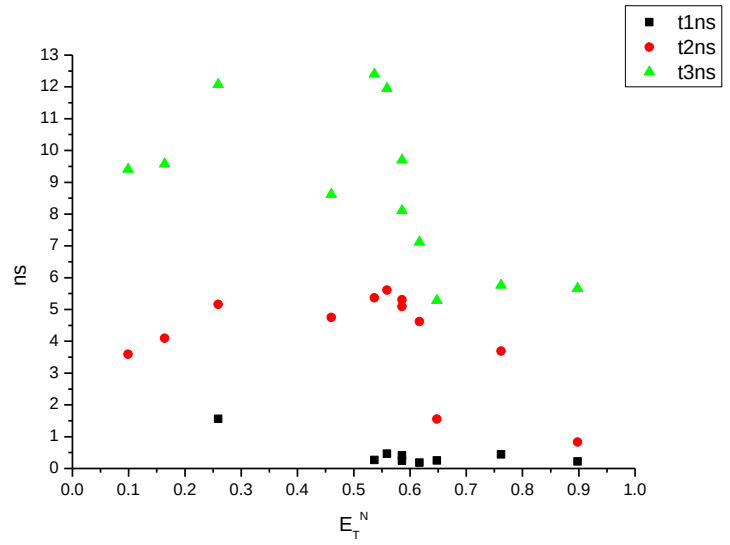

Figure 4.3.91. Intensity weighted components of TCSPC lifetime decay of **25** (470 nm) versus E_T^N.

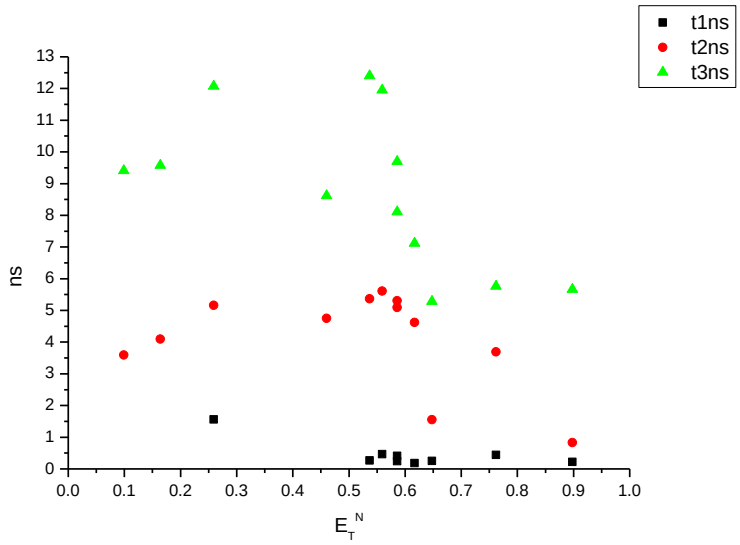

Figure 4.3.92. Amplitude weighted components of TCSPC lifetime decay of **25** (470 nm) versus E_T^N.

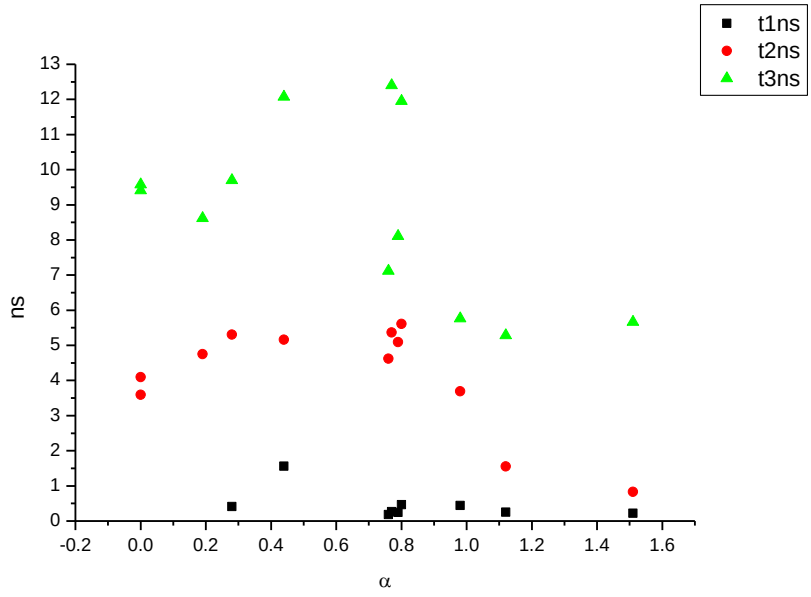

Figure 4.3.93. Intensity weighted components of TCSPC lifetime decay of **25** (470 nm) versus α.

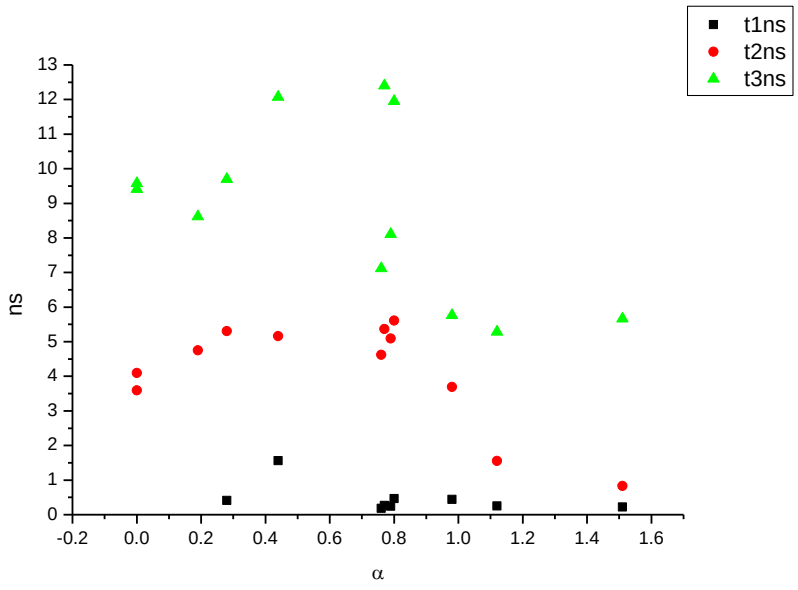

Figure 4.3.94. Amplitude weighted components of TCSPC lifetime decay of **25** (470 nm) versus α.

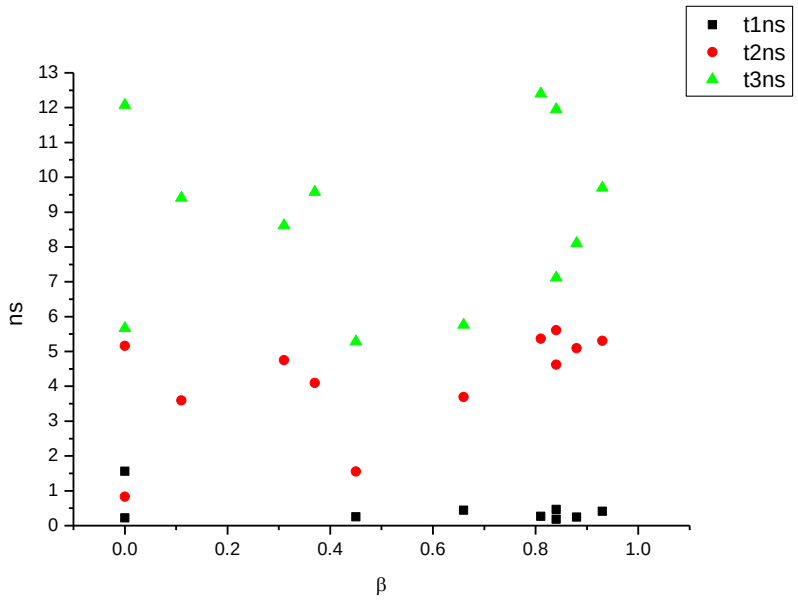

Figure 4.3.95. Intensity weighted components of TCSPC lifetime decay of **25** (470 nm) versus β.

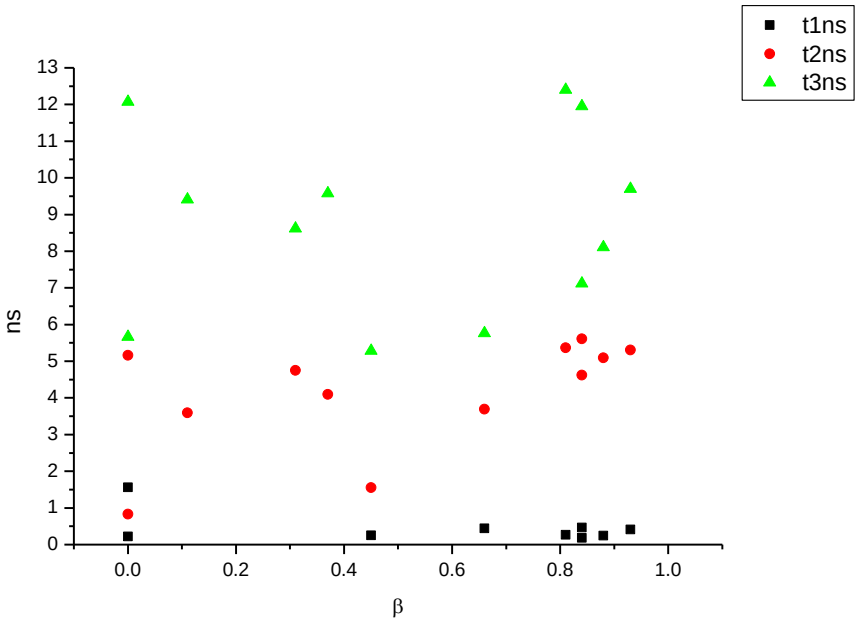

Figure 4.3.96. Amplitude weighted components of TCSPC lifetime decay of **25** (470 nm) versus β.

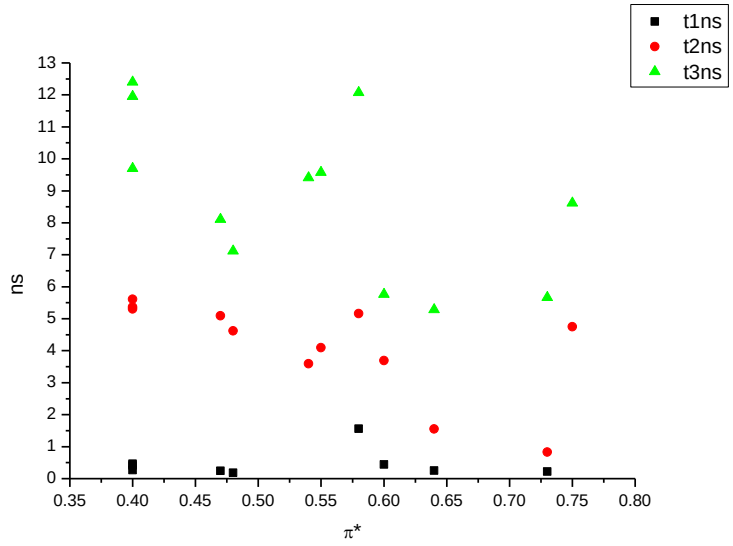

Figure 4.3.97. Intensity weighted components of TCSPC lifetime decay of **25** (470 nm) versus π*.

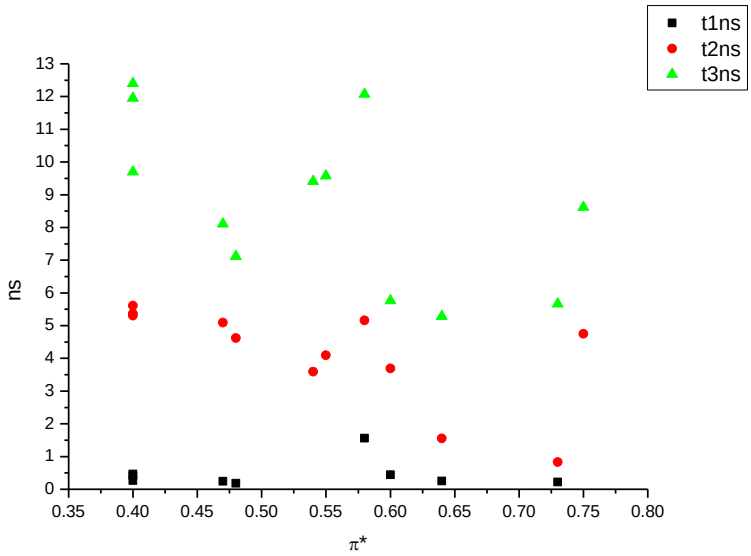

Figure 4.3.98. Amplitude weighted components of TCSPC lifetime decay of **25** (470 nm) versus π*.

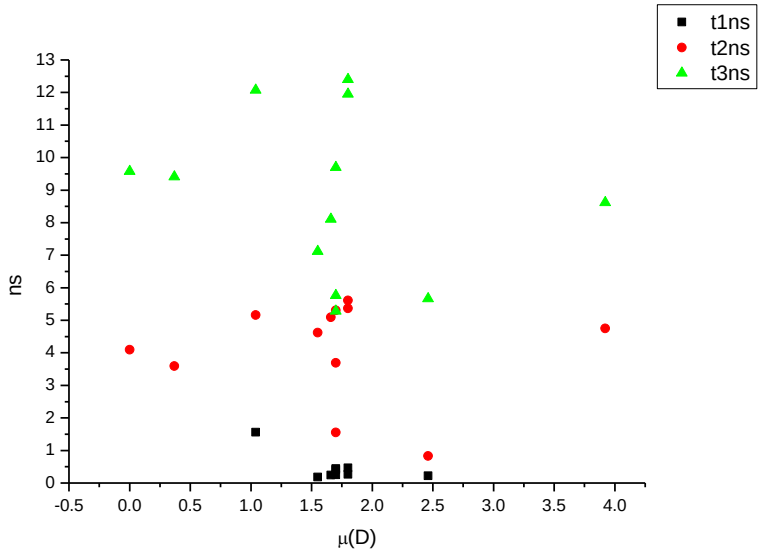

Figure 4.3.99. Intensity weighted components of TCSPC lifetime decay of **25** (470 nm) versus μ(D).

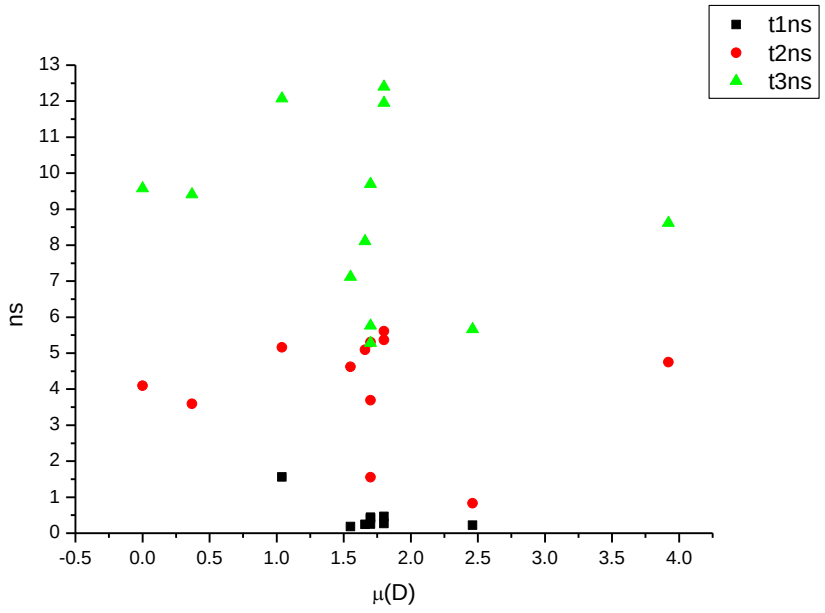

Figure 4.3.100. Amplitude weighted components of TCSPC lifetime decay of **25** (470 nm) versus μ(D).

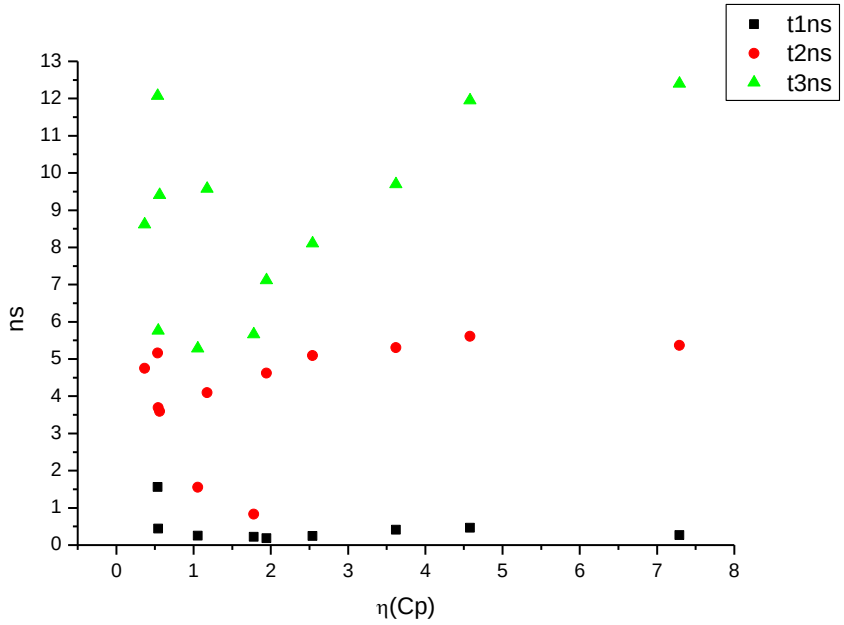

Figure 4.3.101. Intensity weighted components of TCSPC lifetime decay of **25** (470 nm) versus η(Cp).

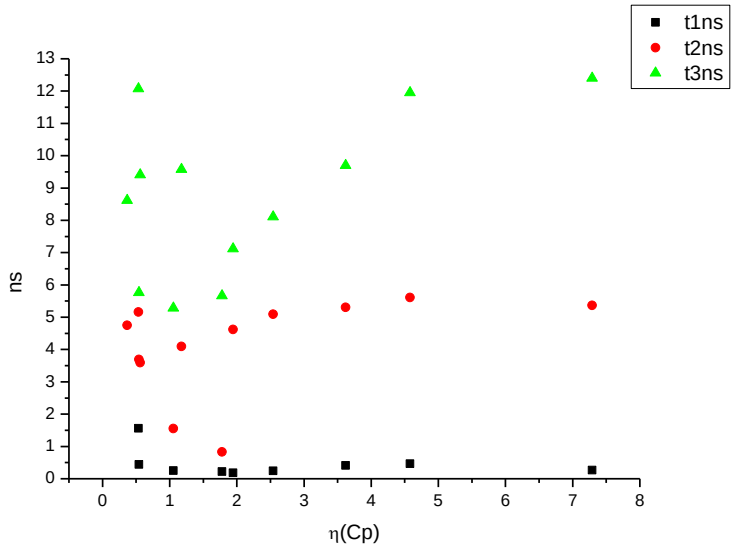

Figure 4.3.102. Amplitude weighted components of TCSPC lifetime decay of **25** (470 nm) versus η(Cp).

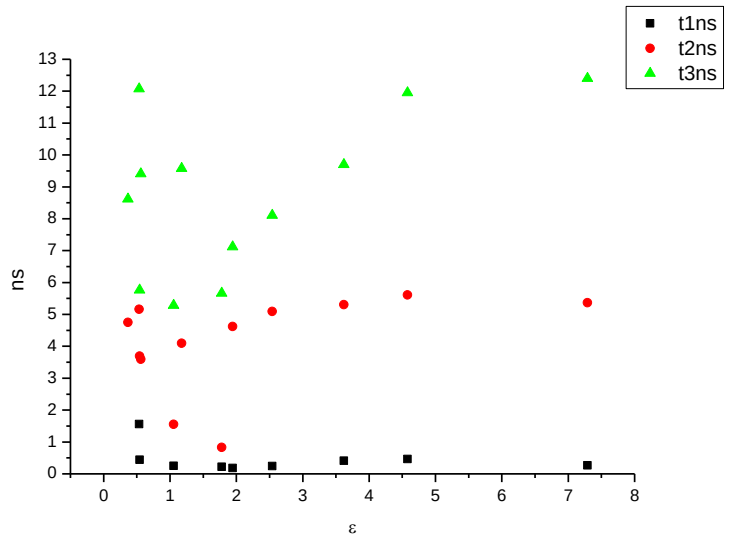

Figure 4.3.103. Intensity weighted components of TCSPC lifetime decay of **25** (470 nm) versus ε.

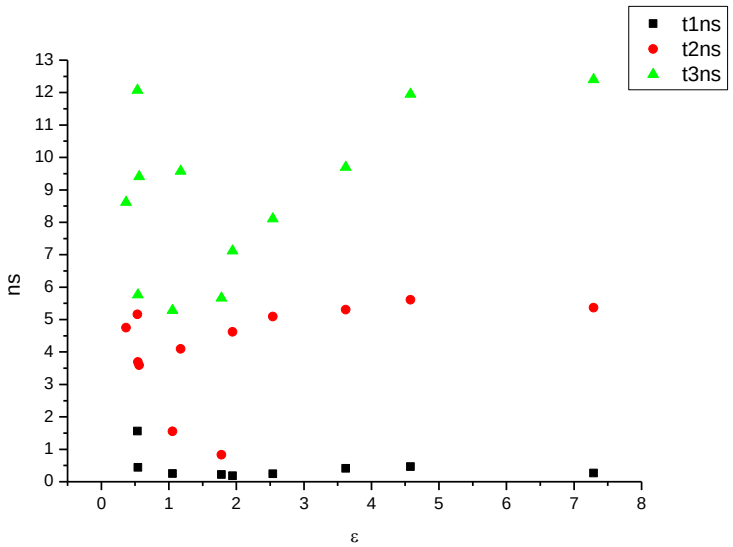

Figure 4.3.104. Amplitude weighted components of TCSPC lifetime decay of **25** (470 nm) versus ε.

4.3.7.2 570 nm Lifetime – Solvatochromic analysis.

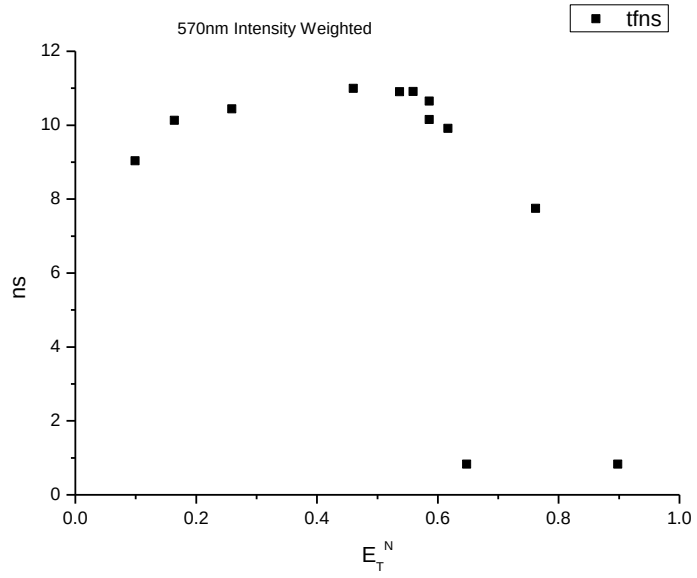

Figure 4.3.105. Intensity weighted average lifetime (τ_f) of **25** at 570 nm versus E_T^N.

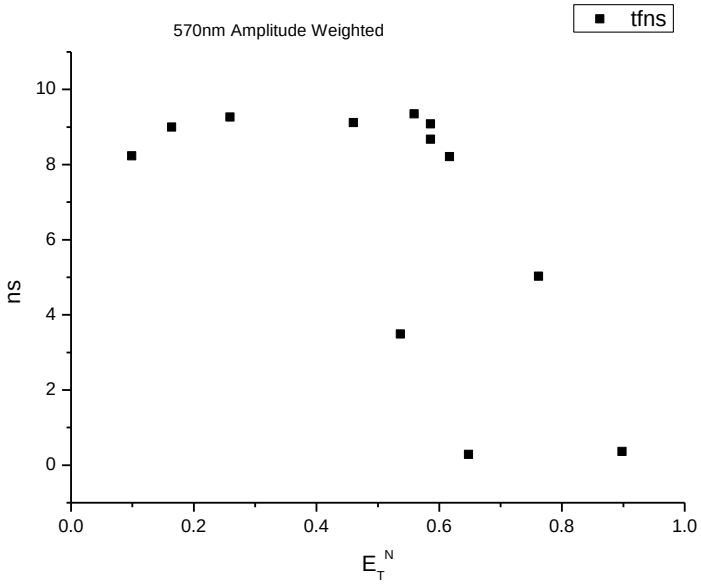

Figure 4.3.106. Amplitude weighted average lifetime (τ_f) of **25** at 570 nm versus E_T^N.

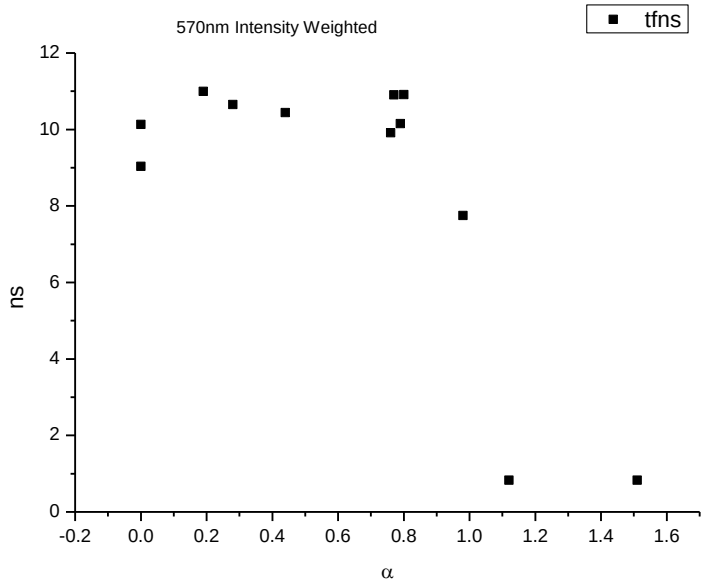

Figure 4.3.107. Intensity weighted average lifetime (τ_f) of **25** at 570 nm versus α.

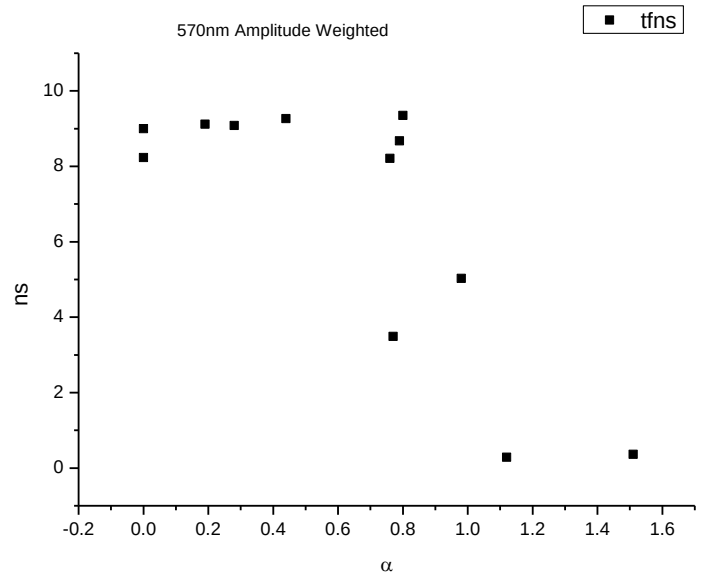

Figure 4.3.108. Amplitude weighted average lifetime (τ_f) of **25** at 570 nm versus α.

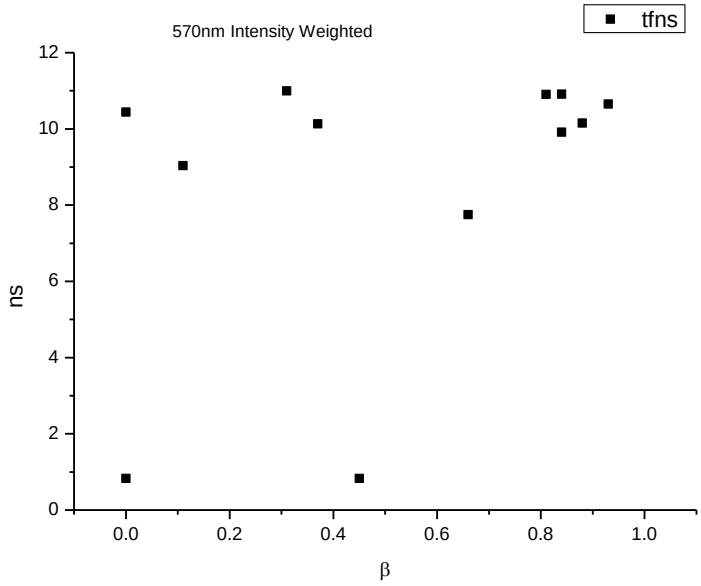

Figure 4.3.109. Intensity weighted average lifetime (τ_f) of **25** at 570 nm versus β.

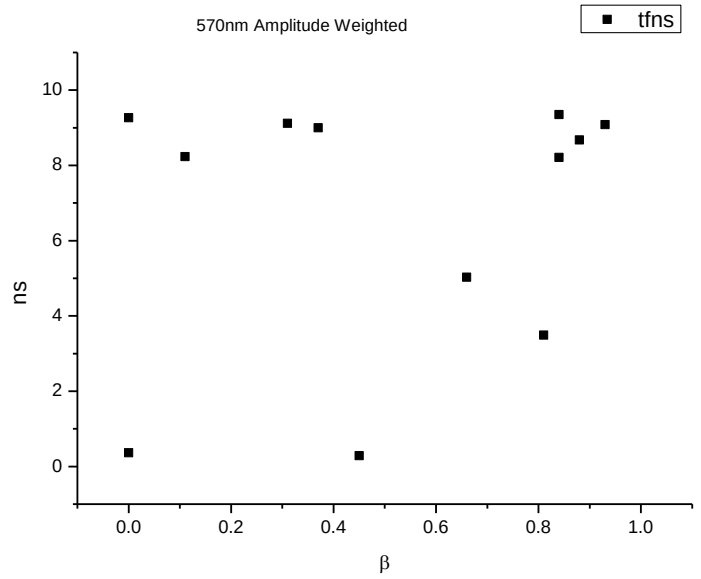

Figure 4.3.110. Amplitude weighted average lifetime (τ_f) of **25** at 570 nm versus β.

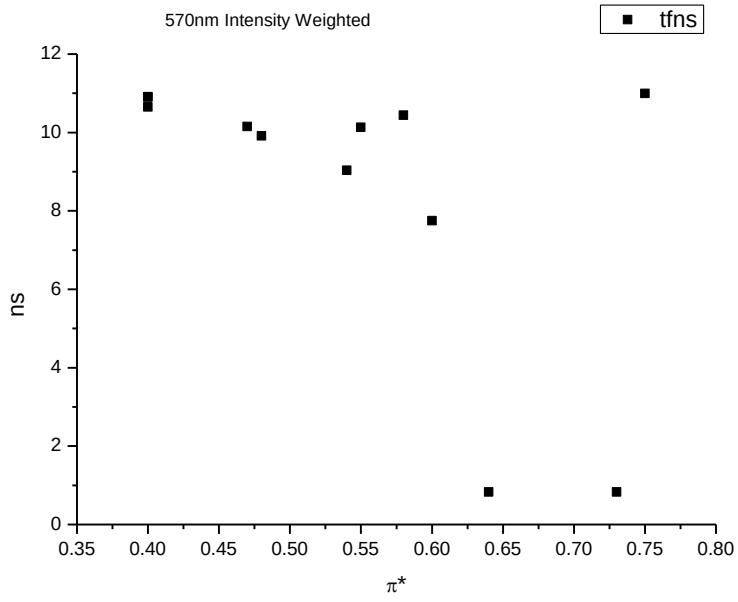

Figure 4.3.111. Intensity weighted average lifetime (τ_f) of **25** at 570 nm versus π*.

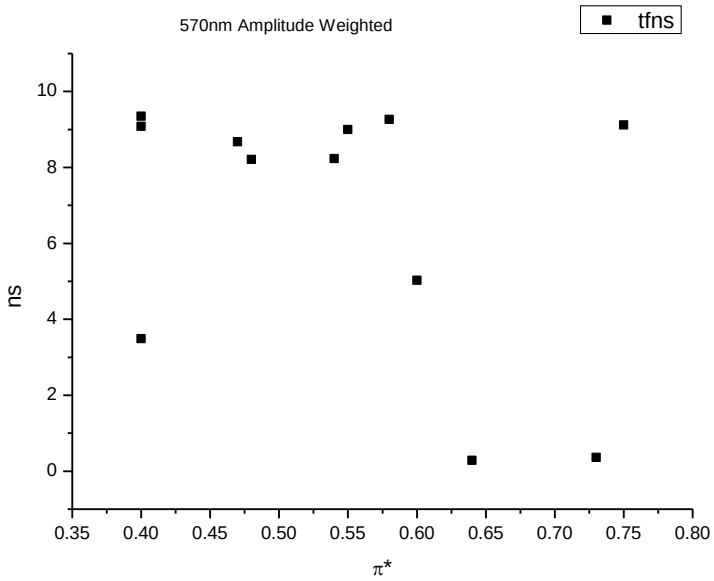

Figure 4.3.112. Amplitude weighted average lifetime (τ_f) of **25** at 570 nm versus π*.

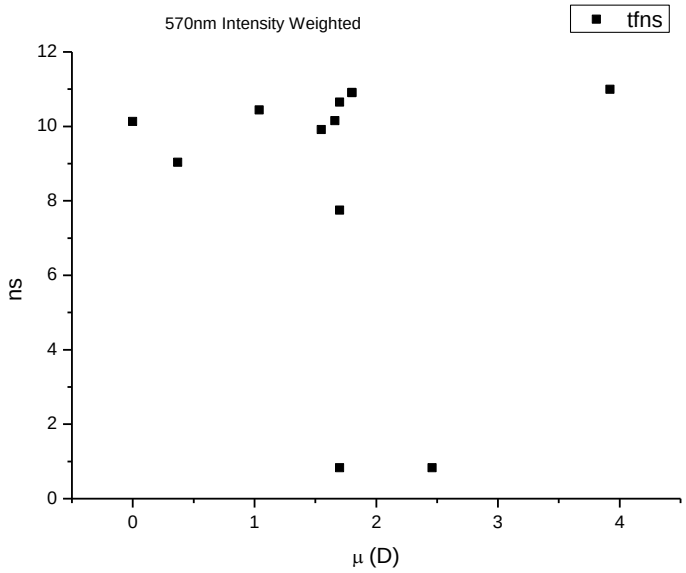

Figure 4.3.113. Intensity weighted average lifetime (τ_f) of **25** at 570 nm versus μ(D).

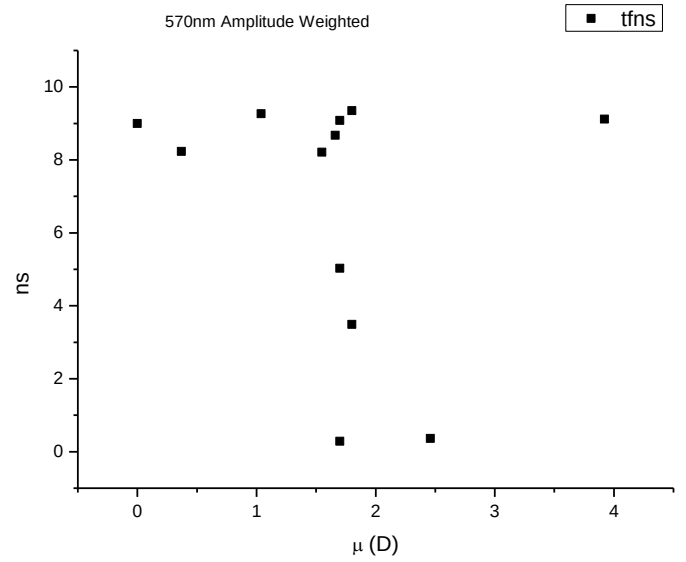

Figure 4.3.114. Amplitude weighted average lifetime (τ_f) of **25** at 570 nm versus μ(D).

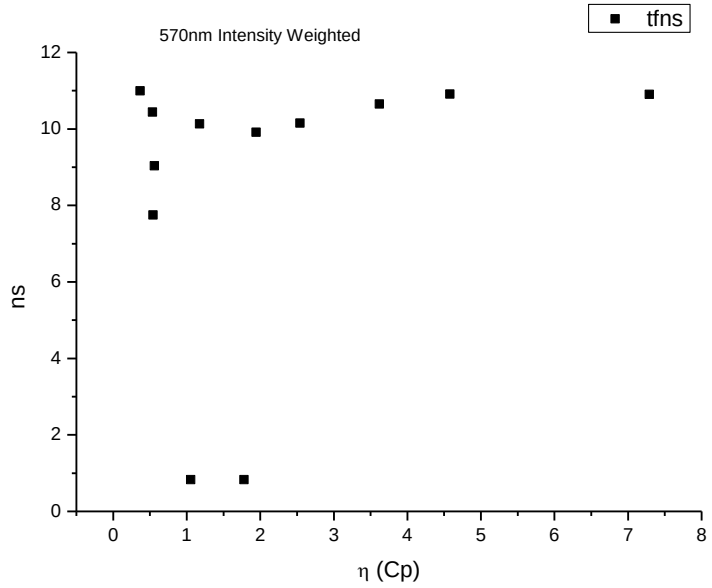

Figure 4.3.115. Intensity weighted average lifetime (τ_f) of **25** at 570 nm versus η(Cp).

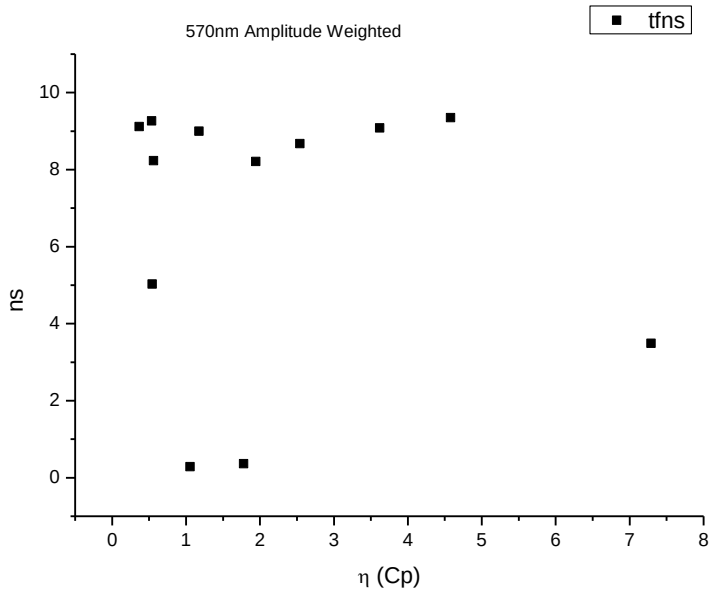

Figure 4.3.116. Amplitude weighted average lifetime (τ_f) of **25** at 570 nm versus η(Cp).

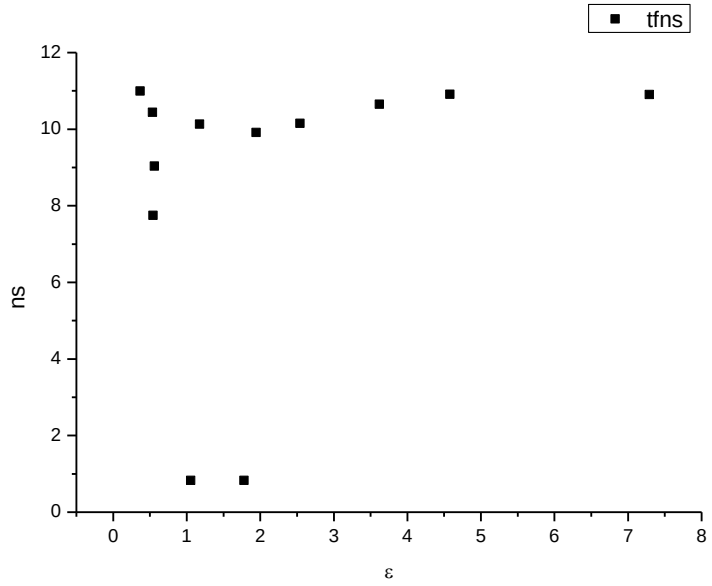

Figure 4.3.117. Intensity weighted average lifetime (τ_f) of **25** at 570 nm versus ε.

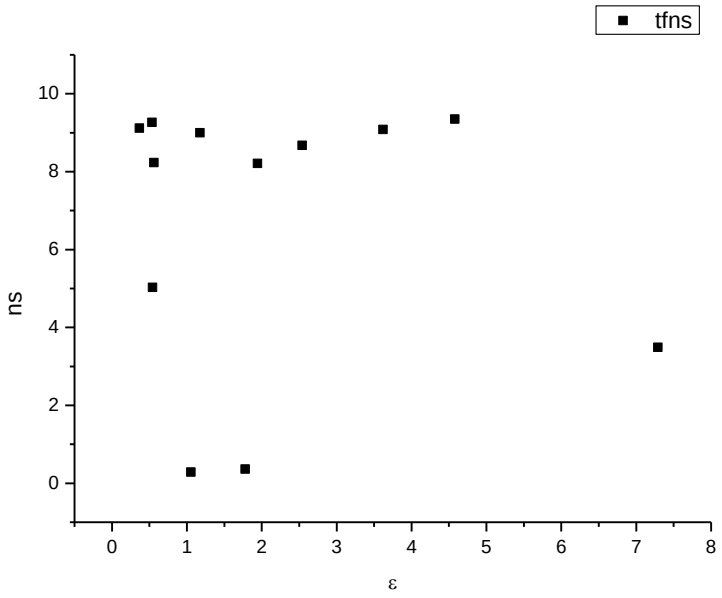

Figure 4.3.118. Amplitude weighted average lifetime (τ_f) of **25** at 570 nm versus ε.

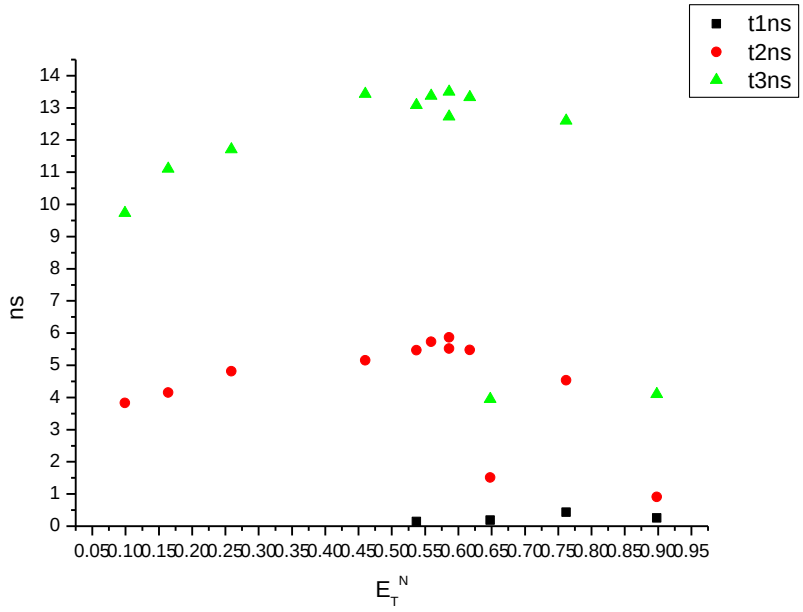

Figure 4.3.119. Intensity weighted components of TCSPC lifetime decay of **25** (570 nm) versus E_T^N.

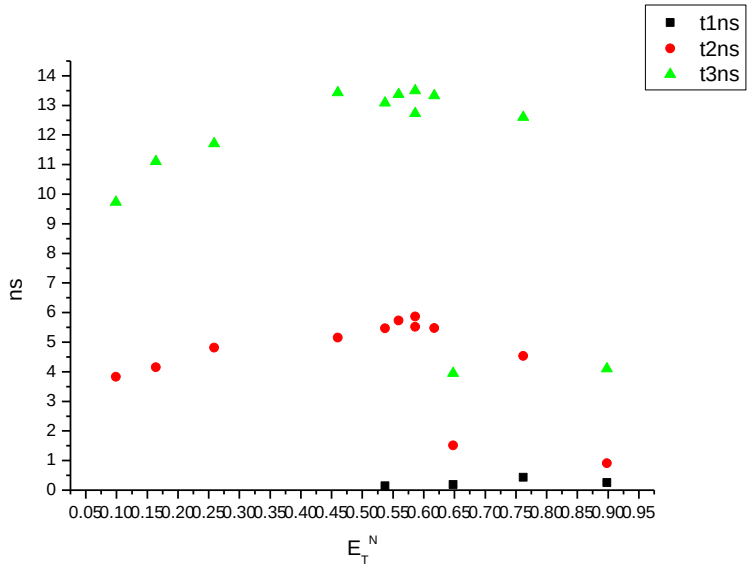

Figure 4.3.120. Amplitude weighted components of TCSPC lifetime decay of **25** (570 nm) versus E_T^N.

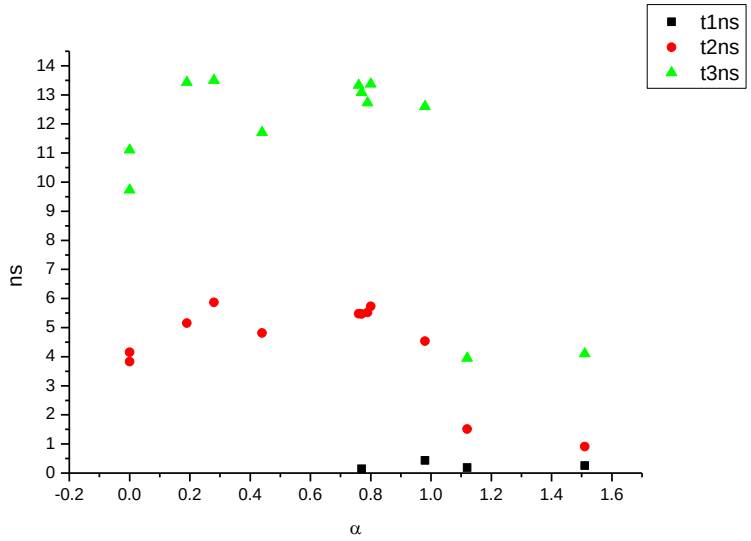

Figure 4.3.121. Intensity weighted components of TCSPC lifetime decay of **25** (570 nm) versus α.

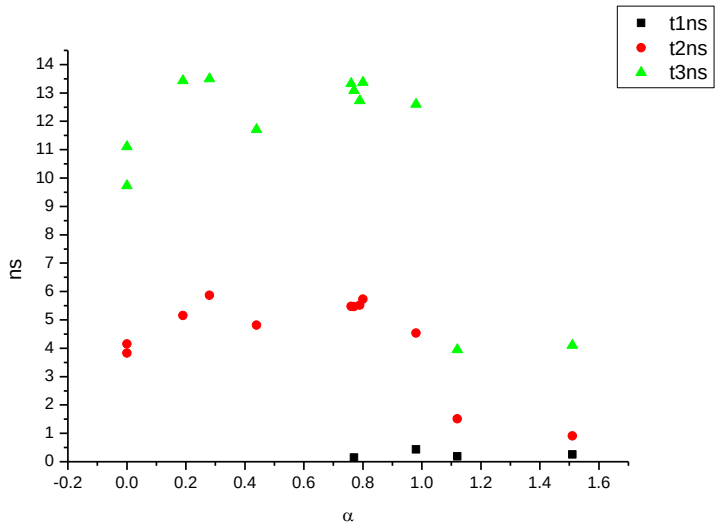

Figure 4.3.122. Amplitude weighted components of TCSPC lifetime decay of **25** (570 nm) versus α.

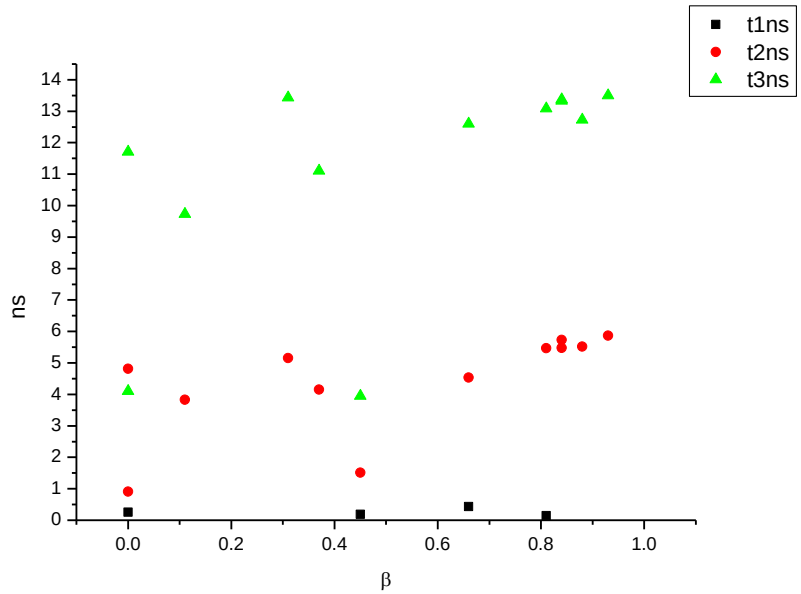

Figure 4.3.123. Intensity weighted components of TCSPC lifetime decay of **25** (570 nm) versus β.

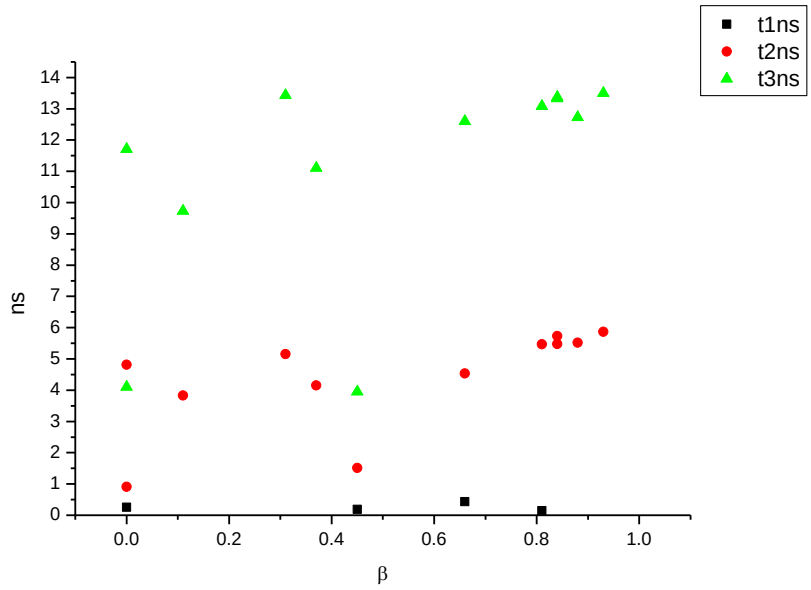

Figure 4.3.124. Amplitude weighted components of TCSPC lifetime decay of **25** (570 nm) versus β.

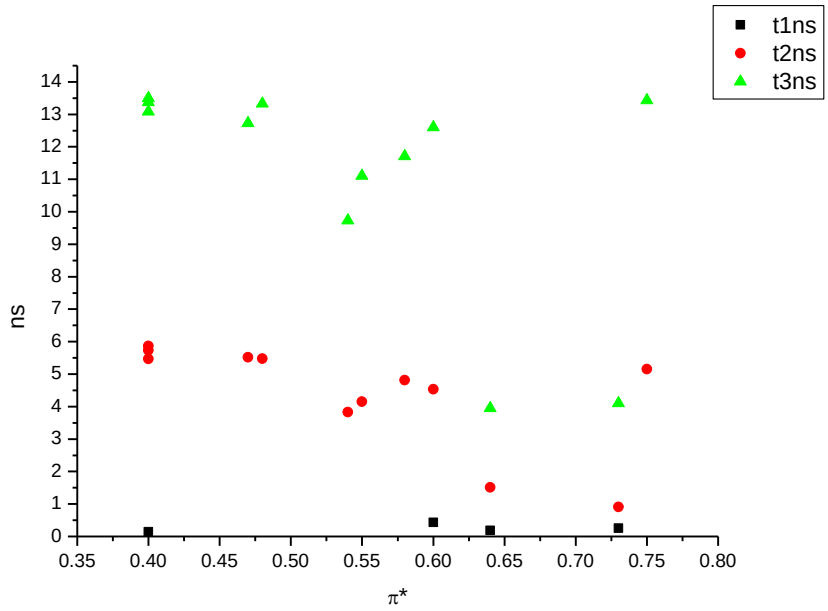

Figure 4.3.125. Intensity weighted components of TCSPC lifetime decay of **25** (570 nm) versus π*.

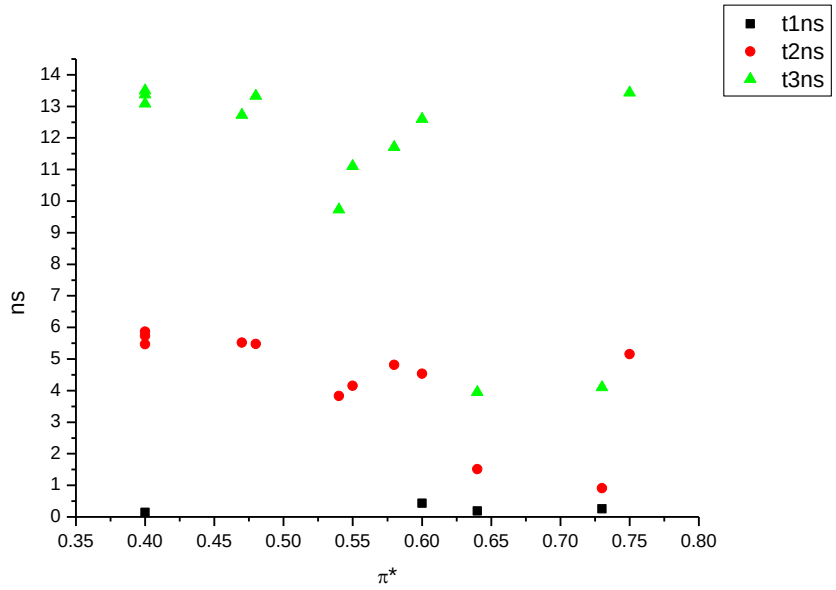

Figure 4.3.126. Amplitude weighted components of TCSPC lifetime decay of **25** (570 nm) versus π*.

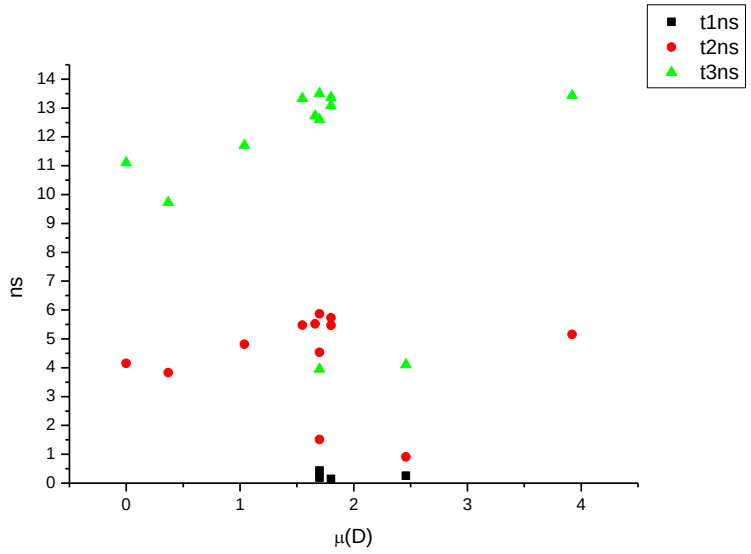

Figure 4.3.127. Intensity weighted components of TCSPC lifetime decay of **25** (570 nm) versus μ(D).

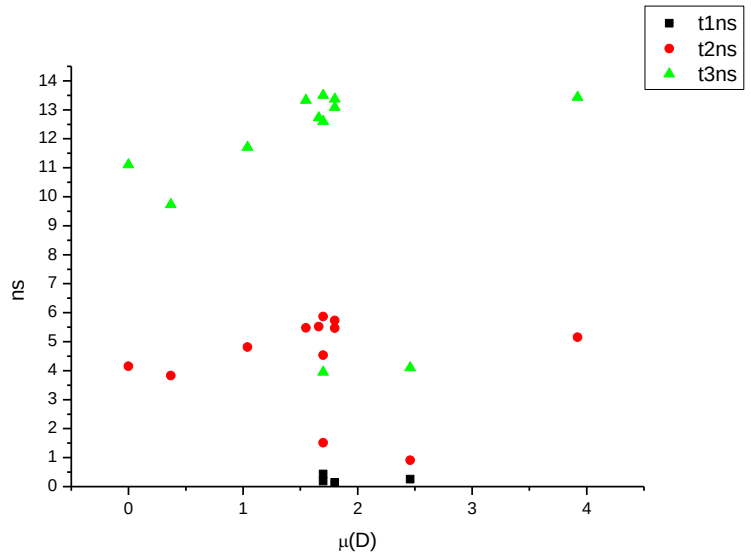

Figure 4.3.128. Amplitude weighted components of TCSPC lifetime decay of **25** (570 nm) versus μ(D).

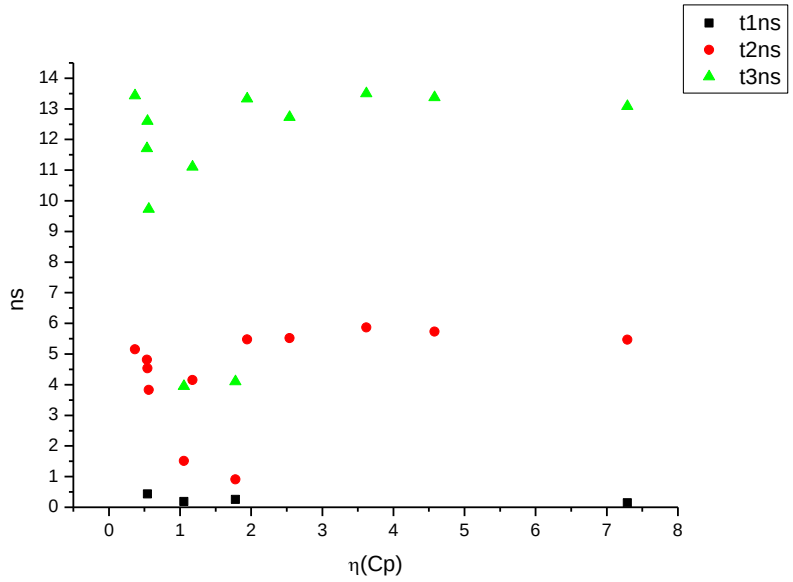

Figure 4.3.129. Intensity weighted components of TCSPC lifetime decay of **25** (570 nm) versus η(Cp).

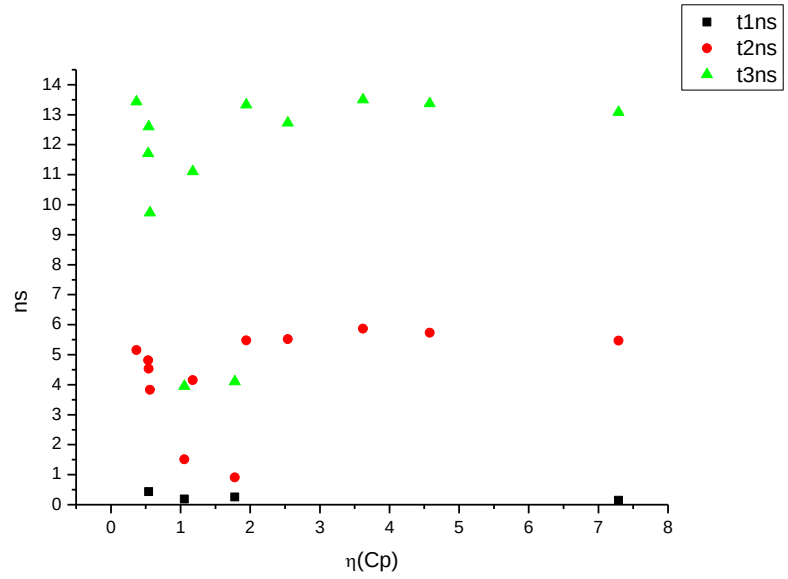

Figure 4.3.130. Amplitude weighted components of TCSPC lifetime decay of **25** (570 nm) versus η(Cp).

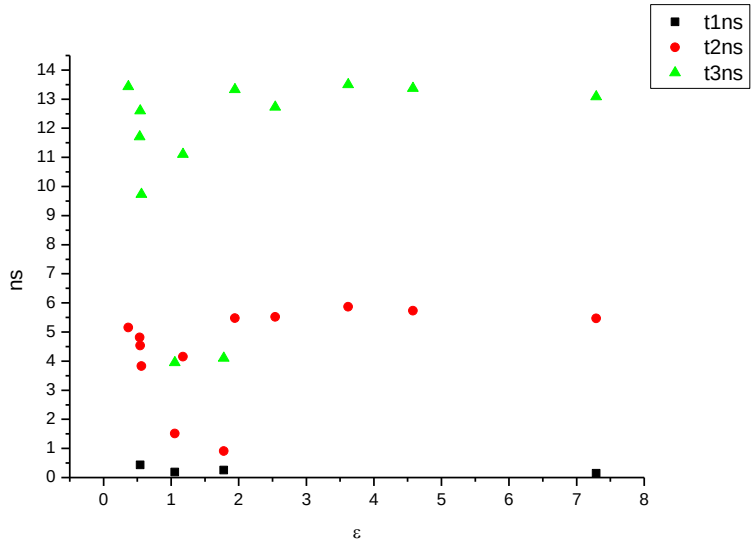

Figure 4.3.131. Intensity weighted components of TCSPC lifetime decay of **25** (570 nm) versus ε.

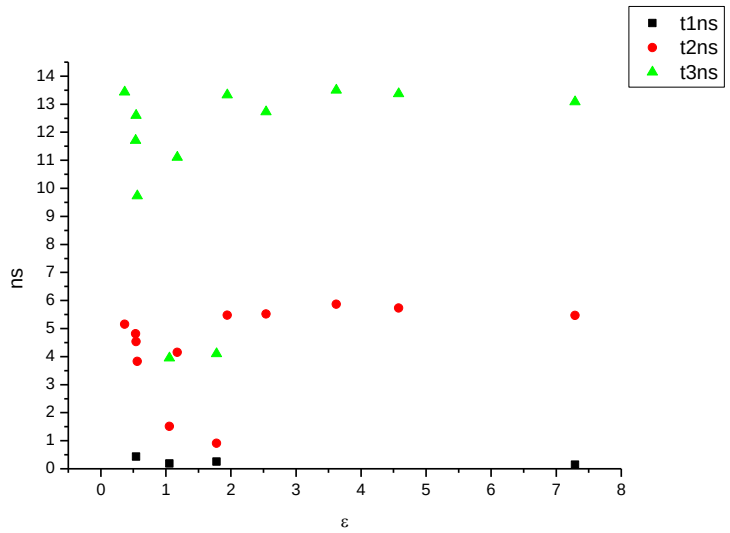

Figure 4.3.132. Amplitude weighted components of TCSPC lifetime decay of **25** (570 nm) versus ε.

4.3.8 Ultraviolet-visible absorption spectra.

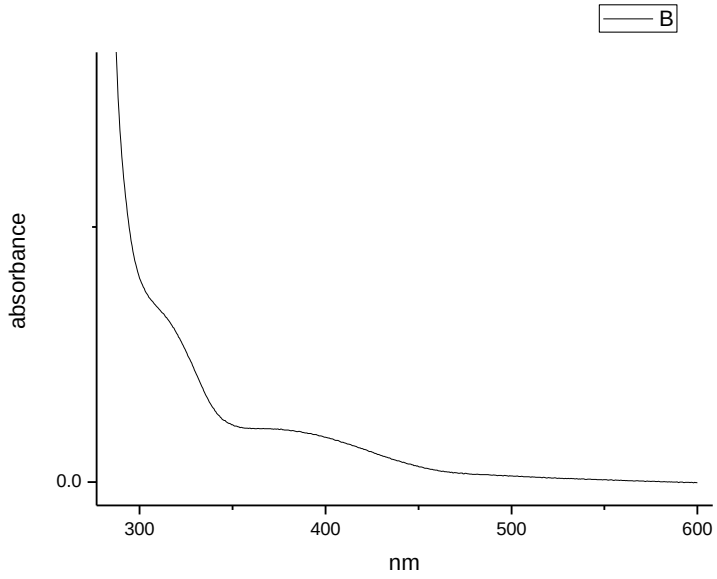

Figure 4.3.133. Ultraviolet-Visible absorption spectrum of **25** recorded in Toluene.

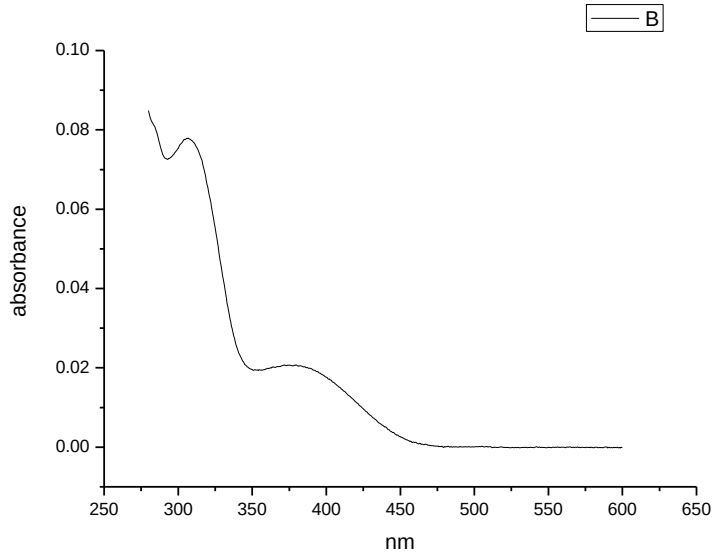

Figure 4.3.134. Ultraviolet-Visible absorption spectrum of **25** recorded in 1,4-dioxane.

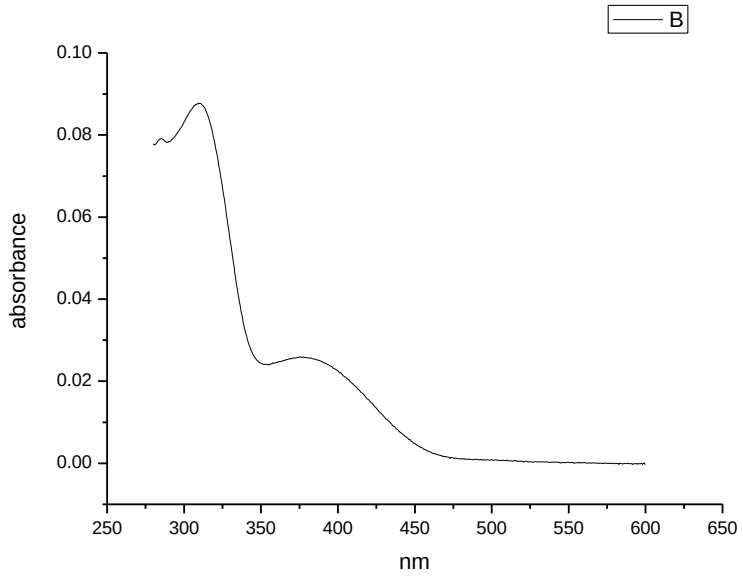

Figure 4.3.135. Ultraviolet-Visible absorption spectrum of **25** recorded in Chloroform.

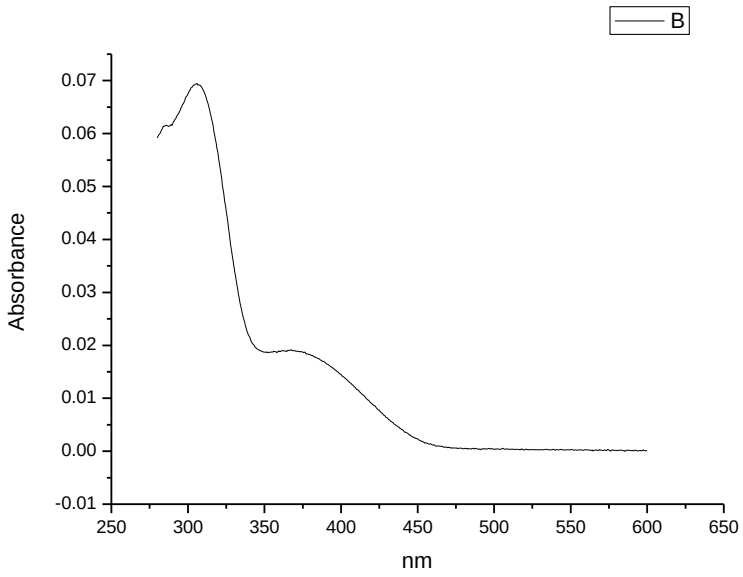

Figure 4.3.136. Ultraviolet-Visible absorption spectrum of **25** recorded in Acetonitrile.

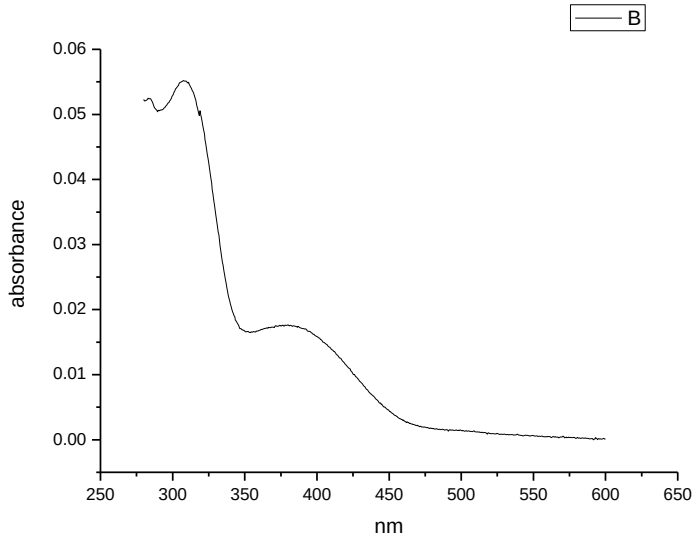

Figure 4.3.137. Ultraviolet-Visible absorption spectrum of **25** recorded in 1-octanol.

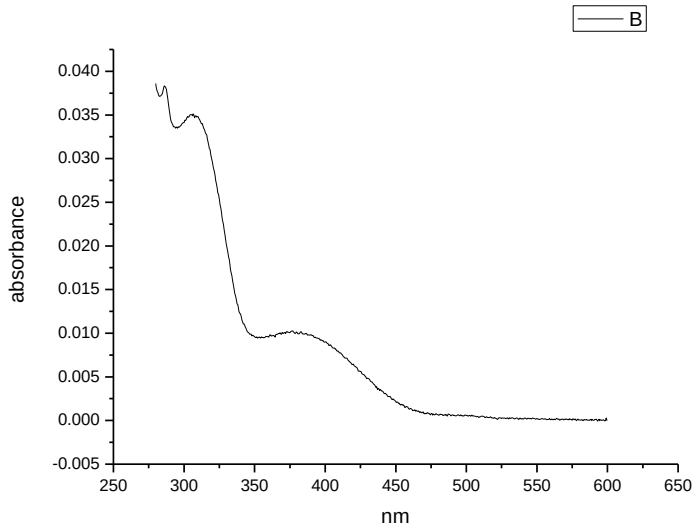

Figure 4.3.138. Ultraviolet-Visible absorption spectrum of **25** recorded in 1-hexanol.

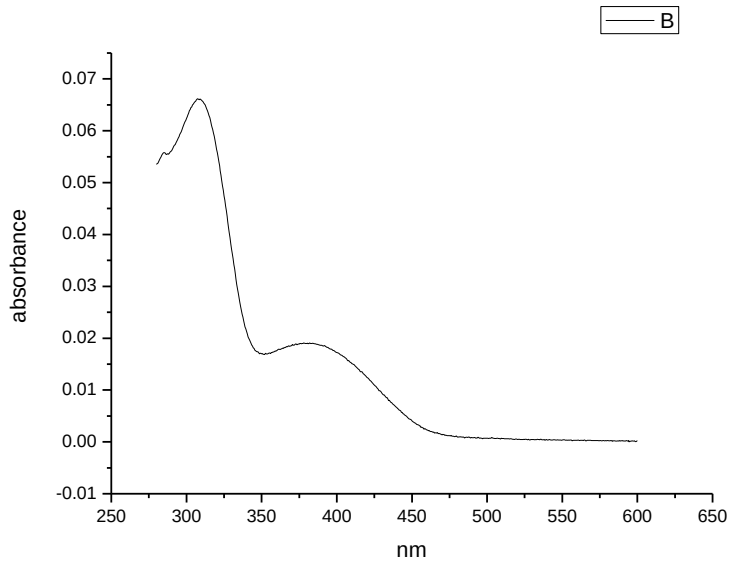

Figure 4.3.139. Ultraviolet-Visible absorption spectrum of **25** recorded in 1-butanol.

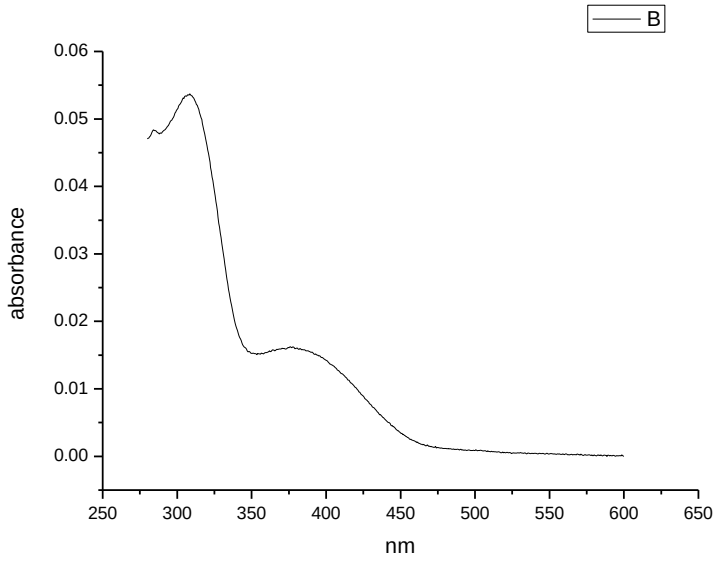

Figure 4.3.140. Ultraviolet-Visible absorption spectrum of **25** recorded in 1-pentanol.

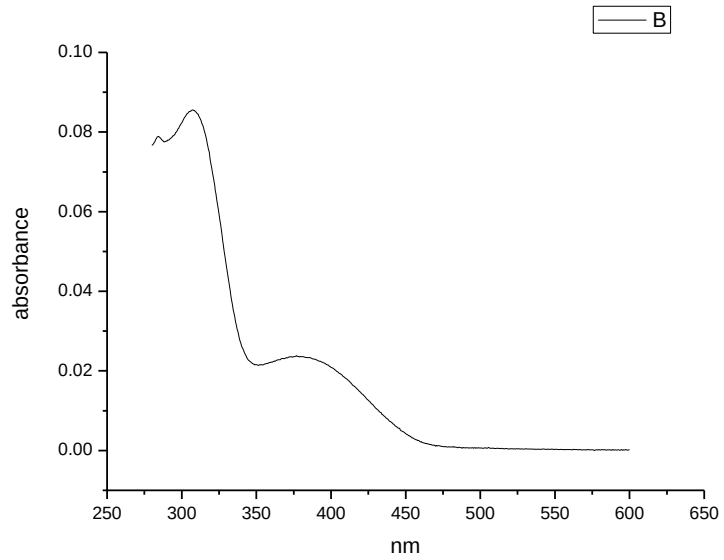

Figure 4.3.141. Ultraviolet-Visible absorption spectrum of **25** recorded in 1-propanol.

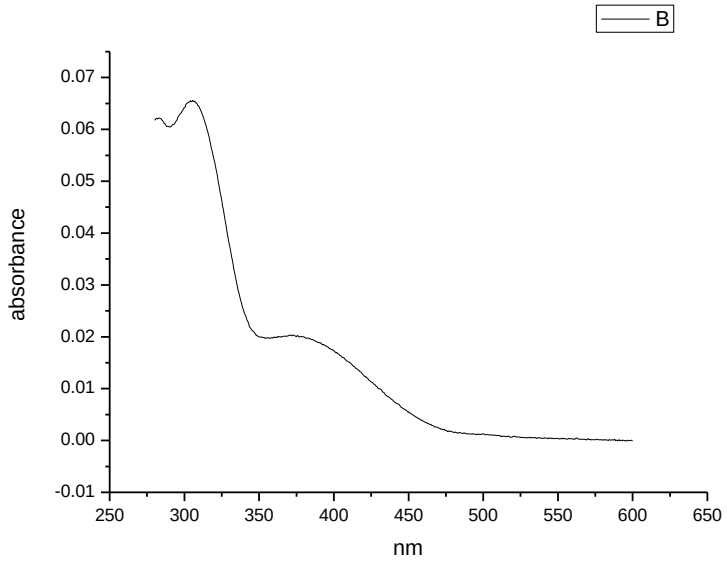

Figure 4.3.142. Ultraviolet-Visible absorption spectrum of **25** recorded in Acetic Acid.

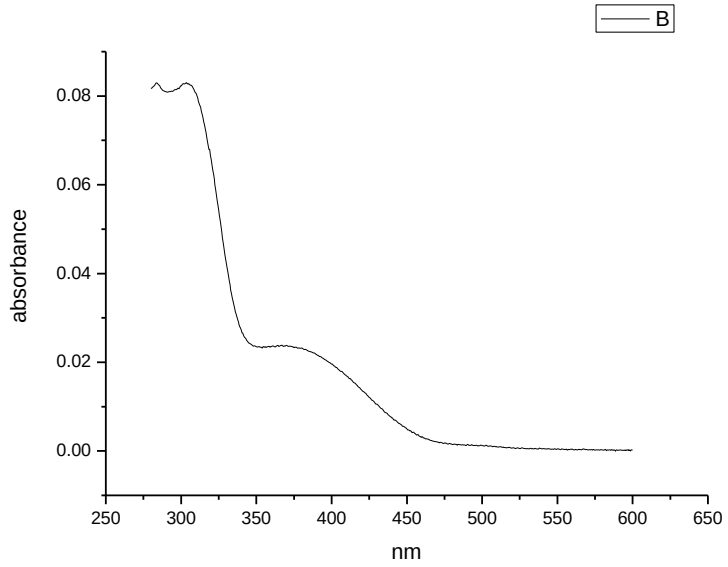

Figure 4.3.143. Ultraviolet-Visible absorption spectrum of **25** recorded in Methanol.

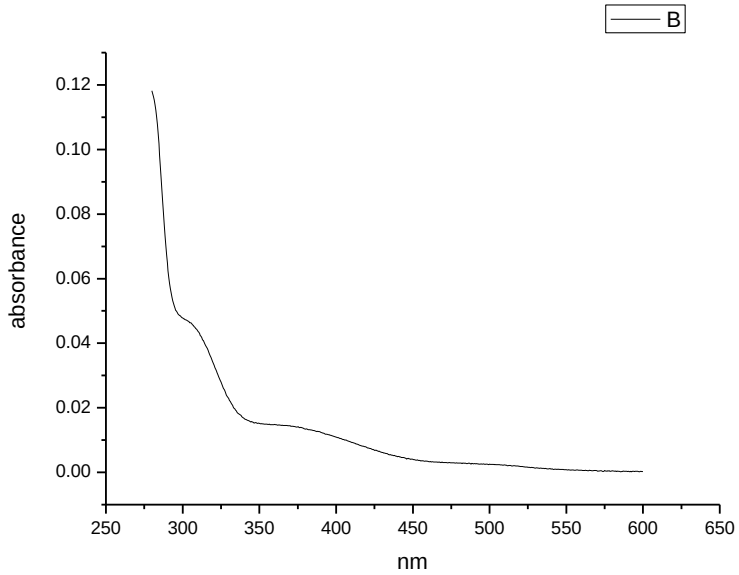

Figure 4.3.144. Ultraviolet-Visible absorption spectrum of **25** recorded in 2,2,2-trifluoroethanol.

4.3.9 Fluorescence Emission spectra.

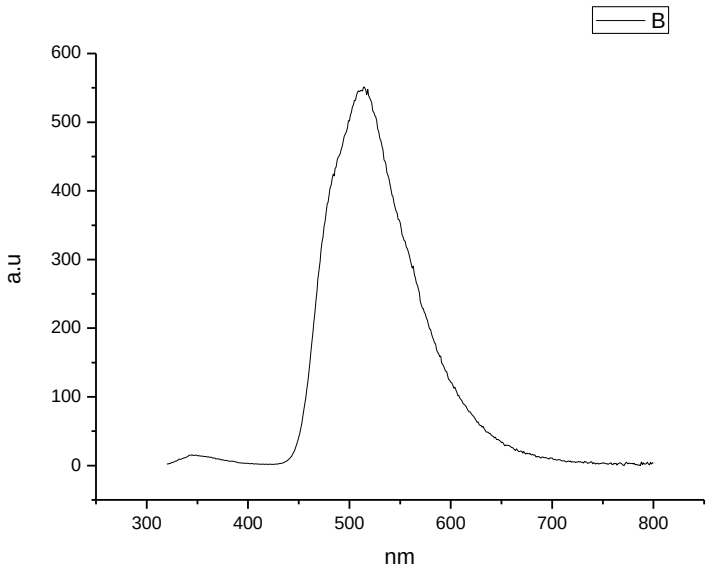

Figure 4.3.145. Fluorescence emission spectrum of **25** recorded in Toluene at 310 nm excitation.

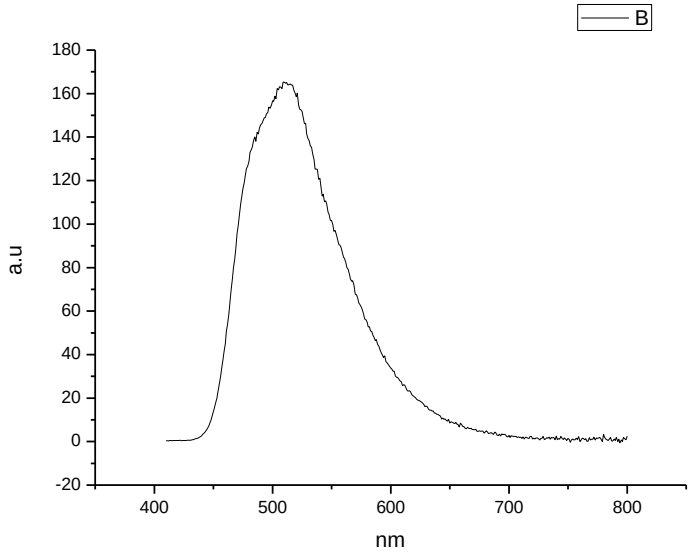

Figure 4.3.146. Fluorescence emission spectrum of **25** recorded in Toluene at 400 nm excitation.

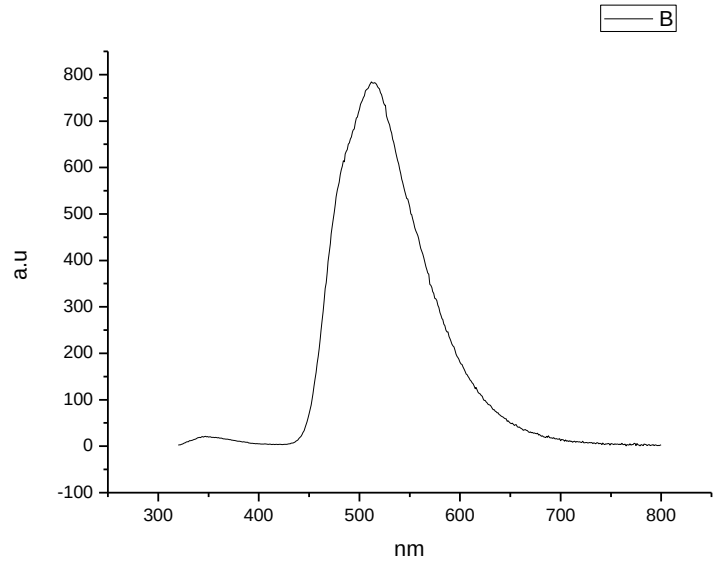

Figure 4.3.147. Fluorescence emission spectrum of **25** recorded in 1,4-dioxane at 310 nm excitation.

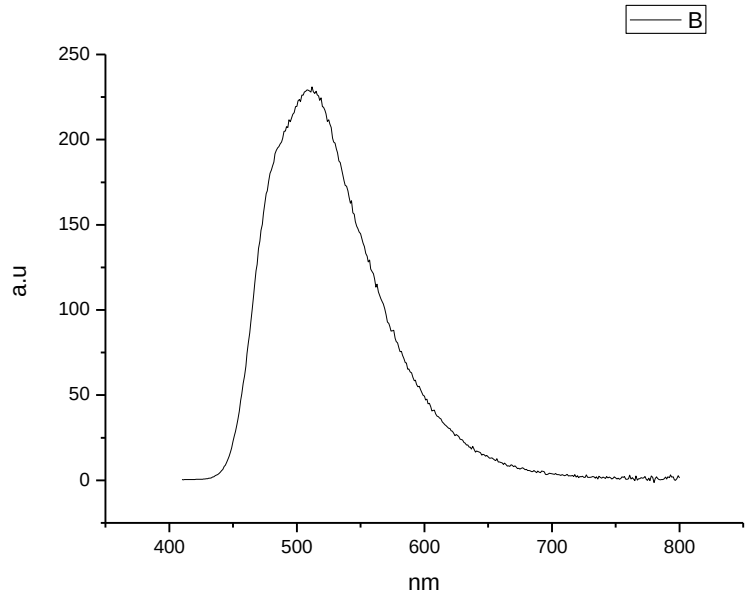

Figure 4.3.148. Fluorescence emission spectrum of **25** recorded in 1,4-dioxane at 400 nm excitation.

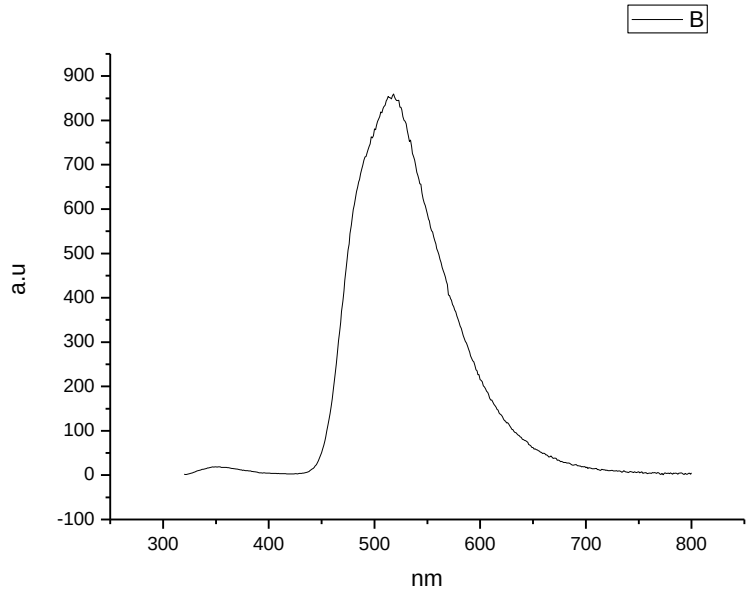

Figure 4.3.149. Fluorescence emission spectrum of **25** recorded in Chloroform at 310 nm excitation.

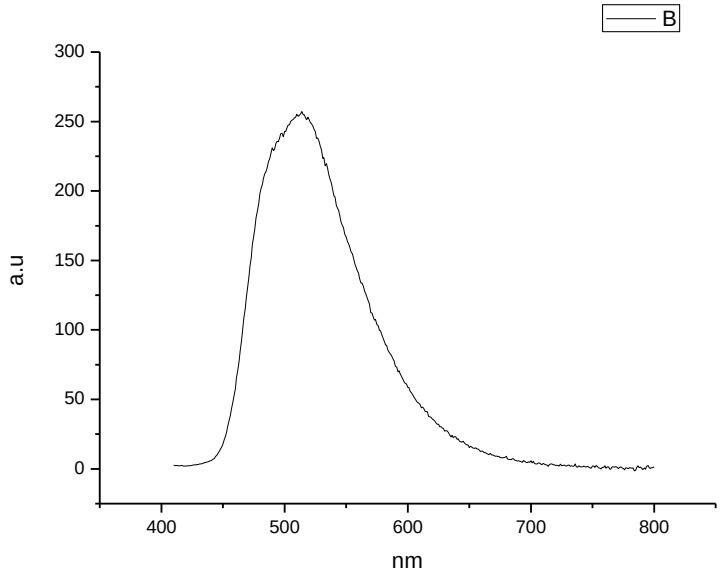

Figure 4.3.150. Fluorescence emission spectrum of **25** recorded in Chloroform at 400 nm excitation.

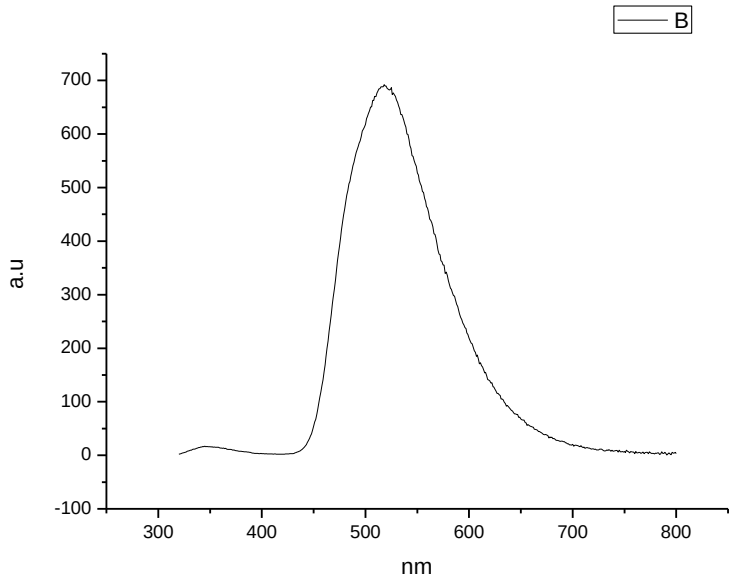

Figure 4.3.151. Fluorescence emission spectrum of **25** recorded in Acetonitrile at 310 nm excitation.

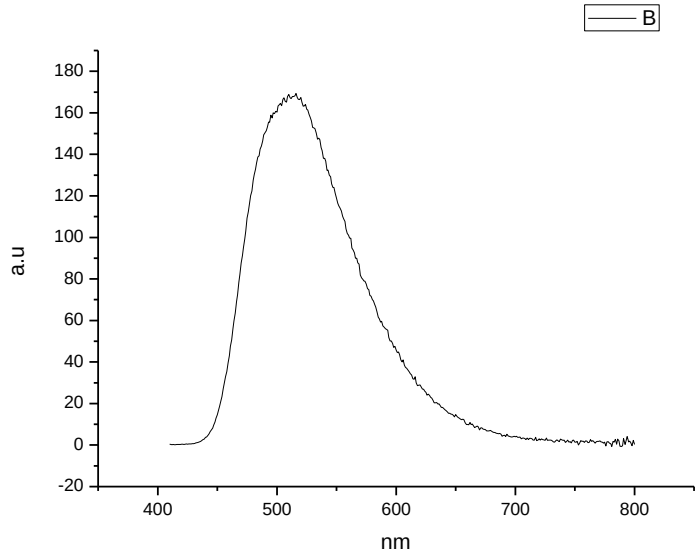

Figure 4.3.152. Fluorescence emission spectrum of **25** recorded in Acetonitrile at 400 nm excitation.

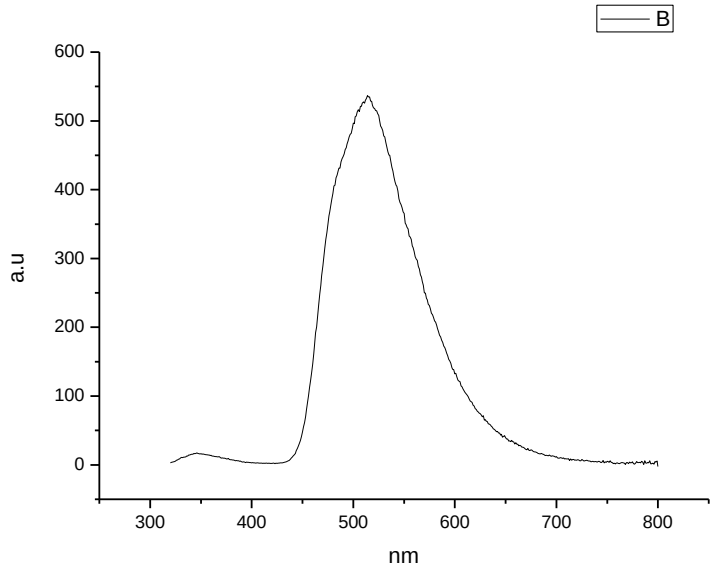

Figure 4.3.153. Fluorescence emission spectrum of **25** recorded in 1-octanol at 310 nm excitation.

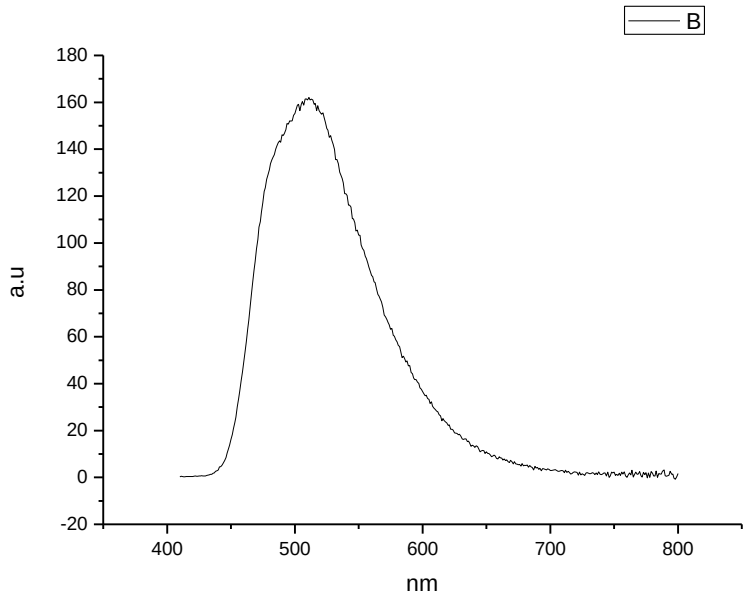

Figure 4.3.154. Fluorescence emission spectrum of **25** recorded in 1-octanol at 400 nm excitation.

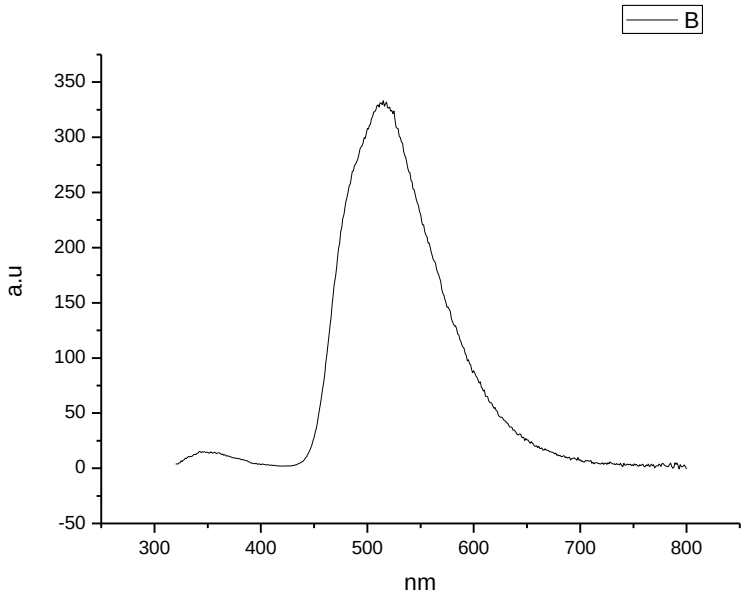

Figure 4.3.155. Fluorescence emission spectrum of **25** recorded in 1-hexanol at 310 nm excitation.

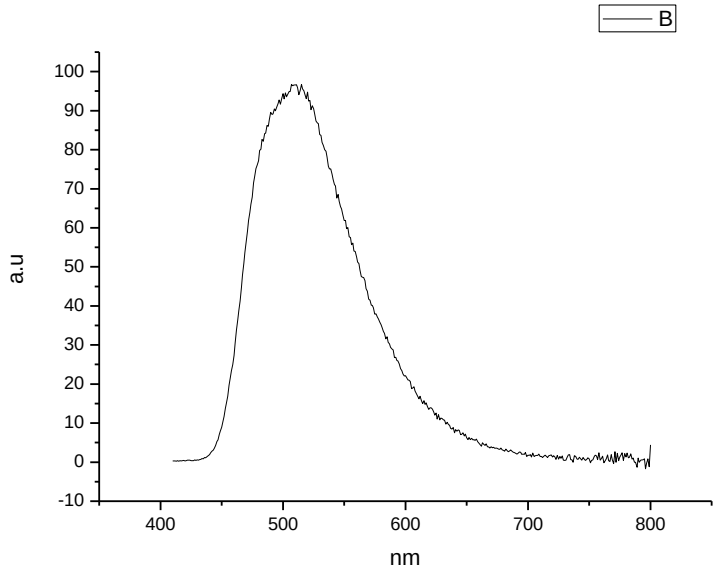

Figure 4.3.156. Fluorescence emission spectrum of **25** recorded in 1-hexanol at 400 nm excitation.

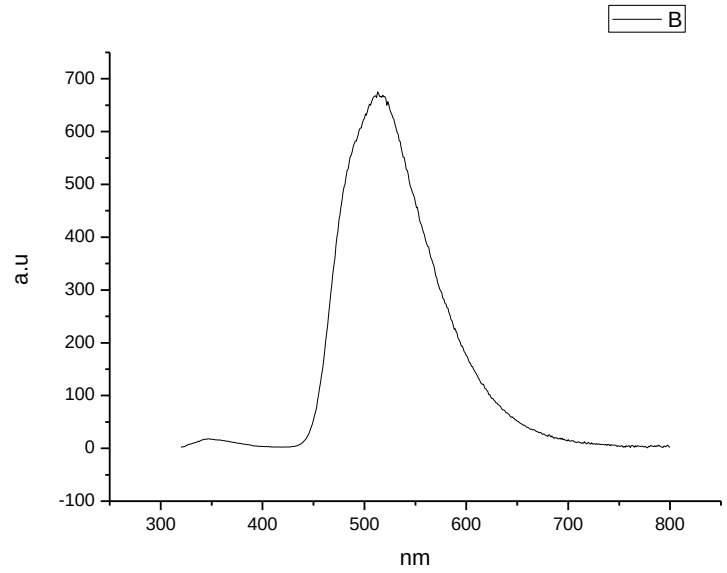

Figure 4.3.157. Fluorescence emission spectrum of **25** recorded in 1-butanol at 310 nm excitation.

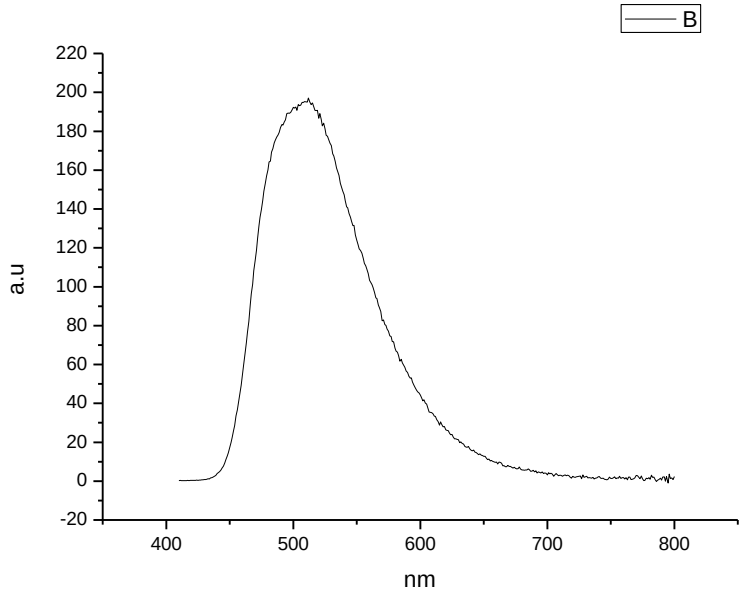

Figure 4.3.158. Fluorescence emission spectrum of **25** recorded in 1-butanol at 400 nm excitation.

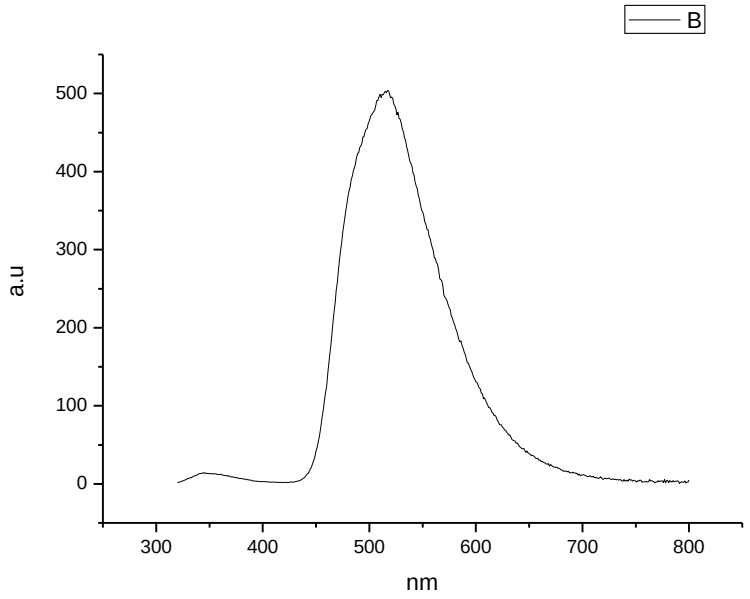

Figure 4.3.159. Fluorescence emission spectrum of **25** recorded in 1-pentanol at 310 nm excitation.

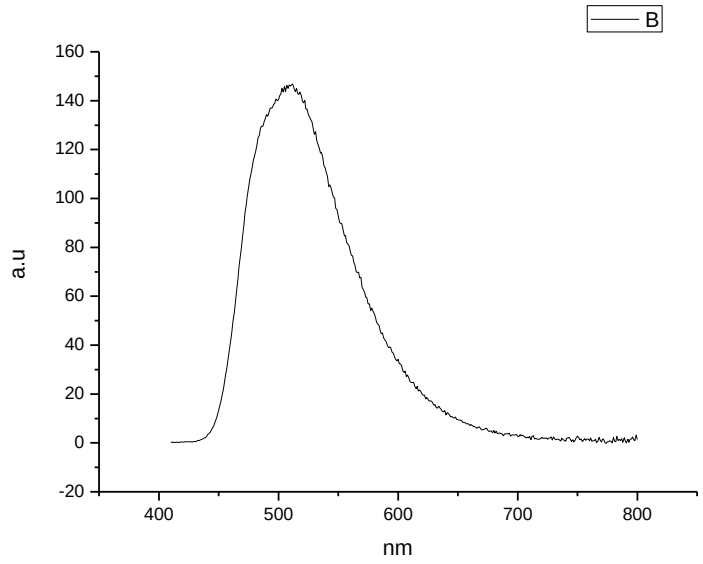

Figure 4.3.160. Fluorescence emission spectrum of **25** recorded in 1-pentanol at 400 nm excitation.

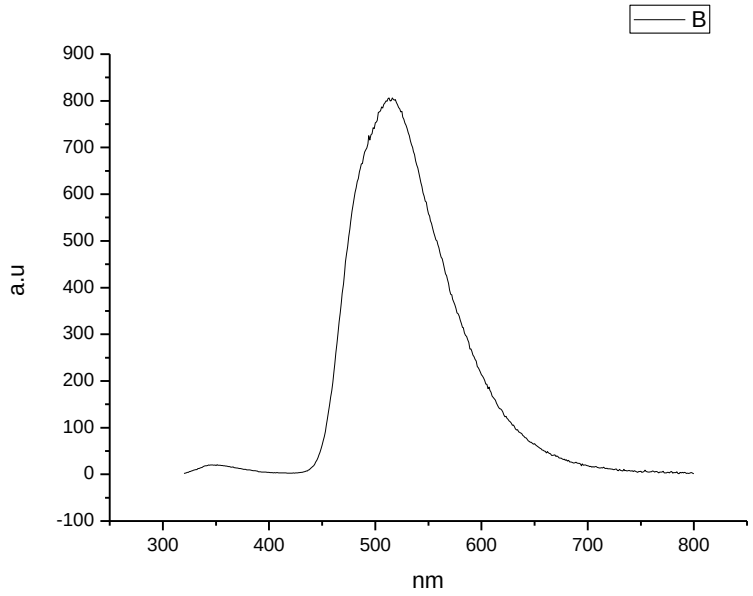

Figure 4.3.161. Fluorescence emission spectrum of **25** recorded in 1-propanol at 310 nm excitation.

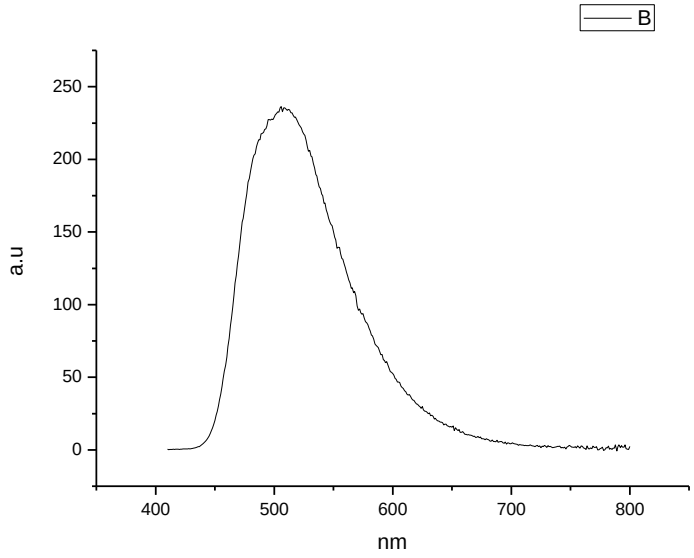

Figure 4.3.162. Fluorescence emission spectrum of **25** recorded in 1-propanol at 400 nm excitation.

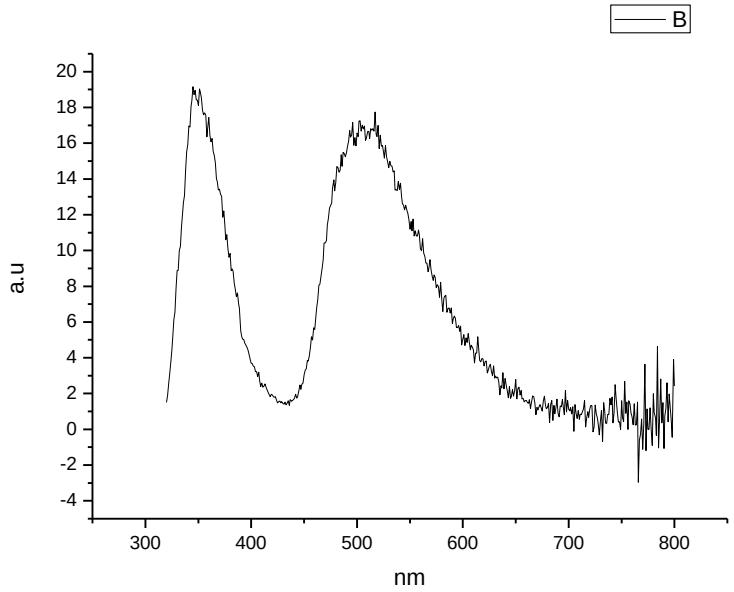

Figure 4.3.163. Fluorescence emission spectrum of **25** recorded in Acetic Acid at 310 nm excitation.

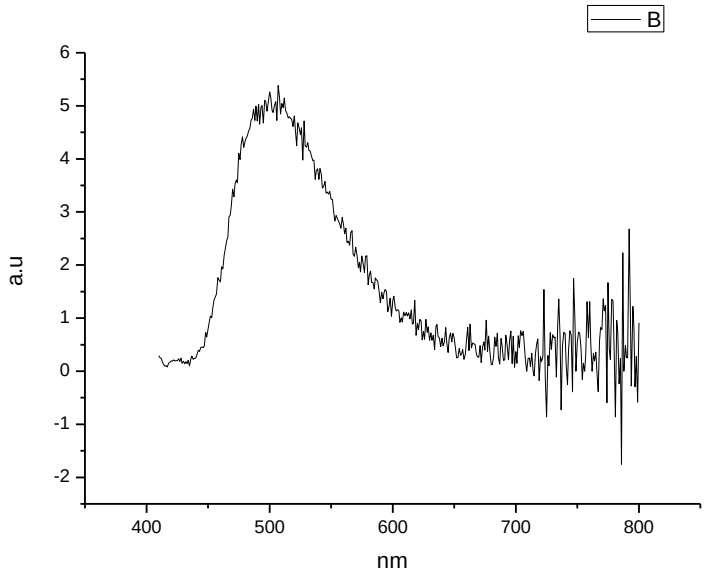

Figure 4.3.164. Fluorescence emission spectrum of **25** recorded in Acetic Acid at 400 nm excitation.

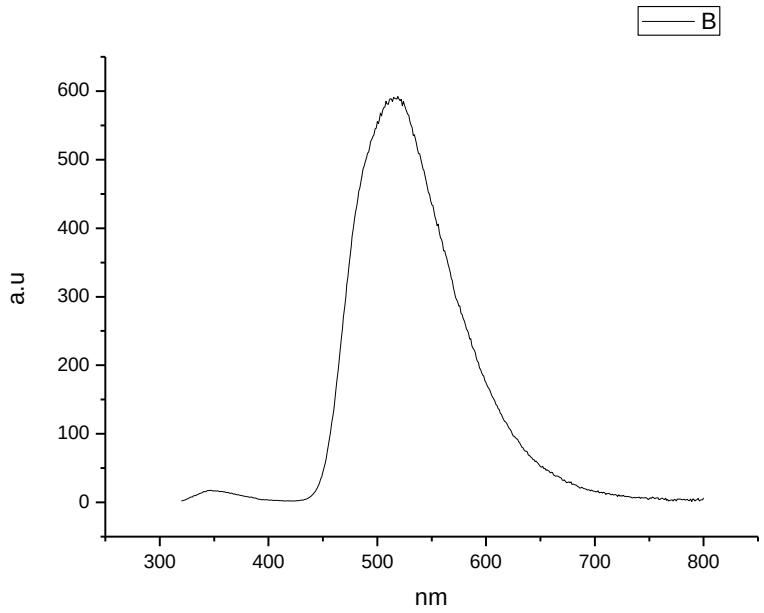

Figure 4.3.165. Fluorescence emission spectrum of **25** recorded in Methanol at 310 nm excitation.

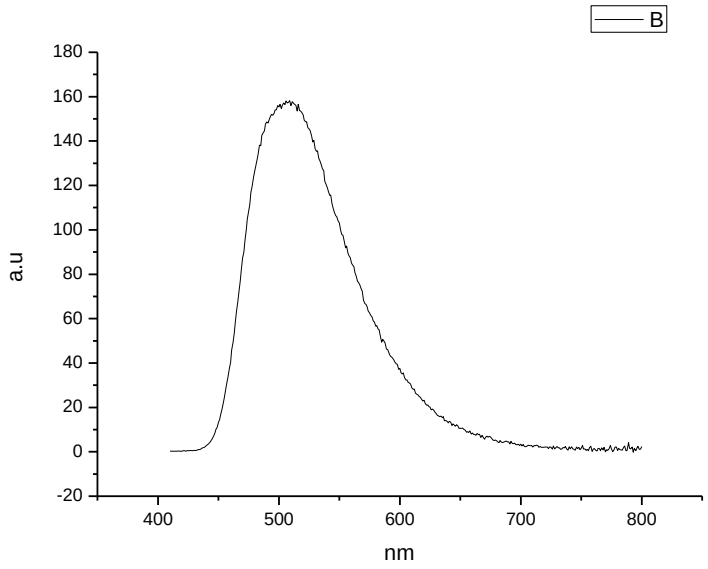

Figure 4.3.166. Fluorescence emission spectrum of **25** recorded in Methanol at 400 nm excitation.

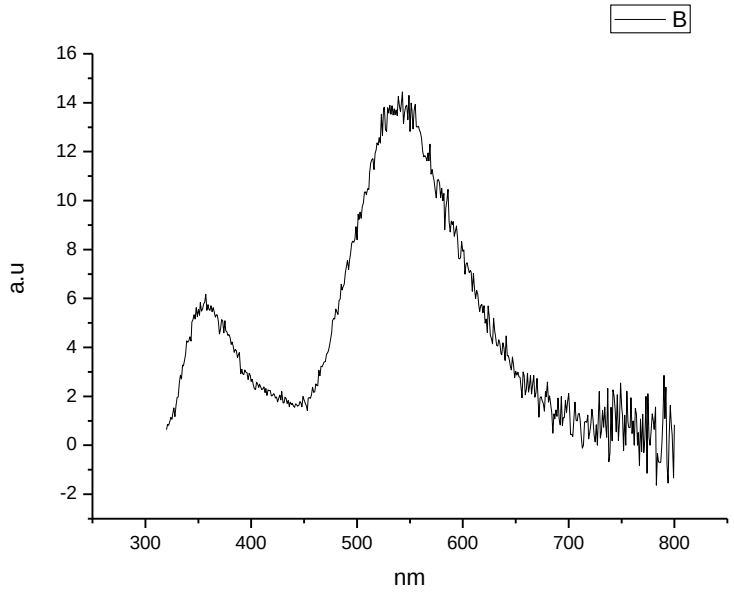

Figure 4.3.167. Fluorescence emission spectrum of **25** recorded in 2,2,2-trifluoroethanol at 310 nm excitation.

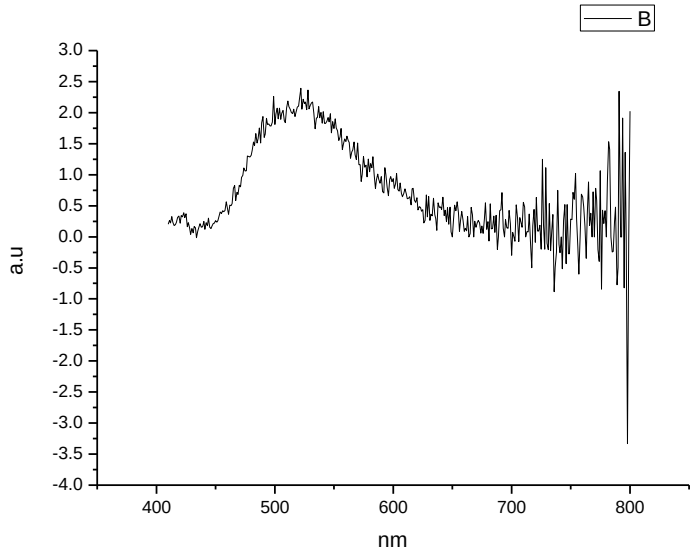

Figure 4.3.168. Fluorescence emission spectrum of **25** recorded in 2,2,2-trifluoroethanol at 400 nm excitation.

4.3.10 Normalised Fluorescence Emission spectra (Gaussian fitted).

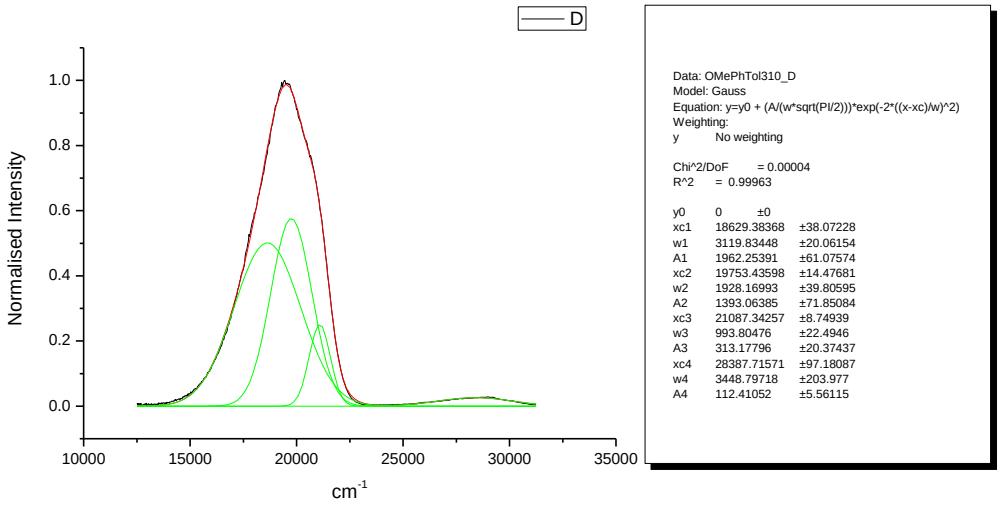

Figure 4.3.169. Gaussian model fit of the normalised fluorescence emission spectrum of **25** recorded in Toluene at 310 nm excitation.

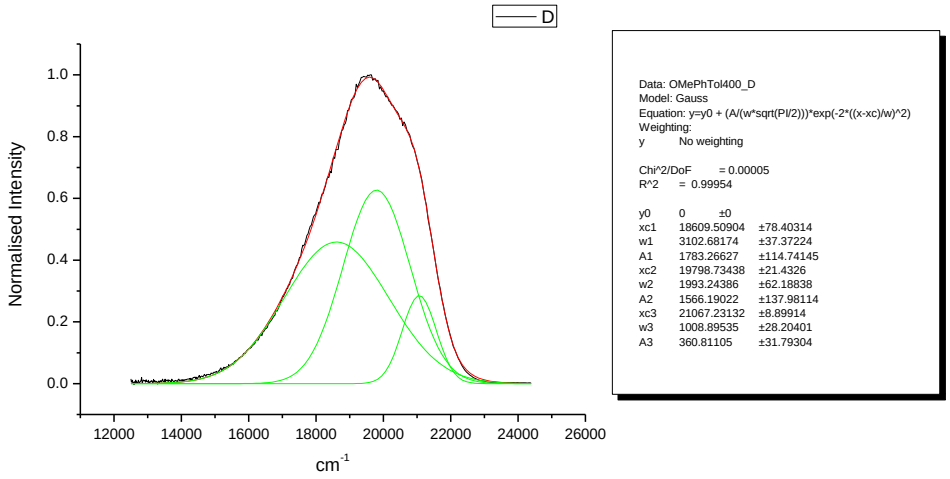

Figure 4.3.170. Gaussian model fit of the normalised fluorescence emission spectrum of **25** recorded in Toluene at 400 nm excitation.

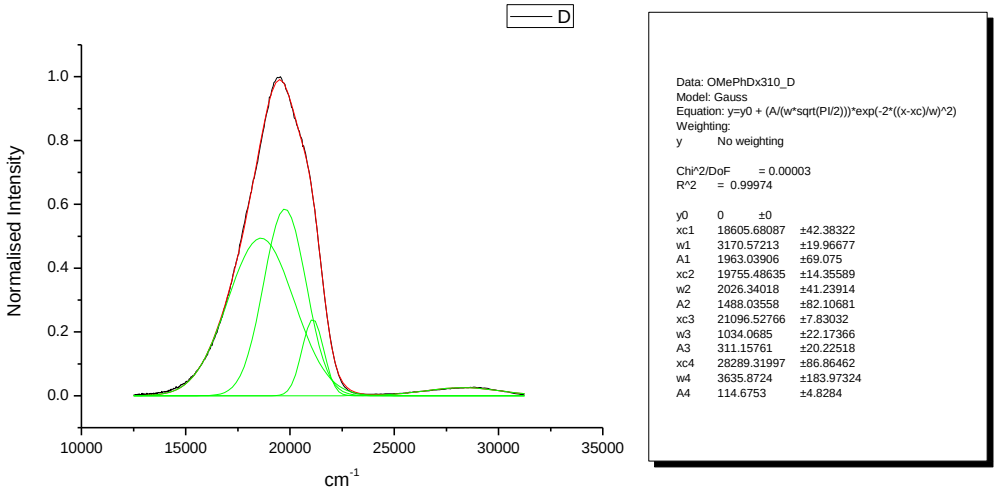

Figure 4.3.171. Gaussian model fit of the normalised fluorescence emission spectrum of **25** recorded in 1,4-dioxane at 310 nm excitation.

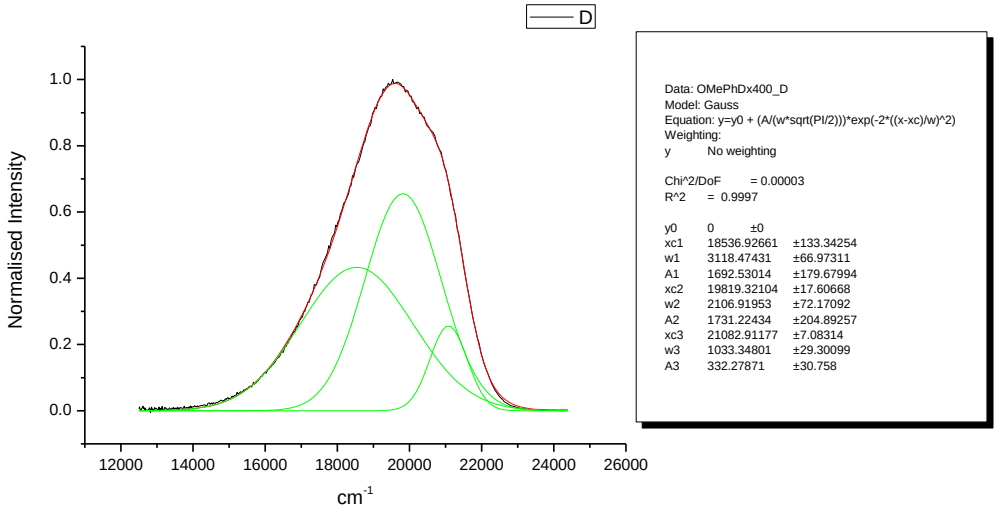

Figure 4.3.172. Gaussian model fit of the normalised fluorescence emission spectrum of **25** recorded in 1,4-dioxane at 400 nm excitation.

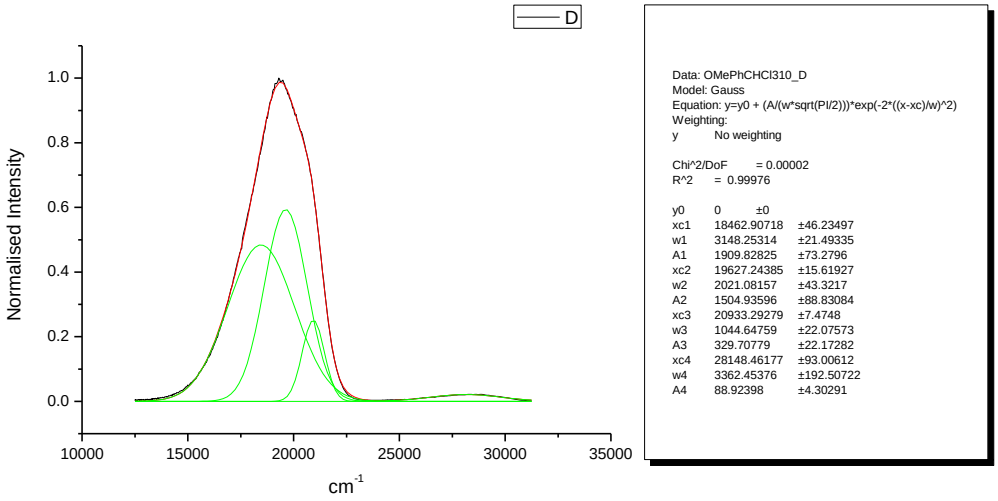

Figure 4.3.173. Gaussian model fit of the normalised fluorescence emission spectrum of **25** recorded in Chloroform at 310 nm excitation.

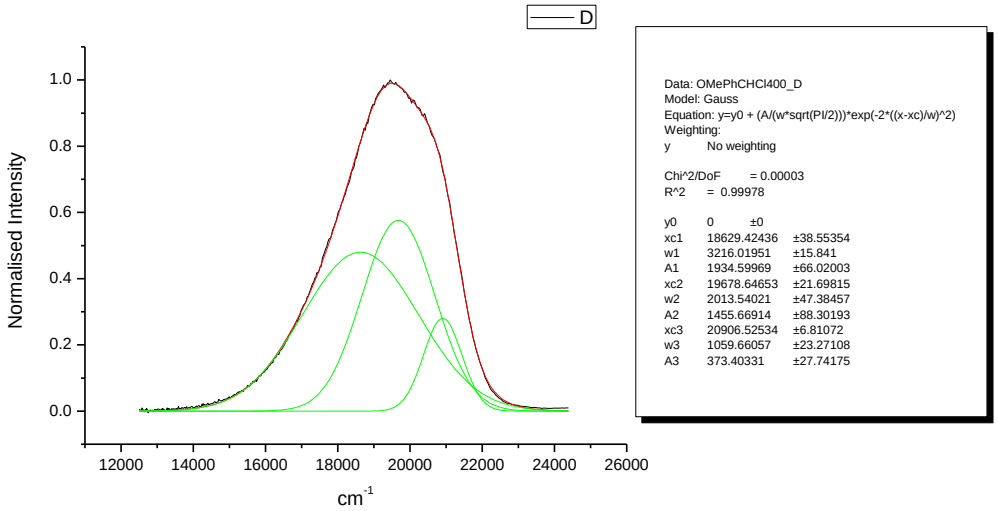

Figure 4.3.174. Gaussian model fit of the normalised fluorescence emission spectrum of **25** recorded in Chloroform at 400 nm excitation.

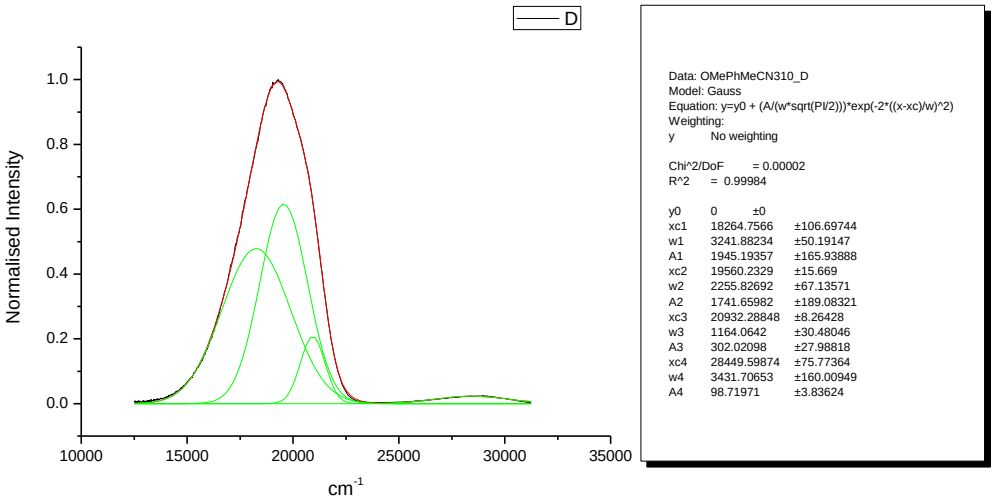

Figure 4.3.175. Gaussian model fit of the normalised fluorescence emission spectrum of **25** recorded in Acetonitrile at 310 nm excitation.

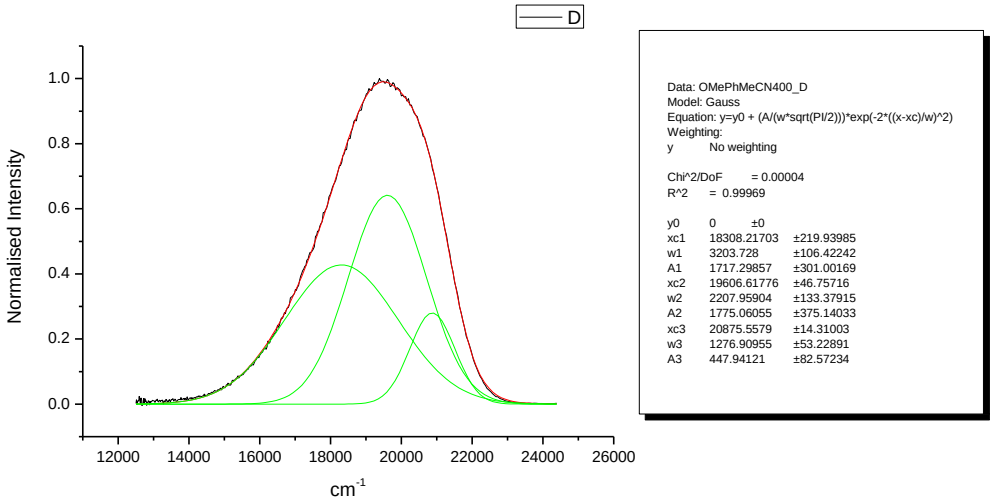

Figure 4.3.176. Gaussian model fit of the normalised fluorescence emission spectrum of **25** recorded in Acetonitrile at 400 nm excitation.

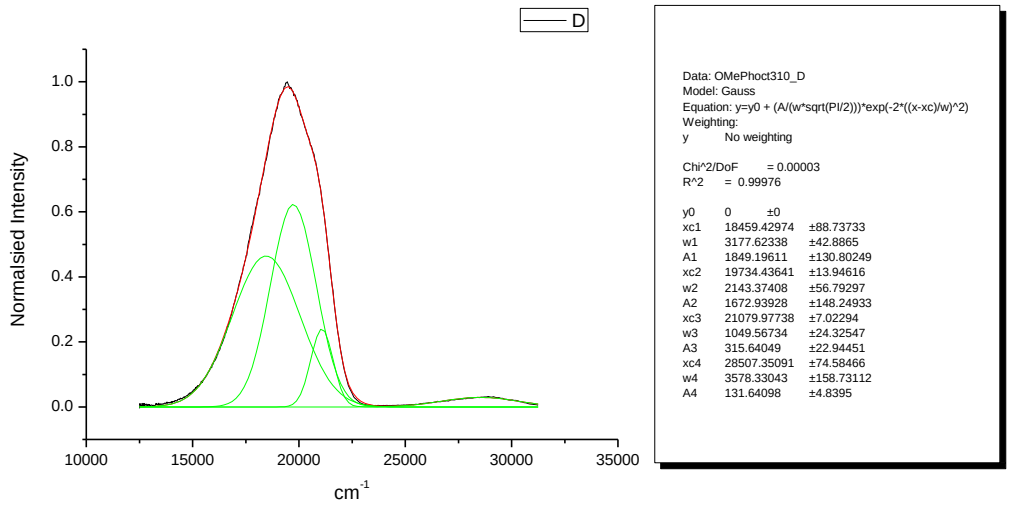

Figure 4.3.177. Gaussian model fit of the normalised fluorescence emission spectrum of **25** recorded in 1-octanol at 310 nm excitation.

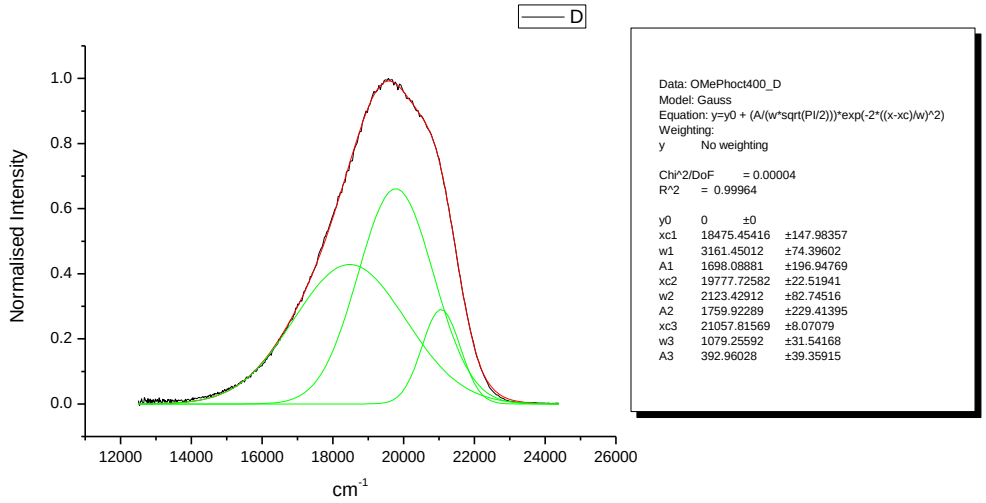

Figure 4.3.178. Gaussian model fit of the normalised fluorescence emission spectrum of **25** recorded in 1-octanol at 400 nm excitation.

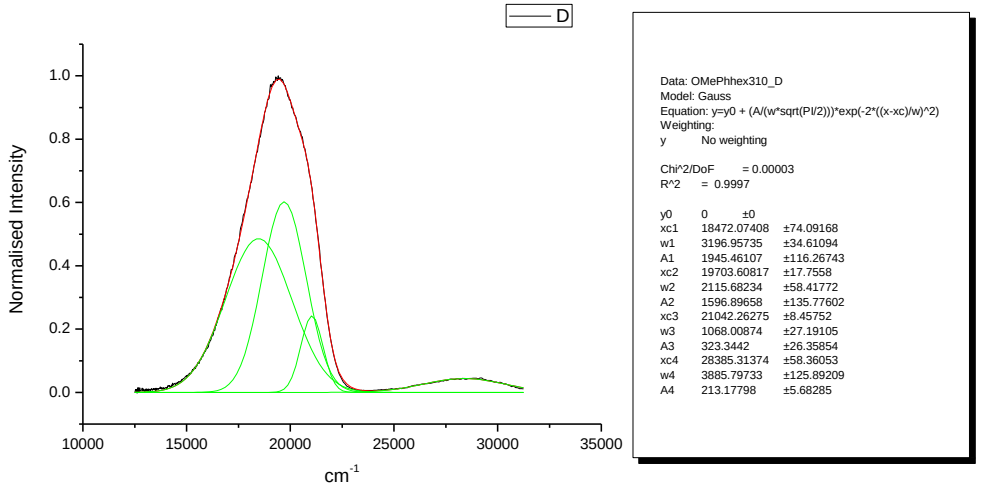

Figure 4.3.179. Gaussian model fit of the normalised fluorescence emission spectrum of **25** recorded in 1-hexanol at 310 nm excitation.

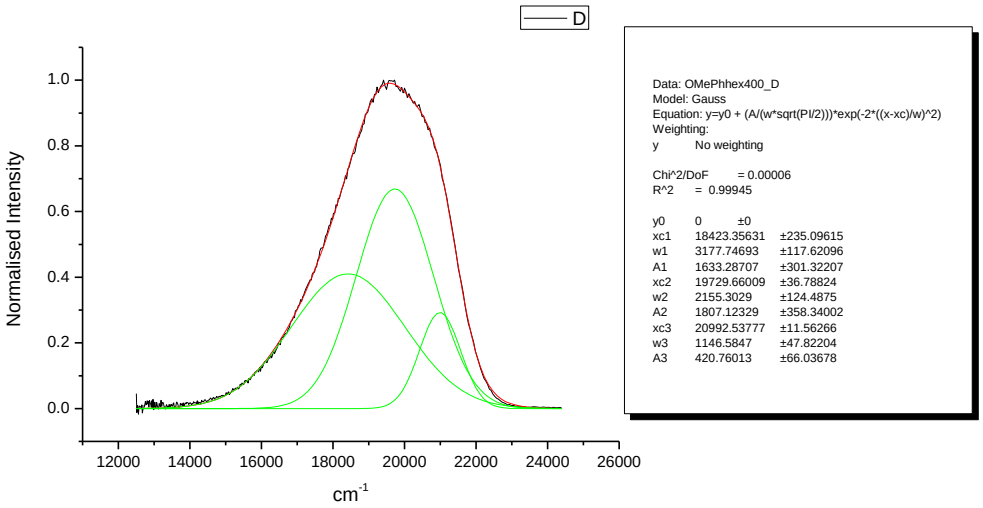

Figure 4.3.180. Gaussian model fit of the normalised fluorescence emission spectrum of **25** recorded in 1-hexanol at 400 nm excitation.

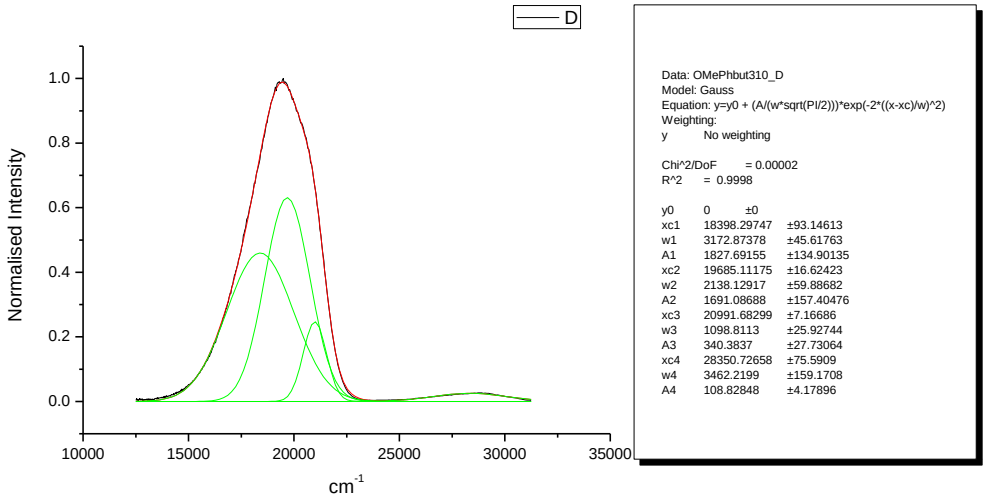

Figure 4.3.181. Gaussian model fit of the normalised fluorescence emission spectrum of **25** recorded in 1-butanol at 310 nm excitation.

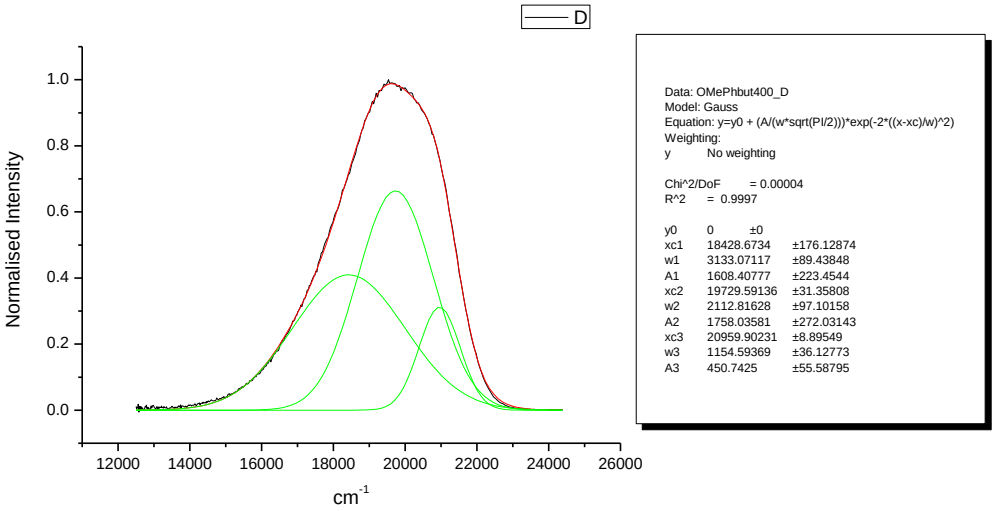

Figure 4.3.182. Gaussian model fit of the normalised fluorescence emission spectrum of **25** recorded in 1-butanol at 400 nm excitation.

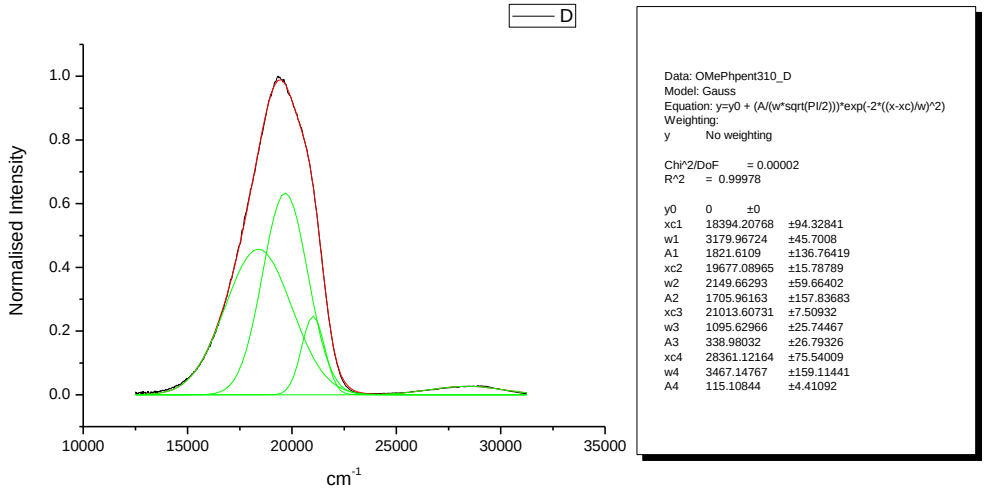

Figure 4.3.183. Gaussian model fit of the normalised fluorescence emission spectrum of **25** recorded in 1-pentanol at 310 nm excitation.

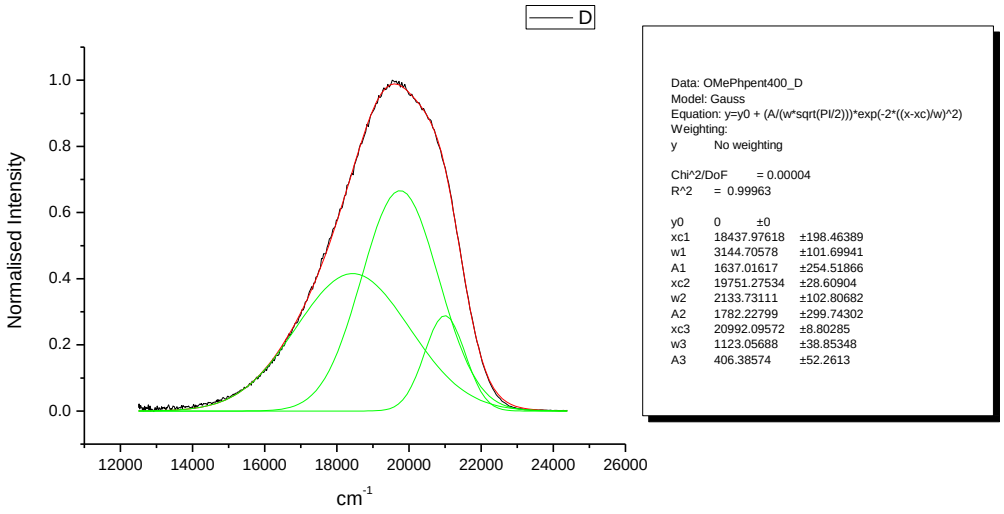

Figure 4.3.184. Gaussian model fit of the normalised fluorescence emission spectrum of **25** recorded in 1-pentanol at 400 nm excitation.

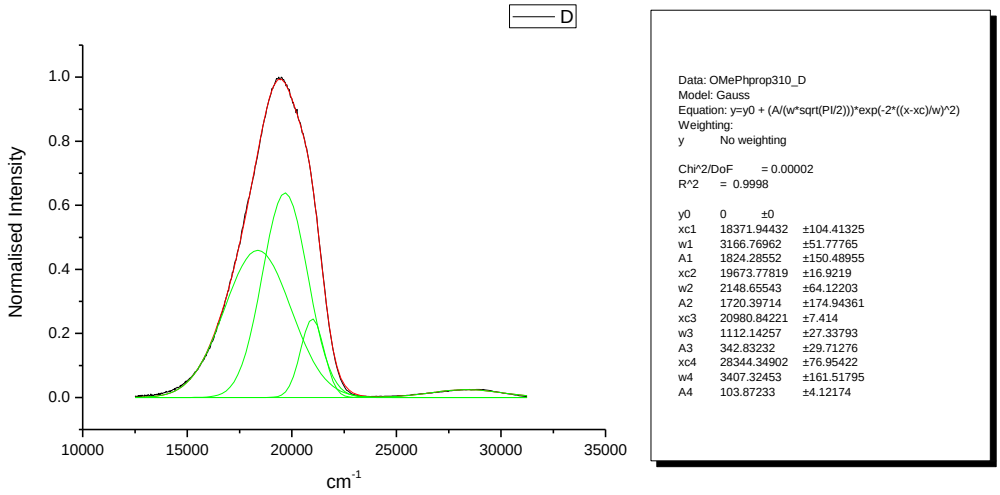

Figure 4.3.185. Gaussian model fit of the normalised fluorescence emission spectrum of **25** recorded in 1-propanol at 310 nm excitation.

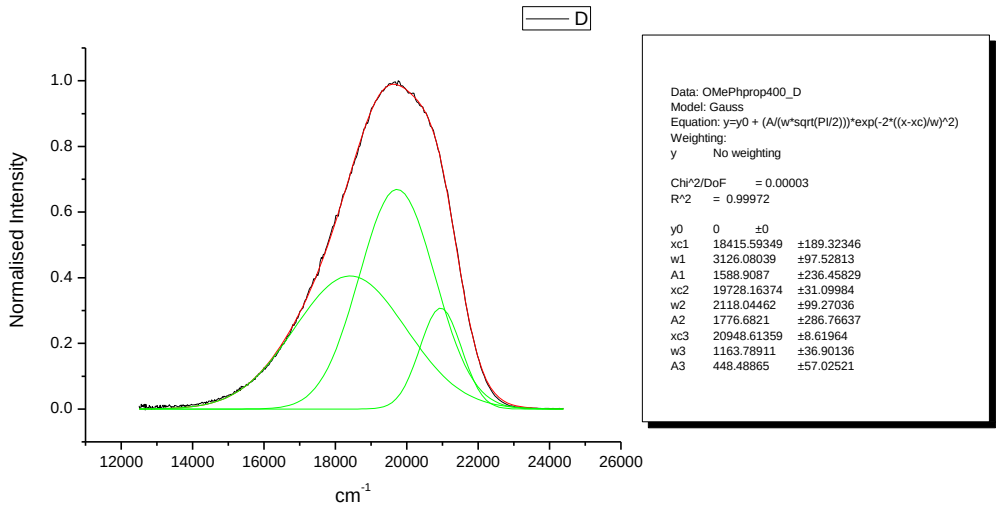

Figure 4.3.186. Gaussian model fit of the normalised fluorescence emission spectrum of **25** recorded in 1-propanol at 400 nm excitation.

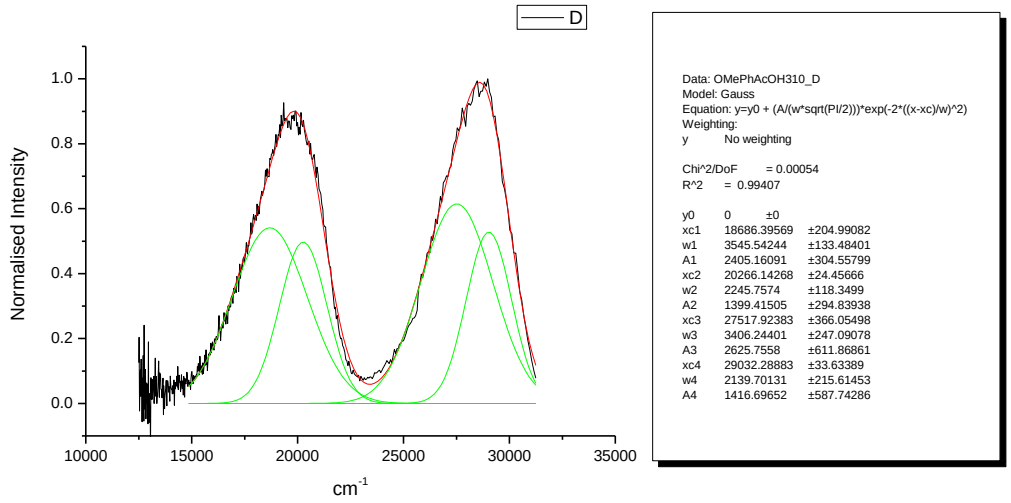

Figure 4.3.187. Gaussian model fit of the normalised fluorescence emission spectrum of **25** recorded in Acetic Acid at 310 nm excitation.

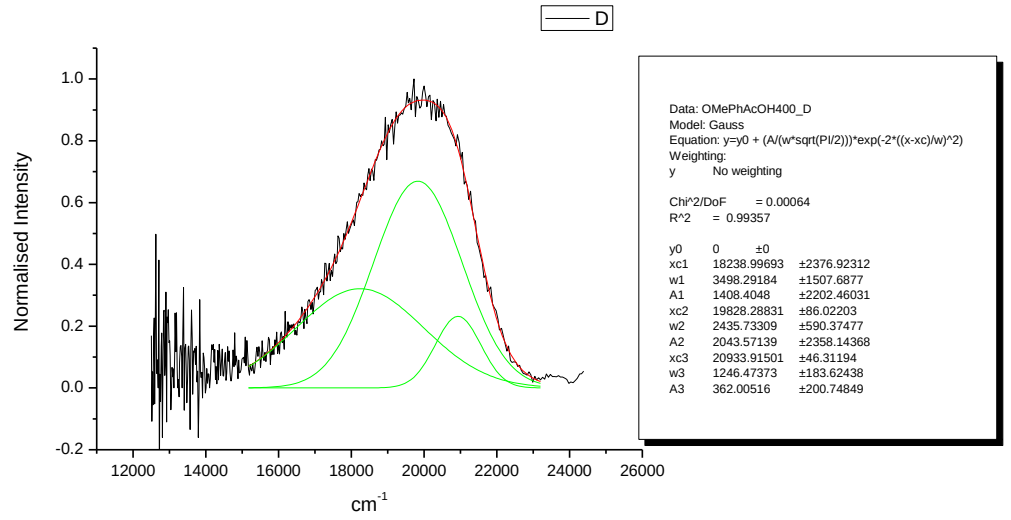

Figure 4.3.188. Gaussian model fit of the normalised fluorescence emission spectrum of **25** recorded in Acetic Acid at 400 nm excitation.

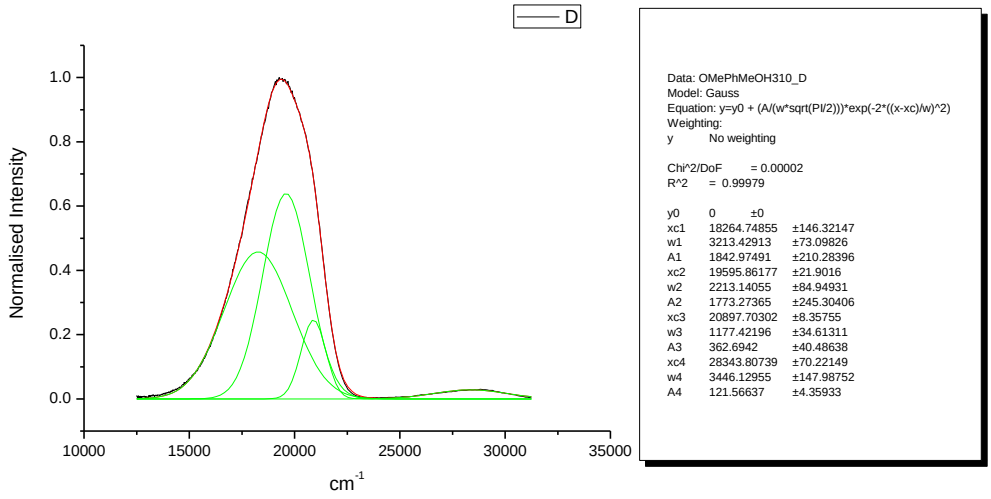

Figure 4.3.189. Gaussian model fit of the normalised fluorescence emission spectrum of **25** recorded in Methanol at 310 nm excitation.

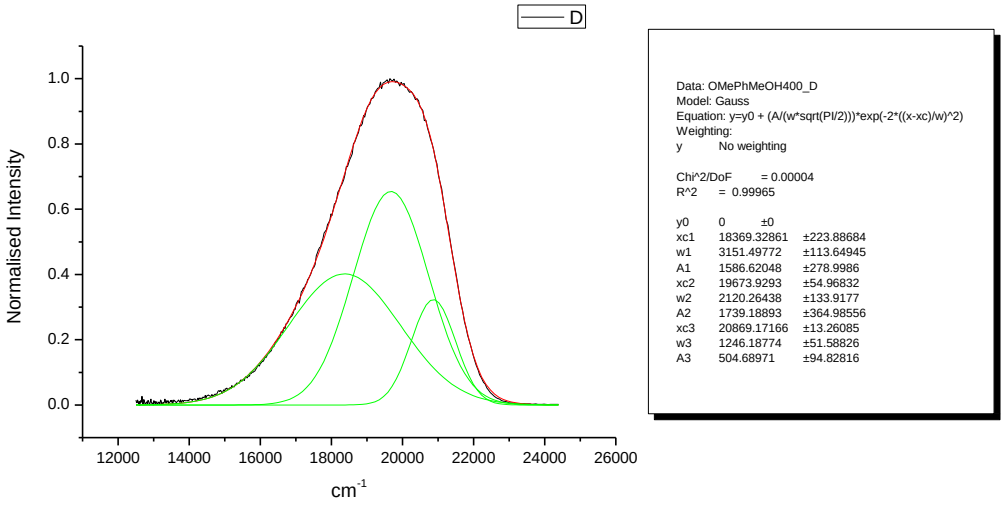

Figure 4.3.190. Gaussian model fit of the normalised fluorescence emission spectrum of **25** recorded in Methanol at 400 nm excitation.

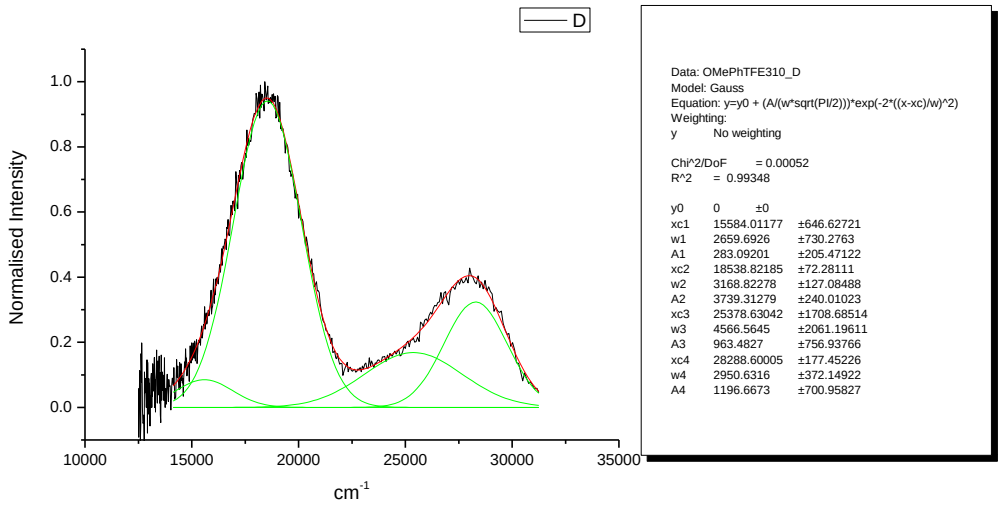

Figure 4.3.191. Gaussian model fit of the normalised fluorescence emission spectrum of **25** recorded in 2,2,2-trifluoroethanol at 310 nm excitation.

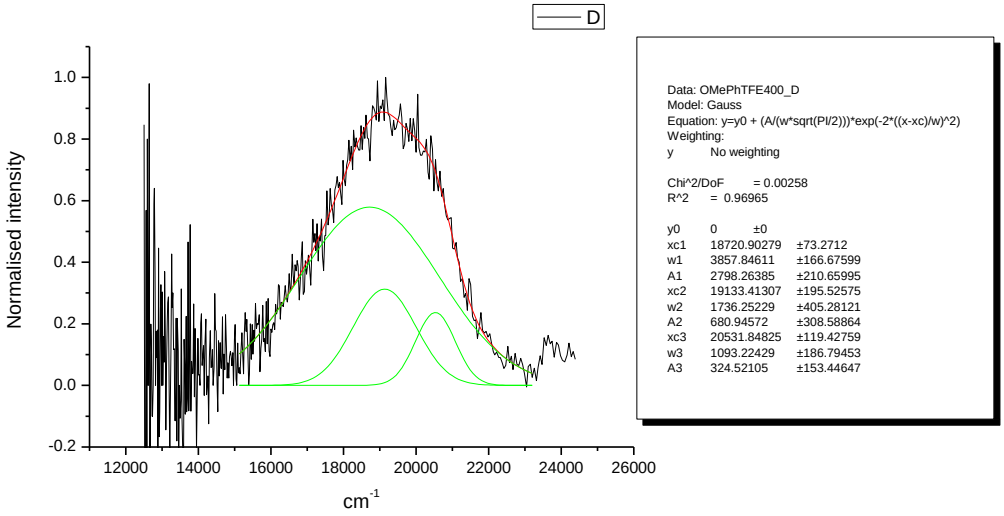

Figure 4.3.192. Gaussian model fit of the normalised fluorescence emission spectrum of **25** recorded in 2,2,2-trifluoroethanol at 400 nm excitation.

4.3.11 Fluorescence Excitation spectra.

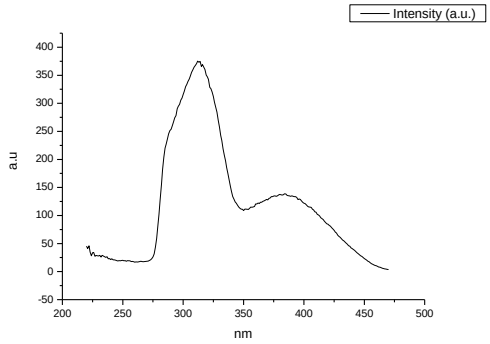

Figure 4.3.193. Fluorescence excitation spectrum of **25** recorded in Toluene with emission fixed at 480 nm.

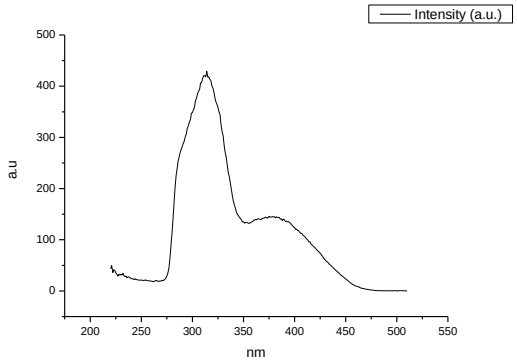

Figure 4.3.194. Fluorescence excitation spectrum of **25** recorded in Toluene with emission fixed at 520 nm.

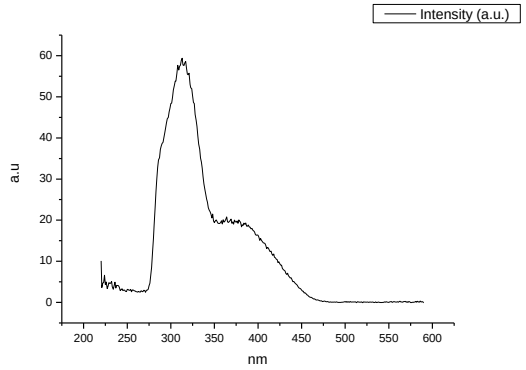

Figure 4.3.195. Fluorescence excitation spectrum of **25** recorded in Toluene with emission fixed at 600 nm.

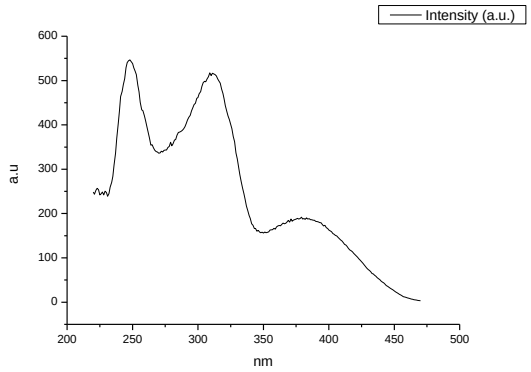

Figure 4.3.196. Fluorescence excitation spectrum of **25** recorded in 1,4-dioxane with emission fixed at 480 nm.

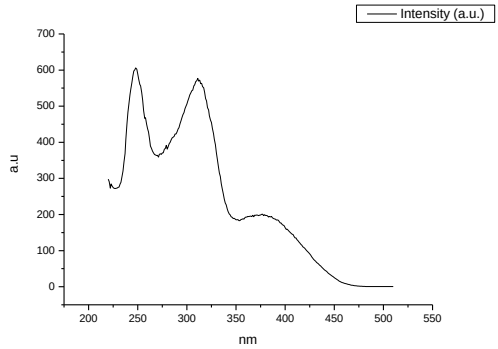

Figure 4.3.197. Fluorescence excitation spectrum of **25** recorded in 1,4-dioxane with emission fixed at 520 nm.

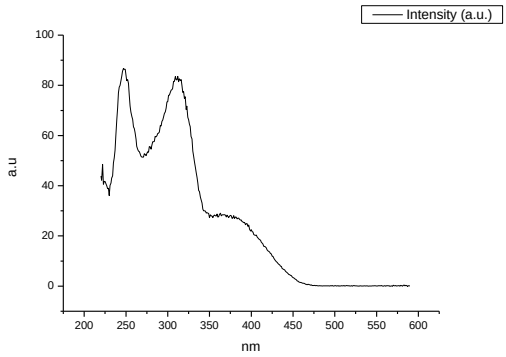

Figure 4.3.198. Fluorescence excitation spectrum of **25** recorded in 1,4-dioxane with emission fixed at 600 nm.

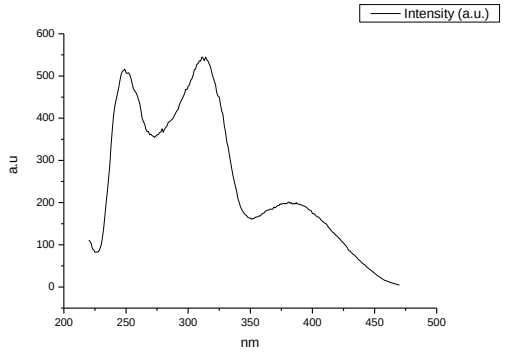

Figure 4.3.199. Fluorescence excitation spectrum of **25** recorded in Chloroform with emission fixed at 480 nm.

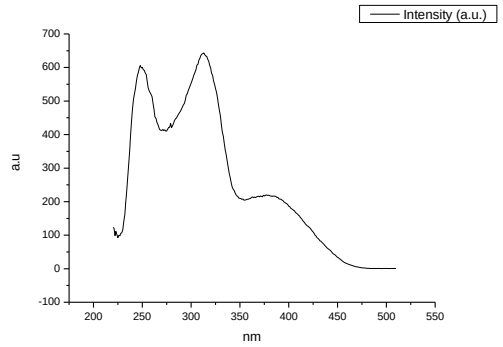

Figure 4.3.200. Fluorescence excitation spectrum of **25** recorded in Chloroform with emission fixed at 520 nm.

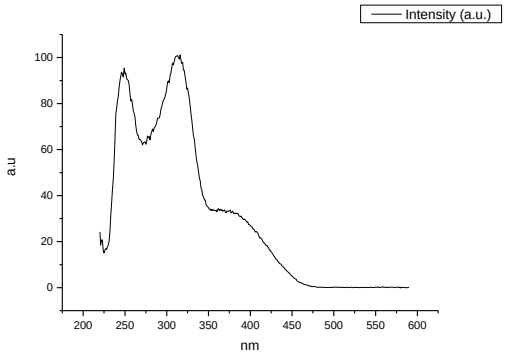

Figure 4.3.201. Fluorescence excitation spectrum of **25** recorded in Chloroform with emission fixed at 600 nm.

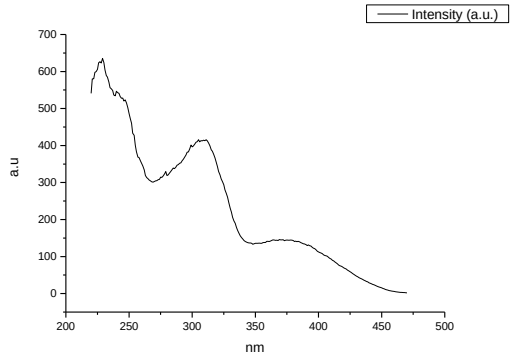

Figure 4.3.202. Fluorescence excitation spectrum of **25** recorded in Acetonitrile with emission fixed at 480 nm.

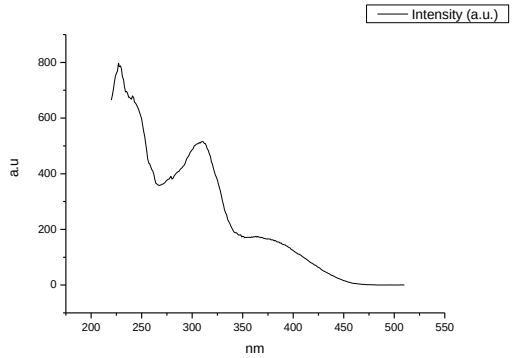

Figure 4.3.203. Fluorescence excitation spectrum of **25** recorded in Acetonitrile with emission fixed at 520 nm.

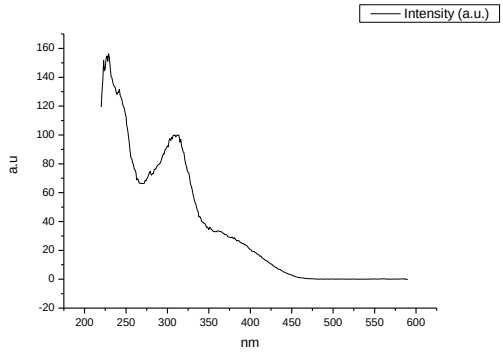

Figure 4.3.204. Fluorescence excitation spectrum of **25** recorded in Acetonitrile with emission fixed at 600 nm.

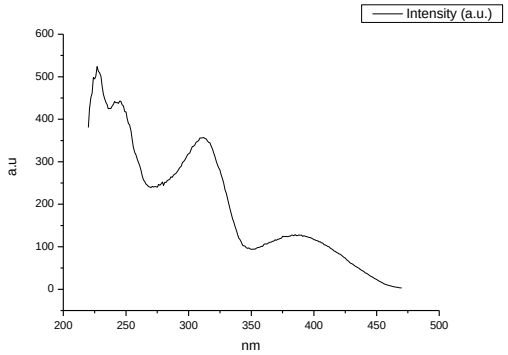

Figure 4.3.205. Fluorescence excitation spectrum of **25** recorded in 1-octanol with emission fixed at 480 nm.

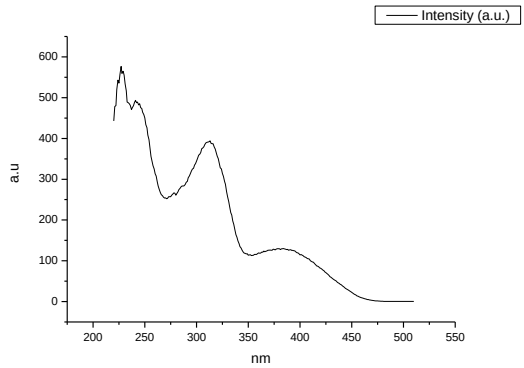

Figure 4.3.206. Fluorescence excitation spectrum of **25** recorded in 1-octanol with emission fixed at 520 nm.

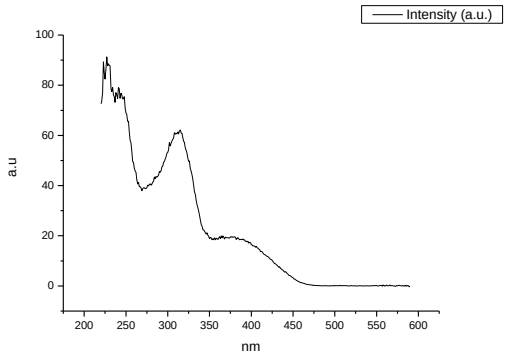

Figure 4.3.207. Fluorescence excitation spectrum of **25** recorded in 1-octanol with emission fixed at 600 nm.

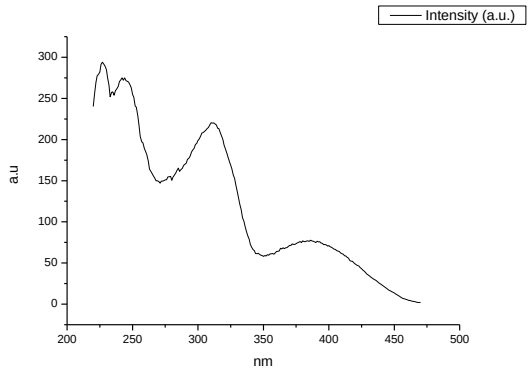

Figure 4.3.208. Fluorescence excitation spectrum of **25** recorded in 1-hexanol with emission fixed at 480 nm.

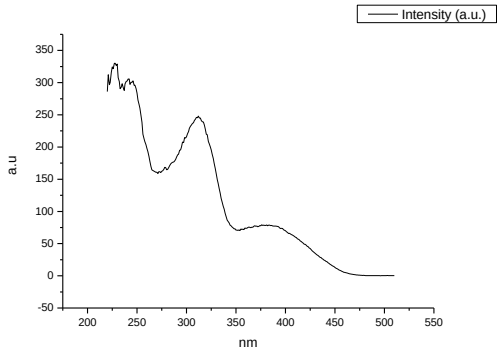

Figure 4.3.209. Fluorescence excitation spectrum of **25** recorded in 1-hexanol with emission fixed at 520 nm.

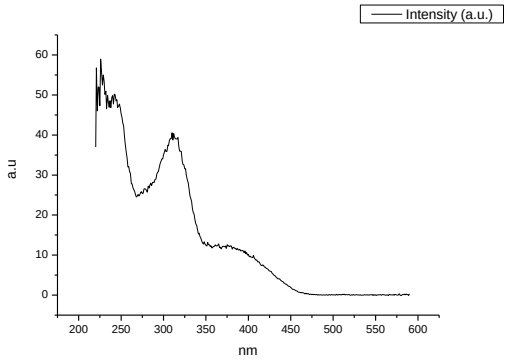

Figure 4.3.210. Fluorescence excitation spectrum of **25** recorded in 1-hexanol with emission fixed at 600 nm.

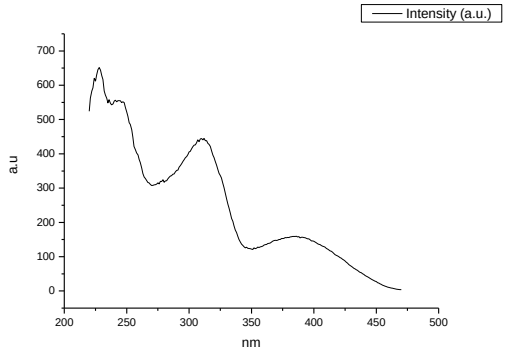

Figure 4.3.211. Fluorescence excitation spectrum of **25** recorded in 1-butanol with emission fixed at 480 nm.

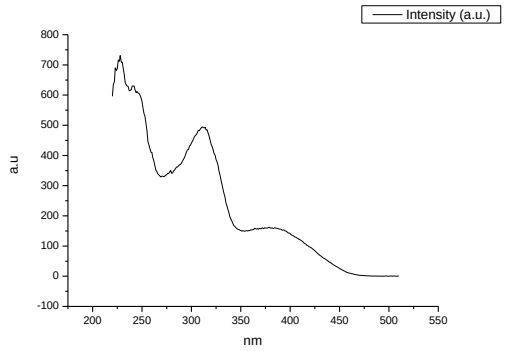

Figure 4.3.212. Fluorescence excitation spectrum of **25** recorded in 1-butanol with emission fixed at 520 nm.

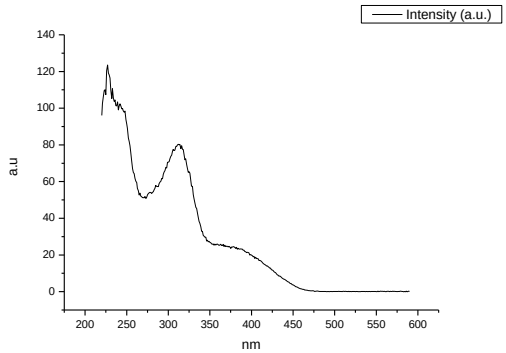

Figure 4.3.213. Fluorescence excitation spectrum of **25** recorded in 1-butanol with emission fixed at 600 nm.

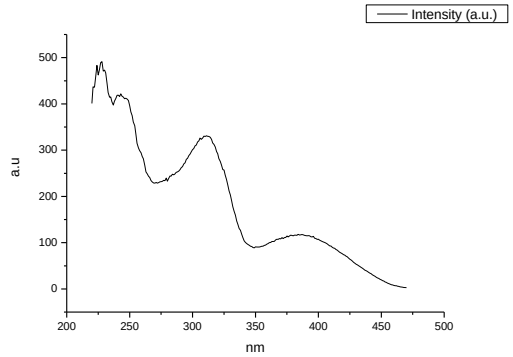

Figure 4.3.214. Fluorescence excitation spectrum of **25** recorded in 1-pentanol with emission fixed at 480 nm.

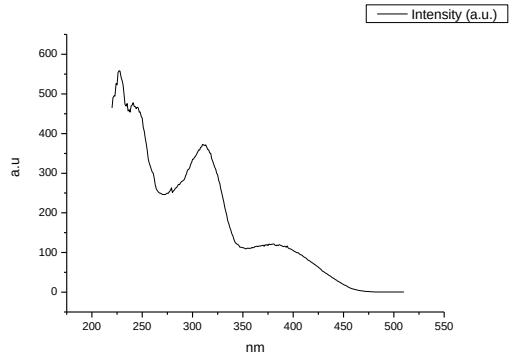

Figure 4.3.215. Fluorescence excitation spectrum of **25** recorded in 1-pentanol with emission fixed at 520 nm.

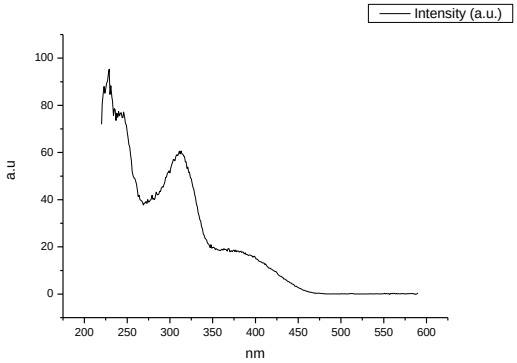

Figure 4.3.216. Fluorescence excitation spectrum of **25** recorded in 1-pentanol with emission fixed at 600 nm.

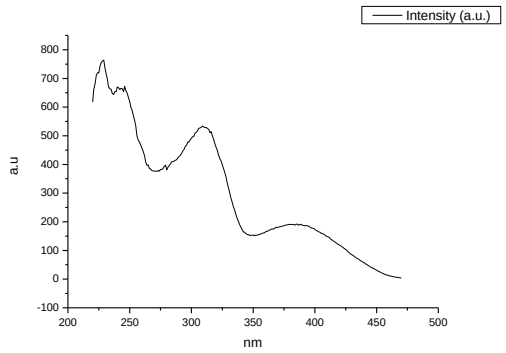

Figure 4.3.217. Fluorescence excitation spectrum of **25** recorded in 1-propanol with emission fixed at 480 nm.

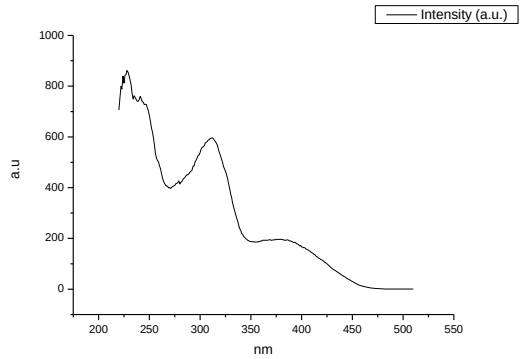

Figure 4.3.218. Fluorescence excitation spectrum of **25** recorded in 1-propanol with emission fixed at 520 nm.

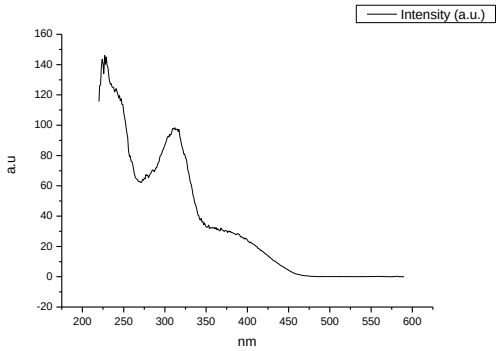

Figure 4.3.219. Fluorescence excitation spectrum of **25** recorded in 1-propanol with emission fixed at 600 nm.

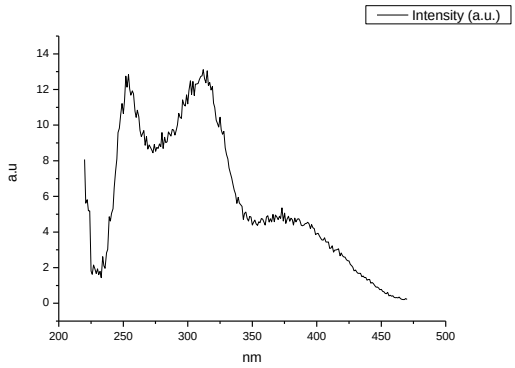

Figure 4.3.220. Fluorescence excitation spectrum of **25** recorded in Acetic Acid with emission fixed at 480 nm.

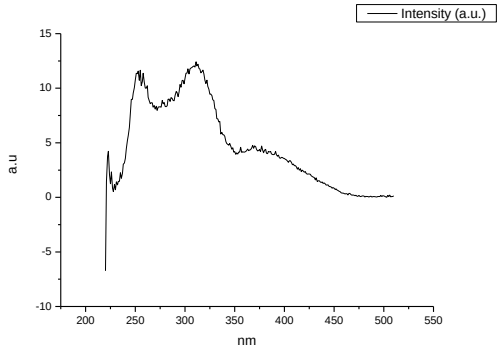

Figure 4.3.221. Fluorescence excitation spectrum of **25** recorded in Acetic Acid with emission fixed at 520 nm.

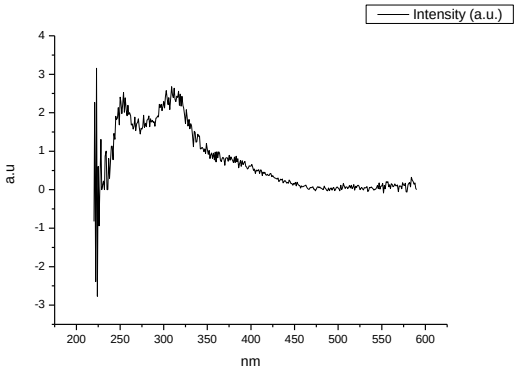

Figure 4.3.222. Fluorescence excitation spectrum of **25** recorded in Acetic Acid with emission fixed at 600 nm.

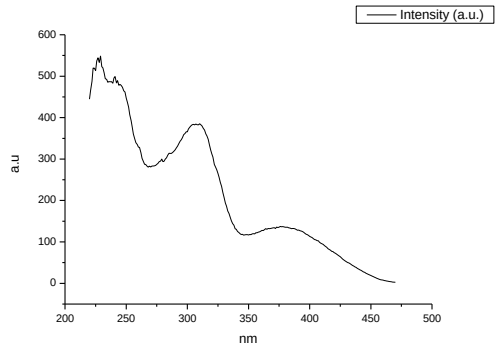

Figure 4.3.223. Fluorescence excitation spectrum of **25** recorded in Methanol with emission fixed at 480 nm.

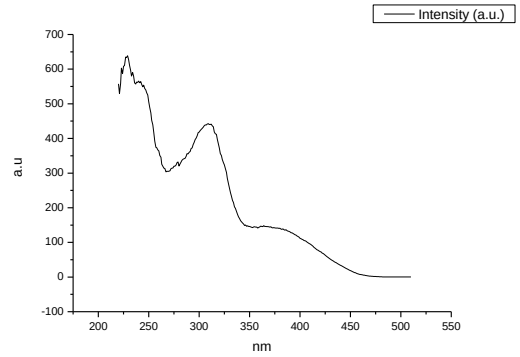

Figure 4.3.224. Fluorescence excitation spectrum of **25** recorded in Methanol with emission fixed at 520 nm.

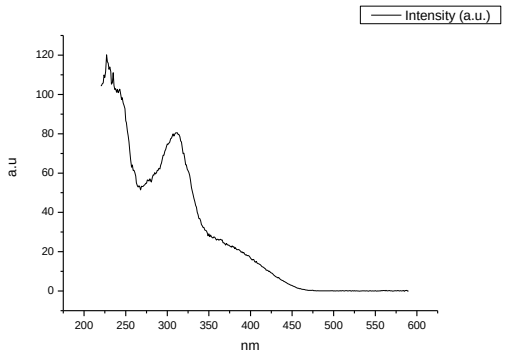

Figure 4.3.225. Fluorescence excitation spectrum of **25** recorded in Methanol with emission fixed at 600 nm.

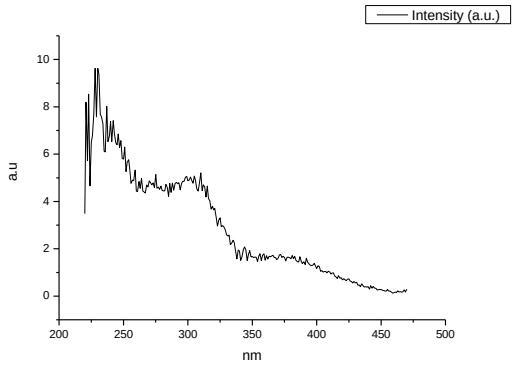

Figure 4.3.226. Fluorescence excitation spectrum of **25** recorded in 2,2,2-trifluoroethanol with emission fixed at 480 nm.

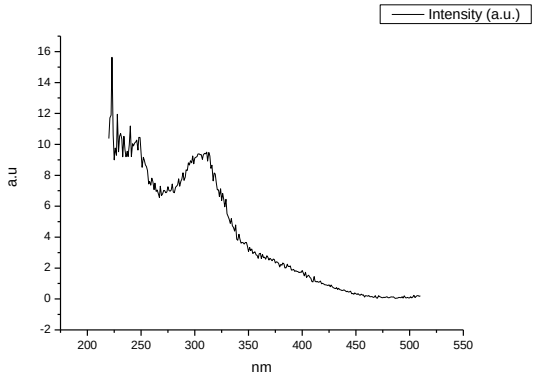

Figure 4.3.227. Fluorescence excitation spectrum of **25** recorded in 2,2,2-trifluoroethanol with emission fixed at 520 nm.

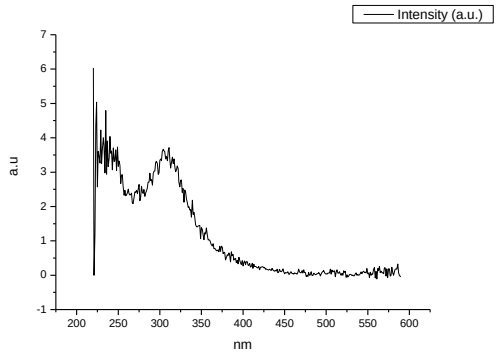

Figure 4.3.228. Fluorescence excitation spectrum of **25** recorded in 2,2,2-trifluoroethanol with emission fixed at 600 nm.

4.4 COMPOUND 27.

4.4.1 Quantum Yield Summary.

Solvent	abs (310 nm)	$\lambda_{ems\ (max)}$	$\Phi_{310\ nm}$	abs (400 nm)	$\lambda_{ems\ (max)}$	$\Phi_{400\ nm}$
Toluene	0.10	517.01	0.43	0.05	515.97	0.42
1,4-Dioxane	0.08	520.00	0.44	0.02	518.95	0.45
Chloroform	0.09	524.02	0.01	0.02	518.38	0.01
Acetonitrile	0.07	508.59	0.01	0.01	518.25	0.01
1-Octanol	0.05	525.07	0.07	0.02	505.07	0.06
1-Hexanol	0.03	522.98	0.04	0.01	505.97	0.03
1-Butanol	0.07	517.01	0.02	0.02	510.00	0.01
1-Pentanol	0.05	525.07	0.03	0.01	508.05	0.02
1-Propanol	0.08	525.07	0.01	0.02	500.00	0.01
Acetic acid	0.06	560.00	0.01	0.02	546.09	0.01
Methanol	0.08	525.07	0.02	0.02	502.98	0.02
2,2,2-Trifluoroethanol	0.04	502.59	0.00	0.01	507.93	0.00

Table 4.4.1. Summary of ultraviolet-visible absorbance values at 310 nm and 400 nm, emission maxima and quantum yield (Φ) of **27** at 310 nm and 400 nm excitation.

4.4.2 310 nm excitation Gaussian band fit summaries.

Solvent	λ max$_{em}$ Band 1 (cm^{-1})	λ max$_{em}$ Band 1 (nm)	λ max$_{em}$ Band 2 (cm^{-1})	λ max$_{em}$ Band 2 (nm)	λ max$_{em}$ Band 3 (cm^{-1})	λ max$_{em}$ Band 3 (nm)
Toluene	18400.66	543.46	19558.82	511.28	20844.09	479.75
1,4-Dioxane	18394.41	543.64	19530.45	512.02	20885.60	478.80
Chloroform	18838.96	530.81	-	-	-	-
Acetonitrile	-	-	19315.15	517.73	-	-
1-Octanol	18146.19	551.08	19610.77	509.92	-	-
1-Hexanol	18526.05	539.78	19854.09	503.67	-	-
1-Butanol	-	-	19222.06	520.24	-	-
1-Pentanol	-	-	19181.53	521.33	-	-
1-Propanol	-	-	19224.94	520.16	-	-
Acetic acid	17598.87	568.22	19399.61	515.47	-	-
Methanol	18337.70	545.32	19848.85	503.81	-	-
2,2,2-Trifluoroethanol	-	-	19017.27	525.84	-	-

Solvent	λ max$_{em}$ Band 4 (cm^{-1})	λ max$_{em}$ Band 4 (nm)	λ max$_{em}$ Band 5 (cm^{-1})	λ max$_{em}$ Band 5 (nm)
Toluene	-	-	-	-
1,4-Dioxane	-	-	-	-
Chloroform	26872.31	372.13	28686.41	348.60
Acetonitrile	23506.38	425.42	28665.45	348.85
1-Octanol	24506.42	408.06	28852.61	346.59
1-Hexanol	28333.96	352.93	29253.43	341.84
1-Butanol	24253.86	412.31	28366.75	352.53
1-Pentanol	24301.13	411.50	28386.81	352.28
1-Propanol	24213.24	413.00	28467.81	351.27
Acetic acid	27939.48	357.92	29190.95	342.57
Methanol	26354.24	379.45	28899.99	346.02
2,2,2-Trifluoroethanol	24725.29	404.44	28393.01	352.20

Table 4.4.2. Summary of band maxima of 5 band fit using Gaussian model for normalised **27** emission spectra recorded at 310 nm excitation.

(a)

Solvent	Width Band 1 (cm^{-1})	Width Band 2 (cm^{-1})	Width Band 3 (cm^{-1})	Width Band 4 (cm^{-1})	Width Band 5 (cm^{-1})
Toluene	3078.31	1952.46	924.38	-	-
1,4-Dioxane	3144.14	2024.26	946.55	-	-
Chloroform	2763.98	-	-	3372.56	2002.62
Acetonitrile	-	3956.09	-	3552.52	3044.08
1-Octanol	3420.48	2691.17	-	1643.66	3754.47
1-Hexanol	2985.63	2524.32	-	4225.15	601.85
1-Butanol	-	3401.79	-	1651.84	3373.75
1-Pentanol	-	3347.98	-	1495.51	3568.34
1-Propanol	-	3462.31	-	2050.94	3251.13
Acetic acid	3050.64	2134.55	-	3510.02	1131.56
Methanol	3341.71	2703.08	-	2585.30	2476.92
2,2,2-Trifluoroethanol	-	3522.32	-	4884.04	2804.14

(b)

Solvent	Area Band 1 (cm^{-1})	Area Band 2 (cm^{-1})	Area Band 3 (cm^{-1})	Area Band 4 (cm^{-1})	Area Band 5 (cm^{-1})
Toluene	1944.64	1426.37	188.45	-	-
1,4-Dioxane	2055.32	1425.41	168.29	-	-
Chloroform	2811.30	-	-	965.24	727.82
Acetonitrile	-	3831.96	-	2669.66	3435.54
1-Octanol	1440.43	2450.45	-	59.45	454.61
1-Hexanol	1941.26	2524.32	-	1514.25	47.03
1-Butanol	-	4007.85	-	117.47	780.50
1-Pentanol	-	3971.33	-	89.35	661.11
1-Propanol	-	4081.60	-	203.24	1016.22
Acetic acid	2785.12	787.90	-	2680.31	330.00
Methanol	1998.96	2091.64	-	158.79	331.63
2,2,2-Trifluoroethanol	-	1447.20	-	2329.48	1599.16

Tables 4.4.3 (a) and (b). Summary band width and band area of 5 band fit using Gaussian model for normalised **27** emission spectra recorded at 310 nm excitation.

Solvent	Band 1 Area Percentage (%)	Band 2 Area Percentage (%)	Band 3 Area Percentage (%)	Band 4 Area Percentage (%)	Band 5 Area Percentage (%)
Toluene	54.63	40.07	5.29	-	-
1,4-Dioxane	56.33	39.06	4.61	-	-
Chloroform	62.41	-	-	21.43	16.16
Acetonitrile	-	38.56	-	26.87	34.57
1-Octanol	32.70	55.63	-	1.35	10.32
1-Hexanol	32.21	41.88	-	25.13	0.78
1-Butanol	-	81.70	-	2.39	15.91
1-Pentanol	-	84.11	-	1.89	14.00
1-Propanol	-	77.00	-	3.83	19.17
Acetic acid	42.31	11.97	-	40.71	5.01
Methanol	43.64	45.66	-	3.47	7.24
2,2,2-Trifluoroethanol	-	26.92	-	43.33	29.75

Table 4.4.4. Total Area Percentages of 5 band fit using Gaussian model for normalised **27** emission spectra recorded at 310 nm excitation.

Solvent	Area Ratio Band 1/2 (310 nm ex)	Area Ratio Band 1/3 (310 nm ex)	Area Ratio Band 1/4 (310 nm ex)	Area Ratio Band 1/5 (310 nm ex)
Toluene	1.36	10.32	-	-
1,4-Dioxane	1.44	12.21	-	-
Chloroform	-	-	2.91	3.86
Acetonitrile	-	-	-	-
1-Octanol	0.59	-	24.23	3.17
1-Hexanol	0.77	-	1.28	41.28
1-Butanol	-	-	-	-
1-Pentanol	-	-	-	-
1-Propanol	-	-	-	-
Acetic acid	3.53	-	1.04	8.44
Methanol	0.96	-	12.59	6.03
2,2,2-Trifluoroethanol	-	-	-	-

Solvent	Area Ratio Band 2/3 (310 nm ex)	Area Ratio Band 2/4 (310 nm ex)	Area Ratio Band 2/5 (310 nm ex)	Area Ratio Band 3/4 (310 nm ex)	Area Ratio Band 3/5 (310 nm ex)	Area Ratio Band 4/5 (310 nm ex)
Toluene	7.57	-	-	-	-	-
1,4-Dioxane	8.47	-	-	-	-	-
Chloroform	-	-	-	-	-	1.33
Acetonitrile	-	1.44	1.12	-	-	0.78
1-Octanol	-	41.22	5.39	-	-	0.13
1-Hexanol	-	1.67	53.67	-	-	32.20
1-Butanol	-	34.12	5.13	-	-	0.15
1-Pentanol	-	44.45	6.01	-	-	0.14
1-Propanol	-	20.08	4.02	-	-	0.20
Acetic acid	-	0.29	2.39	-	-	8.12
Methanol	-	13.17	6.31	-	-	0.48
2,2,2-Trifluoroethanol	-	0.62	0.90	-	-	1.46

Table 4.4.5. Area Ratios of 5 band fit using Gaussian model for normalised **27** emission spectra recorded at 310 nm excitation.

4.4.3 400 nm excitation Gaussian band fit summaries.

Solvent	λ max$_{em}$ Band 1 (cm^{-1})	λ max$_{em}$ Band 1 (nm)	λ max$_{em}$ Band 2 (cm^{-1})	λ max$_{em}$ Band 2 (nm)	λmax$_{em}$ Band 3 (cm^{-1})	λmax$_{em}$ Band 3 (nm)
Toluene	18359.50	544.68	19595.29	510.33	20804.90	480.66
1,4-Dioxane	18315.69	545.98	19572.68	510.92	20833.88	479.99
Chloroform	-	-	19992.11	500.20	-	-
Acetonitrile	-	-	19995.25	500.12	-	-
1-Octanol	18381.22	544.03	19745.87	506.44	20908.78	478.27
1-Hexanol	18641.17	536.45	-	-	20199.16	495.07
1-Butanol	18741.52	533.57	-	-	20241.65	494.03
1-Pentanol	18655.03	536.05	-	-	20211.19	494.78
1-Propanol	18730.60	533.89	-	-	20281.29	493.07
Acetic acid	18519.95	539.96	-	-	-	-
Methanol	18930.31	528.25	-	-	20474.93	488.40
2,2,2-Trifluoroethanol	-	-	19593.17	510.38	-	-

Table 4.4.6. Summary of band maxima of 3 band fit using Gaussian model for normalised **27** emission spectra recorded at 400 nm excitation.

Solvent	Width Band 1 (cm^{-1})	Width Band 2 (cm^{-1})	Width Band 3 (cm^{-1})
Toluene	3059.89	2013.99	968.67
1,4-Dioxane	3100.89	2091.41	1020.24
Chloroform	-	4187.84	-
Acetonitrile	-	4190.20	-
1-Octanol	3308.36	2329.91	1078.40
1-Hexanol	3111.21	-	2227.79
1-Butanol	3129.39	-	2184.40
1-Pentanol	3117.14	-	2188.54
1-Propanol	3075.82	-	2176.24
Acetic acid	3228.19	-	-
Methanol	3059.16	-	1982.57
2,2,2-Trifluoroethanol	-	2772.18	-

Table 4.4.7. Summary of band width of 3 band fit using Gaussian model for normalised **27** emission spectra recorded at 400 nm excitation.

Solvent	Area Band 1 (cm^{-1})	Area Band 2 (cm^{-1})	Area Band 3 (cm^{-1})	Area Ratio Band 1/2 (400 nm ex)	Area Ratio Band 1/3 (400 nm ex)	Area Ratio Band 2/3 (400 nm ex)
Toluene	1749.66	1586.73	240.01	1.10	7.29	6.61
1,4-Dioxane	1774.22	1679.93	238.30	1.06	7.45	7.05
Chloroform	-	2279.19	-	-	-	-
Acetonitrile	-	2276.72	-	-	-	-
1-Octanol	1485.49	2014.39	282.10	0.74	5.27	7.14
1-Hexanol	1982.64	-	1802.51	-	1.10	-
1-Butanol	1994.10	-	1644.64	-	1.21	-
1-Pentanol	1944.84	-	1727.38	-	1.13	-
1-Propanol	1927.77	-	1604.24	-	1.20	-
Acetic acid	1984.22	-	-	-	-	-
Methanol	2339.51	-	1448.52	-	1.62	-
2,2,2-Trifluoroethanol	-	346.06	-	-	-	-

Solvent	Band 1 Area Percentage (%)	Band 2 Area Percentage (%)	Band 3 Area Percentage (%)
Toluene	48.92	44.37	6.71
1,4-Dioxane	48.05	45.50	6.45
Chloroform	-	100.00	-
Acetonitrile	-	100.00	-
1-Octanol	39.28	53.26	7.46
1-Hexanol	52.38	-	47.62
1-Butanol	54.80	-	45.20
1-Pentanol	52.96	-	47.04
1-Propanol	54.58	-	45.42
Acetic acid	100.00	-	-
Methanol	61.76	-	38.24
2,2,2-Trifluoroethanol	-	100.00	-

Table 4.4.8. Band areas, area ratios and total area percentage of 3 band fit using Gaussian model for normalised **27** emission spectra recorded at 400 nm excitation.

4.4.4 310 nm Gaussian band fit - Solvatochromic analysis.

4.4.4.1 E_T^N.

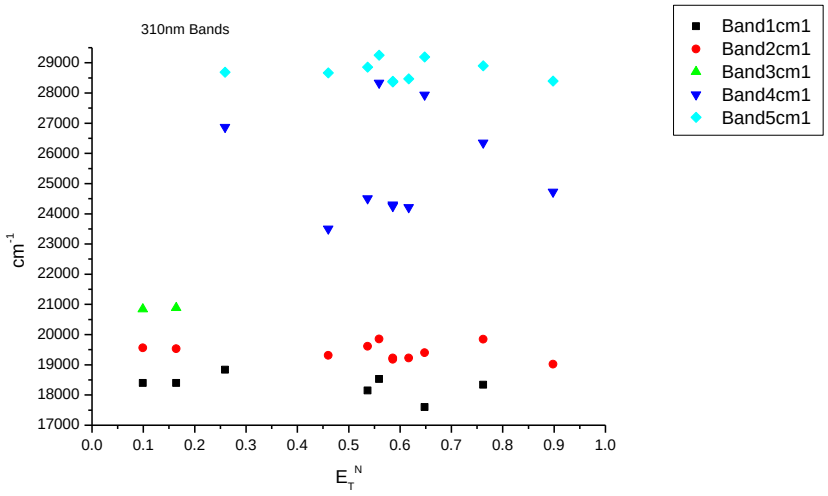

Figure 4.4.1. Band maxima from Gaussian model fit of the normalised fluorescence emission spectra of **27** recorded at 310 nm excitation against E_T^N.

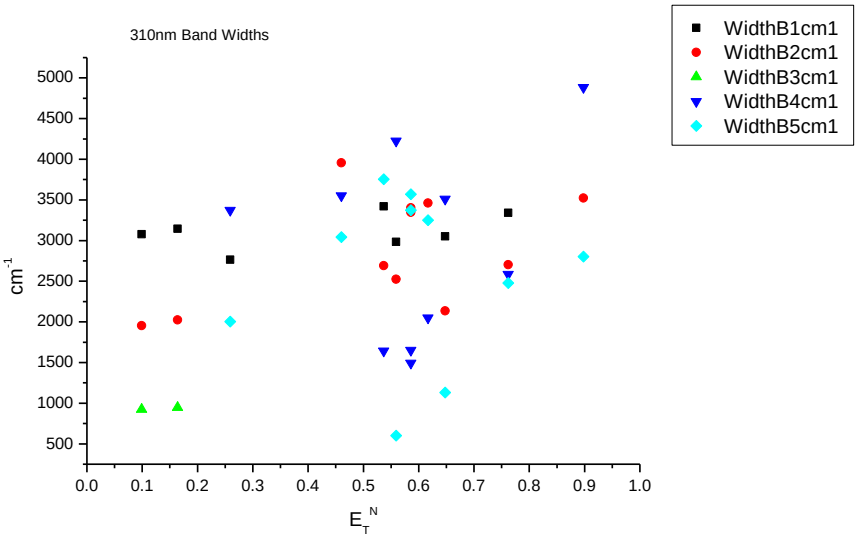

Figure 4.4.2. Band widths from Gaussian model fit of the normalised fluorescence emission spectra of **27** recorded at 310 nm excitation against E_T^N.

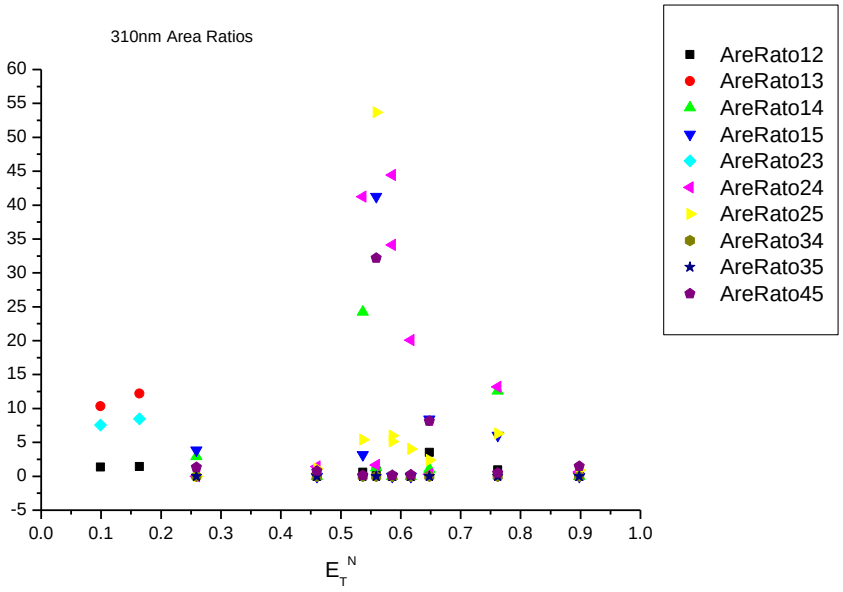

Figure 4.4.3. Area ratios from Gaussian model fit of the normalised fluorescence emission spectra of **27** recorded at 310 nm excitation against E_T^N.

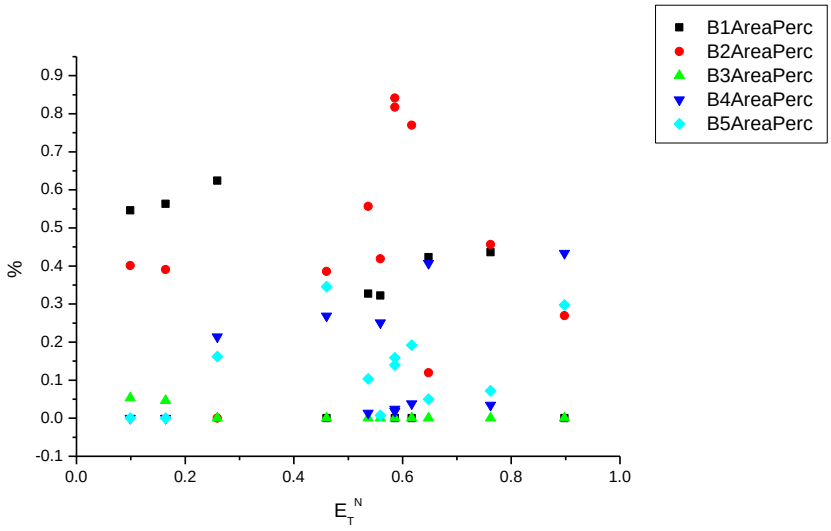

Figure 4.4.4. Area percentages from Gaussian model fit of the normalised fluorescence emission spectra of **27** recorded at 310 nm excitation against E_T^N.

4.4.4.2 α

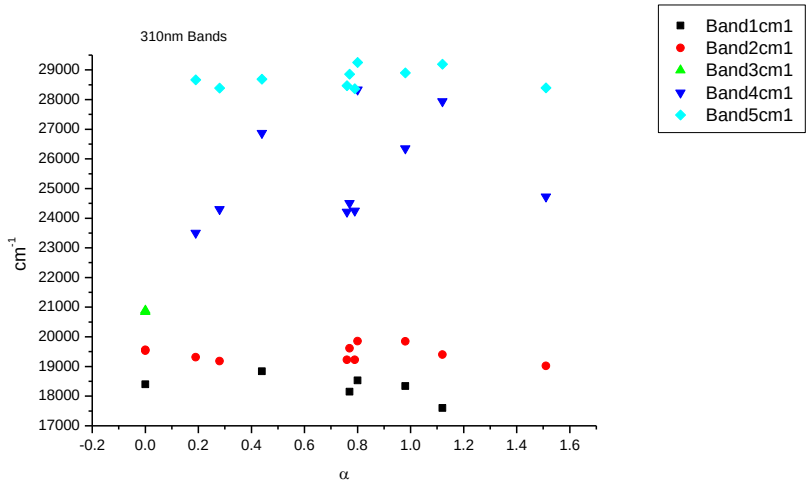

Figure 4.4.5. Band maxima from Gaussian model fit of the normalised fluorescence emission spectra of **27** recorded at 310 nm excitation against α.

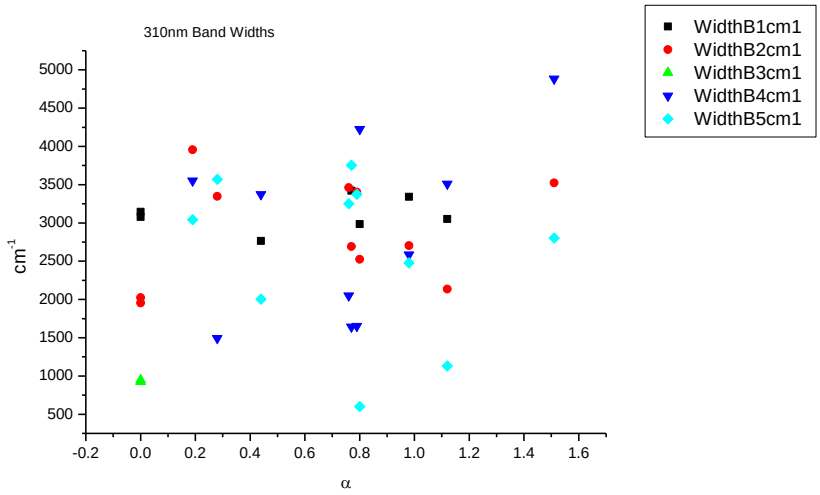

Figure 4.4.6. Band widths from Gaussian model fit of the normalised fluorescence emission spectra of **27** recorded at 310 nm excitation against α.

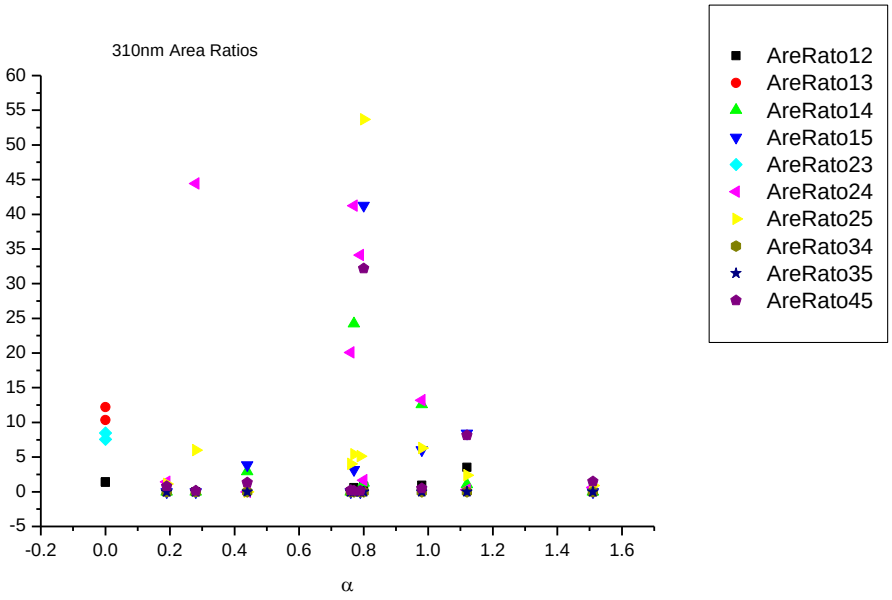

Figure 4.4.7. Area Ratios from Gaussian model fit of the normalised fluorescence emission spectra of **27** recorded at 310 nm excitation against α.

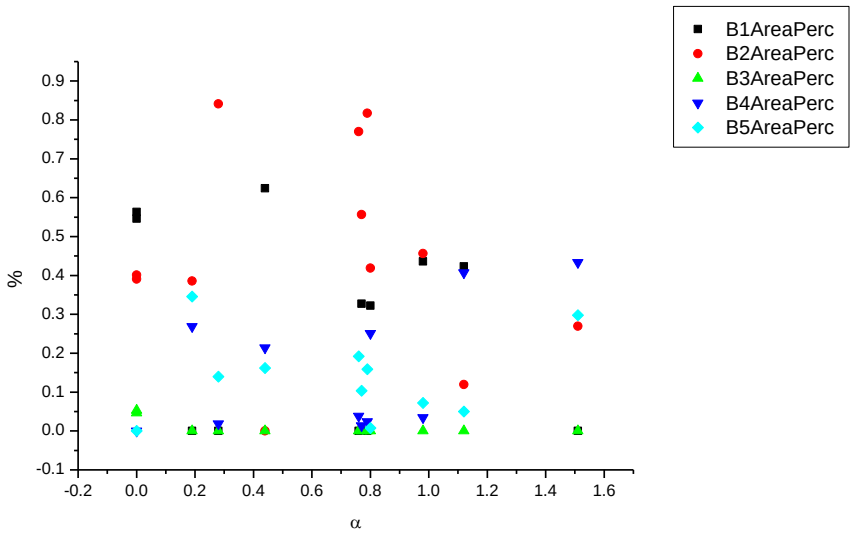

Figure 4.4.8. Area percentages from Gaussian model fit of the normalised fluorescence emission spectra of **27** recorded at 310 nm excitation against α.

4.4.4.3 β.

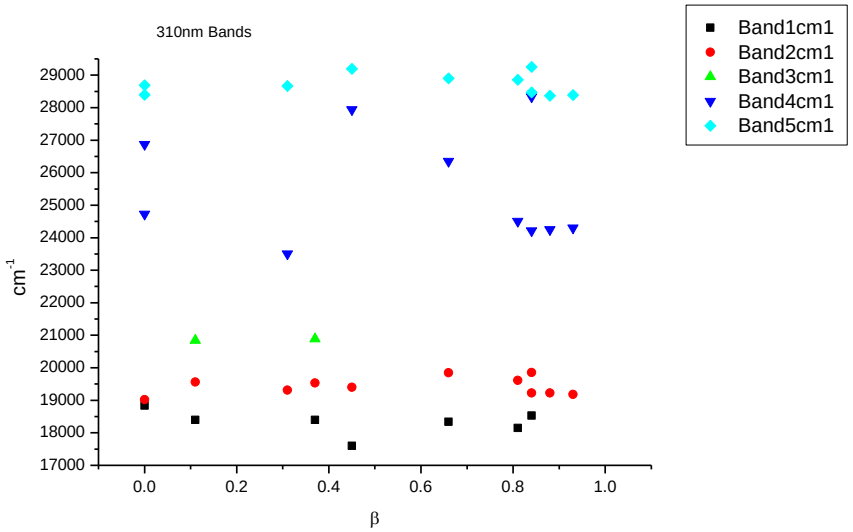

Figure 4.4.9. Band maxima from Gaussian model fit of the normalised fluorescence emission spectra of **27** recorded at 310 nm excitation against β.

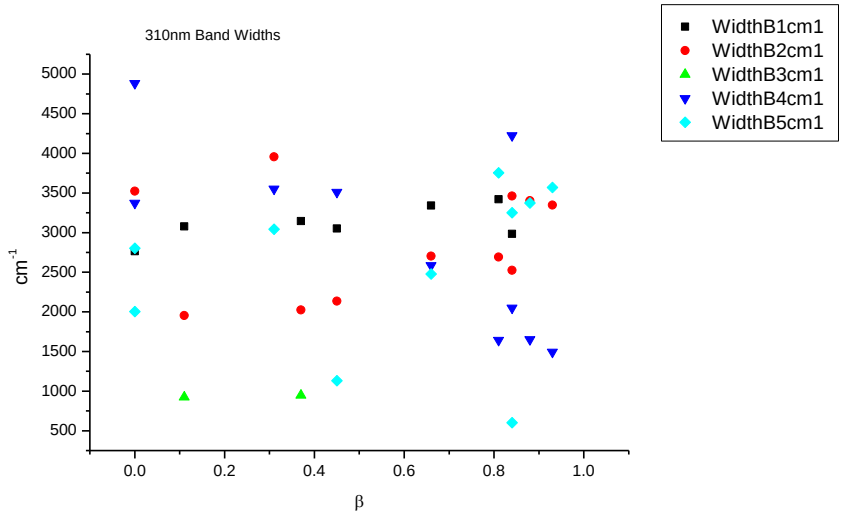

Figure 4.4.10. Band widths from Gaussian model fit of the normalised fluorescence emission spectra of **27** recorded at 310 nm excitation against β.

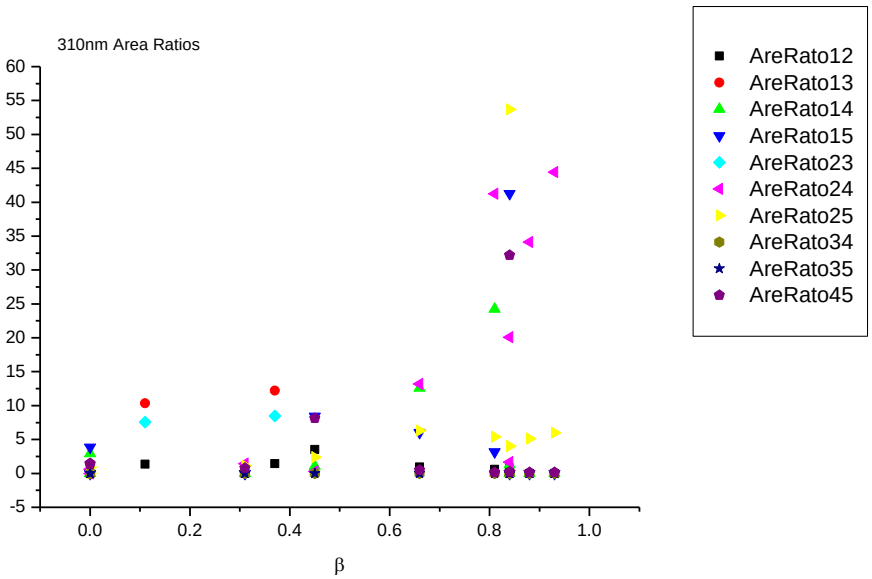

Figure 4.4.11. Area ratios from Gaussian model fit of the normalised fluorescence emission spectra of **27** recorded at 310 nm excitation against β.

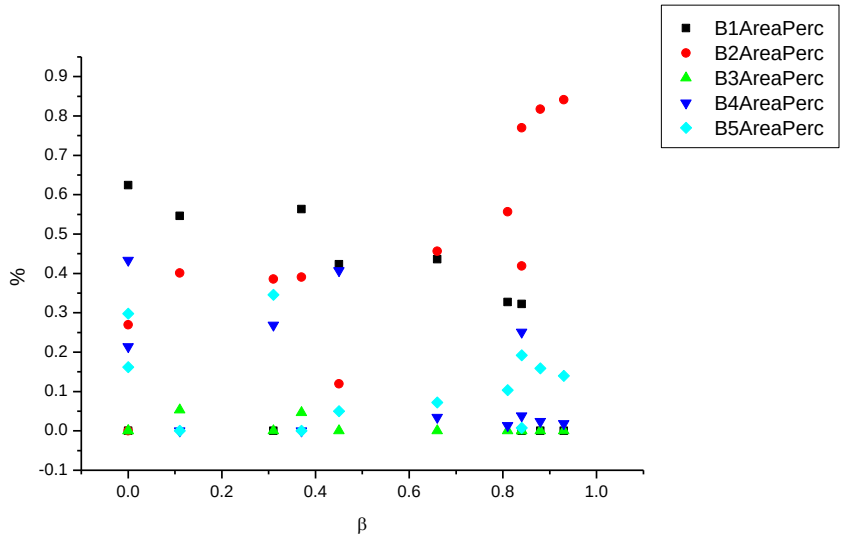

Figure 4.4.12. Area percentages from Gaussian model fit of the normalised fluorescence emission spectra of **27** recorded at 310 nm excitation against β.

4.4.4.4 π.*

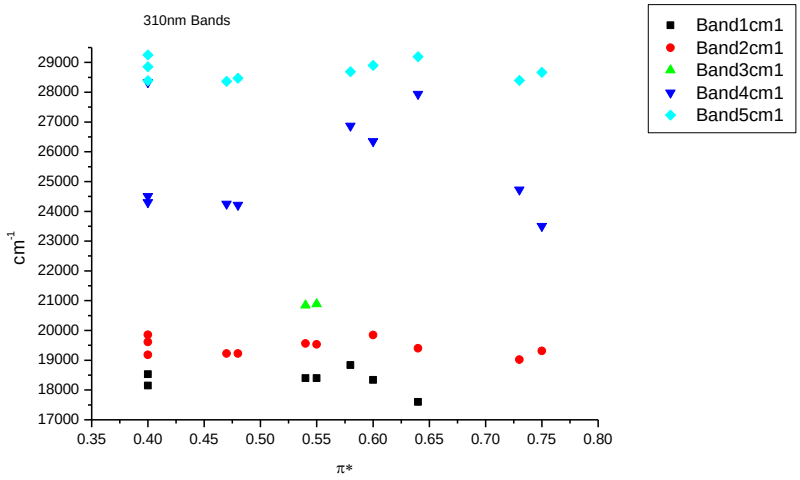

Figure 4.4.13. Band maxima from Gaussian model fit of the normalised fluorescence emission spectra of **27** recorded at 310 nm excitation against π*.

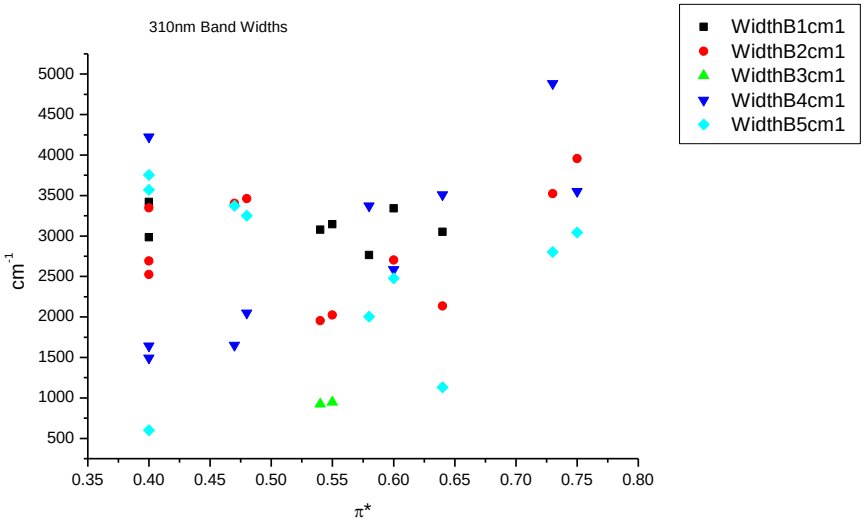

Figure 4.4.14. Band widths from Gaussian model fit of the normalised fluorescence emission spectra of **27** recorded at 310 nm excitation against π*.

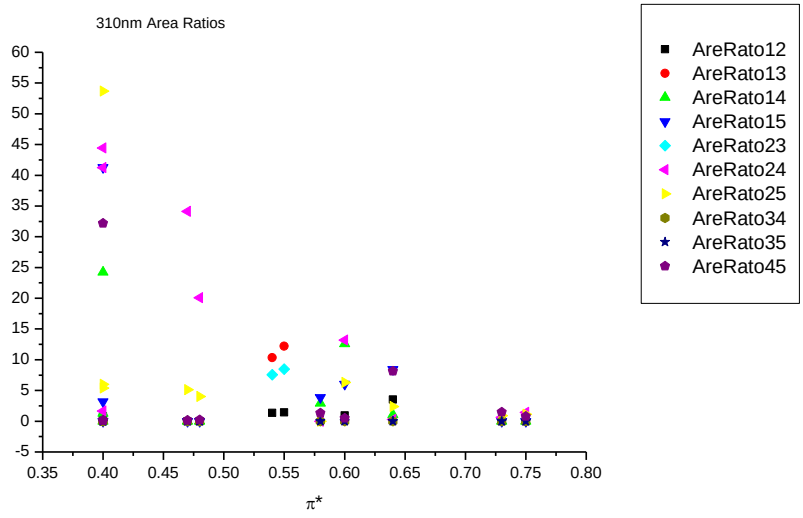

Figure 4.4.15. Area ratios from Gaussian model fit of the normalised fluorescence emission spectra of **27** recorded at 310 nm excitation against π*.

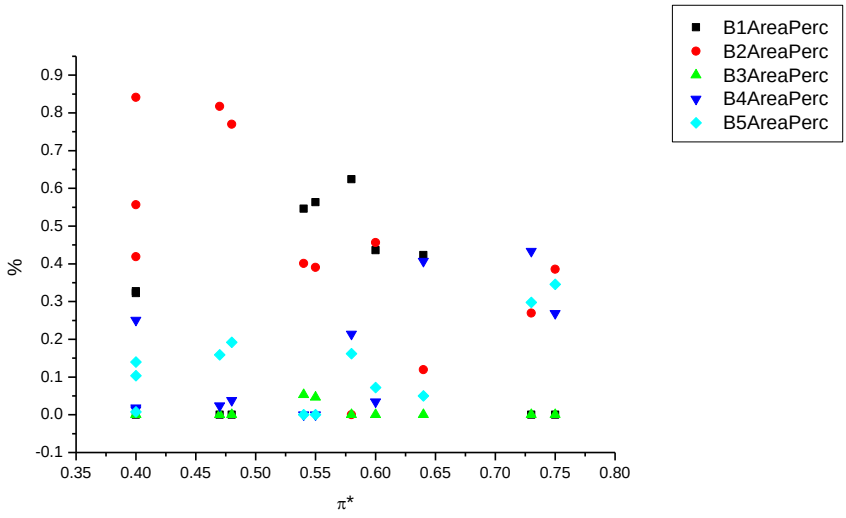

Figure 4.4.16. Area percentages from Gaussian model fit of the normalised fluorescence emission spectra of **27** recorded at 310 nm excitation against π*.

4.4.4.5 μ(D).

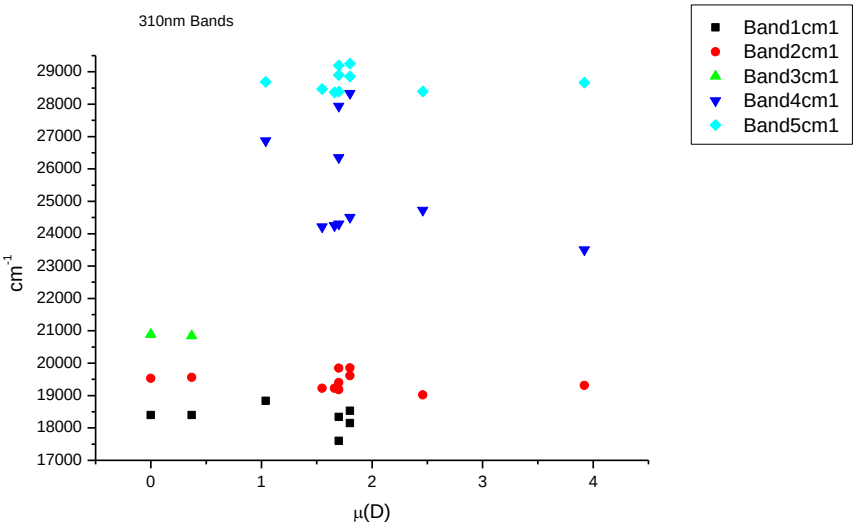

Figure 4.4.17. Band maxima from Gaussian model fit of the normalised fluorescence emission spectra of **27** recorded at 310 nm excitation against μ(D).

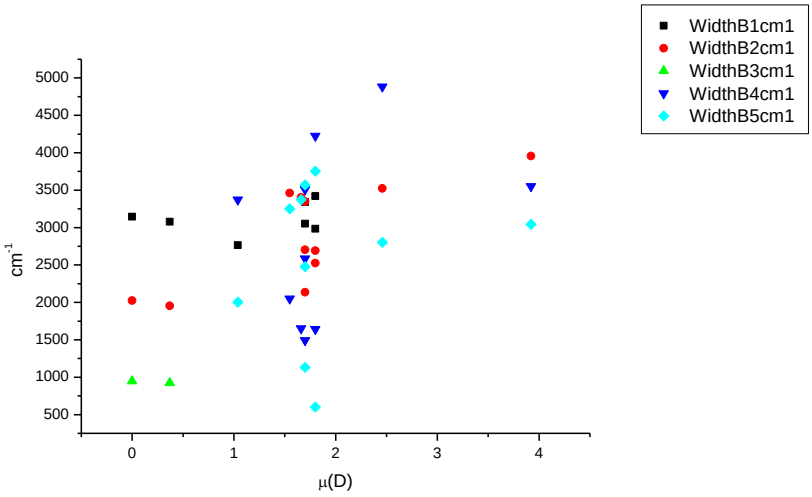

Figure 4.4.18. Band widths from Gaussian model fit of the normalised fluorescence emission spectra of **27** recorded at 310 nm excitation against μ(D).

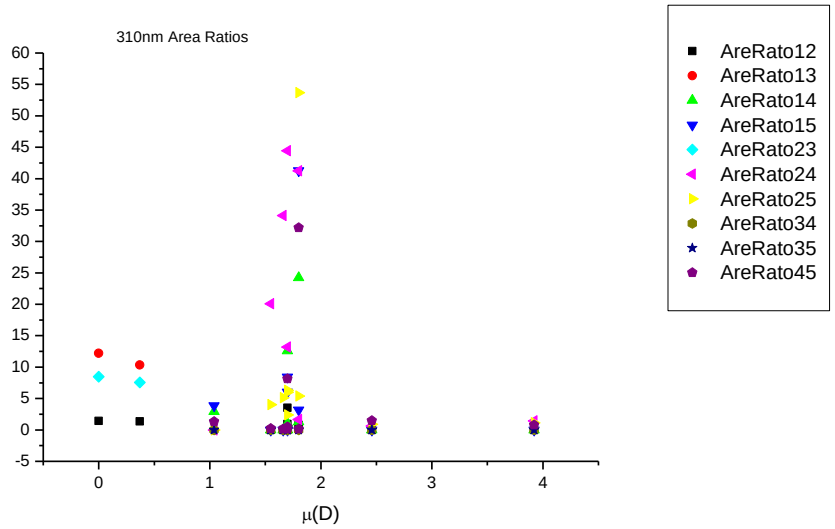

Figure 4.4.19. Area ratios from Gaussian model fit of the normalised fluorescence emission spectra of **27** recorded at 310 nm excitation against μ(D).

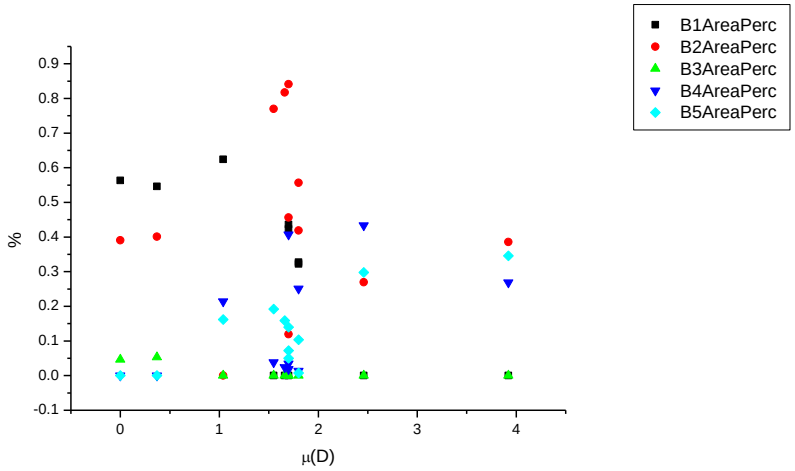

Figure 4.4.20. Area percentages from Gaussian model fit of the normalised fluorescence emission spectra of **27** recorded at 310 nm excitation against μ(D).

4.4.4.6 η(Cp).

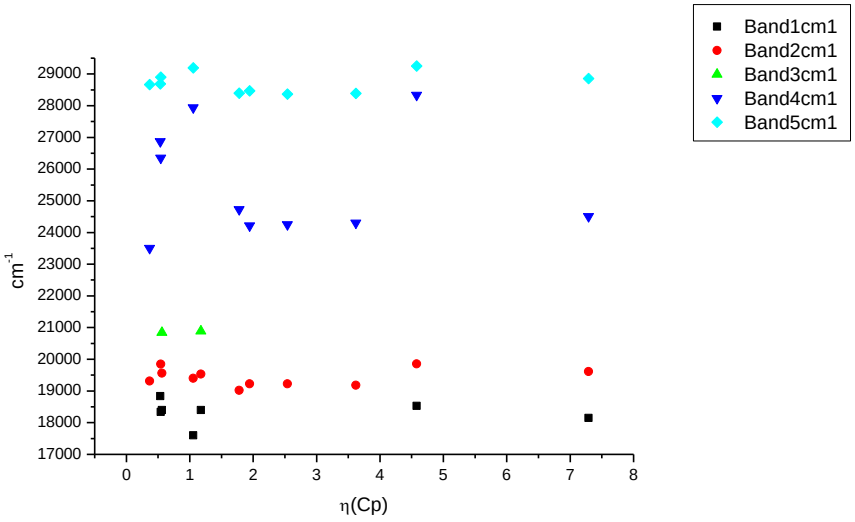

Figure 4.4.21. Band maxima from Gaussian model fit of the normalised fluorescence emission spectra of **27** recorded at 310 nm excitation against η(Cp).

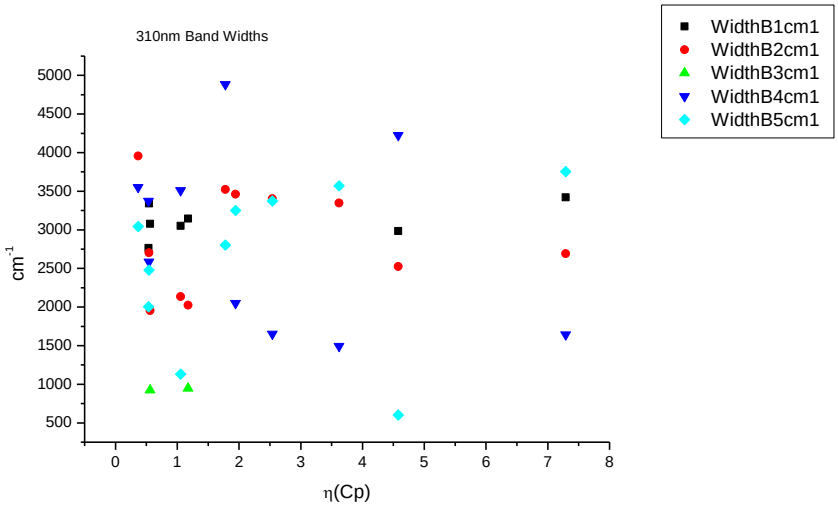

Figure 4.4.22. Band widths from Gaussian model fit of the normalised fluorescence emission spectra of **27** recorded at 310 nm excitation against η(Cp).

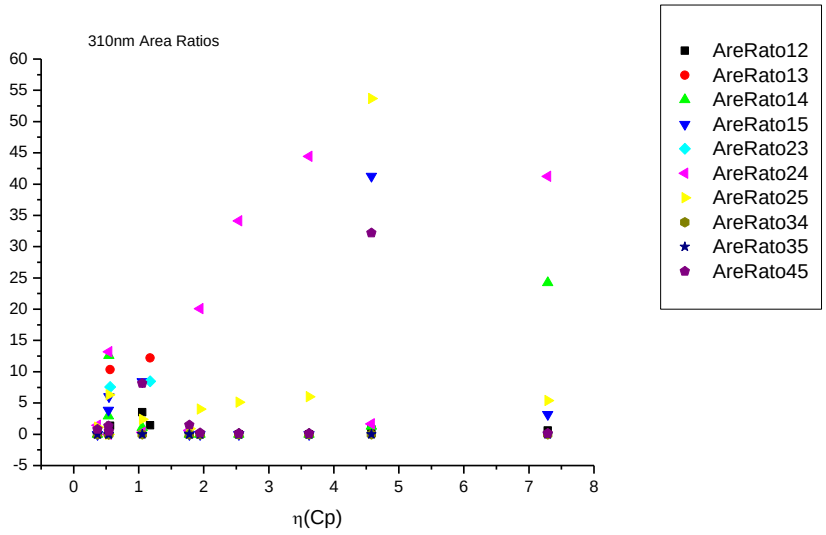

Figure 4.4.23. Area ratios from Gaussian model fit of the normalised fluorescence emission spectra of **27** recorded at 310 nm excitation against η(Cp).

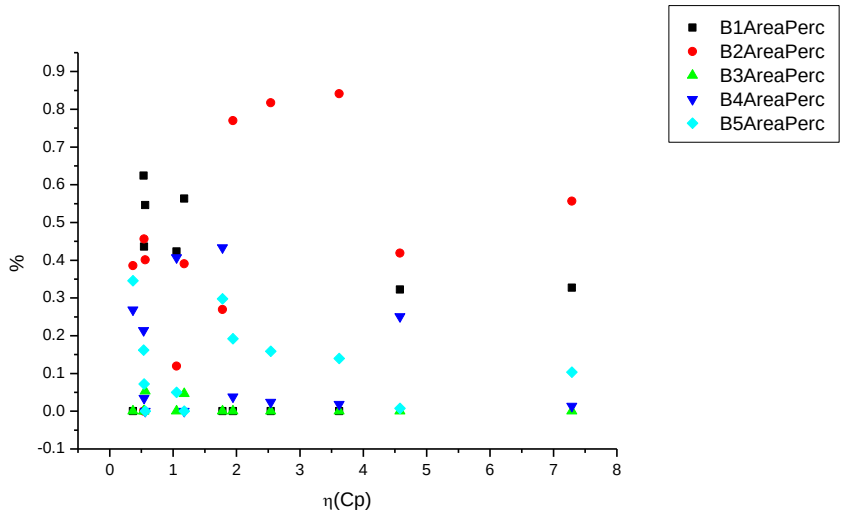

Figure 4.4.24. Area percentages from Gaussian model fit of the normalised fluorescence emission spectra of **27** recorded at 310 nm excitation against η(Cp).

4.4.5 400 nm Gaussian band fit - Solvatochromic analysis.

4.4.5.1 E_T^N.

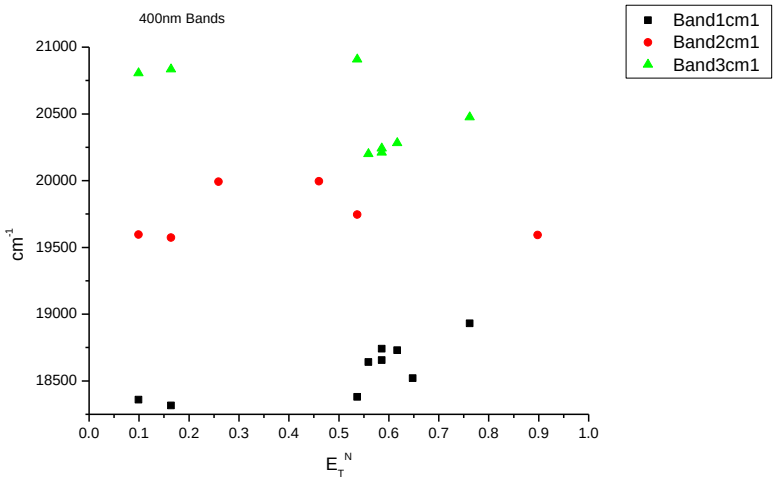

Figure 4.4.25. Band maxima from Gaussian model fit of the normalised fluorescence emission spectra of **27** recorded at 400 nm excitation against E_T^N.

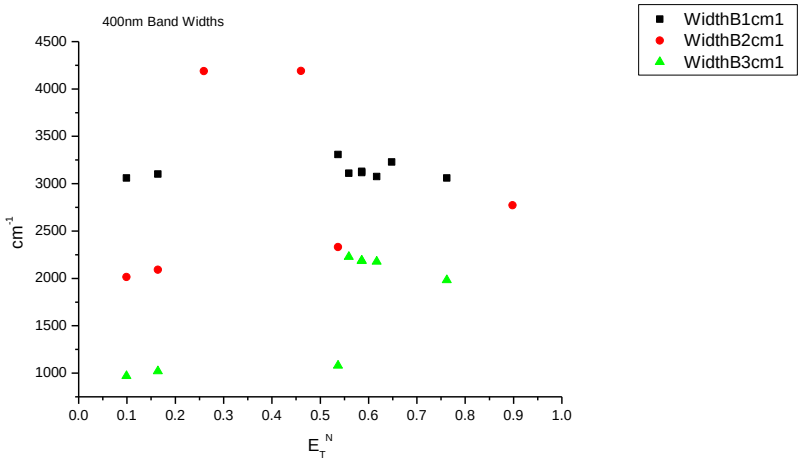

Figure 4.4.26. Band widths from Gaussian model fit of the normalised fluorescence emission spectra of **27** recorded at 400 nm excitation against E_T^N.

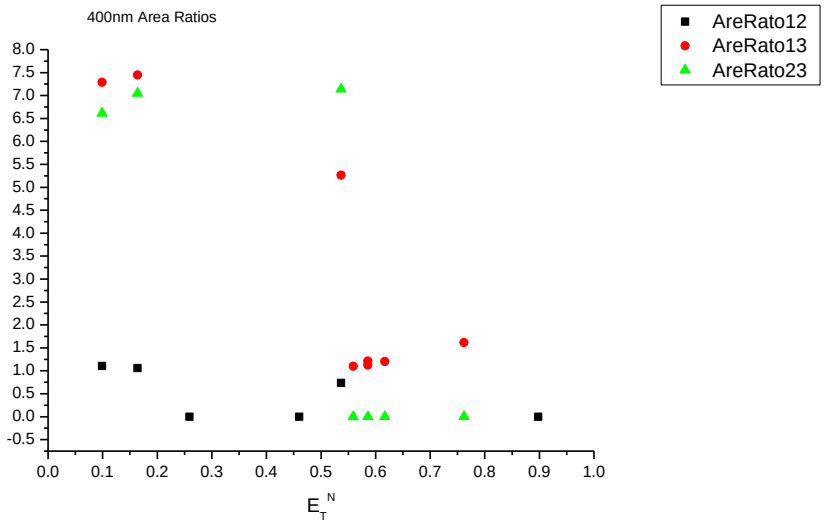

Figure 4.4.27. Area ratios from Gaussian model fit of the normalised fluorescence emission spectra of **27** recorded at 400 nm excitation against E_T^N.

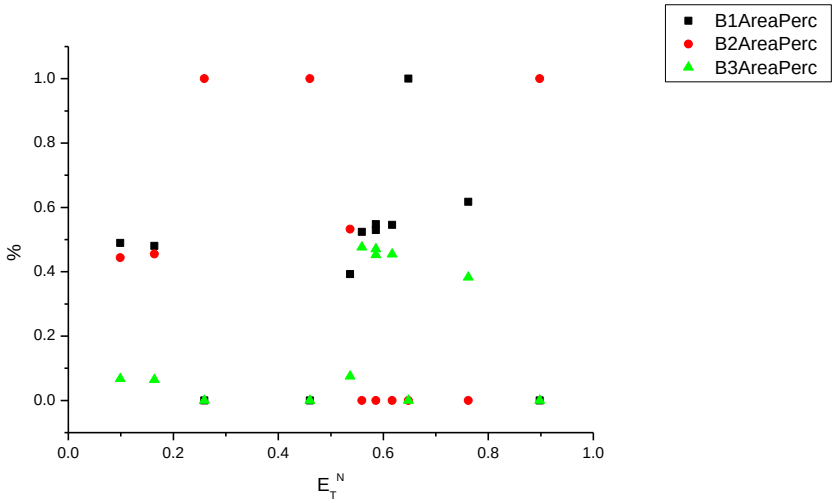

Figure 4.4.28. Area percentages from Gaussian model fit of the normalised fluorescence emission spectra of **27** recorded at 400 nm excitation against E_T^N.

4.4.5.2 α

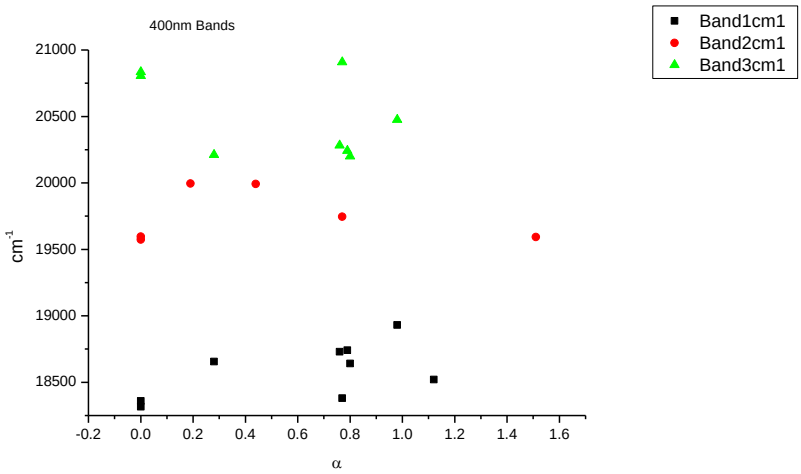

Figure 4.4.29. Band maxima from Gaussian model fit of the normalised fluorescence emission spectra of **27** recorded at 400 nm excitation against α.

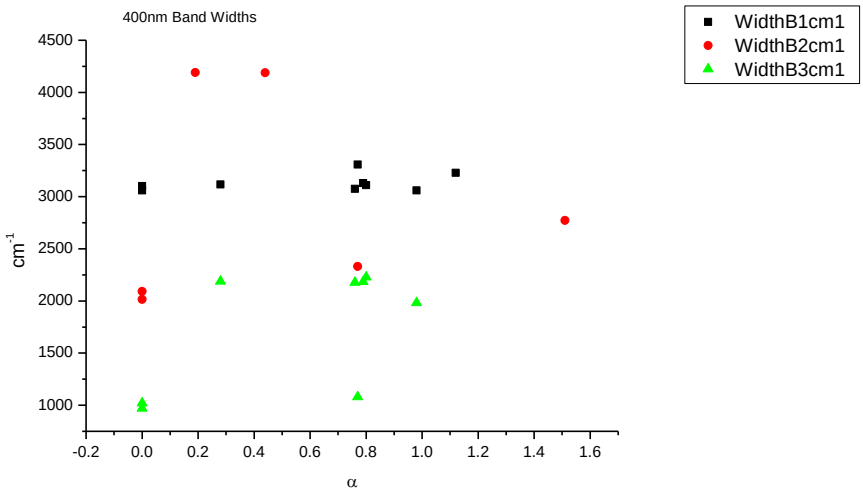

Figure 4.4.30. Band widths from Gaussian model fit of the normalised fluorescence emission spectra of **27** recorded at 400 nm excitation against α.

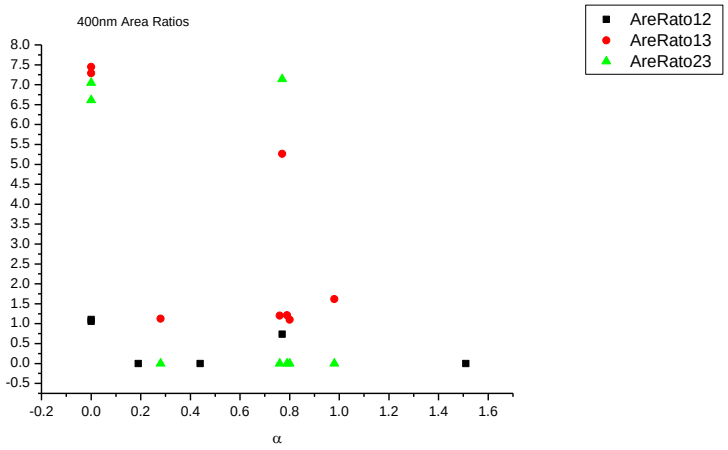

Figure 4.4.31. Area ratios from Gaussian model fit of the normalised fluorescence emission spectra of **27** recorded at 400 nm excitation against α.

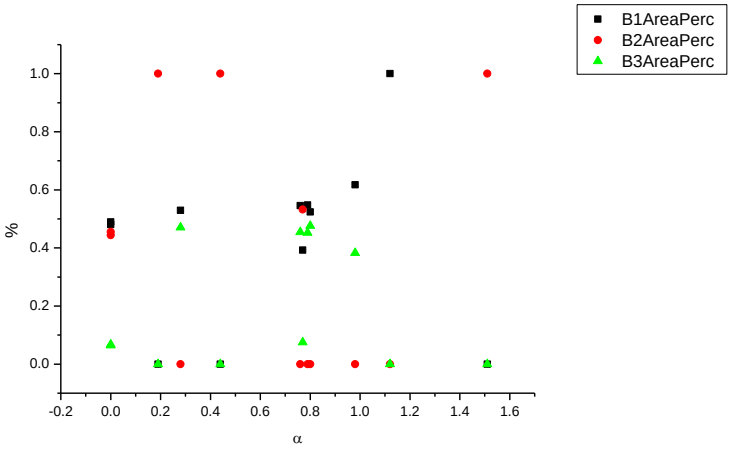

Figure 4.4.32. Area percentages from Gaussian model fit of the normalised fluorescence emission spectra of **27** recorded at 400 nm excitation against α.

4.4.5.3 β.

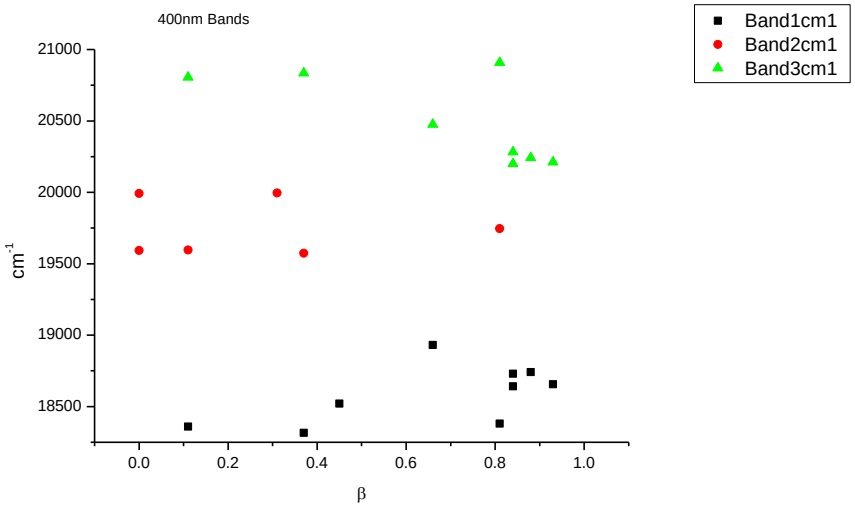

Figure 4.4.33. Band maxima from Gaussian model fit of the normalised fluorescence emission spectra of **27** recorded at 400 nm excitation against β.

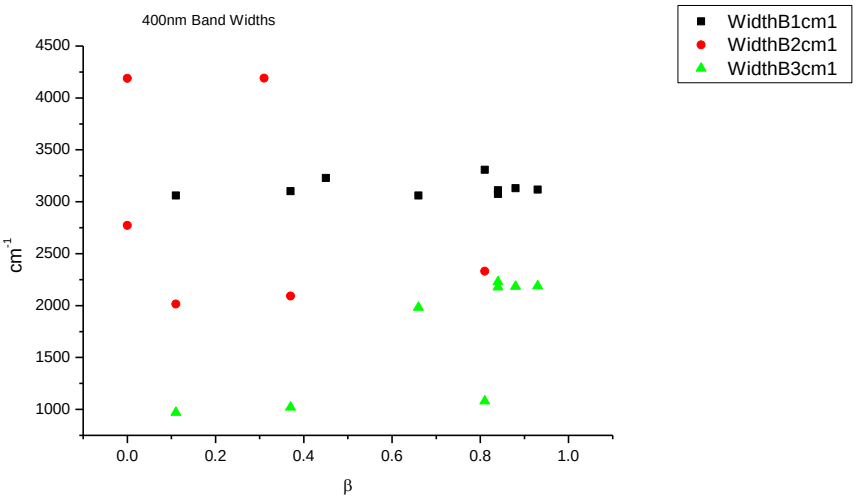

Figure 4.4.34. Band widths from Gaussian model fit of the normalised fluorescence emission spectra of **27** recorded at 400 nm excitation against β.

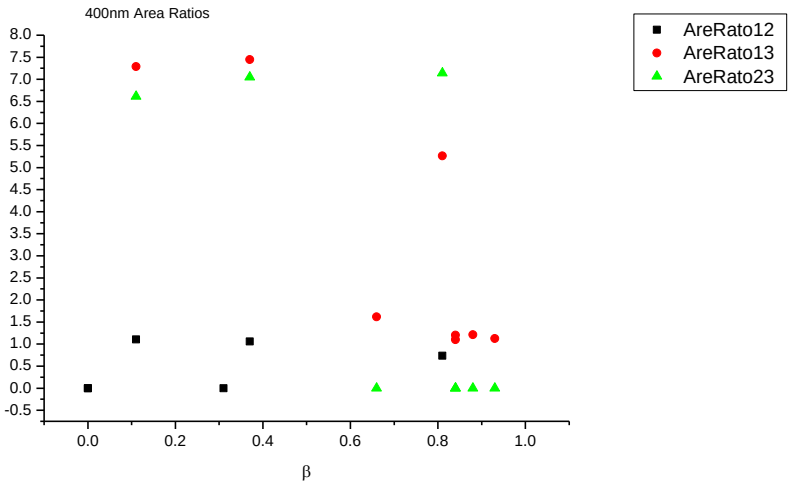

Figure 4.4.35. Area ratios from Gaussian model fit of the normalised fluorescence emission spectra of **27** recorded at 400 nm excitation against β.

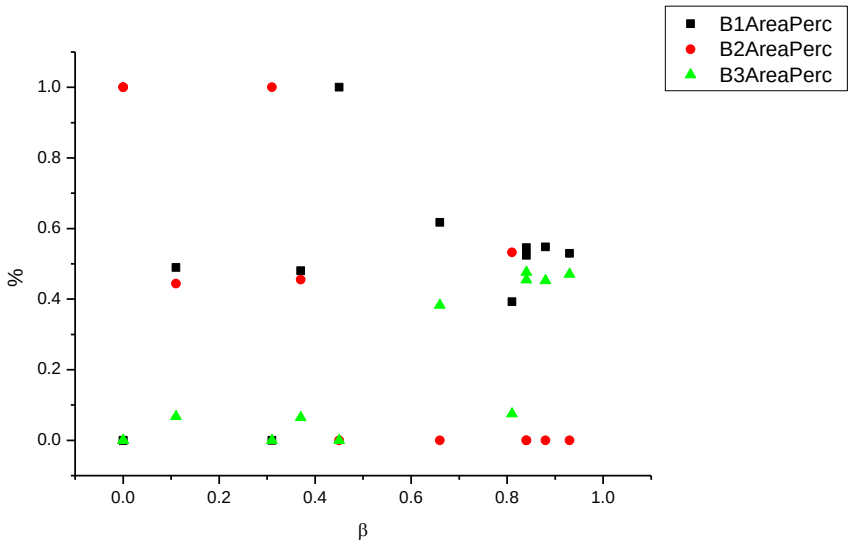

Figure 4.4.36. Area percentages from Gaussian model fit of the normalised fluorescence emission spectra of **27** recorded at 400 nm excitation against β.

4.4.5.4 π.*

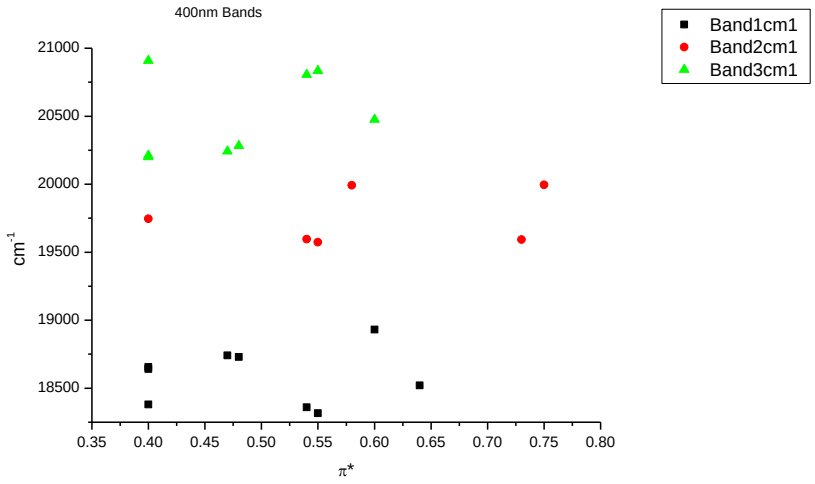

Figure 4.4.37. Band maxima from Gaussian model fit of the normalised fluorescence emission spectra of **27** recorded at 400 nm excitation against π*.

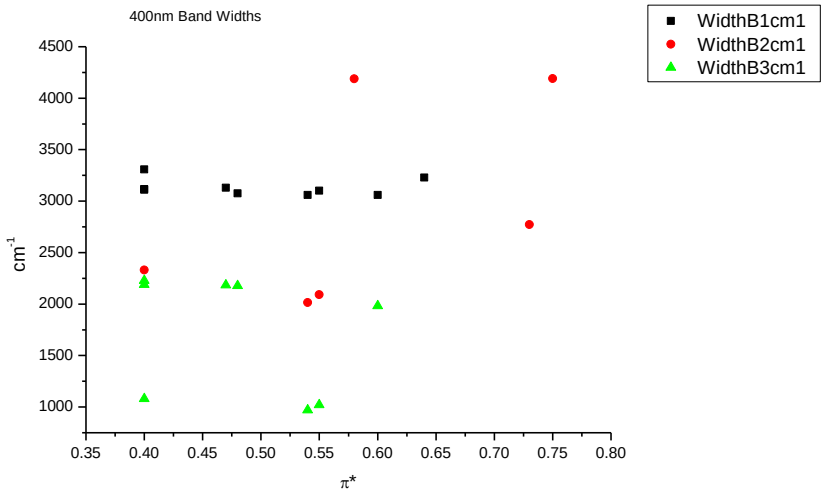

Figure 4.4.38. Band widths from Gaussian model fit of the normalised fluorescence emission spectra of **27** recorded at 400 nm excitation against π*.

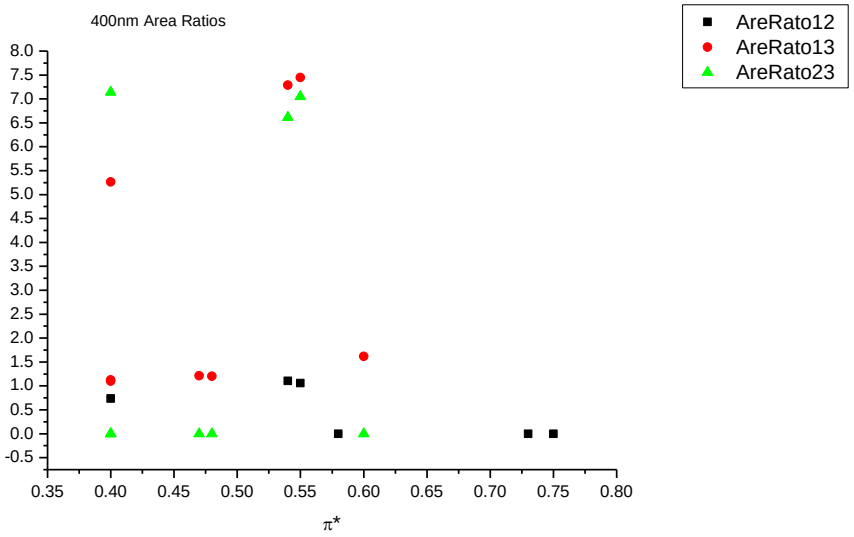

Figure 4.4.39. Area ratios from Gaussian model fit of the normalised fluorescence emission spectra of **27** recorded at 400 nm excitation against π*.

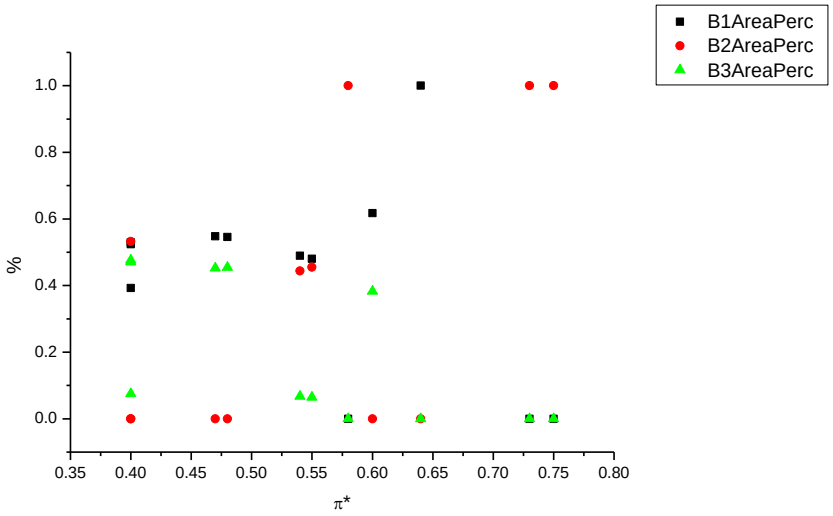

Figure 4.4.40. Area percentages from Gaussian model fit of the normalised fluorescence emission spectra of **27** recorded at 400 nm excitation against π*.

4.4.5.5 μ(D).

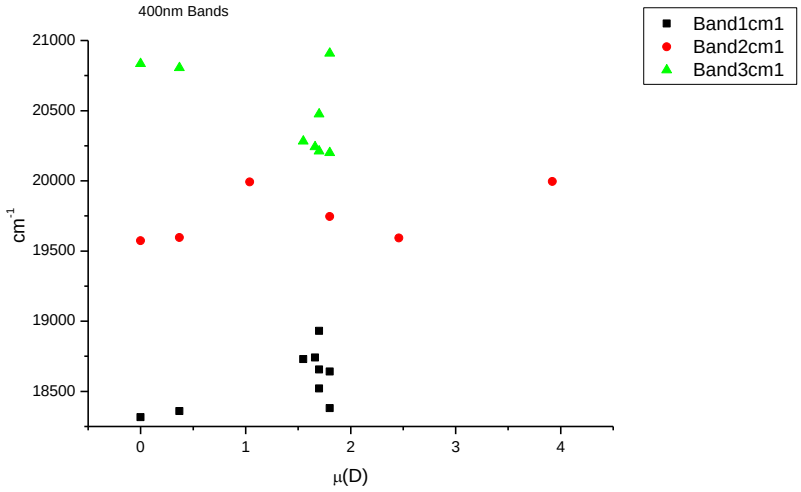

Figure 4.4.41. Band maxima from Gaussian model fit of the normalised fluorescence emission spectra of **27** recorded at 400 nm excitation against μ(D).

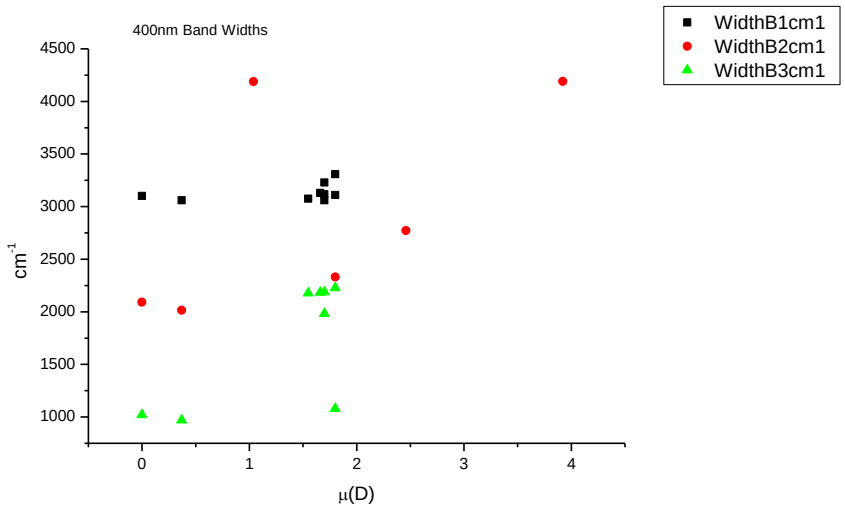

Figure 4.4.42. Band widths from Gaussian model fit of the normalised fluorescence emission spectra of **27** recorded at 400 nm excitation against μ(D).

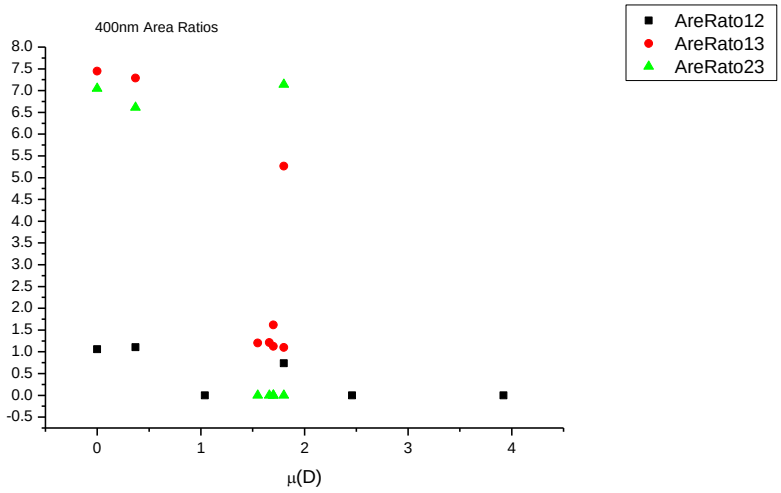

Figure 4.4.43. Area ratios from Gaussian model fit of the normalised fluorescence emission spectra of **27** recorded at 400 nm excitation against μ(D).

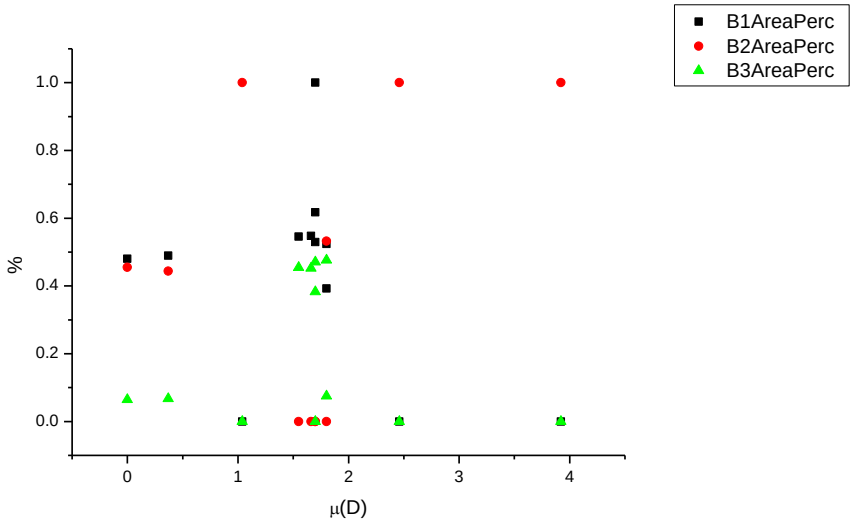

Figure 4.4.44. Area percentages from Gaussian model fit of the normalised fluorescence emission spectra of **27** recorded at 400 nm excitation against μ(D).

4.4.5.6 η(Cp).

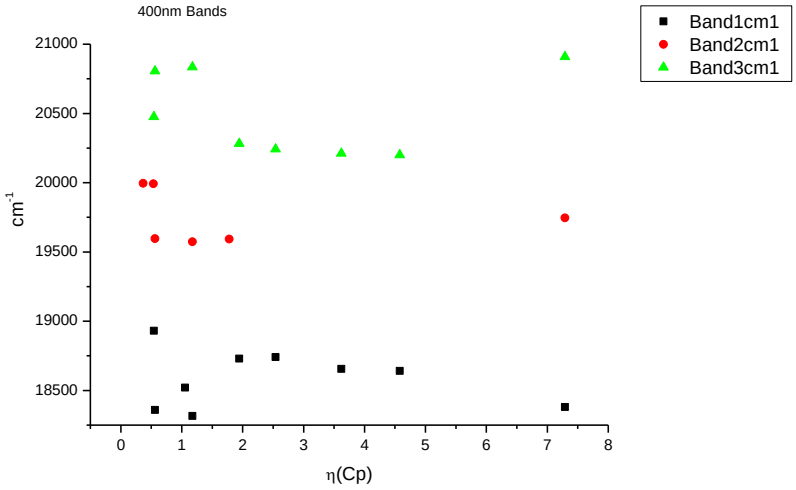

Figure 4.4.45. Band maxima from Gaussian model fit of the normalised fluorescence emission spectra of **27** recorded at 400 nm excitation against η(Cp).

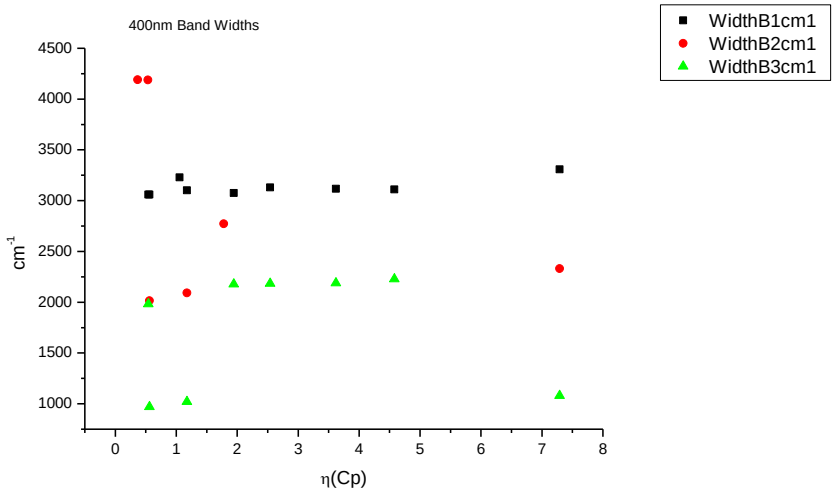

Figure 4.4.46. Band widths from Gaussian model fit of the normalised fluorescence emission spectra of **27** recorded at 400 nm excitation against η(Cp).

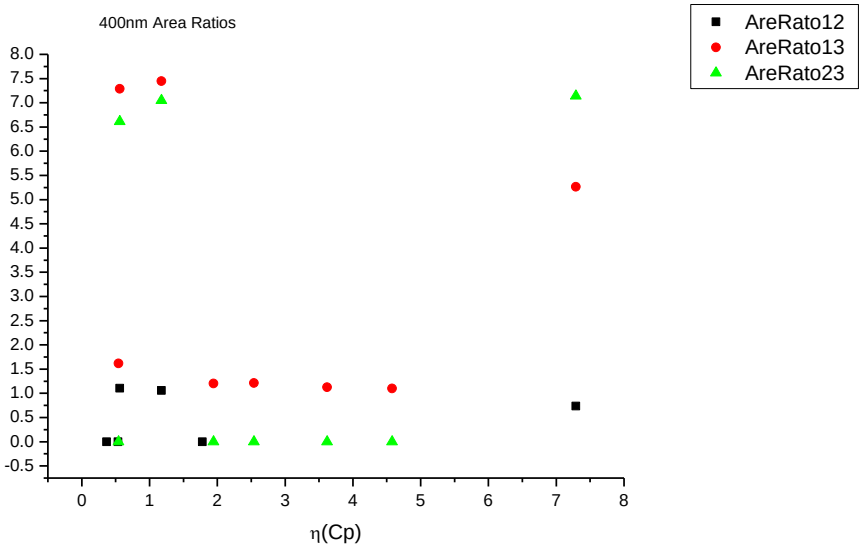

Figure 4.4.47. Area ratios from Gaussian model fit of the normalised fluorescence emission spectra of **27** recorded at 400 nm excitation against η(Cp).

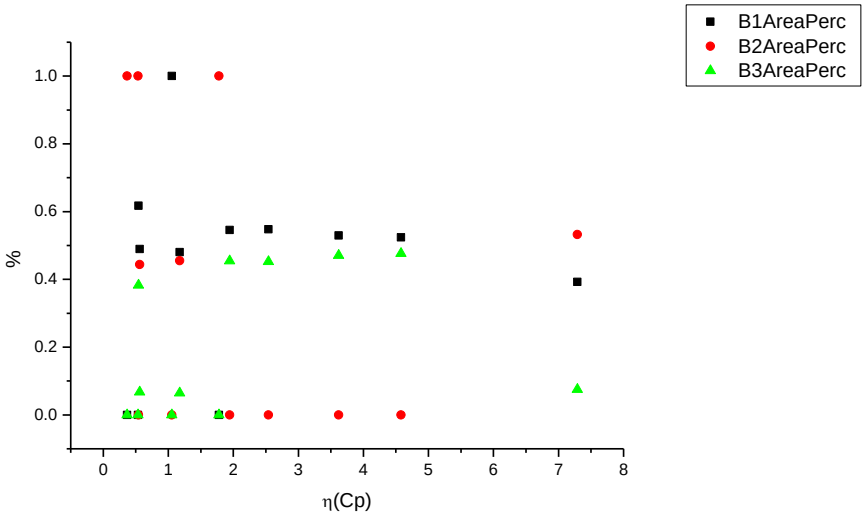

Figure 4.4.48. Area percentages from Gaussian model fit of the normalised fluorescence emission spectra of **27** recorded at 400 nm excitation against η(Cp).

4.4.6 400 nm fluorescent lifetime results.

4.4.6.1 Intensity weighted.

Wavelength (nm)	Solvent	τ_1 (ns)	A_1 (%)	τ_2 (ns)	A_2 (%)	τ_3 (ns)	A_3 (%)	τ_f (ns) (Intensity Weighted)	$1/\tau_f$	χ^2
470	Toluene	-	-	3.94	55.31	10.62	44.69	6.92	0.14	1.21
470	1,4-Dioxane	-	-	3.97	64.34	9.92	35.66	6.09	0.16	1.26
470	Chloroform	0.24	15.03	1.41	80.28	6.22	4.69	1.46	0.69	1.12
470	Acetonitrile	0.23	84.05	1.85	9.38	6.91	6.57	0.83	1.21	1.17
470	1-Octanol	0.10	72.51	0.91	25.09	6.33	2.41	0.45	2.23	1.54
470	1-Hexanol	0.28	70.75	0.94	14.43	5.17	14.82	1.10	0.91	1.06
470	1-Butanol	0.21	22.14	3.37	20.51	6.06	57.35	4.30	0.23	1.01
470	1-Pentanol	0.25	50.68	-	-	5.09	49.32	2.64	0.38	1.29
470	1-Propanol	0.14	4.01	4.45	48.56	6.44	47.43	5.22	0.19	1.07
470	Acetic acid	0.22	85.94	1.36	8.58	6.23	5.48	0.65	1.54	1.30
470	Methanol	0.41	2.06	3.33	63.59	5.30	34.35	3.95	0.25	1.11
470	2,2,2-Trifluoroethanol	0.23	64.15	0.77	31.77	5.24	4.07	0.60	1.66	0.96

Table 4.4.9. Summary of Time Correlated Single Photon Counting (TCSPC) fluorescent lifetimes (intensity weighted) of **27** recorded at 470 nm.

Wavelength (nm)	Solvent	τ_1 (ns)	A_1 (%)	τ_2 (ns)	A_2 (%)	τ_3 (ns)	A_3 (%)	τ_f (ns) (Intensity Weighted)	$1/\tau_f$	χ^2
490	Toluene	-	-	4.13	49.18	10.91	50.82	7.58	0.13	1.11
490	1,4-Dioxane	-	-	4.06	59.05	10.67	40.95	6.77	0.15	1.15
490	Chloroform	0.19	25.69	1.41	64.65	6.63	9.66	1.60	0.62	0.89
490	Acetonitrile	0.23	81.44	2.77	12.07	13.42	6.49	1.39	0.72	1.22
490	1-Octanol	0.22	51.00	0.95	44.29	5.84	4.71	0.81	1.24	1.69
490	1-Hexanol	0.37	74.68	1.25	11.71	5.63	13.61	1.19	0.84	1.16
490	1-Butanol	0.19	19.49	4.24	37.30	7.18	43.21	4.72	0.21	1.02
490	1-Pentanol	0.26	52.89	2.57	7.91	6.21	39.20	2.77	0.36	1.23
490	1-Propanol	0.15	3.43	4.94	75.81	9.37	20.76	5.70	0.18	1.13
490	Acetic acid	0.17	92.52	1.24	4.33	5.28	3.15	0.38	2.62	1.13
490	Methanol	0.41	1.72	3.26	54.21	5.51	44.07	4.20	0.24	1.12
490	2,2,2-Trifluoroethanol	0.23	64.03	0.76	31.87	5.23	4.10	0.60	1.66	0.95

Table 4.4.10. Summary of Time Correlated Single Photon Counting (TCSPC) fluorescent lifetimes (intensity weighted) of **27** recorded at 490 nm.

Wavelength (nm)	Solvent	τ_1 (ns)	A_1 (%)	τ_2 (ns)	A_2 (%)	τ_3 (ns)	A_3 (%)	τ_f (ns) (Intensity Weighted)	$1/\tau_f$	χ^2
520	Toluene	-	-	4.20	20.60	10.87	79.40	9.49	0.11	1.25
520	1,4-Dioxane	-	-	4.14	31.92	11.62	68.08	9.23	0.11	1.10
520	Chloroform	0.27	23.92	1.34	56.34	7.11	19.73	2.23	0.45	1.02
520	Acetonitrile	0.26	80.75	4.11	11.64	21.07	7.63	2.29	0.44	3.42
520	1-Octanol	0.24	38.95	1.02	46.47	5.19	14.59	1.32	0.76	1.30
520	1-Hexanol	0.40	71.17	1.55	13.16	5.43	15.68	1.34	0.75	1.17
520	1-Butanol	0.20	18.35	4.66	46.63	10.58	35.02	5.91	0.17	1.13
520	1-Pentanol	0.29	46.76	3.30	18.75	8.70	34.49	3.75	0.27	1.16
520	1-Propanol	0.16	3.14	4.98	62.69	11.32	34.17	6.99	0.14	1.04
520	Acetic acid	0.16	93.55	1.38	4.08	5.84	2.37	0.34	2.92	1.21
520	Methanol	0.71	1.81	3.82	75.39	10.66	22.80	5.32	0.19	1.05
520	2,2,2-Trifluoroethanol	0.23	62.27	0.78	30.49	4.91	7.24	0.74	1.36	0.97

Table 4.4.11. Summary of Time Correlated Single Photon Counting (TCSPC) fluorescent lifetimes (intensity weighted) of **27** recorded at 520 nm.

Wavelength (nm)	Solvent	τ_1 (ns)	A_1 (%)	τ_2 (ns)	A_2 (%)	τ_3 (ns)	A_3 (%)	τ_f (ns) (Intensity Weighted)	$1/\tau_f$	χ^2
540	Toluene	-	-	4.14	12.54	10.80	87.46	9.96	0.10	1.13
540	1,4-Dioxane	-	-	4.17	22.21	11.53	77.79	9.90	0.10	1.19
540	Chloroform	0.26	20.33	1.14	54.86	5.92	24.81	2.15	0.47	1.14
540	Acetonitrile	0.21	74.96	2.52	10.51	10.32	14.52	1.92	0.52	1.10
540	1-Octanol	0.26	38.25	1.04	43.05	4.98	18.69	1.48	0.68	1.22
540	1-Hexanol	0.42	70.04	2.23	18.28	7.36	11.68	1.56	0.64	0.95
540	1-Butanol	0.20	18.53	4.10	32.05	9.78	49.43	6.19	0.16	1.07
540	1-Pentanol	0.29	45.31	2.50	14.57	8.33	40.12	3.84	0.26	1.21
540	1-Propanol	0.22	2.21	5.09	59.13	12.47	38.66	7.83	0.13	1.14
540	Acetic acid	0.15	91.30	1.05	6.49	5.24	2.21	0.32	3.16	1.15
540	Methanol	1.62	3.42	4.01	70.35	12.29	26.23	6.10	0.16	1.15
540	2,2,2-Trifluoroethanol	0.22	62.00	0.79	29.50	4.77	8.50	0.78	1.29	1.02

Table 4.4.12. Summary of Time Correlated Single Photon Counting (TCSPC) fluorescent lifetimes (intensity weighted) of **27** recorded at 540 nm.

Wavelength (nm)	Solvent	τ_1 (ns)	A_1 (%)	τ_2 (ns)	A_2 (%)	τ_3 (ns)	A_3 (%)	τ_f (ns) (Intensity Weighted)	$1/\tau_f$	χ^2
570	Toluene	-	-	4.02	2.26	10.81	97.74	10.66	0.09	1.19
570	1,4-Dioxane	-	-	4.71	12.46	11.74	87.54	10.86	0.09	1.17
570	Chloroform	0.33	22.65	1.07	49.71	7.03	27.64	2.55	0.39	1.08
570	Acetonitrile	0.24	74.99	2.25	9.35	11.40	15.65	2.18	0.46	1.25
570	1-Octanol	0.14	41.33	0.99	37.28	4.80	21.39	1.45	0.69	1.21
570	1-Hexanol	0.43	66.01	2.24	21.61	7.36	12.39	1.68	0.60	1.02
570	1-Butanol	0.23	20.24	3.93	25.48	10.58	54.28	6.79	0.15	1.07
570	1-Pentanol	0.31	45.28	2.39	15.55	9.43	39.17	4.20	0.24	1.27
570	1-Propanol	0.21	2.97	4.76	41.81	11.60	55.22	8.40	0.12	1.14
570	Acetic acid	0.16	87.64	0.90	10.35	4.44	2.01	0.32	3.13	1.01
570	Methanol	2.36	4.40	4.01	60.11	12.22	35.49	6.85	0.15	1.26
570	2,2,2-Trifluoroethanol	0.22	58.68	0.80	29.78	4.32	11.54	0.87	1.15	1.10

Table 4.4.13. Summary of Time Correlated Single Photon Counting (TCSPC) fluorescent lifetimes (intensity weighted) of **27** recorded at 570 nm.

4.4.6.2 Amplitude weighted.

Wavelength (nm)	Solvent	τ_1 (ns)	A_1 (%)	τ_2 (ns)	A_2 (%)	τ_3 (ns)	A_3 (%)	τ_f (ns) (Amplitude Weighted)	$1/\tau_f$	χ^2
470	Toluene	-	-	3.94	76.93	10.62	23.07	5.48	0.18	1.21
470	1,4-Dioxane	-	-	3.97	81.85	9.92	18.15	5.05	0.20	1.26
470	Chloroform	0.24	51.92	1.41	47.45	6.22	0.63	0.83	1.20	1.12
470	Acetonitrile	0.23	98.34	1.85	1.39	6.91	0.26	0.28	3.64	1.17
470	1-Octanol	0.10	96.44	0.91	3.51	6.33	0.05	0.13	7.87	1.54
470	1-Hexanol	0.28	93.29	0.94	5.65	5.17	1.06	0.37	2.71	1.06
470	1-Butanol	0.21	87.88	3.37	4.41	6.06	7.71	0.82	1.23	1.01
470	1-Pentanol	0.25	95.47	-	-	5.09	4.53	0.47	2.14	1.29
470	1-Propanol	0.14	61.01	4.45	23.27	6.44	15.71	2.13	0.47	1.07
470	Acetic acid	0.22	98.17	1.36	1.60	6.23	0.22	0.25	3.93	1.30
470	Methanol	0.41	16.44	3.33	62.42	5.30	21.24	3.26	0.31	1.11
470	2,2,2-Trifluoroethanol	0.23	87.03	0.77	12.73	5.24	0.24	0.31	3.26	0.96

Table 4.4.14. Summary of Time Correlated Single Photon Counting (TCSPC) fluorescent lifetimes (amplitude weighted) of **27** recorded at 470 nm.

Wavelength (nm)	Solvent	τ_1 (ns)	A_1 (%)	τ_2 (ns)	A_2 (%)	τ_3 (ns)	A_3 (%)	τ_f (ns) (Amplitude Weighted)	$1/\tau_f$	χ^2
490	Toluene	-	-	4.13	71.87	10.91	28.13	6.04	0.17	1.11
490	1,4-Dioxane	-	-	4.06	79.14	10.67	20.86	5.44	0.18	1.15
490	Chloroform	0.19	74.02	1.41	25.18	6.63	0.80	0.55	1.82	0.89
490	Acetonitrile	0.23	98.67	2.77	1.20	13.42	0.13	0.28	3.62	1.22
490	1-Octanol	0.22	83.32	0.95	16.39	5.84	0.28	0.35	2.84	1.69
490	1-Hexanol	0.37	94.56	1.25	4.33	5.63	1.12	0.46	2.16	1.16
490	1-Butanol	0.19	87.25	4.24	7.58	7.18	5.18	0.86	1.16	1.02
490	1-Pentanol	0.26	95.63	2.57	1.43	6.21	2.93	0.46	2.15	1.23
490	1-Propanol	0.15	56.42	4.94	38.09	9.37	5.49	2.48	0.40	1.13
490	Acetic acid	0.17	99.24	1.24	0.65	5.28	0.11	0.19	5.36	1.13
490	Methanol	0.41	14.46	3.26	57.78	5.51	27.76	3.47	0.29	1.12
490	2,2,2-Trifluoroethanol	0.23	86.97	0.76	12.79	5.23	0.24	0.31	3.26	0.95

Table 4.4.15. Summary of Time Correlated Single Photon Counting (TCSPC) fluorescent lifetimes (amplitude weighted) of **27** recorded at 490 nm.

Wavelength (nm)	Solvent	τ_1 (ns)	A_1 (%)	τ_2 (ns)	A_2 (%)	τ_3 (ns)	A_3 (%)	τ_f (ns) (Amplitude Weighted)	$1/\tau_f$	χ^2
520	Toluene	-	-	4.20	40.14	10.87	59.86	8.19	0.12	1.25
520	1,4-Dioxane	-	-	4.14	56.83	11.62	43.17	7.37	0.14	1.10
520	Chloroform	0.27	66.08	1.34	31.81	7.11	2.10	0.76	1.32	1.02
520	Acetonitrile	0.26	98.99	4.11	0.89	21.07	0.11	0.32	3.17	3.42
520	1-Octanol	0.24	76.60	1.02	22.05	5.19	1.35	0.48	2.08	1.30
520	1-Hexanol	0.40	94.01	1.55	4.47	5.43	1.52	0.53	1.90	1.17
520	1-Butanol	0.20	87.56	4.66	9.35	10.58	3.09	0.93	1.07	1.13
520	1-Pentanol	0.29	94.39	3.30	3.31	8.70	2.31	0.58	1.72	1.16
520	1-Propanol	0.16	55.56	4.98	35.85	11.32	8.60	2.85	0.35	1.04
520	Acetic acid	0.16	99.43	1.38	0.50	5.84	0.07	0.17	5.94	1.21
520	Methanol	0.71	10.43	3.82	80.81	10.66	8.76	4.09	0.24	1.05
520	2,2,2-Trifluoroethanol	0.23	86.74	0.78	12.78	4.91	0.48	0.33	3.07	0.97

Table 4.4.16. Summary of Time Correlated Single Photon Counting (TCSPC) fluorescent lifetimes (amplitude weighted) of **27** recorded at 520 nm.

Wavelength (nm)	Solvent	τ_1 (ns)	A_1 (%)	τ_2 (ns)	A_2 (%)	τ_3 (ns)	A_3 (%)	τ_f (ns) (Amplitude Weighted)	$1/\tau_f$	χ^2
540	Toluene	-	-	4.14	27.23	10.80	72.77	8.99	0.11	1.13
540	1,4-Dioxane	-	-	4.17	22.21	11.53	55.92	8.29	0.12	1.19
540	Chloroform	0.26	60.27	1.14	36.54	5.92	3.18	0.76	1.32	1.14
540	Acetonitrile	0.21	98.44	2.52	1.17	10.32	0.39	0.28	3.56	1.10
540	1-Octanol	0.26	76.40	1.04	21.64	4.98	1.96	0.52	1.92	1.22
540	1-Hexanol	0.42	94.42	2.23	4.68	7.36	0.91	0.57	1.75	0.95
540	1-Butanol	0.20	87.57	4.10	7.55	9.78	4.89	0.97	1.03	1.07
540	1-Pentanol	0.29	93.71	2.50	3.44	8.33	2.85	0.59	1.69	1.21
540	1-Propanol	0.22	2.21	5.09	59.13	12.47	38.66	4.02	0.25	1.14
540	Acetic acid	0.15	98.96	1.05	0.97	5.24	0.07	0.16	6.36	1.15
540	Methanol	1.62	9.68	4.01	80.52	12.29	9.80	4.59	0.22	1.15
540	2,2,2-Trifluoroethanol	0.22	87.85	0.79	11.59	4.77	0.55	0.31	3.22	1.02

Table 4.4.17. Summary of Time Correlated Single Photon Counting (TCSPC) fluorescent lifetimes (amplitude weighted) of **27** recorded at 540 nm.

Wavelength (nm)	Solvent	τ_1 (ns)	A_1 (%)	τ_2 (ns)	A_2 (%)	τ_3 (ns)	A_3 (%)	τ_f (ns) (Amplitude Weighted)	$1/\tau_f$	χ^2
570	Toluene	-	-	4.02	5.85	10.81	94.15	10.41	0.10	1.19
570	1,4-Dioxane	-	-	4.71	26.16	11.74	73.84	9.90	0.10	1.17
570	Chloroform	0.33	57.77	1.07	38.93	7.03	3.29	0.84	1.19	1.08
570	Acetonitrile	0.24	98.25	2.25	1.31	11.40	0.43	0.32	3.16	1.25
570	1-Octanol	0.14	87.89	0.99	10.83	4.80	1.28	0.29	3.47	1.21
570	1-Hexanol	0.43	93.14	2.24	5.84	7.36	1.02	0.61	1.65	1.02
570	1-Butanol	0.23	88.50	3.93	6.42	10.58	5.08	0.99	1.01	1.07
570	1-Pentanol	0.31	93.22	2.39	4.14	9.43	2.64	0.64	1.57	1.27
570	1-Propanol	0.21	50.83	4.76	31.88	11.60	17.29	3.63	0.28	1.14
570	Acetic acid	0.16	97.91	0.90	2.01	4.44	0.08	0.17	5.72	1.01
570	Methanol	2.36	9.44	4.01	75.86	12.22	14.69	1.26	0.80	1.26
570	2,2,2-Trifluoroethanol	0.22	87.00	0.80	12.13	4.32	0.88	0.33	3.05	1.10

Table 4.4.18. Summary of Time Correlated Single Photon Counting (TCSPC) fluorescent lifetimes (amplitude weighted) of **27** recorded at 570 nm.

4.4.7 400 nm average fluorescent lifetimes - Solvatochromic analysis.

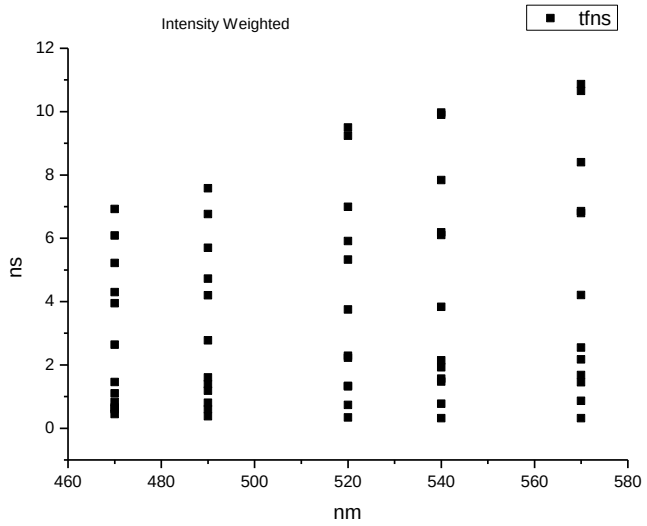

Figure 4.4.49. Intensity weighted average lifetime (τ_f) of **27** versus wavelength (nm).

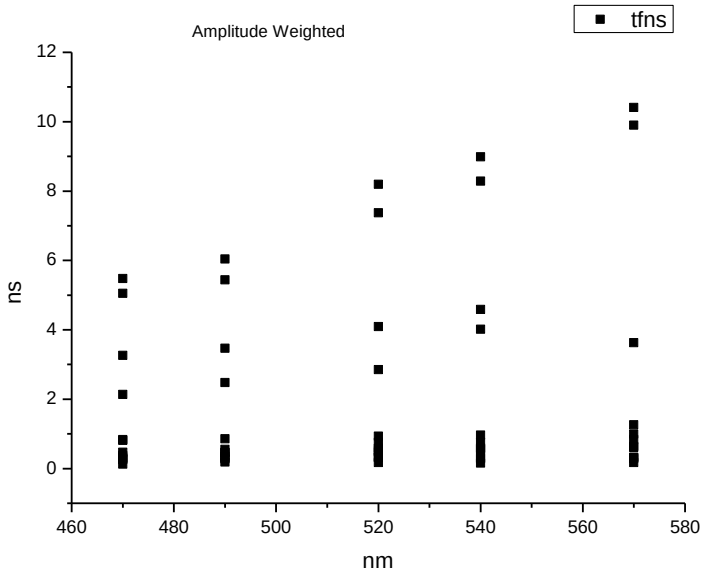

Figure 4.4.50. Amplitude weighted average lifetime (τ_f) of **27** versus wavelength (nm).

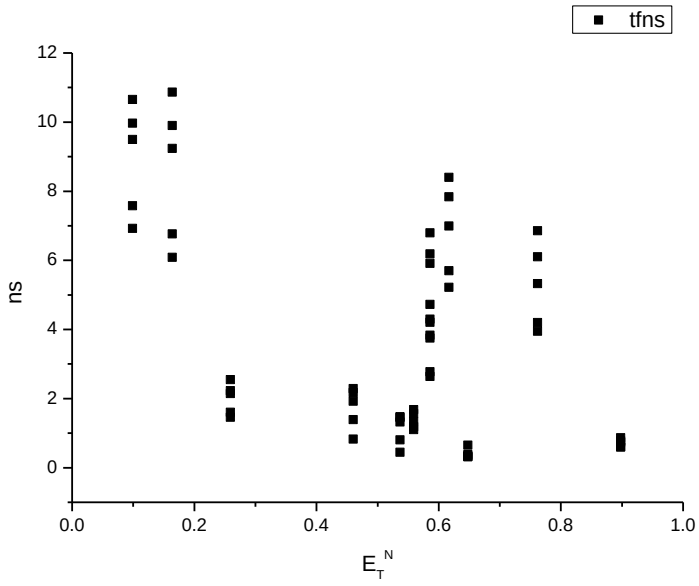

Figure 4.4.51. Intensity weighted average lifetime (τ_f) of **27** versus E_T^N.

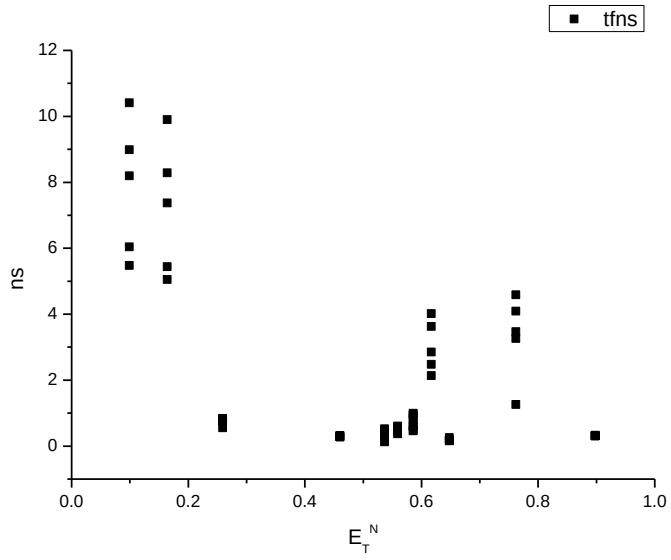

Figure 4.4.52. Amplitude weighted average lifetime (τ_f) of **27** versus E_T^N.

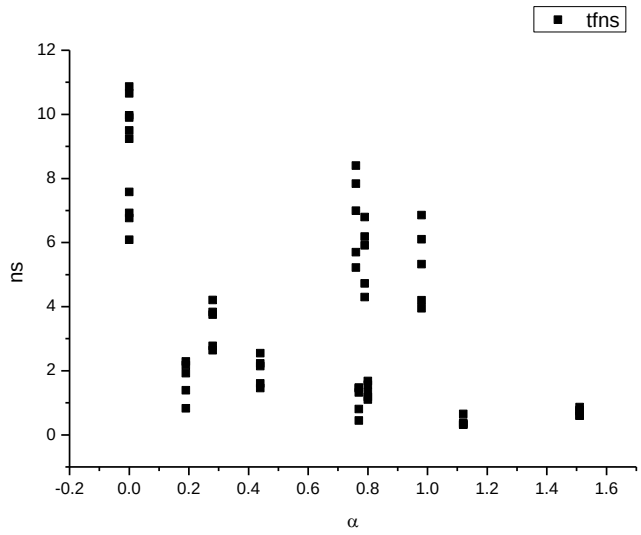

Figure 4.4.53. Intensity weighted average lifetime (τ_f) of **27** versus α.

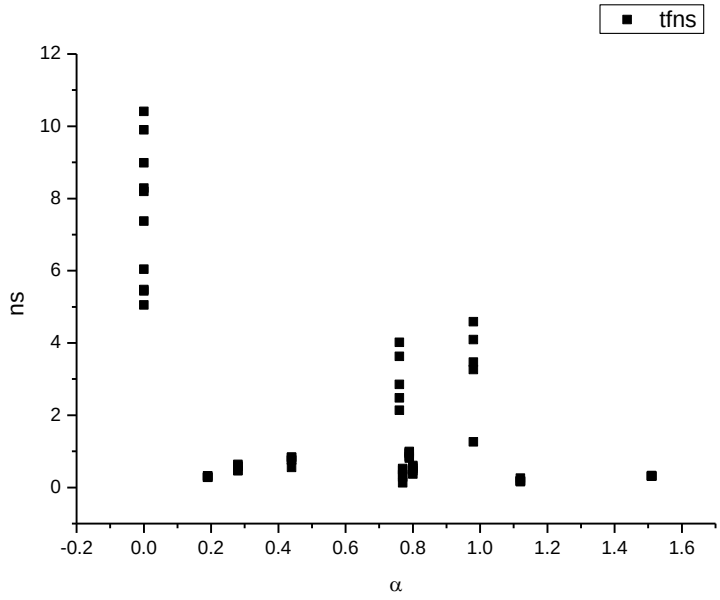

Figure 4.4.54. Amplitude weighted average lifetime (τ_f) of **27** versus α.

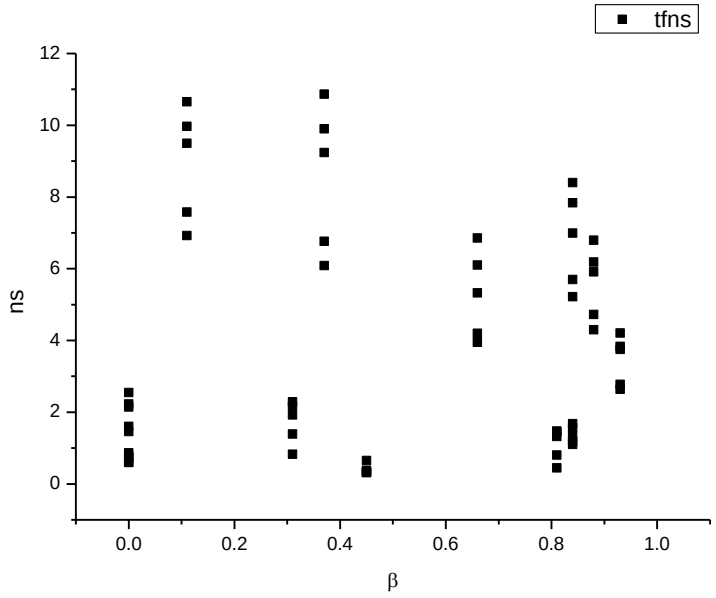

Figure 4.4.55. Intensity weighted average lifetime (τ_f) of **27** versus β.

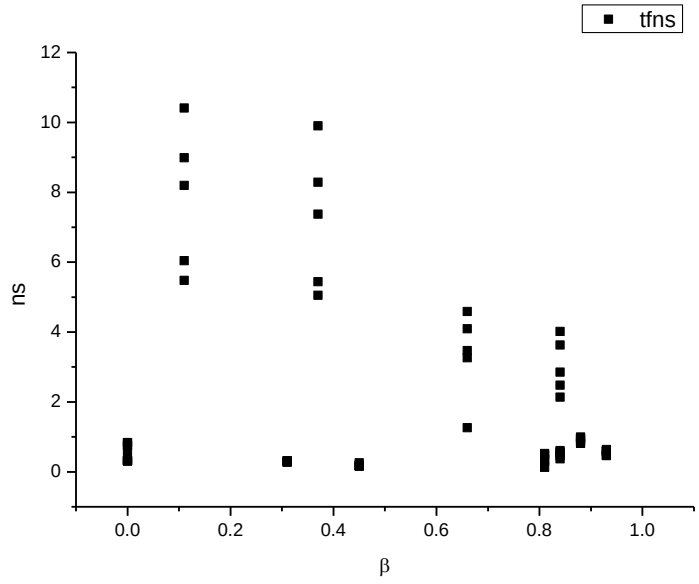

Figure 4.4.56. Amplitude weighted average lifetime (τ_f) of **27** versus β.

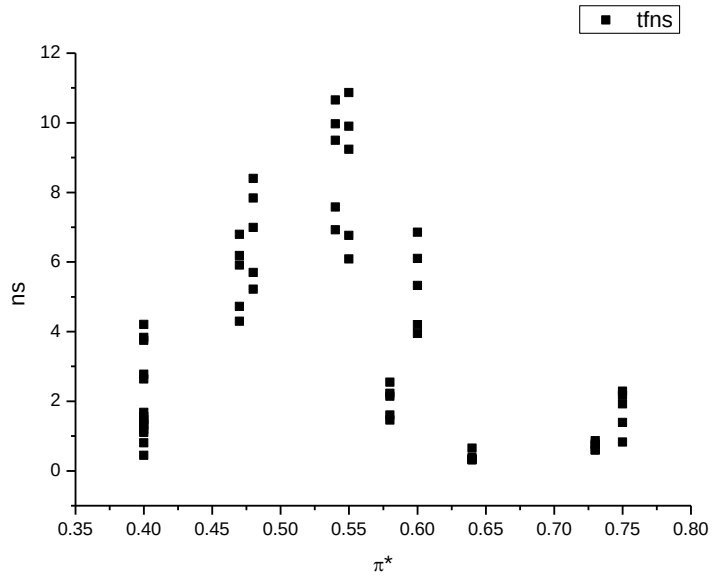

Figure 4.4.57. Intensity weighted average lifetime (τ_f) of **27** versus π*.

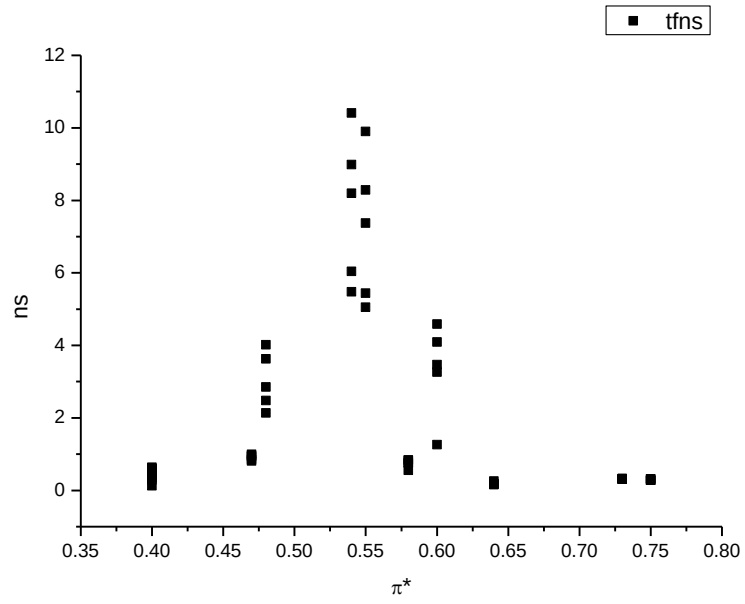

Figure 4.4.58. Amplitude weighted average lifetime (τ_f) of **27** versus π*.

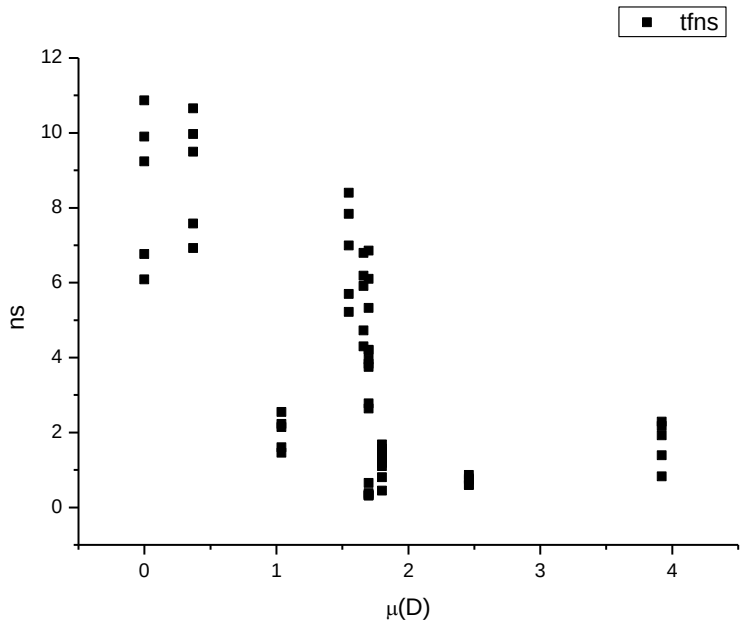

Figure 4.4.59. Intensity weighted average lifetime (τ_f) of **27** versus μ(D).

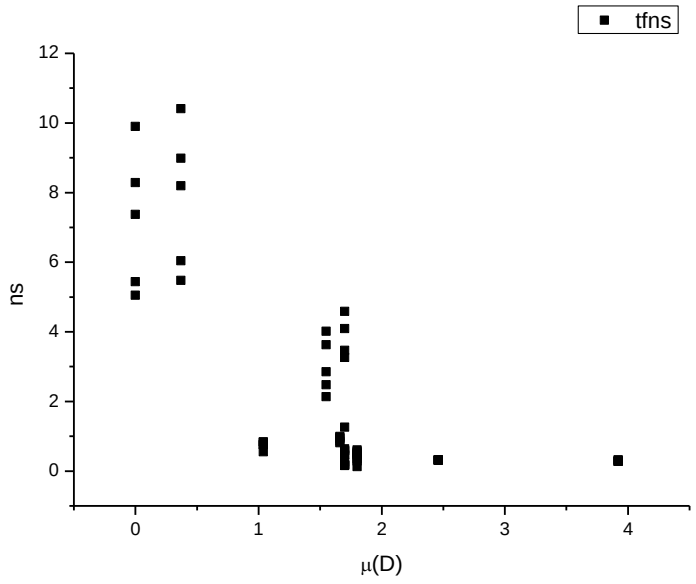

Figure 4.4.60. Amplitude weighted average lifetime (τ_f) of **27** versus μ(D).

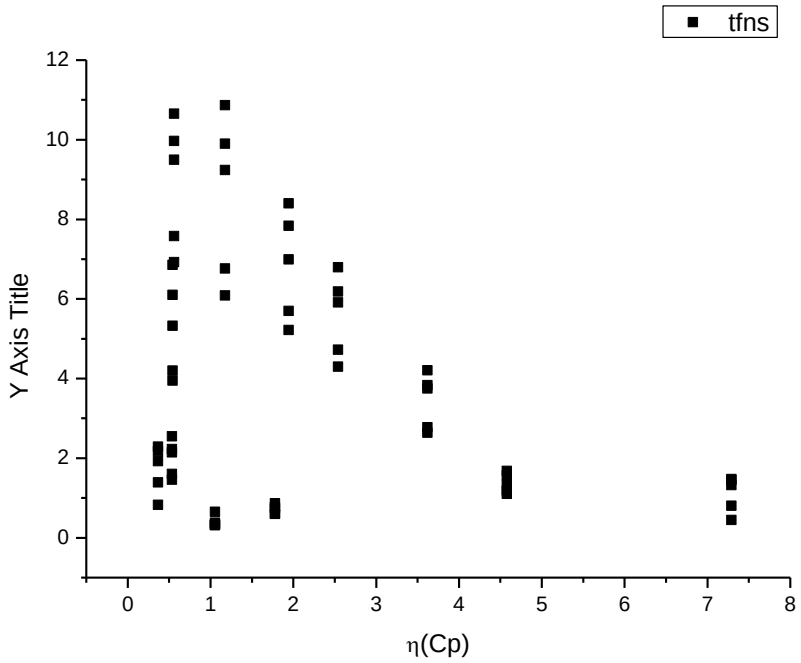

Figure 4.4.61. Intensity weighted average lifetime (τ_f) of **27** versus η(Cp).

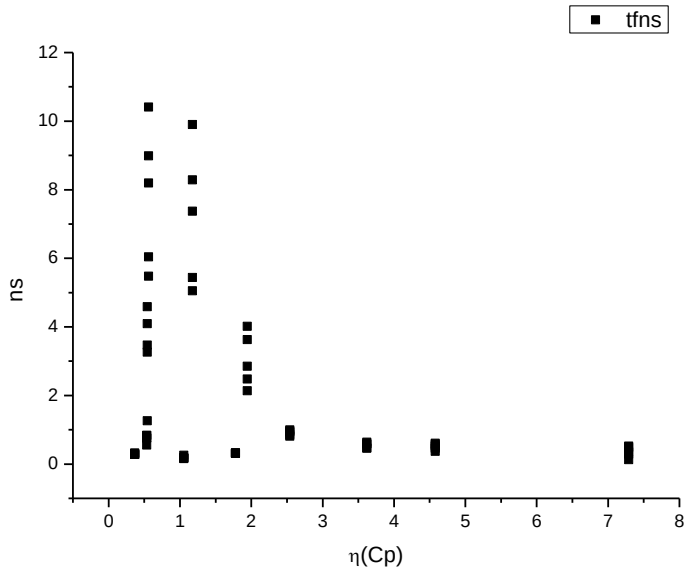

Figure 4.4.62. Amplitude weighted average lifetime (τ_f) of **27** versus η(Cp).

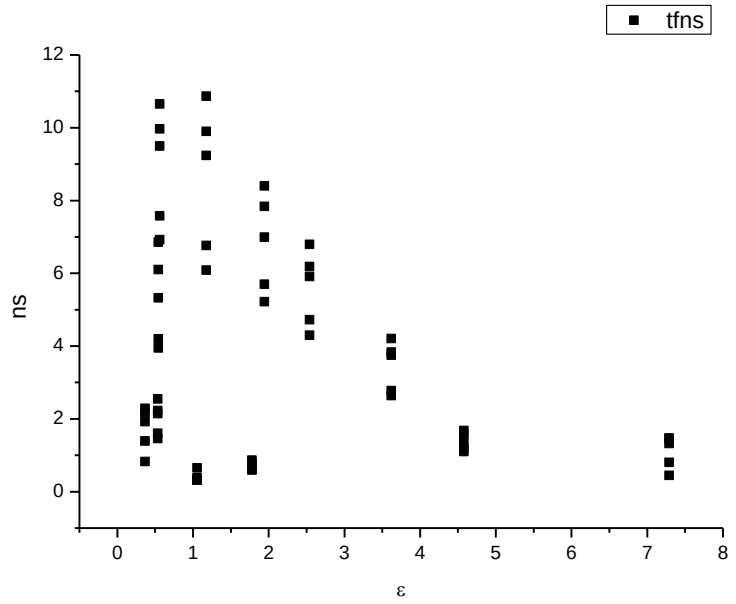

Figure 4.4.63. Intensity weighted average lifetime (τ_f) of **27** versus ε.

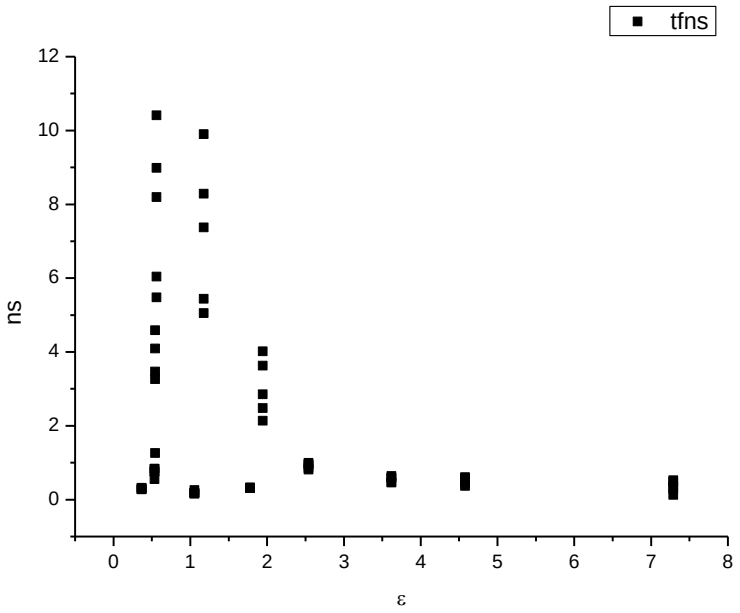

Figure 4.4.64. Amplitude weighted average lifetime (τ_f) of **27** versus ε.

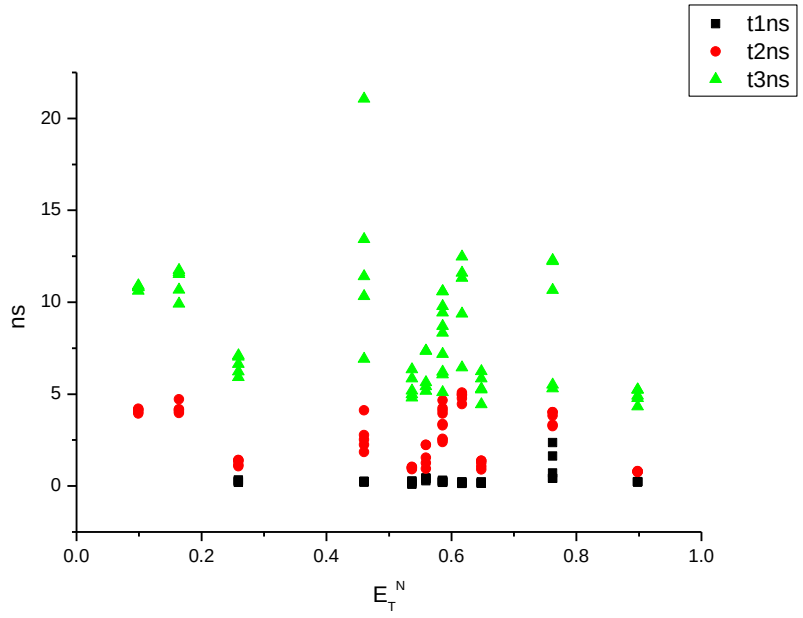

Figure 4.4.65. Intensity weighted components of TCSPC lifetime decay of **27** (470 nm to 570 nm) versus E_T^N.

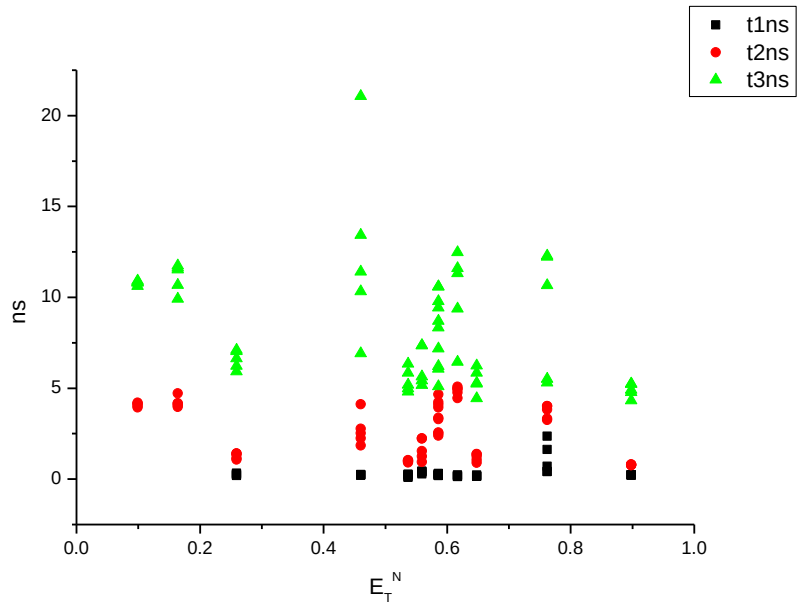

Figure 4.4.66. Amplitude weighted components of TCSPC lifetime decay of **27** (470 nm to 570 nm) versus E_T^N.

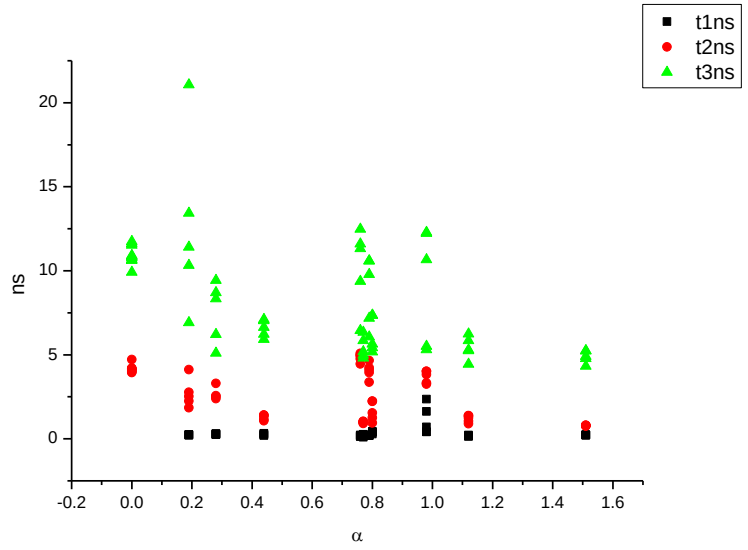

Figure 4.4.67. Intensity weighted components of TCSPC lifetime decay of **27** (470 nm to 570 nm) versus α.

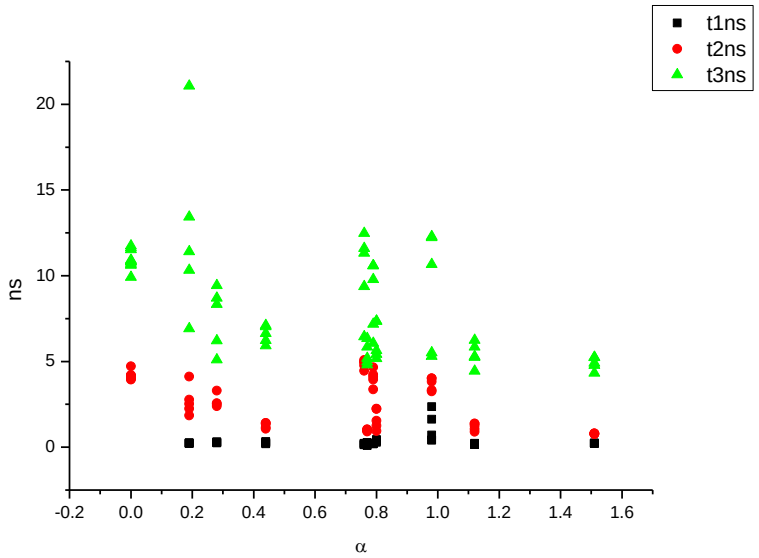

Figure 4.4.68. Amplitude weighted components of TCSPC lifetime decay of **27** (470 nm to 570 nm) versus α.

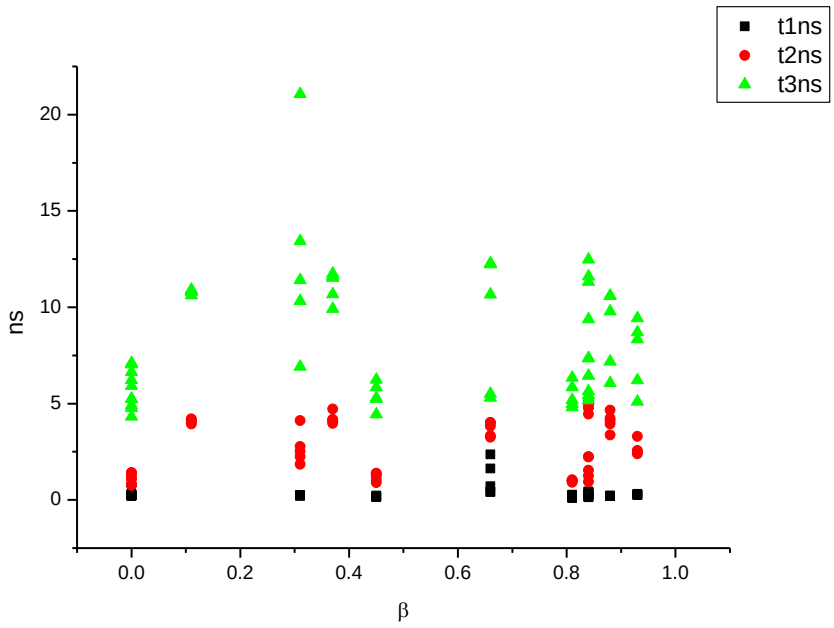

Figure 4.4.69. Intensity weighted components of TCSPC lifetime decay of **27** (470 nm to 570 nm) versus β.

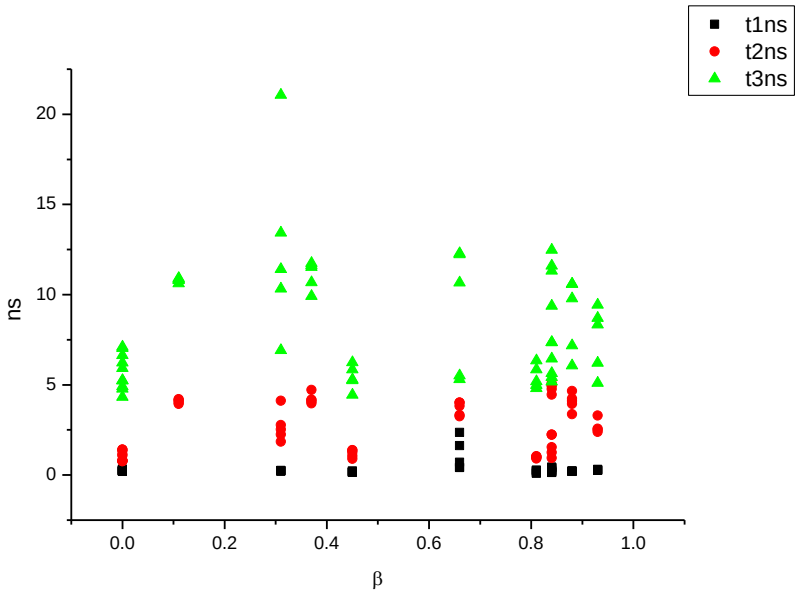

Figure 4.4.70. Amplitude weighted components of TCSPC lifetime decay of **27** (470 nm to 570 nm) versus β.

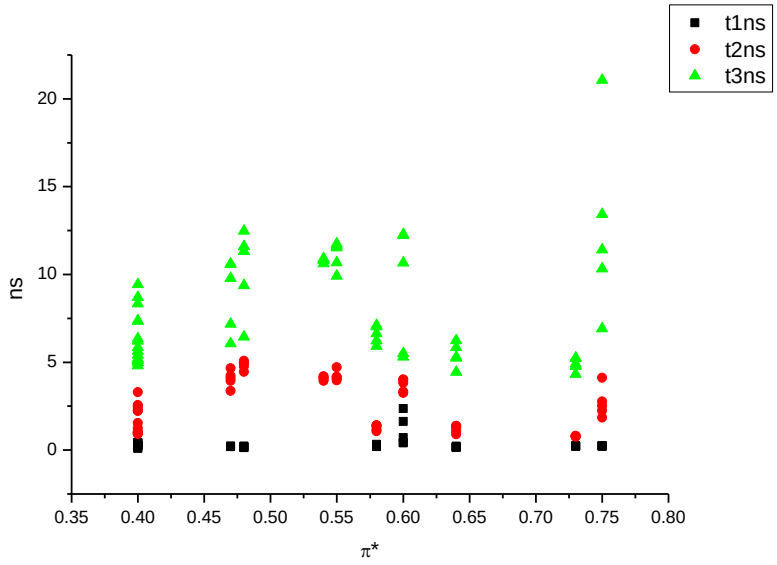

Figure 4.4.71. Intensity weighted components of TCSPC lifetime decay of **27** (470 nm to 570 nm) versus π*.

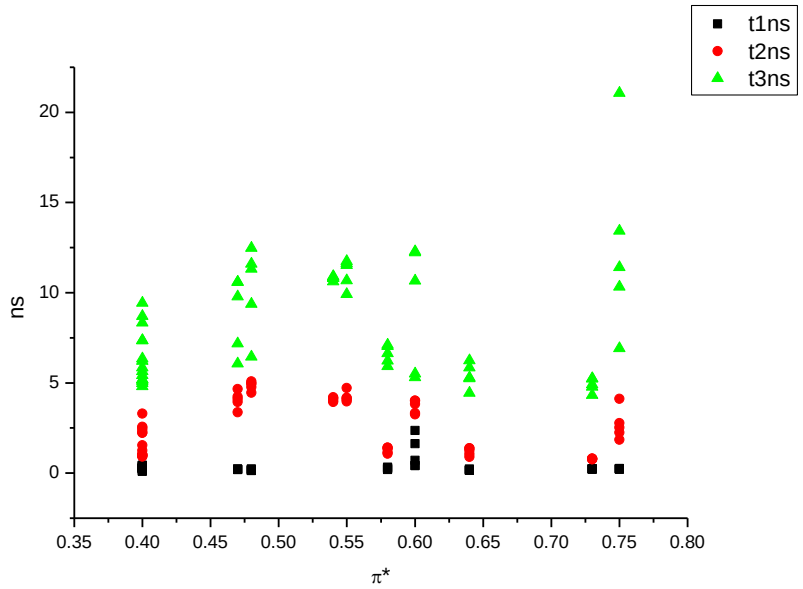

Figure 4.4.72. Amplitude weighted components of TCSPC lifetime decay of **27** (470 nm to 570 nm) versus π*.

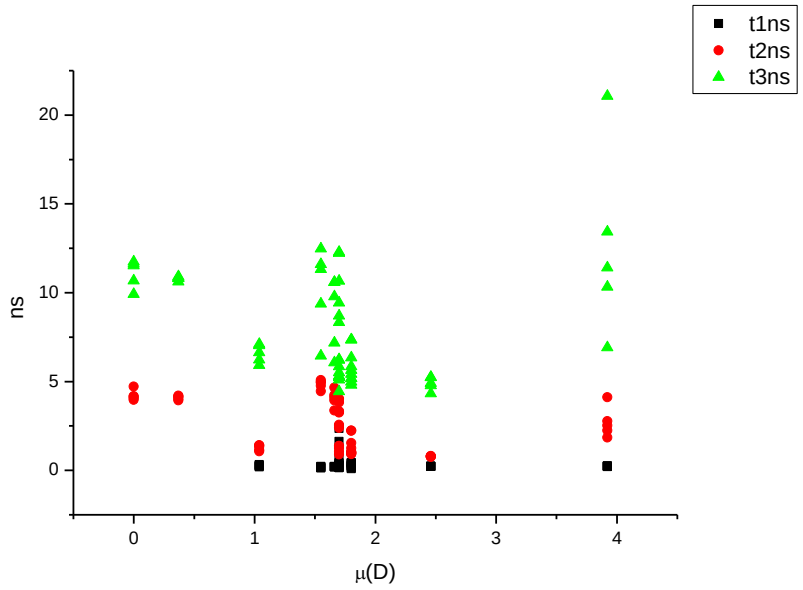

Figure 4.4.73. Intensity weighted components of TCSPC lifetime decay of **27** (470 nm to 570 nm) versus μ(D).

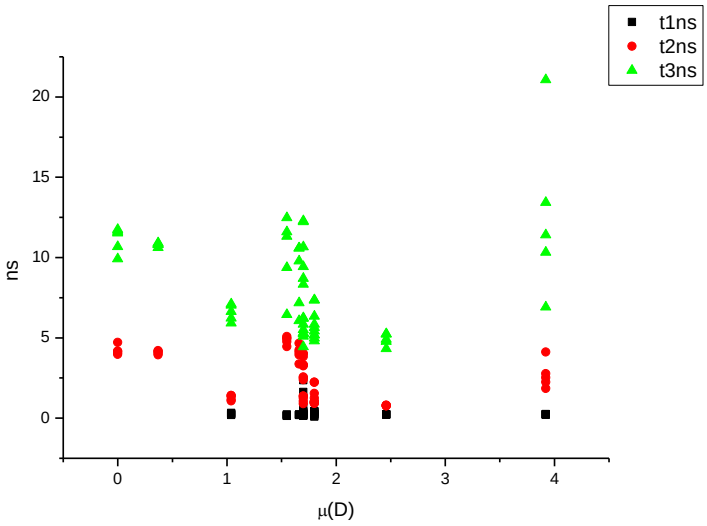

Figure 4.4.74. Amplitude weighted components of TCSPC lifetime decay of **27** (470 nm to 570 nm) versus μ(D).

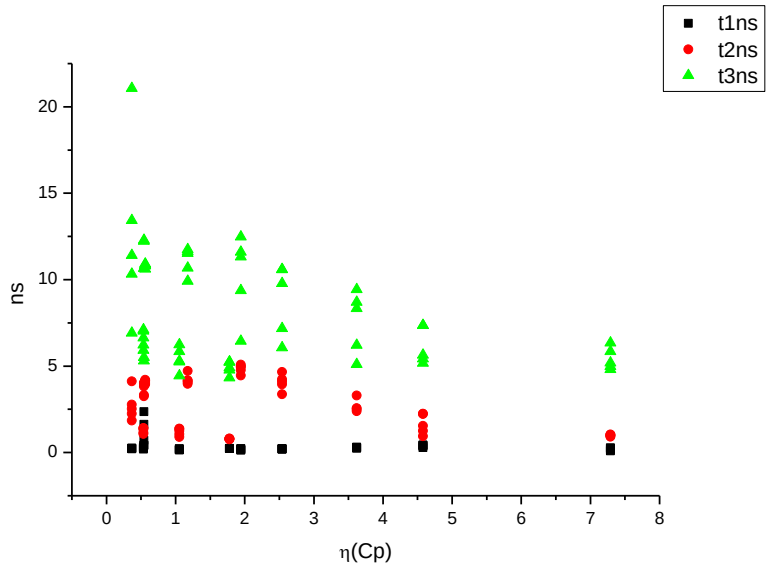

Figure 4.4.75. Intensity weighted components of TCSPC lifetime decay of **27** (470 nm to 570 nm) versus η(Cp).

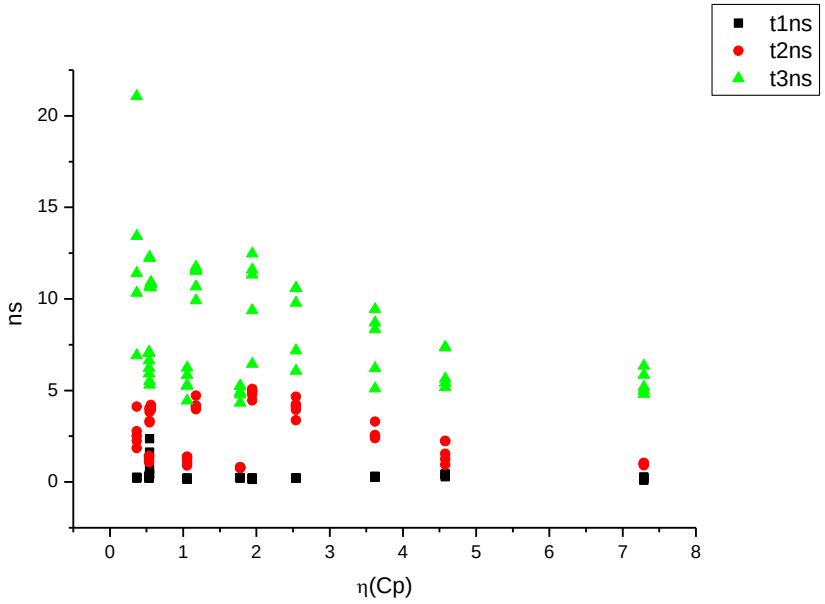

Figure 4.4.76. Amplitude weighted components of TCSPC lifetime decay of **27** (470 nm to 570 nm) versus η(Cp).

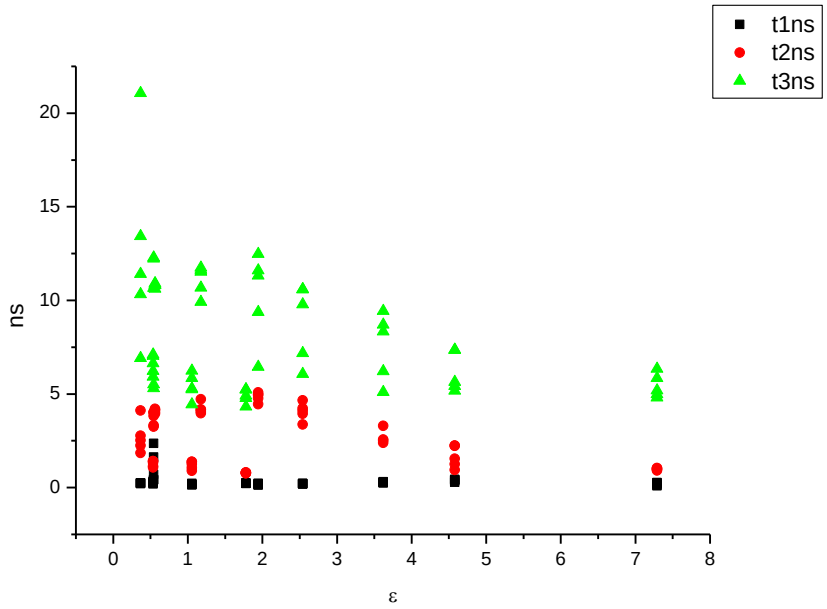

Figure 4.4.77. Intensity weighted components of TCSPC lifetime decay of **27** (470 nm to 570 nm) versus ε.

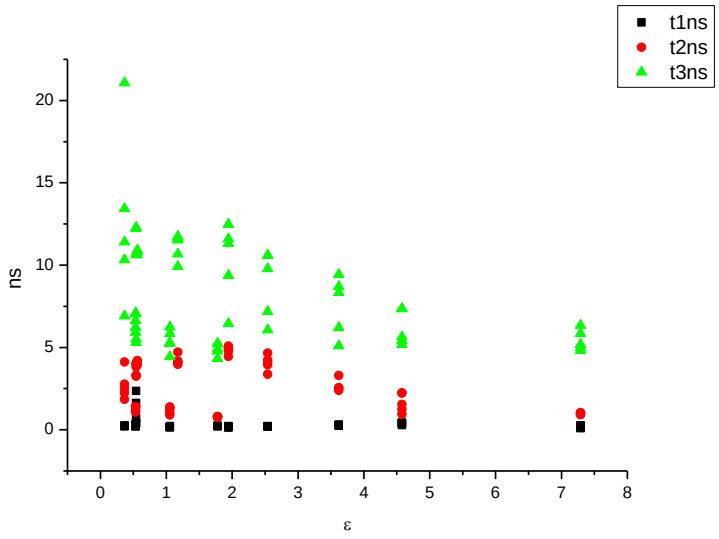

Figure 4.4.78. Amplitude weighted components of TCSPC lifetime decay of **27** (470 nm to 570 nm) versus ε.

4.4.7.1 470 nm Lifetime – Solvatochromic analysis.

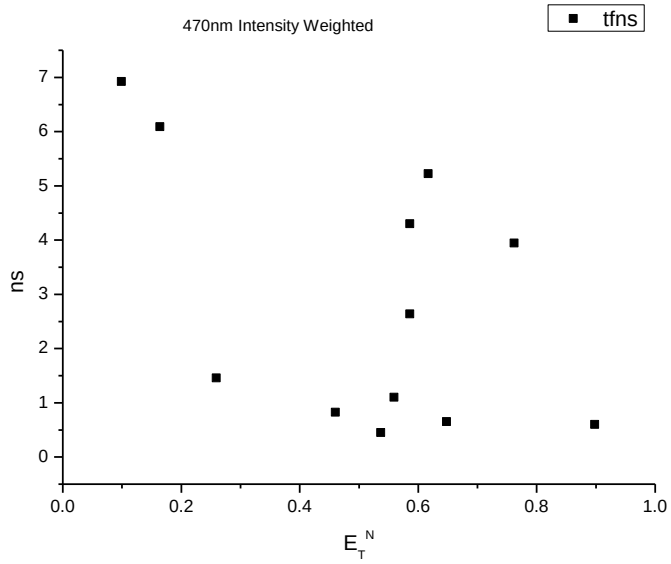

Figure 4.4.79. Intensity weighted average lifetime (τ_f) of **27** at 470 nm versus E_T^N.

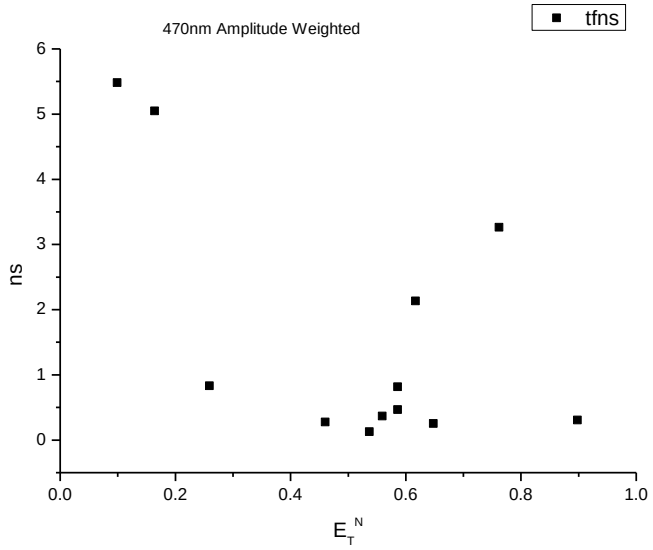

Figure 4.4.80. Amplitude weighted average lifetime (τ_f) of **27** at 470 nm versus E_T^N.

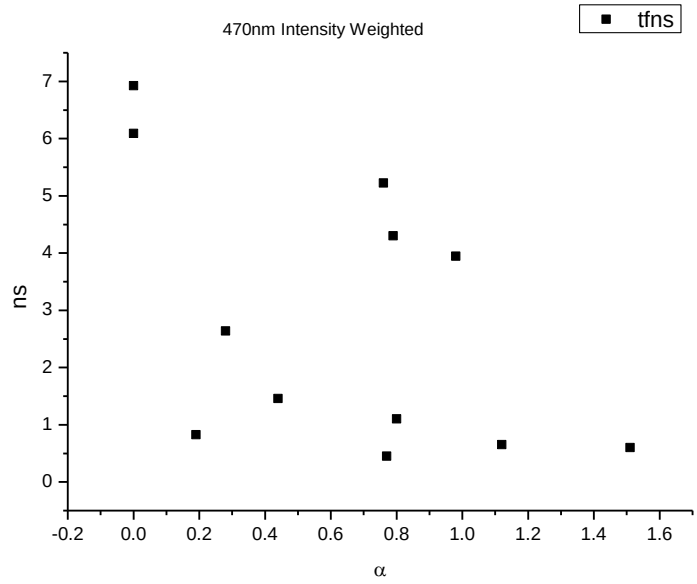

Figure 4.4.81. Intensity weighted average lifetime (τ_f) of **27** at 470 nm versus α.

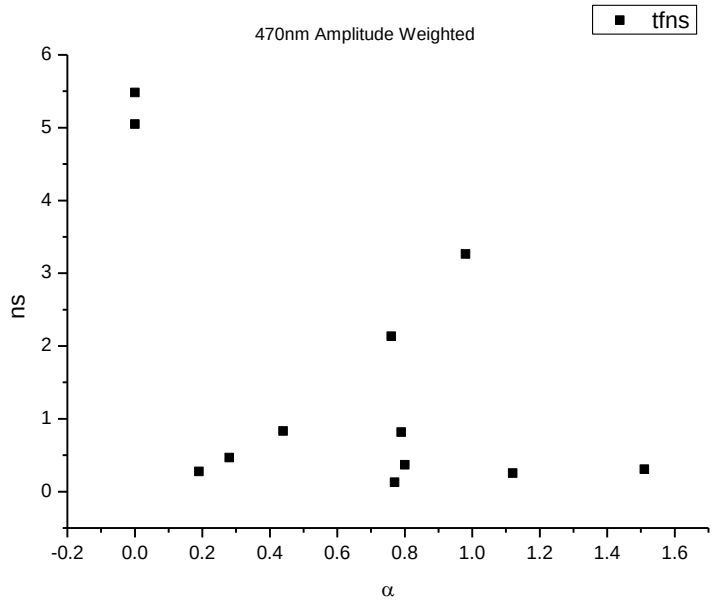

Figure 4.4.82. Amplitude weighted average lifetime (τ_f) of **27** at 470 nm versus α.

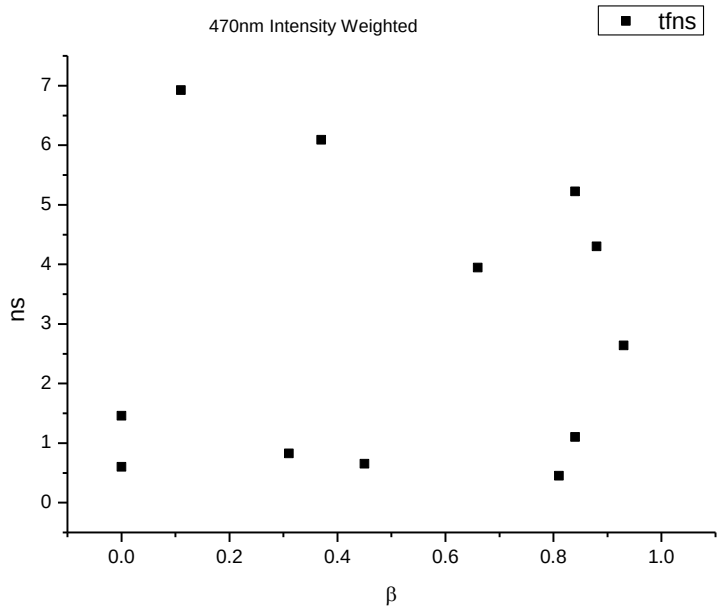

Figure 4.4.83. Intensity weighted average lifetime (τ_f) of **27** at 470 nm versus β.

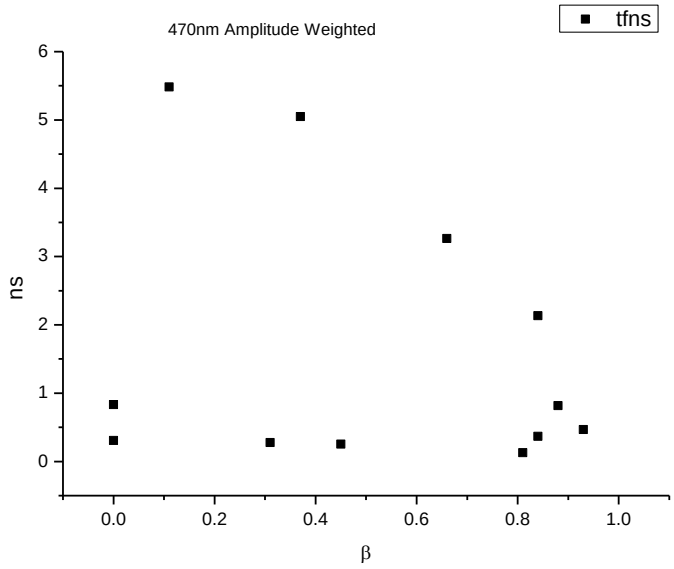

Figure 4.4.84. Amplitude weighted average lifetime (τ_f) of **27** at 470 nm versus β.

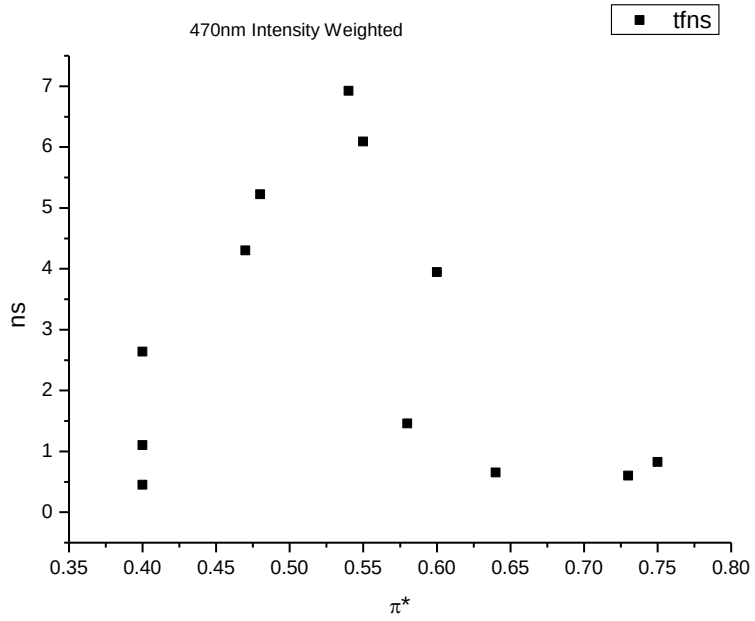

Figure 4.4.85. Intensity weighted average lifetime (τ_f) of **27** at 470 nm versus π*.

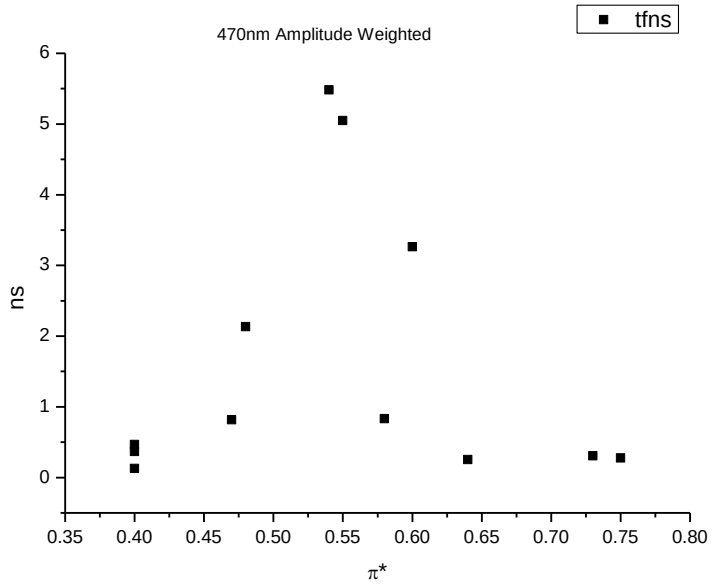

Figure 4.4.86. Amplitude weighted average lifetime (τ_f) of **27** at 470 nm versus π*.

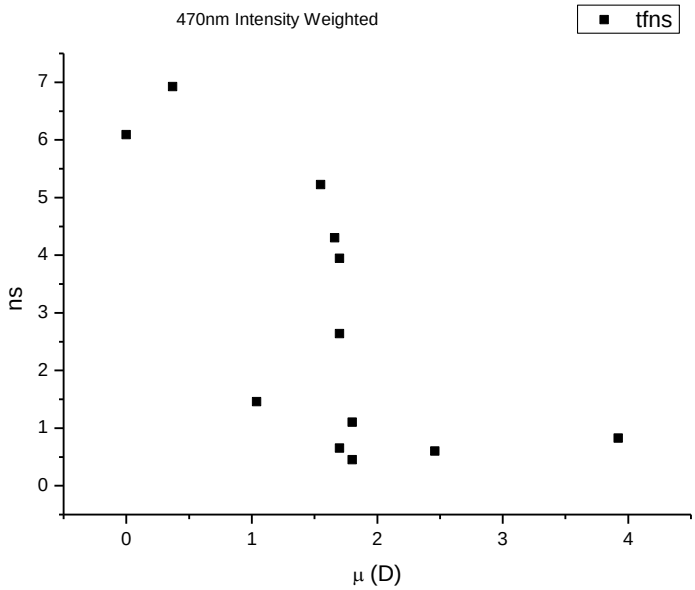

Figure 4.4.87. Intensity weighted average lifetime (τ_f) of **27** at 470 nm versus μ(D).

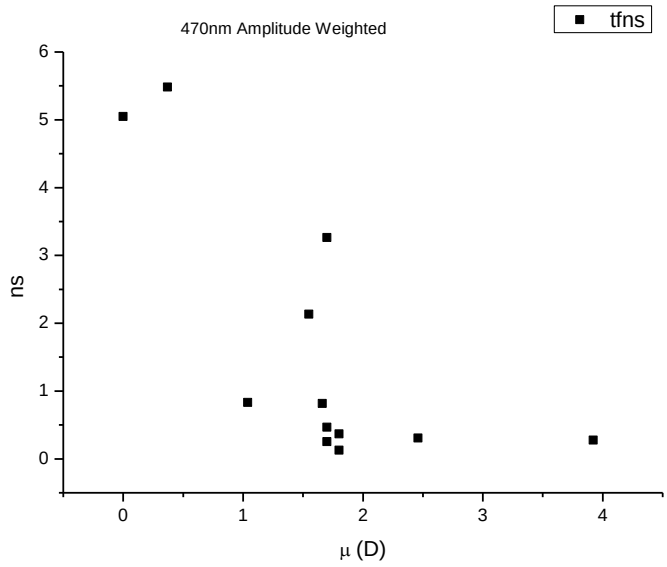

Figure 4.4.88. Amplitude weighted average lifetime (τ_f) of **27** at 470 nm versus μ(D).

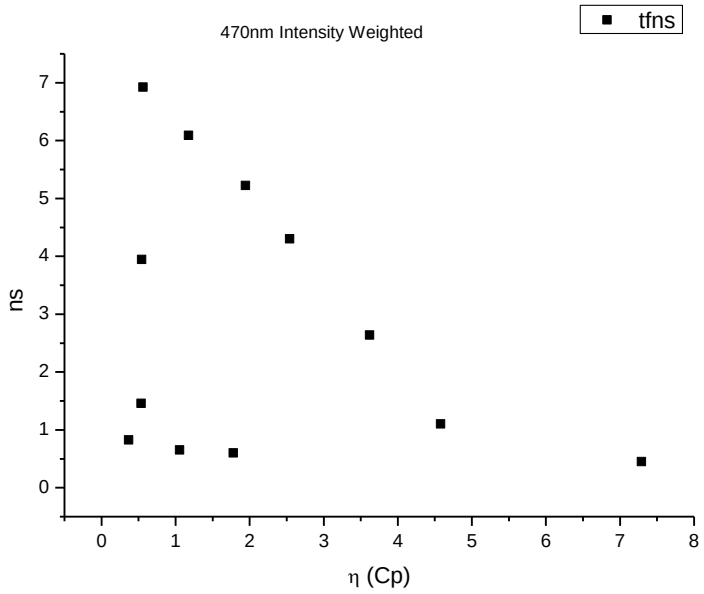

Figure 4.4.89. Intensity weighted average lifetime (τ_f) of **27** at 470 nm versus η(Cp).

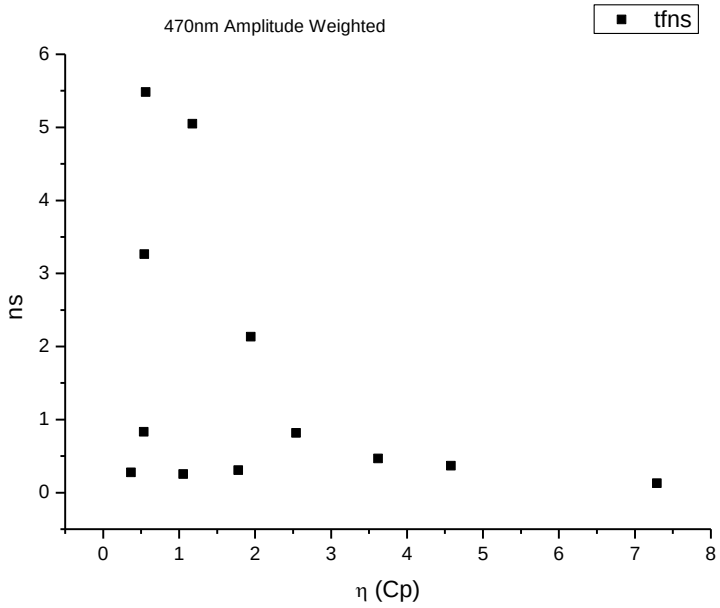

Figure 4.4.90. Amplitude weighted average lifetime (τ_f) of **27** at 470 nm versus η(Cp).

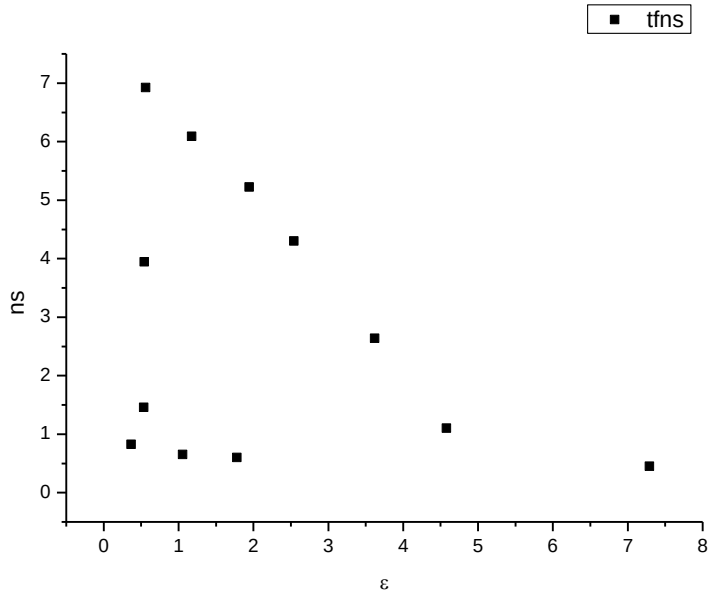

Figure 4.4.91. Intensity weighted average lifetime (τ_f) of **27** at 470 nm versus ε.

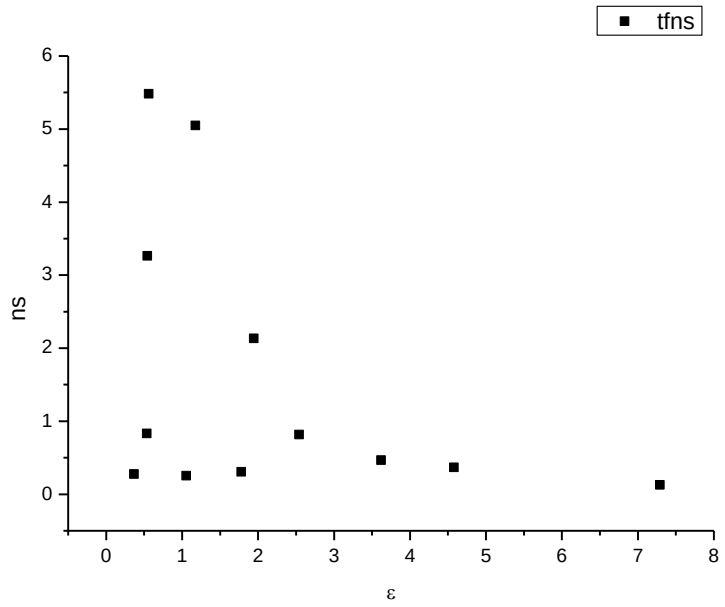

Figure 4.4.92. Amplitude weighted average lifetime (τ_f) of **27** at 470 nm versus ε.

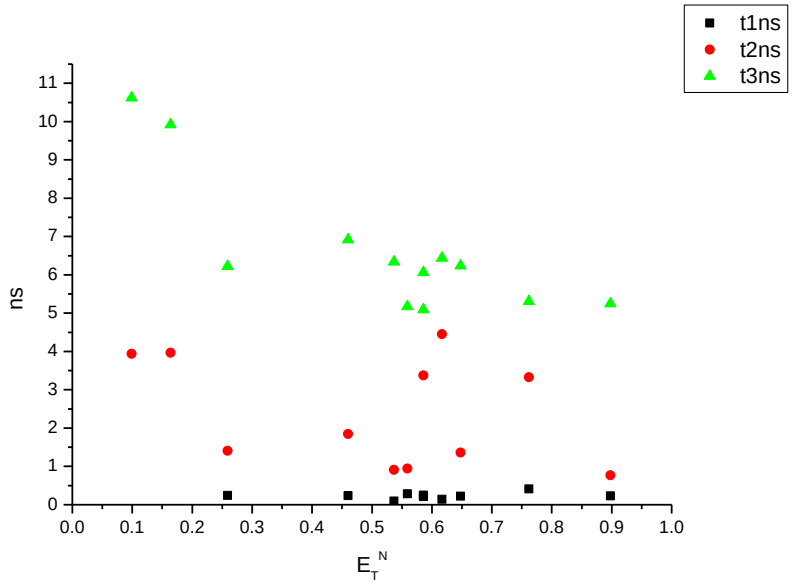

Figure 4.4.93. Intensity weighted components of TCSPC lifetime decay of **27** (470 nm) versus E_T^N.

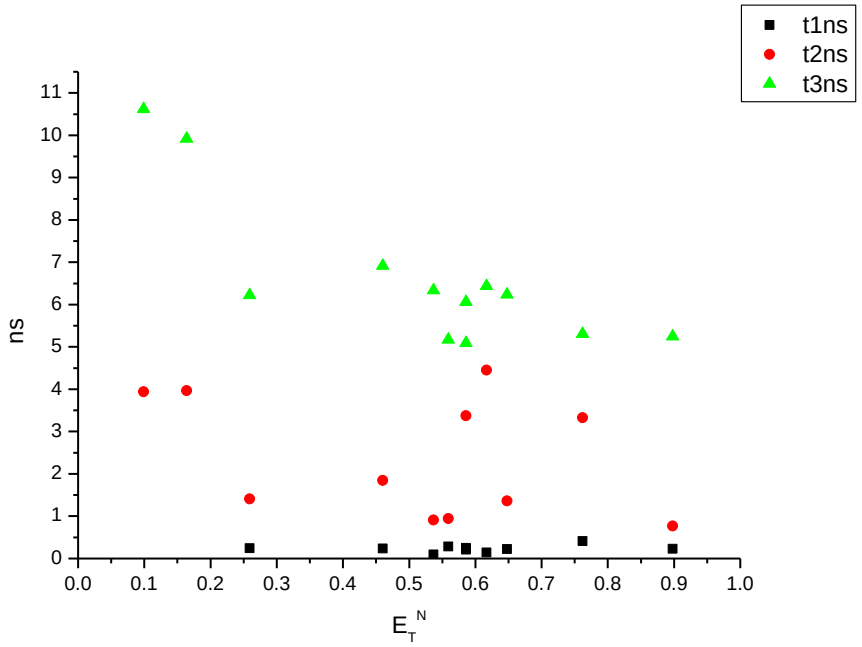

Figure 4.4.94. Amplitude weighted components of TCSPC lifetime decay of **27** (470 nm) versus E_T^N.

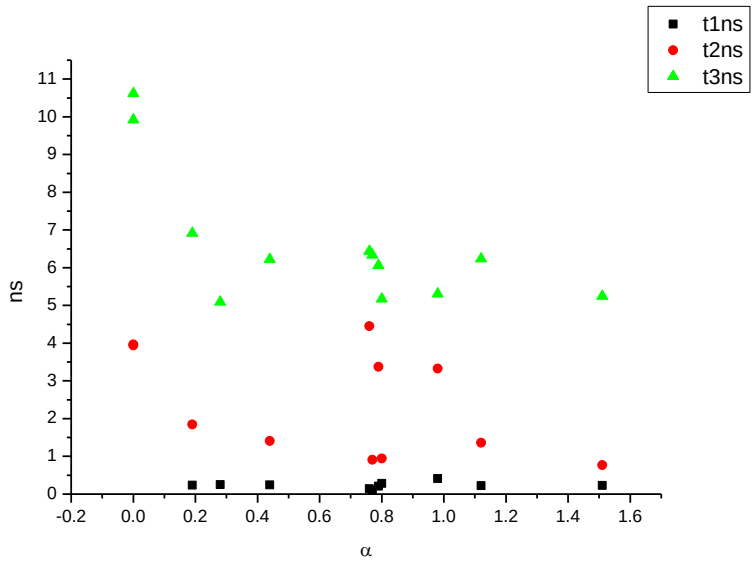

Figure 4.4.95. Intensity weighted components of TCSPC lifetime decay of **27** (470 nm) versus α.

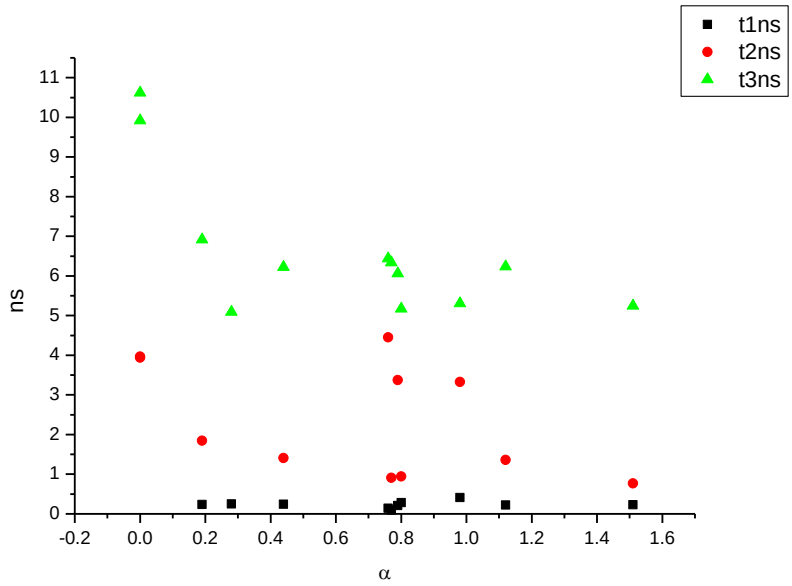

Figure 4.4.96. Amplitude weighted components of TCSPC lifetime decay of **27** (470 nm) versus α.

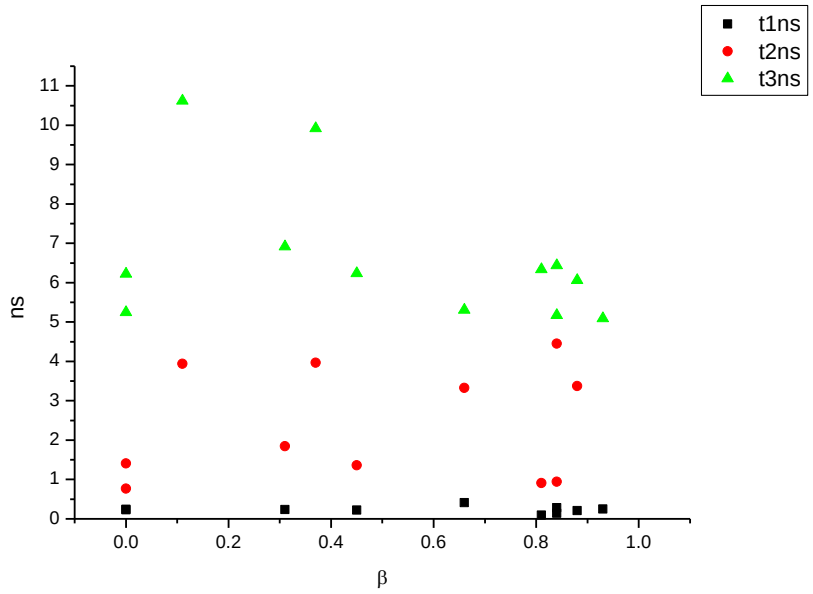

Figure 4.4.97. Intensity weighted components of TCSPC lifetime decay of **27** (470 nm) versus β.

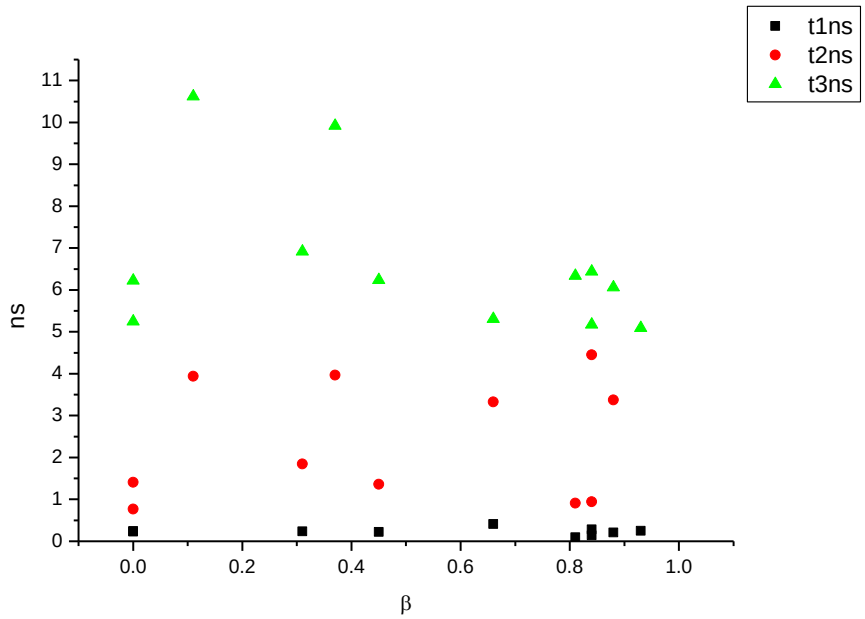

Figure 4.4.98. Amplitude weighted components of TCSPC lifetime decay of **27** (470 nm) versus β.

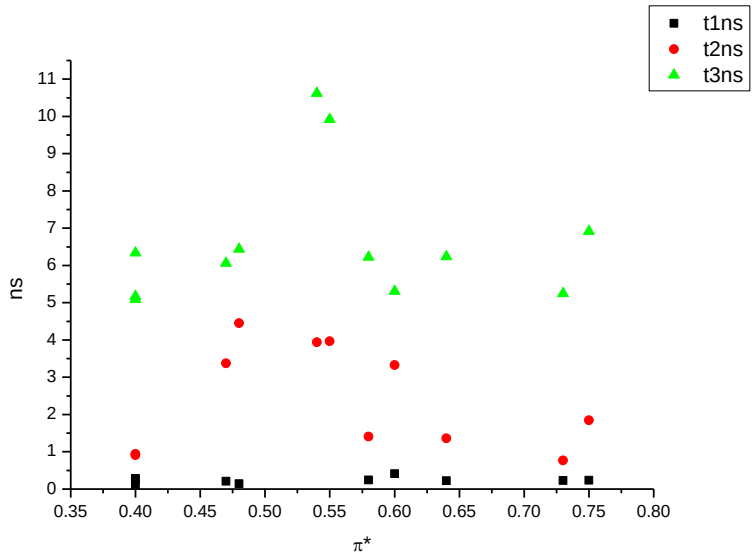

Figure 4.4.99. Intensity weighted components of TCSPC lifetime decay of **27** (470 nm) versus π*.

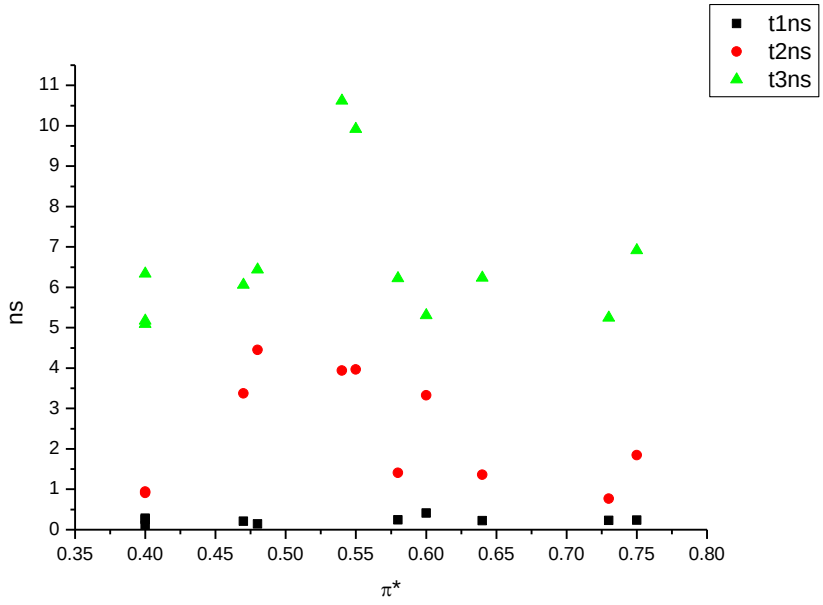

Figure 4.4.100. Amplitude weighted components of TCSPC lifetime decay of **27** (470 nm) versus π*.

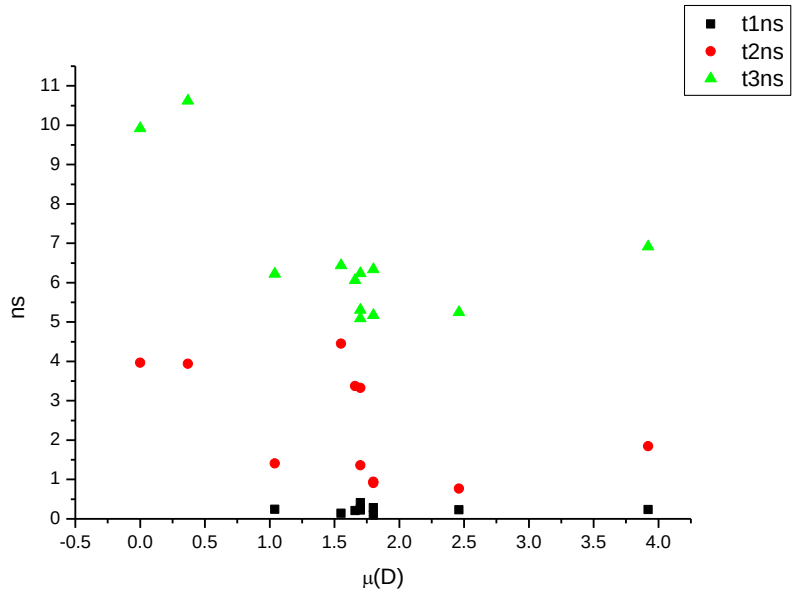

Figure 4.4.101. Intensity weighted components of TCSPC lifetime decay of **27** (470 nm) versus μ(D).

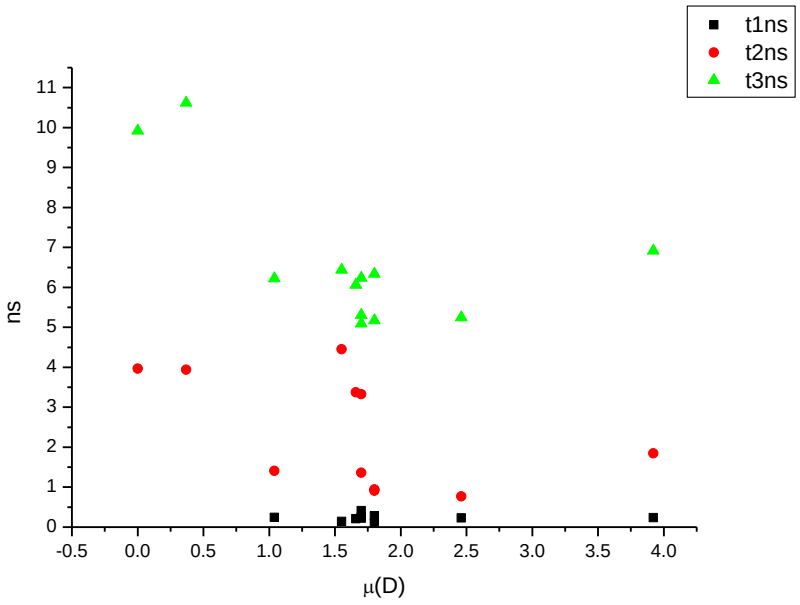

Figure 4.4.102. Amplitude weighted components of TCSPC lifetime decay of **27** (470 nm) versus μ(D).

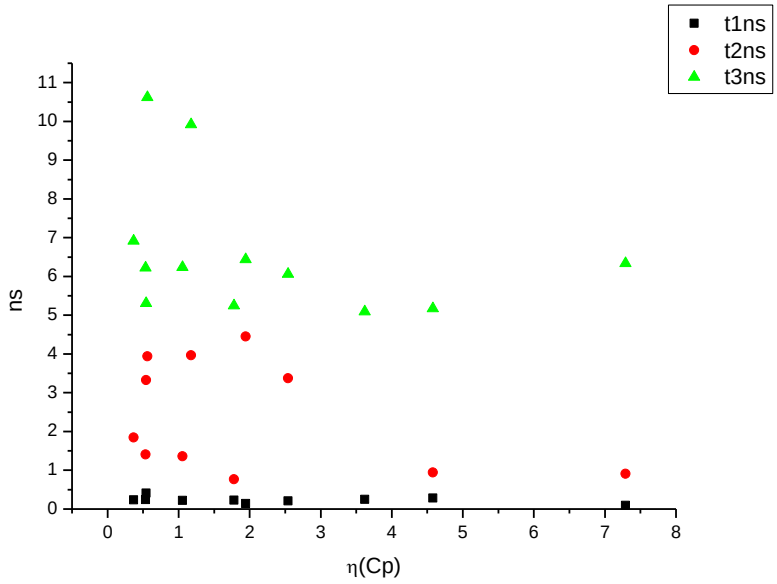

Figure 4.4.103. Intensity weighted components of TCSPC lifetime decay of **27** (470 nm) versus η(Cp).

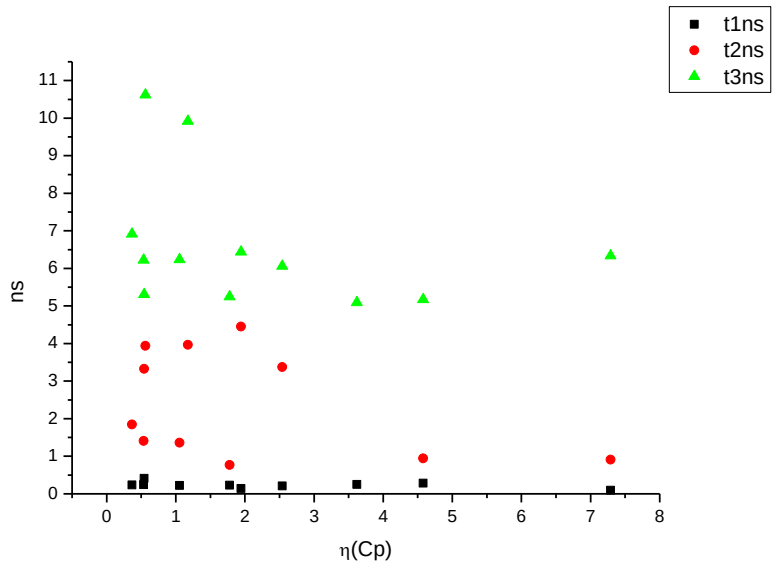

Figure 4.4.104. Amplitude weighted components of TCSPC lifetime decay of **27** (470 nm) versus η(Cp).

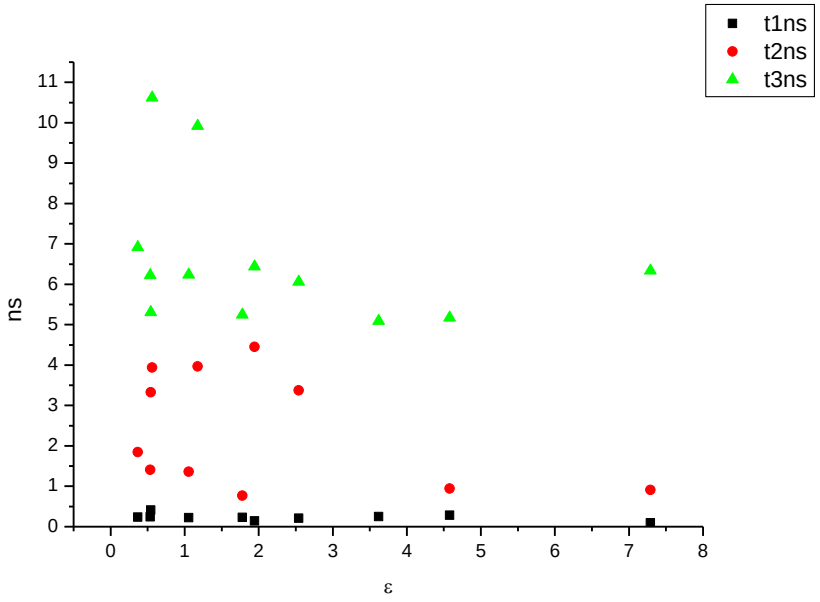

Figure 4.4.105. Intensity weighted components of TCSPC lifetime decay of **27** (470 nm) versus ε.

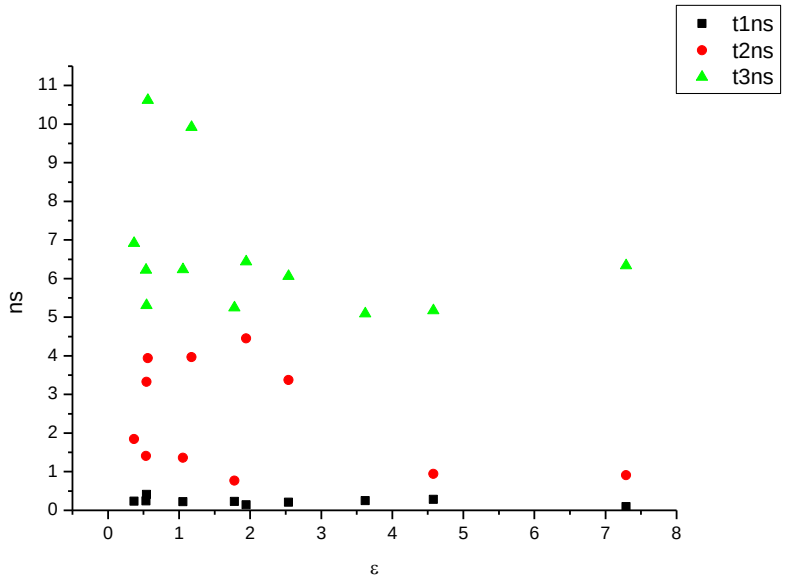

Figure 4.4.106. Amplitude weighted components of TCSPC lifetime decay of **27** (470 nm) versus ε.

4.4.7.2 570 nm Lifetime – Solvatochromic analysis.

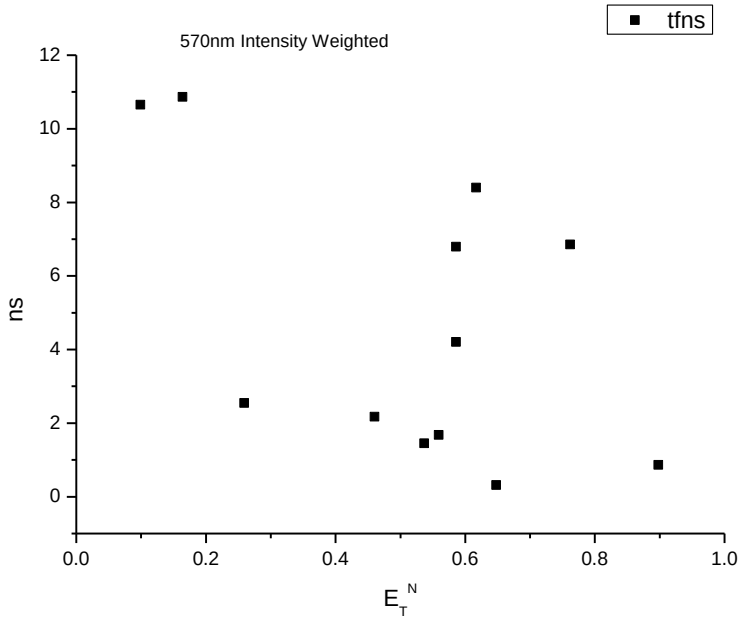

Figure 4.4.107. Intensity weighted average lifetime (τ_f) of **27** at 570 nm versus E_T^N.

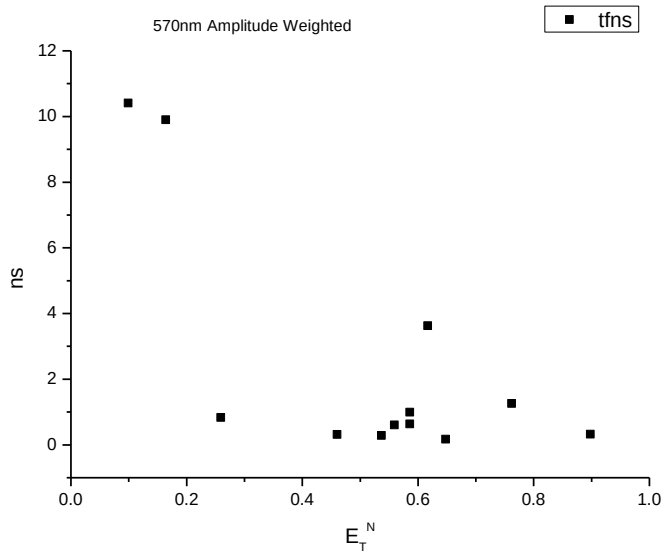

Figure 4.4.108. Amplitude weighted average lifetime (τ_f) of **27** at 570 nm versus E_T^N.

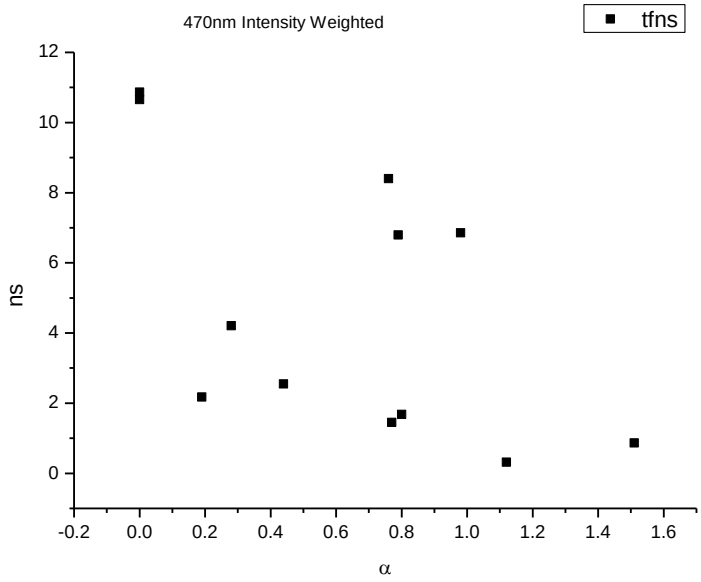

Figure 4.4.109. Intensity weighted average lifetime (τ_f) of **27** at 570 nm versus α.

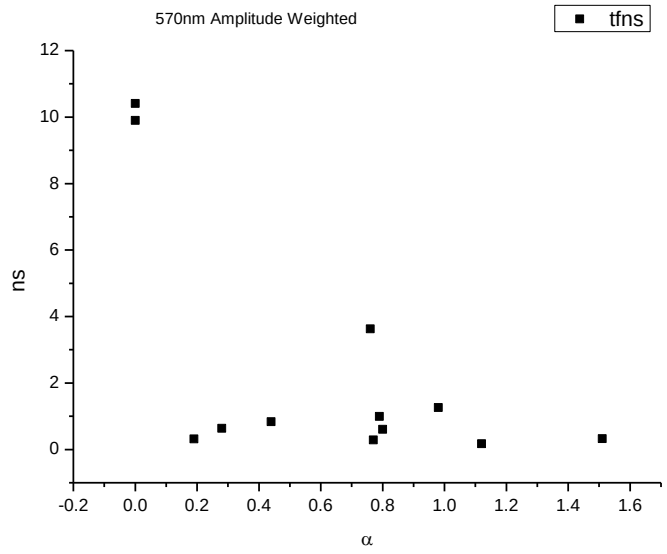

Figure 4.4.110. Amplitude weighted average lifetime (τ_f) of **27** at 570 nm versus α.

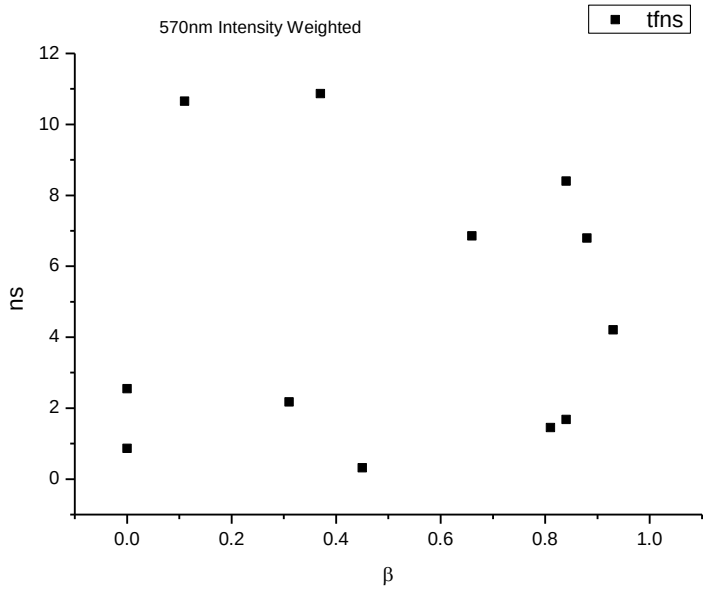

Figure 4.4.111. Intensity weighted average lifetime (τ_f) of **27** at 570 nm versus β.

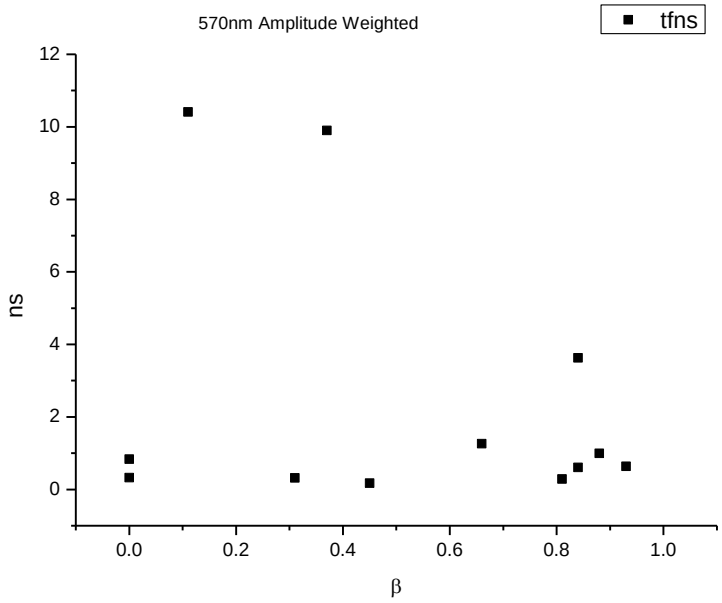

Figure 4.4.112. Amplitude weighted average lifetime (τ_f) of **27** at 570 nm versus β.

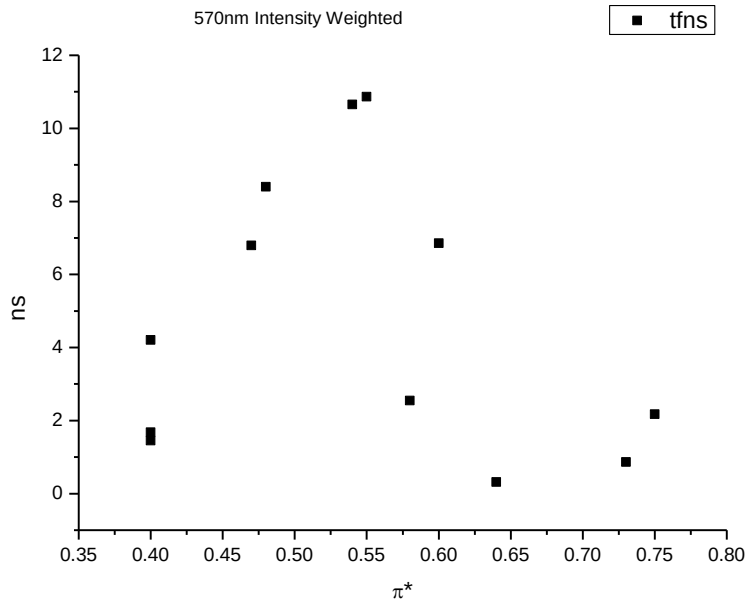

Figure 4.4.113. Intensity weighted average lifetime (τ_f) of **27** at 570 nm versus π*.

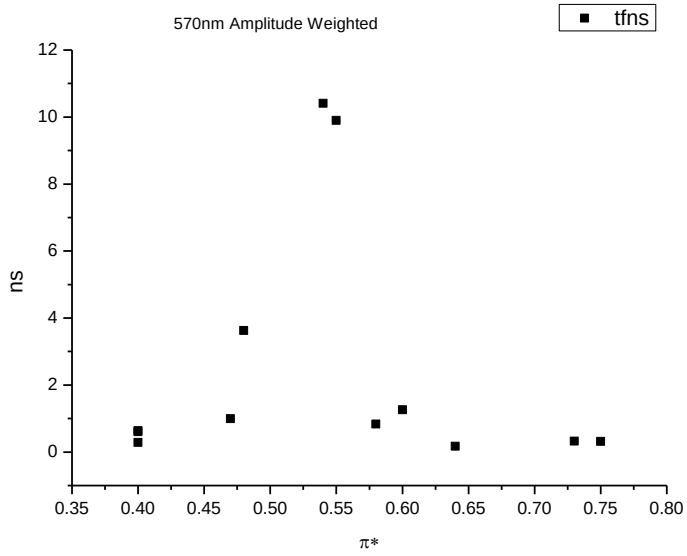

Figure 4.4.114. Amplitude weighted average lifetime (τ_f) of **27** at 570 nm versus π*.

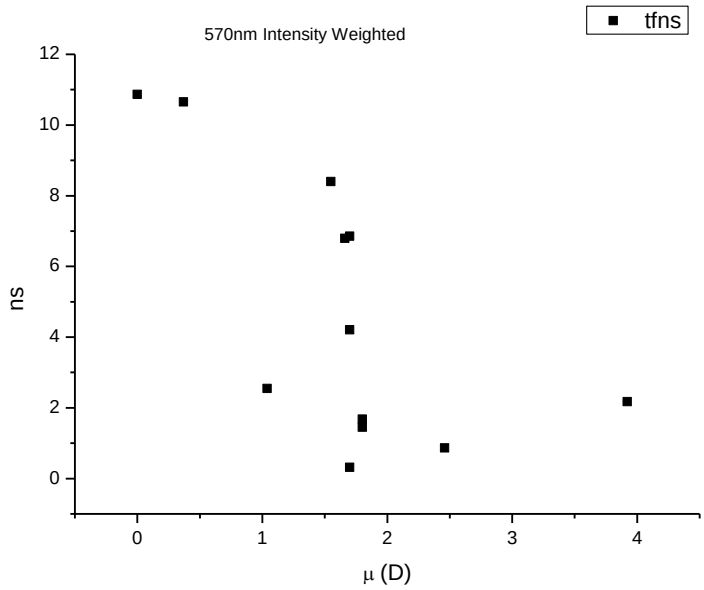

Figure 4.4.115. Intensity weighted average lifetime (τ_f) of **27** at 570 nm versus μ(D).

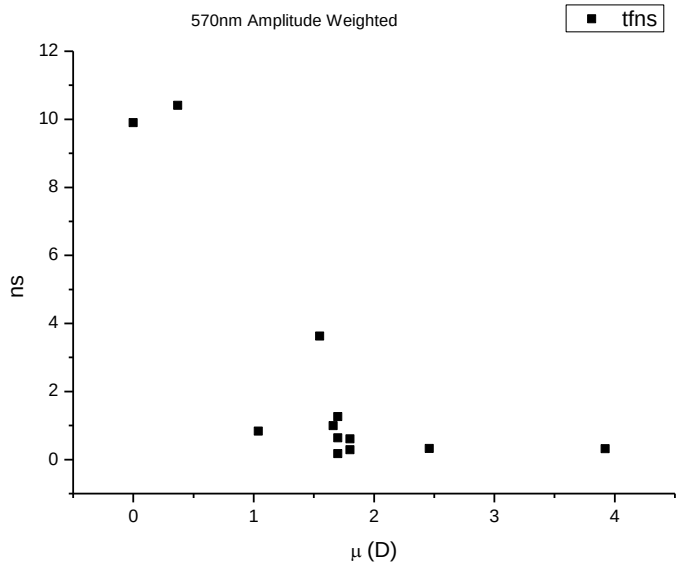

Figure 4.4.116. Amplitude weighted average lifetime (τ_f) of **27** at 570 nm versus μ(D).

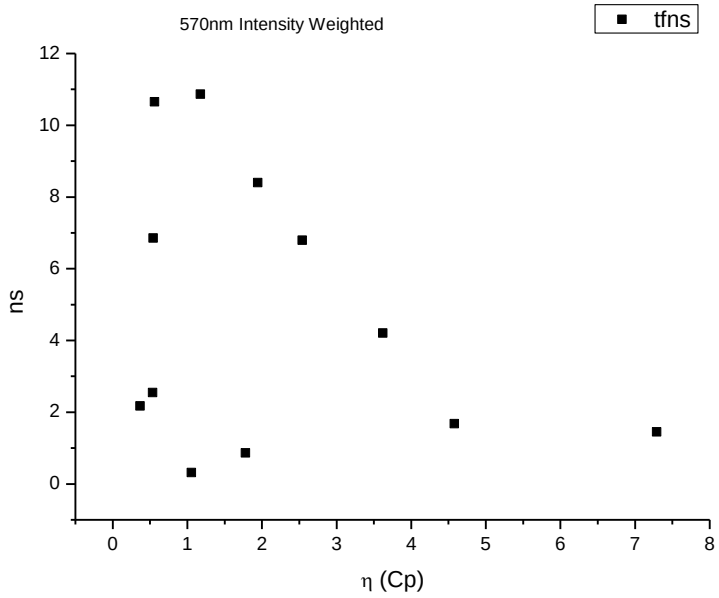

Figure 4.4.117. Intensity weighted average lifetime (τ_f) of **27** at 570 nm versus η(Cp).

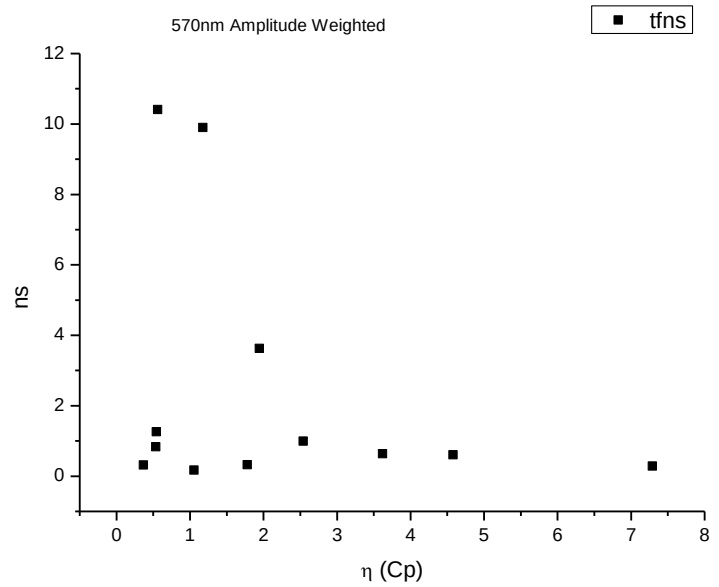

Figure 4.4.118. Amplitude weighted average lifetime (τ_f) of **27** at 570 nm versus η(Cp).

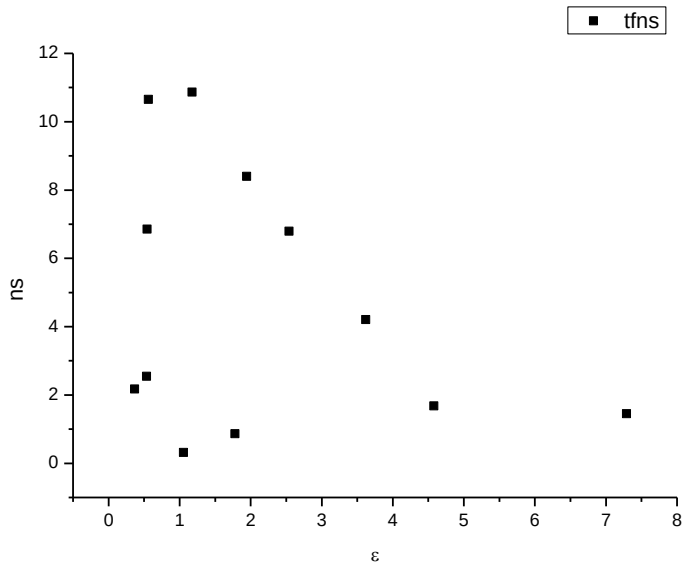

Figure 4.4.119. Intensity weighted average lifetime (τ_f) of **27** at 570 nm versus ε.

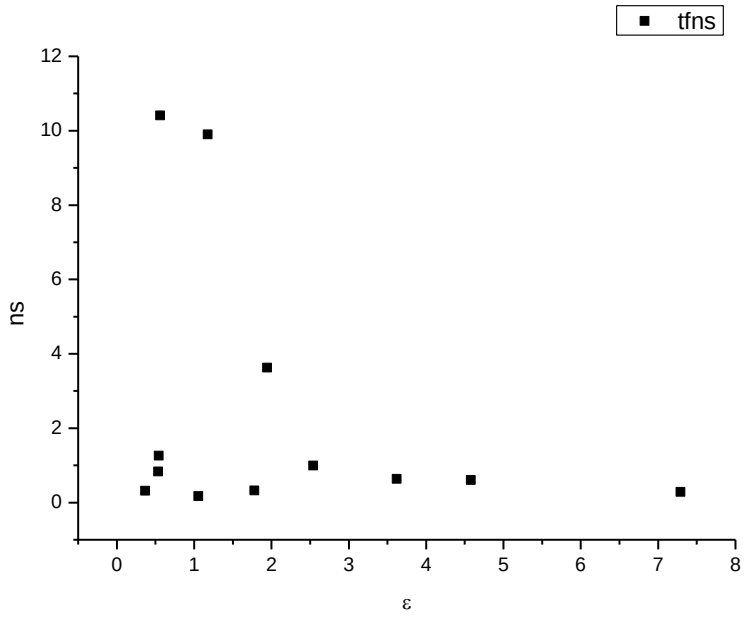

Figure 4.4.120. Amplitude weighted average lifetime (τ_f) of **27** at 570 nm versus ε.

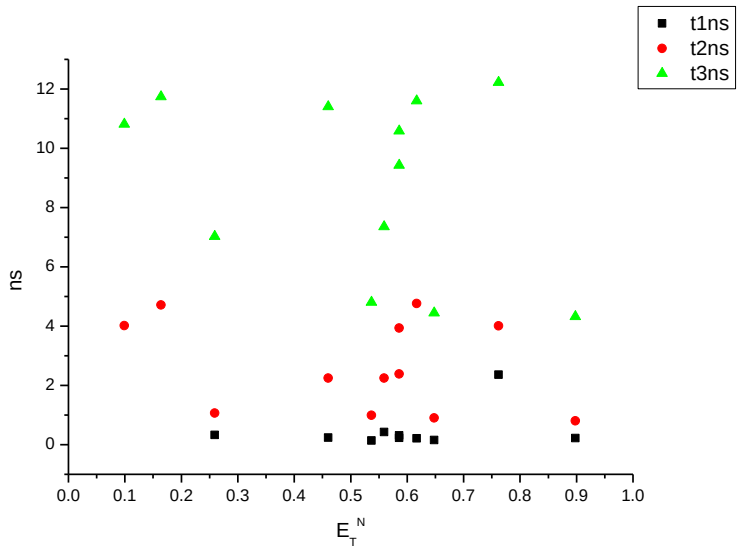

Figure 4.4.121. Intensity weighted components of TCSPC lifetime decay of **27** (570 nm) versus E_T^N.

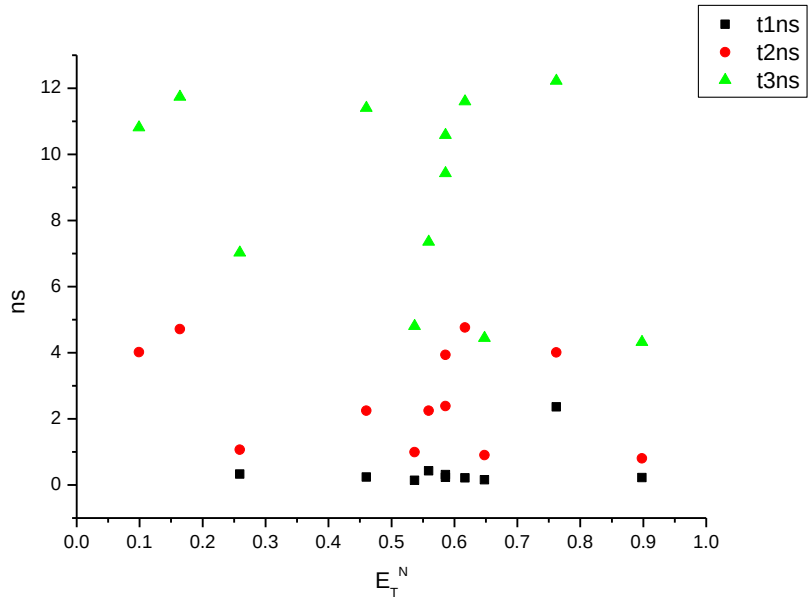

Figure 4.4.122. Amplitude weighted components of TCSPC lifetime decay of **27** (570 nm) versus E_T^N.

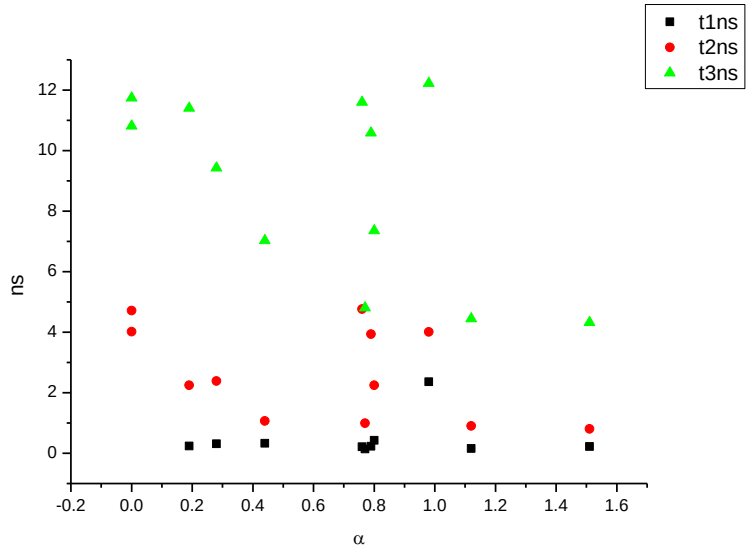

Figure 4.4.123. Intensity weighted components of TCSPC lifetime decay of **27** (570 nm) versus α.

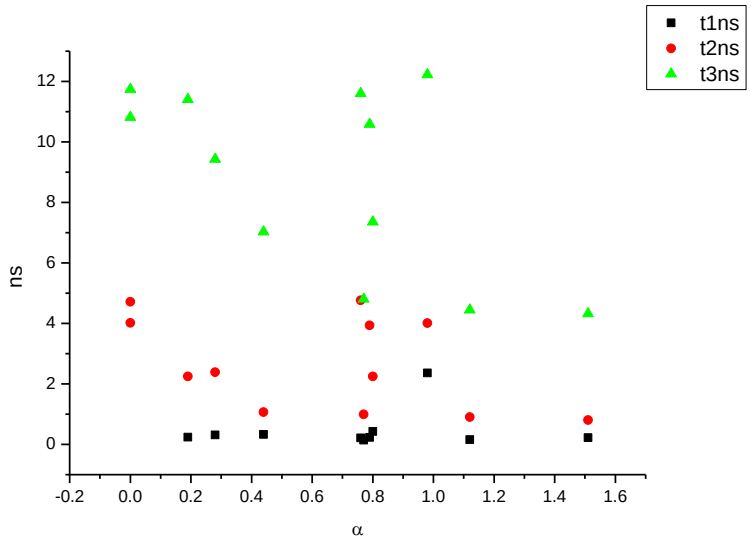

Figure 4.4.124. Amplitude weighted components of TCSPC lifetime decay of **27** (570 nm) versus α.

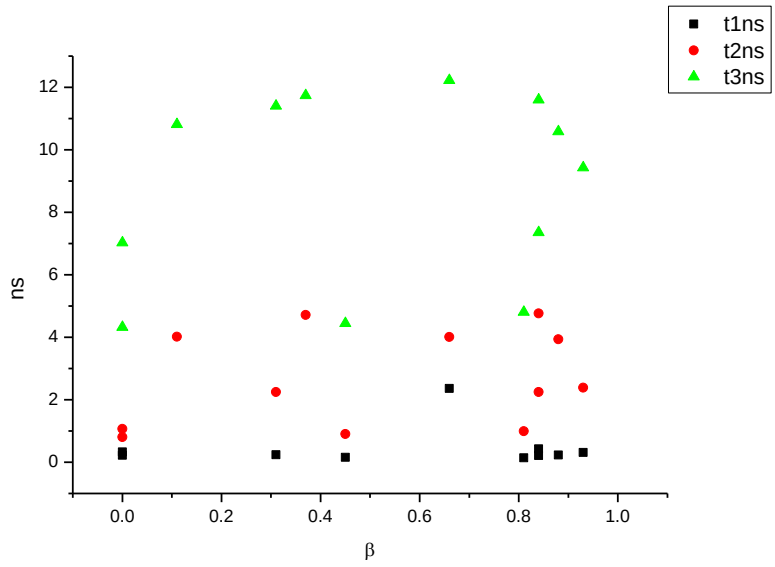

Figure 4.4.125. Intensity weighted components of TCSPC lifetime decay of **27** (570 nm) versus β.

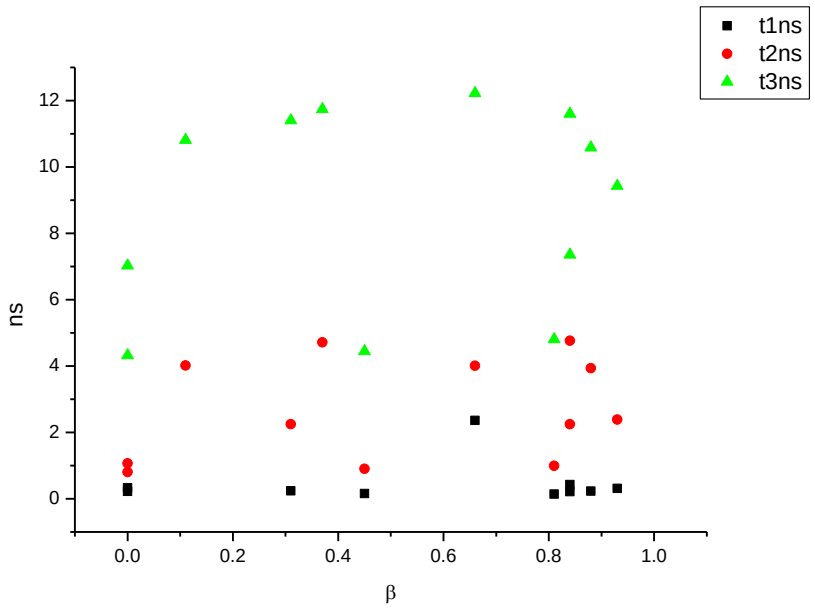

Figure 4.4.126. Amplitude weighted components of TCSPC lifetime decay of **27** (570 nm) versus β.

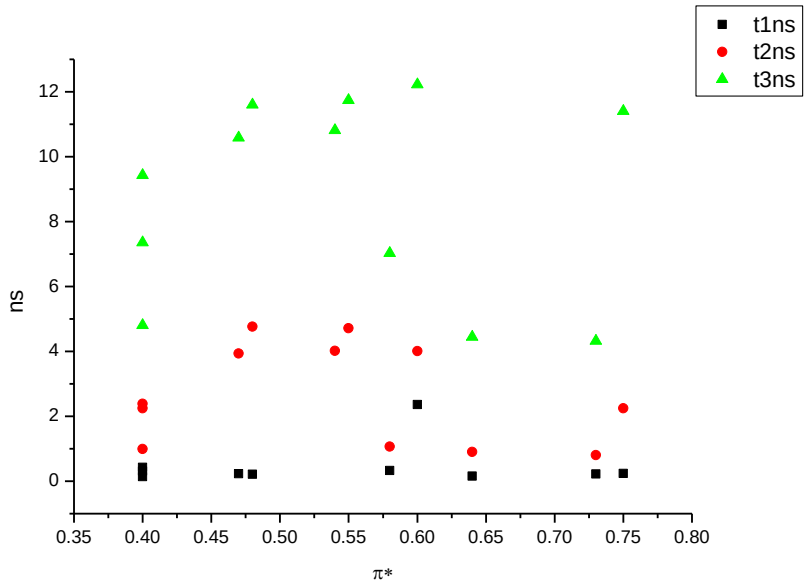

Figure 4.4.127. Intensity weighted components of TCSPC lifetime decay of **27** (570 nm) versus π*.

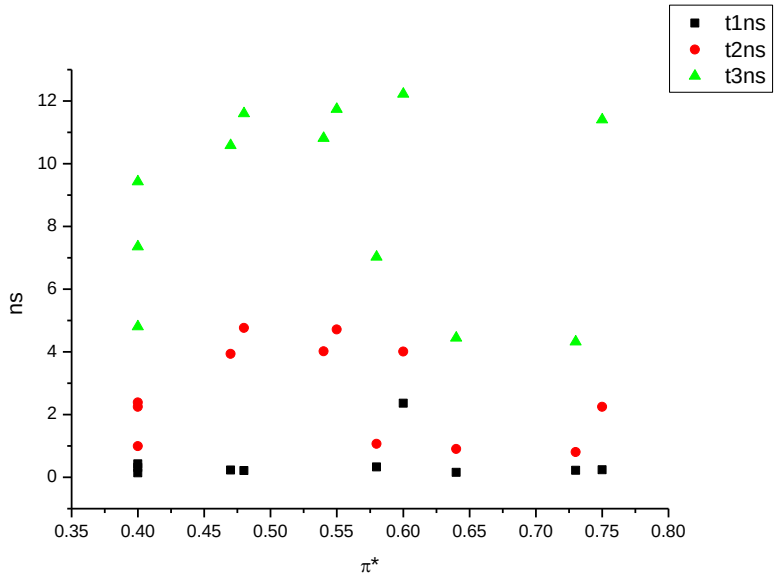

Figure 4.4.128. Amplitude weighted components of TCSPC lifetime decay of **27** (570 nm) versus π*.

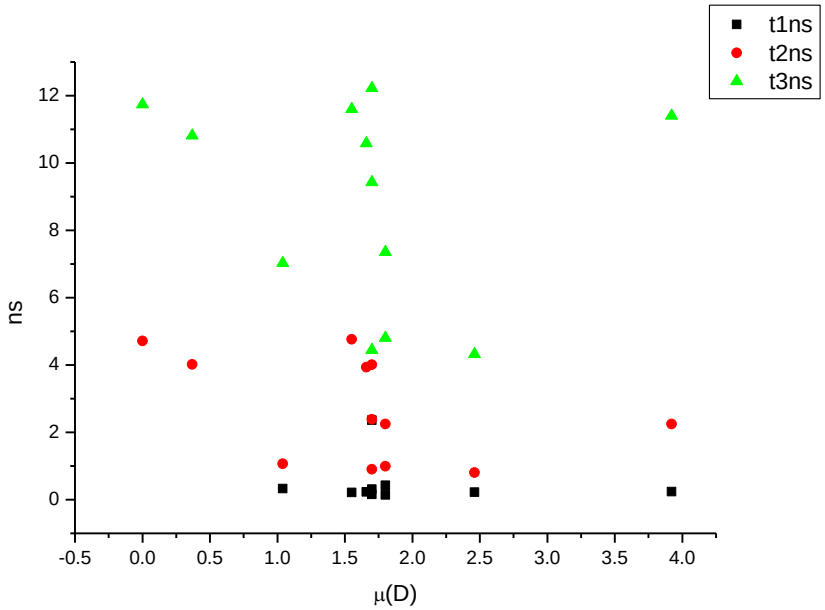

Figure 4.4.129. Intensity weighted components of TCSPC lifetime decay of **27** (570 nm) versus μ(D).

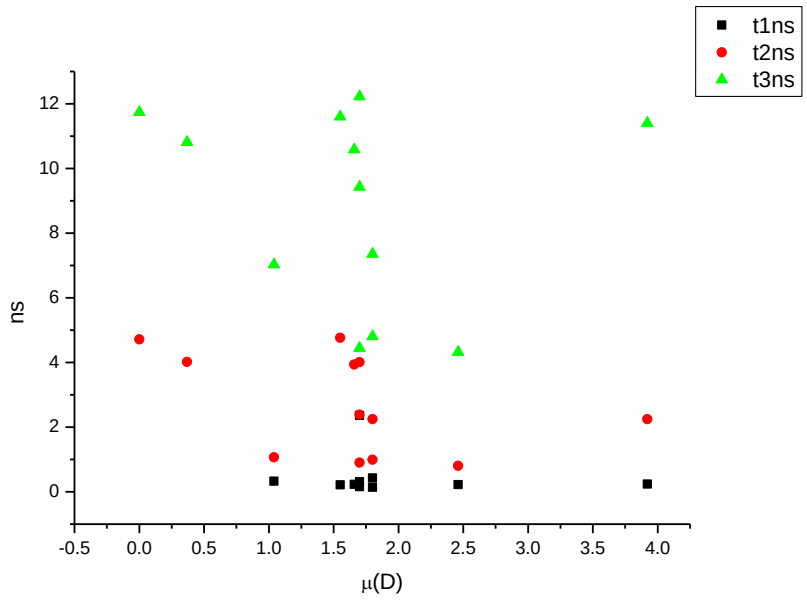

Figure 4.4.130. Amplitude weighted components of TCSPC lifetime decay of **27** (570 nm) versus μ(D).

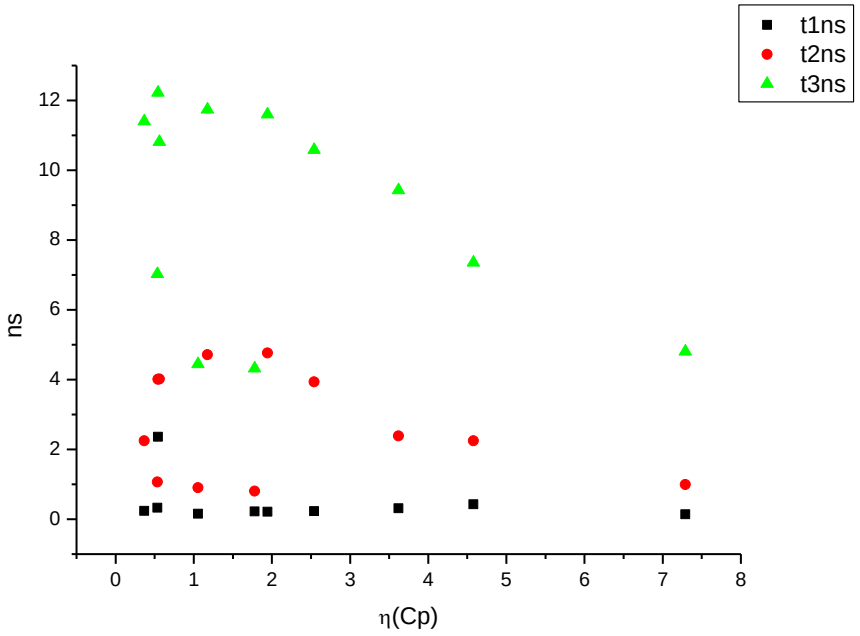

Figure 4.4.131. Intensity weighted components of TCSPC lifetime decay of **27** (570 nm) versus η(Cp).

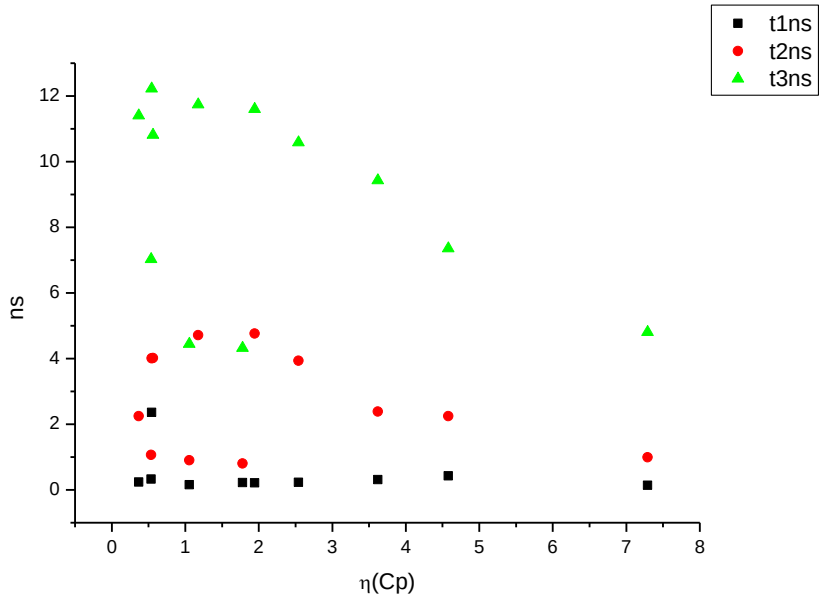

Figure 4.4.132. Amplitude weighted components of TCSPC lifetime decay of **27** (570 nm) versus η(Cp).

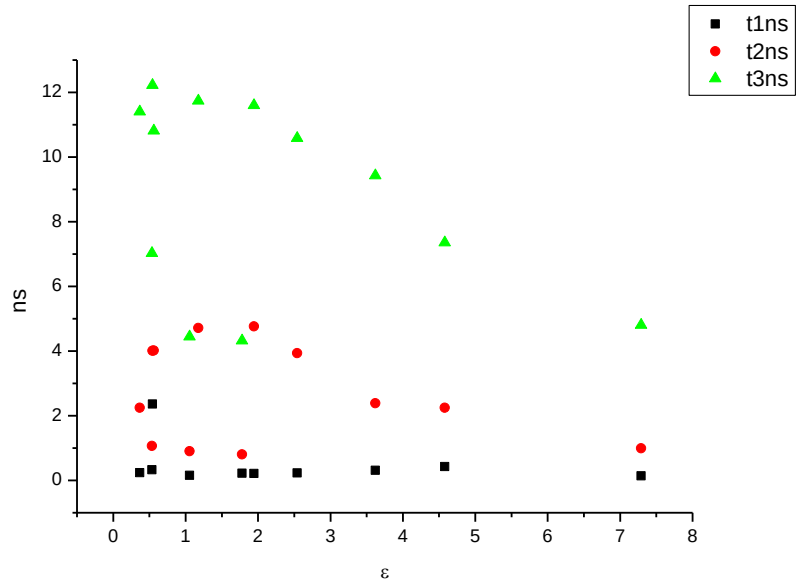

Figure 4.4.133. Intensity weighted components of TCSPC lifetime decay of **27** (570 nm) versus ε.

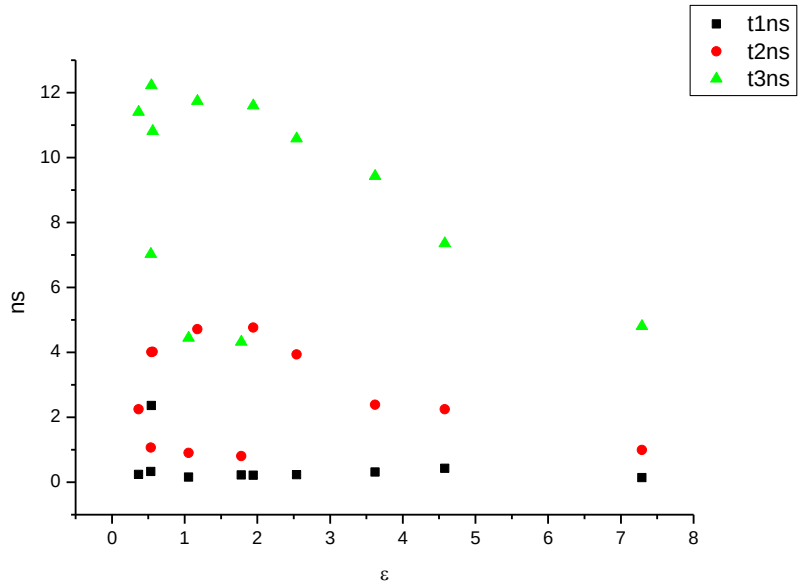

Figure 4.4.134. Amplitude weighted components of TCSPC lifetime decay of **27** (570 nm) versus ε.

4.4.8 Ultraviolet-visible absorption spectra.

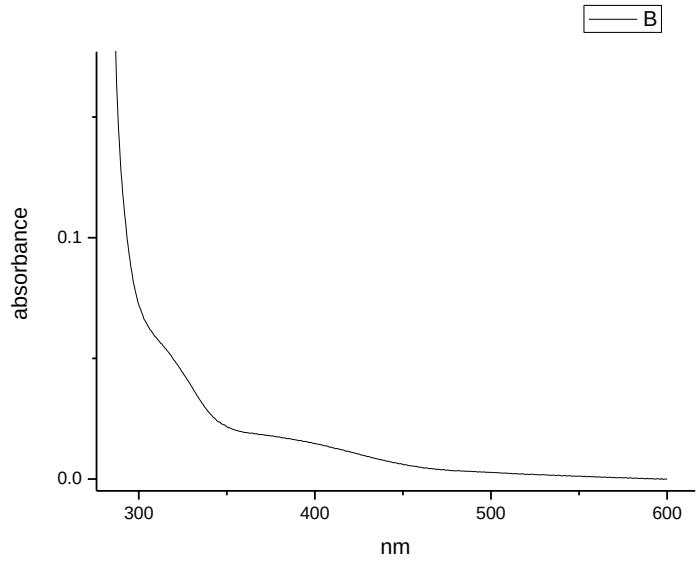

Figure 4.4.135. Ultraviolet-Visible absorption spectrum of **27** recorded in Toluene.

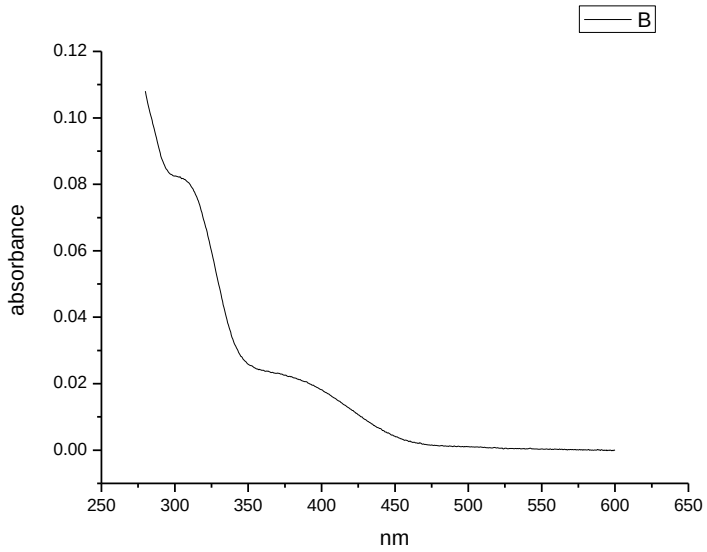

Figure 4.4.136. Ultraviolet-Visible absorption spectrum of **27** recorded in 1,4-dioxane.

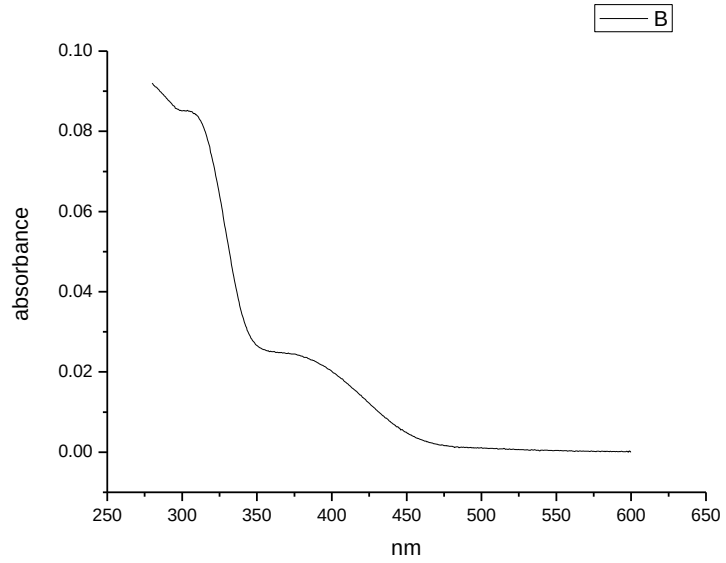

Figure 4.4.137. Ultraviolet-Visible absorption spectrum of **27** recorded in Chloroform.

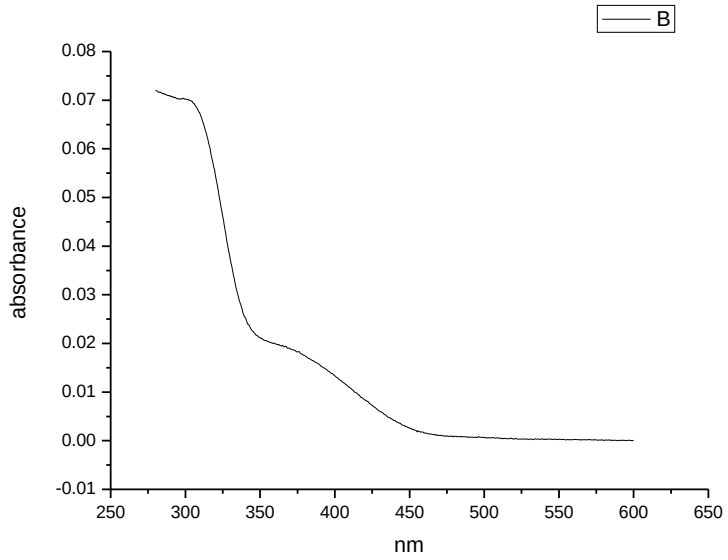

Figure 4.4.138. Ultraviolet-Visible absorption spectrum of **27** recorded in Acetonitrile.

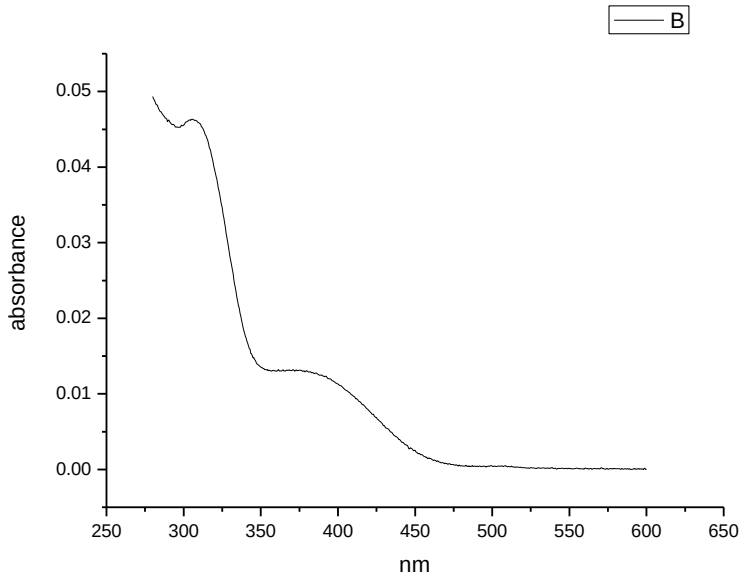

Figure 4.4.139. Ultraviolet-Visible absorption spectrum of **27** recorded in 1-octanol.

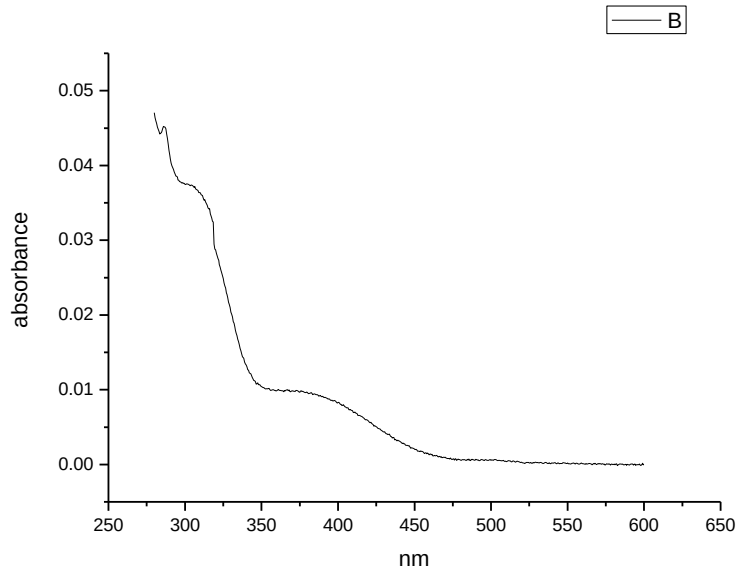

Figure 4.4.140. Ultraviolet-Visible absorption spectrum of **27** recorded in 1-hexanol.

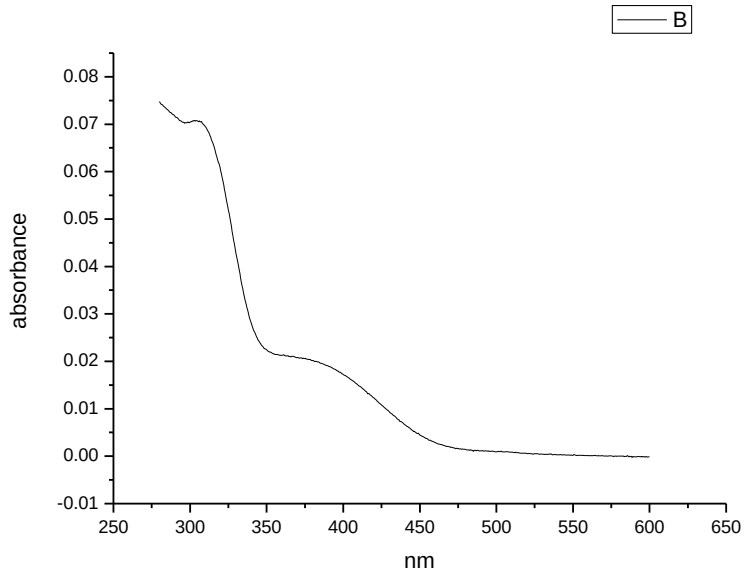

Figure 4.4.141. Ultraviolet-Visible absorption spectrum of **27** recorded in 1-butanol.

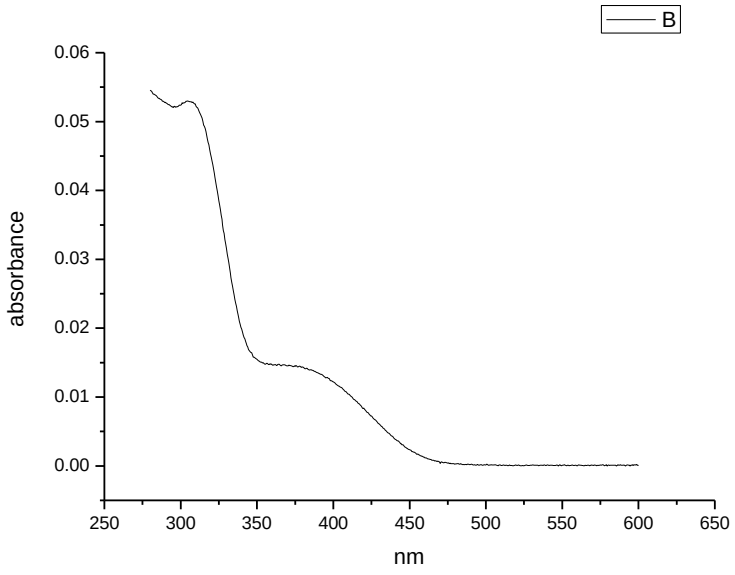

Figure 4.4.142. Ultraviolet-Visible absorption spectrum of **27** recorded in 1-pentanol.

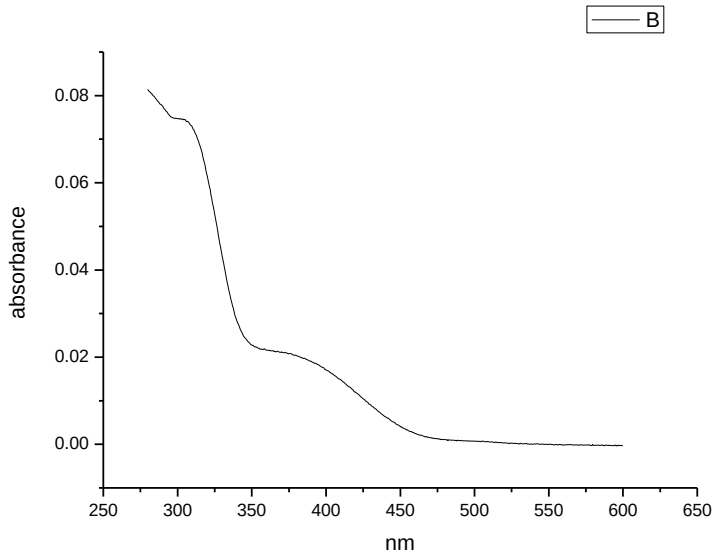

Figure 4.4.143. Ultraviolet-Visible absorption spectrum of **27** recorded in 1-propanol.

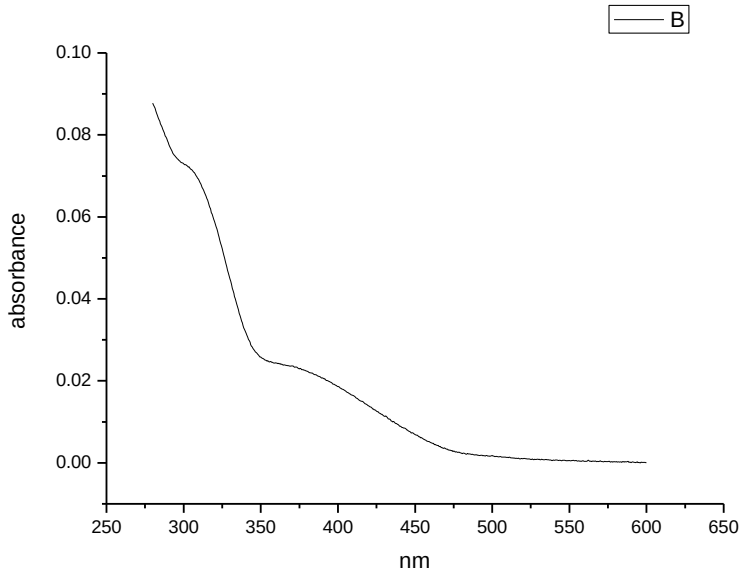

Figure 4.4.144. Ultraviolet-Visible absorption spectrum of **27** recorded in Acetic Acid.

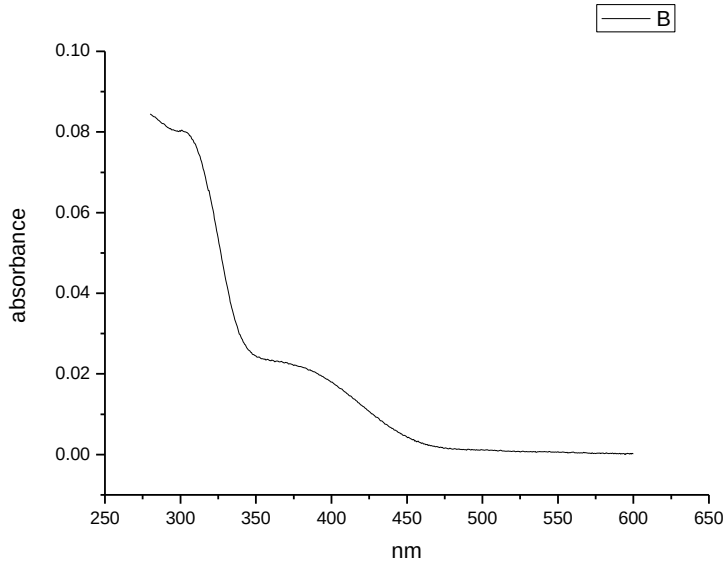

Figure 4.4.145. Ultraviolet-Visible absorption spectrum of **27** recorded in Methanol.

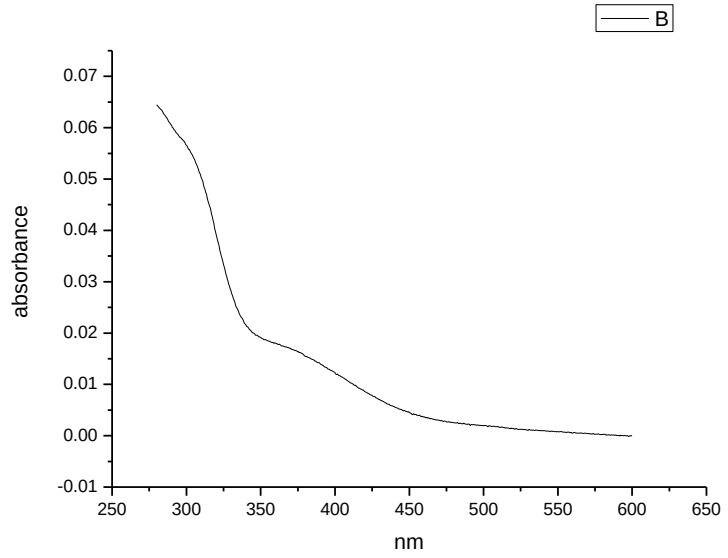

Figure 4.4.146. Ultraviolet-Visible absorption spectrum of **27** recorded in 2,2,2-trifluoroethanol.

4.4.9 Fluorescence Emission spectra.

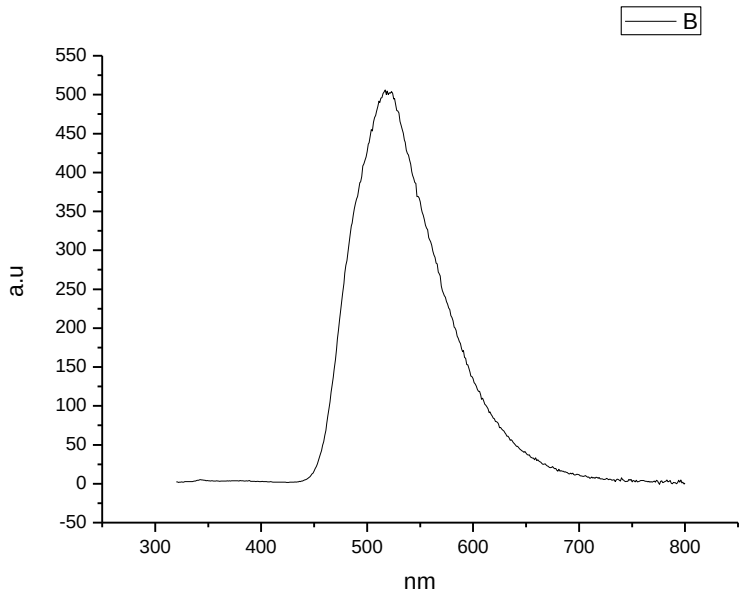

Figure 4.4.147. Fluorescence emission spectrum of **27** recorded in Toluene at 310 nm excitation.

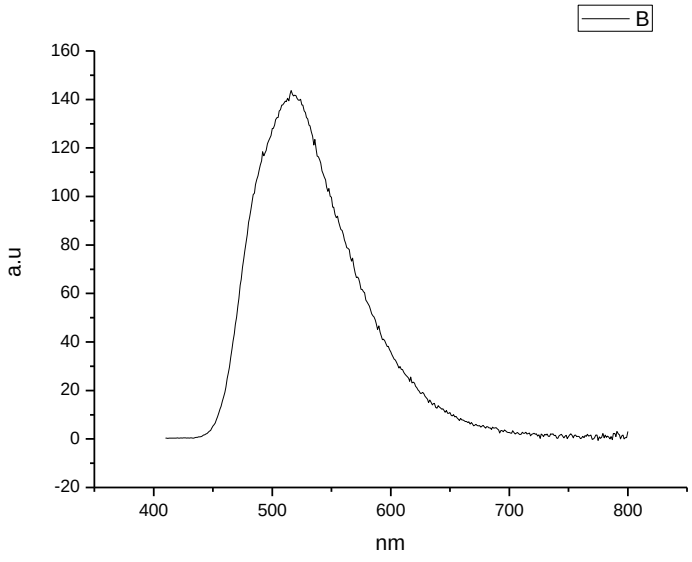

Figure 4.4.148. Fluorescence emission spectrum of **27** recorded in Toluene at 400 nm excitation.

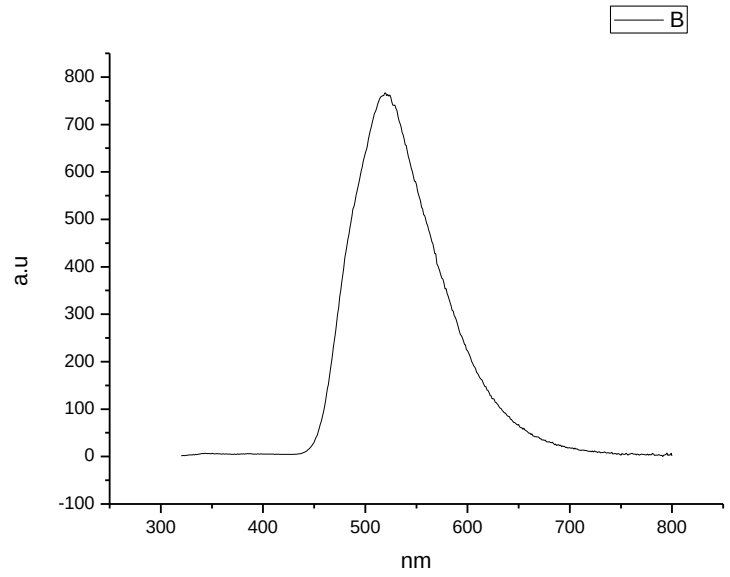

Figure 4.4.149. Fluorescence emission spectrum of **27** recorded in 1,4-dioxane at 310 nm excitation.

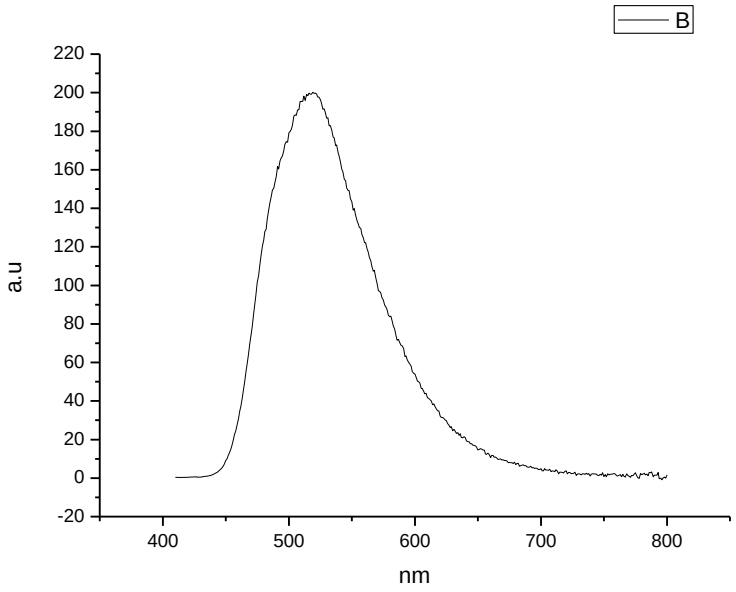

Figure 4.4.150. Fluorescence emission spectrum of **27** recorded in 1,4-dioxane at 400 nm excitation.

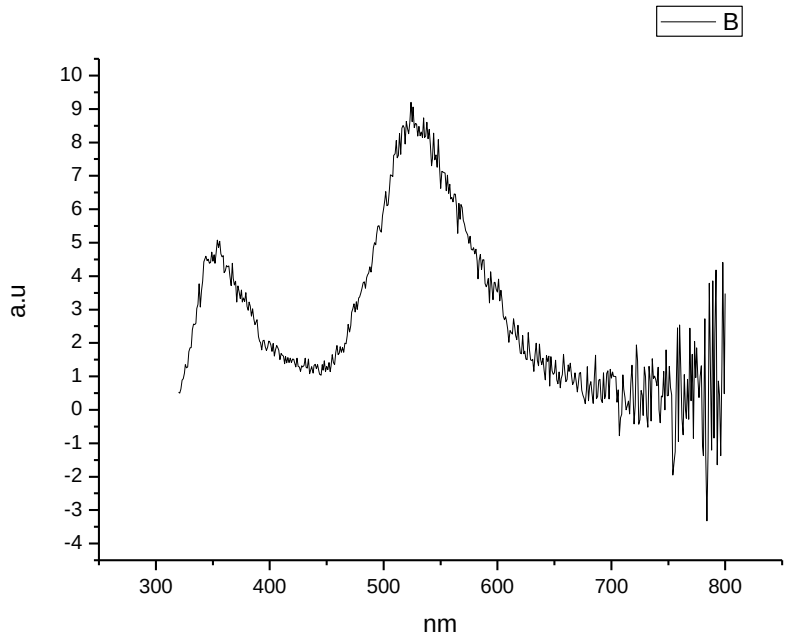

Figure 4.4.151. Fluorescence emission spectrum of **27** recorded in Chloroform at 310 nm excitation.

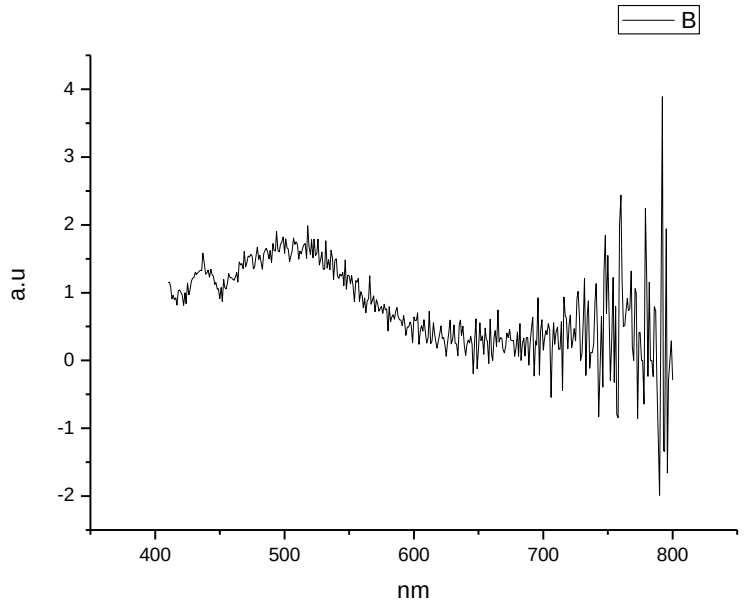

Figure 4.4.152. Fluorescence emission spectrum of **27** recorded in Chloroform at 400 nm excitation.

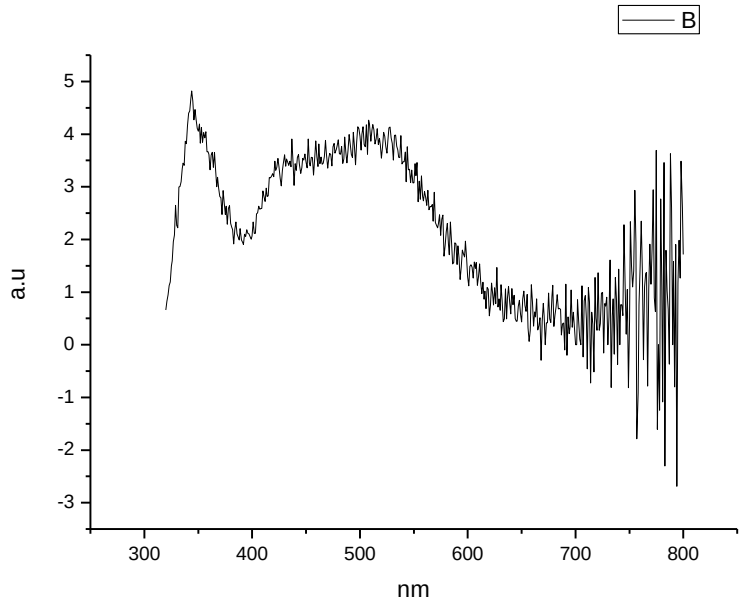

Figure 4.4.153. Fluorescence emission spectrum of **27** recorded in Acetonitrile at 310 nm excitation.

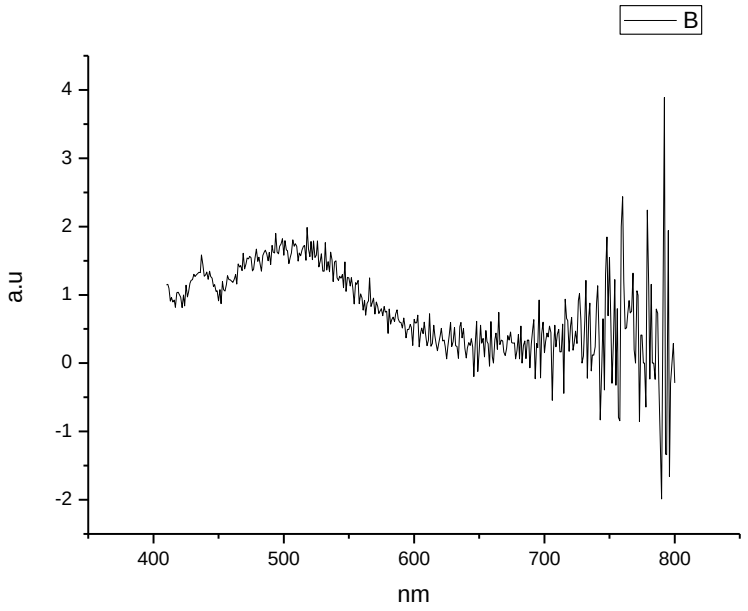

Figure 4.4.154. Fluorescence emission spectrum of **27** recorded in Acetonitrile at 400 nm excitation.

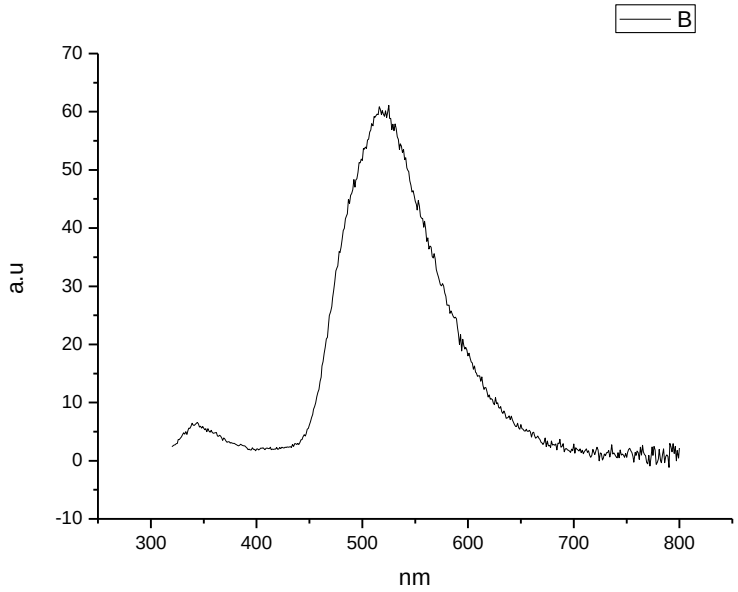

Figure 4.4.155. Fluorescence emission spectrum of **27** recorded in 1-octanol at 310 nm excitation.

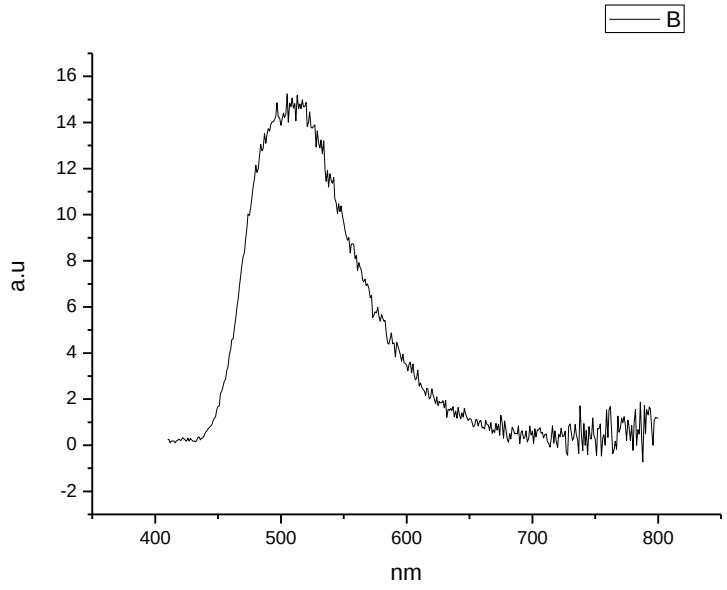

Figure 4.4.156. Fluorescence emission spectrum of **27** recorded in 1-octanol at 400 nm excitation.

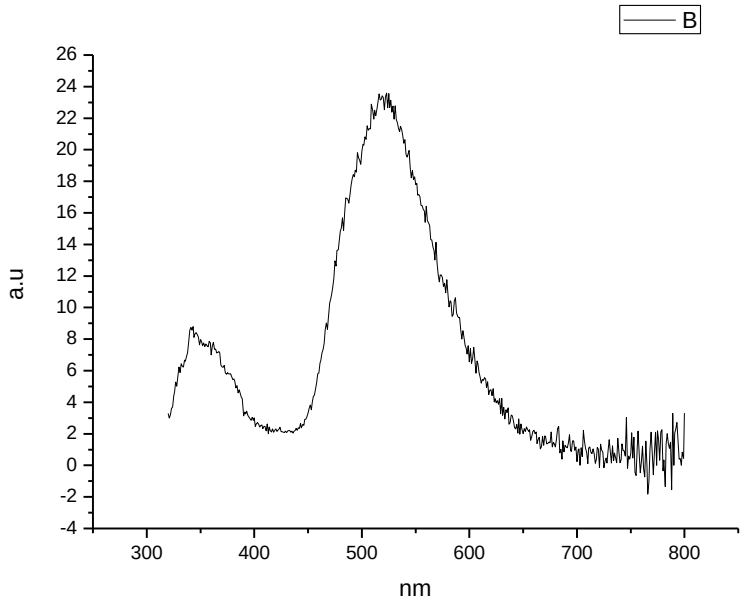

Figure 4.4.157. Fluorescence emission spectrum of **27** recorded in 1-hexanol at 310 nm excitation.

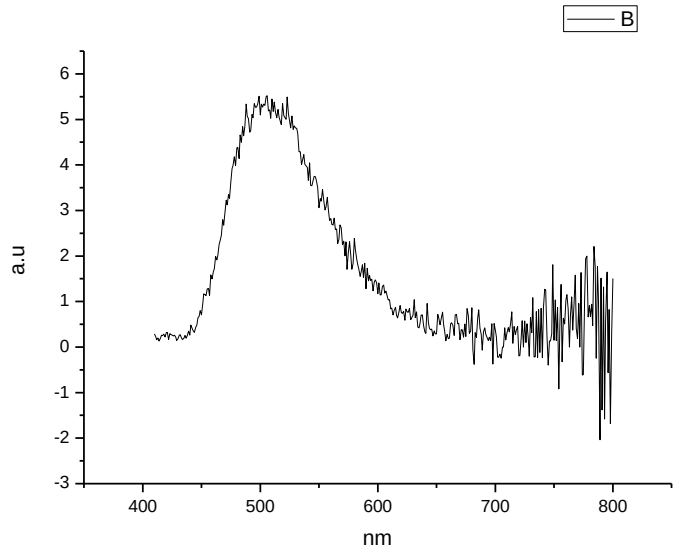

Figure 4.4.158. Fluorescence emission spectrum of **27** recorded in 1-hexanol at 400 nm excitation.

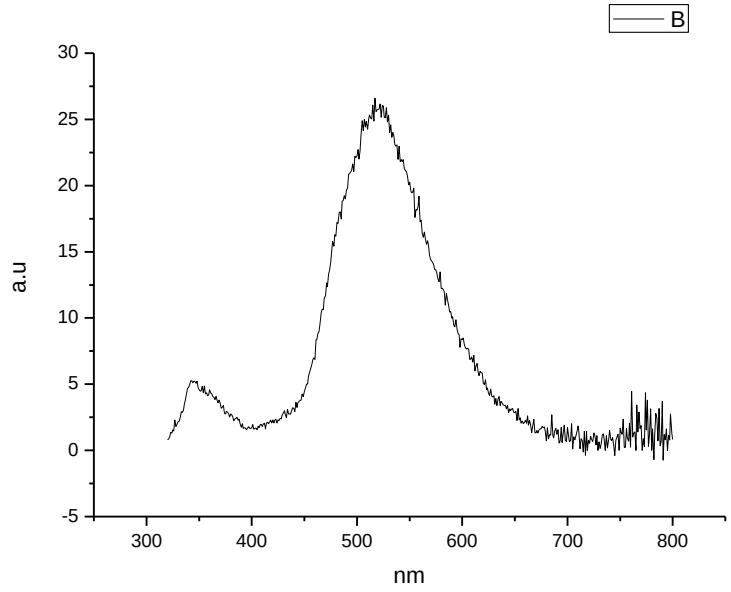

Figure 4.4.159. Fluorescence emission spectrum of **27** recorded in 1-butanol at 310 nm excitation.

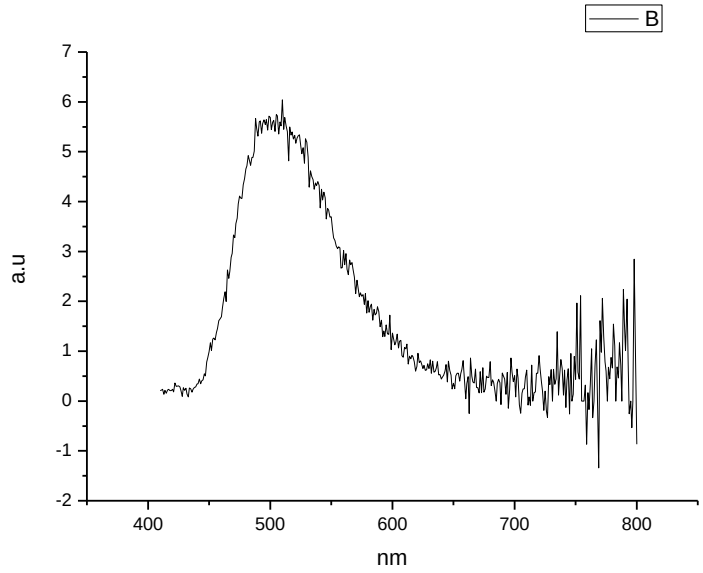

Figure 4.4.160. Fluorescence emission spectrum of **27** recorded in 1-butanol at 400 nm excitation.

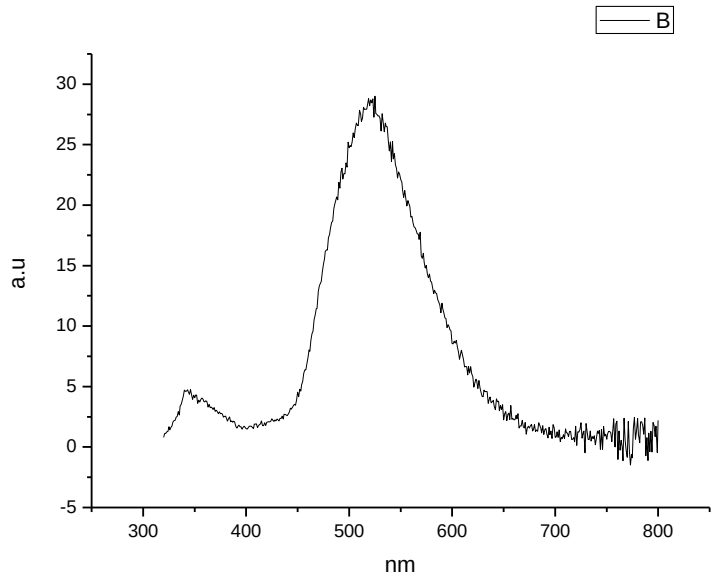

Figure 4.4.161. Fluorescence emission spectrum of **27** recorded in 1-pentanol at 310 nm excitation.

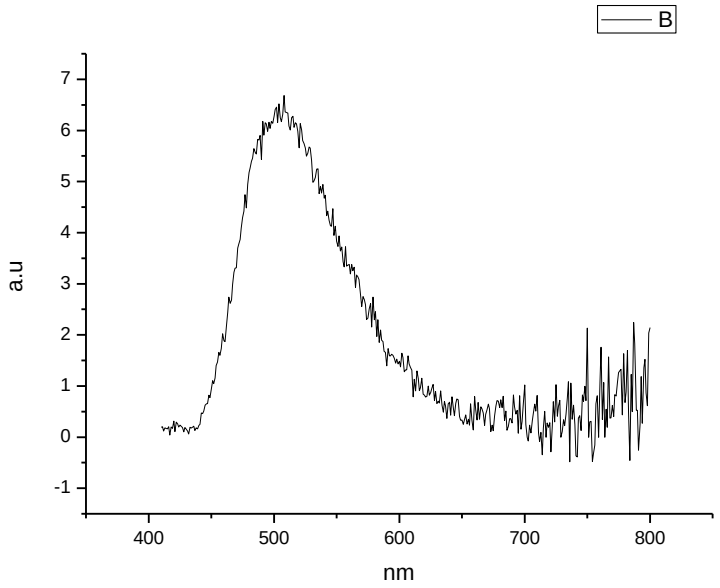

Figure 4.4.162. Fluorescence emission spectrum of **27** recorded in 1-pentanol at 400 nm excitation.

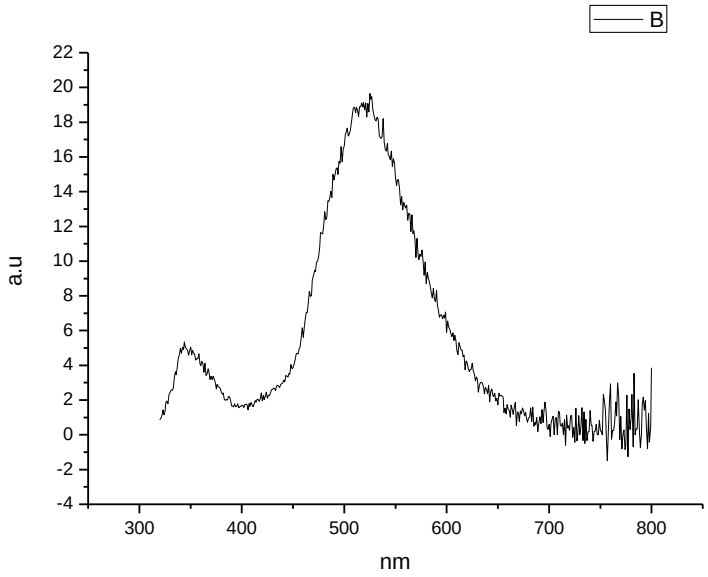

Figure 4.4.163. Fluorescence emission spectrum of **27** recorded in 1-propanol at 310 nm excitation.

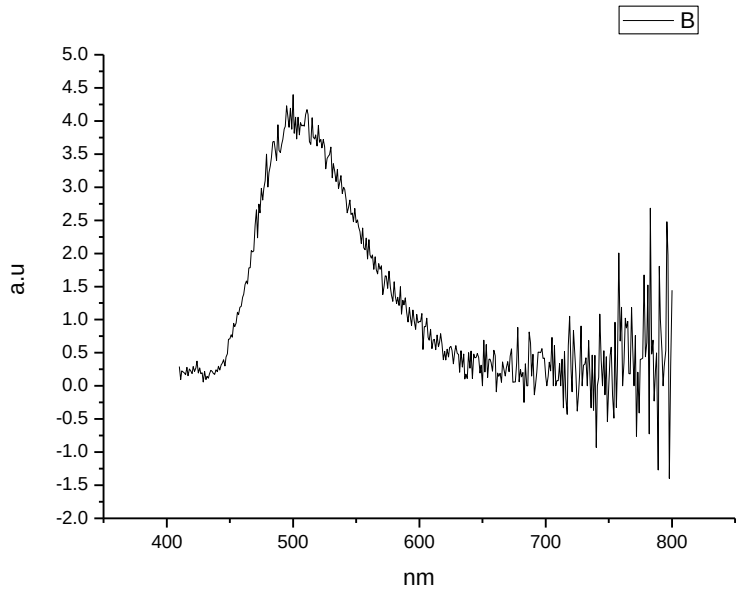

Figure 4.4.164. Fluorescence emission spectrum of **27** recorded in 1-propanol at 400 nm excitation.

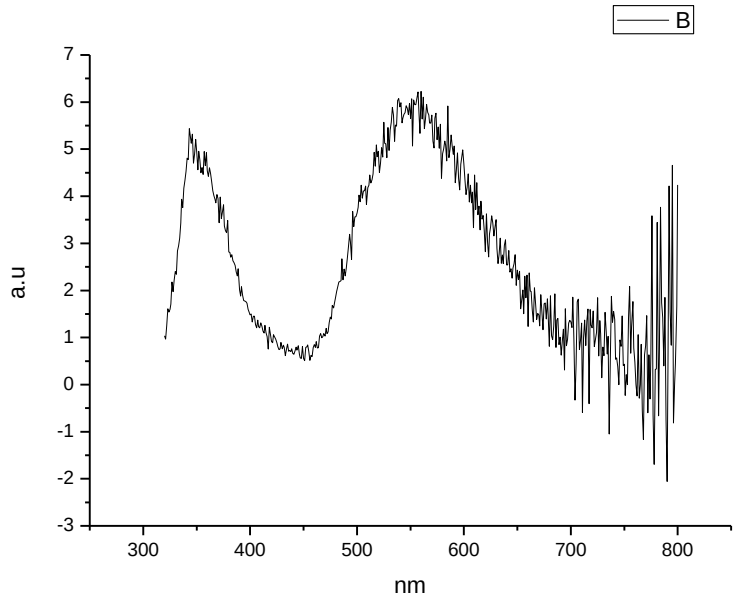

Figure 4.4.165. Fluorescence emission spectrum of **27** recorded in Acetic Acid at 310 nm excitation.

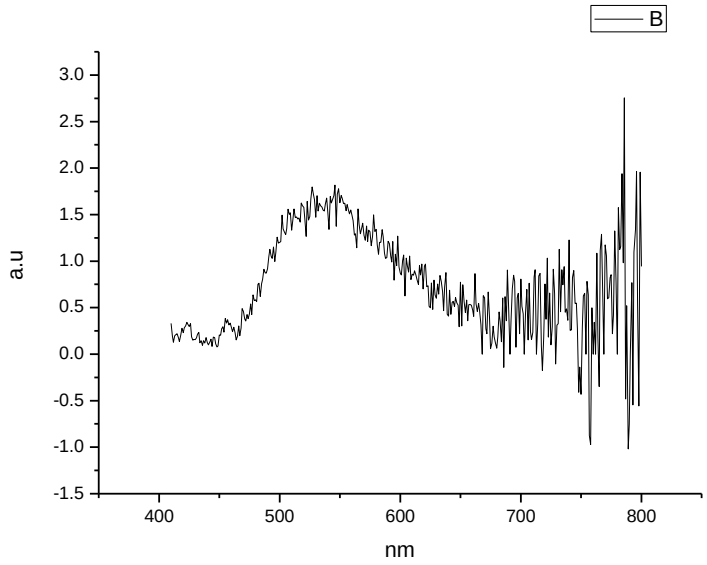

Figure 4.4.166. Fluorescence emission spectrum of **27** recorded in Acetic Acid at 400 nm excitation.

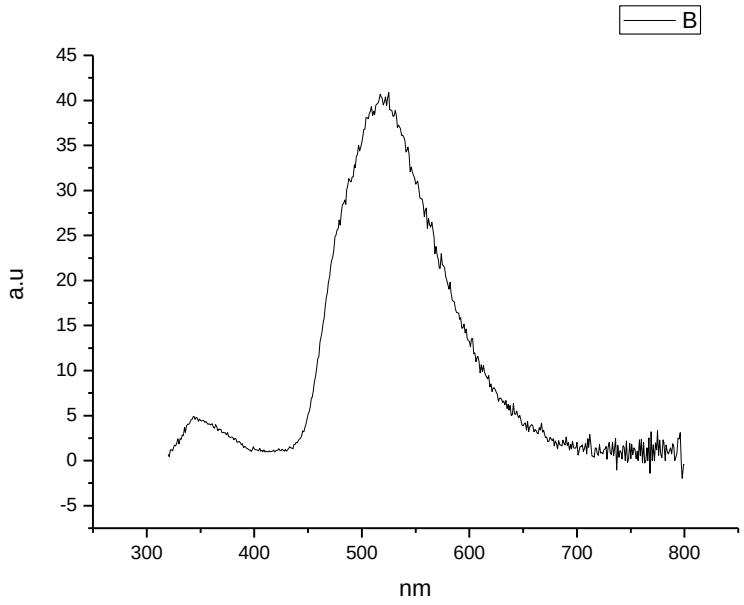

Figure 4.4.167. Fluorescence emission spectrum of **27** recorded in Methanol at 310 nm excitation.

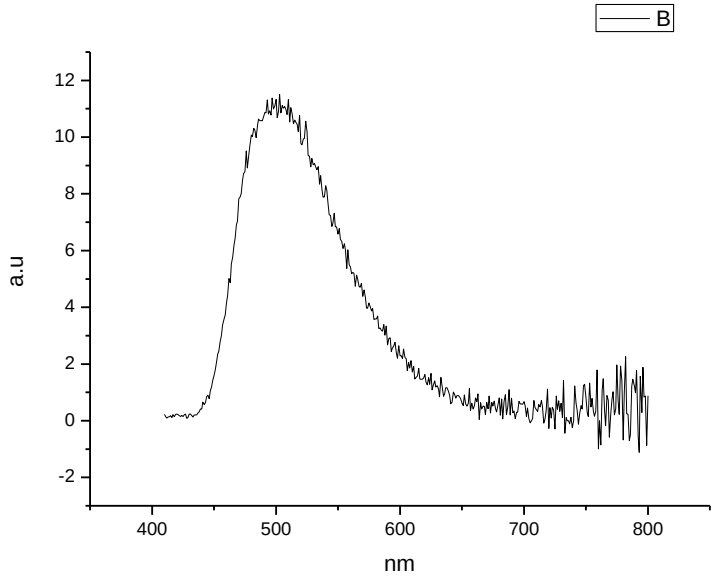

Figure 4.4.168. Fluorescence emission spectrum of **27** recorded in Methanol at 400 nm excitation.

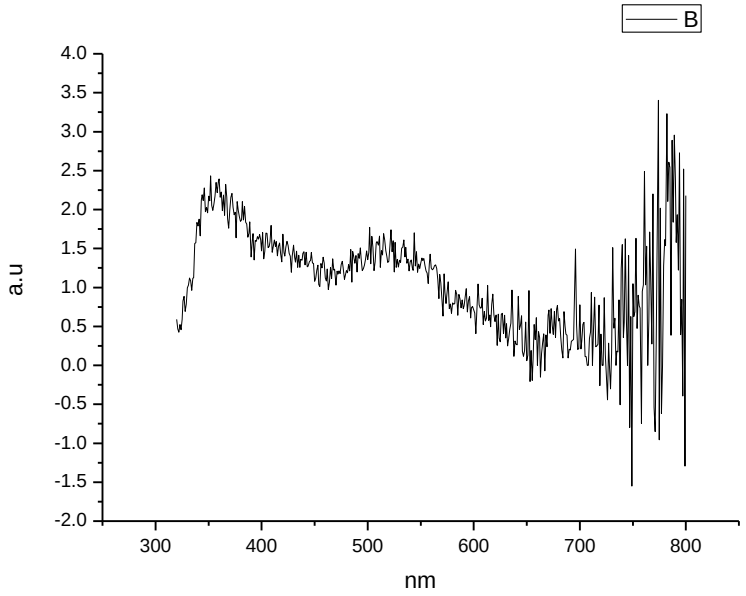

Figure 4.4.169. Fluorescence emission spectrum of **27** recorded in 2,2,2-trifluoroethanol at 310 nm excitation.

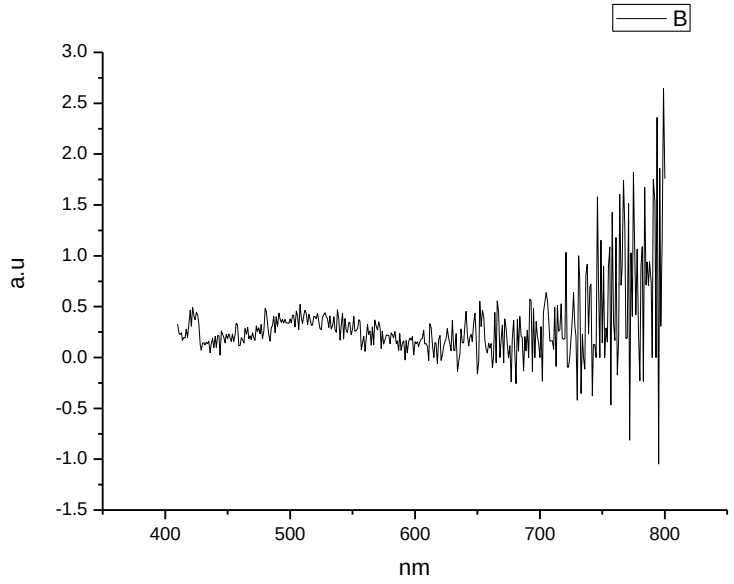

Figure 4.4.170. Fluorescence emission spectrum of **27** recorded in 2,2,2-trifluoroethanol at 400 nm excitation.

4.4.10 Normalised Fluorescence Emission spectra (Gaussian fitted).

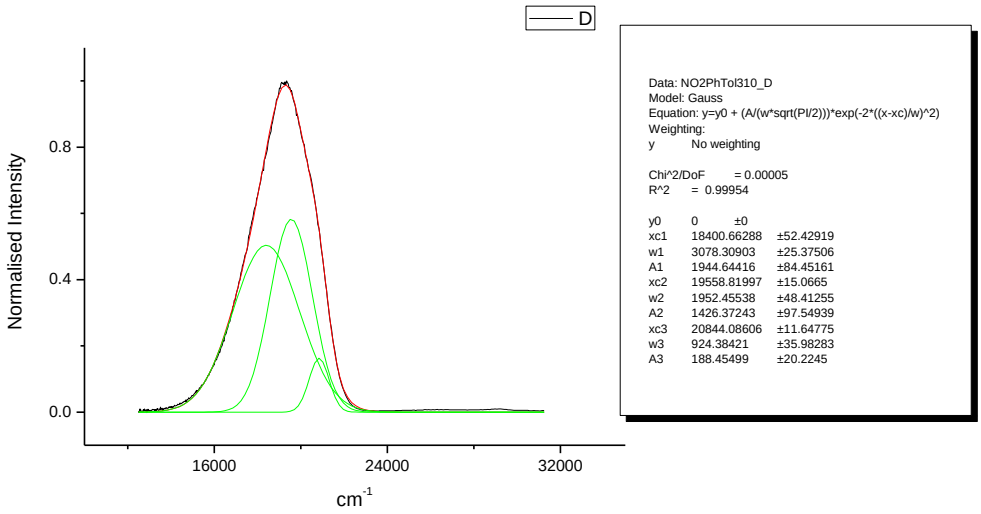

Figure 4.4.171. Gaussian model fit of the normalised fluorescence emission spectrum of **27** recorded in Toluene at 310 nm excitation.

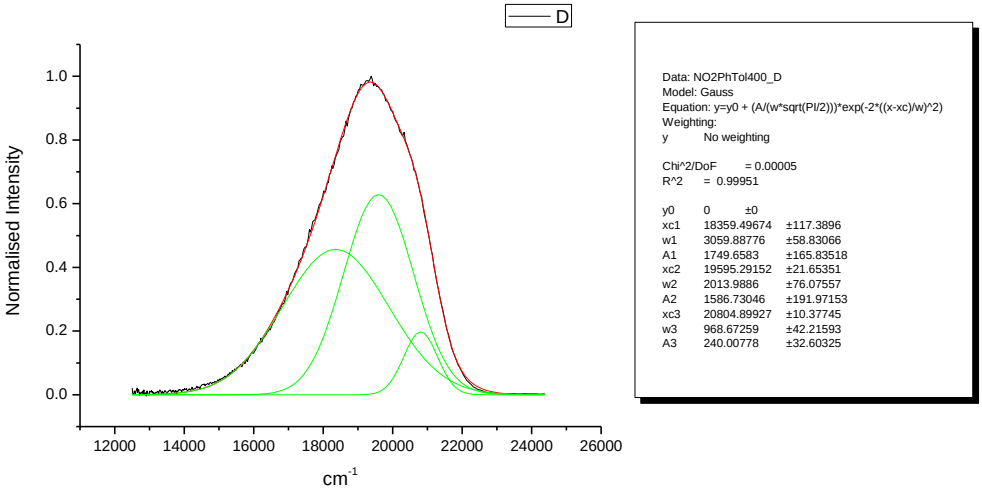

Figure 4.4.172. Gaussian model fit of the normalised fluorescence emission spectrum of **27** recorded in Toluene at 400 nm excitation.

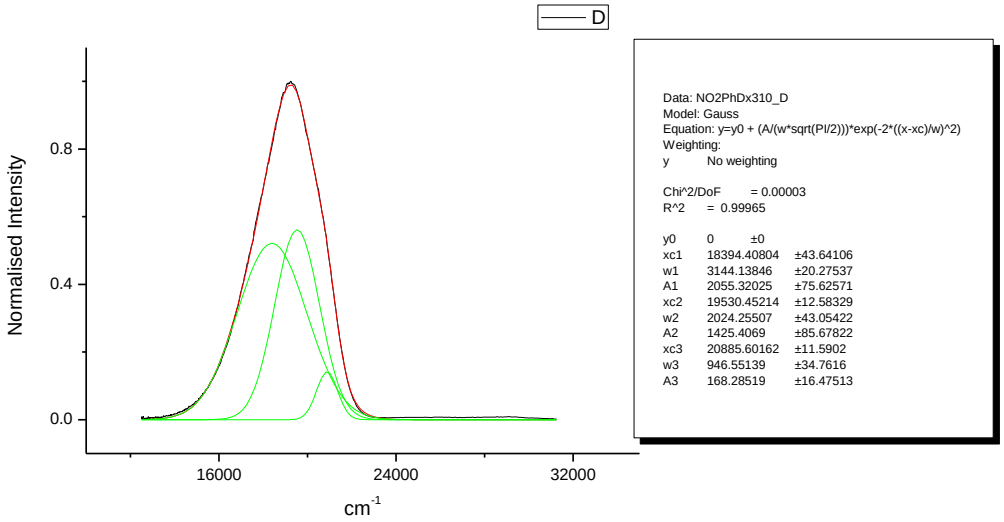

Figure 4.4.173. Gaussian model fit of the normalised fluorescence emission spectrum of **27** recorded in 1,4-dioxane at 310 nm excitation.

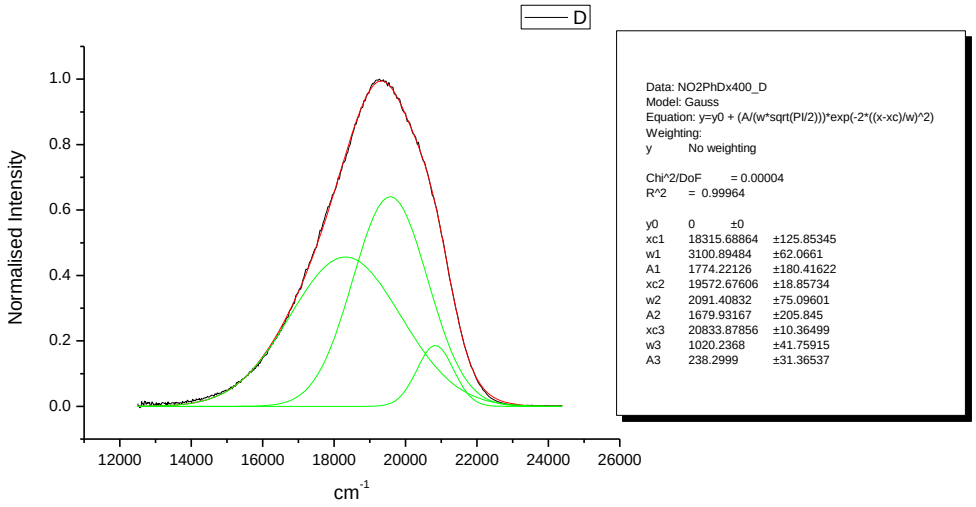

Figure 4.4.174. Gaussian model fit of the normalised fluorescence emission spectrum of **27** recorded in 1,4-dioxane at 400 nm excitation.

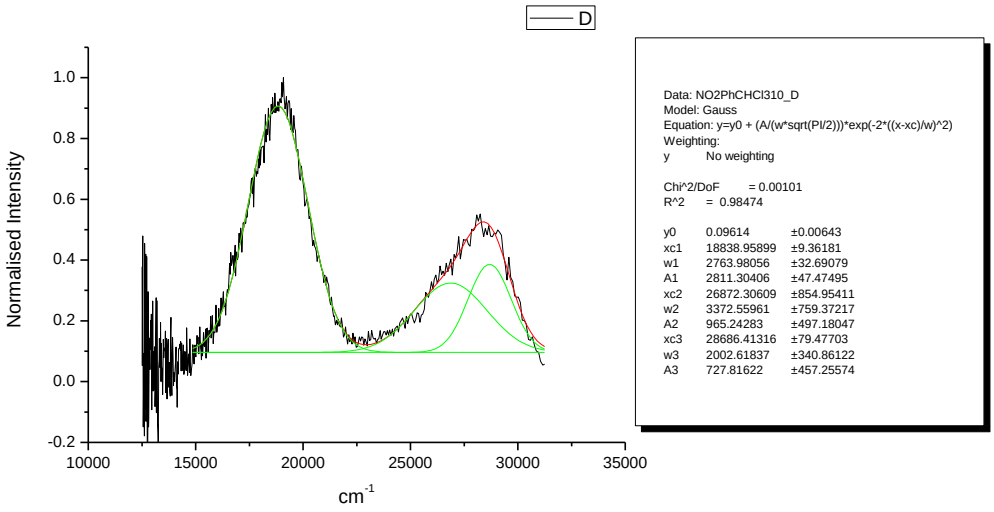

Figure 4.4.175. Gaussian model fit of the normalised fluorescence emission spectrum of **27** recorded in Chloroform at 310 nm excitation.

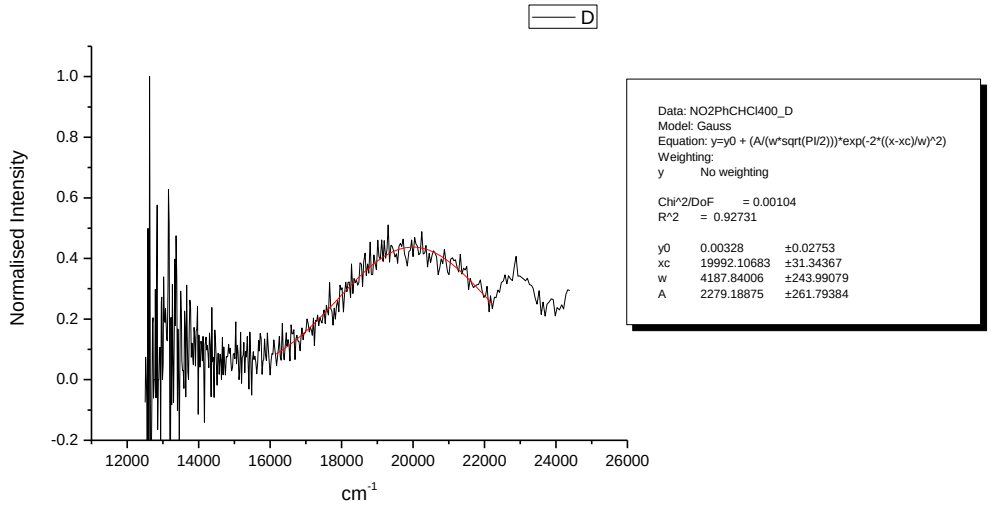

Figure 4.4.176. Gaussian model fit of the normalised fluorescence emission spectrum of **27** recorded in Chloroform at 400 nm excitation.

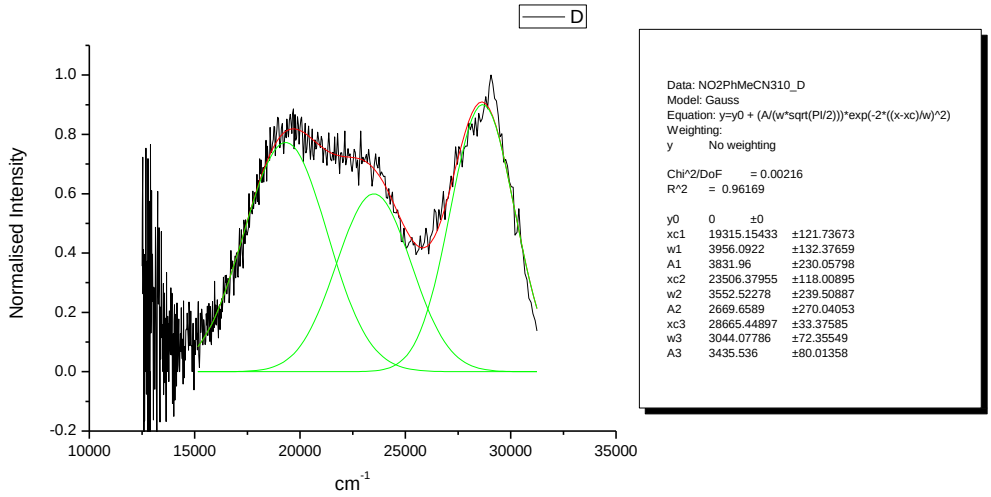

Figure 4.4.177. Gaussian model fit of the normalised fluorescence emission spectrum of **27** recorded in Acetonitrile at 310 nm excitation.

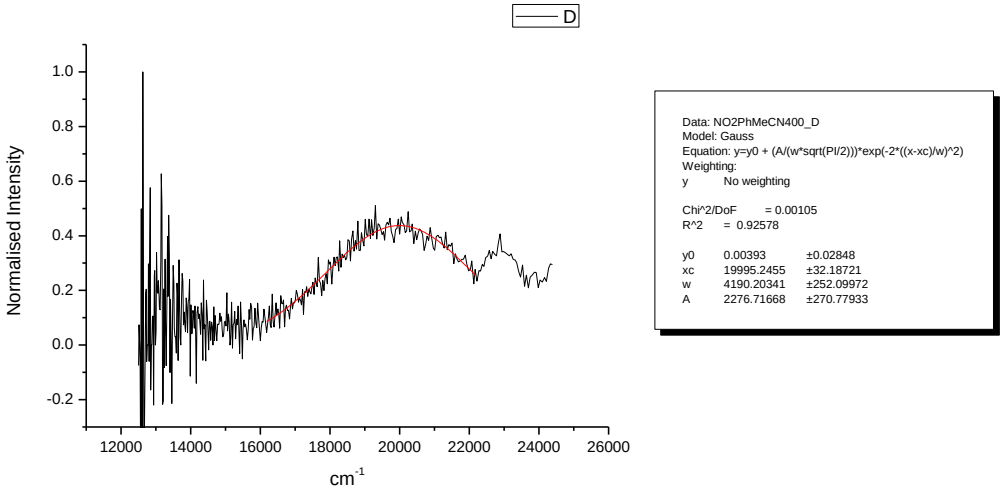

Figure 4.4.178. Gaussian model fit of the normalised fluorescence emission spectrum of **27** recorded in Acetonitrile at 400 nm excitation.

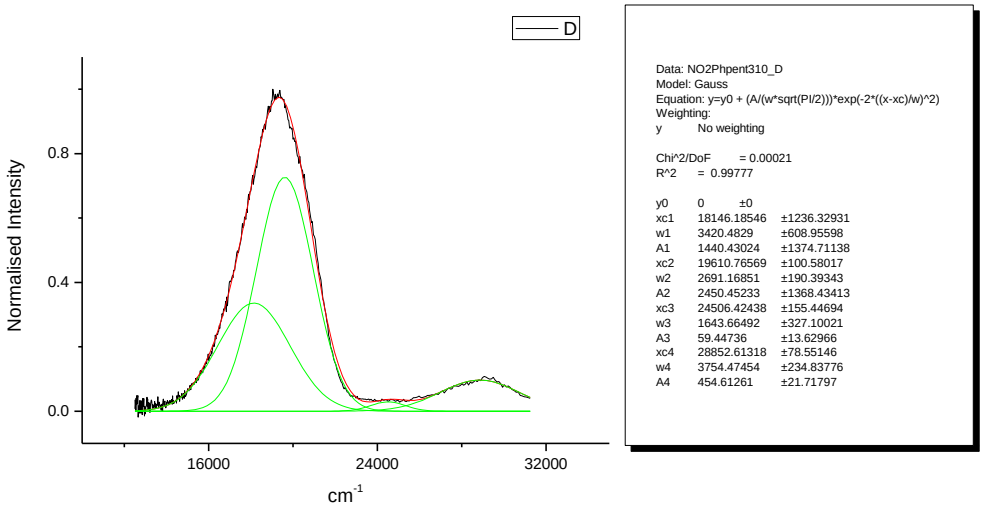

Figure 4.4.179. Gaussian model fit of the normalised fluorescence emission spectrum of **27** recorded in 1-octanol at 310 nm excitation.

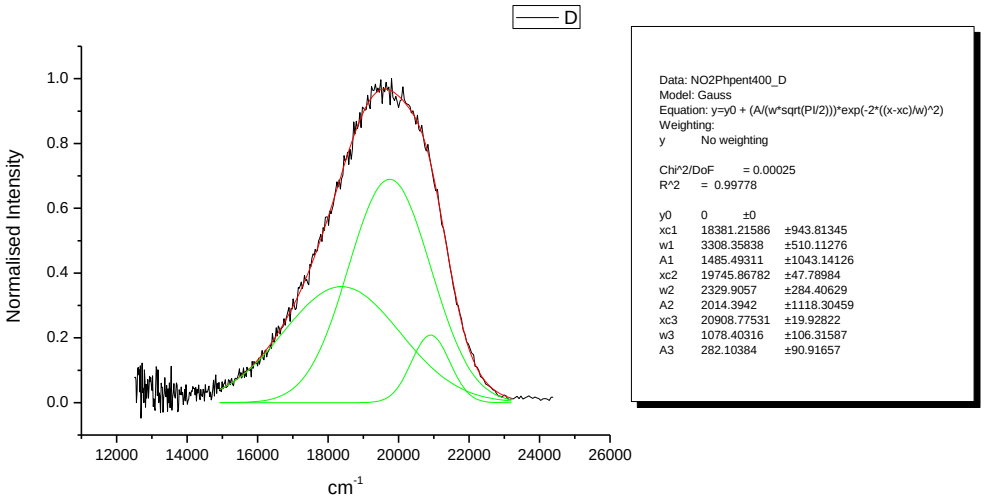

Figure 4.4.180. Gaussian model fit of the normalised fluorescence emission spectrum of **27** recorded in 1-octanol at 400 nm excitation.

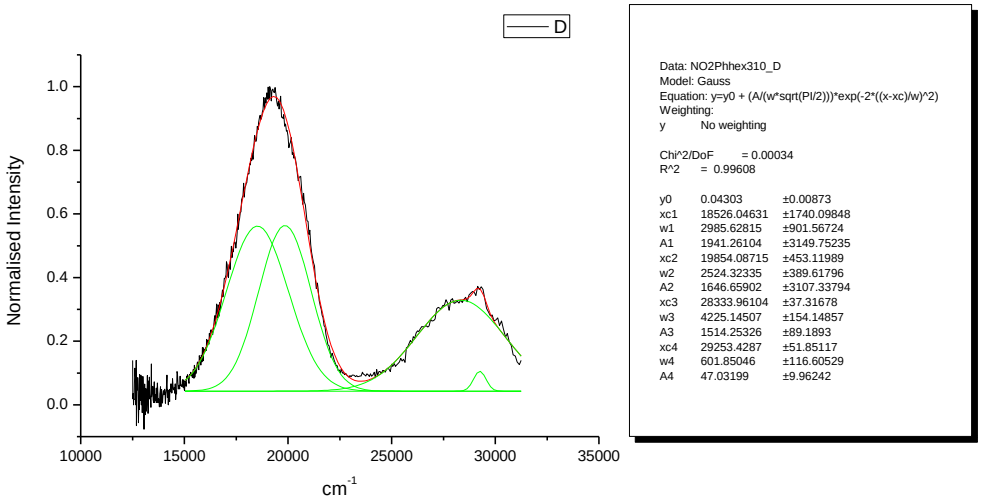

Figure 4.4.181. Gaussian model fit of the normalised fluorescence emission spectrum of **27** recorded in 1-hexanol at 310 nm excitation.

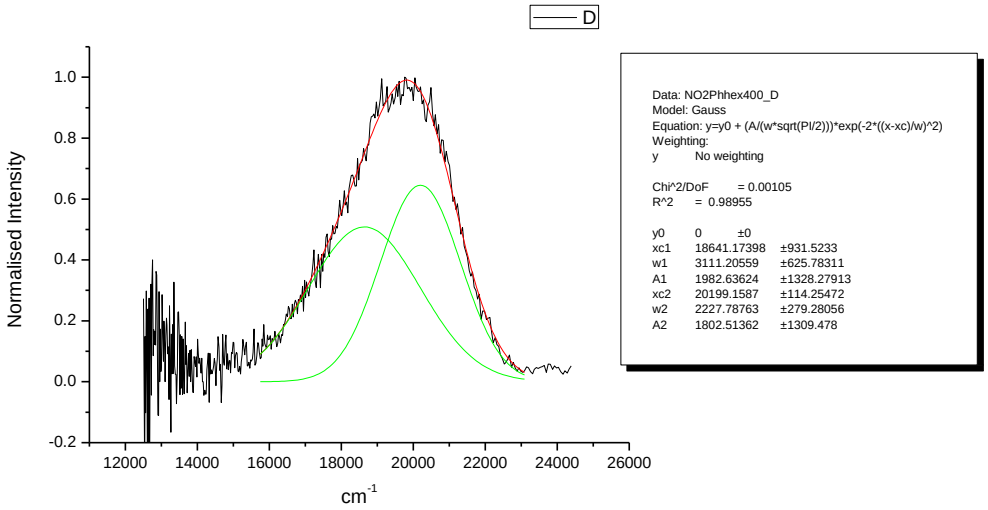

Figure 4.4.182. Gaussian model fit of the normalised fluorescence emission spectrum of **27** recorded in 1-hexanol at 400 nm excitation.

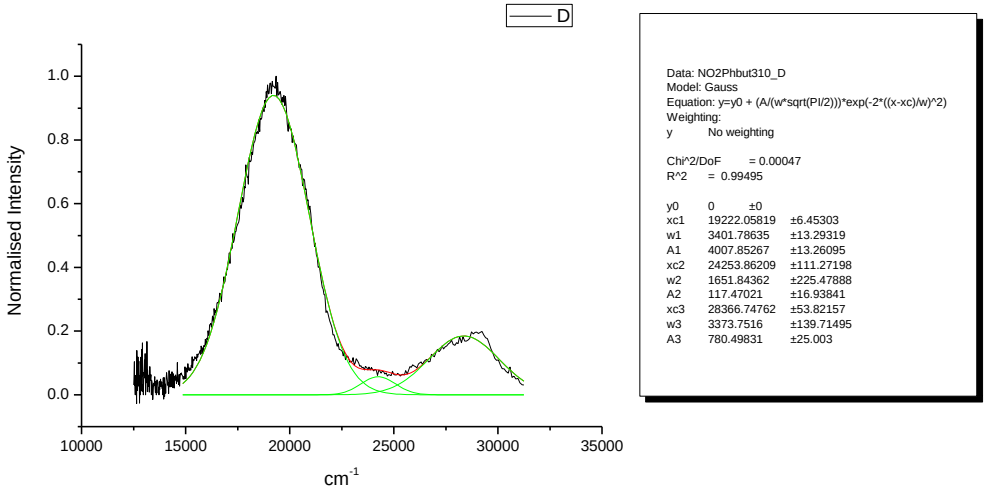

Figure 4.4.183. Gaussian model fit of the normalised fluorescence emission spectrum of **27** recorded in 1-butanol at 310 nm excitation.

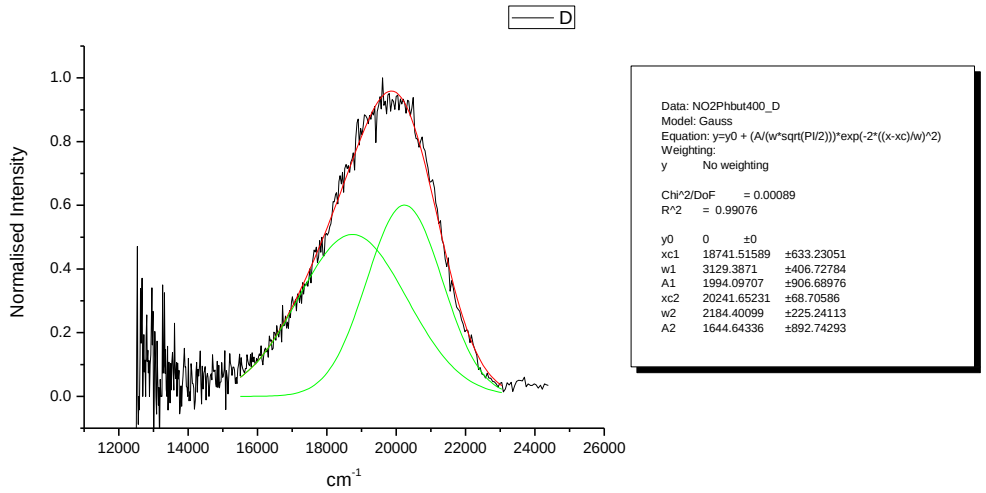

Figure 4.4.184. Gaussian model fit of the normalised fluorescence emission spectrum of **27** recorded in 1-butanol at 400 nm excitation.

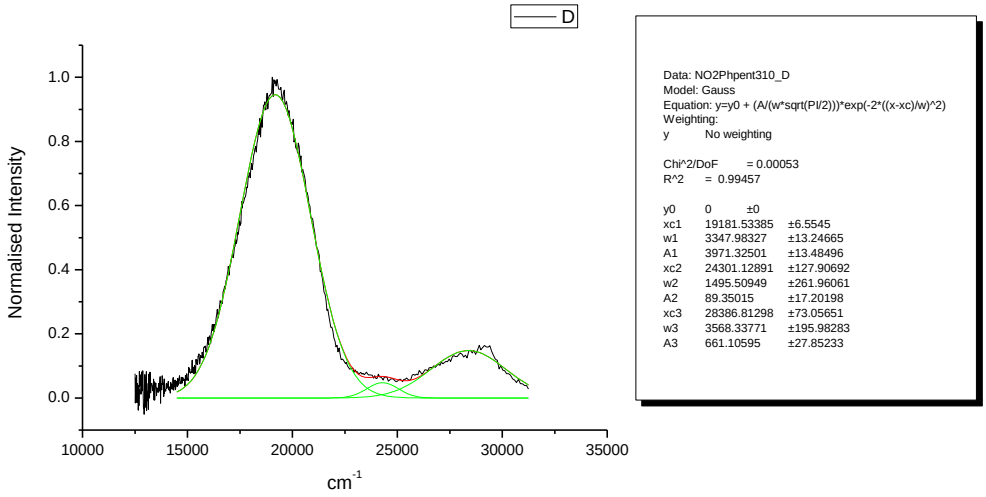

Figure 4.4.185. Gaussian model fit of the normalised fluorescence emission spectrum of **27** recorded in 1-pentanol at 310 nm excitation.

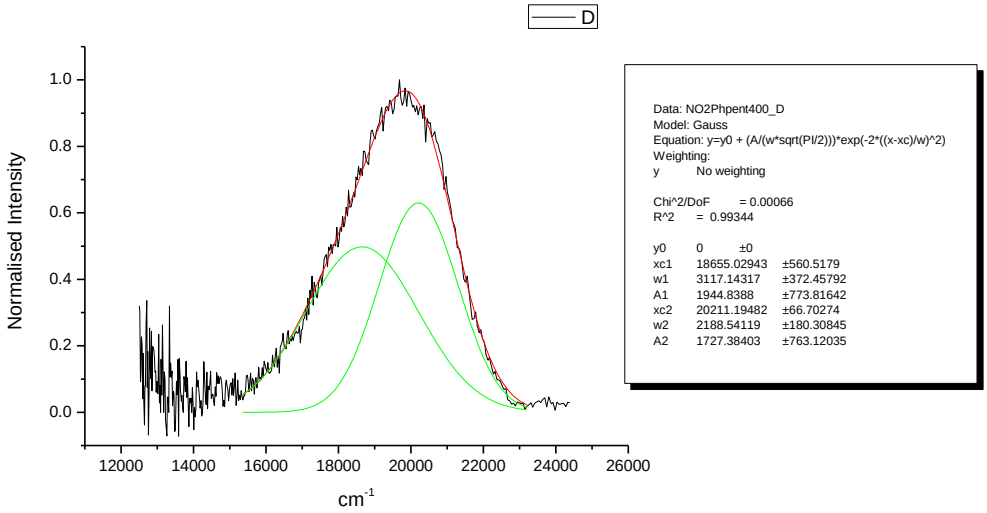

Figure 4.4.186. Gaussian model fit of the normalised fluorescence emission spectrum of **27** recorded in 1-pentanol at 400 nm excitation.

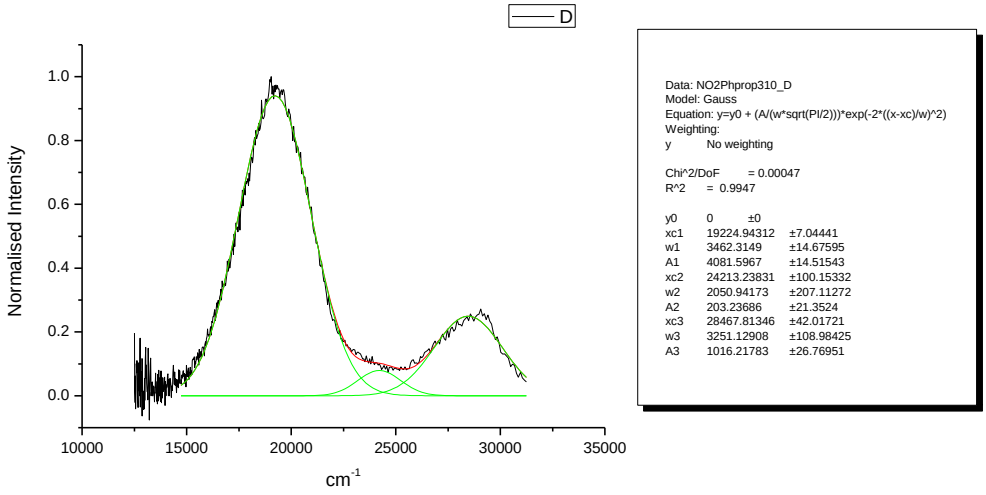

Figure 4.4.187. Gaussian model fit of the normalised fluorescence emission spectrum of **27** recorded in 1-propanol at 310 nm excitation.

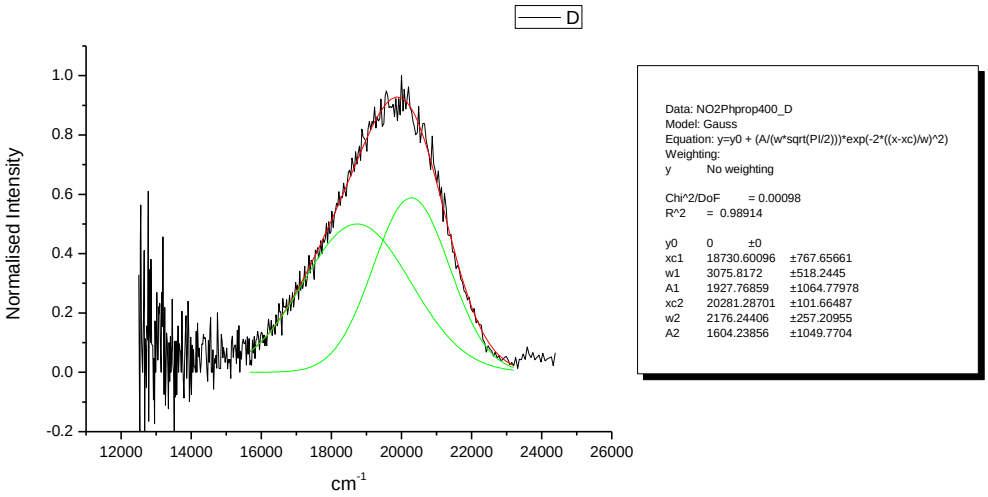

Figure 4.4.188. Gaussian model fit of the normalised fluorescence emission spectrum of **27** recorded in 1-propanol at 400 nm excitation.

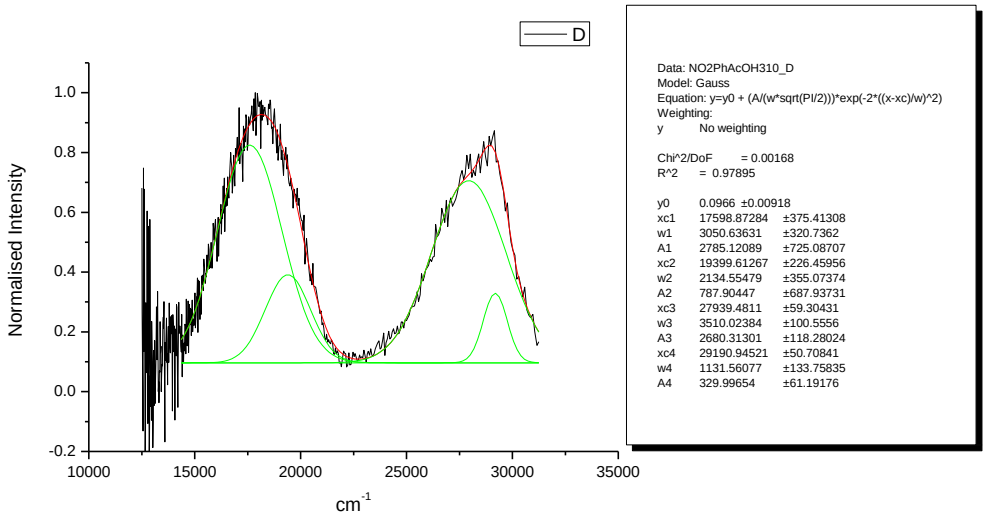

Figure 4.4.189. Gaussian model fit of the normalised fluorescence emission spectrum of **27** recorded in Acetic Acid at 310 nm excitation.

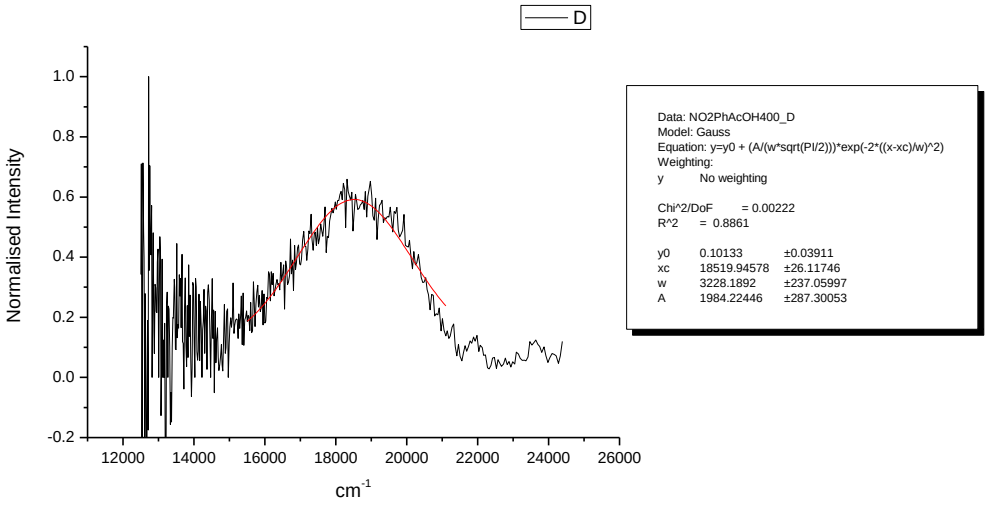

Figure 4.4.190. Gaussian model fit of the normalised fluorescence emission spectrum of **27** recorded in Acetic Acid at 400 nm excitation.

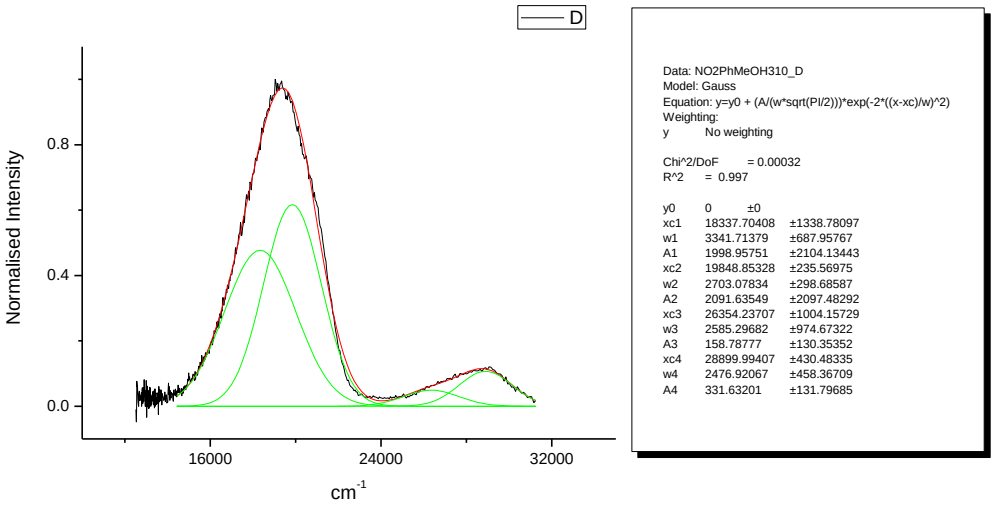

Figure 4.4.191. Gaussian model fit of the normalised fluorescence emission spectrum of **27** recorded in Methanol at 310 nm excitation.

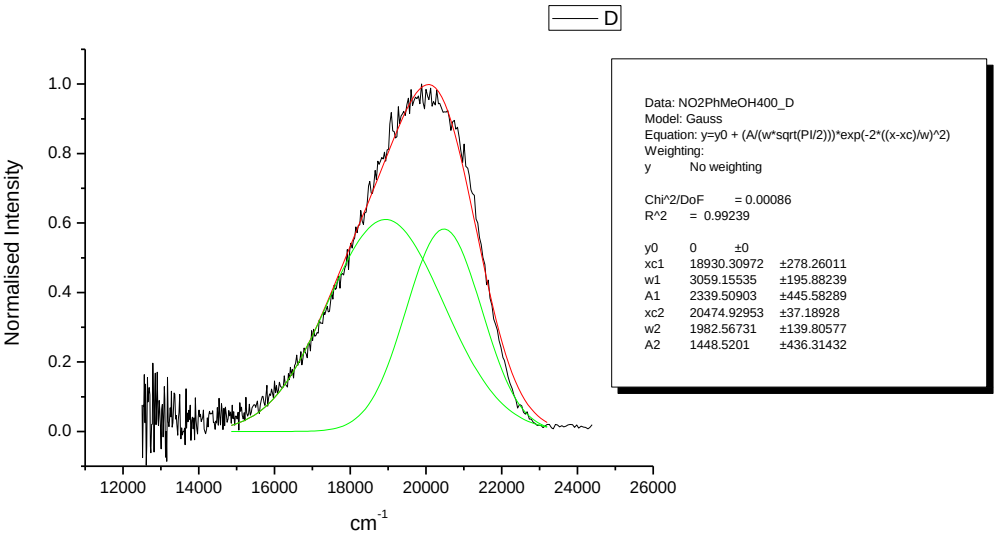

Figure 4.4.192. Gaussian model fit of the normalised fluorescence emission spectrum of **27** recorded in Methanol at 400 nm excitation.

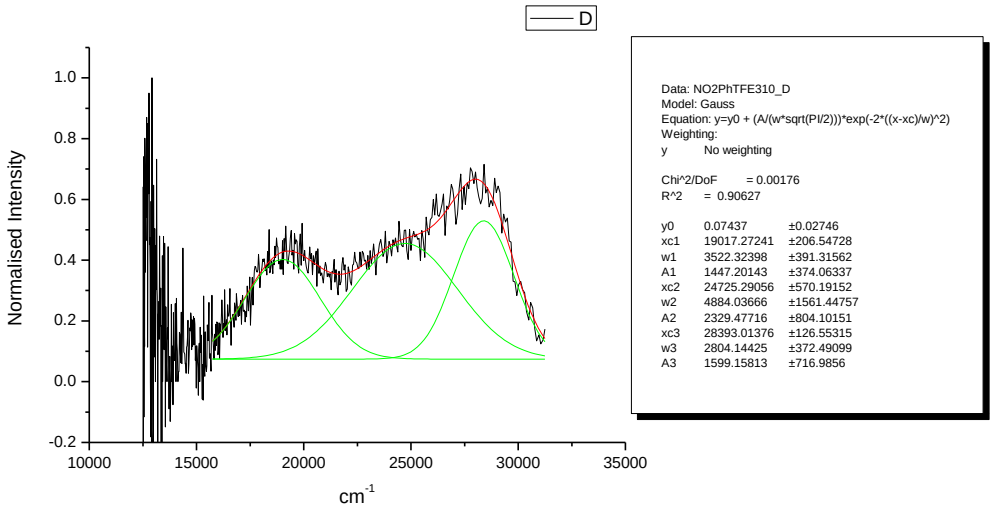

Figure 4.4.193. Gaussian model fit of the normalised fluorescence emission spectrum of **27** recorded in 2,2,2-trifluoroethanol at 310 nm excitation.

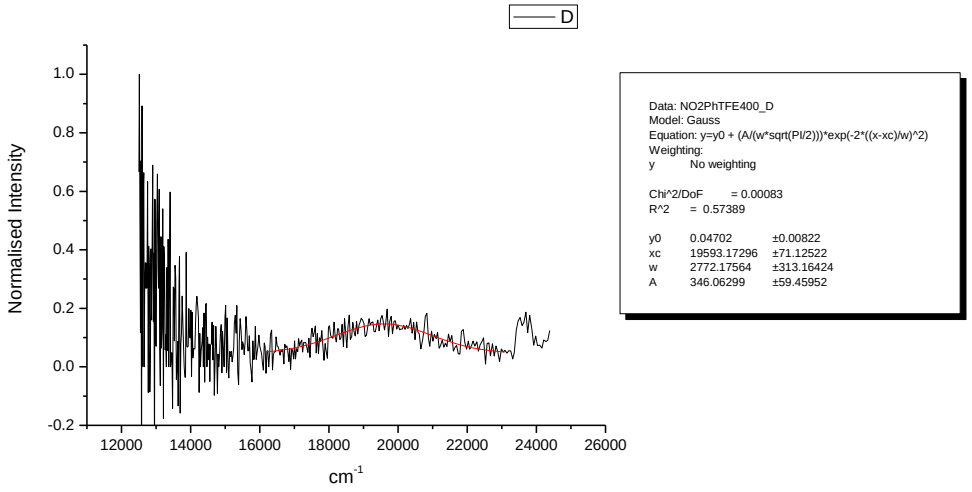

Figure 4.4.194. Gaussian model fit of the normalised fluorescence emission spectrum of **27** recorded in 2,2,2-trifluoroethanol at 400 nm excitation.

4.4.11 Fluorescence Excitation spectra.

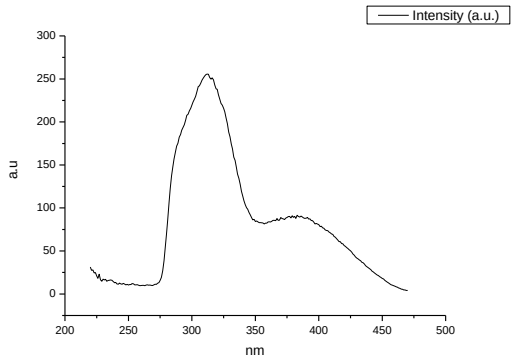

Figure 4.4.195. Fluorescence excitation spectrum of **27** recorded in Toluene with emission fixed at 480 nm.

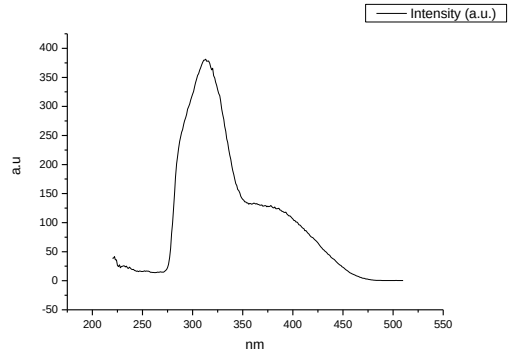

Figure 4.4.196. Fluorescence excitation spectrum of **27** recorded in Toluene with emission fixed at 520 nm.

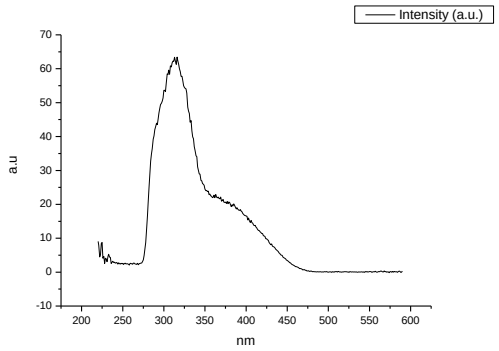

Figure 4.4.197. Fluorescence excitation spectrum of **27** recorded in Toluene with emission fixed at 600 nm.

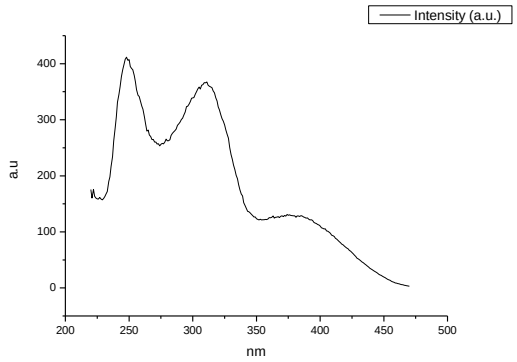

Figure 4.4.198. Fluorescence excitation spectrum of **27** recorded in 1,4-dioxane with emission fixed at 480 nm.

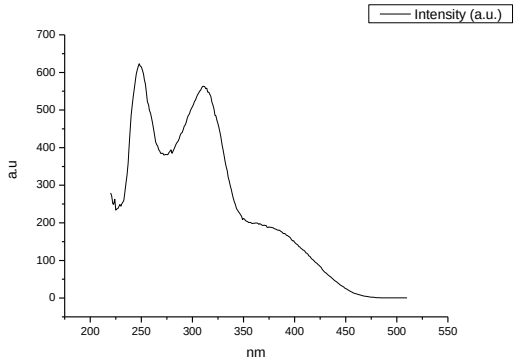

Figure 4.4.199. Fluorescence excitation spectrum of **27** recorded in 1,4-dioxane with emission fixed at 520 nm.

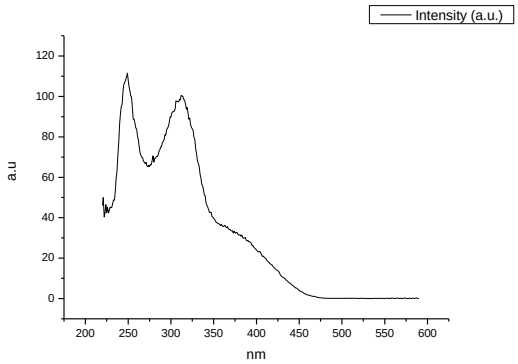

Figure 4.4.200. Fluorescence excitation spectrum of **27** recorded in 1,4-dioxane with emission fixed at 600 nm.

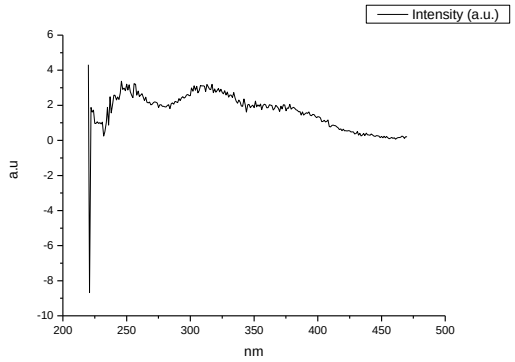

Figure 4.4.201. Fluorescence excitation spectrum of **27** recorded in Chloroform with emission fixed at 480 nm.

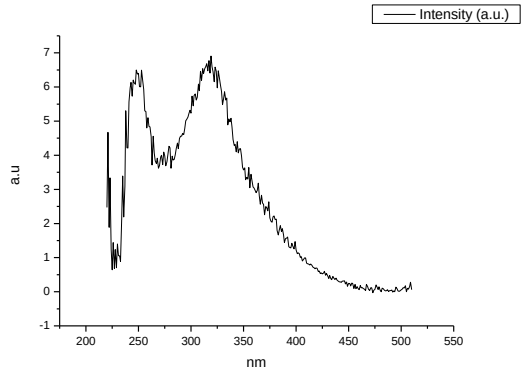

Figure 4.4.202. Fluorescence excitation spectrum of **27** recorded in Chloroform with emission fixed at 520 nm.

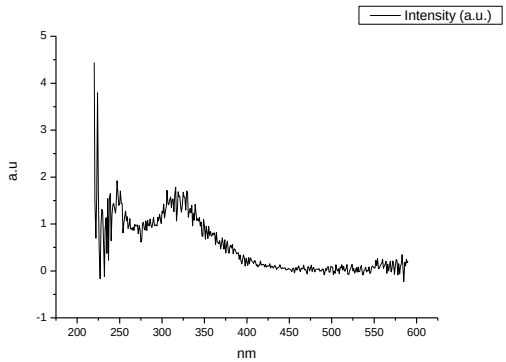

Figure 4.4.203. Fluorescence excitation spectrum of **27** recorded in Chloroform with emission fixed at 600 nm.

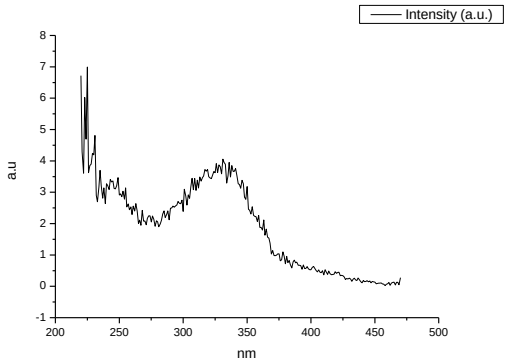

Figure 4.4.204. Fluorescence excitation spectrum of **27** recorded in Acetonitrile with emission fixed at 480 nm.

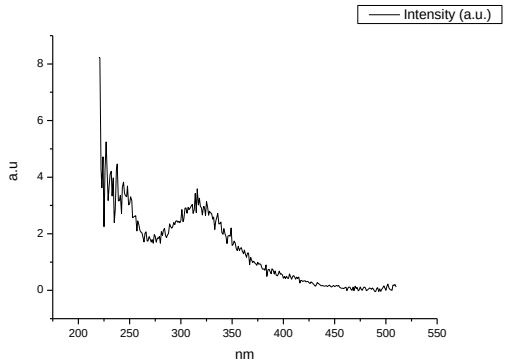

Figure 4.4.205. Fluorescence excitation spectrum of **27** recorded in Acetonitrile with emission fixed at 520 nm.

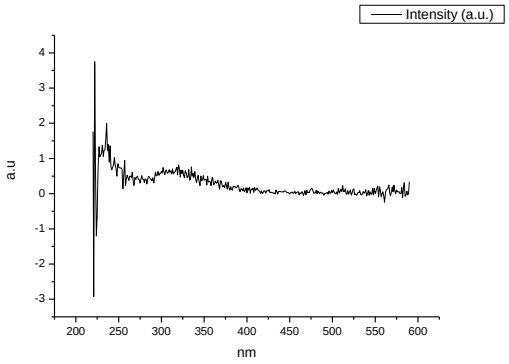

Figure 4.4.206. Fluorescence excitation spectrum of **27** recorded in Acetonitrile with emission fixed at 600 nm.

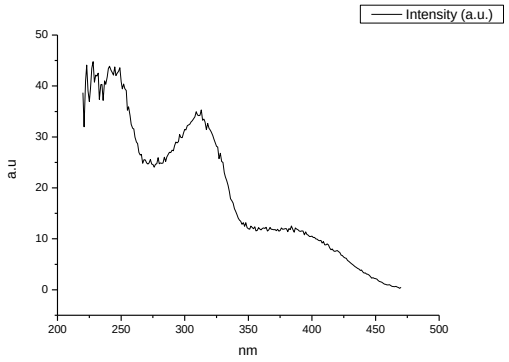

Figure 4.4.207. Fluorescence excitation spectrum of **27** recorded in 1-octanol with emission fixed at 480 nm.

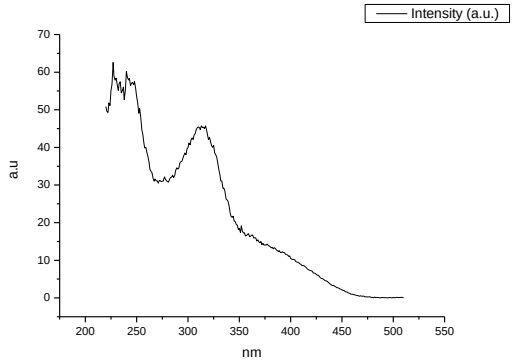

Figure 4.4.208. Fluorescence excitation spectrum of **27** recorded in 1-octanol with emission fixed at 520 nm.

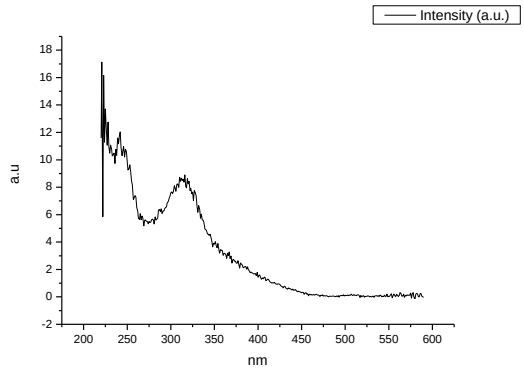

Figure 4.4.209. Fluorescence excitation spectrum of **27** recorded in 1-octanol with emission fixed at 600 nm.

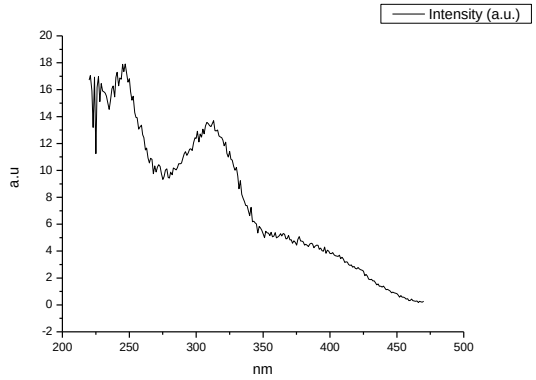

Figure 4.4.210. Fluorescence excitation spectrum of **27** recorded in 1-hexanol with emission fixed at 480 nm.

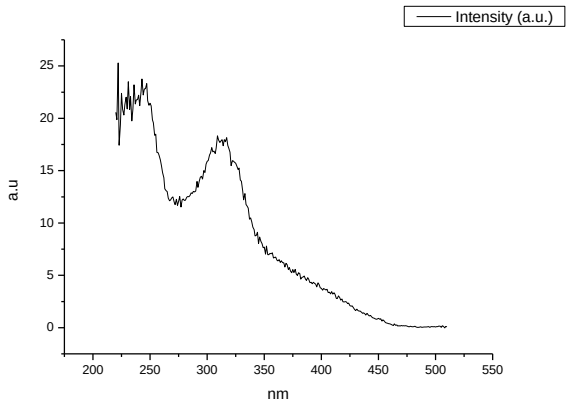

Figure 4.4.211. Fluorescence excitation spectrum of **27** recorded in 1-hexanol with emission fixed at 520 nm.

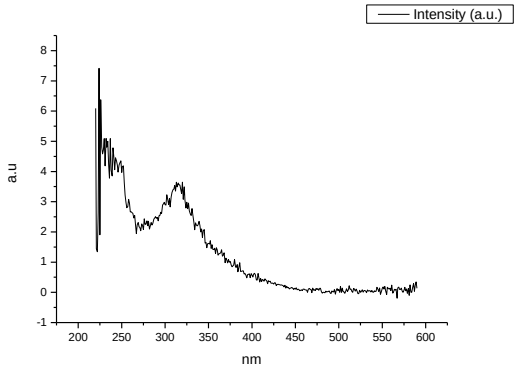

Figure 4.4.212. Fluorescence excitation spectrum of **27** recorded in 1-hexanol with emission fixed at 600 nm.

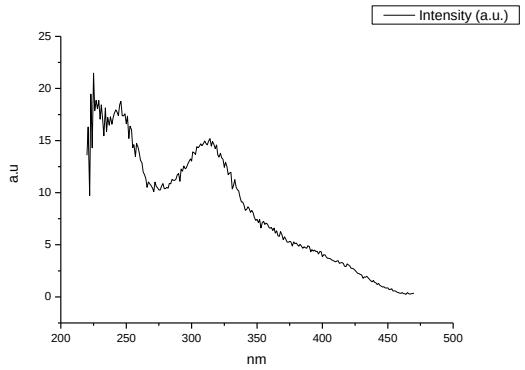

Figure 4.4.213. Fluorescence excitation spectrum of **27** recorded in 1-butanol with emission fixed at 480 nm.

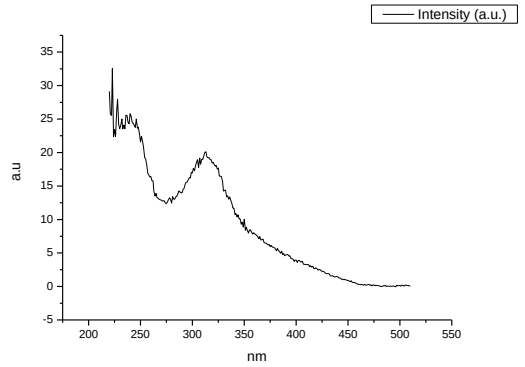

Figure 4.4.214. Fluorescence excitation spectrum of **27** recorded in 1-butanol with emission fixed at 520 nm.

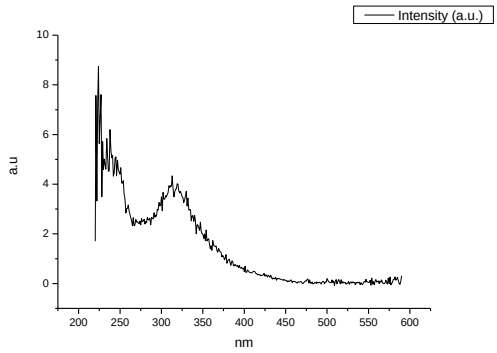

Figure 4.4.215. Fluorescence excitation spectrum of **27** recorded in 1-butanol with emission fixed at 600 nm.

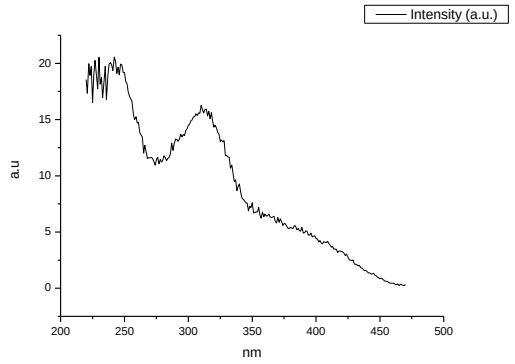

Figure 4.4.216. Fluorescence excitation spectrum of **27** recorded in 1-pentanol with emission fixed at 480 nm.

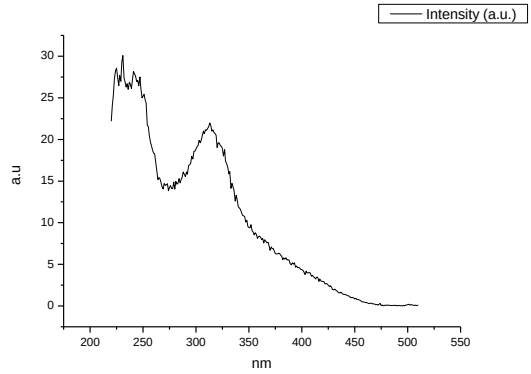

Figure 4.4.217. Fluorescence excitation spectrum of **27** recorded in 1-pentanol with emission fixed at 520 nm.

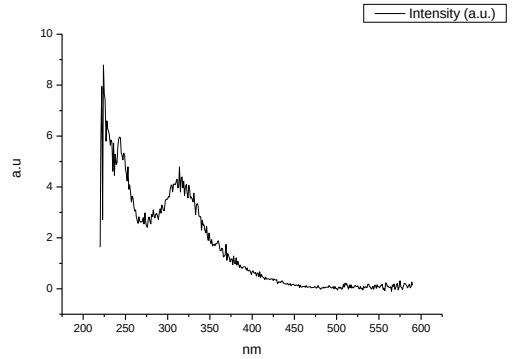

Figure 4.4.218. Fluorescence excitation spectrum of **27** recorded in 1-pentanol with emission fixed at 600 nm.

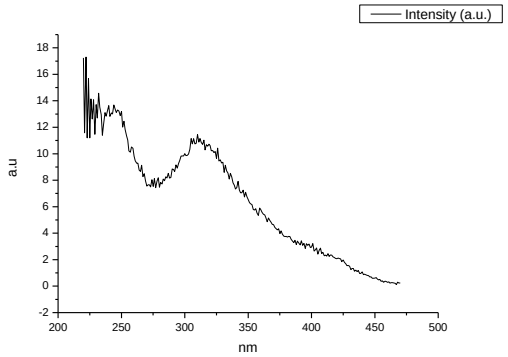

Figure 4.4.219. Fluorescence excitation spectrum of **27** recorded in 1-propanol with emission fixed at 480 nm.

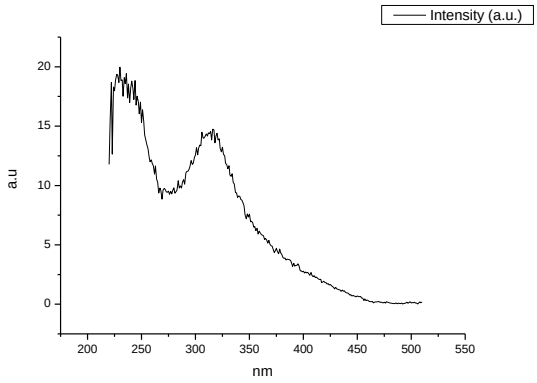

Figure 4.4.220. Fluorescence excitation spectrum of **27** recorded in 1-propanol with emission fixed at 520 nm.

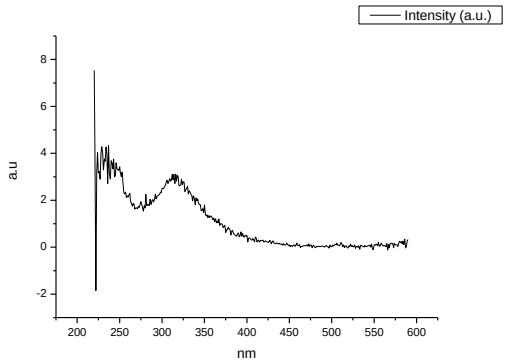

Figure 4.4.221. Fluorescence excitation spectrum of **27** recorded in 1-propanol with emission fixed at 600 nm.

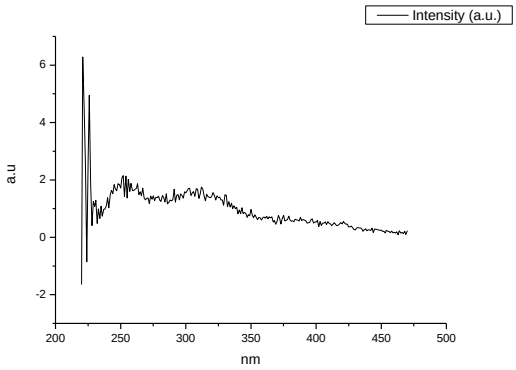

Figure 4.4.222. Fluorescence excitation spectrum of **27** recorded in Acetic Acid with emission fixed at 480 nm.

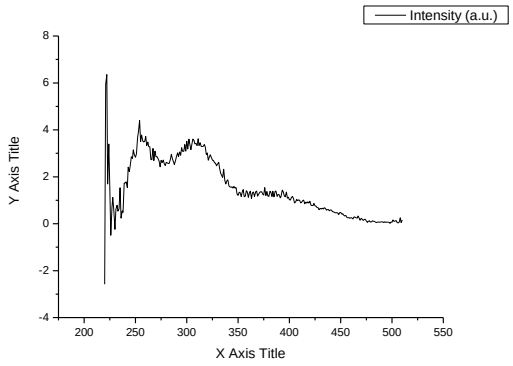

Figure 4.4.223. Fluorescence excitation spectrum of **27** recorded in Acetic Acid with emission fixed at 520 nm.

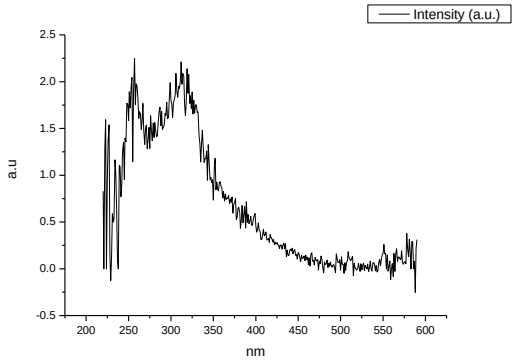

Figure 4.4.224. Fluorescence excitation spectrum of **27** recorded in Acetic Acid with emission fixed at 600 nm.

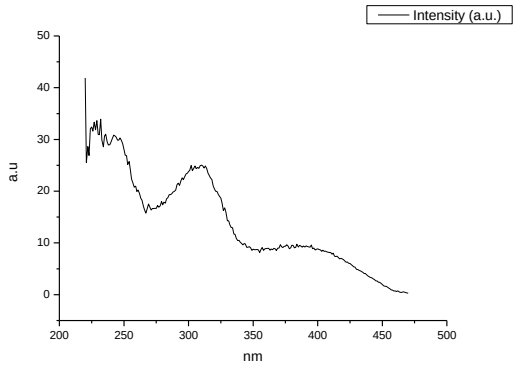

Figure 4.4.225. Fluorescence excitation spectrum of **27** recorded in Methanol with emission fixed at 480 nm.

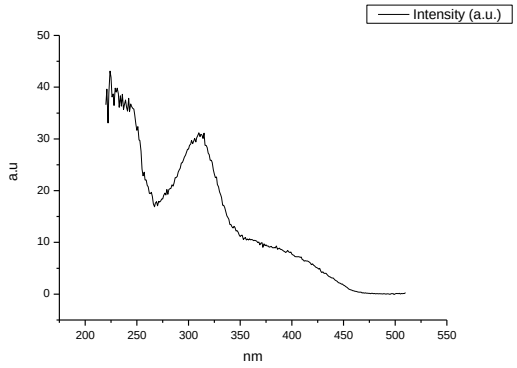

Figure 4.4.226. Fluorescence excitation spectrum of **27** recorded in Methanol with emission fixed at 520 nm.

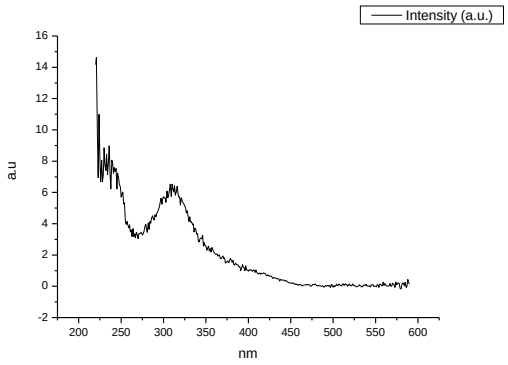

Figure 4.4.227. Fluorescence excitation spectrum of **27** recorded in Methanol with emission fixed at 600 nm.

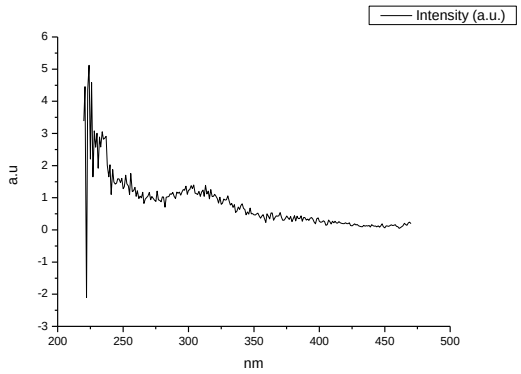

Figure 4.4.228. Fluorescence excitation spectrum of **27** recorded in 2,2,2-trifluoroethanol with emission fixed at 480 nm.

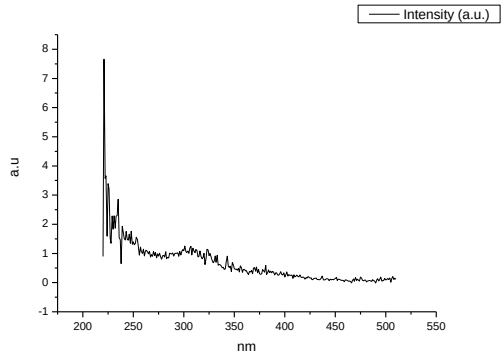

Figure 4.4.229. Fluorescence excitation spectrum of **27** recorded in 2,2,2-trifluoroethanol with emission fixed at 520 nm.

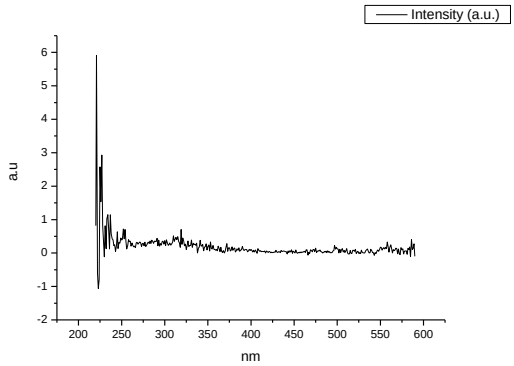

Figure 4.4.230. Fluorescence excitation spectrum of **27** recorded in 2,2,2-trifluoroethanol with emission fixed at 600 nm.